PARIS 1980

7th International Congress on the Chemistry of Cement

VOLUME I
PRINCIPAL REPORTS

PARIS 1980

7th International Congress on the Chemistry of Cement

VOLUME I
PRINCIPAL REPORTS

PARIS 1980 [June 30 – July 4]

EDITIONS SEPTIMA - 14, rue Falguière,
75015 PARIS (France).

Printed in France 1980.

CONTENTS

* First of all, the pagination consists of a roman numeral corresponding to the theme number; it is followed by the number of the appropriate sub-theme, then by the page number in the interior of the principal report; therefore, each one of them starts on page 1, except for sub-themes 1, where all the principal reports begin on page 3.

* This report, received too late, will be published in the volume « Communications ».

SUB-THEME I - 1

Influence of the nature and preparation of raw materials on the reactivity of raw mix

R. BUCCHI,
Italcementi spa, ITALIA

1. INTRODUCTION.

It is said that a cement factory arises where a market of such a product exists and where deposits of raw materials suitable for production are available. In the practice the first condition always (or almost always) keeps its strictness whereas the second one is often compromised by other needs till to be reduced to the banal requisite to merely give the four fundamental oxides in the proportions demanded.

However experience shows that nature and characteristics of rocks and, generally, of the materials used for the raw meal involve important consequences on investments, operating costs and quality of the cement produced.

It seems therefore reasonable that the cement industry devotes grater attention to the study of raw materials and the methods used for their preparation.

2. REACTIVITY AND BURNABILITY.

2.1 Definitions. The raw mix is a system consisting of several components in finely dispersed phases. It transforms into clinker through a series of reactions between about 400° and 1450°C. Its reactivity is defined by the overall rate of these reactions at the temperatures completing them in practically suitable times. So as is defined with reference to a given mix, the reactivity prescinds from every quality attribute of the obtained clinker. On the contrary it has a considerable influence on the energy consumption of the process and the capacity of the plant.

The concept of reactivity differs from that of burnability, as the derivative of a function differs from the function itself (or from the value which the latter takes for given values of the variables).

2.2 Expression of CaO in the mix during burning. Since the fundamental constituents of clinker are all calcium compounds, the transformed CaO gives a suitable measure of the advancement of the overall process. The amount Γ of CaO, in a given form of combination present at any moment and temperature, can be expressed in different terms (the formulas without mark represent concentrations of the corresponding chemical species in the raw meal, in homogeneous unities of mass %):

- between about 400°C and 1000°C, as degree of decarbonation φ (1, 2):

$$\varphi = 1 - \frac{CO_2'}{CO_2}\ , \text{undim.} \qquad [1]$$

where CO_2' is the mass % of CO_2 in the transforming mix;

- between about 700°C and 1450°C, as free CaO:
  - CaO_f, in the l.o.i.-free mix, mass %;
  - F_{CaO_f}, fraction of CaO_f with respect to total CaO_t ($F_{CaO_f} = CaO_f/CaO_t$), undim.;
  - S_{CaO_f}, fraction of CaO_f with respect to the saturation CaO calculated according to Lea and Parker (see TAB. II), undim.;
  - H_{CaO_f}, fraction of CaO_f with respect to the hydraulic factors ($H_{CaO_f} = CaO_f/SiO_2+Al_2O_3+Fe_2O_3$), undim.;
- between about 400°C and 1450°C, as burning degree α (2):

$$\alpha = 1 - \frac{1.27\,CO_2' + 0.7\,SO_3' + CaO_f}{CaO_t}\ , \text{undim} \qquad [2]$$

where CO_2' and SO_3' are the mass % of CO_2 and SO_3 in the transforming mix, in unities homogeneous with those of CaO_f and CaO_t. (The term $0.7\,SO_3'$ must be neglected when $SO_3 \leq K_2O + Na_2O$, in molar concentrations).

Only α, φ and F_{CaO_f} versus the processing time and temperature correctly express a measure of the burnability of the mix. Their derivatives versus time (or, on the average, the ratio of the finite variations of functions to the time intervals when these variations occur) measure the reactivity, for given constant temperatures. The quantities S_{CaO_f} and H_{CaO_f}, considered by Longuet & Courtault (3) and Pfrunder and Wickert (4) respectively, concern in some way the burnability of the components of the mix rather than that of the mix itself.

2.3 Course of the CaO transformation.

2.3.1 $\alpha = f(t, \theta)$ describes the CaO transformation versus the temperature t and the reaction time θ. It is represented, in the space $(+\alpha; +t; +\theta)$, by a curved surface whose intersections by planes almost parallel to $(\alpha; \theta)$ for $t_i \simeq$ const. and to $(\alpha; t)$ for $\theta_i \simeq$ const. (pseudo-isotherms and pseudo-isochrones of reaction respectively (*) are experimentally determined.

2.3.2 The trend deducible from the literature data (5, 6) of a pseudo-isochrone is schematically represented in FIG. 1. The reaction velocity increases in two temperature ranges:

- between t_1 and t_2 (about 850°C and 950°C) when K_p of the $CaCO_3$ dissociation sharply increases (7). The first free CaO appears

(*) Actually, in practice, these planes result not strictly t = const. or θ = const., but more or less inclined with respect to $(\alpha; \theta)$ or $(\alpha; t)$ because of the variability (with t_i) of the time and the temperatures reached to bring a sample to the test temperature t_i.

in this interval whereas $CaCO_3$ has already disappeared at t_2 (8);

- between t_3 and t_4 (about 1250°C and 1300°C) where the C_3S formation starts.

The values t_1, t_2, t_3 and t_4 and those of the corresponding ordinates are typical of the reactive properties of the mix.

2.3.3 The portion of pseudo-isochrone $\varphi = f(t)$ for $\theta_i \simeq$ const. between about 400°C and t_2 is called decarbonation function (9). FIG. 2 shows some examples derived from Vogel's (2) and Ritzman's (9) papers. These functions, characterizing the decarbonation and the first reactions in the solid phase,

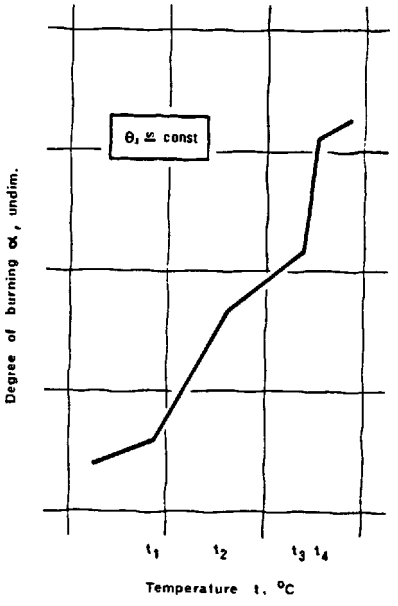

FIG. 1 .PSEUDO-ISOCHRONE OF REACTION.

are greatly important in the study of the calcining processes outside the kiln (10).

2.3.4 The portion of pseudo-isochrone between t_2 and about 1450°C, expressed by $CaO_f = f(t, \theta)$ for $\theta \simeq$ const., is exponential:

$$CaO_f = e^{a-bt} (\theta_i \simeq \text{const.}), \text{ mass \%} \qquad [3]$$

and it has two different trends (different couples of the constants a and b) in the t_2 - t_3 and t_3 - 1450°C ranges. These trends characterize the diffusion processes in the solid phase and in the presence of the liquid phase, respectively. FIGS. 3 and 4 show the functions of four typical mixes of which the literature (11, 12) and other sources (13, 14) give the necessary number of couples of values (CaO_f, t_i).
TAB. I summarizes the values of a, b and t_3.

2.3.5 The portion of pseudo-isotherm between t_2 and about 1450°C, expressed by $CaO_f = f(\theta, t)$ for $t \simeq$ const., is a logarithmic function (4, 13):

$$CaO_f = k - h \ln \theta \quad (t_i \simeq \text{const.}), \text{ mass \%} \qquad [4]$$

(with constant k and h), at least in the $0' \leq \theta \leq 30'$ range for t_i = 1380°C (4). FIG. 5 shows some examples (12, 13).

2.4 Measure of burnability. It is expressed by one

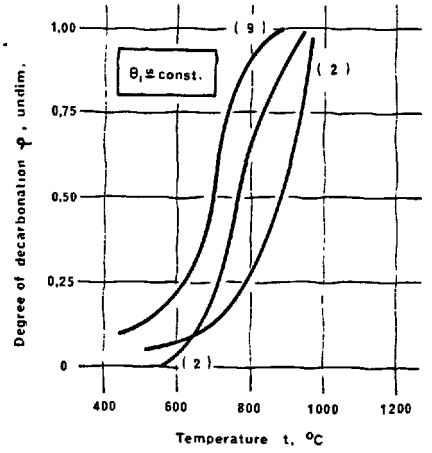

FIG. 2 .FUNCTIONS OF DECARBONATION. AFTER VOGEL(2)AND RITZMANN (9).

of the following quantities (determined under strictly reproducible conditions):

- measure of CaO_f of a pseudo-isochrone at given t_i. Examples: 30' and 1300°C or 1400°C (15); 45' and 1450°C (16); 42' and 1450°C (13); 15' and 1450°C (3); 15' and 1370°C (4); 15' and 1400°C (17); a.s.o. Increasing values of CaO_f correspond to decreasing reactivities (*);
- measure of θ_i of a pseudo-isotherm, necessary so as CaO_f becomes equal to or lower than a fixed value. Example: θ_i for $CaO_f \leq 2\%$ at 1350°C (18). Increasing values of θ_i correspond to decreasing reactivities (*);

(*) Therefore this quantity expresses more precisely a reluctance to burning (13).

factor K_{su}. Sulikowski (11) characterizes the burnability as the ratio of CaO_t to the maximum of $CaO_f = f(t)$ in the 700°C ≤ t ≤ 1400°C range, θ being of few seconds:

$$K_{su} = \frac{CaO_t}{CaO_f max.}, \text{ undim.} \qquad [5]$$

The measure is based on the thesis that the maximum quantity of CaO_f released during the process should be the lower the more reactive the mix. K_{su}, always > 1, increases as the reactivity rises;

factor AC. Blaise et Al. (12) rightly think that the evaluation of the burnability demands

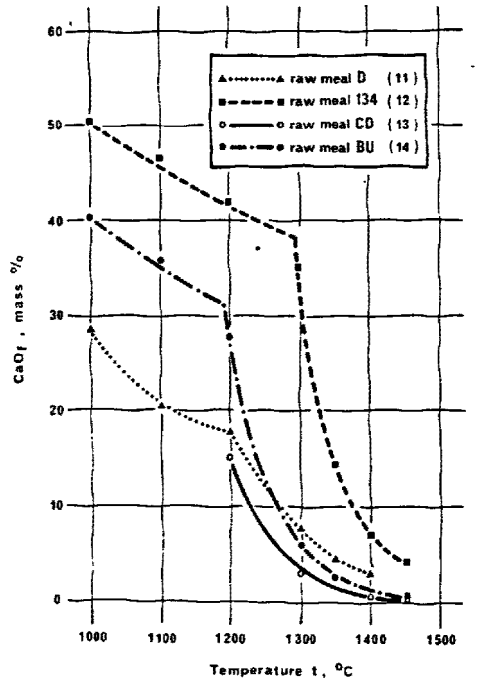

FIG. 3 . FUNCTIONS $CaO_f = e^{a-bt}$ IN LINEAR CO-ORDINATES.

a quantitative expression related to the CaOf= f (t,θ) trend in the overall 1000° et 1450°C range. This requirement is satisfied by the ratio of a constant (=600) reference surface (CaOf; t) area to the one integral (*) of the abo-

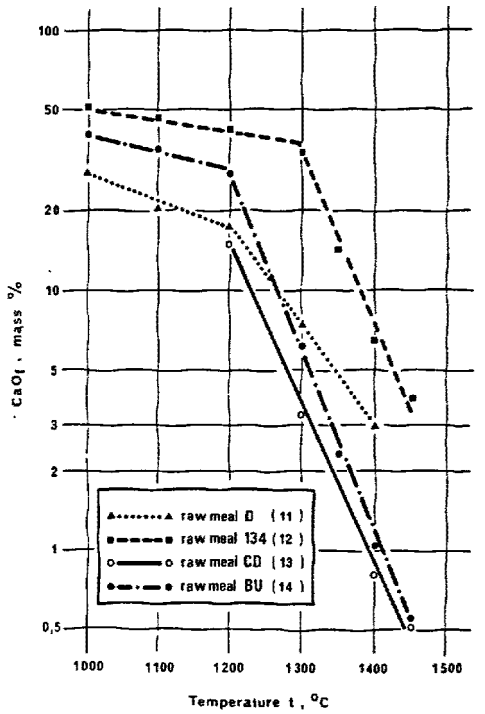

FIG. 4 . FUNCTIONS $CaO_f = e^{a-bt}$ IN SEMILOGARITHMIC CO-ORDINATES.

ve function for fixed θ_i in the aforesaid temperature range:

$$AC = \frac{600}{C_0+2C_1+2C_2+3C_3+4C_4+4C_5+2C_6}, \text{undim.} \qquad [6]$$

where $C_0 \ldots C_6$ are the values of CaO_f at seven different increasing t_1, for $\theta_0 = 20'$, $\theta_1 = 20' + 20' \ldots \theta_6 = (6 \times 20)' + 20'$ (**). The reproduci-

TAB. I. VALUES OF THE CONSTANTS a, b, t3 OF $CaO_f = e^{a-bt}$ (θ_i ≅ CONST.) OF THE FOUR RAW MEALS OF FIG. 3 AND FIG. 4.

raw mix	intervals of t °C	θ_i min.	a	b (x 10^{-2})	t3	ref.
D	1000÷1300 1300÷1400	0	7.56 13.87	- 0.412 - 0.916	1300	(11)
134	1000÷1300 1300÷1450	(*)	5.14 22.88	- 0.120 - 1.493	1300	(12)
CD	1200÷1450	42'	19.21	- 1.380	-	(13)
BU	1000÷1200 1200÷1450	(*)	5.51 22.67	- 0.178 - 1.611	1200	(14)
(*) see factor AC in paragraph 2.4.						

(*) Suitably enlarged for the highest temperatures.

(**) The times necessary to pass from each level of temperature to the next higher one are added to these times. Consequently a $CaO_f = f(t,\theta)$ quite different from both the isochrones and the isotherms is obviously used.

bility of the measure is ensured by strictly controlled working modes.

The inadequancy of the first three methods, expressing the measure of the burnability by means of the co-ordinates of an only point of $CaO_f = f(t, \theta)$ is obvious. On the contrary, the factor AC seems to be more interesting in this connection. It has the advantage of considering the overall course of the CaO combination in the presence of liquid, the trend of the reactions in the solid phase as well as (by the value CO) the extreme portion of the decarbonation function.

It is also clear that the examined measures of burnability give results whose significance, method by method, does not exceed that of the relative comparison, since the technological process develops under quite different conditions from the laboratory ones and different from one another depending on the type of plant.

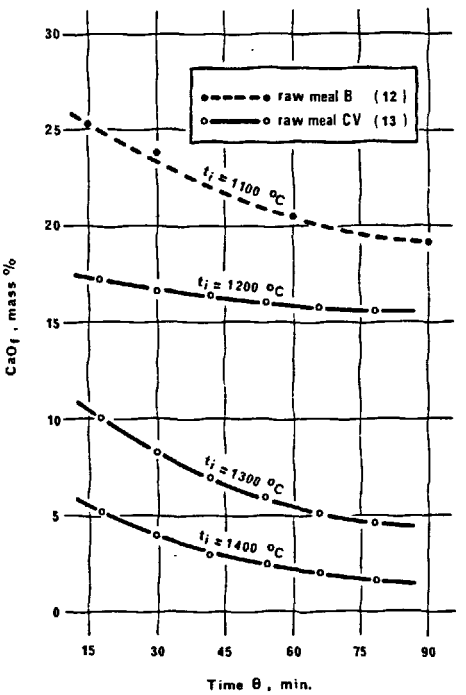

FIG. 5 . FUNCTIONS $CaO_f = k - h \cdot \ln \theta$ IN LINEAR CO-ORDINATES.

2.5 Evaluations of the burnability by calculation. At least three methods allow the burnability of the mix to be calculated (in the absence of mineralizers and other specific additions), by its chemical, mineralogical and physical parameters. These procedures are important since they explain, to some extent, the influence of the different chemical and physical parameters on the burning process.

2.5.1 Ludwig and Ruckensteiner (18, 19, 20) showed that the practical burnability (*) B_{pr} of a mix, determined as time of reaction at 1350 °C needed to reduce the CaO_f content to a value ≤ 2%:

$$\theta_{1350\,°C} \geq e^{\frac{k-2}{h}} \quad , \text{min.} \qquad [7]$$

coincides (correlation coefficient r = 0.985 for 12 mixes) with the value of the theoretical burnability, B_{th}, so called since it can be calculated from:

$$B_{th} = 55.5 + 11.9 H_{k90} + 1.56 (K_{st}III - 90)^2 - 0.43 (SA)^2, \text{ min.} \qquad [8]$$

This equation is obviously valid for $K_{st}III \geq 90$. It has been extended to the temperatures of 1375 °C and 1400 °C in a following paper (21).

The significances of the symbols are:

H_{R90}, "heterogeneity > 90 μm", measured as the amount of raw meal retained on 90 μm sieve lessened of the quantity of multimineral aggregations of elements < 90 μm present in this oversize, mass % of the mix;

SA, amount of liquid phase at 1350 °C after Dahl (22), mass % of the l.o.i.-free mix;

$K_{st}III$, Kalkstandard after Spohn et Al. (23), undim.

The hypothesis on which the determination of H_{R90} is based - namely that the ratio of CaO to hydraulic factors in the multimineral aggregations > 90 μm is equal to the one in the mix - may not occur in all cases.

2.5.2 Kock et Al. (17) determined the correlation between burnability (CaO_f for t_i = 1400 °C and θ_i = 15') of 168 industrial mixes (raw materials of 15 different deposits) and 10 parameters resulted significant out of 15 examined. From a 3rd order-regression it results (correlation coefficient r = 0.949):

$$CaO_{f\,1400\,°C}^{15'} = \frac{0.022y - 1 - \sqrt{(0.022y-1)^2 + 0.0188y^2}}{0.008y} + 5, \quad \text{mass \%} \qquad [9]$$

$$y = y_{ref.} + \sum_{i=1}^{10} a_i x_i \quad , \text{mass \%} \qquad [10]$$

(*) "Practical" means "experimental", without any reference to the technological process.

$$y_{ref.} = \frac{CaO_{ref.} - 5}{-0.004(CaO_{ref.}-5)^2 + 0.022(CaO_{ref.}-5) + 1.174}$$, mass % [11]

where:

$CaO_{ref.}$ = value of reference CaO_f, obtained by burning any mix of the studied raw materials at 1400°C and 15', provided it has values of the parameters within defined limits;

x_i = differences between the value of each parameters and the value of the same for the reference mix;

a_i = (constant) coefficients of x_i defining the regression.

TAB. II. PARAMETERS OF COMPOSITION OF THE RAW MEAL AND CLINKER.

symbol	parameter	denomination	ref.
OG	2.8S+1.65A+0.35F	max. combinable CaO after Guttmann and Gille	(35)
SP	2.8S+1.1A+0.70F	max. combinable CaO after Spohn	(36)
LP	2.8S+1.18A+0.65F	max. combinable CaO after Lea and Parker	(37)
BO	% of C_3S, C_2S, C_3A (C_2F) and C_4AF	"potential composition" after Bogue	(38)
SA	% of liquid at t_i °C	"liquid phase" after Dahl "diagrams of clinkerization"	(22) (39)
SM	S : (A+F)	silica modulu	(40)
TM	A : F	iron modulus	(41)
CM	C*: S	calcare modulus	(35)
MSO_3	$\bar{S}$: 0.85 $\bar{K}$	sulphate modulus	(42)

NOTES. S,A,F,C,$\bar{S}$ and $\bar{K}$ are mass % of SiO_2, Al_2O_3, Fe_2O_3, CaO, SO_3 and $K_2O + Na_2O$ equiv. respectively in the l.o.i.-free raw meal (or in clinker).
C* is mass % of CaO in the l.o.i.-free raw meal (or in clinker), combined in silicates.

The limits of the variables within which the correlation is valid are stated [9].

2.5.3 Christensen (24) reports an empiric relation enabling $CaO^{30'}_{f\,1400°C}$ to be calculated versus the chemical composition, as well as the content in particles of calcite > 125 μm and quartz and flint > 44 μm. This relation is consistent with Ludwig and Ruckensteiner's.

3. CHEMICAL COMPOSITION.

3.1 Composition in raw materials. The mass quantities of n raw materials, having independent chemical composition (*), necessary for the mass unit of raw meal are solutions of linear systems of n simultaneous equations expressing the n-1 conditions of chemical composition assigned to the mix. The methods of algebraic solution, among which (25, 26, 27, 28, 29) and the graphic procedures, out of which Fenaroli's (30, 31, 32) and Glauser's (33) ones are reminded, are based on this principle. A method of optimized solution (for the minimum consumption of fuel for burning) was developed by Xirokostas and Zoppas (34).

3.2 Composition in oxides. The chemical composition of the mix is defined by assigned values of one or more characteristic parameters (TAB. II) suitably chosen on the basis of the composition of the available raw materials.

3.2.1 In the system C - A - S - F, the compositions of the plane C_3S - C_3A - C_4AF (the latter expressed numerically as $C_3A + CF$), contain GG mass % of CaO. GG is fully combinable only under conditions of equilibrium cooling ensuring a complete reaction between free CaO and liquid during the cooling itself. Therefore GG is a limit practically unattainable in any case.
An identical situation occurs for all the BO compositions without C_2S.

According to Spohn (36) SP is the maximum amount (mass %) of CaO combinable in the clinker cooled not in equilibrium. The straight line 2.8 S + 1.1 A - C = 0 joins C_3S with (C_2A) in the plane C - A - S and it is called Wetzel line (43) (**). In the space C - A - S - F, the plane 2.8 S + 1.1 A + 0.7 F - C = 0 contains C_3S, (C_2A) and C_4AF (this time expressed numerically as $C_2A + C_2F$). Kühl (44, 45) defined Kalkstandard, ($K_{st}l$), as the CaO : SP ratio (of a clinker or a raw meal). LP is the maximum quantity of CaO combinable in the clinker cooled not in equilibrium, according to Lea and Parker (37). In the space C - A -

(*) The independence of chemical composition of any raw material (with respect to the compositions of any number of others) is verified by the non-identity condition between suitable ratios of % of oxides expressing the chemical analysis and the homologous ratios of all the other raw materials, including those obtainable by addition or subtraction from one another.
(**) This line is near (but does not coincide with) the line joining C_3S to point Z (Z = invariant at 1470°C among liquid, CaO, C_3S and C_3A, having composition 54.8% CaO, 22.7% Al_2O_3, 6% SiO_2, 16.5 % Fe_2O_3).

S - F, the plane 2.8 S + 1.18 A + 0.65 F - C = 0 contains C_3S, invariant Z at 1470°C and C_4AF (CaO combined with F is $4CaO - 1.18Al_2O_3$). The compositions containing CaO ≤ LP are deprived of equilibrium free CaO. The CaO : LP ratio is called lime saturation factor (LSF) or also modified Kalkstandard ($K_{st}II$).

Spohn et Al. (23) showed that MgO combines in clinker up to the limit of about 2 mass % (of clinker) by releasing 0.75 mass % CaO for each 1 mass % MgO, as a rule. In most cases the amount exceeding 2% does not affect the CaO combinations. For such a reason these Authors proposed $K_{st}III$ as (CaO-0.75 MgO): LP ratio, or (CaO-1.5) : LP when MgO ≤ 2% or MgO ≥ 2% respectively.

Christensen (46) attained a very similar expression of LSF corrected by the presence of MgO (not exceeding ~2%) on the basis of the phase relations in the system C - A - S - F - M:

$$LSF\,I = \frac{CaO - 0.77\,MgO}{2.8\,S + 1.18\,A + 0.66\,F}\ ,\ \text{undim.} \quad [12]$$

3.2.2 The sulphate modulus, recently introduced by Osbaeck (42), determines the fraction of soluble alkalis with respect to the total alkalis in clinker according to the results of Pollit and Brown's research (47).

3.2.3 The reason why the potential compound composition according to Bogue (38) does not correspond to the mineralogical composition of clinker determined by microscope and/or X-ray diffraction is well-known. Above all the calculated amounts of C_3S and C_2S deviate, being the former higher than that of alite and the latter lower than that of belite (23, 48, 49, 50). Nevertheless Bogue's model is a simple and clear reference of unnegligible practical utility. Therefore Hansen (51) proposed its revision by calculating the aluminate as $C_3A_{0.9}F_{0.1}$ and the alumino-ferrite as $C_2A_{0.54}F_{0.46}$ (52, 53, 54).

The interpretation of SM, TM and CM in terms of the potential compound composition was given by Bucchi and Buzzetti (55).

3.3 Chemical composition and reactivity. The effects due to the minor compounds are discussed in Chaps. 6 and 7.

3.3.1 As the lime saturation of the mix increases, the number of $CaCO_3$ particles sterically "co-ordinated" by each particle of acidic oxides increases and therefore the mass fraction of CaO (of the total one present), diffusing into these oxides in the time unit for each temperature below about 1300°C, decreases. All the values of the functions $\varphi = f(t, \theta)$ and $\alpha = f(t, \theta)$, expressing burnability and reactivity decrease.

On the contrary, as the liquid phase appears (above ~1300°C), the kinetics of the dissolution processes in the liquid is affected only to a slight extent - any other condition unchanged by the mass of the present solid CaO. The graphs of the functions $\alpha = f(t, \theta)$ and $CaO_f = f(t, \theta)$ of mixes differing only in the lime saturation, between about 1300° and 1400°C, are roughly parallel and distant from one another of an ordinate value equal (case of CaO_f) or about proportional (case of α) to the difference of free CaO present at temperature and time (t_i, θ_i) when the liquid appears. This trend seems to be confirmed by the data derived and calculated from Heilmann's (56), Toropov and Luginina's (57), Pfrunder and Wickert's (4), Blaise et Al.'s (12) papers. Also Mussgnug (15), Ludwig and Ruckensteiner (19), Kock et Al.'s (17) equations - even if with different dependence - express the increase in CaO_f (for given t_i, θ_i) or in θ_i for $CaO_f \leq 2\%$, when the lime saturation increases.

Therefore above 1300°C, the increase in this parameter determines a decrease in burnability whereas it does not practically affect the reactivity.

3.3.2 The processes occurring in the presence of liquid phase are clearly affected by the amount composition and properties of the latter. The liquid appearing at 1338°C in the system C - A - S - F (1301°C, under MgO saturation conditions) has A : F = 1.23 (1.63 under MgO saturation conditions) (58). Therefore Al_2O_3 and Fe_2O_3 act as agents of first melting for raw meals having TM < 1.23 (<1.63) or TM > 1.23 (>1.63) respectively. At the same SM, the amount of liquid is maximum at TM = 1.23 (=1.63); at the same TM, the amount of liquid increases (22) as SM decreases (*). At constant temperature, the viscosity of the liquid phase decreases as A : F reduces (60) with consequent increase in the rate of the dissolution processes.

These circumstances, and other examined in Chap. 6, explain why the increasing silica modulus-mixes show worse and worse reactivities, at K_{st}, TM and any other condition unchanged (4, 15, 61) (**). On the contra-

(*) Dahl's (22) equations are based on a composition of the liquid, at 1338°C, having A : F = 1.38 (59) instead of 1.23 (or 1.63 under MgO saturation conditions). This difference does not change the kind of reasoning.

(**) Mussgnug (15) showed that the function $CaO_f = f(KS)$ (KS = S : A, Kieselsäuremodul) linearly increases with KS, for constant t_i and θ_i. $CaO_f = f(SM)$ coincides with $CaO_f = f(KS)$, when the angular coefficient of the first function is multiplied by the value $\frac{TM+1}{TM}$.

ry the deductions on the influence of the TM varia - tions badly agree with the results of Mussgnug's (15) and Lehemann et Al.'s (8) works. Neverthe - less it is observed in this connection that raw meals having TM between 1.3 and 1.6 are almost univer - sally judged as the easiest to burn, at any other con dition unchanged.

4. PARTICLE SIZE.

4.1 Demolition of the structure of the clayey minerals. $CaCO_3$ decarbonation.

4.1.1 Both processes proceed according to first order-reactions and they are governed by the rates of this type of reactions. The research of many Au thors (62, 63, 64, 65, 66, 67) shows that the time for the dissociation of a $CaCO_3$ particle is a linear func tion of the particle diameter, in the range of the usual sizes that they have in the raw meal.

4.1.2 The time θ'_M demanded for the isothermal demolition of the mass unit of clayey mineral, di - stributed in quasi-spherical particles having nar - row grading interval, is approximatively proportio nal to the reciprocal of the specific surface S'_M of these particles:

$$\theta'_M \simeq \frac{k'}{S'_M} \quad , s \cdot g^{-1} \qquad [13]$$

where k' is constant ($s \cdot cm^2 \cdot g^{-1}$) at constant temperature and activation energy.

4.1.3 Similarly, the time demanded for the decarbonation of the mass unit of quasi-spherical $CaCO_3$ particles having narrow grading interval is expressed by a [13] type function (except for the diffe - rent numerical value of k') in that stage of the process when the dissociation rate is higher than the diffusion rate of CaO in the acidic oxides. This oc curs starting from the first appearance-temperature of free CaO as far as the temperature of comple te disappearance of $CaCO_3$ ($\leq t_2$). Below the for - mer temperature, the early decarbonation supplies CaO to the reactions with SiO_2, Al_2O_3 and Fe_2O_3 (absence of free CaO); in this stage of the process the dissociation times are controlled by the diffu - sion rate of CaO in the acidic solid phases.

4.2 Reactions between solid phases.

4.2.1 In the simple processes of binary diffusion between the fundamental oxides, the direction of transfer of matter follows De Keyser's rule (68):

$$CaO\ (0.70) \longrightarrow SiO_2\ (2.39)$$
$$CaO\ (0.70) \longrightarrow Al_2O_3\ (1.66)$$
$$Al_2O_3\ (1.66) \longrightarrow SiO_2\ (2.39)$$

(the affinity values of oxygen after Katelaar are within brackets) according to which the oxide having less affinity for the oxygen diffuses on and inside the oxide having a greater affinity (acceptor oxide). The diffusion proceeds by three ways (69):

(a) transfer of matter on the external surface of the particle of acceptor oxide (surface diffusion);

(b) transfer of matter along the surfaces joining the grains of the particles of the acceptor oxide (diffusion at the joints);

(c) transfer of matter inside the grains of the acceptor oxide (lattice or volume diffusion).

The weaker bonds of the atoms and/or ions at the surface and the greater disorder existing at the joints of the grains determine, in these sites, a higher level of free energy than that present inside the lattice. Consequently the activation energies of the process at the surface Q_s, at the joints Q_j and inside the lattice Q_r, increase according to the following order under isothermal conditions (70):

$$Q_s < Q_j < Q_r \quad , cal \cdot moles^{-1} \qquad [14]$$

with corresponding decrease, in the same order - from [15] and [18] - of the diffusion rate of each process. Therefore the processes (a) and (b) are by-pass of (c). The latter being the slowest one, con trols the overall stationary process under isother - mal conditions when the grains of the acceptor oxi - de have size higher by several orders of magnitude than the thickness of the surface layer of matter con cerned in the diffusion according to (a) (equal to some atomic distances of the acceptor).

4.2.2 Under stationary isothermal conditions, the advancement of the front of the diffusion inside the lattice is described by:

$$\frac{dn}{d\theta} = -DA\frac{dc}{dy} \quad , moles \cdot s^{-1} \qquad [15]$$

where n is expressed in moles, θ in s; c in moles $\cdot cm^{-3}$, D in $cm^2 \cdot s^{-1}$, y in cm (direction of propagation of the front) and A in cm^2 (surface across the direction of propagation). The negative sign in dicates the propagation towards the lowest concentrations. If the diffusion front travels y_i cm in θ_i s, from [15] it results:

$$y_i^2 = k\theta_i \quad , cm^2 \qquad [16]$$

or

$$\frac{y_i}{\theta_i} = \frac{k}{y_i} \quad , cm \cdot s^{-1} \qquad [17]$$

where k is constant at constant temperature and activation energy (*).

(*) Only formally the dimensions of k are the same as D.

In the portion of plane $(+\frac{y}{\theta}\ ;\ +y)$, the average rate [17] of propagation along y is represented by a branch of equilateral hyperbola having asymptotes coinciding with the reference axes (FIG. 6).

The diffusion coefficient D (and therefore the rate $dn/d\theta$ of the process) varies according to Hevesy's equation:

$$D = D_o \exp -\frac{Q}{RT} \quad , cm^2 \cdot s^{-1} \qquad [18]$$

where Q ($cal \cdot moles^{-1}$) represents the activation energy of the type of diffusional process considered, T (°K) is the temperature at which this process occurs, and D_o ($cm^2 \cdot s^{-1}$) is a (quasi-) constant, called pre-exponential factor or frequency factor (of the atomic oscillations) formally equal to D when $T = \infty$.

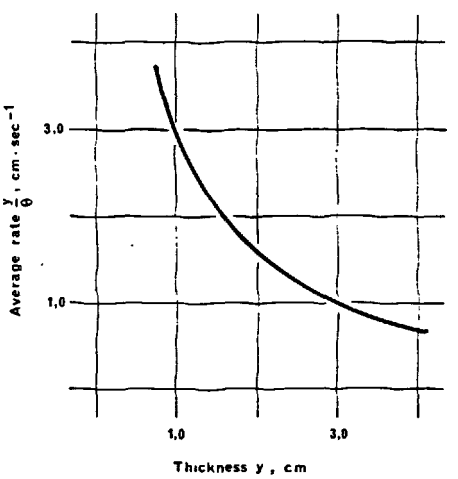

FIG. 6 . AVERAGE RATE OF THE PROGRESSIVE ADVANCEMENT OF THE REACTION FRONT VERSUS THE THICKNESS OF THE MATTER TRANSFORMED (LATTICE DIFFUSION).

4.2.3 From [14] the reactivity in the solid phase is mainly controlled by the size of the grains of CaO acceptors, that is the acidic oxides, SiO_2, Al_2O_3 and Fe_2O_3.

The time θ''_M demanded for the isothermal reaction of the mass unit of acceptor oxide (distributed in quasi-spherical grains having narrow grading interval) is approximatively proportional to the reciprocal of the square of the specific surface of the grains S''_M:

$$\theta''_M \simeq \frac{k''}{S''^2_M} \quad , s \cdot g^{-1} \qquad [19]$$

where k" ($s \cdot cm^4 \cdot g^{-3}$) is constant at constant temperature and activation energy Qr.

As seen, the validity of [19] is based on the hypotheses that the volume diffusion is the bottle neck of the overall process and the grains of acceptor oxides have quasi-spherical shape of very narrow grading interval. Consequently the description of the influence of S''_M on θ''_M the more deviates from [19] the larger the grading interval, the more different the shape of the grains from the spherical one, and the smaller their shortest dimension.

Two remarks on the quantity S''_M are necessary:

- S''_M measures the surface of the mass unit of portions of single-phase matter (acceptor oxides) delimited by crystal joints where the diffusion coefficient D_j is higher than D_r. Briefly, S''_M represents the specific surface of single-phase grains delimited by active joints. Its value can be represented by the results obtained from the usual measure of specific surface of powdered matter only when the particles consist of a single grain of a single mineralogical species. Ludwig and Ruckenstein's (18) concept of heterogeneity > 90 μm, H_{R90}, already seen in 2.5.1, takes into account this criterion.
- S''_{M_1} refers to the fineness that the acceptor oxides have when the reactions develop, instant by instant during the process (and not necessarily to the fineness that they have in the raw meal before the thermal process).

From what considered in 4.2.1, the surface of the free particles, consisting of single - or multi-phase grains, (that is the one referable to the usual measures of specific surface) affects the kinetics of the overall diffusion process in that it is an extent of the by-pass of the lattice process.

4.3 Reactions of clinkerization.

4.3.1 Clinkerization is controlled by the diffusion process in the liquid phase (71, 72).

4.3.2 Rumyantsev (73) and Kondo and Choi (74) showed that the isothermal dissolution of C_2S and CaO in the liquid phase at the temperature of clinkerization is described by equations of the same type as [15], [16], [17], [18] and [19] governing the lattice diffusion (*).

(*) Rumyantsev's equation (73) does not differ from Kondo's and Choi's (74) and both of them do not differ from [16] when, in the former, the due size ($s \cdot cm^{-1}$) is assigned to τ and in the latter α is expressed as the distance covered by the diffusion with regard to the radius of the grain or particle.

Nevertheless, in the isothermal dissolution, S''_M represents the surface of the mass unit of the C_2S and CaO grains wetted by the liquid phase, whereas dc : dy is the gradient of concentration in the contact solution.

4.3.3 Therefore the process rate is controlled by:

- the grain size of the phases produced in the previous reactions between solid phases;
- the size of the CaO grains resulting from decarbonation; (differently from what occurs for the latter process, the time for the dissolution of CaO is proportional to the fourth power of the grain diameter);
- the wetting power (surface tension) of the liquid phase.

4.4 Technological considerations. The described model is an approach that, as such, has only a beginning-value. Nevertheless it allows some deductions useful for the practice to be drawn.

4.4.1 The diameter of the grains of the acidic oxides - at the fourth power in [19] - would have a decisive effect, according to this model, on the kinetics of the reactions both in the solid phase and in the presence of liquid. Thus the considerable importance, for the reactivity of a mix, of the size of quartz here contained is explained. On the contrary, in the reactions in the solid phase, the diameter of the pure $CaCO_3$ particles would have a reduced influence, merely proportioned to the square of its size (see equation [13]). During the dissolution process in the liquid, the diameter of the CaO grains from the decarbonation of $CaCO_3$ would have the same importance as that of the acidic oxides.

These deductions are directly or indirectly confirmed by several data of the literature (56, 16, 75, 76, 77, 78, 79, 80, 81), but not by others (82, 8).

4.4.2 The particles consisting of coarser single-phase grains in the industrial raw meals, are the last to complete the reactions. It becomes obvious that the reactivity is increased by the reduced grading interval, at the same specific surface. In this connection, therefore, methods and equipment to - day used for grinding the raw meal in the technological practice do not seem the most suitable to produce the most reactive grading at the lowest energy consumption. Clearly this inadequacy must be attributed to the poor separation precision of the equipment "cutting" the feed produced in the closed-circuit mills. It is also due to the indifferentiated application of the mechanical grinding energy to materials having different grindability which, because of this, are differently distributed into the different grading intervals (83).

This problem can be solved by separately grinding the component the most difficult to grind (for ex. quartz) (76, 84), according to a method already used in some modern cement factories (85, 86).

5. MINERALOGICAL SPECIES AND THEIR REACTIVITY.

5.1 Activity state of solids.

5.1.1 The ease or hardness of an industrial raw meal to burn must be referred to the petrographic characteristics of the rocks composing it, the present mineralogical species and their state of activity just before being attributed to the different technological parameters, such as chemical composition, fineness of grinding, homogeneity a.s.o.

The two expressions of the previous chapter:

$$D = D_o \exp -\frac{Q}{RT} \quad , cm^2 \cdot s^{-1} \qquad [18]$$

$$Qs < Qj < Qr \quad , cal \cdot moles^{-1} \qquad [14]$$

(of which significance and symbols are specified in 4.2.2 and 4.2.1 respectively) allows the interpretation of the different behaviour that different solids show in the solid-phase reactions and in the presence of liquid. The energy of diffusional activation Q of [18] (or Qs, Qj or Qr, if the elementary processes, on the external surface of the grains, at the joints or inside the lattice are considered) is, to some extent, a measure of the chemical rigidity of the lattice: it is the lower (that is the process is the faster) the higher the level of free energy related to the lattice (or the zone of lattice) involved in the process or - as is briefly said - the higher the activity state of the portion of solid matter considered. Moreover the equation [14] expresses that the active state of a portion of a same solid species is maximum at the delimiting surface, lower at the junctions between grains and minimum inside the lattice.

5.1.1 The active state of solids is evidenced by the measure of suitable quantities which are directly or indirectly related to the lattice disorder as:

- distorsions inside the lattice (87, 88, 89);
- concentration of punctual faults (broadness and intensity of the lines of EPR spectra) (89, 90);
- position, shape and area of DTA effects (82, 91);
- enthalpy and rate of reaction and/or dissolution (88, 6);
- a.s.o.

5.1.3 The aforesaid type of approach justifies a great deal of well-known phenomena (69, 92, 93, 94, 95, 96, 18, 97, 89, 98):

- a mean value of Q, characteristic of the species, is due to each solid matter or mineralogical species carrying one or more oxides into the raw meal. Each mineral, or solid mat-

ter, reacts with its own rate, all the other conditions unchanged;

- for a same species of matter, the value of Q is a function of the particular state of activity that this species assumes from its formation and elapsed vicissitudes. Faults, defective structures and disorder of any origin in the lattice, increase active state and reactivity. Even if not as a rule, higher levels of free energy are often related to the condition of solid solution of substitutive type (especially among ions of different charge and at the limit of the dimensions of replaceability), interestitial and subtractive type. The pseudo-solids and the matter badly crystallized or having limited lattice periodicity (glasses, colloids, a.s.o.) owe the high reactivity to the high content in free energy of these structures;
- similarly the solids in transient state of structural modification (especially if it results from a deep rearrangement) and the chemical species in the nascent state are exceptionally reactive. The 'ageing" of the structures, on the contrary, reduces the concentration of their crystalline faults, increases their stability and grain sizes, and so makes them less reactive;
- the surface extension of an exposed phase as wells as the concentration of junctions among the grains, are liable for great variations in the active state where the same crystalline species, or the same minerals of a rock, can be found.

5.1.4 The application of suitable mechanical stresses to the solid matter can cause distorsions inside the lattice and/or changes to the structural arrangement in the proximity of the free surfaces, which increase its state of activity (mechanical activation) (99, 4, 6, 100).

5.2 Carrier of acidic oxides.

5.2.1 The main minerals, and most of the accessory ones, of argillaceous materials (clays, shales, slates), phyllites, schists, flysh, marls, sandstones are carriers of acidic oxides. The use of metastable glassy volcanic rocks, such as tuffs, pozzolanas, trass, pumice and industrial wastes, such as fly-ashes and blastfurnace slags, is less frequent. When necessary, the raw meal is corrected by small amounts of siliceous materials, laterites, terra rossa, bauxite, limonite, siderite or pyrite cinders, depending on the lacking oxide and the material available at the lowest cost. An exhaustive review of these materials is contained in Wolfe's (101) paper. Kiefer (102) published a synthesis on the structure and properties of the main clay minerals. Of the latter Beutelspacher and Van der Marel (103) presented over 250 electron micrographs of rare evidence. Leroux (104) reported significant notes on the different textures of clayey and marly rocks.

5.2.2 SiO_2 released through thermal amorphization of phyllosilicates has great dispersion and considerable activity because of its nascent state. Therefore it is much more reactive than the several types of natural silica.

As for the clastic quartz of clays, sandstones, sands and veins in limestones, as for chalcedony and/or opal of flint, as well as gels of "aged" natural silica, it is the dispersion and the size of grains, the type of structure and the degree of disorder inside the lattice at the temperature of reaction which control their reactivity anyhow low. The results of Dyckerhoff's (16) and Akatsu and Ikeda's (91) works are very instructive on this subject. According to Makashev (97) the reactivity of the different types of SiO_2, free and combined, increases in the order:

> quartz < chalcedony < opal < α-cristobalite; α-tridymite < silica of feldspars (orthoclase; albite; anorthite) < silica of micas and amphiboles < silica of clay minerals < silica of glassy slags;

whereas Michedlov-Petrosyan et Al. (89) found that silica of volcanic glasses and that of clayey minerals are more reactive than that of blastfurnace slags.

5.2.3 It can be reasonably assumed that an analogous situation to that of SiO_2 occurs for Al_2O_3 and Fe_2O_3. The thermal demolition of the structure of a phyllosilicate gives these oxides in the nascent state at temperatures at which their reaction with $CaCO_3$ can begin and develop at practically useful rates. Gibbsite, bohemite, diaspore, goehtite, a.s.o. - present as accessory minerals in clays, or as main constituents of residual sediments (laterite, terra rossa, bauxites, limonites a.s.o.) - contain, "at the green state", the hydroxides under conditions of poor crystallinity and high configurational energy. However they are unable to offer these hydroxides under this very condition to the reaction with $CaCO_3$ over 500°C during the conventional process of burning. In fact the gradual heating of the raw meal dehydrates these compounds prematurely and it favours their structural rearrangement. Consequently the latter reduces their energy content, activity and reactivity.

In the light of these concepts, the pyrite cinders are the worst carriers of Fe_2O_3, because of the high temperatures at which they form.

5.2.4 Generally the most abundant phyllosilicates in the clayey fraction of the raw meal are illite, chlorite and muscovite (102, 105, 106, 16). Kaolinite is frequent but less abundant. According to Lehmann et Al. (8) montmorillonite would be rare even if it appears to be present and sometimes abundant in raw materials and raw meals examined by other Authors (107, 81). It is mainly found in the alteration products of volcanic ashes and as accessory mineral of recent marls. More common carriers of octahedric layer-Fe^{3+} are glauconite (ferric illite)

and nontronite (ferric montmorillonite). Detailed information on the presence of the different phyllosilicates in the sediments of different origin and nature is found in Grim's (108, 109) and Millot's (110) classical texts.

The lattice stability of these minerals is related to the temperatures of initial and final hydroxyl dehydration. The stability decreases - all the other conditions unchanged - as the simmetry of the sheet decreases and, for a same type of structure, by moving from the alumina terms to the iron ones (102). As Goerg (111), Hill and Schwiete (112), Ludwig et Al. (113), Bereczky (114), Lehmann and Thormann (7) and Mchedlov-Petrosyan et Al. (115) show, it is thought that, as the stability of phyllosilicates decreases, the reactivity with $CaCO_3$ increases, as a rule, according to the order:

muscovite < montmorillonite < chlorite < illite < kaolinite.

Nevertheless there are disagreeing experimental results (116, 117) and opinions (101, 118). Actually, it would seem right to relate the reactivity of a phyllosilicate towards $CaCO_3$ not to the activity of the structure before the demolition of the latter, but more properly to the temperature at which SiO_2, Al_2O_3 and Fe_2O_3 are offered in the nascent state with respect to the temperature at which the $CaCO_3$ dissociation, in their presence, attains practically useful values. Therefore the different phyllosilicates are likely to show different degrees of relative reactivity depending on the nature and texture of the carbonatic rock with which they react.

Anyhow, if the requirements of chemical composition of the industrial raw meals are considered, it must be concluded that the three layer-sialites of pyrophyllitic structure (montmorillonite, a.s.o.), having Si : (Al, Fe) atomic ratio equal to or slightly lower than 2 (SM≃2.3), give more reactive raw meals than those containing other sialites (kaolinite, illite, chlorites, muscovite a.s.o.) which, even if of very different nature, have Si : (Al, Fe) atomic ratio ≤ 1 (SM≃1.2). In fact the latter ones must always be accompained, in the raw meal, by higher contents in poorly reactive free SiO_2 (or combined in another tectosilicate) than the former ones.

5.3 Carriers of CaO.

5.3.1 Calcite (rarely and in negligible amounts, aragonite and ankerite) of the carbonatic rocks is the main carrier of CaO in the raw meal. A contribution in CaO can be sometimes given by blastfurnace slags and wastes from other industries in the form of silicate, hydroxide or oxide. The supply of CaO from dolomite, gypsum, magmatic rocks, and phyllitic silicates having adsorbed or reticular Ca^{2+} is always poor.

The case of raw meals containing quicklime obtained by burning limestone (119) is exceptional.

5.3.2 The state of activity (and therefore the reactivity) of calcium oxide released from $CaCO_3$ for the diffusion in the acidic oxides is determined by the disorder and concentration of defective structures present in the dissociation product which, in their turn, depend on (93, 120, 121, 5, 11, 122, 123, 97, 90):

- the microstructure of the carbonatic rock;
- the temperature of formation of CaO;
- the temperatures and the times during which the produced CaO "ages" before reacting with the other solid phases, or before dissolving in the liquid phase.

The most influential variable is the size of the calcite crystals. As it decreases, the concentration

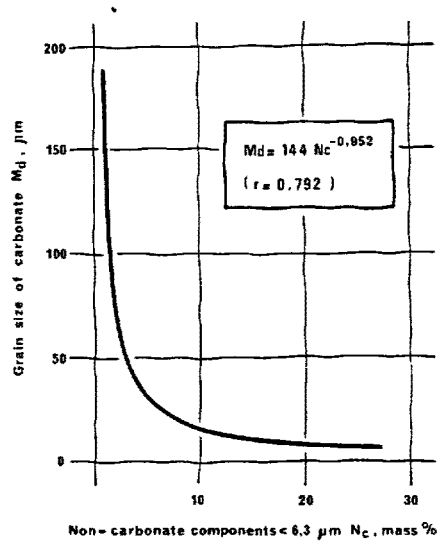

FIG. 7 . GRAIN SIZES OF THE DIAGENETIC CARBONATE SEDIMENTS AND NON-CARBONATE FRACTION (< 6,3 µm). ELABORATION FROM MARSCHNER'S PAPER (124).

of the defective structures of the dissociation CaO increases and the temperature at which - for a given equilibrium of solid phases - p_{CO_2} attains practically useful values, decreases. On the other hand, Marschner (124) proved that, for diagenetic limestones, the sizes of the grains are inversely proportional to the content of clayey minerals (FIG. 7) whose protective coating would prevent the formation of large crystals during the diagenesis.

5.3.3 These concepts explain the great burnability of marls and the preference that the cement manufacturers generally give to limestones of "polluted" microstructure rather than to pure or very pure carbonatic rocks. Subordinately, among these, micrites and micro-and cryptocrystalline limestones are more reactive; the middle-grained sediments are ac-

ceptable. Clearly the worst carbonates used for cement are pure limestones deeply diagenized and containing large crystals, such as marbles.

5. MINOR COMPOUNDS.

6.1 Concentrations of minor compounds in the raw meal. Admixtures.

Minor compounds (*) are chemical species different from the four fundamental oxides which participate in the transformation process of the raw meal into clinker. As a rule, they derive from the accessory minerals of rocks, fuels, refractories, wear parts of equipment; they can also result from admixtures added to the raw meal for specific purposes. Blaine et Al. (125, 126) published the frequency distribution of 17 minor elements into 186 portland cements as well as the results of a research concerning their effects on the properties of cement.

TAB. III gives the significant statistical quantities of the concentrations of 11 minor compounds in 141 industrial raw meals (127, 128, 129, 130). The median values of the concentrations decrease in the order:

$$MgO > K_2O > SO_3 > Na_2O > TiO_2 > Mn_2O_3 > P_2O_5 > SrO > F^{1-} > Cl^{1-} > Cr_2O_3;$$

the frequency distribution is of normal-logarithm type (except for that of TiO_2, approaching the normal one).

TAB. III. CONTENTS IN MINOR COMPOUNDS OF INDUSTRIAL RAW MEALS (127,128,129,130).

minor compound	number of samples	ΔC_E extremes of conc. mass %	ΔC_{fo} interval of fo mass %	fo frequency of ΔC_{fo} %	C_M median content mass %	C_m mean content mass %
MgO	113	0.30 - 4.00	0.50 - 0.80	26	1.00	1.053
K_2O	141	0.05 - 1.50	0.45 - 0.50	13	0.55	0.571
SO_3	122	0.00 - 1.91	0.09 - 0.13	11	0.20	0.306
Na_2O	140	0.03 - 0.63	0.08 - 1.11	19	0.16	0.173
TiO_2	136	0.02 - 0.40	0.14 - 0.17	35	0.15	0.155
Mn_2O_3	77	0.01 - 0.83	0.09 - 0.11	39	0.09	0.116
P_2O_5	136	0.01 - 0.50	0.04 - 0.07	35	0.07	0.093
SrO	77	0.01 - 1.47	0.05 - 0.07	21	0.06	0.074
F^{1-}	89	0.00 - 0.34	0.04 - 0.06	35	0.05	0.055
Cl^{1-}	118	$<1\cdot10^{-4}$ - 0.20	$<1\cdot10^{-4}$ - 0.01	40	0.01	0.021
Cr_2O_3	91	$<8\cdot10^{-3}$ - 0.03	$8\cdot10^{-3}$ - 0.01	46	0.01	0.013

The main purposes that have been stimulating the research on the minor compounds and admixtures for several years are:

- production of more reactive raw mixes;
- improvement of particular technological conditions in order to increase efficiency of the process;
- increase in the allowable levels of impurities and consequently enlargement of the availability of raw materials and types of fuel. There is also the possibility of using industrial wastes or the ones of different source for ecological decontamination purposes;
- production of cements having better quality.

6.2 Modifiers of the properties of the liquid phase.

These are the minor compounds called fluxes and mineralizers acting in the liquid and/or liquid-solid phase. Fluxes are substances which lower the first appearance-temperature of the liquid phase (131). Mineralizers are substances which, through any mechanism, accelerate the rate of the process or reaction between solid phases, or in the liquid phase or at the liquid-solid interface (131). Attributing (84) both properties to fluxes - that is the lowering of the first-melting point and the reduction in the viscosity of the liquid-must be avoided because not always the same substance produces the two effects simultaneously. It does not

(*) Also called: minor components, minor constituents, minor elements, impurities, traces.

even seem suitable to assign (132) the role of mineralizers only to fluxes, since many of these act just in the solid phase.

TAB. IV. COMPOSITION OF THE LIQUIDS OF WHICH BUTT AND TIMASHEV (137) STUDIED THE VARIATIONS OF σ AND η.

	liquid 1 peritectic at 1338°C	liquid 2 saturated at 1450°C
CaO	54.8	57.0
SiO_2	6.0	7.5
Al_2O_3	22.7	22.6
Fe_2O_3	16.5	12.9
a	2.76	2.78
b	0.016	0.025

6.2.1 The important role that fluxes play on the transformation of the raw mix must be referred:

- first of all, to the necessity of the presence of a liquid phase for the rapid C_3S formation (peritectic reaction);

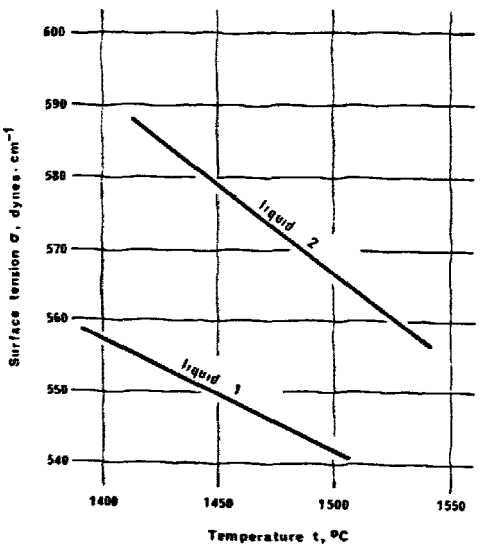

FIG. 8 .POLYTHERMS OF σ OF THE LIQUID PHASES 1 AND 2 OF TAB. IV .AFTER BUTT AND TIMASHEV (137).

- afterwards, to the need to avoid the "ageing" of the CaO and C_2S crystals before dissolving in the liquid;
- finally, to the energy saving of the process, which results to be the higher the lower the first appearance-temperature of the liquid.

It has already been mentioned (paragraph 3.3.2) that this temperature is 1338°C in the most basic part of the system C - S - A - F (59); 1301°C in the same in the presence of 5% MgO (58); 1280°C in the system C - S - A - F - M - N (133). All the minor compounds dissolving in the liquid phase decrease its first appearance-temperature. Nevertheless, since C_3S does not form below 1250°C, this temperature must be considered the lowest (also theoretical) limit for clinkerization.

6.2.2 The substances able to modify the kinetics of the C_2S and CaO dissolution and the rate of ionic diffusion in the same, affect the rate of the peritectic reaction (134, 135, 136, 73). Butt and Timashev

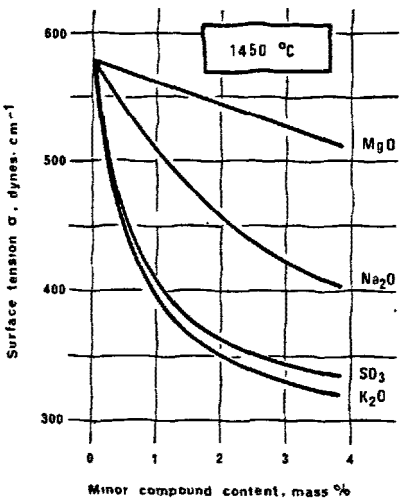

FIG. 9 .ISOTHERMS (1450°C) OF σ OF THE LIQUID PHASE 2 OF TAB. IV FOR INCREASING CONTENTS IN DIFFERENT MINOR COMPOUNDS. AFTER BUTT AND TIMASHEV (137).

(137) have exhaustively reported on the mechanism of formation of clinker. The mineralizers act, at the solid-liquid interface, by increasing the wetting power of the liquid phase - that is by reducing its surface tension - and they increase the fraction of exposed surface of the solid phase which dissolve. On the contrary, the mineralizers in the liquid phase accelerate the ionic diffusion by reducing the viscosity.

The surface tension σ of the liquid phase of clinker is of the order of hundreds of dynes·cm^{-1}, between 1300°C and 1450°C (138); the viscosity η is of the order of poises (60). According to Butt and Timashev (137):

$$\log_{10} \sigma = a - \frac{b}{\eta} \quad , \text{undim.} \qquad [20]$$

is valid between 1400° C et 1500°C for the quaterna

ry liquids having the composition given in TAB.IV. The values of the constant a and b are also shown in the same TAB. IV.

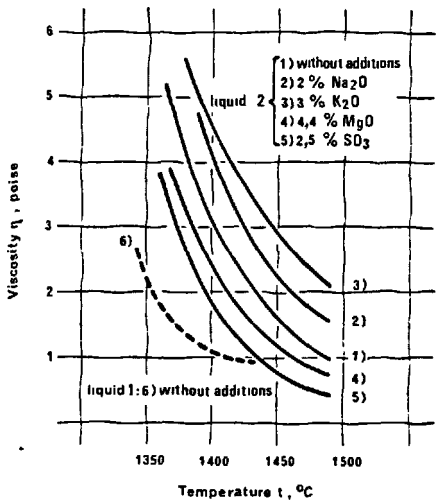

FIG. 10 .POLYTHERMS OF η OF THE LIQUID PHASES 1 AND 2 OF TAB. IV. AFTER BUTT AND TIMASHEV(137).

The variation of σ versus the temperature is shown in FIG. 8, whereas FIG. 9 gives the isotherms σ

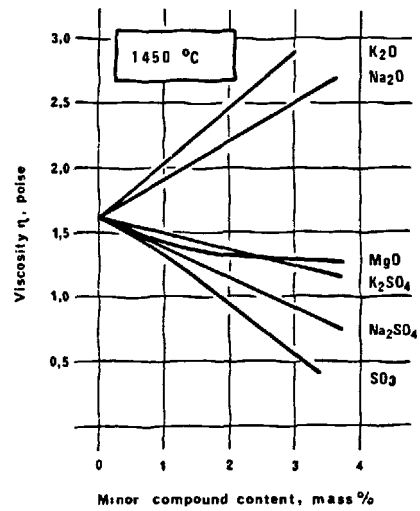

FIG. 11 .ISOTHERMS (1450 °C) OF η OF THE LIQUID PHASE 2 OF TAB. IV FOR INCREASING CONTENTS IN DIFFERENT MINOR COMPOUNDS. AFTER BUTT AND TIMASHEV (137).

of liquid 2 at 1450°C for increasing concentrations in different minor compounds.

The viscosity is caused by the mobility of the ions $Si_xO_y^{z-}$.

In the presence of minor compounds the values of η depend on the equilibrium displacement between the co-ordinative structures of the amphoteric elements:

$$MeO_4^{5-} \rightleftharpoons Me^{3+} + 4\,O^{2-} \qquad [21]$$

FIGS. 10 and 11 show the variations of η versus the temperature and the concentration of different minor compounds. It must be pointed out that increasing K_2O and Na_2O reduce σ but increase η, at the same temperature.

TAB. V. DECREASING ORDER (FROM ABOVE DOWNWARDS) OF THE EFFECTIVENESS IN REDUCING THE VISCOSITY OF THE LIQUID PHASE OF DIFFERENT IONS. VALUES OT THE FIRST COLUMN AFTER GRACHLAN ET AL.(140).

decreasing order of effectiveness	electronegativity χ	field force Z/a_o^2 Å^{-2}	ionic potential Z/a Å^{-1}
Be^{2+}	1.5	0.72	5.71
Mg^{2+}	1.2	0.44	2.50
Sr^{2+}	1.0	0.31	1.65
Li^{1+}	1.0	0.23	1.22
Ba^{2+}	0.9	0.26	1.39
Na^{1+}	0.9	0.18	0.91
K^{1+}	0.8	0.13	0.68
SiF_6^{2-}	4.0	-	-
F^{1-}	4.0	-	-
SO_4^{2-}	3.6	-	-
Cl^{1-}	3.0	-	-

NOTES. Values of χ after Pauling (141) for ions in octahedral co-ordination with O^{2-}; 0.7 ÷ 0.4 scale.
a_o = sum of the cation radius and O^{2-}.
a = cationic R^{VI} after Whittaker and Muntus (142).
Z = number of ionic charge.

5.2.3 The ability of an ion to modify the characteristics of the liquid is a property of the electron configuration of the ion itself. The effectiveness by which the viscosity is reduced, at the same temperature, increases as the electronegativity χ, or the field force Z/a_o^2, or the ionic potential Z/a of the ion increase (137, 139, 140), as shown by the values of TAB.V. Ions like K^{1+} and Na^{1+} having large radius and low charge do not reduce but increase η (137). Also the mineralizing effectiveness, measured by the degree of combination of CaO through the liquid phase, increases as χ, Z/a_o^2 and Z/a increase (143,

144, 145, 146, 147, 148) (FIG. 12); in fact ions having small radius and high charge (Cr, V, Ti, Mn, a.s.o.) are the most effective mineralizers.

This behaviour towards the liquid phase of clinker must be considered as a particular case of a more general rule, valid for all the silicatic magmas (149).

6.3 Equlibrium modifiers between phase and structure modifiers of the clinker minerals.

6.3.1 The minor compounds distribute differently into the clinker phases at high temperature and they determine displacements of the equilibria among the phases. New solid solutions and new compounds often form. In any case the evaluation of the effects

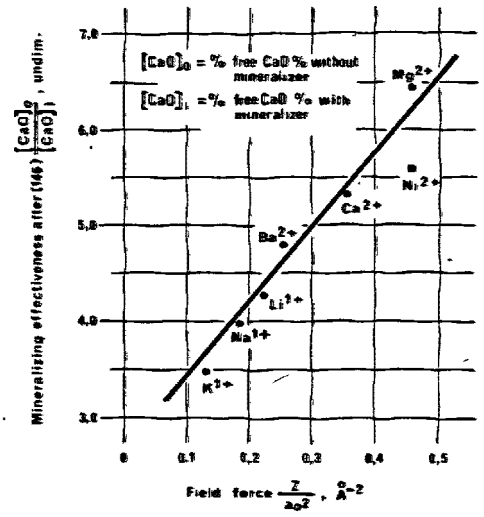

FIG. 12 . MINERALIZING EFFECTIVENESS OF DIFFERENT CATIONS FOR CLINKER LSF=0,96 SM=2,2 AND TM=2,0 BURNT AT 1350°C UNDER LOAD OF g 100 WITH ADDITION OF 0,01 g-% EQUIV. OF F^-. AFTER TEOREANU AND TRAN VAN HUYNH (146).

of one or more minor compounds presume the knowledge of the resulting phase relations, out of which the most important are reported in Chap. 7.

6.3.2 These minor compounds that, in adequate concentration, increase the hydraulic properties of clinker and/or its minerals, are called activators (of hydraulicity) (150, 151, 152). The fundamental papers (137, 138, 153, 154, 155, 156, 49, 157, 158) published on this subject allow two types of model of activation to be designed:

- the presence of an isomorphogeneous substitute in a lattice causes disorder and often increases the concentration of defective structures of any kind (punctual, linear and superficial). This rise can increase the free energy of the structure by reducing its stability and by activating its hydraulicity (*). There are, however, some exceptions: for instance the impurities do not increase the concentration of the imperfections inside the lattice of C_2S (160). Foreign ions, depending on their ionic potential, can make the structure of β -C_2S more stable (and decrease its hydraulic activity) (161);
- when ions having high value of Z/a vary the surface tension, the ionic mobility and the concentration gradients in the liquid, they modify the conditions of formation and growth of the crystals at the same time. In this way the microstructure of clinker varies with possible increase in the relative hydraulic activity (162).

6.4 Mineralizers between solid phases and through formation of atypical liquid phase (**). These are the minor compounds which increase, at the same temperature, the dissociation tension of $CaCO_3$, the rate of the diffusion processes in the solid phase and/or give intermediate compounds favouring or accelerating the C_3S formation.

The mineralizers of this type (NaCl, $CaCl_2$, B_2O_3, $Na_2B_2O_7$, $NaNO_3$, phosphates, fluorides, sulphates, a.s.o.), which gave interesting laboratory results, are numerous. Nevertheless most of them have the disadvantage of yielding technological conditions unfavourable for other aspects, or they involve costs not repaid by the advantages obtained. For this reason, today, the cement industry utilizes only fluorite and gypsum (or anhydrite), in particular cases and for specific purposes.

6.5 Minor volatile compounds.

6.5.1 The minor chemical species, whose vapor tension is unnegligible at the burning temperatures and, at the same time, not high enough at the temperature of the exhaust gases, volatilize in the hotter zones of the kiln and condense in the cooler ones (on the raw mix, on the walls, on the recuperators,

(*) The stability of a structure corresponds to a minimum of the free energy F at temperatures > 0°K (F=U-TS, for isothermal and isochoral systems). Disorder and imperfections increase both the internal energy U and the entropy S. The stability decreases when $\Delta U > T\Delta S$ (159).
(**) Liquid phase different from the typical liquid phase of clinkerization as for composition and properties (i. e. liquid phases of chlorides, sulphates, nitrates, a.s.o.).

a.s.o.). Thus, a cycle of these compounds is established (163, 164, 165, 166, 167, 168, 169, 170, 171, 172, 173, 174). It increases the concentration in the processed material up to the (maximum) level X_i needed to balance the entering and the coming out amounts.

With respect to the concentrations A_i and A_{ki} of the chemical species i, in the fresh raw meal and in the fuel respectively, X_i expresses the intensity of the cycle of that chemical species by the recycling factor K_i (167):

$$K_i = \frac{X_i}{A_i + A_{ki}} \quad , \text{undim.} \qquad [22]$$

with X_i, A_i and A_{ki} in homogeneous units of mass concentration.

K_i depends on the type of process (171) and other different parameters, among which the coefficients of primary volatility ϵ_{1i} and cycle volatility ϵ_{2i} of the considered species (167):

ϵ_{1i} = mass fraction, with respect to the total one, of the species i volatilized from the fresh raw meal having concentration A_i (undim.);

ϵ_{2i} = mass fraction, with respect to the total one, of the species i volatilized from the burning raw meal having concentration X_i (undim.).

The two coefficients are referred to given temperatures.

Ritzman (172) published the quantitative relations from which X_i and the concentration of i in clinker, at steady condition, are calculated versus A_i, A_{ki}, ϵ_{1i}, ϵ_{2i} and other variables of the process. From Locher et Al.'s (170) equations, it is possible to calculate X_i versus the time of recycle, as well as the time necessary to attain the equilibrium concentration X_i in the burning material.

6.5.2 Cl^{1-}, Br^{1-}, J^{1-}, alkalis, sulphates, fluorides and zinc compounds produce cycles. K_i of the two latter species are very low. There is little information on the cycles of Br^{1-} and J^{1-} even if there is evidence of the aggressiveness of these halogens on the electrofilters and their ducts. K_i (and therefore X_i) of chlorides, sulphates and alkalis are high and liable for the direct or indirect formation of most coatings and rings which jeopardize the regularity and the operation continuity of kilns.

In the technological practice, three methods allow the coming out amounts of volatile compounds to be increased in order to reduce X_i:

- shut off of the cycle generally by total elimination of the dust of electrofilter (and sometimes of grate in the lepol kilns) when the volatile compound concentrates in the dust (170, 175). The latter condition, and the necessity to reutilize the recovered dust, limit the practicability of the method only to the kilns producing very reduced amounts of dust (0.04 ÷ ÷ 0.06 kg/kgcli.), that is to the lepol and the nodule-fed kilns. (In order to reduce the production of dust the characteristics of the nodules can be improved by avoiding the presence, in the raw meal, of compounds hydrolyzable in Ca^{2+}, by adding Na_2CO_3, a.s.o.);
- shut off of the cycle by (partial or total) bypass of the exit gases in the suspension preheater kilns (165, 166), especially when they are equipped with precalciner (176, 177, 178, 10);
- reduction in the volatilization of the chemical species which recycles by addition of suitable compounds to the raw meal (see paragraphs 7.3.4 and 7.6.3) and by adopting the measures which enable the burning at lower temperatures. Obviously, in this way, clinker becomes richer in volatile compound. This method is favoured by the semi-dry process since the nodules release fewer compounds than the raw meal, at any other condition unchanged (164, 171).

7. BEHAVIOUR OF SOME MINOR COMPOUNDS.

7.1 Sulphates.

7.1.1 Sulphates (gypsum, anhydrite, celestine, baritine), and exceptionally elementary sulphur, are often present in the evaporitic limestones. On the contrary the ancient limestones can be mineralized by sulphides (prevailingly blende and galena). Clayey sediments, marls, detrital rocks contain both sulphides (pyrites and marcassite) and sulphates. Gypsum and anhydrite are sometimes added to the raw mix as mineralizers and modifiers of the recycle of alkalis (170). Sulphides and sulphur of the raw meal and the fuel are oxidized to sulphates and combined, as such, in the solid phases during burning (179, 169).

7.1.2 Fundamental knowledge of the sulphate-containing systems:

- SO_3 preferably combines as $(K, Na)_2SO_4$. At ordinary temperature, the solid solution contains the two sulphates in the same ratio of the present oxides if (in moles) $SO_3 \geq K_2O + Na_2O$; on the contrary it corresponds to about $3K_2SO_4 \cdot Na_2SO_4$ in the opposite case (180);
- $2CaSO_4 \cdot K_2SO_4$ is stable up to 1011 °C in the system $CaSO_4$-K_2SO_4. The compound can form during the cooling of high potassium and sulphate clinkers (181);
- $3CA \cdot CaSO_4$ (182, 183) is stable up to about 1400 °C. Kostov (184) explains how to calculate its amount, eventually together with C_3A, in the clinkers rich in $CaSO_4$. Alkalis (185) and low A : F ratios (≤ 0.64) (186) prevent its formation;

- $2C_2S \cdot CaSO_4$ (187) forms from the oxides already at 900°C. Above 1298°C it decomposes in α-$CaSO_4$ and α'-C_2S containing 1.1 mole % $CaSO_4$;
- C_3S coexists with $CaSO_4$ in the system CaO-C_2S-$CaSO_4$ (188). The saturated solid solution of $CaSO_4$ in C_3S contains about 2.9% SO_3 (at 1310°C) (189). Sulphatic C_3S has lower hydraulicity (189) and decreasing mechanical strengths as the SO_3 content increases (190);
- the compatibility (coexistence at the equili - brium) among $CaSO_4$, $2C_2S \cdot CaSO_4$ and $3CA \cdot CaSO_4$ and $SCA \cdot CaSO_4$ with CaO, C_2S, $C_{12}A_7$ and Ca - in the 950°/1150°C range and in the

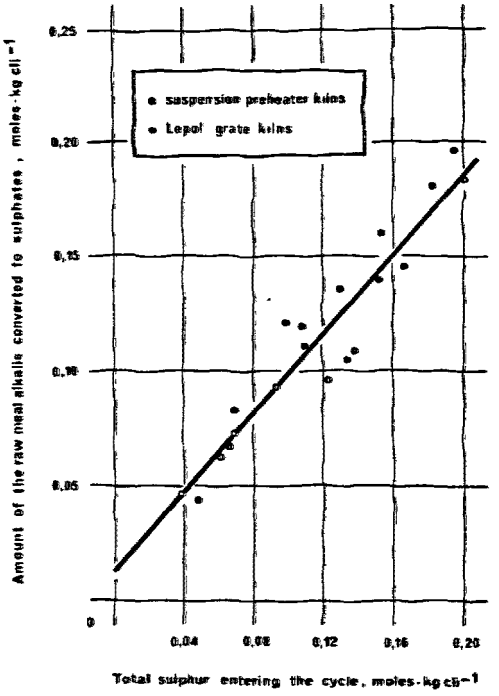

FIG. 13 . FORMATION OF ALKALI SULPHATES IN CEMENT KILNS. AFTER LOCHER ET AL. (170).

absence of K_2SO_4 and C_3S - was established by Pliego Cuervo et Al. (191).

7.1.3 The advantages of the addition of calcium sulphate to the raw meals have repeatedly been reported, especially by Russian Authors (192, 193, 194, 195, 196, 197, 198, 199). $CaSO_4$ is an effective flux and mineralizer: it lowers the appearance temperature of the liquid phase by over 100°C, it decreases its viscosity and surface tension and increases the mobility of Ca^{2+}, $Si_xO_y^{z-}$, Al^{3+}, AlO_4^{5-}, Fe^{3+} (137).

The addition of $CaSO_4$ to raw meals having molarly lower alkali content than SO_3 (including the one of fuel), in the absence of Cl^{1-}, allows the alkalis to be "fixed" in clinker as sulphates and therefore it reduces the internal cycle of the kilns (FIG. 13). Generally the quality (early mechanical strengths) of clinker is favoured by the condition (in moles) $SO_3 > K_2O + Na_2O$ - at least for limited amounts of SO_3 in excess (200, 201, 202, 203, 204). The most effective action of $CaSO_4$ is obtained on raw meals having low A : F ratio (1.2 ÷ 1.5) and moderate lime saturation (~0.8), for contents of 2.3 ÷ 2.5% SO_3 in clinker (186).

Alkali sulphates are less active mineralizers than $CaSO_4$. On the other hand they promote-similarly

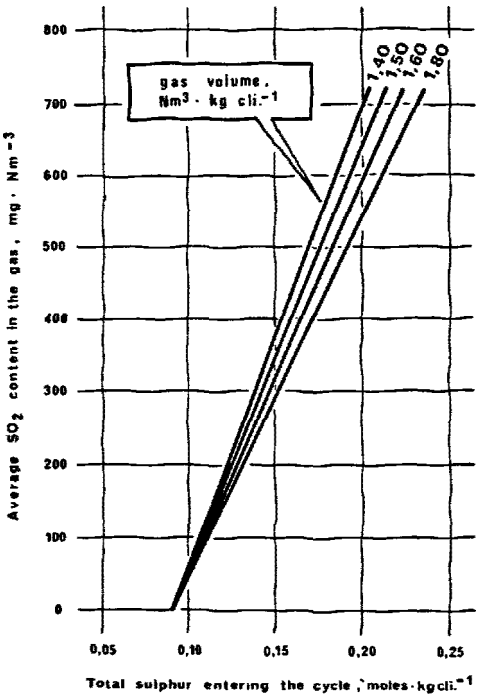

FIG. 14 . SO_2 EMISSIONS WITH THE GASES OF SUSPENSION PREHEATER AND LEPOL KILNS. AFTER LOCHER ET AL. (170).

to F^{1-} and Cl^{1-} - the formation of C_3S (181).

7.1.4 Nevertheless the use of calcium sulphate must be cautious. One must consider the lower hydraulicity of sulphatic alite, as well as the fact that the simultaneous presence of Al^{3+} and SO_4^{2-}, in the absence of MgO, impoverishes the clinker in C_3S, whose formation can even be prevented (189). Still in the absence of suitable concentration in MgO, also Na_2SO_4 and high contents in K_2SO_4 can avoid the C_3S formation (181). The unfavourable effect of the combined action of Al^{3+} and SO_4^{2-} is eliminated, or strongly weakened, by the presence of a sufficient

quantity of MgO. These phenomena are likely to be related to the particular "wetting and penetrating" properties of the liquid phases containing high amounts of alkali sulphates which, in this way, would be able to "mineralize" a very rapid decomposition of C_3S at 1250°C, during the clinker cooling (205). Finally one must remember the role of sulphates in the formation of rings and coatings (206, 207) which, in the upper parts of kilns, prevailingly consist of sulphosilicate, $2CaSO_4 \cdot K_2SO_4$ and Na_2SO_4.

7.1.5 The SO_2 emissions with the kiln gases which process, under normal condition, raw meals and fuels containing sulphur compounds are poor (179, 170, 208, 209). The graph of FIG. 14 shows the SO_2 concentrations in the gases, calculated by Locher et Al. (170) versus the overall amounts of sulphur entering the kiln.

7.2 Fluorides.

7.2.1 The vicariance between F^{1-} and OH^{1-} makes fluorine the most important halogen of the sedimentary rocks. It is contained in carbonatic rocks (100 ÷ 600 ppm F), combined as fluorite and fluor-apatite; in marls, clays, shales (300 ÷ 2500 ppm F); in sandstones, calcareous sands, loess (80 ÷ 360 ppm F). The minerals of the most rich clays are illite (0.1 ÷ 0.3% F), micas (0.1 ÷ 0.2% F), montmorillonite (~0.03% F). Fluorine is always present in the cement raw mix and it is often added to improve its reactivity.

7.2.2 Some aspects of the equilibria in the CaF_2 containing-systems are interesting for the practical implications:

- in the system $C - S - CaF_2$, $(C_2S)_2 \cdot CaF_2$ forms at 950°C and decomposes at 1040°C in α'-C_2S and CaF_2 (210). The compound $11CaO \cdot 4SiO_2 \cdot CaF_2$ (211), or more precisely $19CaO \cdot 7SiO_2 \cdot 2CaF_2$ (212), also called "$(C_3S)_3 \cdot CaF_2$" is stable between 1110°C and 1185°C. Its incongruent melting gives trigonal C_3S, α'-C_2S and liquid, at 1185°C;
- in $C_{12}A_7$, O^{2-} is replaced by F^{1-} at 1300°C in a continuous series of solid solutions (213), $C_{12-x}A_7 \cdot (CaF_2)_x$ ($0 \leq x \leq 1$), whose extreme term contains 2.7% F. The singular term, when $x = 0.8$, contains 2.3% F. In the most basic part of the system $C - A - CaF_2$, the solid solutions of the interval $0.8 \leq x \leq 1.0$ are in equilibrium with CaO at 1300°C; those of the interval $0 \leq x \leq 0.8$, with C_3A (214). In the most basic and F-poorest part of the system $C - A - S - CaF_2$ (215) the solutions of the interval $0.8 \leq x \leq 1.0$ are compatible, each time, with C_2S and C_3S at 1300°C, or with C_3S and CaO, but not with C_3A. On the contrary, the latter is in equilibrium with the solutions of the interval $0 \leq x \leq 0.8$, C_2S and C_3S (FIG. 15). It is therefore wrong to think that, in every case, CaF_2 decomposes C_3A in CaO and a solid solution of F in $C_{12}A_7$ (216); really this occurs only for higher contents in CaF_2 than those of the plane C_2S-C_3S-$C_{11.2}A_7 \cdot (CaF_2)_{0.8}$. In the practice the fluoridized clinkers contain C_3A or $C_{12-x}A_7 \cdot (CaF_2)_x$, or both, depending on the F content and the cooling conditions (217);
- the system $C - A - F - CaF_2$ at 1250°C (218), in its most basic part, has not quaternary compounds but only solid solutions containing a small amount of fluoride;
- in the system $C - C_2S - CaSO_4 - CaF_2$ between 1000°C and 1150°C (212), an only quaternary compound $3C_2S \cdot 3CaSO_4 \cdot CaF_2$ (fluorellestadite) is present. It is incompatible with both C_2S not saturated with $CaSO_4$ (1000°C) and "$(C_3S)_3 \cdot CaF_2$" (1150°C). The two silico-fluorides $(C_2S)_2 \cdot CaF_2$ and "$(C_3S)_2 \cdot CaF_2$" would only form in the raw meals containing $F : SO_3$ (mass %) > 0.158.

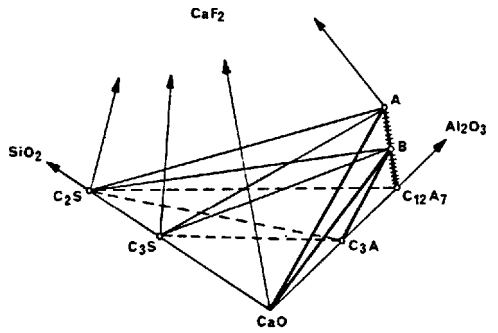

FIG. 15 . MOST BASIC PART OF THE SYSTEM C-A-S-CaF_2 (NOT TO SCALE). AFTER MASSAZZA AND PEZZUOLI(215).

7.2.3 Even small amounts (< 0.3% CaF_2) of fluorides in the raw meal increase the values of $p_{CO_2} = f(t)$ of the carbonatic phase and they modify the kinetics of all the burning reactions deeply (2, 219, 82, 3, 220, 221, 222). The amount of β-C_2S, which forms as from 750°C, increases and a liquid phase, which favours the diffusion processes among the reacting solid phases, appears already at 800°C (223). Therefore, at 850°C (p_{CO_2} = 1 atm), the presence of CaF_2 determines the formation of $(C_2S)_2 \cdot CaCO_3$ which, at 960°C (p_{CO_2} = 1 atm), decomposes by separating CO_2, C_2S and CaO, the two latter in a particularly active state to be combined in C_3S: in this way, spurrite would play a role of intermediate phase which accelerates the formation of alite. These phenomena are evidenced, in the DTA graphs, by the variations in height or area of the thermal effects of the transformations versus the content in CaF_2 (82) (FIG. 16). The de-

creases in the specific effectiveness of fluoride as its concentration increases is also clear, as alrea-

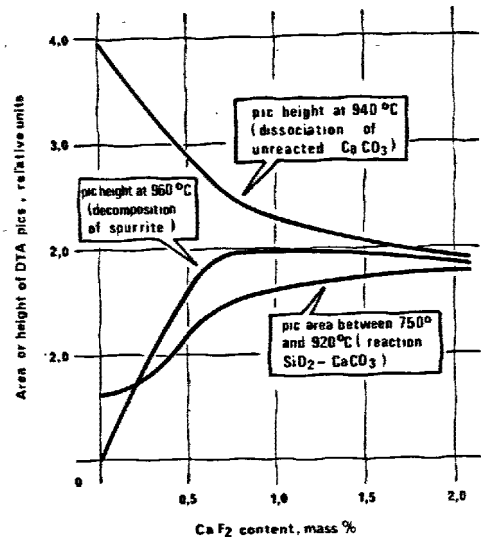

FIG. 16 .DTA EFFECTS OF THE RAW MEAL VERSUS CaF_2 CONTENT. AFTER COURTAULT (82).

dy pointed out by Vogel (2) and recently reconfir - med by Johansen et Al. (224).

Similarly to spurrite, also $(C_2S)_2 \cdot CaF_2$ and $C_{19}S_7 \cdot 2CaF_2$ would give rise, between 950 and 1200°C approx., to a mechanism of formation of alite through incon - gruent melting of $C_{19}S_7 \cdot 2CaF_2$, according to a sche me proposed by Gutt (220). The higher rate of for- mation of C_3S in the presence of CaF_2 is also attri- buted (224) to the larger extention of the primary phase field of C_3S in the C - S - CaF_2 and C - S - A systems. In any case the C_3S formation begins at lower temperatures by at least 150° ÷ 200°C than those in the absence of fluorides.

On the contrary the existence of $C_{19}S_7 \cdot 2CaF_2$ in - volves - during the clinker cooling - the attack of alite and belite by the liquid, with separation of $C_{19}S_7 \cdot 2CaF_2$ because of the peripheral reaction at 1185°C (225). In the practice the rate of cooling is always fast enough so that the reaction does not oc- cur; nevertheless the case of fluoridized clinkers containing $C_{19}S_7 \cdot 2CaF_2$ (as a coating of alite) is not rare. The poor hydraulicity of C_3S fluoridized (226) would explain the low mechanical strengths of clinkers containing more than 0.5 ÷ 0.6% F (227).

7.2.4 The mineralizing action of fluorine com - pounds is attributed to their influence on the stabi- lity of the rhombohedral structure of $CaCO_3$ and on the mobility of the $(SiO_4)^{IV}$ groups of silicates (82). This influence increases as the lattice energy of fluoride increases and therefore, in first approach, as the radius of the cation decreases. For this rea son, at the same concentration in F, MgF_2 and LiF have higher effectivenesses and (in decreasing or - der) NaF, CaF_2, SrF_2 the lower ones. BaF_2 and KF are the less active (82, 147). The fluosilicates, having the same ionic species and equal content in F, have equal (82) or slightly lower (228) effective- ness than that of fluorides.

7.2.5 Fluorite is generally used in the technologi- cal practice for its lower cost and its easy handling. In the last few years its use has extented not only to the manufacture of white clinkers but also of nor- mal ones because of the fuel saving and the increa- se in the kiln capacity that this mineralizer and flux often enables. The advantages obtanable, at the sa me amount added, are not equal for all the raw meals and all the types of kiln: as a rule, the har - der raw meals to burn, containing macrocrystalline rocks, and the short processing-kilns, above all the lepol ones, take the most advantage. The inter nal cycle of fluorine in the burning plants is weak and such that only traces are found in the gases (229). The losses correspond to the eventual shut off of the cycle by extraction of the electrofilter dust which generally has higher (10 ÷ 20%) concentra tion in fluoride than that of the raw meal (values re ferred to the calcined matter).

Experience suggests to limit the additions of fluorite not above 0.5 ÷ 0.6% F of clinker, in order to avoid the dangerous decrease in mechanical strengths. Within this limit the hydraulicity and the strengths of clinker are quite normal if it still contains 1 ÷ 2% free CaO or anyhow it is intended for the produc - tion of high fineness cement.

7.3 Phosphates.

7.3.1 The organogen sedimentary rocks (fossilife- rous limestones, marls and clays of shore-sea fa - cies, a.s.o.) contain varying and sometimes consi derable amounts of phosphates. These minerals are also present in sandstones, sands, and prevailin - gly detrital clays. Phosphorus compounds are con tained in the by-products of the siderurgical indu - stry (blastfurnace slags, slags from electric furna- ces, from converters, a.s.o.) often used in the ce- ment raw meal.

7.3.2 The fundamental knowledge on the phospha- tic clinkers is mainly due to the Researchers (230, 231, 232, 227, 233, 220) of the Building Research Station of Garston (United Kingdom). Schlaudt (234), V'lkov and Tabakova (235), Fix et Al. (236), Salge and Thormann (237) gave further contribu - tions.

P_2O_5 preferably concentrates in belite to the detri ment of alite and the intersitial phase (237): the concentrations in the three phases are in the ratio 4: 2 : 1 approximatively.

In the system CaO - SiO_2 - P_2O_5, a series of solid solutions of CaO and P_2O_5 in C_3S (233) appears as

a primary phase of crystallization. The compositions given in TAB. VI have been assigned to the saturated term (called C_3S") (233, 234, 237). C_3S"

TAB. VI. APPROXIMATE COMPOSITIONS (MASS %) OF C_3S" AFTER DIFFERENT AUTHORS (233,234,237).

	Gutt (1963)	Schauldt (1964)	Salge and Thormann (*) (1973)
CaO %	74.0	73.4	72.9
SiO_2 %	25.5	25.5	25.1
P_2O_5 %	0.5	1.1	2.0
C_3S %	96.9	96.9	95.4
CaO %	2.6	2.0	2.6
P_2O_5 %	0.5	1.1.	2.0

(*) in the presence of Al_2O_3, Fe_2O_3, MgO and alkalis.

has trigonal structure; with respect to C_3S, it shows a distorted elementary cell having reduced dimensions (227). The hydraulic activity ought to be slightly higher than that of C_3S.

Phosphatic belite is a solid solution of $\overline{\alpha}$-C_3P in β-C_2S (for contents $\leq$ 2% P_2O_5) and in α' and α-C_2S (for higher contents in P_2O_5) (227). Since the series of solid solutions C_2S - C_3P shows a lack of subsolid miscibility, a limiting composition called PSS' is in equilibrium with C_3S" at 1500°C. There are still considerable uncertainties for the practical consequences on the composition of PSS' (TAB. VII). It must not even excluded that it falls outside the line joining C_2S to C_3P, towards higher lime contents, because of the marked aptitude of this solution to take hyperstoechiometric CaO (236, 237). The composition of PSS' found by Nurse (230) confirms this hypothesis.

7.3.3 The portion of the system CaO - C_2S - C_3P near C_2S and C_3S, at 1500°C, is shown in FIG. 17 where the compositions deducible from the paper (237) have been assigned to C_3S" and PSS'.

The phases in equilibrium are:

- C_3S and solid solution C_2S - PSS', for lower content in P_2O_5 than the line C_3S - PSS';
- solid solution C_3S - C_3S" and PSS', for content in P_2O_5 between the line C_3S - PSS' and the line C_3S" - PSS';
- CaO, solid solution C_3S - C_3S" and PSS' for higher content in P_2O_5 than the line C_3S" - PSS'.

C_3S" disappears, as an equilibrium solid phase, for higher contents in P_2O_5 than the line CaO - PSS'. In the C_3S - C_2S - PSS' - C_3S" field, the amounts of C_3S and/or C_3S" decrease and that of solid solution between C_2S and PSS' increases as the % of P_2O_5 increases: an experimental confirmation was obtained by Salge and Thormann (237). The opportunity of using very high values of lime saturation (or even supersaturation) for the phosphatic raw meals, consistently with the present content in P_2O_5, is clear.

The hydraulicity of the phosphatic clinkers shows a

TAB. VII. APPROXIMATE COMPOSITIONS (MASS %) OF THE LIMITING SOLID SOLUTION PSS' AT 1550°C AFTER DIFFERENT AUTHORS (230, 233, 234, 237).

	Nurse (*) (1952)	Gutt (1963)	Schlaudt (1964)	Salge and Thormann (**) (1973)
CaO	66.5	63.7	64.1	63.9
SiO_2	26.5	30.3	31.8	31.0
P_2O_5	7.0	6.0	4.1	5.1
C_2S	76.0	86.9	91	88.8
C_3P	15.3	13.1	9	11.2
CaO	8.7	-	-	-

(*) indicated as PSS. In the presence of Al_2O_3, Fe_2O_3, MgO and alkalis, at 1400°C.
(**) from FIG. 14 of (237). In the presence of Al_2O_3, Fe_2O_3, MgO and alkalis.

slight increase for low contents in P_2O_5 (0.5 ÷ 1.0%) (235, 237, 238, 239), probably due to the peculiar structure of C_3S"; afterwards it considerably decreases as the content in P_2O_5 increases. This drop must be related to the decrease in the C_3S/C_2S

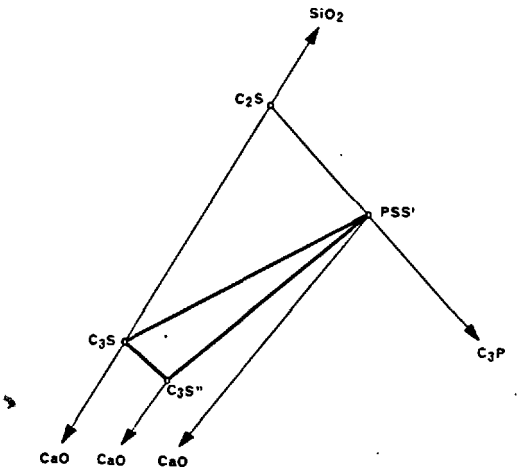

FIG. 17 .MOST BASIC PART OF THE SYSTEM $CaO-C_2S-C_3P$ AT 1500 °C (NOT TO SCALE).

ratio, as well as to the progressive increase in the amount of the structures α' and αC_2S, to the detri - ment of the β-form.

7.3.4 It is recognized (235, 240, 241, 242) that pho sphates have a strong accelerating action on all the reactions occurring during the burning of clinker. The process of combination of CaO in the solid phase is facilitated; conditions favourable for a rapid crystallization of the clinker minerals occur in the presence of liquid phase.

The presence of hydroxyapatite in raw meals con - taining chlorides ought to reduce their intensity of internal recycle in the kilns and in this way it should avoid (or minimize) the formation of spurrite coa -

TAB. VIII. MAXIMUM AND OP TIMUM CONTENTS IN P_2O_5 (MASS % IN THE RAW MEAL) AFTER V'LKOV ET AL. (235).

lime saturation	maximum content	optimum content
0.74	2.0	1.5
0.84	1.5	1.0
0.94	1.0	0.3

tings (207). Therefore the correction of raw meals with suitable amounts of phosphatic additions can be an effective means to improve some technological conditions of the clinker burning.

The uncertainty of the compositions of C_3S" and, above all, of PSS' does not allow the calculation of the maximum content in P_2O_5, practically allowable in a raw meal. V'lkov and Tabakova (235) suggest the limits shown in TAB. VIII.

7.3.5 The favourable influence of CaF_2 on the raw meals containing P_2O_5 was examined by several Au thors among whom Simanovskaya and Vodzinskaya (243) and Gutt (220). Tymashev et Al. (244) studied the effects of concentrations of 0.8 ÷ 1.5% P_2O_5 on the raw meals containing high amounts of alkalis.

7.4 Titanium compounds.

7.4.1 Titanium is present in the clayey sediments and in the detrital ones as both hydrolysis product cooprecipitated with Al, Fe, Be and Zr (bauxites, laterites, a.s.o.) and combined in less alterable re sidual minerals, such as ilmenite, rutile and titanite.

7.4.2 Owing to the great proximity of the ionic rays and the strong energy of the bond Ti-O, Ti^{4+} is vicariant of Fe^{3+} in the tetrahedra $(FeO_4)^V$ of cal - cium alumino-ferrite (245, 246, 247, 248). It also re places Al^{3+} in the same alumino-ferrite and the aluminate (orthorhombic, cubic and tetragonal forms)

TAB. IX. RELATIVE RATIOS OF MASS CONTENT IN TiO_2 IN THE CLINKER PHASES AFTER DIFFERENT AUTHORS.

	Midgley (253) (*)	Hornain (49)	Regourd et Al. (158) (**)	Knöfel (254)(***)
alite	1	1	1	1
belite	1.1	2	1.7	2
aluminate	7.4	0.8	3.3	3
alumino-ferrite		6	10.8	7
TiO_2% of clinker	0.24 ÷ 0.34	0.78	-	1.00

NOTES. (*) Arithmetical mean of the determinations on four industrial clinkers.
(**) Clinker 1 of (158).
(***) Mean of six determinations on one laboratory clinker.

(158, 249). In alite, the vicariance between $(TiO_4)^{IV}$ and $(SiO_4)^{IV}$ is limited (1500 °C) at 13 mole %, equal to 4.53 mass % TiO_2 of C_3 (S, T). The form M_{II} and the form R remain stabilized up to 7 mole % (2.45 mass % TiO_2) and for higher contents respectively (250). The limit of the solid solution in belite corresponds to 0.76 mass % TiO_2 (251). The limits of vicariance of Ti^{4+} instead of Si^{4+}, Al^{3+} and Fe^{3+} in the minerals of pure clinker result from a recent research (252):

	TiO_2 mass %
C_3(S, T)	5.0 ± 0.3
C_2(S, T)	0.7 ± 0.1
C_3(A, T)	1.1 ± 0.2
C_4(AF, T)	18.5 ± 0.5

The distribution in the different phases of clinker appears to be varying (253, 49, 254, 158); neverthe- less the tendency to the enrichment in alumino-ferri te is clear (TAB. IX).

It was reported (254) that increasing amounts (up to 4%) of TiO_2 in a clinker having K_{st} = 90, SM = 2, TM = 1 - not in equivalent replacement of SiO_2 - determine a sharp reduction in the alite content with equal gain in belite without, however, appreciable variations in the amounts of the other phases (FIG.18).

Variations of the same type are much more restrai- ned when TiO_2 is added in place of equivalent a - mounts of SiO_2. It is assumed that either the solid solution of TiO_2 in belite contains hyperstoechiome tric CaO (as is assumed for phosphatic belite) or the presence of TiO_2 displaces the compositions of the invariants at 1338 °C and 1341 °C of the sy - stem C - S - A - F.

In any case, in the practice, it seems suitable to cal

culate the saturation of the raw meals containing TiO_2 (not exceeding ~ 2.5%) by summing the % of SiO_2 to the % of TiO_2 (in equivalent amounts).

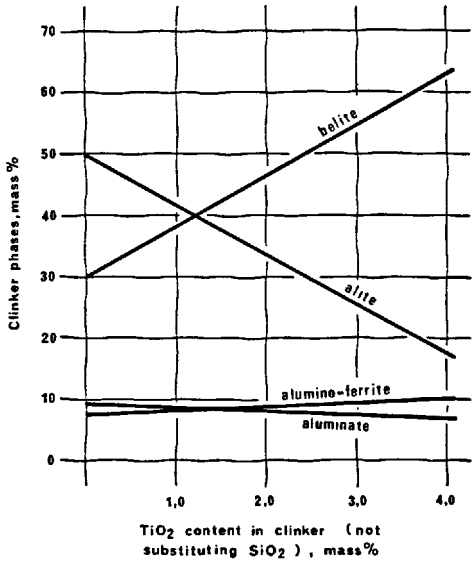

FIG. 18 .PHASES IN THE TiO_2 CLINKERS, AFTER KNÖFEL(254).

7.4.3 1% (of clinker) of TiO_2 is enough to reduce the temperature of incipient melting of the raw meal by 50° - 100°C (254). TiO_2 reduces the surface tension of the liquid phase (138) and causes a drop in the viscosity proportional to its concentration (at least within 4% TiO_2) (255). These conditions facilitate the CaO combination and the alite formation, which are however considerably favoured also by the intermediate formation of CaO - TiO_2 and solid solutions of CaO in the same. The effectiveness of the mechanism of C_3S production would even exceed the one occurring in the presence of CaF_2 (256). The presence of TiO_2 gives clinker a darker colour than the usual one.

7.4.4 TiO_2 retards the initial rate of the clinker hydration (250, 49, 254, 257) with slower setting times and lower early strengths (1 and 2 days). Nevertheless Kondo (250) showed that alite containing TiO_2 has a higher hydraulic activity than ordinary alite for ages over three days. The TiO_2 clinkers examined by Knöfel (254, 252) confirm higher (up to 20%) strengths between 3 and 90 days, for TiO_2 contents of about 1%. The highest increases occur in clinkers having very high lime saturation and high SM (252).

7.5 Chrome compounds.

7.5.1 Generally limestones contain only traces of chrome. Since Cr is an isomorphogenous substitute in the femic silicates, it is found in the sediments from basic and ultrabasic rocks and in the sedimentary products of hydrolysis (laterites, bauxites, a. s.o.). Chrome is sometimes present in the raw meals containing siderurgical slags. The wear of the grinding media and the linings of the raw mix mills as well as the one of the refractory inside the kilns produce only traces.

7.5.2 Although there is a certain disagreement (258, 259, 155, 260) about whether chrome replaces Ca^{2+} or Si^{4+} in C_3S, or both, the latest research (261, 262) seems to indicate that tetrahedra $(CrO_4)^{III}$ and $(CrO_4)^{IV}$ replace $(SiO_4)^{IV}$ according to:

$$2Si^{4+} \rightarrow 2Cr^{5+} + Ca\square^{2-} \quad [23]$$

$$Si^{4+} \rightarrow Cr^{4+} \quad [24]$$

($Ca\square^{2-}$ = lattice vacancy of Ca), with mean state of oxidation of Cr + 4.6 (155). Different Authors fix the limit of solubility at 0.9 (263), 1.4 (264), 1.5 (265, 266), 1.7 (155), 2.0 (259) of Cr_2O_3 mass % of solid solution. The Cr_2O_3 saturation increases the solubility of Al_2O_3 (1.1 to 1.3%) in C_3S and it decreases that of Fe_2O_3 (0.9 to 0.7%) (155). Cr_2O_3 in excess with respect to saturation decomposes C_3S in C_2S and CaO (155, 265, 138). According to Sakurai et Al. (155) the forms T_I and T_{II} (for $Cr_2O_3 \leq 1.4\%$ and $Cr_2O_3 > 1.4\%$, respectively) remain stabilized at ordinary temperature; according to Hornain (49), on the contrary, the hexagonal forms and M_{Ia}do.

Cr^{5+} replaces Si^{4+} in C_2S at 1100°C ÷ 1250°C, by stabilizing the form β at ordinary temperature; the limit of solubility attains at least 8.6 of Cr_2O_3% solid solution (267, 261).

Cr^{6+} replaces Al^{3+} in C_3A (49, 150).

In $C_6A_pF_{1-p}$ $(0 \leq p \leq 0.7)$ Cr^{6+} occupies octahedric sites instead of Fe^{3+} and Al^{3+} (247).

Peters and Hummel (268) studied the relations of subsolid phase in the systems $CaO - Al_2O_3 - 3CaO \cdot 3Al_2O_3 \cdot CaCrO_4 - Al_2O_3$ at 1300°C and $SrO \cdot Al_2O_3 - 3SrO \cdot 3Al_2O_3 \cdot SrCrO_4 - Al_2O_3$ at 1400°C.

In a typical clinker containing 0.55% Cr_2O_3, 76.3% C_3S, 9.1% C_2S, 5.3% C_3A and 8% C_4AF, Hornain (49) found the following distribution of chrome into the different phases (ratios among mass concentrations of Cr_2O_3 in the phases):

alite	:	belite	:	aluminate	:	alumino-ferrite
1	:	2	:	0.1	:	1.4

The limit of solubility of Cr_2O_3 in clinker is about 2% (under oxidizing conditions): considera-

ble amounts of free CaO appear above this concentration (241).

7.5.3 The viscosity of the liquid decreases, at the same temperature, for concentrations up to 2% Cr_2O_3 of liquid (138).
Increasing contents of Cr_2O_3 up to 4 mass% cause also a reduction in the surface tension; this reduction is the greater the higher the A : F ratio (269).
Therefore the lime combinations is favoured in the raw meals which are difficult to burn and have high A : F ratio (270).
Alite forms more rapidly and its crystals become larger (49).
However, also as regards the kinetics of the clinker formation, it is suitable that the Cr_2O_3 content does not exceed 0.5 ÷ 1.0 % of clinker (154, 137).

7.5.4 The solid solution of chrome in C_3S contains, in the lattice, punctual defects due to vacancies and linear faults which, during the reaction with water, favour the detachment of Ca^{2+} from the latyice sites.
Although the data of the literature are discordant on the minimum amount of Cr_2O needed, nevertheless it is accertained that the presence of 0.25 ÷ 0.50 % Cr_2O_3 increase the initial hydraulic activity of clinker (155, 260, 138, 49, 241, 271, 152).
The effect mainly concerns the mechanical strenghs at very short ages (270) of clinkers having high lime saturation (154) and high A : F ratio (270).
Strengths at longer ages are not affected or are negatively influenced (270).
The presence of small amounts of fluorine and manganese favours the action of chrome (272).

7.6 Potassium and sodium.

7.6.1 The main carriers of alkalis into clayey rocks and clastic sediments are orthoclase, albite and plagioclase of magmatic rocks.
K and Na are also contained in the structure of some phyllosilicates, above all the three layer-sialites such as micas, illite, montmorillonite, montronite, a.s.o.
All the sediments, including the carbonatic ones, sometimes contain soluble alkali salts which are residues of the deposit environnement.
K_2O and Na_2O in the raw meals of European cement factories (170) range between 0.5 and 2.0% and between 0.05 and 0.6% respectively (ratio of the mass concentrations between 3 and 10).
Jawed and Skalny (273) have recently revised the knowledge about alkalis in clinker.

7.6.2 Because of their marked volatility, alkalis give rise to a cycle, inside the kilns, which increases their concentration in the processed material with possible danger to the regular course of the process (164, 167, 169, 170, 274).
The intensity of the recycle more concerns the potassium compounds than the sodium ones, being the former more volatile than the latter, at the same temperatures (FIG. 19) (164, 275, 276).
Moreover this intensity depends on the nature of the present alkali minerals and anionic species, on the chemical composition of the raw meal, on the characteristics of the process as well as on the type of kiln (173).
Under normal conditions, the alkali volatility of the raw meals increases, in the order, for feldspars, micas, illite and montmorillonite, that is as the bond energy of the considered silicate decreases (164).
Sulphates determine less intense cycles than carbonates, and these than chlorides (164) (FIG.19).
The nodule-fed kilns (lepol and long with internal recuperators) have poorer recycles than the dry meal-fed ones (both with suspension preheater and long with internal recuperators) and than the wet kilns (171).

7.6.3 Although they act as fluxes, alkalis are the technologically less desiderable compounds among the minor ones. They can be eliminated from the internal cycle through the three systems already mentio

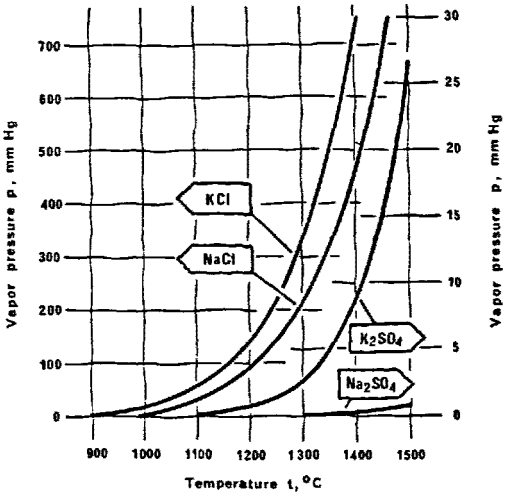

FIG. 19 .VAPOR PRESSURE OF SODIUM AND POTASSIUM SULPHATES AND CHLORIDES (164,275,276).

ned in the paragraph 6.5.2:

- through shut off of the cycle by (total or partial) elimination of the electrofilter dust. This technique is not practicable with the suspension preheater kilns;

- through shut off of the cycle by (partial or total) bypass of the external recuperator. Unfortunately the method involves the wasting of an amount of energy which is proportional to the amount of bypass; this loss can substantially be reduced by the technique of the calcination outside the kiln (10).
  Today the total bypass of the kiln gases with a nearly full precalcination, enables low alkali clinkers to be cheaply produced also from raw meals rich in alkalis (277), eventually by using addition of calcium chloride (278, 279, 280, 281);

- through clinker. The method can be used in all the kilns and demands the conversion of alkalis to sulphates (279, 282). It involves fairly high amounts of recycling phase in the burning material and the production of clinkers having all the alkalis contained in the raw meal and fuel. Therefore it is not practicable with raw meals too rich in alkalis ($K_2O + Na_2O$ > about 1.0% of the calcined material) because of the forming coatings and rings. Moreover it is not even practicable with raw meals not very poor in alkalis ($\leq$ 0.6% Na_2O + + K_2O equiv. of the calcined material) if they are intended for low alkali clinkers. The presence of Cl (>50 ppm of the calcined material) makes the system ineffective.

7.6.4 The alkalis present in clinker as sulphates, particularly K_2SO_4, favourably affect its strengths at early ages (up to 3 days) whereas they lower those at 28 days and over (42, 283).

7.7 Magnesium.

7.7.1 In the practice there are not calcareous rocks deprived of magnesium, which replaces Ca^{2+}, also at random. Generally limestones of the oldest formation are richer. Magnesium is also present in clayey and detrital sediments as a carbonate, as a silicate of primary rocks and finally as an isomorphogenous substitute in some phyllosilicates.

7.7.2 MgO distributes, in the solid solution, into the clinker minerals as far as saturation; the excess remains uncombined as periclase.

In alite, the solid solution is of substitutive type $Mg^{2+} \longrightarrow Ca^{2+}$ (284, 158). Its content in MgO is a constant fraction of MgO of clinker, within the $0 \leq MgO_{cli} \leq 3\%$ range: this fraction is 0.74 according to Yamaguchi and Takagi (285) and 0.63 according to Kristmann (50). As a rule, the richest alites are monoclinic (286); the poorest ones are trigonal (158, 50). The MgO content in belite is 0.25 ÷ 0.35 MgO of clinker, within the $0 \leq MgO_{cli} \leq 2\%$ range (50). The presence of high concentrations in MgO would reduce the activation energy of the conversion $\alpha - C_2S \longrightarrow \alpha' - C_2S$, with consequent stabilization, during cooling, of the hydraulically less active form β (287). Although the liquid phase can contain up to 8% MgO (A : F = = 1.3) (288), the replacement of Ca^{2+} and Fe^{3+} by Mg^{2+}, in C_3A and $C_2A_pF_{1-p}$ ($0 \leq p \leq 0.7$), generally yields matrixes containing 3.5% MgO. In some cases, concentrations of 6% and over have been found (50). The presence of magnesia favours compositions of $C_2A_pF_{1-p}$ having higher values of p, with decrease in C_3A and corresponding increase in C_3S, to the detriment of C_2S (288, 289, 290, 48, 291).

Periclase appears as an independent phase in clinkers containing over 2% MgO (23, 50): depending

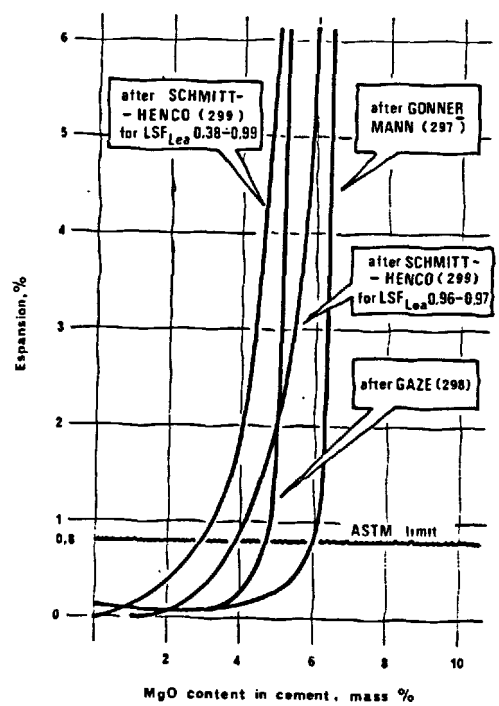

FIG. 20 . AUTOCLAVE EXPANSION FOR INCREASING MgO CONTENT(297,298,299).

on its excess and the rate of cooling, it appears in large roundish crystals arranged in clusters as well as in dendritic shape, finely dispersed and well-distributed into the mass (292, 293, 294).

7.7.3 The reactivity of raw meals is favoured by the presence of MgO only in the range of the higher temperatures (about 1300°C) (228). At any other variable unchanged, the first appearance-temperature of the liquid drops by some tens of °C; viscosity and surface tension of the liquid reduce whereas the mobility of all the present ionic structures increases (137). Under these conditions, the dissolutions in the liquid of C_2S and CaO are more rapid and C_3S forms more quickly (228). Unfortunately - as known - the presence of periclase (especially the one in the form of large crystals in clusters) makes the cement unstable. Therefore the standards of several countries (295) limit its content and/or prescribe a test of unsoundness in autoclave (296).

The results achievable by this test with regard to the % of MgO in clinker, reported by different Authors (297, 298, 299) are shown in FIG. 20.

Nevertheless it is recognized that the test is not probative with every type of cement (288, 298).

Moreover the decrease in the mechanical strengths at medium ages, that some cements containing a limited amount of MgO ($< 4 \div 5\%$) show, also with quite normal volume stability, is worrying (291, 287, 288). According to Soda et Al. (287) this phenomenon would be limited only to clinkers very rich in C_2S, containing over 2% MgO, and it would be attributed to the convertion of α-C_2S to β-C_2S.

7.7.4 Finally it must be noticed a curious relation between MgO and SO_3 present in clinker. It was seen (paragraph 7.1.4) that the impoverishment in C_3S caused by the combined action of SO_4^{2-} and Al^{3+} is hampered by a suitable concentration in MgO. On the other hand, Schmitt-Henco (299) showed that the volume instability of cements containing over 2% MgO is neutralized by the presence of an amount of SO_3 (in clinker) equal to:

$$\% SO_3 = 0.67\ (\%MgO - 2) \qquad [25]$$

when $2 \leq \%MgO \leq 6$ about.

7.8 Strontium.

7.8.1 As a rule, strontium is present in minimum amounts in ancient limestones (and marls), attributable to sediments of skeletons and shells of organisms. On the contrary, even important contents (up to 10% SrO and over) are sometimes found in recent limestones (and marls), especially of evaporitic and chemical origin. The more frequent mineral is celestine ($SrSO_4$). This (together with other evaporitic minerals) is also present, as a cement, in the calcareous and siliceous detrital sediments (sandstones, grauwackes, a.s.o.). Strontianite is relatively rare; it is generally found in veins of limestones and marls.

7.8.2 The phase equilibria of the system CaO - SrO - SiO_2 were reexamined and completed by Brisi and Appendino (300) at 1200°C and, in the most basic part, at 1350°C.

In Ca_2SiO_4, Sr^{2+} is vicariant of Ca^{2+} in all the proportions (with stabilization of the form α'), whereas in Ca_3SiO_5 the vicariance is limited to $1 \div 2$ atomic % Sr, roughly corresponding to $(Ca_{2.95}Sr_{0.05})SiO_5$ (point N of FIG. 21). The structures

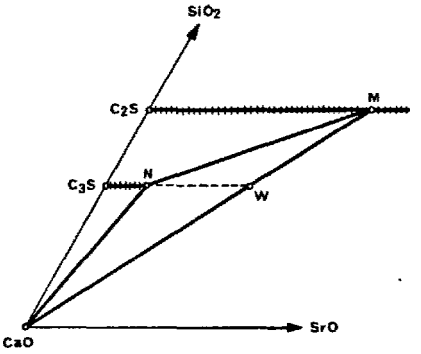

FIG. 21 . MOST BASIC PART OF THE SYSTEM CaO - SrO - SiO_2 (NOT NO SCALE) AFTER BRISI AND APPENDINO (300).

T_I and T_{II} remain stabilized, at room temperature, up to 1 atomic % Sr and at the limiting concentration respectively (301). In the two-phase field C_2S - M - N - C_3S, the solid solutions of SrO in C_2S and SrO in C_3S coexist, whereas in the three-phase field C - M - N, $(Ca_{2.95}Sr_{0.05})SiO_5$ is in equilibrium with the solid solution $(Ca_{1.8}Sr_{0.2})SiO_4$ (point M) and free CaO. It is deduced that the mixes of $C_3S + C_2S$ can carry not more than $2.25 \div 11.40\%$ SrO (segment NM) in the solid solution, depending on the $C_3S : C_2S$ ratio; for contents exceeding these limits, free CaO of equilibrium (coexisting with N and M) always appears. When SrO exceeds a value between 11.40% (point M) and 8.71% (point W) depending on the $C_3S : C_2S$ ratio, the solid solution of $3SrO \cdot SiO_2$ in C_3S disappears and only $(Ca, Sr)_2SiO_4$ and (Ca, Sr)O remain in equilibrium (in the case concerning the composition of portland cement clinker, (Ca, Sr)O is practically pure CaO).

7.8.3 Gilioli, Massazza and Pezzuoli (302, 303) studied the equilibria of the systems CaO-SrO-SiO_2 -SO_3 and CaO-SrO-Al_2O_3-SO_3 at 1330°C. They

found in the former, on the segment $CaSO_4$-$SrSO_4$, three series of solid solutions separated by two lacks of miscibility, and the compound $CaSO_4 \cdot 2SrSO_4$ (304) as a singular term (for x = 0.666) of the series $(Ca_{1-x}Sr_x)SO_4$ with $0.6 \leq x \leq 0.7$. The saturated solution N in the presence of SO_3 is in equilibrium with M, CaO and a solid solution $SrSO_4$ - $CaSO_4$: for this reason, the limits 2.25 ÷ ÷ 11.40% SrO become higher in the presence of SO_3 (in fact, as FIG. 22 shows, a part of SrO forms a solid solution with $CaSO_4$).

The equilibria of the systems CaO - SrO - Al_2O_3 - SO_3 (FIG. 23) evidenced incompatibilities between solid solutions C_3A - $3SrO \cdot Al_2O_3$ and all the sulpha

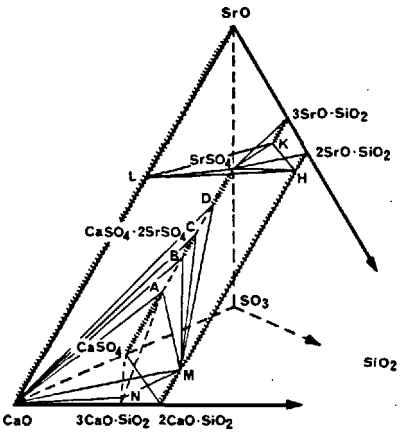

FIG. 22 .MOST BASIC PART OF THE SYSTEM CaO-SrO-SiO_2-SO_3. AFTER GILIOLI ET AL.(302).

tic phases, except for the extreme term $3SrO \cdot Al_2O_3$ with $SrSO_4$: therefore the solid solutions $3(CaO, SrO) \cdot Al_2O_3$ decompose in the presence of SO_3 to form free CaO and a solid solution of the series $4(CaO, SrO) \cdot 3Al_2O_3 \cdot SO_3$, having the compound $3CA \cdot CaSO_4$ (305, 183, 306, 307) and the compound $3(SrO \cdot Al_2O_3) \cdot SrSO_4$ (308) as extremes.

The direct measurements (electron microanalysis) carried out by Massazza and Pezzuoli (309) on industrial and laboratory clinkers confirmed that, for contents of 4 ÷ 5% SrO, this element preferably distributes into belite and, to a lesser extent, into alite. Free CaO is just contaminated.

7.8.4 Although celestine (and probably strontianite) have an accelerating action on the combination reactions of CaO in the solid phase (310) and they lower the appearance-temperature of the liquid (302), their presence in the raw meals is not desirable since they are liable for the release of free CaO of equilibrium and - over certain limits - for the distruction of alite. From this standpoint, $SrCO_3$ is more dangerous than $SrSO_4$ and the clinkers having high degree of lime saturation are more vulnerable than the prevailingly belitic ones.

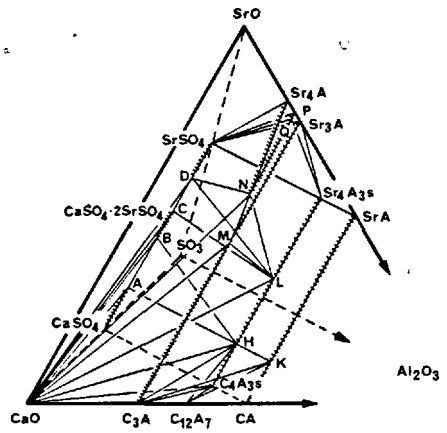

FIG.23 .MOST BASIC PART OF THE SYSTEM CaO-SrO-Al_2O_3-SO_3. AFTER GILIOLI ET AL.(303).

On the other hand $SrSO_4$ - at least in the absence of alkalis - decomposes the solid solutions $3(CaO, SrO) \cdot Al_2O_3$ by releasing CaO in this case too. The limits of acceptability of the SrO concentration in two typical raw meals are given in TAB. X. It would seem that higher concentrations can be allowed in the presence of CaF_2 (310).

Butt et Al. (311) found that hydraulicity and strengths developed by strontium alites are considerably lower than those of the ordinary ones; they attributed this fact to the lower number and the smaller sizes of the lattice voids in strontium alite.

TAB. X. - ACCEPTANCE LIMITS OF SrO CONTENT IN THE RAW MEALS, MASS % OF SrO ON BURNT MATTER (309).

form of combination	$K_{st}I$=0.76	$K_{st}I$=0.96
celestine ($SrSO_4$)	8	3
strontianite ($SrCO_3$)	6	3

7.9 Barium.

7.9.1 Limestones contain varying amounts of ba -

rium (10÷600 ppm Ba), essentially as barite. Evaporitic limestones are rich (up to 1000 ppm) or, exceptionally, very rich. Barium can concentrate in the hydrolysis minerals of clayey sediments also in appreciable amounts. It is found in the detrital rocks, besides as a sulphate, also as a residual femic mineral (amphiboles and pyroxenes).

7.9.2 Ba^{2+} replaces Ca^{2+} in all the minerals of clinker, except for alumino-ferrite (152).
FIG. 24 shows (312) the portion richest in lime of the system CaO - BaO - SiO_2.

It results that:

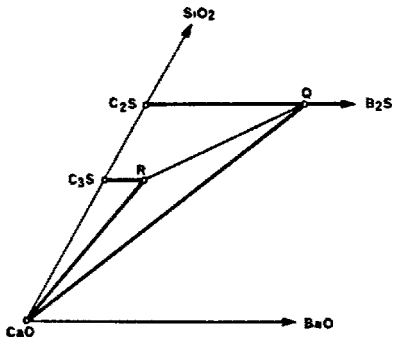

FIG. 24 . MOST BASIC PART OF THE SYSTEM CaO-BaO-SiO_2 (NOT NO SCALE). AFTER BRISI (312).

- in the two-phase field $C_3S - C_2S$ - Q - R: solid solutions $(C,B)_2S$ and solid solutions $(C,B)_3S$;
- in the two-phase field C_3S - R - CaO: solid solutions $(C, B)_3S$ and CaO;
- in the three-phase field CaO - Q - R: solid solution $(C, B)_2S$ having composition Q, saturated solid solution $(C, B)_3S$ having composition R, and CaO;
- on the right of the Q - CaO line: solid solutions $(C, B)_2S$ and CaO;

coexist in equilibrium, in each of these times.

The limiting solid solution R of BaO in C_3S contains 1.5 mole % BaO (2.96 mass %) (313), or 1.0 mole % BaO (1.99 mass %) (301), at 1600°C and 1450°C respectively.

The stabilized form is T_{II} (in the presence of MgO ≥ 2% moles, $M_{Inv.}$) (301). The solid solution Q of BaO in C_2S, in equilibrium with R and CaO, contains 7 mole % BaO (11.55 mass %) at 1350°C (312).

The form α' remains stabilized (314, 315). The limiting solid solution of BaO in C_3A contains about 1.5 mole % BaO (about 2.5 mass %) (152).

7.9.3 In disagreement with other Authors (316, 317), Suleimenov et Al. (318) and Kurdowski (152) believe that the presence of BaO - also in limited amount - affects neither the characteristics of the liquid phase nor the rate of the lime combination.
On the contrary, barium appears to be one of the most effective "activators" of the hydraulicity and strengths of clinker; the latter are higher by 10 ÷ ÷ 20% at any age, all the other conditions unchanged (152, 271, 150, 319, 320).

The optimum concentration is between 0.3 and 0.5 mass % BaO and the clinkers containing few fluxes (SM > 3.0) (152) and having high content in C_2S (150) are more favoured by this concentration.
Barium cements demand suitable additions of gypsum and eventually of K_2SO_4 (320).
This behaviour of clinker is strangely different from that of the solid solution of BaO in C_3S; for this solution, in fact - because of the larger ionic radius of Ba^{2+} with respect to Ca^{2+} - Butt et Al. (311) theorized and experimentally confirmed a reduced hydraulic activity.

The action of $BaCl_2$ on C_3A, between 900°C and 1000°C, was studied by Muminov and Akhmedov (321).

7.10 Zinc.

7.10.1 The content in zinc in the sedimentary rocks does not exceed the tens of ppm, as a rule. It is mainly contained in the detrital and clayey rocks (magnetite and chlorite vectors). Sprung and Rechenberg (322) found amounts ranging between 25 and 62.10^{-4}% ZnO in 23 raw meals from German cement factories. Nevertheless higher concentrations must be expected in raw meals containing limestones mineralized by sulphides or corrected with pyrite cinders rich in blende.

7.10.2 During the burning process, 80 ÷ 90% ZnO (or ZnS) in the raw meal is combined in clinker (322, 323). Therefore clinkers contain between 30 and $100 \cdot 10^{-4}$% ZnO, depending on the content in the raw meal and the amount of electrofilter dust rejected out of the cycle.

Roughly half zinc distributes into silicates (with sharp preference for alite, to the detriment of belite) and the other half does into the matrix (with preference for the ferritic phase) (323, 293). Therefore, for a normal composition of clinker, alumi

no-ferrite and aluminate, alite and belite should result less rich in the decreasing order two by two.

Hornain (49) found concentrations (ZnO mass % of phase) resulting in the ratios:

belite	:	aluminate	:	alite	:	alumino-ferrite
1	:	4	:	8	:	17

According to Knöfel (323), the saturation attains 5 ÷ 6% ZnO in alumino-ferrite, 4 ÷ 5% in aluminate, about 1% in alite, 0.3% in belite.
According to Ono et Al. (324) and Tsuboi et Al. (293), trigonal C_3S would be stabilized; according to Knöfel (323) C_3S M_{II} and β -C_2S, and according to Hornain (49) C_3S M_{Ib} and β -C_2S would.

In the clinkers studied by Knöfel (323) - also containing only 1% ZnO - a new phase probably consisting of free ZnO (zincite) appears together with zinc containing-minerals.

The presence of ZnO reduces the amount of aluminate in favour of alumino-ferrite (323, 293, 325): each 1% ZnO reduces the former and increases the latter by little less than 2%.
Strangely, an increase in alite does not correspond to this variation (323).

7.10.3 Zinc is a very effective flux and mineralizer (323, 293): it lowers the clinkerization temperature and accelerates the lime absorption.
Nevertheless the effect on the properties of clinker (except for a darker colour) are not quite clear.
According to Aktsu (325) just 0.3% ZnO would negatively affect the hydraulicity.

On the contrary, Knöfel's (323) research show that limited contents in ZnO (< 1 ÷ 2%) in a typical clinker having K_{st} = 95, SM = 2.2 and TM = 2.5 determine an improvement in its mechanical strengths by up to 20% and over (especially at short ages).

8. CONCLUSIONS.

8.1 It is important to distinguish reactivity from burnability of a raw mix. In the present paper, the concept of reactivity has been associated to that of rate of reaction, or of a set of reactions, for given conditions of temperature.
On the contrary, burnability expresses an amount of matter transformed or still to transform, at any instant and temperature of the process.
This distinction seems particularly useful to compare raw meals having different lime saturation.

8.2 Reactivity and burnability are fundamental properties having important effects on the capacity of plants and the energy needs of the process.
The choice of the type of kiln and its dimensions, the proportioning of the raw meal, the more suitable admixtures cannot prescind from a right evaluation of such properties.
Nevertheless the knowledge on this matter is not satisfactory, above all for want of a suitable methodology of measurement, universally adopted.
The methods entrusting the evaluation of burnability to the value of CaO_f, that the function $CaO_f = f(t, \theta)$ assumes for only a couple $(t_i; \theta_i)$, or to the values t_i' and θ_i', for which the quantity of CaO_f becomes equal to or lower than an established amount, prove to be insufficient.

On the contrary, Blaise et Al.'s method seems to be rational. It evaluates burnability on the basis of the course of the reactions in the overall range between 1000°C and 1450°C.
For practical purposes, the characterization of the raw mix by three values of average reactivity relevant to three significant temperature intervals (for instance, 500°C ÷ 1000°C, 1000°C ÷ 1300°C, 1300°C ÷ 1450°C), under standard conditions of temperature and time gradients, could result even more useful.

8.3 Reactivity and lime saturation affect the value of the burnability.
In its turn, reactivity is a function of SM, TM, fineness, present mineralogical species and activity state of such species.
The laws governing the diffusion processes among solids and between solids and liquid well explain the influence that those variables have on the reactivity.
Particularly, the dependence of the diffusion coefficients on the activation energy, and the dependence of the value of the latter on the concentrations of defective structures in the solid matter, constitute the basis for a satisfactory model of interpretation of the phenomena. This model also explains the interesting possibilities offered by the so called mechanical, thermal, and chemical activations of the raw meal.

8.4 It seems right to expect that the chemical activation (or however one prefers to call, or must interpret, the action of the minor compounds acting as mineralizers and/or fluxes) constitute the more promising field for the development of new technological methods. The knowledge on the mechanism of action of these compounds, and on the phase relations that they yield, more and more frequently allow higher capacities of the equipment and energy savings to be obtained. Thanks to this knowledge, also the limits of exploitability of raw materials as well as of wastes, which are sometimes introduced into the raw meal for ecological decontamination purposes, are enlarging.

REFERENCES

1.- VOGEL, E. (1953) "Untersuchungen über den Entsäuerungsgrad der Granalien auf dem Le - polrost", Silikattechnik 4, 469.

2.- VOGEL, E. (1959) "Die Wirkung von Flussspat und Kiesabbrand auf den Reaktionsverlauf von Zementrohmehlen unterhalb 1100°C.", Silikattechnik 10, 415.

3.- LONGUET, P. et COURTAULT, B. (1964) "Aptitude à la clinkérisation des crus de ci - menterie", Rev. Mater. Constr. N° 585, 174.

4.- PFRUNDER, V.R. et WICKERT, H. (1970) "Einige Versuche über den Einfluss der chemischen Zusammensetzung und der Mahlung auf die Sinterung von Zement-Rohmehlen", Ze - ment-Kalk-Gips 23, 147.

5.- QUITTKAT, W. (1965) "Die Phasenumbildungsvorgänge beim Zement-Klinkerbrennen aus Rohmehlen mit Branntkalk-, Kalkhydrat- und Kalksteinkomponente und ihre Bedeutung für den technischen Brennprozess", Tonind. Ztg. 89, 351.

6.- PHILIPP, O. et SCHRADER, R. (1974) "Ap - plication of thermal, chemical and mechanical activation in clinker burning", 6th Int. Congr. Chem. Cement, Moscow.

7.- LEHMANN, H. et THORMANN, P. (1963) "Über den Einfluss der Kalksteinkorngrösse auf die Klinkermineralbildung", Tonind. Ztg. 87, 369.

8.- LEHMANN, H., LOCHER, F.W. et THOR - MANN, P. (1964) "Der Einfluss der kalkstein korngrösse auf die Klinkermineralbildung im Temperaturbereich von 850°C bis 1450°C", Tonind. Ztg. 88, 489 et 537.

9.- RITZMANN, H. (1976) "Möglichkeiten und Grenzen der Vorkalzination bei verschiedenen Drehrohrofenverfahren", Zement-Kalk-Gips 29, 207.

10.- BUCCHI, R. (1978) "Calcining systems outside the suspension preheater cement kilns", Il Cemento 75, 411.

11.- SULIKOWSKI, J.P. (1968) "Burnability of raw mixes", Proc. 5th Int. Symp. Chem. Cement, Tokyo P.1, 106.

12.- BLAISE, R., MUSIKAS, N. et TIEDREZ, H. (1971) "Nouvelle méthode de détermination cinétique de l'aptitude à la cuisson d'un cru de cimenterie", Rev. Mater. Constr. N° 674 - 675, 287.

13.- FRANCARDI, M.T. (1962) "Relazione interna Laboratorio Centrale Italcementi", 18 juin.

14.- S.TE DES CIMENTS FRANCAIS (1975) "Private communication", Paris.

15.- MUSSGNUG, G. (1953) "Sinterfähigkeit von Rohmehlen. Tagunsber. der Zementindustrie H. 7, Düsseldorf 14 + 17 Mai 1952 p. 33", Zement-Kalk-Gips 6, 46.

16.- Dyckerhoff, K. (1958) "Untersuchungen an Zementrohmischungen mit sehr hohem Silikatmodul", Zement-Kalk-Gips 11, 196.

17.- KOCK, H., REY, G. et BECKER, F. (1974) "A statistical model for determining the burnability of cement raw mixes", 6th Int. Congr. Chem. Cement, Moscow.

18.- LUDWIG, U. et RUCKENSTEINER, G. (1973) "Einfluss der Phasengrenzen bei der Klinkerbildung", Proc. 11th Conf. Silicate Ind. Budapest P.I, p. 365.

19.- LUDWIG, U. et RUCKENSTEINER, G. (1973) "Einflüsse auf das Brennverhalten von Zementrohmehlen und die Klinkerqualität", Tonind. Ztg. 97, 313.

20.- LUDWIG, U. et RUCKENSTEINER, G. (1974) "Über die Brennbarkeit von Zementrohmehlen", Cem. Concr. Res. 4, 239.

21.- LUDWIG, U. et DÄRR, G.M. (1975) "Über die Brennbarkeit von Zementrohmehl", Zement - Kalk-Gips 28, 421.

22.- DAHL, L.A. (1938) "Estimation of phase composition of clinker in the system C_3S-C_2S-C_3A-C_4AF at clinkering temperatures", Rock Prod. 41, 48, 46, 42, 44 et 42, 38, 46, 50.

23.- SPOHN, E., WOERMANN, E. et KNÖFEL, D. (1968) "A refinement of the lime standard formula", Proc. 5th Int. Symp. Chem. Cement, Tokyo P.I, 172;
(1969) "Eine verfeinerte Kalkstandardformel", Zement-Kalk-Gips 22, 55.

24.- CHRISTENSEN, N.H. (1979) "Burnability of cement raw mixes at 1400°C. I - The effect of the chemical composition", Cem. Concr. Res. 9, 219.

25.- LEGRAND, J. (1961) "Relations entre les caractéristiques d'un clinker et celles des ses matières premierès", Rev. Mater. Constr. N° 554, 469; N° 555, 505; N° 556, 25; N° 557, 50; N° 558, 83.

26.- BUCCHI, R. (1965) "Leganti idraulici", Enciclopedia Scienze e Tecniche SADEA Firenze 6, 51.

27.- GLAUSER, A. (1966) "Berechnungen von Portlandzement - Rohmischungen mittels der Aequivalentnorm von Niggli und Kühls Kalkstandard", I Teil : Zement-Kalk-Gips 19, 238. II Teil: Zement-Kalk-Gips 20, 102. III Teil: Zement-Kalk-Gips 20, 287.

28.- GLAUSER, A. (1970) "Die Auswertung des kühl'schen Silikatmoduls in aequivalentnorma-

tiven Berechnungen von Portlandzement-Roh - mischungen", Zement-Kalk-Gips 23, 312.

29.- GLAUSER, A. (1972) "Der Tonerdemodul in aequivalentnormativen Berechnungen von Roh-mischungen", Zement-Kalk-Gips 25, 202.

30.- FENAROLI, G. (1929) "Rappresentazioni grafiche e calcolo dei leganti idraulici", Ind. Ital. Cem. 26, 85.

31.- SESTINI, Q. (1941) "Il sistema quaternario $CaO - SiO_2 - Al_2O_3 - Fe_2O_3$ e le sue applicazioni", Chim. Ind. (Milan) 23, 163.

32.- BUCCHI, R. (1952) "Procedimento di approssimazione successiva per il calcolo di miscela da cemento mediante il metodo grafico di Fenaroli", Ind. Ital. Cem. 22, 292.

33.- GLAUSER, A. (1974) "Über Methoden der graphischen Darstellung in der Zementchemie unter Berücksichtigung der Aequivalentnorm", Zement-Kalk-Gips 27, 610.

34.- XIROKOSTAS, D.A. et ZOPPAS, C.E. (1977) "Mathematical programming approach to the problem of cement blending optimization", Cem. Concr. Res. 7, 503.

35.- GUTTMANN, A. et GILLE, F. (1929) "Das Mangan im Zementklinker, zugleich ein Beitrag zur Konstitutionsfrage des Zementes", Zement-Kalk-Gips 18, 500, 537 et 570.

36.- SPOHN, E. (1932) "Die Kalkgrenze des Portlandzements", Zement 21, 702, 717 et 731.

37.- LEA, F.M. et PARKER, T.W (1935) "The quaternary system $CaO - Al_2O_3 - SiO_2 - Fe_2O_3$ in relation to cement technology", Bldg. Res. Pap. N° 16.

38.- BOGUE, R.H. (1929) "Calculation of the compounds in portland cement", Ind. Eng. Chem. Anal. Ed. 1, 192.

39.- HERATH BANDA, R.M. et GLASSER, F.P. (1978) "Role of iron and aluminium oxides as fluxes during the burning of portland cement", Cem. Concr. Res. 8, 319.

40.- KÜHL, H. (1913), Zement-Protokoll des V.D. P.Z.F. 405.

41.- KÜHL, H. (1926) "Der junge Zemenchemiker", Zement 15, 636.

42.- OSBAECK, B. (1979) "Der Einfluss von Alkalien auf die Festigkeitseigenschaften von Portlandzement", Zement-Kalk-Gips 32, 72.

43.- WETZEL, E. (1911), Zement-Protokoll des V.D.P.Z.F. 281.; (1912) 217; (1913) 347 et (1914) 145.

44.- KÜHL, H. (1929) "Die Berechnung der besten Zementrohmischung", Zement 18, 833 et 868.

45.- KÜHL, H. (1933) "Der Kalkstandard der Portlandzemente", Tonind. Ztg. 57, 460.

46.- CHRISTENSEN, N.H. (1978) "The effects of magnesia on lime combination in clinker", World Cem. Technol. 9, 223.

47.- POLLITT, H.W.W. et BROWN, A.W. (1968) "The distribution of alkalis in Portland cement clinker", Proc. 5th Int. Symp. Chem. Cement, Tokyo P.I, 322.

48.- KNÖFEL, D. et SPOHN, E. (1969) "Der quantitative Phasengehalt in Portlandzementklinkern", Zement-Kalk-Gips 22, 471.

49.- HORNAIN, H. (1971) "Sur la répartition des éléments de transition et leur influence sur quelques propriétés du clinker et du ciment", Rev. Mater. Constr. N° 671 - 672, 203.

50.- KRISTMANN, M. (1977) "Portland cement clinker. Mineralogical and chemical investigations P.I et P. II", Cem. Concr. Res. 7, 649 et 8, 93.

51.- HANSEN, W.C. (1968) "Potential compound composition of portland cement clinker", J.Mater. 3, 100.

52.- MAJUMDAR, A.J. (1966) "The ferrite phase in cement", Trans. Brit. Ceram. Soc. 64, 105.

53.- TARTE, P. (1966) "Study of interaction between tricalcium aluminate and dicalcium aluminoferrite", Silicates Ind. 31, 343.

54.- SCHLAUDT, C.M. et ROY, D.M. (1965) "Crystalline solutions in $3CaO \cdot Al_2O_3$ in the join $Ca_3Al_2O_3 - Ca_3Fe_2O_3$", Nature 207, 819.

55.- BUCCHI, R. et BUZZETTI, F. (1975) "Interpretation of modules as a function of potential composition of portland cement clinker", Cem. Technol. 6, 71.

56.- HEILMANN, T. (1952) "The influence of the fineness of cement raw mixes on their burnability", Proc. 3rd Int. Symp. Chem. Cement, London, 711.

57.- TOROPOV, N.A. et LUGININA, I.G. (1953) "Effect of the grain size on assimilation of CaO during burning of portland cement", Tsement 19, N° 2, 17.

58.- SWAYZE, M.A. (1946) "A report on studies of: I the ternary system $CaO - C_5A_3 - C_2F$; II the quaternary system $CaO - C_5A_3 - C_2F - C_2S$; III the quaternary system as modified by 5% magnesia", Amer. J. Sci 244, 1 et 65.

59.- LEA, F.M. et PARKER, T.W. (1934) "Investigation of a portion of the quaternary system $CaO - Al_2O_3 - SiO_2 - Fe_2O_3$: the quaternary system $CaO - C_2S - C_5A_3 - C_4AF$", Phil. Trans. R. Soc. 234, N° 731, 1.

60.- SYCHEV, M.M. (1962) "The technological

properties of cement raw mixes", Gosstroy - izdat 131.

61.- JOHANSEN, V. (1977) "Cocciòn de clinker de cemento portland en hornos rotatorios", Mat. de Constr. N° 166 - 167, 85.

62.- VOSTEEN, B. (1971) "Physikalische und chemische Kinetik endothermer topochemischer Gleichgewichtsreaktionen", Chem. Ing. Tech. Z. 43, 478.

63.- ZACHAROV, G.V. (1973) "Das Brennen von gemahlenem Kalkstein in schwebendem Zustand", Stroit. Mater. 19, 11.

64.- VOSTEEN, B. (1974) "Vorwärmung und vollkommene Kalzination von Zementrohmehl in einem Schwebegassystem", Zement-Kalk-Gips 27, 443.

65.- OHME, K., SCHRADER, R. et MÜLLER, A. (1975) "Kinetik der thermischen Dissoziation von Kalkstein und Zemenrohmehl im Flugstaubreaktor", Silikattechnik 26, 403.

66.- MÜLLER, A. (1977) "Zum Einfluss verfahrenstechnischer und stofflicher Parameter auf die Kinetik der thermischen Zersetzung von Kalziumkarbonat", Proc. 12th Conf. Silicate Ind. Budapest P.I, p. 565.

67.- MÜLLER, A., DAHM, B. et STARK, J. (1979) "Beitrag zur Kinetik der Calciumcarbonatzersetzung", Zement-Kalk-Gips 32, 78.

68.- DE KEYSER, W.L. (1965) "Studies on the solid state reactions between SiO_2, Al_2O_3, MgO, CaO, Fe_2O_3, ZrO_2", Proc. 8th Conf. Silicate Ind. Budapest p. 133.

69.- HEDVALL, J.A. (1952) "Einführung in die Festkörperchemie", Vieweg u. Sohn, Braunschweig.

70.- ADDA, Y. et PHYLIBERT, J. (1966) "La diffusion dans les solides", Tome II, chap. XII et XIII pp. 667 et 751. Presses Univ. Paris.

71.- CHRISTENSEN, N.H. et SIMONSEN, K.A. (1970) "Diffusion in portland cement clinker", J. Amer. Ceram. Soc. 53, 361.

72.- JOHANSEN V. et JEPSEN, O.L. (1972) "Burnability of raw mix: Theoretical approach to the particle size of CaO in clinker", 74th Ann. Meet. Am. Ceram. Soc., Whashington.

73.- RUMYANTSEV, P.F. (1968) "On kinetics of formation of portland cement clinker", Proc. 5th Int. Symp. Chem. Cement, Tokyo P.I, 111.

74.- KONDO, R. et CHOI, S.H. (1968) "Mechanisms and kinetics of portland cement clinker formation for an example of the solid state reaction in the presence of a liquid phase", Proc. 5th Int. Symp. Chem. Cement, Tokyo P.I, 163.

75.- SYCHEV, M.M. et ASTAKHOVA, M.A. (1962) "Influence of the limestone fineness on the burnability of the cement mixes", Tsement 28, N° 3, 12.

76.- THORMANN, P. (1968) "Über die Bedeutung der getrennten Vermahlung von Kalkmergel und Sand für die Klinkermineralbildung beim Zementbrennen", Tonind. Ztg. 92, 7.

77.- KAWAMURA, S. et MIZUKAMI, K. (1969) "The influence of quarz and feldspar on the burning process of cement clinker", Rev. 23rd Gen. Meet. Cem. Assoc. Japan, Tokyo p. 50.

78.- KANTSEPOL'SKII, I.S., TEREKHOVICH, S. V. et DROZHZHIN, A. Kh. (1971) "Optimization of the fineness of the grinding of a mixture of raw materials", Tsement 37, N° 9, 16.

79.- CEBRIAN ZALAMA, J.L. (1973) "La sílice libre en los crudos de cemento portland", Cem. Hormigon 44, 295.

80.- CEBRIAN ZALAMA, J.L. (1973) "Química del ensayo de aptitud a cocción de crudos de cemento portland", Cem. Hormigon 44, 693.

81.- FOREST, J. (1973) "Etude de certains minéraux du clinker et de la réactivité des crus de cimenterie", Silicates Ind. 38, 121, 149 et 175.

82.- COURTAULT, B. (1963) "Etude des réactions à l'état solide jusqu'à 1600°C au moyen de l'analyse thermique différentielle", Rev. Mater. Constr. N° 569, 37; N° 570, 67; N° 571, 110; N° 572, 143; N° 573, 190.

83.- RICHARTZ, W. (1971) "Ausschalten von Fehlerquellen bei der Roentgenfluoreszenzanalyse", Zement-Kalk-Gips 24, 72.

84.- LOCHER, F.W. (1975) "Einfluss der Klinkerherstellung auf die Eigenschaften des Zements", Zement-Kalk-Gips 28, 265.

85.- BUCCHI, R., VALOTI, S. et GIOVANETTI, G. (1975) "Visita della cementeria di Bath della Ciments Canada Lafarge. Rapporto Italcementi S.p.A., Bergamo", juin.

86.- BUCCHI R. et GIOVANETTI, G. (1978) "Visita della cementeria di Bussac della S.té des Ciments Français. Rapporto Italcementi S.p.A., Bergamo", octobre.

87.- BECKER, F. (1970) "Einfluss verschiedenlanger Mahldauern auf die Eigenschaften des Rohmehls", Vortrag bei 8. Chemikersitzung der Gruppe Holderbank. Reference (4) de V. R. Pfrunder et H. Wickert in Zement-Kalk-Gips 23, 147.

88.- SCHRADER, R., HOFFMANN, B., PLÄNITZ, H. et HENNEBERGER, J. (1970) "Über aktiviertes Calciumoxyd", Zement-Kalk-Gips 23, 194.

89.- MCHEDLOV-PETROSYAN, O.P., SHCHETKINA, T.YU. et FATALIEV, S.S. (1975) "Die Rolle metastabiler Phasen bei Silikatbildungsprozessen", Silikattechnik 26, 258.

90.- MCHEDLOV-PETROSYAN, O.P., SAPOSHNIKOVA, N.I., SKRYNNIK, L.N. et SHCHETKINA, T. YU. (1977) "Untersuchung des Einflusses der Kalkstruktur auf die chemische Aktivität bei der Klinkerbildung", Silikattechnik 28, 234.

91.- AKATSU, K. et IKEDA, I. (1971) "An expedient method for determining reactivity of siliceous raw materials", Rev. 25th Gen. Meet. Cem. Assoc. Japan, Tokyo p. 47.

92.- BECKER, F. et SCHRÄMLI, W. (1960) "Portlandzement im Lichte neuerer Anschauungen der Festkörperchemie", Zement-Kalk-Gips 13, 222.

93.- SCHRÄMLI, W. et BECKER, F. (1960) "Die Reaktionen zwischen Kalk und Kieselsäure verschiedener Aktivität im Temperaturbereich unter 1100°C", Zement-Kalk-Gips 13, 265.

94.- SCHWIETE, H.E. et HECHLER, R.W. (1965) "Solid state reactions of silicate systems", Proc. 8th Conf. Silicate Ind. Budapest p. 93.

95.- HEDVALL, J.A. (1966) "Solid state chemistry", Elsevier Publ. Co Amsterdam.

96.- MAKASHEV, S.D. (1970) "Burnability of cement raw mixes", Tsement 36 N° 1, 14.

97.- MAKASHEV, S.D. (1974) "Effect of raw material physico-chemical properties on reactivity of raw mix and on clinker minerogeneisis processes", Proc. 6th Int. Congr. Chem. Cement, Moscow.

98.- DASGUPTA, A. (1975) "Burnability of cement raw materials and clinker formation kinetics", Chem. Era 11, 7.

99.- RENNEN, H. et SCHWIETE, H.E. (1963) "Reactions of kaolinite and calcium oxide between 450° and 800°C", Proc. 7th Conf. Silicate Ind. Budapest p. 171.

100.- SCHNEIDER, F.U. (1978) "Untersuchungen zur Darstellung und Analyse aktiver Feststoffzustände als Folge intensiver Mahlbeanspruchung", Aufbereit. Tech. 19, 462.

101.- WOLFE, J.A. (1955) "What to look for in selecting cement raw materials", Rock Prod. 58, aug. 132.

102.- KIEFER, CH. (1950) "Stabilité et classification des minéraux phylliteux. Application aux argiles de cimenterie", Rev. Mater. Constr. N° 422, 335; N° 423, 358; N° 424, 19; N° 425, 53; N° 426, 84; N° 427, 109; N° 428, 141; N° 429, 191; N° 430, 225; N° 431/32, 358.

103.- BEUTELSPACHER, H. et VAN DER MAREL, H.W. (1968) "Atlas of electron microscopy of clay minerals and their admixtures", Elsevier Publ. Co., Amsterdam.

104.- LEROUX, A. (1975) "Les differentes textures et leur influence sur le comportement des sols argileux et marneux", Geologia applicata e idrogeologia Vol. X, P. II, 67.

105.- SCHWIETE, H.E. (1956) "Der Einfluss der Tonminerale auf die Staubbildung beim Klinkerbrand", Zement-Kalk-Gips 9, 351.

106.- LEHMANN, H., WUHRER, J. et LAHN, W. (1958) "Das Brennverhalten von Kalksteinen aus verschiedenen geologischen Formationen", Tonind. Ztg. 82, 434, 486, 542.

107.- SCHWIETE, H.E. et ZIEGLER, G. (1956) "Beitrag zur Thermochemie des Kalkes", Tonind. Ztg. 80, 97.

108.- GRIM, R.E. (1968) "Clay mineralogy", 2nd Edt. McGraw-Hill Book Co., New York.

109.- GRIM, R.E. (1962) "Applied clay mineralogy", McGraw-Hill Book Co., New York.

110.- MILLOT, G. (1964) "Géologie des argiles", Masson et Cie, Edt. Paris.

111.- GOERG, W. (1956) "Reaktionen zwischen Kalk und Tonmineralien", Tonind. Ztg. 80, 219.

112.- HILL, G. et SCHWIETE, H.E. (1958) "Der Einfluss des Mineralbestandes und der Verformung auf das Brennverhalten von Granalien aus Zement-Rohmehlen", Zement-Kalk-Gips 11, 181.

113.- LUDWIG, U., MÜLLER-HESSE, H. et SCHWIETE, H.E. (1960) "Über die Konstitution und das Erhärten hydraulischer Kalke", Zement-Kalk-Gips 13, 449.

114.- BERECZKY, A. (1961) "Die Bestrebungen zur Erzeugung hochwertiger Zemente", Tonind. Ztg. 85, 37.

115.- MCHEDLOV-PETROSYAN, O.P., SAPOSHNIKOVA, N.I. et SHCHETKINA, T. YU. (1975) "Thermodinamic methods for studying the reactivity of raw material mixtures and cements", Tsement 41 N° 10, 17.

116.- BUTT, YU. M., TIMASHEV, V.V. et VOLKOV, V.V. (1964) "Effect of mineralogical composition and structure of initial components on the reaction capacity of initial mixes", Tr. Gos. Vses. Nauch. - Issled. Inst. Tsem. Prom. N° 20, 82.

117.- TALABER, J. (1968) "Solid phase diffusion of CaO in mineral substances", Proc. 9th Conf. Silicate Ind. Budapest p. 171.

118.- RAUSCHENFELS, E. (1976) "Die Sinterbar

keit von Zement-Rohmehl", Zement-Kalk-Gips 29, 78.

119.- ASANO, T. (1965) "Onoda cement company's lime calcination process in cement manufacture", Pit Quarry 58, (1), 184.

120.- FATALIEV, S.A. (1963) "Effect of limestone microstructure on the petrographic characteristics of portland cement clinker and the strength of concrete", Dokl. Akad. Nauk. Azerb. SSR 19 (1), 41.

121.- FATALIEV, S.A. (1965) "Special features of mineral formation in firing of charges with limestones of various microstructures", Tsement 31 N° 3, 9.

122.- PHILIPP, O. (1973) "Einfluss des Aufheizverhaltens auf den Garbrand von Zementklinkern", Silikattechnik 24, 265.

123.- IMLACH, J.A. et HOFMÄNNER, F. (1974) "Investigation of clinker formation by DTA and optical microscopy", 6th Int. Congr. Chem. Cement, Moscow.

124.- MARSCHNER. H. (1968) "Relationship between carbonate grain size and non-carbonate content in carbonate sedimentary rocks. From: "Recent developments in carbonate sedimentology in Central Europe", by G. Müller and G.M. Friedman. Springer-Verlag, New York p. 55.

125.- BLAINE, R.L., BEAN, L. et HUBBARD, E. K. (1961) "Occurrence of minor and trace elements in portland cement", Part 1, Building Science Series 2, National Bureau of Standards. Aug. p. 33.

126.- BLAINE, R.L. (1968) "A statistical study of the effects of trace elements on the properties of portland cement", Proc. 5th Int. Symp. Chem. Cement, Tokyo P.III, 86.

127.- DYCKERHOFF ZEMENTWERKE A.G., WIESBADEN (1979) "Private communication 30.03.1979".

128.- HOLDERBANK MANAGEMENT UND BERATUNG A.G., TECHNISCHE STELLE, HOLDERBANK (1978) "Private communication 20. 12.1978".

129.- LAFARGE CONSEILS et ETUDES, PARIS (1979) "Private communication 23.01.1979".

130.- S.TE DES CIMENTS FRANCAIS, PARIS (1979) "Private communication 25.04.1979".

131.- KLEMM, W.A. et SKALNY, J.(1976) "Mineralizers and fluxes in the clinkering process", Cem. Res. Progr. Chap. 14, 259.

132.- TEOREANU, I. (1974) "The chemistry of white and coloured cements", 6th Int. Congr. Chem. Cement, Moscow.

133.- HANSEN, W.C. (1930) "Influence of magnesia, ferric oxid and soda upon the temperature of liquid formation in certain portland cement mixtures", J. Res. NBS 4, 55.

134.- TOROPOV, N.A. et RUMYANTSEV, P.F. (1965) "Formation of portland cement clinker", Zh. Prikl. Khim. (Leningrad) 38:

I. Factors controlling the rate of clinker formation. (3), 660;

II. A method for the study of the kinetics of solution of clinker minerals in the liquid phase of portland cement clinker. (5), 1129;

III. Kinetics of dissolution of calcium oxide in the liquid phase of cement clinker. (7), 1614;

IV. Kinetics of dissolution of dicalcium silicate in the liquid phase of cement clinker. (8), 1858;

V. Kinetics of dissolution of tricalcium silicate in the liquid phase of cement clinker. (8), 1860 e 1558.

135.- TOROPOV, N.A., RUMYANTSEV, P.F. et FILIPOVICH, V.N. (1964) "Kinetics of dissolution of CaO, C_3S, C_2S and SiO_2 in a molten cement clinker", J. Phy. Chem. 38, 528.

136.- TOROPOV, N.A. et RUMYANTSEV, P.F. (1967) "Über die Bildungskinetik von Zementklinker", Silikattechnik 18, 322 et 349.

137.- BUTT, Y.M., TIMASHEV, V.V., et OSOKIN, A.P. (1974) "The mechanism of clinker formation processes and the modification of its structure", 6th Int. Congr. Chem. Cement, Moscow.

138.- SYCHEV, M.M. (1968) "Problem of admixtures", Proc. 5th Int. Symp. Chem. Cement. Tokyo P.I , 157.

139.- SHMIDT, YU. A. (1959) "Effect of composition on properties of alkali silicate glasses", Structure Glass. Proc. All-Union Conf. Glassy State, 3rd (Leningrad) 274.

140.- GRACHIAN, A.N., ZUBEKHIN, A.P. et LEONOV, V.M. (1971) "Dependence of the liquid phase viscosity of a cement clinker on the characteristics of cations and anions of mineralizers", Zh. Prikl. Khim. (Leningrad) 44, 189.

141.- PAULING, L. (1960) "The nature of chemical bond", Cornell. Univ.Press. New York, p. 644.

142.- WHITTAKER, E.J.W. et MUNTUS, R. (1970) Jonic radii for use in geochemistry", Geochim. Cosmochim. Acta 34, 945.

143.- OKOROKOV, S.D., GOLINKO-VOL'FSON, S.

L., SHEVELEVA, B.I. et YARKINA, T.N. (1957) "Comparison of salts group as potential mineralizers in firing portland cement clinker", Tsement 23, N° 3, 5.

144.- P'YACHEV, V. et TIKHONENKOVA, Z.V. (1966) "Assimilation of lime during synthesis of clinker minerals and calcination of clinker in the presence of addition of Cr_2O_3, B_2O_3, P_2O_5 and V_2O_5", Izv. Vyssh. Ucheb. Zaved. Khim. Khim. Tekhnol. 9, 802.

145.- PONOMAREV, I.F., GRACHIAN, A.N. et ZUBEKHIN, A.P. (1966) "Influence of mineralizing additives on the process of cement clinker formation as a function of the electronegativity of the mineralizer cation and anion", Dokl. Akad. Nauk SSSR 166, 410.

146.- TEOREANU, I. et TRAN VAN HUYNH (1970) "Wechselbeziehungen zwischen der mineralisierenden Wirkung der Stoffe auf die Portlandzementklinkerbildung und dem periodischen System der Elemente", Silicates Ind. 35, 281

147.- TEOREANU, I. et TRAN VAN HUYNH (1971) "L'influence des composés fluorés sur les processus de cristallisation et sur la composition des constituants minéralogiques des clinkers de ciments portland", Rev. Mater. Constr. N° 666, 73.

148.- SHUBIN, V.I. (1974) "Investigation into consolidation of portland cement clinker", 6th Int. Congr. Chem. Cement, Moscow.

149.- HESS, P.C. (1971) "Polymer model of silicate melts", Geochim. Cosmochim. Acta 35, 289.

150.- KURDOWSKI, W. et SZUMMZR, A. (1968) "L'influence des composants mineurs sur les propriétés hydrauliques du clinker portland", Silicates Ind. 33, 183.

151.- TEORENAU, I. et ENCULESCU, M. (1973) "Influence des microadditions d'oxydes des métaux de transition sur les propriétés des silicates du clinker de ciment portland", Rev. Mater. Constr. N° 684, 31.

152.- KURDOWSKI, W. (1974) "Influence of minor components on hydraulic activity of portland cement clinker", 6th Int. Congr. Chem. Cement, Moscow.

153.- ONO, Y. et SODA, Y. (1965) "Effect of the crystallographic properties of alite and belite on the strength of cement", Semento Gijutsu Nempo 19, 93.

154.- BUTT, Y.M., TIMASHEV, V.V. et MALOZOHN, L.I. (1968) "The crystallization of compounds in the presence of Cr_2O_3, P_2O_5, or SO_3 and the properties of the resultant cement", Proc. 5th Int. Symp. Chem. Cement, Tokyo P.I, 340.

155.- SAKURAI, T., SATO, T. et YOSHINAGA, A. (1968) "The effect of minor components on the early hydraulic activity of the major phases of portland cement clinker", Proc. 5th Int. Symp. Chem. Cement, Tokyo P.I, 300.

156.- BOIKOVA, A.I. (1968) "Ordered and disordered structures of tricalcium silicate solid solutions", Proc. 9th Conf. Silicate Ind. Budapest p. 41.

157.- FIERENS, P. et VERHAEGEN, J.P. (1972) "Structure and reactivity of chromium-doped tricalcium silicate", J. Amer. Ceram. Soc. 55, 309.

158.- REGOURD, M. et GUINIER, A. (1974) "The crystal chemistry of the constituents of portland cement clinker", 6thInt. Congr. Chem. Cement, Moscow.

159.- CAROBBI, G. (1971) "Trattato di mineralogia", Vol. I pagg. 347 et segg. USES - Edizioni Scientifiche Firenze.

160.- MAYCOCK, J.N. et MC CARTHY, M. Jr. (1973) "Crystal lattice defects in dicalcium silicate", Proc. 11th Conf. Silicate Ind. Budapest P.I, 389.

161.- PRITTS, I.M., et DAUGHERTY, K.E. (1976) "The effect of stabilizing agents on the hydration rate of β-C_2S", Cem. Concr. Res. 6, 783.

162.- GRZYMEK, J. (1959) "Die Beeinflussung der Alitbildung im Portlandzementklinker", Silikattechnik 10, 81.

163.- VOGEL, E. (1960) "Heterogene Reaktionen im Zementdrehofen", T.I, T. II, et T. III. Silikattechnik 11, 476, 512, 572.

164.- GOES, C. et KEIL, F. (1960) "Über das Verhalten der Alkalien beim Zementbrennen", Tonind. Ztg. 84, 125.

165.- WEBER, P. (1960) "Wärmeübergang im Drehofen unter Berücksichtigung der Kreislaufvorgänge und Phasenneubildung", Zement-Kalk Gips Sonderausgabe N° 9.

166.- MUSSGNUG, G. (1962) "Beitrag zur Alkalifrage in Schwebegaswärmetauscheröfen", Zement-Kalk-Gips 15, 197.

167.- WEBER, P. (1964) "Alkaliprobleme und Alkalibeseitigung bei wärmesparenden Trockendrehöfen", Zement-Kalk-Gips 17, 335.

168.- VIKTORENKOV, V.J. et VOLKONSKII, B. V. (1965) "Circulation of alkalies in furnaces with cyclone exchangers", Tsement 31 N° 6, 12.

169.- RITZMANN, H. (1971) "Kreisläufe in Dre-

hofensystemen", Zement-Kalk-Gips 24, 338.

170.- LOCHER, F.W., SPRUNG, S. et OPITZ, D. (1972) "Reaktionen im Bereich der Ofengase. Kreisläufe flüchtiger Stoffe, Ansätze, Beseitigen von Ringen", Zement-Kalk-Gips 25, 1.

171.- BUCCHI, R. et GANDINI, P.A. (1972) "A contribution to the knowledge of the cycles of some volatile compounds in cement kilns. I - Theoretical considerations. II - Experimental results and their interpretation. III - Wet process", Chim. Ind. (Milan) 53, 819, 825, 54, 1097.

172.- RITZMANN, H. (1972) "Raw meal preheater and alkali problems", Rock Prod. 8th Int. Cement. Ind. Seminar Chicago, dec. 3-6 p. 39.

173.- TEOREANU, I., PURI, A. et GEORGESCU, M. (1975) "Volatility of alkalis from raw materials and raw mixes for portland cement clinkers", Mater. Constr. (Bucharest) 5(2), 55.

174.- LOCHER, F.W. (1978) "Verfahrenstechnik und Zementeigenschaften", Zement-Kalk-Gips 31, 269.

175.- CARLSEN, H.S. (1966) "Behavior of alkalies during the burning process", Rock Prod. 69 (5), 87.

176.- BIEGE, N. et PEARSON, L. (1977) "The theory and development of bypass systems for preheater and flash calcinerkiln system", IEEE 1977 Cement Ind. Techn. Confer. Omaha (U.S.) may 16-19.

177.- SVENDSEN, J. (1978) "Alkaliarmer Zement aus Hochalkali-Rohstoffen mit energiewirtschaftlich günstiger Verfahrenstechnik", Zement-Kalk-Gips 31, 281.

178.- WARSHAWSKY, J. et PORTER, E.S. (1978) "Verminderung des Alkali und Schwefelgehalts im Klinker durch einen Ofen-By pass im Vorcalciniersystem", Zement-Kalk-Gips 31, 284.

179.- SPRUNG, S. (1965) "Das Verhalten des Schwefels beim Brennen von Zementklinker", Tonind. Ztg. 89, 124.

180.- NEWKIRK, T.F. (1951) "Effect of SO_3 on the alkali compounds of portalnd cement clinker", RP 2261. I. Res. N.B.S. 47, 349.

181.- GUTT, W. et SMITH, M.A. (1971) "Studies of sulphates in portland cement clinker", Cem. Technol. 2, 143.

182.- FUKUDA, N. (1961) "Effect of calcium sulphate on the compound composition of portland cement clinker", Semento Gijustu Nempo 15, 26.

183.- FUKUDA, N. (1961) "Constitution of sulphoaluminous clinker", Bull. Chem. Soc. Japan 34, 138.

184.- KOSTOV, B. (1965) "Mineral formation during firing of sulphatized portland cement raw material mixtures", Compt. Rend. Acad. Bulgare Sci. 18, 335.

185.- BUDNIKOV, P.P. (1967) "Effect of alkalies and calcium sulphate on the synthesis of calcium aluminates and of portland clinker", Cement-Wapno Gips 22, 281.

186.- RAGOZINA, T.A. et AKHMEDOV, M.A. (1968) "Influence of calcium sulphate on the mineralization processes during the firing of cement mixtures", Proc. 9th Conf. Silicate Ind. Budapest p. 263.

187.- GUTT, W. et SMITH, M.A. (1966) "A new calcium silicosulphate", Nature 210, 408.

188.- GUTT, W. et SMITH, M.A. (1967) "Studies of the sub-system $CaO-CaO \cdot SiO_2-CaSO_4$", Trans. Brit. Ceram. Soc. 66, 557.

189.- GUTT, W. et SMITH, M.A. (1968) "Studies of the role of calcium sulphate in the manufacture of portland cement clinker", Trans. Brit. Ceram. Soc. 67, 487.

190.- SMITH, M.A. et GUTT, W. (1970) "The effect of magnesium and sulphate ions on the hydraulicity of tricalcium silicate", Cem. Technol. 1, 187.

191.- PLIEGO-CUERVO, Y.B. et GLASSER, F. P. (1979) "The role of sulphates in cement clinkering: subsolidus phase relations in the system $CaO-Al_2O_3-SiO_2-SO_3$", Cem. Concr. Res. 9, 51.

192.- OKOROKOV, S.D., GOLYNKO-VOL'FSON, S.L. et KUKUSHKINA, E.S. (1960) "The mineralizing action of sulphates in the synthesis of separate minerals of portland cement clinker", Tr. Leningr. Tekhnol. Inst. im. Lensoveta (56), 84.

193.- OKOROKOV, S.D., GOLYNKO-VOL'FSON, S.L. et KORNEEV, V.L. (1960) "Change in the strength of dicalcium silicate depending on the nature of the stabilizing admixture", Tr. Leningr. Tekhnol. Inst. im. Lensoveta (56), 93.

194.- AKHMEDOV, M.A. et RAGOZINA, T.A. (1961) "The effect of calcium sulphate on the sintering point of the portland cement clinker", Vop. Ispol'z. Miner. Rast. Syr'ya Srednei Azii, 55.

195.- BUDNIKOV, P.P. et KUSNETSOWA, I.P. (1962) "The effect of gypsum on the formation of the minerals of the portland clinker", Zh. Prikl. Khim. (Leningrad) 35, 939.

196.- RAGOZINA, T.A. et AKHMEDOV, M.A. (1962) "The effect of $CaSO_4$ on the phase com

position of calcium silicates and aluminates at calcination", Uzb. Khim. Zh. 6, 5.

197.- POD'YACHEVA, I.B. (1964) "Gypsum as mineralizer in the firing of portland cement clinker", Tr. Gos. Vses. Inst. Proekt. Nauch. Issled. Rab. Tsem. Prom. 28, 26.

198.- BUDNIKOV, P.P. et AZELITSKAYA, R.D. (1964) "A pretreatment of raw materials and its effect on the properties of cement", Cement-Wapno Gips 11, 285.

199.- BUDNIKOV, P.P., KUSNETSOWA, I.P. et SAWELJEW, W.G. (1965) "Eigenschaften von $3CaO \cdot 3Al_2O_3 \cdot CaSO_4$ und sein Einfluss auf die Festigkeit von Klinkermineralien und Zement", Silikattechnik 16, 414 (Sonderheft).

200.- TANDILOVA, K.B. et DZHADZHANASHVILI, O.S. (1968) "Mineralizeraccelerator of the clinker burning process", Sb. Tr. Tbilis. Gos. Nauch. - Issled. Inst. Stroit. Mater. N° 3, 150.

201.- AZELITSKAYA, R.D., PONOMAREV, I.F., BLONSKAJA, V.M., KARBIKEV, M.G., LOKOT A.A. et STEFANOV, V.M. (1969) "The effect of gypsum on the phase composition of alkali containing clinker", Tsement 35 N° 2, 6.

202.- VOLKONSKII, B.V. et SHTEYERT, N.P. (1970) "The relationship between cement properties and alkali content of clinker", Tsement 36 N° 10, 6.

203.- BUTT, YU. M., KAUSHANSKII, V.E., TURETSKII, A.M. et PANINA, N.S. (1971) "The influence of gypsum on the properties of cement containing alkalis", Tsement 37 N° 4, 14.

204.- ABBASSI, GH. (1974) "Contribution à l'étude de l'influence des métaux alcalins sur la composition et sur l'hydratation des phases du clinker", Rev. Mater. Constr. N° 691, 315.

205.- PLIEGO-CUERVO, Y.B. et GLASSER, F. P. (1977) "The role of sulphates in cement clinkering reactions: phase formation and melting in the system $CaO-Ca_2SiO_4-CaSO_4-K_2SO_4$", Cem. Concr. Res. 7, 477.

206.- AMAFUJI, M. et TSUMAGARI, A. (1968) "Formation of double salt in cement burning", Proc. 5th Int. Symp. Chem. Cement, Tokyo P.I, 136.

207.- SYLLA, H.M. (1974) "Untersuchungen zur Bildung von Ansatzringen in Zementdrehöfen", Zement-Kalk-Gips 27, 499.

208.- HATANO, H. (1972) "Über das Verhalten des Schwefels im Wärmetauscherofen", Zement-Kalk-Gips 25, 18.

209.- ETOC, P. (1976) "Le four de cimenterie: un piège à soufre efficace", Rev. Mater. Constr. N° 701, 210.

210.- GUTT, W. et OSBORNE, G.J. (1966) "The system $2CaO \cdot SiO_2-CaF_2$", Trans. Brit. Ceram. Soc. 65, 521.

211.- AKAIWA, S., SUDOH, G. et TANAKA, M. (1966) "Studies on mineralizing effect of CaF_2 and a ternary compound in the system $CaO-SiO_2-CaF_2$", Semento Gijutsu Nempo 20, 26.

212.- GILIOLI, C., MASSAZZA, F. et PEZZUOLI, M. (1979) "Studies on clinker calcium silicates bearing CaF_2 and $CaSO_4$", Cem. Concr. Res. 9, 295.

213.- MASSAZZA, F. et PEZZUOLI, M. (1970) "Ricerche su $12CaO \cdot 7Al_2O_3$ e sul sistema $12CaO \cdot 7Al_2O_3 - 11CaO \cdot 7Al_2O_3 \cdot CaF_2$", Il Cemento 67, 11.

214.- BRISI, C. et ROLANDO, P. (1966) "Sul meccanismo di decomposizione dell'alluminato tricalcico in presenza di fluoruro e cloruro di calcio", Annali di chimica, 56, 224.

215.- MASSAZZA, F. et PEZZUOLI, M. (1969) "Equilibres à l'état solide dans le système quaternaire $CaO-Al_2O_3-SiO_2-CaF_2$", Rev. Mater. Constr. N° 642, 81.

216.- GOL'DSHMIDT, E.M., KRUGLYAK, S.L., SOKOLOVA, N.A. et SYRKIN, YA.M. (1976) "On the mineralogical composition of white clinker containing fluorine", Tsement 42 N° 1, 17.

217.- IMLACH, J.A. (1974) "The influence of heating conditions on the production of fluorine-containing Portland cement clinker", Cem. Technol. 5, 403.

218.- MASSAZZA, F., PEZZUOLI, M. et GILIOLI, C. (1970) "Relations d'équilibre à l'état solide dans le système quaternaire $CaO-Al_2O_3-Fe_2O_3-CaF_2$", Rev. Mater. Constr. N° 663, 357.

219.- LUGININA, I.G. (1961) "Influence of mineralizers on the clinker formation by rapid firing", Tsement 27 N° 4, 20.

220.- GUTT, W. (1968) "Manufacture of portland cement from phosphatic raw materials", Proc. 5th Int. Symp. Chem. Cement, Tokyo P.I, 93.

221.- SCHLEGEL, E. (1968) "Die Einwirkung von Flussspat auf die Entsäuerung von Magnesit, Calcit und Dolomit", Zement-Kalk-Gips 21, 386.

222.- KLEMM, W.A., HOLUB, K.J. et SKALNY, J. (1977) "The effects of fluxes and mineralizers in lowering cement kiln temperatures",

Progress Report N° 1, July 1977 (Prepared for Div. Adv. Energy and Resources, Research and Technology National Science Foundation Washington.

223.- COURTAULT, B. (1962) "Réactivité des crus de cimenterie", Silicates Ind. 27, 141.

224.- JOAHNSEN, V. et CHRISTENSEN, N.H. (1979) "Rate of formation of C_3S in the system $CaO-SiO_2-Al_2O_3-Fe_2O_3-MgO$ with addition of CaF_2", Cem. Concr. Res. 9, 1.

225.- TANAKA, M., SUDOH, G. et AKAIWA, S. (1968) "New compound $Ca_{12}Si_4O_{19}F_2$ in the system $CaO-SiO_2-CaF_2$ and the role of CaF_2 in the burning of cement clinker", Proc. 5th Int. Symp. Chem. Cement, Tokyo P.I, 122.

226.- NURSE, R.W., MIDGLEY, H.G., GUTT, W. et FLETCHER, K. (1966) "Effect of polymorphism of tricalcium silicate on its reactivity". Symp. on structure of portland cement paste and concrete, Highway Research Board, S.R.90, Washington.

227.- WELCH, J.H. et GUTT, W. (1960) "The effect of minor components on the hydraulicity of the calcium silicates", Proc. 4th Int. Symp. Chem. Cement, Washington, 1, 59.

228.- SKALNY, J., HOLUB, K.J. et KLEMM, W. A. (1978) "Influence of potential interstitial phase composition on clinkering reactions", Il Cemento 75, 351.

229.- SPRUNG, S. et von SEEBACH, H.M. (1968) "Fluorhaushalt und Fluoremission von Zementöfen", Zement-Kalk-Gips 21, 1.

230.- NURSE, R.W. (1952) "The effect of phosphate on the constitution and hardening of portland cement", J. Appl. Chem. 2, 708.

231.- NURSE, R.W., WELCH, J.H. et GUTT, W. (1958) "A new form of tricalcium phosphate", Nature 192, 1230.

232.- NURSE, R.W., WELCH, J.H. et GUTT, W. (1959) "High temperature phase equilibria in the system dicalcium silicate-tricalcium phosfate", J. Chem. Soc. N° 220, 1077.

233.- GUTT, W. (1963) "High temperature phase equilibria in the system $2CaO, SiO_2-3CaO, P_2O_5-CaO$", Nature 197, 142.

234.- SCHLAUDT, C.M. (1964) "Phase equilibria and cristal chemistry of cement and refractory phases in the system $CaO-MgO-Al_2O_3-Fe_2O_3-CaF_2-P_2O_5-SiO_2$", Ph. D. Thesis, Pennsylvania State University.

235.- V'LKOV, V. et TABAKOVA, N. (1967) "The effect of P_2O_5 on clinker formation and the quality of cement", Stroit. Mat. Silik. Prom. 9, 6.

236.- FIX, W., TRÖMEL, G. et HEINKE, R. (1969) "Untersuchung zur Gleichgewichtseinstellung der festen Phasen im System $CaO-2CaO, SiO_2-3CaO, P_2O_5$", Arch. Eisenhuettenw. 40, 979.

237.- SALGE, H. et THORMANN, P. (1973) "Über den Einfluss von P_2O_5 auf die Konstitution von Portlandzementklinker", Zement-Kalk-Gips 26, 532.

238.- GUYE, F. (1954) "Influence du phosphore sur le ciment portland", Rev. Mater. Constr. N° 460, 7.

239.- ARAPOVA, A.S., PAKHOMOVA, V.I., et DEMKINA, L.M. (1969) "Phosphorites increase the strength of portland cement", Tsement 35 N° 1, 10.

240.- BUI VAN TIEN, BUTT, YU. M. et VOROB'EVA, M.A. (1969) "Action of apatite during the firing of cement clinker", Tr. Mosk. Khim. Teckhnol. Inst. N° 63, 165.

241.- AKATSU, K., MAEDA, K. et IKEDA, I. (1970) "The effect of Cr_2O_3 and P_2O_5 on the strength and color of portland cement clinker", Rev. 24th Gen. Meet. Cem. Assoc. Japan, Tokyo, 20.

242.- TEOREANU, I. et TRAN VAN HUYNH (1970) "Mineralizing influence of apatite on the formation of portland cement clinker", Rev. Roum. Chim. 15, 229.

243.- SIMANOVSKAYA, R.E. et VODZINSKAYA, Z.V. (1955) "Effect of fluor on the reaction of clinker minerals cristallization and formation in presence of phosphates", Tsement 21 N° 5, 12.

244.- TIMASHEV, V.V., GALPERINA, T.YA., BYKOVA, S.N., SEVOSTIANOVA, L.I. et YANKOV, N.F. (1979) "Effect of phosphorus on phase composition and properties of cement produced of high-alkali raw materials", Tsement 45 N° 3, 6.

245.- MOORE, A.E. (1965) "Examination of a portland cement clinker by electron probe microanalysis", Silicates Ind. 30, 445.

246.- PONOMAREV, I.F., GRACHIAN, A.N. et ROTYTSCH, N.W. (1968) "Einfluss von Kombinationen der Oxide von Übergangselementen auf die Eigenschaften des Weissen Portlandzements", Silikattechnik 19, 69.

247.- SAKURAI, T. et SATO, T. (1968) "Written discussion on "Analysis of portland cement clinker" Yamaguchi G. et Takagi S.", 5th Int. Symp. Chem. Cement, Tokyo P. I, 221.

248.- SYCHEV, M.M., KOPINA, G.I. et ZHURBENCO, V.B. (1969) "Phase distribution of alloying additives and the modification of clinker microstructure", Tsement 35 N° 4, 3.

249.- FIERENS, P., THAUVOYE, M. et VERHAEGEN, J.P.(1974) "Effects of iron (III) and titanium (IV) on the tricalcium aluminate structure and reactivity", Il Cemento 71, 3.

250.- KONDO, R. et YOSHIDA, K. (1968) "Miscibilities of special elements in tricalcium silicate and alite and the hydration properties of C_3S solid solutions", 5th Int. Symp. Chem. Cement, Tokyo P.I. 262.

251.- EREMIN, N.J., EGEREVA, A.J., DIMITRIEVA, A. et FIRFAROVA, J.B. (1970) "Solid solutions of $2CaO \cdot SiO_2$ with some metal oxides", Zh. Prikl. Kim. (Leningrad) 43, 18.

252.- KNÖFEL, D. (1979) "Der Einbau von TiO_2 in die Phasen des Portlandzementklinkers", Zement-Kalk-Gips 32, 35.

253.- MIDGLEY, H.G. (1968) "The minor elements in alite (tricalcium silicate) and belite (dicalcium silicate) from some portland cement clinkers as determined by electron probe X-ray microanalysis", 5th Int. Symp. Chem. Cement, Tokyo P.I, 226.

254.- KNÖFEL, D. (1977) "Beeinflussung einiger Eigenschaften des Portlandzementklinkers und des Portlandzements durch TiO_2", Zement-Kalk-Gips 30, 191.

255.- SYCHEV, M.M. et ZOZULIA, P.V. (1967) "Clinker liquid viscosity and sintering processes", Tr. Gos. Vses. Proekt. Nauch.-Issled. Inst. Tsem. Prom. 33, 3.

256.- ROYAK, S.M., ASTREYEVA, O.M. et LUKINA, M.N. (1955) "Effect of titanium dioxide on clinker formation processes", Tsement 21 N° 3, 12.

257.- FIERENS, P., THAUVOYE, M. et VERHAEGEN, J.P. (1972) "The influence of iron (III) and titanium (IV) on the structure and reactivity of tricalcium silicate", Il Cemento, 69, 211.

258.- BOIKOVA, A.I. (1964) "Stoichiometry and polymorphism of tricalcium silicate", Dokl. Chem. Technol. 156 (6), 90.

259.- SYCHEV, M.M. et KORNEEV, V.I. (1965) "Cromalite of portland cement clinkers", Zh. Prikl. Khim. (Leningrad) 38, 2642.

260.- FIERENS, P. et VERHAEGEN, J.P. (1972) "Structure and reactivity of chromium-doped tricalcium silicate", J. Amer. Ceram. Soc. 55, 309.

261.- JOHANSEN, V. (1972) "Solid solution of chromium in Ca_3SiO_5", Cem. Concr. Res. 2, 33.

262.- JOHANSEN, V. (1978) "Absorption spectra of CrO_4^{4-} in Ca_3SiO_5 and $Ca_3Al_2O_6$", Cem. Concr. Res. 8, 245.

263.- BUTT, YU.M., TIMASHEV, V.V. et MALOZHON L.I. (1968) "Cristallization of minerals in clinker containing chromium oxide", Inorganic Materials 4 (3), 431.

264.- WOERMANN, E., HAHN, TH. et EYSEL, W. (1963) "Chemische und strukturelle Untersuchungen der Mischkristallbildung von Tricalciumsilikat", Zement-Kalk-Gips 16, 370.

265.- BOIKOVA, A.I. (1968) "The effect of chromium oxide on the structural transformations in tricalcium silicate", Proc. 5th Int. Symp. Chem. Cement, Tokyo P.I, 234.

266.- BOIKOVA, A.I., TOROPOV, M.A., PURUTKO, M.M. et GRUM-GRZHIMAILO, C.V. (1966) "Effect of Cr oxide on structural transformation of tricalcium silicate", Izv. Akad. Nauk. SSSR, Neorg. Mater. 2, 1796.

267.- GLASSER, F.P. et OSBORN, E.F. (1958) "Phase equilibrium studies in the system $CaO-Cr_2O_3-SiO_2$", J. Amer. Ceram. Soc. 41, 358.

268.- PETERS, D. et HUMMEL, F.A. (1979) "Phase studies in the systems $CaO-Al_2O_3-CaCrO_4$ and $SrO-Al_2O_3-SrCrO_4$", Cem. Concr. Rs. 9, 259.

269.- ZOZULIA, P.V. et SYCHEV, M.M. (1972) "Surface tension of portland cement clinker liquid phase", Inzh.-Fiz. Issled. Stroit. Mater. p. 55.

270.- IMLACH, J.A. (1975) "Assessment of the role of chromium in portland cement manufacture", Amer. Ceram. Soc. Bull. 54, 519.

271.- BUTT, YU.M. et TIMASHEV, V.V. (1968) "Technological and physical-chemical characteristics of the manufacture of rapid hardening and high strength cements", Proc. 9th Conf. Silicate Ind. Budapest p. 217.

272.- TERAMOTO, H. et KOIE, S. (1975) "Phasenzusammensetzung und Hydratation eines hochstwertigen Portlandzementklinkers mit Fremdbestandteilen", Zement-Kalk-Gips 28, 370.

273.- JAWED, I. et SKALNY, J. (1977) "Alkalies in cement: a review", Cem. Concr. Res. 7, 719 et 8, 37.

274.- DANOWSKI, W. et STROBEL, U. (1976) "Alkalibelastbarkeitsuntersuchungen in Trockenbrennanlagen", Zement-Kalk-Gips 29, 458.

275.- HALSTEAD, W.D. (1970) " Saturated vapor pressure of potassium sulphate", Trans. Faraday Soc. 66, 1966.

276.- CUBICIOTTI, D. et KENESHEA, F.J. (1972) "Thermodinamics of vaporisation of sodium sulphate", High Temp. Sci. 4, 32.

277.- CHRISTIANSEN, S. et MADSEN, G.M. (1974) "Precalciners for cement kilns: development and applications", Rock Prod. 10th Int. Cement. Ind. Seminar Chicago, dic. 8-11 p. 100.

278.- DAHL, L.A. (1941), Meet. of Portl. Cem. Assoc. St. Louis, Mo. may 15.

279.- WOODS, H.(1942) "Removing alkalies by heating with admixtures", Rock Prod. 45, febr. 66.

280.- HOLDEN, E.R. (1950) "Reduction of alkalies in portland cement", Ind. Eng. Chem. 42, 337.

281.- BOHMAN, R. (1978) "Einfluss von Calciumchlorid-Zugabe zum Ofenmehl auf den Alkali-Haushalt und die Klinkerqualität von Wärmetauscheröfen", Zement-Kalk-Gips 31, 278.

282.- SYLLA, H.M. (1977) "Ansatzbildung durch Salzschmelzen", Zement-Kalk-Gips 30, 487.

283.- GEBAUER, J. et KRISTMANN, M. (1979) "The influence of the composition of industrial clinker on cement and concrete properties", World. Cem. Technol. 10, 46.

284.- NURSE, R.W. (1968) "Phase equilibria and formation of portland cement minerals", Proc. 5th Int. Symp. Chem. Cement, Tokyo P.I, 77.

285.- YAMAGUCHI, G. et TAKAGI, S. (1968) "The analysis of portland cement clinker", Proc. 5th Int. Symp. Chem. Cement, Tokyo P.I, 181.

286.- MAKI, I. et CHROMY, S. (1978) "Characterization of the alite phase in portland cement clinker by microscopy", Il Cemento 75, 247.

287.- SODA, Y., MIZUKAMI, K. et SHIRASAKA, M. (1969) "On the decline in the development of the strength of portland cement by the increase of magnesia", Rev. 22th Gen. Meet. Cem. Assoc. Japan, Tokyo p. 48.

288.- NIKIFOROV, YU. V., ZOZULYA, R.A. et IVANOVA, N.M. (1974) "Role played by magnesia in clinker and cement technology", 6th Int. Congr. Chem. Cement, Moscow.

289.- CIRILLI, V. et BRISI, C. (1955) "Influenza del modulo calcareo sulla composizione della fase ferrica del clinker di portland", Ind. Ital. Cem. 25, 5.

290.- KRÄMER, H. et ZUR STRASSEN, H. (1960) "Discussion. Phase equlibria and constitution of portland cement clinker.(R. W. Nurse)", Proc. 4th Int. Symp. Chem. Cement, Washington 1, sess. II, 32.

291.- MIYAZAWA, K. et TOMITA, K. (1966) "Der Einfluss von MgO auf die Eigenschaften des Portlandzementes", Zement-Kalk-Gips 19, 82.

292.- STAHEL, A. et SCHRÄMLI, W. (1969) "Zum Verhalten des Magnesiums im Klinker unter verschiedenen Abkühlbedingungen", Zement-Kalk-Gips 22, 407.

293.- TSUBOI, T., ITO, T., HOKINOUE, Y. et MATSUZAKI, Y. (1972) "Die Einflüsse von $MgO-SO_3$ und ZnO auf die Sinterung von Portlandklinker", Zement-Kalk-Gips 25, 426.

294.- HOFMÄNNER, F. (1975) "Microstructure of portland cement clinker", Holderbank Manag. and Consul. Ltd.

295.- CEMBUREAU (EUROPEAN CEMENT ASSOCIATION) (1968) "Cement standards of the world".Paris.

296.- ASTM STANDARD BOOK (1971), Design. C 150-71. P. 9, p. 135.

297.- GONNERMANN, H.F., LERCH, W. et WHITESIDE, T.M. (1953) "Investigations of the hydration expansion characteristics of portland cements", Portl. Cem. Ass. Chicago. Res. Dpt. Bull. 45, pp. 168.

298.- GAZE, M.E. et SMITH, M.A. (1973) "High magnesia cements I and II", Cem. Technol. 4, 224, 5, 291.

299.- SCHMITT-HENCO, C. (1974) "Magnesium oxide content of clinker, autoclave test and soundness", 6th Int. Congr. Chem. Cement, Moscow.

300.- BRISI, C. et APPENDINO, P. (1965) "Equilibri allo stato solido nel sistema $CaO-SrO-SiO_2$", Annali di chimica 65, 1213.

301.- APPENDINO, P. et MONTORSI, M. (1971) "Influenza di aggiunte di stronzio, di bario e di magnesio sulle trasformazioni polimorfe del silicato tricalcico", Il Cemento 68, 89.

302.- GILIOLI, C., MASSAZZA, F. et PEZZUOLI, M. (1972) "Relazioni d'equilibrio nel sistema $CaO-SrO-SiO_2-SO_3$", Il Cemento 69, 19.

303.- GILIOLI, C., MASSAZZA, F. et PEZZUOLI, M. (1973) "Studio delle relazioni esistenti allo stato solido nella parte più basica del sistema quaternario $CaO-SrO-Al_2O_3-SO_3$", Il Cemento 70, 137.

304.- MASSAZZA, F. et GILIOLI, C. (1970) "Un nuovo composto nel sistema $CaSO_4-SrSO_4$", Il Cemento 67, 89.

305.- RAGOZINA, T.A. (1957) "Reaction of calcium sulphate with aluminates at 1200° ", Zh. Prikl. Khim. (Leningrad) 30, 1682.

306.- RAGOZINA T.A. et AKHMEDOV, M.A. (1962) "The phase composition of aluminium

ferrates (III) formed in the presence of calcium sulphate", Uzb. Khim. Zh. 6, 30.

307.- HALSTEAD, P.E. et MOORE, A.E. (1962) "The composition and crystallography of an anydrous calcium aluminosulphate occuring in expanding cement", J. Appl. Chem. 12, 413.

308.- GILIOLI, C., MASSAZZA, F. et PEZZUOLI, M. (1971)" A new compound: strontium sulphoaluminate and its relationships with calcium sulphoaluminate", Cem. Concr. Res. 1, 621.

309.- MASSAZZA, F. et PEZZUOLI, M. (1974) "Influenza dello stronzio sulla composizione mineralogica dei clinker", Il Cemento 71,167.

310.- RIO, A., CERRONE, M. et SAINI, A.(1970) "Influenza e meccanismo d'azione della celestina nel processo di cottura del cemento Portland in assenza ed in presenza di un agente mineralizzante", Il Cemento 67, 105.

311.- BUTT, YU. M., TIMASHEV,V.V. et KAUSHANSKI, V.E. (1968) " Properties of tricalcium silicate and its solid solutions", Proc. 9th Conf. Silicate Ind. (Siliconf 1967) Budapest, 59.

312.- BRISI, C. (1963) "Ricerche sul sistema calce-ossido di bario-silice", Ind. Ital. Cem. 33, 397.

313.- KURDOWSKI, W. et WOLLAST, R. (1970) "Solutions solides de BaO dans le silicate tricalcique", Silicates Ind. 35, 153.

314.- TOROPOV, N.A. (1960) "Solid solutions of the minerals of portland cement clinker", Proc. 4th Int. Symp. Chem. Cement, Washington 1, 113.

315.- SUZUKI, K. et YAMAGUCHI, G. (1968)"A structural study on α'-Ca_2SiO_4", Proc. 5th Int. Symp. Chem. Cement, Tokyo P.I, 67.

316.- CHOLIN, I.I., MALININ, J.S. et ENTIN, S.B. (1961)"Über den Einfluss von Bariumoxyd auf die Klinkerbildung, T. II", Silikattechnik 12, 340.

317.- KRAVCHENKO, I.V., ALESHINA, O.K. et GRIKEVICH, L.N. (1967)"Effect of barium oxide on the kinetics of clinker formation", Tr. Gos. Vses. Nauch.-Issled. Inst. Tsem. Prom. N° 22, 133.

318.- SULEIMENOV, A.T., BUTT, YU.M., TIMASHEV, V.V. et RAMANKULOV, M.R. (1969)"Production conditions and some properties of barium-containing portland cements", Tr. Mosk. Khim. - Tekhnol. Inst. N° 59, 242.

319.- KRAVCHENKO, I.V., ALESHINA, O.K. et GRIKEVICH, L.N. (1970)"Barium containing portland cement", Tr. Gos. Vses. Nauch.-Issled. Inst. Tsem. Prom. N° 23, 3.

320.- PEUKERT, J. (1974) "The technology of rapid-hardening or high-strength cements from one clinker", 6th Int. Congr. Chem. Cement, Moscow.

321.- MUMINOV, A.S. et AKHMEDOV, M.A. (1974)"On the interaction of barium chloride with the calcium aluminates in the solid phase conditions at high temperatures", 6th Int. Congr. Chem. Cement, Moscow.

322.- SPRUNG, S. et RECHENBERG, W. (1978) "Die Reaktionen von Blei und Zink beim Brennen von Zementklinker", Zement-Kalk-Gips 31, 327.

323.- KNÖFEL, D. (1978) "Beeinflussung einiger Eigenschaften des Portlandzementklinkers und des Portlandzements durch ZnO und ZnS", Zement-Kalk-Gips 31, 157.

324.- ONO, Y. ,UNO, T. et KANAI, Y. (1965) "Synthesis of five polymorphic modifications of C_3S", Semento Gijutsu Nempo 19, 33.

325.- AKATSU, K., IKAWA, K. et MAEDA, K. (1968)"Some effects of zinc oxide in the raw mix on the portland cement and clinker", Rev. 22nd Gen. Meet. Cem. Assoc. Japan, Tokyo p. 40.

SUB-THEME I-2

Effect of the Burning Process on the formation and properties of the clinker

S. SPRUNG,
Forschungsinstitut der Zementindustrie
Düsseldorf, R.F.A.

1. Introduction

The properties of the cement are essentially influenced by the composition and thermal treatment of the clinker. The clinker composition mainly depends on the composition of the raw material mixture. Besides, it can be affected by the type of fuel used and the ash constituents of the fuel. Depending on the type of burning process applied, material circulations in the kiln and preheater will frequently lead to an enrichment or depletion of volatile substances and thus to a change in composition.

During the thermal treatment the properties of the clinker are mainly determined by the temperature, heating rate and burning period. Equally important are the interactions between the material to be burnt and the furnace atmosphere as well as the cooling rate of the clinker.

The underlying report presents a summary of the recent findings that have been published since 1973/74. Only in a few cases reference is made to older publications. In its first part the report deals with the composition of fuels as far as they have an influence on the properties of the clinker. Subsequently the reactions during heating and sintering of the kiln feed and its interactions with the kiln atmosphere and the resulting material circulations are being discussed. In the last part of the report the influence of the cooling rate is described.

2. Fuels for Cement Production

2.1 Fuel Oil

Mineral oil still is the most important source of energy for the production of cement. For burning heavy oil is used most frequently. In 1978 heavy oil accounted for 64 % of the total fuel consumption in the German cement industry (1). The composition of fuel oils differs according to the origin of the crude oil. The composition of the cement is mainly influenced by the sulphur content which may amount to anything between 1 and 2,5 wt.-% (2) in fuel oil grade S. In fuel oil with residues from cracking even higher sulphur contents have to be expected. During combustion sulphur is converted to SO_2 which reacts with the alkalis and the calcium oxide of the cement raw materials.

Moreover, fuel oils contain small quantities of ash which may amount to .01 to .1 wt.-%, depending on the origin of the oil. The ash constituents mainly are SiO_2, Al_2O_3, K_2O, Na_2O and Ni. If the V-content amounts to .0001 to .0109 wt.-% in the crude oil (3), similar concentrations may be expected in the fuel oil. As far as we know today, other heavy metals, such as Pb and Zn, occur in concentrations of .0016 and .0020 wt.-% (12).

2.2 Coal

Hard coal and lignite are used more and more frequently as sources of energy. Depending on the conditions of its formation, coal may vary in composition very much. Important characteristics are the ash and sulphur content.

The coal ash forms from the mineral admixtures such as the clay minerals of kaolite and illite, some quartz, carbonate minerals and pyrite. The ranges over which the composition of coal ashes may vary in the USA, the U.K. and Germany are shown in Table I (4).

Table I: Composition of Coal Ashes (acc. W. Gunz) (4)

	Hard Coal			Lignite
	USA	U.K.	Germany	Germany
	wt.-%			
SiO_2	20-60	25-50	25-45	8-18
Al_2O_3	10-35	20-40	15-21	4-9
TiO_2	0,5-2,5	0-3	-	-
Fe_2O_3	5-35	0-30	20-45	2-6
CaO	1-20	1-10	2-4	25-40
MgO	0,3-4	0,5-5	0,5-1	0,5-6
Na_2O+K_2O	1-4	1-6	3-4 (6)	0-1 (6)
SO_3	0,1-12	1-12	4-10	0-50

The ash content of coals may vary between about 3 and 30 wt.-%. Acid coal ashes tend to form melts of low viscosity which react with the material to be burnt in the kiln. In this way the tendency of coating and ring formation in cement kilns is enhanced (5).

Besides, the coal ash will change the clinker composition. If high-ash coals with high SiO_2, Al_2O_3 and Fe_2O_3 contents are fired in the kiln, the $CaCO_3$ content of the raw meal must therefore be increased proportionately in order to maintain the standard lime factor or the LSF of the clinker. The homogeneous blending of the ash with the kiln feed is also important. Kilns working as suspension-type preheater kilns offer the most favorable conditions for homogeneous blending. In kilns with grate preheater ash may accumulate on the pellet surface which increases the formation of C_2S and melting phases. This, however, does not seem to change the technical characteristics of the cement (7). A very homogeneous distribution of the ash can be achieved if coal is used as fuel for precalcination. This is the reason why according to E. Steinbiss (8) low-grade fuels from waste materials can be used profitably and without impairing the clinker quality. However, the use of such fuels is limited due to the emission of organic carbon compounds and CO.

Of special importance for the burning process are sulphur and chloride and occasionally alkalis. The sulphur content of the coal frequently amounts to .5 to 1,2 wt.-%. Most of the sulphur is bound in pyrite or marcasite (FeS_2). The proportion of sulphur bound in the organic substance is not significant. Lignite may contain sulphur in the form of calcium sulphate or alkali sulphate. In coals with a higher FeS_2 content the sulphur may also rise to values of more than 2 wt.-% (4).

Contrary to fuel oil, coal may contain as much as .01 to .1 wt.-% of chloride. In coals that are particularly rich in ash and salt, chloride contents of up to .4 wt.-% have been measured (9). A high supply of chloride in the kiln enhances the tendency of coating and ring formation (10).

The amount of alkali fed into the kiln with the coal is low, i.e. about .1 wt.-% at an ash content of 20 wt.-%. The alkalis from the coal together with the alkalis from the raw meal have an effect on the emission of sulphur dioxide (10). Coal also contains traces of other pollutants, i.e. heavy metals such as Pb, Zn, Ni, V, Co, Cr, As and Tl. In coal from West Germany concentrations of .00010 to .0150 wt.-% (10 to 150 ppm) of such elements were found (3, 11, 12). The Pb and Zn contents that have so far been measured in West German lignite amounted to about .0010 to .0030 wt.-% (10 to 30 ppm)(12).

2.3 Alternative fuels

The alternative fuels that are being tested with the purpose of saving fuel oil consist of burnable waste materials from production processes and municipal waste. The calorific value should amount to at least 12,600 to 16,800 kJ/kg (3,000 to 4,000 kcal/kg) (13-18). In general alternative fuels are able to produce 10 to 30 % of the heat supply today.

As far as the composition and properties of the clinker are concerned, it is the ash content of those alternative materials, the ash composition and the content of alkalis, chloride and sulphur that is of importance. No reliable statements can be made about the average composition of alternative fuels. Analytic data that have so far been published are summerized in Table II.

Table II: Composition of Alternative Fuels (13-18)

	Ash	S	K_2O	Na_2O
	wt.-%			
Bleaching earth	48-52	1,0-1,5	0,6	1,2
Acid sludge	2-6	10-15	-	-
Used tyres	4-6	1-2,1	-	-
Delayed coke (Canada)	2,5-4	5-6	0,1	-

Bleaching earths containing about 50 wt.-% of ash require a correction of the $CaCO_3$ content in the raw meal because the ash primarily consists of SiO_2 and Al_2O_3. The ash contents of the other alternative fuels are below 10 wt.-%. Municipal waste, however, may contain more ash depending on the water content (15).

Alternative fuels contain various amounts of sulphur depending on their origin; in the case of acid sludge the sulphur content may rise to as much as 15 wt.-%. In order to avoid SO_2 emissions, the sulphur supply to the kiln must be adjusted to the supply of alkali. For this reason, acid sludge can only be used to a limited extent. The alkali and chloride contents in the materials mentioned in Table II are insignificant with respect to kiln operation and clinker composition. Other alternative fuels, such as shredder waste (13) or chlorinated hydrocarbons (17), were less desirable because the chloride content led to an increase in the chloride circulations in the kiln and interfered with the kiln operation due to coating and ring formation.

The influence of heavy metals on the clinker quality and the emission is not yet known. According to the results of studies made so far, alternative fuels may contain .0100 to 2 wt.-% of Pb, Zn, Cu, Sn, Ni and V. Concentrations of less than .01 wt.-% are reported for Cd, B, Mo and Cr (12, 13, 16, 18). In used oil a bromine content of .15 wt.-% was found (16). The contents of other elements, such as Tl, As and Se, have not yet been studied in a systematic way.

2.4 Fuels with a high content of inert materials

Such fuels that are more and more being used as a substitute for high-grade sources of energy, are oil shale, coal-containing shale, low-grade coal with a high inerts content and charcoal. The typical characteristics of such fuels are the low content of natural burnable substances and, consequently, a high ash content. Therefore these fuels have a low calorific value which, according to B. Mayer (19), amounts to only 9,300 kJ/kg (2,200 kcal/kg) in a Corean coal shale or to as little as 3,900 kJ/kg (930 kcal/kg) in oil shale (Dotternhausen), according to R. Rohrbach (20). Flotation slimes formed during coal preparation have an ash content of 53 to 74 wt.-%, according to W. Poersch (21). The calorific values are low, i.e. 6,500 to 15,800 kJ/kg (1,548 to 3,762 kcal/kg). The values given for the composition of such fuels are summarized in Table III; they may differ so widely from each other that an average composition cannot be stated.

Table III: Composition of Fuels with a High Content of (6, 19-22) Inert Materials

	Ash	K_2O	Na_2O	S	Cl
	wt.-%				
Oil shale	80	2,0	0,3	3,0	-
Coal shale	69	2,7	0,2	1,95	0,04
Coal slime (flotation)	53-74	-	-	1,1-1,3	-

Due to their high content of ash rich in SiO_2 and Al_2O_3, the use of such fuels requires a correction of the $CaCO_3$ content in the raw meal. In addition to continuous monitoring of the raw meal composition, homogenization of the coal in mixed beds and continuous checking of the ash content and ash composition would also be desi-

rable (19).

Coal with a high inerts content can be used as primary fuel up to an ash supply of 50 to 75 kg/t clinker (in all following cases metric ton), according to J. Parisis (23), without coating or ring formation in the transition zone from sintering to calcination. If the coal is very finely ground and injected at high speed, even an ash quantity of 100 to 150 kg/t clinker is considered acceptable. In kilns with grate preheater high-ash coals can usually not be used.

From the angle of process engineering, the use of coal with a high inerts content is more advantageous for precalcination of the raw meal. If enough excess air is present, complete combustion will occur due to high meal and gas temperatures of about 700 to 1,000 °C. The released heat is immediately used for dissociation of the raw meal. Besides, the ash mixes homogeneously with the kiln feed, as the experience with several kilns equipped with a suspension-type preheater has shown. Obviously, complete mixing even occurs if the suspension-type preheater is only charged with limestone meal and the required quantities of SiO_2, Al_2O_3 and Fe_2O_3 are exclusively supplied from the burnt up secondary fuel such as oil shale, bituminous lime marl or washery refuse (19-20, 22-25).

According to Table III, fuels with a high content of inert materials may contain major sulphur quantities which may rise to 3 wt.-% and mainly occur in a chemically bound form as pyrite or marcasite (FeS_2). On the basis of geochemical studies (3), higher contents of heavy metals than in prepared coal and lignite must be expected in such fuels. It is therefore necessary to analyze their composition and decide whether they can be used.

3. Burning of the Clinker

When the cement raw meal is heated, $CaCO_3$ and the clay minerals dissociate first. Even before this reaction is completed, the formation of the clinker phases begins which is accelerated at higher temperatures by the clinker melt. The reaction rate is important for reducing the heat requirements and for the properties of the cement clinker. For this reason, it has often been attempted to predict the burnability of raw meals and to influence it by suitable measures. During burning the clinker composition can be influenced by the kiln atmosphere and may be changed by the type of fuel used and by circulations. Besides, the cooling rate of the clinker which was slowed down by the use of planetary coolers may have an effect on the setting and development of strength in the cement.

3.1 Burnability

3.1.1 Dissociation of raw meal constituents

The dissociation reactions of raw meal constituents occur at temperatures of less than 1,000 °C. When pure calcium carbonate is heated in a CO_2 atmosphere, decomposition will start at a temperature of about 900 °C. With decreasing CO_2 partial pressure, the dissociation occurs at lower temperatures, according to the equilibrium conditions. For technical-scale processes, the reaction time required for complete dissociation is of special importance. In addition to CO_2 partial pressure and temperature, also the particle size and crystalline structure of the calcium carbonate and the reactions of the $CaCO_3$ with the other main constituents of the raw meal are major factors of influence. According to a summary by F.W. Locher (26), the reactions already begin at a temperature of about 550 °C. Due to the reaction of SiO_2, Al_2O_3 and Fe_2O_3 the dissociation pressure of the $CaCO_3$ which is still very low in this temperature range will start to rise. As reaction products C_2S, aluminates with lower calcium content and calcium aluminate ferrite will be formed. Free CaO only forms at temperatures above 900 °C.

The dissociation rate of the raw meal constituents is particularly important from the angle of process engineering. In the modern heat saving kiln installations operating on the basis of the half-wet or dry process, the raw meal is mainly preheated in the grate and suspension-type preheaters in counterflow to the hot kiln exhaust gases; decomposition only amounts to 20 to 40 % in the preheater (27). Dissociation is taking place subsequently in the rotary kiln. According to a summarizing description of the state of the art in the field of process engineering by L. Kwech (28), the output of the kiln could only be improved to a significant extent while maintaining nearly unchanged favorable energy consumption figures when precalcination was introduced. The higher kiln output was due to the fact that, after raw meal preheating in the heat exchanger, an almost complete calcination in an additional calcinator step with secondary firing was taking place so that the only process occuring in the rotary tube was the sintering process. Essential prerequisite for the precalcination technique are an improved heat transfer and a rapid dissociation of the raw meal constituents.

Other possibilities of saving energy may arise from a better burnability of the raw meal. The kinetics of the $CaCO_3$ dissociation were studied in detail by B. Vösteen (29). More recent studies with a laboratory reactor about which A. Müller, B. Dahm and J. Stark (30) reported in a summarized form, showed that the time required for complete dissociation of the $CaCO_3$ decreases with increasing temperature of the kiln feed, declining CO_2 partial pressure in the combustion gases, decreasing load of solid particles in the gas flow, decreasing mean particle size of the $CaCO_3$ and decreasing crystallinity. Although the test results and the mathematical formulas for precalculating the degree of dissociation or the dissociation rate derived from them cannot automatically be transferred to practical conditions, they might be useful for estimating how an in-

crease in material temperature in the calcinator step of the preheater, a decline of the CO_2 content in the combustion gas, if natural gas is used instead of fuel oil, or a greater fineness of the ground $CaCO_3$ in the raw meal would affect the acceleration of precalcination in technical scale installations. The influence of clay minerals and quartz on the dissociation rate of the $CaCO_3$, however, is not considered in this approach.

The impact of the heating-up velocity on the dissociation rate of limestone and cement raw meal was studied by K. Volke (31) in the temperature range of about 100 to 2000 K/min. The heating velocity in technical installations is estimated to amount to a few hundred K per minute. From studies made on a laboratory scale with N_2 as carrier gas it appears that in the case of low heating velocities the dissociation rate of limestone meal mainly depends on the mass transfer. With rising heating velocities and increasing calcite particle size, the inadequate thermal conductivity and a mounting CO_2 partial pressure inside the particle will slow up the dissociation rate. In cement raw meal and a high heating gradient of more than 450 K/min. the $CaCO_3$ dissociation is enhanced by the reaction with the clay containing raw meal constituents, and the delaying effect of the inadequate thermal conductivity is partially offset. Similarly, Y. Nygardas (32) found that by slightly reducing the number of rotations of the kiln to .92 r.p.m. as compared to 1.33 r.p.m., higher heating velocities were observed on the particle surface of the kiln feed which led to a higher degree of calcination at the same mean material temperature. B. Vosteen (35) has developed a formula for precalculating the retention time of cement raw meal for complete decomposition taking into consideration the heat transfer in a suspension-type preheater with a downstream calcination step. These calculations, however, are based on the dissociation equilibrium of pure $CaCO_3$ so that they will only lead to an approximation to the actual conditions even if a large number of parameters are included.

An accelerated heating rate also favors the reactivity of CaO and thus the rate at which clinker phases will form. According to studies by O.P. Mtschedlow-Petrossian and coworkers (33), the increased reactivity of CaO which is formed at 800 to 900 °C and does not recrystallize at short retention periods, is due to a high content of lattice defects and lattice voids. U. Ludwig (34) also emphasizes the technical advantage of a high heating gradient in the temperature range below 1000 °C for the sintering reaction.

K.P. Kacker, R.C. Satiya and D. Chandra (36) as well as H.J. Wächtler (37) have studied the influence of clay minerals and other foreign oxides on the thermal dissociation and dissociation rate of calcite. According to these studies, the lowering of the dissociation temperature of the calcite in the clay containing raw meal by about 90 to 130 K is supposed to be exclusively due to water vapor (36). H.J. Wächtler (37), however found that besides clay minerals alkali salts occurring in quantities of up to 2 wt.-% will reduce the activation energy of the $CaCO_3$ dissociation. Their effect is due to the formation of salt melts or easily melting compounds at the reaction front of the $CaCO_3$. During technical-scale operation alkali compounds are carried into the raw meal by the kiln dust. The most effective substance for reducing the activation energy in cement raw meals is Na_2SiF_6. Additives such as basalt, lead and copper slag, apatite, triphosphate, phosphorite and phosphorous slag have a similar effect. V.V. Timasev, J.A. Fridman and A.L. Polanskij (38) were able to accelerate the raw meal decomposition and increase the kiln output by adding $FeCO_3$ (Siderite).

These investigations thus lead to the conclusion that a high dissociation rate of the raw meal constituents has a favorable effect on the rate of clinker phase formation and, thus, on the output of the kiln. Additives to the raw meal also expedite dissociation. A similar behaviour can be expected of foreign substances which are carried into the kiln system mainly by way of alternative fuels, although this still requires detailed and comprehensive studies. Since, in practice, the retention time of the material in the rotary tube often is too long, the technical benefit of the quick dissociation of the raw meal constituents will be partly or fully lost unless such parameters as length and number of rotations of the kiln are fully adjusted to the conditions of precalcination.

3.1.2 Sintering

The sintering reactions accelerate at temperatures of more than 900 to 1000 °C. Mainly dicalcium silicate, calcium aluminate and calcium aluminate ferrite as well as free CaO are formed in the process. The content of free CaO decreases when clinker melt is formed and C_3S formation may occur at a faster rate at temperatures above 1250 °C. The significance of melt quantity, melt composition and the equilibria that occur as well as the kinetics of the sintering reactions are discussed by V.V. Timasev in his report.

The temperature at which the clinker is burnt must be above 1250 °C to promote the formation of C_3S which is important for the development of strength. In rotary cement kilns the burning temperature usually amounts to about 1450 °C. Higher burning temperatures of up to 1700 °C may be disadvantageous and therefore are of no technical importance for the time being (26). Previous studies by J.M. Butt and V.V. Timasev (30) show in principle the advantage of a high sintering temperature for the rate of clinker phase formation. Below 1450 °C C_3S formation mainly occurs as solid body reaction when the quantity of clinker melt is still relatively small. At a higher temperature the

sintering time is reduced to a few minutes because the amount of melt increases and its viscosity decreases. Japanese studies (40) have led to similar conclusions. If, however, the isothermal holding time at burning temperatures of more than 1350 °C is extended to the extreme value of 120 minutes, the C_3S content will decline. The reason for this is the dissolution of the C_3S in the enlarged amount of melt (41). It is questionable whether sintering at temperatures exceeding 1500 °C will be of any interest at all in future, since substantial energy savings cannot be expected from the acceleration of the sinterung process and the rotary kilns with the present types of linings cannot be automatically used for such processes. Of much greater technical interest might be those processes in future that permit to burn clinker also at temperatures below 1400 °C. Indications in this direction were given by N.P. Kogan, O.P. Mtschedlov-Petrossian and V.I. Satarin (42). It might be worth-while to study the influence of the heating rate in this context.

According to O. Philipp (47), a high heating velocity promotes the sintering of the cement raw meal at temperatures of up to 1450 °C, since the CaO and the other oxides show a high activity due to the fact that no recrystallization occurs; this activity leads to the fast formation of clinker phases at temperatures as low as 1000 °C as soon as the melt begins to form. Studies by J. Stark and D.Q. Phu (48) as well as studies by J.M. Butt, V.V. Timasev and J. Stark (49) on a laboratory scale at temperatures of up to about 1700 °C also show that the clinker obviously has good strength characteristics which are mainly due to a higher C_3S content and a reduced particle size of the C_2S as a function of burning time. The technical significance of the process cannot yet be estimated because no data have so far been given with regard to the energy requirements.

Of a more practical importance for burning is the small particle size of the raw meal constituents and their homogeneous distribution. Sintering is mainly promoted by fine grinding and homogeneous distribution of the raw meal constituents (26,44). At temperatures above 1450 °C the particle size distribution is less important, as studies by U. Ludwig and G. Ruckensteiner (43) have shown. Coarse quartz and calcite particles of a diameter larger than 100 microns should not amount to more than 1 and 6 wt.-%, respectively. H. Lehmann and P. Thormann (45) found that the C_2S forms fastest if the average particle size of the calcite is 15 microns. When standard treatment methods are used, however, quartz sand which is added to the raw mixture is rarely ground more finely than to an average diameter of 50 to 100 microns (46). Due to the poor grinding characteristics of quartz sand, cements from lime stone and quartz with a reduced amount of clinker melt cannot be produced economically, as calculations by F.W. Locher (26) have shown. The energy required for grinding the quartz would be higher than the energy saving that could be made as a result of the better grinding characteristics of a clinker with a lower melt proportion. Similar statements may be made for experiments aiming at a better decomposition and sintering behaviour by mechanical activation and grinding to maximum fineness in vibration mills (50, 51).

The burning of cement clinker may also be promoted by fluxes and mineralizers. Whereas fluxes reduce the temperature at which melt will begin to form and change its viscosity, mineralizers enhance the C_3S formation without any melt. Fluorides act as both fluxes and mineralizers. A summary on the use of fluxes and mineralizers was given by W.A. Klemm and J. Skalny (60). It appears from this summary that not only oxides but also fluorides and silicofluorides have proved to be effective in laboratory and industrial scale studies. Similar conclusions are reported by J. Stark (52) for the production of quick burnt clinker in the laboratory.

Additions of Ba, P, Cr, SO_3, Na, Ti and other elements are supposed to have a mineralizing effect, whereby A.K. Chatterjee (44) mentions an optimum concentration of .2 to 1 wt.-% in most cases. In laboratory scale burning tests a mineralizing effect of the elements Cu, Cr, Mn, Ti, Zn and Pb was observed if these were added in quantities of up to 4 wt.-% (55-59). Substances that act as a flux or mineralizer and which especially promote C_3S formation, are often contained in industrial waste materials. In this context A.M. Dmitriew, M.T. Wlasowa und B.E. Judowitsch (53) as well as Th. Uschold and E. Giesa (54) refer to blast furnace slag, nepheline sludge, phosphorous slag, wollastonite, basalt, power plant ash and heavy metal containing waste such as copper slag and lead slag as raw meal constituents.

In summary, it appears from all these studies that little is known about whether the industrial scale use of such materials, esp. in comparison with modern production methods, would lead to cost and energy savings, production increases or to a marked improvement of the cement quality. When burning mixtures of natural raw materials and standard composition with an Al_2O_3 ratio of 1.38, the optimum quantity of melt will be formed at the lowest possible temperature that leads to complete sintering, according to studies by H.R.M. Banda and F.P. Glasser (61). In such cases the additional expenditures for buying, storing and dosing of the fluxes or mineralizers do not appear to be economically justified. Such expenditures might possibly be useful if raw material mixtures with a high content of lime and a low melt formation are to be burnt which would otherwise require a very high sintering temperature (26).

3.1.3 Testing procedures

For planning new cement kiln installations and deciding about operational measures for reducing the heat requirements of older installations or making specific changes in the clinker quality, it is very important to determine the burnability of the raw meal. The burnability or sinterability depends on the material properties of the raw meal and the process engineering conditions. The material properties include the chemical and mineralogical composition of the raw meal, the particle size distribution and the degree of interstratification of the constituents. The process engineering parameters are the temperature rise over time up to sintering temperature, temperature differentials in the raw meal particle, sintering temperature, retention time at sintering temperature, kiln atmosphere and cooling rate. Tests for characterizing the burnability or sinterability are therefore made with the objective to verify the success of the thermal treatment by examining the clinker or to burn the raw meal unter controlled conditions and observe the process of the reactions.

An appraisal of the burning behaviour by microscopic methods is suggested by Y. Ono (62), M. Kristmann (63), F.A. DeLisle (64) and by J.D. Dorn (65). The influence of the fineness of the calcite and quartz particles, the heating and cooling conditions and the kiln atmosphere on the sinterability can be qualitatively recognized from the micrograph. On certain conditions it is also considered possible to classify the clinker in quality categories (62).

A summary of the studies made so far for the appraisal of burnability was given by E. Rauschenfels (66). The methods used for testing the burnability are characterized by steady-state or dynamic burning conditions, and in some cases the burnability of unknown raw meals is computed on the basis of regression analyses determined previously. In experimental processes using steady-state burning conditions the success of burning is usually measured by the free lime content. The burning temperatures amount to between 1000 and 1500 °C and the retention time remains constant (67-70). In a comparison with a standard meal of known burning behaviour relative conclusions can be drawn with respect to a deviating burning behaviour, and the duration of the sintering process, the rate constant or the activation energy can be computed. The kiln atmosphere and heating rate often are neglected in such calculations.

The experimental procedure suggested by U. Ludwig and G. Ruckensteiner (71) for determining the burnability permits the calculatory prediction of the sintering behaviour (B_p) of raw meals made from limestone, clay and sand, since there is a proved correlation between the practical burnability B_p in minutes at 1350 °C determined experimentally under steady-state burning conditions and the theoretical burnability B_{th}. For such a prediction data on the lime standard III, the proportion of melt including the proportion of alkalis and SO_3 (72) and the particle size distribution of the raw meal constituents are required. With rising burning temperature the burning period (B_p) decreases in a non-linear way (73). The effects of the heating velocity, motions of the kiln feed and kiln atmosphere on the burning period B_p are still unknown.

The studies by N.H. Christensen (74), V. Johansen (75) and E. Fundal (76) basically lead to a similar definition and computation of burnability. The free lime content determined after a 30 minute burning period at 1400 °C shows a linear correlation with the lime saturation factor (LSF), the silica module and the proportion of calcite > 125 microns and of quartz > 44 microns in raw meals that do not very much differ in composition. The influence of the alumina module (.5 to 4) is obviously excluded by the choice of the burning conditions. The alumina module essentially determines the melt point temperature of the clinker melt (61). The effects of the motions of the kiln feed, heating rate and kiln atmosphere are also neglected.

Dynamic methods for testing the burnability of stationary raw meal specimens were suggested by H.-J. Wächtler (77, 78), J. Kieser, A. Krähner and B. Gathemann (79) as well as by H. Hoffmann (80). Such processes are based on thermoanalytical and thermogravimetric studies for determining the raw meal activity and raw meal decompositon rate and the use of a gradient kiln for determining the sinterability or the degree of lime binding. The laboratory burning equipment permits to adjust the heating rate to the temperature curve of a technical-scale kiln installation and the creation of a CO_2 containing atmosphere. This process was also applied for studying the effect of alkali salts and spurrite formations on the burnability by way of a model (79). As with other processes, the burnability of raw meal was calculated on the basis of the standard lime, silicate module, alumina module, screen retainings and heating gradient which are the factors that have an effect on and are correlated to the free lime content (80).

From these studies the conclusion can be drawn that there obviously is a considerable interest in predetermining, by means of suitable testing methods, the burnability and sinterability of raw meals and the effect that additives may have on both. However, with all testing procedures known today simplifications must be made so that a number of parameters that are known from practical burning operations are neglected. Thus, for instance, the motions of the kiln feed, the reactions between the kiln feed and the gas atmosphere and the heat transfer cannot fully be taken into consideration in laboratory tests as yet. Therefore it is to be assumed that the test values found in the

way described can only be considered as relative values to which the burnability of the raw meals is to be compared with practical experience. This means that even with very complex and sophisticated testing procedures only a relative measure might be found for the burnability which could also be found by simpler means.

3.2 Composition

The composition of the raw meal essentially determines its behaviour during calcination and sintering, the economy of the burning process and the properties of the clinker. The most important criterion for the clinker properties is the strength of the cement made from it and its workability characteristics. The economy of the burning process mainly depends on the kiln output and the heat consumption. Besides, the grinding characteristics of the clinker also influence the energy requirements of cement production.

Usually the sinterability of cement raw meals is created in practice by an adequate fineness of grinding, reduction of the silicate module ($S_M = SiO_2/(Al_2O_3 + Fe_2O_3)$) and standard lime ($KST = 100\ CaO/(2.80\ SiO_2 + 1.18\ Al_2O_3 + .65\ Fe_2O_3)$) and by increasing the melt quantity and lowering the melting point temperature of the clinker. The lowest melting temperature occurs at an alumina module ($T_M = Al_2O_3/Fe_2O_3$) of 1.38 (61). Further details as to the influence of the main and minor constituents on raw meal sintering can be found in the literature (66-80). G. Gouda listed the various technical requirements to be met by the raw materials and the raw meal composition (81). Of critical importance is the chemical and mineralogical composition of the raw materials, the energy required for crushing and homogenizing and for drying and burning. Due to the different characteristics of the raw materials, the optimum production conditions have to be determined for each plant separately, whereby the procedures used for testing the burnability may supply the first indications. In this connection attention must be paid to the fact that an improvement of the sintering characteristics due to a higher proportion of melting phase may lead to a decrease of the grinding characteristics of the clinker which is directly proportional to the extent of melting phase. Complete sintering should therefore take place at the lowest possible temperature and the minimum quantity of melting phase (82).

The influence of the clinker composition on the development of strength and workability characteristics of the cement produced on a technical scale was studied by C. Schmitt-Henco (83) and by B. Sutej and K. Vrgoc (84). According to these studies, the setting time can be prolonged and in this way the workability characteristics of the cement can be improved if the C_4AF content of the clinker is increased at the expense of the C_3A content and no change is made in the amount of melting phase. It was observed that the strength of industrially made clinker increased with rising standard lime (KST). A silicate module rising from 2 to 3.2 may lead to particularly high 28 d strength properties if the quartz is present in a finely dispersed form and complete sintering is achieved. Under comparable conditions a rising alumina module will lead to a slight increase in the early strength. The test results obtained in factory-made clinkers can only be transferred to other raw material compositions, factories or even kilns as far as their general tendency is concerned, since in most cases the sinterability and burning conditions (heat transfer, kiln temperature curves, kiln atmosphere and cooling rate) are different. This also applies to tests for determining the strength development in advance on the basis of the chemical composition of the clinker by means of a multiple regression analysis (84) or quantitative phase analysis (85).

The minor constituents also have an effect on the workability and strength characteristics of the cement. Increasing quantities of free lime will reduce the soundness and strength if the CaO has formed in a primary way and recrystallized (83). Free CaO in quantities of up to about 6 wt.-% from weakly burnt shaft kiln clinker, however, did not impair the properties of the cement, according to tests made by K. Nagy (86).

The effect of alkalis bound in the clinker as described by I. Jawed and J. Skalny (87) may differ according to the prevailing conditions. Alkalis that are mainly bound in the C_3A usually increase its reactivity and may therefore contribute to quick setting of clinker that is rich in C_3A and to higher early strength but lower 28 d strength (88). In clinkers in which the alkalis are essentially bound as sulphates (sulphurization) by $CaSO_4$ additions or by burning with high-sulphur fuels, the early strength will increase. The final strength remains unaffected up to a total alkali content of about .8 wt.-% (Na_2O - equivalent). If, however, the total alkali content rises to values of more than 1 wt.-% (Na_2O equivalent) as a result of sulphurization, the 28 d strength may decline (89).

In natural raw meal heavy metals only occur in trace amounts, and it may be assumed that they have no major effect on the clinker properties. However, it is not yet known what the effect of those heavy metals may be that are carried into the cement kiln when substitute or alternative fuels are used. That seems to be of interest assuming that most of the heavy metals are bound in the cement clinker. According to the experiences made so far, clinker may contain heavy metal concentrations of up to about 200 ppm (12 - 18).

A large number of studies many of which, however, were only made in the laboratory, deal with the effect of higher heavy metal

and fluoride quantities added in the form of mineralizers or fluxes. In the older literature (60) the effects of fluorides on the cement properties are assessed in very different ways. According to P. Tewari and P.K. Mehta (90) as well as W. Gutt and M.A. Smith (91), a marked increase in the final strength was observed when fluoride was bound in the clinker. Studies concerning the practical use of fluoride sludge in the cement factory showed a considerable improvement of the 3 d and 28 d strength values, according to G. Stampendahl, H. Tauchmann and Ch. Engelmann (92).

However, the specific energy consumption for cement grinding was 16 to 22 % higher than the energy required for grinding cement which was free of fluxes.

Elements such as Ba, Sr, Ce, Cr, F, Ti and Zn that were added to the clinker in concentrations of up to 3 wt.-% or contained in the raw materials had more or less the same effect on setting and strength. With the exception of Ce which obviously did not influence the properties of the clinker in any way, and Cr which led to higher early strength values, all those elements delayed the hydration of the cement. Besides, it is being assumed that .5 wt.-% of V_2O_5, Cr_2O_3 or BaO in the clinker may improve the grindability (94).

The conclusion to be drawn from those studies is that the effects of trace elements or minor constituents cannot be appraised in a quantitative way. It is practically impossible to compare the results because the production conditions of the various cements differ too much from one another.

3.3 Kiln atmosphere

Experience has shown that, for quality reasons, the burning of the clinker requires an oxidizing atmosphere. This means that especially in the sintering and cooling zone of the kiln there must be an adequately high excess of air. The oxygen content of the kiln atmosphere cannot be controlled by simple means during the burning process in the sintering zone of the kiln. O_2 contents of 1 to 2 vol.-% measured in the kiln exhaust gas before it enters the preheater very often are no reliable indications of the absence of reducing conditons in the sintering zone. This largely depends on the shape of the flame, optimum atomization of the fuel, complete combustion of the fuel after mixing with hot air before it comes in contact with the kiln feed.

The results of older studies dealing with the influence that burning under reducing conditions has on the clinker quality were discussed in a summarized form by F.W. Locher (7) and H.-M. Sylla (98). Sylla again studied these correlations in a systematic way under laboratory conditions. The raw meals were burnt for 30 minutes at 1450 °C in air and in a CO_2 and CO atmosphere. The most striking characteristic of a clinker burnt in a reducing atmosphere was its brown color. This, however, only occurred if the clinker was cooled slowly to 1200 °C also in a reducing atmosphere. Cements made from clinker burnt in a reducing atmosphere and cooled slowly had a shorter setting time and also a considerably lower final strength. The early strength was not affected as strongly. The reason for the fast setting was the much higher C_3A content in the clinker than would have been expected in view of the composition and phase calculations according to Bogue. The increase in C_3A formation is due to the fact that part of the iron is reduced and can therefore not contribute to the formation of aluminate ferrite. The loss of strength is mainly caused by the fact that the C_3S takes up bivalent iron in its lattice during burning and becomes unstable as a result. The increase in the C_3A content and the decrease in the C_3S content is promoted by slow cooling in the temperature range between 1450 °C and 1200 °C.

The conclusion to be drawn from these studies is that, under normal operating conditions, the clinker quality will not deteriorate because in most cases the burning is done with an adequately high excess of air. Reducing burning conditions that may occasionally exist will only affect the clinker properties to any extent if, at the same time, the cooling zone of the kiln is longer and the clinker therefore is not cooled quickly enough.

3.4 Circulations

The gas in the cement kiln which flows in the direction opposite to the direction of the kiln feed, not only contains CO_2, O_2, CO, N_2 and water vapor but also dust from the kiln feed and a number of other gaseous and vaporous compounds. Most of the nitrogen oxides NO and NO_2 formed during combustion are emitted with the exhaust gas (99).

The kiln gas also contains alkali, sulphur, chloride and fluoride compounds which are formed from vapourized and dissociated constituents of the kiln feed and the fuel by reactions in the gas phase. When they react with the kiln feed or condense again in the cooler parts of the kiln, the preheater or in the hot-air drying and grinding plant, an inner circulation is created. An outer circulation is formed when dusts which are separated in the electrical precipitator containing the condensed compounds are added again to the raw meal and fed into the kiln. The circulation is interrupted when separated dusts are rejected.

The reactions of the volatile constituents in the kiln atmosphere were discussed in a summarized form at the 1971 VDZ Congress (10). The most important statement made in the paper was that the alkalis and the sulphur are mainly bound as alkali sulphates in the clinker and in the dust. The SO_2 emission of cement kilns is therefore low if

a stoichiometric alkali surplus exists. Forty investigations of kilns resulted in a mean SO_2 concentration of 30 mg/m³ (1013mbar, 273 °K, dry). When the raw material and fuel composition are changed or when new installations are planned, the SO_2 emission can be predicted by approximation. However, a higher SO_2 emission must be expected if there is an excess of sulphur or when burning is done in a reducing atmosphere. In agreement with R. Frankenberger and J. Matejka (100) it was found that a surplus of sulphur also enhances the tendency of sulphate spurrite coating ($2\ CaO \cdot SiO_2 \cdot CaSO_4$). This often occurs if the cement raw materials are low in alkalis and high-sulphur fuels are used. The use of raw materials richer in alkalis leads to an increased sulphur absorption in the clinker, and thus represents an effective remedial measure in production.

Contrary to the less volatile alkali sulphates, the alkali chlorides evaporate more easily. Only very little of them is bound in the clinker. The mean Cl^- concentration in the clinker amounts to about .01 wt.-%. In clinker with a high proportion of melting phase it may rise to levels of up to .03 wt.-%. Alkali chlorides therefore often build up an inner circulation in the kiln and must be removed via a bypass, if necessary. Studies on suspension-type preheater kilns have shown that a bypass is required whenever the Cl^- content in the raw meal amounts to more than .015 wt.-% and the K_2O supply exceeds 20 g/kg clinker.

The Cl^- concentration in the kiln feed near the kiln inlet may rise to values of 1 to 2 wt.-%. Such a chloride enrichment favours coating and ring formation in the cement kiln and in the area of the lower stage of the preheater (10, 101). According to studies by H.-M. Sylla (102), A.E. Moore (103) and I.G. Luginina (104), this is mainly caused by the formation of salt melts and spurrite and a number of other compounds. W. Danowski and J. Kieser (105) found that in the rotary kiln with shaft preheater the risk of coating is low even if the alkali content amounts to 20 g K_2O /kg clinker and the chloride content is five times higher (106). These studies, however, also indicate that the balances show relatively high deficits on the output side. These may be due to an emission of KCl. An emission of chlorides, however, would have the same effect as a bypass because it would interrupt the circulation. This agrees with later findings by P. Rösner, F. Feige, W. Danowski and J. Kieser (107) according to which the Cl^- concentration in the kiln feed at the kiln inlet was not higher than only 1 to 2 wt.-% and permitted trouble-free kiln operation although the Cl^- content in the raw meal amounted to .05 wt.-%.

Contrary to the reactions of sulphur, chloride and water vapor in the kiln atmosphere lead to an increase in the volatility of the alkalis. It is therefore possible to volatilize alkalis by adding Cl^-, to remove the alkali chlorides via bypass and to reduce the alkali content of the clinker in this way. Tests of this kind were made among others by R. Bohmann (108). However, it was found that the addition of $CaCl_2$ leads to relatively high operating expenses. Additionally, the alkali chlorides in the bypass reduce the efficiency of the electric precipitator which increases the dust emissions (109).

Other measures for reducing the alkali content in the clinker which are easier to carry out from the technical point of view would be to remove dusts with a high alkali load from the kiln system. Especially in grate preheaters with a high alkali supply of over 12 to 15 g K_2O/kg clinker this measure has a chance of success (110). Im suspension-type preheater kilns with precalcination, contrary to kilns without precalcination the size of the bypass can be varied in a wide range. In special cases the use of the kiln exhaust gases for raw meal preheating can be entirely dispensed with (100 % bypass). The design and operation of such kiln systems were described by J. Svendsen (111), J. Warshawsky and E.S. Porter (112) and H. Ritzmann (113). They also gave data as to the amount of energy required for reducing the total alkali content to values below .6 wt.-% Na_2O equivalent. A study made by the Portland Cement Association, USA (114) also contains information about the energy costs to be expected for bypass installations.

Minor alkali and alkali sulphate contents in the cement lead to an increase of the 28 d strength, as investigations by V. Johansen (115) and B. Osbaeck (116) have shown. Besides, the storage and processing characteristics are improved (117-118, 88). If the total alkali content is less than .6 wt.-% Na_2O equivalent, the cement may be used for the production of concrete with alkali-reactive aggregates.

Besides the circulations of alkalis, sulphur and chloride the fluoride and some heavy metal circulations were also studied. It was found that most of the fluoride is bound in the clinker. Gaseous fluorides are not emitted. The emission is limited to fluorides, that are bound predominantly as CaF_2 in the dust of the waste gas having passed the precipitator.

Heavy metals are contained in the raw materials and fuels at lower concentrations. By using substitute or alternativ fuels larger quantities of heavy metals may be supplied to the kiln. So far only the reactions of lead and zinc in the cement kiln have been studied (12). It turned out that, depending on the kiln system, 80 to 95 % of the zinc is bound in the clinker and 5 to 20 % in the dust respectively. Lead shows a behaviour similar to the one of zinc. More recent investigations, however, indicate that the degree of lead bindings in the clinker may

also be somewhat lower so that the lead content in the kiln dust increases and consequently the inner circuit too. In kilns with grate preheaters and in the case of a high chloride load this seems to be a frequent observation.

According to the studies made so far, lead and zinc can only be emitted with the dust which means that the lead and zinc emission depends on the efficiency of the precipitating system of the kiln (12, 16-18). The effects of binding fairly low concentrations of Pb and Zn in the clinker on the properties of the cement have not yet been studied in a complete way. Systematic studies of the reactions of other heavy metals that are contained in the raw materials and especially in the fuels and substitute fuels, have not yet been made. However, it may be assumed that these reactions might prove to be more important in connection with the emissions to the environment than they are to the properties of the cement.

4. Cooling of Cement Clinker

The cooling rate and kiln atmosphere influence the strength development and setting behaviour of the cement. In this part of the report only the effect of the cooling rate on the cement properties will be discussed.

The test results described in older publications (7, 26) show unanimously that fast cooling of the clinker generally leads to higher strength values. Fast cooling has a positive influence on both the early and the final strength. Fast cooling from sintering temperature is required in order to prevent reduction of the C_3S content by resorption which would lead to an increase in the C_2S and C_3A content. Fast cooling is also required to avoid decomposition of C_3S to C_2S and CaO and to obtain a fine-grained periclase crystallization. According to K. Mohan and F.P. Glasser (120), the C_3S decomposition is initiated by slow cooling in the temperature range between 1210 °C and 1025 °C by the formation of C_2S and CaO nuclei on the C_3S surface. The C_2S and CaO in the clinker accelerate the decomposition rate. Only by quenching the reactivity of the C_3A which is essential for setting behaviour can also be reduced. From a technical standpoint, however, quenching ist not practical and would lead to a loss of strength.

Recent studies by H.-M. Sylla (98, 121) have shown that cooling in an oxygen-containing atmosphere generally leads to higher final strength values than cooling in a reducing atmosphere. The effect on the early strength values is less important. Losses of strength will occur if the clinker is cooled from sintering temperature to room temperature by quenching. When the clinker was shortly quenched with water at a temperature level of 1450 °C and then slowly cooled by air without impairing the crystallization of the melt, the highest 28 d strength values were obtained in laboratory-made clinkers. Medium 28 d strength values were reached when the clinker was cooled from 1450 °C to 1250 °C within 30 minutes and then cooled faster by air. The explanation can probably be found in the reactivity of the C_3S which can obviously be influenced more strongly in the temperature range between 1450 °C and 1250 °C. However, these processes have not yet been fully clarified. Evidently the decisive phase of the cooling process still occurs in the kiln between the end of the sintering zone and the entry of the clinker into the cooler. The cooling zone varies in length depending on whether the kiln is equipped with a planetary or grate cooler. The length of the cooler also depends on the insertion length of the burner lance. However, so far no significant differences in strength have been found in technical scale cements that would have been due to different conditions during clinker cooling (7). Similar conclusions are to be drawn from the investigations by T. Enkegaard (122) and O.L. Jebsen (123) who compared the effects of the cooling rates of grate and planetary coolers. The samples taken at the inlet of the cooler and at the cooler outlet, however, primarily characterized the influence of the different cooling zone length in the kiln rather than the effect of the cooler design on the strength of the cement.

The conclusions to be drawn from the results available today show that the difference in the cooling rates may lead to significant changes especially in the final strength of the cement, as laboratory tests have indicated. In this connection only the temperature range from 1450 °C to 1250 °C is of interest. In technical-scale clinkers no effects on the strength could be observed despite the differences that existed in the cooling conditions in the kiln. This, however, may only apply if the clinker is burnt and cooled in an oxidizing atmosphere. In a reducing atmosphere longer cooling periods in the high-temperature range may impair the development of strength and the setting behaviour of industrially made cements.

REFERENCES

1.- Bundesverband der Deutschen Zementindustrie e.V., Köln: Zahlen aus der Zementindustrie, Ausgabe 1979

2.- Hansen, W.: Ölfeuerungen, Springer-Verlag Berlin-Heidelberg-New York 1970

3.- Wedepohl, K.H.: Handbook of Geochemistry, Springer-Verlag Berlin-Heidelberg-New York

4.- Gunz, W.: Kurzes Handbuch der Brennstoff- und Feuerungstechnik, Springer-Verlag Berlin-Göttingen-Heidelberg 1953

5.- Dannenbrink, W.C.,F.I. Kohanowski, P.D. Hess, E.T. Losin: Eigenschaften von Kohlen und deren Einfluß auf den Betrieb von Ofensystemen mit Zyklonvorwärmern, Zement-Kalk-Gips 30 (1977), H. 12, S. 618/619

6.- Keil, F.:Zement - Herstellung und Eigenschaften, Springer-Verlag Berlin-Heidelberg-New York 1971

7.- Locher, F.W.:Verfahrenstechnik und Zementeigenschaften, Generalbericht Fachbereich 7, VDZ-Kongress '77, S. 626/641, Bauverlag GmbH, Wiesbaden und Berlin

8.- Steinbiß, E.:Erfahrungen mit der Vorcalcinierung unter Berücksichtigung von Ersatzbrennstoffen, Zement-Kalk-Gips 32 (1979), H. 5, S. 211/221

9.- Mussgnug, G.:Beitrag zur Alkalifrage in Schwebegaswärmetauscheröfen, Zement-Kalk-Gips 15 (1962), H. 5, S. 197/204

10.- Locher, F.W.,S. Sprung, D. Opitz: Reaktionen im Bereich der Ofengase, Generalbericht Fachbereich 4, VDZ-Kongress '71, S. 149/160, Bauverlag GmbH, Wiesbaden und Berlin

11.- Ruhrkohlen-Handbuch, Verlag Glückauf GmbH, Essen, 5. Auflage 1969, S. 45

12.- Sprung S. und W. Rechenberg: Die Reaktionen von Blei und Zink beim Brennen von Zementklinker, Zement-Kalk-Gips 31 (1978), H. 7, S. 327/329

13.- Hochdahl, O.: Erfahrungen und Gesichtspunkte beim Einsatz von Ersatzbrennstoffen, Zement-Kalk-Gips 31 (1978), H. 9, S. 421/424

14.- Dorn, J.D.: Use of waste and recycled material in the cement industry, IEEE Transactions of Industry Applications IA-13 (1977), No. 6, S. 576/580

15.- Pennel, R., P.E. Giles, A. Hansen: Erfahrungen beim Betrieb von Zementdrehöfen bei teilweisem Ersatz traditioneller Brennstoffe durch Haus- bzw. Gewerbemüll, Zement-Kalk-Gips 31 (1978), H. 7, S. 321/322

16.- Berry, E.E.: Experimental burning of used automotive crankcase oil in a dry-process cement kiln, J. Hazardous Materials 1 (1975/76), S. 137/156

17.- MacDonald, L.P., D.J. Skinner, F.J. Hopton, G.H. Thomas: Burning waste chlorinated hydrocarbons in a cement kiln, Rep.-No. EPS 4 - WP - 77 - 2 Water Pollution Control Directorate - Environmental Protection Service, Canada 1977

18.- MacDonald, L.P., F.J. Hopton: Experimental burning of delayed coke in a wet process cement kiln, Rep.-No. EPS 4 - WP - 77 - 5, Water Pollution Control Directorate - Environmental Protection Service, Canada 1977

19.- Mayer, B.: Erweiterung des Zementwerks Donghoe/Südkorea unter besonderer Berücksichtigung eines Vorkalzinierverfahrens mit minderwertiger Kohle, Zement-Kalk-Gips 30 (1977), H. 3, S. 117/125

20.- Rohrbach, R.: Herstellung von Ölschieferzement und Gewinnung elektrischer Energie nach dem Rohrbach-Lurgi-Verfahren, Zement-Kalk-Gips 22 (1969), H. 7, S. 293/296

21.- Poersch, W.: Wirbelschichtverbrennung von schwierigen, ballastreichen Brennstoffen, VDI-Berichte Nr. 346, 1979, S. 305/318

22.- Rechmeier, H.: Der fünfstufige Wärmetauscherofen zum Brennen von Klinker aus Kalkstein und Ölschiefer, Zement-Kalk-Gips 23 (1970), H. 6, S. 249/253

23.- Parisis, J.: Wirtschaftliche und technische Gesichtspunkte des Einsatzes von Nebenprodukten der Kohleaufbereitung im Zementofen, Zement-Kalk-Gips 31 (1878), H. 5, S. 245/246

24.- Rohrbach, R.: Verfahren zur Herstellung von Zementklinkern, Deutsches Patentamt DAS 1 251 688 v. 26.3.1965

25.- Rechmeier, H., R. Rohrbach, G. Rohrbach: Verfahren zur Wärmebehandlung von staubförmigem Gut, Deutsches Patentamt OS 2 262 213 v. 19.9.1974

26.- Locher, F.W.: Einfluß der Klinkerherstellung auf die Zementeigenschaften, Zement-Kalk-Gips 28 (1975), H. 7, S. 265/272

27.- Pastala, A.L.: The application of precalciner technology for the cement industry of a developing country, World Cement Technology 1977, No. 7/8, S. 131/143

28.- Kwech, L.: Brennverfahren, Generalbericht Fachbereich 3, VDZ-Kongress '77, S. 227/243, Bauverlag GmbH, Wiesbaden und Berlin

29.- Vosteen, B.: Die physikalische und chemische Kinetik der thermischen Zersetzung von Kalk, Dissertation TU Braunschweig 1971

30.- Müller, A., B. Dahm, J. Stark: Beitrag zur Kinetik der Calciumcarbonzersetzung, Zement-Kalk-Gips 32 (1979), H. 2, S. 78/82

31.- Volke, K.: Untersuchung der Dissoziation von $CaCO_3$ im Aufheizgeschwindigkeitsbereich des Schachtvorwärmers, baustoffindustrie 1976, Ausgabe A, Nr. 3, S. 16/21

32.- Nygardas, Y.: Temperaturabhängigkeit der Reaktionen in einem Zementofen und der Einfluß der Umdrehungsgeschwindigkeit, Zement-Kalk-Gips 25 (1972), H. 6, S. 286/288

33.- Mtschedlow-Petrossian, O.P., N.J. Saposhnikowa, L.N. Skrynnik, T.J. Steschetkina: Untersuchung des Einflusses der Kalkzufuhr auf die chemische Aktivität bei der Klinkerbildung, Silikattechnik 28 (1977), H. 8, S. 234/236

34.- Ludwig, U.: Verfahren und Vorrichtung zum Brennen von Zementrohmehlen zu Zementklinkern, Deutsches Patentamt AS 2365152 v. 29.12.1973

35.- Vosteen, B.: Vorwärmung und vollkommene Kalzination von Zementrohmehl in einem Schwebegassystem, Zement-Kalk-Gips 27 (1974), H. 9, S. 443/450

36.- Kacker, K.P., R.C. Satiya, D. Chandra: Einfluß von Tonmineralen auf die thermische Zersetzung von Kalkstein und Dolomit, Zement-Kalk-Gips 25 (1972), H. 1, S. 37/41

37.- Wächtler, H.-J.: Thermoanalytische Untersuchungen in der Zementchemie - Entsäuerung von Zementrohmehlen, Silikattechnik 26 (1975), H. 3, S. 92/98

38.- Timasev, V.V., J.A. Fridman, A.L. Polanskij: Decarbonatisierung der Rohmischung im Wärmetauscher, Cement (Leningrad) 39 (1973), Nr. 12, S. 9/10

39.- Butt, J.M., V.V. Timasev: Die Geschwindigkeit der Klinkerbildung bei hohen Temperaturen, Silikattechnik 23 (1972), H. 3, S.89/92

40.- Suzukawa, Y., H. Kono, K. Fukunaga: High-temperature burning of portland cement clinker, Cem. Ass. Japan, Rev. 18. Ge. Meeting, Tokyo 1964, S. 96/99

41.- Timasev, V.V., J.I. Mituzas, V.V. Montvilla, A.J. Mituzas: Einige Besonderheiten der Mineralbildungsprozesse beim Brennen von Portlandzementrohmischungen im Temperaturbereich von 1000 bis 1500 °C, 6. ibausil, Weimar, 14.-18. Juni 1976, Sektion 2: Bindemittel, Vortrag Nr. 2.2.1 Bauforschung, Baupraxis 12. Bauinformation, DDR, Berlin 1978, S.66/69

42.- Kogan, N.P., O.P. Mtschedlov-Petrossian, V.J. Satarin: Physicochemical processes of clinker burning at reduced temperatures in rotary kilns, VI. Intern. Congr. Chem. Cem., Moskau (1974), Suppl. Paper 22, Sect. I.

43.- Ludwig, U., G. Ruckensteiner: Einfluß der Phasengrenzen bei der Klinkerbildung, Sprechsaal 107 (1974), H. 6, S. 231/234, 236/237, 239/240, 242

44.- Chatterjee, A.K.: Phase composition, microstructure, quality and burning of portland cement clinkers - A review of phenomenological interrelations - Part 2, World Cement Technol. 1979, Nr. 6, S. 165/173

45.- Lehmann, H., P. Thormann: Über den Einfluß der Kalksteinkorngröße auf die Klinkermineralbildung, Tonind.-Ztg. 87 (1963), H. 17/18, S. 369/375

46.- Richartz, W.: Ausschalten von Fehlerquellen bei der Röntgenfluoreszenzanalyse, Zement-Kalk-Gips 24 (1971), H. 2, S. 72/78

47.- Philipp, O.: Einfluß des Aufheizverhaltens auf den Garbrand von Zementklinker, Silikattechnik 24 (1973), H. 8/9, S. 265/268

48.- Stark, J., D.Q. Phu: Beitrag zur Rohmehloptimierung beim Schnellbrand von PZ-Klinker im Hochtemperaturbereich, Wiss. Zeitschr. Hochsch. Arch. und Bauw. Weimar 19 (1972), H. 1, S. 85/88

49.- Butt, J.M., V.V. Timasev, J. Stark: Phasenzusammensetzung und Kristallgröße von Schnellbrand - PZ - Klinkern, Silikattechnik 24 (1973), H. 1, S. 10/12

50.- Hoffmann, B.: Der Einfluß von Mahlhilfsmitteln auf die mechanische Aktivierung von Magnesiumoxid für die Sinterung,
Silikattechnik 23 (1972), H. 7,
S. 224/227

51.- Philipp, O., R. Schrader: Application of thermal, chemical and mechanical activation in clinker burning,
Proc. 6th Intern. Congr. Chem. Cement,
Moskau, 1976, Vol. 1, S. 207/211

52.- Stark, J.: Reaktionszeitverkürzung beim Schnellbrand von PZ-Klinker durch Erhöhung der Rohmehlfeinheit und Zusatz von Mineralisatoren,
Wiss. Zeitschr. Hochsch. Arch. und Bauw. Weimar, 19 (1972), H. 4,
S. 409/412

53.- Dmitriew, A.M., M.T. Wlasowa, B.E. Judowitsch: Verfahren zur Herstellung von schnell erhärtenden Zementen hoher Festigkeit,
Zement-Kalk-Gips 30 (1977), H. 9,
S. 705/707

54.- Uschold, Th., E. Giesa: Einsatz von Mineralisatoren in der Zementindustrie,
baustoffindustrie 1974, Ausg. A.,
Nr. 3, S. 4/7

55.- Knöfel, D.: Beeinflussung einiger Eigenschaften des Portlandzementklinkers und des Portlandzements durch TiO_2,
Zement-Kalk-Gips 30 (1977), H. 4,
S. 191/196

56.- Odler, I., O. Schmidt: Possible use of ZnO as a mineralizer in the manufacture of portland cement clinker,
80th Annual Meeting Amer. Ceram. Soc.,
Paper 4-T-78, 1978

57.- Teramoto, H., S. Koie: Phasenzusammensetzung und Hydratation eines höchstwertigen Portlandzementklinkers mit Fremdbestandteilen,
Zement-Kalk-Gips 28 (1975), H. 9,
S. 370/376

58.- Knöfel, D.: Beeinflussung einiger Eigenschaften des Portlandzementklinkers und des Portlandzements durch ZnO und ZnS,
Zement-Kalk-Gips 31 (1978), H. 3,
S. 157/161

59.- Tashiro, C., J. Oba: The effects of Cr_2O_3, $Cu(OH)_2$, ZnO and PbO on the compressive strength and the hydrates of the hardened C_3A paste,
Cement and Concrete Res. 9 (1979),
S. 253/258

60.- Klemm, W.A., J. Skalny: Mineralizers and fluxes in the clinkering process,
Cements Research Progress 1976, American Ceramic Society, Columbus, Ohio 1977

61.- Banda, H.R.M., F.P. Glasser: Role of iron and aluminium oxides as fluxes during the burning of portland cement,
Cement and Concrete Res. 8 (1978),
S. 319/324

62.- Ono, Y.: Microscopic analysis of clinker,
Central Res. Lab. Onoda Cement Co. Ltd. 1973

63.- Kristmann, M.: Portland cement clinker: Mineralogical and chemical investigations,
Part I: Microscopy, X-ray fluorescence and X-ray diffraction,
Cement and Concrete Res. 7 (1977),
S. 649/658

64.- DeLisle, F.A.: Microscopic analysis of clinker and cement,
Cement Technology 1976, No. 516,
S. 93/99

65.- Dorn, J.D.: Microscopic methods for burnability improvement,
Cement and Concrete Res. 8 (1978),
S. 635/645

66.- Rauschenfels, E.: Die Sinterbarkeit von Zement-Rohmehl,
Zement-Kalk-Gips 29 (1976), Nr. 2,
S. 78/85

67.- Blaise, R., N. Musikas, H. Tiedrez: Nonvelle méthode de determination cinétique de l'aptitude à la cuisson d' un cru de cimenterie,
Rev. Mater. (1971) Nr. 674/675,
S. 287/295

68.- Pfrunder, V.R., H. Wickert: Einige Versuche über den Einfluß der chemischen Zusammensetzung und der Mahlung auf die Sinterung von Zement-Rohmehlen,
Zement-Kalk-Gips 23 (1970), H. 4,
S. 147/151

69.- Butt, J.M., V.V. Timasev, J. Stark: Zur Frage der Beschreibung des Reaktionsfortschrittes beim Brennen von Portlandzementklinker,
Silikattechnik 23 (1972), H. 2,
S. 52/55

70.- Rao, P.B., V.V. Viswanathan: Burnability of cement raw mixes - A new look at the experimental methods,
Cement (Bombay) 9 (1978), No. 2/3,
S. 25/28

71.- Ludwig, U., G. Ruckensteiner: Einflüsse auf die Brennbarkeit von Zementrohmehlen,
Forschungsber. NRW, Westdeutscher Verlag Köln-Opladen Nr. 2373 (1973)
Über die Brennbarkeit von Zementrohmehlen,
Cement and Concrete Res. 4 (1974),
S. 239/246

72.- Ludwig, U., G. Ruckensteiner: Einflüsse auf das Brennverhalten von Zementrohmehlen und die Klinkerqualität, Tonind.-Ztg. 97 (1973) Nr. 12, S. 313/315

73.- Ludwig, U., G.-M. Därr: Über die Brennbarkeit von Zementrohmehlen, Zement-Kalk-Gips 28 (1975), Nr. 10, S. 421/423

74.- Christensen, N.H.: Burnability of cement raw mixes at 1400 °C, I: Effect of chemical composition, Cement and Concrete Res. 9 (1979), S. 219/228 II: The effect of fineness, Cement and Concrete Res. 9 (1979), S. 285/293

75.- Johansen, V.: Anwendung des Gleichgewichtsdiagramms beim Klinkerbildungsvorgang industriell hergestellter Klinker, Zement-Kalk-Gips 32 (1979) Nr. 4, S. 176/181

76.- Fundal, E.: The burnability of cement raw mixes, World Cement Technol. 10 (1979) No. 6, S. 195/196, 199/200, 203/204

77.- Wächtler, H.-J.: Thermoanalytische Untersuchungen in der Zementchemie - Sintern von Zementrohmehlen, Silikattechnik 26 (1975), H. 7, S. 235/240

78.- Wächtler, H.-J.: Einsatz der Thermogravimetrie und eines Laborbrennverfahrens zur Untersuchung der Reaktivität von Zementrohmehl und Kalksteinkomponente, Silikattechnik 30 (1979), H. 2, S. 37/41

79.- Kieser, J., A. Krähner, B. Gathemann: Modell zur Bestimmung der Rohmehlreaktivität unter praxisähnlichen Bedingungen, Zement-Kalk-Gips 32 (1979), Nr. 9, S. 442/447

80.- Hoffmann, H.: Untersuchungs- und Bewertungsmethodik für reaktionskinetische Untersuchungen an PZ-Rohmehlen im Labormaßstab, 6. ibausil, Weimar, 14.-18. Juni 1976, Vortrag Nr. 2.2.22, Bauforschung, Baupraxis 12. Bauinformation, DDR, Berlin 1978, S. 97/99

81.- Gouda, G.R.: Cement raw materials: Their effect on fuel consumption, Rock Products 1977, No. 10, S. 60/64

82.- Gouda, G.R.: Effect of clinker composition on grindability, Cement and Concrete Res. 9 (1979), S. 209/218

83.- Schmitt-Henco, C.: Einfluß der Zusammensetzung des Klinkers auf Erstarren und Anfangsfestigkeit von Zement, Zement-Kalk-Gips 26 (1973), H. 2, S. 63/66

84.- Sutej, C., K. Vrgoc: Zur Abhängigkeit der Zementfestigkeit von der chemischen Zusammensetzung des Klinkers, Zement-Kalk-Gips 26 (1973) Nr. 10, S. 497/500

85.- Knöfel, D.: Beziehungen zwischen Chemismus, Phasengehalt und Festigkeit bei Portlandzementen, Zement-Kalk-Gips 32 (1979), H. 9, S. 448/454

86.- Nagy, K.: Untersuchung des Zusammenhangs zwischen der Menge des freien Kalks im Klinker und den Zementeigenschaften, 6. ibausil, Weimar, 14.-18. Juni 1976, Vortrag Nr. 2.2.21, Bauforschung, Baupraxis 12. Bauinformation, DDR, Berlin 1978, S. 94/96

87.- Jawed, I., J. Skalny: Alkalies in cement: A review. I. Forms of alkalies and their effect on clinker formation, Cement and Concrete Res. 7 (1977), S. 719/729

88.- Locher, F.W., W. Richartz, S. Sprung: Erstarren von Zement, Teil I: Reaktion und Gefügeentwicklung, Zement-Kalk-Gips 29 (1976), H. 10, S. 435/442

89.- Billhardt, H.W.: Über den Einfluß der Alkalien und des Sulfats auf das Erhärten von Zement (Vortragsreferat), Zement-Kalk-Gips 24 (1971), H. 2, S. 91

90.- Tewari, P., P.K. Mehta: Fluorogypsum as a mineralizer in portland cement clinker manufacture, Ceram. Bull. 51 (1972), No. 5, S. 461/463

91.- Gutt, W., M.A. Smith: Calcium fluoride as a mineralizer in the cement/sulfuric acid process, Cement Technology 1971, No. 1/2, S. 9/14

92.- Staupendahl, G., H. Tauchmann, Ch. Engelmann: Einsatz CaF_2-haltiger Mineralisatoren im VEB Zementwerk Harsdorf, baustoffindustrie 1978, Ausg. A, Nr.5, S. 10/12

93.- Gutt, W., M.A. Smith: Studies of phosphatic portland Cements, 6th Intern. Congr. Chemistry of Cement, Moskau 1974, Suppl. Paper I/3

94.- Raugavao, M.V.: Effect of minor components on formation and properties of portland cement clinker, Cement (Bombay) 10 (1977), Nr. 3, S.6/13

95.- Imlach, J.A.: Assessment of the role of chronium in portland cement manufacture,
Ceram. Bull. 54 (1975), No. 5,
S. 419/522

96.- Gutt, W., M.A. Smith: Cerium as a minor component in cement manufacture,
Cement Technology 1970, No. 1,
S. 17/21

97.- Massazza, F., M. Pezzuoli: Influence of strontium on the clinker mineralogical composition,
il cemento 1974, No. 4, S. 167/175

98.- Sylla, H.-M.: Einfluß der Ofenatmosphäre beim Brennen von Zementklinker,
Zement-Kalk-Gips 31 (1978), H. 6,
S. 291/293, 11. Qu.

99.- Rechenberg, W.: Die Bestimmung von Nitrit in Stäuben der Zementherstellung,
Zement-Kalk-Gips 29 (1976), H. 6,
S. 254/258

100.- Frankenberger, R., J. Matejka: Alkali-Schwefelkreislauf in einem Drehofen mit zweistufigem Zyklonvorwärmer,
Zement-Kalk-Gips 31 (1978), H. 1,
S. 30/31

101.- Teoreanu, I., A. Puri: Kreisläufe flüchtiger Stoffe in Zement-Drehöfen,
Zement-Kalk-Gips 28 (1975), H. 9,
S. 277/379

102.- Sylla, H.-M.: Untersuchungen zur Bildung von Ansatzringen in Zementdrehöfen,
Zement-Kalk-Gips 27 (1974), H. 10,
S. 499/508

103.- Moore, A.E.: The sequence of compound formation in portland cement rotary kilns,
Part 1: Cement Technology 1976, No. 5/6, S. 85/91
Part 2: Cement Technology 1976, No. 7/8, S. 134/138

104.- Luginina, I.G., A.N. Luginin, M.A. Schaposchnikowa, V.K. Klassen: Über den chemischen Einfluß von Zusätzen auf die der Klinkerbildung vorangehenden Prozesse,
Silikattechnik 24 (1973), H. 11,
S. 374/377

105.- Danowski, W., J. Kieser: Chemische Reaktionen im ZAB-Vorwärmer bei hoher Alkalibelastung,
Zement-Kalk-Gips 28 (1975), H. 2,
S. 68/71

106.- Danowski, W., U. Strobel: Alkalibelastbarkeitsuntersuchungen in Trockenbrennanlagen,
Zement-Kalk-Gips 29 (1976), H. 10,
S. 458/462

107.- Rößner, P., F. Feige, W. Danowski, J. Kieser: Betriebsergebnisse mit dem ZAB-Vorwärmer im Eichsfelder Zementwerk Deuna unter den Bedingungen hoher Alkali- und Chloridbelastungen,
Zement-Kalk-Gips 30 (1977), H. 12,
S. 616/617

108.- Bohman, R.: Einfluß von Calciumchlorid-Zugabe zum Ofenmehl auf den Alkali-Haushalt und die Klinkerqualität von Wärmetauscheröfen,
Zement-Kalk-Gips 31 (1978), H. 6,
S. 278/281

109.- Ramesohl, H.: Probleme der Elektroentstaubung hochalkalichloridhaltiger Abgase aus Teilgasabzügen bei Wärmetauscher-Trockendrehöfen
Zement-Kalk-Gips 31 (1978), H. 5,
S. 236/238, 2. Qu.

110.- Sprung, S.: Schwefelkreislauf im Zementofen (Vortragsreferat),
Zement-Kalk-Gips 29 (1976), H. 11,
S. 520

111.- Svendsen, J.: Alkaliarmer Zement aus Hochalkali-Rohstoffen mit energiewirtschaftlich günstiger Verfahrenstechnik,
Zement-Kalk-Gips 31 (1978), H. 6,
S. 281/284, 2. Qu.

112.- Warshawsky, J., E.S. Porter: Verminderung des Alkali- und Schwefelgehalts im Klinker durch einen Ofen-Bypass im Vorcalciniersystem,
Zement-Kalk-Gips 31 (1978), H. 6,
S. 284/287, 5. Qu.

113.- Ritzmann, H.: Betriebsergebnisse moderner Vorkalzinieranlagen,
Zement-Kalk-Gips 30 (1977), H. 12,
S. 607/609

114.- Energy conservation potential in the cement industry,
PCA Conservation Paper No. 26, 1975, (USA)

115.- Johansen, V.: Influence of alkalies on strength development of cements,
Symposium on "The effect of alkalies on the properties of concrete", London 1976, Proceedings Cem. and Concr. Assoc., Slough/GB 1977, S.81/96

116.- Osbaeck, B.: Der Einfluß von Alkalien auf die Festigkeitseigenschaften von Portlandzement,
Zement-Kalk-Gips 32 (1979), H. 2,
S. 72/77

117.- Richartz, W.: Einfluß der Lagerung auf die Eigenschaften des Zements,
Zement-Kalk-Gips 26 (1973), H. 2,
S. 67/74

118.- Sprung, S.: Einfluß der Lagerungsbedingungen auf die Zementeigenschaften, Zement-Kalk-Gips 31 (1978), H. 6, S. 305/309

119.- Vorbeugende Maßnahmen gegen Alkalireaktion im Beton, Verein Deutscher Zementwerke, Schriftenreihe der Zementindustrie, H. 40/1973, Beton Verlag GmbH, Düsseldorf

120.- Mohan, K., F.P. Glasser: The thermal decomposition of Ca_3SiO_5 at temperatures below 1250 °C, I. Pure C_3S and the influence of excess CaO or Ca_2SiO_4, Cement and Concrete Res. 7 (1977). S. 1/7

121.- Sylla, H.-M.: Einfluß der Klinkerkühlung auf Erstarren und Festigkeit von Zement, Zement-Kalk-Gips 28 (1975), H. 9, S. 357/362

122.- Enkegaard, T.: The modern planetary cooler, Cement Technology 1972, No. 3/4, S. 45/51

123.- Jepsen, O.L.: Zementfestigkeiten und ihre Beziehung zur Kühlgeschwindigkeit und Kühlertype, Zement-Kalk-Gips 29 (1976), H. 2, S. 62/64

SUB-THEME I-3

The Kinetics of Clinker Formation
The Structure and Composition of Clinker and its Phases

V.V. TIMASHEV,
Professor,
Moscow Mendeleev Chemical Engineering Institute
Moscow, USSR

The problem of the catalysis of the synthesis of Portland cement clinker, especially at the liquid-phase stage, is becoming more and more topical because of the general tendency towards the reduction of energy consumption in chemical engineering. Since the formation of the phase composition and of the micro- and macrostructure of clinker grains depends, to a considerable extent, on the amount of the melt in the sintering system and its physico-chemical properties, the control of these parameters is a very important task. No substantial change in the properties of the melt formed in the C-S-A-F system can be achieved by the control of the modular characteristics of clinker (1). In this connection, many investigators are searching for elements or their combinations that would have an efficient influence on the structure and properties of the melt in the sintering grains of the material, on the microstructure and composition of the crystalline phases in clinker.

THE ACID-BASE EQUILIBRIUM IN THE MELT

The clinker liquid phase belongs to the class of slightly associated and high-basic alumoferrosilicate melts. The low degree of polymerization is confirmed by the low values of viscosity (0.1 to 0.3 Pa · s) and by its nearly exponential dependence on temperature and also by the absence of relaxation effects. The ionic nature of the melt is evidenced by the results of investigations of its physico-chemical characteristics, such as electrical conductivity and surface tension, the values of which correspond to the pa-

Period / Row	I	II	III	IV	V	VI	VII			
2			5 B $2s^2 2p^1$			8 O $2s^2 2p^4$	9 F $2s^2 2p^5$			
3	11 Na $3s^1$	12 Mg $3s^2$	13 Al $3s^2 3p^1$	14 Si $3s^2 3p^2$	15 P $3s^2 3p^3$	16 S $3s^2 3p^4$	17 Cl $3s^2 3p^5$			
4	19 K $4s^1$	20 Ca $4s^2$		22 Ti $3d^2 4s^2$	23 V $3d^3 4s^2$	24 Cr $3d^5 4s^1$	25 Mn $3d^5 4s^2$	26 Fe $3d^6 4s^2$	27 Co $3d^7 4s^2$	28 Ni $3d^8 4s^2$
	29 Cu $3d^{10} 4s^1$	30 Zn $3d^{10} 4s^2$								
5		38 Sr $5s^2$				42 Mo $4d^5 5s^1$				
		48 Cd $4d^{10} 5s^2$								
6		56 Ba $6s^2$				74 W $5d^4 6s^2$				

Fig. 1. The positions of the elements chosen for investigation in the Mendeleyev Periodic System.

rameters characteristic of typical electrolytes--molten salts.

The skeleton structure of the melt is built up of silicon-oxygen radicals which are present predominantly in the form of the complex SiO_4^{4-}, Ca^{2+} ions and amphoteric Al and Fe, which enter, depending on the conditions, into the composition of the groupings $[MeO_4^{5-}]$ or $[MeO_6^{9-}]$. By forming the complex $[MeO_4^{5-}]$, the ions Al^{3+} and Fe^{3+} display the properties of acids, and when they remain as free cations with an octahedral oxygen environment of $[MeO_6^{9-}]$ the ions Al^{3+} and Fe^{3+} exhibit the properties of bases.

In the low-oxygen complexes $[MeO_4^{5-}]$ the Me - O bond is more stable than in the octahedral groupings $[MeO_6^{9-}]$, as a consequence of which the complex $[MeO_4^{5-}]$ moves in the melt predominantly in the undissociated state, whereas the complex $[MeO_6^{9-}]$ dissociates into Me^{3+} and $6O^{2-}$, whose mobility is high.

In the melt there must exist an acid-base equilibrium between the various corrdination forms of amphoteric elements:

$$MeO_4^{5-} \rightleftharpoons Me^{3+} + 4O^{2-} \qquad (1)$$

$$K = \frac{[Me^{3+}]\,[O^{2-}]^4}{[MeO_4^{5-}]} \qquad (2)$$

The elements S, P, B, etc., which form stable silicon-oxygen complexes, $[SO_4^{2-}]$, $[PO_4^{3-}]$, and $[BO_4^{5-}]$, bind O^{2-}, thereby decreasing its concentration in the melt, which causes the dissociation of such an amount of the complexes $[MeO_4^{5-}]$ which is required to restore the upset acid-base equilibrium (1). As a result of the breakdown of part of the complexes $[MeO_4^{5-}]$, the viscosity of the melt is decreased and the diffusion coefficients of its structural units are increased. The elements Ti, Cr, Mn, F, Cl, Ni, etc., combine with O^{2-} in the melt to give groupings, the type of which depends on the value of the Me - O bond energy. For example, the presence of F, Cl, B, and Mo increases the absorption in the region of valence vibrations (400-700 cm^{-1}), which is evidence of the increase of the number of $[AlO_6^{9-}]$ groupings in the melt and of the shift of the equilibrium (1) in the melt to the right. The ions Ba^{2+} and Sr^{2+}, on the contrary, caused a decrease in the absorption in the spectral region indicated, i.e. caused the shift of the equilibrium (1) to the left.

Belov and coworkers (2,3) assume the formation in the melt of neutral angular O=S=O molecules at a deficiency of free oxygen ions in it, which participate in the building-up of the crystal lattices of C_2S and C_3S.

THE STRUCTURE AND PROPERTIES OF A MELT WITH A HIGH CALCIUM CONTENT

The effect of variour elements on the properties of the melt which is formed in clinker at 1450°C and which has the following composition (per cent by mass): CaO = 57, SiO_2 = 7.5, Al_2O_3 = 22.6, Fe_2O_3 = 12.9, has been studied (Fig.1).

The experimental procedures have been described in the literature (5). The elements were introduced into the melt in an amount of 0.1M in the form of oxides, carbonates and ammonium salts. The viscosity of the melt in the presence of s-elements decreased in the order of their decreasing basic properties: K → Ba → Na → Sr → Ca → Mg.

Accordingly, the quantity decreased with increasing acidity of p-elements in the sequence: Al → P → B → S → Cl → F (Fig.2).

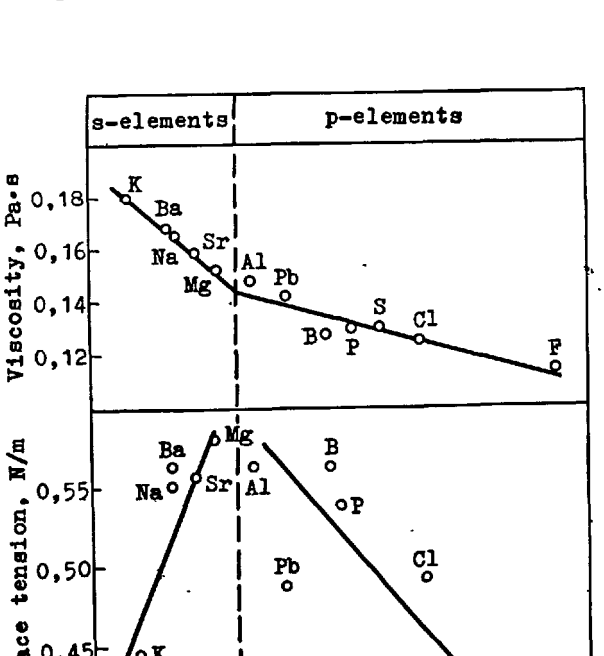

Fig. 2. Effect of the electronegativity of s- and p-elements on the viscosity and surface tension of the melt.

That is, there exists a linear dependence of the viscosity on electronegativity of elements with the same structure of their outer electron shells. In the presence of d-elements the viscosity, η, increased with decreasing state of oxidation (Fig.3) of the elements, which corresponds

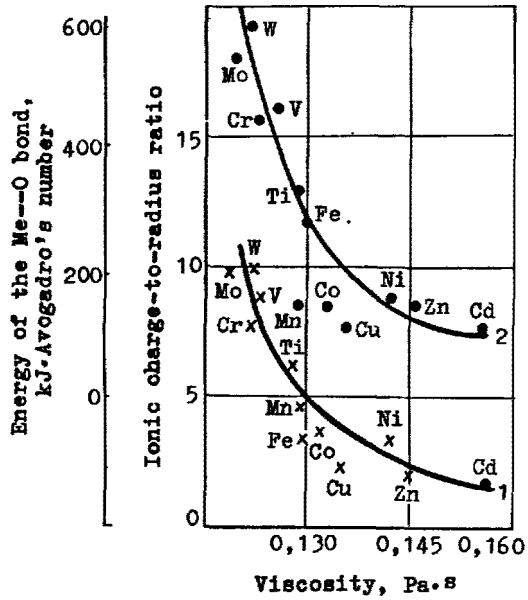

Fig. 3. The viscosity of the melt against the ratio of cationic charge to cationic radius Z/r (1) and against the energy of the bond between the cation and oxygen Me - O (2).

(according to the Kossel scheme) to the weakening of their acidic properties in the sequence: Mo → W → V → Cr → Ti → Mn → Fe → Co → Cu → Ni → Zn → Cd.

As the charge-to-radius ratio of the ion and the Me — O bond energy diminishes the decreasing effect of the element on the viscosity of the melt is weakened. This dependence is characteristic of s- and p-elements as well as of d-elements (Fig.3)

When comparing the effect, on the viscosity η, of s- and p-elements which are situated in the periodic table in the same period but in different groups, it has been established that the viscosity decreases with increasing nuclear charge (Fig.4). An insignificant difference in

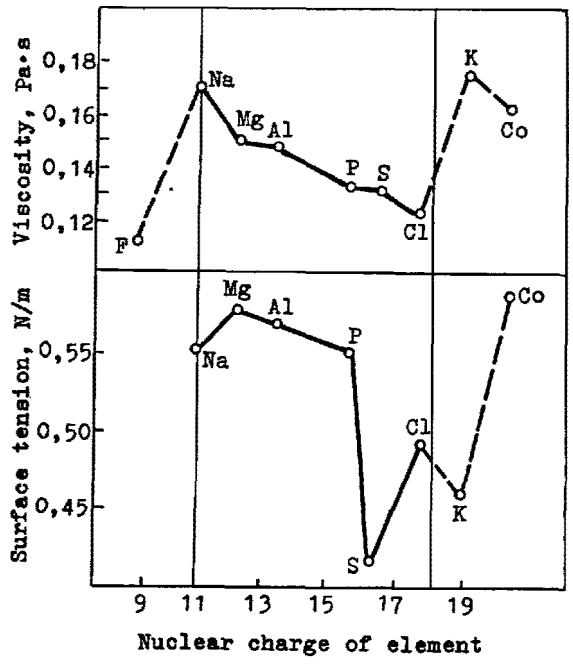

Fig. 4. Effect of the nuclear charge of the element introduced on the surface tension and viscosity of the melt.

the properties of d-elements of the same period, which is accounted for by the identical structure of their outer electron shell (2 s-electrons), is responsible for the fact that the properties of the melt differ little in the presence of these elements. Thus, for example, in the series Mn-Fe-Co-Ni the viscosity of the melt increased from 0.129 (Mn) to 0.143 Pa·s (Ni), and the in the series Ti-V-Cr it increased from 0.123 to 0.128 Pa·s. With increase of the cationic radius in their comparable series, which corresponds to the increase of basic properties, the viscosity of the melt diminishes to a lesser extent.

The activation energy of the viscous flow of the melt, E_η, was equal to 364 kJ/mole. In the presence of s-elements E_η decreased with increasing basicity of the cation within the limits of 317 (Mg) and 193 kJ/mole (K). The quantity E_η of melts containing Cr, Ni, Mo, Mn, V, Cu, W, Ti and Co varied within the limits of 113-155 kJ/mole; in the presence of Zn and Cd the activation energy increased abnormally up to 193 and 251 kJ/mole, respectively. The values of E_η of the melt in the presence of p-elements were very low: from 84 to 147 kJ/mole. An exception is a system with phosphorus, whose E_η increased up to 251 kJ/mole.

The departures of the function $\log \eta = f(1/T)$ from the exponential law, the appea-

rance of points of inflection on the curve and the increase of the quantity E_η can be explained by the onset of crystallization of the melt in the presence of the corresponding elements. The following temperatures of the onset of crystallization of the melt in the presence of individual elements are as follows (in °C): 1432 for P, 1427 for Ni, 1406 for V, 1402 for Cr and Cl, 1400 for Cd and Mn, 1397 for Zn, 1387 for Cu, and 1386 for Co. The viscosity η is decreased most strongly under the influence of elements when their concentration in the melt is 2-3 per cent; higher concentrations of the elements may bring about negative results.

When several elements are jointly present in the melt, the properties of the melt are not additively changed by the ion concentration. The negative effect of K^+ and Na^+ on the viscosity of the melt is well compensated for by Mg^{2+}. According to the data obtained by Osokin and Mironov, the effect of 1.5 per cent of (K_2O + Na_2O) is fully compensated for by 6.5 per cent of MgO. Further increase of the amount of MgO causes the viscosity to decrease due probably to the oversaturation of the melt with Mg^{2+} and to the onset of the crystallization of the latter. The positive effect of SO_4^{2-} on the viscosity of the melt is weakened by Na^+ and K^+; but if these cations are present together in the ratio corresponding to the compounds Na_2SO_4 and K_2SO_4, the viscosity of the melt is nevertheless considerably diminished. After the stoichiometry is exceeded there is observed an intensive increase of η with increasing amount of Na^+ and K^+ in the melt. In such cases the melt undergoes microliquation. The joint presence of Na^+, K^+, Mg^{2+}, and SO_4^{2-} in the melt is accompanied by the change of η from 0.08 to 1.65 Pa·s, depending on the ratio of the ions. The microliquation of the melt in the presence of the given group of elements is retained (fig.5)

The effect of a complex consisting of Ti^{4+}, Mn^{3+}, and SO_4^{2-} on the viscosity of the melt is more complicated: in the respective concentration triangle the viscosity isocoms are broken. A considerable decrease of the viscosity of a melt containing an increased amount of SO_4^{2-} and Mn^{3+} combines with zones of increased viscosity, which are situated closer to the side of Ti-Mn. The increase of the viscosity at a certain ratio of the elements may be accounted for by the formation of stable complexes in the melt. To the lowest η value (0.085 Pa·s) of a melt containing the complex (Mg^{2+} + Ba^{2+} + Mn^{3+}) there corresponds the maximum content of Mn^{3+} and Mg^{2+} and the minimum content of Ba^{2+}. The above-given examples of the effect of a group of elements on the viscosity of the melt are in agreement with the character and specificity of the action of the corresponding individual elements.

The surface tension of the melt is governed by its structure in the bulk and also by the composition and structure of the surface layer. In the presence of various elements the value of σ is changed not only as a result of the change of the activity of the matrix ions of the melt but also because of the high absorption capacity of the ions introduced, which, as compared with viscosity, complicates the dependence of the variation of σ on the nature of the element.

With increasing electronegativity of s-elements there is observed an increase of σ, and, on the contrary, the increase of the electronegativity of p-elements is accompanied by the decrease of the surface tension of the melt (Fig.2). True, in view of a wide spread of experimental data, one should speak only of a tendency in the manifestation of the above-discussed regularities. As the values of ratio Z/r and the Me - O bond energy of elements increase, the following effect of elements is observed: the alkali and alkaline-earth cations increase and acid cations, on the contrary, decrease σ, this being in agreement with the data obtained by Yesin. The cations K^+ and Na^+ are weakly bonded with O^{2-}, which leads to their displacement into the surface layer of the melt, whose σ decreases from 0.58 to 0.35-0.40 N/m with increasing concentration of these cations (Fig.6). As the values of the Me - O

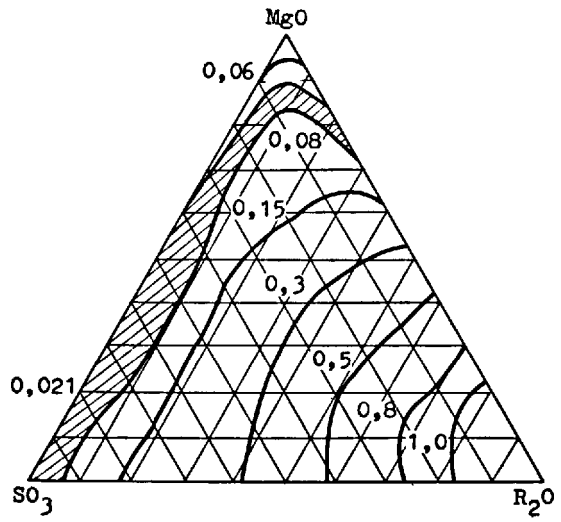

Fig. 5. The isocoms of the viscosity of the melt in the presence of the complex $MgO-R_2O-SO_3$.

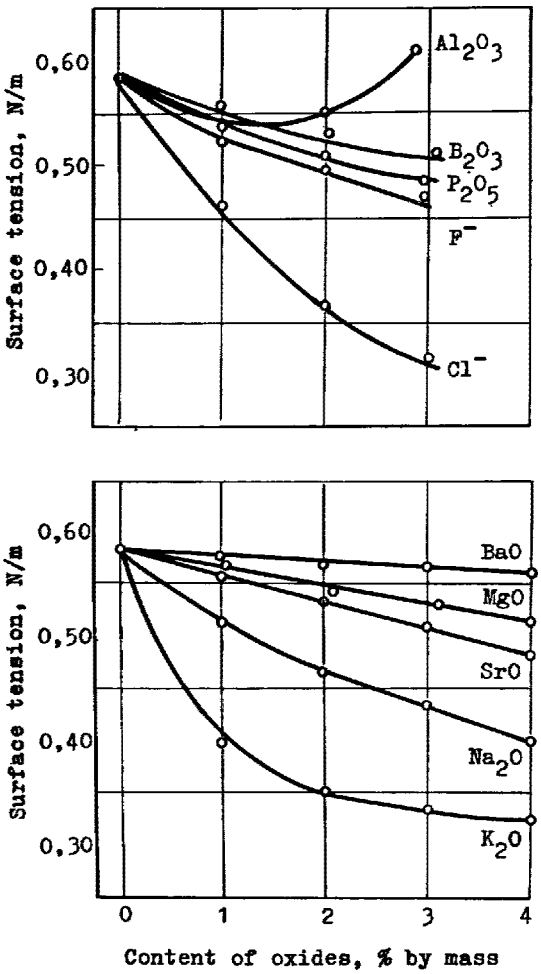

Fig. 6. The isotherms (1450°C of the surface tension of the melt in the presence of s-elements (a) and p-elements (b).

bond energy and Z/r of p-elements increase, their surface activity is enhanced (Fig. 6), this being due to the stability of the complex ions PO_4^{3-}, SO_4^{2-}, and BO_4^{3-}, which cannot be held in the bulk of the liquid and are displaced into its surface layer. The anomalies in the behaviour of F^- and SO_4^{2-} (Fig.4) are accounted for by the liquation phenomena that occur in the melt. The increase of σ caused by the addition of more than 1.5 per cent of Al_2O_3 may be associated with the saturation of the melt with the complex $[AlO_4^{5-}]$ and with the increase of its viscosity. With increase of the acidity of d-elements there is observed the tendency towards the decrease of the surface tension of the melt (Fig.7), just as is the case with the

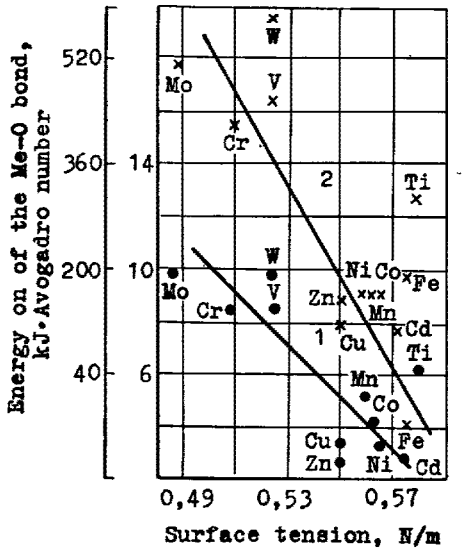

Fig. 7. The surface tension of the melt against the cationic charge-to-radius ratio Z/r (1) and the energy of the bond between the cation and oxygen Me – O (2).

regularity obtained for η (Fig.3). The order of arrangement of elements is evidence that for ions having close radio the surface activity increases with increasing state of oxidation, i.e., with increase of acidic properties: Co → V → Cr → Mo.

According to Appen (6), the introduction of a component having a smaller value of σ brings about a decrease in the surface tension of the system. Such a mode of change of σ caused by mutual replacements of s-, p-, and d-elements in the melt occurs rather regularly.

When the ions K^+, Na^+, and SO_4^{2-} ions are present together in the melt, the observed decrease of the surface tension of the melt is described by the empirical equations (1). In the presence of a group of the elements K^+, Na^+, Mg^{2+} and S^{6+}, because of the screening of the cations Na^+ and especially of K^+ by the anion SO_4^{2-}, there arises an extensive liquation zone with the formation of a liquid characterized by the decrease of σ down to values of the order of 0.1-0.25 N/m (Fig.8).

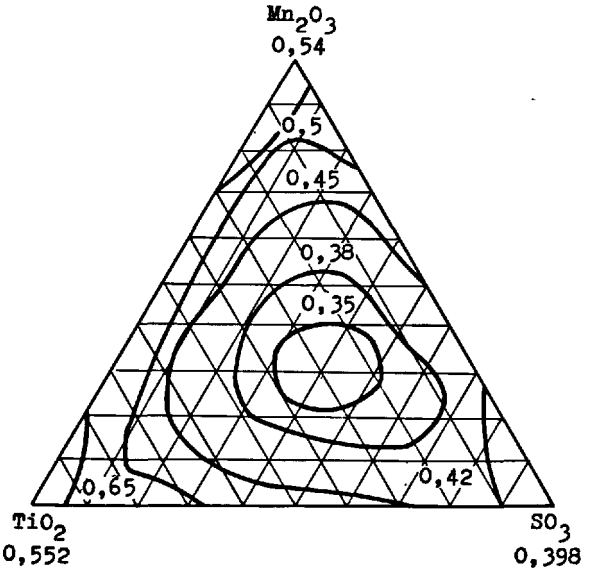

Fig. 8. The isocoms of the surface tension of the melt in the presence of the complex Mn_2O_3-TiO_2-SO_3.

The Mn-Ti complex contributes to the increase of σ up to 0.54-0.60 N/m, but upon addition of S to it and with an optimum ratio of all the three elements the surface tension of the melt may be diminished down to 0.34-0.36 N/m.

The sizes of vacancies (microcavities) in the melt, as calculated from the values of σ, are as follows: at 1450°C the radius of vacancies is 1.1 Å, and at 1525°C it is equal to 1.15Å, which is an indication of the increase of the free volume of the melt upon heating it above the liquidus temperature. The density of the melt at 1450°C is 3020 kg/m^3. As the temperature rises from 1450 to 1475°C the value of ρ drops to 2900 kg/m^3, which confirms that the structure of the melt in the pre-liquidus region has undergone considerable changes.

The clinker melt is characterized by the electronic-ionic conductivity (1). The electronic component is due to the exchange of electrons between the iron ions, and the ionic component is due to the high mobility of the Ca^{2+} cations and also due to the transport of electricity by the octahedrally coordinated ions Fe^{3+} and Al^{3+}. The nature of the effect of the ions introduced into the melt depends on many factors: the size of the ion and its charge, the strength of the Me - O bond, the mutual polarization of oxygen and several cations, the viscometric properties of the melt and the change of the electronic component of conductivity. The joint presence of several charge-transfer agents and the presence of the electronic component complicates the interpretaion of the results obtained.

In the presence of the ions of Mg, Sr, and Ba the electrical conductivity of the melt, which is equal to 63.7 S/m at 1450°C, increases proportionately to their concentration, its value increasing with decreasing field strength of the cation (Fig. 9).

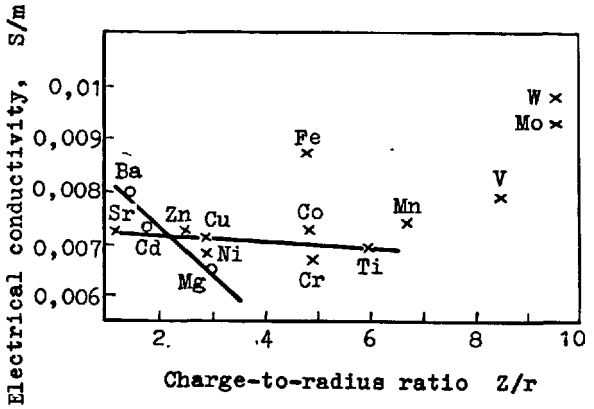

Fig. 9. The electrical conductivity of the melt versus the charge-to-radius ratio Z/r of s- and d-elements.

The observed increase of χ with increasing radius of the cation is accounted for by the fact that the size of vacancies (microcavities) in the clinker melt, which is equal to 1.1 Å at 1450°C, is commensurate with the size of the cations of Mg, Sr, and Ba. Therefore, the most probable mechanism of diffusion for them is the vacancy mechanism and in this case the geometric factor (the quantity r) has no substantial effect. The predominating effect is exerted by the energy factor--as the field strength increases, so does the attractive energy of the cation O^{2-}, which is what lowers the probability of the vacancy mechanism. This increases the mobility of the cation Ca^{2+}.

The Na^+ ions contribute to the growth of χ due to the increase of the concentration of current carrier in the melt, and the K^+ ions reduce χ due to the decrease of the mobility of Ca^{2+} and the reduction of the electronic conductivity (there are formed FeO_4^{2-} ions which are less capable of exchanging electrons).

An analogous dependence is observed for the majority of the d-elements studied (Fig. 9). The abnormally high electrical conductivity of melts containing the ions of V (79), Mo (94), W (97), Fe (87 S/m) is explained by the increase of the electronic conductivity, which has been observed for molten glasses and slags (6). An increase in the content of chromium increases χ, because the energy levels of the transitions $Fe^{2+} \longrightarrow Fe^{3+}$ and $Cr^{2+} \rightarrow Cr^{3+}$ are practically identical and the increase of the

content of Cr increases the number of vacancies and the probability of electronic transitions. But, judging by the results of viscosity measurements, one could have expected a more substantial decrease of electrical resistance in the presence of Cr, but the electrical conductivity increased only up to 76 S/m with the concentration of Cr_2O_3 being 4 per cent.

The incorporation of p-elements into the melt leads to an increase of $\varkappa$ due to the decrease of the viscosity of the system and the attending increase of the mobility of the cation Ca^{2+}. In the presence of phosphorus ions the electrical resistance increases in proportion to the concentration of P_2O_5, which is accounted for by the formation of complex anions of the type (− O − Si − O − Ca − O − P − O), which reduces the number of current carriers.

The electrical conductivity of the melt is enhanced within the temperature range from 1400 to 1500°C, it increasing most intensively in the pre-liquidus region. The activation energy of electrical conduction in the melt, which is equal to 50 kJ/mole, is 3 times lower than E_{Ca} (163 kJ/mole), which supports the fact of transport of electricity in the melt both by ions and electrons.

The diffusion coefficients of the structural components of the melt over the temperature range 1450-1525°C are as follows: D_{Ca} = (5.31 to 8.55) x 10^{9} ; D_{Fe} = (5.70 to 14.2) x 10^{-10}; D_{Al} = (2.35 to 7.10) x 10^{-10} ; D_{Si} = (4.73 to 15.8) x 10^{-11} m^2/s. The diffusion coefficients increase with rise of temperature. A comparison of the size of vacancies in the melt (1.1 to 1.15 Å) with the effective radii of the cations Ca^{2+} , Al^{3+}, and Fe^{3+} (ca. 1 Å) suggests the vacancy mechanism of their diffusion; larger anions, such as $[SiO_4^{4-}]$, $[FeO_4^{5-}]$, and $[AlO_4^{5-}]$ diffuse by way of exchanging places upon rotation of the corresponding groupings relative to each other. In the presence of Na^+ and K^+ ions the diffusion coefficients of all the structural units of the melt were diminished; they increased under the influence of Mg^{2+} and SO_4^{2-}.

The high surface activity of p-elements (F, Cl, Si, P, S) causes the formation in the melt of micro- and macroliquation regions which differ considerably in acidic-basic properties. The segregation of the composition of the liquid phase results from the adsorption of the anionic groupings by the surface layer of the melt and also from the low mobility of the silicon-oxygen complexes, which leads to an increase in their concentration in the melt regions adjacent to the dissolving silicon-containing phases (SiO_2 , C_2S, C_2AS, etc.). The tendency of the ions of Si, Al, and Fe to form a coordination sphere leads to the following: elements such as F, Cl, and S, especially in combination with Ba, Cd, Sr, Na, and K, enhance the liquation phenomena.

According to the theory developed by Weyl (6), the degree of shielding of cations increases with increasing polarizability of anions. Since the F^- ion has a lower polarizability (0.96 A^{o3}) than O^{2-} (2.74 A^{o3}), it is readily displaced from the coordination sphere of the complex-formers (Si, Al) into the coordination sphere of Ca^{2+}, Na^+ and K^+. Therefore, even at a fluorine concentration of about 1 per cent in the melt there is observed the appearance of liquation zones (Fig. 10) which are

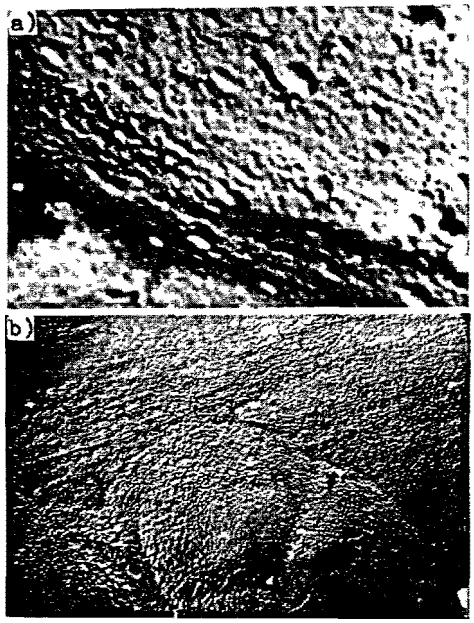

Fig. 10. The liquation regions in the clinker melt at the following concentrations: a — 1.0 per cent F^- by mass; b — 3.0 per cent Cl^- by mass (magnification x 10000).

(2 to 3) x 10^3 Å in size. The appearance of non-miscibility in a fluorine-containing melt has also been confirmed by the appearance of the exo-effect on the thermograms at 850°C, which results from the crystallization of liquating drops and from the presence of two endothermic effects (1200 and 1380°C), which has also been observed in the case of glass-forming systems (7). The fact that the F^- ion is close to Ca^{2+} contributes to the microheterogenization of the melt to regions enriched with groups containing the bonds Si − O and Al − O and to the zones with an increased concentration of modifying cations, where the Me − O bond is predominating.

The chloride ions exhibit a higher polarizability than do the fluoride ions and therefore in their presence the degree of shielding is increased and microliquation

appears at higher concentrations of Cl (2-3 per cent) with the formation of liquation regions of a smaller size. The ions S^{6+} are even more polarizable and therefore in this case the liquation is observed only in the presence of Na^+ and, especially, of K^+. Thus, for example, when the total content of SO_3 and Na_2O in the melt is 2.7 per cent, the observed microliquation (the size of drops being 10^3 Å) changed to complete immiscibility at a 5-per cent concentration of the oxides. In the presence of the complex SO_3—K_2O, macroliquation appeared even when their total concentration was 2.4 per cent. The addition of Mg^{2+} to a melt containing the complex R_2O—SO_3 contributes to the suppression of the liquation phenomena and the phase separation occurs only at high concentrations of sulphur and alkalis in the melt.

Liquation salt melts enriched with F, Cl, K, Na, and S have a viscosity which is lower by about two orders than the viscosity of the matrix liquid phase and low values of surface tension (0.15 to 0.19 N/m). Therefore, the macrosegregation in the system alters, to a considerable extent, the kinetics of dissolution of grains of CaO, C_2S and other minerals, and also hinders the aggregation of the particles of the materials in the sintering zone where clinker grains are formed.

DISSOLUTION AND CRYSTALLIZATION

The liquid phase formed in the sample of the material being burned fills separate pores and capillaries, forming thin films on the particles. Some authors (8-10) presume that the melt in the sintering samples is a continuous phase in which grains of CaO, C_2S and C_3S are distributed. The interaction of the minerals indicated above with the melt takes place in constrained conditions when the diffusion of the ions required for the growth of C_3S crystals limits the course of the synthesis reaction.

At lower temperatures (1000-1200°C) there are formed non-equilibrium melts of acidic nature (11), which arrange themselves in the form of small drops predominantly near the softening quartz grains and which contains the ions of S, F, Cl, Na, K, Ca, Si, Al, Fe, and O. It is through these melts that the Ca^{2+} ion is transferred to the surface of the SiO_2 grains and C_2S is synthesized. In spheres consisting of a shell having the C_2S composition and a kernel of SiO_2 the acidic melts are retained until they are absorbed (pulled) by the melt enriched with Ca^{2+} as a result of the countercurrent diffusion of Ca^{2+} and $Si_nO_m^{z-}$ (a pore is left in place of the SiO_2 kernel). Between the grains of CaO-C_2S, CaO-C_3S, CaO-C_2S-C_3S there are formed zones of the melt enriched with Ca^{2+}, in which crystals of C_3S are generated. The zonally arranged melts characterized by concentration gradients and different acidic-basic properties when brought into contact with each other exchange their ions at the interface, tending to the equilibrium composition. When the melts have large volumes, the averaging of their composition is contributed by convection, but in thin capillaries and films the transport of a substance is accomplished only by diffusion. The retainment of molten volumes of different composition in clinker grains (metastable microliquation) and the development of liquation processes in the presence of impurities lead to the separation of solid phases which are at equilibrium with these liquids.

The kinetics of the dissolution of sintered samples of CaO and C_2S in melts of different composition have been investigated by the equally-accessible-surface through the control of the thickness of the diffusion layer by altering the intensity of rotation of the sample. At 1450°C the rate of dissolution of C_2S in the main melt (n= 600 to 1400 r.p.m.) was equal to (1.94 to 2.78) x 10^{-8} m/s and that of CaO was (6.10 to 8.34) x 10^{-8} m/s, i.e., higher by 3 times. The activation energy of the dissolution process is as follows: E_{CaO} = 264 kJ/mole and E_{C_2S} = 419 kJ/mole. The rate of dissolution of CaO is commensurate with D_{Ca} (E_{Ca} = 163 kJ/mole) and that of C_2S is commensurate with D_{Si} (E_{Si} = 368 kJ/mole). The difference in the values of E_{CaO} and E_{Ca} and also in the values of E_{C_2S} and E_{Si} may be attributed to the complex mechanism of the multi-component diffusion (8,10) within the thin films of the melt. The diffusion mechanism of the dissolution process confirms the dependence of the rate of dissolution of CaO and C_2S on the viscosity of the melt (Fig. 11). The fact the dissolution is

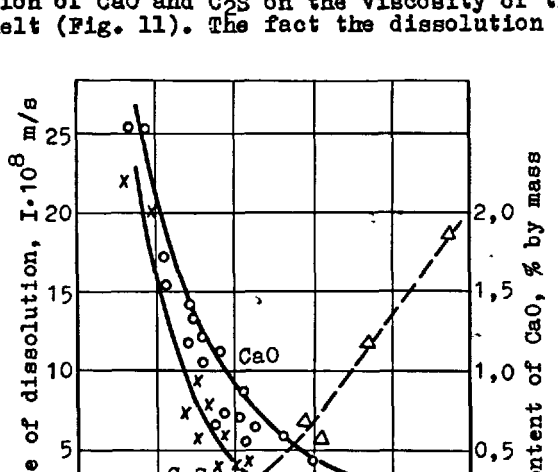

Fig. 11. The rate of dissolution of C_2S and CaO cakes versus the viscosity of the melt.

speeded up with decrease of η is associated with the decrease of the thickness of the diffusion films on the particles being dissolved.

The sulphur, chloride and fluoride ions, which render the melt acidic and lower its viscosity, speed up the dissolution of CaO (by 1.5-2 times) and of C_2S. In the presence of Ba^{2+} and Sr^{2+} the rates of dissolution of CaO and C_2S (I_{CaO} and I_{C_2S}) are somewhat diminished. The rate of dissolution I_{CaO} is very strongly decreased in a melt containing Na^+ and K^+ (by 2 to 4 times at 3-4 per cent R_2O) due to the increase of η. The rate of dissolution of C_2S in an alkali-containing melt increases anomalously: by 3 to 7 times with the content of K_2O being 0.5-1.9 per cent by mass and by 30 to 50 times with the content of Na_2O being 2.2-4 per cent by mass; the rates of dissolution in the latter case are 78 and 133 x 10^{-8} m/s, respectively. The special role of the ions Na^+ and K^+ may consist in the following: being concentrated in the diffusion layer on a particle of C_2S, they also speed up the transport of the low-mobile ions $Si_nO_m^{z-}$. The difference in the effect of Na and K may be ascribed to the sizes of their ions: Na = 0.97 A and K = 1.33 A. When R_2O and SO_3 are present together in the melt, this leading to the microliquation of the melt, I_{C_2S} is lower than in the presence of R_2O alone, but it exceeds I_{CaO} by 3 to 5 times. The kinetics of the expansion of the C_3S zone at the point of contact between of the layers of the composition CaO + C_3S + melt and C_3S + C_2S + melt (1500°C) referred to the rate of formation of C_3S is expressed, according to the literature data (8, 10), by the following parabolic relation:

$$x^2 = Kt \qquad (3)$$

where x is the width of the C_3S zone, t is the reaction time, and K is a constant (cm^2/s). The reaction rate constant increased with increasing amount of the melt from 10 to 30 per cent, upon replacement of part of Al_2O_3 by Fe_2O_3 and with rise of temperature. The proportionality between the amount of the melt and the rate of the processes of binding of CaO in the preparation of clinker has also been established by Butt, Timashev and Osokin (1). The positive effect of the replacement of Al^{3+} by Fe^{3+} is due to the decrease of the viscosity of the melt involved (Figs. 2 and 4). It has been found (12, 13) that with increasing size of the particles of CaO, SiO_2, C_2S, etc., apart from the decrease of the rate of their dissolution, the following anomaly is observed: the process takes place in cycles, this being caused by the formation, on the reacting grains, of fringes of the reaction products (C_2S and C_3S), which retard the synthesis, the formation of these fringes being followed by the rupture of the shell and the onset of a new cycle of the accelerated reaction. The cyclic course of the reaction correlates well with the existence of local melts which differ in composition.

In the zones of the acidic melt (C_2S + liquid) the formation of C_3S is controlled by the rate of diffusion of Ca^{2+} ions from the regions with a larger content of lime to the crystal nuclei and also by the rate of dissolution of C_2S, the alite crystals growing in the direction of the C_2S particles. In basic melts and especially in the presence of Na^+ and K^+ the rate of dissolution of C_2S is high, and the process is limited by the rate of dissolution of CaO grains, the C_3S crystals being formed at various points in the volume of the melt. After the grains of CaO (and also of C SiO_2 are dissolved there are left pores in their place.

For a model system composed of particles of CaO, C_2S and glass, it has been established (20) that the concentration of the liquid phase undergoes change in the direction of the dissolving particles and, for example, at 1450°C the portions of the melt in the CaO-melt and C_2S-melt zones are characterized by different concentrations of Ca and Si because of the difference between the diffusion coefficients of the ions of these elements. The η values of the melts are different: with increasing concentration of Ca^{2+} the viscosity of the melt is decreased. During the course of the synthesis there takes place a mutual diffusion of the melts until there are formed zones of supersaturation with respect to portions of the melt saturated with C_3S. In the supersaturated zones there occurs the crystallization of C_3S with the formation of a saturated melt.

Since the rate of the reaction of formation of C_3S is usually proportional to the concentration gradient (ΔC) in the diffusion layer and the surface area of the latter is equal to that of the dissolving particles (20, 37, 38), the kinetics of the process, at least at the initial stage, is satisfactorily described by diffusion equations of the following type:

$$(1 - \sqrt[3]{1-\alpha})^n = \frac{2D\Delta C}{r^2}\tau = K\tau$$

where α is the fraction of the reacted substance and τ is the time. The fraction of the reacted substance has been found to be proportional to the viscosity of the melt.

In comparing models for the process of sintering from the preliminarily synthesized C_2S, CaO, and C_3S, one should bear in mind that under the influence of the capillary pressure of the melt the porous grains of the minerals can be dispersed, thereby distorting the kinetics of the dissolution process (1, 8).

The presence of 1 per cent of TiO_2 in the batch results in an increase of the amount of the melt and a decrease in the temperature, at which the process of binding of CaO is completed, by 50-100°C, but with a

higher content of titanium the amount of C_3S is diminished (51). The catalytic properties of the complex (R_2O + MgO + SO_3), which is usually present in the composition of raw mix have been analyzed (52-54). According to the literature data (52), the process of binding of CaO is speeded up with the following content of the components: 0.2-1.2% MgO + 1-4% SO_3 + 0-0.3% R_2O; the effect of a complex consisting of 3-5% MgO + 1-1.5% SO_3 + 1% MnO has been found to be positive (53). Complexes having a more complicated composition have also been found to be effective (54); two examples are (MgO + $CaCl_2$ + CaF_2 + $CaSO_4$ + P_2O_5), (MgO + SO_3 + R_2O + MnO + BaO).

In order to prepare a clinker with a saturation coefficient of 0.88 at 1400°C, the original clinker containing 1 per cent of CaO, the optimum concentrations of the components of the complex MgO-$CaSO_4$-R_2O (where R_2O = K_2O/Na_2O = 3/1) must be in the

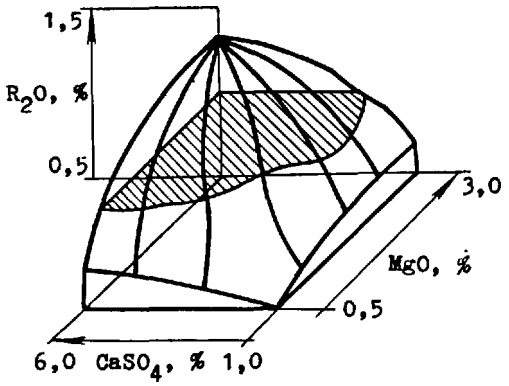

Fig. 12. The region of the optimum ratios of the components of the complex MgO-$CaSO_4$-R_2O (where R_2O-K_2O/Na_2O = 3/1) for producing the clinker with SC = 0.88, n = 2.1, p = 1.2 at 1400°C, containing less than 1 per cent of free CaO.

range presented in Fig. 12. With the increase of the saturation coefficient from 0.88 to 0.96 and of the burning temperature the limiting concentration of R_2O is decreased.

The presence of several elements often has a positive effect on the binding of CaO upon burning. A complex consisting of Na_2SO_4 (0.3%) and MgO (3%), while causing the viscosity of the melt to decrease, contributes to the binding of CaO, though the microliquation of the liquid has also been observed (22). The process of binding of CaO is catalyzed by the complex ($BaSO_4$ + MgO + R_2O), this leading to the decrease of η and the temperature at which a melt is formed (23). The addition of magnesium oxide to R_2O and P_2O_5 eliminates the unfavourable effect of alkalis and phosphorus (24).

Under the action of a flux of accelerated neutrons (200-400 kGy/s) the rate of binding of CaO increased by about 100 times (14), and the process of alite formation is completed at 1100-1300°C in 5-15 seconds with an energy consumption of about 3300J/g.

THE LIQUID-PHASE SINTERING OF CLINKER

The mechanism of the formation of the micro- and macrostructure of clinker granules obeys the general regularities of the process of liquid-phase sintering (15, 16). The process of formation of clinker grains in the presence of an equilibrium melt may be subdivided into three stages: (1) the combination and rearrangement of particles; (2) the packing of granules due to dissolution-crystallization reactions; and (3) the cooling stage followed by the crystallization and freezing of the melt.

The Combination and Rearrangement Stage. When a melt is formed, the particles of the material being fired and their aggregates enter into random contact interactions and combine with one another due to the surface tension of the melt. The rearrangement of the particles in the grain is made possible by the high value of σ (0.5-0.6 N/m) of the melt and its low viscosity (0.1-0.2 Pa·s), and also by the compression of the grains by the overlying layer of the material being burned in the furnace. The intensive rearrangement of the particles, which takes place in the initial period (stage 1) results in the shrinkage, of the granules (Fig. 13). Stage 2 is characteriz-

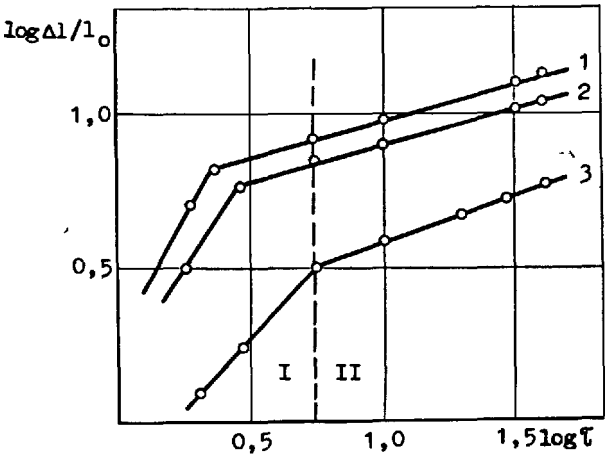

Fig. 13. The relative linear shrinkage of pressed samples against the time of thermal treatment at various temperatures: 1 — 1450°C; 2 — 1400°C; 3 — 1350°C.

ed by the reduced rate of shrinkage and its

lower absolute value; its mechanism consists of dissolution-crystallization reactions. With rise of temperature the amount of the melt increases and there is required less and less time for the rearrangement process to be complete.

The capillary force F, which draws the particles together at the rearrangement stage, is determined by two components: F_1 and F_2. The force F_1 is due to the difference between the pressures on both sides of the meniscus of the melt in the particle contact zone (the Laplace law): the pressure inside the liquid ring is lower than that outside, and the particles are brought nearer to one another. The force F_2 is due to the tendency of the free surface of the liquid to contract and depends on the surface tension of the melt. Having calculated the total driving force of the process, F, one can derive an equation for the kinetics of shrinkage of the sintering grain of the material (dl/l_0), which characterizes the rate of the rearrangement process (17, 18):

$$dl/l_0 = \frac{\sigma}{\eta r \sin\varphi}\left\{\sin\varphi\left[\frac{\cos(\varphi+\theta)}{1-\cos\varphi} - \frac{1}{\sin\varphi} - \frac{(1-\cos\varphi)\left[1-\sin(\varphi+\theta)\right]}{\cos(\varphi+\theta)}\right] + 2\sin\varphi \cdot \sin(\varphi+\theta)\right\} \cdot d\tau \quad (4)$$

Equation (4) take account of the dependence of the rate of shrinkage of grains on the properties of the liquid phase, such as σ, η and θ (the angle of wetting and its amount φ (the angle depending on the amount of the melt) at a certain particle size. After substituting $\Delta l/l_0$ by the total driving force of the process of drawing of particles together (17) Eq. (4) can be used for the computation of the kinetics of the aggregation of the particles of the material being burned into clinker grains in the sintering zone of the rotary furnace. By changing the properties of the melt, the process of aggregation of particles of different mass can be influenced in any desirable way.

The dependence of the predominating size of the clinker grain, as calculated from the modified equation (4), on the surface tension of the melt (Fig. 14) is al-

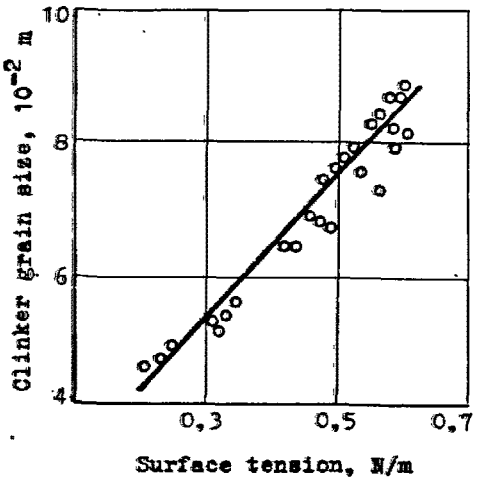

Fig. 14. Dependence of the final size of clinker grains formed in the rotary furnace on the surface tension of the clinker melt.

most linear. An appreciable decrease in the surface tension of the melt achieved under certain conditions in the presence of K^+, Na^+, Sr^{2+}, Mo^{3+}, and S^{6+} was accompanied by a decrease in the final size of the agglomerate (17). A slight decrease of σ, the more so its increase, observed in the presence of Ti^{4+}, Al^{3+}, Fe^{3+}, Mn^{3+}, and Mg^{2+}, contributed to the progress of the aggregation process. The effect of the joint presence of several elements satisfactorily obeys the dependence of F on σ (Fig. 14). Anomalies arise in those cases where the melt undergoes liquation in the presence of impurities. For example, in the presence of $nSO_3 + mR_2O$, as a result of the liquation, there is formed a sulphate-alkaline liquid with a low surface tension (0.3 to 0.35 N/m), which lowers the driving force F of the process of aggregation. The final size of the clinker grain is reduced almost by half in the presence of F^- and Cl^-, which also causes liquation with the formation of salt zones in the melt with decreasing σ. The indicated dependences of the grain size, R, on the surface tension of the melt (σ) are well reproducible in industrial conditions. But in such cases it is necessary to take into account the effect of many technological factors on the process of aggregation: the fluctuations in temperature in the sintering zone; the particle-size distribution of the material before it enters the zone of intensive aggregation; the dimensions of the sintering zone, and the shape of the flame.

The dissolution-crystallization stage involves the formation of stable crystals of minerals and the compaction of the system due to a more compact packing of cry-

stals and to the decrease of the pore volume. At this stage there takes place the crystallization of C_3S from the melt. This is accompanied by the convective transport of the melt between zones with temperature gradients and also the diffusion averaging of the composition of the melts characterized by concentration gradients. The driving force F of the process of rearrangement of crystals and of their approach (i.e., the shrinkage process) is the same as that at the first stage, but with a small correction introduced for the non-spherical shape of the crystals formed.

The kinetics of the shrinkage of clinker grains at the second sintering stage may be expressed by the following equations (15, 20):

$$\Delta l/l_o = (6 K_2 \delta D_o C_o \sigma V_o/K_1 RT)^{1/3} r^{-4/3} \cdot \tau^{1/3} \qquad (5)$$

where K_1 is the ratio of the pore radius to the radius of the particles; K_2 is the proportionality factor; C_o is the equilibrium solubility of C_3S, m/m^3; D_o is the diffusion coefficient for SiO_4^{4-} in the melt, m^2/s; V_o is the molar volume of C_3S, $m^3/kmole$; δ is the thickness of the film of the melt between the C_3S crystals, m; R is the universal gas constant, J/kmole; T is the absolute temperature, °K; r is the size of C_3S crystals, m; τ is the duration of heat treatment, seconds.

At a constant temperature (T) the values of C_o and σ are sufficiently stable, and therefore the amount of shrinkage will depend on the rate of the growth of the volume fraction of C_3S (V_o, δ, D_o), which determines the time of the process, τ. As the grain structure become more and more compact the diffusion of the most slowly moving ions SiO_4^{4-} to the crystal nuclei of C_3S becomes the rate-limiting factor of the process. The decrease of the viscosity of the melt attained in various ways contributes to the increase of $D_{SiO_4^{4-}}$ and speeds up the process of synthesis. The dependence of the clinker microstructure on the viscosity of the melt containing Ti, V, and Cr has been deduced by Kurdowski (21).

Since the packing of the sample at the second sintering stage is associated with the formation and growth of C_3S crystals (r), one can predict, by solving Eq. (5) for r, the size of the crystals of the mineral during the occurrence of the process of shrinkage of the clinker grain.

At the cooling stage (stage 3), the convection of the liquid is increased in the clinker grain (because of the large ΔT), as a result of which there may appear in it zones of increased porosity (usually, a surface layer) in it, and, on the contrary, compact zones (zones in the middle portion). The specific volume of the eutectic melt is lowered when it is frozen to glass. The volume of the hardened melt containing R_2O and Cr_2O_3 also decreases; in the presence of SO_3, MgO, and CaF_2 it is increased (19). The increase of the specific volume of the cooled melt occurs due to the formation of pores in the solid phase of the pores upon crystallization. The compression and expansion deformations that take place upon cooling the melt, especially if they are alternating in the various zones of the grain, develop mechanical stresses in it. These stresses are enhanced by the difference in the thermal linear expansion coefficients of the crystals of the minerals (as determined on sintered samples at 25-600°C): C_2S = 19.5 x; C_3S = 13 x; C_4AF = 10 x; glass = 10.8 x 10^{-6} K^{-1}. Solid solutions of C_2S with P_2O_5 (2.5-3 per cent) are characterized by even higher thermal linear expansion coefficients (39 x 10^{-6} K^{-1}); the thermal linear expansion coefficient also increases upon dissolution of K_2O in the lattice of the mineral and when Cr^{3+} and Ti^{4+} are incorporated the linear expansion coefficient decreases. The crystals of solid solutions formed in the non-equilibrium regions of the melt exhibit, when cooled slowly, the tendency towards chemical and physical breakdown. These processes may lead to a partial (dusting) and complete (crumbling) destruction of clinker grains. Melts with a high content of iron, with a temperature above the liquidus temperature are prone to overcooling by 100-130°C below the solidus temperature (55). The crystallization of the overcooled liquid proceeds spontaneously. It has been shown (56) that on the DTA curves for glass phases being cooled there appear endothermal effects caused by the pre-crystallization nucleation. The heat of crystallization of minerals is as follows: 436 kJ/kg for C_3A; 109-197 kJ/kg for $C_6A_xF_y$; 34 kJ/kg for C_2S; the pre-crystallization effect of the crystallization of C_3S is 155 kJ/kg.

THE STRUCTURE AND COMPOSITION OF CLINKER AND ITS PHASES

The crystallization of minerals from a melt containing various chemical elements as impurities is accompanied by the formation of non-equilibrium multi-component solid solutions. A comparatively large number of elements (about 12-15) are distributed non-uniformly among the main phases of clinker (25, 40-43). Belov and Boikova (25, 40) have found that the least amount of impurities is contained in the crystals of alite (4 per cent), and the largest amount, in the aluminate phase (13 per cent); the belite phase contains 6 per cent of impurities, and the aluminoferrite phase contains 10 per cent. The Mg^{2+} ion is preferentially dissolved in the alumin-

oferrite phase (1.9-3.2 per cent) and enters, in a considerable amount, into the composition of C_3S and C_3A (41). The Na^+ ions are concentrated in C_3A (0.3-4.6 per cent), and the K^+ ions are concentrated in C_2S. In crystals of C_3S and C_2S there are more Na^+ and K^+ ions in the centre than in the surface layers (27). The concentration of Al^{3+} and Fe^{3+} is considerable in C_3S and C_2S, but their concentration in the belite phase is two times higher. The elements Ti, Mn, and Cr dissolve predominantly in the aluminoferrite phase, and S^{6+}, P^{5+}, Ba^{2+}, and Sr^{2+} dissolve in C_2S.

Solid Solutions of Minerals. A new monoclinic modification M_3 of C_3S has been detected by the microscopic method (26): T_1 (ca. 620°C), T_2 (620-920°C), T_3 (920-980°C M_1 (980-990°C), M_2 (990-1060°C), M_3 (1060-1070°C), R (1070°C). * It exists in a narrow temperature range of about 10°C between M_2 and R. The transitions $T_1 \rightleftharpoons T_2$, $T_3 \rightleftharpoons M_1$, $M_2 \rightleftharpoons M_3$ and $M_3 \rightleftharpoons R$ differ from each other by their optical properties, such as birefringence and the orientation of axes, and $T_3 \rightleftharpoons M_1$, $M_2 \rightleftharpoons M_3$ and $M_3 \rightleftharpoons R$ differ by twinning. The transition $M_1 \rightleftharpoons M_2$, which cannot be determined by heating optical microscopy has been identified by the X-ray spectral analysis ($\beta = 90^0$ for M_2 and $\beta < 90^0$ for M_1).

The modification M_3 has also been identified in a solid solution of C_3S + 0.5% ZnO in the temperature range from 1020 to 1090°C (27). It is stabilized in clinker in a solid solution of C_3S + MgO with a content of MgO being equal to or greater than 2 per cent (23). With a lower concentration of MgO there is observed a zonal structure in the alite crystal with M_1 and M3 : a high concentration of Mg^{2+} in the peripheral portions stabilizes the lattice structure corresponding to M_3, and the in the central portion, which is impoverished in Mg^{2+}, there is retained the M_1 modification. Here the zonal boundary is parallel to the outer hexagonal boundaries of the crystal. The transition R $\rightarrow$ M_3 is accompanied, at a temperature of about 1000°C, by the formation of a cyclic twin structure along {1120} for monoclinic crystals of C_3S. The phase transition $M_3 \rightarrow M_1$ is one of the processes of activation of the lattice.

If the content of MgO is low, the stability of monoclinic forms of C_3S depends on the rate of cooling of clinker (43). In the slowly cooled clinker, M_{Ia} or M_{IIa} is stabilized, and in the rapidly cooled clinker the M_{Ia} modification is stabilized in the central portion of the alite crystal, whereas in the surface layer it is the M_{Ib} modification which is stabilized (M_{Ib} is the monoclinic modification of a solid solution containing Al_2O_3 and MgO).

In monocrystals (single crystals) of solid solutions of C_3S with MgO, Al_2O_3 and Fe_2O_3 grown by the Nurse procedure there have been detected a block (39) and a domain structure (29) with the impurity ions being distributed along the domain boundaries. A solid solution of Al and Cl in C_3S has been synthesized in the form of single crystals, which has the composition $C_{11}(Si, Al)_4O_{18}Cl$ or $6Ca_3SiO_5 \cdot {}^4CaO \cdot 2AlOCl$ (30). The chromium spurrite has been identified: $2Ca_2SiO_4 \cdot CaCrO_4$ (46). In the system $CaO-SiO_2-CaCl_2$ there have been isolated (48) $Ca_3SiO_4Cl_2$ in the form of needle-prismatic and monoclinic crystals and Ca_2SiO_3Cl in the form of transparent, almost fibrous crystals. Chloroalite melts at 1040°C and chloro-orthosilicate melts at 920°C. In the system $CaO-SiO_2-Al_2O_3-CaSO_4$ the mineral C_3S is decomposed by the action of Al_2O_3 and SO_3, but in the presence of MgO the decomposition process is slowed down.

Heterovalent replacement of Ca^{2+} ions by Cr^{3+} and of Si^{4+} ions by Cr^{6+} in the system $C_3S-Cr_2O_3$ bring about the stabilization of the T_{III} modification of C_3S over the entire concentration range up to 2.5 per cent of Cr_2O_3 by mass. At 3 per cent of Cr_2O_3 the M_I modification is stabilized. The volume of the unit cell attains a maximum value for a solid solution of C_3S with 1.75 per cent of Cr_2O_3. In the binary systems C_3S-TiO_2, $C_3S-Mn_2O_3$ and C_3S-SO_3 there are formed solid solutions of the substitution type at concentrations of the added impurity reaching 3 per cent by mass. Upon replacement of Ca^{2+} ions by Mn^{3+}, of Si^{4+} by Mn^{3+}, and of Si^{4+} by Ti^{4+} and of the complex ion SiO_4^{4-} by SO_4^{2-} there takes place the stabilization of the T_{II} modification of C_3S. The presence, in the composition of solid solutions, of complexes containing (0.5% TiO_2 + 0.5% Mn_2O_3 + 0.5% SO_3) and (2.0% TiO_2 + 1.0% Mn_2O_3) leads to the stabilization of the M_I modification of C_3S. When the contents of oxides in ternary complexes is increased and also with titanium-sulphur, manganese-sulphur combinations there is formed a triclinic modification of C_3S.

Calcium orthosilicate at an Mn_2O_3 content of more than 1% by mass in a solid solution is stabilized in the β - and α_L - forms; as the content of Mn_2O_3 increases up to 7 per cent the fraction of the α_L - form of C_2S increases up to 60 per cent. This enhances the degree of disorientation of fragments of the block-mosaic structure of belite crystals (44). Sulphosilicate

* In some works (27,43) the polymorphic forms of C_3S are designated as follows: T_I, T_{II}, T_{III}, M_{Ia}, M_{IIa}, M_{IIb}, R.

$2(2CaO \cdot SiO_2)$. $CaSO_4$ (C_5S_2Si) formed at low temperatures is decomposed at 1298°C into α'-C_2S and α-$CaSO_4$. In the presence of the complex $BaSO_4 + Mn_2O_3$ there is formed $2(BaO\ CaO) \cdot SiO_2$ (45).

A study of the symmetry and coordination of the structural units of C_3A and $C_{12}A_7$ has shown that the Al^{3+} ion entering into the composition of these minerals gives rise to tetrahedral complexes which perform the function of anions (31). Belov and Boikova (25) assume the occurence of a "feldspar" balanced substitution $Ca^{2+}Al^{3+} \rightleftharpoons Na^{+}Si^{4+}$ during the formation of solid solutions in C_3A and calcium aluminoferrites. In this substitution the maximum amount of Na_2O in C_3A will be lower than during the formation of a saturated solid solution of NC_8A_3.

There have been synthesized the following halogen-containing compounds: $C_{11}A_7CaF_2$ (T_{melt} = 1550°C), $C_{11}A_7CaCl_2$ ($T_{melt} \cong$ 1520°C $C_{11}A_7CaBr_2$ ($T_{melt} \cong$ 1420°C), $C_{11}A_7CaI_2$ (T_{melt} = 1410°C), $3(CA) \cdot CaF_2$ (T_{melt} = 1505°C), $3(CA) \cdot CaCl_2$ (T_{melt} = 1540°C), $3(CA) \cdot CaBr_2$ (T_{melt} = 1580°C) and solid solutions of the type $C_{11}A_{7-x}Fe_x \cdot CaF_2$ ($0 \leq x \leq 0.7$) The stability of the minerals decreases in the following sequence: F → Cl → Br → I. Minerals that contain Br and I are readily decomposed in air with to the evolution of bromine and iodine vapours. Like the compound $3(CA) \cdot CaSO_4$, the mineral $3(CA) \cdot CaF_2$ is formed at low temperatures (1100-1150°C) (47). In order to prevent the volatilization of the halogens during the firing process, to raw mix there are added salts (say, $NaCl-AlCl_3$, $NaF-MgF_2$), which form thermally stable compounds. A solid solution of $3(Ca_xBa_{1-x}A) \cdot CaSO_4$ has been produced (50). The analysis of the Mössbauer spectra of a complete series of solid solutions of calcium aluminoferrites (32) has shown that the Fe^{3+} ions are uniformly distributed in tetrahedral and octahedral cavities of the crystal laltice of calcium aluminoferrites. The same sites are occupied by the Al^{3+} ions which replace the Fe^{3+} ions. The incorporation of the Fe^{3+} and Mg^{2+} ions in place of Al^{3+} and Fe^{3+} into the crystal lattice of calcium aluminferrites causes the appearance of ionic vacancies in place of Al^{3+} (33). The incorporation of Cr^{3+} and Cr^{2+} ions alters the composition of solid solutions from C_6A_2F to C_4AF; the iron and aluminium have predominantly coordination number of 4 in C_4AF and a coordination number of 6 in C_6A_2F. Upon replacement of Fe^{3+} with Mn^{3+} there are formed solid solutions of the composition $C_2A_p(F, Mn)_{1-p}$; the limiting composition is $C_4AF_{0.3}Mn_{0.7}$ (34, 35). Crystals of $C_6A_xF_y$ have been found to grow in a helical manner (44). In the presence of P_2O_5, calcium aluminoferrite becomes impoverished in iron because of the replacement $FeO_4^{5-} \rightleftharpoons PO_4^{3-}$, and in the presence of F^-, on the contrary, the content of iron increases in it. The Ba^{2+} ions favour the separation of Fe_2O_3 - enriched calcium aluminoferrites from the melt, and the acidic components ZnO, CuO, P_2O_5 favour the separation of Fe_2O_3 -impoverished calcium aluminoferrites (36). The Na^+ ions contribute to the formation of a high-iron aluminoferrite phase and C_3A. The abovementioned changes in the composition of the aluminoferrite phase conform with the acid-base equilibrium (1) of the melt.

Crystal Defects. Real crystals of minerals, the more so their solid solutions, have imperfections or defects. The stresses that arise in crystals upon rapid cooling may be responsible for the formation of supersaturated metastable structures and for the occurrence of the processes of replacement of ions, say, of Ca^{2+} by Mg^{2+} (49). Prolonged annealing reduces the number of defects and stresses in crystals. The mineral C_3S cooled from 1550°C to 25°C was found to display a prominent thermoluminescence peak and high reactivity. The magnitude of the peak decreased upon slow cooling and when the mineral was allowed to stand in air for a prolonged period of time (58). This increased the degree of binding of electrons in traps.

Several types of electron-hole defects have been detected in the formation of solid solutions of clinker minerals;

1. Electron-hole paramagnetic centres on cationic and anionic vacancies, which have been detected from the spectra of gamma-irradiated solid solutions of calcium silicate (57).

2. Free charge carriers-electrons (n-type) and holes (p-type).

3. Thermoluminescence centres, which have been detected for C_3S after heat treatment and ultraviolet irradiation (58).

The changes of the concentration of point defects of the first two types are interconnected and depend not only on the specific features of the crystal lattice structure and the type and chemical nature of the impurity added but also on the arrangement of impurity ions in the crystal lattice of minerals.

The magnitude of electrical conductivity of solid solutions of C_3S, C_2S, and C_3A ranges from 10^{-7} to 10^{-10} ($S^{-1} \cdot m^{-1}$), which is characteristic of dielectrics. Even when its value is increased by addition of impurities, the materials under study cannot be assigned to the class of typical semiconductors. On the basis of measurements of the parameters of the Hall effect in alternating electric and magne-

tic fields carried out by the four-probe method it has been found, however, that solid solutions of clinker minerals exhibit the properties of semiconductors; the properties of semiconductors; in the case of impurity-free minerals the p-type conduction can be changed to the opposite type by introducing certain additives, say Fe_2O_3, NiO, or CaO. The concentration of holes in pure C_3S and C_3A is 2.6×10^{15} and 2.1×10^{18} $1/m^3$, respectively, with the same mobility of charge-carriers (1.2×10^{-6} $m^2/V \cdot s$), which is probably caused by departures from stoichiometry, the presence of cationic and anionic vacancies and by the unsaturation of valence bonds. The introduction of impurities leads not only to an increase in the concentration of charge carriers but also to a change in their mobility, which is evidently associated with the spreading of charges over structural defects, such as dislocations, twins, grain boundaries, etc. It has been established that the mobility of charge carriers ranges from 10^{-5} to 10^{-8} $m^2/V \cdot s$. The concentration of charge carriers and their mobility for the β-and α'-forms of C_2S depend on the nature and content of modifying additives. It should be noted that the concentration of charge carriers is practically always higher in samples of α'-C_2S since for the high-temperature forms to be stabilized, there is required a larger amount of the impurity, which causes additional structural distortions. This regularity is also characteristic of solid solutions of C_3S. The concentration of charge carriers, however, decreases in the following sequence of polymorphic forms: rhombohedral ⟶ triclinic ⟶ monoclinic.

Two types of conduction have been established for the formation of solid solutions of C_3S:

1. Electronic Conduction. In the systems C_3S-Fe_2O_3, C_3S-CoO, and C_3S-NiO upon iso- and heterovalent substitutions, the concentration of charge carriers increases with increasing concentration of additives (up to 1 per cent by weight) (Fig. 15).

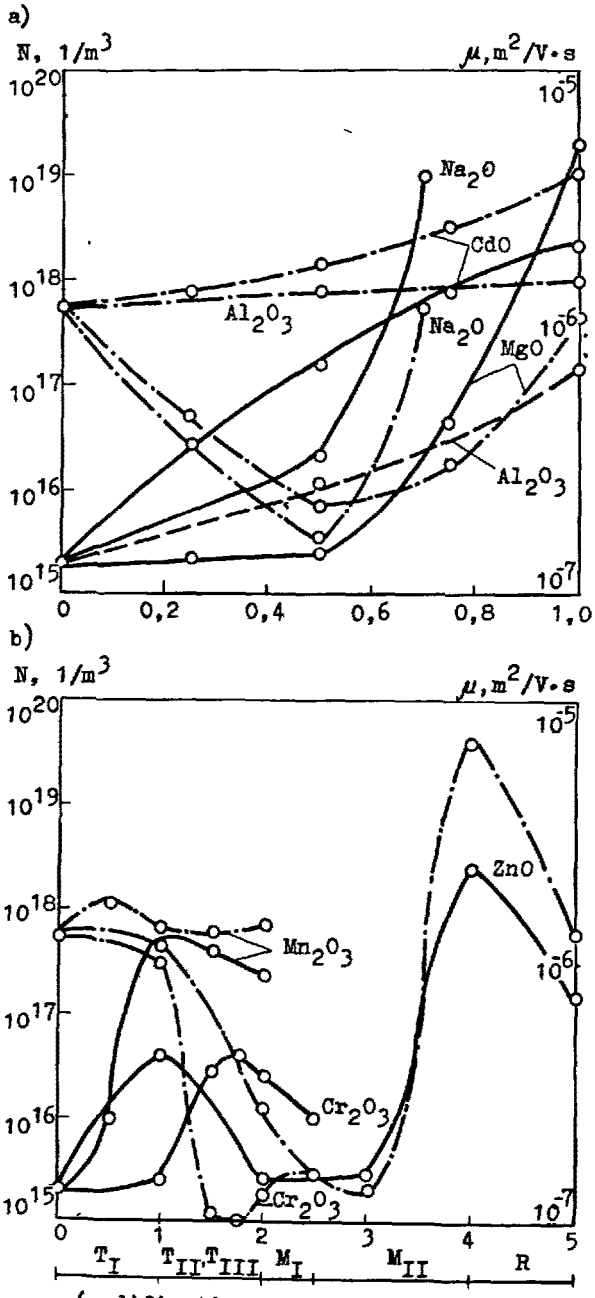

Fig. 15. The concentration of charge-carriers (N) and their mobility (μ) versus the content of the elements dissolved in C_3S

The electronic type of conduction in solid solutions with Fe is associated with the redistribution of the electron density of valence bonds with the Si^{4+} ions being predominantly replaced by Fe^{3+} and the

structural cavities being occupied by Fe^{3+} ions. In other cases, perhaps, not only the replacement of Si^{4+} and Ca^{2+} ions is a decisive factor, but the type of conduction also greatly depends on the specific features of the electronic shell structure, the departures from stoichiometry, and the changes in the concentration of other types of defects, which are difficult to take into account. Sing has determined (59) the electronic conduction in the system C_3S-NiO but the concentration of charge carriers and their mobility differ significantly from the data obtained by the author of the present paper.

2. Hole Conduction. The majority of solid solutions of C_3S of varying composition the display p-type conduction. Upon iso- and heterovalent replacements of Ca^{2+} and Si^{4+} ions by the ions Zn^{2+}, Ba^{2+}, Mg^{2+}, Mn^{3+}, Cd^{2+}, Al^{3+}, Cr^{3+}, Cr^{6+}, and Cu^{2+} and also upon incorporation of Na^{+}, Ba^{2+}, etc., into the crystal lattice of the matrix the concentration of charge carriers increases as a result of a change in the density of valence bonds, different degrees of substitution in the non-equilibrium crystal lattice, the presence of defects, etc. The concentrations of free charge carriers is influenced especially strongly by the replacement of Ca^{2+} by Mg^{2+}, the incorporation of Na^{+} into the structure of C_3S and the addition of complex additives of the type (0.3% by mass of SO_3 + 0.7% by mass of Na_2O) which exert a simultaneous effect on the anionic and cationic parts of the structure. The largest concentration of charge carriers has been found in solid solutions of C_3S+ 0.7% Na_2O and C_3S + 1% MgO (from 1.8×10^{19} to and 3.2×10^{19} $1/m^3$, respectively) The changes in the galvanomagnetic characteristics that take place in the solid solution systems C_3S-Mn_2O_3 and C_3S-Cr_2O_3 are presented in Fig. 15 as examples of what results from heterovalent substitutions.

The density of dislocations in alite crystals ranges from 5×10^{12} to 5×10^{13} m^{-2} (60), and the area occupied by dislocations on the surface of crystals of minerals is as follows, as evidenced by microphotographs: (1/3-1/2) for C_3S and (1/6-1/3) for C_2S (61). The Burgers vector of screw dislocations in alite should be expected to have a value of 0.05 to 0.1 μm since the nucleus of alite upon its crystallization from the melt is of the same order of magnitude (1). As the concentration of dislocations increases, so does the number of surface-active centres on which the hydration starts. The high rate of hydration of α'-C_2S as compared with β-C_2S has been accounted for (62) by the difference in the structure of the crystals and also by the presence of linear dislocations in α'-C_2S. According to Boikova (63), the density of etched pits on the surface of crystals of α'- and α-C_2S is, however, lower by a factor of 2 and 3.5, respectively, than in crystals of β-C_2S. No direct relationship between the amount of impurities in a crystal and the density of etched pits on its surface has been established by Boikova.

Point defects, thermoluminescent centres, and electron-hole defects contribute to the adsorption of charged particles from aqueous solutions on crystal surfaces.

REFERENCES :

1.- Ю.М.БУТТ, В.В.ТИМАШЕВ, А.П.ОСОКИН (1976), "Механизм процессов образования клинкера и модифицирование его структуры", Тр. VI Международного конгресса по химии цемента, М. Стройиздат, т.I, I32-I5I (in Russian).

2.- Н.В.БЕЛОВ, Е.Н.БЕЛОВА, Г.П.ЛИТВИНСКАЯ, Ю.А.ХАРИТОНОВ (I970), "Силификация, силикоз, полимеризация, алюминоз в геокристаллохимии силикатов и алюмосиликатов", Вестн. Московского ун-та, № 4 , 8-25 (in Russian).

3.- В.В.ИЛЮХИН, В.А.КУЗНЕЦОВ, А.Н.ЛОБАЧЕВ, В.С.БАКШУТОВ (I979), "Гидросиликаты кальция" М. "Наука" (in Russian).

4.- В.В.ТИМАШЕВ, А.П.ОСОКИН, С.И.ИВАЩЕНКО, Б.С.АЛЬБАЦ, Л.С.ФИЛИППОВА (I977), "Кислотно-основное взаимодействие в клинкерном расплаве", Тр. XII конференции силикатной промышленности и науки о силикатах, Будапешт, т.I, 25-47 (in Russian).

5.- Ю.М.БУТТ, В.В.ТИМАШЕВ, А.П.ОСОКИН (I973), "Комплексное исследование физико-химических свойств клинкерного расплава", Тр. У международного съезда по стройматериалам и силикатам. Веймар, 55-74 (in Russian).

6.- А.А.АППЕН (I974). Химия стекла, Л., "Химия" (in Russian).

7.- Н.М.РОТИНСКАЯ, Н.М.ПАВЛУШКИН, П.Д.САРКИСОВ, Т.С.МАТВЕЕВА, Г.П.ЛИСОВСКАЯ , Н.С.ЧЕРНЯК (I975), "Влияние фтора на кристаллизацию стекол в системе CaO-Al_2O_3-SiO_2-R_2O ", Изв.АН СССР. Неорганические материалы, т.II, № I, I40-I43 (in Russian).

8.- N.H.CHRISTENSEN, O.L.JEPSEN, V.JOHANSEN, (1978), "Rate of Alite Formation in Clinker Sandwiches, Cem. and Concr. Res., vol. 8, No. 6, pp. 693-702;vol.8, No.3, pp.301-310 (in English).

9.- Yu.M.BUTT, V.V.TIMASHEV, J.STAR (1972) "Description of Progress of Reaction in Firing Portland Cement Clinker" , Silikattechnik, vol. 23, No. 2, pp.52--54; vol. 23, No. 3, pp.89-92 , (in German).

10.- V.JOHANSEN, (1973), "Model for Reaction Between CaO Particles and Portland Cement Clinker", J.Amer.Ceram. Soc., vol. 56, No. 9, pp.450-454 (in English).

II.- С.ХРОМИ (I976), "Механизм образования белого клинкера", Тр. УI Межд.конгресса по химии цемента, М., Стройиздат, т.Ш, 268-273 (in Russian).

I2.- К.В.ВАСИЛЬЕВА, В.В.ТИМАШЕВ, Г.А.ТРОФИМОВ (I969), "Исследование кинетики процессов, протекающих при взаимодействии C_2S с клинкерным расплавом", Тр. Моск. хим.-технолог.ин-та им.Д.И. Менделеева, вып.9, 232-239 (in Russian).

I3.- М.Т.ВЛАСОВА (I976), "Периодичность процессов клинкерообразования", Тр.УI Межд.конгресса по химии цемента. М., Стройиздат, т.I I77-I8I (in Russian).

I4.- И.Г.АБРАМСОН, Б.В.ВОЛКОНСКИЙ, С.И.ДАНЮШЕВСКИЙ, Г.Б.ЕГОРОВ, Ю.В.НИКИФОРОВ, Я.М.ЦЕЙТЛИН, А.Ф.ВАЙСМН (1976), "Радиационно химический способ получения портландцементного клинкера", Цемент, № 9, 6-7 (in Russian).

I5.- У.КИНГЕРИ (I967), "Введение в керамику", М., Стройиздат (in Russian).

I6.- В.Н.ЕРЕМЕНКО, Ю.В.НАЙДИЧ, И.А.ЛАВРИНЕНКО (I968), "Спекание в присутствии жидкой металлической фазы", Киев, изд. Наукова Думка", (in Russian).

I7.- В.В.ТИМАШЕВ, Л.М.СУЛИМЕНКО, Б.С.АЛЬБАЦ (I978), "Агломерация порошкообразных силикатных материалов", М., Стройиздат (in Russian).

I8.- V.V.TIMASHEV, B.S.ALBATS, A.P.OSOKIN, L.S.FILIPPOVA (1979), "Sintering of Silicate Systems in the Presence of the Liquid Phase", "Science of Sintering", 11, 1, pp. 55-70 (in English).

I9.- Ю.М.БУТТ, В.В.ТИМАШЕВ (I974), "Портландцемент", М., Стройиздат (in Russian).

20.- R.KONDO, S.CHOI (1970), "The Reaction of Portland Cement Clinker Formation", Iogyo-Kuokai-Shi, vol. 78, No. 1, pp. 8-13 (in Japanese).

2I.- В.КУРДОВСКИ (I976), "Влияние малых примесей на прочность портландцемента" Тр.УI Межд.конгресса по химии цемента. М.. Стройиздат, т.I, 203-207 (in Russian).

22.- И.Ф.ПОНОМАРЕВ, А.П.ЗУБЕКИН, Р.П.ВАСИЛЬЕВА (I977), "Влияние сульфата натрия и окиси магния на минералообразование и свойства клинкера белого портландцемента", Цемент, № 5, I8-20 (in Russian).

23.- В.В.ТИМАШЕВ, А.Т.СУЛЕЙМЕНОВ, А.Ю.СИЧКАРЕВА, А.И.ТЛЕУБЕРГЕНОВА (I979), "Улучшение качества цемента на основе высокощелочного сырья при помощи барийсодержащей добавки". "Цемент", № 5, 8-9 (in Russian).

24.- М.Г.ЛУГИНИНА, Ю.М.МИХЕЕВ (I978), "Фосфорносодержащая добавка смягчает отрицательное влияние щелочей на прочность цементного камня", Цемент, № I2, I2-I4 (in Russian).

25.- Н.В.БЕЛОВ, А.И.БОЙКОВА (I978), "Структурно-кристаллохимические особенности цементных минералов", Цемент, № 9, I0-II (in Russian).

26.- I.MAKI, S.CHROMY (1978), "Microscopic Study of the Polymorphism of Ca_3SiO_5", Cem. and Concr. Res., vol. 8, No. 3, pp. 407-414 (in English).

27.- M.REGOURD, (1979), "Physique cristalline-Polymorphisme du Silicate tricalcique, nouvelles donnees de la diffraction des rayons X", French Academy of Sciences, (in French).

28.- I.MAKI, S.CHROMY (1978), "Characterization of the Alite Phase in Portland Cement by Microscopy", Il Cemento , vol. 3, pp. 247-252, (in English).

29.- K.V.IOST, (1975), Epitoanyag, 27, 1, pp. 23-26, (in Hungarian) .

30.- В.В.ИЛЮХИН, Н.Н.НЕВСКИЙ, Р.А.ХАУД, М.Я.БИКБАУ, Н.В.БЕЛОВ (I977), "Кристаллохимическая структура алинита", ДАН СССР, № 4, 834-836 (in Russian).

3I.- А.Л.ВОЛКОВА, Т.Ю.ЩЕТКИНА, О.П.МЧЕДЛОВ-ПЕТРОСЯН, В.И.САТАРИН (I977), "Исследование кристаллохимических особенностей некоторых минералов, проявляющих вяжущие свойства" Тр.ВНИИ цемент. промышленности, № 34, 70-83 (in Russian).

32.- С.П.ЕКИМОВ, А.И.БОЙКОВА, Л.В.ГРИЩЕНКО (I979), "Распределение Fe^{3+} в структуре алюмоферритов кальция". Кристаллография, т.24, № I, 90-94 (in Russian).

33.- И.В.КРАВЧЕНКО, Т.В.КУЗНЕЦОВА, М.Т.ВЛАСОВА, Б.Э.ЮДОВИЧ, В.Н.КАЛЬЯНОВА (I977), "Пути повышения качества цемента для производства асбестоцементных изделий", Тр.ВНИИ цемент. пром-сти, № 32, 58-65 (in Russian).

34.- Э.Е.КИРЯЕВА, Т.Ю.ЩЕТКИНА, И.С.КОВШИКОВ, Г.Н.КОРАТАНОВА, Л.Н.СКРЫШНИК (I977), "Влияние марганецсодержащих добавок на фазовый состав и свойства цементного клинкера", Тр.ВНИИ цемент. пром-сти, № 44, 58-72 (in Russian).

35.- В.В.ТИМАШЕВ, Н.И.МАКАРОВ, А.П.ОСОКИН, В.П.РЯЗИН, А.Н.МАКАРОВ (I977), "Формирование, состав и свойства марганецсодержащего портландцемента", Тр.ВНИИ цемент.пром-сти, № 45, I4-23 (in Russian).

36.- С.И.ИВАЩЕНКО, М.Т.ВЛАСОВА, В.Н.КАЛЬЯНОВА, Н.Я.МИХАЛЬЧЕНКОВ, В.Н.КАРНАУХОВ, Е.М.ХАВИН, Г.Б.КУЛАКОВА (I979), "Возможности повышения гидратационной активности портландцемента", Цемент , № 7, I0-II (en Russian).

37.- Р.КОНДО, М.ДАЙМОН (I976), "Фазовый состав затвердевшего цементного теста", Тр.УI Межд.конгресса по химии цемента. М.. Стройиздат, т.II, 244-257 (in Russian).

38.- В.А.ПЬЯЧЕВ, В.Н.ЧЕРЕПАНОВА (I974), "Кинетика образования трехкальциевого

силиката", Тр.Уральск.политехн.ин-та № 223, 81-84 (in Russian).

39.- Ю.М.БУТТ, В.В.ТИМАШЕВ, С.В.НЕСТИК, А.В.УШЕРОВ-МАРШАК (1971), "Процессы гидратации в пасте C_3S и влияние на них дисперсности исходного порошка", Тр.Моск.хим-технолог.ин-та им.Д.И. Менделеева, вып.68, 212-216 (in Russian).

40.- A.I.BOIKOVA (1978), "On the Composition of Clinker Phases", Il Cemento, No. 3, No. 3, pp. 137-146, (in English).

41.- M.KRISTMAN (1978), "Portland Cement Clinker. Mineralogical and Chemical Investigations", Cem. and Concr. Res., vol. 7, No. 6, 1977, pp. 649-658 ; vol. 6, No. 1, 1978, pp. 93-102 (in English).

42.- P.BARNES, N.T.MOORE, J.W.JEFFERY, S.L.SARKAR, (1976), "Characterization of Cement Phases by Energy Dispersive Elemental Analysis", World Cem. Technol., vol. 9, No. 2, pp. 50-51;(1978) vol. 6, No. 5, pp. 559-564 (in English).

43.- M.REGOURD (1979), "The Crystal Chemistry of Portland Cement Minerals. New Data", Engineering Foundation Conferences, (in English).

44.- Ю.С.МАЛИНИН, Ю.Ф.ХНЫКИН, У.И.ПАПИАШВИЛИ, В.П.РЯЗИН (1978), "Модифицирование портландцементного клинкера окисью марганца" Ж. прикл.химии, Т., 51, № 7, 1480-1493 (in Russian).

45.- В.В.ВОЛКОВ, М.М.СЫЧЕВ, А.С.ЧИГОВА, (1977), "Влияние небольших добавок окиси бария и марганца на получение и свойства портландцемента", Ж.прикл. химии,т.50,№ 7, 1433-1436 (in Russian).

46.- F.TROJER, Chr.WARBENOWA (1977), "Chromatspurrit eine neue Spurritphase", Zem-Kalk-Gips, vol. 30, No. 1, pp.40-43 (in German).

47.- М.Т.ВЛАСОВА, Б.Э.ЮДОВИЧ, В.П.РЯЗИН, Г.Н.ВОВЧЕК (1977), "Фазовый состав галогенсодержащих клинкеров для быстротвердеющих цементов" Тр.ВНИИ цемент. пром-сти, № 45, 5-13 (in Russian).

48.- В.Г.ЧУХЛАНЦЕВ (1979), "Хлорсиликаты кальция. Система $CaCO_3(CaO)-SiO_6-6CI_2$", ДАН СССР, т.246, № 5, 1187, (in Russian).

49.- R.A.THOMPSON, D.C.KILLOCK, J.H.FORRESTER (1965), "Crystal Chemistry and Reactivity of the MgO-Stabilized Alites", J.Amer.Ceram.Soc., vol. vol.58, No. 1-2, pp. 54-57 (in English).

50.- А.Ю.СИЧКАРЕВА, В.В.ТИМАШЕВ, А.Т.СУЛЕЙМЕНОВ (1978), "Модифицирование структуры и свойств $Ca_4(AI6O_{12})(SO_4)$ окисью бария", Тр.Моск.хим.-техн.ин-та им.Д.И.Менделеева, вып.100, 52-54 (in Russian).

51.- D.KNÖFEL (1977), "Beeinflussung einiger Eigenschaften des Portlandzementklinkers und des Portlandzementes durch TiO_2", Zem.-Kalk-Gips, vol. 30, No. 4, pp. 191-196 (in German).

52.- Х.Ю.ВЭХТЛЕР, П.В.ЗАЗУЛЯ, М.М.СЫЧЕВ, Ю.И.ШУБИНА (1975) "О влиянии примесей на спекаемость портландцементных сырьевых шихт" Сб. "Химия и технология вяжущих веществ", Ленинград.технол.ин-т им.Ленсовета, 50-59 (in Russian).

53.- Т.Г.АНГЕЛОВА, В.В.ТИМАШЕВ (1978), "Исследование влияния комплекса окислов MgO, R_2O, SO_3, MnO и BaO при получении клинкера", Тр.Моск.хим.-техн. ин-та им.Д.И.Менделеева, вып.100, 42-44 (in Russian).

54.- П.И.СОФИНСКИЙ, В.В.ТИМАШЕВ, В.В.БОЛЬШОВ, Т.В.ПАХОМОВА (1978), "Влияние фторида, хлорида и сульфата кальция на структуру и свойства цемента, Тр. Моск.хим.-техн.ин-та им.Д.И.Менделеева, вып.100, 57-59 (in Russian).

55.- M.MAULTZSCH, H.SCHOLZE (1973), "Zur Bildung der ferritischen klinkerperosse aus der Schmelze, Zem.-Kalk-Gips, 26, 12, 583-587 (in German).

56.- P.W.SOSULJA, H.J.WÄCHTER (1975) "Differentialtermische Untersuchungen der Claskristallisation im System CaO - SiO_2-Al_2O_3-Fe_2O_3", Journal of Thermal Analysis", vol. 7, N 3, s. 643-658, (in German).

57.- В.Г.АКИМОВ, В.В.ТИМАШЕВ, А.И.БОЙКОВА (1976), "Определение концентрации точечных дефектов в твердых растворах трехкальциевого силиката с ZnO", Тр. Моск.хим.-техн.ин-та им.Д.И.Менделеева, вып.92, 112-115 (in Russian).

58.- P.FIERENS, J.P.VERHAEGEN, (1976), "Hydration of Tricalcium Silicate in Paste. The Kinetics of Dissolution of Calcium Ions in the Aqueous Phase", Cem. and Concr.Res., vol. 6, No. 1, pp. 103-112; No. 2, pp. 337-342 (in English).

59.- N.B.SINGH (1976) "Effect of Nickel Doping on the Solid-State Properties of C_2S", Cem. and Concr.Res., vol. 6, No. 3, pp. 409-412 (in English).

60.- Ю.С.МАЛИНИН, У.И.ПАПИАШВИЛИ, Б.Э.ЮДОВИЧ (1977), "Применение растворовой электронной микроскопии для исследования структуры портландцементного клинкера", Тр. ВНИИ цемент, пром-сти, № 32, 211-243 (in Russian).

61.- Г.М.ТАРНОРУЦКИЙ, Б.Э.ЮДОВИЧ, Л.В.КРАВЧЕНКО (1977), "Исследование адсорбции ПАВ на цементе и составляющих его минералах", Тр. ВНИИ цемент. пром-сти, № 32, 79-91 (in Russian).

62.- J.JELENIC, A.BEZJAK, M.BUSAN (1978), "Hydration of B_2O_3-Stabilized α' - and β -Modifications of Dicalcium Silicate", Cem. and Concr. Res., vol.8, No. 2, pp. 173-180 (in English).

63.- А.И.БОЙКОВА (1978), "О взаимосвязи между составом, кристаллохимическими особенностями структуры и свойствами цементных минералов", Успехи физ. и хим. силикатов, Изд. "Наука" Л., 266-292 (in Russian).

SUB-THEME I - 4

Influence of grinding and storage conditions of clinker

J.P. MÉRIC
Général Manager
Centre d'Études et de Recherches
de l'Industrie des Liants Hydrauliques
Paris, FRANCE

The grinding of clinker and secondary components is the ultimate stage in cement manufacture. It is the grinding which, by freeing the surfaces necessary for clinker hydration give the final product the reactivity to water leading to high strengths. Research on grinding was focused on the manufacture of high strength cements for many years.

Since this objective has now been reached, recent research on grinding has concentrated more on the regularity of cement manufacture and towards a reduction in grinding energy consumption. In these two fields, results have been obtained only through reflexion on the physics of comminution applied to cement and after a thorough study of the properties of ground material. These three topics : physics of comminution applied to cement, properties of the ground material and energy utilization are developed in the following paragraphs.

1.- PHYSICAL PRINCIPLES OF COMMINUTION

The physics of comminution is a complex scientific field devoted to the study of modifications in the structure of a material subjected to mechanical stresses.

The most important parameters concerning these stresses are their distribution and the rate at which they are applied, taking into account the mechanical properties specific to the material. Structural modifications include the setting up of free surfaces and defects in the molecular organization within the material.

The surfaces defined by comminution have very different characteristics from those set up by sublimation, diffusion or condensation. The physics of comminution aims at studying these particular features.

The defects in molecular organization caused by comminution also show specific characteristics very different from those induced by temperature variations, chemical actions, ionic bombing. Study of these features constitutes the second aspect of the physics of comminution.

1.1.- Fracture mechanics

Fracture mechanics was introduced by Griffith (1) in 1920. His work underlined the importance of structural defects in the understanding of fracture phenomena, and promoted understanding of why former theoretical calculations, which failed to take structural faults into consideration, revealed strengths 100 to 1000 times higher than those observed in testing of the strongest natural materials. These strengths are only some tens of MPa under tensile stress, whereas calculation founded on chemical energy gives results up to 1000 MPa. Moreover it is only recently that flawless materials were manufactured, revealing the tensile strengths forecast by these calculations. Such materials are essentially fibres produced in such a way that microcracks do not occur.

With fracture mechanics it is possible to determine the mechanical stress conditions in which the microcracks can develop and give rise to fracture of the material. It is possible in this way to calculate the strength of materials with structural flaws, however provided that two determining microcrack propagation parameters are known : the mean dimension of microcracks and the specific fracture energy γ_F.

The specific fracture energy is the energy which has to be used per freed unit surface to propagate the crack. This energy is much higher than the surface energy, that is to say the energy needed to break the molecular bonds present on the surface. Indeed, surface energy is around 0,05 to 0,5 Joule per m2, whilst fracture energy is around 5 Joules per m2 for brittle materials, 10 Joules per m2 for plastics and 500 Joules per m2 for metals. The differences between surface energy and specific fracture energy show that more energy must be used to develop a crack by opening the two edges than is needed to break the molecular surface bonds by an ideal means. This difference finds its explanation in the setting up of high stress concentration near the edge of the crack ; this concentration is due to the application of forces necessary to the propagation of the crack and brings about plastic deformations in the material, themselves sources of irreversible energy losses. These losses are all the higher the more plastic the mechanical behaviour of the material as is shown in the preceding values.

Crack propagation energy is provided by the field of elastic stresses applied to the material. As propagation develops, this stress field decreases in intensity, that is to say in energy, part of energy being transformed into specific fracture energy. This transfer of mechanical stress field towards fracture energy corresponds to a deterioration of mechanical energy into heat. The orders of magnitude involved are as follows.

Q the section, L the length. Transverse fracture requires $2Q\gamma_F$ which must come from this stress field. Consequently it is necessary that

$$2Q\gamma_F < \frac{\sigma^2}{2E} QL$$

$$\text{or again } L > 4\,\frac{E\gamma_F}{\sigma^2}$$

that is to say that the propagation of a crack starting from an elastic stress field is possibly only above a certain dimension of the volume in which this stress is exerted. As an example for glass the preceding

formula gives an order of magnitude to the micron and for a plastic material to the millimeter.

These examples illustrate a point which will be reconsidered later : the difficulty of fine grinding and the importance of a precise determination of γ_F to fix the grinding limits. This parameter can be determined with mechanical tests by applying to the material an appropriately chosen stress field where all the energy transforms into fracture energy. Huet (2) has studied these techniques and applied them to a large number of materials to determine their γ_F coefficient. The values obtained are given in detail in table I.

Material	γ_F Joules/m2
Fired clays	5,5 to 40
Plate glass	3,5
Ceramics	20 to 60
Natural stones	3,7 to 59
Dried clays	7,3 to 25,3
Al_2O_3	20 to 50
Refractory bricks	30 to 50
NaCl + fibres	200

TABLE I

Another particularly important parameter in the study of comminution is the mean size of structural flaws which are responsible for cracking onset. Weber (3) shows that stressing a cylinder by simple compression leads to unstable cracking, that is to say that an excess of elastic energy must be provided to obtain crack propagation, this then occurs in an uncontrolled way and the excess energy is transformed into cinetic energy of fragments. Weber indicates that the effectiveness of the operation, that is to say the proportion of elastic energy transformed into fracture energy, is proportional to a_o, mean dimension of the onsets of fracture in a material.

The overall fracture behaviour of a material can consequently be discribed by two intrinsic parameters γ_F and a_o.

Table II provides as example the values of these parameters for two common materials.

Material	γ_F Joules/m2	a_o microns
Fired clays	5,5 to 40	100 to 1500
Glass	3,5	20

TABLE II

For clinkers very little work has been undertaken up to present to determine γ_F and a_o according to the composition of the material and taking into account its thermal treatment. It would be appropriate to undertake this research with the aim of correlating the manufacturing parameters with the specific fracture energy along the lines of work carried out on alumina by Simpson (12). It would then be possible to explain more thoroughly the differences in grindability observed on industrial clinkers and focus attention on producing more grindable materials.

1.2.- Grinding methods

Crack propagation occurs through stressing of material. This stressing can be brought about in three ways (figures 1, 2 and 3).

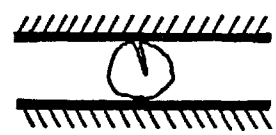

Fig. 1 - By slow compression between two jaws

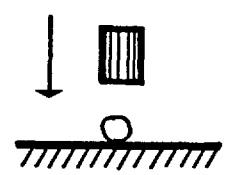

Fig. 2 - By impact compression of a falling body

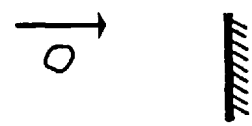

Fig. 3 - By projection against an anvil

These three means of stressing material correspond to three grinding modes which have

defined three technological approaches :

. roller mills,
. rod or ball mills,
. impact or impeller mills.

Rumpf (4) and his school have analysed these grinding modes, giving a very exact description of the stress field in these three cases. Theoretical investigations and testing carried out on glass beads have revealed only few differences in the stress field, even when the kinetic effects linked to the rapidity of stressing were expected as in grinding by projection. This research was carried out by crushing the material grain by grain and measuring the surfaces freed as well as the grinding energy used for this. The grinding energy is the deformation or kinetic energy supplied to the grain.

In this way, Rumpf (5) checks on grain by grain testing the proportionality of the freed surface to the energy spent, that is to say that the Rittinger law, known since the nineteenth century and currently used in the cement industry is still applicable, with a certain approximation to the individual grain scale.

The Rittinger law stipulates more generally that, for a given grinding process, the grinding energy is proportional to the surfaces set up or, in other words, that the output of a grinding process is constant and consequently independant of the fineness of the material. This law proves correct for common finenesses, but it is found that for high finenesses the grinding efficiency falls. This was been attributed to clustering but it happens even when this is prevented. The explanation of this fall in output is undoubtedly dual :

. on one hand, the areas of plastic deformation become extensive compared with the sizes of the grains and the grinding by transfer of elastic energy into surface energy is no longer possible, as was shown previously ;

. on the other hand, successive grinding exhausts the microcracks in the material and when a certain size is reached, the useful microcracks have all been freed. The material is then a monocrystal medium difficult to grind.

The two phenomena limit the law of Rittinger towards the high finenesses. Rumpf (5) by undertaking a dimension analysis has given this phenomenon a new law which takes into account the size of grains in the application of the Rittinger law.

Haese (6) reports on systematic grinding tests on clinker grain by grain. In the light of tests carried out with different modes of grinding the author determines the parameters which indicate the aptitude of a clinker to comminution. He especially studies in detail an essential magnitude : the probability of fracture of a grain of given size according to the load applied on it. He also examines the aspect of grading distributions of ground material and gives a formulation deduced from the testing.

1.3.- Surfaces freed by grinding

The surfaces freed by grinding are generally measured by two methods : the Blaine method which gives an envelope surface and the BET surface which gives the total surface taking into account all the dislocations and surface fractures. Comparison of the two methods gives useful informations on the structure of surface set up by grinding.

Schwenk (72) has found (5) that with vacuum grinding, it is possible to obtain very active surfaces. Grinding was undertaken at 10^{-5} Torr ; the surfaces freed were measured before and after being in contact with the air. This revealed that the action of the air and of its humidity especially lead to a decrease of these surfaces by closing of cracks. The reduction factor was 1,6 in the case of quartz and about 2,6 for glass, therefore the surface reactions during the very grinding are of considerable importance.

This importance has led research scientists to study the influence of the surroundings on grinding performance. Schönert (7) has shown that grinding with liquid water or steam leads to a decrease in specific fracture energy. The decrease only occurs however with low rates of crack propagation : 10^{-3}m/s. When the rate of propagation is higher, the specific fracture energy is identical in vacuum or in water vapour. This gives an evaluation of the kinetics for the fixing of water molecules in the heart of the crack. The very active surfaces set up by grinding can weld together again, this is the phenomenon of clustering which can be avoided by covering the surfaces with a surface active product. This phenomenon will be described later in the case of cement. The structure of the surface set up by grinding is amorphous (8). This statement is explained by the plastic deformations which occur with the crack propagation and also by the very high temperatures which prevail in the crack neighbourhood. Weichert and Schönert (9) have measured these temperatures by basing their calculations on the light emission of grains during grinding and they have found in certain cases temperatures of several thousand degrees.

Other surface phenomena have also been studied by various authors. These phenomena are surface loads and triboluminescence.

Surfaces obtained by grinding have numerous properties ; research scientists have exa-

mined the variations in these properties according to the grinding mode. Schönert (10) has considered that all the grinding modes lead to similar fracture phenomena, therefore to identical surface properties. This conclusion is however challenged by fine grinding where marked differences in surface aspect (11) have been revealed by scanning electron microscopy between impact compression grinding and projection grinding.

1.4.- Structural flaws induced by grinding

It is commonly accepted that fracture onset is necessary for material fragmentation and none the less discutable that grinding can induce extensive dislocations and disorders in the crystalline networks.

Numerous investigations have been undertaken on this subject. Sciora (13) examines the effect of grinding on hydrates and shows that the mechanical forces bring about modifications in the network identificable by the dehydration temperature variations. Certain network modifications can also be made easy to identify by a widening of diffraction X rays. Tekiz (14) studies the zinc oxide and zinc sulphur network modifications. The widening of rays makes it possible to obtain an order of magnitude of dislocations which occur during the grinding and which can be later suppressed by a thermal treatment. Legrand and Nicolas (15) have applied these techniques to clays and have also found extensive transformations in the crystalline network. Opoczky (16) points out similar phenomena for βC_2S to which grinding confers a certain amorphization and therefore a certain activation which must be taken into account in the grinding work index. Using calorimetric tests (16) it has been possible to indicate an order of magnitude of this energy.

The importance of a thorough study of the fundamentals of comminution for the chemistry of cement is also clearly obvious since cement hydration is first of all a surface reaction ; it therefore varies with the quantity of surface freed and the physical nature of these surfaces (73). It is also a transformation reaction of the anhydrous phase transformation whose kinetics is linked to structure. However grinding can modify this structure towards greater activity (16) and concequently, towards an improvement of transformation kinetics.

2.- THE ROLE OF COMMINUTION IN THE CHEMISTRY OF CEMENT

2.1.- Particle size distribution of ground clinker

The aim of grinding is to free the surfaces necessary for the hydration reaction. Measuring these surfaces according to the Blaine method has for a long time constituted the most used parameter to identify the ground state of a cement. However it became obvious that the particle size distribution was also a capital indication towards knowledge of cement properties. The grading curves after comminution do not comply with any theoretical formulae which have been drawn up in the past. So it is necessary to manage with approaching these actual distributions by approximate formulae.

The most used functions are as follows (D(a) is the proportion of undersize at diameter a) :

Function of Gaudin and Schuhmann :

$$D(a) = \left(\frac{a}{k}\right)^m$$

Log-normal function :

$$D(a) = \Phi\left[\ln\left(\frac{a}{d}\right)\right]^p$$

where Φ represents the integral of the Gauss function.

Rosin-Rammler function :

$$D(a) = 1 - \exp - \left(\frac{a}{a_o}\right)^n$$

This later function is widely used. The mean value of the distribution is :

$$A = a_o \frac{1}{\Gamma(n)}$$

The standard deviation is :

$$\sigma = a_o \sqrt{\frac{2}{\Gamma(n)} - \left(\frac{1}{\Gamma(n)}\right)^2}$$

The maximum frequency of the grading distribution corresponds to the diameter :

$$a_m = a_o \left(\frac{n-1}{n}\right)^{\frac{1}{n}}$$

When this function is represented in logarithmic coordonates in

$$\ln a \text{ and } \ln\ln \frac{1}{1-D}$$

a straight line is obtained

$$Y = n(x - x_o) \quad \text{where } x_o = \ln a_o$$

n is the slope of the straight line and notifies the smaller range grading distribution, whilst x_o represents the degree of fineness.

Theoretically the grading distribution should make it possible to calculate the specific surface thanks to the following formula :

$$S = \frac{6}{\rho} \int_0^1 \frac{dD}{a} \quad \text{where } \rho \text{ is the density}$$

In the case of Rosin-Rammler distribution we find :

$$S = \frac{6}{a_o \rho} \Gamma\,\frac{n-1}{n}$$

This function is not defined for $n \leq 1$ and for $n > 1$ it gives values which are very different from surfaces determined by the Blaine method. The two other formulae proposed bring us no closer to obtaining correlation between theory and experience. This is due to the ever approximate nature of the functions proposed, this nature above all obvious for the lower extremity of the grading curve, that is to say for the very low values of a. These are the frequencies corresponding to these values which have the highest weight in calculating S. It is not surprising therefore to find the disagreement mentioned previously. In spite of this, the Rosin-Rammler formula is very useful since, thanks to two parameters a_0 and n, it is possible to identify a grading distribution with enough accuracy for routine grinding.

Closer study must be made on complete grading determinations carried out by sieving with the elutriator or the Andreasen pipette. With a more recent method (17) it is possible to carry out a complete grading determination in a few minutes by using laser beam diffraction. Thanks to this method, grading determination has become routine in laboratories.

The grading curve is used to calculate the specific surface with the formula :

$$S = \frac{6}{\rho} \sum \frac{\Delta D}{a}$$

where ρ is the density and ΔD the proportion of grains in the class characterized by the diameter a. This gives a value of the specific surface which is generally close to that determined by the Blaine method.

It is then possible to compare experimentally as Slegten did (18) this new determination of the specific surface with that carried out according to Blaine and to look for the determination which gives the closest definition of the cement characteristics. In spite of the interest of this research, recent work emphasizes more the grading distribution than the surface determinations to evaluate the cement properties. Indeed it is obvious that the specific surface depends essentially on the finest grains ; however these grains hydrate very quickly and if they play an important part, this remains limited to the initial properties of cements and cannot be extended entirely to their future development.

2.2.- Relation between grading distribution, rate of hydration and strength

According to zur Strassen (19) hydration is a diffusion reaction which propagates on a uniform front of the clinker grain surface towards the core. Measurements carried out on portland cement and on pure C_3S give the following values for depths of penetration of the reaction

1 day	0,5 µm
3 days	2 µm
7 days	3 - 4 µm
28 days	6 - 7 µm

For C_2S zur Strassen admits the following values :

30 days	1 µm
60 days	2 µm
80 days	3 µm

This shows that in a cement rich in alite the 30 micron grains are hydrated at 87,5% at 28 days and that the grains smaller than 3 microns undergo complete hydration shortly after mixing.

This points to two conclusions :

- first, that the 0-3 micron fraction grains (and these contribute to giving the cement a high specific surface) are indispensable for initial strength but make no contribution to final strengths.
- secondly, that the 0-3 micron fraction grains are the only ones to contribute meaningfully to final strength. Grains over 30 microns only partially hydrate ; consequently their contribution to strength is very low.

Beke (20) has checked these conclusions on blends of different classes of cements by replacing missing classes by an inert powder. From this work, he was able to draw useful conclusions on mill adjustment.

Ritzmann (21) checks the relation between the time-dependent development of strength and the grading curve by blending about thirty cements from ten distinct grading classes. This relation can be expressed as a satisfactory theoretical formulation with the hypothesis which zur Strassen used that the hydration reaction is a diffusion reaction. Using a grading curve it is then possible to determine the quantity of hydrated cement as a function of time. Ritzmann shows that quantity determined by calculation is linked to strength by a linear law, however provided that the water/cement ratio is constant. If the cement is mixed at normal consistency, the excess water brings about falls in strength for a given rate of hydration. Nevertheless such decreases in strength can be forecast by calculation taking this excess water into account.

Locher, Sprung and Korf (22) come to the conclusion that with equal specific surface it is the cements with a narrow grading spectrum which offer the best final strength, whilst initial strengths are equivalent. These findings can again be explained by the concept of depth of hydration. The laws drawn from these tests are not however gene-

ral, they are based on the chemistry of cements : so with an identical curve, a cement rich in alkalies will offer an initial strength higher than a cement without alkalies whereas its final strength will be lower. The obvious conclusion is that the increase in specific surface with the aim of improving initial strengths will be more marked for a cement with low alkali content.

Keienburg (33) takes three distinct clinkers to study the relationships between the grading curve, the hydrated fraction of the clinker and the normal mechanical strengths. The quantity of clinker hydrated is determined by measuring the non-evaporable water. Consequently this quantity is no longer dealt with as a calculation intermediary, but as a physical factor whose correlation with strengths has been checked. THis work underlines how the zur Strassen diffusion model explains the correlations between grading curve and quantity of hydrates. The relation between quantity of hydrates and strengths may be linear for a given cement but nevertheless varies a great deal with the composition and structure of hydrated cement. It is shown that with a given composition, the whole kinetic formation process of strengths could be described by two points on the grading curve 10 and 50 microns for example ; but this information is to be added to the specific surface.

The great importance of the structure of hardened pastes in explaining the relationships between rates of hydration and strengths is underlined by Syrkin and coworkers (23) as well as by Butt, Kolbasow and Berlin (24) who have linked fineness to hardened paste porosity. It has been found that the increase in cement fineness beyond a certain threshold would not lead to a marked transformation of cement structure and that the grains more than 10 microns in diameter offer favorable conditions for porosity of the order of the micrometer.

The concept of depth of hydration penetration makes it possible to explain the influence of grading distribution on the quantity of cement hydrated. Explaining the relation between the quantity of hydrated cement and strengths is found more difficult. However we can consider certain the fact that for a cement of given composition and for a fixed water/cement ratio, the rate of hydration is an excellent indication of strengths. It still remains that the structure of hydrates vary with their growth kinetics and that the knowledge of this structure could complete the determination of the hydration rate for improved forecasting of strengths according to grain size. Research on porosity already quoted can open an approach to bring light on this question.

2.3.- Clustering and the role of grinding aids

When grinding in a ball mill is pursued to very high specific surfaces, it is found that beyond a certain limit the specific surface no longer increases in spite of the energy input.

This phenomenon has been interpreted by the recaking of grains whose active surfaces bond together to form large size composite grains. Papadakis (25) has drawn up a formula showing the influence of the ball mill and ball sizes in the understanding of the phenomenon which seems linked to the grinding tool and its working. In extreme cases, continuing grinding will imply a decrease in specific surface (figure 4) and an unacceptable waste of energy.

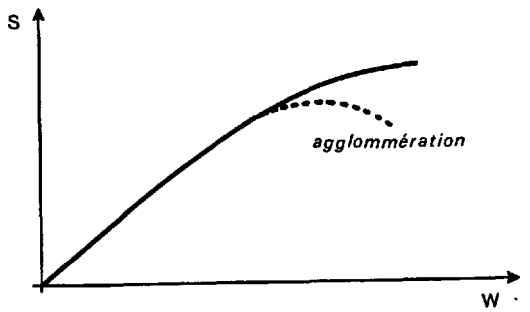

Fig. 4 - Development of specific surface plotted against grinding energy in a ball mill

The phenomenon has been studied in detail by Beke (26) who has measured the development of grading curves in a ball mill plotted against grinding time and energy used. As the grinding progresses, three stages become obvious :

1. The coefficient of uniformity remains constant ; the straight lines represent the grading distribution moving parallel to themselves.
2. The coefficient of uniformity increases; the finest grains are monocrystals difficult to grind ; grinding continues only thanks to failure onsets in the largest grains. The specific surface tends to stagnate at a ceiling.
3. The coefficient of uniformity falls since the fine grains cake together to form larger grains. The specific surface tends to decrease.

Figure 5 shows this development plotted against energy supplied to the material.

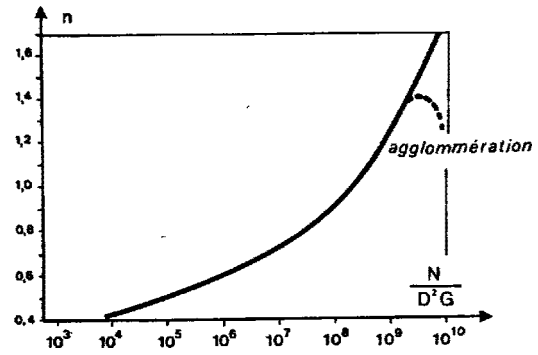

Fig. 5 - Development of the coefficient of uniformity plotted against the number of impacts N, the diameter of the mill D and the mass of balls G according to Beke.

Clustering can be lessened by adding grinding aids. The products used are generally polar surface active which saturate the fresh surfaces set up by grinding. These surfaces consist of free links and electric charges which encourage the grains to come together. The additives composed of poler organic molecules bind with the oxygen ions of these surfaces by hydrogen links. This phenomenon is analysed by Iwabuchi (27) who also comes to the conclusion about a possible action on failure onsets, action which would have a positive effect on grinding efficiency. Von Seebach (28) has carried out grinding in different atmospheres without succeeding in revealing an influence of organic substances of these atmospheres on the grinding output. We must conclude that grinding aids act essentially on the caking and this point of view is properly confirmed (29)(30) by rheology studies on dry powders obtained with and without grinding aids.

Grinding aids of the glycol or ethanolamine type have considerable practical importance since they offer the possibility of pursuing grinding to its technological limits (fixed by sizes or the energy of milling bodies) or its physical limits (limit of plasticity of the material).

Grinding aids also influence the hydration reactions. The covering over of active surfaces by a monomolecular layer of organic material also affects the hydration kinetics and the morphology of hydrates. This influence has been studied on pozzolanas (31) by grinding the material to the same degree of fineness without and with grinding aids. The influence of the aid is then examined according to whether it is added to grinding or in the mixing water. Differences thus become obvious in the kinetics of hydration and in the morphology of hydrates which seem more pronounced when the aid is added during grinding. The mechanisms of this influence are as yet incompletely known ; it is however probable (32) that the hydrogen links set up by the organic molecules with the crystal surfaces orientate the crystalline growth as well as the dissolution of crystals.

It seems then that the role of grinding aids is complex . Their influence is obvious on several parameters :

- the caking rate,
- the Blaine fineness,
- the grading distribution,
- the reactivity of surfaces.

All these parameters influence the kinetics of hydration.

2.4.- Grindability of clinker according to its chemical composition, thermal treatment and storage conditions

The grindability of different clinker phases has been extensively investigated. Beke and Opoczky (34) especially have ground separately synthetic preparations of C_3A, C_4AF, C_2S and C_3S. Grinding carried out in a ball mill has shown how the behaviour of the various cement phases is differentiated. C_3S was particularly grindable, showing only a slight tendency to caking, whilst βC_2S was more difficult to grind with more accentuated likelihood of caking in spite of grinding aids being added. βC_2S was ground a long time but it was impossible to exceed a 5000 Blaine surface. This surface moreover fluctuates during grinding, the phases of increasing surface being followed by caking phases during which the surface decreases. With pure C_3S, 10000 Blaine surfaces were obtained. C_4AF and C_3A show intermediate behaviour. C_3A is close to C_3S and C_4AF similar to βC_2S. X-ray diffraction studies reveal a distinct tendency to amorphization of all phases, except C_3S when grinding is pursued to an extreme limit. It is however noted that when grinding of the phases is simultaneous, this amorphization then also extends to C_3S, which proves an interaction between the phases during grinding in a ball mill. This interaction undeniably leads to less effective grinding of C_3S in the presence of the other phases.

Gouda (35) carries out investigations on four factory clinkers whose grindability improves the lower the liquid phase concentration. Consequently it is advisable to keep to a low liquid phase concentration and a C_3S content as high as possible to improve clinker grindability.

Deckers (36) also studies the influence of physical parameters of clinker on its grindability and especially the influence of its porosity. This parameter has a very marked influence for primary grinding below 2000 cm2/g Blaine.

The presence of free lime which indicates firing conditions and consequently the

structure of clinker, influences grindability to produce an increase in this property with higher free lime content, an increase obvious in the ranges of fine or primary grinding. The influence of cooling systems has been examined by Regourd (supplementary paper) working on industrial and synthetic clinker tempered in air and water. Regourd observes significant differences in the crack network and in grindability. Differences in the latter property which reach 10% can especially be explained by elastic energy stored in a grain put to thermal shock. Hasselman (37) has calculated this energy which corresponds to the gain in elastic energy which has been revealed by experimenting.

Storage conditions act on clinker structure and therefore on its grindability. Exposure has a negative influence on clinker grindability. Cussino and Pintor (38) have analysed the causes of this phenomenon. First it is observed that the specific surface variations no longer follow the grading spectra variations since the very fine particles caused by exposure show a very high specific surface which superposes that of the cement proper. Moreover during grinding the particles formed by exposure cake around clinker grains and absorb a high fraction of grinding energy. Exposure therefore reduces mill efficiency especially ball mills and causes overestimation of the specific surface still hydratable. So it is not surprising that grinding evaporated clinker in a ball mill leads to lower strengths if the fine particles are not extracted from the mill as grinding proceeds and if the fineness determination is not corrected from the specific surface of these same particles. Clinker deterioration through exposure can be avoided by immediate grinding as soon as it leaves the furnace. Schweindig (39) proposes grinding clinker as it leaves the cooler at 400°C and using the roller mill as an exchange unit capable of lowering the clinker temperature to 100°C whilst generating hot gases. Pospisil (40) has investigated the effectiveness of grinding at different temperatures. Using laboratory equipment he finds that grinding energy increases when clinker temperature rises from 20°C to 200°C. This increase is not surprising in so much as it expresses a decrease in the brittleness of the materials with the increase in temperature. The author also notes that clinker grindability decreases with storage time. This fall is attributed to the relaxation of internal stresses whose potential encouraged grinding; it can also be due to a slow reorganization of microstructures leading to microcrack consolidation. It seems therefore that clinker as it leaves the kiln retains a capacity of development which leads it towards a greater stability as grinding tests show. This stabilization is detrimental to grindability especially if it combines with deterioration through exposure to air.

2.5.- Chemical reactions in the ball mill and mineral releasing of clinker phases

The ball mill must be considered as a chemical reactor where complex phenomena occur liable to modify the behaviour of cements.

Up to now this paper has only mentioned clinker proper. In reality grinding clinker in a ball mill is generally carried out simultaneously with that of gypsum and with a certain proportion of alkaline sulphates within the clinker itself. These components definately tend to be unstable when the temperature of the material increases during grinding following degradation of an extensive part of the mechanical energy of grinding accompanied by heat. This rise in heat must be controlled ; in the case of ball mills it can be limited by energetic ventilation or by injecting water. The strong steam-generating heat helps to absorb the surplus thermal units. The thermal work index of such a process has been drawn up by Reuss (41). Hansen and Clausen (42) have checked its harmlessness on the cement properties.

The regulating role of gypsum rests with grinding conditions. Research has shown that when grinding is carried out in a selective way to produce monodimensional grains, the optimal gypsum proportioning is appreciably higher than during traditional grinding in a ball mill. Poijärvi and Matikkala (43) have ground cements in a ball mill, but so as to obtain a clear grading restricted to 30 microns. They found that the optimum gypsum proportioning lies between 9 and 12%. A similar result is found with cements ground in a vacuum spinner type mill grinding by projection (11). This phenomenon had been attributed to more thorough mineral release obtained by projection grinding and especially the mineral release of C_3A. Regourd, Hornain and Mortureux (44) examined the hydration of these cements, showing that projection grinding made it possible to achieve more complete hydration of the different cement phases. They have also found that the texture of these hydrated cements is different from that usually observed, which seems to confirm that the modification of the gypsum optimum corresponds to extensive modifications in the hydration of cements undergoing selective grinding, whether in a ball mill or put to projection grinding.

The increased importance of gypsum for these cements leads to studying the role of dissolution kinetics which varies with its fineness and degree of hydration. These factors were the subject of interest in a study by Kato and Hirose (45) who prepared 27 samples varying the clinker grading distribution, the gypsum porportioning and its degree of hydration. These tests confirm

the negative effects of an excessive solubility of gypsum and the importance of a high proportioning in gypsum for cements with a various grading spectrum.

Gypsum solubility can be checked by regulating the mill atmosphere (temperature and humidity). The complex role of this atmosphere has been examined especially by Sprung (46) who investigated the reactions liable to occur between the aluminates, the gypsum and the alkalines sulphates and leading in particular to ettringite $3CaO.Al_2O_3$, $3CaSO_4$, $32\ H_2O$, to the semi-hydrate and the syngenite $CaSO_4$, K_2SO4, H_2O. These reactions exert an influence not only on the setting of the cement, but also on its hardening and strengths. They vary with the quantities of alkaline sulphates, gypsum and water present, but also with the quantity of aluminates released by grinding and the degree of activation of these aluminates by grinding. Work in progress in different laboratories should make it possible to define more clearly the role of these different parameters and especially their contribution in the rheology and durability of concretes.

3.- GRINDING EFFICIENCY

Grinding consumes large quantities of energy. It is therefore important to study ways of fulfilling grinding objectives with the minimum consumption of energy.

These objectives may include :

- a given specific surface,
- grading distribution,
- strengths on standardized test-pieces,
- concrete strengths.

This last objective is the most important one for industry.

Figure 6, drawn from (47), gives as an example the relationships observed between grinding energy and concrete strength.

Cleemann and Modeweg-Hansen (47) have observed that the different parameters : surface, grading curve, standardized strengths and concrete strengths show precise correlations between them for a given type of grinding. However these correlations are no longer respected when the grinding system is modified, even if there are only minor modifications such as the running of a separator for example. When the grinding mode is basically changed, the relationships between the preceding parameters undergo even more extensive changes. Research on these modifications which has just entered an active stage will lead to improved knowledge of grinding and important technological development in this field.

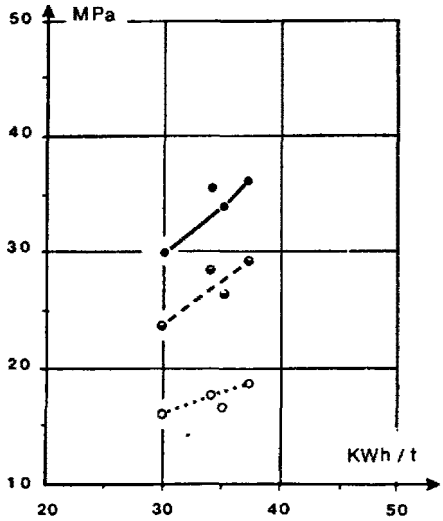

Fig. 6 - Grinding energy plotted against strength measured on concrete, based on results by Cleemann and Modeweg-Hansen

3.1.- Comparison of energy consumed by different modes of grinding clinker

The three modes of grinding mentioned in 1.2 were investigated thoroughly by Rumpf, Schönert and their co-workers. These tests were first carried out grain by grain and then mechanized in the appropriate equipment. The amount of energy consumed is measured for each test.

Haese (6) and Schönert (10) have published these results for clinker.

Figure 7 drawn from (48) sums up results obtained by different authors on quartz.

The tests carried out are :

- slow compression
  - on isolated grains,
  - on a set of grains between a cylinder and a piston,
  - in a roller mill,
- impact compression by a falling mass
  - on isolated grains,
  - in a ball mill,
- projection against an anvil
  - grain by grain,
  - by a plate revolving in vacuum.

For each test measurements were taken of the energy supplied and the surface freed. The surface set up per unit of energy is plotted on the ordinate and the surface on the abscissa.

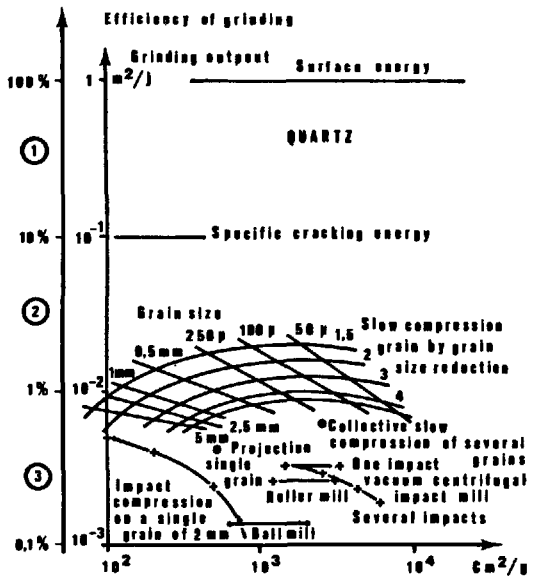

Fig. 7 - Efficiency of different grinding processes expressed in square meters of surface set up per Joule consumed (and in efficiency compared with the theoretical surface energy) plotted against fineness of ground material expressed in square centimeters per gramme using the Blaine method

Since this graph sums up tests carried out in different laboratories, the indications should be taken cautiously. Extrapolating tests carried out on quartz to results obtained on clinker can not be done without taking precautions.

However this graph can be used as a reference to illustrate the general conclusions drawn from the most recent research in the field of grinding.

These conclusions are as follows :

- The efficiency of all the methods in respect to surface energy is low and in any case close or below 1%.
- The efficiency as regards specific cracking energy is around 10%.
- The different modes of grinding and the mechanical equipment implementing these modes fall in a range of efficiency whose extreme values are in an approximate ratio of ten.

The best output is obtained with slow compression grain by grain. The grinding energy here is the compression work of crushing bodies. Unfortunately this process cannot be undertaken industrially : it would lead to minute output. Collective crushing of grains reveals a loss compared with crushing isolated grains but remains one of the best methods from the energy point of view. Moreover it seems possible to mechanize it, which encourages Schönert (10) to consider its application to the cement industry. The roller mill, compared with the preceding process introduces additional losses due to roller friction, but this process proves to be much better than the ball mill. This explains the present development of the latter for clinker grinding (49)(50)(51).

Impact compression by falling mass offers good efficiency for low values of fineness, as shown in the diagram obtained by crushing a 2 mm grain with a falling mass. Here the crushing energy is the kinetic energy behind this mass. If improved fineness is required, the crushing body energy must be increased. It is then found that the efficiency of this grinding mode drops. It moreover joins the efficiency of a ball mill which remains constant for a certain range of fineness. This fall in efficiency can be attenuated if the mass of the crushing body is reduced with naturally lowering the incident energy. This essential adaptation of the size of the crushing bodies to the fineness of the material has been studied by Bombled (52). It is also at the origin of the recent development in small size finishing ball mills (53)(54).

Generally speaking experience has shown that grinding equipment - a ball mill just as a roller mill - reaches maximum efficiency for a well defined grain size. Now, grinding produces a wide spectrum of sizes. It therefore seems advisable to extract the fine particles from the grinder as soon as they have reached the required size to avoid overgrinding and therefore waste of energy. The air separators offer this possibility. In the case of roller mills, the separator is built into the grinder casing ; with the ball mill, it is generally a turbo-separator (55) connected on to the grinder.

The optimal configurations mill-separator, preparatory grinder-mill, mill-finishing mill have been thoroughly studied based on mathematical modelization (56)(57)(58)(59)(60)(61)(62). Beke (63) however states that the development of ball mills now seems to suffer from a limitation due to the principle which results from the impossibility of increasing the concentration of energy to obtain finer grinding at higher outputs.

Projection grinding is not subject to this limitation because the rate of projection of material can be increased to high speeds. Here the grinding energy is the kinetic energy of the material. The graph in figure 7 shows that the efficiency of this grinding mode is high if compared with ball milling. Mechanization of this grinding mode only brings about a slight fall in efficien-

cy if it is carried out according to the process advocated by Planiol (64) who has succeeded in fine grinding by accelerating the material with a wheel turning in vacuum. However this solution raises a certain number of technological difficulties which still have to be faced. It is also possible to accelerate the material by a jet of gas (65) but the transfer of compressive energy of the gas into kinetic energy in the material occurs with a much more mediocre efficiency than in the device advocated by Planiol. The satisfactory output of this grinding mode offers the possibility of planning developing an industrial-scale projection mill which would constitute a third generation of mills after the ball mills and the roller mills.

Having surveyed the output of different grinding processes, it is now possible to check the energy losses which bring down the overall grinding efficiency.

- The first source of losses must be attributed to the propagation of cracks. This mechanism brings about a dissipation of energy by plastic deformation near the surfaces. It was analysed in paragraph 1.

- The second source of losses comes from the surplus elastic energy which must be transmitted to the material for crack propagation. This phenomenon requires a certain amount of energy which is taken from this elastic energy, the surplus is generally lost in the shape of kinetic energy through chipping.

- The third source of losses is a lack of selectivity in the crushing body action. These masses transfer to the material more energy than necessary to obtain the critical elastic energy, that is to say the energy which leads to failure. This lack of selectivity can lead to the material clustering or caking.

Grinding by slow compression is very selective especially if it is carried out grain by grain and at low rates of reduction.

Grinding by projection in a vacuum centrifugal mill is also selective ; since the speed is constant, the kinetic energy varies with the mass of particles. In this way a large grain is worked on more than a fine grain.

Ball milling on the other hand is not selective, the ball falls with the same energy on a large or small grain. This explains the modest output of ball mills which can however be improved by a separator eliminating the fine grains. This elimination makes the lack of selectivity of this equipment less important.

The three sources of losses are traced on the graph figure 7 where the areas in which they exert influence are numbered 1, 2 and 3.

To evaluate the total energy consumption of a mill, those losses due to the machine must be added to the preceding causes. They are analyzed by Sillem (66).

3.2.- Optimization of clinker hydraulic activity by different grinding modes

The preceding comparisons were carried out based on the specific surface. In paragraph 2 the importance of the grading curve was underlined for forecasting the behaviour of clinkers and especially the 3-30 micron class. A precise comparison of the advantages of different grinding modes must consequently be found not only on their capacity to set up surfaces, but also on their aptitude to produce grains in the 3-30 micron range. This approach was adopted by Schönert (10) and has made it possible to emphasize the advantage of slow and collective compression used with declustering equipment and a separator to produce a cement in compliance with the preceding grading criteria.

The selectivity of the projection mill makes it possible to produce cements with various grading spectra. As formally stated, there is a greater probability of the larger grains being crushed than the smaller ones. The comminution modes of these mills therefore makes it possible to obtain narrow spectra (11) which satisfy criteria of not containing grains over 30 microns, that is to say grains which only hydrate partially, at the same time showing no excess of fine grains where hydration would occur too early to really contribute to strengths. These fine grains which have the highest specific surface require high crushing energy out of proportion with their contribution to the quantity of the crushed material. This aspect of crushing effectiveness has been developed in mathematical form by Reuss ([67][68]) with an aim to obtaining maximum clinker hydraulic activity with minimum energy consumption.

Cleemann and Modeweg-Hansen (47) have carried out experimental study on a ball mill working with a separator with an aim to relating the strengths measured on standardized test-pieces to the grinding energy. This research has proved that the most effective crushing equipment from the point of view of mortar strengths is the mill producing 3-30 micron grains with maximum selectivity.

3.3.- Optimization of cement properties by selective crushing of its ingredients

Secondary constituents are of increasing importance in present day cements. They are

generally incorporated in the cement during crushing in a ball mill. This process offers great advantages through its simplicity because the mill also serves as a homogeniser. On the other hand, this process is not very satisfactory from the physico-chemical point of view since there is no possibility of controling the grain sizes of the various cement ingredients. This control is only carried out on the finished product for which the total grading curve can be imposed as well as the specific surface, but it is impossible to control the curves of each of the different ingredients which vary in the grading ranges according to their specific grindability.

In this way, by grinding a blend of clinker and slag (which is less grindable than clinker) (69) a range of grading will be obtained containing large proportions of slag in the coarse sizes and a large quantity of clinker in the finest sizes. Since clinker is intrinsically more active than slag, it is the latter which should be ground finer to develop its hydraulic potential properly. Simultaneous grinding of ingredients leads to the opposite result and consequently to a waste of the hydraulic potential of the materials. To avoid such waste research scientists have explored the possibility of separated or selective grinding, each ingredient being ground according to its reactivity, that is to say the higher the reactivity, the coarser the grinding. As far back as 1965 Bombled (70) carried out separate grindings of slag and clinker, finding improved tensile strengths. Recent X-ray diffraction research attributes this increase to the presence of a high proportion of ettringite.

Iwabuchi and Okaue (71) have studied the parameters which influence the behaviour of cements with slag ground simultaneously or apart, with an aim to determining the influence of the grinding mode on the optimal gypsum content.

When clinker and a very soft pozzolana are ground simultaneously, the latter becomes much finer than the clinker but in this case this fineness is preferable because a pozzolana is improved when activated by thorough grinding, so simultaneous grinding contributes to an optimization of the cement characteristics. However this is a specific case where selectivity is obtained naturally by a fortunate coincidence between the activity of the materials and grindability.

As for fillers, their role can be essential as secondary constituents of a very narrow grading spectrum clinker. Research has shown that such cements (whose grains are monodimensional, therefore impeding an optimal grading filling) hydrate, leaving a porosity of the order of a micrometer (24) This porosity can be filled in by adding a fine filler which thus becomes a granular complement of a narrow spectrum. This combination of a narrow spectrum for the active matter and of a complement of fine and inert material could be an optimal solution for making up a cement which, together with good strengths, offers the possibility of noticeable saving in clinker and therefore in energy. It is hardly likely that simultaneous grinding leads to the required result. Selective grinding of the different ingredients is necessary along with reformulating the cement by blending the ground materials.

3.4.- Optimization of concrete quality in accordance with the cement

The behaviour of cements is usually tested on standardized test-pieces which are mixed with a constant quantity of water, in weight half that of the cement quantity. The concrete test-pieces are made with constant workability, that is to say that the quantity of water to add to the concrete to obtain a given consistency is determined. The influence of water on concrete strengths is capital. Excess water quickly brings down concrete strengths, so cements must give concretes the required rheological properties with as low water contents as possible. Cements which comply best with this objective (74) are those which show a continuous grading curve to ensure optimal filling. If this is so, instead of accumulating in the microcavities, the water moves between the grains and promotes their relative displacement. Good rheological properties are thus obtained with a minimal water content. From this point of view the ideal grading curve is undoubtedly close to a curve discribed by

$$D(x) = \sqrt{\frac{x}{\phi}}$$

where x is the grain diameter, D(x) the undersize at this diameter and ϕ the maximum diameter. The ball mill working in open circuit tends to produce curves of this type. This is not surprising because the ball falling on the material compacts it and contributes to grinding, whilst there are voids in the layer of material. Through its internal working such a mill tends to produce a curve without voids, therefore an optimal curve for rheological behaviour.

Paragraph 2 pointed out that the optimum curve for hydration is on the contrary a narrow grading spectrum curve. So there is opposition between the two imperative requirements : maximum hydraulic activity and optimum rheological properties. This opposition has been noticed by numerous research scientists either on narrow grading spectrum cements made up from separate classes (21), or on narrow spectrum cements obtained in ball mill separators (47), or in roller mills (50) or gas-jet mills (75).

The rheological differences noted usually imply a requirement for a greater quantity of water. This excess water however exerts only limited influence on strengths because of the additional activation of the clinker. The result is generally positive (50); it could undoubtedly be still further improved by better knowledge of the physical parameters which influence the rheology, that is to say apart from the grading distribution, the grain shape, their surface activity, the composition of pore liquid and especially the dissolution of gypsum in this liquid.

It also appears timely to investigate the role of appropriate fillers which could exert a positive influence on rheology as is the case with fly ash. There is reason to hope that fillers which contribute to the compactness of hardened pastes (3.3.) have a favourable influence on rheological properties. This is a field where research has available an extensive field of investigation and where the work to be undertaken will make it possible at one and the same time to reach a better understanding of cements and achieve savings in the manufacture of these products by discerning replacement of certain clinker gradings by less energy-intensive materials.

REFERENCES

1.- A.A. GRIFFITH (1920) - The phenomena of Rupture and Flow in Solids, Phil. Trans. Roy. Soc. (Londres), 221, 16-98.

2.- C. HUET (1973)(1974) - Méthode de détermination de l'énergie spécifique de rupture et application aux céramiques et à divers matériaux - Cahiers du Groupe Français de Rhéologie - I : Bases théoriques, t 3, n° 3 - II : Conséquences pratiques et expérimentation, t 3, n° 4.

3.- Ph. WEBER - Influence de la fissuration des minerais sur leur aptitude de broyage - Rapport D.G.R.S.T. n° 72.7. 0727.

4.- H. RUMPF, K. SCHÖNERT (1971) - Die Brucherscheinungen in Kugeln bei elastischen sowie plastischen Verformungen durch Druckbeanspruchung - 3. Europ. Symp. Zerkleinern, Cannes.

5.- H. RUMPF (1973) - Physikalische Aspekte des Zerkleinern, Ähnlichkeitsgesetz der Bruchmechanik und die Energieausnutzung der Einzelkornzerkleinerung - Aufbereitungs-Technik n° 2, 59-71.

6.- U. HAESE (1978)(1979) - Zerkleinerungstechnische Stoffeigenschaften von Zementrohmaterial und Klinker (Übersicht) - Zement-Kalk-Gips n° 9, 439-446, n° 1, 10-13.

7.- K. SCHÖNERT, H. UMHAUER, W. KLEMM (1969) The influence of temperature and environment on the slow crack propagation in glass - Proc. 2nd Intern. Conf. on Fracture, Brighton, Chapman & Hall.

8.- N.H. MACMILLAN, N. GANE (1970) J. Appl. Phys. 41, 672.

9.- R. WEICHERT, K. SCHÖNERT (1978) J. Mech. Phys. Solids, 26, 151.

10.- K. SCHÖNERT (1979) - Energetische Aspekte des Zerkleiners spröder Stoffe. Zement-Kalk-Gips n° 1, 1-9.

11.- J.P. MERIC (1975) - Perspectives technologiques d'économie d'énergie dans la fabrication du ciment - Rev. Mat. Const. n° 693, 66-72.

12.- L.A. SIMPSON (1973) - Effect of Microstructure on Measurements of Fracture Energy of Al_2O_3 - J. Amer. Ceram. Soc. 56, n° 1, 7-11.

13.- C. SCIORA (1976) - Etude des effets du broyage sur le comportement de quelques hydrates - Thèse Université Dijon.

14.- Y. TEKIZ (1965) - Influence du broyage sur quelques structures cristallines - Thèse Fac. Sciences Université Paris.

15.- C. LEGRAND, J. NICOLAS (1960) - Broyage et structure cristalline - Actes du 7ème Congrès Intern. Céramique, Londres Ed. The British Ceramic Soc., 261-274.

16.- L. OPOCZKY (1974) - Mechanochemical phenomena on the surface of clinker minerals - VI Intern. Cong. Chem. Cement, Moscou, suppl. paper, II.

17.- J.P. MERIC (1972) - Mesure en continu de la granularité par diffraction d'un faisceau laser - Bull. Soc. Fr. Céram. n° 95, 67-76.

18.- J. SLEGTEN (1973) - Über die massenbezogene Oberfläche und ihr Zusammenhang mit der Festigkeitsentwicklung und dem Arbeitsbedarf bei Zement - Zement-Kalk-Gips, n° 7, 320-325.

19.- H. zur STRASSEN (1959) - Zur Frage der nicht-selektiven Hydratation der Zement minerale - Zement Beton, 16, 32-34.

20.- B. BEKE (1960) - Mahlverfahren, Kornaufbau und Festigkeitsverlauf verschiedener Zemente - Zement-Kalk-Gips, n° 9 419-424.

21.- H. RITZMANN (1968) - Über Beziehungen zwischen der Kornverteilung und der Festigkeit von Portlandzement - Zement-Kalk-Gips, n° 9, 390-396.

22.- F.W. LOCHER, S. SPRUNG, P. KORF (1973) Der Einfluss der Korngrössenverteilung auf die Festigkeit von Portlandzement- Zement-Kalk-Gips, n° 8, 349-355.

23.- Ya.M. SYRKIN, I.A. SIBIRYAKOVA, L.P. SHATOKHINA (1974) - The significance of grain size distribution in cement strength formation - VI Intern. Cong. Chem. Cement, Moscou, suppl. paper, III.

24.- J.M. BUTT, W.M. KOLBASOW, L.E. BERLIN (1977) - Einfluss der Zementfeinheit auf die Struktur des Zementsteins - Silikattechnik 28, 104-107.

25.- M. PAPADAKIS (1960) - Contribution à l'étude des broyeurs à boulets industriels - Rev. Mat. Const. n° 542, 295-308.

26.- B. BEKE (1976) - Fine grinding and agglomeration - Cement Technology, sept/oct 165-168 ; nov/dec 199-204.

27.- T. IWABUCHI (1968) - A concept of the Cause of Agglomeration and Mechanism of Grinding Aid Action in Cement Grinding - CAJ Review of the 22nd General Meeting (Techn. session) Tokyo, mai, 95-99.

28.- H.M. von SEEBACH (1969) - Die Wirkung von Dämpfen organischer Flüssigkeiten bei der Zerkleinerung von Zementklinker in Kugelmühlen - Dissertation an der TH Clausthal.

29.- K. GRAICHEN, H. MÜLLER, H. SCHUBERT (1974) - Zur Wirkungsweise von Tensiden als Mahlhilfsmittel - Silikattechnik 25, 169-172.

30.- W. SCHEIBE, H. DOMBROWE, R. HERRMANN (1975) - Die Beeinflussung der Haftkräfte in Mahlprodukten durch Mahlhilfsmittel - Silikattechnik 26, 243-245.

31.- A. RACCANELLI, G. SCARINCI, L. MARCHESINI, D. ROSIGNOLI, S. GUELLA (1972) Effects of grinding aid on the hydration of pozzuolanic cements - Il Cemento 1, 3-18.

32.- H.H. STEINOUR (1952) - Proc. of III Intern. Cong. of Concrete Chem., Londres.

33.- R.R. KEIENBURG (1977) - Kornverteilung und Normfestigkeit von Portlandzement - DÜsseldorf : Beton-Verlag (Schriftenreihe der Zementindustrie H.42).

34.- B. BEKE, L. OPOCZKY (1969) - Feinstmahlung von Zementklinker - Zement-Kalk-Gips n° 12, 541-546.

35.- G.R. GOUDA (1979) - Effect of clinker composition on grindability - Cement and Concrete Research, 9, 209-218.

36.- M. DECKERS (1972) - Über die Mahlbarkeit von Zementklinker - Zement-Kalk-Gips, 25, 445.

37.- D.F.H. HASSELMAN (1963) Elastic energy at fracture and surface energy as design criteria for thermal shock - J. Amer. Ceram. Soc. n° 11, 535-540.

38.- L. CUSSINO, G. PINTOR (1978) - Mahlschwierigkeiten von abgelagertem Klinker - Zement-Kalk-Gips, n° 7, 332-334.

39.- G. SCHWEINDIG (1978) - German tests prove roller mill advantages - Rock Products, august, 60-62.

40.- Z. POSPISIL (1979) - Der Einfluss der Temperatur des Klinkers auf seine Mahlbarkeit - Zement-Kalk-Gips, n° 1, 20-23.

41.- A.K. REUSS (1974) - Die thermische Belastungsgrenze bei der Zementvermahlung - Zement-Kalk-Gips, n° 7, 321-329.

42.- F.E. HANSEN, H.J. CLAUSEN (1974) - Zementfestigkeit und Kühlung durch verdüstes Wasser beim Mahlen - Zement-Kalk-Gips, n° 7, 333-336.

43.- H. POIJÄRVI, J.MATIKKALA (1977) - Über Festigkeitsuntersuchungen an scharf Klassierten Zementen - Zement-Kalk-Gips, n° 11, 586-591.

44.- M. REGOURD, H. HORNAIN, B. MORTUREUX (1978) - Influence de la granularité des ciments sur leur cinétique d'hydratation - Ciments Bétons Plâtres Chaux, n° 3, 137-143.

45.- A. KATO, K. HIROSE (1969) - Factors in Cement Grinding Process Affecting Strength of Cement - CAJ Review of the 23rd General Meeting (Techn. session) Tokyo, mai, 109-112.

46.- S. SPRUNG (1974) - Einfluss der Mühlenatmosphäre auf das Erstarren und die Festigkeit von Zement - Zement-Kalk-Gips, n° 5, 259-267.

47.- J. CLEEMANN, C. MODEWEG-HANSEN (1974) Der Einfluss des Sichters auf den Arbeitsbedarf und die Kornverteilung bei der Kreislaufmahlung - Zement-Kalk-Gips, n° 7, 337-343.

48.- J.P. MERIC (1978) - Le broyage - Annales des Mines, nov.

49.- E.J. KLOVERS (1979) - Energieeinsparungen bei Rollenmühlen - Zement-Kalk-Gips, n° 1, 24-29.

50.- P. TIGGESBÄUMKER, O. KNOBLOCH (1979) - Zementmahlung mit der Rollenmühle - Entwicklung und Aussichten - Zement-Kalk-Gips, n° 4, 166-170.

51.- E.G. LOESCHE, H.G. KLATT (1979) - Zielsetzung beim Zementmahlen mit Wälzmühlen und erste Versuchsergebnisse Zement-Kalk-Gips,n° 4, 171-173.

52.- J.P. BOMBLED (1968) - Recherches des dimensions optimales et de l'échelonnement des corpsbroyants dans les broyeurs à boulets - Rev. Mat. Const. n° 631, 143-153 ; n° 632, 198-205.

53.- B. BEKE (1973) - Grinding body size and the hardening of cement - Cement Technology, march/april, 47-56.

54.- O. FEDDERSEN (1979) - Problèmes et besoins de l'industrie du ciment et du béton - Engineering Foundation Conferences (Cement production and use) Franklin Pierce College, Rindge, New Hampshire, june 24-29.

55.- R. GUYOT (1971) - Contrôle des turbo séparateurs utilisés en cimenterie - Rev. Industrie Minérale, mars, 207-218.

56.- L.G. AUSTIN, P.T. LUCKIE, D. WIGHTMAN (1975) - Steady-state simulation of a cement milling circuit - Intern. J. Mineral Processing, 2, 127-150.

57.- L.G. AUSTIN, P.T. LUCKIE, B.G. ATEYA (1971) - Residence time distributions in mills - Cement Concrete Research, 1, 241-256.

58.- A.M. DMITRIEV, Ju.S. MALININE, Ju.I. DESHKO, T.G. MESHIK, N.S. PANINA Ju.F. KUZNECOVA, L.N. GRIKEVICH (1978) *Description mathématique et algorithmes de calcul des broyeurs de l'industrie cimentière* - Ministère de l'Industrie des Matériaux de Construction de l'URSS, NII Cement.

59.- J. KOLOSTORI (1979) - Einfluss der Mahlguteigenschaften auf die Bestimmung der Mahlkörperzusammensetzung von Kreislauf-Kugelmühlen - Silikattechnik, 30, 88-90.

60.- L.G. AUSTIN, P.T. LUCKIE, H.M. von SEEBACH (1975) - Optimization of a Cement Milling Circuit With Respect to Particles Size - Distribution and Strength Development, by Simulation Models - Symposium de la Fragmentation de Nüremberg.

61.- Clinker pre-crushing (1972) - Cement Technology, july/august, 131-133.

62.- J.P. BOMBLED (1973) - L'usure des corps broyants dans les broyeurs à boulets - Rev. Mat. Const. n° 677, 4-16.

63.- B. BEKE (1977) - L'avenir des broyeurs à boulets et à galets - Rev. Mat. Const. n° 706, 163-167.

64.- R. PLANIOL (1962) - Les broyeurs centrifuges et le vide - Rev. Mat. Const. n° 557, 42-49.

65.- H. GÜHNE, S. de SILVA (1978) - Probleme der Feinmahlung von Hartmineralien und ihre Lösung - Aufbereitungs-Technik, n° 10, 472-480.

66.- H. SILLEM (1977) - Zerkleinerungstechnik - Zement-Kalk-Gips, n° 11, 549-557.

67.- A. REUSS (1970) - Efficacité du broyage de ciment (1ère partie) - Cement Wapno Gips, n° 3, 81-88 ; n° 4, 103-110.

68.- A. REUSS (1970) - Efficacité du broyage du ciment (2ème partie) Cement Wapno Gips, n° 5, 156-163.

69.- H.G. ELLERBROCK (1977) - Mahlbarkeit von Klinker und Hüttensand - Zement-Kalk-Gips, n° 11, 572-575.

70.- J.P. BOMBLED (1965) - Etude du broyage de mélanges clinker-laitier - Rev. Mat. Const. n° 593, 61-75.

71.- T. IWABUCHI, H. OKAUE (1971) - Effects of Particle Size Distribution on the Technical Properties of Portland Blastfurnace Slag Cement - CAJ Review of the 25th General Meeting (Techn. session) Tokyo, juin, 59-63.

72.- W. SCHWENK (1973) - Oberflächenveränderungen von Feststoffen nach Zerkleinerung im Hochvakuum durch die Wirkung feuchter Luft - Dissertation Universität Karlsruhe (TH).

73.- A. GUINIER (Note de J.H. THOMASSIN, M. REGOURD, P. BAILLIF, J.C. TOURAY) (1979) - Etude de l'hydratation initiale du silicate tricalcique par spectrométrie de photoélectrons - C.R. Acad. Sciences Paris.

74.- J.P. BOMBLED (1978) - Rhéologie du béton frais - Ciments Bétons Plâtres Chaux, n° 1, 27-29.

75.- Ju. I. DESHKO, V.I. AKUNOV, V.L. PANKRATOV, N.I. FERENS, V.M. KOLOSOVSKAJA (1973) - Le broyage à jet améliore la qualité du ciment - Cement, n° 5, 16-17.

THEME II

Hydration of pure Portland Cements

SUB-THEME II - 1

Mechanisms of Portland Cement hydration

J. SKALNY
Martin Marietta Laboratories
Baltimore USA

J.F. YOUNG
University of Illinois
Urbana USA

1. INTRODUCTION

This paper presents a review of the literature on the mechanisms of hydration of individual portland cement clinker minerals and portland cements at normal temperatures (i.e., hydration above 60°C is not discussed). The paper is not intended to be comprehensive; rather, it will discuss selected works on the mechanistic aspects of hydration reactions, especially those published after the 1974 Congress in Moscow. Papers discussing hydration in terms of mechanical properties are generally not included, and the structure, morphology, and influence of the various hydration products and their modifications on the engineering properties of cement pastes, mortars, and concretes will be reviewed by other authors. Therefore, these subjects will be addressed only when they bear on mechanistic interpretations.

Our review will consider the mechanisms of hydration with respect to the crystal form of the minerals; the presence of impurities (e.g., solid solutions), minor components (e.g., alkali sulfates), and chemical admixtures (e.g., accelerators, water reducers); and special treatments (e.g., carbonation). The scope of the interpretations given will depend on the importance of the particular mechanism to overall cement performance and on the availability in the literature of appropriate experimental and theoretical data.

2. HYDRATION OF CLINKER MINERALS

2.1 Tricalcium Silicate

We shall pay special attention to the hydration of tricalcium silicate, C_3S, because it is the most important component of portland cements, responsible for most of the engineering properties of hardened cement paste (e.g., strength, dimensional stability). C_3S hydration is also often used as a model for explaining the hydration of cement — an approach that is acceptable after the first few hours of hydration, when the most important reactions of the aluminate and sulfate phases have occurred. Scientific literature published on the subject of tricalcium silicate hydration after 1974 is reviewed yearly in Cements Research Progress. In addition, several review papers discussing the controversial views on the mechanism of C_3S-water interaction have been published (1-3).

2.1.1 Hydration Mechanism

There is a vast amount of literature discussing the basic mechanism of C_3S hydration. This is due to 1) the recognition of C_3S as the main component of portland cements, and 2) the extremely complex and still unresolved details of its reaction mechanism with water. As is the case with other cementitious compounds, hydration of C_3S involves a sequence of overlapping reactions, some slow and others fast. All of these contribute to the technical importance of portland cement concrete: workability at early stages, strength development, and volume stability and durability at mature ages.

C_3S reacts immediately upon contact with water in a short exothermic reaction (pre-induction period), followed by a so-called induction or dormant period of relative inactivity. During the induction period, an exchange of ionic species between the solution and solid anhydrous C_3S occurs, leading to reaction conditions that cause an autocatalytic increase in reaction rate — referred to as the acceleration period. During this reaction stage, large amounts of hydration products with lower density and larger volume than the anhydrous phases deposit into the available (water-filled) space, causing an overall decrease in system porosity, decreased transport of ionic species on the solid-liquid interface, and overall deceleration of hydration. This stage is referred to in the literature as the diffusion-controlled stage of hydration.

Numerous attempts have been made to explain the complex C_3S hydration processes. Calorimetry, analysis of the liquid phase composition, surface area measurements, and electron microscopy have been the most commonly used experimental approaches. In recent years, these have been supplemented by thermoluminescence, spectroscopy (e.g., Raman, ESCA/Auger), electron microscopy (STEM, AEM, high-voltage EM), silicate polymerization analysis, and other techniques. Based on data obtained with these high-precision methods, new mechanisms are being proposed.

The Pre-Induction and Induction Periods

Protective Hydrate Theories. de Jong et al. (4) have proposed the formation of a protective hydrate layer, which inhibits further hydration of C_3S and thus starts the induction period. The "first hydrate", C_3SH_n, which is not readily detectable by direct observation, is converted into a "second hydrate" with a lower C/S ratio (~0.8-1.5) and a thin-film morphology. Since this hydrate is more permeable to diffusion of ionic species to and from the C_3S surface, its formation signals the end of the induction period. Later, during the post-induction acceleration period, it transforms to a fibrous "third hydrate" (C/S = 1.5-2.0).

This proposed sequence embodies many of the ideas of Brunauer and Kantro (5), and a somewhat similar mechanism has been adopted by others (6-9). Barret et al. (10) concluded from a study of concentrations of ions in solution that congruent dissolution occurs initially; but, because the first C-S-H precipitate has C/S < 3, the C/S ratio in solution tends to increase indefinitely. However, in our opinion, congruent dissolution in C_3S pastes is at best a transient state, and a truly congruent solution cannot be said to occur with certainty in the bulk solution. Andreeva

and Keshelava (11) report data indicating the transient nature of congruent dissolution at high solids contents of suspensions.

Shpynova et al. (7) also postulate initial congruent dissolution with subsequent precipitation of C_3SH_n, which is based on a calcium hydroxide structure containing SiO_4 tetrahedra. This material is unstable, and the silica condenses first to Si_2O_7 units and then to infinite silicate chains (as in wollastonite or xonotlite) with the simultaneous release of CaO as $Ca(OH)_2$. Magnan et al. (9) agree that silicate polymerization occurs concomitantly with liberation of lime from the primary C-S-H (first hydrate). Condensation of isolated silicate tetrahedra forms a gel structure which, by pozzolanic effect, reacts with lime in solution to form the final silicate hydrates. Both Rebinder et al. (8) and Andreeva and Keshelava (11) consider the ionic concentrations to be important in crystallizing new C-S-H phases and subsequent structure formation.

Magnan et al. (9) could not detect the formation of a primary hydrate directly, but Fujii and Kondo (12) were able to locate hydration products on the C_3S surface after 20 minutes of hydration. Menetrier et al. (13) also observed the development of hydration products in the first 20 minutes of C_3S hydration; after the initial formation of minute, round or rod-like particles, Type II C-S-H developed on the surface (Fig. 1).

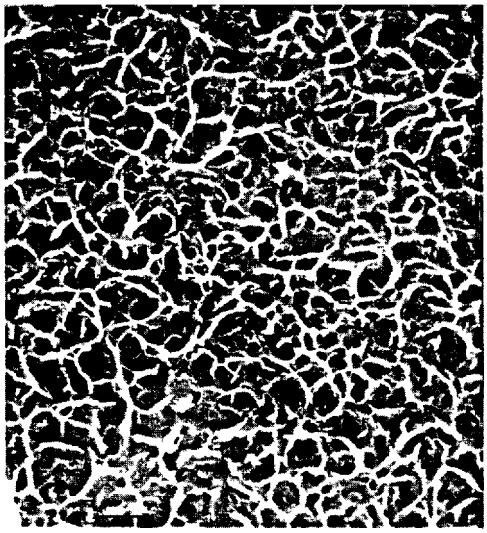

Fig. 1 C_3S hydration products after 1 hour at 25°C (ref. 13).

Lattice Defect Theories. Maycock and co-workers (14) explored the influence of lattice defects on the initial reactions of C_3S with water. They concluded that the number of lattice defects (the degree of crystal disorder), introduced by mechanical grinding or heating and quenching, was directly related to the length of the induction stage of hydration. Using a fast-response calorimeter, they were able to separate the first heat evolution peak into two (believed to correspond to physical adsorption of water and formation of a hydrate) and to show that the induction period shortens with increased concentration of lattice defects. They postulated that this effect was controlled by solid state diffusion within the anhydrous grain rather than by diffusion of species through a "first hydrate" that (and this was considered important) was formed after the introduction of the defects and thus could not be the reason for initiation of the induction period.

In related studies, but with different experimental approaches and interpretations, Fierens and Verhaegen (15-19) attempted to correlate lattice defects, introduced by u.v. excitation, to the early reactivity of C_3S. Using calorimetry and thermoluminescence as the main experimental tools, they found that irradiated C_3S gave two thermoluminescence peaks; however, for C_3S hydrated with water vapor or liquid, one peak diminished with hydration time while the other remained unchanged. The time for complete disappearance of the first thermoluminescence peak was about the same as the induction period determined by calorimetry. The higher the probability of the escape of electrons trapped in the defect structure, as measured by thermoluminescence, the shorter was the induction period. They therefore concluded that the main reaction during the induction period involved participation of the trapped electrons. Using ESR, they showed that the active sites on the surface, originating from lattice defects, were highly nucleophilic and provided preferential sites for chemisorption of water molecules during hydration of C_3S. Menetrier et al. (13), using high-resolution SEM, observed non-uniform attack of the C_3S surface exposed to water. According to Fierens and Verhaegen, the absence of any intensity change in the second peak indicates that the process does not involve the whole C_3S surface.

Fierens and Verhaegen have proposed the following mechanism for C_3S hydration: 1) rapid chemisorption of water on C_3S particles, 2) simultaneous formation of hydrated nuclei on the active sites and dissolution of a small quantity of C_3S, and 3) exothermal growth of C-S-H. The induction period ends when C-S-H nuclei reach their critical size and start growing according to the laws of nucleation kinetics, i.e., as the result of a potential barrier corresponding to the critical size of the C-S-H nuclei on the C_3S surface and not because of a protective layer which would prevent further contact with water. Exposing C_3S to water vapor prior to paste hydration decreases the induction period, apparently because the water vapor produces nuclei, or at least potential nuclei, on the active sites, which can be used in the final step of exothermal growth of C-S-H. The induction period, i.e., the time required for appearance of a sufficient number of stable nuclei, is thus ap-

preciably reduced. Fujii and Kondo (12) also believe that the induction period is terminated by propagative surface nucleation growth of C-S-H initiated by high Ca^{2+} concentration.

According to Stein (3), the above mechanism — although incorrectly interpreted from experimental data — is not necessarily incompatible with the hypothesis of de Jong et al. For instance, if one kind of lattice imperfection is due to an ion that is significantly displaced during the inward diffusion of water into C_3S to form the first hydrate, whereas a different kind of lattice defect is due to an ion unaltered by the first hydrate formation, then the Fierens-Verhaegen and de Jong et al. mechanisms are complementary. A possible model, according to Stein, involves displaced calcium ions on the one hand and imperfections related to silicate ions on the other.

Calcium Hydroxide Nucleation Theories. The arguments of Fierens and Verhaegen and Maycock et al. favor a "delayed nucleation" rather than "protective layer" explanation for the early hydration mechanism. Additional arguments in favor of this view were given recently by Young (20), Young et al. (21), Tadros et al. (22), Dent Glasser et al. (23) and others, but these concentrate more on the question of the nucleation of calcium hydroxide than of C-S-H.

Young et al. (21) have studied the composition of the liquid phase of hydrating C_3S pastes. The ionic product for calcium and hydroxyl ions, $[Ca^{+2}][OH^-]^2$, was calculated as a function of time and correlated with CH crystal growth data and calorimetric measurements of C_3S hydration. The results confirmed that the maximum Ca^{2+} concentration corresponds to the end of the induction period and coincides with the onset of initial nucleation of CH. The onset of maximum crystal growth correlated closely with the period of maximum reactivity (heat evolution). The increase of ionic products after CH nucleation began was attributed to the dominant role of the $[OH^-]^2$ factor, which did not decrease during the subsequent growth of CH. This continued increase in $[OH^-]$ may have resulted from the polymerization of silicate species, which were formed during renewed activity of C_3S at the end of the induction period. According to Young et al., the following scheme for C_3S hydration seems plausible:

Initial hydrolysis:

$$C_3S \xrightarrow{H} \text{"}C_2S\text{"} + Ca^{2+} + OH^- \qquad (1a)$$

(where "C_2S" can be considered a lime-deficient C_3S structure after undergoing initial hydrolysis)

$$\text{"}C_2S\text{"} \xrightarrow{H} 2Ca^{2+} + H_2SiO_4^{2-} + 2OH^- \qquad (1b)$$

$$2H_2SiO_4^{2-} + 2OH^- \rightarrow Si_2O_7^{6-} + 3H_2O. \qquad (1c)$$

At the end of the induction period:

$$Ca^{2+} + 2OH^- \rightarrow CH \qquad (2a)$$

$$2SiO_4^{4-} \xrightarrow{H} Si_2O_7^{6-} + 2OH^- \rightarrow [SiO_3]_n^{2-} + 2nOH^-. \qquad (2b)$$

Young et al. did not have any evidence for C/S = 2 in reaction (1b). It is also unknown if $Si_2O_7^{6-}$ would be unprotonated in reactions (1a) and (2b), but this does not affect their argument. "C_2S" was deduced solely from relative concentrations in solution rather than from experimental evidence, but it could be the "first hydrate" of Stein (3). The end of the induction period may be inferred from both the crystallization of CH and the formation of acicular C-S-H (second hydration product) from "C_2S." A major reaction occurring during the growth of the second hydration product may be the polymerization of monosilicate ions (in C_3S) to disilicate and higher polymers (in C-S-H). As pointed out by Magnan et al. (9), this gel structure of polymers can react with lime solution to form the final hydration products.

Changes in the Ca^{2+} ion concentration with lime have also been studied by Fierens and Verhaegen (24) and Slegers and Rouxhet (25). Fierens and Verhaegen observed that initial release of Ca^{2+} was independent of the reactivity of C_3S as measured by thermoluminescence, but that the $[Ca^{2+}]$ increase depended on the specimen treatment used (Fig. 2). In contrast to Young et al. (21), they found the $[Ca^{2+}]$ peak not to coincide with the end of the induction period. Slegers and Rouxhet (25) have confirmed that the Ca^{2+} ion concentration peak is a real supersaturation peak. However, crystalline CH was detected long before the appearance of this peak. This is surprising but could be due to the crystallization of CH near the grain surfaces. Crystallization of CH at or near grain surfaces of hydrating C_3S, where a high concentration of Ca^{2+} ions would be expected, has also been noted by others (7,26,27).

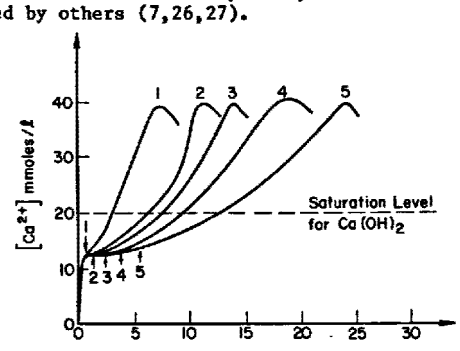

Fig. 2 Variation of Ca^{2+} concentration with time for five different samples of C_3S. Arrows indicate the end of the induction period, determined by conduction calorimetry (ref. 24).

New data by Tadros et al. (22) point to a similar C_3S hydration mechanism. At the beginning of hydration, the Ca/Si ratio in the liquid phase was found to be much higher than 3, and zeta-potential measurements showed the presence of a positive charge on the surface of the C_3S particles. Additionally, CH crystal growth studies showed that that the presence of silicate ions retarded the nucleation and growth of CH crystals and, thus, led to supersaturated CH solutions. Based on these observations, Tadros et al. suggested the following mechanism for early hydration of C_3S. Upon contact with water, C_3S undergoes a rapid hydrolysis, releasing Ca^{2+} and SiO_4^{4-} into solution. The ratio of C/S is much greater than 3, implying that the surface of the original C_3S becomes deficient in calcium. As indicated by zeta-potential data, calcium ions chemisorb on the Si-rich surface, giving it a positive charge:

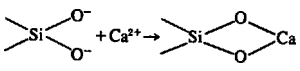

Using ESCA for analysis of surface layers, Thomassin et al. (28) and Menetrier et al. (13) found evidence to support this view. Initially, the C/S ratio at the surface falls rapidly to about 2.5, but quickly rises again to about 2.75 after 1 minute (see Fig. 3). Thereafter, a slow, but continual decrease in C/S ratio with lime is observed over several hours. The high Ca^{2+} concentration in the interfacial region, perhaps aided by the underlying Si-rich layer, reduces further the dissolution of C_3S, thus initiating the induction period (22). The Ca^{2+} and OH^- ions continue to dissolve at lower rates and, since the growth of CH crystals is inhibited by silicate ions, the liquid phases become supersaturated with respect to CH. When the supersaturation reaches a certain limit (1.5-2.0 times the saturation value), CH nuclei are formed and rapid precipitation of CH begins. This marks the end of the induction period. The precipitating ions act as a sink for ions in solution, which, in turn, enhances the further dissolution and reaction of C_3S. The CH crystals incorporate silicate ions and therefore may also act as nuclei for C-S-H. The dissolution of C_3S marks the the beginning of the acceleration period.

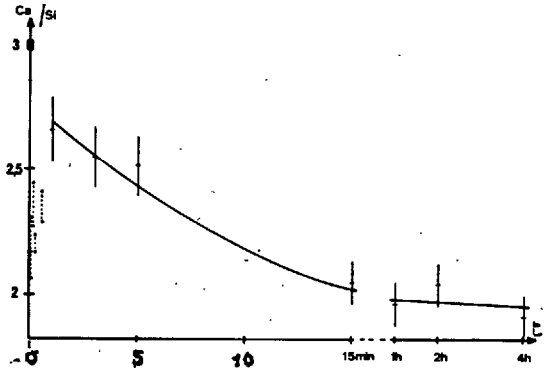

Fig. 3 Changes in C/S of surface of hydrating C_3S as a function of time (ref. 28).

Stein (3) disagrees with the above interpretations; he believes that these observations — a molar C/S >>3 after 1 minute of hydration, a positive zeta-potential indicating an outer layer of chemisorbed Ca^{2+}, and initiation of CH crystallization simultaneous with the end of the induction period — can be more satisfactorily accounted for by using the hypothesis of de Jong et al. (4). He considers the end of the induction period to be the cause rather than the effect of CH crystallization, and feels that the Tadros et al. mechanism cannot explain the experimentally found accelerating effect of amorphous silica on the hydration of C_3S.

Other Theories. The question of the induction period of C_3S hydration is discussed also by Odler and Dorr (29). According to these authors, upon C_3S contact with water, the Ca^{2+} ions are leached out from the surface to form CH in solution. Water molecules are simultaneously taken up by the surface to form a C-S-H of low C/S and high H/S ("first hydrate"). This initial, topochemical reaction terminates upon supersaturation of the liquid phase with respect to CH, so that no more Ca^{2+} can be accommodated. At this point, the degree of reaction has reached about 1-2 percent. Almost simultaneously, nuclei of a "second hydrate" form on preferential C_3S surface sites. The exact reasons for the induction period are not clear. During this period, neither the "first" nor the "second" hydrate can form because of, respectively, the supersaturation of the liquid phase with respect to CH and the size of nuclei, which are smaller than critical. The induction period terminates when the second hydrate nuclei reach the critical size, enabling rapid propagative surface nucleation. The reaction continues until it is decelerated by consumption of anhydrous C_3S and the diffusion-controlled character of the process. The "second hydrate" has a lower H/S and higher C/S than the "first hydrate." However, since both C-S-H forms have a C/S < 3, liberation of free lime is occurring simultaneously. During the formation of the "second" C-S-H, amorphous CH is formed, which, upon conversion to crystalline form, is initially effective in nucleation and growth of CH. During this time, the supersaturation of the liquid phase with respect to CH decreases to the saturation concentration. Formation of detectable solid CH at the beginning of the acceleration period is considered to be the consequence of rather than the reason for the termination of the induction period.

The considerable variation in estimates of the C/S ratio for a "first hydrate" emphasizes the difficulty of obtaining a good measure of its stoichiometry. Dent Glasser et al. (23) noted an apparent discrepancy between the C/S ratios of the C-S-H obtained by the direct and indirect

methods at early ages: for pastes a few days old, their own results from the indirect method gave low values, around 1.0, while direct analyses by analytical electron microscopy gave a mean C/S of about 1.6. They suggested that the C-S-H might exist in two different forms, which they called "surface" and "precipitated" hydrate. The precipitated hydrate was what had been observed by electron microscopy, and included both Type I and Type III Diamond varieties (30). The surface hydrate was formed from the surface regions of reacting C_3S particles as a layer of approximately fixed thickness, which contracted as the C_3S was consumed. Its mean C/S ratio was assumed to be below 1, and the actual value ranged from a maximum value of 3 at the C_3S interface to a minimum well below 1 at the solution interface. Several assumptions are implicit in this hypothesis. First, variations in C/S with degree of hydration are due to changes in the relative amounts of different kinds of C-S-H, rather than to changes affecting the whole of the C-S-H. Second, there is a continuous conversion of surface into precipitated C-S-H. The concept thus differs from that of inner and outer hydrates in that, in the latter model, inner hydrate is never converted into outer or vice versa. The two concepts are not mutually exclusive, however, as the precipitated hydrate could be differentiated into inner and outer products.

A mechanism for portland cement hydration has been proposed (31-33) which also requires the formation of a protective layer around the alite grains. This layer, however, is considered to act as a semipermeable membrane, thereby allowing osmotic pressures to develop. Passage of Ca^{2+} and OH^- through the membrane leaves behind a silica-rich solution. C-S-H grows by a "silicate garden" process as the membrane ruptures and forces out the liquid beneath. These ideas are discussed more fully in the section on portland cement.

According to Taylor (1), the assumptions that some sort of protective layer causes the induction period and that nucleation of C-S-H or CH or both ends it need not conflict. Indeed, in his view, the combination is highly probable. Similarly, the delayed-nucleation theory and the hypothesis that an osmosis-like mechanism plays an important part in the hydration reaction are not necessarily contradictory. This conclusion is based partially on the recognition of the inherent difficulties in the concept (described earlier) of a membrane enclosing a silica-rich fluid through which Ca^{2+} has to pass. It is almost certain that the silica would polymerize to form a gel, and it is difficult to visualize how calcium could migrate through such a gel to form C-S-H. Using an analogy of the behavior of rubber in benzene, Dent Glasser (34) noted that a gel can absorb solvent, develop an inbibition pressure, and swell without being enclosed in a semi-permeable membrane. She seems to be implying the existence of a polymeric gel, although the evidence shows that polymerization occurs during later hydration. Thus, instead of a cement particle coated with a semi-permeable membrane that encloses a Si-rich liquid to which additional water flows by osmosis, we may be dealing with a semi-fluid gelatinous coating that draws water by inbibition. This concept may provide a bridge between the ideas of Fierens, Young, Skalny, and others on the one hand, and those of Jennings and Pratt -- and to some extent of Double, Birchall and others -- on the other hand. In Taylor's view (1), the ultimate driving force of the hydration reaction is twofold: attraction of protons to the basic oxide and silicate ions, and attraction of water molecules to all the ions. A calcium-depleted layer is produced, as suggested by Tadros et al. (22) and others, but this layer may be semi-fluid and based on a mobile, hydrogen-bonded network of highly protonated silicate ions and water molecules. If this layer actually imbibes water, as suggested by Dent Glasser (34), then a continuous hydration of the underlying C_3S surface is feasible. Ca^{2+} ions could diffuse outward through this layer, but would be held back on the surface by an excess of negative charge. This may explain the existence on the surface of a chemisorbed Ca-layer as reported by Tadros et al. (22).

The Post-Induction Periods

Until now we have discussed the experimental data and theories relative to the first few hours of hydration -- a period characterized by a relatively low rate of C_3S-H interaction. However, the main property of cement -- namely, its structural integrity (strength, volume stability, and durability) -- is to a large degree the consequence of an accelerated C_3S hydration during which a substantial amount of C-S-H forms a rigid network. Unfortunately, compared to the pre-induction period, the acceleration and diffusion-controlled stages of hydration are less fully explored. The reasons for this lack of knowledge are inadequate instrumentation and the extremely complex character of the structures formed, both on a micro- and a macro-scale. To illustrate our uncertainty about the post-induction mechanism, note the disagreement of various reported data on the composition of C-S-H as a function of time and temperature of hydration, the degree of hydration, composition of the liquid phase, etc. This issue has been discussed recently by Bentur and Berger (35). The "reactivity" of C_3S is influenced by thermal history, particle size and distribution, polymorphism, form of minor components present, etc., and in turn, influences the post-induction period as well as earlier hydration. Although these issues may seem academic, they are actually the preconditions for full realization of cement potentials. This knowledge could enable prediction and better control of concrete properties on the basis of "microstructural engineering." More experimental evidence is thus needed to better explain this and the decelerating diffusion processes, e.g., the role of porosity and liquid phase composition.

Powers (36), Terrier and Moreau (37), and others have distinguished between "inner" and "outer" hydration products, formed in spaces previously occupied by anhydrous solid and water, respectively. It is not clear how these hydrates relate, if at all, to the types of hydrates recognized by Diamond (30) or to the "precipitated" hydrate discussed by Dent Glasser et al. (23). Stucke and Majumdar (38) have measured C/S ratios for both inner and outer hydrates, but the issue is far from resolved.

Taylor (1), based on previous work of Tadros et al. (22), Dent Glasser et al. (23), and others, proposed a possible mechanism for the post-induction period. It is shown, together with his ideas about the pre-induction period, in Fig. 4. As the C_3S-H reaction progresses, there is necessarily an interface that advances into the diminishing C_3S grain. Behind it follows a semi-solid, Si-rich (low C/S) layer, which, depending on its thickness, may dominate the composition of C-S-H as a whole. Outside this layer, some of the ions from the reacting C_3S form a zone of inner product with increasing C/S. Other ions pass through the inner product to augment the outer product. This hypothesis needs additional experimental proof, however.

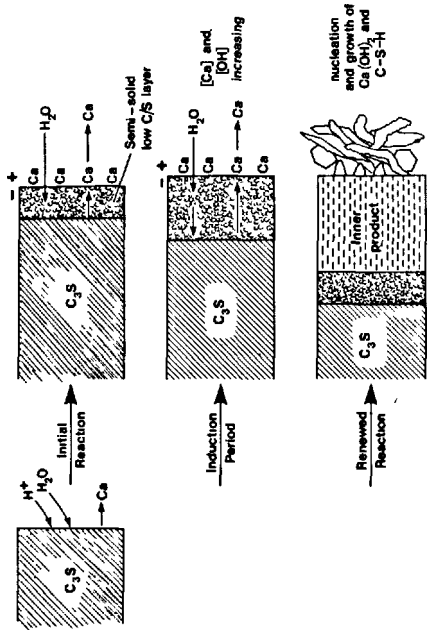

Fig. 4 Mechanism of C_3S hydration proposed by Taylor (1).

2.1.2 Hydration in the Presence of Admixtures

Since a special report on admixtures has not been prepared for this Congress, we will address the subject here. Because of space limitations, we will concentrate on more fundamental aspects of C_3S-admixture interactions and will continue the discussion in the section on cement. There is no single mechanism that will explain the way in which set-modifying admixtures affect the hydration of C_3S, primarily because the reaction rates and products of hydration are controlled by numerous simultaneous chemical and physical processes. For example, the influence of any admixture may affect the length of the induction period, the time of maximum rate of heat evolution, or the area under the main heat peak (total heat evolution) (39). Any of these changes may cause acceleration or retardation. Furthermore, other properties have been used to evaluate set-modifying effects, such as strength development, non-evaporable water content, development of surface area, formation of hydrates, etc. -- properties which are not necessarily related linearly.

Inorganic Electrolytes

It has been suggested in the past that the effect of an electrolyte, e.g., $CaCl_2$, on the hydration process is sequential, i.e., it participates in only one reaction at a time. For example, DeKeyser and Tenoutasse (40), in their study of the ferrite phase, concluded that calcium monochloroaluminate-ferrite, $C_3(A,F).CaCl_2.10H_2O$, is not formed until all the available gypsum is consumed. On the other hand, Rozenberg and Kucheryaeva (41), in agreement with Ratinov and Rozenberg (42), concluded that simultaneous formation of basic salts from a complex hydration system is possible. Using $CaCl_2$, $Ca(NO_3)_2$, and $Ca(NO_2)_2$ with calcium hydroxide (C_3S reaction product) alone and with additions of C_3A, they calculated the reaction rates and yields for the various combinations and concluded that, when two or even three electrolytes are added to a system together, the reaction that has the higher rate constant will have the higher yield. Unfortunately, the authors do not discuss the effect of added salts on the mechanism of C_3S-H reaction.

Despite the long and extensive use of $CaCl_2$ as a commercial accelerator, very little is known about the mechanism of its influence on C_3S hydration (43,44). Many investigators have compared the behavior of different metal chlorides (39, 45-48) and have attempted to correlate the effectiveness of the cations in accelerating C_3S hydration with their ionic radii and electronegativity. However, there is no general agreement on the proper order of rank for cations because, as Kantro's study shows (39), the relative accelerating power of cations depends on the salt concentration and the criterion used for acceleration.

The influence of various anions on the accelerating process has also been studied (39,47,48). Although these studies used different cations, and thus are not completely comparable, it is apparent that chloride ion is not necessarily the best anion for accelerating the hydration of C_3S. Kondo et al. (47,48) related the effect of the anion on the C_3S calorimeter curve to its ionic mobility (Fig. 5a) and found that sulfate, chromate, and thiosulfate ranked ahead of the chloride ions for potassium salts. Kantro (39) observed similar anion rankings for calcium salts (Fig. 5b).

Although there is general agreement between the results of the two studies, there are some notable differences. For example, the calcium salts are generally better accelerators than the potassium salts, and the behavior of I^- and SCN^- is quite sensitive to the cation.

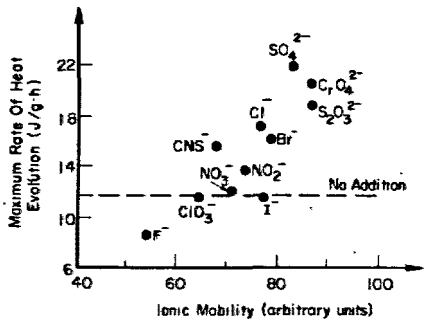

a

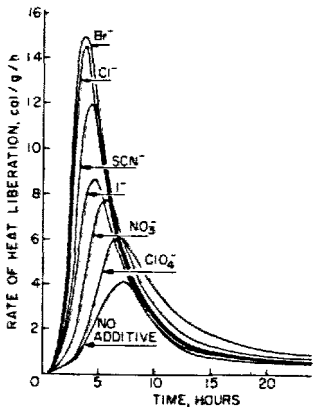

b

Fig. 5 Effect of inorganic anions on C_3S heat evolution: (a) Potassium salts (ref. 47), (b) Calcium salts (ref. 39).

The effects of various other salts have also been studied (21,39,49-51). Most inorganic electrolytes behave as accelerators, with the exception of fluorides (47,48,21), phosphates (52), and those cations that precipitate insoluble hydroxides (39,47,48). It is clear that $CaCl_2$ is not unique in this regard, but has the advantage of being a cheap and readily available material.

Young (53,54) has attempted to explain the influence of soluble salts by considering each stage of C_3S separately and sequentially. The importance of the composition of the liquid phase, particularly with respect to CH supersaturation, is supported to some extent also by work of Teoreanu and Muntean (45). This would explain the higher acclerating effects of calcium salts compared to potassium salts. Kondo et al. (47, 48) considered ion diffusion to be an important property. A highly mobile anion, such as Cl^-, can penetrate the initial protective layer to the underlying C_3S, forcing diffusion of other ionic species (e.g., Ca^{2+}) to maintain electroneutrality, and thus accelerating hydration. The order of Cl^- diffusion coefficients was found to be $D_{MgCl_2} > D_{CaCl_2} > D_{LiCl} > D_{KCl} > D_{NaCl}$, and the values are greater than those of the cations. This order is also approximately that found for their accelerating effect on C_3S hydration.

When cations precipitate insoluble hydroxides, retardation of C_3S hydration is observed (39,47,48). This is attributed by Kondo et al. (47,48) to the formation of an impermeable layer of insoluble hydroxides or other insoluble calcium salts. Young (53,54) has suggested that the precipitation produces the retarding effect by keeping the contact solution from becoming supersaturated with respect to calcium hydroxide. However, neither theory explains why Na_2CO_3 accelerates C_3S hydration (21,51).

Organic Admixtures

Most organic admixtures retard the hydration of C_3S — including those used as accelerators for cement, e.g., triethanolamine. Salts of lignosulfonates, which contain varying amounts of sugars and related compounds, are an important component of commercial retarding admixtures. Milestone (55) investigated the effects of such organics, using fractionated lignosulfonates, glucose, and sodium gluconate. At 0.1% concentration, fractions high in sugar at first retarded C_3S hydration and then accelerated it. The same concentration of fractions high in lignosulfonate caused little delay, but a 0.5% concentration completely inhibited hydration of C_3S. Adding 0.1% glucose delayed hydration for about 11 days, whereas the same amount of sodium gluconate caused complete inhibition. Milestone concluded that the retarding effect of lignosulfonate is due to the presence of sugar acid impurities, which are more effective than sugars alone because of their charge and stability, i.e., the readily ionized, negatively charged sugar acids adsorb on the positively charged surface of the C_3S and retard hydration. Thus, as proposed by Tadros et al. (22,56), the delay in hydration is believed to be caused by poisoning of the CH nuclei. Total inhibition of hydration by sugar acids is perhaps caused by their adsorption on the C-S-H nucleation sites (55).

In a related study, Jawed et al. (57) found that the Na-lignosulfonate delayed or completely inhibited the growth of CH from a supersaturated solution (Fig. 6). At a lignosulfonate concentration of approximately 2.5 ppm, no effect on crystal growth was observed. At somewhat higher concentrations, well-defined induction periods were noticed followed by accelerated growth rate. At concentrations above 200 ppm, the growth, and probably also the nucleation, of CH was com-

pletely inhibited. In a C_3S paste, higher supersaturation was required to overcome the poisoning effect of lignosulfonate. When crystal growth did occur, numerous small crystals formed rather than a few large ones. This may well explain the delayed acceleration observed by Milestone (55). (See also discussion in section on C_3S-temperature effects.)

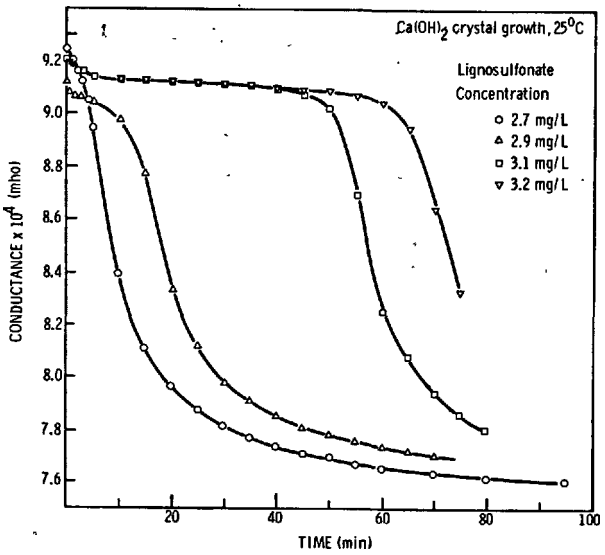

Fig. 6 Effect of lignosulfonate concentrations on growth of CH crystals from supersaturated solution (ref. 57).

2.1.3 Selected Issues

Hydration of C_3S Polymorphs

It has been reported in the past that the various crystal forms of pure C_3S have comparable reactivities with water. In the presence of impurities, minor differences in hydraulic activity are noted, but these are related to lattice and electronic defects rather than to the crystal form (58,59).

An attempt to better characterize the reactivity of the C_3S polymorphs was reported by Harada et al. (60). Using synthetic C_3S preparations at w/c of 0.3 and 0.4 (20°C) and quantitative X-ray diffraction analysis, the authors found the following order of reactivities at early stages of hydration: monoclinic < triclinic < rhombohedral. With time of hydration, the differences diminished, and, at 3 months, the degree of hydration of all three polymorphs reached approximately 70%. According to the authors, the morphologies of the C-S-H formed depended on which polymorph was hydrated:

C_3S	C-S-H
rhombohedral	thin sheets
monoclinic	fibrous
triclinic	amorphous

The reactivity of C_3S may depend on the particular oxide impurity used (61,62). Kaushanskii and Timashev (63) believe that different defects affect reactivity to different extents. At low levels (<0.3%) of Al_2O_3 in C_3S, Al^{3+} replaces Ca^{2+} in the lattice, creating donor centers and releasing conductivity electrons. Above 0.3%, Al^{3+} substitutes for Si^{4+}, and creates acceptor centers or "holes." The presence of holes causes greater reactivity.

Effect of Temperature

C_3S hydration is affected by temperature in the first three stages. The induction period shortens and the heat peak in Stage 3 becomes more intense. Later, when hydration becomes diffusion-controlled, temperature sensitivity decreases. Boyer (64) and Boyer and Berger (65) have found that the temperature of hydration affects the size of calcium hydroxide crystals. At 5°C, relatively large crystals are formed while, at 40°C, a much greater number of small crystals is formed. This change is even more marked when the temperature is raised just prior to the end of the induction period. A large number (~1000 times those formed at 5°C) of very small crystals is formed if the temperature is changed from 20° to 40°C, for example. This effect is believed to be due to the decrease of calcium hydroxide solubility with temperature. Raising the temperature causes the solution in contact to become highly supersaturated with respect to calcium hydroxide.

Seeding

Davis and Young (66) used afwillite to seed C_3S hydration. Addition of afwillite accelerated the hydration of C_3S, but strength development was not influenced to the same degree. Afwillite appeared to form both by conversion from C-S-H and directly from C_3S. Seeding was most effective when the seed material was interground with the C_3S rather than mixed by blending. Mchedlov-Petrosyan et al. (67) observed similar behavior when seeding C_3S with prehydrated C_3S. Stein and Stevels (68) have attributed the accelerating effect of amorphous silica to its influence on the nucleation of the "second" C-S-H.

Carbonation

C_3S carbonation reactions have been pursued by a few authors, but most results are descriptive rather than mechanistic. According to Takagi et al. (69), hydrating C_3S specimens prepared from triclinic, monoclinic, and rhombohedral polymorphs all produce calcite upon carbonation. Goodbrake et al. (70) developed a kinetic equation for the carbonation reaction of both C_3S and β-C_2S in the presence of water vapor:

$$[1-(1-\alpha)^{1/3}]^2 = K_T't \qquad (3),$$

where α = degree of carbonation, K_T' = apparent rate constant, and t = time of reaction. K_T' depends on the actual rate constant, K, the

diffusion coefficient, D, and the average particle size, r_o:

$$K_T' = \frac{KD/r}{r_o^2} \quad (4)$$

The carbonation reaction is exothermic (-83 kcal/mol C_3S) and follows a decreasing-volume, diffusion-controlled kinetic model. The activation energy was found to be 9.8 kcal/mol. The overall equation:

$$C_3S + 3\overline{C} + \overset{H}{} + 3C\overline{C} + SH = SH_z \quad (5)$$

describes the carbonation process satisfactorily.

When liquid water comes in contact with the solid during carbonation (w/s = 0.10-0.20), the course of the reaction changes, and C-S-H (believed to be similar to that formed in normal hydration) is formed and subsequently carbonated:

$$C_3S + (3-x)\overline{C} + yH + C_xSH_y + (3-x)C\overline{C} \quad (6)$$

$$C_xSH_y + x\overline{C} + (z-y)H + xC\overline{C} + SH_z \quad (7)$$

The overall reaction is the same as in Equation 5. A simple rate equation of the form

$$\frac{d\alpha}{dt} = k \log t \quad (8)$$

can be used to describe carbonation. The form is the same as is often used for hydration, but the rate constant is several orders of magnitude larger.

Mathematical Modeling of the Hydration Process

Mathematical modeling of cement hydration processes is the subject of another review; therefore, we will present only a brief discussion here.

Pommersheim and Clifton (71), using mainly experimental data of Kondo and co-workers (6,72) and de Jong et al. (4), developed a mathematical model for C_3S hydration by which the following output variables could be predicted as a function of time: degree of hydration and its rate, core and particle radii, amount of free and combined water, amount of CH and C-S-H formed, intergranular porosity, and the rate of the controlling process. For modeling purposes, the hydration was broken down into several processes: 1) diffusion of chemical reactants through ever-thickening spherical layers of precipitated porous hydrates to the interface between the C_3S core and the innermost hydrate layer, 2) dissolution of ions from C_3S and their hydration near this interface, 3) diffusion of soluble product ions out through deposited hydrate layers, and 4) precipitation of insoluble products (inner, middle, and outer C-S-H). The middle (barrier) product layer forms at early stages of hydration; its later disappearance may mark the end of induction period and the beginning of the acceleration stage.

Tomosawa (73), in an attempt to relate the hydration process to practical engineering properties of concrete (e.g., strength development, heat liberation), developed a model that assumed an induction period at the early stages of C_3S hydration followed by a diffusion-controlled stage. Kinetic models for C_3S and β-C_2S hydration were also proposed by Fujii and Kondo (12, 74).

2.1.4 Proposed Mechanism of Hydration

The following concepts describe processes during the induction and acceleration periods of C_3S hydration:

- o C-S-H nucleation
- o CH nucleation
- o Osmotic pumping
- o Crystal defects.

Table I reviews the different theories on the three main stages of hydration.

An appropriate mechanism should be able to explain the effects of experimental variables on the hydration of C_3S. Table II lists the predictions of the various mechanisms for some of the variables discussed above. Based on the reported experimental data and on Taylor's ideas reconciling some of the conflicting views (1), we propose the following mechanism of C_3S hydration.

Stage 1. Initial hydrolysis with water causes protonation of O^{2-} to OH^-, SiO_4^{4-} to $H_nSiO_4^{(n-4)}$, and Ca^{2+} to $Ca^{2+}(aq)$. Hydrolysis occurs preferentially at active sites, and the number of such sites determines how rapidly this process occurs. As Ca^{2+} and OH^- preferentially leach into solution, a surface layer reaction product forms that can be best described as an assembly of silicate ions, such as $H_3SiO_4^-$ and $H_4Si_2O_7^{2-}$, held together mainly by hydrogen bonds and a few calcium ions (Fig. 7). This layer is certainly amorphous and bears no resemblance to the original crystal structure. It may not be very rigid and might tend to imbibe water and swell (the imbibition pressure which causes swelling is similar to an osmotic pressure, but does not require a specific semi-permeable membrane). Charge balance is maintained by loss of Ca^{2+} into solution to compensate for H^+ taken up from the water during hydrolysis. An electrical double layer sets up between

Table I

COMPARISON OF MECHANISTIC CONCEPTS
FOR C_3S HYDRATION

Initial Hydration (Stage 1)	(i) 1st hydrate (C_3SH_n)	Congruent dissolution
	(ii) Chemisorbed layer ($C_{2-5}SH_n$)	Incongruent dissolution Ca adsorbed on silica-rich hydrolyzed layer
	(iii) Semipermeable membrane C-S-H	$Ca(OH)_2 + Si_2O_7^{6-}$
	(iv) No specific retarding layer	Change in solution composition Change in active sites
	(v) Semi-liquid layer ($C_{\leq 1}SH_n$)	
Induction Period (Stage 2)	(i) C-S-H Nucleation Control	2nd hydrate $C_{1-1.5}SH_n$ (acicular)
	(ii) CH Nucleation Control	Acicular C-S-H also $C_{1.5-2.0}SH_n$
	(iii) Osmotic Pumping	Osmotic pressures burst coating. C-S-H same composition as membrane
	(iv) Crystal Defects	Nucleation of C-S-H at active sites
Acceleration Period (Stage 3)	(i) Growth of C-S-H	Heat peak due to renewed hydration of C_3S and formation of C-S-H. CH is a by-product
	(ii) Growth of CH and C-S-H	Heat peak due to growth of CH which controls renewed hydration of C_3S

Table II

EXPLANATION OF VARIABLES THAT AFFECT HYDRATION OF C_3S
IN TERMS OF PRINCIPAL HYDRATION MECHANISMS

Variable	C-S-H Nucleation	CH Nucleation	Osmotic Pumping	Crystal Defects
Temperature	Affects nucleation of 2nd hydrate	Affects initial rate of hydrolysis; thermal shocking may accelerate hydration	Affects initial dissolution of C_3S and build-up of osmotic pressure	Affects rate at which reactive sites react. Quenching from kiln temperatures affects initial number of sites
Effect of adding $Ca(OH)_2$	Retards by inhibiting nucleation of second hydrate	Should shorten induction period, but crystals may be poisoned. Not always retarding	No predicted effect. Might assist in development of membrane and might influence development of osmotic pressure	No predicted effect
Effect of adding $CaCl_2$	Promotes nucleation of second hydrate	Shortens induction period by adding Ca^{2+} and reaching supersaturation sooner	Not predicted	Not predicted, but may affect reactivity of active sites
Effect of adding a retarder	Not predicted	Lengthens induction period by inhibiting crystal growth. Higher supersaturation is required.	Not predicted	Active sites inhibited by adsorption of retarder molecules
Effect of adding amorphous SiO_2	Aids nucleation of second hydrate	Initial formation of C-S-H will occur which may prevent poisoning of CH	Not predicted but might aid membrane formation	Not predicted

the relatively mobile Ca^{2+} and the immobile silicate surface layer, and is observed as chemisorption.

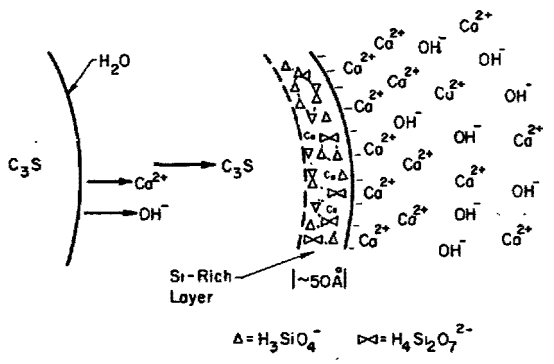

Fig. 7 Initial hydrolysis of C_3S.

Stage 2. The surface layer first formed in Stage 1 continues to develop, and Ca^{2+} and OH^- ions continue to pass into solution. But the process is slow because the ions must pass through the electrical double layer. The characteristics of the double layer will be affected by the concentration of Ca^{2+}, i.e., ions will move more readily through a diffuse double layer (solid line, Fig. 8) than through a condensed layer (dotted line, Fig. 8). Nuclei form from assembly of atoms in solution, but are not able to reach the critical size necessary for growth. The nuclei contain Ca^{2+}, OH^-, and silicate ions, and will form either CH or C-S-H.

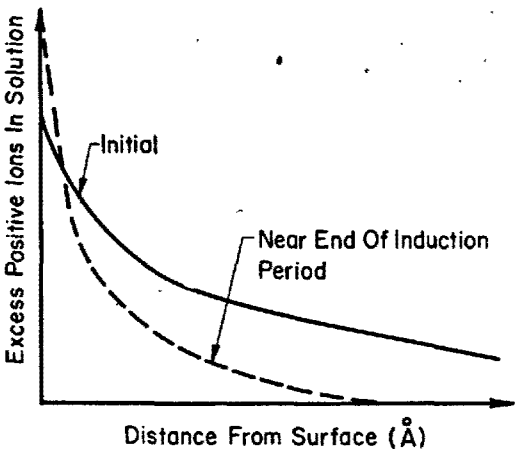

Fig. 8 Variation of double layer with ionic concentration in solution.

Stage 3. Ionic concentrations in solution become large enough for the nuclei to grow. Growth is first observed when the solution becomes supersaturated with respect to calcium hydroxide, and occurs close to the surface of the grain where ionic concentrations are highest (Fig. 9). Growth of C-S-H is confined to the surface because of the difficulties in transporting silica (surface mechanism). Mostly small particles form because of lack of silicate movement. Growth of CH may occur initially at the surface, but some crystals also form in the pores away from the grains. These grow more rapidly because of lack of space constraints, and eventually consume most of the smaller crystals near the surface. Growth of CH is controlled by the supersaturation of the liquid phase. Growth is first achieved at the end of Stage 2, but continues even during Stage 3.

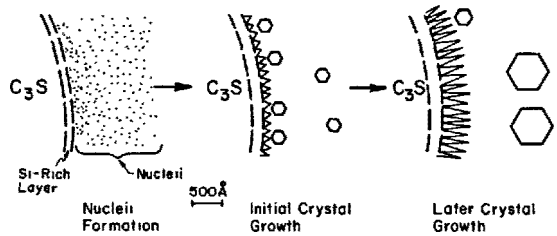

Fig. 9 Nucleation and crystal growth at the end of the induction period.

Stages 4 and 5. Rapid initial growth of CH and C-S-H slows down as supersaturation decreases. Most initial growth takes place outside the original grain boundaries in the water-filled space. Later growth (see Fig. 10) takes place within the original grain boundaries (hence this C-S-H is often called the "inner product"). The interface and Si-rich layer move inward, and C-S-H precipitates predominately beneath the outer acicular because these act as a barrier to ionic transport. However, some additional growth of aciculae will occur during the initial period of Stage 4. The morphology of the inner C-S-H will be different because of lack of space and changes in ionic concentrations (solutions are no longer highly supersaturated). The composition of inner C-S-H may also change because of changes in ionic mobility and space restrictions. Thus, inner and outer C-S-H may be quite different, or there

may be a structural and compositional gradient through the C-S-H layer.

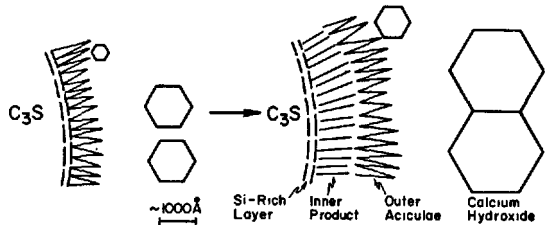

Fig. 10 Formation of inner product C-S-H.

2.2 Dicalcium Silicate

Dicalcium silicate is one of the most important components of portland cement clinker, where it exists mostly as the metastable β polymorph, stabilized by the presence of impurities. Because the hydration rate of β-C_2S is low compared to that of C_3S (alite), β-C_2S does not play an important role in the development of cement properties during the early stages of cement hydration. Consequently, only very limited research is focused on this clinker mineral. However, in view of its substantially lower temperature of formation compared to C_3S, and the subsequent possibility of energy savings, more interest in the chemistry of C_2S has been shown recently. It should also be noted that the hydration products of C_2S play an important role in the development of the ultimate engineering properties of mortar and concrete. Hydration of C_2S polymorphs has been recently reviewed (75,76).

2.2.1 Hydration of γ-C_2S

The γ-form is known to be the least reactive C_2S polymorph at ambient temperature. Under normal conditions, it is not found in industrial clinkers. Danilov (77) explains the differences in the rates of hydration of clinker minerals in terms of the electronegativities and ionic/covalent character of Ca-O-X bonds, and states that the low reactivity of γ-C_2S is caused by inadequate saturation of the liquid phase and subsequent low probability of formation of C-S-H nuclei. Others attribute the low reactivity of γ-C_2S to the regular coordination of its calcium ions with oxygen atoms in the olivine-type (Mg_2SiO_4) orthorhombic structure, to the absence of holes of atomic dimensions, or to the differences in hydration mechanism between the γ and β forms. In the view of Sychev et al. (78), the limited hydration of γ-C_2S proceeds by a "through solution" mechanism, whereas β-C_2S reacts by a "topochemical" mechanism. Lea (79) questions some of these explanations for the relative reactivity of C_2S polymorphs. He argues that the absence of "holes" and a highly coordinated structure are much less important than the impurities used to stabilize the high-temperature polymorphs for the hydration studies. He uses the highly reactive C_3S (six-coordinated Ca-ions) and very soluble NaCl (no "holes" in its structure) to prove his point. There is no accepted and experimentally proven explanation for the differences in the reactivity of the various polymorphs. Any future mechanistic research would have to consider all the above factors.

DTA and IR investigations by Bensted (80) of FeO-stabilized and pure γ-C_2S have shown that the γ-form does hydrate to form C-S-H and calcium hydroxide, but that the rate and degree of hydrahydration is much lower than for the other polymorphs, especially β-C_2S. The C-S-H was similar to that formed by the hydration of α, α′, and β modifications. At the end of five years, only approximately 20-25% of the material had hydrated. At elevated temperatures, especially in the presence of steam, γ-C_2S is known to react rapidly to form various calcium silicate hydrates (81). γ-C_2S also reacts rapidly with high concentrations of CO_2 (82), nearly as rapidly as β-C_2S under the same conditions.

2.2.2 Hydration of β-C_2S

Effect of Solid Substitutions

Pritts and Daugherty (83) studied the effect of incorporation of small quantities of metal oxides (V^{5+}, Cr^{6+}, B^{3+}, S^{6+}, Na^{+}, K^{+}) on the rate of β-C_2S hydration, and developed a model relating β-C_2S to the charge/radius ratio of the stabilizing metal ion. As expected, they found the hydration of β-C_2S to be temperature dependent and the activation energies of the acceleration stage of hydration to be 14 and 12 kcal/mol for the Cr_2O_3-doped and pure C_2S, respectively. According to these authors, the data were consistent with a silicate polymerization rate-determining step for the acceleration stage of hydration. They concluded that, although it is possible to significantly alter the hydration rate of β-C_2S by doping it with metal oxides, it still hydrates much more slowly than C_3S and undoped β-C_2S. Their data showed that, in all cases, both the calcium and silicon-substituted samples hydrated at lower rates that were inversely proportional to the charge/radius ratio. They concluded that partial replacement of C_3S (alite) in industrial clinkers by activated β-C_2S was not possible -- a view which is not universally accepted.

In a related study, Maycock and McCarty (84) explored the mechanism of β-C_2S stabilization by metal oxides and discussed the subsequent reactivity of the doped product. Using a solid

state physics approach — interpreting the electrical conductance of the solids — they concluded that generation of point defects by adding impurities is not as important to the stabilization process as is the precipitation of impurity phases during the cooling process. The influence of lattice defects, generated by mechanical grinding and heating of β-C_2S (and C_3S), was studied by Maycock et al. (14) and Opoczky and Juhasz (85). Maycock et al. showed that lattice imperfections influenced both the pre-induction and the induction stages of hydration by enhancing the diffusion of ions within the solid particle. They argued that introduction of lattice defects in the unhydrated solid could not affect the solution processes or the diffusion through a "first hydrate" layer. Using thermoluminescence and quadrupole mass spectrometry, Fierens and Trilocq (86) have shown that the differences in the rate of hydration of β and γ modifications are not related to the very first stage of hydration (chemisorption of water on the anhydrous surface) because the sorption of water vapor is the same for both polymorphic forms.

Reaction Mechanisms

It is our opinion that the experimental evidence indicates substantial similarities between the hydration mechanisms of C_3S and β-C_2S. The different hydration rates are believed to be a consequence of the differences in crystal structure between the two silicates. Therefore, the hydration of β-C_2S and C_3S can be discussed in similar mechanistic terms. Major differences are the lack of high supersaturation with respect to CH and the low rate of heat evolution, which makes it difficult to study the reaction calorimetrically. The overrall composition and morphology of C-S-H formed from C_2S and C_3S appear to be similar, but there are definite differences in micro-structural details (87).

Tong and Young (88) have shown that, during hydration of β-C_2S, the rate of release of ionic species is slow, with a consequent low degree of supersaturation and slow increase in the ionic product, $K_{1p}[CH]$. If, as is assumed, the degree of supersaturation is related to the nucleation of CH and C-S-H, then the small supersaturation observed for β-C_2S will mean slow rates of hydration. It has been found (87) that larger CH crystals are formed in β-C_2S than in C_3S pastes, as would be expected from a low degree of supersaturation. With small amounts of C_3S in the β-C_2S, the crystallization of $Ca(OH)_2$ and, thus, the β-C_2S hydration proceed at a higher rate (89) because the faster hydrolysis rate of C_3S essentially restores the high degree of supersaturation needed for rapid formation and growth of nuclei.

The usefulness of liquid phase studies has also been demonstrated recently by Fujii and Kondo (74). They consider the early hydration of β-C_2S and C_3S to proceed in a similar manner. After initial congruent dissolution of the silicate, water molecules adsorb on the surface of the particles, and "CSH(I)" precipitates from solution, thereby causing a decrease in silicate ion concentration. Eventually, nuclei of calcium silicate hydrate, with a time-variable C/S, form and grow on the surface of the particles, while Ca^{2+} and OH^- diffuse into the solution and cause a supersaturation with respect to calcium hydroxide. At the maximum supersaturation (~80 hours after contact with H_2O), the hydration of β-C_2S, unlike that of C_3S, starts to accelerate; when the degree of hydration reaches approximately 20%, deceleration, followed by a renewed acceleration, is observed.

In saturated lime solution, the deceleration stage was found to be more pronounced, but no explanation for this phenomenon was given. Based on liquid phase and microscopic experimental data, and several assumptions (some of them, unfortunately, contradicted by experimental evidence, e.g., fixed C-S-H composition independent of time and temperature of hydration, and congruent dissolution of β-C_2S), the authors conclude that 1) the early β-C_2S hydration may be a "propagative surface-nucleation-growth reaction," 2) the second acceleration stage is peculiar to β-C_2S, and 3) in contrast to C_3S, the precipitation of CSH(I) at the very early stages of interaction with water does affect the hydration rate.

Recently, β-C_2S hydration was studied (90) using ESCA and high-resolution SEM. As has been reported for C_3S (13), non-uniform etching of the surface was observed. Hydration products were observed on the surface at times as short as 15 seconds after contact with water (Fig. 11).

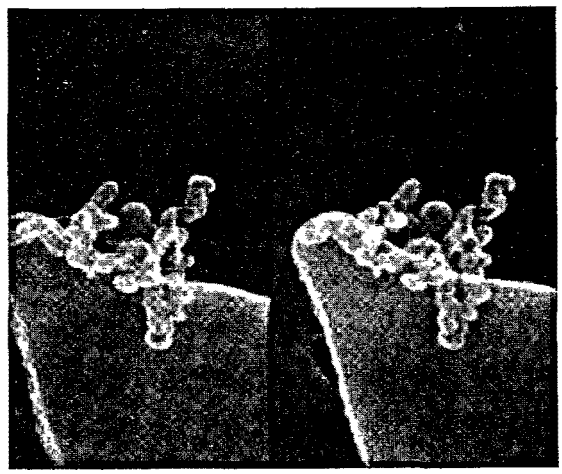

Fig. 11 Stereomicrograph of hydration products observed on the surface of β-C_2S, after 15 sec of hydration at 25°C. Scale: 0.1 μm

Influence of Admixtures and Special Treatments

Compared to the voluminous literature on the effect of admixtures on the hydration of tricalcium silicate and cement, relatively few studies have been performed in recent years on the hydration of dicalcium silicate in the presence of admixtures.

Effect of Calcium Chloride. It is assumed that the effects of $CaCl_2$ on the hydration of β-C_2S and C_3S are similar (43,44), although mechanistic interpretations are virtually nonexistent. It is generally agreed, however, that $CaCl_2$ accelerates β-C_2S to a lesser degree than C_3S. According to Zharov and Demel (91), the dissolution of β-C_2S in the initial stages of hydration, both with and without $CaCl_2$, is incongruent. This result contradicts data given by others (11,74,84). The authors (91) found the 28-day strengths of $CaCl_2$-doped C_2S pastes to be 10-15 percent higher than those of chloride-free samples, whereas Young and Tong (87) did not observe significant differences in tensile strength. Klyusov et al. (92) studied the effect of $CaCl_2$ and NaCl upon β-C $\underline{S}$ hydration at temperatures of 20°, 5°, 0° and -5°C. As expected, the rate of reaction with water at lower temperatures decreased, and NaCl, but not $CaCl_2$, decelerated hydration. Young and Tong believe that, as in the case of C_3S, $CaCl_2$ controls the composition of the solution.

Effect of Carbonation. Studies of the effect of $\overline{CO_2}$ on calcium silicate hydration, initiated in the early 1970's (93-95), have been continued. The most recent work published on carbonation of β-C_2S and C_3S was by Goodbrake et al. (70, 96). As was the case for C_3S, the β-C_2S reaction with CO_2 and water followed a decreasing-volume, diffusion-controlled kinetic model. The activation energy of this exothermic reaction was found to be approximately 17 kcal/mol and the heat of formation -44 kcal/mol. The degree of carbonation increased with increasing reaction temperature, particle surface area, reaction time, relative humidity, and partial pressure of CO_2. The ultimate reaction products were identified as aragonite and silica gel. In the presence of water vapor, only very small amounts of C-S-H were found in the early stages of carbonation; but, when liquid water was present, considerable quantities of C-S-H were formed (96). It is believed that the initial reaction is:

$$C_2S \text{ (or } C_3S) + (2-x)\overline{C} + yH \rightarrow C_xSH_y + (2-x)C\overline{C} \quad (9)$$

followed by carbonation of the C-S-H:

$$C_xSH_y + x\overline{C} \rightarrow SH_y + xC\overline{C}. \quad (10)$$

The reaction is similar to Equations 6 and 7 for C_3S, and the composition of the initial C-S-H is probably similar to that formed in ordinary hydration. Calcite is now the predominate form of calcium carbonate.

Highly reactive β-C_2S. Roy and co-workers (97, 98), using the evaporative decomposition of solutions (EDS) technique, succeeded in preparing β-C_2S with a reactivity 10 times higher than that of a comparable, conventionally prepared β-C_2S. By pumping a fine mist of solution of $Ca(NO_3)_2$•aq and colloidal SiO_2 into a long hot zone at a temperature of 750° to 1050°C, they formed C_2S by the reaction:

$$2Ca(NO_3)_2 + SiO_2 \rightarrow C_2S + 4NO_x. \quad (11)$$

Similar experiments were done with $CaCl_2$. The preliminary data showed that the quality of the C_2S formed depended on the choice and concentration of the feed solution and on the temperature of its decomposition. Attempts to form C_3S at low temperature failed: a feed solution of C:S = 3:1 yielded C_3S only at temperatures above 1250°C.

Under hydrothermal conditions, the β-C_2S produced by EDS was found to be much more reactive than than β-C_2S prepared by usual techniques (99). Reactive, finely divided β-C_2S has also been obtained (100) by calcining carbonated wollastonites at 700-900°C.

2.2.3 Hydration of α'- and α-C_2S

As is the case with the γ and β polymorphs, the reactivity of the high-temperature α' and α forms depends on the impurities used to stabilize the structure. Although earlier studies reported the α-C_2S to be non-reactive, Ono et al. (101) showed that doped α' and α forms could react with water.

According to Bensted (80,102-104), α'- and α-C_2S are less reactive than the β form but much more reactive than the γ-C_2S. It has been reported that the reactivity of the C_2S polymorphs can be correlated with the concentration of lattice defects (105); the density of pits in the etched surfaces was found to be β-C_2S > α'-C_2S > α-C_2S. This finding does not agree with those reported by Maycock and McCarty (84).

Jelenic et al. (106) found B_2O_3-doped α'-C_2S more reactive than a comparable sample of β-C_2S: both the degree of hydration and the compressive strengh were found to be higher in the α' form. Using electron microscopy and diffraction techniques, the authors attributed the larger reactivity of α'-C_2S to differences in crystal imperfections.

The reactivity of α- and α'-C_2S thus must be considered to be sensitive to specimen-specific conditions, such as its thermal history, and type and level of stabilizing oxides. It is possible that exsolution of impurities during the phase transformations at lower temperature could cause reactive grain boundary precipitates as well as crystal defects.

2.3 Tricalcium Aluminate

2.3.1 Mechanisms of Hydration

A well-established theory is that the rate-controlling step of C_3A hydration is diffusion through a layer of "hexagonal hydrates" (C_4AH_{13} and C_2AH_8), which forms rapidly at the surface of each grain (107). Since these hydrates convert rapidly to C_3AH_6 — due to the large heat of hydration of C_3A which raises the temperature of pastes to critical levels — this barrier does not persist, and the C_3A rapidly hydrates completely, primarily to C_3AH_6.

Corstanje et al. (107) have deduced from studies of mixtures of $C_3S + C_3A + C\bar{S}H_2$ that the primary cause of C_3A retardation is not the sulfate ion but the precipitation of amorphous $Al(OH)_3$ on the surface of the C_3A grain. The formation of the hexagonal hydrates (C_4AH_{13}, $C_4A\bar{S}H_{12}$, and their solid solutions) provides an "insulating layer" that isolates each grain from the bulk of the solution. This layer is not sufficient in itself to severely retard C_3A hydration since water and ions can move through it. However, their flow is sufficiently slow to allow the solution beneath the layer, in contact with the surface, to maintain a different composition from the bulk. Thus, subsequent formation of C_4AH_{13} depletes the solution in contact with the C_3A grain in Ca^{2+}, thereby causing $Al(OH)_3$ to precipitate:

$$4C_3A + 24H$$

$$\downarrow$$

$$12Ca^{2+} + 8Al(OH)_4^- + 16OH^-$$

$$\downarrow H$$

$$3C_4AH_{13} + 2Al(OH)_3. \qquad (12)$$

Although $C_4A\bar{S}H_{12}$ can act as an "insulating layer", its formation will not cause the precipitation of AH_3 since Ca^{2+} ions are supplied by the gypsum present. Breakdown of the insulating layer, e.g., by conversion to C_3AH_6, will cause the AH_3 layer to be broken down by the high concentrations of Ca^{2+} and OH^- in the bulk solution, and C_3A will continue to hydrate. In the absence of sulfate ions, this happens quite readily.

It can be seen from Fig. 12 that the conduction calorimetric curves can be quite complex and are significantly influenced by the different amounts of C_3S and gypsum present. Evidence is presented for a sequence of unusual reactions that occur in the presence of these additional compounds:

$$C_3AH_6 + CH + 6H \rightarrow C_4AH_{13} \qquad (13)$$

$$C_3A + 6H \rightarrow C_3AH_6 \qquad (14)$$

$$3C_4AH_{13} \rightarrow 3C_3AH_6 + 3CH + 18H. \qquad (15)$$

The last reaction gives an endothermal effect (Fig. 12). This sequence apparently is most noticeable at intermediate gypsum additions for reasons that are not clear. If the insulating layer were not present, then the diffusion of ions into the surrounding solution would not allow concentrations sufficient for the precipitation of AH_3 when C_4AH_{13} first forms. Periodic breakdown of the insulating layer, e.g., by conversion to C_3AH_6, would allow the AH_3 retarding layer to be attacked by Ca^{2+} and OH^- in the bulk solution, and C_3A would continue to hydrate.

Tadros et al. (108) suggested that retardation by the hexagonal hydrates does not play a significant role. They studied the kinetics and stoichiometry of C_3A dissolution in water and HCl and found initial dissolution to be incongruent by both solution and surface analyses: more calcium and fewer aluminum ions were released into solution compared to the stoichiometry of C_3A. In the experiments in which C_3A was reacted with HCl solution, an induction period was observed, at the end of which the pH rose sharply (Fig. 13). The authors suggested that the primary retardation of the dissolution was caused by formation of an Al-rich layer, and that the induction period represented the process responsible for the removal of the Al-rich layer. The time required for these processes to occur was long in the presence of HCl but was short when C_3A was reacted with neutral water. Hydrolysis of Al^{3+} to form polynuclear complexes such as $[Al_8(OH)_{20}]^{4+}$ and $Al(OH)_4^-$ may represent such processes.

Both of these theories, while ultimately predicting the formation of some kind of aluminum hydroxide, approach the problem from quite different perspectives and must be considered to be speculative at this time. Surface analysis, high resolution SEM, thermal analysis, and solution chemistry will all have their part to play in unraveling the complexities of C_3A hydration, particularly the early formation of precipitates. The initial formation of an amorphous gel, first observed by Breval (109) (see Fig. 14), is perhaps pertinent here. It can be considered to be either AH_3 or the precursor of C_4AH_{13} through reaction with Ca^{2+} and OH^- from solution. Knowing that crystalline hexagonal hydrates grow from the gel layer, we may not be have to invoke the special conditions of precipitation suggested by Corstanje et al. (107).

The exact role of the Al-rich layer in the overall hydration of C_3A is not yet clear. Does it persist through the hydration process, or is it no longer capable of forming once C_3AH_6 nucleates and grows? In pure water, the induction period will be quite short, as observed by Spierings and Stein (110), and the gel (or aluminum hydroxide) may be responsible for the later retardation of C_3A. To further understand the consequences of initial hydrolysis and early formation of precipitates, we will need to investigate this part of the reaction in considerably greater detail, drawing on a wide range of solid state

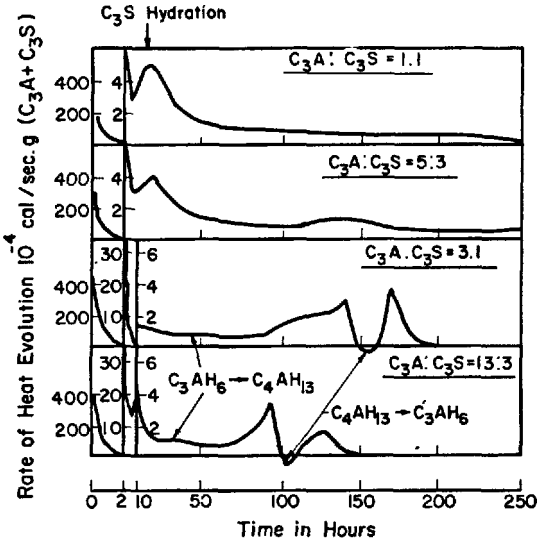

(a)

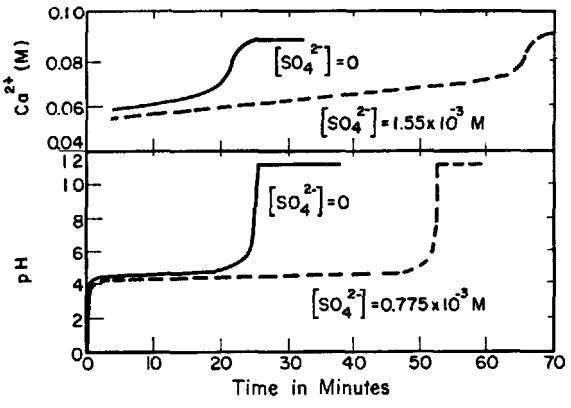

Fig. 13 Rates of dissolution of C_3A in 0.155 M HCl, with and without gypsum (adapted from ref. 108)

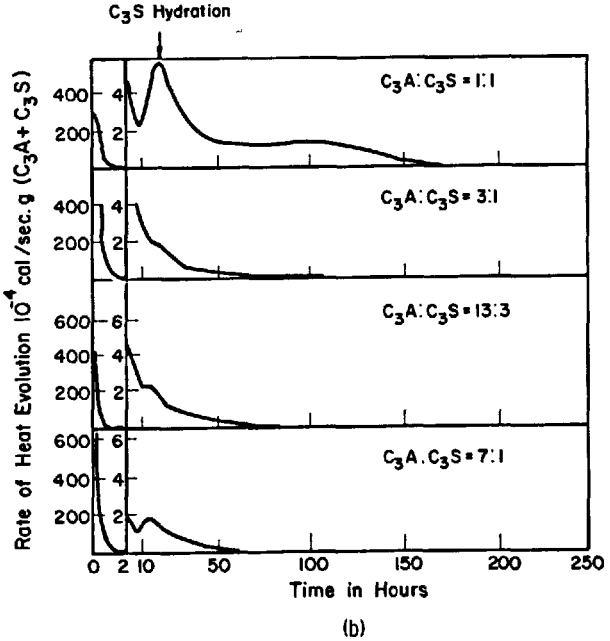

(b)

Fig. 12 Conduction calorimetric curves for pastes containing C_3A, C_3S and $C\bar{S}H_2$ (adapted from ref. 107): (a) Variable C_3A:C_3S weight ratios, no $C\bar{S}H_2$, (b) Variable C_3A:C_3S weight ratios at constant C_3A:$C\bar{S}H_2$ weight ratio of 25:1

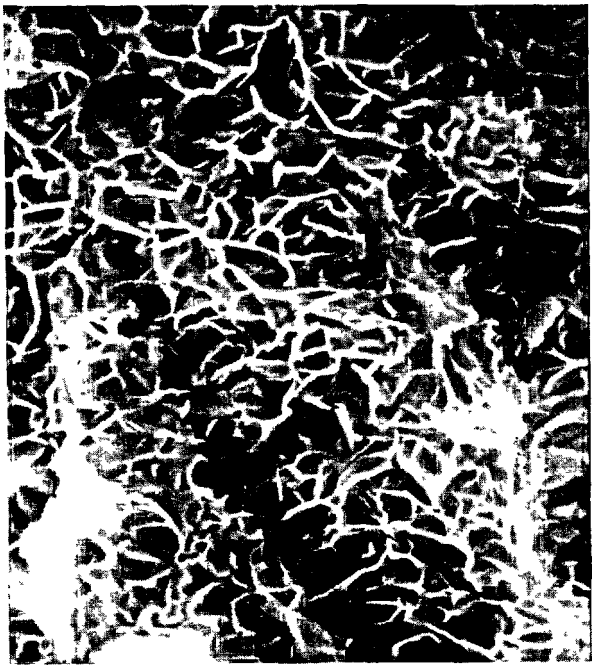

Fig. 14 Formation of gel on the surface of hydrating C_3A (ref. 109)

analyses. These early reactions are of considerable importance in characterizing the retardation by sulfate ions and organic molecules.

2.3.2 Hydration Products

Breval (109) has exhaustively studied the sequence of product formation in C_3A hydration and has confirmed the overall findings of numerous early studies. She has, however, developed some new interesting details (see Fig. 15). Gel formation is apparently the precursor of the hexagonal hydrates, which grow first as thin, irregular flakes with poor X-ray diffraction patterns. With time, these flakes can grow to better crystallized, hexagonal forms, but this process competes with the transformation to C_3AH_6 at normal ambient temperatures. Breval suggests that thin hexagonal plates, which are observed only at low hydration temperatures, may be formed from a secondary precipitation process rather than by growth from the gel. According to Breval's data, C_3AH_6 forms at or below 20°C, somewhat lower than the generally accepted transformation temperature. This may well indicate that even when very small quantities of C_3A are hydrated in large quantities of water (~2 mg C_3A/100 mg water), local temperature rise at the surface of grains may nucleate C_3AH_6 in the gel layer. The fact that C_3AH_6 has been reported in pastes hydrated as low as −5°C (111), where its formation is excluded thermodynamically, lends credence to this view. Once nuclei have formed, it is likely that they can slowly grow at this low temperature to form large isolated crystals. The gel persists above 60°C as a transient phase, but then C_3AH_6 forms directly from C_3A as an aggregate, or matrix, around the grain. Breval's data re-emphasize the importance of the heat of hydration in controlling the hydration products in small quantities of pastes or slurries (~100 mg C_3A/100–500 mg H_2O), since C_3AH_6 is the major hydration product even at −5°C. Simulating the hydration of C_3A under conditions that might approximate those of a cement paste would consequently present considerable difficulties.

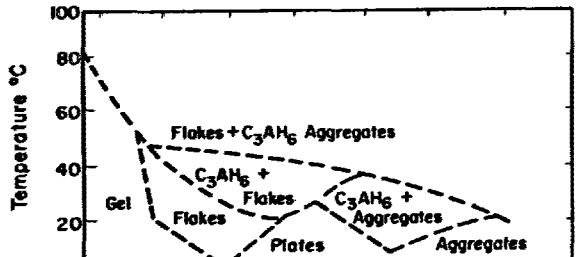

Figure 15. Sequence of formation of C_3A hydration products (adapted from ref. 109).

2.3.3 Effect of Prehydration

Another topic of potential technological significance is the effect of prehydration of C_3A upon contact with water vapor. This phenomenon can have a profound influence on the subsequent performance of the cement because changing the course of C_3A hydration can affect the sulfate balance and the way admixtures interact with cement. Since no liquid water is involved, at least some of the C_3A can interact without sulfate ions being present, as was found by Breval (112,113). From this study, she concluded that, if the bound water (W_k) is less than 3%, the hydration products formed do not interfere with subsequent hydration in water. If, however, $W_k > 3\%$, the hydration products profoundly influence the products during subsequent hydration, leading primarily to the formation of C_3AH_6.

Wittmann (114), using thermoluminescence to study the vapor hydration of C_3A, has reported that initially metastable hydration centers are created, which can be destroyed by subsequent heating or drying. With increasing relative humidity, these centers become stable. No other studies of this nature have been reported, although the influence of prehydration on the subsequent reaction with sulfates and other admixtures is clearly of interest. Studies of prehydration could be quite valuable in helping to elucidate hydration mechanisms.

2.3.4 Effect of Admixtures

Alkalies

It is now well known that sodium can substitute readily in C_3A, thereby inducing different crystal modifications. There seems to be general agreement (110,115-117) that the reactivity of C_3A markedly decreases as the Na_2O content in the crystal increases. This has been attributed (116, 118) to the formation of a less reactive structure as Na^+ ions fill the holes in the lattice. Spierings and Stein (110), on the other hand, believe that the lower reactivity is due to the effects of Na^+ after it is released into solution. When Na_2O was incorporated into C_3A, the time of conversion to C_3AH_6 during hydration, as observed by calorimetry, increased considerably, and the size of the heat peak was markedly reduced. With increasing Na_2O content, this effect was much less pronounced.

To further understand the reactions, Spierings and Stein (110) hydrated pure C_3A in various concentrations of NaOH. The calorimetric data were rather complex and suggested that both OH^- and $Al(OH)_4^-$ were influencing the reaction, but the effects appeared to be independent of the cation. As the concentration of NaOH increased up to 0.1 M, the early reactivity of C_3A decreased markedly. On the basis of conductivity measurements, this result was attributed to the precipitation of a retarding, amorphous $Ca(OH)_2$ precipitate, promoted by the highly alkaline conditions. The formation of $Al(OH)_4^-$ would, in this case, tend

to prevent precipitation of AH_3 and to favor the formation of C_2AH_8 rather than C_4AH_{13}. The calorimeter peak corresponding to conversion to C_3AH_6 became increasingly retarded and smaller as NaOH was added, suggesting that the hexagonal hydrates, or gel, were stabilized with respect to C_3AH_6. This peak occurred earlier at high concentrations of NaOH, and it also became sharper, although the area under the peak did not change very much. Spierings and Stein (110) attributed this result to the decreasing stability of the hexagonal hydrates, but their calorimetry data indicated that the overall hydration of C_3A decreased as the concentration of NaOH in solution increased.

Sulfates

Tadros et al. (108), Skalny and Tadros (119), and Mehta (120) have recently questioned the role of ettringite in the retardation of C_3A by sulfate ions. In studies of the dissolution of C_3A in acid media, it was found (108,119) that the induction period, discussed above (Fig. 12), was significantly increased in the presence of sulfate ions. This was attributed to the adsorption of sulfate ions on the positively charged surfaces, and a Langmuir-type adsorption isotherm was found to apply. Increasing the concentration of sulfate ions resulted in a decrease in the positive surface charge, but charge reversal did not occur. At the concentrations used, no precipitation of ettringite was observed, although substantial retardations were found. Similar results were obtained with additions of $CaSO_4$ or Na_2SO_4.

Fierens et al. (121) observed from thermoluminescence studies that the initial reactivity of C_3A did not influence its reaction with gypsum, in contrast to its behavior in pure water. This observation could be explained by a rapid adsorption of sulfate ions on active surface sites. For C_3A in cements, Locher et al. (122) found an induction period lasting several hours, which was independent of sulfate concentration (the clinkers contained some alkali sulfates) and the formation of ettringite and hexagonal hydrates (monosulfoaluminate?).

Collepardi et al. (123) have challenged these conclusions in a new study of the system C_3A-CH-$C\bar{S}H_2$-H. They observed that retardation of C_3A, as determined by isothermal conduction calorimetry and by DTA, occurred only when ettringite was formed. Thus, when Na_2SO_4 was added, there was little early retardation because ettringite did not form. The effect of the sulfates on later hydration is not clear from this study. Retardation was greatest when both $C\bar{S}H_2$ and CH were present, a fact attributed to the presence of small, colloidal-sized crystals of ettringite that form under such conditions (124,125). Mehta (124) suggests that this is a gel-like form of ettringite. It is noteworthy that, in such systems, a gel-like coating apparently precedes the growth of identifiable ettringite crystals (126) and appears remarkably similar to that observed by Breval (109) in sulfate-free systems.

Corstanje and co-workers (107) took a slightly different point of view. At S/A molar ratios where ettringite can be detected, retardation was observed; but, at $\bar{S}$/A ratios less than 0.10, when ettringite does not form, $C\bar{S}H_2$ tended to promote C_3A hydration. As discussed above, monosulfoaluminate can form an "insulating layer," but its formation does not promote AH_3 precipitation to the same extent as C_4AH_{13} formation.

These various studies come to disparate conclusions; clearly, more work needs to be done to clarify the situation. As in the case of sulfate-free hydration, the evidence indicates that, after the initial hydrolysis, a gel forms which can cause retardation. In this case, the gel undoubtedly contains SO_4^{2-} ions, and the relative proportions of calcium, aluminum, and sulfate may well determine how readily the gel may recrystallize to other hydration products — ettringite, hexagonal hydrates, or C_3AH_6. Such a hypothesis is an extension of that suggested by results of studies on sulfate-free systems and considers ettringite formation to be the process following the initial retardation.

The apparent contradiction between the studies discussed here can be reconciled if it is remembered that the conditions of hydration were very different. Skalny and Tadros (119) studied suspensions, whereas Collepardi et al. (123) studied pastes. A brief induction period of about 15 sec was observed (126) in pastes and could well have occurred in Collepardi's systems also. Corstanje and his associates investigated C_3A hydration in the presence of C_3S, and Locher et al. studied C_3A in portland cement. It might be useful to consider three sequential retarding steps, any one of which may be the dominant mechanism for a given set of conditions:

1) Formation of a hydrolyzed double layer, which is important in dilute suspensions

2) Formation of an amorphous hydration product (gel), which may be most important in cement pastes

3) Formation of ettringite, which dominates retardation in pastes of C_3A and gypsum.

Recent studies (126,127) have confirmed earlier observations that monosulfoaluminate may form even when gypsum is still present. Evidently, the crucial factor is the reactivity of C_3A compared to the rate of release of sulfate ions from the gypsum crystals, i.e., the sulfate balance must be assessed from a kinetic viewpoint as well as from stoichiometric considerations.

Chlorides

Although calcium oxychloride has not been recognized as a normal hydration product of

C_3A in the presence of chlorides, its formation has been reported by Lepnev et al. (111) in pastes containing $CaCl_2$ — but not NaCl. However, Traetteberg and Grattan-Bellew (127) confirmed earlier conclusions that $C_3A \cdot CaCl_2 \cdot 10H_2O$ forms along with C_4AH_{13}, and that the formation of oxychloride is dubious, or, at best, occurs only under special conditions. $C_3A \cdot CaCl_2 \cdot 10H_2O$ has an X-ray diffraction pattern very similar to that of C_4AH_{13}, and a solid solution may exist between the two (127). The chloroaluminate hydrate may be mistakenly identified as α-C_4AH_{13}. Calcium chloride accelerates the formation of ettringite (127). With high proportions of chloride (16 wt.%), the chloroaluminate hydrate forms before ettringite converts to monosulfoaluminate. This finding agrees with previous results of Tenoutasse (128).

Other Inorganic Admixtures

Holten and Stein (129) studied the effects of finely divided quartz on the reactions between C_3A and $C\bar{S}H_2$ under conditions where ettringite was the stable phase. They found that the quartz significantly increased the rate of reaction of C_3A and concluded that this was primarily due to the formation of ettringite on quartz particles, which prevented it from acting as an "insulating layer" of the type described earlier. This explanation ignores the possibility of any reaction between quartz and the solution, even though some chemical activity might be expected. A similar phenomenon might be expected in the case of natural pozzolanic silicas, but, in this case, the initial reaction of C_3A was retarded compared to that with quartz (130). The effect of the pozzolans was to increase the conversion to C_3AH_6 in gypsum-free systems, and to increase the rate of consumption of calcium hydroxide whether or not sulfate was present. It is even more likely in this case that the silica was chemically active in the system, and it is thus tempting to attribute the accelerated consumption of CH to the formation of calcium silicoaluminate hydrate, recently reported by Regourd et al. (131).

Tashiro and Oba (132) reported that oxides that retarded the hydration of C_3A (e.g., $Cu(OH)_2$ and ZnO) stabilized the hexagonal hydrates with respect to C_3AH_6, while those that accelerated hydration (e.g., PbO) increased the rate of conversion. This result is analagous to the influence of organic admixtures (133). Both Cr_2O_3 (132) and $CaCrO_4$ (134,135) also retard the hydration of C_3A. The effect of $CaCrO_4$ is attributed to the initial formation of the chromate analog of ettringite, which later transforms to the hexagonal $C_3A \cdot CaCrO_4 \cdot nH_2O$. The X-ray diffraction pattern of this compound appears to be similar to that of C_2AH_8, and the peaks attributed by Tashiro and Oba to C_2AH_8 may actually result from the presence of $C_3A \cdot CaCrO_4 \cdot nH_2O$ or the cuprate and zincate analogs. Tl_2CO_3 retarded the reaction of C_3A with gypsum (136), and calcium carboaluminate hydrate was detected in the system.

Organic Admixtures

Ramachandran (137) reported that triethanolamine accelerated the hydration of C_3A both with and without sulfate, increasing the amount of C_3AH_6 or ettringite formed in the first few minutes. No changes in the nature of the hydration products were observed. Milestone (138) showed that sugar acids such as gluconic acid, which are formed as oxidation products of sugars, were very effective retarders of C_3A hydration. Gluconic acid was about 10 times more effective than glucose, for example. The retarding power of commercial lignosulfonate admixtures was attributed (139) to the presence of small, but significant, quantities of sugar acids.

Milestone's study confirms that retardation is accompanied by the stabilization of the hexagonal hydrates due to organic molecules entering the crystal lattice. Since it has been shown that the hydrates are poorly crystalline in the presence of retarders, it could be argued that organic retarders impede the crystallization of the initial gel layer to the hexagonal hydrates and C_3AH_6. The effect will depend on both the concentration and the alkaline stability of the admixture. Compounds that retard the hydration of pure C_3A also retard its reaction with calcium sulfate. This would be expected if the admixtures affect the initial gel layer, regardless of whether it contains sulfate ions. This would also explain why accelerators such as triethanolamine react the same way in both systems.

Normally, a retarder is added with the mixing water; but, when it is added after a few minutes of hydration, retardation increases (133). The degree of retardation is assumed to be controlled by the concentration of the admixture in solution which, in turn, is controlled by the degree to which the retarder is removed from solution by sorption on the solid materials. Sorption is greater when the retarder is added during the initial formation of the hydration products. In a recent study (126), a retarder, citric acid, was allowed to contact the solid surfaces of a C_3A-$C\bar{S}H_2$-C mixture before water was added. The result was a longer induction period followed by increased reactivity and then prolonged retardation (Fig. 16). When the citric acid was allowed to come in contact with C_3A only, early reactivity increased even more, but no subsequent retardation occurred. Clearly, the competition between citric citric acid and water at different solid surfaces is an important factor.

What causes some organic compounds to be accelerators and some retarders? It has previously been shown (133) that retarders are good chelating agents; yet, accelerators, such as triethanolamine or 8-hydroxyquinoline, are also excellent chelating agents. An accepted view is that chelation with the aluminate ion $[Al(OH)_4^-]$ may accelerate the initial hydrolysis of C_3A by changing the chemical potential of species in solution and thereby preventing immediate precipitation of a gel. Evidence for the formation of aluminate complexes has been summarized elsewhere (133). Once preci-

pitation of a gel starts, removal of some of the admixture by adsorption in the gel or crystalline hydration products will allow further rapid precipitation, thereby causing flash set. The initial acceleration is usually followed by retardation of later reactions, as would be expected if the adsorbed admixture can interfere with recrystallization of the hydration products. As postulated by Skalny and Tadros (119) for sulfate retardation, the organic molecules in very strong retarders may adsorb on the Al-Ca double layer, which would inhibit even initial hydrolysis. Adsorption of this kind has been suggested by Jawed et al. (57) for lignosulfonate-alkali carbonate combinations in cement. The relative importance of adsorption on hydration products in any particular case will depend on the molecular structure and concentration of the admixture.

2.3.5 The Nature of the Retarding Layer

The recent results discussed above clearly require a reformulation of the previously accepted view of retardation. Although the formation of an Al-rich layer at the surface of each C_3A grain may occur initially, other evidence points to the formation of a second retarding layer by precipitation processes, which probably accounts for secondary, extended retardation. It may not be necessary to postulate the existence of precipitates of distinct chemical composition as suggested by Stein and co-workers. The retarding layer can be considered as a co-precipitate of aluminum and calcium hydroxides and sulfates, the exact composition of which depends on the surrounding solution. The degree of condensation of the alumina phase will also depend on the nature of the solution. From this amorphous precipitate — Breval's gel phase -- can grow C_4AH_x, C_2AH_8, $C_4A\bar{S}H_{12}$, $C_6A\bar{S}_3H_{32}$, or C_3AH_6, depending on the particular circumstances. However, the gel phase could be a hydrolyzed layer similar in principle to the protective layers suggested for C_3S hydration. Minor components or admixtures, such as alkalies, chlorides, organic molecules, etc., may also enter the gel and modify crystal growth by random substitution in the lattice of the hexagonal hydrates. This mechanism would have much in common with other cementitious systems, that of C_3S and C_2S, monocalcium aluminate, or magnesium oxychloride.

2.4 The Ferrite Phase

Recent studies (140-150) have confirmed previous conclusions that hydration of the ferrite phase (Fss) is very similar to that of C_3A, both in the presence and absence of sulfate. Reactivity increases with increasing A/F ratio (140,141), but Fss reacts more slowly than C_3A (141,142).

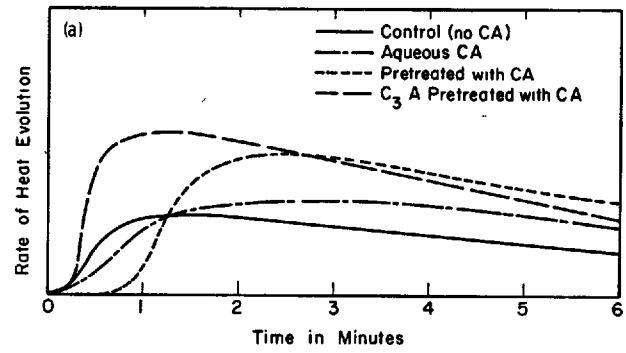

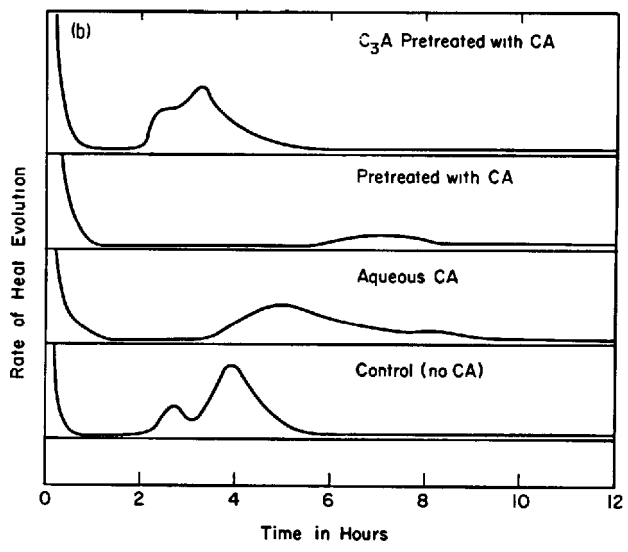

Figure 16. Hydration of C_3A-$C\bar{S}H_2$-C mixture with citric acid (CA) added at different times (adapted from ref. 126): (a) Rate of heat evolution in the first few minutes, (b) Rate of heat evolution over several hours.

2.4.1 Hydration Studies

Hydration Without Sulfate

At low temperatures, $C_4(A,F)H_{19}$, usually detected as $C_4(A,F)H_{13}$, is the stable product; but, at about 20°C, it soon converts to $C_3(A,F)H_6$. Ramachandran and Beaudoin (150) considered the conversion of $C_4(A,F)H_{19}$ to $C_3(A,F)H_6$ to be slower than in C_3A hydration — possibly because C_3A pastes may reach very high temperatures due to the high heat of hydration. Thus, the conversion of the hexagonal hydrates to C_3AH_6 cannot be

distinguished calorimetrically unless the reaction is retarded. In contrast, the conversion to $C_3(A,F)H_6$ in C_4AF pastes can be readily separated (see Fig. 17) (67), and the process C_4AF in which $C_3(A,F)H_6$ has already formed. At higher temperatures (>50°C), only $C_3(A,F)H_6$ is formed. Although Bensted (142) claims that the hydration of the ferrite phase should be studied only in the presence of calcium hydroxide to simulate conditions in a portland cement paste, others (140,141) have shown that its presence has very little effect on the hydration kinetics and does not change the hydration products. Sanzhaasuren and Andreeva (148) found, however, that calcium hydroxide retarded the conversion of $Ca_4(A,F)H_{13}$ to $C_3(A,F)H_6$.

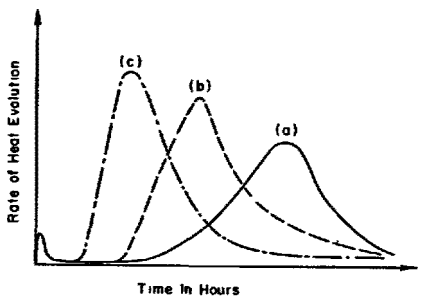

Fig. 17 - Influence of seeding on hydration of C_4AF (ref. 67): (a) No seeding, (b) seeds mixed with C_4AF, (c) seeds ground with C_4AF.

Two unresolved questions concerning the hydration of the ferrite phase have been:

1) Is amorphous ferric hydroxide (or aluminum hydroxide) formed as required by stoichiometry?

$$C_4AF + 22H \rightarrow C_4(A,F)H_{19} + (A,F)H_3 \qquad (16)$$

2) What is the degree of iron substitution in the hydration products?

Rogers and Aldridge (143) provided direct evidence on these two points. Using the SEM, they observed finely divided particles that contained only iron and must therefore have been ferric hydroxide (or more likely, hydrated ferric oxide). This phase could not be detected by XRD and was therefore amorphous, as is usually assumed. Since no aluminum hydroxide was observed, the reactions must be (143):

$$C_6A_2F + 30H \rightarrow C_4AH_{19} + C_2AH_8 + FH_3 \qquad (17)$$

$$C_4AF + 22H \rightarrow C_4AH_{19} + FH_3 \qquad (18)$$

$$2C_6AF_2 + 60H \rightarrow 3C_4(A_{2/3}F_{1/3})H_{19} + FH_3. \qquad (19)$$

These reactions are in general agreement with the degree of Fe-substitution found in the hexagonal hydrates and determined by variations in the d-spacings (Table III). Since there was a small substitution of iron in all cases, a little Al was probably included in the FH_3. By contrast, Sanzhaasuren and Andreeva (148), using the same method, estimated 60% F in $C_3(A,F)H_6$ at 20°C and 50% F at 50°C. Klyusov et al. (151) reported the presence of gibbsite in C_4AF pastes. It is not clear why different results were obtained for iron substitution in the hydration products.

Table III

DEGREE OF SUBSTITUTION OF Fe IN $C_3(A,F)H_6$ (Ref. 143)

Temp. of Formation	C_6A_2F	C_4AF	C_6AF_2
21°C	2.5 ± 1%	6 ± 3%	30 ± 3%
50°C	3.0 ± 2%	—	2 ± 2%

Neither Rogers and Aldridge (143) nor Teoreanu et al. (146) found evidence for the formation of C_3FH_6 in these systems, in contrast to the claims of Tamas and Vertes (144). They also found less Fe-substitution than assumed by Vertes and Ranogajec-Komor (145). The interpretations by Vertes and co-workers were based on Mossbauer measurements alone, but Rogers and Aldridge were not able to distinguish between any hydration products -- $C_4(A,F)H_{13}$, C_4FH_{13}, C_3AH_6, C_3FH_6, or FH_3 — by Mossbauer measurements. C_4FH_{13} and C_3FH_6 formed only in C_2F hydration (see below). $C_3(A,F)H_6$ was unstable at high temperatures and will break down to C_3AH_6, hematite (α-Fe_2O_3), and lime; thus, decomposition was complete at 150°C. In contrast, Teoreanu et al. (146) did not observe Fe_2O_3 above 75°C.

Hydration With Admixtures

Sulfates. When gypsum is present, the hydration sequence is the same as for C_3A (141,142,147,152); ettringite is first formed and later converts to monosulfoaluminate when the gypsum is exhausted. The calorimetric curve has the same features as observed for C_3A (142). However, early hydration of C_4AF is much more strongly retarded by gypsum than is C_3A, and, when calcium hydroxide is also present, early hydration practically ceases. It is not clear why this difference occurs; perhaps sulfate adsorption, as discussed for C_3A hydration, is very effective in first step retardation.

At high gypsum contents, Ramachandran and Beaudoin (152) observed conversion of ettringite to monosulfoaluminate before all the gypsum was exhausted. This may have been caused by local depletions due to the screening action of ettringite. The effect was more noticeable with high temperatures and low porosities.

Hydration With Chlorides. When hydrated with <3N $CaCl_2$ solution (151,153), C_4AF forms $C_3(A,F)\cdot CaCl_2\cdot 10H_2O$ as a major hydration product. Stukalova and Andreeva (153) considered this compound to contain only about 10% F at

concentrations of $CaCl_2$ >4.5N. The chloride analog of ettringite forms, but not if NaCl is used instead of $CaCl_2$ (151). Also, $C_4(A,F)H_{19}$ does not form in the presence of chloride, and only $C_4(A,F)\underline{H}_{13}$ is observed. As in the case of the C_3A-$C\overline{S}H_2$ system, $CaCl_2$ accelerates the formation of ettringite from C_4AF-$C\overline{S}H_2$ mixtures (154). After the sulfate is consumed, $C_3(A,F)\cdot CaCl_2\cdot 10H_2O$ forms rather than monosulfoaluminate. These results are in general agreement with earlier studies for C_3A pastes (140). The presence of chloride does not change the stoichiometry of ettringite. The Fe-substitution remains at about 35%.

2.4.2 Hydration of Calcium Ferrites

Hydration of C_2F forms C_4FH_{13} (140,143), which has been shown to initially form as C_4FH_{19}, and amorphous FH_x (143). At 38°C, C_4FH_{13} converts to C_3FH_6 within 1 day, but the latter rapidly breaks down to CH and hematite. At 80°C, C_3FH_6 has never been observed, only its decomposition products. Teoreanu et al. (146) did not observe either C_4FH_{19} or C_3FH_6 in their study of C_2F hydration. However, it has been pointed out (143) that these hydrates give the same Mossbauer spectra as FH_x, and that XRD is not sensitive unless a good monochromator is used to filter out iron fluorescence. Aldridge and Rogers also studied "C_3F" and "C_4F," which are really intimate mixtures of C_2F and C. As expected, they behave similarly. CF also hydrates in the same way, but much more slowly.

2.4.3 Competition with C_3A

Since their hydration is so similar, C_3A and the ferrite phase must compete for sulfate ions during the hydration of portland cement. This interaction has not been adequately studied, but Jawed et al. (141) added small quantities of C_3A to $C_4\overline{AF}$ + gypsum and found that conversion of ettringite occurred much sooner, depending on the amount of C_3A. The calorimetric curves showed what appeared to be a conversion peak for C_3A followed by one for C_4AF. These results indicate that C_3A competes more effectively for sulfate ions and suggest that local exhaustion of SO_4^{2-} may occur near the more reactive C_3A grain. When hemihydrate was used instead of gypsum, the conversion reactions were retarded. It was not clear why this happened, but the more soluble hemihydrate will release SO_4^{2-} at a greater rate, thereby allowing C_4AF to form more ettringite initially and so retard its hydration more effectively.

It must be remembered that impure phases are present in portland cement. C_3A may contain up to 10% F (corresponding to $C_6A_{8/3}F_{1/3}$), while the ferrite phase contains Si, Mg, and alkalies. The effect of these substitutions might be to lower the reactivity of C_3A (155) and increase the reactivity of the ferrite phase (156), thereby making competition easier.

3. HYDRATION OF PORTLAND CEMENTS

Portland cements are composed of clinker minerals and smaller amounts of minor components, e.g., alkali sulfates and MgO. In addition, a limited amount of calcium sulfate, usually in the form of gypsum, is added for set regulation. The main clinker minerals in cement are impure forms, containing small quantities of every element that is present in the raw materials.

3.1 Hydration Mechanisms

Selected mechanistic studies performed on cement-water, rather than on pure clinker mineral-water system will be discussed in this section. Because the early development of C-S-H is primarily due to the hydration of alite, a direct correlation is generally made between the hydration of cements and alite. However, we do not know the precise influence of the C_3A and C_4AF phases on the hydration of the silicates. Neither do we know the exact effect of gypsum, alkalies, MgO, etc., on the above interrelationships.

3.1.1 Mechanisms Suggested by Soviet Scientists

The basic cement hydration mechanisms are given special attention in the U.S.S.R. (157). The cement-water system is generally handled as a heterogeneous liquid-solid system with interacting components, in which the development of hardened cement paste properties is the result of condensation of disperse systems. General conclusions regarding the solidification of all cementitious systems are based on theoretical considerations.

Sychev (158) presents views very similar to those discussed earlier in the C_3S section. The low coordination of some surface atoms plays an important role. Thus, for example, the formation of the first hydrates on the surface of an alite particle may well initiate at these active centers. The first hydrate, formed on the surface and initiating the induction period, is believed to be an unstable, semi-permeable film of $C_3S\cdot H_2O$. For structural reasons, some of the Ca atoms, not coordinated with the silicate tetrahedra, react with water, thus enabling transfer of Ca^{2+} into the liquid phase. The $C_3S\cdot H_2O$ membrane changes into a layer of hydrates with $C/S < 3$, which is more permeable, and the hydration reactions resume to form a cementitious phase with high surface area (acceleration period).

The formation of new phases is related to the surface protonation of calcium silicate particles (which produces an increase of pH), ionization of silica tetrahedra, and formation of a double layer. These phenomena are considered important during the paste structure development. As the $[Ca^{2+}]$ in the liquid increases, saturation level is reached, and adsorption of Ca^{2+} on the surface leads to formation of hydrates outside the originally formed primary hydrate ("outer product"). Water molecules diffuse through the hydrates to the anhydrous surface forming the

"inner product." The solidification of a cementitious paste is the result of condensation of the solid particles and formation of hydrogen and donor-acceptor bonds at the interparticle contacts. The adhesive and strength properties of the cementitious system are strongly dependent on the electrostatic properties of the cations and their ability to form covalent bonds. In hydrated portland cement, hydrosilicates with lower C/S should have increased strength.

According to Danilov (77), the initial step in the hydration is the transfer of a proton (from water) to the oxygen ions at the cement mineral surface (e.g., C_2S, C_3S, C_3A). The ions thus formed (e.g., Ca^{2+}) transfer into the solution where they react with water to reach an equilibrium distribution of complexes. These complexes adsorb on the surface, thus passivating it and initiating an induction period. The relative reactivity of the various clinker minerals is ascribed to the differences in the electronegativity of the metal ions and the ability of the double oxide to protonate. This approach is used to explain the higher hydraulic activity of C_3S (characterized by the Ca-O-Ca bond) compared to that of β-C_2S, as well as to explain the increased reactivity of Al_2O_3-substituted alite and the inhibited hydration rate of P_2O_5-substituted alite. The induction period ends when hydrate nuclei are formed and disrupt the adsorption equilibrium. The kinetics of the crystallization are determined by the location of the new nuclei formed (bulk liquid phase, surface of impurities, or adsorption film). Kapranov (159) and Polak (160) have presented quantitative treatment of the initial hydrolysis and formation of crystal nuclei. Usherov-Marshak and Urzenko (161) also conclude from thermodynamic considerations that nucleation controls cement hydration.

Vyrodov (162) considers the hydration of cement to be a topochemical process characterized by the formation on the anhydrous surface of layers consisting of thermodynamically unstable hydrate. These layers can form because the rate of primary hydrate formation is greater than the rate of its concurrent dissolution. The induction period is thus caused by a decrease in the anhydrous surface-to-water interaction. The renewed reactivity (acceleration period) is ascribed by Vyrodov to recrystallization of the primary hydrate layer into new hydrates or to its disruption by "internal mechanical stresses of a physico-chemical nature." The hydration process is described as topochemical also by Sorochkin et al. (163)

3.1.2 Osmotic Pressure Mechanisms

Double et al. (31), using high-voltage electron microscopy (HVEM), postulated an analogy with "silicate gardens" and developed the following mechanism. Within minutes after the initiation of hydration, a semi-permeable silicate hydrate envelope forms around the anhydrous silicate grains. The gelatinous envelope separates the anhydrous material from the bulk liquid, thus initiating the induction period. Whereas calcium ions can diffuse through the membrane, the silicate ions, formed by dissolution of the anhydrous material beneath the membrane, cannot penetrate the membrane and, thus, increase the osmotic pressure. This mechanism, according to the authors, is evidenced by the sharp increase in the Ca^{2+} concentration but a low silicate concentration in the bulk liquid during the induction period of hydration. When the osmotic pressure is sufficient to rupture the membrane at weak points, the calcium-depleted hydrosilicate is squeezed into the bulk liquid where it recombines with the Ca^{2+} ions to precipitate tubular fibrils and, possibly, other morphologies. This event marks the initiation of the acceleration period. The mechanism is based mostly on microscopic evidence.

Decrease of the pressure within the membrane enables further dissolution of the cement grains with deposition of C-S-H material (of different morphology and, possibly, composition from that formed in the outer spaces) inside the original grain boundaries. The authors believe that the two different but simultaneous precipitation processes account for the difference in the morphology and composition of the "inner" and "outer" hydration products. However, the mechanism does not address the question of various morphologies as distinguished by Diamond (30). The formation of calcium hydroxide and aluminate hydrates proceeds by the conventional dissolution-nucleation-crystal growth mechanism. A similar mechanism, schematically shown in Fig. 18, was proposed by Birchall and co-workers (32). According to this model, the early hydration of the calcium silicates involves neither nucleation and growth of C-S-H nor a "through solution" mechanism.

Whereas Double et al. and Birchall et al. used diluted suspensions in a special environmental cell, Jennings and Pratt (27,33) were able to examine pastes of normal consistency in a differentially pumped specimen stage. Their HVEM data also showed the formation of a membrane which they considered permeable to water and Ca, but, in contrast to the above authors, they believed that the end of the induction period, indicated by the disruption of the membrane, was caused by $Ca(OH)_2$ nucleation on its surface. Solutions rich in Ca^{2+} and silicate mixed, forming C-S-H of thin-foil morphology, which subsequently rolled up during drying to form acicular Type I C-S-H. Although neither of the above "protective membrane" mechanisms addresses explicitly the function of the aluminate, ferrite, and minor clinker phases in the overall cement hydration mechanism, Jennings and Pratt acknowledge the presence of minor components in the membrane, and suggest that they are responsible for the differences in hydration, as well as in the morphology of hydrates formed from pure C_3S and portland cements. In contrast to Double et al. (31), who reported the existence of hollow C-S-H needles formed by an osmotic mechanism, Jennings and Pratt found hollow acicular needles containing Ca, Si, Al, and S, implying ettringite composition. The situation is unclear, and much

more evidence is needed to explain the available data. Care must be taken in extrapolating observations made on suspensions at high w/s to pastes at normal w/s. High water-solids ratios extend the induction period of C_3S and may change the mode of formation of C-S-H.

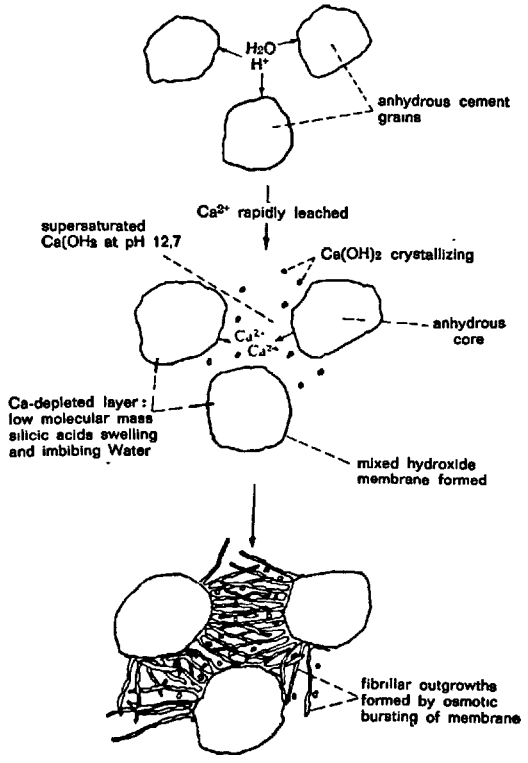

Fig. 18 - Mechanism of hydration proposed by Birchall et al. (32)

3.1.3 Hollow-Shell Hydration

Barnes et al. (164,165) have recently reported the occurrence of "hollow shell" hydration of cement particles. Although first observed at glass-cement interfaces (164), this feature is also found in the bulk of the paste and may occur also in pure silicates. The mode of hydration leading to the observed structure formation is not known, but it is an additional factor that must be ultimately explained in any description of hydration.

3.2 Selected Issues

3.2.1 Early Structure Formation

The practical implications of the early hydration reactions of cement are found in the setting behavior and early strength development. Specific examples of how these properties are affected by such factors as alkalies, crystal modifications, admixtures, etc., are discussed in the next sections. Here we briefly review the more general aspects of the subject. The wealth of information available on cement hydration clearly indicates that alite hydration controls early strength development and probably normal setting behavior, although Gebauer (166) has suggested that highly reactive alite may contribute to abnormal setting behavior in certain cases. Adams (167) and Previte (168) have found good correlation between the end of the induction period and the initial set determined by standard ASTM tests; final set occurs about midway through the acceleration period. However, Locher et al. (122) believe that normal setting occurs upon the recrystallization of ettringite, rather than by the formation of new hydration products of C_3S. Schramli (169), considering the effect of C_3A on the setting of portland cement, points out that such an analysis is complicated by lack of uniformity in 1) methods of determining setting, 2) measurements of C_3A content, 3) material on which experiments are conducted, i.e., paste, mortar, or concrete, and 4) the changes in cement composition that occur when when C_3A contents are changed.

Locher et al. (122) have concluded that the effects of gypsum on setting behavior are due not to changes in the rate of hydration of C_3A, but to the way the hydration products form. With the correct amount of gypsum, small crystals of ettringite cover the surfaces of the grains and do not affect the rheology of the system. Setting will occur when the ettringite recrystallizes to form larger crystals which bridge the cement grains. If too much sulfate is present, large crystals of ettringite will form initially and cause premature stiffening. Recrystallization of gypsum or precipitation of syngenite will cause the same effect but generally more rapidly. If too little ettringite is present, large crystals of the hexagonal hydrates can form and bridge particles in the same way. In extreme cases, flash setting may occur. Thus, C_3A causes "abnormal" setting behavior if the SO_3-C_3A balance is not corect. Either the reactivity of the sulfate or of the C_3A (117) or the presence of admixtures (170-173) can affect this balance. In low-C_3A, Type V cements, C_4AF may play the same role as C_3A. Frigione (174) has studied the false set caused by gypsum dehydrated in the grinding mills.

It must be remembered that the effects on setting and early hardening may be quite different because of the concomitant effects on C_3S hydration (117, 172). The rate of early strength development is of course determined by the rate of C_3S hydration in the acceleration period, but the processes occurring at this stage may also affect later strength development. For example, $CaCl_2$ influences the properties of C-S-H and the pore size distribution. Similarly, Bentur (175) has shown that the presence of sulfate ions can reduce the "intrinsic strength" of C-S-H, and thus affect the optimum gypsum content of a cement. Such influences on C-S-H may also change the diffusion coefficient of the C-S-H layer around the cement grains and, hence,

the rate of later hydration.

3.2.2 Interactions Between Hydrating Cement Compounds

The main cement compounds do not react in isolation, and interactions between them can be important. For example, it is known that C_3S hydration is retarded when C_3A is involved in uncontrolled initial reactions. This behavior is believed to be one of the factors affecting optimum gypsum content (176) and the low rate of C_3S hydration attributed to a high lime demand during the formation of hexagonal hydrates. However, Cottin (177,178) attributes retardation to the release of small amounts of soluble alumina when sufficient gypsum is present. A similar explanation is offered by Bobrov and Shikiryansky (179) to explain the adverse effect of C_4AF on C_3S hydration in the absence of sulfate. Conversely, C_3S will slow the rate of hydration of C_4AF by the liberation of large quantities of lime into the solution. The formation of calcium silicoaluminates (131) indicates interaction of C_3S and C_3A during the hydration.

Young and Tong (87) have shown that only small quantities of C_3S are necessary to control the concentration of Ca^{2+} in the contact solution. They argue that the faster nucleation of CH in the presence of C_3S should speed up the hydration of β-C_2S, as has been observed earlier.

3.3 Factors Affecting Hydration Behavior

The reactivity of cement depends on parameters such as crystal size, solid state impurities, stabilization of polymorphs, presence of minor components, etc. The way these factors are affected by manufacturing processes is discussed in the review papers of Theme I of this conference. The mechanistic implications of some of these factors have already been addressed; other parameters, which are important in cement hydration, are discussed below.

3.3.1. Effect of Minor Components

Alkalies

Jawed and Skalny (180) have written a comprehensive review on the effect of alkalies on the hydration and properties of cement. Although release of alkalies from the silicate phases may be slow, within a month or so, alkali concentrations in the pore fluid of pastes made with low-alkali cement may rise to about 0.2 M and may exceed 0.7 M in pastes of high-alkali cements. However, in many modern clinkers, a substantial fraction of the alkalies is present as sulfates. These pass into solution very rapidly, leading to a continuous rise in alkali concentration and complete dissolution of almost all the alkalies after about 28 days. The high alkali concentrations thus raise the pH of the solutions and lower the concentration of Ca^{2+} ions and the solubility of $Ca(OH)_2$ accordingly. Alkalies must therefore influence the hydration processes and modify the setting and hardening of cement pastes.

Alkali sulfates accelerate the hydration of cement (117,181-186) and may lower their activation energy (181). They principally affect alite hydration, which agrees with results of studies on pure C_3S (175). Cottin (178) concludes that K_2SO_4 accelerates alite hydration by preventing the alumina poisoning that occurs when C_3A is present without sulfate ions. However, K_2SO_4 is known to accelerate C_3S hydration in the absence of C_3A. Collepardi et al. (187) have confirmed previous studies that sodium carbonate is an accelerator. Since $CaCO_3$ was found in the system, they postulated that sodium sulfate forms according to the reaction:

$$Na_2CO_3 + CaSO_4 \cdot 2H_2O \rightarrow CaCO_3 + Na_2SO_4 + aq. \quad (20)$$

Luginina et al. (188) reported that alkali silicates also increased the rate of cement hydration. From these various studies, it can be concluded that alkali salts increase the hydration rate by affecting alite hydration, presumably through their influence on $Ca(OH)_2$ solubility. The anion might influence C_3A hydration and could lead to setting problems as discussed below.

Alkalies can promote flash setting of cements, and this phenomenon has been the subject of recent research. Richartz (189) and Sprung (190) found that rapid setting by potassium sulfate was due to the formation of syngenite:

$$K_2SO_4 + CaSO_4 \cdot 2H_2O \rightarrow K_2SO_4 \cdot CaSO_4 \cdot H_2O + H_2O. \quad (21)$$

Syngenite not only causes a plastic-type set, but the reduction of SO_4^{2-} in solution prevents satisfactory retardation of C_3A hydration. Regourd (117) also observed syngenite formation when C_3A hydration in a cement was accelerated by the presence of K_2SO_4. Rapid stiffening and lower early strength observed in certain cements have been attributed (191) to the presence of alkali carbonates in the clinker. Rapid setting with alkali carbonates (187,191) was also attributed to lowered Ca^{2+} concentrations, which hindered the formation of a retarding ettringite layer and thus accelerated C_3A hydration.

Although alkali sulfates present in clinkers will increase the rate of alite hydration, and hence early strength, strengths at 28 days or later generally decrease (192-194). This is in keeping with the general observation that more rapid early hydration results in lower ultimate strengths. Johansen (193) obtained good correlation between the amount of K_2SO_4 in a clinker and 28-day strengths. Increasing the K_2SO_4 content decreased 28-day strength but increased the amount of water combined after 3 minutes of hydration. Changes in optimum gypsum requirements (see discussion below) may have a bearing on this behavior (186,195).

Effect of SO_3 and C_3A

Hobbs (195) has recently reviewed the earlier literature concerning optimum gypsum content in cements. Although optimum content can be correlated

with the C_3A and alkali contents of the cement, Ost (196) used a standard multiple regression analysis to show that Lerch's original data (197) could be correlated primarily with cement fineness and secondarily with alkali content. Further, there was correlation with Fe_2O_3 content rather than with C_3A. Hobbs (195) re-analyzed earlier data on SO_3 concentrations that caused large expansions during moist curing up to 7 days and found a correlation with cement fineness or, less probably, with alkali content. From these studies, it can be concluded that fineness is the major parameter controlling optimum gypsum content, but, with the tendency for some modern clinkers to contain larger quantities of alkali sulfates, a new study of this subject could be of value. Smith and Matthews (198), for example, have shown that alkali sulfates in the clinker are more effective in controlling C_3A reactions than is added gypsum, although this contradics the results of Collepardi et al. on pure C_3A (123). When other parameters are equal, optimum gypsum content depends primarily on clinker sulfate levels. A reasonable correlation exists between 3-day heat evolution and total SO_3 content.

Other Minor Components

Minor components can have three effects on the hydration of cement:

1) They can affect the reactivity of the cement minerals by influencing their defect structure (see discussion in earlier sections of C_3S and β-C_2S hydration and References 60,199,200).

2) Their release into solution can accelerate the hydration of the silicates. Chromium (201,202), which exists primarily as K_2CrO_4, accelerates C_3S hydration. Phosphorus causes C_3S to be more reactive (200), but, in the presence of P-substituted C_3A, C_3S hydration is retarded unless gypsum is also present. This can be explained by assuming that the rapid hydration of C_3A releases phosphate ions, which are known (52) to retard the C_3S hydration.

3) Minor components may change the relative amounts of each cement compound in a clinker. Thus, TiO_2 (203) lowers the amount of C_3S formed and hence reduces early strength. Similarly, P_2O_5 in raw materials is known to decrease alite in the clinker.

3.3.2 Grinding and Prehydration

The effect of grinding on defect structures has already been discussed (14,85) and has been used to explain the effects of prolonged grinding (85). Grinding by jet milling (204) was observed to increase the hydration of the clinker compounds, particularly C_3S.

Prehydration of cement is the cause of "silo set" or "pack set" that can occur in storage silos. This is most likely to occur if the cement is stored while still warm, and too much water has been carried over from the grinding process (189); but, in certain circumstances, gypsum may dehydrate in the silo to provide additional moisture. Under the near-adiabatic conditions of a silo, the warmth of the cement combined with heat of prehydration may push the temperatures above 100°C, causing partial or complete dehydration of the gypsum. A cement temperature of ~70°C may be sufficient (205). Sprung (190) has shown that gypsum dehydration depends on 1) local temperature (temperature gradients in the silo result in greatest dehydration in the center), 2) C_3A content, and 3) alkali content of the C_3A. Dehydration is thus apparently aggravated by the dessicating action of hydrating C_3A. Water given off by the dehydrating gypsum can condense in cooler parts of the silo where prehydration without dehydration can occur.

There is general agreement that high-alkali, high-C_3A cements are very sensitive to the effects of prehydration. It appears that alkali substitution in C_3A increases its initial reactivity towards water. If alkali contents are low or most of the alkali is in the form of sulfates, the effects of prehydration are low. This result is in apparent conflict with observations that alkali-substituted C_3A is less reactive. Most probably, if the crystal structure is not changed, substitution will enhance crystal imperfections.

Prehydration delays setting times because a coating of hydration products grows on the C_3A grains. Although ettringite is generally cited as a major hydration product, Theisen and Johansen (206) did not observe it in their studies. The relative humidity must be high (> 80% rh) (113) to form the water films between grains that allow the transport of sulfate ions necessary for the rapid formation of ettringite. In addition, premature stiffening can sometimes occur due to the reduced reactivity of C_3A after prehydration: syngenite (KCS_2H) can form when there is a high alkali sulfate content, or gypsum dehydration can be enhanced (189,190,207). Prehydration also reduces 1-day and 28-day strengths, particularly with high-C_3A and high-alkali cements. Most cements will have normal setting and strength development if the loss on ignition at 500°C due to prehydration (corrected for gypsum and CH) is less than 0.35% (113). This can be done by keeping cements cool, mill humidities low, or using a grinding aid (207).

Storage of unground clinker can also cause problems with strength development. Cussino and Pinter (208) have attributed this to the influence of prehydration on the grinding of the clinker. Small clinker particles that are significantly prehydrated become easier to grind, thus producing a preponderance of fine material with low reactivity. The good, unhydrated clinker is more coarsely ground, and thus reacts more slowly than expected.

3.3.3 Effect of Temperature on Hydration

Sub-Zero Temperatures

The hydration of cement at temperatures below zero is of particular interest to Russian scientists because of their need to place concrete in severe climates. Cement and cement compounds will hydrate at -5°C (92,151,209-211), but hydration essentially stops at -10°C (151,211). Hydration is very slow at sub-zero temperatures, particularly in the case of β-C_2S (92,210), and accelerating admixtures, such as $CaCl_2$ are used. Logodia et al. (210) believe that hydration can be initiated at temperatures as low as -15°C by supercooled water: the heat of hydration then causes localized melting at the surface of the cement grain, which allows further hydration to proceed. The data in Table IV support this concept since most hydration takes place in the first 3 days when it is relatively rapid and temperature sensitive. β-C_2S does not hydrate appreciably because it is inherently less reactive and has a much lower heat of hydration than the other compounds. Hydration of cement at -20°C is dependent on the length of time the fresh paste is held at ambient temperature before being frozen (211); the critical period appears to be 4-6 hours (Fig. 19), which is sufficient time for alite hydration to pass through the induction period.

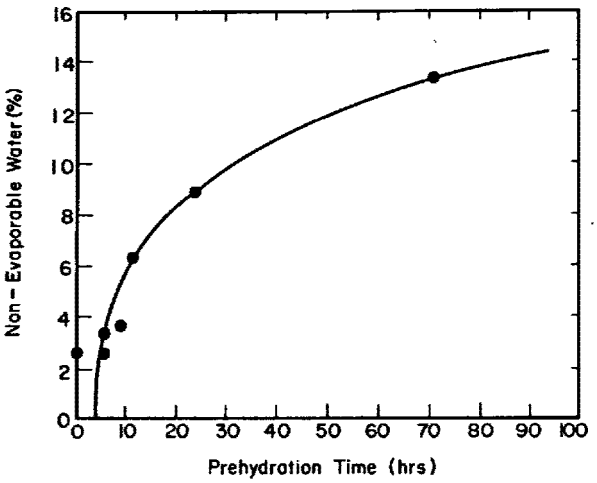

Fig. 19 - Influence of prehydration (at ambient temperatures) on the hydration of cement at -20°C (ref. 211).

Table IV

DEGREE OF HYDRATION IN FROZEN SUSPENSIONS AT -15°C (QXDA data) (from Ref. 210)

Compound	Percent Hydrated 3 days	90 days
C_3S	44	53
β-C_2S	3	4
C_3A	71	86
C_4AF	64	79

The mechanism of hydration does not appear to be radically altered by lower temperatures. The induction period in C_3S hydration is lengthened, but subsequent hydration can be quite rapid (Table IV). The hydration products are generally the same as those observed at normal temperatures; C-S-H, however, has somewhat different properties when formed at low temperatures (209,212). Measurements on C-S-H formed at 4°C (77) suggest that the changes in properties result from slower aging processes.

Above-Ambient Temperatures

C_2S hydration is reported to be accelerated more than that of C_3S at higher temperatures (213). Hydration of C_3S is accelerated to a greater extent above 60°C than between 20° and 60°C (213-215). Since the solubility of silica increases more rapidly above 60°C, and the solubility of calcium hydroxide decreases approximately linearly in the range of 30°-80°C, the dissolution of silica may be a controlling factor. No changes in hydration mechanism have been reported in the temperature range up to 90°C. The induction period is shortened (214,215), and the second heat peak is sharper and more intense, indicating very rapid hydration at the end of the induction period (213-216). After the initial rapid hydration, the rate of C_3S hydration decelerates at elevated temperatures (214-216), the apparent result (214) of a dense C-S-H layer around the C_3S grains due to accelerated aging processes. Bentur et al. (212) have reported data on the properties of C-S-H at 65°C that support this view.

A long-standing question concerning the hydration of C_3A is the stability of ettringite at elevated temperatures. It has variously been reported unstable at many different temperatures ranging from 40°C to above 100°C. Recent studies have not clarified the situation. Barvinok et al. (217) found ettringite to be unstable in the range 50-70°C, while Lach and Burev (213) observed ettringite up to 90°C, which is the limiting temperature of stability according to Moldovan and Butucescu (218).

3.3.4 Influence of Admixtures on Cement Hydration

Research programs assume, either tacitly or explicitly, that the effect of admixtures on cement hydration is due only to their influence on the hydration of C_3S and/or C_3A, and that C_2S and C_4AF can be ignored. The validity of this assumption has been justified by experience, since the precise action of a "set-modifying" admixture depends on how it affects the hydration of C_3S and C_3A. Under normal circumstances, it is the hydration of C_3S that affects setting, while C_3A is responsible for unusual setting behavior and changes in water requirements.

The classification of accelerators and retarders poses some problems of definition. An accelerator is generally described as a material that hastens the setting time and/or strength

development of portland cement. However, such a definition does not specify the exact nature of the measurement being used to develop the criteria, nor does it indicate the effects on the basic hydration processes. For the purposes of this review, we will classify accelerating admixtures into those that primarily accelerate the hydration of C_3S to achieve their effect and those that primarily accelerate C_3A hydration. The exact effect on cement will depend on the relative acceleration or retardation of each component (219). Such a classification is of more fundamental value than one based on inorganic/organic or setting/hardening distinctions, even though these have practical advantages.

Accelerating Admixtures

Since calcium chloride is the most widely used commercial accelerator, it has been extensively studied. A review article (43) and a book (44) summarize the influences of calcium chloride on hydration and properties of cement compounds and pastes.

Admixtures Accelerating C_3S Hydration. As discussed earlier, most inorganic electrolytes accelerate the hydration of C_3S, with soluble calcium salts being the most effective due to their greater effect on the crystallization of calcium hydroxide. It is clear from Kantro's extensive survey (39) that there is no single mechanism that can explain all observations. A salt may change the length of the induction period, the time of maximum heat output, or the area under the main heat peak (Fig. 20). Young (53,54,133) has attempted to analyze admixture interactions in terms of possible C_3S hydration mechanisms.

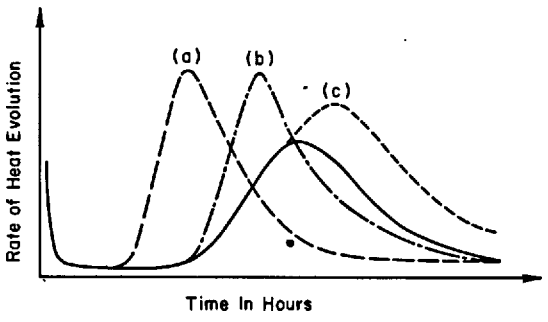

Fig. 20 - Effects of accelerating admixtures on cement hydration (solid line: normal hydration): (a) Shortened induction period, (b) faster rate of heat evolution in stage 3, (c) increased amount of heat evolution in stages 3 and 4.

The accelerators of C_3S hydration may affect also the hydration of C_3A. For example, $CaSO_4 \cdot 2H_2O$ retards the hydration of C_3A more than Na_2SO_4 (123), while calcium chloride can accelerate the formation of ettringite in the presence of gypsum (127,128,220). It should be noted, however, that many salts can form complex hexagonal calcium aluminate hydrates of the type $C_4AX_2H_n$ [$C_3A \cdot CaX_2 \cdot nH_2O$]. Thus, if C_3A forms hexagonal hydrates in the early stages of hydration, then the possibility exists for complex formation with the admixture. In such instances, overall C_3A hydration would probably be retarded. Because of this retardation, there is no good correlation between temperature rise and cement setting times.

Admixtures Accelerating C_3A Hydration. Although most organic compounds retard the hydration of cement, some are considered to be accelerators. Triethanolamine (TEA) is a case in point and has been the focus of much interest since it is also extensively used commercially. Recent studies (172,221) have shown that the accelerating characteristics of TEA are due to its effect on C_3A hydration, since it retards C_3S hydration. In small quantities, TEA has little effect on the setting times of cement and strength development. Cements containing more than 0.1% TEA tend to flash set and show reduced strength after 3 days. This effect of TEA is similar to that of sugars (172), which also tend to cause flash setting in large quantities, but which are strong retarders of C_3S hydration.

It is thus questionable whether we should consider TEA (and similar molecules) an accelerating admixture because of its influence on C_3S; yet, it is often included in an admixture formulation to offset the retarding action of a water-reducing component. This strategy presumably works because an increase in the rate of hydration of C_3A will allow the hydration products to absorb larger quantities of the retarding molecules (53,133). TEA can be used successfully since the concentration needed to achieve adequate acceleration of C_3A does not cause excessive retardation of C_3S and flash setting. This conclusion is supported by data summarized in Table V. Nevertheless, flash setting induced by TEA in the commercial admixture has been reported (172).

Retarding Admixtures

Studies on the hydration of pure cement compounds have shown that retardation of cement depends primarily on retardation of alite. As has been mentioned above, a retarder may retard or accelerate the hydration of C_3A. Again, the overall hydration of pure C_3A may be retarded while initial reactions may be accelerated, thus leading to the practical problems of premature set or excessive slump loss (171,172,173,222,223). Studies of such problems (170,172,222) have clearly demonstrated that, in many cases, an admixture can upset the aluminate-sulfate balance so that the cement behaves as if it were undersulfated. Addition of sulfate to attain the optimum sulfate content for the cement-admixture combination can often alleviate the problem. The situation is somewhat complex since no two cements behave in the same way. The amount and reactivity of the C_3A are clearly important, as is temperature. Sometimes the potential for false set arising from dehydrated calcium sulfates

can be changed by the addition of an admixture. On the other hand, although sugar-based admixtures are most commonly implicated in setting problems, the potential exists for most retarding admixtures to cause difficulties under the right circumstances. In view of the practical implications and scientific interest in the problem, the lack of basic studies is somewhat surprising.

TABLE V

EFFECT OF TRIETHANOLAMINE AND SUGAR ON CEMENT HYDRATION

Admixture	Concentration (wt. %)	% Change in Setting Time Initial	Final[a]	Ref.
Triethanol-amine	0.025	+ 13	+ 2	221
	0.05	+ 12	+ 1	221
	0.1	F.S.[b]	+200	221
	0.1	F.S.	[c]	172
	0.2	F.S.	[c]	172
	0.3	F.S.	[c]	172
Sucrose	0.05	+125	+130	257
	0.1	+325	+330	257
	0.1	- 31	+ 28	172
	0.2	F.S.	[c]	172
	0.3	F.S.	[c]	172

NOTES: Negative sign indicates shorter setting time.
a) Changes > 200% indicate excessive retardation of C_3S.
b) F.S. = flash setting indicating uncontrolled reactions of C_3A.
c) Final set according to ASTM C-266 even though C_3S has not yet completed the induction period.

If the mechanism of retarding action is to be elucidated, it is useful to know how different organic compounds affect the hydration of C_3S. Taplin (224) reported such a survey for a commercial cement, and Milestone (225) has made a similar survey using conduction calorimetry. The two studies are in good qualitative agreement, but we must assume that the observations for cement reflect the combined influence of C_3S and C_3A hydration. It can be concluded that a molecule must have a strong chelating group if it is to be a good retarder. The best chelating unit is typified by the β-hydroxyl-carboxylate grouping (Fig. 21a), which forms a strong 6-membered ring with a metal ion. For example, tartaric acid, which contains the grouping, is a strong retarder, while succinic acid, which does not have the β-hydroxyl group, is not; maleic acid retards, but fumaric acid, which cannot chelate, does not; and, similarly, glyceric acid is retarding, but propionic acid is not. Groupings which form larger or smaller chelate rings have less retarding power (Fig. 21b). Electronic effects are also important as can be seen in comparing pyruvic and glyceric acids or different hydroxylbenzoic acids (Fig. 21c). The retardation effect is related to the molecule's ability to chelate at more than one site, shown by the difference in retarding power between the dihydroxylbenzoic acids (Fig. 21c) and also between ketoglutaric acid and gluconic acid (Fig. 21d). More detailed comparison of retarders require studies of their effects on the hydration of pure C_3S. Milestone (55), for example, has shown that 0.1 wt % gluconic acid has greater retarding power than glucose for pure C_3S, although this is not true for all cements (225,226). Undoubtedly, the C_3A content is an important factor in determining relative behavior.

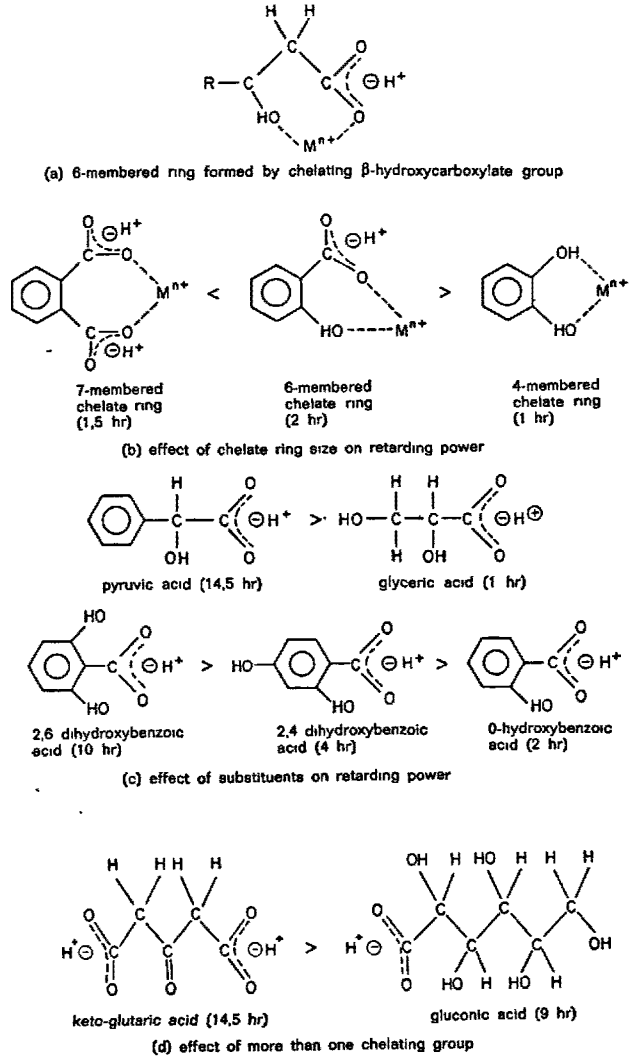

Fig. 21 - Effect of different molecular structures on retarding ability. Times represent the retardation of the main heat evolution peaks at 0.1 wt. % additions.

A few inorganic salts are known to retard C_3S hydration -- water-soluble diphosphates and polyphosphates (52), and fluorides (21,217,219) are recent examples. However, fluorides apparently accelerate C_3A hydration (217).

Water-Reducing Admixtures

With the introduction of the new "superplasticizing" admixtures, considerable interest has centered on the effects of these materials on cement performance. Unfortunately, few investigations have looked specifically at the influence of such admixtures on cement hydration, but it is clear from various observations (227) that interactions with the hydrating compounds must be important: 1) water reduction is most effective when the admixture is added after the mix water, 2) C_3S content and sulfate levels affect the degree to which superplasticizers increase workability, 3) subsequent slump loss is also affected by cement composition, and 4) excessive slump loss can be ameliorated by the concomitant use of a retarding admixture.

Little is known about the mechanism of action of high-range water reducers, although a vast amount of literature is available on their effects on the physical properties of mortars and concretes (227). They are believed to act by: 1) decreasing the surface tension of water, 2) charging the cement particles with equidirectional charges, or 3) producing a lubricating film at the particle surfaces. An interesting basic work, addressing the effects of surface-active chemicals on the viscosity of cement suspensions, has been published by Petri (228), but the effects on hydration are not discussed. Kondo and co-workers (229,230) have studied the effects of various dispersing surfactants, including a "superplasticizer," on the hydration of cement. Quaternary ammonium chlorides, representing cationic surfactants, caused some acceleration due to the influence of the chloride ion. Polyvinyl alcohols, representing non-ionic species, showed only slight retardation. Sodium p-n-dodecylbenzene-sulfonate represented various sulfonate anionic surfactants; generally, alite was much more strongly retarded than cements, particularly at high concentrations when the admixture contained long-chain aliphatics, and some hydrophilic substituents were present in the hydrophobic component. However, studies (229) have indicated that adsorption of these compounds is relatively low, and that absorption into calcium aluminate hydrates is not as strong as that observed for other retarding molecules. It has been hypothesized that differences in adsorption behavior due to molecular structure determine the extent to which adsorbed layers of these admixtures will affect the access of water to the surface.

Suzuki et al. (231) also studied the interaction of surfactants with C_3S and came to similar conclusions. Non-ionics, such as polyethenes, have little effect on hydration, whereas anionics, such as sodium gluconate or laurate, have retarding properties. Sodium gluconate strongly retards the hydration of C_3S at concentrations >0.1% and changes the surface charge to a positive value. affects surface charge less. These results are explained in terms of different adsorption characteristics. Tarnarutsky (232) found that additions of high molecular weight fatty acids as hydrophilic admixtures tended to retard hydration of cement and of the individual cement compounds. The effect on cement hydration depended on the alite content. Sugi et al. (233) considered lignosulfonate and polyol water reducers to influence gypsum solubilities and hence to affect false-setting tendencies of a cement. However, more work is necessary to further refine their ideas.

"Superplasticizers" can be used to either improve workability or lower w/c ratios to achieve strength. Another approach to attaining low w/c, high-strength concretes has been to work with ground clinkers using conventional lignosulfonate admixtures along with an alkali carbonate. The combination of lignosulfonate and sodium carbonate produces greater dispersing power and retardation of both ground clinker and cement than does lignosulfonate alone (57,234,235): the presence of carbonate apparently maintains higher concentrations of lignosulfonate for longer periods (57,234). The precipitation of $CaCO_3$ decreases lignosulfonate in solution and causes the onset of C_3A hydration and eventually C_3S hydration. It has been hypothesized (57) that a negatively charged lignosulfonate carbonate complex forms, which can adsorb effectively on the cement grains to form negatively charged surfaces that repel each other. This adsorption strongly retards C_3A hydration even in the absence of sulfate, but does not prevent Ca^{2+} ions from passing slowly into solution. When Ca^{2+} concentration exceeds a normal level, $\overline{CC}$ precipitates, destroying the lignosulfonate complex. C_3A can now hydrate more normally, and lignosulfonate is gradually removed from solution either by precipitation as calcium lignosulfonate or by absorption into calcium aluminate hydrates. Removal of lignosulfonate from solution overcomes its poisoning effect on calcium hydroxide crystallization, and C_3S can proceed to hydrate normally.

3.4 New Experimental Techniques

It is evident from the foregoing discussions concerning the mechanism of hydration of portland cements and its compounds that we are dealing with a complex system. It is therefore desirable to assess the potential of new experimental methods that might provide additional insight into the physico-chemical processes occurring. A number of papers that explore these possibilities will be reviewed in this section. We can divide these into four classes: new analytical methods, electrical measurements, spectroscopic investigations, and miscellaneous techniques. Theoretical intepretation of the data obtained by many of these methods is difficult because of the complex nature of pastes. Comparisons with established techniques would be helpful in many instances, but are not always available. From a practical point of view, a method may provide useful comparative data, for example on the effect of admixtures on setting behavior, even when complete theoretical interpretations are not possible.

3.4.1 Analytical Methods

The application of silicate polymerization analysis as an alternative means of assessing the degree of hydration in C_3S pastes has been suggested (23). This idea is based on the assumption that no monosilicate occurs in C-S-H; it remains to be seen whether this holds true for cement paste.

The composition of the liquid phase is known to be an important consideration in the hydration process. In the calculation of ionic equilibria, activities should be used in preference to concentrations. Specific ion electrodes measure activities directly, and the calcium ion electrode has been used in the analysis of hydrating systems (25,236). Concentration-time profiles determined by this method agree well with those from conventional methods. pH changes with time can be measured using a glass electrode, but, once pH rises above 12, the method does not seem to be sensitive (25). This may be due to potential errors that can occur at high pH, and it has been suggested (237) that metallic electrodes can be used successfully. Other specific ion electrodes could be of use for investigating admixture interactions.

3.4.2 Electrical Methods

Measurements of electric conductivity of cement pastes have been used for many years in hydration studies. A number of other parameters based on electrical measurements have also been evaluated in recent years. Changes in the dielectric constant of a paste are observed (238,239) during hardening and can be used to follow the setting process. Dielectric changes have been correlated with other measurements during early hydration (238). Podkin and Rozenthal (240,241) and Rozenthal and Fedingin (242) have also measured both dielectric constant and electrical conductivity in the radiofrequency range (5-100 MHz). The dielectric constant at 5 MHz is very sensitive to the dipole orientations that lead to thixotropic behavior, and changes in its value are observed on redispersion of pastes during the first few hours. In contrast, the dielectric constant at 100 MHz is insensitive to such changes. Conductivity measurements correlate with hydration behavior rather than with physical changes within the paste. Reboul (243, 244) has determined complex electric permittivities of pastes from microwave resonance measurements (permittivity depends on free water content; it decreases with time and can be used to estimate setting). At 3 kHz and -20°C, permittivity is affected by water adsorbed on surfaces. It has been shown that adsorption of water on C_3S or cement surfaces is complete in 10-15 minutes, even though no hydration products are observed within 30 minutes.

3.4.3 Spectroscopic Investigations

Nuclear magnetic resonance (NMR) has been used in the study of cement pastes, and Lahajnar et al. (245) have surveyed the various applicable NMR methods. Proton relaxation data (either spin-lattice, T_1, or spin-spin, T_2) of adsorbed water, as distinct from crystalline water in a structural lattice, change with time and can be used to follow hydration (246-249). Pulsed NMR methods are better than spin-echo techniques for determining these parameters. Other NMR methods that can be used are line-shape measurements, proton-free induction decay, multiple pulse method, and ^{27}Al NMR studies. The intent of all these methods is to separate signals due to adsorbed water and crystalline H_2O or OH^-.

Blinc and co-workers (246) studied the proton and deuteron relaxation times in hydrating C_3S and cement pastes. They concluded that the H_2O molecules were highly mobile in the adsorbed monolayer and exchanged rapidly with pore water in contact with the monolayer. They also showed that the relaxation times directly reflected the number of active surface sites and could be used to follow the hydration process. These studies (using T_1) have been applied to probing the effect of admixtures on the hydration of cement. The results are encouraging: setting times and rate of hardening can be estimated. Unfortunately, correlations with other hydration studies do not appear to have been explored. Palkin et al. (249) used line-shape studies to follow hydration of cements and concluded that the formation of structured liquid layers preceded the development of microstructure.

Infrared (IR) spectroscopy has been used to study compounds of interest in cement chemistry, but line broadening and difficulties in quantitative measurements have precluded its use in detailed hydration studies. Bensted and Bansted and Varma (250,251) have drawn attention to the possible application of laser Raman spectroscopy and the complementary nature of the two techniques. It is likely that IR and Raman spectroscopic studies could be used more in hydration studies than has been the case, but experimental methods and approaches may have to be further developed to utilize their full potential.

3.4.4 Miscellaneous Techniques

Changes in ultrasonic pulse velocity measurements during setting and hardening have been studied on cement (252) and C_3S (253) pastes. The pulse velocity rapidly changes from 1400-1500 m/s in the fluid state to over 3000 m/s in the first few hours after setting. Velocity then continues to increase more slowly to above 4000 m/s. The method has been shown (252) to correlate well with heat evolution and changes in voltage between electrodes embedded in the paste. The maximum rates of change in pulse velocity, voltage change, and heat evolution agree well with the final set as measured conventionally. The method is useful to distinguish between the influence of admixtures in hydration (252,253) and on microstructural development (253).

Taylor (254) has described a method of hydrating undisturbed specimens for subsequent SEM observations. Advantages claimed are high sensitivity to early hydration, detection of

both amorphous and crystalline phases, and a capability for following the hydration of individual phases in a mixture. However, the method entails the use of a very high w/c ratio. Other workers (13,126) have hydrated, premounted, and compacted specimens in a similar way to follow early hydration reactions of cement compounds.

Thermoluminescence studies are described in the discussions of reaction mechanisms, and Mossbauer spectroscopy has been used to study the hydration of the ferrite phase and cement. Shchurov et al. (255) have used low angle X-ray scattering (LAXRS) to study the hydration of C_3S and C_3A. They point out that LAXRS can detect volume heterogeneities in anhydrous cements with similar BET surface areas but different LAXRS surface areas. Slegers and co-workers (256) have studied radial electron density distributions (RED) of hydrating C_3S. Interpretation of the complex curves supports the idea that silicate polymerization occurs during hydration.

4. CONCLUSIONS

Considerable progress has been made in our understanding of cement hydration since the last Congress. There is general agreement on the main features of hydration, although there is still considerable disagreement over details of interpretation. We have a sufficient body of knowledge to be used to advantage in the cement and concrete industries; however, technology transfer is the major limiting factor in our progress.

The large gaps remaining in our knowledge concern the cement-water interactions occurring in the first few hours of hydration. If precise control over the development of microstructure is to be achieved, the hydration process that directs it must be understood in more detail. Control of microstructure will lead ultimately to the greater realization of the potential of portland cement and, perhaps, to new uses of concrete not yet imagined. The developments of modern-day metallurgy and ceramics are good examples of the powerful effects of microstructural control on engineering properties.

To achieve these aims, we should try to answer the following practical questions in the indicated areas:

1) Controlling the reactivity of calcium silicates

   How can we increase the reactivity of C_3S of C_2S? How do we measure reactivity? Can two plants (or even laboratories) produce cements with exactly the same properties?

2) Cement-admixture interactions

   Are there alternative materials to gypsum for set regulation? Can we scientifically design admixtures? Can we better predict rheological behavior?

3) Control of microstructure formation

   How do alkalies and minor components affect the course of hydration? How do interactions between clinker compounds affect the course of hydration and structure formation? How can we use external factors to direct the formation of microstructure?

We already have some partial answers to many of these questions. To make further progress, we must make greater use of techniques used in other disciplines, such as ESCA, NMR, Raman spectroscopy, etc., and develop research programs that will probe the fundamental behavior of the cement-water system.

Acknowledgements

We would like to thank all those who helped in preparing the manuscript for publication. Special thanks are due to L. Struble and J. Marcus for their invaluable contribution in checking and correcting the text.

5. REFERENCES

1.- H.F.W. TAYLOR (1979), "Cement hydration reactions: the silicate phases," in Cement Production & Use, Proc. Eng. Found. Conf., in press.

2.- J. SKALNY, I. JAWED et H.F.W. TAYLOR (1978), "Studies on hydration of cement -- recent developments", World Cem. Technol., 9, 183.

3.- H.N. STEIN (1977), "The initial stages of the hydration of C_3S", Il Cemento, 74, 3.

4.- J.G.M. de JONG, H.N. STEIN et J.M. STEVELS (1967), "Hydration of tricalcium silicate", J. Appl. Chem., 17, 246.

5.- S. BRUNAUER et D.L. KANTRO (1964), "Hydration of tricalcium silicate and β-dicalcium silicate from 5° to 50°C", in Chemistry of Cements, Vol. I, Ed. H.F.W. Taylor, 287.

6.- R. KONDO et M. DAIMON (1969), "A solid reaction with induction and acceleration periods: early hydration of tricalcium silicate", J. Am. Ceram. Soc., 52, 503.

7.- L.G. SHPYNOVA, N.V. BELOV, M.A. SANITSKII et V.I. CHIKH (1977), "Mechanism of alite hydration", Dokl. Akad. Nauk SSSR, 236, 168; Chem. Abstr., 88:65139.

8.- P.A. RHEBINDER, E.E. SEGALOVA, E.A. AMELINA, E.P. ANDREEVA, S.I. KONTOROVICH, O.I. LUKYANOVA, E.S. SOLOVYEVA et E.D. SCHUKIN (1976), "Physico-chemical aspects of hydration hardening of binders", Proc., Sixth Int. Congr. Chem. Cement, 1974, Moscow, Vol. II Book 1, 58.

9.- R. MAGNAN, B. COTTIN et J.J. GARDET, (1975), "Initial hydration of calcium binders", Cim., Betons, Platres, Chaux, 692, 41.

10.- P. BARRET, D. MENETRIER et D. BERTRANDIE (1977), "Calcium aluminate and silicate hydration kinetics relative to the process of cement hardening", Rev. Hautes Temp. Refract., 14, 127.

11.- E.P. ANDREEVA et B.F. KESHELAVA (1976), "Study of the kinetics of dissolution and crystallization in suspensions of di- and tricalcium silicates", Usp. Kolloidn. Khim., 230; Chem. Abstr., 88:11041.

12.- K. FUJII et W. KONDO (1974), "Kinetics of the hydration of tricalcium silicate", J. Am. Ceram. Soc., 57, 492.

13.- D. MENETRIER, I. JAWED, T.S. SUN et J. SKALNY (1979), "ESCA and SEM studies on early C_3S hydration", Cem. Concr. Res., 9, 473.

14.- J.N. MAYCOCK, J. SKALNY et R. KALYONCU (1974), "Crystal defects and hydration I. Influence of lattice defects", Cem. Concr. Res., 4, 835.

15.- P. FIERENS et J. VERHAEGEN (1976), "Microcathodoluminescence of C_3S", Il Cemento, 73, 39.

16.- P. FIERENS et J. VERHAEGEN (1974), "Thermoluminescence applied to the kinetic study of the chemisorption of water by tricalcium silicate", Silic. Ind., 39, 125.

17.- P. FIERENS et J.P. VERHAEGEN (1976), "Properties nucleophiles de surfaces de silicate tricalcique", Cem. Concr. Res., 6, 103.

18.- P. FIERENS et J.P. VERHAEGEN (1976), "Induction period of hydration of tricalcium silicate", Cem. Concr. Res., 6, 287.

19.- P. FIERENS et J.P. VERHAEGEN (1975), "The effect of water on pure and doped tricalcium silicate using the techniques of adsorboluminescence", Cem. Concr. Res., 5, 233.

20.- J.F. YOUNG (1972), "A review of the mechanisms of set-retardation in portland cement pastes containing organic admixtures", Cem. Concr. Res., 2, 415.

21.- J.F. YOUNG, H.S. TONG et R.L. BERGER (1977), "Compositions of solutions in contact with hydrating tricalcium silicate pastes", J. Am. Ceram. Soc., 60, 193.

22.- M.E. TADROS, J. SKALNY et R.S. KALYONCU (1976), "Early hydration of C_3S", J. Am. Ceram. Soc., 59, 344.

23.- L.S. DENT GLASSER, E.E. LACHOWSKI, K. MOHAN et H.F.W. TAYLOR (1978), "A multi-method study of C_3S hydration", Cem. Concr. Res., 8, 733.

24.- P. FIERENS et J.P. VERHAEGEN (1976), "Hydration of tricalcium silicate in paste - kinetics of calcium ions dissolution in aqueous phase", Cem. Concr. Res., 6, 337.

25.- P.A. SLEGERS et P.G. ROUXHET (1977), "The hydration of tricalcium silicate: calcium concentration and portlandite formation", Cem. Concr. Res., 7, 31.

26.- R.L. BERGER et J.D. McGREGOR (1973), "Effect of temperature and water-solid ratio on growth of $Ca(OH)_2$ crystals formed during hydration of Ca_3SiO_5", J. Am. Ceram. Soc., 56, 73.

27.- H.M. JENNINGS et P.L. PRATT (1979), "An experimental argument for the existence of a protective membrane surrounding portland cement during the induction period", Cem. Concr. Res., 9, 501.

28.- J.H. THOMASSIN, M. REGOURD, P. BAILLIFF et J.C. TOURAY (1978), "Study of the early hydration of tricalcium silicate by X-ray photoelectron spectrometry", C.R. Hebd. Seances Acad. Sci., Ser. C, 288, 93.

29.- I. ODLER et H. DORR (1979), "Early hydration of tricalcium silicate", Cem. Concr. Res., 9, 239 and 277.

30.- S. DIAMOND (1976), "Cement paste microstructure - an overview at several levels", Proc. Conf. Hydraulic Cement Pastes: Their Structure and Properties, Sheffield, April 1976, 2.

31.- D.D. DOUBLE, A. HELLAWELL et S.J. PERRY (1978), "The hydration of portland cement", Proc. Roy. Soc. London, Ser. A, 359, 435.

32.- J.D. BIRCHALL, A.J. HOWARD et J.E. BAILEY (1978), "On the hydration of portland cement", Proc. Roy. Soc. London, Ser. A, 360, 445.

33.- H. JENNINGS et P. PRATT (1979), "On the hydration of portland cemnt", Proc. Brit. Ceram. Soc., in press.

34.- L.S. DENT GLASSER (1979), "Osmotic pressure and the swelling of gels", Cem. Concr. Res., 9, 515.

35.- A. BENTUR et R.L. BERGER (1979), "Chemical composition of C-S-H gel formed in the hydration of calcium silicate pastes", J. Am. Ceram. Soc., 62, 117.

36.- T.C. POWERS (1961), "Some physical aspects of the hydration of portland cement", J. PCA R&D Labs, 3, 47.

37.- D. TERRIER et M. MOREAU (1966), "Study on the mechanism of pozzolanic reaction of fly ash with cement", Rev. Mater. Constr. Trav. Publics, 613, 379 and 614, 440.

38.- M.S. STUCKE et A.J. MAJUMDAR (1976), "The composition of the gel phase in portland cement paste", Proc. Conf. Hydraulic Cement Pastes: Their Structure and Properties, Sheffield, April 1976, 31.

39.- D.L. KANTRO (1975), "Tricalcium silicate hydration in the presence of various salts", J. Test. Eval. 3, 312.

40.- W.L. DeKEYSER et N. TENOUTASSE (1969), "The hydration of ferrite phase of cements", Proc., Fifth Int. Symp. Chem. Cement, 1968, Tokyo, Vol. II, 378.

41.- T.I. ROZENBERG et G.D. KUCHERYAEVA (1976), "Concurrent reactions of C_3S and C_3A with the addition of electrolytes", Proc., Sixth Int. Congr. Chem. Cement, 1974, Moscow, Vol. II Book 2, 54.

42.- V.B. RATINOV et T.I. ROZENBERG (1973), Concrete Additives, Strojizdat, Moscow.

43.- J. SKALNY et J.N. MAYCOCK (1975), "Mechanism of acceleration by calcium chloride: a review", J. Test. Eval., 3, 303.

44.- V.S. RAMACHANDRAN (1976), Calcium Chloride in Concrete, Science and Technology.

45.- I. TEOREANU et M. MUNTEAN (1976), "Calcium silicates-water-electrolyte systems", Proc., Sixth Int. Congr. Chem. Cement, 1974, Moscow, Vol. II Book 2, 51; see also (1974), Silic. Ind., 39, 49.

46.- M. COLLEPARDI, G. ROSSI et M.C. SPIGA (1971), "Hydration of tricalcium silicate in the presence of electrolytes", Ann. Chim. (Rome), 61, 137.

47.- R. KONDO, M. DAIMON, E. SAKAI et H. USHIYAWA (1977), "Influence of inorganic salts on the hydration of tricalcium silicate", J. Appl. Chem. Biotechnol., 27, 191.

48.- R. KONDO, M. SATAKE et H. USHIYAWA (1974), "Diffusion of various ions in hardened portland cement", Rev. 28th Gen. Mtg., Cem. Assoc. Japan, 41.

49.- L. BEN-DOR et D. PEREZ (1975), "Hydration of cement minerals with various admixtures studied by differential thermal analysis and infrared spectrometry", Thermochim. Acta, 12, 81.

50.- L. BEN-DOR, D. PEREZ et S. SARIG (1975), "Thermal study of the effect of additives on the hydration of tricalcium silicate", J. Am. Ceram. Soc., 58, 87.

51.- J.N. MAYCOCK et J. SKALNY (1974), "Hydration of Ca_3SiO_5-K_2CO_3 system", Thermochim. Acta, 8, 167.

52.- W. LIEBER (1976), "The influence of phosphates on the hydration of portland cement", Proc., Sixth Int. Congr. Chem. Cement, 1974, Moscow, Vol. II Book 2, 51.

53.- J.F. YOUNG (1978), "A discussion of the interactions between hydrating calcium silicates and set-modifying admixtures", Silic. Ind., 43, 209.

54.- J.F. YOUNG (1976), "Interactions of admixtures with portland cement", Cement (Zagreb), 2, 55.

55.- N.B. MILESTONE (1979), "Hydration of tricalcium silicate in the presence of lignosulfonates, glucose, and sodium gluconate", J. Am. Ceram. Soc., 62, 321.

56.- M.E. TADROS, J. SKALNY et R.S. KALYONCU (1976), "Kinetics of calcium hydroxide crystal growth from solution", J. Colloid Interface Sci., 55, 20.

57.- I. JAWED, W.A. KLEMM et J. SKALNY (1979), "Hydration of cement-lignosulfonate-alkali carbonate system", J. Am. Ceram. Soc., 62, 461.

58.- M. REGOURD et A. GUINIER (1976), "The crystal chemistry of the constituents of portland cement clinker," Proc., Sixth Int. Congr. Chem. Cement, 1974, Moscow, Vol. 1, 25.

59.- A.K. CHATTERJI (1979), "Phase composition, microstructure, quality and burning of portland cement clinker - a review of phenomenological interrelations, Parts 1 & 2", World Cem. Technol., 10, 124 and 165.

60.- T. HARADA, M. OHTA et S. TAKAGI (1978), "Effect of polymorphism of tricalcium silicate on hydration and structural characteristics of hardened paste", Yogyo Kyokai Shi, 86, 7.

61.- G.L. VALENTINI, V. SABATELLI et B. MARCHESE (1978), "Hydration kinetics of tricalcium silicate solid solutions at early ages", Cem. Concr. Res., 8, 61.

62.- G. MASCOLO et V.S. RAMACHANDRAN (1975), "Hydration and strength characteristics of synthetic Al- Mg- and Fe-alites", Mater. Constr. (Paris), 8, 373.

63.- V.E. KAUSHANSKII et V.V. TIMASHEV (1978), "Imperfections in the crystal lattice of an aluminum oxide solid solution in tricalcium silicate", Izv. Akad. Nauk SSSR, Neorg. Mater., 14, 1094; Chem. Abstr., 89:94157.

64.- J.P. BOYER (1976), "Influence of temperature increases during the induction period of C_3S hydration on the microstructure and strength of C_3S mortars", M.S. Thesis, University of Illinois, Urbana.

65.- J.P. BOYER et R.L. BERGER (1979), to be published.

66.- R.W. DAVIS et J.F. YOUNG (1975), "Hydration and strength development in tricalcium silicate pastes seeded with afwillite", J. Amer. Ceram. Soc., 56, 67.

67.- O.P. MCHEDLOV-PETROSYAN, A.M. URZHENKO et A.V. USHEROV-MARSHAK (1977), "Calorimetric studies of the crystal chemical activation of binder hardening processes", Dokl. Akad. Nauk SSSR, 233, 439; Chem. Abstr., 86:194024.

68.- H.N. STEIN et J.M. STEVELS (1964), "Influence of silica on the hydration of $3CaO \cdot SiO_2$", J. Appl. Chem., 14, 338.

69.- S. TAKAGI, G. YAMAGUCHI et M. SAITO (1975), "Hydration and carbonation of cement minerals in solid-gas reaction and their texture", Rev. 29th Gen. Mtg., Cem. Assoc, Japan, 44.

70.- C.J. GOODBRAKE, J.F. YOUNG et R.L. BERGER (1979), "Reaction of beta-dicalcium silicate and tricalcium silicate with carbon dioxide and water vapor", J. Am. Ceram. Soc., 62, 168.

71.- J.M. POMMERSHEIM et J.R. CLIFTON (1979), "Mathematical modeling of tricalcium silicate hydration", Cem. Concr. Res., 9, 765.

72.- R. KONDO et S. UEDA (1969), "Kinetics and mechanisms of the hydration of cements", Proc., Fifth Int. Symp. Chem. Cement, 1968, Tokyo, Vol. II, 203.

73.- F. TOMOSAWA (1974), "A kinetic model of the hydration process of cement", Rev. 28th Gen. Mtg., Cem. Assoc. Japan, 38.

74.- K. FUJII et W. KONDO (1979), "Rate and mechanism of hydration of β-dicalcium silicate", J. Am. Ceram. Soc., 62, 161.

75.- S.N. GHOSH, P.B. RAO, A.K. PAUL et K. RAINA (1979), "Review: the chemistry of dicalcium silicate mineral", J. Mater. Sci., 14, 1554.

76.- M. GAWLICKI et W. NOCUN (1979), "Hydration of β-Ca_2SiO_4", Cem.-Wapno-Gips, 32/46, 81.

77.- V.V. DANILOV (1976), "On hydration mechanism in cement pastes", Proc., Sixth Int. Congr. Chem. Cement, 1974, Moscow, Vol. II Book 1, 73.

78.- M.M. SYCHEV, V.I. KORNEEV, E.N. KAZANSKAYA et I.N. MEDVEDEVA (1973), "Interaction of the β and γ forms of calcium orthosilicate with water", Zh. Prikl. Khim. (Leningrad), 46, 502.

79.- F.M. LEA (1970), The Chemistry of Cement and Concrete, 3rd ed.

80.- J. BENSTED (1978), "γ-dicalcium silicate and its hydraulicity", Cem. Concr. Res., 8, 73.

81.- J. JERNEJCIC et I. JELENIC (1974), "Properties of autoclaved and thermally treated molds made from γ-Ca_2SiO_4 and quartz at C/S ratios 0.5 to 1.5", Cem. Concr. Res., 4, 123.

82.- J.M. BUKOWSKI et R.L. BERGER (1979), "Reactivity and strength development of CO_2-activated non-hydraulic calcium silicates", Cem. Concr. Res., 9, 57.

83.- I.M. PRITTS et K.E. DAUGHERTY (1976), "The effect of stabilizing agents on the hydration rate of β-C_2S", Cem. Concr. Res. 6, 783.

84.- J.N. MAYCOCK et M. McCARTY, Jr. (1973), "Crystal lattice defects in dicalcium silicate", Cem. Concr. Res., 3, 701.

85.- L. OPOCZKY et Z. JUHASZ (1976), "Mechanochemical phenomena on the surface of clinker minerals", Proc., Sixth Int. Congr. Chem. Cement, 1974, Moscow, Vol. II Book 1, 173.

86.- P. FIERENS et J. TRILOCQ (1978), "Application of thermoluminescence in the hydration studies of dicalcium silicate", Cem. Concr. Res., 8, 397.

87.- J.F. YOUNG et H.S. TONG (1977), "Microstructure and strength development of beta-dicalcium silicate pastes with and without admixtures", Cem. Concr. Res., 7, 627.

88.- H.S. TONG et J.F. YOUNG (1977), "Composition of solutions in contact with hydrating β-dicalcium silicate", J. Am. Ceram. Soc., 60, 321.

89.- N. KAWADA et A. NEMOTO (1967), "Calcium silicates in the early stages of hydration", Zem.-Kalk-Gips, 21, 65.

90.- D. MENETRIER, T.S. SUN, I. JAWED et J. SKALNY (1979), to be published.

91.- E.F. ZHAROV et G. DEMEL (1978), "Hydration of dicalcium silicate and effect of calcium chloride additive on this process", Izv. Vyssh. Uchebn. Zaved., Khim. Khim. Tekhnol., 21, 404; Chem. Abstr., 89:116745.

92.- A.A. KLYUSOV, E.N. LEPNEV, V.N. NIKITIN V.S. BAKSHUTOV et V.V. ILYUKHIN (1977), "Study of the hydration of β-dicalcium silicate at lowered temperatures", Izv. Akad. Nauk SSSR, Neorg. Mater., 13, 1876; Chem. Abstr., 88:65164.

93.- W.A. KLEMM et R.L. BERGER (1972), "Accelerated curing of cementitious systems by carbon dioxide", Cem. Concr. Res., 2, 567 and 647.

94.- R.L. BERGER, J.F. YOUNG et K. LEUNG (1972), "Acceleration of hydration of calcium silicates by carbon dioxide treatment", Nature (London), Phys. Sci., 240, 16.

95.- J.F. YOUNG, R.L. BERGER et J. BREESE (1974), "Accelerated curing of compacted calcium silicate mortars on exposure to CO_2", J. Am. Ceram. Soc., 57, 394.

96.- C.J. GOODBRAKE, J.F. YOUNG, R.L. BERGER (1979), "Reaction of hydraulic calcium silicates with carbon dioxide and water", J. Am. Ceram. Soc., 62, 488.

97.- D.M. ROY et S.O. OYEFESOBI (1977), "Preparation of very reactive Ca_2SiO_4 powder", J. Am. Ceram. Soc., 60, 178.

98.- D.M. ROY, T.P. O'HOLLERAN et R.R. NEURGAONKAR (1978), "Preparation and hydration studies of reactive β-Ca_2SiO_4 prepared by the EDS technique", Il Cemento, 75, 337.

99.- S.O.OYEFESOBI et D.M. ROY (1977), "Hydrothermal cements: studies of special types of cement-quartz mixes", Cem. Concr. Res., 7, 95.

100.- W.A. KLEMM et R.L. BERGER (1972), "Calcination and cementing properties of $CaCO_3$ - SiO_2 Mixtures J. Am. Ceram. Soc., 55, 485.

101.- Y. ONO, S. KAWAMURA et Y. SODA (1969), "Microscopic observations of alite and belite and hydraulic strength of cement", Proc., Fifth Int. Symp. Chem. Cement, 1968, Tokyo, Vol. I, 275.

102.- J. BENSTED (1974), "Some applications of infrared and Raman spectroscopy in cement chemistry, Part I - examination of dicalcium silicate", Cement Technol., 5, 256.

103.- J. BENSTED (1975), "α-dicalcium silicate and its hydraulic behavior", Chem. Ind. (London), 20, 885.

104.- J. BENSTED (1976), "Raman spectroscopic study of α'-dicalcium silicate hydration", Cim. Betons, Platres, Chaux, 703, 335.

105.- A.I. BOIKOVA, M.G. DEGEN et V.A. PARAMONOVA (1976), "Defect state of solid solutions of dicalcium silicate", Proc., Sixth Int. Congr. Chem. Cement, 1974, Moscow, Vol. I, 68.

106.- I. JELENIC, A. BEZJAK et M. BUJAN (1978), "Hydration of B_2O_3 stabilized α' and β-modifications of dicalcium silicate", Cem. Concr. Res., 8, 173.

107.- W.A. CORSTANJE, H.N. STEIN et J.M. STEVELS (1973 and 1974), "Hydration reactions in pastes C_3S + C_3A + $CaSO_4 \cdot 2aq$ + water at 25°C. I, II, and III", Cem. Concr. Res., 3, 791; 4, 193; and 4, 417.

108.- M.E. TADROS, W.Y. JACKSON et J. SKALNY (1976), "Study of the dissolution and electrokinetic behavior of tricalcium aluminate", in Colloid and Interface Science, Ed. M. Kerker, IV, 211.

109.- E. BREVAL (1976), "C_3A hydration", Cem. Concr. Res., 6, 129.

110.- G.A.C.M. SPIERINGS et H.N. STEIN (1976), "The influence of Na_2O on the hydration of C_3A I. Paste hydration and II. Suspension hydration", Cem. Concr. Res., 6, 265 and 6, 487.

111.- E.N. LEPNEV, A.A. KLYUSOV, V.S. BAKSHUTOV, V.V. ILLYUKHIN et V.N. NIKITIN (1977), "Hydration of tricalcium aluminate in electrolyte solutions at lowered temperatures", Izv. Akad. Nauk SSSR, Neorg. Mater., 13, 1872 and Inorg. Mater., 13, 1505.

112.- E. BREVAL (1977), "Gas-phase and liquid-phase hydration of C_3A", Cem. Concr. Res., 7, 297.

113.- E. BREVAL (1979), "The effects of prehydration on the liquid hydration of $3CaO \cdot Al_2O_3$ with $CaSO_4 \cdot 2H_2O$", J. Am. Ceram. Soc., 62, 394.

114.- F.H. WITTMAN (1977), "Observation of early hydration by means of luminescence experiments", CEMBUREAU Seminar on Reaction of Aluminates During the Setting of Cements, Eindhoven, The Netherlands.

115.- A.I. BOIKOVA, V.A. PARAMONOVA, A.I. DOMANSKY et M.M. PIRIUTKO (1976), "On the composition and hydration activity of a clinker aluminate phase", Tsement, 1976, n°8, 20.

116.- A.I. BOIKOVA, A.I. DOMANSKY, V.A. PARAMONOVA, G.P. STAVITSKAJA et V.M. NIKUSHCHENKO (1977), "Influence of Na_2O on the structure and properties of $3CaO \cdot Al_2O_3$", Cem. Concr. Res., 7, 483.

117.- M. REGOURD (1978), "Crystallization and reactivity of tricalcium aluminate in portland cements", Il Cemento, 75, 323.

118.- M. REGOURD (1979), "Fundamentals of cement production: crystal chemistry of portland cement minerals, new data", in Cement Production & Use, Proc. Eng. Found. Conf., in press.

119.- J. SKALNY et M.E. TADROS (1977), "Retardation of tricalcium aluminate hydrate by sulfates", J. Am. Ceram. Soc., 60, 174.

120.- P.K. MEHTA (1976), "Scanning electron micrographic studies of ettringite formation", Cem. Concr. Res., 6, 169.

121.- P. FIERENS, A. VERHAEGEN et J.P. VERHAEGEN (1974), "Thermoluminescence study of tricalcium aluminate hydration", Cem. Concr. Res., 4, 381.

122.- F.W. LOCHER, W. RICHARTZ et S. SPRUNG (1976), "Setting of cement I. Reaction and development of structure", Zem.-Kalk-Gips, 29, 435.

123.- M. COLLEPARDI, G. BALDINI et M. PAURI (1978), "Tricalcium aluminate hydration in the presence of lime, gypsum or sodium sulfate", Cem. Concr. Res., 8, 571 and II Cemento, 75, 169.

124.- P.K. MEHTA (1973), "Effect of lime on hydration of pastes containing gypsum and calcium aluminates or sulfoaluminates", J. Am. Ceram. Soc., 56, 315.

125.- P.K. MEHTA (1973), "Mechanism of expansion associated with ettringite formation", Cem. Concr. Res., 3, 1.

126.- J. TINNEA et J.F. YOUNG (1977), "Influence of citric acid on reactions in the system $3CaO \cdot Al_2O_3$-$CaSO_4 \cdot 2H_2O$-CaO-H_2O", J. Am. Ceram. Soc., 60, 387.

127.- A. TRAETTEBERG et P.E. GRATTAN-BELLEW (1975), "Hydration of $3CaO \cdot Al_2O_3$ and $3CaO \cdot Al_2O_3$ + gypsum with and without $CaCl_2$", J. Am. Ceram. Soc., 58, 221.

128.- N. TENOUTASSE (1969), "The hydration mechanism of C_3A and C_3S in the presence of calcium chloride and calcium sulfate", Proc., Fifth Int. Symp. Chem. Cement, 1968, Tokyo, Vol. II, 372.

129.- C.L.M. HOLTEN et H.N. STEIN (1977), "Influence of quartz surfaces on the reaction C_3A + $CaSO_4 \cdot 2H_2O$ + water", Cem. Concr. Res., 7, 291.

130.- M. COLLEPARDI, G. BALDINI et M. PAURI (1978), "The effect of pozzolans on the tricalcium silicate hydration", Cem. Concr. Res., 8, 741.

131.- M. REGOURD, H. HORNAIN et B. MORTUREUX (1976), "Evidence of calcium silicoaluminates in hydrated mixtures of tricalcium silicate and tricalcium aluminate", Cem. Concr. Res., 6, 733.

132.- C. TASHIRO et J. OBA (1979), "The effects of Cr_2O_3, $Cu(OH)_2$, ZnO and PbO on the compressive strength and the hydrates of the hardened C_3A paste", Cem. Concr. Res., 9, 253.

133.- J.F. YOUNG (1976), "Hydration mechanisms of organic admixtures with hydrating cement compounds", Transportation Research Record, No. 564, 1.

134.- C. TASHIRO et FUKUYAMA (1975), "The hydration of C_3A in $CaCrO_4$ solution", Rev. 29th Gen. Mtg., Cem. Assoc. Japan, 42.

135.- R. KRZYWOBLOCKA-LAUROW et E. ZIELINSKA (1978), "The effect of CrO^{2-} ions upon the hydration of C_3S and C_3A mixture in the presence of gypsum" Cem.-Wapno-Gips, 32/46, 206.

136.- N.B. SINGH (1977), "Study of C_3A-gypsum-Tl_2CO_3-H_2O system", Cem. Concr. Res., 7, 195.

137.- V.S. RAMACHANDRAN (1973), "The action of triethanolamine on the hydration of tricalcium aluminate", Cem. Concr. Res., 3, 41.

138.- N.B. MILESTONE (1977), "The effect of glucose and some glucose oxidation products on the hydration of tricalcium aluminate", Cem. Concr. Res. 7, 45.

139.- N.B. MILESTONE (1976), "The effect of lignosulfonate fractions on the hydration of tricalcium aluminate", Cem. Concr. Res., 6, 89.

140.- A. NEGRO et L. STAFFIERI (1979), "The hydration of calcium ferrites and calcium aluminoferrites", Zem.-Kalk-Gips, 32, 83.

141.- I. JAWED, S. GOTO et R. KONDO (1976), "Hydration of tetra-calcium aluminoferrite in presence of lime and sulfates", Cem. Concr. Res., 6, 441.

142.- J. BENSTED (1976), "The ferrite phase - an infrared spectroscopic study", Il Cemento, 74, 45.

143.- D.E. ROGERS et L.P. ALDRIDGE (1977), "Hydrates of calcium ferrites and calcium aluminoferrites", Cem. Concr. Res., 7, 399.

144.- F.D. TAMAS et A. VERTES (1973), "A Mossbauer study on the hydration of brownmillerite", Cem. Concr. Res., 3, 575.

145.- A. VERTES et M. RANOGAJEC-KOMOR (1976), "Brownmillerite hydration by Mossbauer spectrometry", Proc., Sixth Int. Congr. Chem. Cement, 1974, Moscow, Vol. II Book 2, 180.

146.- I. TEOREANU, G. FILOTI, C. HRITEU, L. BUCEAU, V. SPANU, S. CIOCANEL et M. IVASCU (1979), "Interaction mechanism of $2CaO \cdot Fe_2O_3$ and $4CaO \cdot Al_2O_3 \cdot Fe_2O_3$ with water at various pressures and temperatures", Il Cemento, 76, 19.

147.- E.P. ANDREEVA et R. SANZHAASUREN (1977), "Investigations of the process of chemical interaction in aqueous suspensions of $4CaO \cdot Al_2O_3 \cdot Fe_2O_3$ in the presence of $CaSO_4 \cdot 2H_2O$", Kolloidn. Zh., 39, 227 and Colloid J. USSR, 39, 197.

148.- R. SANZHAASUREN et E.P. ANDREEVA (1977), "Study of the chemical interaction processes in tetracalcium aluminoferrite pastes during hydration in the presence of calcium hydroxide", Kolloidn. Zh., 39, 802 and Colloid J. USSR, 39, 715.

149.- M. COLLEPARDI, S. MONOSI, A. MORICANI et M. CORRADI (1979), "Tetracalcium aluminoferrite hydration in the presence of lime and gypsum", Cem. Concr. Res., 9, 431.

150.- V.S. RAMACHANDRAN et J.J BEAUDOIN (1980), "Hydration of C_4AF + gypsum: study of various factors", to be published in Proc., Seventh Int. Symp. Chem. Cement, 1980, Paris.

151.- A.A. KLYUSOV, E.N. LEPNEV, V.S. BAKSHUTOV, V.V. ILYUKHIN et V.N. NIKITIN (1977), "Study of the hydration of tetracalcium aluminoferrite at lowered temperatures", Izv. Acad. Nauk SSSR, Neorg. Mater., 13, 2070 and Inorg. Mater. (USSR), 13, 1655.

152.- V.S. RAMACHANDRAN et J.J. BEAUDOIN (1976), "Significance of water/solid ratio and temperature on the physico-mechanical characteristics of hydrating $4CaO \cdot Al_2O_3 \cdot Fe_2O_3$", J. Mater. Sci., 11, 1893.

153.- N.P. STUKALOVA et E.P. ANDREEVA (1977), "Study of structure formation and chemical reactions in aqueous suspensions of tetracalcium aluminoferrite in the presence of calcium chloride", Kolloidn. Zh., 39, 508 and Colloid J. USSR, 39, 437.

154.- N.P. STUKALOVA et E.P. ANDREEVA (1977), "Investigation of processes of structure formation and chemical interaction in aqueous suspensions of tetracalcium aluminoferrite in presence of calcium chloride and sulfate", Kolloidn. Zh., 39, 718 and Colloid J. USSR, 39, 630.

155.- N. NAGASHIMA et M. SAITO (1977), "Some aspects of hydration of $3CaO \cdot Al_2O_3$ solid solutions", Rev. 31st Mtg., Cem. Assoc. Japan, 37.

156.- A.I. BOIKOVA et L.V. SMIRNOVA (1977), "Composition and properties of the aluminoferrite phase of a clinker", Tsement, 1977, n°9, 18.

157.- A.F. POLAK (1976), "Comparative review of the theories of mineral binder hardening", Usp. Kolloidn. Khim., 223; Chem. Abstr. 88: 11008.

158.- M.M. SYCHEV (1978), "Chemistry of setting and formation of strength properties of hardened cement paste", Tsement, 1978, n°9, 4.

159.- V.V. KAPRANOV (1976), "Interaction of the liquid and solid phases in the process of cement hydration", Proc., Sixth Int. Congr. Chem. Cement, 1974, Moscow, Vol. II Book 1, 80.

160.- A.F. POLAK (1976), "On the capability of binder hydration in hardened phase", Tsement, 1976, n°9, 15.

161.- A.V. USHEROV-MARSHAK et A.M. URZHENKO (1976), "Thermokinetic analysis of early stages of binder hydration", Proc., Sixth Int. Congr. Chem. Cement, 1974, Moscow, Vol. 2 Book 1, 31.

162.- I.P. VYRODOV (1976), "On some main aspects of hydration theory and hydration hardening of binders", Proc. Sixth Int. Congr. Chem. Cement, 1974, Moscow, Vol. II Book 1, 68.

163.- M.A. SOROCHKIN, M.B. LIPKIND et A.F. SCHUROV (1978), "Periodicity of cement hydration process under nonequilibrium conditions and changing solution pH", Zh. Prikl. Khim. (Leningrad), 51, 1205.

164.- B.D. BARNES, S. DIAMOND et W.L. DOLCH (1978), "The contact zone between portland cement paste and glass 'aggregate' surfaces", Cem. Concr. Res., 8, 233.

165.- B.D. BARNES, S. DIAMOND et W.L. DOLCH (1978), "Hollow shell hydration of cement particles in bulk cement paste", Cem. Concr. Res., 8, 263.

166.- J. GEBAUER (1978), "Technological possibilities of avoiding the early setting of cement", Zem.-Kalk-Gips, 31, 302.

167.- L.D. ADAMS (1976), "The measurement of very early hydration reactions of portland cement by a thermoelectric conduction calorimeter", Cem. Concr. Res., 6, 293.

168.- R.W. PREVITE (1971), "Some insights on the mechanism of saccharide set retardation of portland cement", Cem. Concr. Res., 1, 301.

169.- W. SCHRAMLI (1977 and 1978), "An attempt to assess beneficial and detrimental effects of aluminate in the cement on concrete performance", World Cem. Technol., 8, 46.

170.- S.M. KHALIL et M.A. WARD (1978), "Influence of SO_3 and C_3A on the early reaction rates of portland cement in the presence of calcium lignosulfonate", Am. Ceram. Soc. Bull., 57, 1116.

171.- B. ERLIN et W.G. HIME (1979), "Concrete slump loss and field examples of placement problems", Concr. Int.: Des. & Constr., 1, 48.

172.- L.M. MEYER et W.F. PERENCHIO (1979), "Theory of concrete slump loss as related to the use of chemical admixtures", Concr. Int.: Des. & Constr., 1, 36.

173.- H.A. NEWLON, Jr. (1979), Discussion to Ref. 172, Concr. Int.: Des. & Constr., 1, 67.

174.- G. FRIGIONE (1978), "False set in portland cement pastes", Il Cemento, 75, 207.

175.- A. BENTUR (1976), "Effect of gypsum on the hydration and strength of C_3S pastes", J. Am. Ceram. Soc., 59, 210.

176.- L.E. COPELAND et D.L. KANTRO (1969), "Hydration of portland cement", Proc., Fifth Inter. Symp. Chem. Cement, 1968, Tokyo, Vol. II, 387.

177.- B. COTTIN (1976), "Poisoning of hydration of C_3S by soluble alumina", Cem.-Wapno-Gips, 30/42, 193.

178.- B. COTTIN (1978), "Hydration kinetics of portland cement in the presence of gypsum and potassium sulfate", Il Cemento, 75, 177.

179.- B.S. BOBROV et A.M. SHIKIRYANSKY (1976), "Mutual influence of C_3S and C_4AF in portland cement hydration", Proc., Sixth Int. Congr. Chem. Cement, 1974, Moscow, Vol. II Book 1, 163.

180.- I. JAWED et J. SKALNY (1978), "Alkalies in cement: a review II. Effects of alkalies on hydration and performance of portland cement", Cem. Concr. Res., 8, 37.

181.- O. HENNING et R. STIELER (1976), "Alkaline-rich cement dust in portland cement", Proc., Sixth Int. Congr. Chem. Cement, 1974, Moscow, Vol. II Book 2, 27.

182.- A.E. SHEYKIN, I.I. KURBATOVA, A.E. FYODOROV et V.N. SHVEDOV (1976), "Effect of sulphate-bearing phases on cement stone strength", Proc., Sixth Int. Congr. Chem. Cement, 1974, Moscow, Vol. II Book 1, 166.

183.- F.W. LOCHER et S. SPRUNG (1974), "Influence of the setting properties of cement", Tonind. Ztg., 98, 273.

184.- F.W. LOCHER (1973), "Setting and early strength of cement", Zem.-Kalk-Gips, 26, 53.

185.- J.E. MANDER et J.P. SKALNY (1977), "Calcium alkali sulfates in clinker", Am. Ceram. Soc. Bull., 56, 987.

186.- I. JELENIC, A. PANOVIC, R. HALLE et T. GACESA (1977), "Effect of gypsum on the hydration and strength development of commercial portland cements containing alkali sulfates", Cem. Concr. Res., 7, 239.

187.- M. COLLEPARDI, A. MARCIALIS et L. MASSIDDA (1973), "The influence of sodium carbonate on the hydration of cements", Ann. Chim. (Rome), 63, 83.

188.- I.G. LUGININA, A.N. LUGININ et G.P. POLYAKOV (1974), "Effect of alkali metal salts on the setting of portland cement pastes", Tsement, 1974, n°7, 14.

189.- W. RICHARTZ (1973), "Effect of storage on the properties of cement", Zem.-Kalk-Gips, 26, 67.

190.- S. SPRUNG (1974), "Effect of mill atmosphere on the setting and strength of cement", Zem.-Kalk-Gips, 27, 259.

191.- U. COSTA et F. MASSAZZA (1975), "Interstitial mass composition and setting irregularities of portland cements", Il Cemento, 72, 181.

192.- H. MORI, G. SUDOH, K. MINEGISHI et T. OHTA (1976), "Some properties of C-S-H gel formed by C_3S hydration in the presence of alkali", Proc., Sixth Int. Congr. Chem. Cement, 1974, Moscow, Vol. II Book 1, 223.

193.- V. JOHANSEN (1976), "Influence of alkalies on the strength development of cements", Proc. Conf. Effect of Alkalis on Properties of Concrete, London, 1976, 81.

194.- J. GEBAUER et J. KRISTMANN (1979), "The influence of the composition of industrial clinker on cemen and concrete properties", World Cem. Technol., 10 44.

195.- D.W. HOBBS (1977), "The influence of SO_3 content on the behavior of portland cement mortars", Worl Cem. Technol., 8, 75.

196.- B.W. OST (1974), "Optimum sulfate content of portland cements", Am. Ceram. Soc. Bull., 53, 579.

197.- W. LERCH (1946), "The influence of gypsum on the hydration and properties of portland cement pastes", PCA R&D Bull., 12.

198.- M.A. SMITH et J.D. MATTHEWS (1974), "Conduction calorimetric studies of the effect of sulphate on the hydration reactions of portland cement", Cem. Concr. Res., 4, 45.

199.- A.I. BOIKOVA, M.G. DEGEN, V.A. PARAMONOVA et V.V. SUDINA (1978), "Defect nature and hydration activity of solid solutions of tricalcium silicate with zinc oxide", Tsement, 1978, n°5, 305.

200.- I.G. LUGININA, V.D. BARBANYAGRE, V.K. KLASSEN, K.A. RYABCHENKO et O.A. DRUGOVA (1976), "The effect of phosphorus on cement stone properties", Proc., Sixth Int. Congr. Chem. Cement, 1974, Moscow, Vol. II Book 2, 43.

201.- H. TERAMOTO et S. KOIE (1975), "Phase composition and hydration of a very high grade portland cement clinker with foreign constituents", Zem.-Kalk-Gips, 28, 370.

202.- H. TERAMOTO et S. KOIE (1976), "Early hydration of a superhigh-early-strength portland cement containing chromium", J. Am. Ceram. Soc., 59, 522.

203.- D. KNOFEL (1977), "Modifying some properties of portland cement clinker and portland cement by means of TiO_2", Zem.-Kalk-Gips, 30, 191.

204.- M. REGOURD, H. HORNAIN et B. MORTUREUX (1978), "Effect of cement fineness on its hydration kinetics", Cim., Betons, Platres, Chaux, 712, 137.

205.- P. HAWKINS (1979), Private communication.

206.- K. THEISEN et V. JOHANSEN (1975), "Prehydration and strength development of portland cement", Am. Ceram. Soc. Bull, 54, 787.

207.- F.W. LOCHER (1978), "Process technology and cement properties", Zem.-Kalk-Gips, 31, 269.

208.- L. CUSSINO et G. PINTER (1978), "Problems associated with the grinding of clinker stored in the open air", Zem.-Kalk-Gips, 31, 332.

209.- P. WLASSACK (1975), "The course of the process of hydrolysis and hydration of tricalcium silicate at lowered temperatures", Cem.-Wapno-Gips, 29, 129.

210.- A.V. LAGODIA, YU. M. BUTT, G.V. TOPIL'SKII et V.N. BUYANOV (1977), "Hydration and hardening of portland cement at negative temperatures", J. Appl. Chem. USSR, 49, 2375.

211.- S.A. MIRONOV (1976), "Hydration and hardening of cement at minus temperatures", Proc., Sixth Int. Congr. Chem. Cement, 1974, Moscow, Vol. II Book 1, 182.

212.- A. BENTUR, R.L. BERGER, J.H. KUNG, N.B. MILESTONE et J.F. YOUNG (1979), "Structural properties of calcium silicate pastes II. Effect of curing temperatures", J. Am. Ceram. Soc., 62, 362.

213.- V. LACH et J. BURES (1976), "The phase composition and microstructure of cement pastes hydrated at elevated temperature", Proc., Sixth Int. Congr. Chem. Cement, 1974, Moscow, Vol. II Book 2, 129.

214.- V. ALUNNO-ROSSETTI, G. CHIOCCHIO et M. COLLEPARDI (1974), "Low pressure steam hydration of tricalcium silicate", Cem. Concr. Res., 4, 279.

215.- B. COURTALT (1974), "Influence of temperature on the thermal evolution of cement pastes", Rev. Mater. Constr. Trav. Publics, 687, 117.

216.- I. ODLER et J. SKALNY (1973), "Hydration of tricalcium silicate at elevated temperatures", J. Appl. Chem. Biotechnol., 23, 661.

217.- M.S. BARVINOK, P.G. KOMOKHOV et N.F. BONDAREVA (1976), "Effect of temperature and additives in the early stage of hardening", Proc., Sixth Int. Congr. Chem. Cement, 1974, Moscow, Vol. II Book 2, 151.

218.- V. MALDOVAN et N. BUTUCESCU (1976),"Essential aspects concerning the effects of temperature (20-90°C) on the hydration of the main mineralogical components of portland cement", Mater. Constr. (Bucharest), 6, 65; Chem. Abstr., 86:144645.

219.- P.A. ROSSKOPF, F.J. LINTON et R.B. PEPPLER (1975), "Effect of various accelerating chemical admixtures on setting and strength development of concrete", J. Test. Eval., 3, 322.

220.- J. BENSTED (1978), "Early hydration behavior of portland cement in water, calcium chloride and calcium formate solutions", Silic. Ind., 43, 117.

221.- V.S. RAMACHANDRAN (1976), "Hydration of cement - role of triethanolamine", Cem. Concr. Res., 6, 623.

222.- K. T. GREENE (1976), "A setting problem involving white cement and admixture", Transportation Research Record, No. 564, 21.

223.- Z.H. TUTHILL (1979), "Slump loss", Concr. Int.: Des. & Const., 1, 30.

224.- J.H. TAPLIN (1962), Discussion to the paper, "Some chemical additions and admixtures in cement paste and concrete", Proc., Fourth Int. Symp. Chem. Cement, 1960, Washington, 924.

225.- N.B. MILESTONE (1976), Unpublished results.

226.- N.B. SINGH (1975 and 1976), "Influence of calcium gluconate with calcium chloride or glucose on the hydration of cements", Cem. Concr. Res., 5, 545 and 6, 455.

227.- V.M. MALLUSTRA, E.E. BERRY et T.A. WHEAT, eds. (1978), "Superplasticizers in concrete", Proc. of an International Symp., 1979, Ottawa (2 volumes), ACI-SP62.

228.- E.M. PETRI (1976), "Effect of surfactant on the viscosity of portland cement-water dispersions", Ind. Eng. Chem., Prod. Res. Dev., 15, 242.

229.- R. KONDO, M. DAIMON et E. SAKAI (1978), "Interaction beween cement and organic polyelectrolytes", Il Cemento, 75, 225.

230.- R. KONDO, M. DAIMON, E. SAKAI et S. YAMANAKA (1976), "The influence of the organic compounds on the hydration of alite and cement", Rev. 30th Gen. Mtg., Cem. Assoc. Japan, 32.

231.- K. SUZUKI, Y. TSUCHIDA, I. MONTA, H. SHIN et S. ITO (1978), "Actions of anionic and nonionic surfactants on the hydration of $3CaO \cdot SiO_2$", Yogyo Kyokai Shi, 86, 398.

232.- G.M. TARNARUTSKY (1976), "The influence of hydrophobic additives on the hydration of portland cement", Proc., Sixth Int. Congr. Chem. Cement, 1974, Moscow, Vol. III, 310.

233.- T. SUGI, N. KAMESHIMA, S. YAMADA et K. OKADA (1974), "The effect of water-reducing admixtures on the solubility of gypsum in cement", Rev. 28th Gen. Mtg., Cem. Assoc. Japan, 61.

234.- I.ODLER, R. SCHONFELD et H. DORR (1978), "On the combined effect of water soluble lignosulfonates and carbonates on portland cement and clinker pastes II. Mode of action and structure of the hydration products", Cem. Concr. Res., 8, 525.

235.- S. DIAMOND et C. GOMEZ-TOLEDO (1978), "Consistency, setting and strength gain characteristics of a 'low porosity' cement paste", Cem. Concr. Res., 8, 613.

236.- S.S. D'YANCHENKO et E.A. MATEROVA (1977), "Determination of the activity of Ca^{2+} ions in cement suspensions using an ion selective elctrode", J. Appl. Chem. USSR, 50, 1219.

237.- R. KRSTULOVIC, P. KROLO et I. VUJNOVIC (1978), "Hydration process of cement studied by electrochemical methods", Cement (Zagreb), 20, 6.

238.- M. POP et S. POPOVICI (1976), "The dielectric constant method aplied to the kinetic study of hydration processes of cement pastes", Bul. Stiint. Teh. Inst. Politeh. Timisoara, 21, 121; Chem. Abstr., 86:175937.

239.- E.I. KOPYTOV et O.M. ROZENTAL (1976), "Dielectric properties of cement pastes at superhigh frequencies", Izv. Vyssh. Uchebn. Zaved., Khim. Khim. Technol., 19, 1751; Chem. Abstr. 86: 160081.

240.- YU. G. PODKIN et O.M. ROZENTAL (1976), "Dielectrometry of binder materials", Izv. Akad. Nauk. SSSR, Neorg. Mater., 12, 1099; Chem. Abstr., 85:197108.

241.- YU. G. PODKIN et O.M. ROZENTAL (1978), "Radiofrequency dielectrometry of cement pastes - methodological basis", Colloid J. USSR, 40, 137.

242.- O.M. ROZENTAL et E.I. FEDINGIN (1979), "Radiofrequency dielectrometry of cement pastes, coherent molecular relocation processes of thixotropic cement pastes", Kholloidn. Zh., 41, 171.

243.- J.P. REBOUL (1977), "Adsorption as the first hydrating phase of portland cement pastes", C.R. Hebd. Seances Acad. Sci. Ser. B., 284, 409; Chem. Abstr., 87:89446.

244.- J. REBOUL (1978), "The hydraulic reaction of tricalcium silicate observed by microwave dielectric meaasurements", Rev. Phys. Appl., 13, 383.

245.- G. LAHAJNAR, R. BLINC, V. RUTAR, V. SMOLEJ, I. ZUPANCIC, I. KOCUVAN et J. URSIC (1977), "On the use of pulse NMR techniques for the study of cement hydration", Cem. Concr. Res., 7, 385.

246.- R. BLINC, M. BURGER, G. LAHAJNAR, M. ROZMARIN, V. RUTAR, I. KOCUVAN et J. URSIC (1978), "NMR relaxation study of adsorbed water in cement and C_3S pastes", J. Am. Ceram. Soc., 61, 35.

247.- I. KOCUVAN, J. URSIC, G. LAHAJNAR, R. BLINC et M. ROZMARIN (1978), "Evaluation of various cement additives by pulse NMR", Silic. Ind., 43, 223.

248.- A.M. SAZONOV, M.M. SYCHEV, V.G. SHIBALLO et A.B. PORAI-KOSHITS (1976), "Hydration of cement studied by NMR methods", Zh. Prikl. Khim. (Leningrad), 49, 1915; Chem. Abstr., 86:46700.

249.- A.P. PALKIN, O.M. ROZENTAL et A.S. SOBOLEV (1979), "Hardening of cement pastes at positive and negative temperatures based on proton NMR data", Izv. Akad. Nauk. SSSR, Neorg. Mater., 15, 347; see also (1977), 13,580.

250.- J. BENSTED (1976), "Use of Raman spectroscopy in cement chemistry", J. Am. Ceram. Soc., 59, 140.

251.- J. BENSTED et S.P. VARMA (1977), "Infrared and Raman spectroscopy in cement chemistry miscellaneous application", World Cem. Technol, 8, 16.

252.- F. RAOULT, J. LEBOT et A. BARON (1976), "Hydration and hardening of concrete immediately after mixing with water", Cim., Betons, Platres, Chaux, 698, 37.

253.- F.W. LAWRENCE, J.F. YOUNG et R.L. BERGER (1976), "Hydration and properties of calcium silicate pastes", Cem. Concr. Res., 7, 369.

254.- D.H. TAYLOR (1977), "A new technique for the study of cement hydration by scanning electron microscopy", J. Test. Eval., 5, 102.

255.- A.F. SHCHUROV, M.A. SOROCHKIN et T.A. ERSHOVA (1976), "Physical models of the early stages of hardening of binders", Proc., Sixth Int. Congr. Chem. Cement, 1974, Moscow, Vol. II Book 1, 76.

256.- P.A. SLEGERS, M. GENET, A.J. LEONARD et J.J. FRIPIAT (1977), Structural transformation of tricalcium silicate during hydration", J. Appl. Crystallogr., 10, 270.

257.- G.M. BRUERE (1972), Some influences on admixture requirements in concrete", Div. Bldg. Res., CSIRO (Australia), Report L-19.

SUB-THEME II - 2

Structure and composition of hydrates

H.F.W. TAYLOR
University of Aberdeen, Scotland, U.K.
D.M. ROY
Pennsylvania State University U.S.A.

I. PRODUCTS FORMED AT ORDINARY TEMPERATURES

The reaction of portland cement with water in pastes at ordinary temperatures gives as the main products a nearly amorphous form of C-S-H, $Ca(OH)_2$, and smaller amounts of an AFm (hexagonal plate) phase or an AFt (ettringite-type) phase or both. We review here current knowledge and hypotheses of the compositions and structures of these phases in the forms in which they exist in cement pastes. We shall deal also with C_3S and β-C_2S pastes, but not with mechanisms of formation, morphology, microstructure or relations to properties.

C-S-H COMPOSITION: INDIRECT OR DIFFERENCE METHODS

The Ca/Si ratio of the C-S-H in a C_3S or β-C_2S paste can be obtained by difference, using determinations of unreacted starting material and of $Ca(OH)_2$ formed. Such methods give values usually between 1.5 and 2.0 for fully-reacted pastes, depending somewhat on water/cement ratio and other factors. For low degrees of reaction, results vary widely. Some workers have reported that the Ca/Si ratio passes through a minimum for C_2S but not C_3S pastes (1,2), but this is not universally agreed; for a discussion, see Odler and Dörr (3). The results at low degrees of reaction are very sensitive to small experimental errors, and different methods of determining the $Ca(OH)_2$ tend to give different results; some or all of the published results may be wrong. However, it has also been suggested that the Ca/Si ratio in the early stages of reaction, and whether or not it passes through a minimum, may depend on the reactivity of the starting material (1,3,4).

DIRECT OR ELECTRON-OPTICAL METHODS

Indirect methods give an average Ca/Si ratio for all the C-S-H in a sample and can thus eliminate sampling errors, but they have serious limitations. Their reliability at low degrees of reaction has already been mentioned. In addition, they cannot give information about possible differences in composition between different regions, such as "inner" and "outer" products, or between individual particles within a given region. They cannot safely be applied to cement pastes, because of uncertainties connected with subsidiary components and phases.

Direct or electron-optical methods can avoid these drawbacks. Electron probe microanalysis (EPMA) and scanning electron microscopes (SEM) fitted with X-ray detectors have been in use for some time. These methods allow ready correlation of composition with microstructure, but have limitations. The volume analyzed (about 2 μm in each direction) is probably too large for the scale of heterogeneity of the material, and certainly too large for the study of between-particle variability. Corrections for absorption and other effects can be difficult, especially if rough surfaces are used. The identity of the sample analyzed, or its freedom from crystalline impurities, cannot be checked by a diffraction pattern. Some newer instruments overcome these limitations. In the analytical electron microscope (AEM), a transmission electron microscope is fitted with an X-ray detector; analyses can be obtained from regions a few hundreds of Å in each direction (5). The scanning transmission electron microscope (STEM) offers further possibilities (6), but these have thus far scarcely been exploited in the analysis of cement hydration products.

ELECTRON-OPTICAL ANALYSES OF C_3S PASTES

EPMA and SEM studies of the C-S-H in C_3S pastes (7-9) have mostly indicated Ca/Si ratios of 1.6 - 1.9, in general agreement with results of indirect methods for mature pastes. Some have distinguished between inner and outer products: Goto *et al.* (10) found 1.8 - 2.0 for the inner product of a mature paste, and 4 - 4.5 for the outer product; this latter value presumably relates to a mixture with $Ca(OH)_2$. Stucke and Majumdar (11), studying a 1-month old paste, obtained values of 1.9 and 1.6 for the inner and outer products respectively.

Using AEM, Gard *et al.* (12) found mean Ca/Si ratios of 1.5 - 1.7 for the C-S-H in C_3S pastes cured for 1 - 180 days. The means for two different C_3S preparations were 1.5 and 1.6, but no significant correlations with curing time, degree of reaction, or morphological type of C-S-H were found. All the samples showed significant compositional variation between particles; the range of Ca/Si ratio over the 161 particles analyzed was 1.21 - 1.96. For high degrees of reaction, the results agreed broadly with those obtained for the same samples by an indirect method, but for low degrees of reaction the latter gave lower Ca/Si ratios. Two possible explanations were suggested: either the indirect results were wrong, or the AEM results related to only a part of the C-S-H. The specimens were prepared for electron microscopy by grinding and redispersing, and this procedure could have enriched them in material easily detached from the cores of unreacted C_3S. This question will remain unanswered until a better method of specimen preparation, such as ion-thinning, has been developed.

C-S-H COMPOSITION IN CEMENT PASTES

This could not be reliably determined before electron-optical methods were available, but some useful indications were nevertheless obtained. Kalousek (13) concluded from thermal analysis that the amounts of AFm and AFt phases were too small to account for all the sulfate ion present, and that some of it must enter the C-S-H. Copeland and coworkers, in studies summarized by Copeland and Kantro (14), concluded from indirect evidence that the C-S-H could accommodate Al^{3+}, Fe^{3+} and SO_4^{2-} ions, in each case to the extent of about 1 ion per 6 Si, and that their presence in the C-S-H was associated with an increase in Ca/Si ratio. SEM studies have supported some of these conclusions: Diamond (15) found Ca/Si ratios of 2-3 and evidence of significant S substitution, while Stucke and Majumdar (16) reported a bimodal distribution of Ca/Si ratio with maxima at 1.90 and 2.15.

Lachowski *et al.* (17) analysed 365 particles of C-S-H, $Ca(OH)_2$, AFm phase and AFt phase from pastes of cements and clinkers using AEM. All the phases other than $Ca(OH)_2$ showed significant compositional variation between different paste specimens and also between different particles within each specimen. Fig. 1 gives a general indication of this variability in a typical case. Nearly all the C-S-H particles analyzed contained significant amounts of Al, Fe and S, and smaller amounts of Mg. Many contained a little Na or K, and a few contained traces of Ti or Cl. For the pastes to which Fig. 1 refers, the mean atomic contents, expressed as ratios relative to 10(Ca + Mg), were :

Na	Mg	Al	Si	S	Cl	K	Ca	Ti	Fe
<0.1	<0.1	0.5	5.7	0.8	<0.1	0.1	10.0	<0.1	0.1

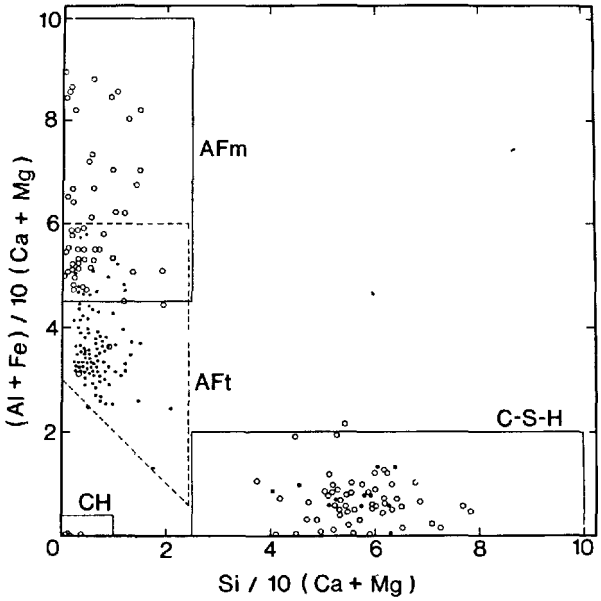

Fig. 1 - Atomic ratios in particles of hydration products in some cement pastes, determined using analytical electron microscopy (17). Open and full circles denote S/10(Ca+Mg) ratios below and above 1.5 respectively. Water/cement ratio = 0.7, curing times 1 - 28 days.

For 156 C-S-H particles from these and other pastes, the mean Ca/Si ratio was 2.0.

THE WATER CONTENT OF THE C-S-H IN PASTES

For the C-S-H of fully reacted and D-dried C_3S or cement pastes, H_2O/Si ratios are typically about 0.5 below Ca/Si ratios[14]; *i.e.*, H_2O/Ca is about 0.7. Heating to 150-200°C under dynamic (∓G) conditions leaves a similar amount of water in the C-S-H, though the effect on the structure is not necessarily the same. In either case, the water retained presumably occurs partly as molecules and partly as OH groups bound in various ways, but the respective amounts are unknown. Opinions differ as to whether the H_2O/Si ratios of C-S-H in partly reacted pastes are higher or lower than in the case of fully reacted pastes, and for this and other reasons, the use of 'fixed water' as a measure of the degree of reaction is of uncertain validity.

The terms 'chemically' and 'physically' bound water have no intrinsic meaning, but it is legitimate to enquire about the mobility of water molecules lost under given conditions, the part they play in the structure, or the way in which the latter is affected by their loss. The results of Feldman and others indicate that substantial and partly irreversible changes begin to occur at water contents much above those produced by D-drying.

STRUCTURE OF THE C-S-H IN CEMENT AND CALCIUM SILICATE PASTES

Because the C-S-H formed in pastes cured at ordinary temperatures is almost amorphous, X-ray or other diffraction methods provide only slight structural information and there have been no significant recent developments in this respect. Mather (18) and Diamond (19) have reported typical X-ray powder patterns, which show only a very weak, diffuse band at 2.6 - 3.1 Å and a somewhat sharper one at 1.8 Å. A 20-year old C_3S paste gave a closely similar pattern (20) and there appears to be no foundation for occasional suggestions that the crystallinity of the C-S-H increases significantly over a period of some decades.

Of other methods used to provide structural information, trimethylsilylation (TMS) has proved the most useful. This is a chemical method that provides information on the distribution of Si among different anionic species. It was first applied by Lentz (21), who showed that the monomeric anions (SiO_4) initially present are replaced in the course of reaction by dimer (Si_2O_7) and ultimately by polymer. Recent improvements in TMS procedures (22,23) have led to a more exact and detailed understanding of this process.

ANION-SIZE DISTRIBUTION IN C_3S AND β-C_2S PASTES

The silicate anions in C_3S and β-C_2S are monomeric, and recent TMS studies have shown that for calcium silicate pastes cured at room temperatures the amount of monomer corresponds to that of unreacted starting material found using QXRD (2,4,24,25). Little or no monomer is therefore present in the C-S-H. This does not hold, however, for C_3S pastes cured at 4°C. Bentur *et al.* (24) found that such pastes contained much more monomer than could be attributed to unreacted C_3S. They suggested that the C-S-H formed initially contained monomer, which was later converted into dimer and then into polymer; at room temperatures, the dimerization step was sufficiently rapid that the concentration of monomer was very low.

It is now widely agreed that the C-S-H of C_3S pastes cured at room temperature contains much dimer, a very little linear trimer (Si_3O_{10}), virtually no cyclic trimer (Si_3O_9) or cyclic tetramer (Si_4O_{12}), and varying amounts of polymer (2,4, 23 - 25). Unless otherwise stated, this latter term will be used here to include all silicate species larger than those listed above. Dent Glasser *et al.* (4) found that for degrees of reaction up to about 20% the Si in the C-S-H was present entirely as dimer, but that at later stages of reaction polymer was also present. The absolute amount of dimer increased throughout the period studied (about 15 months); a nearly fully-hydrated paste of this age contained about equal amounts of Si as dimer and as polymer. Comparison with electron-microscope evidence suggested that Type I C-S-H (nomenclature of Diamond, 19) contained only dimer and that Type III C-S-H contained either polymer, or a mixture of dimer and polymer. Mohan (20) later extended this study to a 20-year old C_3S paste provided by Dr. D.L. Kantro (Portland Cement Association); of the total Si, 2% was recovered as monomer, 36% as dimer and 47% as polymer (total yield, 85%).

ANION-SIZE DISTRIBUTION IN CEMENT PASTES

In the main, results obtained by TMS procedures have been similar to those for calcium silicate pastes. The most important difference is that for pastes hydrated at ordinary temperatures, the C-S-H contains an appreciable amount of monomer (26, 27). For three fully-hydrated cement pastes 1.8 - 6.3 years old, Lachowski (26) found 9 - 11% of the Si to be recoverable as monomer, 22 - 30% as dimer, and 44 - 51% as

polymer. Polymer here includes 1 - 2% as linear trimer, and the total yields were 80 - 88%. As with C_3S pastes, little or no cyclic trimer or cyclic tetramer has been found, but Sarkar and Roy (27) observed peaks in the GLC curves of the TMS derivatives which they attributed to linear tetramer (Si_4O_{13}) and cyclic pentamer (Si_5O_{15}). Berger *et al.* (2) found that, for cement pastes cured for short times, the proportion of the Si in the C-S-H present as polymer was less than for comparable C_3S or C_2S pastes. The higher proportions of monomer in cement pastes could be associated with partial replacement of Si by other elements (2,27,28). A little monomeric silicate could also occur in the AFm and AFt phases.

ANION-SIZE DISTRIBUTIONS WITHIN THE POLYMER FRACTION

These have so far been studied most effectively by gel-permeation chromatography (GPC) of the TMS derivatives (26,27); thin-layer chromatography also appears promising (29). It is also possible, from chemical analysis of the TMS derivatives, to determine the mean connectivity ($\bar{Q}$) of the polymer fraction; this quantity is defined as the mean number of Si-O-Si linkages formed by each Si atom and is, for instance, 1.6 for linear pentamer, 2.0 for a ring or infinite chain, and 3.0 for the finite, three-dimensional ion Si_8O_{20}.

For fully-reacted cement pastes, both Sarkar and Roy (27) and Lachowski (26) found anion-size distributions within the polymer fraction peaking at a molecular weight of about 1100 for the TMS derivatives. Sarkar and Roy considered the main component of the polymer to be cyclic pentamer. They found no evidence of anionic species larger than this, but Lachowski's distributions (Fig. 2) for the three pastes mentioned in the previous section showed tails on the high molecular weight sides, with minor peaks or shoulders indicating significant contributions from anions with 6 - 9 Si. The number and weight means for the anion size corresponded to 8 - 9 Si and 14 - 17 Si atoms respectively, and the mean connectivities were 2.3. Later work using a different GPC instrument indicated the slightly higher modal molecular weight of 1300 (30).

Mohan (20) has applied Lachowski's methods to C_3S pastes (w/c = 0.45 or 0.47). He obtained GPC curves which broadly resembled those in Fig. 2, and which gave the results shown in Table I. Some tentative interpretations are are follows. First, for the 7-day old paste, about a half of the Si in the polymer fraction is present in anions containing less than

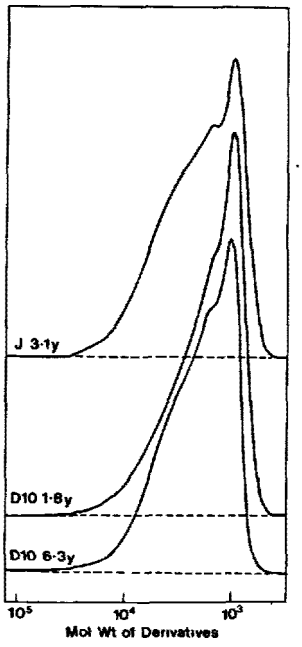

Fig. 2 - Gel permeation chromatograms of polysilicate derivatives from cement pastes aged 1.8 - 6.3 years (Lachowski, 26)

8 Si, possibly mainly linear pentamer; much of the rest is in anions with 8 - 9 Si. Second, during the next 3 months, there is little change in the fraction present in anions with less than 8 Si, but the fraction present in highly-polymerized anions (> 10 Si) increases at the expense of that present in anions with 8 - 9 Si. Third, changes continue over a period of years, during which time the fraction of the Si present in anions with less than 8 Si also decreases considerably; in the 20-year old paste, possibly half of the Si in the polymer fraction is present in highly-polymerized anions. The connectivity results are also of interest, and their significance is discussed later.

Ono *et al.* (25) have obtained somewhat higher molecular weights for the polymer TMS derivatives obtained from alite pastes with and without added Na_2O. They reported values of about 3000 for pastes 3 - 28

TABLE I

C_3S Pastes : Anion-Size Distributions Within the Polymer Fraction (Mohan, 20).

Curing Time	Molecular Weight of TMS Derivatives			No. of Si Atoms in the Anion		Mean
	Mode	Number Mean	Weight Mean	Number Mean	Weight Mean	Connectivity ($\bar{Q}$)
7 days	1300	1600	1900	7	8	1.8
14,30,42 "	1300	1600	2100	7	9	1.8 - 1.9
84 "	1300	1700	2400	7	10	1.8
180 "	1300	1800	2600	8	11	1.8
20 years	1300	2500	7000	11	33	2.1

days old, rising to nearly 4000 for the Na_2O-free paste at 91 days.

STRUCTURAL MODELS FOR C-S-H

Two assumptions about the structure of the C-S-H of cement and calcium silicate pastes are widely accepted: first, that it is a layer structure, and second, that when the silicate ions polymerize, they do so in a way that produces chains. Both assumptions derive, at least in part, from the suggestion made over 20 years ago by one of us (H.F.W.T.) that the structure resembles that of tobermorite. The view that there is any close relationship to tobermorite is now generally rejected, but the assumptions of a layer structure and of silicate chains remain, and it is timely to examine whether they are soundly based.

Four arguments for a layer structure may be considered, *viz:*

(i) *Diffraction.* The most obvious interpretation of the weak x-ray peaks or bands at 1.8 and about 3 Å is that they are *hk* reflections from layers similar to those in $Ca(OH)_2$, but possessing only short-range order and distorted because many of their oxygen atoms are shared with silicate tetrahedra in a particular way. Very occasionally, particles have been found that give selected-area electron-diffraction patterns (31,32), and these patterns are also consistent with the above explanation (33).

(ii) *Surface-Area Studies.* Differing structural models have been advanced to account for the results of studies of specific surface areas and related properties, but nearly all share the common feature of a layer structure. It is not clear whether layer structures are the only ones that can explain the data, or whether they have been adopted because of the other arguments outlined here.

(iii) *Morphology.* Some, though not all electron-microscope studies suggest that Types I and II C-S-H, which predominate at early ages, are composed of either flakes or foils, in some cases either rolled into scrolls or joined to form honeycombs (31,32, 34 - 36). For Types III and IV C-S-H, which seem to predominate in mature pastes, the morphology gives little clue to the underlying structure, though the description of Type III C-S-H as "irregularly equant or flattened particles" (19) could possibly be considered as suggesting a layer structure.

(iv) *Analogy with Other Basic Salts.* Many, though by no means all basic salts are known to have layer structures, and analogy suggests that these could include the C-S-H of cement and calcium silicate pastes.

None of this evidence is conclusive, but taken as a whole it suggests that there is indeed a tendency towards formation of layers, which is possibly stronger in Types I and II than in Types III and IV C-S-H. The diffraction evidence shows that it is no more than a tendency. As Diamond (19) has emphasized, the structure possesses only short-range order, and the absence of any X-ray powder spacing in the 9 - 15 Å region shows that there is no close approximation to a set of regularly spaced layers. The structure must differ markedly from those of such crystalline or quasi-crystalline phases as tobermorite, jennite, C-S-H(I) or C-S-H(II), and the use of any of these as models is likely to be misleading.

The only significant argument for a chain-type anion appears to be the diffraction evidence; condensation of the SiO_4 tetrahedra into chains would distort the Ca-O sheets in a way that would produce the observed diffraction effects. However, some other patterns of condensation, including the mere formation of dimer, would probably have the same effect.

The TMS evidence gives no support to the hypothesis that polymerization produces chains, and affords some indications against. Sarkar and Roy's (27) view that the main constituent of the polymer fraction is cyclic pentamer has already been mentioned. The combination of relatively low mean molecular weight and relatively high connectivity found by Lachowski (26) and Mohan (20) does not support the view that the higher molecular-weight constituents of the polymer have chain structures. It suggests rather that they are rings or, perhaps more probably, compact and roughly equidimensional anionic species similar to, though not necessarily the same as those known to exist in silicate solutions (37).

These arguments suggest that most and perhaps all of the models that have been suggested indicate a higher degree of crystalline order than really exists. In Types I and II C-S-H, there may well be an approximation to continuous Ca-O layers, in which the oxygen atoms form parts of Si_2O_7, OH, and, for the C-S-H of cement pastes, SO_4 and Aℓ- and Fe-containing groups. For Types III and IV C-S-H, such sub-crystalline order as exists could be confined to the neighborhood of small fragments of Ca-O layers, perhaps only some tens of Å large and only rarely parallel to each other (Fig. 3). The intervening spaces could be totally amorphous and any silicate ions in them might well be of compact types. It is by no means certain that Types III and IV C-S-H are particulate in nature, and Fig. 3 has been drawn in a manner intended to show this.

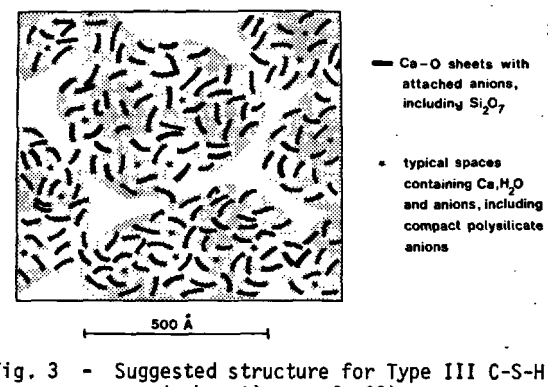

Fig. 3 - Suggested structure for Type III C-S-H (schematic; ref. 38)

A model of this type would appear compatible with some other data, such as the densities of 2.3 - 2.4 g cm^{-3} found for material equilibrated to 11% R.H. (39). Nitrogen specific surfaces of about 60 m^2g^{-1} could reasonably apply to the C-S-H particles, and the much higher values of around 950 m^2g^{-1} found using low-angle x-ray scattering (40) to the Ca-O sheet fragments and the anions directly associated with them.

CALCIUM HYDROXIDE IN CEMENT PASTES

Analytical electron microscope analyses of $Ca(OH)_2$ crystals from cement pastes showed that most contain a little Si, S and Fe and that a few contain a little Aℓ; maximum contents of any of these elements relative to Ca were 0.02 - 0.03 (17). The relative

abundance of Fe compared with Aℓ suggests that it may be present as Fe^{2+}, which could replace Ca. It is not clear whether the other elements are present in the $Ca(OH)_2$ structure or in inclusions, although no indications of a second phase were observed.

AFM PHASES

These are crystalline phases of hexagonal-plate morphology and are typified by monosulfate, $[Ca_2A\ell(OH)_6]_2(SO_4).6H_2O$. The basic crystal structure and other data are well established; several reviews exist (41 - 43). AFm phases have layer structures related to that of $Ca(OH)_2$; every third Ca is replaced in an ordered way by a tripositive cation, which causes considerable distortion, and anions and H_2O molecules are intercalated between the layers. The general formula is $Ca_2M(OH)_6.X_x aq.$, where M is an octahedral cation (normally $A\ell^{3+}$ or Fe^{3+}), and X is the interlayer anion. Many anions can occupy these sites, including among others OH^-, CO_3^{2-}, SO_4^{2-} $C\ell^-$, $A\ell(OH)_4^-$ (in C_2AH_8), $H_2A\ell SiO_5^-$ (in C_2ASH_8) and a silicate ion of unknown constitution. Up to one interlayer anion can be accommodated per unit of $[Ca_2A\ell(OH)_6]^+$.

The AFm phase of cement pastes has often been regarded as monosulfate or as a mixture or solid solution of this phase with its hydroxide analog, C_4AH_x, but this view is an oversimplification. Regourd *et al.* (44) studied C_3S-C_3A - gypsum pastes by SEM and EPMA. They found that both AFm and AFt phases can be formed which contain Si but no S. Lachowski *et al.* (17) studied the AFm phase in portland cement pastes with w/c 0.7, hydrated for 7 days at 25°C; they found the following atomic ratios :

Mg	Aℓ	Si	S	K	Ca	Fe
0.01	1.06	0.11	0.15	0.02	1.99	0.03

These are mean ratios for 30 particles and are given relative to 2(Ca + Mg). Assuming the Fe to be in octahedral sites, and ignoring minor replacements, this gives the ionic constitution

$[Ca_2A\ell_{0.97}Fe_{0.03}(OH)_6](SO_4)_{0.15}A\ell_{0.79}Si_{0.11}O_xH_y$.

The constitution of the interlayer is not given in more detail because the forms in which the Aℓ and Si occur are not known. Marked compositional variation between particles was observed (Fig 4a) and the AFm phase clearly has aspects of both a mixture and a solid solution. The mean composition corresponds to that of a mixture or solid solution of which the components are C_4AH_x (about 50 mole %), monosulfate ($C_3A.C\bar{S}.H_x$; about 30 mole %) and a composite component with interlayer Aℓ and Si (about 20 mole %), all with some replacement of Aℓ by Fe. With increase in time to 28 days (Fig. 4b), the proportion of this composite component increases, at the expense largely of C_4AH_x; a major part of it is $2[C_2AH_x]$. Lachowski *et al.* also analyzed the AFm phase formed in pastes of finely-ground clinkers; as might be expected, the interlayer sites were occupied largely by OH^- and by Aℓ- or Si-containing species, with relatively little sulfate.

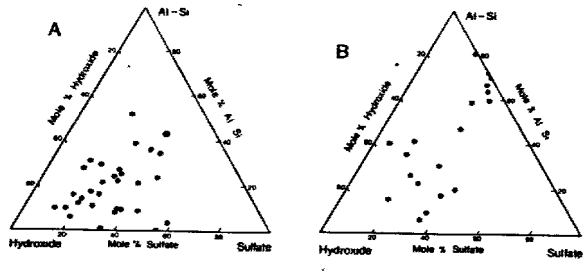

Fig. 4 - Compositions of individual particles of AFm phases in pastes of a cement hydrated for (a) 7 days and (b) 28 days. The components are defined as $C_4A\bar{S}.aq.$, $C_4A.aq.$ and $C_4A(A,AS_2,S_2).aq.$, with substitution of Fe for Aℓ in each case (ref. 17).

AFT PHASES

These are crystalline phases of hexagonal prism or needle morphology, and typified by ettringite, $[Ca_3A\ell(OH)_6.12H_2O]_2(SO_4)_3.2H_2O$. As with AFm phases, the basic structure and other data are well established; for reviews, see refs. 41 - 42. AFt phases have columnar structures, the material enclosed in the square brackets forming the columns and that outside them occupying the intervening channels. The Aℓ can be replaced by Fe^{3+} or, in thaumasite, $[Ca_3Si(OH)_6.12H_2O](SO_4)(CO_3)$, by Si. Various anions can occupy the channel sites, including SO_4^{2-}, CO_3^{2-}, $C\ell^-$, a silicate ion of unknown constitution (45) and possibly OH (45). Under some conditions, solid solutions between ettringite and thaumasite can be made (46).

The AFt phase in cement pastes has usually been regarded as ettringite, but the work of Regourd *et al.* (44) suggests that it may contain Si. Lachowski *et al.* (17), in their AEM study, had difficulty in obtaining reliable analyses of AFt phase because of suspected loss of S and Ca in the beam; for a typical portland cement hydrated for 1 - 28 days, the mean atom ratios were Ca 4.74, K 0.09, Mg 0.03, Aℓ 1.64, Fe 0.06, Si 0.30, S 1.60. These are means for 100 particles and are given relative to (Aℓ + Fe + Si) = 2. The theoretical contents of Ca and S are 6 and 3 respectively; the deficiency in S is probably too large to be wholly attributable to loss in the beam and some of the channel-anion sites may be occupied by OH^- or CO_3^{2-}. The results confirm the presence of Si, and it was only possible to explain them rationally by assuming that this largely or wholly replaced Aℓ.

DISTRIBUTION OF SUBSIDIARY ELEMENTS IN CEMENT PASTES

The AEM studies of Lachowski *et al.* (17) give tentative indications of the distribution of the Aℓ, Fe and S among the product phases. Comparison of the mean C-S-H composition with that of the cement suggests that about a third of the Aℓ and by far the greater part of the S ends up in the C-S-H; the mean composition and probable amount of AFm phase are compatible with this. The data did not justify such calculations for the Fe, but suggested that this tends to enter C-S-H in preference to AFm and AFt phases.

Copeland *et al.* (47) obtained X-ray evidence of the formation of a hydrogarnet phase from a wide range of cements. It had a = 12.4 Å, and they concluded that it may have been silica-containing and of approximate composition $C_6AFS_2H_8$. Relatively few other workers seem to have detected hydrogarnet phases in normally cured portland cement pastes (18).

Seligmann and Greening (48) concluded from indirect evidence that the C-S-H formed at early ages should be high in SO_4 and low in Aℓ, and that it should lose SO_4 and gain Aℓ as reaction proceeded. There is probably no direct evidence for or against this view in the case of Aℓ. Evidence for a decrease in SO_4 content was found by Lachowski *et al.* (17).

II. PHASES FORMED AT ELEVATED TEMPERATURES

INTRODUCTION

The hydration products of portland cement, C_3S or β-C_2S in pastes at temperatures up to or somewhat above 100°C do not differ essentially from those formed at ordinary temperatures, though there are differences in morphology and microstructure. Odler and Skalny (49) studied C_3S hydration at 25 - 100°C; the C-S-H Ca/Si ratio increased (from 1.88 to 2.04), while the H_2O/Si ratio for D-dried material decreased from 1.52 to 0.98. Bentur *et al.* (24) found more polysilicate in C-S-H formed at 65°C than in that formed at 25°C. The upper stability limit of ettringite has been studied, because of the importance of this phase for expansive cements; from static experiments, Roy *et al.* (50) placed the transition temperature for decomposition to monosulfate plus hemihydrate at 105 ± 5°C at 690 - 1380 KPa. Satava and Veprek (51), using dynamic hydrothermal analysis, placed the onset of the DTA peak in liquid water at 111°C, in reasonable agreement; taken together, these studies define the maximum stability temperature at relatively low confining water pressures. Izozaki and Nakagawa (53) found that various inorganic salts failed to stabilize ettringite at 180°C under saturated vapor pressure. Monosulfate is reported stable up to 190°C (51), and in an Fe-substituted form has been obtained from C_4AF and Fe-Aℓ-ettringite at 190°C (52).

The phases described in the remainder of this review are formed in autoclaved or hot-pressed materials, or hydrothermally, as in deep oil-well or geothermal cementing operations. They range from X-ray amorphous to highly crystalline phases. Because of their varying degree of crystallinity and sometimes also difficulties of isolation, many uncertainties remain about compositions and structures, especially in regard to products formed in autoclaved cement-based materials, which typically result from reactions lasting only a few hours. Nevertheless, there has been progress since the Moscow Congress review (42), in both synthetic and structural studies. Taylor and associates in Aberdeen have obtained new powder diffraction data from many of the phases for inclusion in the JCPDS file; these revisions have emphasized the use of calculated patterns whenever the structures are known, to permit recognition of impurity peaks, reliable indexing, checks on intensities, and unit-cell refinements. New combinations of analytical and structural tools have been applied to help elucidate relationships between initial phase compositions, reaction conditions, and structures and compositions of products; of particular interest is the development of a microscope for direct observation of autoclave processes (54). Some new mineral localities have been investigated that contain an abundance of hydrothermal calcium silicates and related minerals, of which the chief are the Hatrurim Formation in Israel and the Fuka locality in Japan, which have been studied by Gross (55) and by Henmi and associates in Okayama respectively.

Table II lists the phases that either have been found in cements hydrated at elevated temperatures, or which from other evidence could possibly be found in such materials, and summarizes new data. Fuller accounts of some of these recent studies follow.

WOLLASTONITE GROUP

Xonotlite has assumed increasing importance from its persistent formation in higher-temperature autoclaved materials and presumably in deep oil-well and geothermal cements. Kudoh and Takéuchi (56) determined the crystal structure of the A$\bar{1}$ polytype; it basically resembles the much more approximate structure found earlier by Mamedov and Belov. Kalousek *et al.* (57) studied 15 natural and synthetic xonotlites by X-ray diffraction, TG and AEM. An earlier suggestion (58) that xonotlites can be defective in Ca was confirmed; the deficiency is balanced by presence of SiOH groups, which partly or wholly explains observations that samples made at low temperatures contain more water than that indicated by the formula C_6S_6H. The results also showed that Aℓ can enter the structure and that this affects the cell parameters. Tashiro and Kawaguchi (59) studied the effects of Ca/Si ratio and added Cr_2O_3 on xonotlite synthesis. The formation temperature is increased either by departure from the 1:1 composition; or by adding Cr^{3+}. The formation temperatures at 0% and 10% Cr_2O_3 were, respectively, 210° and 450°C at C/S 0.83, 160° and 280°C at C/S 1.0, and 250° and 270°C at C/S 1.2. The Cr appears to enter the C-S-H(I) structure and to interfere with formation of tobermorite.

A new polytype of wollastonite (7T) has been discovered (60). Foshagite has been proposed as a feasible constituent of geothermal cements; it appears to contribute favorably to the mechanical properties due to its fibrous habit (61, 62). Hillebrandite can also occur under conditions relevant to geothermal cements (62).

TOBERMORITE GROUP

11 Å Tobermorite. Considerable effort has been directed to both synthesis and properties of tobermorite phases. Many of the studies center on 11 Å tobermorite, which is a major component of many autoclaved building materials and is also formed in cementing deep oil wells. Mitsuda and Taylor (63) discussed 'normal' and 'anomalous' behavior in natural tobermorites (in normal tobermorite the basal spacing decreases to about 9.3 Å on heating at 300°C while in the anomalous variety it does not). Normal behavior is associated with defective silicate chains and Ca/Si ratios above the theoretical 5:6, while in the natural anomalous tobermorites studied, all of which contained Aℓ and alkalies, the structure was defective in Ca and the Ca/(Si + Aℓ) ratios were below 5:6. Eℓ-Hemaly *et al.* (64) reported on the synthesis of normal and anomalous tobermorites; they found reaction to pass through the sequence semi-crystalline C-S-H → normal tobermorite → anomalous tobermorite. Addition of $Aℓ^{3+}$ generally favored growth of normal tobermorite, while $Aℓ^{3+}$ plus alkali yielded anomalous or intermediate varieties.

Other Crystalline Tobermorite Phases. 14 Å tobermorite has been synthesized (64, 65); Hara *et al.* (65) obtained it from prolonged reactions at 60°C under conditions similar to those used originally by Kalousek and Roy (66). The occurrence of 10 Å tobermorite as a natural mineral has been confirmed; Ca/Si ratios of 1.3 - 1.7 have been found (55, 67). Tacharanite appears closely related to the tobermorite minerals; it contains essential Aℓ and may be identical with the previously reported 12.6 Å tobermorite (55, 68).

Hydrothermally-Produced C-S-H and its Conversion into Tobermorite. In autoclaved materials and cements hydrated under hydrothermal conditions, various forms of C-S-H can occur either as intermed-

TABLE II Hydrothermally Produced Calcium Silicates, Aluminosilicates and Related Phases

Compound	Composition	Constitutional Formula	Comments, New Data, and References
Wollastonite Group			
Nekoite	$C_3S_6H_8$	$3CaSi_2O_5.8H_2O$	Natural mineral, not synthesized
Okenite	$C_3S_6H_6$	$3CaSi_2O_5.6H_2O$	Ditto; new occurrence[55]
Xonotlite	C_6S_6H	$Ca_6Si_6O_{17}(OH)_2$	Structure[56] composition and substitution [57-59], geothermal cements[61 62 89 94]
Wollastonite	CS	$CaSiO_3$ (β-)	New polytype[60]
Foshagite	C_4S_3H	$Ca_4(SiO_3)_3(OH)_2$	Geothermal cements[61 62]
Hillebrandite	C_2SH	$Ca_2(SiO_3)(OH)_2$	Geothermal cements[62]
Tobermorite Group			
14 Å Tobermorite	$C_5S_6H_9$	$Ca_5(Si_6O_{18}H_2).8H_2O$	Synthesis[64-66]
Tacharanite	$C_{12}AS_{18}H_{18}$	$Ca_4(Si_6O_{18}H_2)Al_{2/3}.5H_2O$ (?)	Crystal data, relation to tobermorites[68] new occurrence, ?=12.6Å tobermorite[55]
11 Å Tobermorite	$C_5S_6H_5$	$Ca_5(Si_6O_{18}H_2).4H_2O$	Normal & anomalous[63 64], autoclaved products[69-78]; geothermal uses[79-84 88 89]
10 Å Tobermorite	$\sim C_5S_4H_5$(?)	(?)	New natural occurrence, composition[55 67]
9 Å Tobermorite	C_5S_6H	$Ca_5(Si_6O_{18}H_2)$	Natural occurrence[55]; = riversideite
C-S-H(I)	$C_5S_{4-6}H_X$ (?)	Complex: $(SiO_3)_\infty$ and Si_2O_7 (?)	Autoclaved products[69-78], TMS & TG[72]; transition to tobermorite[73-80], geothermal applications[79-84 88 89]
Jennite Group			
Jennite	$C_9S_6H_{11}$	$Ca_9(Si_6O_{18}H_2)(OH)_8.6H_2O$	New occurrence[55]; composition[55 85 86]
Metajennite	$C_9S_6H_7$	$Ca_9(Si_6O_{18}H_2)(OH)_8.2H_2O$	Composition[85]
C-S-H(II)	$C_9S_{4-6}H_X$	Complex: $(SiO_3)_\infty$ and Si_2O_7	Composition, crystal data, silicate anion type, TG, relation to jennite[33]
Gyrolite Group			
Gyrolite	$C_2S_3H_{\sim 2}$	$Ca_8(Si_4O_{10})_3(OH)_4.\sim 6H_2O$	Formation, stability relations, and geothermal cements[61 62 87-91]
Truscottite	$C_7S_{12}H_{\sim 3}$	$Ca_7(Si_4O_{10})(Si_8O_{19})(OH)_4.\sim 1H_2O$	Truscottite composition[92]
Reyerite	$(N,K)C_{14}S_{22}AH_{\sim 8}$	Substituted truscottite	
Z-Phase (Assarsson)	$\sim CS_2H_2$	$Ca(Si_2O_5).2H_2O$ (?)	Crystal data, relation to gyrolite[93]
γ-C_2S Group			
Kilchoanite	C_3S_2	$Ca_6(SiO_4)(Si_3O_{10})$	Geothermal cements[94], TMS study[27]
C_8S_5	C_8S_5	$Ca_8(SiO_4)_2(Si_3O_{10})$	Formation from γ-C_2S + quartz[96]
Calciochondrodite	C_5S_2H	$Ca_5(SiO_4)_2(OH)_2$	Hot-pressed cements[95]
Other Calcium Silicate Phases			
"3.15 Å Phase"	$\sim C_4S_5H$	(?)	Synthesis & crystal data of new phase[97] geothermal cements[84 90]
Suolunite	CSH	$Ca_2(Si_2O_7H_2).H_2O$	Structure[100]
Rosenhahnite	C_3S_3H	$Ca_3(Si_3O_{10}H_2)$	High-pressure phase
Afwillite	$C_3S_2H_3$	$Ca_3(SiO_4H)_2.2H_2O$	Structure refinement[101]
Killalaite	$\sim C_{3.2}S_2H_{0.8}$	$Ca_{3.2}(Si_2O_7H_{0.6})(OH)$	Structure, relation to "Phase F"[102]
α-C_2S Hydrate	C_2SH	$Ca_2(SiO_4H)(OH)$	Formation[83 98], natural mineral[55], structure of Ge-analog[99]
Dellaite	C_6S_3H	$Ca_6(SiO_4)(Si_2O_7)(OH)_2$	Geothermal cements[61 62]
Tricalcium silicate hydrate	$C_6S_2H_3$	$Ca_6(Si_2O_7)(OH)_6$	Hot-pressed cements[95]; structure[103]
Other High-Temperature Cement Phases			
Scawtite	$C_7S_6\bar{C}H_2$	$Ca_7(Si_6O_{18})(CO_3).2H_2O$	Formation, geothermal cements[61 62 84 90]
Fukalite	$C_4S_2\bar{C}H$	$Ca_4Si_2O_6(OH,F)_2(CO_3)$	New mineral; crystal data[104]
Pectolite	NC_4S_6H	$NaCa_2(Si_3O_9H)$	Geothermal cements[62 78-80]
Rustumite	$C_5S_5H.CaCl_2$	$Ca_{10}(SiO_4)(Si_2O_7)_2(OH)_2Cl_2$	Composition, structure[105]
Hexagonal CAS_2	CAS_2	$Ca(Al_2Si_2O_8)$	Geothermal cements[61 62 90 107]
Stratlingite	C_2ASH_8	$[Ca_2Al(OH)_6][AlSiO_5H_2].4H_2O$	Crystal data[106]
Bicchulite	C_2ASH	$Ca_2(Al_2SiO_6)(OH)_2$	Geothermal cements[61 62 90]; structure[108]
Hydrogarnet	$C_3(A,F)(H_6,S_3)$	$Ca_3[Al,Fe]_2[(SiO_4),(OH)_4]_3$	Autoclaved materials, geothermal cements[61 62], hot-pressed cements[95]

iates in the formation of 11 Å tobermorite or as the final product. The designation "C-S-H" denotes any sub-crystalline or amorphous calcium silicate hydrate and includes a wide variety of phases, many of which probably differ markedly in structure both from the C-S-H of normally-cured cement pastes and from the tobermorite phases. The term 'C-S-H(I)' refers more specifically to forms of C-S-H with a relatively high degree of crystallinity and a composition and structure approaching those of the crystalline tobermorites. Šauman (69) explored the conditions of formation and character of the binding phases in autoclaved cement-silica materials; imperfectly developed 11 Å tobermorite and CSH_n (a form of C-S-H) were reported to be the major phases in compact silicate concretes, but cellular (aerated) concretes contained well-developed crystals of tobermorite; Mitsuda and Chan (70) showed this to be anomalous. Crennan *et al.* (71) and Eℓ-Hemaly *et al.* (72) also studied dense lime-quartz materials. They found the binder to be a poorly crystalline C-S-H, and TMS studies showed a gradual change from monomer and dimer to polysilicate as reaction proceeded and the binder Ca/Si ratio decreased. The binder H_2O/Si ratio was related to its Ca/Si ratio, very much as in the C-S-H of normally cured cement.

Several studies have been made on the transition from C-S-H into tobermorite, in reactions starting from various combinations of lime, colloidal silica and quartz (73 - 77). In the lime-quartz-water reaction, the reaction of the lime is controlled by the rate of dissolution and that of the quartz by diffusion through the coating of reaction products (76). The role of $Aℓ_2O_3$ in this reaction is complex; kaolinite can retard the reaction of the quartz, perhaps through the formation of dense, surface coatings (76, 77), but it can also accelerate the crystallization of tobermorite from C-S-H (74, etc.). Alkali accelerates reaction of quartz but retards conversion of C-S-H into tobermorite (78,79), which can take up K (80). Formation of C-S-H and tobermorite from mixtures of cement or β-C_2S with quartz has also been studied with reference to geothermal and other borehole applications (79, 81-84). Reaction passes through successive formation of various types of C-S-H to tobermorite, and high strengths have been obtained both with C-S-H(I) and with tobermorite as the binder.

JENNITE GROUP

Jennite has not been synthesized, but Gard and Taylor (33) showed a possible relationship to the semi-crystalline, fibrous C-S-H(II), which can be made by aging dilute aqueous suspensions of β-C_2S or C_3S. They reported that W. Wieker had shown using paper chromatography and molybdate methods that C-S-H(II) contains di- and polysilicate anions. Three independent studies show that jennite does not contain any significant amount of Na, as previously supposed (55, 85, 86). Jennite and its dehydration product metajennite have layer structures, with the possible constitutional formulae given in Table II.

GYROLITE GROUP

Recent interest in phases of this group has arisen mainly because of their formation in potentially useful geothermal cements. Buckner *et al's* (87) observation that they form particularly readily from starting materials that include high-surface area silica has been confirmed in several recent studies (61, 62, 88-91); however, contrary to some previous suggestions, they can also form from mixtures of cement or β-C_2S with quartz or fly-ash (61, 90) and when once formed can persist in runs as long as 98 days at 350°C and 69 MPa. Concern over the suitability of truscottite as a phase in geothermal cements centers around its stability relative to the alternate assemblage containing xonotlite and quartz (89,90).

AEM and X-ray studies of natural and synthetic truscottites show that in absence of substitution, the formula is $Ca_7(Si_{12}O_{29})(OH)_4.\sim 1H_2O$ and that the phase can accommodate Aℓ and K in absence of each other to the extents of about 0.7 Aℓ or 0.25 K in the above formula (92). Substitution of Aℓ causes a small increase in cell dimensions, which can approach those of reyerite. The latter phase is structurally very similar to truscottite, to which it appears to be related by ordered replacement of one Si in the above formula by Aℓ and incorporation of alkali cations in otherwise vacant sites. The molecular water is zeolitically held and for any given temperature and humidity the water content of reyerite is probably at most only slightly higher than that of truscottite.

X-ray and electron-diffraction studies of Assarsson's Z-phase confirm that it is structurally related to gyrolite (93), in the formation of which it can be a precursor.

PHASES STRUCTURALLY RELATED TO γ-C_2S

This group includes kilchoanite, C_8S_5, calcio-chondrodite and the indefinite mixture or intergrowth of these phases known as $C_2SH(C)$ or C_2S γ-hydrate. TMS studies confirm the presence of monomer and linear trimer in kilchoanite (27). Eilers and Nelson (94) have shown that kilchoanite can form from mixes of portland cement and quartz hydrated in heavy brines under simulated geothermal conditions, its formation being favored by use of finely ground cement with relatively coarse silica and concentrated brine. Calciochondrodite has been found in very strong, dense, hot-pressed cement pastes reacted for 30 min at 250°C, where its relatively high density is consistent with that of the microstructure (95). Jernejčič and Jelenić have confirmed that kilchoanite and C_8S_5 ("P-phase") can be prepared from γ-C_2S and quartz at ∿200°C (96).

OTHER CALCIUM SILICATE HYDRATE PHASES

"3.15 Å Phase". This phase. the name of which refers to the strongest powder reflection, was first described by Bezjak *et al.* (97), who determined the composition and the unit cell or pseudo cell, and studied the thermal decomposition behavior. It has also been obtained by Kalousek and Nelson (84). In both these cases the starting materials included γ-C_2S, but it has also been formed, together with truscottite, from mixes of $Ca(OH)_2$ and silicic acid (90). It forms typically at 250 - 300°C under hydrothermal conditions and, while possibly a purely metastable product, has been found to persist in runs of up to 28 days' duration.

α-*Dicalcium Silicate Hydrate.* This dense, orthorhombic phase forms in portland cement pastes that have been autoclaved without added silica, or in autoclaved lime-quartz pastes of suitable composition. Its presence in autoclaved building materials is normally, though not always associated with low mechanical strength, presumably caused by relatively high porosity. Chiocchio *et al.* (98) autoclaved

β-C_2S with small amounts of C_3A and C_3F, and showed that some Aℓ and Fe can enter the α-C_2SH structure and that this generated resistance to sulfate attack. α-C_2SH can form as a first product on autoclaving β-C_2S even in presence of quartz if the β-C_2S is extremely finely divided (83). The crystal structure of the Ge analog has been determined (99); the constitution $Ca_2(HSiO_4)(OH)$ found in Heller's original determination was thereby confirmed but some of the atomic positions were significantly in error. α-C_2SH has been found as a natural mineral (55).

Other Phases. New crystal structure determinations or refinements have been reported on suolunite (100), afwillite (101), killalaite (102), and tricalcium silicate hydrate (103). Killalaite is identical with, or closely similar to the "Phase F" which has been found in autoclaved products. Tricalcium silicate hydrate has been found in hot-pressed cement pastes prepared at 250°C and 350 MPa (95). Dellaite has been found in reaction products of materials under investigation for high-temperature geothermal cements (61,62) but the cement compositions yielding it are probably not the most favored.

MISCELLANEOUS PHASES

Scawtite is a ubiquitous phase in hydrothermal calcium silicate reaction products obtained in the presence of minor concentrations of CO_2 up to about 350°C (61, 84, 90). Its formation in geothermal cementing seems to be impeded by Aℓ (84, 90) or alkalis (62). In moderate quantities it can apparently be a satisfactory binder. A new CO_3-containing phase, fukalite, has been discovered (104). Pectolite, a fibrous phase, can form in large amounts in Na-bearing hydrothermal systems (62, 78 - 80). It has been reported to coexist with truscottite, gyrolite, tobermorite, xonotlite and foshagite. Rustumite, contrary to earlier reports, contains essential Cℓ; its crystal structure has been determined (105).

Several calcium aluminate and aluminosilicate phases are readily formed in autoclaved materials or hydrothermally processed cements. Hydrogarnets and strätlingite (C_2ASH_8) have long been known; new thermal and structural data for the latter have been obtained (106). Both triclinic anorthite and its hexagonal polymorph have been found in geothermal cements (61,62, 90, 107). The hexagonal form can be a dominant phase, having cementing properties (61,62). A product called X-phase is now believed to be closely similar to hexagonal CAS_2 (61). Bicchulite (C_2ASH) is another common product in high-temperature geothermal cements (61,62, 90). Its crystal structure is related to that of sodalite but differs in symmetry (108). It is also related to that of $C_4A_3H_3$, with which bicchulite probably forms solid solutions in which Aℓ + H replaces Si; $C_4A_3H_3$ forms hydrothermally and also (95) in hot-pressed cements.

Contrary to some earlier reports that it cannot be made, the hydrogarnet end-member C_3FH_6 has been obtained by hydration of ferrite phase at temperatures up to 80°C (109), but at 110°C only $Ca(OH)_2$ and hematite were obtained. Mössbauer spectra were found useful as an aid for characterization in this system.

Hydrogarnet phases can be a major constituent of very strong pastes made either by hot-pressing (95, 110), or by hydration, with or without autoclaving, of dense C_4AF compacts (111). Both studies showed that strength depends not only on the structure and morphology of individual phases, but also on the density and microstructure of the material.

REFERENCES

1. - D.L. KANTRO, S. BRUNAUER and C.H. WEISE (1962) "Development of Surface in the Hydration of Calcium Silicates. II. Extension of Investigations to Earlier and Later Stages of Hydration", J. Phys. Chem. 66, 1804 - 9.

2. - R.L. BERGER, A. BENTUR, N.B. MILESTONE and J.H. KUNG (1979) "Structural Properties of Calcium Silicate Pastes: I, Effect of the Hydrating Compound", J. Am. Ceram. Soc. 62, 358 - 362.

3. - I. ODLER and H. DÖRR (1979) "Early Hydration of Tricalcium Silicate. I. Kinetics of the Hydration Process and the Stoichiometry of the Hydration Products", Cement Concr. Res. 9, 239 - 248.

4. - L.S. DENT GLASSER, E.E. LACHOWSKI, K. MOHAN and H.F.W. TAYLOR (1978) "A Multi-Method Study of Cement Hydration", *ibid.* 8, 733 - 740.

5. - G.W. LORIMER and G. CLIFF (1976) "Analytical Electron Microscopy of Minerals" Chapter 7.3 in Electron Microscopy in Mineralogy [H.-R. Wenk, Ed.] Springer, Berlin.

6. - J.B. VANDER SANDE and E.L. HALL (1979) "Applications of Dedicated Scanning Transmission Electron Microscopy to Nonmetallic Materials", J. Am. Ceram. Soc. 62, 246 - 254.

7. - P. TERRIER (1969) "Contribution of Analysis by Means of an Electron Microprobe to the Cement Chemistry", Proc. 5th. Int. Symp. Chem. Cement, Tokyo, 1968, 2, 278 - 284.

8. - M.W. GRUTZECK and D.M. ROY (1969) "Electron Microprobe Studies of the Hydration of $3CaO.SiO_2$ [Tricalcium Silicate]", Nature (Lond.) 223, 492 - 4.

9. - S. DIAMOND (1976) "C/S Mole Ratio of C-S-H Gel in a Mature C_3S Paste as Determined by EDXA", Cement Concr. Res. 6, 413 - 6.

10. - S. GOTO, M. DAIMON, G. HOSAKA and R. KONDO (1976) "Composition and Morphology of Hydrated Tricalcium Silicate", J. Am. Ceram. Soc. 59, 281 - 4.

11. - M.S. STUCKE and A.J. MAJUMDAR (1977) "The Morphology and Composition of an Immature C_3S Paste", Cement Concr. Res. 7, 711 - 8.

12. - J.A. GARD, K. MOHAN, H.F.W. TAYLOR and G. CLIFF (1980) "Analytical Electron Microscopy of Cement Pastes. Part I. Tricalcium Silicate Pastes", J. Am. Ceram. Soc., submitted.

13. - G.L. KALOUSEK (1965) "Analyzing SO_3-Bearing Phases in Hydrating Cements", Mater. Res. Stand. 5, 292 - 304.

14. - L.E. COPELAND and D.L. KANTRO (1969) "Hydration of Portland Cement", Proc. 5th. Int. Symp. Chem. Cement, Tokyo, 1968, 2, 387 - 420.

15. - S. DIAMOND (1972) "Identification of Hydrated Cement Constituents Using a Scanning Electron Microscope-Energy Dispersive X-Ray Spectrometer Combination", Cement Concr. Res. 2, 617 - 632.

16. - M.S. STUCKE and A.J. MAJUMDAR (1976) "The Composition of the Gel Phase in Portland Cement Paste", *in* Hydraulic Cement Pastes: Their Structure and Properties, Cement and Concrete Assoc., Slough, pp. 31 - 51.

17. - E.E. LACHOWSKI, K. MOHAN, H.F.W. TAYLOR and A.E. MOORE (1980) "Analytical Electron Microscopy of Cement Pastes. Part II, Pastes of Portland Cements and Clinkers", J. Am. Ceram. Soc., submitted.

18. - K. MATHER (1972) "Examination of Cement Pastes, Hydrated Phases and Synthetic Products by X-Ray Diffraction". Misc. Paper C-72-5, U.S. Army Waterways Experiment Station.

19. - S. DIAMOND (1976) "Cement Paste Microstructure - An Overview at Several Levels", *in* Hydraulic Cement Pastes: Their Structure and Properties, Cement and Concrete Assoc., Slough, pp. 2 - 30.

20. - K. MOHAN (1980) New data.

21. - C.W. LENTZ (1966) "The Silicate Structure Analysis of Hydrated Portland Cement Paste", Symp. Structure of Portland Cement Paste and Concrete, Sp. Report 90, (U.S.) Highway Res. Board, 269 - 283.

22. - N.B. MILESTONE (1977) "A New Method for Qualitative Silylation of Silicates", Cement Concr. Res. 7, 345 - 6.

23. - F.D. TAMÁS, A.K. SARKAR and D.M. ROY (1976) "Effect of Variables upon the Silylation Products of Hydrated Cements", *in* Hydraulic Cement Pastes: Their Structure and Properties, Cement and Concrete Assoc., Slough, pp. 55 - 72.

24. - A. BENTUR, R.L. BERGER, J.H. KUNG, N.B. MILESTONE and J.F. YOUNG (1979) "Structural Properties of Calcium Silicate Pastes: II, Effect of Curing Temperature", J. Am. Ceram. Soc. 62, 362 - 6.

25. - M. ONO, M. NAGASHIMA and K. OTSUKA (1979) "Studies of the Alite-Alkali-Water System by the Trimethylsilylation Method" (Japanese), 33rd. General Meeting, Japan Cement Association.

26. - E.E. LACHOWSKI (1979) "Trimethylsilylation as a Tool for the Study of Cement Pastes. (2) Quantitative Analysis of the Silicate Fraction of Portland Cement Pastes", Cement Concr. Res. 9, 337 - 342.

27. - A.K. SARKAR and D.M. ROY (1979) "A New Characterization Technique for Trimethylsilylated Products of Old Cement Pastes", *ibid.* 9, 343-352.

28. - A. RIO (1976) "Approaching a Macromolecular Characterization of the C_3S Hydration Process" (Russ. with Eng. preprint), Proc. 6th. Int. Cong. Chem. Cement, Moscow, 1974, 2 (1), 145-157.

29. - F. TAMÁS and L. AMRICH (1978) "Layer Chromatographic Separation of Silicate Oligomers Formed During the Hydration of Portland Cement", Il Cemento, 75, 357 - 362.

30. - E.E. LACHOWSKI (1980) New data.

31. - A. GRUDEMO (1962) "The Microstructure of Hardened Cement Paste", Proc. 4th Int. Symp. Chem. Cement, Washington, 1960, 2, 615 - 647.

32. - L.E. COPELAND, E. BODOR, T.N. CHANG and C.H. WEISE (1967) "Reactions of Tobermorite Gel with Aluminates, Ferrites and Sulfates", J. Portland Cement Ass. Res. Dev. Labs. 9 (1) 61 - 74.

33. J.A. GARD and H.F.W. TAYLOR (1976) "Calcium Silicate Hydrate (II) ("C-S-H(II)"), Cement Concr. Res. 6, 667 - 678.

34. - W. RICHARTZ and F.W. LOCHER (1965) "A Contribution to the Morphology and Combination with Water of Calcium Silicate Hydrates and to the Structure of Hardened Cement Paste" (Germ.), Zement-Kalk-Gips 18, 449 - 459.

35. - H.M. JENNINGS and P.L. PRATT (1979) "On the Hydration of Portland Cement" Proc. Brit. Ceram. Soc. (28), 179 - 193.

36. - D. MÉNÉTRIER, I. JAWED, T.S. SUN and J. SKALNY (1979) "ESCA and SEM Studies on Early C_3S Hydration, Cement Concr. Res. 9, 473 - 482.

37. - L.S. DENT GLASSER, E.E. LACHOWSKI and G.G. CAMERON (1977) "Studies on Sodium Silicate Solutions by the Method of Trimethylsilylation", J. appl. Chem. Biotechnol. 27, 39 - 47.

38. - H.F.W. TAYLOR (1979) "Cement Hydration Reactions: the Silicate Phases", Proc. Conf. Cement Production and Use, Engineering Foundation, N.Y., *in press.*

39. - R.F. FELDMAN (1972) "Helium Flow and Density Measurement of the Hydrated Tricalcium Silicate - Water System", Cement Concr. Res. 2, 123 - 136.

40. D.N. WINSLOW and S. DIAMOND (1974) "Specific Surface of Hardened Portland Cement Paste as Determined by Small-Angle X-Ray Scattering", J. Am. Ceram. Soc. 57, 193 - 7.

41. - H.F.W. TAYLOR (1973) "Crystal Structures of Some Double Hydroxide Minerals", Miner. Mag. 39, 377 - 389.

42. - H.F.W. TAYLOR, (1976) "Crystal Chemistry of Portland Cement Hydration Products" (Russ. with Eng. Preprint), Proc. 6th. Int. Cong. Chem. Cement, Moscow, 1974, 2 (1), 192 - 207.

43. - R. ALLMANN (1970) "Double-Sheet Structures with Brucite-Like Sheet Ions $[Me(II)_{1-x}Me(III)_x(OH)_2]^{x+}$ " (in German), Chimia 24, 99 - 108.

44. - M. REGOURD, H. HORNAIN and B. MORTUREUX (1976) "Evidence of Calcium Silicoaluminates in Hydrated Mixtures of Tricalcium Silicate and Tricalcium Aluminate". Cement Concr. Res. 6, 733 - 740.

45. - E.P. FLINT and L.S. WELLS (1944) "Analogy of Hydrated Calcium Silicoaluminates and Hexacalcium Aluminate to Hydrated Calcium Sulfoaluminates", J. Res. Nat. Bur. Stand. 33, 471-8.

46. - H. KOLLMANN and G. STRÜBEL (1978) "Experimental Studies on the Question of Solid Solution Formation Between Ettringite and Thaumasite", Fortschr. Mineral., Beih. 56, 25 - 6.

47. - L.E. COPELAND, D.L. KANTRO and G. VERBECK (1962) "Chemistry of Hydration of Portland Cement", Proc. 4th. Int. Symp. Chem. Cement, Washington 1960, 1, 429 - 465.

48. - P. SELIGMANN and N.R. GREENING (1969) "Phase Equilibria of Cement-Water". Proc. 5th. Int. Symp. Chem. Cement, Tokyo, 1968, 2, 179 - 200.

49. - I. ODLER and J. SKALNY (1973) "Hydration of Tricalcium Silicate at Elevated Temperatures", J. appl. Chem. Biotechnol. 23, 661 - 7.

50. - D.M. ROY, S. OYEFESOBI and A.K. SARKAR (1977) "Ettringite Stability and Related Hydration Studies", Am. Ceram. Soc. Bull. 56, 305. (Abstr.)

51. - V. SATAVA and O. VEPREK (1975) "Thermal Decomposition of Ettringite under Hydrothermal Conditions", J. Am. Ceram. Soc. 58, 357 - 9.

52. - R. SANZHAASUREN and E.P. ANDREEVA (1978) "Study of Structure Formation Processes in Aqueous Suspensions of Tetracalcium Aluminoferrite in Presence of Gypsum and Calcium Hydroxide" (Russ.) Vestn. Mosk. Univ., Ser. 2: Khim. (2) 160 - 4.

53. - K. IZOZAKI and K. NAKAGAWA (1977) "Hydrothermal Reactions Between Ettringite and Inorganic Salts", Rev. 31st. Gen. Mtg., Cement Assoc. Japan, Tokyo, 47 - 8.

54. - S. UDAGAWA and K. URABE (1978) "Looking into the Autoclave" (Japanese), Ceramics (Tokyo) 13, 542 - 552.

55. - S. GROSS (1977) "The Mineralogy of the Hatrurim Formation, Israel", Geol. Surv. Israel Bull., #70.

56. - Y. KUDOH and Y. TAKÉUCHI (1979) Private Communication.

57. - G.L. KALOUSEK, T. MITSUDA and H.F.W. TAYLOR (1977) "Xonotlite: Cell Parameters, Thermogravimetry and Analytical Electron Microscopy", Cement Concr. Res. 7, 305 - 312.

58. - A.-R. GRIMMER and W. WIEKER (1971) "Determination of the Type of Water Binding in Xonotlite $6CaO.6SiO_2.H_2O$" (Germ.) Z. anorg. allg. Chem. 384, 34 - 42.

59. - C. TASHIRO and K. KAWAGUCHI (1977) "Effects of the CaO/SiO_2 Ratio and Cr_2O_3 on the Hydrothermal Synthesis of Xonotlite", Cement Concr. Res. 7, 69 - 76.

60. C. HENMI, I. KUSACHI, A. KAWAHARA and K. HENMI (1978) "7T Wollastonite from Fuka, Okayama Prefecture", Mineral. J. (Tokyo) 9, 169 - 181.

61. - D.M. ROY, E.L. WHITE, C.A. LANGTON and M.W. GRUTZECK (1979) "Potential New High Temperature Cements for Geothermal Wells", Proc. Int. Symp. Oilfield and Geothermal Chem., Houston, 1979 (S.P.E. Pub. 7877) 153 - 161.

62. - C.A. LANGTON, E.L. WHITE, M.W. GRUTZECK and D.M. ROY (1980) "High Temperature Cements with Geothermal Applications", this Cong., Theme V.

63. - T. MITSUDA and H.F.W. TAYLOR (1978) "Normal and Anomalous Tobermorites", Miner. Mag. 42, 229-235.

64. - S.A.S. EL-HEMALY, T. MITSUDA and H.F.W. TAYLOR (1977) "Synthesis of Normal and Anomalous Tobermorites", Cement Concr. Res. 7, 429 - 438.

65. - N. HARA, C.F. CHAN and T. MITSUDA (1978) "Formation of 14 Å Tobermorite", *ibid.* 8, 113-6.

66. - G.L. KALOUSEK and R. ROY (1957) "Crystal Chemistry of Hydrous Calcium Silicates: II, Characterization of Interlayer Water", J. Am. Ceram. Soc. 40, 236 - 9.

67. - C. HENMI (1979). Private communication.

68. - G. CLIFF, J.A. GARD, G.W. LORIMER and H.F.W. TAYLOR (1975) "Tacharanite", Miner. Mag. 40, 113 - 126.

69. - Z. ŠAUMAN (1975) "Formation Conditions and the Character of Binding Phases in Autoclaved Building Materials", Cement (Zagreb) 18, 9 - 18.

70. - T. MITSUDA and C.H. CHAN (1977) "Anomalous Tobermorite in Autoclaved Aerated Concrete", Cement Concr. Res. 7, 191 - 4.

71. - J.M. CRENNAN, S.A.S. EL-HEMALY and H.F.W. TAYLOR (1977) "Autoclaved Lime-Quartz Materials. I. Some Factors Influencing Strength", *ibid.* 7, 493 - 502.

72. - S.A.S. EL-HEMALY, K. MOHAN and H.F.W. TAYLOR (1978) "Autoclaved Lime-Quartz Materials. II. Thermogravimetry and Trimethylsilylation". *ibid.* 8, 671 - 6.

73. - T. MITSUDA and H.F.W. TAYLOR (1975) "Influence of Aluminium on the Conversion of Calcium Silicate Hydrate Gels into 11 Å Tobermorite at 90°C and 120°C", *ibid.* 5, 203 - 210.

74. - M. SAKIYAMA and T. MITSUDA (1977) "Hydrothermal Reaction Between C-S-H and Kaolinite for the Formation of Tobermorite at 180°C, *ibid.* 7, 681 - 6.

75. - C.F. CHAN and T. MITSUDA (1978) "Formation of 11 Å Tobermorite from Mixtures of Lime and Colloidal Silica with Quartz", *ibid.* 8, 135 - 8.

76. - R. KONDO, K. LEE and M. DAIMON (1976) "Kinetics and Mechanism of Hydrothermal Reaction in Lime-Quartz-Water System", Yogyo-Kyokai-Shi (Jap.) 84, 573 - 8.

77. - K.H. LEE, M. DAIMON, K. ASAGA, T. NISHIKAWA, S. GOTO and R. KONDO (1977) "Role of the Microstructure of Reaction Products on Hydrothermal Reaction Rate in Lime-Quartz-Water System", (Jap.) *ibid.* 85, 14 - 9.

78. - E.A. BLAKEMAN, J.A. GARD, C.G. RAMSAY and H.F.W. TAYLOR (1974) "Studies on the System Oxide - Calcium Oxide - Silica-Water", J. appl. Chem. Biotechnol. 24, 239 - 245.

79. - E.B. NELSON and G.L. KALOUSEK (1977) "Effects of Na_2O on Calcium Silicate Hydrates at Elevated Temperatures", Cement Concr. Res. 7, 687 - 694.

80. - R. KONDO, K. ASAGA and M. SHIMURA (1978) "Effects of Alkali on the Hydrothermal Reaction of $Ca(OH)_2$ or $CaCO_3$-SiO_2-H_2O Systems", Rev. 32nd. Gen. Mtg., Cement Assoc. Japan, 45 - 6.

81. - G.L. KALOUSEK (1976) "CSH(I)-Binder of Potentially Superior Strength", Cement Concr. Res. 6, 417 - 8.

82. - S.O. OYEFESOBI and D.M. ROY (1976) "Hydrothermal Studies of Type V Cement-Quartz Mixes", *ibid.* 6, 803 - 810.

83. - S.O. OYEFESOBI and D.M. ROY (1977) "Hydrothermal Studies of Special Types of Cement Mixed with Quartz", *ibid.* 7, 95 - 102.

84. - G.L. KALOUSEK and E.B. NELSON (1978) "Hydrothermal Reactions of Dicalcium Silicate and Silica", *ibid.* 8, 283 - 290.

85. - J.A. GARD, H.F.W. TAYLOR, G. CLIFF and G.W. LORIMER (1977) "A Re-Examination of Jennite", Am.Mineral. 62, 365 - 8.

86. - J.N. MAYCOCK, J. SKALNY and R.S. KALYONCU (1974) "Thermal Decomposition of Cementitious Hydrates", Analytical Calorimetry 3, 697-711.

87. - D.A. BUCKNER, D.M. ROY and R. ROY (1960) "Studies in the System CaO-Al_2O_3-SiO_2-H_2O. II, The System $CaSiO_3$-H_2O", Am. J. Sci. 258, 132-147.

88. - G.L. KALOUSEK (1978) "Factors Affecting Hydrothermal Formation of Hydrous Calcium Silicates, Int. Symp. Lime-Sand Products, Karlsruhe.

89. - G.L. KALOUSEK and S.Y. CHAW (1976) "Research on Cements for Geothermal and Deep Oil Wells", Soc. Pet. Engrs. J. 16, 307 - 9.

90. - K. LUKE, H.F.W. TAYLOR and G.L. KALOUSEK (1979) "Geothermal-Well Cements: Formation of Truscottite, Xonotlite and Scawtite", Amer. Ceram. Soc. Bull. 58, 334 (Abst.), and new data.

91. - E.L. WHITE, C.A. LANGTON, M.W. GRUTZEK and D.M. ROY (1979) "High Temperature Cements for Geothermal Applications", Am. Ceram. Soc. Bull. 58, 334 (Abst.).

92. - E.E. LACHOWSKI, L.W. MURRAY, H.F.W. TAYLOR (1979) "Truscottite: Composition and Ionic Substitutions", Miner. Mag. 43, 333-6.

93. - J.A. GARD, T. MITSUDA and H.F.W. TAYLOR (1975) "Some Observations on Assarsson's Z-Phase and its Structural Relations to Gyrolite, Truscottite and Reyerite", *ibid.* 40, 325-333.

94. - L.H. EILERS and E.B. NELSON (1979) "Effect of Silica Particle Size on Degradation of Silica Stabilized Portland Cement", Soc. Pet. Engrs. J. (S.P.E. Publ. 7875).

95. - G.R. GOUDA and D.M. ROY (1976) "Characterization of Hot-Pressed Cement Pastes", J. Am. Ceram. Soc. 59, 412 - 4.

96. - J. JERNEJČIČ and I. JELENIĆ (1974) "Properties of Autoclaved and Thermally Treated Moulds Made from γ-Ca_2SiO_4 and Quartz at C/S Ratios 0.5 to 1.5", Cement Concr. Res. 4, 123 - 132.

97. A. BEZJAK, I. JELENIĆ and J. JERNEJČIČ (1974) "New Calcium Silicate Phase in Hydrothermally Treated γ-Dicalcium Silicate-Quartz Mixtures", Nature (Lond.) 248, 581 - 2.

98. - G. CHIOCCHIO, M. COLLEPARDI and R. TURRIZIANI (1975) "Substituted Hydrated Calcium Silicates Obtained in Autoclave Hydration", J. Am. Ceram. Soc. 58, 185 - 8.

99. - S. UDAGAWA, K. URABE and K. HIYAMA (1979) "Synthesis and Crystal Structure of $Ca_2(GeO_3(OH))OH$" (Jap.) Ann. Mtg. Ceram. Soc. Japan (Preprint).

100. - X-RAY LAB., HUPEH GEOL. COLLEGE (1974) "Crystal Structure of Suolunite" [Chinese], Sci. Geol. Sinica, 117 - 132.

101. - K.M.A. MALIK and J.W. JEFFERY (1976) "A Re-Investigation of the Structure of Afwillite", Acta Cryst. B32, 475 - 480.

102. - H.F.W. TAYLOR (1977) "The Crystal Structure of Killalaite", Miner. Mag. 41, 363 - 9.

103. - B.F. KAZAK, V.A. BLINOV, V.V. ILYUKHIN and N.V. BELOV (1974) "Crystal Structure of Hydrated Tricalcium Silicate" (Russ.) Doklady Akad. Nauk SSSR, 219, 340 - 3.

104. - C. HENMI, I. KUSACHI, A. KAWAHARA and K. HENMI (1977) "Fukalite, a New Calcium Carbonate Silicate Hydrate Mineral", Mineral. J. (Tokyo) 8, 374 - 381.

105. - R.A. HOWIE and V.V. ILYUKHIN (1977) "Crystal Structure of Rustumite", Nature (Lond.) 269, 231.

106. - H.-J. KÜZEL (1976) "Crystallographic Data and Thermal Decomposition of Synthetic Gehlenite Hydrate $2CaO.Al_2O_3.SiO_2.8H_2O$", Neues Jb. Miner. Mh. 7, 319 - 325.

107. - D.M. ROY, E.L. WHITE, C.A. LANGTON and K.G. ZIMMERMAN (1978) "Hydrated Calcium Aluminosilicate Cements for Hydrothermal Bonding", Cement Concr. Res. 8, 509 - 511.

108. - K. SAHL, N.D. CHATTERJEE (1977) "Crystal Structure of Bicchulite, $Ca_2[Al_2SiO_6](OH)_2$", Z. Krist. 145, 369 - 375.

109. - D.E. RODGERS and L.P. ALDRIDGE (1977) "Hydrates of Calcium Ferrites and Calcium Aluminoferrites", Cement Concr. Res. 7, 399 - 410.

110. - D.M. ROY and G.R. GOUDA (1975) "Optimization of Strength in Cement Pastes", Cement Concr. Res. 5, 153 - 162.

111. - V.S. RAMACHANDRAN and J.J. BEAUDOIN (1976) "Significance of Water/Solid Ratio and Temperature on the Physico-Mechanical Characteristics of Hydrating Calcium Oxide-Alumina-Iron(III) Oxide ($4CaO.Al_2O_3.Fe_2O_3$)", J. Mater. Sci. 11, 1893 - 1910.

* * * * *

ACKNOWLEDGEMENTS

H.F.W. Taylor contributed to this work as part of a program financed by the U.S. Army Research Office and sub-contracted through Martin Marietta Laboratories. D.M. Roy, who is also affiliated with the Department of Materials Science and Engineering, The Pennsylvania State University, contributed to it as parts of programs supported by the Department of Energy Office of Nuclear Waste Isolation, and the Department of Energy Brookhaven National Laboratory, Upton NY, Sub-contract # 422272-S.

THEME III

Structure of slags and hydration of slag cements

SUB-THEME III - 1

Slag structure and identification of slags

H.G. SMOLCZYK
Forschungsgemeinschaft
Eisenhüttenschlacken
Duisburg R.F.A.

1. INTRODUCTION

Slags arising from metallurgical and similar industrial processes differ characteristically in their chemical compositions, their mineralogical and physical structure and, therefore, also in their typical properties and the possibilities of their utilization /1/ /2/ /3/ /4/ /5/. Some typical analyses of well-known types of slag are compared in TABLE I. It can be seen that even the two most important slags of iron and steel making, as there are blastfurnace slag and steel slag (LD slag in this special case), are basically different. On the other hand, blastfurnace slag can be rather similar to phosphorus slag.

The best known and quantitative most important slag is the blastfurnace slag. It arises besides the pig iron during the metallurgical treatment of iron ores and leaves the blastfurnace as a highly viscous rock melt of 1350 to 1550 °C. The specific quantity of slag which 30 years ago still amounted up to 1 t/t pig iron decreased more and more in the last years. Today slag quantities of about 0.3 t/t pig iron are sufficient for modern blastfurnaces. In 1974 the world production of pig iron was 513 Mt/year. This comes up to more than 250 Mt blastfurnace slag.

2. GENERAL CHARACTERIZATION OF BLASTFURNACE SLAGS

The molten blastfurnace slag is formed out of the gangue and the secondary constituents of the iron ores, the combustion residue of coke and the necessary additions as there are limestone or dolomite. Their chemical main components are CaO, SiO_2, Al_2O_3, and MgO. At a given ore base a relative small range of the chemical composition has to be kept, because otherwise the blastfurnace operation would be disturbed or too much thermal energy would be necessary. F. SCHRÖDER reported in detail /6/ on the most useful composition of these slag melts, their liquid structures,and their liquidus temperatures. Also V.I. SATARIN referred to it once more/7/ /8/.

This slag melt has a high content of thermal energy of about 1700 kJoule/kg (406 kcal/kg). If this energy is fully dissipated by slow cooling a stabil crystalline CaO-MgO-Al_2O_3-silicatic rock product is formed with mechanical properties similar to basalt and being used for a long time as road construction material to a very large extent and also being suitable as concrete aggregate /1/ /2/ /3/ /4/.

The location of the blastfurnace slags within the quaternary system CaO-SiO_2-Al_2O_3-MgO at the 10 % MgO level is shown in FIGURE 1.

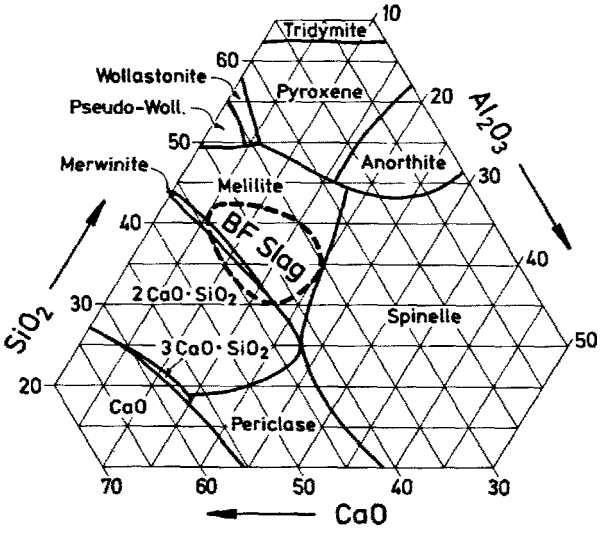

FIG. 1 - Main Field of Chemical Compositions of Blastfurnace Slags with 10 wt-% MgO.

TAB. I - Characteristical Compositons of Metallurgical Slags in wt-%

	Non-Ferrous Slags				Ferrous Slags	
	Lead -Zinc Un. Kingdom	Nickel Canada	Copper South Africa	Phosphorus-furnace USA	Steel BOF (LD Slag) Germany	Iron Blast-furnace Europe
SiO_2	18	29	34	41	13	34
CaO	20	4	9	44	47	41
MgO	1	2	4	1	1	7
Al_2O_3	6	1	6	9	1	13
FeO_x + MnO_x	38	53	44	1	31	1
CaO/SiO_2	1.1	0.1	0.3	1.1	3.6	1.2

The most important minerals of blastfurnace slag which were found so far are given in TABLE II. The main part of the basic blastfurnace slags consists of melilite and merwinite. If the CaO/SiO_2-ratio becomes smaller than 1.0, pyroxene can occur increasingly. Contrary to some other slags and to Portland cement clinkers, blastfurnace slags never develop free oxides, such as free FeO, free CaO or free MgO. Also the lime rich clinker minerals $3CaO \cdot SiO_2$ and $3CaO \cdot Al_2O_3$ do not arise.

TAB. II - Mineral Compositions of Chrystallized Blastfurnace Slags

Possible main components	
Melilite	solid solution of
Gehlenite and Akermanite	$2CaO \cdot Al_2O_3 \cdot SiO_2$ and $2CaO \cdot MgO \cdot 2SiO_2$
Merwinite +	$3CaO \cdot MgO \cdot 2SiO_2$
Diopside ++ and other Pyroxenes	$CaO \cdot MgO \cdot 2SiO_2$
Possible minor components	
Dicalcium silicate + ($\alpha, \alpha', \beta, \gamma$)	$2CaO \cdot SiO_2$
Monticellite +	$CaO \cdot MgO \cdot SiO_2$
Rankinite	$3CaO \cdot 2SiO_2$
Pseudo-Wollastonite	$CaO \cdot SiO_2$
Oldhamite	CaS
Seldom observed minor components	
Anorthite ++	$CaO \cdot Al_2O_3 \cdot 2SiO_2$
Forsterite	$2MgO \cdot SiO_2$
Enstatite ++	$MgO \cdot SiO_2$
Perowskite	$CaO \cdot TiO_2$
Spinelle	$MgO \cdot Al_2O_3$

+only in basic slags ++only in acid slags

Fully crystallized blastfurnace slags of the usual composition have either no or only very weak hydraulic or latent hydraulic properties. If, however, caused by quick cooling, this lowest energy level of the crystallized stage is not reached, then an unregular slag glass, richer in energy is formed (heat of crystallization about 200 Joule/g). This granulated blastfurnace slag is latent hydraulic. The lower energy level is obtained by forming solid hydration products under heat evolution when activated by lime and sulphate. These are principally the same hydrates as we have in Portland cements /7/ /9/.

The yearly production of granulated blastfurnace slags in Western Europe amounts to approx. 22 Mt /2/. The tendency to use their hydraulic properties for cement, concrete, and road building material is increasing.

3. GRANULATED BLASTFURNACE SLAG

3.1 Granulation

It was in 1953 when the granulation of the blastfurnace slag was started in order to produce a granular bulk material out of the slag melt which can easily be transported. In doing so a sand with a more or less high content of glassy constituents was formed. In 1962 EMIL LANGEN found out that this product showed certain hydraulic properties. Some time later it was proved that the glassy constituents of granulated blastfurnace slag, namely the super cooled slag melt, was the carrier of the latent hydraulic properties. Thereupon, the granulation processes were improved to obtain granulated blastfurnace slags with a high glass content for the production of slag cements. The glass content of modern cement slags amounts to 90 wt-% and more.

Since 1953 many granulation processes were tested and applicated /1/ /10/. It was the aim of all these processes to abstract as much heat as possible from a large quantity of molten slag in the shortest possible time. For that purpose in all cases the slag is broken into small droplets or grains up to a size of 3 or 5 mm which then are brought into contact with a lot of air or water as coolants. Processes running with compressed air have the advantage of a dry product. By this dry-granulation process, however, glass contents of only 60 to maximum 80 wt-% are obtained and, therefore, granulation is mainly done with water today.

In case of basic blastfurnace slags suitable for the cement production it is especially important to reach very quickly temperature ranges $< 800\ ^{o}C$ in order to keep the glassy state /6/. The glass already starts to recrystallize between 800 and 900 ^{o}C, and merwinite is precipitated as the first phase /6/. High quantities of water or an increased water pressure are necessary for prevention. Mostly both methods are combined. Water quantities of up to 10 m^3/t of slag are reported for granulation in water channels. If granulation is carried out with spraying jets the water jets are under compressions up to 6 bar. In this case the water quantity could be reduced to 3 m^3/t of slag. The most modern German granulation plant is situated at a blastfurnace with a pig iron production of 9500 t/day. The capacity of this plant is to granulate 3000 t of 1550 ^{o}C hot blastfurnace slag a day at a hydrostatic pressure of 2.2 bar and a water quantity of about 10 m^3/t of slag /11/. The glass content of the granulated slag reaches 95 to

100 wt-%.

After granulation the water content of slags can be undesirably high and can exceed 30 wt-%. The greatest portion of the water will, therefore, be removed by intermediate storage in gravel filter basins /11/ or in interposed water extraction tanks /12/. Another part is still lost during transport to further treatment. Subsequently the granulated blastfurnace slags still have water contents of 8 to 12 wt-% and can directly be grinded to slag cements in dryer-mills /11/ /12/. For grinding in usual cement mills or for producing supersulphated cements the slag is dried up to a residual moisture of wt-%.

A new granulation equipment named "Pelletizer" was developed in Canada and is operating in some other countries, too /10/ /13/ /14/. It is a half-dry granulation process by which the molten slag is pre-cooled with water and is flung into the air by a rotary drum (300 r.p.m.). As it is shown in FIGURE 2 different fractions result from this process. The large pellets up to 15 mm have a lower glass content and are suitable as lightweight aggregate. The smaller fractions up to 3 or 5 mm have a higher glass content and are reported to be suitable for the production of blastfurnace slag cements. The process seems to be advantageous because of the low water consumption of about 1 m^3/t of slag and the small residual moisture of the pelletized material of about 10 wt-%.

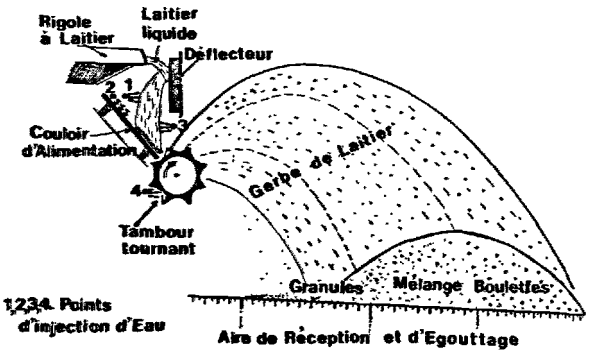

FIG. 2 - Slag Pelletizer (System GALEX /14/)

Tests of CERILH showed an even lower water consumption by this thermomechanical granulation method. Even at a total dry thermomechanical treatment blastfurnace slags still had satisfying hydraulic properties /15/ /16/.

According to prevailing opinion a hydraulic active blastfurnace slag should have a high glass content, if possible ≥ 90 wt-%. On the other hand, it seems that small amounts of crystalline material in the vitreous slag will not have very detrimental effects /15/. From other investigations it is even reported that crystal nuclei in the vitreous slag have an advantageous effect /7/ /8/ /17/.

3.2 The Structure of Vitreous Blastfurnace Slag

The network theory of ZACHARIASEN /18/ proved a suitable basis to describe the structure of the vitreous slag and some of its properties /5/ /19/. At this the glass consists of a more or less disturbed three-dimensional net of oxides of network forming elements. They are characterized by small ionic radii and by highest possible ionic valencies. They are surrounded by 4 oxygen atoms only (co-ordination number 4) in the form of a tetrahedron. The network is formed that way that distinct oxygen atoms belong to two tetrahedra at the same time. One typical network former is silicium. Within the vitreous blastfurnace slag it forms SiO_4^{4-}-tetrahedra, $Si_2O_7^{6-}$-groups, chains, and other polymerization products /20/.

The negative valencies of these anionic-groups become neutralized by the positive valencies of cations. They are called network modifiers. In general, they have larger ionic radii and higher co-ordination numbers than the network formers and are mostly situated in the cavities of the network. A typical network modifier within the vitreous blastfurnace slag is the Ca^{++}-ion with the co-ordination number 6.

The higher the part of network modifiers is the smaller the polymerization grade of the network-forming SiO_4-tetrahedra will be. That means that the glass has a smaller stability and a higher chemical reactivity. The state of bond of the other two main components of the blastfurnace slag, as there are aluminium and magnesium is said to play an important role. These two amphotere metals appear in silicates, both in fourfold co-ordination and in sixfold co-ordination /6/ /19/. Their bond within the vitreous slag as network former (AlO_4^{5-} and MgO_4^{6-}) or as network modifier (Al^{+++} and Mg^{++}) has been investigated with different results for a long time /6/ /7/ /19/ /20/.

Today it is proved that aluminium and magnesium can also arise in the vitreous slag both in fourfold co-ordination and in sixfold co-ordination at the same time /6/ /7/ /20/. In this case the ratio of MeO_6/MeO_4 depends on the chemical composition and the thermal treatment (granulation) of the glass /7/ /20/.

The kind of bond of the MgO as a constituent of the three-dimensional glass network makes it understandable why no free MgO was found in granulated blastfurnace slags even not at MgO-contents of 10 to 20 wt-% /21/ /22/ /23/. In case of hydration of the vitreous slag the magnesium will be incorporated into the hydration products and even at high MgO-contents up to 20 wt-% no $Mg(OH)_2$ and no expansion phenomena were observed /7/ /8/ /20/ /24/ /25/ /26/ /27/ /28/ /29/.

The minor components of the blastfurnace slag, such as manganese, titanium and sulphur, are also constituents of the glass structure in the granulated slag. Sulphur is probably incorporated homogeneously as S^{--} in the places of oxygen into the network. The precipitation of sulphides starts first at contents of > 3.3 wt-% /30/. Manganese was found in sixfold co-ordination in synthetic vitreous slags with MnO-contents up to 7.5 wt-% /19/. Titanium seems to exist in sixfold co-ordination at TiO_2-contents up to 4 wt-%. At > 4 wt-% TiO_2 it becomes a network former with fourfold co-ordination /20/.

The opinions on the influence of the glass structure on the hydraulic properties of the blastfurnace slag are not always uniform. This is due to different reasons. First of all it depends on the method by which the hydraulic properties are tested. The following properties of the slag can be measured: rate of solution, reactivity at alkaline and/or sulphatic activation, strengths of test cements after a few days or after months.

In case of different slags the reactivities mostly have another sequence than the strengths of the cements. Cements with low early strength often develop a higher final strength than early strength cements. Furthermore, besides the thermal pretreatment the glass structure is very strongly influenced by the chemical composition /7/ /20/ /31/. Therefore, the influence of the chemical composition on the hydraulic properties of the slag can mostly be recognized much clearer than the influence of the glass structure on the hydraulic properties /32/.

The strength forming constituents of the hydrated slag cement are the calcium silicate hydrate phases as it is with Portland cement. Consequently, pure $CaO-SiO_2$-glasses should reach the highest strengths. They would, however, react too slowly at normal temperature. It is therefore, important that the network of SiO_4^{4-}-tetrahedra within the blastfurnace slag is disordered by additional constituents, such as aluminium and magnesium. As a result, the glass is on a higher energy level, is less stable and has a higher reactivity.

For this case, the way in which these amphotere elements become effective by modificating the glass structure was estimated in different ways. They are reported to have a high effectiveness if they are present in sixfold co-ordination and thus in form of network modifiers they reduce the degree of polymerization of the SiO_4^{4-}-tetrahedra /20/ /33/. Thus the reactivity of the glass is increased. It has, however, to be taken into account that not all network modifiers have this function. Manganese for example is present in sixfold co-ordination at contents up to 7.5 wt-% MnO /19/, but nevertheless it stabilizies the slag glass and reduces its hydraulic activity /34/. According to a different opinion aluminium in fourfold co-ordination as a network former is of high effectiveness because the cations of the AlO_4^{5-}-tetrahedrea in the network are bound more weakly as for example by the SiO_4^{4-}-tetrahedra and, therefore, they become dissolved more easily /35/.

The investigation of 15 Russian blastfurnace slags with same Al_2O_3-contents (5.3 to 6.1 wt-%) and comparable chemical compositions (4.4 to 6.3 wt-% MgO) showed that the highest effectiveness can be expected in case of a certain ratio of Al and Mg in sixfold co-ordination to Al and Mg in fourfold co-ordination /7/. The highest strengths were obtained at a

$$\frac{MeO_6}{MeO_4} \text{ - ratio of } 0.35$$

There not always exists unanimity on the significance of the states of bond and co-ordination numbers in the glass structure of the blastfurnace slag and the measuring methods are partly quite complicated. On one point, however, all experts agree: the glass structure of the slag has to be disordered as strongly as possible to get a high hydraulic effectiveness.

There is also the opinion that the beginning of crystallization can result in a more disordered glass structure and in an increased reactivity of the slag /17/ /36/. In this connection, however, various investigation methods and effects have to be taken into consideration. The solubility of certain elements, such as Ca, Na, K, and S, increases with increasing amount of crystalline constituents in the granulated blastfurnace slag /36/. This, however, is no argument for better hydraulic properties of the glassy constituents.

If, however, the influence of the crystalline constituents on the strength of a blastfurnace slag cement is tested, their kind and distribution will certainly be of importance. If parts of the ground slag are present in form of totally crystallized grains, the strength will accordingly be lower. If, on the other hand, crystals of smaller size ar tightly intergrown with the vitreous slag, they will most likely be of unessential influence on the strength. A higher strength could be expected if the crystalline constituents are homogeneously distributed in the vitreous slag as submicroscopic crystal nuclei.

Finally it has to be considered that by crystalline influences the grindability of the slag will improve. Advantageous and detrimental effects have possibly to be discussed altogether in case there are mentioned good hyraulic properties of blastfurnace slags containing noticeable crystalline portions /7/ /15/ /37/ /38/.

An additional view is based upon the opinion that even without crystalline separations the vitreous slag will not have a homogeneous structure but consists of micro heterogeneous ranges (500 to 4000 Å) of different

glass phases /39/ /40/. The highest hydraulic effectiveness is expected if the different ranges are not too large and if there is an optimum phase separation /41/.

The investigation of the microstructure of the vitreous blastfurnace slag is very important from the scientific angle of view. It cannot be expected, however, that the hydraulic behaviour of glasses is mainly based on their structure /42/. Due to the fact that the test methods are rather complicated, they did not reach much importance for the valuation and the control of cement slags. It is more essential to control the glass content of the granulated blastfurnace slag by well-known microscopic or X-ray methods in a relatively simple way.

One testing method by which also structural properties of the blastfurnace slag can indirectly be evaluated, too, is the well-known investigation of their fluorescence in the ultra-violet radiation /6/ /7/ /43/. The reason for this fluorescence in the light pink and red range of the spectrum are defects in the glass structure which also increase the reactivity of the slag. This ultra-violet test is an approved method to control well-known blastfurnace slags. In case of more different slags a combination with the CaO/SiO_2-ratio proved appropriate /43/. Ultra-violet tests with unknown slags should also consider the chemical analysis.

3.3 Influence of the Chemical Composition

In case of evaluating the hydraulic properties of the blastfurnace slag in practice besides the glass content the chemical composition is of great importance. It is a characteristical attribute, for it determines the basicity and the kind of reaction of the slags and also influences the structure of the vitreous slag.

In TABLE III analyses of blastfurnace slags from different areas of the world were summarized which are used as hydraulic active components of cements or concretes. It has to be considered that within the various ranges increasing MgO-contents generally coincide with decreasing CaO-contents. The ranges of CaO + MgO are, therefore, smaller than the ones of CaO. It can be seen that generally the ranges of SiO_2, CaO + MgO and Al_2O_3 are rather similar. The on an average high MgO-contents of the slags from South Africa and the very high Al_2O_3-contents of the slags from India are remarkable.

As chemical analyses can be carried out in rather a simple and quick way a lot of attempts were made to characterize the blastfurnace slags by chemical hydraulic-factors or -moduli. For the discussion of these factors and formulas the following abbreviations are used:

$SiO_2 = S \quad CaO = C \quad MgO = M \quad Al_2O_3 = A$

The basicity ratios p of the slag /1/, well-known from the blastfurnace practice, were the starting-point for most of the hydraulic identification values.

$$p_1 = \frac{C}{S} \qquad p_2 = \frac{C + M}{S} \qquad p_3 = \frac{C + M}{S + A}$$

These basicity ratios- however, are not very suitable as hydraulic factors because the alumina is not taken into account in the proper way. Furthermore, the common name "acid slag" for $p_1 < 1$ is no limiting value for hydraulic slags, if the lower CaO-contents are compensated by corresponding higher contents of MgO and Al_2O_3.

TAB. III - Ranges of Chemical Composition of Granulated Blastfurnace Slags in wt-%

Area	SiO_2	CaO	MgO	Al_2O_3	Reference
USSR	30/40	30/50	14/2	5/17	(7)
USA and Canada	33/42	36/47	16/1	6/16	(2) (44) (45)
Australia	33/38	39/44	4/1	15/19	(2) (45)
Japan	31/40	38/45	8/2	13/17	(45)
India	27/39	30/40	17/0	17/33	(2) (27) (45)
South-Africa	30/36	30/40	21/8	9/16	(2)
Western Europe + Yugoslavia +)	30/38	33/47	10/2	9/18	(2) (10) (45) (46)
Ranges of minor components generally less than 4 % TiO_2, 2 % MnO, 3 % FeO, 2 % S, 2 % $Na_2O + K_2O$					

+) average ranges of granulated BF-slags from Yugoslavia, Italy, Spain, France, Belgium, Netherlands, United Kingdom, and Germany-West

The best-known hydraulic factors are listed in TABLE IV. The first group F_1 to F_7 consists of the main components of the blastfurnace slag only. F_1 is also included because in a comprehensive comparison the ratios F_1 to F_6 showed the same statistical significance of insignificance, respectively. F_2 and F_3 anyhow contain nearly the same statement /17/. F_3 is the best-known modulus which was incorporated into the regulations of various countries (e.f. $F_3 \geq 1.0$ in Western Germany, $F_3 \geq 1.4$ in Japan). F_7 was developed for the 28-day strength of MgO rich slags with Al_2O_3-contents in the range of 10 to 35 wt-% and is not relevant for the usual blastfurnace slags.

In the factors F_8 to F_{10} MnO and other minor components are taken into consideration, too. F_{10} was proposed for MnO-contents up to 14 wt-%. In the case of the moduli F_{11} and F_{12},

the hydraulicity of the slag is reduced by increasing Al_2O_3-contents. F_{11} was originally developed for the 28-day strengths. In the case of F_{12} it is especially stated that this modulus is valid for strengths after 28 days and more only, whereas F_3 and F_6 are more suitable for the 2-day strengths /10 /32/.

The applicability of the ratios F_3, F_5, F_6, F_8, and F_{11} to 26 blastfurnace slag cements with 50 wt-% slag was statistically tested in a comprehensive program with 13 different granulated blastfurnace slags /53/. For the early strengths up to 3 days no correlations could be determined. In the case of the strengths after 7 and 28 days, F_3 and F_8 showed the best correlations. The coefficients of determination (square of the correlation coefficient r in %) were

$$r^2 = 35 \text{ to } 83 \text{ \%}.$$

TAB. IV - Well-Known Hydraulic Factors for Granulated Blastfurnace Slag

$F_1 = 100-S$ (1)	$F_2 = \frac{100-S}{S}$ (1) $\quad F_3 = \frac{C+M+A}{S}$ (1)
$F_4 = \frac{C+M+A-10}{S+10}$ (47)	$F_5 = \frac{C+1.4M+0.6A}{S}$ (22)
$F_6 = C+0.5M+A-2.0S$ (48)	$F_7 = \frac{6C+3A}{7S+4M}$ (49)
$F_8 = \frac{C+0.5M+A+CaS}{S+MnO}$ (1)	$F_9 = \frac{C+0.5M+A}{S+FeO+(MnO)^2}$ (50)
$F_{10} = \frac{C+M+A+BaO}{S+MnO}$ (51)	
$F_{11} = \frac{C+M+0.3A}{S+0.7A}$ (52)	$F_{12} = \frac{C+M}{S+0.5A}$ (32)

A similar experiment was made in the Forschungsinstitut Eisenhüttenschlacken during an extensive test series with 24 granulated blastfurnace slags (glass contents > 95 %) the chemical analyses of which covered the whole range of Western-European slags listed in Table III /46/. 192 blastfurnace slag cements were made (2 clinkers, 2 specific surfaces, 60 wt-% and 75 wt-% granulated slag) and strengths according to German Cement Standard DIN 1164 were measured from 2 up to 91 days. The linear correlations to a lot of hydraulic factors were tested on the basis of the compressive strengths after 2 and 28 days of the 96 blastfurnace slag cements with 75 wt-% granulated slag. The ratios F_1, F_2, F_3, F_4, F_6, F_8, and F_9 showed the best coefficients of determination r^2. They all were low and there was no significant difference between the 7 moduli. After 2 days r^2 ranged from 51 to 61 % and after 28 days from 44 to 50 %. In this case the average results of the simple ratios F_1 and F_2 considering SiO_2 only were not worse than the more complicated ones. This phenomenon was referred to by F. KEIL a long time ago already /1/.

By the calculation of coefficients for each of the chemical components on the basis of multiple regressions, the items F_3 and F_6 could be extended to hydraulic ratios with r^2 from 60 to 75 %. A decisive improvement was obtained only after the basis of linear influences was neglected. The compressive strengths of 2, 7, 28, 56 and 91 days then resulted in the complicated empiric interpolation formula

$$D = a_o + a_1 \cdot f(C+M) + a_2 \cdot f(A) + a_3 \cdot f(MnO) + a_4 \cdot f(Na_2O + 0.66\,K_2O) + a_5 \cdot f(P_2O_5)$$

The individual terms "(f(X))" of this formula are non-linear functions of the chemical components. The coefficients "a" strongly depend on the type of clinker component especially at early strengths. All the coefficients of determination r^2 were better than 90 %. After 2 days they amounted to 93 % and after 28 days to 94 %.

This formula practically represents only the mathematical description of the strength development of 192 blastfurnace slag cements (960 data). SiO_2 does not appear in the formula, for it is implicated as a completion to 100 wt-%. Because of the high statistical significance the following results were safely proven:

a) An increase of the Al_2O_3-content above 13 wt-% increased the early strengths only. FIGURE 3 shows that the 91-day strengths were even lower at higher Al_2O_3-contents. This tendency is indicated in Table IV by the factors F_{11} and F_{12}.

b) MgO in the range up to 11 wt-% had quantitatively the same effectiveness as CaO had.

c) If the minor components MnO (up to 1.4 wt-%), P_2O_5 (up to 0.2 wt-%), and alkali (up to 1.9 wt-%) were not considered, r^2 decreased to a value of 80 to 85 %. In every case MnO had a negative effect. The influences of P_2O_5 and alkali depended on the kind of the clinker used and on the testing age. After 28 days P_2O_5 always proved positive. Partly the effect of the minor components was so strong that after 7 days already some blastfurnace slags with 11 wt-% Al_2O_3 showed higher strengths than those with 15 wt-% Al_2O_3.

d) The statistical examination of TiO_2 (up to 1 wt-%), FeO (up to 2 wt-%), and sulphur (up to 2 wt-%) did not prove any significant influence.

e) Besides the clinker-content and the fineness, the strength developments of the blastfurnace slag cements also considerably depended on the kind of clinker.

For the investigated range of the chemical compositions these results conform well to the general state of knowledge upon the hydraulic properties of granulated blastfurnace slag:

All experts agree that increasing SiO_2-contents generally have a negative effect and

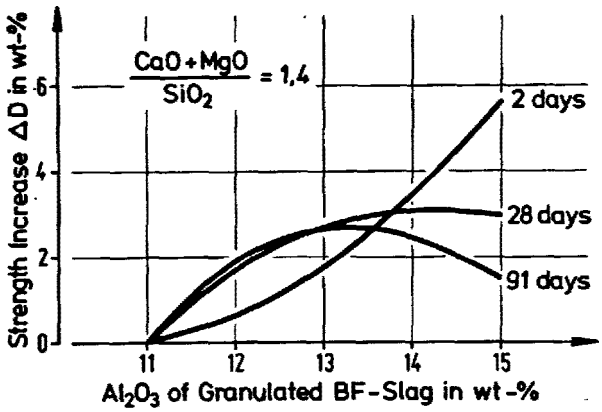

FIG. 3 - Average Variation of Compressive Strengths of Blastfurnace Slag Cements with Increasing Al_2O_3-Content of the BF Slag. Cements with 75 wt-% slag and 3850 Blaine.

that CaO usually has a positive influence. With the exception of a few special cases also MgO is said to have a positive influence up to contents of 18 wt-% /20/ /53/, 15 wt-% /22/ /54/ and, for sure up to contents of 12 wt-% /46/ /55/. According to Russian authors the most suitable MgO-content depends on the Al_2O_3-content /56/. In the case of MgO-contents of 10 to 12 wt-% /55/ or 13 to 18 wt-% /20/ accordingly higher Al_2O_3-contents of 14 to 18 wt-% are recommended. For the hydraulic moduli (see Table IV) MgO is added to CaO by multiplying it with factors of 0,5 to 1.4. The most often used factor is 1,0 which was statistically confirmed for MgO-contents up to 11 wt-% /46/.

The two publications reporting on a strength-diminishing influence of MgO cannot be compared with the other literature. In the first publication blastfurnace slags with 25 to 28 wt-% Al_2O_3 from India were investigated which apparently react in a different way /27/. In the second publication synthetic glasses of the system $CaO-MgO-Al_2O_3-SiO_2$ were activated with $Ca(OH)_2$, only /49/. A comparison with the strengthening of slag cements is impossible because the important components sulphate and alkali are missing. In blastfurnace slag cements sulphate is added not only as a set-regulating component but is also used for the optimum activation of the slag /6/ /9/. Furthermore, pore solutions in hardening Portland cements and blastfurnace slag cements are no $Ca(OH)_2$-solutions at all but highly concentrated alkali hydroxide solutions with $Ca(OH)_2$ as a precipitate /57/ /58/.

The interpretations of the influence of Al_2O_3 are apparently contradictory because the influence depends on the testing age /32/ /46/ and on the Al_2O_3-range investigated /46/ /53/. The considerably positive influence up to contents of 18 to 21 wt-% /20/ /22/ /55/, also expressed in most of the hydraulic factors is evidently restricted to the early strengths /32/ /46/. At testing ages of 28 days and more a diminishing of the effectiveness of Al_2O_3 is reported /53/ and a negative influence begins if the Al_2O_3-contents will exceed a maximum of 13 to 14 wt-% /46/. According to other investigations contents of more than 11 wt-% already can cause a distinct decrease of the strengths after 7 and 28 days /32/. These results prove that the influence of Al_2O_3 in a hydraulic formula cannot be described as a linear term.

MnO is commonly said to have a detrimental influence /1/ /7/ and according to this it appears as a strength diminishing term in all hydraulic moduli (see Table IV). Nevertheless, there is also a report on good hydraulic properties of blastfurnace slags containing up to 14 wt-% MnO /51/. In case of a special form of the glass structure /34/ or at higher Al_2O_3-contents /59/ no effect was found at all or even advantageous effects were observed at MnO-contents up to 6 wt-% /60/.

As reported TiO_2 distinctly diminishes the strength in case of contents of more than 4 wt-% /61/. The detrimental influence can be reduced by adding alkali to the slag melt /62/.

Finally it must be considered that the kind of the clinker component has a great influence on the strength development of blastfurnace slag cements /46/ /63/ /65/. Little is known of quantitative correlations so far. Generally, clinkers with high CaO-contents or high C_3S-contents or with highest possible early strengths are preferred. While discussing the clinker components of blastfurnace slag cement the fact was often neglected that not only the clinker activates the slag but that vice versa the slag itself and its minor components can have great influence on the strength development of the clinker component.

Summarizing, it has to be taken into account that a hydrating blastfurnace slag cement is a complicated multi-material system. Therefore, it cannot be expected that the resulting strength development can be predetermined by aid of simple hydraulic factors. In the regulations of several countries these hydraulic moduli are referred to for a rough classification into different groups of blastfurnace slags and they have also proved suitable for the control of known slags within relatively small ranges. This applies especially to blastfurnace slags coming from one steel plant only. They, however, neither have the grade of generally valid functional correlations between hydraulicity and chemical composition nor are they suitable to quantitatively classify blastfurnace slags coming from different plants.

4. CHARACTERISTIC PROPERTIES OF BLASTFURNACE SLAG CEMENTS

Blastfurnace slag cements with slag contents in the range of 36 to 80 wt-% (Western

Germany) or up to 95 wt-% (France) can be produced in the same strength classes (28 days) as Portland cements except those of the highest strength class getting more than 60 N/mm² after 28 days (ISO). Blastfurnace slag cements, however, have a somewhat different strength development than Portland cements. Having the same 28-day strength the 2-d strength of blastfurnace slag cements in general is lower, but the strength increase after 28 days is higher and more continuous than the one of Portland cements. FIGURE 4 shows the characteristic strength developments of a Portland cement and a blastfurnace slag cement containing 65 wt-% slag.

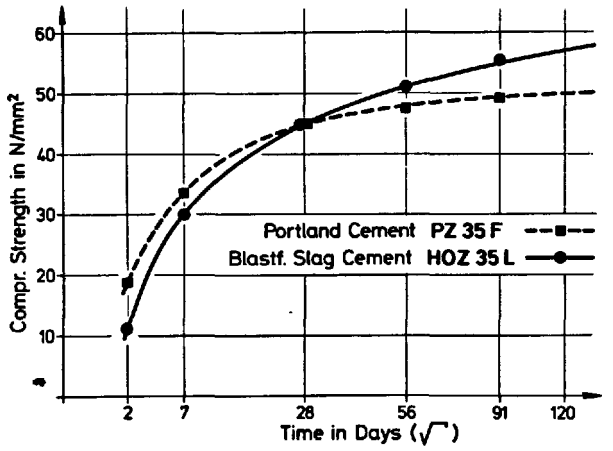

FIG. 4 - Average Strength Development of Cements Z 35.
Reference point: 45.0 N/mm² after 28 days

For a long time these specialities are as well-known as the low hydration heat of blastfurnace slag cements and their higher resistance against various chemical attacks /6/ /7/, which only recently has been proved by new investigations /66/ /67/. Also the special qualification of blastfurnace slag cements for marine constructions was verified again by evaluating extensive long-time studies with mortar and concrete /68/ /69/, as well as by research works on seawater desalination equipments /70/.

Discussions on steel corrosion in connection with blastfurnace slag cements are not to be repeated here for they are mostly based on theoretical suppositions only. In practice any damages of this kind are not known, and in the meantime respective apprehensions have proved unfounded /6/ /71/ /72/ /73/. In Western Germany blastfurnace slag cement is used for all kind of prestressed concrete /67/. One of the most modern big engineering structures made entirely from blastfurnace slag cement (HOZ 35L and HOZ 45L) is the prestressed posttensioned concrete bridge over the river Rhine at Köln-Deutz. The bridge was built as unsupported cantilever construction with lightweight concrete /74/.

Three important characteristic properties of blastfurnace slag cements less known up to now were investigated quantitatively only recently:

Blastfurnace slag reduces the reactivity of the cement with alkali reactive aggregates /75/ /76/ /77/ /78/. For the quantitative correlation between the effective alkali content A_{eff}, decisive for the alkali reaction, and the total alkali content A of the cement in dependence of its content of granulated blastfurnace slag H the formula

$$A_{eff} = A \cdot \left[1 - \left(\frac{H}{H_o}\right)^2\right]$$

was proposed /79/. H_o is a constant, which means that in case of $H \geq H_o$ no expansion phenomenon will occur. The examination of 40 Portland and blastfurnace slag cements executed by a working group of the Verein Deutscher Zementwerke e.V., confirmed this formula. Provided that Portland cements with $\leq$ 0.60 wt-% alkali (Na_2O-equivalent) in practice do not cause any alkali damages (low alkali cements) - that means, in case of $A_{eff} \leq$ 0,60 wt-% - the permitted alkali content of low alkali cements resulted in /80/

$$A \leq \frac{0.60}{1 - 1.8 \cdot (H/100)^2}$$

The effect of blastfurnace slag in this formula is plotted in FIGURE 5. TABLE V shows the limitting values for NA-cements (low alkali cements) fixed in German regulations /81/.

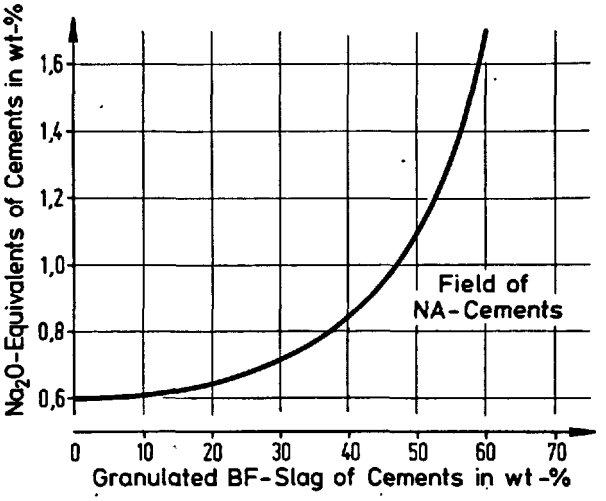

FIG. 5 - Alkali Contents of NA-Cements.
(Cements with $\leq$ 0.60 wt-% effective alkali)

One property being of importance for the corrosion protection of the reinforcement as well as for the prevention of alkali aggregate reactions, is the high resistance of concrete made from blastfurnace slag cement against the diffusion of chlorides /68/ /82/ /84/ /85/ and alkalies /84/ /86/. The diffusion resistance increases considerably with an increasing content of granulated blastfurnace slag /84/ /86/ /88/. At this

TAB. V - Cements with Low Effective Alkali		
	Total alkali in wt-% Na_2O equivalent	Granulated blastfurnace slag in wt-%
Portland cement	≤ 0.60	-
Blast-furnace slag cement	≤ 1.10	≥ 50
	(≤ 2.00)	≥ 65

the composition of the cement has a distinctly stronger influence than even the w/c-ratio of the concrete has /87/ /88/. If blastfurnace slag cements containing > 70 % slag are used, concrete layers of more than 2 cm thickness become practically impermeable for NaCl /67/ /86/. The graph in FIGURE 6 shows the influence of the blastfurnace slag in the cement on the progress of Cl-diffusion in concrete bars 10 x 10 x 50 cm. The relative intensity of the influence is characteristic for blastfurnace slag /83/ /84/ /87/.

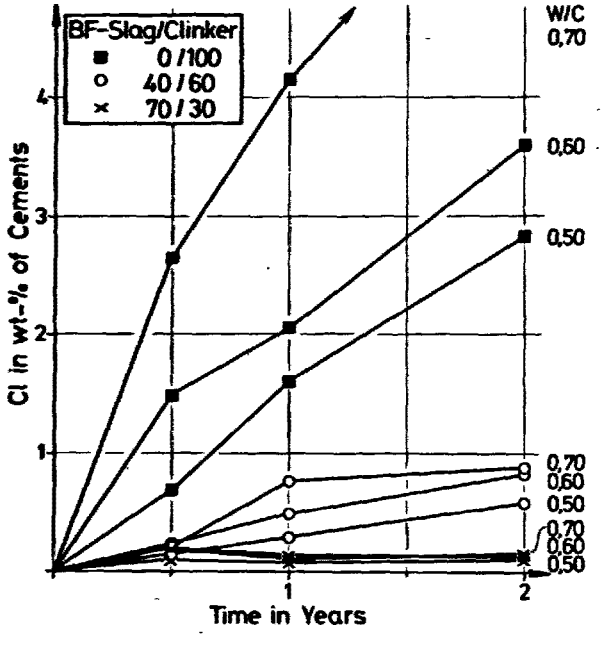

FIG. 6 - Chloride Diffusion into Concrete Bars.
NaCl-solution: 3 mol/l - Test layer: 2/4cm

The third typical property of concrete made from blastfurnace slag cement is the increasing impermeability with increasing content of blastfurnace slag /6/ /89/ /90/. Some special properties of blastfurnace slag cements are closely connected with this higher density. In this case not the total pore volume, which highly depends on the w/c-ratio, is decisive, but the more advantageous pore-size distribution of the blastfurnace slag cements /87/ /91/. The hardened cement paste of Portland cements has a higher quantity of capillary pores (radius > 300 Å), whereas blastfurnace slag cements develop more gel pores. That means that in the paste of blastfurnace slag cements the average pore size is smaller /87/. The results of an extensive test series with 6 cements with graduated contents of blastfurnace slag and with different storage conditions of the test specimens could be evaluated statistically /91/. With increasing content of blastfurnace slag, the pores > 300 Å decreased continuously. With increasing slag content of 0 to 76 wt-% slag, the quantity of these pores expressed as volume-% of the hardened paste were reduced from 30.5 to 22.5 volume-% (after storage in water) or from 37.0 to 25.0 volume-% (after dry storage). That means a relative reduction of the capillary porosity of about 25 to 30 %.

5. REVIEW ON THE UTILIZATION OF GRANULATED BLASTFURNACE SLAG

Besides Portland cement clinker, granulated blastfurnace slag is the only cement component which corresponding to its hydraulic effectiveness can be used as well as a secondary constituent of the cement as also a main constituent with more than 50 wt-% up to 80 wt-% (Germany) or even 95 wt-% (France). Such high slag contents should only be used, however, if these slag cements are produced in the cement plant from the definite single components in the same way as all the other cements, and if they are tested and controlled in the same way. In countries where suitable blastfurnace slags and sufficient experience with slag cements are available, blastfurnace slag cements are used in the same way as other cements and in certain cases they are favoured /6/ /7/ /68/ /69/ /81/. The tendency is increasing for there is no other cement component by which more energy and natural resources can be saved than it is with the granulated blastfurnace slag /3/ /53/ /92/. In case of a modern fabrication technique for the production of 1 t Portland cement about 1.5 t raw meal and 3.53 G Joule ($840 \cdot 10^3$ kcal) energy are necessary. For the production of 1 t blastfurnace slag cement containing 65 wt-% slag which originally had a residual moisture of 15 wt-%, only 0.5 t raw meal and 1.67 G Joule ($400 \cdot 10^3$ kcal) are necessary. In this calculation the drying of the slag was considered as well as the different demands of electrical energy which are necessary to grind either the raw meal and the clinker, or the slag /93/. Calculations with similar results are reported for North America where it is expected that the blastfurnace slag component of all cements will rise to about 30 wt-% within the next decade /92/.

It is nearly impossible to list up the total utilization of granulated blastfurnace slag quantitatively, for in many countries also Portland cements are allowed to contain slag (for instance in Germany ≤ 5 wt-%, in Austria ≤ 15 wt-%, in Yugoslavia > 15 wt-%). In other countries (for instance South Africa and Great Britain) most of the granulated blastfurnace slag is mixed into the concrete at the building site. In France about 10 to 15 million t "Graves-Laitier" are used for road construction yearly /2/ /3/. This hydraulic hardening material contains 15 to 20 wt-% granulated blastfurnace slag and about 1 wt-% $Ca(OH)_2$ as an activator /94/ /95/ /96/ /97/. In 1977 in France 3.0 million t granulated blastfurnace slag were used for road construction and 2.9 million t were used for cement production /3/. At last blastfurnace slags are used in multicomponent mixtures, too, which besides clinker and slag contain also natural or artificial pozzolanas. The production of super sulphated cement has been very much reduced.

For these reasons statistics about worldwide production data and applications of granulated blastfurnace slag often differ very much. Even data given for slag cements are not in good accordance. To allow at least a rough orientation for the cements, in TABLE VI data are summarized for those countries which produce more than 2 million t slag cement a year. Data for 1977 were asked for by personal correspondence /45/, whereas data for 1978 were taken from official statistics /98/. Table VI was completed with known data for 1971 /7/.

TAB. VI - BF-Slag Cement Production of Countries with Amounts of > 2 Mt/year

Country	Slag cement production in Mt/year	Percentage of total production	Year
USSR	27.1 30.0	27	1971 1973
France			1977
>35 % slag	2.0	7	
<35 % slag	10.0	35	
Germany-West			1978
>35 % slag	5.4	16	
≤35 % slag	2.7	8	
Poland	5.2	40	1971
CSSR	4.3	54	1971
Japan	3.3	4	1977
India	3.3	17	1977
Roumania	3.0	36	1971
Italy	2.7	7	1977
Netherlands	2.2	55	1977
Belgium	2.2	32	1977

REFERENCES

1.- F. KEIL: "Hochofenschlacke", 2. Auflage, Verlag Stahleisen, Düsseldorf 1963.

2.- W. GUTT and P.J. NIXON: "Use of Waste Materials in the Construction Industry", Matériaux et Constructions 12 (1979) p. 255/306.

3.- J. DUSSART: "Blastfurnace and Steel Slags in France", Symposium on the Utilisation of Steelplant Slags, Illawarra 1979, published by The Australasien Institute of Mining & Metallurgy (1979) p. 25/34.

4.- G. BLUNK: "Utilisation of Blastfurnace Slag and Steelmaking Slag in the Federal Rebublic of Germany", Slag Symposium, Illawarra 1979, p. 35/39.

5.- G. BLUNK und J. GEISELER: "Verwendung von Stahlwerksschlacken, dargestellt an ausgewählten Beispielen", Stahl und Eisen 100 (1980).

6.- F. SCHRÖDER: "Blastfurnace Slag and Slag Cements" with discussions and author's closure, Proceed. of THE V INTERNATIONAL SYMPOSIUM ON THE CHEMISTRY OF CEMENT (V ISCC), Tokyo 1968, Vol. IV, p. 149/207. (The Cement Association of Japan, Tokyo 1969).

7.- V.I. SATARIN: "Slag Portland Cement", THE VI INTERNATIONAL CONGRESS ON THE CHEMISTRY OF CEMENT (VI ICCC), Moscow 1974, Principal Paper p. 1/51. (Summaries in /8/).

8.- M. VENUAT: "Les ciments contenant du laitier ou des cendres volantes", Synthèse des communications du VI ICCC, Moscou 1974, Rev. des Matériaux de Construction N° 692 (1975) p. 30/33.

9.- H.-G. SMOLCZYK: "Die Hydratationsprodukte hüttensandreicher Zemente", Zement-Kalk-Gips 18 (1965) p. 238/246.

10.- R. GALIBERT: "Le laitier granulé en technique cimentière", CILAM-Informations N° 25 (1978) p. 1/8.

11.- H. MAAS und K.H. PETERS: "Der Einfluß der Granulation auf die hydraulischen Eigenschaften des Hüttensands", VDZ-Kongress '77 über Verfahrenstechnik der Zementherstellung, Verein Deutscher Zementwerke, Düsseldorf 1979, p. 678/681. (germ. and engl.).

12.- H. KISTER und H. WYSOCKI: "Neuartiges System zur Herstellung von granulierter Hochofenschlacke mit hohem Glasgehalt und geringer Restfeuchte" VDZ-Kongress '77, p. 674/678. (germ. and engl.).

13.- J.J. EMERY, R.P. COTSWORTH and R.D. HOOTON: "Pelletized Blastfurnace Slag", NSA-Meeting, Florida 1978, Paper 4.1, p. 1/23.

14.- M. KUNICKI: "La production des laitiers GALEX bouletê ou granulê et leurs applications", Silicates Industriels 42 (1977) p. 91/98.

15.- B. COURTAULT: "Traitement thermomécanique du laitier de haut fourneau", Rev. des Matêriaux de Construction N° 699 (1976) p. 108/110.

16.- M. REGOURD: "Cements Research in France" Ciments Bêtons Plâtres Chaux N° 2 (1978) p. 83/90.

17.- S. SOLACOLU: "Die Bedeutung der thermischen Gleichgewichte des Systems $MgO-CaO-Al_2O_3-SiO_2$ für Schmelzen und Granulieren der Hochofenschlacken", Zement-Kalk-Gips 11 (1958) p. 125/137.

18.- W.H. ZACHARIASEN: "The Atomic Arrangement in Glass", J. Amer. chem. Soc. 54 (1932) p. 3841/3851.

19.- K. CHOPRA and C.A. TANEJA: "Co-Ordination State of Aluminium, Magnesium and Manganese Ions in Synthetic Slag Glasses", VISCC, Tokyo 1968, Vol. IV, p. 228/236.

20.- S.M. ROYAK: "Blastfurnace Slag Hydraulic Activity and Structure", Tsement N° 8 (1978) p. 4/5. (in Russian).

21.- N. STUTTERHEIM: "The Risk of Unsoundness Due to Periclase in High-Magnesia Blastfurnace Slags", Proceed. of The IV International Symposium on the Chemistry of Cement, Washington 1960, Vol. II, p. 1035/1041.

22.- M. CHERON and C. LARDINOIS: "The Role of Magnesia and Alumina in the Hydraulic Properties of Granulated Blast-Furnace Slags", V ISCC, Tokyo 1968, Vol. IV, p. 277/285.

23.- A. NEGRO und B. BACHIORRINI: "Einfluß des Magnesiumoxyds auf die Entglasung synthetischer Hochofenschlacken", Zement-Kalk-Gips 26 (1973) p. 448/450.

24.- N. STUTTERHEIM: "MgO in Blastfurnace Slag Cements" (Oral discussion) V ISCC, Tokyo 1968, Vol. IV, p. 200/201.

25.- K. KÜHLE und U. LUDWIG: "Über die Verwendung MgO-reicher Hüttensande in Hochofenzementen", Sprechsaal für Keramik Glas Email Silikate (1972) p. 421/432.

26.- G. MASCOLO: "Hydration Products of Synthetic Glasses Similar to Blast-Furnace Slags", Cement and Concrete Research 3 (1973) p. 207/213.

27.- C.A. TANEJA: "Role of Magnesia on Hydration of High Alumina Slags", VI ICCC, Moscow 1974, Supplem. Paper, Section III/2 (Summary in /8/).

28.- M. REGOURD, B. MORTUREUX, H. HORNAIN: "Hydratation et microstructure des ciments au laitier", 7 CONGRES INTERNATIONAL DE LA CHIMIE DES CIMENTS (VII CICC), Paris 1980, Communication Thème III.

29.- R. SERSALE: "Produits à haut teneur en MgO par l'hydratation des ciments sidérurgiques", VII CICC, Paris 1980, Communication Thème III.

30.- H. SALGE: "Untersuchungen zur Löslichkeit von Schwefel in Hüttenschlacken (System $CaO-Al_2O_3-SiO_2$)", Tonindustrie Ztg. 86 (1962) p. 586/589.

31.- R. DRON: "Relation entre la composition potentielle des laitiers et leur reactivité", VII CICC, Paris 1980, Communication Thème III.

32.- P. TERRIER: "Recherche sur l'hydraulicitê des laitiers granulès de haut Fourneau", CILAM-Informations N° 8 (1973) p. 1/6, N° 9 (1973) p. 1/6, N° 10 (1973) p. 1/7.

33.- S.M. ROYAK, Y.S. SHKOLNIK, N.V. ORININSKY, V.V. ORLOW, L.A. ORLOVA: "Electron Paramagnetic Resonance Investigations of Slag Glasses", Building and Architecture N° 5 (1972) p. 75/79 (in Russian).

34.- S.M. ROYAK, V.F. KRYLOV, V.S. KLIMENTEVA: "Investigations on Hydraulic Reactivity of Slags with High Contents of Manganese and Barium", Stroitelniye Materialy N° 3 (1965) p. 37/39 (in Russian).

35.- V. POKH: "On Bonds of Alkaline Ions in Various Glasses", Glassy State, Nauka (1971) p. 354/356 (in Russian).

36.- H.-E. SCHWIETE, W. KRÖNERT und M. NUSselein: "Zum Säureangriff auf Oberflächen glasiger Hochofenschlacken", Glastechnische Berichte 42 (1969) p. 471/473.

37.- S.M. ROYAK, G.S. ROYAK: "Special Cements", Stroyizdat (1969) p. 137/155 (in Russian).

38.- P.P. BUDNIKOV, V.S. GORSHKOV, T.A. KHMELEVSKAYA: "Evaluation of Binding Properties of Slags on the Basis of Chemico-Mineralogical Composition", Stroitelniye Materialy N° 5 (1960) p. 29/33 (in Russian).

39.- H.-E. SCHWIETE, W. KRÖNERT und M. NUSSELEIN: "Beitrag zum Säureangriff auf Oberflächen glasiger Hochofenschlacken", Glastechnische Berichte 41 (1968) p. 451/455.

40.- H. BUSCH und A. PETZOLD: "Phasentrennung in basischen Schlackengläsern", Silikattechnik 20 (1969) p. 47/49.

41.- H. BUSCH und A. PETZOLD: "Struktur und Hydraulizität basischer Hochofenschlakken", Silikattechnik 22 (1971) p. 13/14.

42.- F.W. LOCHER (Personal Information).

43.- F. SCHRÖDER: "Über die hydraulischen Eigenschaften von Hüttensanden und ihre Beurteilungsmethoden", Tonindustrie Ztg. 85 (1961) p. 39/44.

44.- J.C. YANG: "Chemistry of Slag-Rich Cements", V ISCC, Tokyo 1968, Vol. IV, p. 296/309.

45.- Personal Informations (1979) from L. ANDERSON, H. BOUILLON, W. BUIST, J. CALLEJA, J. DUSSART, R. GALIBERT, N. HARA, L.J. HUSS, T. IKEDA, W. VAN KLAVEREN, R. KONDO, Z. KOSTRENCIC, P.G. LANIGAN, G. RAMASESHAN, R. SERSALE, A. THOMAS.

46.- H.-G. SMOLCZYK: "Zum Einfluß der Chemie des Hüttensands auf die Festigkeiten von Hochofenzementen", Zement-Kalk-Gips 31 (1978) p. 294/296.

47.- H.-E. SCHWIETE und F.C. DÖLBOR: "Einfluß der Abkühlungsbedingungen und der Zusammensetzung auf die hydraulischen Eigenschaften von Hämatitschlacken", Forschungsberichte des Landes Nordrhein-Westfalen Nr. 1186 (1963).

48.- J. CLERET DE LANGAVANT: "Considérations théoretiques sur la nature du laitier de cimenterie", Rev. des Matériaux de Construction (1949) p. 77/81.

49.- R.D. COALE, C.W. WOLHUTER, P.R. JOCHENS and D.D. HOWAT: "Cementitious Properties of Metallurgical Slags", Cement and Concrete Research 3 (1973), p. 81/92.

50.- H. SOPORA: "Bewertung von Hochofenschlacken für die Zementherstellung im Betriebslaboratorium", Silikattechnik 10 (1959) p. 361/363.

51.- I.S. VYLKOVA: "On Binding Properties of Blast-Furnace Slag with High Content of Barium and Manganese", VI ICCC, Moscow 1974, Supp. Paper, Section III/2 (Summary in /8/).

52.- T.W. PARKER and R.W. NURSE: "Investigations on Granulated Blast-Furnace Slags for the Manufacture of Portland Blast-Furnace Cement", Nat. Build. Stud. Techn. Paper N° 3, London 1949.

53.- S.E. JOHANSSON: "Relation between Strengths of Slag Cement and Properties of Slag", Silicates Industrielles 43 (1978) p. 139/143.

54.- K. BERGT: "Effect of Magnesia Content of Blast-Furnace Slags on the Strength of Slag Cements", Proceed. of the VII Conference of the Silicate Industry, Budapest 1965, p. 661/668.

55.- V.L. PANKRATOV: "Hydraulic Activity of Blast-Furnace Granulated Slags", Tsement N° 1 (1971) p. 19/20 (in Russian).

56.- S. ROYAK, Y. CHOLNIK: "L'effet des particularités physicochimiques du laitier de haut fourneau sur son activité hydraulique", VII CICC, Paris 1980, Communication Thème III.

57.- P. LONGUET, L. BURGLEN et A. ZELWER: "La phase liquide du ciment hydraté", Rev. des Matériaux de Construction N° 676 (1973) p. 35/41.

58.- S. DIAMOND: "Long-Term Status of Calcium Hydroxide Saturation of Pore Solutions in Hardened Cements", Cement and Concrete Research 5 (1975) p. 607/616.

59.- R.K. DATTA, D. LAHIRI: "Einfluß kleiner Beimengungen auf die hydraulischen Eigenschaften von Hochofenschlacke. Teil I: Einfluß von MnO", Zement-Kalk-Gips 25 (1972) p. 344/346.

60.- C.A. TANEJA, S.P. THERI, M. SINGH: "Investigations on High Alumina Slags for Cement Manufacture", VII CICC, Paris 1980, Comminication Thème III.

61.- V.Y. DOVGOPOL, S.M. ROYAK, M.F. CHEBUKOV, Y.S. SHKOLNIK: "Utilization of Titanous Blast-Furnace Slags in Cement Production", Tsement N° 11 (1971) p. 7/8 (in Russian).

62.- S.M. ROYAK, Y.S. SHKOLNIK, N.V. ORININSKY, Z.E. SLEPTSOV, F.K. ADMAKIN, T.M. FEDOROVA: "Crystallization of Magnesia in High Magnesia Blast-Furnace Slags", Stroitelnye Materialy N° 2 (1972) p. 33/34 (in Russian).

63.- V.L. PANKRATOV, V.P. IGNATOVA, R.Y. CHERNES: "Super Rapid-Hardening Slag Portland Cement", Proceed. of NII Tsement N° 23 (1968) p. 79/83 (in Russian).

64.- V.I. SATARIN, Y.M. SYRKIN, M.B. FRENKEL: "Rapid Hardening Slag Portland Cement", Stroyizdat (1970) p. 105/125 (in Russian).

65.- V.I. SATATIN, A.G. KHOLODNY, O.G. SHINKARENKO, L.V. TEREKOVA: "Hardening of Slag Portland Cements Prepared on the Basis of Low-Temperature-Kiln Clinker", Budivelni materialy i konstruktsii N° 3 (1971) p. 3/5 (in Russian).

66.- Y. EFES und H.P. LÜHR: "Beurteilung des Kohlensäure-Angriffs auf Mörtel aus Zementen mit verschiedenem Klinker-Hüttensand-Verhältnis", Institut für Bauforschung der RWTH Aachen, Bericht F 49 (1978) p. 1/40 und Anhang (publication in 1980).

67.- H.-G. SMOLCZYK: "L'emploi du ciment de laitier de haut fourneau dans le bêton armé et le bêton précontraint", Revue de Mêtallurgie (1978) p. 275/280.

68.- H.T. SCHRÖDER, O. HALLAUER und W. SCHOLZ: " Beständigkeit verschiedener Betonarten im Meerwasser und in sulfathaltigem Wasser", Deutscher Ausschuß für Stahlbeton, Heft 252 (1975)p. 1/100.

69.- M. REGOURD et al (see /99/).

70.- S. SPRUNG: "Beton für Meerwasserentsalzungsanlagen", beton 28 (1978) p. 241/245.

71.- P. GUNKEL und H.-G. SMOLCZYK: "Untersuchung der Reaktionsmöglichkeiten von Sulfiden bei der Einwirkung von Kohlensäure und Sauerstoff auf sulfidhaltigen Zementstein", Werkstoffe und Korrosion 27 (1976) p. 297/303.

72.- V. VANDEN BOSCH: "Connaissance actuelles sur le comportement des aciers dans les bêtons de ciments mêtallurgiques"(avec discussion et rêponse de l'auteur). Silicates Industriels 42 (1977) p. 145/149.

73.- P. PONTEVILLE: "Le bêton hydraulique de granulat de laitier", Laitiers de Haut Fourneau (CTPL) 31 (1978) N° 43, p. 5/143.

74.- H. GRUBE und W. HEROLD: "Der Beton der Rheinbrücke Köln-Deutz", Beton-Informationen, Heft 2 + 3/79 (1979) p. 32/35.

75.- L. PEPPER and B. MATHER: "Effectiveness of Mineral Admixtures in Preventing Excessive Expansion of Concrete due to Alkali Aggregate Reaction", 62. ASTM-Meeting (1959) preprint p. 1/25.

76.- P. KLIEGER and A.ISBERNER: "Laboratory Studies of Blended Cements. Portland Blastfurnace Slag Cements", Journal PCA Research and Develop. Lab. 9 (1967) p. 2/22.

77.- Forschungsinstitut der Zementindustrie: Vorbeugende Maßnahmen gegen Alkalireaktion im Beton", Schriftenreihe der Zementindustrie, Heft 40 (1973) p. 1/98.

78.- F.W. LOCHER und S. SPRUNG: "Einflüsse auf die Alkali-Kieselsäure-Reaktion im Beton", Zement-Kalk-Gips 28 (1975) p. 162/169.

79.- H.-G. SMOLCZYK: "Slag Cements and Alkalireactive Aggregates", VI ICCC, Moscow 1974, Suppl. Paper Section III/2 (Summary in /8/).

80.- VDZ-Arbeitskreis Alkalien im Zement: "Zement mit niedrigem wirksamen Alkaligehalt", Verein Deutscher Zementwerke, Tätigkeitsbericht 75-78 (1978) p. 49/50.

81.- G. WISCHERS: "Bautechnische Eigenschaften des Zements. Widerstand gegen Alkalireaktion", Verein Deutscher Zementwerke, Zement-Taschenbuch 1979/80, p. 96/97.

82.- Forschungsinstitut der Zementindustrie: "Diffusion von Chlorid- und Sulfationen im Zementstein", Verein Deutscher Zementwerke, Tätigkeitsbericht 65-66 (1966) p. 71/72.

83.- M. COLEPARDI, A. MARCIALIS, R. TURRIZIANI: "La cinetica di penetrazione degli ioni cloruro nel calcestruzzo", Il Cemento 67 (1970) p. 157/164.

84,- R.F.M. BAKKER en W.I.M. THOMASSEN: "Diffusiesnelheid van ionen in beton", Cement 29 (1977) p. 419/421.

95.- W.L. SLUIJTER and P.C. KREIJGER: "Corrosion of Reinforcement in Concrete due to Calcium Chloride", Stress Corrosion in Prestressing Steel, Heron 22 (1977) p. 28.

86.- H.-G. SMOLCZYK: "Investigation on the Diffusion of Na-Ion in Concrete", Symposium on Alkali-Aggregate Reaction, Reykjavik 1975, Proceed. (1975) p. 183/188.

87.- O.E. GJØRV and Ø. VENNESLAND: "Diffusion of Chloride Ions from Seawater into Concrete", Cement and Concrete Research 9 (1979) p. 229/238.

88.- G. BLUNK and H.-G. SMOLCZYK: "Discussion to the Principal Paper Slag Portland Cement", VI ICCC, Moscow 1974, Written Discussion Section III/2 (1974) p. 1/3.

89.- R.H. MILLS: "Molcular Sieve Effect in Concrete", V ISCC, Tokyo 1968, Vol.III, p. 74/84.

90.- H. ROMBERG: "Einfluß der Zementart auf die Porengrößenverteilung im Zementstein", Tonindustrie Ztg. 95 (1971) p. 105/115.

91.- H.-G. SMOLCZYK und H. ROMBERG: "Der Einfluß der Nachbehandlung und der Lagerung auf die Nacherhärtung und Porenverteilung von Beton", Tonindustrie Ztg. 100 (1976) p. 349/357 and 381/390.

92.- R.H. MILLS: "Significance of Latent Energy in Hydraulic Slags to the Cement and Concrete Industry", Slag Symposium, Illawarra 1979, p. 51/57.

93.- H. BRODERSEN: "Zum Energiebedarf verschiedener Zemente unter besonderer Berücksichtigung von schwerem Heizöl", Forschungsinstitut Eisenhüttenschlakken, Interner Bericht, März 1974 (unpublished).

94.- Ministère de L'Amenagement du Territoire de l'Equipment, du Logement et du Tourisme: "DIRECTIVE pour la réalisation des assises de chaussées en grave-laitier et sables-laitiers", Service d'Etudes Techniques des Routes et Autoroutes (SETRA), Laboratoire Central des Ponts et Chaussées (L.C.P.C.), Octobre 1973.

95.- M. PONTEVILLE: "Evolution de l'emploi du laitier en France de 1973 à 1976", Silicates Industriels 42 (1977) p. 193/208.

96.- K. KRASS: "Verfestigte Tragschichten in Frankreich - Alternative für den deutschen Straßenbau?", Strasse und Autobahn 27 (1976) p. 255/258.

97.- J. DUSSART, CH. CIMPELLI, J.P. COURANT, J. IFERGAN, G. FONTAINE, R. BLOIS: "Graves-laitier, sables-laitier, graves-laitier tout laitier", Laitiers de Haut Fourneau (CTPL) 32 (1979) N°44, p. 1/63.

98.- Bundesverband der Deutschen Zementindustrie: "Zement, Zahlen und Daten 78-79", BDZ, Köln 1979.

99.- M. REGOURD, H. HORNAIN et B. MORTUREUX: "Résistance à l'eau de mer des ciments au laitier", Silicates Industriels 42 (1977) p. 19/27 (see /69/).

SUB-THEME III - 2

Mecanism and kinetics of slag Cement Hydration

M. DAIMON
Tokyo Institute of Technology
JAPAN

INTRODUCTION

Blastfurnace slags are the most useful latent hydraulic materials, because the amount produced is very large and its properties are very stable compared with other industrial byproducts.

Slag cements have been an important topic in the previous symposiums, and are reviewed at each time (1. 2). Many reviews concerning the utilization of slag (3-6) are written after the previous symposiums, showing the importance of slag utilization in every country. There are also several attempts to find new way (7-11) to utilize blastfurnace slags.

The present authors wish to take this opportunity to introduce results obtained in this field especially after the previous symposium in 1974. They will welcome comments on their own research work, as well as on this review paper.

DETERMINATION OF THE DEGREE OF HYDRATION

Slag hydration should be determined by the similar methods to those used for cement hydration (12). There are two differences; (i) slags are in glassy state, and (ii) the hydration of slag is generally very slow.

The general problem in determining the cement hydration is the change in the compositions of the produced hydrates with the progress of the hydration. Therefore several kinds of experimental techniques must be used in order to get a full picture of cement hydration.

Quantitative Analysis of Slag

The degree of hydration is usually shown by the amount of residual reactant, in the usual hydration of cements, when produced hydrates change in their compositions with the progress of hydration. X-ray diffractometry can be used when reactants are crystalline. As slag used in cement are in glassy state, it is necessary to find a suitable method for the quantitative analysis of slag.

Kondo and Ohsawa (13) introduced an extraction technique; 0.5g sample is put into a beaker together with 2.5g of salicylic acid, 35cc of aceton and 15cc of methanol at room temperature for 1 hour. After 1 day, it is filtered and residue is washed with methanol, dried and heated at 850°C for 10 minutes. The original slag sample should be treated in the same way before hand, in order to correct the experimental results. Fig.1 is the typical results obtained by authors (14). Mironov, Kurbatova and Vysotskie (15) recommended this method.

At elevated temperature hydration products are well crystallized and dissolved into acid solution very slowly, and so extraction method is not available. Authors adopted X-ray quantitative analysis of melilite crystallized by heating at 900°C for 5 min. (16). A density separation method (17) and an infrared spectroscopy (18) have been also proposed, but these techniques are only for the original mixes of slag cements or for the semi-quantitative analysis. The thermoluminescence measurement was also applied to study slag hydration (19)(20).

Non-evaporable water, free lime and free gypsum

The amount of the non-evaporable water (21) in cement paste increases with the curing time to give a similar results as the curve of the reduction of reactant slag. But two results do not coincide exactly, as the stoichiometry is not constant in the course of slag hydration. It must be noted that the sample should not be heated up to too high temperature in order to avoid a weight increase due to the oxidation.

Mikhail, Abo-El-Enein and Gabr (22) adopted the non-evaporable water value to evaluate the hydration degree of slag cements. The amount of combined water should be closely related to the strength of hardened body. Because hydrated cement is a typical porous material, and porosity is the main factor to determine the mechanical strength. Pore space which was originally occupied by water decreases with the formation of hydration products.

$Ca(OH)_2$ and $CaSO_4$ are the most typical activating component of slag hydration. It has been reported (23) that activators play role in slag hydration not only as glass attacking catalysts but also as reagents in hydrate formation reactions. Therefore it is very important to know the residual amount of $Ca(OH)_2$ and $CaSO_4$. There have been proposed many extraction methods for free lime (24,25), and Forén's method (13,26) for free gypsum.

Fig. 2 shows the reaction rate of gypsum in the same high sulphated slag cement as in Fig.1. Both graphs exhibit similar tendency, and suggest that the gypsum is not an exciter, but an important reactant in this system.

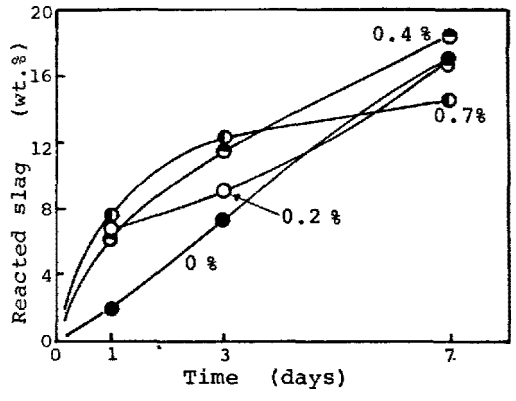

Fig. 1 - Percentage of reacted slag as a function of time in slag + 10wt.%$CaSO_4 \cdot 2H_2O$ + various amount of $Ca(OH)_2$ (14)

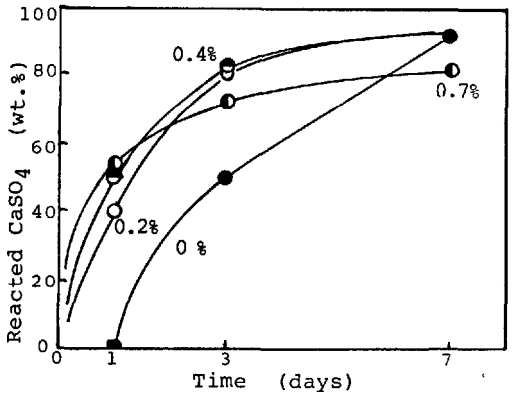

Fig. 2 -Percentage of reacted $CaSO_4$ as a function of time in slag + 10wt.% $CaSO_4 \cdot 2H_2O$ + various amount of $Ca(OH)_2$ (14)

Calorimetry

The heat of solution, the adiabatic and the conduction calorimeters are frequently used for the calorimetric determination. Among those, the conduction calolimeter have been used for the measurement of the heat of hydration, as heat can be obtained continuously at almost constant curing temperature for a long period. Many investigators have made conduction calorimeters (12,27,28), in which determination is possible using small amounts of cement samples for the convenience of using synthesized samples. But larger amount of sample should be used in the case of slag hydration for slag hydrates slowly.

The results of conduction calorimetric measurements also show the parallel tendency with the degree of slag hydration obtained by extraction method, although they are not exactly identical (14). De Jong (29) studied slag hydration mainly with this method.

LATENT HYDRAULIC PROPERTY OF SLAG

Certain activators such as sodium hydroxide, calcium hydroxide and gypsum have been known to accelerate the hydration of slag. The activation mechanism on the hydration of slag has not been adequately reported.

Hydration of Slag

Kondo (12,30) studied the hydration of calcium alumino-silicate glass powders and found that glasses with composition of above 50% CaO and below 20% SiO_2 content had hydraulic properties. In the suspension hydration of C_2AS glass, a low permeable coating which was approximately ASH_6 in composition and 0.2 μm in thickness was formed on their surfaces, and the liquid concentration was kept low as shown in Fig. 3. Fig. 4 showed that the suspension hydration of C_2AS glass was accelerated by the addition of $Ca(OH)_2$, because SiO_2 and particularly Al_2O_3 were apt to be liberated from above mentioned coating, and the solubility of hydrate decreases under this condition. These results were reconfirmed by the authors (31).

Such activating effect seems similar to the effect of $MgCl_2$ in magnesia cement. Table 1 shows the MgO concentration in liquid phase, after mixing MgO and $MgCl_2$ solution (32). MgO dissolves very rapidly into $MgCl_2$ solution of higher concentration. Main difference between the hydration mechanisms of slag and magnesia cement might be that the former hydrates topo-chemically and the latter with through solution mechanism (30,31). Regourd (33) considerd that the poorly crystallized hydrated layer around the slag grains could be called "pseudomorphic" layer.

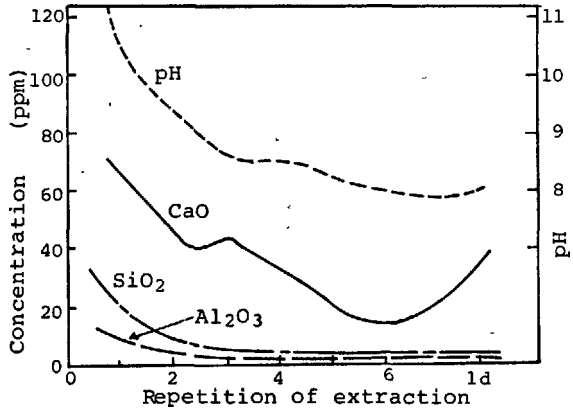

Fig. 3 - Repeated extraction of C_2AS glass (5g of C_2AS per 100ml of water) (12,30)

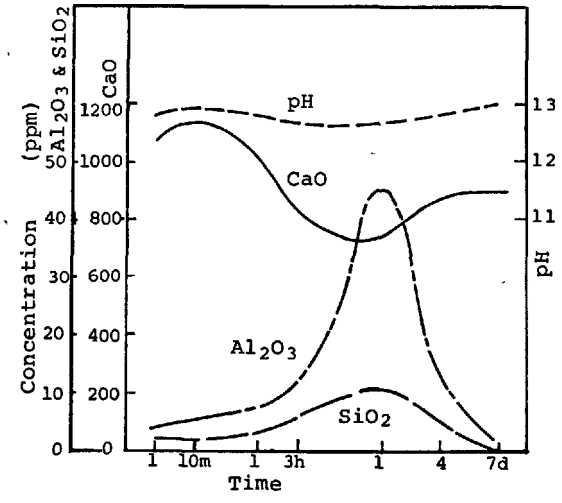

Fig. 4 - Solubility of C_2AS glass with 2 moles of $Ca(OH)_2$ (1g of solid per 100ml of water) (12,30)

Table 1. Dissolution of MgO into $MgCl_2$ solutions (5g of MgO per 450ml of solution) (29)

Conc. of $MgCl_2$	5min	1h	2h	3h	4h	5h	6h
10.72%	.059	.011	.007	.005	.003	.004	.005
20.22%	.078	.313	.487	.596	.622	.130	.086
29.49%	.155	.433	.632	.754	.835	.895	.905

Hydraulic Reactivity of slag

Reactivity of slag has been considered to be determined by the glass content (34) and chemical composition, which can be represented by a number called hydraulic moduli or basicity such as $(CaO + MgO + Al_2O_3) / SiO_2$.

When other conditions than chemical composition are in good controll, certain trends can be shown in hydraulic activity and composition. Coal, Wolhuter, Jochens and Howat(35) reported the iso-strength plots of lime activated slag cement, in SiO_2-Al_2O_3-MgO-CaO system. Teoreanu and Georgescu(36) also presented such iso-strength plots for slag cements, with 15% portland cement clinker and 2% $CaCl_2$. Miyairi and Takaki(37) concluded that CaX_2 accelerate the hydration of portland cement. Taneja(38) discussed the role of Al_2O_3, MgO and MnO contents in slag.

Taneja(39) observed, that the incorporated MgO up to 2.5% improved the hydraulic behaviour MgO in slag have been supposed to behave very differently from that in portland cement. Mascolo(40) suggested the formation of a solid solution between C_4Aaq and M_4Aaq, and explained the volume stability of slag portland cement with slags having very high MgO content. But, according to Casselouri and Parissakis(41), blastfurnace slag did not stabilize the volume unstability of high magnesia cement, while a certain fly ash had a stabilizing effect.

But it has recently been found that two values, i.e. hydraulic moduli and glass content can not describe the latent hydraulic property of slag. Akatsu, Ikeda and Sadatsune(42) studied on glass with the composition between C_2AS and C_2MS_2. The results could not be explained by basicity. Smolczyk(43) reported none of the well known fomulas was able to give generally. valid information of the hydraulic activities of 192 laboratory cements. Totani, Saito, Kageyama and Tanaka(44) studied using three different slags with similar glass content and chemical composition and found that the reactivities are very different each other. This is supposed to be one of the most important problem in this field which must be solved. Detailed studies should be performed on the structure of glass.

Activators for Slag Hydration

Fig. 5 is the changes in the amount of combined water of hydrated slag with various activators(45). In the case of $Ca(OH)_2$ (a), the curves showed that slag hydration was not largely dependent on $Ca(OH)_2$ content when it was more than 5%. In the case of NaOH (b) and $CaSO_4 \cdot 2H_2O$ (c), the combined water continuously increased with the amount of additives. When NaOH was used, the reaction proceeded to a considerable extent within one day and almost the same as those of 3 and 7 days. The curves for $Ca(OH)_2 + CaSO_4 \cdot 2H_2O$ (d), showed an optimum lime content, which was very low value.

It was found that the activators, $Ca(OH)_2$, $Ca(OH)_2$ + gypsum, and NaOH remarkably promoted the hydration of slag (45). $Ca(OH)_2$ represents slag portland cement, and $Ca(OH)_2$ + gypsum represents high sulphate slag cement. NaOH is a powerful activator, but this has not frequently been utilized until now. New techniques using such alkaline activators have recently been attempted (10,11).

Voinnovitch and Dron(23) proposed the stoichiometric formulas in the first approximation for the slag hydration as follows.

$$C_5S_3A + 2C + 16H \longrightarrow C_4AH_{13} + 3CSH \cdots (A)$$

$$C_5S_3A + 2C_S + 76/3H \longrightarrow$$

$$3CSH + 2/3 \cdot C_3A \cdot 3C_S \cdot H_{32} + 2/3Al(OH)_3 \cdots (B)$$

It can be seen that lime and gypsum are not simple "activators" but main reactants. But in the case of NaOH activation, NaOH seemed to play a role as a simple catalyst(23). Sersale, Aiello and Colella(10) recognized C-S-H and hydrogarnet as hydration products in this system. Regourd(46) gave more details on different activators.

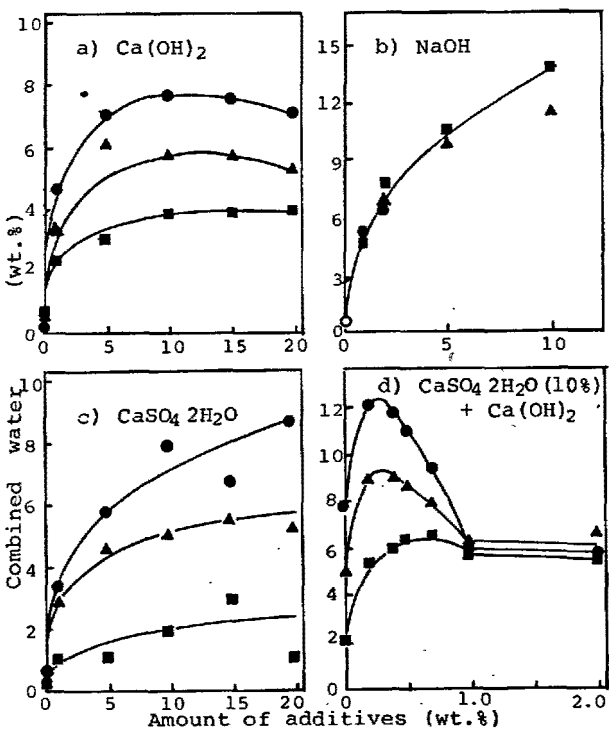

Fig. 5 - Amount of combined water during the hydration of granulated blastfurnace slag with various activators (■ 1d, ▲ 3d, ● 7d)(45)

HYDRATION OF SLAG IN SLAG CEMENTS

Gypsum and lime are the most typical activators. Lime has activating effect by dissolving Al_2O_3 and SiO_2 from slag. Gypsum, on the other hand, does not have such effect, although it is an important reactant to form AFt phase. And so gypsum is always used with a certain alkaline activator. Accordingly, lime and gypsum + lime are the most typical activating system, and they are related to the most important slag cements, i.e. slag portland cement and super sulphated slag cement.

Slag Portland Cement

Slag portland cement is the most popular way to utilize granulated blastfurnace slag. Slag portland cements with higher slag contents are frequently used for mass concrete because of their low heat evolution. And those with lower slag content are generally used as a substitute of portland cement. Smolczyk(47) reported this cement was very suitable to be used with alkaline active aggregates. Slag have been permitted to be added in portland cement in several countries (1,2), and Japanese Industrial Standard has also permitted the addition of 5% slag or other latent hydraulic or pozzolanic materials.

For slag portland cements, activation of slag is accomplished by the $Ca(OH)_2$ liberated during the hydration of portland cement. Therefore $Ca(OH)_2$ has been generally used instead of portland cement in fundamental studies of kinetics and mechanisms of hydration, in order to simplify the experimental system.

Table 2 is the results obtained by Abo-El-Enein, Daimon, Ohsawa and Kondo(25). 20 wt% $Ca(OH)_2$ was used as the activator. Slag hydration is not such a simple reaction as shown in formula(A). A high lime product with molar $C/(S + A)$ ratio of 2.5 - 2.6 is formed during the early stage of the hydration process. Then the molar $C/(S + A)$ ratio drops to a value around 1.6.

Table 2 shows, slag was hydrated at relatively high rate during the first 7 days, but thereafter the reaction extremely delayed. The calculated depth of the hydrated layer on the slag grains was found to be as little as 0.3 μm in the later stages. This coincided well with the previous results by Kondo and Ohsawa (13), and they concluded that the reaction rate became very slow when compact sheath had grown around the slag grains to a certain thickness.

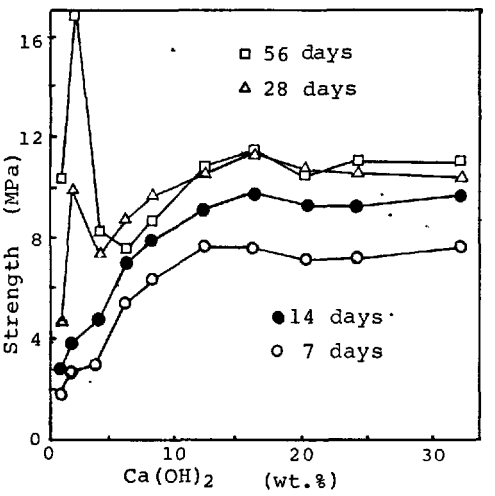

Fig. 6 - Effect of $Ca(OH)_2$ activator content on the compressive strength developed by blastfurnace slag (35)

Thus the slags have been supposed to hydrate very slowly, so that the strength developments of slag portland cements are smaller than usual portland cement. But there are two papers reporting that slags hydrate fast in some cases when they are activated by portland cement or $Ca(OH)_2$.

Coale, Wolhuter, Jochens and Howat(35) found slag hydrated, in the presence of very small amount of lime, rather rapidly especially at later periods. Fig, 6 is their results. Nagataki and Tanaka(48) observed the microstructure of hardened concrete with slag aggregates, and found very thick reacted layers around each aggregate grains.

Table 2. Hydration of the low porosity paste of blastfurnace slag and 20 wt.% $Ca(OH)_2$ (25).

Hydration time (days)	1/4	1	3	7	28	90	180
Combined water (wt.%)	1.132	2.120	3.124	4.013	5.628	7.168	8.799
Combined slag (wt.%)	3.13	5.19	6.70	11.09	16.05	20.14	20.55
Combined lime(CaO) (wt.%)	1.81	3.11	3.28	3.33	3.54	3.82	5.24
Ignited products (wt.%)	4.94	8.30	9.98	14.42	19.59	23.96	25.79
Reaction ratio of lime	0.114	0.195	0.206	0.209	0.222	0.240	0.329
Reaction ratio of slag	0.038	0.062	0.081	0.134	0.193	0.243	0.248
Depth of reacted layer (μm)	0.040	0.065	0.080	0.150	0.220	0.260	0.280
$CaO/(SiO_2 + Al_2O_3)$	2.507	2.563	2.295	1.825	1.630	1.553	1.714

Those two results were obtained in very different experimental conditions. The former occured at very low ratio of activator to slag, and the latter at very high ratio of activator amount to slag surface. Further studies are desirable to clarify those phenomena.

High Sulphated Slag Cement

High sulphated slag cement is not such a common cement, as slag portland cements, but has been used successfully for concrete in soil involving sulphate in Europe for a long time. As it contains 80 - 90% of slag, it should be the best way for the full utilization of latent hydraulic property of blast-furnace slags.

A small amount of lime or portland cement is commonly used in supersulphated slag cement, as an activator together with calcium sulphate. Van Haute(49) proposed to use a combination of aluminous cement + $Ca(OH)_2$ + K_2SO_4 as alkali agitator. Uchida, Nomi and Minegishi(50) obtained a good results by using hauyne type clinker.

Fig. 7 shows the results of calorimetric study with different lime contents(51). It can be seen that the hydration processes are much influenced by the amount of lime. The curve of low lime content, $<0.3\%$ $Ca(OH)_2$, shows a small but sharp peak which corresponds to the main hydration in a short period of time (less than 9h) and after 3d, it approximates to that of 0% $Ca(OH)_2$. On the other hand, the curve of high lime content, $>1.0\%$ $Ca(OH)_2$, shows a broader peak and after 3d, drops below that of 0% $Ca(OH)_2$. The time for the appearance of the main hydration peak tends to be delayed with the amount of lime.

It is suggested from these results that, in the presence of lime, the early reaction rate is greatly accelerated. In the case of low lime content, the reaction is steadily accelerated throughout the test period (5d). This behaviour is sharply contrary to that of the high lime. From the results obtained, it can be estimated that the optimum lime content for activating supersulphated slag cement is very small (around 0.3%). Similar results have been reported by Tashiro and Urushima(52).

Fig. 8 shows the effect of lime content on the amount of reacted slag. This appears to support those from the calorimetric study. Fig. 9 is the result of free lime determination. It is seen that the consumption of $Ca(OH)_2$ in the early stage is rapid especially in the case of 0.3% $Ca(OH)_2$ addition, the $Ca(OH)_2$ is almost consumed within the first 3h. After this, the concentration of free $Ca(OH)_2$ gradually increases. The trends in free lime curves are generally similar for all the lime added samples. Moreover, free lime is detectable in the unadded sample (0% $Ca(OH)_2$) after 1d and also shows a slightly increasing trend. This suggests that free lime can also be extracted from other hydrated phases in the system, as reported by Bentur

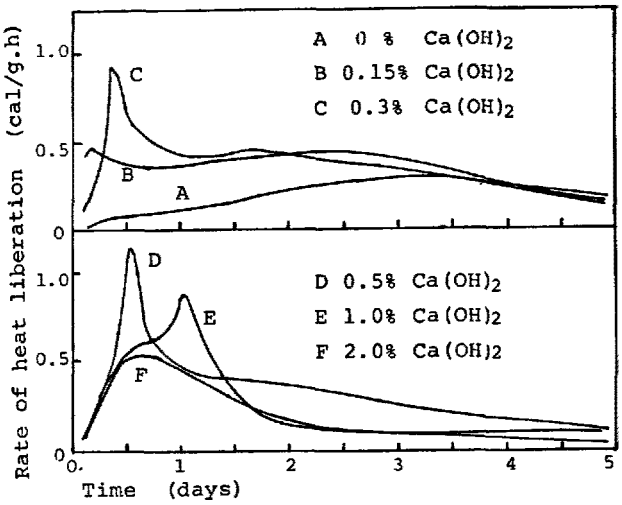

Fig. 7 - Conduction calorimetric curves of slag hydrated with 10 wt.% $CaSO_4$ and various amount of $Ca(OH)_2$ (51).

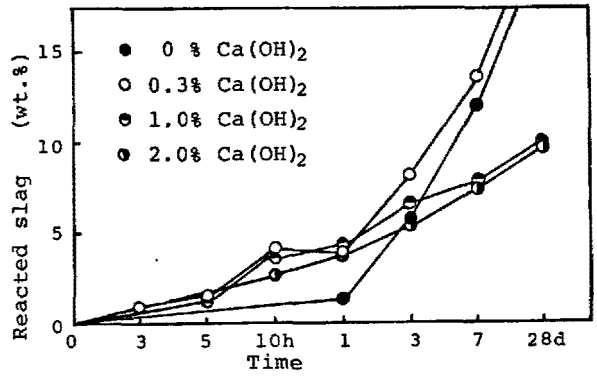

Fig. 8 - percentage of reacted slag as a function of time in slag + 10 wt.% $CaSO_4$ + various amount of $Ca(OH)_2$ (51).

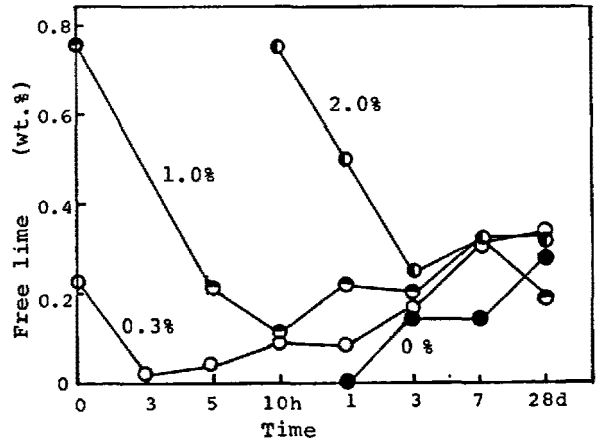

Fig. 9 - Percentage of free lime as a function of time in slag + 10 wt.% $CaSO_4$ + various amount of $Ca(OH)_2$ (51).

and Berger(53).

The above mentioned results indicate the following mechanism. In the case of no $Ca(OH)_2$ addition, it may be considered that calcium silicate hydrate (C-S-H) is formed, and thereby Al_2O_3 is liberated from the slag. $CaSO_4$ slowly reacts with the liberated Al_2O_3 to form AFt phase (54,55) and the reaction proceeds with a controlled rate throughout the process. With $Ca(OH)_2$ addtion, the reaction in the early stage, in comparison with the former, is considerably rapid as seen in Fig. 1. This may be explained by that Al_2O_3 is rapidly dissolved under high basic condition, and the AFt phase is formed by a violent and rapid reaction of $CaSO_4$ and Al_2O_3 released into the solution. As time goes by, reaction products increasingly coats the surface of unhydrated slag grains and resluts in the inhibiting hydration reaction of slag.

These discussion are coincided with the results by Tashiro and Urushima(52), Yang(56) and Midgley and Pettifer(57), they concluded that the hydration products in this system were C-S-H and ettringite, or AFt phase.

REFERENCES

1.- F. Schröder, "Blast furnace slags and slag cements", 149-207, vol. IV, proceedings of 5th International Symposium on the Chemistry of Cement, Tokyo 1968.

2.- V.I. Satarin, "Slag portland cement", (in Russian) 45-56, vol.III, Proceedings of 6th International Congress on the Chemistry of Cement, Moscow 1974.

3.- P. Ponteville, "Blast-furnace slag in France. Road uses and other uses. Present aspects of utilization", (in French) Silic. Ind., 41 193-206 (1976).

4.- M. Ponteville, "Evolution de l'emploi du laitier en France de 1973 á 1976", (in French) Silic. Ind., 42 193-208 (1977).

5.- J.J. Emery, "Slags as industrial minerals", Proceedings of 3rd Industrial Minerals In ernational Congress.

6.- R. Kondo, "Chemistry of iron and steel slags", (in Japanese) Sekko to Sekkai No. 147 (Special issue for slag) 1977, pp.13-21.

7.- A.H. Kamel, Hassanein, Abdel-Azim, "High-Slag cement mortars for brickwork and renderings", (in Russian) Appl. Chem. Biotechnol., 24 469-73 (1974).

8.- I.S. Finogenov, N.F. Drepin, G.N. Girilovich, Ya.D. Stasyuk, "Slag portland cement for reinforcing deep wells", (in Russian) Tsement, 1972, No.11, pp.15-16.

9.- E.I. Ved, E.F. Zharov, A.V. Satarin, "Expanding slag-portland cement based on wastes of kaolin processing", (in Russian) Tsement, 1976, No.10, pp.15.

10.- R. Sersale, R. Alello, C. Colella and G. Frigione, "Alternative uses of blast-furnace slag", (in French) Silic. Ind., 41 513-19 (1976)

11.- M.A. Smith, G.J. Osborne, "Slag/fly ash cements", World Cem. Technol., 8 223-33 (1977).

12.- R. Kondo and S. Ueda, "Kinetics and mechanisms of the hydration of cement", 203-255 vol.II-4, Proceeding of 5th International Symposium on the Chemistry of Cement, Tokyo 1968.

13.- R. Kondo and S. Ohsawa, "Studies on a methed to determine the amount of granulated blast furnace slag and the rate of hydration of slag in cement", 255-262, vol.IV, Proceeding of 5th International Symposium on the Chemistry of Cement, Tokyo 1968.

14.- C.T. Song, S. Jinawath, M. Daimon and R. Kondo, "Hydration of supersulphated slag cement", (in Japanese) Sekko To Sekkai, 1979, No.163, pp.2-6.

15.- S.A. Mironov, I.I. Kurbatova, S.A. Vysotskii, "Extraction method to determine the blast-furnace slag content in cements", Tsement, 1976, No.12, pp.11-12.

16.- R. Kondo, S.A. Abo-El-Enein and M. Daimon, "Kinetics and mechanisms of hydrothermal reaction of granulated blast furnace slag", Bull. Chem. Soc. Japan, 48 222-226 (1975).

17.- P. Catharin, "Quantitative determination of blastfurnace slag in cements", (in German) Zem.-Kalk-Gips, 29 71-77 (1976).

18.- I.I. Kurbatova, S.A. Vysotskii, M.A. Averbukh, "IR spectroscopic determination of slag content of cements", (in Russian) Tsement, 1978, No.7, pp.14-15.

19.- P. Fierens and P. Poswick "Kinetic study on the hydration of synthetic slags", Silicates Industriels, 42, 235-245 (1977).

20.- P. Poswick "Contribution to the study of synthetic and industrial slags", Thesis, Mons, Belgique (1979).

21.- L.E. Copeland and J.C. Hayes, "Determination of non-evaporable water in hardened portland cement paste", ASTM Bull, 194 70-74 (1953)

22.- R.Sh. Mikhail, S.A. Abo-El-Enein, N.A. Gabr, "Hardened slag-cement pastes of various porosities: I. Compressive strength, degree of hydration, and total porosity", J. Appl. Chem. Biotechnol., 24 735-43 (1974).

23.- I.A. Voinovitch, R. Dron, "Effect of various activators on the hydration of granulated slag", (in French) Silic. Ind., 41 209-12 (1976).

24.- S. Brunauer and S.A. Greenberg, "The hydration of tricalcium silicate and β-dicalcium silicate at room temperature", 135-165, Proceedings of the Fourth International Symposium on the Chemistry of cement, Washington 1960.

25.- S.A. Abo-El-Enein, M. Daimon, S. Ohsawa

and R. Kondo, "Hydration of low porosity slag-lime pastes", Cement and concrete, Res., 4 299-312 (1974).

26.- L. Forsén, "The chemistry of retarders and accelerators", 298-381, Proceedings of 2nd Intern. Symp. on Chemistry of Cement, Stockholm 1938.

27.- De Jong, "Mechanisms of the slag cements hydration", (in French) Silicate Industriels, 42 5-11 (1977).

28.- K. Minegishi and M. Daimon, "Studies on mechanisms of cement hydration by means of calorimeter", (in Japanese) Seramikkusu, 11 408-415 (1976).

29.- R. Kondo and M. Daimon, "Phase composition of hardened cement paste", (in Russian) 45-56, vol.III, Proceedings of 6th International Congress on the Chemistry of Cement, Moscow 1974.

30.- R. Kondo, "Fundamental study on the manufacture of slag cement", Dr. Thesis in Tokyo Institute of Technology (1958).

31.- C.T. Song, M. Daimon and R. Kondo, to be published.

32.- J. Kasai, M. Ichiba and M. Nakahara, "Hydration mechanism of magnesia cement", (in Japanese) Kogyo Kagaku Zashi, 63 93-96 (1960).

33.- M. Regourd, private communication.

34.- K. Akatsu, I. Ikeda, N. Shiga and K. Maeda, "Investigation on the so-called glass content of granulated blast-furnace slag", 64-66, CAJ Review of 28th General Meeting 1974, Semento Gijutsu Nemppo (in Japanese) 28, 1974.

35.- R.D. Cale, C.W. Wolhuter, P.R. Jochens and D.D. Howat, "Cementitious properties of metallugical slags", Cement and Concrete Res., 3 81-92 (1973).

36.- I. Teoreanu and M. Georgescu, "Behaviour of synthetic and industrial blast furnace slags in the presence of activators", (in Germany) Zem.-Kalk-Gips., 27 308-312 (1974).

37.- H. Miyairi and R. Takaki, "Influence of calcium halide on the early hydration of portland blast-furnace slag cement", 40-41, CAJ Review 30th General Meeting 1976, 62-69, Sement Gijutsu Nempo 30 1976.

38.- C.A. Taneja, "Role of alumina, magnesia, and manganese oxide on the hydration and hardening of slag glasses", Trans. Indian Ceram. Soc., 32 (5) 109-124 (1973).

39.- C.A. Taneja, "Role of magnesia on hydration of high alumina slag", (in Russian) 60-63 vol.III, Proceedings of 6th International Congress on the Chemistry of Cement, Moscow 1974.

40.- G. Mascolo, "Hydration products of synthetic glasses similar to blast furnace slag", Cement and Concrete Res., 3 207-213 (1973).

41.- W. Casselouri, G. Parissakis, "Stabilization of cements with a high magnesia content by additions of fly ash and slag", Silic. Ind., 42 (1) 13-17 (1977).

42.- K. Akatsu, I.Ikeda and K. Sadatsune, "Practical properties of slag cement prepared with a series of glasses of the gehlenite-åkermanite system", 57-58, CAJ Review of 32nd General Meeting, 1978, 97-99, Semento Gijutsu Nempo (in Japanese) 32, 1978.

43.- Heinz-Guenter Smolczyk, "Effect of the chemistry of the slag on the strengths of blast furnace cements", (in Germany) Zem.-Kalk-Gips, 31 (6) 294-96 (1978).

44.- Y. Totani, Y. Saito, N. Kageyama and H. Tanaka, "The hydration of blast-furnace slag cement", submitted to this symposium.

45.- R. Kondo, C.T. Song, S. Goto and M. Daimon, "The ltent property of granulated blast furnace slag by various activators", (in Japanese) Tetsu to Hagane, 65 1825-1829 (1977)

46.- M. Regourd, "Microstructure and behaviour of hydrated slag cements", submitted to this symposium.

47.- H.-G. Smolczyk, "Slag cement and alkali-active aggregates", 57-60, vol.III, Proceedings of 6th International Congress on the Chemistry of Cement, Moscow 1974.

48.- S. Nagataki and M. Tanaka, "Effect of interface reaction between blast-furnace slag and cement paste on the physical properties of concrete", submitted to this sympsium.

49.- A.A. Van Haute, "Anhydrate cement", 286-295, vol.IV, proceedings of 5th International Symposium on the Chemistry of Cement, Tokyo 1968.

50.- I. Uchida, S. Nomi and K. Minegishi, "Exiting effect of hauyne type clinker on hydration of sulfated slag cement" to be printed in CAJ Rev. 33nd Gen. Met. 1979, and Semento Gijutsu Nempo (in Japanese) 1979.

51.- R. Kondo, M. Daimon, C.T. Song and S. Jinawath, J. Amer. Cer. Soc., to be published.

52.- C. Tashiro, H. Urushima, "Compressive strength and hydrates of hardened cement paste of the system blast-furnace, slag-gypsum-slaked lime", (in Japanese) Sekko To Sekkai, 1977, No.147, pp.8-12.

53.- A. Bentur and R.L. Berger, "The Chemical Composition of C-S-H Gel Formed in the Hydration of Calcium Silicate Pastes", J. Amer. Chem. Soc., 62, 117-120 (1979).

54.- H.-G. Smolczyk, "Hydration products of cements with high contents of blast-furnace slag", Zement-Kalk Gips, 18 238-246 (1965).

55.- H.E. Schwrite and U. Ludwig, "Crystal structure and properties of cement hydration products (hydrated calcium aluminates and ferrites)", 37-78, vol.II, proceedings of 5th International sympo-

sium on the Chemistry of Cement, Tokyo 1968.

56.- J.C. Yang, "Chemistry of slag-rich cements", 296-309, vol.IV, proceedings of 5th International Symposium on the Chemistry of Cement, Tokyo 1968.

57.- H.G. Midgley and K. Pettifer, "The Microstructure of Hydrated Supersulphated Cement", Cement and Concrete Res., 1, 101-104 (1971).

SUB-THEME III - 2

Structure and behaviour of slag Portland cement hydrates

M. REGOURD
Microstructure Department
C.E.R.I.L.H.
Paris, FRANCE

1. INTRODUCTION

According to the principal report on slag Portland cement presented at the Moscow Congress in 1974, by SATARIN (1), two lines of research on cement hydration can be determined : in one case the reaction mechanisms between the slag and the water and the other the development process of the structure during the setting and hardening. The Paris Congress will continue these two themes of which the first is given to DAIMON.

This report highlights the work done on the microstructure of slag cements published since the Moscow Congress. These studies concerning the hydrate structures and their comportment was accomplished by varying a certain number of parameters such as the composition and the granularity of vitreous slag, the mode of activation (alkaline, sulfatic), the thermal treatments and the aggressive agents (sulfates, chlorides, sea water).

2. SLAG CEMENTS HYDRATION

2.1 Activated slag hydration

The thermodynamic study by DRON (2) of the quaternary system $CaO - SiO_2 - Al_2O_3 - H_2O$ has shown that the hydrated phases that coexist with the aqueous phase in slag pastes are limited to three. The system of three compatible hydrates shows on the ternary diagram lime-silica-alumina a unique mode of subdivisions in triangular domains (fig. 1) but no matter which activator is used, the hydrated calcium silicate is always present.

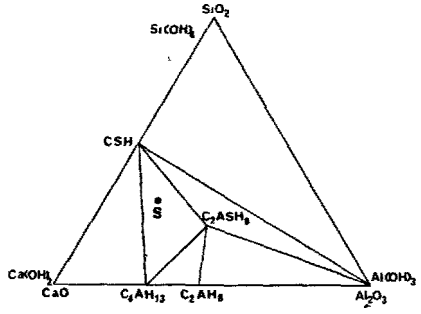

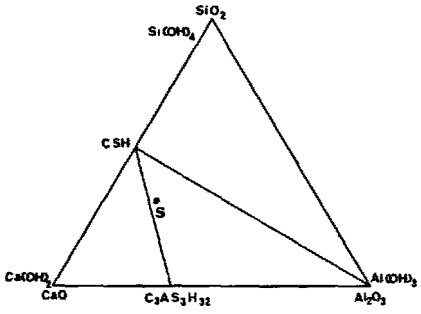

Fig. 1 - Triangulation of the ternary diagram of slag hydration in presence or not of gypsum (ref. 2).

2.1.1 Alkaline Activation

Alkaline activation can be either soda or lime activation. Activated by soda, the slag gives C-S-H, C_4AH_{13} and C_2ASH_8. The C_4AH_{13} and C_2AH_8 are hexagonal plates which play the role of crystalline bridges between the slag grains. Electronprobe microanalysis reveals that the plates of C_4AH_{13} contain silicon (3). The C-S-H covers the slag grains but by the intermediary of the solution, it is found equally on the inert supports such as a metallic (4) or a glass (fig. 2) blade on which was placed a drop of slag-soda solution suspension. TERRIER (5) has found its CaO/SiO_2 ratio to be weaker than that of the clinker C-S-H : it is around 1 according to the electronprobe microanalysis measurements by DRON et al (6).

The soda activation in the preceding examples was obtained with NaOH solutions. The soda can be replaced by sodium carbonate (7) or sodium silicate (8, 9).

In the lime activation the hydrated phases compatible with $Ca(OH)_2$ are C-S-H and C_4AH_{13}. The hydrated gehlenite C_2ASH_8 does not show itself in the presence of calcium hydroxide. In slag-lime cements with a low porosity (w/c = 0.20), ABO-El-ENEIN et al (10) found a first hydrate rich in lime $\frac{C}{S+A} = 2.5$ but at 180 days, this ratio was only 1.7.

2.1.2 Sulfate Activation

According to D'ANS and EICK (11), sulfate activation due to gypsum leads to the formation of C-S-H, ettringite $C_3A.3CaSO_4.32H_2O$ and aluminum hydroxide $Al(OH)_3$.

The sulfate activation is slow during the evolution of pastes composed of slag (90 %) + gypsum (10 %), w/c ratio = 0.5, ground between 40 and 63 µm and observed at 2, 7, 15 and 28 days. The ettringite is only detected after 15 days and X-ray diffraction lines of gypsum are still present at 28 days. At that time the slag grains are surrounded by a thick layer of C-S-H and ettringite needles (fig. 4). The adherence of the C-S-H to the smooth slag grains is not good : a part of the hydrate layer detaches from the anhydrous grain during the breaking of the sample by traction. The feeble adherence of C-S-H to the slag grain is an unfavorable factor in the case of slags coarsely ground. The same observation has been reported by SYRKIN et al (12).

Sulfate activation can be obtained with other sulfates than gypsum, for example hemihydrate, anhydrite and phosphogypsum. The sulphur present in the slag can also be an autoactivant.

2.1.3 Mixed Activation

In the presence of gypsum and lime or gypsum and soda, the alumina $Al(OH)_3$ is transformed into ettringite. The sodium is found in the form of sulfate Na_2SO_4.

The sample of slag paste containing 90 % slag + 10 % gypsum and mixed with a normal soda solution is covered with C-S-H fibers and ettringite from the second day at which time half the gypsum is already consumed. The sodium sulfate is detected on the X-ray diffraction diagram : the soda, therefore, has played an important activating role and has given a notable proportion of hydrates. According to the theoretic formulas of VOÏNOVITCH and DRON (8), the soda

activation uses five times more activant than the lime activation, but the quantity of hydrates formed is twice as great. The soda plays the simple role of a catalyzer while the lime and gypsum enter into the hydration reaction.

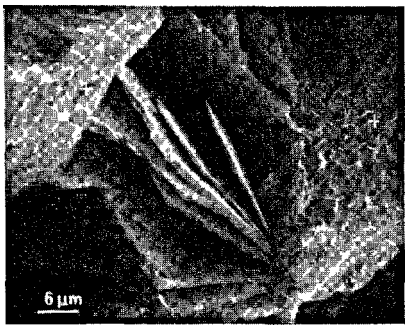

Fig. 2 - Soda activation : C_4AH_{13} (o), slag (+)

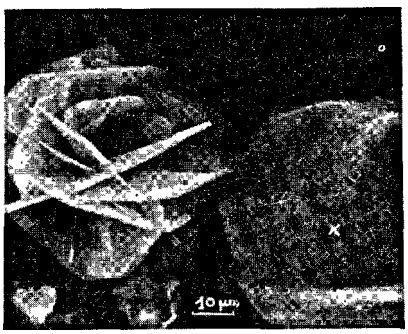

Fig. 3 - Soda activation : C_2ASH_8, C-S-H (x)

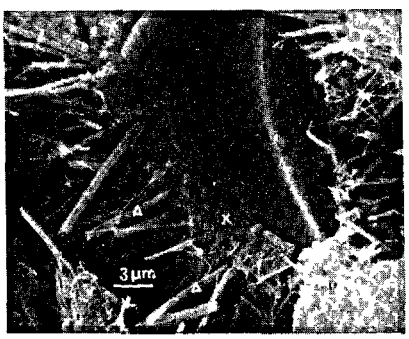

Fig. 4 - Sulfate activation : Ettringite (Δ), C-S-H (x)

2.2 Slag cements hydration

Two slag activants are present in cements : the gypsum and the lime liberated by the hydration of the clinker silicates.

In all samples of industrial slag cement, the Portland cement clinker is the first to hydrate. The C-S-H hydrated silicate due to the dissolution of the tricalcium silicate covers both the clinker and the slag grains. The portlandite $Ca(OH)_2$ is present in layers of hexagonal plates (fig. 5). The ettringite is spread out in non dense needles in the C-S-H, but rather localized around the clinker grains (fig. 6).

In the 2, 7 and 28 days study of industrial slag cement pastes, w/c ratio 0.5, the beginning of the slag hydration was only observed at 28 days. It shows on the X-ray diffraction diagrams by a lessening of the $Ca(OH)_2$ content in samples containing 20 and 50 % slag and by the disappearance of portlandite in cements with an 80 % slag content. Slag grains already covered by the clinker C-S-H are surrounded by a compact hydrated zone (fig. 7). Elementary analysis with the aid of X-ray energy dispersive analysis shows the difference in composition of Mg, Al and Si between the slag grain, its hydrate and the clinker C-S-H in a hydrated paste at six months : the slag hydrate is richer in MgO and Al_2O_3 than that of the clinker. The slag C-S-H is poorly crystallized. According to the infrared absorption spectrometry studies of BENSTED (13), the silica tetrahedra of this C-S-H are only slightly polymerized.

Along with the lime activation, there is also a sulfate activation which first of all gives ettringite. The morphology of the ettringite needles depends upon the slag content. The needles are shorter and more fixed in the samples rich in slag and in 80 % slag cement, they seem to play the role of a binder (fig. 8). At later dates, when the gypsum is completely combined, the ettringite transforms into monosulfoaluminate which forms solid solutions with tricalcium aluminate C_4AH_{13} (fig. 8).

According to DE JONG (14) and following the theory of D'ANS and EICK (11), sulfate is the principal slag activator. The alkaline reactions cause, in the beginning, the formation of acid hydrates surrounding the slag grains. These first hydrates can block the slag hydration. The sulfate ions dissolve the first hydrate and favorize the formation of a second hydrate of a rougher structure that does not oppose the penetration of water.

Hydrogarnets C_3ASH_4 have been identified by TANEJA (15), SERSALE et al (16) and DASGUPTA (17) in cements with a low magnesium content. To the contrary, in the products with a high MgO content, the hydrated aluminates C_4AH_x transform into M_4AH_x (15, 18). The hydrotalcite $Mg_6Al_2CO_3(OH)_{16}4H_2O$ has been found by KÜHKLEand LUDWIG (19) in slag cement pastes containing up to 29 % MgO. KOERTH (20) has detected the vicatite $C_3S_2H_3$: it is a transformation of the afwillite C_3SH_3. It can contain MnO, ZnO, FeS, MnS, CaS which in its crystalline lattice substitute for CaO.

HYDRATION OF A SLAG PORTLAND CEMENT

1. Hydration of Portland cement

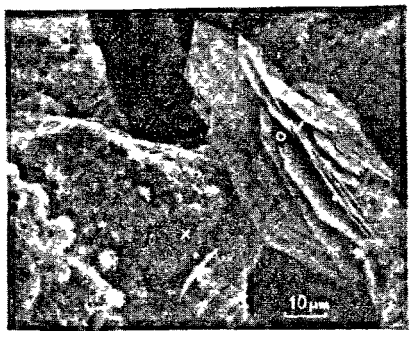

Fig. 5 : Portlandite (o), C-S-H (x)

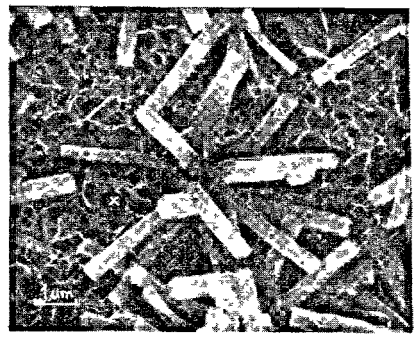

Fig. 6 : C-S-H (x), Ettringite (Δ)

2. Slag hydration

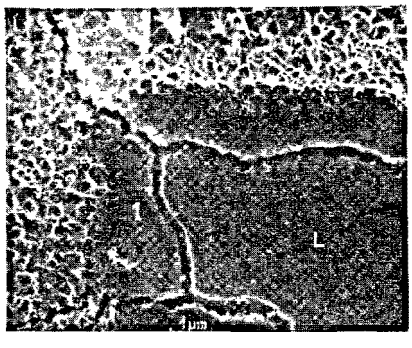

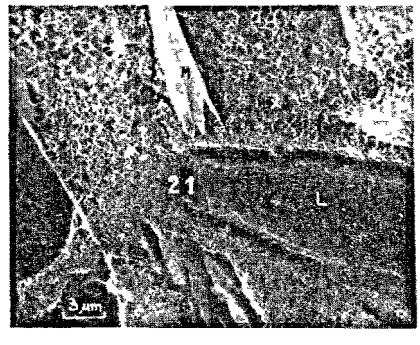

Fig. 7 : Slag grain S, monosulfoaluminate (M), C-S-H (x).

Two layers of hydrate (1, 2) surround the slag grain.

The X-ray energy dispersive analysis shows that the "pseudomorphic" slag hydrate (1) is richer in Al_2O_3 and MgO than that of clinker (2).

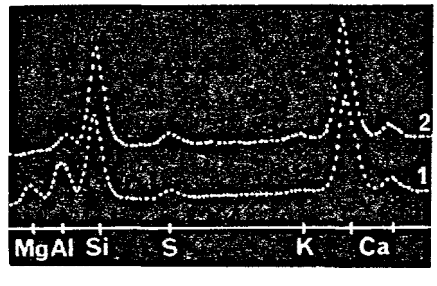

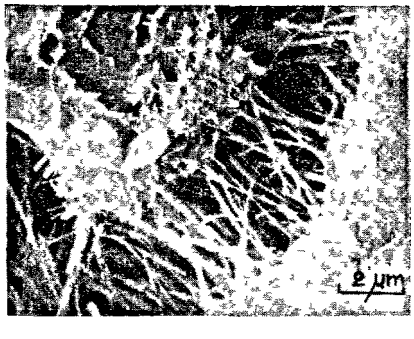

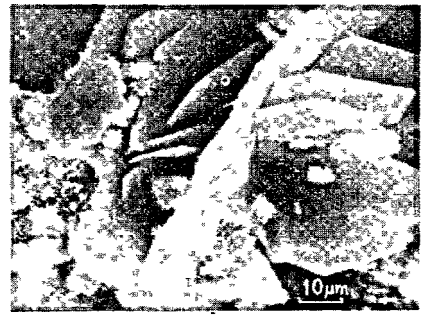

Fig. 8 : Binding ettringite (Δ) and monosulfoaluminate - C_4AH_{13} solid solution (o).

2.2.1 Influence of the glass structure

In his principal report at the Moscow Congress, SATARIN (1) discussed the relation between the hydraulic properties of slags and the structure of their glassy phase. Silica tetrahedra coexist in slag glass. These tetrahedra can present a certain degree of polymerization which, if too high, can lead to a lessening of the hydraulic activity. Aluminum ions are coordinated either tetrahedrally or octahedrally with the oxygen ions. The Al-O liaison in the tetrahedron $(AlO_4)^{5-}$ is less covalent than the liaison Si-O in the tetrahedron $(SiO_4)^{4-}$ and therefore is weaker. It is a fact that there must be an optimal rate of octahedral and tetrahedral coordination for a maximal hydraulic activity. The $Si_2O_7^{6-}$ or $SiAlO_7^{7-}$ complex seem to be a base structural unit of melilite glasses of high hydraulic activity.

The depolymerization of silica-oxide complexes has been studied by ROYAK et al (21) by electron paramagnetic resonance and infrared spectroscopy. The authors have concluded that the slag activity is in function to the degree of depolymerization of the oxide-silica complexes, the energy of the Me-O liaison of the depolymerizing cation and the coordination of this last factor which could differentiate between two slags with an identical chemical composition but with different hydraulic properties.

The highest mechanical resistances were obtained by SABATELLI et al (22) with slags which, during the devitrification study, recrystallized only in melilite. An increase in the MgO and CaO content diminishes the degree of polymerization of slags and increases the SiO_4^{4-} fraction (23) favorable to a diffusion of Mg^{2+} and Al^{3+} ions from the moment of the devitrification and the formation of melilite. In the same way, VAN LOO (24) has shown that the merwinite is unfavorable to the hydration of slag.

These ideas on the polymerization of the tetrahedra have just been precised by DRON (25, 26). The silicate glasses with an average basic oxide content, such as slags, can, like the glasses with a high oxide content studied by MASSON (27), be represented by statistical methods.

The silicate melts are formed of isolated linear elements (straight chains) or branched (internal or external ramifications) of which the numeric distribution form geometric series. It is the creative probability of the singly bonded oxygen atoms on the silicon and the other tetracoordinated structural elements (Al and Mg) which determine these structures. In the domain of average basicity, the silicon atoms at zero or four atoms of singly bonded oxygen are practically nonexistant. The Si atoms with one, two or three singly bonded oxygen atoms are distributed following a binomial law and constitute respectively the following elements :

1) Element of simple ramification Y :

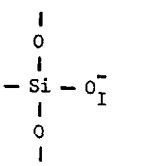

2) Chain element E :

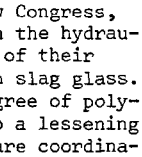

3) Element of chain ending Z :

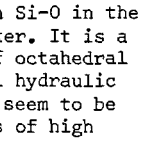

Because of its more metallic character, aluminium would essentially be surrounded by four doubly bonded oxygen atoms and would constitute an element of double ramification designated by the symbol X.

4) Chain crossing element X :

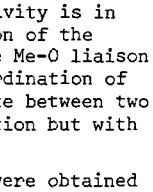

This chain crossing element carries a negative charge $(AlO_2)^-$. The aluminium atoms surrounded by four doubly bonded oxygen atoms have the same tetrahedral configuration as that of monocalcium aluminate.

The magnesium atoms are tetrahedrally coordinated to the doubly bonded oxygen atoms as in the crystalline structure of akermanite C_2MS_2. The chain crossing element X carries two negative charges $(MgO_2)^{2-}$.

To the contrary, calcium only leads to ionic bonds. It is the oxygen atom brought by the CaO which, in forming bonds of the covalent type with the structural elements in the degree of their affinity, determines the reduction in the degree of chain branching. This idea identifies with that which has been called degree of depolymerization, an expression which is not precise since the monomers of the type $(SiO_4)^{4-}$ and more surely those of $(AlO_4)^{5-}$ do not exist in the domain of granulated blast furnace slags. The octahedral coordination does not exist for Al or Mg.

The hydration of the granulated slag leads to its dissolution in the aqueous phase and to the recombination of the liberated ions in this solution conforming to the schema of LE CHATELIER. In the initial phase, that is to say before the first C-S-H precipitations, it is the most basic structural elements of glass which pass preferentially into solution such as $(SiO_{3,5})^{3-}$ or $\frac{1}{2}(Si_2O_7)^{6-}$ and $(AlO_2)^-$. This dissolution is hydrolytic and non hydroxylic. It explains the basic reaction of the slag. It is to be noted that one finds the same entities in the crystalline lattices of rankinite C_3S_2 and monocalcium aluminate CA.

Following and especially in normal reaction (dissolution-precipitation of C-S-H) the dissolution becomes approximately congruent. The C-S-H C/S ratio is inferior to that of the slag, the solution therefore becomes richer in calcium and corelatively weakens in silicon to respect the product of solubility constant.

Further, the aluminium accumulates in the solution up to the beginning of the crystallization of the aluminates which is late in occurring (28).

The microstructure study of seven blast furnace cements containing the same Portland cement but slags of a different chemical composition has shown that there is a correlation between the amount of akermanite of the recrystallized slag and the degree of hydration of the granulated slag (29). The variation of the crystalline parameters of the recrystallized melilite has given akermanite contents varying from 20 to 55 % for seven slags. A coefficient of linear relation equal to 0.98 was found between the akermanite content and the rate of slag hydration. This was determined by chemical analysis using the dissolution method of KONDO and OHSAWA (30) : the richer the slag is in C_2MS_2 the slower it is to hydrate.

Foreign ions Mn, Ti, P, in solid solution in the recrystallized melilite enlarged the X-ray diffraction reflections and thusly created substitution or addition disorders but they did not displace the angular position of the maximum of the chacteristic reflections. The amorphous phase halo of the granulated slag is proof that a certain degree of local order already exists in the liquid and it was fixed by the quench. The long distance order, to the contrary, does not exist.

The influence of the quench on the hydraulic reactivity of slags has been studied by FIERENS et al (31, 32, 33) with the aid of electron thermoluminescence, exoemission and thermogravimetry. The products used were gehlenite, synthetic slags and industrial slags (32). The thermoluminescence is well adapted to the study of synthetic products. It proves that the quench influences the superficial excited centers and allows, by the lowering of its characteristic peaks, to study the degree of advancement of the hydration. The study of the lessening of the thermoluminescence peaks of gehlenite shows that the hydration is effectuated following a nucleation reaction auto-inhibited by the hydrate which progressively covers the grains. The deep hydration is produced following a process of diffusion shown by the thermogravimetry. The same mechanism can be applied to synthetic slags : there is a relation between the kinetic coefficient of diffusion and the cooling speed estimated by thermoluminescence. The quench is very important in the case of basic slags. For industrial slags, only the photostimulated exoemission results were used : for the same industrial slag, the number of exoemitted electrons varies in function with the quench and the long term hydration occurs according to a process of diffusion. The quench also influences the texture of the hydrated product and for a same degree of progress in the hydration reaction, the mechanical resistances are in function to the cooling process. The same techniques were used in the study of aged products which hydrate slower than the fresh. The hydration mechanism remains unchanged. A three year old gehlenite is not devitrificated but the loss of a part of its hydraulic power is probably due to a progressive deactivation of the excited centers of the surface.

2.2.2 Influence of the fineness

Slag cements finely ground hydrate quicker than ordinary cements and give more compact structures (1, 12, 34). The fineness of the clinker influences the first mechanical resistance while the fineness of the slag enters into the final resistance (1). However, the simultaneous grinding of the clinker and the slag to a high degree of fineness gives a clinker very finely ground and a slag still too coarse. A separate grinding of the slag and the clinker will allow a much finer slag.

The hydration of a slag cement, Blaine specific surface equal to 5720 $cm^2.g^{-1}$ composed of 85 % slag ground to 6310 $cm^2.g^{-1}$, 13 % Portland cement clinker ground to 3500 $cm^2.g^{-1}$ and 2 % $CaSO_4$ has been followed by X-ray diffraction (fig. 9) and scanning electron microscope. The samples studied were fragments of ISO mortar samples (4 x 4 x 16 cm) having served for the measure of mechanical resistance at 2, 7 and 28 days.

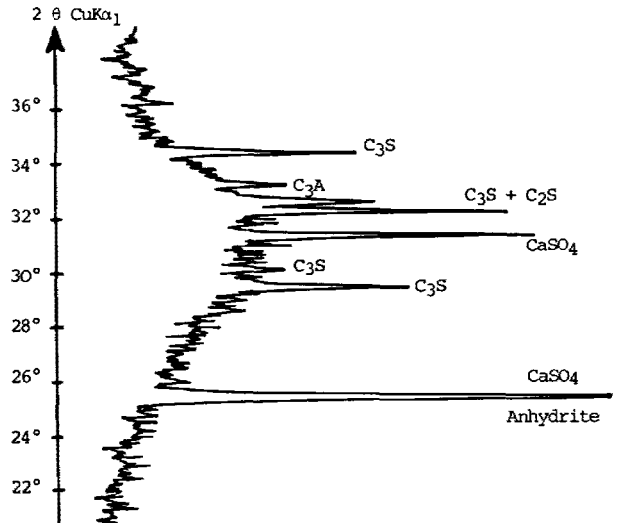

Fig. 9 : X-ray diffraction pattern of the anhydrous slag cement.

The slag cement was compared to the Portland cement that entered into its composition :

- from the second day, there is a greater quantity of ettringite in the mortar of the slag cement than in the mortar of the Portland cement (fig. 10). This ettringite was formed by the reaction of $CaSO_4$ with both the C_3A of the clinker (on the order of 1.5 % in the slag cement) and the alumina of the slag. The C-S-H comes from the simultaneous hydration of the C_3S of the clinker and the slag. The proof of the early reactivity of the slag is illustrated by the diminution by 30 % in the intensity of the amorphous phase halo. Scanning electron microscope observations reveal that a large quantity of ettringite is spread throughout the sample in contact with the slag grains and in the pores.

- at seven days, the ettringite is partially transformed into sulfoaluminate $C_3A.CaSO_4.12H_2O$ and hydrated aluminate C_4AH_{13} in Portland cement. On the slag cement X-ray diagram, one can observe the increase in the C-S-H reflections. $CaSO_4$ and all the clinker phases have disappeared. Ettringite is still abundant and microscopic examination shows it to be crystallized in fine needles.

- between 7 and 28 days, the hydrates continue to develop. The size of the slag grains that have not yet reacted with water at 28 days is between 10 and 20 µm.

The early hydration of the slag gives a compact material after short periods. In tests accelerated by

soda, the slags 6310 $cm^2.g^{-1}$ are well separated from the slags 3500 $cm^2.g^{-1}$ (Table I).

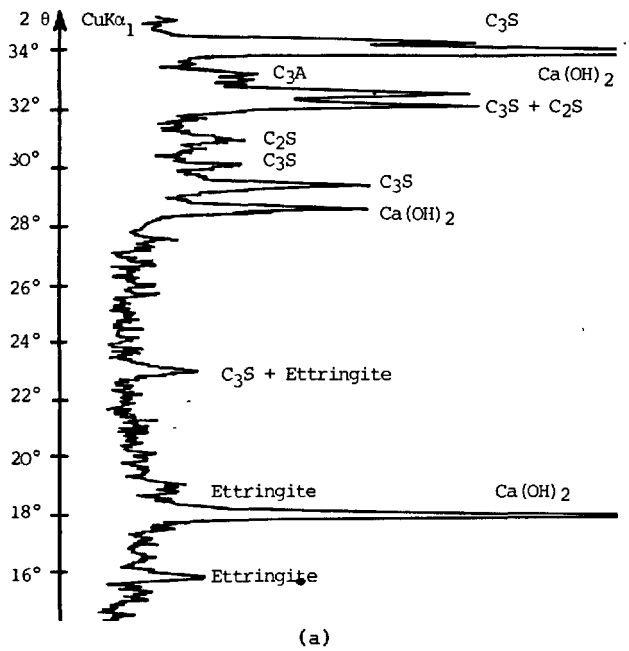

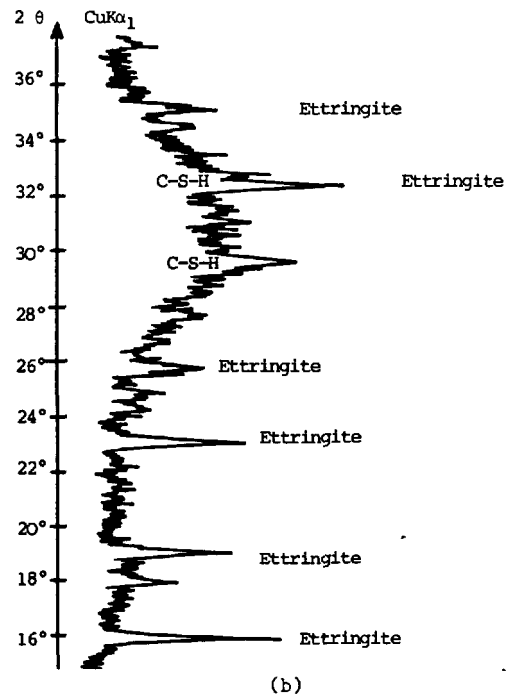

Fig. 10 : X-ray diffraction patterns of Portland cement (a) and slag cement (b) at 2 days.

Table I : Compressive resistance (R_c) and flexure resistance (R_f) for the same slag ground to two degrees of fineness. Test accelerated with soda.

Time of hydration	6310 $cm^2.g^{-1}$		3500 $cm^2.g^{-1}$	
	$R_{c\,MPa}$	$R_{f\,MPa}$	$R_{c\,MPa}$	$R_{f\,MPa}$
6 hours	23.7	5.7	8.5	2.2
24 hours	32.2	8.8	15.7	4.5

In the same conditions and for a specific surface of 3500 $cm^2.g^{-1}$, a reactive slag gives R_c = 7 to 8 MPa at 6 hours and 12.5 to 15 MPa at 24 hours.

A finely ground slag cement presents a feeble bleeding, a good plasticity, an early but relatively minor heat liberation, a slight shrinkage (fig. 11) and an increased resistance to flexure as well at 20 °C as at 5 °C (fig. 12).

The crystallization of ettringite into fine needles can explain the minor shrinkage as well as the high traction resistance. The shrinkage, generally tied to the presence of fine grains, would be compensated by the crystallization of trisulfoaluminate with 32 molecules of water. This crystallization into fibers would be more favorable to the flexure resistance (35). Such a correlation between the flexure strength and the formation of fibrous ettringite has also been reported by SUGI et al (36).

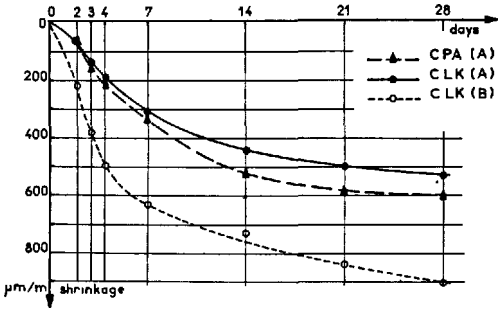

Fig. 11 : Shrinkage of slag cement (A) finely ground, compared to those of OPC and slag cement (B) ground to 3500 $cm^2.g^{-1}$.

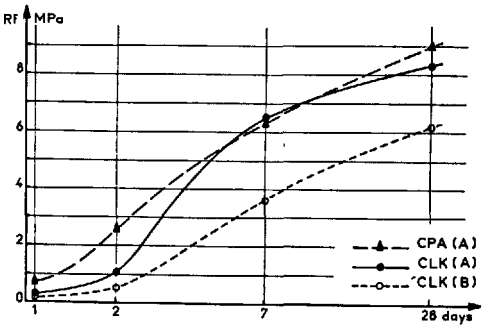

Fig. 12 : Flexure strength at 5 °C of slag cement (A) compared to those of OPC and slag cement (B).

2.2.3 Influence of thermal treatments

The temperature is at the same time a thermodynamic and a kinetic factor : it modifies the values of the free enthalpy of the hydrate formation and accelerates the hydration reaction.

(i) Thermal treatment

Hydration reactions of cements are exothermic. At a given instant, the quantity of heat liberated can characterize the overall state of the advancement of the reactions. If the dormant period is excluded, that is to say if one considers the heat liberation from the beginning of the setting process, the calorimetric isotherms at 20, 40, 60 and 80 °C are affine. The heat production, therefore, acts like a system of separated variables, temperature and time. The affinity ratios follow the ARRHENIUS law (37). The energy value of activation E of the hydration reaction of cement can be easily determined from the calorimetric curves if one keeps in mind a certain lessening which increasesin relation to temperature. The same affinity ratios have been found in the evolution of mechanical resistances of ISO mortars.

After about 4 hours at 20 °C, the calorimetric curve of a Portland cement presents an important thermal effect which characterizes the beginning of the setting and hardening process during the course of which precipitate hydrated silicates, portlandite and sulfoaluminates. The same cement hydrated at 60 °C gives an earlier and narrower signal. If we consider the heat liberation from the beginning of the set to the end of the thermal effect, we notice that to obtain the same degree of advancement α, ittakes ten times less time at 60 °C than at 20 °C and 26 times less time at 80 °C than at 20 °C. The energy activation value E determined from these three experiments is 46 kJ.mol $^{-1}$. However, it must in all cases be precised that the calorimetric curves show a lessening in the total quantity of heat liberated at 60 °C and 80 °C. This diminution is 5 % at 60 °C and 10 % at 80 °C. According to X-ray diffraction measurements, this corresponds to a lesser rate of C_3S hydration (37).

The evolution of the compressive strengths of ISO mortar samples has been followed at the same temperatures. The resistances were measured up to 45 days at 20 °C in order to encompass the major part of their growth. At 60° and 80 °C the measurements were continued up to the point where the variations became very weak from on day to another, that is to say 10 days at 60 °C and 7 days at 80 °C. A study of the evolution of these resistances shows that the maximum values obtained at 60 °C and 80 °C are less than those obtained at 20 °C. The curves corresponding to the temperatures of 60 and 80 °C cross the curve traced at the ambient temperature. However, when one represents the variations of resistance in relative values giving a value to α equal to 1 when the resistances no longer vary in a significant manner, onenotices that the curves are affine. A coefficient must be utilized to compensate for the lessening in resistance from 20 % at 80 °C. It is observed that the affinity ratios are the same as in the case of the evolution of the heat of hydration.

In the same manner, the variation curves of the heat of hydration (fig. 13) and the resistance to compression (fig. 14) at 20, 60 and 80 °C of a clinker slag cement (CLK) containing 80 % slag permit the deduction of affinity ratios which are higher than those of OPC (12 instead of 10 at 20 °C, 34 instead of 26 at 80 °C) and a greater energy of activation (50 kJ.mol^{-1} instead of 46). Therefore, thermal treatment shows itself to be favorable to slag cements.

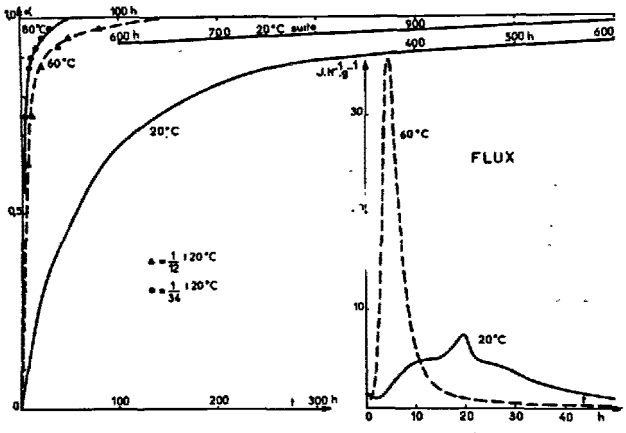

Fig. 13 : Heat liberation of a slag cement at 20 and 60 °C. The left curves, in relative coordinates, are affine.

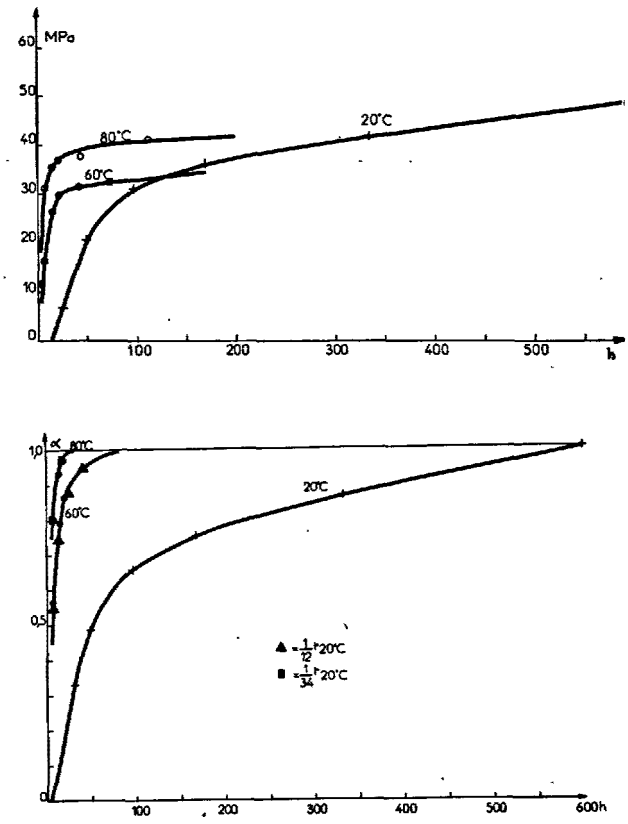

Fig. 14 : Compressive strengths of a slag cement at 20, 60, 80 °C. The bottom curves, in relative coordinates, are affine.

However, all granulated slags do not react in the same manner during a thermal treatment. Three slags, A, B, C, were used in the composition of three blast furnace cements CHF (70 % slag) beginning with a Portland cement containing 62 % C_3S and 12 % C_3A. The table II of the resistances obtained after a treatment at 80 °C compared to resistances measured at 28 days at 20 °C show a prolonged thermal treatment is not favorable to cement A.

Table II : Compressive strengths of ISO mortars thermally treated.

CHF cement 70 % slag	ISO mortar compressive strengths (MPa)		
	28 days at 20 °C	7 h at 80 °C	14 h at 80 °C
A	54	21	22
B	46	26	30
C	39	22	27

If,after the treatment 7 h at 80 °C, the three cements are placed in water at 20 °C for 28 days, the resistance will be :

- Cement A : 27 MPa
- Cement B : 37 MPa
- Cement C : 36 MPa

Cement A only reaches half its resistance at 20 °C. X-ray diffraction analysis of the mortar samples show that there is a large quantity of monosulfoaluminates. Microscopic examination shows these monosulfoaluminates to be compactly grouped in the form of hexagonal plates (fig. 15). A very dense layer of C-S-H surrounds the slag grains and covers the grains of sand with a thick layer which ends up as foils (fig. 16). The rather brutal hydration of this cement over short periods at 80 °C, only progresses feebly after the thermal treatment is discontinued. To the contrary, with the two other cements, the hydration continues up till 28 days. The essential difference between the three slags concern their chemical composition and especially their content in alumina (Table III). The slag C-S-H contains less lime than the anhydrous grain. The differences in the chemical composition between the slag and its hydrate are more important for alumina and magnesia. With the same thermal treatment the C/S ratio of the Portland cement C-S-H is 1.4 at 20 °C and 1.7 at 80 °C.

The favorable role of thermal treatment on the setting and hardening of slag cements was equally noticed by KUREPA et al (38) : 70 % of the final projected resistance were reached after 12 hours of thermal treatment at 40 °C. According to MIRONOV (39), in 20 % slag cements a short treatment at 95 °C diminishes the difference in the resistance between Portland cement and slag cement. However, some precautions are always necessary concerning the composition of slag cement and the gypsum content. HATO et al (40) have thermally treated concretes prepared with cements containing 0 to 60 % slag for either 1 hour at 65 °C or 3 hours at 80 °C. If the gypsum is not consumed during the course of the thermal treatment, the ettringite formation which takes place at the end of the treatment results in unstable concretes.

Fig. 15 : Monosulfoaluminate in a slag cement after 7 hours at 80 °C.

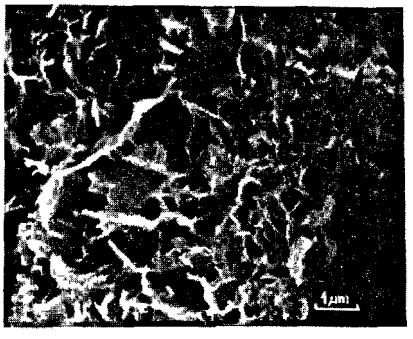

Fig. 16 : C-S-H in a slag cement mortar after 7 hours at 80 °C.

Table III : The C/S, C/A, C/M ratios values in the anhydrous slag grain and in the C-S-H of the three blast furnace cements (70 % of slag) surrounding the slag grain.

Slag		CaO/SiO_2	CaO/Al_2O_3	CaO/MgO
Anhydrous	A	1.4	5.6	6.9
	B	1.4	6.4	3.7
	C	1.3	6.6	3.8
20 °C (28 days)	A	1.0	4.6	3.2
	B	0.9	4.8	1.9
	C	1.3	4.8	1.4
80 °C (6 days)	A	1.0	5.4	3.5
	B	1.3	5.0	1.4
	C	1.1	4.4	1.5

(ii) Autoclavage

Autoclavage associates the elevation of the temperature to pressure. The work done since the Moscow Symposium concerns synthetic slag and industrial products.

With the aid of infrared absorption spectrometry, conductimetry , X-ray diffraction and differential thermal analysis, GOVOROV (41) has identified four types of synthetic glasses giving different hydrates in the case of finely ground slag pastes treated 2 days at 150, 200 and 250 °C in an atmosphere of saturated water vapor. The highest mechanical resistances were measured on samples with a composition approaching that of wollastonite or anorthite. The structure contain a limited number of silica tetrahedra and form during hydration essentially tobermorite or gyrolite. Higher alumina contents tend to reduce the resistance of slag pastes in particular for treatments at 150 to 200 °C, with the exception of glasses containing isolated silica tetrahedra which favorize the development of hydrogarnets. Xonotlite was found by BASH (42) in slag + loess mixes autoclaved above 250 °C. Its formation leads to an increase in mechanical resistances. The lessening of resistances observed at temperature superior to 200 °C can be tied to the presence of C_2SH and to a too violent crystal growth of the hydrates.

In a 95 % slag mix (ground to less than 100 µm) and 5 % gypsum, compacted to 200 MPa and autoclaved at 180 °C, MASSIDDA and SANNA (43) have tied the increase in the resistance to compression to the fact that the material is less porous. Plazolite was identified by X-ray diffraction, the crystals filled the spaces between the slag grains. In slag pastes + activator (lime, sodium carbonate) studied by SERSALE et al (7, 16), the hydrates formed in the course of a steam treatment at 205 °C are amorphous or slightly crystallized silicates and hydrogarnets. The resistances are tied to the microstructure of the materials : at 20 °C there are many spaces in the paste which are filled after autoclavage. Sodium carbonate is proven more efficient than calcium hydroxide. It gives a more compact material from which the possibility to produce molded products (100 MPa) and the hydrothermal treatment of slag. Molding pressure and fineness of the grind favorably influence the mechanical comportment of slag mixes + $Ca(OH)_2$, but high temperaturesare not always favorable to mechanical resistances.

According to a study by KONDO et al (44), the initial stage of the hydrothermal reaction in the system slag + lime + water corresponds to the formation of C-S-H with a low lime content. The ulterior formation of crystallized C-S-H and hydrogarnet diminish the mechanical resistances. In the system slag + lime + quartz + water, a C-S-H rich in lime is the first to form, but after the free lime is completely consumed, this C-S-H weakens in calcium. The slag is very reactive but it inhibits the reactivity of the quartz especially in the initial phase of the reaction.

Tobermorite at 11 Å was identified by X-ray diffraction in cements with a high slag content that were treated for 5 hours with saturated water vapour at 1.3 MPa. KAMEL (45,46) found hillebrandite, tobermorite and xonotlite in samples only containing slag that were treated in the same manner as slag cements.

ABO-El-ENEIM et al (47, 48, 49) have reported the following from their systematic study of autoclaved mixes slag + lime, slag + lime + sand, slag + clinker + sand. The hydrated phases obtained in the different mixes are :

- Slag + lime : C-S-H + hydrogarnets C_3ASH_4
- Slag + lime + sand optimum composition : first, the tobermorite poorly crystallized, then the tobermorite at 11 Å crystallized in plates. The acceleration of the slag hydration inhibits the reactivity of the quartz.
- Slag + clinker : C-S-H + C_3ASH_4 + $Ca(OH)_2$
- Slag + clinker + sand : semi-crystallized tobermorite, then tobermorite at 11 Å (fig. 17).

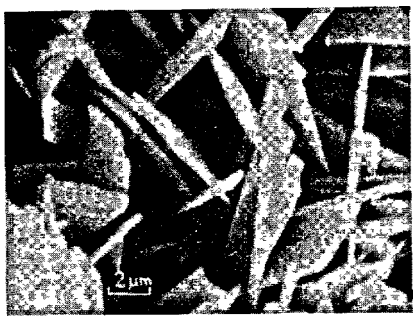

Fig. 17 : Tobermorite in an autoclaved mortar (ref.47)

The resistance of autoclaved slag + clinker + sand paste samples could be linked to the pore structure and their distribution in relation to the microstructure of the hydrates formed. Mesopores with a hydraulic radius (surface of the water molecule = 11.4 Å2) between 18 and 23 Å of lamellar structure (36 - 46 Å) have more effect on the resistance to compression than micropores with a hydraulic radius between 3 and 4 Å or lamellar structure (7 Å). The number of mesopores diminishes up to the sixth hour of treatment (10 atmospheres saturated vapor pressure) and correspond to an increase in R_c. After 6 hours the number of mesopores increases to a maximum at 12 hours and simultaneously, the resistance diminishes.

MIYAIRI and MYOJIN (50) confirmed the previous results : the compressive strength is maximal after 6 hours of autoclavage at 180 °C in the case of Portland cements containing 60 % slag. The optimum alumina content of the cement must not be greater than 9 %.

According to NAKAHARA et al (51), a water vapour treatment at 75 °C is favorable to slag cements with a high gypsum content (10 % OPC, 65 % slag, 25 % gypsum) but an autoclavage at 90 °C causes an expansion and a cracking for mixes containing less than 50 % slag and more than 20 % gypsum.

The good resistance of autoclaved cements containing 8.5 % MgO from blast furnace slags has been tied by NIKIFOROV et al (52) to the very fine periclase crystallization. MASCOLO et al (18) have shown the crystallization of M_4AH_n which causes no expansion during autoclavage and the formation of $5MgO.Al_2O_3.SiO_2$.

This review of the work on hydration of slag cements has revealed that these products give the same hydrates as Portland cement. They are slow to react with water but they can be activated chemically (alkaline or sulfate activation), mechanically (over grinding) and thermally. Slag cements to the contrary are

well known for their resistance toaggressive chemical agents.

3. BEHAVIOUR OF SLAG CEMENTS

All long term tests have shown the good performance of slag cements in aggressive environments such as sulfate water, sea water and pure water.

3.1 Resistance to sulfate water

The attack on cements by sulfates like $MgSO_4$ is double. The magnesium takes the place of the calcium of the cement hydrates such as $Ca(OH)_2$ and C-S-H and gives respectively $Mg(OH)_2$ and M-S-H without binding properties. The SO_4^{2-} ions react with the Ca^{2+} ions displaced by the Mg^{2+} ions and form a secondary gypsum $CaSO_4.2H_2O$ which reacts itself with the aluminates giving birth to an expansive ettringite.

This series of reactions can be observed in samples of synthetic mixes containing 50 % C_3S + 15 % C_3A + 5 % gypsum + 30 % quartz immersed in a solution of 5 % $MgSO_4$. From the first day, the samples showed a large swelling, they were destroyed at the end of 7 days. The hydrates formed, detected by X-ray diffraction and scanning electron microscope were $Mg(OH)_2$, $CaSO_4.2H_2O$ (high quantity of gypsum, much superior to the 5 % in the anhydrous mix), $C_3A.3CaSO_4.32H_2O$(secondary ettringite) and C-M-S-H (fig. 18).

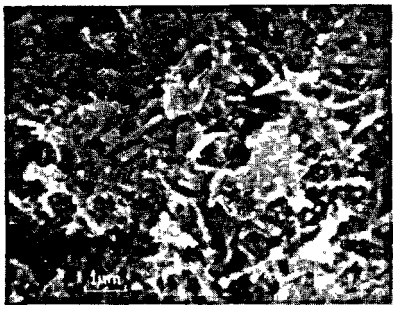

Fig. 18 : Secondary gypsum and cracked C-M-S-H

In a second series of samples, the 30 % quartz was replaced by 30 % granulated blast furnace slag. After seven days of immersion in sulfate water, the samples were still in good condition. The hydrates observed were a dense C-S-H (fig. 19), crystals of $Ca(OH)_2$ and monosulfoaluminate and some dispersed needles of ettringite of which the size was only about µm (fig. 20). The hydrated slag grain are surrounded by a layer of C-S-H. It is partially a lime activation : the quantity of $Ca(OH)_2$ is less after 7 days than after 1 day according to the X-ray diffraction diagram on which is detected neither $Mg(OH)_2$ or secondary $CaSO_4.2H_2O$. Here, the denseness of the material and the low lime content are both favorable to the sample resistance to sulfate attack.

According to SMOLCZYK (53), the good chemical resistance of 65 % slag cements remains even if the concrete is in contact with sulfate water after its preparation. KODAMA and KITAMURA (54) have also shown the good resistance of cements containing 60 % slag ground to a Blaine specific surface of 4000 $cm^2.g^{-1}$. A finer than normal slag granulatiry, on the order of 5000 $cm^2.g^{-1}$, however, increases its chemical resistance in decreasing its porosity (55).

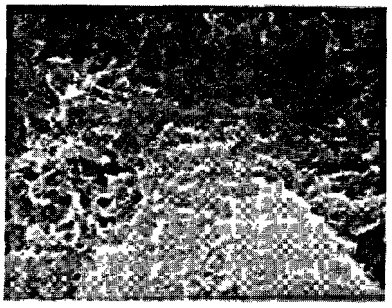

Fig. 19 : Dense C-S-H in presence of slag.

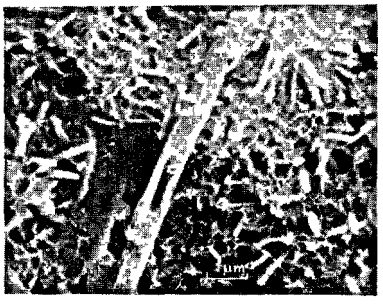

Fig. 20 : $Ca(OH)_2$ (o) and finely crystallized ettringite (x) in presence of slag.

3.2 Resistance to chloride waters

Mortar samples of slag and Portland cements were immersed in different solutions of $MgCl_2$ by KOBAYASHI and OKABAYASHI (56). The penetration of the Cl^- ion in successive layers has been estimated by chemical analysis at :

- 20 mm after 4 weeks for OPC,
- 10 mm after 52 weeks for the cement containing 65 % slag,

both having been immersed in a solution containing 25 g of $MgCl_2$ per liter.

Chloroaluminates $C_3A.CaCl_2.10H_2O$ have been characterized by X-ray diffraction. VIRODOV et al (57) have detected hydrotalcite $Mg_6Al_2(OH)_6.CO_3.4H_2O$ in the presence of $MgCl_2$.

3.3 Resistance to sea water

When a Portland cement, totally immersed in sea water, shows a large swelling, it would be the same for slag cements containing less than 60 % slag. This result was obtained on ISO mortar samples (4 x 4 x 16 cm) conserved in the same conditions for one year (58).

OPC	1000 µm/m
OPC + 50 % slag	750
OPC + 30 % slag	690
CLK (80 % slag)	190

Table IV : Evolution, in function of percentage of slag, of the compressive resistances of 4 x 4 x 16 cm mortar samples immersed in sea water, compared to the compressive resistances of the same samples immersed in fresh water (59).

$$\frac{R_c \text{ compression 6 months fresh water}}{R_c \text{ compression sea water}} \text{ in \%}$$

Portland cements			Slag Cement type A S < 30 %			Slag Cement type B 30 % < S < 60 %			Slag Cement type C S > 60 %		
6 months	1 year	3 years	6 months	1 year	3 years	6 months	1 year	3 years	6 months	1 year	3 years
* 73	57	x	66	51	33	68	86	118	99	124	191
** 64	33	x	59	41	x	63	63	52	95	140	193
*** 58	24	x	53	25	x	68	63	x	108	133	160

x : destruction of the sample, S : slag.

Potential composition of Portland cement (% in weight)

	C_3S	C_2S	C_3A	C_4AF
*	46	32	6	16
**	55	22	10	13
***	60	17	10	13

Further, the compressive resistance of samples of the same type compared by MIYAIRI et al (59) to their resistance at six months in fresh water (Table IV) showed that for a non marine cement, only the addition of more than 60 % slag will give an increase to resistance over a period of time.

The aggressive sea water salts are magnesium sulfate and magnesium chloride. The secondary products are therefore $Mg(OH)_2$, M-S-H, $CaSO_4.2H_2O$ and $C_3A.3CaSO_4.32H_2O$ (60).

In sea water as in fresh water, the clinker hydrates first in slag cements. The chlorine and the sulfur coming from the dissociation of the chlorides and the sulfates dissolved in sea water diffuse in the sample forming chloroaluminates and sulfoaluminates.

The figure 21(a) shows the polished section of a pure paste slag cement sample examined by electronprobe microanalysis after three years of immersion in fresh water. A comparison with the same sample immersed three years in sea water [fig. 21(b)] reveals that the material is just as compact in the two cases and that in sea water there was neither the dissolution of CaO nor a diffusion of Mg^{2+} ions. To the contrary, in the Portland cement which enters into the composition of the clinker slag cement (CLK), the Mg^{2+} ions were able to progress and formed M-S-H around the clinker grains [fig. 21(c)].

The penetration of chlorine into the samples leads to the formation of chloroaluminate [fig. 21(b)] However, it is limited in slag cement if compared to that of Portland cement [fig. 21(c)]. The reticulated C-S-H containing Cl^- ions in their crystalline network were not observed in slag cements. Ettringite is finely crystallized and more disseminated in the clinker slag cement (CLK) than in the Portland cement where it is more localized around the C_3A crystals where the alumina saturation is the strongest. Figure 21(c) also shows two zones superimposed around a grain of C_3A, the interior zone is composed of chloroaluminate and is the first to form, the exterior is composed of ettringite. Chloroaluminates are not stable in sea water. In decomposing, they permit a new crystallization of ettringite. Trisulfoaluminate can also be obtained at later dates by a delayed hydration of C_3A crystals which are in the large clinker grains ; this leads to a cracking of the C-S-H.

In clinker slag cement (CLK), all the alumina of the slag grains does not combine with the chlorides and the sulfates, it also enters into a solid solution in the C-S-H which remains compact (60).

The kinetics and the mode of crystallization of ettringite are different from those of Portland cement. Trisulfoaluminate appears by a relatively slow process of the passage into solution, its distribution is diffused (61). Its content is less because of the low percentage of $Ca(OH)_2$ which could give rise to a secondary gypsum.

Fully immersed, the samples are covered by a white film composed of brucite $Mg(OH)_2$ and $CaCO_3$ in the form of a calcite and aragonite mixture. MARCHESE and SERSALE (62) found more aragonite than calcite in Portland cements. To the contrary, in blast furnace cements, the calcite content is greater than the aragonite. The vaterite $\mu CaCO_3$, which could come from the carbonation of the hydrated silicates in fresh water (63) is not observed in sea water.

In alternate immersion, the attack is both physical and chemical. The degradation of certain blast furnace (CHF) and clinker slag (CLK) cements that had insufficiently resisted to the conjugated action of sea water, waves, sand, wind, sun and freezing has been tied to the slow hydration speed of the slag grains. In this sense, T. IDEMITSU et al (64) have shown that the comportment of slag cements is very sensible to the initial conditions of conservation. Certain precautions are therefore necessary in a marine environment : surface protection, a longer hydration period than that for Portland cements before immersion in sea water, dense concretes or mortars with a heavy cement content (65). After having tested

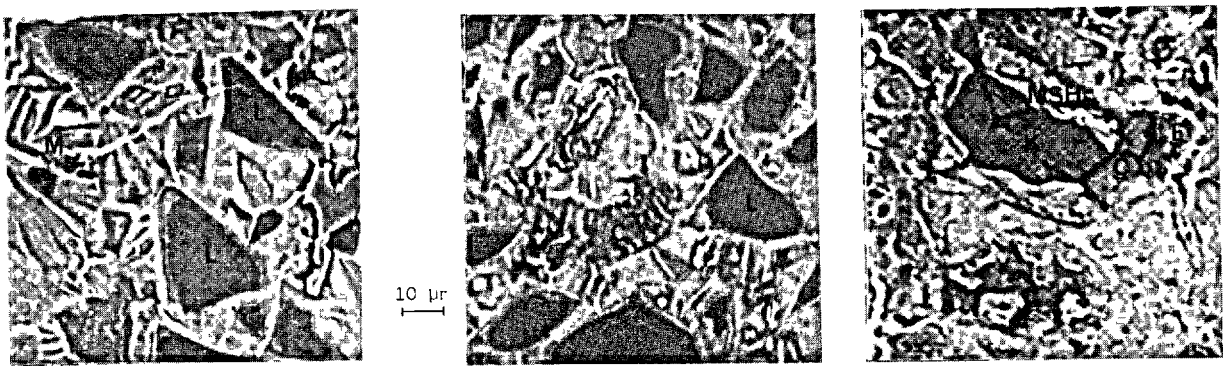

Absorbed Electrons : S = slag, M = monosulfoaluminate, C = chloroaluminate, E = ettringite, K = clinker.

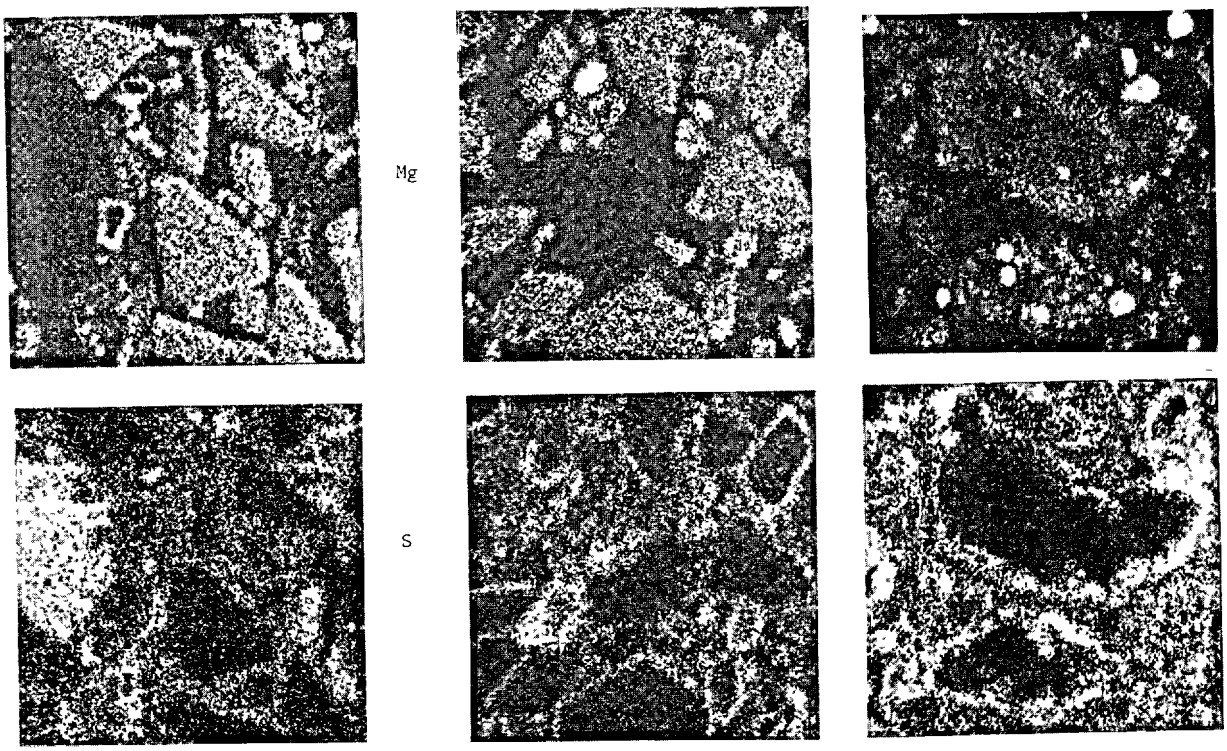

(a)
Fresh water : Slag Cement

(b)
Sea water:Slag Cement (b)

(c)
OPC (c)

Fig. 21 : Electron Probe Microanalysis. Elemental distribution of Mg, S, Cl in a slag cement (80 % slag) after three years immersion in fresh water (a) and sea water (b) compared to that of OPC immersed under the same conditions.

different types of cement for seven years, l'Electricité de France selected a blast furnace cement (CHF) for the construction of the Rance tidal power station started up in 1966. The total surface exposed to sea water is 90,000 m^2. This work of civil engineering remains in excellent condition. Slag cements are also used in the form of injection grouts in marine environment (66).

3.4 Resistance to carbonation

The carbonation of slag cements which, in the case of reinforced concretes, leads to the depassivation of the steel reinforcing, is no greater than that of Portland cement if the concrete is compact and conserved in an atmosphere sufficiently humid (53). The results of SMOLCZYK (53) are confirmed by YODA et al (67), after seven years conservation in an atmosphere of 100 % relative humidity, the carbonation is zero in cylindrical samples 15 x 30 cm.

In carbonated cements, the steel rusts at the same speed in a slag cement containing sulfur and a cement without sulfur (53). Electrochemical measurements (pH, conductance, redox potential, corrosion potential, potentiometric curves) taken by LONGUET (68) on the aqueous interstitial phase of concretes have proven that the clinker slag cements (CLK) containing more than 80 % slag protect the steel reinforcing as well as Portland cements.

Slag cements have a good resistance to thermal carbonated waters. The CO_2 dissolved in the water can only penetrate very slowly because of the compactness of the material (69).

Short term carbonation does not sensibly modify the crystalline texture of the hydrates according to MURAT and NEGRO (70), the reaction with CO_2 would be a true pseudomorphosis. Carboaluminates were observed by FRIGIONE and SERSALE (71). Their quantity is in function to the gypsum content of the cement. In the case of a high gypsum content (> 4 %), the carboaluminates give way to ettringite.

3.5 Comportment at low temperatures

Slag cement is not as favorable as Portland cement in countries with long and rigourous winters because it hydrates slower at temperatures lower than 20 °C (72). However, it is possible to increase its resistance to freezing and its mechanical performance by accelerating its hydration with chemical activators such as sulfoaluminosilicate (73).

Portland cement accelerators admixtures are not always as good with slag cements : $CaCl_2$ is fixed in a greater quantity by the slag (74) but it increases the porosity (more "open structure")of the cement paste (75). The accelerating effect of $CaCl_2$ decreases from tricalcium silicate to dicalcium silicate (principal constituants of Portland cement) to rankinite C_3S_2 and to wollastonite CS, silicates with a composition close to that of the slags (76).

The addition of air entrainers equally increases the porosity and diminishes the rate of hydration of the cement (77).

3.6 Resistance to the alkali-aggregate reaction

In concretes containing reactive siliceous aggregates, slag cements are preferable to Portland cements which are rich in alkalines. Tests conducted by SMOLCZYK (78) on 30 different types of cement mixed with ground Pyrex glass show that the expansion due to the alkali-silica reaction decreases in function to the slag content. An addition of 70 % slag to a Portland cement can move the admitted limit of Na_2O from 0.6 % to 2 % without risk of degradation to the concrete.

4. CONCLUSION. FUTURE RESEARCH

The hydrates of slag cements are the same as those of Portland cements : C-S-H, $C_3A.3CaSO_4.31H_2O$, $C_3A.CaSO_4.12H_2O$, C_4AH_{13}. The granulated slag reacts slower than the constituents of Portland cement but it can be activated. The activation can be chemical, mechanical (overground) or thermal. Whichever form of activation is used, hydrosilicate C-S-H is always present. It is not as well crystallized but denser than the fibrous C-S-H of Portland cement. The ettringite is present in fine binding needles more disseminated in the paste than the ettringite of Portland cement localized close to the C_3A crystals. The alumina of the slag grains is also found in the C-S-H in solid solution.

In the hydration of slag cements, the alumina plays a role which has not yet been completely elucidated and which has already been signaled by SCHRÖDER (79) at the Tokyo Symposium in 1968. In certain cases, the increase in mechanical resistance from one slag to another has been tied to a higher alumina content. In other cases, alumina shows itself to be unfavorable to the development of these same resistances at the ambient temperature as well as during thermal treatment or autoclavage.

Two vitreous slags of identical chemical composition can present different hydraulic properties which leads to the difficulty of using one or the other of the hydraulicity modules proposed in the last few years (80). The difference in reactivity seems to be tied to the structure of the glass. Current studies on the polymerization of silica, alumina and magnesia tetrahedra by bridging oxygen atoms will permit a better understanding of the mechanism of slag hydration.

Cements with a high slag amount contain little or no $Ca(OH)_2$, their C-S-H is compact and contains alumina in solid solution. These cements offer a strong resistance to chemical attack.

The medium and long term performance of slag cements are equal or greater to those of Portland cement and their short term performance can be improved.

The utilization of blast furnace slags, by-products of the metallurgical industry, enters in the framework of the savings energy and will be necessary developed in the near future. Europe and Japan have already acquired a large experience in their use.

Current studies involving other by-products are : slags from the steel industry or LD converted slags (81, 82, 83, 84), copper slags (85,86), electrothermophosphorous glasses (87), slags containing foreign elements such as Ti (88), Mn (89) and Ba (90). Certain of them, much less hydraulic than blast furnace slags, call for a greater activation the conditions of which are yet to be defined.

Acknowledgements

The author would like to thank the members of the Microstructure Department of C.E.R.I.L.H. who were of great assistance in the preparation of this report and especially J. VOLANT who took charge of the bibliographic review.

I am equally very greatful to Prof. Dr. R. Sh. MIKHAIL for having provided the scanning electron microscope photos of autoclaved mortars and to Dr. R. DRON for having transmitted the results of his study on the structure and hydration of slag glasses before its publication.

5. REFERENCES

1.- V.I. SATARIN (1974) : "Slag Portland Cement", VIth Internat. Congress Chem. Cement, Moscow, 23-27 Sept., principal paper.

2.- R. DRON (1974) : "Experimental and theoretical study of the $CaO-Al_2O_3-SiO_2-H_2O$ system", VIth Internat. Congress Chem. Cement, Moscow, 23-27 Sept., suppl. paper, sect. II.

3.- M. REGOURD, H. HORNAIN et B. MORTUREUX (1976) : "Microstructure des ciments de laitier", Rev. Matér. Constr., 699, 83-6.

4.- R. DRON (1973) : "Mécanisme de la prise du laitier granulé sous activation alcaline", Thèse de docteur-ingénieur, Université de Paris VI, 12 novembre. Rapport de Recherche L.C.P.C., n° 38 (sept. 1974).

5.- P. TERRIER (1973) : "Recherche sur l'hydraulicité des laitiers granulés de haut fourneau", CILAM-Inform., n° 8, 9 et 10, 1er, 2ème et 3ème trim.

6.- R. DRON, H. HORNAIN et P. PETIT (1975) : "Localisation du silicate de calcium hydraté dans les pâtes de laitier granulé". C.R. Acad. Sc. Paris, 280, série C, 187-8.

7.- G. FRIGIONE, R. AIELLO, R. SERSALE and C. COLELLA (1977) : "Manufacts obtained by compaction and hydrothermal treatment of powdered blastfurnace slags", Sil. Industr. 42, 4-5, 219-22.

8.- I.A. VOINOVITCH et R. DRON (1976) : "Action des différents activants sur l'hydratation du laitier granulé", Sil. Industr., 41, 4-5, 209-12; Bull. Liaison Lab. Ponts Chauss., 83, 55-8.

9.- I. TEOREANU and A. PURI (1975) : "Exciting blastfurnace slag with sodium silicate", Silikattechnik, 26, 6, 209-10.

10.- S.A. ABO-EL-ENEIN, M. DAIMON, S. OHSAWA and R. KONDO (1974) : "Hydration of low porosity slag-lime pastes", Cement Concr. Res., 4, 2, 299-312.

11.- J. D'ANS and H. EICK (1953) : "The system $CaO-Al_2O_3-CaSO_4-H_2O$ at 20 °C". Zement-Kalk-Gips, 6, 9, 302-11.

12.- Ja. M. SYRKIN, I.A. SIBIRJAKOVA and L.P. SHATOKHINA (1974) : "The significance of grain size distribution in cement strength formation", VIth Internat. Congress Chem. Cement, Moscow, 23-27 Sept., suppl. paper, sect. III.

13.- J. BENSTED (1976) : "Examination of the hydration of slag and pozzolanic cements by infrared spectroscopy", Il Cemento, 73, 4, 209-14.

14.- J.G.M. DE JONG (1977) : "Le mécanisme de réaction de l'hydratation des ciments métallurgiques", Sil Industr., 42, 1, 5-11.

15.- C.A. TANEJA (1974) : "Role of magnesia on hydration of high alumina slags", VIth Internat. Congress Chem. Cement, Moscow, 23-27 Sept., suppl. paper, sect. III.

16.- R. SERSALE, R. AIELLO, C. COLELLA et G. FRIGIONE (1976) : "Utilisations alternatives des laitiers de haut fourneau", Sil. Industr., 41, 12, 513-9.

17.- A. DASGUPTA (1975) : "Nature of the hydrated phases formed during hydration of slag glasses as revealed by thermogravimetry", Indian J. Technol., 13, 8, 355-8.

18.- G. MASCOLO, A. NASTRO and V. SABATELLI (1977) : "Study of the hydration and hydraulic behaviour of vitreous blastfurnace slags in relation to the MgO content", Il Cemento, 74, 2, 45-52.

19.- K. KÜHKLE and U. LUDWIG (1972) :."On the use of foundry sands high in MgO in blastfurnace cements" Sprechsaal für Keramik Glas Email Silikate, 105, 10, 421-32.

20.- W. KOERTH (1976) : "Volume stoichiometry of the formation of hydrated cement - a contribution to developing a practicable theory of hardening", Silikattechnik, 27, 7, 244-6.

21.- S.M. ROJAK, Ja. Sh. SHKOLNIK and W.W. ORLOW (1975) : "Crystallochemical structure and hydraulic properties of blastfurnace slags", Cement Wapno Gips 12, 355-9.

22.- V. SABATELLI, A. NASTRO and G. MASCOLO (1975) : "On the relation between the devitrification behaviour and the hydraulic activity of synthetic blastfurnace slags", Rend. Accad. Sci. Fis. Mat., Napoli, 42, série IV, 229-37.

23.- G. MASCOLO, A. BURI, A. MAROTTA and V. SABATELLI (1976) : "Devitrification behaviour of industrial and synthetic slags", Ann. Chim. 66, 5-6, 251-60.

24.- W. VAN LOO (1977) : "Factors determining the hydraulicity of granulated blastfurnace slag", "Reaction of aluminates during the setting of cements", Seminar CEMBUREAU, Univ. Technol. Eindhoven, 13-14 April.

25.- R. DRON (1979) : "Structure des silicates fondus : interprétation statistique de la théorie de Masson", C.R. Acad. Sc., Paris, à paraître.

26.- R. DRON (1979) : "Théorie statistique des silicates fondus à forte et moyenne teneurs en silice", C.R. Acad. Sc., Paris, à paraître.

27.- C.R. MASSON (1968) : "Ionic equilibria in liquid silicatès", J. amer. Ceram. Soc., 51, 3, 135-43.

28.- R. DRON et F. BRIVOT (1980) : "Approche du problème de la réactivité du laitier granulé", Communication à ce Congrès.

29.- M. REGOURD, B. MORTUREUX, H. HORNAIN, E. GAUTIER, J. VOLANT (1980) : "Hydratation et microstructure des ciments au laitier. Influence de l'étuvage", Communication à ce Congrès.

30.- R. KONDO and S. OHSAWA (1968) : "Studies on a method to determine the amount of granulated blastfurnace slag and the rate of hydration of slag in cements", Proceedings of the Fifth International Symposium on the Chemistry of Cement, The Cement Association of Japan, Tokyo, 7-11 Oct., part IV, 255-62.

31.- P. FIERENS et P. POSWICK (1977) : "Etude cinétique de l'hydratation de laitiers synthétiques", Sil. Industr., 42, 4-5, 235-45.

32.- P. POSWICK (1979) : "Contribution à l'étude de l'hydratation de laitiers synthétiques et industriels", Thèse Docteur en Sciences, Univ. de l'Etat à Mons.

33.- P. FIERENS, P. POSWICK et J.P. VERHAEGEN (1975) : "Influence du traitement thermique sur les caractéristiques des centres excités de constituants de laitiers de hauts fourneaux", Sil. Industr., 40, 10, 253-8.

34.- G. FRIGIONE and R. DI LEVA (1975) : "Size distribution of granular components in Portland and blastfurnace cement", Il Cemento, 72, 1, 13-24.

35.- J.P. BOMBLED et M. REGOURD (1978) : "Compte rendu d'étude sur un CLK à très fine mouture". Rapport interne C.E.R.I.L.H.

36.- T. SUGI; K. KATAOKA, H. YANAGIHARA and S. KOBAYASHI (1976) : "Fundamental experiments on gypsum -blastfurnace slag- alumina cement systems", CAJ Rev. 30th Gen. Meet., Tokyo, June, 73-5.

37.- M. REGOURD et E. GAUTIER (1979) : "Comportement des ciments soumis au durcissement accéléré", Journée d'étude "Traitements thermiques des bétons", Paris 15 nov., à paraître dans les Annales de l'I.T.B.T.P.

38.- R.N. KUREPA, T.V. JURINA and T.A. PLOTNIKOVA (1976), "Thermal treatment of slag - alkali concrete", Beton i Zhelezobeton, 12, 21-2.

39.- S.A. MIRONOV, S.A. VYSOCKIJ, I.I. KURBATOVA and M.G. BUGRINA (1978) : "On effect of hydration activity of slag Portland cements on physical and mechanical features of concrete", Cement, U.S.S.R., 6, 8-9.

40.- Y. HATO, T. MIZUNO, T. GOTO and T. DEGUCHI (1978): "Properties of concrete with mixed cement of blastfurnace slag, gypsum and ordinary Portland cement in steam curing", CAJ Rev. 32nd Gen. Meet., Tokyo, May, 70-1.

41.- A.A. GOVOROV (1974) : "Hydrothermal hardening of slag glasses dispersions", VIth Internat. Congress Chem. Cement, Moscow, 23-27 Sept. suppl. paper, sect. III.

42.- S.M. BASH (1975) : "Hardening of silicate materials of low hydration activity", Zh. prikl. Khim. 48, 9, 1926-32; J. appl. Chem. U.S.S.R., 48, 9, 1999-2003.

43.- L. MASSIDDA and U. SANNA (1979) : "Structure and characteristic of compacts of blastfurnace slag activated by $CaSO_4.2H_2O$", Cement Concr. Res., 9, 1, 127-33.

44.- R. KONDO, S.A. ABO-EL-ENEIN and M. DAIMON (1975): "Kinetics and mechanisms of hydrothermal reaction of granulated blastfurnace slag", Bull. Chem. Soc. Jap., 48, 1, 222-6.

45.- A.H. KAMEL (1973) : "High-pressure steam curing of high-slag cement", J. appl. Chem. Biotechnol., 23, 7, 483-8 and 489-92.

46.- A.H. KAMEL (1975) : "Strength of autoclaved Portland blastfurnace cement", J. appl. Chem. Biotechnol., 25, 1, 57-62.

47.- S.A. ABO-EL-ENEIN, N.A. GABR and R. Sh. MIKHAIL (1977) : "Morphology and microstructure of autoclaved clinker and slag-lime pastes in presence and in absence of silica sand", Cement Concr. Res., 7, 3, 231-8.

48.- S.A. ABO-EL-ENEIN, N.A. GABR and R. Sh. MIKHAIL (1977) : "Morphology and microstructure of autoclaved slag-clinker pastes in presence and absence of silica-sand", Cement Concr. Res., 7, 4, 363-8.

49.- S.A. ABO-EL-ENEIN, R. Sh. MIKHAIL, M. DAIMON and R. KONDO (1978) : "Surface area and pore structure of hydrothermal reaction products of granulated blastfurnace slag", Cement Concr. Res., 8, 2, 151-60.

50.- H. MIYAIRI and S. MYOJIN (1974) : "The development of strength Portland-blastfurnace slag cement under autoclave curing condition", CAJ Rev. 28th Gen. Meet., Tokyo, May, 214-6.

51.- Y. NAKAHARA, F. AMANO and H. YANAGIHARA (1975) : "Studies on strength development of ordinary Portland cement - blastfurnace slag-gypsum systems in steam curing", CAJ Rev. 29th Gen. Meet., Tokyo, May, 70-2.

52.- Ju. V. NIKIFOROV, R.A. ZOZULJA and N.M. IVANOVA (1974) : "Role played by magnesia in clinker and cement technology", VIth Internat. Congress Chem. Cement, Moscow, 23-27 Sept., suppl. paper, Sect.I.

53.- H.G. SMOLCZYK (1977) : "L'emploi du ciment de laitier de haut fourneau dans les bétons armé et précontraint", 6ème Journée Internationale de Sidérurgie : "Utilisation des laitiers", Paris, 13 oct.

54.- K. KODAMA and M. KITAMURA (1978) : "Properties of concrete containing granulated slag powder", CAJ Rev. 32nd Gen. Meet., Tokyo, May, 152-4.

55.- C.A. TANEJA (1975) : "Effect of alumina content and fineness of blastfurnace slag on the sulphate resistance of slag cements", Zement-Kalk-Gips, 28, 2, 76-9.

56.- W. KOBAYASHI and S. OKABAYASHI (1975) : "Study on chloride resistance of various types of cement", CAJ Rev. 29th Gen. Meet., Tokyo, May, 51-3.

57.- I.P. VYRODOV, D.F. NOVOKHATSKIJ, N.A. IVANOVA, V.V. ZHORIN and A.F. MASHTAKOV (1975) : "Physico-mechanical properties of slag hardening products and their differential thermal analysis", Zh. prikl. Khim, 48, 12, 2619-26.

58.- M. REGOURD, H. HORNAIN et B. MORTUREUX (1977) : "Résistance à l'eau de mer des ciments au laitier" Sil. Industr., 42, 1, 19-27.

59.- H. MIYAIRI, R. FURUKAWA and K. SAITO (1975) : "The influence of chemical composition of granulated blastfurnace slag and Portland cement clinker of various Portland-slag cement on resistance to sea water", CAJ Rev. 29th Gen. Meet., Tokyo, May, 73-5.

60.- M. REGOURD (1975) : "L'action de l'eau de mer sur les ciments", Ann. Inst. techn. Bâtim. Trav. publics, 329, 85-102.

61.- M. REGOURD, H. HORNAIN, P. LEVY et B. MORTUREUX (1980) : "Résistance du béton aux attaques physico-chimiques", Communication à ce Congrès.

62.- B. MARCHESE and R. SERSALE (1978) : "Constitution of the products originating by attack of sea water on cement pastes", Il Cemento, 75, 3, 253-62.

63.- A. NEGRO, L. STAFFERI, M. REGOURD, H. HORNAIN et B. MORTUREUX (1973-1974) : "Application du microscope électronique à balayage à l'étude du ciment et de ses produits d'hydratation", Rev. Matér. Constr., 1973, 684, 6-14 et 1974, 686, 17-25.

64.- T. IDEMITSU, S. TAKAYAMA, S. OKABE and S. MORI (1977) : "Basic study on slag cement", CAJ Rev. 31st Gen. Meet., Tokyo, May, 75-7.

65.- M. REGOURD (1977) : "Comportement des bétons à la mer", Travaux, 512, 74-8.

66.- M. FUJITA, S. ADACHI, T. TANEMURA and T. IWABUCHI (1976) : "Effect of the amount of granulated blastfurnace slag on the properties of cement milk-sodium silicate system", CAJ Rev. 30th Gen. Meet., Tokyo, June, 78-80.

67.- A. YODA, K. KODAMA, M. NAKAJIMA and H. NAKAGAWA (1978) : "Effect of salt water on Portland blastfurnace slag cement used in concrete - Results after seven years -", CAJ Rev. 32nd Gen. Meet., Tokyo, May, 148-9.

68.- P. LONGUET (1976) : "La protection des armatures dans le béton armé élaboré avec des ciments de laitier", Sil. Industr., 41, 7-8, 321-8.

69.- K. OKADA, R. FURUKAWA and H. MIYAIRI (1977) : "Some observations on the durability of slag cements to the action of thermal water", CAJ Rev., 31st Gen. Meet., Tokyo, May, 142-4.

70.- M. MURAT et A. NEGRO (1974) : "Application de la microscopie électronique à balayage à l'étude des laitiers et de leurs produits d'hydratation à court terme", Matér. et Constr., RILEM, 7, 40, 253-63.

71.- G. FRIGIONE and R. SERSALE (1976) : "Relation between gypsum content and mechanical behaviour of high slag blastfurnace cements" - Hydraulic cement pastes : their structure and properties". Proceedings of a Conference held at Tapton Hall, University of Sheffield, 8-9 April, Cement and Concrete Association, Ed., Wexham Springs, G.-B., 326-9.

72.- S.E. JOHANSSON (1978) : "Relation between strengths of slag cement and properties of slag", Sil. Industr., 43, 7-8, 139-43.

73.- Ja. M. SYRKIN, B.G. SHOKOTOVA, T.I. ENGORN, V.A. TOKAR and M.I. ZUBIK (1976) : "Increase of hydration activity and improvment of building and engineering characteristics of slag Portland cement, Cement, U.S.S.R., 4, 19-21.

74.- H. MIYAIRI and R. TAKAGI (1976) : "Influence of calcium halides on the early hydration of Portland blastfurnace slag cement", CAJ Rev. 30th Gen. Meet., Tokyo, June, 40-2.

75.- R. Sh. MIKHAIL, W.E. MOURAD and V.K. GOUDA (1974) "Hardened Portland blastfurnace slag cement pastes, Cement Concr. Res., 4, 5, 807-20.

76.- I. TEOREANU and M. GEORGESCU (1973) : "The role of clinker and of calcium chloride in the hardening process of some silicate slags", Rev. roum., Chim., 18, 4, 623-34.

77.- R. Sh. MIKHAIL, A.M. YOUSSEF and M. SHATER (1977) "Air entrainment in Portland blastfurnace slag cement pastes : effects on strengths and pore structure", Cement Concr. Res., 7, 5, 515-22.

78.- H.G. SMOLCZYK (1974) : "Slag cements and alkali-reactive aggregates", VIth Internat. Congress Chem. Cement, Moscow, 23-27 Sept., suppl. paper, sect. III.

79.- F. SCHRÖDER (1968) : "Blastfurnace slags and slag cements", Proceedings of the Fifth International Symposium on the Chemistry of Cement, the Cement Association of Japan, Tokyo, 7-11 Oct., part IV, 149-207.

80.- H.G. SMOLCZYK (1978) : "The effect of the chemistry of the slag on the strengths of blastfurnace cements", Zement-Kalk-Gips, 31, 6, 294-6.

81.- F. SORRENTINO et C.M. GEORGE (1977) : "Etude de l'hydratation des laitiers d'aciérie L.D.", Sil. Industr., 42, 4-5, 249-54.

82.- A. PANIS (1976) : "Les scories L.D.", Sil. Industr., 41, 4-5, 253-8; Bull. Liaison Lab. Ponts Chauss., 83, 99-104.

83.- K. GUSTAW, W. ROSZCZYNIALSKI and A. PTAK (1978) : "Study on the usefulness of slag from steelworks as addition to cement", Cement Wapno Gips, 10, 274-6 and 11, 305-8.

84.- R. KONDO and Y. ASO (1977) : "New material obtained by carbonation of L.D. slag", Gypsum & Lime, 52, 147, 3-7; Sekko To Sekkai, 147, 61-5.

85.- A. DERDACKA, E. PALUCH and M. GAWLICKI (1975) : "Copper slag as admixture for cement", Cement Wapno Gips, 8-9, 229-36.

86.- A. DERDACKA, E. PALUCH and J. MALOLEPSKY (1977) : "The production and properties of cements with addition of cupric slag", Cement Wapno Gips, 10, 273-80.

87.- A.W. SATARINE, E.F. ZHAROV, T. Ju. SHCHETKINA and E.I. VED (1977) ; "Structure and hydraulic activity of slags obtained by the electrothermal production of phosphorus", Silikattechnik, 28, 2, 43-4.

88.- V.L. PANKRATOV, Ju. S. MALININ, N.V. ALIMOVA and N.D. KLISHANIS (1974) : "Hydraulic activity and phase composition of titanium-containing blastfurnace slags", Tr. Ural Nauchno-Issled. Inst. Chern. Met., 20, 65-72.

89.- I.S. VYLKOVA and R.G. DOGANDZHIEVA (1974) : "On binding properties of blastfurnace granulated slag with high content of barium and manganese", VIth Internat. Congress Chem. Cement, Moscow, 23-27 Sept., suppl. paper, sect. III.

90.- I.P. VYRODOV, D.F. NOVOKHATSKIJ, N.A. IVANOVA, V.V. ZHORIN and A.F. MASHTAKOV (1975) : "X-ray examination and general analysis of products of hardening of slag and slag-barite mixtures", Zh. prikl. Khim., 48, 12, 2627-31.

THEME IV

Structure of pozzolana and fly-ash and the hydration of pozzolanic and fly-ash cements

SUB-THEME IV-1

Structure and characterisation of pozzolanas and of fly-ashes

R. SERSALE
Napoli University
ITALY

This paper is a normal state-of art of a part of the reports submitted by Massazza (1) and by Kokubu and Yamada (2) at the 6th International Congress on Chemistry of Cement. Consequently it will not deal with the knowledge already acquired with certitude, but will be limited to giving an account of the subsequent addition to our knowledge, by defining, where possible, the practical results of the scientific and technological progress, whilst endeavouring to give specific emphasis to the problems which call for further research.

1. INTRODUCTION

Table I represents the classification of the principal materials having the property of fixing lime. This classification takes the origin into account.

TABLE I

Classification of the principal lime-combining materials

Natural				Artificial		
Sialic material		Siliceous	Mixed type	Traditional		Non traditional
Unaltered Pozzolanas	Diagenetic: Lithoid tuffs (zeolitic)	Clay (clay minerals)		Fly ash	Clays Shales Burnt diatomaceous earths	Plant ash

It can be observed that the natural materials can be divided into: sialic, siliceous and mixed-type products.
The former groups include materials rich in silica and alumina, such as: volcanic glass, zeolites and clay minerals, but the latter do not yield an appreciable hardening when they fix lime.
The latter groups are characterized by materials of organogeneous origin, extremely porous and crumbly, formed mostly by the siliceous remains of radiolarites and diatoms. As a group, these types of earths are very reactive to lime but, being formed by angular, porous and spindle-shaped skeletons, they need a considerable quantity of water when they are mixed with the cement and the resulting pastes and mortars present, consequently, a decrease in the resistance to atmospheric agents and an increase in drying shrinkage. Therefore they are not considered as materials of quality (3) even if sometimes they are used in the production of binders (4).
The reactivity of diatomites can be increased by thermal treatment at 500°-600°C (5)(6). The class of the mixed-origin materials, sialic and siliceous, includes Gaize (Ardenses and Mense) and Moler, a tertiary deposit of diatomaceous earth with a rather high clay content (Denmark). French gaizes, polluted by clay, can be used after the thermal treatment.

2. SIALIC MATERIALS

2.1 Unaltered materials

2.1.1 Pozzolanas

This term must be reserved solely for essentially vitreous pyroclastic material easily zeolitizable. It is well known that one of the fundamental conditions for a rapid zeolitization is the structure of finely subdivided volcanic glass (7). Equally familiar is the fact that the zeolitization process of pozzolanas causes cementation of the incoherent material so that (true) pozzolanas must be considered as the non-zeolitized equivalents of volcanic tuffs. In this connection it is interesting to note that not all pozzolanas zeolitize with the same ease. In fact the most easily zeolitizable pozzolanas are precisely those which have a more marked hydraulic activity (trachytic or leucitic pozzolanas (8)).

2.1.2 Selection of pozzolans

This can be done on the basis of the vitreous phase content, by the difference between the silica and lime content respectively, which is determined by the usual chemical methods. A limit value around 34% would reveal the absence of the vitreous phase (9). Colour of pozzolanas would only result from the degree of iron oxidation without implying reactivity. Therefore black pozzolanas are not inferior in quality to red pozzolanas (11).

2.1.3 Composition of pozzolanas

It fluctuates between the following limits: SiO_2: 45--60%; $Al_2O_3+Fe_2O_3$: 15-30%; CaO+MgO+alkali $\sim$ 15%: loss on ignition up to 10%.
A true pozzolana is formed essentially of a small quantity of crystalline minerals (feldspar, leucite, augite etc.) plunged into an abundant vitreous mass, more or less altered by atmospheric agents, porous to such a point that it simulates a gel and with wide internal surface. Beside solubilizable silica, it contains significant quantities of solubilizable alumina.

2.1.4 Origin of pozzolanas

They form (12)(13) as a result of volcanic, explosive-type eruptions, because of the violent projection of melted magma into the atmosphere, in the form of minute particles which bring about a phenomenon of tempering responsible for producing a vitreous state. They are made up of elements of different aspect and dimensions: pumice, scoria etc. which can be distinguished by grading.
On the contrary non-explosive eruptions produce volcanic ash, much less reactive with lime than pozzolanas even if identical in composition and grading, since the quick tempering process has not occurred. Indeed only once has Vesuvius produced pozzolanas, during the well-known eruption which destroyed Pompeii and Herculanum in AD 79 and which Pliny the Younger described in his letter to Tacitus (14). Following this and failing explosive phenomena, it has only produced ash.

2.1.5 Dosage of the vitreous phase of pozzolanas

The reactive fraction of pozzolanas is the vitreous one, since the partially altered minerals react to a lesser extent.
By X-ray diffraction it was found that the diffused band which can be attributed to glass is directly proportional to the vitreous phase content, therefore it could be determined after appropriate calibration of the instrument with an obsidian whose mineralogical composition is as close as possible to the sample to examine (15).
A vitreous state index, calculated on the basis of the width of the diffused band of diffractograms around d = 4 - 5 Å appeared to give good correlation with scanning electron microscope observations and with values of mechanical strength by making it possible

to classify pozzolanas according to reactivity (16).

2.1.6 Detection of pozzolana texture

The observation under the optical microscope at low magnification (50 x) allows pozzolanas to be classified into scorias and pumice.
The scanning electron microscope cannot reveal the differentiation of the feldspar from the vitreous phase because of a transgranular break in the crystals, given the common conchoidal aspect of the elements (17).

2.1.7 Internal structure of pozzolanas

The absorption infrared spectroscopy has been used to underline the variations in structure determined by a chemical attack or by a thermal treatment of pozzolanas (18). Although pozzolana spectra are difficult to interpret, since the high degree of vitreous state allows the recording of only slight differences, however the interferences between atomic vibrations and infrared rays seem to be the most appropriate means for studying components formed by amorphous and crystalline fractions and they give useful information on their reactivity.

2.2 Diagenetic materials

2.2.1 Lithoid tuffs

The term tuff must be reserved to pyroclastic rocks which form because of diagenetic phenomena acting on the vitreous, incoherent fraction which has settled in different circumstances because of volcanic explosions (7).
Volcanic materials, mostly vitreous, accumulating in all the different sedimentary basins, represent in fact in most cases the cradle of zeolitization phenomena. Silicate glasses with their higher content in free energy are particularly sensitive to any sort of reaction especially in a wet medium and, by hydration, solubilization, hydrolysis, they can give rise to phenomena of zeolitization, feldsparization or transformation into clay which are responsible for the cementation of the original material.
Therefore we can only call tuffs the zeolitized equivalents of pozzolanas. The most compact compounds, therefore, show a lithoid aspect and have a compressive strength of about 100-300 kg/cm^2; from early times this property determined their use in building. Once ground, these tuffs show an aptitude to combine with lime similar to that of non zeolitized equivalents (true pozzolanas) and sometimes an increased aptitude, since the zeolitic fraction is more easily attacked by lime than the pozzolana glass.
As for characteristics of quality, cements made with trass, for example, make very plastic, compact concretes which are impermeable to water and have low heat of hydration (19).

2.2.1.1 Origin of tuffs

It seems logical to attribute the process which governed the genesis of the best known and best studied formations - such as the Rhine "trass", the Naples yellow tuff, the tawny tuff of the Alban Hills, the Grand Canary tuff etc., to the category of diagenetics, set up by the action of meteoric waters on volcanic glass.
The zeolitization mechanism has been interpreted in the light of the factors which encourage this process and also assumptions justifying the contemporany presence in some formations of zeolites and clay minerals have been proposed (7).

2.2.2 Clays

Pyroclastites are also liable to transform into clays (20); as we have already emphasized, this process is sometimes combined with zeolitization, in turn determined by diagenetic phenomena. The development of volcanic glass in one or other direction is probably determined by a series of factors: chemical composition, microstructure, grading and permeability of sedimentary materials, the pH of the sedimentary medium, the type of ions present in the solution, the age of deposits, the pressure and temperature, the composition of pore waters.
Clays do not interest the cement industry as materials capable of reacting with lime. Indeed although the decomposition of clay minerals under the action of lime causes the neoformation of the same hydrated phases which can be observed from non clayified equivalents (pozzolanas and tuffs) and although the combining rate as well as the quantity of reacting lime generally have higher values (21), their use with clinker lowers mechanical strength. This confirms the fact that the quantity of lime reacting with the compounds having this property, is not enough to foresee the development of the mechanical strengths (22)(23). Their plasticity implies that clays are not adapted to be incorporated in cement (13).
The mechanism prevailing in the processing by lime at ambient temperature is a long alteration process of the crystalline lattice. This process affecting more directly the octahedric strata of the structure was revealed by means of infrared spectrometry.
In the field of neoformation compounds roentgenographic analysis carried out on materials originated by reaction at 39°C during 250 days of lime on kaolinite has allowed C-S-H hydrated calcium aluminates and hydro-garnets to be identified (25).

3. ARTIFICIAL MATERIALS

As shown in table I, these can be classified in two categories: traditional materials and those of more recent use. The first comprises in order: fly ash, burnt clays and shales.

3.1 Fly ash

The term "artificial pozzolana", adopted to describe these important materials as well as those obtained by thermal treatment of clays and earths, in general must be dropped, because it only sets up confusion between categories of materials which have in common the aptitude of reacting with lime, but which present substantial differences in origin, formation and microstructure (13). This term went through a period of validity of course, since in the past there was a need to overcome the distrust of introducing on the market little known products, little known especially in their behaviour. Today it is no longer meaningful because fly ash proved to be not inferior to the best pozzolanas. Indeed they were successfully tested in several cases: as secondary components to cements(26)(27)(28)(29) added to mortars and concretes (30) (31) as raw materials (32)(33) in the precast industry and in road works (34)(35).
Consequently, the residues from combustion of pulverised coal in power stations must be called fly ashes. They represent an industrial product of growing interest, especially if we take into account the fact that world production reaches about 180 million tonnes(36) with a rate of use of approximately 16-17%.
This production will probably increase since less liquid and gas fuels are being used in power stations. Power station boilers can be of two types with melted ash and dry ash. In the first case 85-99% of solid residue is collected in a state of fusion and quench-

ed rapidly in water. The unburnt carbon content is extremely low. In the second case, a fraction (10-15%) of solid waste settles at the bottom of the combustion chamber; it is removed mechanically and is made up of small size particles (30 μ - 30 mm cinders); the remains(85-90%) collects along the exaust path, to be removed afterwards by the electrofilters (37). This is true ash, sold either in a dry state, or humidified (8-12%).
The vitreous state of the material is due to the combustion temperature and then to the quenching. Ash formed at temperatures from 1200-1400°C can be used in cements but higher quality ash is obtained only at 1500-1700°C (38).
About 45 million tonnes of fly ashes are produced per year in the U.S.A., with a yearly increase of 10%.
The cement industry uses about 10% of the annual production (3). France is in second position behind the U.S.A. amongst the countries which devote vast quantities of ash to their production of hydraulic binders. About 95% of production comes from coal ashes (39)(40) with a very low calcium content and a Blaine specific surface between 2500 and 4000 cm^2/g. Out of 5 million tonnes produced in 1976, 2.5 were used in the building industry (41).
On a lesser scale France also produces ashes from lignite combustion (42) characterized by higher calcium content and specific surface (5000-8000 cm^2/g) called sulphocalcic ashes. It also produces ashes containing a high percentage of calcium ($\sim$ 44%)called hydraulic ashes. Both are used in the hydraulic binder industry.
England produced 10 million tonnes of fly ash in 1971-72. About half of this production was used (43) mostly as filler and a small quantity in cement production.

3.1.1 Composition of fly ashes

Coal ash is basically composed of silica and alumina. The composition is approximately: 50% SiO_2, 30% Al_2O_3, 2% CaO, 5% alkalies, 7% Fe_2O_3. The unburnt matter ranges between 1 and 6%. These are therefore silico-aluminous products with a high degree of vitrification and few crystalline elements.
Electronic probe investigation reveals extensive variability in the particle composition, variability which has no influence on the overall chemical composition for ash produced by a single well-tuned power station burning coal from one mine.
Lignite or hydraulic ashes are richer in lime and their composition varies within the following limits (44) SiO_2: 23-50%; Al_2O_3: 8-14%; Fe_2O_3: 8-20%; CaO: 18-50%. Its hydraulic reaction increases in proportion to the lime content and from ashes richer in lime, the neoformation compounds are identical to those obtained from Portland cement, the reaction occurring with heat evaluation. The light colour of this ash is a proof of good quality.
As regards the most interesting ashes, the more important chemical characteristics taken into consideration by standards in different countries are those indicated below in the prescribed limits (45).
Loss on ignition, directly limited to the unburnt matter (1-6%) varies between 5 and 12%. The sulphate content which can cause volume instability of concretes falls between 2.5 and 5% as SO_3. This content,as well as that of the unburnt matter, is an element to be taken into consideration for ashes used in reinforced concretes (46). The percentage of main oxides(SiO_2 +Al_2O_3+Fe_2O_3) should not fall below 70%. The magnesia content can reach a maximum of 5%, since we have not yet checked with certainty if its methods used to estimate volume stability of Portland cement are valid for fly ash cements. The alkali content, such as Na_2O should not exceed 1.5% for concretes made with reactive aggregates. The humidity content must lie between 1 and 3% since a higher content favours loss of reactivity.
The quantity of the unburnt material which varies with furnace design, regulation of combustion and the coal volatile matter content, should be kept as low as possible. Unburnt matter is generally found in the smallest fractions, is inert and although it causes no damage up to a maximum content of 12%, it can influence the colour of the concrete. Lean coals leave a higher rate of combustible material than the rich coal. It can be eliminated by sieving, by mechanical ventilation or by both methods combined. Black stains occur because the residual carbon contained in ash used in manufacturing cements may rise to the surface. These stains can be prevented from forming by adding a tensio-active agent (sodic alkhilnaftalenesulphonate(47)) with absorption of organic molecules at the surface of carbonated fractions, lowering of the solid-water interface tension and consequently elimination of the spontaneous flottation phenomenon.

3.1.2 Physical properties of fly ash

Fineness is one of the principal parameters to define the aptitude of ash to be added to cement since it influences the rate of development of mechanical strength and the relative values to be attained. There is an optimal fineness above which the increase in strength becomes less significant because of the increase in the specific surface (48).
This fineness which can be determined by the Blaine method varies from country to country from 270 m^2/kg to 425 m^2/kg. Because of its porous nature the presence of combustible material distorts this determination since it gives higher specific surface values if the air permeability measurement methods are used. This is why the sieve procedure is preferable (45).
Laboratory tests carried out on fly ashes containing slightly reactive forms of MgO and CaO (49) have shown that grinding lasting 10-15 minutes under suitable conditions in a planet mill gives rise to chemical activation linked to a phenomenon of agglomeration and amorphization of the structure producing hydrates of higher mechanical strength.
The influence of the ground material fineness is underlined by research carried out on lignite fly ashes of Greek origin (50).Mechanical strength tests on mortars have shown that the ash can replace 20% of Portland cement if ungraded material is used. The quantity to add can reach 45% if only the $< 45\,\mu$ fraction is used. It is preferable to grind ungraded material rather than to sieve. Optimal grinding time is about 10 minutes (51).

3.1.3 Structure of fly ash

The specific characteristics of each ash are revealed by scanning electron microscope investigation (52).
Ash is seen as a powder made up of fine spherical particles whose sizes vary from 0.5 to 200 μ. Shape and colour are variable. There are indeed small hollow or solid spheres, angular grains with bulges and hollows, open shells. The grain surface is generally smooth and glossy.
From the mineralogical point of view they consist mostly (53) of vitreous alumino-silicates with modest quantities of iron, sodium, potassium, calcium, magnesium, titanium. The other predominant phases are mullite, quartz, hematite and magnetite as well as combustible material. Traces of mullite in the residue aft

er diluted chlorhydric acid attack seem to be a means to differentiate ash from pozzolana in cements (13).

3.2 Clays, shales, burnt diatomaceous earths

Heating clays, at temperatures corresponding to those of the thermal destruction of minerals which characterize them, brings about rupture in the lattice and consequently the formation of a mixture of amorphous silica and alumina in the stoechiometric proportions of the original minerals. Since the increase in structural disorder brings about an increase in the instability of the system, reactivity with lime and loss of plasticity become noticeable. Cement pastes with appropriate proportion can offer mechanical strengths of the same magnitude as those obtained using pozzolanas or fly ashes.

The use of burnt clays added to cement is not widespread owing to the energy needs and the eventual competition of fly ashes which have already undergone thermal treatment and require no further energy consumption, not even for grinding. From this point of view they prevail over pozzolanas.

Even spent oil shales (ashes) can be used to combine with lime (54). Ungraded material with density above 2 can be competitive if used in an area not exceeding a distance of approximately 30 km from the production or the collecting point; which explains how ternary blends of shales (85%) fly ashes (13-15%) and lime(1--2%) are used in road works.

Finally the main consequence of the thermal treatment on diatomaceous earths is the activation of clay minerals which makes them polluted.

3.3 Non traditional artificial materials

Amongst plant-based materials which can be used as a source of active silica, rice husk seems the most appropriate. Rice growing is extensive all over the world, particularly in developing countries (55).This use of husk appears very timely since a tonne of raw rice produces 200 kg of husk which, because of its low specific gravity, is very bulky. Without counting the calories which can be retrieved for energy purposes, burning rice at about 800°C will produce 20% of its weight as ash containing a high percentage (80-95%)of very reactive silica and 1-2% of potash. The remaining part is unburnt matter.

It was stated that by adding 50% of this ash to clinker, mechanical strengths higher than those of Portland cement are obtained even in the case of short curing (56) and the mortar gains resistance to attack by diluted acids, whether organic or inorganic.

Other reactive forms of silica are dusts trailed by fumes from ferrous alloy production furnaces;the Blaine fineness is about 20.000 cm^2/g (57). Their use increases cement hardness and chemical resistance(58).

Very interesting projects also concern the use of by-products and manufacturing wastes which lead to savings in natural raw products (59).

4. POZZOLANIC ACTIVITY

Pozzolanic activity - that is to say the phenomenon which determines the neo-formation of phases likely to show mechanical strength after hardening - occurs through the effect of the reaction of lime on compounds formed by the alkaline attack of acid silicates (60). The reaction produces hydrated phases similar to phases neoformed by clinker/granulated blastfurnace slag reaction (61) - hydrated calcium silicates and aluminates with excess lime - and is very advantageous from the industrial point of view when the basis material contains silica and alumina easily mobilized, which is typical of amorphous structures and particularly acid glasses. This explain why pozzolanas, fly ashes and burnt clays are preferred as active additions.

In the case of zeolitic type crystalline structures, reactivity which is sometimes even higher than that of vitreous equivalents (12) is probably due to the more open porous structure, therefore more likely to be attacked. Indeed these pores allow chemical agents to penetrate, attacking their crystalline structure through destruction and freeing of silica,alumina and alkalies, the first two of which combine with lime.

In an alkaline medium, zeolitic minerals as well as glass are subjected to a hydrolysis process which brings silicate and aluminate ions into the solution. With Ca^{+2} and Mg^{+2} ions, very low solubility product phases form, such as silicates and aluminates. Their precipitation promotes the passage of other silicate and aluminate ions into the solution, so that the hydrolysis process can continue, differently from what would happen if the attacking agent were only water. With this last assumption the system tends to balance after a certain time.

A pozzolanic reaction mechanism was recently proposed with reference to the structure of feldspar (60). It is well-known that the $K AlSi_3O_8$ orthoclase consists of three SiO_2 units and one AlO_2^- unit, the aluminate ion charge being compensated by K^+. These units are tetrahedrons.

Within the feldspar structure, a SiO_2 unit can be represented as in figure 1. Each of the four oxide O^{-2} ion is linked to the central Si^{+4}, as well as to others which are not on the figure but lie along the dotted line.

On the contrary the situation is quite different for a unit on the outside surface: instead of an oxide ion there is an hydroxile according to:

$$O^{-2} + H_2O \longrightarrow 2OH^-$$

This allows the $^{-2}$ charge to find compensation outside the external surface. The contact with a water solution also allows the other O^{-2} ions to transform progressively into OH^-. The tetrahedron is thus less and less bonded and at a given moment breaks away from the original position and passes in solution as $H_3SiO_4^-$. If this solution contains Ca^{+2} ions, insoluble, hydrated calcium silicates are formed.

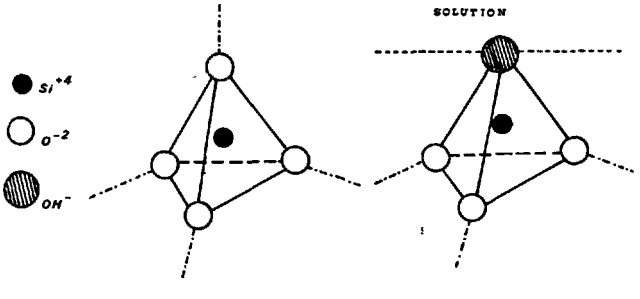

The glassy structure of a pyroclast is more predisposed to the replacement of O^{-2} ion by OH^{-} ion since less intense links allow progressive detaching of units from the tetrahedron.
These would not be topochemical-type reactions since the hydrated phases would occur through total disintegration of the glass silico-aluminous lattice (60).
Very probably for stable crystalline structures such as in feldspars, the surface attack by the lime-saturated solution proceeds in an orderly way, layer by layer. With more labile crystalline structures of the zeolitic type, the attack starting here again on the external surface where the links are less intense, would penetrate more easily inside, because of the "open"-type structure, leading to grain gelification and swelling.
This assumption would be confirmed by the trend of curves showing lime combination by zeolitic minerals and powdered tuffs (62); these curves go up suddenly even after short attack times. The calcium/alkali exchange cannot totally explain this development.
The lime solution attack is made easier by the subdivision of the solid and by its porosity (63) even though (as already pointed out) this is on the molecular level.
With short periods of curing, the specific surface plays a fundamental role on the reaction kinetics; with long periods of curing, the chemical composition predominates, that is to say the silica and alumina (vitreous and zeolitic phase components)determine the behaviour (64).
Research on kinetics and mechanism of reaction of pulverised zeolitic tuffs subjected to combining with lime in water solutions and at a temperature of 65°C (65) seems to prove that the attack by the lime-saturated solution brings about surface dissolution of the grains from the very beginning of the reaction, with rapid local formation of C-S-H gel. The dissolution of the original compound would continue at the interface C-S-H solid/grain surface in a favourable medium to reach levels of sursaturation. Then the development of gelatinous silicate toward forms of greater crystallinity would be regulated by a process of controlled diffusion.
Without forgetting that each pyroclast has specific characteristics and must be studied individually(66), with the aim at bringing light on the complex chemico-physical phenomena which cause pozzolanic activity, solids with simple structure and constitution have been used. The reaction of silica gel with lime has been studied (67) by determining its reactivity as a function of prior thermal treatment and the relative modifications in its structure. The temperature used and the contact time with the solution at first saturated with lime were obviously the determining factor for the activity of the solid. Research also checked that the silica gel selectively combines with potassium and in general the alkalies (68), so that its behaviour can simulate that of a pozzolana only when no alkali is present.
As shown in industrial practice, colloidal silica combines with lime (69) by increasing the strength of cement pastes after short curing, even if they call for a quantity of water which can only be reduced by incorporating the appropriate admixtures.

4.1 Factors which influence "pozzolanic" activity

4.1.1 Incoherent lithoid pyroclasts. Other natural products

Apart from the structure, the morphology and the chemical composition, it is the fineness of the ground material which determines the reactivity of pyroclasts (11)(64). The quantity of lime added, without however disregarding its type (16), plays a fondamental role on the binder hardening kinetics, as well as the water content which intervenes in the composition of neoformed phases bringing about cohesion.
The development of mechanical strength can be mainly attributed to the low basicity hydrated calcium silicates (11) with high water content, whilst alumina-tes seem to play only a secondary role.
Thermal treatment would not appear to be a useful means of increasing pyroclast reactivity. In any case there is no convincing explanation for a possible increase in reactivity (70), but the treatment can be positive if the basic product is polluted with clay. This treatment is negative if it determines a lowering of specific surface (71) as probably happens for powdered volcanic tuffs or in an extreme case if it brings on crystallization of any kind.
With lithoid pyroclasts (tuffs), reactivity is also determined by the quantity and type of zeolitic mineral diffused in the matrix, by its amorphous fraction and pumice content (13) as well as by the more or less noticeable presence of stable crystalline phases.
In Italy vitreous pyroclasts (pozzolanas) found extensively in Campania and Latium are used for binder production more often than lithoids (tuffs) since the former require less costly grinding. In other countries the use of lithoid materials is investigated with interest and recently it is referred to in the case where the materials available for cement production have high alkali content (72) in order to prevent alkali/aggregate reaction.
Tuffs and ignimbrytes comparable to the former, although their composition is different from the genetic point of view, have proved to be appropriate in pozzolanic cement production (73).
Fineness of grinding (74) and the particular nature of the basic component also determine the reactivity of some compact, effusive rocks (which are found amongst others in the Massif Central) made up of a myriad of microcrystals surrounded by amorphous glass. Their composition is similar to that of pozzolanas,even if their basicity is higher. Indeed blends of basalt, lime and water in cylindrical specimens have shown the same values of compressive strength as the best pozzolanas (75).

4.1.2 Fly ash

The reactivity of ash varies with: the type and source of coal, the chemical and above all mineralogical composition, the vitreous phase quantity, the combustion temperature, grinding fineness as already emphasized and low unburnt carbon content.Fineness of grinding and carbon content again determine the mixing water demand (53). As in the case of pyroclasts, reactivity becomes high after a period of latency (76) even if the ash and the pyroclast are not inert even with the shortest curing periods (2)(77).
Mechanical strengths of mortars increase with fineness of grinding and the decrease in carbon content percentage (78).
It seems that the particles of ash most easily attacked by lime are those which are not entirely vitreous (79) containing inclusions of mullite and quartz. However the latter show low reactivity (78).
The grains of ash seem to be covered by a glassy film which shows down the action of the water but sets up the reactivity. The grinding process by breaking this film would accelerate the reaction with water (80).

Chemical analysis of ash determines the inert and reactive fraction percentages, as well as that of soluble silica (total silica minus the inert fraction percentage) and makes possible the classification of the material according to an activity factor resulting from the sum: soluble silica + alumina + lime + + magnesia + sulphuric anhydride.
Ash reactivity is favoured by temperature (81), by certain setting time accelerators (Na_2SO_4, Na_2CO_3, NaOH etc.) as well as by the use of slightly acidified or alkalized water (36). Ash can just,as well, be actified by immersion in a concentrated solution of $Ca(OH)_2$ (82) at 60°C, followed by desiccation, which causes decomposition of the grain surface vitreous layer. The fixing activity of the lime increases, but there is no corresponding increase in mechanical strength, at least as regards mixtures with 20% ash.
According to research concluded on synthetic silico-aluminous ashes (83) aimed at determining the influence of fineness, crystalline structure and chemical composition on reactivity, the results show that the properties of combining with lime would be influenced by the vitreous phase contents much more than by fineness. The state of tension in the vitreous phase (68) would influence reactivity. The iron content would reduce it, the calcium increase it. The soluble components in HCl and HF would give an approximate evaluation of the reactive fraction in ashes. Moreover it seems that the pozzolana activity is put directly in correlation with the Al_2O_3 content (85).
The reactivity of ash in cement is shown by a surface "corrosion" of active particles (86) by lime released during hydration. Consequently the formation of bonds with the hydroxide yields mechanical strength because of the neoformation of calcium silicate insoluble in water and hydrated calcium aluminates. At first hydration is slower than in the case of pure Portland cement (87) and then becomes faster so that at the end the nature of hydration products are quite similar to those of Portland cement (88) even if the reciprocal ratios between the resulting new formed phases are different (53).
The time necessary to achieve the equilibrium condition depends on the quantity of ash and its activity as well as fineness and other factors; generally it is about three months. The reactions are identical to those of pure Portland cement in the initial period, ashes having high fineness and activity,or when the material is further ground if the quantity of ash falls under 25-30% (89).
Light has been brought on the hydraulic behaviour of ash with high lime content (90). Most of it is silico-aluminous and badly crystallized. First contact with water causes portlandite crystallization followed by considerable formation of ettringite due to high calcium sulphate content (91). The vitreous fraction releases silica and alumina slowly and without interruption, causing formation of C-S-H and hydrated gehlenite at the expense of a part of portlandite.

5. EVALUATION OF POZZOLANIC ACTIVITY

Preparing a simple and quick test to estimate pozzolanic activity with certainty is still today a complex unsolved problem (92).Many research groups including CERILH, the Laboratoire des Ponts et Chaussées (French civil engineering laboratories)and the cement manufacturers are at present studying this question (93).
To determine the activity of a pyroclast or a fly ash, it can be tested on mortar or concrete (3) by continuing strength tests up to a year if necessary (94).
However it is possible to obtain useful information from simple compressive strength on pozzolana binder /lime (80% pozzolana + 20% slaked lime) specimens(95). These considerations result from a survey on recently completed chemical, physical and mechanical methods.
Tests were undertaken to correlate pozzolana activity and the soluble component content in acids or bases.
As regards pyroclasts, the soluble silica content - which can be related to the capacity of the material to combine lime rather than its mechanical strength potential properties - can in any case be considered proportional to the compressive strength only by a comparison between the products of same origin and nature. For curings up to 28 days a difference of 10% in the soluble silica content would have repercussions on the strengths determined on lime mortar following the ASTM Standard C 595 but not on blends with Portland cement (96).
The methods appropriate for correlating the lime reaction kinetics to the dissolution heat in a nitro-hydrofluoric mixture are apparently not suitable for fly-ash. Considering the fact that the mixture of 2 molar of nitric acid and 0.6 molar of hydrofluoric acid would be too aggressive (97), by hiding the differences in particle reactivity, a determination of pozzolana activity is proposed by means of measuring the electrical conductivity of a fly ash suspension in 0.1 molar hydrofluoric acid (non-ionic) following the increse in conductivity due to the new formation of hydrofluosilicic acid (ionic) proportional to the quantity of dissolved silica. Assuming that for ashes the silica dissolution follows a diffusive phenomenon, a pozzolana index in agreement with mechanical behaviour is obtained.
However objections have been raised (98), namely that, beside silica, other ash components are soluble in hydrofluoric acid and that consequently the electrical conductivity cannot be put directly in correlation with the active silica content of ashes.
There is also uncertainty as regards the methods of determining pozzolana activity on the basis of the quantity of combinable lime. This lime can be added as it is or as clinker. Having carried out tests to determine the quantity of lime consumed by pyroclasts or by fly ashes after 16 hours'boiling of a gram of the compound, with a gram of lime and 200 cm^3 of water, they need to be completed by chemical analysis of the solid and by a balance between the lime in solution and that still in solid state (99).
To obtain the kinetics curve of the process of lime combining by vitreous or lithoid pyroclasts and properly pulverised zeolitic minerals, a constant quantity of the material must be kept shaken in contact with the same quantities of distilled water,without CO_2, having different initial quantities of calcium oxide (62). With rapid sampling, at determined intervals of time, of a certain quantity of clear liquor above the bottom deposit and the following determination of alkali and lime concentration, it is possible to determine the moment from which the contact solution becomes unsaturated. By subtracting from the total quantity of lime the amount still present in the solution which is no longer saturated,as well as that removed by the successive liquor,sampling, the operator finds the quantity of stably combined lime, taking into account the influence of alkalies. This process ensures to obtain a certain differentiation in the behaviour of the above-mentioned components towards time.
A possible objection to this method is that for su-

spensions it requires delays and therefore considerably deviates from the actual water/cement ratio condition.
To evaluate the activity of pozzolanas, the ISO pozzolanicity test was used improperly. It was conceived to verify whether a ciment can be considered pouzzolanic without requiring the knowledge of the base portland cement.
The validity of the test for pozzolanic cements has been recently confirmed (101).
On the contrary the test is less suitable for characterizing the activity of pozzolanas (53) since it undergoes the influence of many factors depending on the working modes (101)(100), the clinker composition (102)(103)(104)(105) and the difficulty, typical of the systems made up of hydraulic binders, of attaining complete equilibrium conditions (99)(100).
By trials, the pozzolanicity test allows the determination of the minimum quantity of pozzolana or fly ash necessary to prepare a really pozzolanic cement (53).
Some useful indications concerning activity of fly ash have been obtained by analyzing the concentration of a lime-saturated solution at room temperature and at higher temperature (82).
As regards evaluating pozzolanic activity on the basis of the nature of hydration products, it is impossible to differentiate those of clinker from those of pozzolanas since the latter are quite identical to the former, except for calcium hydroxide.
Mechanical strength tests are still today the indispensable complement to chemical and physical methods. Of course it is impossible to differentiate the clinker fraction from that of the pozzolana fraction in their contribution to mechanical strength. It is nevertheless possible to determine at ordinary temperature the mechanical strength of mortar specimens prepared with blended cements and to compare the resulting values with those obtainable in standardized conditions with mortar specimens prepared with the same neat cement or with the equivalent quantities of effectively inert material (106).
The most meaningful mechanical tests seem to be those carried out on mortar of normal consistency, prepared with active materials and lime, although the results are affected by the amount of inert fraction and porosity. From one country to another in fly ash investigation there is a certain variability in the test terms as well as in the percentage to add to the binder.
Accelerating the setting and hardening process by curing the specimens in an atmosphere with vapour saturated at 100°C or in an autoclave cannot be considered a practical approach (100). It is possible to extend the Chapelle test to cements, by testing a pozzolanic cement and by comparing the quantity of remaining lime with that due to hydration of the corresponding quantity of binder without additions (99).
To intensify this phenomenon a gram of pure lime can be added and the mixture shaken magnetically.
It was shown that at the end of the test the quantity of lime measured is under one gram, that is to say that the pozzolana combines with more lime than that released by the clinker. However the quantity of combined lime will not increase in proportion to the quantity of active additions.
By considering that the rate of lime combining (as well as the contribution of fly ash to the development of mechanical strengths) is sensitive to temperature changes and, even if slow at low temperature, it increases more quickly than Portland cement, the introduction of a determination of the lime combining aptitude of the same type as that proposed for pyroclasts (107) is looked favourably (45). It advocates a comparison between the compressive strength of a mortar hardened at 18°C and at 50°C. The increase in strength recorded on the specimen hardened at ordinary temperature, can be practically attributed to the additions. With this test it is possible to obtain in seven days a useful indication of the contribution which a particular ash added to the cement can give to the development of mechanical strengths with long curing times (53).
To assess the quality of ash it was proposed to take into account tests on concrete, bearing in mind that for an equal level of replacement of cement by fly ash, the water/cement ratio decreases and the compressive strength increases in relation to the mortar (80)(108).
As regards certain ash where the SO_3 content is below 1% (36) a good correlation coefficient has been noted between the quantity of combined lime after three hours and the compressive strength. If the SO_3 content increases up to 2-3% there is no longer any possible relationship.
Investigations have even been carried out on the correlation existing between Blaine specific surface, Chapelle test, percentage of the quantity of material sieved at 40 μ and compressive strength. The best correlation would be that between the percentage of material sieved at 40 μ and the compressive strength in the case of ash treated with 10% lime or blends of sand, ash and lime.
Finally it was proposed (109) to express the hydraulic value of an ash by a factor (K) so as to determine the quantity of ash necessary to replace a certain quantity of cement. This factor depends on the curing temperature, as well as on the fly ash/cement ratio and the water/cement ratios of concretes with or without ashes having the same strength.

6. NEW MATERIALS FORMED FOLLOWING THE REACTION OF PYROCLASTS AND FLY ASH WITH LIME

In a lime-pozzolana mortar, the quantity of lime is generally in excess, so because of the presence of hydroxide, there is no possibility that hydrated gehlenite forms and there are formations of calcium silicate and hydrated tetracalcic aluminate (13). The gehlenite can form from products such as calcined kaolin, following the consumption of the whole quantity of added lime and therefore to the detriment of the lime produced by the decomposition of aluminate.
For sulphoaluminates to form there must be sulphates, obviously present in fly ashes. With excess lime (60) two phases will develop: hydrated calcium silicate and ettringite. The monosulphate will occur only after total consumption of calcium sulphate during the formation of ettringite. It will form to the detriment of the latter.
According to the similitude between hydration products of Portland, slag, pozzolanic and fly ash cements, binding properties are attributed to new formation compounds. However morphology, microstructure, stoechiometry, quantity etc. which contribute, each differently, to the formation of bonds also contribute at different levels to make up the mechanical strength and the chemical stability of the conglomerate.
With roentgenographic analysis on lime-pozzolana pastes from Auvergne (10) prepared with 10 to 34% of lime and 8% water, it is possible to define, among the various crystalline phases, only the $4CaO.Al_2O_3.11H_2O$, probably carbonated. This analysis takes care of the fineness, since the vitreous fraction more finely ground, tends to concentrate in the finest part. The

hydrated calcium silicate was detected by scanning electron microscope and by microprobe it was possible to determine that the CaO/SiO_2 ratio was below 1.The quantity of combined lime and the compressive strength increased till a year.
Investigation of pozzolanic cement hydration by the observation of the main infrared spectral bands allowed the identification of the hydrated calcium silicate of a type similar to that formed by the hydration of alite and belite of ordinary Portland cement.
Research on some Roman and Flegrean pozzolanas, mixed with different quantities of lime, wetted with water, formed and cured with steam at 50-90°C (112) has revealed that the reaction is influenced by the temperature and by the pozzolana treatment, by the quantity of added lime and that the amorphous calcium silicate similar to that neoformed at ordinary temperature, represents the main reaction product (113).
It has also been observed (114) that beside the well-known combinations between lime and pozzolana, it is possible to obtain other reactions between pozzolana and C_3A or its hydration products through a mechanism governed by the presence of gypsum.
It was also noticed (53) that the fly ash-lime product tends towards a C-S-H (I) with a lower CaO/SiO_2 ratio than the final Portland cement hydration product which is of the C-S-H (II) type. The quantity of C-S-H gel in a hydrated fly ash cement is higher than that occurring with Portland cement, which causes a fall in the permeability of the conglomerate. This phenomenon together with the decrease in calcium hydroxide concentration explains the better resistance to the chemical attack, especially of sulphates. The gelatinous C-S-H increases in proportion with the ash content, whilst the portlandite phase decreases.
The hydrated pastes of ash-based cements are better predisposed to carbonation than those of Portland cement (89)(115) when ashes exceed 30%.
The reactions between fly ash and calcium oxide have also been studied in hydrothermal conditions (116). Blends with fly ash/lime weight ratio = 3:1, treated at 175°C have revealed, after 2-4 hours heating, the presence of C-S-H (I), of 11 Å tobermorite and of a hydrogarnet whose composition is close to ASH_4. After four hours'processing, the C-S-H (I) develops into 11 Å tobermorite.
As the ash SiO_2 content increases there is also an increase in the quantity of new formed 11 Å tobermorite and a decrease in hydrogarnet, whilst Fe_2O_3 and Al_2O_3 would have a contrary effect.
The alkalies making up the vitreous phase up to a content of about 3% would promote the formation of tobermorite. Beyond this value it would decrease.
As regards the link between the nature of phases and mechanical strength, tests carried out on pastes containing 15-30% lime, 65-85% ash and 0-5% gypsum, autoclaved between 140 and 185°C have shown (118) that the highest compressive strength values around 300--400 kg/cm^3 can be reached with a very low hydrogarnet content (< 5%) and a considerably high gelatinous hydrated calcium silicate content, with partial isomorphous replacement of Si^{+4} by Al^{+3}.

7. IDENTIFICATION OF PYROCLASTS AND FLY ASH IN CEMENT

To combine with lime, an addition must meet certain specific conditions, for example it must be acid,that is contain a high percentage of silica and alumina; it must have a high percentage of vitreous fraction and a high specific surface. By treating it with hydrochloric acid at 1:50, it will be possible to set aside the basic fraction (cement) and in this way determine the percentage of addition and, if need be, its specific surface (99).
The presence of a band which can be determined by X rays, included between 2.5 Å and 5 Å (16) with a maximum at 3.5 Å, will characterize the vitreous phase and after preliminary calibration of the apparatus, will give indications on quantities. The determination of feldspar and pyroxene phases leads to the definition of vitreous pyroclasts. The presence of zeolites disseminated in the matrix which can only be revealed by using X rays (7)(12) allows the pyroclasts of lithoid origin to be determined; traces of mullite lead to recognize the acid fly ashes (119).
If the insoluble fraction in the acid exceeds the normal quantity, the pyroclast can be differentiated from siliceous additions by infrared spectroscopy provided that the spectra of the materials used are known. In the case of vitreous pyroclasts quantitative analysis uses infrared spectroscopy at the 697 cm^{-1} band or titration with an alcohol solution of salicylic acid (120).
The direct determination of the quantity of siliceous addition in the cement can also be carried out on the basis of the different solubility of the components (clinker and additions) in sulpho-salicylic acid. The method could also be used when each component is not available separately (121).
It was also proposed a analysis method by X ray diffraction (122) which is appropriate for rapid detection of phases characterizing fly ashes and other materials of industrial interest.

8. PRESENT DAY INTEREST FOR ACTIVE ADDITIONS

Beside the positive specific effects which fly ash and pozzolana determine on binders, the interest concerning their use and consequently the promotion of scientific and technological research in this field is obvious when reference is made, for example, to the energy aspect of binder production (123)(124).
Ten tonnes of addition represent a saving of a tonne of fuel (76). In Italy pozzolana cement production has brought about a saving of half a million tonnes of fuel.
Adding more than a million tonnes of fly ash to cement has enabled the French cement industry to save 120.000 tonnes of fuel per year (125).
About 15 million tonnes of pozzolanic cement were produced in Italy in 1977, that is to say approximately 40% of the total cement production, by using at least 5 million tonnes of pozzolana.

9. EFFECTS OF VITREOUS PYROCLASTS AND FLY ASHES ON CEMENT

Pyroclasts added to cement in optimal quantity make pastes more workable (126), reducing the heat of hydration (127), thermal expansion, increasing water proofing, resistance to sulphate attack, and lowering expansion due to the alkali reaction with aggregates (128), so cutting production costs.
Another point of interest concerns the influence on the freezing-thawing behaviour, especially as regards lime,pozzolana and aggregate mixtures used in road construction (129).
Unfavourable effects will be found if materials with a mediocre hydraulic value are used or if the ratios between the mix components are not appropriately chosen.
Adding pyroclasts also produces cements with a good capacity for stopping chlorides - which are a danger to steel reinforcement - by a mechanism setting up the formation of hydrated calcium chloro-aluminate and, subordinately, chloride compounds of hydrated calcium silicates (130). Different reactions are ob-

tained in the case of materials of another origin containing active silica but incapable of producing hydrated calcium aluminates owing to the reaction with lime.
In the same way adding fly ashes to clinker lowers the amount of water demand (131) compared with that needed for concretes prepared with Portland cement; it also reduces heat evolved (132), shrinkage-expansion and improves resistance to corrosion (133)(134) either from aggressive of pure waters, and also the freezing-thawing behaviour (135). This latter advantage is however considerably diminished if there is a quantity of carbon residue (136). All fly ashes can also lower mortar expansion owing to the alkali-aggregate reaction (137).
Adding ash is yet again beneficial as regards the reduction in expansion of cements containing 7-10% MgO (138)(139)(140). Further more there is an increase in sulphate resistance (141), it rises in proportion to the C_3A content of Portland cement, reaches its maximum with 50% ash and falls beyond this content. The positive influence of ash is due on one hand to the reactivity of lime and the formation of stable compounds, and on the other to the reduction in water content with identical consistency and to the resulting increase in compactness of the concrete.
The presence of ash also brings about an increase in the rate of hydration of calcium silicates, as compared with the case of Portland cement (142). It also makes the mix more sensitive to hardening with steam curing, therefore the curing of relative cements can occur at higher temperatures (89).
Steam curing also improves concrete surface hardness. However this hardness is compromised when the quantity of ash added to the cement reaches 40% (143).
Finally if ash is added to aluminous cement (144), by lowering the CaO content, it modifies the CaO/Al_2O_3 ratios.
When ashes rich in lime are added to cement, they further lower the heat of hydration as regards the silico-aluminous ashes. This decrease varies with the quantity added (145). The corresponding binders have slightly longer setting times and a small drop in mechanical strength compared with cement.

10. CONCLUSIONS

The general trend of research completed since the Moscow International Congress suggests the following statements:

1. It is time to draft an orderly terminology of the range of materials used in the industry for their aptitude of combining lime. Therefore it seems timely to restrict the term of pozzolanas to vitreous pyroclasts and that of tuff only to pyroclasts changed into lithoids by a zeolitization.
   For other materials with equally high characteristics of quality, such as properly called fly ashes, the most apt term must be reserved to express their origin, composition and microstructure.
   The term "artificial pozzolana" must therefore be dropped, since up to now it was used to identify very different materials, setting up unnecessary confusion which still continues today.
2. The prospects for using the vast range of materials adapted to the cement industry through their property of combining with lime seem very promising. Amongst these materials particular emphasis is placed on fly ashes and pozzolanas as cement addition, not only for aspects linked with the shortage of fuel and the possible use of by-products, but essentially for the very positive effects these materials produce in the respective binders. This implies that research in this field should be particularly fostered.
3. Modern analytical methods for identifying materials reactive with lime can give useful indications for their differentiation in homogeneous groups and for assessing the combining kinetics and the quantity of combinable lime. These indications are however insufficient to foresee the mechanical behaviour with certainty.
4. The most appropriate way to determine the reactivity with lime of industrially interesting materials is still the test on mortar or concrete obviously limited by long delays in obtaining results. Moreover useful information can be deduced on the basis of compressive strength tests carried out on pastes prepared with hydrated lime.
5. The rapid and quantitative determination of pozzolanic activity therefore remains a complex and unsolved problem, requiring the preparation of a test exempt of any uncertainty.
6. The quantity of combinable lime in active materials is not generally correlatable with the values of mechanical strength (146), even if the factors which govern this process have been identified sufficiently.
7. There are valid bases for assuming the mechanisms of attacks by lime on vitreous or lithoid pyroclasts and on related materials, but the subject deserves research to develop further experimental tests, whilst neoformation products have already been identified to a satisfactory degree.
8. The probable activation of the materials used in the industry as additions sets up problems worthy of further research.

REFERENCES

1.- F. MASSAZZA (1974), "Chimie des additions pouzzolaniques et des ciments mélangés", VI Congrès International de la Chimie des ciments, 1-65 (en anglais); (1976) Il Cemento; 73, 1, 3-38 (en italien et en anglais).

2.- M. KOKUBU et J. YAMADA (1974), "Ciments aux cendres volantes", VI Congrès International de la chimie des ciments, 1-51 (en anglais).

3.- W.H. PRICE (1975), "Les pouzzolanes-une-revue", Journ. Amer. Concrete Inst., 5, 225-232 (en anglais).

4.- J. GRZYMEK, W. ROSZCZYNIALSKI et G. KRYSTYNA (1974), "Les diatomites polonaises comme addition pouzzolanique aux liants hydrauliques", Cement-Wapno-Gips, 29, 3, 61-67 (en polanais).

5.- W. ROSZCYNIALSKI, K. GUSTAW, J. SARNA et B. GRZELEC (1977), "Les diatomites de Leszczawka comme addition pouzzolanique au ciment", Cement-Wapno-Gips, 2, 25-30 (en polonais).

6.- H.S. ROBERT ROBERTSON (1973), "Utilisations industrielles des minéraux des argiles", Silicates Industriels, 38, 2, 33-43 (en anglais).

7.- R. SERSALE (1978), "Gisements et utilisations des zéolites en Italie", en Natural zéolites occurrence, properties, use", L.B. Sand et F.A. Mumpton, Pergamon Press, 285-302 (en anglais).

8.- R. SERSALE (1959-1961), "Recherches sur la zéolitisation des verres volcaniques par traitement hydrothermal", 1. "Herschelite par traitement d'un verre preparé par fusion d'une roche sanidinique". 2. "Zéolitisation d'obsidiennes leucititiques artificielles", Rend. Acc. Sci. Fis. et Mat., Napoli, 26, 15-22; 28, 317-336 (en italien).

9.- R. DRON et F. BRIVOT (1977), "Bases minéralogiques de sélection des pouzzolanes", Bull. Liaison Labo. P. et Ch., 92, 105-112 (en français).

10.- J.M. GEOFFRAY et R. VALLADEAU (1977), "Morphologie et couleur des pouzzolanes", Bull. Liaison Labo. P. et Ch., 92, 91-94 (en français).

11.- M. FOURNIER et J.M. GEOFFRAY (1978), "Le liant pouzzolanes-chaux", Bull. Liaison Labo. P. et Ch. 93, 70-78 (en français).

12.- R. SERSALE (1958), "Genèse et constitution du tuf jaune napolitain", Rend. Acc. Sci. Fis. et Mat., Napoli, 25, 181-207 (en italien).

13.- R. DRON (1975), "Les pouzzolanes et la pouzzolanicité", Rev. Mat. Constr., 692, 27-30 (en français).

14.- C. PLINIUS minor, Epist., VI, 16 (en latin).

15.- J. MILLET, R. HOMMEY et F. BRIVOT (1977), "Dosage de la phase vitreuse dans les materiaux pouzzolaniques", Bull. Liaison Labo. P. et Ch., 92, 101-104 (en français).

16.- J. MILLET, A. FOURNIER et R. SIERRA (1976), "Rôle des chaux industrielles dans leur emplois avec les matériaux à caractère pouzzolanique", Silicates Industriels, 41, 4-5, 245-252 (en français).

17.- M.H. TINTURIER (1977), "Observation des pouzzolanes au microscope électronique à balayage", Bull. Liaison Labo. P. et Ch., 92, 95-100 (en français).

18.- M. PILAR de LUXAN (1976), "Etude des pouzzolanes d'origine volcanique à l'aide de la spectroscopie d'absorption dans l'infrarouge", I.E. Torroja C.C. Quadernos de investigaccion,32, 5-22 (en espagnol et en anglais).

19.- S.M. ROJAK et G.S. ROJAK (1974), "Ciments spéciaux", Tsement, 9, 31-33 (en russe).

20.- M. FORNASERI et A. SCHERILLO (1963), "Pétrographie des Cols Albani", en La Regione Vulcanica dei Colli Albani, par M. FORNASERI, A. SCHERILLO, U. VENTRIGLIA, Ed. Bardi, Roma (en italien).

21.- V. AMICARELLI, R. SERSALE et V. SABATELLI (1966), "Activité "pouzzolanique" des produits pyroclastiques "argilifiés", Rend. Acc. Sci. Fis. et Mat., Napoli, 33, 257-278 (en italien).

22.- C.N. BABATSCHEV (1965), "Über bewertungsverfahren der Aktivität mineralischer Zement-zusätze", Zement-Kalk-Gips, 12, 631-635 (en allemand).

23.- F. MASSAZZA et U. COSTA (1979), "Aspects de l'activité pouzzolanique et propriétés des ciments pouzzolaniques", Il Cemento, 76, 1, 3-18 (en italien et en anglais).

24.- A. BARON (1967), "Spectrometrie infrarouge. Application à l'étude d'argiles traitées à la chaux",

Rapp. Labo. C.P. et Ch., dec. (en français).

25.- J.H.P. VAN AARDT et S. VISSER (1977), "Attaque des feldspaths par la chaux: possible rapport avec la reaction alcalis-agrégat", Cement and Concrete Research, 7, 6, 643-648.

26.- "Les cendres volantes des centrales thermiques à charbon" (1975), Charbonnages de France, Electricité de France, 1-41 (en français).

27.- "Cendres volantes en France et dans le monde" (1975), Rev. Techn. Bâtiment, 22, 49, 19-20 (en français).

28.- M.M. MURAT (1975), "Les déchets et sous produit industriels en chimie et technologie des ciments, bétons et autres matériaux de construction", Journ. Inform. Déchets et sous produits industriels", Lyon INSA, 1-20 (en français).

29.- YU.N. PERMINOVA et T.I. NEMYKINA (1975), "Utilisation des résidus solides de la combustion comme additions", Tsement, 7, 16-17 (en russe).

30.- J.F. YOUNG (1977), "Chaux de construction", Cement Research Progress 1976, Columbs, Ohio, Amer. Ceram. Soc., 207-216 (en anglais).

31.- J.A. CHAPELLE (1974, 1975), "Dix ans d'utilisation des laitiers et des cendres volantes sur les aménagements d'Electricité de France du Nord et de l'Est de la France", Laitiers de Hauts Fourneau, 27, 32, 7-60; 28, 33, 5-71 (en français).

32.- S.S. REHSI et S.K. GARG (1974), "Production de clinker de ciment en employant des cendres volantes", VI Congrès International de la chimie des ciments, 1-12 (en anglais).

33.- J. BERETKA et T. BROWN (1977), "L'utilisation des cendres volantes dans l'industrie du bâtiment", Journ. Aust. Ceram. Soc., 13, 2, 24-30 (en anglais).

34.- E. BARENBERG (1975), "Chaux de construction", Cement Research Progress, American Ceramic Soc., 153-158 (en anglais).

35.- S.I. PAVLENKO,A.I.CHIRKINE,N.I.FEDYNINE,V.M.MEDVEDEV (1977), "Processus de durcissement du mortier de ciment et du béton additionnés de grandes quantités de cendres de centrale", Beton i Zelezobeton, 11, 16-18 (en russe).

36.- P. ANDRIEUX et J.H. COLOMBEL (1976), "Utilisation des cendres volantes en technique routière. Les graves-cendres volantes", Silicates Industriels, 41, 4-5, 227-244 (en français).

37.- M.P. ZUBCHENOK (1978), "Amélioration du dépoussierage par électrisation des cendres volantes", Tsement, 2, 19-20 (en russe).

38.- A. PAPROCKI (1978), "L'emploi des cendres volantes dans l'industrie du bâtiment", Tonind. Zeit. Keram. Rund., 102, 8, 453-456 (en allemand).

39.- M. VENUAT (1976), "L'utilisation des cendres volantes en cimenterie", Rev. Industrie Minèrale, 58, 5, 217-224 (en français).

40.- M. VENUAT (1975), "La valorisation des cendres volantes dans la fabrication des ciments et des bétons", Journ. Inform. Déchets et sous produits industriels, Lyon INSA, 1-8 (en français).

41.- P. MARIE (1978), "Un matériaux économique: les cendres volantes. Utilisation et perspectives", L'Equipement Mécanique Carrières et Materiaux, 167, 53-6 (en français).

42.- PIRNER JOCHEN (1977), "Filtres de cendres de lignite - un déchet utilisable", Silikattechnik,28, 3, 84 (en allemand).

43.- W. GUTT, P.J. NIXON, M.A. SMITH, W.H. HARRISON, et A.D. RUSSEL (1974), "Une revue des possibilités d'utilisation et des perspectives des principaux sous produits et déchets", B.R. E. Current Paper, 19, 1-81 (en englais).

44.- P. PONTEVILLE (1976), "Liant hydrauliques et pouzzolaniques", Syndicat Professionnel des Entrepreneurs de Travaux routiers de France, 1-28 (en français).

45.- M.A. SMITH (1977), "Sept standards nationaux pour comparer les cendres volantes pulverisées", Precast Concrete, April, 191-193; May, 257-258 (en anglais).

46.- Z.B. ENTINE, E.T. JASHINA, N.Z. RJAZANCEVA, et G.G. LEPESHENKOVA (1976), "Corrosion de l'armature dans les ciments aux cendres volantes", Tsement, 12, 12 (en russe).

47.- B. THURET (1976), "Le traitement des cendres volantes", Rev. Mat. Constr., 699, 110-111 (en français).

48.- A.M. PURI (1975), "Aspects concernant l'utilisation de cendres de centrale thermique comme addition lors du broyage du ciment", Materiale de Constructii, 5, 1, 27-30 (en roum).

49.- M.A. SAVINKINA et A.T. LOGVINENKO (1974), "Activation mécanique des materiaux liant silicatés", Izvest. Sibir. Otdel. Akad. Nauk SSSR, Khim. Nauk URSS, 6, 14, 141-144 (en russe).

50.- E.VOYATZAKIS, K.M. SIPITANOS et A. CHRISTAKI-PAPAGEORGIOU (1976), "Etude sur le cendres volantes des lignites grecs. Utilisation dans le ciment. Region de Ptolémaide", Rev. Mat. Constr. 703, 6, 341-344 (en français).

51.- K.M. SIPITANOS, E. VOYATZAKIS et S.B. MELIDIS (1977), "Etude sur les cendres volantes des lignites grecs. Utilisation dans les ciments.Influence du degré de finesse. II. Region de Ptolémaide", Rev. Mat. Constr., 707, 4, 211-213 (en français).

52.- M. MURAT et A. NEGRO (1974), "Quelques exemples d'utilisation de la microscopie électronique à balayage pour l'étude morphologique des materiaux vitreux", Rev. Physique Appl., 9, 403-418 (en

français).

53.- J.D. MATTHEWS et W.H. GUTT (1978), "Recherches sur les cendres volantes comme matériau pour le ciment", Inter. Conf. on Ash technology and marketing, London, 1-21 (en anglais).

54.- E. HANQUEZ (1976), "Utilisation des cendres volantes et des schistes houillers: procédés surschistes et surex", Cement-Béton, Rev. Mat. Constr., 703, 336-339 (en français).

55.- P.D. CADY et P.R. GRONEY (1976), "Ciments hydrauliques à base d'écorse de riz", Cement Technology, 7, 6, 215 (en anglais).

56.- P.K. MEHTA (1977), "Propriétés de ciments composés à base de cendre de balle de riz", Journ. Amer. Concrete Inst., 9, 440-442 (en anglais).

57.- H. ASGEIRSSON et G. GUDMUNDSSON (1979), "Activité pouzzolanique de la poussière de silice", Cement and Concrete Research, 9, 2, 249-252 (en anglais).

58.- A. TRAETTEBERG (1978), "Poussières de fumés siliceuses comme matière pouzzolanique", Il Cemento, 75, 3, 369-376 (en anglais).

59.- P. FIERENS (1976), "Perspectives de valorisation des sous-produits industriels", Silicates Industriels, 41, 10, 395-400 (en français).

60.- R. DRON (1978), "L'activité pouzzolanique", Bull. Liaison Labo. et Ch., 93, 66-69 (en français).

61.- R. DRON, J.C. VAUTRIN et F. VERHEE (1978), "Les différents liants hydrauliques et pouzzolaniques. Obtention et mode d'action", Bull. Liaison Labo. P. et Ch., 94, 73-83 (en français).

62.- R. SERSALE et V. SABATELLI (1960), "Activité pouzzolanique des zéolites. Reactivité à la solution saturée de chaux par l'herscelite", Rend. Acc. Sci. Fis. e Mat., Napoli, 27, 263-282 (en italien).

63.- J. MILLET, A. FOURNIER et R. SIERRA (1976), "Rôle des chaux industrielles dans leur emplois avec les matériaux à caractère pouzzolaniques", Silicates Industriels, 41, 4-5, 245-252 (en français).

64.- U. COSTA et F. MASSAZZA (1974), "Les facteurs qui réglent la reaction entre la chaux et les pouzzolanes italiennes", Il Cemento, 71, 3, 131-139.

65.- B. DRZAJ, S. HOCEVAR, M. SLOKAN et A. ZAJC (1978), "Cinetique et mécanisme de reaction dans le système tuf zéolitic - $CaO-H_2O$ à température élevée", Cement and Concrete Research, 8, 6, 711-720 (en anglais).

66.- M. DE LUXAN BAQUERO (1973), "D'autres liants à base de portland: les ciments ternaires", Cemento Hormigòn, 44, 476, 1155-1161; 1164-1170 (en espagnol).

67.- M. PILAR DE LUXAN et T. VAZQUEZ (1974), "Le gel de silice comme pouzzolane de rèpere: sa remarquable activité et ses limites", Il Cemento, 71, 3, 113-130 (en italien et en anglais).

68.- M. PILAR DE LUXAN (1976), "Comportement du gel de silice au cours de l'essai de pouzzolanicité", Materiales de Construccion, 161, 1-20 (en espagnol).

69.- J.A. NELSON et J.F. YOUNG (1977), "Addition de silice colloidale et de silicates aux pâtes en ciment Portland", Journal of Concrete Research, 7, 3, 277-282 (en anglais).

70.- G. ROSSI et L. FORCHIELLI (1976), "Structure poreuse et absorption de chaux de certaines pouzzolanes naturelles italiennes", Il Cemento, 4, 215-221 (en italien).

71.- U. COSTA et F. MASSAZZA (1977), "Influece du traitement thermique sur la réactivité à la chaux de quelques pouzzolanes naturelles", Il Cemento, 74, 3, 105-122 (en italien et en anglais).

72.- G. GUDMUNDSSON et H. ÅSGEIRSSON (1975), "Recherches sur la reaction alcalis agrégat", Cement and Concrete Research, 5, 3, 211-220 (en anglais).

73.- G. GUDMUNDSSON (1975), "Recherches sur le pouzzolanes islandaises", Symposium on alkali aggregate reaction. Preventive measures, Reykjavik, 65-71 (en anglais).

74.- B. FAURE et J.M. GEOFFRAY (1978), "Planches expérimentales basalte-chaux", Bull. Liaison Labo. P. et Ch., 94, 53-59 (en français).

75.- J.C. MONTVENOUX et J.M. GEOFFRAY (1975), "Mise en évidence des proprietés pouzzolaniques des basaltes", Bull. Liaison Labo. P. et Ch., 78, 21-24 (en français).

76.- P. LONGUET (1975), "Les ajouts au clinker de ciment", Rev. Mat. Constr., 693, 113-116 (en français).

77.- M. VENUAT (1975), "Les ciments contenant du laitier ou des cendres volantes", Rev. Mat. Constr. 692, 30-35 (en français).

78.- C. OSTROWSKI (1976), "Hydroxide de calcium et plâtre - leur action sur les propriétés pouzzolaniques des cendres volantes", Baustoffindustrie, Ausg. A., 19, 6, 13-17 (en allemand).

79.- Z.B. ENTIN, G.G. LEPESHENKOVA et E.T. YASHINA (1976), "Hydratation et durcissement des ciments portland aux cendres", Tsement, 1, 15-16 (en russe).

80.- M.B. ZLATANOS (1976), "Recherches helléniques sur l'amelioration des cendres volantes de lignite ou de houille, en vue de leur utilisation en cimenterie", Ciment Béton, Rev. Mat. Constr., 702, 5, 281 (en français).

81.- P. TERRIER et M. MOREAU (1975), "Mécanisme de l'action pouzzolanique des cendres volantes dans le ciment", Cement-Wapno-Gips, 29, 8-9, 269-277 (en polonais).

82.- K. GABOR (1976), "Recherches sur l'activité et sur l'activation chimique des cendres volantes", Epitoanyag, 28, 7, 253-257 (en hongrois).

83.- R.C. IOSHI et E.A. ROSAUER (1973), "Activité pouzzolanique de cendres volantes synthetiques: II. Comportement pouzzolanique", Amer. Ceram. Soc. Bull., 52, 5, 459-463 (en anglais).

84.- E.A. ROSAUER et R.S. MASTERS (1973), "Cendres volantes synthetiques: I. Caractère pouzzolanique. II. Rôle du calcium", Fortschr. Mineral., 50, 312-325 (en anglais).

85.- W. KURDOWSKI et M. POLESZAK (1978), "Utilisation de cendres volantes dans la production de ciment", Tonind.-Zeit. und Keram. Rundschau, 102, 12, 696-700 (en allemand).

86.- Z.B. ENTIN, E.T. YASHINA, G.G. LEPESHENKOVA et N.Z. RYAZANTSEVA (1974), "Hydratation et durcissement du ciment avec addition de cendres volantes", VI Congrès International de la chimie des ciments, 1-11 (en anglais).

87.- J. PAKO' et R. KOVACS (1974), "Utilisation du derivatographe pour l'etude des ciments aux cendres volantes", Thermal. Analysis, 3, Proc. Fourth ICTA, Budapest, 459-470 (en anglais).

88.- R. KOVACS (1975), "Influence des produits d'hydratation sur les propriétés des ciments aux cendres volantes", Cement and Concrete Research, 5, 1, 73-82 (en anglais).

89.- R. KOVACS (1976), "Utilisations des cendres volantes en Hongrie", Proceeding Fourth Int. ash utilisation Symposium, St. Louis, Mo., 24-25 march, 70-79 (en anglais).

90.- A. CARLES-GIBERGUES (1978), "Propriétés hydrauliques des cendres volantes sulfocalciques de Gardanne", Bull. Liaison Labo. P. et Ch., 93, 5-8 (en français).

91.- A. CARLES-GIBERGUES et A.VAQUIER (1973), "Comportement pseudo-pouzzolanique d'une cendre volante de centrale thermique", Materiaux et Constructions Rilem, 6, 32, 141-147 (en français).

92.- J. CALLEJA (1977), "Ciments pouzzolaniques", Materiales de Construccion, 165, 1-14 (en espagnol).

93.- M. REGOURD (1978), "Recherches sur les ciments en France", Ciments Betons Platres Chaux, 2, 711, 82-90 (en français).

94.- C. PAULI (1977), "Détermination du module d'efficacité des pouzzolanes incorporées au ciment portland", Cemento Hormigon, 48, 528, 1299-1302; 1307-1308 (en espagnol).

95.- J.M. GEOFFRAY et R. VALLADEAU (1978), "Traitment des sables alluvionnaires par le liant pouzzolanes-chaux", Bull. Liaison Labo. P. et Ch., 93, 86-91 (en français).

96.- J. SOROKA et Ch. IAEGERMANN (1974), "Comportement mécanique et teneur en silice soluble de certaines roches volcaniques", Journ. Amer. Ceram.Soc., 57, 12, 534 (en englais).

97.- E.RAASK et M.C. BHASKAR (1975), "Activité pouzzolanique des cendres volantes pulvérisées", Cement and Concrete Research, 5, 4, 363-376 (en anglais).

98.- A.J. MAJUMDAR et L.J. LARNER (1977), "L'évaluation de l'activité pouzzolanique", Cement and Concrete Research, 7, 2, 209-210 (en anglais).

99.- R. LARGENT (1978), "Estimation de l'activité pouzzolanique. Recherche d'un essai", Bull. Liaison Labo. P. et Ch., 93, 61-65 (en français).

100.- R. LARGENT (1975), "Estimation de l'activité pouzzolanique. Recherche d'un essai", Thèse de doctorat Univeristé Paris VI (en français).

101.- M.P. DE LUXAN et F. SORIA (1975), "Etude et revue critique de l'essai de pouzzolanicité", Cement and Concrete Research, 5, 5, 461-480 (en anglais)

102.- J. BENSTED (1977), "Une discussion sur l'exposé: Etude et revue critique de l'essai de pouzzolanicité par M.P. de Luxan and F. Soria", Cement and Concrete Research, 7, 4, 461-462 (en anglais).

103.- J. BENSTED (1976), "La phase ferrite. Un étude spectroscopique à l'infrarouge", Il Cemento, 73, 1; 45-51 (en italien et en anglais).

104.- M.P. DE LUXAN et F. SORIA (1977), "Une réponse à la discussion du dr. Bensted sur l'étude et revue critique de l'essai de pouzzolanicité", Cement and Concrete Research, 7, 4, 463-464 (en anglais).

105.- F. BONOMI et M.T. FRANCARDI (1975), "Contribution supplémentaire en vue d'améliorer l'essai de pouzzolanicité", Il Cemento, 72, 4, 163-172 (en italien et en anglais).

106.- J. CALLEJA (1977), "Les additions aux ciments", Materiales de Construccion, 165, 1-7 (en espagnol).

107.- F.M. LEA (1973), "L'essai des ciments pouzzolaniques", Cement Technology, 4, 1, 21-25 (en anglais).

108.- M. KOKUBU (1975), "Essais en commun de différents cendres volantes", Studies on Materials for Concrete Structures, Tokyo, 77-116 (en anglais).

109.- R.K. DHIR, E.S. DARFOUR et J.G.L. MUNDAY (1979), "Caractéristiques de résistance de bétons additionnés de cendres volantes", Silicates Industriels, 44, 1, 23-9 (en anglais).

110.- J. MILLET et R. HOMMEY (1974), "Etude minéralogique des pâtes pouzzolanes-chaux", Bull. Liaison Labo. P. et Ch., 74, 59-63 (en français).

111.- J. BENSTED (1976), "Examen de l'hydratation des ciments de laitier et des ciments pouzzolaniques par spectrometrie infrarouge", Il Cemento, 73, 4,

209-214 (en italien et en anglais).

112.- M. COLLEPARDI, A. MARCIALIS, L. MASSIDDA et U. SANNA (1976), "Traitement à la vapeur basse pression de mélanges chaux-pouzzolane compactés", Cement and Concrete Research, 6, 4, 497-506 (en anglais).

113.- Z. SAUMAN et M. HLOZEK (1978), "Explication de l'influence des matières siliceuses ajoutées au ciment, de l'hydratation des pâtes et de la température de traitement sur la quantité de chaux dégagée par réhydratation", Il Cemento, 75, 3, 343-350 (en anglais).

114.- M. COLLEPARDI, G. BALDINI, M. PAURI et M.CORRADI (1978), "L'influence des pouzzolanes sur l'hydratation de l'aluminate tricalcique", Cement and Concrete Research, 8, 741-752 (en anglais).

115.- R. KOVACS (1974), "Le processus d'hydratation et la durabilité des ciments aux cendres volantes", VI Congrès International de la chimie des ciments, 1-18 (en anglais).

116.- Z. SAUMAN (1975), "Les reactions entre cendres volantes de centrales thermiques et la chaux en conditions hydrothermales", Silikaty, 19, 3, 193-202 (en anglais).

117.- Z. SAUMAN (1973), "Rôle et caractéristiques de la phase vitreuse des cendres volantes de centrale thermiques", Siliconf. Budapest, 1, 461-475 (en anglais).

118.- I. STEBNICKA-KALICKA (1974), "Interdépendance entre effects thermiques et resistance des pâtes cendres volantes chaux", Thermal. Analysis, 3, Proc. Fourth ICTA, Budapest, 497-512 (en anglais).

119.- F.X. DELOYE, C. CHEZEAUD et M.I. BUISSON (1975), "Identification rapide des ciments sur chantier", Bull. Liaison Labo. P. et Ch., 77, 65-70 (en français).

120.- P. DE LUXAN GOMEZ DEL CAMPILLO (1978), "Méthodes d'évaluation quantitative et qualitative des additions de type siliceux présents dans le ciment", Cement Hormigòn, 49, 530, 531, 91-98, 101-111, 202-214, 217-224, 229-234 (en espagnol).

121.- M.I. KAMAEVA et A.I. TOLPA (1978), "Détermination directe de la quantité d'additions siliceuses dans le ciment", Tsement, 5, 9 (en russe).

122.- J. CZUBA et A. DZIEDZIC (1978), "Méthode d'analyse minéralogique quantitative par diffraction X, des materiaux de construction", Cement-Wapno--Gips, 5, 158-160 (en polonais).

123.- A. JOISEL (1974), "Ciment d'hier, d'haujourd'hui, de demain", Rev. Mat. Constr. 690, 257-263 (en français).

124.- P.M. MEHTA (1978), "Energie, ressources et environnement - une revue de l'industrie cimentière aux Etats-Unis", World Cement Technology, 9, 5, 144-160 (en anglais).

125.- M.E. HANQUEZ (1975), "Utilisation des cendres volantes et des schistes houillers", Journr. Informations "Dechets et sous produits industriels", Lyon INSA, 1-12 (en français).

126.- I. CIB SOROKA (1976), "Utilisation des scories volcaniques pulvérisées dans le bétons", Bâtim. Internat., 9, 5, 297-303 (en français).

127.- A. DERDACKA-GRZYMEK, W. ROSZCZYMIALSKI et K. GUSTAW (1976), "Influence des additions sur les propriétés des ciments", Baustoffindustrie, A, 19, 3, 14-16 (en allemand).

128.- S. SPRUNG et M. ADABIAN (1976), "Influence des additions sur la reaction alcalis-agrégat dans le béton", Symp. on the effect of alkalies on the properties of concrete, London, sept., 125-137 (en anglais).

129.- G. CUMBERLEDGE, G.L. HOFFMAN et A.C. BHAJANDAS (1976), "Propriétés de durcissement et de résistance en traction des mélanges de granulats--chaux-pouzzolanes", Stabilization, Transp. Res. Rec., 560, 21-30 (en anglais).

130.- C. GORIA et F. FINELLO (1978), "Sur la participation de la pouzzolane ou de matériaux à comportement pouzzolanique à bloccage partiel des chlorures chez le ciments pouzzolaniques", Il Cemento, 75, 2, 49-58 (en italien et en anglais).

131.- W. PERENCHIO et P. KLIEGER (1976), "Etudes supplementaires des ciments pouzzolaniques", PCA Research and Development Bull., RD041 -01T, 1-9 (en anglais).

132.- A. PAPROCKI et C. WOLSKA-KOTANSKA (1979), "Influence des additions de cendres volantes sur la chaleur d'hydratation et sur des autres propriétés du ciment Portland", Part. I, Tonindustrie Zeitung, 7, 408-413; Part. II, Tonindustrie Zeitung, 8, 474-479 (en allemand).

133.- V. Kh. KIKAS, E.I. PIKSARV, A.A. KHAIN et I.A. LAUL (1974), "Ciments aux cendres volantes sur la base des cendres de combustible solide", VI Congrès International de la chimie des ciments, 1-10 (en anglais).

134.- P. SCHUBERT (1974), "Une contribution sur la resistance aux solutions de sulphates de prismes de mortier de ciment aux cendres volantes", VI Congrès International de la chimie des ciments, 1-15 (en anglais).

135.- R.J. ANDRES, R. GIBALA et E.J. BARENBERG (1976), "Quelques facteurs influant sur la durabilité des mélanges de chaux-cendre volante-granulats", Stabilisation, Transp. Res. Rec., 560, 1-10 (en anglais).

136.- A.V. VOLZHENSKIJ, L.B. GOLDENBERG et G.F. VOLVODA (1977), "Influence du combustible imbrûlé sur la rèsistance au gel des bétons de sable ad

ditionnés de cendre", Béton i Zelezobeton, 5, 29-30 (en russe).

137.- W.F. PERENCHIO et P. KLIEGER (1976), "Nouveaux essais de laboratoire sur le ciments portland pouzzolanique", PCA Research and Development Bull., RD041 -01T, 1-8 (en anglais).

138.- W. CASSELOURI et G. PARISSAKIS (1977), "Stabilisation des ciments à haute teneur en magnésie par addition de cendres volantes et de laitier", Silicates Industriels, 42, 1, 13-17 (en anglais).

139.- J. MALOLEPSZY (1973), "L'addition de cendres volantes garantit la stabilité de volume du ciment portland contenant 7% MgO", Cement-Wapno-Gips, 6, 207-209 (en polonais).

140.- S.S. REHSI et S.K. GARG (1975), "Stabilisation des ciments riches en magnésie, à l'aide de cendres volantes", Zement-Kalk-Gips, 28, 2, 84-87 (en allemand).

141.- P. SCHUBERT et M.P. LÜHR (1979), "La résistance aux sulfates des mortiers et bétons contenant des cendres volantes", Béton+Fertigteil-Technik, 45, 3, 177-182 (en allemand).

142.- S.I. PAVLENKO, M.V. KARPENKO, N.I. FEDYNIN, V.M. MEDVEDEV et B.A. KRYLOV (1977), "Caractères de l'hydratation du ciment portland à haute teneur en cendres volantes de centrale thermique", Tsement, 2, 7-8 (en russe).

143.- TRAN-THANH-PHÁT (1973), "La dureté des bétons de ciments aux cendres", Rev. Mat. Constr. 676, 10-20 (en français).

144.- M. KOBAYASHI, N. MIYAKE et M. KOKUBU (1974), "Cendres volantes pour la rèsistance à long délai du ciment alumineux", VI Congrès International de la chimie des ciments, 1-13 (en anglais).

145.- Cz. WOLSKA-KOTANSKA (1978), "Influence des cendres volantes sur la chaleur d'hydratation et sur les propriétés des ciments Portland", 2, Cement-Wapno-Gips, 1, 20-27 (en polonais).

146.- F. MASSAZZA et U. COSTA (1977), "Les facteurs qui determinent la développement des rèsistances mécaniques dans les pâtes chaux-pouzzolane", XII Conference on Silicate Industry and Silicate Science-Sili-Conf., Budapest, 537-552 (en anglais).

147.- R. KONDO et S. OHSAWA (1979), "Réactivités de différents silicatès avec la chaux et l'eau", Journ. Amer. Ceramic. Soc., 62, 9-10, 433-544 (en anglais).

SUB-THEME IV - 2

Hydration of pozzolanic cement

K. TAKEMOTO
H. UCHIKAWA
Onoda Cement Co, JAPAN

1. POZZOLANIC REACTIVITY

"Pozzolana" is defined as natural or artificial solids involving constituents which react with Ca^{2+} or $Ca(OH)_2$ and form new binding compounds under the presence of water. "Constituents", we say, means minerals, crystals, noncrystalline materials, glasses and "artificial"means chemical or physical treatment for natural materials. Fly ash is one of pozzolanas in this meaning.

"Pozzolanic reactivity" is defined as index of reaction degree at ordinary temperature between pozzolanas and Ca^{2+} or $Ca(OH)_2$ with water or between pozzolanas, water and material which produces $Ca(OH)_2$ under the presence of water.

As the definition of "pozzolana" says, the mere physical absorption is excluded from pozzolanic reaction because this term means the formation of binding compounds by the reaction. In general, the chemical reaction has absorption process as one of reaction processes and after that process forms new compounds, but we interpretate here such a physical absorption process as so-called induction period and evaluate the degree of pozzolanic reaction of this period as zero.

In the definition of "pozzolanic reactivity", properties of reaction products or aggregate system which involves raw materials and reaction products are not mentioned. The reason is that the properties of paste which involves reaction products are substantially independent from pozzolanic reactivity. For example, strength, which is one of the representative properties of paste, is strongly influenced by the kinds, shapes, sizes and distribution of hydration products and pores, has not so good correlation with the degree of reaction.

The base of pozzolanic reactivity can be defined so that the difference of free energy between source system and products system or magnitude of activation energy from source system to products system, in the reaction system of pozzolanas, Ca^{2+} (or $Ca(OH)_2$) and water, or pozzolanas, water and materials which form $Ca(OH)_2$ under the presence of water. The nature of pozzolanic reactivity is determened by the character of pozzolanas, that is, the composition and structure of pozzolanas.

In the many papers, the term of "pozzolanic activity" or "pozzolanicity" other than reactivity has been used. Some of them (1), (2) used the pozzolanic activity for the test results of strength of pozzolanic cements. ISO (3) uses the "pozzolanicity" for the test results of $Ca(OH)_2$ concentration in the liquid of cement suspension. The concept of these terms is not always authorized or standardized and gives us unnecessary confusion. In this paper, the authors uses only the term of "pozzolanic reactivity", as defined at the first.

2. THE CHARACTER OF SEVERAL JAPANESE POZZOLANAS

2.1 Progress in Analytical Method

In general, since ceramics is the mixtures of fine particles composed of single crystal, polycrystal and amorphous phase, for the methods of characterization, it is necessary not only to know chemical and mineral composition of micro area, the micro texture and surface state but also to gather wide range information from micro to macro, besides understanding conventional average chemical and mineral composition of the object. The recent development of analysing method for that purpose is remarkable and it is indispensable to take in and apply those new analysing method to the study of cement for the advance of cement chemistry. The detailed explanation in this field was recently done by Uchikawa (4).

2.1.1 The classification of analysing method

The analysing methods mainly used at present is classified roughly as compositional separation method and compositional analysis, indentification method. Compositional separation method is further divided into two groups, that is, chemical separation method which dissolves or leaves desired composition in the sample by the difference of pH or the complex formation constant using aqueous solution such as acid, alkali and complex formation agents, or nonaqueous solution, and physical separation method which utilizes the difference of specific gravity, surface property, magnetic susceptibility and electrical property.

For the compositional analysis and identification of substance, method is divided into two main classes, for macro character and for micro character. Average chemical composition is one of the main factors of macro character. Though the methods change with the property and the shape of the sample, the kind and the quantity of coexisting component and required precision, main component is determined mainly with chemical analysis such as gravimetric and volumetric analysis, fluorescent X-ray and emission spectrochemical analysis, for the analysis of trace component atomic absorption and spectroscopic analysis are widely used. As for new analysing methods, inductively coupled plasma method, radio activation analysis, anodic elusion voltammetry are going to be in practice. For the average structure analysis and state analysis, there is powder X-ray diffraction which is used for analysis of solid solution (peak shift), crystallinity (peak profile), low crystalline materials (radial distribution function method) and long-range order crystal (small angle scattering method). UPS (ultraviolet rays) and XPS (soft X-rays excitation) are used for the methods to examine atomic bond state from the position, the shape and the intensity of spectrum of X-ray, electron beam, ultraviolet and

infrared absorption.

As the methods for the determination of micro character, the apparatus which can determine the variance of composition of micro area without separation procedures of the sample are going to be widely used. Electron Probe Microanalysis (EPMA) is the apparatus that can analyse elements qualitatively or quantitatively and estimates the state of electron of atom by measuring characteristic X-rays generated with mutual interaction between accelerated electron beam and material. Analytical electron microscope (AEM) is very useful tool for the analysis of micro area as it has high resolving power especially for thin sample which has less matrix effect. Scanning electron microscope (SEM) is effective for observation of micro surface structure with back scattered electron and secondary electron generated from the sample. Elemental analysis can be also made with the image of Auger electron, and cathode luminescence (7) of wave length 4,500-10,000Å can make elemental analysis and clarify the state of atomic bond. Ion microprobe mass analyser, which makes mass analysis of secondary ions generated by ion bombardment instead of electron beam, is utilized for surface analysis.

2.1.2 The progress in several characteristic methods

The extention of measurement to ultra soft X-rays area, which have large amounts of information owing to the improvement and the development of apparatus and soft ware, and the application to microquantitative analysis are considered to be one of the remarkable progresses in the field of fluorescent X-ray analysis. In recent years synchrotron orbital radiation (8) comes to be used for excitation of X-rays which has higher intensity than conventional source of X-ray, high degree of parallel, polarized ray. Quantitative analysis and state analysis of $_6C$, $_8O$, $_9F$ (9) can also be made by the progress of analysing crystal such as TAP and RAP, and organometalic thin film analysing element such as LMD (Lead Myristate Dicanoate). Semiconductor X-ray detector that Li is doped into Si or Ge and has high sensitivity is developed and is used for trace analysis as energy dispersive spectrometer.

Inductively coupled plasma spectroscope (ICP) also comes to be used for trace analysis of cement and related samples. It measures the intensity of emission generated by the excitation of elements of atomized sample heated at 7,000°K by plasma and has higher sensitivity compared with conventional atomic absorption analysis (5), (6). Burman, Ponter and Bostron (10) used ICP for the analysis of Si, Al, Ti, Ca, Mg, Na, Fe, Mn, Cr, Ba, Zn, Cu in quartzite and Scott and Kokot (11) applied ICP to quantitative analysis of Cu, Zn, Ni, Co, Pb, Mg, Fe, Al in soil and obtained good result.

In laser micro emission spectrochemical analysis, laser light is gathered at the analysing point and generated emission is recorded. It has characteristics that the component of extremely microquantities can be analysed since temperature of generated plasma is above 10,000°K, that the effects of the shape of sample the state of chemical bond and formation process of plasma are small because the vaporization of sample is very rapid that the quantity of sample is less than 1 ug and it needs little time for analysis. Bensted (12) investigated the structural inhomogeneities of clinker mineral particles, characterization of clinker minerals, the identification of calcium sulfate and the detection of carbonation of cement hydrates by Raman spectroscopy using laser.

EPMA is most widely used for micro area analysis with electron beam, but the space resolution of obtained information is not so high because incident beam diffuses into thick sample. To overcome this problem AEM was developed recently. AEM is designed to analyse excited X-rays generated with transmitted electron through thin sample before it diffuses, and has practically space resolution of 100Å. Since X-rays are generated from extremely micro area of very thin sample and very weak, energy dispersive spectrometer with semiconductor detector is used in stead of analysing element for wave dispersion which is applied in EPMA. The trace analysis of fine crystal can be made with this method and is utilized for identification of Mg, Si, Fe and so on in calcium aluminate sulfate hydrates, sizes of which are about 100 x 500 μm, existing in hardened cement paste (13) and for compositional analysis of each phases in rock minerals.

Though the resolving power of Transmission Electron Microscope (TEM) is dependent on the wave length of electron beam and spherical aberration, in recent years TEM of which resolving power is about 1.4Å (100KV) can be designed with the progress of high power magnetic field object lens. Lattice image can be observed sufficiently with that resolving power and many kinds of lattice images are explained with diffraction theory and imaging theory. The observation of SiO_4 chain arrangement of calcium silicate hydrate (13) and the direct observation of the lattice image of cordierite (14) provide effective data for the studies of lattice defects, dislocation, crystal growth and so on.

As for NMR, conventional method which uses continuous high frequency magnetic field, is modified to pulse Fourier transformation NMR with the introduction of computor and the means of Fourier transformation. Since the amounts of information in definite time is increased highly with that method, the observation of the nuclides which have low natural existence rate or have low sensitivity such as ^{13}C, ^{15}N becomes easy. In the field of cement chemistry, adsorbed water was analysed quantitatively by pulsed proton NMR and the

information about hydration and structure of cement was obtained (15).

The precision of X-ray diffraction recently rises and the delicate difference of radial distribution of glass phase comes to be able to be discussed by means of computor and measurement technique of high precision. Yasui, Hasegawa and Imaoka (16) analysed radial distribution of $K_2O \cdot SiO_2$ using MoK_α X-ray monochromatized by graphite monochromator and balanced filter and showed that experimental curve well coincided with calculated radial distribution considering various conditions. That method is desired to apply to structural study of glass phase in pozzolana.

New information and epoch-making progress on the studies of cement chemistry are very largely due to development and establishment of new analysing methods. The authors expect that a lot of outcomes of studies which are obtained using those new apparatuses and methods will be presented on Paris Congress.

2.2 Characterization of Japanese Pozzolanas

2.2.1 The geological consideration and microscopic observation of natural pozzolanas

(a) Beppu white clay (V)

Beppu white clay is collected at the district of Beppu hot spring, Ōita prefecture. The rock, which constitutes the neighborhood of mineral deposite of Beppu white clay, is made of hornblended andesite. Silicate minerals in hornblended andesite decomposed to silica gel by the action of hot spring and formed opal. That opal stayed original position and formed irregular massive fairly-soft ore deposite.

Observing by microscope, Beppu white clay is constituted mainly of amorphous silica, and small quantities of quartz, cristobalite and opaque minerals.

(b) Higashi-Matsuyama tuff (G)

Higashi-Matsuyama tuff yields in the neighborhood of "Yoshimi Hyakketsu", Saitama prefecture. The lithofacies of that acidic tuff has no bedding and is homogeneous. The surface of outcrop is like white powder, the inner is tinged with blue-gray.

Higashi-Matsuyama tuff is constituted mainly of glass phase and small quantities of quartz, plagioclase, clay minerals and very small quantities of zeolite. Main composition of volcanic glass is SiO_2 and Al_2O_3. Fe_2O_3 and K are also contained.

(c) Furue shirasu (F)

"Shirasu" was formed by a large quantity of eruptions which fell down after Pleistocene (the secondary glacial age) from two caldera volcanos, Aira and Ata, south part of Kyūshū. That eruptions have several rock faces which are pumice fall, pumice flow and welded tuff, and shirasu was formed from pumice fall.

In general, shirasu is constituted of volcanic ash, volcanic sand and pumiceous lapilli. As the mineral composition, shirasu is made up with glass phase mainly and has small quantities of quartz, feldspar and hypersthene.

With optical microscope, almost particles are made with glass phase and quartz and plagioclase are slightly observed.

(d) Tominaga Masa-soil (M)

"Masa" is a term of geology or engineering work. Masa-soil exists abundantly in Aich and Gifu prefecture and is the sand of weathered granite and contains feldspar, quartz, mica, kaolinite limonite and so on.

In the six kinds of rocks which constitute that district granodiorite is closely connected with masa-soil. Granodiorite is in general constituted of coarse-grained and relatively homogeneous. The color of granodiorite is dark-green or black and it contains amphibole and biotite. Granodiorite is decomposed easily by the weathering action and forms masa-soil.

(e) Kanto loam (Hachiōji loam) (R)

"Kanto loam" layer exists widely in the diluvial upland of Kanto plain. Kanto loam is considered to be formed with falling ash by volcanic activity of Diluvial age.

Several terraces are observed in Kanto loam layer, Tachikawa Terrace, Musashino Terrace, Simo-Sueyoshi Terrace and Tama Terrace and the collected loam is corresponded to upper Musashino loam layer.

Musashino loam layer contains pyroxene and olivine as colored minerals, and hypersthene and magnetite are also contained. As noncolored minerals, much quantities of feldspar, small quantities of quartz are contained. Allophane and less than 20% of hydrated halloysite exist as clay minerals. Under optical microscope, quartz, plagioclase hypersthene and weathered olivine are main minerals, the rest are fine opaque minerals.

2.2.2 Characterization of natural and artificial pozzolana

Characterization was made for five kinds of Japanese natural pozzolanas and one kind of artificial pozzolana of fly ash which used in the present study.

As the item of characterization, the means, which investigate the composition and the structure of pozzolanas itself directly, are adopted. That is, the structure was observed with optical microscope, SEM and

Table I Chemical composition of pozzolanas

	(%)	Natural pozzolana					Artificial pozzolana
		Beppu white clay (V)	Higashi-Matsuyama tuff (G)	Furue shirasu (F)	Tominaga masa-soil (M)	Kanto (Hachioji) loam (R)	Takehara fly ash (T)
	H_2O (-)	1.18	1.33	0.36	0.72	15.25	0.40
	ig.loss	4.09	6.50	1.85	3.11	12.07	4.62
	insol.	84.38	85.38	87.99	65.78	13.61	52.09
Hot HCl soluble part analysis	SiO_2	8.48	4.02	4.72	12.90	23.94	16.87
	TiO_2	0.10	0.04	0.16	0.48	0.69	0.47
	Al_2O_3	0.38	0.95	1.73	8.94	18.70	10.35
	Fe_2O_3	0.29	0.46	0.88	2.17	10.15	3.24
	FeO	0.01	0.03	0.42	1.17	0.79	0.79
	MnO	0.01	0.14	0.07	0.30	0.37	0.10
	MgO	0.02	0.33	0.21	1.07	2.07	1.15
	CaO	0.05	0.15	0.58	0.54	0.74	5.35
	Na_2O	0.01	0.22	0.23	0.03	0.07	1.12
	K_2O	0.04	0.12	0.13	1.20	0.06	0.51
	P_2O_5	0.01	0.00	0.04	0.14	0.07	0.18
	Total	99.68	99.67	99.37	98.55	98.58	97.24
Total analysis	SiO_2	87.75	71.77	69.34	65.21	33.03	49.06
	TiO_2	1.10	0.14	0.25	0.56	1.05	1.23
	Al_2O_3	2.44	11.46	14.56	16.43	20.86	24.37
	Fe_2O_3	0.41	1.14	1.02	2.20	10.24	4.20
	FeO	0.05	0.56	0.83	1.19	0.83	0.93
	MnO	0.02	0.32	0.23	0.33	0.61	0.13
	MgO	0.23	0.54	0.71	1.19	2.35	1.76
	CaO	0.19	1.10	2.61	1.67	1.07	6.15
	Na_2O	0.11	1.53	3.00	1.47	0.42	2.22
	K_2O	0.11	2.55	2.39	2.79	0.17	1.27
	P_2O_5	0.03	0.02	0.06	0.16	0.11	0.21
	S	0.11	0.00	0.00	0.00	0.03	0.51
	Total	98.45	98.96	97.21	97.03	98.09	97.06

( ); notation

TEM, the composition was determined with chemical analysis and powder X-ray diffraction. In addition to those examination, the physical tests, which are thermal analysis, IR analysis and measurement of cation exchange capacity (CEC), were made. Results are shown in Table I, II and Fig. 1.

3. HYDRATION REACTION BETWEEN LIME, CEMENT COMPOUND, PORTLAND CEMENT AND POZZOLANA

3.1 Hydration in the system pozzolana-$Ca(OH)_2$

3.1.1 The process of hydration

The crystalline hydrates formed in the reaction between lime and pozzolana in the presence of water were summarized by Massazza (17) as hexagonal calcium aluminate hydrate (C_4AH_x), calcium carboaluminate hydrate ($C_3A \cdot CaCO_3 \cdot H_{12}$), calcium aluminate monosulfate hydrate ($C_3A \cdot CaSO_4 \cdot H_{12}$), calcium silicoaluminate hydrate which were identified by means of DTA, powder X-ray diffraction and electron diffraction analysis.

The kinds and compositions of produced hydrates are generally related to the character, that is, chemical composition, crystal structure of constituents of pozzolana, and the conditions of hydration. However, there

Table II Characters of pozzolanas

Pozzolana	Shape		Specific surface area (BET) (m^2/g)	Density (g/cm^3)	Mineralogical composition(%)		Chemical composition	Size of grain (%)	Thermal properties		IR	CEC
	SEM	TEM			Glass phase	Crystalline (XRD,OM)			DTA	TG		
Furue shirasu (F)	glass phase (conchoidal fracture)	shape-edged glass like (conchoidal fracture)	2.95	2.48	95	quartz 1 anorthite 3	high Al_2O_3 alkali	<80μ 98.8 <10μ 35.4	460-515°C removal of OH in glass	r.t.-540°C weight loss 3.3%	shifted SiO_4 peak	5
Higashi-Matsuyama tuff (G)	glass phase (small uneveness rod shaped projection)	glass particle (conchoidal fracture)	2.42	2.29	97	quartz 1 anorthite 1	high alkali	<80 96.2 <10 21.8	200-500°C removal of OH in glass	r.t.-200°C 2.3 200-1100°C 9.4	same as Furue shirasu	
Kanto loam (Hachioji loam) (R)	massive irregular particles	winding ball pipe-like	199	2.10	<10	allophane halloysite olivine hypersthene plagioclase quartz	low SiO_2 high Al_2O_3 Fe_2O_3	<80 56.5 <10 12.7	r.t.-190°C combustion of organic compounds, removal of OH in clay formation of mullite	r.t.-190°C 17.5	Si-OH H-O-H peaks	26
Beppu white clay (V)	irregular particles	fine round particle	14.7	2.14	62	quartz 1 cristobalite 39	high SiO_2 low Al_2O_3 alkali	<80 56.5 <10 19.6	480-550°C removal of OH in glass	r.t.-500°C 4.4	SiO_4 cristobalite	4
Tominaga masa-soil (M)	needle-like irregular particles	pipe-like	17.3	2.68	<10	feldspar quartz mica halloysite	high Al_2O_3 alkali	<80 92.9 <10 19.6	260-290°C removal of OH in glass, α-β transformation		similar to Kanto loam	6
Takehara fly ash (T)	empty sphere rod-like particle	sphere small irregular particle	2.25	2.42	86	quartz 5 mullite 7	high Al_2O_3 CaO low SiO_2	1-50 100 <10 57.5	600-720°C combustion of carbon, 1014°C sintering of glass phase	456-830°C 4.2	shifted SiO_4 peak (broad)	2

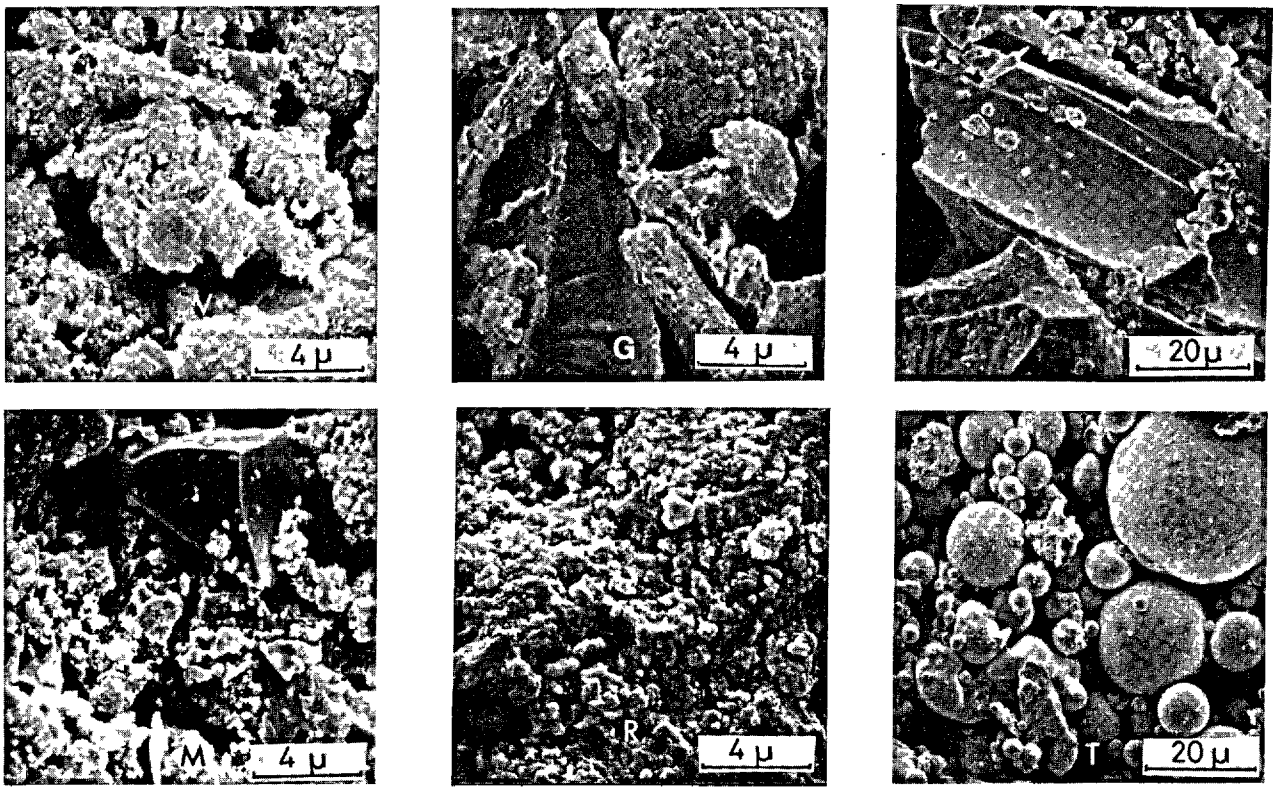

Fig. 1 - Scanning electronmicrograph of pozzolanas

are no remarkable difference between hydrates formed in paste and those of suspension hydration at later age.

Ludwig and Schwiete (18) studied the hydration in the system $Ca(OH)_2$ and two kinds of trasses containing 50-70% of glass phase, feldspar, quartz analcite etc. in suspension and paste. They confirmed the formation of C_4AH_{13} and C_3S_2 hydrate in the case without gypsum, and ettringite and monosulfate hydrate with gypsum.

Amicarelli, Sersale and Sabatelli (19) studied the suspension hydration of argillified pyroclasts in lime saturated solution. They found C_2ASH_8, C_4AH_{13} and tobermorite-like calcium silicate hydrate in clayish pozzolana containing large amount of halloysite, C_2ASH_8 and tobermorite in zeolitic pozzolana containing chabazite and $C_3A{\cdot}CaCO_3{\cdot}H_{12}$ and tobermorite in tuff containing leucite and halloysite at the age of 20 days. The amount of combined lime was 17% by weight of added lime. Hydrogarnet, or C_2ASH_8 and hydrogarnet, were formed at the later stage of 70-150 days, when the combined lime was from 46 to 60%.

In the five years old paste initially containing 40% of lime and 60% of calcined pozzolana, Sabatelli, Sersale and Americarelli (20) observed two typical different cases consisting of C-S-H (I) and C_2ASH_8, and C-S-H (I), C_2ASH_8, C_4AH_{13} and $C_3A{\cdot}CaCO_3{\cdot}H_{12}$.

In the authors' study, the hydrates produced in the paste hydration of pozzolana-$Ca(OH)_2$ in W/S=0.56-0.46 at 20°, 40° and 60°C using five kinds of Japanese natural pozzolanas and one kind of fly ash were classified into three cases according to pozzolanas, that is, (1) C-S-H only, (2) C-S-H, (C_3A $CaCO_3$ H_{12}-C_4AH_{13})ss and hydrogarnet in later age, (3) C_2ASH_8, hydrogarnet, and a little amount of C-S-H. The first case was Beppu white clay consisting of opal. The second case was tuff containing volcanic glass and shirasu containing volcanic glass and plagioclase. The third case was Kanto loam containing much allophane. The formation of hydrogarnet in allophane rich pozzolana was accelerated in the increased amount of $Ca(OH)_2$ and in the rise of temperature.

The hydrates formed in the paste hydration in the system pozzolana-$Ca(OH)_2$ are shown in Table III.

Regourd, Hornain and Mortureux (21) recognized silicoaluminates of $C_3A{\cdot}CS{\cdot}H_{12}$ and $C_3A{\cdot}3CS{\cdot}H_{31}$ near C_3A grains in the hydrated paste of C_3S-C_3A and C_3S-C_3A-$CaSO_4{\cdot}2H_2O$ at 28 days by SEM with energy dispersive X-ray analysis (EDX). These hydrates might be produced in the pozzolana system.

Table III Hydrates formed in the paste hydration in the system pozzolana-$Ca(OH)_2$

Pozzolana	Curing temp. (°C)	Age (days)	C-S-H	C_3AH_6 $C_3AS_2H_2$	$C_3A \cdot CaCO_3 \cdot H_{12}$ C_4AH_{13}	C_2ASH_8
Furue shirasu(F)	20,40,60	7	+	-	+	-
		180	+++	(+)	+++	(+)
Higashi-Matsuyama tuff(G)	20	7	-	-	(+)	-
		180	+++	-	+	-
	40	7	(+)	-	(+)	-
		180	+++	-	(+)	-
	60	7	+	-	-	-
		180	+++	-	-	-
Kanto (Hachioji) loam(R)	20	7	-	(+)	+++	+
		180	(+)	-	+++	+++
	40	7	(+)	+++	+	(+)
		180	(+)	+++++	(+)	(+)
	60	7	(+)	++++	(+)	-
		180	+	+++++	-	-
Beppu white clay(V)	20,40,60	7	+	-	-	-
		180	+++	-	-	-
Tominaga masa-soil (M)	20	7	-	(+)	+++	-
		180	-	-	++	-
	40	7	-	(+)	+	-
		180	-	++	+	-
	60	7	-	+	+	-
		180	(+)	+++	(+)	-
Takehara fly ash(T)	20,40,60	7	+	-	-	-
		180	++	-	+	(+)

Table IV CaO/SiO ratio of formed C-S-H in the system pozzolana-Ca(OH) estimated by FESEM with EDX

Accelerating voltage ; 20kV

Pozzolana	CH/P ratio	Curing Temp. (°C)	Age (M.)	Ca/Si molar ratio
Beppu white clay(V)	25/75	20	3	0.87-0.77
		40		0.85-0.80
		60		0.81-0.75
Higashi-Matsuyama tuff(G)	25/75	20	3	1.49-1.35
		40		1.75-1.60

The concentration of Ca^{2+} in the liquid of the system pozzolana-$Ca(OH)_2$ is kept between 2 m mole/l and 9 m mole/l (22). The former corresponds to the value equilibrating to C-S-H and the latter corresponds to the value in the liquid equilibrating to $Ca(OH)_2$ coexisting with alkalies. The molar CaO/SiO_2 ratio is closely related to the concentration of Ca^{2+} in the liquid. Some of the authors' results are shown in Table IV. In the case of of Beppu white clay the CaO/SiO_2 ratio was about 0.8, because the added lime was consumed before 3 months and in the case of tuff the ratio was 1.4-1.7, coexisting with remained lime.

3.1.2 Kinetics of hydration in the system pozzolana-$Ca(OH)_2$

Drzaj, Hocevar, Slokan and Zajc (23) studied kinetics and mechanism of reaction in the system zeolitic tuff-$CaO-H_2O$ at 65°C using the 1:1 mixture of CaO and three kinds of tuffs and one kind of heulandite hydrated in W/S=50/6 at 65°C. They determined the relative decrease of the minerals in reactants and the relative increase of the amounts of CSH(I), tobermorite, tetracalcium aluminate hydrate, nekoite, osumilite in products by powder X-ray diffraction referring the SEM observation. They described that the initial

reaction was the diffusive dissolution of zeolite and $Ca(OH)_2$ as it agreed with Fick's first low, and that the reaction was diffusion-controlled topochemical reaction limited by the diffusion of Ca^{2+} and OH^- through the membrane of CSH(I) gel, which formed on the surface of zeolite grain in the processes of zeolite + $Ca(OH)_2$ → CSH(I) → tobermorite, and the interface layer between zeolite and CSH (I) gel membrane. They also pointed out that CSH(I) formed in the early stage of reaction and that tobermorite formed as final product through heterogeneous nucleation on the solid (CSH(I))-liquid (solution) interface.

Kondo, Lee and Daimon (24) studied the hydrothermal reaction at 181°C in the system quartz-$Ca(OH)_2$-H_2O. They classified the reaction by the N in the modified Jander equation : $(1-\sqrt[3]{1-\alpha})^N = kt$. They explained that N = 1 meant the surface reaction on the grain boundary and rate determining step was the dissolution and precipitation, and that N = 2 was the diffusion, of which rate determing step was diffusion of material through the reacted layers. Dividing these into two parts they considered that N<2 implied the reaction of which reacted layer became less dense with age and N>2 implied the reaction of which reacted layer became denser with age. They speculated by the calculation of N that dense hydrated layer with high CaO/SiO_2 was kept in the presence of $Ca(OH)_2$ solid and less dense hydrated layer with low CaO/SiO_2 was formed when solid $Ca(OH)_2$ was completely consumed.

In the authors' study, the amounts of reacted $Ca(OH)_2$ per unit weight of pozzolana in each pastes prepared under the condition described in 3.1.1 with varing the mixed amounts of $Ca(OH)_2$ are shown in Fig. 2.

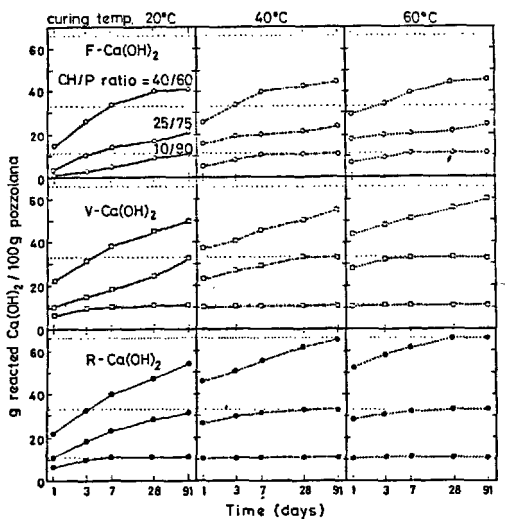

Fig. 2-Reacted $Ca(OH)_2$ in the system pozzolana-$Ca(OH)_2$ estimated by X-ray diffraction analysis varying the mixing ratio and curing temperature

In all pastes regardless of the kind of pozzolana and curing temperature, the more $Ca(OH)_2$ was mixed, the more the amount of reacted $Ca(OH)_2$ became. That is, the rate of pozzolanic reaction is accelerated by mixing more $Ca(OH)_2$. And it was decreased with age in logarithmic relation.

Judging from the N calculated from modified Jander equation, the reaction in early stage is considered to be controlled by the dissolution of atom or atomic groups from the surface of $Ca(OH)_2$ grain and the precipitation of hydrates on the surface of pozzolana grain as a rate determing step (N<1) and after a week, N attains above 2, it is also considered to be governed by the diffusion of atoms and atomic groups through denser layer of hydrates formed between pozzolana and $Ca(OH)_2$ grain as a rate determining step.

On the other hand the degree of reaction of pozzolana was the order of Kanto loam, Beppu white clay and Furue shirasu as shown in Fig. 3.

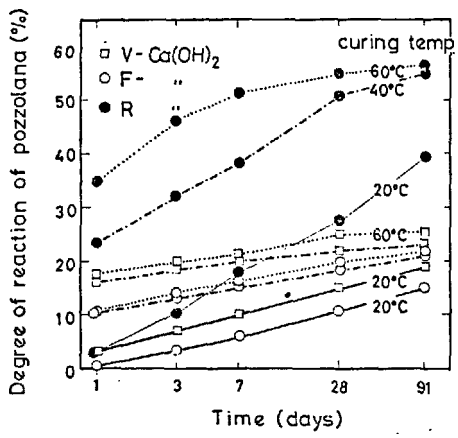

Fig. 3-Degree of reaction of pozzolana in the system pozzolana-$Ca(OH)_2$

These data coincide with the rate of reaction estimated from the amounts of reacted $Ca(OH)_2$.

Raask and Bhaskar (25) thought that the rate of the dissolution of silica fraction in pulverized fuel ash was governed by the diffusion of silica through insoluble layers on the surface of grain and that this process could be adopted by the equation of diffusion-controlled dissolution for uniform spherical particles.

$$W_r/W_o = 1-6/\pi^2 \sum_{n=2}^{\infty} 1/n^2 . \exp(-D_n^2 \pi^2 t/a^2)$$

$$= 1-6/\pi^2 \cdot \exp(-D\pi^2 t/a^2) \qquad -(1)$$

where a is the radius of particles, D is the diffusion coefficient, n is an integer, t is time, W_r is the amount of silica reacted at time t. W_o is the total silica. When d represents the density of grain and S represents

specific surface area, the equation becomes

$$W_r = W_o(1-\beta e^{-\alpha t}),\ \alpha = D\pi^2/a^2 = \pi^2 Dd^2S^2/9$$
$$\beta = 6/\pi^2 \qquad -(2)$$

Considering $\log(1-W_r/W_o) = \log\beta - \alpha t$, the relation shown in Fig. 4 are obtained by plotting $\log(1-W_r/W_o)$ against age from the author's data.

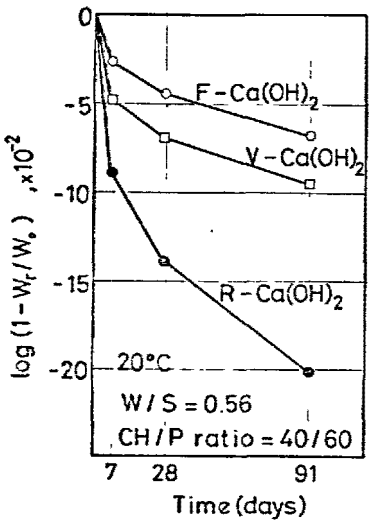

Fig. 4-Logarithmic plott of $(1-W_r/W_o)$ against age

The slope of the curve was the largest in the Kanto loam which has the largest specific surface area and that of Beppu white clay and Furue shirasu followed in this order, which indicate the good fit to the equation of diffusion controlled dissolution. The value of α, the slope of the curve, decreased with age. This implies the decrease of specific surface area of pozzolana which has far great contribution to α. After very fine particles are completely consumed, the rate of reaction is governed by the diffusion coefficient, which has close relation to the nature of amorphous film on the surface of pozzolana grain attributed to its structural factor and by the character of precipitated hydrates layer outside the film.

3.1.3 The mechanism of the hydration in the system pozzolana-$Ca(OH)_2$

The mechanism of the hydration in the system pozzolana-$Ca(OH)_2$ has been studied mainly on suspension hydration and few researches on paste hydration were published.

Drzaj, Hocever, Slokan and Zajc (23) studied the suspension hydration on the system zeolitic tuff and $Ca(OH)_2$ at 65°C and reported that the hydration proceeded by the diffusive dissolution of zeolite and $Ca(OH)_2$ and by topochemical reaction of the precipitation of hydrates on the surface of zeolite from the experimental fact that CSH(I) precipitated on the surface of zeolite grains.

Diamond and Kinter (26) found that the adsorbed amount of $Ca(OH)_2$ molecules on the surface of clay grains is at most 3% by weight of mixture while the consumption of $Ca(OH)_2$ proceeds over 3% with age. From these results they thought that $Ca(OH)_2$ molecules are adsorbed on the surface of clay grains at first, then adsorbed $Ca(OH)_2$ molecules and clay grains dissolve into water precipitating hydrates near the clay grains.

It is well known that the concentration of $Ca(OH)_2$ in the liquid is lowered towards zero when allophane is dispersed in the $Ca(OH)_2$ solution.

Berrell and Gradwell (27) considered that cations are adsorbed on the surface of allophane as the adsorption equilibria followed BET equation.

Wada and Ataka (28) considered that cations were adsorbed on the surface of allophane as salt from the fact that CEC was related to the concentration of exchanged salt and pH value of the solution. On the other hand, Iimura (29) described that cation adsorption of allophane was an ion exchange phenomenon based on the dissociation of weak acidic group of the grain surface.

Greenberg (30) studied the reaction between silica and calcium hydroxide solution and concluded that the reaction could be divided into six elementary processes, that is, the adsorption of $Ca(OH)_2$ to silanol group of silica surface, the dissolution of silica, the reaction of $H_4SiO_4 + Ca(OH)_2 \rightarrow C\text{-}S\text{-}H$, the formation of nuclei, the growth of nuclei and the precipitation of crystal. They also emphasized that the dissolution of silica was the rate determining step of overall reaction. And the rate of reaction was influenced by the surface area of silica and its free energy state but it was not influenced by the concentration of $Ca(OH)_2$ above 3.6 m mol/l.

Van Aardt and Visser (31) studied the reaction between feldspar and $Ca(OH)_2$ relating to the alkali-aggregate reaction of cement and described as follows : $Ca(OH)_2$ liberated by the hydration of cement precipitates on the surface of feldspar grains and dissolves alkalies in feldspar. The alkalies exist in the liquid phase as KOH and NaOH or from alkali silicates to precipitate on the surface of feldspar grains as gel. Alkali silicate film is destroyed by the repetition of expansion and shrinkage caused by the adsorption and the adsorption of water. The fragments of destroyed film of alkali silicates are flown into opening and crack of aggregate as viscous fluid and repeat the expansion and shrinkage.

Many pozzolanas contain fairly large amount of glass phase and a little amount of alkalies. It is easy to imagine that glass phase plays an important role and alkalies are related strongly to the reaction between pozzolana and $Ca(OH)_2$.

Sanders and Hench (32) showed that, on contact with water, alkalies in the glass dissolved preferentially into water leaving the thin layer of silica gel. They also said that dissolution proceeded more actively in soda glass than in soda-lime glass, and that the inhibition of dissolution in soda-lime glass, was due to the formation of Ca and Si rich layer where Na^+ was leached off.

El-Shamy (33) studied the reaction between potassium glass and water. He showed that the surface of glass was protonically attacked remarkably in the high alkaline solution of pH>9 and SiOH group dissociated to SiO^- and H^+ making electric double layers between the surface of glass and the solution, and that the resulting negatively charged glass attracted alkali ions in the solution. He described that the diffusion of ions through the reacted surface layer was the rate determining step of the erosion reaction of glass by alkalies.

These previous researches are very suggestive in considering the mechanism of hydration in the system pozzolana-$Ca(OH)_2$.

In the hydration in the system pozzolana-$Ca(OH)_2$, C-S-H precipitated near the pozzolana grains and Ca-Al hydrate Ca-Al-Si hydrate etc. precipitated apart from pozzolana grains as shown in Fig. 5.

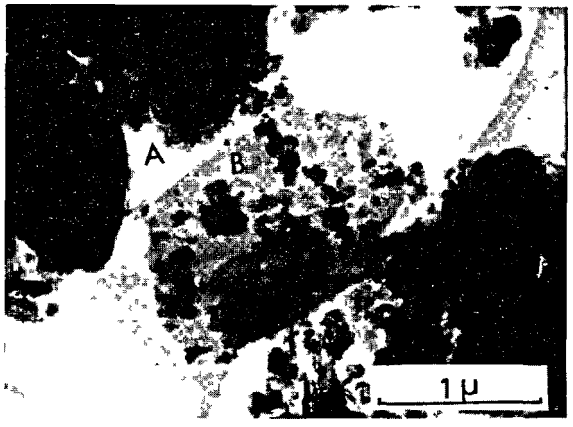

A. C-S-H B. Ca-Al hydrate

Fig. 5-Transmission electronmicrograph of the hydrates formed in the system pozzolana-$Ca(OH)_2$

Ultra fine particles of Å-order suggesting the dissociation of SiO_4 from the pozzolana grains were recognized in high resolution transmission electron microscopic observation as shown in Fig. 6.

As shown in Fig. 2, regardless of the kind of pozzolana, the amount of hydrates formed by the reaction between pozzolana and $Ca(OH)_2$ was proportional to the added amount of $Ca(OH)_2$ even in the age when solid $Ca(OH)_2$ coexisted.

Clifton, Brown and Fronsdorff (34) reviewed the works for the reaction of fly ash with

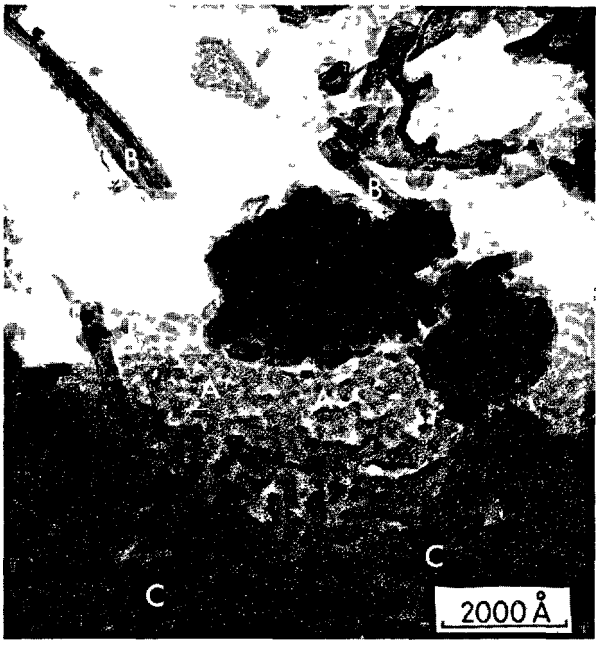

A. SiO_4 group product
B. precipitated type I C-S-H
C. pozzolana grain

Fig. 6-SiO_4 group released from pozzolana grain observed in high resolution transmission electronmicrograph

cement, as follows : the adsorption of calcium hydroxide on the surface of fly ash particles occurs initially, and forms a membrane over fly ash particle. Water gap exists between the membrane and fly ash particle. The pozzolanic reaction products are precipitated in the water gap and cover the fly ash particle to form a reaction rim.

Summarizing these experimental results and the previous works, the mechanism of the paste hydration in the system pozzolana-$Ca(OH)_2$ is considered as follows :

After mixing with water the liquid is saturated with $Ca(OH)_2$ in the short time and pH of the liquid is kept above 12.7. Pozzolana grains are protonically attacked by water in high caustic solution dissociating the SiOH group on the surface of the grains to SiO_4^{4-} and H^+ leaving negatively charged grains. Ca^{2+} is adsorbed on the surface of pozzolana grains by electrostatic force and alkalies in pozzolana dissolve into the liquid phase. The disolving-out of alkalies and so on remains a thin amorphous Si, Al-rich layer on the surface of pozzolana grain. SiO_4^{4-} and AlO_2^- in the layer gradually begin to dissolve and combine with Ca^{2+} to increase the thickness of the layer. The expansion and destruction of the layer due to the osmotic pressure caused by the difference of concentration between outside and inside of the thin layer proceed following the mechanism

mentioned-later (31).

SiO_4^{4-} is considered to diffuse more slowly than AlO_2^-, as the former has larger electric charge and has more oxygen atoms than latter. The concentration of Ca^{2+} enables Ca-Al hydrate to precipitate is generally higher than that of C-S-H. For these reason, Ca-Al hydrate precipitates at the place apart from pozzolana grains.

Pozzolana having large dissolving surface area, wide precipitating site of hydrates and high free energy state gives high rate of pozzolanic reaction.

3.2 Hydration in the System Pozzolana-Cement Compound

3.2.1 Hydration in the system pozzolana-C_3S

Few papers are published on the hydration of the pozzolana cement compound.

Stein and Stevels (35) investigated the influence of amorphous silica on hydration of C_3S using C_3S, amorphous silica, quartz and portland cement. The conduction calorimetry on the hydration of C_3S and cement paste, TEM observation of pastes and suspension and the measurements of calcium and silicate ion concentration, electrical conductivity and pH in C_3S suspension brought them to the following conclusion. Amorphous silica accelerates the rate of hydration of alite in cement pastes and that of C_3S. By lowering calcium and hydroxyl ion concentration in the liquid phase for a few minutes after mixing with water silica converts the C-S-H film on the surface of C_3S or alite into less protective film composed of low Ca/Si ratio which accelerates the hydration of C_3S and cement paste. In portland cement pastes not only the hydration of alite but also the consumption of sulfate by the formation of ettringite are accelerated by the addition of amorphous silica. As calcium ion concentration is low, ettringite crystalizes generally apart from C_3A particles.

Lukas (36) investigated the rate of hydration of each clinker compound by X-ray diffraction and quantitative analysis of $Ca(OH)_2$ by DTA using the specimens prepared from 30% of fly ash and 70% of cement with W/S ratio of 0.4 from two kinds of cements and one kind of fly ash. Fly ash accelerates the early hydration of C_3S phase. But after three days it inhibits the hydration of C_3S. Though the rate of hydration of C_3A in cement is not so fast as that of pure C_3A, fly ash accelerates its hydration. Ettringte was not found by X-ray diffraction in early stage owing to its low content. But it increased from the first day to 14 days and then decreased. At the age of 14 days monosulfate hydrate was detected. The amount of $Ca(OH)_2$ is lower than that calculated from the stoichiometrical equation, so C-S-H has higher Ca/Si ratio than 1.5 shown in the stoichiometry. The decrease of $Ca(OH)_2$ in paste at the later age is attributed to the absorption by fly ash over than the amount of $Ca(OH)_2$ released by hydration.

Nelson and Young (37) investigated the additions of colloidal silicas and silicates on the hydrations of the Type I cement and C_3S pastes. The amount of added four kinds of colloidal silicas and silicates were based on percentage of the theoretical amount required to convert all the $Ca(OH)_2$ to C-S-H gel. Water was added to achieve given workability and water reducing agent was used when necessary. C_3S with colloidal silicas needed a higher W/S ratio than that without colloidal silicas to achieve given workability and its strength decreased with increase in W/S ratio. The decrease in $Ca(OH)_2$ content occurs in all cases especially in quite early age such as within one day. Amount of silica added to portland cement were 6.6% of cement by weight, which is 25% of theoretical amount required to complete the pozzolanic reaction with $Ca(OH)_2$ produced. The W/S ratio was adjusted 0.45 adding much water reducing agent. While one day strengths were improved by addition of colloidal silicas and silicates, later strengths were not affected by them. The reduction of $Ca(OH)_2$ in portland cement pastes by given amount of colloidal silicas and silicates is greater than in C_3S pastes which indicate the occurence of other reaction than C-S-H formation.

Takemoto, Uchikawa, Ogawa and Yasui (38) studied the hydration of the 6:4 mixture of C_3S and pozzolana with 0.4 of water solid ratio. Five kinds of Japanese pozzolanas and one kind of Japanese fly ash were used in this experiment. From the conduction calorimetry at initial and early stage of hydration, estimation of the rate of hydration of clinker compound by X-ray diffraction, quantitative analysis of unreacted pozzolanas by salicylic acid-methanol extraction method and observations of broken surface of hardened paste by SEM, they concluded that the addition of pozzolana and fly ash to C_3S accelerated the initial hydration within an hour. This tendency is remarkable in Beppu white clay and Kanto loam which are mainly consisted of opal and allophane, respectively. Degree of hydration of C_3S after the induction period was increased by the addition of pozzolana. Pozzolanas consisting mainly of opal and allophane were more reactive with C_3S than that consisting mainly of volcanic glass and fly ash. C_3AH_6 and C_4AH_{13} are found by DTA at the age of 28 days in case of the pozzolanas rich in allophane and aluminum-rich fly ash, respectively. But in the other pozzolanas no Ca-Al hydrate was found at 91 days. They also showed that there exists the void between the surface of pozzolana or fly ash and the layer of hydration products so that the hydrates tend to be stripped easily in the form of shell as shown in Fig. 7.

Summarizing above-mentioned previous works: Additions of pozzolanas accelerate the hydration of C_3S. Acceleration of hydration

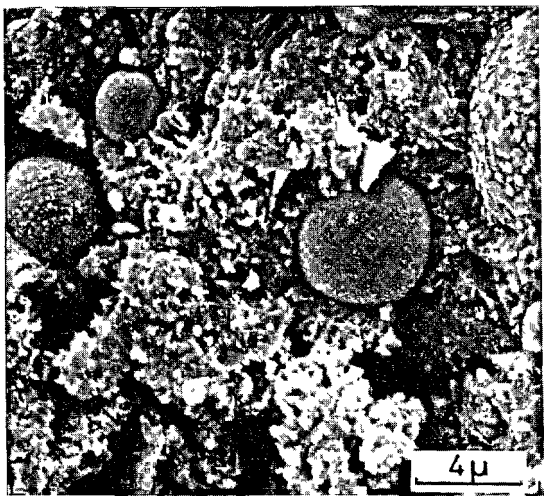

T - C_3S 91d

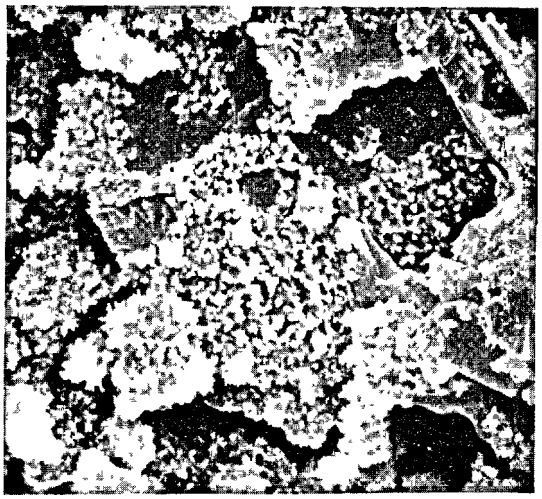

G - C_3S 91d

Fig. 7-Scanning electronmicrograph of the fracture surface of hardened pozzolana-C_3S paste showing the clearance between pozzolana and hydrates

after induction period by pozzolana is due to the stimulation of C_3S dissolution by the adsorption of Ca^{2+} in the liquid with pozzolana and due to the increase of surface by the addition of pozzolana which is preferable to the precipitation of C-S-H. C-S-H preciptated after induction period has higher Ca/Si ratio than 1.5, when sufficient amount of $Ca(OH)_2$ exists. C-S-H and Ca-Al hydrate etc. are generally formed by the pozzolanic reaction between $Ca(OH)_2$ and pozzolana after one day and the physical properties, for example strength of paste, develops in later age. Aluminate hydrates are formed later and their period of formation depends on the characters of pozzolanas, that is, aluminum content and their solubility. Addition of pozzolanas also accelerates hydration of alite and C_3A phase in cement.

3.2.2 Mechanism of the hydration in the system pozzolana-C_3S

Studies on the mechanism of the hydration of C_3S are actively performed recently.

Dent Glasser, Lachowski, Mohan and Taylor (39) reported informative work, and recent works on this field were reviewed by Skalny, Jawed and Taylor (40). They suggested that the reaction of hydration proceeded in the following cycle, that is releasement of calcium ion from the surfaces of C_3S particles and formation of amorphous silica rich layer by protonic attack of water, swelling and opening of surface film by osmotic pressure, formation of inner hydrates by movement of calcium ions from outside to the inside of the film by passing through the opening, precipitation of $Ca(OH)_2$ on outside of the film. This view is accepted as a whole to be right.

Takemoto, Uchikawa, Ogawa and Yasui (38) carried out the observation of the polished surface of hardened paste in the system pozzolana-C_3S and the analysis of hydrates between C_3S-C_3S grains, C_3S-pozzolana grain and pozzolana-pozzolana grains by FESEM with EDX. Considering the data obtained by FESEM with EDX and the results of analysis of liquid phases at initial and early stages and SEM observation of C-S-H precipitation on the surface of quartz grain in C_3S-quartz and that in C_3S-alkali treated quartz systems, they obtained the following results. C-S-H formed between C_3S and pozzolana grain precipitated in spherical structure wrapping C_3S grain which extended from C_3S grain to pozzolana grain and showed zonal structure. Each zone had its own chemical composition. Stepwise decrease in Ca/Si ratio from C_3S grain towards pozzolana grain was clearly observed.

$Ca(OH)_2$ crystals could be observed where Ca/Si ratio was abnormally high. The dissolution of alkali from pozzolana was higher in the system C_3S-pozzolana than in the case of pozzolana alone. C-S-H precipitated on the surfaces of all C_3S and quartz grains in the system C_3S-quartz, while C-S-H did not seen occationally on the surface of alkali treated quartz grain though it was observed on the surface of C_3S without exception in the system C_3S-alkali treated quartz.

Considering above mentioned results they proposed the following mechanism of the hydration in the system pozzolana-C_3S.

As shown in Fig. 9, calcium ions dissolved from C_3S run about freely in liquid are captured by collision to the negatively charged pozzolana grains and are adsorbed on the surfaces. C-S-H formed by hydration of C_3S precipitates as the hydrates of high Ca/Si ratio on the surface of C_3S grains and

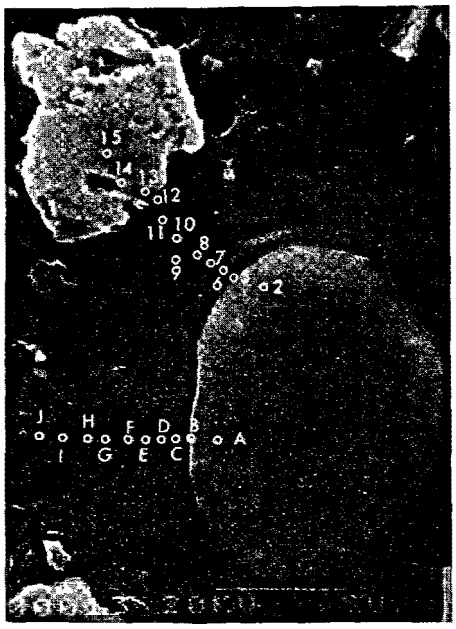

Age 91day

Electronmicrograph of hardened C_3S-Beppu white clay paste after etching with 2%HCl-ethanol solution and coated by carbon

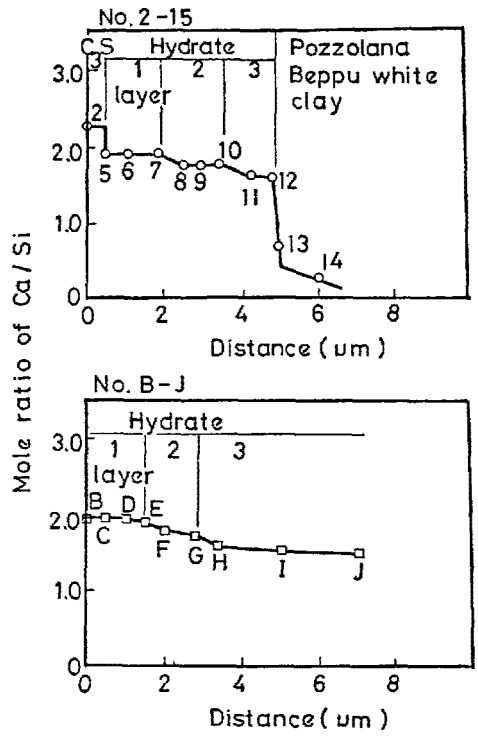

(Accelerating voltage: 20 kv, sample current : 10 μμA , carbon coating)

Age 3 days

C_3S - fly ash past, no etching

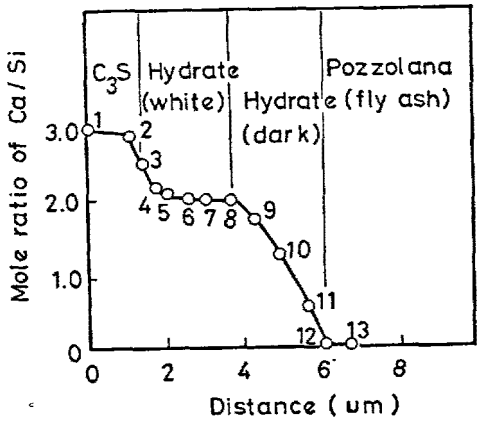

Fig. 8-Field emission scanning electron micrograph of pozzolana-C_3S paste showing zonal structure of hydrates and the distribution of calcium and silicon between pozzolana grain and C_3S grain.

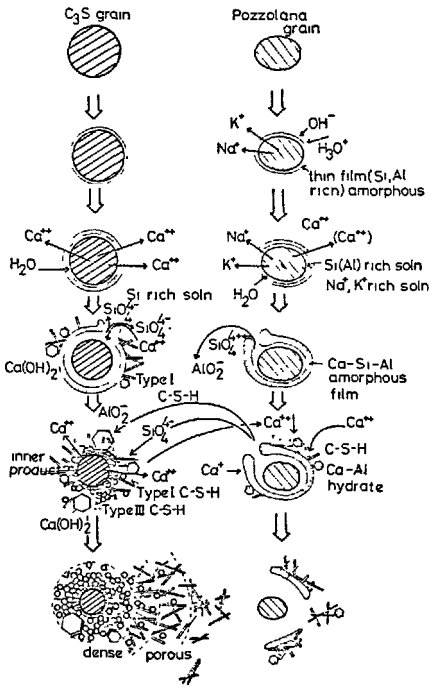

Fig. 9 - Schematic explanation of the mechanism of hydration in the system pozzolana-C_3S (38)

as the porous hydrates of low Ca/Si ratio on the surfaces of pozzolana grains. On contacting with water, surfaces of pozzolana grains are protonically attacked by H_3O^+ formed by the dissociation of water. It brings gradual dissolution of Na^+ and K^+ etc., resulting si and Al rich amorphous layer on the surfaces. Dissolved Na^+ and K^+ accelerate the dissociation of water, intensify the protonic attack of water and accelerate the dissolution of SiO_4^{4-} and AlO_2^- which combine with Ca^{2+} and increase the thickness of layer. Due to the osmotic pressure generated by the difference of concentration of ions, such as alkalies, SiO_4^{4-}, AlO_2^-, between inside and outside of layers, the layer swells gradually and the void between layer and pozzolana grain is formed. The void is filled with Si, Al, Na^+ and K^+ rich liquid. When osmotic pressure attains certain pressure, the film is broken and SiO_4^{4-} and AlO_2^- diffuse outside through the openings to meet Ca^{2+}. The condition of precipitation being satisfied, C-S-H and Ca-Al hydrate precipitate on the surface of outer hydrates of C_3S. Solution near the outer surfaces of destroyed film becomes poorer in Na^+ and K^+ than inside and Ca^{2+} is apt to be adsorbed on the film resulting in the precipitation of C-S-H and Ca-Al hydrate. Considering the thickness of film and the distribution of Ca ion concentration, the amount of the precipitated C-S-H and Ca-Al hydrate is, however, very small compared with the amount of outer hydrates of C_3S. Vacant space remains inside the film as the hydrate do not precipitate there because of high concentration of alkalies. The hydration proceeds according to the repetition of above mentioned cycle. Accordingly vacant space always exists between the film and pozzolana grain.

When alkalies do not exist, destruction of amorphous Si, Al rich film enables Ca^{2+} to move into the inside of the film from the openings and to precipitate C-S-H and Ca-Al hydrate on the surface of pozzolana grain and filled the clearance. Therefore no clearance is observed between pozzolana grains and hydrates.

Pozzolana is a mixture composed of alkali containing minerals and glasses and those without alkali. In paste hydration, some places become rich in alkali and others are poor. Therefore, the hydrates produced in alkali rich region tend to be stripped off from pozzolana surface and the hydrates produced in alkali poor region attached closely to pozzolana grain. The glass such as in fly ash contains homogeniously much alkali, so the typical stripping off of the hydrates from pozzolana grain is often clearly observed.

3.2.3 Hydration in the system pozzolana-C_3A

Few investigations have been made on hydration reaction in the system pozzolana-C_3A.

Holten and Stein (41) examined the influence of quartz surface upon hydration in the system of C_3A-$CaSO_4 \cdot 2H_2O$- H_2O by measuring the heat of hydration by conduction calorimetry, the identification of formed phases by X-ray diffraction and the observation of hydrated specimen by SEM. They found that heat evolution peaks are divided into four stages. The first peak corresponds to the formation of ettringite, the second one to perfect consumption of $CaSO_4 \cdot 2H_2O$, the third to a part of formation of AFm and the fourth to the formation of monosulfate hydrate and 8.2Å carboaluminate coexisting with ettringite. Quartz prevents ettringite from precipitating on C_3A surface by presenting the site of its precipitation and lowers the retardation by SO_4^{2-}. Surface of C_3A particles is covered with layer having similar composition to $Al(OH)_3$, because Ca^{2+} on C_3A surface is preferentially extracted by dissociated hydronium ion. The the hydration in NaOH solution, disturbed surface layer having similar composition to that of $Ca(OH)_2$ is formed on surface of C_3A particles by the preferential extraction of aluminate ion by OH^-.

Collepardi, Baldini, Paure and Corradi (42) examined the hydration in the system C_3A, $CaSO_4 \cdot 2H_2O$, $Ca(OH)_2$ and volcanic and diatomaceous silica rich pozzolana at 20 ± 0.5°C and W/S = 0.8 by carrying out the measurement of the heat evolution, DTA and SEM observation. They found that the heat evolution in the system of C_3A hydration decreases with addition of pozzolana, especially in diatomaceous silica rich pozzolana. This effect is rather small when the rate of hydration of C_3A is retarded by $CaSO_4 \cdot 2H_2O$ and/or $Ca(OH)_2$.

They concluded that retardation of hydration of C_3A by pozzolana was caused by the absorption of pozzolana to surface of C_3A particles. $Ca(OH)_2$ in C_3A paste decreases rapidly when pozzolana exists. This decrease can not be related to the lime-pozzolana reaction, which is much slower. They described that ettringite, lime and C_3A reacted to form hexagonal solid solution when gypsum existed and that hexagonal hydrates were easy to convert to C_3AH_6 in the C_3A sample containing $Ca(OH)_2$ and volcanic pozzolana. These facts show that reactions between pozzolana and C_3A or pozzolana and hydrates from C_3A proceed besides well known reaction between lime and pozzolana.

Uchikawa and Uchida (43) studied the hydration in the system C_3A-$CaSO_4 \cdot 2H_2O$-$Ca(OH)_2$ containing 40% by weight of five kinds of Japanese pozzolanas or one kind of Japanese fly ash at 20 ±1°C and W/S=0.60. The identification and quantitative analysis of formed hydrates by DSC-TG under Ar atomosphere, conduction calorimetry in hydration, quantitative analysis of C_3A by X-ray diffraction, SEM observation and the measurement of cation exchange capacity of pozzolana brought them following results. In the absence of $Ca(OH)_2$, hydration of C_3A, formation of ettringite and conversion of ettringite to monosulfate hydrate were accelerated by the addition of pozzolana especially pozzolanas mainly composed of allophane, volcanic glass and opal. The acceleration was roughly proportional to the added amount of pozzolanas. The formation of ettringite and conversion of ettringite to monosulfate hydrate were retarded by the addition of $Ca(OH)_2$. Pozzolana containing much alkalies (Na, K) accelerated the formation of C_3AH_6. They deduced that the reaction of acceleration of hydration of C_3A by addition of pozzolana was adsorption of Ca^{2+} to the surface of pozzolana and that the acceleration of the dissolution of C_3A particles was due to less formation of ettringite film on C_3A grains caused by the precipitation of ettringite on the surface of pozzolana grains. As the hydration of C_3A is accelerated by the addition of pozzolana, so that the complete consumption of solid calcium sulfate is also accelerated, which make the ettringite convert to monosulfate hydrate. The reason why conversion to C_3AH_6 was accelerated in pozzolana containing much alkalies is probably the decrease of the stability of hexagonal hydrate with increasing alkalies concentration as reported by Spierings and Stein (44).

Summing up above mentioned previous works, hydration of C_3A is accelerated by addition of pozzolana. The degree of acceleration is larger in pozzolana with larger specific surface area and higher CEC value. The reason for acceleration of the hydration of C_3A by pozzolana is adsorption of Ca^{2+} in liquid phase to the surface of pozzolana and acceleration of C_3A dissolution due to the precipitation of ettringite on the surface of pozzolana. Accelerated conversion to C_3AH_6 under coexistence of pozzolana containing much alkali is responsible for decreased stability of hexagonal hydrates under high alkali concentration. Decrease of $Ca(OH)_2$ in initial and early stages of hydration may not be due to pozzolana reaction but another elementary process of reaction such as adsorption.

3.2.4 Mechanism of the hydration in the system pozzolana-C_3A

There are many studies on the hydration of C_3A and on the effect of Na_2O (44) (45) and SO_4^{2-} (46) (47). Summing up these reports, Skalny, Jawed and Taylor (40) presented the mechanism of the hydration of C_3A as follows:

On contact with water, C_3A dissolves incongruently leaving Al rich surface. Ca ions chemisorb on this surface producing positively charged particles. The formation of such a structure decreases the number of active dissolution sites and thus, the rate of C_3A dissolution decreases. Sulfate ion is adsorbed on the positively charged C_3A particles resulting in further reduction of dissolution sites. This blocking effect retards rate of hydration further more.

There are few reports, however, on the mechanism of hydration on the system containing pozzolana-C_3A.

Uchikawa and Uchida (43) presented the following mechanism of the hydration on the system C_3A-$CaSO_4 \cdot 2H_2O$-$Ca(OH)_2$-pozzolana combining the idea of Skalny et al (40) on C_3A and the mechanism of the hydration of pozzolana as shown in Fig. 10.

On contact with water, C_3A is protonically attacked by H_3O^+ formed by the dissociation of water releasing Ca^{2+} and leaving amorphous Al rich layer on C_3A grain surface. Amorphous layer is expanded by osmotic pressure and formes slight clearance between hydrated C_3A particle and itself. This clearance is filled with AlO_2^- rich solution. There exists Ca^{2+}, SO_4^{2-} rich solution at the near outside of the layer brought by the coproceeding dissolution of calcium sulfate and calcium hydroxide. Ca^{2+} is adsorbed on the amorphous Al rich layer on the surface of C_3A. The grain charges positively and the active sites on the surface of C_3A decreases. Therefore, hydration of C_3A is stopped temporarilly. SO_4^{2-} is adsorbed on the surface of positively charged grain and play a part of blocking against protonic attack of hydronium ion. Amorphous Al rich film is brocken at the weakest point by osmotic pressure. From the openings Ca^{2+} and SO_4^{2-} introduced into inner side of film. AlO_2 moves towards outer side of film and ettringite precipitates on both sides of film. On inner side of film, monosulfate hydrate often precipitates as SO_4^{2-} is apt to be in shortage. Monosulfate hydrate on the inner side is generally small in size because of the narrow precipitation space. Precipitated hydrates have high crystallinity, so it is easy for Ca^{2+}, AlO_2^-, SO_4^{2-} etc. to diffuse through the hydrate

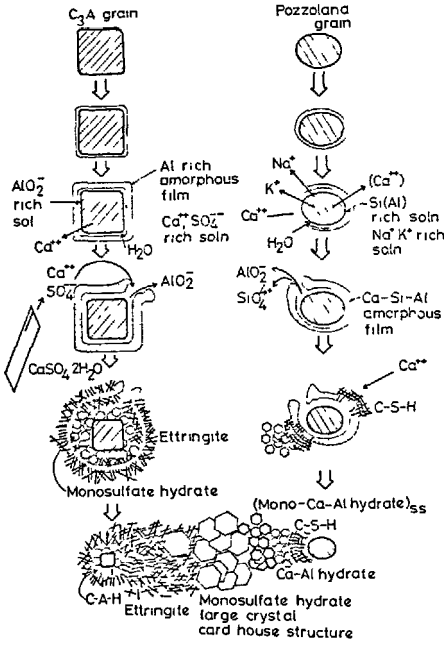

Fig. 10 - Schematic explanation of the mechanism of hydration in the system pozzolana-C_3A under the existence of $Ca(OH)_2$ and $CaSO_4 \cdot 2H_2O$ (43)

layer covering the C_3A grain. The porous ettringite layer is broken by the expansion of itself to make the contact of water to C_3A easy.

Hydration of C_3A proceeds repeating above mentioned process as one cycle. When solid $CaSO_4 \cdot 2H_2O$ is consumed completely and concentration of SO_4^{2-} lowers, monosulfate hydrate or solid solution of monosulfate hydrate and C_4AH_{19} precipitates on the outside of film. Void in the paste outside the grain is usually large, so hexagonal monosulfate hydrate or its solid solution precipitate as large crystal towards large void to build the well known card house structure.

Ettringite once formed converts to hexagonal hydrate, monosulfate hydrate or its solid solution. The time of conversion of hexagonal Ca-Al hydrate to cubic C_3AH_6 depends upon the concentration of alkali ion. Negatively charged grains of pozzolana, on the other hand, adsorb Ca^{2+} formed by the hydration of C_3A, $CaSO_4 \cdot 2H_2O$ and $Ca(OH)_2$ on their surface. By the adsorption of Ca^{2+} in liquid phase and by presenting the site of precipitation of ettringite, pozzolana accelerates the hydration of C_3A.

General features of hydration of pozzolana are about the same as those of pozzolana-C_3S system.

SiO_4^{2-} and AlO_2^- near at the outside of film precipitate as ettringite, monosulfate hydrate, Ca-Al hydrate and C-S-H on the surface film of the outside of pozzolana grain or on the surface hydrate layer of C_3A grain according to the concentration of Ca^{2+} and SO_4^{2-} in the liquid. As the rate of diffusion of SiO_4^{4-} is slow and the concentration of Ca^{2+} is rather high even at the neighbour of pozzolana grain. C-S-H is observed in the paste containing negatively charged acidic pozzolana with low alkali and high SiO_2.

Concentration of SO_4^{2-} in the liquid near the pozzolana grain is low, so the nearest hydrate to the pozzolana grain consists mainly of Ca-Al hydrate and towards outside, the solid solution of Ca-Al hydrate and monosulfate hydrate and monosulfate hydrate precipitate in this order. Ettringite, precipitated in the early stage of hydration, is not observed in the later stage.

3.3 Hydration in the System Pozzolana-Cement

There is no essential difference between the hydration in the system pozzolana-cement and that in the system pozzolana-$Ca(OH)_2$ and pozzolana-cement compounds. Here the authors' results are shown.

Pozzolanic cement, 4:6 mixture of five kinds of Japanese natural pozzolanas, one kind of fly ash and ordinary portland cement, was hydrated at 20°C with W/S=0.3.

Heat evolution curve by conduction calorimetry, degree of hydration of alite in the pozzolanic cement paste estimated by X-ray diffraction analysis and the degree of pozzolanic reaction with curing time are shown in Fig. 11, Fig. 12 and Fig. 13.

The degree of pozzolanic reaction was expressed in term of the difference between the amount of estimated $Ca(OH)_2$ which might be formed in the case when no pozzolanic reaction occurs and that formed actually in pozzolanic cement paste. The amount of former was determined by measuring the degree of hydration of alite in ordinary portland cement by X-ray diffraction using the predetermined relation between the degree of hydration of alite and the amount of $Ca(OH)_2$ formed in the ordinary portland cement paste hydrated in the same conditions as pozzolanic cement.

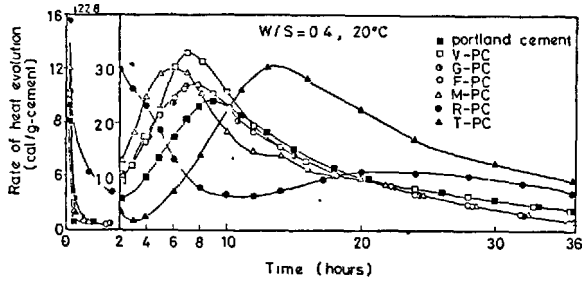

Fig. 11 - Heat evolution curve in hydration of pozzolanic cement

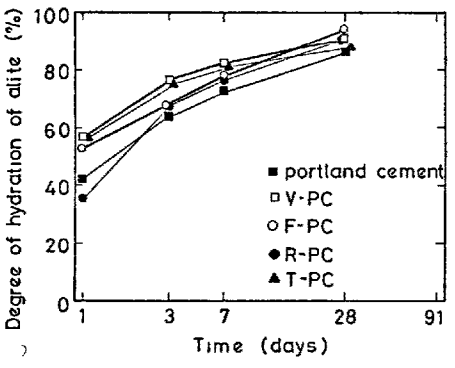

Fig. 12 - Degree of hydration of alite in pozzolanic cement

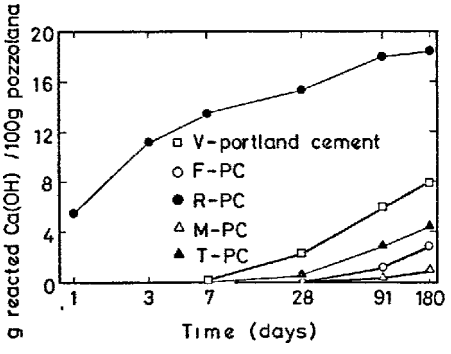

Fig. 13 - Degree of pozzolanic reaction expressed in term of the quantity of reacted $Ca(OH)_2$

The hydration of pozzolanic cement,especially the hydration of alite, was accelerated by the addition of pozzolana, except for the initial stage of Kanto loam and fly ash.

The pozzolanic reaction in general is considered to proceed the hydration of cement from the early stage. But it took 7 days for Beppu white clay mixed pozzolanic cement and Takehara fly ash mixed fly ash cement, and 28 days for Furue shirasu mixed pozzolanic cement, Higashi-Matsuyama tuff mixed pozzolanic cement and Tominaga masa-soil mixed pozzolanic cement to be able to recognize clearly the pozzolanic reaction by the amount of reacted $Ca(OH)_2$. In Kanto loam mixed pozzolanic cement, the pozzolanic reaction seems to proceed even in the initial stage.

There were no difference in the kinds of produced hydrates among the kinds of pozzolanic cement within 180 days. In the early age ettringite, solid solution of monosulfate hydrate-C_4AH_{13} and $Ca(OH)_2$ were produced. Ettringite disappeared at three days. C-S-H attained to the detectable amount by X-ray diffraction at 28 days. In the Kanto loam mixed pozzolanic cement containing much amount of alumina, C_3AH_6 were observed at 40°C. Gehlenite hydrate (C_2ASH_8), which appeared in the system pozzolana-$Ca(OH)_2$, was not detected.

4. STRENGTH OF POZZOLANIC CEMENT

4.1 Microstructure of Pozzolanic Cement Paste

In the study for morphology, composition and structure of cement paste and particles which constitute cement paste, the analytical method, experimental means and interpretation of obtained results are significantly different with the sizes of the objects.

In this report, to avoid the complexity, Diamond's classification (48) is used with some modification, as follows:

(1) the problem for texture level (μm order); remarking the texture of hardened paste

(2) the problem for particle level (0.1 μm order); remarking gel structure with hydrates particles and unhydrated particles which constitute paste structure

(3) the problem for atomic level (unit cell order); remarking atomic arrangement and crystal structure of hydration products which constitute hydrates particles

Texture level corresponds to the order of paste structure as texture. The composition can be analysed by EPMA, and the morphology can be observed by SEM as the macro structure. The objects of texture level are aggregate texture of C-S-H particles, aggregate texture of crystalline hydrates particles, that is, $Ca(OH)_2$, ettringite, monosulfate hydrate, hydrogarnet, unhydrated particles and capillary space.

Particle level corresponds to gel structure, the composition can be analysed by AEM and the morphology can be observed by SEM or TEM as the micro structure. Type I to type IV C-S-H particles, polycrystalline particles like $Ca(OH)_2$, ettringite, monosulfate hydrate, hydrogarnet and gel pore are the object of this level.

Atomic level structurally corresponds to crystal structure, which is observed by TEM as lattice image. We now have no tool to analyse the composition directly such micro area. The objects of this level are solid solution, lattice defect, atomic arrangement, strain of lattice and so on.

4.1.1 Texture level

Cement gel and unhydrated particles make characteristic aggregation according to water material ratio, degree of hydration, morphology and size of hydrate, precipitation time and form characteristic paste structure.

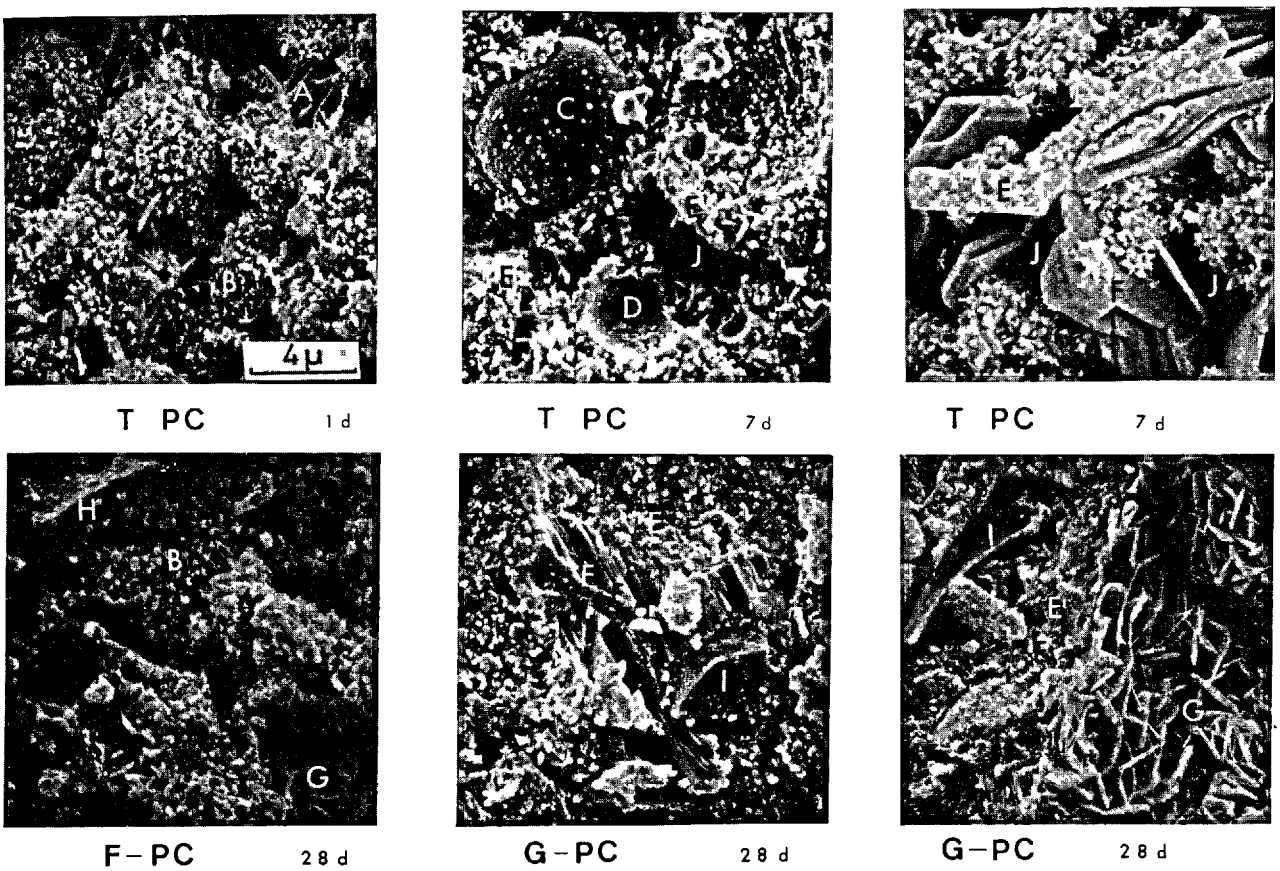

Fig. 14 - Scanning electronmicrographs of the fracture surface of hardened pozzolanic cement paste

A. ettringite
B. type I C-S-H
C. fly ash grain
D. cast-off shell of fly ash
E. type III C-S-H
F. calcium hydroxide
G. monosulfate hydrate
H. pozzolana grain
I. pozzolana grain
J. capillary space

Ciach, Gillott, Swenson and Sereda (49), who studied hardened C_3S paste structure with electron microscopy, showed that fibrous grain, formed around C_3S particles, interlocked each other and made mesh structure of pseudohexagonal arrangement, and that amorphous C-S-H particles of high CaO/SiO_2 particles filled the pores of mesh structure to form platy particles. This platy particles bound unhydrated particles each other or bound amorphous particles formed at the position of unhydrated particles.

Not only $Ca(OH)_2$ but also C-S-H particles formed platy particles having high compressive strength. It was due to fibrous network in amorphous materials, and the reason of low tensile strength was that those platy grains didn't interconnect each other but merely overlapped.

Collepardi, Marcialis, Massiddo and Sanna (50) studied the reaction between $Ca(OH)_2$ and four kinds of Italian pozzolanas. Hardened pastes had textures consisting of low crystalline, irregular shaped grains. The texture become closely with the higher CaO/SiO_2 ratio and the pore size distribution was divided into two parts, $1 \sim 0.2$ μm and $0.2 \sim 0.02$ μm with the measurement of mercury penetration porosimeter of the pressure between 100 to 10,000 atom. The former was the pores in pozzolana, the latter was the pores in the particle texture formed with the reaction between CaO and pozzolana.

On the other hand it is known that $Ca(OH)_2$ forms on the surface of fly ash like a film in the reaction process between fly ash and cement or $Ca(OH)_2$, Kokubu (51) showed that the $0.5 \sim 1.0$ μm water gap (capillary space) existed between unhydrated fly ash particle and hydrates with the observation of fracture surface of concrete cured for 3.5 years, and assumed that Ca^{2+} was supplied to fly ash surface through the gap.

In the early stage of pozzolana cement reaction, the hydrates texture mainly consists of type I and type III C-S-H particles,

needlelike crystal of ettringite, card house structure of monosulfate hydrates formed towards pores just like as in portland cement paste. With the curing time, type III C-S-H becomes predominant phase and the piled large $Ca(OH)_2$ crystal often penetrates the aggregate texture.

In the reaction between fly ash cement, even in the early stage, hexagonal $Ca(OH)_2$ crystals penetrate the hydrate texture can be seen. Type III C-S-H forms on the surface of fly ash, and card-house structure of monosulfate forms toward pores. The shape of $Ca(OH)_2$ crystal becomes irregular and makes piled crystal with the curing age.

There are very few studies for hardened paste, not only pozzolanic cement, fly ash cement but also portland cement in texture level though those play an important role on the properties of hardened paste. Those problems will become much more apparent by SEM and the new tools in near future.

4.1.2 Particle level

When cement paste is considered in hydrated particles order, C-S-H is morphologically classified (48) type I (fibrous particle), type II (reticular network), type III (small equant grains) and type IV (inner product). Each particle is usually polycrystal.

Calcium hydroxide forms as hexagonal or irregular accumulating shape. Ettringite is columnar. Monosulfate hydrate is hexagonal plate and forms far apart from each other or makes card house structure. Calcium aluminate hydrates have the same morphology as monosulfate hydrate or can rarely be observed as a trapezohedron, those hydrates have high crystallinity in general and some are considered to be consisted of single crystals.

Recently the composition of particle level, that is 0.1 μm (1,000Å) order, is frequently determined with the spread of AEM (13) (39). Diamond (52) showed, using SEM-EDX, that C-S-H of cement contained SO_3. Uchikawa, Uchida and Mihara (13) showed, using TEM-EDX, that in the case of ultra rapid hardening cement, C-S-H contained sulfur and aluminum and monosulfate hydrate and ettringite contained silicon.

Lukas (53) analysed, using EDX, composition of ettringite which showed the higher intensity of SiKα in the hydration of fly ash cement than that in the case of ordinary portland cement. Though we do not have works on these matter for pozzolanic cement, similar invasion of the "third" ions to the hydrates could be occured for pozzolanic cement.

TMS (trimethylsilylation) analysis (54) has given the better understanding of the structure of C-S-H in these days. Dent Glasser, Lachowski, Mohan and Taylor (39) suggested, in the hydration of C_3S, that C-S-H contained dimer and polymer and the latter increased with curing time using TMS analysis. The authors found by TMS analysis, in the hydration in the system pozzolana-C_3S, that the paste containing the pozzolana of higher reactivity yielded more quantity of polymer at the same curing age.

4.2 Pore Structure of Pozzolanic Cement Paste

4.2.1 Total porosity, capillary space and gel pore space

Pozzolanic cement, mixture of five kinds of Japanese natural pozzolanas and one kind of fly ash with 40% of ordinary portland cement, was hydrated at 20°C with W/S = 0.3. Hardened paste was D-dried and total porosity, capillary space, gel pore space and compressive strength which changed according to the curing time was determined. The result was shown in Fig. 15.

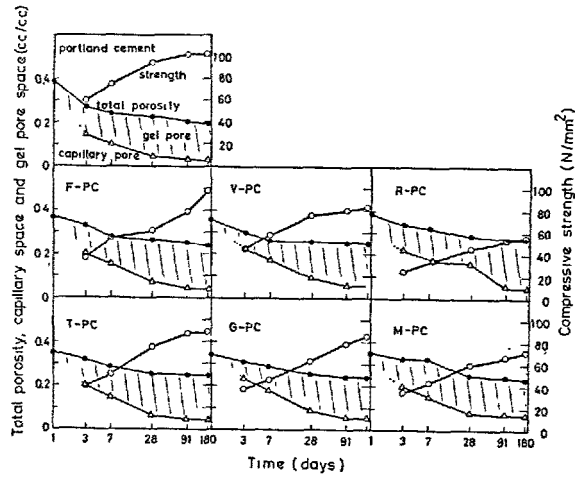

Fig. 15-Change in total porosity, capillary space and gel pore space of pozzolanic cement paste with age

Total porosity was determined with the method by Yudenfreund, Older and Brunauer (55) and the volume of capillary space which was corresponded to the pores above 75Å radius was measured with mercury penetrating porosimeter. Gel pore space was calculated as the difference between total porosity and capillary space. Therefore, gel pore, mentioned here, contains pores above 20Å which is average distance of C-S-H particles.

Total porosity was increased according to the quantity of added pozzolana in the early and middle age. That phenomena is considered to be mainly according that the increase of added pozzolana causes less formation of hydrates. Though total porosity decreases with the curing time, it shows still higher value than that of portland cement at about 180 days.

The volume of capillary space decreased remarkably with the curing time and the degree of decrease has characteristic tendency with the kinds of pozzolanas. This means that hydration products are liable to precipitate

selectively on the surface of particles surrounding relatively large pores, and shows the process that larger pores are in turn filled with hydration products. Therefore the decrease of volume of capillary space is remarkable in the early age when reaction of cement hydration is active and large pores mainly exist. The decrease of volume of capillary space is small in pozzolanic cement made of Kanto loam or Tominaga masa-soil which has large amounts of soluble alumina. The reason for this is supposed that besides C-S-H, large crystals of calcium aluminate hydrates or/and gehlenite hydrates precipitate significantly and form porous structure of hydration products. Though fly ash has large amounts of soluble alumina, the volume of capillary space is similar to natural pozzolanas which have small amounts of soluble alumina, because pozzolanic reaction of fly ash is rapid and large amounts of hydration products are formed.

Gel pore increases with the curing time in the early stage, but turns to decrease between 91 days and 180 days. The fact shows that along with filling capillary space by hydration products formed in the early and middle age, fine gel pores are newly formed in the filled capillary space and gel pore space bigins to decrease in the láter age when the amounts of filling of gel pore with fine crystals, such as C-S-H, exceeds the volume of formed gel pore. Therefore, the ratio of the amounts of gel pore and total porosity, that is G/T, increases rapidly till 91 days, then decreases after that. The change of gel pore ratio accompanied by the curing time is similar in the following couples, that is, Beppu white clay mixed pozzolanic cement and Higashi-Matsuyama tuff mixed pozzolanic cement, Furue shirasu mixed pozzolanic cement and Takehara fly ash mixed fly ash cement, Tominaga masa-soil mixed pozzolanic cement and Kanto loam mixed pozzolanic cement.

4.2.2 The shape of gel pore

Adsorption-desorption isotherms with N_2 gas

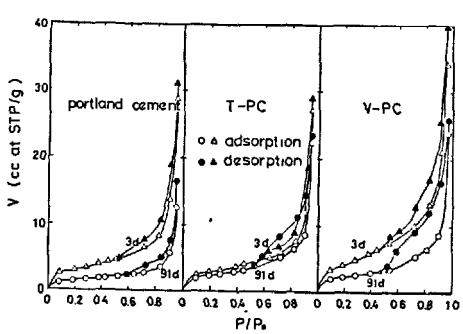

Fig. 16 - Adsorption - desorption isotherms with N_2 gas of hardened pozzolanic cement paste and hardened ordinary portland cement

of Beppu white clay mixed pozzolanic cement, Takehara fly ash mixed fly ash cement and ordinary portland cement paste are shown in Fig. 16.

In the pozzolanic cement, pronounced hysterisis of adsorption-desorption is observed with the curing time and the tendency that can easily adsorb but hardly desorb, is noticed. This result is cosidered to show that the proportion of fine pore or pore which has small opening to gel pore increases with the curing time and the order is in turn Beppu white clay mixed pozzolanic cement, Takehara fly ash mixed fly ash cement and ordinary portland cement.

Calculating the ratio of height and radius of pore using the data of specific surface area determined by BET method and adsorption isotherms and assuming the shape of pore as cylinder (56), in Beppu white clay mixed pozzolanic cement paste, the ratio is 4 at 3 days and 11 at 91 days, in Takehara fly ash mixed fly ash cement paste, the ratio is 4 at 3 days and 7 at 91 days and in portland cement paste, the ratio is 3 regardless of the curing time. That is, in the pozzolanic cement the shape of gel pore changes to be slender with the curing time.

4.2.3 Pore size distribution

The data of pore size distribution above 75Å radius in pozzolanic cement by mercury penetrating method is shown in Fig. 17.

Pore size distribution and change of pore size distribution with time is divided into three groups. In Beppu white clay mixed pozzolanic cement and Higashi-Matsuyama tuff mixed pozzolanic cement, pore size distribution has peaks at 125-375Å and above 1,870Å at 3 days. Though the peak at 125-375Å decreases and shifts to small radius with the curing time, the amounts of decrease of the pores above 1,870Å is small and a significant amount of pores remains even at 180 days.

Tominaga masa-soil mixed pozzolanic cement and Kanto loam mixed pozzolanic cement paste have higher peak at 125-375Å at 3 days compared with above case and have a smaller amount of pores above 1,875Å. Though the peak shifts to small radius, the amounts of decrease of peak height is small. The considerable amounts of pore about 100Å exists even at 28 days.

In Furue shirasu mixed pozzolanic cement and Takehara fly ash mixed fly ash cement paste, pore size distribution is similar to that of Tominaga masa-soil mixed pozzolanic cement paste till 3 days, but after 7 days it changes like that of Beppu white clay mixed pozzolanic cement and Higashi-Matsuyama tuff mixed pozzolanic cement paste.

These pore size distributions of pozzolanic cement pastes are different from that of portland cement paste, therefore, it is supposed that the difference of the peak

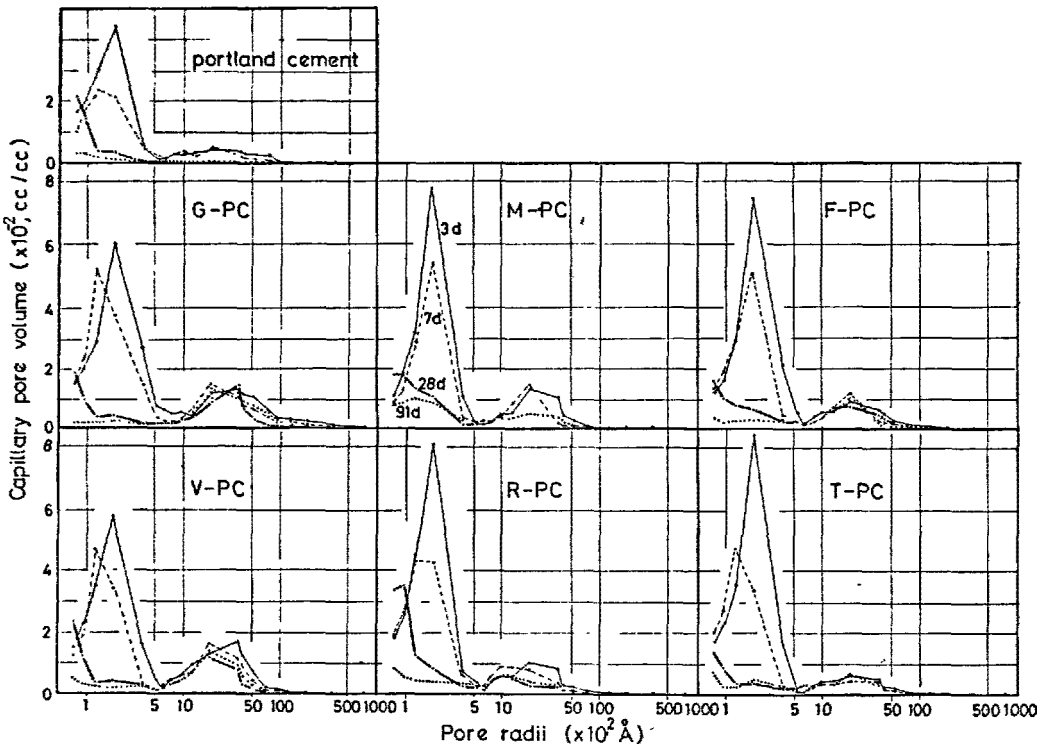

Fig. 17 - Pore size distribution curve of hardened pozzolanic cement paste measured by mercury penetration

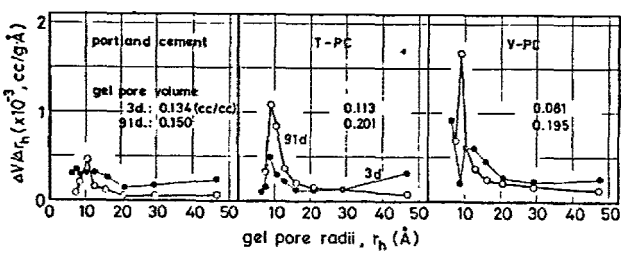

Fig. 18 - Gel pore size distribution curve of hardened pozzolanic cement measured by BET method using N_2 gas

height of 125-375Å and above 1,875Å at 3 days is due to the amounts of produced hydrates and the pore size distribution of mixed pozzolana itself.

Pore size distribution of gel pore measured by N_2 gas adsorption of BET method is shown in Fig. 18.

Though the quantity of gel pore is different with the kinds of pozzolanic cement, that is 0.195 cc/cc in Beppu white clay mixed pozzolanic cement paste, 0.201 cc/cc in Takehara fly ash mixed fly ash cement and 0.150 cc/cc in portland cement, in all the cases pore size distribution shifts to small radius with the curing time and the peak appeares at about 10Å radius at 91 days.

4.3 The Strength of Pozzolanic Cement Paste and the Character of Pozzolana

There are many studies which have tried to connect the strength of pozzolanic cement with the character of pozzolana.

Hanna and Afify (2) described that definite relation existed between 91 days mortar strength of pozzolanic cement and the ratio of the quantity of soluble $SiO_2 + R_2O_3$ in pozzolanic cement paste to the quantity of $SiO_2 + R_2O_3$ in the starting materials except for diatomaceous earth and granulated slag.

Battaglino and Shippa (57) stated that there existed correlation between the strength of pozzolanic cement and the change with time of specific surface area and the quantity of adsorbed CaO by pozzolana, that is, $\Delta s/\Delta t$ and $\Delta c/\Delta t$, till 3 days and that $\Delta s/\Delta t$ had higher correlation with the strength, and concluded that pozzolana, which was rich in amorphous silica and glassy silica, was desirable.

Jambor (58) stated that there existed the relation expressed in equation of tertiary order between compressive strength of pozzolana-lime mixture and the volume of hydration products except for burnt kaoline which formed different hydration products, and porous silica gel.

Chatterjee and Lahiri (59) showed that, though mortar strength of pozzolana-$Ca(OH)_2$ mixture had correlation with the specific surface area of the same pozzolana, the correlation was varied by the kind of pozzolana.

Thorne and Watt (60) showed that the strength of 2.5:1::2 mortar of fly ash, CaO and sand had correlation with the specific surface area of fly ash till 91 days, and after 91 days, with the content of SiO_2 + Al_2O_3 in fly ash.

Joshi and Rosauer (61) reported that the strength of 2 : 1 paste of synthesized fly ash and $Ca(OH)_2$ had correlation with the specific surface area of fly ash and that CaO in fly ash increased the strength but Fe_2O_3 decreased the strength.

Spitanos, Voyatzakis and Melidis (62) stated that the mortar strength of fly ash cement mixed with 30% of classified fly ash had correlation with grain size of fly ash and the finer the grain size of fly ash, the higher the strength was.

Summing up the result of above mentioned previous studies, it is showed that the character of pozzolana such as chemical composition, SiO_2, Al_2O_3, Fe_2O_3, etc. in pozzolana, the quantity of amorphous silica and glassy silica, and specific surface area,and the factor which have relations with the character of pozzolana such as the amount of formed hydration products, the quantity of CaO absorption in paste and the increment of specific surface area of paste, have some correlation with the strength. Those correlations, however, are mere results obtained under restricted condition as there exist not a few exceptions and the result is restricted to the case of the same pozzolana.

The fact clearly shows how difficult to connect the character of pozzolana with the strength of pozzolanic cement unequivocally and universally is. Therefore in the present study, the relation between character of pozzolana and the strength of pozzolanic cement should be connected by mediating other properties which have better-defined relation with character of pozzolana such as pozzolanic reactivity or properties concerning with the pore of paste of which correlation with the strength have been clarified to some extent.

4.4 The Strength and the Pore of Pozzolanic Cement Paste

It is well known that there exists fair linear correlation between the strength of the material and the porosity, and it is confirmed that the strength of cement paste also has a similar relation with the porosity (63).

Uchikawa and Tsukiyama (64) showed in the studies on the hydration of ultra rapid hardening cement that the slope of strength-porosity correlation curve changed by the size and shape of pores dependent on the size and morpholohy of crystals of hydration products and stated that in the early stage the strength remarkably developed but decrease of the porosity was small with formation of the large amount of prismatic crystals of ettringite and in the later stage in spite of relatively small strength development, porosity decreased remarkably with the formation of C-S-H.

Crennan, El-Hemaly and Taylor (65) studied that the relation between porosity and coarse dense crystalline material using the strength as parameter and showed that the lower the porosity, the higher the strength of the same amount of coarse dense crystalline material, the porosity increased to a constant value and beyond that decreased with the increase of the amount of coarse dense crystalline material. Therefore, there exists the amount of coarse dense crystalline material which makes porosity maximum and that in general the strength is higher when the amount of coarse dense crystalline material large.

Uchikawa and Tsukiyama (66) analysed the relationship between the shape of pore and the degree of stress-concentration under the loading by finite element method and showed that the strength of cement paste was influenced by the shape of pore.

The relation between compressive strength of pozzolanic cement, made with Japanese natural pozzolanas and fly ash, and total porosity is shown in Fig. 19.

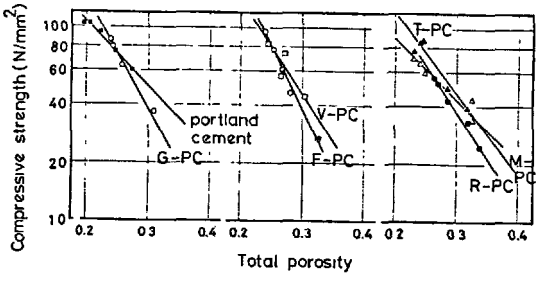

Fig. 19- Relation between total porosity and compressive strength of hardened pozzolanic cement paste

From the result of Fig. 19 and Fig. 15, it became clear that the strength of pozzolanic cement paste had good correlation with total porosity and it had particularly good correlation with capillary space in the early and middle age, and with gel pore space in the later age.

The value of developed strength, however, is different even if the value of porosity is the same. For example, in Beppu white clay mixed pozzolanic cement and Higashi-Matsuyama tuff mixed pozzolanic cement, though the change of porosities with curing time are nearly the same, the early strength of the

former is extensively higher and the latter attains to nearly same value at 180 days. In Furue shirasu mixed pozzolanic cement and Takehara fly ash mixed fly ash cement, though the change of porosities with curing time are approximately the same, the development of the strength of the former after 28 days is larger than the latter and the strength of the latter is higher till 91 days than the former.

The fact suggests that besides porosity, pore size distribution and the shape of pore have the effect on the strength.

As shown in Fig. 17 in the early age Higashi-Matsuyama tuff mixed pozzolanic cement has larger amounts of pores of which size is between 0.2 ∿ 0.02 μm but on the contrary Beppu white clay mixed pozzolanic cement has larger amounts of pores of that size in the later age, therefore it can be understood that pore size distribution and strength have close relation. In Furue shirasu mixed pozzolanic cement and Takehara fly ash mixed fly ash cement, the difference in the strength of the two is considered to have closer relation to the difference of pore shape than pore size distribution.

The strength of Tominaga masa-soil mixed pozzolanic cement is low and that of Kanto loam mixed pozzolanic cement is the lowest, that difference of strengths is too large to explain only with porosity, pore size distribution and the shape of pore.

That is, as other factors than above mentioned, it is supposed that the strength of nonporously coagulated hydration products participates.

Duckworth (67) showed that there existed following relation between the strength of a porous brittle polycrystalline body (S) and specimen porosity (P):

$$S = S_o e^{-bp} \qquad -(3)$$

where S_o is calculated strength of a brittle nonporous polycrystalline body and b is constant. The strength for pozzolanic cement and the data of total porosity is substituted in above equation and the value of calculated strength of a brittle nonporous polycrystalline body (S_o), that is, the case of total porosity is zero and the constant (b) is obtained as Table V.

Considering from the equation for the calculation of total porosity, zero total porosity means the case that there exists no water except for the combined crystalline water and the paste is constituted only with unhydrated cement particles, unreacted pozzolana particles and nonporously coagulated hydration products, and S_o means the strength of the aggregation of those particles. If the strength of unhydrated particles is supposed to be higher than the hydration product, S_o is considered to be the value which reflect the strength of nonporously coagulated hydration products. The fact, that the value of S_o is high in Higashi-Matsuyama tuff mixed pozzolanic cement, Beppu white clay mixed pozzolanic cement and Furue shirasu mixed pozzolanic cement, and low in Kanto loam mixed pozzolanic cement, Tominaga masa-soil mixed pozzolanic cement and fly ash cement, is considered to show that S_o is related to the S/A ratio of acid soluble part of pozzolana and the strength of nonporously coagulated C-S-H is relatively higher compared with that of nonporously coagulated Ca-Al hydrate. The reason why S_o of the high siliceous pozzolanic cements are higher than that of pure portland cement is the same as above mentioned.

Though the constant b is different with the kind of material, the kind of measured strength, the relation between the shape of pore and the direction of load and so on, for compressive strength, it is said that in the case of idealized cubic closest packing of sphere, b = 6 and in the case of hexagonal closest packing, b = 9 (68) and large b value means the increase of contact points of mutual particles, that is the increase of the contact surface. The b value was about 11 in most of natural pozzolana mixed cements and was lower value in fly ash cement. These differences in b value are not clear at present.

4.5 The Evaluation of Pozzolana

It is considered that there exists following

Table V. S_o and b calculated from the strength and total porosity of paste using the equation (3).

Cement	W/S	S_o (N/mm^2)	b
Portland cement	0.30	421	7.0
Portland cement	0.40	657	7.6
F-PC	0.30	1088	10.6
G-PC	0.30	1421	11.9
R-PC	0.30	941	10.7
V-PC	0.30	1303	11.2
M-PC	0.30	304	6.3
T-PC	0.30	559	7.6

Table VI. Weighting constant (w) and correlation coefficient (r) in equation (4)

System	Curing temperature (°C)	Age (day)	$C = w_o + w_1f_1 + w_2f_2 + w_3f_3 + w_4f_4$					r
			w_o	w_1	w_2	w_3	w_4	
Pozzolana-$Ca(OH)_2$ (W/S=0.56, 0.46)	20	7	-0.62	0.159	0.268	0.601	0.070	0.99
		28	16.68	0.020	0.021	0.418	0.060	0.89
		91	21.5	0.064	0.100	0.589	0.106	0.98
	40	7	-7.41	0.267	0.225	0.845	0.226	0.99
	60	7	2.80	0.217	0.127	1.03	0.274	0.99
Pozzolana-Cement (W/S = 0.30)	20	91	-2.69	0.030	0.057	0.219	0.086	0.99
		180	-2.44	0.066	0.264	0.264	0.086	0.99

C : amount of $Ca(OH)_2$ reacted (g/100g pozzolana)
f_1 : amount of glass (wt%)
f_2 : amount of acid soluble part (wt%)
f_3 : S/A in acid soluble part
f_4 : specific surface area (m^2/g)
r : correlation coefficient

unequivocal proportional relationship between the characters, such as chemical composition, the kind and the quantity of glass, the kind and the quantity of mineral, specific surface area and so on, and pozzolanic reactivity represented by reacted $Ca(OH)_2$.

$$C = \sum wifi \qquad -(4)$$

where C is the quantity of reacted $Ca(OH)_2$, f is the factor of character and w is weighting constant. Satisfactory linear relationship between the quantity of reacted $Ca(OH)_2$ and the character of pozzolana was obtained in the case mentioned 3.1. The weighting constant of each factor and correlation coefficient are shown in Table VI.

Since in the calculation not all the characters of pozzolana are used, the value of r is considered to approach to 1, when the new factors of characters obtained by advanced characterization are added to the calculation.

On the other hand the correlations between the quantity of reacted $Ca(OH)_2$ and the strength, are low in general as shown in Fig. 20 except for a few cases.

The correlations between pozzolanicity by ISO method for five kinds of Japanese pozzolanas and one kind of fly ash and the strength are also low in general as shown in Fig. 21 except for a few cases.

Therefore, to evaluate the quality of pozzolana by measuring the pozzolanic reactivity is not appropriate and it is considered that pozzolana should be evaluated with direct measurement of the most important properties in many pozzolanic properties and if the strength is assumed to be representative property, evaluation should be done by strength test itself although there are some inconveniences that it takes long time to obtain the result of evaluation (69).

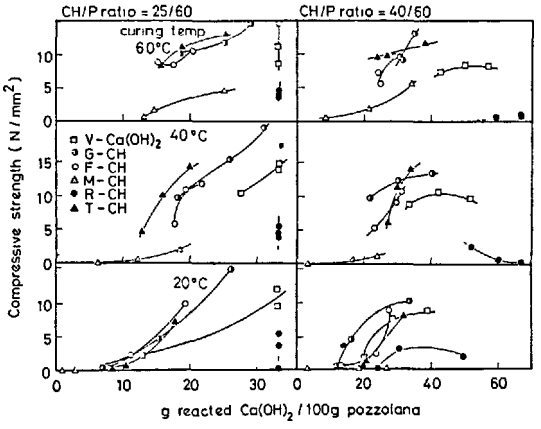

Fig. 20 - Relation between reacted $Ca(OH)_2$ and compressive strength of hardened paste in the system pozzolana-$Ca(OH)_2$

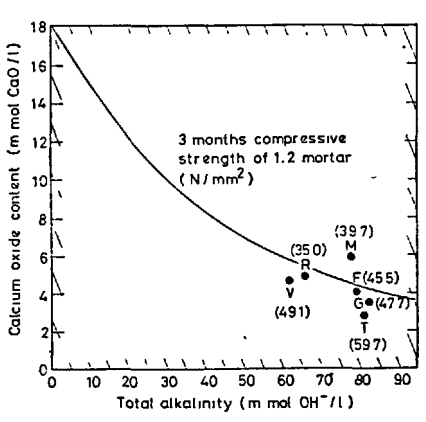

Fig. 21 - Pozzolanicity test for pozzolanic cement (P/C = 20/80) by ISO

5. CONCLUSION

On the hydration of pozzolanic cement, following results were clarified referring the previous studies mainly after Moscow Congress and by the authors' investigation.

(1) Though the character of pozzolana has correlation with the quantity of reacted $Ca(OH)_2$, that is, pozzolanic reactivity, the correlation between the character of pozzolana and strength of pozzolanic cement is low. The correlation between pozzolanic reactivity and the strength of pozzolanic cement paste is also low.
Therefore, the quality of natural or artificial pozzolana for pozzolanic cement should be evaluated by strength test, not by reactivity test.

(2) The new analytical methods and sample preparation techniques such as ESCA,AEM,ICP, TMS and ion thining etc. are giving great progress to cement chemistry, but their application to pozzolanic cement are poor at present. They will bring us more extensive information of cement chemistry in near future.

(3) The decrease of $Ca(OH)_2$ in the early stage is not due to pozzolanic reaction but to other elemental processes such as adsorption. With the consideration of the kinetics of pozzolanic reaction from the both sides, the quantity of reacted $Ca(OH)_2$ and reacted pozzolana, it could be seen that pozzolanic reaction is diffusion-controlled dissolution reaction which rate determining step is the dissolution of unhydrates and the precipitation of hydration products in the early stage, and the diffusion of ions or ion radicals through amorphous surface layer of pozzolana and precipitated hydrates layer on the surface of pozzolana in later stage.

(4) Though the hydration products in pozzolana-$Ca(OH)_2$ system are slightly different according to the kind of pozzolana, condition of hydration and so on. Those were either combination of C-S-H, $C_3A{\cdot}CaCO_3{\cdot}H_{12}$-$C_4AH_{13}$ solid solution, C_2ASH_8 and hydrogarnet.

(5) In the hydration of pozzolana-C_3S system, addition of pozzolanas accelerate the hydration of C_3S. Acceleration of hydration after induction period is due to the stimulation of C_3S dissolution by the adsorption of Ca^{2+} in the liquid with pozzolana and due to the increase of surface by the addition of pozzolana which is preferable to the precipitation of C-S-H. C-S-H precipitated after induction period has a higher Ca/Si ratio than 1.5, when sufficient amount of $Ca(OH)_2$ exists. C-S-H and Ca-Al hydrate are generally formed by the pozzolanic reaction between $Ca(OH)_2$ and pozzolana after one day but the physical properties, for example mechanical strength, develops in later age. Aluminate hydrates are generally formed later and their period of formation depends on the characters of pozzolanas, that is aluminum content and their solubility.

(6) In the hydration of pozzolana-C_3A system under the existence of $Ca(OH)_2$ and $CaSO_4{\cdot}2H_2O$, hydration of C_3A is accelerated by the addition of pozzolana. The degree of acceleration is larger in pozzolana with larger specific surface area and higher CEC value. The reason why hydration of C_3A is accelerated, is the stimulation of C_3A dissolution by the adsorption of Ca^{2+} in the liquid with pozzolana and the precipitation of ettringite on the surface of pozzolana grain. When pozzolana which contains much alkali are used, C_3AH_6 are formed earlier, the reason is considered to be the decrease of the stability of hexagonal hydrates under the existence of alkalies.

(7) The hydration in the pozzolana-C_3S system and pozzolana-C_3A system under the existence of $Ca(OH)_2$ and $CaSO_4{\cdot}2H_2O$, proceeds through the processes, that is, alkali dissolution from the surface of pozzolana grain, formation of negatively charged amorphous layer rich in Si, Al, collision of Ca^{2+} in the solution with pozzolana grain, swelling of the amorphous layer on the surface of pozzolana grain by osmotic pressure, destruction of film and so on. In the pozzolanic reaction, alkali in pozzolana plays an important role and has an influence on the state of precipitation of hydration products.

(8) Total porosity of pozzolanic cement paste is larger than that of portland cement paste in the early age. Capillary space decreases with the curing time, but gel pore space defined as below 75Å in radius increases till definite age, then turns to decrease. Pore size distribution shifts to small diameter with the curing time. Those change has the characteristics according to the kind of pozzolana. Though the shape of gel pore comes to be slender with curing age in pozzolanic cement paste and fly ash cement paste, there is almost no change with age in portland cement paste.

(9) The strength of pozzolanic cement paste has good correlation with total porosity in the same pozzolanic cement, especially with capillary space. When the kind of pozzolana is different, however, developed strength is different even if total porosity is the same. The strength is influenced by pore size distribution and the shape of pore besides total porosity. The factor which has influences on the strength besides above mentioned, is the strength of assumed nonporously coagulated hydrates and it was suggested that the strength of nonporously coagulated C-S-H is higher than that of nonporously coagulated Ca-Al hydrate.

REFERENCE

1.- R.C. ROSHI and E. A. ROSAUER (1973) "Pozzolanic activity in the synthetic fly ashes, II. Pozzolanic behavior", Am. Cerm. Soc. Bull., 52, 459-463.

2.- K. M. HANNA and A. AFIFY (1974), "Evaluation of the activity of pozzolanic materials", J. Appl. Biotechnol., 24, 751-757.

3.- ISO Recommendation R-863 (1968) "Pozzolanicity test for pozzolanic cements", 1st ed.

4.- H. UCHIKAWA (1979), "Technology of ceramics-Texture and microstructure of ceramics-Recent progress in analysis", pp. 197-213, Sangyo Gijutsu Center Tokyo.

5.- V. A. FASSEL and R. N. KNISELIY (1974), "Inductively Coupled Plasma", Anal. Chem., 46, 1110A-1118A, 1120A, 1155A-1158A, 62A, 64A.

6.- K. KAWAGUCHI (1975), "Emission spectroscopy using high frequency plasma", Bunseki, 34, 612-618.

7.- T. HIRAI, H. SOEJIMA and H. YONEZU (1975), "Cathode luminescence apparatus for X-ray microanalysis", Shimadzu Hyoron, 32, 89-94.

8.- H. KAMATA and Y. GOHSHI (1977). "Synchroton orbital radiation and X-ray spectroscopy", Preprint for 14th symposium on X-ray analysis, pp. 51-56.

9.- H. UCHIKAWA and M. NUMATA (1973), "X-ray spectroscopy for chemical bonding on oxygen, chromium and manganese compounds" J. Ceram. Soc. Japan, 81, 189-196.

10.- J. O. BURMAN, C. PONTER and K. BOSTRON (1978), "Metaborate digestion procedure for inductively coupled plasma-optical emission spectroscopy", Anal. Chem., 50, 679-680.

11.- R. H. SCOTT and M. L. KOKOT (1975), "Application of inductively coupled plasma to the analysis of geochemical sample", Anal. Chim. Acta, 75, 257-270.

12.- J. BENSTED (1976), "Use of Raman Spectroscopy in cement chemistry", J. Am. Ceram. Soc. 59, 3-4, 140-143.

13.- H. UCHIKAWA, S. UCHIDA and Y. MIHARA (1978), "Characterization of hydrated ultra rapid hardening cement pastes", il cemento, 2, 59-70.

14.- P. R. BUSECK and S. IIJIMA (1974), "High resolution electron microscopy of silicates", Am. Mineral., 59, 1-21

15.- G. LAHAJNAR, R. BLINC, V. RUTAR, V. SMOLEJ, I. ZUPANCIC, I. KOCUVAN and J. URSIC (1977), "On the use of pulse NMR techniques for the study of cement hydration", Cem. and Conc. Res., 7, 385-394.

16.- I. YASUI, H. HASEGAWA and M. IMAOKA, (1979), "X-ray Diffraction Study of K_2O. SiO_2 glass", J. Ceram. Soc. Japan, 87, 242-247.

17.- F. MASSAZZA (1974), "Chemistry of pozzolanic additions and mixed cements", 6th Int. Cong. Chem. Cem. Moscow.

18.- U. LUDWIG and H. E. SCHWIETE (1963), "Untersuchungen an Deutschen Trassen", Silicate Ind. 28, 439-447.

19.- V. AMICARELLI, R. SERSALE and V. SABATELLI (1966), "Pozzolanic activity of argillified pyroclasts", Rend. Accad. Sci. Fis. e Mat. 33, 257-282.

20.- V. SABATELLI, R. SERSALE and V. AMICARELLI (1967), "Researches on the lime-pozzolana paste constitution cured for a long time in fresh water", Rend. Accad. Sci. Fis. e Mat. 34, 243-252.

21.- M. REGOURD, H. HORNAIN and B. MORTUREUX (1976), "Evidence of calcium silico-aluminate", Cem. Conc. Res., 6, 733-740.

22.- A. CELANI, P. A. MOGGI and A. RIO (1968), "The differential action mechanism of pozzolanic materials and slag in hydraulic binder", 5th Int. Symp. Chem. Cem. Tokyo, V, pp. 140-147.

23.- B. DRZAJ, S. HOCEVAR, M. SLOKAN and A. ZAJC (1978), "Kinetics and mechanism of reaction in the zeolitic tuff-CaO-H_2O system at increased temperature", Cem. Conc. Res., 8, 711-720.

24.- R. KONDO, K. LEE and M. DAIMON (1976), "Kinetics and mechanism of hydrothermal reaction in lime-quartz-water system", J. Ceram. Soc. Japan, 84, 573-580.

25.- E. BAASK and M. C. BHASKER (1975), "Pozzolanic activity of pulverized fuel ash", Cem. Conc. Res., 5, 363-376.

26.- S. DIAMOND and M. KINTER (1966), "Mechanisms of soil-lime stabilization, an interpretative review", Public Road, 33, 260-265.

27.- K. S. BIRRELL and M. GRADWELL (1956), "Ion exchange phenomena in some soils containing amorphous mineral constituents", J. Soil Sci., 7, 130-147.

28.- K. WADA and H. ATAKA (1958), "The ion-uptake mechanism of allophane", Soil and Plant, 4, 12-18.

29.- K. IIMURA (1961), "Acidic property and ion exchange in allophane", Clay Sci., 1, 40-44.

30.- S. A. GREENBERG (1961), "Reaction between silica and calcium hydroxide solution, I. Kinetics in the temperature range 30 to 85°C", J. Phys. Chem. 65, 12-16.

31.- T. H. P. VAN AARDT and S. VISSER (1977), "Calcium hydroxide attack on feldspar and clays, possible relevance to cement -aggregate reactions", Cem. Conc. Res., 7, 643-648.

32.- D. M. SANDERS and L. L. HENCH (1973), "Mechanisms of glass corrosion", J. Am. Ceram. Soc., 56, 373-377.

33.- T. M. EL-SHAMY (1973), "The Rate-determining step in the dealkalization of silicate glasses", Phys. Chem. Glass, 14, 18-19.

34.- J. R. CLIFTON, P. W. BROWN and G. FRONSDORFF (1977), "Reactivity of fly ashes with cement", Cements Research Progress pp. 321-341 American Ceramic Society.

35.- H. N. STEIN and J. M. STEVELS (1964), "Influence of silica on the hydration of $3CaO \cdot SiO_2$", J. Appl. Chem., 14, 338-336.

36.- W. LUKAS (1976), "The influence of an Austrian fly ash on the reaction process in the clinker phases of portland cement", Mater. et Const., 9, 331-337.

37. J. A. NELSON and J. F. YOUNG (1977), "Additions of colloidal silicas and silicates to portland cement pastes", Cem. Conc. Res., 7, 227-282.

38.- K. TAKEMOTO, H. UCHIKAWA, K. OGAWA and I. YASUI, in preparation, "Mechanism of the hydration in the system pozzolana-C_3S".

39.- L. S. DENT GLASSER, E. E. LACHOWSKI, K. MOHAN, and H, F, W, TAYLOR (1978), "A multi-method study of C_3S hydration", Cem. Conc. Res., 8, 733-740.

40.- J. SKALNY, I. JAWED and H. F. W. TAYLOR, (1978), "Studies on hydration of cement-recent developments", World Cement Technology, 2, 183-195.

41.- C. L. M. HOLTEN and H. N. STEIN (1977), "Influence of quartz surfaces on the reaction $C_3A + CaSO_4 \cdot 2H_2O$ + water", Cem. Conc. Res., 7, 291-296.

42.- M. COLLEPARDI, G. BALDINI, M. PAURI and M. CORRADI (1978), "The effect of pozzolanas on the tricalcium aluminate hydration", Cem. Conc. Res., 8, 741-752.

43.- H. UCHIKAWA and S. UCHIDA (1980), "Influence of pozzolana on the hydration of tricalcium aluminate", Presented at the 7th International Congress on the Chemistry of Cement, Paris

44.- G. A. C. M. SPIERINGS and H. N. STEIN (1976), "The influence of Na_2O on the hydration of C_3A, I paste hydration", Cem. Conc. Res., 6, 265-272.

45.- G. A. C. M. SPIERINGS and H. M. STEIN (1976), "The influence of Na_2O on the hydration of C_3A. II. suspension hydration", Cem. Conc. Res., 6, 487-496.

46.- J. SKALNY and M. TADROS (1977), "Retardation of tricalcium aluminate hydrate by sulfate", J. Am. Ceram. Soc., 60, 174-177.

47.- F. LOCHER, W. RICHARTZ and S. SPRUNG (1976), "Erstarren von zement-Teil I. Reaktion und Gefügeentwicklung", Zement-Kalk-Gips, 29, 435-442.

48.- S. DIAMOND (1976), "Cement paste microstructure-An overview at several, levels", Proceeding of a conference held at university of Sheffield 8-9 April, pp. 2-30, Cement and Concrete Association.

49.- T. D. CIACH, J. E. GILLOTT, D. G. SWENSON and P. J. SEREDA (1971), "Microstructure of calcium silicate hydrate", Cem. Conc. Res., 1, 13-25.

50.- M. COLLEPARDI, A. MARCIALIS, L. MASSIDDO and U. SANNA (1976), "Low pressure steam curing of compacted lime-pozzolana mixtures", Cem. Conc. Res., 6, 497-506.

51.- M. KOKUBU (1974), "Fly ash Cements", 6th Intern. Cong. on the Chem. Cem., Moscow.

52.- S. DIAMOND (1972), "Identification of hydrated cement constituents using a scanning electron microscope", Cem. Conc. Res., 2, 617-632.

53.- W. LUKAS (1976), "Substitution of Si in the lattice of ettringite", Cem. Conc. Res., 6, 225-234.

54.- F. D. TAMAS, A. K. SARKAR and D. M. ROY (1976), "Effect of variables upon the silylation products of hydrated cements", Hydraulic cement pastes their structure and properties, pp. 55-72. Cement and Concrete Association.

55.- M. YUDENFREUND, I. ODLER and S. BRUNAUER (1972), "Hardened portland cement pastes of low porosity 1. Materials and experimental method", Cem. Conc. Res., 2, 313-330.

56.- E. P. BARRET, L. G. JOYER and P. P. HALENDA (1951), "The determination of pore volume and area distributions in porous substance, I. Computions from nitrogen isotherms", J. Appl. Biotechnol. 24, 175-178.

57.- G. BATTAGLINO and G. SCHIPPA (1968), "New method for evaluating pozzolanic material", Ind. Ital. Chem., 38, 175-178.

58.- J. JAMBOR (1963), "Relation between. phase composition, over-all porosity and strength of hardened lime-pozzolana pastes" Mag. Conc. Res., 15, 131-142.

59.- M. K. CHATTERJEE and D. LAHIRI (1967), "Pozzolanic activity in relation to specific surface area of some artificial pozzolanas, part I and part II", Trans. Indian. Ceram. Soc., 26, 65-70.

60.- D. J. THORNE and J. D. WATT (1965), "Composition and pozzolanic properties of pulverized fuel ashes, II. Pozzolanic properties of fly ashes as determined by crushing strength test on lime mortars", J. Appl. Chem., 15, 595-604.

61.- R. C. JOSHI and E. A. ROSAUER (1973), "Pozzolanic activity in synthetic fly ashes, II. Pozzolanic behaviour", Am. Ceram. Soc. Bull., 52, 457-463.

62.- K. M. SPITANOS, E. VOYATZAKIS and S. B. MELIDIS (1977), "Etude sur les cendres volantes des lignites grecs-Utilisation dans le cement-Influence du degre de finess II-Region de ptolemide", Rev. des Mater, de Const., 211-213.

63.- R. F. FELDMAN and J. J. BEAUDOIN (1976), "Microstructure and strength of hydrated cement", Cem. Conc. Res., 6, 389-400.

64.- H. UCHIKAWA and K. TSUKIYAMA (1973), "The hydration of jet cement at 20°C", Cem. Conc. Res., 3, 263-277.

65.- J. M. CRENNAN, S. A. S. EL-HEMALY and H. F. W. TAYLOR (1977), "Autoclaved lime-quartz materials I. Some factors influencing strength", Cem. Conc. Res., 7, 493-520.

66.- H. UCHIKAWA and K. TSUKIYAMA (1975), "Studies on the influence of shape of pore and aggregate on the stress-strain distribution in hardened cement paste by finite element method", J. Ceram. Soc. Japan, 83, 117-121.

67.- W. DUCKWORTH (1953), "Discussion of Ryshkewitch paper", J. Am. Ceram. Soc., 36, 68.

68.- F. P. KNUDSEN (1959), "Dependence of mechanical strength of brittle polycrystalline specimens on porosity and grain size", J. Am., Ceram. Soc., 42, 376-387.

69.- ASTM C595-76, "Standard specification for blended hydraulic cements".

THEME V

Special Cements

SUB-THEME V-1

Aluminous Cements A review of recent literature (1974 - 1979)

C. M. GEORGE
Lafarge Fondu International
Paris FRANCE

SUMMARY

World wide use of many different types of aluminous cement continues to increase and with it the interest in the chemistry of calcium aluminates. The type of cement most frequently encountered is still that made by fusion of natural bauxite and limestone and containing approximately 40 % alumina. Generally known as cement Fondu, this was the first to be produced industrially, the original patent dating from 1908, and is the main subject of this, and previous reviews. High alumina cements containing up to 80 % alumina, used almost exclusively for refractory applications (to approximately 1800°C) are made by both fusion and sintering processes, but the overall pattern of manufacture has not changed appreciably during the period in question (1974 - 1979). Publications concerning these special cements are mentioned only in-so-far as they contribute to general understanding of the chemistry of the alkaline-earth aluminates.

The principal hydraulic constituents of the aluminous cements, $C_{12}A_7$, CA, CA_2 are generally, but not exclusively reported to melt incongruently : in particular the melting point of $C_{12}A_7$ appears to be affected by oxygen partial pressure or water vapour. Iron oxide, in the lower purity cements, is soluble in all the calcium aluminates to a significant degree, and can replace up to 50 % of the alumina in gehlenite, which occurs in silica containing aluminate cements. Further studies of pleochroite now prove that it requires a fairly high ratio of ferrous to ferric ion for its formation as a stable phase. The iron oxide content of 40 % alumina cement is however greater than can be accommodated in the above manner, so that calcium alumino-ferrites of the C_2A - C_2F solid solution series, and even free wustite, appear in the crystallised product.

The reactivity of the calcium aluminates with water increases with the C/A ratio, but the predominance of CA in aluminous cements makes this the most important hydraulic constituent. Pleochroite is largely inert in comparison, but the alumino-ferrite solid solutions display significant reactivity. Gehlenite is inert, however stratlingite does appear as a hydration product of the lower purity cements, due to the interaction of mono-calcium aluminate hydrate and calcium silicate hydrate formed from the small quantities of β-C_2S found in these cements. CAH_{10} is the principal hydrate formed from CA at temperature of 20°C or less, C_2AH_8 predominates at temperatures around 30°C, and both 'convert' increasingly rapidly to C_3AH_6 as temperatures are further increased. Stochiometry is maintained by the formation of AH_3 and free water. The free water released by conversion (or by carbonation) is taken up by further hydration of residual cement in mixes made at or below the critical water/cement ratio, so that changes in porosity are minimised. The hydration of C_4AF leads to the formation of $C_4(A,F)H_{13}$ at room temperature, and to $C_3(A,F)H_6$ later or at higher temperatures.

The $Ca_2Al(OH)_6^+$ cationic layers in the C_4AH_n structure are separately by aqueous anionic interlayers in which many mono-and-di-valent anions can be substituted from solution, $Al(OH)_4^-$ being a special case which shows C_2AH_8 as a solid solution product of C_4AH_{13}. Substitution of certain anions in the C_2AH_8 interlayers confers a degree of stability to the structure, and reduces the rate at which conversion to C_3AH_6 occurs.

Hydration of CA in the presence of carbonate leads to the formation of mono-carbo aluminate and a lower rate of conversion of the hexagonal aluminates to the cubic form. The ultimate products of carbonation are calcite and gibbsite. The reaction of atmospheric CO_2 with hardened cement, and that of solutions of sulphates to produce ettringite and chlorides to produce mono-chloro aluminates, is a very slow surface phenomenon at low water/cement ratios, and does not adversely affect strength. Chemical attack is thus associated with permeable high water/cement ratio mixes which are in any case to be proscribed for reasons of strength alone.

It has been shown that precipitation of calcium aluminate hydrates from solutions in contact with CA or aluminous cement does not occur through heterogeneous nucleation by the anhydrous grains. Nevertheless, the nature of the hydrate which crystallises is influenced by the C/A ratio of the solution and, as hydration proceeds, apparently by the nature of the hydrate initially precipitated. Another new result is that the hydration of amorphous CAH_n ($10 > n > 1.5$) does not lead to cementitious bonding although the hydrate formed, CAH_{10} is chemically the same as that produced from CA. Morphology is thus also a critical factor in strength development.

A high proportion of publications continues to deal with the effects of conversion on long term behaviour. Some authors appear to maintain support for the view that the initial extremely high strength of aluminous cements due to CAH_{10} can be exploited in permanent structures provided precautions are taken to prevent conversion, while others still regard conversion as an inevitable cause of vulnerability. Yet there is virtually universal recognition of the importance of temperature and water/cement ratio on the durability of aluminous cement concrete, although failure to distinguish between free and total water/cement ratio causes confusion in some cases. The most important publications relating long term strength and conversion however, clearly show that aluminous cements will convert relatively rapidly (a few months or years) under nearly all service conditions, so that the rapid hardening properties should be used only by designing to the converted strength of low water/cement ratio mixes. Much work on measuring conversion by derivatographic methods has appeared. Although this is a valuable technique under strict control, its wide adoption as a quick method of assessing concrete quality in the field is far from reliable. To use degree of conversion as function of age to infer water/cement ratio is to rely on an effect which is difficult to quantify even in the laboratory, and to ignore the overriding effect of temperature. Thus heating, deliberate or not, will cause rapid conversion whether a low or a high water/cement ratio has been employed.

Some alternative approaches to quality assessment are mentioned and data is given to show that the porosity of converted aluminous cement concrete is not greater than that of Portland cement concrete of the same water/cement ratio. In relating conversion to mechanical properties several recent publications provide further information on

the modulus of elasticity and creep of aluminous cement concrete.

1. COMPOSITION

1.1. Manufacture

Since the original French patent of 1908, a variety of methods have been reported for the manufacture of aluminous cements involving sintering, fusion under oxidizing conditions, reductive fusion in the Blast Furnace or by cupola, and melting in electric furnaces, (1). However, over the last 5 years, no major changes are apparent in the pattern or methods of manufacture of aluminous cements, although the increasing preoccupation with the use of waste products as raw materials is to be noted.

The literature concerning manufacture which has appeared since 1974, frequently in the form of patents, has been concerned mainly with the production of high alumina cements containing 70 % or more aluminium oxide, and it is not appropriate to discuss this extensively in the present paper : brief mention only will be made of some of the publications in this area.

Sintering is difficult to control when raw materials containing appreciable quantities of iron oxide are used. For this reason the preferred process is still fusion for the manufacture of the most widely encountered type of aluminous cement, the raw materials being red bauxite and limestone ; hence the origin of the name ciment Fondu for this product. To the author's knowledge, and contrary to an earlier report, (2), fusion in electric furnaces has not been used for many years for the manufacture of this type of cement containing approximately 38 % CaO, 39 % Al_2O_3, 16 % iron oxide and 4 % silica.

A laboratory study of the use of ferrous sulphate as a mineraliser for the sintering of lime or limestone and alumina has been reported by TEOREANU and co-workers (3) and the same research institute has also described (4), the properties of sintered mixtures of alumina and combinations of magnesium, calcium and barium carbonates. The mixtures were chosen to give either 20 % or 50 % magnesia spinel in the fired material. From the study of the porosities of the clinkers produced it was found that compositions in the partial system BA-BA_6-BC_2A_4 sintered without formation of a liquid phase and thus gave clinkers of higher refractoriness, although harder to grind to cement fineness.

DROZDZ and WOLEK, (5) have extended earlier studies of barium aluminate cements prepared by sintering. The principal mineralogical phase formed is BA which has considerable hydraulicity - a heat of hydration between 200 and 300 cal/g, ≃ twice that of commercial aluminous cements, is reported. In preparing refractory concretes from such cements, if more than the minimum amount of gauging water needed to form barium aluminate hydrates is used, alumina hydrate and barium hydroxide are formed, or barium carbonate in the presence of atmoshperique CO_2. Contrary to calcium aluminates, the carbonation of barium aluminate cements does not improve strength. The rapid setting characteristics of barium aluminate can be retarded by citrates and borates, for example but apparently not by halide salts, phosphates or sugar. Despite its high refractoriness barium aluminate cement does not appear to have yet achieved any industrial success.

KRAVCHENKO et al (6) have investigated the manufacture by sintering of high alumina cements (alumina contents, 70 to 80 %) using various metallurgical slags. The use of alumina rich slags containing only small quantities of silica minimises the amount of gehlenite, C_2AS formed thus increasing the CA content of the final clinker and hence its cementitious behaviour.

KONDRASHENKO (7) discusses the preparation of a cement composed primarily of CA_2. This is produced by melting, either as a slag during the production of ferro-titanium or ferro-chrome by alumino-thermic reduction or by remelting of such slags in an electric furnace, with suitable additons of alumina and lime. The product contains 70 to 80 % alumina with CA_2 as the principal phase, and is thus intrinsically more refractory than cements based on CA. However its rate of hydration and hence bonding efficiency, is much less than that of the mono-calcium aluminate cements since the hydraulic activity of the calcium aluminates increases with the lime/alumina ratio.

Another publication, (8) also discusses the manufacture of aluminous cements from metallurgical slags produced in the smelting of aluminium. One of the difficulties normally associated with using such slags (60 -90 % Al_2O_3 content) is due to the presence of AlN or Al_4C_3, which evolve ammonia or hydrocarbon gases in contact with water. By sintering such slags with a complement of lime in the presence of manganese carbonate or oxide, these impurities are removed.

Alternatively the slags can be remelted in an electric furnace and ferro-manganese or ferro-silicon added together with the necessary lime. This study was not restricted to high purity cements, the range of compositions produced being CaO 20 - 35 %, Al_2O_3 40 - 65 %, SiO_2 2 - 10 %, together with small amounts of Fe_2O_3, MgO and other impurities. Setting times in the range 40 to 150 minutes are reported, with reasonable subsequent strength development.

1.2. Mineralogy

The calcium aluminates, $C_{12}A_7$, CA and CA_2 encountered in industrial aluminous cements as well as the calcium alumino-ferrites, were reviewed by ROBSON (9) at the 1974 International Symposium on the Chemistry of Cements (Moscow). All the calcium aluminates can take up appreciable quantities of ferric oxide in solid solution, the remaining iron appearing as calcium alumino-ferrites. Ferrous oxide can appear as wustite and may also be combined in pleochroite.

The alumino-ferrites are solid solutions between the end members, C_2A - C_2F. The general formula C_4AF is thus frequently given. However, in aluminous cements of the Fondu type, the composition is most often on the iron rich side of the solid solution range, represented by the formula, $C_{10}AF_4$, (9).

$C_{12}A_7$ in dry conditions, CA and CA_2 are all reported to melt incongruently. $C_{12}A_7$ however, takes up moisture at high temperatures and melts at 1390°C so that in air, for example, it appears to melt congruently. In a paper (10) which examines the

formation of CA from C_3A and α-Al_2O_3, $C_{12}A_7$ is reported as an intermediate product :

$C_3A + 3/4\ \alpha\text{-}Al_2O_3 \rightarrow 1/4\ C_{12}A_7$

$1/4\ C_{12}A_7 + 5/4\ \alpha\text{-}Al_2O_3 \rightarrow 3CA$

The rate of formation of CA was accelerated in the presence of water vapour.

However, in another paper UDALOV, CHEMEKOVA and APPEN, (11) working on pure materials, state that water vapour does not affect the melting of calcium aluminates and that $C_{12}A_7$ melts congruently in oxidising atmospheres. C_5A_3, which decomposes above 820°C to $C_{12}A_7$ and CA under oxidising conditions, is stable under reducing conditions and also melts congruently. Congruent melting of CA and CA_2 is also claimed.

PETZOLD and RIEDEL (12) discuss the phase compositions of aluminous cements made by reductive fusion of bauxite and limestone with coke, in electric arc furnaces. An optimum coke utilisation produced low iron (0.4 to 0.6 %) cement, without appreciable formation of calcium carbide, suitable for high temperature applications. Under the conditions used, the silica content of the raw materials appeared as β-C_2S in the products, which on cooling transformed spontaneously to γ-C_2S below 600°C, with disintegration due to the associated volume increase. The C_2S could be stabilised in the β-form by the addition of boric oxide or vanadium oxide. Many other materials are known to have the same effect. In relating the strength development of the cements to their mineralogy, these authors assimilate TiO_2 with SiO_2. The best results are reported for compositions which when $SiO_2 + TiO_2$ is considered as SiO_2, lie on the line CA-C_2S of the C-A-S diagram. This is consistent with earlier observations where SiO_2 is considered alone (13) for which the maximum utilisation of alumina to form CA is obtained for compositions close to the line CA - C_2S.C_2AS.CA.

GLASSER and SORRENTINO,(14),(15) have considerably extended the study of the phase diagram corresponding to aluminous cements of the Fondu type, (≃ 40 % alumina).

The lime-alumina-silica-iron oxide system of aluminous cements, under oxidising conditions (pO_2 = 0.2 atmos - free air) has a ratio of ferrous oxide to total iron oxide which does not exceed 1.5. In this system, pleochroite is not formed on solidification. The same observation applies to the study of the subsolidus at these levels of oxidation. It follows, that since the pleochroite phase is occasionaly encountered in practice, its existance as a stable phase requires the higher ferrous to ferric oxide ratios found in aluminous cements, (12). This is directly confirmed by a further publication, (16). At the same time these studies demonstrate that the SiO_2 concentration at which large quantities of gehlenite are formed, is lower than in the lime-alumina-silica diagram alone. This is important in explaining the upper limit to the SiO_2 level in these types of cement, beyond which a significant proportion of the alumina is used in forming C_2AS at the expense of CA, thus seriously reducing hydraulic activity.

In practice this limit is found at about 6 % SiO_2, whereas it would not be expected from the C-A-S diagram alone until the CA/C_2AS boundary is reached at ≃ 10 %. Thus pleochroite formation has been, in the past, considered as the factor responsible. The recent studies show that in the presence of iron oxide, the CA/C_2AS boundary moves to lower silica concentrations and indeed, to about the 6 % level under practical conditions.

Several researchers have made further studies of pleochroite. A phase of composition 22CaO.$13Al_2O_3$.3MgO.SiO_2 found (17) in the CaO-Al_2O_3-MgO-SiO_2 system is considered equivalent to pleochroite if MgO is replaced by FeO and some Al_2O_3 by Fe_2O_3. Using electron microprobe analysis three possible compositions for synthetic pleochroite are proposed, (16) : 22CaO.$13Al_2O_3$.3FeO.$4SiO_2$, 23CaO.$13Al_2O_3$.3Fe.$3.5SiO_2$, 23CaO.$13(Al_2O_3.Fe_2O_3)$ 3FeO.$4SiO_2$.

Finally, from the analysis of this phase in industrial aluminous cement clinkers, a general formula is suggested, (18) of the type : $(Ca,Na,K,Fe^{II})_A\ (Fe^{III}Al)_B\ (Al_2O_7)_8\ (AlO_4)_{6-x}\ (SiTiO_4)_x$, where A and B take on various values to maintain ionic balance. Typical values are given as A = 28, and B = 13 but wide variations were observed : A = 31, B = 10 to A = 20, B = 17.

1.3. Siliceous aluminate cements

Some studies of aluminous cement compositions with high silica contents are reported by OHTA and AKIYAMA, (19). In general, cements containing 10 to 16 % SiO_2 showed the presence of C_3A, $C_{12}A_7$ and CA. Those with more than 18 % SiO_2 contained large quantities of C_2S and C_2AS, and exhibited much less hydraulic activity. All the compositions studied contained little or no iron oxide. The behaviour of mixtures of some of these cements with a CA/CA_2 cement of composition 33 % CaO, 60 % Al_2O_3, 3 % SiO_2 and 4 % Fe_2O_3 is also described. The 1, 7 and 28 days strengths of the high silica cements alone were much lower than for the CA/CA_2 cement, but when added (20 %) to the latter, strengths were higher than those of the CA/CA_2 cement itself. The improvement was greatest with siliceous cements having the highest C/A ratio but it is to be noted that the addition of pure SiO_2 was also beneficial :

Table I : Summary of results from reference (19)

R* = Ratio of 1 day strength of 80 : 20 mixtures of CA/CA_2 and siliceous cements to the 1 day strength of CA/CA_2 cement alone.

R*	1	1.2	1.27	1.5	1.9	2.3
SiO_2 content of siliceous cement	20%	20%	16%	100%	16%	16%
C/A ratio of siliceous cement	1.35	1.85	1	-	1.3	1.33
Reported mineralogical compositions of siliceous cement	CA C_2AS C_2S	CA $C_{12}A_7$ C_2S	CA C_2AS C_2S	pure silica	CA C_2AS C_2S	CA $C_{12}A_7$ C_2S
R	0	0.64	0.56	0	0	1

R = Ratio of 1 day strength of siliceous cement to the 1 day strength of CA/CA_2 cement.

Mixtures containing more than 20 % of the siliceous cements showed progressively poorer performances except in the case of the highest C/A ratios. The above results are somewhat difficult to explain except perhaps an increase in the strength at ages less than 1 day which occured with the cement having a C/A ratio of 1.85 but not with that having a C/A ratio of 1.35 - accelerating effect of $C_{12}A_7$?

ZAKHAROV (20) has described the preparation of an alumina-belite cement with a chemical composition intermediate between that of aluminous cement and ordinary Portland cement. The raw materials, limestone and alumina rich clays, with a small quantity of gypsum as a mineraliser, are sintered at a relatively low temperature and then quenched. By this means (arresting the reaction before equilibrium is reached) a clinker is produced containing principally β-C_2S and CA and avoiding the formation of the inert phase, C_2AS. β-C_2S contents of 60 % can be obtained but the CA content is quite low. Most of the iron oxide in the raw materials appears to be in solid solution in the silicate and aluminate phases, while the gypsum is combined in the form of $C_4A_3\bar{S}$.

This cement is further examined in another publication (21) under the title 'Porsal' cement. The clinker produced, also on a laboratory scale, contained approximately 60 % β-C_2S, 15 % $C_4A_3\bar{S}$, 9 % $C_{12}A_7$ and about 6 to 7 % CA. Sintering was at approximately 1300°C for 20 minutes after which the product was air quenched.

As may be expected from its mineralogical composition this type of cement displays hydration kinetics more typical of Portland than aluminous cements. Thus a standard mortar made with Porsal cement at a water/cement ratio just below 0.5 attained 14 MPa in compression after 3 days normal curing, and 26.5 MPa after 28 days. So although this material contains nearly 20 % alumina, considerably more than is encountered in Portland cement, its chemical and physical characteristics are not those of the aluminous cement class.

SORRENTINO, (22) describes the preparation of a β-C_2S - $C_{11}A_7.CaX$ cement by sintering at approximately 900°C in the presence of water vapour and mineralisers such as fluorides, chlorides or bromides. This approach differs from that of ZAKHAROV in that equilibrium is established during the heating process. The presence of substantial quantities of the $C_{11}A_7.CaX$ phase leads to very rapid setting and considerable amounts of gypsum are added to provide workable properties. Early strength development intermediate between that of Portland and aluminous cements is reported, but the system appears somewhat difficult to control.

2. HYDRATION

The general chemistry of aluminous cements has been extensively reviewed in past publications ; eg. ROBSON, 1962 (1), LEA, 1970 (23), TALABER, 1974 (2), - and the papers on this subject which have appeared from 1974 onwards, while extending previous knowledge substantially confirm many of the views previously presented.

It should be remembered that aluminous cements of the most generally encountered type (Fondu type), although containing mono-calcium aluminate as the principle phase, do not contain more than 50 % of this compound. Thus in understanding the hydration and other characteristics of this type of material, it is important to take due account of the several other hydraulic constituents present : $C_{12}A_7$, C_2S, C_4AF. Recent studies have not ignored this fact, but more work, particularly on the iron containing phases, is undoubtedly desirable.

2.1. Calcium aluminates

BARRET and co-workers (24) (25), have investigated the processes occuring during the initial period of contact of calcium aluminates with water - ie the period up to the time of initial set. Pure CA and an aluminous cement (Fondu) were studied.

In a first series of experiments curves of the Wells type are compared with the behaviour of filtrates (B curves) obtained after the first 5 to 10 minutes of contact (21°C with agitation) which leads to the maximum solution concentrations of lime and alumina. When the solids are placed in contact with distilled, CO_2 free water, the W curves (heterogeneous system - excess solid present) and the B curves (homogeneous system - solids removed by filtering) for pure CA, both exhibit a dormant period which is characterised by stability in solution concentrations of lime and alumina. By contrast, using cement, while the B curve shows a dormant period the W curves do not. This suggests that pure CA grains present during the determination of the W curves are not providing nucleation surfaces for hydrate formation, whereas a nucleation mechanism may occur when cement is used instead of synthetic CA. However, when the cement is shaken with a saturated filtrate obtained from CA and water or cement and water, both W and B curves show a dormant period. The lack of a dormant period in the cement-pure water system cannot therefore be attributed to heterogeneous nucleation by the cement grains.

In a second series of experiments, aluminous cement is pretreated with water for various periods (up to half an hour) before being placed in contact with a saturated filtrate. The longer the period of pretreatment the shorter the subsequent dormant period observed in the Wells curve. It is also observed that the length of the dormant period for fresh aluminous cement (not previously treated with water) in contact with filtrates, decreases as the degree of undersaturation of the filtrate increases. This clearly points to the initial dissolution of the cement as the critical factor which triggers bulk hydrate precipitation.

These results represent an important step forward in the understanding of the behaviour of calcium aluminates on first contact with water.

Another publication (26) (27), relates the initial dissolution of calcium aluminates to the pH of the solution phase. The process is seen to be diffusion controlled both from the kinetics of concentration change and the acceleration induced by agitation. Like that of BARRET, this work also used high liquid/solid ratios but also mono-crystals as a means of slowing the process down to more readily measura-

ble rates. Both CA and $C_{12}A_7$ were studied. The pH of 11.5 developed is attributed to hydrolysis of aluminate ions formed from the dissociation of dissolved calcium aluminate :

$$CaO.Al_2O_3 \rightarrow Ca^{2+} + 2AlO_2^-$$

$$2AlO_2^- + 4H_2O \rightarrow 2Al(OH)_4^-$$

$$2Al(OH)_4^- \rightarrow 2Al(OH)_3 + 2OH^-$$

In agreement with this, the solution concentration of aluminate increases with pH and achieves the same values for the CA-water system as is found in the alumina gel-water system. Also, artificially increasing the pH of the solvent phase reduces the rate at which calcium aluminate dissolves.

The lime/alumina ratio in solution was 1.1 to 1.2 irrespective of the nature of the starting aluminate and these results agree well with the papers previously described, where pure CA and aluminous cement each gave values at saturation in the same range. However it may be noted that the initial C/A ratio of solutions in contact with Fondu type cement is slightly higher than that obtained with pure CA.

The dissolution of $C_{12}A_7$ is extremely rapid, more so than that of CA or CA_2 (indeed the rate of solution increases with the lime/alumina ratio of calcium aluminates). Thus, without prejudice to the mechanism of hydrate formation suggested by BARRET (24) (25), the shorter dormant period for aluminous cement (containing some $C_{12}A_7$) compared with that of pure CA, in the B curves shown in his publications, may be due, at least in part to this effect. Consistent with the above idea, is the known acceleration of the setting time of calcium aluminate cements when $C_{12}A_7$ is present, as reported anew by SMITH, (28).

Reference (26) also reports that C_2AH_8 is the hydrate first precipitated when CA is put in contact with water at 25°C (or C_4AH_{19} if nucleation is slow compared to the rate of solution of the anhydrous material), thus the CA is never in equilibrium with its own solution.

BERGER and PUSHNYAKOVA (29) studied the solubility of C_3AH_6 in solutions of alkali metal hydroxides. Solubility increased with the concentration of alkalis (and hence pH) with Li preceeding Na, preceeding K, in order of activity. The effect of adding calcium hydroxide was to reduce the solubility. Solution concentrations of dissolved C_3AH_6 reached a maximum value and then fell to a quasi-equilibrium level in which the solution coexisted with a solid phase in which some C_4AH_{13} was apparent by DTA analysis, and in proportions which increased with the concentration of hydroxide employed.

COSTA, MASSAZZA and TESTOLIN (30) describe the hydration of $C_{12}A_7$ and $C_{11}A_7.CaF_2$. Although this study was directed towards the behaviour of Portland cements, the results are of interest for aluminous cements which frequently contain small percentages of $C_{12}A_7$. Calorimetric and X-ray diffraction experiments showed a dissolution, nucleation and bulk precipitation process qualitatively similar to that reported by other workers for CA and for aluminous cements. At 20°C the initial hydrate formed was C_2AH_8 from $C_{12}A_7$ and C_3AH_6 from the fluoro-aluminate. This correlated well with a higher lime/alumina ratio developed initially in the solutions of the latter material. At later stages (3 days or more) C_3AH_6 also formed from solutions in contact with $C_{12}A_7$. Small quantities of CAH_{10} were apparently formed, which could be explained on the basis of stochiometric differences between the composition of the anhydrous starting materials (C/A = 1.7) and that of the hydration products (C/A = 2 or 3). However, the conconmittant formation of alumina gel (undetectable by X-ray diffraction)is an alternative mechanism.

2.2. Calcium alumino-ferrite

Aluminous cements of the Fondu type contain appreciable quantities of calcium alumino-ferrite. Although the contribution of these ferrites to the hydration of aluminous cement is generally eclipsed by that of the more active mono-calcium aluminate, they should not be regarded as an inert constituent.

A detailed study of the hydration of C_4AF is reported by RAMACHANDRAN and BEAUDOIN, (32). Neat pastes at water/cement ratios of 0.3 to 1.0, and pressed discs with water/cement ratios of 0.08 and 0.13 were studied by thermogravimetry and X-ray techniques to identify the products of hydration. The accompanying changes in porosity, micro-hardness, hydrate morphology, surface area and specimen dimensions were also measured over periods up to 45 days. Hydration temperatures were 23 and 80°C, and 216°C in an autoclave in some cases. Hydration was rapid, with $C_4(A,F)H_{13}$ the intiial reaction product, which predominated at the lower temperature. However at the higher temperature of 80°C, C_3AH_6 was increasingly formed, and the cubic hydrate was also favoured by the very low water/cement ratios achieved in the pressed discs. Of course, as may be expected, the degree of hydration was lower than in the higher water/cement ratio pastes. The hexagonal hydrate $C_4(A,F)H_{13}$, reported from the DTA analyses was not detected by X-ray diffraction.

At 23°C the surface area of the hydrated specimens decreased markedly with water/cement ratio. At 80°C the pattern is less clear since although a predominance of cubic hydrate tends to reduce surface area, the greater degree of hydration has an opposite effect. Complementary scanning electron micrographs showed a more compact hydrate structure associated with the lower surface areas, and with the higher hydration temperatures. Such structures are considered typical of a strong cementitious material. Porosity decreased with decreasing water/cement ratio and increasing degree of hydration. A parallel increase in microhardness was observed and a correlation between porosity (p) and microhardness (h) was found of the form, $\log h = k_1 - k_2 p$, where k_1 and k_2 are constants. The coefficient of correlation was 0.978. This compares well with the results of COTTIN & REIF (31) on aluminous cement and synthetic CA.

The overall conclusion is that the formation of $C_3(A,F)H_6$ as the hydration product of C_4AF, in place of the hexagonal hydrate $C_4(A,F)H_{13}$ of lower density, which appears to an important degree at lower temperatures and high water/cement ratios, need not be detrimental to the mechanical properties of cements containing C_4AF - Portland cement, and aluminous cement made from red bauxite. This paper thus provides valuable evidence in support of the contribution

of the ferrite phase to the strength development of aluminous cements. It can obviously contribute to the long term strength of this material at 'normal' service temperatures, and more so to massive aluminous cement structures which develop high internal temperatures during the initial cure, or concretes which are deliberately heat cured.

2.3. Calcium alumino-silicate

Another hydrate which may play a significant role in the later age strength of aluminous cement is C_2ASH_8, (33). Thus MIDGLEY describes the formation of stratlingite from the reaction between CAH_{10} and CSH.

CAH_{10} is of course, a major product of the low temperature hydration of aluminous cement, while CSH is intrinsically available due to the presence of β-C_2S as a minor constituent. The reaction of aluminium gel with CSH to form C_2ASH_8 only occurs in the presence of CH, which is absent in hydrated aluminous cement. Although the formation of C_2ASH_8 was demonstrated with experimental cements of an aluminous character formulated to encourage its presence, the contribution to strength could not be conclusively demonstrated.

The use of fly-ash as an addition to aluminous cement is advocated in another publication, (34). The authors suggest that C_2ASH_8 and CSH are formed by such additions, and show that the solution concentrations in contact with such modified cements exhibits a lower than normal C/A ratio. The presence of these calcium silicate hydrates may enhance strength but the lower C/A ratio, by discouraging the formation of C_3AH_6 in favour of the hexagonal hydrates of lower density is considered to be the main advantage of the fly-ash addition.

While it is undoubtedly true that the addition of a material which absorbs calcium ions will modify the pattern of the normally produced hydration products of aluminous cement, the use of fly-ash for this purpose is of doubtful value since its principal effect is as a diluent of otherwise more active hydraulic material. Also while the presence of fly-ash may hinder, it is unlikely to permanently prevent conversion. Moreover, fly-ash is an intrinsically variable material. So, although the addition of this material to aluminous cement may be of chemical interest, support for such a combination in practice is difficult to find.

A study of the hydration of Porsal cement (21) presents C_2ASH_8 and C_4AH_{13} as the initial products formed. However, as mentioned in section 1.3., the chemical composition of this type of cement is more typical of Portland than aluminous cement, and more detailed consideration of this paper is not warranted in the present review.

2.4. Hydrate solid-solutions

The formation of complex hydrates from C_4AH_{13} and C_2AH_8 has continued to attract research interest. The ionic constitution of these hydrates is : $Ca_2Al(OH)_6^+ . OH^- . 3H_2O$, ($C_4AH_{13}$), and $Ca_2Al(OH)_6^+ . Al(OH)_4^- . 3H_2O$, ($C_2AH_8$). A solid solution between these two end members occurs when, for example, C_4AH_{13} absorbs aluminate ions from sodium aluminate solution, (35). However, such solid solutions are only reasonably stable at low temperatures (0°C) and tend to decompose in alkaline solutions, to C_3AH_6.

The structure of these types of hydrates consists of cationic layers of $Ca_2Al(OH)_6^+$, separatedly by interlayers containing anions surrounded by water. The OH^- anion, or the aluminate anion can be substituted by a wide range of other mono or divalent anions, giving complex hydrates of the general formula : $\left[Ca_2Al(OH)_6\right] + \left[m/n\ X^{n-} . (1 - m)Al(OH)_4^- . mAl(OH)_3 . aq.\right]^-$. In this formula, n is the valency of the substituting anion X, and m is the degree of substitution.

KUZEL and SCHELLER, (36) show that α and β-dicalcium aluminate hydrates are not polymorphs as previously proposed, but differ slightly in their water content : α-C_2AH_8 and β-$C_2AH_{7.5}$. The $\alpha \rightleftharpoons \beta$ transformation temperature lies near 20°C (18°C at 36 % relative humidity, 26°C in nitrogen at more than 45 % relative humidity). The stacking of the $Ca_2Al(OH)_6^+$ layers differs in the two forms.

DOSCH and KELLER, (35) have studied a wide range of anions, both inorganic and organic which can be introduced into C_4AH_{13} without modification of the cation layers, as shown by X-ray diffraction. The C_4AH_x-C_2AH_8 solid solution range is given as lying between m = 0.5 and m = 0.7, in contrast to the range 0.66 to 1 previously reported.

The stabilization of C_2AH_8 is also described by DOSCH and KOESTEL, (37). A number of anions, and particularly CrO_4^{2-} and SO_3^{2-} from the calcium salts are shown to form complex hydrates, stable in moist conditions up to 70° or 80°C, conditions under which C_2AH_8 alone is very rapidly transformed into C_3AH_6 and AH_3. This is suggested as a basis for preventing the conversion of aluminous cement. In support of this, the strengths of aluminous cement specimens, with and without the addition of these compounds ($CaSO_3.1/2H_2O$ and $CaCrO_4$) are compared after 1, 7 and 28 days storage under water at 30°C. Specimens without the additives showed the highest strength at 7 days but the lowest at 28 days, compared to the stabilised product. A stabilising effect was thus evident, but longer term tests would be needed before any conclusion could be drawn about durability. From a practical point of view the quantities of 'stabilising' agent required (2.2 to 10.7 % by weight) are rather large.

HOUTEPEN and STEIN, (38) have studied the dehydration of C_2AH_8 hydrates containing substituted mono-valent anions, by calorimetry and using a thermo-balance. The enthalpy of dehydration, ΔH_{deh}, determined calorimetrically from the heats of solution of the hydrate and the dehydrated compound, were significantly lower than those calculated using the Clausius-Clapeyron equation, from the hydration and dehydration curves observed thermogravimetrically. This is explained by hysteresis in the hydration-dehydration curves associated with the change in the layer spacings of the crystals, necessary to accommodate the interlayer water. It is concluded that the heat of dehydration cannot be determined as isosteric heat of adsorption (i.e thermogravimetrically) because the dehydrated material is not an inert adsorbent.

BENSTED, (39) reports an investigation of calcium nitro-aluminate hydrate using infra-red spectroscopy, X-ray diffraction, DTA and chemical analysis. Calcium nitrate is shown to react with C_3A to form compounds of the general type : $C_4\left[Al(OH)_6\right]_2.(NO_3)_2.3H_2O$ or $C_3A.Ca(NO_3)_2.9H_2O$. Furthermore, the aluminium ion can be substituted by other trivalent cations, Cr, Mn or Fe. The nitro-aluminates thus resemble the chloro-aluminates and do not form higher substitution products, isomorphous with ettringite, at normal temperatures, probably for steric reasons.

The incorporation of chloride (from $CaCl_2$) in various calcium aluminate hydrates, is reported by DARR and LUDWIG, (40). C_4AH_{13}, $C_4(A_{0.5},F_{0.5})H_{13}$, $C_3A.CaSO_4.12H_2O$ and $C_3A.3CaSO_4.32H_2O$ were prepared by mixing appropriate proportions of C_3A, C_4AF, $Ca(OH)_2$ and $CaSO_4$ in water at a water/solids ratio of 2. Additions of $CaCl_2$ were then made at 5°C, 20°C and 40°C. The highest $CaCl_2$ addition was 1 mole/mole and C_4AH_{13} and $C_3A.CaSO_4.12H_2O$ both proved capable of absorbing up to 0.9 moles of chloride. The mono-sulphate hydrate reached equilibrium later and took up slightly less than the tetra-calcium aluminate hydrate. Ettringite appears in increasing quantities when the mono-sulpho aluminate hydrate takes up $CaCl_2$. The iron substituted tetra-calcium aluminate hydrate absorbed only about half the quantity of chloride added. Up to 0.8 moles of $CaCl_2$ were incorporated in ettringite at 5°C after 28 days. At 20°C, only 0.4 moles were absorbed after 100 days and 0.3 moles at 40°C, also after 100 days. In general, both the rate of incorporation of chloride in these hydrates and the total equilibrium quantity absorbed increases with the solution concentration of chloride added, but decreases as temperatures are raised.

2.5. Some effects of heat and pressure

BARRET and DUFOUR, (41) discuss the solubility of dehydrated mono-calcium aluminate hydrate. Dehydration under vacuum at temperatures up to 90°C removes water from the CAH_{10} structure progressively and the solubility in water of the dehydrated product increases from that of CAH_{10} to that of CA. When dehydration is carried out above 90°C (100 to 900°C), subsequent re-solution takes the form of a rapid increase in solution concentrations, to a maximum greater than that shown by CA itself, followed by abrupt precipitation and a decrease in concentrations to a normal and steady level. A few hours later, further precipitation occurs and solution concentrations fall to low values.

The dehydration products of CAH_{10} are amorphous until 900°C is reached, when X-ray diffraction and infra-red spectroscopy show the appearance of the CA structure. The re-solution is understood to take place through an initial hydroxylation of the solid surface and not through bulk solution of the dehydrated material. Since the precipitated hydrates formed by CA at room temperature are both CAH_{10} and C_2AH_8 + AH_3 gel, while that of dehydrated, amorphous CAH_x is exclusively CAH_{10}, it is suggested that the 'amorphous' product still reflects the original hydrate structure and thus seeds the precipitation of CAH_{10}. High resolution electrom microscopy and electron diffraction appears to confirm this conclusion. It is also observed that the precipitation of CAH_{10} from solutions formed by the dehydrated product does not lead to setting and hardening unless the original dehydration has been accomplished above 900°C - ie., resulting in the formation of CA. Thus while precipitation of hydrate is a necessary condition for strength development it is not sufficient. This supports the view that hydrate morphology is also a critical factor for hydraulic bonding.

KUZEL, (42) suggested that the thermal dehydration of C_3AH_6 occurs by the formation of $C_{12}A_7$ and CH, and BALL, (43) provides confirmation with thermogravimetric and infra-red studies : for the reaction $7C_3AH_6 \rightarrow C_{12}A_7H + 9CH$ at 527°C the weight loss measured, 21,7 % agrees well with that calculated, 21.77 %.

Another study, (44) of the dehydration of C_3AH_6 and γ-AH_3 shows that gibbsite present in high alumina cement, CA or CA_2 hydrated at 100°C (in which C_3AH_6 is the other hydrate formed) looses its water without passing through the monohydrate (boehmite) stage, whereas in synthetic mixtures of separately prepared C_3AH_6 and γ-AH_3, boehmite appears as a transition phase during dehydration. Further results on the dehydration of hydrated neat high alumina cements used in refractory formulations, are reporded by WAGNER, (45).

Iron free high alumina cements containing less than about 0.2 % SiO_2 are frequently employed as binders for cracking catalysts used in the manufacture of hydrogen by steam reforming of hydrocarbons, at temperatures approaching 1000°C, and the development of one such cement specifically for this purpose is reported, (46). Because of destruction of hydraulic bonding and the relatively slow rate of ceramic bond formation in this service temperature range, MILLS and HUGHES, (47) have studied the effects of curing such cements in steam and in carbon dioxide atmospheres : the effects of curing conditions on the intermediate temperature strength of aluminous cements is known to be important, (48), (49), (50). A cement consisting primarily of CA, cured at room temperature in air at 0.5 W/C is only partially hydrated in the first 2 days. Its 20°C strength, due to CAH_{10}, is good but its performance in steam at 850°C is indifferent. Curing in steam produces C_3AH_6 and AH_3 with complete hydration and its behaviour as a catalyst support binder is good. Curing in CO_2 at normal temperatures produces $CaCO_3$ and C_3AH_6 with green strengths as high as those obtained from CAH_{10} at similar levels of hydration. Because of the high reactivity of the decomposition products, the performance at 850°C exceeds that obtained by steam curing with full hydration.

The effects of curing Fondu aluminous cement (approximately 40 % Al_2O_3) and Secar, high alumina cement (approximately 70 % Al_2O_3) under even more drastic conditions, is described by GOUDA and ROY, (51), who used a hot-pressing technique. Hot-pressing at 250°C for 1/2 hour at approximately 350 MPa produced C_3AH_6, and virtually all the gauging water was combined. At longer periods, $C_4A_3H_3$ was also formed. No CH was detected with either cement even after 1 year. Hot-pressing at 150°C did not lead to the formation of $C_4A_3H_3$. Very high strengths and low porosities were obtained by this method with both cements, but it is noteworthy that the high alumina

cement gave less good strengths than the ordinary type, despite its greater calcium aluminate content. (The CA + CA_2 content of the Secar cement studied is approximately 50 % greater than that of Fondu cement). The water/cement ratios used were the same in both cases and much lower than the critical values (*), and virtually all (approximately 99 %) of the water provided was combined. The possible conclusion that the morphology of the hydration products and hence their contribution to mechanical properties, is favorably affected by the non-aluminous contents of the lower purity cement remains to be proved.

FARRIS and MASARYK, (53) investigated the mineral products formed in dense massive refractory concretes made from high alumina cement. The initial hydrates normally found in 110°C dried concrete, C_3AH_6 and γ-AH_3 were present, but progressively towards the centre of massive specimens, $C_4A_3H_3$ and AH (boehmite) were detected. These phases are known to form under pressure and it is concluded that conditions within the body of a large concrete specimen approach that of an autoclave. This is because the initial rapid heat evolution during hydration cannot be quickly dissipated. The effect is intensified at lower water/cement ratios. However, comparisons between small and large specimens revealed no influence of the different mineralogies on the strengths of the concretes.

3. CARBONATION

The equations for carbonation of calcium aluminate hydrates may be written :

$CaO.Al_2O_3.10H_2O + CO_2 \rightarrow CaCO_3 + 2Al(OH)_3 + 7H_2O$

$3CaO.Al_2O_3.6H_2O + 3CO_2 \rightarrow 3CaCO_3 + 2Al(OH)_3 + 3H_2O$

In both cases, water is released and it may thus be expected that a decrease in strength with increase in porosity will result. This is not the case in practice, indeed, the reverse occurs and one explanation is that of further hydration of anhydrous cement by the water released. The overall effect would thus be :

$CaO.Al_2O_3.10H_2O + CO_2 \rightarrow CaCO_3 + 2Al(OH)_3 + 7H_2O$

$7/10CaO.Al_2O_3 + 7H_2O \rightarrow 7/10CaO.Al_2O_3.10H_2O$

$3/10CaO.Al_2O_3.10H_2O + 7/10CaO.Al_2O_3 + CO_2 \rightarrow CaCO_3 + 2Al(OH)_3$

In these circumstances the total weight of solid reaction products after carbonation is greater due to the incorporation of atmospheric CO_2, and this would be expected to decrease porosity and increase strength : the increase in the volume of solids represented by the above reaction is about 10 %.

A study of the hydration of synthetic CA in the presence of silica or of $CaCO_3$ is reported, (54). DTA and X-ray diffraction were used to identify the reaction products at 5, 20 and 40°C. In the presence of silica CAH_{10} was formed at 5°C, and traces of C_3AH_6 became detectable after 45 days. Alumina gel and gibbsite were present at all ages. At 20°C both CAH_{10} and C_2AH_8 were formed together with the alumina hydrates while some C_3AH_6 was apparent earlier (28 days) than at 5°C. At 40°C, CAH_{10} and alumina gel formed at ages less than 1 day were no longer apparent at later ages, while large quantities of C_3AH_6 and gibbsite were observed. This pattern of behaviour is entirely consistent with the results of earlier investigations.

In the presence of $CaCO_3$, CAH_{10} was less in evidence at all temperatures but the appearance of C_3AH_6 was also depressed in favour of the appearance of mono-carbo aluminate hydrate, $C_3A.CaCO_3.11H_2O$. It is concluded that the rate of conversion is lower in the presence of $CaCO_3$ and that the formation of carbo-aluminate in place of C_3AH_6 must reduce porosity and hence improve the strength of aluminous cement concrete.

Support for the above conclusion is given by RAASK, (55) who studied the absorption of CO_2 by hydrated aluminous cement paste with water/cement ratios of 0.38 to 1.0, at temperatures of 17°C and 37°C. From laboratory measurements of the rate of uptake of CO_2, an equation was derived which predicted well the measured penetration of CO_2 into a 5 year old aluminous cement concrete beam assuming a service temperature of 22°C. However, beams which had been in service for 8 years at 37°C showed a much lower than predicted depth of CO_2 penetration. This is explained by lack of liquid water in the latter case, which virtually prevents the carbonation reaction. In a further series of tests at 0.38 total water/cement ratio carbonation was shown to decrease the degree of conversion and increase the strength of aluminous cement concrete treated in a CO_2 atmosphere at 52°C.

KUZEL and FISCHER, (56) have restudied the carbonation of tetra-calcium aluminate hydrates at various temperatures and relative humidities. No evidence of solid solutions was found in the system $C_4A.nH_2O$ - $C_3A.CaCO_3.nH_2O$. Starting from C_4AH_{19} or C_4AH_{13} crystals, carbonation leads only to a surface zone of half carbonate, $C_4A.1/2CO_2.12H_2O$ while the bulk of the crystals remain unaffected.

FIERENS et al, (57) have studied the formation of tricalcium aluminate mono-carbonate hydrate from mixtures of C_3A and $CaCO_3$, or C_3AH_6 and $CaCO_3$, in water at 25°C. The formula $C_3A.CaCO_3.11H_2O$ is given. This compound is known, (58) to form as the interface material between the cement paste phase and limestone aggregate in aluminous cement concretes, and may explain the higher strength of such concretes compared to those made using siliceous aggregates. The very rapid formation of the carbo-aluminate from C_3A and $CaCO_3$, together with the simultaneous presence of C_4AH_{13} is taken to imply the reaction scheme : $C_3A + H \rightarrow C_4AH_{19} \rightarrow C_4AH_{13} + CO_2 \rightarrow C_3A.CaCO_3.11H_2O$. It is believed that the hydration of C_3A in the presence of $CaCO_3$ does not lead to the formation of C_3AH_6 as a precursor to the carbo-aluminate. FIERENS also demonstrates that the attack of $CaCO_3$ in the presence of C_3A/H_2O is greatest on those crystals faces with the highest density of $CO_3^=$ ions.

(*) The critical water/cement ratio for an aluminous cement has been defined by ALEGRE (52) as that needed for complete hydration in the fully converted state.

An extensive study of carbonation of aluminous cement concrete was reported by VASQUEZ and co-workers (59) at the 1974 International Symposium on the Chemistry of Cement (Moscow), and published in 1975. Here again a reduction in the rate of conversion is observed in the presence of CO_2. Short periods (2 weeks) of carbonation at relatively low temperatures (20°C) appeared to show reversibility, wherein carbo-aluminate could be decomposed under vacuum to reform C_3AH_6. Longer periods of carbonation, and particularly higher temperatures, (43°C) produced a carbo-aluminate which was stable. Thermogravimetric analysis, X-ray diffraction and infra-red spectroscopy were used to identify reaction products and evidence is presented to show that CO_2 substitutes step wise for 2, 4 and ultimatly 6 molecules of water in the C_3AH_6 hydrate in a manner analogous to the formation of hydraogarnets in the presence of silica. The final products of the reaction between C_3AH_6 and CO_2 are calcium carbonate and alumina hydrate.

As a general rule it may be stated that a carbonation of aluminous cement will only proceed at a significant rate in the presence of liquid water and when sufficient porosity exists to accommodate this water and allow penetration of CO_2. It thus follows that dense, low water/cement ratio material will show only very small depths of reaction even after many years. Recent studies, (60) of 25 aluminous cement concrete beams aged less than one year to up to 20 years showed exceptionally 60 mm penetration in the oldest beam, less than 5 mm in the youngest but 5 to 10 mm on average at ages up to 17 years. The water/cement ratios of these beams are not accurately known but are estimated to be generally 0.5 to 0.55 total, (61) which is relatively high.

RAUEN, (62) commenting on the failure of prestressing wires in some aluminous cement concrete of Bavarian origin (1962), reports depths of carbonation of several centimetres in 1 year old samples. Such a degree of attack is only conceivable in extremely porous, wet concrete made at very high water/cement ratios, but no information on this point is given. At the levels of attack reported by RAUEN the prestressing wires were inevitably in the carbonated zone and this may have contributed to one of the several forms of steel corrosion observed. By contrast, significant corrosion of prestressing wires was not observed in the very large number of concrete units of widely different ages, examined in the UK in recent years, (60), despite evidence of higher than recommended water/cement ratios. There is thus no evidence for depassivation of reinforcement due to carbonation in well made aluminous cement concrete.

Carbonation in the presence of alkalis (sodium and potassium hydroxides), in contrast to normal carbonation, can seriously weaken aluminous cement bonded materials. This has been known for a long time and the mechanism, usually referred to as alkaline hydrolysis, was explained by RENGADE, L'HOPITALIER and DURAND DE FONTMAGNE, (63) working in the Lafarge laboratories as early as 1935. The alkali is regenerated in the process so that relatively small quantities can sustain the reaction. The final reaction products, $CaCO_3$ and AH_3 are the same as when carbonation occurs in the absence of alkalis, but the effect on strength is reversed. It is therefore highly probable that the two different mechanisms involved in the presence or in the absence of alkalis affect the morphology of the reaction products, but this remains to be proved.

From a practical point of view carbonation only reaches significant proportions when porosity or permeability is high, so that while alkaline hydrolysis was a problem in some early uses of aluminous cement concrete, it is very rarely encountered today, as NEVILLE, (64) points out. Now that the importance of maintaining a low water/cement ratio is recognised, aluminous cement concrete manufactured with a porosity high enough to engender alkaline hydrolysis must be considered unacceptable for long term applications whether alkalis are present or not.

4. CONVERSION AND ITS EFFECTS

As in the past, so during the period covered by this report a high proportion of publications concerning aluminous cement discuss conversion and its effects on durability. Several papers (65), (66), (67) report the results of long term laboratory tests on aluminous cement concrete under various storage conditions, both artificial and natural. The effects observed are then explained in terms of conversion, wherein strength changes are related to changes in porosity of the cement paste phase. However, direct measurements of porosity are regrettably rare.

The overall consequence of recent publications is a substantial confirmation of previous knowledge.

Quantitative comparisons of the results of different workers is difficult due to different choices of experimental conditions : cement contents, mixing procedures, methods of compaction, curing and storage environments and water/cement ratio.

4.1. Rate of conversion

MIDGLEY and MIDGLEY, (68) give a comprehensive account of conversion, bringing together a large amount of experimental data, some of which was reported prior to 1974. From laboratory tests on neat cement pastes, mortars and concretes a number of empirical relationships are developed relating conversion to both compositional factors (mineralogy and water/cement ratio) and environmental factors, (temperature, humidity, age). Rate of conversion is seen to be increased by temperature and humidity of curing and storage of specimens, as previously established. These authors also present evidence, (69) to show that, other factors constant, the rate of conversion increases with water/cement ratio. For concrete specimens stored under water at 18°C this appears to be the case with total water/cement ratios of 0.5 or more, at ages of 5 years and later. The effect is shown in figure 1. It is swamped by the effect of temperature when similar concretes are stored at 38°C.

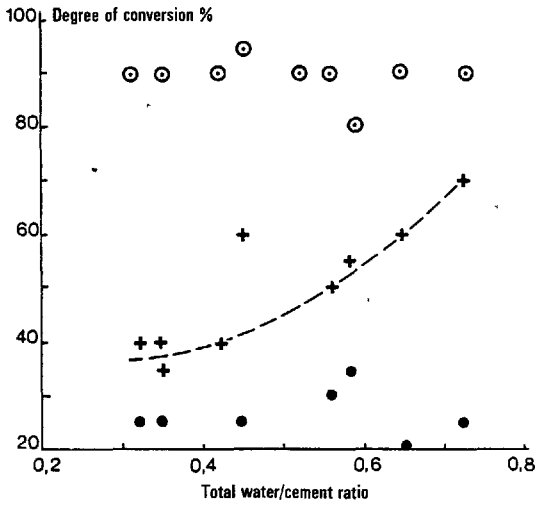

● concrete after 1 year at 18°C
+ concrete after 8 1/2 years at 18°C
⊙ concrete after 8 1/2 years at 38°C
Data from reference 66

Fig. 1 - Water/cement ratio related to degree of conversion

The effect of conversion on the compressive strength of aluminous cement is then discussed and extensively illustrated. The results confirm that the minimum strength of aluminous cement increases with decreasing water/cement ratio, and also that the minimum strength is higher the slower the conversion takes place. Note that the rate of conversion is dependent on temperature, an increase in one being accompanied by an increase in the other. Consequently minimum strengths are higher when conversion takes place at lower temperatures. This is well known, (1).

A general expression, $S = (k \log_e R + p) + q(w - m)$, is given, where S is the minimum strength expressed as a percentage of the 1 day unconverted strength, w is the water/cement ratio (the water/cement ratio used would appear to be total water/cement ratio) and k, p, q and m are constants. R is the rate of conversion defined as : $R = \log_e Dc / \{\log_e \text{age (years} \times 10^6)\}$, Dc being the degree of conversion, determined by DTA.

BRADBURY, CALLAWAY and DOUBLE, (70) have studied conversion in neat high alumina cement pastes of the 'Secar' type, containing CA, CA_2 and free alumina. Low, (0.2) and high, (0.6) water/cement ratios were used and curing temperatures of 18°C and 40°C. The hydrates produced were examined by DTA and electron microscopy. The initial formation of CAH_{10} and C_2AH_8, followed by conversion to C_3AH_6 exhibited the normal pattern. There was qualitative evidence that conversion was less rapid at the lower water/cement ratio and the size of the C_3AH_6 crystals was smaller than at the high water/cement ratio. An examination was also made of variations in the degree of conversion through a section of an aluminous cement concrete beam. Within the bulk of the concrete the degree of conversion was high (70 % typically) but near, or at the surfaces, values of 40 to 50 % occured. This accords well with the frequently observed 'skin' effect on aluminous cement concretes due to a lower rate of conversion as a result of drying, or to the superficial effects of carbonation.

The authors also remark that substantial variations in the water/cement ratio may occur from point to point in a concrete due to segregation effects before hardening commences, and that in aluminous cement concrete this can cause important differences in the degree of conversion and hence strength. The implication is, of course, that deleterious localised weakening will result and that the effect will be aggravated by errors in the control of water/cement ratio.

Two points may be made : (1), aluminous cement concretes should be designed on converted strrength, (2), when the converted strength is taken as that resulting from rapid conversion (at 38°C) - severe in practice - this strength is not more sensitive to water/cement ratio than in the case of a corresponding Portland cement concrete, (66).

4.2. Long term behaviour

TEYCHENNE, (66) reports the results up to 9 years of a major programme aimed at characterising the long term strength (in compression) of aluminous cement concrete. Concretes with total water/cement ratios ranging from 0.3 to 0.8 were stored under water at 18°C and also, after 24 hrs curing at 18°C, under water at 38°C (100°F). This latter temperature is considered a realistic maximum in practice for concrete in buildings in temperate climates. The cement used displayed converted strengths in the lower range of normally encountered values as was demonstrated by shorter term repeat tests on a number of other cements of the same origin. Its behaviour corresponded in fact, to the characteristic strength (95 % confidence) of the product tested. The data reported clearly reproduces the now well known sigmoidal strength development curve of aluminous cement concretes, although some doubt is left about the degree of strength increase beyond the minimum, due to the fact that the test age had not exceeded 8 1/2 to 9 years at the time of publication.

In view of this, and the importance of a real and significant increase in strength beyond the so-called minimum converted strength of aluminous cement concretes, the opportunity is taken to extend the results reported by TEYCHENNE, and also by GEORGE, (67) with the data shown in figure 2. The test programme represented by figure 2 was initiated in 1955, and in appreciating the value of the results today it is important to realise that 25 years ago, the relationship between the unconverted and converted properties of aluminous cement was considerably less well established and understood. Thus while it was evident that if porosity increased due to conversion this increase would not exceed that corresponding to complete conversion, the results shown in figure 2 and other long term tests which have now become available, are important : they establish with a degree of confidence never provided by accelerated tests, that there is a significant strength gain beyond the minimum converted value, and that this gain is considerable at lower water/cement ratios.

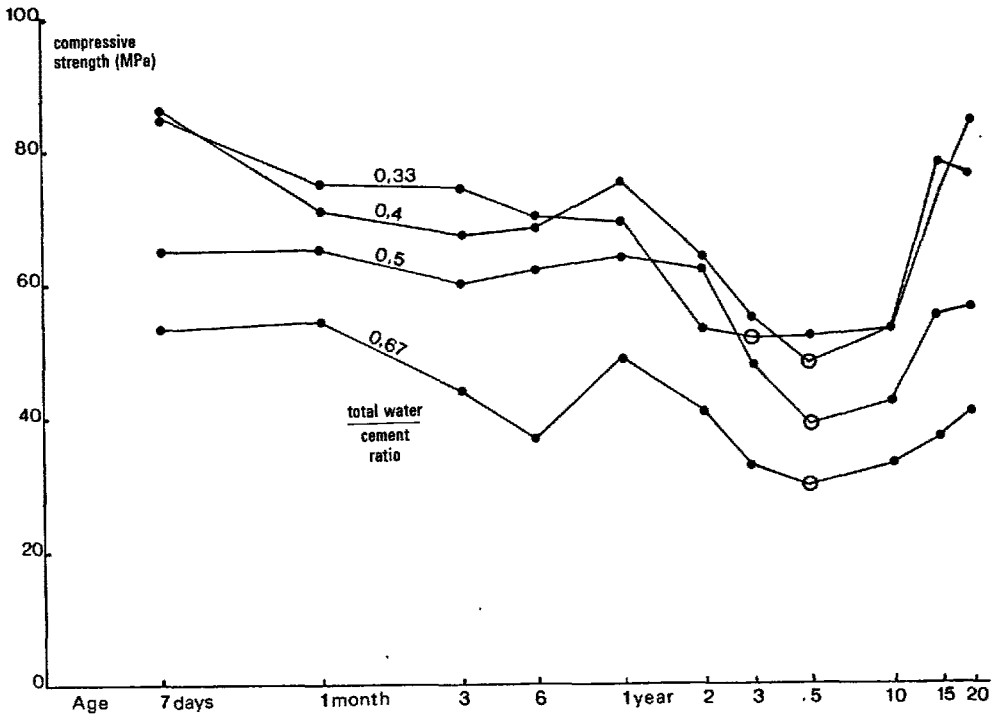

O indicates minimum strength when the effects of conversion are complete

Fig. 2 - Concretes cured 24 hours in moist air at 18°C then stored outdoors (S. France)

4.3. Conversion and curing

An interesting feature of the work reported by TEYCHENNE is the effect of different curing regimes on subsequent strength development. The experimental procedure was to cure concrete cubes under water either at 18°C or at a higher temperature (25, 35 or 50°C). The period at the higher temperature was varied from 3 hours to 24 hours and began immediately after placing the concrete, or after different periods (up to 21 hours) of curing at 18°C. It was found that the temperature of 25°C had relatively little effect, but the higher temperatures induced lower strengths at earlier ages, if imposed immediately after placing, than if delayed for 3 to 6 hours. Accompanying DTA estimates of the degree of conversion show a consistent pattern. Some examples are given in table II.

TEYCHENNE offers no explanation of this effect.

COTTIN and GEORGE, (71) studied the effect of steady and oscillating curing and storage temperatures on neat aluminous cement pastes. Seales pastes (to prevent carbonation) at a water/cement ratio of 0.4 were stored from time of gauging continuously at 30°C and 38°C. Other equivalent specimens were cured for 24 hours at 20°C, then for 24 hours at 30°C, at 20°C the following day, and so on. Finally the cyclic temperature test was repeated but with the initial 24 hours being at 30°C, followed by 20°C, etc. X-ray diffraction, DTA and infra-red spectroscopy were used to identify the hydrates formed and the proportion of cement reacted, while the percentage bound water was also measured. In parallel,

Table II : The effect of different curing regimes on degree of conversion and compressive strength of concrete

Data from reference (66)	Curing regime under water		T°C	Strength ratio (%) after 3 months, regime X/ regime Y Total water/cement ratio		
	6 hours at T°C, then 18 hours at 18°C (regime X)	18 hours at 18°C then 6 hours at T°C (regime Y)		0.4	0.5	0.6
Degree of conversion after 3 months %	75	15	50	37	38	31
	40	10	35	95	49	36
	20	15	25	99	107	109

compressive strengths and penetration resistance of the specimens was recorded. At 38°C, C_2AH_8 formed initially, was fully converted after 2 days and C_3AH_6 and AH_3 were the principal phases. The CA and alumino-ferrite contents of the cement were rapidly reacted. At 30°C the same effects occured more slowly with C_2AH_8 finally disappearing after about 2 weeks. No CAH_{10} was detected in either case.

The behaviour under cyclic curing depended on whether the first 24 hours curing took place at 20°C or at 30°C. In the latter case, the behaviour was qualitatively identical to that observed for continuous curing at 30°C. Despite subsequent 24 hour curing periods at 20°C, no CAH_{10} was detected. By contrast when the initial curing was at 20°C, CAH_{10} formed, and continued to form during later periods at 30°C, for up to 4 months. Beyond this age, with virtually complete hydration of the cement, the C_3AH_6 and AH_3 contents continued to rise while the CAH_{10} gradually converted. C_2AH_8 formed only during the first 24 hours and disappeared after 2 days curing.

All this suggests that there is some sort of seeding or epitaxial effect whereby the form of the hydrate initially precipitated at the end of the dormand period, (initial set) or during the early stages of hydrate development, influences the further hydrate form, and hence both the measured degree of conversion and the associated mechanical properties. This hypothesis is also consistent with the effects mentioned above, observed by TEYCHENNE.

Another observation, (66) which appears to reflect the same phenomenon is that conversion is slower at a given temperature if the initial curing temperature is low. Thus concretes cured at 18°C for 24 hours and then stored at 38°C reach their minimum converted strength at a degree of conversion of 80 - 85 % after 3 months. Equivalent concretes cured and stored continuously at 38°C after placing, reach the same minimum strength after a few days. The inference is that the hexagonal hydrate, or CAH_{10} at least, after a few hours ageing, is more resistant to conversion than at its time of formation. However, from a practical point of view the fact that the effect on strength is the same whether conversion is immediate or delayed, is the most important conclusion. This is another way of saying that the dominating factor for conversion is temperature ; whether a concrete is subjected intermittently to an elevated temperature or continuously, immediately or later, the overall result will be the same.

This is one of the less widely known features of aluminous cement. It should not be confused with the fact that conversion occurs faster, and minimum strengths are lower and earlier, the higher the curing or storage temperature, (68), (72).

The long term tests reported by GEORGE, (67) involve a range of curing conditions (10 to 90°C), total water/cement ratios from 0.33 to 0.67 and 3 different storage conditions : - under water at 18°C, outdoors and in ano outdoor hangar where specimens are protected from direct rain water. This last condition proves the most severe since not only did the concrete cubes experience climatic temperature variations from at least - 10°C to at least + 40°C, but the effects of drying-out are not alleviated by liquid water. By contrast, storage under water at 18°C gave the highest and least variable strengths. The results over 10 years are in very good agreement with the 20 year test results reported for the first time in the present review and extend the work of TEYCHENNE to a wider range of storage conditions. They also show that if initial curing temperatures are sufficiently high to bring about a major degree of conversion the concrete increases in strength thereafter. It is suggested, (65), (72) that this offers a method of producing high strength concrete.

4.4. Porosity

Although there is virtually universal agreement that porosity changes accompany conversion, relatively little experimental information (30), (60), (68) on this point has been published since 1974. The subject was very thoroughly studied earlier, (31) and it was demonstrated that the compressive strength of aluminous cement paste is related to porosity by an expression of the form : $\log C = a - bP$, where C is compressive strength and P is the percentage porosity.

Table III : Results from reference (31)

Curing temperature	Constants a	Constants b	Coefficient of correlation	Conditions
10°C	3.331	0.085	0.997	unconverted
70°C	3.714	0.105	0.976	converted

The porosity of concrete will depend on that of the aggregates used, voids due to entrained air or inadequate compaction, but primarily on that of the cement paste phase. Porosity will thus depend on cement content and water/cement ratio. Figure 3 shows results obtained, (73) through laboratory and field tests, on converted aluminous cement concretes. Some data on Portland cement concrete is included for comparison. Qualitatively, these results confirm earlier findings that conversion causes an increase in porosity and that this effect is greater the higher the water/cement ratio. However, from a quantitative point of view it is important to see that the fully converted porosity of aluminous cement concrete is not greater than, but if anything, less than that of a Portland cement concrete at the same water/cement ratio. Such a finding is clear indication that conversion does not automatically imply lack of durability. Water/cement ratio and temperature taken together are the decisive factors.

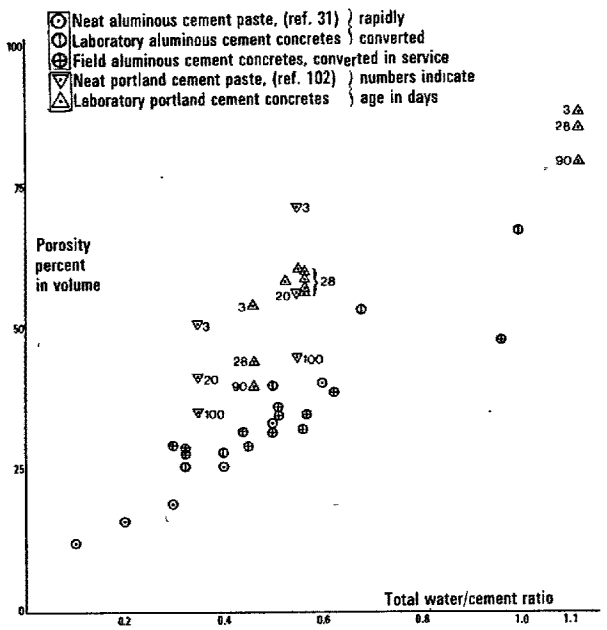

Fig. 3 - Porosity of cement paste as a function of water/cement ratio

5. ALUMINOUS CEMENT CONCRETE IN SERVICE

5.1. Mineralogical characterisation

Many publications have appeared describing methods of measuring the degree of conversion of aluminous cement. In most cases they have been developed as tools for assessing the quality of concretes made with this cement. Thermogravimetric and derivotographic techniques have received the most attention, and in particular the procedure reported by MIDGLEY, (74). It is clear from this work that the DTA method, and similar techniques such as differential scanning calorimetry DSC, semi-isothermal gravimetry and derivative thermo-gravimetry, DTG (75), offer a high degree of reproducibility, (0.5 %). Errors due to sampling are more significant and when interlaboratory differences are taken into account the overall result is to estimate the degree of conversion to within ± 15 % (at 95 % confidence limits). In other words, if a measurement of the degree of conversion of a sample of aluminous cement concrete by the method described by MIDGLEY yields a value of 50 % for example, there is apparently no more than one chance in 20 that the actual degree of conversion is less than 35 % or greater than 65 %.

Semi-isothermal thermogravimetry is a technique which appears to facilitate the identification of the hydrate phases as their water content is progressively driven off, (76). In this method, the instrument is switched from the dynamic mode (constant specimen heating rate) to the isothermal mode (specimen held at constant temperature) as each maximum in the DGT curve is reached. Continued weight loss is then recorded until the curve has again reached its base line. A return to the dynamic mode is then made, and so on. Results are given to show that this provides a more accurate measure of the quantities of individual calcium aluminate hydrates present in an aluminous cement specimen, and a better separation.

REVAY and WAGNER, (77) use DTG to measure degree of conversion in conjunction with a modified sample treatment designed to overcome difficulties due to overlap in the dehydration temperatures of different hydrates. Their procedure involves measuring the TG and DTG curves for the sample in the as-received state, and again after autoclaving. The autoclave treatment crystallises the alumina hydrate to boehmite with a dehydration peak near 500°C, well removed from the others. During the same autoclave treatment, the hexagonal hydrates, CAH_{10} and C_2AH_8 are converted to C_3AH_6 and further AH. From a comparison of the results before and after autoclaving it is thus proposed to calculate the amounts of hexagonal hydrates which could exist in the material, and which may thus convert at some stage in the service life of the concrete.

STROBEL, (78) also points out the problem of peak identification using DTA due to overlap at dehydration temperatures below 200°C.

A number of points needs to be made about the use of the above techniques and the interpretation of the results obtained.

Semi-isothermal DTG appears to be the best method of overcoming assignment problems associated with overlap between different hydrates.

REVAY's studies aimed at assessing the ultimate porosity due to conversion which could arise in an aluminous cement concrete in service, and hence an estimate of its minimum converted strength. However the autoclave method gives a false picture since there is evidence, (68) that the minimum strength of aluminous cement concrete under most service conditions is passed before conversion is complete. Furthermore autoclaving changes the degree of hydration of the sample. Nevertheless REVAY's approach does not rely only on thermogravimetry : the cement content and as-received porosity in his samples is also measured. With this information some assessment of the quality of the concrete is indeed possible, as discussed later.

Most authors (74), (75), (76) calculate the degree of conversion from the formula :

$$Dc\ \% = \frac{100 \times AH_3 \text{ peak height}}{AH_3 \text{ peak height} + CAH_{10} \text{ peak height}}$$

Although strictly speaking, peak areas should be used, since Dc is expressed as a ratio better reproducibility between different laboratories was obtained using peak heights. The above formula is based on the equation :

$$3CAH_{10} \rightarrow C_3AH_6 + 2AH_3 + 18\ H$$

1 g 0.378 g 0.308 g

from which it can be seen that the weights of C_3AH_6 and AH_3 produced by the conversion of CAH_{10} are rather similar. As MIDGLEY points out, (68) such an approximation is not justified in laboratory studies. However it has been widely adopted in field studies of aluminous cement concrete.

It must be pointed out that the measurement of AH_3 as an indicater of C_3AH_6 ignores the fact that AH_3 in aluminous cement can arise from sources other than the conversion of CAH_{10}. At temperatures of 20°C and above, the initial hydration of aluminous cement produces both CAH_{10} and C_2AH_8. The precipitation of C_2AH_8 is accompanied by that of AH_3 ; $2CA + 11H \rightarrow C_2AH_8 + AH_3$. (see for example references (65) and (79)). If any CA_2 is present in the cement (rare in aluminous cement of the Fondu type) this will also produce AH_3 during hydration. Finally the carbonation of calcium aluminate hydrates, results in the formation of AH_3 as well : $C_3A.CaCO_3.12H + 3CO_2 \rightarrow 4CaCO_3 + AH_3 + 9H$

Thus although techniques such as DTA, DSC and DTG give excellent reproducibility, the values of Dc obtained from AH_3 are by no means an infallible measure of conversion.

The use of DTA to study the reaction of aluminous cement concrete with sulphates, chlorides and carbon dioxide is also recommended by MIDGLEY, (80). The reaction products, ettringite, $C_3A.CaCl_2.nH_2O$, AH_3 and $CaCO_3$ have characteristic endotherms which may be quantitatively determined by this technique. However, the peak temperature increases with the amount of material being estimated. Thus greater precision is obtained by calibration with synthetic mixtures of controlled increments of composition. Ettringite has a peak temperature at $\simeq$ 100°C which can overlap with that of gypsum. However the above refinement enables the two compounds (product and reactant), to be distinguished. The peak temperature for $C_3A.CaCl_2.nH_2O$ is in the range 150 to 170°C approximately, depending on concentration. Attempts to distinguish between forms of AH_3 produced as a result of carbonation in the presence or absence of alkalis, were unsuccessful.

This work was carried out in the context of disruptive chemical attack of highly porous aluminous cement concrete. While porosity (or permeability) is undoubtedly the dominant factor governing chemical attack (in any type of concrete), attention is drawn to the information on the porosity of converted aluminous cement concrete given in section 4.4. Conversion and vulnerability to chemical attack are not synonymous, and the fundamental importance of maintaining a low water/cement ratio in the manufacture of durable aluminous cement concrete cannot be over emphasised.

Thermogravimetric analysis has also been used by DAY and LEWIS, (81) to analyse the products of autoclaved refractory high alumina cements and concretes. Quantitative estimates of the phases present were made and mass balance calculations agreed well with the known chemical compositions of the starting materials : calibrations were carried out with pure samples of boehmite, gibbsite, portlandite and C_3AH_6. The results obtained also demonstrated the decomposition of C_3AH_6 at approximately 200 to 260°C, to $C_4A_3H_3$ and CH. $C_4A_3H_3$ did not form directly from CA. By contrast, a commercial high alumina cement containing predominantly CA and free alumina produced $C_4A_3H_3$ directly from the CA present. The reason for the difference in behaviour between laboratory and industrial materials is not known.

X-ray diffraction is an alternative method of determining the phase composition of set aluminous cement and is recommended by PLOWMAN and GYLLENSPETZ, (82). It has the advantage of more reliable identification of the various hydrates but is generally less quantitatively reproducible than thermogravimetric methods, (30). The use of both methods is generally more instructive than either one alone.

Infra-red spectroscopy has been usefuly applied as a complementary technique.

LEJAWKA, (83) describes the use of quantitative X-ray diffraction to measure the CA, CA_2 and free α-alumina content of aluminous cements, mainly of the purer type employed in refractory concretes. For cements containing less than 2 % of materials other than lime and alumina, an external calibration standard is considered satisfactory. Pure laboratory prepared samples of CA, CA_2 or α-Al_2O_3 are used as standards. For less pure cements an internal standard (quartz) is employed. In both cases the conditions of sample preparation are critical : grinding to crystal sizes less than 5µ is considered necessary.

5.2. The assessment of quality

The use of degree of conversion calculated from the DTA peak heights of AH_3 and CAH_{10} has been made the basis of a method of assessing the quality of aluminous cement concrete and has been extensively applied, (60), (68), (84). This method, which it must be stressed is intended only as an initial rapid guide to quality and not a definitive assessment, is based on relating the degree of conversion to its age, from which the rate of conversion is then inferred.

Since laboratory studies had shown that the rate of conversion of aluminous cement concrete depends, in part, on water/cement ratio (see section 4.1.) a classification was made of concrete based on rate of conversion. This classification recognises three broad classes of concrete - those with minimum strengths greater than the 1 day strength, those with minimum strengths less than half the 1 day strength and an intermediate class. The limits are approximately

Table IV : Relative converted minimum strength and rate of conversion

S, minimum converted strength as a fraction of 24 hours 20°C strength	S>1	0.5 <S<1	S<0.5
Rate of conversion, R*	R<0.24	0.24<R<0.27	R>0.27
Approximate degree of conversion % and age (years)	from 30 % at 1 year to 50 % at 20 years	intermediate	from 50 % at 1 year to 75 % at 20 years

* R as defined in section 4.1.

In assessing the quality of aluminous cement concrete it is suggested that concrete having a value of R of 0.24 or less is good, while values of R in the intermediate range give cause for suspicion. Concretes with values of R above 0.27 are classified as 'highly converted' and this is assumed to generally imply poor quality, because it results from a high water/cement ratio.

The dependence of rate of conversion on water/cement ratio is not very pronounced and, as shown in figure 1., the trend is only really noticeable at high water/cement ratios. However the most serious criticism of this classification is that it takes no account of the dominant effect of temperature on rate of conversion. The relative importance of temperature compared to water/cement ratio can be judged from the fact that a change in curing temperature from 20 to 30°C can cause a bigger increase in this rate than that predicted at constant temperature, for a change in water/cement ratio of 0.27 to 0.6. Consequently a low water/cement ratio concrete which was been subjected to heat either during curing or at an early age will show a degree of conversion which would be considered on the above basis to imply a high water/cement ratio. The conclusions drawn as a result about the quality of the concrete would be quite wrong.

Another feature of the above method is the procedure used in sampling the concrete. This procedure involves drilling the concrete with masonry drills to give a powder specimen, (74). The well-known 'skin' effect on aluminous cement concretes, in which, due to dry surface conditions the degree of conversion is normally lower than in the bulk of the concrete, is allowed for by discarding the material produced during the drilling of the first 4 to 5 mm. Only the material extracted below this level is used for analysis, and results are presented to show that by this procedure a representative sample of the concrete is obtained. The results of two different drilling methods are described - rotary and rotary-percussion and compared with those obtained by crushing the concretes and taking internal samples.

These different drilling methods do not appear to give equivalent data. Admitting that each individual estimate of the degree of conversion is subject to an error of at least 5 %, one way legitimately analyse differences of 5 % or more observed between the degree of conversion of drilled and crushed samples. The results analysed in this way are shown in figure 4. - the dotted line is purely conjectural.

It is quite evident that the estimated degree of conversion is higher for drilled samples than crushed samples, and the difference is more pronounced the less the total degree of conversion. The most immediately obvious explanation is that the heat of drilling causes conversion and such an effect will evidently be greatest in those specimens which are initially the least converted. The determination of degree of conversion as a function of age must therefore be considered as a very imperfect preliminary measurement and not in itself a reliable guide to the quality of aluminous cement concrete. But in taking high rates of conversion to imply high water/cement ratios it correctly recognises the overriding importance of water/cement ratio.

The above method is put forward because no reliable direct method of assessing the water/cement ratio of a hardened aluminous cement concrete has yet been published. At this point therefore the opportunity is taken to report some previously unpublished attempts to make such an estimate. The test procedure involves measuring several related properties of a concrete sample : porosity (by water impregnation under vacuum), cement content (by chemical analysis) and density, which is a property determined incidentally during the measurement of porosity. Also needed is a knowledge of the chemical composition of the aluminous cement employed and the amount of porosity in the sample due to air entrained while mixing the concrete, or resulting from inadequate compaction. Manufacturer's records normally provide a reliable estimate of the cement composition. The degree of air entrainment or lack of compaction cannot be established directly, and this is the only weakness of the method. However the degree of uncertainty which this imparts to the overall result is not necessarily serious.

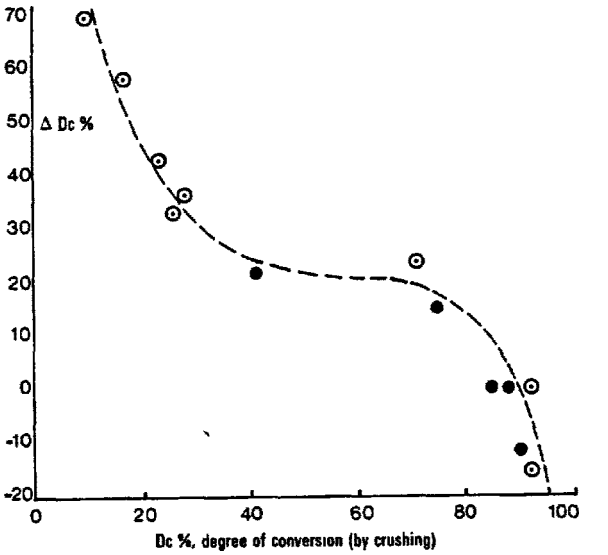

Fig. 4 - Influence of sampling method (drilling or crushing) on the apparent degree of conversion of concrete

The general formula for calculating the total water/cement ratio is :
W/C = (P - A + L.d) 10/C where P is the porosity (% by volume), A is the estimated entrained air (% by volume), L is the loss on heating under nitrogen at 550°C (% by weight), d is the density of the concrete (kg/litre) and C is the cement content, (kg/m^3).

Table V : Comparison of measured and actual water/cement ratios of hardened aluminous cement concrete

Concrete	Total water/cement ratio Actual	Measured	Measured / Actual	% Air entrained
Partially converted	0.33	0.33	1.00	1.8
Fully converted		0.37	1.12	
Partially converted	0.4	0.38	0.95	2.1
Fully converted		0.455	1.14	
Partially converted	0.5	0.465	0.93	3.1
Fully converted		0.575	1.15	
Partially converted	0.67	0.67	1.00	6.0
Fully converted		0.70	1.04	

Table V shows the results of a series of experiments based on the above procedure on concretes prepared at known water/cement ratios, and for which the air entrained in the freshly placed concrete was also measured. For an unknown concrete it would be prudent to use a value of 2 % for the air entrained (see also reference (85)) and table V shows that the method provides quite a reasonable estimate. Any systematic errors tend to give an overestimate of the water/cement ratio.

A disadvantage of this method, and that of REVAY (77), (86), is that a relatively large specimen of concrete is needed for analysis, which in many cases in practice must imply the destruction of the unit under investigation. Also several experimental procedures must be carried out in order to arrive at the final answer. A more simple, non destructive, though less rigorous approach, consists of estimating only the cement content of the concrete. This can be done with considerable accuracy by classical chemical analysis, as the following results show :

Table VI : Comparison of known cement contents with cement contents of hardened concrete estimated by chemical analysis

Cement content kg/m^3 Measured	Actual	Average Measured / Actual	Total water/cement ratio
651, 640, 647	616	1.05	0.33
469, 495, 517	491	1.01	0.40
375, 345, 378	402	0.92	0.50
303, 310, 309	302	1.02	0.67

It is well established that the workability of concrete in general, for a given cement content, is very sensitive to water/cement ratio. Since in practice, workability is probably the most consistently controlled parameter in precast concrete manufacture, it follows that variation in water/cement ratio will closely mirror variations in cement content. Figure 5 constructed from data in the publication by TEYCHENNE, (66) is illustrative :

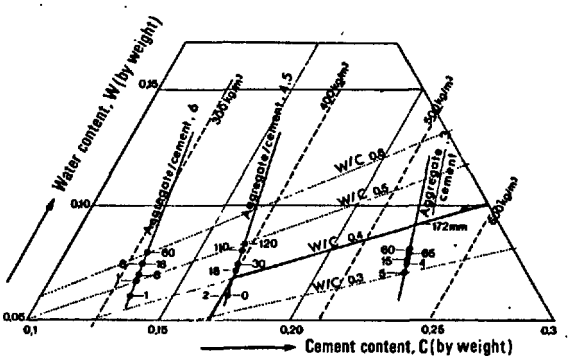

Fig. 5 - Aluminous cement concrete : slump (mm) and mix proportions

In view of this a simple estimate by chemical analysis of the cement content of an aluminous cement concrete, might provide quite a useful guide to water/cement ratio, and hence quality.

Acoustic emission as a non destructive technique for assessing concrete quality has been applied to aluminous cement based materials, (87), (88). Tests on beams during proof loading showed a correlation between acoustic activity, load and deflection. Laboratory prepared cubes cured at 20°C and at 40°C were monitored in compression. Acoustic emission increased with load but total levels of emission were lower for the samples cured at the higher temperature. These samples, due to conversion, also showed lower crushing strengths.

The acoustic emission of neat aluminous cement pastes at water/cement ratios of 0.35 and 0.65 was recorded during curing at 60°C. There was very little activity from the lower water/cement ratio sample indicating that conversion under these conditions does not cause acoustic emission. At the higher water/cement ratio, acoustic emission increased to a maximum after about 25-30 hours at 60°C (preceeded by 24 hours curing at 17°C) and then decreased to reach negligible levels after about 40 hours. This activity is thus most probably associated with microcracking during conversion of the higher water/cement ratio, intrinsically weaker, specimen.

Recent mention has also been made of the assessment of aluminous cement concrete quality by measuring ultra-sonic pulse velocity, (65), (67), (89). It provides a broad non-destructive guide to

the quality of concrete in service but is only really reliable in cases where the many factors, water content, aggregate content, reinforcement, porosity, etc. affecting velocity can be individually allowed for through calibration tests on equivalent laboratory concretes of known composition. The USPV method is thus not adapted to comparisons between different concretes, or to the absolute determination of mechanical properties, but is certainly a useful tool for monitoring changes with age of a given specimen.

It is suggested that methods such as acoustic emission, pulse velocity, velocity of sound or gamma-ray absorption for example, could well find wider application in laboratory studies aimed at following the changes in properties of aluminous cement during hydration and aging. By such techniques the most important stages in property development might be more precisely identified and thus provide a means of choosing the most appropriate moments to carry out destructive tests, such as cube crushing. In this way better data might be aquired, from fewer specimens.

5.3. Modulus of elasticity and creep

The relationships between such mechanical properties of concretes as creep, modulus of elasticity and compressive or flexural strength change relatively little with the chemistry of the cement. The largest differences between Portland cement and aluminous cement concretes are found at early ages and are a consequence of the rapid hardening character of aluminous cements, (1).

Recent work, (66) on the modulus of elasticity of aluminous cement concrete confirms that it increases with compressive strength : values at the higher end of the range normally encountered with Portland cement concretes are reported. Results obtained for aluminous cement concrete with total water/cement ratios in the range 0.35 to 0.6 fall on the same curve, with higher values in the unconverted state (storage at 18°C) and lower values in the converted state, (storage at 38°C). Furthermore, it has been shown, (90) that the relationship between static and dynamic modulus is not affected by conversion, and is the same, for practical purposes, for Portland cement concretes and aluminous cement concretes.

The modulus of elasticity of aluminous cement-granite concretes, and an ultra-fine Portland cement-granite concrete were measured in accordance with British Standard 1881 (1970), by SWAMY, IBRAHIM and ANAND, (91) who give the equations : $E = 4.87 \sqrt{C}$ (aluminous cement), $E = 4.07 \sqrt{C}$ (Portland cement), where E is the static modulus and C is the cube crushing strength.

NEVILLE, (64) quoting the work of CUSENS and JACKSON, (92) in a review of aluminous cements, states that the elastic modulus in the unconverted state is slightly higher than that of Portland cement concretes of the same strength, and at the lower end of Portland cement values in the converted state.

SWAMY and co-workers, (91) have also compared the shrinkage and creep of Portland cement and aluminous cement concretes. The initial shrinkage and creep in the aluminous cement-granite concrete (first 24 hours), associated with the development of compressive strengths approaching 100 MPa, is necessarily high. The longer term characteristics however, are equivalent for the different types of cement. The specific creep of the aluminous cement concretes measured over a period when compressive strengths dropped from 109 MPa at 120 days age to 77 MPa at 390 days age due to conversion, was in the range 40 to 60 x 10^{-6} m/m per MPa, compared to a range of 50 to 80 for Portland cement concretes. Since the long term deformation characteristics are normal it is suggested that heat curing of aluminous cement concretes may be used. This produces concrete in the fully converted condition with early strength development and no possible subsequent strength changes due to conversion. Allowance should be made in design of prestressed units for the enhanced initial creep.

In another paper, SWAMY and ANAND, (93) report shear strain and some loss of prestress in the end zones of aluminous cement concrete beams. It is suggested that this is a consequence of conversion. If loss of strength due to conversion is large, and no shear reinforcement is provided, the effect could be serious if the concrete has been specified in terms of its unconverted characteristics.

It is pointed out here, as elsewhere in the present review, that the design of structural aluminous cement concrete should be based on the converted properties, which can be predicted and controlled through water/cement ratio.

5.4. Water/cement ratio

Water/cement ratio can be defined as total water content (that absorbed in the aggregates at the time of mixing plus the gauging water) divided by cement content, or free water content (that not taken up by the aggregates) divided by cement content. It follows that free water/cement ratio is equal to total water/cement ratio only in a neat paste, and becomes progressively less than total water/cement ratio as sand and aggregate is added. For concretes in practice the difference can be quite substantial :

Table VII : Relationship between free and total water/cement ratio of concrete

Ratio of cement to aggregate	R, Ratio of free to total water/ cement ratio	Coefficient of variation % of R	Range of water/cement ratios used
1 : 3	0.852	1.6	0.30 - 0.40
1 : 4.5	0.820	3.7	0.35 - 0.50
1 : 6	0.810	2.4	0.45 - 0.60
1 : 7.5	0.819	2.1	0.59 - 0.80

Data from reference (66).

Failure to distinguish between free and total water/cement ratio can thus lead to significant errors. For example, in a report (94) on the quali-

ty of samples of an aluminous cement concrete which failed in service, it is stated that failure may have been due to the use of a free water/cement ratio greater than the value of 0.4 aimed at in practice, when the Code of Practice, (95) governing the manufacture of such concretes clearly specified a maximum total water/cement ratio not exceeding 0.4. Thus if the concrete in question had a free water/cement ratio greater than 0.4 it would have had a total water/cement ratio of 0.5 or more.

The difference between average and characteristic strength (mean - 1.67 standard deviations) has been mentioned elsewhere in this review, (section 4.2.) and like the difference between free and total water/cement ratio, must not be forgotten when comparing experimental results. These points are well illustrated by figures 6A and 6B.

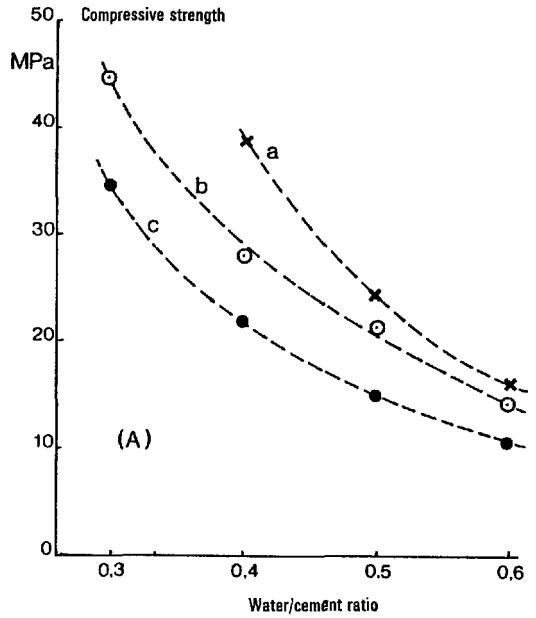

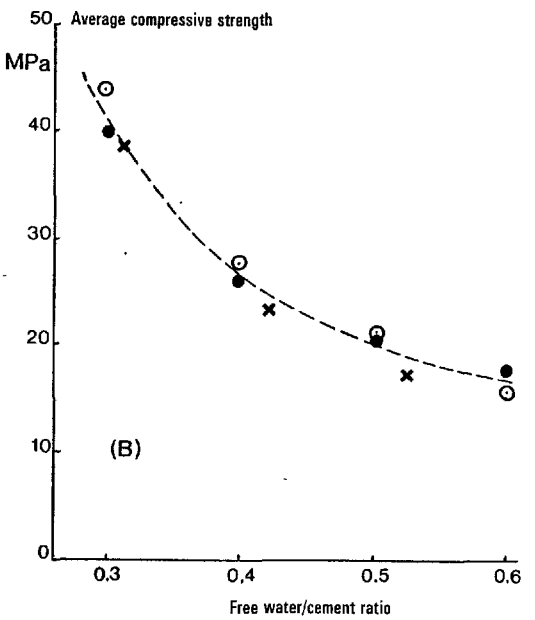

Data from 3 different sources presented in 2 different ways

a. Reference (95) ×
average strength, total W/C
b. Reference (96) ⊙
average strength, free W/C
c. Reference (97) ●
characteristic strength, total W/C

a. Reference (95) ×
b. Reference (96) ⊙
corrected to total W/C
c. Reference (97) ●
corrected to average strength

Fig. 6 - Influence of water/cement ratio on compressive strength of aluminous cement concrete converted at 38°C

NEVILLE, (98) comparing curves a, b and c presented in the manner shown in figure 6A, concludes that there is a considerable lack of agreement between different workers, which implies that the converted strength of aluminous cement is unpredictable and may be lower than is generally reported. On the contrary, when the confusion between total and free water/cement ratio and between average and characteristic strength is eliminated, the converted strength is seen, figure 6B, to be highly reproducible and clearly fixed by water/cement ratio.

In concluding this section it is appropriate to provide an indication of the reproducibility obtained in the manufacture of aluminous cement. The example given is of a 40 % Al_2O_3 cement of the 'Fondu' type manufactured in compliance with the British Standard, 915. Spot checks made on 39 different production batches gave the following results :

Table VIII : Compressive strength (MPa) of 100 mm Fondu cement concrete cubes made from 39 different production batches of cement

	24 hours curing at 18°C			Fast conversion by curing for 5 days at 38°C		
Total water/ cement ratio	0.35	0.40	0.50	0.35	0.40	0.50
Mean strength	74.8	66.8	59.4	51.0	40.5	25.6
Standard deviation	5.2	5.2	6.4	5.3	4.4	3.3

5.5. Recent recommendations

In 1974, the collapse of an aluminous cement concrete beam in the roof of a swimming pool led to very extensive investigations of many structures in Britain. The conclusions reached as a result are given in several reports (60), (61), (94) published by the government Building Research Establishment and the Department of the Environment. It is apparent from these investigations that service temperature in the UK can frequently exceed 30°C and may at times exceed 35°C so that conversion occurs more rapidly than was earlier believed. Consequently the previous practice of designing on unconverted strengths, assuming that in service conversion will be so slow that it will have a negligible effect on strength, must be revised. It is also apparent that much structural concrete had been made with total water/cement ratios in excess of the maximum of 0.4 prescribed (95).

It is because of these two conclusions that the recommendation was made (61) to assume a minimum compressive strength for aluminous cement structural units of 21 MPa when appraising buildings made with this material. It must be strongly emphasised that this figure applies to concretes for which the water/cement ratio is unknown but assumed to be above 0.4 total, and which have been converted relatively rapidly in service. The value of 21 MPa is consistent with a total water/cement ratio of 0.5 to 0.55, (95). By contrast, regular long term monitoring of structural aluminous cement concretes made at total water/cement ratios of 0.4 or below has demonstrated the excellent durability in practice that laboratory tests predict, (67), with a minimum converted strength of at least 40 MPa in compression.

The failure of structural concrete during service must always be the subject of serious investigations which should lead to more clear and reliable prescriptions for its future use. In the United Kingdom it was considered that the guidance given in the 1972 Code of Practice, (99) was inadequate for the manufacture of durable aluminous cement concrete and reference to this material was withdrawn from that Code in 1975 while the Building Research Establishment investigations were being carried out, and has not been reintroduced up to the present time. It seems clear that future recommendations must limit the water/cement ratio to 0.4 total as required by the earlier code (CP 116, 1965 - reference (95)) and not 0.4 free. Furthermore a minimum not a maximum cement content of 400 kg/m3 is preferable to ensure adequate workability. Finally design should be on the basis of converted not unconverted strengths.

The Ministerial circular of 1970, (100) governing the structural use of aluminous cement concrete in France, was also reexamined after 1974 and this led, in 1979 to a new official circular, (101). The 1979 French circular fully confirmed the view reached in 1970, that aluminous cement concrete manufactured at low water/cement ratios (0.4 total or less) is a durable structural material. It also takes advantage of work since 1970, including the UK findings, to extend the scope of the prescriptions to be followed in using this material and to require manufacturers of this type of cement to guarantee certain fundamental characteristics as well as to provide a complementary guide to its properties and applications. Such guarantees and guidance now exist for the aluminous cement known as ciment Fondu Lafarge, (103).

ACKNOWLEDGEMENTS

The author is indebted to the many researchers whose publications it has been his priviledge to review.

At the same time, apologies are extended to all whose work, due to the limitations of time and space, has been omitted or given but scant or inadequate coverage.

REFERENCES

1. T.D. ROBSON, (1962), "High alumina cements and Concretes", Contractors Record Limited, London.

2. J. TALABER, "High-alumina cements", VI International Symposium on the Chemistry of Cement, Moscow, (1974).

3. I. DRAGNEA, M. MUNTEAN and I. TEOREANU, (1976), "The action of $FeSO_4$ at burning oxidic mixtures in the system CaO ($CaCO_3$)-Al_2O_3", Silicates Industriels, 9, 357-362.

4. I. TEOREANU, N. CIOCEA, (1976), "Spezielle Tonerdezemente, Mechanismus des Sinterprozesses und technische Eigenschaften von Rohstoffen aus Aluminatsystemen mit verschiedenen Erdalkalimetallen", Baustoff., 29-32, A.3 (Mai).

5. M. DROZDZ, W. WOLEK, (1975), "Le ciment alumineux de baryum. Ses propriétés et ses applications", Bull. Soc. Française Ceram., 107, 39-52.

6. I.V. KRAVCHENKO, I.V. KUZNETSOVA, S.G. BEZRUKOVA, Brevet Soviétique n° 512188 du 08.08.1974, "Mélange de matières premières pour l'obtention d'un ciment alumineux".

7. A.A. KONDRASHENKO, G.I. ZADAT, B.S. KISHKO, (Jan. 1977), "Ciment fortement alumineux à base de laitiers alumino-thermiques", Tsement russe, N°1, 5-6.

8. K. AKIYAMA, Y. TSUMURA, S. ONUKI, T. YOSHIDA, (June 1976), "Preparation of aluminous cements from aluminium smelting residues", CAJ-Rev. 13th gen. meetg. Techn. Sessn, Jap., Tokyo, 81-1.

9. T.D. ROBSON, "Chemistry of calcium aluminates and their relating compounds", VI International Symposium on the Chemistry of Cement, Moscow, (1974), Part 1, Section 4.

10. S. ITO, S. SHIBATA, K. SUZUKI, M. INAGAKI, (1975), "Kinetic studies on the formation of calcium monoaluminate", J. Ceram. Soc. Japan, 93, 5, 239-43.

11. Yu. P. UDALOV, T. Yu. CHEMEKOVA, Z.S. APPEN, "On the character of the CaO-Al_2O_3 system diagram", VI international Symposium on the

Chemistry of Cement, Moscow, (1974), Section III-4, Suppl. paper.

12. A. PETZOLD, K. RIEDEL, (1975), "Action des conditions de cuisson fortement réductrices sur le ciment alumineux Fondu", Baustoff., Series A, 19, 1, 12-14.

13. T.D. ROBSON, Discussion, III International Symposium on the Chemistry of Cement, London, (1952), 521-524.

14. F.P. SORRENTINO and F.P. GLASSER, (1976),"Phase relations in the system $CaO-Al_2O_3-SiO_2-Fe-O$. The system $CaO-Al_2O_3-Fe_2O_3-SiO_2$", Trans. Jour. Br. Ceram. Soc. 5, 95-103.

15. F.P. SORRENTINO and F.P. GLASSER, (1975), "The system $CaO-Fe_2O_3-Al_2O_3-SiO_2$. I. The pseudo ternary section $Ca_2Fe_2O_5-Ca_2Al_2O_5-SiO_2$". Ibid. 74(7), 253.

16. F.P. SORRENTINO, (1973), "Studies in the system $CaO-Al_2O_3-SiO_2-Fe-O_2$", Ph.D. Thesis, University of Aberdeen.

17. F.P. GLASSER and J. MARR, (1975), "Quaternary phase in the system $CaO.MgO.Al_2O_3.SiO_2$", Trans. Jour. Brit. Ceram. Soc., 74, 113.

18. H.D. MIDGLEY, (1979), "The composition of pleochroite in high alumina cement clinker", Cement and Concrete Res., 9, 623-630.

19. M. OHTA, K. AKIYAMA, (1975), "Studies on high siliceous aluminous cements", Gyspsum and Lime, 137, 139-143.

20. L.A. ZAKHAROV, "Alumina-Belite cement", VI International Symposium on the Chemistry of Cement, Moscow, (1974), Section III-4, Suppl. paper.

21. V.N. VISWANATHAN, S.J. RAINA, A.K. CHATTERJEE, (May/June 1978), "An exploratory investigation on Porsal cement", World Cement Techny., 109-118, see also Zement KAL.GIPS, 10, 516-518, (1978).

22. F. SORRENTINO, Brevet français n° 74 23137 du 3 Juillet 1974, "Nouveau liant hydraulique, procédé pour sa fabrication et ses applications".

23. F.M. LEA, (1970), "The chemistry of cement and concrete", Arnold, 3rd Ed.

24. P. BARRET, D. MENETRIER, D. BERTRANDIE, (1974), "Contribution to the study of the kinetic mechanism of aluminous cement setting. I - Latent periods in heterogeneous and homogeneous milieus and the absence of heterogeneous nucleation", Cement and Concrete Res., 4, 545-556.

25 P. BARRET, D. MENETRIER, (1974), "Contribution to the study of the kinetic mechanism of aluminous cement setting. II - Release of the factor responsible for breaking the latent period by the dissolution of a fraction of the initial cement", Ibid 4, 723-733.

26. V.M. NIKUSHCHENKO, P.F. RUMYANTSEV, V.S. KHOTIMCHENKO, "On mechanism of interaction of alumina cement minerals with water", VI International Symposium on the Chemistry of Cement, Moscow, (1974), Section III-4, Suppl. paper.

27. V.S. KHOTIMCHENKO, V.M. NIKUSHCHENKO, (1974), "Role of the pH of the medium and hydrolysis of aluminate ions during hydration of calcium monoaluminate", Izvest. Akad. Nauk SSSR, Neorganich. Mat., 10, N°1, 91-95.

28. T.E. SMITH (Jan. 1977), "The reasons for fast-setting of calcium aluminate cements", Ceram. Eng. Dept. Clemson Univ. Clemson, S. Carolina, USA.

29. A.S. BERGER, N.P. KOTSUPALO, V.A. PUSHNYAKOVA, "On metastable equilibrium of calcium hydroaluminates in solutions of hydroxides of alkali metals", VI International Symposium on the Chemistry of Cement, Moscow, (1974), Section III-4, Suppl. paper.

30. U. COSTA, F. MASSAZZA, M. TESTOLIN, (1974), "Comparaison entre le procédé d'hydratation du $12CaO.7Al_2O_3$ et du $11CaO.7Al_2O_3.CAF_2$", Ind. Chim. Belg. 39, N° 6, 579-586.

31. B. COTTIN, P. REIF, (1970), "Paramètres physiques régissant les propriétés mécaniques des pâtes pures de liants alumineux", Rev. Mats. Constr., 661, 293-305.

32. V.S. RAMACHANDRAN, J.J. BEAUDOIN, (1976), "Significance of water/solid ratio and temperature on the physico-mechanical characteristics of hydrating $4CaO.Al_2O_3.Fe_2O_3$", J. Mats. Sci., 11, 1893-1910.

33. H.G. MIDGLEY, P. BHASKARA RAO, (1978), "Formation of stratlingite, $2CaO.SiO_2.Al_2O_3.8H_2O$, in relation to the hydration of high alumina cement", Cement and Concrete Res., 8, 169-172.

34. M. KOBAYASHI, N. MIYAKE, M. KOKUBU, "Fly-ash for long-term high-alumina cement strength", VI International Symposium on the Chemistry of Cement, Moscow, (1974), Section III-3, Suppl. paper.

35. W. DOSCH, H. KELLER, "On the crystal chemistry of tetracalcium aluminate hydrate", VI International Symposium on the Chemistry of Cement, Moscow, (1974), Section III-4, Suppl. paper.

36. H. KUZEL, Th. SCHELLER, "Studies on dicalcium aluminate hydrates", VI International Symposium on the Chemistry of Cement, Moscow, (1974), Suppl. paper.

37. W. DOSCH, C. KOESTEL, Patent US. 4095989, 20 June, 1978, "Stabilized dicalcium aluminate hydrates".

38. C.M. HOUTEPEN, H.N. STEIN, (1976), "The dehydration of some calcium aluminate hydrates, with univalent anions", J. Coll. Interf. Sci., USA, 56, 370-376.

39. J. BENSTED, (Jan./Feb. 1976), "An investigation of calcium nitratoaluminate hydrate and its derivatives", Cem. Techy., 3-6.

40. G.M. DARR, U. LUDWIG, (1974), "The incorporation of chloride in calcium aluminate hydrates", Ind. Chim. Belg., 39, 687-692.

41. Ph. DUFOUR, P. BARRET, (Mars 1979), "Thermodynamique chimique - Solubilité et propriétés hydrauliques du produit de déshydratation de l'aluminate monocalcique décahydraté CaO, Al_2O_3, $10H_2O$", C.R. Acad. Sc. Paris, t. 288, Série C, 343-345.

42. H.J. KUZEL, (1969), "Über die orientierte Entwässerung von Tricalciumaluminathexahydrat $3CaO.Al_2O_3.6H_2O$", Neues Jb. Min. Mh., 397.

43. M.C. BALL, (1976), "The thermal dehydroxylation of C_3AH_6", Cement and Concrete Res., 6, 419-420.

44. A.A. KONDRASHENKOV, I.G. ZHIGUN, E.V. ZALIZOVSKIJ, S.M. KUKIJ, (1974), "Transformation au cours d'un traitement thermique des phases contenues dans la pâte durcie d'un ciment fortement alumineux", Zh. Prikl. khim., 47, 12, 2633-39

45. R.A. WAGNER, "The effects of dehydration on the microstructure of calcium-aluminate cement pastes", presented at 78th ann. meet. g., Amer. Ceram. Soc., Cincinnati, Ohio, USA, 5, May, 1976.

46. I.V. KRAVCHENKO, T.V. KUZNETSOVA, Yu. F. KUZHETSOVA, I.E. GERGERT, V.I. SHUSTINA, (1975) "Production d'un ciment fortement alumineux", Tsement, 5, 15-2.

47. B.E. MILLS, D.O. HUGHES, (1976), "Effects of carbonation and hydrothermal treatments on some properties of calcium monoaluminate mortars", J. appl. chem. Biotechnol., 26, 506-512.

48. A.C. TSEUNG, T.G. CARRUTHERS, (1963), "Refractory concretes based on pure calcium aluminate cement", Trans. Brit. Ceram. Soc., 62, 305.

49. G.V. GIVAN, L.D. HART, R.P. HEILICH, G. MacZURA, (1975), "Curing and firing high purity calcium aluminate-bonded tabular alumina castables", Bull. Amer. Ceram. Soc., 54, N° 8, 710.

50. C.M. GEORGE, (Avril/Juin 1979), "Cinétique de l'hydratation des ciments alumineux et influence sur les propriétés du béton", Bull. Soc. Française Ceram., N°123.

51. G.R. GOUDA, D.M. ROY, (1975), "Properties of hot-pressed calcium aluminate cements", Cement and Concrete Res., 5, 551-564.

52. R. ALEGRE, (1968), "Etude des effets sur les ciments alumineux hydratés de la transformation de $CaO.Al_2O_3$ 10 H_2O sous l'action de la température", Rev. Mater. Constr., N° 630, 101-108.

53. J.S. MASARYK, R.E. FARRIS, (1976), "High purity refractory concretes : behaviour during manufacture of massive shapes", Bull. Amer. Ceram. Soc., 55, N° 11, 996-998.

54. A. NEGRO, L. CUSSINO, A. BACCHIORINI, (1978), "The hydration of monocalcic aluminate in the presence of quartz and calcium carbonate", Il Cemento, 3, 285-290.

55. E. RAASK, (April 1976), "Carbonation of high alumina cement (HAC) concrete", Seminar on Carbonation of Concretes, Slough, UK, RILEM Procs.

56. R. FISCHER, H. KUZEL, (1978), "Carbonated tetracalcium aluminate hydrates", Fortschr. D. Mineral. Beih. 56, 1, 25-26.

57. P. FIERENS, A. VERHAEGEN, J.P. VERHAEGEN, (1974), "Etude de la formation de l'hydrocarboaluminate de calcium", Cement and Concrete Res., 4, 695-707.

58. J. FARRAN, (1956), "Contribution minéralogique à l'étude de l'adhérence entre les constituants hydratés des ciments et les matériaux enrobés", Rev. Mats. Constr. N° 490/491, 155, N° 492, 191.

59. A. RUIZ de GAUNA, F. TRIVINO, T. VAZQUEZ, (1975), "Etude des transformations du ciment alumineux hydraté au moyen de la diffraction des rayons X de la spectrimétrie infra-rouge et de l'analyse thermique. Action de l'anhydride carbonique, de la température,de l'humidité et des additions de la chaux en poudre", Mater. Constr. Espagnol, 157, 43-64.

60. "High alumina cement concrete in buildings", Building Res. Est. (UK), Current paper N° 34, (1975).

61. "High alumina cement concrete", Building Regulations Advisory Committee, (UK), Report by Sub-Committee, P 40, (1975). The Struct. Engr. 54, N° 9, 352-361.

62. A. RAUEN, (1975), "Dommages survenus à des éléments de construction en béton précontraint de ciment alumineux", Betonwerk + Fertigteil-Technik, 12, 591-593.

63. E. RENGADE, P. LHOPITALIER, P. DURAND de FONTMAGNE, (1936), "Recherches sur les causes de certains phénomènes d'altération des bétons de ciment alumineux", Rev. Mater. Constr. et Trav. Pub., N° 318, 52-55, N° 319, 78-82.

64. A. NEVILLE, (1978), "High-alumina cement - A current review", Il Cemento, 3, 291-301.

65. D.H.H. QUON, V.M. MALHOTRA, (June 1978), "Performance of high-alumina cement concrete stored in water and dry heat at 25, 35 and 50°C", CANMET Report, N° 78-15.

66. D.C. TEYCHENNE, (1975), "Long-term research into the characteristics of high alumina cement concrete", Mag. Concr. Res., 27, N° 91, 78-102.

67. C.M. GEORGE, (1976) "The structural use of high alumina cement concrete", Lafarge Aluminous Cement Co. Ltd., Grays, Essex, UK, Rev. Mater. Constr. 701, 4, 3-11.

68. H.G. MIDGLEY, A. MIDGLEY, (1975), "The conversion of high alumina cement", Mag. Concr. Res., 27, N° 91, 59-77.

69. Reference 66, Table 5, P. 84.

70. C. BRADBURY, P.M. CALLAWAY, D.D. DOUBLE, (1976), "The conversion of high alumina cement/concrete", Mater. Sci. Eng., 23, 43-53.

71. B. COTTIN, C.M. GEORGE, "The effects of temperature cycling on the hydration of aluminous cement paste", to be published.

72. P.J. FRENCH, R.G.J. MONTGOMERY, T.D. ROBSON, (Aug. 1971), "High concrete strength within the hour", Concrete, 3-8.

73. C.M. GEORGE, "High alumina cement with special reference to ciment Fondu Lafarge", Seminar Cement and Concrete Science, Thames Polytechnic, London, 9-10th April, 1979, available from Lafarge Fondu International, 157, ave Ch. de Gaulle, 92521 Neuilly-sur-Seine Cedex, France.

74. H.G. MIDGLEY, (1978), "The use of thermal analysis methods in assessing the quality of high alumina cement concrete", J. Therm. Analy., 13, 515-524.

75. P.A. BARNES, J.H. BAXTER, (1978), "A critical analysis of the application of derivative thermogravimetry to the determination of the degree of conversion of high alumina cement", Thermochimica Acta, 24, 427-431.

76. B. EL JAZAIRI, (1977), "The semi-isothermal thermogravimetric technique and the determination of the degree of conversion of high alumina cement concrete", Ibid, 21, 381-389.

77. M. REVAY, Zs. WAGNER, (1976), "Determination of expectable decrease in the strength of high-alumina cement concrete by derivatography", 1st. European Symposium on Thermal Analysis, 374-377.

78. U. STROBEL, (1977), "Qualitative und quantitative Untersuchungen der Hydratation von Portlandzement und Tonerdeschmelzzement sowie der Zersetzung von Kalziumaluminatdekahydrat mittles DTA", Wissench. Z. Hochsch. Archit. Bauwes Weimar, 24, 4/5, 423-426.

79. K. MISHIMA, "Relation between the hydration of alumina cement mortars and their strength in the early stages", Proc. V Internat. Conf. Chem. Cement., Tokyo, (1968), Part III-88, 167-174.

80. H.G. MIDGLEY, (1978), "The use of thermoanalytical technique for the detection of chemical attack on high alumina cement concrete", Thermochimica Acta, 27, 281-284.

81. D.E. DAY, G. LEWIS, (1979), "Quantitative thermogravimetry of calcium aluminate compounds and cements after hydrothermal treatment", Bull. Amer. Ceram. Soc., 58, 441-447.

82. C. PLOWMAN, J. GYLLESPETZ, (1976), "X-ray analysis of high alumina cement concrete", Analyst. 101, 1199, 141-2.

83. W. LEJAWKA, (1974), "Analyse phasée quantitative des ciments alumineux par rayons X", Cement, Wagno, Gips, 6, 171-175.

84. Document BRA/1082/2, 20 July, 1974, Department of the Environment, UK.

85. D.H.H. QUON, V.M. MALHOTRA, (May 1977), "Effect of elevated temperatures on compressive strength, pulse velocity and conversion of high alumina cement concrete", CANMET report N° 77-49.

86. M. REVAY, "The pre-estimation of the expected decrease of strength of high alumina cement concretes", VI International Symposium on the Chemistry of Cement, Moscow, (1974), Section III-4, Suppl. paper.

87. C.T. PETERS, R.W. PARKINSON, "Acoustic emission activity during accelerated conversion of high alumina cement pastes", J. Material Science, (1977), Vol. 12, 848-850.

88. M. ARRINGTON, B.M. EVANS, (April 1977), "Acoustic emission testing of high alumina cement concrete", NDT International, 81-87.

89. B. MAYFIELD, M. BETTISON, (Sept. 1974), "Ultrasonic pulse testing of high alumina cement concrete, in the laboratory", Concrete, 36-38.

90. J.H. BUNGEY, (June 1976), Discussion of reference 66, Mag. Concr. Res., 28, N° 95, 105-106.

91. R.N. SWAMY, A.B. IBRAHIM, K.L. ANAND, (1976), "The strength and deformation characteristics of high early strength structural concrete", Mater. Constr., 8, N° 48, 413-423.

92. A.R. CUSENS, N. JACKSON, (June 1975), "Flexural behaviour of highly converted prestressed high-alumina cement concrete", Mag. Concr. Res., 27, N° 91, 103-110.

93. R.N. SWAMY, K.L. ANAND, (1975), "Losses in transmission length and prestress in high alumina cement concrete", Proc. Inst. Civ. Engrs., Part 2, 59, 293-307.

94. S.C.C. BATE, (1974), "Report on the failure of roof beams at Sir John Cass's Foundation and Red Coat Church of England Secondary School, Stepney", Buildg. Res. Est., UK, Current paper 58/74.

95. Brit. Standards Inst. (1965), "The structural use of precast concrete", Code of Practice CP 116 : Part 1, Fig. 7, p. 128.

96. K. NEWMAN, (Mar. 1960), "Design of concrete mixes with high-alumina cement", Reinf. Conc. Rev., 5, N° 5, 269-294.

97. Reference 94, Table 5, p. 15.

98. A.M. NEVILLE, P.J. WAINWRIGHT, (1975), "High alumina cement concrete", Construction Press, UK, Fig. 3.15, p. 47.

99. British Standards Institution, "Nov. 1972), "The structural use of concrete", Code of Practice, CP 110.

100. Circulaire N° 70-31, 6 Mars 1970, Ministère de l'Environnement, France.

101. Circulaire N° 79-34, 27 Mars 1979, Ministère de l'Environnement, France.

102. A. AUSKERN, W. HORN, (1973), "Capillary porosity in hardened cement paste", J. Testing Evaluation, 1, N° 1, 74-79.

103. Guide d'Emploi du Ciment Fondu Lafarge en Eléments de Structure de Génie Civil, (Jan. 1979), copies obtainable from Lafarge Fondu International, 157, ave Ch. de Gaulle, 92521 Neuilly-sur-Seine Cedex, France.

SUB-THEME V - 2

Expansive Cements

W. KURDOWSKI
Research Center of the Industry
of Binding Materials
Krakow, Poland

INTRODUCTION

Commercial production of expansive cements was undertaken over 30 years ago /1/. In the last decade it had been expanded substantially in three countries: United States, Japan and Soviet Union /2-4/. In the United States about 300 000 tons per year of shrinkage-compensating cement is produced, in Japan - 50 000 tons of expansive additive, corresponding to 500 000 tons of the cement /3/. In the USSR 63 000 tons of self-stressing expansive cement only was produced in 1977 /5/, to say nothing of other types of these cements.

The develpment of expansive cements production is connected with an important progress in structural engineering, as well as with the necessity to eliminate the well-known shortcomming of Portland cement, consisting in the formation of cracks in the concrete, due to natural drying shrinkage.

Shrinkage-compensating cements are used wherever a prevention of the shrinkage cracking, as well as of the changes in initial dimensions of concrete units is required, namely for the manufacturing of structural concrete units, airfields, runways, pavements water tanks, slabs of skating rinks, underground garages, warehouses, parkings, railroads etc.

The second field of expansive cements employment comprises the production of self-stressing concretes, in which the preliminary compressive stresses are obtained as result of so-called chemical stressing. This cement serves for fabrication of structural elements requiring a low optimum prestress, such as pipes, wall panels, thin slabs for floors and roofs, shells and folded plates, water tanks, pavements, sport objects etc. Recently the possibility of utilization of expansion potential of these cements to generate the jacking forces in concrete constructions was mentioned /6/.

Both the types of expansive cement differ in the magnitude of expansion potential. The level of compressive strengths developed is in the range of 25 to 100 psi /2 to 7 kg/cm^2/ for shrinkage-compensating cements and up to 1000 psi /about 70 kg/cm^2/ for self-stressing cements.

Generally it can be said, that the shrinkage compensating cements are the most commonly used and their technology is almost entirely acquired. The best experience in self-stressing cements manufacturing falls to the Soviet Union/4/.

An excellent review of theoretical foundations of expansive cement technology, properties of these cements as well as fields of application of expansive concretes was presented by Mehta at the Sixth Congress on the Chemistry of Cement in Moscow in 1974 /2/ and actualized recently /3/. Ever since not any new hypotheses concerning the theoretical basis of manufacturing these cements, especially the expansion mechanism, have been appeared.

However, the industrial practice has been developed considerably and the position of expansive cements in structural engineering is being now well established /7/. This allowed to collect detailed material on the properties of expansive concretes in various conditions and environments.

Also the growth of interest in other, than ettringite, expansive additives appeared, in particular in free CaO, which has found already a practical application in Japan /8/.

In this paper a review of recent opinions on the physical-chemical relations, governing the properties of expansive cements, as well as of suppositions tending to explain the mechanism of expansion is given.

Purely technological questions of expansive cements manufacturing as well as the problems related to expansive concretes and their miscellaneous applications were reduced to a minimum. However a list of any attainable bibliography in this subject is annexed.

TYPES OF EXPANSIVE CEMENTS

As mentioned before, the most of all developed expansive cements are these in which the expansion phenomenon is originated by the reaction of ettringite formation. Their technologies differ only in utilized raw materials, which introduce the aluminium compounds, calcium sulphate and calcium oxide.

The most widely applied technology is that developed by Klein in the United States. This cement, so-called Type K, is based on $C_4A_3\bar{S}$ as alumina-bearing compound. It is usually produced by intergrinding ordinary Portland cement clinker, an expansive clinker containing $C_4A_3\bar{S}$ and gypsum /or a mixture of gypsum and anhydrite/. Besides $C_4A_3\bar{S}$ the expansive clinker generally contains alite, belite, C_4AF, anhydrite and some free lime. Its manufacturing is developed also in Japan /3/, and now in the Soviet Union the works go on to start in its production /9/.

The K-Type cement can be manufactured by two means. Expansive additive is sintered separately in the form of calcium sulphoaluminate clinker, which is then interground with Portland cement clinker and gypsum. One can also obtain - in a single process - a Portland-like expansive clinker with suitable tetracalcium sulphoaluminate content, by addition of calcium sulphate to raw materials, serving to ordinary Portland cement clinker manufacturing.

The grinding of this clinker with addition of gypsum and/or anhydrite gives the expansive cement. As yet a technology consisting in the separate preparation of the expansive clinker prevails. This method is applied in two variants: in the United States the components of expansive cements are ground jointly, giving a commercial product - expansive cement, while in Japan other way is choosed: an adequately ground expansive

additive rather than expansive cement is produced and marketed. This additive is added to concrete at the time of mixing, in amounts necessary to produce either a shrinkage-compensating or a self-stressing concrete.

The second type of expansive cements is obtained by addition of aluminous cement to Portland cement. This is so-called M-Type cement and its production has been developed particularly in the Soviet Union, owing to Mikhailov's works. In this technology the aluminous cement or aluminous slag as alumina-bearing component is utilized; in this latter case lime addition is applied /4/.

The first of these cements, SCT cement, is composed of Portland cement, calcium aluminate cement and gypsum in the ratio of 66: 20:14 respectively; the second, SCN cement - of Portland cement, calcium aluminate cement, gypsum and lime in the ratio of 67: 22:9:2.

The SCT cement concrete is exposed to hydrothermal curing and then to water curing at normal temperature. According to Mikhailov, during the heating stage of the curing process calcium monosulphoaluminate hydrate is formed, and then - during normal curing - it is transformed into ettringite, that is responsible for expansion. This technology is being applied in precast units plants.

The SCN cement contains an aluminous slag and lime. It hydrates in natural conditions and the formation of ettringite in the paste is retarded in early ages due to the presence of lime.

In elaborated by Mikhailov and produced in the USSR since 1948 so-called WEC cement, the high-alumina cement occurs as predominant component /4/. This cement is a mixture of high-alumina cement, gypsum and calcium aluminate hydrate C_4AH_{13} in the ratio such as 65:22:13 respectively. Calcium aluminate hydrate is obtained by hydration of a mixture of high-alumina cement and lime at 100°C. The annual production of this cement is about 15 000 tons.

Elaborated by Budnikov and Kravchenko and produced in the USSR expansive cement, unique in the world, being a mixture of aluminous slag and gypsum in the ratio of 70:30 respectively, can be included also to this group /4/.

All the expansive cements produced in the USSR are ordered in three grades: 20, 40 and 60, as the expansive potential generated in these cements is about 20, 40 and 60 kg/cm^2 /280, 570 and 860 psi/, respectively. The cement n° 20 is a shrinkage- compensating one and the two other are self-stressing cements.

The third type of expansive cement is S-Type cement, manufactured from Portland cement clinker with increased C_3A content. This technology finds limited applications, first of all by reason of the difficulties in the getting under control the steadiness of ettringite formation rate from tricalcium aluminate. This means the difficulties with controlling expansion. Ettringite is formed very rapidly from C_3A phase in early hydration age and then the reaction becomes to be slowed down to very low rate at later age. In this connection even after 7 days the unreacted aluminate content is still appreciable.

At early age the $C_4A_3\bar{S}$ phase hydrates more rapidly than C_3A and the rate of this reaction remains relatively high till the depletion of this compound. Fig. 1 shows the curves of ettringite formation from different anhydrous aluminate phases, plotted by Mehta /10/. After 1 day of $C_4A_3\bar{S}$ hydration the rate of reaction is still appreciable, which results in complete transformation of this phase into ettringite within 7 days. Examination of the curves given in this figure allows also to account for the advantage of M-Type cement over S-Type one: in aluminous cement the aluminium occurs mainly in calcium monoaluminate phase and this phase transforms into ettringite at considerably earlier ages than 7 days.

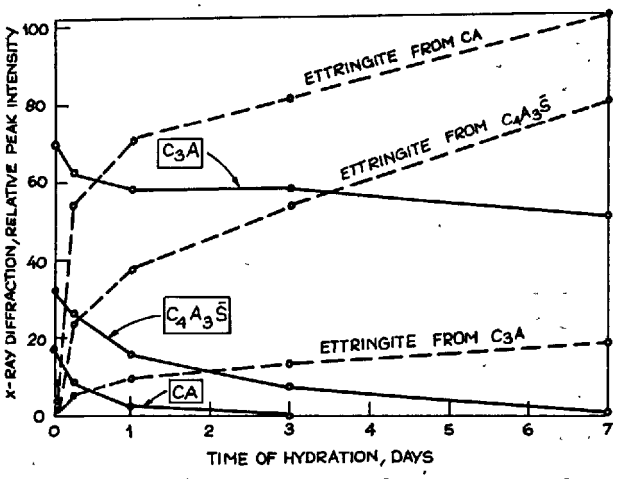

Fig. 1 - Relative rates of ettringite formation and depletion of CA, $C_4A_3\bar{S}$, or C_3A in pastes containing both gypsum and lime /Mehta/

The separate group is made by expansive cements with addition of activated alunite. Studies in this field are conducted by Bulgarian as well as Georgian investigators. Alunite containing raw materials utilized for this purpose are activated at 600° to 800°C, and then interground with Portland cement clinker and gypsum. Alunite gives - as a product of reaction with other constituents - the ettringite phase. This cement is manufactured in Bulgaria and USSR /11-14, 9/.

In the USSR a technology of expansive cement had been elaborated in which the by-

product from aluminium sulphate manufacturing process is utilized as alumina-bearing component /15-18/.

Further, entirely separate type of expansive cement encloses a group of cements, made in Japan, with calcium oxide as expansive component. Kawano et al. /8/ developed an expansive additive that contains predominantly uncombined calcium oxide; the additive can be obtained by sintering a mixture of limestone, clay and anhydrite. The principal phases of the additive are alite /about 38%/, free lime /about 44-47%/ and $CaSO_4$ /about 6-10%/. This additive is interground with the Portland cement clinker. The CaO phase occurs in great part as inclusions of 10-30 um large crystals in developed up to 100-900 μm alite grains, thus undergoing hydration more slowly, gradually as the alite itself hydrates, which ensures controlled expansive properties of the cement. Recently a new expansive additive is developed, which contains large alite crystals and small /5-20 μm/ free CaO crystals dispersed in an amorphous calcium sulphate matrix /3/. The composition of a mixture with 40-70% of alite, 20-30% free lime and 10-20% $CaSO_4$ gives good expansion characteristic.

Pollitt and Brown in Great Britain /19/ and Allen et al. in the United States /20/ developed expansive cements based on similar principe as the first of the cements mentioned above, proposed by Kawano. English investigators believe the most preferred range of free CaO content to be 3-12%. According to Allen more than about 2% of free CaO in an ordinary Portland cement could lead to undesirably delayed hydration, when the free CaO is enclosed by less reactive compound, such as C_2S.

A method of producing CaO and MgO containing expansive cements was given by Collepardi /21/. Also Daugherty et al. /22/ patented a process for preparing expansive cement with addition of free CaO and/or MgO. Expansive clinker containing 2-7% MgO and 1-70% CaO as well as C_3S is interground with Portland cement clinker. Utilization of MgO powder as expansive additive was also the matter of studies of Komendant et al. /3/.

MECHANISM OF EXPANSION

In the Portland cement technology a destructive phenomenon of volume change, resulting in failure of the concrete, has been well known for a long time. The three reactions cause this volume change: the formation of ettringite, portlandite and brucite. This phenomenon influences negatively the properties of mortars and concretes, if the process of formation of these phases occurs after the hardening of the cement paste is over. At that time high stresses appear in the material, exceeding often its strength, which results in disruption of the concrete.

Numerous studies allowed to state, that the factors influencing this unfavourable volume change are not only the content of harmful components, but also their grain-size distribution and repartition in the material. For example Gille /23/ as early as in 1952 stated that periclase in the form of crystalline grains not greater than about 5 um in size, do not gives unfavourable volume change even by its content of 4-6% of cement. Similar observations concern free calcium oxide /24/. Most of the studies on the expansion phenomenon dealed with ettringite formation, as that was the first, consciously utilized expansive reaction. The first hypothesis on the mechanism of expansion was suggested in 1929 by Lafuma /25/. He theorized, that possible mechanism of expansion consists in solid state hydration of tricalcium aluminate to ettringite in saturated solution of calcium hydroxide, thus in topochemical reaction, whereas ettringite formation by through-solution reaction do not causes expansion. This hypothesis provoked large discussions and finally had been rejected in result of works carried out by Mehta, who demonstrated, basing on scanning electron microscopy, that the ettringite is formed, as a rule, by through-solution crystallization /26/.

The next attempt to elucidate the expansion phenomenon resulted in hypothesis in which essential role was attributed to osmotic pressure /27/. It has been stated /28-29/ that electrically charged colloidal particles show the ability to swelling, due to osmotic "suction" of water by charged surface.

As follows from the work of Moore and Taylor /30/, the crystals of ettringite have a negative surface charge and according to Mehta /26/ a colloidal nature of this phase in solutions saturated with lime is quite sure. Thus the experimental results are not out of accord with the osmotic hypothesis of expansion.

The most comprehensively supported by experimental evidence is Mehta's hypothesis, developed in early seventies /31/. This author is of opinion, that negatively charged colloidal ettringite grains with high specific surface attract the polar molecules of water, which surround the crystals of this phase and cause interparticle - perhaps double-layer type - repulsion. This results in overall expansion of the system.

In order to confirm this hypothesis experimentally, Mehta realized a complete hydration of the mixture $C_4A_3\overline{S}+8C\overline{S}+6C+96H$ with formation of ettringite in conditions preventing moisture loss or carbonation of the sample. Ettringite sample obtained was then exposed to water; volume changes after various curing ages were determined. The curve, given in Fig. 2, shows quite a large expansion of the sample, which is accompanied by no difference in the X-ray diffraction pattern /32/. This mechanism is res-

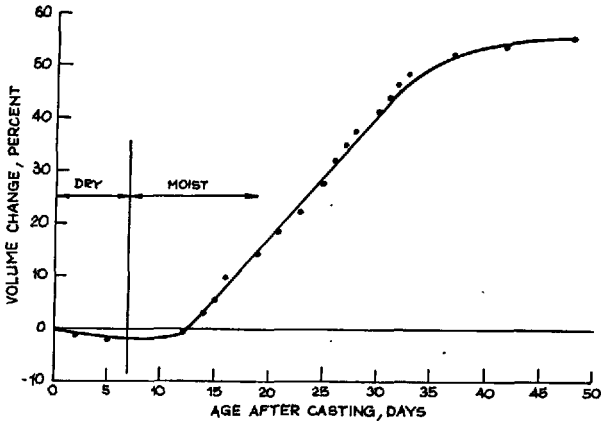

Fig. 2 - Uniaxial expansion of ettringite on moist curing /Mehta/

ponsible also, according to Mehta, for expansion of other colloidal hydrates, as $Ca/OH/_2$, $Mg/OH/_2$ and alkali silicates. A further increase in the length of CaO samples after the hydration is completed, stated by Ramachandran et al. /33/, is the case for this opinion.

Independently of Mehta's hypothesis, many authors continue to consider, that the expansion can be caused by local transformation of anhydrous phases into hydrates /34-36/. Electrolyte solution migrates through capillary pores to the grain of anhydrous phase surrounded with hydrates, entailing an expansive reaction in situ. The hydrate, formed in situ, has substantially greater volume as porous anhydrous phase and this generates stresses, leading to volume change of the sample. This hypothesis is in a way a recurrence to the known Lafuma's conception. Experimental data supporting this hypothesis are rather scarce. One can here mention the scanning pictures of compact ettringite phases, forming the envelopes on C_3A grains /36/. Japan investigators suggested the formation of $C_4A\bar{S}H12$ on $C_4A_3\bar{S}$ grains /37/. This hypothesis is not contradictory to the increase in porosity of pastes in the range of pore sizes from 0.2 to 0.8 µm, typical of ettringite formation. These pores appear in the mortar as early as after 1 day of hardening, exist up to 7 days and finally disappear between 7-th and 28-th day of hardening /Fig. 3/. In non-expansive cement pastes no maximum is observed in this range of pore size distribution /36/. Generally speaking, expansive mortars are always more porous than Portland cement mortars /36/. Well-known fact of high ability of portlandite and ettringite to crystallization, two most easily detectable crystalline phases of the paste, is not out of accordance with this hypothesis.

Important experimental data supporting the hypothesis of expansion as result of the formation of hydrates in place of anhyd-

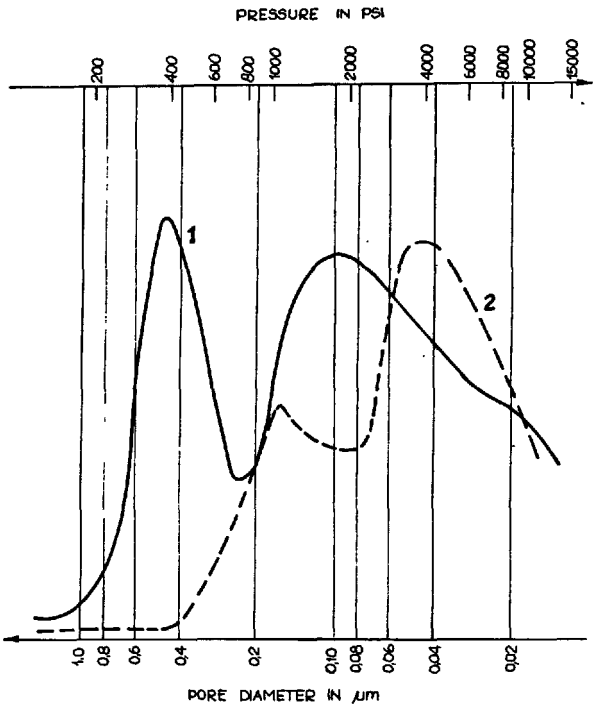

Fig. 3 - Pore size distribution of /1/ expansive and /2/ non-expansive cements /Gaspar/

rous compounds, thus in too small volume, has been presented by Cottin /38/.

Fig. 4 shows, according to this author, calculated as well as determined experimentally expansion of a mixt of aluminous

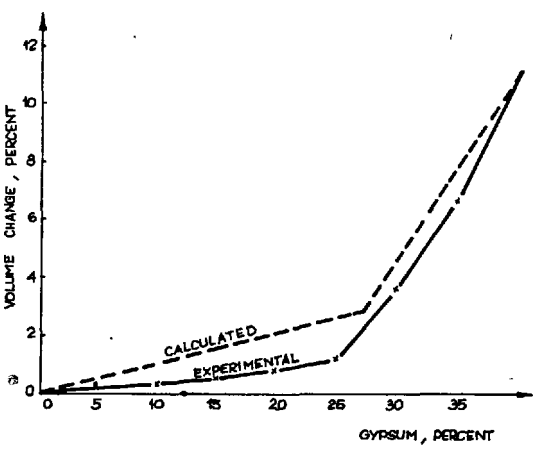

Fig. 4 - Expansion of a mixt of high-alumina cement with gypsum /Cottin/

cement with gypsum, hydrating with insufficient /30%/ water addition. Theoretical

expansion was calculated basing on the known phase composition of the hydration product.

Similar expansion characteristics were observed by Cottin for the samples exposed to water after a long period of preliminary moist storage /Fig. 5/.

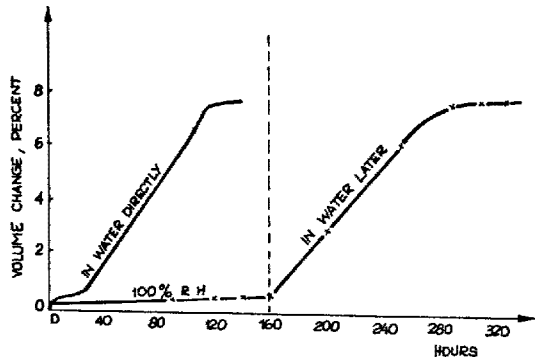

Fig. 5 - Expansion characteristics of the samples exposed to water directly or after 160 hours of preliminary moist storage /Cottin/

Also Isogai's work /39/ seems to confirm this hypothesis. This author advances an opinion, that the calcium trisulphoaluminate hydrate is formed mainly by topochemical reaction in case of water curing, but chiefly formed by through-solution reaction in case of air curing.

The study of concrete corrosion processes, carried out by Regourd /40/ indicated, that the appearance of cracks was in relation to the formation of compact masses of amorphous ettringite, not detectable by X-ray diffraction, but also was accompanied with the formation of large crystals of this phase /Fig. 6/. This seems to show, that rather the amount of ettrigite formed than the size of crystals determines the expansion level.

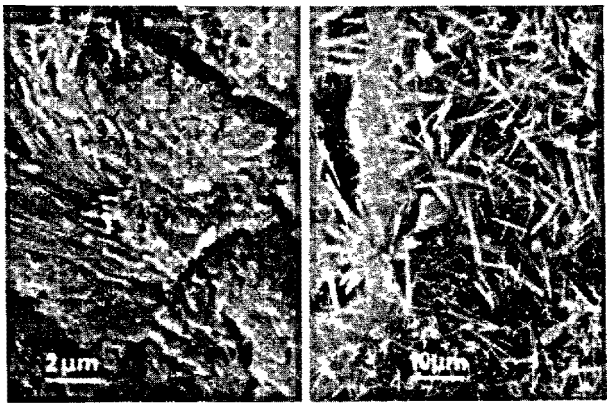

/a/ /b/

Fig. 6. - Different forms of ettringite in destroyed concrete. a - amorphous, b - crystalline /Regourd/

Finally, the most recent investigations by Collepardi et al. /41/ concerning the C_3A hydration proved, that an outside source of water is not indispensable for occurence of expansive process; though in the sealed system it occurs less intensively. Collepardi relates this fact with transformation of the liquid water, present in capillary pores, into a low density configuration with water molecules, adsorbed on ettringite crystals. Nevertheless these observations do not refute the hypothesis of the conversion in situ of C_3A grains, coated by a low-permeable ettringite layer, into hydrated calcium sulphoaluminate.

Bentur and Ish-Shalom /42/, examining the mixtures of $C_4A_3\bar{S}$, $C\bar{S}H_2$ and CH, proposed a model of this process, based on the growth of a porous ettringite layer around the $C_4A_3\bar{S}$ grains. This growth causes expansion of the sample as a result of spherically overgrowing ettringite layers pushing against each other.

As follows from this review, it is necessary to obtain further experimental data, in order to elucidate completely and explain conclusively the mechanism of expansion phenomenon.

SOME FACTORS INFLUENCING EXPANSION

Free lime

All the authors agree in the matter of fact, that the free lime content influences favourably the expansion process. This finds its expression in the compositions of industrial expansive cements. It has been found /37/, that the lime retards hydration of $C_4A_3\bar{S}$ and C_3A, and accelerates hydration of C_3A /43/. The role of lime will therefore consist in a reduction of the amount of ettringite formed at early age, and first of all within 5 hours of hydration. In this connection the phases, giving ettringite, are not consumed in the period of plastic state of the paste, in which its formation is not followed by expansion. Lime addition gives beneficial expansion characteristics, with higher level of volume change not only at early ages, but till the end of the process /Fig. 7/. The curves of the content of some components in liquid phase of the paste confirm also such a course of the process /Fig. 8/. In a free lime containing cement the lime concentration of liquid phase is substantially higher; the concentration of SO_4^{--} ions is higher too. This indicates the retardation of the process of ettringite formation, which becomes accelerated after 5 hours, simultaneously with the start of alite hydration. In a cement with very low content of free CaO the process of ettringite formation runs continuously since the moment of cement mixing with water.

According to Mehta's results and hypothesis,

lime content in the solution promotes the formation of fine-crystalline ettringite /26/.

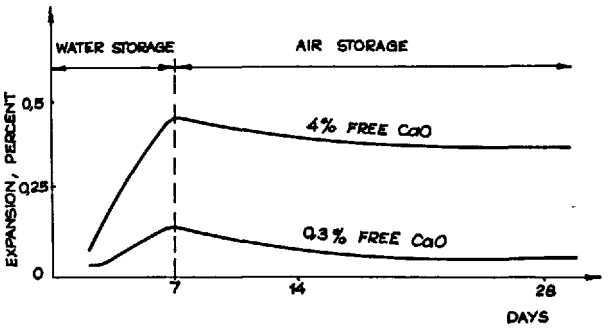

Fig. 7 - Effect of lime addition on expansion characteristic

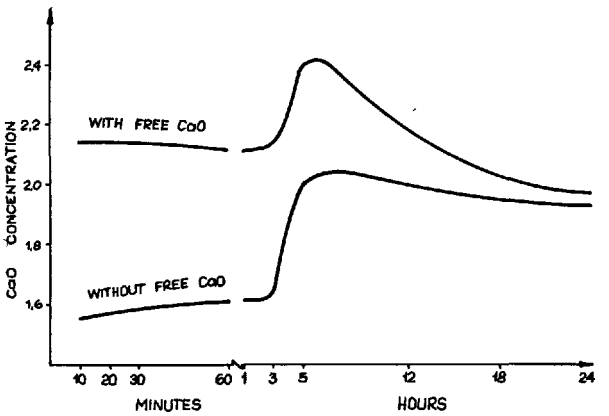

Fig. 8 - CaO concentration in liquid phase of expansive cement pastes without and with free CaO

Portland cement

Not many data are available on this subject. It seems to be evident that an increase in the amount of C_3A and alkalis in Portland cement clinker is unfavourable. The effect of alkalis can be easily explained by reduction in Ca^{++} ions content of the liquid phase in the paste and - as its consequence - acceleration of ettringite formation.

Higher C_3A content will make difficult the control of expansion, as in this case the latter appears to be extended in time.

Similar informations with respect to M-Type cements gives Gaspar /36/. He calls attention to the advantageous effect of CO_2, which promotes the expansion; on the other hand the ability to clinkerization of the raw materials as well as the high fineness of Portland cement are unfavourable /Fig. 9/.

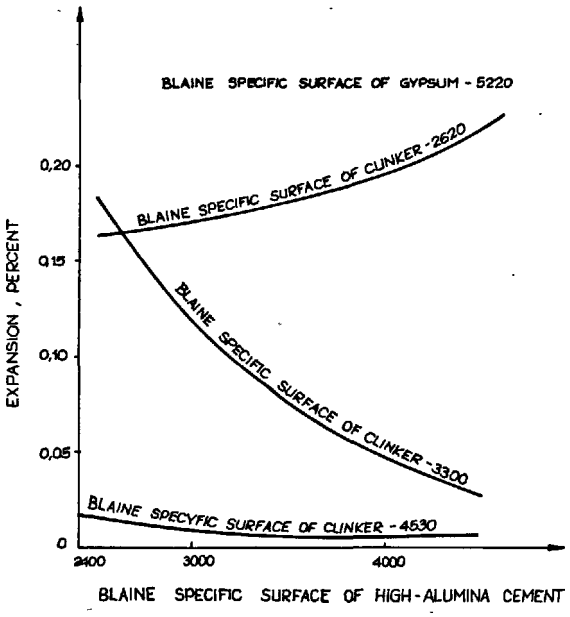

Fig. 9 - Effect of fineness on expansion for M-Type cements /Gaspar/

Expansive components

Tetracalcium sulphoaluminate is the only known ternary compound in the system $CaO-Al_2O_3-SO_3$ /44/. It forms easily at temperature as low as 1300°C and shows good stability up to melting temperature, 1600°C.

In the mixtures rich in lime it reacts with CaO with formation of C_3A and anhydrite /2/. In this connection an excess of the latter in industrial mixes is favourable.

The $C_4A_3\overline{S}$ is formed by sintering in rotary kilns, at temperatures not exceeding 1300 °C. As raw materials limestone, various alumina-bearing materials and gypsum are utilized. A large number of informations on the manufacturing of the clinker containing calcium sulphoaluminate was given at the Symposium in Tokyo /45, 46/. The K-Type clinker contains, apart from phases typical of Portland cement, $C_4A_3\overline{S}$ and small amounts of free lime and anhydrite. Expansive clinkers manufactured in the United States contain 8-50% of $C_4A_3\overline{S}$, depending on the degree of purity of used raw materials.

The computing procedure of mineral composition of K-Type clinker has been given by Mehta /2/. Adams and Larkin have elaborated a chemical method for determining the $C_4A_3\overline{S}$ content of cement and clinker of K-Type. It consists in a combination of two separation procedures, a maleic acid-methanol leach and an ammonium chloride-water leach /45/. Occasionally, in the expansive clinkers burnt at low temperatures, the calcium silicosulphate $/C_2S/_2C\overline{S}$ has been detected, which at temperature about 1300°C is known to decompose to belite and anhydrite /46/.

Substantial amount of this compound reduces the expansion potential of the cement.

Japanese expansive components for cement contain 15-20% $C_4A_3\overline{S}$, 45-50% $C\overline{S}$ and 20-30% CaO. Belite is present as minor phase in these products /2/.

In the USSR expansive clinker differs in composition from known expansive clinkers produced in the United States and in Japan; it contains also a few percent of $C_{12}A_7$ and a higher amount of C_2S /9/.

As regards the expansion process, the content of free lime is - as was stated above - advantageous, however the $/C_2S/_2C\overline{S}$ phase should not to be present.

The specific surface of this component should be high; this can be obtained easily even by intergrinding of this clinker with Portland cement clinker, due to a good grindability of the former.

In the case of M-Type cement, as expansive additive either ordinary aluminous cement or refractory high-alumina cement - as SECAR - can be utilized /36/. The latter is more advantageous since as little as 1.5% of this additive gives a sensible expansion /36/. High fineness of aluminous cement has a beneficial effect, as is evident from Fig. 9.

EXPANSIVE CONCRETES

Many years of the practice in utilization of expansive concretes allowed to collect a comprehensive experimental material as well as to examine carefully their properties. These acquirements had been presented at the Klein Symposium in Hollywood in 1972. Also Mehta /2, 3/ discussed widely the properties of these concretes, and ACI Committee 223 proposed recommended practice for the use of shrinkage-compensating concretes /7/.

Limiting oneself to essential problems only one should state, that shrinkage-compensating concretes are designed similarly to ordinary concretes with Portland cement and that, in general, their properties are in most respects close to those of Portland cement concretes.

Attention however should be called to the fact, that the type of aggregate utilized has sensible effect upon expansion /46/.

Recently Polivka and Mehta /47/ have emphasized the advantage of shrinkage-compensating cement, which is capable to give a concrete with very low drying shrinkage, even from high-absorption aggregates.

A higher water requirement of the shrinkage- compensating concretes makes additional problem; in the case of these concretes a water-cement ratio higher by 0.05 is employed /2/.

These concretes exhibit also somewhat greater slump loss, especially at elevated temperatures, than that of corresponding Portland cement concretes. It can be eliminated in practice by designing a concrete mix with increased initial slump or by addition of retarding agents. Mehta ascertained very good action of 0.05% citric acid /2/ and Collepardi et al. of other hydroxy acids and polyalcohols /48/. Nevertheless these concretes should be protected against drying in early stages of the hardening, as the drying shrinkage influences very unfavourably the expansion level and can cause shrinkage cracks.

For behaviour of expansive mortars and concretes in various conditions, especially during thermal curing as well as during drying, a great importance of the stability of ettringite has been emphasized. As reported by Mehta, no changes in X-ray diffraction pattern of a synthetic ettringite specimen have been observed when heating under dry conditions up to 65°C /51/. On the other hand, under moist conditions the ettringite phase is unaffected even when exposed to 93°C for 1 hour. Similar results were obtained by Šatava and Veprek /52/. They found, that in the atmosphere saturated with water vapour the ettringite decomposes at 111°C, with formation of $C_4A\overline{S}H_{12}$ and $C\overline{S}_{0.5}$.

Ludwig /53/ and four years later Skoblinskaya and Krasilnikov /54/ examined desorption isotherms and corresponding X-ray diffraction patterns of ettringite samples. Ludwig reported, that the crystalline structure of ettringite shows no detectable changes in XRD pattern up to 12% relative humidity. At this humidity ettringite loses about 10 molecules of water. Also Berman and Newman stated that X-ray diffraction pattern of the specimen of ettringite after the removal of 9 H_2O remains unchanged /55/. On the other hand Mehta and Klein observed no significant differences in the X-ray diffraction pattern of ettringite, which loses as many as 15 molecules of water /3/.

A detailed analysis of desorption isotherm of ettringite based on its crystalline structure, determined by Moore and Taylor /30/ has been carried out by Skoblinskaya and Krasilnikov /54/. They found, that two of 32 molecules of water do not enter into the structure of ettringite; these molecules withdraw over a wide range of vapour pressures, which is characteristic of water in the lattice defects as well as of adsorbed water. Thus the structure of ettringite contains 30 molecules of water. In the first step of dehydration ettringite loses 12 molecules of water.

X-ray examination gives no changes in the structure and the microscopic observations indicate the presence of two hydrates: 30 H_2O hydrate and 18 H_2O hydrate. The 12 water molecules removed are probably these molecules from calcium polyhedra, which make additional vertices of the trigonal prisms.

In the second step of dehydration, ettringite loses further 12 molecules of H_2O.

That will be, at first, the third molecule of water from the main vertex of the trigonal prism, whereupon the last molecule of water leaves the Ca polyhedron, and n falls to 6. As early as the amount of water molecules decreases to 16, the 18 H_2O hydrate ceases to exist and regular crystalline structure appears to disintegrate.

The third, last step of the dehydration is concerned with the most strongly bound 12 hydroxyl groups.

As is evident from all these investigations, the structure of ettringite is stable, and the curing of concrete under hydrtothermal conditions, even at temperatures exceeding 90°C, will cause not any decomposition of this phase. On the other hand, high-pressure steam curing will produce a decomposition of ettringite. Under these conditions calcium monosulphoaluminate hydrate can be stable, as it decomposes in saturated vapour atmosphere at temperatures exceeding 190°C /52/.

Resistance of expansive concretes to sulphate solutions depends on the type of expansive cement; only K-Type cement shows good resistance /2, 56/. Durability of these concretes is very high, as has been discovered by Polivka et al. /57/.

Self-stressing concretes should be designed with extreme care, basing on laboratory tests. The effect of the type and amount of steel reinforcement should be taken into account.

Polivka /58/ pointed out, that for successful application of self-stressing concrete triaxial restraints of its expansion are needed, except such elements as slabs, in which biaxial restraints are sufficient, if the concrete is kept at relatively low prestress level.

CONCLUSIONS

The position of expansive cements and concretes produced with these cements has been evidently fortified. At the same time a substantial progress is made in the understanding of the chemistry of these cements. It is to be expected, that in near future new factory produced types of these cements will appear, especially these with MgO as expansive component.

New prospects for application of the K-Type clinkers or very similar ones have been pointed out by Mehta /59/. They repose on the possibility of manufacturing of clinkers with modified compound composition at temperature substantially lower as Portland clinkers, but which would be similar in performance to Portland cement.

Acknowledgement

I gratefully acknowledge the assistance of the many research-workers who have communicated their results to me and have been helpful in more complete presentation of the problem of expansive cement in this paper, and especially to Prof. Mehta, Prof. Mather, Prof. Calleja, Dr Cottin and Dr Skalny.

REFERENCES

1. - G.L. Kalousek /1973/ "Development of expansive cements", ACI Publ. n° SP-38, pp. 1-20.

2. - P.K. Mehta and M. Polivka /1974/ "Expansive cements", Proc. of the Sixth Int. Congress on the Chemistry of Cement, Moscow 1974.

3. - P.K. Mehta /1979/ "Expansive cements and their engineering application", Canadian Department of Energy, Mines and Resources, Ottawa.

4. - V.V. Mikhailov and S.L. Litver /1974/ "Expanding and stressing cements and self-stressed reinforced structures", Stroyizdat, Moscow /in Russian/.

5. - A.M. Dmitriev /1979/ "Quality of cement and the ways of its improvement", Tsement n° 9, 16-17 /in Russian/.

6. - J. Timusk and S. Sheik /1977/ "Expansive Cement Jacks", J.Amer.Concr.Inst. 74, n°2, 80-84.

7. - ACI Committee 223 /1976/ "Recommended Practice for the Use of Shrinkage-Compensating Concrete", ACI Journal 73, n° 6, pp. 319-339.

8. - T. Kawano, K. Hitotsuya and T. Mori /1974/ "The role of $CaSO_4$ in /Alite-CaO-$CaSO_4$-Interstitial substance/ System Expansive Component for Cement", Proc. of the Sixth Int. Congress on the Chemistry of Cement, Moscow 1974.

9. - T.V. Kuznietsova /1979/ "The Chemistry and Technology of Expanding and Stressing Cements", Tsement n° 2, 10-11 /in Russian/.

10. - P.K. Mehta /1973/ "Effect of Lime on Hydration of Paste Containing Gypsum Calcium Aluminates or Calcium Sulfoaluminate", J.Amer.Ceran.Soc. 56, n° 6, 315-319.

11. - V. Volkov et al. /1974/ "Effect of Activated Alunite Quartzite Expansive Cements Properties", Proc. of the Sixth Int. Congress on the Chemistry of Cement, Moscow 1974.

12. - V. Volkov et al. /1974/ "Production of Quick-Setting, Fast-Hardening and Expansive Portland Cements Based on Secondary Alunite Quartzite", Stroit. Mat.Silik.Prom. 15, n° 2, 3-9 /in Bulgarian/.

13. - V. Volkov and S. Zamanchev /1975/ "Effect and Relations between Several Basic Factors in the Production of Shrinkage-Compensating Cements from Alunitized Quartzites", Stroit.Mat. Silik.Prom. 16, n° 1, 117-121 /in Bulgarian/.

14. - K.S. Kutateladze, T.G. Gabadadze and N.G. Nergadze /1974/ "Alunite Non-Shrinkage, Expansive and Stressing Cements", Proc.of the Sixth Int. Congress on the Chemistry of Cement, Moscow 1974.

15. - E.I. Ved et al. /1976/ "Expansive Slag Cement on the Waste Products of Caolin Transformation", Tsement n° 10, 15 /in Russian/.

16. - I.A. Kryzhanovskaya et all. /1977/ "Rapid-Setting Expanding Cements", Tsement n° 2, 5-6 /in Russian/.

17. - I.F. Ponomarev et al. /1978/ "The properties of Cements on the Basis of All-purpose Additive, Tsement n° 8, 5-6 /in Russian/.

18. - I.F. Ponomarev /1977/ "Special Modifications of Cements on the Basis of All-purpose Additive", Tsement n° 9, 7-8/In Russian/.

19. - H.W.W Pollitt and A.W. Brown /1975/ "Portland Cements", U.S. 3,883,361.

20. - J.H. Allen, W.A. Klemm and J.P. Luker /1975/ "Expansive Cement", U.S. 3,884, 710.

21. - M. Collepardi /1977/ "Method of Producing Expansive and High Strength Cementitious Pastes, Mortars and Concretes", U.S. 4,046,583.

22. - K.E. Daugherty, J.P. Luker, J.H. Allen and W.A. Klemm /1977/ "Expansive Cement", U.S. 4,002,483.

23. - F. Gille /1952/ "Untersuchungen über das Magnesia-Treiben von Portlandzement", Zement-Kalk-Gips 5, 142-151.

24. - F.M. Lea /1971/ "The Chemistry of Cement and Concrete", Chemical Publ. Co., New York, p. 368.

25. - H. Lafuma /1929/ "Théorie de l'expansion des liants hydrauliques", Rev. Mat.Constr.Trav.Publ. n° 243, 441-444, n° 244, 4-8.

26. - P.K. Mehta /1976/ "Scanning Electron Micrographic Studies of Ettringite Formation", Cem.Concr.Res. 6, n° 2, 169-182.

27. - W.C. Hansen /1944/ "Mechanism of the Expansion of Concrete, ACI Journal 15, 213-227.

28. - A.E. Sheikin and T.Yu. Yakub /1966/ "Non-Shrinkage Portland Cement", Stroyizdat, Moscow /in Russian/.

29. - V.I. Babushkin, L.P. Mokritskaya et al. /1974/ "A Study of Physico-Chemical Processes During Hydration and Hardening of Expansive Cements", Proc.of the Sixth Int.Congress on the Chemistry of Cement, Moscow 1974.

30. - A.E. Moore and H.F.W. Taylor /1968/ "Crystal Structure of Ettringite", Nature 218, 1048; /1970/ "Crystal Structure of Ettringite", Acta Cryst. Sect. B, 26, 386.

31. - P.K. Mehta /1973/ "Mechanism of Expansion Associated with Ettringite Formation", Cem.Concr.Res. 3, n° 1, 1-6.

32. - P.K. Mehta and F. Hu /1978/ "Further Evidence for Expansion of Ettringite by Water Adsorption", J.Amer.Ceram. Soc. 61, n° 3-4, 179-181.

33. - V.S. Ramachandran, P.J. Sereda and R.F. Feldman /1964/ "Mechanism of Hydration of Calcium Oxide", Nature 201, 288-289.

34. - K.G. Krasilnikov, L.V. Nikitina and N.N. Skoblinskaya /1974/ "Physico-chemistry of Cement Expansion Processes", Proc.of the Sixth Int.Congress on the Chemistry of Cement, Moscow 1974.

35. - B. Mather /1973/ A Discussion of the Paper "Mechanism of Expansion Associated with Ettringite Formation" by P.K. Mehta, Cem.Conr.Res. 3, n° 5, 651-652.

36. - J.P.Gaspar /1979/ "Cinétique d'hydratation des ciments expansifs de Type M", Lafarge, France /to be published/.

37. - M. Okushima, R. Kondo et al. /1968/ "Development of Expansive Cement with Calcium Sulphoaluminous Cement Clinker", Proc.of the Fifth Int.Symposium on the Chemistry of Cement, The Cement Ass.of Japan, Tokyo 1968, Vol. IV, pp. 419-438.

38. - B. Cottin /1979/ "Hydratation et expansion des ciments", Lafarge, France /to be poblished/ and private communication.

39. - I. Isogai /1975/ "Properties of Long-Term Ages of Hardened Mortar of $3CaO.3Al_2O_3.CaSO_4$ - $CaSO_4$ - CaO Expansive Cement", Rev. 29-th Gen.Mtg., Cement Ass.of Japan, pp. 85-88.

40. - M. Regourd, H. Hornain and B. Mortureux /1978/ "Microstructure of Con-

crete in Aggressive Environments", The First Int. Conference on Durability of Building Materials and Components", Ottawa, 21-23 August 1978 /to be published by ASTM/.

41. - M. Collepardi at al /1978/ "Tricalcium Aluminate Hydration in the Presence of Lime, Gypsum or Sodium Sulfate", Cem.Concr.Res. 8, n° 5, 571-580.

42. - A. Bentur and M. Ish-Shalom /1974/ "Properties of Type K Expansive Cement of Pure Components. II. Proposed Mechanism of Ettringite Formation and Expansion in Unrestrained Paste of Pure Expansive Component", Cem.Concr. Res. 4, n° 5, 700-721.

43. - P.K. Mehta /1973/ "Studies on Slump Loss in Expansive Cement Concretes", ACI Publ. n° SP-38, pp. 57-68.

44. - P.E. Halstead and A.E. Moore /1962/ "The Composition and Crystallography of an Anhydrous Calcium Aluminosulphate occuring in Expanding Cement", J.appl.Chem. 12, 413-417.

45. - N. Fukuda /1968/ "Fundamental Studies on the Expansive Cement", Proc.of the Fifth Int.Symposium on the Chemistry of Cement, The Cement Ass.of Japan, Tokyo 1968, Vol. IV, pp. 341-350.

46. - T. Nakamura, G. Sudoh and S. Akaiwa /1968/ "Mineralogical Composition of Expansive Cement Clinker Rich in SiO_2 and Its Expansibility", Ibid., Vol. IV, pp. 351-365.

47. - L.D. Adams and E.E. Larkin /1978/ "Determination of $C_4A_3\bar{S}$ in Type K Cement and Clinker Using Maleic Acid-Methanol and Ammonium Chloride-Water as Extracting Agents", Cem.Concr.Res. 8, n° 5, 539-544.

48. - J.A. Epps and M. Polivka /1970/ "Effect of Aggregate Type on the Properties of Shrinkage-Compensating Concrete", Highway Research Board, Highway Research Record n° 316, pp. 82-90.

49. - M. Polivka and P.K. Mehta /1976/ "Use of Aggregates Producing High Shrinkage with Shrinkage-Compensating Cements", Special Technical Publ. n° 597.

50. - M. Collepardi et al. /1975/ "L'idratazione in pasta del $4CaO.3Al_2O_3.SO_3$ in presenza di $Ca(OH)_2$, $CaSO_4.2H_2O$ ed alcuni Composti Organici", Il Cemento n° 2, 53-60.

51. - P.K. Mehta /1972/ "Stability of Ettringite on Heating", J.Amer.Ceram. Soc., 55, n° 1, 55-56.

52. - V. Šatava and O. Vepřek /1975/ "Thermal Decomposition of Ettringite Under Hydrothermal Conditions", J.Amer.Ceram. Soc. 58, n° 7-8, 357-358.

53. - H. Ludwig /1969-1971/ "Combined Water in Cement Hydration Products", Tätigkeitsbericht des Forschungsinstituts der Zement Industrie, pp. 80-82 /in German/.

54. - N.N. Skoblinskaya and K.G. Krasilnikov /1975/ "Changes in Crystal Structure of Ettringite on Dehydration", Cem.Concr.Res. 5, n° 4, 381-394.

55. - H.A. Berman and E.S. Newman /1962/ "Heat of Formation of Calcium Trisulfoaluminate at 25°C", Proc.of the Fourth Int.Symposium on the Chemistry of Cement, Monograph 43, Nat.Bur.of Standards, pp. 247-257, Washington DC.

56. - P.K. Mehta and M. Polivka /1975/ "Sulfate Resistance of Expansive Cement Concretes", ACI Publ. n° SP-47, pp. 367-379.

57. - M. Polivka, P.K. Mehta and J.A. Baker /1975/ "Freeze-Thaw Durability of Shrinkage-Compensating Cement Concrete", ACI Publ. n° SP-47, pp. 79-87.

58. - M. Polivka /1973/ "Self-Stressing Concrete", ACI Publ. n° SP-38, pp. 483-487.

59. - P.K. Mehta /1978/ "Energy, Resources and the Environment - a Review of the US Cement Industry", World Cement Technology 9, n° 5, 144-160.

SUB-THEME V - 3

Other cements (cements with high content of active C_2S) and their application

A.S. BOLDYREV
Ministry of the building material industry of U.S.S.R.

INTRODUCTION. Mankind today is facing two global problems - apart from others - whose successful solution is going to affect not only the economic affluence of the peoples in the modern world but the health and well-being of future generations as well. They are the necessity to protect the environment against pollution and that of conserving energy.

The cement industry is one of the most material- and energy-consuming branches, and its contribution to the solution of these two problems can be very considerable. According to forecasts made by some scientists, the world production of cement by 1985 will reach 1 billion tons (1) which will require more than 1.5 billion tons of raw materials and some 200 million tons of fuel.

The chemical, metallurgical, coal and other industries yield hundreds of tons of technogenic by-products and waste materials which are not sufficiently utilized as yet. Many of these materials may be successfully used as raw materials and active mineral admixtures in cement industry (2). The utilization of by-products is one of the main means of saving energy in cement industry (3,4).

Blast-furnace granulated slags have been extensively used in the Soviet Union for a long time. Their yearly consumption in cement industry is from 28 to 30 million tons. Calculations show that out of all possible ways of utilizing blast-furnace slags their use in cement industry is, from the economic point of view, the most profitable one. The valuable experience accumulated in this field in the USSR was summarized in a paper presented by V.I.Satarin at the Sixth International Congress on Cement Chemistry in Moscow (5).

Fuel ashes and slags are used more and more in the production of Portland cement. Extensive research and experimental work is carried out to utilize of other kinds of technogenic by-products produced by a number of industries (chemical gypsum, electrothermophosphorous slags, non-ferrous metallurgy slags, etc.).

I. UTILIZATION OF TECHNOGENIC INDUSTRIAL BY-PRODUCTS CONTAINING $2CaO \cdot SiO_2$ IN CEMENT PRODUCTION

The present paper deals with the experience of utilizing technogenic by-products, mainly dicalcium silicates formed during the production of alumina, in cement industry.

In contrast to foreign countries, the main trend in alumina industry in the USSR is more extensive use of highly siliceous kinds of alumina-containing raw materials, like siliceous bauxites, nephelines, alunites and some other minerals. Nephelinic ores are of special practical interest in this respect.

The nephelinic ores which are found in unlimited quantities in the USSR are poorer in alumina and richer in silica than bauxites and differ from the latter in that they have a higher alkali content (10 to 20 percent R_2O). Such a composition makes them, according to Soviet researchers, a valuable raw material complex for the production of alumina, soda and cement.

In the USSR, following research by Soviet scientists (I.L. Talmud, O.N. Zakharzhevski, V.P. Pochivalov, N.I. Vlodavets, V.A. Krochevski, F.N. Strokov and others (6), for the first time in world practice, an all-round and practically waste-free processing of nephelinic ores and concentrates into alumina, soda and potash using the so-called sintering method has been realized. It is done on an industrial scale, at three enterprises. The by-product of this process is a nephelinic slurry containing up to 50 percent water and 80 to 90 percent of β -C_2S in the solid component.

The possibility of producing binders using the solid component of nephelinic slurry was first studied by V.A. Kind, N.I. Voronin and P.I. Bozhenov as early as 1932-1935. Their purpose was to produce a non-calcinated binder which they called "nephelinic cement" and which consisted of 80 percent of dried slurry and 20 percent of lime, with an admixture of gypsum. But because this cement was found to quickly loose its activity during storage and transportation, it was not accepted industrially. The authors also pointed to the possibility of utilizing this reject material as raw material in the production of Portland cement.

This work was continued by S.D. Makashev (7) and in the postwar years by L.S. Kogan (8), S.M. Royak and others. They discovered some specific physico-chemical properties of the belite product, which considerably differ from those of the traditional raw materials in current use in cement production and which to use this product both in the production of Portland cement clinker at considerably lower energy consumption levels and as a hydraulically active component in cements which, according to the authors, closely resembled common Portland cement.

Though investigations in the field of comprehensive processing of nephelinic ores into alumina, soda and potash, with the belite by-product being utilized in the production of cement, were completed on the whole, in the USSR, in 1938-1940 (8,9), the industrial realization of the resultant technology had to be put off because of the World War II and was carried into effect in 1948 in Volkhov, near Leningrad.

Apart from nepheline, Soviet scientists in 1939-1941 investigated other raw materials suitable for the production of alumina and cement.

For example, I.S. Lileyev, B.I. Kogan, A.F. Dumskaya, S.D. Makashev and others studied the ash of the Moscow brown coals for possible use as a new alumina raw material. The ash, when processed by the alkaline method, yields, besides alumina, the so-called "ash slurry" whose solid part contains as much as 70 to 75 percent of β-C_2S. S.D. Makashev (1939-1940) found that this technogenic by-product, just like nephelinic slurry, made a very effective raw material for producing clinker and a good component of Portland cement (7).

The same author obtained similar results for technogenic belite materials (slurries) formed during alumina extraction using the same method of extraction from new alumina raw materials like kaolin, mica slate, colliery dump rock etc. which were investigated at V.A.M.I. and G.I.P.Kh. It should also be remembered that the "Svobodny Sokol" plant in Lipetsk produced in 1938-1940 - 225 thousand tons of aluminate-silicate cement. The basic component of this cement was γ-C_2S obtained by slow cooling of blast-furnace slags having a high percentage of alumina. The cement required no grinding due to the autopulverization effect during inversion (β-C_2S ⟶ γ-C_2S) and was of 250 to 400 grade.

Following the method and technology worked out by Ch.De Sey assisted by K. Dickerhoff, alumina was industrially produced from TPS ash at a cement factory in Rüdersdorf. The TPS was using brown coal, and the "black" slurry formed in the process and consisting for the most part of γ-C_2S was utilized in cement production as a raw mix component (10).

So, the beginning of the industrial utilization of technogenic C_2S in cement production dates back to the '30ies and '40ies.

The alumina industry in the USSR uses nephelinic ores from various deposits.

According to N.V. Belov (11), the crystal cell of nepheline has the following formula:

$$2Na_2Al_2Si_2O_8 \cdot 2SiO_2 = Na_4Al_3[AlSi_5O_8]$$

The chemical principle of extracting alumina from nepheline is based on formation of soluble alkali aluminates, $Na_2O \cdot Al_2O_3$ and $K_2O \cdot Al_2O_3$, and on conversion of silica into the insoluble compound $2CaO \cdot SiO_2$ in the course of reaction:

$$(Na,K)_2 \cdot Al_2O_3 \cdot 2SiO_2 + 4CaCO_3 \longrightarrow$$

$$2(Na,K) \cdot Al_2O_3 + 2(2CaO \cdot SiO_2) + 4CO_2$$

Here the following optimum ratios must be maintained in the alumina charge between the basis oxides (6):

$CaO : SiO_2 = 2$ and

$Na_2O + K_2O : Al_2O_3 = 1$

I. STRUCTURE AND PROPERTIES OF DICALCIUM SILICATE IN TECHNOGENIC BY-PRODUCTS OF ALUMINA INDUSTRY. It is now accepted that C_2S exists in five polymorphic forms: α, α'_H, α'_L, β and γ, with different stability intervals at heating and cooling.

Transition of modifications is accompanied by complete reconstruction of the crystal lattice (12) or an insignificant structure shift (13), which affects enthalpy and conversion rate (14).

The structure of crystal lattices of all the polymorphic forms of calcium orthosilicate has been studied fairly well. The α-form features hexagonal (or, according to some reports, trigonal) symmetry, while the α'_L, α'_H and γ-C_2S forms are orthorhombic and the β-form is monoclinic. The structure of all the modifications is made up of independent SiO_4 tetrahedrons linked together by calcium atoms whose coordination changes from 6 to 10 during transition from the γ- to the α-form. Hydraulic activity of dicalcium silicate modifications varies. γ-C_2S is considered hydraulically inactive, although it is reported (15,16) that it shows binding properties in the presence of alkalis and in alumosilicate cements. Alumosilicate slags with compositions within the crystallization field of dicalcium silicate in the $C_{12}A_7$ - C_2S - CA elementary triangle of the CaO - SiO_2 - Al_2O_3 system were industrially produced in a blast furnace.

When cooled gradually, the slags disintegrated into powder due to the transformation of β-C_2S into the hydraulically active γ-form.

The strength of cement solution at 28 days reached 250-400 kgs/cm^2. This was a fast-hardening cement with daily strength of 100-150 kG/cm^2. Until then it was thought that only β-C_2S was hydraulically active. At present activity has been found to exist in high-temperature forms of dicalcium silicate as well. Properties were found to depend on the composition and quantities of admixtures used for stabilization.

Stabilization of C_2S modifications is due to isomorphism in cationic and anionic parts of the structure (16, 17). Isomorphic substitutions of Ca and Si lead to disarrangement of the structure which is accompanied by changes in lattice symmetry and results in corresponding changes in the physical, chemical and technical properties of C_2S solid solutions. An important factor in the formation of C_2S properties is the ability to form solid solutions with a great number of oxides. The C_2S lattice may comprise ions of Al, Fe, K, Na, Ti, Cr, B, P, oxides or their combinations (12-14, 18, 19). Dissolution of CaO or SiO_2 in C_2S lattice is also possible leading to deviation from the stoichiometric composition of C_2S. In the case of CaO β-C_2S is stabilized,

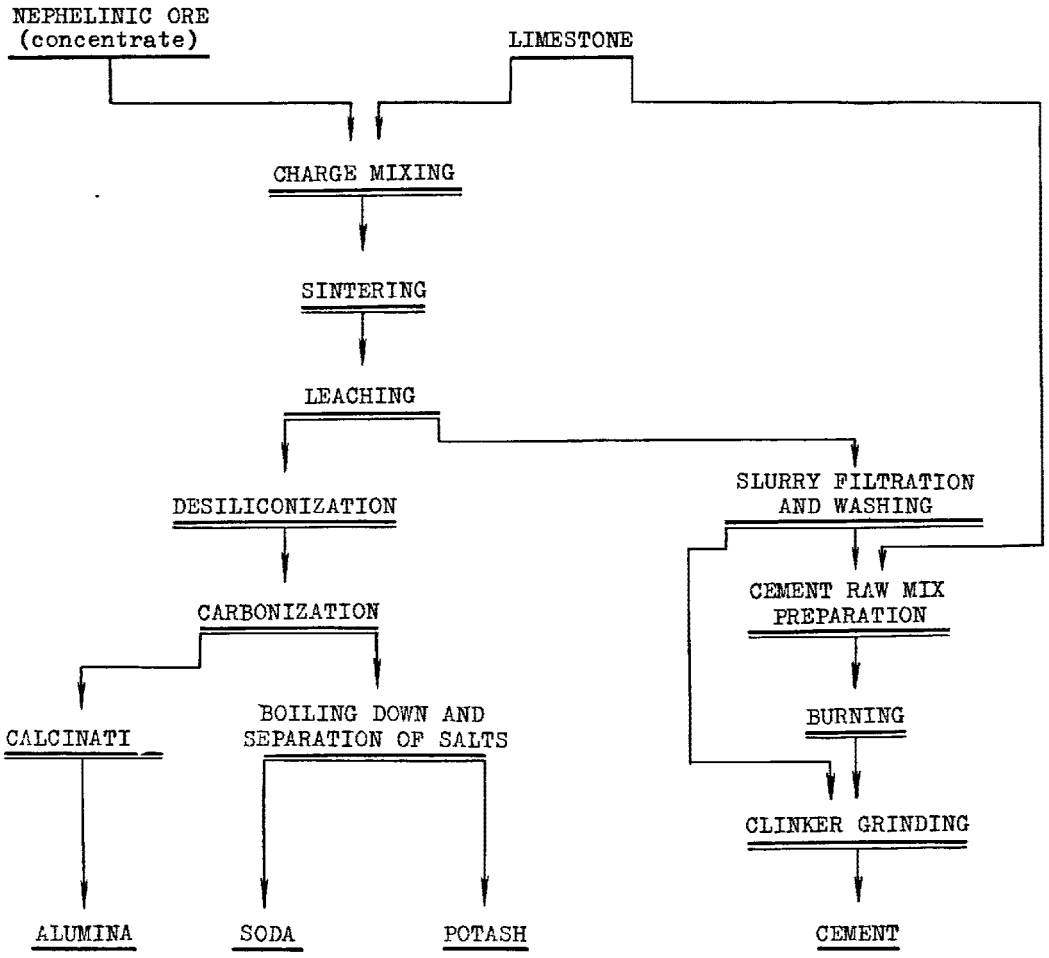

Fig. 1. Basic diagram of integrated processing of nepheline.

in the case of SiO_2, the $\beta \rightarrow \gamma$ inversion is made easier.

In technogenic products of apatite or phosphorite, processing undecomposed residues of basic rocks are always present.

P_2O_5 present in these products, depending on quantity, may cause stabilization of α, α' or β -forms of C_2S (18, 19). Although the presence of the α and α' modifications together with β -C_2S does not reduce hydraulic activity of nephelinic slurries, it can lessen considerably their reactivity in burning.

Of particular importance to the structure of calcium orthosilicate in technogenic products are solid solutions with Al_2O_3 and Fe_2O_3 (red slurries) which facilitate the $\beta \rightarrow \gamma$ inversion (15). K_2O at slow cooling was shown (20) to stabilize the β-form, while quick quenching resulted in the formation of an α' -and β -C_2S mixture.

According to reports (21), solubility in C_2S drops in the series Fe_2O_3 > MgO > TiO_2 and is, respectively, 1.8%, 0.75 - 1.5% and 0.75%. These admixtures facilitate the $\beta \rightarrow \gamma$ inversion progressively in the same order. Solubility of Na_2O in C_2S does not exceed 0.6% but, unlike the above mentioned oxides, alkali stabilizes β -C_2S.

It was shown (22) that Na_2O may be included in the C_2S lattice in considerable quantities (up to 5% or more) if alkali is introduced as a carbonate or sulphate. The alkali-stabilized β -form, however, possesses reduced hydraulic activity in comparison to the α -and α' - modifications. Higher hydraulic activity in α - and α' -forms of C_2S and the possibility of their stabilization by chemical admixtures was reported by other authors as well.

It follows then that in alkali-containing technogenic products it is the β -form that is stabilized, whereas alkali-free

sinters contain mainly the γ-form of C_2S. On the other hand, alkalis should be removed as completely as possible because of the adverse effect they have on the quality of cement. It should be pointed out that in the presence of small quantities of fluorine not even sodium aluminate can stabilize the β-form, and inversion becomes very intensive. (23)

Kh.N. Nurmagambetov, S.A. Tscherban and V.A. Belousova studied phase composition of orthosilicate on sinters and slurries from alumina factories by infra-red spectrography and X-ray structure analysis (24). Fig. 2 which is based on their findings gives the infra-red spectra of β - and γ-C_2S, as well as those of some nephelinic and bauxite sinters. According to the results obtained, in nephelinic sinters and slurries C_2S is present mainly in its β - form, whereas in bauxite sinters and slurries the C_2S form was not found to correspond to any of the known modifications. The authors ascribe this phenomenon to large quantities of ferric oxide dissolved in the C_2S lattice. But a more natural supposition is that the bauxite sinters studied by the authors were heterophase and contained, apart from C_2S, admixtures of alumoferritic nature. An indirect confirmation of this, as the same study points out, is chemisorption of Al_2O_3 by low-modulus solution whereas β-C_2S from nephelinic sinter practically did not absorb a Al_2O_3. Formation in nephelinic slurry of practically only the β-form is also reported in (25), but in the same study it is also noted that β-C_2S absorbs alumina from solution with formation of hydrogarnets.

According to other data, nephelinic sinters and slurries contain, apart from the β-form, also α - and α'-modifications of C_2S (26).

According to some reports, the presence of a particular form or forms of C_2S in slurries depends on the quantity of admixtures (see Table I).

Phase composition of slurries in this paper (26) was studied using X-ray, thermographic, crystallooptical, IR-spectrum and chemical methods.

The α-form of C_2S in slurries resulting from the processing of highly siliceous bauxites was identified on the basis of X-ray data and by the presence of a broad absorption band in the 800- to 1000 cm^{-1} region of the IR spectrum. When heated up to 800°C, α-C_2S-containing slurry samples showed an intensive $\alpha \rightarrow \beta$ conversion. This process was accompanied either by separation of the admixtures and their localization around C_2S grains or by formation of a new phase of the mellite type. Stabilization of the α-form of C_2S by alkalis was also reported in (27); the α-C_2S content of clinker was found to be closely connected with the quantity of insoluble alkalis.

It should be stressed in summarizing the above reports, that the crystallochemical structure of C_2S in the technogenic belite products of nephelinic slurries depends on the quantity of admixtures and the degree of leaching and of alkali aluminates extraction, i.e. on the physico-chemical and technological particulars of alumina production. On the other hand, the latter determines the hydration activity of the technogenic belite product in cement and its reactivity in cement raw mixes, i.e. exactly those properties which are of primary importance to the chemistry, technology and technical properties of cement. Consequently, an optimum technology for the all-round processing of nephelines can result only from combining the interests of both alumina and cement industries.

2. REACTIVITY OF CEMENT RAW MIXES BASED ON TECHNOGENIC PRODUCTS CONTAINING DICALCIUM SILICATE. The above discussion concerned the composition and properties of the solid substance of nephelinic slurries, mainly from the point of view of hydration activity generation which makes them suitable for cement production.

Of considerable interest is also utilization of this belite product as an ingredient of raw mixes used to produce cement clinker. One of the first reports concerning prospects of such an utilization was contained in the Makashev paper (7).

The same paper also discussed the main technological aspects of using nephelinic slurries as raw material to produce Portland cement clinker by the wet method.

As a raw material for clinker production, nephelinic slurry formed as a coarse suspension containing 40% of water, has the following technologically important features:

- all the silica and most of the calcium oxide in the solid substance of the slurry are present in the form of belite;
- a higher silicate modulus in comparison to the commonly used clays;
- a fairly considerable percentage of residual alkalis, Na_2O and K_2O.

The first factor is responsible for higher reactivity of the slurry, a lower level of carbonate raw material consumption and, consequently, an increased output capacity of kilns and a reduced heat consumption required for burning . In contrast, the two other features make the utilization of nephelinic slurries as raw material somewhat difficult.

Table 2 gives typical chemical compositions of the solid substance of industrial nephelinic slurries used by the cement industry (28).

The Achinsk slurry has a very high Al_2O_3 and alkali content which points to worse conditions of sodium aluminate extraction from the sinter.

TABLE I

Chemical composition and modification of technogenic C_2S in slurries

Slurry	Oxides in slurries, %									Cristal structure C_2S
	SiO_2	Al_2O_3	Fe_2O_3	CaO	MgO	SO_3	TiO_2	Na_2O	K_2O	
After processing:										
clays	22.38	4.0	1.08	54.65	1.64	0.21	0.17	0.33	0.11	γ
nephelins	28.79	2.48	2.89	54.67	2.55	0.93	0.33	0.93	1.16	β
highly siliceous bauxites	25.90	3.41	9.05	48.03	1.29	0.57	2.33	2.13	0.50	α

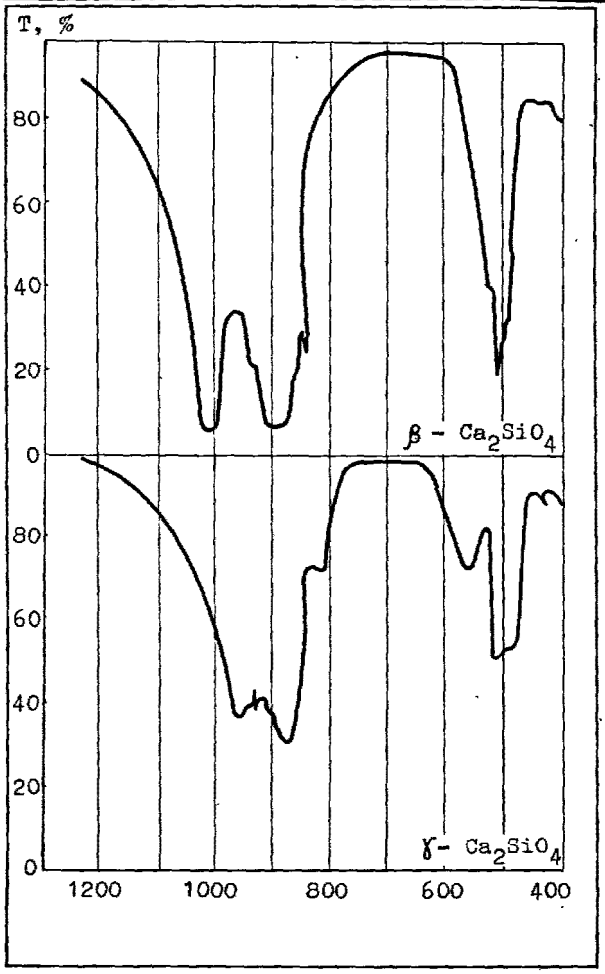

Fig. 2a. Infrared spectra of the β and γ -modifications of dicalcium silicate.

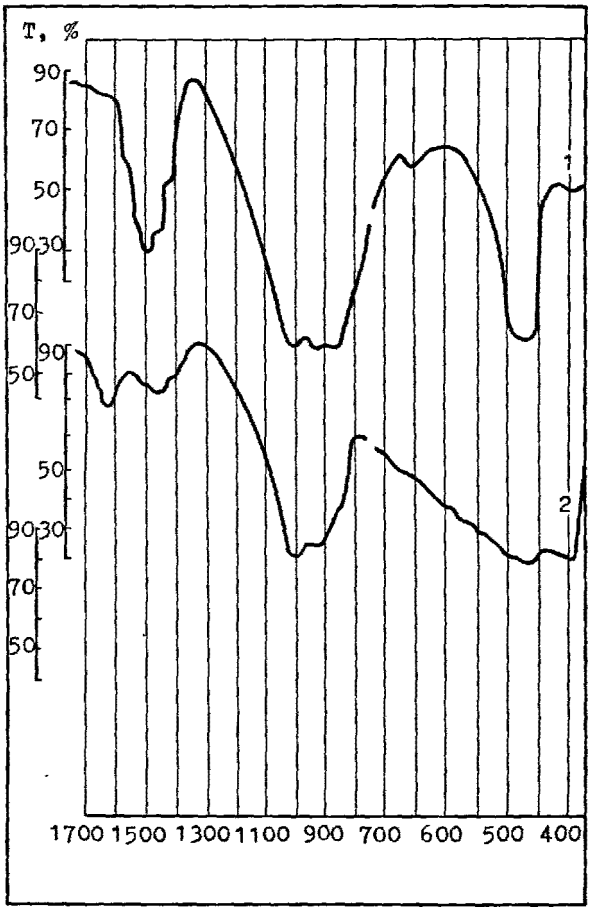

Fig. 2b. Infrared spectra of the solid substance of slurries after the leaching of sinters: 1-nephelinic sinter; 2-bauxitic sinter.

Fig. 2. IR spectra of β and γ -C_2S and sinters of nephelines and bauxites.

All of the solid substance of slurries is mainly composed by β -C_2S crystals. The C_2S grains in all the slurries do not differ greatly in size (up to 12-18 μm).

Judging by X-ray photographs, C_2S in the Achinsk slurry has the most defective structure of all.

In the course of heating, recrystallization of C_2S grains is observed, starting at about 900-1000°C and rapidly proceeding at 1100°C. Belite-grains grow to up to 35-50 μm. The belite product of the Achinsk slurry shows simultaneous disintegration of solid solutions and isolation, at grain boundaries, of ferric oxide which forms the alumoferritic phase. According to P.I. Bozhenov (29), admixtures in C_2S crystals are originally adsorbed along the boundaries of mosaic blocks, in intercrystallite zones, where their concentration is much higher than in the crystal volume. At a change of temperature, disintegration of solid solutions may occur in these zones even before the solubility limit is reached in the crystal volume. When the cooling regime is changed, the admixture may be either isolated forming a new phase or "dissolved" in the crystal volume. Clinker properties thus become controllable. It should be noted that the presence of amorphized intercrystallite films in clinker phases, and their influence on clinker properties was confirmed by electronic microscopic investigations carried out by U.I. Papiashvili (30).

Recrystallization of C_2S grains on heating and decomposition of solid solutions somewhat reduces the reactivity of raw mixes based on nephelinic slurry. That is why the heating should be carried out as quickly as possible. Because of a higher silicate modulus, bicomponent mixes of nephelinic slurry and limestone are inferior, as far as reactivity is concerned, to mixes containing clay or marl and fluxes. That is why a tetra-component raw mix is in common use consisting of nephelinic slurry, limestone, and aluminous and ferriferous correction admixtures. This results in an unwanted reduction of slurry consumption per ton of clinker in comparison to bicomponent mixes (31).

Use of 0.4 - 0.5% CaF_2 admixture as a mineralizer allows to carry out successfully the burning of a bicomponent raw mix having a silicate modulus of 4.5. This increases the nephelinic slurry percentage in raw mix from 38-40 to 50%, while that of limestone is reduced from 55-57 to 50%.

Total raw material consumption is reduced by about 10 percent by mass (32).

Of particular importance to the reactivity of a raw mix and the quality of clinker obtained is the percentage of alkali oxides present, especially that of Na_2O, whose sublimation during burning does not take place as easily as in the case of K_2O. That is why the Achinsk slurry, as far as reactivity goes, is very inferior to the other two.

According to some authors, the unavoidable recrystallization of belite in the preparatory zones of rotary kilns results in such a substantial drop of reactivity in raw mixes based on nephelinic slurries that it affects the quality of clinker (33). Alite which is formed in such clinkers shows poorly defined crystallization and a defective structure with crystal sizes of 20 to 30μm, while the hydration activity of clinker is about 15 percent lower than when clay is used. However, the cause of the inferior microstructure and reduced activity of clinker is not the reduced reactivity of the raw-mix but rather the adverse effect of Na_2O on the alite structure.

Fig. 3 gives changes in CO_2 and CaO content in roast material along the length of the 175-meter kiln of the Achinsk factory (34). As can be seen, the amount of CaO does not exceed 5 percent in any part of the kiln, whereas in the case of the usual charge it reaches 15 to 18 percent at the end of the decarbonization zone. Assimilation of lime by the belite product of nephelinic slurry takes place parallel to decomposition of $CaCO_3$.

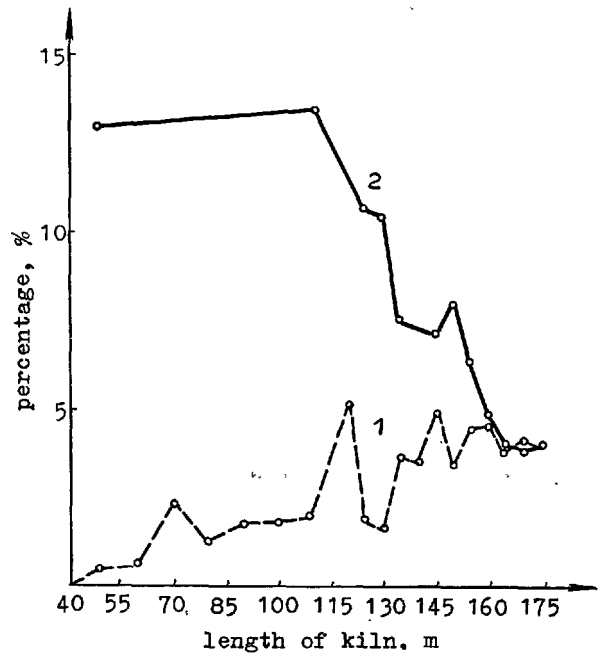

Fig. 3. Change in content of (1) CO_2 and (2) free CaO in roast material along the length of the kiln

A high Na_2O concentration in the charge of the Achinsk factory is responsible for the formation of large quantities of spurrite $2(C_2S)\cdot CaCO_3$ in the roast material. At the 135th meter of the kiln it accounts for 46.7 percent of the roast material mass. Decomposition of spurrite takes place at a temperature above 940°C according to the reaction:

$$(C_2S)_2 \cdot CaCO_3 \longrightarrow 2C_2S + CaO + CO_2$$

The newly-formed belite and CaO in statu nascendi have adequate reactivity so that the formation of spurrite is, from this point of view, even useful. But at the same time intensive clinker dust generation

TABLE II

Composition of solid substance of nephelinic slurries which are utilized in the USSR cement industry, in percentages, and its modulus

Slurry	SiO_2	Al_2O_3	Fe_2O_3	CaO	MgO	Na_2O	K_2O	Silicate modulus	Alumina modulus
Pikalevo slurry	28.8	2.5	2.9	54.7	2.5	1.2	0.9	5.36	0.85
Volkhov slurry	28.4	2.8	2.6	55.2	1.7	1.1	0.8	5.17	1.06
Achinsk slurry	27.3	4.6	3.4	52.2	1.2	0.7	1.4	3.42	1.33

is observed which makes it much more difficult for the kilns to function. At other factories which use nephelinic slurries of a lower general percentage of alkali and especially lower Na_2O content, the operation of kilns presents no snares caused by the dusting effect.

At higher content of water-soluble alkalis, rheological properties of raw slurry deteriorate as well when the wet method is used.

Table III gives average data (1973) on the mineralogy and strength (activity) of clinker at factories which use nephelinic slurry as a main component of raw mixes.

These data show that all these clinkers have high alite percentages.

The Achinsk clinker is inferior to the other ones in quality despite a higher C_3A percentage, because of a higher alkali content both in nephelinic slurry and clinker. The Volkhov clinker is in the most active category and is superior in quality to most of the clinkers produced from traditional raw materials.

At all the above factories the output capacity of rotary kilns is at least 30 percent higher and the specific fuel consumption is 20 to 25 percent lower than for kilns of the same type used for the processing of traditional raw materials.

Earlier we discussed some of the investigation results and the main lines of practical utilization in cement industry of technogenic belite products which are formed during the all-round processing of nephelines into alumina, soda and potash.

In future, other technogenic belite products with similar physico-chemical properties can be obtained from the all-round processing of other alkaline alumosilicate mineral rocks. Large deposits of such minerals are found in Siberia and the Far East, and in particular in the area through which the Baikal-Amur railway line is being built.

Similar belite by-products may also be obtained in alumina production using the alkaline charge sintering method, with soda added, from such materials as fuel ashes, kaolins, clay and mica dump slate and other materials containing sufficient amounts of alumina.

But, in utilizing TPS ashes and kaolins, clays and clay slate and other alumina-containing materials, a non-alkaline method of processing may be preferable, like that proposed by the Polish academician E. Grzymek.

The non-alkaline method of processing such materials for alumina which yields γ-C_2S powder, with γ-product grain sizes of about 10 to 20 μm, to be used as a component of cement raw mixes, was discussed by E. Grzymek in detail at the 6th International Congress on Cement Chemistry in Moscow (35). One of its major advantages is the absence of alkali admixtures in its γ-product, and is the corresponding difficulties in clinker burning. It should be said, however, that ensuring a steady and complete pulverization of alkali-free alumina sinters, when the original raw material is of unstable composition, is not a simple matter.

Original raw materials almost always contain P^{5+}, B^{3+}, Mn^{4+}, Cr^{6+}, V^{5+} and some other ions in various combinations which, though present in relatively small quantities, can have a stabilizing effect on C_2S and thus obstruct the full polymorphic conversion on $\beta \rightarrow \gamma$-C_2S. This can be prevented, according to E. Grzymek, if the sinter is burned in a reducing atmosphere.

Slower dispersion rates of alumina sinters may also be caused by melts of a certain composition, which facilitate formation of finely crystalline C_2S where the formation of γ-C_2S nucleus is somewhat hindered, by rapid cooling of the sinter as well as by other factors.

From 1954, experimental industrial production of alumina and cement utilizing fuel ashes has been in progress in the Polish People's Republic. Taking into account the experience accumulated over the years in this field, a factory is being built there with an output capacity of about 100 thousand tons of alumina and 1270 thousand tons of cement. A similar factory is being built in the Hungarian People's Republic in co-

TABLE III

Mineralogy and strength of clinker

Factories (large production units, plants)	Composition of clinker, mass percentages					Compression strength at 28 days, MPa
	C_3S	C_2S	C_3A	C_4AF	R_2O	
Pikalevo	62	18	4	12	1.3	47.6
Volkhov	59	18	5	14	1.04	58.2
Achinsk	58	19	8	11	1.5	44.0

operation with the PPR.

Following reports on the possibility of utilizing a number of new alumina-containing non-bauxitic raw materials, Soviet scientists have been engaged in extensive research of the technogenic γ-product for its possible use in raw mixes in cement clinker production.

For instance, researchers at V.A.M.I., Leningrad ascertained the basic possibility of utilizing, as an alumina raw material, the mineral part of coals and enclosing rocks from the Ekibastus coal field in the Kazakh SSR.

Around this unique coal field, a number of large TPStations have been planned and partly built which, apart from alumina-containing dump rock with as much as 35 percent of Al_2O_3, yield ashes and slags containing up to 25-32 percent of Al_2O_3 and 62-68 percent of SiO_2. The overall output of these materials from 3.3 million tons a year is to reach 30 million tons by 1990.

The self-pulverizing alumocalcium sinter (dispersion degree of up to 95-99%) produced from the above materials by the non-alkaline sintering method, subjected to leaching, yields a γ-product containing as much as 60 - 65 percent of γ-C_2S (36, 37).

Research at Giprotsement (38) showed this material to be a highly reactive component of raw mixes for obtaining a highly active clinker, analogous in this respect to the γ-product which is formed during the extraction of alumina from the previously studied kaolin from the Angren deposit.

It should be noted however that, notwithstanding its positive properties discussed here, the γ-product produced by the above method, is lacking in, or, according to some reports, has a very weak hydration activity. This prevents, its use as an active component of Portland cement, until methods of activization are found.

3. BUILDING AND TECHNICAL PROPERTIES OF PORTLAND CEMENTS WITH ADMIXTURES OF TECHNOGENIC DICALCIUM SILICATE. Before turning to the discussion of the existing data concerning properties of cements which, apart from clinker, contain various quantities of technogenic dicalcium silicates as an active component, the term used to describe there cements should be discussed since it is not generally recognized yet.

The term used at present by some authors (39-41) "nephelinic cement". It was used previously to designate a binder produced by grinding together a mixture of dried nephelinic slurry, lime and gypsum.

Apart from this, a cement based on the mixture of Portland cement clinker and technogenic belite product can be produced, according to the above discussion, by the method of alkaline sintering not only from nephelinic raw materials, but also from other kinds of alumina-containing materials, like highly siliceous bauxites, fuel ashes, clay and clay slate, kaolin. To avoid introducing new names to designate the latter kinds of cement which are quite similar, as far as composition and properties are concerned, to the ones produced by processing of nepheline, cement which is composed of clinker and technogenic belite product in excess of 20 percent is called "belite Portland cement", shortened to BPC, throughout the discussion that follows. Portland cements with lower percentages of technogenic belite and clinker which is produced by burning a raw mix with nephelinic slurry in it require no special designation.

These cements are produced in the USSR at the factories in Volkhov and Achinsk, where technogenic belite product is used as an active mineral admixture in the production of Grade 400 and 500 Portland cements (with admixtures) and of the GOST 10178-76 fast-hardening Portland cement. The high-quality clinker from the Volkhov factory allows to produce mostly cements of enhanced strength. Building and technical properties of BPC with over 20 percent of technogenic belite were studied in detail at Giprotsement and L.I.S.I., Leningrad, under the guidance of P.I. Bozhenov (39-40).

Fig. 4. shows how the quantity of belite product in nephelinic slurry affects the strength of cement produced at the Pikalevo factory (42).

At initial hardening stages, BPC with a higher belite percentage is found to be somewhat inferior in strength to cement wit-

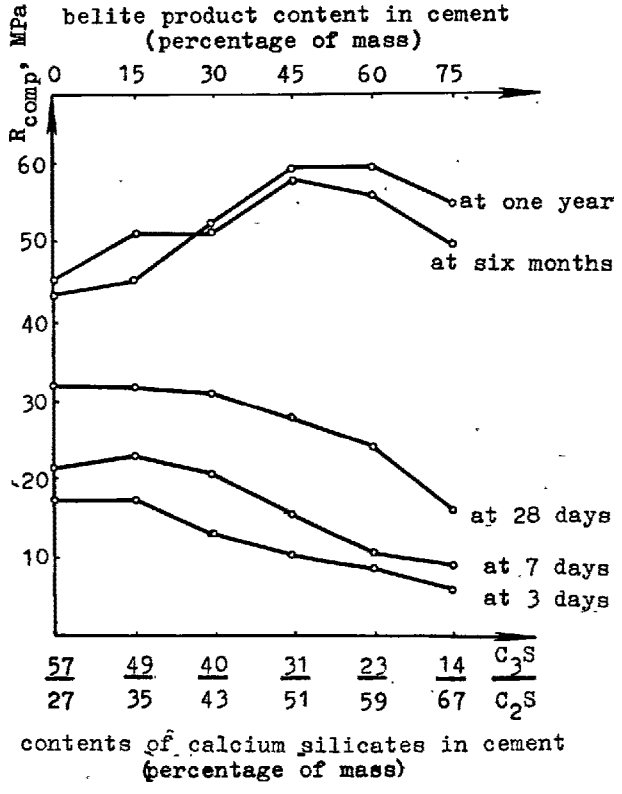

Fig. 4. The influence of nephelinic-slurry belite product and calcium silicate on BPC strength (R comp.).

hout admixtures, but at one to three months (and even at 7 days in the case of cement from the Volkhov factory) BPC having 40 to 45 percent of nephelinic slurry catches up with the strength values of control samples of Portland cement without admixtures and even surpasses them at later hardening stages.

At greater percentages (60-80%) of belite product, BPC reaches the strength of cement without admixtures at six months. But high alkali content (as in some of the cements from the Achinsk factory) keeps the strength values down (below 20 MPa) at all hardening stages. However, cements with up to 80 percent of belite, after wet-heat treatment and especially after autoclave treatment, allow to obtain articles of superior strength (39, 43).

Despite the different physico-mechanical conditions under which β-C_2S is formed in belite products and Portland cement clinkers, these belites are so similar that their hydration processes are very much alike both in kinetics and in the phase composition of new formations.

BPC strength values in Fig. 4 are shown to depend not only on belite product content, but also on the quantity of C_3S and the overall C_2S content in cement, including belite contained both in clinker and in belite product (42).

It follows that starting at three to seven days, technogenic belite takes an active part in cement stone strength formation.

As the overall C_2S content grows and the C_3S quantity is accordingly reduced, cement hardening rate slows down, but at later hydration stages strength values grow, e.g. at six months to one year, the maximum strength is observed in cements containing 20 to 30 percent of alite and 50 to 60 percent of belite.

It should be mentioned, however, that water-consumption rates in BPC, estimated on the basis of water content in normal consistency paste, are increased by 3 to 4 percent in the presence of 40 to 60 percent of belite product. But, according to P.I. Bozhenov, this has no effect on the water-consumption rates in the case of BPC-based concretes.

A special problem, as far as BPC is concerned, is a considerable reduction of setting time at higher belite product content. Already at 30 to 40 percent the setting time drops to the lowest level of 45 minutes allowed by GOST 10178-76. At 45 to 60 percent, setting starts 20 or 30 minutes after mixing.

An additional washing of slurry to remove the residual alkali aluminates permits to maintain the standard setting times in BPC containing 50 to 60 percent of belite product, but even in this case the beginning and the end of setting are observed much earlier than in control samples.

Fig. 5 shows the effect of water-soluble alkalis present in nephelinic slurry on the content of oxides, in particular of Al_2O_3, in the liquid phase during the hydration of slurry (44).

These data show that in the initial stages, water-soluble alkalis cause a sharp increase in the extraction of aluminate ions from the slurry and in their transition to the liquid phase, which results in the reduction of setting time. At the same time, the hydration of β -C_2S grains is considerably accelerated.

In order to avoid producing cements with non-standard setting times the industry still gives preference to the production of cements with up to 15 percent of belite product. General characteristics of industrial cements are given in Table 4.

All the cements are characterized by high bending strength which is 10 to 20 percent higher than in control Portland cements.

TABLE IV

Cement characteristics

Factory	Grade	Setting time, hours, minutes		Normal consistency, %	Strength, R comp.,MPa			
		Start	Finish		3d.	7d.	28d.	1 day (steaming)*
Achinsk factory	400	2^{02}	3^{10}	27.04	28.8	38.4	45	32.7
Volkhov factory	500	2^{50}	3^{40}	25.88	28.7	38.7	51.4	39.7

* As per schedule: 2+3+6+2hrs (preliminary curing + temperature rise + warming up at 85°C + cooling).

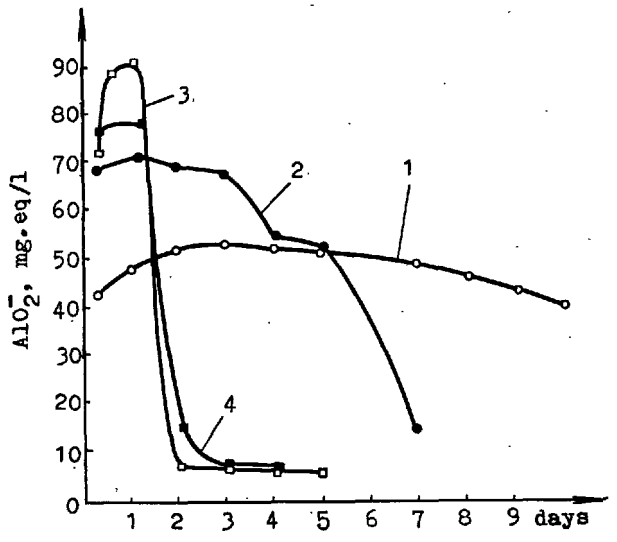

Fig. 5. The influence of water-soluble alkali content in the liquid phase during the hydration of belite product on Al_2O_3 content: 1-0.21%, 2-0.5%, 3-1.0% and 4-2.0% of R_2O (for Na_2O).

Cements having higher belite-product contents (30 to 60 percent) were produced at the Volkhov factory. At contents up to 30 percent cements were of Grade 400 to 500; at 40 percent, Grades 300 to 400 were obtained, and at 50 to 60 percent, cements were of Grade 300 (45).

Standard setting times were observed only in cements containing up to 30 percent of belite product. But the somewhat accelerated setting did not prevent the experimental cements from being successfully used by Leningrad factories producing prefabricated reinforced-concrete articles. High-quality articles were also produced from lightweight aggregate concrete. Despite some increase in the specific consumption of cement, economy in clinker used to produce concrete, if we consider the reduction of its content in cement, was 30 to 50 kg/cu.m.

Among other properties of BPC as a building and technical material a reduced heat-evolution during hydration, a lower water-separation rate, a sufficiently high corrosion and frost resistance and an ability to provide an increased water-tightness of concretes should be noted (40).

Concretes based on this type of cement are now intensively studied in particular their creep.

It should be noted that there is considerable progress in the technology of leaching of alumina sinters at Soviet alumina factories where nepheline is used. These improvements allow to raise the degree of alumina and alkali extraction and, what is of major importance to cement chemistry, to reduce accordingly the alkali content in the belite product.

A very interesting paper is presented at this congress (NIITsement) by Akunov, Dmitriyev, Makashev et al. concerning the possibility of increasing the strength of BPC by the method of jet pulverization instead of by grinding in traditional ball mills (46).

The authors also obtained positive results in applying this method to increase the strength of Portland cement containing 30 percent of γ-product.

At present nephelinic slurries are being used in cement industry mainly to produce clinker and to a lesser extent as an active mineral admixture for cements.

4. SPECIAL CEMENTS BASED ON TECHNOGENIC DICALCIUM SILICATE (BELITE PRODUCT). A low C_3A content in clinkers produced on the basis of nephelinic slurry, as well as high corrosion-resistence in cements with an admixture of technogenic belite product have drawn attention to the problem of using them to produce a sulphate-resistant cement.

To this end, the sulphate-resistance of the common Pikalevo clinker and that of an experimental highly siliceous clinker having a silicate modulus of 5.3 were studied. The latter was obtained by burning a bicomponent raw mix which was composed of nephelinic slurry and limestone (47). The common clinker and the highly siliceous clinker con-

tained, respectively, 4 and 2 percent of C_3A.

Cements based on these clinkers proved to be sulphate-resistant according to USSR standards, although the expected advantage of the experimental composition was not confirmed.

Practical application of clinkers based on belite slurry raw materials, and of belite product as an active component of sulphate resistant cements is difficult because of the high alkali content.

In order to overcome the adverse alkali effect, it is proposed to add small quantities of phosphorites to nepheline-containing raw mixes (0.8 to 1.5 percent of P_2O_5 in the mix) (48).

In control clinker, formation of C_8A_3 and $KC_{23}S_{12}$ alkali-containing phases was observed, with considerable presence of free lime. In phosphorous clinker, C_8A_3 or $KC_{23}S_{12}$ phases were not observed, but the presence of the $Na_4P_2O_7$ and $Mg_2(PO_4)F$ was noted. The aluminate phase, along with C_3A, contained $C_{12}A_7$, while the alumoferritic phase showed a shift towards C_6A_2F formation.

This controlled phase modification caused clinker strengths to increase by 4 to 13 MPa (28-day samples), while corrosion resistance which was tested in a 5-percent Na_2SO_4 solution and in sea water, was considerably improved. Longer setting times were also observed.

This method of overcoming the adverse alkali effect, although has not yet found practical application, is undoubtedly interesting.

The speedily developing production of oil and gas brought to the foreground the necessity of increasing the production of oil-well cements.

Oil and gas extraction from deep strata seems to be generally favoured throughout the world. This entails drilling of deep and superdeep wells in which temperature reaches hundreds of degrees and pressure is up to a thousand atmospheres. Common oil-well cements, including those used in hot wells, cannot be used under such conditions because they thicken easily and loss their mobility before plugging is completed and because of their low resistance in the extreme conditions of superdeep wells.

The Soviet practice is to use for such purposes cements based on blast-furnace granulated slags.

Investigations which have been carried out in the USSR show that oil-well cements with all the required technical properties may be obtained using technogenic belite products.

Several oil-well cement compositions for super-deep wells, their basic component being the technogenic belite by-product of alumina production from nepheline, were proposed by S.M. Royak and A.M. Dmitriyev (49).

The belito-siliceous oil-well cement (BSC) was prepared from a mix containing technogenic belite product and quartz sand at ratios from 70:30 to 30:70, which was ground to a specific surface of 2 to 4 thous.sq. cm/g.

It was found that at temperatures from 150 to 300°C and pressures from 500 to 700 atm. this cement hardened well without activizers such as Portland cement or gypsum. Setting times of BSC depend on the temperature of the medium. At temperature elevation from 105 to 200°C, the onset of setting was accelerated from 4 hrs 15 min to 1.5 hrs, which is within permissible limits. Additional retardation of the onset of setting (1.5 to 2 times) and an increased flow of oil-well mortars can be effected by adding up to 3 percent of bentonitic clay.

The strength of oil-well mortars was increased when the quartz sand content of BSC was raised to 30 percent. BSC prepared from a 70:30 mix of belite product and quartz sand reached its maximum strength of 45 to 50 MPa at 200°C. As the temperature and pressure were increased further, its strength decreased though it remained sufficiently high, up to 15-17 MPa at 300°C and 700 atm. A prolonged curing of hardened samples at this temperature did not cause any strength reduction.

Another BSC composition, along with belite product and quartz sand, includes acid blast-furnace slags. By changing the composition of cement, a product is obtained which can satisfy consumers both in terms of strength and in terms of setting time.

The composition of the new formations resulting from a prolonged steaming of BSC in an autoclave was studied by the method of X-ray structural thermography. The findings showed that both of the two basic components - belite product and quartz sand - take part in the processes of hydration and stone structure formation. Basic hydration products are low-base calcium hydrosilicates of the tobermorite type with minimum basicity of 0.8 (50). There are also unreacted β-C_2S grains and some quartz. No free lime was found in cement stone.

CONCLUSIONS

The present paper summarizes mostly research data and experience industrial utilization of technogenic dicalcium silicate (belite products) which have been so far accumulated in the USSR.

Unfortunately, at the time this paper was prepared, rather few sources were known in which similar work done in other countries was discussed. That is why the present review is not as complete as it could have been.

It is to be hoped, however, that in the course of the 7th International Congress on Chemistry of Cement, in discussing corresponding papers, this shortcoming will be overcome.

This hope seems to be well-founded, if one is to take into consideration the continually expanded production of aluminium, that "20th-century metal", from new kinds of alumina-containing raw materials and the insufficient resources of low-siliceous bauxites which still remain the basic source of alumina for aluminium production.

Extensive research by Soviet scientists and the practical experience of all-round utilisation of nephelines and in the future of similar alkaline alumosiliceous minerals in producing Portland cements in addition to alumina and alkali carbonates, will make it possible:
- to considerably extend the raw material base for the alumina, chemical and cement industries;
- to obtain, during the processing of nepheline into alumina and alkali carbonates, a technogenic belite by-product composed mainly of dicalcium silicate in the form of β-phase, which, on the strength of its physical and chemical properties, is the most effective material for the production of cement clinker and Portland cement;
- using the technogenic belite product, to realize a more economical, in terms of fuel, energy and raw materials, production of cement in relation to the traditional production based on carbonate and clay rocks;
- using the belite product, to develop an efficient production of (a) general-purpose cements of varying activity, including highly alitic and siliceous cements, and (b) special-purpose cements, such as sulphate-resistant cements, low-thermic cements, hydrotechnical and oil-well cements, where this technogenic material can be used as an active component both in cement raw mixes and in Portland cement.

Possibilities exist for extensive use of γ-products which are formed during the processing of alumina-containing materials by the non-alkaline method as a component in raw mixes.

On the strength of these research findings the USSR, for the first time in world practice acquired, apart from an industrially integrated, large-scale processing of nephelines by the alkaline sintering method into alumina, soda and potash, another large-scale and highly efficient production of cement from the technogenic belite by-products of the above-mentioned processing of nephelines.

According to the existing economic estimates, the combined nepheline-based production of alumina, soda products and cements allows to reduce specific investments by 20 to 25 percent and raw-material consumption by 25 to 30 percent, as compared to having a separate production of alumina and bauxites, of calcinated soda from salt solutions (sodium chloride) and limestone, and a separate production of cement based on traditional raw materials - carbonate and clayey rocks.

At the same time, an integrated and practically waste-free processing of nephelinic and similar, alkaline and non-alkaline, alumosiliceous rocks for alumina, cement and other products, stands for the maximum utilization of natural resources and is therefore, from the point of view of ecology, a more effective production process than the two separate processes of obtaining these products which result in the accumulation of many tons of unused waste (red slurry) from bauxite-based production of alumina, and of distillation slurries resulting from the production of soda out of limestone and rock salt.

ACKNOWLEDGEMENT

The author is grateful to Z.B. Entin and S.D. Makashev for assistence in preparation of this paper.

REFERENCES

1.- P.K.MEHTA (1978) "Energy, resources and the environment - a review of the US cement industry". World Cement Technology, 9, N° 5, 144-160 (en anglais).

2.- А.С.БОЛДЫРЕВ (1978) "Слово об отходах". Химия и жизнь, № 2 (1979) "Второй продукт" Социалистическая индустрия № 168 (en russe).

3.- Н.М.ЖАВОРОНКОВ, А.С.БОЛДЫРЕВ, Н.П.КОГАН, С.Д.МАКАШЕВ, О.П.МЧЕДЛОВ-ПЕТРОСЯН, А.А.ПАЩЕНКО, С.А.ФАТАЛИЕВ, Т.Ю. ШЕТКИНА (1979) "Теоретическое обоснование применения новых видов сырья в цементной промышленности". Доклады АН СССР, 245, № 3, 666-669 (en russe).

4.- В.Е.ОРЛОВ (1978) "Резервы народного хозяйства в использовании отходов производства" финансы СССР № 3, 11-15 , (en russe).

5.- В.И.САТАРИН (1976) "Шлакопортландцемент" УІ Международный конгресс по химии цемента, т. Ш, Москва, Стройиздат, (en russe).

6.- И.Н.КИТЛЕР, Ю.А.ЛАЙНЕР (1962) "Нефелины - комплексное сырье алюминиевой промышленности", Москва, "Металлургиздат", (en russe).

7.- С.Д.МАКАШЕВ (1946) "Комплексное производство цемента и окиси алюминия" Цемент (Ленинград), № 11-12, 8-15 , (en russe).

8.- Л.С.КОГАН, К.Н.ЗИЛЬБЕРМАН, Е.В.РЕБРИК (1956) "Применение в цементном производстве отхода алюминиевой промышленности - белитового шлама", Ленинград, "Промстройиздат", (en russe).

9.- А.С.БОЛДЫРЕВ (1938) Комплексное производство окиси алюминия, соды и портландцемента из нефелина, Цемент , Ленинград, № 3, (en russe).

10- А.И.БЕЛЯЕВ (1947) Производство легких

металлов. Алюминиевая промышленность. В кн. "Цветная металлургия центральной и восточной Германии" Под редакцией В.А. Флорова. Гос.научно-техн. изд. литературы по черной и цветной металлургии, Москва, (en russe).

II.- Н.В.БЕЛОВ (1954) Труды Института кристаллографии АН СССР, вып. 10, 6, (en russe).

I2.- R.W.NURSE (1954) III International Symposium on the Chemistry of Cement. London, (1952) General Report, London , HMSO, (en anglais).

I3.- А.И.БОЙКОВА (1974) "Твердые растворы цементных минералов", Ленинград, "Наука", (en russe).

I4.- M.REGOURD, A.GUINIER (1974) "The Crystal Chemistry of Portland Cement Clinker Components", VI International Congress of the Chemistry of Cement, Moscow, 1974, General Report, ed. VNIIESM, (en anglais).

I5.- П.П.БУДНИКОВ, В.А.БРОН, Л.Б.ХОРОШАВИН (I96I) "Двухкальциевый силикат и его свойства" Труды МХТИ им.Д.И.Менделеева, № 36, I5-43, (en russe).

I6.- D.K.SMITH, A.J.MAJUMDAR, F.ORDWAY (1965) "The crystal structure of γ-C_2S", Acta Crystallographica, v.18, 785-795, (en anglais).

I7.- H.LEHMANN, K.NIESEL, P.THORMANN (1969) "Der Modifikationsstabilitätgereich von Dicalcium Silicates", Tonindustrie - Zeitung , B. 93, N° 6, 197-209 (en allemand).

I8.- Ю.Ф.ХНЫКИН, В.В.ТИМАШЕВ, Ю.С. МАЛИНИН, В.П.РЯЗИН (I97I) "Влияние P_2O_5 на фазовый состав портландцементного клинкера" Сб. "Силикаты". Труды МХТИ им.Д.И.Менделеева № 68, (en russe).

I9.- Ю.Ф.ХНЫКИН, В.В.ТИМАШЕВ, Ю.С.МАЛИНИН, В.П.РЯЗИН (I973) "О фосфорсодержащих фазах портландцементного клинкера", Сб. "Силикаты", Труды МХТИ им.Д.И.Менделеева № 72, (en russe).

20.- M.HIRAI, M.YANAGI (1968) "Formation of belite burned in the presence of Al_2O_3 and Na_2SO_4", Revue of the 22-th Gen. Meeting of Cement Association Industry, Tokyo, (en anglais).

2I.- Н.И.ЕРЕМИН, А.И.ЕГОРОВА, Г.Г.ДМИТРИЕВА, И.Б.ФИРФАРОВА (I970) "Исследование твердых растворов C_2S с окислами некоторых металлов", Журнал прикладной химии, Ленинград, № 43, № I, (en russe).

22.- И.В.ГОРШКОВА, В.Г.САВЕЛЬЕВ, Т.Н.КИШИШЯН (I976) "Стабилизация структуры неустойчивых при нормальной температуре форм ортосиликатов кальция соединениями натрия", Сб."Структура технических силикатов", Труды МХТИ им.Д.И.Менделеева № 92, (en russe).

23.- Х.Н.НУРМАГАМБЕТОВ, С.А.ШЕРБАН (I97I) Журнал прикладной химии, Ленинград , 44, № 7, I467, (en russe).

24.- Х.Н.НУРМАГАМБЕТОВ, С.А.ШЕРБАН, В.А.БЕЛОУСОВА (I972) "Исследование структуры двухкальциевого силиката в спеках и шламах глиноземных заводов". Цветные металлы № 8, 37-4I, (en russe).

25.- Н.С.МАЛЫЦ, Ж.Д.ЗИНКЕВИЧ, О.И.АРАКЕЛЯН (I975) "Влияние условий выщелачивания спека на степень разложения β-C_2S, соотношение образующихся фаз и состав гидрогранатов", Цветные металлы № I, 36-40, (en russe).

26.- М.В.КОУГИЯ (I978) "Двухкальциевый силикат в шламах-отходах глиноземного производства", Краткие тезисы докладов на У Всесоюзном научно-техническом совещании по химии и технологии цемента (Москва, 26-29 сентября I978г.), НИИЦемент, ВНИИЭСМ, (en russe).

27.- Т.М.БЕРКОВИЧ, Г.С.БЛОХ, Т.И.ГРАЧЕВА, Г.С.МАРГОЛИНА, Л.С.ГРИШИНА, А.А.ШЛОМЕНКО, С.И.КАЗАНЦЕВА (I978) "Кристаллохимические особенности портландцементов для производства асбестоцементных изделий", Краткие тезисы докладов на У Всесоюзном научно-техническом совещании по химии и технологии цемента (Москва, 26-29 сентября I978г.) НИИЦемент, ВНИИЭСМ, (en russe).

28.- А.А.ЧИСТЯКОВА, М.В.КОУГИЯ "Свойства нефелиновых шламов, получаемых при переработке различного исходного сырья" Цемент, Ленинград, № I0, 20-2I, (en russe).

29.- П.И.БОЖЕНОВ, Б.А.ГРИГОРЬЕВ, Г.И.ОВЧАРЕНКО (I978) "К проблеме вяжущих свойств на основе ортосиликата кальция", Краткие тезисы докладов на У Всесоюзном научно-техническом совещании по химии и технологии цемента (Москва, 26-29 сентября I978г.) НИИЦемент , ВНИИЭСМ, (en russe).

30.- У.И.ПАПИАШВИЛИ (I974) "Электронномикроскопическое исследование особенностей структуры портландцементного клинкера и продуктов его взаимодействия с водой" Диссертация, НИИЦемент, Москва, (en russe).

3I.- М.М.СЫЧЕВ, В.И.КОРНЕЕВ, Н.С.ШМОРГУНЕНКО и др. (I974) "Комплексная переработка нефелинового шлама", Москва , "Металлургия", (en russe).

32.- Л.А.КРОЙЧУК, В.Н.НЕСТЕРОВА, С.М.РОЯК, Е.М.СТЕШЕНКО (I963) "Обжиг двухкомпонентной шихты" Цемент, Ленинград, № 3, 8-I0, (en russe).

33.- Н.А.САФОНОВ, И.А.СЕМЧЕНКО, Е.А.ЗОТОВА (I979) "Особенности переработки сырьевых шихт, содержащих белитовый шлам", Цемент, Ленинград, № 3, I3-I4, (en russe).

34.- В.К.КЛАССЕН, В.И.БЕЛЯЕВА (I976) "Особенности процессов клинкерообразования в мощных вращающихся печах при обжиге шихты на основе нефелинового шлама" Труды Московского инженерно-строительного института (сокращенно - МИСИ) им.Куйбышева и Белгородского технологического института строительных материалов (сокращенно - БТИСМ) № 23, (en russe).

35.- Е.ГЖИМЕК (I976) "Комплексные методы производства цемента" (Основной доклад) УI Международный конгресс по химии цемента, Москва, "Стройиздат", т. Ш, 328-345, (en russe).

36.- Н.И.ЕРЕМИН, Г.З.НАСЫРОВ, П.С.ПЕТЕЛЬКО и др. (I978) "Переработка минеральной части угля Экибастузского месторождения на глинозем и цемент методом спекания", "Комплексное использование минерального сырья", ноябрь № 5, стр.62-68, (en russe).

37.- Д.Г.ЯРОШЕНКО, Л.А.ПРОШИНА, С.Б.ШАЖНИКОВ (I979) "Пути использования экибастузских зол и шлаков в народном хозяйстве", Комплексное использование сырья, июль, № 7, стр. 72-77, (en russe).

38.- И.А.СЕМЧЕНКО, Е.А.ЗОТОВА, М.М.СЫЧЕВ (I978) "Особенности получения высокоактивного клинкера на основе γ-C_2S - шлама. Краткие тезисы докладов на У Всесоюзном совещании по химии и технологии цемента. (Москва, 26-29 сентября I978г.), НИИЦемент, ВНИИЭСМ, (en russe).

39.- П.И.БОЖЕНОВ, В.И.КАВАЛЕРОВА (I966) "Нефелиновые шламы", Ленинград, Стройиздат, (en russe).

40.- П.И.БОЖЕНОВ, А.Р.АЛЛИК, М.А.АСТАХОВА, Б.И.ПОДОБРЯНСКАЯ, Б.З.ЧИСТЯКОВ, Н.П. ШТЕЙЕРТ (I974) "Технические свойства нефелиновых цементов", Труды Гипроцемента № 42, 70-85, (en russe).

4I.- М.А.АСТАХОВА, Н.П.ШТЕЙЕРТ, Б.И.ПОДОБРЯНСКАЯ, Б.З.ЧИСТЯКОВ (I970) "Нефелиновые цементы" Цемент, Ленинград, № I2, II-I2, (en russe).

42.- Б.В.ВОЛКОНСКИЙ, С.Д.МАКАШЕВ (I976) Дискуссия, УI Международный конгресс по химии цемента, Москва, I974, Стройиздат, т. Ш, 346-347, (en russe).

43.- Б.З.ЧИСТЯКОВ (I978) "Особенности и преимущества использования нефелинового цемента в строительстве" Цемент, Ленинград, № 5, I0-II, (en russe).

44.- И.И.КУРБАТОВА, В.С.КОШИЛЕВИЧ, В.Г.АБРАМКИНА (I979) "Влияние щелочей на гидравлическую активность белитового шлама" Цемент, Ленинград, № 2, 2I-22, (en russe).

45.- В.М.ДОРОДНОВ (I978) "Опыт использования на Волховском алюминиевом заводе белитового шлама в качестве добавки при помоле цемента", Краткие тезисы докладов на У Всесоюзном совещании по химии и технологии цемента, (26-29 сентября I978г.) НИИЦемент, ВНИИЭСМ, (en russe).

46.- В.И.АКУНОВ, Ю.И.ДЕШКО, С.Д.МАКАШЕВ, Г.П.ЛИТВИНОВ (I978) "Струйное измельчение - эффективный метод повышения гидратационной активности белитового шлама", Ibid., (en russe).

47.- С.И.ДАНЮШЕВСКИЙ, Н.А.САФОНОВ, Е.В. РЕБРИК, Д.А.МИХАЙЛОВА (I974) "О некоторых технических свойствах высококремнеземистых клинкеров на основе белитового шлама" Труды Гипроцемента, № 42, I0I-I26, (en russe).

48.- В.В.ТИМАШЕВ, Т.Я.ГАЛЬПЕРИНА, С.Н.БЫКОВА, Л.М.СЕВОСТЬЯНОВА, Н.Ф.ЯНЬКОВ (I979) "Влияние фосфора на фазовый состав и свойства цемента, получаемого из высокощелочного сырья" Цемент, Ленинград, № 3, 6-7, (en russe).

49.- С.М.РОЯК, А.М.ДМИТРИЕВ (I96I) "О вяжущем материале для цементирования глубоких скважин", Нефтяное хозяйство № 7, (en russe).

50.- Ю.М.БУТТ, Л.Н.РАШКОВИЧ (I96I) "Твердение вяжущих при повышенных температурах", Москва, Стройиздат, (en russe).

THEME VI

Cement pastes : rheology, evolution of the properties and structures

SUB-THEME VI-1

Structure formation and development in hardened cement pastes

P. J. SEREDA
R. F. FELDMAN
V. S. RAMACHANDRAN

Conseil National de
Recherche du Canada
Ottawa - CANADA

1. FORMATION OF CEMENTITIOUS BONDS

1.1 INTRODUCTION

A binder is defined in the Handbook of Adhesives (1) as "a component of an adhesive composition that is primarily responsible for the adhesive forces which hold two bodies together." In cements the property that enables a binder to act in this capacity is also responsible for the formation of a cohesive structure and, because it is usually a multi-component system, it is not obvious which component is the binder. Of course, it may be that the same component, or combination of components, may serve both as the structure (grain or micro unit) and the binder (intergranular material).

In cement research, the strength and modulus of the unit or system, rather than its bond strength, has special significance. This is understandable because the cementitious binders based on portland cement consist of submicroscopic, colloidal-like particles, produced from supersaturated solutions, and which form a porous, interconnected network. The structure formation is a very complex process and it is difficult to define the grain, micro-unit or particle and the product at the boundary. Where these are crystalline and single component as in gypsum, the interparticle bond may resemble the grain boundary in ceramic materials. Because of this complexity, it is useful to maintain the concept of intraparticle and interparticle bonds.

It is the porous nature coupled with the indefinable stress concentration regime of the cementitious binders that undoubtedly presents the greatest difficulty in defining and measuring the nature of the bond. The measured value of strength cannot be reduced to a value of bond strength without a measure of bond area, a parameter difficult to measure. Many of the mechanical properties correlate with porosity and this, along with other data, enables comparison of results obtained by various workers.

Because hydration products are colloidal in size when first formed, models of other colloidal systems or gels (xerogel) have often been used to describe the nature of the structure of hydrated cement, especially to explain the nature of the bonds. Whether such models represent the structure of hydrated cement depends on whether their physical and mechanical behaviour is similar with respect to all the available experimental evidence. In such complex systems one cannot accept evidence of similarity on the basis of one type of measurement. The authors have strived to provide a body of experimental evidence for a variety of similar and dissimilar cementitious systems, including compacted porous materials, showing physical and mechanical similarities and differences, to provide a basis for an evaluation of the structures of these different systems.

This paper will attempt to assess the available information with these criteria in mind. Mention will also be made of those parts of the knowledge system in this area which are as yet unknown.

1.2 BINDING SYSTEMS - NATURE OF BONDS

It is useful to use the term "binders" as it emphasizes the importance of the nature of bonds in a cementitious material. The question as to what kinds of bonds exist in cement paste has been discussed for a long time but little progress has been made because the greatest emphasis for practical applications has always been on strength and because the problem of measuring bond strength is very difficult.

Rehbinder et al (2) formulated theories for hardening of binders and stated that crystallization contacts are associated with the process of crystal coalescence, which is controlled by a given level of supersaturation. They suggested that there is a balance between the supersaturation level in the surrounding medium and the mechanical effort to maintain the crystals in a certain fixed position relative to each other. Thus internal strain is related to the pressure associated with the constrained crystal growth in a supersaturated solution. Strength increase is observed under conditions conducive to reduce internal strain. Presence of strain in hydrating systems is possible since all such reactions result in a molar volume increase. A study by Gillott and Sereda (3) showed that $Ca(OH)_2$ crystals undergo considerable strain during the hydration process. Evidence of this was found in X-ray diffraction transmission Laue photographs of $Ca(OH)_2$ crystals.

Sychev (4) has dealt with the structure formation as a synthesis of a solid body through condensation of a disperse system. He tried to link the binding property of the hydrating system with products having polar groups, and also to verify that the first step of hardening is associated with the "constrained state" when particles are brought together so close that long-range forces can begin to act and the polar groups in the surfaces can serve as a crystallization contact or valency nature.

This theory suggests that bonds are based on the superficial chemical "stitching-up" by water molecules and thus saturate the ionic fields of the surfaces brought close together. According to Sychev, this bond can be strong only when there is a low concentration of water at the contact faces; this is possible during the active hydration

(reaction) stages due to the withdrawal of water to the reacting material.

Ubelhack and Wittman (5) concluded that thin films of water occupy the interparticle bond area. These water films exhibit a high degree of ordering due to surface force interaction, creating the so-called disjoining pressure. The work of these authors, based on measurements of Mossbauer spectrum on samples of "xerogel of hydrated cement doped with calcium ferrite hydrates," is difficult to assess because they do not characterize the samples adequately to enable comparison with work of other researchers.

Wittman et al (6) obtained from Mossbauer measurement values of the coupling constant for samples of hydrated cement hydrogel. These values were found to decrease from 2×10^5 dyn/cm at 0% relative humidity (RH), 1.4×10^5 dyn/cm at 55% RH, to 0.8×10^5 dyn/cm at 100% RH, which is consistent with the idea that water enters the system (including the interlayer spaces) and separates surfaces. That the modulus increases to a highest value at 100% RH, as observed by Wittman (7), can be explained, based on the fact that the water enters interlayer spaces where it reinforces the system by its interaction with the two layers. However, Wittman and Setzer (8) consider that the strength originates partly in chemical bonding which is not influenced by moisture. They estimate that about 50% of the total bond strength can be attributed to van der Waals' interactions, but give no explanation for this. Their explanation of the increased modulus in the high relative humidity region is based on a two-component system, with water constituting one of the components.

These theories do not appear to have considered the theory of bond formation that involves consolidation of a dispersed system to form solid-to-solid contacts followed by polymerization of SiOH groups of the silicic acid. Collepardi (9) proposed the formation of Si-O-Si bonds by the interaction of SiOH + HO-Si. This conclusion is based on a study of pore sizes and surface area (N_2 adsorption) and the changes with time, temperature and admixtures. For example, Collepardi attributes the decrease in porosity and surface area to the formation of solid-solid contacts.

Various ideas regarding the structure formation and its bonds admit the possibility of both the chemical and physical nature of bonds and does not make any clear-cut distinction between the nature of the intraparticle bonds and interparticle (intergranular) bonds.

Sereda et al (10) studied the effect of different levels of relative humidity on the elastic modulus and also applied the cold compaction technique of breaking and making bonds. This study showed that Young's modulus increased as the dry cement paste was exposed to progressively higher levels of relative humidity beyond about 50%, as was also reported by Wittman (7). This was unexpected because it does not fit the description presented by most previous authors of the nature of this system, namely, that the structure was formed from "gel"-sized particles coalescing but maintaining layers of water at points of contact (although some chemical bonds were postulated because of the limited swelling). Such a system should show a decreasing modulus as water is adsorbed unless it is assumed that this water is interlayer water and has characteristics different than that of sorbed water. Sorbed water causes a decrease in modulus in the case of hydrogen bonded systems, such as acetate silk or cellulose.

A comparison of the behaviour of cement paste at different levels of relative humidity with that of a high surface area material such as porous glass demonstrates that, although the porous glass has a surface area of 175 m^2/g and pore radius of 20Å (similar to cement "gel"), its modulus does not change over the entire range of relative humidities from 0 to 100% despite an expansion of 0.25% (11).

From these considerations, it must be concluded that water adsorbed in cement paste does not behave simply as surface adsorbed water, as in the case of porous glass, nor does it attenuate the bonds, as in the case of cellulose, but that most probably water enters the intraparticle bond area where it acts to reinforce the bonds. This conclusion was the basis for a model for the hydrated cement paste system presented by Feldman and Sereda (12). This model accounts for the highest modulus at 100% RH due to maximum influence of water on intraparticle bonds and no influence on the interparticle bond or contacts. Strength from interparticle bonds is highest at the dry state and suffers a moderate decrease when approximately a monolayer of water is introduced due to the crack propagation process that is characteristic of bodies with "fused" contacts.

The technique of cold compaction and recompaction of hydrated products has been used to provide evidence regarding the nature of bonds and structure that can be produced in this way and enable comparison of the bonds resulting from the structure formation during the hydration reations (13).

In the case of the cement paste material, the modulus and microhardness give the same values for a significant range of porosities whether the material samples are compacted, recompacted or cast-in-situ. This can be explained by considering that the micro-units or particles made up of a system of interlayer C-S-H sheets with their complement of interlayer water were the same in each case because none was dried below a condition of 30% RH. The compaction process produced interparticle bonds similar in nature to those produced by the hydration process; this might lead to the conclusion that these bonds represent contacts of random nature between solid surfaces. Recent work by Marchese (14) presents evidence, using the scanning electron microscope, of fracture surfaces that present strong adhesion between C-S-H gel and $Ca(OH)_2$ masses in alite paste, confirming the above idea.

Using the compaction technique, Feldman (15) has studied the contribution of interlayer water on bond formation as measured by Young's modulus. Two series of compacted samples in the porosity range of 10 to 60% were made: Series B made from bottle hydrated cement dried to 30% RH, and Series A from the same material dried to d-dried condition. Figure 1.1 gives the sequence of wetting and drying to which the two series of compacted samples, prepared at 11% porosity, were exposed. The values for Young's modulus at each condition are given.

Series B, hydrated cement compacted with interlayer water intact, and Series A, compacted with interlayer water removed (d-dried) both give high values of modulus. However, when series B samples are dried the modulus decreases by about one half. No change occurs to the modulus of series A samples on wetting but they, too, suffer a loss in modulus when dried again.

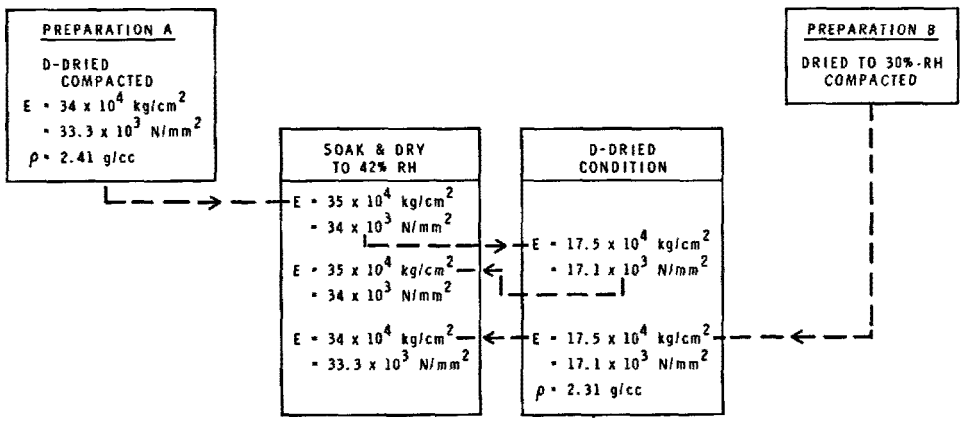

Fig. 1.1 - Sequence of conditioning and testing (15)

The role of interlayer water in this sequence of measurements is that of contributing to the bonding, perhaps by coordinating with calcium ions which are present between the sheets. It is also evident that compaction of the d-dried material can bring the layers close together and so increase the surface-to-surface interaction. The result of this is that the value of modulus is about the same as obtained for the system with interlayer water. The higher density product of 2.41 g/cc obtained when compacting d-dried hydrated cement (Fig. 1.2), confirms the explanation given above.

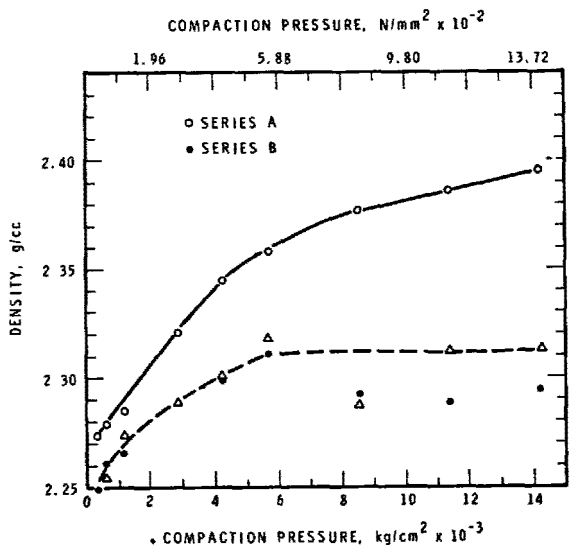

Fig. 1.2 - Density vs compaction pressure for bottle hydrated cement.

1.3 BOND STRENGTH AND MATERIAL STRENGTH

From the practical point of view, bond strength as such may not have any significance. It is the material strength, which is the value obtained in tests, that can be used in all design calculations.

If it were possible to obtain by measurement the total interparticle contact area, it would be easy to relate the material strength to bond strength. Although this is impossible as yet, some indirect measurements such as change in surface area have been made by Collepardi (9).

When strength of a material is related to the total porosity, one obtains a characteristic that is probably related to bond strength and contact area. Where modulus, hardness or strength is determined for samples at any one porosity, the results do not characterize that property and cannot be used to compare such a material as a binder with any other material. This is a feature of porous materials that does not apply to non-porous materials, and must not be overlooked. Much information in the current literature has not considered this and is, therefore, of limited use.

When considering contact (bond) area, it must be remembered that size of particles plays a very important role. For example, when a model of uniform diameter particles is considered in a hexagonal, close-packed arrangement, the surface area per unit mass (assuming a density of 2.4 g/cm^3) is related to particle diameter (Fig. 1.3). It is obvious that, for the same porosity, as the particle diameter decreases

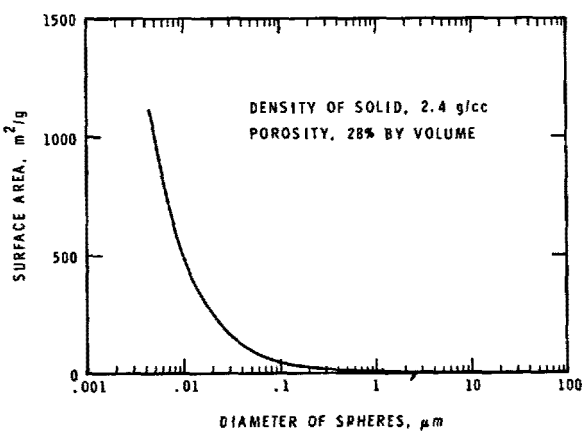

Fig. 1.3 - Relation of diameter of spheres to their surface area in a hexagonal close-packed system

and surface area increases, the area of effective contact (where surfaces are within the field of force of long-range forces) increases.. This is the situation with cement gel which is first produced as sub-microscopic particles of various shapes and includes silicate sheets with a surface area of over 700 m^2/g (Winslow and Diamond (16)). This fact and the presence of stress generated by the hydrating reaction (as discussed in 1.2), provides the conditions for the formation of a structure that has considerable contact area between particles.

Most binders can be characterized by a relationship of the mechanical properties to porosity. This relationship may represent the bond strength or nature of the bond. In this regard the microhardness appears particularly useful because it seems to give the characteristic behaviour that is observed with flexure strength when the material is tested at different levels of relative humidity. Microhardness measurement must involve, wholly or in part, the progressive breaking of bonds between particles as well as fracturing of particles as the pyramid indenter penetrates the porous material. The work by Sereda (17) has shown that even different preparations of gypsum representing different morphologies of the crystals when compacted could be characterized by the hardness-to-porosity relationship, as shown in Fig. 1.4.

Using microhardness techniques, Beaudoin (18) characterized various binding cements by a hardness-to-porosity relationship (Fig. 1.5). From this relationship it can be seen that magnesium oxychloride provides the strongest structure, with normal portland cement ranking second, and magnesium oxysulfate cement ranking the lowest.

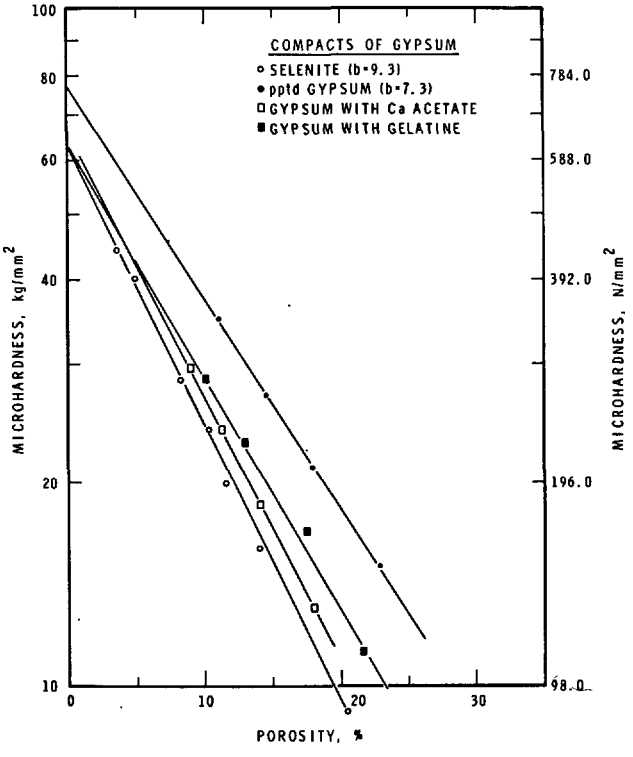

Fig. 1.4 - Microhardness vs porosity for compacts of different samples of gypsum (17)

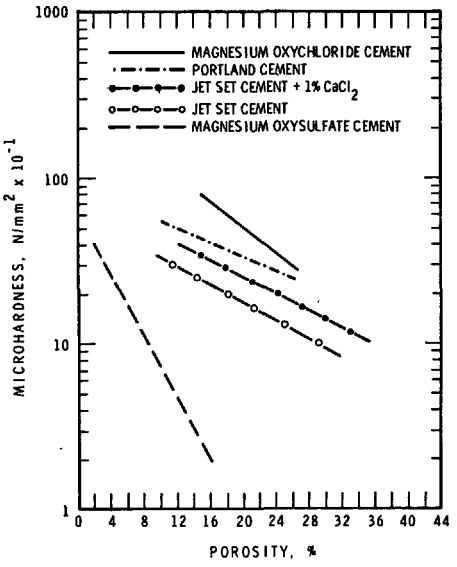

Fig. 1.5 - Microhardness vs porosity for several inorganic cementitious systems (18)

Bache (19) developed a model for the strength of a brittle material built up of particles joined at points of contact. In this model, the particles are large in relation to contact area. In the derivation of the equation to represent strength, the assumption is made that the mechanical properties of the contact area are the same as that of the particle. This is essentially the assumption made in dealing with polycrystalline ceramic materials. The relation between strength and the volume concentration of cement in mortars made from silica "fines" and cement as obtained by Bache, agreed well with his theoretical equation.

Attempts have been made to predict the strength of cement paste by analysing various parameters of this system. Polak (20) derived a series of equations where the strength of the hardened system is a function of 12 parameters forming 4 dimensionless complexes. In this analysis the structure is defined by chemical and mineralogical composition, system geometry and force bonds derived from the structure of the material and the structure of its porous space. He suggests that 14 experiments are required to determine the parameters for use in the mathematical analysis but it is not clear what these experiments are. Grudemo (21) stated that, "The theoretical treatment of the strength vs structure relationship of such a system containing several solid phases in a non-random arrangement, and pores of various types in unknown proportions, is certainly very complex, if not impossible." However, he subsequently derived equations to relate properties with porosity. In this analysis (22) he does not include the influence of stress concentrations, or variation in stress intensity factors due to differences in pore shape or due to the heterogeneous distribution of matter in the solid phase including internal microstructural arrangements.

Lawrence et al (23) studied physical properties of hydrated tricalcium and β-dicalcium silicate pastes where the microstructures were altered by the use of

admixtures and by temperature variations during hydration. Thus tensile strength was compared for a range of microstructures and was found to be uninfluenced by large changes in outer C-S-H morphology induced by admixtures. They concluded that strength development in C_3S pastes appears to depend primarily on the total capillary porosity and that changes in microstructure have little influence on strength. Although this result agrees with those of others--that porosity is an important parameter in determining strength--their conclusion appears to be in conflict with work where unique strength vs porosity curves were obtained for different preparations representing different morphologies (as discussed in Section 2). Perhaps the result of Lawrence et al (23) is fortuitous due to the fact that only one W/C ratio was used in the preparation of the samples.

1.4 MICROSTRUCTURE AND BONDS

Since the emergence of the scanning electron microscope, a large number of micrographs have been published which show a range of morphologies of hydrated cement products. Diamond (24) summarized the information and proposed a classification based on 4 types of morphologies. It should be recognized, however, that it would be useful if an estimate were provided of the amounts of the different products characterized by a type of morphology in the microstructures, as stressed by Grattan-Bellew et al (25). In examining a system so lacking in distinct features as hydrated C-S-H, there is a tendency to concentrate on certain morphological features that may not represent the whole subject.

Most of the evidence from microstructural examination can be used to compare or characterize the particular samples under study but fails to indicate, even semi-quantitatively, when a given material is strong or weak, stable or unstable. When microscopic examination is used as evidence for structure formation, there is a tendency to use the information obtained at the beginning of the hydration process (at the time when the morphologies of the different products are distinct). Thus it is assumed that the microstructure and the process responsible for it are the same at the beginning and at the end. All evidence points to the conclusion that this assumption is invalid and that the nature of the first product formed and the process causing it to form is more than likely very different from the final product and process. For example, work by Double and Hellawell (26) concluded that, at the start, the hydration process is driven by osmotic pressure occurring in fibrils which are tubular. This may not be a property that is relevant to the mature structure.

1.5 COMPACTION - STRUCTURE FORMATION

As an aid to a better understanding of the behaviour and properties of porous materials, the authors have used cold compaction of various powders for the past 15 years to produce porous bodies as "models" from various materials, ranging from sodium chloride, gypsum, sulfur, to a variety of cementitious binders. In the numerous experimental studies where this technique was used to prepare samples, the purpose was to provide a series of rigid, porous samples of varying porosity, thus enabling this parameter to be tested in relation to other properties such as sorption, dimensional change, modulus, hardness, and response to changing environmental conditions of various materials available as powders.

Compacted samples of calcium carbonate, silica gel, and molecular sieves were used successfully by Sereda and Feldman (27) and compacted samples of hydrated portland cement, by Feldman (28) to show the relation between sorption of water and dimensional change and to confirm the Bangham relation where simple adsorption occurs.

Compacted samples have been used effectively to study volume changes associated with hydration reactions of such materials as MgO (29) where it was shown that the expansion of the compact is related to the concentration of MgO in lime. Similarly, the expansion of gypsum plaster on hydration was determined by means of compacts (30) where it was shown that expansion was related to initial porosity and temperature as shown in Fig. 1.6.

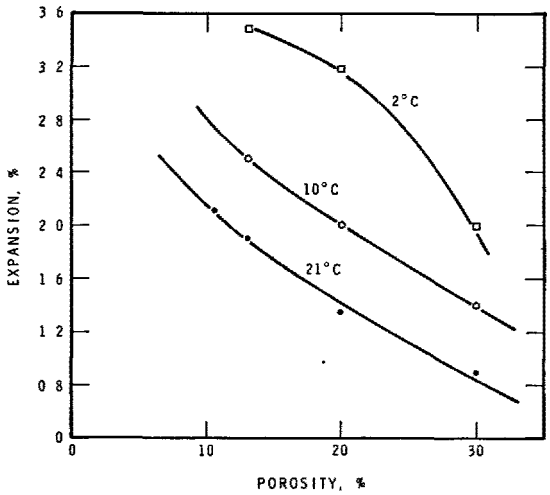

Fig. 1.6 - Expansion of pottery plaster as a function of porosity and temperature (30)

The compaction technique was also used to study the nature of bonds in portland cement system and gypsum system, as discussed in the previous section (13,31).

To show the significance of microhardness measurement in characterizing different binders, Sereda (17) used compacted samples where it was possible to distinguish between different preparations of gypsum (see Fig. 1.4).

Hot pressing of unhydrated cement followed by hydration was shown by Roy et al (32) to be a successful technique to produce samples of hydrated cement of very low porosity and very high strength.

It can be concluded that compaction technique can be a useful tool to study porous materials, especially the hydrated cementitious sytems.

REFERENCES (SECTION 1)

1.- I. SKEIST (1963), "Handbook of adhesives," Reinhold Publishing Corp., Chapman and Hall Ltd., London, p.x of Glossary.

2.- P.A. REHBINDER, E.E. SEGALOVA, E.A. AMELINA, E.P. ANDREEVA, S.I. KONTOROWICH, O.I. LUKYANOVA, E.S. SOLOVYEVA, and E.D. SHCHUKIN (1974), "Physico-chemical aspects of hydration hardening of binders," Proc. Sixth Int. Congr., Chem of Cement, Moscow, Vol. II, book 1, 58-64.

3.- J.E. GILLOTT and P.J. SEREDA (1966), "Strain in crystals detected by X-rays," Nature, 209 (5018), 34-36.

4.- M.M. SYCHEV (1974), "Regularities of binding property manifestation," Proc. Sixth Int. Congr., Chem. of Cement, Moscow, Vol. II, book 1, 42-57.

5.- H.J. UBELHACK and F.H. WITTMAN (1976), "Dynamics of the development of structures in colloids and Brownian motion," J. de Phys., p. C6-269 to C6-271; also "Coupling of colloid particles and recoilless fraction," J. de Phys., p. C6-273-276.

6.- F.H. WITTMAN, U. PUCHNER and H. UBELHACK (1975), "Properties of colloidal particles in hardened cement paste and the relation to mechanical behaviour," Int. Proc. Congr., Colloid and Surface Chemistry (IUPAC), Budapest/Ungarn.

7.- F.H. WITTMAN (1973), "Interaction of hardened cement paste and water," J. Amer. Ceram. Soc. 56, 409-415.

8.- M.J. SETZER and F.H. WITTMAN (1974), "Surface energy and mechanical behaviour of hardened cement paste," Appl. Phys. 3, 403-409.

9.- M. COLLEPARDI (1973), "Pore structure of hydrated tricalcium silicate," Proc. Int. Congr., Colloid and Surface Chemistry (IUPAC), Prague, Vol. 1, B25-B49.

10.- P.J. SEREDA, R.F. FELDMAN and E.G. SWENSEN (1966), "Effect of sorbed water on some mechanical properties of hydrated portland cement pastes and compacts," Highway Research Board, Special Report 90, Washington, p. 58-73.

11.- P.J. SEREDA (1978), "The instability of hydrated portland cement," published in Epitoanyag 40, 147-153.

12.- R.F. FELDMAN and P.J. SEREDA (1968), "A model for hydrated portland cement paste as deduced from sorption length change and mechanical properties," Matériaux et Constructions 1, 509-520.

13.- I. SOROKA and P.J. SEREDA (1968), "The structure of cement-stone and the use of compacts as structural models," In Proc. Fifth Int. Symp., Chem. of Cement, Part III, Vol. III, 67-73, Tokyo.

14.- B. MARCHESE (1977), "SEM topography of twin fracture surfaces of alite pastes 3 years old," Cem. Concr. Res. 7, 9-17.

15.- R.F. FELDMAN (1972), "Factors affecting the Young's modulus-porosity relation of hydrated portland cement compacts," Cem. Concr. Res. 2, 375-386.

16.- D.N. WINSLOW and S. DIAMOND (1974), "Specific surface of hardened cement paste as determined by small-angle X-ray scattering," J. Amer. Ceram. Soc. 57, 193-197.

17.- P.J. SEREDA (1972), "Significance of microhardness of porous inorganic materials," Cem. Concr. Res. 2, 717-729.

18.- J.J. BEAUDOIN,"Porosity measurement by high pressure mercury intrusion - microstructural limitations," (In preparation.)

19.- H.H. BACHE (1970), "Model for strength of brittle materials built up of particles joined at points of contact," J. Amer. Ceram. Soc. 53, 654-658.

20.- A.F. POLOK (1974), "Kinetics of cement stone structure formation," Proc. Sixth Int. Congr., Chem. of Cement, Moscow, Vol. II, book 1, 64-73.

21.- A. GRUDEMO (1974), "Strength vs structure in cement paste," Proc. Sixth Int. Congr., Chem. of Cement, Moscow.

22.- A GRUDEMO (1979), "Microcracks, fracture mechanics and strength of the cement paste matrix," Cem. Concr. Res. 9, 19-34.

23.- F.V. LAWRENCE, J.F. YOUNG and R.L. BERGER (1977), "Hydration and properties of calcium silicate pastes," Cem. Concr. Res. 7, 369-377.

24.- S. DIAMOND (1976), "Cement paste microstructure - an overview at several levels," Proc. of a Conference on Hydraulic Cement Pastes: Their Structure and Properties, held at Univ. of Sheffield, p. 2-30.

25.- P.E. GRATTAN-BELLEW, E.G. QUINN and P.J. SEREDA (1978), "Reliability of scanning electron microscopy information," Cem. Concr. Res. 8, 333-342.

26.- D.D. DOUBLE and A. HELLAWELL (1974), "The solidification of cement," Scientific Amer. 237, 82-90.

27.- P.J. SEREDA and R.F. FELDMAN (1963), "Compacts of powdered materials as porous bodies for use in sorption studies," J. Applied Chem. 13, 150-158.

28.- R.F. FELDMAN (1968), "Sorption and length-change scanning isotherms of methanol and water on hydrated portland cement," Proc. Fifth Int. Symp., Chem. of Cement, Part III, Vol. III, p. 53-66, Tokyo.

29.- V.S. RAMACHANDRAN, R.F. FELDMAN and P.J. SEREDA (1965), "An unsoundness test for limes without cement," Materials Research and Standards, 5, 510-515.

30.- P.J. SEREDA, R.F. FELDMAN and V.S. RAMACHANDRAN (1965), "Hydration of gypsum plaster by the compact technique." Bull. Amer. Ceram. Soc. 44, 151-155.

31.- I. SOROKA and P.J. SEREDA (1968), "Interrelation of hardness, modulus of elasticity, and porosity in various gypsum systems," J. Amer. Ceram. Soc. 51, 337-340.

32.- D.M. ROY, G.R. GOUDA and A. BOBROWSKY (1972), "Very high strength cement paste prepared by hot pressing and other high pressure techniques," Cem. and Concr. Res. 2, 349-366.

2. POROSITY AND PORE-SIZE DISTRIBUTION IN ORDINARY PORTLAND CEMENT PASTE

This section of the paper will deal with some of the more important techniques used to measure porosity and pore-size distribution, which have helped determine the structure of hydrated portland cement. Pore structure is one of the most important parameters controlling the properties of porous materials. Many procedures to determine the pore structure of a solid have involved mercury porosimetry and nitrogen or water-vapour adsorption isotherms. Calculations based on these have been relatively successful for materials with pore structures that remain stable on removal or addition of water.

Measurements for unstable materials such as hydrated portland cement, however, have been difficult to interpret. Water used as a medium always gives a higher porosity for hydrated portland cement than that obtained by other media, e.g., nitrogen, methanol and helium (1,2). In order to measure many of the properties of hydrated portland cement, it must be dried; this presents a major problem since decomposition of some of the hydrates will occur. One may expect changes in porosity, surface area and other physical properties (3-10). Also, on exposing the material to water, rehydration of the decomposed hydrates may occur (11).

In recent years, several advances have been made in the application of two techniques that have been widely used on a variety of materials for measuring porosity and pore-size distribution. These are the capillary condensation method, which uses several different adsorbates (mainly nitrogen and water on cement paste), and mercury porosimetry. These will be presented and discussed.

However, since the Moscow Symposium, two new techniques have been applied to the hydrated portland system. These are:

(i) the quasi-elastic or inelastic neutron-scattering method (12);

(ii) the helium inflow and helium pycnometric technique (13).

With the first technique, the fractions of free and bound water can be determined to quite a good approximation. Previously, nuclear magnetic resonance had been used on these types of hydrated silicates to distinguish between protons having different induction decay times caused by different types of bonding (14,15), but the relative amounts of differently bonded protons for samples containing appreciable fractions of free water, as occurs in a saturated cement paste, were not measured.

With the second technique, changes to the structure can be followed as water is removed from the system or as water re-enters the system. This is important because much work has been done with the aim of relating porosity determined by water with that determined by other techniques. The difference has been termed "missing porosity" or "gel pores." The helium flow technique has detected this missing porosity, which is, in fact, the interlayer space normally occupied by approximately one layer of water when the material is in the wet condition. On drying and removal of the interlayer water, this space partially collapses. The effort and controversy related to the study of the "missing porosity" and its importance relating to mechanical properties has justified its inclusion in a discussion on porosity.

2.1 INELASTIC NEUTRON-SCATTERING METHOD

Neutron inelastic scattering is sensitive to the mobility of atomic nuclei, especially those of hydrogen, which has an exceptionally large neutron-scattering cross-section. A bound molecule undergoes vibration with some particular frequency, characteristic of the particular mode, and gives rise to an inelastic scattering distribution of neutron energies, which reflects the density of vibrational states, together with elastic peaks reflecting the time-averaged position of the molecule. In contrast, a mobile molecule has no particular time-averaged position and so gives rise to no strictly elastic peak in the spectrum, but rather a quasi-elastic distribution that reflects the Doppler shifts in frequency caused by the molecular motions.

In the context of a water phase in a cement, Harris, Windsor and Lawrence (12) considered it plausible to postulate a multi-component structure, each component obeying Fick's law individually (16), having a distribution of diffusion constants. In the analysis of water in vermiculite clays, workers fitted their results to a single diffusion constant (17).

The cement paste spectra correspond quite accurately to those of two-component systems with free components given by the pure-water spectrum and bound components by a resolution function. There is no evidence from the shape of the quasi-elastic frequency distribution that any more complicated model than a two-component system with free and bound water states should be used.

Table 2.I (based on ref. 12) contains a summary of experimental measurements by neutron scattering and conventional methods, on four saturated cement pastes approximately 2 years old. The weight losses incurred by drying at 100°C and by evacuation at room temperature are consistently greater than the amount of free water calculated from neutron scattering measurements on the saturated pastes (Rows 2 and 3 respectively). This can be explained if one concludes that some combined water has been removed during drying.

The volume fraction of free water calculated from the neutron scattering estimate of free water is approximately equal to the calculated (18) capillary water content (Rows 5 and 8). Other data (19) show that this capillary volume is approximately equal to the total volume available to liquid nitrogen in pre-dried pastes. As previously mentioned, the free water volume by drying at 100°C is much more than that determined by neutron scattering (Rows 7 and 5 respectively).

These results are very significant because they agree with nitrogen adsorption data, suggesting that nitrogen adsorption gives realistic values and that evaporable water is partly combined. They also suggest that the neutron-scattering technique can be used to elucidate the structure of saturated cement pastes because it avoids the uncertainties associated with drying.

The results from this work are illustrated in Fig. 2.1 (12), which shows the volume fractions of

TABLE 2.I - Estimation of free and combined water by neutron scattering and conventional methods (based on ref. 12)

Row	Properties - saturated pastes	w/c = 0.66	w/c = 0.33	Compact	Compact
1	Ignition loss, weight fraction at 1000°C	0.4371	0.2880	0.2032	0.1209
2	Drying loss, weight fraction at 100°C	0.3006	0.1565	0.0933	0.0597
3	Free water by weight by neutron scattering	0.223	0.081	0.045	0.019
4	Cement volume	0.305	0.465	0.595	0.726
5	Free water volume by neutron scattering	0.394	0.172	0.109	0.052
6	Combined water volume by neutron scattering	0.301	0.363	0.296	0.222
7	Free water volume by loss on drying at 100°C	0.531	0.334	0.228	0.161
8	Capillary water volume, from weight loss on drying	0.379	0.135	0.063	0.064

cement, combined water and free water determined from (a) neutron scattering data, and (b) from traditional concepts using the usual drying techniques. The over-estimate of the porosity by the conventional techniques is obvious in this illustration.

2.2 HELIUM FLOW AND HELIUM PYCNOMETRIC TECHNIQUE

This technique involves the normal pycnometric measurement of the solid volume of a body during which the helium surrounding the body is compressed to 2 atm. Immediately after this period (a total of 2 min from the time helium is first admitted to the sample) the rate at which helium penetrates the body under an absolute pressure of 2 atm is measured for a period of 40 h (13). In other techniques such as sorption, weight or volume changes are measured as a function of partial pressure of sorbate, which does not take into account removal or replacement of, in this case, water from or to the molecular structure. The helium flow technique is capable of following these changes and has been used to study hydrated C_3S and portland cement as well as some relatively well-defined systems (20).

The study of the C-S-H gel found in hydrated portland cement by the helium flow technique has revealed that much of what was formerly thought to be adsorbed water is associated with the solid as interlayer water. The removal or replacement of the interlayer water results in changes to the solid volume, density and porosity, which can be measured. Ageing effects that occur during wetting and drying treatments can also be detected.

The volume of interlayer space and the change in volume due to water removal or re-entry can be readily monitored by a combination of solid-volume and helium-inflow-change measurements. These measurements, together with those of other properties such as surface area, can determine hydraulic radius or average surface-to-surface separation and shape of the interlayer spaces.

Several of the pertinent experimental observations and types of calculations made through this technique are described in the following three sections.

2.2.1 Density and Porosity Measurements

Several types of density measurements can be made on hydrated portland cement (2). The most obvious density is that where most hydrates have been left intact. This can be partially obtained by measuring the solid volume of specimens conditioned at 11% RH, using the helium pycnometer. However, a constant procedure has to be adopted where the time-to-helium exposure is limited because of the problem of helium

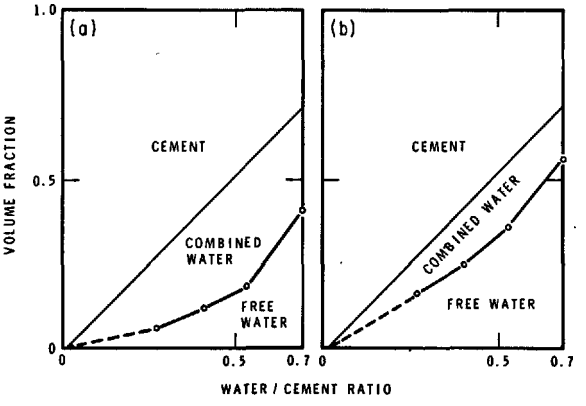

Fig. 2.1 - The volume fractions occupied by cement, combined water and free water in saturated cement pastes (12). (a) Composition from neutron scattering; (b) Composition from drying loss

flowing into vacated interlayer spaces. The value for this density at different water contents drying from 11% RH is shown in Fig. 2.2 (2).

Once density has been measured, porosity can be calculated from the apparent volume. Porosity was calculated for d-dried hydrated portland cement from the data in Fig. 2.2 (2) and compared with that obtained with methanol and with water. The results, shown in Fig. 2.3 (2) for several water/cement ratio pastes, indicate that the porosities obtained with helium and methanol are very similar over the whole range. When water is used, porosity is about 8% more at a water/cement ratio of 0.4. This corresponds approximately to the value estimated by scanning isotherms (21) for the quantity of interlayer or hydrated water. When water is used to measure porosity or density of hydrated portland cement dried only to 11% RH, the values are similar to those obtained with both helium and methanol (2). This shows that most of the interlayer water is retained in the solid at this condition.

Density may also be calculated by including as pore space the volume of interlayer space that is free of water and in an uncollapsed state (22). In order to calculate this volume, the total volume of helium inflow at 40 h is subtracted from the solid volume measured by the helium pycnometer. The results

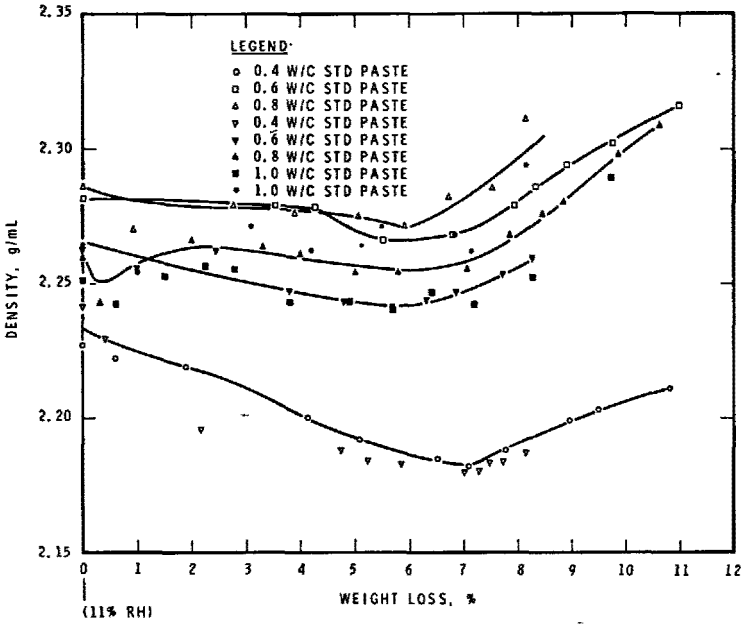

Fig. 2.2 - Relationship between density and weight loss for cement pastes with w/c ratios of 0.4, 0.6, 0.8 and 1.0 (2)

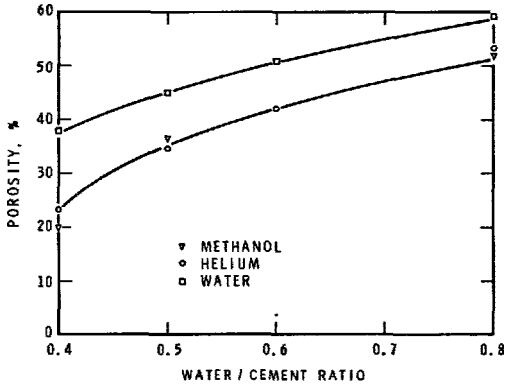

Fig. 2.3 - Relationship between porosity and w/c ratio for portland cement pastes (2)

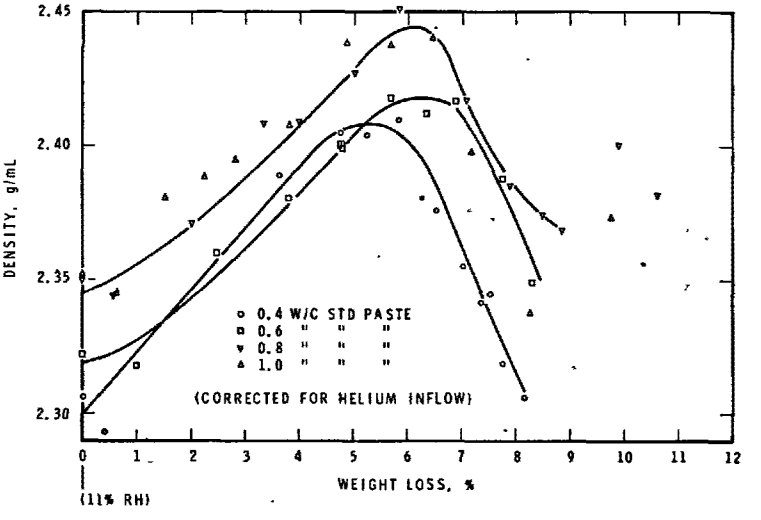

Fig. 2.4 - Relationship between density (corrected for helium inflow) and weight loss for cement pastes with w/c ratios of 0.4, 0.6, 0.8 and 1.0 (2)

plotted in Fig. 2.4 (2) show that density increases with weight loss up to 5 to 6% after which it decreases. The maximum density occurs because collapsing sheets retard the inflow of helium into the interlayer space and in the 40 h of measurement complete filling of the volume does not occur. The low final density at the dry state is a result of the layers only partially collapsing which prevents helium from fully entering the space.

2.2.2 Collapse of Layered Structure on Drying

Figure 2.5 (2) shows typical helium flow curves with time for a hydrated portland cement dried from the initial 11% RH condition to a final condition obtained by heating at 140°C under vacuum for 6 h. Weight losses are recorded from the 11% condition.

Individual rate curves are functions of the volume of vacated interlayer space remaining and the size of the entrances. When the size of the entrances are large, rate of flow will be rapid but because collapse occurs initially from the entrances, the rate will decrease even though more vacated space may exist. This is illustrated by the crossing over of the rate curves in Fig. 2.5 (2).

The effect of the withdrawal of water may be more clearly observed in Fig. 2.6 (23). The total inflow after all moisture is withdrawn is less than that at the initial 11% condition, mainly because there is an abrupt reduction in inflow over a very low weight-loss range. This is due to partial collapse of the interlayer spaces.

Solid volume and total interlayer space vacated by water on drying. - Removal of interlayer water leads to a change in "solid volume" (ΔV) and to a change in total helium inflow, ΔD. Because part of the vacated interlayer space has collapsed, resulting in a change in solid volume, an assessment of the space occupied by the water molecules can

only be made by combining these parameters. Thus, a parameter ΔV-ΔD is obtained where, owing to increased weight loss, the decrease in volume is a negative ΔV, and increased inflow, ΔD, is regarded as positive. This then accounts for the space vacated by the water if helium enters all the space in 40 h.

Figure 2.7 (23) shows a plot of ΔV-ΔD and ΔV against weight loss, for 10 different samples. The ΔV-ΔD plot is linear up to 5.5% weight loss of slope 0.7886 mL/g, which is the space occupied by 1 g of water; the inverse is 1.27 g/mL (±0.08 g/mL), which is the density of the water.

Between 6 and 11% weight loss, there is very little change in ΔV-ΔD even though there is an increase in rate of change of ΔV. The departure from linearity of the plot in Fig. 2.7 (23) is due to the reduction in helium inflow because of a restriction in the entrances of the interlayer spaces and their partial collapse.

2.2.3 Reopening of Layered Structure

When strongly dried hydrated portland cement is exposed to water vapour, water molecules re-enter between the sheets (6,11); as the material is exposed to higher humidities, more water molecules re-enter the structure. This re-entry can be investigated by exposing material to various humidities before measuring helium inflow at 11% RH; helium inflow increases with re-entry and as the interlayer space becomes filled, helium inflow decreases. Evidence of repenetration of water molecules has also been obtained from low-angle X-ray scattering measurements (24).

The penetration of the layered structure by water molecules leads to a variation of solid volume and density. Drying and wetting cycles result in a significant increase in solid volume, an example of ageing of the structure.

Measurement of total space occupied by repenetrating water. - The ΔV-ΔD vs weight change plot for re-exposure to water vapour is presented in Fig. 2.8 (6). It records an increase in ΔV-ΔD of only 1.75 mL/g for weight gain of up to 6.0%, on exposure up to 42% RH. The helium is not fully measuring the volume of the water that has entered structure. Beyond 6.0% a good linear correlation is obtained, resulting in a density calculation of 1.20 g/mL for the interlayer water.

The weight gain up to 42% RH would imply an impossibly high density for the water, and it is obvious that the water molecules are mainly entering the interlayer structure

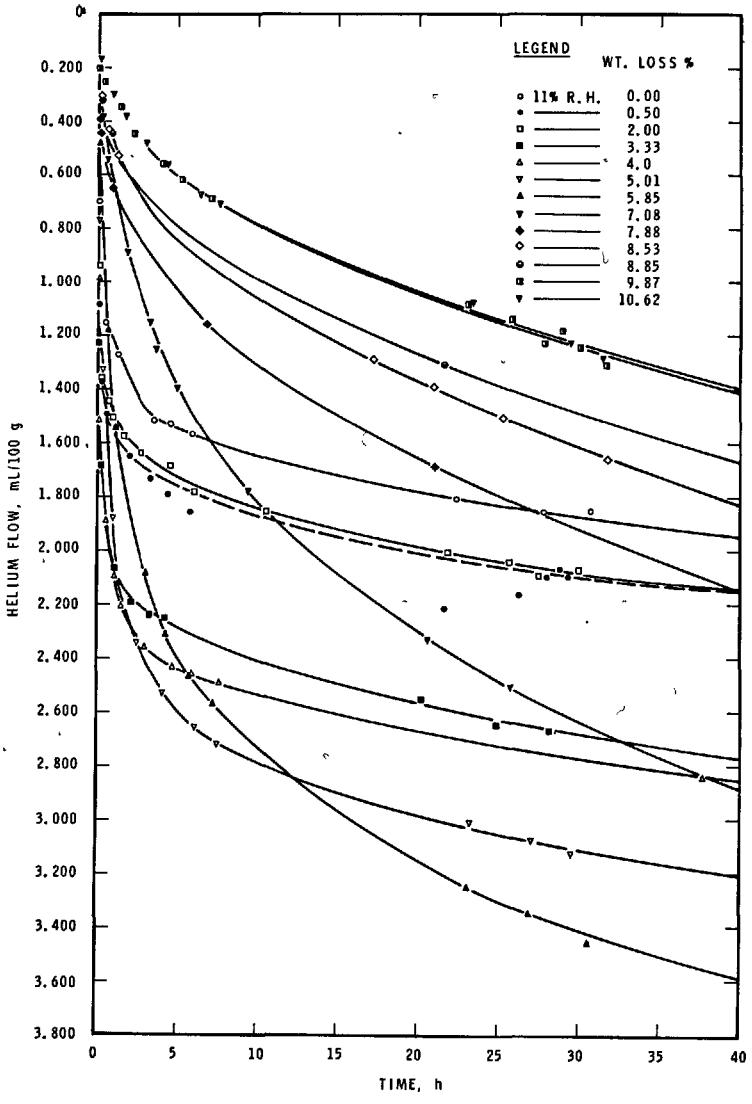

Fig. 2.5 - Helium flow into 0.8 w/c ratio cement paste at different water contents as a function of time (2)

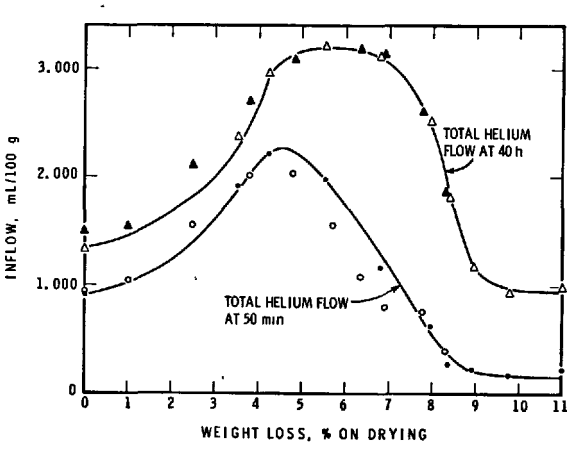

Fig. 2.6 - Helium flow at 50 min and 40 h, plotted as a function of weight loss for 0.6 w/c ratio cement paste (23)

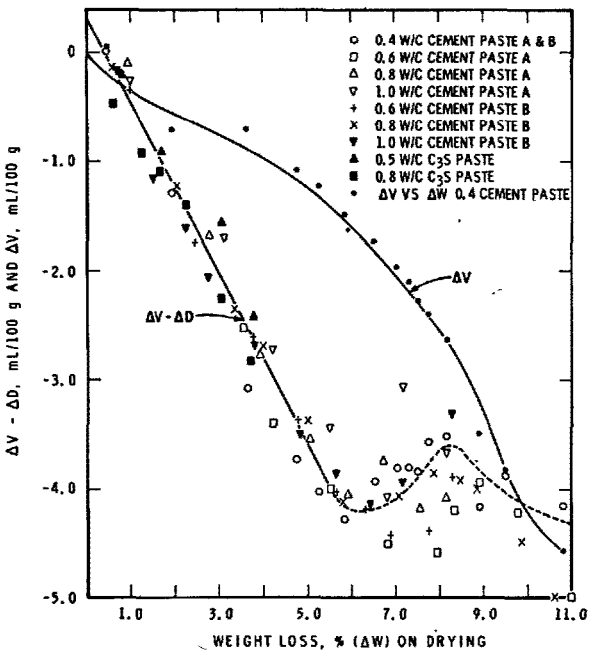

Fig. 2.7 - Plot of ΔV-ΔD and ΔV as a function of weight loss for 10 different pastes (23)

that had partially collapsed on drying. This also indicates that the monolayer of adsorbed water on the open surface is a relatively minor part of the 6.0% sorbed up to this stage.

Beyond this point, the water is completely held in interlayer positions because all these measurements are made at 11% RH, and a monolayer on the exterior surface is complete at 11% RH. The linear plot in this region indicates that helium fully enters the interlayer space (after exposure to 42% RH and up) and measures the volume of the interlayer water and the remaining space.

Hydraulic radius and surface area of capillary porosity. - When d-dried hydrated portland cement paste is exposed to water vapour, the water molecules enter the pores, adsorb on the solid that is bounding the pores, and some molecules penetrate the layered structure within the solid. The solid particles swell, not only because of the interlayer penetration, but also because of the physical interaction of water on the surface of the solid. This is called Bangham swelling and is due to a decrease in surface tension forces that compress the solid. This swelling should be transmitted through the porous body and is referred to as $\Delta\ell/\ell$, which is the measured linear expansion of the porous body. If $\Delta\ell/\ell$ is small, $3\,\Delta\ell/\ell$ is the volumetric expansion. If there is no change in porosity or packing during changing conditions, then $3\,\Delta\ell/\ell$ is equal to the fractional volume change of the solid phase of the body.

A measurement of the solid volume by helium pycnometry would include the adsorbed water, as well as the solid in the expanded state. By measuring the solid volume at the dry state and at 11% RH, where the adsorbed water is approximately equal to a monolayer, one would obtain the volume of a monolayer of adsorbed water plus the increase of the solid. This is referred to as $\Delta V/_V$.

The difference of the volume changes would then be equal to the volume of the adsorbed water as a fraction of the total volume of the solid. This may be written as follows:

$$\Delta V/_V - 3\,\Delta\ell/\ell = v/_V$$

where "v" is the volume of adsorbed water and "V" the volume of the solid (25).

The measurement of both these volume changes assumes that during the change of condition from 0 to 11% RH, no ageing occurs. Previous work (7) has shown this to be the case.

Because "v" is the volume of the monolayer of adsorbed water on the surface bounding the porosity, the surface area can be readily calculated. The hydraulic radius of a pore system is computed by dividing the total pore volume of the system by its surface area; thus the hydraulic radius can also be readily calculated, as shown in Table 2.II for hydrated portland cement paste of w/c = 0.4, 0.6 and 0.8.

Results were obtained for 10 different samples of hydrated portland cement and C_3S of various water/cement ratios. The surface areas of these samples were also determined by nitrogen adsorption, using the same drying technique. These quantities are plotted in Fig. 2.9 (based on unpublished work by one of the authors.) Although a deviation occurs at

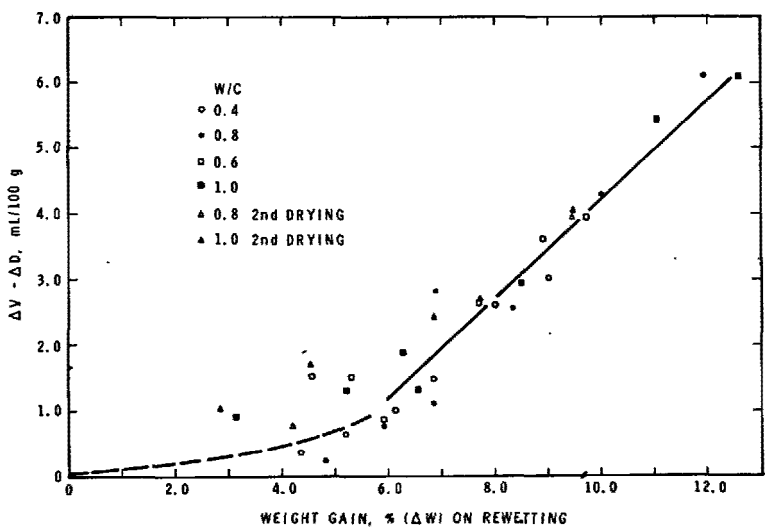

Fig. 2.8 - Plot ΔV-ΔD as a function of weight change for 4 different pastes on rewetting (6)

TABLE 2.II - Surface area and hydraulic radius of hydrated portland cement by helium pycnometry

Water/cement ratio	Surface area, m^2/g	Hydraulic radius, Å
0.4	35.0	39.4
0.6	49.0	64.2
0.8	44.0	107.0

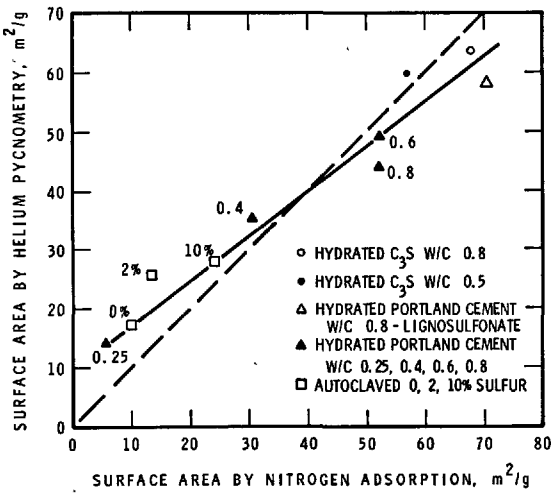

Fig. 2.9 - Surface area by nitrogen adsorption and by helium pycnometry (Feldman, in process)

the lower surface areas, the agreement justifies the assumptions and confirms the general validity of the equation. The concept that the instantaneous helium pore volume is the same as the pore volume determined by nitrogen, and that the remaining pore volume is that of the partially collapsed interlayer space is sound. This confirms the validity of the inelastic neutron scattering experiments already discussed (2).

Hydraulic radius of the interlayer space. - As mentioned previously, the hydraulic radius of a pore system is computed by dividing the total pore volume of the pore system by its surface area. Until recently, this calculation could not be made without assuming a particular structure for the C-S-H gel, but the low-angle scattering data of Winslow and Diamond (24) has provided this value. In addition, as discussed earlier, the interlayer space is re-opened by exposure to 42% RH; at this condition, helium can fully enter the internal space within 40 h of flow time. The volume of the interlayer space can thus be measured on the partially-open or fully-open state depending on the relative humidity of exposure, using helium to measure the remaining volume.

The results from measurements on a hydrated cement paste cured at a water/cement ratio of 0.6, using the helium-volume-change method reported here, give a value of 1.35% of water for the monolayer on the external surface which gives a surface of 49 m^2/g. After exposure to 100% RH, 10.8% water was retained at 11% RH (11). This leaves 9.45% in the interlayer structure. A space of 2.4 mL unoccupied by water was also measured in the structure by helium inflow. Using 1.20 g/mL as the density of the water, referred to earlier, results in a volume of 10.28 mL as the internal space. The surface area for the internal space is 670 m^2/g, determined by Winslow and Diamond (24), resulting in 670-49 = 621 m^2/g for the interlayer surface, and a hydraulic radius of 1.65 Å (0.165 nm).

Assuming that the pores are bounded by two parallel plates, the average separation between the plates is 3.3 Å (0.33 nm) (twice the hydraulic radius). This model is consistent with the internal system composed of layers separated by, on the average, one water molecule. The impact of this calculation may be enhanced by another simple calculation. If 9.45% of water is held as a single layer between two sheets, it will cover twice the normal area per molecule, i.e., 10.8 × 2 $Å^2$ (0.216 nm^2). This results in a surface area of 687.2 m^2/g compared to 621 m^2/g given by low angle X-ray scattering. This, however, assumes that all the water is held as a single layer, while in fact there may be "kinks" in the alignment of the sheets, leaving room for more than one layer of water. On the other hand, a coverage of 10.8 $Å^2$ (0.108 nm^2) per molecule may be too high.

The hydraulic radius can be calculated for the sample when exposed only to 42% RH and where 5.15% water and 2 mL of space exist between the sheets. One obtains an average hydraulic radius of 1.0 Å (0.1 nm), obviously a result of a partially collapsed state.

Calculations of this type have also been obtained from data of Brunauer, Odler and Yudenfreund (26), and Mikhail and Abo-El-Enein (27). In these cases, the internal volume was obtained by measuring the difference between the total water and the total nitrogen porosity; the surface areas were determined by the difference between the surface areas given by Winslow and Diamond (24) and the surface area determined by nitrogen adsorption.

The results calculated from the data of Brunauer, Odler and Yudenfreund (26) are shown in Table 2.III; an average of 1.23 Å (0.123 nm) was obtained for the four pastes at water/cement ratios between 0.35 and 0.57.

In Table 2.IV, the data of Mikhail and Abo-El-Enein (27), corrected for degree of hydration, give an average value of 2.51 Å (0.251 nm) when the first value at 18.50% hydration is excluded. These data were obtained for pastes cured at a water/cement

TABLE 2.III - Surface areas, porosities and hydraulic radii of portland cement paste

Water/cement ratio	S_{N_2}, m^2/g	$S_T - S_{N_2}$, m^2/g	$V_{H_2O} - V_{N_2}$, mL/g	$\frac{V_{H_2O} - V_{N_2}}{S_T - S_{N_2}}$ (Å)	
0.35	56.7	580-56.7	0.0516	0.99	avg = 1.23
0.40	79.4	642-79.4	0.0717	1.28	
0.50	97.3	642-97.3	0.0823	1.51	
0.57	132.2	670-132.2	0.0617	1.14	

TABLE 2.IV - Internal radius of low porosity pastes

Sample No.	Degree of Hydration, %	V_{H_2O}-V_{N_2},	676-S_{N_2}, m^2/g	Hydraulic radius, Å	
I	18.50	0.92	644	14.4	
II	33.80	0.175	628	2.78	
III	49.30	0.144	.646	2.22	
IV	57.1	0.155	655	2.36	avg =
V	62.0	0.184	667	2.78	2.51
VI	74.1	0.168	668	2.51	
VII	78.1	0.166	671	2.48	

ratio of 0.2. This value is much higher than that obtained from the other data (Table 2.III) but is consistent with other results for low water/cement ratio pastes. Very low surface areas (27) and relatively low densities (28) are obtained for these pastes, and it must be concluded that there are many kinked regions in the stacking of the sheets and trapped space, due to lack of space during hydration. This is illustrated in Fig. 2.10, a further modification of a modification by Daimon et al (29) of a model by Feldman and Sereda.

2.3 MERCURY POROSIMETRY

The mercury porosimetry method enables the widest range of pore-size distribution to be measured. The upper diameter limit can be as high as 1000 µm; the lower limit can be as small as 30 Å (3 nm), depending on the pressure available and the contact angle used in the calculation.

A review of the porosimetry technique was published by Orr (30). More recently, Liabastre and Orr (31) assessed the structure of a graded series of controlled pore glasses and Nucleopore membranes, both of which have pores with right-cylinder characteristics, using both electron microscopy and mercury penetration. The data showed good comparison if a simple pressure correction was applied. It was suggested that pores are compressed to an hour-glass shape, thereby exhibiting an effectively smaller diameter until mercury actually enters them. Upon the entrance of mercury, the pores expand because of the equalisation of hydrostatic pressure, and return to nearly their original volume. The partial closing and reduction in diameter accounts for the apparent entry of mercury into pores smaller than they actually are, and the subsequent return to shape explains correct volume measurements.

A survey of the method as applied to cement systems and some results for cement pastes at different water/cement ratios was made by Winslow and Diamond (32). It was observed that the pore volume left unintruded by mercury at 15 000 psi (102 MPa) was significantly less than the 28% by volume that should represent gel pores.

Diamond and Dolch (33) again addressed themselves to the problem of whether there is a separate class of "gel pores" in the range of tens of ångströms. They showed that for a mature paste (318 days old) the pore volume, intruded below about 60 Å (6 nm) in diameter, is not only less than that predicted by a log normal plot, which suggests that all the pores intruded belong to a single pore-size distribution, but is almost negligible in absolute terms. The plot of cumulative percentage of pore volume intruded vs pore diameter is given in Fig. 2.11 (33) for this sample. The total pore volume in this sample was measured as 0.306 cm^3/g. The volume intruded between pressures corresponding to pore diameters of 77 Å (7.7 nm) and 25 Å (2.5 nm) is only 0.011 cm^3/g.

In their study of capillary porosity, Auskern and Horn (34) showed that the addition of a small amount of water does not affect the porosity measured by mercury, contrary to the findings of Winslow and Diamond (32). The porosity by mercury intrusion of an oven-dried sample up to 50 000 psi (340 MPa) was 0.108 cc/g; the oven-dried sample exposed to 5% RH had a porosity of 0.115 cc/g. This type of result was also observed by Beaudoin (35). As a result, Auskern and Horn (34) used 117 deg as the contact

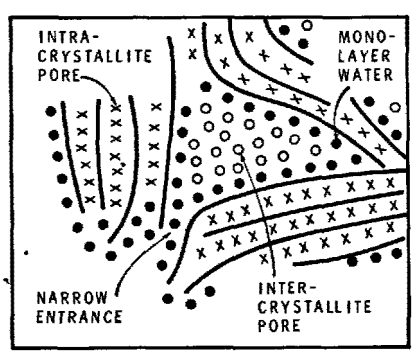

Fig. 2.10 - Modification of Feldman and Sereda model (29)

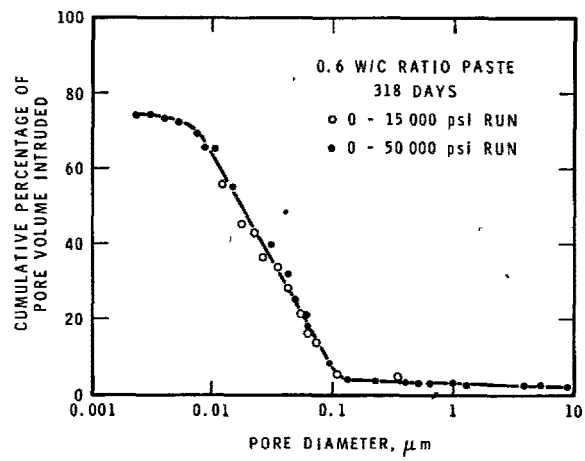

Fig. 2.11 - Cumulative mercury pore-size distribution for 0.6 w/c paste 318 days old (33)

angle for all their work. They also found limited penetration below about 80 Å (8 nm) and concluded that the "missing porosity" relative to the porosity as determined by water adsorption must be smaller than 35 Å (3.5 nm). They found that the porosity measured by carbon tetrachloride saturation is close to, but a bit larger than, the porosity measured by mercury penetration. Beaudoin (35) measured total porosity by mercury porosimetry up to 60 000 psi (408 MPa) pressure and found that mercury porosimetry and helium pycnometric methods could be used interchangeably to measure porosity if the water/cement ratio was equal to or greater than 0.40. These results are shown in Fig. 2.12 (after ref. 35). Included in this Figure are results for other materials, including porous glass in which mercury was able to penetrate only 69% of the pore space. Average pore diameter of this material was measured by other techniques (36) to be between 50 and 60 Å (5 and 6 nm).

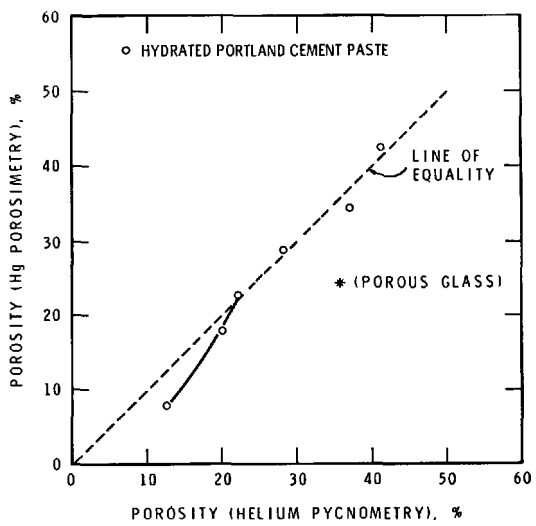

Fig. 2.12 - Mercury porosity vs helium porosity for hydrated portland cement paste (after ref. 35)

It is apparent that the results from the mercury intrusion method agree with those of other techniques described previously, and especially with the helium inflow measurements. The results showed that the porosity was made up of a pore structure into which helium could rapidly enter, and of interlayer spaces of hydraulic radius less than 1 Å (0.1 nm) when the paste is oven dried.

In a study of capillary porosity during hydration of C_3S and the effect of admixtures, Young (37) found that, on measuring the mercury intrusion, the pastes showed a threshold diameter that decreased with hydration; the results are shown in Fig. 2.13. This was in agreement with the finding of Winslow and Diamond (32). It was suggested by Young that the large intrusion immediately below the threshold diameter results from filling of the void spaces between C-S-H gel needles, and the filling of larger pores accessible only through intergrowth of needles.

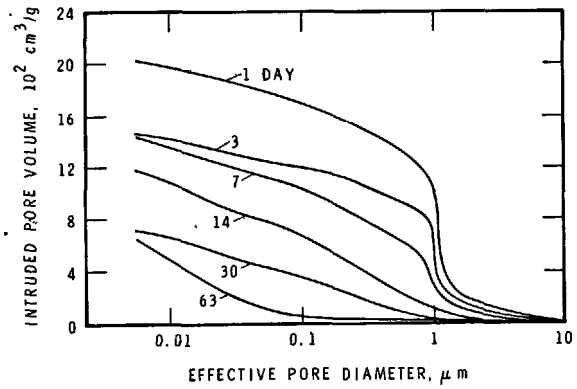

Fig. 2.13 - Intrusion curves for a series of hydrating C_3S pastes (w/c = 0.4) (37)

Diamond (38) investigated the evolution of pore structure of cement paste at two temperatures and two water/cement ratios, 0.4 and 0.6. Results for w/c = 0.6 in Fig. 2.14 (38) show that there is a slight difference in the character of the product formed slowly at low temperatures as compared to that formed rapidly at higher temperatures; this shows up in the pore structure. After about one year of hydration, the pore volume of the paste cured at 40°C is higher than that cured at 6°C because of greater volume of pores smaller than 500 Å (50 nm).

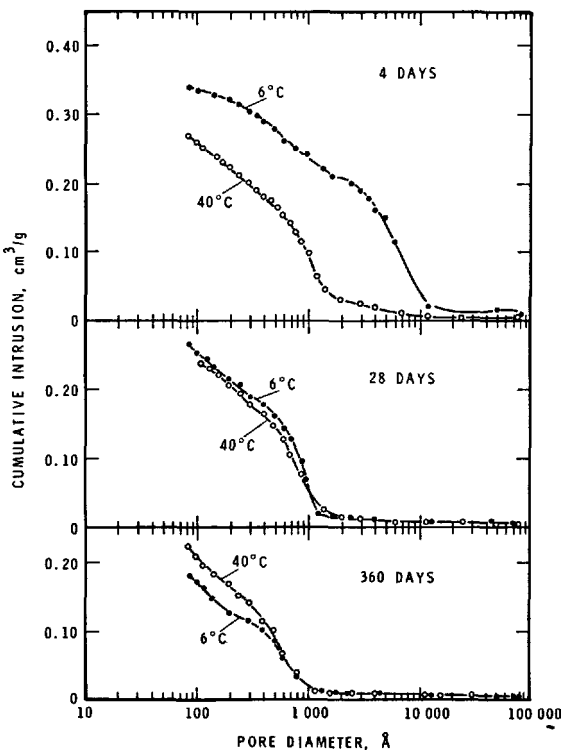

Fig. 2.14 - Cumulative pore-size distributions of 0.6 w/c cement pastes hydrated at 6°C and at 40°C (38)

2.4 PORE-SIZE DISTRIBUTION BY NITROGEN ADSORPTION AND CAPILLARY CONDENSATION METHODS AND COMPARISON WITH MERCURY POROSIMETRY

Studies have been made (39-41) of pore structure as determined by water vapour adsorption. It has been shown in the previous sections that porosity determined by water is quite different from that determined by other fluids, largely because of the interaction of water molecules with the solid and their penetration into partially collapsed interlayer spaces. Several authors (42,43) have now confirmed, however, "that the high degree of specificity of water adsorption does not allow water vapour to be used as an alternative to nitrogen for determination of surface area and pore size distribution." It should, therefore, be exploited only to "provide information concerning the chemistry of the solid surface rather than its surface area and texture." This section will thus deal primarily with nitrogen adsorption.

The common method in use is that of "capillary condensation." The pore-size distribution data is obtained by applying the Kelvin or similar equation to either the adsorption or desorption isotherm. A number of different assumptions as to pore shape and thickness of the adsorbed film at each stage have been used (44-50), leading to some variation in calculation methods. However, in contrast to the wide range of sizes that can be determined by mercury porosimetry, capillary condensation methods are limited essentially to pores of diameters between a few tens to several hundreds of ångströms. The lower limit associated with capillary condensation methods depends on the particular isotherms, but it is generally accepted that the Kelvin equation tends to break down for micropores. Kadlec and Dubinin (51) presented data suggesting that the Kelvin equation does not apply for pore diameters as small as 35 to 40 Å (3.5 to 4 nm). They concluded that this equation is inapplicable at relative vapour pressures slightly higher than those at which the adsorption-desorption hysteresis loop closes, and appears to be a characteristic of the adsorbate. The limiting diameters range from 20 to 35 Å (2 to 3.5 nm) for various adsorbates.

Recently Winslow (52) reported results that showed satisfactory agreement between mercury porosimetry and nitrogen adsorption for porous alumina in the pore range 500 to 40 Å (50 to 4 nm).

In a comprehensive study of a variety of pastes of portland cement and C_3S, Bodor et al (53) found a maximum for the pore-size distribution at around 12 Å (1.2 nm) hydraulic radius, i.e., 48 Å (4.8 nm) diameter with the assumption of cylindrical pores. In a review, Diamond (54) observes that most plots in the literature display strong maxima between 30 and 50 Å (3 and 5 nm). Bodor states that no micropores are measured in hydrated portland cement by this technique nor by the "t-method." However, Diamond (54) observed that the cumulative volume determined by mercury intrusion was not too different from that by capillary condensation for pores 100 to 400 Å (10 to 40 nm) in diameter; below 100 Å (10 nm) this is not the case. The capillary condensation data by some workers show steep slopes and considerable pore volume below 100 Å (10 nm) and particularly below 50 Å (5 nm). This fact led Diamond (54) to suggest that large amounts of the C-S-H were encapsulated by calcium hydroxide and unintrudable by at least mercury, but the work of Auskern and Horn (34) and the helium pycnometric work dispels this idea and, in any event, the pore-size distribution by mercury intrusion should still be reasonably representative of the whole of the distribution. Diamond (54) used radius of gyration results obtained by Winslow (52) in his low-angle X-ray scattering work, and calculated mean diameters, assuming various models. He obtained a mean diameter of approximately 300 Å (30 nm) assuming a cylinder of equal length and diameter. Mikhail, Turk and Brunauer (55) later refuted this work on the basis that the calculated surface area was too low. They used both radius of gyration and hydraulic radius to calculate the dimensions of an average cylindrical pore and obtained a diameter of 47.2 Å (4.72 nm) and a length of 466 Å (46.6 nm). These authors, however, had obtained their hydraulic radius by water adsorption which, as stated previously, is not valid.

Most recent work by Daimon et al (29) presented results on leached and unleached C_3S. Accordingly, the pore volume of an unextracted $Ca(OH)_2$ sample should be multiplied by 1.43 to compare it with the extracted paste. In fact, it was found that the pore volume determined by nitrogen adsorption was 1.39 times the values of the unextracted pastes, suggesting that $Ca(OH)_2$ does not engulf any appreciable volume of C-S-H. Work by Feldman and Ramachandran (56) with the helium flow technique lead to the same conclusion.

The pore-size distributions obtained by Daimon et al (29) are presented in Fig. 2.15 and Table 2.V. In this table, columns are given for the calculation of pore distribution using both the adsorption and desorption isotherm, and for parallel plate (S_{pp}, V_{pp}) or cylindrical pores (S_{cp}, V_{cp}). Best fit is given by the adsorption curve, and both models give a reasonable fit although the cylindrical model is better for the extracted paste. This is determined by comparing calculated values with S_{BET} and V_p in the upper part of Table 2.V (29). The hydraulic radius gives the pore diameter down to about 60 Å (6 nm), assuming a cylindrical model.

Results by Collepardi (57) are shown in Fig. 2.16. Pore-size distribution by nitrogen capillary condensation shows that room temperature cured C_3S

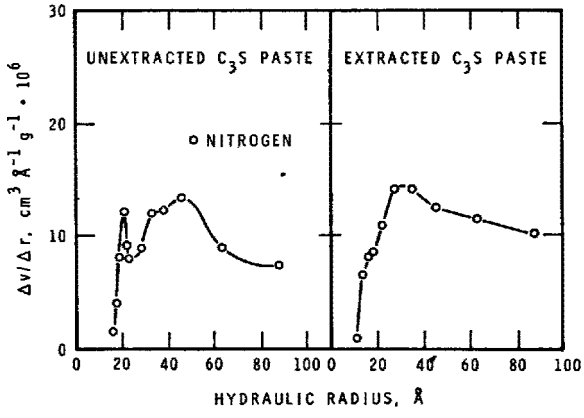

Fig. 2.15 - Pore-size distribution derived from adsorption isotherms (adsorption branches of N isotherms were used for calculation) (after ref. 29)

TABLE 2.V - N_2 adsorption data (29)

Parameter		Unextracted C_3S paste		Extracted C_3S paste	
V_m	(cm^3/g)	4.177		8.135	
S_{BET}	(m^2/g)	18.17		26.69	
S_t	(m^2/g)	17.5		25.5	
V_p	(ml/g)	0.1342		0.1862	
		Adsorption	Desorption	Adsorption	Desorption
S_{pp}	(m^2/g)	18.09	33.43	24.32	43.78
S_{vp}	(m^2/g)	21.09	42.00	28.53	48.37
V_{pp}	(ml/g)	0.1340	0.1412	0.1832	0.1942
V_{ep}	(ml/g)	0.1358	0.1453	0.1851	0.1994

paste has a maximum at about 20 Å (2 nm) pore radius, although the average value appears to be much higher. It is also shown that by hydrating at different temperatures the reduction in pore volume is due almost exclusively to the decrease in volume of the smaller pores down to about 60 Å (6 nm) radius. These results show general agreement with mercury intrusion, although nitrogen capillary condensation techniques indicate, in some cases, greater volumes in small pores. This difference may be explained, however, by the fact that "t"-curves are important in the calculation of the small pore distribution and measuring the appropriate "t"-curve is difficult for hydrated portland cement. In addition, the validity of their application for small pores is debatable.

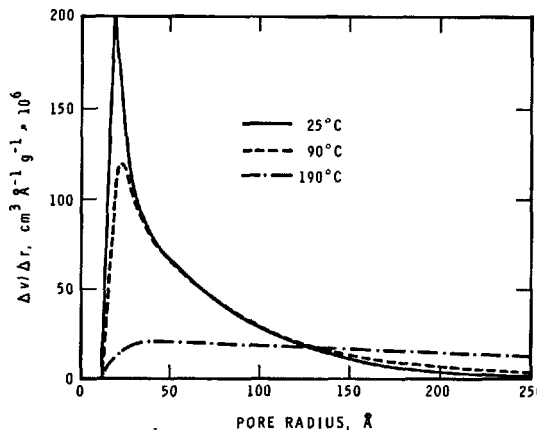

Fig. 2.16 - Pore-size distribution in $3CaO.SiO_2$ hydrated for 1 day at different temperatures (57)

REFERENCES (SECTION 2)

1.- R. Sh. MIKHAIL, L.E. COPELAND and S. BRUNAUER (1964), "Pore structure and surface areas of hardened portland cement pastes by nitrogen adsorption," Can. J. Chem. 42, 426-438.

2.- R.F. FELDMAN (1972), "Density and porosity studies of hydrated portland cement," Cem. Technol. 3, 5-14.

3.- G.G. LITVAN (1976), "Variability of the nitrogen surface area of hydrated cement paste," Cem. Concr. Res. 6, 139-144.

4.- R.F. FELDMAN and V.S. RAMACHANDRAN (1974), "A study of the state of water and stoichiometry of bottle-hydrated Ca_3SiO_5," Cem. Concr. Res. 4, 155-166.

5.- R.F. FELDMAN and J.J. BEAUDOIN (1976), "Structure and properties of porous cement systems and their modifications by impregnants," Proc. Conf. Hydraulic Cement Pastes: Their Structure and Properties, held at Univ. Sheffield, Cem. Concr. Assoc., pp. 150-165.

6.- R.F. FELDMAN (1973), "Changes to structure of hydrated portland cement on drying and rewetting observed by helium flow techniques," Cem. Concr. Res. 4, 1-11.

7.- R.F. FELDMAN (1975), "Mechanism of creep of hydrated portland cement paste," Cem. Concr. Res. 5, 577-586.

8.- B. HOPE and N. BROWN (1975), "A model for the creep of concrete," Cem. Concr. Res. 5, 577-586.

9.- N. BROWN and B. HOPE (1976), "The creep of hydrated cement paste," Cem. Concr. Res. 6, 475-486.

10.- A. BENTUR, N.B. MILESTONE, J.F. YOUNG and S. MINDESS (1979), "Creep and drying shrinkage of calcium silicate pastes. IV. Effects of accelerated aging," Cem. Concr. Res. 9, 161-170.

11.- R.F. FELDMAN (1973), "Helium flow characteristics of re-wetted specimens of dried portland cement paste," Cem. Concr. Res. 3, 777-790.

12.- D.H.C. HARRIS, C.G. WINDSOR and C.D. LAWRENCE (1974), "Free and bound water in cement pastes," Mag. Concr. Res. 26, (87), 65-72.

13.- R.F. FELDMAN (1973), "Volume change, porosity and helium flow studies of hydrated portland cement," Proc. RILEM/IUPAC Int. Symp. Pore Structure and Properties of Materials, Prague, Vol. I, pp. C101-116.

14.- P. SELIGMAN (1968), "Nuclear magnetic resonance studies of the water in hardened cement paste," J. PCA Res. Develop. Lab. 10, 52-65.

15.- H. OCHIAI, H. YAMAMURA, K. HUKENAGA, I. MAKI and K. WATANABE (1965), "A nuclear magnetic study of the water in calcium silicate pastes," Bull. Amer. Soc. Japan, 38, 945-948.

16.- C.G. WINDSOR and B.T.W. WILLIS (Editor) (1973), "Chemical applications of thermal neutron scattering," London, Oxford Univ. Press, p.130.

17.- S. OLEJNIK, C.G. STIRLING and W. WHITE (1970), "Neutron scattering studies of hydrated layer silicates," Faraday Society special discussion on thin liquid films and boundary layers, London, Academic Press, pp. 194-201.

18.- R.A. HELMUTH and D.H. TURK (1966), "Elastic moduli of hardened cement and tricalcium silicate pastes: effect of porosity," Symp. Structure of Portland Cement Paste and Concrete, Washington, D.C., Highw. Res. Bd. Spec. Rep. 90, pp. 135-144.

19.- G.J. VERBECK and R.A. HELMUTH (1968), "Structures and physical properties of cement pastes," Proc. Fifth Int. Congr. Chemistry of Cement, Tokyo, Vol. III, pp. 1-32.

20.- J.J. BEAUDOIN and R.F. FELDMAN (1978), "The significance of helium diffusion measurements in studying the removal of structural water in inorganic hydrated systems," Cem. Concr. Res. 8, 223-232.

21.- R.F. FELDMAN (1968), "Sorption and length-change scanning isotherms of methanol and water on hydrated portland cement," Proc. Fifth Int. Congr. Chemistry of Cement, Tokyo, Vol. III, pp. 36-44.

22.- R.F. FELDMAN (1972), "Helium flow and density measurement of the hydrated tri-calcium silicate-water system," Cem. Concr. Res. 2, 123-136.

23.- R.F. FELDMAN (1971), "The flow of helium into the interlayer spaces of hydrated portland cement paste," Cem. Concr. Res. 1. 285.

24.- D.N. WINSLOW and S. DIAMOND (1974), "Specific surface of hardened portland cement paste as determined by small-angle X-ray scattering," J. Am. Ceram. Soc. 57, 193-197.

25.- R.F. FELDMAN (1971), "Assessment of experimental evidence for models of hydrated portland cement," Highw. Res. Bd. Rec. 370, pp. 8-24.

26.- S. BRUNAUER, I. ODLER and M. YUDENFREUND (1970), "The new model of hardened portland cement paste," Highw. Res. Bd. Rec. 328, pp. 89-107.

27.- R.SH. MIKHAIL and S.A. ABO-EL-ENEIN (1972), "Studies of water and nitrogen adsorption on hardened cement pastes. I. Development of surface in low porosity pastes," Cem. Concr. Res. 2, 401-414.

28.- R.F. FELDMAN and J.J. BEAUDOIN (1976), "Microstructure and strength of hydrated cement," Cem. Concr. Res. 6, 389-400.

29.- M. DAIMON, S. ABO-EL-ENEIN, G. HOSAKA, S. GOTO and R. KONDO (1977), "Pore structure of calcium silicate in hydrated tricalcium silicate," J. Am. Ceram. Soc., 60, 110-114.

30.- C. ORR (1970), "Application of mercury penetration to materials analysis," J. Powder Technol. 3, 117-123.

31.- A.A. LIABASTRE and C. ORR (1978), "An evaluation of pore structure by mercury penetration," J. Colloid and Interface Sci. 64, 1-18.

32.- D.N. WINSLOW and S. DIAMOND (1970), "A mercury porosimetry study of the evolution of porosity in portland cement," ASTM J. Mater. 5, 564-585.

33.- S. DIAMOND and W. DOLCH (1972), "General log-normal distribution of pore sizes in hydrated cement paste," J. Colloid and Interface Sci. 38, 234-244.

34.- A. AUSKERN and W. HORN (1973), "Capillary porosity in hardened cement paste," ASTM J. Test. Eval. 1, 74-79.

35.- J.J. BEAUDOIN (1979), "Porosity measurements of some hydrated cementitious systems by high pressure mercury-intrusion - microstructural limitations," Cem. Concr. Res. 9, 771-781.

36.- C.H. AMBERG and R. McINTOSH (1952), "A study of hysteresis by means of length changes of a rod of porous glass," Can. J. Chem. 30, 1012.

37.- J.F. YOUNG (1974), "Capillary porosity in hydrated tricalcium silicate pastes," J. Powder Technol. 9, 173-179.

38.- S. DIAMOND (1973), "Pore structure of hardened cement paste as influenced by hydration temperature," Proc. RILEM/IUPAC Int. Symp. Pore Structure and Properties of Materials, Prague, Vol. I, pp. B73-88.

39.- R. Sh. MIKHAIL, S. BRUNAUER and E.E. BODOR (1968), "Investigations of a complete pore structure analysis. I. Analysis of micropores," J. Colloid and Interface Sci. 26, 45.

40.- J. HAGYMASSY and S. BRUNAUER (1970), "Pore structure analysis by water vapor adsorption. II. Analysis of five silica gels," J. Colloid and Interface Sci. 33, 317.

41.- J. HAGYMASSY, I. ODLER, M. YUDENFREUND, J. SKALNY and S. BRUNAUER (1972), "Pore structure analysis by water vapour adsorption. III. Analysis of hydration calcium silicates and portland cements," J. Colloid and Interface Sci. 38, 20-34.

42.- R. Sh. MIKHAIL, S. NASHED and K.W. SING (1973), "The adsorption of water by porous hydroxylated silicas," Proc. RILEM/IUPAC Int. Symp. Pore Structure and Properties of Materials, Prague, Vol. IV, pp. C157-164.

43.- K.S.W. SING (1973), "A discussion of the paper 'Complete pore structure analysis' by S. Brunauer, J. Skalny and I. Odler," Proc. RILEM/IUPAC Int. Symp. Pore Structure and Properties of Materials, Prague, Vol. 4, pp. C209-210.

44.- E.P. BARRETT, L.G. JOYNER and P.P. HALENDA (1951), "The determination of pore volume and area distribution in porous substances. I. Computations from nitrogen isotherms," J. Am. Chem. Soc. 73, 373-380.

45.- C. PIERCE (1953), "Computations of pore sizes from physical adsorption data," J. Phys. Chem. 57, 149-152.

46.- W.P. INNES (1957), "Use of a parallel plate model in calculation of pore size distribution," Anal. Chem. 29, 1069-1072.

47.- R.W. CRANSTON and F.A. INKLEY (1957), "The determination of pore structures from nitrogen adsorption isotherms," Adv. Catal. 9, 143-154.

48.- D. DOLLIMORE and G.R. HEAL (1964), "An improved method for the calculation of pore size distribution from adsorption data," J. Appl. Chem. 14, 109-114.

49.- B.F. ROBERTS (1967), "A procedure for estimating pore volume and area distributions from sorption isotherms," J. Colloid and Interface Sci. 23, 266-273.

50.- S. BRUNAUER, R. Sh. MIKHAIL and E.E. BODER (1967), "Pore structure analysis without a pore shape model," J. Colloid and Interface Sci. 24, 451-463.

51.- O. KADLEC and M.M. DUBININ (1969), "Comments on the limits of applicability of the mechanism of capillary condensation," J. Colloid and Interface Sci. 31, 479-489.

52.- D. WINSLOW (1978), "The validity of high pressure mercury intrusion porosimetry," J. Colloid and Interface Sci. 67, 42-47.

53.- E.E. BODOR, J. SKALNY, S. BRUNAUER, J. HAGYMASSY and M. YUDENFREUND (1970), "Pore structures of hydrated calcium silicates and portland cements by nitrogen adsorption," J. Colloid and Interface Sci. 34, 560-570.

54.- S. DIAMOND (1971), "A critical comparison of mercury porosimetry and capillary condensation pore size distributions of portland cement pastes," Cem. Concr. Res., 1, 531-545.

55.- R. Sh. MIKHAIL, D. TURK and S. BRUNAUER (1975), "Dimensions of the average pore, the number of pores and the surface area of hardened portland cement paste," Cem. Concr. Res. 5, 433-442.

56.- R.F. FELDMAN and V.S. RAMACHANDRAN, unpublished data.

57.- M. COLLEPARDI (1973), "Pore structure of hydrated tri-calcium silicate," Proc. RILEM/IUPAC Int. Symp. Pore Structure and Properties of Materials, Prague, Vol. 1, pp. B25-49.

3. PHYSICAL FACTORS CONTROLLING STRUCTURE AND STRENGTH DEVELOPMENT

Strength, modulus of elasticity, and permeability are important properties that determine the relative applicability of hydrated cement products. When portland cement paste is hydrated at room temperature and to a high degree of hydration, there is a fairly consistent relation between its mechanical properties and its porosity. If these data are extended to very low porosity, however, it is obvious that porosity by itself does not fully define the system (1-3).

Autoclaved cement pastes and pastes mixed with quartz and other sources of silica have been studied extensively by several investigators (4-12) and the sequence of reactions and nature of the products are reasonably well understood. It has generally been concluded that low strengths are associated with the formation of α-C_2S hydrate or hydrogarnets at medium to high porosities and that high strengths are associated with the formation of 11 Å tobermorite together with poorly crystallized CSH(I) and CSH(II). The high strength compounds are formed when a sufficient quantity of ground quartz or equivalent material is added to the cement. On the basis of their work on a variety of materials Feldman and Beaudoin (10), Crennan et al (7) and Taylor (13) concluded that there exists an optimum ratio of crystalline to poorly crystallized products for a high strength product; others considered that porosity alone could account for strength differences (14).

These approaches made it apparent, however, that several significant factors should also be considered in studying the mechanical properties of hydrated cements. Accordingly, a porosity study should include the following:
(i) The relation of pore structure to bonding between crystallites and bonding within crystallites.
(ii) The effect of pore size or shape and total porosity on mechanical properties.
(iii) The effect of the nature of the solid; its mineralogical and chemical composition, its crystal size and density on the relation between porosity and mechanical properties.

These factors were discussed by Polak (15) in his study of the kinetics of structure formation of cements and by Jambor (5) in his study of porosity. Significant findings in these areas will be discussed later.

3.1 MODULUS, STRENGTH AND BONDING

One of the first studies to indicate the type of bonding in hydrated portland cement is the compaction work of Sereda et al (16) and Soroka and Sereda (17). This showed that by merely compacting hydrated powder, bodies of strength and rigidity equal to hardened paste at this same porosity could be made; in addition it was shown that the bodies formed did not decrease in hardness or strength significantly when wetted from 15 to 100% RH. In fact, the modulus of elasticity increased significantly above 50% RH due to interlayer rehydration.

Further work by Feldman (18) showed that by compacting bottle hydrated powder in a d-dried state with dehydrated interlayer spaces, a body could be obtained with Young's modulus of a magnitude equal to that with interlayer water present. This was shown to be due to the sheets being forced closer together. Normally, without interlayer water, Young's modulus is low. A higher Young's modulus indicates that either some new solid bonds have been established or simply that the proximity of surfaces, which results in increased van der Waals' forces (as suggested by Wittman (19)) is contributing. The fact that the water compensates exactly for any decrease in Young's modulus when the layers move apart emphasizes the bridging role of the water. It probably participates in bonding, perhaps by coordinating with calcium ions between the sheets.

It seems possible that the type of bonds that appear to form between sheets within a layered system might form between individual particles of C-S-H by compaction, or between different particles of C-S-H, originating from separate nuclei during hydration. The concept of cement paste as a continuous mass around pores, when the paste is reasonably mature rather than particles joined by special bonds may be a more useful concept with regard to models. Thus, the area of contact may be the critical factor in determining mechanical properties, and this is related to pore size and shape.

These concepts explain the particular ability of hydrating portland cement in filling space without large expansive strains. The very low surface areas observed by Mikhail and Abo-El-Enein (20) for pastes with low water-cement ratios and Hedin's views about pore filling (21) illustrate this point. Other bonds due to silica polymerization will form subsequently (22,23). Bentur et al (24) also observed increased silica polymerization with specimens under load.

The strength of a brittle material as opposed to Young's modulus is controlled by critical flaws according to Lawrence et al (25). These may occur mainly at regions of inhomogeneity, such as at the interface of C-S-H gel and calcium hydroxide crystals. Care should thus be taken in relating measured strength of such a body in terms of strength of a specific bond.

3.2 EFFECT OF PORE SIZE, SHAPE AND POROSITY ON MECHANICAL PROPERTIES

The need to understand and improve strength and rigidity of portland cement and other concretes has led to the study of the influence of porosity on its mechanical properties. Correlation of porosity with mechanical properties has led to three types of equations, mainly semi-empirical. These are:

$$\sigma = \sigma_0(1-p)^A \qquad (3.1)$$

derived by Balshin (26);

$$\sigma = \sigma_0 e^{-Bp} \qquad (3.2)$$

derived by Ryskewitch (27). In these equations σ_0 is strength at zero porosity and p is the porosity. In the equation

$$\sigma = D \ln \frac{P_{CR}}{p} \qquad (3.3)$$

which was derived by Schiller (28), P_{CR} is zero strength porosity. A, B, C and D are constants.

Equations (3.1 and 3.2) were also used to relate Young's modulus to porosity. Schiller (28) showed that Eqs. (3.2 and 3.3) deviated only slightly at the two extremes of porosity: Eq. (3.2) is accurate at low porosities and Eq. (3.3) at high porosities.

Roy et al (1) and Roy and Gouda (2,29) used an equation similar to (3.3) to correlate data from specimens made to very low porosities and with high strengths by 'hot' and other forms of pressing.

These results are presented in Fig. 3.1.

Data from Yudenfreund et al (3) and Verbeck and Helmuth (14) are included in the figure. The results of Verbeck and Helmuth refer to capillary porosity and do not fit into the main curve. The rest of the data, plotted as porosity determined by water adsorption, is linear over a wide range of porosities.

Fagerlund (30) correlated data for paste using Eq. (3.1), but with different constants for each paste with a different degree of curing. In this case, σ_0 was around 500 N/mm^2 and the constant A about 3.

Danyushevsky and Djabarov (31) studied the total porosity, pore-size distribution and phase composition versus strength of hardened paste from oil well cements, C_3S, β-C_2S and mixtures of these with silica flour, diatomite earth and bentonite. The pastes, which were made at several water-cement ratios, were hydrated at room temperature and autoclaved. It was found that with these cements at a CaO/SiO_2 ratio of 2, a large crystalline structure of low strength was formed after autoclaving. With the CaO/SiO_2 ratio down to 0.8, however, material with smaller pores and of high strength and low permeability was formed. The products were tobermorite, xonotlite or CSH(B). The spread of pore-size distribution found in this work is shown in Fig. 3.2. Data were correlated according to Eq. (3.1) by plotting data as a function of capillary porosity. σ_0 was found to vary between 1.5 to 3.0×10^2 N/mm^2. These authors concluded that optimal strength at fairly high porosities was found with medium size crystals, such as xonotlite.

Dyczek and Petri (4) prepared specimens of tobermorite, xonotlite and CSH(I), and correlated data with an equation analogous to Eq. (3.2)

$$E = E_0 \, e^{-Bp} \qquad (3.4)$$

where E is Young's modulus and E_0 is Young's modulus at zero porosity. They found E_0's to be 5.01, 0.097, and 0.762×10^5 (N/mm^2) respectively and discussed the results in terms of the very low value for xonotlite. The value for tobermorite seems excessively high. Porosities were measured by water adsorption and the values are not realistic because tobermorite loses and regains large amounts of structural water on drying and wetting.

Jambor (5), recognizing the importance of pore size as well as the type of product and total porosity, prepared a variety of materials using $Ca(OH)_2$, several siliceous materials, C_3S, and C_3A. He measured pore-size distribution, pore volume and compressive strength. The five types of products formed and a plot of compressive strength vs volume fraction of each solid is shown in Fig. 3.3. It was found that pastes containing the same type of hydration products had similar pore-size distributions.

Pore-size distributions are tabulated in Table 3.I with the approximate pore radius range as determined by the mercury porosimeter. Figure 3.3 also shows that there can be a considerable spread in compressive strength for the variety of materials at the same solid volume fraction or, in other words, at the same porosity. Jambor concluded that these

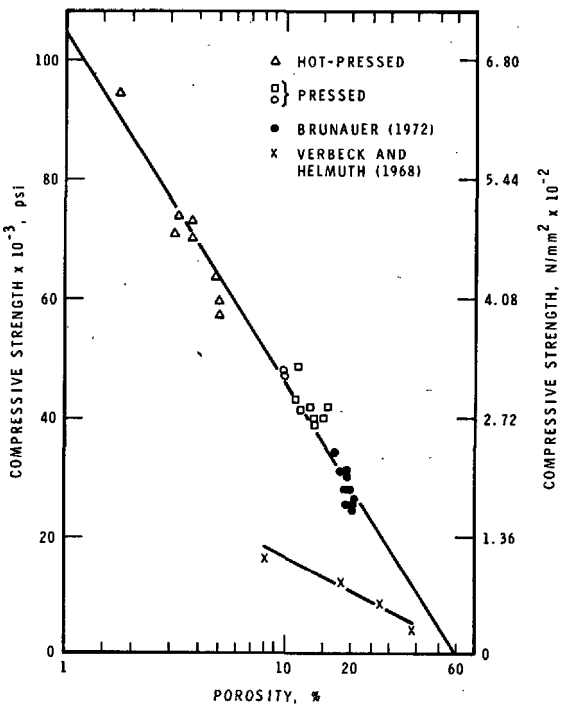

Fig. 3.1 - Relation of compressive strength and log porosity cement pastes (29)

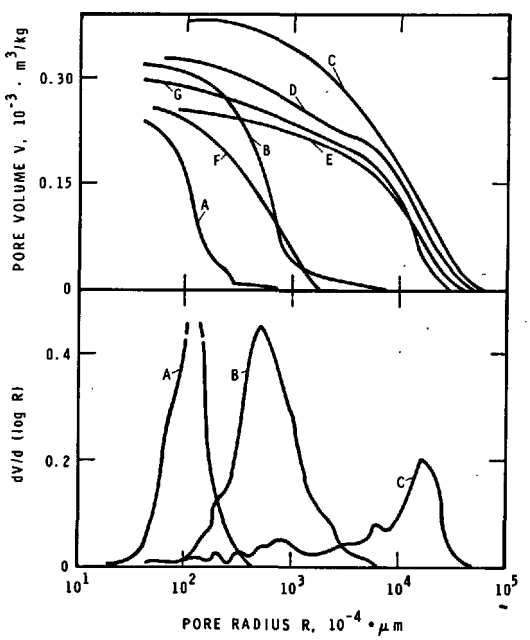

Fig. 3.2 - Pore-size distributions curves hydrated at various temperatures (31)

differences were primarily due to the average pore size within each characteristic composition; the smaller the pore size, the higher the compressive strength, at a given porosity. This is illustrated in Fig. 3.4.

Feldman and Beaudoin (10,32) measured and correlated strength and modulus data for several systems over a wide range of porosities. They measured compressive strength and Young's modulus of paste hydrated at room temperature, autoclaved cement paste with and without additions of fly ash and also included data of other workers (1,3). Measurements of porosity were obtained either from a helium pycnometer or from a capillary porosity calculation. Correlation was based on Eq. (3.2). Plots for strength data are shown in Fig. 3.5.

There are essentially three curves. Curve AB, representing all the pastes cured at room temperature, covers porosities from 1.4 to 41.5% and terminates at about 230 N/mm^2 at zero porosity. The second line, CD, represents the best fit for most of the autoclaved preparations exclusive of those made with fly ash. This line intersects AB at 27% porosity (w/c ratio: 0.45). At porosities above 27%, the room temperature pastes, when compared at the same porosity, are stronger than those made by autoclaving. This confirms Jambor's view that porosity is not the only factor that controls strength, but it may be related to the pore-size distribution. In addition, it may also be related to the type of bonding within the bulk material or between crystallites. This type of behaviour was also shown in the work of Beaudoin and Ramachandran (33), in which they compared the

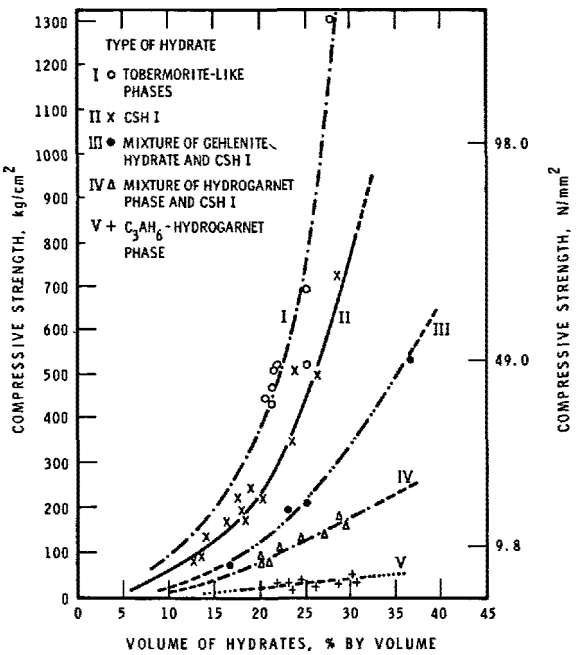

Fig. 3.3 - Relation between compressive strength and type as well as volume of binding hydration products developed in the hardened paste (5)

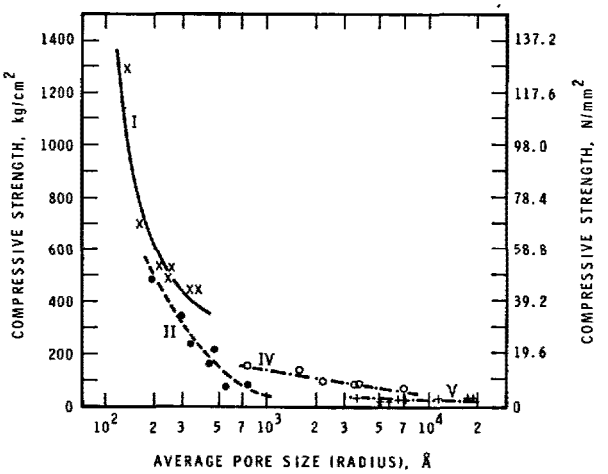

Fig. 3.4 - Relationship of compressive strength vs average pore size of hardened pastes containing hydration products (Types I, II, IV, and V) (5)

TABLE 3.I - Values of average pore size defining the pore size distributions of the hardened pastes containing hydration products of Types I to V (5)

Type of hydration product in paste	Approximate average radii of pores (Å)
I. Mostly tobermorite and tobermorite-like phases	100 - 400
II. Mostly CSH(I)	200 - 800
III. Mixture of about 70-80% gehlenite hydrate and 20-30% CSH(I)	500 - 1 000
IV. Mixture of about 70-80% hydrogarnet phase and 20-30% CSH(I)	700 - 7 000
V. C_3AH_6 - hydrogarnet phase	3 000 - 20 000

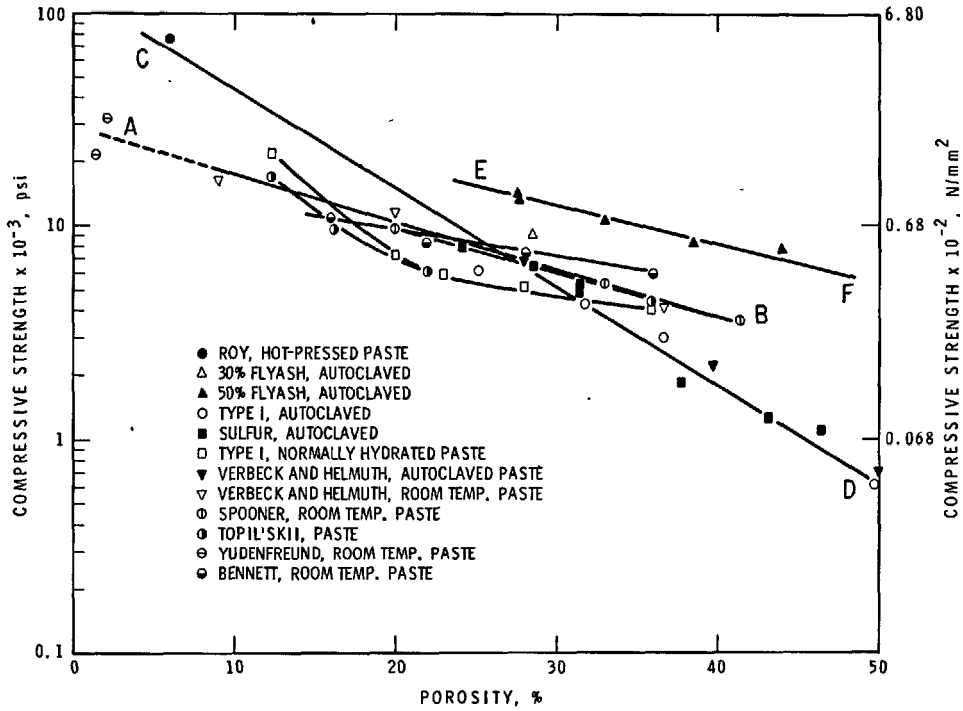

Fig. 3.5 - Strength vs porosity for autoclaved and room-temperature cured preparations (10)

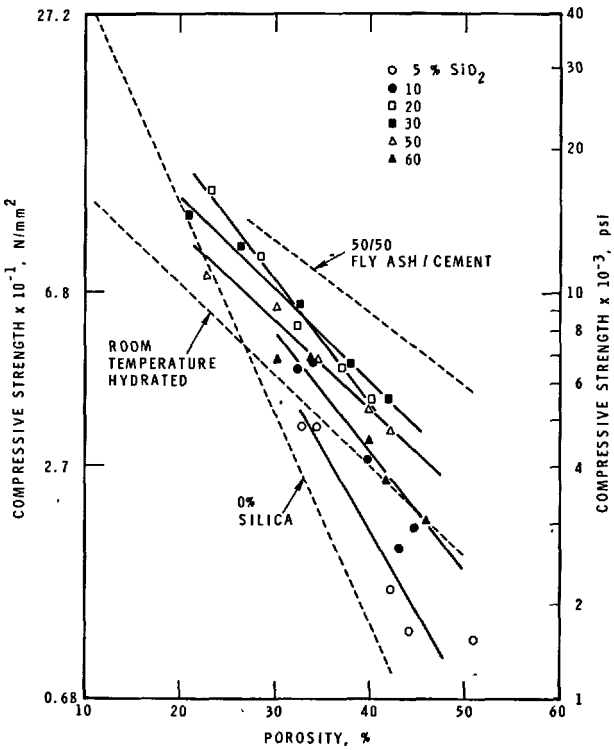

Fig. 3.6 - Compressive strength vs porosity for various autoclaved and room temperature hydrated cement and cement-silica preparations (11)

mechanical properties of several cements including magnesium oxychloride, gypsum and portland cement (see Fig. 1.5).

On the third curve, CD, points representing cement containing sulfur and those of hot-pressed data of Roy et al (1) are represented. At zero porosity a strength of over 800 N/mm^2 would be obtained for this series.

3.3 - EFFECT OF MINERALOGY AND SPECIFIC VOLUME ON THE RELATION BETWEEN POROSITY AND MECHANICAL PROPERTIES

Beaudoin and Feldman (10,11) prepared a variety of silicates by mixing different amounts of ground silica and normal type I cement and autoclaved each mixture at several water-cement ratios. Mechanical properties including microhardness, which approximately represents strength (34), were measured as a function of porosity. These results are plotted in Fig. 3.6 according to Eq. (3.2), $\sigma = \sigma_0 e^{-Bp}$; a family of mechanical property-porosity lines results. The σ_0 values and the B constant (the slope for each set of preparations) are presented in Table 3.II. The data of Danyushevsky and Djabaro (31) fall into the range of these data. As the silica content is varied, the slope B of the line changes.

In Fig. 3.7 are shown the range of specific volumes obtained in this series of preparations. Results show that mixtures with low silica content contain a predominance of well crystallized, high density α-C_2S when hydrated, while those with 20 to 40% silica contain predominantly CSH(I) and CSH(II) and tobermorite. The mixtures with 50 and 65% silica contain an excess of silica with tobermorite, CSH(I) and CSH(II).

The changes in slope and density support the view that an optimum amount of poorly crystallized hydrosilicate and well crystallized dense material provides maximum values of strength and modulus of

TABLE 3.II - Regression analysis of compressive strength vs porosity data (33)

$\sigma = \sigma_0 e^{-Bp}$

% SiO_2	σ_0 ($N/mm^2 \times 10^{-2}$)	B*	r**
0	9.500	0.1085 ±0.0142	0.949
5	3.105	0.0683 ±0.0138	0.945
10	6.223	0.0767 ±0.0138	0.967
20	5.200	0.0649 ±0.0038	0.995
30	2.952	0.0479 ±0.0018	0.988
50	2.254	0.0444 ±0.0053	0.977
65	2.838	0.0560 ±0.0067	0.987

* gives 90% confidence limits

** correlation coefficient

elasticity at a specified porosity. At high porosity, it is very evident that not only porosity but also the bonding of individual crystallites plays a role in controlling the strengths.

It is apparent that disorganized, poorly crystallized material tends to form a higher contact area of bonds, resulting in smaller pores. As porosity decreases, better bonding will develop between high density, well crystallized and poorly crystallized material and consequently higher strengths will result; the potential strength of the high density and high strength material is manifested. This explains how very high strength can be obtained by hot-pressing, because a small but adequate quantity of poorly crystallized material at these low porosities provides the bonding for the high density clinker material. Work by Ramachandran and Feldman (35) with C_3A and CA systems has shown that at low porosities, high strength could be obtained from the C_3AH_6 product because increased area of contact forms between crystallites than is possible at higher porosities. Work with fly ashes of a variety of compositions has confirmed these concepts (12).

Taylor (13) and later Crennan et al (7), in a discussion of these ideas, suggested that the distribution of crystallinity in CSH formed in autoclaving can have a major effect on strength.

Increase in C-S-H crystallinity can either raise or lower strength, depending on the amount of unreacted quartz. This concept is presented in Fig. 3.8. Lines P to T present results obtained for 5 different quartz particle sizes by Crennan et al (7). The diagram illustrates that the effect of particle size may outweigh that of porosity. Alexanderson (36) also observed maxima in strength with crystallinity of calcium silicate hydrates.

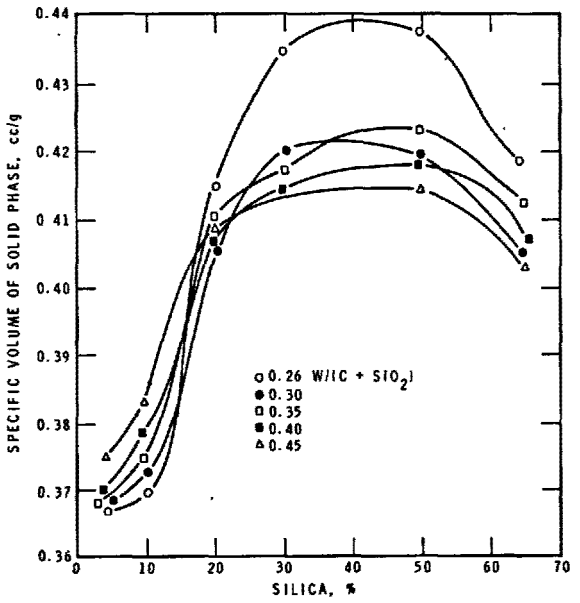

Fig. 3.7 - Specific volume of solid phase vs silica content for various autoclaved cement-silica preparations (11)

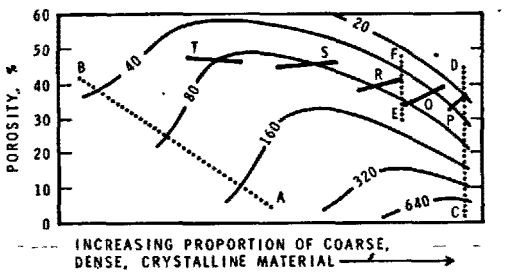

Fig. 3.8 - Compressive strengths (MPa) as a function of porosity and particle crystallinity distribution. Lines AB, CD, EF are as in Fig. 3.5 (7)

3.4 - PORE REDUCTION BY IMPREGNATION AND ITS EFFECT ON MECHANICAL PROPERTIES

The effect of porosity on modulus of elasticity can be described by Eq. (3.4). This equation has a theoretical base for its derivation (37,38) but contains several assumptions. The constant B depends on pore geometry and orientation of the pores with respect to stress. As explained in the last section, B varies with different preparations. Equation (3.4) predicts that filling of the pores, even with a foreign material, would lead to greatly improved mechanical properties.

The technique of impregnation has been performed on many materials such as cement paste, concrete (39 to 42) and porous ceramic tile (43) with methyl methacrylate, epoxy resins (44), and sulfur (45 to 47). Mechanical properties have been found to increase by several hundred percent and large improvements in water impermeability and resistance to corrosion have also been achieved.

Several workers have applied mixing rule equations to the concrete impregnation system to explain results (42,46,48,49). However, a high degree of impregnation has not been achieved owing to the size of the specimens, and thus bodies approximating non-porous, uniformly impregnated specimens were not obtained. The main conclusions were that the elastic modulus and compressive strength of the impregnated cement paste or concrete are functions of the residual porosity after impregnation and that the increase of fracture energy of impregnated cement is due entirely to the polymer itself and is independent of the initial strength of the porous body.

Hasselman et al (50) and Hasselman and Pentry (51) noted that large increases in elastic moduli are surprising in the light of present theories of elastic behaviour of composites with fibrous, cylindrical or spherical inclusions. They concluded that the pore geometry must deviate considerably from these models and they theoretically analyzed flat or elliptic inclusions. Expressions were derived relating the effect of a second phase on elastic behaviour to the stress concentrations in the matrix phase, e.g., for porous ceramic bodies having flat pore geometry major changes in elastic moduli resulting from polymer impregnation can be explained even when the elastic modulus of the impregnant is considerably less than that of the matrix.

Simplified equations used were:

$$E_c = E_{01}\,[1+\{\alpha V_s\,/(1+\gamma V_s)\}] \qquad (3.5)$$

$$H_c = H_{01}\,[1+\{\alpha V_s\,/(1+\gamma V_s)\}] \qquad (3.6)$$

where V_s is the volume fraction of the impregnant, α and γ are terms incorporating stress concentration factors, E_c and H_c are the Young's modulus and microhardness respectively of the composite, and E_{01} and H_{01} are these properties at zero porosity.

When the stress concentration term reduces to one, Eq. (3.5) reduces to

$$E_c = 1/\left(\frac{V_1}{E_{01}} + \frac{V_2}{E_{02}}\right) \qquad (3.7)$$

where subscript 1 refers to the matrix phase and subscript 2 to the impregnant phase. This equation is the same as that derived from Reuss' model.

Portland cement paste and autoclaved cement-silica mixes from which mechanical property vs porosity data have been obtained (Table 3.II and Fig. 3.9), were impregnated with either sulfur or methyl methacrylate (41,45). Specimens were discs of 3.2 cm diameter and 1.3 mm thick to facilitate complete and homogeneous impregnation. The residual pore volume of the specimens, measured by helium pycnometry, was, in most cases, lower than 3% of the volume of the sample.

Young's modulus and microhardness were plotted as a function of the volume fraction of sulfur. Linear regression of the results for Young's modulus are shown in Fig. 3.9. Each composition has a distinct

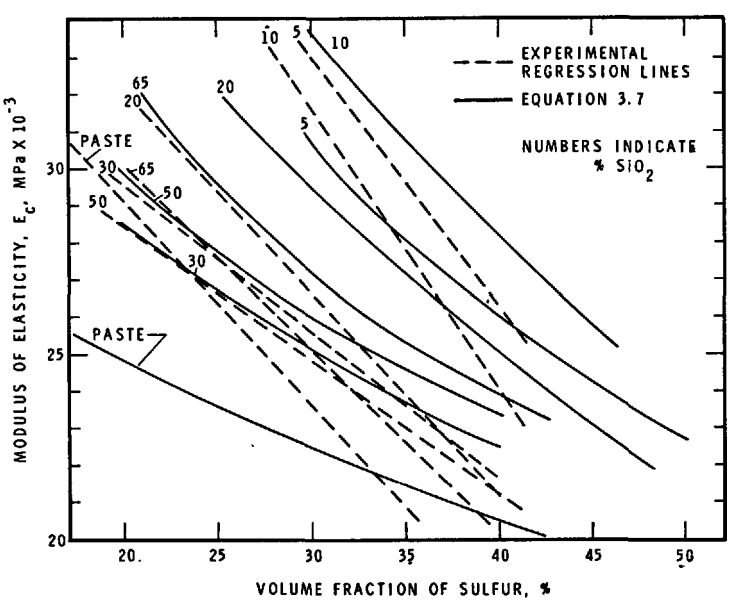

Fig. 3.9 - Young's modulus of composite vs volume fraction of sulfur for preparations with different initial silica contents (45)

curve; for each curve a theoretical curve was plotted. Best fit for Young's modulus was with the stress concentration term $\beta \to 1$, thus in effect using Reuss' model equation (Eq. 3.7). Values of E_{01} were obtained from Table 3.II; they in turn had been obtained by extrapolating data according to Eq. (3.4). Curves for the specimens containing the high proportion of weakly bonded α-C_2SH have the greatest value for Young's modulus at a given sulfur content.

Equation (3.7) provides an independent method for calculating E_{01} for the various matrices. All the terms in this equation are measurable. If these values are substituted using the experimentally determined point with the lowest sulfur content, E_{01} can be calculated for each composition (52). This is shown in Fig. 3.10; the values differ by an average of 13.5% from those determined by Eq. (3.2). These results support the view that Eq. (3.4) is a valid expression to predict the effect of porosity on Young's modulus.

Microhardness data, however, could not be correlated with a Reuss-type equation. Unlike modulus of elasticity, microhardness measurements involve failure processes; if stress concentration factors are not included the agreement of Eq. (3.6) is very poor. However, despite the use of stress concentration terms, there is greater deviation between theory and experiment for microhardness than there is for modulus.

The results from these impregnation experiments provide some data for understanding the role of pores in these cement systems. The fact that Eq. (3.7) does not contain any stress concentration term suggests that impregnation is effective in modifying local stress concentrations so that they do not significantly affect the calculation of the elastic modulus of the composite. This of course was not true for microhardness, which involves failure processes and much higher stress levels than were used for Young's modulus determinations. Nevertheless, significant improvements were attained in microhardness through impregnation. The ratio of microhardness, before and after impregnation, H_c / H_u, is plotted in Fig. 3.11.

Improvements were greater by a factor of 5 for the specimen autoclaved with 5% silica, while predictions from Eq. (3.6) and an equation of the type $H_u = H_0 e^{-B_H P}$ amounts to a factor of 4.25 at the same volume fraction of sulfur. Improvements for room temperature paste are about a factor of 3. This confirms that the shape of pores and the area of bonding are important in the strength formation of these systems. The systems containing α-C_2S were the weakest at intermediate porosities and had the lowest Young's modulus despite the high strength crystals (Fig. 3.6). However, after impregnation, they had the highest mechanical properties because impregnation provided the bond. Before impregnation, at these porosities, the bond between crystallites was very weak compared with pastes cured at room temperature and specimens autoclaved with 20 to 50% silica.

Much work has been done with methyl methacrylate as the impregnant (40,53) and impregnation has been performed with mixtures of polymers, e.g., n-butyl acrylate to methyl methacrylate (54) to give more ductility to the impregnant and thus to the composite. Thus, potential material properties can be tailored to particular structural service requirements as shown in Fig. 3.12. However, there is still much that is not known with regard to the state of the polymer in the pore, since the actual polymerization takes place

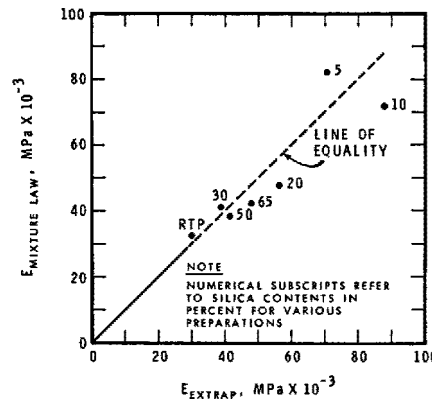

Fig. 3.10 - E_{01} calculated from mixture law vs E_{01} determined by extrapolation of log E vs porosity (52)

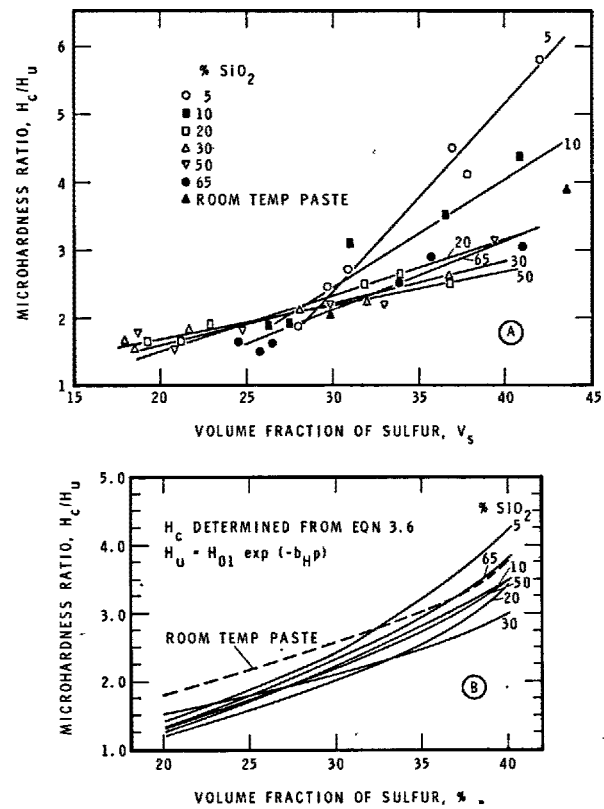

Fig. 3.11 - Ratios H_c / H_u (microhardness of impregnated sample to that of unimpregnated sample) vs volume fraction of sulfur of composite. (A - Experimental; B - Theoretical) (45)

in this confined space and it is unlikely that it will be the same as the polymer found under normal conditions. Little is known about the role of adhesion of the polymer to the matrix surface and about the durability of the composite. In an attempt to answer some of the questions the cement-silica systems were impregnated with methyl methacrylate (41). A calculation of E_0 for the polymer from

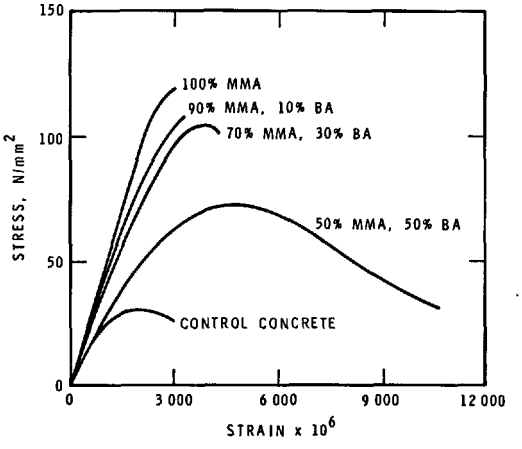

Fig. 3.12 - Compressive stress-strain curves (54)

Eq. (3.6) results in values varying from 6.3 to 11.8 x 10^3 MPa (N/mm^2). This is two to three times the value of the polymer formed in the bulk phrase. The paste samples hydrated at room temperature covered a wide range of porosities and the 0.7 and 1.1 water/cement ratios contained a high proportion of large pores. The calculated values for E_{02} for the water/cement ratios of 0.25, 0.45, 0.7 and 1.1 were 11.84, 11.54, 7.52 and 6.33 x 10^3 N/mm^2 respectively. Young's modulus of the bulk polymer is largely determined by van der Waals' forces between entangled long chains. However, when these long chains are formed in pores that have diameters of the same size as the length of the chains they may bond on both sides of a pore or crack. As a result, the properties of the polymer as it affects the composite may depend on the covalent bonds within a chain resulting in a higher composite modulus. As pores increase in size, the mean Young's modulus will decrease. Manson (in Ref. 53) has reported changes in the glass transition temperature of about 50 C deg for the polymethyl methacrylate in the pores. This may be due to the effects just discussed.

The values of Young's modulus for the polymer composite are similar to those for sulfur with regard to relative improvement for the various compositions but, quantitatively, the improvement ratios for the sulfur composites are higher. This is probably a result of the higher E_0 for sulfur. These results, however, are reversed in the case of the microhardness measurements, suggesting that the polymer has a much greater facility for bonding with the surface of the matrix and is more effective in modifying regions of stress concentration in the composite. This factor is more important for improved microhardness than for improved modulus.

REFERENCES (SECTION 3)

1.- D.M. ROY, G.R. GOUDA and A. BOBROWSKY (1972), "Very high strengths cement pastes prepared by hot pressing and other high pressure techniques," Cem. Concr. Res., 2, 349-366.

2.- D.M. ROY and G.R. GOUDA (1974), "Optimization of strength in cement pastes," Proc. Sixth Int. Congr. Chem. of Cement, Moscow, Vol. II, book 1, 310-314.

3.- M. YUDENFREUND, K.M. HANNA, J. SKALNY, I. ODLER and S. BRUNAUER (1972), "Hardened cement pastes of low porosity, V. Compressive strength," Cem. Concr. Res. 2, 731-743.

4.- J. DYCZEK and M. PETRI (1974), "The mechanical properties of calcium silicate hydrates existing in autoclaved cement-quartz materials," Proc. Sixth Int. Congr. Chem. of Cement, Moscow, Vol. II, book 2, 159-161.

5.- J. JAMBOR (1973), "Influence of phase composition of hardened binder pastes on its pore structure and strength." Proc. Conf. "Pore structure and properties of materials," Prague, Vol. II, p. D-75 - D-96.

6.- V.V. SIMONOV, I.F. TOLSTYKH, V.S. BAKSHUTOV, PIN-KHUAN TJAO, "Investigation and control of pore structure of oil well cement-store," Proc. Conf. "Pore structure and properties of materials," Prague, Vol. II, p. D-115 - D-128.

7.- J.M. CRENNAN, S.A.S. EL-HEMALY and H.F.W. Taylor (1977), "Autoclaved lime-quartz materials, I. Some factors influencing strength," Cem. Concr. Res. 7, 493-502.

8.- J. ALEXANDERSON (1979), "Relations between structure and mechanical properties of autoclaved aerated concrete," Cem. Concr. Res. 9, 507-514.

9.- V. SATAVA (1967), "Hardening of lime and silica at 175°C," Proc. Int. Symp. Autoclaved Calcium Silicate Building Products, London, p. 148-151.

10.- R.F. FELDMAN and J.J. BEAUDOIN (1974), "Microstructure and strength of hydrated cement," Proc. Sixth Int. Congr. Chem. of Cement, Moscow, Vol. II, book 1, 288-293.

11.- J.J. BEAUDOIN and R.F. FELDMAN (1975), "A study of mechanical properties of autoclaved calcium silicate systems," Cem. Concr. Res. 5, 103-118.

12.- J.J. BEAUDOIN and R.F. FELDMAN (1979), "Partial replacement of cement by fly-ash in autoclaved products - theory and practice," J. Mat. Sci. 14, 1681-1693.

13.- H.F.W. TAYLOR (1977), Discussion of paper, "Microstructure and strength of hydrated cements," by R.F. Feldman and J.J. Beaudoin, Cem. Concr. Res. 7, 465-468.

14.- G. VERBECK and R.A. HELMUTH (1968), "Structures and physical properties of cement pastes," Proc. Fifth Int. Symp. Chem. of Cement, Tokyo, Vol. III, 1-31.

15.- A.F. POLAK (1974), "Kinetics of cement stone structure formation," Proc. Sixth Int. Congr. Chem. of Cement, Moscow, Vol. II, book 1, 58-64.

16.- P.J. SEREDA, R.F. FELDMAN and E.G. SWENSON (1966), "Effect of sorbed water on some mechanical properties of hydrated portland cement pastes and compacts," Highway Research Board, HRB Special Report 90, 58-73.

17.- I. SOROKA and P.J. SEREDA (1968), "The structure of cement stone and the use of compacts as structural models," Proc. Fifth Int. Symp. Chem. of Cement, Tokyo, Vol. III, p. 67-73.

18.- R.F. FELDMAN (1972), "Factors affecting the Young's modulus-porosity relation of hydrate portland cement compacts," Cem. Concr. Res. 2, 375-386.

19.- F.H. WITTMAN, A. PUCHNER, and H. WELBACK (1975), "Properties of colloidal particles in hardened paste," Int. Congr. Colloid and Surface Chem., Budapest.

20.- R. SH. MIKHAIL and S.A. ABO-EL-ENEIN (1972), "Studies on water and nitrogen adsorption on hardened cement pastes; development of surface in low porosity pastes," Cem. Concr. Res. 2, 401-414.

21.- R. HEDIN (1974), "Strength and structure of mortar with mixtures of hydraulic compounds," Proc. Sixth Int. Congr. Chem of Cement, Moscow, Vol. II, book 1, p. 283-287.

22.- A.K. SARKAR and D.M. ROY (1979), A new characterization technique for trimethyl-silylated products of old cement pastes," Cem. Concr. Res. 9, 343-352.

23.- E.E. LACHOWSKI (1979), "Trimethylsilylation as a tool for the study of cement pastes, 2. Quantitative analysis of the silicate fraction of portland cement pastes," Cem. Concr. Res. 9, 337-342.

24.- A. BENTUR, N.B. MILESTONE, J.F. YOUNG and S. MINDESS (1979), "Creep and drying shrinkage of calcium silicate pastes, IV. Effects of accelerated curing," Cem. Concr. Res. 9, 161-170.

25.- F.V. LAWRENCE, J.F. YOUNG and R. BERGER (1977), "Hydration and properties of calcium silicate pastes," Cem. Concr. Res. 7, 369-378.

26.- M.Y. BALSHIN (1949), "Relation of mechanical properties of powdered metals and their porosity and the ultimate properties of porous metal," Dokl Adad. Nauk. SSSR, 67, 831-834.

27.- E. RYSHKEWITCH (1953), "Compression strength of porous sintered alumina and zirconia," J. Amer. Ceram. Soc. 36, 65-68.

28.- K.K. SCHILLER (1971), "Strength of porous materials," Cem. Concr. Res. 1, 419-422.

29.- D.M. ROY and G. GOUDA (1973), "Porosity-strength relation in cementitious materials with very high strengths," J. Amer. Ceram. Soc. 56, 549-550.

30.- G. FAGERLUND (1973), "Strength and porosity of concrete," Proc. Conf. "Pore structure and properties of materials," Prague, Vol. II, p. D-53 - D-73.

31.- V.S. DANYUSHEVSKY and K.A. DJABAROV (1973), "Interrelation between pore structure and properties of hydrated cement pastes," Proc. Conf. "Pore structure and properties of materials," Prague, Vol. II, p. D-97 - D-114.

32.- R.F. FELDMAN and J.J. BEAUDOIN (1976), "Micro-structure and strength of hydrated cement," Cem. Concr. Res. 6, 389-400.

33.- J.J. BEAUDOIN and V.S. RAMACHANDRAN (1975), "Strength development in magnesium oxychloride and other cememts," Cem. Concr. Res. 5, 617-630.

34.- P.J. SEREDA (1972), "Significance of microhardness of porous inorganic materials," Cem. Concr. Res. 2, 717-729.

35.- V.S. RAMACHANDRAN and R.F. FELDMAN (1973), "Significance of low water/solid ratio and temperature on the physico-mechanical characteristics of hydrates of tricalcium aluminate," J. Appl. Chem. and Bio. Tech. 23, 625-633.

36.- J. ALEXANDERSON (1979), "Relationship between structure and mechanical properties of autoclaved aerated concrete," Cem. Concr. Res. 9, 507-514.

37.- S.P. BROWN, R.B. BIDDULPH, and P.D. WILCOX (1964), "Strength-porosity relation involving different pore geometry and orientation," J. Amer. Ceram. Soc. 47, 320.

38.- D.P.M. HASSELMAN (1963), "Relation between effects of porosity on strength and on Young's modulus of elasticity of polycrystalline materials," J. Amer. Ceram. Soc., 46, 564.

39.- A. AUSKEN and W. HORNE (1971), "Some properties of polymer impregnated cements and concretes," J. Amer. Ceram. Soc. 54, 282.

40.- M. STEINBERG, L.E. KUKACHKA, P. COLOMBO and B. MANOWITZ (1971), Multi-component polymer systems, Ed. R.F. Gould, Advances in Chemistry, Series No. 99, Amer. Chem. Soc., Washington, D.C.

41.- R.F. FELDMAN and J.J. BEAUDOIN (1978), "Studies of composites made by impregnation of porous bodies, 2. Polymethyl methacrylate in portland cement systems," Cem. Concr. Res. 8, 425-432.

42.- D. MANNING and B. HOPE (1971), "The effect of porosity on the compressive strength and elastic modulus of polymer impregnated concrete," Cem. Concr. Res. 1, 631.

43.- J. GEBAUER, D.P.H. HASSELMAN and R.E. LANG (1972), "Effect of polymer impregnation on physical and mechanical behavior of ceramic tile bodies," Amer. Ceram. Soc., Bull 51, 471-473.

44.- D WHITING and D.E. KLINE (1976), "Internal friction in poly-mer-impregnated cement paste," J. Appl. Polymer Sci. 20, 3337-3351

45.- R.F. FELDMAN and J.J. BEAUDOIN (1977), "Studies of composites made by impregnation of porous bodies, I. Sulphur impregnant in portland cement systems," Cem. Concr. Res. 7, 19-30.

46.- J.A. SOLES, G.G. CARETTE, and MALHOTRA, V.M. (1978), "Stability of sulphur infiltrated concrete in various environments," Advances in Chem., Series 165, Amer. Chem. Soc., "New Uses of Sulphur," Washington, D.C. p. 79-97.

47.- N. THAULOW (1974), "Sulphur impregnated concrete," Cem. Concr. Res. 4, 269.

48.- A. AUSKERN and W. HORN (1974), "Fracture energy and strength of polymer impregnated cement," Cem. Concr. Res. 4, 785.

49.- J.T. DIKEOU (1972), "Concrete-polymer materials, Fourth topical report," Brookhaven National Laboratories, Upton, N.Y., and U.S. Bureau of Reclamation, USBR-REC-ERC-72-10 and BNL 50328, Denver, Col.

50.- D. HASSELMAN,-J. GEBAUER and J.A. MANSON (1972), "Elastic behavior of polymer-impregnated porous ceramics," J. Amer. Ceram. Soc. 55, 588.

51.- D. HASSELMAN and R.A. PENTRY (1973), "Stress concentrations in polymer-impregnated porous brittle materials," J. Amer. Ceram. Soc. 56, 105.

52.- R.R. FELDMAN and J.J. BEAUDOIN (1977), "Impregnation as a technique for measuring zero porosity modulus of elasticity of porous materials," Cem. Concr. Res. 7, 143-148.

53.- POLYMER CONCRETES (1976), First Int. Congr. Polymer Concretes, London, 1975. Ed. The Concrete Society, Construction Press.

54.- WAI-FAH CHEN and E. DAHL-JORGENSEN (1974), "Polymer-impregnated concrete as a structural material," Mag. Concr. Res. 26, 16-20.

4. INFLUENCE OF ADMIXTURES ON THE STRUCTURE AND STRENGTH DEVELOPMENT

In the previous sections the nature and significance of bonds, porosity and other structural aspects of portland cement pastes have been discussed. Introduction of admixtures to the hydrating cement influences to different extents, changes in setting, strength, morphology, porosity, density, surface area, volume, etc. In this section such changes are discussed with particular reference to more recent contributions. It must be recognized that variations in results reported in the literature for apparently similar systems are not unexpected, especially where commercial admixtures are used. In the presence of admixtures, the structure of the hydrating cement or cement mineral depends on the type and amount of admixture, chemical and mineralogical composition of cement, surface area, reactivity, w/c ratio, period of hydration, temperature and humidity.

4.1 STRENGTH

4.1.1 Cement Minerals

A direct study of the influence of admixtures on the hydration and structuration of cement, although a useful approach from the practical point of view is not easy to interpret because the admixture may act in a complex way to affect the hydration of the individual phases and their hydration products. Hence, much attention has been directed to a study of the role of admixtures on the strength development in individual cement minerals.

Addition of $CaCl_2$ to portland cement results in a significant reduction in setting times and acceleration of strength development. Because of its ready availability, low cost and predictable performance characteristics and application over several decades, $CaCl_2$ is more widely studied than other accelerators (1). Compared with many other complex admixtures, $CaCl_2$ is relatively simple in terms of its chemical and physical nature. However, there is not only much controversy regarding the actual mechanism of its action but also a persistent disagreement on its effects on concrete (2).

The reactivity of cement minerals C_3S and C_2S to H_2O may be enhanced by increasing their fineness. In an examination of the strength development in C_3S and C_2S ground to different fineness values, Balazs and Boros (3) found that increased dosages of $CaCl_2$ and fineness resulted in higher strengths (Fig. 4.1). In the presence of citric acid, the strengths decreased with increased dosages. However, as the fineness increased the strengths were enhanced. The main factors promoting strength development at increased fineness values are the initial compactness of the structure and higher reactivity.

It is generally recommended that the dosage of $CaCl_2$ in concrete should not exceed 1.5% by weight of portland cement. This does not necessarily mean that strengths are lowered at higher dosages in cement pastes or in silicate phases. It has been observed by Traetteberg and Ramachandran (4) that in the system C_3S-$CaCl_2$-H_2O, at a w/s ratio = 0.5, addition of 2% $CaCl_2$ gives better strength than that obtained by 5% $CaCl_2$. However, at a w/s = 0.3, addition of 5% $CaCl_2$ yields even higher strengths than those obtained by 2% $CaCl_2$ at a w/s = 0.5 (Table 4.I) (4). This indicates that in a more compacted system proximity of the particles would promote better bonding on the surfaces and therefore higher than normal amounts of $CaCl_2$ can be tolerated for achieving strengths.

TABLE 4.I - Microhardness for C_3S pastes containing different amounts of $CaCl_2$ (4)

Hydration time, days	Microhardness (N/mm^2)			
	Water/solid = 0.5		Water/solid = 0.3	
	C_3S+2% $CaCl_2$	C_3S+5% $CaCl_2$	C_3S+2% $CaCl_2$	C_3S+5% $CaCl_2$
1	113	13	132	98
2	83	23	221	155
3	98	27	271	225
7	117	41	292	284
10	150	57	360	346
15	186	92	311	353

Modulus of elasticity of a cementitious system can be obtained by the ultrasonic pulse velocity technique. In a study of C_3S hydrated with calcium salts of thiocyanate, propionate, maleate, perchlorate and chloride, Lawrence et al (5) found that the velocities were higher with pastes containing admixtures. The velocity-time behaviour could partly be explained by the higher degree of hydration. Results with $CaCl_2$ were anomalous; compared to other admixtures, it gave lower velocities and lower porosity at equal degrees of hydration. Since the velocity depends on the density of the product and the number of contact points,

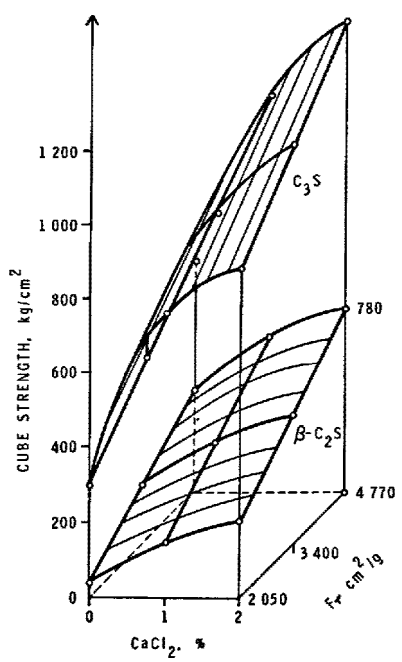

Fig. 4.1 - Effect of $CaCl_2$ on cube strength of C_3S and βC_2S pastes (3)

it is possible that in the presence of $CaCl_2$ the higher density product that is formed reduces the contact points. Hence the applicability of the ultrasonic technique for the cementitious systems containing admixtures should be re-examined especially since the structure of the hydrate product is changed.

The silicate structure changes occurring in the hydrated cements was followed by Lentz (6) using the trimethylsilylation reaction. He found that with time of hydration the orthosilicate content gradually decreased, giving rise to disilicate and polysilicate structures. As an extension of this idea, polymerization of silicates in pastes containing C_3S or C_2S and admixtures $CaCl_2$, citric acid and thionyl chloride was examined by Tamas et al (7). The hydrated products were found to contain mainly the dimeric $Si_2O_7^{6-}$ ions with small amounts of trimeric chains and tetrameric rings. In both C_3S and βC_2S, the ratio of the monosilicate/disilicate peak heights were lower for pastes containing $CaCl_2$ (Fig. 4.2) (7) indicating the increase in the disilicate formation with the progress of hydration. As it is known that there is an increase in strength in the pastes containing $CaCl_2$, it is possible that strengths tend to be higher in pastes containing larger amounts of polymerized silicates. The citric acid admixture which is a retarder shows less polymerization effect at very early ages. More work should be done before it can be stated that polymerization is directly related to strength development.

A comparison of the strengths developed in pastes containing different types of admixtures are usually compared at equal times of hydration. This method

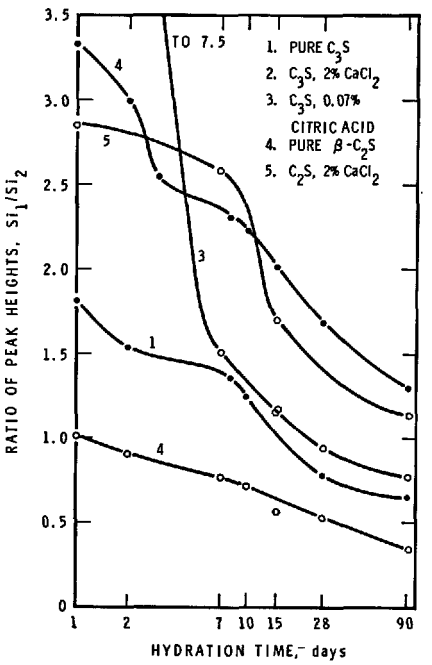

Fig. 4.2 - Peak height ratios in chromatograms of silylated reaction product of C_3S and C_2S pastes, with and without admixtures, as a function of hydration time (7)

does not provide information on the intrinsic property of the product. The intrinsic property can be studied by comparing the strengths at equal degrees of hydration. In an investigation of tensile strengths developed by βC_2S containing $CaCl_2$, NaF, $NaHCO_3$, NaH_2PO_4 and NaCl, comparison at 60% hydration showed different values (8). This would indicate that the nature of the products formed in the presence of these admixtures is different.

Admixtures also influence the strengths developed in C_4AF and C_3A pastes. In suspensions containing $CaCl_2$ concentrations of more than 3N, early strength of C_4AF can increase with the formation of a high chloride complex (9). Similar observations have been reported in the C_3A-$CaCl_2$-H_2O system containing 16% $CaCl_2$ (10). These results would indicate that depending on the conditions of hydration and the materials, a much higher than normal amount of $CaCl_2$ prescribed in cement can be used without detrimental effects to strengths.

4.1.2 Cement Pastes

The relative importance of factors influencing strength in a cement paste containing $CaCl_2$ is not completely resolved. Although it is recognized that $CaCl_2$ yields high early strengths, there is no agreement on its influence on long-term strength development; the values may increase, decrease or remain the same as that of the reference cement paste. It is not even clear what the optimum dosage of $CaCl_2$ is for achieving the maximum strength. For example, contrary to general belief, Wolhutter and Morris (11) have found that the maximum strength at 28 days is achieved with 4 to 6% anhydrous calcium chloride. This indicates the existence of many factors that influence the strength development in concretes. As described already, comparison of the properties at equal degrees of hydration forms a good basis to study the intrinsic property of pastes hydrated in the presence of different amounts of admixtures. This approach was adopted by Ramachandran and Feldman (12) for an examination of strength development in portland cement pastes hydrated in the presence of 0, 1, 2 and 3½% $CaCl_2$. Figure 4.3 (12) shows that at any one degree of hydration the sample with 3½% $CaCl_2$ has the lowest strength; at lower degrees of hydration the sample containing 0% $CaCl_2$ is the strongest, although with the progress of hydration samples containing 1 to 2% $CaCl_2$ form stronger bodies than all others. Porosity, density and bonding are factors that affect these results. It is thus evident that addition of $CaCl_2$ not only changes the rate of hydration but also the intrinsic nature of the hydration products.

The Soviet literature contains references to the use of many complex admixtures (13,14). For example, by using nitrites and nitrates in combination with $CaCl_2$ higher strengths are reported at below-freezing temperatures. Mchedlov-Petrosyan et al (15) found that among the combinations used, a mixture of 1.1% $CaCl_2$ and 1.2% $Ni(NO_3)_2$ developed maximum strength. The higher strengths were attributed to a more complete hydration, low basic C-S-H formation and complex formation of the salt with the hydrating cement. Strengths are not a linear function of the degree of hydration and caution should be exercised when comparison is made of pastes containing complex admixtures. For example at 50% hydration of cement, the strengths developed with the $Ca(NO_3)_2$-$CaCl_2$ combination and the reference cement were, respectively, 160 to 230 kg/cm^2 (15.69 to 22.56 N/mm^2) and 100 kg/cm^2 (9.8 N/mm^2) (16).

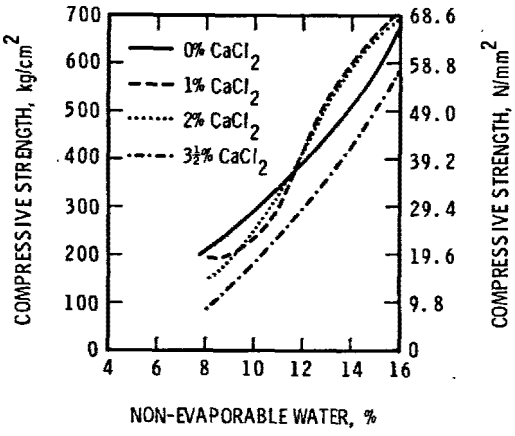

Fig. 4.3 - Strength vs non-evaporable water relationship for cement paste containing calcium chloride (w/c = 0.4) (12)

A number of organic and inorganic compounds, such as aluminates, sulfates, formates, thiosulfates, carbonates and amines, have been suggested as alternatives to the $CaCl_2$ accelerator. None of them has been found to be as efficient and economical as $CaCl_2$. Using chlorides of Ca, Ba, Mg and Fe, Ranga Rao (17) found that 1.6% $BaCl_2$ gives 1-day strength equivalent to that obtained with 2% $CaCl_2$. However, the 28-day strength with $BaCl_2$ was lower than that obtained with $CaCl_2$. It was also found that $BaCl_2$ is not as efficient an accelerator as $CaCl_2$ at 10 to 15°C. It is likely that the differences in the solubility of $BaCl_2$ and $CaCl_2$ play a role in the mechanism of acceleration and strength development.

Triethanolamine is a constituent in certain admixture formulations in concrete and its addition is thought to reduce the excessive retarding action of a water-reducing admixture. Consequently, it is assumed that when used alone it should act as an accelerator. It may act as an accelerator for C_3A, C_3A + gypsum hydration (18) and as a retarder for the hydration of C_3S (19). When added to portland cement, triethanolamine decreases its strength at all ages and also alters the setting characteristics (20). Fig. 4.4 (20) shows the strength development in cement pastes containing 0, 0.1, 0.25, 0.35, 0.5 and 1% triethanolamine. Strength decreases as the amount of triethanolamine is increased. Complex factors that may be involved for low strengths are: formation of C-S-H with higher C/S ratio, retardation of C_3S hydration, rapid initial setting followed by large heat development and a more porous structure. Sodium carbonate is also found to be an accelerator for the setting of cement. Strengths (1 to 28 days), however, seem to decrease by the addition of 2% Na_2CO_3 (21). In addition, there is an increase in the water requirement caused by the quick initial hydration of C_3S and C_3A components and the precipitation of $CaCO_3$. The slow strengths are attributed mainly to decreased rate of subsequent hydration.

Water reducers, such as lignosulfonates, hydroxycarboxylic acids and, more recently, superplasticizers have been used widely in concrete practice either to achieve higher water reductions while maintaining the same workability or to obtain higher workability at the same w/c ratio. Use of superplasticizers permits production of flowing concrete without any loss in strength. They can also be used to reduce water requirements by about 30% for the development of high strengths. Using 1 to 4% of a sulfonated melamine formaldehyde-based admixture, strength increases of the order of 50% over the control concrete have been obtained at the same slump value (Fig. 4.5) (22). There is still controversy as to whether the ultimate strength achieved, using a low w/c ratio (at nominal consistency) in the presence of a water reducer, is equal to or higher than the reference cement paste or concrete made at the same w/c ratio but at low workability (23-25). There is also some disagreement as to the relative strength values of cement pastes made with or without water reducers made at the same normal w/c ratio but with different workability characteristics. Generally the mix containing the water reducer yields higher strengths. The cement paste containing the water

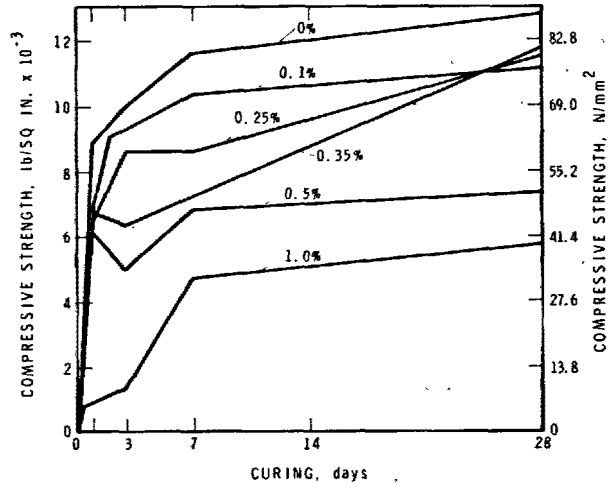

Fig. 4.4 - Compressive strengths of cement pastes containing triethanolamine (20)

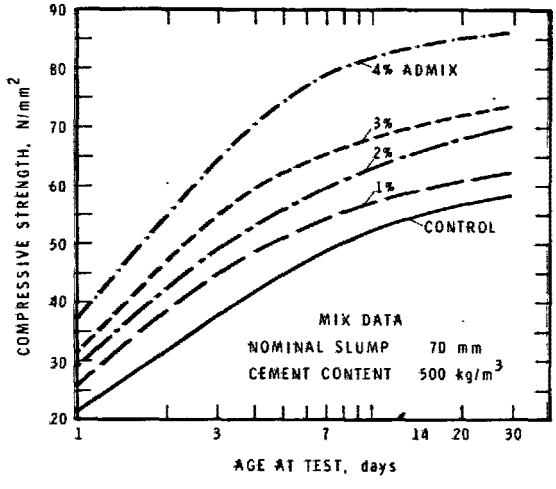

Fig. 4.5 - The variation in strength development of constant initial slump concrete with a superplasticizer (22)

reducer will have higher workability and will be better compacted, resulting in a better bonding of the hydrated products. Collepardi and Massida (26) have observed that a reduction in porosity occurs in such pastes containing the water reducer. In these pastes a higher degree of hydration has also been observed. It is thought that the water layer surrounding the cement particles in the presence of water reducers provides a source of efficient hydration (27).

Renewed interest has recently been shown in preparing cement pastes at a very low w/c ratio. This is achieved by using a high surface area clinker (6000 to 7000 cm^2/g) and a mixture of lignosulfonate with a carbonate or bicarbonate of K or Na. By this method a w/c ratio of 0.20 to 0.25 is possible and strengths of the order of 19 000 lb/sq in. (131 N/mm^2) have been obtained (28-31). Typically at a w/c = 0.22, the strengths at 15 h, 24 h and 3 days are, respectively, 2000, 9500 and 12 500 lb/sq in. (13.8, 65.5 and 86.2 N/mm^2). Strength gain follows the kinetics of hydration, unlike what was observed in the hydration of portland cement containing gypsum. It has also been reported that addition of the Na_2CO_3 + Na-lignosulfonate combination to clinker or clinker + gypsum at the same w/c ratio results in 1-day strength being higher and 28-day strength lower for gypsum-containing clinkers (30). The mechanism responsible for these effects is not immediately apparent.

Roy and co-workers (32) have been able to obtain strengths as high as 95 000 lb/sq in. (655.0 N/mm^2) in cement pastes by using the technique of hot-pressing. The resultant reaction products formed using this technique are different from those obtained in normal hydration reactions. Also a substantial portion of the cement remains unhydrated. In an investigation of the effect of various admixtures, viz., triethanolamine, $CaCl_2$, citric acid, sulfonated naphthalene condensate and a polymer resin on hot pressed type I and type III cements, $CaCl_2$ was found to give higher strengths (33,34). Generally strengths increased as the hydration progressed. Citric acid did not improve early strengths and triethanolamine gave very low strengths. The effect of admixture seems to be to change the rate of hydration and form a product that bonds the high density matrix of varying porosity. The presence of $CaCl_2$ seems to result in the inhibition of crystalline products (34) and a change in the nature of the polymerization of the silicates.

4.2 PORE STRUCTURE

Total porosity and pore-size distribution are important parameters that provide information on the possible strength and durability characteristics of cementitious materials. A plot of strength vs porosity plotted on a linear scale or as a semi-log plot shows the dependence of strength on porosity. Although such a relationship appears to exist over a range of porosity values, its use for prediction purposes is limited because the relation is different for different materials prepared in different ways. Some work has been carried out to determine the effect of admixtures on the pore structure of hydrating cement and cement minerals. Porosity and pore size distribution data for apparently similar materials may show significant differences depending on what methods are adopted for their determination.

4.2.1 Cement Minerals

A considerable amount of work has been done on the influence of $CaCl_2$ on the porosity and pore-size characteristics of C_3S paste. Working on C_3S containing 1% $CaCl_2$, Berger et al (35) found that at equal degrees of hydration the porosity of the paste containing $CaCl_2$ was lower than that of the reference paste. A plot of gel space ratio vs compressive strength indicated a linear relationship for pastes with or without $CaCl_2$ hydrated to different degrees. It was assumed that the specific volume of the pastes was not changed by the addition of $CaCl_2$. Recent work of Ramachandran and Feldman (12) on cement pastes has shown, however, that $CaCl_2$ influences the specific volume of the pastes. Since these workers (12) used Hg porosimetry with a maximum intrusion pressure of 30 000 lb/sq in. (206.9 N/mm^2), only pores of diameter >0.0065 μm could be registered. However, it is known that pastes containing $CaCl_2$ can have a substantial portion of total porosity in pores of diameter below 0.0065 μm (36-38). Collepardi (39) found that in C_3S hydrated with 2% $CaCl_2$ at 1 day, at a w/c = 0.5, the hydrated product had most of the pores in the range of 10 to 50Å radius. Skalny and co-workers (40) using N_2 isotherms also concluded that C_3S hydrated in the presence of $CaCl_2$ for 28 days has a lower hydraulic radius (31.8Å) than that of the reference paste (53.3Å).

Figure 4.6 (41) shows the total porosity and effective pore diameter relationship obtained for C_3S hydrated to different times in the presence of 1% $CaCl_2$. As hydration progresses, porosity decreases because the hydration products fill the pores, and at 30 days the product contains mainly pores of smaller diameter.

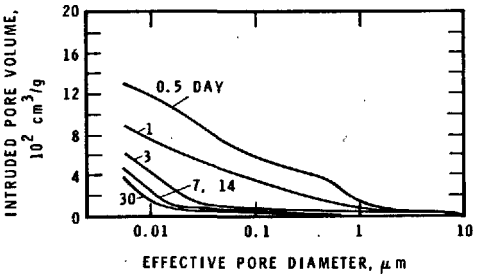

Fig. 4.6 - Intrusion curves of a series of C_3S pastes hydrated with calcium chloride (41)

In a study of the effect of 2 to 5% $CaCl_2$ on the properties of C_3S hydrated at w/s ratios of 0.3 and 0.5, Traetteberg and Ramachandran (4) found that an approximate linear relationship exists between porosity and logarithm of microhardness (Fig. 4.7). Lack of perfect linearity may be attributed to differences in pore-size distribution, composition and morphology.

Some work has been carried out on porosity and pore-size distribution characteristics of C_3S pastes hydrated in the presence of non-chloride admixtures such as calcium lignosulfonate, Na_2CO_3, polymers and calcium salts of maleate, perchlorate, propionate and thiocyanate. According to Collepardi (39,42), in C_3S pastes hydrated to 1 day the porosity and pore-size distribution data for the reference paste and that containing calcium lignosulfonate are almost the same. However, in the presence of Na_2CO_3 the total porosity decreases from 0.091 to 0.06 cm^3/g, and the volume of pores in the range 10 to 50Å is lower than that of

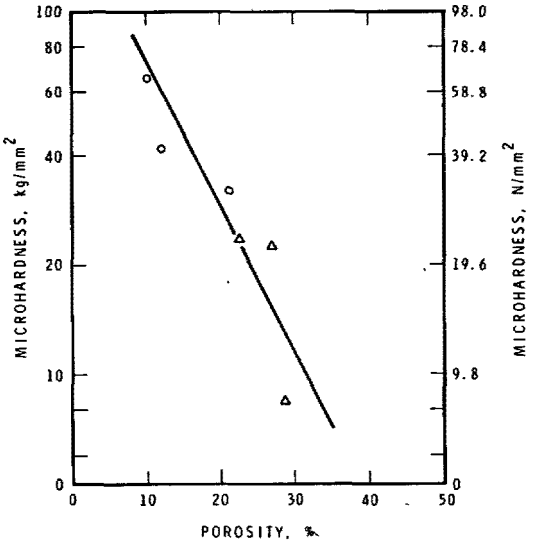

Fig. 4.7 - Microhardness vs porosity relationship for C_3S paste; w/s = 0.5 (Δ), w/s = 0.3 (o) (4)

the reference. The lower porosity was attributed to the precipitation of $CaCO_3$ on the pore entrances due to the reaction between Na_2CO_3 and $Ca(OH)_2$. No data were collected for these systems to assess how the porosity and pore-size effects determine strength. Although the pore structure is similar for the reference paste and that treated with calcium lignosulfonate, the intrinsic structure may have been different if the results had been obtained at the same degree of hydration.

Young and co-workers (5,41) have measured the porosity and pore-size distribution values of C_3S pastes hydrated with various calcium salts. Using mercury porosimetry, pore diameter only above 0.0065 μm could be determined. At a constant degree of hydration the intruded volume, as well as the pore-size distribution, varied from one sample to the other. The differences were ascribed to variations in gel porosity, isolated large pores, air-entrainment, etc., assuming that they should have the same porosity. As already discussed, there is no reason to assume that the paste containing an admixture should have the same porosity as the reference material at the same degree of hydration.

4.2.2 Cement Pastes

In an investigation on the effect of different amounts of $CaCl_2$ (0, 1, 2 and 3½%) on the properties of cement pastes, Ramachandran and Feldman (12) found that the product shows a decrease in porosity as hydration progresses (Fig. 4.8). Helium pycnometry was used to determine the absolute density of discs of the pastes, and the porosity was computed from absolute and apparent densities. When cement is mixed with water it sets into a rigid body. Water in the pores slowly reacts with the unhydrated particles forming the hydrated products; these products fill the spaces originally occupied by the water molecules as well as spaces originally held by the unhydrated particles. Because the density of the hydrated cement is lower than that of the unhydrated cement a decrease in porosity results during hydration. The decrease is steep during the first 24 h, and at the same time

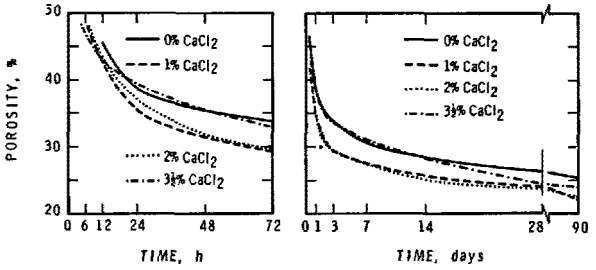

Fig. 4.8 - Porosity of cement pastes containing different amounts of calcium chloride (w/c = 0.4) (12)

there is a rapid rate of hydration. After 28 days most samples show a 50% decrease in porosity.

In Fig. 4.9 (12) the porosity of cement pastes is expressed as a function of the non-evaporable water content. Porosity decreases as the degree of hydration increases. The main factor causing this decrease is the filling of pores by the low density hydrated cement. A plot of absolute density vs

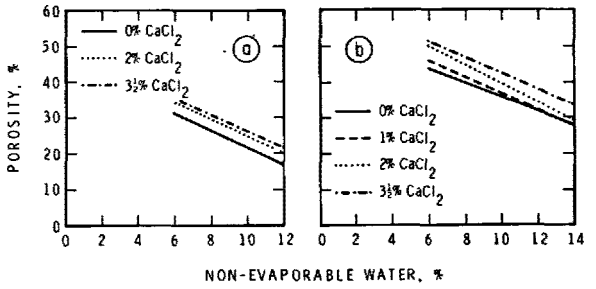

Fig. 4.9 - Porosity vs non-evaporable water relationship; (a) w/c = 0.25, (b) w/c = 0.4 (12)

porosity shows a linear relation (Fig. 4.10) (12). The relatively higher porosity values for pastes with a w/c = 0.4 are due to the higher initial amounts of water. A completely hydrated cement formed at w/c = 0.4 has an absolute density of 2.19 g/cm³ (43). An extrapolation of the line representing the sample made at a w/c = 0.4 to a density of 2.19 g/cm³ corresponds to a porosity of 22.5%. This is the minimum porosity that can be attained with a cement paste prepared at a w/c = 0.4 (made with or without admixtures). At the same degree of hydration for samples made at a w/c ratio of 0.4, porosity decreases as follows: Cement + 3½% $CaCl_2$ > Cement + 2% $CaCl_2$ > Cement + 1% $CaCl_2$ > Cement + 0% $CaCl_2$. Collepardi et al (44) compared the porosity of cement hydrated for 7 days with and without $CaCl_2$ and found that the total porosity was higher in the paste containing $CaCl_2$. The differences in the porosity obtained at the same degree of hydration indicate that the types of hydration products formed in pastes containing different

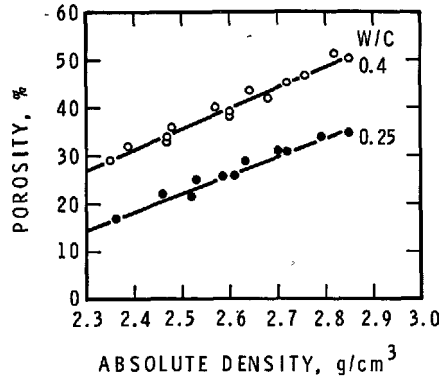

Fig. 4.10 - The influence of absolute density on the porosity of cement pastes hydrated with calcium chloride (12)

amounts of $CaCl_2$ are intrinsically different in nature. It can also be concluded that in this system the differences in porosity are mainly due to the variation in the absolute densities of the hydration products.

Although a substantial amount of work has been carried out on the effect of superplasticizers on the physico-mechanical characteristics of concrete, only meagre information is available on their effect on cement pastes. Collepardi (26) compared the porosity and pore-size distribution characteristics of cement pastes (with or without a superplasticizer) made at the same w/c ratios of 0.30, 0.35 and 0.44. The study covered only pore diameters in the range 0.01 to 1 μm. Porosity values were lower in samples containing the admixture and this was partly due to a higher degree of hydration (Fig. 4.11) (26). The results do not

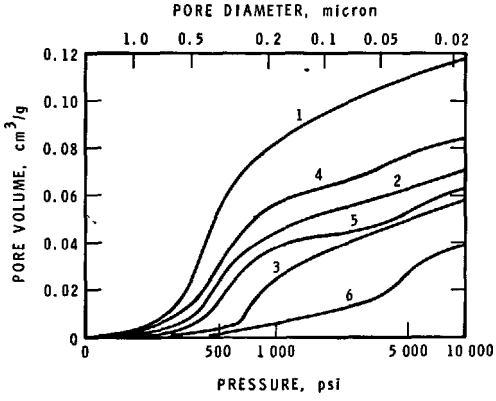

Fig. 4-11 - Cumulative pore volume in function of pore diameter or pressure of intruded mercury. The cement pastes were hydrated for 3 days with the following w/c ratios:

1 - w/c = 0.44; 2 - w/c = 0.35;
3 - w/c = 0.30; 4 - w/c = 0.44;
5 - w/c = 0.35; 6 - w/c = 0.30.
1-2-3 without Rheomac;
4-5-6 with Rheomac (26)

permit an evaluation of the intrinsic nature of the paste because pore volume was not determined for pore sizes below 0.01 μm. In another study, however, Collepardi et al (23) investigated the pore volume vs pore radius (down to 10Å) relationship for cement hydrated with calcium lignosulfonate. In the pore radius range 10 to 70Å, both the reference specimen and that containing lignosulfonate showed a similar relationship. The lignosulfonate-treated sample showed a larger volume of pores of radius >70Å than the reference paste. Similar trends were obtained in C_3S pastes containing lignosulfonate. The higher shrinkage rate observed in pastes containing lignosulfonate was explained by the presence of larger amounts of pores from which water can escape more rapidly.

Sodium carbonate can be used as an accelerator of setting. Addition of this admixture to cement changes the intrinsic nature of the hydrated product. Total porosity and pore-size distribution values of hydrated cement containing Na_2CO_3 are not the same as that of the reference paste. In the presence of Na_2CO_3 smaller pores (r = 10 to 100Å) are decreased and larger pores (r >150Å) are increased slightly (21). The reduction in small pores may be due to the precipitation of $CaCO_3$. A decrease in total porosity of cement pastes from 19.2 to 8.1% was observed by Butt and Kolbasov (45) when $NaNO_2$ was used as an admixture. The decrease in porosity was attended by an increase in compressive strength.

Uchikawa and Tsukiyama (46) compared the porosity of two regulated set cements A and B containing citric acid and $CaSO_4 \cdot \frac{1}{2}H_2O$, respectively. When strength was compared at different times, cement A containing citric acid appeared stronger than B containing $CaSO_4 \cdot \frac{1}{2}H_2O$. However, a comparison of strength at equal porosity values showed that cement B mix was stronger than cement A mix. This implies that the internal structure of mix B was different from that of mix A.

4.3 SURFACE AREA

Surface area studies of a hydrated cement may yield information on the reactivity, strength, shrinkage and volume changes of the paste. The unhydrated portland cement has a Blaine surface area of about 3000 to 4000 cm^2/g. In a set cement (saturated condition) the values, determined by the small-angle X-ray scattering technique (47), are as high as 600 m^2/g. This figure is even higher if computed for the C-S-H portion of hydrate. The specific surface area determined by H_2O vapour yields a value of about 250 m^2/g and that by N_2 decreases to 50% of this value or less. The large surface area indicates that the individual particles comprising the hydrated cement are of colloidal dimensions. It is generally observed that the surface area of a cement paste determined by H_2O vapour gives a reasonably constant value independent of the method of preparation or history. Surface area determined by N_2 gives values that differ for different preparations and accounts for changes occurring as a result of sample history and ageing processes. Addition of admixtures influences significantly the N_2 surface area of pastes; in this section these effects will be discussed.

4.3.1 Tricalcium Silicate

The N_2 surface area of hydrated C_3S or C_2S is increased in the presence of $CaCl_2$ (37,39,40,48-52). The extent of this increase differs, depending on factors such as particle size and purity of the silicate, w/s ratio, amount of $CaCl_2$ added, extent of hydration, temperature

of hydration and drying conditions. If water is used as the adsorbate, surface area values are found to be much higher than N_2 values. The H_2O surface areas of C_3S pastes containing calcium chloride are not much different from those hydrated without it.

Figure 4.12 shows the N_2 surface area values as a function of the time of hydration for C_3S (51). In the presence of $CaCl_2$ in the first day, the surface area is about 220 m^2/g, which decreases to a value of about 80 m^2/g in 3 months. This value is still about three times that determined for C_3S + 0% $CaCl_2$. Nitrogen area for C_3S + 5% $CaCl_2$ is even higher than that for C_3S containing 2% $CaCl_2$ (53,54). Though surface area decreases as the temperature of hydration is increased, at any temperature, samples containing $CaCl_2$ show higher surface areas than those without it (54). In Fig. 4.12, C_3S samples show a decrease in surface area as hydration progresses, and this is due to the "ageing" effect involving formation of physical and/or chemical interlayer bonds.

Surface area (by H_2O vapour) of hydrated C_3S carried out at a hydration degree of 64% shows a value of 324 m^2/g for C_3S + 0% $CaCl_2$ and a value of 261 m^2/g for C_3S + 2% $CaCl_2$ (40). The lower surface area is explained by the formation of C-S-H of higher c/s ratio and increased average thickness of the gel unit (55). A higher c/s ratio in the gel need not necessarily mean that it would have a lower surface area. For example, the gel with 5% $CaCl_2$ has a surface area of about 15 m^2/g larger than that formed with 2% $CaCl_2$, though the c/s ratio of the gel at 5% $CaCl_2$ is higher.

Shrinkage of a C_3S paste is increased in the presence of $CaCl_2$. If the measurements are carried out at a particular time, the values may reflect the extent to which the hydration has progressed. Hence, Berger et al (35) compared the shrinkage of the C_3S paste and C_3S paste + 1% $CaCl_2$ at constant degrees of hydration. At any degree of hydration the paste containing $CaCl_2$ showed a higher shrinkage. Though the higher shrinkage values have been thought to be due to an increase in the finer pore size range, it can be considered that a higher surface area promotes greater shrinkage.

The non-chloride admixtures may also influence the surface area of the C_3S pastes. At 1 day of hydration the specific surface areas of the hydrated portion of the reference C_3S paste, and that containing $CaCl_2$, Na_2CO_3 and calcium lignosulfonate, are, respectively, 45, 198, 26 and 47 m^2/g (39). Since C_3S is hydrated to different extents at 1 day, the results do not mean that the values will be similar if compared on this basis at all levels of hydration. Addition of triethanolamine (TEA) results in an increase in the surface area of C_3S paste. At 28 days of hydration N_2 surface areas of C_3S + 0% TEA, C_3S + 0.1% TEA and C_3S + 1% TEA are, respectively, 24.8, 30.9 and 44.6 m^2/g (19). It may be envisaged that the chemisorption of TEA on freshly formed C-S-H inhibits the orderly growth of plates in a tubular form and thus promotes the formation of a higher surface area product. Triethanolamine also increases the amount of non-crystalline $Ca(OH)_2$, and this factor may partly account for the increased area.

4.3.2 Cement Pastes

The addition of $CaCl_2$ increases the surface area of hydrated C_3S and hence it follows that a similar effect should also operate in portland cement paste. In the presence of $CaCl_2$, the surface area values of portland cement, pozzolanic cement and blast furnace cement increase from initial values of 43.2, 45.4 and

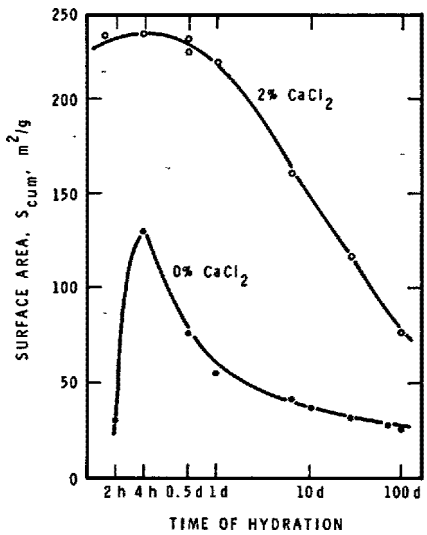

Fig. 4.12 - Surface area of a C_3S paste containing calcium chloride (51)

45 m^2/g to 76.3, 61.0 and 198 m^2/g, respectively (44). Calcium chloride is more effective in increasing the surface area of C_3S paste than that of portland cement paste. Part of the explanation is that $CaCl_2$ increases only marginally the surface area of the βC_2S component of cement. The small increase in surface area of the pozzolanic cement is due to the negligible influence of $CaCl_2$ on the lime-pozzolana reaction. The activation of the slag by $CaCl_2$ may explain its significant influence on this system.

The surface area of various cement pastes, determined at a particular degree of hydration, was reported by Ramachandran and Feldman (12). At a particular degree of hydration the surface area generally increases as the amount of $CaCl_2$ is increased (Table 4.II) (12). Chemisorption of Cl-ions on the

TABLE 4.II - Specific surface areas of cement pastes containing $CaCl_2$ at a particular non-evaporable water content (12)

$CaCl_2$, %	Non-evaporable Water, %	
	8.2	14.4
	Surface Area, m^2/g	
0	20.5	22.1
1	20.3	24.3
2	37.9	28.7
3½	37.3	32.2

hydrating surfaces may be responsible for this effect (53). The significant differences in the surface area values for the same degree of hydration suggest the existence of differences in the intrinsic properties of samples. At higher degrees of hydration, any decrease in surface area of pastes

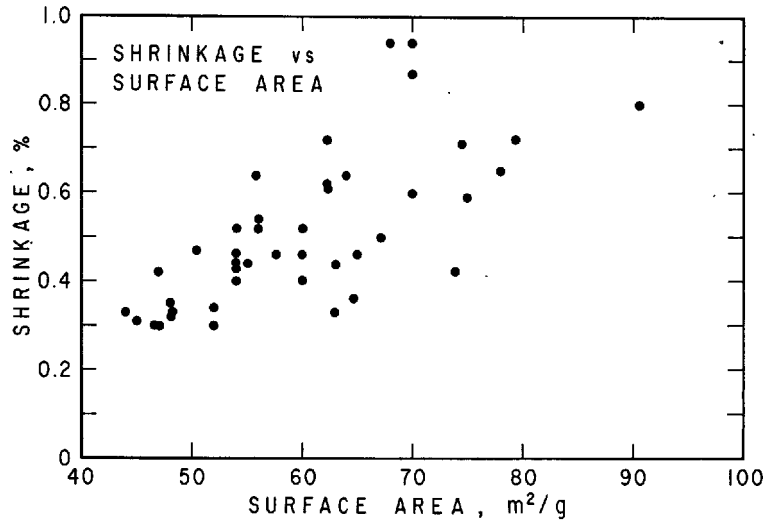

Fig. 4.13 - Shrinkage vs surface area for several admixtures (56)

containing 2 and 3½ $CaCl_2$ may be due to ageing. The shrinkage of a cement paste containing $CaCl_2$ depends on its surface area and the degree of hydration (44). If the degree of hydration is constant, the shrinkage values should depend on surface area. In Table 4.II (12), the surface areas of pastes containing $CaCl_2$ are larger than those containing no $CaCl_2$, indicating that shrinkage values should be higher in pastes containing $CaCl_2$. This has been verified for the system C_3S-$CaCl_2$-H_2O (35).

The significance of surface area on shrinkage in cements hydrated with calcium lignosulfonate, hydroxycarboxylic acid and triethanolamine has been investigated by Feldman and Swenson (56). A plot of shrinkage (drying from 100 to 50% RH) vs surface area (N_2) for various samples showed that samples producing higher shrinkages had significantly higher surface areas (Fig. 4.13) (56). It appears that shrinkage is associated more with the degree of dispersion of the pastes than with the chemical composition or morphology.

As stated earlier, $CaCl_2$ at normal dosages increases the surface area substantially. At normal dosages calcium lignosulfonate increases only marginally the surface area of cement paste. Collepardi et al (23) found that with calcium lignosulfonate the areas increased from 43-48 to 48-53 m^2/g. This increase was partly attributable to a higher degree of hydration in the presence of calcium lignosulfonate. Under similar conditions, addition of Na_2CO_3 decreased the surface area of cement paste from 43-48 to 22.7 - 26.0 m^2/g because of the blocking of pores by precipitated $CaCO_3$. The shrinkage values were also lower in these pastes.

4.4 MICROSTRUCTURE

The microunits formed in the cement paste are too small to be amenable to investigation by the optical microscope and consequently the electron microscope capable of very high resoltuion has received recognition for the examination of the microstructure of cementitious materials. Radczewski et al (57) were probably the first to apply this technique for investigating cementitious systems and since then several refinements to the technique have been made, resulting in the publication of innumerable micrographs. It is beginning to be recognized that comparison of results by different workers has an inherent limitation because of the small number of micrographs usually published and the correspondingly small area represented by these micrographs, which may indicate a non-representative view of the structure. What may be selected by one researcher as the representative structure may differ from that selected by another. Even the description of apparently similar features becomes subjective (58). Consequently, speculations on the origin of strength and other properties, when based on these observations, have limited validity, especially since many properties of cement paste are influenced at a much lower microlevel than can be observed by the electron microscope.

In spite of human and instrumental limitations, electron microscopic techniques have provided useful information on morphological features and an estimate of the elements contained in the microunits of various products. Depending on the starting materials and conditions of hydration, addition of admixtures to cements and cement minerals modifies to different extents the microstructure of the hydration products.

4.4.1 Tricalcium Silicate

The tricalcium silicate phase, constituting the major component in portland cement, greatly influences its strength characteristics and hence has received greater attention than other phases. A number of investigators have studied the effect of different concentrations of $CaCl_2$ on the morphological characteristics of hydrated calcium silicate. There has, however, been a variance in the actual description of the morphology (1). According to Odler and Skalny (55), hydrated C_3S normally forms spicules or sheets rolled into cigar-shaped fibres 0.25 to 1.0 μm long and in the presence of $CaCl_2$ a spherulitic morphology is facilitated. Kurczyk and Schwiete (59) reported that needle-like products change to spherulites in the presence of $CaCl_2$. Young (41) found that the morphology of hydrated C_3S + 0% $CaCl_2$ was needle-like whereas that of hydrated C_3S + 2% $CaCl_2$ was lace-like in structure. In contrast to the above, Murakami and

Tanaka (1) found the existence of a fibrous cross-linked structure in C_3S pastes treated with $CaCl_2$.

Using transmission electron microscopy, Ramachandran (53) found that C_3S hydrated at a w/s ratio = 0.5 showed needle-like morphology, whereas that hydrated in the presence of 1% or 4% $CaCl_2$ exhibited a platy or crumpled foil-like morphology (Fig. 4.14). Collepardi and Marchese (51) and Berger et al (60) came to similar conclusions. These changes in morphology may have resulted from the chemisorption of Cl^- ions on the C-S-H surface and introduction of these ions into the C-S-H lattice.

The morphological features become less distinct when the hydrated products are formed in a confined space, as for example, when the pastes are prepared at low w/s ratios. This is because the particles are so close to each other that there is not enough space for crystals to grow into larger dimensions. In Fig. 4.15 (12) are shown the micrographs of C_3S hydrated at a w/s ratio of 0.3 and obtained with 0, 2 and 5% $CaCl_2$. A dense structure for pastes with 2 and 5% $CaCl_2$ is evident and this feature may be responsible for a 50 to 150% increase in microhardness values over the paste containing no $CaCl_2$. It may, however, be argued that a lower porosity and better contact or bonding of the particles are factors causing strength increases. Bendor and Perez (61) have ascribed the higher strengths in C_3S pastes with $CaCl_2$ to the honeycomb nature of the paste as opposed to the sponge-like feature in the reference C_3S paste. Berger et al (35, 41) compared the microstructure of C_3S hydrated with and without $CaCl_2$ at the same degree of hydration and concluded that differences in external morphology indicated the differences in pore-size distribution. Porosity and pore-size distributions are recognized as important parameters affecting the strength development. However, in this work (35), it is not easy to assess pore sizes below 0.1 μm from the morphological features. Lawrence et al (5), on the other hand, have concluded that the outer morphology observed by SEM is not as important as the contact points closest to the unhydrated grains (which cannot be resolved by SEM) in assessing the mechanical properties of the C_3S paste. It is important, therefore, to recognize that morphology, porosity, density and chemical composition are mutually dependent factors that determine strength characteristics.

Addition of $CaCl_2$ modifies the morphology of autoclaved C_3S. Fibrous crystals and rectangular block-shaped crystals normally present are not found with $CaCl_2$. In the presence of $CaCl_2$, $C_3SH_{1.5}$ and α-C_2SH are not formed (62).

Changes in the C_3S paste microstructure occurring in the presence of admixtures containing Ca are well documented but their relevance to strength development is still largely unknown. Young and co-workers (5,63) studied the effect of various anions containing Ca^{++} as the common cation. The anions included perchlorate, thiocyanate, propionate, maleate and chloride. There was a change in the C-S-H morphology from an acicular to a lacey and honeycomb structure in the presence of some admixtures. Other changes such as the number of CH crystals per square millimetre, their relative sizes and crystal axis ratios, also occurred (Table 4.III) (63). The relevance of these changes to strength development is not completely clear and the results suggest that capillary porosity is the dominant factor controlling the tensile strength. The importance of the role of anions in modifying the morphology of βC_2S pastes has also been examined using sodium salts of fluoride, bicarbonate, chloride and orthophosphate (8).

Berger and McGregor (64) have made an extensive study of the microstructure of C_3S paste, with particular reference to the CH component. The pastes that

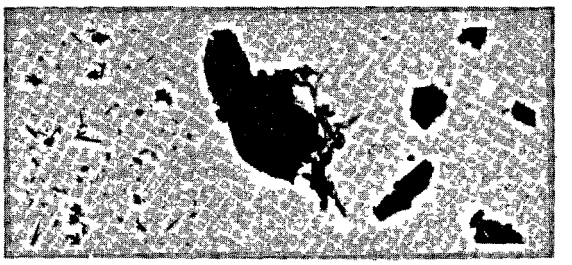

C_3S+0% $CaCl_2$ C_3S+1% $CaCl_2$ C_3S+4% $CaCl_2$

Fig. 4.14 - Electron micrographs of tricalcium silicate hydrated for one month (magnification × 1500) (53)

TABLE 4.III - Influence of admixtures on the microstructure of C_3S pastes (63)

Admixture	Effect on Hydration Kinetics (24 h)	Effect on Morphology		Approximate number of CH crystals/mm^2
		CSH Phase	CH	
Calcium chloride	Strong accelerator	Modified	Large c<<a	-
Calcium thiocyanate	Accelerator	Modified	Large c<<a	2.5
Calcium propionate	Accelerator	Unchanged	Small irregular	14.0
Calcium perchlorate	Weak accelerator	Unchanged	Large c<<a	3.0
Calcium sulfate dihydrate	Weak accelerator	Unchanged	Small c<a	4.0
Calcium maleate	Retarder	Modified	Large c<a	9.0

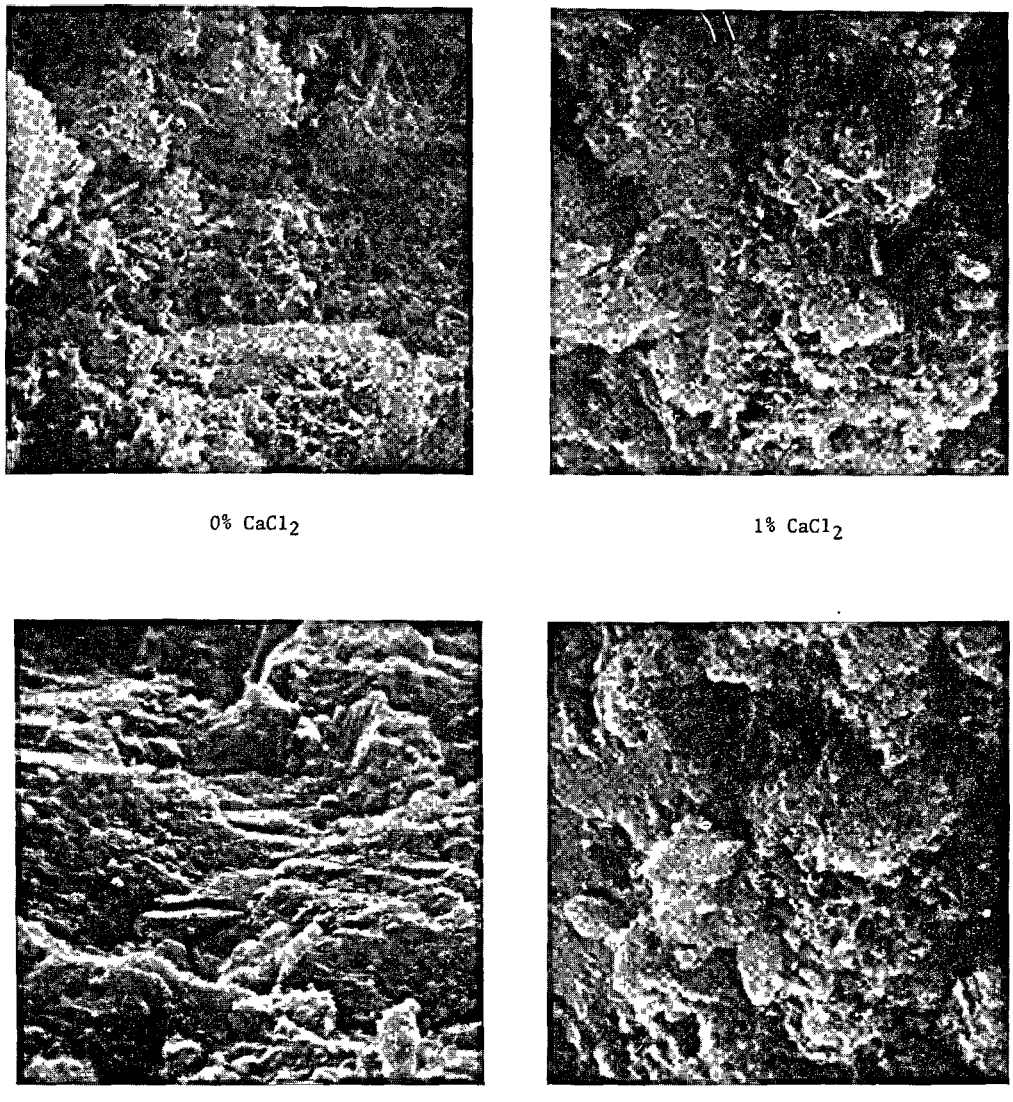

0% $CaCl_2$ 1% $CaCl_2$

2% $CaCl_2$ 3½% $CaCl_2$

Fig. 4.15 - Microstructural features of cement pastes containing calcium chloride and hydrated to a non-evaporable water content of 8.2% (magnification × 2400) (12)

resulted by using 62 admixtures could be divided into four groups, based on the c/a axis ratios. The morphology was found to be dependent more on the type of anion than on the type of cation. There is need to investigate how these differences influence the engineering properties. It has often been reported that in C_3S pastes containing various admixtures, the hexagonal phase typical of CH may or may not be present. According to Bendor and Perez (61), in pastes containing CdI_2 the hexagonal CH phase formed, whereas it was absent in the presence of $CaCl_2$ and $CrCl_3$. The mechanism responsible for these differences is not clear. In some instances the CH crystals may be obscured by the C-S-H gel.

4.4.2 Cement Pastes

Addition of $CaCl_2$ to the hydrating cement affects the microstructural features of the paste. Without the admixture, the paste may consist of clusters of sheets mixed with fibres, the fibres being much more abundant than in C_3S pastes. With the addition of 2% $CaCl_2$ the fibrous particles may be completely absent (23).

Ramachandran and Feldman (12) compared the microstructural features of cements containing 0, 1, 2, and 3½% $CaCl_2$, all hydrated to the same degree. At lower degrees of hydration (corresponding to a constant non-evaporable water content of 8.2%) pastes

containing 0% $CaCl_2$ showed well-defined needles representing C-S-H and ettringite formation. Columnar particles of CH, identified by energy-dispersive X-ray analysis, were also present. At 1% $CaCl_2$ addition, however, thin plates of C-S-H appeared. At 2% $CaCl_2$ the structure became more consolidated and contained plates and small particles. A sponge-like mass was evident at 3½% $CaCl_2$ addition. Specific area, density, porosity and strength differences existing between samples could not be explained on the basis of microstructure. Some of these may depend on microstructural features that are not easily resolved by the SEM. Also some of the features may be obscured by the deposition of a gel-like hydration product. Micrographs, however, showed that there were some morphological differences, especially at lower degrees of hydration. In hot pressed cements containing admixtures such as $CaCl_2$, triethanolamine and citric acid, Sarkar and Roy (34) found differences in strength development but the microstructural investigation yielded no useful information to explain the strength variations.

Cement pastes containing a normal water-reducing agent, as well as a superplasticizer, and formed at w/c ratios in the range 0.30 to 0.50 may not show any morphological changes with reference to the cement paste containing no admixture (23,65,66). This would imply that the differences observed in creep and shrinkage with calcium lignosulfonate cannot be explained by the microstructural examination using the SEM technique (66).

A study of the low porosity portland cement paste (containing no gypsum) prepared at w/c ratios of 0.22 to 0.24 with Na-lignosulfonate and Na-bicarbonate admixture has shown that the admixtures modify the microstructure (67). In place of fibrous and reticular network-type structure, normally found in a cement paste, the admixture-treated paste appeared as thin sheets in the first few hours and than as small equant grains. The presence of the admixtures promoted a more massive type of structure, implying improvement in mechanical properties. Odler et al (68) used a mixture of lignosulfonate and carbonate with clinker and portland cement and found no distinct differences in morphological characteristics of pastes (with or without admixtures) though there were differences in the composition of the hydrated products.

It is generally difficult to study the microstructure of pastes formed at very low w/s ratios. Further difficulty is experienced when the pastes are formed using the hot-pressing technique. Because of high pressure, high temperature and low amounts of water, the structure becomes dense and nearly 70% of portland cement remains unhydrated. Using the hot-pressing technique, Oyefesboi and Roy (33) made compacts of cement in the presence of various admixtures. Although substantial differences in strengths were observed, SEM showed no obvious differences.

REFERENCES (SECTION 4)

1.- V.S. RAMACHANDRAN (1976), "Calcium chloride in concrete," Applied Science Publishers, U.K., 216 p.

2.- V.S. RAMACHANDRAN (1978), "Calcium chloride in concrete - applications and ambiguities," Can. J. Civil Eng., 5, 213-221.

3.- GY. BALAZS and M. BOROS (1978), "Effect of calcium chloride and citric acid on the hydration of C_3S and βC_2S pastes," Periodica Polytechnica, 22, 29-35.

4.- A. TRAETTEBERG and V.S. RAMACHANDRAN (1974), "The microstructural and hardening behaviour of tricalcium silicate pastes in the presence of calcium chloride," J. Appl. Chem. Biotechnol., 24, 157-170.

5.- F.V. LAWRENCE, J.F. YOUNG and R.L. BERGER (1977), "Hydration and properties of calcium silicate pastes," Cem. Concr. Res., 7, 369-378.

6.- C.W. LENTZ (1966), "The silicate structure analysis of hydrated portland cement paste," Symp. Structure of Portland Cement Paste and Concrete, Highway Research Board, Special Rept. 90, pp. 269-283.

7.- F.D. TAMAS, A.K. SARKAR and D.M. Roy (1976), "Effect of variables upon the silylation products of hydrated cements," Proc. Conf. Hydraulic Cement Pastes - Their Structure and Properties, Univ. Sheffield, Cem. Concr. Assoc., pp. 55-72.

8.- J.F. YOUNG and H.S. TONG (1977), "Microstructure and strength development of beta dicalcium silicate pastes with and without admixtures," Cem. Concr. Res., 7, 627-636.

9.- N.P. STUKALOVA and E.P. ANDREEVA (1977), "Structure formation and chemical reaction in aqueous suspensions of tetracalcium aluminoferrite in the presence of calcium chloride," Kolld. Zh., 39, 508-512.

10.- A. TRAETTEBERG and P.J. SEREDA (1976), "Strength of C_3A paste containing gypsum and $CaCl_2$," Cem. Concr. Res., 6, 461-474.

11.- C.W. WOLHUTTER and R.M. MORRIS (1973), "Strength-imposed limitations on admixed calcium chloride content of concrete," Civil Eng., S. Africa, 15, 129-131.

12.- V.S. RAMACHANDRAN and R.F. FELDMAN (1978), "Time-dependent and intrinsic characteristics of portland cement hydrated in the presence of calcium chloride," Il Cemento, 75, 311-322.

13.- V.S. RAMACHANDRAN (1978), "Admixtures," Cements Research Progress, Amer. Ceram. Soc., Chapt. VI, pp. 119-157.

14.- V.S. RAMACHANDRAN (1977), "Admixtures," Cements Research Progress, Amer. Ceram. Soc., Chapt. VI, pp. 97-140.

15.- O.P. MCHEDLOV-PETROSYAN, A.G. OL'GINSKII and YU. M. DOROSHENKO (1977), "Influence of certain combined chemical additives on hydration and mechanical properties of clinker cement," Zh. Prik. Khim., 51, 1493-1498.

16.- V. RATINOV, T. ROZENBERG and V. TOKAR (1973), "The structure of the concrete pore space with CNN and CNNC admixtures," Proc. Int. Symp. Structure and Properties of Materials, Prague, pp. 205-215.

17.- M.V. RANGA RAO (1976), "Investigation of admixtures for high early strength development," Indian Concr. J., 50, 279-289.

18.- V.S. RAMACHANDRAN (1973), "Action of triethanolamine on the hydration of tricalcium aluminate," Cem. Concr. Res., 3, 41-54.

19.- V.S. RAMACHANDRAN (1972), "Influence of triethanolamine on the hydration characteristics of tricalcium silicate," J. Appl. Chem. Biotechnol, 22, 1125-1338.

20.- V.S. RAMACHANDRAN (1976), "Hydration of cement - role of triethanolamine," Cem. Concr. Res., 6, 623-631.

21.- M. COLLEPARDI, A. MARCIALIS and L. MASSIDA (1973), "The influence of sodium carbonate on the hydration of cements," Annali di Chimica, 63, 83-93.

22.- W.G. RYAN and R.L. MUNN (1978), "Some recent experiences in Australia with superplasticizing admixtures," Proc. Int. Symp. Superplasticizers in Concrete, Ottawa, Canada, pp. 279-293.

23.- M. COLLEPARDI, A. MARCIALIS and V. SOLINAS (1973), "The influence of calcium lignosulfonate on the hydration of cements," Il Cemento, 70, 3-14.

24.- R.C. MIELENZ (1968), "Use of surface active agents in concrete," Proc. V Int. Symp. Chem., Cem., Tokyo, Vol. IV, pp. 1-29.

25.- W.F. PERENCHIO, D.A. WHITING and D.L. KANTRO (1978), "Water reduction, slump loss and entrained air void systems as influenced by superplasticizers," Proc. Int. Symp. Superplasticizers in Concrete, Ottawa, Canada, pp. 295-323.

26.- M. COLLEPARDI and L. MASSIDA (1976), "The influence of water-reducing admixtures on the cement paste and concrete properties," Proc. Conf. Hydraulic Cements - Their Structure and Properties, Univ. Sheffield, Cem. Concr. Assoc., pp. 256-267.

27.- M.J. McCARTHY (1979), "Tests on set retarding admixtures," Precast Concr., 10, 128-130, 1979.

28.- S. DIAMOND and C. GOMEZ-TOLEDO (1978), "Consistency, setting and strength gain characteristics of a 'low-porosity' portland cement paste," Cem. Concr. Res., 8, 613-622.

29.- K.M. HANNA (1977),"Application of experience with low-porosity cement pastes and mortar," Zement-Kalk-Gips, 30, 140-142.

30.- J. SKALNY and I. ODLER, "Use of admixtures in production of low porosity pastes and concretes," Transp. Res. Rec. 564, pp. 27-38.

31.- I. ODLER, U. DUCKSTEIN and TH. BECKER (1978), "On the combined effect of water solubles, lignosulfonates and carbonates on portland cement and clinker pastes. I. Physical properties," Cem. Concr. Res., 8, 469-480.

32.- D.M. ROY and G.R. GOUDA (1973), "High strength generation in cement pastes," Cem. Concr. Res., 3, 807-820.

33.- S.O. OYEFESBOI and D.M. ROY (1977), "Effect of admixtures on hot-pressed cements," Cem. Concr. Res., 7, 165-172.

34.- A.K. SARKAR and D.M. ROY (1977), "Hot-pressed cements prepared with admixtures," Amer. Ceram. Soc. Bull., 56, 984-986.

35.- R.L. BERGER, J.H. KUNG and J.F. YOUNG (1976), "Influence of calcium chloride on the drying shrinkage of alite paste," J. Test. Eval., 4, 85-93.

36.- M. COLLEPARDI, G. ROSS and G. USAI (1968), "The paste and ball mill hydration of tricalcium silicate in the presence of calcium chloride," L'Industria Ital. Cem., 38, 657-663.

37.- J. SKALNY and I. ODLER (1972), "Pore structure of calcium silicate hydrates," Cem. Concr. Res., 2, 387-400.

38.- J.F. YOUNG (1973), "Effect of calcium chloride on the capillary porosity distribution in tricalcium silicate pastes," RILEM Proc. Int. Symp., Prague, pp. 197-204.

39.- M. COLLEPARDI (1973), "Pore structure of hydrated tricalcium silicate," Proc. Int. Symp. Pore Structure and Properties of Materials, Prague, pp. 25-49.

40.- J. SKALNY, I. ODLER and J. HAGYMASSY (1971), "Pore structure of hydrated calcium silicates. I. Influence of calcium chloride on the pore structure of hydrated tricalcium silicate," J. Colld. Interface, 35, 434-440.

41.- J.F. YOUNG (1973), "Capillary porosity in hydrated tricalcium silicate pastes," Powder Technol., 9, 173-179.

42.- M. COLLEPARDI (1974), "Porous structure of pastes of hydrated tricalcium silicate," Il Cemento, 71, 11-22.

43.- R.F. FELDMAN (1972), "Density and porosity studies of hydrated portland cement," Cem. Technol. 3, 5-14.

44.- M. COLLEPARDI, A. MARCIALIS and V. SOLINAS (1973), "The influence of calcium chloride on the properties of cement pastes," Il Cemento, 70, 83-92.

45.- YU. M. BUTT and V.M. KOLBASOV (1975), "Features of structure formation during the solidification of cements in the presence of water-soluble chemical additives," Khim. Met. Metall. Khim. Tekhnol. Silik., Mendelecusk. S'ezd. Obshch. Prikl. Khim., 11th pp. 186-187; Chem. Absts., 85, 197073, (1977).

46.- H. UCHIKAWA and K. TSUKIYAMA (1973), "The hydration of jet cement at 20°C," Cem. Concr. Res., 3, 263-277.

47.- D.N. WINSLOW and S. DIAMOND (1974), "Specific surface of hardened portland cement paste as determined by small angle X-ray scattering," J. Amer. Ceram. Soc., 57, 193-197.

48.- M. COLLEPARDI and L. MASSIDA (1971), "Hydration of tricalcium silicate in suspension," Annali di Chimica, 61, 160-168.

49.- A. RIO (1974), "Approaching to macromolecular characterization of the C_3S hydration process," VI Int. Congr. Chem. Cem., Moscow, Supp. paper, Section II, pp. 53.

50.- J. SKALNY and I. ODLER (1973), "Pore structure by nitrogen and/or water vapour of calcium silicate hydrates formed under different conditions," XI SILICONF, Budapest, pp. 505-519.

51.- M. COLLEPARDI and B. MARCHESE (1972), "Morphology and surface properties of hydrated tricalcium silicate pastes," Cem. Concr. Res., 2, 57-65.

52.- I. ODLER and J. SKALNY (1971), "Pore structure of hydrated calcium silicates. II - Influence of calcium chloride on the pore structure of β-dicalcium silicate," J. Colld. Interface Sci., 36, 293-297.

53.- V.S. RAMACHANDRAN (1971), "Possible states of chloride in the hydration of tricalcium silicate in the presence of calcium chloride," Matériaux et Constructions, 4, 3-12.

54.- M. COLLEPARDI, L. MASSIDA and G. USAI (1971), "The kinetics and the mechanism of ageing of tobermorite gel," Il Cemento, 68, 3-8.

55.- I. ODLER and J. SKALNY (1971), "Influence of calcium chloride on paste hydration of tricalcium silicate," J. Amer. Ceram. Soc., 54, 362-363.

56.- R.F. FELDMAN and E.G. SWENSON (1975), "Volume change on first drying of hydrated portland cement with and without admixtures," Cem. Concr. Res., 5, 25-35.

57.- O.E. RADCZEWSKI, H.O. MULLER and W. EITEL (1939), "On the hydration of tricalcium silicate," Naturwissenschaften, 27, 807.

58.- P.J. SEREDA and V.S. RAMACHANDRAN (1975), "Predictability gap between science and technology of cements. II. Physical and mechanical behaviour of hydrated cements," J. Amer. Ceram. Soc., 58, 249-253.

59.- H.G. KURCZYK and H.E. SCHWIETE (1960), "Electron microscopic and thermochemical investigations on the hydration of calcium silicates $3CaO.SiO_2$ and $\beta 2CaO.SiO_2$ and the effects of calcium chloride and gypsum on the process of hydration," Tonind. Ztg., 84, 585-598.

60.- R.L. BERGER, J.F. YOUNG and F.V. LAWRENCE (1972), Discussion of Ref. 51, Cem. Concr. Res., 2, 633-636.

61.- L. BENDOR and D. PEREZ (1976), "Influence of admixtures on strength development of portland cement and on the microstructure of tricalcium silicate," J. Mater. Sci. 11, 239-245.

62.- G. CHIOCCHIO and M. COLLEPARDI (1974), "Autoclave hydration of the constituents of portland cement in the presence of calcium chloride," Il Cemento, 71, 57-66.

63.- J.F. YOUNG, R.L. BERGER and F.V. LAWRENCE (1973), "Studies on the hydration of tricalcium silicate pastes. III. Influence of admixtures on hydration and strength development," Cem. Concr. Res., 3, 689-700.

64.- R.L. BERGER and J.D. McGREGOR (1972), "Influence of admixtures on the morphology of calcium hydroxide formed during tricalcium silicate hydration," Cem. Concr. Res., 2, 43-55.

65.- S.M. KHALIL and M.A. WARD (1977), "Microstructure of cement hydrates containing Ca-lignosulfonate admixture," Mater. Struct., 10, 67-72.

66.- S.M. KHALIL and M.A. WARD (1977), "Effect of degree of hydration upon creep of mortars containing calcium lignosulfonate," Mag. Concr. Res., 29 (98), 19-25, 1977.

67.- S. DIAMOND and C. GOMEZ-TOLEDO (1978), "The microstructure of low porosity portland cement paste," Il Cemento, 75, 189-194.

68.- I. ODLER, R. SCHONFELD and H. DORR (1978), "On the combined effect of water soluble lignosulfonates and carbonates on the portland cement and clinker pastes. II. Mode of action and structure of the hydration products," Cem. Concr. Res., 8, 525-538.

SUB-THEME VI - 2

Properties of hardened cement paste

F.H. WITTMAN
Delft University
NETHERLAND

1. INTRODUCTION

The state of the art of knowledge on structure and properties of hardened cement paste has been compiled by Copeland /1/, Kondo /2/ and Taylor /3/ for the 6th International Congress on the Chemistry of Cement held in Moscow in 1974. In this contribution it will be tried to point out some new developments and major achievements of the last six years.

It is not the aim of this report to provide a comprehensive literature survey of all papers published on properties of hardened cement paste. This task is being done by the contributors to the annual "Cements Research Progress" which is published by the Cements Division of the American Ceramic Society and threfore this literature is easily accessable to everybody.

Instead of summing up all contributions on different properties it is tried to concentrate on the work done on the characteristic behaviour which is directly related to engineering applications. Special emphasis is placed on the interaction of hardened cement paste with water, because all properties are influenced by a change of water content.

The real structure of hydration products forming the xerogel of hardened cement paste is still not yet understood well enough. Therefore all relations between macroscopically observed behaviour and processes in the microstructure remain tentative and should not be overestimated.

Until now most contributions have concentrated on physical and chemical properties of C-S-H gel. It will be shown that mechanics of solids has to be taken into consideration to avoid erraneous conclusions derived from simple test data. The writer feels that this is one of the most important new aspects of materials science of hardened cement paste.

Another comparatively young branch concentrates on probabilistic aspects. This may mean the formulation of a statistically representative characterisation of the complex microstructure but it may also mean a probabilistic description of materials properties. In this context computer simulation methods will play an important role.

Further development in this field will largely depend on a closer contact and a better mutual exchange of ideas between the different disciplines involved.

2. STRUCTURE OF HARDENED CEMENT PASTE

2.1. General Remarks

One of the general aims of materials science is to relate relevant properties with the corresponding materials structure. In this way much success has been achieved in metallurgy. Experimentally observed behaviour could not only be explained satisfactorily by means of elementary processes but some properties could be ameliorated in a systematic way. In concrete technology comparatively little improvement has been reached by fundamental approach.

This fact may partly be attributed to lack of knowledge on the structure of hardened cement paste. Although more than 30 years ago Powers and his coworkers started with serious investigations into the microstructure of hardened cement paste /4/, we are still far form fully understanding the system which is built up when cement is being mixed with water. Some recent trends of research on the microstructure will be briefly summarized in this section. It may be hoped that compilation of all results eventually may provide a solid basis for a materials science approach to study the most widely spread building material, concrete.

The structure of hardened cement paste can be subdivided into three major components: solid phase, pores and water.

The solid phase essentially consists of hydration products and remaining unhydrated clinker particles. A considerable amount of a given volume is occupied by pores with varying pore size distribution. Under normal conditions the pores are partly filled with water. The interaction of the solid phase with the surrounding adsorbed or capillary condensated water has a significant influence on all properties of hardened cement paste. Therefore water is considered to be a seperate component. In contrast air and water vapour within the pore system are being neglected. The three essential components just mentioned will be treated consicutively.

2.2. The Solid Skeleton : xerogel

The solid phase of hardened cement paste consists of crystalline and smaller amorphous particles, with respect to X-ray spectrometry. The structure and composition of hydration products will be dealt with elsewhere in this volume /5/. In this context we shall concentrate on the solid skeleton which is built up by hydration products thus forming a xerogel.

Sorption measurements once meant a real break through /4/. The importance of the information which has been gathered by means of sorption techniques can hardly be overestimated. Yet there remain serious limitations. It was early recognized that the hydration products are not stable with respect to drying and subsequent rewetting /6/. That means, the system which is being studied changes during the measurements. The high internal surface is reduced as the adsorbed water films are removed. In this way the total energy of the system is lowered. In addition to this effect some hydrate compounds loose some of their hydrate or interlayer water as the vapour pressure is reduced. Only after several drying-wetting cycles the system stabilizes /7/. This hygral instability of hydration products is one of the reasons that sorption measurements have often been disputed and interpreted in different diverging ways.

By introducing simplifying assumptions a model for the structure of hardened cement paste has been developed 8, 9/. This model (Munich Model) is essentially based on sorption measurements but additional information has been drawn a series of different approaches such as direct measurements of van der Waals forces at low distances, thermodynamic calculations and experiments to determine creep, shrinkage and strength as function of relative humidity.

With the help of this model the behaviour of hardened cement paste under different hydral conditions can be predicted quantitatively. In fact based on this model the time dependent deformation of concrete has been calculated and this method is now being applied to the design of real structures /10/.

The Munich Model suggests that the influence of water content on the properties of hardened cement paste can be explained by means of two different phenomenons, the surface energy of the colloidal particles and the disjoining pressure. In the region below 50 % relative humidity all properties are predominantly influenced by the surface energy of the gel particles. The surface energy changes due to sorption as the hygral equilibrium is changed. At higher relative humidities gel particles are separated by thin water films due to the action of spreading pressure of water. In the high humidity region therefore the xerogel, that means the structure of the soild phases, is mechanically less stable than in the dry state.

This model describing the interaction of the xerogel of hardened cement paste with water and the consequences for the mechanical behaviour has proved to be succesful in predicting quantitatively properties of concrete. The heterogeneity of elements within the actual xerogel is replaced by a statistical average. The model does not take into consideration properties such as morphology of individual gel particles. By means of Scanning Electron Microscopes some information on this aspect can be gained. A huge number of papers describe observations with this technique. The benefit to further developement of our knowledge, however, may sometimes be questioned. It must also be kept in mind that usual preparation techniques may alter the microstructure.

Diand classifies four morphological distinct varieties of C-S-H gel /11/. At the early ages fibrous particles are observed. Following a suggestion of Berger et al. /12/ Diamond calls these acicular particles Type I = fibrous particles. A second type of morphology is characterized by Type II = reticular network. Rather common in hardened cement paste are irrgularely equant or flattened particles. C-S-H particles of this form are designated by Diamond as Type III = equant grain. Finally there exists a phase which is normally maintained to an outer shell of other hydration products. This type is possibly filling the space which was originally occupied by C_3S. This type of morphology therefore is called Type IV = inner product.

The huge variety of different morphological details all present in hardened cement paste is not completely covered of course by these four types. There are many more details to be observed which may or may not be important for the properties of the system. Furtheremore one has to realize that a fractured surface does not necessarely represent a three-dimensional micristructure.

As scanning electron microscopes are further developed more information may be expected. Puchner has shown that visual inspection can be inaccurate and rather misleading /13/. He used conventional scanning electron microscopy in combination with scanning transmission electron microscopy.

Just one additional pecularity of the solid skeleton shall be mentioned here. It is well-known that most particles within the xerogel are not well defined chemical or mineralogical compounds. The calcium/ silica ratio for example may vary and many impurities have been detected /14/. As a result the actual composition varies locally and intergrowth takes place. In some cases the growth of fibrous particles (type I) is oriented in a fairly regular way by intermashing platelike material. In fig. 1 an example of this type of structure is shown /15/.

Considering the huge morphological variety in hardened cement paste it seems impossble to relate mechanical or non-mechanical properties directly with these structural details. It will probably turn out that the only way to approach this problem is to find appropriate statistical average representations. Computerized image analysing techniques may provide valuable information for a quantitative characterization of different microstructures.

As mentioned above X-ray spectroscopy gives only little information on the structure of elements in the xerogel of hardened cement paste. Based on earlier work by Lentz /16/ Tamas et al. /17/ used trimethylsilylation to determine the degree of polymerization of Si in hydration products.

This method proved to be most succesful and is now being applied by several groups of researchers. In a comparatively short time basically new information on the structure of C-S-H has been compiled /18 - 22/. Now it seems that the structure of hydration products markedly differs from quasi-crystalline calcium silicate hydrates such as tobermorite or jennite as has been earlier believed. There is no reason to believe that there in a layered structure.

It is not yet quite clear what the presence of dimer, linear or cyclic trimer, tetramer, and pentamer really implies for the properties of the xerogel. In any way the fruitless discusiion on postulated structural details used in simplifying models will come to and end. The quantitative determination of polymerization by means of trimethyl silylation provides a rational basis for a better understanding of gel properties. At this moment it cannot be differentiated whether polymerization exists within a gel unit or also across boundaries.

The mechanical properties depend on both the strength of the gel particles and their mutual coupling. Possibly further polymerization studies may lead to a better understanding of the link between structure and mechanical properties.

Since 1974 another method has been applied to study colloidal properties of the xerogel in hardened cement paste and that is MöBbauer spectroscopy. Usually the stiffness of a lattice immediately surrounding a MöBbauer isotope is determined by recoilfree resonance. It can be shown that in colloidal substances the recoilfree resonance is also influenced by the mutual coupling of gel particles /23 - 26/.

If the MöBbauer spectrum is measured as function of temperature the coupling force can be determined. It is of special interest to study the influence of porosity and adsorbed water layers on the mutual coupling within a xerogel. So far no other method can provide similar data.

Ubelhack /24/ has clearly pointed out that the porosity dependence of the elastic modulus of hardened cement paste is essentially caused by the interaction between colloidal particles. This result has to be taken into consideration if one tries to explain Young's modulus of xerogels as function of porosity and of structures having different gel particles.

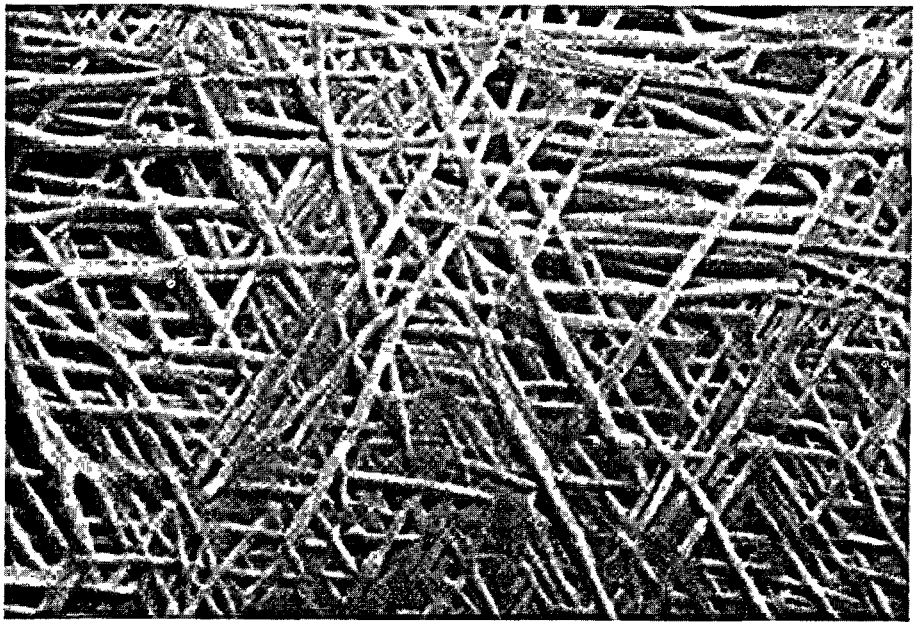

Fig. 1 : Micrograph taken with a Jeol ISM 35 with a magnification of 20.000x. The hardened cement paste was prepared using blast furnace slag cement. The orienting effect results in fairly regular fabric. (taken from Réf. /15/).

In concentrated suspensions the resonance lines of the MöBbauer spectrum are broadened by Brownian motion of the colloidal particles. As the Brownian motion of the gel particles gets obstructed the resonance lines become narrower. This effect was used to study the mobility of hydration products in water /27/. It was found that mechanical agitation destroys the gel structure in the suspension. After a few days, however, the metastable structure is rebuilt. This can be attributed to be ordering effect of thin wtaer layers between the colloidal particles.

It is obvious that by means of MöBbauer spectroscopy the compiling of particles in a xerogel as well as in a suspension can be determined. If one combines this new and non-destructive method with polymerisation studies it might be possible to develop a conclusive description of the structure of hardened cement paste. Furthermore it might be advisable to incorporate more of those techniques common in classical studies of colloids (see for example /28/) into the investigations on C-S-H.

2.3. Pore System

In the previous section it was tried to point out some recent developments of investigations into the solid skeleton of the porous material. In some respect a complementary branch of research is porology. The aim of porology is to characterize a porous system by indications such as total porosity, pore size distribution, and pore geometry. Related values are hydraulic radius and internal surface.

The is not one universal method to study porous systems but different techniques are being used in different ranges of pore size. Until an average pore radius of 20 nm sorption methods are widely used. As the hydration products are not stable with respect to drastic changes of vapour pressure results of water sorption measurements necessarely involve some uncertainty. But this is true for all other techniques. Pore size distributions calculated from water sorption measurements possibly do not differ far from reality and can be interpreted for instance in terms of degree of hydration /29/. Winslow and Diamond /30, 31/, however, found values for the internal surface by small angle X-ray scattering far in excess of those determined by water sorption. At this moment the meaning of this discrepancy is not clear.

Pores with a diameter between 10 m and 10 um can be observed by mercury intrusion techniques. Here again an inherent inaccuracy must be mentioned. The method assumes cylindrical pores with a constant taper. It is obvious that this condition is never fulfilled. As a consequence a characteristic pore size distribution is measured instead of the real one. The results can, however, be used for comparison of similar systems and to study different influences on the pore system. Kayyali et al. /32/ as well as Rostasy et al. /33, 34/ have used mercury intrusion method to determine the influence of temperature on the porous structure. Beaudoin has compared results of mercury intrusion method with those of helium pyconemetry /35/. He also discusses his findings critically.

Even larger pores can be observed with optical methods. Computerized image analyzing techniques have become popular /36/. Artificiel sphere-shaped pores caused by air entraining agents can be detected in this way. The preparation technique, however, remains difficult.

As most mechanical properties such as strength and Young's modulus are directly related to the pore system of a material several attempts have been made to investigate the pore structure of modified cement pastes. The influence of superplasticizers on the structure has been studied by Wittmann /29/. Diamond

and Gome-Toledo studied the microstructure of low porosity Portland cement paste /37/. Using a somewhat more finely ground clinker instead of gypsum, lignosulfonate and alkali-carbonate or bicarbonate is added to regulate setting behaviour. They found that the microstructure of low porosity cement paste is quite different from what is known about ordinary cement pastes. Mikhail et al. studied the influence of fibre reinforcement on the microstructure /38/. The total porosity and the specific surface area have been determined and discussed in comparison with mechanical properties.

2.4. Water in Hardened Cement Paste

All properties of concrete are severely influenced by the interaction of the porous hardened cement paste with water. The interaction of gel particles with adsorbed water molecules, however, is not yet satisfactorily understood even in much simpler systems. Therefore there still exist widely differing views on this subject.

By means of luminescence experiments it has been shown recently that the first adsorbed layers interact energetically with the surface of the xerogel. Monolayers also interact with clinker but no hydration does take place and the sorption process is reversible /39/. Only at much higher vapour pressures irreversible interactions can be observed.

A comprehensive report on the interaction of water with concrete has been published by Setzer /40/. He concentrates especially on thermodynamic aspects and develops a modified method to calculate pore size distribution from sorption measurements. Furthermore Setzer discusses mechanical properties of hardened cement paste on the basis of the Munich Model /8, 9/ as function of water content.

Lahajnar et al. /41/ have applied pulse NMR techniques for the study of water in hydrating cement. Their results clearly show that there are several modifications of differently bound water which essentially verifies earlier measurements /42/. The problem with NMR techniques, however, remains the comparatively poor resolution. In general these findings can be used in combination with other methods of investigation.

Winslow /43/ tried to apply the photoacustic effect to study properties of water in hardened cement paste. With this method the thermal expansion of a thin gas layer surrounding a specimen is measured. This small pressure pulse is caused by a chopped incident light beam. From the presented results one can conclude that the photoacustic effect is linearely increased as the water content decreases until D-drying state is reached. Further removal of water (heating) leads again to a linear increase of photoacustic effect but with a higher slope. At this moment it is not yet quite clear what actually affects the photoacustic signal. Probably it is mainly the absorption coefficient of the drying material. Anyhow the observed behaviour can at least qualitatively be explained on this basis and especially the further increase of the signal as hydration products are thermally decomposed is then a consequence of the changed optical properties /7, 44/.

With the major aim to study frost action and ice formation in hardened cement paste several authors determined phase transitions of water held in the pore system /45 - 48/. A typical example of measurements of the transition temperatures is shown in Fig. 2. Stockhausen et al. /48/ summarized these findings and they concluded that four different modifications of adsorbed and capillary condensated water can be distinguished.

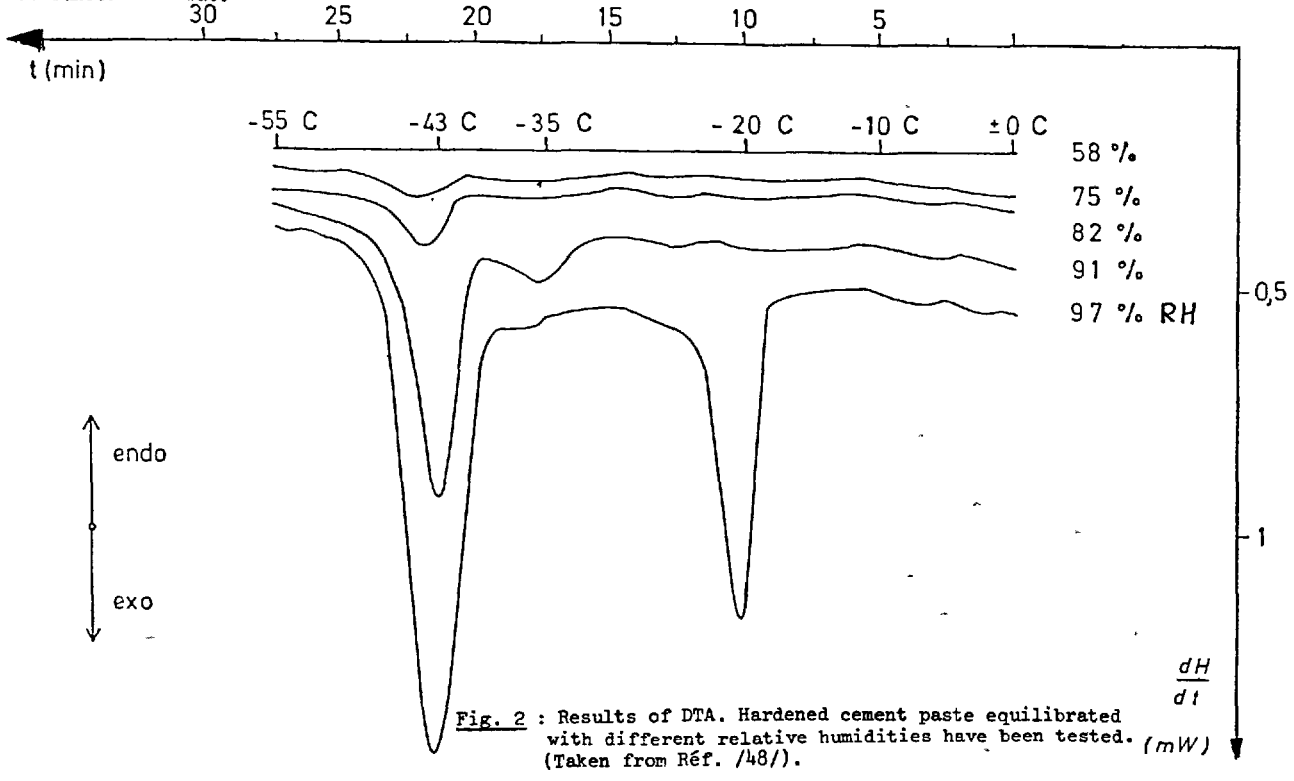

Fig. 2 : Results of DTA. Hardened cement paste equilibrated with different relative humidities have been tested. (Taken from Réf. /48/).

In capillaries with a radius bigger than 100 nm normal bulk water is observed.These big pores are only filled if the sample is in direct contact with water.

Water condensated in capillaries with a radius bigger than 10 nm has a reduced chemical potential because of the interaction with the solid surfaces. As a consequence the freezing point of this second modification is shifted towards lower temperatures. This type of water is taken up by capillary condensation at high vapour pressures : 90% $\leq$ RH $\leq$100 %.

In still smaller capillaries the condensated water is structured. The corresponding capillary radius may range between 3 and 10 nm. These pores are filled by condensation between 60 % and 90 % RH. The third modification undergoes a phase transition at a temperature around -43C.

Finally there is a fourth modification and that is water adsorbed in layers not thicker than 2,5 monolayers. This type of water does not freeze until a temperature of at least -160°C. The adsorbed films are firmly held on the surface but water molecules are very mobile within the layer. Therefore sometimes this fourth modification is called a two-dimensional van der Waals gas /9/. The comparatively high mobility along the surface has also been found by Vignes-Adler /49/.

This subdivision of adsorbed and capillary condensated water in hardened cement paste into four categories is based on experiments at temperatures below 0 C. It seems reasonable to assume that these conclusions hold true also at room temperatures.

3. MECHANICAL PROPERTIES

3.1. General Remarks

The study of details of the microstructure of hardened cement paste is fascinating. Advanced modern measuring techniques can be and are applied. Next to the methods mentioned above results of techniques such as Raman spectroscopy /50/, ESCA /51/ and high resolution electron microscopy /52/ are described in the literature. The aim of all these studies, however, is to provide gradually a solid basis for a better understanding of properties of concrete. By means of computerized structural design complicated load histories and multi-axial states of stress can be taken into consideration in a realistic way. But the advantage of these methods can only be fully utilized if the corresponding materials data are available. In this respect fundamental research on concrete properties has recently gained a great deal of importance.

We have just pointed out that the structure of hardened cement paste is a complicated colloidal system and that many details are still not really understood. The chemical and mineralogical complexity of the xerogel in hardened cement paste necessarily leads to a certain smearing effect. The discovery of a close relation between structural details and macroscopic properties is thereby hampered. This may be one of the reasons that some authors prepare pastes with pure cement clinker compounds. Strength development and drying shrinkage have been measured by Lawrence et al. /53/ and by Mehta et al. /54/ using tricalcium and β-dicalcium silicate pastes. Young and Tong /55/ investigated the microstructure and strength develop development of β-dicalcium silicate pastes with and without admixtures.

Certainly pure clinker pastes are generally easier to be described quantitatively but it may be questioned whether all results are characteristic for the material in which we are actually interested.

3.2. Load Induced Deformation

First of all we will deal with deformation of hardened cement paste under sealed conditions. If it were possible to model the complex structure of hardened cement paste realistically, by means of an enormous computer study the stress distribution within the solid skeleton could be evaluated. On principle the total, that means the instantaneous and the time dependent deformation, could then be calculated. Considering the actual microstructure it becomes quite clear that there is no hope that this aim will ever be achieved. This one may choose between a phenomenological and a statistical approach.

Several authors tried to relate what they call measured Young's modulus with properties of the microstructure. In the dry state hardened cement paste approximately reacts like a linear elastic material. But even then bending tests of small samples will lead to erraneous results because of crack formation in the surface zone. At higher relative humidities hardened cement paste reacts like a linear viscoelastic material with relaxation times in the order of magnitude of seconds. Therefore a quasi-static measurement cannot provide all the necessary information to characterize the material. This has been clearly pointed out by Sellevold /56/. Instead of simple Young's modulus the complex form, that is storage and loss modulus, have to be used to describe materials behaviour. The internal friction which is given by the loss modulus is most probably caused by water redistribution within the solid skeleton.

In Fig. 3 the deformation modulus as measured at samples with a water/cement ratio of 0,4 is plotted

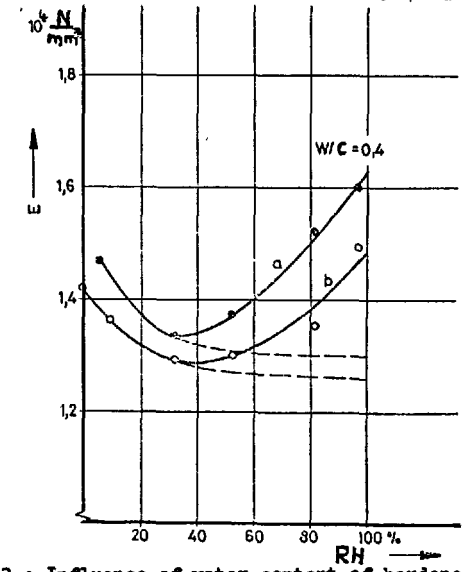

Fig. 3 : Influence of water content of hardened cement paste in equilibrium with different relative humidities on Young's modulus. Results of two test series are being shown. (Taken from Ref. /9/).

as function of relative humidity /8/. Dashed lines indicate the expected behaviour if only adsorbed water would interact with the xerogel. This behaviour is predicted by the Munich Model /8, 9/. The observed increase at higher relative humidities is caused by the above mentioned transition within the microstructure. The existence of internal friction and relaxation times in the order of magnitude of a test duration is an excellent example to point out how careful one has to be if one tries to correlate results of simple mechanical tests with microprocesses or properties of microstructure.

In many materials creep mechanism can be described in a statistical way by means of rate theory. This approach has been applied to hardened cement paste by several authors. Klug and Wittmann determined the activation energy and the activation volume of creep of hardened cement paste /57/.

The activation energy of the creep process has been experimentally determined by Straub /58/. He found a value of 4,45 kcal/Mol in the temperature range of -70C to +20C. Furthermore the activation volume has been evaluated from measurements of creep strain under compressive and tensile stress /59/. The activation volume depends on water/cement ratio and on age of loading. As can be anticipated the activation volume decreases as the microstructure becomes denser.

With the help of rate theory creep of hardened cement paste under sealed condition can be described satisfactorily. The influence of water content on creep in equilibrium can also be taken into consideration. Under practical conditions, however, creep is most often accompanied by drying shrinkage. This case will be dealt with in the following section.

3.3. Drying Shrinkage and Creep

As matured hardened cement paste is dried a volume change called drying shrinkage is observed. Here we shall not discuss chemical shrinkage or capillary shrinkage of fresh concrete /60, 61/.

Many authors have tried to correlate the macroscopically observed shrinkage with structural processes in the hydration products (see for example /62/). These attempts necessarily involve a great deal of ambuigity because as has been discussed above the structure itself is not well enough understood.

Young et al. /63/ came to the conclusion that shrinkage is caused by two different mechanisms and these are capillary drying and gel drying. Their subdivision is based on the measured length change plotted as function of weight loss. There is, however, no data point which would clearly indicate two regions of different mechanisms. But more important, the curve of length change as function of weight loss does not represent equilibrium points. The inner core of a sample may still be staturated while the outer shell is already dried to equilibrium with the ambiant water vapour pressure. The moisture gradient is essentially dependent on the diffusion coefficient and on geometry. That means the total deformation measured cannot be linked directly to the shrinkage mechanisms involved. The only materials property which can well be related with properties and processes of the microstructure is unrestrained shrinkage. This value has to be determined by extrapolation of measured data to zero thickness. Probably the extensive studies by Young et al. /63/ on the microstructure using among other methods mercury intrusion porosimetry, nitrogen adsorption, and determination of polysilicate content may be reinterpreted taking real shrinkage data as a basis for discussion.

By evaluating equilibrium shrinkage strain values at different relative humidities Wittmann /8, 9/ suggested on the basis of the Munich Model that hygral length change at low vapour pressure (RH < 50 %) is caused by a change of surface energy of the xerogel. At higher water content (RH > 50 %) the surface energy is not influenced drastically by drying or rewetting. It is assumed that in this region spreading pressure of water between gel particles causes additional length change. At very high humidities near saturation the action of capillary action can be observed.

It is well known that the xerogel of hardened cement paste is thermodynamically instable. The high potential energy which is stored in the large surface area tends to reach a minimum. Thus most changes around the xerogel will lead to a caorsening of the microstructure. Drying and change of temperature are two possibilities to influence the metastable state of the xerogel.

There is a long lasting discussion in the literature whether or not mechanical loading has a similar influence. Several authors suggested triggering processes caused by an external stress. Recently Gamble and Illston /64/ raised this argument again. Parrott /65, 66/ explained his experimental findings by introducing transient thermal creep. He found some analogy between polysilicate formation and transient thermal creep as defined by Illston and Sanders /67/. By means of an extensive experimental investigation Mindess et al. /68 - 71/ observed changes in the microstures of pure calcium silicate pastes as function of drying and loading. They subdivide the structure of calcium silicate paste into four groups. According to this classification the "C-S-H component" consists of C-S-H particles and the micropores (d < 2,6 nm), the "Pore Component" includes all mesopores and macropores (d > 2,6 nm). Besides of these two components they have characterized "Calcium Hydroxide" and "Unhydrated Silicate Residue" as two crystalline components. They conclude that irreversible strains are caused by changes in the "Pore Component" and the "C-S-H Component". Under load microshearing between C-S-H particles is believed to occur.

In this study /68 - 71/ very valuable data on the influence of drying and loading on the microstructure have been gathered. If, however, all the data available are condensed in a simple model, questionable assumptions on the microstructure have to be made. The actual meaning of all the data on changes in microstructure will probably only become clear when more quantitative details on the xerogel are at our disposal.

So far we have neglected one aspect which cannot be separated from considerations on shrinkage and that is crack formation. It is well-known that tensile strength of hardened cement paste is comparatively low. Stresses caused by the contraction of the drying outer shell rapidly overcome tensile strength. As mentioned above shrinkage strain of a tested specimen is not directly caused by shrinkage mechanisms but by the stress distribution which is given by the moisture gradient.

It can be shown that the stress distribution and as a consequence the measured shrinkage strain are severely influenced by crack formation. By means of a computer study shrinkage strain has been calculated /10, 72/. The approach is also mentioned in /73/. In Fig.4 the obtained shrinkage strain, taking crack formation into consideration, is plotted by a solid line. Dashed lines represent calculated shrinkage strain as an external load of 2 and 10 N/mm^2 is applied respectively.

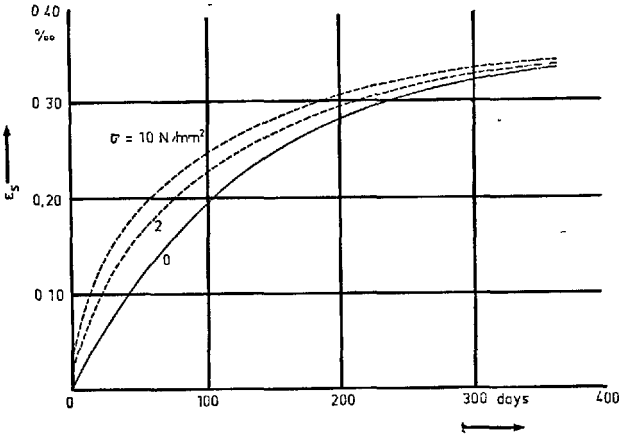

Fig. 4 : Calculated shrinkage strain as function of time. A solid line indicates the behaviour of an unloaded specimen. If crack formation is prevented by an external load of 2 and 10 N/mm^2 respectively dashed lines are obtained. (Taken from Ref. /10/).

An external load of 10 N/mm^2 prevents crack formation in the outer shell of a specimen. As can be seen from Fig. 4 the shrinkage strain under load at a certain duration of drying (50 days) is nearly doubled. The time when the external load has a maximum influence is dependent on geometry and on water permeability. It should be mentioned that creep deformation is not taken into consideration in Fig. 4. The only reason why shrinkage is increased if measured under load is thus the prevention of microcraking.

At this moment it cannot be decided whether this purely mechanical effect accounts for all the transient drying creep. In any case the deformation which might be caused by triggered processes within the microstructure is much less than usually assumed and possibly it is zero.

3.4. Crack Formation and Failure

Strength of concrete is undoubtedly related to crack formation and failure of hardened cement paste. Therefore a huge number of papers on this subject has been published and the already existing number increases with a considerable rate. Excluding purely phenomenological papers, the main attempts can be differentiated into four methotological different approaches. These are (1) microstructural investigations, (2) application of stochastic theories, (3) mathematical crack theory, and (4) application of fracture mechanics. Of course there are studies which incorporate more than one of the above mentioned concepts. Grudemo /74 - 76/ studied the microstructure of Portland cement paste and pastes prepared with pure compounds by means of several classical methods of investigation such as mercury intrusion porosimetry and sorption weight change. He related his findings to results of tensile, compression and circular plate loading tests. In supplementary test series microhardness of hydrating samples has been measured. Grudemo pays special attention to statistical aspects of microstructures and he applies Weibull's distribution function. Summarizing his results Grudemo /76/ sketches possible crack path elements through the microstructure.

Higgins and Bailey /77, 78/ used a special optical microscopy technique taking advantage of diffuse illumination. By means of this method it is possible to detect stable crack growth in stressed samples of hardened cement paste. Higgins and Bailey did not find a zone microcracks in front of a crack tip as they expected. According to their observation the crack follows smaller microcracks in a line ahead of it.

In a homogenous material under tensile stress a crack propagates catastrophically once the stress has reached a critical value. In a composite material cracks may be arrested and thus failure take place in a less brittle way. It has been mentioned above that the complex structure of hardened cement paste can never be described analytically in a realistic way. Therefore a statistical representation seems to be a reasonable approximating approach. Several authors tried to describe failure of cement bonded materials as a statistical series of independent steps /79 - 82/.

Mihashi et al. /80, 81/ developed a stockastic theory for fracture of hardened cement paste and concrete. A speciment is subdivided into n units and each unit contains one crack. The orientation and the crack length may be distributed at random. The external stress field is markedly disturbed by the structural defects. As a consequence really acting stresses in a given unit are also randomly distributed within the solid skeleton. On these two basic assumptions a stochastic theory is developed.

The formulae obtained by Mihashi et al. /80, 81/ describe failure of hardened cement paste as function of various loading histories such as sustained load, high rate of loading, and cyclic loading. The variance of strength of porous materials is also taken into consideration. Experimental investigations essentially verify this extremely interesting approach /81, 82/.

In Fig. 5 results from experiments to study the lifetime of hardened cement paste under high sustained load are shown. The age at loading of the specimens varies between 1 day and 90 days. With a solid line the theoretical prediction of Mihashi's approach is shown. It seems that with this concept the influence of porosity and pore size distribution on strength and variability of hardened cement paste can be formulated quantitatively for the first time.

Wittmann and Zaitsev /83, 84/ have applied crack theory to describe the behaviour of hardened cement paste under load. Crack length in a porous matrix is studied as function of load. It is assumed that failure can be related to a critical total crack length. That means that the structure desintegrates under compressive load if the sum of all microcracks reaches a critical value. Under high sustained load

cracks propagate and the lifetime of a given sample is dependent on the time necessary to reach critical crack length in the microstructure by stable crack growth. For reasons of comparison in Fig. 5 the lifetime of hardened cement paste calculated on this basis is shown by dashed lines.

mined K_{IC} of hardened cement pastes, aggregates and the interface.

J_{IC} and K_{IC} are measured by Mindess et al. /90/ at cement pastes, plain concrete and eight different steel and glass fibre reinforced concretes. They

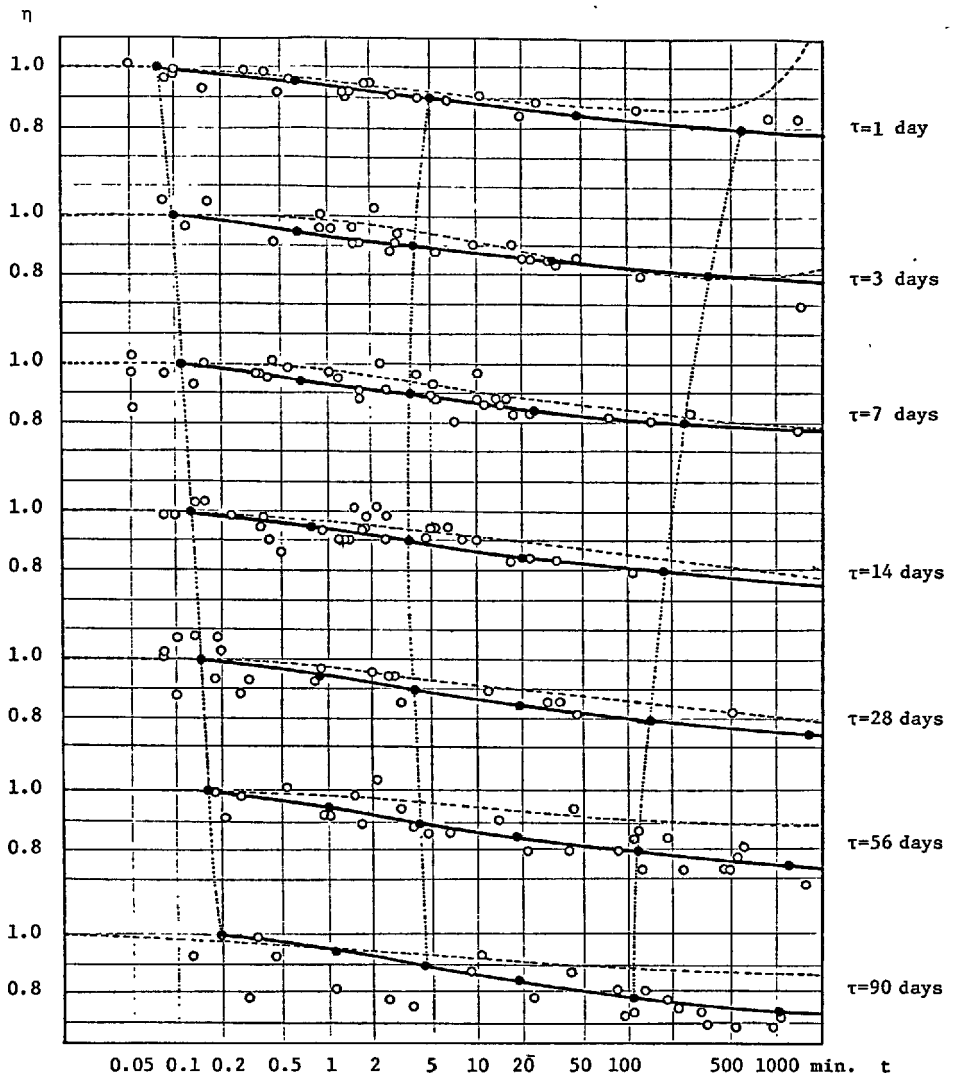

Fig. 5 : Lifetime of hardened cement paste under high sustained load. The solid line is calculated by means of the stochastic approach of Mihashi et al. /80, 90/. Dashed lines are obtained by formulae given by Zaitsev et al. /83/.

Failure of hardened cement paste is comparatively brittle. Therefore the application of fracture mechanics seems to be justified. Fracture mechanics parameters have been determined by various authors /85 - 87/. Hillemeier /88, 89/ concentrated his investigations on the interface between cement paste and aggregate. Using a wedge loaded CT-specimen he deter-

conclude that the values of K_{IC} for concrete is not meaningful whereas J_{IC} can be used to characterize failure process of all cement bonded materials. Solz and Baron /91/ stated at the end of a thorough literature study that K_{IC} has to be measured at large concrete specimens. As a consequence they started experiments with specimens having a height of two meters.

They suggest that K_{IC} should not be considered to be a fixed value but rather a function of crack length.

Finally another approach to describe failure of concrete should be mentioned and that is endochronic theory. Bazant et al. /92/ have applied this very elegant method probably for the first time in this field.

4. OTHER PROPERTIES

The term "other properties" is very wide and therefore a selection has to be made. Again major trends shall be outlined.

Schulte et al. /93/ investigated the electrical conductance of hardened cement paste as function of moisture content. Dry cement paste is a typical semiconductor. The change of electrical conductance by adsorbed and capillary condensated water can be explained in terms of the interaction of water with a xerogel.

In colloidal suspensions usually a Zeta-potential can be observed. Wittmann et al. /94/ have shown that movement of the diffuse double layer in the xerogel can be achieved by mechanical deformation. In fact on opposite sides of a bended bar a mechanically induced streaming potential can be measured.

Puchner et al. /95, 96/ measured luminescence at clinker components as well as at hydrated pastes. It can be concluded that surface luminescence is observed. Therefore the measured intensity is dependent on the amount of adsorbed molecules.

Due to agressive industrial atmosphère and the increased use of concrete under severe climatic conditions such as in marine technology the durability of hardened cement paste gains importance rapidly. Marchese /97/has studied chemical resistance of different hardened pastes. Durability of hardened cement paste as well as of reinforced concrete depends essentially on the permeability of the pore structure. Some preliminary results of a comprehensive study are to be found in /98/. Chen et al. /99/ have measured the diffusion of methane through concrete.

Measurements of the complex permitivity of hydraulic cement pastes can be performed with two different aims. First of all the dielectric behaviour of hardened cement paste and concrete has to be known for special applications. Besides the determination of materials properties dielectric measurements can also be evaluated analytically. The interaction of adsorbed molecules with the surface of the xerogel can be studied /100 - 102/. The range of frequencies used has been extended in the meantime until the microware region /103/. This method can also be used as a fast and nondestructive way to determine the degree of hydration of hydraulic binders.

Internal friction of hardened cement past is dependent on moisture content. In /56/ low frequency internal friction has been related to short-time creep of hardened cement paste. There are reasons to suggest that low frequency internal friction is caused by water movement and that the mechano-electrical effect described in /94/ as well as the above mentioned increase of Young's modulus at high relative humidities can be attributed to the same physical phenomenon. The effect of drying and resaturation on internal friction has been investigated by Sellevold and Radjy /104/.

Microhardness of hydrating pastes with or without additions can be used to characterize the gradual development of mechanical properties. In /105/ Traetteberg et al. tried to relate microhardness with special features of the microstructure.

Finally the position anihilation as measured in hardened cement paste shall be mentioned /106, 107/. At a first glance this method seems to be rather exotic. There is, however, a possibility that by means of this approach new and valuable information on the microstructure can be provided.

REFERENCES

1. L.E. Copeland and G.J. Verbeck, "Structures and Properties of Hardened Cement Paste", The VI. International Congress on the Chemistry of Cement, Moscow 1974, A. principal paper.

2. R. Kondo and M; Diamon, "Phase Composition of Hardened Cement Paste", The VI. International Congress on the Chemistry of Cement, Moscow, 1974, A principal paper.

3. H.F.W. Taylor, "Crystal Chemistry of Portland Cement Hydration Products", The VI. International Congress on the Chemistry of Cement, Moscow 1974, A principal paper.

4. T.C. Powers and T.L. Brownyard, "Studies of the Physical Properties of Hardened Portland Cement Paste", Portland Cement Association, Res. Bull. 22 (1947).

5. H.F.W. Taylor, "Hydrate Structure and Composition", Theme 2.2. of this Congress

6. L.A. Tomes, C.M. Hunt and R.L. Blaine, "Some Factors Affecting Surface Area of Hydrates in Portland Cement Paste as Determined by Water Vapor and Nitrogen Adsorption", J. Res. Nat. Bur. Stand. 59, 357 - 364 (1957)

7. F.H. Wittmann, "Bestimmung physikalischer Eigenschaften des Zemensteins", Deutscher Ausschuss für Stahlbeton, Schriftenreihe, Heft 232 (1974)

8. F.H. Wittmann, "The Structure of Hardened Cement Paste - a Basis for a better Understanding of the Materials Properties", Proc. Conf, Hydraulic Cement Pastes : Their Structure and Properties, Sheffield, pp. 96 - 117 (1976)

9. F.H. Wittmann, "Grundlagen eines Modells zur Beschreibung charakteristischer Eigenschaften des Betons", Deutscher Ausschuss für Stahlbeton, Schriftenreihe, Heft 290 (1977)

10. F.H. Wittmann and P.E. Roelfstra, "Rekenmodel ter bepaling van de totale tijdsafhankelijke vervorming van uitdrogend beton", Cement (Dutch to be published 1980)

11. S. Diamond, "Cement Paste Microstructure - An Overview at Several Levels", Proc. Conf. Hydraulic Cement Pastes : Their Structure and Properties, Sheffield, pp. 2 - 30 (1976)

12. R.L. Berger, F.J. Young and F.V. Lawrence, "Discussion of the Paper Morphology and Surface Properties of Hydrates in Tricalcium Silicate Paste by M. Collepardi and B. Marchese", Cem. Concr. Res. 2, 633 - 636 (1972)

13. U.F.E. Puchner, "Untersuchung der Physi- und Chemisoption von Wasser an den Mikrokristallen der Hydratationsprodukte des Zements mit Hilfe der Lumineszenz", Dissertation, Technische Universität München (1976)

14. H.F.W. Taylor, "Mechanism and Products of Portland Cement Hydration", Contribution to the Annual Meeting of Japan Cement Association (1979)

15. J. Cabrera and F.H. Wittmann, "Orientation Mechanism in Fibrous Hydration Products of Cement" (to be published 1980)

16. C.W. Lentz, "The silicate structure analysis of hydrated Portland cement paste", Highway Research Board, Washington D.C., Special Report No. 90, pp. 209 - 283 (1966)

17. D.D. Tamas, A.K. Sarkar and D.M. Roy, "Effect of Variables Upon the Silylation Products of Hydrated Cements", Prof. Conf. Hydraulic Cement Pastes, Their Structure and Properties, Sheffield, pp. 55 - 72 (1976)

18. A.K. Sarkar and D.M. Roy "A New Characterization Technique for Trimethylsilyated Products of Old Cement Pastes", Cem. Concr. Res. 9, 343 - 352 (1979)

19. E.E. Lachowski, "Trimethylsilylation as a Tool for the Study of Cement Pastes. (1) Comparison of Methods of Derivatisation", Cem. Concr. Res. 9, 111 - 114 (1979)

20. E.E. Lachowski, "Trimethylsilylation as a Tool for the Study of Cement Pastes. (2) Quantitative Analysis of the Silicate Fraction of Portland Cement Pastes", Cem. Concr. Res. 9, 337 - 342 (1979)

21. L.S. Dent-Glasser, E.E. Lachowski, K. Mohan and H.F.W. Taylor, "A Multi-Method Study of C_3S Hydration", Cem. Concr. Res. 8, 733 (1978)

22. F. Tamas und L. Amrich, "Layer Chromatographic Separation of Silicate Oligomers formed during the Hydration of Portland Cement", Il Cemento 75, 357 - 362 (1978)

23. F.H. Wittmann, U. Puchner, and H. Übelhack, "Properties of Colloidal Particles in Hardened Cement Paste and the Relation to Mechanical Behaviour", Proc. Int. Conf. on Colloids and Surface Science, Budapest, Vol. 2 pp. 205 - 212 (1976)

24. H. Übelhack, "On the Mutual Coupling of Colloidal Particles as Determined by MöBbauer Effect and its relation to the Elastic Modulus of a Xerogel", Proc. Conf. Hydraulic Cement Pastes : Their Structure and Properties, Sheffield, pp. 166 - 174 (1976)

25. H.J. Übelhack, "Einfluss der Kopplung der kolloidalen Hydrate auf die mechanischen Eigenschaften von Zementstein - Eine MöBbauereffekt Studie -", Dissertation, Technische Universität München (1976)

26. H.J. Übelhack and F.H. Wittmann, "Coupling of Colloidal Particles and Recoilless Fraction", Journal de Physique, Colloque C6, supplément au no. 12, Vol. 37, 273 - 276 (1976)

27. H.J. Übelhack and F.H. Wittmann, "Dynamics of the Development of Structures in Colloids and Brownian Motion", Journal de Physique, Colloque C6, supplément au no. 12, Vol. 37, 269 - 271 (1976).

28. K. te Nijenhuis, "Dynamic Mechanical Studies on Thermo-Reversible Ageing Processes in Gels of Polyvinyl Chloride and of Gelatin", Dissertation, Technische Hogeschool Delft (1979)

29. F.H. Wittmann, "Influence of Water Reducing Admixtures on the Rheological Behaviour, Capillary Shrinkage and Structures of Cement Paste", Silicates Industriels 44, 5 - 12 (1979)

30. D.N. Winslow, "The Specific Surface of Hardened Portland Cement Paste as Measured by Low Angle X-ray Scattering", Thesis, Purdue University (1973)

31. D.N. Winslow and S. Diamond, "Specific Surface of Hardened Portland Cement Paste as determined by Small Angle X-ray Scattering", J. Amer. Ceram. Soc. 57, 193 - 197 (1974)

32. D.A. Kayyali, C.L. Page and A.G.B. Ritchie, "The Effects of Freezing and Thawing Cycles on the Microstructure and Strength of Portland Cement Paste", Proc. Conf. Hydraulic Cement Pastes : Their Structures and Properties, Sheffield, pp. 204 - 218 (1976)

33. F.S. Rostasy, U. Schneider, and G. Wiedemann, "Behaviour of Mortar and Concrete at Extremely Low Temperatures", Cem. Concr. Res. 9, 365 - 376 (1979)

34. F.S. Rostasy, R. Weiss and G. Wiedelann, "Changes of Pore Structure of Cement Mortars dus to Temperature", Cem. Concr. Res. 10, (1980)

35. J.J. Beaudoin, "Porosity Measurement of Some Hydrated Cementitious Systems by High Pressure Mercury Intrusion - Microstructural Limitations", Cem. Concr. Res. 9, 771 - 781 (1979)

36. H. Gudmundsson, S. Chatterji, A.D. Jensen, N. Thaulow, and P. Christensen, "The Measurement of Paste Content in Hardened Concrete Using Automatic Image Analysing Technique", Cem. Concr. Res. 9, 607 - 612 (1979)

37. S. Diamond and C. Gomez-Toledo, "The Microstructure of Low Porosity Portland Cement Paste", Il Cemento 75, 189 - 194 (1978)

38. R.S. Mikhail, D. Dollimore and R. Stino, "Microstructure and Mechanical Properties of Fibre Reinforced Cement Pastes", Il Cemento 75, 277 - 284 (1978)

39. F.H. Wittmann, "Observation of Early Hydration by Means of Luminescence Experiments", Proc. CEMBUREAU-Seminar, Reaction of Aluminate During The Setting of Cements, Eindhoven, April 1977

40. M.J. Setzer, "Einfluss des Wassergehaltes auf die Eigenschaften des erhärteten Betons", Deutscher Ausschuss für Stahlbeton, Heft No. 280 (1977)

41. G. Lahajnar, R. Blinc, V. Rutar, V. Smolej, I. Zupanic, I. Kocuvan, and J. Ursic, "On the Use of Pulse NMR Techniques for the Study of Cement Hydration", Cem. Concr. Res. 7, 385 - 394 (1977)

42. G. Englert, F.H. Wittmann and M. Nussbaum, "Studium der Bildungsverhältnisse des Wassers im Zementstein", Zement-Kalk-Gips 24, 165 - 174 (1971)

43. D.N. Winslow, "A Photoacustic Study of the Water in Hydrated Cement Paste", Cem. Concr. Res. 9, 563 - 572 (1979)

44. F.H. Wittmann, "Farbmessungen an erhärtendem Zementstein", Optik 23, 400 - 408 (1966)

45. U.G. Meier and A.B. Harnik, "Das Gefrieren von Wasser im Zementstein bei verhinderter Verdunstung", Cem. Concr. Res. 8, 545 - 552 (1978)

46. C. Fontenay and E.J. Sellvold, "Ice Formation in Hardened Cement Paste I. Water Saturated Pastes", Proc. I. International Conf. on Durability of Building Materials and Components, Ottawa (1978)

47. G.G. Litvan, "Adsorption Systems at Temperatures below the Freezing Point of the Adsorptive", Adv. Coll. Interface Sci. 9, 253 - 302 (1978)

48. N. Stockhausen, H. Dorner, B. Zech and M.J. Setzer, "Untersuchung von Gefriervorgängen in Zementstein mit Hilfe der DTA", Cem. Concr. Res. 9, 783 - 794 (1979)

49. M. Vignes-Adler, "On the Origin of the Water Aspiration in a Freezing Dispersed Medium", J. Coll. Interface Sci. 60, 162 - 171 (1977)

50. J. Bensted, "Raman Spectral Studies of Carbonation Phenomena", Cem. Concr. Res. 7, 161 - 164 (1977)

51. D. Ménétrier, I. Jawed, T.S. Sun, and J. Skalny, "ESCA and SEM Studies on Early C_3S Hydration", Cem. Concr. Res. 9, 473 - 482 (1979)

52. H.M. Jennings and P.L. Pratt, "An Experimental Argument for the Existence of a Protective Membrane Surrounding Portland Cement During the Induction Period", Cem. Concr. Res. 9, 501 - 506 (1979)

53. F.V. Lawrence, J.F. Young, and R.L. Berger, "Hydration and Properties of Calcium Silicate Pastes", Cem. Concr. Res. 7, 369 - 378 (1977)

54. P.K. Mehta, D. Pirtz, and M. Polivka, "Properties of Alite Cements" Cem. Concr. Res. 9, 439 - 450 (1979)

55. J.F. Young and H.S. Tong, "Microstructure and Strength Development of Beta-Dicalcium Silicate Pastes With and Without Admixtures", Cem. Concr. Res. 7, 627 - 636 (1977)

56. E.J. Sellevold, "Low Frequency International Friction and Short-Time Creep of Hardened Cement Paste : An Experimental Correlation", Proc. Conf. Hydraulic Cement Pastes : Their Structure and Properties, Sheffield, pp. 330 - 334 (1976)

57. P. Klug and F.H. Wittmann, "Activation Energy and Activation Volume of Creep of Hardened Cement Paste", Mat. Sci. Eng. 15, 63 - 66 (1974)

58. F. Straub, "Physikalische Messungen an Zementstein bei tiefen Temperaturen", Techn. University of Munich, Building Materials Physics, Report No. 7 (1975)

59. F. Straub and F.H. Wittmann, "Activation Energy and Activation Volume of Compressive and Tensile Creep of Hardened Cement Paste", Proc. Conf. Hydraulic Cement Pastes : Their Structure and Properties Sheffield, pp. 227 - 230 (1976)

60. F.H. Wittmann "Zur Ursache der sogenannten Schrumpfrisse", Zement und Beton, Heft 85/86, 10 - 16 (1975)

61. F.H. Wittmann, "On the Action of Capillary Pressure in Fresh Concrete", Cem. Concr. Res. 6, 49 - 56 (1976)

62. B.B. Hope and N.H. Brown, "The Creep of Hydrated Cement Paste", Cem. Concr. Res. 5, 475 - 486 (1975)

63. J.F. Young, R.L. Berger and A. Bentur, "Shrinkage of Tricalcium Silicate Pastes : Superposition of Several Machanisms", Il Cemento 75, 391 - 398 (1978)

64. B.R. Gamble and J.M. Illston, "Rate of Deformation of Cement Paste and Concrete during Regimes of Variable Stress, Moisture-Content and Temperature", Proc. Conf. Hydraulic Cement Pastes : Their Structure and Properties, Sheffield pp. 297 - 310 (1976)

65. L.J. Parrot, "Basic Creep, Drying Creep and Shrinkage of a Mature Cement Paste after a Heat Cycle", Cem. Concr. Res. 7, 597 - 604 (1977)

66. L.J. Parrot, "A Study of Transitional Thermal Creep in Hardened Cement Paste", Mag. Concr. Res. 31, 99 - 103 (1979)

67. J.M. Illston and P.D. Sanders, "The Effect of Temperature Change upon the Creep of Mortar under Torsional Loading", Mag. Concr. Res., 25, 136 - 144 (1973)

68. S. Mindess, J.F. Young and F.V. Lawrence, "Creep and Drying Shrinkage of Calcium Silicate Paste. I. Speciment Preparation and Mechanical Properties", Cem. Concr. Res. 8, 591 - 600 (1978)

69. A. Bentur, N.B. Milestone and J.F. Young, "Creep Drying Shrinkage of Calcium Silicate Pastes. II. Induced Microstructural and Chemical Changes", Cem. Concr. Res. 8, 721 - 732 (1978)

70. A. Bentur, R.L. Berger, F.V. Lawrence, M.B. Milestone, S. Mindess, and J.F. Young, "Creep and Drying Shrinkage of Calcium Silicate Pastes. III. A Hypothesis of Irreversible Strains", Cem. Concr. Res. 9, 83 - 95 (1979)

71. A. Bentur, N.B. Milestone, J.F. Young, and S. Mindess, "Creep and Drying Shrinkage of Calcium Silicate Pastes. IV. Effect of Accelerated Curing", Cem. Concr. Res. 9, 161 - 169 (1979)

72. F.H. Wittmann and P.E. Roelfstra, "Drying Shrinkage and Creep of Concrete", (to be published in 1980)

73. F.H. Wittmann, "Trends in Research on Creep and Shrinkage of Concrete", Proc. Eng. Found. Conf., Rindge, New Hampshire 1979

74. A. Grudemo, "Strength-Structure Relationships of Cement Paste Materials; Part I : Methods and basic data for Studying phase composition and microstructure", Swedish Cement and Concrete Research Institute CBI, Froskning 6 : 77 (1977)

75. A. Grudemo, "Strength-Structure Relationships of Cement Paste Materials; Part 2 : Methods and Basic Material Data for Studying Strength and Failure Properties", Swedish Cement and Concrete Research Institute CBI, Forskning 8 : 79 (1979)

76. A. Grudemo, "Microcracks, Fracture Mechanism and Strength of the Cement Paste Matrix", Cem. Concr. Res. 9, 19 - 34 (1979)

77. D.D. Higgins and J.E. Bailey, "A Microstructural Investigation of the Failure Behaviour of Cement Paste", Proc. Conf. Hydraulic Cement Pastes : Their Structure and Properties, Sheffield, pp. 283 - 296 (1976)

78. D.D. Higgins and J.E. Bailey, "Fracture Measurements on Cement Paste", Journal of Materials Science 11, 1995 - 2003 (1976)

79. M. Kawamura, "Internal Stresses and Microcrack Formation caused by Drying in Hardened Cement Pastes", J. Amer. Ceram. Soc. 61, 281 - 283 (1978)

80. H. Mihashi and M. Izumi, "A Stochastic Theory for Concrete Fracture", Cem. Concr. Res. 7, 411 - 422 (1977)

81. F.H. Wittmann and H. Mihashi, "Stochastic Approach to Study the Influence of Rate of Loading on Strength of Concrete", Heron (to be published 1980)

82. B. Zech and F.H. Wittmann, "Influence of Rate of Loading on Strength of Concrete", (to be published in 1980)

83. F.H. Wittmann and J. Zaitsev, "Verformung und Bruchvorgang poröser Baustoffe bei Kurzzeitiger Belastung und Dauerlast", Schriftenreihe Deutscher Ausschuss für Stahlbeton, Heft 232 (1974)

84. F.H. Wittmann "Micromechanics of Achieving High Strength and other Superior Properties", Proc. NSF-Workshop, Chicago Dec. 1979

85. S. Mindess, J.S. Nadeau and J.M. May, "Effects of Different Curing Conditions on Slow Crack Growth in Cement Paste", Cem. Concr. Res. 4, 953 - 965 (1974)

86. K.L. Watson, "The Estimation of Fracture Surface Energy as a Measure of the "Toughness" of Hardened Cement Paste", Cem. Concr, Res. 8, 651 - 656 (1978)

87. O.S. Kayyali, C.L. Page and A.G.B. Ritchie, "Frost Action on Immature Cement Paste-Effects on Mechanical Behavior", ACI-Journal, 87, 1217 - 1225 (1979)

88. B. Hillemeier, "Bruchmechanische Untersuchungen des Rissfortschnitts in zementgebundenen Werkstoffen", Universität Karlsruhe, Dissertation (1976)

89. B. Hillemeier and H.K. Hilsdorf, "Fracture Mechanics Studies on Concrete Compounds", Cem. Concr. Res., 7, 523 - 536 (1977)

90. S. Mindess, F.V. Lawrence and C.E. Kesler, "The J-Integral as a Fracture Criterion for Fibre Reinforced Concrete", Cem. Concr. Res. 7, 731 - 742 (1977)

91. Ch. Solz and J. Baron, "Mecanique de la Rupture Appliquée au Beton Hydraulique", Cem. Concr. Res. 9, 641 - 648 (1979)

92. Z.P. Bazant and P.D. Bhat, "Endochronic Theory of Inelasticity and Failure of Concrete", J. Eng. Mech. Div. ASCE 102 (EMU) 701 - 722 (1976)

93. Ch. Schulte, H. Mader and F.H. Wittmann, "Elektrische Leitfähigkeit des Zementsteins bei unterschiedlichem Feuchtigkeitsgehalt", Cem. Concr. Res. 8, 359 - 368 (1978)

94. F.H. Wittmann and C. Hollenz, "On the Significance of Electroosmosis in Hardened Cement Paste", Cem. Concr. Res. 4, 389 - 397 (1974)

95. U. Puchner, "A Model for Sorption Effects on the Surface of Hydrated Cement Derived from Luminescence Experiments" Proc. Conf. Hydraulic Cement Pastes: Their Structure and Properties, Sheffield, pp. 73 - 81, (1976)

96. U. Puchner and F.H. Wittmann, "Lumineszenz röntgenbestrahlter Klinker-komponenten", Cem. Concr. Res. 4, 623 - 640 (1974)

97. B. Marchese, "Chemical Resistance of Cement Pastes I, Patina Alterations" Cem. Concr. Res. 8, 501 - 508 (1978)

98. E.V. Srensen and F. Radjy, "Permeability of Hardened Cement Paste in Relation to Pore Structure", Proc. Conf. Hydraulic Cement Pastes : Their Structure and Properties, Sheffield, pp. 52 - 54 (1976)

99. L.C. Chen and D.L. Katz, "Diffusion of Methane through concrete", J. Amer. Concr. Inst. 75, 673 - 679 (1978)

100. R. Sierra, "Contribution à l'étude de l'hydratation des silicates calciques hydrauliques", Dissertation, Université de Rennes (1974)

101. B. Zech and F.H. Wittmann, "Studium des dieelektrischen Verhaltens von dünnen adsorbierten Wasserfilmen, Z. Phys. Chem., Neue Folge 92, 45 - 62 (1974)

102. V.V. Kapranov and A.I. Stukov, "Dielectric Measurements of Cement and Gypsum", Tr. Chelyab. Politekn. Inst. 169, 29 - 41 (1977) see also Chem. Abstr. 87, 188456 (1977)

103. F.H. Wittmann and F. Schlude, "Microware Absorption of Hardened Cement Paste", Cem. Concr. Res. 5, 63 - 69 (1975)

104. E.J. Sellevold and F. Radjy, "Drying and Resaturation Effects on Internal Friction in Hardened Cement Pastes", J. Amer. Ceram. Soc. 59, 256 - 258 (1976)

105. A. Traetteberg and P. Sereda, "Strength of C_3A Paste Containing Gypsum and $CaCl_2$" Cem. Concr. Res. 6, 461 - 474 (1976)

106. Y. Ito and T. Yamashina, "Structure of Porous Vycar Glass and its Adsorption Characteristics of Water - An Application of Positron Annihilation Method", Appl. Phys. 6, 231 - 326 (1975)

107. R. Myllyla and M. Karras, "Positron Annihilation Probing for the Hydration Rate of Cement Paste", Appl. Phys., 7, 303 - 313 (1975)

SUB-THEME VI - 3

Mathematical models of alteration of the properties of cement paste with time

V. I. SHEIN
Institute of Civil Engineering
Kharkov, U.S.S.R.

Modern methods of applied mathematics in combination with computer techniques open up possibilities for elucidating the general regularities of strength synthesis in cements with various physico-chemical characteristics. Solution of such problems will make it possible to forecast the physico-chemical properties of cement by calculation, to estimate the efficiency of the existing methods of production, to indicate the paths for further improvement of manufacturing processes and, in the final run, to establish more precisely the nature of manifestation of the binding properties of mineral materials.

At present, however, it is difficult to forecast the effect of the application of mathematical methods to cement manufacture. It is therefore natural that the problems of mathematical models of variation of cement paste properties in time are discussed for the first time as a separate topic at the 7th International Congress on the Chemistry of Cement.

The discrepancy between the possibilities of mathematical methods and practical results is due to the lack of rigorous systematization of the determining characteristics of the composition and structure of initial binders and hydration products, to the absence of definitions and methods of calculation of the kinetic characteristics of strength development in time with account taken of the hardening conditions, and also to the relative nature of estimation of parameters of the disperse structure of the cement paste and mortar. The application of mathematical methods in such circumstances is often reduced to description of the results within the framework of investigations carried out, supporting, as a rule, those scientific conceptions which were used to plan the given experiment. The number of factors that are taken into account in such experiments is limited, and the generalization of the results is qualitative; that is why there is the same gap between the science and practice of cement manufacture and application.

In this connection, in studying the variation of cement paste properties using mathematical methods, we shall consider successively the strength characteristics of clinker and clinker-based cement on the basis of plant data for a 11-year period, with emphasis on the features which are of methodological nature and allow one to treat unambiguously the results of investigations of the increase of strength of clinker and cement.

The duration of the time series of clinker strength is determined by the constancy of standard methods of determination of its physico-mechanical characteristics and chemical composition. Daily sampling was carried from the hot end of the furnace and was followed by averaging and testing. For monthly samplings, using the methods of mathematical statistics with a reliability level of P = 0.95 with a two-sided restriction, the upper and lower confidence limits were set up and the average monthly values (X_i) and empirical dispersions calculated. The correspondence of the average monthly characteristics of clinker to the total set for the 11-year period was estimated by the Student criterion, and the homogeneity of empirical dispersions (spreads) was evaluated by the Bartlett criterion. The thus obtained characteristics of the strength of clinker are treated as individual values of the dynamic time series for the time period concerned. Analogous determinations of the successive values of the dynamic series have been carried out for the 3-day strength and mineral composition of clinker.

Graphs of the time series of compressive strength at an age of 28 days the activity of clinker(R_{28}, in MPa) and 3 days (R_3, MPa) and also of the content of C_3S, C_2S, C_3A, and C_4AF, are given in Fig. 1.

The solid lines represent the initial values, and the dashed lines, the trend and seasonal fluctuations.

In order to analyse the dependence of the activity of clinker on the factors indicated, the modified method of spectral analysis of random processes with subsequent correlation of the dynamic series was used (1-3).

At the first step, the mathematical expectation of the initial time series, the empirical dispersion (S^2) are determined and with the aid of the Durbin-Watson criterion (the DW criterion) the necessity of picking out a trend of development of the phenomenon is estimated. In contrast to the accepted linear approximation of a trend, in all cases we made use of a trigonometric polynomial of fourth order, and its coefficients were determined with the aid of the Bessel formulas for the best (in the sense of the method of least squares) approximation. The amplitude characteristics of the trend (X_{ti}) and the dispersion introduced by the trend (S_t^2) are determined from the polynomial. The difference between X_i and X_{ti} is the starting quantity for determining seasonal variations (X_{si}), which is also evaluated by the DW criterion, and then the dispersion introduced by a seasonal variation (S_s^2) is calculated. After the amplitude of seasonal fluctuations is subtracted, the dynamic series is expanded, with the aid of the Bessel formulas, into a Fourier series for K = N/4 harmonics, which provides a good approximation for practical purposes. In this particular case, the amplitude characteristics of Fourier series (X_{hi}) and the corresponding value of dispersion (S_h^2) are calculated at K = 33. After X_{hi} is subtracted the values of the residual terms of the series are determined, which do not exceed in absolute magnitude the values of the procedural error in determination of the respective characteristics. The residual dispersion (S_{res}^2), which is not taken into account by the trend, the seasonal fluctuations and the K harmonics of the Fourier series is determined for the residual terms. Thus, the

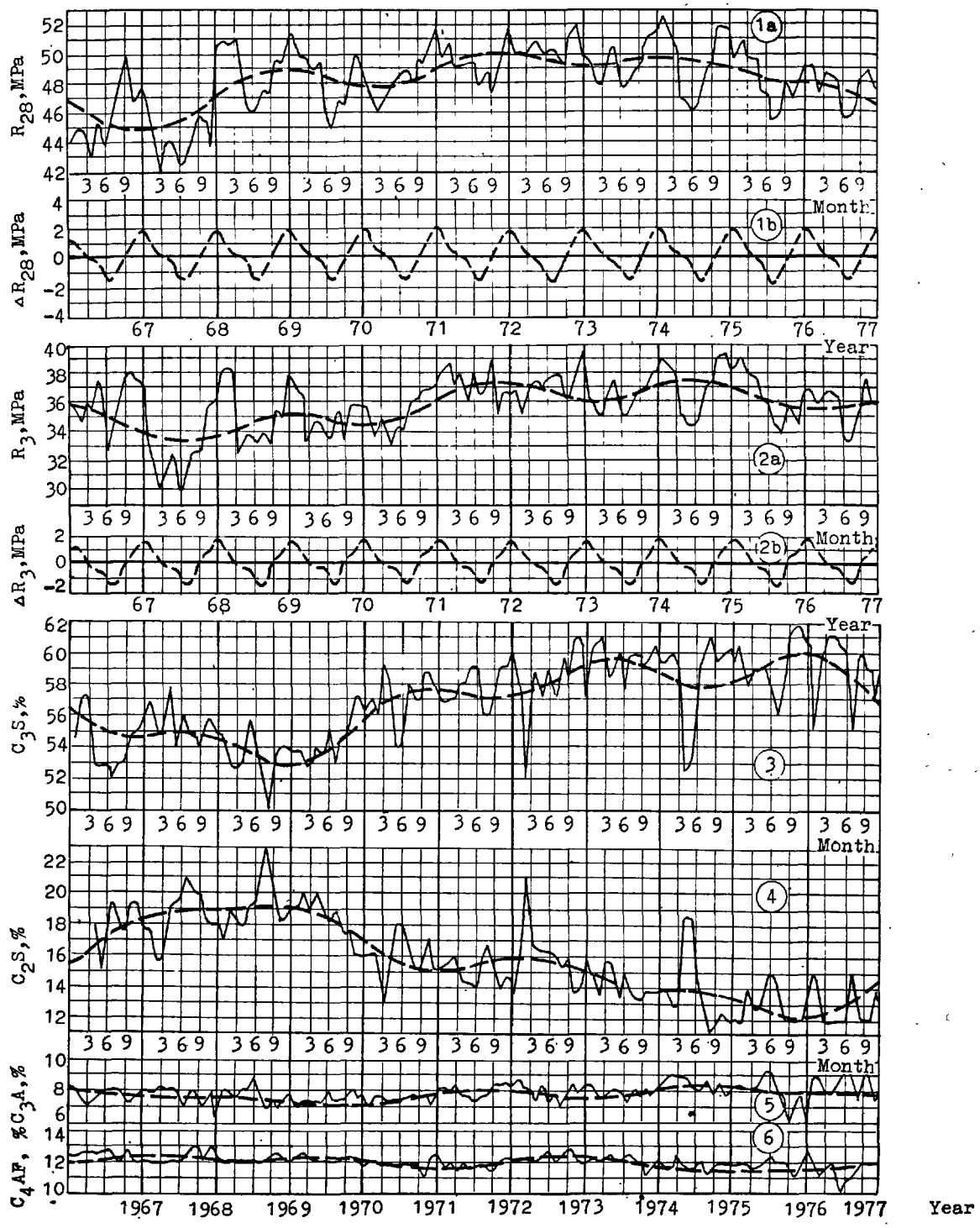

Fig. 1. Time series of the physico-chemical characteristics of clinker: 1a—the initial dynamics series and the trend of clinker activity; 1b—seasonal fluctuations of clinker activity; 2a—the original dynamic series and the trend of 3-day strength; 2b—seasonal fluctuations of 3-day strength; 3, 4, 5, and 6—the time series and trend of the content of C_3S, C_2S, C_3A, and C_4AF in clinker, respectively

TABLE 1

Factor	Mean values	Empirical dispersions (above the line are given the absolute value, below the line, %%)				
		S^2	S_t^2	S_s^2	S_h^2	S_{res}^2
R_{28}, MPa	48.10	5.593 / 100	2.244 / 40.1	1.083 / 19.4	1.846 / 33.0	0.420 / 7.5
R_3, MPa	35.58	4.118 / 100	1.380 / 33.5	0.741 / 18.0	1.594 / 38.7	0.403 / 9.8
C_3S, %	56.93	7.453 / 100	4.471 / 60.0	0.425 / 5.7	1.667 / 22.4	0.886 / 11.9
C_2S, %	15.79	7.152 / 100	4.917 / 68.8	0.231 / 3.2	1.497 / 20.9	0.505 / 7.1
C_3A, %	8.03	0.406 / 100	0.121 / 29.8	0.036 / 9.0	0.163 / 40.3	0.085 / 20.9
C_4AF, %	12.06	0.189 / 100	0.053 / 28.2	0.006 / 3.2	0.075 / 39.7	0.055 / 28.9

spectrum of the initial time series is distributed among the constituent dispersions in the form:

$$S^2 = S_t^2 + S_s^2 + S_h^2 + S_{res}^2 \qquad (1)$$

The distribution of the values of empirical dispersions for the characteristics presented in Fig. 1 are tabulated in Table I.

Emphasis should be placed on the presence of significant seasonal fluctuations for the activity of clinker, which are +1.71 MPa for winter months and -1.81 MPa for summer months; for the 3-day strength the respective figures are +1.4 and -1.58 MPa, in relation to the trend of the time series.

At the second stage, cross-spectrum analysis is performed, which allows one to determine the coherence between the harmonic components of the clinker activity and the factors being investigated and to calculate, the intensification factor and the overall correlation using Parzen weights. Considering that almost 60 per cent of the dispersion value of clinker activity is determined by the trend and seasonal fluctuations, we give the corresponding values of the correlation together with characteristics of mineral composition (see Table II).

TABLE II

Factor	Trend	Seasonal fluctuations
C_3S	0.4836	0.7934
C_2S	-0.4341	-0.8166
C_3A	0.4198	-0.3518
C_4AF	-0.2914	0.3361

Let us note the significant correlation only for the seasonal fluctuations of the clinker activity and the content of C_3S and C_2S. The use of this correlation for construction a mathematical dependence will not, however, be of practical value since, according to Table I, the dispersion values per seasonal fluctuations of C_3S and C_2S are only 5.7 and 3.2 per cent of the total values of the corresponding dispersions. An almost analogous picture is characteristic of the 3-day strength of clinker.

Hence, for the entire time period being analysed it is impossible to establish a significant correlation in a linear approximation between the activity of clinker and its mineral composition and, therefore, one cannot control the activity of clinker, taking into account only on the chemical and mineralogical characteristics.

Let us now consider the possibility of constructing a mathematical model for the strength of cement, using as an example rapid-hardening Portland blast-furnace cement M 400, depending on the amount of clinker (C, per cent), slag (Sl, per cent), gypsum (G, per cent), and on the specific surface area (S, cm^2/g), which is determined by the air-permeability method according to State standard GOST 310-60. "Cements. Methods of Physical and Mechanical Testing".

The content of clinker, slag, gypsum in cement and the magnitude of specific surface area are the determining factors for cement strength. A requisite condition is the constancy of clinker activity. Otherwise, the activity of clinker must be known in advance and incorporated into the mathematical model for calculating cement strength. In other words, in the case considered it is impossible to find an ade-

quate mathematical dependence of cement strength for the entire time series of the clinker activity of clinker which was used to prepare rapid-hardening Portland blast-furnace cement (BTShPTs-400). If the period of time is limited to constant clinker activity, it is practically always possible to determine the dependence of cement strength on its determining factors in the form of an adequate linear equation of regression. Thus, to plot of the strength of cement versus its composition and the specific surface area, we chose the last quarter of 1975 and the first quarter of 1976 (this time period is indicated in Fig. 1 by an arrow).

During this six-month period all the characteristics of the cement under study have a normal distribution with the parameters given in Table III.

The composition of cement is given in Fig. 2 as a ternary C-Sl-G diagram. The shown range of cement composition is restricted by the respective values of confidence limits which were calculated for P=0.95 and two-sided restriction.

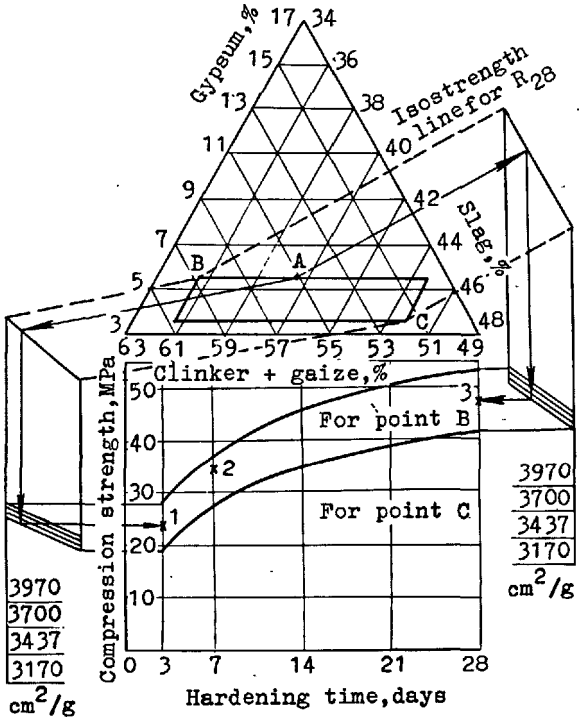

Fig. 2. Phase diagrams and strength increase of rapid-hardening Portland blast-furnace cement M 400.

Using the known methods (4), we find regression equations for the 3-day and 28-day strength:

$$R_3 = -350.0 + 3.8862 \cdot C + 3.2650 \cdot Sl + 4.3608 \cdot G + 0.002036 \cdot S \quad (2)$$

$$R_{28} = -1102.9 + 11.6881 \cdot C + 10.8713 \cdot Sl + 12.5853 \cdot G + 0.002971 \cdot S \quad (3)$$

which are adequate, have a significant coefficient of multiple correlation and take into account the condition

$$C + Sl + G = 100 \text{ per cent} \quad (4)$$

By constructing iso-strength and reflection lines for the 3-day and 28-day strength, we may "relate" to the composition diagram the time dependence of the strength characteristics of BTShPTs-400. The effect of specific surface area on R_3 and R_{28} is pictured graphically with a 267 cm^2/g step. Such a diagram allows one to easily trace the variation of cement strength in time as a function of its composition for different specific surface.

Arrows in Fig. 2 illustrate the possibility of graphical determination the increase of cement strength, using a sample having a composition designated by the point A : C = 55.2 per cent, Sl = 34.0%, G = 5.30% at S = 3147 cm^2/g. The calculated values at age of 3 and 28 days are 23.0 and 47.7 MPa. The actual values of cement strength determined by the method described by USSR (GOST 310-60) State Standard at the age of 3, 7 and 28 days are 24.5, 34.2, and 47.1 MPa, respectively, which are designated in Fig. 2 by the points 1, 2, and 3.

Hence, at constant clinker activity, it is always possible to determine the dependence of cement strength on its composition and specific surface at a given moment by hardening. However, to determine strength variation in a continuous time scale a characteristic which takes into account the increase of cement strength should be introduced.

Investigations show that specific features of strength increase of various clinkers and types of cement are described by expression:

$$R_\tau = R_3 + A_s \cdot \log \tau / 3 \quad (5)$$

where R_τ is the compressive strength of cement at the age of $\tau > 3$ days, MPa; R_3 is the compressive strength at the age of $\tau > 3$ days, MPa; A_s is a coefficient which characterizes the increase of cement strength at the later stages of hardening; τ is the time from the moment of mixing the cement paste with water, days.

From formula (5) the characteristic of the increase of the strength of cement at the later stages of hardening is calculated

$$A_s = \frac{R_\tau - R_3}{\log \tau / 3} \quad (6)$$

TABLE III

Statistical characteristic	Factors, dimensions				
	R_{28}, MPa	R_3, MPa	Sl, %%	G, %%	S, cm^2/g
Mean values	47.65	22.95	40.41	4.55	3612
Lower limit	43.50	19.40	35.60	4.53	3170
Upper limit	51.77	26.49	44.80	5.30	3970
Empirical dispersion	4.69	3.16	5.85	0.21	43298
Coefficient of variation	4.55	7.74	5.98	10.20	5.76

For our sample of cement we obtain $A_s = 23.29$, therefore the 7-day strength is:

$$R_7 = 24.5 + 23.29 \cdot \log 7/3 = 33.1 \text{ MPa}$$

By substituting formulas (2) and (3) into formula (6), we may determine the dependence of the intensity of strength increase of the cement on the composition and specific surface area:

For our example we obtain

$$A_s = -776.18 + 8.0424 \cdot O + 7.8407 \cdot Sl + 8.4779 \cdot G + 0.0009643 \cdot S \quad (7)$$

If the strength of cement is expressed in relative units R_τ/R_{28}, the dependence of the intensity of strength increase on its determining factors will be fractional-linear by virtue of the relation:

$$A_s = \frac{1 - R_3/R_{28}}{\log 28/3} \quad (8)$$

It should be noted that if the absolute and relative values of intensity of strength increase is determined by composition and specific surface area then the hardening temperature has only relative effect on the magnitude of A_s. Studies of various types of cements showed that the relative effect of hardening temperature in the range 0-40°C is characterized by dependence:

$$K_t = 0.58 + 0.021\,\bar{t} \quad (9)$$

where K_t is the coefficient of the relative effect of hardening temperature on the intensity of strength increase; $\bar{t}$ is the weight-average hardening temperature in a logarithmic time scale determined by formula

$$\bar{t} = \frac{\sum_{i=1}^{n} t_i \cdot \log \frac{\tau_{i+1}}{\tau_i}}{\sum_{i=1}^{n} \log \frac{\tau_{i+1}}{\tau_i}} \quad (10)$$

where τ_i and τ_{i+1} are the periods of variation of hardening temperature of standard samples under moist conditions, days; t_i is the hardening temperature in the time interval from t_{i+1} to t_i, °C.

Therefore, the strength of cement at the age of $\tau \geq 3$ can be determined by the formula:

$$R_\tau = R_3 + K_t \cdot A_s \cdot \log \tau / 3 \quad (11)$$

where R_3 and A_s depend on the composition of cement and the specific surface area, and the relative effect of temperature on the increase of the strength is given by formula (9).

The intensity of increase of the strength of cement at the later stages of hardening can be determined more precisely from experimental data by the method of least squares.

Of considerable theoretical and practical interest is the problem of the applicability of relation (11) in the range of at $\tau < 3$ days. Here it becomes necessary to solve the problem of the determination of the kinetic characteristics of cement strength increase at the early stages of hardening. The early period of hardening is here the time commensurable with the periods of the beginning (τ_{beg}, days) and the end (τ_{end}, days) of cement setting. Special investigations have shown that the strength of 4 x 4 x 16 cm samples from cement mortar of 1:3 composition using normal sand produced in accordance with the USSR State Standard (GOST 310.4-76) "Cements". "Methods of Determination of the compressive strength and modulus of rupture", is $R_{beg} = 0.2 \pm 0.03$ MPa at the beginning of setting and $R_{end} = 0.42 \pm 0.02$ MPa at the end of setting. The zero hardening time is the time when the cement mortar is mixed with water. The characteristics indicated make it possible to estimate the increase of cement strength, from the beginning of setting of the cement paste.

It has been found that at the initial periods of hardening the best approximation of experimental data on the increase of strength at the early period of hardening is provided by equation of the type:

$$R_\tau = R_1 (1 - e^{-B\tau^{A_{in}}}) \quad (12)$$

where R_τ is the strength of the cement mortar at $\tau > \tau_{beg}$, MPa; R_1 is the one-day strength used for normalization in determination of coefficients A_{in} and B, MPa; A_{in} and is the coefficient characterizing the kinetics of the increase of cement strength at the initial stages of hardening.

After linearization

$$\log \ln \frac{R_1}{R_1 - R_\tau} = \log B + A_{in} \cdot \log\tau \quad (13)$$

coefficients A_{in} and B are determined by least squares method.

Knowing coefficients A_{in} and B, one can find the time of the most intensive strengthening of the original (primary) structure of the hardening cement:

$$\tau_m = \left(\frac{A_{in} - 1}{A_{in} \cdot B}\right)^{\frac{1}{A_{in}}}, \text{ (days)} \quad (14)$$

Thus, the kinetic equation (12) for strength increase during the initial periods of hardening (R_I) reflects the process of formation of the primary structure, and Equation (5) written in the general form

$$R_\tau = B_s + A_s \cdot \log \frac{\tau}{\tau_0} \quad (15)$$

describes the strengthening of the primary structure in subsequent periods of hardening (R_{II}).

To make these equations consistent in time one must determine the time (τ_0) when the irreversible process of strengthening of the primary structure begins.

This may be solved taking into account the additive nature of actual compressive strength which includes strength due to formation of primary structure (adhesion forces, forces of weak chemical interaction) and strength due to further strengthening of primary structure (concretion of hydration products).

Knowing that

$$R_\tau = R_I + R_{II} \quad (16)$$

with R_I being the advanced strength, we can determine τ_0 from formula

$$\tau_0 = 1/\ \text{EXP}\ \left(\frac{B_s}{M \cdot A_s}\right). \quad (17)$$

Thus, the overall equation for the kinetics of increase of cement strength in time takes the form:

$$R_\tau = R_1 \cdot \left[1 + \text{EXP}\ (-B \cdot \tau^{A_{in}})\right] + K_t \cdot A_s \cdot \log \frac{\tau}{\tau_0} \quad (18)$$

where the second term is taken into account only for $\tau > \tau_0$.

If we take into account that the intensity of strength increase at the later stages of hardening (A_s) depends, as has been shown above, on the composition and specific surface of cement, then, knowing the setting times and, hence, R_{beg} and R_{end}, and also the one-day strength, we can calculate the strength of cement at any moment of time by means of Equation (18). It should be noted that Equation (18) may also be used for describing strength increase of clinker.

The procedure described here for the calculation of the strength in time is illustrated on the example of the clinker studied and rapid-hardening Portland blast-furnace cement M 400 prepared on from this clinker.

The periods of the beginning and end of clinker setting are 0.059 and 0.121 day respectively. The results of testing of clinker strength in time are listed in Table IV and are indicated by dots in Fig. 3.

Performing linearization according to formula (13), we can determine, using the method of least squares, the coefficients $A_{in} = 2.1656$ and $B = 2.1053$ for ratio correlation $r = 0.9842$.

From Equation (14) we find the period when the primary structure is strengthened most strongly:

$$\tau_m = 0.5327 \text{ day}$$

The kinetic equation for the initial period of strength increase has the form:

$$R_\tau = 24.6 \cdot \left(1 - e^{-2.1053 \cdot \tau^{2.1656}}\right) \quad (19)$$

The values of strength calculated by means of this equation are given in Table IV (column 3) and in Fig. 3 (R_{kl}). By subtracting the values in Equation (19) from the initial values of strength and employing the method of least squares, the parameters of Equation (15) which describes strength increase in the subsequent hardening periods and is valid at correlation ratio $r = 0.9974$

$$R_\tau = 3.6417 + 14.8516 \cdot \log\tau$$

Equation (17) is used to calculate the beginning of strengthening of the primary structure:

$$\tau_0 = 0.5685 \text{ day}$$

TABLE IV

Time of hardening τ, days	Actual strength, R_τ, MPa	Strength due to formation of primary structure, MPa, to equation (19)	Strength due to strengthening of structure, MPa, to equation (20)	Total strength according to equation (18)
0.058	0.20	0.112	0	0.112
0.121	0.42	0.529	0	0.529
0.250	1.29	2.443	0	2.443
0.330	3.51	4.273	0	4.273
0.500	8.78	9.213	0	9.213
0.667	14.90	14.354	1.029	15.384
0.833	20.30	18.638	2.463	21.101
1.000	24.60	21.604	3.642	25.245
3.000	36.10	24.600	10.728	35.328
7.000	41.10	24.600	16.193	40.793
28.000	49.30	24.600	25.134	49.734

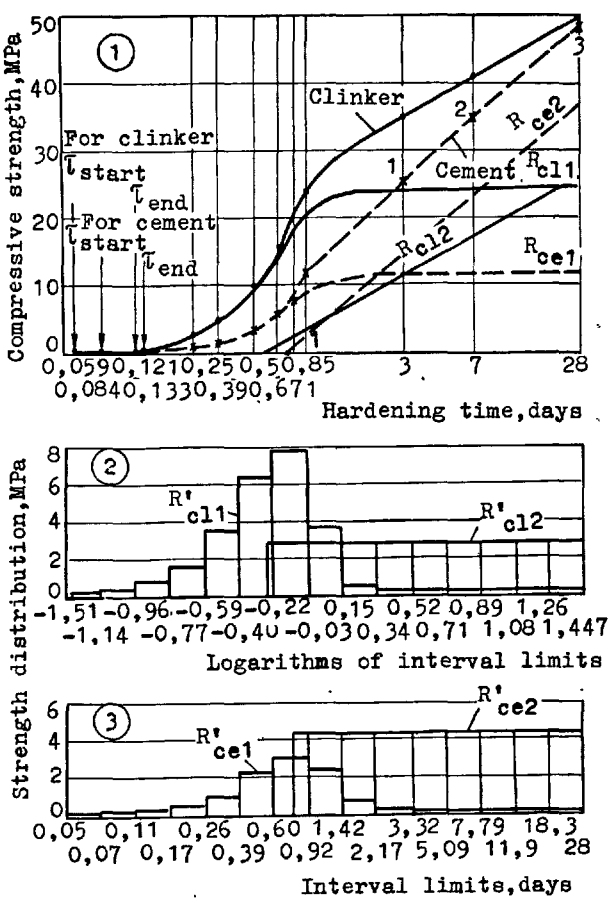

Fig. 3. The kinetics of strength increase of clinker and quick-hardening Portland blast-furnace cement M 400.

Using the determined value of τ_0, the equation of strength increase in the subsequent periods may be written as:

$$R_\tau = 14.8516 \cdot \log \frac{\tau}{0.5685} \qquad (20)$$

The calculated values of strength are presented in Table IV (column 4) and in Fig. 3 (R_{k2}, $\tau > 0.5685$).

The differential values of these strength characteristics are given in the form of a histogram in Fig. 3.2.

The overall kinetic equation of strength increase for clinker is

$$R_\tau = 24.6 \cdot (1 - e^{-2.1053 \cdot \tau^{2.1656}}) + 14.8516 \cdot \log \frac{\tau}{0.5685} \qquad (21)$$

where the second term is used when $\tau >$ 0.5685 day.

The values of strength calculated from equation (21) for clinker are presented in Table IV (column 5) and in Fig. 3 by a solid line. It should be noted that the root-mean-square deviation (the adequacy dispersion) is 0.62 MPa.

For the rapid-hardening Portland blast-furnace cement we can obtain, in an analogous manner, the following kinetic equation for strength increase:

$$R_\tau = 24.5 \cdot (1 - e^{-1.4264 \cdot \tau^{1.8456}}) + 23.1383 \cdot \log \frac{\tau}{0.7641} \qquad (22)$$

where the second term is used when $\tau > 0.7641$ day.

The adequacy dispersion for this equation is only 0.361 MPa. The general form of strength increase of the cement with composition represented by the point A in Fig. 2, is shown in Fig. 3 by a dashed line. The differential values of the strength characteristics of the cement are given in Fig. 3.3.

It should be noted that the intensity of cement strength increase at the later stages of hardening, as calculated by the procedure described here and by means of Equation (7), as a function of the amount of slag, gypsum and clinker as well as the specific surface area, practically coincide.

Analysis of kinetic equations of strength increase of clinker (21) and cement (22) shows the intensity characteristics of strength increase differ considerably at the initial and later periods of hardening, while 28-day strengths values differ only slightly and are 49.30 and 47.1 MPa respectively.

Hence, the kinetic equation of strength increase (18) makes it possible to employ calculations for determination of strength characteristics of hardening cements, discarding tedious and crude methods of rapid (accelerated) determination of activity.

In conclusion we would line to stress that the necessity of developing methods of calculation of cement strength was repeatedly noted at the VI International congress on the Chemistry of Cement (5).

REFERENCES

1.- Дж.БЕНДАТ, А.ПИРСОЛ (1974) Измерение и анализ случайных процессов (Пер. с англ.), М., "Мир", 1974, 463 с., (in Russian).

2.- Я.Я.-Ф.ВАЙНУ (1977) Корреляция рядов динамики. М., "Статистика", 1977, 116с. (in Russian).

3.- К.ГРЕНДЖЕР, М.ХАТАНАКА (1972) Спектральный анализ временных рядов в экономике (Пер. с англ.), М., "Статистика", 312 с., (in Russian).

4.- Прикладная статистика. Анализ и оценка на ЭЦВМ регрессионных зависимостей, М., "Изд-во стандартов", 1975, 46 с., (in Russian).

5.- П.ДЮТРОН, К.Б.ПЕТЕРСЕН, С.КРАЛЬ (1976) Современные методы механических испытаний цемента. Основной доклад. Труды VI международного конгресса по химии цемента, М., "Стройиздат", (in Russian).

THEME VII

Interface reactions between cement and aggregate in concrete and mortar

SUB-THEME VII-1

The bond between aggregates and hydrated cement paste

J.C. MASO
Professor INSA
Toulouse, France

INTRODUCTION

For a very long time, the idea prevailed that a top-grade concrete from a mechanical point of view resulted, for the main part, of the filling, at maximum compactness, of the volume to cast with fragments of rocks embedded in a matrix, both phases having mechanical strengths as high as possible. Obviously, it was taken for granted from the outset that the bond was supposed to be established between these two compounds. Nevertheless, the adherence seemingly satisfying at work and the rocks not being able to be extracted far away from the place of use -which always makes a limited choice- the main research effort bore quite naturally on the matrix, not however on its binding ability, but on its embedding and filling ability..

However consider a concrete element subjected to a traction. Suppose, for simplicity's sake, that the grains of rocks and matrix possess identical deformability, that the element has a constant cross-section and sufficient length. Then, should there be adherence between the aggregates and the matrix, the strain and stress fields are uniform, except for the end sections. All around the aggregates, the stress shifts from traction to shear. Suppose that the bond between the two phases breaks down without either the aggregate or matrix being damaged. Then, the matrix alone bears the total stress ; it, however, only occupies a small fraction in any section of the element and the system behaves as if the aggregates were voids. They are almost completely useless, following the breakdown of the bonds.

In traditional concrete, the matrix is more deformable than the aggregates. The consequence thereof, as shown by DANTU [1] is a concentration of isostatics towards and inside these latter. The bond breaking then takes place at an earlier stage than in the theoretical example mentioned above.-

Suppose, on the other hand, that the breakdown starts in the matrix. The aggregates, less deformable, slow down the crack propagation provides the strength of the bond is sufficient ; however, the propagation will increase if the bond is weak.

Yet, the failure surfaces of concretes in traction follow the contour of aggregates (MASO [2], DHIR and SANGHA [3]). Some research carried out earlier, shows that if the bond does not exist or is very weak, its failure does not bring about that of the whole. The resistance depends only on the matrix, it is the first type of failure. If the bond is beyond a given value, its breakdown brings about the collapse of the whole because the matrix alone is unable to support the total loading. It represents the second type of failure (fig. 1). For equal composition, the strength in traction following the second type is higher than the one following the first type. Therefore, the bond plays a major role in the crack propagation process and the failure of the concrete. The concrete strength in traction is higher, all other things being equal, when the bond strength is higher.

These two types of breakdown are found also in compression but the aggregates continue to contribute to the strength, even beyond the rupture of the bonds. Furthermore, this process occurs for much higher loads than in traction. Indeed, the bonds stressed directly in traction are only stressed indirectly in compression, due to the differences in strength between the

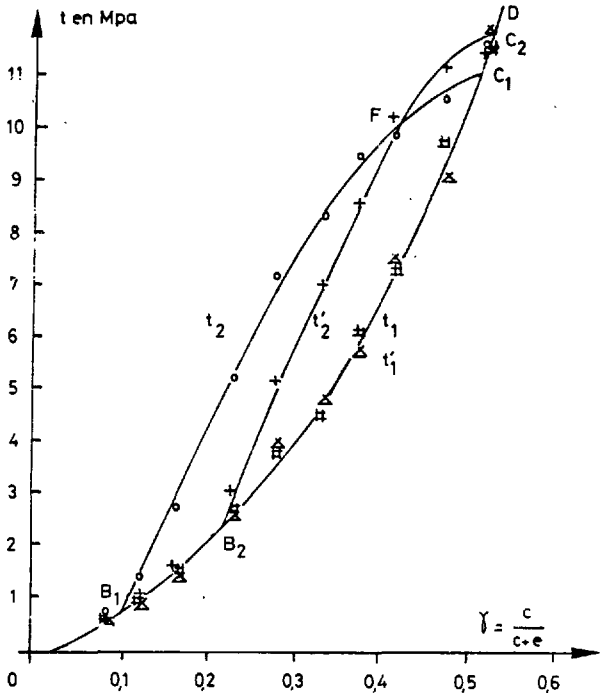

Fig. 1 : Strength in traction by bending (t) of calcite and quartz mortars
calcite : O clean (t_2) Δ coated with silicones (t_1)
quartz : + clean (t'_2) □ coated with silicones (t'_1)

c and e proportions, in volumes, of cement and water of the set-cement. Mortars have been mixed with W = constant = 0,314 and the samples tested at 28 days.

matrix and the aggregates. These phenomena account to a great extent for the strength in compression being much higher than that in traction.

If engineers had not invented reinforced concrete and pre-stressed concrete to supply the weakness of concrete in traction, it is likely that researchers would have taken an interest in the bond between the matrix and the aggregates earlier, even if, as it will be seen further on, the study thereof proves more difficult.

Therefore, those physico-chemists who took an interest in the cement-aggregate bond were few, more because of lack of motivation than tools. But it is likely that research in this field will develop, for the benefits to be excepted by the engineer are seen more and more clearly nowadays. In effect, the mechanics of composites, non-existent until recently, allows the analysis of the influence of bonds between phases on the mechanical properties of the concrete. Moreover, a greater and greater number of research investigations are being undertaken in the world on the internal mechanisms of crack propagation and failure of concrete. The necessity of analyzing the phenomena with fine resolution in order to understand and model them better, will lead inevitably to a greater number of researchers having an interest in the structure of bond.

We will not discuss the adherence, i. e. the mechanical aspect of the problem. The purpose of our paper is mainly to present the current state of knowledge on the structure and the formation of the bond. The mechanical aspects and the alteration under the action of corrosive agents will only be briefly discussed, to show to the physicists and chemists, how interesting is the physico-chemical study of the hydrated set cement-granulate bond for the mechanicians as well as engineers.

It is with regard to the techniques used that we present the chief attainments of scientific research in that field among the works of which we have knowledge. In effect, the results available, if they enable us to form an idea of the mechanisms of bond formation, are still very incomplete and their interpretation very dependent on these techniques.

I - THE BOND WITH NON-POROUS MATERIALS THE TRANSITIONAL RING

I.1 - Determination of the bond closeness by the impregnation method and observation by optical microscopy

This technique used by FARRAN [4] consists in taking a sample of mortar and planing a flat face. The sample is then dried in an oven, set in a vacuum to remove the water and the entrained air and, then, impregnated with a coloured resin (Canada balm diluted in benzene, coloured with fuschine, red, or violet of gentian). Thin sections parallel to the plane face are cut and observed in optical microscopy.

FARRAN has studied, by this way, the closeness of bonds between artificial, blast-furnace, supersulphated and aluminous cements, on the one hand, and defined minerals issued from recent crushing of calcite, dolomite, quartz, silex, orthoclase, muscovite, biotite and anhydrite, on the other.

With a water-cement ratio W/C = 0,42 and a one month curing period in water at 15°C, he noticed the lack of any coloured edge around the grains of calcite and dolomite, for all cements concerned. Edge developments of increasing size in the following order were observed : quartz, silex, orthoclose, mica and anhydrite.

Rings are thinner with aluminous cements than with artificial or blast-furnace cements. When anhydrite is used, the ring is thinner with supersulphated cement.

We give in table I the chemical composition of the cements used by all the authors quoted in this paper.

Authors	Cement	SiO_2	Al_2O_3	Fe_2O_3	CaO	MgO	SO_3	Na_2O K_2O TiO_2	Fire loss
J. FARRAN	Aluminous	4,0 6,4	38,9 42,0	17,1 15,7	38,0 34,7	1,3 0,2	0,5 0,2		0,9 0,3
	Portland	21,8 21,3	5,3 5,6	4,3 3,5	64,1 64,4	1,1 1,4	1,9 1,7	(1)	1,2 2,4
	Blast-furnace	27,8	12,3	2,9	47,0	3,0	3,4		2,9
	Supersulphated	25,8 28,2	9,5 10,7	5,1 0,6	46,7 43,9	4,4 4,7	9,0 8,3		0,1 3,1
J. GRANDET J. P. OLLIVIER B. PERRIN	Portland	21,5	5,0	2,3	64,3	2,0	3,2	(1)	1,4
S. DIAMOND	Portland Type I	20,8	5,4	3,0	62,9	2,8	3,0	1,17	0,81
	Type II	20,9	5,0	2,5	66,1	1,2	3,0	0,75	0,65
	Type IS (2)	21,2	5,4	2,8	64,6	3,5	2,4	0,11	0,04
	Type V	22,7	3,5	2,8	65,5	1,2	2,1	0,74	1,32
J. GRANDET J. P. OLLIVIER	Portland	21,4	5,3	2,3	64,0	1,4	2,98	0,53	1,02
A. VAQUIER	Portland	21,5	5,0	2,3	64,7	2,2	3,2	1,0	0,1

TABLE I - Chemical composition (per cent) of the different cements

(1) non indicated
(2) chemical analyses for the cement phase (cement 65 %, slag 35 %)

The rings widen, attaining their maximum values around the grains of calcitic nature. These experiments have been repeated with numerous samples and with cemented ottawa sand. The same results are found again except for the grains of cemented quartz sand, which are surrounded by a similar contact ring. The microcrystalline minerals offer an almost total lack of bond with the hydrated set-cement in contact with them.

This technique can be criticized for the oven-drying followed by the vacuum treatment which certainly produces an important microcracking of samples before impregnation. Nonetheless we can say that when no coloured ring is observed, the bond will be very tight. When a coloured ring is observed one cannot be certain that there existed a defect of the bond in the non-treated sample, but we can, however, conclude that the bond, if it did exist, was more fragile than in the case of calcite or dolomite. It had to have been broken by the initial treatment.

A more recent technique will be described now which enabled us to specify partly these results.

II. - Study of the bond by electron microscope of transmission by a replica technique

A concrete plane section is attacked by hydrofluoric acid. After cleaning, this surface is cast in the form of a thin film of bioden. In order to clear the surface of the particles loosened by abrasion and to make it more plane after cleaning, several prints are taken in a row, before the final print is effected. In a metallization cell, carbon is pulverized on the bioden film under normal incidence while chrome undergoes 45° incidence. The double film metal-bioden is subsequently placed in an acetone bath which dissolves the bioden. The metallic film left is observed by T. E. M.

The resolution thus increases from a few microns for usual optical microscopy to 150 Å by the double-replica technique.

We give as an example, in figure 2, a micrography of a calcite and portland cement mortar.

Fig. 2 : Calcite mortar cured for 4 weeks
G = calcite grain ; W/C = 0,48

By means of this method, PERRIN et al. [5] studied the bond between grains of quartz or calcite and Portland cement, in which W/C and the hardening time were made to vary. In most cases a first layer of hydrated finely crystallized compounds was observed, tightly clinging to the aggregate surface. Subsequently, a zone containing dark blotches tends to spread outwards, followed then by the matrix of hydrated set-cement. The dark blotches are due to grains clinging to the set-cement by the bioden film, then trapped by the metallic film. These grains undissolved by acetone continue to cling to the metallic film. Their thickness is sufficient that the electrons emitted by the microscope are unable to pass through.

It appears, therefore, that the aggregates are surrounded by a particular matrix, varying in structure, composition and cohesion, between the surface of the aggregate and the matrix of hydrated set-cement, which we will call transitional ring.

For given material and cement, its thickness increases with the W/C ratio and decreases with the hardening time until about seven weeks after the mixing under normal curing conditions.

For an identical W/C and identical time of curing, its thickness depends on the mineralogical nature of the aggregate : it is thinner with calcite than quartz (fig. 3). The loss of cohesion, allowing the film of bioden to trap fragments of paste, is due to the machining of the plane surface of the mortar by abrasion.

The spreading and the number of particles removed (i. e. of the zone containing black blotches) are therefore quite representative of the set-cement in part of the transitional ring.

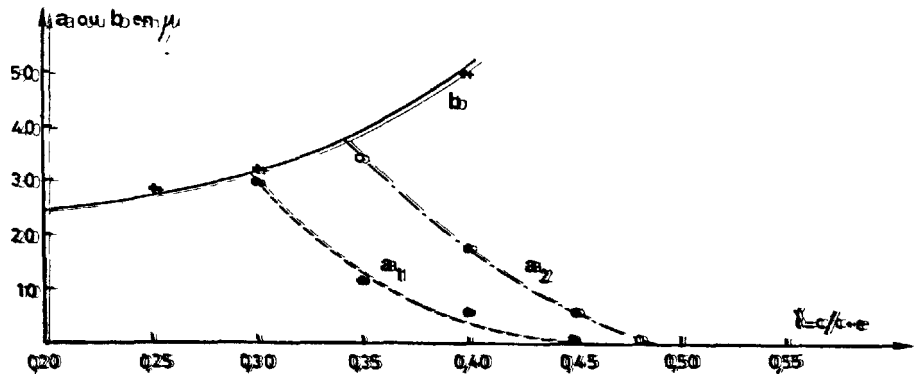

Fig. 3 : Calcite and quartz mortars cured for 4 weeks
curve a : variation in thickness of the transitional ring
(a_1 : calcite mortars ; a_2 : quartz mortars)
curve b : variation of half-distance between aggregates
(mortars have been mixed with W = constant = 0,314)

In figure 4, we can observe that for the lowest W/C, the area of low cohesion disappears. It will be noticed however that cohesion still exists for normal W/C. The coloured edge observed by FARRAN certainly corresponds to the area of lowest cohesion of the ring, cracked by thermic treatment, vacuum action and mechanical action of preparation of the polished section.

Fig. 4 : Calcite mortar cured for 4 weeks
G : calcite grain ; $\gamma = 0,55$

In the case of calcite or quartz in association with Portland cement, it is not the interface proper. On the contrary, it is perhaps very likely the case with micaceous minerals.

PERRIN et al. were unable to determine the nature of fragments lifted by the bioden. Their research ought to be extended to include other aggregates and different cements.

We pointed out that at the interface of calcite and quartz, a finely crystallized layer tightly clinging to the aggregate could be observed. The double replica technique neither allows them to be identified nor permits their observation on a higher resolution scale. However, this is possible, to some extent, using the method mentionned hereafter.

I.3 - Study of the part of the transitional ring in close proximity of the aggregates by direct observation in T. E. M.

It is necessary to obtain sections of mortar thin enough to be crossed by the electrons in a T. E. M. OLLIVIER et al. [6] achieved this by ionic etching.

A first thin section of mortar, a few hundredth millimeters in thickness is obtained after the technique traditionally used for the preparation of samples intended to be observed in optical microscopy.

Fragments of this section including hydrated set-cement - aggregate bonds are subjected to the bombardment by a twin argon - ions beam (fig. 5). We can thus remove successive monoatomic layers on both faces of the sample. The intensity of beams being maximum in the center, we get samples the thickness of which varies from the center to the edges between 0 and about 1 000 Å.

The samples thus prepared are then observed by T. E. M. The resolution herein is in the range of 20 Å for normal use. This technique has only been used so far for mortars associating grains of quartz or calcite to Portland cement or to C_3S. With normal W/C ratios, hardening times and modes of curing, there is no loss of cohesion of grains which would destroy the samples and would make the observation impossible.

The micrography of figure 6 gives, as an example, a picture of the first layer of a bond of hydrated set Portland cement with a grain of calcite.

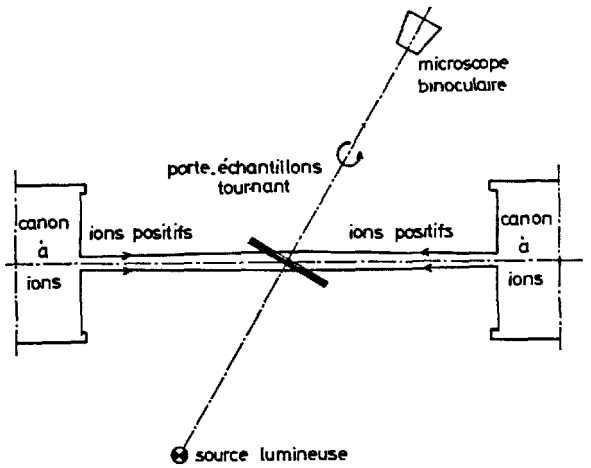

Fig. 5 : Diagram of the ionic etching apparatus

The chief results provided by these studies are summarized below :

- no gap can be observed between the aggregates and the hydrated set-cement. If one does exist, its thickness is less than ten Å, which implies quite high attractive forces of the Van der Waals type, and excludes any gap at the interface.

- no crystal of portlandite can be observed in the immediate vicinity of calcite or quartz.

There can always be found, between the aggregate and the first portlandite crystals a thin film of tiny crystals causing a blurred ring around 3 Å by electron diffraction. This can be accounted for by the fact that the species observed are very tiny and do not present a sufficient number of crystalline networks to provide a distinct diagram in electron diffraction.

These two statements reinforce an hypothesis, already formulated by FARRAN in the case of calcite associated to Portland cement and to aluminous cement, about the formation of compounds by combination of ions emanating from the aggregates and of ions coming from the dissolution of anhydrous constituents of cements. We will consider this hypothesis again later.

The diminutive thickness of the first layer of the transitional ring, the smallness of formed species, the combined action of vacuum and heat in the etching apparatus, and in the microscope limit the possibilities of this method of study because it does not allow, except in a few well defined cases, the establishment of the diagnosis of the constituents found in the first layer at the interface.

However, other means have brought complementary views, X-ray diffractometry and scanning microscopy which we will examine in turn.

I.4 - Study of bond by X-ray diffractometry and optical microscopy

Composite samples are fabricated according to the diagram of figure 7.

Fig. 6 : Calcite (c)-set cement (p.c.) interface in a mortar cured for 6 months
$\gamma = 0,45$

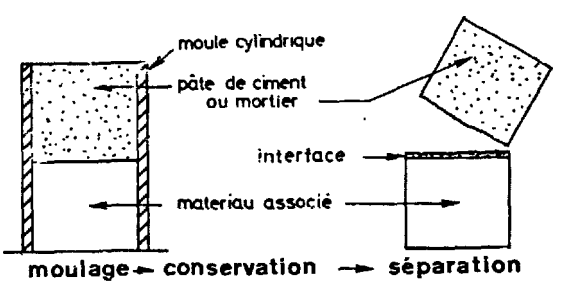

Fig. 7 : Preparation of mixed samples

The face of the adjoining part in contact with the set-cement or the mortar was previously polished so as to facilitate the forthcoming splitting of the two parts of the sample. The latter is kept under specified conditions, until the desired hardening time is reached. The two half-samples are then separated. The rupture occurs, either at the very interface or in the immediate vicinity, in the set-cement or in the adjoining part. In the two former cases, one can observe both faces (adjoining part side and hydrated set-cement side) by means of metallographic optical microscope and, by determination of refractive indices, identify the well crystallized compounds. A layer several μ in thickness can also be obtained by scraping, on either side of the interface, and analysing it by X-ray diffractometry (powder diagram). This technique was used by FARRAN [4] to determine the components laid in contact with samples of glass, calcite, quartz, orthoclase and stainless steel during the hydratation of cements mentionned in I.1. All the samples were kept in water at 15°C.

With aluminous cement and associated materials other than calcite, the contact film is constituted after a fortnight, of a non-identificated gel and bicalcium aluminate, C_2AH_8.

With ageing, the gel progressively disappears, to give way to a finely crystallized mat of hydrated monocalcium aluminate C A H_x ($x \sim 8$) which constitutes the main part of the film observed at the interface. The non-identificated gel would be constituted almost exclusively of alumina and lime in an equimolecular ratio and water.

With calcite the previous formation of hydrated monocalcium aluminate is observed, which disappears progressively to give way to a solid solution of hydrated tetracalcium aluminate and calcium carbo-aluminate, also observed by FIERENS [7] . Corrosion patterns are also noticed on the surface of calcite, which clearly confirm the partial dissolving of this mineral in contact with aluminous cement.

With artificial cement, one is still led to distinguish between calcite and other associated minerals. With the latter, FARRAN observed that the interfacial film was either constituted of portlandite alone or of portlandite associated with a non-identificated gel. He did not observe any visible evolution beyond a fortnight's hardening.

With calcite, FARRAN was unable to observe the interfacial film and by way of consequence, unable to identify the components because the rupture always took place in calcite. He assumed that, in this case again, the bond was insured for the most part of portlandite crystals. In order to justify the top-grade quality of the adherence between calcite and Portland cement, he formulated the hypothesis of epitaxial arrangements between calcite and Portland cement. We can observe in effect, on the one hand, that within 10 % the hexagonal base of portlandite crystals by association of three diamond-shaped faces of calcite rhombohedron can be obtained and, on the other hand, that calcite is etched, which results in bringing to light cliveage planes crystallographically blank. The conditions necessary to the forming of epitaxial coupling, according to ROYER [8], are thus reunited.

With blast-furnace cement, FARRAN does not point out the differences in behaviour between calcite and the other associated materials studied. The interface film is constituted of portlandite, ettringite in abundance, hydrated calcium aluminates and non-identificated gel.

With supersulphated cement, FARRAN noticed at the interface of all associated materials a very thick tangle of ettringite crystals and a non-identificated gel.

At the time, this research was carried out (1950-1955) and with the means at his disposal, FARRAN was unable to recognize the C. S. H. Besides, he could not establish whether the identificated compounds were effectively in direct contact with the associated material, or at a certain distance, albeit very short, from the latter.

The principle of the identification method used by FARRAN, the results of which we have just presented, was employed again by BARNES, DIAMOND and DOLCH, replacing the optical microscope and X-ray diffractograms on powder by the scanning microscope and the E. D. X. A.

I.5 - Study of the bond by scanning microscopy and E. D. X. A.

BARNES, DIAMOND and DOLCH [9] studied the bond of glass with various cements. The optical microscopy is replaced by the scanning microscopy and the resolution thus increases from a few microns to a hundred Å. Furthermore, the analysis by X-ray diffractometry is no longer global on the over-all layer gathered by scraping but is local owing to E. D. X. A.

BARNES, DIAMOND and DOLCH brought to light the existence in close vicinity of the glass, of a twin layer which they called duplex film constituted of portlandite crystals the axes of which are perpendicular to the aggregate and layers of C. S. H. Beyond this film about one micron thick, they observed a highly porous zone bearing portlandite crystals the axes of which run parallel to the glass aggregate, well-formed and rather large in size, leaving between them large spaces partially filled afterwards with heaps of secondary portlandite crystals with their axes perpendicular to the glass-surface, smaller in size, and of C. S. H. Moreover, this zone contains a large quantity of HADLEY's grains [10] . The latter, as mentioned earlier are constituted by a C. S. H. shell about one micron thick, the inside of which is either empty or partially filled with a remainder of anhydrous cement grains or, sometimes, of hydrated compounds.

These authors do not mention the presence of ettringite. However, they mention lime-sulphate ratios ranging from 13 to 22 according to the sites.

BARNES, DIAMOND and DOLCH repeated these studies with siliceous sand mortars (OTTAWA - ILLINOIS). They find the same results again, but the preciseness of the contact area being smaller they were unable to bring to notice possible interactions at the aggregate-cement interface.

The schematic representation of the bond of figure 8, can be given from the observations of BARNES, DIAMOND and DOLCH.

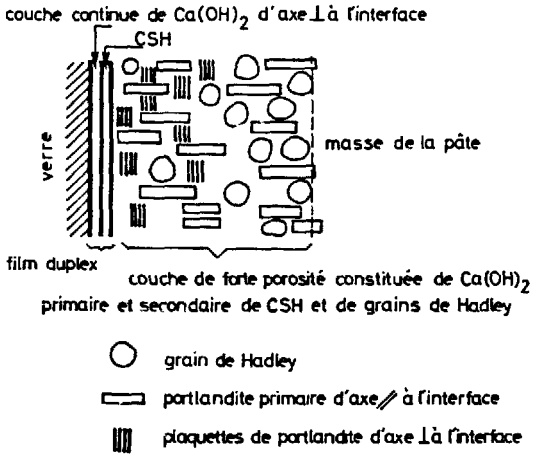

Fig. 8 : Schematic representation of the bond according to BARNES, DIAMOND and DOLCH.

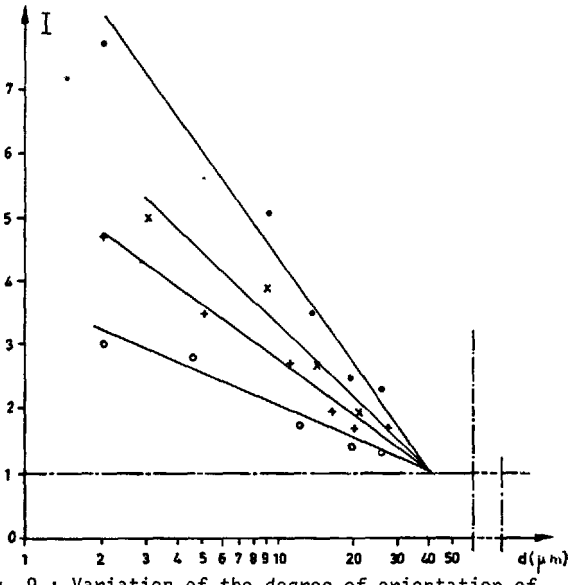

Fig. 9 : Variation of the degree of orientation of portlandite as function of distance to the the interface and for different types of aggregates

O : Mosset marble (FRANCE) x : quartz
+ : Calacata marble (ITALY) • : polyethylene

The phenomena of preferential orientation of portlandite by the glass-surface associated to the set-cement or by the aggregates is worthy of investigating.

I.6 - Study of the orientation of portlandite crystals by X-rays diffractometry

Utilizing again the technique used by FARRAN consisting of separating and splitting mixed cylindrical samples, GRANDET and OLLIVIER [11] followed the evolution of the intensity of the two beams at 4,90 Å and at 2,628 Å of portlandite as a function of the distance to the interface. Both half-cylinders obtained after separation are placed directly on the goniometer of the diffractometer and the ratio :

$$I = \frac{I_{(001)}/I_{(101)}}{0,74}$$

$I_{(001)}$ = intensity of the beam at 4,90 Å of the 001 planes of portlandite

$I_{(001)}$ = intensity of the beam at 2,628 Å of the 101 planes of portlandite

for layers about 1 micron apart, the surfaces successively analyzed being brought to light by minute scraping. Figure 9 gives the evolution of ratio I, characteristic of the degree of orientation for a given cement and different adjoining part.

The degree of orientation varies linearly with the distance to the interface. The distance at which the adjoining part has no longer an influence on the orientation of portlandite is important and independent of its nature.

(*) The ratio $\frac{I_{(001)}}{I_{(101)}}$ equals 0,74, when there is no preferential orientation.

On the contrary, the slope of straight lines changes with the latter. It appears that the degree of orientation is smaller when the reactivity of the adjoining part is higher which would tend to reinforce the hypotheses of formation of solid solutions between the set-cement and the aggregates.

Lastly, the discontinuity of orientation of portlandite indicated by BARNES, DIAMOND and DOLCH is not observed here. There is disagreement on this point between the observations of these authors and those of GRANDET and OLLIVIER.

I.7 - Hypotheses concerning the formation mechanisms of the transitional ring

When the mixing takes place, the aggregates become coated by a film of water several microns thick, in which grains of anhydrous cement can be found only in very limited numbers, if at all. The concentration in anhydrous cement, null in the vicinity of aggregates, progressively increases afterwards with the distance to the latter.

When the anhydrous components are dissolved, the most mobile ions are the first to diffuse in the water-film. With the Portland cements, for example, the order of diffusion is as follows : sodium and potassium ions, sulphate ions, aluminium ions probably issued from an earlier dissolution of C_3A before fixation of sulphate ions on their surface, followed by calcium ions. Silicon ions remain at first fixed by the anhydrous grains of the cement and spread only later on in the water film surrounding the aggregates.

If the latter are insoluble, these phenomena can be expressed as indicated on the theoretical diagram of figure 10-a. On the contrary, if they are partially soluble, a maximum concentration of ions issued from the aggregates is obtained at the surface of the latter ; this concentration decreases quickly with distance. It is represented in the theoretical diagram of figure 10-b.

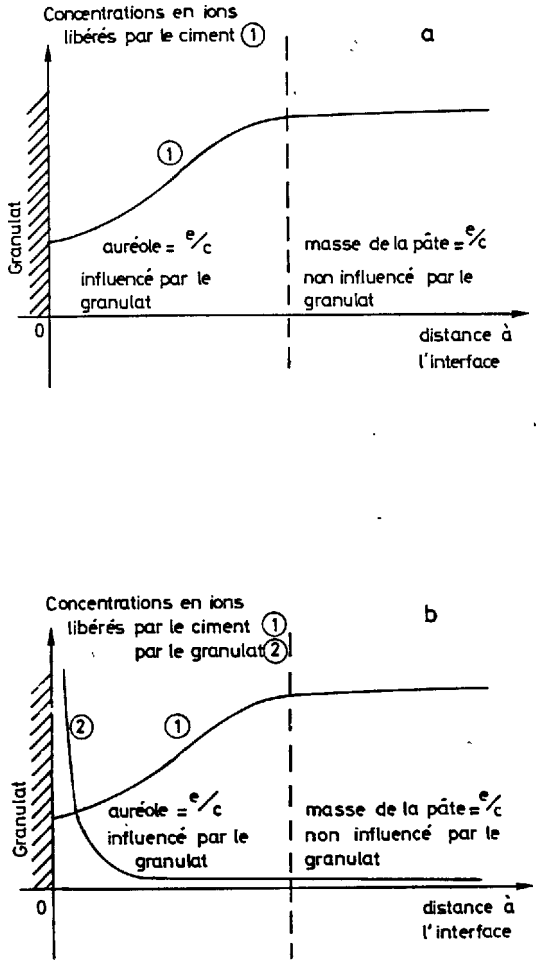

Fig. 10 : Schematic representation of concentration of ions liberated by the cement and by the aggregates for a given time (1 curve type 1 or type 2 resembling those given for each ion)

a : case where aggregates are non-soluble

b : case where aggregates dissolve partially

In the water surrounding the aggregate the first nucleii to form are those of the hydrated components corresponding to the most mobile ions ; ettringite and portlandite in the case of Portland cement.

Development of crystals is not hindered, and they reach considerable size, larger than in the body of the set where supersaturation is much higher and space more limited. They form a looser network the pores of which are progressively saturated with less mobile ions, such as silicon and aluminum ions for Portland cements. A second generation of crystals then develops in the voids left by those of the first generation. Taking again the example of Portland cements, we find C. S. H., and again ettringite and portlandite in crystals of smaller size.

One can think, as a consequence of the experiments of OLLIVIER et al., that first generation crystals do not develop in continuous layer in direct contact with the aggregates.

Furthermore, the latter always being partially soluble, the space left between the first generation crystals and the aggregates progressively fills with a very tight crystallite network formed by the ions issued from the anhydrous cement and those coming from the aggregates which are able to combine.

HADLEY'S grains observed by BARNES, DIAMOND and DOLCH, could have arisen from the hydratation of the first, not very dense, layer of anhydrous grains of cement.

From GRANDET and OLLIVIER'S experiments one can deduce that the thickness of the water film surrounding the aggregates at the time of mixing depends little or not at all on the nature of the latter. On the contrary, it would play a non negligible part in the orientation of the first generation crystals and, as a consequence, of those of the second generation.

Therefore, the hydratation process, when the transitional ring is formed, would occur according to LE CHATELIER'S theory, and not, as in the body of the matrix, by formation of a crystallized coagulated network.

It is therefore important to stress the probable existence of an area of minimal concentration (figures 10-a and 10-b). It is in that part of the ring that the largest crystals and the highest porosity will be found. It must correspond to the coloured edges observed by FARRAN, to the zone of reduced cohesion pointed out by PERRIN and to that of maximum porosity beyond the duplex film shown by BARNES, DIAMOND and DOLCH.

Lastly, the partial dissolution of the aggregates increases the roughness of surfaces, which favours the mechanical clinging of hydratation products, increases the interface, which increases the effect of bond forces of a physical type, can cause a formation of chemical type bonds by a combination of ions issued both from aggregates and cement.

I.8 - Relationships between the transitional ring and the properties of concrete - Perspectives

A material is all the less resistant to mechanical actions as it is more porous ; therefore, the transitional ring is more porous than the matrix of the hydrated set-cement.

Crack initiation and its propagation is easier in large size crystals than in the arrays of crystals of small dimension tightly entangled ; therefore, the transitional ring contains crystals larger than those found in the body of the hydrated set-cement and in greater quantities.

Moreover, these crystals show a preferential orientation, an aspect favourable to the propagation of cracks.

For these three above stated reasons, the transitional ring is the weakest part of the granular cohesive material which constitutes hardened concrete.

In traditional concretes, the aggregates are less deformable than the matrix of hydrated cement. Under the action of external forces, there is always a concentration of stresses in the aggregates and, as a result, in the transitional ring.

The latter, therefore, happens to be both the most highly stressed part, and the weakest region of the concrete. It is then in the transitional ring that the first irreversibilities will occur, by packing, resulting from microruptures and the closing of pores, if it is compressed, by cracking when subjected to tractions or shears. The cracking, once initiated, then propagates from ring to ring. The observation of concrete fracture surfaces confirms this. In most cases, these follow the contour of aggregates.

Numerous authors think, however, that the shrinkage cracks or microcracks the set-cement. It is to be pointed out that the experiments seemingly confirming this fact, normally lead one to submit the concrete to treatments which amplify the phenomenon to a great extent. However, it appears that the cracks resulting from shrinkage initiate at the aggregates and cause as a consequence ruptures of the transitional rings. If the concrete is effectively fissured initially by the shrinkage, it is then the roots of the fissures which are subjected to the highest stress. The transitional ring would then no longer play a part in the first irreversibilities under the action of the external forces (beginning of crack propagation).

But its role would remain unchanged after the beginning of propagation for fissures would develop throughout the transitional rings.

On the other hand, the action of corrosive chemical agents depends not only of the nature of the elements in contact but also on the exposed surface. Yet, the transitional rings, through higher porosity, and if they are effectively connected by a network of capillaries or of microfissures resulting from shrinkage or from the action of external forces, contitute a preferential way for attack by aggressive agents since they offer a considerable amount of internal exposed surface.

In the case of Portland cements, furthermore, the elevated concentration of portlandite in the transitional ring is an extra factor of alteration.

The objective of research directed towards a better understanding of the composition and structure of the transitional ring is therefore obvious. It is important then to broaden the research efforts to include various types of cements and aggregates. It would also be necessary to shed light on the influence of curing temperatures, admixtures, slags and pozzolanas. Finally, processes aimed at decreasing the ring porosity, at diminishing the size of crystals developping thereon and at preventing their preferential orientations would probably have very favourable consequences on the behaviour of concrete under mechanical, physical or chemical actions.

II - THE BOND WITH POROUS MATERIALS

Two cases are to be examined. In the first, one of the faces of the porous material is in contact with the cement, while the other is in contact with the atmosphere. In the second case, the porous materials are completely embedded in the set-cement.

II.1 - Case of porous materials with only one face in contact with cement

Studies by GRANDET et al. [12] have been undertaken on this topic using bricks and a Portland cement. They made up composite cylindrical samples associating a cylinder of brick to a cylinder of set-cement or mortar. The samples of brick were chosen so as to cover a domain of capillary patterns as wide as possible.

Furthermore, for each sort of brick, they varied the initial water content from 0 to 100 %. The samples were stored until testing in atmospheres saturated with water, devoid of CO_2 at the beginning.

After separating the brick from the set-cement, the two exposed faces were analyzed by X-ray diffractometry. They were subjected to successive scrapings, each time removing a layer a tenth of millimeter thick. The new surfaces so obtained were in turn analyzed by diffraction. These researchers were thus able to draw diagrams presenting the variations of concentration in crystallized components as a function of the distance to the interface.

With initially dry brick, one can observe that the percentage of ettringite, maximum at the interface, decreases towards the body of the set-cement or of the mortar. The portlandite concentration follows an inverse law of variation (fig. 11). The phenomenon is all the more obvious as the internal specific surface of the brick is higher. The analysis of X-ray diffractograms reveals the existence of a low hydrated area in the vicinity of the interface.

As the initial water content of the brick increases, the suction decreases and a diffusion of the ions from the water phase of the set-cement to that of the brick takes place. This results in an increase in the maximum concentration of ettringite at the interface, the diffusion effect augmenting that of suction. The portlandite concentration increases but still offers, even for the brick initially saturated with water, a value lower than one that would be in contact with a porous material.

Moreover, it can be observed that the delay of hydratation in the vicinity of the interface also decreases when the initial water content of the brick increases.

Lastly, no noticeable preferential orientation of portlandite crystals in the vicinity of the brick is observed.

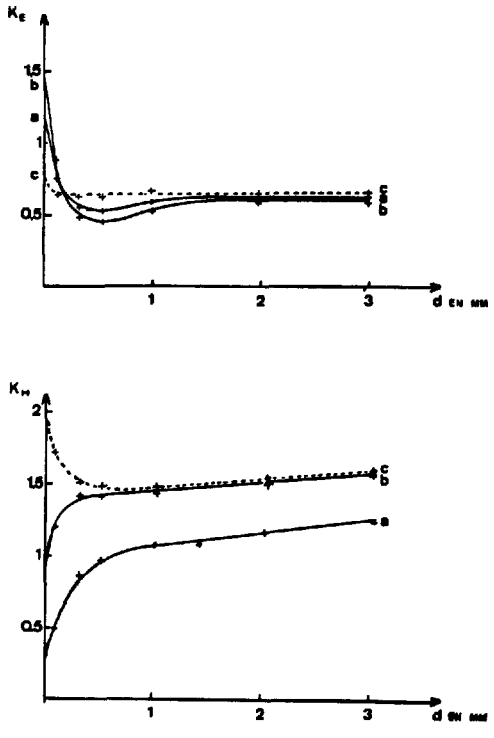

Fig. 11 : Variation in concentrations of ettringite and portlandite in contact with a porous material as function of distance to the interface

a : brick initially dry
b : brick initially saturated with water
c : glass (given for comparison)

$$KE = \frac{IE}{IC_3A} \qquad KH = \frac{IP}{IC_3S}$$

IE = intensity of the beam at 9,73 Å of ettringite
IC_3A = intensity of the beam at 2,70 Å of C_3A
IP = intensity of the beam at 4,90 Å of portlandite
IC_3S = intensity of the twin beam at 2,764-2,739 Å of C_3S

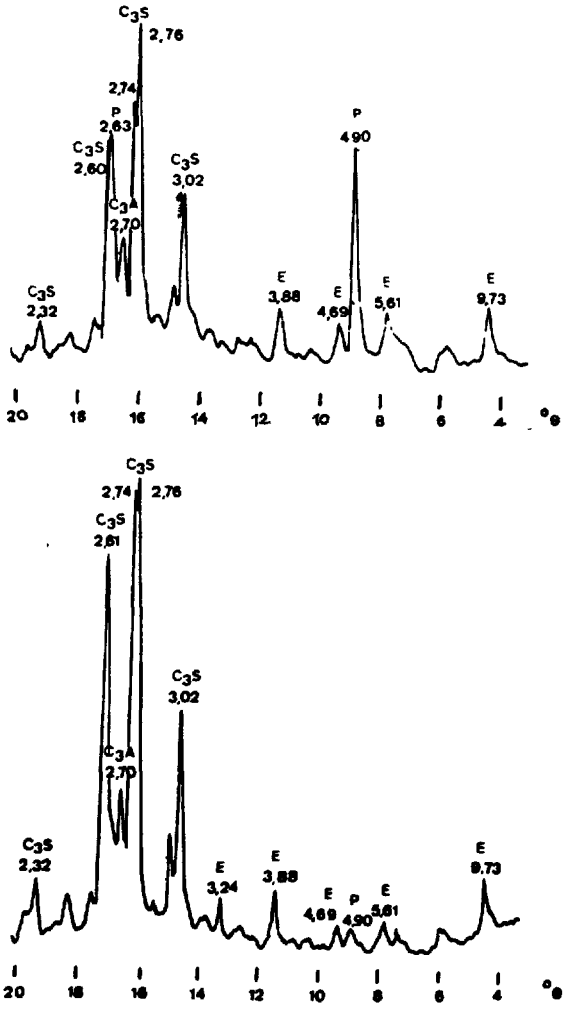

Fig. 12 : Diffractogram relative to set-cement in association with brick initially dry

a) at 10 mm from the interface
b) at the interface

The mechanism of bond formation would be as follows. With the initially non-saturated brick, the set-cement water is drawn by the brick, and this all the more as the level of initial impregnation of the latter is lower and its internal specific surface higher. This occurs fairly quickly, upon casting, therefore prior to the beginning of the cement setting. The consequences of this suction phenomenom are, on the one hand, a diminution of the porosity of the set-cement or of the mortar, until the force of water retention by the set-cement balances that of suction by the brick, and on the other hand, the lack of a water film of considerable thickness in the vicinity of the interface.

We thus have important variations in water content between the brick and the body of the set-cement. For an initial W/C = 0,26, the W/C at the interface can be reduced to values from 0,14 to 0,11 with initially dry bricks.

In the course of time, the water may migrate, from the body of the set-cement to the brick thus allowing a progressive but very slow hydratation of still anhydrous silicates.

The phenomenom is less pronounced as the initial water content of the brick is higher and its pores larger in size.

The hygrometry of the environment in contact with the side of the brick facing the set-cement or mortar plays an important role due to the evaporation resulting thereof.

When the composite sample is exposed to atmospheric carbon dioxide previous to total hydratation of the set-cement, carbonation of ettringite and portlandite from the interface liberates water in significant quantities, thus resulting in an acceleration of hydratation of the less hydrated zone.

The very uneven surface of the porous material, owing to the large number of capillaries opening onto it, would prevent any preferential orientation. The clinging is of an essentially mechanical type, through formation of ettringite crystals at the opening of the pores of the brick.

II.2 - Case of porous materials completely embedded in the set-cement

Whenever the porous material is completely embedded in the set-cement, as is the case with porous lightweight concretes, identical phenomena occur, excepting the evaporation of water in the atmosphere. They are therefore much less strong due to their having limited absorption capacities of water by the aggregates. Moreover, this absorption reverses after a few hours, the aggregates yielding back all or part of the water absorbed from the set-cement. No delay in hydration by lack of water in the vicinity of the aggregates can be observed.

Attempts made to observe a transitional ring by the techniques previously cited were all unsuccessful. This can be mostly accounted for, by the very intricate geometry, on the surface, of the porous aggregates. Methods of study adapted to this case then remain to be elaborated upon and put to work.

It is also to be noted that with some light aggregates, the migration into the set-cement, by the diffusion of ions issuing from the partial dissolution of aggregates can have noxious effects on hydration. This is the case with pumice aggregates and Portland cement. VAQUIER et al. [13] noticed that under wet curing, setting did not occur. They ascribed this phenomenom to the freeing, by pumice, of SO_4Na_2 which considerably lowers the pH of the solution (to about 10) thus preventing setting to take place.

It should be pointed out, last of all, that, as against aggregates used in traditional concretes, porous aggregates are, except for new concretes, generally more deformable than the matrix. Under the action of external forces, isostatics move aways from the aggregates and those, as well as their bond to the hydrated set-cement, are less stressed than the latter. There is no longer any risk of rupture at the interface. On the contrary, any crack occuring in the matrix is attracted by the aggregates.

III - CONCLUSIONS

At the time of mixing, the non-porous aggregate becomes surrounded by a water-film several microns thick, and hydration occurs mainly in accordance with the mechanisms described by LE CHATELIER. Around these aggregates, a transitional ring appears, different in its composition and its structure from that of the body of the set-cement - more porous and lower in cohesion. The mineralogical nature of the aggregates is of major importance.

In contact with porous materials not completely embedded, the suction of the set-cement water by these materials plays an essential part in the formation of the bond.

Around the completely embedded porous materials (case of lightweight concretes) no zone of composition different from that of the body of the set-cement can be observed.

Numerous studies remain to be done, in order to clarify, among others, the natures of the components formed immediatly in contact with non-porous aggregates, the influence of temperature, of admixtures, of slags and of pozzolanic materials. One can hope, by diminishing the porosity of the transitional ring, the size and the orientation of the crystals which develop thereon, to improve significantly the mechanical properties of concretes and their resistance to corrosive agents.

REFERENCES

1 - P. DANTU (1958) "Etude des contraintes dans les milieux hétérogènes. Applications au béton" Annales de l'I. T. B. T. P., n° 121

2 - J. C. MASO (1969) "La nature minéralogique des agrégats, facteur essentiel de la résistance des bétons à la rupture et à l'action du gel" Doctorat ès Sciences, Université de TOULOUSE Revue des Matériaux de Construction, n° 647-648 et 649, pp. 247-276 et 321-330

3 - R. K. DHIR et C. M. SANGHA (1974) "Development and propagation of microcracks in plain concrete" Matériaux et Constructions n° 37, pp. 17-23.

4 - J. FARRAN (1956) "Contribution minéralogique à l'étude de l'adhérence entre les constituants hydratés des ciments et les matériaux associés" Doctorat ès Sciences, Université de TOULOUSE Revue des Matériaux de Construction, n° 490-491 et 492.

5 - B. PERRIN, J. C. MASO, J. FARRAN et R. JAVELAS (1972) "Existence d'une auréole de transition entre les granulats d'un mortier ou d'un béton et la masse de la pâte de ciment hydraté. Conséquences sur les propriétés mécaniques" C. R. Ac. Sc. PARIS, t. 275, série D, pp. 1 467 - 1 468

6 - J. P. OLLIVIER, R. JAVELAS, J. C. MASO et B. THENOZ (1975) "Observation directe au microscope électronique par transmission de la liaison pâte de ciment-granulats dans des mortiers de calcite et de quartz" Cement and Concrete Research, vol. 5 pp. 285 - 294

7 - P. FIERENS (1974) "Etude de la formation de l'hydrocarboaluminate de calcium" Cement and Concrete Research, vol. 4, pp. 695-707

8 - L. ROYER (1928) "Recherches expérimentales sur l'épitaxie ou orientation mutuelle de cristaux d'espèces différentes" Bul. Soc. Fr. Min., t. 51, pp. 7
L. ROYER (1954) "De l'épitaxie ; quelques remarques sur les problèmes qu'elle soulève" Bul. Soc. Fr. Min., t. 77, pp. 1 004

9 - B. D. BARNES, S. DIAMOND and W. L. DOLCH (1978) "The contact between Portland cement paste and glass "aggregate" surfaces" Cement and Concrete Research, vol. 8, pp. 233-244
B. D. BARNES, S. DIAMOND and W. L. DOLCH (1979) "Micromorphology of the interfacial zone around aggregates in Portland cement mortar" Journal American Ceramic Society, vol. 62, n° 1-2, pp. 21-24

10 - D. W. HADLEY (1972) "Nature of the paste-aggregate interface" Ph. D. Thesis, School of Civil Eng., Purdue University

11 - J. GRANDET et J. P. OLLIVIER (1980) "Orientation des hydrates au contact des granulats" Septième Congrès International de la Chimie des Ciments PARIS (à paraître)

12 - J. GRANDET, J. FARRAN et J. C. MASO (1970) "Variations des concentrations de portlandite et d'ettringite dans les pâtes de ciment Portland au contact des terres cuites poreuses" C. R. Ac. Sc. PARIS, t. 271, série D, pp. 4-7

13 - A. VAQUIER et B. THENOZ (1974) "Conservé en atmosphère saturée d'eau, le béton ponce ne fait pas prise" Matériaux et Constructions, n° 691, pp. 347-349.

SUB-THEME VII - 2

Durability

J. CALLEJA
IETCC
Madrid, SPAIN

1. - GENERAL INTRODUCTION

Even when it is intended to apply the term DURABILITY referred only to CEMENT as component, it would be erroneous to mislead CONCRETE as compound, and so much so when durability of any component of concrete and concrete itself may be affected by any other component of it (sulfate-bearing aggregates, reactive silica, reactive silica, reactive silicate or reactive carbonate-bearing aggregates and alkali-bearing cements) (1). Moreover, the main and even the only finality of cements are cement derivatives, i.e., concrete in its different modalities.

Mechanical strength of concrete is not -not always should be- the only or the main factor to be considered. On the contrary, durability should be always a factor to be taken in due account as it greatly and some times decisively influences and determines the strength of concrete and the general behaviour and performance of it in each moment, at shorter or longer terms (2).

Concrete durability and the reverse concrete deterioration respond to very complex phenomena according to the very many causes and to their several possible combinations acting simultaneously or successively (3).

Anyway, durability, as referred to cement or to concrete, is a term which needs to be clearly and precisely defined. Several arbitrary and conventional definitions of it are possible and some of them have already been expressed.

Durability may be defined in a most general way as the capability of material to mantein its good behaviour and performance in safety conditions and in the foreseen service circunstances during the foreseen service time (4).

In a more specific manner, durability may be defined as the resistance of cement and concrete to either internal (*intrinsic*) or external (*extrinsic*) physical, phisico-chemical or chemical actions (5) (6).

Whatever may be its definition, durability is a so broad matter that needs to be limited if it is to be treated within given disponibilities of time and/or space. So, as far as the purpuse of this paper is concerned, durability is conventionally defined as the resistance of cement and cement derivatives -pastes, mortars and concretes- against external actions merely chemical in nature, acting only chemically on hydrated cement paste. Nevertheless, durability even defined as resistance to chemical attack, to so limitate in some way the broad general problem of it, is by far complex (3).

Consequently, the (in origin) physical actions on cement or concrete such as the freezing of absorbed or adsorbed water; the causes and effects of damages due to reinforcement corrosion -though chemical or electrochemical in nature and external or internal in origin-; the disruptive actions and effects owing to volume changes of internal -though chemical- origin (free lime and periclase expansive hydration), or external -though physical- origin (expansion, shrinkage, swelling due to rapid and big changes of temperature and/or humidity), are deliberately discarted in principle and as much as possible, as considered not directly belonging to the content of the bare chemistry of cement, which is the main -the only- matter of this 7th Congress. Alkali-aggregate reaction could fit in the group of internal chemical actions, but very specific in character. Protection and protective materials and treatments are also obviously excluded.

Nevertheless, chemical, physico-chemical and physical -even mechanical- internal and/or external actions are so narrowly and indissolubly linked together, at least in practice, that not always is either possible or convenient to separate from one another and to take into consideration only some of them, neglecting the rest. On the other hand, most of work done and papers written on durability of cement and concret seem to show in average an eclectic position in this aspect. Unfortunately, according to the reality, neither "pure" actions (whatever their nature) take place, nor single unitary effects are observed in practive, but exceptionally. This reality implies an enormous complexity of durability problems and a huge difficulty to study and solve them, at least as far as the finding of general solutions is concerned. This has been -and perhaps still is- the aim of a certain number of research workers on durability, even as it has been defined above. And the question arises: is it possible to reach such a purpose?. Before attempting to give an answer let us tray to evaluate the progress attained up tu date, taking as a reference the ratio of definite knowledge gained and practical -technical- problems solved, to the time devoted, the persons involved and the papers written and published, in the general research work done on cement durability. Probably it could be said about it something similar to what has been opportunely said as referred to shrinkage (7): many hundreds -perhaps much more than a thousand- of significant papers dealing with durability have been published in the last fifty years, and some basic knowledge has been gained with them; but the real and practical durability of today's concretes is not very different from that of the concretes in the thirties. At least it is not better to the extent which would to be expected, considering the effort done. But possibly the same thing to one or another extent could be also said as referred to expansion, swelling, reinforcement corrosion, alkali-aggregate reaction, high-alumina cement conversion and alkaline hydrolisis and so many chief problems within a more extended field of durability.

What does it mean?. First of all and simply that a high proportion of the total effort has been vain or but scarcely profitable. And why?. The answer cannot be so simple, but a certain number of reasonable causes could be mentioned: a) repetition of tasks

owing to lack of communication and coordination; b) discordant or even contradictory results -at least apparently- as attributed to the same of very similar experimental conditions, when in reality very different, but anyway very frequently not (or not sufficient ly) specified; c) difficulty or impossibility to compare results obtained in conditions to be considered as different enough to permit an acceptable comparison; d) conclusions hardly admissible or even erroneous as a consequence of an incorrect or undue evaluation and/ /or comparison of results; e) conclusions drawn through unadvised criterions of simplification, extrapolation, generalization or exaggeration applied to what is complex, specific, particular or normal; f) a certain "orientation" of the experimental work from the very beginning of it in order to reach with a given (higher) probability some expected results. This latter possibility is obviously unconceivable and inadmissible in a pure scientific and technical work, but it is not su much so in some other type of applied "research", the results of which being -obviously- also published, when interests other than those concerning pure and true knowledge are involved.

Present knowledge slowly accumulated along the time on durability is nonethelesss very valuable and litterature is extremely copious even as referred only to chemical attack on cement by whatever aggressive medium. Periodically and recently compilations and summaries of the copious references found in the general abstracts have been made in a very conscious and efficient manner (1). But even if it is intended in such compilations to deal with durability as referred only or mainly to cement, it is impossible to neglect concrete, as mentioned above, as otherwise the survey would be limited and unrealistic. On the other hand, selective criteria must be applied, as the number of references collected is really very high (1) (8) (9) (10). This is the reason why, as pointed out, it is intended in this paper to deal only with the main and more common chemical aspects on durability.

Despite the superabundant litterature on the item, many dark and dubious aspects still remain without an adequate answer, so that a satisfactory and complete doctrine summarizing the fundamental matter is far from being reached (3). Nevertheless, interest in concrete corrosion themes is permanent. In recent times research lines and directions have been exposed and proposed (11); attempts have been made to solve the difficult problem of describing the complex corrosion process on concrete (12); methods for quantitative analysis of such processes have also been described (13); and criteria for evaluating either the aggressivity of the environment or the concrete resistance to it, have been dealt with too (14).

When trying to evaluate consciously the relative influence of all kind of factors (physical, mechanical or chemical in nature) affecting the chemical attack on concrete and the corresponding chemical resistance of the material, a sort of disorientation arises from considerations found in the extense bibliography existing on the subject. The reason in the author's opinion may be the very different importance quantitatively given to such factors, depending on the various points of view based on several distinct mentalities or professionalities of the authors. So, authors in which an engineering formation predominates, "authomatically" or "instinctively" tend to focuse the problems from mechanical or physical standpoints rather than from chemical bases. And so, one tends to pay greater attention to density, homogeneity, compacity, porosity, permeability, etc., in connection with penetrability, diffusion, capillary suction and capillary raise, osmotic pressure, etc., referred to pore size distribution -maximum, medium and minimum pore size-, evolution of porosity, intercommunication and accessibility of the pore system, etc. All the main paremeters of concrete and concrete materials such as cement content, cement fineness, water/cement ratio, aggregate grading, etc., are considered as factors determining the foregoing characteristics and properties of the concrete itself, as it is really the case.

On the other hand, authors possessing a more basically scientific -perhaps chemical- formation will naturally tend to emphasize the importance of factors of chemical nature, such as composition of cements, reactivity of aggregates, etc., in connection with potential and actual reactions in any of the materials or between them, or even of them with external and/or internal aggressive substances. So, one tends to consider all these factors at least as important coadjuvants of the characteristics, properties and performance of concrete, as is really the case too.

But in any case -in both cases- the effects such as losses in wight and/or in strength either by leaching of soluble products or by formation of non-hydraulic compounds with softening of the resistant structure; or by expansion (crystallization and crysyal-growth pressure cracking) causing disruption; or by reinforcement (electro) chemical corrosion, etc., must be equitatively considered at the ligth of all the possible causes and influencing factors.

Dealing with chemical attack on concrete very many authors begin, very many others finish -or both- invoking the compactness of the material as the first and by far the main condition to resist. This is really so to such extent that it is superfluous to afford particular references. Thus, the nature of the cement as far as its intrinsic resistance is concerned, is considered in many cases as secondary or not operative, except in cases of leaner mixes, so that a high compacity obtained through a high cement content permits for instance to use with similar results cements either of high or low content in C_3A (in sea--water attack), whereas lower cement contents impose the use of specifically resistant cements. Moreover, when differences in behaviour not easy -or not possible- to be explained are detected, variations in compacity are generally invoked as a valid explanation (15) (16).

A clear example of conscious eclecticism to be applied in this sense has still been exposed (17) when considering that kinetics of gas and water penetration in concrete, depending on its structure as determined by porosity and penetrability of aggregates and paste, in turn determining absorption, capillary rise and diffusion in the material, is decisive for durability. So that the knowledge of true coefficients of permeability, either correctly calculated or determined in laboratory tests carried out duly in real conditions, is absolutely necessary (17). But absorption tests, permeability tests and capillary rise tests must be designed on scientific bases in such a way that they do permit to describe the actual behaviour of a porous system as far as water penetration in concrete is concerned (18) (19). On the other hand, it must be added that not only physical factors as homogeneity, porosity, permeability, absorptivity, capillarity, etc., with their respective features and implications are important for durability; cement composition in anhydrous state, degree of hydration of cement paste, bond strength between paste and aggregates, and several others, are also factors affecting decisively concrete durability, which so becomes a very important but most complex and difficult problem (20), either in real practice or in the field of more basic laboratory research work.

On the basis of the foregoing considerations the task of this paper will mainly be centered on the more outstanding specific aspects of the chemical attack on cement and concrete, and on the chemical resistance of concrete to external aggressivity of them on it.

2. - TYPES OF CHEMICAL ATTACK ON CONCRETE

Firs of all it must be said that chemical attack on concrete needs water or at least humidity to proceed, and so the very many different aggressive media are mainly liquid (aqueous solutions): soil-waters, surface-waters, sea-waters, waste (industrial)-water, etc., containing acids, sulfides, sulfates, chlorides and in general salts of sodium, potassium, calcium, magnesium, ammonium, etc., in each case, and even organic compounds.

Much has been written on mechanisms of attack on concrete. Two main types of such mechanisms have been simply proposed for interaction between hardened cement paste and aggressive media in contact with it (2): dissolution (leaching, lixiviation) of water soluble products formed first on surface and consecutively in mass as the attack progresses inwards (21), and expansion. Dissolution may be caused in acid or soft waters and/or by ion-exchanging salt solutions. In turn, it causes a loosening and softening of the structure of the cement paste. Expansion may take place when sparingly soluble products are formed and crystallization pressure due to crystal growth of salts acts causing structural disruption. This is the case of sulfates, ettringite and/or thaumasite formed successively (2) (21).

The possibility and the intensity of chemical attack depend, on the one hand, on solubilities, concentrations and dissociation constants of aggressive media; on the other hand, on the same parameters corresponding to the reaction products, all referred to ordinary, "normal" or stagnant conditions. Extraordinary or "abnormal" conditions such as higher temperatures, freezing, water pressure or renewal of aggressive agents, as well as mechanical actions, may accelerate and intensify the chemical attack (2).

So, in such conditions the concentration or proportion of an aggressive substance in an aggressive medium is not the only parameter determining the rate, intensity and effects of any specific attack. This depends also on other factors as those mentioned, so that a given concentration may behave as innocuous or as highly aggressive (3). This is one reason of the uncertainty (and therefore of the lack of agreement) concerning the establishment of general limits of concentration for safety. It also explain the -to a great extent- probabilistic character of the chemical attack. On the other hand, not always the action of an aggressive substance is proportional to its concentration. Moreover, changes in it may affect even qualitatively the process involved in the attack. This if, among many others, a possible cause of failure of the accelerated methods of testing based on high concentrations of aggressive media (3).

Many types of chemical attack on concrete may be considered according to the specificity of the aggressive agent and its chemical nature. From this latter point of view, either inorganic and organic types of aggression may be foreseen, or acid, basic and saline attacks can be considered. Schematically this is very simple, but the reality is much more complex, as various simultaneous or consecutive chemical actions may take place in an aggressive process.

From equilibrium solubility studies in the system C-S-H it has been shown that $Ca(OH)_2$ is the least stable component of the hydrated cement paste, its solubility depending on the pH-value. Pore liquid in the paste as far as its Ca^{2+} and OH^- ionic concentrations are concerned, is in equilibrium with $Ca(OH)_2$, provided this is present and in contact with the liquid phase. Otherwise, equilibrium establishes between liquid phase and $C_xS_yH_z$, the more complex solubility of the latter depending on the x/y ratio (22).

Parameters governing a pure acid attack are the acid strength and the concentration, i.e., the pH-value (22) (23). So, acid attack on cement acts on bases and basic salts formed in hydrated paste and causes deterioration provided that soluble salts are formed in it and leaching of them take place. In the case of organic acids it seems to be so to such extent that the order of aggressivity more of less coincides with the order of solubility of salt formed (23). But acid attack proceeds in a different way if less soluble salts are formed, which in turn can react with other

hydrated components of the paste -this is the case of sulfuric acid attack forming gypsum (24)-.

The great influence of the pH-value is the reason why it is to be expected that acid waters of low pH ($\leq$4. 5) attack very strongly concretes, whatever their cement may be, but more particularly if it is a portland cement. To such extent it is so, that as far as mineral acid attack on cement is concerned it has been roughly stated that none of the cements used resists the action of waters with pH-values lower than 4 (25) and even lower than 5 (23); that ordinary portland cements may resist without heavy damages waters with pH-values higher than 6, and that high-alumina cements may resist waters with pH-values between 4 and 6 without any special protection (25).

But not only the pH-value as such is to be considered in the attack of cement by acids; the rate of their diffusion and/or replenishment from the surrounding environment (for instance, soil), particularly if hydrostatic pressures are operative, must be taken into account. Possibilities of removal of the more or less soluble reaction products must also be considered in practice (26). This is another of the innumerous cases in which factors other than those closely related to the chemical attack itself influence its kinetics and determine the rate and the extent of the damage, the chemical parameters of the aggressive process being constant.

Sulfuric acid attack from bacteriological origin is a typical one acting on the surface of sewer concrete pipes, producing softening by loss of adherence between aggregate and cement paste. Destruction of concrete is caused by complex reactions of acid with hydrated lime and other basic hydrated compounds of cement to form sulfates (mainly of calcium), amorphous silica and calcium sulfoaluminates (ettringite). Sulfuric acid is produced by a bacteriological oxidation -at normal temperatures- of hydrogen sulfide, which in turn is formed by a bacteriological reduction of sulfates (24). Oxidation of hydrogen sulfide needs an almost neutral pH which can be reached through carbonation (weathering) of the fresh hydrated cement paste. Deterioration due to this type of acid attack is produced in two steps: first, formation of gypsum; second, formation of ettringite. So, portland cements low in C_3A are, at least in theory, more resistant to this type of aggression. In fact, it has been stated that there is little difference in behaviour and performance of ASTM cements of type I and type II. This seems to indicate that disruption caused by crystallization of gypsum formed in the first step may have a decissive importance (24).

Basic attack on concrete takes place when caustic bases such as sodium hydroxide penetrates the cement paste and undergoes a carbonation, or when alkali carbonates directly penetrate, particularly if penetration continues and wetting and drying alternations take place. In the case of sodium hydroxide and/or sodium carbonate penetration, hydrated sodium carbonates may be formed and damage may be produced by crystalization and crystal growth pressure (27).

Saline attack produced by salts other than chlorides and sulfates may take place and produce effects depending on the chemical nature of the salt involved and on its interaction with hydrated cement compounds. For instance, ammonium carbonate, fluoride and oxalate form fairly insoluble products with cement paste and consequently they are not harmful to it (27).

Destructive effects may be produced by nitrates through the formation and crystallization of calcium nitroaluminates in the pores of the cement paste. The corrosive action depends on the nature and concentration of the nitrate involved, on the time of contact and on the nature of the cement. In this respect, pastes made with blast-furnace slag cements with slag contents higher than 70 % have shown higher relative resistances to nitrate attack. Portland cement pastes are relatively less resistant (28).

A special type of attack with internal origin in concrete is that produced by sulfuric acid and/or sulfates formed by oxidation of sulfides -generally iron sulfides (pyrite and marcasite FeS_2 and pyrrhotite $Fe_{x-1}S_x$- contained in some aggregates or -calcium sulfide- present in slag aggregate or in blast-furnace slag cements. Oxidation may take place prior to the use of the material or once it has been incorporated to concrete (29).

Saline attacks more common are those involving chlorides and/or sulfates (sea-water). They are specifically treated. Nevertheless, mention must be made here on the influence of cations and anions, as saline components, in general attack, as well as in some specific type of attack as for instance that of sulfates.

In this latter respect three types of cations may be considered: those forming soluble hydroxides; those forming sparingly soluble hydroxides; and those forming volatile or neutral compounds.

The former -alkali cations- form gypsum (expansive or not by crystal growth pressure, depending on the initial sulfate concentration). In addition, they increase the OH^--ion concentration lowering that of $Ca(OH)_2$ in solution and facilitating an accomodative expansion process. On the other hand, at the same time the increase of OH^--ion concentration facilitates the attack of other cement constituents and reduces the strength of the paste (30).

Cations forming low solubility hydroxides (earth-alkali cations as Mg^{2+}) form expansive gypsum and hydroxide gels, some of them potentially expansive and some others potentially protective by coating, specially in the case of compact pastes rich in cement.

The third group of cations (NH_4^+) neither favour accomodative processes nor protect by coating. They may cause a strong attack not only through expansion, but also by solubilization of cement components (30).

But, if it is true and well known that cation greatly influences the action and the corresponding effect of sulfate attack on cement, the reciprocal seems to be also true: anion influences the action and effects of cations, particularly those of Mg^{2+}. In the case of attack by $MgCl_2$ the formation of the FRIEDEL's salt retards the corrosion of cement, so that portland cements with no C_3A are more affected than ordinary portland cements. Whereas in the case of attack by concentrated $MgSO_4$ solutions ordinary portland cements, independently of their C_3A content, may be stable, due to a rapid formation of gypsum and gel products which difficult and retard the penetration of Mg^{2+} and SO_4^{2-} -ions (31).

As far as organic matter attack on cement is concerned, it could be made the following general consideration: if chemical attack on cement and concrete is a very difficult theme, it is much more so when the aggressive medium is organic matter, as most commonly this matter is a complex mixture almost never sufficiently well defined as far as its composition is concerned. So, empiricism dominates the studies and research work on chemical resistance of concrete against aggressive matters of organic nature, much more than when dealing with inorganic attack. An example of the complexity inherent to the organic attack on concrete, even when the aggressive product can b · precisely identified with a well defined chemical compound, is offered by the deterioration caused by urea, or better, by its hydrolitic products in alkaline solutions. The damaging effects are attributed to dissolution (even through the hygroscopicity of the urea), penetration, crystallyzation and disruption, i.e., to a series of phenomena physical in nature. But really, the exact nature of the chemical attack of urea in concrete is unknown (32). It seems not to be exagerated to think that much more difficulties and consequently much more lack of knowledge exist when organic aggressives are more complex and their composition is variable and not well defined. Nevertheless, these are the cases actually present in practice.

On the other hand, it is difficult to find a method of general and uniform application to assess the attack caused on concrete by organic compounds or matters. Only on the basis of wide laboratory and industrial empirical experience has been possible an attempt to group organic aggressives into three classes: a) compounds causing reversible deterioration; b) water-soluble and non dissociable products forming calcium compounds; and c) water-soluble and well--dissociable compounds (33). This classification has been introduced in some national standards (for instance, in the new Hungarian Standards).

Some regularity seems to exist in the case of attack caused by organic acids, in the sense that the order of their aggressivity more o less agrees with the order of solubility of their salts formed in the attack (23). Phenols in aqueous solutions affect concrete as weak acids, so that water containing more than 1000 mg/l of phenols should be considered aggressive (34).

Carboxilic acids, alcohols, esters, etc., may attack cement paste depending on their ability to penetrate rapidly into the concrete, and on their more or less intensive acid properties. Dichlorobutene, for instance, has a pronounced acidic behaviour, so that it fully attacks the $Ca(OH)_2$, leaching it in the form of $CaCl_2$ (which in turn causes reinforcement corrosion) (1). This migth unduly induce to simplify, in the way of attributing the main capacity of attack by organic compounds to their acidic properties and to their possibility to form soluble calcium salts, particularly $CaCl_2$ (in the case of chlorinated compounds).

3. - CARBONATION

Carbonation covers all the actions carried out and effects caused by carbon dioxide on cement and concrete. Carbonation may be spontaneous -that achieved by normal athmospheric CO_2- or forced -that artificially created by "pure" or "concentrated" CO_2 even under pressure. Carbonation may act on anhydrous or hydrated cements, neutralizing their basic calcium compounds.

As far as hydrated cement pastes are concerned, it is obvious that the compound more susceptible to carbonation is calcium hydroxide. But it is also well known that other hydrated compounds -every hydrated compound (35)- can be affected to some extent by carbonation, being decomposed to form finally calcium carbonates and hydrated silica, alumina and ferric oxide, as ultimate products of a total carbonation (36) (37) (38) (39). For instance, total carbonation of tobermorite gels according to the schema

$$C_3S_2H_3 + 3\,\bar{C} \longrightarrow 3\,\bar{C}\bar{C} + 2\,S + 3\,H \qquad (40)$$

has been suggested that proceeds by steps:

$$C_3S_2H_3 + \bar{C} \longrightarrow C\bar{C} + 2\,CSH + H \qquad (39)$$

$$CSH + \bar{C} + H \longrightarrow C\bar{C} + SH_2 \qquad (41)$$

A proof that compounds other than $Ca(OH)_2$ may undergo simultaneous carbonation is that the decrease in non-evaporable water of cement after carbonation is lower than corresponding increase in carbon dioxide, taking into account that there is a correspondence mol-to-mol in the fixation of CO_2 and the liberation of H_2O when $Ca(OH)_2$ carbonates (42) (43). So, carbonation affects to hydrated and even unhydrated compounds, for instance C_3S, tending to form calcite with the hydrated products of C_3S, and vaterite with unhydrated C_3S (44). Alkalies and aluminates carbonate very fast and fast, respectively (35).

Different opinions have been exposed as to the "selective" action of carbonation on hydrated phases of calcium silicates and on cement pastes, as well as in connection with the products formed in it according to the degree of hydration of the starting products. It has been stated that CSH is attacked and decomposed by carbonation, whereas hydrogarnets are much

more resistant to it (1). XRD and IR data show that vaterite is formed in greater amount than aragonite when the degree of hydration of C_3S previous to carbonation is higher (45) (46). Carbonate phases have been detected by IR in carbonated CSH gel together with amorphous silica, the hydrated calcium silicate tending to desappear by further carbonation, whereas portlandite is still present, as XRD reveals. This seems to indicate that carbonation acts on hydrated calcium silicates rather than on portlandite, according to

$$C_3S \xrightarrow[H]{\text{hydration}} \begin{matrix}CSH\\CH\end{matrix} \xrightarrow[\overline{C}]{\text{carbonation}} \begin{matrix}C\overline{C}\\CH\\S\ \text{gel}\end{matrix} \quad (45)$$

Probably this is not the usual case (47) (48) (49) (50).

Other opinions consider that carbonation of cements affects preferently to silicates and aluminates, all the forms of calcium carbonate being formed in it, as well as ettringite (51). But on the other hand, other results conclude that ettringite is trasformed into calcite under the action of carbonic water (45).

It has been assumed that calcium ions in hydrated products other than $Ca(CH)_2$ may be in two forms: one relatively susceptible, and the other non-susceptible to carbonation. The former reacts topochemically with CO_2, but remaining attached to the gel structure. So, only a small part of the hydrated compounds other than CH may undergo a slow carbonation (36) (48) (52). This is a chemical reason why the situation of full carbonation is practically never reached in concrete; another (physical, mechanical) reason is that many factors hinder the carbonation progress.

Not always concrete carbonation has been related to free CH and, consequently to different types of cements involved. Carbonation penetration in blast-furnace slag cements and even in portland cement is determined by permeability of concrete, so that a high content of CH -as in the case of portland cements- cannot always protect concrete from carbonation, as has been stated (53).

As to the form in which silica liberated by carbonation appears, amorphous silica insoluble in hydrochloric acid has been suggested (38) and confirmed (54) (55), the ratio of soluble to insoluble rescue of cement paste in hydrochloric acid decreasing with the intensity and degree of carbonation (40).

Calcium carbonate may appear as mixtures of vaterite, calcite and/or aragonite (35) in different proportions according to variable conditions. Hydrated alumina, firstly amorphous, is transformed afterwards into bayerite and finally into gibbsite (56). Gypsum may also appear together with aragonite, as result of carbonation of calcium solfoaluminates (35).

Carbonation of concrete depends on many internal and external factors such as relative humidity, temperature and pressure, concrete porosity and permeability, depending on water/cement ratio, cement content, nature and fineness and secondary components of the cements (15) (35) (37) (53) (56) (57) (58) (59), as well as on hydration conditions, age, strength and moisture content of the concrete. For instance, carbonation of normal or of hydrothermically hardened concrete is different, due to the different nature and composition of the calcium silicate hydrates in each case, and to the corresponding different structure of the paste (37) (40).

As far as carbonation of calcium silicate hydrates and its effects are concerned, the composition and the structure of the hydrated silicates are, as mentioned, particularly important. At first sight one could think that the higher the basicity of the hydrated silicates, the faster and deeper the effects of carbonation. Nevertheless, carbonation of less basic (tobermoritic) calcium silicate hydrates, in spite of their high density, is much faster than that of the more basic and less dense ones, as for instance those formed in hydrothermal treatments of cements (60) as mentioned (40). The explanation given is based on the high specific surface and the laminar structure of the less basic hydrates, together with the different nature of carbonation products, mainly $CaCO_3$, which depends in turn of the carbonation conditions: low concentration of CO_2 and slow carbonation give large calcite crystals with better structure, whereas at much higher concentrations of CO_2 small crystals equal in size are formed, which give place to a worse structure. This affects the strength as well as the degree of crystallization of the calcium silicate hydrates undergoing carbonation. In the case of tobermorite, the less crystallized product forms loose calcite crystals, whereas the more crystallized one forms large solid and strongly linked crystals (60).

Moreover, there is a great difference in initial carbonation of cements with lower early strength and high "afterhardening", on the one hand, and that of cements with higher early strength and lower afterhardening, on the other hand (53). This difference tends to disappear with the age of the concrete. In any case, taking into account the influences of permeability, cement content, strength development, etc., on carbonation, it has been stated that it is safer to make concretes with sufficiently high contents of normal or even slow-hardening cement, than concretes with lower contents of high-early stength cements, provided that concretes in both cases have similar initial strengths (53).

Compaction is also decisive for carbonation, as, depending on it, a retardation of 20 to 25 times in reaching a given depth may be observed. Assuming theoretically that the amount of CO_2 penetrating to the depth x at a given time t is inversely proportional to x, i.e., that the time t required to carbonate (neutralize) the concrete at the depth x is $t = k.x^2$ (the constant k depending on concrete characteristics and mainly on compaction), it has been found for a concrete with w/c = 0,60 poorly compacted that: t (years) = $7.2\ x^2$(cm), whereas for the same concrete thoroughly compacted k = 167. So, 167/7.2 = about 23 (36). In practice it has been observed that carbonation may be retarded by full compaction of dry-consistent concretes, as carbonation proceeds along voids, and easier and faster in concretes.

of higher w/c ratios and lower cement contents.

As to the influence of the moisture content, soaked concrete or periodically rain moistened concrete is more resistant to carbonation than concrete stored in normal conditions, as far as relative humidity is concerned (61). An optimun moisture content in concrete is necessary for carbonation (35).

As far as ambiental circumstances are concerned, relative humidity is equally decisive, as carbonation advances at very high rates for RH values between 50 and 75 % (being much slower for RH 75-100 % or 0-45 %). The reason is that another optimum humidity is necessary (35): values higher than optimum fill the cement pores with water and CO_2 must first dissolve and thendiffuse to penetrate, which is much slower; values lower than optimum retard the process, probably because at such lower values water has not the liquid characteristics corresponding to ordinary water for dissolving either $Ca(OH)_2$ or CO_2 (36), according to old ideas (52) (62).

As far as carbonation kinetics is concerned, several empirical equations have been proposed, in function of carbonation speed (depth of carbonation -cm, mm-) or of carbonation intensity (amount of CO_2 fixed -grams- versus time -from days to years-), w/c ratio, compressive strength and some experimental constants depending on cements, degree of neutralization, induction period, etc. Speed of carbonation of concrete depends on the nature of the cement and on the porosity of its paste -indirectly on the cement fineness, the cement content and the w/c ratio- as intrinsic factors of concrete. Also, as mentioned, on the relative humidity as extrinsic factor (57) (59).

A summary of much of the mentioned equations, as well as an ennumeration of the methods and devices used to determine the depth of carbonation has been recently exposed (40). Among such methods and devices can be mentioned those consisting on coloured indicators (63), radioactive tracer elements and neutronic radiography (64), porosity measurements (65) (66) and diffusion techniques (67), all of them summarily described as well (40).

One of the last equations proposed for carbonation kinetics, very similar to others previously suggested has been $x = a.t^{1/2} + b$ (35) (37) (53), in which x (cm) is the depth of carbonation, t (years) the time and a and b coeficients variable with a great number of factors and parameters. Other equations relate the amount of CO_2 fixed to the square root of CO_2 concentration (45).

The depth of carbonation of a fully compacted and normal cured concrete is largely determined by temperature (45) and by the w/c ratio in an almost linear relationship (61), through other opinion is that optima w/c ratios -low in general- favour maximum carbonation (45). Depth is also determined by the type of cement: other things equal, carbonation penetrates deeper in concretes made with blast-furnace slag cements and pozzolanic cements (and so much so the higher their contents of pozzolan or slag) than in portland cement concretes. The reason seems to be the different proportion of "carbonatable" products in portland cements and in cements other than portland (61) -lower content of $Ca(OH)_2$ in the latter-. These relationships are qualitatively valid either for spontaneous outdoor or indoor carbonation, or for accelerated carbonation in chamber. In general, blended cements containing slags, pozzolans or fly-ashes carbonate faster than portland cements, and ordinary portland cements quiker than high-early strength portland cements. In fact, in blast-furnace slag cement concretes or in pozzolan cement concretes depths of carbonation have been observed one and half to twice than those corresponding to similar portland cement concretes (36).

Studies on artificial carbonation of hydrated as well as anhidrous portland cements submitted to later hydration have been recently carried out. In the case of hydrated cements ettringite, portlandite, vaterite, calcite, anhydrous C_3A and (in short term hydration) gypsum are present. The non-carbonated phases are in proportion lower than in the case of not carbonated cements. As far as ettringite is concerned, it has been suggested that a decomposition process such as:

$$C_3A\,(C\bar{S})_3H_{32} + 3\,\bar{C} \longrightarrow 3\,C\bar{C} + AH_x + 3\,C\bar{S}H_2 + (32-x-6)\,H$$

could take place (49) (50). If CO_2 acts on the same cement paste cured in humid conditions during much longer period, portlandite and ettringite are present in lower proportions, whereas calcite and vaterite show a considerable increase. Moreover, monosulfoaluminate present in notcarbonated paste cured in the same conditions disappears. This has been attributed to a decomposition by CO_2 similar to that suggested for ettringite (49).

In the case of carbonation of anhydrous cement previous to its hydration, anhydrous C_3A, ettringite, carboaluminates, portlandite and calcite have been found in pastes cured during short periods; in addition, vaterite and monosulfoaluminate are also present but anhydrous C_3A is absent in pastes cured during longer periods. Carbonated phases are more abundant in this latter case. On the other hand, carboaluminates have not been detected in pastes of the same portland cement previously submitted to a longer and more intensive carbonation. It has been also suggested that water liberated in carbonation (from $Ca(OH)_2$ mol-to-mol with respect to CO_2 fixed) according to:

$$\underset{\text{solid}}{CH} \overset{H}{\longleftarrow} \underset{\text{solution}}{CH} \overset{H}{\longleftarrow} Ca^{2+} + 2\,OH^- \xrightarrow{\bar{C}} \underset{\text{solid}}{C\bar{C}} + H$$

aids to the hydration. Nevertheless, carbonation of anhydrous cement seems to slow the hydration in bulk. This is patent in the lowering of tensile strength of the corresponding pastes of carbonated anhydrous cements (48) (49) (50).

Carbonation mechanisms in clinker minerals -pure compounds- seem to lead to products of different nature and texture, depending on conditions and parti-

cularly on humidity. Early carbonation of C_3S-solid solutions gives granular products which further on turn into calcite, except in low humidity conditions. At early carbonation whisker products are formed in the case of α-C_2S and angular plates are developped in the case of α' and β -C_2S, which grow to form stick structures in the case of β-C_2S. All these formations correspond to the simultaneous formation of aragonite accompanied by vaterite (68).

Carbonation affects in one or another sense to several properties of cements themselves and of concretes, depending on particular conditions and on the fact that it may act spontaneously or in a forced and controlled manner, either on anhydrous or on hydrated products with different degrees of hydration (40) (48).

Carbonation of hydrated cement may be beneficial in some cases (69). So, it may enhance strengths -which is known since long time ago and has been more and more confirmed (38) (40) (70) (71) (72) (73) (74) (75); it may also improve the durability in different aggressive media (75) (76) (77) (78) (79) (80).( ). In fact, either spantaneous or previously induced carbonation of concrete may protect it to some extent against acid attack in a similar way -and by similar reasons- as does the use of limestone aggregates in concrete (23). Benefits may extend to resist aggressive sulfate waters, mainly if the attack is produced in conditions of total immersion, for in alternative immersion a cracking may be produced depending on the C_3A content of the cement. This is attributed to differential shrinkage due in turn to differences in deformation modul of external carbonated and internal non-carbonated zones of specimens (59) (81). Improvements in sulfate resistance may also be obtained by superficial carbonation of sufficiently consolidated concrete (27) (77).

In alkali sulfate attack on concrete leaching of lime may take place to some extent, which increases alkalinity:

$$SO_4^{2-} + 2\,Na^+ + Ca(OH)_2 + 2\,H_2O \longleftrightarrow$$

$$\longleftrightarrow CaSO_4.2H_2O + 2\,Na^+ + 2\,OH^-$$

if carbonation does not take place:

$$Ca^{2+} + 2\,OH^- + CO_2 \longrightarrow CaCO_3 + H_2O$$

But more intensive carbonation could form thaumasite and plazolite, specially at much longer terms (82).

As far as shrinkage is concerned, and old knowledge confirmed along the time indicates that carbonation seems to increase it, depending on previous curing conditions and drying treatments of concrete, and also on the conditions of the carbonation itself (75) (83) (84) (85). Carbonation is worse when acting on fresh, not yet sufficiently consolidated concrete, as softening of its surface takes place (27).

Artificial (provoked) carbonation of anhydrous portland cements impairs them causing increases in their water demand for pastes of normal consistency and in the time of setting (more for final than for initial set); it also causes decreases in specific surface, compressive strengths (specially at shorter terms) and heat of hydration (48). The action depends on realative humidity (being stronger at RH of 60-70 % than of 30-40 %). It manifests chemically in the formation of calcium carbonates, carboaluminates and carbosilicates (51).

At higher RH values more ettringite and calcium carbonates and less carboaluminates are formed. It has been suggested that this is probably due in part to the process (51):

$$C_3AC\bar{C}H_{12} + 3\,\bar{C} \longrightarrow 4\,C\bar{C} + A + 12\,H$$

As "aeration" is intended the atmospheric action (spontaneous or not) on anhydrous cements through CO_2 and H_2O. CO_2 content in the air may vary in a range from 1 to 10, between values of 0.01 to 0.1 per cent in volume (0.03 in average) (35). Air moisture expressed as relative humidity may vary between very broad limits from low RH % to RH 100 %. Both CO_2 and H_2O in air may act conjointly on anhydrous cements, so that their components may undergo either a partial hydration or (and) a carbonation depending on the chemical nature and fineness of cements. Studies based on IR spectroscopy on anhydrous portland cements submitted to humid at - morpheres have revealed that hydration and carbonation may perhaps be interpreted as follows:

$$\text{Free } C + H \longrightarrow CH \qquad \text{(I) rapid}$$

$$C_3S + n\,H \longrightarrow CSH_{(n-2)} + 2\,CH \qquad \text{(II) slow}$$

$$CH + \bar{C} \longrightarrow C\bar{C} + H \qquad \text{(III) more rapid}$$

Terms "rapid" and "slow" are relative. Processes (II) and (III) are respectively controlled (other things equal) by diffusion of moisture through hydrated products and by protection afforded by calcium carbonate covering particles and closing their pores. Process (III) could explain the tendency of C and CH to disappear by aeration of cements, though it could be also explained (in the case of a strong humidification of cement) by a process such as:

$$C_4AF + 6\,C\bar{S}H_2 + 2\,CH + 50\,H \longrightarrow 2\,C_3(A,F)(C\bar{S})_3H_{32}$$

as alternations observed in IR-bands corresponding to water and gypsum coincide with the formation of ettringite. On the other hand, strong aeration seems to affect to the ferritic phase, lowering its A/F ratio to form ettringite (48).

Carbonation may affect to high-alumina cements during and after their hydration in such a way that in C_3AH_6, 2, 4 or 6 water molecules may be gradually replaced by 1, 2 or 3 molecules of CO_2 to form successively "CO_2-hydrogarnets" such as $C_3A\bar{C}H_4$ and $C_3A\bar{C}_2H_2$, and finally $CaCO_3$ in a matrix of $Al(OH)_3$ (86) (87).

4. - CARBONIC WATER ATTACK

Almost pure waters -natural acid waters, but not highly carbonic mineral waters- from mountains and snow melting may be aggressive, not only by their pH-value, but mainly by their contents of "total", "excess" and particularly "aggressive" dissolved carbon dioxide, and by their "temporary" -calcium bicarbonate in solution- and "permanent" hardness.

All "pure" waters contain a certain amount of "total" dissolved CO_2, depending on ambiental conditions. A part of it is "fixed" as calcium bicarbonate; another part is "free". In turn, a part of this latter -"equilibrant" CO_2- mantains calcium bicarbonate in solution, according to the equilibrium:

$$(CO_2 + H_2O)\ H_2CO_3 + CaCO_3 \longrightarrow Ca(HCO_3)_2$$

Free carbon dioxide in the form of carbonic acid, in excess over the amount needed to mantain the equilibrium -i.e., the difference between "total free" CO_2 and "equilibrant" CO_2: "excess" CO_2- may attack and dissolve calcium carbonate, if the solution is not saturated with calcium bicarbonate, shifting the equilibrium to the right. But this attack progresses only up to reach saturation in calcium bicarbonate, so that only a part of the "excess" CO_2 (the so-called "aggressive" CO_2) acts more or less depending on the lower or higher initial concentration of $Ca(HCO_3)_2$. The "remainder" dissolved CO_2, if any, does not act in this way. Conversely, if "total free" CO_2 in solution is less than the corresponding "equilibrant" CO_2 -as is the case in "incrustant" (non-aggressive) waters-, the equilibrium shifts to the links and calcium carbonate precipitates. Consequently, the equilibrium determines in each moment the aggressivity of a carbonic water and hence the possible extent of its attack on calcium carbonate.

Excess CO_2 of aggressive waters may attack $Ca(OH)_2$ from cements, but calcium carbonate formed precipitates in the pores of the paste. This is a way to compact concrete and, consequently, carbonation by carbonic waters may have a beneficial effect for concrete, provided that no leaching of calcium bicarbonate occurs and attack stops by a compaction effect near to the surface of the concrete (23) (27).

Anyway, all the "excess" CO_2 can be considered as aggressive for concrete and a considerable leaching of lime is the outstanding result of an intense and continous carbonic acid attack through aggressive carbonic water. (88).

A schematic exposition of all the preceeding relationships has been developped (23), which slightly modified could be presented as follows:

Total CO_2 = fixed CO_2 + (total) free CO_2 (I)

(total) free CO_2 (I) = equilibrant CO_2 (II) +

\+ excess CO_2 (III)

excess CO_2 (III) = aggressive CO_2 + remainder CO_2.

Considering excess CO_2 as aggressive for cement, classification of carbonic waters as far as attack to concrete is concerned, may be as follows (23):

when $I > II$ $III > 0$ (aggressive water)
$I = II$ $III = 0$ (equilibrated water)
$I < II$ $III < 0$ (incrustant water)

It follows that for a given total CO_2, the higher the calcium content in water (hardness) the lower its aggressivity. This is specified in standards and recommendations in terms of "nul", "very weak" (or negligeable), "weak", "strong" and "very strong" aggressivity, according to the content of aggressive (in this case "excess") CO_2 -mg/l. - It could be added that a sure and serious attack is to be expected when aggressive (excess) CO_2 concentration is higher than 60 mg/l (23).

So, natural water aggressivity depends conjointly on pH, on lime in solution and on aggressive (excess) CO_2 content in it. The aggressivity may be lower at lower pH-values if the initial concentration of calcium bicarbonate in water is higher; conversely, it may be higher at higher pH- values if the initial concentration of calcium bicarbonate is lower. In sum, lower pH waters (if highly mineralized: with much dissolved CaO) may be less aggressive than waters of higher pH (if less or not mineralized) (25) (27).

Other dissolved salts may modify quantitatively the relationships so far exposed, as calcium salts increase and alkali salts decrease the dissolved carbon dioxide required to mantain equilibrium, so that for given equilibrium conditions the aggressive CO_2 and the corresponding attack is lower in calcium solutions -for instance, in the presence of gypsum in solution-, and higher in sodium or potassium salts solutions (27).

Furthermore, other factors which may modify the extent (intensity) and the speed of the attack are the renewal of aggressive CO_2 of waters containing it and the percolation of carbonic waters through concrete (25). In practice, and other things being equal, attack on concrete and concrete resistance to carbonic aggressive waters depend conjointly on the thickness of the concrete member attacked and on the time of action of the aggressive water (89). Thickness and time could be considered as conjugated parameters as far as effects and importance of the damages caused by carbonic waters are concerned.

Carbonic compounds present in water may influence other types of aggressivity on cement. For instance, sulfate attack depends on sulfate concentration and also on the pH of the aggressive media, so that when both -and even the HCO_3-ion concentration- change, it is difficult to explain the aggressive action on the basis of only one unitary process of attack. In the case of a sulfate-bicarbonate combined action, corrosion products such as ettringite, gypsum and calcium carbonate (calcite) are formed in three main different zones from the not yet attacked surface of cement paste outwards, as follows: a first inner zone where sulfate action begins, in which the amounts

of ettringite and gypsum increase, and portlandite decreases outwards to a minimum; a second zone in which ettringite and gypsum have reached their maximum concentration and the amount of portlandite increases to some extent; a third zone in which Ca $(OH)_2$ decreases to a practically null value, gypsum and ettringite also decrease, and the amount of $CaCO_3$ increases to a high value (90). From thermodynamic considerations to explain the formation of ettringite and that of gypsum it has been concluded that both may take place together, predominating the latter when cement is richer in C_3A. The rate of penetration of the attack and the absolute and relative thickness of the zones depend on the rate of diffusion of SO_4^{2-}-ions, which in turn depends on the chemical nature of the cement paste (90).

Similar thermodinamic considerations and calculations have also permitted to determine the (relative) stability of hydrated cement minerals and corrosion products in terms of their solubilities in aggressive media, depending on the composition (anions, cations, pH) of their saturated solutions. So, further experimental results have confirmed the theoretical previsions as to the formation of calcite and gypsum in the surface attack of cement paste by simultaneously carbonic and sulfate waters (91).

5. - ALKALI-CARBONATE REACTION

This type of reaction involving alkalies of cement affects to some carbonate rock aggregates, as for instance very fine grained dolomitic limestones containing clay, which are reactive and expansive. The problems in this field seems to be to differentiate by suitable methods expansive and non-expansive, among reactive rocks (27) (92).

In the expansive reaction considered as a "dedolomitization" (93) according to the schema:

$$MCC_2 + XH \longrightarrow MH + C\bar{C} + X\bar{C}$$

dolomite alkali brucite calcite alkali carbonate

brucite is formed to which expansion and corresponding effects are attributed, through processes based on inhibition of water and creation of osmotic pressure by semipermeable membrane actions. Contribution to it is afforded by the weakening of bonds between rhombic crystals of dolomite. In all these processes the clay accompaying dolomite is thought to be involved (94).

Other point of view consider that transformation of dolomite into calcite and brucite according to:

$$M\bar{C} + CH \longrightarrow C\bar{C} + MH$$

has expansive effects if magnesium hydroxide crystallizes forming brucite instead of remaining in gel form acting as a binder (1).

A reflexion of the writter at this point is that, as in the case of alkali-silica reaction, alkali-carbonate reaction seems to take place with injurious character preferently if the concrete is easily -continously or periodically- submitted to wet conditions. It should be thought if the true main mechanism of expansion might be adscribed first of all to osmotic pressure phenomena, in which clays may act as semipermeable membranes, or to which they may cooperate by contributing to the formation of such membranes -for instance, affording ions necessary to give them a semipermeable character-. This point of view could aid perhaps to solve the problem of differentiating expanding and non-expanding reactive dolomites, in function of their content of clays and of the nature of the clays (92).

6. - ALKALI-AGGREGATE REACTION

Alkali-silica reactions as concrete unsoundness causing internal autodestruction is different from that caused by an external chemical attack (9) and similar to that caused by expansive free-lime or free magnesia -periclase- in cements. It is not intended to deal here in detail with alkali-aggregate (alkali-silica, alkali-silicate (95) and/or alkali-carbonate) reactions and much less so when so many technical papers and excelent compilations, reviews and summaries of very interesting papers have been issued along the time (8) (96) (97) (98) (99) (100) (101) (102) (103) (104) (105)

Among them two have been recently issued. The one is a bibliographic compilation of 569 references of papers published from 1923 up to 1975, classified according to dates of publication, countries affected, test methods, laboratory investigations, performance of structures and case studies, cracking and pop-outs, pozzolans, aggregate performance, cement types, preventive measures, remedial action, bibliographic reviews and comprehensive papers and general articles (104). The other is a CEMBUREAU confidential "state of the art" report on alkali-aggregate reactivity in concrete, of about hundred pages, containing three appendixes dealing with glossary of terms, rock names and silica forms involved in reaction, references on aggregate classification and description, additional references -to (104)- on alkali-silica reactivity and figures, maps, graphics and photographs (105). Technical papers not only dealing with the current prospects on the possible future trends in alkali-aggregate reactions and expansions, mainly as far as their mechanisms are concerned, have been published by some of the main personalities specialized in the theme (106) (107) (108).

Nevertheless, some considerations will be made on the outstanding chemical mechanisms, as the not well known but extensively described alkali-silica reaction presents many peculiar aspects not easy to explain and not yet fully or satisfactory explained.

Two types of alkali-aggregate reactions have been traditionally considered: alkali-carbonate (dealt with elsewhere in this paper) and alkali-silica reaction. As far as the possibility of a third type, that of alkali-silicate reaction, it seems to be adscribed to some phyllosilicates, and when attributed to some

"argillaceous dolomitic limestones" is not to be either confused or mixed with the alkali-carbonate (second type) of alkali-aggregate attack (109) (110). Each of them are possible, wether isolately or conjointly. Alkali-silicate seems to proceed much more slowly and with but very little or negligible gel formation. But this is also possible in specific cases of alkali-silica reaction which may take place simultaneously. Nevertheless, the mechanisms and kinetics of controverted alkali-silicate reactions are far from being known and explained (109). Calcium hydroxide attack on clays and feldspars, in which tetracalcium aluminate hydrates, alkali silicates, hydrogarnets and free alkalies are formed depending on the type of feldspars involved, has been suggested as possibly related to cement (alkali)-aggregate reaction (111).

Some principal factors have been mentioned as governing the expansive alkali-silica reaction: crystallinity and (induced) changes in crystallinity of active parts of aggregates (112); "opaline" nature, amount and particle or grain size of reactive materials; amount and alkali content of cements; and water availability. As to the nature of the reactive materials, those containing glassy amorphous (hydrated), cryptocrystalline and microcrystalline forms of silica, or crystalline silica with lattice defects able to absorb water (21) are the more active. Studies on specific reactivity of rocks and minerals have revealed that, depending on materials, the degree of strain, the microstructure, the crystallite size, the degree of disorder in the structure, the amorphous character, the hydrated condition and the acidic nature of natural volcanic glasses, the alkali cation -sodium or potassium- of syntetic glasses and the microporous channel system of materials, are factors influencing the reactivity. The combination of some of the more decisive factors among those mentioned may explain the higher susceptibility of certain materials such as opal, as well as their expansive and damaging actions, even when in very low proportions in aggregates (98). In fact, it has been found that silicious aggregates showing a high IR absortion corresponding to OH bands, probably are alkali reactive. This seems to be in agreement with the hydrated character of the amorphous reactive silica, as in the case of opal (1) (113).

On the other hand, it has been stated that expansion is not always proportional either to the alkali content of cements or to the cement content of concretes -both determining mainly the total content of alkalies in concrete- (27) (114) (115). So, the heating-cooling and the wetting-drying exposure in accelerated testing of cement-aggregate combinations show a lack of close correlation between expansion measured and alkali content of cements. This means that although alkali-silica reaction may contribute to produce expansion during the testing, the incompatibility of the cement and the aggregate in combinations tested is independent -or not only dependent- on the expansive alkali-aggregate reaction, as very large expansions may be observed in specimens containing cement of very low alkali content, whereas reaction rims may not appear on potentially alkali reactive aggregate particles (29).

The limits of alkalies (equivalent Na_2O contents) in cements causing sensible expansions recently seem to tend to be enhanced -about 20 % from 0, 9 to 1, 1- (21). This might lead to consider if a similar criterion should be applied to the specification limits in cement standards, as far as the present limits -in general 0, 6 %- are concerned, affecting to the so-called low-alkali cements. Such a consideration would be consequent with the spare of energy and lowering of fuel consumption in cement manufacture recomended by the International Energy Agency.

As far as the nature, amount and particle size of reactive material in aggregate are concerned, it has been claimed that there is no clear quantitative relationship between them and expansion caused: expansion is sometimes greater for lower amounts and medium-size particles than for higher amounts and smaller or greater particle sizes. Moreover, increases of reactive materials in concrete may sometimes cause decreases in expansion (1). All this -and sometimes the reverse- depends in turn on the degree of reactivity of the material itself (27) (114) (115), i.e., on the nature of the rocky material or artificial product, for instance, pyrex glass (1). Some standard test methods show that highly reactive aggregates may produce a smaller expansion than do considerable less reactive aggregates. This seems to depend on the content of reactive constituents and on their proportion as compared with that corresponding to the most unfavourable ratio of available alkalies to reactive silica. Nevertheless, it is not advisable to use highly reactive aggregates with high alkali cements, even though they may show a small expansion in a given standard test, whatever may be it (29).

Other different points of view consider that there seems to be an amount -concentration- and a range of particle sizes for which expansion is maximum. Mention is usually made since many years ago to "pessimun condition" of an active aggregate: maximum expansion for each size range, depending on the proportion of susceptible material in it; or for a given proportion, variable with size range -and depending on total content of susceptible material in total aggregate- (116). So, pessimum condition appears easier and with higher values of expansion: i) for higher proportions of reactive aggregate, the coarser it is; ii) for lower proportions of it, the higher its reactivity and/or the higher its density (the lower its porosity), as dense pore-free structures of reactive aggregates favour expansion; iii) for different (decreasing) proportions of reactive aggregate, depending on cement nature (portland, blast-furnace slag cements with increasing slag proportions); iv) for different (increasing) total alkali contents in cement, depending also on the cement nature; v) the higher the cement content in concrete (116).

The external manifestations, i.e., the appearance of the expanded specimens is different depending on the size of the expansive aggregate particles: exudation over them appears as an uniformly distributed fine white powder when expansive aggregate is fine, whereas

the exudation is transparent and presents a spot-pattern distribution when the aggregate is medium to coarse; the coarser the particles, the larger the sponts. Generation and size of cracks also depend on the grain size (1) (117).

Not only the appearance and aspect, but also the composition of the alkali-silica gels -as well as that of the rims- formed in alkali-opal reaction and deposited in cracks, may be very significant to interpretate the expansion mechanism, in function of the distance of gels to the reaction sites. Exudations of specimens containing opal show calcium, potassium and silicon, whereas those of specimens free of opal only show both cations (118). So, opal is transformed into a calcium silicate hydrate of low basicity, but the calcium content of the gels formed and accumulated in cracks is lower in the zones of gels close to reaction sites, whereas it increases greatly in the zones more distant from the sites (119).

Nevertheless, despite the generally accepted opinion that critical reactive aggregate particle size ranges -variable with the nature of the material (1)- are necessary for the expansive action, modern results show that fineness of aggregate -size particle under a given value even lower than 50 microns down to 30-20 microns- is not a guarantee that an active (opaline) material will be innocuous, though customarily it is thought that innocuity refers to expansion, not to alkali-aggregate reaction.

As to the lack of a general direct relationship between the extent and rate of the chemical alkali-silica reaction and the expansion -not always involved in it-, one of the difficulties has been the problem (not well solved) of measuring the extent and rate of the reaction, for the measurement of the expansion is solved. A proposal has been made to determine the extent of reaction based on determinations (and corrections) of total alkali content in pore liquid of reacting mortars and in that of blank mortars. Differences between the latter and the former values referred to the corresponding ages, expressed as percentages of the total alkali provided by the cement and plotted against time give the trend of the alkali consumption in reaction. Further hypothesis on stoichiometry (average value of $(K_2O + NaO_2)/ SiO_2$ mol ratio of 0,25) of the alkali-silica product formed permits to calculate the active silica consumed at each age by reaction in some given experimental conditions (120). Among the several factors influencing the method, one of them, that of the possible "reciclation" of alkalies displaced by calcium after reaction with silica -to form a more stable calcium-alkali silicate (that of a semi permeable membrane? -see later-) needs further consideration, as it may cause an underestimation of the extent of the alkali-silica reaction (120).

On the other hand, large expansion is not always accompanied by severe local cracking (10) (118). Differences to be attributed to grain size, as far as expansion is concerned, are more related to the rates and relative amounts of expansion than to the character of it. So, there seems not to be a limiting size of aggregate over 20-30 microns below which expansion will not take place, though expansion due to the finer particles is sudden and complete in short periods, whereas that of larger particles is slower and more gradual and delayed. In the author's opinion the influence of the grain size is one of the many dark points in the alkali-aggregate problem, and this seems not to be consistent with the use of very finely ground expansive aggregate rocks and other materials -pozzolans, fly-ashes and slags- added to cement to avoid the effects of alkali-silica expansive reaction (27).

Another very important factor determining alkali-silica expansive reaction is the initial moisture content of the aggregate and the availability of water to be absorbed and fixed -in the presence of alkalinity (OH^-)- causing expansion (1). In any case it seems that permanent or almost permanent wet conditions are necessary for expansive reaction (21). The extent to which the presence of water is determinant for the reaction -other necessary conditions for it being fulfilled; highly reactive particles in proportions, sizes and amounts favourable for expansion, and high contents of high-alkali cement in concrete- has been emphasized by the fact that inhibition of drying in concrete samples shows that the moisture content of massive concrete is sufficient -but also necessary- to cause deleterious alkali-aggregate reaction (121).

An important paper has been attributed to the OH^--ions in the mechanism of the reaction, as it has been claimed that they may attack silicious aggregates more intensively after the early reactions of hydration, when the depletion of sulfate-ions permits a higher OH^- concentration due to the higher solubility strength and dissociation of the alkali hydroxides formed with alkali cations (97). This is the mechanism by which alkalies forming sulfates -according to the writter in "saline" form- may pass to act as alkalies in "caustic" form. In fact, the expansive reaction seems to be conditioned by the pH of the liquid phase, determined in turn by the type and amount of dissolved alkali ions (21). But OH^--ion concentration seems to be the main governing factor, rather than alkali cations, which can influence the physical nature of the products formed and the rate of the expansive reaction and cracking. In fact, the experience seems to indicate that it is only in concretes with high hydroxil-ion concentration where attack on reactive aggregates can be expected. Such high concentrations are easier and earlier reached with high-alkali cements, as are those favoured by new manufacturing technologies developped even prior to fuel shortage (97).

All these complex and seemingly contradictory facts. as well as the stresses and "map cracking" resulting from reaction between some silicas and alkalies have been more or less convincingly but logically and generally interpreted (27) (122), as several mechanisms have been proposed to explain reaction and even expansion due to it (95) (97) (110). Among them, some assume that reactive silicious material may form with alkali and $Ca(OH)_2$ wether

a solid non-expansive complex calcium-alkali-silica compound, or a solid complex alkali-silica compound able to expand by water imbibition. The formation (and the order of formation) of the one or the other of both complex compounds seem to depend on the relative concentrations of alkalies and calcium hydroxide, and on the surface of the reactive material: in low alkali concentrations the non-expansive compound forms first and the process may continue without expansion, if the amount of reactive material is either negligeable or higher than a critical value, which depends on the alkali available and on the fineness of the active material. In high alkali-ion concentrations the expansive product first formed is a more or less fluid alkali silicate gel, whose imbibition and osmotic swelling may develop pressure depending on the proportion of reactive silica and available alkalies (29). The expansion may be stopped only when the active material presents a surface for reaction great enough (very many reactive particles and/or sufficiently fine) to substitute the expansive reaction by the non-expansive one (27).

The swelling of susceptible aggregates to alkali hydroxide solutions or that of gelly alkali silicates by water imbibition (123) have also been invoked, more or less in connection with the lack of space to accomodate alkali silicate reaction products of greater volume than that of the original reactive particle (95) (124). The osmotic pressure created in dilution of concentrated alkali-silicate solutions formed in reaction, by passing water through a silicate semipermeable membrane -see later- has been also proposed and sustained (95) (124).

The higher expansion produced in specimens containing mainly sodium rather than potassium (1) has been explained on the basis of a much greater increase of volume in the case of hydrated sodium silicate formation. In a similar manner, the lower expansions observed when litium or barium salts are present have been explained in terms of the lower solubilities of the respective silicates formed (99).

In the writter's opinion -see later- a complementary -more detailled- explanation could be perhaps that a true semipermeable membrane of a complex silicate (of calcium and other cation) giving place to a "true" osmotic cell is more easyly and effectively formed when the cation is mainly sodium. Then, the osmotic pressure action of the "true" cell is maximum, as well as the corresponding expansive and disruptive effects (125) (126).

Suggestive explanations of expansive alkali-silica reaction have been given and recently actualized considering the nature of the reaction products formed in rims and cracks of reaction zones (96) (126): hydrated silica gels, alkali silicates of sodium and/or potassium, and complex alkali-calcium silicates. Not all of them are considered as producers of expansion, for sodium and potassium silicates, when in vitreous condition or in solution are stable. On the other hand, it has been invoked that when SiO_2 reacts with alkali hydroxides the volume of the alkali silicates formed is smaller than that of the original reacting products. So, no expansion should be expected based on the formation of pure alkali silicates. Moreover, silica gels are also stable, so that expansions from that alkali-silica reaction should be based mainly on physicochemical schemas other than hydration or imbibition of alkali silicates or silica gels, such as the following:

$$SH_n + MH \longrightarrow MSH_{n+1} = MS.(n+1)H$$

$$S_xH_n + MH \longrightarrow MS_xH_{n+1} = MS_x.(n+1)H$$

(here M is either Na_2O or K_2O and x = 3 in general)

or: $$S + nH \longrightarrow SH_n = S.nH$$

$$SH_x + yH \longrightarrow SH_{x+y} = S.(x+y)H$$

A point of view widely shared among many authors considers that expansion is primarily a consequence of the formation and widening of cracks due to mechanical pressure exerted by reaction products (127). But this sees not to be in accordance with experimental results showing expansions with no significant crack formation (118).

Osmotic pressure effect has been also suggested many years ago and supported by many authors since then, as causing expansion (128) (129). For it it is necessary the existence (the formation) of a semipermeable membrane through which diffusion of ions and molecules may take place, so creating a high differential pressure between both sides of it. It has been suggested that the membrane may consist in complex alkali-calcium silicates of variable and not well defined composition or stoichiometry -polysilicic complexes with metalic ions, oxides and hydroxides adsorbed- (96) (126), formed according to the schema (126).

$$xS + yCH + zMH + (n-m)H \longrightarrow S_xC_yM_zH_{(y+z+n-m)}$$

probably in two steps. In the first one the disperse alkali in solution acts on a localized alkali silicate

$$xS + zMH + nH \longrightarrow S_xM_zH_{(n+z)}$$

In the second one the disperse calcium hydroxide in solution may act on the alkali silicate first formed to give by partial cation exchange the localized complex compound previously mentioned, with liberation of alkali, ready for further action:

$$S_xM_zH_{(n+z)} + yCH \longrightarrow S_xM_{(z-m)}C_yH_{(n+z+y-m)} + mMH$$

This schema is consistent with a point of view concerning the role of calcium. It states that in solutions highly concentrated in alkali ions and hydroxil ions from moderately high-alkali cements the calcium ion concentration drops in a few days to a very low value corresponding to saturation of $Ca(OH)_2$. Afterwards it drops again to vanishingly small levels in a few months. It implies a possible isolation of portlandite from the pore solution, probably caused by a low-lime calcium silicate. This induces to think that calcium

should not significantly participate in the initial reaction product of alkalies with susceptible aggregates. Instead of it, it seems that sols first produced, flowing through open cracks (130) (131) (132)(133). In their way outwards take from portlandite crystals calcium, which they finally fix, simultaneously lossing a part or their content in alkalies which diffuse all around (130). In fact, complex compounds of the type CKNSH in the form of amorphous "expansive" gels are produced in the alkali-silica reaction (134).

On the other hand, the possible decisive influence of abundant calcium ion has been previously recognized and since widely accepted (97) through a somewhat different interpretation: that of the "safe" reaction products corresponding to limited -swelling gels rich in calcium and "unsafe" reaction products corresponding to osmotically active gels richer in alkali cations (122) potassium and sodium (but not lithium -another dark point in alkali-aggregate reaction- (135).

It is well known that semipermeable membranes consisting in insoluble amorphous gelly masses of polysilicic anions with adsorbed metalic ions, oxides and hydroxides showing undefined compositions (96) (126) may be formed when polivalent metal (Fe, Ni, Co, Mn, Ca, etc.) salts are put in contact with solutions of alkali silicates (96), according to a schema more or less like this:

$$n\ Na_2SiO_3 + n\ FeCl_3 + (3/2n + x + y + z)\ H_2O \longrightarrow$$

$$\longrightarrow (m-r)\ SiO_2 \cdot (m-3/2n)Na_2O \cdot xH_2O + rSiO_2 \cdot yH_2O +$$

$$+ nFe(OH)_3 \cdot zH_2O + 3n\ NaCl$$

Other important factors conditioning the semipermeable and ion-interchanging character of the membrane able to create osmotic pressure are temperature, time of contact, and more particularly the proportion of its components. Membranes rich in highly and rapidly reactive silica are impermeable. To lower concentration of alkalies correspond higher concentrations of CH in the liquid phase and consequently highly calcic impermeable membranes. Therefore, there seems to exist a relatively narrow range of proportions and compositions most favourable to the semipermeability and hence to the creation of osmotic pressure. This range, depending on the composition and concentration of reactants in the liquid phase, corresponds to a sort of new notion of the concept of "pessimum" advanced long time ago (136) to express the highest probability of destructive expansion.

The statement that early cracking precludes the formation -or the permanence- of "true" osmotic cells should be taken in the sense of "classical" osmotic cells formed by an intact and "real" semipermeable membrane. Otherwise, it is possible to imagine the formation and the permanence of "virtual" osmotic membranes from gel structures, in such a way that solute ions electrically or chemically attracted by the gel framework are hindered to move freely, according to decreasing concentration gradients; consequently, the solvent -water molecules- moves in opposite direction so generating osmotic pressure in confined zones, even in the absence of "intact" membranes (100). In the author's opinion this could be an acute eclectic interpretation linking swelling of gels by water absorption and true cells acting by osmotic pressure.

Finally, other things related to concrete characteristics being equal, an important last condition is necessary for osmotic pressure expansion to proceed: the presence of water -liquid water- to be diffused by endosmosis through the semipermeable membrane. This implies a "permanent" contact of concrete with water; otherwise, even if the remainder favourable circumstances for "pessimum" condition are given, expansion by alkali-silica reaction does not take place (96) (126)

This vision of the alkali-silica expansive reaction mechanism enables interpretations of factors otherwise difficult to explain: the action of inhibitors such as pozzolans or other finely ground and highly active silicious materials -even the reactive aggregate itself- in shifting the membrane composition from its "pessimum" condition, and dispersing the intensive local actions changingthem by much numerous and much weaker diffuse actions; smaller expansions observed with higher alkali cements and conversely; absent or much lower expansion when external water is not sufficientely available, etc. (96) (126).

According to the foregoing, some questions arise to the author's consideration. One first is the possible influence of the form in which akalies are present in cements (97) -"neutral saline" form (as sulfates) and "basic saline" form (combined with calcium silicates and aluminates)- on the composition of membranes, and therefore on the possibility of expansion. A complete bibliographic compilation on alkali compounds in clinker, as well as on crystalline modifications of clinker phases by alkalies has been recently published (137). In the same way, a similar compilation on the influence of alkalies on the morphology and structure of hydration products, as well as on other aspects affecting stability and durability of cement pastes has been recently issued too (138).

If the influence of the form in which alkalies are present exists -and it is considered to be so (97)- another second question to be considered is wether the total content of alkalies in cements or the partial content of them in one or another of the mentioned forms are mainly responsible for expansive reaction. If one of the two mentioned partial contents is more determinant of the expansion than the other -and if the value of the ratio K_2O/Na_2O is also decisive-, a third question arises concerning the justification of limiting to 0.6 % in cement standards the total alkali content (as equivalent Na_2O) of the so-called low- alkali portland cements considered as more safe, as far as alkali-silica expansive reaction is concerned. In fact, it has been still claimed that the effect of the alkali content of a given cement

should be at least partially a function of the state of combination of the sodium and potassium in the cement, as well as of their total content. Most of the soluble portion of alkalies occurs as sulfates, either in the form of aphthitalites $NK_4\overline{S}_5$ to $NK_5\overline{S}_6$ or calcium langbeinite $KC_2\overline{S}_3$, or in the form of carbonates, equivalent to hydroxides. Insoluble -less rapidly soluble- portion of alkalies is combined in silicate $(K,N)C_{23}S_{12}$ and aluminate -ferrite- $(K,N)C_8A_3$ phases and the respective solid solutions, their speed of solution depending on their rates of hydration (97).

Moreover, alkalies may come not only from cement -clinker- but also from added materials (pozzolans, slags, fly-ashes), weathered aggregate constituents, concrete admixtures, sea-water or deicing salts, so that variable limits specified in standards for cements seem to be of less value than the effective amount of alkali present in a given volume of concrete -kg of eq. Na_2O/m^3-in order to assess the extent of alkali--aggregate reaction. In fact, for given "pessimum" conditions not always cements of higher alkali content give maximum expansion. Nevertheless, expansion is higher in general the higher the cement content in concrete. On the other hand, concretes with medium to low contents of high-alkali cements may not always show deleterious alkali-aggregate reaction according to actual results in practice (116) (139). Furthermore, some other laboratory tests have shown that their results either correspond to those observed in practice or -if not- they are placed on the safety side (140).

Laboratories are making progress in the development of more rational guidelines governing specifications limiting the alkali content of cements. Attempts are being made to specify the total amount of alkalies per cubic meter of concrete, rather than to fix limitations to the total alkali content of cements (141). All this is duly justified because it has been claimed that high alkali content in cement -even together with a highly reactive aggregate- does not necessarily produce relative great expansion and damage, but even may reduce them. Despite that the rate of silica reaction is increased, when increments in alkali content in cement are higher than an arbitrary and variable value they do not increase expansion, but reduce it. Then, large amounts of alkali react rapidly to form gelly reaction products with a Na_2O/SiO_2 ratio high enough to be fluid -or even to pass quickly from gel to sol state by water adsorption-. The sol formed or the fluid gel, if not fully confined, penetrate and accomodate in pores and free spaces around reacting particles, neither exerting mechanical pressure nor producing damage (131) (132). Thismay make difficult to consider, at least in general, that the factor governing the kinetics of expansion is either the formation of alkali-silica compounds or their swelling (118).

All these aspects among others have been recently exposed (126). It seems that they claims for attention on further research in order to proof if the present limitation of total alkali content in cement standards is operative and justified or not, as compared with the influence of other various factors involved in the expansive alkali-silica reaction. If not, there is no reason to mantain limitations affecting adversely the fuel consumption, particularly in most of the present more economical cement manufacturing processes (126). In any case, according to the preceeding considerations, it seems to be clear that in the case of a possible and probable expansion to be fear by the use of susceptible silicious aggregates, portland cements, either low in alkalies or not, are not the most adequate to make concrete free of damages by expansion. Anyway, blast-furnace slag cements -and pozzolanic cements- seem to be more idoneus, partially because they permit a higher total alkali content in clinker, as established in most of the standards (142).

As final considerations it is worth wile to expose some of the more recent observations and conclusions concerning alkali-aggregate reactions. Among them (108): i) that the increase in reports of reactions during last years in several countries is important; ii) that more parameters and a variety of climatic conditions wider than that so far considered seems to be involved in reaction; iii) that very quick and very delayed reactions have been reported, not corresponding to long term field performance or to laboratory test behaviours of specimens; iv) that these facts, as well as many other factors question the reliability of the testing methods and criteria to detect, to evaluate, to foresee and to prevent damages from alkali-aggregate reaction. This could be precised as follows: i) low-alkali portland cements may cause deterioration -the opposite could also be invoked-, so that the limit of 0,6 % equivalent Na_2O does not constitute a guarantee, and so less so as the alkali content of pozzolanic materials, slags and certain rocks -an overlooked factor- seems to be potentially operative; ii) aggregates earlier considered safe must be reconsidered, as they may react and cause expansion and even deterioration, depending on their mineralogy and chemical (soluble) constituents other than SiO_2 -another overlooked factor out of control-; iii) the mechanical simplicity of tests based on expansion of mortar or concrete bars does not correspond to the physicochemical complexity of the reaction and expansion kinetics, in which many internal and external factors and parameters not (duly) taken into account or out of control do in fact influence (108).

A critic and objetive panoramic exposition of alkali--silica problem recently presented (107) states that the more extensive and deeper the partial knowledge about it, the more complex and difficult seems to be its solution. Questions not yet solved, among others, are: i) how and why disperse alkali-silica gels formed on discrete active particles of aggregates create locally accumulated expansions, as expansive imbibition of gels would exige integration of local efforts to produce fracture; ii) the true influence of the "pessimum" proportion (amount and granulometry) of reactive aggregates and the ratio of inactive to expansive aggregate giving maximum expansion, as well as the dependence of pessimum proportion on many other

different and variable factors; iii) the difficulty to establish a classification of different aggregates in types according to their alkali susceptibility (which does not permit to generalize testing methods, crite ria for evaluation and preventive measures); iv) the preventive effect of pozzolans and the influence of their nature, as well as that of their alkali content, which makes it difficult to classify pozzolanic materials according to therir more or less beneficial action. The paradoxal conclusion to be drawn from the dark points preceedingly exposed is that the broad knowledge obtained up to date only serves to recognize the enormous complexity and difficulty of the problem, but it hardly aids either to foresee better the alkali--silica expansion or to prevent it. A secondary conclusion in which the writter agrees is that much sys tematic and cooperative basic and applied research is needed, as well as a better application of the know ledge still gained and to be gained in the future on the chemistry of silicates (107).

Many aspects of cement research, some of them dealing with durability, are or seem to be in conflict with some of the main present guidelines in cement development. This is particularly the case of alkali--aggregate reaction as far as fuel consumption and profit of certain raw materials and by-products in cement manufacture are concerned (7). On the other hand, in the field of durability as well as in many other fields, most of research work runs around the same themes, using the same methods, applying the same ideas and arriving repeatedly almost always to the same partial and not decisive conclusions. As mentioned somewhere (7), as far as shrinkage is concerned, our present knowledge on durability either in general or in whatever specific aspect of it such as alkali-aggregate reaction in particular-, it is by no means proportional to the effort made and to the number of papers published since the beginning of the century. In fact, up to the present time the problem of alkali reactivity has been studied during more than thirty years. No clear conclusions have been reached on the mechanisms of reactions, expansions and deteriorations, neither in the more common case of alkali-silica reaction nor in the more complex one of alkali-silicate reaction. Reasons for it may be the many variables involved and their simultaneous inter actions creating feed-back problems which must be necessarily taken into account to establish test methods and criteria to evaluate test results (95). These also depend on many other factors involved in active materials to be tested, even other things being equal (143) (144).

This is perhaps, among many others, a case in which a work of synthese on the basis of a wide interdisciplinary cooperative research, in addition to an almost exclusive basic research would be of profit to go onwards. Probably such a synthese would serve to fix directions and guidelines according to which further research should be orientated (7).

7. - ATTACK BY CHLORIDES AND DE-ICING SALTS ON CONCRETE

It has been examined and described the actions (mainly physical) and the effects of chlorides -$CaCl_2$ and NaCl- used as ice-removing salts on concretes. Studies on de-icing salts and concrete resistance to them have been recently carried out and published (145). The characteristics of the concrete void and cement paste pore systems, the presence of admixtures (particularly air-entraining agents) and the nature of the tests (based either on immersion or in surface application) have influence on the effects caused by the crystallization pressure created on ice formation. Several papers on this matter have been reviewed recently (1).

As far as the influence of the void structure of concretes is concerned, it seems that a sufficient (minimum) amount of micro-air voids in concretes is needed to impart them an adequate de-icing salts resistance, provided that the void distribution and the maximum distance between voids are also adequate (21).

Two different mechanisms have been proposed to explain the attack of concrete by saturated calcium chloride solutions, depending on its low or high w/c ratio, and without taking into consideration freezing and thawing cycles. In the case of low w/c ratio large weight losses and degradations are observed, which cause loss in strength without expansion. This has been attributed to leaching. In the case of high w/c ratio weight gains and large expansions are produced, and degradations and loss in strength are observed due to crystallization. Nevertheless, more complicated seems to be the explanation in the case of (practical) intermediate w/c values (146).

On the other hand, two factors must be taken into account to explain the successive actions of de-icing salts -$CaCl_2$, NaCl- in concrete, according to more recent points of view. The one, physical in nature, consist in a change (lowering) of the evaporable water content of the specimens, caused by an osmotic pressure action between the strongly concentrated salt solutions and the specimens in contact with them. This lowering of evaporable water firstly causes an increase of strength.

The other factor, chemical in nature, consists in a real attack which brings about a leaching and the corresponding losses in weight and decreses of strength. This leaching is caused by calcium chloride solutions, due to their low pH, which may produce the formation of soluble compounds with the cement paste. This is not -or this is much less- the case of strong NaCl solutions, and this may explain why these do not show the trend to reduce concrete strength, at least to the same extent as $CaCl_2$ solutions do it (147).

Of course, both mechanisms are independent of some others based on hydraulic pressure, which may be superimposed when freezing-thawing actions take

place simultaneously. The author calls attention on the importance given to the osmotic pressure actions also in other fields such as that of alkali-silica expansive reaction (96) (126).

From the chemical point of view, in the attack of portland cement by solutions of $CaCl_2$ of various concentrations and at different temperatures, monochloroaluminate hydrate $C_3A.CaCl_2.H_x$ (x=10) is always formed. And in addition to leaching of CH the formation of other complex salts containing both CH and $CaCl_2$ -and even calcium carbonate $C\bar{C}$- may be formed, depending on time, temperature and concentration of the $CaCl_2$ solution. Thus, it could be inferred that the attack on cement by calcium chloride used as de-icing salt is caused by crystallization and crystal growth pressure of the mentioned complex salts formed. This action is facilitated by an increase of porosity due to the simultaneous leaching of CH (146) (148).

The attack of $CaCl_2$ to concrete seems to depend greatly on temperature, as a rapid deterioration is produced at 5°C, which is neither observed at 20°C nor at 40°C. The explanation given for it is that an expansive product stable at low temperature is formed at 5°C, causing disruption (9) (149).

An interesting viewpoint concening de-icing salt attack is that attributing destructive effects not so much to chemical as to physical causes involving alterations in the frost mechanism through opposite actions conducting to an intensified freezing and to a stronger thermal shock, which produces serious contractions and the corresponding scaling (150).

In fact, independently of the chemical actions which de-icing salts may produce in hydrated cement pastes, the stronger damage observed in frost action when salts are dissolved in the freezing water has been physically explained by the lowering of the vapour pressure and the freezing point of the solvent. This makes, on the one hand, that the degree of water saturation of a porous body (cement paste) corresponding to equilibrium at a given relative humidity is higher when the porous body is impregnated with a salt solution than when it is imbibed with pure water. On the other hand, at lower temperatures the viscosity of the solution may be very high and pure solvent may crystallize, so that flow of pure liquid is hindered and the frost resistance thus impaired (151).

Anyway, *though much research work has been done* even in recent time (152) (153), and much practical experience has been gained, damages caused by freezing of water and crystallization of de-icing salts have been not yet fully explained, and it is admitted that all of the several factors involved must be taken into consideration (154). This point of view is supported even at present. In the author's opinion, this is one more of the innumerous cases of durability in which factors, actions and effects purely chemical or purely physical in nature cannot be separated from one another, as they are linked together in an indissoluble manner, acting either simultaneously or successively. The importance attributed to the one or to the other of both factors will depend on conditions and circumstances, and on the evaluation made of them in each particular case by each individual author.

Reaction of ions from different salts penetrating a cement paste depends on the permeability of the paste to the diffusion of the ions involved ( ). Attack of chlorides proceeds by ionic penetration of Cl^- in ordinary concrete. It has been stated that this penetration seems to follow the FICK's diffusion law, and that it is independent of the chloride concentration, and hence of the concrete penetrability to the salt solution as a whole, or even to pure water. Diffusion seems to be to some extent independent -or not only dependent- of the porosity of the material. Moreover, it seems to depend more on the nature of the cement paste. An explanation given for it has been the "primary adsorption" of Ca^{2+}--ions (and the "secondaty adsorption" of Cl^--ions) by materials added to cement, or by combination products of them with the hydrolitic lime produced in hydration. This explanation may be valid in the case of pozzolanic cements (156).

If no gradient of electrical potential is established in the cement paste, diffusion and adsorption of bothe Ca^{2+} and Cl^--ions (one of the former to two of the latter) must be simultaneous.

It has been stated that chloride penetration is greater in concretes with low C_3A cements, though the decrease in strength caused by sea-water attack, for instance, is greater with increasing C3A content of the cement (1), for other factors are involved.

It has been quite recently stated that for ordinary portland cements the time is determinant for the Cl^--ion penetration, even through high quality concrete; that w/c ratio influences the Cl^--ion penetration to concrete surface layer and for short duration of concrete contact with chlorides; and that the type of cement has a major influence in deeper penetration and for longer durations of contact. Furthermore, in portland cements penetrations of Cl^---ions have been observed being from 2 to 5 times greater than those observed in blended cements. Moreover, Cl^--ionic diffusion depends not only on the permeability and binding capacity of the Cl^--ions, but also on the ion-exchange capacity of the system, i.e., of the cement paste (157).

Apparent diffusion coefficients of Cl^--anion and various cations from different salts (Li, Na, K, Ca, Mg) and salt mixtures (Li + Na + K) experimentally determined through hardened plates of portland cement paste have shown, in the case of the cations, to increase in the order:

$D_{Li^+} < D_{Na^+} < D_{K^+}$ in approximate ratios of

1 : 1.5 : 2 This order is nearly the reverse to that of the radii of solvated -hydrated- ions (155) (158). On the other hand, other things being equal, in the case of chlorides the diffusion and penetrabi-

lity of Cl^--anion is greater when linked to divalent cations than when combined with monovalent cations, the order being:

$$D_{Cl^-(MgCl_2)} > D_{Cl^-(CaCl_2)} > D_{Cl^-(LiCl)} >$$

$$> D_{Cl^-(KCl)} > D_{Cl^-(NaCl)} .$$

Moreover, the diffusion of Cl^--anion is much greater than that of the cations.

$$D_{Cl^-} \gg D_{K^+} > D_{Na^+} > D_{Li^+}$$

despite almost equal mobilities of Cl^- and K^+ -ions; this is invoked as a proof of the electropositive character of the hardened cement paste considered as a semipermeable membrane (155) (158) (159).

These differences in ionic diffusion explain that in contact with $CaCl_2$ or $MgCl_2$, $Ca(OH)_2$ and $Mg(OH)_2$ -and even LiOH, NaOH and KOH in contact with the respective chlorides- are formed on the surface of the cement paste by a mechanism of exchange between penetrating Cl^--ions and OH^--ions present in the paste, the latter reacting either with Ca^{2+} or Mg^{2+}-ions of lower mobility in solution. This exchange may be considered as mutual diffusion (counter-diffusion) of Cl^- and OH^--ions (155) (158).

OH^--ions come out as a result of the deeper and rapid penetration of Cl^--ions which interchange with OH^- in the bulk of the paste. Once in the external part of this, OH^--ions compensate the alkali or earth-alkali cations previously left in excess by the more diffusive Cl^--ions (155).

So, if it is accepted that the diffusion coefficients of alkali and earth-alkali cations decrease in the order:

$$Mg^{2+} < Ca^{2+} < Li^+ < Na^+ < K^+$$

it must be accepted that the destructive effect of Cl^--ion decreases in the order:

$$MgCl_2 > CaCl_2 > LiCl > NaCl > KCl$$

according to the valency and the radii of hydrated cations (155).

Deep penetration by diffusion of Cl^--ions into the paste from a solution of a divalent-cation chloride accelerates the dissolution of $Ca(OH)_2$, which explains the acceleration effect on setting and hardening (hydration) of the cement paste caused by $CaCl_2$ solutions.

Furthermore, the diffusion rate of Cl^--ions is 10 to 100 times faster than that of SO_4^{2-}-ions. Nevertheless, sulfate attack caused by Na_2SO_4 solutions is much greater than chloride attack produced by NaCl solutions on cement, as calcium sulfoaluminate hydrate is less soluble than calcium chloroaluminate hydrate (159).

During hydration of portland cement in the presence of chlorides it has been claimed that ettringite is always first formed, untill all the gypsum has been consumed. Only then monochloroaluminate is formed. On the other hand, in the case o tricalcium aluminate and tetracalcium aluminate hydration in the presence of chlorides, sulfates may act on monochloroaluminate previously formed to transform it into ettringite, with new formation of chloride. So, ettringite seems to be a more stable phase (159 bis).

Monochloroaluminate first formed and crystallized in chloride attack to concrete, due to the more rapid diffusion of Cl^--ions, is unstable in the presence of SO_4^{2-}-ions, so that afterwards it is transformed into expansive ettringite. This occurs in sea-water attack and this is also a reason why the use of sea-water as mixing water is not recommended for cement rich in C_3A, since chloroaluminates first formed are transformed later on into ettringite. Moreover, Cl^--ions also enter to form a reticular and porous solid solution in an initially fibrous CSH of the hydrated cement paste (15) (58) (59).

In attack on surface of either alite pastes or portland cement pastes by NaCl solutions and sea-water, different forms of calcium carbonate such as calcite, aragonite and vaterite have been detected as products of carbonation. The preferential formation of either of these forms depends on experimental or natural conditions (160).

Among salts other than sulfates and sodium and calcium chlorides, comporting conditions and properties to be aggressive to cement paste -such as water solubility, a corresponding base weaker than $Ca(OH)_2$ and an anion forming water-soluble calcium compounds-, magnesium chloride and ammonium chloride should be mentioned. Both react with $Ca(OH)_2$ to form calcium chloride and insoluble magnesium hydroxide (brucite) and volatil ammonia, respectively. In the latter case ammonia evolution rapidly deteriorates the cement paste (23).

Different expanding products are formed on portland cements with low (less than 1 %) or high (about 12 %) contents of C_3A as well as on blast-furnace slag cements (with about 75 % of slag) when attacked by 3M $MgCl_2$ and $CaCl_2$ solutions and by saturated NaCl solutions (161). Magnesium and calcium chlorides attack strongly to portland cement mortars, the expanding reaction products being $MgO.Mg(OH)Cl.5H_2O$ and $CaO.CaCl_2 2H_2O$, respectively. Both are formed from free CH, causing a total loss of alkalinity. Astonishingly this affects more to denser than to less denser concretes. Slag cements do not form expanding oxichlorides and consequently they do not suffer deterioration. This may be one of the several explanations of the better performance of slag cements in sea-water attack and so much so the higher the slag content of the cement (162).

Sodium chloride, as stated (146) (148), forms $3CaO(Al, Fe)_2O_3.CaCl_2.10H_2O$ with either portland or slag cements and the alkalinity of the paste is not lowered (147) (161).

As far as magnesium chloride attack on different cements is more particularly concerned, it has been pointed out that Mg^{2+}-ions form $Mg(OH)_2$ on the surface of the concrete (specimens). The amount of brucite formed -as well as penetration of Cl^--ions to

form chloroaluminate are higher in portland and fly-ash cements than in slag cements. Consequently, the strength of the former decreases considerably, whereas that of the latter shows very little change. All this seems to be in accordance with the exchange of Ca by Mg in $Ca(OH)_2$, causing leaching of calcium, which leads to an increase of porosity and pore volume in specimens. This may aid to explain the more remarkable loss in strength in the case of magnesium chloride attack on portland cement mortars and concretes (163).

But, on the other hand, magnesium hydroxide formed may protect the cement paste -by coating its surface- from further attack, provided that $MgCl_2$ concentration is not very hig, so that crystallization of brucite may disrump the structure of the paste (23). This is one of the many examples of compounds formed in aggressive reactions which may either cause damage or afford protection, depending on different conditions and circumstances. And this is also one of the several reasons by which durability problems are, at least apparently, so complicated, and their actions and effects so different and even so contradictory.

In opposition to what has been generally accepted (at least in the case of sea-water attack), i.e., that the presence of chlorides reduces the sulfatic action, the contrary effect has been postulated in the case of attack in the severe conditions in hot arid internal areas, where soil contains chlorides and sulfates, for climatic factors seem to influence decisively the nature and extent of the attack. Anyway, opinions on favourable, unfavourable or indifferent influence of chlorides on sulfate attack are very diverse, as shows the bibliography on this item, particularly in the last twenty years. Arguments based on variations of solubility of gypsum (in general sulfate compounds) in chloride solutions, and on their influence in inhibiting the formation of ettringite seem not to be valid in arid regions. On the contrary, the growth of attringite crystals in the presence of chloroaluminate has been invoked, as well as the stability of the latter in the presence of an excess of the former. These facts could explain the higher expansion and damage of cement pastes, sometimes observed, caused by mixtures of chlorides and sulfates (164).

It has been proposed a schema to explain all these facts It consists in the formation of $CaCl_2$ and NaOH by reaction between $Ca(OH)_2$ and NaCl. Calcium chloride forms chloroaluminate and simultaneously ettringite is formed which in the presence of it experiments a crystal growth. If there is an excess of NaCl, more $CaCl_2$ may be formed which, if not reacting with C_3A, may be leached, so increasing concrete porosity and permeability (164). As previously mentioned, the action of chlorides is reinforced by the much faster and deeper penetration of Cl^--ions into the cement paste and by their greater adsorption in it, as compared with those of SO_4^{2-} -ions (59).

Summarizing, in the author's opinion it could be assumed that penetration of Cl^--ions take place more or less always (partially depending on the nature of the cement -portland, fly-ash cements pozzolan cements, slag cements- in all the cases). But serious deteriorations occur only when the chloride containing compounds formed are highly expansive in nature. The extent of the deterioration caused by them may be greater in some denser concretes, probably due to a more intensive and efficient effect of the expansive pressure created. On the other hand, it seems to be evident that conditions for chloride actions in sea-water attack and in dry and hot arid regions in connection with a simultaneous sulfate attack are not the same. The mechanisms of attack as well as the resulting damages of it are also probably different. So, no contradiction seems to exist necessarily between both types of aggressivity, not comparable to one another.

8.- SULFATE ATTACK

Taking into account the chemical nature of the hydration products of the cements, it is easy to foresee the types of aggressivity to which they can be subjected (165). The more or less basic character of them implies the possibility of an acid attack at pH below a certain variable value. On the other hand, a base exchange may take place between $Ca(OH)_2$ and salts of cations giving weaker and/or less soluble hydroxides and anions forming soluble calcium salts, as for instance magnesium salts. And finally more complex attack is possible by interaction of hydrated aluminates and ferrites with sulfates (23). It has been estimated that about 75 % of publications on concrete corrosion deal with sulfate attack (23).

All the knowledge accumulated on sulfate attack to cement has been mainly centered in the chemical reaction of C_3A with external sulfates, by complex mechanisms even not yet quite clear due to confusing or contradictory results leading to different, opposite or erroneous conclusions. Something similar could be said as far as the limits of C_3A in cement are concerned, to guarantee an immunity or an admisible degree of attack (166).

Nevertheless, chemical reactions and processes involved in sulfate attack to cements, as well as their effects, on concretes, depend basically on the nature of all three: sulfates, cements and concretes; on salts concentration, external conditions and time. Cations linked to sulfate anion, mixtures of different sulfates (and their relative proportions), the presence or absence of chlorides and the more or less abundant C_3A in anhydrous cement and of CH in hydrated paste may determine various isolated or conjoint -simultaneous or successive- types of attack. This may be significant for sulfate concentrations starting from limits widely and diversely established by differents authors -in general about 1000 ppm- (167). Anyway, a strong attack is always to be expected when concentration of SO_4^{2-}-ions is higher than 3000 ppm (23).

The effects of mixtures of sulfates are sometimes unexpected. They cannot be foreseen, as they are not additive; on the contrary, they are in some way "substractive", for additions of $N\bar{S}$ to $M\bar{S}$ or conversely reduce the attack of each of the two salts acting alone (166) (168).

Most abundant sulfates in soils are those of calcium (gypsum, selenite), magnesium (epsomite), sodium--calcium (glauberite) and sodium (thenardite), which have very different solubilities. Soluble alkali and earth-alkali sulfates produce different effects on cement paste, as they act in different ways. Sodium sulfate react mainly with hydrated aluminates to form ettringite, whereas magnesium sulfate also reacts with hydrated silicates to form gypsum, brucite and silica gel (27). Ettringite formed in stronger attack (169), being instable in the presence of $M\bar{S}$, the attack of this produces even more gypsum, so that damages caused by $M\bar{S}$ are in general greater than those produced by other sulfates -apparent on real exceptions have been duly explained (27)-. Calcium sulfate as such, due to its lower solubility affects to cement to a lesser extent than other more soluble sulfates.

Sulfuric acid and other sulfates may be formed in soils by oxidation in acidic media of iron sulfides such as pirite, pyrrhotite, marcasite (29) (170). Sulfates may reach concrete in different ways and to different extents by several mechanisms conditioning the rate of attack, such as penetration, osmotic pressure, capillary rise, etc., depending mainly on concrete porosity and permeability, in turn related to the quality of construction materials and technologies (170).

The diffusibility of SO_4^{2-}-ions through hydrated cement pastes. as compared with that of cations (Li^+ Na^+, K^+), is smaller towards pure water and greater towards saturated lime solution. This indicates, as stated elsewhere in this paper, that hardened cement paste behavies as a semipermeable electropositive membrane facilitating diffusion of anions (155) (158) (159), depending on their nature. So, the rate of diffusion of SO_4^{2-}-ions is 10 to 100 times lower than that of Cl^--ions; in spite of it, chloride attack is always much weaker than sulfate attack, due to the different nature and solubility of the main products formed in each case (higher solubility for calcium chloroaluminate than for sulfoaluminate) (159). So, internal physical parameters of concrete, such as density, compacity, porosity, permeability, capillarity, etc., depending on factors other than (but in addition to) the chemical nature of the cements, complicate the problem of sulfate attack -and those of durability in general- to such an extent that it is very often difficult to establish clear and even logical relationships between chemical composition of cements and its influence on their chemical resistance (171). This is also valid as far as results of methods to study and to test durability are concerned.

Pore size distribution and amount of capillary pores over a given size (2500 Å) after a sulfate ($M\bar{S}$) attack varies very much depending on the nature of the (pure portland or blended) cement. In the case of blended cement the amount and nature of admixtures have also an influence, so that cements suffering more severe attack present more and larger pores than do better resisting cements (169). This may condition the further course of the attack on either of the two types of cements.

All these factors influence greatly the sulfate attack because in it two different processes are involved. One being of chemical nature is very rapid, whereas the other, physical in nature -ionic diffusion as mentioned- is much slower and governs the rate of reaction. This is a reason why the physical state of the mortar of concrete is decisive in determining the effects of sulfate attack and the resistance to it (172) (173). This also makes that the time before attack being very important (174), may be very variable and even very long, but once the attack starts, the destructive process runs very fast (2) (172) (175). Both processes may explain that the most important factor in the attack by sulfates is, in given circumstances, a combination -the product, as far as regression coefficient is concerned- of the (high) C_3A content in cement and the (high) w/c ratio in the paste (172).

Even external physical factors such as temperature are important in sulfate attack on cement, though this is not always taken into due consideration. Temperature may condition the type and the nature of hydrated aluminates and also those of sulfoaluminates formed in the attack of cements by sulfates. In addition, changes of these compounds once formed may be caused by changes in temperature, as they are stable phases in different equilibria which may be shifted in one or another direction depending on temperature variations (171) (176). This might explain the different (better) behaviour (but not immunity) of thermically treated cement products in sulfate attack. These different behaviours are not always sufficientely clear on the basis of a reduction of CH forming with silica compounds, in thermal treatment, more resistant calcium silicate hydrares of different composition and physical nature, or on the basis of the formation of a more crystalline tobermorite or hydrogarnets (171). Nevertheless, an indirect evidence of the protective effect of $C_xS_yH_z$ tobermoritic gels on cements against (sodium) sulfate attack determined by expansion measurements is given by the better behaviour of industrial cement pastes and pastes obtained from mixtures of different calcium silicates and aluminates with gypsum, all of them treated in autoclave. An interpretation of the good behaviour has been proposed in terms of a covering of sensible Al^{3+} and Fe^{3+} ions in the weaker parts so resulting isolated from contact and interaction with SO_4^{2-}-ions (177). Moreover, steam curing affects better than normal curing to cements exposed to (magnesium) sulfate attack, specially if their silica content is high -low C_3S and probably relatively low C_3A contents- (178). In the same or similar sense could be invoked a higher difficulty of dif-

fusion of sulfates in solution through pastes poorer in CH and richer in tobermoritic gels, in the case of slag cements (179). The case of thermal treated -steam cured concrete- is one in which it seems that sulfate resistance (and durability in general) is much more affected by the nature and composition of the cement than by other physical factors -including thermal curing conditions- (180). On the other hand, it seems that sulfate attack on cement is more usual and impontant in cold than in warm weather conditions (171).

Sulfate attack is centered on calcium aluminates. Nevertheless, some points of view consider that though cement susceptibility to sulfate attack depends on its C_3A content, concrete mixes rich in cement even of medium to high content of C_3A are less attacked by gypsum waters than are poorer mixes made with low C_3A cements (181). Research work and publications on the effect of C_3A on cement behaviour is copious, as mentioned, but not always very useful to asses it duly, because of the lack of precission in describing real and/or experimental conditions (182). This is a general handicap in many features dealing with durability. Even more beneficial actions have been attributed to higher contents of C_3A in cements, in the case of a complex attack by Cl^- and SO_4^{2-}-ions in sea-water (183).

On the other hand, the reaction mechanism of aluminates with sulfates and particularly with gypsum is far from being simple (171). Free energy calculations for possible reactions of various calcium aluminate hydrates -and calcium aluminate double salt hydrates- as C_4AH_{13}, $C_4A\bar{S}H_{12}$, $C_4A\bar{C}H_{11}$, $C_4A\bar{N}_2H_{10}$ and $C_3A.CaCl_2H_{10}$ with sulfate ions show the possibility of their transformation into ettringite, on the basis of the corresponding negative free energy changes (45). Hydration of anhydrous C_3A may form hydrates of different calcium contents depending on the calcium concentration in the liquid phase. The more basic of them, C_4AH_{13}, may react in solid state even with very low sulfate concentrations to form expansive ettringite. The less basic CAH_8 may be hydrolized to give CH and AH_3, which in solution may also react with sulfates to give ettringite as well, but not expansive, as it is formed from not crystallized compounds and it may accomodate in pores and free spaces (184).

According to different authors tree or five main mechanisms have been invoked as causing sulfate attack, depending on the fact of taking into account or not the influence of cations (166) (185) (186). Such mechanisms seem to be:

1) formation of sulfoaluminates (ettringite) -schematically-:

$$C_3A + CH + 12\,H \longrightarrow C_4AH_{13}$$

$$C_4AH_{13} + 3\,C\bar{S}H_2 + 14\,H \longrightarrow C_3A(CS)_3H_{32} \quad CH$$

$$C_3A + 3\,C\bar{S}H_2 + 26\,H \longrightarrow C_3A(C\bar{S})_3H_{32}$$

2) formation of gypsum (schematically):

$$N\bar{S} + CH + 2\,H \longrightarrow NH \quad C\bar{S}H_2$$

the acidic nature of sulfate attack causing surface deterioration by softening without expansion;

3) other reactions in which sulfate ions or sulfates are involved, as for instance formation of alkali sulfate crystals (when alkali sulfate concentration is high and conditions are propitious, for instance: $N\bar{S} + 10\,H \longrightarrow N\bar{S}H_{10}$ (mirabilite) also contributing to surface deterioration by spalling or splitting (166) (186);

4) formation of brucite (in the case of magnesium sulfate) with simultaneous formation of gypsum: $M\bar{S} + CH + 2\,H \longrightarrow MH + C\bar{S}H_2$ both contributing to deterioration;

5) formation of hydrated silica (in the case of magnesium sulfate) with simultaneous formation of gypsum and brucite (schematically):

$$C_xS_yH_z + x\,M\bar{S} + (3x + 0,5y - z)\,H \longrightarrow$$

$$\longrightarrow x\,MH + x\,C\bar{S}H_2 + 0,5y\,S_2H$$

causing effects corresponding to 2) and 3) conjointly (166) (186).

Process 1) adscribed to C_3A is operative for very variable contents of it, according to different opinions and circumstances, but it seems that expansion is due to the water imbibing character of colloidal ettringite formed in the presence of CH at lower concentrativon of sulfates (187). Process 2) can also take place when sulfate concentration is high -more than 1000 ppm- (167), as for instance in some $N\bar{S}$ and $M\bar{S}$ more concentrated solutions of ground, sea-water and industrial waters (188). Processes 4) and 5) can take place simultaneously in some highly concentrated natural waters and some times in sea-water attack too. They are respectively characterized by elimination of portlandite and tobermorite (189). They can also take place simultaneously with processes 1) and/or 2) in the most complex cases of sulfate attack. Either of the two processes 4) or 5) or both are found in some long term sea-water attack on cements with medium contents of C_3A (188), but also in some laboratory tests carried out with very concentrated $M\bar{S}$ solutions. The results of such tests in general may not agree with the real ones in practice, as taking place in different conditions (189). Process 3) purely physical in nature, takes place by evaporation and concentration of salts in pores (186). As to the limit of C_3A content in cement determining the degree of acceptability of expansion due to process 1), opinions differ widely -from less than 2, 3 or 5 % till less than 7, 9, 10 or even 12 %- (166). This indicates the great influence of other not always or not well considered factors (189).

Aside from the old and well known theory on the formation of expansive ettringite -through a solid state reaction mechanism when the liquid phase containing

sulfate ions at sufficiently high concentration is oversaturated or saturated with CH (185)-, and that of the formation of non-expansive ettringite (by a through--solution process when the liquid phase is not saturated with CH), other mechanisms discarding ettringite action have been proposed to explain sulfate expansion (30). So, some opinions have been exposed in favour of monosulfoaluminate as causing sulfate expansion and deterioration instead of trisulfoaluminate. On the basis that in a paste of $C_3A + C + C\bar{S}H_2$ expansion takes place when ettringite dissapears and monosulfoaluminate forms, it has been assumed that expansive monosulfate is formed in cement pastes by reaction of C_4AH_{13} with sufficiently concentrated SO_4^{2-} - ions by an anion exchange process (30) which could be schematically represented as follows:

$$C_4AH_{13} = \left[C_3A\,(Ca^{2+} + 2\,OH^-)\right] H_{12}$$

$$CaSO_4 = (Ca^{2+} + SO_4^{2-})$$

$$\left[C_3A\,(Ca^{2+} + 2\,OH^-)\right] H_{12} + \left[Ca^{2+} + SO_4^{2-}\right] \longrightarrow$$

$$\longrightarrow (Ca^{2+} + 2\,OH^-) + \left[C_3A\,(Ca^{2+} + SO_4^{2-})\right] H_{12}$$

Further increase of SO_4^{2-}-ion concentration may transform monosulfate into secondary harmless ettringite by a through-solution process, its crystals precipitating in pores. The character (expansive or not) of the monosulfate depends -as in the case of ettringite- on the CH concentration in the liquid phase (185): if it is high, the lowered solubility of C_4AH_{13} hinders the accomodation of monosulfate in pores. And the exchanging-ion (anion) character of the process, essential for expansion, is confirmed on the basis of the replacement of SO_4^{2-}-anions in monosulfate by other anions, for instance Cl^-, in $CaCl_2$ solutions, according to the schema:

$$\left[C_3A\,(Ca^{2+} + SO_4^{2-})\right] H_{12} + \left[Ca^{2+} + 2Cl^-\right] \longrightarrow$$

$$\longrightarrow Ca^{2+} + SO_4^{2-} + \left[C_3A\,(Ca^{2+} + 2\,Cl^-)\right] H_{10} + 2H$$

This might explain expansion of cement pastes in chloride ($CaCl_2$) solutions by releasing of SO_4^{2-} -ions, which once free and reaching the concentration needed to react with more C_4AH_{13}, may form more expansive monosulfate (30). These assumptions lead to a solution for avoiding sulfate expansion: the transformation of C_4AH_{13} into other more stable compound with a lower basal spacing, for instance, monocarboaluminate, by the action of finely ground $CaCO_3$ added to cement (30).

Changes in ionic concentrations of solutions in contact with cement paste are important to interpretate the mechanics of the attack, as aggressive waters may leach calcium hydroxide from the paste and introduce anions in it. In the case of sulfate attack the greater amount of sulfate anions introduced corresponds to magnesium and ammonium sulfate solutions, which affords an explanation of the higher aggressivity of them (82).

In this respect three types of cations regarding sulfate attack may be considered: those forming soluble hydroxides; those forming sparingly soluble hydroxides; and those forming volatile or neutral compounds. Differentations and effects take place in each case, as pointed out when dealing with the different types of attacks to concrete (30).

Sulfate attack seems to be produced through formation of gypsum, if this is not originally present:

$$3\,CH + 3\,X\bar{S} + 6\,H \longrightarrow 3\,C\bar{S}H_2 + 3\,XH$$

to form ettringite:

$$C_3AH_6 + 3\,C\bar{S}H_2 + 20\,H \longrightarrow C_3A(C\bar{S})_3H_{32}$$

and in total (23):

$$3\,CH + C_3AH_6 + 3\,X\bar{S} + 26\,H \longrightarrow C_3A(C\bar{S})_3H_{32} + 3\,XH$$

In the attack of sodium sulfate or magnesium sulfate on cement, gypsum in both cases and sodium hydroxide or magnesium hydroxide are respectively formed at early ages (less than 3 days) according to:

$$CH + N\bar{S}H_2 \longleftrightarrow C\bar{S}H_2 + NH \qquad (I)$$

$$CH + M\bar{S}H_7 \longrightarrow C\bar{S}H_2 + MH + 5\,H \qquad (II)$$

But few ettringite is then formed (176).

In the case of sodium sulfate solutions, if the solubility product of CH is not depassed, more gypsum is formed according to (schematically):

$$C_{2n}A_{n-1}F + 3n\;C\bar{S}H_2 + n\;C + (24\text{ to }26)\,n\,H \longrightarrow$$

$$\longrightarrow n\left[C_3A_{1-1/n}F_{1/n}(C\bar{S})_3H_{30\text{ to }32}\right]$$

(for phases between C_2F and C_6A_2F), and:

$$C_{2n}AF_{n-1} + 3n\;C\bar{S}H_2 + n\;C + (24\text{ to }26)\,n\,H \longrightarrow$$

$$\longrightarrow n\left[C_3A_{1/n}F_{1-1/n}(C\bar{S})_3H_{30\text{ to }32}\right]$$

(for phases beween C_2A and C_6AF_2).

Increases of alkali concentration and/or of temperature make decrease the lime solubility according to I. Then gypsum precipitates, the formation of ettringite is at least stopped and ettringite still formed tends to dissolve. This explains the continous growing of gypsum and the maximum attained by ettringite when comparing expansion by sulfate attack with the sulfate (ettringite and/or gypsum) contents in expanding speciments (176).

Leaching of lime takes also place to some extent:

$$SO_4^{2-} + 2\,Na + Ca(OH)_2 + H_2O \longleftrightarrow CaSO_4.2H_2O +$$

$$+ 2\,Na + 2\,OH^-$$

increasing the alkalinity in solution if carbonation $Ca^2 + 2\,OH^- + CO_2 \longrightarrow CaCO_3 + H_2O$ does not take place. Intensive carbonation could form thaumasite (especially at much longer terms) and plazolite $CA.CS.C\bar{C}.H_2$. In each case, when the solution has reached the conditions for gypsum precipitation, gypsum crystallizes (82). Thaumasite formation as nedleshaped crystals forming big masses with high silica content and low contents in SO_3 and CO_2 has been reported as taking place in concrete deterioration by sulfate attack (190).

In the case of magnesium sulfate solutions ettringite first formed is decomposed by the salt to form gypsum, and magnesium and aluminium hydroxides according to:

$$C_3(A,F)\,(C\bar{S})_3H_{31} + 3\,M\bar{S} \longrightarrow 6\,C\bar{S}H_2 + (A,F)H_3 + 3\,MH + 13\,H$$

Brucite is also formed (82) and in greater amount when the alkalinity of the paste is greater than normally; this is the case when sodium silicate is added to portland cement to form grouts, as it affords an extra alkalinity depending on the molar ratio Na_2O/SiO_2. Seepage of Na_2O making the grout less compact may also contribute to facilitate magnesium sulfate attack in this case (191).

The better resistance to magnesium sulfate of portland cements with high iron-compound contents has been related to the fact that on hydration of brownmillerite in the presence of $MgSO_4$, Fe is displaced from places in the hydrated cubic phase (9).

A suggestive explanation has been given on the stronger but slower attack of calcium silicate hydrates (especially those of low basicity) by $MgSO_4$ solutions than by Na_2SO_4 solutions, on the basis of heterovalence and ionic radii of Mg^{2+} and Na^{+} ions (60) as follows: heterovalence and difference in ionic radii difficult or hinder the substitution $2\,Na^{+} \longleftrightarrow Ca^{2+}$ whereas it favour the substitution $Mg^{2} \longleftrightarrow Ca^{2}$, the latter cations having the same valence and similar radii. On the other hand, adsorptive capacity of bivalent Mg^{2+} ions on calcium silicate hydrates is greater than that of monovalent Na^{+} ions. Furthermore, reaction products of calcium silicate hydrates with $MgSO_4$, i.e., $Mg(OH)_2$ (brucite) and $CaSO_4$ (gypsum) are in bulk much less soluble than those with Na_2SO_4, i.e., NaOH and $CaSO_4$. And finally, the protective action against ionic diffusion afforded by films of products formed by interaction of sulfates and calcium silicate hydrates depends on the structure of such films. This structure seems to be continuous, denser and more impervious for films formed from the more basic calcium silicate hydrates than for those formed from less basic tobermoritic compounds (60). In fact, it was known that the attack due to magnesium ion seems to be more intense on low C_3A cements and in the presence of higher amounts of hydrated lime (high C_3S cements), which today is clearly explained by the exchange between Ca and Mg in $Ca(OH)_2$ and CSH to form $Mg(OH)_2$ and MSH, the former potentially expansive, the latter much less or not hydraulic (58) (192).

In the case of ammonium sulfate attack an exchange of lime equivalent to the ammonium content takes place (82).

In conclusion, the mechanism of the alkali and/or magnesium sulfate attack on concrete seems to proceed through a front of ettringite penetration which causes cracks. Afterwards gypsum and/or brucite crystallize in the cracks causing either further expansion or the filling of cracks and pores (176).

In the case of gypsum attack on aluminates the kinetics as well as the nature of the intermediate and final products depend on the characteristics of the starting materials, on the presence, amount and concentration of $Ca(OH)_2$, on temperature, time, etc., even though the final compound causing deterioration be also ettringite. Differences have been attributed to variations in the d-spacings of hydrated starting, intermediate and final products (171). In the writter's opinion, if it is so when dealing with well defined (or better defined) and controlled more simple reacting compounds as are bare calcium aluminates, it is to be though that the complexity must be necessarily much greater when dealing with not always well defined mixtures of compounds, as is the case of cements.

An early succint summary of the hypothesis concerning expansion due to ettringite formation has been exposed (187). According to it, increases of volume have been invoked (193) (194) or questionned (195); crystallization pressure as a factor determining concrete rupture has been supported by the measurement of pressures created in the formation of calcium sulfualuminates in different conditions, reaching values up to 200 kg/cm^2 (196); solid-state (194) (197) (198) or throug-solution mechanisms (195) (199) have been proposed; suggestive osmotic pressure actions have been supported (200) or considered doubful (201); thrust by anosotropic crystal growth has been advanced (202) or refused (203) More recently new points of view have taken into consideration another alternative hypothesis (187), according to which only colloidal ettringite of high specific surface formed in the presence of lime is highly expansive, if it is in contact with outer water. The expansion mechanism may be then a double-layer type of interparticle repulsion caused by a considerable adsorption of water around the ettringite, without changing its crystal lattice. This may also afford an additional explanation of why pozzolanic or slag cements and high-alumina cements with little or no $Ca(OH)_2$ in their pastes exhibit much less expansion due to ettringite formation in sulfate attack (187). The conclusion is that attack involving ettringite formation not only depends on the (crystalline) nature of C_3A (182) -as pointed out elsewere- but also on the nature of the ettringite formed, to the extent that its formation may produce either deleterious (disruptive) expansions or beneficial phenomena and effects -shrinkage compensation and self-stressing- (187). Other somewhat different viewpoint in the same sense is that ettringite formed in hydration at pH 11.5-12.0 by a through-solution reaction contributes to the strength and is not expansive, whereas secondary ettringite formed at pH 12.5-13.0 by a topochemical reaction may be expansive and destructive (159). It seems that ettringite formation by the one or the other mechanism depend upon the (ratio of) diffusions of SO_4^{2-}-anion and cations. This ratio being nearly 1 in the case of the lower pH-values, SO_4^{2-}, Al^{3+} and Ca^{2+} ions meet together and form ettringite in spaces between grains -without

expansion-, whereas in the case of higher pH values the ratio is also higher and SO_4^{2-} and Ca^{2+} ions meet together with Al^{3+} ions around and on the cement grains containing aluminates (159).

In addition to what has been exposed more in detail elsewere in this paper as regards of standard specifications and sulfate resisting cements, it is to be said here that limitations of C_3A and C_4AF do not solve the problem of sulfate attack, so that restriction of the condition of sulfate resisting cements to those meeting specifications for ASTM type V seems not to be justified. Instead, pozzolanic (fly-ash) cements made with clinker of less than 6,5 % C_3A and less than 12 % C_4AF have been proposed as sulfate resisting cements (204).

9.- SEA-WATER ATTACK

Much work has been done and very many publications on it have been produced dealing with sea--water attack to concrete and concrete behaviour in sea-water. Several International Congresses on Chemistry of Cements, on Navigation, RILEM Colloquia and Symposia, etc., have monographically devoted a good deal of paper to these themes. The treatment of them is obviously very difficult due to their great complexity. There is -or at least there has been- a tendency to consider sea-water attack on concrete as a well defined and homogeneous topic within the general field of concrete durability. It seems doubtful to accept such a homogeneity as being general, as potentially very variable physical factors such as climate -temperature or frost-; or mechanical factors such as erosion, streams, surfs, tidal and wave alternating actions, total or partial alternative immersion or biological factors, etc., join indissolubly their contribution to the mere chemical action due to salinity, to the corrosion of concrete by sea-water.

The mechanism of sea-water attack on concrete is a leatory and very complex, as many parameters difficult to isolate may contribute to the total damage (205). The attack acting on concrete submitted to alternative immersion and emersion in tidal zones manifests itself mainly as a physical effect of salt crystallization combined with carbonation and, of course, with mechanical, erosional and frost actions depending on local circumstances (206). In particular circumstances erosion actions of sea-water on concrete are strong. Their effects superimpose to chemical attack and facilitate it. Isolated or combined actions affect more to poor and/or to bad cured concretes (207). Combinations of physical and chemical actions correspond always to alternate immersion, whereas chemical attack alone is produced in total and permanent immersion (208). In the tidal zone alternative cycles of drying and wetting may produce concentration, crystallization and dehydration of salts (drying) and recrystallization (wetting) processes in concrete mass, to which may contribute hygrometric and thermal action, insolation etc., as well as concrete porosity. Crystallization pressure of Na_2SO_4 for instance creates an expansive force in the exposed part of specimens, similar to that caused by ettringite formation in the immersed part of them (25). Moreover, in the tidal zone a complicated process of cement deterioration takes place based on diffusion mechanisms. Diffusion is negligeably slow when considering the penetration of water in concrete, but not always in the case of salt solutions, as gradients may be considerable if salt concentration in some pores and voids is much higher than in others. Complication may be even greater if either the water or the dissolved components react chemically with the hydrated compounds of the cement paste. Anyway, high gradients of osmotic pressure may be created and much more so if salt concentration increases by evaporation. If saturation is raised, crystal formation and crystal growth may take place so generating hydraulic and/or crystallization pressure similar to that of the ice formation, with the corresponding disruptive effect (209). Furthermore, complexity of sea-water attack on concrete, as referred to prestressed ocean structures has been exposed in a not exhaustive manner (210).

On the contrary, it has been timidly claimed that the attack of sea-water on cement and even the resistance of cement paste to sea-water attack seem often to be imprevisible and highly variable. In any case, so far they are considered as matters not yet elucidated, from VICAT and MICHAELIS onwards (211) (212). The reason is the great complexity of sea-water attack on concrete as the result of a number of superimposed mechanical, physical and/or chemical actions, which take place in very different conditions. It is impossible to avoid in practice such an overlapping of actions and thus many variables are simultaneously operative, and as many parameters are affected in various ways and to different extents in each moment and circumstance.

The total effect produced by sea-water attack is in general neither that corresponding to the sum of individual effects of each cause (as it is sometimes higher or much higher), nor proportional to a given (isolated) action. For instance, sea-water attack is in most cases weaker than that to be expected from the SO_4^{2-}-ion concentration, as compared with that of sulfate solutions (213). Attack by sea-water weaker than that of $MgSO_4$ solutions of similar concentration has been attributed to a greater solubility of ettringite and gypsum in chloride solutions rather than to a lower level of reaction of sulfates in the presence of chlorides (214). Anyway it seems to be clear that sulfate attack is different in the presence than in the absence of chlorides (215). To such an extent, that in the presence of chlorides (sea-water) a positive action of C_3A in cement has been attributed to retardation of Cl^--ion diffusion and reinforcement corrosion, quite appart from SO_4^{2-}-ion aggressivity (183). The greater solubility of ettringite in the presence of chlorides makes it to crystallize from solution in pores, in a harmless form without causing expansion (214). Though the presence of chlorides in the attack of cement by sulfates (as in the case of sea-water attack) has been considered in general as beneficial, other opinions are in support of an activation of the

aggression, the intermediate chlorinated compounds formed being noxious, as they finally form ettringite. (208).

The fact that sea-water attack is weaker than that of sulfate solutions of similar concentration would seem to shift partially the deterioration mechanism of cement paste by sea-water to the side of leaching and solution (non-expansive) processes (27). Anyway, distinction has to be made between degree of reaction -even expansive in nature-, real expansion produced, and damaging effects of it, as in fact, observed swelling and deterioration are not always proportional to the amount of ettringite formed, though expansive ettringite formation and leaching of calcium hydroxide by dissolution in the presence of magnesium salts seem to be the two principal factors conditioning the attack (205).

In fact, sea-water attack may respond to each of the several accepted mechanisms of sulfate attack or, what is more probable and general, to various of them simultaneously (167), as concentrations of sulfates may reach from less than 4000 to 7000 ppm (189).

The most general, wide ranging and complete attack by sea-water on cement up to its ultimate consequences is characterized:

a) by elimination of calcium, either by solution of substitution for magnesium -cation exchange-, i.e., leaching of portlandite CH, formation of brucite MH or transformation of the $C_xS_yH_z$ type of calcium silicate hydrates into the more complex and less or not hydraulic $C_x.M_x..S_y.H_z$. magnesium type of compounds (15);

b) by formation of secondary dense expansive ettringite through reaction of sulfates with CH giving first secondaty gypsum $C\overline{S}H_2$;

c) by (subsequent) strong carbonation converting ettringite into thaumasite $C\overline{C}.C\overline{S}.CS.H_{15}$ (16) (212) with previous formation of silica (70) (190), calcite and/aragonite (216) (217);

d) by crystallization of gypsum;

e) by formation of $C_3A.CaCl_2.H_{10}$ which first prevents the inmediate formation of ettringite, but being unstable in the presence of sulfates finally tends to form ettringite;

f) by penetration of Cl^--ions in tobermoritic gels $C_xS_yH_z$ (15) (16).

Processes a) and b) due to the action of SO_4^{2-} and Mg^{2+} ions seem to be in general more important, though action c) -moderate carbonation- and d) may also take place to some extent. So, calcite and aragonite may be formed in a progressive attack on the surface and in the paste, either of portland or slag cements, and either for short or for long periods of contact with sea-water. Brucite -solide MH- is formed on the surface or in the mass of portland cements only (218) -other previous opinions are that even in slag cements pastes MH may appear in the attack of them by synthetic sea-water (214), mainly in short contacts, whereas secondary gypsum has been detected in surface attack of both cements during long contacts, and in mass attack of them during shorter contacts. Sometimes ettringite formed in the attack of pastes during short contacts is not found in surface attack, neither during short or long contacts, probably due to its unstability and/or to a low or very low content of C_3A in cement (219). In other aspect, processes e) and f) are favoured by the fact that penetration of Cl^--ions in pastes progresses deeper and more rapidly than that of SO_4^{2-}-ions (220).

In deep and prolongated attack by sea-water on cement calcite, aragonite, secondary gypsum, ettringite and thaumasite in addition to brucite are formed (212). Gypsum and thaumasite are more abundant in the more longly and/or deeply attacked cement pastes, whereas ettringite predominates in the more slowly and slightly damaged ones. The ratio ettringite/thaumasite is lower in the former than in the latter. This seems to indicate that ettringite is formed first and transformed later into (isostructural) thaumasite by a carbonation process -also responsible for the formation of calcite and aragonite- and probably by a more or less simultaneous substitution of Al by Si, the silicium being afforded either by formation of more or less alkali and/or earth-alkali (expansive) silicates containing alkalies from either the aggregate or the cement (or both), or by silica gel formed in the carbonation itself, affecting the calcium silicate hydrates (212). This generally very slow transformation could be imagined as taking place by steps, with formation of intermediate compounds (190). In a parallel way, regarding compounds formed and destroyed by a complex attack of sea-water, ettringite, gypsum and brucite, as well as hydrocalumite may appear, and portlandite crystals and tobermorite gels may dissappear. This indicates on the one hand, that acidic action by carbonation may also take place; on the other hand, that slag cements and pozzolanic cements can be, as in practice they are, more resistant to long term action of sea-water (189).

Processes involving ettringite formation can be reduced or eliminated by using cements of no or very low content of C_3A; but when processes involving lime dissolution occur over long terms, cements with low content of C_3A -even lower than 3 %- may be affected. This shows that in preventing sulfate acidic action in long term sea-water attack a low content of CH in the hydrated cement paste, i.e., a low C_3S/C_2S ratio in clinker (188) is even more important than a low content of C_3A in anhydrous cement, at least in general (166).

At this point it should be interesting to emphasize the -at least potentially- very good performance of ternary pozzolanic (fly-ash)-slag cements made with clinkers of low C_3A content having an adequate C_3S/C_2S ratio. All this means that the prescription of a type V ASTM portland cement to prevent long attacks by sulfate concentrations higher than 1000 ppm may not be sufficient in all the cases. As far as performances of different types of cements in sea-water

are concerned, results of long term French experiences have recently been reported (15) (208) (221).

Sea-water attack has been also centered in the action of magnesium sulfate reacting with calcium hydroxide to form gypsum -through an irreversible process (222) (223)-, which, in turn, reacts with calcium aluminate to form the well known expansive ettringite:

$$Mg^{2+} + SO_4^{2-} + Ca(OH)_2 + H_2O \longrightarrow Mg(OH)_2 + CaSO_4 \cdot 2H_2O$$

$$3\ CaSO_4 \cdot 2H_2O + 3\ C_3A + 30\ H \longrightarrow C_3A(\bar{C}S)_3H_{32} \quad \text{or:}$$

$$C_4AH_{13} + CaSO_4 + 18\ H \longrightarrow C_3A(\bar{C}S)_3H_{31} \qquad (25)$$

The depressing action of chlorides in the sulfate attack may be attributed not only to an increase of the solubility of expansive calcium compounds (222) (223) but even to a greater instability and decomposition of them in chloride solutions when the content of C_3A in cement and the sulfate concentration are high. For smaller contents of C_3A it is possible that no ettringite is formed in the presence of chlorides and no attack of sea-water on cements take place (209).

The fixation of Mg^{2+} -obviously- and the loss of Ca^{2+} by cement pastes are greater in sea-water (as in $MgCl_2$ and $MgSO_4$ solutions) than in pure water, and they are also greater the higher the initial content of calcium compounds in cements (224). Moreover, in cements attacked by sea-water it has been stated that no monosulfoaluminate is formed, because of the lack of CH necessary to form C_4AH_{13}, necessary in turn to transform slowly the trisulfoaluminate previously and rapidly formed into monosulfoaluminate, thus

$$C_4AH_{13} - 3\ C\bar{S}H_2 - 14\ H \longrightarrow C_3A(CS)_3H_{32} + CH$$

$$C_3A(\bar{C}S)_3H_{32} + 2\ C_4AH_{13} \longrightarrow 3\ C_3A\bar{C}SH_{12} + 2\ CH + 20\ H$$

This is another of the main differences between attacks by sea-water and mere sulfatic waters: the presence of stable trisulfoaluminate and the absence os monosulfoaluminate -and portlandite- (222). An additional difference is connected with carbonation. Carbonation is insignificant under sulfate solutions and under sea-water due to the lower solubility of CO_2 in them; but in any case aragonite is preferently formed in sea-water carbonation instead of vaterite and/or calcite, due perhaps -basicity appart- to the higher solubility of vaterite in chloride solutions. These do not permit, even in basic media, either the formation of vaterite or its subsequent transformation into calcite (222). Moreover, aragonite is the denser, harder and less soluble form of crystallized calcium carbonate, and consequently the more apt to be formed stably in the more difficult conditions. Anyway, protection by carbonation is practically absent on cement in contact with sea-water (222).

Insoluble brucite may also be formed by another mechanism such as

$$MgCl_2 + Ca(OH)_2 \longrightarrow Mg(OH)_2 + CaCl_2$$

which may accumulate in pores and voids of a fairly dense concrete, so reducing further action of sea-water on it. But the solubility of $CaCl_2$ is high and those of $Ca(OH)_2$ and $CaSO_4$ are much higher in sea-water than in plain water. This may explain a much greater leaching of lime from porous and permeable concrete in sea-water (209).

As far as an explanation of the weaker attack of sulfates in the presence of chlorides is concerned, as is the case in sea-water attack- it has been invoked that a part of the aluminate in the cement paste forms the FRIEDEL's salt, and only the remainder aluminate forms ettringite (214). Nevertheless, whatever the explanation may be, experiments carried out with portland and blastfurnace slag cements submitted to sodium and magnesium sulfate solutions, either pure or each of them containing sodium chloride or sodium bicarbonate, have revealed the following facts: first, that the stronger attack corresponds to the greater formation of ettringite, particularly in the case of magnesium sulfate attack; second, that the FRIEDEL's salt is formed from monosulfate and/or from aluminate hydrate, or even from anhydrous aluminate, but not from the trisulfate; third, that the monochloroaluminate thus formed (by penetration and diffusion of Cl^--ion more rapid and deep than those of SO_4^{2-}-ion and more than those of K^+ and Na^+ --ions) is not stable in the presence of sulfates, which transform it into trisulfate on attack (59) (214) -this transformation dissapoint the use of sea-water for mixing concrete (a very controverted matter (208) particularly if cement is rich in C_3A (59)-; and fourth, that as a main consequence of the preceeding results, the high content of Cl^--ion in sea-water has no essential effect on sulfate attack. Much greater influence seems to be attributable to the presence of sodium bicarbonate dissolved in sea-water, as it reacts with CH forming calcite on surface, so hindering or retarding the penetration and diffusion of attacking sulfates (214). Calcite may also be formed in the absence of previously dissolved sodium bicarbonate, or by the action of athmospheric CO_2, but its formation is much slower and takes place to a much lower extent, so that it cannot hinder sulfate penetration, attack and damage. In the same way $Mg(OH)_2$ formed in the attack by $MgSO_4$ does not influence the sulfate attack; but if $Mg(OH)_2$ and $CaCO_3$ are formed together, a protective effect similar to that of calcite is afforded (214).

Anyway, chlorides, sulfates and magnesium ions may form chloroaluminate, sulfoaluminate, brucite and magnesium silicate without visible expansion, while free pore space permits the free growing of crystals -mainly of those of ettringite-. Afterwards, delayed hydration of C_3A crystals closed in anhydrous silicates of the bigger grains of clinker gives place to a new formation of ettringite near to and all around of the C_3A crystals. This "secondary" ettringite enables further penetration and diffusion of attacking SO_4^{2-}--ions (58).

Observations carefully carried out have shown that the layers of concrete attacked from outside to inside contain successively aragonite (the form of calcium carbonate formed in the presence of magnesium salts), brucite, CSH + MSH sourrounded by chloroaluminates and sulfoaluminates. Sometimes aragonite in the first layer and brucite in the second one have protective effects as mentioned (214), by enhancing compaction and imperviousness of the attacked paste (205). On the other hand, in superficial attack either of alite pastes or of portland cement pastes exposed to water, NaCl and $MgSO_4$ solutions, and sea-water, calcite, aragonite and varite have been observed as products of carbonation, and gypsum and brucite as products resulting from the action of $MgSO_4$. In each case calcium hydroxide and calcium silicate hydrates are affected to different extents, and different forms of calcium carbonate are preferentlly formed depending on experimental conditions (160).

Whatever may be, sea-water attack is quite different from that of pure sulfate solutions -and generally smaller due to surface protection of concrete (by brucite formation and carbonation, if so), by the simultaneous presence of anions other than sulfates (chlorides) and different cations. Moreover, the relative influence of cations in aggressivity depends on the SO_4^{2-}-ion concentration (23).

Isolated mineral components of portland clinker submitted to sea-water attack show that penetration of Cl^- accelerates the hydration of C_3S and β-C_2S pastes, and that penetration of SO_4^{2-}-ions (and the consequent formation of gypsum) depends on the density or porosity -related to the degree of hydration and to the morphology- of the pastes in which may have, as mentioned, a beneficial influence as far as silicate hydration is concerned (225). But sea-water action on hydrated C_3A and C_4AF pastes consists mainly and primarily in the formation of monosulfate-like phases $C_3A.Ca(SO_4, Cl_2).xH_2O$, which in the presence of $Ca(OH)_2$ and by penetration of SO_4^{2-}-ions finally form ettringite. Almost the same occurs in magnesium sulfate solutions free from Cl^--ions (a solid solution of monosulfate and C_4AH_{13} is first formed). The chemical changes in pastes of C_3A and/or C_4AF produced by sea-water action cause morphological changes of structure accompanied by an increase of porosity, especially in the case of C_4AF. These changes are to be added to the pure chemical action in the case of sea-water attack to hydrated silicates, aluminates and ferrite-aluminates (225). On the other hand, secondary ettringite formed at later ages from C_3A occluded in anhydrous silicate crystals may cause local strains and cracks in concrete, which may in turn facilitate further penetration and diffusion of SO_4^{2-}-ions (58) (59).

Attack by sea-water brine at 80ºC on mortar of ordinary portland cement, fly-ash cement and high-alumina cement shows damages attributed to expansive crystallization of gypsum and to lime leaching by ionic exchange of Ca by Mg in tobermorite (or in hydrated calcium compounds of the high-alumina cement pastes), in which a solft talk-like product is also formed. In the case of high-alumina cements the proportion in which both mechanisms participate in the attack may be variable, depending on the composition and nature of the cement. The product of the attack seems to correspond to a complex double hydroxide of Mg^{2+} and Al^{3+} , that ratio Mg/Al in it being also variable. (225 bis).

In general, as to the influence of the temperature on the attack by saline solutions and artificial sea-water, it has been recently reported that the penetration of SO_4^{2-}-ions, the attack of $MgSO_4$ solutions and the corresponding expansions and damages by ettringite and gypsum formation are more intense at lower temperatures; conversely, in penetration of Cl^--ions, formation of chloroaluminate and attack by $MgCl_2$ no influence of temperature has been observed (226).

As far as cements are concerned, it is difficult to establish correlations and to drow conclusions relating cement types and their resistances to sea-water, as whatever the type of cement, strong attack always leads to the destructive formation of calcite, aragonite and non-hydraulic magnesium silicate (205). Being obvious that sea-water attack may act leaching lime from cement and forming ettringite with hydrated aluminates, it seems that portland cements resisting sea-water attack must be low in C_3S and C_3A (25). Some recent interesting results have been reported according to which ASTM type II portland cements -and to some extent type V cements also- mixed with water containing different amounts of either $CaCl_2$ or NaCl, or some other salts to compose artificial sea-water ("ocean mixtures"), give at 28 days higher strength than the same cements mixed with plain water. Moreover, cements mixed with NaCl solutions and cured in "ocean mixtures" give even much higher resistances. This last result is surprising and no satisfactory explanation seems to be for it, at least for the moment (227).

It has been invoked that ettringite from ASTM type I cement (mainly formed in sea-water and by action of sodium and magnesium sulfate on C_3A) crystallizes with expansion, whereas that of ASTM type V cement, resulting from C_4AF precipitates and remains as a non-expansive gel (202 ·). On the other hand, laboratory and field experience have shown that under certain conditions sulfate resisting portland cements may be damaged at long terms by sulfates (228).

Ettringite, other complex hydrated calcium aluminates, gypsum, brucite, MSH formation and leaching of CH in cement paste by sea-water action depend mainly on the various proportions of the different crystalline forms of C_3A: cubic, orthorrhombic and tetragonal in cement, and on their texture and grain size, rather than on the total amount of C_3A, as each of these forms reacts in different way. Attack and damage depend consequently on this, as well as on the fact that the C_3A crystals may be more or less sourrounded and protected by other big silicate crystals (58) (59) (205). As mentioned elsewhere one could perhaps in-

fluence the crystalline condition of the C_3A in cement through a deeper knowledge of the stability relationships of C_3A at higher temperatures by mineralization with fluorite in clinker formation by fusion or by other non traditional burning processes. In fact, in the substitution of Ca^{2+} by Na^{+} -ions in the cubic C_3A a part of this is converted into stabilized orthorrhobic and tetragonal solid solutions. Two of the three possible forms in cement coexist. The hydration kinetics of each of them being different in pure water, the speed of hydration of the cubic form is greater than that of the orthorrohobic form and this in turn is greater than that of the tetragonal form. Moreover, to a faster hydration of C_3A corresponds a faster hydration of C_3S too. In contact with sea-water cements with cubic C_3A give more ettringite than chloroaluminate; the opposite is valid for cements with orthorrhobic or tetragonal C_3A. Ettringite formed at short terms (as still mentioned) may be non-expansive, as crystallized from solution and with free space at disposal; whereas that formed much later may cause expansion, as formed locally in solid phase, without previous solubilization of alumina, and without free space for accomodation (15).

On the other hand, the penetration of Cl^{-}, SO_4^{2-} and Mg^{2+} -ions in the reticulated $C_xS_yH_z$ tobermoritic compound -though more compact than the corresponding fibrous compound- makes the former more porous, and weaker as far as the substitution of C by M to form partially less hydraulic (or non-hydraulic) $C_x \cdot M_x \cdot \cdot S_yH_z$ is concerned. This leads to a greater friability of the paste (15).

As far as synthetic mixtures of C_3S, C_3A and CSH_2 are concerned, C_3S hydrates faster and C_3A slower in sea-water than in pure water. Proportions of hydration products in sea-water (ettringite, gypse, brucite and magnesian tobermorite) depend on the crystalline form of C_3A too. Cubic C_3A gives more of the three former products, tetragonal C_3A gives more of the latter, and orthorrhombic C_3A behavies in an intermediate manner (15).

A question arises here as to the greater or smaller harmfulness of the weakening due to the more abundant magnesian tobermorite formed in the case of cements or synthetic mixtures richer in tetragonal C_3A, in comparison with that due to expansion caused by the more abundant ettringite formed in the case of cements richer in cubic C_3A. In the author's opinion this uncertainty, joined to the interdependence of both causes of degradation -among others and together with several others- could clear some of the abnormal, uncommon, unexpected and always inexplicable results and behaviours of some cements in some circumstances.

To the potential multiple variability so far exposed as far as the chemistry of cements, is concerned it is to be added those of the enviromment and of the concrete as regards its composition, permeability, capillarity and capillary suction, absorption capacity, pore system, etc. All the possible combinations of such potentially very variable factors intrinsic and extrinsic to concrete, overlapping to each other in all the very many possible forms and proportions, lead us, theoretically at least, to an extremely complicated picture of the real and practical sea-water attack on concrete. And probably they also lead us to the discouraging conclusion that the doubful homogeneity invoked for sea-water attack as one of the main topics in concrete durability does not exist in a great majority of cases. This may be one of the reasons why some results of research work done in real practical conditions and/or of testing methods carried out in laboratories do not agree with each others, or even they are -or seem to be- mutually contradictory, when otherwise expected. As a result it is really difficult to establish correlations between cement types and their performances -for instance on the basis of short term losses in strength- the main guarantee for resistance to chemical attack being in general a high degree of compacity obtained, other things being equal, with a high cement content in concrete. The probability of such guarantee may increase by using intrinsically more resistant cements. Regarding portland cements nominally resisting sulfate and sea-water attack, some doubts already exposed have arised many years ago on their guarantee, which now-a-days are well justified and explained (15) (229).

In the perhaps extreme but possible and even very probable complex situation of sea-water attack to concrete, simplifications, generalizations and extrapolations may be very dangerous. For instance, as far as the pure chemical aspects of the problem is concerned, attempts have been made as it has been already pointed out, to assimilate sea-water attack to sulfate attack, despite the knowledge that the action of SO_4^{2-} -ions of sea-water on cement is but very slow and secondaty, due to the presence of Cl^{-} -ion at a high concentration (223) (224). If not so, portland cements with lower contents of C_3A would resist sea-water action better than those richer in C_3A, according to the largely supported opinion. But it is not always so, as portland cements with very low, low and high C_3A contents have been almost equally and strongly damaged, as in the case of attack by $MgCl_2$ concentrated solutions (224).

This is so because in the case of sea-water attack a so-called "intrinsic" resistance of cements to SO_4^{2-}-ions depending on the nature and amount of their C_3A is not the only operative one. The resistance of cements to very high concentrations of Cl^{-}-ions and the possibility that brucite is formed filling the pores are probably much more important in the corrosive processes in sea-water as a whole. On the other hand, in very cold sea-water the action of sulfates is even much less important (230).

In the case of specially high saline sea-water, as for instance that of the Dead Sea (231) -much more concentrated in alkaline, calcium and chloride ions and less concentrated in sulfate ions-, in addition to brucite calcium chloroaluminates and magnesium oxychlorides instead of sulfoaluminates are also formed during cement attack. Something similar occurs when the attack on cement is produced by highly concentrated sea salt deposits in which strongly

corrosive kainite $KCl.MgSO_4.3H_2O$ is formed, and a severe threefold corrosion process produced by SO_4^{2-}, Cl^- and Mg^{2+}-ions takes place (232).

These facts explain, as mentioned elsewhere, the much better behaviour in sea-water of cements containing highly silicic slags over a certain proportion -to be fixed between 65 and 80 %- compared with that of ordinary portland cements, and even of other sulfate resisting cements -including portland, pozzolanic and high-alumina cements (224) (231) (232) (233) (234) (235). And much more so if the portland clinker has a low conten of C_3A, a high $S/(A+F)$ ratio and a low A/F ratio (234).

Even better results are obtained by using ternary cements composed with low C_3A portland clinker, slag and pozzolan of adequate nature and composition, and in adequate proportions (232).

From a strict chemical point of view all these well known experimental facts are logical. Slag cements with 60-70 % of a highly silicic slag; pozzolanic cements -even made with a clinker rich in C_3S, provided that the pozzolan has a high content of active silica (about 90 %) and a low content of reactive alumina and iron compounds- (234); and ternary cements, on the one hand they all have a low content of C_3A; on the other hand they are able to fix CH, so eliminating or reducing the formation of solid portlandite (additionally they make difficult the formation of ettringite). Moreover, they are able to form tobermoritic gels in higher proportions (234).

In conclusion, corrosion produced by solutions of $MgSO_4$ and $MgCl_2$ containing NaCl, as is the case in sea-water, is lower on binary or ternary composed (blended) cements. This is much more so the lower the content of free CH and/or of the more basic hydrated aluminates in their pastes, other things being constant (236).

From a more physical point of view, the higher amount of tobermoritic gels formed contributes to increase the imperviousness and to lower the penetrability of the cement paste, so protecting it from further attack. Furthermore, gels cover other sensible phases isolating them from the contact with aggressive media and inhibiting or retarding their corrosion.

In the case of pozzolanic cements as compared with normal portland cements, the effect of this physical .ction has been adscribed to a different proportion of phases, more than to a different nature of the phases formed. This difference in proportion of phases -particularly portlandite and tobermorite- leads to a structure of the cement paste with different physical characteristics. Among them, a greater impermeability and a greater resistance to ionic diffusion of SO_4^{2-}-ions through the more abundant tobermoritic gels (234).

In different aspect, very variable external and generally not well known circumstances condition the behaviour of different cements in such a way that it is not always sufficient to make reference to portland, pozzolanic or slag cements in terms of their chemical composition and that of their constituents. This is sometimes less important as compared with other influencing physical factors considered either favourable or not (236) (237). But it seems clear that when the attack progresses from outside to the inside of the material, depending on its initial porosity and absorption increasing with time, this attack is weaker if the cement is adequately resistant (238).

The result is a combination of physical and chemical factors which mutually combine and reinforce, acting together simultaneously and indissolubly. A question arises: in which way and relative proportion do the whole of each of these two factors operate in each circumstance and moment?. Otherwise, which of the two factors is temporarily more important and finally decisive?. It seems obvious that there cannot be a general answer to this question. Each particular case will have its own answer, though unknown in most of them. Anyway, the importance is relative; it cannot be absolute.

This is one of the reasons why the influence of the porosity of cement pastes, mortars and concretes -open and total porosity, size and geometry of the pores, pore size distribution- seems to be so decisive in sea-water durability studies. Particularly when the behaviour of different types of cements and concretes is investigated. This has lead to affirm that if the compacity of the material is high, its behaviour is good, independently of the nature of its cement; but if the compacity is low, then the nature of the cement may have a greater influence on the chemical resistance of the material to corrosion (239). More drastically it has been expressed that when the volume of pores is less than 30 %, no attack is produced by sea-water, whatever the cement may be (235), particularly if good concrete is permanently placed under low waters. In addition, this may lead to understand a series of facts difficult to explain, as for instance the different and sometimes opposite results as far as the behaviour of cements of the same type, class and quality in sea-water is concerned; the different behaviour of one and the same cement when other variables -for instance, porosity- are involved; the alternations in the order of the behaviour -from better to worse- of different types of cements when the porosity of their respective pastes -or some other factor, including the nature of the aggressive medium (5)- varies in different aspects.

And finally this may lead to the discouraging but interesting conclusion that it will not be possible lawfully to compare results of studies and research work done in common in different countries or institutions, as far as the real and practical behaviour of different cements in various conditions is concerned, if these studies and research work are not based on the knowledge, measurement and control of the porosity of the materials involved; or at least on the guarantee that porosity is acceptably similar in all the cases and consequently it is not a variable to be taken into consideration as such.

Otherwise, one cement with a lower "intrinsic" chemical resistance might behave better than another one with a higher "intrinsic" chemical resistance, provided that the porosity and penetrability of the material made with the former be lower than that of the similar material made with the latter. The same could be said of capillary suction and rise, of absorption (233) and of many other physical factors more or less related to porosity -not always well defined and differentiated, as for instance, hygroscopicity-, when external conditions are propitious to the influence of such factors.

Furthermore, it must be added that when corrosive dislocations are mainly produced by mere physical actions due to crystallization of salts from very concentrated solutions, the behaviour of the material involved depends much more on its physical structure and of its cement paste than on the chemical nature of the cement itself.

And nevertheless things are not always so simple as to generalize and accept without caution the preceeding observations. For instance, in the mentioned case of the Dead Sea, materials with a higher w/c ratio -and consequently with a higher porosity- have given better results, because they had more free space to accommodate with less or no dislocation the large amount of salts formed in a very complex process of crystallization (231).

In connection with the studies whose aim is to establish an order of behaviour of different cements in given experimental -laboratory or external field- conditions, it must be said that sometimes some not well known or uncontrolled influence may act. If the order obtained is that to be expected, then there is a tendency to minimize the importance of such influences, because one does not think about them, even if there is a certain probability that they may invalidate the comparison of results; but if the resulting order is different from that to be expected, then it is more probable that such influences are taken into account, and a greater importance is attributed to them (235).

Moreover, the order may depend on very peculiar circumstances. For instance, in the repeatedly mentioned case of the Dead Sea, mass concrete made with an ordinary portland cement behavies better than similar mass concrete made with a sulfate resisting portland cement, provided that the former is mixed with Dead Sea water instead of pure or distilled water. The explanation seems to be clear: in an ordinary portland cement richer in C_3A mixed with water containing a high concentration of Cl^--ions a great proportion of chloroaluminate is formed; whereas in a sulfate resisting portland cement poorer in C_3A, mixed with pure water, normal calcium aluminate hydrates are formed, which are able to experiment subsequent expansive complex reactions causing dislocation (231). At least one of the factors contributing to corrosion -that depending on the deteriorating reactions of C_3A- is minimized in the former case and manteined at its expected level in the latter case. In dependtly that probably some other factors may be involved, this particular result is obviously not to be generalized.

10.- METHODS OF TESTING

Much controversy has been developped and much more could be still promoted on the item of test methods for cement and concrete durability. Complication, poor effectiveness, difficulty to reproduce real conditions, to interpretate and evaluate results and to apply statistical methods to them, as well as the need of a scientific basis either for destructive or non-destructive accelerated testing procedures for durability in order to guarantee a minimum of reliability, reproducibility and simplicity of them, have been aspects clearly exposed (4). A relatively recent and detailled summary of testing methods for sulfate attack has been published in connection with the extensive work on sulfate resistance carried out by the U.S. Bureau of Reclamation (240).

Some studies have been conducted to put in clear if different methods of testing lead to the same or similar results, specifically as far as the behaviour of different cements is concerned. Such studies are interesting when comparing methods based on the same or similar (comparable) principles. The results of such comparisons not always are concordant. An interesting conclusion in this respect is that LE CHATELIER-ANSTETT-BLONDIAU method (241) and ASTM C 452-68 method lead to results which seem to be concordant (242). In the author's opinion this is precisely due to the fact that in both methods the condition of similarity of principles is accomplished. Nevertheless, such concordance not always is in good agreement with the real behaviour of cements in practice, or even in other different test conditions, as far as some types of cements other than portland are concerned; for instance, pozzolanic cements containing good silicious natural pozzolans (5) (241).

In general, the methods used to study, to test or to evaluate concrete durability are indirect methods in which some parameters of the material more or less related to its "durability" are considered. This is so because of the ambiguity of the definition of durability, and this in turn because of the empiricism which considers that effects are by fare more important than causes and mechanisms (3). In this sense the main difficulty in comparing results is that methods to assess durability may operate on various types of specimens of neat cement pastes, mortars or concretes, submitted to different aggressive media, in field or in laboratory, in very different experimental conditions. These methods may consider changes in weight, volume or length, strength or composition -detected in each case by chemical, XRD, IR spectroscopy, thermal analysis, etc.-, or they may be based on techniques of ultrasonic pulse time, optical microscopy, energy dispersive X-ray analysis, etc. Most of the methods show either weakness or drawbacks in measuring progressive deteriora-

tion of concrete, and according to their experimental conditions they may cause very variable degrees of damage depending on the different mechanisms of attack involved in them, either isolately or conjointly, simultaneously or successively (243). These appreciations are in agreement with the author's opinion on the difficulty and the risk to interpretate and evaluate test results, and, what is probably more important, to generalize and extrapolate them in all the cases to real practice.

The examples of the criticism made to different types of test methods could be innumerous, but the main of them refer to the adequation or inadequation of the methods to particular types of cements. One of such examples: some viewpoints on methods of testing sulfate resistance consider that in the case of slag cements those accelerated methods based on introduction of sulfate ions (gypsum) in specimens producing a deterioration "from inside" are not adequate. Otherwise, methods based on contact of specimens with aggressive sulfate solutions, which cause an attack "from outside" give reliable results as applied to slag cements. These results, when referred to specific conditions, may be related to the C_3A content in clinker and/or to the slag content in cement involved (244). But as far as the influence of the C_3A content is concerned, it must be taken into account that each of the polymorphic forms of C_3A in clinker behavies differently -as detailled elsewhere- in sea--water attack, as cubic form seems to be more sensible than tetragonal form. Independently of the little knowledge about the factors governing the formation of individual forms in clinker, the foregoing considerations claim for an idoneous method to determine the different polymorphic forms of C_3A. In this respect the fact that calculation of C_3A content by BOGUE's formulae gives results in general higher than those obtained by X-ray difraction -and also different than those resulting from optical microscopy- seems to be important. All these difficult problems are related to the limiting specifications for C_3A in cement standards (182).

In the author'opinion it should be clearly declared in each case what must be understood by "an adequate testing method": one favouring some given types of cements, though its results are not clearly in agreement with their behaviour in practice, or another one in which the situation is the contrary?. Independently of the fact that some methods seem to favour to some cements -and consequently to impair others- as far as their real performance in practice is concerned, the so-called "accelerated" methods of testing generally do not give sufficiently reliable results.

As far as accelerated methods of testing durability are concerned, based on increasing of tensions and stresses, temperature, pressure, concentration, porosity, percolation, surface of contact, surface-to-mass ratio; on decreasing of specimen size; on alternating (wetting-drying, freezing-thawing or immersion-emersion) conditions or renewal of aggressive media; on previous introduction of the attacking agent into the cement paste, etc., and in general on all what tend to enhance intensively and/or extensively the contact between cement or concrete and aggressive media, it must be considered if they really (technically and scientifically) represent natural or practical conditions, or if (on the contrary) their arbitrary empiricism introduces new disturbing factors not present in practice, which may alter the mechanisms and/or the kinetics of the real aggressive process. If so, the methods may affect (at least quantitatively when not also qualitatitively) the results, so that no realiability can be expected (3) (245). Other aspect concerns the relationships between the properties and parameters observed or measured in tests, the processes (mechanisms and kinetics) taking part in the attack and the damaging effects produced, as these latter, for given processes even expansive and disruptive in nature may be absent, depending -often mainly- on real and testing conditions and/or materials, rather than on processes themselves (245). All this may have important consequences when comparing behaviours of materials which otherwise -i.e., in practice- would perhaps show a different performance (3).

Methods have been proposed as being of general application to almost every type of cement using medium-size bars of normal mortar semi-immersed in magnesium sulfate solutions and measuring the stregth of both, immersed and exposed part (172). Nevertheless, accelerated tests generally do not provide a quantitative measure of the prospective service life of concrete, even under ordinary conditions. They are intended to evaluate rapidly in either absolute or relative terms the resistance of concrete to specified exposures and they may be helpful in comparing the prospective durability of individual concretes. The value of such tests depends on their degree of simulation of service conditions in practice, and on the extent to which they reproduce the responses of concrete in such conditions. They are needed because of the lack of possibilities to evaluate quantitatively those properties of concrete which control its response to environments, and consequently they must produce the same or very similar effects than those occurring in practice, on the same material as used in practice. Such conditions are always difficult to be accomplished (29). Approaches to it can be reached if accelerated methods of testing take into account: type and nature of the attack (weakening by leaching -lixiviation- or by chemical reactions involving ion exchange; disruption by volume changes due to crystallizations); the corresponding type of laboratory exposure; the criterium to evaluate the attack, so that laboratory results can give reliable indications on resistance of cements and concretes to specific aggressions, consistent with field experience (29).

To such extent it is so considered that suggestions have been made in the sense that even by theoretical considerations on sulfate attack on concrete, it should be possible to foresee its resistance, better than by results based on accelerated tests carried out in highly concentrated aggressive solutions (82). So, it is thought that the problem is to select those accelerated methods the "more adequate" in each case for each

particular purpose. For instance: it seems to be evident that in comparing the relative chemical resistance of different types of cements, elongation measurements are not always sufficiently indicative, and the same could be said about methos based on neat paste testing and/or on "internal" attack (172). More useful in this respect seem to be methods based on indexes of aggressivity defined as the ratio of flexural strength of prisms in aggressive media and in pure water at the same ages. And much more so if the age is not excessively short (better 180 days than 56 days, for instance). In this reaspect, as far as differential behaviour of several types of cements is concerned, relatively short periods of observation do not permit to establish any clear conclusion, as results are not sufficiently discriminative; even they may be contradictory (246). Improvements in results can be obtained if these ratios of strengths are represented in function of the logarithm of the age (days), or if a mean value of them at different ages is taken as representative of the comparative behaviour of different cements. In this respect KOCH & STEINEGGER method more or less modified (improved) in its application seems to be of more general use than are other methods determining only the cement resistance to calcium sulfate, either acting "from inside" or "from outside" (247). An interesting alternative developped to assess cement resistance to sulfate attack is that based on the measurement of the compressive strength of small cubes immersed in sulfate solutions at constant pH-value (9) (245). Another new method proposed seems to be rapid, giving reliable results which permit to evaluate the behaviour of different cements, so contributing to solve the problem of lack of correlation between laboratory testing and field performance of concrete (228).

The method of K&S permits to evaluate and interpretate the influence of C_3A content in portland cements (249) -always with the reserves and limitations exposed elsewhere in this paper-. It also permits to evaluate the influence of the slag content in slag cements, that of the cation in the case of different sulfates, that of the concentration in the attack by sulfates or sea-water, etc. Thus its results seem to be in agreement with logical considerations on the composition of portland and slag cements and, as far as such cements are concerned, the method seems to agree with appreciations and conclusions of other more controverted methods such as LE CHATELIER-ANSTETT-BLONDIAU and ASTM (247) (250). Other methods seem to be particularly appropriated to assess on cement resistance to sea-water attack (251).

Some of the more drastic tests for cement susceptibility to sulfates (gypsum) -for instance the mentioned LE CHATELIER-ANSTETT-BLONDIAU method- operate with hydrated neat pastes. Their results may depend on the degree of hydration of the paste at the time of mixing it with gypsum, which in turn may depend on the type and other characteristics of the cement. So, in order to operate always in the same or very similar conditions of very advanced (if not total) hydration of the cements, a method has been developped to accelerate hydration maintaining all the other experimental conditions of the test. Acceleration is provoked by chemical action of vibration and percussion on the hydrating paste (252).

Some other points of view on accelerated methods state that all of them based on acceleration procedures other than those consisting in the increase of the surface/volume ratio of the speciments risk of great deviations from real conditions and consequently their results may lead to highly erroneous interpretations and conclusions (25). This consideration advices that it is indispensable to compare every accelerated method with one or several slow methods during sufficiently long periods of time, before taking the rapid one into consideration, as the slower methods are generally much more in accordance with real results in practice (246). On the other hand, long term testing is recomended on concrete specimens submitted to semi-immersion conditions in saturated $CaSO_4$ solutions and/or in sea-water; lean concrete of high w/c ratio and rich concrete of low w/c ratio, as well as monthly renewal of aggressive medium are also recommended (25).

As far as accelerated test methods for alkali-aggregate reaction are concerned, one of them has been quite recently proposed (253). Those based on heating-cooling or wetting-drying exposure do not show a close correlation between their results in terms of expansion observed and alkali content of cements, other influencing factors being simultaneously involved. Other standard methods of testing show a similar lack of correlation between expansion measured and susceptibility of aggregates, all depending in addition on the ratio of reactive silica to available alkalies, as compared with the most unfavourable ratio (29).

In the author's opinion all these facts put the question of wether specifications for low-alkali cements in cement standards and those for aggregates in some of the corresponding standards are sufficiently justified or not, specially the former ones implying harder and antieconomical conditions in cement manufacture, particularly nowadays when sparing energy and reducing fuel consumption in seriously recommended.

Finally, in order to overcome the insuficiency of present methods of testing durability in general, several proposals have been made -and are continuously made- to elaborate common test methods based on general (scientific and practical) principles, real experimental conditions, reliable results easy to evaluate and interpretate, to which statistics can be applied. In these aspects, pessimism due to the difficulty of the task, and optimism based on the work done and now running have been manifested (254) (255).

11.- STANDARD SPECIFICATIONS

Most countries produce and standardize cements resisting to some type of attack: sulfate attack (gypsum and/or other sulfates), sea-water attack, carbonic acid attack, etc.. Some other countries tend to this type of standardization and so in recen time Japan, among others, has included in the Japanese portland cement standards those corresponding to the chemical composition of sulfate resisting cements, comparing their requirements whith those of many other foreing standards (256).

In general, the problem of standard specifications for chemically resisting portland cements is linked to that of the recommendations for using one or another type of portland cements, or of cements other than portland, in each particular case of foreseable aggressivity. This is a point in which some confusion may be created due to differences in criteria of different countries, not precisely based on scientific and/or technical viewpoints, but sometimes on commercial interests.

In the case of portland cements it seems to be a general qualitative agreement as to the conditions to be fulfilled for their chemical resistance to sulfates or to sea-water attack, for instance. Something different occurs in the case of cements other than portland, as countries posessing natural pozzolans claim for the use of pozzolanic cements, whereas other countries lacking of such pozzolans invoke the use of fly-ash cements, and finally other countries with traditionally produce and use successfully blast-furnace slag cements consider them as the more adequate. This may create confusion to an impartial observer and much more so because each of the mentiones cements has properties which make it at least partially apt to be used in some given cases of aggressivity. The confusionism may arise when trying to generalize and extrapolate the use of one or another of such cements in all the instances.

It is very difficult to explain, among others, the fact that very large variations are observed in the behaviour of good concretes made with more o less sulfate resisting portland cements in contact with (sodium) sulfate. On the other hand, such laboratory results agree with field results. Moreover, some pozzolans with low water requirement in pozzolanic cements of moderately low C_3A and C_4AF contents improve substantially the behaviour of cements in sulfate attack. All these facts lead to question the perhaps excessive importance attributed to the more stringent limitations of C_3A and C_4AF contents, as far as the sulfate resistance of portland cements is concerned (182) (204).

In a recent general report on sulfate resistance of cements, concerning last works published up to 1977 it is stated that, according to the litterature, sulfate resisting portland cements should be used when sulfate resisting concrete is required; that phase composition of cements does have a significant influence on sulfate resistance of concretes, though not so much as the bibliography and the standards indicate (1).

In the author'opinion this is an important point for consideration as, generally speaking, some papers probalby tend to overestimate some experimental results, and some standard specifications tend to secure and to guarantee -perhaps too emphatically- the performance of some cements in some aggressive conditions. If so, this leads to consider once more if the (excessive?) rigour of some standard specifications is always sufficiently justified. And so much so as the problem of limitating the C_3A content of portland cement in standards to make it more resistant to sulfate attack may have implications in cement manufacture, cement properties and cement behaviour, other than those concerning durability. So, the limitation of C_3A content in cement standards should be considered very carefully (182). On the other hand, limitations of C_3A and/or of $x\,C_3A + y\,C_4AF$ and/or C_3S in standards do not consider influences of clinker burning and clinker cooling conditions (257).

From practical points of view, as far as cements resisting sulfate attack are concerned, it is obvious the much emphasis put in aluminate phases. Nevertheless, ferritic phases are also affected, and this has been also emphasized in discussing the chemistry of sulfate attack in terms of differences in C_3A and ferrite phase contents of cement clinkers (8) (240). In the author's opinion this leads to the conclusion that specifications concerning portland cements resisting sulfate attack must take into account not only the C_3A content, but also the C_4AF content, either as the bare sum or as some sort of "composed" sum. In fact, portland cement resistance against attacks of different degree has been expressed in terms of chemical and/ /or potential composition. More particularly in terms of the A/F ratio and in terms of C_3A and/or $(xC_3A + yC_4AF)$ -and some times C_3S- contents. (6) (23) (257). (Concrete Yearbooks, ACI Manuals of Concrete Practice, DIN 1164 Standards, ASTM, Soviet, Spanish, etc. Standards). Consequently, portland cements low in all of the mentioned parameters are considered as being adequately sulfate resistant, and in each case different specified limits for C_3A and/or for the ("composed") sum of C_3A and C_4AF, depending on country standards and local conditions as mentioned are fixed. For instance, resistance to sea-water attack is defined in the French specifications by the following two prescriptions: $C_3A \leq$ 10 % and $C_3A + 0.27\,C_3S \leq 23.5$ %. Other similar prescriptions are imposed by several other standards; those of ASTM are: $C_3A \leq 8$ % and $C_3A + C_3S \leq 58$ %. Different limitations of C_3A in norms seem not to be always fully justified, as it has been broadly observed that there is no close correlation between C_3A content of portland cements and their resistance to sea-water attack (25). A closer correlation seems to exist between C_3A content and resistance of portland cements to gypsum attack (gypsy soil waters). So, portland cements resistant to soil waters with sulfate contents above certain limits must be low in C_3A and C_4AF, the

maximum contents of them being variable with national standards. As in the previous case they affect to the C_3A content and to a simple or "composite" sum of C_3A and C_4AF. For instance, ASTM and French Standards specify $C_3A \leqslant 5$ % and $2\,C_3A + C_4AF \leqslant 20$ %; and Soviet and Spanish Norms prescribe $C_3A \leqslant 5$ % and $C_3A + C_4AF \leqslant 22$ % (6) (25). All these limitations, particularly those concerning C_3A are always subjeted to the criticism based on the decisive influence of the different crystalline forms of C_3A in cement, on durability (205) (258). So, it seems not possible to consider the attack on C_3A without discrimination. The various forms of it still identified and characterized: cubic orthorhombic and tetragonal react in different way with sea-water. Cubic C_3A gives more ettringite, gypsum and brucite, whereas tetragonal C_3A induces the formation of more MSH than the other two forms in the cement paste as already mentioned, (182) (205).

In the author's opinion the difference is important, as it may affect even to the qualitative nature of the attack: gypsum, ettringite and brucite formation imply mainly a disruptive action by expansion due to crystallization pressure and crystal growth, whereas the formation of non-hydraulic magnesian tobermorite compounds by cation exchange implies a lixiviating action causing softening and weakening of the structure of the cement paste.

As far as limitations of C_4AF in one or another form are concerned, they seem to contradict in any way the statement that portland cement rich in iron compounds resist better the magnesium sulfate attack (9).

"Synthetic" portland cements obtained by mixing pure phases have shown that for a moderate content of C_3S (50 %) and even for a low content of C_3A (1 %) the susceptibility of the cement is higher (its behaviour is worse) when $2\,C_3A + C_4AF$ exceeds than 20 %. The performance is improved if the C_3S content is lowered to 35 %. Nevertheless, great differences have been observed between behaviours of laboratory cements obtained as mentioned and industrial cements (257), due to minor components (manganese, phosphorous, titanium) absent in the former (27) (257), as stated elsewhere in this paper. Such differences cannot be neglected when stipulating values and limitations of potential composition of portland cements in standards, as they may qualify quite differently the same cement according to a given limitaing specification. For it, results obtained with industrial cements seem to be much more independent -or even contradictory- as related to those to be expected from "theoretical", "rational" or "logical" considerations. Among industrial cements such differences are not only due to minor components, but also to the manufacturing processes -burning, cooling, etc.-, which determine the glassy or crystalline condition of C_3A and other aluminate and/or ferrite solid solutions (257). So, specifications based on calculated potentital composition are of little significance, as similar compositions may correspond to different behaviours. The question arises of wether these differences based on minor components and on manufacturing process peculiarities, generally not taken into account in standards, may explain some or many of the sometimes apparently confuse or contradictory results. The author's opinion in this respect is inclined to be moderately affirmative.

Cements containing slag, or natural pozzolan, or fly-ash, generally in high proportion -much higher in the case of slag cements (always over 50 %) (25) may be adequate as far as durability is concerned. The mechanism by which such materials are operative may be common to all of them or specific of each of them. The common mechanism is the dilution of the clinker portion of cement, and hence that of C_3A and C_4AF, and the different nature of the calcium silicate hydrates formed. The specific mechnisms are based on the hindering of the formation of $Ca(OH)_2$ saturated solutions -and hence that of highly basic C_4AH_{13}-, as well as the fixation of (almost) all the $Ca(OH)_2$ in the case of pozzolanic and fly-ash cements (23) (184): and on the much less $Ca(OH)_2$ formed in the case of blast-furnace slag cements, which consequently form much less gypsum and secondary ettringite (59). So, the performance of slag cements in saline attack (chlorides, sea-water) is in general much better than that of portland cements, and so much so the higher their slag content (162). But on the other hand, such slag cements perform well in sea-water provided that concretes are fully immersed; not as well if concretes are (partially) exposed to air (25).

In a similar way to what happens with limitations established in cement standards for composition of portland cements, the limits established to fix the aggressivity degree of sulfatic water and soils are very variable and depend on countries and organizations. Those of DIN 4030 and of ancient CEMBUREAU Working Party, as well as those of TGL Standards (DDR) seem to be sufficiently explicit and detailled (23). It can be said in a summarizing and general manner that attack on concrete is sure and its consequences may be important if one or several of the following conditions are fulfilled: $pH \leqslant 4.5$; aggressive $CO_2 > 60$ mg/l; SO_4^{2-}-ion concentration > 3000 mg/l.

12.- CEMENT

One of the main problems in durability of concrete is that of the more suitable cements for a given type of attack depending on aggressive media and conditions. In a general maner it can be said for instance that, independently of the well known conditions to be fulfilled by any concrete to resist better whatewer type of chemical attack, neither high-early strength cement nor ordinary portland

should be used for concrete resisting sulfate attack, owing to the two more important mechanisms of deterioration: lime leaching and expansive sulfoaluminate formation, depending on the nature and amount of sulfates (calcium, magnesium, sodium, ... with very different solubilities in the ratios of 1 to 150 to 200) and on the nature and composition of the cements (170). On the other hand, sulfate resisting portland cement or better, blast-furnace slag cements or pozzolanic cements should be used (170). In some special cases supersulfated cements or high-alumina cements are more adequate (170). The same conclusion has been reached as to the behaviour of sulfate resisting and moderate heat portland cements and fly-ash cements in contact with magnesium sulfate solutions (169).

As almost always, not only chemical but also physical factors are involved in durability, and hence the difficulty and the incertitude of some results in laboratory testing and in practice. For instance, the importance of the age of test pieces (or that of real concrete) -i.e., the degree of hydration and hardening-, as well as the influence of testing conditions has been revealed by studies made in Germany (as well as in many other countries) on concretes exposed to sea-water attack at Wilhelmshaven. Conclusions were drawn contrary to real practical results, as far as the behaviour of portland and slag cements containing pozzolanic ("trass") materials. Premature erosion on concretes of low maturity -so much so as pozzolans behavie in general as inerts at early ages in hard thermal and weathering conditions-may explain the abnormal results observed (259). So, the hardening rate of the cement -as well as its curing conditions- as factors determining the early strength, have a great influence in the performance of the cement, independently of its chemical nature. This is the reason why some slag cements show sometimes a worse behaviour, and also why the performance of pozzolanic and slag cements specially -but in general of every cement- is better the longer the curing period in adequate curing conditions (2) (260).

When attempting to correlate the chemical nature of the cements, either in terms of their chemical analysis or of their calculated potential composition, (in the case of portland cements) with their performance in aggressive media, attention must be paid to the nature and proportion of the possible added materials, as well as to the chemical nature of the clinker. In fact, additions may modify the fineness (granularity, granulometry) of the resulting blended cements as compared with that of the corresponding portland cements, so that the former may give more capillary adsorptive -and hence less durable- pastes in function of their higher content of finer particles than the latter (261). But, on the other hand, additions may afford chemical properties and actions in benefit of a better durability.

The behaviour in sea-water of synthetic slag cements obtained from synthetic clinkers with various contents of C_3S and C_3A and slags with various C/S ratios -basicities-, mixed in different proportions, shows that the influence of the clinker composition is greater than that of the slag. The clinker influence depends on its contents of C_3S and C_3A, and that of the slag on its C/S ratio and/or on its A content. In both cases the relationship is inverse. The influence of the cement itself depends on the ratio slag/clinker, particularly for ratios lower than 65 %. Moreover, it seems that for higher ratios slag cements resist sea-water attack regardeless of the compositions, either of clinker or of slag (262).

One reason for it may be that the cation exchange of Mg by Ca between $C_xS_yH_z$ and sea-water to give a non-hydraulic $C_x . M_x . . S_yH_z$ (in the limit $M_xS_yH_z$) is much more restricted in the case of slag cements than in the case of portland cements (15) (208).

On the other hand, slag cements are also more resistant than portland cements to saline and thermal water containing alkaline and magnesium sulfates and chlorides, as salinity accelerates the development of their strength. They resist also better to carbonic attack, fairly rapid on them but not progressing (263). To saline solutions of $MgCl_2$, $MgSO_4$ and mixtures at different temperatures slag cements behavie much better than sulfate resisting cements, and these better than ordinary portland cements (264).

Nevertheless, some doubts have been expressed as to the resistance of slag cements to sulfate attack when the Al_2O_3 content of the slag is high. Increasing substitutions of SiO_2 by Al_2O_3 in artificial vitreous slags reveal increasing drops in strength of laboratory slag cements. Such cements with normal blast-furnace slags perform considerably better when the slag content increases from 35 to 50 %, particularly if their fineness increases too (179). Moreover, cements with 50 % of slag content seem to be able to resist sulfate attack if the alumina content of the slag is low and the C_3A content of the clinker is lower than 10 %. This means that a normal portland cement clinker may be used to produce a sulfate resisting cement provided that at least 50 % of a slag poor in Al_2O_3 is added to it and the mixture is ground to sufficient degree of fineness. This also means that the chemical composition of the slag and its proportion in the slag cement condition the behaviour of the slag cement in sulfate attack more than does the clinker nature (265). This, as applied to normal (commercial) slag cements as far as their resistance to sulfate attack is concerned, seems to be at least partially different from -in opposition with?"-similar considerations as applied to special (synthetic) slag cements -both slag and clinker being synthetic- as far as their resistance to sea-water attack is concerned, as above mentioned (262). Nevertheless, much lower contents of slag -about 10 to 15 %- have been invoked as being beneficial to the sulfate resistance of portland cements made with clinkers with up to 7 to 9 % of C_3A (266).

Portland cements with low C_3A and/or low ($x\ C_3A + y\ C_4AF$) content -limits depending on country stand-

ards- are considered resistant to sulfate attack (23) (25) (184) (257). This chemical resistance of portland cements has been attributed to the formation, on their hydration, of more complex hydrates with a more resisting structure, containing simultaneously lime, alumina and silica, or lime, alumina, iron oxide and silica (267) (268).

In connection with the increase of sulfate resistance of portland cements, improvements have been achiev ed by using additions containing phosphorous (P_2O_5) and fluorine (electro-thermo-phosphorous slags) to clinkerizing raw mixtures. The effect is the lowering of both C_3A content and C_3S/C_2S ratio, to a considerable extent (269) (270). Very special cements highly resistant to sulfates are those portland cements containing barium in proportions of about 4 to 6 % of BaO (271).

An interesting observation has been made concerning the generally accepted resistance of cements with A/F ratios lower than 0, 64 and consequently exempt of C_3A, at least "nominally" (FERRARI cements). It is considered that Na_2O not combined as sodium sulfate may form in the clinker, as is well known, NC_8A_3, but according to:

$$3\ C_4AF + N + 2\ C_3S \longrightarrow NC_8A_3 + 3\ C_2F + 2\ C_2S$$

the consequence is the lowering of C_3S content in favour of C_2S, and that of C_4AF in favour of C_2F, with simultaneous formation of an unexpected and undesirable phase (in general $N_xC_{(9-x)}A_3$ in which $x > 0.3$), which is susceptible to sulfate attack. This may lower the sulfate resistance of cements free from C_3A, particularly when high Na_2O and low SO_3 contents are present in raw material and raw mixes. This could also afford an explanation, at least in some cases, of the abnormally bad behaviour of some cements free from C_3A (272).

Really it has been but very little advanced in deciding whether portland cements with lower contents of C_3A -eventually with lower contents of C_3S too- or cements other than portland -slag cements, pozzolanic cements- behavie better or worse when exposed to sulfate or sea-water attack. A brief but very significative discussion has been developped ten years ago (27). According to it, independently of the nature and concentration of the sulfate(s) involved and of the details and circumstances of test pieces and test procedures, etc., the behaviour of "pure" portland cements or that of "composite" cements will depend, other things being equal or similar, on the composition of clinkers and additions. Variability observed -even in terms of contradictory or not logical results- is fatally due to the fact that neither clinkers nor additions are chemically pure and easily defined compounds and that finally, cement chemistry is far from being a chemistry based on pure substances reacting through simple and well defined processes obeying to well known kinetics and stoichiometry. So, not always the experimental results permit to accept that, for instance, portland blast-furnace slag cements perform better than portland cements or conversely (27) (273).

But in general, systematic studies on portland cements with null (0 %), medium (about 8 %) and high (about 12 %) contents of C_3A, as well as on slag cements containing (relative) high (75-80 %), medium (65 %) and low (50 %) slag contents have clearly revealed that, for example, the attack by sodium and magnesium sulfates, either alone or containing sodium chloride or sodium bicarbonate, is always related to the amount of ettringite formed in each case. The better behaviour of the cements is inversely related to the content of C_3A of portland cements and directly related to the slag content of slag cements (214).

In the case of sulfate resistance in general many good arguments have been invoked in favour of the better behaviour of pozzolanic cements (and slag cements). Surveys of them have been afforded (274) (275) emphasizing different possible actions. Thus the fixation of Ca $(OH)_2$ with formation of more complex hydrates (267) (268) (276). Or the higher protective action on susceptible alumina compounds exerted by impervious films of different calcium silicate hydrates (204) (277) -with higher S/C and S/A ratios in the case of pozzolanic cements and with higher S/C and lower S/A ratios in the case of blast-furnace slag cements- (15). Protection also causes retention of lime from leaching (274). Or the more abundant gels lowering ionic diffusion (particularly that of SO^{2-} -ions) through pastes (278) of lower penetrability and higher impermeability (279) (280), despite their higher porosity and water demand (156) (274). Emphasis has also been put on the instability of ettringite in the presence of pozzolans (281) and in the absence of $Ca(OH)_2$ (274).

All these explanations in addition to some others (268) (277), seem to show that not only a mechanism alone of the several possible is always responsible for the higher resistance of some cements to sulfate attack, but probably various of them acting together are responsible in most of cases.

From a strictly chemical point of view sea-water attack should be stronger on pozzolanic cements than on portland cements. The reason could be that sea salts in bulk, and more particularly magnesium salts, cause a substantial decrease of pH in saturated solutions of $Ca(OH)_2$ up to 9.5, unless solid $Ca(OH)_2$ in excess or hydrated cement paste are present in contact with solutions or sea-water. When hydrated paste is that of a pozzolanic cement, excess of $Ca(OH)_2$ may not be available, and pH may not be maintained at a high value (282).

Pozzolanic cements with 25 to 35 % of pozzolan (or an adequate fly-ash instead) and slag cements with no less than 65 to 70 % of slag -considered as equivalent to portland cements with less than 3 % C_3A and 5 % Al_2O_3- may be estimated as sulfate resisting cements, specially if their clinker component corresponds to that of a sulfate resisting portland cement (26). Another similar statement indicates that for sulfate contents in water higher than 400 mg/l or in soils higher than 300 mg/kg, portland cements with less than 3 % C_3A, slag cements with high content of slag (25) -more than 70 % (162)- and slag cements from

clinker with less than 3 % C_3A and slag with less than 13 % Al_2O_3 are considered as being resistant (283).

Slag cements submitted to sea-water attack form much less secondary ettringite than portland cements due to the much lower content of $Ca(OH)_2$ in their hydrated pastes (1) (59). The same is valid for pozzolanic cements through a mechanism of fixation of $Ca(OH)_2$ (58).

It has been stated that differences in behaviour of more resistant pozzolanic cements to sulfate attack are observed, depending more on the quality of the pozzolan than on the clinker composition as referred to ASTM II and V types of portland cements (8) (240). On the other hand, fly-ashes considered as pozzolanic materials may afford higher resistance to sulfate attack. But it has been also claimed (284) that some fly-ashes act in the reverse sense, so that specifications of requirements for fly-ashes are needed, as for instance those of ASTM. Moreover, it has been observed that when fly-ashes act positively, the increase in sulfate resistance is greater the higher the content of their fine fraction. This leads to think in a physical effect of enhanced compacity in the cement paste caused by the fly-ash, superimposed to its pozzolanic -chemical- action (8). This is also in the line of some patents of sea-water resistant concretes of low porosity, made with very finely ground cements.

Favourable modifications in the structural compactness of the cement pastes may be achieved by adding "water (soluble) glass", either to portland or to slag cements. In the case of the former significant amounts of $Ca(OH)_2$ are present in their pastes, which facilitates a marked attack by acid waters and soil waters containing alkali and earth-alkali sulfates and chlorides, owing to the well known formation of ettringite due to water and ionic penetration. In the case of slag cements no $Ca(OH)_2$ is present in their denser pastes. In both cases additions of water glass contribute to densify the cement paste so difficulting the penetration and diffusion of aggressive agents (285).

Sodium chloride accelerates the hydration of slag in slag cements, so contributing to a more rapid formation of abundant tobermoritic gel phases of lower basicity, and to reduce the porosity and permeability -penetrability- of the cement paste. This is a reason why in some cases, as for instance, that of cements for boring oil-wells -i.e., used at higher temperatures and pressures- their performance is better when mixed with salt solutions -specially sodium and magnesium chlorides- similar to those found in the ground, to which oil-well cements must resist (286).

The chapter dealing with the behaviour of cement pastes modified by the presence of synthetic resins, plastics polymers and in general organic materials added to cements or concretes would be extremely wide if treated. This is not the case now and here, but by the way it could be said that the performance of such differrently modified binding materials is very variable depending mainly on the behaviour of the organic modifying materials, as far as its alkaline hydrolisis is concerned, in the presence of cement alkalinity in aqueous pastes (287). The performance may be no good, unless the material is resistent to the hydrolitic action of $Ca(OH)_2$ (288).

The improvements afforded by heat treatments (steam curing) of cements at normal pressure and specially at higher pressures (autoclave) to their sulfate resistance is greater for cements originally not highly resistant, i.e., for those having a fairly high content of C_3A (27). Hydrothermal treatments modifying the composition and the structure of hydrates formed may also alter the behaviour of cement pastes against corrosion. Silicate hydrate phases may undergo different actions, not only due to their higher or lower basicity and density, but also depending on their higher or lower specific surface. Less basic tobermoritic calcium silicate hydrates of higher density have also a higher specific surface than the less dense and more basic ones. This implies a different behaviour, for instance as far as carbonation is concerned. This may also affect the nature of the more or less protective films formed in the attack by alkaline or magnesium sulfates; this explains the better behaviour of the more basic calcium silicate hydrates resulting in hydrothermal treatments of cements when in contact with such sulfates (60).

As special cements presenting the main advantages of portland cements and high-alumina cements (with none of the major inconvenients of either of them) as far as general chemical resistance is concerned, the so-called "alumina-belite cements" have been proposed (289). These cements are defined by a special lime-saturation factor and by silica and alumina moduli corresponding to ordinary portland cements. Their prevailing phases are CA, β-C_2S and $C_{12}A_7$. Other phases as $(CA)_3\overline{CS}$ and $(CS)_2\overline{CS}$ are considered responsible for the increased chemical resistance of such cements manifested in sodium, calcium and magnesium sulfate solutions, as well as in sea-water (chlorides). Thus, these cements have been proposed for sea-water works and dam construction (289). On the other hand, it has been recently stated the very good performance of high-alumina cements in soil water and sulfate attack (25).

It would appear that in sulfate attack at early ages the type of cement is less significant than the quality of the concrete. Nevertheless, the use of a sulfate resisting cement is even then better, particularly if concrete quality is not exceptional, though it is doubful if this assertion is equally valid for longer term behaviour of such cements in the same conditions (26).

Anyway, one of the more efficient measures to prevent the rapid and intense effects of a chemical attack (whatever it may be) on cement and concrete is to avoid a premature contact of aggressive media with the material, when this has not yet reached an adequate degree of hardening (2) (259) (260).

When relating sulfate resistance of portland cements to their potential calculated C_3A contents, observations have been made on the convenience of correcting

cement analysis for minor oxides of titanium, phosphorous and manganese, as the criteria (limiting values of C_3A) to separate cements of good or poor sulfate resistance may substantially vary (27). Anyway, cement composition and particularly C_3A content is much more important -with the cautions and reserves exposed elsewhere in this paper- in intermediate and lean concrete mixes than in rich mixes, according to the previously exposed (26). This is once more a proof of the greater importance of compacity as a physical factor, as compared with the chemical composition of the cements (27). Better resistance to magnesium sulfate attack is offered by portland cements of high iron-compounds content (9). This seems to contradict in part the standard limitations affecting C_4AF content.

In addition to classical opinions of the reasons for higher resistance of cements other than portland to sulfate attack, an original hypothesis has been advanced according to which the scarcity or the lack of calcium hydroxide in hydrated pastes of pozzolanic, slag or high-alumina cements induces the formation of non colloidal and non expansive ettringite. The ultimate reason seems to be the lack of a double-layer-type interparticle repulsion, otherwise produced by a large water adsorption (187).

Expansive cements have been proposed as more adequate to resist sulfate attack, due to their higher content of calcium sulfoaluminate hydrates and more particularly ettringite, as monosulfate is susceptible to react with sulfates to form at longer terms secondary (expansive) ettringite causing cracking:

$$C_3A\bar{C}\bar{S}H_{12} + 2\,C\bar{S}H_2 + 16\,H \longrightarrow C_3A(C\bar{S})_3H_{32}$$

The behaviour is much better in the case of expansive (shrinkage compensated) cements made with ASTM type II or type V, than in the case of those made with type I cement clinker,

Anyway, for equal C_3A content expansive cements behavie better than ordinary portland cements from the same clinker, and so much so the lower the C_3A content in each case. The different behaviour of different expansive (shrinkage-compensated) cements in sulfate attack is probably to be related to Al_2O_3/SO_3 ratio, i.e., to the different contents of reactive alumina in them. Reactive alumina is defined as total alumina minus "relatively" inactive alumina (that combined as C_4AF or in solid solution with calcium silicates), minus alumina fixed in the form of ettringite by SO_3 of cement, on hydration. Reactive alumina may act on ettringite previously formed to convert it in monosulfate, ready to form the undesirable secondary ettringite at longer terms.

$$C_3A(C\bar{S})_3H_{32} + 2\,C_3A + 4\,H \longrightarrow 3\,C_3A\bar{C}\bar{S}H_{12}$$

When desintegration of concrete has an internal origin due to attack by sulfates contained in the aggregates -exceptionally by excess of gypsum in cement too- a general realionship seems to exist between expansion, C_3A content of the cement and total SO_3 present in concrete, including that of the cement itself. Nevertheless, the many exceptions as far as the content of C_3A is concerned, indicate that other factors of the cement composition may have a great influence on the sulfate resistance of cement. The influence of C_3A is more evident for the higher concentrations of SO_3 in concrete. Even in this type of attack pozzolanic cements show better performance (260).

In the case of alkali-silica reaction, and consistent with the explanation generally accepted for the corresponding expansive process (27) (122), the use of adequate very finely ground mineral admixtures and reactive materials in concrete, in addition to, or in substitution of a part of cement (which is equivalent to add pozzolanic materials to clinker), may avoid or reduce the expansive effects of the reaction. So, natural pozzolans (trass) blast-furnace slags and fly-ashes -and even cristobalite and silica glass- in cements may be effective, as well as true expansive materials contained in natural rocky reactive aggregates when finelly ground to form powders of high specific surface and mixed with concrete (21) (27).

As far as acid attack by waters with pH-values lower than 4.5 is concerned, it is always strong on any type of cement, so that whatever this may be, it behavies more or less in the same manner, i.e., bad (283). Nevertheless, waters with pH-values higher than 6 do not cause strong deterioration on ordinary portland cements, and high-alumina cements without any protection may resist waters with pH-values between 4 and 6 (25).

Pozzolanic cements and slag cements are considered to be more resistant to lixiviation of $Ca(OH)_2$ caused by soft waters (1) than are portland cements, particularly if these are rich in C_3S (25). Portland cements are not adequate for very pure waters or for mineral or aggressive CO_2 containing waters (25), specially if these are considered as very strongly or strongly aggressive ones (23). High-alumina cements perform well for extremely aggressive pure waters, as some spring waters may be (25). But recent conclusions show that slag cements with higher contents of slag resist much better than portland cements intense attack produced by continous and prolonged carbonic acid action (88).

Among the many physical factors influencing the durability of concrete, in addition to the chemical and mineralogical composition of the cements and partially depending on it, it must be mentioned the porosity of the paste, partially depending on the fineness of the cement as well. Both, composition and fineness do in fact determine the strength characteristics of the cement paste. Furthermore, the porosity is in a narrow relationship with the strengh (290) (291), and in turn with the durability of hydrated pastes.

All these relationships may be even more complex due to the fact that (total) porosity, size of pores, pore-size distribution and kinetics of pore formation in cement pastes -influencing their permeability and penetrability- depend to some extent on the chemical and mineralogical composition of the cement, as men-

tioned. Thus, total (integral) porosity of portland cements high in alumina is greater than that of portland cements of lower alumina content, due to a slightly higher formation of contration pores. Moreover, at 28 days of hydration the total porosity in pastes of portland cements richer in C_3S is lower than that of cements richer in C_2S, though large pores and gel pores are more abundant in the former case than in latter case. On the other hand, variations in pore-size distribution take place along the time, so that at latter ages the pore content in the range of 100 to 1000 Å diminishes. This occurs mainly and sooner in cement pastes of portland cements rich in C_3S and C_3A.

This interdependence between cement composition, cement fineness and pore structure of the paste is even more complex due to the influence of other variable factors on the paste itself and on concrete, such as w/c ratio, concrete compaction, concrete curing, etc. This is another factor contributing to difficult the understanding of concrete behaviour in chemical attack.

The influence of the voids and pore systems of concrete, as well as their modification caused by admixtures (air-entraining agents) is also discussed when dealing with de-icing salts and chloride attack (1). Optimum amount of micro-voids, void distribution and distance between voids seem to be necessary for an adequate resistance of concrete (21).

Anyway, it seems to be clear that the nature and structure of the cement paste, as far as its porosity and chemical composition are concerned, determine its permeability and also the penetrability of salts and different ions in it. Details of these influences on ionic diffusion and penetration are also given when dealing with de-icing salts attack (155).

13. - FINAL CONSIDERATIONS AND FUTURE PROSPECTIVES

The obvious considerations derived from the foregoing exposition, from the General Introduction onwards, are: a) that whatever the definition and limitation of the subject on cement and concrete durability, this is a very complex matter not always possible or easy to simplify; b) that many variable factors of very different nature are almost always indissolubly involved in durability problems; c) that the influence -isolated or superimposed actions and effects- of these factors not always are either quantitatively -or sometimes even qualitatively- in a clear and direct relationship with the factors themselves.

As a consequence, empiricism has predominated in a good deal of the research work carried out on durability, and confusing or contradictory results not easy to explain or even erroneous have been obtained. These facts, in addition to repetitive tasks not always conducting to the same or similar conclusions, may explain the relatively poor progress reached in the studies on durability, as compared with the effort made to achieve them. This would seem to be a pessimistic appreciation.

So, when prospecting the future of cement durability research one might express a hope and a wish, rather than make any sort of prophecy or prediction, which is always risky.

Remembering the considerations in the General Introduction of this paper, the author's hope is that research, from now on, progress along rational paths on basic scientific foundations, avoiding empiricism as much as possible. Interdisciplinary cooperation is needed, as physical, physicochemical and chemical aspects are involved in cement and concrete durability, so that all the possible different ideas and points of view must be taken into due consideration to cover all the many different features of the problem.

Fundamentals of inorganic chemistry of silicates, colloidchemistry, physico-chemistry of surfaces, adsorption phenomena, electrochemistry, crystal-chemistry, etc., must be applied to cement and concrete corrosion studies in a systematic and rational manner. On the other hand, doctrine on physics of porous bodies and capillary systems, solid-state physics applied to complex solid macro-systems, etc., must also be focused in due way to such studies.

Intensive intercommunication between specialists in such disciplines working on cement is always absolutely necessary. Even better should be a previous consensus between them at world level to set the bases of a general scientific -long term- research project on durability. Within it, partial research programs should be developped by groups, either in parallel or complementarily, to put in clear the many dark points and unknowns still standing. In fact it should be necessary a sort of "normalization" or "standardization" of the research lines and procedures, in a similar way as it is admitted the convenience and the need of applying standard methods to test durability even empirically.

In these partial research programs it should be convenient to proceed by induction starting from the simplest problems in which as many variable factors as possible should be eliminated as such. Ideally only one variable factor should be investigated in each program, which in principle could be the cement in a series of programs, and the aggressive medium in another series of them. The result of the combination of both series of programs would be the knowledge of several orders of intrinsic chemical resistance of the various types of cements to different kinds of attacking chemicals and media in given -and successively variable- conditions. This or something similar depending on the priorities established in the research programs should be prior to attempt to draw dubious conclusions from work carried out under much more complex circumstances involving two, three or more variable factors.

Certainly, this does not correspond in principle to real situations in practice, in which many variable factors are involved in a very complex manner, overlapping each other. Certainly too that some specific and practical problems of durability require rapid and effective solutions easier to achieve in general

by empirical ways and means. But this must never be confused with what should be the "science of chemical attack on cement", as a part of a broader "science of building materials and construction". On the other hand, induction procedure obviously implies further consideration of all the many and important factors involved, which cannot be neglected and either overestimated or underestimated.

Of course, this is not the first time that similar ideas have been exposed, but in the author's opinion it is worth insisting on them once again, mainly because previous warnings in the same sense seem not to have been sufficiently taken into consideration.

It is clear that such a systematic research method may appear tedious and discouraging, as it is really arduous. Furthermore, everybody is inclined to think that his own ideas, projects and methods are a sort of panacea which may lead to total and general solutions. But really there are but two alternatives: one is to organize and "standardize" a scientific, rational and systematic work in common, so that each conclusion of it can be considered with a high level of probability as firmly established and having a validity the most general possible, without resorting to undue and enthousiastic extrapolations and generalizations; other is to continue as before and even now, which implies much (unprofitable) work and repetitive tasks dubiously efficient, with the risk to reach in this way the only valid conclusions already well known for many years ago and almostalways invoked, particularly when no other clear and interesting conclusionsare possible: the main if not the only property which determines the durability of concrete is a good compacity as a guarantee of low porosity, penetrability, absorption, capillary raise, etc.; and the main (elemental) rules to protect cement and concrete from chemical attack are those being in opposition to the well known ones normally applied to accelerate durability tests: to preclude or to reduce as much as possible the time and/or the surface (mass) contact between cement and aggressive media, either isolating and protecting the former or draining the latter; to neutralize or to weaken as much as possible the aggressive agent and the aggressive conditions before the former may enter in contact with concrete and before the latter -temperature, concentration, pressure, circulation, percolation, etc. - may act accelerating the attack.

But this sort of "rules of thumb" obviously true in a great part, do not solve the problem of durability as considered from the strict point of view of the chemistry of cement and that of the chemical attack on cement and concrete.

And finally, the author's wish is that if the foregoing ideas repeatedly exposed in one or another way in previous occasions are really valid, they be put in practice as soon as possible with the highest care, interest, enthousiasm, perseverance and efficiency.

REFERENCES

1. - R. HELMUT (1977), "Durability", Cem. Res. Progr., 195-230.
2. - A. MEYER (1974), "Anleitung für die Herstellung von dauerhaften Beton", Beton 24 (7), 261-264.
3. - J. PORRERO (1969), "Estabilidad química del concreto (Chemical stability of concrete)", Bull. Techn. INME, Central Univ. of Venezuela (Caracas), nº. 28, 5-36.
4. - O. VALENTA (1969), "General analysis of the methods of testing the durability of concrete", RILEM Symp. Durability of Concrete (Prague), Part I, A 3-28.
5. - J. CALLEJA and P. GARCIA DE PAREDES (1970), "Sobre los métodos para el estudio de la durabilidad de los conglomerantes hidráulicos (On the methods to study durability of cements)", Materiales de Construcción (IETCC-Spain) nº. 137, 51-77.
6. - J. CALLEJA (1971), "Código de buena práctica para hormigón resistente a sulfatos. Consideraciones sobre los cementos portland utilizables (Code of Practice for sulfate resisting concrete. Considerations on requirements for suitable port land cements)", Mat. de Constr. (IETCC-Spain), nº 144, 85-96.
7. - G.M. IDORN (1973), "L'antagonisme entre la nécessité de travailler aujour'hui et pour après-demain", CEMBUREAU (París), Oct. 1973.
8. - R. HELMUT (1976), "Properties of fresh pastes. Durability of hardened pastes", Cem. Res. Progr., 159-183.
9. - R. HELMUT (1975), "Properties of hardened pastes", Cem. Res. Progr., 97-130.
10. - R. HELMUT (1974), "Properties of hardened pastes", Cem. Res. Progr., 93-132.
11. - J. JAMBOR and V. ZIVIKA (1976), "Forschung saufgaben auf der Gebiet der Korrosion von Beton und Betonkonstruktionen", Inz. Stavebny 26 (10), 482-487.
12. - S. PRUDIL (1976), "Ein Betrag zur allgemeinen Darstellung des Verlaufs der Betonkorrosion", Mono/Slovak/Ochr/Stavebn Diela Koroz., 24-31.
13. - F. M. IVANOV (1976), "Methodologie der quantitativen Untersuchung der Prozesse der Betonkorrosion", Mono/Slovak/Ochr. Stavebn Diela Koroz., 73-79.
14. - J. JAMBOR (1976), "Die Einschätzung der Aggressivität des Mediums und der Widerstandfähigkeit des Betons", Mono/Slovak/Ochr. Stavebn Diela Koroz., 105-113.
15. - M. REGOURD (1975), Ann. ITBTP, nº 329, 86-102.
16. - M. REGOURD, H. HORNAIN and B. MORTUREUX (1978), "Microstructure of concrete in aggressive environments", 1st. Int. Conf. on Durability of Building Materials and Components, Nat. Res. Council Canada, Ottawa 1978.
17. - O. VALENTA (1970), "Water permeability and penetration into concrete", Stavebnicky Casopis (Slovenskej Akademie Vied-Bratislava), XVIII 8, 626-639.

18. - O. VALENTA (1972), "Basic problems and conditions of long term performance of materials and structures", NBS Special Publ. 361, Vol. I Proc. Joint RILEM-ASTM-CIB Symp., May 1972.
19. - O. VALENTA (1969), "Kinetics of water penetration into concrete as an important factor of its deterioration and reinforcement corrosion" RILEM Symp. Durability of Concrete (Prague), Part I, A 177-193.
20. - O. VALENTA (1968), "General observations on the durability of concrete structures", Proc. V ISCC (Tokyo), 193-228.
21. - W. RICHARTZ and F. W. LOCHER (1977), "Cement Research in Germany", Cem. Res. Progr., 303-319.
22. - V. V. SAVENKOV and V. L. CHERNIAVSKII (1974), "Investigation of the solubility of calcium hydrosilicates and hydrogarnets in the system C-S-A-H", Proc. VI ICCC (Moscow), Sect. II-9.
23. - F. DUTRUEL and R. GUYADER (1975), "Etude de la corrosion des canalisations en béton", Monographie nº 7 du CERIB (France).
24. - A. H. MEYER and W. B. LEDBETTER (1970), "Sulfuric acid attack on concrete sewer pipe", Journ. Sanitary Eng. Div., 96 (SA5), 1167-1182.
25. - R. ALEGRE (1978), "Comportement des ciments en milieu agressif", Ann. ITBTP, nº 374, 72-81.
26. - W. H. GUTT and W. H. HARRISON (1977), "Chemical resistance of concrete", Concrete 11 (5), 35-37.
27. - H. WOODS (1968), "Durability of concrete construction", ACI Monograph nº 4.
28. - V. ZIVIKA (1971), "Über die korrosive Wirkung von Cálcium-nitrat-lösungen auf erhärtet Zementpaste", Zement-Kalk-Gips nº 4, 175-179.
29. - R. C. MIELENZ (1969), "Significance of accelerated durability tests of concrete", Highway Res. Record, nº 268, 17-34.
30. - S. K. CHATTERJI (1969), "Mechanism of sulfate expansion of hardened cement pastes", Proc. V ISCC (Tokyo) III-138, 336-341.
31. - W. RIEDEL (1973), "Die Korrosionbeständigkeit von Zementmörteln in Magnesiumsalzlösungen", Zement-Kalk-Gips nº 6, 286-296.
32. - T. V. SWAMINATKAN and B. S. NAGRAJ (1974), Ind. Concr. Journ. 48 (9), 277-279.
33. - I. MEDGYESI (1976), "Investigation of concrete corrosion caused by some organic acids", Epitöanyag 28 (11), 410-418.
34. - V. A. FEDEROV (1971), "The effect of phenols on concrete", Beton i Zhelezobeton nº 10, 13-17.
35. - M. VENUAT (1978), "Relation entre la carbonatation du béton et les phénomènes de corrosion des armatures du béton", Ann. ITBTP, nº 364, 42-47.
36. - M. HAMADA (1969), "Neutralization (carbonation) of concrete and corrosion of reinforcement steel", Proc. V ISCC (Tokyo), 343-369.
37. - M. VENUAT and J. ALEXANDRE (1968-1969), Rev. Mat. Constr. nº 638, 421-427; nº 639, 469-481; nº 640, 5-15.
38. - S. L. MEYERS (1949), Rock Products, 52,96-98.
39. - J. M. FERNANDEZ PARIS (1973), "La carbonatación de la pasta hidratada de cemento portland (Carbonation of hydrated portland cement paste)", IETCC-Spain, Monograph nº 310.
40. - D. GASPAR and M. MUÑOZ-PLAZA (1977), "Acción del CO_2 sobre un cemento portland. I (Action of CO_2 on a portland cement. I)", Mat. de Constr. (IETCC-Spain) nº 165, 37-53.
41. - A. JOISEL in references 37 and 39.
42. - R. KONDO, M. DAIMON and T. AKIBA (1969), "Mechanisms and kinetics on carbonation of hardened concrete", Proc. V ISCC (Tokyo), III-16, 402-409.
43. - C. M. HUNT and L. A. THOMES (1962), "Reaction of hardened portland cement paste with carbon dioxide", Journ. Res. NBS 66, 473-481.
44. - F. SCHROEDER (1962), "Vaterit das metastabile Calcium-karbonat als sekundärer Zementstein-mineral", Tonind. Ztg., 86, 354-360.
45. - J. J. BEAUDOIN (1976), "Special reactions of portland cement", Cem. Res. Progr., 45-64.
46. - P. A. SLEGERS and P. G. ROUXHET (1976), "Carbonation of the hydration products of tricalcium silicate", Cem. Concr. Res., 6 (3), 381-388.
47. - J. BENSTED (1976), Discussion of Ref. 46, Cem. Concr. Res., 6 (6), 817-818.
48. - P. GARCIA DE PAREDES, J. CALLEJA and J. L. CEBRIAN (1969), "Estudio de la meteorización de los cementos por espectroscopia infrarroja (IRS study of the weathering of cements)", Mat. de Constr. (IETCC-Spain) nº 136, 17-27.
49. - D. GASPAR, M. MUÑOZ-PLAZA and F. TRIVIÑO (1978), "Acción del CO_2 sobre un cemento portland. III (Action of CO_2 on a portland cement. III)", Mat. de Constr. (IETCC-Spain) nº 169, 63-73.
50. - D. GASPAR, M. MUÑOZ-PLAZA and T. VAZQUEZ (1977), "Acción del CO_2 sobre un cemento portland. II (Action of CO_2 on a portland cement. II)", Mat. de Constr. (IETCC-Spain) nº 168, 75-87.
51. - D. GASPAR, C. DEL OLMO and T. VAZQUEZ (1976), "Influencia del CO_2 sobre un cemento portland anhidro (Influence of CO_2 on an anhydrous portland cement)", Mat. de Constr. (IETCC-Spain), nº 161, 17-25.
52. - T. C. POWERS (1962), PCA Res. Dept., Bull. nº 146.
53. - H. G. SMOLCZYK (1969), Discussion of Ref. 36, Proc. V ISCC (Tokyo) III-3, 343-369.
54. - D. GASPAR, T. VAZQUEZ and M. MUÑOZ-PLAZA (1976), RILEM Symp. Concrete Carbonation (Wexham-Springs, England), Comm. 1.4.
55. - M. REGOURD (1976), RILEM Symp. Concrete Carbonation (Wexham-Springs, England), Comm. 3.5
56. - D. GASPAR (1976), "Carbonatación del hormigón (Concrete carbonation)", Mat. de Constr. (IETCC-Spain) nº 163, 43-49.
57. - J. ALEXANDRE (1976), "Rate of carbonation", RILEM Symp. Concrete Carbonation (Wexham-Springs, England).
58. - M. REGOURD (1976), "Cement Research in France", Cem. Res. Progr., 235-258.
59. - M. REGOURD (1978), "Recherches sur les ci-

ments en France", Ciments, Bétons, Plâtres and Chaux, nº 2, 83-90.
60. - K. K. KUATBAYEV (1974), "Characteristics of phase components of hydrothermally hardened cement", Proc. VI ICCC (Moscow), Sect. II-7, II-8.
61. - A. MEYER (1969), "Investigations on carbonation of concrete" Proc. V ISCC (Tokyo), III-52, 394-401.
62. - G. VERBECK (1956), Special Techn. Publ. nº 205, 17-36.
63. - A. MEYER (1968). See reference 61.
64. - H. REYJONEN and S.E. PIHLAJAVAARA (1972), Cem. Concr. Res., 5, 607-615.
65. - K. ESSIG and H. K. HILSDORF (1976), RILEM Symp. Concrete Carbonation (Wexham-Springs, England), Comm. 2.3.
66. - N. K. ROZENTAL and S.N. ALEKSEEV (1976), RILEM Symp. Concrete Carbonation (Wexham-Springs, England), Comm. 2.4.
67. - P. LONGUET and P. COURTAULT (1976), RILEM Symp. Concrete Carbonation (Wexham-Springs, England), Comm. 2.2.
68. - S. TAKAGI, G. YAMAGUCHI and M. SAITO (1975), "Hydration and carbonation of cement minerals in solid-gas reaction and their texture", Rev. 30th Gen. Meeting Cem. Assoc. Japan, 44-46.
69. - J. CALLEJA (1976), "Topics on beneficial aspects of concrete carbonation", RILEM Symp. Concrete Carbonation (Wexham-Springs, England), April 1976.
70. - H. HORNAIN (1976), RILEM Symp. Concrete Carbonation (Wexham-Springs, England), Comm. 5.2.
71. - S. E. PIHLAJAVAARA (1976), RILEM Symp. Concrete Carbonation (Wexham-Springs, England), Comm. 4.5.
72. - O. LEBER and F. A. BLAKEY (1956), Journ. ACI 3, 295-308.
73. - W. MANNS and O. SCHATZ (1957), Betonstein Ztg., 4, 148-156.
74. - Z. SAUMAN and V. LACH (1972), Cem. Concr. Res., 4, 435-446.
75. - H. T. TOENNIES and J. S. SHIDELER (1963), Journ. ACI, 5, 617-633.
76. - O. FERNANDEZ PEÑA (1971), Private Communication.
77. - T. VAZQUEZ and O. FERNANDEZ PEÑA (1973), "Durabilité du mortier de cement portland carbonaté et non carbonaté face aux sulfates", Cahiers de Recherche (IETCC-Spain) nº 27.
78. - O. FERNANDEZ PEÑA (1972), Private Communication.
79. - I. IONESCU (1976), RILEM Symp. Concrete Carbonation (Wexham-Springs, England), Comm. 6.8.
80. - M. G. ARBER and H. E. VIVIAN (1961), Australian Journ. of Appl. Sc., 3, 330-338.
81. - M. REGOURD (1976), RILEM Symp. Concrete Carbonation (Wexham-Springs, England), (Ref. 55).
82. - R. GRESCHUCHNA (1974), "Cement paste crystals in sulfate and acid solutions", Proc. VI ICCC (Moscow), Sect. II-6.
83. - E. SCHWIETE (1935), Zement 27, in reference 37, p. 425.
84. - B. KROONE (1959), Journ. ACI, 6, 497-510.
85. - S. E. PIHLAJAVAARA (1976), RILEM Symp. Concrete Carbonation (Wexham-Springs, England), Comm. 4.6.
86. - A. RUIZ DE GAUNA, F. TRIVIÑO and T. VAZQUEZ (1975), "On the carbonation mechanism of calcium aluminate hexahydrate in hardened high-alumina cement", Research Paper (IETCC-Spain) nº 31.
87. - T. VAZQUEZ, F. TRIVIÑO and A. RUIZ DE GAUNA (1975), "Study of transformations in hydrated high-alumina cement by XRD, IRS and TA techniques. Effect of CO_2, temperature, humidity and added limestone powder", Mat. de Constr. (IETCC-Spain) nº 159, 63-92.
88. - Y. EFES (1978), "Influence of blast-furnace slag on the durability of cement mortar by carbonic acid attack", 1st. Int. Conf. on Durability of Build. Mat. and Components, Nat. Res. Council Canada, Ottawa 1978.
89. - L. SZABADOS and S. SLANICKA (1976), "Die Widerstandfähigkeit von Betonkonstruktionen gegenüber kohlensäurehaltigem aggressiven Wasser in Abhängigkeit von der Dicke der Konstruktion und der Einwirkungsdauer des aggressiven Mediums", Mono/Slovak/Ochr. Stavebn Diela Koroz., 114-124.
90. - O. P. MTSCHDLOV-PETROSSYAN, V. A. KURTJATSKAYA, A. G. OLGINSKY and W. L. TSCHERNJAVSKY (1973), "Korrosion von Zementmaterialien in flüssigen sulfathaltigen Medien", Baustoffindustrie 16, 6B, 15-18.
91. - O. P. MTSCHDLOV-PETROSSYAN, W. L. TSCHERNJAVSKY and V. V. SAVENKOV (1976), "Über die Beständigkeit der Zementsteinmineralien in Sulfat- und Karbonathaltigen Wasser-lösungen", Baustoffindustrie 19, 3A, 24-25.
92. - A. D. BUCK (1975), "Control of reactive carbonate rocks in concrete", Techn. Report C-75-3, US Waterways Experimental Station.
93. - D. W. HADLEY (1961), "Alkali reactivity of carbonate rocks expansion and dedolomitization", Proc. Highway Res. Board 40, 462-474.
94. - D. W. HADLEY (1964), "Alkali reactivity of dolomite carbonate rocks", Highway Res. Record 45, 1-19 (Bibliographic Index).
95. - P. E. GRATTAN-BELLEW and G. G. LITVAN (1976), "Testing canadian aggregates for alkali expansivity", Nat. Res. Council Canada, Div. of Build. Res., Paper nº 723.
96. - D. J. E. VERONELLI (1978), "Durabilidad de los hormigones: Reacción árido alkali (Durability of concrete: Alkali-aggregate reaction)", IETCC-Spain, Monograph nº 352.
97. - S. DIAMOND (1975), "A review of alkali-silica reaction and expansion mechanism. 1. Alkalies in cements and in concrete pore solutions", Cem. Concr. Res. 5 (4), 329-346.
98. - S. DIAMOND (1976), "A review of alkali-silica reaction and expansion mechanism. 2. Reactive aggregates", Cem. Concr. Res. 6 (4), 549-560.

99. - W. C. HANSEN (1976), Discussion of Ref. 97, Cem. Concr. Res. 6 (2) 323-325.
100. - S. DIAMOND (1976), Reply to Ref. 99, Cem. Concr. Res., 6 (2), 327.
101. - S. DIAMOND (1975), "Article de synthese sur la réaction alcaki-silice et les mécanismes d'expansion. 1. Alcalis contenus dans les ciments et dans les solutions remplissant les pores du béton", See ref. 97.
102. - U. LUDWIG (1976), "Einflüsse auf die Alkali--Zuschlag-Reaktion", Cem. Concr. Res., nº 6, 762-772.
103. - U. LUDWIG and W. BAUER (1976), "Untersuchungen zur Alkali-Zuschlag-Reaktion", Zement-Kalk-Gips, nº 9, 401-411.
104. - J. W. FIGG (1977), "Alkali-aggregate (alkali--silica and alkali-silicate) reactivity in concrete -Bibliography-", CEMBUREAU (Paris).
105. - CEMBUREAU (1977), "Alkali-aggregate reactivity in concrete. A state of the art report", Paris.
106. - S. DIAMOND (1975), Reference to the Symp. on Alkali-Aggregate Reaction: Preventive Measures (1975), Proc. Int. Symp. Reykjavik, August 1975, Build. Res. St. Keldnaholt. H. Asgeirsson Ed., Reykjavik (Iceland).
107. - G. M. IDORN (1978), "Alkali-silica reactions: simplicity and complicity", 4th. Int. Conf. on the effects of alkalis in cement and concretes, Purdue University, June 1978.
108. - G. M. IDORN (1978), Private communication on "Preparatory conclusions from discussion at the 4th. Int. Meeting on Alkali-aggregate reactions, Purdue University, June 1978.
109. - S. DIAMOND (1976), "A reply to Bryant MATHER's discussion of the paper of Ref. 98, Cem. Concr. Res., 6, 549-560.
110. - R. LESAGE and R. SIERRA (1977), "Reactions between alkalies and aggregates in hydraulic concretes", Bull. Liaison Labs. Ponts et Chaussées, nº 90, 103-107.
111. - J. H. P. VAN AARDT and S. VISSER (1977), "Calcium hydroxide attack on feldspars and clays: possible relevance to cement-aggregate reactions", Cem. Concr. Res. 7 (6), 643-648.
112. - S. HASABA, M. KAWAMURA and M. OKADA (1977), "A fundamental study on alkali-silica reaction", Rev. 31st. Gen. Meeting Cem. Assoc. Japan, p. 58.
113. - D. HIRCHE (1976), "Infrarot-spectroskopie zur Untersuchung von Kieselsäurezuschlagen des Betons auf ihre Alkaliempfindlichkeit", Zement-Kalk-Gips, 9, 412-415.
114. - H. E. VIVIAN (1950), "Studies in cement-aggregate reaction", CSIRO Melbourne (Australia), Bull. nº 256 (X), 13-20.
115. - H. E. VIVIAN (1951), "Cement-aggregate reaction", Austral. Journ. Appl. Sc., 2 (4), 488-494.
116. - S. SPRUNG (1975), "Influences on the alkali--aggregate reaction in concrete", Proc. Int. Symp. on Alkali-Aggregate Reaktion: Preventive Measures (Reykjavik -Iceland- Aug. 1975), 231-244.
117. - S. HASABA, M. KAWAMURA and M. OKADA (1976), "A fundamental study of alkali aggregate reaction", Rev. 30th. Gen. Meeting Cem. Assoc. Japan, 81-83.
118. - S. DIAMOND and M. THAULOW (1974), "A study of expansion due to alkali-silica reaction as conditioned by the grain size of the reactive aggregate", Cem. Concr. Res., 4 (4), 591-607.
119. - T. KNUDSEN and M. THAULOW (1975), "Quantitative microanalises of alkali-silica gel in concrete", Cem. Concr. Res., 5 (5), 443-453.
120. - S. DIAMOND and R. S. BARNEYBACK, Jr. (1976), "A prospective measure for the extent of alkali-silica reaction", Prod. Symp. on the effect of alkalies on the Properties of Concrete (London), C. & C. A., Sep. 1976.
121. - J. DAHMS (1977), "Influences on the alkali-aggregate reaction under field conditions", Proc. Symp. on the Effect of Alkalies on the Properties of Concrete (London) C. & C. A., Sep. 1976, 277-289.
122. - T. C. POWERS and H. H. STEINOUR (1955), "An interpretation of some published researches on the alkali-aggregate reaction", Journ. ACI 51 (6), 497-516; 51 (8), 785-812.
123. - J. E. GILLOT, M. A. DUNCAN and E. G. SWENSON (1973), Cem. Concr. Res., 3, 521--525, in Ref. 95.
124. - F. W. LOCHER (1973), "Ursache und Wirkungsweise der Alkalireaktion", in "Vorbeugende Massnahmen gegen Alkalireaktion in Beton", Verein Deutscher Zementwerke, Heft 40/1973.
125. - D. J. E. VERONELLI (1978), "Durabilidad de los hormigones: Reacción árido-álcali (Durability of concrete: Alkali-aggregate reaction)", Mat. de Constr. (IETCC-Spain) nº 171, 5-33.
126. - J. CALLEJA (1979), "La reacción árido-alcalis. Disquisition on the text of a conference by D. J. E. VERONELLI (see Refs. 96 and 125), Cemento-Hormigón (Spain) nº 542, 35-52.
127. - H. E. VIVIAN (1947), CSIRO Bull. (Australia) nº 229, 67.
128. - W. C. HANSEN (1944), Journ ACI Proc. 44, 625.
129. - W. C. HANSEN (1944), "Studies relating to the mechanism by which the alkali-aggregate reaction produces expansion on concrete", Journ. ACI, Proc. 40, 213-227.
130. - S. DIAMOND (1975), "Pore solutions and alkali--aggregate attack" (see Ref. 106).
131. - S. DIAMOND (1975), in Ref. 133.
132. - H. VIVIAN (1975), in Ref. 133.
133. - H. ASGEIRSSON (1975), "An epilogue", Proc. Int. Symp. on Alkali-Aggregate Reaction: Preventive Measures, Reykjavic Aug. 1975, 269-270.
134. - J. E. GILLOT (1975), in Ref. 95.
135. - W. J. McCOY and A. G. CALDWELL (1951), Journ. ACI, Proc. 47, 693.
136. - H. E. VIVIAN (1950), "The effect on mortar expansion of amount of reactive component in the aggregate", Commonwealth Sc. and Ind. Res. Organization (Melbourne), Bull. 256.
137. - I. JAVED and J. SKALNY (1977), "Alkalies in cement. I: Form of alkalies and their effect on

clinker formation", Cem. Concr. Res., nº 6, 719-729.
138. - I. JAVED and J. SKALNY (1978), "Alkalies in cement. II: Effects of alkalies on hydration and performance of portland cements", Cem. Concr. Res., nº 1, 37-52.
139. - F. W. LOCHER and S. SPRUNG (1973), "Ursache und Wirkungsweise der Alkalireaktion", Beton--Herstellung-Verwendung 23 (7), 303-306; 23 (8), 349-353. See also ref. 124.
140. - F. W. LOCHER and S. SPRUNG (1975), "Einflüsse auf die Alkali-Kieselsäure -Reaktion in Beton", Zement-Kalk-Gips 28 (4), 162-169.
141. - PCA (USA) Annual Report (1977), Concrete Materials Research. Alkali-Aggregate reactivity, p. 10.
142. - H. G. SMOLCZYK (1974), "Slag cement and alkali-reactive aggregates", Proc. VI ISCC (Moscow) Suppl. Paper III-2.
143. - B. MATHER (1976), Discussion of Paper 95 (see Ref. 95).
144. - G. M. IDORN (1976), Discussion of Paper 95 (see Ref. 95).
145. - J. BONZEL and E. SIEBEL (1977), "Recent studies of the frost-melting-salts resistance of concrete", Beton-Herstellung-Verwendung 27 (4), 153-158.
146. - A. M. NEVILLE (1969), "Behaviour of concrete in saturated solutions and weak solutions of magnesium sulfate of calcium chloride", Journ. of Mat., 4 (4), 781-816.
147. - F. P. BROWNE and P. D. CADY (1975), "Deicer scaling machanisms in concrete", Durability of Concrete: ACI Pub. SP-47, 101-109.
148. - S. CHATTERJI (1978), "Mechanism of the $CaCl_2$ attack on portland cement concrete", Cem. Concr. Res., 8 (4), 461-468.
149. - S. CHATTERJI and A. DAMGAARD (1975), "Studies of the mechanism of calcium chloride attack on portland cement concrete", Nordisk Betong, 19 (5), 5-6.
150. - A. D. HEROLDT (1975), "Concrete and de-icing salts", Nordisk Betong, nº 1, 29-36.
151. - G. G. LITVAN (1974), "Frost action in cement in the presence of de-icers", Proc. VI ICCC (Moscow), Sect. II-6.
152. - E. WURTH (1977), "Action of de-icing salt on concrete", Betonstein Ztg., 43 (11), 542-548. "Sollicitation de béton par le sel de déverglaçage", Wiesbaden, Betonwerk-Fertigteil Technik, nº 11, 542-548.
153. - A. HEROLDT (1975), "Le béton et les sels de dégel", Nordisk Betong nº 1, 29-36.
154. - J. BONZEL (1973), "Beton mit hohem Frost- und Tausalzwiderstand", Betonwerk-Fertigteil Technik, 39 (12), 888-894.
155. - S. USHIYAMA and S. GOTO (1974), "Diffusion of various ions in hardened portland cement paste", Proc. VI ICCC (Moscow), Sect. II.
156. - M. COLLEPARDI, A. MARCIALIS and R. TURRIZIANI (1970), "La cinetica di penetrazione degli ioni chloruro nel calcestruzzo", Il Cemento 67 (4), 157-163.
157. - O. E. GJORV and O. VENNESLAND (1979), "Diffusion of chloride ions from sea-water into concrete", Cem. Concr. Res., 9 (2), 229-238.
158. - R. KONDO, M. SATAKE and H. USHIYAMA (1974), "Diffusion of vaious ions in hardened portland cement", Rev. 28th. Gen. Meeting Cem. Assoc. Japan, 41-43.
159. - H. USHIYAMA, H. IWAKURA and T. FUKUNAGA (1976), "Diffusion of sulfate ion in hardened portland cement", Rev. 30th. Gen. Meeting Cem. Assoc. Japan, 47-49.
159-bis. - W. RICHARTZ (1969), "Die Bindung von Chlorid bei der Zementhärtung", Zement-Kalk--Gips, 22 (10), 447-456.
160. - B. MARCHESE (1978), "Chemical resistance of cement pastes. I. Patina alterations", Cem. Concr. Res., 8 (4), 501-508.
161. - H. G. SMOLCZYK (1969), "Chemical reactions of strong chloride solutions with concrete", Proc. V ISCC (Tokyo), III-31, 274-278.
162. - A. YODA, K. GOSHOKUBO and O. NAKAGAWA (1976), "Effect of salt water on portland blast-furnace slag cement used in concrete", Rev. 30th. Gen. Meeting Cem. Assoc. Japan, 243-244.
163. - W. KOBAYASHI and S. OKABAYASHI (1975), "Study on chloride resistance of various types of cement", Rev. 29th. Gen. Meeting Cem Assoc. Japan, 51-53.
164. - M. BEN YAIR (1974), "The effect of chlorides on concrete in hot and arid regions", Cem. Concr. Res., 4 (3), 405-416.
165. - M. WEINZSTEIN and L. P. TRAVERSA (1975), "Aspectos relativos a la durabilidad de hormigones (Aspects related to concrete durability)", Ann. LEMIT (Argentina), Serie II, nº 286, pp. 45-100.
166. - T. J. READING (1975), "Combating sulfate attack in Corps of Eng. Concrete Construction", ACI SP-47, 343-366.
167. - I. BICZOK (1967), "Concrete Corrosion, Concrete Protection", Chem. Publ. Co., New York, pp. 178 & 353.
168. - G. VERBECK (1968), Symp. in honour of T. THORVALDSON, Univ. Toronto Press, Canadian Build. Series.
169. - W. KOBAYASHI, S. OKABAYASHI and N. KATAOKA (1974), "Study on sulfate resistance of various types of cement", Rev. 28th. Gen. Meeting Cem. Assoc. Japan, 78-80.
170. - BUILDING RESEARCH STATION -UK- (1968), "Concrete in sulfate-bearing soils and groundwaters", Digest nº 90.
171. - J. H. P. VAN AARDT (1969), "The influence of temperature on sulfate attack on portland cement mortars", Proc. V ISCC (Tokyo), III-25, 250-259.
172. - J. EUSTACHE and R. MAGNAN (1972), "Method for determining resistance of mortars to sulfate attack", Journ. ACI, 55 (5), 237-239.
173. - O. E. GJORV (1971), "Long time durability of concrete in sea-water", Journ. ACI, 68 (1), 60-67.
174. - W. REICHENBERG (1975), "Junger Beton in "stark" angreifendem Wasser", Beton Herstellung und Verwendung, 25 (4), 57-66.

175. - G. J. VERBECK (1968), "Performance of Concretes", ed. E. G. Swenson, Univ. Toronto Press, 113-124.
176. - G. M. DARR, M. PUNZET and U. LUDWIG (1977), "On the chemical and thermal stability of ettringite", CEMBUREAU Seminar on Reaction of Aluminates during the Setting of Cements, Eindhoven (Netherlands).
177. - V. ALUNNO-ROSSETTI, V. CHIOCCHIO and M. COLLEPARDI (1973), "Stagionatura a vapore e resistenza dei cementi portland in soluzione di solfato sodico", Il Cemento, nº 1, 23-32.
178. - M. F. CHERBUKOV and N. G. DOLINSKAYA (1970), "The influence of the silica ratio on chemical resistance of high silica cements to magnesium sulfate corrosion", Journ. Appl. Chem. (SSSR) 43 (9), 1928-1930.
179. - C. A. TANEJA (1975), "Über den Einfluss des Tonerdegehaltes und der Mahlfeinheit der Hochofenslacke auf die Sulfatbeständigkeit von Hüttenzementen", Zement-Kalk-Gips nº 2, 76-79.
180. - K. H. McGHEE and H. E. BROWN (1969), U.S. Clearinghouse, PB 184 946, Springfield (Build. Sc. Abstr. 1969, 42 (12), 69-1b 321.
181. - W. SCHRAMLI (1979), "An attempt to assess beneficial and detrimental effects of aluminate in the cement on concrete performance", Part 2, World Cement Technol., nº 3, 75-80.
182. - W. SCHRAMLI (1978), "An attempt to assess beneficial and detrimental effects of aluminate in the cement on concrete performance", Part 1, World Cement Technol., nº 2, 35-42.
183. - G. G. VERBECK (1967), PCA Res. Dept. Bull. 227, 113-124.
184. - G. FRIGIONE and R. MAROTTA (1975), "I cementi nelle opere marittime", Giorn. Genio Civile, nº 7-9, 311-316.
185. - S. DIAMOND (1977), "The status of calcium in poresolutions of mature hardened portland cement paste", Il Cemento, 74, 149-155.
186. - E. M. WINKLER and Ph. C. SINGLER (1972), "Crystallization pressure of salts in stone and concrete", Geol. Soc. Amer., Bull. 83 3509-3514.
187. - P. K. MEHTA (1973), "Mechanism of expansion associated with ettringite formation", Cem. concr. Res., 3 (1), 1-6.
188. - P. K. MEHTA (1967), Discussion of a paper of T. J. READING, Journ. ACI, April 1967.
189. - P. K. MEHTA and H. H. HAYNES (1975), "Durability of concrete in sea-water", Journ. Structural Div. ASCE 101/ST 8, Proc. 1679-1686.
190. - W. LUKAS (1975), "Concrete determination by sulfate attack through formation of thaumasite and woodfordite", Cem. Concr. Res., 5 (5), 503-518.
191. - S. ADACHI (1976), "Study on durability of grout for long undersea tunnel" Rev. 30th. Gen. Meeting Cem. Assoc. Japan, 141-143.
192. - F. M. LEA (1970), "The Chemistry of Cement and Concrete", 3rd. ed. London, 346-347 and 350.
193. - W. C. HANSEN (1961), "Discussion on significe of tests for calcium sulfate in hydrated portland cement mortar", ASTM Proc., 61, 1039.
194. - B. MATHER (1973), Discussion of Ref. 187, Cem. Concr. Res., 3 (5), 651-652.
195. - P. K. MEHTA (1972), "Chemistry and microstructure of expansive cements", Conference, Univ. of California, Berkeley.
196. - F. HENKEL (1975), "On the crystallization pressure of concrete-corrosive sulfate", Zement un Beton nº 85/86, 26-28.
197. - H. LAFUMA (1929), Rev. Mat. Constr., nº 243, 441.
198. - W. C. HANSEN (1973), Discussion of Ref. 187, Cem. Concr. Res., 3 (5), 655-657.
199. - S. CHATTERJI and J. W. JEFFERY (1963), Journ. Amer. Ceram. Soc., nº 46, 187-191.
200. - T. THORWALDSON (1952), "Chemical aspects of the durability of cement products" Proc. III ISCC (London), 463.
201. - F. M. LEA (1970), "The Chemistry of Cement and Concrete", 3rd. edition, London, p. 348.
202. - G. L. KALOUSEK and E. J. BENTON (1970), "Mechanism of sea-water attack on cement pastes", Journ. ACI, 67 (8), 646-648.
203. - L. S. BROWN (1970), Discussion of Ref. 202, Journ. ACI, 67 (8), 646-648.
204. - G. L. KALOUSEK, L. C. PORTER and E. J. BENTON (1972), "Concrete for long-time service in sulfate environment", Cem. Concr. Res., 2 (1), 79-89.
205. - M. REGOURD, H. HORNAIN and B. MORTUREUX (1975), "Compte rendu d'activité du Dept. Microstructures (CERILH) 1974", Ciments, Bétons et Plâtres, nº 693, 87-95.
206. - T. BROCARD and R. CIRODDE (1962), RILEM Intern. Coll. on Concrete Durability (Prague).
207. - H. W. REINHARDT (1978), "Erosie van beton", Cement nº 6, 282-285.
208. - R. PELTIER (1976), "Le comportement des ciments à l'eau de mer", Ciments et Chaux, nº 653, 21-25.
209. - O. E. GJORV (1968), "Durability of reinforced concrete wharves in Norvegian harbours", The Norvegian Committee on Concrete in Sea-Water, Ingeniørforlaget A/S, Oslo.
210. - B. C. GERWICK (1975), "Practical methods of ensuring durability of prestressed concrete ocean structures", Durability of Concrete: ACI Publ. SP-47, 317-324.
211. - M. REGOURD, H. HORNAIN and B. MORTUREUX (1977), "Resistance à l'eau de mer des ciments au laitier", Silicates Industriels, nº 1, 19-27.
212. - M. REGOUR, H. HORNAIN, P. BISSERIE and G. EVERS (1978), "Ettringite et Thaumasite dans le mortier de la digue du large du port de Cherbourg", Ann. ITBTP Série LH nº 28, 3-13.
213. - K. R. LANER and C. V. GRAY (1969), "Durability of concrete using Monte Carlo simulation", Proc. V ISCC (Tokyo) 1968.
214. - F. W. LOCHER (1969), "Influence of chloride and hydrocarbonate on the sulfate attack", Proc. V ISCC (Tokyo), III-124, 328-335.
215. - J. JAMBOR and V. ZIVIKA (1976), "Die Aggressivität von schwefelsäurem Wasser und die

Beton-Korrosion beim Vorhandensein von Chloriden", Mono/Slovak/Ochr. Stavebn. Diela Koroz. (Czechoslovakia), 6-13.
216. - N. TENOUTASSE, A. VAN BEMST and W. L DE KEYSER (1965), Coll. RILEM sur le Comportement des Bétons à l'eau de Mer (Palerme), Cahiers de la Recherche nº 27, ITBTP, Paris, 1968.
217. - F. CAMPUS (1968), Coll. RILEM sur le Comportement des Bétons à l'eau de Mer (Palerme), Cahier de la Recherche nº 27. ITBTP, Paris 1968.
218. - W. C. HANSEN (1968), "The chemistry of sulfate resisting portland cements", Toronto Press. p. 18.
219. - B. MARCHESE and R. SERSALE (1978), "Natura dei prodotti di neoformazione originati per contatto di acqua marina con le paste cementizie", Il Cemento, 75 (3), 253-261.
220. - M. REGOURD, H. HORNAIN and B. MONTEREUX (1977), (see Ref. 211).
221. - M. REGOURD (1977), "Le comportement des bétons à la mer", Travaux nº 512, 74-78.
222. - N. TENOUTASSE, A. VAN BEMST and W. L. DE KEYSER (1968), (see Refs. 216 and 224).
223. - A. GJORV, I. GUKILD and H. P. SUNDH (1968), (see Ref. 224).
224. - H. G. SMOLCZYK (1968), Coll. RILEM sur le Comportement du Béton à l'Eau de Mer (Palerme), Cahier de la Recherche, nº 27 ITBTP, Paris 1968.
225. - J. ISOGAY (1974), "Hardened cement paste affected by sea-water", Proc. VI ICCC (Moscow), Supp. Paper Sect. II-6.
225 bis. - W. KONDO (1974), "Corrosion resistance of cement mortar and concrete in hot sea-water brine at 80°C", Rev. 28th. Gen. Meeting Cem. Assoc. Japan, 88-90.
226. - W. KOBAYASHI and S. OKABAYASHI (1977), "Effect of curing temperature on chemical resistance of cement", Rev. 31st. Gen.Meeting Cem. Assoc. Japan, 47-48.
227. - M. A. TAYLOR (1978), "Effects of ocean salts on the compressive strength of concrete", Cem. Concr. Res., 8 (4), 491-500.
228. - P. K. MEHTA and R. B. WILLIAMSON(1973), "Durability of cement concrete in sulfate environment", Techn. Report nº 7, Univ. of California, Berkeley.
229. - M. REGOURD, H. HORNAIN and B. MONTUREUX (1974), "Influence du mode de crystallization de l'aluminate tricalcique sur la résistance des ciments à l'eau de mer", Rev. Mat. Constr., nº 687, 69-79.
230. - K. E. C. NIELSEN (1968), (see Ref. 224).
231. - M. BEN YAIR and L. HELLER (1968), (see Ref. 224).
232. - C. GORIA and L. CUSINO (1968), (see Ref. 224).
233. - L. DUHOUX and A. TESSIER (1968), (see Ref. 224).
234. - A. RIO and C. CELANI (1968), (see Ref. 224).
235. - K. WESCHE (1968), (see Ref. 224).
236. - A. MIGLIARDI TASCO (1968), (see Ref. 224).
237. - F. CAMPUS (1968), (see Ref. 224).
238. - F. CAMPUS, R. DANTINNE and M. DZULINSKY (1968), (see Ref. 224).
239. - J. BROCARD and R. CIRODDE (1968), (see Refs. 206 and 224).
240. - G. L. KALOUSEK, L. C. PORTER and E. M. HARBOE (1976), "Past, present and potential developments of sulfate resisting concretes", Journ. Test. Eval., 4 (5), 347-354.
241. - J. L. SAGRERA (1971), "Estudios sobre sulfato-durabilidad. Aplicación del método Le Chatelier Anstett a un cemento puzolánico y a un cemento PAS-puzolánico (Studies on sulfate durability. Application of Le Chatelier-Anstett method to a pozzolanic and a PAS-pozzolanic cement)", Rev. ION (Spain), nº 361, 419-425.
242. - J. M. JASPERS (1970), "Contribution à l'étude expérimentale de la mesure de la résistance aux sulfates des ciments selon la méthode ASTM C452-68", Rev. Mat. Constr., nº 656, 135-143.
243. - O. E. GJORV and S. P. SHAH (1971), "Testing methods for concrete durability", Matériaux et Constructions, 4 (23), 295-304.
244. - G. STAUPENDAHL (1974), "Prüfverfahren zur Bestimmung der Sulfatbeständigkeit von Hochofenzementen", Baustoffindustrie, nº 17, A1, 6-9.
245. - O. VALENTA (1969-1970), From the 2nd. RILEM Symp. on Durability of Concrete (Prague). Build. Res. Inst., Techn. University in Prague.
246. - H. SEKI and T. NOGI (1976), "Research on durability of concrete to sea-water - Interim Report on 5-years age specimens", Rev. 30th. Gen. Meeting Cem. Assoc. Japan, 239-242.
247. - M. J. JASPERS (1977), "Contribution à l'étude expérimentale de la résistance chimique de microprismes en solution agressive", Rev. Mat. Constr., nº 704, 51-58.
248. - P. K. MEHTA (1975), "Evaluation of sulfate resisting cements by a new method", Journ. ACI, 72 (10), 573-575.
249. - H. STEINEGGER (1970), Zement-Kalk-Gips nº 2, 67-71.
250. - M. J. M. JASPERS (1968), "Contribution à l'étude expérimentale de la mesure par l'éssai Le Chatelier-Anstett de la résistance de ciments aux sulfates et chlorures", Rev. Mat. Constr., nº 633-634, 244-256.
251. - D. TEODORESCU, D. MORARU and F. TAFLAN (1969), "Contribution to the establishement of a method to determine corrosion resistance of cements in sea-water", Rev. de Constr. et Mat. de Constr. (Rumania), nº 7, 365-368.
252. - P. GARCIA DE PAREDES and J. L. SAGRERA (1970), "Hidratación acelerada de conglomerantes hidráulicos utilizados en el ensayo Le Chatelier-Anstett (Accelerated hydration of cements for Le Chatelier-Anstett test)", Rev. ION (Spain), nº 353, 677-680.
253. - S. CHATTERJI (1978), "An accelerated method for the detection of alkali-aggregate reactivities of aggregates", Cem. Concr. Res., nº 5, 647-650.

254. - M. VENUAT (1969), "Questions générales de la durabilité du béton", Rev. Mat. Constr., nº 650, 371-374.
255. - M. VENUAT (1969), "Effet de certains paramètres sur l'essai de durabilité aux eaux sulfatées", Rev. Mat. Constr., nº 650, 376-381.
256. - STANDARD STUDYING COMMITTEE of The Cem. Assoc. Japan (1978), "About the revised JIS R5210 relative to sulfate-resisting cement", Cem. and Concr., nº 378, 26-28.
257. - M. NADU (1974), "On the sulfate resistance of the hardened cement paste", Proc. VI ICCC (Moscow), Sect. II.
258. - A. K. CHATTERJI (1974), "Stability of tricalcium aluminate in the lime-alumina-fluorite system", Proc. VI ICCC (Moscow), Sect. I-1-2.
259. - H. KREMSER (1968), "Die Wilhelmshavener Versuche von Beton und Zement im Seewasser aus der Sicht der Trassverwendung", Zement--Kalk-Gips, 21 (3), 134-137.
260. - M. A. SAMARAI (1976), "The desintegration of concrete containing sulfate-contaminated aggregates", Magaz. Concr. Res., 28, nº 96, 130-142.
261. - M. RAVERDI (1969), "Etude de la corrosion des liants en eaux agressives", Bull. de Liaison des Laboratoires Routiers, nº 41, 69-81.
262. - H. MIYAIRI, R. FURUKAWA and K. SAITO (1975), "The influence of chemical composition of granulated blastfurnace slag and portland cement clinker of various portland slag cements on resistance to sea-water", Rev. 30th. Gen. Meeting Cem. Assoc. Japan, 73-75.
263. - K. OKADA, R. FURUKAWA and H. MIYAIRI (1977), "Some observations on the durability of slag cements to the action of thermal water", Rev. 31st. Gen. Meeting Cem. Assoc. Japan, 142-144.
264. - W. KOBAYASHI and S. OKABAYASHI (1977), (see Ref. 226).
265. - D. DIMIC (1973), "The influence of the amount and chemical composition of slag on the resistance of cements to sulfates", Cements (Yugoeslavia) nº 4, 185-188.
266. - G. M. BAKLANOV, L. M. SIDOCHENKO et al. (1973), "Defects in the standard specifications for sulfate resistant portland cement", Tsement, nº 3, 20-21.
267. - W. RICHARTZ (1966), Chem. Ing. Techn. 38, 1099-1105.
268. - H. G. SMOLCZYK (1965), Zement-Kalk-Gips, 18, 238-246.
269. - I. A. KRYZHANOVSKAYA, E. E. KIRYAEVA, Yu. L. GALOCHINETSKAYA and G. N. KARATANOVA (1974), "Additions containing phosphorous and fluorine in cement production", Proc. VI ICCC (Moscow), Sect. II.
270. - E. E. KIRYAEVA, I. D. BERKHOER et al. (1974), "The influence of P_2O_5 + F on the sulfate resistance of cement", Tsement nº 2, 17-18.
271. - I. V. KRAVCHENKO and V. I. ZHARKO (1975), "The manufacture of highly sulfate resistant barium-bearing portland cement", Tsement, nº 9, 17-18.
272. - F. TROJER (1968), "Beiträge zur Ferrari-Zementen", Zement-Kalk-Gips, nº 3, 124-130.
273. - A. MEYER (1962), "The resistance of portland and slag cements to sulfate solutions", RILEM Int. Symp. on Durability of Concrete (Prague) 1961), Final Report RILEM, Paris 1962.
274. - F. MASSAZZA (1974), "Chemistry of pozzolanic additions and mixed cements" VI ICCC (Moscow).
275. - F. MASSAZZA (1978), "L'attaque des sulfates et le comportement des ciments pouzzolaniques", Private Communication to the 32 RCA RILEM Committee Meeting, Athens 1978.
276. - P. SCHUBERT and H. P. LÜHR (1979), "Zum sulfatwiderstand flugaschehaltiger Mörtel und Betone", Betonwerk Fertigteil-Technik, nº 3 177-182.
277. - F. M. LEA (1970), "The Chemistry of Cement and Concrete", 3rd. ed., London, p. 442.
278. - F. W. LOCHER (1966), Zement-Kalk-Gips, 19, 395-401.
279. - R. TURRIZIANI and A. RIO (1960), "High chemical resistant pozzolanic cements", Proc. IV ISCC (Washington) pp. 1067-1073.
280. - A. RIO, A. CELANI and L. ANGELETTI (1961), "La composizione dei cementi pozzolanici e la loro resistenza alle acque solfatiche", L'Ind. Ital. del Cemento, nº 4, 184-193.
281. - R. TURRIZIANI, A. RIO and A. CELANI (1962), "Ricerche sull'azione protettiva esercitata dalla silice reattiva dei cementi pozzolanici nei confronto delle acque solfatiche" L'Ind. Ital. del Cemento, nº 6, 313-320.
282. - O. E. GJORV and O. VENNESLAND (1976), "Sea-water salts and alkalinity of concrete" Journ. ACI, 73 (9), 512-516.
283. - H. O. LAMPRECHT (1969), "Widerstandfähikeit von Rohrbeton gegen chemische Angriffe", Betonstein Ztg., 35 (9), 543-546.
284. - E. R. DUNSTAN (1976), "Performance of lignite and subbituminous fly-ash in concrete. A Proggres Report", U. S. Bureau of Reclamation, Eng. and Res. Center, Report REC-ERC-1.
285. - M. G. TOLOCHKOVA and G. P. GERASIMOVA (1974), "On hardening of oil-well cements in aggressive media of high mineralization", Proc. VI ICCC (Moscow), Sect. III-6, III-7.
286. - A. I. BULATOV (1974), "Oil-well cements for high temperature wells", Proc. VI ICCC (Moscow), Sect. III-6, III-7.
287. - R. C. DE VEKEY and A. J. MAJUMDAR (1974), "Durability of cement pastes modified by polymer dispersions", Proc. VI ICCC (Moscow).
288. - Ja. KOOS (1974), "Stability of plastic materials in hydrated portland cement", Proc. VI ICCC (Moscow), Sect. III-9.
289. - L. A. ZAKHAROV (1974), "Alumina-belite cement", Proc. VI ICCC (Moscow), Sect. III-4.
290. - S. POPOVICS (1974), "Strength development of portland cement paste", Proc. VI ICCC (Moscow), Sect. II.
291. - D. M. ROY and G. R. GOUDA (1974), "Optimization of strength in cement pastes", Proc. VI ICCC (Moscow), Sect. II.

7e Congrès International de la Chimie des Ciments

7th International Congress on the Chemistry of Cement

VOLUME II
COMMUNICATIONS

PARIS 1980

7e Congrès International de la Chimie des Ciments

7th International Congress on the Chemistry of Cement

VOLUME II
COMMUNICATIONS

PARIS 1980 [June 30 - July 4]

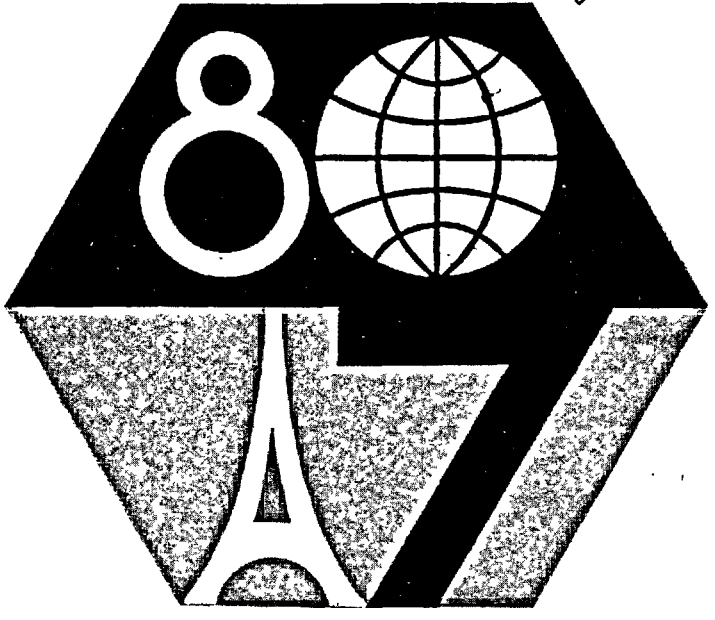

Le Secrétariat Général laisse à leurs auteurs la responsabilité de la forme et du fond des communications publiées dans cet ouvrage.

The General Secretariat are not responsible either for the substance or for the form of the communications contained in this volume.

EDITIONS SEPTIMA - 14, rue Falguière,
75015 PARIS (France).

Imprimé en France - 1980.

TABLE DES MATIERES
CONTENTS

* La pagination comporte tout d'abord un chiffre romain correspondant au numéro du thème, suivi d'un numéro de page à l'intérieur du thème. Dans chaque thème, les communications ont été publiées dans l'ordre où elles sont parvenues au Secrétariat Général du Congrès pour permettre une publication plus rapide.
The pagination consists of a roman numeral corresponding to the theme number, followed by a page number in the interior of the theme. In each theme the communications have been published in the order they reached the General Secrétariat of the Congress, in order to accelerate the publication.

I-90	I. Teoreanu, H. Balasoiu, C. Radovici, D. Ciomartan (Roumanie)	Influence des micro-additions d'oxyde de chrome (III) sur la composition chimique et minéralogique des clinkers de ciment portland. The influence of chromium sesquioxide micro-additions on the chemical and mineralogical composition of portland cement clinkers.
I-95	V. Valkov (Bulgarie) M.M. Sitchiov (URSS) L. Gigova (Bulgarie) Yu. V. Nikiforov URSS)	Common influence of BaO and Mn_2O_3 on the obtaining and the properties of the portland cement. Influence des additions de BaO et Mn_2O_3 sur la fabrication et les propriétés des ciments portland.
I-99	Udo Ludwig, Albrecht Wolter (R.F.A.)	Formation and stability of C_3S and alites. La formation et la stabilité du C_3S et des alites.
I-104	K. Karibayev, A. Paschenko, K. Bekishev, D. Aldiarov, B. Taymasov (URSS)	Dispersing and plasticizing admixtures to cements. Des ajouts disperseurs et plastifiants des ciments.
I-108	S.K. Sinha, S.K. Handoo, A.K. Chatterjee (India)	Comminution and dissociation characteristics of Indian limestones. Broyabilité et décarbonatation des calcaires indiens.
I-114	U. Ludwig, S.E. Ibrahim (R.F.A.)	Burnability of industrial Portland cement raw mixes. Cuisabilité des crus du ciment de Portland industriel.
I-119	M.V. Ranga Rao, Kamal Kumar, (India)	A comparative study of the effect of heating rate in 2-stage and 4-stage suspension preheater kiln installations. Etude comparée de l'influence de la vitesse de chauffe dans les fours avec préchauffeurs à deux et à quatre étages.
I-124	M. Ono, M. Akita, K. Hikita (Japan)	Effect of Na_2O on the stability of calcium aluminoferrite under the reducing atmosphere. Effet du Na_2O sur la stabilité de l'aluminoferrite de calcium sous atmosphère réductrice.
I-128	Dr. M. Maultzsch, M. Gierloff, Dr. P. Schimmelwitz (RFA)	Aging of cement through long term storage. Vieillissement du ciment lors du stockage à longue durée.
I-134	A. Derdacka-Grzymek, J. Grzymek (Pologne)	Mécanisme de la stabilisation dans la transformation polymorphique beta-gamma C_2S. Polymorphic Phase change of beta-gamma Ca_2SiO_4.
I-140	O.P. Mtchedlov-Petrossian, V.I. Satarine, N.P. Kogan, A.G. Kholodny, E.P. Kostinski (URSS)	Intensification du processus physico-chimique de clinkérisation. Intensification of physico-chemical process of clinker formation.
I-145	B.S. Albats, L.S. Filippova, Y.R. Krivoborodov (URSS)	Physical and chemical grounds for granulation of clinker. Bases physico-chimiques de la formation des granules de clinker.
I-150	W.A. Klemm, I. Jawed (USA)	Minéralisateurs et fondants dans le processus de clinkérisation. III. Aptitude à la cuisson de mélanges synthétiques et industriels. Mineralizers and fluxes in the clinkering process. III. Burnability of synthetic and industrial raw mixes.
I-156	V.Z. Pirotski (URSS)	Problèmes physico-chimiques du broyage du clinker portland. Physico-chemical problems of grinding of portland cement clinker.
I-161	M. Gawlicki, W. Nocun-Wczelik (Pologne)	L'influence du traitement thermique sur la transition $\beta \rightarrow \gamma$-C_2S. Influence of thermal treatment on the transition $\beta \rightarrow \gamma$-C_2S.
I-166	I.F. Ponomarev, P.O. Gaydjourov, A.P. Zoubekhine, V.V. Kitaev (URSS)	Particularités cristallochimiques et propriétés des phases du clinker de ciment portland en fonction des conditions de cuisson et de refroidissement. Crystal chemical peculiarities and phase properties of portland cement clinker depending on the conditions of burning and cooling.
I-170	T. Knudsen (Danemark)	On particle size distribution in cement hydration. L'effet de la granulométrie sur l'hydratation du ciment.
I-176	A. Pachtchenko, G. Baklanov (URSS)	Influence des basaltes sur la clinkérisation et les propriétés des ciments. Basalt influence on the clinker formation process and cement properties.
I-182	B. Werynski, A. Werynska (Pologne)	Raw material effect on clinker quality. L'influence de matières premières sur la qualité de clinker.
I-189	B. Matkovic, V. Carin, T. Gacesa, R. Halle (Yougoslavie)	Reactivity of belite stabilized by $Ca_5(Po_4)_3OH$. Réactivité de la bélite stabilisée avec $Ca_5(Po_4)_3OH$.
I-195	Asok K. Sarkar, Della M. Roy, Roderick M. Smart (USA)	Mineralizers and fluxes in the clinkering process. I. Phase equilibria in the CaO-Al_2O_3-Fe_2O_3-SiO_2 system with calcium fluosilicate. Minéralisateurs et fondants dans la formation des clinkers. I. Equilibre des phases dans le système CAFS avec du fluosilicate de calcium.
I-201	P.V. Zozulja, E.A. Rodionov (URSS)	Mineral formation and reactive capacity of portland cement raw mixtures. Influence de la composition du cru sur la clinkérisation et la réactivité du ciment.

I-206	Y. Ono (Japan)	Microscopical estimation of burning condition and quality of clinker. Estimation microscopique de la résistance du ciment.
I-212	E. Demoulian, P. Gourdin, F. Hawthorn, C. Vernet (France)	Anomalies de cuisson - structures microscopiques - propriétés des clinkers et ciments. Burning anomalies - microscopic structures - clinkers and cements properties.
I-218	J. Moisset, B. Cottin, A. Rouanet, A. Petit (France)	La célite dans les ciments portland obtenus par fusion. Celite phase in portland cements from molten products.
I-223	P. Gourdin, E. Demoulian, F. Hawthorn, C. Vernet (France)	Polymorphisme de l'alite et du C_3A. Statistiques. Alite and C_3A polymorphism. Statistics.
I-229	I.V. Kravtchenko, A.M. Dmitriev, I.E. Kovaleva (URSS)	Influence de la température d'apparition des bains fondus eutectiques et des particularités de la structure cristalline des phases réagissantes sur la structure et les propriétés du clinker. Influence of melt eutectic temperature and pecularities of crystalline structure of reacting phases on structure and properties of clinker.
I-235	G.R. Gouda (USA)	Effect of raw materials on cement process and properties. Influence des matières premières sur la fabrication du ciment et ses propriétés.
I-241	V.V. Timachev, A.P. Ossokine, E.N. Potapova (URSS)	Sur le mécanisme de la cristallogenèse dans les microzones des grains de clinker. Mechanism and kinetics of crystal formation in the microvolumes of clinker grains.
I-247	M. Kovacs, K. Benei (Hongrie)	Caractéristiques de la matière adhérente causant des troubles de fontionnement et leur élimination. Characterisation and elimination of adherent layers causing operational troubles.
I-252	Y. Le Jean (France)	Influence du mode de broyage du clinker et des constituants secondaires sur la réactivité des ciments et sur la rhéologie. Clinker grinding method and secondary components - their effect upon cement reactivity and rheology.
I-259	I. Luginina (URSS)	Neutralisation des additions indésirables dans la matière première. Neutralisation of undesirable admixtures in raw materials.
I-264	L. Opoczky, T.K. Mrakovics (Hongrie)	Problems of the simultaneous and separate grinding at the production of blast furnace slag cement. Problèmes du broyage simultané ou séparé dans la production des ciments de laitier.
I-272	O.P. Mtchedlov-Petrossian, T.Y. Chtchetkina (URSS) N.I. Sapojnikova I. Talaber, K. Bosci (Hongrie)	Corrélation de la cinétique des réactions de clinkérisation à l'état solide avec les constituants minéraux et les conditions du traitement thermique. Correlation between kinetics of solid-phase reactions of clinker formation and mineral composition and thermal treatment conditions.
I-276	H. Hornain, M. Regourd (France)	Fissuration et broyabilité du clinker. Cracking and grindability of clinker.
I-282	W. Kurdowski, M. Handke, G. Sieminska (Pologne)	The effect of Al_2O_3, BaO and B_2O_3 admixtures on C_3S structure. L'effet des additions Al_2O_3, BaO et B_2O_3 sur la structure du C_3S.
I-288	W. Kurdowski, Z. Weliszek (Pologne)	Formation of syngenite during cement grinding. Formation de la syngénite au cours de broyage du ciment.
I-292	S. Takagi, A. Kawashima (Japan)	Processing characterization on the industrial scale cement production. Prévision de la qualité d'un ciment, en production industrielle.

II-0 **THEME II – Hydratation des ciments portland sans constituants secondaires.**
Hydration of pure Portland Cements.

II-1	J. Bensted (Grande-Bretagne)	Early hydration behaviour of sulphate resisting and white portland cement. Comportement initial lors de l'hydratation de ciment portland à haute résistance aux sulphates et de ciment blanc.
II-7	P. Kittl, C. Suchicital, A. Goldschmidt (Chili et Brésil)	Study on the evaporation product of the liquid phase of a cement paste. Etude du produit de l'évaporation de la phase liquide d'une pâte de ciment.
II-12	I.P. Vyrodov (URSS)	On physico-chemical foundations of hydration and setting of binding systems. Phases physico-chimiques de l'hydratation et de la prise de liants hydrauliques.
II-18	Surendra Nath Gosh (Inde)	Some applications of infrared spectroscopy in the fields of cement and concrete. Quelques applications de la spectroscopie infrarouge dans le domaine du ciment et du béton.
II-25	V.S. Ramachandran, J.-J. Beaudoin (Canada)	Hydration of C_4AF + gypsum : study of various factors. Hydratation du C_4AF + gypse : étude des divers facteurs.

II-31	F. Hannawayya (Suède)	Study of the structure and crystallization properties of tricalcium silicate (C_3S) and β-dicalcium silicate (β-C_2S) hydrate and the new calcium silicate hydrate. C-S-H (III), C-S.H (I^1) and C-S-H (II^2). Etude de la structure et de la cristallograhie du silicate tricalcique (C_3S), du silicate bicalcique β (β-C_2S), et du silicate calcique hydraté C-S-H (III), C-S-H (I^1) et C-S-H (II^2).
II-37	C. Tashiro (Japon)	The effects of several heavy metal oxides on the hydration and the microstructure of hardened mortar of C_3S. Effets de quelques oxydes de métaux lourds sur l'hydratation du C_3S et sur la structure fine des corps durcis.
II-43	F.G. Buttler, S.R. Morgan (Grande-Bretagne)	A thermoanalytical method for the determination of the amount of calcium hydroxide in systems containing hydrated Portland cement. Une méthode de l'analyse thermique pour la détermination quantitative de l'hydroxyde de calcium dans des systèmes contenant du ciment portland hydraté.
II-47	Kazutaka Suzuki, Suketoshi Ito, Sumio Shibata, Namitsugu Fujii (Japon)	Hydration and strength of α-, α'-, and β-dicalcium silicates stabilized with Na-Al, K-Al, Na-Fe, and K-Fe. Hydratation et Résistance de α-, α'-, et β-dicalcium silicates stabilisées par Na-Al, K-Al, Na-Fe, et K-Fe.
II-52	S.A. Mironov, I.I. Kourbatova, O.S. Ivanova, S.A. Vyssotsky (URSS)	Durcissement du ciment à des températures au-dessous de zéro. Cement hardening under below zero temperature.
II-58	C. Tashiro, J. Oba (Japon)	The effects of $Cu(OH)_2$ on the hydration of C_3A. Action du $Cu(OH)_2$ sur l'hydratation du C_3A.
II-64	D.L. Rayment, A.J. Majumdar (Grande-Bretagne)	The composition of CSH phase(s) in hydrated C_3S paste. Composition des phases HSC dans la pâte hydratée de C_3S.
II-71	I.B. Zacedatelev (URSS)	Caractéristiques thermochimiques du ciment et accélération de durcissement du béton. Thermochemical characteristics of cement and acceleration of concrete setting.
II-76	Z.M. Larionova, L.P. Kourassova, (URSS)	Les variations de phase et les propriétés du ciment durci. Phase change and properties of hardened cement paste.
II-82	Zonghan Lou, Xianyu Xu, Ren Han (Chine Populaire)	On ettringite and modification of slag cement. Sur l'ettringite et l'amélioration des ciments de laitier.
II-88	Feipeng Zhang, Zhifa Zhou, Zonghan Lou (Chine Populaire)	Solubility product and stability of ettringite. La stabilité de l'ettringite et le "produit de solubilité".
II-94	Tang Ming-Shu, Han Su-fen, (Chine Populaire)	Effect of $Ca(OH)_2$ on alkali-silica reaction. Effet de $Ca(OH)_2$ sur l'alcali-réaction.
II-100	N.B. Singh, P.N. Ojha (Inde)	Effect of glucose on the hydration of portland cement. Action du glucose sur l'hydratation du ciment portland.
II-106	Z. Sauman, F. Vavrin (Tchécoslovquie)	Conditions of the Hydroxyl Ellestadite Formation in Mixtures containing Calcium Sulphate. Les conditions de la formation de l'hydroxyle-ellestadite dans les mélanges comprenant du sulfate de calcium.
II-111	A. Bezjak, I. Jelenic, V. Mlakar, A. Panovic (Yougoslavie)	A Kinetic Study of Alite Hydration. Etude cinétique de l'hydratation de l'alite.
II-117	Z.B. Entine, Ou I. Papiachvili L.S. Klioneva (URSS)	Formation de la structure des ciments avec fausse prise. Structure formation of cements with false setting.
II-123	M. Regourd, J.H. Thomassin, P. Baillif et J.C. Touray (France)	X-Ray photoelectron spectrometry investigation of the early stages of C_3S hydration. The role of NaF admixture. Etude par la spectrométrie de photoélectrons XPS des stades initiaux de l'hydratation de C_3S. Rôle de l'adjuvant NaF.
II-129	V.D. Glukhovsky, P.V. Krivenko, R.F. Runova (URSS)	Condensation properties of dispersed products of portland cement hydration and rehydration. Propriétés agglomérantes des composants dispersés du ciment, après leur hydratation ou leur réhydratation.
II-135	B. Osbaeck and E.S. Jons (Danemark)	The Influence of the Content and Distribtuion of Alkalies on the Hydration Properties of Portland Cement. Influence du contenu et de la répartition des alcalis sur les propriétés d'hydratation du ciment Portland.
II-141	H.M. Jennings, P.L. Pratt, (Grande-Bretagne)	On the reactions leading to calcium silicate hydrate, calcium hydroxide and ettringite during the hydration of cement. A propos des réactions produisant le silicate de calcium hydraté, l'hydroxyde de calcium et l'ettringite pendant l'hydratation du ciment.

II-147	A. Zelwer (France)	Propriétés électrocinétiques à la surface des minéraux du ciment portland. Electrokinetic surface properties of portland cement minerals.
II-153	R. Krstulovic, T. Feric, P. Krolo (Yougoslavie)	Study of kinetics of industrial cements hydration. Vitesse d'hydratation des ciments industriels.
II-161	Slanicka Stefan (Tchécoslovaquie)	Influence of Water-Soluble Melamine Formaldehyde Resin on Hydration of C_3S,C_3A + $CaSO_4$.$2H_2O$ mixes and cement pastes. L'influence de la résine hydrosoluble de mélamine-formaldehyde sur l'hydratation des pâtes préparées de C_3S, du mélange C_3A + $CaSO_4$.$2H_2O$ et des pâtes de ciment.
II-167	E.D. Shchukin, E.A. Amelina, E.P. Andreeva, S.I. Kontorovich (URSS)	Agglutination (bridging) of Particles during Hydration Hardening and the Effect of Surface Active Additives. Agglutination des particules pendant l'hydratation et le durcissement des ciments. Influence des ajouts tensio-actifs.
II-172	M. Ono, M. Nagashima, M. Saito (Japon)	The stiffening of mortar accompanied with the early hydration of cement. Le raidissement du mortier accompagnant l'hydratation initiale du ciment.
II-176	R. Sanzhaasuren, E.P. Andreeva, N. Stukalova (URSS)	On the mechanism of Hydration Hardening of Portland Cement Ferrite Phase. Mécanisme de l'hydratation et du durcissement de la phase ferritique des ciments Portland.
II-182	I. Jawed, D. Ménétrier, J. Skalny (USA)	Early hydration of calcium silicates : surface phenomena. L'hydratation initiale des silicates de calcium : phénomènes de surface.
II-188	T. Ciach, J. Dyczek, M. Petri, L. Westfal (Pologne)	Materials from the Synthetic Tobermorite. Matériaux comportant de la tobermorite de synthèse.
II-192	K. Nakagawa, K. Isozaki, Y. Watanabe (Japon)	Hydration and strength of normal portland cement admixed with anhydrous calcium sulfate. Hydratation et résistance du ciment portland normal additionné d'anhydrite.
II-198	T.V. Kouznetsova, I.V. Kravtchenko, (URSS)	Le rôle des aluminates et des sulfoaluminates de calcium dans l'élaboration de propriétés de la pierre de ciment. Part played by aluminates and calcium sulfoaluminate in formation of properties of cement stone.
II-203	E. Sakai, M. Daimon, R. Kondo (Japon)	Very early hydration of tricalcium silicate. L'hydratation aux premiers âges du silicate tricalcique.
II-209	A. Bonin (France)	Eventement et raidissement des ciments. Air aging and stiffening of Portland cements.
II-214	P. Galtier et B. Guilhot, M. Murat (France) A. Bachiorrini et A. Negro (Italie)	Réactivité de l'aluminate monocalcique vis-à-vis de l'eau. Reactivity of monocalcium aluminate.
II-219	C. Vernet, E. Demoulian, P. Gourdin, F. Hawthorn (France)	Cinétique de l'hydratation du ciment portland. Hydration kinetics of portland cement.
II-225	F.G.R. Gimblett, K.S.W. Sing, Z. Mohd. Amin (Grande-Bretagne)	Influence of pretreatment on the microstructure of calcium silicate hydrate gels. Influence du prétraitement sur la microstructure des gels de silicate de calcium hydraté.
II-232	D. Menetrier, B. Cottin, P. Barret (France)	Etude analytique des C-S-H obtenus par action de la chaux sur la silice. Analytical study of C-S-H obtained by the action of lime on silica.
II-237	A.V. Oucherov-Marchak, A.M. Ourjenko, O.P. Mtchedlov-Petrossian (URSS)	Calorimétrie des liants. Calorimetry of binders.
II-242	D.M. Roy, (USA) M. Daimon, K. Asaga (Japon)	Effects of Admixtures upon Electrokinetic Phenomena During Hydration of C_3S, C_3A and Cement. Effet des adjuvants sur les phénomènes électrocinétiques au cours de l'hydratation de C_3S, C_3A et du ciment.
II-247	V.M. Kolbasov, N.A. Kozyreva, (URSS)	Modifications of Structure and Properties of Cement Stone. La modification de la structure et propriétés des ciments hydratés.
II-252	P. Longuet, G. Bellina (France)	Comportement de l'aluminate tricalcique en milieu glycol - Comparaison avec l'hydratation. Tricalcium aluminate behaviour in glycol - Comparison with water.
II-256	D.D. Double, N.L. Thomas, D.A. Jameson (Grande-Bretagne)	The Hydration of Portland Cement. Evidence for an Osmotic Mechanism. L'hydratation des ciments Portland. Intervention évidente d'un processus osmotique.
II-261	P. Barret, D. Bertrandie, D. Ménétrier (France)	Etude comparée de la formation de C-S-H à partir de solutions sursaturées et de mélanges C_3S-solution. Comparative study of C-S-H formation from supersaturated solutions and C_3S solution mixtures.

L'index des auteurs se trouve en fin du volume III
The author index is at the end of the volume III

THÈME I

Influence des matières premières des combustibles et des procédés de fabrication sur la structure et les propriétés des clinkers

Influence of raw materials, fuels and manufacturing processes on clinker structure and properties

Présidents : M. BUCCHI (Italie)
M. MÉRIC (France)

Mineralizers and Fluxes in the Clinkering Process. II. Kinetics Effects on Alite Formation

Minéralisateurs et fondants dans la clinkérisation. II. Effets cinétiques sur la formation d'alite

N.H. CHRISTENSEN F.L. Smidth et Co.A/S
V. JOHANSEN COPENHAGUE, Danemark.

RESUME : L'influence de certains produits d'addition sur la vitesse de la réaction $C + C_2S \rightarrow C_3S$ a été étudiée dans des conditions isothermes à des températures comprises entre 1350 et 1500°. Sont exposés, dans cette communication, des résultats expérimentaux concernant l'effet cinétique du spathfluor, du gypse et des alcalis sulfatés ou non sulfatés. Alors que le spathfluor a un effet accélérateur, les autres produits essayés ont une action retardatrice sur la formation de l'alite.

Ces effets chimiques sur la formation de l'alite peuvent être attribués à des modifications dans la composition de la phase liquide, de son coefficient de diffusion, de la force qui engendre cette diffusion, ou d'une combinaison de ces facteurs. Les effets cinétiques observés sont, pour une grande part, sous l'influence de cette force. Les résultats semblent indiquer qu'il existe une relation entre ces effets et les concentrations relatives, dans la bélite et l'alite, des produits ajoutés.

SUMMARY : The effects of some additives on the rate of the reaction $C + C_2S \rightarrow C_3S$ have been studied under isothermal conditions between 1350°C and 1500°C. Data on the rate effects of fluorspar, anhydrite, and sulfated and unsulfated soda and potassia are presented. Whereas fluorspar acts as an accelerator, all the other additives studied are observed to retard alite formation.

Chemical effects on the alite formation reaction can be attributed to changes in melt content, melt diffusivity, and driving force for diffusion, or combinations of these. The rate effects observed in the present study are to a large extent associated with influences on the driving force. The results suggest a relationship between the effects of these additives and their relative concentrations in C_2S and C_3S.

INTRODUCTION

In this presentation we shall report on results of kinetic studies of the alite formation reaction, $C + C_2S \rightarrow C_3S$. In particular, effects of various fluxing or mineralizing agents upon this reaction will be discussed. The need for kinetic studies on this particular reaction step, separate from the other reactions occurring in burnability studies, was pointed out by R.Kondo twenty years ago (1). Results from his study (2) have greatly improved our insight into the mechanism of the alite formation reaction and, indeed, of the overall clinkering process. By applying a modification of a sandwich (diffusion couple) technique introduced by Kondo and Choi (2), we have been able to collect further information concerning the effects of alumina, ferric oxide and magnesia on the reaction rate (3), and the same technique has also been applied in the present investigation. The advantages of this method are that results are easily interpretable in terms of the fundamental principles for diffusion controlled reactions, and that fineness of the reactants has no influence on the reaction rate measured.

EXPERIMENTAL PROCEDURE

Batches of about 200 g were prepared from analytical grade reagents with known ignition losses; the ignited batch compositions are given in Table I. At the high temperatures, A-compositions with LSF>100% consist of $C + C_3S$ + melt, whereas B-compositions with LSF≈80% consist of $C_3S + C_2S$ + melt.

TABLE I

Tablet type	weight %				
	CaO	SiO_2	Al_2O_3	Fe_2O_3	MgO
1 A	72	22	3	2	1
1 B	66	28	3	2	1
2 A	72	22	6	0	0
2 B	66	28	6	0	0

Each batch was homogenized, calcined at 1050°C, compacted into tablets (1 cm · 1 cm Ø), heated at 1500°C for one hour, ground into a powder, and divided into portions of ~20 g. To some of these portions the required amount of CaF_2, Na_2CO_3, K_2CO_3, Na_2SO_4, K_2SO_4 or $CaSO_4$ was added. At least one portion of each batch was left undoped as a reference sample. After further grinding, the portions (including the reference) were again compacted, heated at 1500°C for one hour, and then air-quenched. One flat surface of each tablet was polished as the final preparation for the isothermal diffusion couple burn.

An A- and a B-tablet were stacked with their polished surfaces in contact. The couple was introduced into an electrically-heated vertical tube furnace, whose temperature stability over 20 hours was ±3°C. After a known period of heating time, t seconds, the couple was air-quenched, cut perpendicularly to the original join, polished, etched and studied under the reflection microscope. A region consisting of C_3S + solidified melt, sharply demarcated from the A- and B-zone, had developed, and its width, x cm, was measured optically at 5-10 positions. Further details of this technique are given in Ref. (3).

Analysis of the fluorspar-doped samples showed that about 10% of the added fluoride had evaporated during the latter part of the preparation of the tablets. Such minor evaporation was not considered important for the interpretation of these studies.

Samples associated with the study of the effects of alkalies and sulfates were analysed for SO_3, Na_2O and K_2O, at the stage prior to the diffusion couple experiments, as well as after further heat-treatment duplicating that of the couple experiments. Here the volatility of the alkalies and SO_3 often was >30%, and differences between volatilities of potassia and soda, sulfated and unsulfated, in A-tablets or B-tablets, were conspicuous.

For various reasons, the alkali and sulfate contents chosen to characterize each couple were those measured in the corresponding B-tablet, just prior to the diffusion couple burn. The actual concentrations during the burn of interest have thereby been overestimated; the magnitude of this error is greater for the more volatile than for the less volatile constituents. Since the more volatile constituents proved to have the most marked rate effects, the errors associated with adoption of the procedure selected tend to diminish, rather than to accentuate, the differences in rate effects.

RESULTS

According to the theory for diffusion couples (3), the width, x, should increase with the square root of the heating time, $t^{\frac{1}{2}}$. Plots of x versus $t^{\frac{1}{2}}$ or of x^2 versus t, should therefore be linear, and this was found to be the case for most series, cf. Fig. 1.

The rate constants, k, which are related to the slopes of these lines ($x^2 = kt$), should be a function of sandwich composition and temperature only. Dividing the rate constant for a doped sandwich, k_d, by the rate constant for an undoped sandwich from the same batch, k_o, both measured at the same temperature, gives a measure for the rate effect caused by the added agent. Values of k_d/k_o, together with other important parameters, are shown in Table II.

The data for CaF_2 in Table II show that fluorspar doping causes a marked increase in rate, although the further effect upon

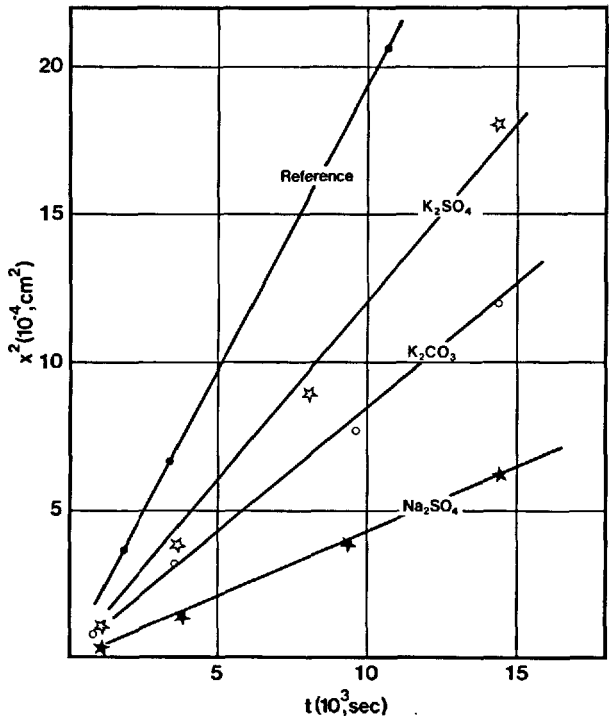

Fig. 1 - Plots of the square of product layer width, versus heating time for some couples specified in Table II, 1450°C.

TABLE II			
Sandwich type	Additive wt.%	Temp. °C	k_d/k_o
1	0.44 CaF_2	1350	2.4
1	0.84 -	1350	2.6
1	1.80 -	1350	2.9
1	0.44 -	1500	1.4
1	0.84 -	1500	1.6
1	0.64 K_2O a)	1400	0.42
1	0.64 -	1450	0.42
1	0.64 -	1500	0.38
2	0.60 -	1475 d)	0.41
2	0.60 -	1500	0.43
1	1.00 K_2O b)	1400	0.74
1	1.00 -	1450	0.66
1	1.00 -	1500	0.55
2	0.90 -	1475 d)	0.63
2	0.90 -	1500	0.60
1	0.46 Na_2O a)	1450	0.59
1	0.86 Na_2O b)	1450	0.23
1	0.90 SO_3 c)	1450	0.46
1	1.10 -	1450	0.39

a) added as carbonate, no sulfate present

b) added as sulfate, a roughly equivalent SO_3 amount still present after firing

c) added as $CaSO_4$

d) sandwich type 2 (A2/B2) did not grow together at temperatures ≤ 1450°C

increasing the concentration above 0.5-1% is small, indicating that some saturation is being approached. The factor 2.4-2.6 is almost the same as that caused by raising the reaction temperature from 1350° to 1500° without fluorspar addition (3). Thus these results corroborate Klemm et al.'s finding (4) that addition of 1% CaF_2 permits achievement of the same rate of alite formation at a temperature 150°C lower than without CaF_2.

Dusting, caused by the beta/gamma belite transformation, completely excluded the preparation of couples having 5% CaF_2, and somewhat complicated the measurements of the product width in the couples with 2% CaF_2, due to crack formation. With 2% CaF_2, growth of the product layer was markedly slowed down after one hour, probably owing to an excessive solid-state sintering of the alite grains, which was observed at 1500°C.

The addition of alkalies and gypsum always retarded alite formation, i.e. $k_d/k_o < 1$. No significant difference in rate effects was observed between the type 1 and type 2 samples examined, cf. Table II. The retarding effect of K_2SO_4 appeared to increase slightly with rising temperature.

In order to normalize the various effects measured at 1450°C to a common scale, it has been assumed that k_d/k_o varies linearly with additive concentration. k_d/k_o can then be calculated for either 1 g of oxide in 100 g of clinker, or for the weight of oxide equivalent to 1 g of K_2O per 100 g of clinker. The results are given in Table III.

TABLE III					
k_d/k_o calc. for	K_2O		Na_2O		SO_3
	$+SO_3$	$-SO_3$	$+SO_3$	$-SO_3$	+CaO
1 g oxide	0.66	0.09	0.10	0.11	0.43
1 g K_2O equiv.	0.66	0.09	0.41	0.41	0.53

It is seen from Table III that on a simple weight basis, unsulfated potassia and soda in both forms are most effective, while sulfated potassia is much less effective. This finding is in good agreement with observations of KRAMER and ZUR STRASSEN (6). However, on the potassia equivalent basis the picture is somewhat modified.

DISCUSSION

Our data on CaF_2 effects agree well with literature findings. However, certain of the reports on the alkali and sulfate effects previously recorded are not consistent with our findings (7). Although it appears that all authors have found unsulfated alkalies to be retarding agents, some have found that alkali sulfates and gypsum (anhydrite) may act as accelerators.

These discrepancies may at least partly be accounted for by noting that in some instances quoted in ref. (7), the undoped reference samples contained little or no melt phase at the chosen burning temperatures, while melt may have been formed when additive was present. In such a case, an acceleration of the reaction is to be expected.

It should also be borne in mind that, when sulfate is present, alkalies, in particular potassia, tend to accumulate in a separate sulfate phase (8,9). Addition of gypsum to a reference material containing unsulfated alkalies may therefore cause transformation of the alkali from a more inhibiting to a less inhibiting state, i.e. an improvement of burnability is to be expected. On the other hand, addition of excess gypsum may again cause regression in the burnability.

Differences in volatility, and the fact that these studies (7) related to the overall clinkering process, rather than to C_3S formation alone, may also have contributed to the discrepancies.

Growth of the product layer in a diffusion couple is governed by the term $\alpha \cdot D' \cdot \Delta c$ (3). Here α is the volume fraction melt in the product layer (C_3S + melt); D' is the effective binary diffusion coefficient for the melt; $\Delta c = c_a - c_b$, c_a is the concentration of CaO in the melt in equilibrium with C + C_3S, and c_b the concentration of CaO in the melt in equilibrium with C_2S + C_3S. Δc is the driving force for diffusion through the melt in the product layer; hence, changes in Δc are to some extent representative of changes in the driving force for the alite formation reaction (10).

In the present study, little change in α is to be expected as a consequence of the added compounds, and microscopic examination of our samples has confirmed this expectation. The observed changes in rate constants must therefore be attributed to changes in D' and/or Δc.

Butt et al. (11) reported that the viscosity of a clinker melt increased, and the tracer diffusivity for Ca in the same melt decreased, when the concentration of unsulfated soda or potassia in such melt was increased. If these relations also represent changes in D' for melts remaining in equilibrium with C_3S while additive concentration varies, then the rate effects observed in our investigation may be accounted for through variations in D', as far as the unsulfated alkalies are concerned.

However, Butt et al. (11) also observed that the melt viscosity decreased for increasing content of Na_2SO_4, K_2SO_4 and $CaSO_4$. These observations are not consistent with our findings that these additives act as retarders, unless we accept that Δc has been negatively affected.

In fact, the occasional observation that the alite formation reaction is totally inhibited, or even reversed, by the addition of alkalies (6,8,12), cannot be explained as a result of a change in D', but must be caused by a marked decrease in driving force, so that lime and belite can coexist in equilibrium, i.e. Δc is zero.

Δc can be deduced from a relevant phase diagram; the width of the C_3S primary field at the temperature in question is determined by Δc. Unfortunately, no diagram is available for the sulfate-containing systems of interest. However, D.M. Roy et al. (part I, preceding paper) have shown that the C_3S primary field is widened when (A+F) is partially replaced by CaF_2. Similarly it is also known that alkalies cause a narrowing of the C_3S primary field (13). It therefore appears that effects on Δc contribute to the observed effects of CaF_2 as an accelerator, and of alkalies as retarders.

Since Δc is related to the thermodynamic driving force, it is also affected by the partitioning of the added constituents between the solid phases C, C_3S and C_2S; CaF_2 preferentially dissolves in C_3S, while alkalies preferentially dissolve in C_2S. Such considerations also help to explain other examples of chemical effects upon alite formation reaction rates (10).

CONCLUSION

The addition of a modest quantity of a foreign constituent may cause a change, positive or negative, in the rate of the alite formation reaction at constant temperature. Such effect is the net result of changes in: Content of melt, diffusivity of melt, driving force for diffusion. The most marked negative rate effects are associated with decrease in driving force. The most marked positive effects on the rate are associated either with increase in melt content from zero, or with increase in driving force. It would be reasonable to link the traditional terms fluxing and mineralizing effects to these two mechanisms, respectively.

ACKNOWLEDGMENTS

The efficient technical assistance of Dorthe Lotz Clasen and Kenn Svanlundh is gratefully acknowledged. F. MacGregor Miller's critical remarks helped to clarify linguistic and conceptual difficulties.

REFERENCES

1.- R. KONDO (1962), "Reaction velocity in Portland cement clinker formation", Proceedings of the 4th International Symposium on the Chemistry of Cement, Washington D.C., 1960, Vol. I pp. 107-112, National Bureau of Standards Monograph 43. U.S. Printing Office, Washington D.C.

2.- R. KONDO and S. CHOI (1969), "Mechanism and kinetics of Portland cement clinker formation", Proceedings of the 5th International Symposium on the Chemistry of Cement, Tokyo, 1968, Vol. I pp. 163-171, The Cement Association of Japan, Tokyo.

3.- N.H. CHRISTENSEN, O.L. JEPSEN and V. JOHANSEN (1978), "Rate of alite-formation in clinker sandwiches", Cem. Concr. Res. 8, 6, 693-701.

4.- W.A. KLEMM, K.J. HOLUB and J. SKALNY (1978), "The effect of fluxes and mineralizers in lowering cement kiln temperatures", Progress report 3, Martin Marietta Corp. Maryland.

5.- V. JOHANSEN and N.H. CHRISTENSEN (1979), "Rate of formation of C_3S with addition of CaF_2", Cem. Concr. Res. 9, 1, 1-5.

6.- H. KRÄMER and H. ZUR STRASSEN (1962), "Discussion", Ref. (1) pp. 32-33.

7.- I. JAWED and J. SKALNY (1977), "Alkalies in cement, a review", Cem. Concr. Res. 7, 6, 719-730.

8.- H.W.W. POLLITT and A.W. BROWN (1969), "The distribution of alkalies in Portland cement clinker", Ref. (2) pp. 322-333.

9.- J.E. MANDER and J.P. SKALNY (1977), "Calcium alkali sulfates in clinker", Bull. Amer. Ceram. Soc., 56, 11, 987-990.

10.- N.H. CHRISTENSEN and V. JOHANSEN (1979), "Chemical effects on ceramic reactions" J. Amer. Ceram. Soc. 62, 5-6, 313-315.

11.- Y.M. BUTT, V.V. TIMASHEV and A.P. OSOKIN (1974), "The mechanism of clinker formation processes and the modification of its structure", The 6th International Congress on the Chemistry of Cement, Moscow 1974, preprint.

12.- E. WOERMANN (1962), "Decomposition of alite in clinker containing potassium", Ref. (1) p. 128.

13.- R.H. BOGUE (1955), "The chemistry of Portland cement", 2nd ed., pp. 431, 444, Reinhold Publ. Corp., New York.

I-6

Cement minerals of complicated composition

Composants complexes des clinkers

A BOIKOVA Doctor, Institute of Silicate Chemistry of the Academy of the USSR, Leningrad.

RESUME : On a effectué la synthèse et l'étude physico-chimique des alites, bélites, aluminates et aluminoferrites provenant de divers crus ou mélanges complexes; ces éléments peuvent être considérés comme des solutions solides multicomposant dans C_3S, dans C_2S, des oxydes de Na_2O, K_2O, MgO, Al_2O_3, Fe_2O_3, TiO_2, P_2O_5, dans C_3A de Na_2O, K_2O, MgO, Fe_2O_3, SiO_2; et dans C_6A_2F de Na_2O, K_2O, MgO, MnO, SiO_2, TiO_2.

Les compositions synthétiques ont été choisies en partant des résultats de l'analyse à la microsonde électronique des phases du clinker des produits industriels. Le traitement à haute température des compositions choisies provoque la formation d'alite monoclinique, de bélite α -, α'_z -, β , de la phase aluminate cubique et d'aluminoferrite orthorhombique avec la matrice composée de C_6A_2F.

Les compositions chimiques des produits finals synthétiques sont indiqués. Les diagrammes de diffraction des rayons X montrent que les phases complexes sont dérivées de C_3S, C_2S, C_3A et C_6A_2F. Les paramètres cristallins ont été calculés et la densité a été mesurée. L'examen microscopique a été effectué sous lumière transmise et sous lumière réfléchie. Une distinction claire entre les cristaux α -, α'_z, β de la bélite a été faite.

La particularité des phases contenant des impuretés est la capacité de former des cristaux imparfaits et des produits mal cristallisés. De telles phases possèdent une activité plus grande à l'action de l'eau, que les mêmes phases bien cristallisées. Des phases activées peuvent être obtenues par le choix des mélanges d'impuretés et du régime thermique approprié.

L'hydratation aux premiers et derniers âges a été étudiée. L'analyse des courbes cinétiques montre que le cours du processus d'hydratation de chaque phase est particulier et différent de celui des composants purs : C_3S, C_2S, C_3A et C_6A_2F et des phases de composition simple.

SUMMARY : The synthesis and the physico-chemical investigation have been made of alites, belites, aluminates and aluminoferrites of complicated composition which can be regarded as multicomponent solid solutions of C_3S and C_2S with oxides Na_2O, K_2O, MgO, Al_2O_3, Fe_2O_3, TiO_2, P_2O_5; of C_3A with Na_2O, K_2O, MgO, Fe_2O_3, SiO_2; of C_6A_2F with Na_2O, K_2O, MgO, MnO, SiO_2, TiO_2.

The synthesized compositions have been chosen according to the results of electron-probe microanalysis of the clinker phases of commercial products. The high-temperature treatment of the chosen compositions led to the formation of the monoclinic alite, the α -, α'_z -, β - modifications of belite, the cubic aluminate phase, the orthorhombic aluminoferrite whose matrix is composed of C_6A_2F.

The chemical compositions of the final synthesis products are given. The X-ray diffraction patterns show that the complex phases are derivatives of C_3S, C_2S, C_3A, C_6A_2F. The unit cell parameters have been calculated and the density has been measured. Microscopic examinations in transmitted light and in reflected light have been made. A clear distinction between α -, α'_z - and β modifications of belite has been observed.

The peculiarity of the phases containing the complex of impurities is the capability to form imperfect crystals and poorly crystallized products. Such phases show a greater activity to the action of water compared to the same phases which are well crystallized. The activated phases can be obtained by choosing the set of impurities and the appropriate thermal schedule.

Early and later hydration has been studied. The analysis of kinetic curves show that the course of hydration process of each phase is peculiar compared to "pure" C_3S, C_2S, C_3A, C_6A_2F and to the phases of a more simple composition.

A study of cement minerals of complicated composition analogous to phases of commercial clinkers is one of the main tasks of the common problem of composition, structure and properties of the real clinker phases. The formation of these complex phases is first of all possible owing to the crystal chemical structural peculiarities of "pure" matrix compounds C_3S, C_2S, C_3A, C_4A_2F. Cement minerals consist of such elements (Ca, Al, Fe, Si) which possess the greatest ability (compared to others) to substitutions by various isomorphic elements.

The real conditions of cement production - the chemical composition of raw materials and the heat treatment schedule - provide the formation of cement minerals containing many impurities.

The minerals were synthesized by annealing the batch of initial components the amounts of which were calculated according to compositions chosen from results of the electron-probe microanalysis of the phases of commercial clinkers. The annealing schedule (temperature, exposure, cooling rate) varied depending on the mineral synthesized.

The compositions of all products obtained were determined by chemical analysis. The identification of the phases, the determination of the homogeneity of the samples were made using microscopic and X-ray methods.

ALITES OF COMPLICATED COMPOSITION

Table 1 gives the compositions of complex alites A,B,C, alite D with five impurity atoms - Na, K, Mg, Al, Fe, and alite E with three impurity atoms - Mg, Al, Fe. For comparison purposes the samples of C_3S were synthesized and studied.

TABLE I

Sample / Oxide	Alites				
	A	B	C	D	E
CaO	71.13	71.03	71.62	71.89	71.58
SiO_2	25.72	24.95	25.24	24.83	26.40
Na_2O	0.20	0.23	0.28	0.18	-
K_2O	0.11	0.14	0.15	0.12	-
MgO	0.70	0.91	0.71	1.05	0.51
MnO	0.04	-	-	-	-
Al_2O_3	0.80	1.21	0.88	1.21	1.05
Fe_2O_3	0.72	0.95	0.73	0.44	0.55
TiO_2	0.22	0.31	0.22	-	-
P_2O_5	0.16	0.25	0.10	-	-
L.of Ig.	0.27	0.57	0.37	-	-
Σ	100.07	100.55	100.30	99.72	100.09
Σ impur.	2.95	4.00	3.07	3.00	2.11

As an example we give the formula of one of the complex alites in atomic and in the generally accepted form:

alite B: $Ca_{103.87}Si_{34.05}Na_{0.61}K_{0.24}Mg_{1.85}Al_{1.95}Fe_{0.98}Ti_{0.32}P_{0.29}O_{180}$;

$3.04CaO \cdot SiO_2 \cdot 0.009Na_2O \cdot 0.004K_2O \cdot 0.054MgO \cdot 0.029Al_2O_3 \cdot 0.014Fe_2O_3 \cdot 0.009TiO_2 \cdot 0.004P_2O_5$.

Microscopic examination showed that each alite is a homogeneous well-crystallized phase with slightly increased refractive indices compared to pure C_3S and with higher birefringence. $N_g - N_p$ for alites is 0.005-0.008 and for pure C_3S is 0.003.

X-ray analysis showed that all alites are monoclinic; the unit cell parameters for them and refractive indices are given in Table II.

TABLE II

Alite	a, Å	b, Å	c, Å	β°	N_g	N_p
A	12.261	7.059	25.064	89°44′	1.729	1.722
B	12.252	7.054	25.018	89°23′	1.728	1.720
C	12.263	7.056	25.049	89°54′	1.727	1.720
D	12.249	7.048	24.988	89°57′	1.728	1.722
E	12.243	7.050	25.018	89°43′	1.724	1.719

The unit cell parameters for C_3S calculated by us are: a = 12.218 Å; b = 7.119 Å; c = 25.148 Å; α = 89°54′; β = 89°42′; γ = 89°43′. The refractive indices are: N_g = 1.717, N_p = 1.714.

The X-ray diffraction pattern of complex alite B resembles that of pure C_3S (Fig. 1). X-ray patterns of the other alites are not given as they are of the same type.

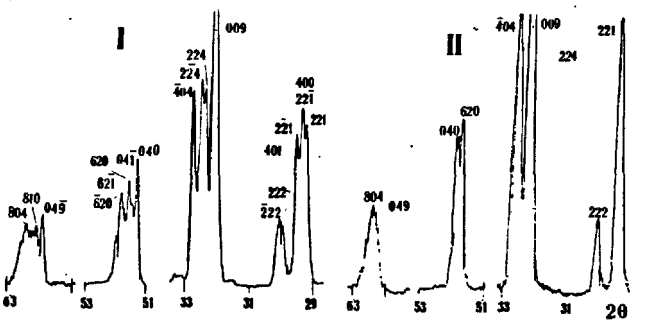

Fig. 1 - Fragments of the X-ray diffraction pattern of C_3S (curve I) and alite B.

The melting temperatures of alites measured on a heating microscope are close to each other: 2055°C ± 10° (for C_3S 2070°C + 10°). The experimental density of alites is 3.18-3.20 g/cm³, the calculated density 3.13-3.17 g/cm³.

The IR spectra demonstrate (Fig.2) that the lattice distortion caused by impurities shows up in the diffuse character of the curves. The decrease of intensity of the bands in the absorption maximum, the broadening of the bands, and as a result, the merging of some of them are due to disorder in distribution of cations in the lattice of the solid solutions and to the distortion of the structural elements.

The hydration kinetic curves (Fig.3) were obtained using the results of X-ray analysis. The parallel runs permitted to make sure of the reproducibility of the process the general character of which can be revealed with sufficient accuracy by X-ray analysis.

The samples were prepared in paste form with a w/c=0.4, the experimental temperature was 20°C. The observation over the course of hydration during the first days was made every two hours and further in the standard terms.

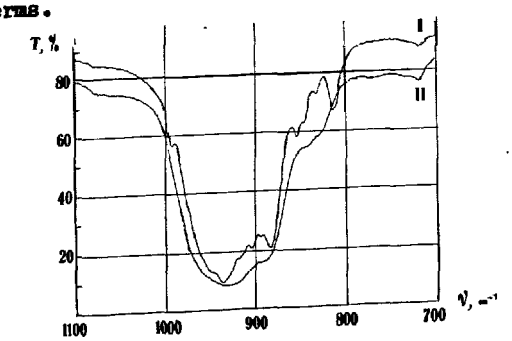

Fig. 2 - IR spectra of C_3S (curve I) and alite B.

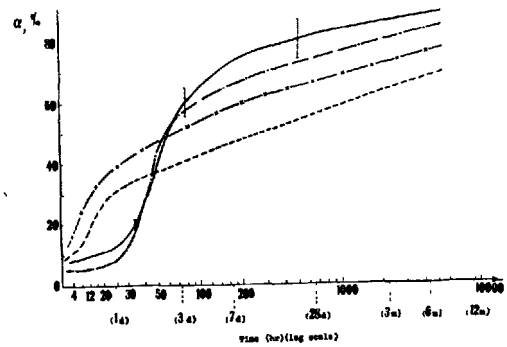

Fig. 3 - Degree of hydration of C_3S (- - -) and alites B (——), A (-·-) and C (-x-).

The analysis of the hydration process shows that at early hydration (in the given experiment for the first 1-2 h) the values of the degree of hydration of alites and C_3S are close to each other. The hydration of alites A and B proceeds slower. But further it is with these alites that the stage of acceleration of the hydration reaction proceeds most intensely. After completion of this period all complex alites hydrated to a considerably greater extent than C_3S; the value of α was greatest for alites A and B.

Although in structural relation the complex of impurities causes the usual transformation of triclinic C_3S to monoclinic alite, the influence of impurities on the hydration activity appears to be rather effective. Complicated monoclinic alites are more reactive than those with one or two impurities. Thus after 28 days the degree of hydration of the monoclinic alite B is twice that of the monoclinic solid solution of C_3S with ZnO.

BELITE

The compositions of α-, α'_x-, β-modifications of belite with a complex of impurities in the lattice are shown in Table III. The preparation of each of the modifications appeared to be possible by choosing an appropriate heat treatment schedule. Belites can be produced homogeneous if the total amount of impurities does not exceed 6 %. The amount of impurities in the different modifications can vary but not significantly.

TABLE III

Belites / Oxide	α	α'_x	β	β	β	β
	A	B	C	D	E	F
CaO	61.97	62.88	62.48	65.70	60.68	61.71
SiO_2	31.52	31.58	31.25	28.50	33.20	31.76
Na_2O	1.00	0.45	0.26	0.38	0.22	0.25
K_2O	0.74	1.15	0.65	0.37	0.61	0.76
MgO	0.50	0.52	0.94	0.17	0.76	0.80
MnO	0.05	-	0.04	-	0.02	0.02
Al_2O_3	1.44	1.68	1.87	2.58	1.89	1.53
Fe_2O_3	1.97	1.22	0.76	1.22	1.07	1.36
Cr_2O_3	-	-	-	-	-	0.029
TiO_2	0.27	-	0.45	-	0.30	0.56
P_2O_5	-	-	0.45	-	0.55	0.79
SO_3	-	-	0.13	0.53	0.18	-
L.of Ig	0.60	0.94	0.34	0.38	0.34	0.49
Σ	100.06	100.42	99.62	99.83	99.82	100.05
Σ imp.	5.97	5.02	5.55	5.25	5.60	6.10

The formula of α-, α'_x-, β-belites in atomic and oxide forms can be represented as follows:

α(A): $Ca_{1.94}Si_{0.92}Na_{0.06}K_{0.03}Mg_{0.02}Al_{0.05}Fe_{0.04}Ti_{0.006}Mn_{0.001}O_4$;

$2.11CaO.SiO_2.0.03Na_2O.0.015K_2O.0.024MgO.0.027Al_2O_3.0.023Fe_2O_3.0.006TiO_2.0.001MnO$;

α'_x(B): $Ca_{1.97}Si_{0.92}Na_{0.02}K_{0.04}Mg_{0.02}Al_{0.06}Fe_{0.03}O_4$;

$2.13CaO.SiO_2.0.014Na_2O.0.023K_2O.0.024MgO.0.03Al_2O_3.0.014Fe_2O_3$;

β(C): $Ca_{1.94}Si_{0.91}Na_{0.01}K_{0.02}Mg_{0.04}Mn_{0.001}Al_{0.06}Fe_{0.02}Ti_{0.01}P_{0.01}S_{0.003}O_4$;

$2.14CaO.SiO_2.0.008Na_2O.0.013K_2O.0.045MgO.0.001MnO.0.035Al_2O_3.0.009Fe_2O_3.0.011TiO_2.0.006P_2O_5.0.003SO_3$.

The unit cell parameters of belites are:

α-(A): a = 5.435Å; c = 6.983Å;

α'_x-(B): a =11.047Å; b =18.730Å; c = 6.764Å;

β-(C): a = 5.520Å; b = 6.799Å; c =11.169Å; β= 123°48';

β-(D): a = 5.517Å; b = 6.777Å; c =11.182Å; β= 123°39';

β-(E): a = 5.509Å; b = 6.770Å; c =11.189Å; β= 123°57';

β-(F): a = 5.526Å; b = 6.771Å; c =11.195Å; β= 123°56'.

Microscopic examination permitted to clearly distinguish α-, α'_x- and β-belites; the α-form represents crystals with low birefringence. The refractive indices are N_g = 1.720, N_p = 1.717. At the edges and in the center of the crystals are strips of crystals of the other phase which can be distinctly observed

under polarizing light owing to higher birefringence.

α'-belite differs from α - and β-forms in striations of the surface in one, two and three directions. The refractive indices are as follows: N_g=~1.732 and N_p= 1.719; N_g-N_p=0.013. The exact determination of N_g and N_p is difficult.

β-belite are crystals of a yellowish color with a rough spotty surface (not striated). N_g=1.733-1.735; N_p= 1.714-1.718. Each modification contains some amount of belites of the other form.

X-ray diffraction patterns of α-, α'_χ - and β - belite are shown in Fig.4. The presence of reflections 350,341,122,231 permits to assign α' to α'_χ.

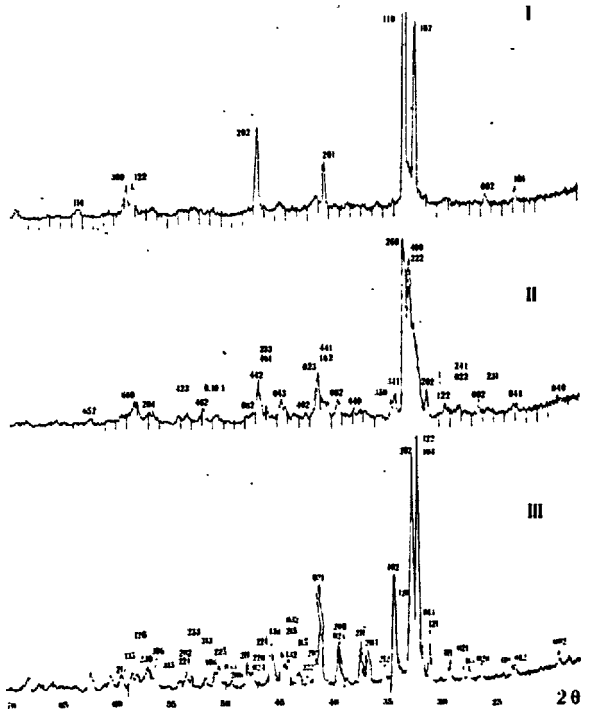

Fig.4 - X-ray diffraction patterns of polymorphic modifications of belite: I - α-(A); II - α'_χ(B); III- β-(C).

Noteworthy is the β - belite (D). The broadening of many reflections in the X- ray pattern is evidence of imperfect crystallization. It is apparently such a belite that is structurally most close to belites of commercial clinkers which are usually called "products of imperfect crystallization". The change in the heat treatment schedule of this belite leads to form either α'- or well crystallized β -modification. This unstable form of belite is closer in hydration activity to the α' -form.

The α'-form is the most "sensitive" modification to the lattice rearrangement. The accurate regulation of the heat treatment schedule and impurity concentrations can lead to obtain, in our opinion, more than two varieties of the α' -form.

The IR spectra of belites (Fig. 5) indicate structural transformations due to the influence of impurities and heat treatment conditions. The diffuse character of the spectra increases from one modification to another and demonstrates disorder in distribution of cations in the lattice and the distortion of the structural elements.

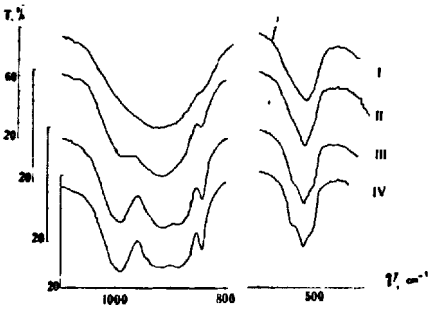

Fig. 5 - IR spectra of α - (curve I), α'_χ - (II), β-(III) belites and of β-belite with B_2O_3 (IV).

The hydration kinetic curves of belites (the averaged curves from the parallel runs) were obtained using the X-ray method (Fig. 6). The curves show a considerably higher reactivity of α - and α'-belites compared to β - belites. Attention is drawn to the high active β-belite D (curve III) imperfectly crystallized.

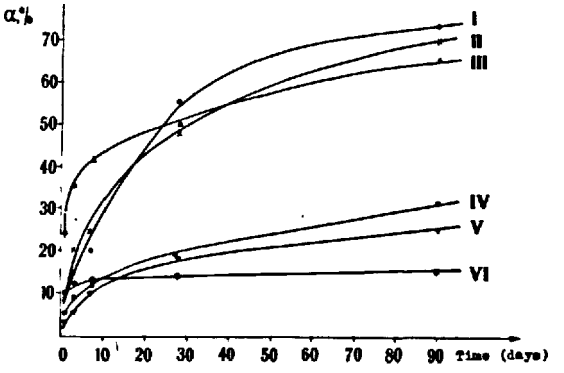

Fig. 6 - Hydration kinetic curves of belites: I -α-(A); II -α'_χ(B); III -β-(D); IV -β-(C) V - β-(E); VI -β-(F).

The increase of hydration activity of belites can be attained not only by providing the appropriate conditions for the formation of most reactive α - and α' - modifications of complicated composition but also by producing imperfect crystals.

The study of belite phases is of interest due to their high content in some cements. A valuable property of belite is the capability to yield active forms.

ALUMINATE PHASE

The peculiarities of the fine structure of C_3A provide the most favourable conditions for distribution in the lattice of a considerably greater amount of impurities than in the silicate phases. The presence of large holes in the C_3A lattice promotes the realization of different schemes of heterovalent isomorphic substitutions and permits the distribution of elements with larger ionic radii.

The synthesized homogeneous samples of the aluminate phases contain not more than 13 wt % of impurity oxides. It was observed that if the initial batch contained more than 5 wt % Fe_2O_3, then a certain amount of the aluminoferrite phase well identified microscopically and by X-rays always appeared in the product formed. Most often the aluminoferrite phase crystallized in the form of fine intergrowths with the aluminate phase.

The composition of the synthesized cubic aluminate phase after the data of chemical analysis is as follows (wt %): CaO - 56.68; Al_2O_3 - 29.31; Fe_2O_3 - 5.75; Na_2O - 0.48; K_2O - 0.64; MgO - 0.67; SiO_2 - 5.84; TiO_2 - 0.12; P_2O_5 - 0.08. The total amount of impurity oxides is 13.58 %.

The formula of this phase in atomic and oxide forms has the following appearance:

$Ca_{2.74}Al_{1.56}Na_{0.042}K_{0.037}Mg_{0.045}Fe_{0.20}Si_{0.26}Ti_{0.004}P_{0.003}O_6$;

$3.52CaO \cdot Al_2O_3 \cdot 0.03Na_2O \cdot 0.02K_2O \cdot 0.06MgO \cdot 0.12Fe_2O_3 \cdot 0.34SiO_2 \cdot 0.005TiO_2 \cdot 0.002P_2O_5$.

The density of the phase is 3.14 g/cm^3 (for pure C_3A 3.09 g/cm^3). The parameter a = 15.234 Å (for pure C_3A a=15.255 Å).

The phase contains some amount of calcium aluminoferrite detected microscopically and by X-ray analysis. The X-ray diffraction patterns for C_3A and for cubic aluminate phase are analogous (Fig. 7).

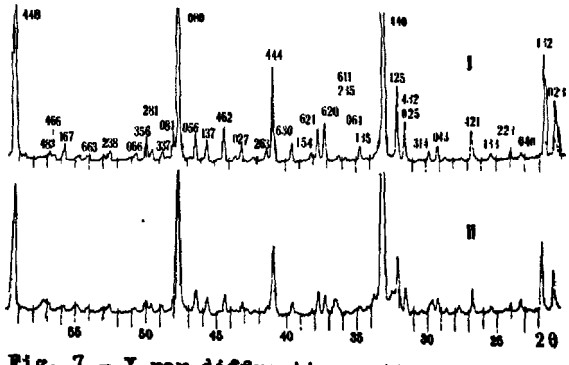

Fig. 7 - X-ray diffraction patterns of C_3A (I) and of the aluminate phase (II).

As shown by kinetic curves of Fig. 8, the hydration process of the aluminate phase (curve II) proceeds like that of pure C_3A and solid solutions of C_3A with Na_2O.

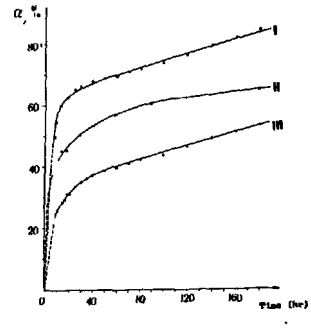

Fig. 8 - Hydration kinetic curves of C_3A(I), aluminate phase (II) and monoclinic solid solution of C_3A with Na_2O (III).

The peculiarity of the aluminate phases is that in the formation process of different crystalline forms the main role belongs to alkalis, whereas the hydration activity depends on the set of all impurities. Detailed results on the study of the aluminate phases will be reported at the Seminar A.

ALUMINOFERRITE PHASE

The aluminoferrite phase, like the aluminate phase, is capable to distribute in its lattice a considerably greater amount of impurities than alite and belite owing to the peculiarities of structure. The occurrence of octahedral and tetrahedral positions with Fe^{3+} and Al^{3+} in the aluminoferrite lattice promotes the variety of substitutions of these atoms for isomorphic impurities. The structure of aluminoferrites is most favourable for occupancy of the lattice sites by Mg, Si, Mn, Cr and Ti.

The compositions of the synthesized homogeneous phases are given in Table IV.

TABLE IV

Oxide \ Sample	AF-2	AF-3	AF-4	AF-6
CaO	46.60	50.02	50.15	49.98
Al_2O_3	23.54	19.41	21.30	18.08
Fe_2O_3	23.86	20.83	20.97	19.80
Na_2O	-	0.25	0.11	0.18
K_2O	-	0.18	0.11	0.26
MgO	0.66	3.21	2.96	3.30
MnO	1.56	1.04	0.27	0.56
SiO_2	2.17	3.87	3.62	6.78
TiO_2	2.48	1.99	1.04	1.34
P_2O_5	-	0.08	-	0.26
Σ	100.87	100.88	100.53	100.54
Σ impur.	6.87	10.62	8.11	12.68

As an example, the formula of aluminoferrite AF-2 in atomic and oxide forms is as follows:

$Ca_{1.94}Al_{1.08}Fe_{0.70}Mg_{0.04}Mn_{0.05}Si_{0.08}Ti_{0.07}O_5$;

$5.56CaO \cdot 1.54Al_2O_3 \cdot Fe_2O_3 \cdot 0.11MgO \cdot 0.15MnO \cdot 0.24SiO_2 \cdot 0.21TiO_2$.

The unit cell parameters of AF-2 are: a = 5.29 Å; b = 14.57 Å; c = 5.54 Å; for C_6A_2F: a = 5.27 Å; b = 14.54 Å; c = 5.53 Å.

All aluminoferrite phases obtained are of the same type, possess analogous X-ray patterns and are similar to the aluminoferrite C_6A_2F. Figure 9 demonstrates as an example the X-ray diffraction pattern of the aluminoferrite AF-2 and that of C_6A_2F for comparison. The matrix of all synthesized aluminoferrites whose compositions were chosen according to the electron-probe microanalysis of commercial products appeared to be the aluminoferrite C_6A_2F.

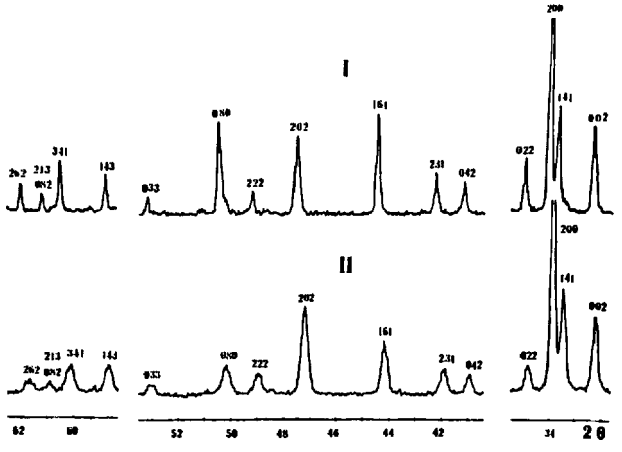

Fig. 9 - Fragments of the X-ray diffraction patterns of C_6A_2F (I) and AF-2 (II).

Aluminoferrites of complicated composition are often distinguished by an imperfect crystallization. The most imperfectly crystallized is the aluminoferrite AF-6. But the quality of the crystals is influenced not only by the set of impurities but also by thermal conditions. Although the structure of AF-6 is so distorted that all reflections are strongly broadened and some of them diffused, nevertheless the character of the whole X-ray pattern remains similar to that of C_6A_2F (Fig. 10).

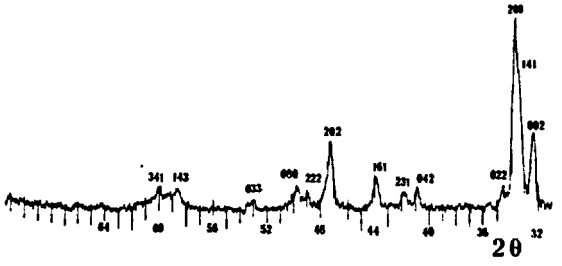

Fig. 10 - X-ray diffraction pattern of AF-6.

The X-ray diffraction pattern of AF-6 is distinguished also by the irregular shift of reflections at angle 2θ of 32-35°, 45-50° and 58-61° what is due to the unit cell distortion.

Aluminoferrites of commercial clinkers are also poorly crystallized. One of the significant causes of the lattice distortion is mainly the heterovalence type of isomorphic substitutions which requires the charge balance, disturbs the microsymmetry and electrostatics of the structure. The distortion is due to the different sizes and different valency of the substitute pairs of atoms, such as Si^{4+} - Al^{3+}, Ti^{4+} - Al^{3+}, Ti^{4+} - Fe^{3+}, Mn^{2+} - Fe^{3+}, Mg^{2+} - Al^{3+}, Mg^{2+} - Fe^{3+}, Si^{4+} - Fe^{3+}.

The influence of a complex of impurities affected first of all the hydration properties of the aluminoferrite phase (Fig. 11). The phase of complicated composition AF-2 appeared to be most reactive during the first days of hydration and its reactivity at all stages of hydration exceeds that of the studied aluminoferrite solid solutions of a more simple composition.

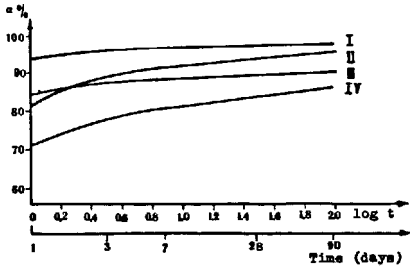

Fig. 11 - Degree of hydration of aluminoferrites: I - AF-2; II - C_6A_2F; III - C_6A_2F with 3.8% MgO and 2.4% SiO_2; IV - C_4AF with 3.5% MgO and 1.2% SiO_2.

CONCLUSION

Cement minerals of complicated composition analogous to phases of commercial clinker can be regarded as multi-component solid solutions.

The preferential location of each impurity in that or another matrix mineral and the total amount of impurity oxides in the limiting solid solutions depend on the peculiarities of fine structures of C_3S, C_2S, C_3A and C_6A_2F.

The contents of impurity oxides in the limiting solid solutions do not exceed the following approximate quantities (wt %): 4.0-4.5% in the alite; 6% in the belite; 10-11% in the aluminoferrite and 13% in the aluminate.

The presence of a complex of impurities and the appropriate thermal conditions may lead to form cement minerals with strongly distorted structure. In industrial conditions the clinker phases (especially belite and aluminoferrite) are most often products of imperfect crystallization. Imperfectly crystallized phases are most active in the process of interaction with water.

The present paper reports the results of unaccomplished investigations. In further work attention will be paid to the preparation and study of the activated phases.

Synthesis of dicalcium silicate and tricalcium silicate phases

Synthèse du silicate bicalcique et du silicate tricalcique.

Surendra Nath GHOSH Ph. D. Cement Research Institute of India, New Delhi.

RESUME : En chauffant les mélanges crus contenant un corps réactif (gel de silice) et en y ajoutant des minéralisateurs, le taux de formation des phases C_2S et C_3S peut être considérablement augmenté. Des minéralisateurs tels que le CaF_2 et le Na_F ont été utilisés et on a fait varier le temps de cuisson d'une demi heure à une heure. La conversion du mélange cru en ces phases était supérieure à 90 % dans le cas d'une seule cuisson.

On a aussi étudié la température de décomposition du $CaCO_3$ dans le mélange par la méthode ATD/ATG. L'effet des cations sur la décomposition du $CaCO_3$ a été observé et mis en corrélation avec le rayon ionique des cations.

SUMMARY : The rate of formation of C_2S and C_3S phases can be increased considerably by heating the raw mixes containing reactive material (silica gel) and addition of mineralizers. Mineralizers, such as CaF_2, NaF were used and total retention time varied from 1/2 hour to 1 hour. The conversion of raw mix to these phases was above 90 % in a single firing.

The decomposition temperature of $CaCO_3$ in the raw mix was also studied by DTA/TGA. The effect of cations on the decomposition of $CaCO_3$ was observed and correlated with the ionic radius of the cations.

INTRODUCTION

The synthesis of the silicate phases, C_2S and C_3S attracted the author's attention during the course of studying the action of mineralizers on the formation of ordinary Portland cement (OPC). Reports on obtaining a fairly good strength OPC with low percentage of alite (1) and on the preparation of reactive - belite (2) were of special interest. Considerable work has been reported in the past by various authors on the synthesis, reactivity, etc, of C_2S phase and this has been covered recently (3). The synthesis of C_3S phase of high purity has been a subject of interest over the years and among others had been dealt elegantly by Odler and Dorr (4). The present research was undertaken to:

i/ increase the kinetics of formation of these phases,

ii/ stabilize the phases in certain desirable polymorphic/solid solution states, and

iii/ understand qualitativly the kine tics and stabilization characteristics.

Preliminary results of the work carried out over a period of one year or so are being presented here, some of which were communicated as short notes earlier (5-7). Needless to mention the complexities and involvement for carrying out this work are quite demanding.

EXPERIMENTAL

Techniques, such as rapid heating to the sintering temperature, use of rective starting materials, e.g. silica gel and additions of mineralizers were adopted. Reagent grade $CaCO_3$, mineralizers (2%) and commercially available silica gel (colourless) were used to make the batches (5g. each). These batches(passing 40μ) in the form of pressed pellets, were introduced in a platinum holder in a quench furnace normally preheated to the temperature of sintering and kept for a period of 1/2 hours to 1 hour in general. The sintered materials were air-quenched and analysed by chemical, XRD, IR, microscopy, etc.

RESULTS

The dissociation temperatures of $CaCO_3$ in mixes containing $CaCO_3$ and SiO_2 (2:1) in presence of NaF were studied by DTA and TGA. These results are shown in Fig. 1. Decomposition temperatures corresponding to the DTA peaks with the highest weight loss were taken though several peaks with weight losses were observed in DTA/TGA traces of the samples (5). The decomposition temperatures of $CaCO_3$ in mixes containing $CaCO_3$ and SiO_2 (3:1) with different mineralizers were studied as shown in Table - I.

The synthesis of β-C_2S phase with the addition of 2% NaF was studied over the temperature range 800-1100°C and some details of the results are given in Table - II and Fig. 2.

TABLE - I

Mineralizer	Percentages of addition		
	2%	4%	6%
LiF	540 (w) 620 (w) 850 (m)	560 (m) 710 (s) 880 (m)	530 (m) 675 (s) 830 (m)
NaF	790 (s) 825 (m) 859 (m)	560 (vw) 595 (w) 745 (s) 1020 (m)	540 (vw) 575 (w) 705 (s) 845 (m) 930 (m)
CaF_2	875 (s) 1110 (vw)	865 (s) 890 (m) 1015 (vw)	850 (s) 1010 (w)
SrF_2	845 (vw) 917 (s)	820 (s) 870 (m)	835 (s) 870 (m) 1010 (vw)
BaF_2	785 (w) 875 (s)	830 (s) 880 (m) 980 (vw)	810 (s) 870 (m) 980 (vw)

W = Weak, m = medium, vw = very weak, s = strong

All are endothermic peaks. DTA peaks without any mineralizer are at 560 and 940°C.

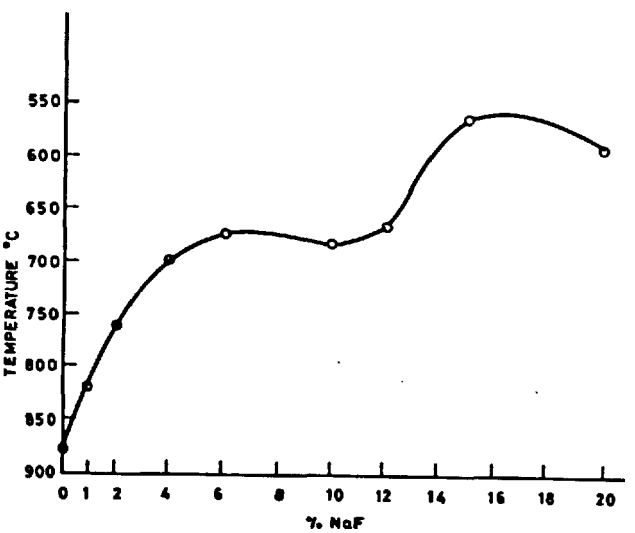

Fig. 1. Dissociation temperature of $CaCO_3$ in mixes of $CaCO_3$ and SiO_2 (2:1) with various amounts of NaF. Endothermic DTA peaks corresponding to the highest Wt. loss considered.

TABLE - II

Slow heating (10°C/min)		Abrupt heating to sintering temperatures	
800°C	1000°C	Raw mix decarbonated at 800°C and fired abrupty at high temperature	Raw mix fired at 1000°C and above
Formation of β-C_2S phase with 5% free lime	Formation of β-C_2S phase with free lime 4%; no reduction in free lime content with increasing retention time	At 850, 900 and 1000°C, the quality of free lime was around 2%	Up to 1000°C free lime content was around 2% but it increased at higher temperature

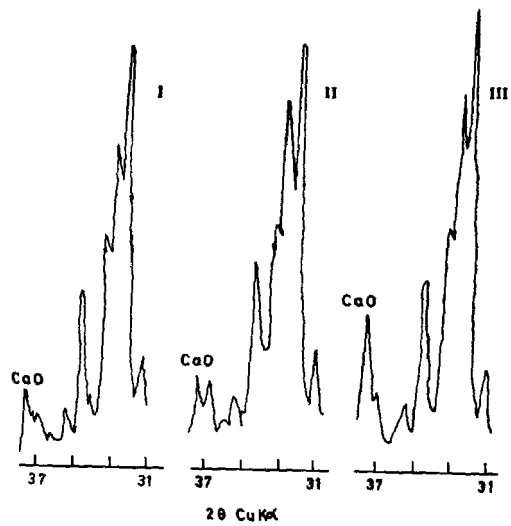

Fig. 2. XRD traces of raw mixes of $CaCO_3$ and SiO_2 (2:1) and 2% NaF. Mix I heated abruptly to 1000°C for 1/2 hr; Mix-II fired abruptly at 1000°C for 1/2 hr after decarbonation at 800°C and Mix-III heated to 1000°C for 1/2 hr (10°C/min).

With a retention time of 1-2 nours, the formation of α'-phase in presence of B_2O_3 (1-3%), and γ-phase in presence of Fe_2O_3 and excess CaO were also studied.

The formation characteristics of C_3S phase in the presence of different mineralizers are outlined in Table -,III. The total percentage of addition of mineralizers was kept to 2% and the batches were heated abruptly to sintering temperatures.

DISCUSSION

The lowering of the decomposition temperature of $CaCO_3$ by the addition of mineralizers is not only important from the viewpoint of heat saving but also from the fact that CaO released at a lower temperature is more reactive which is quite well known.

A number of intermediate compound formations is indicated which leads to the decomposition of $CaCO_3$ in stages. Imlach (8) observed two types of mechanism in the decomposition of $CaCO_3$ in some plant raw mixes. The decomposition of $CaCO_3$ in the presence of NaF is of considerable interest (Fig. 1). The temperature has been lowered to 555°C from 880°C (0% NaF) and further up to 6% of addition of NaF, there was a continuous fall in temperature and then again from 12 to 16%. The effect of cations on the decomposition of $CaCO_3$ in mixes of $CaCO_3$: SiO_2 (3:1) is presented in Figs. 3 and 4.

The formation of α'-C_2S along with β-C_2S in the presence of NaF was observed and it was found that with the addition of gypsum or CaS, the α'-phase disappeared. High conversion rate (~ 96%) for the formation of α'- and γ- C_2S phase was observed (2 hours retention at 1450°C in a single firing).

The formation of C_3S phase in the presence of CaF_2 was observed at as low a temperature as 850°C with a retention time of 2 hours. The free lime contents as determined chemically are 3.9% (1300°C), 2.13% (1350°C) and 2.32% (1400°C) with total retention time of 1 hour. An XRD trace of a mix heated to two hours (total retention time) is shown in Fig 5. Recent work (9) has shown that the percentage of CaF_2 addition could be reduced to as low 0.5%. This indicates that a still purer C_3S sample can be synthesized. The formation of C_3S in the presence of flourides and other mineralizers in shown Fig. 6. The line marked 'A' represents a raw mix containing MgO (0.5%) and Al_2O_3 (0.25%) besides CaF_2.

TABLE - III

Temperature of heating	CaF_2			NaF			$CaSO_4 \cdot 2H_2O$			$CaHOP_4$			CrO_3			$F^- + PO_4^{-3}$			$F^- + PO_4^{-3}$		$+SO_4^{-2}$	$+ CrO_3$
	*A	B	C	A	B	C	A	B	C	A	B	C	A	B	C	A	B	C	A		B	C
1200°C	G	W	L	G	VW	H	W	F	H	-	-	-	W	W	H	W	F	H	W		F	H
1300/ 1350°C	VG	W	L	VG	VW	M	W	F	H	1300° W	W	VH	F VG	W w	H H	G	W	L	G		W	L
										1350° G	W	VH										
1400°C	VG	w	VL	G	VW	M	W	F	H	G	W	VH	W	W	H	G	VW	L	G		-	L

G = Good; VG = Very Good; W = Weak; * C_3S = A

L = Low; H = High; F = Fair; C_2S = B

VH = Very High; VG = Very fair; VL = Very low; Free lime = C

These are relative value as obtained from XRD line intensities.

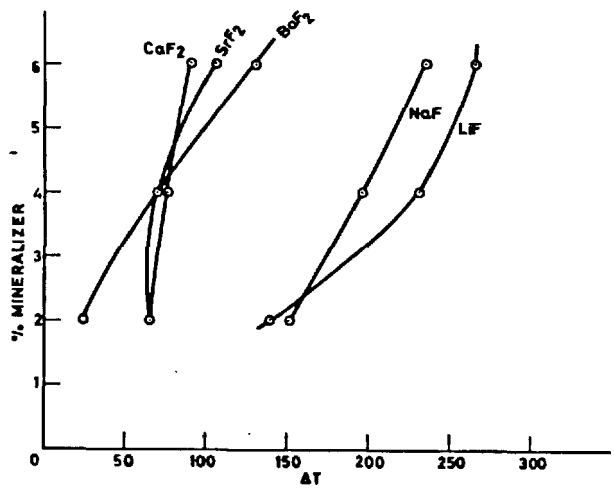

Fig. 3. The lowering of decomposition temperature of $CaCO_3$ in mixes containing $CaCO_3$ and SiO_2 (3:1) and mineralizers.

The kinetics for this mix (alite composition) is the fastest as observed qualitatively on a comparative basis. The lines marked 'M' represent batches containing CaF_2 + $CaHPO_4 2H_2O$ + CrO_3 (1:0.5 : 0.5:0.5); and (0) represents CaF_2 + $CaHPO_4$ (1:1). LiF is apparently volatilized away at higher temperatures.

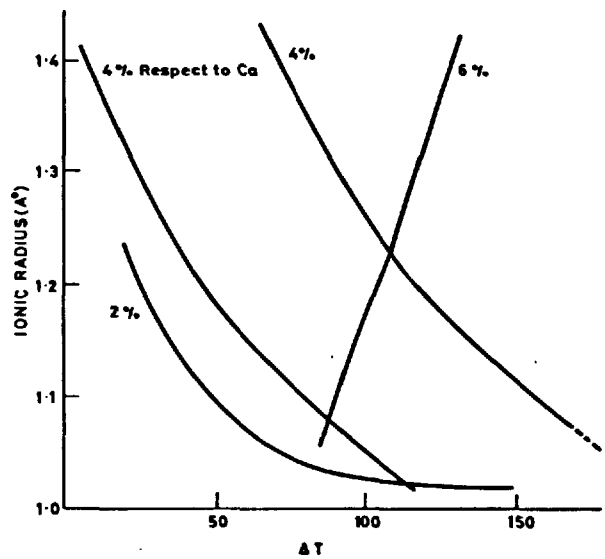

Fig. 4. Effects of ionic radii of cations of mineralizers (as mentioned in Fig. 3) on the dissociation temperature of $CaCO_3$).

The kinetics of C_3S formation process cannot be expressed by a single kinetic equation (10,11). In the presence of CaF_2, the primary phase field of C_3S gets enlarged and this may be one of the reasons for increased kinetics (9). The formation of intermediate compounds, such as $(C_2S)_2$ or $(C_3S)_3$ CaF_2 as reported (12) besides reactive polymorphic form of C_2S at higher temperatures (10,11) may influence the kinetics of formation. The early liquid formation (in the case of C_3S) is also deemed responsible for the increased kinetics of C_3S formation. Details of some of which has been reviewed recently (13). A theoretical approach using polyhedral model to understand the stabilization of orthosilicate system has been

outlined by Moore (14) but the recent experimental work by Barnes et al (15) is rather interesting to note. They found it difficult to correlate any affinity of a particular ion to go into solid solution in the lattice of a particular C_2S form.

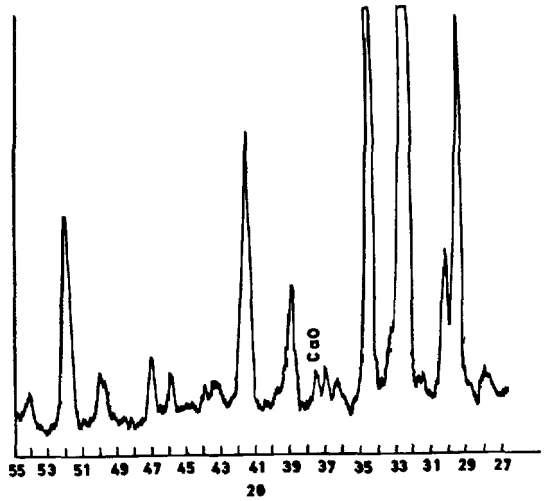

Fig. 5. An XRD trace of C_3S obtained by the rapid heating technique (total retention time-2 hr at 1400°C)

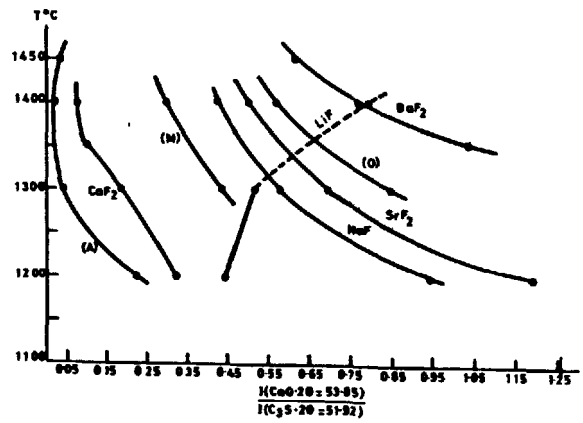

Fig. 6. The formation of C_2S phase in presence of mineralizes using rapid heating technique. XRD line intensity ratio of CaO and C_3S used.

CONCLUSION

The rate of formation C_2S and C_3S phases can be increased considerably by rapidly heating the mix containing reactive material (silica gel) and by additions of mineralizers. The purity of these materials can be improved by a judicious combination of these techniques.

REFERENCES

1. - B.S. RANGNAKAR, V.R.G. SRINIVASAN and V.N. PAI (1974), "An early hardening C_2S phase made by rapid heating technique,". The VIth international congress on the chemistry of cement (MOSCOW) Section 1, 1-4.

2. - D.M. ROY and S.O. OYEFESOBI (1977), "Preparation of very reactive Ca_2SiO_4 Powder," J. Am. Ceram. Soc., 60, 178 - 180.

3. - S.N. GHOSH, P.B. RAO, A.K.PAUL and K. RAINA, "The chemistry of dicalcium silicate - a review" J. Mater, Sci. (in Press).

4. - I. ODLER and H. DORR (1977), " Tricalcium Silicate formation by solid state reactions" Am. Ceram. Soc. Bull., 56 (12) 1086 - 1089.

5. - S.N. GHOSH, A.K. PAUL and A.K. THAKUR (1978), "Thermal decomposition of $CaCO_3$ and formation of β Ca_2SiO_4" J. Mater. Sci, 13, 1602 - 1606.

6. - S.N. GHOSH, (1978), "The thermochemical effects on the formation of Ca_3SiO_5" J. Mater. Sci, 13, 2739-1741.

7. - S.N. GHOSH, A.K. PAUL and H.K. HANDOO (1979) "Thermal decomposition of $CaCO_3$ and formation of Ca_3SiO_5, "J Mater. Sci., 14, 1011-1013.

8. - J.A. IMLACH (1976), "Non-isothermal investigation of the kinetics of reactions occuring during clinker formation, "Cem. and Conc. Res., 6,747-755.

9. - V. JOHANSEN and N.H. CHRISTENSEN (1979), "Rate of formation of C_3S in the system $CaO-SiO_2-Al_2O_3-Fe_2O_3-MgO$ with addition of CaF_2, "Cem. and Conc. Res., 9, 1-5.

10. - C. TRO"MEL, W. FIX and R. HEINKE (1969) "High temperature investigation up to 1900°C of calcium orthosilicate and tricalcium silicate," Tonind. - Ztg. Keram. Rundsch, 93, 1-8.

11. - J.M.P. LOPEZ, H.P. THOMAS and E. PEREIRA (1976), "Kinetic study of the chemical step in the C_3S formation Reaction" Lat. Am. J.Chem. Eng. Appl. Chem., 6 (1), 33-43.

12. - W.GUTT and G.J. OSBORNE (1966), "The system $2CaO.SiO_2.CaF_2$, "Trans. Brit. Ceram. Soc., 65, 521-34.

13. - S.N. GHOSH (1978), "Physico-chemico-mechanical methods to reduce clinkering temperature of portland cement raw mixes", Ind. Ceram., 21, 117-121.

14. - P.B. MORRE (1973), "Bracelets and pinwheels, a topological geometrical approach to the calcium orthosilicate and alkali sulfate structures." Am. Miner, 58, 32-42.

15. - P.BARNES, J.W. JEFFERY and S.L. SARKAR (1978), "Composition of portland cement belites, "Cem. and Conc. Res., 8 (5), 559-64.

Contrôle de la microstructure et de l'activité des clinkers

Control of microstructure and activity of clinkers

B.V. VOLCONSKI, candidat ès sciences techniques, sous-directeur de l'Institut,
L.G. SOUDAKAS, candidat ès sciences techniques, chef du laboratoire de recherches physico-chimiques,
A.F. KRAPLIA, candidat ès-sciences techniques, collaborateur scientifique en chef,
L.G. BERNSTEIN, collaborateur scientifique en chef, "Giprotzement", Léningrad, U.R.S.S.

RESUME :
On a procédé aux études microscopiques de plus de dix mille échantillons prélevés dans des fours rotatifs de sept cimenteries préparant la masse crue par la voie humide et sèche.

On a analysé les conditions thermiques de production de ces échantillons, dont plus de deux mille ont été soumis aux essais physico-mécaniques.

On a établi, pour les clinkers industriels, l'identité de types de microstructures qui ont ensuite été classés. On a montré que la succession des passages d'un type à l'autre est régulièrement liée à la variation de l'intensité du traitement thermique. D'autre part, on a apprécié quantitativement l'influence directe de la microstructure sur l'activité hydraulique (R_{28}). C'est sur cette base qu'ont été mis au point et introduits dans l'industrie les principes de contrôle de la cuisson du clinker, en s'appuyant sur la microstructure en qualité de principal paramètre d'estimation.

SUMMARY:
Over 10 thousands samples from rotary furnaces at seven cement plants with wet and dry production processes have been subject to microscopic investigations.

The thermal conditions of sampling have been analyzed and over 2 thousands of said samples have been subjected to physical and mechanical tests.

The uniformity of types of the industrial clinker microstructures have been found out with corresponding classification provided. It has been proved that the sequence of transfer from one type to another is regularly dependent on variations of thermal treatment intensity. On the other hand, the direct influence of the microstructure on the hydraulic activity (R_{28})has been quantitatively estimated. On this basis the clinker calcination control principles have been developed and implemented in the production to be used as the basic criterion of clinker activity.

L'interdépendance entre la microstructure du clinker et son activité hydraulique a été l'objet d'études de nombreux chercheurs depuis Le Chatelier et Thornebom (1, 2). Après les années 30 et, surtout, ces dernières temps les études en cette direction se sont développées de façon suffisamment intense, mais en dépis de ces efforts l'utilisation pratique de cette interdépendance dans l'industrie est restée jusqu'à aujourd'hui très limitée.

Les études de plus de 10 mille couches minces prélevées dans 7 usines différentes simultanément aux essais physico-mécaniques de plus de 2 mille éprouvettes de clinkers, la confrontation des conditions concrètres d'obtention de ces éprouvettes aux états de phase des minéraux du clinker ont permis d'établir une série de régularités.

Il s'est avéré que malgré la diversité des matières premières et des conditions technologiques des productions concrètes, la microstructure de leurs clinkers présente des traits communs. Cette communité est avant tout la conséquence de l'identité de méthode utilisée pour l'obtention du clinker : la cuisson. Notons toutefois, que les microstructures des clinkers fondus ou des clinkers obtenus par la voie radiative diffèrent en principe des clinkers cuits.

Les résultats de l'étude menée permettent de distinguer quatre types principaux de microstructures embrassant pratiquement tous les cas étudiés (fig. 1a, b, c, d).

Le 1-er type (fig. 1a) se caractérise par une cristallisation incomplète et peu prononcée des principales phases, allant jusqu'à l'absence complète de formes morphologiquement déterminables. En règle générale il s'accompagne d'une distribution irrégulière des minéraux.

Le 2-ème type (fig. 1b) présente une abondance de phases silicates finement cristallisées (moins de 20 μm). Deux variantes se rencontrent à répartition irrégulière (en amas) et régulière de minéraux.

Le 3-ème type (fig. 1c) est constitué de microstructures avec de formations assez volumineuses d'alite et de bélite aux contours flous. Ce type se caractérise par des agrégations au sein d'une même granule. Les secteurs du type 3 sont souvent associés aux secteurs du type 2 et 4.

Le 4-ème type (fig. 1d) comprend des cristaux d'alite et de bélite aux formes nettes en majorité de dimension supérieure à 30μm. Le trait essentiel de ce type de clinkers est la régularité de distribution des phases. La limite supérieure des dimensions des cristaux ne dépasse pratiquement pas 60 μm malgré la présence quelquefois de gros cristaux (jusqu'à 200μm) isolés.

Il est nécessaire de souligner que, pratiquement, chaque éprouvette de clinker constitue une association d'éléments différents en microstructure. Aussi dans nos études a-t-on, au préalable, apprécié l'homogénéité des éprouvettes pour n'analyser que celles d'entre elles dans lesquelles l'apport de l'un des 4 types était dominant et constituait au moins 70 %.

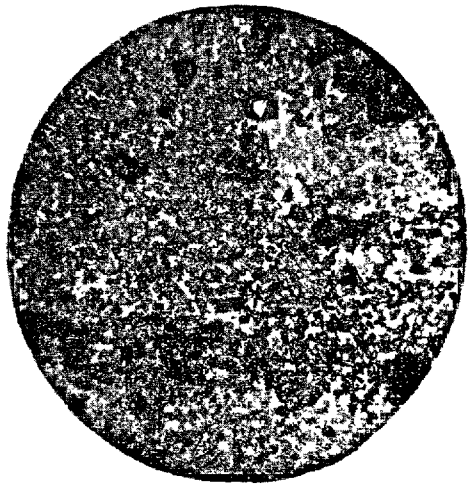

Fig. 1a

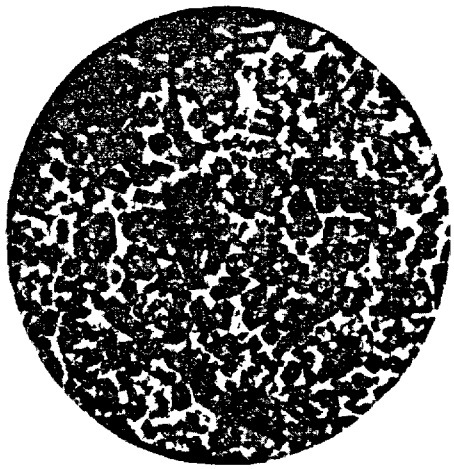

Fig. 1b

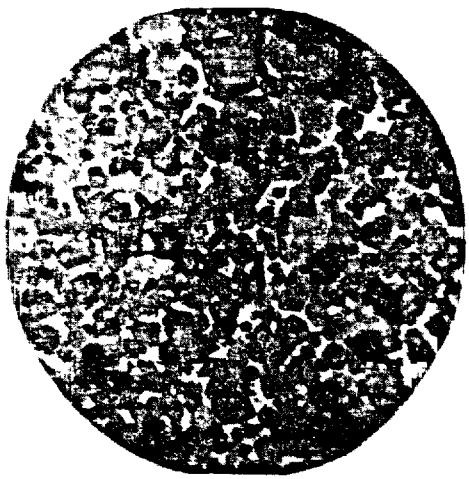

Fig. 1c

Fig. 1d

Les différences limites dans la resistance des clinkers (R_{28}) en rapport avec les variations de microstructure établies par nos études atteignent 120 à 180 kgf/cm^2. Ces chiffres correspondent à ceux trouvés par d'autres auteurs (3, 5). Les meilleurs clinkers, sous l'angle de la résistance à 28 jours, sont les clinkers du 4-ème type.

L'influence des conditions spécifiques à l'entreprise se manifeste principalement dans le niveau de l'activité hydraulique du clinker mais ne se répercute pas sur l'importance du rôle de la microstructure. C'est ainsi, par exemple, qu'on a établi qu'avec une teneur moyenne en alcali dans la matière première de l'ordre de 1,5 % la marge de variation de la résistance, due au changement de la microstructure, était de 370 à 510 kgf/cm^2, tandis qu'à l'usine utilisant une matière première de faible teneur en alcalis (environ 0,5 %) cette marge oscillait de 420 à 600 kgf/cm^2. Une attention particulière était attachée aux problèmes de stabilité de la phase alitique. Il a été établi que même les stades initiaux de la désintégration, observés le plus souvent au sein des microstructures parfaites, entraînaient des chutes de résistance de l'ordre de 30 à 50 kgf/cm^2.

L'expérience de postcombustion en laboratoire des clinkers du 1-er type à 1450 °C a montré que l'amélioration de la microstructure est le corollaire logique d'un traitement thermique poussé du matériau. L'étude des régimes thermiques de fonctionnement des fours a montré que la séquence des variations de la microstructure, résultant de l'intensification de la cuisson par l'élévation de la température dans la zone de cuisson ou du temps de maintient du matériau à des températures dépassant 1300°C, de même que de l'accroissement de la "réceptivité thermique" du mélange brut, constitue une constante de l'entreprise considérée, et, pour les entreprises différentes, ne varie qu'en détails, en principe, de nature non substantiels. La marche générale des variations du type 1 au type 4, en passant par les structures du type 2 et 3, se conserve dans ce cas. On est ainsi arrivé pour la première fois à établir une échelle de microstructures traduisant la liaison de l'état de phases des clinkers avec la résistance et le régime thermique. Une telle échelle (à 8 degrés) nous a servi de critère pour le contrôle de la cuisson du clinker, opération qui dans tous les cas (plus d'une dizaine) nous a permis d'élever la résistance moyenne du clinker dans les entreprises de 30 à 40 kgf/cm^2.

La nature de l'influence de la microstructure sur la résistance se manifeste essentiellement dans la différence de l'état de la surface des particules de ciment obtenues après mouture. (Il est bien entendu qu'on compare des ciments moulus dans les mêmes conditions et jusqu'à obtenir les mêmes caractéristiques standard.) La figure 2 fournit les différences caractéristiques entre les formes des particules obtenues a) à partir du clinker du type 1 et b) à partir du clinker du type 4. Vraisemblablement le développement du contour des particules dans le second cas est le facteur contribuant à l'élévation de la résistance du matériau en voie de durcissement. En tout cas la différence de forme des particules observée constamment s'accompagne de variations dans les caractéristiques de la poudre de ciment telle la chaleur de mouillage, la cinétique de dégagement de chaleur (6).

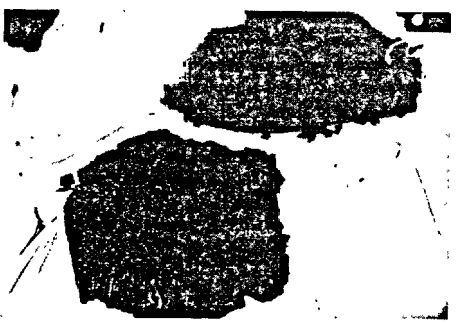

Fig. 2a

Fig. 2b

En conclusion de l'étude menée on peut dire que la microstructure du clinker est justement le critère qui doit être utilisé pour la commande des fours de cuisson et le contrôle du processus. Il faut en outre souligner les avantages majeurs de la microstructure devant la teneur en résidus d'oxyde de calcium, utilisés jusqu'à aujourd'hui comme critère principal.

BIBLIOGRAPHIE

1.- H. LE CHATELIER, Comptes rendus, 96, 1056, 1883.

2.- A.E. THORNEBOM, Die Petrographie des Portlandzements, t. 1, 1887, 31, 1148, 1157.

3.- В.В. ТИМАШЕВ (1957) "Влияние режимов обжига и охлаждения на структуру и свойства цементов", Автореферат кандидатской диссертации, М., (en russe).

4.- Т.В. КУЗНЕЦОВА (1968) "Исследование факторов, влияющих на микроструктуру и технические свойства клинкера", Автореферат канд.диссертации, М., (en russe).

5.- И.В. КРАВЧЕНКО, М.Г. ВЛАСОВА, Ю.Э. ЮДОВИЧ (1971) "Высокопрочные и особобыстротвердеющие цементы", М., Стройиздат, (en russe).

6.- Л.Г. СУДАКАС, А.Ф. КРАПЛЯ, М.М. СЫЧЕВ и др. (1977) "Связь микроструктуры и гидравлических свойств портландцементных клинкеров", Изв.АН СССР Неорганические материалы, № 11, 2103-2107, (en russe).

Spectroscopic studies of Ca_3SiO_5 polymorphism

Les études spectroscopiques du polymorphisme du Ca_3SiO_5

M HANDKE, Cz PALUSZKIEWICZ, G. SIEMINSKA, School of Mining and Metallurgy, Institute of Materials Science, Krakow, Poland.

RESUME : On a étudié sur des échantillons pulvérisés, les modifications polymorphiques du Ca_3SiO_5 stabilisé par ZnO, en utilisant les méthodes de Raman au rayon laser et la spectroscopie infrarouge avec transformation de Fourier. Les modifications polymorphiques ont été déterminées par la diffraction aux rayons X. La spectroscopie vibrationnelle constitue une méthode complémentaire à la diffraction aux rayons X et donne des informations sur l'arrangement des atomes dans les couches superficielles des cristaux. On a proposé une hypothèse, déduite des résultats spectroscopiques, sur la structure réelle du Ca_3SiO_5 ainsi que le mécanisme de sa transformation polymorphique. Conformément à cette hypothèse, on peut considérer la structure du Ca_3SiO_5 comme composée de couches silicatées et de couches d'oxyde de calcium. Quelques polymorphes du Ca_3SiO_5 présentent des structures polytypes.

SUMMARY : Laser Raman and Fourier transform IR investigations have been performed on powdered samples of Ca_3SiO_5 polymorphs obtained by stabilization with ZnO. Types of polymorph have been established by X-ray measurements. Vibrational spectroscopy is a complementary method in comparison with X-ray diffraction and gives information about short range order in crystal. The hypothesis deduced from spectroscopical results concerning real structure of Ca_3SiO_5 crystals has been proposed as well as the mechanism of polymorphic transitions of Ca_3SiO_5 forms. According to this hypothesis Ca_3SiO_5 structure can be regarded as layer structure consisting silicate and calcium oxide layers. Some of Ca_3SiO_5 polymorphs are polytypic forms.

INTRODUCTION

There are many papers /1,2,3,4,5/ concerning phase transitions of the tricalcium silicate and structure of its different forms. The fundamental work is Bigare's et al. paper /4/. The polymorphism of the C_3S using X-ray and thermal analysis methods as well as microscopic investigations have been established. On the base of these papers an existence of six crystalline forms should be accepted up to decomposition temperature of C_3S /1250°C/. Three of these forms are tridlinic, two - monoclinic and one is rhombohedral /the highest-temperature phase/. The phase transition cycle of the C_3S can be shown as follows :

$$T_I \overset{620}{\leftrightarrow} T_{II} \overset{920}{\leftrightarrow} T_{III} \overset{980}{\leftrightarrow} M_I \overset{990}{\leftrightarrow} M_{II} \overset{1050}{\leftrightarrow} R$$

Trömel, Fix and Heinke /6/ have confirmed that the C_3S is the stable phase also at the 1300 - 1800°C temperature range but the existence of another forms at these temperatures is not confirmed. It is possible to find, in some papers, information about other C_3S modifications; for example Uchikawa /7/ has found five additional weak effects on the DTA curves and has attributed them to additional phases structurally close to basic C_3S modifications.

X-ray studies carried out using Guinier camera /1/ at different temperatures have shown that at the temperature 1100°C the crystal lattice of the C_3S is hexagonal one and about 30 reflections on the diffractogram are ascribed to the R3m /C_{3v}^5/ space group which corresponds to the structure proposed by Jeffery /8/. A temperature decrease causes characteristic changes of the $\bar{2}01$, 204 and 220 reflection shapes in the $2\theta = 31^0\text{-}33^0$ and $51^0\text{-}52^0$ angle range. In this angle range the changes connected with the C_3S polymorphic transitions are especially easy to observe. During the phase transition at 1050°C the crystalline symmetry changes from rhombohedral to monoclinic /$R \rightarrow M_{II}$/; this transition is only a small displacement of the elements in a unit-cell but the symmetry reduces rapidly from R3m /C_{3v}^5/ to Cm /C_s/. Considering the hexagonal symmetry R3m it can be confirmed that only two its subgroups exist : C_3-trigonal and C_s-monoclinic. The splitting of the $\bar{2}04$ and 220 reflections shows the change of a crystal system and this decides of the monoclinic system. The parameters of the monoclinic unit-cell expressed by the hexagonal system differ minimally i.e.

$\Delta a = 0{,}02$ Å, $\Delta c = 0{,}13$ Å and γ by $0{,}12^0$.

The phase transition at 990°C is not connected with the symmetry change, so the second monoclinic phase of C_3S /M_{II}/ is of the same space group Cm /C_s/. On the diffractogram more distinct splitting of the $\bar{2}01$, $\bar{2}04$ and 220 doublets is observed. The $M_I \rightarrow M_{II}$ transition is connected with a very small thermal effect.

At the 980°C temperature occurs the transition with considerable thermal effect and change of the symmetry from monoclinic to triclinic /$M_I \rightarrow T_{III}$/. On the diffractogram next splitting is observed of the mentioned above reflections to the triplets. There are more reflections of this form on the diffractogram and it is impossible to explain them without an increase of the unit-cell parameters. In this case pseudo-hexagonal parameters a and b should be doubled to about 14 Å, so the structure of the T_{III} form must be described as super-unit-cell with four times quantity of atoms in comparison to the previous structures.

At the 920°C the strongest thermal effect is observed connected with the $T_I \rightarrow T_{II}$ transition but without change of the symmetry and the unit-cell parameters. The unit-cell of this system is of trivial symmetry. On the diffractogram further splitting of the triplets can be seen.

The phase transition at the 600°C does not cause the change of the symmetry, but diffractograms change significantly that certifies further increase of the unit-cell parameters by the next double a and b parameters.

Now the unit-cell has four times more of the atoms than the unit-cell of the T_I and T_{II} forms, and sixteen times more than the M_{II}, M_I and R forms.

Among these five general accepted polymorphic transitions of the C_3S, only the $R \rightarrow M_{II}$ is the transition of the second type without thermal effect. The $T_{III} \rightarrow T_{II}$ transition is practically unobserved in the X-ray diffraction /the same diffractograms/ but it is accompanied by the strong thermal effect connected with the transition to the second super-lattice.

The C_3S crystals can form solid solutions with different additional cations. The investigations of Bigare et al./4/ have shown that many of these cations can stabilize different crystalline modifications of the C_3S.

PREPARATION OF THE DIFFERENT CRYSTALLINE MODIFICATIONS OF THE C_3S AND THEIR DEFINITION USING X-RAY DIFFRACTION

The samples have been prepared by the stabilization with admixed ZnO. The stabilizer concentration has been chosen as in the paper /4/. For better comparison of the results ZnO has been introduced to the low-temperature T_I form the structure of which does not require the stabilization. Owing to this procedure the sample defected by additional admixture has been obtained but its concentration did not cause structural changes. There were samples prepared with the following ZnO concentration /% weight/: 0,5 , 1, 2, 3 and 5 that corresponds to the T_{III}, T_{II}, M_I, M_{II} and R modifications. The zinc has been introduced as the water

solution of $Zn/COOCH_3/\cdot 2H_2O$. To the adequate quantity of the zinc acetate water solution the mixture of the $CaCO_3$ and the SiO_2 has been introduced in the molar ratio 3:1. This suspension was dried at the temperature 100°C, further holded at the 1000°C /decarbonization/ and next after grinding - 1500°C. The heating at 1500°C was repeated up to getting the clean phase of C_3S, which was controlled using X-ray diffraction and IR spectra.

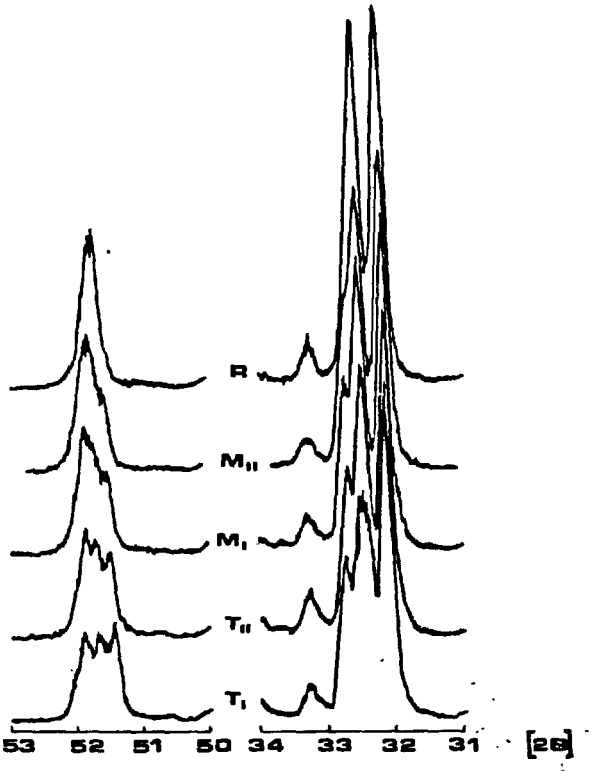

Figure 1. X-ray diffractograms of the C_3S polymorphic modifications stabilized by ZnO.

Figure 1 shows diffractograms of the different C_3S forms stabilized by ZnO of different concentration. The diffractograms were registered in the ranges most characteristic for these forms : $2\theta = 31^0-34^0$ and 50^0-53^0. The indices of the reflections were found accordingly to the paper /2/. It is easy to remark that the reduction of the crystal symmetry and increase of the unit-cell dimensions cause the splitting of the singlet 204 reflection in the rhombohedral structure to the doublet in the monoclinic and to the triplet in the triclinic one. The behaviour of the singlet 220 reflection is the same. The same angle range registered using Guinier camera could show more complicated, fine structure of these two reflections which confirms the formation of the superlattice for the [illegible] temperature modifications. These measurements agree with the results of previous works and synonymously define the samples and allow to confirm the getting of T_{III}, T_{II} or T_I, M_I, M_{II} and R forms. This identification is necessary for basic spectroscopic investigations.

SPECTROSCOPIC RESULTS

Figures 2a and 2b show the spectra of the same samples the diffractograms of which were presented in fig.1. On these spectra

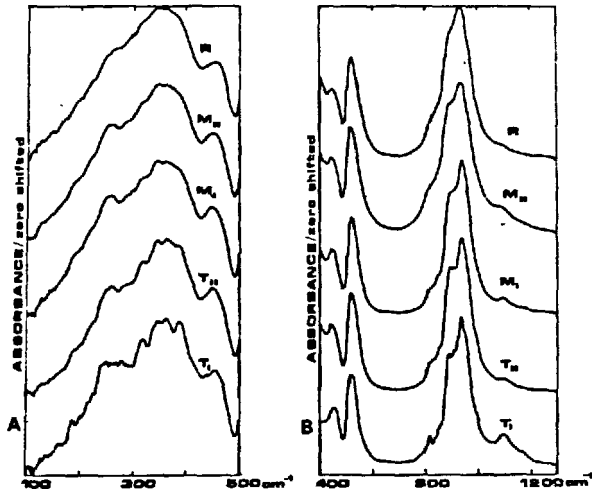

Figure 2. a/ FIR spectra of the C_3S polymorphic modifications stabilized by ZnO; b/ MIR spectra of the C_3S polymorphic modifications stabilized by ZnO.

continuous changes with the increase of the stabilizer concentration are observed. According to the selection rules of the vibrational transition the disappearance of some bands with the increase of the crystal symmetry is not observed. Instead of this the characteristic band broadening is observed. It is especially visible in the 800-1050 cm^{-1} /Si-O bond stretching vibrations in the SiO_4 tetrahedron/ and 100 - 400 cm^{-1} /lattice vibrations/ ranges. This observation shows the broadening of the vibration energy levels so, the selection rules do not operate. These could be only one explanation of this experimental fact- the increase of disorder of crystalline lattice. It has been shown in the paper /9/ that in the medium infrared range spectra the Si-O bond vibrations are observed, which are mostly effected by the arrangement of oxygen ions, because in the vibrations mainly these atoms motions are observed in relation to more static cations. The increase of the lattice disorder -

-which is shown by the spectroscopic data - concerns mainly the sublattice of the oxygen ions, less - the cation sublattice.

From the theory group calculations made for the rhombohedral structure of C_3S /10/ it results that in the stretching vibration range should be observed three A_1-type vibrations from the fully symmetric stretching vibration of the isolated SiO_4 tetrahedron and six vibrations / $3A_1 + 3E$ / from the remained stretching vibrations. This quantity of the bands in the spectrum of the low-temperature C_3S modifications is observed. In the spectra of highly symmetric modifications the mean of these bands is observed and as the result for the rhombohedral modification three weak separated bands are observed; for fully symmetric vibration at about 840 cm^{-1} and for remained vibrations two bands : 890 and 930 cm^{-1}. In the high-temperature modifications the splitting in the corelation field for SiO_4 tetrahedron is not observed, and the observed splitting in the crystal field /activation of the A_1 vibration and reduction of the degeneration of F_2 vibration to E and A_1/ show the position symmetry of the SiO_4 tetrahedra in the crystal structure accordingly to Jeffery - C_{3v}. These conclusions are confirmed by the Raman spectra for the same samples. The Raman spectra have been obtained in the Si-O stretching vibration range /800 - 1050 cm^{-1}/, in the remained range there are no characteristic bands for the C_3S. The weak intensity and broadening of these bands increases strongly with the quantity of the admixed stabilizer. On this base it is possible to conclude that in the FIR range the spectra of the high-temperature modifications are similar to the spectra of amorphous state. The position of the peaks of the complexed 800-950 cm^{-1} band are almost the same like the bands in the IR spectrum and the same changes of the band shape during the increase of the stabilizer concentration are observed /fig.3/. For the rhombohedral modification only three weak separated bands are observed, similar to the IR spectrum.

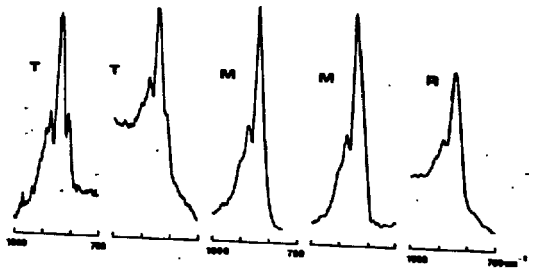

Figure 3. Raman spectra in the 700 -1000 cm^{-1} range of the C_3S polymorphic modifications stabilized by ZnO.

DISCUSSION AND CONCLUSIONS

On the base of the IR and Raman spectra the following conclusions can be drawn :

- the symmetry of the tetrahedra in the structure of all polymorphic modifications is close to C_{3v} symmetry and during the phase transitions the tetrahedron does not deform and its dimensions are almost the same,
- in the stabilized crystallochemically structures of the high-temperature modifications higher symmetry is obtained by the reduction of the oxygen sublattice order,
- the disorder of the oxygen sublattice is a consequence of the orientation disorder of the SiO_4 tetrahedra in the C_3S structure /no splitting in the corelation field/.

In the paper /10/ we have put forward a hypothesis on the real structure of C_3S, which can be now extented to explain the complicate polymorphism of the C_3S. According to our hypothesis the base symmetry of the short range order in the C_3S crystals is the same or very close to the rhombohedral symmetry /high-temperature form/ and the crystal is of "sandwich" structure with the layer by turn : silicate of C_2S and oxide of CaO.

The dicalcium silicate layer is probably of α-C_2S structure in the rhombohedral modifications and in the low-temperature modifications α'- and β- C_2S. About the symmetry of the whole crystal and about the size of the unit-cell in the C_3S polymorphic modifications decides mutual arrangement of the oxide layer respecting to the silicate one.

During the polymorphic transition cycle of C_3S the positions of oxygen ions are at first a little displaced what is the result of tetrahedra reorientation. This mechanism could be explanation of the small thermal effect of $R \leftrightarrow M_{II}$ transition and rapid reduction symmetry from C_{3v} to C_s with practically unchanged parameters of the unit-cell. It is necessary to suppose that during this transition calcium and silicon cations do not displace.

The $M_{II} \rightarrow M_I$ transition is of similar character and as a result the new tetrahedra orientation is established. During the further $M_I \leftrightarrow T_{III}$ transition the cations are displaced what can be presented as a shift of the silicate layer respecting to the oxide layer. The consequence is the increase of the unit-cell parameter of T_{III} form. Now is clear the significant thermal effect of this transition.

During the $T_{III} \leftrightarrow T_{II}$ transition the significant structural changes do not occur.

During last $T_{II} \leftrightarrow T_I$ transition occurs again the change of sequence of silicate and oxi-

de layers causing further increase of the unit-cell dimensions and considerable thermal effect.

On the basis of our hypothesis we can distinguish two kinds of the transitions during the polymorphic transition cycle of the C_3S :

- with little only reorientation of SiO_4 tetrahedra
- with the change of the mutual positions of the silicate and oxide layer being the structure elements of C_3S.

The transitions of second type are : $M_{II} \leftrightarrow T_{III}$ and $T_{II} \leftrightarrow T_I$. Noting double layer C_2S and CaO by letters we can illustrate R, M_I and M_{II} forms like : AAA...; T_{III} and T_{II} forms like : ABAB..; and T_I form : ABCABC... .

Supporting on this hypothesis it is possible to explain the mechanism of the stabilizing operation such ions like Zn^{2+}, Mg^{2+} and Al^{3+}. Stabilizing Zn^{2+} and Mg^{2+} ions substitute larger Ca^{2+} ions in the C_3S lattice causing loosening of the structure. Because substituted is mainly calcium from the oxide layer, admixed ions cause change of the oxide layer orientation respecting to neighbouring silicate layer. The kind of the layer arrangement depends on the admixture concentration.

More complicate is character of Al^{3+} ions in the C_3S structure what is a subject of our another paper /10/.

It is necessary to remark that the stabilization mechanism of the C_3S forms is different from the stabilization mechanism of the C_2S modifications. There is a correctness that the ions stabilizing for C_3S are destabilizing for C_2S and vice versa.

REFERENCES

1. N.YANNAQUIS,M.REGOURD,Ch.MAZIERS,A.GUINIER, Bull.Soc.Franc.Miner.Crist.,85, /1962/,271.
2. M.REGOURD, ibid.,87,/1964/,241
3. A.I.BOIKOVA,N.A.TOROPOV, Dokl.ANSSSR, 156,/1964/,1428.
4. M.BIGARE,A.GUINIER,Ch.MAZIERS,M.REGOURD, N.YANNAQUIS,W.EYSEL,Th.HAHN,H.WOREMANN, J.Amer.Ceram.Soc., 50,/1967/,609.
5. W.EYSEL,Th.HAHN,Zeit.Krist.,131,/1970/, 40.
6. G.TRÖMEL,W.FIX,R.HEINKE, Tonind.Ztg., 93,/1969/,1.
7. H.UCHIKAWA,K.TSUKIYAMA,M.YAMAMOTO, C.A.J. Review of the 23rd General Meeting Tokyo /1969/,31.
8. J.W.JEFFERY, Acta Cryst.,5,/1952/,26.
9. M.HANDKE,M.E.JURKIEWICZ, Ann.Chim.Fr., 4,/1979/,145.
10. W.KURDOWSKI,M.HANDKE, will be publie shed on this Congress.

Formation du clinker dans un grand flux d'électrons accélérés

Clinker formation in high-energy flux of accelerated electrons

I.G. ABRAMSON, candidat ès sciences techniques, chef du laboratoire de radio-isotopie,
B.V. VOLCONSKI, candidat ès sciences techniques, sous-directeur de l'institut,
S.K. DANIOUCHEVSKI, candidat ès sciences techniques, collaborateur scientifique en chef,
G.B. EGOROV, candidat ès sciences techniques, collaborateur scientifique en chef,
Y.V. NIKIFOROV, candidat ès sciences techniques, chef du laboratoire technologique, "Giprotzement", Leningrad, U.R.S.S.

RESUME: Dans le but de produire le clinker de ciment Portland on a procédé à de nombreuses expériences sur des accélérateurs d'électrons de types divers. On décrit la méthode utilisée ainsi que les installations montées au laboratoire. Pour une puissance de dose retenue de 20 à 40 Mrad/s et une pression atmosphérique normale la décomposition totale du carbonate de calcium et, pratiquement, le développement complet de la réaction de synthèse du clinker de ciment de Portland n'ont exigé qu'environ 10 s. Les mesures de l'énergie consommée avec ce procédé ont donné 3300±300 J ou 800±70 cal/g ce qui est d'environ 100 cal/g inférieur à la consommation avec le procédé purement thermique. On a déterminé les caractéristiques de résistance du ciment (50 MPa ou 500 kgf/cm^2 et plus) ainsi que le caractère extrême du rapport entre la résistance et la grandeur de la dose retenue. On a étudié les caractéristiques physiques et chimiques du clinker obtenu par le procédé radiatif. On a détecté une importante irrégularité de phases, un contenu superstoechiométrique et une cristallisation fine de l'alite. On a émis une hypothèse sur le mécanisme des transformations engendrées dans le mélange par un grand flux d'électrons accélérés.

SUMMARY: A plurality of experiments for obtaining a portland-cement clinker have been conducted at electron accelerators of various types. A technique with description of laboratory installations is presented. At an absorbed dose power of 20–40 Mrad/s and normal atmospheric pressure, total decomposition of calcium carbonate and substantially complete synthesis of the portlandcement clinker take about 10 s. The energy consumption measured at this method was 3300±300 J, or 800±70 cal/g, which is about 100 cal/g as low as in case of a purely thermal method. The strength characteristics of the cement (50 MPa or 500 kgf/cm^2 and above) and the extreme nature of strength-to-absorbed doze relationship have been discovered. The physical and chemical features of the clinker obtained by the radiation method have been studied. Considerable non-uniformity of phases, superstoichiometric composition and fine crystallization of alite have been detected. Suppositions of the mechanism of transfers caused in the mixture by a powerful flux of accelerated electrons have been put forward.

Dès qu'on a commencé à produire le clinker de ciment Portland son développement technique se base exclusivement sur le procédé thermique et consiste au perfectionnement de la technologie et des équipements. Quant à l'utilisation de la méthode de haute intensité telle que le procédé radiatif, considéré d'un grand avenir dans nombre de domaines de la technologie chimique, on la jugeait impossible pour les processus exigeant beaucoup d'énergie. Pourtant la nécessité de l'intensification de la technologie du ciment Portland, de l'abaissement capital des dépenses en combustible naturel de haute qualité pour sa production ainsi que des prescriptions écologiques ont incité à une reconsidération minutieuse des arguments avancés.

En abordant l'étude des possibilités d'obtenir le clinker de ciment Portland au moyen du procédé radiatif on s'est basé sur certains succès de la technologie radiative en matière de l'utilisation du flux d'électrons accélérés et de la possibilité de leur introduction condensée dans le système de réaction.

De nombreuses expériences sur des accélérateurs d'électrons de types divers assurant une puissance de dose retenue de 20 à 40 Mrad/s, ont montré que l'irradiation du mélange brut de ciment de Portland permet d'aboutir à la formation du clinker pendant quelques secondes ou, au cas de flux d'électrons moins puissants - en quelques dizaines de seconde. Le processus s'achève à une température d'environ 200°C inférieure à l'ordinaire. Cela se solde par une diminution de l'énergie dépensée. Des mesures réalisées dans des conditions quasi-adiabatiques ont permis de l'estimer à 3300±300 J/g ou 800±70 cal/g.

Par une voie analogue on a obtenu des silicates tri et bi-calciques purs. On a également synthétisé une série d'aluminates composant les agglomérés d'alumine de l'industrie d'aluminium.

La technologie radiative utilisée pour la production du clinker de ciment Portland exige une préparation de la matière première par la voie sèche. On peut soumettre à l'irradiation soit la farine brute, soit le mélange brut granulé. Ayant étudié un grand nombre d'échantillons de clinker en laboratoire, on a obtenu les résultats suivants.

Les paramètres de résistance du ciment sont suffisamment élevés: résistance du ciment durci 50 MPa et plus; l'accroissement de résistance au cours du durcissement suit le rythme commun au ciment Portland ordinaire (fig.1). La dépendance des indices de résistance du ciment de la dose retenue (fig.2) a un caractère extrême. La surabondance comme l'insuffisance des doses retenues au cours de la formation du clinker se traduit par des indices de résistance du ciment inférieurs à ceux obtenus pour le clinker fabriqué avec des doses optimales. Le palier des doses optimales est toutefois suffisamment large et ne présente pas de difficultés technologiques.

Le clinker obtenu par synthèse radiative est proche de celui du ciment Portland par sa composition en phases et ses caractéristiques physico-chimiques. Toutefois, la vitesse assez grande des transformations chimiques au sein du matériau soumis à l'action d'un flux puissant d'électrons accélérés entraîne une série de caractéristiques physico-chimiques du clinker obtenu. S'y rapporte le déséquilibre des phases du clinker, la teneur superstoechiométrique en alite, la quantité insuffisante du composant intermédiaire comprenant parmi d'autres aluminates à basse basicité.

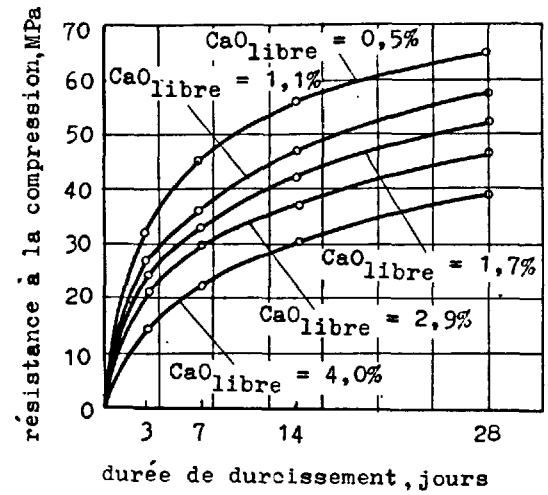

Fig.1. Cinétique du durcissement du ciment obtenu à partir du clinker par le procédé radiatif pour des valeurs différentes de CaO libre

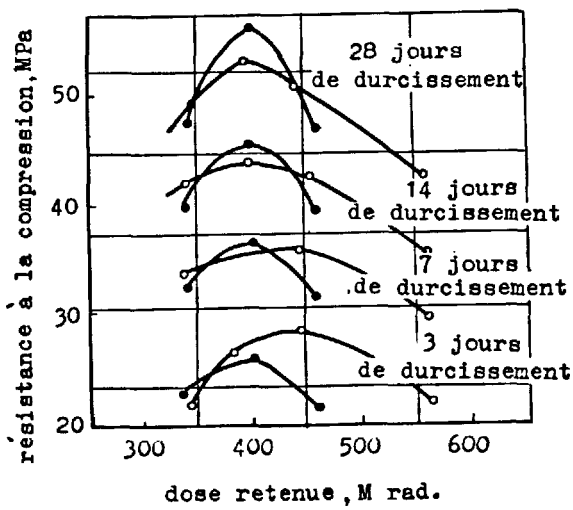

Fig.2. Variation des indices de résistance du clinker du ciment Portland en fonction de la variation de la dose retenue (y compris les pertes en chaleur):
—o— FS = 0,91 n = 2,0 p = 1,0
—•— FS = 0,86 n = 5,7 p = 2,3

On observe souvent une structure cristalline hétérogène (sur une seule coupe mince on peut enregistrer des secteurs de cristallisation très fine peu prononcée à côté de secteurs de grands cristaux aiguillés de l'alite). La cristallisation de l'alite comme du bélite est très fine (de 3 à 7 jusqu'à 10 à 15 μm, rarement de 20 μm), l'alite ayant les cristaux en prismes allongés, on rencontre des cristaux de forme isométrique, irrégulière et en prismes courts.

Le clinker obtenu dans le flux d'électrons accélérés a une broyabilité plus élevée.

Le mécanisme des transformations chimiques de haute température engendrées par les radiations propres aux flux puissants amorcés au sein du corps solide est aujourd'hui insuffisamment connue; les méthodes d'étude expérimentale de ces flux sont loin d'être parfaites. Aussi ne peut-on faire que des hypothèses sur le mécanisme de développement des processus physico-chimiques au cours de la formation du clinker par la voie radiative. Selon l'une de ces hypothèses on peut supposer qu'à côté des processus d'ionisation et d'excitation ainsi que de formation d'une quantité assez grande de défauts de radiation dans le matériau irradié on voit de nombreuses zones submicroscopiques de surchauffage local en forme de coins et d'avalanches thermiques. L'énergie de chaque coin thermique se disperse presque instantanément dans le microvolume du matériau environnant et n'entraîne pas d'élévation de la température moyenne (pour des doses de 250 à 300 Mrad on n'a jamais enregistré de températures dépassant 1300°C). Cependant en chacune de ces zones il se crée des conditions très favorables à la décomposition ultra-rapide de la matière première ainsi qu'à la synthèse également très rapide de phases de hautes températures (vraisemblablement sous forme de germe ou de prémice de germe). Ainsi que la formation du clinker dans un grand flux d'électrons accélérés doit semble-t-il être interprétée comme un phénomène de radiation thermique dont l'originalité réside en une transformation très efficace de l'énergie de radiation en énergie des transformations chimiques avec pertes minimales (devant les processus purement thermiques) d'énergie dans le milieu environnant. Un tel complexe de phénomènes assure le transfert direct de l'énergie du flux d'électrons au matériau irradié; les phénomènes purement thermiques ne jouant qu'un rôle subsidiaire. C'est la raison qui nous autorise de soutenir la thèse que la voie radiative d'obtention du clinker de ciment Portland présente non seulement du point de vue cinétique mais également énergétique un procédé de fabrication du clinker dont le rendement est en principe supérieur à celui basé sur des procédés d'utilisation directe de l'énergie électrique. Ses principaux avantages sont:

- absence de besoin d'utiliser le combustible organique naturel au cours du processus technologique, ce qui est particulièrement important eu égard à l'orientation actuelle du développement des techniques des courants forts;

- coïncidence dans le temps des différents stades de formation du clinker, ainsi qu'une vitesse très grande de déroulement du processus, qui l'intensifie dans son ensemble et crée des conditions favorables à la diminution des gabarits et des besoins en métal du matériel;

- possibilité de limiter l'empoussiérage au cours de la fabrication du clinker et, partant, l'abaissement très important de poussière et de produits nocifs évacués dans l'atmosphère.

Le niveau actuel et les tendances de la technique des accélérateurs autorisent à croire que le problème de la mise au point d'accélérateurs surpuissants pour des applications techniques sera résolu dans un proche avenir. Pour un rendement de la chaîne de fabrication de 1800 à 3000 t de clinker par jour il est nécessaire de disposer d'un complexe d'accélérateurs de puissance de 60 à 90 MW composé de 7 accélérateurs d'une puissance de 10 à 15 MW chacun (un accélérateur est en réserve).

Les orientations principales des études de fabrication du clinker par la voie radiative se concentrent actuellement sur la mise au point de l'équipement technologique du processus.

Nous croyons que la première chaîne industrielle de fabrication du clinker par la voie radiative qui correspondrait aux exigences énergétiques et écologiques actuelles pourrait voir le jour dans les années 90 du siècle courant.

BIBLIOGRAPHIE

1. – И.Г.АБРАМСОН, Б.В.ВОЛКОНСКИЙ, С.И.ДАНЮШЕВСКИЙ, Г.Б.ЕГОРОВ, Ю.В.НИКИФОРОВ, Я.М.ЦЕЙТЛИН, (1976), Получение портландцементного клинкера в пучке ускоренных электронов. Доклады АН СССР т. 230, № 6, (en russe).
2. – И.Г.АБРАМСОН и другие, (1976), Радиационно-химический способ получения портландцементного клинкера, "Цемент", № 9, (en russe).
3. – И.Г.АБРАМСОН и другие, (1976), Основы технологического воплощения радиационно-химического способа получения портландцементного клинкера, "Цемент" , № 11, (en russe).

Modèles mathématiques et leur application à des fins d'optimisation des processus de broyage et d'élévation de la qualité du produit,

Mathematic models and their application for optimizing crushing processes and improving quality of products

V.V. KAFAROV, membre de l'Académie des Sciences de l'U.R.S.S., chef de chaire de la cybernétique des processus chimico-techniques de l'Institut chimico-technique Mendéléev de Moscou,
M.A. VERDIAN, candidat ès sciences techniques, chef de laboratoire de simulation mathématique du "NIITzement", Moscou, U.R.S.S.

RESUME : On étudie au niveau macrocinétique les processus de broyage des corps solides. Toutes les études sont réalisées au moyen de calculateurs électroniques permettant ainsi de ne traiter que les variantes optimales d'organisation du processus qui garantissent une haute activité aux produits de broyage ainsi que des dépenses en énergie minimales.

On a mis au point des modèles mathématiques types de moulins à tambour ; les broyeurs variés et les processus de broyage qui s'y déroulent ont été classés d'après les formes de leurs modèles mathématiques.

En conformité avec les nouveaux principes d'analyse et de calcul des processus et des broyeurs de corps solides la répartition des particules suivant la dimension est considérée comme l'aboutissement d'une interaction compliquée entre la cinétique de la mouture et la structure hydrodynamique du courant de matériau dans le broyeur, c'est-à-dire comme la distribution du temps de séjour des particules du matériau broyé.

On montre la liaison naturelle et continue existant entre la distribution des particules du matériau en temps de séjour et en dimensions. D'où la possibilité d'appréciation qualitative et de prévision de la granulométrie du produit broyé d'après l'arrangement dans les broyeurs de la structure hydrodynamique du courant de matériau.

SUMMARY : The macrokinetic level of solid crushing processes investigations is considered. All the investigations are carried out with the use of computers, which provides for optimizing the variants of the process organization with high activity of crushed products and minimum power consumption.

Typical mathematical models of the drum mills have been developed and the diversity of mills and crushing processes occuring therein have been classified with respect to their mathematical models.

In accordance with novel principles of analysis and calculations of the solid crushing processes and apparatuses, distribution of particles in size is considered as a result of intricate correlation of crushing kinetics with hydrodynamic structure of the material flow in the mill, i.e. with distribution of the exposure time of the crushed material flow particles.

The natural interrelation and inseparability of distribution of material particles by the exposure time and size is shown. This provides for qualitatively estimating and forcasting the grain composition of the crushed product depending on the organization of the material flow hydrodynamic structure in the mill.

L'élévation de la qualité des produits industriels sur la base d'agrégats de grande puissance unitaire est un trait caractéristique du fonctionnement des entreprises de ciments modernes. On sait quelle importance a acquis du point de vue pratique et théorique le degré de dispersion du produit broyé dans la production du ciment ainsi que son rôle déterminant dans l'élévation de l'activité des produits moulus et l'abaissement des frais en énergie dépensés à leur production. Sur l'élucidation de la nature de cette interdépendance repose en grande partie l'efficacité du processus technologique dont l'élévation est en rapport avec l'organisation maximale de ce dernier ce qui exige des conditions optimales pour la marche du processus les frais d'établissement demeurant constants et les dépenses en travail mis en oeuvre, pour atteindre le but posé, restant minimales.

Pour une grande part cette interdépendance a été établie dans la première phase en laboratoire au niveau appelé conventionnellement études microcinétiques et à un moindre degré dans seconde phase, lors des études macrocinétiques sur des unités industrielles d'essai et des complexes industriels mis en oeuvre. Il est évident qu'en pratique la mise en oeuvre du processus dans les conditions établies au cours de la première phase d'études s'avère difficile et le travail qu'il est nécessaire de dépenser pour le développement du processus est de beaucoup plus grand que celui du processus idéal. Il est donc bien entendu que plus le processus réel est proche du processus idéal moins grande est l'énergie qu'il faut dépenser à sa réalisation. C'est sur ces prescriptions qu'on s'est appuyé dans des études entreprises dans seconde phase.

Les études macrocinétiques incluent le choix de la dimension du broyeur et de son modèle mathématique. Toutes les études sont menées également avec l'aide de calculateurs électroniques ce qui permet de ne faire intervenir que des variantes optimales garantissant la production du ciment avec un produit broyé d'une haute activité et pour une dépense d'énergie minimale.

Les études théoriques et expérimentales du processus de broyage des corps solides en recourant à la nouvelle méthodologie de leur analyse (1) ont permis de déterminer les traits caractéristiques des processus se déroulant dans les broyeurs à grande puissance unitaire (2). S'y rapporte la réalisation du broyage dans des broyeurs dont le rapport de leur longeur au diamètre est différent de la valeur optimale ; l'aggravation des conditions cinétiques et hydrodynamiques de la marche du processus; l'introduction d'un recyclage afin d'élever l'efficacité du broyage, mesure nécessaire, mais insuffisante ; le besoin impérieux de recourir aux systèmes automatiques de réglage et exigences élevées envers ces systèmes.

Il va de soi que même de petits écartements du régime de fonctionnement optimal ou de la construction optimale d'agrégats de broyage de grands diamètres entraînent des pertes sensibles et abaissent les paramètres techniques et économiques de leur travail.

Un rôle important dans l'optimisation du processus de broyage et dans l'élévation de la qualité du produit des broyeurs de grande puissance revient à la mise au point de modèles mathématiques de broyeurs types (1, 3).

Le fondement de la description mathématique du processus technologique du broyage se compose des équations concernant l'hydrodynamique des courants (3). Le mouvement du courant de matériau broyé dans les moulins à tambours utilisés dans l'industrie du ciment est très compliqué. Les différents éléments du courant se déplacent suivant des trajectoires variées. La direction de leur mouvement devient même quelquefois opposée à celle du mouvement principal du courant. Il s'ensuit que certains éléments du courant peuvent traverser le broyeur très rapidement. Le séjour de ces éléments dans le broyeur est très restreint et inférieur au séjour moyen des éléments du courant dans le broyeur. Pour les particules du matériau traversant le plus vite le broyeur le temps de séjour dans ce dernier est insuffisant pour acquérir le degré de broyage nécessaire. En cas de présence dans le courant d'un grand nombre de ces éléments une partie de volume utile proportionnelle à la fraction de ces éléments dans le courant total est utilisée de façon inefficace.

Le temps de séjour de certains éléments du courant dans le broyeur peut dépasser de plusieurs fois celui de séjour moyen et abaisser également l'efficacité du broyeur.

Ainsi donc la méconnaissance dans les calculs des broyeurs industriels de la structure réelle du courant qui les parcourt peut être la cause d'importantes erreurs aussi bien dans le calcul du rendement que dans celui du degré de broyage.

Les études expérimentales de la nature du mouvement des matériaux broyés dans les broyeurs de dimensions diverses (1, 3) ont établi que les broyeurs industriels constituent des installations (des systèmes) se caractérisant par une hétérogénéité nettement exprimée de la distribution du temps moyen de séjour du matériau. On a défini les causes de cette hétérogénéité de distribution du temps de séjour du matériau dans les broyeurs. En leur nombre citons : l'existence au sein du courant de régions de stagnation ; des courants de by-pass ; le transport d'une partie du matériau dans le sens opposé au mouvement général de ce dernier ; la diffusion turbulente ; le profil irrégulier des vitesses du matériau. Les causes mentionnées se manifestant en diverses combinaisons dans les broyeurs conditionnent la spécificité de l'irrégularité dans chaque cas particulier.

Les études réalisées pratiquement pour toute la classe des moulins à tambours,

ont permis de mettre au point des modèles mathématiques types de la structure hydrodynamique des courant de matériaux broyés. Ces modèles traduisent l'essence physique des processus de broyage ainsi que les traits spécifiques de ces derniers au cours de l'utilisation pour le broyage de broyeurs de dimensions variées. Les modèles mathématiques types de la structure du courant dans les moulins à tambours comprennent (3) :

- le modèle de déplacement idéal ;
- le modèle de malaxage idéal ;
- le modèle de diffusion ;
- le modèle de maillage ;
- le modèle de déplacement idéal avec zone de stagnation ;
- le modèle de déplacement idéal parallèlement à la zone de malaxage idéal ;
- le modèle de malaxage idéal suivi de la zone de déplacement idéal ;
- le modèle de déplacement idéal avec by-pass ;
- le modèle de déplacement idéal avec recyclage interne ;
- le modèle de malaxage idéal avec zone de stagnation ;
- le modèle de malaxage idéal avec contre-courant et zone de stagnation ;
- le modèle de malaxage idéal avec by-pass;
- le modèle de malaxage idéal suivi de la zone de déplacement idéal connectant avec la zone de stagnation ;
- le modèle de malaxage idéal avec zone de stagnation et celle de déplacement idéal;
- le modèle de malaxage idéal avec zone de stagnation, suivi de celle de déplacement idéal, soumises au by-pass ;
- le modèle de malaxage idéal suivi de la zone de déplacement idéal, connectant à la zone de stagnation et soumis au by-pass ;
- le modèle du maillage avec zones de stagnation ;
- le modèle du maillage avec contre-courants ;
- le modèle du maillage avec by-pass et zones de stagnation.

Au cours de la mise au point de modèles mathématiques du processus de broyage dans les moulins à tambours on s'est appuyé sur les modèles hydrodynamiques de la structure des courants passés en revue plus haut. Le processus de transformation du matériau brut en un produit broyé est étudié sous l'angle pseudochimique, la cinétique du broyage constituant une réaction du premier ordre :

$$\frac{dR}{d\tau} = -kR,$$

où k est une constante de la vitesse de transformation,
R, la dispersité caractérisée par la teneur en grosses particules (refus sur le tamis).

Le domaine d'application de modèles passés plus haut en revue est fonction du broyeur type mis en oeuvre, de sa géométrie, des propriétés du matériau utilisé et des régimes de fonctionnement de l'installation de broyage. Les études ont montré que pour les broyeurs tubulaires on peut recourir aux modèles de déplacement idéal et à leurs combinaisons, le modèle de diffusion, le modèle du maillage et ses modifications. Pour les installations à autobroyage - le modèle de malaxage idéal et ses combinaisons, le modèle du maillage et ses modifications. Pour l'établissement du schéma technologique de broyage on construit le modèle mathématique général en accord avec le schéma structural sur la base des modèles types de ses éléments constituants.

C'est ainsi qu'après des études de plusieurs années des structures de courants hydrodynamiques de moulins à tambours industriels on a mis au point et classé les modèles mathématiques types des processus de broyage des corps solides susceptibles de perfectionner la technologie et de promouvoir des installations de grande puissance unitaire. L'application concrète de modèles consiste dans la simulation de schémas technologiques de broyage permettant ainsi de démontrer le rôle de différents facteurs variables et de déterminer les meilleures variantes de structure des schémas ; dans l'élaboration de projets optimisés de moulins à tambours à grande puissance unitaire, ainsi que de systèmes technologiques de broyage sur la base du fonctionnement d'installations pilotes ; dans l'étude de l'efficacité et de mise au point de système de contrôle du processus de broyage (1, 3).

On examine plus loin une des applications pratiques des modèles mathématiques consistant dans le calcul du degré de dispersion du produit fini (4).

Le problème se pose de la façon suivante : les propriétés du matériau brut étant connues si l'on connaît la géométrie et les conditions de fonctionnement de l'unité de broyage déterminer la dispersité du produit R_{sor} à la sortie du broyeur. On utilise les modèles de malaxage idéal (1), de déplacement (2), de diffusion (3) et du maillage (4) dont les équations prennent la forme :

$$R_{sor} = R_{en} \frac{1}{1 + k\tau} \qquad (1)$$

$$R_{sor} = R_{en} \cdot e^{-k\tau} \qquad (2)$$

$$R_{sor} = R_{en} \frac{4a \cdot \exp(\frac{Pe}{2})}{(1+a)^2 \exp(\frac{a}{2} \cdot Pe) - (1-a)^2 \cdot \exp(-\frac{a}{2} \cdot Pe)} \qquad (3)$$

où $a = \sqrt{1 + 4k\tau/Pe}$

$$R_{sor} = R_{en} \cdot \frac{1}{(1 + \frac{k\tau}{N})^N} \qquad (4)$$

Les paramètres des modèles mathématiques mentionnés nécessaires au calcul de la dispersité du produit sont : le temps moyen de séjour dans le broyeur $\bar{t}$; le nombre Pe, caractérisant le degré de malaxage longitudinal du matériau dans le broyeur ; la constante de la vitesse de broyage k et le nombre de maille N. Les valeurs quantitatives de ces paramètres ont été obtenues par l'expérience ou le calcul dans des conditions de fonctionnement concret des broyeurs industriels.

La technique de calcul de la finesse de mouture du matériau à l'aide de modèles mathématiques (1, 4) a été vérifié sur les broyeurs de matériau brut de voie humide de dimensions 7,0x2,3 ; 4,0x5,5 ; 4,0x13,5 ; 3,0x14,0 et 2,6x13,0 m et les broyeurs à ciment de dimensions 2,6x13,0 ; 3,0x14,0 et 4,0x13,5 m. L'erreur de calcul maximal ne dépasse pas 9 % ce qui constitue une précision suffisante pour des calculs d'ingénieurs. Cette technique à la différence de la technique courante (5) est plus souple (le type de modèle utilisé est fonction de celui de l'appareil et des conditions de son fonctionnement exigées par la précision du calcul) et universelle (s'applique à tous les broyeurs à tambours), aussi est-elle typique (4).

En accord avec les nouveaux principes d'analyse et le calcul des processus et des installations de broyage de corps solides la distribution des particules en dimension (DPD) est étudiée comme un résultat compliqué d'interaction de la cinétique de broyage et de la structure hydrodynamique du courant de matériau dans le broyeur, c'est-à-dire de la distribution du temps de séjour (DTS) des particules du courant de matériau broyé.

Si l'on admet dans le cas général que dans les broyeurs différents est moulu un matériau aux propriétés identiques ou très proches, c'est-à-dire si l'on pose pour hypothèse que la cinétique de broyage demeure toujours identique ce qui est très vraisemblable, alors il devient évident qu'un rapport naturel et continu s'établit entre la DTS et la DPD.

Cela autorise de juger de la DPD du produit fini obtenu sur la base de modèles mathématiques de la structure hydrodynamique de courants de broyeurs concrets, c'est-à-dire d'après la DTS. Il est évident que dans ce cas la DPD sera pour l'essentiel fonction du type de broyeur, de ses paramètres géométriques et de régimes, vu que tous ces paramètres peuvent en règle générale être présentés sous forme de différentes fonctions d'une même grandeur, la DTS des particules au sein du broyeur.

Ce qui vient d'être dit reçoit une confirmation d'autant plus évidente si l'on tient compte du fait que les courbes de densité de distribution des particules en dimension et en temps de séjour pour des degrés de malaxage des particules variés présentent une nature stochastique identique, obéissent à certaines lois de probabilité identiques et, partant, sont analogues. Cela signifie qu'entre les paramètres de ces courbes de distribution, par exemple, les dimensions caractéristiques des particules du produit et la dispersion de la distribution d'une part, et le temps moyen de séjour et le malaxage longitudinal d'autre part, il existe un rapport univoque.

La dimension moyenne des particules du produit fini est fonction du temps moyen de séjour du matériau dans le broyeur, tandis que la dispersion de la distribution de la granulométrie l'est de la grandeur du coefficient de malaxage longitudinal.

Il s'ensuit la possibilité d'appréciation qualitative et de prévision d'obtention d'une granulométrie voulue dans des broyeurs de dimensions différentes d'après l'arrangement dans ces derniers de la structure hydrodynamique du courant de matériau. C'est d'autant plus important que jusqu'à présent on manquait de classification de broyeurs suivant la forme de leurs courbes de distribution des particules en dimension.

La mise au point de modèles mathématiques types de structures hydrodynamiques de courants et leur concrétisation pour les moulins à tambours rendent possible une telle systématisation, la solution du problème devenant ainsi suffisamment générale et rigoureuse. Vu la continuité de la liaison entre DTS et DPD, le domaine d'application de modèles mathématiques, les dépendances de leurs paramètres des caractéristiques géométriques et des régimes des broyeurs déterminent les dimensions des broyeurs dans lesquels on s'entend à obtenir la DPD, ainsi que la liaison entre les caractéristiques du broyeur et les paramètres de la DPD. Donc le spectre de distribution des dimensions de particules le plus large correspond aux broyeurs de malaxage idéal, tandis que le spectre le plus étroit à celui de broyeurs de déplacement idéal.

En conséquence à ce cas limite de réalisation du broyage dans des broyeurs de déplacement et de malaxage idéaux correspondent des cas limites de distribution de particules en dimension, bref, toutes les particules sont dans le premier cas d'une même dimension et dans le second la teneur en toutes les particules est la même. Les résultats obtenus sont confirmés par les publications de données théoriques et expérimentales (5-8). Il semble évident que l'utilisation complexe et l'apport mutuel de la méthode traditionnelle et de la nouvelle méthode d'analyse de la DPD renferment de grandes possibilités d'élévation de l'efficacité de la solution du problème fondamental de la production du ciment : l'obtention du produit broyé d'activité désirée avec une dépense minimale en énergie.

BIBLIOGRAPHIE

I.- М.А. ВЕРДИЯН, В.В. КАФАРОВ (I977), "Процессы измельчения твердых тел". В кн. "Итоги науки и техники. Процессы и аппараты химической технологии". М., ВИНИТИ, т.5, стр. 5-89, (en russe).

2.- М.А. ВЕРДИЯН, В.В. КАФАРОВ (I978), "Эффективность процессов измельчения материалов в агрегатах большой мощности", Цемент, 8, стр. 9-II, (en russe).

3.- В.В. КАФАРОВ, М.А. ВЕРДИЯН (I978) "Математическое описание и алгоритмы расчета мельниц цементной промышленности", М., НИИЦемент, стр. 93, (en russe).

4.- М.А. ВЕРДИЯН, В.В. КАФАРОВ, Е.А. КАНДЫБЕИ, А.И. ЛЕСИХИНА (I979), "Определение тонкости помола материала в барабанных мельницах на основе их математических моделей", Цемент, 3, стр. 7-9,(en russe)

5.- С.Е. АНДРЕЕВ, В.В. ТОВАРОВ, Б.А. ПЕРОВ (I959), "Закономерности измельчения и исчисление характеристик гранулометрического состава", М., Металлургиздат, стр. 437, (en russe).

6.- Л.А. БАХТИН, О.А. ГОРДЕЦОВА, Я.М. ШУЛЬМАН (I972), "Некоторые математические модели аппаратов для процесса роста частиц", ТОХТ, т.6, 3, стр. 389-399, (en russe).

7.- D. NOVAK, A. KOZLOWSKI (1973), "Kornaufbau und Festigkeiten von Zementen aus unterschiedlichen Mahlanlagen" , Zement - Kalk - Gips, N 7, 312-315 , (en allemand).

8.- М.М. ИВАНОВ, Г.С. КРЫХТИН (I976), "Пути повышения производительности каскадных мельниц мокрого самоизмельчения", М., НИИЦемент, 36, стр. I5-22, (en russe).

Cristallisation du périclase et constance du volume des ciments

Crystallization of periclase and soundness of cements

Y.V. NIKIFOROV, chef de laboratoire, candidat ès sciences techniques,
R.A. ZOSOULIA, collaborateur scientifique en chef, candidat ès sciences techniques, Institut d'Etat de recherches scientifiques de l'industrie du ciment de l'U.R.S.S., "Giprotzement".

RESUME: De nombreuses études (Sérov V.V., Boudnikov P.P., Roiak S.M., Schmitt-Henco C., etc.) ont établi qu'il existe une série de mesures qui permettent d'atténuer fortement l'influence nocive du magnesium dans le clinker.

Un des facteurs conditionnant la constance du volume des ciments magnésifères est le mode de cristallisation du periclase. Il a été établi qu'avec un periclase finement dispersé (1 à 7µm) et régulièrement réparti la teneur limite en MgO dans le clinker peut être élevée jusqu'à 8,5%. Une telle cristallisation s'observe lorsqu'on utilise en qualité de matière première des laitiers magnésifères de haut fourneau ainsi que des materiaux divers contenant du silicate de magnesium.

SUMMARY: Numerous investigations (by Serov V.V., Budnikov P.P., Royak S.M., Schmitt-Henco C., etc.) have proved that there are a number of measures which considerably decrease detrimental influence of magnesia in clinker.

One of the principal factors dictating the soundness of magnesium-containing cements is the nature of periclase crystallization. It has been found out that when periclase is finely dispersed (1-7 microns) and uniformly distributed in the mix, maximum content of MgO in the clinker may be increased to 8,5%. Such a crystallization of periclase is observed when using magnesium blast furnace slags and various magnesium silicate containing materials as a raw material ingredient.

Les déformations volumétriques des ciments conditionnées par l'hydratation du périclase sont essentiellement fonction de la dimension de ses grains et de la nature de leur distribution (1,2). Aussi en utilisant des procédés technologiques assurant une dispersité élevée du périclase peut-on accroître la limite admissible de la teneur en oxyde de magnésium dans le ciment sans altération de sa qualité. C'est ainsi, par exemple, que les ciments, obtenus à partir des clinkers fondus présentant des cristaux de périclase de dimension de 1 à 5μm, supportent des essais en autoclave sous 2 MN/m^2 pour une teneur en oxyde de magnésium de 7 à 8% (3,4).

Habituellement dans les clinkers industriels à concentration élevée en oxyde de magnésium le périclase se présente sous forme de grains isolés de dimension de 15 à 20μm formant des accumulations compactes et constituant des pseudomorphoses sur des cristaux de dolomite du mélange brut (5,6).

On a montré que la dispersion du périclase et, partant, l'accroissement de la teneur admissible en MgO dans le clinker au cas de l'utilisation comme composant du mélange brut du calcaire dolomitique sont favorisés par son broyage plus fin (7), ainsi que par la diminution de la valeur du module d'alumine dans le clinker (8,9). Le ciment Portland magnésifère contenant jusqu'à 10% d'oxyde de magnésium (dans le clinker) et dont la production a été mise en oeuvre dans l'usine de ciment de Podolsk sur proposition de V.VSerov (10,11) possède également un bas module d'alumine (0,6-0,9). Le ciment a résisté aux essais en autoclave sous une pression de 0,8 et 1,4 MN/m^2. Sur la base de cette méthode technologique l'usine de ciment citée a produit pendant longtemps un ciment Portland magnésifère ainsi qu'un ciment Portland au laitier avec 10% d'oxyde de magnésium dans le clinker.

Les études ultérieures, réalisées par "Giprotzement" ont été orientées vers la recherche de voies d'atténuation de l'influence nocive du périclase sur la variation régulière du volume. On a établi que les composés fluorés (en particulier, CaF_2, Na_2SiF_6) une fois introduit en quantité dosée dans le mélange brut contribuent à diminuer les dimensions moyennes de cristaux du périclase et, partant, les ciments (sans adjuvants minéraux actifs) arrivent à supporter l'essai en autoclave (pression 2 MN/m^2) pour une teneur en MgO jusqu'à 6% (2).

Toutefois ni l'introduction dans la matière brute de composés de fluor, ni l'abaissement (dans les limites indiquées) du module de l'alumine ne s'opposent à la possibilité d'accumulation du périclase (par suite de la dissolubilité limitée de l'oxyde de magnésium dans la fusion de clinker) et ne permettent donc pas d'élever la teneur en oxyde de magnésium dans le clinker au-dessus de 6%.

Mais la cristallisation devient de nature toute différente au cas d'utilisation en qualité de composants magnésifères de base des laitiers magnésiens de haut fourneau.

Le périclase dans ces clinkers se répartit régulièrement sur toute la coupe mince sous forme des grains de dimension de 1 à 7μm. Rien que 20 à 30% de tout le périclase possèdent des grains de dimension de 7 à 15μm. Les accumulations de cristaux (de 80μm et plus) si communes aux clinkers formés de calcaires dolomitiques et d'argiles ne s'y observent pas. La nature de la cristallisation mentionnée du périclase peut avoir pour cause deux circonstances. Tout d'abord, en utilisant des laitiers magnésiens l'oxyde de magnésium libre se forme par interaction de CaO avec les minéraux magnésifères du laitier de haut fourneau à des températures relativement élevées - 1200-1400°C et, par suite, la période de récristallisation du périclase se raccourcit fortement. Ensuite, la concentration en ions de magnésium dans les minéraux des laitiers de haut fourneau est inférieure à celle rencontrée dans les minéraux de carbonates (dolomite).

Il s'ensuit que pour la même teneur en oxyde de magnésium dans les mélanges bruts le volume des minéraux magnésifères est de beaucoup supérieur lorsqu'on utilise dans la matière crue des laitiers magnésiens au lieu du calcaire dolomitique. C'est la raison de la répartition régulière des grains de périclase parmi les granules du clinker.

La haute dispersité de la cristallisation du périclase dans le clinker à base de laitiers magnésiens de haut fourneau ainsi que sa répartition régulière permet d'accroître sensiblement la teneur admissible en MgO sans entraîner des changements irréguliers dans le volume du ciment. Au cours de nos expériences les ciments à base de ces clinkers ont bien résisté au traitement en autoclave (sous 2 MN/m^2) pour une teneur en oxyde de magnésium ne dépassant pas 8,5%, se sont avérés satisfaisants. Tandis que le ciment à base de clinker contenant 6,65% MgO et fabriqué à partir du calcaire dolomitique et de l'argile n'a pas résisté aux épreuves de régularité de la variation de volume (Tabl.I).

Tableau I

Dénomination du composant argileux	MgO dans le clinker en %	Dilatation linéaire, %	
		Bouillissage	Traitement en autoclave
Laitier N.1	7,02	0,04	0,19
Laitier N.2	8,00	0,04	0,29
Laitier N.3	11,2	0,04	~14
Laitier N.4	6,82	0,02	0,16
Laitier N.6	7,53	0,04	0,23
Laitier N.7	7,70	0,02	0,15
Laitier N.9	9,30	0,04	5,4
Laitier N.10	6,94	0,06	0,41
Laitier N.11	7,85	0,03	0,57
Argile	6,65	0,02	~11

Donc la limite admissible de la teneur en oxyde de magnésium dans les clinkers à base de laitiers magnésiens de haut fourneau peut être élevée par rapport aux normes existantes sans altération de la qualité du ciment en ce qui concerne la régularité de variation du volume.

BIBLIOGRAPHIE

1. - F.GILLE, (1952), "Zement - Kalk - Gips", N.5 (en allemand)
2. - Л.С.КОГАН, Ю.В.НИКИФОРОВ, (1965), "Цемент", № I (en russe).
3. - С.М.РОЯК, В.Ф.КРЫЛОВ, М.М.МАЯНЦ, (1962), "Научные сообщения НИИЦемента", № 13 (44), 33-39, (en russe).
4. - М.КИЙЛЕР, (1961), "Известия АН ЭССР, т.10, серия физико-математических и технических наук, № 2, 143-149, (en russe).
5. - П.Ф.КОНОВАЛОВ, Б.В.ВОЛКОНСКИЙ, А.П.ХАШКОВСКАЯ, (1962), Атлас микроструктур цементных клинкеров, огнеупоров и шлаков. Л-М, (en russe).
6. - С.Д.ОКОРОКОВ, Ю.В.НИКИФОРОВ, Р.А.ЗОЗУЛЯ, М.В.ЛОГИНОВА, (1970), "Цемент" , № 5, (en russe).
7. - E.PAULAT, P.SCHREITER, (1977), Baustoffindustrie, A-20, N 5, 5-7, (en allemand).
8. - L.CZARNIK, (1961), Cement, Wapno, Gips, N 12, (en polonais).
9. - В.А.ЧЕРНЯХОВСКИЙ, В.П.РЯЗИН, (1966) , "Научные сообщения НИИЦемента", вып.21 (52), (en russe).
10. - И.Л.ЛЕФАНД и В.В.СЕРОВ, (1935), "Цемент", № 7, (en russe).
11. - В.В.СЕРОВ, (1957), Сб. статей памяти В.А.Серова, НИИЦемент, М., (en russe).

Activation mécanique des matières premières pour la fabrication du ciment

Mechanical activation of cement raw materials

M.E. NOUDEL, candidat ès sciences techniques, collaborateur scientifique,
G.S. KRYKHTINE, candidat ès sciences techniques, chef de laboratoire, NIITzement, Moscou, U.R.S.S

RESUME: Les auteurs exposent les résultats des recherches qui avaient pour but de mettre au point les principes de la rationalisation du procédé de préparation des matières brutes à la cuisson. Ces principes sont fondés sur l'étude des propriétés des matières premières, propriétés qui peuvent être modifiées par fragmentation de ces matières et exercer une influence considérable sur leur transformation ultérieure, en réduisant la consommation du combustible pour la cuisson et en augmentant l'activité du clinker. Par fragmentation on entend la dispersion et l'activation mécanique, c'est-à-dire, l'accroissement du nombre de défauts cristallins (destruction). On décrit les trois stades principaux de modification de la réactivité des matières premières pendant leur broyage, on établit les limites conventionnelles de ces stades et la possibilité de leur réalisation, on donne les formules pour déterminer le degré et l'efficacité de l'activation mécanique des matières premières. On donne la définition des notions de "degré" et d'"efficacité" de l'activation mécanique. On expose succinctement les principes de fonctionnement d'un activateur destiné à augmenter les défauts de la structure et la surface de contact des grains des matières broyées.

SUMMARY: The work deals with development of a systematic approach to rationalizing the technology of preparation of cement raw materials for calcination. It is based on study of properties of raw materials which may be changed during crushing and exert a considerable effect on further processing, on reduction of fuel consumption for calcination and increase of clinker activity. Crushing is considered as a process of dispersing and mechanical activation - increase of the number of defects in the crystalline structure (destruction). Three main stages of conversion of reaction capacity of the cement production raw materials during crushing are described, conventional boundaries of there stages and the possibility of their achivement are given, formulae for determining the degree and efficiency of mechanical activation of raw materials are given. The notions of "degree" and "efficiency" of mechanical activation are defined. The operating principles of the activator intended to increase defects in the structure and contact surface of the raw mix grains are briefly discussed.

L'efficacité, la qualité et la stabilité de la fabrication du ciment dépendent pour beaucoup de la manière dont on prépare les matières premières à la cuisson. La présente communication a pour objet l'étude des propriétés des matières premières, lesquelles peuvent être modifiées au cours de la fragmentation de ces dernières et exercer une influence considérable sur le processus de traitement thermique des produits broyés. La connaissance de ces propriétés et des lois qui régissent leur modification au cours de la fragmentation des matières premières permettront de choisir les procédés les plus efficaces de préparation de celles-ci à la cuisson avec utilisation du matériel tant existant qu'inédit.

Nos recherches ont porté sur l'argile kaolinitique et les calcaires de composition chimique voisine: un calcaire compact à gros cristaux, un calcaire poreux à gros cristaux et un calcaire compact à cristaux fins. Les calcaires ont subi la réduction séparément et conjointement avec l'argile dans un broyeur à boulets de laboratoire à fonctionnement discontinu. Les produits du broyage ont été soumis aux analyses granulométrique, thermique différentielle, calorimétrique, aux rayons X, chimique et microscopique. A partir des résultats des analyses, on a calculé: la taille caractéristique des particules des matières broyées (δ 36,8); l'énergie d'activation pour la décarbonation des calcaires (E); les effets thermiques globaux de la clinkérisation du mélange brut (Q_c) et de la dissolution dans l'eau de l'oxyde de calcium résultant de la décarbonation des calcaires (Q_{CaO}); le rapport de la hauteur à la largeur (dans leur partie située à mi-hauteur) des pics représentant, sur les radiogrammes, la structure de la calcite (β_{CaCO_3}) et de l'oxyde de calcium (β_{CaO}) pour des quantités invariables de ceux-ci.

La figure 1 représente graphiquement, en coordonnées sans dimensions, les relations généralisées entre les variations des grandeurs δ 36,8, E et Q_c et la durée de la réduction des calcaires et de leurs mélanges avec de l'argile. Il ressort de ces courbes que la vitesse maximale des décroissement de la taille caractéristique des particules est observée pendant les premières minutes de leur réduction (le premier stade conventionnel de fragmentation). Ensuite, la vitesse de la variation du degré de dispersion commence à baisser (c'est le deuxième stade conventionnel) et, enfin, il arrive un moment (le début du troisième stade conventionnel) où une réduction prolongée ne provoque aucun accroissement appréciable du degré de dispersion des produits à broyer.

La vitesse minimale de la variation des grandeurs E et Q_c, qui traduisent respectivement la réactivité des calcaires et des constituants de base lors de leur traitement thermique, est observée au premier stade de fragmentation, et la vitesse maximale, au deuxième. L'accroissement de la durée de réduction des matières au troisième stade favorise la variation des grandeurs E et Q_c, bien que la dispersité des produits broyés

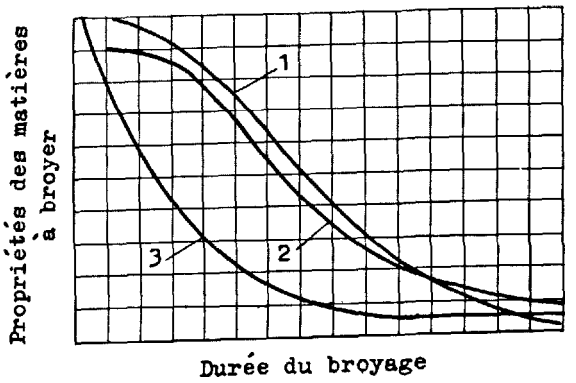

Fig.1. Variations, au cours de la réduction des matières premières, de l'effet thermique global de la clinkérisation (1), de l'énergie d'activation du processus de décarbonation (2) et de la taille caractéristique des particules (3).

reste pratiquement inchangée. Il existe donc une certaine disproportion entre les variations de la dispersité et de la réactivité des matières premières au cours de leur réduction.

Pour pouvoir expliquer ce phénomène, nous avons étudié la variation de la réactivité des matières premières au cours de la réduction, leur dispersité restant invariée. On a prélevé dans le broyeur des prises d'essai du calcaire, en faisant varier la durée de la réduction de celui-ci. On a achevé le broyage pendant un court laps de temps (30 s) dans un broyeur de porcelaine en présence de 50% d'eau, ce qui entraîne, comme il ressort de l'analyse microscopique, la désagrégation d'agglomérations secondaires constituées de particules très fines. Les prises d'essai ainsi désagrégées ont été divisées par tamisage en fractions qui ont été ensuite mélangées dans une proportion assurant une distribution logarithmique de la composition granulométrique avec un coefficient d'uniformité de 0,7 et une taille caractéristique δ 36,8 = 30 microns. On a ainsi obtenu une série de prises d'essai des calcaires, ayant des compositions granulométriques voisines mais ayant subi un broyage de durées différentes.

Comme il ressort des courbes 1 à 3 (Fig.2), l'accroissement de la durée de réduction des calcaires au premier stade conventionnel aboutit à l'obtention de produits qui présentent une valeur accrue de E à condition de maintenir invariable la dispersité. Cette baisse de la réactivité des calcaires peut être attribuée au décroissement, au cours de leur réduction à ce stade, du nombre de défauts des particules ayant des degrés de dispersion égaux. Ce décroissement est dû au fait qu'au premier stade de réduction il se produit essentiellement une dégradation fragile de la matière par suite de l'ouver-

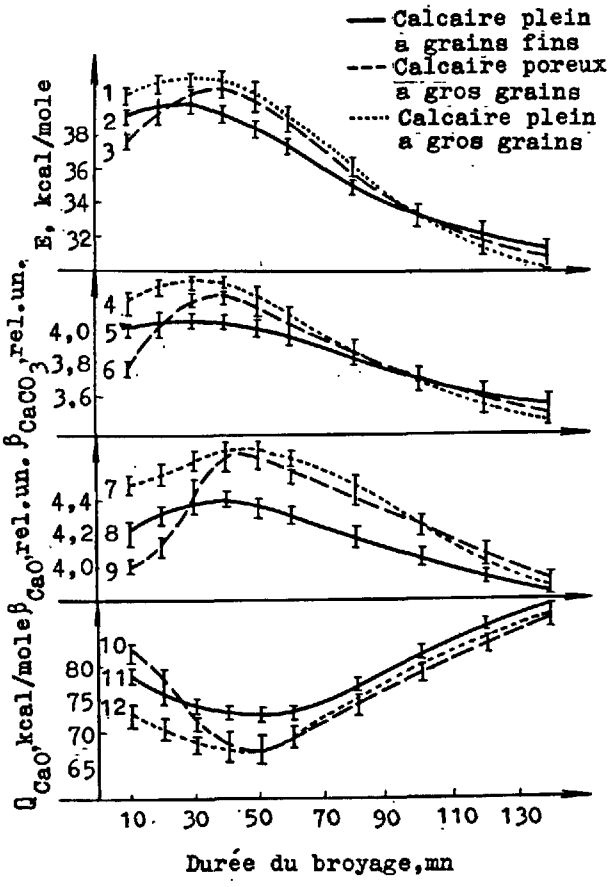

Fig.2. Variations des valeurs de E, de β_{CaO}, de β_{CaCO_3} et de Q_{CaO} des échantillons de calcaire obtenus à la suite des fragmentations de différentes durées, le degré de dispersion restant invarié.

ture des défauts volumiques naturels de sa structure (pores, fissures, etc.), sans qu'il y ait une formation appréciable de défauts nouveaux. Cette hypothèse est étayée par l'accroissement relatif maximal, parmi les calcaires examinés, de la valeur E du calcaire poreux (de plus de 3 kcal/mole), ainsi que par l'accroissement, au premier stade de réduction, de la valeur β_{CaCO_3} (Fig.2, courbes 4 à 6).

La diminution du degré de destruction des calcaires favorise la formation, à l'issue de leur décarbonation, d'un oxyde de calcium présentant lui aussi une structure plus ordonnée (Fig.2, courbes 7 à 9). Ce phénomène est, à son tour, responsable de la diminution de la réactivité de l'oxyde de calcium, ce dont témoigne, d'une manière indirecte, le décroissement de sa chaleur unitaire de dissolution dans l'eau (Fig.2, courbes 10 à 12).

La vitesse de la fragmentation au deuxième stade se voit baisser par suite du décroissement, au sein de la matière, du nombre de défauts volumiques qui ne sont autres que des "fissures de destruction" résultant des contraintes de déformation créées dans le broyeur. La dégradation des particules à ce stade s'effectue en deux étapes: l'apparition de la fissure (par suite de la déformation plastique) et la propagation de celle-ci. Les divers défauts (dislocations, hémitropies, etc.) qui apparaissent et se déplacent lors de la déformation plastique d'un solide n'y donnent des "fissures de destruction" qu'en partie, à cause d'une redistribution non uniforme des contraintes au sein du solide. C'est pourquoi au deuxième stade de fragmentation des calcaires on constate un décroissement de la grandeur β_{CaCO_3}. Au cours du deuxième stade de fragmentation il se forme un grand nombre de particules dont la taille est inférieure à celle des grains cristallins constituant la roche. S'agissant des calcaires étudiés, la solidité des liaisons intracristallines est supérieure à celle des liaisons intercristallines. Aussi, au cours du deuxième stade de fragmentation, y a-t-il rupture de liaisons plus solides qu'au cours du premier. Il en résulte un accroissement de la réserve d'énergie libre des surfaces en cours de formation, tandis qu'une tendance à sa diminution a pour effet un déplacement plus intensif des atomes superficiels vers l'intérieur, c'est-à-dire une destruction plus forte de la matière. L'intensification de la destruction des calcaires accentue leur réactivité, ce dont témoignent les variations correspondantes des valeurs E et Q_{CaO}, constatées en cas de prises d'essai aux degrés de dispersion voisine au cours du deuxième stade de fragmentation.

Au troisième stade de fragmentation intervient un équilibre entre la formation d'agrégations de petites particules et leurs désagrégation, aussi un prolongement de l'action des effets sollicitant la matière n'entraîne-t-il pas de changements de son degré de dispersion. Toutefois, la destruction de la matière résultant essentiellement de la déformation plastique des particules dans les zones adjacentes aux endroits de leurs contacts superficiels continue à s'accentuer, ce qui entraîne un accroissement de la réactivité des calcaires réduits à ce stade avec l'augmentation de la durée de leur broyage (Fig.2).

En partant des données ainsi obtenus, on peut calculer qu'au premier stade de fragmentation l'accroissement de la réactivité résulte totalement de l'augmentation du degré de dispersion des calcaires et se voit freiner pour 20 à 40% par la diminution du degré de leur destruction. Au deuxième stade de fragmentation, l'accroissement du degré de dispersion des calcaires donne 35 à 60% de la contribution totale à l'augmentation de leur réactivité, le reste résultant de la destruction. L'accentuation de 85 à 90% de l'activité des calcaires avec l'accroissement de la durée de fragmentation au troisième stade est due à l'augmentation du degré de destruction des produits broyés.

En conséquence, la fragmentation des constituants de base doit être considérée non

point comme une modification de leur degré de dispersion mais comme une opération d'activation mecanique. Pour l'étude de ce phenomène, nous recommandons de faire usage des indices de degre (I_d) et d'efficacite (I_e) de l'activation mecanique des matières premières, qui peuvent etre calcules d'apres les formules suivantes:

$$I_d = \frac{Q_c' - Q_c}{Q_c'} \cdot 100 \qquad (1)$$

$$I_e = \frac{1,16\ (Q_c' - Q_c)}{E} \qquad (2)$$

où Q_c' et Q_c sont les effets thermiques globaux de clinkerisation, determines pour la matière de charge, respectivement avant et apres sa reduction; cal/g;

E représente les dépenses d'énergie pour la reduction de la matiere de charge, kW.h/t.

L'indice I_d indique la part qui revient à l'activation mecanique dans l'abaissement de la consommation unitaire de chaleur pour la clinkerisation lors du traitement thermique des matieres premieres, alors que l'indice I_e montre l'efficacite avec laquelle s'effectue cette operation dans l'unite considerée. Pour determiner les valeurs de I_d et de I_e on prepare plusieurs echantillons obtenus a differentes depenses d'energie unitaires pour la reduction, on les soumet a une analyse thermique differentielle et on calcule les valeurs correspondantes de Q_c. En mettant les valeurs de Q_c et de E dans l'equation suivante, qui traduit le phenomene d'activation mecanique, on peut déterminer la valeur de Q_c:

$$Q_c = Q_c' \exp\left(-\frac{K_1 E}{K_2 + E}\right) \qquad (3)$$

Etant donné que les indices I_d et I_e traduisent bien les principales transformations utiles intervenant au cours de l'activation mecanique des matieres premieres, la mise en oeuvre de ces indices permet de mener a bien avec plus de certitude les principaux problemes de rationalisation du procede de preparation a la cuisson des matieres premieres, par rapport a l'utilisation des caracteristiques liees au degre de dispersion. Une meilleure precision est notamment obtenue quand il s'agit de déterminer le degre de reduction optimal de la matiere de charge ou bien de choisir le materiel le plus efficace et le schema technologique le plus rationnel. En outre, en faisant varier le degre d'activation mecanique par modification des parametres de fonctionnement des broyeurs, on parvient a obtenir a leur sortie un produit avec une valeur constante de Q_c.

Une analyse du fonctionnement des unités de broyage actuellement en usage a montre qu'elles ne fonctionnent efficacement (I_e = 1) qu'au premier et au deuxième stades conventionnels et n'atteignent pas de ce fait le degre limite d'activation mecanique. C'est pourquoi nous avons mis au point un dispositif special dans lequel la matière issue des deux premieres stades de fragmentation subit une destruction intensive sans donner lieu a une variation du degre de dispersion. Dans ce dispositif, les matieres premieres broyees subissent des chocs qui ne desagregent point les particules mais les deforment seulement d'une manière plastique aux endroits des contacts superficiels. Il en résulte une augmentation brusque (de presque 100 fois) de la surface de contact des particules et leur destruction considérable. La matière sort de l'activateur sous forme de granules secs de 0,5 a 5,00 mm.

L'accroissement du nombre de défauts de structure et de la surface de contact des particules dans l'activateur permet d'augmenter de 20 a 30% l'activite mecanique des matieres broyees. L'indice d'efficacite I_e est d'ailleurs 12 a 15 fois plus grand qu'avec le meme degre d'activation mecanique des matieres premieres dans un broyeur a boulets a fonctionnement discontinu, alors que realiser ce niveau d'activation mecanique dans les broyeurs a boulets a fonctionnement continu est tout a fait impossible. L'activation plastique sous l'effet de coups, subie par les matieres premieres broyees, contribue a augmenter l'activité hydraulique du ciment fabrique a partir de celles-ci, ce qui est du a un deroulement plus complet des réactions de formation d'alite et a une structure particulière des mineraux constituant le clinker.

La mise en oeuvre de la farine brute sous forme de granules actives secs offre la possibilite d'augmenter l'intensite de combustion dans le four et de reduire la quantité du melange pulverulent de ciment et de matieres premieres qui circule dans le systeme "four - echangeur de chaleur". Tout cela contribue a accroitre considerablement le rendement de l'unite, a stabiliser et ameliorer la qualite du clinker de le ciment Portland et a réduire les émanations de poussieres rejetees a l'atmosphere.

On voit donc que l'accroissement de l'activite mecanique des matieres premieres n'est pas proportionnel a l'augmentation de leur degre de dispersion dans tout l'intervalle possible de variation de ce dernier. Plus developpee est la surface du melange brut, plus grande est l'efficacite qui peut être atteinte dans l'augmentation de la reactivite par destruction de ses particules, et moindre est celle qui s'obtient par accroissement ulterieur de leur degre de dispersion. Des lors, il existe des limites de l'activation mecanique des matieres premieres qu'on a interet a atteindre dans les unites qui dispersent efficacement la matiere. L'activation ulterieure peut être avantageusement effectuee dans des unites

dont la fonction principale est une destruction intensive des matières divisées. Les limites de l'utilisation de ces unités dépendent de leur conception, des propriétés et des particularités technologiques du traitement thermique ultérieur des matières premières. Ces limites peuvent être mises en évidence avec recours aux indices de degré et d'efficacité de l'activation mécanique.

Etude thermodynamique de la cinétique de la formation de l'alite

Thermodynamic studies of alite formation kinetics

A.V. BESSMERTNYKH, collaborateur scientifique,
V.K. KHOKHLOV, chef de section,
V.V. CHELOUDKO, chef de laboratoire, "NIITzement", Moscou, U.R.S.S.

RESUME: On analyse la cinétique de la formation du silicate tricalcique en présence de la phase liquide par des méthodes thermodynamiques de processus irreversibles. Les équations cinetiques sont presentées sous forme d'equations lineaires d'Onsager pour les differents domaines de deroulement de la reaction: la reaction est limitée a) par la vitesse de dissolution des deux composants de base en phase liquide, b) par la vitesse de la reaction en phase liquide, c) par la vitesse de cristallisation à partir de la fusion, d) par la vitesse de dissolution d'un des composants de base. Dans ce dernier cas les équations d'Onsager sont bilineaires et possedent des coefficients phenomenologiques croisés negatifs. On analyse les conditions de dominance de la saturation par la chaux en phases solide ou liquide du silicate bicalcique.

SUMMARY: The kinetics of formation of tricalcium silicate in the presence of a liquid phase have been analyzed by the irreversible process thermodynamics methods. The kinetic equations are presented in the form of linear Onsager equations for different reaction regions; the reaction is limited; (a) by the rate of dissolving of both starting substances in the liquid phase; (b) by the rate of the liquid phase reaction; (c) by the rate of crystallization from the melt; (d) by the rate of dissolving of one of the starting substances. In the latter case the Onsager equations are bilinear and feature negative cross-coupling phenomenological coefficient. The conditions of prevailing solid- or liquid-phase saturation of bicalcium silicate with lime have been analyzed.

Le processus complexe de formation du silicate tricalcique en phase liquide (fusion de silicate) peut se subdiviser en une serie de processus élementaires se déroulant simultanement, parmi lesquels on degagera les processus suivants:

- dissolution de C_2S et de CaO de base en phase liquide,
- réaction de formation du C_3S en phase liquide,
- cristallisation de C_3S à partir de la fusion.

Ces processus interagissant mutuellement, aussi juge-t-on utile d'en donner une description simultanee. La liaison entre deux ou plusieurs processus en marche peut être etablie sous l'angle de la thermodynamique des processus irreversibles (TPI), dont les methodes seront frequemment mis en œuvre plus loin.

Soit un système isothermique hétérogène fermé comprenant des phases solide (s) et liquide (l) ainsi que des phases de l'alite cristallin. Vu qu'entre les phases il se produit des phenomènes d'échange de masse, ces dernieres seront considerees comme ouvertes.

Les principes généraux de la description cinetico-thermodynamique de ces systemes sont, en particulier, exposés dans (1).

En se servant de l'équation fondamentale de Gibbs pour chaque phase du système, en tenant compte du bilan massique et energetique, ainsi que de la propriete d'additivite de l'entropie, on peut montrer que la fonction dissipative du système considéré prend la forme

$$\theta = \frac{d_i S}{d\tau} T = -\left(\mu^{s}_{CaO} \frac{dn_{CaO}}{d\tau} - \mu^{s}_{C_2S} \cdot \frac{dn_{C_2S}}{d\tau} + \mu^{l}_{CaO} \frac{dn_{CaO}}{d\tau} + \mu^{l}_{C_2S} \frac{dn_{C_2S}}{d\tau} - \mu^{l}_{CaO} \frac{d\xi_l}{d\tau} - \mu^{l}_{C_2S} \frac{d\xi_l}{d\tau} + \mu^{l}_{C_3S} \cdot \frac{d\xi_l}{d\tau} - \mu^{l}_{C_3S} \frac{dn_{C_3S}}{d\tau} + \mu^{s}_{C_3S} \frac{dn_{C_3S}}{d\tau}\right) =$$

$$= \Delta\mu_{CaO} W_{CaO} + \Delta\mu_{C_2S} W_{C_2S} + A_l W_l + \Delta\mu_{C_3S} W_{C_3S} \quad (1)$$

Analysons l'équation (1) pour différents domaines de déroulement de la réaction de formation du C_3S cristallin, avec la prise en compte des limitations imposées à sa cinetique.

A. La vitesse de la réaction est limitée par celle de la dissolution des substances de base, les vitesses molaires de dissolution constituant un rapport des proportions stoechiometriques :

$$\frac{dn_{CaO}}{d\tau} = \frac{dn_{C_2S}}{d\tau}$$

Dans ce cas

$$\frac{dn_{C_3S}}{d\tau} = \frac{d\xi_l}{d\tau} = \frac{dn_{CaO}}{d\tau} = \frac{dn_{C_2S}}{d\tau},$$

soit,

$W_{CaO} = W_{C_2S} = W_l = W$ et l'équation (1) prend la forme:

$$\theta = W(\Delta\mu_{CaO} + \mu_{C_2S} + A_l + \mu_{C_3S}) = WA_s \quad (2)$$

où

$$A_s = \mu^{s}_{CaO} + \mu^{s}_{C_2S} - \mu_{C_2S}$$ qui est l'affinité pour la réaction en phase solide.

Les méthodes TPI montrent que la fonction dissipative a toujours la forme:

$$\theta = \sum X_i Y_i \quad (3)$$

en outre, entre les flux généralisés et les forces generalisées on retrouve, avec l'application de la methode lineaire TPl, la relation lineaire uniforme d'Onsager:

$$Y_i = \sum_{j=i}^{m} L_{ij} X_j \quad (i = 1, 2...m) \quad (4)$$

Les données expérimentales accumulées autorisent d'admettre que dans la grande majorite des cas les phenomenes de transfert (conductibilite thermique, diffusion, phénomènes électrocinetiques, etc.) peuvent être décrits avec un haut degré de precision par les equations du type (4). Au cas de réactions chimiques soumises à la loi d'action des masses l'application des methodes lineaires TPI se limite au domaine de la realisation approchée de l'égalite:

$$1 - e^{-A/RT} = \frac{A}{RT} - \frac{1}{2!}\left(\frac{A}{RT}\right)^2 + \frac{1}{3!}\left(\frac{A}{RT}\right)^3 - ... \approx \frac{A}{RT} \quad (5)$$

A étant l'affinité maximale pour l'une des réactions élementaires.

D'après les données fournies par (2) il est possible de calculer l'affinite pour la re-

action

$CaO(s) + C_2S(s) \rightleftarrows C_3S(s)$ pour T=1700K

$A = -\Delta Z = 3939$ cal/mol

Les données thermochimiques de base pour le calcul de l'affinité pour les réactions élémentaires manquant, en posant ces dernières égales l'une à l'autre, on obtient A = 1313 cal/mol.

Donc, en tenant compte de deux premiers termes dans le développement en série de la fonction exponentielle, il est possibles de décrire la vitesse de la réaction par des relations linéaires dans le domaine de températures posées avec une précision allant jusqu'à 7,5%.

En revenant à (2) écrivons la relation linéaire

$$W = LA_s \qquad (6)$$

Dans l'équation cinétique on ne trouve pas sous une forme explicite les termes marquant l'influence de la phase liquide. Cette relation, comme la fonction dissipative qui lui correspond, est analogue par sa forme aux équations décrivant la cinétique de la saturation par la chaux en phase solide du silicate bicalcique, autrement dit la phase liquide se manifeste par une action purement catalytique que traduit la grandeur du coefficient phenomenologique a propos duquel on peut remarquer ce qui suit:

si la réaction résultante

$$CaO(s) + C_2S(s) \rightleftarrows C_3S(s),$$

la relation linéaire étant $W = LA$,

se déroule à des stades quelque peu élémentaires

1. $CaO(s) + C_2S(s) \rightleftarrows CaO(l) + C_2S(l)$ $\quad (W_1 = L_1A_1)$
2. $CaO(l) + C_2S(l) \rightleftarrows C_3S(l)$ $\quad (W_2 = L_2A_2)$
3. $C_3S(l) \rightleftarrows C_3S(s)$ $\quad (W_3=L_3A_3)$

alors on a entre les coefficients la relation

$$\frac{1}{L} = \frac{1}{L_1} + \frac{1}{L_2} + \frac{1}{L_3} \qquad (7)$$

Les termes additionnés dans le second membre, par analogie avec les resistances thermique et de diffusion, peuvent être appelés résistances chimiques des réactions élémentaires. Si l'on peut, par rapport à l'une quelconque des resistances, négliger autres resistances, il est possible de tirer de (7), en posant, par exemple, $L_2 \gg L_1$ et $L_3 \gg L_1$ que $L=L_1$. Dans l'étude des réactions en phases solides sans la phase liquide la résistance principale est la résistance à la diffusion des reactifs à travers la couche du produit qui est de beaucoup supérieur à celle s'opposant à la dissolution. Aussi la vitesse de la réaction en présence de la phase liquide est-elle superieure à celle des réactions dans des phases solides.

B. La vitesse de la réaction est limitée par celle de la dissolution de l'un des reactifs (par exemple, CaO):

$$\frac{dn_{CaO}}{d\tau} < \frac{dn_{C_2S}}{d\tau}$$

Dans ce cas, on obtient de l'équation (1):

$$\theta = W(\Delta\mu_{CaO} + A_l + \Delta\mu_{C_3S} + \Delta\mu_{C_2S}) + \Delta W \Delta\mu_{C_2S} \qquad (8)$$

Les équations linéaires correspondantes compte tenu de la relation de reciprocité d'Onsager sont:

$$\left.\begin{aligned} W &= L_{11}A_s + L_{12}\Delta\mu_{C_2S} \\ \Delta W &= L_{21}A_s + L_{22}\Delta\mu_{C_2S} \end{aligned}\right\} \quad L_{12}=L_{21} \qquad (9)$$

Dans les relations (8) et (9)

ΔW est la différence des vitesses de dissolution des substances de base en phase liquide.

Donc la vitesse de la réaction est dans ce cas une fonction bilineaire, c'est-a-dire qu'il se produit une superposition d'influences de forces thermodynamiques generalisees - de l'affinité chimique et de l'affinité pour la dissolution de la substance de base dont la vitesse stoechiometrique molaire de dissolution est la plus grande. Il est en outre important de souligner que les deux forces thermodynamiques constituent des tenseurs d'ordre zero, c'est-a-dire des scalaires.

Pour l'utilisation pratique de la relation (9) il est important d'établir le signe du coefficient croise $L_{21} = L_{12}$. Il est connu que les coefficients directeurs des relations lineaires d'Onsager sont toujours positifs. Quant aux coefficients croises ils ne possèdent pas, en general, de signe determine et il est necessaire de le determiner dans chaque cas concret.

Pour établir le signe du coefficient croisé dans le système (9), rapportons-nous au mecanisme de la marche de la reaction aboutissant à la formation de C_3S. La signification physique de ΔW est la vitesse du cumul de C_2S en phase liquide. Si la phase liquide est prise pour une solution diluée obeissant à la loi de Henry, on peut affirmer que l'affinite pour la dissolution

$$\Delta\mu_{C_2S} = -RTl_n \frac{C_{C_2S}}{C^{Sat}_{C_2S}} \qquad (10)$$

où $C^{Sat}_{C_2S}$ est la concentration de saturation.2

Donc, à mesure de l'accumulation dans la phase liquide du composant a dissolution plus rapide, son affinite pour la dissolution diminue et, partant, sa vitesse de dissolution s'abaisse: le système evolue vers un etat (appelons-le stationnaire) pour lequel $\Delta W \longrightarrow 0$. Mais dans ce cas il est important qu'on ait:

$$\Delta\mu_{C_2S} = \Delta\mu^{st}_{C_2S} > 0.$$

En profitant de l'indépendance des coefficients phenomenologiques de la grandeur de l'affinite, on tire de la seconde equation du systhème (9):

$$L_{21} = -L_{22} \frac{\Delta\mu^{st}_{C_2S}}{A_s} < 0 \qquad (11)$$

En portant (11) dans la première équation du systeme (compte tenu de la relation de reciprocité), il vient:

$$W = L_{11}A_s - L_{22} \frac{\Delta\mu^{st}_{C_2S} \cdot \Delta\mu_{C_2S}}{A_s} \qquad (12)$$

Notons l'importance de cette équation pour l'appreciation de l'influence de la quantité de la phase liquide sur la cinetique de la formation de C_3S. En laissant tomber les details indiquons que l'equation (12) se caracterise par l'existence d'un maximum de la fonction

$$W = f(\sum_i N_i)$$

pour une valeur optimale de la quantité de la phase liquide $\sum N_i$; avec l'accroissement subsequent de cette derniere la vitesse de formation de C_3S diminue.

C. La réaction se déroule dans un domaine cinetique, autrement dit est limitee par la vitesse de la reaction dont tous les participants sont en phase liquide. Vraisemblablement ce cas se presente pour un cuisson ultrarapide, se traduisant par la formation d'un oxyde de calcium et de silicates en état metastable qui se dissolvent rapidement. Le systeme de relations lineaires qui s'y rapporte est:

$$\left.\begin{aligned} W &= L_{11}A_s + L_{12}\Delta\mu_{CaO} + L_{13}\Delta\mu_{C_2S} \\ \Delta W_{CaO} &= L_{21}A_s + L_{22}\Delta\mu_{CaO} + L_{23}\Delta\mu_{C_2S} \\ \Delta W_{C_2S} &= L_{31}A_s + L_{32}\Delta\mu_{CaO} + L_{33}\Delta\mu_{C_2S} \\ L_{12} &= L_{21},\ L_{23} = L_{32},\ L_{31} = L_{13} \end{aligned}\right\} \qquad (13)$$

On peut également montrer que ce système tend vers un certain etat stationnaire correspondant a la vitesse minimale de l'apparition de l'entropie.

La première équation peut également être etudiee en rapport avec l'extrémum.

D. La réaction est limitée par la vitesse de cristallisation de la substance produite. Dans ce cas il y a plusieurs variantes de rapports entre les vitesses des processus elementaires. Par exemple, pour

$$W < W_{CaO} = W_1 < W_{C_2S}$$

le système d'équations linéaires prend la forme:

$$\left.\begin{aligned} W &= L_{11}A_s + L_{12}A_{sl} + L_{13}\Delta\mu_{C_2S} \\ \Delta W_1 &= L_{21}A_s + L_{22}A_{sl} + L_{23}\Delta\mu_{C_2S} \\ \Delta W_2 &= L_{31}A_s + L_{32}A_{sl} + L_{33}\Delta\mu_{C_2S} \end{aligned}\right\} \qquad (14)$$

où

$A_{sl} = \mu^{s}_{CaO} + \mu^{s}_{C_2S} - \mu^{l}_{C_3S}$ est l'affinité pour la formation de C_3S en phase liquide a partir de CaO et C_2S solides. Au cours des raisonnements precedents on a admis l'existence d'un model de saturation en chaux a l'etat liquide. On peut alors sur la base de considerations thermodynamiques generales affirmer qu'il se cristalise a partir de la fusion une certaine modification stable de C_3S (appelons la modification α).

Toutefois dans le système C_2S - CaO, pour des conditions thermodynamiques appropriees, il peut y avoir lieu à formation d'une autre modification α par reaction de saturation en phase solide. En présence de la fusion la modification α est metastable, car elle doit se dissoudre rapidement dans la fusion pour cristalliser ensuite a partir de cette dernière en une modification α stable.

Il est connu que la dissolution de la phase metastable est de beaucoup superieure a celle de la phase solide (3), assurant ainsi continument le retablissement des surfaces reagissant suivant le mode de la phases solides de CaO et C_2S. En posant que la marche

des réactions élémentaires s'écoule sous la forme

1. $CaO\ (s) + C_2S\ (s) \rightleftharpoons y - C_3S\ (s)$
2. $y - C_3S\ (s) \rightleftharpoons C_3S\ (l)$
3. $C_3S\ (l) \rightleftharpoons x - C_3S\ (s)$.

on peut montrer que dans ce cas l'équation cinetique est analogue par la forme a l'equation (6):

$$W' = L'A_s \qquad (15)$$

Toutefois le coefficient L' est différent de L et se détermine au moyen de la relation

$$\frac{1}{L'} = \frac{1}{L'_1} + \frac{1}{L'_2} + \frac{1}{L'_3}$$

Donc la question de dominance de la saturation en phase liquide ou solide se reduit à l'établissement du rapport entre les vitesses de dissolution de CaO, C_2S et y - C_3S dans la fusion. Ce rapport est en premier lieu fonction du régime de cuisson, du melange de composants de base et, dans chaque cas concret, peut amener la dominance de l'un des mecanisme de saturation.

CONCLUSION

L'application des méthodes TPI à l'étude de la cinetique de la reaction hetérogène de formation du C_3S peut conduire à de nouveaux resultats fort importants. La vitesse de formation du C_3S peut être decrite par des relations lineaires de forme très simple dont l'aspect varie suivant le domaine de deroulement de la reaction. On admet generalement que si la vitesse est limitee par celle de la dissolution de l'un des composants, la vitesse de dissolution de l'autre composant (et, partant, l'affinité pour cette dissolution) n'exerce pas d'influence sur la cinetique de la réaction. Or l'analyse par les methodes TPI montre que ce point de vue est en principe faux. Cet analyse permet egalement d'etablir les conditions de dominance du mecanisme de saturation par la chaux de C_2S en phase liquide ou bien solide.

SIGNES SPECIAUX:

$\frac{d_i S}{d\tau}$ - entropie dégagée;

$\Delta\mu$ - affinité pour la dissoulution (cristallisation);

x_i, y_i - forçes et flux thermodynamiques generalisees;

A - affinités pour les réactions selon Donder;

$W = \frac{dn}{d\tau}$ - vitesses de dissolution ou de cristallisation;

n - nombres de moles;

ξ - variable chimique;

L_{ij} - coefficients phénomènomlogiques.

BIBLIOGRAPHIE

1.- S.R. DE GROOT, P. MAZUR (1962) Non-equilibrum Thermodynamics, Amsterdam, (en anglais).

2.- В.И. БАБУШКИН, Г.М. МАТВЕЕВ, О.П.МЧЕДЛОВ-ПЕТРОСЯН (1972) Термодинамика силикатов, М., (en russe).

3.- A. SWOLIN RICHARD (1962) Thermodynamics of Solids, N-Y-Lnd, (en anglais)

L'oxyde ferreux dans le clinker

Ferrous iron in clinker

M.G. TOLOTCHKOVA, candidat ès sciences techniques,
V.P. RIASINE, candidat ès sciences techniques,
K.G. KOLENOVA, candidat ès sciences techniques,
V.N. SERGUEEV, ingénieur NIITzement, Moscou, U.R.S.S.

RESUME : Il s'est avéré que des clinkers du même type, à teneur en oxyde ferreux identique, présentent une activité hydraulique différente. Dans nombre de cas la présence de 0,6 à 0,8% de FeO n'impliquait pas l'altération de propriétés des clinkers de cuisson industrielle.

Des études ont été menées pour définir la composition quantitative et qualitative des phases du clinker avec la variation de la teneur en FeO de 0 à 1,8%. On a montré, en particulier, comment varie la composition de la phase alumoferrite sous l'angle du rapport A/F et la présence dans cette dernière du FeO; Les résultats obtenus sont mis en rapport avec les conditions de formation du Fe^{2+} au cours de la synthèse du clinker dans un milieu gazeux oxydant.

On a avancé une hypothèse sur l'influence de la formation du fer bivalent et de sa répartition en phases du clinker caractérisée par le rapport FeO_{total}/FeO_{alite} sur les propriétés des clinkers contenant de l'oxyde ferreux.

SUMMARY : It has been found out that single-type clinkers comprising equal amounts of ferrous iron are characterised by different hydraulic activity. In a number of cases with 0.6-0.8% of FeO present, no deterioration of plant-calcinated clinker properties has been detected.

Investigations of qualitative and quantitative composition of clinker phases have been performed with FeO content changing from 0 to 1.8%. Changes in the composition of the alumoferrite phase are in particular shown, said phases being characterised by the A to F ratio and presence of FeO therein. The results obtained are correlated with the conditions of formation of Fe^{2+} in the process of clinker synthesis in odixizing gas medium.

A supposition is made on the influence of the bivalent iron formation and distribution thereof among clinker phases, characterised by the FeO_{total} to FeO_{alite} ratio, on the properties of the FeO-containing clinkers.

On attribue souvent à la présence d'oxyde ferreux l'altération de la résistance limite du clinker. Cependant les teneurs limites recommandées en FeO (0,3 à 0,4%) ne sont pas toujours suffisamment argumentées. Le mécanisme de formation du Fe^{2+}, sa teneur quantitative ainsi que les propriétés des clinkers contenant du FeO sont fonction de la composition et des propriétés de la matière première, du régime et du milieu dans lequel s'effectue la cuisson et le refroidissement du clinker.

Au cours de la synthèse du clinker l'oxyde ferreux peut se former dans le milieu réducteur de la cuisson ainsi que par transformation à hautes températures des composés ferrugineux. Le FeO peut également se former par oxydation incomplète du fer métallique introduit avec la matière première. Le wustite introduit avec les minéraux de la matière première ou formé au cours de leur destruction exerce une influence favorable sur la réactivité du mélange brut en accélérant la dissociation des carbonates et les réactions topochimiques (1). La réduction de l'oxyde ferrique par dissociation thermique s'effectue suivant le principe des transformations successives en passant par des stades intermédiaires

$$Fe_2O_3 \rightarrow Fe_3O_4 \rightarrow FeO \rightarrow Fe$$

La décomposition de la modification paramagnétique α de Fe_2O_3, la plus stable, se réalise aux températures de 1350-1500 °C et pratiquement Fe^{2+} est identifié en présence d'une phase gazeuse neutre et même oxydante. La formation du fer métallique dans ces conditions est peu probable, vu que FeO n'est dissocié qu'à des températures beaucoup plus élevées (2500 °C).

Pratiquement la dissociation thermique à cause de la nécessité d'augmenter l'intensité de combustion dans la zone de cuisson s'observe souvent avec l'utilisation de matières premières de basse réactivité, avec la composition de mélanges crus à cuisson difficile, au cas d'une préparation insuffisante du matériau à la cuisson, de même que lors d'un long séjour du matériau dans la zone de cuisson, où il est mis en contact avec la flamme des chalumeaux.

L'accroissement de l'intensité de combustion au stade de la cuisson active entraîne l'élévation de la teneur en FeO ainsi que l'accentuation de l'influence négative sur les propriétés du clinker par suite de l'abaissement de l'activité hydraulique des silicates de calcium comprenant dans leur structure Fe^{2+} sous forme d'impureté isomorphe (2-4). La phase $C_6A_xF_y$ s'appauvrit en fer.

L'accroissement de Fe O dans les clinkers industriels jusqu'à 1,8% s'accompagnait d'une variation du rapport molaire A/F dans la composition des alumoferrites de calcium de 0,96-1,05 à 1,45-1,76 (fig.1). Pour des teneurs en Fe^{2+} maximales la phase alumoferrite possède les compositions suivantes :

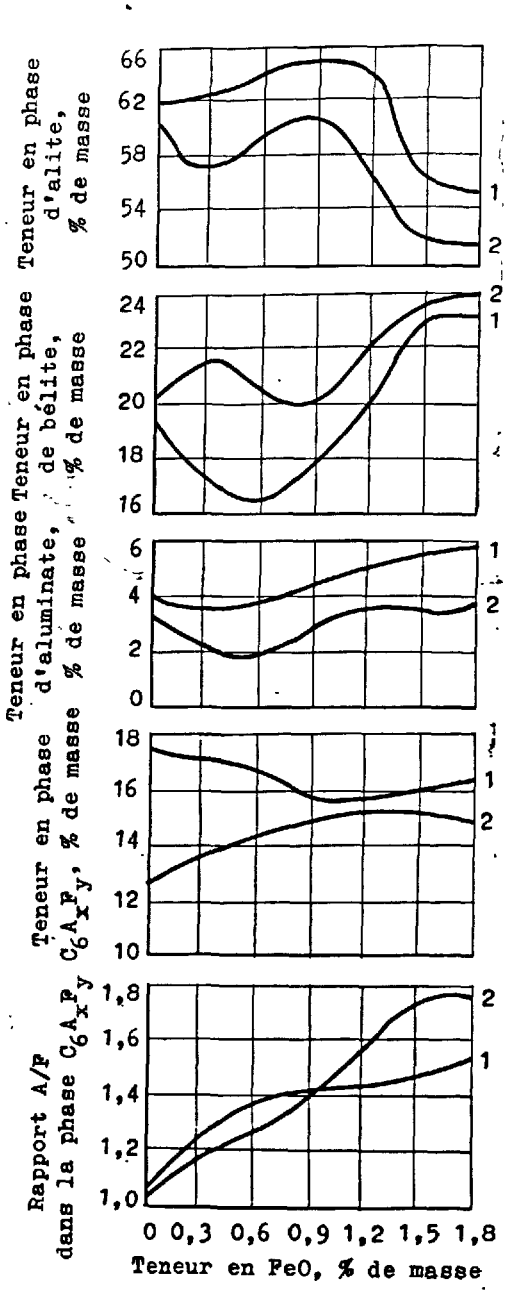

Fig.1. Influence de FeO sur la composition réelle du clinker : 1 - dans les fours rotatifs de longueur 185 m; 2 - dans les fours rotatifs de longueur 150 m (production par la voie humide).

$C_6A_{1,75-1,77}F_{0,94-1,09}f_{0,10-0,13}$ x)

Pour une teneur en FeO égale dans le clinker à 1% on observait la divergence maximale entre la composition théorique (selon Bogue) et expérimentale (obtenue par analyse aux rayons X) de $C_6A_xF_y$, atteignant 3,8-5,5%.

L'ion du fer bivalent en pénétrant dans la structure des silicates vient se placer en position octaédrique (4,5). Avec un lent refroidissement du clinker Fe^{2+} est capable de détruire la structure de l'alite en formant jusqu'à 3-8% de C_2S. Toutefois, dans nombre de cas, surtout avec la présence dans le clinker de FeO pour 0,6-0,8% la teneur en alite au lieu de diminuer augmentait quelque peu (fig.1). Ce fait est à ce qu'il paraît un témoignage de l'existence de conditions dans lesquelles FeO ne fait qu'amorcer la clinkérisation (en abaissant la viscosité de la phase liquide) et joue le rôle de modificateur des compositions de phases de bélite, d'aluminate et d'alumoferrite.

Il y a également formation de FeO au cas d'utilisation d'un combustible de bas pouvoir calorifique. La combustion incomplète du combustible est décrite par l'équation connue de Boudoire selon laquelle le transport dans la couche du matériau du système $CO-CO_2$ à travers la phase gazeuse au cours de la cuisson favorise la formation d'oxydes inférieurs. La réduction de Fe^{3+} par le carbone solide ou les produits de combustion incomplète présente un caractère local.

En présence de clinker fondu on assiste à la réduction del'oxyde ferrique dit "actif" qui modifie de façon efficace la composition en phases du clinker. En contact avec les agglomérats de clinker suffisamment formés (par exemple, avec du charbon à partir du chalumeau) la réduction s'effectue principalement à partir de la surface des granules. Plus la dimension des granules est petite, plus grande est la surface de contact avec le réducteur et partant, plus grand est le degré de réduction. Le transfert $Fe^{3+} \rightarrow Fe^{2+}$ s'effectue alors au sein des phases déjà formées et contenant l'oxyde ferrique dissous. Plus les granules sont grosses moins grande est l'intensité de la réduction nocive de Fe_2O_3 dans l'alite.

Dans les clinkers où dominent des grosses granules de Fe^{2+} on n'observe pas en général d'abaissement de la quantité d'alite ainsi que de l'activité même pour des teneurs en FeO de 0,8-1,0%. D'un autre coté plus la quantité totale d'oxyde ferreux est importante plus on a de chance de le trouver dans les petites granules du clinker.

Les essais sur les clinkers industriels à teneur en FeO de 0 à 1,8% ont montré la nature variable de l'influence de Fe^{2+} sur les paramètres de résistance (Tabl.1). C'est ainsi que l'abaissement de la résistance limite pouvait s'observer même pour une teneur en FeO dans le clinker de 0,3-0,6%, la présence de 0,6-0,8% de FeO étant souvent sans effet sur les propriétés des produits cuits. L'apparition d'une quantité de FeO supérieure à 1% se traduisait toujours par une chute de résistance. Vraisemblablement selon les conditions de formation de FeO et, partant le mode de distribution de Fe^{2+} suivant les phases du clinker, l'influence de l'oxyde ferreux sur les propriétés du clinker se modifiait.

TABLEAU I

Teneur en FeO, % de masse	Facteur de saturation	Module siliceux	Module alumineux	Résistance à la compression 28 jours kgf/cm²
0,00	0,90	1,86	1,29	506
0,00	0,92	1,95	1,50	525
0,00	0,95	2,07	1,35	531
0,00	0,97	2,00	1,28	520
0,18	0,89	1,85	1,30	500
0,25	0,90	1,83	1,27	509
0,28	0,95	2,05	1,40	523
0,30	0,90	1,86	1,30	511
0,31	0,92	1,96	1,48	497
0,32	0,96	2,00	1,13	528
0,38	0,91	1,82	1,35	502
0,39	0,97	1,98	1,22	471
0,44	0,92	1,77	1,40	470
0,44	0,93	1,79	1,38	430
0,49	0,93	1,81	1,38	489
0,56	0,90	1,85	1,24	492
0,60	0,93	1,91	1,19	469
0,64	0,96	2,17	1,46	553
0,65	0,83	1,83	1,39	454
0,73	0,95	2,05	1,35	423
0,75	0,90	1,84	1,20	489
0,78	0,96	1,89	1,10	514
0,80	0,93	1,98	1,22	528
0,86	0,94	1,98	1,34	511
0,86	0,91	1,92	1,25	424
0,92	0,92	1,84	1,23	461
0,96	0,94	2,16	1,47	452
1,03	0,97	2,10	1,38	514
1,15	0,91	1,81	1,19	457
1,33	0,97	2,21	1,56	451
1,36	0,92	1,96	1,54	456
1,39	0,90	1,86	1,20	420
1,44	0,95	2,05	1,35	429
1,53	0,90	1,89	1,29	433
1,74	0,98	2,26	1,65	474
1,77	0,90	1,88	1,28	444
1,80	0,97	2,20	1,50	463

La teneur en FeO dans la partie non siliceuse des clinkers étudiés est à peu près la meme et constitue 0,18 à 0,25%. La présence de Fe^{2+} dans la phase d'aluminate et d'alumoferriete ne peut pas etre rangée parmi les facteurs négatifs, de meme que sa détection dans la phase du bélite au cas où il ne se produit pas, de déstabilisation de la forme β. L'ion Fe^{2+} devient le plus nocif dans la phase de l'alite (5,6). En admettant que FeO se dissout de préférence dans C_2S (selon (7) jusqu'à 0,8-1,2%) et tenant compte de sa présence obligatoire dans la phase intermédiaire (0,2-0,3%), on peut supposer qu'avec l'observation de conditions déterminées de synthèse seule une petite fraction

x) Symbole f - FeO

de la quantité totale de l'oxyde ferreux sera contenu dans C_3S. Autrement dit on est autorisé à supposer qu'au moins jusqu'à 1% de FeO peut se trouver dans le clinker hors la phase de l'alite.

D'après les données fournies par l'expérience, en raison de cette (ou très proche) distribution de FeO dans les phases de clinker une teneur en FeO de 0,6-0,8% n'altérait pas l'activité du produit. Par constre une sensible baisse de l'activité pour de petites (0,2-0,4%) teneurs en oxyde ferreux est conditionnée à ce qu'il parait, par le fait que dans ce cas Fe^{2+} entre dans la structure de l'alite non pas par suite de la distribution en phase (à partir de la fusion) mais en qualité de produit de réduction de Fe^{2+} dissous dans l'alite.

La possibilité de fixer FeO dans la phase vitreuse inerte (5) ou sous forme de magnétite (3, 5) change également nos idées sur l'interdépendance entre l'activité hydraulique et la teneur en oxyde ferreux dans le clinker. Le FeO s'écartant du composé stoechiométrique par un manque d'ions métalliques peut etre représenté sous forme d'un système, où coexistent des ions de fer bi- et trivalents :

$$Fe^{2+}_{1-x} \quad Fe^{3+}_{2x} \quad \square_x \quad O^{-2},$$

où $\square$ est la lacune anionique, x - la concentration de lacunes dans le sous-réseau métallique (8). Plus encore la similitude de liaison chimique (liaison ionique), le rapprochement de dimensions des mailles élémentaires et des rayons ioniques conditionnent la solubilité réciproque et l'apparition d'isomorphisme dans les solutions solides non limitées (substitution) entre FeO et les oxydes de métaux bivalents. Aussi l'assimilation du composé FeO à une phase de wustite peut-elle etre admise que de façon toute conventionnelle. Donc le mécanisme de formation du fer bivalent ainsi que sa distribution en phases du clinker (et avant tout la valeur du rapport f_{total}/f_{alite}) sont les facteurs qui déterminent les propriétés des clinkers contenant FeO.

1. - С.Д.Макашев (1976). "Влияние физико-химических свойств сырья на реакционную способность сырьевой смеси и процессы минералообразования клинкера". Всборнике трудов: Шестой международный конгресс по химии цемента. М.,Стройиздат, том I, 156-162, (en russe).

2. - К.Г.Коленова, В.П.Рязин (1972). "Меры по снижению клинкерного пыления". Цемент, № 7, 7-8, (en russe).

3. - И.В.Кравченко, К.Г.Коленова, Б.С.Альбац, А.П.Малышев (1968) "Причины образования закиси железа в клинкере мощных вращающихся печей с колосниковыми холодильниками". Научные сообщения НИИЦемента.М.,№ 23(54), 3-8, (en russe).

4. - Е.Воерманн (1964) "Разложение алита в техническом портландцементном клинкере". В сборнике трудов: Четвертый международный конгресс по химии цемента.М.,Стройиздат, 108-116, (en russe).

5. - И.Ф.Пономарев, А.Н.Грачьян, П.П.Гайджуров (1965) "Влияние различных газовых сред на свойства клинкера". Цемент, № 3, 18-21, (en russe).

6. - Ю.М.Бутт, В.В.Тимашев (1974) "Портландцемент".М.Стройиздат, 64,86 (en russe).

7. - Н.А.Торопов,Б.В.Волконский (1960)."Полиморфные превращения $3CaO\,SiO_2$ и влияние закиси железа на $3CaO\,SiO_2$ и другие клинкерные минералы".Цемент,№6, 17-20, (en russe).

8. - Г.И.Чуфаров, А.Н.Мень, В.Ф.Балакирев, М.П.Журавлева, А.А.Щепеткин (1970). "Термодинамикапроцессов восстановления окислов металлов". М.,Металлургия, 19-22, (en russe).

Sur les solutions solides dérivant du C_2F par remplacement des atomes Fe par Mn et Al

Researches on the phase originated from C_2F by substitution of iron atoms with Mn and Al

C. BRISI, professeur, et B. DE BENEDETTI, professeur assistant, Istituto di Chemica Generale e Applicata e di Metallurgia del Politecnico di Torino, Italie.

RESUME : On a étudié l'étendue de la phase qu'on peut obtenir à partir du ferrite bicalcique par remplacement des atomes de fer par des atomes de manganèse et d'aluminium. Cela dans le but de vérifier la possibilité d'avoir dans le clinker des phases du type de l'aluminoferrite, riches en manganèse.

Dans les solides obtenus par trempe dans l'air, à partir de 1300°C, le remplacement du fer par le manganèse se borne seulement au 25% atomique, celui par l'aluminium au 70%. Il est cependant possible d'obtenir des solutions solides dans lesquelles tous les atomes de fer du C_2F sont remplacés en partie par l'aluminium et en partie par le manganèse; dans ces solutions solides, le pourcentage atomique de manganèse, en relation au total Mn+Al, se situe entre 32 et 44%.

Le manganèse introduit dans le réseau cristallin du C_2F présente toujours, dans les solides trempés dans l'air, un dégré d'oxydation moyen supérieur à trois.

SUMMARY: The stability field of the phase obtainable from dicalcium ferrite by substitution of iron atoms with manganese and aluminium was studied. This with the aim to verify the possibility to obtain in the clinker phases of the aluminoferrite type rich in manganese.

In the solids quenched in air from 1300°C, the replacement of iron with manganese alone is limited to 25% atomic, while the replacement with aluminium is limited to 70%. It is, however, possible to obtain mixed crystals in which all the iron atoms of C_2F are partly replaced by aluminium and partly by manganese; in these solid solutions the atomic percentage of manganese in relation with the total Mn+Al ranges from 32 to 44%.

The manganese introduced in the crystal lattice of C_2F always presents, in the solids quenched in air, a mean number of oxidation higher than three.

La phase ferritique, c'est à dire la série de solutions solides $2CaO.(Fe,Al)_2O_3$ qui dérivent du ferrite bicalcique par remplacement partiel des atomes de fer par des atomes d'aluminium, représente un des constituants principaux du clinker de ciment portland.

En réalité celle écrite ci-dessus est seulement une formule idéale parce que dans le système très complexe correspondant au clinker une petite partie des atomes de calcium, fer et aluminium peut être remplacée par d'autres éléments. Dans cette communication nous étudierons la possibilité d'introduire dans le reseau cristallin de la phase ferritique des atomes de manganèse, même en proportions bien plus élevées que celles qu'on peut rencontrer dans les matières premières employées pour la fabrication du ciment portland.

Quelques indications isolées sur ce problème sont deja contenues dans la littérature scientifique.

Au cours du troisième symposium sur la chimie du ciment Parker (1) a signalé l'existence d'une phase de formule $4CaO.Al_2O_3.Mn_2O_3$ qui dériverait de l'ainsi-dite brownmillérite ($4CaO.Al_2O_3.Fe_2O_3$) par remplacement complet des atomes de fer par des atomes de manganèse. Entre cette phase et la brownmillerite on aurait, toujours selon Parker, une serie continue de solutions solides. Parker ne fournit aucune donnée sur la structure cristalline du $4CaO.Al_2O_3.Mn_2O_3$ duquel il donne cependant un diagramme de poudres aux rayons X.

Les résultats auxquels parvient Parker ne sont cependant pas en accord avec ceux d'une recherche antérieure conduite par Guttmann et Gille (2), selon laquelle en partant de la brownmillerite le remplacement du fer par le manganèse serait limité à la composition $4CaO.Al_2O_3.0,4Fe_2O_3.0,6Mn_2O_3$.

A la même conclusion semblent parvenir aussi Okorov et Peskina (3) qui eux aussi affirment que la formule $4CaO.Al_2O_3.0,4Fe_2O_3.0,6Mn_2O_3$ correspond à un solide monophasé.

Une phase de composition $4CaO.Al_2O_3.Mn_2O_3$ a été au contraire à nouveau signalée par Gharpurey et Pai (4) qui l'auraient obtenue par échauffement à 1310-1330°C de mélanges de CaO, Al_2O_3 et MnO_2. Pour cette phase ils donnent les paramètres réticulaires a_o=5,23, b_o=14,68 et c_o=5,44 A; il n'est pas toutefois clair si cettes valeurs ont été mesurées directement par les auteurs ou ont été calculées en prenant pour base le diagramme de poudres donné par Parker.

A côté des travaux cités au dessus on doit signaler deux autres notes concernant les solutions solides qu'on peut obtenir du ferrite bicalcique par remplacement des atomes de fer par des atomes de manganèse en absence d'aluminium.

Selon Coates et McMillan (5), qui ont travaillé sur des solides échauffés à l'air à 1350°C, un tel remplacement serait possible jusqu'à une limite maximale du 25% atomique. Les produits ainsi obtenus présentent un excès d'oxygène en comparaison de celui demandé par un degré d'oxydation égal à trois soit pour le fer soit pour le manganèse. La solution solide limite, en particulier, prend la composition $2CaO.Fe_{1,5}Mn_{0,5}O_{3,13}$. Pour cette phase on donne les paramètres réticulaires a_o=5,40, b_o=14,97, c_o=5,54 A; en comparaison du ferrite bicalcique on a ainsi une augmentation de b_o et une diminution de a_o et c_o.

Les résultats obtenus par Coates et McMillan on été confirmés plus récemment par Bando et coll. (6), qui trouvent la même limite de solubilité et une même variation des paramètres réticulaires, mais qui ne donnent aucune indication sur le degré d'oxydation du manganèse.

° ° °

Tous les solides examinés ont été obtenus à partir de mélanges de carbonate de calcium, sesquioxyde de manganèse, hydroxyde d'aluminium et sesquioxyde de fer purs pour analyse. Le rapport atomique Ca/(Fe+Mn+Al) a été maintenu toujours constant et égal à 1, tandis qu'ont été modifiés les pourcentages relatifs de fer, manganèse et aluminium.

Les mélanges, broyés par voie humide en presence d'alcool étilique absolu, ont été échauffés à l'air à 1300°C.

La réalisation des conditions d'équilibre a été plutôt lente, surtout pour les produits plus riches en oxyde d'aluminium; pour cette raison l'échauffement a été prolongé pour des temps allant de 300 à 600 heures. A la fin de la cuisson les solides étaient soumis à trempe en l'air. On passait ensuite à la determination par voie analitique du degré d'oxydation moyen du manganèse. Dans ce but 0,2 grammes de substance étaient dissus dans une solution aqueuse d'acide perchlorique et d'acide oxalique, en titulant après avec permanganate de potassium l'excès du dernier acide.

On a examiné d'abord les produits obtenus par échauffement de mélanges de carbonate de calcium, sesquioxyde de fer et sesquioxyde de manganèse.

Les résultats de l'analyse aux rayons X (diagrammes de poudres, radiation Fe$K\alpha$) sont en accord avec les indications de Coates et McMillan. Les solides avec un pourcentage atomique de manganèse (à l'égard de la somme Fe +Mn) situé entre zero et 25 sont constitués par une seule phase à symétrie rombique semblable à celle du ferrite bicalcique, on a ensuite une zone biphasée et après, entre 50 et 100% de manganèse, une deuxième zone monophasée dans laquelle on rencontre une solution solide $Ca(Mn,Fe)O_{3-x}$ avec une structure du type perovskite, qui dérive du composé de formule idéale $CaMnO_3$ par remplacement partiel des atomes de manganèse par des atomes de fer.

Pour la solution solide rombique de composition limite on a mesuré les paramètres réticulaires suivants: a_o=5,38$_5$, b_o=15,03, c_o=5,54$_0$ A.

L'analyse chimique a donné un degré d'oxydation moyen de fer et manganèse égal à 3,14. Puisque on peut supposer que tous les atomes de fer maintiennent le degré d'oxydation trois, cela entraîne un degré d'oxydation moyen du manganèse égal à 3,56. La composition du produit trempé de 1300°C correspond ainsi à la formule $2CaO.Fe_{1,5}Mn_{O,5}O_{3,14}$.

On pourrait penser qu'un tel degré d'oxydation pour le manganèse soit lié à la presence de lacunes dans le réseau des ions trivalents, c'est à dire à la formation d'une phase du type $2CaO.(Fe,Mn)_{2-x}O_3$; cela paraît toutefois à exclure parce que dans ce cas, avec la composition des mélanges de départ, on devrait constater dans les produits examinés la presence de quantités pas négligeables d'autres phases à rapport (Ca/Fe+Mn) inférieur à 1, phases qui n'ont pas été remarquées à l'examen aux rayons X.

D'autre part la structure du ferrite bicalcique, qui correspond à celle d'une perovskite déformée avec des lacunes anioniques ordonnées (7) n'exclut pas la possibilité d'introduire dans le reseau cristallin des ions tétravalents. On a en effet récemment signalé (8) des phases du type $Ca_2Fe_{2-x}Ti_xO_{5+0,5x}$ dans lesquelles, au moins pour des pourcentages de titanium pas trop élévés, les paramètres réticulaires changent régulièrement avec l'augmentation de la fraction d'ions fer remplacés par des inns titanium.

L'examen des solides obtenus par échauffement de mélanges renfermant (en plus du carbonate de calcium et de deux sesquioxyde de fer et de manganèse) aussi de l'hydroxyde d'aluminium a montré que la solution solide à symétrie rombique provenant du ferrite bicalcique peut admettre le remplacement simultané des atomes de fer par atomes d'aluminium et atomes de manganèse. On a ainsi des solides monophasés representés par la formule $2CaO.(Fe,Al,Mn)_2O_{3+x}$.

L'étendue de la zone de stabilité de cette phase, toujours pour solides trempés à l'air à partir de 1300°C, est représentée dans la figure 1.

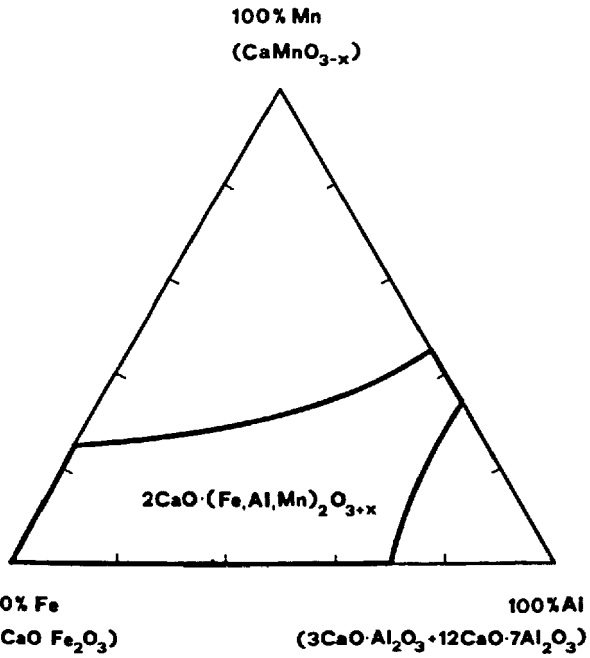

Fig. 1 - Domaine de stabilité des solutions solides provenant du ferrite bicalcique en fonction des pourcentages relatifs de fer, manganèse et aluminium.

La zone de stabilité des solutions solides provenant du ferrite bicalcique occupe la partie centrale du diagramme. Les produits plus riches en manganèse sont formés par une mélange mécanique de ces solutions solides avec la phase $Ca(Mn,Fe)O_{3-x}$, tandis que celles plus riches en oxyde d'aluminium correspondent à des mélanges triphasées de $2CaO.(Fe,Al,Mn)_2O_{3+x}$, $3CaO.Al_2O_3$ et $12CaO.7Al_2O_3$.

Le remplacement dans le ferrite bicalcique des atomes de fer par des atomes de manganèse entraîne, comme dejà dit, une augmentation du paramètre b_o et une diminution de a_o et c_o; un phenomène tout à fait analogue arrive aussi en presence d'atomes d'aluminium, comme on peut bien voir dans le graphique de la fig. 2 où sont montrés les paramètres réticulaires des solides à pourcentage constant d'aluminium.

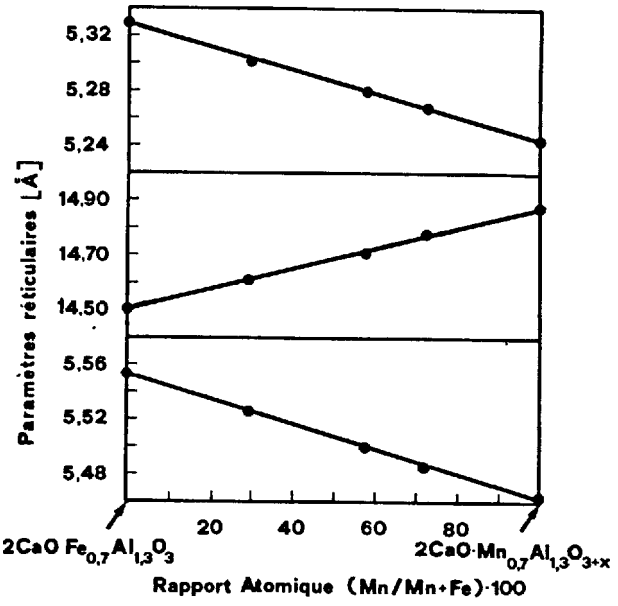

Fig. 2 - Paramètres réticulaires des solutions solides $2CaO.(Fe,Al,Mn)_2O_{3+x}$ à pourcentage fixe d'aluminium: Al/(Fe+Al+Mn)=65%.

L'introduction d'atomes d'aluminium à la place des atomes de fer entraîne au contraire une diminution de tous les paramètres réticulaires, soit lorsque elle a lieu à partir du ferrite bicalcique pur, comme l'on connaît bien des nombreuses études sur les solutions solides $2CaO.(Fe,Al)_2O_3$ (9,10,11,12), soit

lorsque un tel remplacement a lieu en presence d'atomes de manganèse, comme l'on voit sur le graphique de la fig.3, qui montre les paramètres réticulaires mesurés sur des produits dans lesquels on maintenait constant le pourcentage atomique de manganèse.

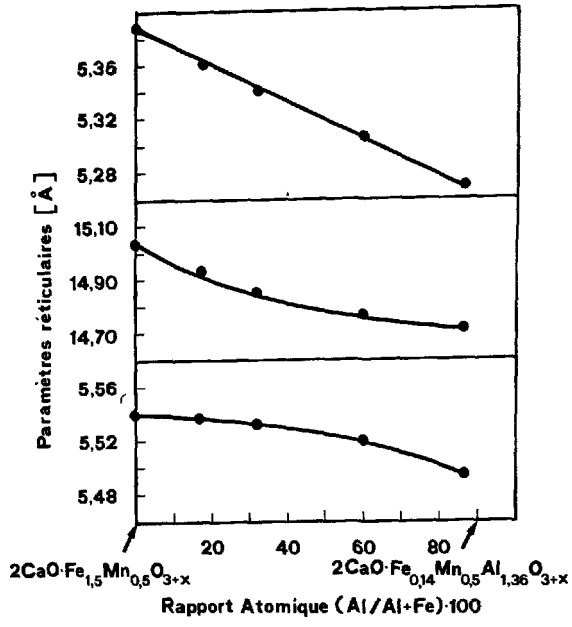

Fig. 3 - Paramètres réticulaires de solutions solides $2CaO.(Fe,Al,Mn)_2O_{3+x}$ à pourcentage fixe de manganèse: Mn/(Fe+Al+Mn)=25%.

Le remplacement des atomes d'aluminium par des atomes de manganèse entraîne à son tour une augmentation assez marquée du paramètre b_o, tandis que a_o et c_o demeurent pratiquement inchangés.

Le degré d'oxydation du manganèse va graduellement en diminuant avec l'augmentation du pourcentage d'atomes de fer remplacés par l'aluminium. On passe en effet de la valeur deja indiquée de 3,56 pour $2CaO.Fe_{1,5}Mn_{0,5}O_{3+x}$ jusqu'à des valeurs pas beaucoup plus elevées que trois pour les produits complètement dépourvus de fer. En maintenant constant le rapport entre atomes de fer et atomes d'aluminium, le degré d'oxydation du manganèse montre au contraire une augmentation avec l'accroissement du pourcentage de manganèse.

En regardant le graphique de la fig.1 on peut observer qu'il est possible d'obtenir des solutions solides avec une structure semblable à celle du ferrite bicalcique dans lesquelles tous les atomes de fer ont été remplacés par des atomes d'aluminium et de manganèse. Ce fait est assez remarquable puisque un composé $2CaO.Mn_2O_3$ n'est pas connu; l'aluminate bicalcique $2CaO.Al_2O_3$, du même type structural du ferrite bicalcique, a été préparé récemment (13), il a été toutefois obtenu en travaillant sous une pression de 25.000 bar. L'échauffement à pression ordinaire de mélanges $2CaO + Al_2O_3$, au contraire, donne naissance, comme il est bien connu, à un mélange mécanique de $3CaO.Al_2O_3$ et de $12CaO.7Al_2O_3$.

Le domaine d'existence des solutions solides rombiques $2CaO.(Al,Mn)_2O_{3+x}$ est très limité. Dans les produits trempés à l'air de 1300°C il s'étend environ de 32 a 44% de manganèse à l'égard de la somme Al+Mn.

Pour des teneurs en manganèse plus élevés la solution solide limite est en équilibre avec la phase $CaMnO_{3-x}$, pour des teneurs plus petites avec $3CaO.Al_2O_3$ et $12CaO.7Al_2O_3$. La solution solide en équilibre avec $CaMnO_{3-x}$ présente les paramètres reticulaires $a_o=5,25_0$, $b_o=14,96$, $c_o=5,47_5$ A; la solution solide en équilibre avec les aluminates présente les paramètres $a_o=5,24_5$, $b_o=14,81$, $c_o=5,46_5$ A.

Des données rapportées ci-dessus on voit bien que, au contraire des indications de Parker et de Gharpurey et Pai, il ne nous a pas été possible d'obtenir le remplacement complet dans la brownmillerite des atomes de fer par des atomes de manganèse. L'échauffement des mélanges de carbonate de calcium, sesquioxyde de manganèse et hydroxyde d'aluminium avec un rapport Mn/Al égal à 1 a en effet toujours amené à la formation de mélanges mécaniques de $CaMnO_{3-x}$ avec la solution solide limite. Les mêmes résultats ont été obtenus aussi conduisant l'échauffement à 1350 et 1400°C.

CONCLUSIONS

On peut obtenir des phases dérivant du ferrite bicalcique par remplacement total des atomes de fer par des atomes de manganèse et d'aluminium.

Lorsque le manganèse remplace le fer dans le C_2F il présente toujours, dans les solides trempés dans l'air, un degré d'oxydation moyen superieur à trois.

BIBLIOGRAPHIE

1 - T.W. PARKER (1952), Proc.Third Int.Symposium on the Chemistry of Cement, London, pp. 143-149.

2 - A. GUTTMANN et F. GILLE (1929), Zement 18, pp. 500,537,570.

3 - S.D. OKOROV et F.S. PESKINA (1957), Trudy Leningrad Tekhnol.Inst. im Lesonveta, pp. 93-98. Cfr. C.A. (1959) 53, 2569 d.

4 - M.K. GHARPUREY et V.N. PAY (1968), Proc. Fifth Int. Symposium on the Chemistry of Cement, Tokio, Vol. I, pp. 289-299.

5 - R.V. KOATES et J.W. McMILLAN (1964), J. Appl.Chem. 14, pp. 346-350.

6 - Y. BANDO, T. TAKADA et T. AKIYAMA (1971), Bull.Inst.Chem.Res. Kyoto University 49, pp. 342-348.

7 - E.F. BERTAUT, P. BLUM et A. SAGNIERES (1959), Acta Cryst. 12, pp. 149-159.

8 - J.C. GRENIER, G. SCHIFFMACKER, P. CARO, M. POUCHARD et P. HAGENMULLER (1977), J.-Solid State Chem. 20, pp. 365-379.

9 - V. CIRILLI et A. BURDESE (1951), Ricerca Scientifica 21, pp. 1185-1191;

10 - T.F. NEWKIRK et R.D. THWAITE (1958), J. Res.Nat.Bur.Stand. 61, pp. 233-245.

11 - D.K. SMITH (1962), Acta Cryst. 15, pp. 1146-1152.

12 - E.WOERMANN, T. HAHN et W. EYSEL, cités par A. GUINIER et M. REGOURD (1968), Proc. Fifth Int. Symposium on the Chemistry of Cement, Tokio, pp. 1-32.

13 - P.S. AGGARWAL, J.A. GARD et F.P. GLASSER (1972), Cement and Concrete Res. 2, pp. 291-297.

Granularity Influence of Limestone and Quartz on the Reactivity of Cement Raw Material

Influence de la finesse de broyage du calcaire et du quartz sur la réactivité du cru

S. CHROMY, RNDr, CSc, Research Institute of Building Materials, Brno, CSSR (Tchécoslovaquie).

RESUME : On a utilisé une méthode cinétique basée sur l'analyse microscopique des phases de clinkers cuits isothermiquement à la température de 1400°C et de farines de matière première ne différant que par la teneur en grains de calcite ou de quartz plus grands que 40µ m. On a montré la dépendance linéaire de la réactivité avec la valeur inverse du carré du rayon de la particule moyenne de calcite, en définissant cette valeur moyenne, comme celle qui a 25 % de grains plus gros. On a déterminé une dépendance analogue pour la grandeur médiane de la particule de quartz contenu dans la farine de matière première. Seuls les grains de calcite les plus grands donnent naissance aux amas de grains de CaO libre; et d'une matière analogue, les grains de quartz les plus grands donnent naissance aux amas des grains de bélite.

Aux corrélations ci-dessus correspond la similitude géométrique de la réaction des amas de CaO et de bélite libres dans le processus de formation de l'alite, qui joue un rôle décisif du point de vue de la réactivité. Pour les farines de matière première de même composition chimique, et dans lesquelles tous le SiO_2 se trouve sous forme de quartz, la réactivité est inversement proportionnelle au produit des rayons médians de calcite et de quartz.

SUMMARY : The reactivity of a series of raw meals, differing only in the calcite or quartz grain contents larger than 40 µm, was determined by a kinetic method based on quantitative microscopic phase analyses of clinkers isothermally fired at 1400°C. It was shown that there exists a linear relationship between the reactivity and the reciprocal value of the square of the average calcite particle radius, if the size of the average particle is determined employing 25% of the coarsest calcite particles. An analogical dependence was determined for the average particle size of all the quartz in the raw meal. Only from the larger calcite grains there are formed agglomerations of free CaO grains and similarly the agglomerations of belite grains are formed from larger quartz grains. To the above relationship corresponds a geometrical similarity of the reactions of the free CaO and belite agglomerations in the process of alite formation which is decisive from the point of view of reactivity. For raw meals of the same chemical composition, in which all the SiO_2 is in the form of quartz, the reactivity varies linearly with the reciprocal value of the product of average diameter squares of calcite and quartz.

INTRODUCTION

Large limestone and quartz grains are the source of chemical inhomogeneity in the clinker formation process and therefore their size is one of the main factors of the raw meal reactivity. On rapid heating there occurs simultaneously with the formation of the liquid clinker phase at a high rate the formation of belite, during which there are reacted the fine fractions of free CaO and all the SiO_2. Out of the larger quartz grains there are formed belite agglomerations with the increased contents of more acidic interstitial melt. The agglomerations of free CaO grains left for the reaction of alite formation are formed from the originally largest limestone grains (1,2). The following reaction $C + C_2S = C_3S$ is a slow process of free CaO and belite dissolution and alite crystallization, controlled by the diffusion of CaO in the liquid phase, and its rate can be described by the modified Kondo and Choi equation (3,4)

$$\left(1-\sqrt[3]{1-\alpha}\right)^2 = \frac{2D.\Delta C.y}{r_o^2} = Kt = F(\alpha) \quad /1/$$

where α = degree of conversion of free CaO in the reaction $C + C_2S = C_3S$

D = diffusion coefficient of CaO in the liquid clinker phase

ΔC = CaO concentration gradient in the reaction zone

y = liquid phase quantity in the clinker

r_o = radius of average sized free CaO agglomeration in the reaction $C + C_2S = C_3S$

K = rate constant of the reaction

t = duration of isothermal firing

With regard to the great difference in the rate of the two following processes, the raw meal reactivity (Rm) can be determined as the relative value of the rate constant of the kinetic description of the second reaction (3)

$$Rm = \frac{K^+}{K^+_s} \quad /2/$$

where K^+_s = rate constant of the reference raw meal. After the elimination of the influences of the liquid phase quantity and lime saturation onto the rate constant (3), it is possible to determine simultaneously also the "reactivity of the raw materials source" (Rq)

$$Rq = \frac{K'' r_{o_C}^2}{K''_s r_{o_S}^2} \quad /3/$$

where K''_s = rate constant of the reference raw meal

r_{o_C} = radius of an average sized $CaCO_3$ particle for the reaction $C + C_2S = C_3S$ (approx. 25% of the coarsest particles)

r_{o_S} = analogically for the reference raw meal.

Through a change in raw meal granulometry there is changed the rate of clinker formation (Rm), but the value Rq does not change, as long as jointly ground identical raw components are employed. The above kinetic methods for the determination of the reactivites can be utilized for an objective influence assessment of the size of limestone and quartz particles onto Rm. The information obtained represents a precondition for a simplified reactivity assessment and can be utilized also for influencing the reactivity of cement raw materials.

RAW MEALS

As raw components there were employed coarse-grained natural calcite, quartz, Al_2O_3 and Fe_2O_3. All raw meals had an identical chemical (Table I) as well as mineralogical composition, and differed only in their contents of calcite (C 1-C 6) or quartz (S 1-S 6) particles larger than 40μm (Table II). The CS raw meal was prepared only from components that passed through the 40 μm sieve.

TABLE I Chemical composition of raw meals

Ignition loss	SiO_2	Al_2O_3	Fe_2O_3	TiO_2
34,61	13,86	3,97	2,33	0,01
Ignition loss	CaO	MgO	K_2O	Na_2O
34,61	43,66	1,32	0,02	0,06

The granulometric composition of the fractions was determined, with the exception of the 90-200 μm fraction, by the Coulter Counter Method and the average particle sizes (Table III) were calculated as the geometrical mean value from the relationship

$$\log d_v = \sum p_i \cdot \log d_i \quad /4/$$

where d = cross section of particle
p = mass of fraction.

For the 90-200 μm fraction was carried out a partial sieve analysis and for the average grain size of the individual fractions was taken the arithmetic mean of the marginal values.

TABLE III Average grain sizes of the calcite and quartz fractions

Fraction (μm)	0-40	40-63	63-90	90-200
d - calcite	20,03	54,65	72,61	67,00
d - quartz	20,33	51,37	74,42	68,00

The average raw meal grain sizes were computed from the values listed in Table III and from the cumulative curves of fractions according to equation /4/ on the basis of values in Table II.

TABLE II Contents of limestone and quartz sieve fractions in the raw meals

	CALCITE						QUARTZ					
Fraction(/um)	C 1	C 2	C 3	C 4	C 5	C 6	S 1	S 2	S 3	S 4	S 5	S 6
0 - 40	71,22	71,22	71,22	76,22	66,22	61,22	7,65	7,65	7,65	9,65	2,65	-
40 - 63	10						5					
63 - 90		10		5	15	20		5		3	10	12,65
90 - 200			10						5			

RESULTS

In accordance with the methods for the determination of reactivities (3), from each raw meal clinkers were fired with an effective isothermal holding period at 1400°C of 1.6 and 5.6 minutes. The clinkers were subjected to a quantitative microscopic analysis (5) and the reactivities listed in Table IV were computed.

TABLE IV Reactivity (Rm), conversion ($\alpha = \frac{C_3S}{C_3S\ max}$) of experimental firings and ratii of average calcite (r_{o_C}) and quartz (r_{o_Q}) particles in raw meals

	CS	C 1	C 2	C 3	C 4	C 5	C 6	CS	S 1	S 2	S 3	S 4	S 5	S 6
Rm	3,03	2,44	2,00	1,34	2,37	1,61	1,29	3,03	1,92	1,01	0,74	1,81	0,41	0,25
Rq	0,46	0,47	0,50	0,47	0,43	0,53	0,55	0,46	0,40	0,24	0,21	0,38	0,13	0,10
1.6	0,668	0,649	0,591	0,586	0,644	0,591	0,578	0,668	0,525	0,508	0,451	0,598	0,344	0,244
5.6	0,883	0,850	0,806	0,751	0,845	0,776	0,743	0,883	0,779	0,681	0,614	0,794	0,489	0,384
r_{o_C}(/um)	18,38	20,66	23,47	28,13	20,2	27,11	30,91							
r_{o_q}(/um)								10,16	14,67	16,97	21,53	13,82	28,33	37,20

The dependence of the reaction grade (α) expressed as the ratio of the alite quantity in the clinker to is maximum possible quantity is shown in Fig.1,and the dependence of Rm on the average particle sizes in Fig. 2.

A satisfactory linearity of the dependence of the raw meal reactivity (Rm) on $1/r_o^2$, assumed from equation /1/, was obtained for the determination of the average particle size from 25% of the coarsest particles of the raw meals C 1-C 6, and for the raw meal series S 1-S 6 for the determination of the average particle size of all the quartz in the raw meal (Table IV,Fig.2). The elimination of granulometric differences in raw meals with coarser calcite is therefore effective and for considerable differences in the Rm values, the differencies in the raw materials source reactivities (Rq) are slight (Table IV). The quartz granulometry is a factor of the raw materials source reactivity and therefore both reactivity values in raw meals with coarser quartz particles are changing concurrently. An analogy of the dependence of Rm on the size of calcite and quartz particles (Figs.1,2) points to a geometrical analogy of the belitic agglomerations degrading process with the dissolution of free CaO agglomerations. A different slope of dependence lines in Fig.1 may be caused by a different size of the belite and free CaO agglomerations formed from equally large calcite and quartz grains. Microscopic studies have shown that in the reaction course of the isothermal alite formation in the clinkers C 1-C 6 there is formed rapidly a homogenous belitic environment, in which the free CaO agglomerations are reacting (Fig.3).This corresponds to the geometrical model of equation /1/, the free CaO grain agglomerations being somewhat smaller than the original calcite particles. On the contrary, on heating the raw meals of the S 1-S 6 series are formed very rapidly belite agglomerations after larger quartz grains, whereas the free CaO is uniformly scattered (Fig.4). The degradation process of these agglomerations through an internal CaO diffusion is a geometrical analogy of

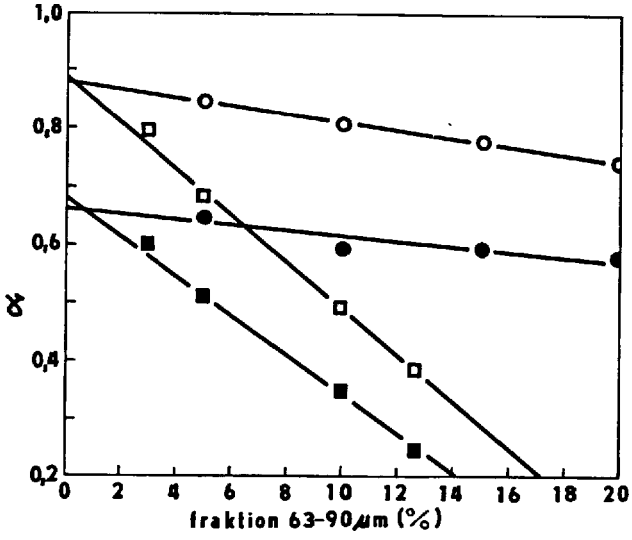

Fig. 1 - Conversion change with the quantity of coarse $CaCO_3$ (O) and quartz (□) particles, isothermal firing of raw meals C 4-C 6 and S 4-S 6, 1400°C, 1.6 and 5.6 minutes.

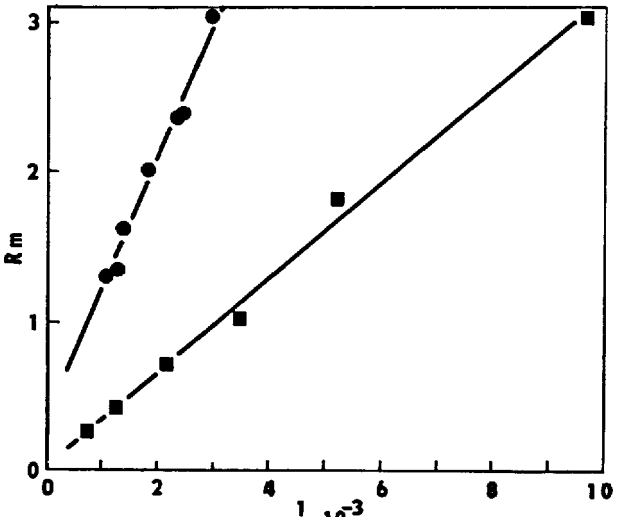

Fig. 2 - Change of reactivity (Rm) with the size of the average calcite and quartz particle. ● -CS, C 1-C 6, ■ -CS, S 1-S 6.

the Jander and Ginstling-Bronstein model, and for the description of its rate for lower conversions there can also be employed equation /1/.The volume of the belitic agglomerations is more than three times as large as the oritinal quartz grains and the largest agglomerations are only being partially reacted, since they represent the source of residual belite,especially in clinkers with a lower lime saturation.

From Fig. 5 can clearly be seen the linear dependence of Rm on the reciprocal value of the products of squares of average

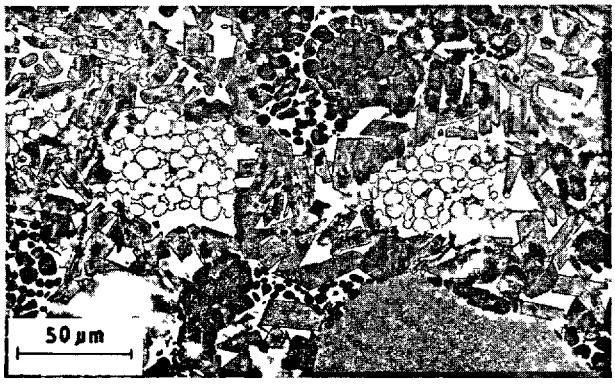

Fig. 3 - Free CaO agglomerations in C 2 clinker, firing at 1400°C, 1 minute, Phases according to blackening of photograph : Interstitial mass, free CaO, alite,belite. Lage homogenous area - epoxide.(CH_3COOH vapour)

Fig. 4 - Belite agglomerations in S 5 clinker, firing at 1400°C, 1 minute. Phases same as in Fig. 3.

limestone and quartz particle radii that have been determined as described above. This dependence holds true only for raw meals of identical chemical composition in which all the SiO_2 is in the form of quartz. Since in industrial raw meals the ratio SiO_2/quartz is always > 1,it is necessary to take into account for the practical utilization of the above findings also the influence of the quartz quantity onto the rate of clinker formation. The raw meal reactivity can be influenced only by the quartz grains which cause the formation of such local SiO_2 concentrations in the belitic clinker that hinder the following alite formation process. With intensive heating, this effect of the smallest quartz particles is suppressed already in the course of the formation of the liquid phase, and therefore there exists a critical size, below which all forms of SiO_2 can for practical purposes be considered as approximately identically reactive. This fact has been established already in previous investigations and the critical size can be found closely bellow 40 µm (6,7). Since the reaction mechanism of larger silicates grains as well as their influence onto the reactivity is analogical to quartz,it is possible to propose a

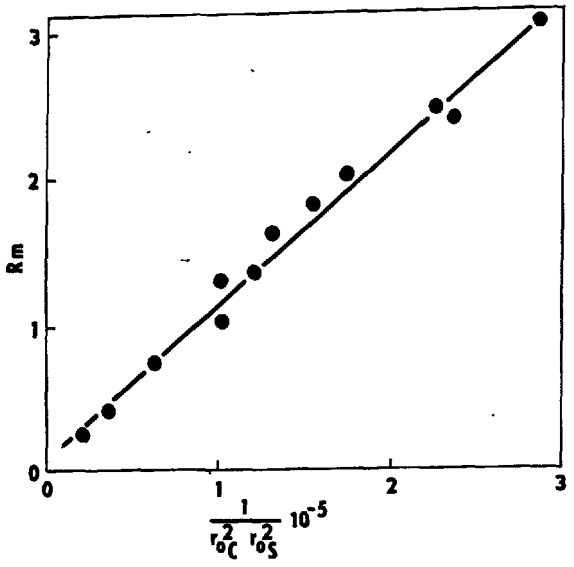

Fig. 5 - Change of reactivity with the size of the average calcite and quartz particle.

simplified method for the determination of the raw meal reactivity on the basis of sieve analyses of the raw meal, the insoluble residue and the chemical composition :

$$Rm' = \frac{L}{r_{oC}^2 \cdot r_{oQ}^2 \cdot C_3S\ max} \cdot \frac{1}{s} \qquad /5/$$

where L = computed liquid phase quantity in the clinker

C_3S max = computed equilibrium C_3S content in the clinker

r_{oC} = average particle radius out of 25% of the coarsest raw meal particles

r_{oQ} = average particle radius of the insoluble residue of the raw meal in HCl

s = expression value in the brackets of the equation /5/, computed for the reference raw meal.

The influences of the liquid phase quantity in the clinker and of C_3S max onto the reactivity of the raw meal are well known (8, 3), and in the course of the assessment of the insoluble residue the average grain size is determined experimentally only for the rest on the 40 µm sieve, and for the computation of r_{oQ} there is assumed an average grain size of the remaining SiO_2 d_{0-40}=20 µm. The proposed method for determining the reactivities of raw meals neglects the influence of side admixtures and is loaded with the systematic error of the differences between the actual and calculated contents of alite and the liquid phase and the simplified assessment of the insoluble residue. It is therefore suitable especially for investigating the reactivity of raw meals prepared from components out the same locality, i.e. for solving the problems of a cement plant, in the laboratory of which it can easily be realized.

CONCLUSION

The reactivity of the cement raw meal decreases linearly with the reciprocal value of the product of the squares of the average calcite and quartz grains. This relationship, together with certain findings concerning the mechanism of clinker formation, hape made it possible to present a simplified method for the operational determination of reactivity which can be realized in cement plant laboratory. The reactivity is determined from the chemical composition of the raw meal, its sieve analysis and the sieve analysis of the insoluble residue.

BIBLIOGRAPHIE

1.- S. CHROMÝ (1974), "Mechanism of White Clinker Formation", Proc.6th Int. Congress Chem.Cement, Vol. III, 268-273.

2.- S. CHROMÝ (1980), "Mechanismus der Entstehung von Portlandzementklinker", Zement-Kalk-Gips (in print).

3.- S. CHROMÝ (1980), "Reaktivität von Zementrohstoffen", Zement-Kalk-Gips (in print).

4.- R. KONDO et S.H. CHOI (1969), "Mechanism and Kinetics of Portland Cement Clinker Formation for an Example of the Solid State Reaction in the Presence of a Liquid Phase", Proc. 5th Intern.Symp. Chem.Cement, I-Suppl.Paper, 1-98, 163-171.

5.- S. CHROMÝ (1978), "Correctness and Accuracy of the Microscopic Quantitative Phase Analysis of Portland Cement Clinkers", Silikáty 22, 3, 215-226(in Czech).

6.- J.L.C. ZALAMA (1973), "La silice libre en los crudos de cemento portland", Cemento-Hormigon 44,469, 295-313.

7.- M. PERNICA (1975), "Study of Reactions in the Course of Firing of Raw Materials for the Production of Portland Cement Clinker", Research Institute of Building Materials, Brno, M-508 (in Czech).

8.- V. JOHANSEN (1973), "Model for Reaction Between CaO Particles and Portland Cement Clinker", J.Amer.Ceram.Soc. 56, 9, 450-454.

Thermodynamics of closed systems applied to the annealing of clinker

Thermodynamique des systèmes clos appliquée à la cuisson du clinker

M. SHULTZ, Academician, Institute of Silicate Chemistry of the Academy of Sciences of the USSR, Leningrad, U.R.S.S.

RESUME : En thermodynamique, il a été convenu d'appeler "clos" des systèmes dans lesquels les processus se développent sans échange de matière avec le milieu extérieur; c'est à dire dans des conditions d'isolation matérielle. Dans la cuisson du clinker de ciment, il y a des stades appropriés qui, quoique approximativement, peuvent être assimilés aux processus ayant lieu dans les systèmes clos. Nous voulons parler des réactions de formation des minéraux et des processus de redistribution de matière entre les phases qui continuent de se développer après l'achèvement de la déshydratation et de la décarbonisation, suivant les variations de la température dans chacune des zones du four.

Malgré le fait que, dans les conditions réelles, les états d'équilibre ne sont pas atteints, une considération thermodynamique permet de mettre en évidence les directions essentielles les plus probables de développement des processus à la cuisson du clinker.

Dans cette communication deux questions corrélées sont considérées. En se basant sur des concepts thermodynamiques généraux, il a été montré comment les changements de température influencent les compositions des phases du clinker (les phases liquides et solides), pour une composition atomique donnée du système, et en cas d'isolation matérielle.

Dans la deuxième partie de la communication une étude est faite, par la méthode des "séries isomolaires" sur la stabilité relative des combinaisons des systèmes $CaO-SiO_2$, $CaO-Al_2O_3$, $MgO-SiO_2$ dans des conditions isothermiques et isobariques, les oxydes dont sont constitués les clinkers étaient, dans cette étude, dans les mêmes proportions que dans les diagrammes de phase habituels bien connus.

SUMMARY : In thermodynamics it is customary to call "closed" the systems in which the processes develop without exchange of material with the outer medium, i.e. under conditions of material isolation. During the annealing of cement clinker there are appropriate stages which, although approximately, can be attributed to the processes taking place in the closed systems. We mean concretely the formation reactions of minerals and the redistribution processes of the material between phases which continue to develop also after the completion of dehydration and decarbonization in accordance with changing temperature in each zone of the cement kiln.

Despite the fact that under real conditions the equilibrium states are not attained, a thermodynamic consideration permits to reveal the most probable basic directions of the development of processes during annealing the clinker.

Two interrelated questions are dealt with in the present paper. When solving one of these questions on the basis of general thermodynamic concepts, we tried to show how the temperature changes influence the compositions of the coexisting clinker phases (liquid and solid solutions) at a given brutto-composition of the system, what corresponds to the conditions of material isolation.

In the second part of the paper a consideration is given, using the method of "isomolar series", of the relative stability of compounds in the systems $CaO-SiO_2$, $CaO-Al_2O_3$, $MgO-SiO_2$ under isothermal-isobaric conditions and at either but at a given mass correlation of the constituent oxides of clinker minerals with respect to the known phase diagrams.

INFLUENCE OF TEMPERATURE ON PHASE RELATIONS IN THE CLOSED SYSTEMS

A thermodynamic consideration of the heterogeneous systems includes as a base, along with the principles of equilibrium and conditions of its stability, the concept of phase as combination of complexes of bodies the equilibrium properties of which can be described by the general thermodynamic equation - an equation of phase. By Gibbs, the latter can be represented as follows:

$$S^r dT - v^r dp + \sum_{i=1}^{n} m_i^r dM_i = 0 \qquad (1)$$

where S^r and v^r are the entropy and the volume of the phase; m_i^r is the mass of each of the components of phase V_r; T,p,M_i are the temperature, the pressure and the chemical potentials, respectively; r is the index of phase. By solving the system of equations (1) for two phases, the generalized differential Van-der-Waals equation is obtained which is considered in detail in /2/ and written as follows:

$$\frac{Q^{12}}{T} dT - v^{12} dp + \sum_{k=1}^{n-1} \sum_{i=1}^{n-1} (x_i^2 - x_i^1) G_{ik}^1 dx_i^1 = 0 \qquad (2)$$

where Q^{12} and v^{12} are the thermal and volume effects of phase transformation; x_i^1 and x_i^2 are the mole fractions of i-components in the solid and liquid phases, respectively;

$G_{ik}^1 = \left(\frac{\partial^2 G}{\partial x_i \partial x_k}\right)^1$ is the second derivative of the Gibbs free energy by mole fractions of components in the phase. The symbols of phases V_1 and V_2 are then introduced.

Equation (2) is written in the variables of the composition of phase V_1; analogous equation can be written in the variables of phase V_2.

At full description of the equilibrium processes in the heterogeneous systems, the following equalities are also taken into consideration /2/:

$$d\left(\frac{\partial G^1}{\partial x_i^1}\right)_{T,p,x_j} = d\left(\frac{\partial G^2}{\partial x_i^2}\right)_{T,p,x_j} \qquad (3)$$

$$(i = 1,\ldots, n-1)$$

which are reduced to the form

$$-\left(\frac{\partial S^1}{\partial x_i^1}\right) dT + \left(\frac{\partial v^1}{\partial x_i^1}\right) dp + \sum_{k=1}^{n-1} G_{ik}^1 dx_k^1 =$$

$$= -\left(\frac{\partial S^2}{\partial x_i^2}\right) dT + \left(\frac{\partial v^2}{\partial x_i^2}\right) dp + \sum_{k=1}^{n-1} G_{ik}^2 dx_k^2 \qquad (4)$$

The total number of independent equations from system (4) together with equation (2) is established using the phase rule and is equal to "n". For the closed systems, equations (2) and (4) are complemented by conditions of material isolation, e.g., in the following form:

$$x_i^1 m^1 + x_i^2 m^2 = m_i^o = \text{const}$$
$$m^1 + m^2 = m^o = \text{const} \qquad (i=1,\ldots n) \qquad (5)$$

where m^1 and m^2 are the masses of phases V_1 and V_2; m_i^o is the full mass of i-component; m^o is the full mass of the system.

Differentiation of the system of equations (5) leads to the following expressions:

$$m^1 dx_i^1 + m^2 dx_i^2 = (x_i^2 - x_i^1) dm_i^1 \quad (i=1,\ldots n) \qquad (6)$$

A consideration of combination of equations (2),(4),(6) often leads to rather bulky and difficult for interpretation expressions. However, as it follows from the works of Filippov /3/, the representation of the appropriate systems of equations in the form of vector expressions permits to easily draw rather clear and visual conclusions. To this purpose, vectors of phase compositions (or generalized vectors of the directions of changes in phase composition), dx_1, are introduced as well as vectors of tie-lines $(\vec{x}_2 - \vec{x}_1)$ connecting the figurative points of the coexisting phases V_1 and V_2. The concentrational space is represented in the metrics of Gibbs free energy; operators G_1 and G_2 are introduced to which the matrices $\|G_{ik}^2\|^r$ (r=1,2) correspond; and finally, use is made of the general expressions for the concentration gradients of the entropies of phases ∇S^1 and ∇S^2. This results, as discussed in detail in /3-6/, in the following expressions for isobaric conditions:

$$m^1 d\vec{x}_1 + m^2 d\vec{x}_2 = (\vec{x}_2 - \vec{x}_1) dm^1 \qquad (7)^*$$

$$G_1 d\vec{x}_1 - \nabla S^1 dT = G_2 d\vec{x}_2 - \nabla S^2 dT \qquad (8)$$

$$(\vec{x}_2 - \vec{x}_1) G_1 d\vec{x}_1 = \left[S^1 - S^2 - (\vec{x}_2 - \vec{x}_1) \nabla S^1\right] dT \qquad (9)$$

After making several transformations of the system of equations (7)-(9) and after introducing the additional term - the concentration gradient of the entropy of the heterogeneous system as a whole, ∇S, (the proper entropy of the heterogeneous system is expressed as $S = S^1 m^1 + S^2 m^2$) one obtains, as shown in /4/-/6/, the following expression characterizing the influence of temperature on the composition of one of the coexisting phases, e.g., of the phase V_1 :

$$G_1 \frac{d\vec{x}_1}{dT} = \nabla S^1 - \nabla S \qquad (10)$$

Scalar product of equation (10) by the vector $\vec{e}_1$ lying at the tangent to the isotherm-isobar of phase V_1 (the straight line $T_1(V_1 - V_2)$ in Figure 1) gives

$$\vec{e}_1 G_1 \frac{d\vec{x}_1}{dT} = \vec{e}_1 (\nabla S^1 - \nabla S) \qquad (11)$$

The left part of equation (11) is a projection of vector $\frac{d\vec{x}_1}{dT}$ against the tangential

* With vector values the phase index stands below

vector $\vec{e}_1$ and characterizes the shift of the composition of phase V_1 in relation to the primary position or, in other words, the motion of the end of the tie-line (or its turn) with the isobaric change of temperature (Figure 1).

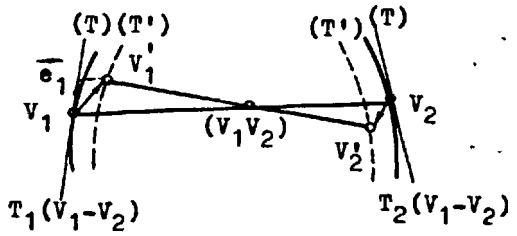

Fig. 1 - Change in position of the isotherm -isobar and of the tie-line in the closed system V_1-V_2 with changing temperature.

As seen from equation (11), the direction of the vector of the tie-line turn at the fixed brutto-composition of the system is determined by the correlation of projections (in a common sense) of the entropy gradients of phase V_1 and of the system V_1-V_2 against vector $\vec{e}_1 \in {}^1T_1(V_1-V_2)$ or, what is the same, by the correlation of the corresponding concentration derivatives. Actually, it can be shown that

$$\vec{e}_1(\nabla s^1 - \nabla s) = \left(\frac{\partial s^1}{\partial x_i^1}\right)_{\vec{e}_1} - \left(\frac{\partial s^2}{\partial x_i^2}\right)_{\vec{e}_1} \qquad (12)$$

where x_i^1 is the mole fraction of i-component in the phase V_1 and x_i is the brutto-mole fraction. The following general conclusion can be formulated: If the difference of the derivatives characterizing the entropy change of the phase V_1 and of the system V_1-V_2 in the direction of vector $\vec{e}_1 \in T_1(V_1-V_2)$ tangential to the isotherm-isobar is positive, then with isobaric increase in temperature of the system the shift of composition of phase V_1 and consequently the turn of the tie-line will occur in the direction of vector $\vec{e}_1$, and on the opposite.

Let us note that in a particular case when the tangents and the isotherms-isobars of the coexisting phases are parallel (such a case will be dealt with somewhat later), the following equation can be obtained:

$$\vec{e}_1(\nabla s^1 - \nabla s) = m^2\left[\left(\frac{\partial s^1}{\partial x_i^1}\right)_{\vec{e}_1} - \left(\frac{\partial s^2}{\partial x_i^2}\right)_{\vec{e}_1}\right] \qquad (13)$$

Due to the equilibrium conditions which are, in particular, expressed by equality (3), the differences of the entropy derivatives in equations (12) and (13) can be replaced accordingly by those of the enthalpy derivatives by concentration attributed to the absolute temperatures. The correlations considered here are of special interest for such cases when the coexisting phases are of variable composition. During the annealing of clinker one often deals with the cases when many phases of variable composition enter into interaction as the clinker phases represent different solid solutions. However, there is a paucity of concrete data on the compositions of coexisting phases.

As it follows from /7/, two equilibrium solid solutions, $(MgO,FeO)SiO_2$ and $(MgO,FeO)_2SiO_2$, form in the MgO-FeO-SiO_2 system for which, although schematically, the positions of tie-lines are given for different temperatures. Based on these data to illustrate consequences (12) and (13), we show in Figure 2 how the temperature influences the position of one of the tie-lines connecting the figurative points of two solid solutions $(MgO,FeO)SiO_2$ - phase V_1 and $(MgO,FeO)_2SiO_2$ - phase V_2.

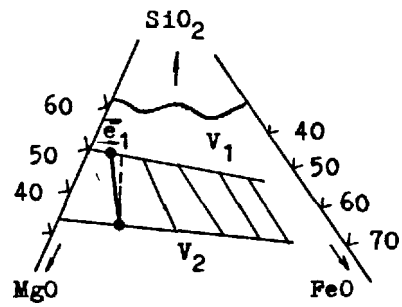

Fig. 2 - Positions of tie-lines of two-phase equilibria of the solid solutions $(MgO,FeO)SiO_2$ and $(MgO,FeO)_2SiO_2$ in the MgO-FeO-SiO_2 system at 955°C and 1250°C.

As follows from Figure 2 and equations (12) and (13), the entropy and enthalpy derivatives by concentration in the equilibrium phases are larger for phase V_1 than for phase V_2, but they are probably rather close in value.

It should be noted that the results given above are first of all of practical significance serving as strict (precise) thermodynamic criteria of the reliability of experimental data. It is obvious that such criteria are quite necessary for experimental investigations of the systems of refractory oxides. This will be evidenced, in particular, by the material to be discussed in the next paragraph.

RELATIVE STABILITY OF COMPOUNDS FORMING THE MINERALS OF CEMENT CLINKER

One of the main questions of the thermodynamic consideration of the formation processes of clinker is that concerning the most probable reactions of mineral formation under given particular conditions. This question is often answered by comparing the values of the Gibbs free energy decrease for different reactions and by asserting that the process with the greatest decrease of this function will be most probable. However, the mass correlations of the participants of the process should also be taken into consideration, as shown on many examples by Mchedlov-Petrossian et al /8/.

Long ago Shchukarev /9/ came to the conclusion that if in a system of two different elements a series of compounds is formed, then the thermal effects of compounds formation calculated per one gram-atom (in the total), represented graphically as a function of composition, should be described by smooth curves without sharp inflections. This concept was illustrated by many examples; for oxide systems they are given in /10/. The analysis of the above-mentioned generalization of experimental data leads to the conclusion that under certain conditions these data can be regarded as consequences of the principle of equilibrium stability developed in the most complete and strict form by Gibbs /1/, if the concept mentioned is related not to enthalpy but to free energy /11/. We shall not concern here the details of the known conceptions but remind only of the following. In the most general form the conditions of equilibrium stability are expressed by the inequality

$$(\Delta E)_{s,v,m_1,\ldots,m_n} > 0 \qquad (14)$$

where ΔE is the internal energy of the system; s is the entropy; v is the volume; $m_1,\ldots, m_n$ are the masses of components.

The fulfilment of inequality (14) is a necessary and sufficient condition for equilibrium stability with respect to any arbitrary changes of the state. This inequality means that under indicated conditions (at a *given mass of components included*), if the system is in the state of stable equilibrium, any change of the state which disturbs the equilibrium should be accompanied by an increase of internal energy. For the isothermal-isobaric conditions, analogous concept is applicable to the standard Gibbs free energy, i.e. under given conditions for a system being in the equilibrium state, the following inequality should be fulfilled

$$(\Delta G)_{T,p,m_1,\ldots,m_n} > 0 \qquad (15)$$

at all changes which disturb the equilibrium of the system. Getting off the point let us note that inequality (15) can be used to derive the following requirement for the states of stable equilibrium:

$$\left[d^2G(x_1,\ldots,x_{n-1})\right]_{T,p} > 0 \qquad (16)$$

(if the composition is expressed in mole fractions).

For the states of stable equilibrium, inequalities (15) and (16) require that in graphic representation the surface of the free energy would be prominent in relation to the coordinate axes of the system composition. This principle is widely used in the study of solutions, i.e. at a continuous change of composition. In the form of inequality (15) it can also apply to the series of compounds formed by the same substances which enter into interaction in the different proportions. The only peculiarity is that in this case a comparison of states discontinuous in composition is made, as shown schematically in Figure 3 /11/.

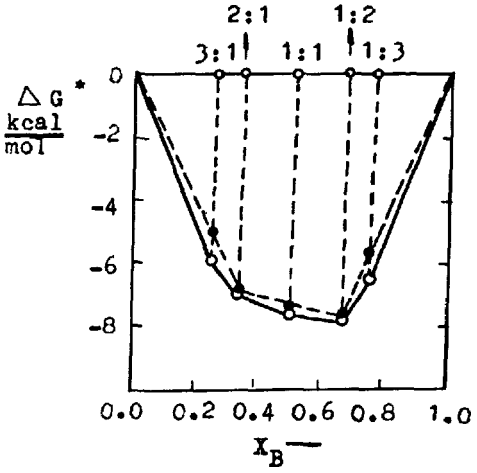

Fig. 3 - Free energies of formation of stable compounds in the system A-B. Composition is given in mole fractions of B (X_B).

This figure is drawn in such a way that each compound is stable with respect to the decomposition into any other compounds being formed in the system. The point is in what concentration range the brutto-composition of the mixture lies: in one range some pairs of compounds are stable, in the other the different ones. This principle extends also to more complex systems where the number of coexisting stable compounds is determined by the phase rule. Without drawing such a diagram or without an appropriate numeric calculation one cannot be sure that the experimental or calculated data are consistent with thermodynamic requirement of stability. Recently, for example, analogous diagrams were used to the same purpose in /12/. Graphic representation is not always convenient but it can be replaced by appropriate calculations. Any complex compound which can be composed of "n" less complex compounds or simple substances will not decompose into them, if the following inequality is fulfilled:

$$\left[\sum_{i=1}^{n} x_i \Delta G_i^* - \Delta G^*\right]_{T,p} > 0 \qquad (17)$$

where x_i is the fraction of the compound chosen as component of the complex compound; ΔG_i^* is the free energy of the component (or of the compound); ΔG^* is analogous value for the complex compound calculated per one mole of the total amount of interacting substances. In all cases the values ΔG_i^* and ΔG^* are obtained by dividing the molar free energies of compounds formation by the total number of particles forming the compound ($\Delta G_i^* = \frac{\Delta G_i}{n_i}$; $\Delta G^* = \frac{\Delta G}{n}$).

Let us turn our attention to several particular examples and consider first of all the data for one of the major systems of interest to the technology of cement, namely for the $CaO-SiO_2$ system. Several compounds

form in this system: C_3S, C_2S, C_3S_2, CS, the thermodynamic data for which are reported in /8/ and presented in the well-known phase diagrams /13, p.33/. The thermodynamic data were used to draw Figure 4 which shows the composition dependence (in mole fraction of SiO_2(X_S)) of the free energy of compounds formation calculated per one mole of the total oxides (ΔG^*).

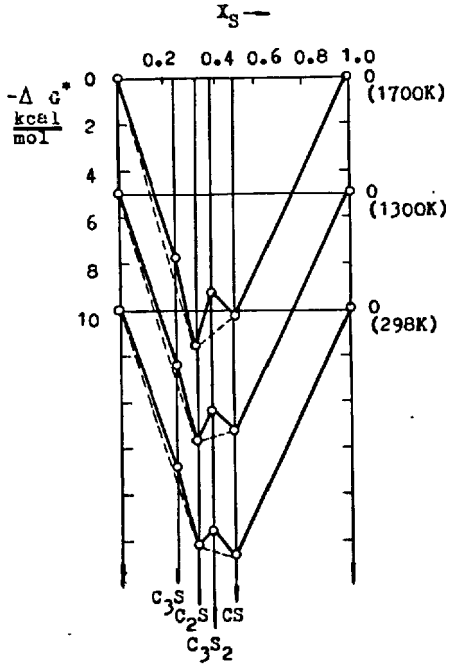

Fig. 4 - Free energies of formation of the oxide compounds in the $CaO-SiO_2$ system as a function of mole fraction of SiO_2. The temperatures are 298K, 1300K, 1700K.

As seen from Figure 4, only two compounds, C_2S and CS, show consistency with requirements of stable equilibrium given by inequalities (15) and (16). At all temperatures indicated in the figure the compounds C_3S and C_3S_2 must decompose into pairs of compounds adjoining in composition. The compound C_3S must decompose into CaO and C_2S, and C_3S_2 into C_2S and CS. However, the compound C_3S owing to the small difference effect of the free energy decrease according to equation (17), which apparently lies within the limits of experimental error, is probably located somewhere at the stability boundary as regards the process of decomposition into phases CaO and $(CaO)_2SiO_2$. It should be noted that we have no data which would permit to attribute the phases C_3S and C_3S_2 to metastable phases. To this end, it would be necessary to obtain and study the stability of solid solutions based on C_3S and C_3S_2 at variable contents of CaO and SiO_2 in them.

If one turns attention to the corresponding phase diagram for the $CaO-SiO_2$, it will be possible to attribute all compounds shown in Figure 4 to equilibrium compounds and assume that all of them should coexist in equilibrium with the adjoining in composition compounds without decomposition over the temperature range studied, except for C_3S below 1250°C. It ought to be concluded that thermodynamic data for this system do not agree fully with the phase diagram. Further checking of thermodynamic data and probably a more critical evaluation of results given in the phase diagram are needed.

The slowing down of the processes in solid bodies is probably responsible for the formation of unstable compounds which are presented in the diagram along with stable compounds. However, to draw final conclusions, further precision of the experimental data discussed here is needed.

Analogous conception can be related to another system of importance for the technology of cement: $CaO-Al_2O_3$. Figure 5 which was drawn using data of paper /8/ shows the dependence of the free energy of formation of the calcium aluminates calculated per one mole of the total oxides on the mole fraction of Al_2O_3 in the compound.

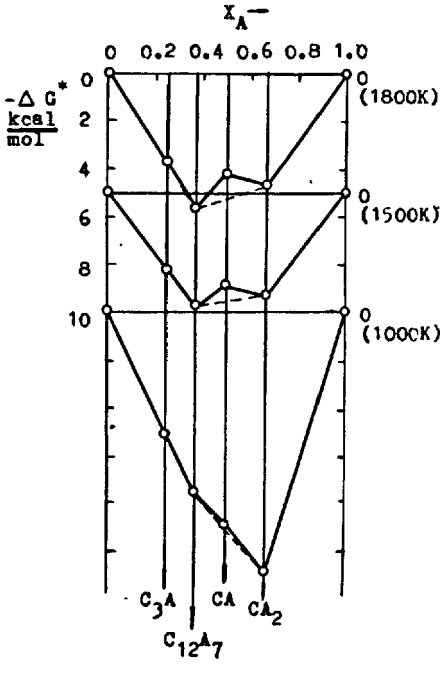

Fig. 5 - Free energies of formation of the oxide compounds in the $CaO-Al_2O_3$ system as a function of mole fraction of SiO_2. The temperatures are 1000K, 1500K, 1800°K.

As it is obvious from Figure 5 and condition (15), the compound CA is unstable with respect to the process of decomposition into compounds CA_2 and $C_{12}A_7$ adjoining in composition at temperatures of 1500 and 1800K. But if we turn our attention to the corresponding well-known phase diagram /13, p.210/, we shall see that in the temperature range considered in Figure 5 all the compounds

shown are equilibrium in themselves and can coexist with the adjoining compounds. Obviously, there is also some contradiction here.

Finally, to complement the picture under discussion, data on the $MgO-SiO_2$ system are presented in Figure 6. Here also in contradiction to the appropriate phase diagram /13, p.28/, the compound MS is unstable.

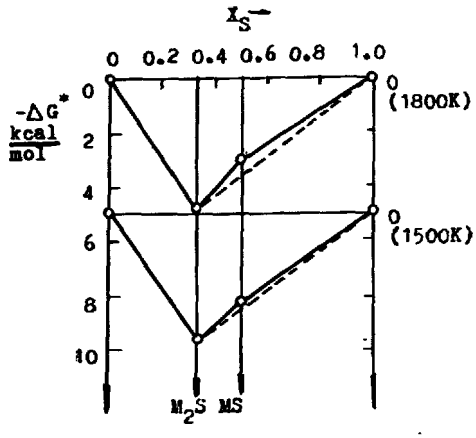

Fig. 6 - Free energies of formation of the oxide compounds in the $MgO-SiO_2$ system as a function of mole fraction of SiO_2. The temperatures are 1500 and 1800K

Many examples could be given to illustrate the point when the phases are presented in the diagrams as equilibrium whereas by thermodynamic properties they should be attributed to unstable phases. The indicated facts, firstly, set the task of a simultaneous study of phase diagrams and thermodynamic functions of formation of the compounds and solid solutions. Together with this, it is apparently of great scientific interest and of practical significance to develop concrete quantitative characteristics of the thermodynamic non-equilibrium "freezed" solid phases and to study the factors of stabilization of the non-equilibrium states.

CONCLUSIONS

Further development of the physico-chemical bases of cement technology implies the deepening of concepts in the field of thermodynamics of the heterogeneous processes and accumulation of appropriate data. It also sets the task of a critical analysis of thermodynamic data on the compounds formation in cement clinker and of the appropriate phase diagrams. It is necessary to coordinate both data with respect to the equilibrium stability of the phases of cement clinker.

REFERENCES

1.- D.V. Gibbs (1950) "Thermodynamic Works", Publ. House of Techn.-Theoret. Literat., Moscow-Leningrad (in Russian).

2.- A.V. Storonkin (1967) "Thermodynamics of the Heterogeneous Systems", Leningrad Univ. Publ. House.

3.- V.K. Filippov (1979) "Metrics of Gibbs Potential and Theory of Monovariant Equilibria", In: Problems of Thermodynamics of the Heterogeneous Systems and of the Theory of Surface Phenomena, Issue 2, Leningrad Univ. Publ. House, 20-35.

4.- V.K. Filippov and M.M. Shultz (1977) "On the Relation between the Parameters of Closed Multiphase Systems", Doklady Akad. Nauk SSSR 235, n°2, 414-416.

5.- V.K. Filippov and M.M. Shultz (1978) "Application of the Thermodynamic Systems to the Study of Phase Separation in Multicomponent Glasses", Fizika i Khim. Stekla 4, n°1, 56-60.

6.- V.K.Filippov and M.M. Shultz (1978) "Temperature Dependence of the Compositions and Masses of Phases in Phase-Separated Glasses", Fizika i Khim. Stekla 4, n° 2, 149-154.

7.- N.L.Bowen and J.F. Schairer (1935) "The System $MgO-FeO-SiO_2$", Am. J. Sci.(5)29, n° 170, 151-217.

8.- V.I. Babushkin, G.M. Matveev and O.P. Mchedlov-Petrossian (1972) "Thermodynamics of the Silicates", Publ. House of Literature on Building, Moscow.

9.- S.A. Shchukarev (1945) "On the Thermodynamic Stability of Oxides of Manganese and Iron", Uchenye Zapiski Leningradsk. Univ. n° 79, issue 7, 197-254.

10.-V.B. Glushkova and E.N. Isupova (1965) "Thermodynamic Calculations of the Solid-State Reactions between Oxides of the Elements of the Second and Fourth Groups of the Periodic System", Izv. Akad. Nauk SSSR, Ser. Neorgan. Materialy 1, n° 7, 1143-1151.

11.-M.M. Shultz (1976) "Thermodynamic Functions of Formation of the Double and More Complex Compounds in the Light of Criteria of Equilibrium Stability", In: Thermodynamics and Properties of Condensated Silicate and Oxide Systems, VEDA, Slovak Acad. Sci., Bratislava, 9-17 (in Russian).

12.-G. Rog, B. Langanke, G. Borchardt and H. Schmalzried (1974) "Determination of the Standard Gibbs Free Energy of Formation of the Silicates of Cobalt, Magnesium and Strontium by E.M.F. Measurements", J. Chem. Thermodyn. 6, n° 12, 1113-1119.

13.-N.A. Toropov, V.P. Barzakovskii, V.V. Lapin and N.N. Kurtseva (1969) Handbook "Phase Diagrams for the Silicate Systems", Issue 1, Nauka, Leningrad.

Fonction généralisée de clinkérabilité

Generalized clinkerability function

P. GOMA, docteur ès sciences chimiques. Laboratoire de zone de Catalogne, Asland S.A., Espagne.

RESUME : On a établi une méthode pour déterminer les températures de clinkérisation des crus de clinker portland à partir des courbes de l'abaissement de la teneur en chaux libre en fonction de l'augmentation de température jusqu'à 1.600°C dans une calcination dans des conditions contrôlées proches de celles d'un four réel.

Cette méthode, qui a déjà été employée par des auteurs précédents, est associée ici, pour la première fois, à une nouvelle méthode d'analyse chimique absolue due à l'auteur. Elle élimine les erreurs encore inconnues dans le procédé gravimétrique traditionnel pour la détermination de la silice ou dans ses variantes.

L'exactitude et la reproductivité ainsi obtenues ont permis de voir l'influence quantitative des variables qui influent sur la température maximum nécessaire pour la clinkérisation des crus industriels.

On établit une fonction généralisée qui donne le degré de clinkérabilité des crus.

Son application aux crus, dans un processus concret, permet de connaître indirectement, en fonction de la chaux libre obtenue, la température maximum équivalente qu'a atteint le matériau dans la zone de clinkérisation et d'évaluer indirectement le degré de concentration de la combustion obtenue, équivalent à la valeur de l'échange "flamme-clinker".

SUMMARY: We establish a method which can be used to determine the clinkerability temperatures of portland clinker raw mixes from the curves corresponding to the mowering of the free lime value depending on the temperatura up to 1.600°C by means of burnability under controlled conditions similar to those of a given kiln.

The base of the method, which has been used by other former authors, is combined here for the first time with a new method of absolute chemical analysis for the gravimetric determination of silica due to the author which avoids errors which are still unknown in the traditional gravimetric process or its variants.

The accuracy and reproducibility obtained in this way have allowed us to see the quantitative influence of the variants which affect the burning temperature maximum that it is necessary for clinkerizing the industrial raw mixes.

Its application on the raw mixes in a concrete process alow to determine indirectly, in relation with the free lime obtained, the maximum equivalent temperature reached by the material in the zone of clinkerization and to know indirectly the concentration degree of flame reached, equivalent to the "flame-clinker" interchange value.

I- Difficultés a surmonter pour connaître le degré d'optimisation énergétique d'une installation de clinkérisation.

L'utilisation énergétique d'une installation dépend de deux facteurs importants: de la valeur des pertes de chaleur de l'ensemble de l'installation et de la valeur obtenue au moyen des transmissions de chaleur au matériel au cours de ses trois étapes principales ,celle de l'échangeur,et dans le four,celle des zones de calcination et clinkérisation,étant cette dernière celle qui permettra d'obtenir,selon sa valeur, un niveau de qualité suffisant pour une production donnée et de laquelle nous parlerons dans ce travail.

La valeur globale de ces facteurs est déterminée d'habitude par les bilans thermiques basés sur des mesures thermodynamiques et physiques,mais ces mesures ne suffisent pas pour évaluer sans interférence la valeur de l'échange entre la flamme et le produit syntherisant dans la zone de clinkérisation que nous appelons échange "flamme-clinker".

Le degré de cet échange serait obtenu en connissant la valeur de la température du matériel dans la zone de clinkérisation en fonction du temps. Cela n'est pas possible dans la technologie actuelle,mais nous essaierons d'expliquer comment on peut déterminer la valeur de cet échange en fonction de la température maximun qui est mesurée indirectament à partir de ce qu'on appelle les courbes de combinabilité obtenues dans le laboratoire dans des conditions déterminée.

La temperatura maximum du clinker dépend- en quantité de combustible constante- du degré de concentration de la zone de combustion obtenu dans le four,qui permet d'aumenter le nombre de calories et d'énergie de radiation par unité de surface intérieure de la zone.

Le degré de concentration de la combustion dépent des parametres de la combustion dans le procès et de la stabilité de son équilibre thermique.

Dans la practique du proces industriel,ces variantes se cachent et interfèrent de manière qu'il n'est pas possible de conaître avec certitude,de façon systématique, quel est le cru le plus approprié a une installation, quand il y a des conditions forcée,quel est le facteur qui limite la production dans chaque cas ou si celui-ci dépend des conditions chimiques du cru ou physico-mécaniques de l'installation. Ces difficultés empêchent l'ajustement énergétique des installations industrielles.

Nous croyons qu'il est possible de connaître, dans des conditions déterminées que nous essaierons d'expliquer, le degré de clinkérabilité d'un cru de façon suffisamment exacte et reproductible et que nous pauvons déduire de celui-ci la temperature maximun équivalente" que doit atteindre le cru dans la zone en un temps constant pour obtenir sa clinkérisation correcte avec une faible teneur en chaux libre et que cette température est,a son tour, une mesure de sa demande d'énergie.

La connaissance de ces points permet de repérer le facteur qui limite la production dans chaque cas et trouver le chemin pour réussir a l'aumenter.

Nous nous basons dans le fait que le temps de clinkérisation soit sensiblement constant pendant le proces en equilibre et que des petites variations de sa valeur dans le laboratoire ne parviennent pas a varier ou diminuer remarquablement le taux de chaux libre et si,au contraire, l'augmentation sensible de la "temperature maximum atteite dans le matériel" nous a permis de pendre comme variante principale cette température pour les mesures que nous prenons au cours de l'analyse du procès.

II- Jugement analytique des antecedents

Parmi les premiers travaux systématiques se trouve celui de HEILMANN (1) fondé sur la détermination de la teneur en chaux libre en fonction de la témperature. Les témperatures employées ont été de 1400 a 1500 °C ce qui amené l'obtention d'une chaux libre inferieure à 2%. BLAISE(2) emploie des cycles de témperature entre 1000 et 1450 °C et mesure l'aptitude à la calcination comme l'inverse de l'integrale de la courbe de chaux libre en fonction de la témperature. SULIKOWSKI (4) utilise des témperatures entre 900 et 1400°C et définit la calcinabilité par des paràmetres arbitraires. KOCH (5) avec des témperatures de 1350-1450 °C propose un modele d'analyse statistique pour déduirela valeur de chaux libre en fonction de dix variantes. LUDWIG et RUCKENSTEINER (6) emploient une témpérature de 1350 °C et expriment la chaux libre au moyen d'une fonction exponentielle. CRISTENSEN (7)établit par calcination a 1400°C une function pour déduire la chaux libre a cette témpérature. KONDO (3) a utilisé des températures entre 1100 et 1450°C et a déterminé le comportement de différentes matières premières et RAUSCHENFELS (8) a résumé une étude comparative de procédés.

Les températures employées dans tous les travaux précédents sont remarquablement basses par rapport à celles qu'on a réellement "dans le materiel" dans les zones de clinkérisation des fours avec les crus d'aujourd'hui.

Dans notre travail nous employons des températures plus hautes jusqu'a 1600°C du même ordre des réelles. Les réactions,en l'absence de phase liquide, ont une cinétique de réaction différente à celle qu'on a dans la cristallisation par le rafroidissement de la phase liquide selon les études à partir des diagrammes de phase,et les composés formés,avant son apparition,son modifiés en fonction de la température maximum atteinte.

L'influence de la composition chimique sur le degré de clinkérabilité est la plus importante et dans sa détermination on n'a pas tenu compte de l'influence, que les méthodes choisies pour l'analyse ont sur les résultats,à cause de ses limitations et d'erreurs encore inconnues aux quelles nous nous rapporterons.

La solution d'avoir recours à l'analyse mathématique par régression renfermera tous ces inconvénients parmi d'autres dont nous n'avons pas tenu compte,puisque nous ne croyons pas qu'ils puissent fournir,d'eux-mêmes, de nouvelles connaissances sur la physico-chimie du procès.

Nous n'avons remarqué aucune fonction qui rapporté le degré de clinkérisation a la température maximum réelle atteinte par le matériel,mais nous croyons qu'il est beaucoup plus intéressant se référer de la valeur de la clinkérabilité a cette température pourquoi nous croyons que ceci permet d'évaluer indirectement le degré de l'échange "flamme- clinker".

III- Conditions pour réussir à ce que la température de clinkerabilité soit reproductible et corresponde a la composition chimique du cru.

Le procédé que nous proposons essaie de mesurer le degré de clinkérabilité par la température que le cru a besoin d'atteindre,pendant 25 minutes,pour réussir la valeur de sa chaux libre à 2%(déterminée par la methode au glycol).

Le figure n°1 ci-dessous illustre la diminution de la chaux libre en function de la température maximum

a temps constant sur des crus a différent degré de clinkérabilité. Les courbes ci-dessous ont été obtenues en laboratoire par calcination a différentes températures jusqu'a 1.600°C

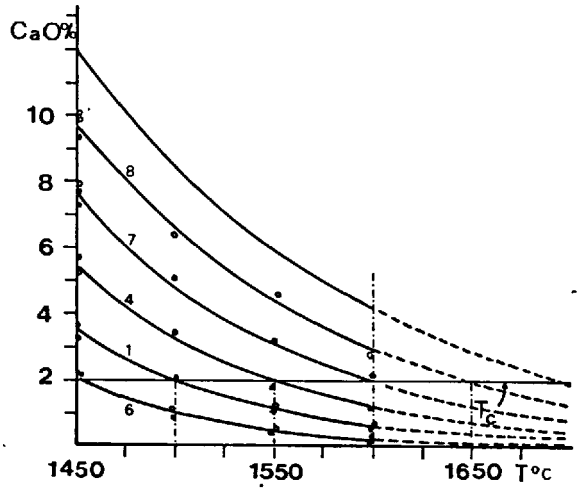

Fig. n°1 Variation de la valeur de la chaux libre en function de la température du materiel pour crus à différentes températures de clinkérabilité

Les courbes expérimentales suiven une fonction exponentielle de type général :

$$\text{CaO libre\%} = A.\ e^{\frac{1450-t}{a}} \qquad [1]$$

où les paràmetres A et a dépendent du degré de clinkérabilité dans des marges étroit. Leurs valeurs dèduites s'expriment dans le tableau I

TABLEAU I

T°C	1450	1500	1550	1600	1650	1700
a	80	92	104	116	130	140
A	2,0	3,4	5,2	7,4	9,5	12,0

1- Exactitude et precision dans la determination de la composition chimique.

Il faut choisir les procédés d'analyse par le fait connu que différentes méthodes d'analyse mènent a des résultats différents sur une même échantillon homogénéisé.CHALMERS (9). Quand il s'agît de la détermination de la silice ,cette dispersion est encore plus grande,a la suite de l'éxistence d'erreus encore inconnues dans la méthode classique traditionelle ou méthode de réference. GOMA (10) et(11).

L'auteur a étudié cette méthode de façon systématique ainsi que le comportement des gels de silice analytiques et a fait apparraître les variantes qui produisent le passage de silice au filtrage qui sont: l'insécurité de l'insolubilisation et la température haute pendant l'extraction (d'usage répandu et generalisé);la basse concentration d'acide et le volume élevé en elle-même et pendant les lavages ,tous s'emploient couranment. Par contre, l'extraction doit être faite en froid avec acide ClH 1:1 ,le volume minimum et lavage a eau froide seulement. L'insolubilisation avec anhydride acétique et évaporation a 160 ± 5°C .La teneur de la silice quipasse au filtrage,selon cette méthode se mesure en fonction du contenu en SiO_2.

L'emploi de ce procédé;celui de méthodes d'analyse pour l'aluminium dont le résultat ne soit pas alteré par des impuretés d'autres sesquioxides ,silice phosphor,etc comme per exemple la complexométrie par retur avec pyridine-azo-naphtol et l'emploi de la complexométrie pour la determination de la CaO et MgO, permetten d'obtenir les paràmetres Lsf,Ms,et Mf(Lsf-facteur de saturation en chaux,Ms-module de silicates,Mf-module de fondants) avec l'exactitude,précision et reproductibilité exigées pour déterminer le degré de clinkérabilité. L'écart standard obtenu dans les résultats des oxides majoritaires est de 0,04 et sa repercussion dans la détermination des paràmetres du cru donne lieu aux variations suivantes Lsf : 0,8; Ms:0,07, Mf : 0,07.

2-Conditions de l'homogeneisation

Dans les études de l'auteur mentionées (10) il en est arrivé a la conclusion qu'il est indispensable d'employer une capsule vibratoire pour la preparation des crus

3-Conditions fondamentales pour obtenir les courbes de clinkérabilité

Le four employé a été électrique a élément de chauffage vertical de SiC de 44 mm de Ø interieur,58mm Ø exterieur et une longueur de 400mm. Muni de relais de réglage automatique de température.On mesure la température avec un pyrométre Pt/Rh-Pt en contact avec le matériel et la température vérifiée par moyen de substances de point de fusion connu $CaSO_4$, Pd ,

Une quantité constante de 10g.de cru cómprimée en forme de pastilles est clinkerizée dans un creuset du Pt selon les courbes standard établiees dans le fig.-2

La pression a utiliser doit être entre 50-100 Kp/cm^2

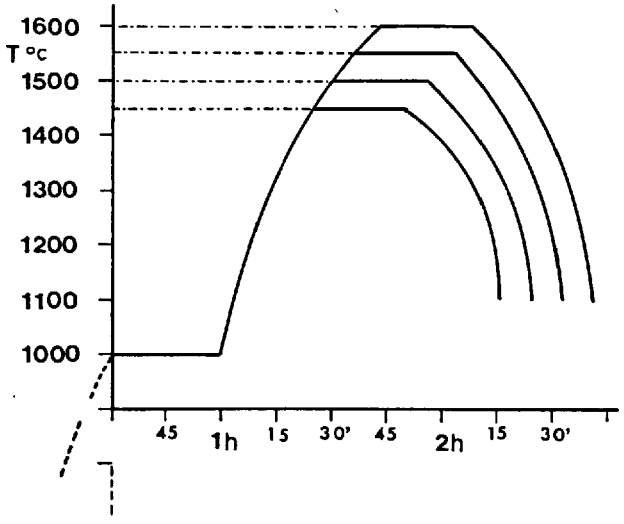

Fig. n°2 Courbes standard de température et pentes des courbes de refroidissement en fonction du temps pour obtenir les clinkérisations en laboratoire à différentes températures maximum

Apres avoir refroadi,on détermine la valeur de la chaux libre,dans un échantillon representatif par la méthode de l'étilenglycol -après broyage manuel a"finesse extrême"

IV- La fonction de la clinkerabilité

Dépend de nombreuses variantes parmi lesquelles les plus importantes sont: lacomposition chimique ,la granulométrie de l'ensamble et de chaque composant,

la composition minéralogique et la présence ou non de substances fondantes, etc. D'autres qui n'ont pas été mentionnées comme par exemple, la quantité de phase liquide est déjà implicité dans le module de silicates Ms et, sa viscosité, dans le module de fondants.

Les oxides étrangers au systeme SiO_2.Al_2O_3.Fe_2O_3.CaO modifient ces dernieres et nous en tenons compte comme variante par la somme de leurs pourcentages comme F.

$$F = (MgO, K_2O, Na_2O, SO_3, MnO, P_2O_5)\% \qquad [2]$$

Grâce a l'étude des crus au cours de cette derniere décade nous avons pu en arriver à la conclusion qu'il est possible, a notre avis, de généraliser une fonction a six variantes comme influences plus importantes qui ont un effet "sensible" sur le degré de clinkérabilité. En plus, par les raisons ci-dessus, nous croyons d'intérêt technique la mesure du degré de clinkérabilité par la température maximum, Tc, dont le cru a besoin pour sa transformation en clinker.

$$T_c = T_i + (Lsf, Ms, Mf, F, R_{92\mu}, R_{200\mu}) \qquad [3]$$

si $R_{>92\mu}$ et $R_{>200\mu}$ sont pourcentages des particules superieures aux respectifs Ø en microns

La généralisation de cette fonction se fonde sur les points suivants:

- sur le fait que les matières premières employées a tous les essais pour la détermination de celles-ci ont été naturelles parmi les calcaires et silicates habituels dans les exploitations et en l'absence d'agents d'addition comme les silicates artificiels, fluorures ou d'autres dont l'effet pourra être déterminé, a posteriori, par le même procédé que nous proposons.
- sur le fait que l'application est pour crus en Portland gris a composition variable dans de limites étroites des compositions habituelles : Lsf=90-100%, Ms=2,0=3,5, Mf=1,5-3,0, F=1-5%, $R_{>92\mu}$=5-25% et $R_{>200\mu}$= 0-2%
- sur le fait que dans cette zone de compositions restreite, l'influence des fonctions partielles de chaque variante apparaît pratiquement comme linéaire et uniquement l'effet de la finesse, se rattachant au rejet de dimensions plus grandes de 92μ, se montre de type exponentiel
- et que dans ces conditions l'influence de la composition minéralogique est beaucoup plus petite que celle de la composition chimique

D'après nos recherches, nous avons déduit, par le procédé que nous décrivons dans III, que les températures maximum équivalentes atteintes par le clinker dans des différentes lignes de procès à fuel et, avec ou sans précalcination, qui avaient un degré de concentration de flamme optimisé, sont comprises entre 1550 et 1650°C. Nous avons constaté que quand la Tc est tres proche de 1600 °C on obtient un déroulement de procès régulier et en équilibre thermique stable et cette régulation devient difficile pour des températures plus hautes ce qui détériore fortement les réfractaires.

Nous avons pris cette valeur comme point de repère et avons constaté que les compositions de crus les plus courantes ayant cette Tc sont très proches à la suivante ou sont iso-combinables avec elles:

Lsf=95%Ms=2,5, Mf=2,2, F=2,1, $R_{>92u}$=18%, $R_{>200u}$ =0 [4]

Dans une série de crus obtenus en laboratoire avec des matières premières naturelles et avec des courbes granulométriques analogues à celles des crus obtenus dans les circuits fermés usuels, on a modifié chacune de ces variantes tout en gardant toutes les autres constantes, dans les marges établies, pour obtenir les quotiens des accroissements partiels finis correspondant a chaque variante.

Les valeurs moyennes obtenues à partir d'un grand nombre d'essais sont exposées sur le tableau II

TABLEAU II

$\frac{\Delta Tc}{\Delta Lsf}$	$\frac{\Delta Tc}{\Delta Ms}$	$\frac{\Delta Tc}{\Delta Mf}$	$\frac{\Delta Tc}{\Delta R_{92}}$	$\frac{\Delta Tc}{\Delta R_{200}}$	$\frac{\Delta Tc}{\Delta F}$
+10,9	+113	+50	+6,7	+31,6	-41,0

si $R_{>92\mu}$ est la valeur moyen pour l'intervalle considéré.

Le sens du terme indepépendant Ti est la valeur de température de clinkérabilité Tc qui correspond à un cru aux caratéristiques données sur [4], obtenu à partir d'oxydes purs, cas dans lesquels tous les autres termes de la fonction donnée sont annulés puisque F es pratiquement zéro.

Un cru avec ces caractéristiques [4], avec des substances pures naturelles, a été obtenu en laboratoire. Il est composé d'un quartz de 99,8% avec une granulométrie continue dont la grandeur maximum est de 30 microsn, une calcite du 99,7% avec une distribution granulométrique continue et dont la grandeur maximum est de 200 microns et un rejet sur tamis de particules supérirures a 92 microns de 18%, une gamme alumine et une sidérite, très pures aussi, dont la grandeur maximum est de 10 microns.

La valeur de sa température de clinkérabilité a été de 1.655°C, valeur moyenne de plusieurs déterminations, que nous avons prise comme valeur de Ti (terme indépendant).

L'application des coefficnets partiels de chaque variable (Tableau II) qui a de l'influence sur la valeur de Tc trouvée dans les crus que nous avons étudiés et la valeur du terme indépendant trouvée expérimentalement, nous a permis d'établir la fonction polynomique ci-dessous:

$$T_c = 1655+(Lsf-95).10,9+(Ms-2,5).113+(Mf-2,2).50+ +(R_{>92\mu}-18).R^{0,65} +31,6.\alpha.R_{>200\mu}-41,0.F \qquad [5]$$

L'application de cette fonction à des crus différents, obtenus a partir de matières premières naturelles a différente nature dont les parametres ont été obtenus à partir des analyses chimiques faites par moyen des procédés décrits dans ce travail, donne les valeurs de leurs respectives températures de clinkérabilité Tc. Celles-ci sont comparées avec celles obtenues par le procédé sur III et sont exprimées sur la Tableau III ci-dessous:

Les numeros des courbes de la fig.n°1 correspondent aux crus du même n°dans le tableau III.

TABLEAU III

Crus ref.	1	2	3	4	5
Lsf	90,2	91,7	95,4	91,1	98,5
Ms	2,84	2,56	3,00	2,27	2,60
Mf	2,52	2,33	2,20	2,21	1,51
$R_{>92\mu}$ %	14,2	18,3	6,9	19,9	18,0
$R_{>200\mu}$ %	1,6 0,9	2,5 0,9	0 -	2,2 0,9	0 -
F %	4,1	2,8	3,2	2,3	3,4
T_c calculée en °C	1507	1596	1545	1565	1565
T_c Trouvée " "	1500	1571	1526	1545	1582
Dif. en°C	+7	+25	-19	-20	+17

Crus ref.	6	7	8	9	10
Lsf	92,0	98,5	98,5	90,6	93,3
Ms	2,41	2,82	2,80	3,40	2,43
Mf	1,60	1,69	1,71	2,50	2,05
$R_{>92\mu}$ %	17,9	20,2	22,7	16,5	17,6
$R_{>200\mu}$ %	0 -	0 -	1,3 0,9	0 -	0 -
F %					
T_c calculée en °C	1441	1634	1643	1590	1545
T_c Trouvée " "	1462	1622	1662	1568	1534
Dif. en °C	+21	-12	+19	-22	-11

L'application de cette fonction a des procédés avec des paramètres connus et fixes permet de la ramener a un nombre de variables plus petit selon les circonstances.

Quand la valeur de $R_{>200\mu}$ est plus grande que 2%, nous avons essayé de déterminer comment réagit sa fraction calcaire $R_{>200\mu}$ quand le calcaire qui la compose est à haut titre (supérieur a 90%).

En introduisant un 5% de particles de calcaire du 95% plus grandes que 200 microns a un cru aux caractéristiques suivantes Lsf = 90% Ms = 2,3, Mf = 2,0 et F = 2,5% avec une Tc de 1.450°C, il a été clinkérisé à différentes températures. La valeur de la chaux libre résiduelle en fonction de la T° est exprimé sur la figura n° 3.

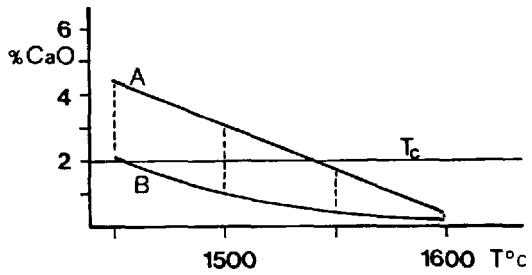

Fig. n° 3. A- Courbe de la diminution de la chaux libre du cru avec $R_{>200\mu}$ et T_c 1.450°C en fonction de la température.

B- Courbe de la diminution de la chaux libre du cru avec $R_{>200\mu} = 0$ en fonction de la température.

De ces résultats on peut déduire que quand la température atteinte par le clinker dans une installation mesurée par le procédé proposé, est plus grande que 1.550°C, le $R_{>200\mu}$ du cru peut être relativement haut ce qui confirme les résultats de Heilmann (1).

La valeur de l'accroissement de ΔTc du a la valeur de $R_{>200\mu}$ quand le calcaire qui la compose a >90% en CO_3Ca peut être exprimée a peu pres par la fonction suivante:

$$T_c = 31{,}6.R_{>200\mu}.\alpha.\left[1-(T_m-1450).6.10^{-3}\right] \quad [6]$$

Etant α la fraction du calcaire exprimé a tant pour 1, et Tm la température du matériel.

V - Evaluation de la température maximum equivalente atteinte par le clinker dans un four donné.

Malgré tout les limitations qu'il y a pour trouver cette température nous croyons qu'il existe una énergie thermique qui peut etre mesurée uniquement a travers la chaux libre résiduelle, qui est équivalente à celle donnée dans l'essai en laboratoire et que nous rapportons à la température maximum atteinte a temps constant.

Nous avons pris comme composition chimique de référence celle qui correspond au clinker obtenu parce qu'elle est la plus proche de celle de la clinkérisation et aussi de sa teneur en fondants. Quant à la composition granulométrique nous avons pris comme point de repère celle du cru à son entrée dans l'échangeur. Ceci bien que n'étant pas rigoureusement exact, est techniquement utile.

La séquence d'opérations a effectuer, en somme, pour évaluer quelle est la température maximum équivalente dans une ligne de proces est la suivante:

- Une fois obtenu un régime de marche en équilibre et stable dans le proces, on extrait un échantillon représentatif du cru (A) qui entre dans l'échangeur (moyenne de plusieurs intervalles pendant une demie-heure). On y détermine la composition chimique par moyen des méthodes indiquées, les pourcentages de R>92 microns, R>200 microns et sa fraction de chaux soluble en acide et la courbe de clinkérabilité sur trois points T° 1.500, 1.550 et 1.600°C.

- Au bout du temps pendant lequel ce matériel a été clinkérisé, on extrait un échantillon représentatif du clinker obtenu (B) et on détermine sa composition chimique et sa chaux libre par moyen des mêmes méthodes et on déduit les valeurs: Lsf, Ms, Mf et le somme de fondants F. On déduit sa température de clinkérabilité par moyen de la fonction polynômique que nous avons rapportée avec les valeurs R>92µ et R>200µ correspondantes au cru (A) et on déduit les valeurs de CaO à différentes températures au moyen de l'équation [1] avec les paramètres correspondants donnés dans le tableau I et on obtient le diagramme de la figure n°[4]

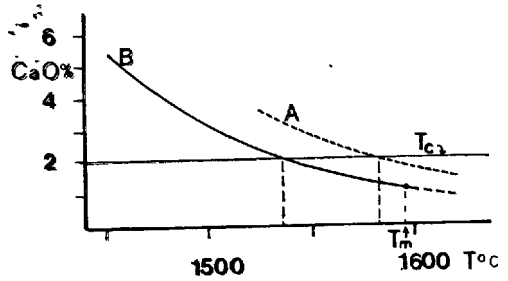

Fig.n° 4 B- Courbe de clinkérabilité du cru qui a la composition chimique du clinker et les valeurs de R>92µet R>200µ qui correspondent au cru qui entre dans l'échangeur.
A- Courbe de clinkérabilité qui correspond au cru qui entre dans l'échangeur.
Tm- Température équivalente atteinte par le clinker/ dans la zone de clinkérabilité du four industriel.
La déviation standard pour la mesure de la température Tc est de ± 20°C.

Celui-ci permet de déduire la valeur de la température maximum équivalente en interpolant la valeur de sa chaux libre dans sa courbe correspondante.

Expérimentalement on en est arrivé à la conclusion que la concentration de flamme optimum est obtenue quand la température maximum équivalente est proche a 1.600°C. Le dépassement de cette température comportera conditions de marche forcée.

VI - Conclusions.

1- On établit les conditions et les méthodes d'analyse pour obtenir l'exactitude et la reproductibilité convenables spécialement a la détermination de la silice par la méthode gravimétrique classique modifiée par l'auteur.

2- On a trouvé une fonction généralisée pour déduire la valeur de la température de clinkérabilité des crus dans les marges des compositions usuelles avec une erreur de ± 20°C et une fonction exponentielle pour déduire la teneur en chaux libre en fonction de la température du matériel et dè la température de clinkérabilité du cru.

3- Il est possible de déterminer la valeur d'une température maximum équivalente atteinte par le clinker dans la zone d'une installation donnée. Cette connaissance ainsi que celle de la température du clinker permet l'analyse du procès: évaluer indirectement le degré de concentration de la combustion, la valeur de l'échange "flamme-clinker" et la température de clinkérabilité maximum possible du cru pour tirer le plus grand profit de l'énergie en jeu.

Je suis reconnessant a Asland S.A pour l'aide qu'elle à bien voulu m'apporter.

BIBLIOGRAPHIE

(1) T.HEILMANN (1952). The influence of the fineness of cement raw mixes on their burnability. Symposium of London. 1952. (i).

(2) BLAISE,R. MUSIKA,S.N. and TIEDREZ,H. (1971) Nouvelle méthode de déterminarion cinétique de l'aptitude a la cuisson d'un cru de cimenterie. Rev.Mater. Nr. 674/675, S. 287-295 (f).

(3) KONDO,R. (1960). Reaction Velocity in portland cement clinker formation. Fourth International Symposium on the Chemistry of Cement. Washington DLC. 1960. (i).

(4) SULIKOWSKI, J.P. (1968). Burnability of Raw mixes. Proceedings of the Fifth International Symposium on the Chemistry of Cement. Tokyo, 1968. (i).

(5) KOCH,H. REY G. and BECKER,F. (1974). A statistical model for determining the burnability of cement raw mixes. VI International Symposium Congr. on the Chemistry of Cement.Moskau. 1974. Suppl. Pap. 31, Sect. I-4. (i).

(6) LUDWIG,U. and RUCKENSTEINER, G. (1973). Einflusse auf die Breunbarkeit von Zementrohmehlen. Forschungsbericht des Landes Nordrhein -Westfalen Nr. 2372. Westdeutscher Verlag.Opladen 1973. (g).

(7) CRISTENSEN,N.H., SMIDTH F.L. and Co. (1978). Burnability of Cement raw mixes at 1.400°C. The effect of the Chemical composition Cement and Concrete Research. Vol.9 p.p. 219-228, 1979 and ibid. Vol. 9 p.p. 285-294.

(8) RAUSCHENFELS, E. (1976). Clinkerability of Cement raw meal. Cement-Kalk-Gips, n° 4, 1976 (g).

(9) CHALMERS R.A. (1964) Chemical Analysis of Silicates. The Chemistry of Cements. Vol. II- H.F.W. TAYLOR. Academic press. London and New-York (i).

(10) GOMÁ,F. (1975) Acerca de la determinación gravimétrica de la sílice. Tesis doctoral Universidad de Barcelona. Dep. de Química Analítica. 4-12-75 (e). Resumen CEMENTO-HORMIGON, n° 505, Marzo 1976. Barcelona (e).

(11) GOMÁ, F. (1976) Nuevo método gravimétrico, esencialmente modificado, para la determinación de sílice en silicatos atacables por ácido. Instituto Eduardo Torroja. Materiales de Construcción n° 164. 1976. (e).

The pore structure and the grindability of clinkers

La structure poreuse et la broyabilité des clinkers

I.F. PETERSEN, F.L. Smidth & Co. A/S Vigerslev Alle 77, DK-2500 Valby Copenhagen, Denmark.

RESUME : On a recherché l'influence de la structure poreuse des clinkers sur leur broyabilité, les essais ayant porté sur des clinkers sans poussières. Des mesures quantitatives au microscope et des mesures de la broyabilité ont été utilisées. Pour un broyage à 3000 Blaine, on a observé une réduction de l'énergie de broyage, lorsque la surface spécifique des pores augmente.

En utilisant un modèle basé sur la physique capillaire, on a montré que la structure des pores des clinkers dépendait de l'importance de la phase liquide, de la finesse des cristaux de C_3S et de C_2S, et des espaces intercristallins. Des expériences faites pour confirmer le modèle ont décelé une cause supplémentaire : la coalescence des cristaux de C_3S. Ces effets sont, dans une large mesure, commandés par la composition chimique et minéralogique du cru, et par sa finesse de broyage.

L'influence de la poussière des clinkers a aussi été examinée.

SUMMARY: The relationship between clinker pore structure and grindability has been investigated, for clinker that do not contain clinker dust. Quantitative microscopy and grindability determinations were the techniques employed. A decrease in the specific power requirement for grinding clinker to 3000 Blaine was observed when the specific surface area of the clinker pore system increased.

Using a model based on capillary physics, it is possible to attribute changes in the clinker pore system to a combination of changes in melt content, fineness of C_3S and C_2S crystals and space between these crystals. Experiments associated with the model indicate an additional effect, caused by a coalescence of C_3S crystals. These effects are to a large extent dependent on chemical and mineralogical composition together with fineness of the raw mix.

The effect of the content of clinker dust on grindability is also discussed.

INTRODUCTION

Clinker grindability is a relative measure of the ability of a given clinker to resist grinding forces. Previous investigations by Gouda (1) and by Butt et al (2) have emphasized the importance to clinker grindability of melt content, clinker microstructure and especially clinker pore structure.

In this study the relationship of the pore structure of industrial clinker nodules to their grindability is investigated microscopically by determination of the specific surface of the pore system.

The clinker pore system results from the processes within the burning zone, where the charge, consisting of crystals and melt, is agglomerated. Therefore, factors affecting the specific surface of the clinker pore system are conveniently elucidated by a model which considers the clinker nodules as agglomerates in which the liquid phase has been frozen.

EXPERIMENTAL

The grindability index used here is the specific power requirement (kWh/t) for grinding the clinkers to a specific surface of 3000 Blaine in a standardized grinding test. This test consists of grinding a batch of 20 kg clinker in a tumbling mill, using three different charges of grinding media simulating three chambers. Two ball charges and one cylpebs charge are employed. The first ball charge is used until 85 wt % of the ground material is finer than 0.5 mm; the second ball charge is then used until 85 wt % of the ground material is finer than 0.25 mm, and finally the cylpebs charge is used until the desired fineness is attained.

The specific surface area of the clinker pore system is determined microscopically in clinker polished section. Two measurements are carried out: A point count of the porosity ε, and a measurement of N_L (mm^{-1}), where N_L is the number of intersections of the pore surface with a random test line of unit length. According to DeHoff and Rhines (3) the specific pore surface area O_s (mm^2/mm^3) equals:

$$O_s = \frac{2\,N_L}{1-\varepsilon} \qquad (1)$$

Seven industrial clinker samples ranging from ordinary Portland clinkers to special types including white clinkers were investigated by grindability testing and microscopy. These clinker samples consisted of pure clinker nodules and contained no clinker dust finer than 0.5 mm.

Fig. 1 shows the results. A decrease in the specific power consumption for grinding to 3000 Blaine is observed with increasing specific clinker pore surface.

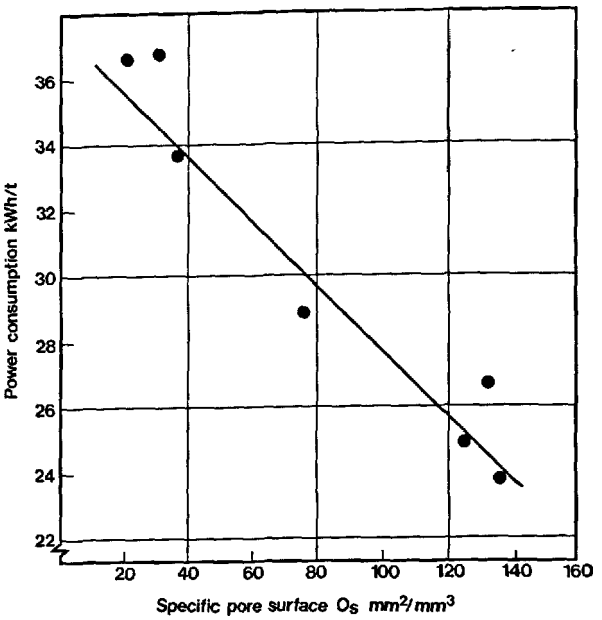

Fig. 1 - Power consumption for grinding clinkers to 3000 Blaine versus specific pore surface of clinkers.

PORE SYSTEM MODEL

To identify parameters influencing the specific pore surface of clinkers, it is appropriate to consider a model. The basic assumption in this model is that the pore system in the cooled clinker nodules can reflect the pore system at high temperature in the burning zone. At high temperature, the clinker nodules may be considered as agglomerates consisting of solid particles (CaO, C_2S and C_3S crystals) and melt phase, where the melt more or less fills out the void volume between these crystals.

Microscopic investigations of clinkers indicate that the melt is effective in wetting the crystals. It is, therefore, appropriate to analyse the specific pore surface in an agglomerate consisting of solid particles and a wetting liquid. In such an agglomerate there will exist a difference in pressure between the surrounding gas phase and the liquid, and the pressure will be lowest within the liquid itself. Provided that changes in liquid volume can be carried out reversibly, isothermally, and without compression, the following equation is a consequence of the first law of thermodynamics, as shown by Morrow (4).

$$-P_c \cdot dV_\ell = \gamma_{\ell v} \cdot d(A_{\ell v} + \cos\theta \cdot A_{pv}) \qquad (2)$$

P_c, the capillary pressure, is the difference in pressure between gas and liquid phase, V_ℓ is the liquid volume, $\gamma_{\ell v}$ is the specific surface energy of the liquid-gas

surface, $A_{\ell v}$ is the area of the liquid-gas surface, A_{pv} is the area of the solid-gas surface, Θ is the contact angle of the liquid against the solid and d denotes differential change.

The liquid volume V_ℓ within the agglomerate is appropriately expressed by means of the liquid saturation S_ℓ, defined as the fraction of the void volume between the solid particles occupied by the liquid.

$$V_\ell = V_p \cdot \frac{\emptyset}{1-\emptyset} \cdot S_\ell \qquad (3)$$

V_p is the volume of solid particles and $\emptyset$ is the void fraction in the packing of the solid particles.

Within an agglomerate with a low liquid saturation the liquid is found in discrete liquid bridges between the particles. In this case, changes in liquid volume cannot be considered reversible. At a certain liquid saturation S_ℓ^*, termed the irreducible liquid saturation, the liquid phase within the agglomerate becomes continuous. From S_ℓ^* up to a liquid saturation close to unity, it is realistic, at least to a first approximation, to consider changes in the liquid volume as reversible and thus to use expression (2). Within this range of liquid saturation, the capillary pressure varies little with liquid saturation, and may be considered constant (cf. for example measurements by Dodds and Lloyd (5)). According to Rumpf (6), the capillary pressure may be calculated:

$$P_c = \gamma_{\ell v} \cdot \frac{1-\emptyset}{\emptyset} \cdot \frac{A_p}{V_p} \cdot \cos\Theta \qquad (4)$$

A_p is the surface area of the solid particles; thus A_p/V_p becomes the specific surface area of the solid particles.

Since clinker melt wets the crystals effectively, the contact angle Θ must be small; thus $\cos\Theta$ must be close to unity. Use of this value of $\cos\Theta$ and substitution of expressions (3) and (4) into (2) give:

$$-A_p \cdot dS_\ell = d(A_{\ell v} + A_{pv}) \qquad (5)$$

The quantity $(A_{\ell v}+A_{pv})$ is the surface area of the pore system, and can be obtained by integration of (5) using S_ℓ^* and the corresponding surface area $(A_{\ell v}^*+A_{pv}^*)$ as lower limits. Integration gives after rearrangement:

$$\frac{A_{\ell v} + A_{pv}}{A_p} = K - S_\ell \qquad (6)$$

Where K is given by:

$$K = \frac{A_{\ell v}^* + A_{pv}^*}{A_p} + S_\ell^* \qquad (7)$$

Equation (6) describes the ratio of the pore surface to the surface of solid particles, as a function of the liquid saturation.

The magnitude of the dimensionless quantity K has been estimated by simple calculations. The system considered consists of equally-sized spheres, varying in packing between the two extremes: Three-dimensional close packing and simple cubic packing as described by Mayer and Stowe (7). In these packings, liquid bridges corresponding to the irreducible liquid saturation have been introduced at particle contacts, using the circle approximation for the form of the liquid bridges as described by Pietsch and Rumpf (8). The calculated values of K, between 0.84 and 0.88, indicate that K, at least to a first approximation, may be considered constant.

EXPERIMENTS ASSOCIATED WITH MODEL

In order to investigate the model, six industrial raw meals produced for the manufacture of Portland cement clinkers were burned at 1400°C for 30 minutes in the laboratory. The surface of the pore system, and that of the CaO, C_2S and C_3S crystals considered as single crystals, were measured using the line-intercept method previously mentioned. These measurements make it possible to calculate the ratio of the pore surface to the surface of the crystals. The liquid saturation was determined based on point counting of interstitial phase and pores. A plot of the pore surface relative to the surface of the crystals is shown in fig. 2.

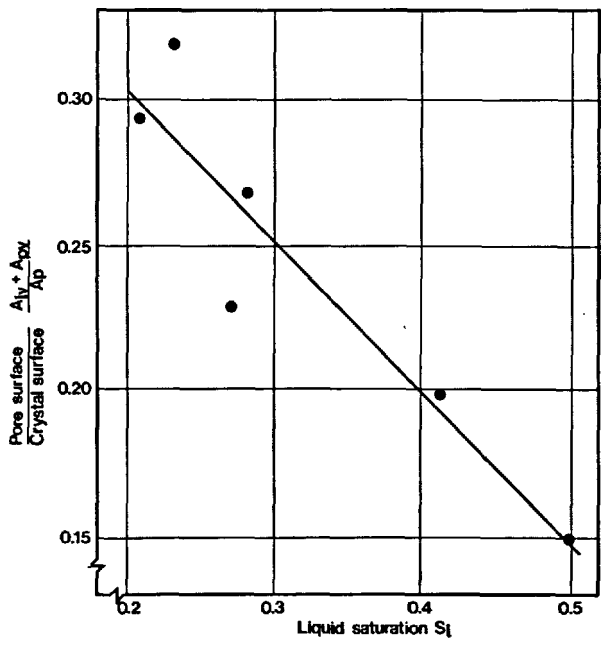

Fig. 2 - Ratio of pore surface to crystal surface versus liquid saturation.

A linear regression analysis on the data in fig. 2 gave the following expression with correlation coefficient 0.93:

$$\frac{A_{\ell v} + A_{pv}}{A_p} = 0.52 \cdot (0.79 - S_\ell) \qquad (8)$$

The relationship of this result to the corresponding expression (6) from the model may be interpreted in the following way: The ratio of the pore surface to the surface of the crystals is a linear function of the liquid saturation, as predicted by the model, but the derivative with respect to S_ℓ is found to be -0.52 and not -1. This can be explained as a result of a coalescence of crystals within the clinker, reducing the surface area of these crystals. This sintering effect appears to be especially important for C_3S-crystals. This is supported by numerous observations from clinker polished sections showing C_3S areas of irregular shape, indicating that a growing-together of several individual C_3S crystals has occurred. Finally the quantity 0.79 in expression (8) is close to the values of K found in the simple model calculations.

Now it is possible to obtain an expression for the specific surface of the clinker pore system. The total condensed volume within a clinker nodule is the sum of the volumes of solid crystals V_p and of melt phase. Using expression (3) this sum becomes:

$$V_p + V_\ell = V_p \cdot (1 + \frac{\emptyset}{1-\emptyset} \cdot S_\ell) \qquad (9)$$

By multiplication by A_p on both sides of equation (8) followed by division by expression (9), the specific surface of the pore system O_s becomes:

$$O_s = \frac{A_{\ell v} + A_{pv}}{V_p + V_\ell} = 0.52 \cdot \frac{A_p}{V_p} \cdot \frac{(0.79 - S_\ell)}{(1 + \frac{\emptyset}{1-\emptyset} \cdot S_\ell)} \qquad (10)$$

From expression (10) it is apparent that the specific surface of the clinker pore system is influenced by the specific surface of the crystals A_p/V_p, the liquid saturation S_ℓ and the void fraction $\emptyset$ between the crystals.

The more common quantities clinker porosity (ε) and wt%(L) of melt phase can be introduces by the following relations:

$$\varepsilon = \emptyset \cdot (1 - S_\ell) \qquad (11)$$

$$S_\ell = 1.16 \cdot \frac{1-\emptyset}{\emptyset} \cdot \frac{L}{100-L} \qquad (12)$$

In equation (12) a density of 2.8 g/cm^3 for clinker melt and an average density for 3.25 g/cm^3 for the crystals is assumed.

DISCUSSION

Data given by Butt et al (2) show that an increase in clinker porosity occurs when the amount of melt is reduced. Using the value 0.43 for $\emptyset$ found from these data and a combination of equation (10) and (12), it is possible to calculate expected values for the specific surface of the clinker pore system as a function of the amount of clinker melt and of the fineness of the crystals. By means of the data given in fig. 1, results from these calculations can be used as an aid in the prediction of clinker grindability (fig. 3).

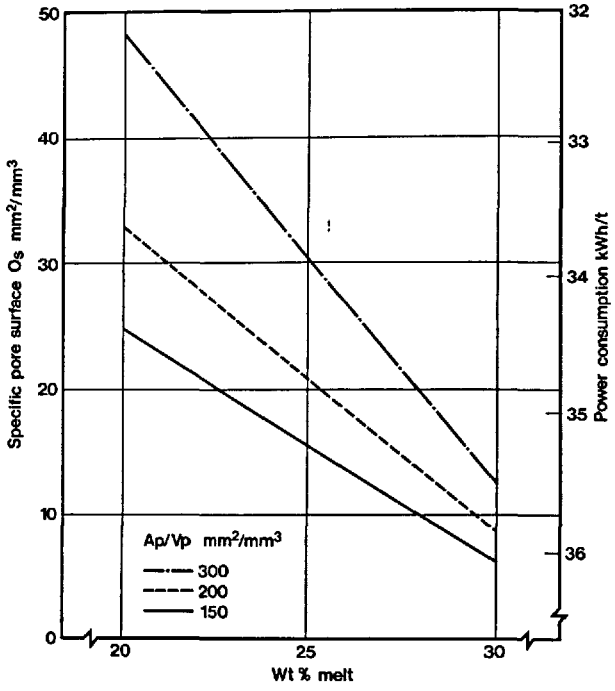

Fig. 3 - Expected specific pore surface and grindability of clinker as function of wt % melt for various crystal finenesses.

The various values for the specific surface of crystals A_p/V_p (300, 200 and 150 mm^2/mm^3) used in fig. 3 are in accordance with microscopic investigations of ordinary Portland cement clinkers, and correspond to Sauter mean diameters of 20, 30 and 40µm respectively. The range of melt contents corresponds to values obtained with Lea and Parkers formulae (9) using compositions corresponding to ordinary Portland cement clinkers.

The crystal fineness has the strongest influence on the specific surface of the clinker pore system and thereby on grindability.

An increase in specific crystal surface increases the specific pore surface and reduces the power requirement for grinding. A reduction in the amount of melt has a similar, but less marked, effect.

It seems reasonable to expect finer crystals within the clinker when the fineness of the raw mix is increased. Very small C_3S and C_2S crystals are obtained in special-type clinkers with silica ratio about 10, for

which the raw mix has to be ground extremely fine in order to compensate for the otherwise difficultly burnable material.

The mineralogy of the raw mix also influences the specific surface of clinker crystals. The finest crystals are in general obtained by burning of a marl-type raw mix, which nature has provided with a high degree of homogeity in distribution of the components. In the investigation from which fig. 2 was derived, the specific surface of clinker crystals decreased from 200 mm^2/mm^3 to 150 mm^2/mm^3 when the raw mix changed from a marl- to a sandy type.

The amount of melt formed is influenced mainly by the chemical composition of the raw mix, with the silica ratio as the most important parameter. When the silica ratio increases, the amount of melt decreases and according to fig. 3 the power consumption for clinker grinding decreases. However, burnability and kiln operation considerations set a limit to the benefit obtainable from this effect, because decreasing the amount of melt without simultaneously ensuring fine crystals will increase the chance of a dusty clinker product.

Hitherto, the investigations and the discussion concerning clinker grindability have dealt with nodule clinkers, which contain no clinker dust finer than 0.5 mm. However, when clinker becomes dusty, grindability will suffer. For the first stage grinding with large-size balls, the fine clinker actually requires less energy than does coarse clinker, as the normal criteria for transferring the material to final stage grinding are based on coarse sieve residues. However, as a consequence of the reduced extent of grinding in the first and second chambers, the material leaving the second chamber actually becomes coarser, with larger residues on sieves finer than, for instance, 0.25 mm; as a result the power consumption in the third chamber, for grinding to 3000 Blaine, increases. Table I, which summarizes the results obtained in separate grinding tests of two size fractions of the same clinker, shows that the total power consumption for grinding to 3000 Blaine is about 25% higher for the fine clinker fraction than for the coarse one.

TABLE I

Size fraction, mm	-8 +0.5	-0.5
kWh/t in chamber I+II	10.0	2.6
% residue on 0.045 mm after chamber II	53	87
kWh/t in chamber III	24.9	41.4
Total kWh/t to 3000 Blaine	35.0	44.0

As long as the amount of clinker dust is modest, the increase in total specific power requirement for grinding to 3000 Blaine is not great, because the decrease in power requirement in the first stage of grinding partially counterbalances the increase in the third chamber. However, with high dust content a drastic increase in total power requirement is to be expected. Particularly at plants with major variations in content of clinker dust, the specific power consumption in the cement mills will increase, as in this case it is not possible consistently to take advantage of a low specific power consumption in the first chamber.

CONCLUSIONS

The fineness of C_3S and C_2S crystals in well-burned nodule clinker, together with the amount of melt phase, are important parameters for the structure of the clinker pore system and hence for the power requirement for clinker grinding. To optimize clinker grindability, it is essential to avoid too large an amount of fine-grained clinker dust.

BIBLIOGRAPHY

1. - G.R. GOUDA (1979), "Effect of clinker composition on grindability", Cement and Concrete Research, Vol. 9, pp. 209-218.

2. - J.M. BUTT, V.M. KOLBASOV and G.A. MELNIEKIJ (1974), "Zur Wechselbeziehung zwischen der Porenstruktur und Mahlbarkeit von Klinkern aus verschiedenen Brenn- und Abkühlungsverfahren", Zement-Kalk-Gips, 27, No.1, pp. 27-32.

3. - R.T. DEHOFF and F.N. RHINES (1968), "Quantitative microscopy", Chap. 4, pp. 87-91.

4. - N.R. MORROW (1970), "Physics and Thermodynamics of capillary action in porous media", Industrial and Engineering Chemistry, 62, No. 6, pp. 32-56.

5. - J.A. DODDS and P.J. LLOYD (1971), "A model for the void structure in multicomponent sphere packs applied to capillary pressure curves", Powder Technology, 5, pp. 69-76.

6. - H. RUMPF (1958), "Grundlagen und Methoden des Granulierens", Chemie-Ingenieur Technik, 30, No. 3, pp. 144-158.

7. - R.P. MAYER and R.A. STOWE (1965), "Mercury porosimetry - Breakthrough pressure for penetration between packed spheres", Journal of Colloid Science, 20, pp. 893-911.

8. - W. PIETSCH and H. RUMPF (1967), "Haftkraft, Kapillardruck, Flüssigkeitsvolumen und Grenzwinkel einer Flüssigkeitsbrücke zwischen zwei Kugeln", Chemie-Ingenieur Technik, 39, No. 15, pp. 885-893.

9. - F.M. LEA and T.W. PARKER (1935), "The quarternary system CaO - Al_2O_3 - SiO_2 - Fe_2O_3", Building Research Technical Paper, No. 16, H.M.S.O., London.

Producing Portland cement clinker using blast-furnace barric-manganese slag

Utilisation de laitiers contenant BaO et MnO, dans la fabrication du clinker de ciment Portland

I.S. VALKOVA, Senior Research, Associate, Master of Science, Institute for Scientific Researches of Construction Materials, Sofia, Bulgarie.

R.G. DOGANDZHIEVA, Senior Research Associate, Institute for Scientific Researches of Construction Materials, Sofia, Bulgarie.

SUMMARY : The investigations conducted show that slags containing basic oxides necessary to form portland cement clinker - CaO, Al_2O_3, SiO_2, Fe_2O_3 and in some cases also alloying oxides BaO and Mn_2O_3, are valuable raw material for portland cement clinker.

The high-temperature treatment at which the slags have been subjected permits the same to be equalized with the raw cement mixture at temperature 1000-1100°C, i.e. when the interaction in the solid phase is already completed with formation low-basic clinker minerals.

It is proved that, introducing of slags both in vitreous, or in crystalline state, intensifies clinker formation and in the same time the processes of lime saturation are accelerated and the formation of clinker minerals is relieved. The presence of BaO and MnO in the slag contributes for the increase and modification of alite crystals, which leads to increased strength values of the cement.

RESUME : Des essais ont montré que des laitiers contenant les oxydes de base nécessaires à la fabrication du clinker de ciment portland (CaO, Al_2O_3, SiO_2 et Fe_2O_3) et dans certains cas contenant aussi des mélanges des oxydes de Baryum et de Manganèse, peuvent être utilisés comme crus des ciments Portland.

La haute température à laquelle les laitiers ont été soumis, au cours de leur fabrication, les rend équivalents aux crus chauffés à la température de 1000 à 1100°C; notamment lorsque les interactions entre phases solides sont déjà achevées, avec formation d'un clinker faiblement basique.

Il a été montré qu'en utilisant du laitier à l'état vitreux, ou à l'état cristallisé, la formation du clinker était activée et qu'en même temps le processus de la saturation en chaux était accéléré et la formation des composants minéraux du clinker aidée. La présence de BaO et de MnO dans le laitier augmente et modifie la cristallisation de l'alite, ce qui conduit à une augmentation des résistances du ciment.

One of the effective directions, ensuring considerable economy of the consumption of fuel (solid or liquid) and electric power for the portlant cement production and increase of the rotary furnace activity, is the use of slags as raw-material for the portland cement clinker production, by feeding directly the cold end of the furnaces.

The insuflation of the grinded slag (used in pure form or as a mixture) in the hot end of the furnace, which method (way of feeding) has been patented in Germany as early as 1929, and the first realization is put into practice in 1944, in the cement plant in Maastricht - Holland. On account of a number of difficulties this method had not been applied to very great extent.

In SSSR, the additional feeding of the furnaces has been applied first in Giprocement by E.I. Tsivileva (1), and at this, the additional component having been fed at the upper end of the furnace. Later, this practice was developed in the scientific works of I.V. Kravtchenko and coll. (2, 3). Their method treats the additional feeding of the furnaces, beginning from their cold end, in case of wet production way.

The aim of our investigations was the study of the processes of the clinkerforming, in case of additional feeding of the furnaces, beginning from the cold end, with blast furnace slag, using the dry method for portland cement production.

At the time of the slag feeding, at the cold end of the furnace, the joint baking of the materials is being effected, which are not been homogeneized in advance, and differ by their chemical composition, in connection of which the following factors have been studied :

- The influence of the phase and chemical composition of the blast furnace slag on the processes of the clinkerforming;
- The influence of the fed quantity of slag on the processes at the moment of the baking of the portland cement clinker and the properties of the portland cement clinker.

For the carrying out of the experimental work are used blast furnace granulated and non-granulated slag with varied make-up, limestone, marl and pyrites slags, the characteristics of which are given on TABLE 1.

Blast furnace slags differ in chemical as well as in phasal composition. Thus, furnace slag - 1 contains BaO and MnO, but slag - 2 does not contain these oxides. The petrographical analysis of slags shows the following :

Blast furnace granular slag - 1. The predominant component of the slag, in quantity 89-93 per cent, represents glass of homogeneous composition - compact sometimes porous with N - 1,68;

Blast-furnace non-granular slag-1. By contrast with the granular slag, here the crystal phase is much more and gets to 40-45 per cent. Predominant mineral here are bicalcium silicate and olchamide in dendritic form and size to 100 microns. Granules of melilite and alabandite are observed in some places.

Blast-furnace granular slag-2. By contrast with slag - 1, slag - 2 contains a great part of crystal phase 25-30 per cent. It is presented predominantly by melilite. The glass phase is homogeneous.

Blast-furnace non-granular slag - 2. By contrast with non-granular slag-1, blast-furnace non-granular slag - 2 consists predominantly of crystal phase, the quantity of which gets to 60-70 per cent. The basic mineral which it contains are: ochermanite and gelenite, in the form of rectangular and square tablets with light-blue interference colouring. Dendrites of oldhamite and larnite crystals are observed in some places.

Some raw compounds characterized by the same chemical composition and the following module characteristics: KH = 0,921, n = 2,70, p = 1,60 were prepared in order to investigate the influence of the phasal and chemical composition of the blast-furnace slag on its interaction into the portland cement raw materials.

The mixture was ground in a laboratory ball mill until 10 % residuum on sieve with 4900 mesh/cm^2 was obtained. Then was added to it slag in quantity 10 per cent of the weight of the raw flour. Some briquettes were made out of the mixture obtained and they were baked in a laboratory supercantal furnace at 1100; 1200; 1300; 1400 and 1450°C and an isothermic delay of two hours.

It is known that the reactivity of the raw material mixture depends on a number of factors, mostly on the physicochemical nature of the initial raw material; the dispersion of the blend, the raw material mixture; on the temperature and duration of baking; on account of which, all enumerated factors, during the experiments carried out, were equal except the chemical and phasal composition of the feeding slag. Table 2 shows the kinetics of the combined calcium oxide, depending of the kind of feeding slags, the chemical composition of which is shown in Table 1.

From the data in Table 2 it can be seen that, when introducing the blast-furnace slags into the raw material mixture, the kinetics of the clinkerforming is accelerated and a considerable difference is observed in the annealing of the calcium oxide.

In the raw material mixtures containing slags, the quantity of the free CaO varies

TABLE I

Chemical composition of the starting materials in %

Materials	Ign.loss	SiO_2	Fe_2O_3	AL_2O_3	CaO	MgO	BaO	MnO	SO_3	Na_2O	K_2O
Limestone -1	42,99	1,26	0,36	0,26	54,40	0,21	-	-	-	0,40	0,09
Limestone -2	31,06	2,56	0,80	1,86	38,93	0,40	-	-	-	0,92	0,45
Marl	25,15	28,96	2,83	8,67	31,05	1,43	-	-	-	0,51	1,40
Pyrite dross	2,38	18,28	60,27	5,69	1,32	1,00	-	-	9,81	0,45	0,80
Bl.furn.sl.gr.-1	-	34,19	0,30	8,94	40,08	2,48	5,66	2,9	3,9	0,86	0,67
Bl.furn.sl.gr.-2	-	34,46	1,96	8,70	42,69	4,55	-	-	4,17	0,79	0,82
Bl.furn.sl.nongr. - 1	-	35,80	0,60	8,79	40,67	2,29	4,8	1,17	3,9	1,29	0,70
Bl.furn.sl.nongr. - 2	-	32,60	1,81	9,28	42,84	5,71	-	-	5,48	0,72	6,48

between the limits of 18,23 to 15,90 per cent. Simultaneously, the raw material mixtures not containing slags, have a content of free CaO, getting to 23,67 per cent, which can be explained by the fact that the slag melting temperature, and especially that of slag - 1, is considerably lower (850-900°C) than that of the raw material mixture. From the data in Table 2 it can be seen that this regularity is kept with the further increase of temperature.

The phasal composition of the slags used does not exert a particular influence on the kinetics of clinkerforming. The combining of the free CaO is almost equal when introducing granular as well as crystal slags (Table 2).

The chemical composition of the slags used exerts considerable influence on the combining quickness of CaO. Thus, in a raw material mixture containing slag-1, the combining of CaO passer faster than in mixtures containing slag - 2, which can be explained

TABLE II

Assimilation of the CaO according to the art the slag

№	Sort slag	% slag	Free lime, %				
			1100°C	1200°C	1300°C	1400°C	1450°C
1.	----------	0	24,90	23,67	16,04	1,75	0,70
2.	Bl.furn.sl.gr. - 1	10	24,89	15,99	13,48	0,60	trace
3.	Bl.furn.sl.nongr.- 1	10	24,81	15,90	13,50	0,68	trace
4.	Bl.furn.sl.gr. - 2	10	24,70	18,23	14,01	0,82	trace
5.	Bl.furn.sl.nongr. - 2	10	24,73	18,15	13,90	0,88	trace

with the lower melting temperature of slag-1 in comparison with the melting temperature of slag - 2 (1000-1100°C), which brings an earlier appearance of a liquid phase and accounts for the acceleration of clinker forming.

Comparing the results of the petrographic investigations, one sees that the produced clinkers from mixture containing slag - 1, are characterized by a more clearly expressed crystallization of the alite and the belite, the crystals of which are with regular crystallographic outlines. Crystals with the size of about 40-60 microns predominate.

The physical and mechanical testings of the cements obtained after grinding of the clinkers, with an addition of 5 per cent gypsum stone and a specific surface 4000 cm^2/g show that, according to their characteristics, they are almost identical

The results of the testing of the specimens

from the cement flour with density according to norm and sizes 2 x 2 x 2 cm are given on Table 3.

TABLE III

Phasical and mechanical characteristics of the cement

No.	Specific surface cm^2/g	Norm density %	Regime of preserving under water											
			Strength of the pressure, kg/cm^2, after under water											
			1 day	3 days	7 days	28 days	3 mnths	6 months	1 year	4 hours	28 days			
1.	4020	28,5	470	650	720	900	1290	1310	1400	373	681			
2.	4050	29,0	485	667	790	920	1294	1340	1450	380	708			
3.	4060	30,0	478	665	790	950	1300	1350	1470	395	700			
4.	4040	29,0	475	657	713	880	1280	1318	1445	388	683			
5.	4010	30,0	469	630	700	893	1250	1313	1400	375	688			

REMARK: The numbers in this Table correspond to those in Table II.

From the data in Table 3, one can see that the cements on the basis of clinkers with utilization of slag-1, show higher strength of pressure than these utilizing slag-2. Prabably that is due on the influence of the introduced with slag-1 oxides: Mn_2O_3 and BaO, which, at liquid phase baking, contribute to the increase of the alite phase quantity of a clinker with increased activity.

In such a manner, the investigations carried out show that blast furnace granulated slags represent a valuable raw material for the portland cement clinker production and their utilization will permit the increase of the activeness of his production thanks to the intensification of the processes of the baking. The introduction of the complex of oxides BaO and Mn_2O_3 in the the raw material mixture, corresponds to the increasing of the alite quantity in the clinker, the enlarging of its crystals and increasing of the strength indices of the cement.

At the examining the influence of the introduced slag on the processes of the forming of the clinkers and the characteristics of the portland cement clinker, are utilized the same raw materials (Table 1). The blast-furnace slag - 1 is introduced in quantities 5, 10, 15 and 20 per cent. The raw material mixture was prepared from the following modulus characteristics : KH = 0,92; n = 2,80; p = 1,65. The methods for the preparation of the raw material mixture and the baking of the clinker, are as described here above.

On Table 4 are given the data of the kinetics at the time of the combining the free calcium oxide. It is seen that with the increase of the slag from 5 to 20%, the speed of the CaO increases and at 1400°C, in the mixture containing slag, the free CaO is almost absent.

TABLE IV

Kinetics for the combining of free CaO

No.	Quantity of slag %	free CaO - %			
		1300°C	1350°C	1400°C	1450°C
1.	0	16,42	7,22	2,42	0,70
2.	5	10,67	3,43	0,85	0,35
3.	10	8,91	3,09	0,68	0,28
4.	15	7,80	3,00	0,42	-
5.	20	7,63	2,85	0,20	-

The petrographic analysis of the clinker obtained shows that the samples of clinker No. 1 (without slag) is of a non-uniform, granular structure, with mostly alite crystallization. The alite crystals are of an irregular form and sizes of 60 to 70 microns, average 40-50 microns. In almost all grains there are belite inclusions. The belite is found foremostly as inclusion and rarely as separate grains. The intermediate mass is about 15%, with the alumoferrite sensibly predominating.

Clinker No.2 (with 5% slag). In comparison with sample No.1, a crystallization with bigger crystals is watched (average 60-65 microns) and better formed crystals.

Clinker No.3 (with 10% slag). It is identical to sample No.2, with still larger crystallization.

Clinkers No.No. 4 and 5 (with 15 and 20% slag) are almost equal, with large crystallization, almost of alite type. The alite crystals with hypidiomorphic form and sizes to 120 microns. In some of them there are belite inclusions. The belite is presented in separate grains also, with sizes to 60 microns. Many pores.

From the petrographic analysis is seen that at introduction of slag the process of formation of clinkers is considerably intensified and the alite synthesis is accelerated. Apart of that, an enlargement of the alite and balite crystals is observed.

The activity of the clinkers, which are obtained through using slag, in comparison with the common clinkers, is almost equal (table 5).

TABLE V

The results of physical and mechanical researches in clinkers in laboratory petrol furnace

No.	Addition of slag	Specific surface cm/g	Norm density %	Time of hardening hour minute beging	Time of hardening hour minute end	Strength of pressure kg/cm^2 1 day	3 days	7 days	28 days	1 year
1.	0	4100	28	2-30	4-05	140	320	404	558	688
2.	5	4150	28	2-20	4-15	144	325	410	566	675
3.	10	4250	28	2-10	3-50	142	330	415	602	690
4.	15	3950	28	2-40	4-20	150	310	435	616	685
5.	20	4050	28	2-00	4-40	151	325	428	609	697

The intensifying influence of the slags at the time of the forming of the clinkers was examined in industrial conditions of plants working according to the dry and semidry ways, among which which, the furnaces with cyclone heat-exchangers, type "Humbold", "Polysius" and "Lepold". The high furnaces were consequently fed with different quantities of slag - from 5 to 25 per cent, as regards the clinker.

In plant conditions was established:

- full assimilation of the slag introduced;
- increase of the productivity of furnaces;
- considerable decrease of the specific consumption of fuel and electric power;
- bettering the structure and increase the hydraulic activity of the clinker.

CONCLUSIONS

1. It has been proved that the blast-furnace slags, containing the basic oxides necessary for the forming of the portland cement clinker - CaO, Al_2O_3, SiO_2, Fe_2O_3, and, in individual cases also alloying oxides BaO and Mn_2O_3, represent valuable raw material for the production of portland cement clinker.

2. The introduction of the slag in the raw material mixture through additional feeding of the furnace, makes possible the intensification of the processes of the clinker formation; in order to increase the furnace productivity and to lower considerably the specific expenses of fuel and electric power for the portland cement production.

BIBLIOGRAPHY

1. - E.I. TSIVILEVA (1964), "Issledovanie sposoba dopolnitelnogo pitaiya vrashchayushchikhsya pechej poroshkoobraznym shlakom so stotony golovok", Trudy Giprotsement, XXIX, 89. (In Russian).

2. - I.V. KRAVCHENKO, E.I. KOVALEVA, V;I; ZHARKO, I.D. GORBACHEVICH (1979), "Dopolnitelnoe pitanie vrashchayushchikhsya pechej - ehffektivnyj sposob povysheniya ikh proizvoditelnosti", Tsement, nº 2, 6-7. (In Russian).

Clinker-Raw Meal-Coal Interrelations in some Indian Cement Plants

Corrélations entre clinker, cru et charbon dans certaines cimenteries indiennes

A.K. CHATTERJEE, V.K. ARORA, T.N. VERMA, D.V. RAMANA RAO et D. GHOSH, Cement Research Institute of India, New Delhi, India.

RESUME : Une série de recherches sur les corrélations entre clinker, cru et charbon dans certaines cimenteries indiennes est expliquée à l'aide de résultats obtenus dans deux fours à préchauffeurs, d'une capacité de 600 tonnes par jour et de 900 tonnes par jour dans un four Lepol d'une capacité de 1000 tonnes par jour et dans deux fours à voie humide d'une capacité de 600 tonnes par jour (l'un avec des chaînes et l'autre avec un concentreur). On a essayé de corréler les variations de la composition chimico-minéralogique des crus, leur finesse et les caractéristiques des cendres du charbon avec les caractéristiques principales du clinker telles que la distribution des phases, la composition et la microstructure. On a démontré que la qualité du clinker obtenu dans de tels fours, utilisant des charbons riches en cendres (cendre 21-29 %, MV 25-36 %) peut être représentée sous l'angle des microstructures par une combinaison d'indices quantitatifs tels que l'indice chimico-minéralogique, l'indice de grain et l'indice d'agglomération.

On a également démontré que, dans les conditions ci-dessus, la qualité du clinker, telle qu'évaluée à l'aide des indices indiqués ci-dessus, pouvait être prévue, avec une bonne probabilité, en utilisant un autre indice, basé empiriquement sur le cru; cet indice est calculé en tenant compte de la composition du cru, après calcination, de l'influence des cendres du charbon, de sa teneur potentielle en liquide et de sa fraction retenue sur le tamis de 150 microns.

SUMMARY : A course of investigations on CLINKER-RAW MEAL-COAL INTERRELATIONS in some Indian Cement plants has been illustrated with the help of results obtained from two suspension preheater kilns of 600 TPD and 900 TPD capacity, one lepol kiln of 1000 TPD capacity and two wet kilns of 600 TPD capacity (one with chains and another with concentrator). Attempts have been made to interrelate the variations in chemico-mineralogical composition of the raw meals, their fineness, coal ash characteristics, and ash influence with the major clinker characteristics such as phase assemblage, composition and microstructure. It has been demonstrated that the quality of clinker that is obtained from such kiln systems, using high ash coals (ash 21-29 %, VM 25-36 %) can be represented by a combination of quantitative indices such as Chemico-mineralogical Index (CMI), Grain Index (GI), Clustering Index (CI) alongwith the micro-structural features.

It has been further shown that under the given conditions, the acceptable quality of clinker, as assessed by the above indices can be forecast with an element of certainty with the help of an empirical Raw meal index (RMI) defived from the composition of ignited raw mixes with coal ash influence, together with its potential liquid content and fraction retained on 150 µm.

INTRODUCTION

Within about six decades of its existence and development, the Indian cement industry today has 56 production units with an installed capacity of 22.75 million tonnes. The production comes from a wide variety of kiln systems that differ from one another in their processes, designs and rated outputs. In addition, the industry has of necessity to use hard crystalline or sedimentary limestones—often quartzose or siliceous—in most of the plants along with high-ash coal. In an average cement plant the relative shares of raw materials and fuel (including power) in the aggregate cost structure obtain at 26.2 and 38.6 percentage (1). Therefore, one of the immediate needs of the industry is to optimise clinker quality and output by balancing the inputs of coal and raw meal.

The present communication is based on a systematic investigation undertaken in this regard. Although the data and results presented below relate to five selected plants, the generalisations, reported here, have been arrived at from a wider set of data which have been excluded for the sake of brevity.

PLANT CHARACTERISTICS

The kiln, raw meal, fuel, and clinker characteristics of the plants in question are presented in Tables I & II. The plants were chosen on the following considerations:

To cover the three major processes of raw meal preparation.

The kiln capacity range to represent the general run i.e. 600-1000 tonnes per day (tpd), which indeed is the range of 50 percent of the operating kilns.

The limestone characteristics to represent a cross section of the material used. Thus plants A,D and E make use of coarse grained quartzose limestone with a host of accessory minerals, while plant B utilises a compact crypto-crystalline fine-grained siliceous limestone, and plant C depends on a high-grade miliolitic limestone. Further, while plants A,D and E make use of limestones of the same geological horizon, they differ in their raw meal preparation and preheating systems.

To represent different additives and correctives used (Plant A, sandstone 6%, clay 2%; Plant B, bauxite 1%, laterite 4%; Plant C, clay 20%; Plant D, bauxite 2%, iron ore 2%, and Plant E, lime sludge 5%, red mud 2%).

TABLE I

Distinctive Features of the Kiln system

Plant	A	B	C	D	E
Capacity TPD	600	900	1000	600	600
Process	Dry (4-SP)	Dry (4-SP)	Semidry (Lepol)	Wet (Concentrator)	Wet (Chains)
Cooler	Grate	Planetary	Grate (Recupol)	Grate	Planetary
Heat consumption Kcal/kg cl	1100	1100	950	1500	1350

TABLE II

Plant Raw Meal, Coal and Clinker Characteristics

		A	B	C	D	E
Raw Meal Composition %	Raw Meal Characteristics					
	LOI	36.10	35.61	34.98	34.69	34.83
	SiO_2	13.70	13.40	14.53	13.95	14.12
	Fe_2O_3	1.40	1.90	1.82	2.76	2.81
	Al_2O_3	2.80	3.25	3.13	1.47	1.77
	CaO	41.53	43.60	43.51	44.53	44.82
	MgO	2.88	0.83	0.68	0.91	1.02
	Na_2O	0.28	0.15	0.10	ND	0.75
	K_2O	0.96	0.33	0.14	ND	0.22
	Mn_2O_3	0.97	ND	ND	ND	ND
	SO_3	ND	0.17	0.20	ND	ND
Coal Analysis %	Coal Characteristics					
	Moisture	3.51	2.06	2.45	1.46	2.98
	VM	36.05	31.26	28.90	24.91	28.93
	FC	34.09	40.37	47.26	44.73	42.55
	Ash	25.89	26.91	21.39	28.90	25.54
	C.V. K.Cal/kg	5290	5480	5870	5010	5366
Coal Ash Analysis %	SiO_2	59.82	63.08	58.71	61.14	58.94
	Fe_2O_3	6.01	7.45	6.37	8.56	6.89
	Al_2O_3	24.50	21.99	22.40	20.60	21.65
	CaO	5.13	3.48	6.11	4.25	6.53
	MgO	0.44	0.51	1.33	1.25	0.60
Oxide Composition %	Clinker Characteristics					
	LOI	0.84	1.58	2.36	0.69	0.72
	SiO_2	21.78	20.96	21.48	24.80	24.82
	Fe_2O_3	2.80	3.69	3.58	4.70	3.60
	Al_2O_3	5.64	6.35	4.58	3.50	4.20
	CaO	60.66	64.99	64.96	63.45	63.92
	MgO	5.80	0.94	1.40	1.25	1.32
	Na_2O	0.05	0.12	0.50	0.36	0.49
	K_2O	1.52	0.51	0.71	0.30	0.37
	Mn_2O_3	1.10	ND	ND	ND	ND
	SO_3	0.77	0.49	ND	0.33	ND
	CaO_f	1.32	0.18	4.83	0.72	0.30
Phase Composition %	C_3S	44.30	48.11	43.00	21.00	50.37
	C_2S	38.30	23.31	38.80	64.40	32.97
	C_3A	4.50	7.67	10.00	3.40	4.45
	C_4AF	12.90	10.91	8.20	11.20	12.20

CLINKER QUALITY:

From the phenomenological inter-relations of phase composition, microstructure, quality, and burning of portland cement clinkers (2) it is known that in addition to their chemical composition, the quality of clinker is defined by the optimum proportions of the major phases, grain size of clinker minerals and overall microstructural characteristics. However, no quantitative indices correlating the above parameters have yet been established. Nevertheless from a study of a fairly large number of Indian plant clinkers it has been observed that the overall quality can be represented by the combination of the following parameters.

Chemico-Mineralogical Index (CMI)

$$CMI = 60(0.05 - K) - (BI_{Exp} - 3) \qquad (1)$$

where

$$K = \frac{1 - \sqrt[3]{1-x}}{T}$$

$$X = \frac{CaO - CaO_f}{CaO}$$

T = burning time taken as 20 min

$$BI_{Exp} = \frac{C_3S\%}{C_3A\% + C_4AF\%} \text{ as determined}$$

experimentally, for example by QXRD.

With high-ash coal firing in Indian plants, the chemico-mineralogical quality of a clinker appears to be acceptable so long as CMI lies within $\pm$ 0.5 with the BI_{Exp} ratio limited to 3.5. Any value of CMI beyond the above range indicates either high free lime, or low alite content, or disproportionate presence of the nonsilicate phase or their combination.

Grain Index (GI)

$$GI = \frac{C_3S\%XP + C_2S\%XQ}{80^2} \qquad (2)$$

Where P and Q refer respectively to the proportion of alite and belite grains lying in the range 21-40 micron.

The closer the index to unity, the better is the clinker quality, when other quality indices are the same.

Clustering Index (CI)

The clustering index is given by the cluster size and frequency. The cluster size is given in millimeters by their average length of linear intercepts obtained from a larger number of traverses across polished sections of clinker samples under the microscope with the help of an integrating stage. Parallely the cluster frequency can be denoted by the number of clustersper millimeter. The higher the intercept length or the lower the frequency, the poorer is the quality. With high-ash coal firing, clustering phenomenon appears to be very common in the plant clinkers and, hence, the significance of this index.

Microstructure

The microstructural characteristics are presented in qualitative and relative terms to cover the grain shape and outline, inclusions within grains, rimming, zoning and twinning. Under Indian conditions, Type I monadoblastic microstructure is rarely achieved and the clinkers generally display Type II monadoblastic and Type III glomeroblastic features (2).

The above quality indices of the clinkers produced by the five plants are illustrated in Table III. For better comprehension, the crystal size distribution of alite and belite as well as the nature of clustering in the above clinkers are presented in Fig 1 and 2. From Table III and Fig 1 and 2, one may conclude that the clinker of plant B is of the best quality with the only deficiency that the grain growth is not entirely satisfactory. In an overall grading of clinker quality plant B is followed by plants E, A, C and D although on the basis of CMI one may observe that the clinkers of plants A, C and D are below the acceptable limits, which is also corroborated by the facts that the free lime in clinker A is high, in clinker C very high and the alite content in clinker D is very low.

RAW MEAL COMPOSITION AND COAL ASH INFLUENCE

The raw meal characteristics of the five plants in terms of moduli values, burnability factor and potential liquid content are presented in Table IV, which also shows the average ash absorption in

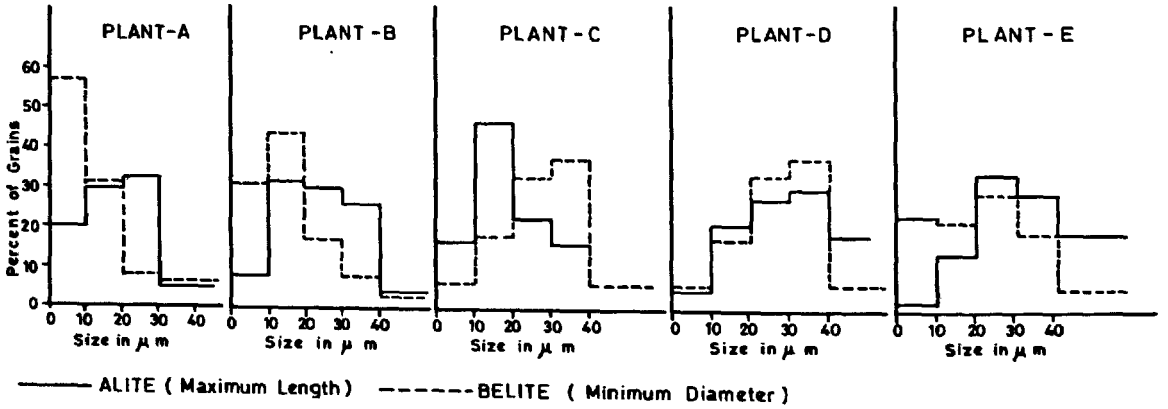

Fig.1. ALITE AND BELITE SIZE DISTRIBUTION

TABLE III

Clinker Quality

Plant	A	B	C	D	E
CMI	1.29	0.29	1.96	2.22	0.46
GI	0.32	0.22	0.41	0.72	0.64
Cluster Size (Av)	0.55	Negligible	0.32	0.90	0.87
Cluster Frequency (Av)	1.68	-	2.97	1.12	1.17

Description of Microstructure

Plant A : Irregular grains of alite with profuse inclusions of belite. Belite grains twinned and zoned. Rims of belite around alite present.

Plant B : Well developed alite and belite. No zoning or twinning of belite. Rims of belite around alite and inclusions of belite within alite rare.

Plant C : Regular grains of alite and belite. Belite better developed than alite. Belite rims around alite present. Some alite have irregular margins. Twinning and zoning rare. Inclusions of belite within alite not very frequent.

Plant D : Alite grains with wavy outline and inclusions of belite. Two generations of belite noticed, one regular and moderately coarse grained and another irregular and fine grained. Twinning in belite present. Rims of belite around alite rare.

Plant E : Alite with irregular outline and inclusions of belite. Belite better developed with twinning.

clinker produced through the given kiln systems. The average ash absorption has been derived from the plant records of specific heat consumption in clinkerisation, compositional differences between raw meal and clinkers, and ash compositions for long periods of plant operation.

The effective changes in all the parameters due to ash absorption are also shown in Table IV. For an additional indirect assessment of the relative burnability of the raw mixes, the theoretical heat requirement (H_{TH} in K Cal/Kg) for clinkerisation with and without coal ash influence has also been carried out following the methods of Strassen (3).

It is obvious from Table IV that the relative burnability of the raw meals cannot be clearly assessed from the set of data individually or in combination. The data is still more confusing if one tries to correlate them with the quality of clinker produced by the plants as summarised in Table III. For example, the relatively inferior quality of clinkers of plants C and D can hardly be envisaged from these indirect burnability indices. This led to the study of granulometry of raw mixes.

TABLE IV

Raw Meal Composition and Coal Ash Influence

Plant	A	B	C	D	E
LSF	0.97	1.02	0.94	1.05	1.03
SM	3.26	2.60	2.31	3.30	3.08
AM	2.00	1.71	1.98	0.53	0.63
BF	110.31	121.91	112.84	131.52	124.65
L_C%	21.96	23.79	22.18	18.41	20.86
H_{TH}	433	439	428	426	434
Ash Absorption%	5.5	5.5	3.5	6.5	7.0
Effective changes due to Ash Absorption					
LSF	0.83	0.87	0.87	0.86	0.85
SM	2.98	2.52	2.83	3.00	2.84
AM	2.28	1.87	1.86	0.76	0.90
BF	94.50	106.35	111.07	109.82	105.39
L_C%	25.63	27.06	24.27	22.53	24.87
H_{TH}	402	403	408	386	394

RAW MIX GRANULOMETRY

The broad pattern of granulometry of the raw mixes of different plants including the five selected was studied by finding out the slopes of lines from the log-log plots of cumulative weight fractions retained on different sieves (Table V) and correlating the slopes with fraction retained on 150, 90 and 53 micron sieves on a semi-log scale (Fig 3). It is evident from Fig 3 that there is a break in the slope of lines beyond ~5% retention on 150 micron sieve and corresponding to ~14% and ~37% retentions on 90 and 53 micron sieves respectively—all against a slope factor range of about 2. But the break in the case of 150 micron is smoother than in the other cases with a detectable trend of approaching a linear relation.

TABLE V

Raw Meal Particle Size Distribution

Plant		A	B	C	D	E
In Microns						
+150		3.05	4.70	3.90	8.49	3.26
-150+ 90		10.85	8.30	8.79	12.46	9.14
- 90+ 75		5.80	4.10	5.86	6.83	6.84
- 75+ 53		40.81	19.40	14.50	27.37	49.94
- 53		39.43	63.50	66.95	44.85	30.82

Further, since modern trends of granulometric studies of raw mixes (4,5) have revealed that the size fractions retained in the 125-150 micron range have an appreciable effect on burnability, the mineral constitution of the coarser fractions of the raw meals and their effect on burnability were separately studied.

The mineral phases present in the +90 and +150 micron sieve fractions in their order of abundance as well as the relative concentrations of calcite and quartz in these size fractions are presented in Table VI. It is evident that the patterns of mineral concentration in both the coarse fractions are more or less identical but in certain cases there is some increase in the concentration of calcite grains in the + 150 micron fraction. Therefore, the effect of increase in the coarsest fraction i.e. + 150 micron range on residual free lime was further investigated, the results of which have been reported later in this paper.

TABLE VI

Mineral Distribution in Raw Meal Coarse Fractions

Plant A		Plant B		Plant C		Plant D		Plant E	
+150 micron	-150+90 micron	+150 micron	-150+90 micron	+150 micron	-150+90 micron	+150 micron	-150+90 micron	+150 micron	-150+90 micron
Calcite, Dolomite, Muscovite, Chlorite, Bytownite, Labradorite, Mn-minerals, Sphene, Apatite, Zircon	Calcite,, Dolomite, Quartz, Muscovite, Chlorite, Bytownite, Labradorite, Mn-minerals, Apatite Sphene	Calcite, Quartz, Diaspore, Kaolinite, Gibbsite, Goethite	Calcite, Quartz, Montmori-llonite, Kaolnite, Gibbsite, Goethite	Calcite, Quartz, Labradorite, Sphene, Kaolinite	Calcite, Quartz, Kaolinite, Labradorite, Sphene	Calcite, Quartz, Musco-vite Biotite, Hematite, Goethite, Sphene	Calcite, Quartz, Musco-vite, Hematite, Biotite, Sphene	Calcite, Quartz, Musco-vite, Tremo-lite, Opaque Minerals	Calcite, Quartz, Musco-vite, Tremo-lite, Opaque Miner-als
Calcite %									
80.32	83.58	86.72	91.22	83.70	79.00	72.94	70.25	68.36	77.34
Quartz %									
19.68	16.41	13.20	8.70	16.30	21.00	27.05	29.74	31.63	22.65

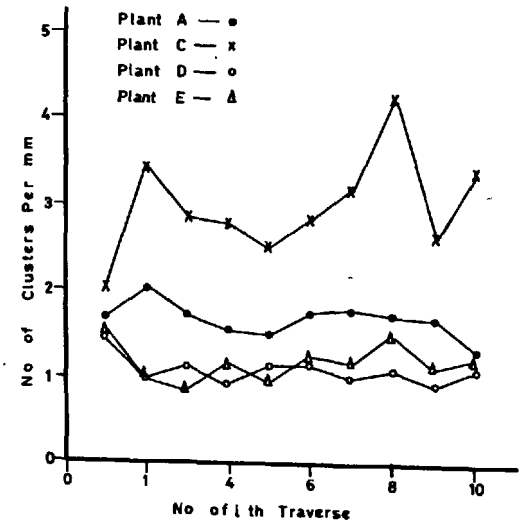

Fig 2 NUMBER OF CLUSTERS PER MM AS OBSERVED IN TEN TRAVERSES.

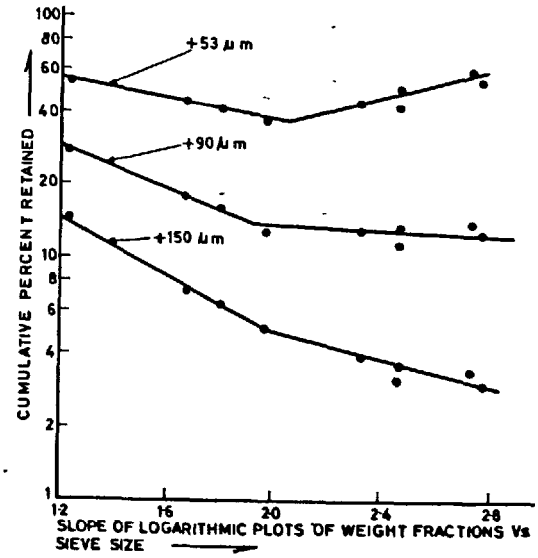

FIG.3 RELATIONS OF DIFFERENT SIZE FRACT- - IONS WITH TOTAL GRANULOMETRY

CLINKER-RAW MEAL-COAL INTER-RELATION BASED ON AN EMPIRICAL RAW MEAL INDEX

Since the normally adopted moduli values on the burnability factor derived from them did not yield an acceptable approach to envisage clinker quality and relative burnability as highlighted earlier in this paper, attempts were made to study the Indian plant raw mixes so as to establish the equivalence in terms of the burnability effect of moduli values vis-a-vis potential liquid of raw meals with coal ash influence, on the one hand, and vis-a-vis raw mix fraction retained on 150 micron sieve on the other. In the context of such equivalence studies it was revealed that for the type and range of kiln systems under investigation the normally favourably working ranges of potential liquid and size fraction retained on 150 micron sieve are about 22.5-27.5% and 0-5% respectively. The disturbance in burnability with potential liquid exceeding the limiting values is such that no equivalence can be established while the effect on account of the higher proportion of coarser fraction is regular and additive. Based on such observations a raw meal index could be derived which is given below:

$$RMI = 100\ LSF + 10SM - (L_c - 25) - 2(5 - R) \qquad (3)$$

Where LSF and SM are derived from the ignited raw mix with average coal ash influence, L_c is the potential liquid content of that raw mix with coal ash (lying in the range 22.5-27.5) and R is the fraction retained on 150 micron sieve.

It has been further observed that so long as this index lies between 105 and 110 approximately, a fairly acceptable quality of clinker that is achievable with high-ash coal firing can be ensured with CMI lying in the range of ± 0.5. The raw meal indices of the five selected plants are given in Table VII.

TABLE VII

Raw Meal Indices					
Plant	A	B	C	D	E
RMI	107.2	105.3	115.2	130.5	109.7

It may be worthwhile to mention here that so far as plant A is concerned, although RMI=107.2, CMI is not favourable. This is explained by the fact that the raw mix of this particular plant contains an appreciable amount of manganese oxide in addition to magnesia and iron oxide. If now LSF is recalculated in accordance with Spohn's formula taking into account the magnesia content, it increases substantially (from 83 to 91) and if manganese oxide is added with iron oxide to obtain the other moduli value, then the potential liquid of this raw mix becomes almost 29%, as a result of which Equation (3) becomes untenable for this raw mix and consequently, the difficulty in obtaining a clinker of acceptable quality can be forecast.

CONCLUSIONS

With the type of raw materials and fuel used in Indian cement plants of 600-1000 tpd capacity, the quality of clinkers produced can be characterised by a combination of four parameters: Chemico-mineralogical Index (CMI), Grain Index (GI), clustering size and frequency, and microstructural features. A CMI range of ± 0.5 with high GI, low clustering, the Type II/III microstructural variety normally indicates an acceptable quality of clinker. Such prognostication of clinker quality cannot always be envisaged with certainty from the conventional moduli values, burnability factors and potential liquid contents, either independently or in combination. The plant raw mixes generally contain an appreciable proportion of fraction retained on 150 micron sieve, which, as expected, has a strong bearing on the overall burnability of raw mixes. From experimental and plant data an equivalent effect of chemical composition and potential liquid content of ignited raw meals with coal ash influence as well as of the raw meal fraction retained on 150 micron sieve, a raw meal index (RMI) has been worked out with certain limiting conditions. It has been observed that when the index lies within the range 105 to 110, an acceptable quality can be achieved for the clinkers under the given conditions.

ACKNOWLEDGEMENT

The work reported here is part of the R & D programme of the Institute and the report is being communicated with the permission of the Director General, Cement Research Institute of India, New Delhi.

BIBLIOGRAPHY

1. - Cement Industry in India--Problems & Prospects, (1979) New Delhi, NCAER.

2. - Chatterjee, A.K., (1979) "Phase Composition, Microstructure, Quality and Burning of Portland Cement Clinker - a Review of Phenomenological Inter-relations" Pt 1 World Cement Technology, 10,4, 124-135.

3. - Strassen H. (1957) "Der theoretische Warmebaday des Zement - brand", Zement-Kalk-Gips 10, 1, 1-12.

4. - Chatterjee, A.K., "Physico-Chemical Characteristics of Cement Raw Materials and Reactivity of Raw Mixes - A Review of Diagnostic Inter-relations",. Pit & Quarry (in press).

5. - Erling Fundal, (1979) "The burnability of Cement Raw Mixes", World Cement Technology, 10,6, 195-204.

Influence des microadditions d'oxyde de chrome (III) sur la composition chimique et minéralogique des clinkers de ciment portland

The influence of chromium sesquioxide microadditions on the chemical and mineralogical composition of portland cement clinkers

I. TEOREANU, H. BALASOIU, C. RADOVICI et D. CIOMARTAN, Roumanie.

RESUME : Le travail est une analyse de la façon dont la composition chimique et minéralogique des clinkers de ciment portland est influencée par des microadditions d'oxyde de chrome (III) (jusqu'à 3 %). Les auteurs ont examiné les modifications de la composition chimique des constituants majeurs du clinker, par suite de la solubilisation du chrome (III) et de la variation des proportions d'autres oxydes inclus dans les réseaux de base, et donnent des solutions solides complexes. La distribution du chrome (III) entre les phases cristallines du clinker, en fonction de sa solubilité dans chaque phase, est aussi analysée. On décrit la façon dont la présence du chrome (III) influence la texture des clinkers et le polymorphisme de leurs constituants silicates.

ABSTRACT:

In the present work is analyzed the way the addition of variable amounts of chromium sesquioxide (as microadditions up to 3 wt.%) exerts an influence on the chemical and mineralogical composition of portland cement clinkers. The changes in the chemical composition of the main components of clinker as a consequence both of the chromium(III) dissolution and of the variations in the amount of other ions inclusion in the basic lattices, resulting in complex solid solutions formation, are examined. The distribution of chromium(III) in the crystalline phases of clinker as a function of its solubility in each phase is analyzed. The way in which the chromium(III) presence influences the clinker texture and the polymorphism of the silicate constituents in clinker is examined, too.

A. INTRODUCTION

Dans une publication précédente /1/ ont été examinées les conséquences de la présence des ions de chrome(III) sur la formation et la stabilité des phases silicatique dans le clinker de ciment portland. Des modifications assez importantes peuvent avoir lieu dans la composition chimique des phases majeures du clinker par suite de la distribution différente des ions de chrome (III) et par les modifications de la solubilité des autres ions dans ces phases. La structure du clinker en général et la structure de ses phases minéralogiques en particulier, peuvent aussi subir des modifications notables.

Le but de ce travail est d'apporter des informations nouvelles en ce que concerne les questions indiquées plus haut, étant donné que des modifications chimiques et structurelles du clinker et de ses constituents peuvent engendrer des variations importantes des proprietés liantes des ciments respectifs.

B. PARTIE EXPERIMENTALE

Afin d'obtenir ces informations (s'ajoutant à celles déjà présentes dans la littérature) ont été utilisées comme matières premières pour les clinkers à contenu en oxyde de chrome(III) variable (c'est à dire 0; 0,5; 3 % en poids) carbonate de calcium, bioxyde de silicium, oxyde d'aluminium, oxyde de fer(III) et oxyde de chrome (III) de pureté chimique (réactifs Merck). Les paramètres modulaires des clinkers synthetisés sont suivants : S_K=0,96; M_{Si}=2,2; M_{Al}=2. Les mélanges brutes, sont caractérisés par des surfaces specifiques élevées, résultat des dimensions granulaires réduites des matières premières (le résidu sur le tamis de 0,063 mm est nul). La cuisson a été effectuée dans un four électrique à 1350°C, pour 30 minutes.

L'analyse qualitative de la composition minéralogique des clinkers a été faite par la diffraction des rayons X, à la temperature ambiante et aussi par diffractométrie à haute temperature, entre 500-1200°C, pour chaque hausse de 100°C de la température. Ont été utilisés un appareil de type DRON-2,0 à un goniomètre horizontal GUR-5 (USSR) et une chambre de hautes températures de type GPVT(USSR). Dans tous les cas on a travaillé avec la radiation $Cu_{K\alpha}$.

L'analyse chimique des échantillons a été faite par la fluorescence des rayons X, avec un appareil de type VRA-2 (Freiberger Präzisionsmechanik-R.D.A.). Pour identifier Ca, Fe, Cr on a travaillé avec un tube de W; le crystal analyseur a été de LiF. Pour identifier Al et Si on a utilisé le tube de Cr, et crystal analyseur de pentaerytritol. Pour éliminer l'instabilité à court terme de l'appareil, on a utilisé un système de mesure à moniteur. Pour éliminer les erreurs à long terme, on a remplacé pour l'étalonnage et les mesures, le nombre des impulsions correspondant au maximum du peak analytique, par le rapport entre le nombre des impulsions au sommet du peak et le nombre des impulsions au fond du même peak (I_L/I_F). Pour chaque système ont été préparées cinq pastilles étalon et pour compenser les effets matriciaux, les concentrations des élements dans chaque pastille ont été calculées jusqu'à 100 % utilisant un programme de calcul adéquat.

Les résultats des analyses par fluorescence des rayons X ont été verifiés et complétés par analyse chimique.

La co-existence des quatre phases crystallines et de la phase vitreuse rend tres difficile l'analyse chimique quantitative des constituents minéralogiques du clinker. Pour écarter en partie au moins ces obstacles, les constituents minéralogiques du clinker, ont été séparés par attaque chimique sélectif. On a utilisé une solution d'acide salicilique en alcool éthylique qui rend solubles les phases silicatiques, les phases célitique et vitreuse restant insolubles. Les phases silicatiques ont été reprécipitées par ébullition à sec. Les réseaux crystallines attaqués ou labilisés par l'attaque chimique, et surtout les phases reprécipitées, deviennent susceptibles de réagir (se carbonater, etc.), avec l'environnement. Pour éviter les erreurs produits par ces réactions, les produits résultant après l'attaque chimique ont été soumis à une cuisson supplémentaire, à 1350°C pour 2 heures.

Ont été aussi effectuées des analyses semiquantitatives avec une microsonde électronique Jeol de type JXA-3A.

Pour obtenir des informations concernant la texture des clinkers à contenu variable en oxyde de chrome(III) ont été effectuées des mesures de porosité pour toute la gamme des clinkers synthetisées, utilisant un microscope analyseur d'images Quantimet 720.

C. RESULTATS ET DISCUSSIONS

Les analyses diffractométriques ont mis en évidence la diminution jusqu'à une disparition quasi-totale de l'alite dans les échantillons à 3 % oxyde de chrome(III) (résultat qu'on attendait d'ailleurs d'après /1/), la phase bélitique étant la plus importante; dans les clinkers exempts d'oxyde de chrome(III) ou à 0,5 % d'oxyde de chrome(III) la phase alitique est la plus abondante.

Les résultats des investigations de diffractométrie à haute température ont montré que l'inclusion du chrome(III) dans les réseaux des minéraux du clinker, n'implique pas des différences essentielles dans leur comportement envers les variations de température, comparées à celles des minéraux du clinker étalon (exempts de Cr); on a remarqué l'abaissement de la température de transition polymorphique $\beta \rightarrow \alpha'_H$ du bélite par rapport à l'orthosilicate de calcium pur (mais ce phénomène est determiné pas seulement par l'inclusion dans le réseau de l'orthosilicate de calcium des ions de chrome(III), mais aussi des ions d'aluminium et de fer(III)).

Tableau I - La composition chimique des clinkers et des phases majeures pour : A - 0% Cr_2O_3; B - 0,5% Cr_2O_3; C - 3% Cr_2O_3

A

Oxydes	Clinker		Phases alitique et bélitique		Phases célitique et vitreuse	
	%	c	%	c	%	c
SiO_2	23,76	0,21	28,96	0,35	10,02	1,40
Al_2O_3	7,89	0,36	1,04	0,40	16,98	0,40
Fe_2O_3	3,66	0,76	1,15	0,01	9,65	1,31
CaO	64,45	0,58	68,73	0,62	62,48	0,39
Total	99,78		99,88		99,33	

B

Oxydes	Clinker		Phases alitique et bélitique		Phases célitique et vitreuse	
	%	c	%	c	%	c
SiO_2	23,68	0,43	29,70	0,36	9,49	0,45
Al_2O_3	7,39	0,38	0,33	0,14	21,96	0,64
Fe_2O_3	3,79	0,01	0,26	0,01	10,98	0,04
CaO	63,95	0,62	68,16	0,72	56,77	0,66
Cr_2O_3	0,48	0,08	0,64	0,08	0,30	0,08
Total	99,29		99,06		99,50	

C

Oxydes	Clinker		Phases alitique et bélitique		Phases célitique et vitreuse	
	%	c	%	c	%	c
SiO_2	23,52	0,46	25,89	0,41	8,96	0,30
Al_2O_3	7,48	0,22	1,75	0,12	19,94	0,10
Fe_2O_3	3,39	0,24	1,62	0,02	7,87	0,31
CaO	62,56	0,65	66,33	0,46	59,98	0,42
Cr_2O_3	2,97	0,12	3,94	0,16	2,39	0,16
Total	99,93		99,53		99,14	

-On a noté par "c" l'erreur absolue et par "%" les pourcentages en poids.

Les compositions oxydiques des phases separées et analysées par la fluorescence des rayons X et par la voie chimique (tableau I), montrent que le chrome (calculé comme oxyde de chrome(III)) est distribué surtout dans les phases alitique et bélitique. Le contenu en chrome est presque double dans les phases déjà mentionnées par rapport à celui determiné dans les phases célitique et vitreuse.

La distribution préferentielle des ions chrome(III) dans les phases alitique et bélitique est aussi démontrée par les images obtenus à l'aide de la microsonde électronique; dans la figure 1 (a et b) sont présentées les distributions des ions de silicium, aluminium, fer(III) et chrome (III), correspondant aux clinkers à 0,5 et 3 % oxyde de chrome(III) respectivement.

L'inclusion du chrome dans le réseaux des minéraux silicatiques entraîne des modifications dans les rapports établis entre les oxydes qui les composent, c'est à dire les oxyde de base (oxydes de silicium et de calcium) et les oxydes solubilisés dans les minéraux de base, formant des solutions solides (oxyde d'aluminium et oxyde de fer (III)) en fonction des modifications de la stabilité des ces minéraux.

Dans le cas du clinker à 0,5 % oxyde de chrome(III), l'inclusion d'une quantité relativement importante de chrome dans les réseaux des silicates dicalcique et tricalcique ne modifie pas essentiellement le rapport gravimétrique entre les oxydes de calcium et de silicium, mais détermine une diminution importante de la quantité des oxydes d'aluminium et de fer(III) solubilisés dans les constituents silicatiques du clinker de ciment portland.

Dans le clinker à 3 % oxyde de chrome (III) on a determiné une diminution nette du rapport gravimétrique des oxydes de chrome et de silicium, dans les conditions d'une diminution de la quantité d'oxyde de calcium et d'une augmentation visible du contenu en oxydes d'aluminium et de fer (III), allant jusqu'à 3,37 % en poids, par rapport à 2,19 % en poids dans le cas du clinker sans chrome; le contenu en chrome (déterminé comme oxyde de chrome(III)) atteint 3,94 % en poids. Par conséquence, le rapport gravimétrique entre l'oxyde de calcium et les oxydes acides diminue, par rapport au clinker étalon, de 2,21 jusqu'à 2.

Les modifications des rapport oxydiques dans les minéraux silicatiques du clinker, lorsque le contenu en oxyde de chrome(III) est variable, sont certainement correlées avec les changements de la composition minéralogique des phases silicatiques. Les modifications, bien que peu importantes par rapport à l'étalon pour le cas du clinker à 0,5 % oxyde de chrome(III), deviennent importantes pour les clinkers à 3 % oxyde de chrome(III) (dans ce cas, on ne trouve pratiquement pas d'alite).

Pour la composition des phases célitique et vitreuse (phases interstitielles) des clinkers obtenus à partir d'un mélange brut (sans microadditions d'oxyde du chrome) un contenu élevé en oxyde de calcium est caractéristique, probablement par suite de la solubilisation de cet oxyde dans la phase liquide du clinker (qu'on retrouve après la solidification comme phase vitreuse).

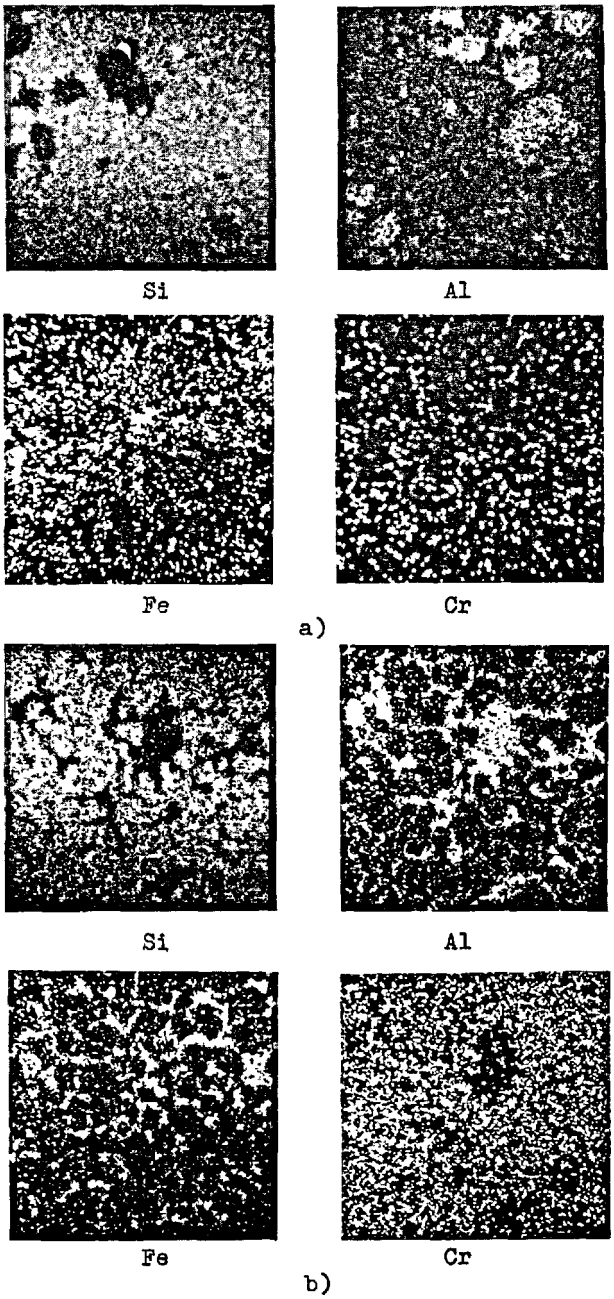

Figure 1 - La distribution élementaire des atomes de silicium, aluminium, fer et chrome dans deux sortes de clinker: a) à o,5% en poids oxyde de chrome(III); b) à 3% en poids oxyde de chrome (III).

Les clinkers à additions d'oxyde de chrome (III) se distinguent par un contenu plus bas en oxyde de calcium dans les phases interstitielles, surtout dans le cas du clinker à o,5% oxyde de chrome(III). Cette constatation est en accord avec le fait que le contenu en phases silicatiques dans ce clinker est plus grand /1/. Dans les phases interstitielles du clinker à chrome on observe aussi un abaissement du contenu en oxyde de silicium. En même temps, on observe une augmentation du contenu en oxyde de fer(III) et surtout, en oxyde d'aluminium. L'oxyde de fer(III) se trouve dans les phases interstitielles dans une proportion plus grande que dans le clinker étalon, seulment dans le cas du clinker à o,5% oxyde de chrome. Quand le contenu en oxyde de chrome(III) dans le mélange brut atteint 3% les pourcentages des oxydes de fer(III) et d'aluminium dans les phases interstitielles sont plus bas par rapport aux phases interstitielles des clinkers à o,5% oxyde de chrome(III). La somme des pourcentages des oxydes de fer et d'aluminium incorporés est pourtant plus grande que dans le cas des clinkers étalon; ceci peut être atribué au contenu relativement élevé en chrome(2,39% en poids, calculé comme oxyde de chrome(III)).

On peut conclure que les variations des proportions des phases célitique et vitreuse dans les clinkers sont directement influencées par les processus ayant lieu dans les phases silicatiques à l'incorporation de proportions variables en oxyde de Cr (III), et par la tendence de solubiliser, notée dans le cas des phases interstitielles surtout dans le ferrite-aluminate de calcium /2,3/.

Les additions en oxyde de chrome(III) conduisent aux changements importants de la texture résultant des modifications de la composition et des influences sur les processus physiques et chimiques pendant la formation du clinker de ciment portland. Les résultats des mesures de porosité effectuées sur les clinkers à contenu variable en chrome, utilisant le microscope-analyseur des images, confirment les suppositions enoncées plus haut, et en même temps, sont en accord avec les modifications dans la composition minéralogique et dans la morphologie des minéraux des clinkers /1/.

Tableau II - Mesures de porosité pour les clinkers étudiés

Les proprietés examinées	Clinkers à:		
	o% Cr_2O_3 en poids	o,5% Cr_2O_3 en poids	3% Cr_2O_3 en poids
La répartition volumique des pores (%vol.)	2o,56	14,09	12,31
Le diamètre moyen des pores(mm)	o,o169	o,oo85	o,oo96

Les données présentées dans le tableau II montrent que la présence du chrome conduit à une vitrification assez importante des clinkers. Ceci est en bonne concordance avec les conclusions occasionnées par les mesures de la composition oxydique des phases majeures du clinker. En même temps avec l'abaissement de la porosité totale a lieu une modification de la distribution des dimensions des pores (tableau III): la

proportion en petits pores augmente.

Tableau III - La distribution des pores pour les clinkers étudiés

Distribution du nombre des pores ayant le diamètre compris dans l'interval (% du nombre total des pores)	Clinkers à:		
	0% Cr_2O_3 en poids	0,5% Cr_2O_3 en poids	3% Cr_2O_3 en poids
0 - 3 µm	30,12	64,93	26,47
3 - 8 µm	30,93	20,03	33,69
8 -15 µm	17,09	5,28	20,13
15 - 20 µm	3,66	1,95	6,66
20 - 30 µm	5,02	2,89	7,22
30 - 50 µm	6,65	3,40	3,98
50 - 80 µm	4,88	1,08	1,54
plus de 80 µm	1,76	0,43	0,32
nombre total des pores/mm^2	575	1079	961

D. CONCLUSIONS

La présence du chrome dans le clinker entraîne des modifications de la composition minérale des clinkers et aussi des modifications notables de la composition chimique des phases majeures; ces modifications peuvent être correllées avec celles qui sont observées dans la composition minéralogique des clinkers, interessant surtout les phases silicatiques. Ces modifications sont plus importantes quand l'oxyde de Cr(III) est incorporé dans des proportions supérieures à 0,5% en poids. Lorsque cette proportion augmente, la phase alitique diminue, jusqu'à une disparition quasi-totale dans les clinkers à 3% oxyde de chrome(III). Les modifications dans les proportions relatives des phases silicatiques et dans leur composition chimique impliquent des modifications dans la composition et les proprietés des phases silicatiques.

La présence du chrome dans les clinkers détermine une vitrification plus intense; à l'augmentation du contenu en oxyde de chrome(III) correspondent un abaissement de la porosité totale et une modification de la distribution des pores (les petits pores deviennent beaucoup plus nombreux).

E. BIBLIOGRAPHIE

1. Teoreanu I., Bălăşoiu M., Sălăgeanu I., et Bălăşoiu Lirella,(1979), Revue Roumaine de Chimie, 24, 225 - 235,(Angl.)
2. Hornain H., (1971), Revue des Matériaux des Constructions, 671-672, 203 - 214, (Franç.).
3. Korneev V.I., (1971), Trudy Giprotzementa, 38, 105 - 110, (Russe).

Common influence of BaO and Mn_2O_3 on the obtaining and the properties of the portland cement

Influence des additions de BaO et Mn_2O_3 sur la fabrication et les propriétés des ciments Portland

V. VALKOV, Associate Professor, Master of Science, Higher Chemical and Technological Institute, Sofia, Bulgarie,
M.M. SITCHIOV, Professor, Doctor of Science, LTI, Leningrad, USSR,
L. GIGOVA, Senior Technical Assistant, Master of Science, NIISM, Sofia, Bulgarie,
Yu. V. NIKIFOROV, Senior Technical Assistant, Master of Science, Giprocement, Leningrad, USSR.

RESUME : Pour étudier l'influence de BaO et Mn_2O_3 sur les processus de formation du clinker et les propriétés du ciment, on a fabriqué et étudié des mélanges de matériaux à partir de ces composés chimiques et de matières premières naturelles.

Il a été établi que BaO et Mn_2O_3 accélèrent la calcination de la pierre à chaux, améliorent la structure cristalline du clinker et augmentent leur teneur en alites.

Le clinker obtenu se caractérise par une mouture améliorée et par une activité chimique et hydraulique augmentée. Les ciments portland contenant une addition de baryum-manganèse ont un durcissement plus rapide et une résistance plus grande de 80 à 120 kg/cm2 que les ciments sans cette addition.

Cette addition exerce une action complexe sur la formation des composants du ciment et leur minéralisation.

SUMMARY : For the investigation of the common influence of BaO and Mn_2O_3 on the clinker-forming processes and the properties of the cement obtained, raw material mixtures of chemical reactives and natural materials are made up and studied.

It is established that BaO and Mn_2O_3 accelerate the lime absorption, better improve the crystal structure of the clinker and increase the alite contents in it.

The clinker obtained is characterized by a bettered grinding ability, increased chemical and hydraulic activity. The portland cements containing a baryum-manganese addition harden faster and muster strength by 80-120 kg/cm^2 higher higher in comparison with cements without addition.

The addition has a complex, alloying and mineralizing action.

The utilization of the alloying and mineralizing additions increases very much the possibilities of accelerating the processes of the mineralforming and regulation the structure of the portland cement clinker and its products. (1, 2). The action of BaO and Mn_2O_3 is of particular interest and each one of them has contradictory data (3-6).

In the present communication brief data will be given concerning the simultaneous action of $BaO + Mn_2O_3$, the use of which becomes real especially when utilizing different natural raw materials or industrial wates. The action of the addition is studied in laboratory, semi-industrial and industrial conditions.

The oxide of barium is introduced as $BaSO_4$ (baryte or concentrate of baryte), the Mn_2O_3 as $MnCO_3$, manganese containing ore or wastes. Additions containing 0,5 ÷ 2,0% BaO and 0,4 ÷ 2,0% Mn_2O_3 in different correlation, have been studied.

I. OBTAINING AND STRUCTURE OF THE PORTLAND CEMENT CLINKER

In the Portlant cement constituents the dissociation of $BaSO_4$ takes place at lower temperatures in comparison with the clean salt, and practically comes to his end at 1400°C. The acid oxides SiO_2, Al_2O_3 and Fe_2O_3 (7) contribute for this. The separating barium oxide has alkaline comportment and appears as analogous to CaO. The manganese compounds most often fully pass into Mn_2O_3, which replaces Fe_2O_3 in the constitients of the Portland cement clinker. This fact was accounted for at constituting the raw material mixtures and the calculation the mineral constituent of the clinker.

In the presence of $BaO + Mn_2O_3$ accelerated annealing of the calcium lime (CaO) was observed. In clinkers with different constituent (KH = 0,85-0,95 - according to Kind-Yong, n = 1,7-3,2 and p = 1-2,5), the full absorption of the lime terminates at temperature by 20 - 40°C lower in comparison with the samples without addition.

In industrial conditions the obtaining of clinker is carried out without any deviation from the technological regime. More uniform and granulometrical clinker constituent is established, with absence of fine and most corse fractions. The clinker obtained is of a decreased strength and increased Brittleness and with ~ 30% ameliorated grind capacity.

The microscopic observations in laboratory and industrial clinkers show that the in the presence of $BaO + Mn_2O_3$: the porosity of the clinker increases; improves the crystallization of the basic phases - of alites and belites (Fig. 1 and 2). Often the alite crystals show additional sectility, some admixtures are included in them, or alteration of their surface is observed. The quantity of the alite phase is by 3 to 8% bigger.

Microphotography of clinkers, containing BaO and Mn_2O_3, obtained in laboratory conditions
(reflected light, Magnitude 90 x)

Fig. 1

Microphotography of clinkers, containing BaO and Mn_2O_3, obtained in factory conditions
(reflected light, Magnitude 90 x)

Fig. 2

The observations with microtester bear witness of practically uniform distribution of BaO in the Portland cement clinker structure, while Mn_2O_3 remain mainly in the constituent of the interstitial substance which surrounds the alite and belite crystals.

It is obvious that the action of the addition $BaO + Mn_2O_3$ begins as early as the reactions of the solid phases, with a partially formed aluminate of barium and a manganate of barium and calcium.

However, its presence in the clinker melt is the determining factor, the quantity and the activity of which is increasing, while the viscosity decreases (8, 9). For this contributes the increased components of the system and the specific modifying influence of Ba^{2+}, Mn^{3+} and SO_4^{2-}. (1)

The presence of BaO concerns, to the utmost

degree, the balite phase and contributes for the stabilization of ß, while increased concentrations of α'-C_2S also, a fact confirming the data of (10).

The manganese, before all, forms a complexe alluminium-ferro-manganese phase, but some though very small part of it, is to be found in the alite and belite phases, something confirmed by data of microtester.

2. HYDRATATION AND HARDENING OF THE CEMENTS CONTAINING $BaO+Mn_2O_3$ IN THE CLINKER

The increased defectiveness of clinker silicate phases, as well as the increased quantity of alite, are a prerequisite for an increased hydraulic activity. This is also favoured by the chemically more active varium ion, especially that from the surface areas of the clinker particles.

An established fact is the increase of the degree of hydratation of cements containing $BaO+Mn_2O_3$ in comparison with cements without addition, including the three month term of hydratation in grout with norm density. This is also accompanied by an increase of the activity of the liquid phase, which in our estimation, activates the hardening.

The laboratory data concerning clinker cements of different constituents (KH, n and p) and different content of $BaO+Mn_2O_3$ show an increase both of the initial (1-7 day) and the later strength. In single instances the difference ranges from 80 to 160 kg/cm^2.

The best strength of cements is obtained when the content of BaO is from 0,5 to 1,5% and for Mn_2O_3 - from 0,4 to 1,6%. The data were confirmed with obtaining clinker in semi-plant furnace (0,7 x 8,0 m) working with liquid fuel.

The positive influence of $BaO+Mn_2O_3$ is manifested both in trials of grout and in reference solutions. This contributes to increasing the adhesive and cohesive properties.

The laboratory and semi-plant trials have been carried out in different cement plants including those working by the dry, semi-dry and aqueous method with liquid or hard fuel.

The necessary quantity of BaO and Mn_2O_3 is introduced with the help of an appropriate industrial waste matter, obtained when dressing the ironstone (11, 12)

When calculating the raw material mixtures, the content of Mn_2O_3 was equalized to that of Fe_2O_3, while that of BaO - to CaO.

The strength standard determinations show an increase of the hydraulic activity towards the 28th day with an amount of 80 to 120 kg/cm^2 (Table 1).

These data were confirmed by the corresponding tests of concretes with various compositions.

TABLE 1

Physical and mechanical testings of the cements, obtained from industrial clinkers, containing BaO and Mn_2O_3

No. of sample	Method of production	Contents of SO_3 %	Residue of the sieve 4900 gaps/cm^2 %	Density according norm %	Connection time according to BSR 72-74+ begining hour	Connection time according to BSR 72-74+ end min	Strength according to BSR 72-74+ kg/cm^2 bending after days 1	3	7	28	stress after days 1	3	7	28
1.	wet	3,5	10	26	2-10	4-40	30	58	76	81	116	289	480	588
2.	wet	3,3	11	27	2-05	3-55	20	47	64	82	78	207	415	610
3.	semidry	3,7	10	25	2-00	4-15	36	61	67	74	187	216	411	583
4.	semidry	3,5	9	25	1-55	4-10	45	68	80	83	169	381	518	636
5.	dry	3,6	10	26	2-00	4-00	50	70	82	88	195	370	520	707
6.	dry	3,4	10	27	1-50	4-20	40	61	70	80	156	374	496	676

+ The testings according to the Bulgarian State Railways (for short = BST) correspond to the Instructions of ISO.

CONCLUSIONS

The introduction of $BaO+Mn_2O_3$ in the composition of the portland cement raw material mixtures gives us the possibility to conduct the prpcess of the clinkerformation.

The addition has complex, alloying and

mineralizing action, through which a clinker with a better crystalization and with an increased contents of alite, is achieved.

The clinker os characterized by an increased chemical and hydraulic activity.

BIBLIOGRAPHY

1. - Trudy Mezhdunarodnogo Kongressa po Khimii Tsementa - tom.I., Strojizdat, Moskva, 1976 (In Russian).

2. - Yu.M. BUTT and V.V. TIMASHEV, (1974), "Portlandtsiment", Moskva, Strojizdat (In Russian).

3. - G.V. KUKOLEV and M.G. MELNIK (1960), "Vliyanie dobavok Cr_2O_3, P_2O_5, V_2O_5, BaO na Mikrostruktutu Portlandtsementnogo klinkera", DANSSSR 132, No.1, 168-171 (In Russian).

4. - I.V. KRAVCHENKO, O.K. ALESHINA and L.N. GRIKEVICH (1967), "Issledovanie vliyaniya okisi bariya na kinetiku klinkeroobrazovaniya", Trudy NII Tsement, No.22, 138-151 (In Russian).

5. - R.A. KENNERLEY (1977), "Sostav Vysokomargantsevistogo portlandtsementa", Cement and Concrete Research, No 5, 565-574.

6. - M.M. SITCHIOV and V.I. KORNEEV (1964), "Vliyanie Primesej Syrya Legiruyushchikh dobavok na tekhnicheskie svojstva trekhkaltsievogo silikata", Trudy Giprotsement, vyp.29, 3-12 (In Russian).

7. - V.M. GRAPJYANOV, L.S. GIGOVA, M.M. SITCHIOV and V.V. VALKOV (1974), "Kinetika na Razlaganeto i Vzaimodejstvieto na $BaSO_4$ s Fe_2O_3, SiO_2 i Al_2O_3 v Intervala 1250-1400°C", Str.Materiali i Silikatna Prom., XV, No.6, 3-5 (In Bulgarian).

8. - I.B.KHOLIN, Z.B. EhTIN and Yu.S. MALININ (1961), "Vzaimodejstvii beta-C_2S i C_3S s okisyu bariya", Nauchnye soobshcheniya NIITsement 10(41), 24-29 (In Russian).

9. - M.M. SITCHIOV, V.I. KORNEEV, A.B. ZOZULYA, (1973), "Protsesy Klinkeroobrazovaniya i Rol Primesej", Sb.Statej Formirovanie Portlandtsementnogo Klinkera, Leningrad (In Russian).

10. - M.Ya. BIKBAU, Yu.M. BUTT and V.V. TIMASHEV (1975), "Issledovanie Stabilnosti Tverdykh Rastvorov v Dvukhkaltsievogo Silikata s Okislami Razlichnykh Ehlementov", Trudy MKhTI, No.87, 10-13 (In Russian).

11. - V.V. VALKOV, M.M. SITCHIOV and L.S. GIGOVA (1977), "Vliyanie Nebolshikh Dobavok Okisi Bariya i Mangantsa na Poluchenie i Svojstva Portlandtsementa", Zhurnal Prikladnoj Khimii, No.7, 1433-36 (In Russian).

12. - V.V. VALKOV (1977), "Izpolzuvane na 'cherniya barit' kato Surovina v Tsementovata Promishlenost", Str.Materiali i Silikatna Prom., No.9, 3-5, (In Bulgarian).

Formation and Stability of C_3S and Alites

La formation et la stabilité du C_3S et des alites

Udo LUDWIG and Albrecht WOLTER, Institut für Gesteinshüttenkunde, RWTH Aachen, R.F.A.

RESUME : La synthèse du C_3S d'une haute pureté a été réalisée pour la première fois au-dessous de 1300°C par l'application de nouveaux modes de préparation, comme le séchage au pétrole chaud (HPT), la synthèse hydrothermale (HTS) et le séchage avec pulvérisation (SPR).

De plus, une technique de cuisson a été mise au point, permettant, non seulement de chauffer très rapidement et de maintenir la température constante pendant un très long temps, à un niveau prédéterminé, mais aussi de faire varier cette température d'une façon programmée. C'est ainsi que la température de stabilité du C_3S pur, en présence de C_2S et de chaux libre, a pu être déterminée à 1264 ± 3°C.

Ensuite des solutions solides courantes de C_3S ont été essayées. Ce que l'on appelle l'alite normale est une solution solide dans le C_3S, d'Al_2O_3, de Fe_2O_3 et de MgO. La réaction solide qui produit cette alite à partir de C_2S, de CaO, de MgO et de C_4AF se produit à environ 1200°C et est beaucoup plus rapide que celle qui produit le C_3S pur. L'addition de phophate de zinc et de sulfate de baryum à l'alite normale n'a qu'une faible influence sur la température de formation de l'alite et sur la vitesse de la réaction. Mais l'addition de 2 % de MnF_3 à l'alite normale abaisse cette température à 1100°C.

La formation de l'alite a aussi été étudiée dans des crus industriels de ciment Portland. Dans ces matériaux, la température limite de formation du C_3S est inférieure de quelques degrés à 1200°C. Il n'y a que de faibles différences dans la formation du C_3S, selon le taux de saturation en chaux du cru.

Ces résultats montrent l'intérêt technique d'utiliser des crus très actifs. Une résistance comparable à celle des ciments Portland peut être obtenue même à une température relativement basse de cuisson et un cru faiblement dosé en chaux. Des économies d'énergie peuvent aussi être faites dans le broyage du clinker.

SUMMARY: The syntesis of very pure C_3S was made for the first time in the temperature range below 1300°C by using new preparation techniques such as "hot kerosene drying" (HPT), "hydrothermal synthesis" (HTS) and "spray drying" (SPR). In addition a burning technique was developed, which allowed not only to heat up very rapidly and keep the temperature constant at a prefixed point for a very long time, but also to change the sample temperature for distinct amounts. In this way the stability temperature of pure C_3S from C_2S plus free lime could be determined as 1264 ± 3°C.

After that some common solid solutions of C_3S were investigated. A so-called "normal alite" represents the solid solution limit of C_3S with Al_2O_3, Fe_2O_3 and MgO. The solid state reaction of this alite from C_2S, CaO, MgO and C_4AF occurs at about 1200°C and proceeds much faster than the formation of pure C_3S. Admixtures of zinc phosphate and bariumsulphate to the normal alite had only a small influence on the formation temperature and reaction rate of alite. But the addition of 2 % MnF_3 to normal alite reduced the formation temperature to 1100°C.

In specially prepared technical Portland cement raw mixes the alite formation was investigated too. In these materials the temperature limit for C_3S-Formation was some degrees lower than 1200°C. There were only small differences between C_3S-formation in a raw mix with a high and a low lime saturation factor.

These results point out the technical importance of the use of high active raw mixes. A strength similar to Portland cement is attained in spite of a lower burning temperature and a lower lime dosage. Additionally energy can be saved in the clinker milling.

INTRODUCTION

The system $CaO - SiO_2$ is well known by work carried out by RANKIN and WRIGHT (1), LEA and PARKER (2), WELCH and GUTT (3) and many other authors. In the past with a high lime content of this system the calcium oxide (C) coexists with dicalcium silicate (C_2S). At higher temperatures the tricalcium silicate is formed from these phases (see Fig. 1).

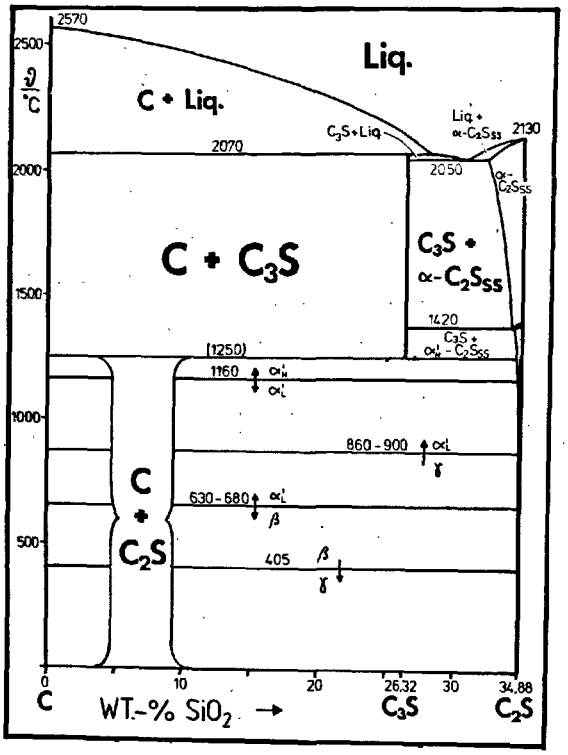

Fig. 1 The subsystem $C - C_2S$ of the system $CaO - SiO_2$

Much research work was done to determine the lower stability limit of C_3S (2,4,5). They all synthesized pure or doped C_3S at temperatures between 1450 and 1600°C and observed the decomposition of C_3S to C_2S and free lime in the temperature range from 1300 to 1000°C. In this way, 1250°C could be extrapolated from the decomposition rate at lower temperatures, but there has not as yet been an exact determination of the stability temperature of C_3S.

The main difficulty the investigations of C_3S-formation come up against is the very low free energy (ΔG) of the reaction $C + C_2S \rightleftharpoons C_3S$ of about 8 to 13 kJ/mol at room temperature to circa - 4 to - 10 kJ/mol at 1800°C.

Figure 2 shows the free energy over the temperature (6,7,8,9). It is easy to see that the tolerances of the thermodynamical data do not allow a good calculation of the stability range of C_3S.

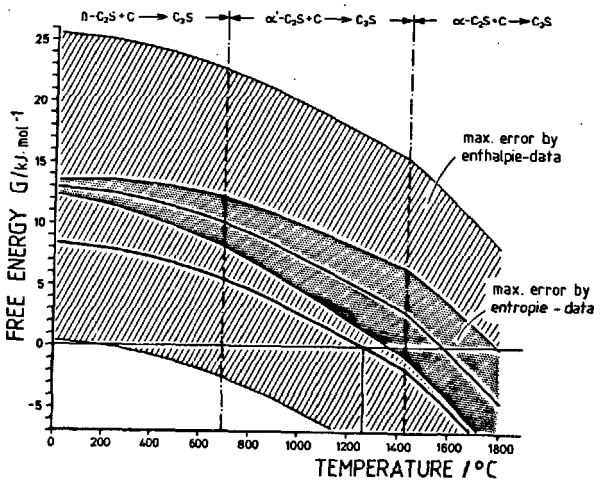

Fig. 2 Free energy (ΔG) for the reaction $C_2S + C \rightarrow C_3S$ (starting with β-C_2S)

Another difficulty is created by the strong influence of impurities on the C_3S-reaction rate. Only a few authors gave information about the purities of their starting materials for C_3S-synthesis. But nobody did report on the purity of his synthesized C_3S.

The affinity of Al_2O_3, Fe_2O_3 and MgO to C_3S in the form of solid solutions ("alites") is well known (10,11,12). The solution limit is about 2 wt-% of MgO, 1 wt-% of Al_2O_3 and 1 wt-% of Fe_2O_3 in C_3S. This alite we call "normal alite".

In technical Portland cement clinker there are a lot of other minor compounds such as alkalies (Na, K), heavy metal oxides (TiO_2, Cr_2O_3, Mn_2O_3, ZnO, NiO, PbO etc.) and anion groups (F, Cl, SO_4, P_2O_5 etc.) present.
To investigate the special influences of these compounds on alite formation we took the following scheme (Fig. 3):

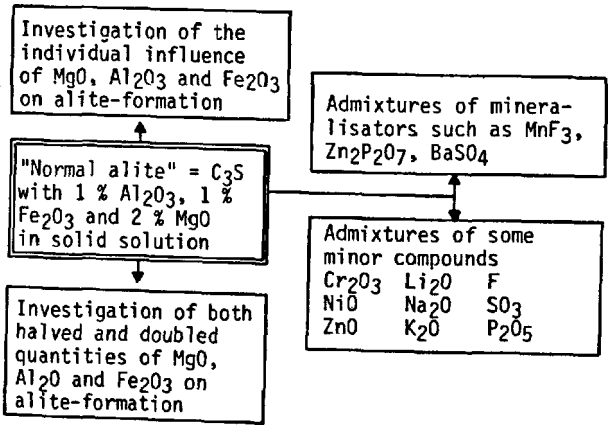

Fig. 3 Working scheme for qualitative investigations on alite-formation

At first the stability temperature of normal alite was examined. The second part concerns the influence of the minor compounds, single and in combinations, on the alite formation temperature, reaction rate and sintering mechanisms in normal alite. To complete this research work, alite formation was observed in homogenized technical Portland cement clinker too. In the literature there is only one piece of information, that Fe^{++}-rich alite decomposes spontaneously at 1173°C (13).

EXPERIMENTAL

For the comparison of common preparation techniques such as homogenisation of heterogeneous compounds by milling and the new ones such as "hot kerosene drying" (HPT), "hydrothermal syntheses" (HTS) and "spray drying" (SPR) a series of samples was taken all with the same CaO/SiO_2-ratio = 3/1:

Preparation	SiO_2 - part	CaO - part	specific surface (BET) m^2/g
Milling	Quartz	$CaCO_3$	1,3
Milling	Aerosil	$Ca(OH)_2$	24,5
Milling	β-C_2S	$CaCO_3$	1,9
HPT	Ethylsilicate	$Ca(CH_3COO)_2$	41,6 +) 20,3 ++)
SPR	Aerosil	$Ca(CH_3COO)_2$	24,3 +) 32,2 ++)
HTS	C_3SH		17,1

+) 200°C - dried - material
++) 450°C - treated - material

The values of specific surface (BET) from 1.3 to 41.6 m^2/g indicate distinct activities of these mixtures, but it is not the sole characteristic of the activity, as the reaction rates in the temperature range from 1200 - 1300°C show (see Fig. 4).

The worst activity can be seen in the mixture of quartz with $CaCO_3$. The best "mixture" is the tricalcium silicate hydrate (C_3SH). But as it was not possible, to make really pure C_3SH, the HPT-material was used for the determination of the C_3S-stability temperature. The low activity of the Aerosil - $Ca(OH)_2$-mixture in response to its high specific surface is attributed to big inhomogeneities between Ca- and Si-distribution in the mixture.

For the very fast heating of the pressings to the prefixed temperature in 2 or 5 min, a new burning procedure, was developed for samples with a volume of 1 cm^3 which also facilitated the temperature change in the gradient of a chamber kiln with tubes. After burning the samples were quenched in air and examined for the free lime content according to the FRANKE-method and also for the phase-composition with x-ray-analyses. The reaction grade (UGR) was calculated from free lime value (C_{free}) according to the formula:

$$UGR = \frac{100 - (C_{free} \times 4.072)}{100}$$

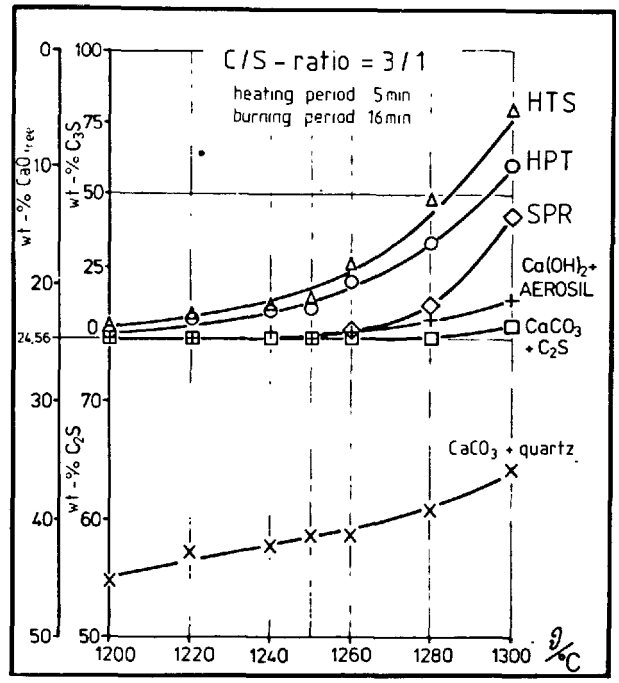

Fig. 4 Reactivity of various lime silica mixtures

and from the x-ray intensities of C_3S, C_2S and C by using a computer programme.

For the investigations of alite formation in technical Portland cement clinker two technical cement raw mixes with Kalkstandard III (KSt) = 100 and 107 were calcined at 900°C and homogenized by hydrothermal treatment in water suspension at 310°C/100 bar for 5 hours. After drying at 160°C a very homogeneous and fine-grained mixture of tricalciumsilicatehydrate, hydrogarnet and calcium hydroxide with small amounts of brucite was left behind.
All materials were pressed into small compacts with 1 cm^3 volume.

RESULTS AND DISCUSSION

After a burning period of 20 minutes at a temperature of 1300°C the reaction degree of pure C_3S was 0.54. After the 20 minutes the sample was rearranged to a temperature of between 1220 and 1300°C. Figure 5 shows the increase or decrease in the reaction rate with the square root of time.

The stability temperature lies between 1260°C and 1270°C. The exact temperature value of 1264,2°C can be extrapolated from the formation- and decomposition-rate over the temperature (Fig. 6). The error margin of this value is ± 3°C, produced by the uncertainties of the thermocouple, the temperature measurement and the positioning of the sample in the temperature gradient.

The reason why the gradient of the increasing reaction rate is much higher than that of the decreasing reaction rate lies in the difference in the density of C_2S + C and C_3S. The C_3S-decomposition produces

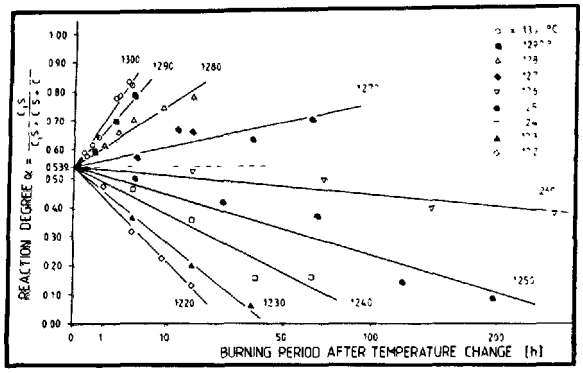

Fig. 5 Degree of C_3S-conversion as a function of burning period and temperature

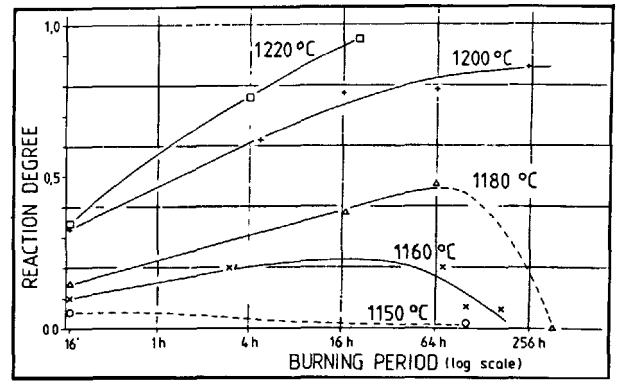

Fig. 7 Reaction degree of normal alite at various temperatures (HPT)

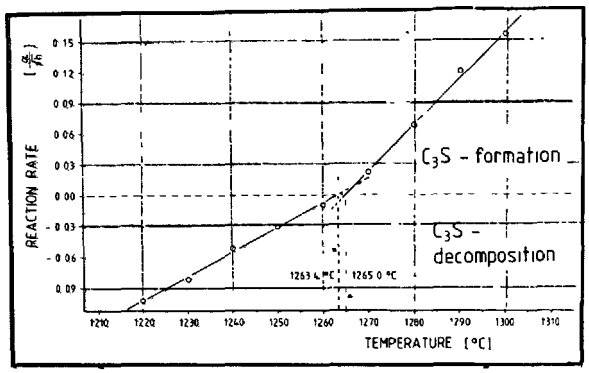

Fig. 6 Temperature dependence of the rate of formation and of decomposition of pure C_3S

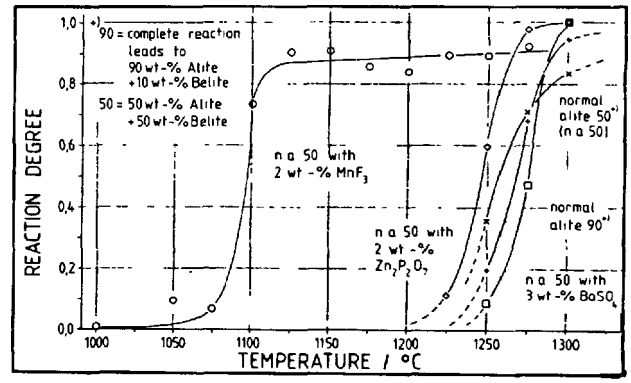

Fig. 8 Influence of low lime-dosage and of mineralisators on formation of normal alite (SPR)

more dense phases and so micro-fractures are originated, at which the solid state diffusion stops. On the other hand the newly formed C_3S occupies a greater volume than the starting phases and so C_3S-formation proceeds faster than C_3S-decomposition.

On the basis of 1264,2°C as the lower stability limit of C_3S, the free energy of C_3S-formation from β-C_2S + C at normal temperature in air was calculated to be 8.32 kJ · mol^{-1}.

The formation of alite could be observed without a temperature change programme, because the alite formation is sharply accelerated as opposed to pure C_3S. The synthesis of normal alite was carried out at temperatures of 1100 to 1280°C (Fig. 7).

Up to 1200°C the alite forms metastably and decomposes after some 10 - 100 h again. At 1220°C a stable alite is formed. So, the stability temperature should be something higher than 1200°C.

Both halved and doubled quantities of the admixtures of Al_2O_3, Fe_2O_3 and MgO had no effect on the stability temperature.

Figure 8 shows the influence of a lower lime dosage (alite : belite = 50 : 50) and of some mineralisators on the alite formation in the temperature range of 1000°C to 1350°C. The burning period in each case was 16 minutes. A lower lime content retards the alite formation. 3 wt.- barium sulfate accelerates the formation rate, but raises the formation temperatures by about 10°C. 2 wt.- zinc phosphate also accelerates the formation rate, but it lowers the formation by about 20°C. The biggest influence was observed by addition of 2 MnF_3. The stability limit of this fluor-bearing alite is short under 1100°C. At lower temperatures a "pseudo-alite" is formed, which gives x-ray patterns similar to the $3C_3S \cdot CaF_2$-phase. At temperatures higher than 1100°C a solid solution of alite and pseudo-alite phase develops.

The alite synthesis in homogenized technical cement raw mix (KSt = 100) was carried out in the temperature range of 1185 - 1250°C. Figure 9 shows the reaction grade against burning time.

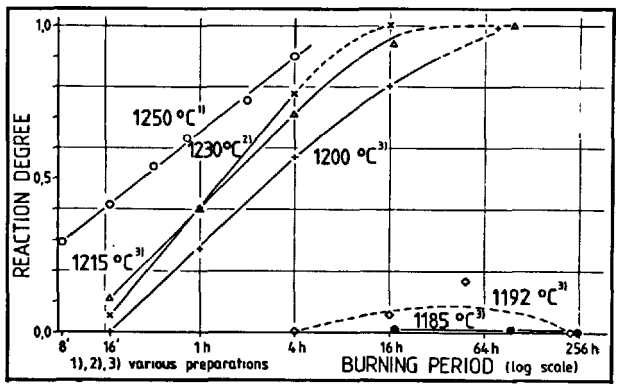

Fig. 9 Reaction degree of hydrothermal homogenized industrial Portland cement raw mix (KSt = 100)

The reaction proceeds in a clearly logarithmic fashion:

$$UGR = a + b \ln t \quad \Big| \quad 0 \leq UGR \leq 0.95 \quad t \geq 1 \text{ min}$$

with the temperature depending constants a for the initial alite content after heating + 1 min burning time and b for the materials activity. That is to say alite formation in a very homogeneous mixture proceeds like a chemical reaction. The error margin of the above equation in the technical cement burning process is attributed to the comparatively high heterogeneity of the compounds in normal cement raw mixes (14,15,16).

For the 1250°C series a material with lower activity than for the other temperatures was used. The stability temperature of technical alite is determined by the very strong difference in reaction between 1200 and 1192°C. The alite formation in the second technical raw mix with KSt = 107 was very similar to the former raw mix. This result is in good correspondence to the behaviour of synthetic normal alite.

ACKNOWLEDGEMENTS

We thank the government of the Nordrhein-Westfalen country for the sponsoring of this research work.

REFERENCES

1. - G.A. Rankin and F.E. WRIGHT 1915), "The ternary system $CaO - Al_2O_3 - SiO_2$", Am. J. Sci., (4th series), 39, 1-79.

2. - F.M. LEA and T.W. PARKER (1934), "Investigations of portion of the quaternary system $CaO - Al_2O_3 - SiO_2 - Fe_2O_3$; the quaternary system $CaO - 2CaO \cdot SiO_2 - 5CaO \cdot 3Al_2O_3 - 4CaO \cdot Al_2O_3 \cdot Fe_2O_3$", Phil. Trans. Roy. Soc. (London), A 234 (731), 1-41.

3. - J.H. WELCH and W. GUTT (1959)m "Tricalcium silicate and its stability within the system $CaO - SiO_2$", J. Am. Cer. Soc., 42, 11-15.

4. - E.T. CARLSON (1931), "The decomposition of tricalcium silicate in the temperature range 1000°C - 1300°C", J. Res. U.S. Bur. Stand., 7, 893-912.

5. - K. MOHAN and F.P. GLASSER (1977), "The thermal decomposition of Ca_3SiO_5 at temperatures below 1250°C. Part I: Pure C_3S and the influence of excess CaO or Ca_2SiO_4", Cem. Concr. Res., 7, 1-7.

(1977), "Part II: The influence of Mg, Fe, Al, and Na oxides on the decomposition", Cem.Concr. Res., 7, 269-276.

(1977), "Part III: The influence of water and sulphate on the decomposition", Cem. Concr. Res., 7, 379-384.

6. - E.G. KING (1951), "Heats of formation of crystalline calcium orthosilicate, tricalcium silicate and zinc orthosilicate", J. Am. Chem. Soc., 73, 656-658.

7. - S.S. TODD (1951), "Low temperature heat capacities and entropies at 298,16 K of crystalline calcium orthosilicate, zinc orthosilicate and tricalcium silicate", J. Am. Chem. Soc., 73, 3277-3278.

8. - J.P. COUGHLIN and C.J. O'BRIEN (1957), "High temperature heat contents of calcium orthosilicate", J. Phys. Chem., 61, 767-769.

9. - S. BRUNAUER and S.A. GREENSBERG (1960), "The hydration of tricalcium silicate and β-dicalcium silicate at room temperature", IV. Int. Symp. Chem. Cem., Washington 1960, 135.

10. - W. LOCHER (1960), "Die Einlagerung von Al_2O_3 und MgO in Tricalciumsilikat", Zement - Kalk - Gips, 13, 389-394.

11. - E. WOERMANN, W. EYSEL und Th. HAHN (1969), "5. Bericht: Die Alitphase im Fünfstoffsystem $CaO - MgO - Al_2O_3 - Fe_2O_3 - SiO_2$", Zement - Kalk - Gips, 22, 414-422.

12. - V. JOHANSEN and O.L. JEPSEN (1978), "Ternary diffusion in cement clinker at 1500°C" Cem. Concr. Res., 8, 301-310.

13. - E. WOERMANN (1960), "Decomposition of alite in technical Portland cement clinker", IV. Int. Symp. Chem. Cem., Washington 1960, 119-129.

14. - U. LUDWIG und G. RUCKENSTEINER (1973), "Einflüsse auf die Brennbarkeit von Zementrohmehlen", Forschungsbericht des Landes NRW, Westdeutscher Verlag Opladen, Nr. 2372.

15. - S.E. IBRAHIM (1979), "Zur Optimierung des Brennens von Zementrohmehlen", Diss. TH Aachen.

16. - N.H. CHRISTENSEN (1979), "Burnability of cement raw mixes at 1400°C. Part I: The effect of chemical composition", Cem. Concr. Res., 9, 219-228.

(1979), "Part II: The effect of the fineness", Cem. Concr. Res., 9, 285-294.

Dispersing and Plasticizing admixtures to cements

Des ajouts disperseurs et plastifiants des ciments

K. KARIBAYEV, Doctor-Engineer, A. PASCHENKO, Professor, K. BEKISHEV, Doctor-Engineer,
D. ALDIAROV, Doctor-Engineer, B. TAYMASOV, Doctor-Engineer,
Kazakh Institute of Chemical Technology, U.R.S.S.

RESUME : On a cherché à obtenir du ciment plastifié par addition de tanins synthétiques et de lignosulfonate du magnesium technique. Ces ciments plastifiés possèdent de hautes propriétés physico-mécaniques et constructives.

L'addition de 0,15-0,5 % de ces plastifiants abaisse l'eau de mouillage nécessaire de 14 à 30 %. La résistance des ciments plastifiés au gel et au sulfate est respectivement 0,93-0,96 et 0,94-1,00. Les processus d'hydratation sont étudiés par les méthodes de radiographie, de thermographie, de spectrographie infrarouge et d'analyse chimique. On a constaté la régularité de l'hydratation des ciments en présence des ajouts indiqués. Les additions de lignosulfonate de magnesium et de syntane améliorent la broyabilité des clinkers.

On a étudié des ajouts de triéthanolamine, de diéthanolamine et monoéthanolamine comme agents de broyage des clinkers. On a constaté que le diéthanolamine et le monoéthanolamine (qui sont des homologues de la triéthanolamine) sont des ajouts disperseurs très actifs. Nous avons étudié l'adsorption des additifs par les différents ciments et son influence sur la broyabilité. En ajoutant 0,3 à 0,5 de triéthanolamine à des ciments différents par leur composition chimico-minéralogique, nous avons obtenu des ciments pour le bétonnage sans coffrage. Le ciment pour le bétonnage sans coffrage peut aussi être obtenu avec du ciment sursulfaté normal et du ciment super-blanc. On peut l'utiliser pour la consolidation des excavations et pour la décoration des bâtiments. La durée de prise de ces ciments est 8 à 15 minutes, leur résistance à la compression est de 2,0 à 2,3 MPa au bout de 2 heures et de 25,2 à 36,3 MPa au bout de 28 jours.

SUMMARY : Possibility of plasticized cement obtaining at the base of synthetic tannic acids and technical magnesium lignin sulfonate admixtures is studied. Plasticized cements possess high physical, mechanical, building and technical properties.

Introduction of plasticized admixtures (o,I5 -o,5%) lowers the water requirement of cements by I4 - 30%, it increases the strength of cement. solutions by I7 - 20%. Plasticized cements freeze and sulfate resistance is respectively 0,93 - 0,96 and 0,94 - I,00. Processes of hydration are studied by X-ray method, thermographical method, method of infrared spectroscopy and by chemical analysis. Regularities of cement hydration in the presence of mentioned admixtures are established. Magnesium lignin sulfonate and syntan admixtures improve clinker grindability.

Triethanolamine, diethanolamine and monoethanolamine admixtures as intensifiers of clinker grinding process are studied. Triethanolamine homologs-diethanolamine and monoethanolamine are established. to be very effective dispersing admixtures. Adsorptive activity of mixtures is studied on different cements, its influence upon the dispersity of powders is also studied. Possibility of cement obtaining for the tubbingless cementation by introducing 0,3 - 0,5 triethanolamine admixtures into the different (according to their chemical-mineralogical composition) cements is established. Cement for the tubbingless cementation can be produced at the base of normal sulfate resistant white cement, it can be used for the rock manufactures strengthening and for the building decoration. Cement setting is 8-I5 minutes, strength at compression in 2 hours of solidification is 2,0-2,3MPa in 28 days - 25,2 - 36,3 MPa.

It is possible to obtain special plasticized cements and intensify clinker grinding process with a help of organic surfactants.Some scientists decided to divide the organic surfactants according to their water affinity and their influence upon cement and cement stone surface properties into two big groups: water-retaining surfactants and water-repellent surfactants(I)

The first group consists of sulfite-cellulose liquor, sulphite yeast converter mash and their derivatives, which increase the cement water affinity. The second group consists of the additives of silicone liquids compositions, fatty naphthenic acids. resin acids and their alkali salts. Adsorption of these substances is accompanied by chemical fixation of additive polar groups with formation of unsoluble caicium soaps at the cement particle surfaces. Water-repellent additives act as plasticizers in the solution and concrete mixtures.

Besides, superplasticizing and superdiluting additives are widely used. Sulfonated melamine-formaldehyde and naphthalene-formaldehyde resins, modified and purified lignin sulphonates, polybenzene aromatic and other compounds are used.

Plasticizing surfactants improve the cement mixtures and concrete properties. High plasticity and packing increase the concrete quality and its ageing.

We used synthetic tannic acids (syntan), SPS and technical magnesium lignin sulfonate as surfactant for obtaining plasticized cement. Plasticized capacity of additives and cement solution water requirement lowering was studied. Tests were carried out according to GOST 310-60. The results are shown in table I.

TABLE I

Admixture	Admixture quantity,%	Deliquescence pyrocone	Water requirement lowering
Without admixture	0	I05	0
Syntan	0,I	I23	I0
	0,I5	I30	I4
	0,20	I45	20
	0,5	206	30
Magnesium lignin sulfonate	0,I	II4	7,5
	0,I5	I20	I0
	0,25	I30	I4
	0,5	I87	25

In the studied concentrations of surfactants the cement solutions plastisity increases permanently. Syntan plasticizing capacity is higher than it is with sulphite-cellulose liquor and technical magnesium lignin sulfonate. To obtain plasticizing Portland cement with deliquescence pyrocone of no less than I25mm it is necessary to use 0,I5% SPS or 0,25% magnesium lignin sulfonate. The best surface activity of syntan SPS in comparison with magnesium lignin sulfonate is proved by the data of determination of surfactanta aqueous solutions surface tension.

Water-requirement lowering of plasticizing cements was determined according to the degree of decreasing the normal density value. Syntan SPS additive is the most effective. If SPS concentration is o,I-0,2-0,5% the lowering pf Portlandcement solution water requirements is I0,2o,30% and that of magnesium lignin sulfonate is 7,5-I2,5-25% respectively. The admixtures used did not increase the plasticity and didn't low the water requirement of high aluminous white cement.

Process of solidification of plasticized cement hydration were studied. Cement strength and the degree of hydration according to the content of $Ca(OH)_2$ and water in solid solution content are determined. Results are shown in table II.

TABLE II

Admixture	Strength of compression			$Ca(OH)_2$, % in 28 days
	I	7	28	
Without admixture	6,9	4I,4	60,7	8,22
Syntan SPS	5,2	44,6	69,0	9,I5
Magnesium lignin sulfonate	2,8	36,8	63,8	8.7I

Plasticized cement strength and the degree of its hydration in a day is less than that of the control cement. In the course of further cement solidification the velosity of $Ca(OH)_2$ liberation and its strength increase and in 7-28 days they will surpass the control samples by 5-I4%. It is in good agreement with X-ray, thermographic and infrared spectroscopic analyses data $Ca(OH)_2$ peaks intensity of the X-ray patterns (4,90Å), end-effect surface of the thermogram (480-500°C) and adsorption lines intensity on the spectra (3648cm^{-1}) of theplasticized cements in a day of solidification is lower than that of control samples.

Strength of the plasticized cement-sand solutions in 28 days is higher by I7-20% thah that of the control samples.

Stregth of the plasticized cement-sand solutios in 28 days is higher by I7-20% than that of control samlpes.

Slowing of hydrolysis reaction and of plasticized cement hydration at the beginning of setting is explained by the surfactant absorption film formation on the surface of cement particles and new formations. This film makes water combination with cement granules difficult. This slowing of plasticized cements hydration with the age increasement of samples is compensated by higher hydration process velocity during this period.

It was also determined that plasticited cements with syntan SPS and MLS admixtures are highly freeze and sulfate resistant. Thus, they may be used in the strict exploitation conditions. Plasticized cement freeze resistance coefficient is 0,93-0,96 (control sample - 0,67-0,80), firmness coefficient in the aggressive media 0,94-I,00 (control sample - 0,64-o,78).

Syntan SPS and magnesium lignin sulfonate admixtures intensify clinker grinding process. Of grinding time is the same, plasticized cement residue on the control sieves is 3-5%, while control cement residue is I0%, specific surface increases by 300 - 400cm^2/g.

Different surfactants as clinker grinding process intensifiers were studied. Amino alcohols-monoethanolamine (MEA), diethanolamine (DEA) and triethanolamine(TEA) were used as surfactants. Cement powder dispersity is determined by percentage residue on the control sieve, by the spacific surface and by granule composition. Results of surfactants influence upon cement residue on the control sieves are given in table III.

TABLE III

Admixture	Admixture quantity	Residue on sieve 008,%
Without admixture	0	I0
Monoethanolamine (MEA)	0,025	4,50
	0,05	4,75
	0,I0	5,00
	0,20	5,50
Diethanolamine (DEA)	0,025	3,75
	0,05	4,00
	0,I0	4,25
	0,20	6,00
Triethanolamine (TEA)	0,025	4,00
	0,05	4,25
	0,I0	4,50
	0,20	4,75

According to their intensifying influence on grinding process, surfactants may be arranged as follows: MEA, DEA, TEA. If we take into account the adsorption activity value of these amino alcohols their arrangement will be the same: MEA, DEA, TEA.

Aminoalcohols usage in a certain quantity also promotes the increasing of grinding product specific surface. However, dispersity increasing determined by specific surface quantity, is much lower than that of the value by the residue on the sieve 008. Dispersity increasing of grinding products with surfactants additives, is obviously connected with the adsorption of strength and with the disaggregation of the surfactants.

Thus, triethanolamine analog-monoethanolamine and diethanolamine highly intensify the clinker grinding process, that's why they can be used for cement mills intensification.

Possibility of obtaining the special cement for tubbingless cementation with triethanolamine admixture was determined. Sulfate resistant, normal and white cements were the initial substances for the tubbingless cementation. Triethanolamine admixtures were added into the make up water of the cement paste with water-cement ratio of0,40

Triethanolamine considerably accelerates cement settig time. Admixture optimal quantities for cement obtaining are: for the sulfate resistant and white Portland-cement - 0,3% TEA, for normal - 0,5. Here setting time is 8-I5 minutes, it meets the technical condition requirements. Beams (4x4xI6 cm) were formed form cement paste with water -cement ratio of 0,40, with triethanolamine admixtire 0,3 - 0,5%. Tests were carried out according to GOST 3I0-60. Results are given in table IV.

TABLE IV

Cements	Strength of samples(waber-cement ratio - 0,40), MPa			
	at bending in...		at compression in....	
	2hours	28days	2 hours	28 days
Sulfate resistant	0,9	4,4I	2,5	25,2
Normal	I,0I	4,48	2,2	36,3
White	0,95	4,05	2,3	30,8

The results of physico-mechanical tests showed that the strength of sulfate-resistant, normal and white cements with respective quantities of triethanolamine met the requirements of conditions for the tubbingless cementation. Thus, the strength of compression of sulfate resistant cement samples (triethanolamine optimal concentration is 0,3%) in two hours of solidification is 2,0 MPa, and in 28 days - 25,2MPa that of normal and white Portlandcement samples in 2 hours of setting is 2,2 and 2,3 MPa, and in 28 days - 36,3 and 30,8 MPa (4,5). Cement for tubbingless cementation can be manufactured directly at the cement mills by introducing triethanolamine while clinker grinding.

CONCLUSIONS

Our studies showed that plasticized cements with syntan SPS and magnesium lignin sulfonate admixtures had high physico-mechanical, building and technical properties. The admixtures surfactants studied favourably influences the hydration and cement setting process.

Triethanolamine analogs-monoethanolamine and diethanolamine are very effective intensifiers of clinker grinding process.

Possibility of cement manufacturing for the tubbingless cementation by using higher triethanolamine admixtures for different cements was determined.

REFERENCES

I.- V.RATINOV, F.IVANOV (I977) "Chemistry in building", Moscow, Stroyisdat, p. 220.

2.- K.KARIBAYEV, A.PASCHENKO, B.TAYMASOV (I975) "Plasticized admixture to cement", USSR Author's Certificate N 47I325.

3.- K.TAZHIBAYEV, K.KARIBAYEV (I974) "Ethanolamine influence on the cement specific surface", Cement N II, pp. I5 - I6.

4.- K.KARIBAYEV, A.PASCHENKO (I977) "Binder", USSR Author's Certificate N 560851.

5.- K.KARIBAYEV, K.TAZHIBAYEV, A.PASCHENKO, B.TAYMASOV (I975) "New method of cement obtaining for the tubbingless cementation", Cement, N 6, p. I7.

Comminution and Dissociation characteristics of Indian limestones

Broyabilité et décarbonatation des calcaires indiens

S.K. SINHA, S.K. HANDOO et A.K. CHATTERJEE, Cement Research Institute of India, New Delhi, India.

RESUME : Etant donné que l'industrie indienne du ciment utilise des calcaires de presque tous les âges géologiques, depuis la période Précambrienne jusqu'à la période Pléistocène, des échantillons représentant des horizons géologiques caractéristiques des différents âges ont été rassemblés dans différentes cimenteries indiennes pour une étude systématique. La présente communication rend compte de la variation de la résistance au concassage, de l'aptitude au concassage, de la broyabilité et des caractéristiques de désintégration de la calcite et du quartz libre en fonction de leur assemblage minéral et de leur répartition granulométrique. Tout en essayant de corréler les paramètres ci-dessus mentionnés, on a étudié et on a comparé la réactivité de différents calcaires après leur désintégration, et les causes de leurs variations ont été établies.

SUMMARY : Since the Indian cement industry has been using limestones of almost all the geological ages starting from Precambrian to Pleistocene period, representative samples of typical geological horizons of different ages were collected from various Indian cement plants for a systematic study. The present paper reports the variation in the crushing strength, crushability, grindability, and dissociation characteristics vis-à-vis their mineral assemblage and grain size distribution of calcite and free quartz. While attempts have been made to interrelate the above parameters, the reactivity of different limestones after dissociation has been investigated and compared, causes for the variations established.

INTRODUCTION

The total reserves of cement-grade limestones in India, estimated at more than 59000 million tonnes are distributed in geological time scale from precambrian to recent times. At present, the contributions of precambrian and postcambrian limestones in cement production are estimated at about 78% and 22% respectively but the future expansion programme of the industry is likely to increase the utilization factor of postcambrian limestones to some extent. Because of this changing pattern of utilization of limestones of diferent geological ages as well as to ascertain the degree of intrinsic difference in the process response of limestones having different characteristics, a systematic investigation had been undertaken to establish the basic relationship between the property and characteristics of different limestones. Some of the significant trends of results obtained are illustrated with the help of eight varieties of limestones belonging to different geological ages and horizons.

LIMESTONE CHARACTERISTICS

Chemical Composition

The composition of the limestones is presented in Table I. The compositional variability of these limestones is reflected in the ratios of CaO to SiO_2 (C/S), (CaO +SiO_2) to (Al_2O_3+ Fe_2O_3), and (CaO+SiO_2+Al_2O_3+Fe_2O_3), designated as ϵ, to (100-ϵ) denoted as B. The C/S ratio varied from about 3 to 30, C+S/A+F ratio from 13.5 to 21.5, and ϵ/B from 13.7 to 47.1. However, no specific correlation ould be established either amongst the above three atios or individually between the ratios and the eological age of the limestone horizons.

Mineral Constituents

The major and minor minerals detected in the limestones by X-ray diffractometry and optical microscopy are listed in Table II. Apart from calcite, which is predominantly present, quartz and dolomite constitute the other important phases. The contribution of feldspathic, micaceous and clay minerals to thetotal composition of the limetsones if of minor significance and more or less comparable in all the varieties. The quartz accounts for the major proportion of silica present in the limestones while the magnesia present in limestone S(5-8) comes mostly from dolomite and in S(1-4) from clay minerals.

Textural Features

The significance of crystal size of calcite and quartz in limestones has been fairly well established (1). The grain size ranges of calcite and quartz in the limestones under study along with their average size, determined from the frequency of grains occurring in different size ranges, are given in Table II. Depending on the average size of calcite grains (1) and comparing the grain size of calcite and quartz the limestones under reference can be classified as follows:

A
- S 7 : Medium-grained (0.5-0.25mm) inequigranular
- S 8 : Medium-grained equigranular

B
- S 2 : Fine-grained (0.25-0.10mm) equigranular
- S 4 : Fine-grained inequigranular

C
- S 1 : Very fine-grained (0.10-0.01mm)
- S 3 :
- S 6 : equigranular

D
- S 5 : Microcrystalline (<0.01 mm) equigranular

Limestone S1 and S5 display poor compaction.

CRUSHABILITY AND GRINDABILITY

The crushing strength of the limestone and their relative grindability (with respect to a standard clinker) are presented in Table III. The difficulties of correlating these parameters with the composition or textural characteristics of limestones have been indicated earlier. Nevertheless, in the present situation for the given set of limestones a qualitative relation between grain size plus C/S ratio on the other, was observed.

So far as the crushing strength is concerned, it increased with decrease in grain size in the range of medium to very fine grain size. The anomalously low strength obtained for the very fine-grained and cryptocrystalline limestones S1 and S5 could be explained by the degree of weathering and poorer compaction. Within each range of the empirical crushing strength scale the limestones with inequigranular distribution of calcite and quartz showed lower strengths than those with equigranular texture.

The relative grindability factor (2) of the limestones, in which the easier grindability is denoted by higher indices, appears to have a joint relationship with the grain size and silica content. The coarser and less quartzose limestones displayed easier grindability (for example, S-7 and S-5). No quantitative relation could be established as the individual effects of grainsize and C/S ratio on the grindability were apparently interactive and not additive.

Constituents % \ Sample No	51 (Pleistocene)	52 (Miopliocene)	53 (Cret)	54 (Perm. carb)	55 (U.Camb)	56 (L.Camb)	57 (U.Pre.Camb)	58 (L.Pre.Camb)
LOI	41.17	42.44	39.42	40.54	36.41	40.99	42.15	35.64
SiO_2	3.70	1.76	6.82	4.86	13.25	6.46	1.72	14.92
Al_2O_3	1.05	0.15	2.52	1.24	2.54	1.00	0.27	1.61
Fe_2O_3	1.24	0.11	1.83	0.75	1.59	0.81	0.45	0.85
CaO	51.63	53.87	47.93	51.44	42.72	47.90	51.43	45.08
MgO	0.96	0.66	1.10	0.53	2.94	2.16	2.69	1.32
Na_2O_3	0.05	0.06	0.05	0.04	0.58	0.58	0.50	0.03
K_2O	0.02	traces	0.04	0.02	0.10	0.03	traces	0.03
SO_3	Nil	traces	Nil	traces	0.01	traces	traces	traces
Cl	0.008	traces	traces	traces	0.01	traces	traces	traces
Variability Indices								
C/S	13.95	30.63	7.03	10.59	3.22	7.42	29.86	3.02
$\frac{C+S}{A+F}$	24.12	215.08	12.58	28.32	13.54	30.04	73.57	24.35
ϵ/B	41.74	33.97	39.16	47.08	16.73	16.73	13.73	30.45

TABLE I - CHEMICAL COMPOSITION OF LIMESTONE

TABLE II
Mineral Composition

	Sample No.							
	S_1	S_2	S_3	S_4	S_5	S_6	S_7	S_8
Major	Calcite Quartz	Calcite Quartz	Calcite Quartz	Calcite Quartz	Calcite Dolomite Quartz	Calcite Dolomite Quartz	Calcite Quartz Dolomite	Calcite Dolomite Quartz
Minor	Iron Oxide Sphene Chlorite Organic remains	Plagio-clase, Chlorite, Tremolite Iron Oxide	Montmo-rillo-nite Illite Iron Oxide	Ortho-clase Montomor-illonite Illite Iron Oxide	Ortho-clase Chlorite Musco-vite Iron Oxide	Othoclase Mascovite Chlorite	Tremolite Iron Oxide	Kaolinite Chlorite Tremolite

Grain Size

Calcite								
Range (in mm)	0,05-0.40	0.06-0.30	0.01-0.15	0.02-0.50	0,005-0.01	0.15-0.25	0.25-0.06	0.01-0.90
Average	0.09	0.12	0.05	0.20	0.005	0.20	0.40	0.45
Quartz (in mm)								
Range (in mm)	0.05-0.47	0.06-0.18	0.01-0.10	0.01-0.50	0.005-	0.01-0.07	0.11-0.57	0.22-0.53
Average	0.07	0.09	0.03	0.07	0.005	0.04	0.17	0.37

TABLE - III

Sample No	Crushing strength	Relative Grindability factor
S_1	S	1.20
S_2	H	1.25
S_3	VH	1.18
S_4	H	1.28
S_5	S	1.10
S_6	VH	1.20
S_7	MH	1.65
S_8	MH	1.40

S=Soft (0-50); MH= Moderately hard (50-400)
H = Hard (400-700); VH = Very hard (700 - 1000)

DISSOCIATION CHARACTERISTICS

The dissociation characteristics of the limestones were investigated by differential thermal analysis carried out with the help of a Hungarian MOM Derivatograph. In order to study the effect of particle size on the dessociation phenomena, each limestone was ground separately to three different finenesses (-45 μm, -150 μm, and - 250 μm) and the samples of each fineness were subject to thermal decomposition separately. The rate, temperature maximum (T max) and temperature range of decarbonisation of the limestones ground to different finenesses are presented in Table IV. From the table it is evident that: (i) no double stage decomposition (3) was observed even in the case of coarsely ground medium-grained limestones, and (ii) there was no consistent trend of increase in T max or decrease in the decarbonisation rate with decrease in the fineness of the limestones. The highest rates od decarbonisation or the lowest T max did not necessarily tally with the finest grinding. In a large number of cases the limestones ground to 150 μm and sometimes to 250 μm shows relatively lower temperature of decarbonisation or higher rates of decomposition.

Activation Energy of Dissociation

It has been reported (4) that activation energy of limestone dissociation has a strong effect on the activation energy of clinker mineral formation. The lime combination at 1300°-1400°C was observed to be higher in those cases where the activation energy of carbonate dissociation was lower.

Following the method of Imlach (5) the activation energies (Ea) of dissociation of the limestone smaples under investigation were determined (Table V). As reported by Imlach for the plant raw mixes, a two-stage decomposition with different values of Ea for the lower and upper stages could be obtained for most of the limestones. The ultimate activation energies of all the limestones lay within the range of 30-60 kcal/mole as reported by Petrosyan (4). But at the same time, no well defined relationship could be observed

between Ea and impurity alone. However, a similar interactive effect of grain size and impurity, as observed in the case of grindability, was apparent in the case of activation energy as well. The finer the grain size and the more impure a limestone, the lower is the activation energy of dissociation. Further, barring a few exceptions, which could not be readily explained, an apparent relation could be seen between Ea-Tmax and Ea-decomposition rate (Fig.1)

TABLE V
Activation energy of Dissociation

Sample No (-45 m)	Activation Energy (Kcal/Mole)	
	Lower Stage	Upper Stage
S_1	22.74	42.42
S_2	36.18	39.91
S_3	16.13	45.80
S_4	27.73	49.91
S_5	22.01	32.91
S_6	-	51.67
S_7	46.90	59.31
S_8	-	58.56

TABLE IV

Dissociation Characteristics

Sample N°	Fineness (μm)	Rate of Decomposition X 10^3 (g ms/min)	Temp. max (°C)	Temp. range of Decomposition (°C)
S_1	- 45	8.37	870	375
	-150	10.11	920	360
	-250	11.0	925	360
S_2	- 45	13.03	930	340
	-150	14.26	940	295
	-250	13.88	920	320
S_3	- 45	9.12	940	400
	-150	11.05	940	335
	-250	9.0	935	290
S_4	- 45	11.52	910	290
	-150	15.0	925	270
	-250	14.11	980	320
S_5	- 45	7.95	915	400
	-150	9.86	960	390
	-250	11.42	900	325
S_6	- 45	12.57	895	285
	-150	13.82	905	290
	-250	13.97	935	305
S_7	- 45	13.66	920	270
	-150	15.60	930	270
	-150	13.38	930	295
S_8	- 45	13.75	945	250
	-250	13.0	925	250
	-250	6.83	915	260

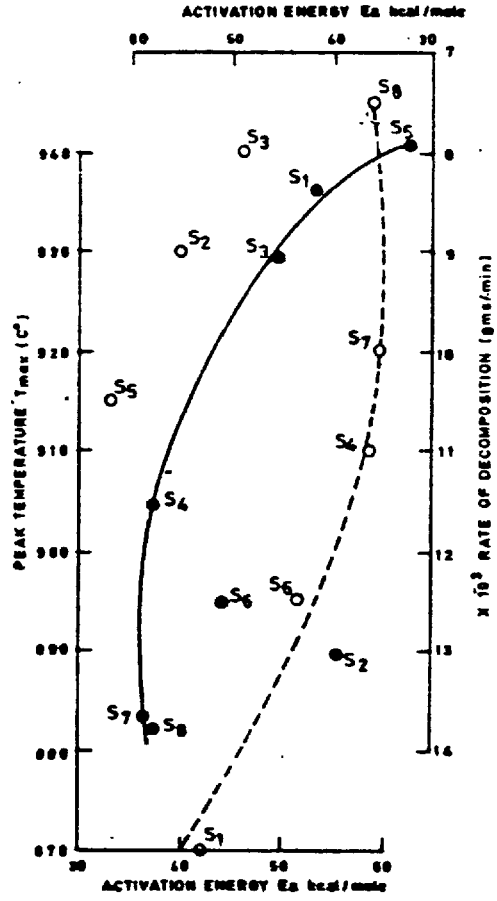

FIG.1 ACTIVATION ENERGY Ea Vs RATE OF DECOMPOSITION (——, ●) AND PEAK TEMPERATURE T_{max} (----, ○)

HIGH-TEMPERATURE REACTIVITY

In order to establish the intrinsic reactivity of the limestones, samples of each variety ground to a fineness of -150 μm, were fired at temperatures ranging from 600° to 1100°C at intervals of 100°C and the phase changes taking place at different temperature were studied by X-ray diffractometry (Table VI and Fig. 2).

It is evident from this investigation that the early formation of C_2S is favoured by relatively lower

activation energy of carbonate dissociation simultaneously with the presence of fluxes along with silica. With higher activation energy the appearance of C_2S takes place at higher temperatures. In the absence of fluxes the C_2S formation is pushed to high temperatures and the released lime crystals after dissociation tend to grow with loss of reactivity. The new mineral formation was detected, as a rule, at temperatures above 800°C and depending on the limestone characteristics the first phases detected were C_2F, C_2AS, C_2S and C_3A. The presence of dolomite did not show any significant effect on the kinetics of dissociation and mineral formation.

TABLE VI

Changes in Phase Composition of Limestone with Temperature

Sample No.	Temperature Range (°C)					
	600	700	800	900	1000	1100
S_1	Calcite Quartz	Calcite Quartz	Calcite Quartz	Calcite Quartz	Calcium Hydroxide Quartz Calcite	Calcium Hydroxide Calcite Quartz
S_2	Calcite Quartz	Calcite Quartz	Calcite Quartz	Calcite Calcium Hydroxide Quartz	Calcium Hydroxide Calite Quartz	Calcium Hydroxide Calcite Quartz
S_4	Calcite Quartz	Calcite Quartz	Calcite Quartz	Calcite Quartz	Calcium Hydroxide Quartz Tricalcium- aluminate calcite	Calcium Hydroxide Quartz Calcite Tricalcium- aluminate
S_5	Calcite Quartz Dolomite	Calcite Quartz Dolomite	Calcite Quartz Dolomite	Calcite Calcium Hydroxide Dicalcium Silicate Quartz	Calcite Calcium Hydroxide Dicalcium Silicate Quartz	Calcium Hydroxide Calcite Dicalcium Silicate Quartz
S_6	Calcite Quartz	Calcite Quartz	Calcite Quartz	Calcite Quartz Calcium- Hydroxide	Calcium Hydroxide Calcite Quartz Dicalcium Silicate	Calcium Hydroxide Calcite Dicalcium Silicate Quartz
S_7	Calcite Dolomite Quartz	Calcite Dolomite Quartz	Calcite Quartz Dolomite	Calcite Tricalcium Aluminate Quatz	Calcite Calcium Hydroxide Tricalcium Aluminate Quartz	Calcium Hydroxide Calcite Tricalcium Aluminate Quartz
S_8	Calcite Quartz Dolomite	Calcite Quartz Dolomite	Calcite Quartz Dolomite	Calcite Quartz Calcium Hydroxide	Calcium Hydroxide Quartz Calcite Dicalcium Silicate	Calcium Hydroxide Quartz Calcite Dicalcium Silicate

CONCLUSIONS

A wide variety of limestones belonging to different geological ages and horizons as well as differing in their chemicomineralogical and textural characteristics showed that, although no direct correlation of reactivity and dissociation characteristics of limestone is possible with their geological age and genesis, they can be linked up with their chemicomineralogical and textural features. For the given set of limestones the crushing strength and grindability have displayed an apparent relation with grain size and impurities present in limestones. These two parameters also appear to have a significant effect on the activation energy of carbonate dissociation. The formation of dicalcium silicate at relatively lower temperature is favoured in limestones with lower activation energy of dissociation and simultaneous presence of fluxing oxides; otherwise the new phases that form are C_2F, C_2AS and C_3A, depending on the limestone characteristics. For the given limestone the first appearance of new phases was a temperature above 800°C. The dolomite did not show any

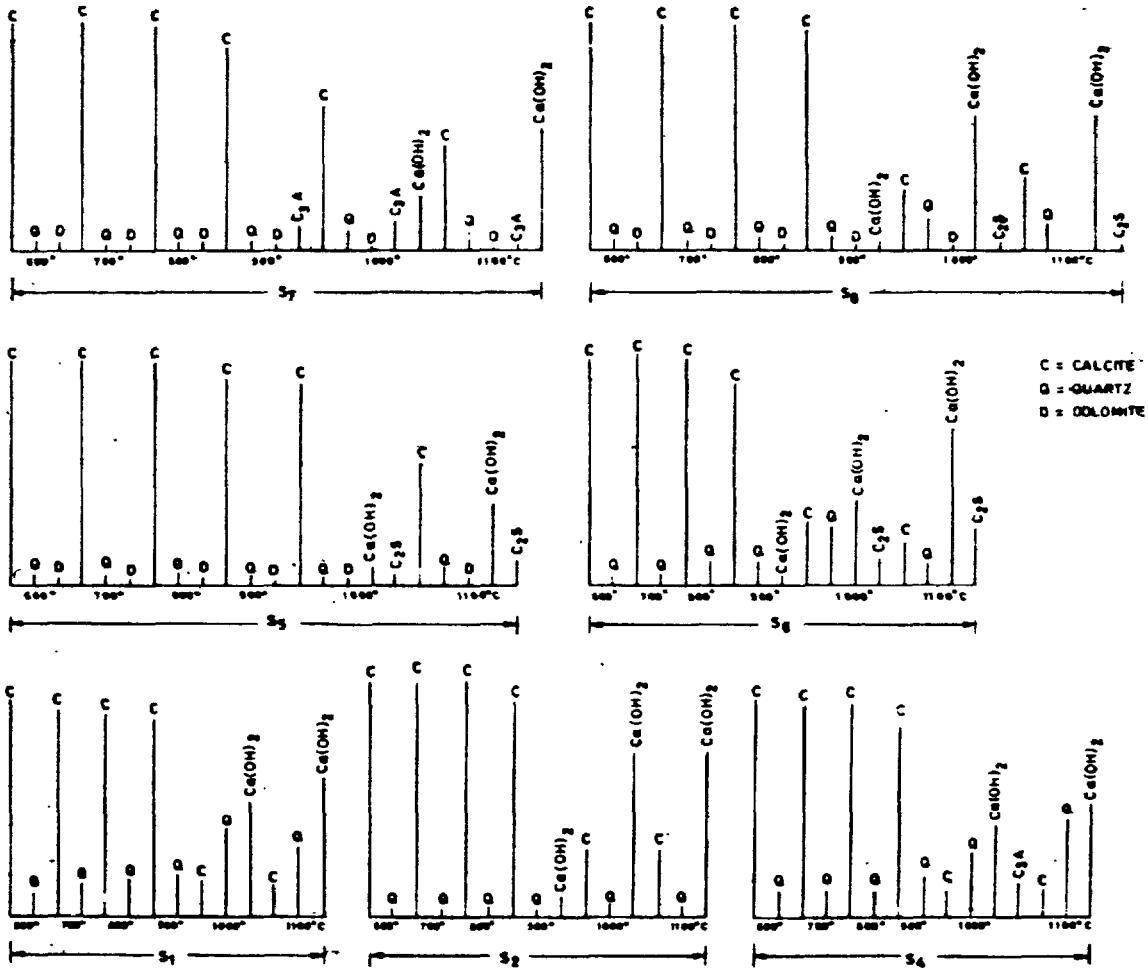

FIG. 2 CHANGES IN PHASE COMPOSITION OF LIMESTONE WITH TEMPERATURE

significant effect on the dissociation or reaction kinetics. On the whole, the grain size jointly with the impurities present in limestones controls their process response.

ACKNOWLEDGEMENT

The work rerported here is part of the R&D programme of the Institute and the report is being communicated with the permission of the Director-General, Cement Research Institute of India.

BIBLOGRAPHIE

1. A K CHATTERJEE "Physicochemical Characteristics of cement raw materials and reactivity of raw mixes - A review of diagnostic inter relations", Pit and quarry (in press)
2. V S KOLOKOLNIKOV and T AOLOKINA (1974) "Manufacture of cement", Visshaya Shkola, Moscow
3. M T VLASOVA (1976) " Periodicity of clinker formation processes". Proceedings of the Sixth International Congress on Cement Chemistry, Vol. I pp 127 - 151.
4. O P MCHEDLOV-PETROSYAN, T Yu SHCHETKINA et N I SERPOXHNIKOVA (1978) Tsement; No. 9, 8
5. J A IMLACH (1976) "Non thermal investigation of the Kinetics of reactions occuring during clinker formation", Vol 6 p 747.

Burnability of industrial Portland cement raw mixes

Cuisabilité des crus du ciment de Portland industriel

U. LUDWIG, Institut für Gesteinshüttenkunde, RWTH Aachen, Allemagne Fédérale,
S.E. IBRAHIM, Bagdad.

RESUME : La cuisabilité de 14 crus granulés industriels a été déterminée pour des températures comprises entre 1340 et 1420°C.

La cuisabilité, pour une certaine température, a été définie comme étant le temps de cuisson en minutes qui est nécessaire pour obtenir une teneur de la chaux libre de 2m-%.

Pour une température de cuisson de 1360°C

- l'hétérogénéité du cru élève ce temps de 19 à 525 minutes, soit en moyenne 100 minutes,
- la teneur en chaux le monte de 34 à 109 minutes, soit en moyenne 65 minutes, et
- la teneur en liquidus l'élève de 22 à 78 minutes, soit en moyenne 50 minutes.

L'élévation de la température de cuisson de 1360°C à 1420°C effectue une réduction du temps de cuisson de moitié.

La cuisson des farines non granulées cause des états actifs près de la température de déhydratation et de calcination, et par là la formation spontanée de dépôts adhérant aux réfractaires et la formation de grenailles.

A notre avis, ces états actifs sont la cause des dépots adhérents, et des annéaux dans les fours.

SUMMARY: The burnability of 14 different granulated industrial raw mixes was measured in the temperature range between 1340 and 1420°C. The burnability is the required burning period in minutes at a given burning temperature to reach a free lime content of 2 wt.-%.

At a given burning temperature of 1360°C

- the influence of the heterogeneity of the provided mixes amounts to between 19 and 525 minutes, 100 minutes on average
- the influence of the standard lime amounts to between 34 and 109, 65 minutes on average and
- the influence of the melt content amounts to between 22 and 78 minutes, 50 minutes on average.

The increase in the burning temperature from 1360 to 1420°C effects a lowering of the burning period by half.

The burning of non-granulated powder leeds in the temperature range of dehydration and decarbonization to active states and thereby to spontaneous formation of adhesions on the lining of the kiln and to the formation of granules. In our opinion they are the cause of adhesions and ringformation in the technical kiln process.

INTRODUCTION

The prediction of the burnability of a technical raw mix and of the factors influencing it is for the design and the management of cement plants of great technical and economical importance.

For determination of the burning behaviour of a raw mix the residue of free lime after a given burning period (1, 2) or the required period to achieve a given content in free lime is normally measured (3,4,5). In a paper wich has just been published (6) the authors proposed to measure the ratio between the lime combined in the clinker minerals and the total lime of the mix in relation to a temperature-range of 800 to 1450°C.

Mostly the burnability is valued only qualitatively. Quantitative valuations have existed for several years for calculating the residue of free lime or the required burning time at a given temperature from the different characteristics of a raw mix. A formula which has been used for some time in our work group (4) for the prediction of burnability was improved (7). Here the burnability again is marked as the burning period needed to achieve a residue in free lime of 2 wt.-%.

EXPERIMENTAL

Mainly the burning experiments were performed in a discontinuous working electrically heated laboratory rotary kiln. The heating was achieved by a partially sawn through coal bar inside the burning room of the kiln. The kiln is designed with a speed control. Mainly the raw mix feeding was done through the non-rotating stopper of the front wall. The stopper contains a second bore hole for temperature measurement. The depletion was done through a lateral opening.
With 600 g raw mix pellets the required period to reach the desired burning temperature amounts to 9 minutes. The burning of granulated material did not give rise to difficulties. The output was nearly 100 % of the theoretical.

Most of the raw mixes were well burned at 1360°C within 10 to 120 minutes. Mixes that needed a longer period of burning lateron were put into an electrical chamber furnace for long term burning.

Besides the measurement of free lime in the well burned clinkers, the content of alkali-, sulphate- and calcium-aluminate-ferrite phases were determined.

More details of the experimental equipment and procedure is given in (7).

Up to now we have not succeeded in burning powdered raw mix in the above-mentioned rotary kiln. The formation of active states within the raw mixes during dehydration of clay minerals and much more during decarbonization of limestone leads to raw mix deposits on the lining of the laboratory kiln. In practice the crust and ring formation in the preheater system and in the rotary kiln respectively are caused primarily in the same way. In addition we directly watched the formation of loose pellets after decarbonization at 1050°C (fig. 1).

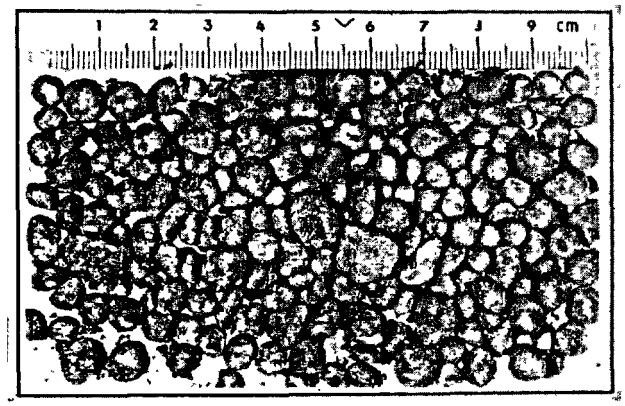

Fig. 1 - Loose raw mix pellets formed at 1050°C in the laboratory rotary kiln

RESULTS

Chemical data

For the 14 examined technical raw mixes the following variations were derived from the chemical analysis:

lime standard III	94,3	- 107,6	
silica ratio	2,1	- 4,7	
alumina ratio	0,55	- 3,8	
calculated melt content at 1360°C according to Dahl	15,0	- 28,4	wt.-%

By thermo-chemical measurement the melt formation was found to be in the range between 1270 and 1345°C. The latter value was found only at low alumina ratio and low impurity content.

Granulometrical data

The deviations in granulometric data are shown in fig. 2. A good characterisation is achieved by the gradient n and the most frequent grain diameter d' from the Rosin-Rammler-Sperling-Bennet (RRSB) diagram. -

Here as a new value the ratio between hete-

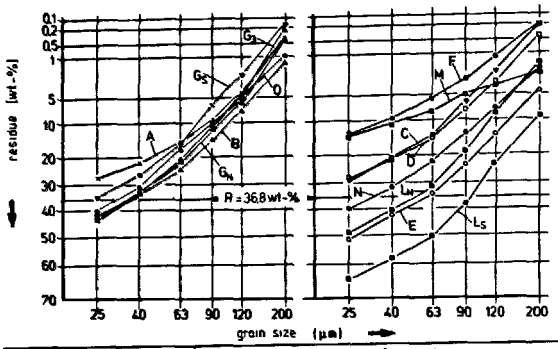

parameter	delivery state	ranges of parameters 1 1	<90 µm
gradient (n)	0,32 - 0,83	0,35 - 0,88	0,60 - 1,17
grain size (d' in µm) at R = 36,8 wt-%	3,3 - 84,4	2,3 - 47,4	2,2 - 27,7
H_{R90} [wt-%]	1,2 - 33,5	0,6 - 16,75	0
$HG = \frac{H_R}{R}$		0,11 - 0,88	

Fig. 2 - Data derived from granulometric measurement

rogenous H_R and total coarse grain content R is introduced as heterogeneity ratio HG. HG in this paper is assumed to be constant for the coarse grain fractions. For better valuation of the influence of HG raw mixes with 50 wt.-% and totally pulverized coarse fraction > 90 µm were prepared. In the table they are designated as "1:1" and "< 90 µm". The residues $R_{200\,\mu m}$ and $R_{90\,\mu m}$ which are used in pratice are directly readable from the RRSB-diagram.

Burnability data

Burnability data are derived from free lime determination dependent on the time. Four typical graphs show the time dependent decrease in free lime at several burning temperatures and also contents of coarse raw mix.

It is impossible to get raw mix A well burned within 13 hours because of the high standard lime of c. 108. Experimental work with this raw mix shows that maximum standard lime could be c. 104 to get well burned clinker (≤ 2 wt.-% free lime).

A burning period of 2 1/2 hours at 1360°C was needed to get raw mix B with standard lime of 103 and the heterogenous portion > 90 µm (H_{R90}) of 7,6 wt.-% well burned. The additional milling of the coarse fraction > 90 µm leads to a reduction of the burning period to 70 minutes.

Raw mix G_S with the lowest alumina ratio of 0,55 was less burnable at 1340°C because of the formation of the clinker melt at higher temperature. That was also established with thermo-chemical analyses.

Improved burnability was measured with raw mix C because of its favourable chemical and granulometric data.

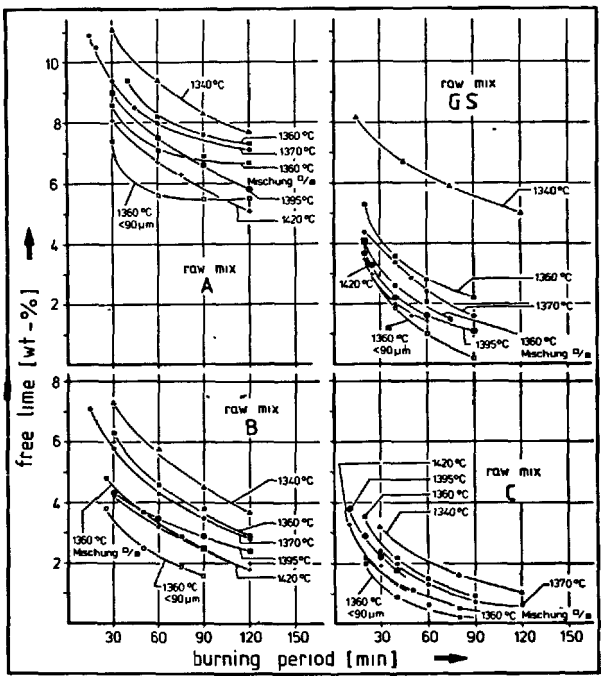

Fig. 3 - Typical free lime - time - curves at several temperatures and H_{R90}-contents

The temperature dependent inter- and extrapolated practical burnability B_T derived from the free lime - time - slopes follow an exponential equation:

$$B_T = B_{1360} e^{0.0126(1360-T)}$$

The correlation coefficient between the measured data and the data calculated from the above equation amounts to 0,95.

Fig. 4 shows a parabolic slope of the practical measured burnability as function of the

heterogeneity H_{R90}. On the other hand from the values of the burnability of 5 raw mixes with additional milling of grain fraction >25 µm the conclusion can be drawn that there is a marked influence of heterogenous particles up to this small grain size.

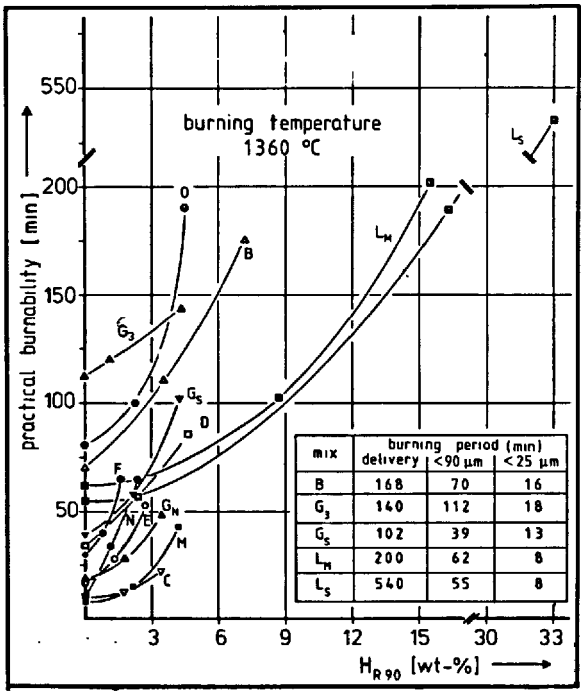

mix	burning period (min) delivery	<90 µm	<25 µm
B	168	70	16
G_3	140	112	18
G_S	102	39	13
L_M	200	62	8
L_S	540	55	8

Fig. 4 - Practical burnability as function of the heterogeneity

With a constant heterogeneity ratio HG the sum of the heterogeneity influences Σ HE are put together by HG, the gradient n, the most frequent grain diameter d' and the value of the maximum grain diameter d_{max} from RRSB-diagram.

A total prediction of the burnability of the raw mixes by computation shows besides the influences from heterogeneity an increase in the needed burning period with the square of the standard lime and a decrease with the square of the melt content. The coefficient of correlation beween the experimental data and the data calculated from the raw mix amounts to 0,96.

For all the burnability series together with the coefficient of temperature the connection represented in fig. 5 was found. The coefficient of correlation amounts to 0,94. Excluding the series with a burning temperature of 1340°C with incomplete melt formation the correlation coefficient was 0,96.

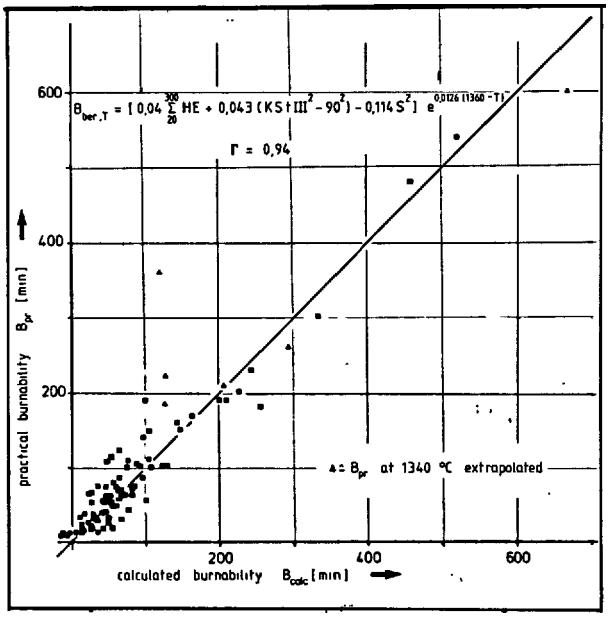

Fig. 5 - Practical and theoretical burnability

CONCLUSIONS

The time dependent measured practical burnability B_{pr} in the range of 1340 to 1420°C of 14 technical Portland cement raw mixes was set in relation to their chemical and granulometric characteristics. This results in the possibility of the prediction of a theoretical burnability B_{cal}.

The time dependent free lime content at a given burning temperature and the thereof derived B_{pr} are of great importance for the design and the operation of cement kilns. In contrast the measurement of the chemical and granulometric characteristics shows the separate influences of the heterogeneity, the lime standard, and of the melt content of a given raw mix on the burnability. This can help to optimize the composition of raw mixes.

ACKNOWLEDGMENT

The authors want to express their thanks to A. Wolter for his help in questions of mineralogical and mathematical content. - The work was supported by some cement plants that delivered the raw mixes and by the Deutsche Forschungsgemeinschaft that financed the project.

BIBLIOGRAPHIE

1.- H. KOCK, R. REY and F. Becker (1974), "A statistical model for determining the burnability of cement raw mixes", VI Intern. Cong. on the Chemistry of Cement, Moscow, Suppl. pap. 31 sect. I-4

2.- E. FUNDAL in, N.H. CHRISTENSEN (1979), Burnability of Cement Raw Mixes at 1400°C, I. The Effect of the Chemical Composition,Cement and Concrete Research, Vol. 9, 219-228

3.- N.A. TOROPOW and J.G. LUGININA (1953), "Über den Einfluß der Granaliengröße der Rohmischung auf den Bindungsprozeß des Calciumoxydes beim Brennen von Portlandzement", Silikattechn. 4 Nr. 10 470/471

4.- U. LUDWIG and G. RUCKENSTEINER (1973), "Einflüsse auf die Brennbarkeit von Zementrohmehlen", Forschungsbericht des Landes NRW, Westdeutscher Verlag Opladen, Nr. 2372

"Einfluß der Phasengrenzen bei der Klinkerbildung", XI. Siliconf., Budapest Vol. p. 365

"Einflüsse auf das Brennverhalten von Zementrohmehlen und die Klinkerqualität Tonind.-Ztg. 97, 313

(1974) "Über die Brennbarkeit von Zementrohmehlen", Cement and Concrete Res. 4, 239

5.- O. PHILIPP (1973), "Einfluß des Aufheizverhaltens auf den Garbrand von Zementklinker", Silikattechn. 24, 265-68

6.- J. KIESER, A. KRÄHNER and B. GATHEMANN (1979), "Modell zur Bestimmung der Rohmehlaktivität unter praxisähnlichen Bedingungen", Zement-Kalk-Gips 32, 442-47

7.- S.E. IBRAHIM (1979), "Zur Optimierung des Brennens von Zementrohmehlen", Dissertation Rheinisch-Westfälische-Technische Hochschule Aachen.

A comparative study of the effect of heating rate in 2-stage and 4-stage suspension preheater kiln installations

Etude comparée de l'influence de la vitesse de chauffe dans les fours avec préchauffeurs à deux et à quatre étages

M.V. RANGA RAO and KAMAL KUMAR, Cement Research Institute of India, New Delhi, India.

RESUME : Des résultats expérimentaux, obtenus sur des fours à préchauffeurs à deux et à quatre étages, installés en Inde, ont été analysés, compte tenu du traitement thermique du cru. Cette analyse a mis en évidence l'effet de la vitesse de chauffe du cru sur la structure et les propriétés du clinker produit. Après avoir tenu compte de l'effet important de la composition chimique du cru sur la structure et les propriétés du clinker produit dans ces usines (utilisant du charbon pulvérisé de qualité plus ou moins constante), on a pu identifier l'effet de la vitesse de chauffe, considérée isolément. On a constaté qu'en plus de l'effet sur la porosité et la texture, une vitesse de chauffe élevée permettait d'obtenir les principaux constituants du clinker sous la forme de cristaux très petits, ce qui a une influence favorable sur la cinétique de formation du C_2S; il en résulte aussi une productivité plus grande.

SUMMARY : Operational data obtained from one 2-stage suspension preheater kiln system and two 4-stage suspension preheater kiln systems in India have been analyzed with respect to the thermal treatment received by the raw meal in these systems. The analysis highlights the effect of the different rates of heating of the raw meal on the structure and properties of the clinker produced. After giving due weightage to the effect of differences in chemical characteristics of raw meal on the structure and properties of clinker produced in these installations (using pulverised coal of more or less similar characteristics) the effect of heating rate alone on these properties has been identified. It is observed that, besides the effect on porosity, texture, etc. higher heating rate gives rise to relatively small size crystals of the major minerals and has a favourable influence on the kinetics of C_3S formation, thus resulting in relatively higher productivity.

INTRODUCTION

The formation and properties of Portland Cement clinker in rotary kilns are influenced by a number of parameters such as (i) Raw Meal chemical composition, its particle size distribution and homogeneity, (ii) Rate of heating of the Meal and the temperature at the time of occurrence of reactions, (iii) Fuel type and quality and (iv) Ash composition and absorption in the case of solid fuels containing inorganic mineral matter. Of the above (ii) is an inbuilt feature of System Design largely dependent on the type of fuel. With solid fuels of the grade mentioned in the text, reactions have proved to be more complex and any attempt to analyse data obtained from such systems is likely to lead to conflicting conclusions. Nevertheless an attempt is made in this paper to analyse the effect of the parameter on the microstructure of clinkers obtained from 3 different dry process suspension preheater kiln systems one of which has a 2 stage preheater kiln. All these systems used semi-Bituminous coal as fuel.

SYSTEM DETAILS

The system details of the 3 plants are given in Table I. The two 4 stage SP installations are herein designated as S_I, S_{II} and the two stage SP installation is designated as S_{III}. These three units have different rated capacities and these range from 300 tpd to 900 tpd. The clinker samples examined for this paper were taken when the operation was stable.

TABLE I

Kiln System Details

Sl. No.	Parameter	Systems I	II	III
1.	L/D_E*	15.69	16.62	23.95
2.	Slope of kiln	3.5%	3.0%	3.0%
3.	Preheater fan capacity (m^3/min at 350°C)	1400	3400	1810
4.	Pressure (mm of Wg)	650	550	720
5.	Type of Coller	Grate	Unax	Unax
6.	RPM of kiln			
	Max	2	1.5	1.5
	Min	0.3	0.5	0.5

D_E* = Effective kiln Diameter (inside brick lining)

RAW MEAL AND CLINKER CHEMICAL CHARACTERISTICS

Table II shows the character of the kiln feed used as meal in the different systems and the chemical characteristics of the corresponding clinkers produced therefrom. The inherent character of the coals used in these systems is given in Table III.

TABLE II

Character of Kiln feeds and Chemical Characteristics of Corresponding Clinkers

	S_I		S_{II}		S_{III}	
	KF	CL	KF	CL	KF	CL
LOI	36.04	1.12	35.92	1.02	35.66	0.88
SiO_2	10.87	22.17	12.60	21.08	13.67	22.79
CaO	42.76	61.24	44.59	65.51	43.90	64.20
Al_2O_3	3.30	5.05	3.54	6.20	2.45	4.66
Fe_2O_3	1.75	2.59	1.80	3.10	2.10	3.55
MgO	3.20	4.71	0.86	1.31	1.07	1.60
Mn_2O_3	1.55	Balance	-	Balance	-	Balance
Na_2O	-	0.18	0.09	0.14	0.22	0.34
K_2O	-	1.45	0.50	0.73	0.60	0.88
SO_3	-	-	-	-	0.33	0.49
Moduli values						
LSF	1.17	0.88	1.09	0.98	1.03	0.88
SM	3.2	2.90	2.35	2.00	3.00	2.77
AM	1.9	1.95	1.97	2.00	1.17	1.31
LC	24.09	27.07	24.87	27.48	21.94	25.00

TABLE III

Inherent Characteristics of Coals

Parameter	System I	II	III
% Residue 170 mesh	17.0	16.0	17.0
% Moisture	5.78	1.62	2.6
% Volatile matter	36.46	27.90	29.50
% Ash	29.34	25.44	26.0
% Fixed Carbon	28.40	45.08	41.90
Net calorific value	3960	5200	5090

OPERATIONAL DATA

The operational data relating to the threee installations S_I, S_{II} and S_{III} are reproduced in Table IV.

EFFECT OF RAW MEAL CHARACTER AND ASH ABSORPTION ALONE ON CLINKER STRUCTURE

It may be seen from Table II that the characteristic Moduli values of the raw material and the corresponding clinkers do not follow the same trend as is normally to be expected provided the operational parameters and coal quality, ash composition and fusion point System Design, are similar. The chemical characteristics of clinker, would not alone reflect how much of ash might have been absorbed in them. As such it may not be correct to infer that the effect of differences in the Moduli values of meal in these systems has not been any significant in respect of ash absorption and thereby the clinker structure. Thus the effect of differences in the characteristic values, viz. LSF, SM, AM of the rawmeal on the texture and porosity of the clinkers produced could be attributed to differences in the system design and operational parameters and could be delineated as follows:

a) On the basis of SM values, the size of alite crystals formed from RM_{III} would be larger than those from RM_{I} and smaller than those of RM_{II}

b) On the basis of AM values, the size of alite crystals formed from RM_{III} would be larger than those of both RM_{I} and RM_{II}

c) On the basis of LSF also, the size of alite crystals from RM_{III} would be larger than those of RM_{I} & RM_{II}. The nett deduction of a,b, & c would thus be that much larger sized alite crystals would have been formed in S_{III} than in S_{II} & S_{I}.

TABLE IV

Operational Data

Sl No	Parameter	Systems I	II	III
1.	Kiln speed RPM	1.8	1.5	1.5
2.	Temperature Primary Air °C	60	70	60
	Secondary Air °C	760	710	700
3.	Coal Consumption kg/kg-cl	0.29	0.18	0.21
4.	Temp of gas at kiln inlet °C	920	930	780
	at Preheater outlet °C	395	350	400
5.	% Calcination at kiln inlet	25	35	NIL
6.	Temp of rawmeal at Feed Point to S.P °C	60	70	60
	Kiln inlet °C	775	830	580
7.	Residence time of meal in kiln (Minutes)	41.6	65.2	100
8.	Temp Profile in the kiln			
	i) Gas	1720°C→1560°C→920°C	1680°C→1495°C→930°C	1720°C→1555°C→780°C
	ii) Material	1450°C←1000°C←820°C	1450°C←1000°C←870°C	1450°C←1000°C←580°C
9.	Gas temperature corresponding to meal temperature of 1260°C	1560	1495	1555
10.	Velocity of Gases (m/sec)			
	i) Calcining Zone	8.0	8.6	6.5
	ii) Transition Zone	6.7	11.3	7.6
	iii) Burning Zone	6.2	12.5	8.0
11.	Temperature rise of meal			
	i) Calcining Zone	1000-775 = 225°C	100-830 = 170°C	100-530 = 420°C
	ii) Transition Zone	1260-1000= 260°C	260°C	260°C
	iii) Burning Zone	1450-1260= 190°C	190°C	190°C
12.	Heating rate (°C/min) in			
	i) Calcining Zone	8.8	5.8	7.6
	ii) Transition Zone	36.3	19.6	15.9

ACTUAL OBSERVATIONS

On the otherhand from microscopic observations of the clinker from these systems under an optical microscope it was seen that the relative sizes of the alite and belite crystals in different clinkers revealed that clinkers from S_{III} are smaller in size than those from S_I & S_{II}. The photo micrographs of the 3 clinkers are shown in Figures 1, 2 and 3 respectively.

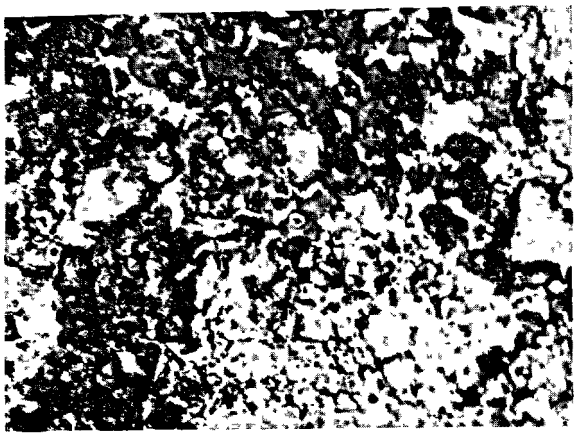

Fig. 1

Fig. 2

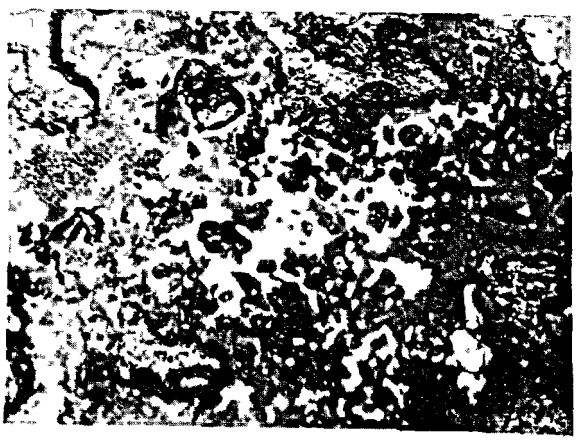

Fig. 3

INFERENCE

One may infer from the above that operational parameters such as the heating rate of meal have predominantly influenced the rate of growth of alite and belite grains and thereby the clinker's structure, porosity and to some extent texture also. How this could have happened is discussed in next section.

DISCUSSION

The deviation from the expected behaviour as derived from the chemical character of the mixes in the different systems may be summed up as follows:

Effect of operational parameters and mechanical condition of the equipment in the systems:

The parameters that influence all the rotary kiln reactions are:

i) Velocity of flue gases

ii) Temperature and Partial pressures of radiant gases.

iii) Residence time of the meal as derived from the rates of heat transfer.

The effect of above parameters on the course of the reactions in the kiln are discussed in the following sub sections.

Velocity of Gases

Due to the counter-current flow of gas and meal, the relatively higher velocity of gas entrains the solid particles, the quantity of particles entrained depending on the physical characteristics such as shape, density and texture. The density of calcium oxide being greater than silicon dioxide, sometimes it remains in the mass of meal as SiO_2 is lifted up due to the turbulent action of the gas stream in the loosely packed surface of the mass of meal exposed to it. Another parameter which is of great significance and importance is the origin of SiO_2. If it is present as free α-quartz, its particle size, shape and texture being different from silica obtained from in-situ dissosiation of argillaceous components in the meal is not so easily carried by the gas except for the finer fractions.

Temperature and Partial Pressure of the Gases

Although partial pressure of CO_2 & H_2O in the gases suppress the calcining reaction as it progressively increases unstream of the kiln and then upto the 2nd stage of the preheater. The retardation in the decarbonation reaction is made up by the increase in radiant heat supplied to the meal by CO_2 and H_2O in the gas stream along with SO_2 and other diatomic gases. (Stefan-Boltzman's law still forms a basis for all radiant heat exchange calculations. Although the view factor & the product of absorptivity and emissivity explain the mechanism of radiant heat transfer, certain hitherto uninvestigated phenomena, which in our view account for the differences in the crystal sizes of C_2S and C_3S, are promoted by relatively higher temperature prevailing in the sintering zone.)

In S_I, pco_2 at the boundary of Tr I and calcining zones was less than in S_{II} & S_{III} whereas at kiln inlet the gases in S_{III} had comparatively a higher value. The PH_2O values were more or less the same

at the corresponding points in the systems.

CONCLUSION

Reactions occurring in the kiln

The sequence of reactions in the burning zone finally alter the grain sizes and boundaries depending on the operating sintering zone temperature. The quantum of heat transfer in the zone depends on the CO_2 and water vapour partial pressure in the combustion products. The thermodynamics of combustion of coal are inturn responsible for the changes in the values of partial pressure in the zones specially of CO_2. The thermodynamics of combustion inturn depends on the quality of coal, fineness and ash content. Coal finness seems to play a vital role in the clinkerisation process. What comes into the sintering zone viz. C_4AF, C_3A and C_2S, CaO (uncombined) forms the nucleus for further reactions in the zone. The two fluxing compounds melt and along with CaO form the vehicle for the remaining mineral C_2S to react with the balance unsatisfied CaO both in the liquid and solid states. The differences in the reaction times of the partially combined oxides of CaO, Al_2O_3 and Fe_2O_3 on one hand and the complete combination of SiO_2 with the CaO already liberated in the calcining zone on the other, obviously explain the differences observed in the microstructure of the clinkers obtained in the sintering zones of the respective systems produced as a result of disintegration/dissosiation phenomena occurring in the transition zone with the C_2S transformation to C_3S being promoted at the relatively higher temperatures prevailing in the sintering zone.

From the heating rates, as can be deduced from the temperature and pressure conditions at the boundaries of the reaction zone, it is to be inferred that low heating rates prevailed in calcining and burning zones and thus allowed the formation of more number of nuclei which ultimately result in smaller sized grains of C_2S and C_3S as is evident from the photomicrograph in Fig.3.

ACKNOWLEDGEMENT

The work reported here is part of the R&D programme of the Institute and the report is being communicated with the permission of the Director General, Cement Research Institute of India, New Delhi.

BIBLIOGRAPHY

1. A.K. CHATTERJEE (1979) "Phase composition, microstructure, quality and burning of portland cement clinkers - A review of phenomenological inter-relations - Part I" World Cement Technology, 10, 4, 124, 127-8, 131-5.
2. A.K. CHATTERJEE (1979) "Phase composition, microstructure, quality and burning of portland cement clinkers - A review of phenomenological inter-relation - Part II", World Cement Technology, 10, 5, 165-8, 171-3.

Effect of Na_2O on the stability of calcium aluminoferrite under the reducing atmosphere

Effet du Na_2O sur la stabilité de l'aluminoferrite de calcium sous atmosphère réductrice

M. ONO, Senior Research Engineer, Research and Development Laboratory,
M. AKITA, Research Engineer, Mitsubishi Ming and Cement Co., Ltd.,
K. HIKITA, Research Engineer, Tokyo, Japan.

RESUME : La phase aluminate contenue dans le clinker de ciment portland, produit dans des fours à atmosphère réductrice, augmente avec la réduction de la phase ferrite. Pour en comprendre le mécanisme, la stabilité de l'aluminoferrite de calcium (C_4AF), avec ou sans Na_2O, a été étudiée à 1420°C dans l'air et dans différentes atmosphères réductrices.

Sans Na_2O dans le système, l'aluminate tricalcique se forme à partir de la ferrite quand la pression partielle de l'oxygène est maintenue à moins de 10^{-4} atm. En présence de Na_2O l'aluminate se sépare de la ferrite dans n'importe quelle condition de cuisson, sans relation avec la pression partielle d'oxygène, mais la quantité d'aluminate formé augmente avec la diminution de la pression partielle d'oxygène.

Les phases cubique, orthorhombique et monoclinique de l'aluminate sont formées à partir de la ferrite suivant la quantité de Na_2O contenue dans le système.

On détermine également la solubilité solide du fer dans cette phase aluminate.

SUMMARY : Aluminate phase content in portland cement clinker increases with the reduction of ferrite phase burning under the reducing atmosphere. To clarify the mechanism, the stability of calcium aluminoferrite (C_4AF) with or without Na_2O was investigated at 1420°C in air and several reducing conditions.

Without Na_2O in the system, tricalcium aluminate phase is formed from ferrite phase when the partial pressure of oxygen is kept less than 10^{-4} atm. In the presence of Na_2O, aluminate is seperated from ferrite in all heating conditions having no connection with the oxygen partial pressure, but the amount of aluminate formed increases with lower oxygen partial pressure.

Cubic, orthorhombic and monoclinic phases of aluminate is formed from ferrite depending upon the Na_2O content in the system.

The solid solubility of iron in these aluminate phase is also determined.

INTRODUCTION

It is very important for the cement technology to make clear the atmospheric effect on the formation of clinker minerals. Most of the investigations which have been carried out in this field are as for the silicate phases, and only a few investigations, on the contrary, have been done to the interstitial materials. Some workers reported that the quantitave ratio of the dark and light interstitial materials was changed in accordance with the oxygen partial pressure (1),(2),(3). J.A.Imlach and F.P.Glasser gave many investigations in regard to the effect of oxygen partial pressure on the formation of the clinker minerals in CaO-Al_2O_3-FeO-Fe_2O_3 system under 10^{-5} and 10^{-8} atm. of the oxygen partial pressure (4). In this report, the stability of ferrite phase with Na_2O at the elevated temperature under 0.21, 10^{-4},10^{-7} and 10^{-9} atm. of the oxygen partial pressure is dicussed from some experimental results.

EXPERIMENT

C_4AF burned at 1380°C in air and Na_2O (as Na_2CO_3) were mixed in various ratios and reheated under 0.21(in air), 10^{-4}(in dry N_2), 10^{-7} and 10^{-9} (in CO/CO_2 mixture) atm. of the oxygen partial pressure(Po_2).
Samples were kept 30 min. at 1420°C in the platinum crucibles put into the alumina tube furnace (50 mmϕ). The fused samples were cooled to 900°C at the rate of 5°C/min. and then allowed to cool to room temperature. The total gas flow rate was 400ml/min.. The samples were subjected to the exminations by X-ray powder diffraction, electron probe microanalysis, microscopic observation and chemical analysis.

RESULTS

It is shown for the X-ray powder diffraction that any phase except ferrite can not be detected from the sample without Na_2O which is burned under 0.21 and 10^{-4} atm. Po_2. However in the presence of Na_2O, orthorhombic C_3A is formed from C_4AF. In proportion as Na_2O content the quentity of C_3A increases and its crystal system changes from orthorhombic to monoclinic. If Na_2O content of the samples reaches over 2.8%, C_3A formed from C_4AF is decomposed into free CaO and β-$NaAlO_2$. When the samples without Na_2O are burned under the condition of 10^{-7} atm. Po_2, cubic C_3A is formed from the ferrite phase. In this case, free CaO and α-Fe are also detected. However burning C_4AF with Na_2O under the same condition, the quantity of C_3A increases and its crystal system changes from cubic to monoclinic through orthorhombic in proportion as Na_2O content in the system. Under the condition of 10^{-9} atm. Po_2, FeO is detected having no connection with Na_2O content in addition to the minerals described above.
Small amount of the C_3A phase which is not detected by X-ray diffraction, is observed in the samples burned under 10^{-4}atm. Po_2 by reflective microscopy. It is shown in Fig.1 that the parameter P of the residual ferrite phase ($C_2A_PF_{1-P}$) decreases with lower Po_2 at the reheating condition and the analytical value of the reheated sample.
As shown in Fig.2 and Fig.3, the content of

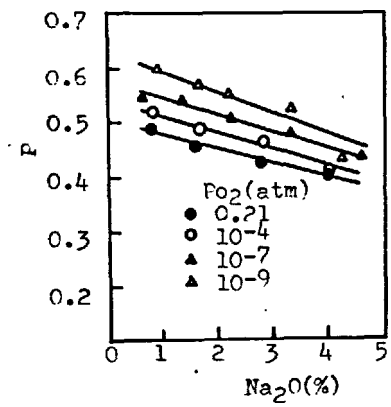

Fig.1 Relation between the residual ferrite phase composition($C_2A_PF_{1-P}$) and Na_2O content in the reheated sample.

Na_2O and Fe_2O_3 in the C_3A phase formed from the initial C_4AF are related to the quantity of Na_2O in the reheating sample and Po_2 at the reheating condition. In the case of Po_2 above 10^{-9} atm., Na_2O content of the C_3A phase reaches the maximum value of 6.2% when Na_2O is included more than 2.8% in the reheated sample.

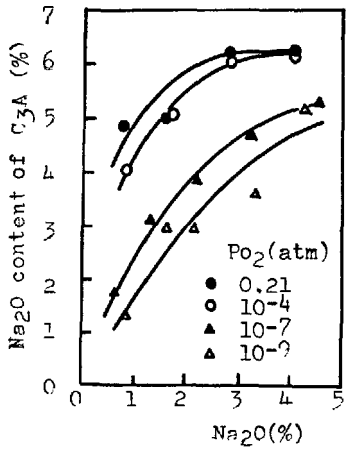

Fig.2 Relation between Na_2O content of C_3A and the quantity of Na_2O in the reheated sample.

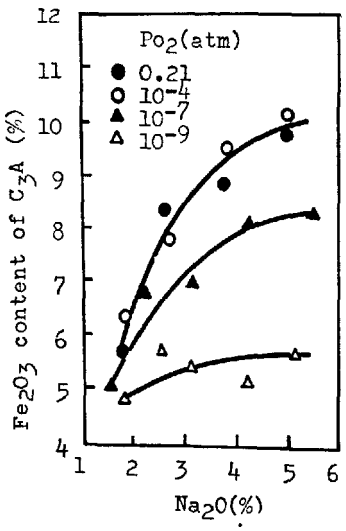

Fig.3 Relation between Fe_2O_3 content of C_3A phase and the quantity of Na_2O in the reheated sample.

It can be read off from Fig.4 that linear relationship exists between Na_2O and Fe_2O_3 content of the C_3A phase under every Po_2 except 0.21 atm., and its slope decreases with the lower Po_2.

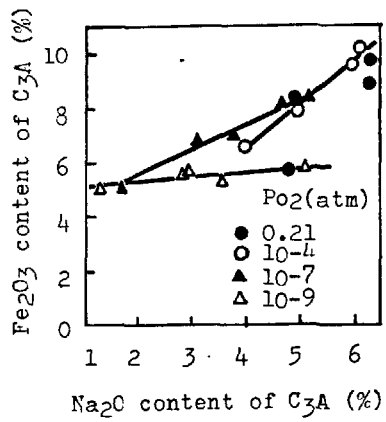

Fig.4 Relation between Fe_2O_3 content and Na_2O content of the C_3A phase.

DISCUSSION

Ferrite phase is unstable under the reducing atmosphere. Therefor, without Na_2O it bigins to decompose under 10^{-4} atm. and C_3A, free CaO, α-Fe and FeO phase are formed below 10^{-7} atm. Po_2. In the presence of Na_2O, the formation of C_3A from ferrite phase is promoted and the composition of the residual ferrite phase shifts to higher Fe composition. The C_3A phase formed from the initial ferrite phase contains Fe_2O_3 and its quantity changes lineally depending upon the Na_2O content which is included in the C_3A phase simultaneously. G. Yamaguchi et al.(5) estimated that the distribution of Fe^{3+} ion extend to the Al^{3+} sites as well as the Ca^{2+} sites in cubic C_3A. Therefor the results of the present study are sufficint to understand that the substitution of Fe^{3+} by Ca^{2+} ion in the C_3A phase obeys following equation in the presence of Na^+ ion.

$$2Ca^{2+} \longrightarrow Na^+ + Fe^{3+}$$

If the above substitution could be occur Fe_2O_3 content might be increased in proportion as the content of Na_2O in the C_3A phase.

CONCLUSION

The stability of C_4AF with or without Na_2O was investigated at the elevated temperature in air and several reducing conditions. The ferrite phase without Na_2O bigins to decompose under 10^{-4} atm. Po_2 and C_3A, free CaO, -Fe and FeO phase are formed below 10^{-7}atm.. In the presence of Na_2O, the formation of C_3A phase from ferrite phase is promoted in all heating condition having no connection with Po_2. The C_3A phase formed from the initial ferrite phase contains Fe_2O_3 and its quantity changes lineally depending upon the Na_2O content which is included in the C_3A phase simultaneously.

REFERENCE

1.- E. WOERMANN ; "Decomposition of Alit in Technical Poltrand Cement Clinker", Proc. IV. Int. Symp. Chem. Cem., Washington Vol.1, 119-129, (1960)

2.- Y. SUZUKAWA and T. SASAKI ;" Influence of Reducing Atmosphere on the Constitution of Clinker", Proc. IV. Int. Symp. Chem. Cem., Washington Vol.1, 83-85, (1960)

3.- H. M. SYLLA ; " Einfluss der Ofenatmosphare beim Brennen von Zementklinker", Zement-Kalk-Gips, 31 (6), 291-293, (1978)

4.- J. A. IMLACH and F. P. GLASSER ; "Phase Relation in the System CaO-Al_2O_3-Fe_2O_3-FeO at Liquidus Temperature", Trans. Brit. Ceram. Soc., 72 (5), 221-228, (1973)

5 - G. YAMAGUCHI, K. SHIRASUKA and T. MORITA; "The X-ray Study on the Tricalcium Aluminate with the Fe^{3+} Ions Substitution", Yogyo-Kyokai-Shi, 78 (7), 221-223, (1970)

Aging of cement through long term storage

Vieillissement du ciment lors du stockage à longue durée

Dr. M. MAULTZSCH, M. GIERLOFF and Dr. P. SCHIMMELWITZ, Federal Institute for Testing Materials (Bundesanstalt für Materialprüfung (BAM) Berlin, R.F.A.

RESUME : Jusqu'à présent, on n'a étudié la stockabilité du ciment que pendant des durées de 3 à 12 mois. On communique ici des recherches effectuées sur des ciments stockés de 7 à 15 ans. Des ciments ayant été stockés en sacs de papier revêtus furent légèrement hydratés de façons variées. D'analyses de phases par thermogravimétrie, il ressort qu'il s'était formé pendant le stockage, avant tout, des silicates hydratés de calcium, de l'ettringite et de la syngénite. Dans des zones marginales solidifiées du contenu des sacs, apparurent, de façon importante, du silicate hydraté de calcium et de la calcite. On a pu considérer la teneur en eau évaporable jusqu'à 180°C (par des analyses thermogravimétriques) comme mesure du degré d'hydratation des ciments stockés. Ce paramètre fut mis en relation avec le développement de la résistance mécanique; il a servi aussi pour la représentation de la répartition locale de l'eau de hydrate dans des sacs de ciment individuels. Comparée avec des ciments frais, l'évolution de l'hydratation des ciments de stockage est caractérisée par une portion moins importante de silicates hydratés de calcium et d'ettringite nouvellement formés durant les premières heures après le gâchage et par la formation initiale de gypse secondaire. Là se trouve la raison de valeurs de résistance amoindries, spécialement dans la phase initiale. Cependant, on a pu constater clairement que des ciments stockés pour une durée de 15 ans atteignent aussi des résistances finales encore satisfaisantes.

SUMMARY: The storage possibility of cement was tested till now only for the period of 3 to 12 months, whereas here tests were made on cement stored for a period of 7 to 15 years. The cements, stored in laminated paper bags were differently pre-hydrated. Thermogravimetrical phase determinations showed that principally calcium silicate hydrate, ettringite and syngenite were formed during the storage, Calcium silicate hydrate and calcite could be found especially in the hardened exterior parts of the bags. Through the thermogravimetrical analysis the water content was defined as reference for the hydration degree, as the water evaporable up to 180 °C. This reference unit can be related to the strength development; aswell the unit serves to describe the space distribution of the hydration water in various cement bags. In comparison to fresh cements the process of hydration of stored cement is characterized by smaller contents of new-formed calcium silicate hydrate and ettringite during the first hours after the addition of water and an initial formation of secundary gypsum. Herein lays the reason for the partially lower values of the strength, especially of early strength. Nevertheless it was established definitely that 15 years long stored cement reaches a satisfactory final strength.

INTRODUCTION

It is well known that the storage of cement may impair its most important property, the strengthening of mortar and concrete. The extent of strength reduction depends on the type of the cement, the condition and the duration of storage. For cements in silos or in bags, stored for 3 months in a dry shed, the loss of strength may be about 10 % (1), in another study values of 10 - 20 % are mentioned for 3 months storage and 20 - 30 % for 6 months storage (2).

Some of the earliest investigations on the aging of cements are those of Gary and Burchartz (3,4), carried out in the former Royal Office for Testing Materials, now Federal Institute for Testing Materials (BAM) in Berlin. The cements, spread out on the floor or filled in paper bags, were exposed to laboratory atmosphere for three or six months. They showed retardation of setting, lower hydration heat development and lower density than the samples of fresh cements, and they contained lumps. The strength values after 28 d hardening were up to 40 % but after 5 years hardening only about 15 % lower than those of fresh cements. In other studies cement bags were stored for 12 months. The early strength development was reduced by 30 %, while the reduction in strength after 28 d and 2 years was only 22 % and 15 % respectively (5). Favorable to strength development is to screen out the lumps (6). Later on cement in 5-ply paper bags was exposed to a rather humid climate. The strength values decreased by nearly 30 %, but only by 12 % if the bags were wrapped in polyvinyl cloth (7). There are only few studies on long term storage. One of these was carried out for up to 4 years. The 28-d-strength of the cements stored in paper bags in rather humid climate came up to only 30 % compared to that of fresh cement samples (8). Most of strength reduction occurred in the early period of storage. In general the authors hardly enter into the reasons for strength reduction.

INVESTIGATIONS ON CEMENTS STORED FOR LONG TERMS

During the last years the Federal Institute for Testing Materials (BAM) in Berlin had the chance to test cements stored for at least 7 years, but mostly for 10 - 15 years. The cements in 5-ply paper bags, one ply covered with bitumen or polyethylene, were piled up to 40 bags in height in large sheds. More than 300 samples were at this investigation's disposal (9).

Many thermogravimetric analyses were made to answer the question whether the stored cements were partially hydrated or not. For example Fig. 1 (bottom) shows the differential thermogravimetric (d.t.g.) curves for samples of a 15 years old cement, taken from the outer and the inner zones of the bag. The peaks appearing with rising temperature mark the portions of adsorbed water (H), calcium silicate hydrates (C-S-H), ettringite (E), gypsum ($Cs\cdot H_2$), calcium aluminate hydrates (C-A-H), syngenite (Sy), calcium hydroxide (CH), and calcium carbonate (Cc). Fig. 1 (top) includes the corresponding curves for fresh portland cement in

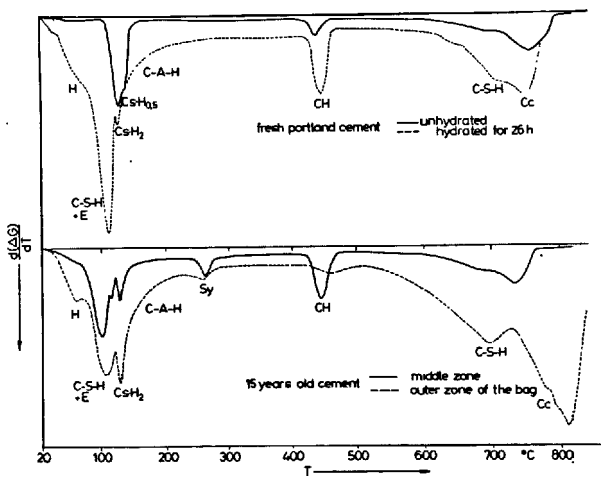

Fig. 1 - Differential thermogravimetric curves of fresh portland cement (top) and stored cement (bottom).

unhydrated and partially hydrated state. The resemblance to the curves for the partially hydrated sample and for the stored cement is evident. Related to fresh cements the stored cement contains increased portions of calcium hydroxide and ettringite, probably a certain portion of such calcium silicate hydrates too which dehydrate at the same temperatures as ettringite, though tobermorite phases dehydrating at about 700 °C do not increase in general. Aluminate hydrates could not be identified definitely. In the outer zones of the bags above all such phases which dehydrate up to 180 °C occur in higher amounts, moreover a strong carbonation is significant. Furthermore the potassium calcium sulphate "syngenite" was found in quantities of 1,1 - 1,4 % by mass, sporadically up to 4 % by mass, in all stored cements. The mineral syngenite is held responsible for the formation of lumps and for the false set (10, 11, 12). In this investigation increased portions of syngenite were found mostly in lumps. As it crytallizes in needles similar to the ettringite the syngenite may cause a certain consolidation of the cement. The strengthening or hardening of the cement in the outer zones of the bag, however, should be attributed to beginning hydration, especially the formation of ettringite, and to carbonation, as the dotted line in fig. 1 (bottom) shows. Furthermore long term stored cements may be compacted by the pressure due to the high piles of bags.

The thermogravimetric analyses of the stored cements showed essential differences for all samples in the behaviour of dehydration up to 180 °C. The weight loss in this temperature

range includes the loss of adsorbed water, the partial dehydration of C-S-H phases (and slightly of a C-A-H phases too) and of ettringite, also the complete dehydration of gypsum. Provided that each cement has a nearly constant content of gypsum due to the manufacturing process, the loss of weight at 180 °C may be seen as a measure for the degree of hydratation. For simplification it is called "water content" in the following.

The "water content" of nearly 100 samples taken from two different cement types here called A and B were determined by drying at 180 °C. In fig. 2 the "water content" values of the cements stored for various terms are compared with the compressive strength after 2 and 28 days respectively. There is a good reciprocal correlation between the values, especially with regard to the 2-d-strength. A minimum value for the "water content" of about 0,4 % by weight may be recognized, referring to the original gypsum content of the cements. If reference values are available it seems possible to infer the strength development by this simple method.

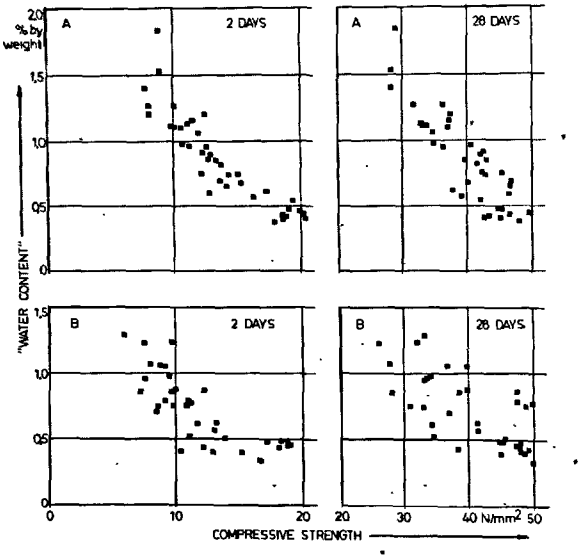

Fig. 2 - Correlation of "water content" to compressive strength after 2 and 28 days respectively, plotted for the cements "A" and "B".

It was mentioned already that the outer zones of the cement bags were partially more hydrated than the inner zones. By determining the "water content" the hydration degree of cements was examined depending on the location in the bags. Fig. 3 shows the distribution of the "water content" values in longitudinal sections of three bags piles one upon another, stored for 15 years. The maximum hydration degrees were found near the ends of the bags, above all at the filling valves on the right side of the figure. Besides the "water content" increases if the air could not circulate because of the adjacent piles of bags. In this case the probability is greater that moisture from the air would condensate on the paper bags and water diffusion would take place.

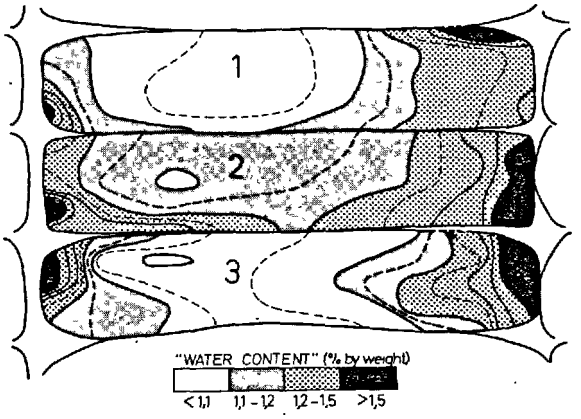

Fig. 3 - Distribution of the 180 °C-evaporabl "water content" of cement in bags stored for 15 years (longitudinal section).

The cement bags shown in longitudinal section were stored in a shed that was not heated and badly ventilated. Thus the cement was exposed to a relatively humid climate at least for some time, and to alternating temperatures. Other bags stored in a rather dry, heated shed for 15 years too were examined in the same manner. High "water contents" were found in this case only in narrow zones at the edges of the bags. Consequently the storage conditions are very important for quality decrease of long term stored cements.

A simple test ascertained the amount of time that moisture needs to penetrate the 5-ply bitumen coated paper bags and to impair the quality of cement. Samples of fresh portland cement PZ 35 F was wrapped in original paper bag material and then exposed to an ambient humidity of 95 % at 22 °C. The relative humidity inside the test bags was measured continuously (fig. 4 top). It rose quickly, and it came up to 80 % r.h. within 10 days and to more than 90 % r.h. within 40 days. That mean that the protective effect of this packing is small with regard to penetration of moisture.

At the same time the density of the cement samples decreased continuously from 3,06 g/cm to 3,01 g/cm³ within 10 weeks, as was also stated in other investigations (3, 4, 13). Furthermore samples were taken after 6, 20, 71 d respectively for tests on strength development (central part of fig. 4). In relation to the strength values of the origina cement the 2-d-strength values decreased to 40 - 60 %. The 28-d-values were not reduced before a longer period of storage; after 10 weeks the reduction was about 20 %. Alterations of mineral phases of the same cement samples were examined thermogravimetrically.

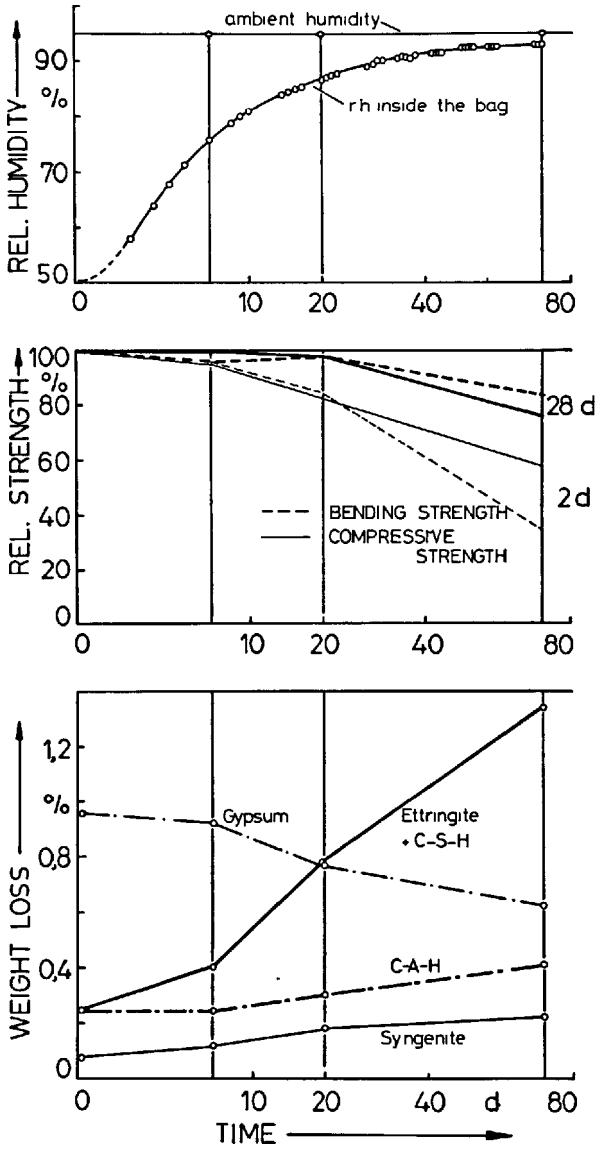

Fig. 4 - Tests by artificial storage: development in time of relative humidity inside the bag, strength values, and mineral phases expressed as weight loss (determined by thermogravimetric method)

The weight loss found by these analyses correlates to the portions of the phases, thus only the weight loss values for certain phases are taken for fig. 4 bottom. Syngenite content increases while gypsum content decreases. The beginning of hydration is shown by formation of more and more ettringite and silicate hydrates dehydrating in the same temperature range. Aluminate hydrates increase slowly. The results found after a rather short but unfaborable storage agree qualitatively with those of long term stored cements.

Alterations of mineral phases by long term storage of cements affect the process of hydration, especially during the initial period. In general the hydration process of stored cements will be retarded. In fig. 5 the contents (as weight loss by thermogravimetric analyses) of gypsum and ettringite with C-S-H respectively in various cement pastes are shown in relation to the time of hydration. The fresh portland cement is continuously forming C-S-H phases and ettringite combining gypsum at the same time. Depending on the various types of cements, the extent and the velocity of the formation of new hydrates in long term stored cements are lower. The content of gypsum even increases slightly in the beginning, probably by redissolution of some ettringite and syngenite in the mixing water. This may cause "false set" in some cases. The slow hydration proceeding within the first hours after mixing with water presumably is responsible for the lower strength values of stored cements, particularly for the early strength development.

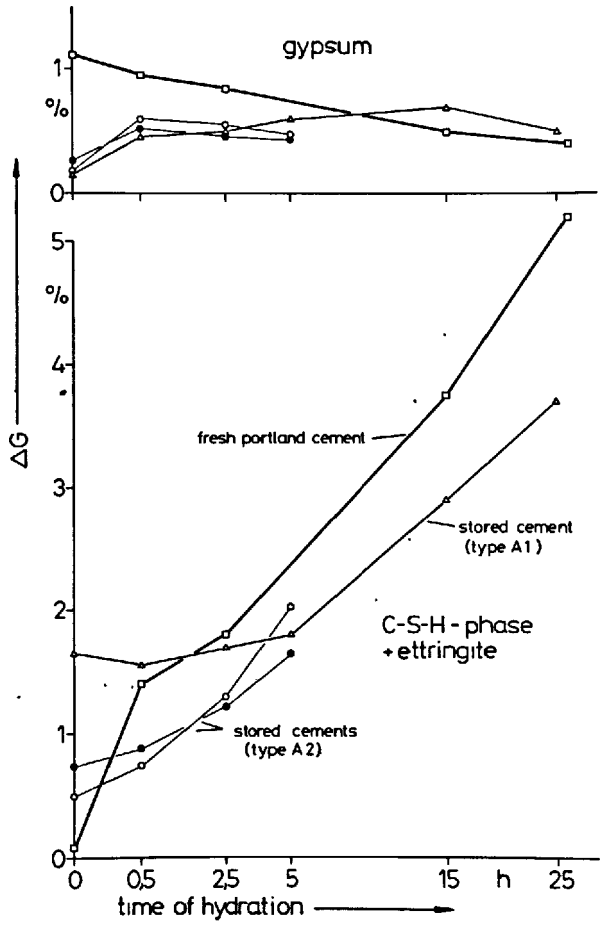

Fig. 5 - Thermogravimetrically determined weight loss Δ G referred to gypsum (top) and to C-S-H and ettringite (bottom) dependent on time of hydration.

Strength values of cements stored for 7 - 15 are spread over a large range. Classified by the age in years, the frequency of 2-d- and 28-d-compressive strength values is plotted in fig. 6. It is conspicuous that a greater number of strength values for the 11 - 15 years old cements fall below the minimum values required for comparable fresh cements. On the other hand many samples of this age reach a rather high compressive strength. Cements stored up to 10 years altogether show a higher strength than the older ones. One of the reasons may be the packing. For the younger cements one ply of the 5-ply paper bags was coated with polyethylene instead of bitumen. The moisture permeability of this material seems to be lower than that of the bitumen coated paper.

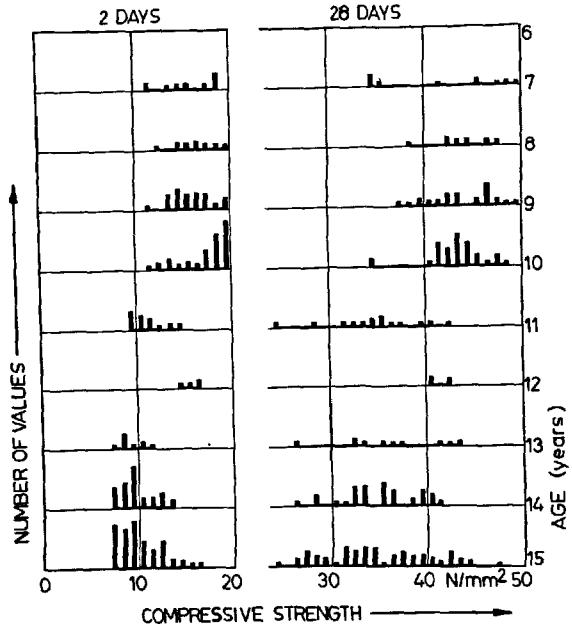

Fig. 6 - Frequency of compressive strength after 2 d and 28 d. Number of values separately plotted for the different ages of the stored cements.

The test on strength were made with unsieved samples. Further 300 partially lumpy samples recently taken from the same stores were passed through the 1-mm-sieve. In this case all values of strength exceeded the minima of 10 N/mm² after 2 d and 35 N/mm² after 28 d. Besides it is possible to obtain better strength development by adding chemical reagents or regrinding the stored cements (9).

During the storage period strength development of the cements could only be observed insufficiently because sampling by statistical point of view was impossible. The number of bags in each store amounted to 20.000 - 100.000, and the storage conditions were various and mostly undefined. Another cause is the change of the method of test according to the German standard in 1970. Nevertheless, based on all the present values one may estimate the annual reduction of the 28-d-compressive strength to 1 N/mm² or 2 % on an average with regard to long term storage in 5-ply paper bags.

CONCLUSIONS

If cements packed in coated paper bags are stored for a long term their quality will be less seriously affected than presumed on the basis of short time investigations. Even 15 years old cements are useable. In this case, however, it is recommended to screen out the lumps. Long term storage affects hydration on cement particle surfaces and formation of syngenite and ettringite. The loss of reactivity by partial hydration and particularly the changes in sulphate compounds affects a more or less retarded hydration within the first hours after mixing with water. This results in reduction of strength, expecially of early strength. One of the most important factors for preservation of quality is the storage condition. Air humidity should be low, and the stores should be provided with good ventilation.

REFERENCES

1. - G. WISCHERS (1975), "Bautechnische Eigenschaften des Zements", Zement-Taschenbuch 1976/77, pp. 75-95.

2. - F. KEIL (1963), "Zement und Zementindustrie", Zement-Taschenbuch 1964/1965, pp. 35-89.

3. - M. GARY and H. BURCHARTZ (1909), "Prüfung von Eisenportlandzement im Vergleich zu Portlandzement", Mitt. Königl. Materialprüfungsamt, 27, 338-372.

4. - H. BURCHARTZ (1920), "Versuche mit Hochofenzement", Mitt. Materialprüfungsamt 38, 163-182.

5. - R. GRÜN (1925), "Die Ablagerung von Zement", Tonind.-Z., 49, 6-7 and 475-480.

6. - R. GRÜN and H. MANECKE (1930), "Der Einfluß der Lagerung auf die Eigenschaften von Normenzementen", Zentralbl. Bauverwaltung, 50, 485-491.

7. - F. L. FITZPATRICK and W. SERKIN (1949), "Storage of Portland cement in 5-ply paper bags", J. Amer. Concr. Inst., 21, 298-300.

8. - F. MATOUSCHEK (1963), "Lagerung von Zement unter verschiednenen Bedingungen", Zement-Kalk-Gips, 16, 483-485.

9. - M. GIERLOFF and M. MAULTZSCH, (1979), "Untersuchung des Verhaltens von Lagerzementen", Forschungsber. Bundesanst. Materialprüfung.

10. - W. RICHARTZ (1973), "Einfluß der Lagerung auf die Eigenschaften des Zements", Zement-Kalk-Gips, 26, 67-74.

11. - F. MATOUSCHEK (1972), "Beitrag zur Erklärung der Knollenbildung im Zement", Zement-Kalk-Gips, 25, 395-396.

12. - H.C. ALSTED NIELSEN (1973), "Falsches Erstarren von Portlandzement und Klumpenbildung im Silo", Zement-Kalk-Gips, 26, 380-384.

13. - M. VENUAT (1965), "Propriétés des ciments chauds, refroidis ou éventés", Rev. Matér. Constr., 597, 283-297.

Mécanisme de la stabilisation dans la transformation polymorphique beta-gamma C_2S

Polymorphic Phase change of beta-gamma Ca_2SiO_4

A. DERDACKA - GRZYMEK
J. GRZYMEK, Pologne.

RESUME : Dans cette communication, on présente les résulltats des recherches faites sur l'influence de microquantités de cations étrangers et de grandes quantités d'aluminate de calcium à l'état vitreux sur le mécanisme de stabilisation du β orthosilicate de calcium. En se basant sur des résultats expérimentaux, on a proposé une formule pour estimer l'abaissement de la température de l'autodésintégration de l'orthosilicate de calcium.

La discussion des résultats a démontré que l'activité des cations dans le mécanisme de stabilisation dépend de l'intensité du champ ($e/\pi r^2$), de l'électronégativité de la configuration des électrons de valence et du nombre de charges positives des cations. Les cations qui stabilisent la modification βC_2S ont été subdivisés en deux groupes. Au premier appartiennent les cations qui stabilisent la modification βC_2S au-dessous de 0,5 % mol. par gmole C_2S. Au second appartiennent les cations dont l'effet stabilisant est observé au-dessous de 1 % mol/gmole C_2S. Les auteurs en concluent que la stabilisation résulte des surtensions dans l'intérieur des cristaux sous l'influence du champ électrostatique à cause du phénomène de la polarisation, et même de l'influence de la pression extérieure exercée sur les cristaux du βC_2S.

Le plus grand effet thermique sur les transformations polymorphiques du C_2S a été observé dans le cas de la transformation $\alpha = \alpha'_H$ (3,28 kcal/mole). La transformation la plus rapide est celle de $\beta \rightarrow \gamma$(0,22 kcal/gmole). L'autodésintégration est accompagnée d'un effet thermique de 1,2 kcal/gmole. Si pendant la transformation polymorphique on élève, puis on abaisse la température, le C_2S peut perdre 25 % de son énergie interne. Les auteurs ont constaté que l'énergie interne du réseau de C_2S atteint 4700 kcal/gmole.

SUMMARY: In this paper study of the influence of microamounts of foreign cations and of larger amounts of the glassy calcium-aluminate phase on the stabilization of calcium orthosilicate was performed. Basing on experimental results and theoretical considerations anempirical formula has been proposed for the quantitative evaluation of the decrease of the temperature of self-disintegration of calcium orthosilicate.

The discussion on the results shows that the activity of cations in the stabilization is primarily dependent from the force of the cation field ($e/\pi r^2$), electronegativity and valences. The stabilizing cations have been divided into two groups. To the first belong cations which stabilize totally the β - Ca_2SiO_4 in amounts up to 0.5% mol/gmol. To the second belong cations in case of which a stabilizing effect is observed only after addition of amounts above 1% mol/gmol Ca_2SiO_4.

Authors suggest that the directly reason of stabilizing effect are rising the strains under the effect of increasing electrostatic field inside the crystals as well as an external influence of pressure on crystals of β calcium orthosilicate phase. The network energy of calcium orthosilicate amounts about 4700 kcal/gmol.

In the paper, that the most heat effect among of the polymorphic processes of investigated Ca_2SiO_4, mark out, the two-way process of polymorphic transformation of $\alpha \rightleftarrows \alpha'_H$ /3.28 kcal/gmol/ itself was determine. The shortest one is polymorphic transformation of $\beta \rightarrow \gamma$ /0.22 kcal/gmol/. The emission of 1.2 kcal/gmol heat during self-disintegration phenomena is the consequence of polymorphic transformation. When reheating and recooling, during the polymorphic transformation, calcium orthosilicate loses about 25% heat energy emission.

Le grand intèret auprès de polymorphisme de Ca_2SiO_4, dont la preuve sont de nombreux travaux de récherche, resulte certainement d'une grande importance de ce problème pour la pratique industrielle. Les travaux de Bredig /1/ sur fluoroberylene de sodium modèle sont des premiers dans ce domaine.

L'éxistence des différentes formes polymorphes α-α_H-α_L-β-γ qui cristallisent sous structures; romboédrique, monoclinique et hexagonale dans le ciment portland, le laitier de haut fourneau et aussi dans les materiaux réfractaires de dolomite stabilisés est d'une importance exceptionelle de point de vue des propriétés de ces materiaux. Ce problème est surtout relié au phénomène connu depuis plusieurs années sous le nom de "décomposition calcique" qui se produit à la transition de la phase β en forme polymorphe basse température γ Ca_2SiO_4. Ce phenomène est accompagné d'une abaissement de poids specifique et d'une transition de la symetrie monoclinique de cristal beta C_2S à la symetrie romboédrique de la phase gamma avec une reduction simultanée de nombre de coordination d'atomes de calcium.

Le phenomens d'autopulverisation de l'orthosilicate de calcium en grains d'une taille de quelques ou plusieurs microns comme le résultat de la transition polymorphique beta en gamma est d'une importance élémentaire si ce phénomène soit utilisé pour la méthode complexe de production d'alumine et des ciments portland à haute teneur d'alites à partir de materiaux à la base des aluminosilicates. Le principe de ce procédé elaboré en Pologne /2, 3, 4, 5/ se traduit par la clinkerisation de calcaire broyée en présence d'aluminosilicates afin d'obtenir un aggloméré aluminofère contenant l'orthosilicate de calcium et des aluminates de calcium. On fait l'extraction de l'oxyde d'aluminium de l'aggloméré refroidi et decomposé en poudre avec des solutions dilués de carbonat de sodium. Le résidu de l'extraction, obtenu au cours de la production de l'alumina, contenant principalement Ca_2SiO_4 sous la forme gamma est le matière première pour la cuisson du clinker portland après l'addition de carbonate de calcium broyé. A partir de solution de l'aluminate de sodium on obtient l'hydroxide d'aluminium, qui après la carbonisation devient l'oxyde d'aluminium de haute qualité pour l'industrie metallurgique.

On a profité de ce phénomène d'autopulverisation de Ca_2SiO_4 pour le développement des méthodes de production des sables de moulage et des ciments colorés de revètement /brevets polonais no. 62637 rt 62386/. Ce sont des examples uniques dans le monde entier de " broyage cristallochimique des materiaux " en utilisant dans ce but l'énerdie declenché par la transformation polymorphe de phase.

Il est evident, que non seulement pour des besoins scientifiques mais egalement pratiques, la connaissance du mécanisme de la stabilisation de la phase beta et l'examination de la cinétique de transformation de la phase beta en gamma Ca_2SiO_4 sont d'une importance considerable.

En années cinquantièmes nous avons commencé en cimenterie Groszowice des recherches de retardation ou même d'arret de la formation des germes stables de la forme polymorphe gamma dans la phase beta. les efforts étaient basés sur l'introduction des quantités limitées des oxydes étrangers dans l'orthosilicate de calcium synthetisé pendant la clinkerisation à la temperature 1450°C. Ces additifs peuvent avoir même une influence sur certains changements structurals de la phase beta dont la preuve sont postérieures travaux de Goerlich /6/ portants sur des propriétés thermodynamiques de cette structure ou des autres changements existants dans cette phase de l'orthosilicate de calcium. En utilisant le microscope à chauffage equipé d'echelle de temperature, nous avons reussi de saisir à l'aide de photographie continue, des moments caractéristiques du procéssus d'autopulverisation superficielle se produisant sous l'influence de transformation beta en gamma Ca_2SiO_4.

Le charactère du type de nucleation de changement de phase polymorphe beta en gamma Ca_2SiO_4 relié à l'autopulverisation de la phase gamma a été examiné par Bethke et Grzymek /7/, Bielański et Nedoma /8/. L'affirmation du charactère du type de nucléation des trnsformation de phase mentionnés et la determination de la vitesse de ces changements avait une importance considérable pour l'explication du mécanisme de ces transformation de phase.

Dans nos experiments nous avons observé que des oxydes introduits dans l'orthosilicate de calcium synthetisé - en tenant compte de leur influence sur la marche du procéssus d'autopulverisation - peuvent être classés en deux groupes. le premier comprend les oxydes ayant des cations avec le potential ionique plus elévé et plus eléctronégatifs. Ces oxydes provoquent la reduction de la temperature d'autopulverisation de l'orthosilicate de calcium de 525°C à la temperature inferieure de 400°C. L'autre groupe comprends les oxydes contenants des cations avec des potentiaux ioniques sensiblement plus faibles et moins eléctronégatifs. Les cations appartenants à ce groupe ont une moindre influence sur l'abaissement de la température d'autopulverisation de l'orthosilicate de calcium. qui est comprise dans ce cas entre 525°C et 400°C.

Nous avons cependant constaté la discontinuité de la fonction entre l'abaissement de la temperature de l'autopulverisation et le potential ionique et l'eléctronégativité des cations introduits pour la synthèse de Ca_2SiO_4. Dans cette situation nous avons essayé de deriver la formule mathématique empirique, qui dans la manière plus precise permettrai de trouver une relation continue entre les propriétés des cations utilisés et l'abaissement de la température d'autopulverisation de l'orthosilicate de calcium. Pour des calculs des éléments supplementaires ont été introduits, en tenant compte de la structure des cations considerés. La formule prends egalement en consideration le coéfficient

d'activité relié à l'action des charges positives sur les niveaux energetiques individuels. Avec une formule mathématique ainsi elaborée il est possible d'evaluer quantitativement l'influence des cations utilisés sur l'abaissement de la température $/\Delta_m/$ d'autopulverisation de l'orthosilicate de calcium.

$$\Delta_m = E[W_n \cdot \Phi_n \cdot (e_s + e_p + e_d)_n + \sqrt[2]{W_{(n-1)} \cdot \Phi_{(n-1)} (e_s + e_p + e_d)_{n-1}} \cdot \frac{e}{\pi r^2}$$

E = éléctronégativité du cation,
W_n = nombre quantique principal de cation stabilisant correspondant a sa couche éléctronique,
$W_{(n-1)}$ = nombre quantique correspondant au niveau energetique interieur voisin à la couche éléctronique du cation consideré,
Φ = coéfficient d'activité relative des charges élémentaires positives placées sur des niveaux energetiques respectifs,
Φ_n = coéfficient d'activité relative des charges élémentaires positives localisées sur la couche éléctronique determinée par le nombre quantique principal $/W_n/$,
$\Phi_{(n-1)}$ = coéfficient d'activité relative des charges élémentaires positives localisées au niveau energetique le plus proche à la couche éléctronique du cation $/W_{(n-1)}/$.

Dans l'evaluation de l'activité des charges élémentaires positives qui depends de la repartition aux niveaux energetiques respectifs, nous avons pris pour l'activité des charges positives dans la couche L une valeur de 0,8.

Cette activité relative correspond à celle de charges positives disposées sur la couche du cation B^{+3}, qui dans notre cas, possède le nombre quantique principal le plus bas = 2. Afin de determiner des activités relatives des charges elémentaires positives localisées

TABLEAU I

CATIONS	As^{+5}	P^{+5}	B^{+3}	As^{+3}	V^{+5}	Cr^{+6}	P^{+3}	K^{+1}	Na^{+1}
t_d .....°C	<0	<0	350		320	400		505	500
Δd.....°C	>525	>525	175		205	125		20	25
r ..... Å	0.46	0.35	0.23	0.58	0.59	0.52	0.44	1.33	0.97
$\frac{e}{\pi r^2}$ ..... $\frac{e}{(Å)^2}$	7.52	12.98	18.05	2.84	4.57	7.06	4.93	0.179	0.338
STRUCTURE ATOMIQUE	Argon	Néon	Hélium	Argon	Argon	Argon	Néon	Argon	Néon
	$3d^{10}$	$3p^8$	$2p^1$	$3d^{10}$	$3d^3$	$3d^5$	$3p^3$	$4s^1$	$3s^1$
	$4p^3$	$3s^2$	$2s^2$	$4p^3$	$4s^2$	$4s^1$	$3s^2$		
	$4s^2$			$4s^2$					
KI / w(n)	$4s^2 4p^3$	$3s^2 3p^3$	$2s^2 2p^1$	$4s^2 4p^1$	$4s^2$	$4s^1$	$3s^2 3p^1$	$4s^1$	$3s^1$
KI / w(n-1)	—	—	—	—	$3d^3$	$3d^5$	—	—	—
e	5	5	3	3	5	6	3	1	1
$(e_s+e_p+e_d)(n)$	2+3	2+3	2+1	2+1	2	1	2+1	1	1
$(e_s+e_p+e_d)(n-1)$	—	—	—	—	3	5	—	—	—
$\Phi(n)$	2.3	1.4	0.8	2.3	2.3	2.3	1.4	2.3	1.4
$\Phi(n-1)$	—	—	—	—	1.4	1.4	—	—	—
ε	2.20	2.06	2.01	2.20	1.63	1.56	2.06	0.82	0.93
tm .....°C	-236	-37	350	353	360	373	397	524	524
Δm.....°C	761	562	175	172	165	152	128	1	1

aux niveaux energetiques consecutifs, nous avons pris un multiple de nombre 0,3. Or, conformement a l'hypothese acceptée, suivant des resultats experimentaux, l'activité relative des charges positives localisées aux niveaux energetiques respectifs des cations etudiés, doit correspondre pour la couche K etant la plus proche du noyau d'atome à une valeur;

pour la couche K = $\Phi_{(1)}$ = 0,5 0,3 x 0 = 0,5
" " " L = $\Phi_{(2)}$ = 0,5 0,3 x 1 = 0,8
" " " M = $\Phi_{(3)}$ = 0,8 0,3 x 2 = 1,4
" " " N = $\Phi_{(4)}$ = 1,4 0,3 x 3 = 2,3
" " " O = $\Phi_{(5)}$ = 2,3 0,3 x 4 = 3,5
" " " P = $\Phi_{(6)}$ = 3,5 0,3 x 5 = 5,0

r - rayon de cation en Å,

e - valence de cation = somme de charges positives localisées dans les cages sur la couche electronique $W_{(n)}$ et de charges positives localisées au niveau energetique $W_{(n-1)}$ voisin à la couche electronique

$$e = (e_s + e_p + e_d)_n + (e_s + e_p + e_d)_{n-1}$$

t_d - température du debut d'autopulverisation de l'orthosilicate de calcium, determinée experimentale, en °C,

t_m - température d'autopulverisation de C_2S, calculée à l'aide de la formule mathématique derivée en °C,

$\frac{e}{\pi r^2}$ - expression pour le potentiel de la surface ionique, introduits par les auteurs.

Tableau I resume les resultats experimentaux sur l'abaissement de la température d'autopulverisation de l'orthosilicate de calcium au - dessous de 525°C en présence de cations stabilisants introduits en quantité 0,3 % mole/gramme mole Ca_2SiO_4 au agglomeré synthetisé à 1450°C. A partir des résultats presentés dans le tableau ci-dessus, le caractère stabilisant la forme β Ca_2SiO_4 possèdent les cations ayant à la même fois des valeurs elevées de potential de surface ionique, eléctronégativité et surtout les cations se caractérisant d'un nombre de charges positives plus elévé, localisés sur les couches eléctroniques avec le nombre quantique plus elévé. Outre cela, ces cations doivent en même temps se caracteriser d'une stabilité thérmique au cours de leur synthése en présence de l'orthosilicate de calcium aux temperatures atteignants 1500°C.

Le cation As^{+5} est un example d'une activité stabilisante considerable. Ce cation possède en même temps une stabilité thermique importante, eléctronégativite exceptionellement elévé = 2,2 et le potential de surface de section ionique elévé = 7,5 e/Å^2. En même temps la couche eléctronique localisée dans ce cation et correspondante à un nombre quantique elévé = 4 est privée de 5 electrons, ce qui implique à ce cation le rôle d'un stabilisateur le plus fort parmi tous examinés. Malgré une stabilité thermique exceptionelle et le nombre quantique elévé = 6 de cation Ba^{+2}, l'oxyde de baryum a prouvé des ptopriétés stabilisantes relativement faibles. L'abaissement de l'activité stabilisante de BaO est l'effét de sa éléctronégativité basse E = 0,89 et du potential de surface de section ionique exceptionellement faible 0,354 e/Å^2. En plus, le nombre des charges élémentaires positives limité, situées sur la couche éléctronique extérieure exclue l'activité stabilisante plus étendue.
Les plus faibles ou pratiquement sans aucune influence sur l'abaissement de la température d'autopulverisation de l'orthosilicate de calcium, sont des cations Na^+ et K^+. On peut expliquer cette faible activité de sodium et de potassium par leur éléctronégativité la plus faible E = 0,82 et 0,93 respectivement. Ce caractère est en plus dû au potential de surface de section ionique faible de 0,179 a 0,338 e/Å^2 avec le minimum, soit une seule charge élémentaire positive située dans la couche éléctronique de ces cations. En outre, nous avons constaté, que tous les plus forts stabilisateurs pour le processus d'autopulverisation polymorphique de Ca_2SiO_4, qui sont selon nous les suivants, classées dans l'ordre d'activité diminuisante; As^{+5}, P^{+5}, B^{+3}, V^{+5}, Cr^{+6}, perdent ces propriétés après que leur valence ionique est reduite.

Les cations As^{+3}, P^{+3}, V^{+3}, B^{+}, Cr^{+3} obtenues par la reduction chimique avec le charbon introduit au cours de la cuisson de l'agglomeré de l'orthosilicate de calcium en limitant en l'air, perdent leur propriétés de l'abaissement de la temperature d'autopulverisation.

On peut expliquer ce phenomène à partir de la formule mathématique derivée. Or, à cause de reduction chimique des oxydes ayant le degré d'oxidation plus eléve, le nombre de charges élémentaires positives situées sur les couches éléctroniques de ces cations est reduit. La reduction des oxydes de ces cations augmente en même temps leur taille, ce qui possède une influence sur l'abaissement de leur potentiel de surface de section ionique. La reduction du potentiel de surface de section ionique, conformement à la formule derivée, provoque l'augmentation de la temperature d'autopulverisation de l'orthosicate de calcium plus sensiblement en présence des oxydes ayant le degré d'oxydation plus faible qu'en cas de présence des oxydes des mêmes cations mais avec le degré d'oxydation plus elévé. On peut conclure alors, que dans les procédés industriels il faut maintenir pendant la clinkerisation l'atmosphére reductrice afin d'obtenir une l'autopulverisation complète des agglomérés aluminoferes contenants l'orthosilicate de calcium.

Afin d'obtenir une évaluation quantitative, qui pourrai nous indiquer plus précisément le mecanisme de changements de phase dans l'orthosilicate de calcium, on a utilisé l'analyse derivatographique des phénomènes qui accompagnent les changements de phase polymorphes à l'aide de l'analyseur "Setaram". Les effets calorifiques obtenus - au cours de la synthése et de refroidissement de l'orthosilicate de calcium echéants à 1 gramme mole de l'échantillon examiné de Ca_2SiO_4 ont été presentés dans le tableau II.

TABLEAU II

		T_1	T_2	T_m	t	ΔC	ΔQ
$CaCO_3 \rightarrow CaO + CO_2$	Réchauffage	725	1023	958	28,0	- 54410	- 46800
$2CaO + SiO_2 \rightarrow Ca_2SiO_4$	Réchauffage	1430	1478	1450	5,0	+ 12230	+12230
$\alpha \rightarrow \alpha'_H$	Refroidissement	1446	1397	1411	5,0	+ 3285	+3285
$\alpha'_H \rightarrow \alpha'_L$	Refroidissement	1193	1055	1175	24,0	+ 185	+ 185
$\alpha'_L \rightarrow \beta$	Refroidissement	707	625	684	8,0	+ 370	+370
$\beta \rightarrow \gamma$	Refroidissement	550	539	546	1,5	+ 220	+ 220
$\gamma \rightarrow$ l'autodés.	Refroidissement	525	384	515	12,0	+ 1110	+1110
Réchauffement au total					33,0	-42180	
Refroidissement au total					50,5	+ 5170	
Grand total					83,5	-37010	

T_1 - temperature /°C/ d'initiation de l'effet calorique de processus qui se produit dans l'echantillon étudié dans le temps t_1

T_2 - temperature /°C/ finale de l'effet calorifique de processus qui se produit dans l'echantillon étudié dans le temps t_2

T_m - temperature /°C/ correspondante à l'intensité maximum de processus qui se produit pendant rechauffement et refroidissement de l'echantillon

$t = t_2 - t_1$ duré /exprimé en minutes/ de processus qui se produit dans l'echantillon etudié entre temperature T_1 et T_2

ΔC - effets calorifiques /exprimés en calories/gramme mole/ de mineraux individuels présents dans des proportions determinées dans l'echantillon étudié, se produisant au cours de rechauffement ou refroidissement de l'echantillon

ΔQ - effet calorifique unitaire /exprimé en calories/ resultant au cours de rechauffage et refroidissement de l'echantillon, converti pour 1 gramme mole des des composants mineraux individuels compris dans l'echantillon.

L'echatillon a été soumis à la temperature de 1500°C pendant 60 minutes. Vitesse d'échauffement ou de refroidissement 10°C/min.

Les observations et conclusions qui se posent en tenant compte des données comparatives du tableau II annexé des différences observées qu'on a obtenues entre effets calorifiques et intervalles de temperature dans lesquels se produisent ces effets pendant réchauffement et réfroidissement de l'echantillon etudié. L'effet calorifique le plus important se produit pendant le processus même de la synthèse de l'orthosilicate de calcium et il atteint 12230 cal/gramme mole du Ca_2SiO_4. Ce processus a lieu pendant réchauffement de l'echantillon dans l'intervalle étroit de 1430 à 1478°C. Cette synthèse parcourt avec une intensité importante et se caractérise d'une vitesse relativement élevée du degagement du chaleur égale a 2445 cal/gramme mole/minute. Le plus lents parmi des processus polymorphes ayant en même temps les effets calorifiques les plus faibles par l'unite de temps sont des changements de phase bidirectionnels $\alpha'_H \rightleftharpoons \alpha'_L$. Le processus de changement de phase bidirectionel $\alpha \rightleftharpoons \alpha'_H$ est un processus rapide, ayant l'effet calorifique le plus elevé des processus polymorphes. Le changement polymorph unidirectionnel $\beta \rightarrow \gamma$, isolé par nous, est un processus de changement de phase d'une durée la plus courte. Les transformations polymorphes bidirectionnelles dans l'orthosilicate de calcium pur, sans additions stabilisantes, se produisent rapidement /dans un intervalle de 1,5 a 6 minutes/. Cependant cette observation ne s'applique pas au changement de phase de longue durée $\alpha'_L \rightleftharpoons \alpha'_H$ /qui dure 24 minutes/, ce qui mantrait, qu'il faudrait reviser les données de la literature portantes sur des changements de structure qui accompagnent cette transformation polymorphe. Les transformations de phase polymorphes endothérmiques unidirectionnelles sont d'une durée longue et se caractérisent d'une marche plus moderée se traduisant par un degrée d'intensité plus faible.

A partir de nos données experimentales, nous avons calculé, en utilisant la formule de Kapustyński et le valeur de ek de A.E.Fersman, l'energie de réseau des cristaux de l'orthosilicate de calcium

$$E = E_1 + E_2 + E_3$$

E_1 - énergie de réseau du SiO_2

E_2 - énergie de réseau du CaO

E_3 = ΔQ = calories degagées au cours de la synthèse $2CaO + SiO_2$ = 12,23 kcal/gramme mole du Ca_2SiO_4 - évaluées par nous.

La valeur moyenne de l'énergie de réseau calculée selon le deux méthodes pour un gramme mole du Ca_2SiO_4 est égale à 4696,53 kcal.

En appliquant pour A dans la formule de Born Mayer une valeur de 4,439 pour β quartz et en assument B = 9 pour tous les combinaisons

binaires - l'énergie de réseau pour β quartz calculée selon la formule de Born Mayer est égale à E_1 = 3042 kcal/mole SiO_2. D' ou la valeur de l'energie de réseau;

E = 12,23 + 3042 + 2 x 825,15 = 4704,53 kcal/ gramme mole du Ca_2SiO_4.

En considerant ces calculs on peut assumer que l'énergie de réseau moyenne des cristaux de l'orthosilicate de calcium doit être environ 4700 kcal/gramme mole du Ca_2SiO_4. A partir de ces données on peut conclure, que les transformation /ΔQ/ se produisant dans l'ensemble de l'énergie de réseau /E/ et resultant du phénomène de changement de phase polymorphe $\beta \rightarrow \gamma$ Ca_2SiO_4 qui provoque une désintégration totale des cristaux de l'orthosilicate de calcium, sont très faibles par rapport à l'énergie de réseau totale des cristaux de l'orthosilicate de calcium, car ils ne depassent pas une valeur de 1,5 kcal/gramme mole. Néamoins ces changements ont une influece importante sur autodésintégration de ces cristaux. Il faut expliquer cette efficacité considerable des changements énergétiques relativement faibles par le degrée exceptionnellment élevé de l'intensité de la marche des changements de phase polymorphes se produisant dans un système fortement sursaturé resultant de surfusion considerable de la phase β par rapport à la phase γ Ca_2SiO_4. L'autodésintégration totale du β orthosilicate de calcium conduisant aux grains d'une taille moyenne de 20μm est provoquée par une reduction de l'énergie de réseau totale de 0,032 % seulement. D'ou vient que la quantité de l'énergie de réseau nécessaire pour désintégrer une tonne d'un mineral composé de β Ca_2SiO_4 sous la forme des grains d'une taille de 30 mm environ au cours de son transformation en poussière /taille moyenne de 20μm/ est 8720 kcal.

Si l'on compare cette énergie à l'énergie consommée par des installations mécaniques /broyeurs à boulets rotatifs/ où il est nécessaire d'assurer 200 kilowattheures par tonne, ce qui est equivalent à 172 000 Kcal, on voit bien qu'il est possible de faire des èconomies de l'energie d'un facteur de 20 environ grâce a l'utilisation du phénomène de polymorphisme dans les opérations de broyage.

BIBLIOGRAPHIE

1.- M.A. BREDIG / 1950/ "Polymorphism of calcium orthosilicate", J.Amer. Ceram. Soc., 33, 188.

2.- J. GRZYMEK /1959/ "Sposób otrzymywania samorozpadowego klinkru krzemianu dwuwapniowego lub materiałów zawierających go", Patent polski n° 43443.

3.- J. GRZYMEK /1959/ "Sposób wytwarzania wysokosprawnego cementu portlandzkiego przy jednoczesnym otrzymywaniu tlenku glinu jako produktu ubocznego", Patent polski n° 43444.

4.- J. GRZYMEK /1961/ "Sposób wytwarzania szybkosprawnego cementu portlandzkiego", Patent polski n° 44998.

5.- A. DERDACKA, Z. KONIK, A. JAWOROWICZ, B. WERYNSKI, /1977/, "Produkcja tlenku glinu i cementu metodą spiekowo rozpadową J.Grzymka", IPWMB Opole, 89 - 121.

6.- E.GORRLICH et M. HANDKE /1975/, "Polimorfizm Ca_2SiO_4 w świetle badań metodami spektroskopii w podczerwieni i spektroskopii Ramana", n° 7, 201, n° 8-9, 236, n° 10, 299.

7.- S. BETHKE /1971/, "Kinetyka niskotemperaturowych przemian polimorficznych krzemianu dwuwapniowego", Thése de chimie, L'Acad. de Minnes et de Metalurgie.

8.- A. BIELANSKI, A. NEDOMA et W. TUROWA /1964/, "Studies on the polimorphic transformation of sodium fluoroberylate", International Symposium on the Reactivity of Solids, Monachium.

Intensification du processus physico-chimique de clinkérisation

Intensification of physico-chemical process of clinker formation

O.P. MTCHEDLOV - PETROSSIAN, professeur, docteur ès sciences techniques,
V.I. SATARINE, professeur, docteur ès sciences techniques,
N.P. KOGAN, candidat ès sciences techniques,
A.G. KHOLODNY, candidat ès sciences techniques,
E.P. KOSTINSKI, ingénieur, Youjguiprotzement, U.R.S.S.

RESUME : L'objet de l'étude a été l'analyse des principaux aspects théoriques de l'intensification de la cuisson du clinker dans les fours rotatifs. Le recours aux flux dispersifs au stade préparatoire de décarbonatation du matériau modifie le mécanisme des réactions en phase solide. Il a été établi par l'expérience que pour des échanges de chaleur et de masse poussés la vitesse de dissociation des carbonates est de beaucoup supérieure à celle de la fixation de la chaux par les oxydes acides. L'accroissement de la concentration du CaO_{lib} actif au cours du traitement thermique ultérieur en couche contribue à l'intensification du processus d'interaction des oxydes. Au stade final, à une température de 1623°K, on peut obtenir un clinker de structure perturbée avec une certaine quantité de CaO_{lib} et de grande activité hydraulique.

SUMMARY : Theoretical fundamentals of intensification of clinker burning in rotary furnaces are considered. Use of disperse flows at the stage of preparation of material for decarbonization changes the mechanism of solid-phase reactions. It has been determined experimentally that at high heat and mass exchange the rate of dissociation of carbonates considerably exceeds the rate of binding of lime with acid oxides. Increase of concentration of active CaO_{free} at further thermal treatment in the bed intensifies the reaction of oxides. At the final stage at a temperature of 1623°K, clinker with distorted structure may be obtained, this clinker includes a certain amount of CaO_{free} and features high hydraulic activity.

Une organisation rationnelle des processus physico-chimiques de clinkérisation dans le four est la condition essentielle de l'intensification de la cuisson et de l'abaissement des dépenses spécifiques d'énergie en production du clinker. Dans les fours modernes on utilise au stade préliminaire de préparation de la matière le procédé de flux dispersifs assurant une vitesse maximale à l'apport de chaleur et l'utilisation de cette dernière avec un haut rendement. Un rôle particulièrement important revient aux procédés technologiques et physico-chimiques d'action aux stades suivants de clinkérisation. L'addition au mélange brut de composants capables d'abaisser la chaleur théorique de clinkérisation ainsi que le mode d'amenée de la chaleur exercent une influence sur l'ordre et la séquence des réactions en phases solide et liquide, ce qui au cas d'une cuisson dans des fours rotatifs, se répercute de façon imminente sur la résistance limite du ciment.

Le nombre de réactions dont il faut tenir compte dans le système chimique - mélange brut - le nombre de phases engagées et l'orientation d'interaction entre les phases, peuvent être déterminés par la règle des phases. Toutefois, en cas de la cuisson rapide le rôle décisif appartient aux particularités de la cinétique chimique.

Il est connu que la vitesse de transformation des matières dans les systèmes se trouvant en phase solide est fonction de la surface de contact des phases, de la concentration des agents chimiques, c.-à-d.:

$$\frac{dq}{d\tau} = KC_1^m \cdot C_2^n \cdot F_1 \cdot F_2 , \qquad (1)$$

où m, n sont les ordres des réactions; F_1, F_2 - la surface des particules; C_1, C_2 - la concentration des agents chimiques.

L'ordre apparent des réactions peut varier en fonction de l'activité catalytique de l'un des constituants, tandis que les substances gazeuses intermédiaires permettent d'améliorer l'échange de matière entre les phases.

La haute valeur de la constante de vitesse de décarbonatation aboutit à ce que la vitesse de transformation du constituant calcique se trouve limitée par la vitesse de l'apport de chaleur.

Les calculs ont établi que le temps de réchauffement des particules de matière première servant à la production du ciment et ayant les propriétés d'un corps fin, pour un diamètre équivalent à 0,000025; 0,00005; 0,0001 m et une température dans le four de 1273, 1373, 1473°K, se mesure en centièmes de seconde.

La vitesse de synthèse des composés du calcium avec les oxydes acides est de plusieurs degrés inférieure à celle de la dissociation du $CaCO_3$, ce qui au stade préparatoire de clinkérisation dans les courants dispersifs des fours industriels implique une haute teneur en CaO_{lib} dans le matériau. De plus, dans ce cas, le constituant argileux s'avère convenablement préparé à l'interaction subséquente avec la chaux.

Les produits finement dispersés ainsi obtenus possèdent de grandes réserves d'énergie interne et, vraisemblablement, sont susceptibles d'influencer la marche des réactions en phase solide au cas d'un réchauffement dans la couche roulante du four rotatif, où la surface de contact des phases entrant en réaction est grande.

Après l'apparition du bain fondu eutectique la clinkérisation se poursuit suivant l'équation des réactions hétérogènes

$$W = \frac{D \cdot S}{V} \cdot \frac{dC}{dx} \qquad (2)$$

où S est la surface; V - le volume du liquide; C - la concentration, D - le coefficient de diffusion, X - la distance.

On peut admettre que la concentration poussée de chaux formée aux dépens d'une rapide dissociation de $CaCO_3$ et une intensification de son interaction avec les oxydes acides peut également engendrer un écartement sensible du processus équilibré de formation des minéraux à des températures plus basses.

La vitesse de croissance des cristaux (période de récristallisation accumulative) est une fonction exponentielle de la température, aussi faut-il s'attendre à une élévation de l'activité hydraulique des phases générant le clinker-portland, y compris celle de la chaux libre.

A des fins de vérification de l'hypothèse formulée, on a utilisé, dans des conditions de laboratoire, un mélange brut à deux constituants avec un facteur de saturation=0,85; n = 3,3; p = 1,8. Le mélange cru était broyé jusqu'à la traversée complète du tamis à 5476 mailles/cm^2. Ensuite, on préparait des pastilles de 10 mm de hauteur et de 8 mm de diamètre qui étaient chauffées jusqu'à 1473°K. Les éprouvettes obtenues étaient de nouveau broyées puis passées à travers un tamis de 5476 mailles/cm^2 et pressées en pastilles. Les pastilles étaient placées dans un four de platine chauffé jusqu'à 1473°K et y étaient réchauffées jusqu'à 1623°K au rythme de 12°/mn. Les constituants du mélange cru étaient également soumis à la cuisson séparément jusqu'à la température de 1473°K, puis broyés, passés au tamis de 5476 mailles/cm^2 et servaient à la confection de pastilles de composition chimique identique au premier mélange cru. Ces pastilles étaient, elles aussi, cuites jusqu'à la température de 1623°K. Les résultats des déterminations en éprouvettes du CaO_{lib} avec l'alcoole et glycérat sont donnés au tableau I.

Il découle du tableau que la vitesse absolue de l'assimilation de la chaux est supérieure dans les éprouvettes se caractérisant

par leur teneur en chaux plus élevée dans les échantillons de départ. L'accélération de l'assimilation de la chaux est due à l'augmentation de la différence entre sa concentration dans les phases en interaction. La teneur absolue en CaO_{lib} est plus grande dans les éprouvettes dont les constituants étaient cuits séparément. Toutefois, à la température de cuisson de 1673°K la chaux est totalement assimilée indépendamment de la teneur en CaO_{lib} à des stades intermédiaires.

Les analyses aux rayons X, comme les études pétrographiques d'éprouvettes cuites, ont montré que l'alite se forme à des températures plus basses dans des matériaux à teneur élevée en chaux libre.

Tableau I

Quantité de CaO_{lib} dans des éprouvettes cuites

Mélange cru homogène		Mélange cru à partir de constituants cuits séparément	
Régime de cuisson	Teneur en CaO_{lib} %	Régime de cuisson	Teneur en CaO_{lib} %
T = 1473°K	32,59	T=1473°K	56,46
de 1473 à 1523°K avec temporisation de 5 min	11,31	de 1473 à 1523°K avec temporisation de 5 min	27,38
de 1473 à 1523°K avec temporisation de 15 min	9,24	de 1473 à 1523°K avec temporisation de 15 min	18,03
de 1473 à 1573°K	2,49	de 1473 à 1573°K	6,33
de 1473 à 1623°K	-	de 1473 à 1623°K	2,03
de 1473 à 1673°K	-	de 1473 à 1673°K	-

Afin d'élucider les raisons possibles de l'apparition précoce de l'alite dans les éprouvettes, on a procédé à la comparaison d'échantillons cuits à des températures s'élevant jusqu'à 1573°K. Il s'est avéré que la bélite, principal minéral formé à ce stade de cuisson., apparaît dans le mélange homogène sous une seule forme et dans le mélange comprenant des constituants cuits séparément, sous deux formes (Fig.1).

La variante commune pour les deux types d'éprouvettes est la bélite à "faible" relief. La bélite à "fort" relief n'apparaît

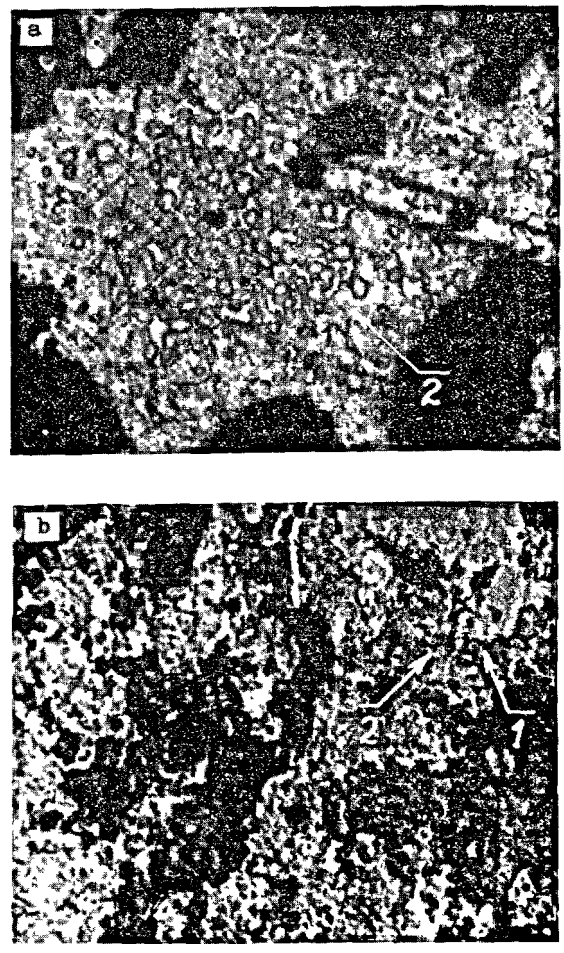

Fig.1 La bélite dans des éprouvettes du mélange cru homogène (a) et du mélange cru formé à partir de constituants cuits séparément (b) I - bélite à "fort" relief. II - bélite à "faible" relief (500 x).

que dans les éprouvettes obtenues par cuisson séparée des constituants. Vraisemblablement, à en juger par la texture des éprouvettes cuites à 1623°K (Fig.2) la bélite à relief fort constitue une source d'alite.

Il est typique que dans les éprouvettes en mélange homogène la bélite à fort relief n'apparaît qu'une fois atteinte la température de 1623°K.

Des recherches pilotes on été réalisées dont le schéma comprend un four rotatif de 1 m de diamètre et long de 15 m, une installation de décarbonatation à cyclone de 1,25 m de diamètre et d'une capacité de 1,1 m^3, un précipitateur de 1,45 m de diamètre, deux étages d'échangeurs de chaleur à cyclones, un dispositif de dépoussiérage et un refroidisseur à tambours. L'installation de décarbonatation est munie de quatre brûleurs à gaz. La matière destinée à la décarbonatation est transportée par le courant d'air utilisé

Fig.2. Alite (1) des éprouvettes en mélange formé de constituants cuits séparément à 1623°K (grossissement 500x).

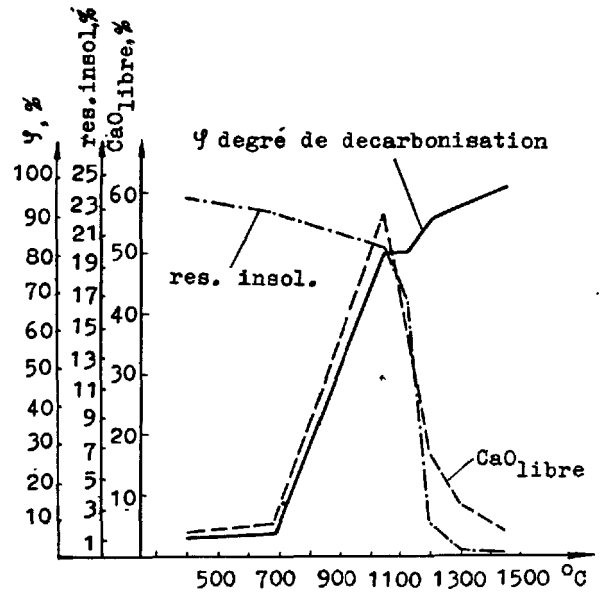

Fig.3. La marche de la clinkérisation.

pour la combustion.

La matière, après avoir traversé le système d'échangeurs de chaleur, est dirigée vers l'installation de décarbonatation, d'où la partie précipitée du mélange cru passe par le conduit à gaz du four rotatif pour rentrer au précipitateur, tandis que la partie restante est, elle aussi, emportée par les fumées vers le précipitateur; ensuite, toute la matière, après avoir subi un traitement thermique préalable, est introduite dans le four rotatif. L'installation d'essai ne prévoit pas de cycle complet d'utilisation de la chaleur. Les études étaient menées sur des mélanges de matières premières dont le facteur de saturation oscillait entre 1,0 et 1,13 à des températures de décarbonatation de 1123 à 1323°K; la consommation en mélange cru étant de 960-1788 kg/h.

L'accroissement du facteur de saturation est dû à un entraînement sélectif du constituant calcique. Le module silicique variait de 3,2 à 3,3 et celui d'alumine, de 1,55 à 1,8. Le degré de décarbonatation atteint sur cette installation après cuisson se montait à 80%.

Le processus de clinkérisation a été étudié sur l'installation d'essai en recourant aux méthodes d'analyse chimique, aux rayons X et aux déterminations pétrographiques.

Les valeurs moyennes de déterminations chimiques sont rapportées sur le graphique de la figure 3. Les données fournies montrent que la clinkérisation sur l'installation utilisée diffère du processus se déroulant dans le four rotatif courant par une décarbonatation accélérée.

Le CaO_{lib} apparaît aussitôt que commence la décarbonatation puis, à mesure que le processus se poursuit, la quantité de CaO_{lib} augmente proportionnellement au degré de décarbonatation, tant que ce dernier monte jusqu'à 80%. Ensuite, on observe une brusque chute de la quantité de CaO_{lib} dans le matériau cuit. Le point d'inflexion de la courbe de variation de CaO_{lib} correspond au déplacement du mélange cru vers le four rotatif court, marquant ainsi la fin du traitement thermique du matériau en suspension et le début de cuisson en couche.
L'aspect des courbes de la figure 3 implique qu'au cours de la décarbonatation en suspension les processus en phase solide sont quelque peu ralentis par rapport à ceux observés lors de la cuisson en couche.

La diminution sensible des résidus indissolubles est constatée simultanément au début de la baisse de la teneur en CaO_{lib}.

Les données d'analyse aux rayons X et des déterminations pétrographiques sont en accord complet avec les résultats d'analyse chimique.

Donc, les études à l'échelle industrielle ont confirmé qu'à l'état de suspension la décarbonatation s'effectue de façon intense: quant aux réactions en phase solide entre CaO et les constituants argileux elles n'ont pas le temps de se produire.

La concentration, de beaucoup plus grande qu'au cas d'une cuisson ordinaire, de CaO_{lib} et des produits de transformation des constituants argileux ayant subi un traitement thermique préalable est le facteur qui augmente la vitesse de marche des processus en phase solide dans le tronçon court du four rotatif.

Au cours de l'élévation subséquente de la température jusqu'à 1573°K, la concentration

Tableau II

Propriétés physico-mécaniques des clinkers

N°N°	Facteur de saturation de la matière première	Facteur de saturation de clinker	CaO_{lib} %	Surface spécifique cm^2/g	Consistance normale, %	Rapport E/C, %	Délais de prise, h-mn		Limite de résistance à la compression, kgf/cm^2			Limite de résistance à la flexion		
							début	fin	3 jours	7 jours	28 jours	3 jours	7 jours	28 jours
1	1,00	0,90	4,72	3574	23,0	0,4	0-55	1-40	313	402	562	46,7	52,8	66,4
2	1,00	0,92	4,24	3492	22,75	0,4	1-10	1-50	283	397	551	46,4	52,3	64,2
3	1,08	1,02	6,18	3574	24,0	0,4	1-10	1-55	320	394	611	45,8	46,7	56,2
4	1,08	1,04	4,51	3589	22,75	0,4	0-55	1-45	318	377	624	44,3	47,9	70,8
5	1,13	1,01	3,57	3271	24,75	0,4	1-30	2-40	309	393	559	45,1	54,4	62,0
6	1,13	1,01	3,68	3213	24,5	0,4	2-05	3-50	324	390	572	44,3	49,4	62,8

des masses en réaction étant grande et les transformations structurales se poursuivant, on observe d'intenses interactions entre les constituants, ce que confirment les données de déterminations physico-chimiques.

Il est intéressant que les formations nouvelles, comme le confirment les diagrammes radiographiques, contiennent à côté de la bélite d'importantes quantités d'alite avant même l'apparition de la phase liquide.

Les clinkers ainsi obtenus se caractérisent par une activité hydraulique élevée (500-600 kgf/cm^2) quoiqu'ils contiennent une petite quantité de CaO_{lib} (tableau II).

Comme il s'ensuit du tableau II, malgré une certaine teneur en CaO_{lib} à la température de 1623°K le clinker obtenu possède une grande activité hydraulique dont la raison, d'après les diverses méthodes d'étude, tient à l'irrégularité de la structure perturbée des minéraux du clinker.

Il faut noter qu'avant on obtenait également des ciments d'une résistance limite élevée à base de clinkers à haute teneur en CaO_{lib} en abaissant la température de cuisson dans la zone d'agglomération. Mais ces clinkers exigeaient une mouture beaucoup plus fine.

CONCLUSION

Les études entreprises montrent que l'intensification de la décarbonatation est le résultat d'accélération, dans les courants dispersifs, des échanges de chaleur et de masse, engendrant une haute teneur en chaux libre dans la matière cuite.

En continuant d'élever la température de la masse fluide dans le four rotatif, on arrive à accélérer la clinkérisation à tous les stades suivants du processus grâce à la grande concentration de CaO_{lib} et aux transformations des matériaux argileux.

Au stade final, à la température de 1623°K, on peut obtenir un clinker de structure désordonnée contenant une certaine quantité de CaO_{lib} et dont l'activité hydraulique est très grande.

Bases physico-chimiques de la formation des granules du clinker

Physical and chemical grounds for granulation of clinker

B.S. ALBATS, candidat ès sciences techniques, chef de laboratoire,
L.S. FILIPPOVA, collaborateur scientifique, NIITZement,
Y.R. KRIVOBORODOV, collaborateur scientifique, Institut Chimico-Technique, Mendéléiev, Moscou, U.R.S.S.

RESUME : Le processus de formation des granules du clinker repose sur les lois d'agglomération en phase liquide des poudres et avant tout sur la relation entre la quantité, la tension superficielle, la viscosité de la matière fondue, son pouvoir mouillant, la dimension initiale des particules et le retrait linéaire relatif.

L'accroissement de la dimension des particules de la matière à l'entrée de la zone de cuisson et la variation de tension superficielle et de viscosité des matières fondues exercent l'influence la plus efficace sur le processus de formation des granules.

L'accroissement de la tension superficielle des matières fondues dans le système $CaO-Al_2O_3-Fe_2O_3-SiO_2$ jusqu'à 540-580.10^{-3} N/m pour les valeurs de la viscosité de 1,2 à 1,6.10^{-1} Pa.s, dû à l'introduction des oxydes de titane, d'aluminium, de magnésium, de cadmium, de nickel et de manganèse, entraîne l'augmentation de la dimension des granules du clinker. Les relations quantitatives obtenues permettent de régler la composition granulométrique du clinker des fours rotatifs par variation de la composition chimique du mélange cru et du traitement thermique.

SUMMARY : The process of clinker granulation is determined by conditions of liquid-phase sintering of powders and, first of all, interrelation between the amount, surface tension, viscosity of the melt, its wettability, initial particle size and relative linear shrinkage.

The most effective method of controlling the granulation process is increase of the size of the material particles before the sintering zone and variation of surface tension and viscosity of the melt.

The surface tension of the melts in the $CaO-Al_2O_3-Fe_2O_3-SiO_2$ system is increased to 540-580·10^{-3} N/m at a viscosity of 1;2-1,6·10^{-1} Pa·s by introduction of oxides of titanium, aluminium, magnesium, cadmium, nickel, manganese resulting in increase of dimensions of the clinker granules. The quantitative relationship obtained make it possible to regulate the granulometric composition of clinker in rotary furnaces by changing the chemical composition of the raw mix and thermal parameters in the furnace.

Actuellement la masse principale du clinker-portland est soumise à la cuisson dans les fours puissants avec une large gamme de réglage des paramètres thermotechniques et technologiques. Cela permet de combiner de façon rationnelle le niveau de température de la cuisson avec la composition chimico-minéralogique du mélange cru pour obtenir le clinker ayant la composition et les propriétés optimales. Dans ce cas c'est la stabilité du fonctionnement des fours qui est le plus importante; elle dépend fortement de la composition granulométrique du clinker car la présence dans le clinker d'une grande quantité de fines particules (de la poussière de clinker) et de grands agglomérés provoque les perturbations dans le fonctionnement de l'équipement et la déstabilisation de la cuisson. C'est pour cette raison que l'étude de la formation des granules du clinker présente un grand intérêt scientifique et pratique.

Le processus de formation des granules du clinker repose sur les lois d'agglomération en phase liquide des poudres et avant tout sur la relation entre la quantité, la tension superficielle, la viscosité de la matière fondue, son pouvoir mouillant, la dimension des particules de départ et le retrait linéaire relatif. Les paramètres indiqués déterminent la dimension finale des grains du clinker et la vitesse du processus d'agrégation.

Nous avons montré précédemment [1] que la dimension des grains du clinker dans les fours rotatifs se détermine par le rapport de deux forces : la force serrant les particules de la matière soumise à la cuisson (F) et la force de pesanteur (P), sous la forme suivante :

$$\frac{F}{P} = \frac{3\cdot\sigma}{4r^2\cdot\gamma\cdot g}\left\{\sin^2\varphi\left[\frac{\cos(\varphi+\theta)}{1-\cos\varphi} - \frac{1}{\sin\varphi - \frac{(1-\cos\varphi)[1-\sin(\varphi+\theta)]}{\cos(\varphi+\theta)}}\right] + 2\sin\varphi\cdot\sin(\varphi+\theta)\right\}, \quad (1)$$

où σ est la tension superficielle de la matière fondue, N/m;
r - le rayon des particules, m;
γ - la densité des particules, kg/m^3;
g - l'accélération de la force de pesanteur, m/s^2;
θ - l'angle de mouillage, degrés;
φ - l'angle dépendant de la quantité de la phase liquide, degrés.

On prend la grandeur F/P pour paramètre d'agrégation sans dimension.

Il est évident que les particules cessent d'être agrégées dans les cas où $F \leq P$ et le paramètre d'agrégation $F/P \leq 1$. Cette valeur du paramètre est critique [2];

La vitesse du processus d'agrégation peut être exprimée en fonction de la vitesse de retrait du conglomérat des particules en cours d'agglomération :

$$\frac{\Delta l/l_0}{\tau} = \frac{\sigma}{\eta\cdot r}\left\{\left[\frac{\cos(\varphi+\theta)}{1-\cos\varphi} - \frac{1}{\sin\varphi - \frac{(1-\cos\varphi)[1-\sin(\varphi+\theta)]}{\cos(\varphi+\theta)}}\right] + 2\,\frac{\sin(\varphi+\theta)}{\sin\varphi}\right\} \quad (2)$$

où $\Delta l/l_0$ est le retrait linéaire relatif ;
τ - le temps, s;
η - la viscosité, Pa·s.

Lors du passage de la matière par la zone de préclinkérisation, plusieurs variantes du processus d'agrégation, dépendant de la valeur initiale (avant l'agglomération) du paramètre d'agrégation et de la vitesse d'agrégation, sont possibles. Pour évaluer la grandeur F/P et la vitesse d'agrégation nous avons utilisé les valeurs expérimentales de la tension superficielle et de la viscosité des matières fondues modèles, préparées sur la base de la matière fondue de composition suivante: CaO - 57,0; SiO_2 - 7,5; Al_2O_3 - 22,6 et Fe_2O_3 - 12,9% en masse, avec additions des différents oxydes. Les données expérimentales sont obtenues avec la participation de A.Ossokin et S.Ivachtchenko et citées dans le tableau.

Tableau

Addition, % en masse	Viscosité, Pa·s·10^{-1}	Tension superficielle, N/m·10^{-3}
Matière fondue	1,6	580
1,0 de K_2O	1,8	455
2,0 de K_2O	2,4	350
2,5 de SO_3	0,7	350
1,9 de SO_3 + 3,0 de K_2O	1,6	150
1,0 de MoO_3	1,2	490
1,0 de BaO	1,7	565
1,0 de CdO	1,6	577
1,0 de MgO	1,5	573
1,0 de Al_2O_3	1,5	565
2,0 de Na_2O	2,2	457
1,0 de Na_2O	1,7	555
1,0 de Ni_2O_3	1,4	560
1,0 de Fe_2O_3	1,3	577
1,0 de Mn_2O_3	1,3	560
1,0 de B_2O_3	1,6	570
1,0 de TfO_2	1,3	577

Envisageons les variantes possibles du processus d'agglomération.

1. La grandeur F/P atteint la valeur critique à l'entrée de la zone de préclinkérisation, quand le processus commence et la dimension des granules est faible. Cela est possible lorsque la tension superficielle de la matière fondue est très basse (150 à 350·10^{-3} N/m) et la valeur de F/P est de 1,5 à 4, par exemple si le bain fondu contient 2,5% en masse de SO_3 ou 1,9 % en masse de SO_3 + 3% en masse de K_2O et la vitesse d'agrégation est grande (pour la viscosité du bain fondu de 0,7 à 1,2·10^{-1} Pa·s). Dans ce cas l'agrégation s'achève à peine commencée et la matière passe toute la zone de cuisson sous forme d'une masse finement dispersée.

2. La grandeur F devient égale à P au milieu de la zone de cuisson , lorsque le processus

d'agrégation est assez développé et les granules formés atteignent la valeur commensurable avec la dimension des granules du produit fini (de 8 à 10 mm). Cette variante du processus d'agrégation a lieu si la tension superficielle des matières fondues est de 540 à 580·10^{-3} N/m et le paramètre d'agrégation est égal à 6-9, par exemple en présence des oxydes de Ti, Mg, Ba, Al, et la vitesse d'agrégation est assez élevée (pour les valeurs de la viscosité de la matière fondue de 1,2 à 1,6·10^{-1} Pa·s). Les granules ainsi formés seront compactés pendant un temps assez long en présence de phase liquide, par suite de quoi il se forme le clinker de composition granulométrique serrée (sans particules fines).

3. La grandeur F/P devient égale à l'unité dans la deuxième moitié de la zone de préclinkérisation, lorsque le processus de cristallisation des minéraux à partir du bain fondu est intense. Cette situation apparaît si la tension superficielle des matières fondues est assez élevée (390 à 520·10^{-3} N/m), le paramètre d'agrégation est de 4,5 à 6, par exemple en présence de 1 à 2 % en masse de K_2O ou de Na_2O, et la vitesse d'agrégation est petite (pour les valeurs de la viscosité de 1,6 à 2,6·10^{-1} Pa·s). Dans ce cas le processus d'agrégation ne s'achève que vers la sortie de la zone de préclinkérisation, lorsque la teneur en phase liquide de la matière baisse brusquement. Par suite, les grains ainsi formés se trouvent sous l'action des tensions thermomécaniques.

On peut influer sur le processus d'agrégation, en déplaçant son achèvement vers le milieu de la zone de préclinkérisation, à l'aide de la variation des paramètres entrant dans les équations (1) et (2). Nos recherches ont permis d'analyser l'influence des paramètres indiqués et de choisir les paramètres les plus efficaces pour la commande du processus d'agrégation.

Influence de la quantité de la matière fondue. Les valeurs de l'angle φ, caractérisant la quantité de la matière fondue dans le système de préclinkérisation, étaient calculées d'après sa tangente qui, à son tour, était déterminée d'après le rapport de la longueur de l'isthme entre deux granules, agglomérés au cours de la cuisson, au diamètre du granule. Les mesures des grandeurs mentionnées étaient effectuées pour les granules des mélanges de composition chimique différente (avec la teneur en phase liquide de 11 à 35 % en volume). Ainsi on a établi que les angles mesurés ne dépassent pas 40 degrés. Comme le montrent les calculs d'après l'équation (1), la variation des angles φ dans l'intervalle de 10 à 40° conduit à la diminution du paramètre d'agrégation de 18-25 % (Fig.1).

Influence de l'angle de mouillage. Des angles de mouillage, formés par les bains fondus de clinker de composition différente sur les surfaces des agglomérés denses de CaO et C_2S, ne dépassent pas 30° [3].

Les calculs faits d'après l'équation (1) montrent que la grandeur F/P diminue de

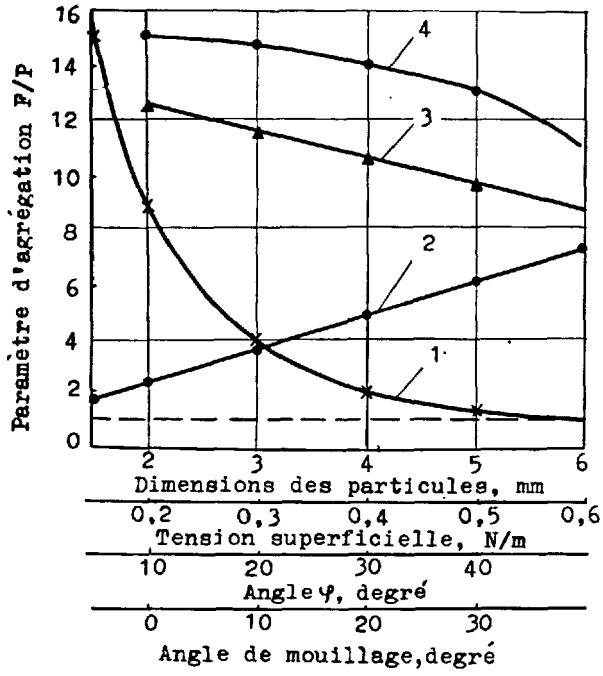

Fig.1; Influence des caractéristiques du système de frittage sur le paramètre d'agrégation

20-25 % lors de la variation de θ de 0 à 30° (Fig.1). Dans les conditions réelles les angles de mouillage peuvent être sensiblement inférieurs aux angles mesurés ou même égaux à zéro grâce à la rugosité de la surface des particules dispersées solides et à l'interaction chimique des phases solide et liquide, ce qui conduit à la diminution de l'influence de l'angle de mouillage sur le paramètre d'agrégation.

Influence de la tension superficielle. La tension superficielle des matières fondues dépend fortement du type et de la quantité des additions et peut varier de 150 à 580·10^{-3} N/m à la température de 1723°K (voir le tableau). La valeur du paramètre d'agrégation est proportionnelle à la tension superficielle (équation (1)) et si cette dernière varie dans les limites indiquées, elle augmente d'environ 75 % (Fig;1).

Influence de la dimension des particules. L'influence principale sur le paramètre d'agrégation est exercée par la dimension des particules, car la grandeur F/P est inversement proportionnelle au carré de leur rayon. La variation de 2 à 6 mm entraîne la diminution du paramètre d'agrégation d'environ 95% (Fig.1). Pour une dimension "maximale" déterminée des particules en amont de la zone de préclinkérisation (près de 10 mm), elles ne forment pas d'agrégats.

Influence de la viscosité. La viscosité de la matière fondue influe sur la vitesse du processus d'agrégation (équation (2)) et en fin de compte sur la dimension des granules du clinker. Les grandes vitesses d'agréga-

tion sont dues aux petites valeurs de la viscosité des matières fondues (0,7 à 1,2·10^{-1} Pa·s) et les petites vitesses, aux valeurs élevées de la viscosité (1,7 à 2,6·10^{-1} Pa·s).

L'analyse effectuée montre que le procédé le plus efficace d'action sur le processus de formation des granules consiste dans la variation de la tension superficielle, de la viscosité des matières fondues et de la dimension des particules de la matière en amont de la zone de cuisson.

Il est préférable d'utiliser les matières fondues ayant une tension superficielle élevée qui assure de grandes valeurs initiales du paramètre d'agrégation (6 à 9) pour pouvoir déplacer la fin du processus d'agrégation vers le milieu de la zone de préclinkérisation en faisant varier sa vitesse. La variation de la dimension des granules du clinker en fonction de la tension superficielle des matières fondues est représentée sur la figure 2.

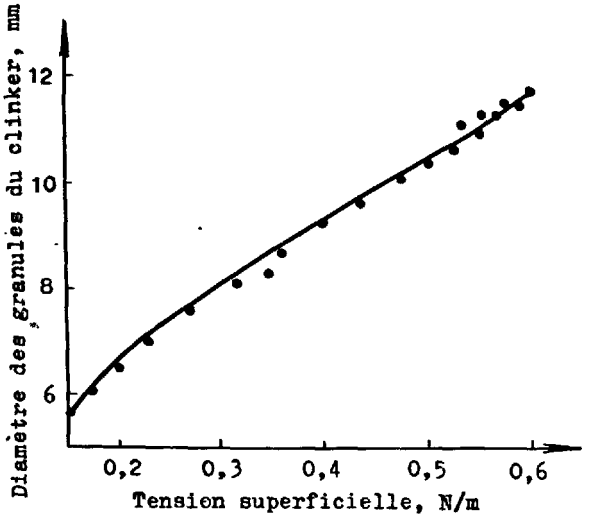

Fig.2. Variation de la dimension des grains du clinker en fonction de la tension superficielle

On peut accroître la vitesse d'agrégation par l'introduction complémentaire dans le mélange cru de Fe_2O_3 (le module alumine diminue) ainsi que des oxydes de titane et de manganèse en quantité de 1% en masse (en recalculant pour la matière fondue). Des résultats analogues peuvent être obtenus en augmentant la quantité de matière fondue.

On peut diminuer la vitesse d'agrégation en augmentant le module alumine par l'introduction dans le mélange cru d'une quantité supplémentaire d'Al_2O_3 ou des oxydes de magnésium, de cadmium, de nickel en proportion de 1% en masse.

Dans les conditions industrielles, on a contrôlé expérimentalement l'influence des additions d'Al_2O_3, SO_3, Fe_2O_3, MgO, Na_2O + K_2O, MnO sur la composition granulométrique du clinker. La teneur élevée en SO_3 et R_2O, les autres conditions étant égales, empira la granulation du clinker; par contre la teneur élevée en Al_2O_3, Fe_2O_3, MnO, MgO améliora la granulation.

En plus de l'augmentation de la plasticité du mélange cru, on peut influer sur la dimension des particules de la matière en amont de la zone de préclinkérisation en faisant varier la position et la longueur de cette zone. Ainsi, si la zone de préclinkérisation est courte, la température de la matière diminue dans la zone de calcination tandis que la dimension des particules augmente (Fig.3).

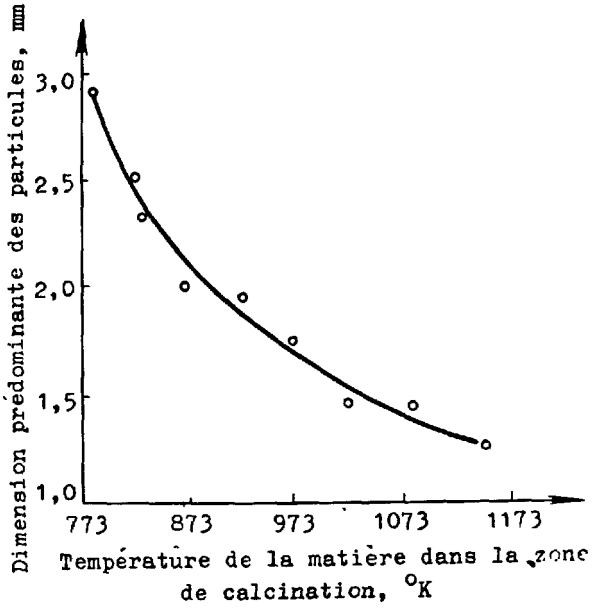

Fig.3. Variation de dimension des particules en fonction de la température dans la zone de calcination.

La composition granulométrique du clinker se trouve donc bien améliorée. Les compositions granulométriques des clinkers obtenues pour la zone de préclinkérisation courte (courbe 2) et longue (courbe 1) sont représentées sur la figure 4.

La commande du processus de formation des granules du clinker n'est pas seulement importante du point de vue de la stabilité du fonctionnement du four mais aussi du point de vue de l'accroissement de l'activité du clinker.

Les recherches effectuées dans plusieurs cimenteries ont permis d'établir les dépendances extremes entre la température théorique du courant gazeux dans la zone de préclinkérisation d'une part et la dimension dominante des granules du clinker et son activité à l'age de 28 jours d'autre part (Fig.5).

Le caractère des courbes témoigne de la dépendance proportionnelle entre la composition granulométrique du clinker et son activité.

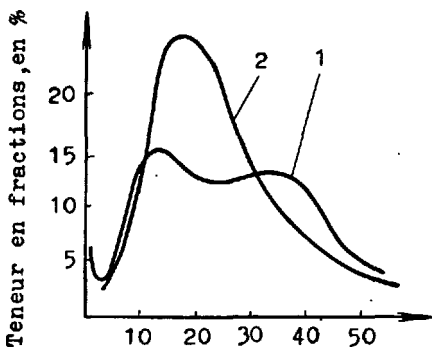

Fig.4. Courbes de répartition granulométrique du clinker.

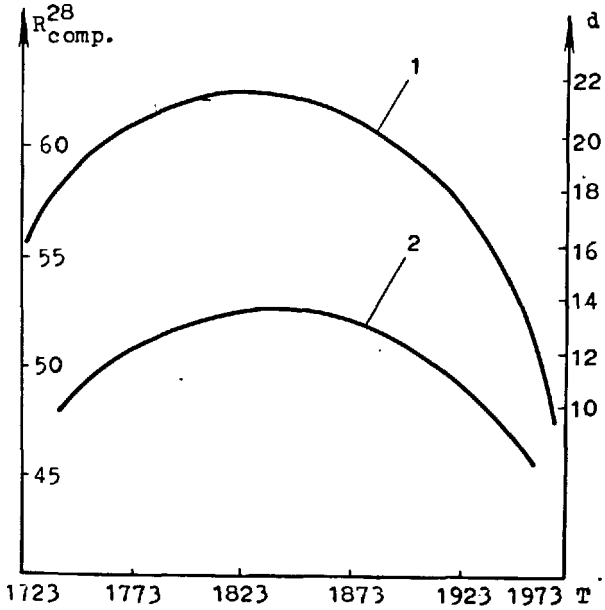

T – Température calculée du courant gazeux dans la zone de cuisson du four rotatif, °K

d – Dimensions prédominantes des grains du clinker, mm

$R^{28}_{comp.}$ – activité du clinker, MPa

Fig.5. Variation de la dimension dominante des granules du clinker (courbe 1) et son activité (courbe 2) en fonction de la température théorique du courant gazeux

Aux températures abaissées du courant gazeux dans la zone de préclinkérisation, on obtient un clinker qui a une grande teneur en particules fines et dont l'activité est généralement peu importante par suite du caractère inachevé des processus de formation des minéraux. En plus d'un grand pourcentage de petites particules dans le clinker aux températures élevées, on observe de gros boules. L'activité de ce clinker est également peu importante, ce qui est lié à la décomposition de l'alite (d'après les données de l'analyse des phases aux rayons X).

Enfin, il existe le domaine optimal de températures qui correspond aux grains de clinker relativement gros (la dimension prépondérante étant de 10 à 15 mm) à granulométrie serrée. C'est justement ce clinker qui présente l'activité maximale.

CONCLUSIONS

La commande du processus de formation des granules du clinker peut être réalisée sur la base des dépendances quantitatives obtenues, par modification de la composition chimique des mélanges crus et des paramètres thermotechniques du fonctionnement des fours rotatifs. L'action dirigée sur la formation des granules assure des caractéristiques techniques et économiques élevées du fonctionnement des fours et le clinker ainsi obtenu est de haute qualité.

Les recherches théoriques effectuées sont confirmées dans les conditions industrielles lors de la production des clinkers portlands dans les fours rotatifs puissants.

BIBLIOGRAPHIE

1. – В.В.ТИМАШЕВ, Б.С.АЛЬБАЦ (1976) "Процесс жидкофазного спекания портландцементного клинкера", Труды VI Международного конгресса по химии цемента", т.I, 165-169 (en russe)

2. – В.В.ТИМАШЕВ, Б.С.АЛЬБАЦ, А.П.ОСОКИН, С.И.ИВАЩЕНКО, Л.С.ФИЛИППОВА (1977), "Кислотноосновное взаимодействие в клинкерном расплаве", Труды XII конференции силикатной промышленности и науки о силикатах, т.I, 25-48. (en russe)

3. – V.V.TIMASHEV, B.S.ALBATS, A.P.OSOKIN, L.S.FILIPPOVA (1979), "Sintering of silikate system with presence of liquid phase", Science of sintering, vol.11, n.1, 55-70 (en anglais).

Mineralizers and fluxes in the clinkering process III. Burnability of synthetic and industrial raw mixes

Minéralisateurs et fondants dans le processus de clinkérisation III. Aptitude à la cuisson de mélanges synthétiques et industriels

W.A. KLEEM and I. JAWED, Martin Marietta Laboratories, Baltimore, Maryland, U.S.A.

2
Kleem

RÉSUMÉ: On a déterminé les effets de minéralisateurs et de fondants contenant du fluor sur l'aptitude à la cuisson d'une série de mélanges crus, allant du système quaternaire $CaO-Al_2O_3-Fe_2O_3-SiO_2$ à des mélanges plus complexes et industriels. On a trouvé de nouveaux indices qui montrent que les additifs contenant du fluor ont une influence importante sur la composition de la phase liquide, laquelle accélère la formation des silicates entre 1200°C et 1300°C. MgO et K_2SO_4 influencent la répartition du fluor entre les phases silicate et intersticielle. Le processus de cristallisation de C_3S entraîne un départ de fluor des phases intersticielles, ce qui provoque un changement de composition de $C_{11}A_7 \cdot CaF_2$ à C_3A. Les résultats expérimentaux montrent les interactions entre le pourcentage de fluor, la température de clinkérisation, le rapport Al_2O_3/Fe_2O_3 et les vitesses de réaction. On a mis en évidence les facteurs qui influencent l'hydratation et le développement des résistances. Ces résultats ont des implications directes sur la production du clinker et la conservation de l'énergie.

SUMMARY: The effects of fluorine-containing mineralizers and fluxes on the burnability of a series of raw mixes, ranging from the quaternary system $CaO-Al_2O_3-Fe_2O_3-SiO_2$ to more complex mixtures and industrial mixes, were determined. New evidence has been found to show that fluorine-containing additives have a major influence on the composition of the liquid phase which, in turn, accelerates silicate mineral formation between 1200° and 1300°C. MgO and K_2SO_4 influence the partitioning of fluorine between silicate and interstitial phases. The C_3S crystallization process results in removal of fluorine from the interstitial phases, and causes a compositional shift from $C_{11}A_7 \cdot CaF_2$ to C_3A. Data are given which show the relationships between fluorine content, clinkering temperature, Al_2O_3/Fe_2O_3 ratio, and rates of reaction. Factors that influence hydration and strength development are shown. These results have direct implications on commercial clinker production and energy conservation.

INTRODUCTION

A potentially attractive approach to energy conservation in the cement industry is through the addition of mineralizers and fluxes to the cement raw feed to enhance its burnability. This could result either in a decrease of the required kiln temperature or in an increase of the clinker production rate. Although for many years substantial efforts have been devoted to various aspects of this problem, most, for one reason or another, have been peripheral to gaining a fundamental understanding of the effects of mineralizers and fluxes on clinker formation (1).

The purpose of this present work was to establish the fundamental relationships and relative importance of fluorine-containing substances and minor oxides on mineral formation and clinkering reaction mechanisms. This was approached by starting with the basic quaternary system, $CaO-Al_2O_3-SiO_2-Fe_2O_3$, and progressing to more complex compositions, including industrial raw mixes, to determine the reaction kinetics of liquid and compound formation under dynamic or nonequilibrium conditions.

EXPERIMENTAL

Reagent-grade calcium carbonate, silicic acid, aluminum oxide, and ferric oxide were used to prepare three experimental quaternary compositions. The total of $Al_2O_3 + Fe_2O_3$ was held at 10% in each composition, but the ratio Al_2O_3/Fe_2O_3 was varied, as shown in Table I, along with the potential amounts of $C_{11}A_7 \cdot CaF_2$ that could be formed if sufficient fluorine were available.

TABLE I

Quaternary Composition	CaO/SiO_2	Al_2O_3/Fe_2O_3	% Potential $C_{11}A_7 \cdot CaF_2$
A	3	0.67	0.36
B	3	1.50	6.82
C	3	4.00	13.28

Further additions to each experimental composition, on a loss-free clinkered basis, were made with reagent-grade magnesium oxide and potassium sulfate. Calcium fluoride and calcium fluosilicate dihydrate were used as mineralizers for the above synthetic raw mixes, whereas fluosilicic acid was used for an industrial raw mix. Free CaO, C_3S, and $C_{11}A_7 \cdot CaF_2$ contents in clinker were determined by a quantitative X-ray diffraction procedure (2). The silicate phases were removed from the clinker by the selective dissolution of interstitial compounds with a hot aqueous KOH-sugar solution (3). The fluorine contents of both the original clinker and the separated silicate phases were determined by a method based on an initial lithium metaborate fusion, followed by dissolution in dilute HNO_3 and measurement with a fluoride-specific ion electrode (4).

RESULTS AND DISCUSSION

The most readily observed improvement from adding fluorine to a cement raw mix is due to its interaction with the liquid phase during the clinkering process. The importance of this liquid phase on clinker burnability has been discussed in detail in recent publications (5,6). The fluorine-containingliquid, which after solidification usually contains $C_{11}A_7 \cdot CaF_2$, is formed at a lower temperature and exhibits a lower viscosity, thus permitting the more rapid diffusion of reactive species and the accelerated formation of C_3S.

Clinkering Kinetics. Previous clinkering studies (7) on the three basic quaternary compositions containing 0.5% F^- as CaF_2 and $CaSiF_6$, at 1200° and 1300°C, established that as the ratio A/F was decreased, the clinker burnability was somewhat improved. Furthermore, at the same level of fluorine, CaF_2 appeared to be a slightly more effective mineralizer than $CaSiF_6$. Using either the progressive decrease in free CaO, or the corresponding increase in C_3S in the clinker, as an indicator of the clinkering reaction, it was found that the reaction rate of mineralized compositions at 1300°C was generally comparable to compositions without mineralizer additions at 1450°C. These findings are supported by Johansen and Christensen (8), who studied the kinetics of the reaction ($C + C_2S \rightarrow C_3S$) in the presence of CaF_2, by means of diffusion-couple experiments.

To determine the effectiveness of mineralizers on more complex mixtures, minor oxide additions were made to the basic quaternary compositions. The effects of CaF_2 and 1% additions of MgO and SO_3 (as K_2SO_4) on the burnability of composition B are shown in Figure 1.

In the absence of a mineralizing additive, essentially no C_3S is formed at temperatures as low as 1200°C, and only a small amount is formed at 1300°C. The addition of minor oxides to a non-mineralized composition produces two different effects. MgO functions as a flux because it lowers the temperature of liquid formation and significantly increases the rate of C_3S formation at 1300°C. A comparable addition of K_2SO_4 decreased the rate of C_3S formation to below that of the basic composition.

Mineralization with CaF_2 (0.5% F^-) greatly accelerated the clinkering reaction, and permitted the rapid formation of C_3S at 1200°C, a temperature well below the usual stability range of 1300° to 1800°C for C_3S. This is in aggreement with work by Mukherji (9), who reported that in the presence of CaF_2 the lower limit of decomposition of C_3S is reduced from 1000°-1300°C to

800°-1030°C. Roy and Sarkar (10) also observed C_3S formation at 1200°C in the presence of $CaSiF_6$, and have shown the enlargement of the C_3S primary phase field in the fluorine-containing ternary system $CaO-Al_2O_3-SiO_2$.

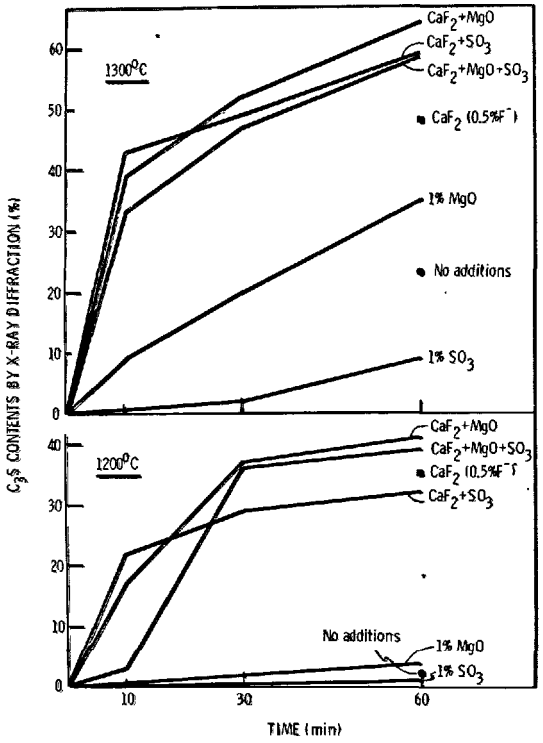

Figure 1. Rates of C_3S formation in composition B.

The previously observed negative effect of SO_3 additions on the clinkering reaction rate is not apparent with the mineralized compositions. Minor oxide additions, particularly at 1300°C, seem to have a further fluxing effect and give a slightly higher C_3S content than the composition with only CaF_2. In every case, however, mineralized compositions exhibit a very rapid initial reaction rate during the first 10-30 minutes, followed by a greatly reduced rate of C_3S formation. Selected clinkering tests conducted for up to four hours duration indicated that the C_3S content leveled off to about the same amount for each burning temperature. Approximately 40% C_3S was formed at 1200°C, and 60% C_3S formed at 1300°C.

Fluorine Partitioning. The finding of limits to maximum C_3S content obtained at a given clinkering temperature raises the question of whether the limits are due to a chemical constraint such as a change in melt composition or depletion of a reacting species, or perhaps a physical constraint such as inhomogeneities within the raw mix and localized regions of melt formation, which could restrict the diffusion processes.

To minimize burnability problems resulting from poor raw mix homogeneity, three samples of composition B, all containing CaF_2 (0.5% F-), 1% MgO, and 1% SO_3 (as K_2SO_4), were burned for 30 minutes, ground, and subsequently reburned for an additional 15 minutes, one each at 1100°, 1200°, and 1300°C. The resulting analyses of major clinker phases and fluoride contents of the total clinker as well as the separated silicate phases, are shown in Table II.

TABLE II

	Burning Temperature (C°)		
	1100	1200	1300
Free CaO (%)	16.8	5.8	0.7
C_3S (%)	9	42	59
$C_{11}A_7 \cdot CaF_2$*	+++	++	0
F^- in Clinker (%)	0.48	0.44	0.39
F^- in Silicates (%)	0.08	0.14	0.35
Fluorine Loss (%)	4	12	22

* Amounts are relative; 0 = none, + = detectable, ++ = moderate, +++ = substantial.

Again, although a steady-state condition was reached more rapidly, the C_3S content was limited to about 40% at 1200°C and 60% at 1300°C. Furthermore, the amount of $C_{11}A_7 \cdot CaF_2$ which was originally formed at 1100°C, decreased at 1200°C, and could not be detected at 1300°C. At this higher temperature, X-ray diffraction showed that C_3A was the only aluminate phase present. The loss of $C_{11}A_7 \cdot CaF_2$ was accompanied by an increase of fluorine in the silicate phases. Additionally, as has been reported by other researchers (8,11), about 20% of the fluorine appears to have volatilized.

Based on the observed partitioning of fluorine between the interstitial and silicate phases, the following reaction sequence was proposed (12) to clarify the clinkering process in the presence of fluorine-containing mineralizers:

1) Fluorine (as CaF_2 or $CaSiF_6$) reacts with the raw mix components to form a ferrite and aluminate liquid phase below 1200°C.

2) The clinker liquid phase is required for low temperature formation of C_3S. Accordingly, C_3S rapidly forms at temperatures below 1200°C. As C_3S crystallizes from the melt, it continuously removes with it a small quantity of fluorine.

3) Depletion of fluorine results in a change of the liquid phase composition, quali-

tatively depicted as (Fss + $C_{11}A_7 \cdot CaF_2$ + Fss + C_3A). Such a change in melt composition varies with initial fluorine content and clinkering temperature, and may limit the amount of C_3S that will form at a given temperature.

4) At higher temperatures (e.g., 1300°C), sufficient fluorine may be removed from the clinker liquid to result in the complete decomposition of $C_{11}A_7 \cdot CaF_2$ and formation of C_3A.

Calcium Fluosilicate and Minor Oxides. The effect of changes in interstitial phase composition on clinker burnability and on the effectiveness of mineralization was determined on quaternary compositions A, B, and C. The three compositions, representing alumina ratios of 0.67, 1.50, and 4.00, were prepared with minor oxide additions of 1% MgO, 1% SO_3 (as K_2SO_4), and a combination of MgO and SO_3. Each mixture contained $CaSiF_6$ (0.5% F^-) as the mineralizing agent. For comparison, the most complex mixture, containing both MgO and SO_3, was prepared with CaF_2 (0.5% F^-). After burning each for 30 minutes at 1300°C, the clinkered products were analyzed, and the results are given in Table III.

The amount of free CaO remaining after clinkering may be used as an index of the progress of the clinkering reactions and, therefore, the relative burnability. It appears that the compositions burn with somewhat more difficulty as the alumina content is increased. In all cases, however, the addition of minor oxides results in an improvement of burnability, and the combination of MgO and SO_3 gives the lowest free CaO contents. A comparison with those compositions containing CaF_2, suggests that, at equivalent fluorine concentrations, $CaSiF_6$ is the more effective mineralizing agent. This is the opposite of what had been previously found in the absence of minor oxide additions.

An analysis of the clinkers for total fluorine content indicates that the amount of fluorine found in the basic quaternary compositions A, B, and C are essentially the same, and that about a 20% loss occurs during the clinkering process. Those samples containing MgO alone seem to have retained slightly more fluorine, and those containing SO_3 have somewhat less. This could perhaps be attributed to the influence of K_2O on fluorine volatilization.

Some interesting effects were observed in the partitioning of fluorine between the silicate and interstitial phases in the clinker. MgO additions tend to increase the amount of fluorine passing into the silicate phases, whereas SO_3 additions have a negative influence on the process. In the absence of SO_3, the higher alumina ratio compositions also exhibit less fluorine in the calcium silicate minerals.

There is a poor correlation between the amount of fluorine that can be calculated as being in the interstitial phase and the $C_{11}A_7 \cdot CaF_2$ content estimated from X-ray diffraction measurements. This is particularly true with composition A, which is capable of forming only a very small quantity of $C_{11}A_7 \cdot CaF_2$. A substantial amount of fluorine is clearly associated with the predominate ferrite phase. In composition B, partitioning of fluorine seems to occur between the aluminate and ferrite phases, as well as the silicate phases. Little has been done to charac-

TABLE III

Composition	Clinker				Silicate Phase
	Free CaO (%)	C_3S (%)	$C_{11}A_7 \cdot CaF_2$*	F^- (%)	F^- (%)
A + $CaSiF_6$	4.8	50	+	0.39	0.31
A + MgO + $CaSiF_6$	3.4	55	+	0.42	0.38
A + SO_3 + $CaSiF_6$	3.0	55	+	0.36	0.21
A + MgO + SO_3 + $CaSiF_6$	2.8	52	+	0.41	0.23
A + MgO + SO_3 + CaF_2	3.7	55	+	0.36	0.23
B + $CaSiF_6$	7.2	52	++	0.40	0.23
B + MgO + $CaSiF_6$	3.8	52	++	0.41	0.30
B + SO_3 + $CaSiF_6$	4.2	57	+	0.37	0.19
B + MgO + SO_3 + $CaSiF_6$	3.0	52	+	0.37	0.23
B + MgO + SO_3 + CaF_2	4.0	30	+	0.37	0.24
C + $CaSiF_6$	7.4	56	++	0.39	0.21
C + MgO + $CaSiF_6$	5.2	53	+++	0.41	0.24
C + SO_3 + $CaSiF_6$	5.2	63	++	0.34	0.19
C + MgO + SO_3 + $CaSiF_6$	3.6	54	++	0.37	0.20
C + MgO + SO_3 + CaF_2	7.2	33	++	0.38	0.18

* Amounts are relative; 0 = none, + = detectable, ++ = moderate, +++ = substantial.

terize these fluorine-containing Fss phases, but Yamaguchi and co-workers (13) have reported that in a high calcium fluoroaluminate clinker, the ferrite phase approaches the alumina-rich end of the solid solution series and contains about 1% fluorine.

Industrial Raw Mixes. An industrial portland cement raw mix was chosen for study that broadly resembled composition B. The chemical composition is given in Table IV.

TABLE IV

Oxide	%
SiO_2	13.88
Al_2O_3	3.27
Fe_2O_3	1.42
CaO	42.67
MgO	2.03
SO_3	0.70
K_2O	0.67
Na_2O	0.16
Ignition loss	35.52
	100.32

It has been reported (14) that improved burnability is achieved when the fluorine-containing mineralizing agent is added to the raw mix as a free mineral acid rather than as a salt. Therefore, all fluosilicate additions were made in the form of H_2SiF_6, as a 24% aqueous solution. This was accomplished in two ways. First, the acid solution was added to a slurry of the raw material, which was subsequently dried and identified as raw mix I. In the second way, the acid solution was well mixed with the dry powdered raw material, which was called raw mix II. The fluorine contents of both raw mixes were 0.30 and 0.60%. Each mix composition was burned for one hour at 1300°C. The amounts of free CaO and C_3S in the clinker were determined by X-ray diffraction, and are shown in Table V.

TABLE V

Composition	H_2SiF_6 Addition (% F^-)	Free CaO (%)	C_3S (%)
Raw Mix I (slurry)	0.30	2.3	58
	0.60	1.5	58
Raw Mix II (powder)	0.30	4.2	48
	0.60	2.3	52

Both raw mixes had good burnability characteristics, with the actual free CaO content depending upon the amount of fluosilicic acid originally used for mineralization. When compared with raw mix II containing the same amounts of fluorine, raw mix I had lower free CaO contents, and higher amounts of C_3S formed, which are attributed to the greatly improved homogeneity brought about by slurry mixing. This has permitted the same degree of clinkering to be achieved with 0.3% F^- in a slurry-derived mix as could be achieved with 0.6% F^- in a mix prepared as a powder.

Hydration and Strength Development. It has been established that portland cement clinker can be produced at temperatures of 1300°C, if fluorine-containing additives are used as mineralizing agents. Furthermore, fluorine will partition between the interstitial and the silicate phases during clinker formation. The effect this will have on the subsequent hydration and strength development of cement produced from such clinkers is, therefore, of great importance. Welch and Gutt (15) and Nurse and co-workers (16) showed that the increasing fluorine content in C_3S resulted in reduced strength and rates of strength development. However, this work was conducted on pure C_3S preparations, and the effect of fluorine on C_3S produced in normal clinker at lower temperatures had not been determined.

Cement from selected compositions was prepared with laboratory-burned clinkers and 5% gypsum, and ground to a Blaine fineness of about 3500 cm2/g. These clinkers consisted of compositions A, B, and C, all containing 1% additions of MgO and SO_3 (as K_2SO_4), and burned for 30 minutes at 1450°C. Similar compositions, mineralized with CaF_2 (0.5% F^-), were burned for 30 minutes at 1300°C. Industrial raw mix I, mineralized with H_2SiF_6 (0.3% F^-), and raw mix II, mineralized with H_2SiF_6 (0.6% F^-), were each burned for 60 minutes at 1300°C.

Mortar cubes, prepared according to ASTM C109 procedures were made from all cements. Twelve 25-mm cubes were produced with cements containing compositions A, B, and C, and four each were subsequently tested at 1, 7, and 28 days. Similarly, nine 50-mm cubes were produced with the cements made from the two industrial raw mixes, and three each were tested at 1, 7, and 28 days. The results of these compressive strength tests are given in Table VI.

TABLE VI

Composition	Compressive Strength (MPa)		
	1 day	7 days	28 days
A + MgO + SO_3	6.2	23.1	31.6
A + MgO + SO_3 + CaF_2	10.1	29.2	34.8
B + MgO + SO_3	7.3	22.6	33.6
B + MgO + SO_3 + CaF_2	9.1	26.7	38.4
C + MgO + SO_3	5.6	28.1	38.3
C + MgO + SO_3 + CaF_2	1.2	20.8	32.5
Raw Mix I + H_2SiF_6 (0.3% F^-)	10.8	31.1	35.6
Raw Mix II + H_2SiF_6 (0.6% F^-)	6.3	28.1	33.6

Compared to the nonmineralized cements, compositions A and B exhibit significant strength increases, particularly at 1 day. Composition C, however, which has the highest alumina ratio and the most $C_{11}A_7 \cdot CaF_2$, is highly retarded at 1 day, and also remains below the rate of strength development of the control samples at 7 and 28 days.

The two cements made from industrial raw mixes mineralized with fluosilicic acid also show good strength development characteristics. The effect of fluorine level, however, is evident in that the composition containing 0.6% F- is somewhat retarded at 1 day compared to the composition containing 0.3% F-.

CONCLUSIONS

Fluorine-containing mineralizers greatly accelerate the clinkering reaction, permitting C_3S formation at temperatures below the usual stability range for C_3S. Minor oxide additions such as MgO, K_2O, and SO_3 have a further fluxing effect. Clinker burnability is also somewhat improved as the Al_2O_3/Fe_2O_3 ratio is decreased.

Mineralizers have a major influence on the liquid phase of the clinker. At about 1100°C, the liquid phase contains a significant amount of $C_{11}A_7 \cdot CaF_2$, which subsequently transforms to C_3A at 1300°C as a major portion of fluorine is preferentially taken up by the silicate phase. The fluorine loss due to volatilization is about 20%. The presence of MgO seems to favor the partitioning of fluorine into the silicate phase, whereas K_2SO_4 seems to increase its volatilization. Studies of the interstitial phase further indicate that partitioning of fluorine also takes place between the aluminate and ferrite phases.

Cement produced with mineralizers show, in some cases, significant increases in compressive strength as compared to nonmineralized cements. This was found to be true for both synthetic and industrial raw mixes. The results, therefore, indicate the possibility of producing clinker at lower temperatures with compressive strengths comparable to ordinary portland cements.

ACKNOWLEDGMENT

This work was suported by the National Science Foundation Division of Applied Research, under Grant No. DAR 77-07471 A01. The authors thank J. Skalny, L.J. Struble, C.H. Locher, and H.J. Holub for their valuable contributions.

REFERENCES

1. W.A. KLEMM and J. SKALNY (1977) "Mineralizers and Fluxes in the Clinkering Process," Cements Research Progress 1976, pp. 259-291 (American Ceramic Society, Columbus, Ohio).

2. W.A. KLEMM, K.J. HOLUB, and J. SKALNY (1977) The Effect of Fluxes and Mineralizers in Lowering Cement Kiln Temperatures, Grant AER 77-07471 National Science Foundation, Progress Report No. 1.

3. W. GUTTERIDGE (1979) "On the Dissolution of the Interstitial Phases in Portland Cement," Cem. Concr. Res. 9(3), 319-324.

4. W.A. KLEMM, K.J. HOLUB, and J. SKALNY (1978) The Effect of Fluxes and Mineralizers in Lowering Cement Kiln Temperatures, Grant DAR 77-07471 A01, National Science Foundation, Progress Report No. 3.

5. N.H. CHRISTENSEN and V. JOHANSEN (1979) "Role of Liquid Phase and Mineralizers," in Cement Production and Use, Proc. of Engineering Foundation Conf.

6. W.A. KLEMM (1979) "Influence of Clinker Liquid on Burnability," in Cement Production and Use, Proc. of Engineering Foundation Conf.

7. J. SKALNY, K.J. HOLUB, and W.A. KLEMM (1978) "Influence of Potential Interstitial Phase Composition on Clinkering Reactions," Cemento, 75(3), 351-356.

8. V. JOHANSEN and N.H. CHRISTENSEN (1979) "Rate of Formation of C_3S in the System $CaO-SiO_2-Al_2O_3-Fe_2O_3-MgO$ with Addition of CaF_2," Cem. Concr. Res. 9,(1), 1-6.

9. J. MUKHERJI (1965) "Phase Equilibrium Diagram $CaO-CaF_2-2CaO \cdot SiO_2$," J. Am. Ceram. Soc. 48(4), 210-213.

10. D.M. ROY and A.K. SARKAR (1979) "Effects of Fluoride Fluxes and Mineralizers upon Phase Equilibria," in Cement Production and Use, Proc. of Engineering Foundation Conf.

11. S.G. AMPIAN and E.P. FLINT (1973) "Effect of Silicofluorides on the Formation of Calcium Silicates, Aluminates and Aluminoferrite," Bull. Am. Ceram. Soc., 52(8), 604-620.

12. W.A. KLEMM, I. JAWED, and K.J. HOLUB (1979) "Effects of Calcium Fluoride Mineralization on Silicates and Melt Formation in Portland Cement Clinker," Cem. Concr. Res., 9(4), 489-496.

13. G. YAMAGUCHI, H. UCHIKAWA, S. TAKAGI, and K. TSUKIYAMA (1972) "Studies on Calcium Fluoroaluminate and Ferrite Phase in Jet Cement Clinker," Rev. of 26th Gen. Mtg., pp. 29-34 (Cement Association of Japan, Tokyo).

14. J.P. SKALNY AND W.A. KLEMM (1979) "Process for the Production of Portland Type Cement Clinker," U.S. Patent 4,135,941.

15. J.H. WELCH and W. GUTT (1962) "The Effect of Minor Components on the Hydraulicity of the Calcium Silicates," Proc. Fourth Intern. Symp. Chemistry Cement, Vol. I, pp. 59-67 (National Bureau of Standards, Washington, D.C.).

16. R.W. NURSE, H.G. MIDGLEY, W. GUTT, and K. FLETCHER (1966) "Effect of Polymorphism of Tricalcium Silicate on its Reactivity," Symp. Structure of Portland Cement Paste and Concrete, Spec. Rept. 90, pp. 258-262 (Highway Research Board, Washington, D.C.).

Problèmes physico-chimiques du broyage du clinker-portland

Physico-chemical problems of grinding of portland cement clinker

V.Z. PIROTSKI, candidat ès sciences techniques, NIITzement, Moscou, U.R.S.S.

RESUME : Le processus de broyage du clinker-portland s'accompagne d'effets physico-chimiques et se caractérise par la variation par stades de la constante de la vitesse de broyage et des propriétés physiques de la poudre, ce qui est dû à l'hétérogénéité macro et microscopique de la structure du clinker et aux interactions superficielles. L'efficacité du processus et la distribution granulométrique du ciment sont déterminées par l'interaction et l'influence mutuelle des propriétés physico-chimiques du clinker, des conditions thermiques d'humidité et d'adsorption. On a établi des relations qualitatives et quantitatives entre les indices de cinétique du broyage et la distribution granulométrique et les propriétés de cohésion des clinkers-portlands; ceux-ci se différencient par leurs caractéristiques minéralogiques et structurales, notamment si l'on utilise un agent de mouture. On a établi une possibilité de principe de contrôler les caractéristiques de dispersion et les propriétés du ciment en utilisant comme agents de mouture des surfactifs, qui se distinguent par leur action sélective sur les constituants. L'accroissement de l'efficacité des méthodes physico-chimiques d'intensification des processus doit être fondé sur l'optimisation du régime énergétique et hydrodynamique relativement aux propriétés du matériau et du milieu.

SUMMARY : The process of portland cement clinker grinding is accompanied by various physico-chemical effects and is characterized by stepwise variation of the grinding rate constant and of physical properties of the powder due to macro- and micro- inhomogenienties in the clinker structure and to surface interactions. The effectiveness of the process and the granular distribution of cement are determined by the interaction and interdependence of physico-chemical properties of clinker, heat-moisture and adsorption conditions. Qualitative and quantitative dependences of grinding kinetics, of granular distribution, adhesive-autohesive properties were determined for portland cement clinkers with different minerological and structural characteristics, including grinding in the presence of surface-active compositions.

The possibility of controlling dispersion characteristics and properties of cements by using surface-active compositions with selective action of the components is established. Increase of the effectiveness of physico-chemical methods of intensifying processes should be based on optimization of the energy and hydrodynamic conditions in relation to properties of the material and medium.

Le broyage du clinker-portland s'accompagne d'effets profonds et variés des interactions superficielles, qui sont caractéristiques des processus physico-chimiques et influent sensiblement sur les indices énergétiques, les caractéristiques de dispersion et sur l'activité du ciment. Ces effets consistent dans :

l'adhésion et l'autohésion dues à l'interaction des particules de clinker entre elles et avec les surfaces de broyage ;

la diminution de résistance d'adsorption (résistance au broyage) et la désagrégation dues à l'interaction entre les particules de clinker et le milieu actif adsorbant ;

la déformation plastique de la structure cristalline de la couche superficielle (destruction) et les réactions mécano-chimiques qui se manifestent en cas de dispersion très profonde.

La valeur et la contribution des effets sont déterminées par les propriétés physico-chimiques du clinker et des additions, les paramètres technologiques et les caractéristiques de régime ainsi que par les conditions thermiques et d'humidité et d'adsoprtion (1 à 6). Les procédés physico-chimiques d'intensification du processus, fondés sur la création du milieu actif adsorbant dans le broyeur par addition de surfactifs, et sur le réglage de la température du processus donnent dans les conditions réelles un effet de 15 à 20 %. Théoriquement et expérimentalement cet effet est évalué à 30-60 % et est obtenu par optimisation des paramètres et des régimes du processus relativement aux propriétés du clinker et du milieu (1, 3, 6). Dans cette optique, l'étude de la cinétique du broyage et de la distribution des grains acquiert une importance primordiale. On a montré auparavant (6, 7) que pour la plupart des clinkers, la dépendance des dépenses d'énergie spécifiques par rapport à la dispersion E = f(S) se caractérise par des stades consécutifs : broyage grossier (<1500 cm^2/g), moyen (1500 à 2500 cm^2/g) et fin (>2500 cm^2/g). La grandeur E/S déterminant l'efficacité du processus est respectivement de (6 à 10)·10^{-9}, (10 à 14)·10^{-9} et (14 à 40)·10^{-9} kWh/cm^2 (6).

Au cours des études de la cinétique du broyage et de la distribution granulométrique de 10 clinkers industriels, qui se distinguent par la composition minéralogique ($C_3S \approx 50 \pm 5$ % ; $C_2S \approx 24 \pm 6$ % ; $C_3A \approx 9 \pm 5$ % ; $C_4AF \approx 10 \pm 3$ %) et la microstructure, on a révélé la variation par stades de la constante de vitesse de broyage relative (K) dans l'équation de la cinétique du broyage :

$$R_\tau = R_o \cdot e^{-Kt^m}. \qquad (1)$$

La fonction K = f(τ) se caractérise par une courbe à trois portions : accroissement, constance relative et diminution des valeurs de K (fig. 1). La valeur du rapport $\frac{K_{max}}{K_{min}}$ est de 1,15 à 1,22. Les valeurs de dispersion des points caractéristiques de la courbe K = f(τ) coïncident avec les points correspondants de la fonction E = = f(S).

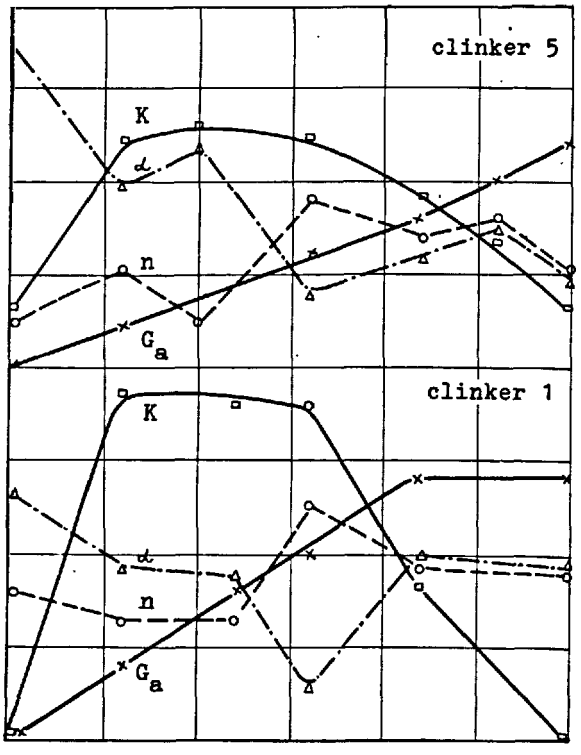

Fig. 1 - Variation de la constante de vitesse K, du coefficient d'uniformité n, de l'angle de talus naturel α ° et de la valeur d'adhésion G_a en fonction de la durée de broyage

La valeur relative de G_a (%) et la cinétique de l'adhésion $G_a = f(\tau)$ dépendent des particularités chimico-minéralogiques et structurales du clinker. Toutefois, on n'a pas réussi à suivre l'interdépendance entre le contenu de certaines phases de clinker et la grandeur G_a. D'après la valeur de G_a on a identifié trois groupes de clinkers : à valeur maximale, moyenne et minimale, respectivement de >0,6 ; 0,6 à 0,4 et <0,4 % (par rapport à la masse des corps broyeurs). D'après la cinétique, on a également établi trois groupes, caractérisés par la courbe exponentielle, la courbe de "maximum saturé" (fig. 1) et la courbe d'accroissement par gradins.

En fonction de la classe granulométrique, la grandeur K varie (fig. 2) non seulement de façon absolue mais aussi de façon relative. Dans le domaine de la fraction de

20 à 40 μm a lieu une brusque diminution de K et la "redistribution" de ses valeurs par rapport aux classes de 40 μm, ce qui est lié au début du broyage des minéraux-silicates dont la dimension prépondérante correspond à cette gamme, et aux différentes propriétés mécaniques des phases de clinker (résistance et fragilité), ainsi qu'à l'influence des phénomènes d'adhésion et d'autohésion.

Le caractère par stades des processus se voit également dans la variation de densité apparente γ_v (g/cm^3).

La relation $\alpha^\circ = f(\tau)$, qui traduit les propriétés "rhéologiques" de la poudre et caractérise indirectement sa fluidité (mobilité) présente un intérêt particulier. On a identifié trois groupes de clinkers : à allure de variations graduelle, par sauts (fig. 1), ou extrême (fig. 3) de $\alpha = f(\tau)$.

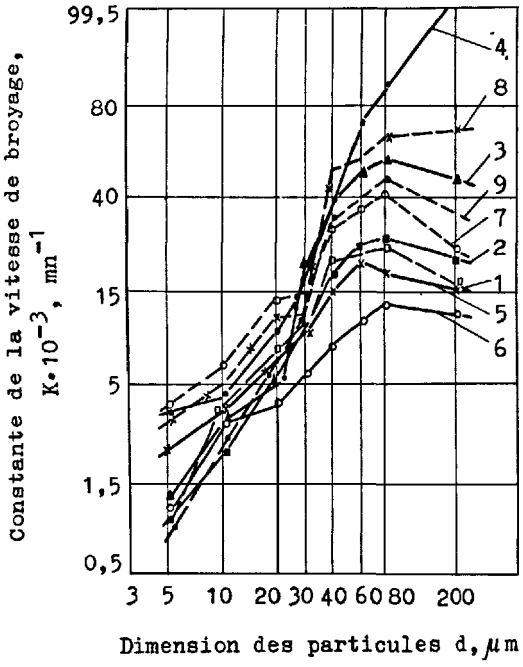

Fig. 2 - Dépendance de la constante de vitesse de broyage K de la classe granulométrique. 1 à 9 - clinkers-portlands.

Le coefficient d'uniformité de distribution granulométrique n dans l'équation RRB

$$R_d = R_o\, e^{-(\frac{d}{d'})^n} \qquad (2)$$

varie dans la plupart des cas à peu près de la même façon que α°, mais les points extrêmes sont d'une orientation opposée. La coïncidance des valeurs extrêmes du coefficient d'uniformité n , caractérisant indirectement la capacité d'agrégation, avec la grandeur α° ainsi que l'accroissement du degré d'adhésion G_a au voisinage de ces valeurs témoignent de l'interdépendance entre la distribution granulométrique et les propriétés d'adhésion et d'autohésion du ciment, ce qui est en accord avec les données de Beke, Opoczky et Mrakovitchne (4, 8). Notons que les dépendances généralisées citées dans (9) n'épuisent pas toute la diversité des régularités de broyage n et α° au fur et à mesure de la dispersion.

Il est tout à fait évident que la variation par stades de la constante de vitesse, l'influence des propriétés d'adhésion et d'autohésion sur les caractéristiques de dispersion et l'efficacité du processus commandent d'en tenir compte lors de la simulation et l'optimisation du processus.

Relativement aux stades établis, l'influence de la température s'exprime par un accroissement du degré d'adhésion et d'agrégation (6, 7). L'optimum de température se situe entre 90 et 110 °C. L'influence de l'humidité s'exprime par une baisse de la fluidité (mobilité) aux premiers stades et une diminution du degré d'adhésion et d'agrégation au dernier stade. L'optimum d'humidité est alors égal à 0,5-1,0 % (6, 7).

L'intensification du processus dans les conditions du milieu actif du point de vue de l'adsorption est liée aux effets de diminution de la résistance, qui se manifestent aux stades initiaux ainsi qu'aux effets de réduction de l'adhésion et de l'agrégation au stade de broyage fin (3, 7) et d'accroissement de la fluidité (mobilité) du ciment.

En présence de surfactifs, le caractère de $\alpha^\circ = f(\tau)$ et $n = f(\tau)$ est plus calme et la courbe ne présente pas de variations par sauts de α° et n (fig. 3), ce qui est dû à la diminution de l'agrégation.

L'efficacité des surfactifs devient plus importante lors du broyage des clinkers ayant une défectuosité élevée ; elle baisse lors de broyage simultané avec des additions poreuses faciles à broyer ainsi qu'avec des additions minérales à propriétés antiadhésives (sable, tripoli, laitiers, etc.) lorsque l'humidité devient supérieure à 1,5-2 %. Le dosage optimal des agents tensio-actifs est de 0,01 à 0,03 % (par rapport à la masse du ciment).

Pour le dosage de 0,05 à 0,1 %, l'efficacité du processus soit ne varie pas soit diminue ; pour le dosage > 0,1 %, l'efficacité baisse brusquement dans la plupart des cas, ce qui est lié aux conditions empirées du processus (diminution du coefficient de frottement, accroissement de la vitesse de mouvement du matériaux, etc.).

L'interaction des surfactifs avec les particules de clinker et le milieu broyeur influe sensiblement sur la cinétique du processus et la composition granulométrique du ciment, ce qui s'exprime par va-

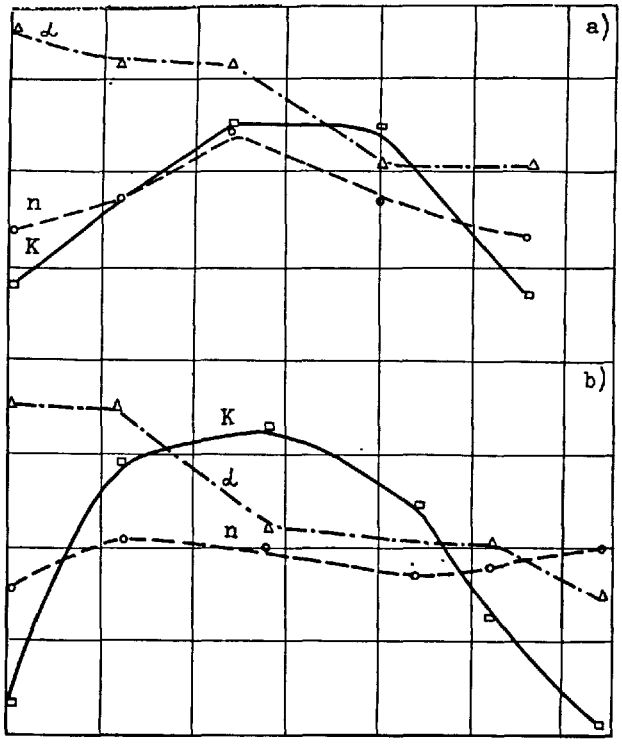

Durée de broyage - τ, mn

Fig. 3 - Variation de la constante de vitesse de broyage K, du coefficient d'uniformité n et d'angle de talus naturel α ° en fonction de la durée de broyage en présence de surfactifs (a - LST ; b - TEA + + LST ; 1:1)

riation des constantes K et n (fig. 1 à 3).

Sous cet angle, l'étude des compositions de surfactifs présente un intérêt certain; il s'agit avant tout des compositions à base de triéthanolamine et de lignosulfonate technique (TEA + LST), dans lesquelles, à côté de l'évaluation des dépenses d'énergie spécifiques, des propriétés de résistance et de dispersion du ciment, on a étudié l'influence sur les indices K, n, d', α ° et γ_v (Tableau I).

On a établi la sélectivité d'action des surfactifs complexes (leur quantité est de 0,025 % de la masse du ciment) par rapport aux paramètres de la cinétique du broyage et de la distribution granulométrique.

Ainsi, lors du broyage du clinker sans addition de surfactifs, la valeur de n et de d' est égale respectivement à 1,2 et 34 µm, avec TEA à 1,38 et 23, avec LST à 1,51 et 34. Lors du broyage avec surfactif complexe (TEA + LST), ces indices sont de 1,6 à 1,7 et de 35 à 40. Lorsque la part de LST dans la composition augmente, les valeurs de n

TABLEAU I

Influence des surfactifs sur la cinétique du broyage et la distribution granulométrique du ciment

Indice	Sans surfactifs	TEA	LST	Compositions de surfactifs			
				1:1	1:5	1:10	1:25
$K \cdot 10^{-2}$	6,41	2,87	5,15	4,15	4,52	4,73	5,58
γ_v	1,20	1,45	1,23	1,25	1,22	1,23	1,24
α	48	60	53	49	46	57	53
n	1,23	1,38	1,51	1,71	1,62	1,62	1,62
d'	34	28	34	38	45	45	40
$\frac{E_R}{R_{comp28}} \cdot 10^{-1}$	1,06	0,85	1,04	0,82	0,83	0,83	0,84

et d' s'élèvent. La sélectivité d'action des agents tensio-actifs se manifeste par un rapport différent des dépenses d'énergie spécifiques lors de l'évaluation de la dispersion d'après la teneur en grosse classe et la surface spécifique. Lors du broyage avec TEA, ce rapport est plus bas et avec LST plus élevé que lors du broyage sans surfactifs. La même régularité est caractéristique de α ° et γ_v. Les valeurs maximales de α ° et de γ_v correspondent aux ciments broyés avec TEA et atteignent 60° et 1,45 g/cm³. Pour les ciments avec LST, elles sont respectivement égales à 53 et à 1,25. Lors du broyage avec TEA + LST en différentes proportions, ces indices s'expriment pour la plupart des compositions par des valeurs intermédiaires.

L'évaluation complexe de l'action de la composition de surfactifs sur les indices énergétiques et de résistance, E_R/R_{comp28}, a montré leur efficacité dans le domaine des rapports TEA + LST de 1:5 à 1:25.

Ainsi on a établi une possibilité de principe de contrôler le processus, les caractéristiques de dispersion et les propriétés du ciment sur la base des surfactifs complexes dont les constituants ont une action sélective par rapport au pouvoir dispersif et aux propriétés du ciment. Outre les propriétés du matériau et les paramètres du procédé (type, dosage, distribution des agents tensio-actifs), l'efficacité des procédés d'intensification physico-chimiques dépend aussi des régimes énergétique et hydrodynamique.

En partant de la conception de l'influence dominante des propriétés physiques, physico-chimiques du matériau et du milieu, la mise en étude, le contrôle et l'intensification du processus doivent être fondés sur une "adaptation" des régimes énergétique et hydrodynamique ainsi que des conditions thermiques et d'humidité et d'adsorption aux particularités de la cinétique du broyage et de la distribution granulométri-

que. Les paramètres des régimes énergétique et hydrodynamique doivent être établis de manière à assurer à chaque stade une densité énergétique optimale exprimée par le rapport de l'énergie des actions broyantes à l'unité de volume du matériau :

$$q = \frac{E'}{V_m}, \text{ kWh/m}^3.$$

Le niveau de la densité énergétique est déterminé par les dimensions du boulet et de la particule, le diamètre du broyeur et le régime de vitesse de la charge broyante ainsi que par la vitesse et le caractère du mouvement du matériau (régime hydrodynamique), définissant la concentration du matériau dans le volume libre de l'espace utile. On a formulé les principes d'optimisation du processus :

l'énergie, la fréquence et le type des actions broyantes doivent être optimisés par rapport à la grosseur, à la broyabilité et aux propriétés d'adhésion du clinker ;

les résistances hydraulique et aérodynamique de la charge broyante et des diaphragmes doivent assurer une concentration et une vitesse de mouvement du matériau optinales, compte tenu des propriétés physiques, d'adhésion et d'autohésion et de la distribution granulométrique requise ;

les caractéristiques d'adsorption ainsi que celles de température et d'humidité du milieu doivent assurer une manifestation optimale des effets de diminution de la résistance et de la désagrégation.

La réalisation du premier principe est possible par les procédés suivants : utilisation des schémas de broyage en plusieurs stades dans les cycles ouvert et fermé ; maintien du régime différentiel de vitesse et de la classification des corps broyants sur la base du blindage à coefficient d'adhérence variable (12) ; application au stade de broyage fin de corps broyants de petites dimensions (système "Minipebs").

La réalisation du deuxième principe consiste dans l'application des sections efficaces et rationnelles de diaphragmes des broyeurs, un rapport optimal entre longueurs des chambres et degrés de remplissage L_1/L_2 et φ_1/φ_2, le choix judicieux de la valeur L/D, de l'intensité d'aspiration et de la composition granulométrique des corps broyants. La valabilité d'une telle conception est confirmée par le travail (10) où l'on a proposé une méthode de calcul des broyeurs, compte tenu de la cinétique du broyage et de la distribution granulométrique. Les travaux (11), où l'hydrodynamique du processus a été étudiée de façon minutieuse, donnent des résultats théoriques et pratiques importants.

Enfin, le troisième principe se réalise par l'introduction des compositions de surfactifs-intensificateurs du broyage et par le maintien de la température du processus dans les limites de 90 à 110 °C.

L'optimisation des conditions physico-chimiques est surtout d'actualité pour les broyeurs de grande capacité dans lesquels la puissance et le débit augmentent proportionnellement à $D^{2,5}$ et à $D^{2,7}$ et l'intensité d'aspiration, proportionnellement à D^2. A côté d'une énergie élevée de l'action unitaire, aux dernières étapes du broyage ceci entraîne une élévation de la température du processus et conduit à l'accroissement du degré d'adhésion et d'agrégation et à la diminution de l'efficacité du processus.

BIBLIOGRAPHIE

1- П.А. РЕБИНДЕР и др. (1944), Понизители твердости в бурении, М., изд. АН СССР, (en russe).

2- С.Е. АНДРЕЕВ, В.В. ТОВАРОВ, В.А. ПЕРОВ (1959) Закономерности измельчения и исчисления характеристик гранулометрического состава, М., (en russe).

3- Т.С. ХОДАКОВ (1972) Физика измельчения, М., (en russe).

4- B. BEKE, L. OPOCZKY (1967) Dechema Monographien , 57, 495, (en allemand).

5- М. ПАПАДАКИС (1966) Европ. Совещан. по измельч. М., Стройиздат, с. 307, (en russe).

6- С.М. РОЯК, В.З. ПИРОЦКИЙ (1960) Труды НИИЦемента, вып. 14, (en russe).

7- С.М. РОЯК, В.З. ПИРОЦКИЙ (1963) Труды НИИЦемента, вып. 19, (en russe).

8- Л. ОПОЧКИ, Т.К. МРАКОВИЧНЕ (1978) Epitöanyag, 30, II, 430-434, (en hongrois

9- М.Е. НУДЕЛЬ (1978), Epitöanyag, 30, II, 426, (en hongrois).

10- T. ТАНАКА (1977), Zement-Kalk-Gips, 7, (en allemand).

11- В.В.КАФАРОВ, М.А. ВЕРДИЯН (1978) Процессы и аппараты химической технологии, вып. 5, (en russe).

12- В.З. ПИРОЦКИЙ, Г.Ф. КОНЬКОВ и др.(1976) Труды НИИЦемента, вып. 36, (en russe).

L'influence du traitement thermique sur la transmission $\beta \rightarrow \gamma$-C_2S

Influence of thermal treatment on the transition $\beta \rightarrow \gamma$-C_2S

M. GAWLICKI, docteur, L'Académie de Mines et de Métallurgie, Cracovie, Pologne
et W. NOCUN-WCZELIK, ingénieur.

RESUME : L'importance particulière de la transition polymorphique du β-C_2S en γ-C_2S consiste dans le fait que cette transition, outre l'augmentation du volume spécifique, provoque la perte des propriétés hydrauliques du C_2S. Cette transition peut être arrêtée par un traitement thermique convenable qui limite la croissance des cristaux du β-C_2S aux dimensions auxquelles la nucléation et la croissance des germes du γ-C_2S n'est plus possible. La synthèse du β-C_2S à la température au-dessous de 1150°C ainsi que la cuisson du C_2S à grains fins aux températures au-dessous de 1400°C assurent les conditions convenables de la stabilisation du β-C_2S. Le dépassement, pendant la synthèse du C_2S, de la température de la transition $\alpha'_H \rightleftarrows \alpha$ /1420-1450°C/ joue un rôle particulier dans le processus de la transition du β-C_2S en γ. Aux températures 1420-1450°C le frittage du C_2S est rapidement accéléré et les grains du C_2S atteignent les dimensions si grandes que pendant le refroidissement suffisamment lent on obtient de grands cristaux de β-C_2S qui se transforment facilement en γ. Simultanement le refroidissement rapide des échantillons du C_2S cuits aux températures supérieures à 1450°C provoque la formation d'un grand nombre des cristaux du α'-C_2S très fins et conséquemment des cristaux du β-C_2S également fins dans lesquels la probabilité de la formation et de la croissance des germes de γ-C_2S est faible. La microstructure spécifique des agrégats des grains du γ-C_2S composés d'un grand nombre des paillettes et des aiguilles couvertes d'un réseau des profondes fissures permet de supposer que la dimension critique des cristaux du β-C_2S qui peuvent conserver la stabilité relative dans les conditions normales peut être estimée à 0,2-0,3 µm.

SUMMARY : The polymorphic transition of β-C_2S to γ form involving the great increase of specific volume and the loss of hydraulic properties of C_2S is of particular importance in the polymorphism of C_2S. One of the ways of suppressing this transition is by limiting the growth of β-C_2S crystals. It can be realized by proper thermal treatment β-C_2S can be stabilized when synthesis from oxides is performed at temperatures up to 1150°C or when finely ground γ-C_2S is fired for a short time at temperatures below 1400°C. When the temperature corresponding the transition $\alpha'_H \rightleftarrows \alpha$-$C_2S$ /1420-1450°C/ is exceeded, processes of sintering and crystal growth are rapidly accelerated. If, then, the cooling proceeds slowly, β-C_2S forms thin crystals which easily invert to γ-C_2S. The rapid cooling of the C_2S samples from temperatures higher than the transition temperature, that is 1420-1450°C, results in the material which has large proportion of very small crystals of α'-C_2S. These crystals transform to β form on cooling. The probability of the transition of small β-C_2S crystals to γ crystals is negligible. The aggregated γ-C_2S grains are composed of numerous needle - and platelike crystals. The smallest dimension of these crystals can be estimated as to be equal to 0.2-0.3 µm. It suggests that the dimension of the β-C_2S crystals which can be transformed to γ-C_2S crystals should be at least some about 0.3 µm.

La transformation polymorphique de β-C_2S en γ-C_2S est une transition monotrope de la phase métastable en phase thermodynamiquement stable. Le traitement thermique, c'est-á-dire la température et le temps de la cuisson aux températures detérminées ainsi que la vitesse du refroidissement des échantillons du C_2S joue un rôle important dans ce processus. L'analyse des publications consacrées au problème du polymorphism de C_2S /1-6/ suggère la nécessité des études de l'influence du traitement thermique ainsi que de la composition granulométrique des matériaux examinés sur la transition $\beta \rightarrow \gamma$-C_2S.
Le problème de la granulométrie est dans ce cas particulièrement compliqué car γ-C_2S forme des agrégats très caractéristiques, composés des aiguilles et des paillettes très minces, couvertes d'un réseau des fissures /figure 1/.

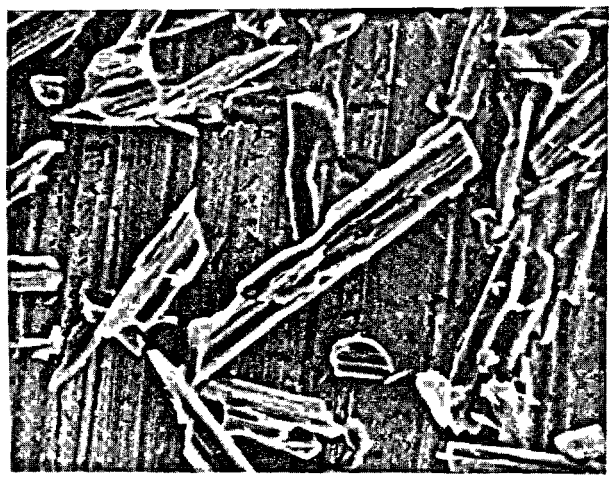

Fig. 1 - Microscope à balayage. γ-C_2S synthétisé á 1500°

Cette microstructure de γ-C_2S ainsique la cohésion assez faible entre les parts des agrégats rend pratiquemment impossible la détermination de la composition granulométrique des échantillons et des produits de frittage et d'autopulvérisation. Pour cette raison les données comprises dans ce travail sont limités aux fractions granulométriques prédominant dans les échantillons analysés.

Dans la majorité des études éffectuées on a utilisé, comme la matière de départ, la γ-modification - l'orthosilicate de calcium très pure. La concentration du β-C_2S dans le matériau analysé a été déterminée pour 1-2% au microscope.

Dans la première série des études on a déterminé les températures de l'autopulvérisation ainsi que la composition minéralogique des échantillons du C_2S cuits aux températures differéntes et dans les temps variables. Les observations étaient éffectuées à l'aide du microscope aux températures élevées et la composition minéralogique était déterminée après le refroidissement par la diffraction aux rayons X en utilisant la méthode d'étalon externe /d_γ=3,01 Å/. Dans les études on a utilisé C_2S des grains de moins de 60 µm. La fraction prépondérante était celle de 10-30 µm.

Pour les observations au microscope aux températures élevées on a formé les petits cubes à partir du C_2S sous la pression constante. La vitesse de l'échauffement et du refroidissement était constante - 10°/min. Les données obtenues sont montrées dans les tableaux I, II.

TABLEAU I

Température de la cuisson du C_2S °C	Température de l'autopulvérisation en function du temps de la cuisson:				
	10'	30'	60'	120'	180'
1500	480	480	480	500	500
1450	460	460	470	470	480
1400	370	380	380	400	400
1350	360	380	380	390	390
1300	320	330	360	380	380
1250	300	320	320	360	360
1200	280	300	330	340	340
1150	Les échantillons ne s'autopulvérisaient pas.				
1100					

TABLEAU II

Température de la cuisson du C_2S °C	% γ-C_2S après le refroidissement. Temps de la cuisson:				
	10'	30'	60'	120'	180'
1500	100	100	100	100	100
1450	100	100	100	100	100
1400	78	80	82	83	85
1350	75	75	78	80	80
1300	60	65	70	75	80
1250	60	60	65	70	75
1200	55	55	60	60	65
1150	40	45	45	46	47
1100	40	40	45	45	45

Des données placées dans les tableaux I, II résulte, que la température de l'autopulvérisation des échantillons et leur composition minéralogique sont liées avec la température de la cuisson ainsi qu'avec le temps de la cuisson à la température établie. Dans tous les échantillons cuits à la température 1450°C et 1500°C on n'a constaté, après le refroidissement, que la phase γ-C_2S. L'abaissement de la température du traitement provoquait l'abaissement de la température de l'autopulvérisation des échantillons et de la teneur en γ-C_2S des produits obtenus. Ces variations n'étaient pas proportionelles à l'abaissement de la température du traitement, les plus grandes différences ont été constatées pour la variation de la température de 1450°C à 1400°C. En même temps il faut remarquer que la température d'autopulvérisation, déterminée par l'observation au microscope n'est qu'une mesure de la vitesse

de la transition $\beta \rightarrow \gamma$-C_2S et ne peut pas être considérée comme la température du commencement de cette transition. Les températures du commencement de la transition $\beta \rightarrow \gamma$-C_2S en registrées aux thermogrammes d'ATD ne dépendaient que faiblement de la température du traitement du C_2S, n'atteignaient que 15° de différence pour les échantillons cuits à 1200°C et à 1500°C.

Les variations des températures de l'autopulvérisation du C_2S et de sa composition minéralogique sont liées avec le degré du frittage des échantillons examinés. On a établi, que la contraction des préparations observée au microscope aux températures élevées pendant l'échauffement peut servir de la mesure de ce processus /figure 2/.

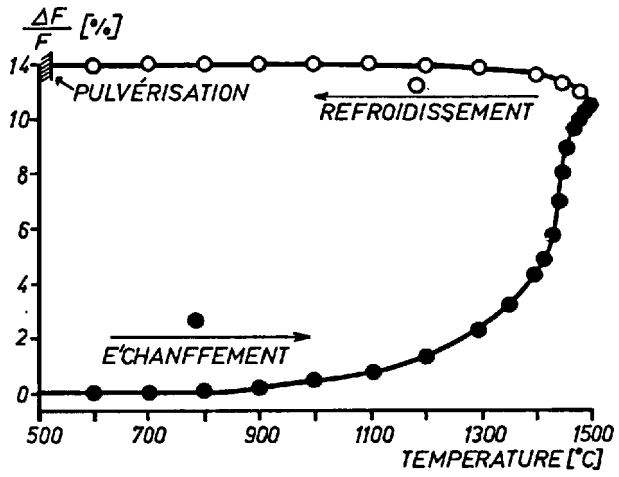

Fig. 2 - Les changements de surface de l'échantillon du C_2S observés au microscope thermique. $\Delta F = F - F_t$. F - la surface de l'échantillon de départ, F_t - la surface de l'échantillon à la température établie

Les résultats presentés montraient la contraction rapide au voisinage de la température de l'inversion $\alpha'_H \rightarrow \alpha$-$C_2S$ et s'accordaient avec ceux de S.Chromy /4/. Les études au microscope à la température élevée ne montraient pas au-dessous de 900°C des changements remarquables bien que l'augmentation de la masse spécifique accompagne la transition $\gamma \rightarrow \alpha'_L$-$C_2S$ /7/. Les études effectuées dans le même intervalle de température à l'aide du microscope à balayage à la température élevée ont montré, que les contractions des fibres conduisaient à la diminution de sonadhésion mutuelle et au lâchage de la microstructure fibreuse des agrégats des grains du C_2S sans augmentation des dimensions de ces agrégats. Ces changements n'étaient pas décélable au microscope à la température élevée à cause de la considérable porosité des échantillons examinés. On pouvait remarquer quand même, que les échantillons du C_2S cuits à 700-900°C étaient considérablement moins cohérents que ceux de départ.

La composition granulométrique du matériau de départ exercait l'influence sur le degré de la transition $\beta \rightarrow \gamma$-C_2S particulièrement quand l'échantillon était cuit à une température au-dessous de 1450°C. L'augmentation du degré de dispersion provoquait l'abaissement de la température de l'autopulvérisation ainsi que l'abaissement de la teneur en γ-C_2S du matériau refroidi. Les différences étaient plus poussées pour les températures de traitement du C_2S plus basses. Les résultats des études effectués à 1300°C et à 1500°C /2 heures de la cuisson, refroidissement lent/ sont groupés au tableau III.

TABLEAU III

No.	Fraction prédominante >70% µm	%γ-C_2S après le refroidissement. Température de la cuisson du C_2S: 1500°C	1300°C
1	60 - 80	100	87
2	10 - 30	100	85
3	5 - 10	93	35
4	2 - 5	84	10
5	< 2	72	-

La désintégration des agrégats des grains du γ-C_2S de départ en petits fragments rend le processus du frittage et de la recristallisation du C_2S difficile. Pendant le refroidissement un grand nombre de petits cristaux de β-C_2S se forme et dans cette masse les germes de la phase γ-C_2S ne peuvent ni se produire ni se développer. Par contre si les agrégats des grains du γ-C_2S de départ ne furent pas désintégrés les grains peuvent se fritter et recristalliser pendant l'échauffement, surtout dans les régions des agrégats. Les grandes surfaces d'adhésion des fibres et des paillettes ainsi que la concordance de l'orientation de leur structure favorisent ce processus. La phase qui paraît en train de refroidissement se compose des cristaux sufisamment grands qu'elle peut se transformer en γ. Pendant la cuisson du C_2S à la température supérieure de 1450°C le processus du frittage comprend des espaces plus grandes que l'ensemble des fibres et des paillettes appartenant aux mêmes agrégats et il est favorisé par la transition de α'_H en α-C_2S à 1420°C. Si le temps du traitement à une température élevée est sufisamment long, on obtient pendant le refroidissement les cristaux du β-C_2S tellement grands, qu'aussi bien la nucléation que la croissance des germes du γ-C_2S en sont possibles.

Prenant en considération des résultats obtenus jusqu'au présent il faut admettre que la répétition des cycles "cuisson - refroidissement" du C_2S conduit à la désintégration des agrégats des grains et en conséquence à l'augmentation de la teneur en β-C_2S et à l'arrêt de l'autopulvérisation à condition que la température de la cuisson soit sufisamment basse. Cette hypothèse a été confirmée par la répétition des cycles "cuisson-refroidissement" du C_2S dans les intervalles de température les suivants: 20° - 1200° - 20°, 20° - 1300° - 20°, 20° - 1400° - 20°C.

Les études au microscope, par la diffraction aux rayons X et par l'ATD ont montré, qu'après avoir répété les cycles "cuisson - refroidissement" la teneur en β-C_2S du matériau refroidi systématiquement augmentait et l'autopulvérisation était arrêtée tandis que la teneur en γ-C_2S ne dépassait pas 40%. Le nombre des cycles "cuisson - refroidissement" nécessaires pour arrêter l'autopulvérisation dépandait de la température et du temps de la cuisson et il avait valeurs les suivantes: 1200^{o}/2h - 2, 1300^{o}/2h - 3, 1400^{o}/2h - 7. La répétition des cycles "cuisson - refroidissement" aux températures 1450°C et 1500°C ne provoquait pas des variations de la température de l'autopulvérisation et de la composition minéralogique.

Les synthèses du C_2S effectuées en partant du mélange de silicagel et de $CaCO_3$ ainsi que de silicagel et de $Ca/OH/_2$ ont confirmé l'influence du degré du frittage et de la recristallisation du C_2S sur sa composition minéralogique.

TABLEAU IV

Temp. de la synthèse du C_2S °C	% γ-C_2S après le refroidissement. Matériaux de départ utilisés dans la synthèse:	
	$CaCO_3+SiO_2.nH_2O$	$Ca/OH/_2+SiO_2.nH_2O$
1500	100	100
1400	85	83
1300	80	75
1200	65	60
1180	45	35
1160	15	5
1140	5	-
1120	-	-
1100	La synthèse du	-
1000	C_2S de $CaCO_3$	-
900	et de silica-	-
800	gel n'a pas été effectuée aux 800°- 1000°C	-

Le temps de la cuisson a été établi en fonction de la teneur en CaO libre et allait de 48 jusqu'à 150h.

La série suivante des études a montré que la vitesse du refroidissement à la température de l'inversion de α-C_2S en α'_H avait de l'influence importante sur l'autopulvérisation ainsi que sur la composition minéralogique après le refroidissement d'un échantillon. On a obtenu les conditions du refroidissement rapide en immergeant des échantillons cuits au nitrogène liquide, ce qu'a donné les produits composés des cristaux du β-C_2S si fines que la probabilité du développement dans cette masse des germes stables du γ-C_2S était très faible. La cuisson des échantillons à la température supérieure à 1450°C, le refroidissement lent jusqu'à la température 1400°C et puis le refroidissement rapide dans le nitrogène liquide ne provoquaient pas de stabilisation du β-C_2S mais conduisaient à l'obtention du mélange du β et γ-C_2S.

Les relations entre les conditions du traitement thermique et la stabilisation du β-C_2S presentées dans le travail permettent de déterminer les conditions dans les quelles les cristaux du β-C_2S n'atteignent pas de dimension critique, ce que rend possible la nucléation ainsi que la croissance des germes du γ-C_2S. Les données presentées indiquent, que cette dimension doit être au-dessous de 2 µm. Cette estimation coincide avec des observations de l'autopulvérisation du C_2S dans les agglomérés contenant à côté de C_2S des aluminates de calcium /figures 3, 4/.

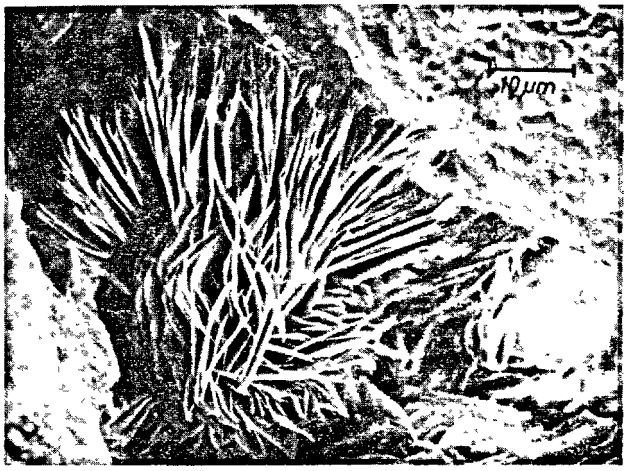

Fig. 3 - Microscope à balayage. Les formes du γ-C_2S très caractéristiques pour les agglomérés contenant les aluminates de calcium à côté du C_2S

Fig. 4 - Fragment de la figure 3

L'épaisseur des paillettes du γ-C_2S dans ces échantillons, et par cela même le plus petites dimensions des grains du β-C_2S, va de 0,2 à 0,3 µm. On peut confirmer cette hypothèse en déterminant les dimensions des cri-

stallites du β-C_2S stabilisé par l'addition de bore, d'arsenic ou de phosphore, par la méthode de la diffraction des rayons X. Ces dimensions, rapprochés à la limite d'utilité de cette méthode attaignent les valeurs 0,2-0,3 µm.

BIBLIOGRAPHIE

1. - N. YANNAQUIS et A. GUINIER /1959/ "La transformation polymorphique $\beta \longrightarrow \gamma$ de l'orthosilicate de calcium", Bull. Soc. Franc. Miner. et Cristal., 82, 126-136.
2. - A. GUINIER et M. REGOURD /1975/ "Structure of Portland Cement Minerals", VI Int. Congr. on the Chem. of Cem., Moscow, Vol. 1 pp. 25-51.
3. - A. DERDACKA-GRZYMEK /1978/ "Polymorphic Phase Change of Ca_2SiO_4", Polish Academy of Sciences, Papers of the Comission of Ceramics, 29, pp. 5-39.
4. - S. CHROMY /1970/ "Zur Umwandlung der Modifikationen $\beta \longrightarrow \gamma$ des Dikalziumsilikats", Zement-Kalk-Gips, 23, n° 8, 382-389.
5. - M. GAWLICKI /1977/ "The Factors Influenced the Polymorphic Transition $\beta \longrightarrow \gamma$-$Ca_2SiO_4$", These.
6. - J. GRZYMEK et J. SKALNY /1967/ "Beitrag zur Polymorphie von C_2S", Tonind. Ztg., 91, n° 4, 128-130.
7. - M. REGOURD, M. BIGARE, J. FOREST, A. GUINIER /1969/ "Synthesis and Crystallographic Investigation of Some Belites", Congr. on the Chem. of Cem. Tokyo, Vol. 1, pp. 44-48.

Particularités cristallochimiques et propriétés des phases du clinker de ciment portland en fonction des conditions de cuisson et de refroidissement

Crystal chemical peculiarities and phase properties of portland cement clinker depending on the conditions of burning and cooling

I.F. PONOMAREV, professeur, docteur ès sciences techniques,
P.O. GAYDJOUROV, candidat ès sciences techniques,
A.P. ZOUBEKHINE, candidat ès sciences techniques,
V.V. KITAEV, ingénieur, Institut Polytechnique de Novotcherkassk, U.R.S.S.

RESUME : On a examiné des particularités cristallochimiques et des propriétés des phases essentielles de clinker des solutions ferrifères solides et leur composition en fonction du moyen de cuisson et de refroidissement du clinker. On a établi, par effet Mössbauer, la position des ions de fer Fe^{3+} et Fe^{2+} dans la structure de C_3S et C_2S, leur coordination, les limites de la solubilité et la distribution par phases en fonction de la vitesse de refroidissement. Le caractère fortement désordonné de la structure de l'alite et l'augmentation de son activité hydraulique sont conditionnés par l'introduction, dans les limites de solubilité, de l'oxyde ferreux dans C_3S. Mais une quantité élevée de FeO conduit à la destruction de l'alite ainsi qu'à une forte diminution de la résistance du ciment. La dissolution des oxydes de fer dans les silicates, dans les conditions d'une cristallisation en équilibre instable lors d'un brusque refroidissement du clinker, est examinée. Les composés ferreux sont fixés dans la phase vitreuse, ce qui contribue à l'élévation de la qualité du ciment.

SUMMARY : Chrystal chemical peculiarities and properties of the main clinker phases, ferriferrous solid solutions and their composition have been studied depending on the method of burning and clinker cooling. Crystal chemical sites of ions Fe^{3+} and Fe^{2+} in the structure of C_3S and C_2S, their coordination, limit solubility and phase distribution depending on the cooling rate have been established by Mössbauer spectroscopy. The introduction of ferrous oxide into C_3S within the solubility rang accounts for a high disorder of alite structure and the increase of its hydraulic activity. However the increased amount of FeO results in destruction of alite and significant decrease of cement strength. On rapid cooling of clinker non-equilibrium phase crystallization prevents the solution of ferrous oxides in silicate minerals while ferriferrous compounds are fixed in the vitreous phase which promotes the increase of cement quality.

Les phases ferrifères déterminent dans une grande mesure le processus de la clinkérisation et exercent une influence importante sur les propriétés du ciment portland, en fonction de leurs quantités, conditions de cuisson et de refroidissement. On a étudié des particularités cristallochimiques des phases de clinker contenant les oxydes de fer au cours de la formation des ciments portlands à faible teneur en fer (blanc) et ordinaire. On amis en évidence, par effet Mössbauer, que la formation des phases ferrifères au cours de la cuisson du mélange brut à faible teneur en fer (fig. 1b) diffère au plus haut degré de leur formation dans le mélange ordinaire (fig. 1a).

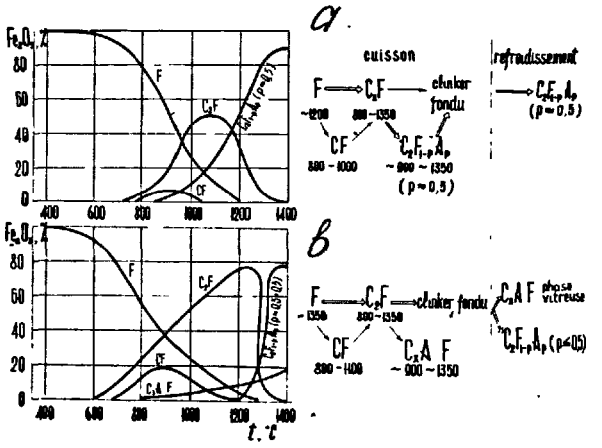

Fig. 1 - Répartition de fer par phases et schémas de formation des phases ferrifères au cours de la cuisson du clinker de ciment portland ordinaire (a) et blanc (b).

L'absence de la phase alumoferrite dans la charge en cuisson, au cours de la formation du ciment portland blanc et l'existence séparée de C_2Fe et de la solution solide C_2A:F sont une des causes de la formation de la phase fondue de clinker aux températures élevées et du ralentissement de la formation des minéraux du clinker blanc. La composition des phases ferreuses est, dans ce cas, fonction du mode de refroidissement. Dans le cas de refroidissement lent par air, quelque 50 à 60 % des oxydes de fer entrent dans la composition de la solution solide C_2A:F et de la phase vitreuse (dissolution des quantités microscopiques de Fe_2O_3 dans C_3S et C_2S n'est pas exclue), alors que le reste de Fe_2O_3 forme une phase alumoferrite indépendante dont la composition est voisine de C_4AF (fig. 2b). Par contre, en cas de refroidissement rapide par eau, l'oxyde ferrique se fixe essentiellement (90-100 %) dans la composition de la phase vitreuse et de la solution solide C_2A:F (fig. 2a). La fixation des oxydes de fer dans la composition de la phase vitreuse ou dans C_2A conditionne l'augmentation de la blancheur du clinker de 10 à 20 % en fonction de la quantité d'oxyde ferrique dans le mélange.

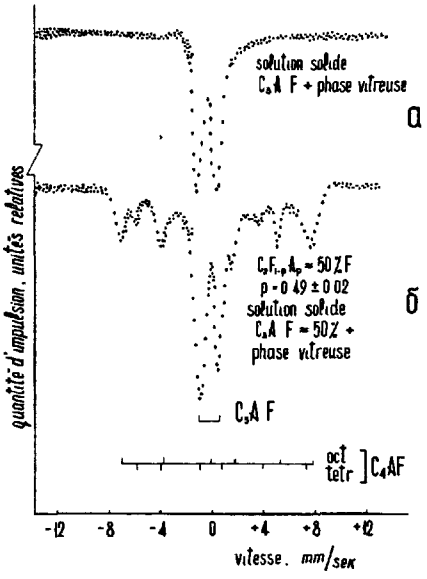

Fig. 2 - Spectres Mössbauer du clinker de ciment portland blanc au refroidissement par eau (a) et par air (b).

Les conditions de cuisson réductrice du clinker à faible teneur en fer (blanc), lorsque se forment les ions Fe^{2+}, exercent un effet positif sur la rapidité de la formation des minéraux et sur les propriétés du clinker (blancheur, résistance) dans les conditions de refroidissement rapide par eau.

Quant à l'influence de FeO se formant dans le clinker de ciment portland ordinaire pendant la cuisson réductrice dans des fours industriels, elle dépend essentiellement de sa quantité et sa répartition par phases.

Nous avons établi les particularités de la formation du clinker et mis en évidence les conditions prévenant une action négative de FeO sur la résistance du ciment. En l'absence de la phase liquide, l'oxyde ferreux pénètre à C_3S et C_2S et compose des solutions solides de substitution du type :

$$Ca^{2+} \rightleftharpoons Fe^{2+}$$

Il a été établi, par effet Mössbauer, que la limite de la solubilité de FeO dans C_3S ne dépasse pas 1.0 %. C'est que, malgré la présence d'isomorphisme isovalent, les paramètres cristallochimiques des ions Ca^{2+} et Fe^{2+} sont essentiellement différents, en particulier leurs rayons, leur charge négative et leur potentiel polarisant qui présentent pour Ca^{2+} et Fe^{2+} respectivement

1,04 et 0,80 Å ; 1,04 et 1,70 eV ; 0,66 et 0,89.

Lors de la pénétration d'une quantité de FeO supérieure à 1,0 %, l'oxyde détruit C_3S et il se forme des phases indépendantes : triferrite $CaO \cdot FeO \cdot Fe_2O_3$ et la composition $0{,}54CaO \cdot 1{,}46FeO \cdot SiO_2$ (fig. 3).

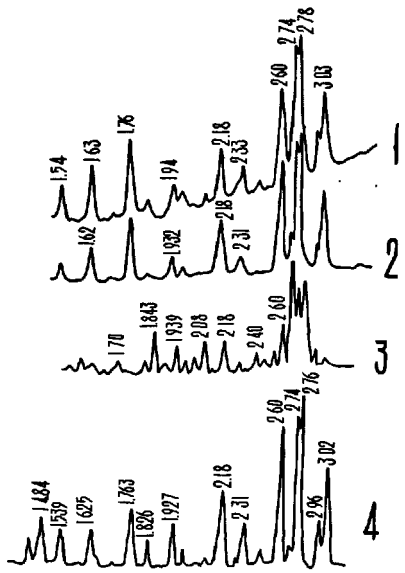

Fig. 3 - Radiogrammes des échantillons C_3S cuits dans un milieu réducteur et refroidis (1-3 - lentement, 4 - vite) : 1 - C_3S ; 2 - C_3S + 1 % FeO ; 3, 4 - C_3S + 3 % FeO.

Le chimisme du processus destructif peut être représenté par l'équation :

$$3(3CaO \cdot SiO_2) + 2{,}46FeO + Fe_2O_3 =$$

$$= 2(CaO \cdot SiO_2) + 3{,}46CaO + CaO \cdot FeO \cdot Fe_2O_3 +$$

$$+ 0{,}54CaO \cdot 1{,}46FeO \cdot SiO_2 .$$

Lorsque la teneur en FeO est excédentaire, la destruction de C_3S peut s'expliquer par les particularités de sa structure composée selon N.V. Bélov (1, 2), des couches d'octaèdres CaO_6 ou d'unités structurales à sept sommets $^6CaO_7$, reliés entre eux et aux tetraèdres SiO_4 par leurs arêtes et plans.

Lorsqu'on substitue Fe^{2+} à Ca^{2+}, sensiblement différents par leur charge négative et leur potentiel polarisant, il se produit des changements importants du type de la liaison et des déformations du réseau cristallin ce qui conduit, en fin de compte, à la destruction de la structure.

C_2S est plus stable que C_3S lorsqu'il y a pénétration de FeO. La limite de la solubilité de FeO dans C_2S est de 3 %. Du fait de la structure en îlots de C_2S, composée de tetraèdres isolés SiO_4 et de polyèdres CaO_6 ou CaO_8, C_2S possède une plus grande capacité de déformation et modification du réseau cristallin. Ceci rend possible la pénétration d'une plus grande quantité de FeO sans destruction du réseau cristallin de C_2S.

La présence de la fusion de clinker modifie substantiellement l'effet de FeO sur les minéraux-silicates. Dans ce cas, la solubilité de l'oxyde ferreux étant limitée dans le minéral siliceux C_2S cristallisant, en premier lieu, à des températures élevées, il se produit une redistribution de FeO par phases dans la fusion de clinker. L'oxyde ferreux est essentiellement fixé dans la phase vitreuse. La vitesse de refroidissement y joue un rôle très important : plus est grande la vitesse de refroidissement du clinker à partir des températures les plus élevées possible et plus est élevé le degré de solubilité de FeO dans la phase vitreuse. Lors de la fixation de l'oxyde ferreux dans la phase vitreuse la pénétration de FeO dans l'alite peut être limitée et même nulle ce qui prévient l'effet négatif de l'oxyde ferreux sur la résistance de la pierre de ciment.

Des essais physico-mécaniques des minéraux siliceux ferrifères (tableau I) ont montré que l'introduction jusqu'à 1 % de FeO dans C_3S et C_2S augmente la résistance de la pierre de ciment de 25 % à 30 % du fait de la formation de la structure défectueuse chimiquement plus active. Si l'on augmente la quantité de FeO dans les conditions de refroidissement lent, il se produit un décroissance de la résistance de C_3S et de C_2S ; elle est plus forte chez C_3S du fait de la destruction de sa structure.

TABLEAU I

Dépendance de la résistance de C_3S et C_2S de la teneur en FeO et de la vitesse de refroidissement au cours de la cuisson réductrice

Minéral	Teneur en FeO, %	Refroidissement	Limite de la résistance à la compression (kgf/cm^2) après, jours			
			3	7	28	90
C_3S	sans addition	lent	146	304	315	319
-"-	1	-"-	185	401	406	404
-"-	3	-"-	98	180	193	189
-"-	5	-"-	0	0	15	37
C_3S	sans addition	rapide	167	325	340	343
-"-	1	-"-	192	418	435	437
-"-	3	-"-	165	389	395	403
-"-	5	-"-	150	366	378	387
C_2S	sans addition	lent	8	16	54	260
-"-	1	-"-	20	38	97	318

1	2	3	4	5	6	7
C_2S	3	lent	18	29	80	305
-"-	5	-"-	16	26	85	306
C_2S	sans addition	rapide	10	22	69	287
-"-	1	-"-	25	56	112	335
-"-	3	-"-	23	50	108	330
-"-	5	-"-	17	45	97	318

Par contre dans les conditions de refroidissement rapide, on n'observe pas de diminution de la résistance ce qui est lié à la fixation de FeO dans la fusion et, par conséquent, l'effet négatif d'oxyde ferreux ne se produit pas. Ceci est bien confirmé dans le cas des clinkers industriels obtenus lors des essais dans les fours rotatifs 4,5x170 m dans les conditions de cuisson réductrice est oxydante (tableau II).

TABLEAU II

Relation entre la résistance des clinkers industriels et les conditions de cuisson et de refroidissement

Conditions de cuisson	Refroidissement	Teneur en FeO, %	Limite de résistance (kgf/cm2) après, jours					
			à la flexion			à la compression		
			3	7	28	3	7	28
oxydante	par air	0,07	49	51	59	265	310	470
oxydante	par air-eau	0,07	52	57	68	296	347	528
réductrice	par air	1,30	45	47	54	239	278	422
réductrice	par air-eau	1,37	48	52	58	300	345	530

Comme il apparaît du tableau II, le refroidissement lent du clinker de cuisson réductrice, diminue la résistance de 10 %. Par contre dans le cas de refroidissement rapide la résistance est loin de baisser et même elle augmente un peu.

CONCLUSIONS

1.- On a établi les particularités cristallochimiques des phases ferrifères, la composition et la structure des clinkers à faible teneur en fer et des clinkers ordinaires dans les cas de cuisson réductrice et oxydante.

2.- L'introduction de l'oxyde ferreux dans C_3S, dans les limites de solubilité (moins de 1 %), conditionne une forte perturbation de la structure de l'alite et une élévation de son activité hydraulique. L'augmentation de la quantité de FeO au-delà de la limite de solubilité conduit à la destruction de l'alite et à une diminution sensible de la résistance de la pierre de ciment.

3.- Le refroidissement rapide du clinker fixe une composition optimale des phases ferreuses, détermine une répartition voulue des oxydes de fer par phases et prévient un effet négatif de l'oxyde ferrifères sur la résistance du ciment.

BIBLIOGRAPHIE

1.- BELOV N.V., BELOVA E.N. La chimie et la cristallochimie des minéraux de ciment. Le VI-ième Congrès international de chimie du ciment, Moscou, Stroïizdate, 1976, v.I, p.p. 19-24 (en russe).

2.- GOLOVASTIKOV N.I., MATVEEVA R.G., BELOV N.V. Structure cristalline du silicate tricalcite. Cristallographia, 1975, v. 20, 4e éd., p.p. 721-729 (en russe).

On particle size distribution in cement hydration

L'effet de la granulométrie sur l'hydratation du ciment

Torben KNUDSEN, Technical University of Denmark, Lyngby, Denmark.

RESUME : Le temps que met une pâte d'un ciment Portland pour arriver à un degré d'hydratation donné, dépend de sa finesse. Par cette publication, nous désirons démontrer que la forme de la courbe du degré d'hydratation-temps du ciment Portland est étroitement liée à la granulométrie du matériau. Les détails de la cinétique de base (laquelle détermine la réaction chimique) ont moins d'importance. Il est capital de comprendre ce fait quand on veut essayer d'interpréter des essais d'hydratation du ciment Portland du point de vue cinétique, car la large granulométrie de ce matériau ne permet pas d'obtenir des informations détaillées sur la cinétique des réactions. Par des exemples numériques et des déductions mathématiques, nous cherchons à établir une base qui explique l'influence de la granulométrie sur l'hydratation du ciment Portland. Une équation sous une forme analytique simple, de l'hydratation-temps, dérivée de la transformation de Laplace, se conforme bien aux résultats expérimentaux et peut avoir une importance dans la pratique.

SUMMARY : The time for a Portland cement paste to reach a certain degree of hydration is a function of its fineness. We tend to show in the present paper that the form of the hydration degree-time curve for Portland cement is closely related to the form of the particle size distribution for this material. The detailed form of the underlying kinetics governing the reaction of the single particles is of minor importance. Recognition of this fact is important, when trying to interpret hydration experiments with Portland cement in terms of reaction kinetics. Detailed information about reaction kinetics is prohibited by the broad particle size distribution of this material. By numerical examples and mathematical derivations we attempt to establish a foundation for the understanding of the influence of particle size distribution on hydration-time behaviour of Portland cement. A hydration-time equation of a simple analytical form, derived from a Laplace transformation formulation of the problem, compares favorably with experimental data, and may prove to be of practical value.

INTRODUCTION

Specific surface has generally been used as the practical measure of the fineness of Portland cement. Further parameters for a more detailed representation of the particle size distribution (p.s.d.) have not found technical recognition. Recently however, the approach has been broadened. Locher et al (1) and Frigione et al (2) have studied the influence of p.s.d. on compressive strength. Cements with various p.s.d.'s, but the same specific surface were tested, and the narrow distributions were found to result in higher strength. Frigione et al explain this observation by showing, that the narrower the distribution the higher the degree of hydration, and thus the higher the strength.

In the Tokyo symposium 1968 on the chemistry of cement John H. Taplin presented work on hydration kinetics of various hydraulic cements (3). In the quantitative evaluations of the data he included explicitely the influence of the p.s.d.. In his discussions of the works of other authors in the field of hydration he stressed the importance of p.s.d. in the interpretation of kinetic experiments (4).

The aim of the present investigation is to establish the general relation between p.s.d. and the hydration-time curve for Portland cement. The numerical examples and formal derivations presented in this paper will show, that the form of the broad p.s.d. of a Portland cement is very dominating in its influence on the form of the hydration-time curve. The form of the kinetic equation governing the reaction of the single particle is of comparatively smaller influence. Only the fundamental characteristics of the kinetic equation, i.e. whether of linear or parabolic form (3) is not effectively blurred by the influence of the broad p.s.d..

As an introductory illustration of the kind of relations we shall deal with in this paper, consider Table I. Measured values of the degree of hydration of a rapid hardening Portland cement at 20°C is given as a function of time. To compare with these values the cumulative p.s.d. of the same cement is presented in the last row. Values of the p.s.d. have been chosen such that 1 hour corresponds to 0.4μm, i.e. time is multiplied by 0.4μm/h to give the corresponding grain size. The cumulative p.s.d., when subjected to this simple transformation from grain size to time, is seen to predict the hydration-time curve with fair approximation.

Table I. Degree of hydration of a rapid hardening Portland cement at 20°C compared with the cumulative p.s.d. of the cement. Time and size values are in constant proportions.

Time, hours	5	10	20	30	40	60	80	160
Degree of hydration, %	5	21	46	58	66	75	81	90
Fraction passing, w%	10	20	37	50	60	73	83	98
Grain size, μm	2	4	8	12	16	24	32	64

THEORETICAL PART

Formulae for p.s.d. of Portland cement

Many formulae relating to p.s.d. of tube milled products have been suggested in the litterature (5). Some have an empirical nature, some are derived from theoretical considerations. In this work we shall make use of the Rosin and Rammler's law (6) in the form:

$$W(r) = B\exp(-Br)\ ;\ C(r) = 1-\exp(-Br) \qquad (1)$$

where r is the grain size, B a constant, C(r) is the cumulative weight distribution, which is the integrated form of W(r). We shall also make use of an extension of eq.(1) originally suggested by Gille (7), but here in a modified form:

$$W(r) = \frac{BC}{C-B}\{\exp(-Br) - \exp(-Cr)\} \qquad (2)$$

$$C(r) = 1 - \frac{C}{C-B}\exp(-Br) + \frac{B}{C-B}\exp(-Cr)$$

Experimental data for p.s.d. for normal and rapid hardening Portland cement from ref.(5) were used to test eq.(1) and (2). Eq.(1) was found to be accurate down to r≈1μm, whereas eq.(2) gave a perfect fit down to r≈0.1μm. This is verified in Fig.1.

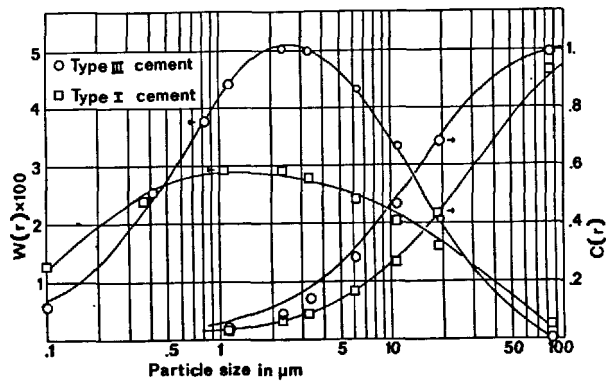

Fig.1. Particle size distribution of a normal and a rapid hardening Portland cement, from ref.(5). Lines representing eq.(2), with constants: B=0.0297, C=5.05 for normal, and B=0.0595, C=1.28 for rapid hardening cement.

A formula for specific surface S can be derived from eq.(2):

$$S = \frac{6}{\rho}\int_0^\infty\{W(r)/r\}dr = \frac{6}{\rho}\frac{BC}{C-B}\ln\frac{B}{C} \qquad (3)$$

Here we have adopted the definition of r used in ref. (5): particle shape is a cube, with edge length r. ρ is density. Inserting the constants found in Fig.1 we get for the specific surface of the normal and rapid hardening Portland cement respectively: 2950 cm^2/g and 3830 cm^2/g. These values are close to the blaine values for the two cements.

Kinetics of hydration

In his work on hydration kinetics of hydraulic cements, Taplin (3) tested his experiments against the kinetic equations:

$$1-(1-\alpha_1)^{1/3} = \frac{kt}{r}\ ;\ \alpha_1 = 1 \text{ for } \frac{kt}{r} > 1 \qquad (4a)$$

$$3-3(1-\alpha_2)^{2/3}-2\alpha_2 = \frac{kt}{r^2}\ ;\ \alpha_2 = 1 \text{ for } \frac{kt}{r^2} > 1 \qquad (4b)$$

where α_i (i=1,2) is the degree of reaction, t the reaction time and k a reaction constant. Both equations can be derived from a shrinking core model (8), eq. (4a) by assuming the resistance to be in the chemical

reaction at the reaction boundary and eq.(4b) by assuming the diffusion through the inner product to be the rate controlling factor.

By writing eqs.(4) in the form:

$$\alpha_i(k,t,r) = \alpha_i(kt/r^i) \; ; \; (i=1,2) \qquad (5)$$

we do not confine ourselves to any specific form of the kinetic equation, but merely state the function α_i to be a function of the single variable kt/r^i. In accordance with Taplin we shall designate the cases $i = 1$ and 2 linear and parabolic kinetics respectively, although we use this designation in a somewhat broader sense, as no explicit form is given to α_i. The case $i = 1$ will be of special importance to us since Portland cement, according to our findings hydrate according to linear kinetics. It should be noted, that reaction time t is measured from the end of the dormant period.

Combining kinetics and p.s.d.

We shall in the following make use of the basic equation:

$$\alpha_i(k,t) = \int_0^\infty \alpha_i(k,t,r)W(r)dr \qquad (6)$$

which relates the degree of hydration for the total system $\alpha_i(k,t)$ to the degree of hydration for the single particle $\alpha_i(k,t,r)$ and the weight distribution function $W(r)$. Eq.(6) is based on at least two basic assumptions about the hydration of the total particulate system:

a) Particles react independently.

b) Particles need be classified only according to their size r.

Assumption a) are expected to be violated for very low water/cement ratios. Assumption b) excludes the influence of factors such as particles having different chemical compositions.

Numerical example of the use of eq.(6)

In the numerical example of the use of eq.(6) to follow, the particle system was divided into 127 size classes, with size range 1μm, and weight fractions according to the p.s.d.: $W(r) = 0.03\exp(-0.03r)$. This p.s.d., as shown earlier, is typical of normal hardening Portland cement.

We wanted to see the effect of the analytical form of eq.(5) on the hydration behaviour of the total system. Therefore we included several different kinetic equations in our calculations. These kinetic equations are shown in Fig.2. Kin.1-4 were primarily chosen so as to cover a broad range of functional forms. Only kin.2 and 3 have an obvious physical meaning. They are all examples of linear kinetics.

The results of the calculation is shown in Fig.3. The constants in kin.1-4 was chosen so as to make the curves cross at $\alpha_1 = 0.5$. The small differences between the curves are striking from this calculation. Especially curve 2 and 3 are hardly different on the graph, and yet they correspond to two distincly different forms of kinetics. This is a numerical demonstration of hydration behaviour of Portland cement being insensitive to the form of kinetics of the single grains. The broad p.s.d. of Portland cement blurs the kinetic details. Parabolic kinetics can be differed from linear, as demonstrated on Fig.4.

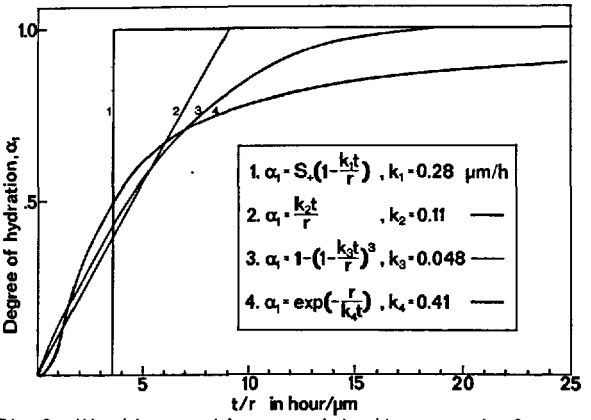

Fig.2. Kinetic equations used in the numerical example of calculation of eq.(6).

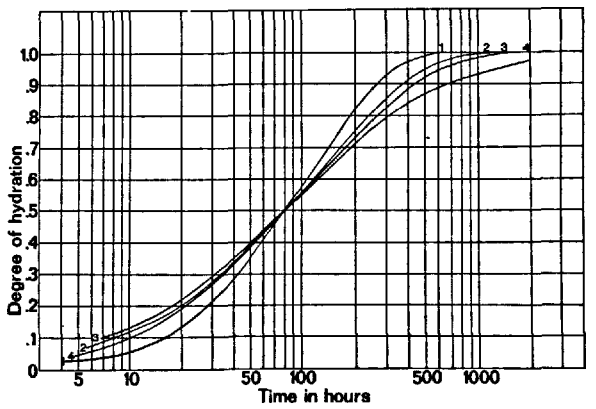

Fig.3. Results of calculations using eq.(6), the kinetic equations from Fig.2 and $W(r) = 0.03\exp(-0.03r)$. Log scale on abscissa axis.

In Fig.3 curve 1 and 4 are of special interest to us. Curve 1, as will be proved later, is conformal with the cumulative p.s.d. curve. Curve 4 can be given exact analytical form, which will prove of practical value in the numerical representation of hydration data for Portland cement.

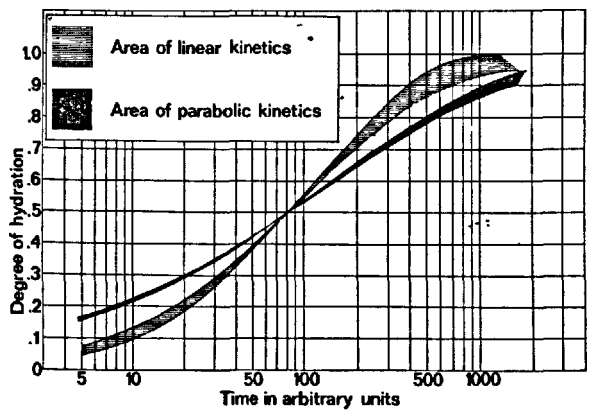

Fig.4. Approximate areas for linear and parabolic kinetics of ordinary Portland cement.

Convolution theorem

In the following we shall derive a general relationship of formal and conceptual significance for the understanding of the influence of the form of the p.s.d. on reaction degree-time curves. We have called it the convolution theorem. We start from the basic eq.(6) and assume that particle kinetics obey eq.(5):

$$\alpha_i(\tau) = \int_0^\infty \alpha_i(\tau/r)W(r)dr \qquad (7)$$

where $\tau \equiv kt^{1/i}$, (i=1,2). Using the relation between weight distribution W(r) and cumulative weight distribution C(r): $dC(r) = W(r)dr$, and integrating by parts we get:

$$\alpha_i(\tau) = \alpha_i(\tau/r)C(r)\Big|_0^\infty - \int_0^\infty C(r)d\alpha_i(\tau/r) \qquad (8)$$

By virtue of $C(0) = 0$ and $\alpha_i(0) = 0$ this reduces to:

$$\alpha_i(\tau) = -\int_0^\infty C(r)d\alpha_i(\tau/r)$$

The differential of α_i can be written:

$$\frac{d\alpha_i(\tau/r)}{d(\tau/r)} \frac{\partial(\tau/r)}{\partial r} dr = -\alpha_i'(\tau/r) \frac{\tau}{r} \frac{dr}{r} \qquad (9)$$

where:

$$\alpha_i'(\tau/r) \equiv \frac{d\alpha_i(\tau/r)}{d(\tau/r)}$$

and by insertion into eq.(9) we get:

$$\alpha_i(\tau) = \int_0^\infty C(r)\alpha_i'(\tau/r) \frac{\tau}{r} \frac{dr}{r} \qquad (10)$$

Changing now the variable of integration, r to lnr we finally arrive at:

$$\alpha_i(\ln\tau) = \int_{-\infty}^{\infty} C(\ln r)\alpha_i'(\ln\tau - \ln r)\exp(\ln\tau - \ln r)d\ln r \qquad (11)$$

It should be noted, that changing the independent variables should result in a corresponding change of the functions. For the sake of physical clarity we do not make a change of function symbols, as the physical meaning of the functions are unchanged.

This final relation has the form of a convolution integral:

$$f(y) = \int_{-\infty}^{\infty} h(x)g(y-x)dx \qquad (12)$$

with y corresponding to lnτ and x to lnr.

It should be noted, that:

$$\alpha_i'(\ln\tau - \ln r)\exp(\ln\tau - \ln r) \to 0 \text{ for } \ln r \to +-\infty \qquad (13)$$

which of course is a necessary condition for the integral in eq.(11) to have meaning.

The content of eq.(11) may be stated in words: When the cumulative weight distribution function is plotted against lnr the degree of hydration-lnτ function can be derived from this function by convolution with $\alpha_i'(x)\exp(x)$, a function depending solely on the single particle reaction kinetics. This convolution formalism illustrates the relation between the three fundamental curves: $\alpha_i(k,t)$, $\alpha_i(k,t,r)$ and C(r) in a illuminative way, and its only condition is, that particle kinetics should obey eq.(5).

The change in shape from $C(\ln r)$ to $\alpha_i(\ln\tau)$ accomplished by convolution according to eq.(11) depends mainly on the width of the convolution function $\alpha_i'(\ln\tau - \ln r)\exp(\ln\tau - \ln r)$ relative to the width of the cumulative weight distribution $C(\ln r)$. A small relative width of the convolution function will result in a small change of shape and vice versa. In the extreme case of kin.1 in Fig.2 the convolution function is infinitely narrow, as it is the first derivative of a step function. In this case the $C(\ln r)$ is not changed in shape by convolution according to eq.(11), but $\alpha_i(\ln\tau)$ is merely a replica of this function, in the new variable lnτ. This proves our earlier postulate, that curve 1 in Fig.3 was the cumulative p.s.d. after the change of variables t to r. Thus for Portland cement the change in shape from $C(\ln r)$ to $\alpha_i(\ln\tau)$ can be seen in Fig.3, namely the change in shape from curve 1 to curves 2-4, as the latter three represents more realistic approaches to the particle kinetics.

Increasing the width of the p.s.d. tends to decrease the difference between $C(\ln r)$ and $\alpha_i(\ln\tau)$ which means, that the kinetic information tends to be lost.

In closing this paragraph it should be mentioned, that when we use the independent variable lnτ, the position of the α_i function along the lnτ-axis is determined by eq.(11). The position along the lnt-axis depends on the value of k.

The Laplace transformation formalism

In the preceding paragraph the derivation of the convolution theorem assumed single particle kinetics to obey eq.(5). In the derivation of the Laplace transformation formalism we shall further assume the p.s.d. to be of the form: $W(r) = B\exp(-Br)$, i.e. a form typical of Portland cement.

With this additional assumption our basic eq.(6) can be written:

$$\alpha_i(B,\tau) = \int_0^\infty \alpha_i(\tau/r)B\exp(-Br)dr \qquad (14)$$

Changing the integration variable we get:

$$\alpha_i(B\tau) = \int_0^\infty \alpha_i(r/\tau)B\tau\exp(-B\tau(r/\tau))d(r/\tau) \qquad (15)$$

The integral on the R.H.S. is the Laplace integral with the dummy variable r/τ. With the accepted notation for this integral:

$$L\{F(x)\} \equiv \int_0^\infty F(x)\exp(-yx)dx \qquad (16)$$

we finally arrive at:

$$\alpha_i(B\tau) = B\tau L\{\alpha_i(r/\tau)\} \qquad (17)$$

Formula (17) is convenient, as it puts the problem of finding the influence of the p.s.d. of Portland cement on hydration measurements into a solid mathematical framework. Consider the way the variables B, k and t enter into the equation. They enter as factors in the variable $Bkt^{1/i}$, which means, that the material variables B and k have the same influence on the $\alpha_i(B\tau)$-curve. This explains the often made observation, that a change of fineness and a change in temperature (k is a function of temperature) has the same effect on the $\alpha_i(B\tau)$-curve. This can be more clearly seen by a change of variables:

$$\alpha_i(B\tau) = \alpha_i(\exp(\ln B + \ln k + (1/i)\ln t)) \qquad (18)$$

Now it is apparent, that a change of B and k works in the same direction, i.e. it translates the $\alpha_i(B\tau)$-curve along the lnt-axis without a change in the shape of the curve.

Exact solutions to the Laplace transform

The importance of the Laplace transformation formalism presented by eq.(17) lies in the fact, that it represents a well-known mathematical problem with well-established methods of solution.

Consider for instance kin.1 in Fig.2. This is a step function having the properties:

$$\alpha_i(r/\tau) = 0 \text{ for } r/\tau > 1$$
$$\alpha_i(r/\tau) = 1 \text{ for } r/\tau < 1 \qquad (19)$$

In tables of Laplace transforms the solution to eq.(17) for this function can be found, giving a hydration-time curve of the form:

$$\alpha_i(B\tau) = 1 - \exp(-B\tau) \qquad (20)$$

As expected from our earlier results, for this limiting case of kinetics the hydration-time curve is identical to the p.s.d., except for a change of variables τ to r.

Of a more practical value is the fact, that we can find an exact solution to kin.4. This form of a kinetic equation has realistic features, and does not give rise to a hydration-time curve deviating much from kin.2 or 3 as seen from our numerical example. The solution of eq.(17) applying kin.4 is given by:

$$\alpha_i(B\tau) = \frac{B\tau}{B\tau+1} \qquad (21)$$

This equation is of an attractive simple mathematical form, which makes it useful in practice as will be shown in the following paragraph.

Properties of eq.(21)

We shall start by rewriting eq.(21), using i = 1 in the definition of τ:

$$\alpha_1(t_R) = \frac{1}{1+t_R^{-1}} \qquad (22)$$

where $t_R \equiv t/t_{1/2}$ and $t_{1/2} \equiv 1/Bk$ is the time to reach 50% hydration. t_R is called reduced time.

According to eq.(22) a plot of α_1 versus t_R for hydration experiments with Portland cements of different finenesses and carried out at different temperatures should fall on the same curve, if Portland cement hydrates according to linear kinetics. This is seen to be the case for the examples given in Fig.5. The data presented on this figure comprises different kinds of measurements of α, different temperatures and different finenesses. α_1 has been calculated in all cases by dividing the property by the value of this property after infinite time, thus $\alpha_1 \equiv P/P_\infty$. Reaction time is measured from the end of the dormant period t_0, such that $t_M = t + t_0$, where t_M is reaction time from the mixing with water.

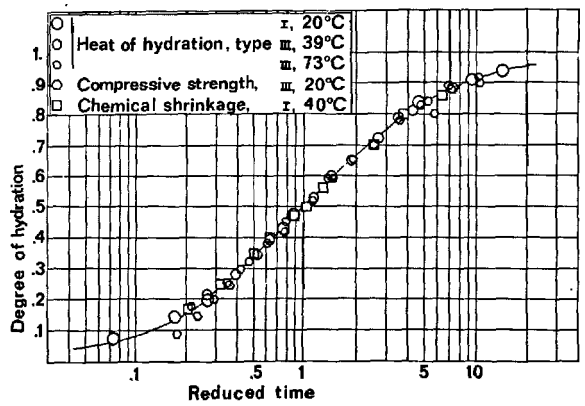

Fig.5. Degree of hydration versus reduced time in a single log diagram for 5 different hydration experiments. The line represents eq.(22). Data are from refs.(9,10) and our own unpublished results.

As the correct determination of the measured property at infinite time P_∞ and the duration of the dormant period t_0 is important for the success of the plot in Fig.5, we shall go through the use of eq.(22) to fit experimental data. We insert P_∞ and t_0 into eq.(22) and get:

$$P = P_\infty \frac{t_M - t_0}{t_M - t_0 + t_{1/2}} \qquad (23)$$

For $t_M \gg t_0$ we neglect t_0 and eq.(23) can be written:

$$\frac{1}{P} = \frac{t_{1/2}}{P_\infty}\frac{1}{t_M} + \frac{1}{P_\infty} \qquad (24)$$

Thus a plot of 1/P against $1/t_M$ will give a straight line, and the extrapolation $t_M \to \infty$ will give $1/P_\infty$. A plot of this kind is shown in Fig.6.

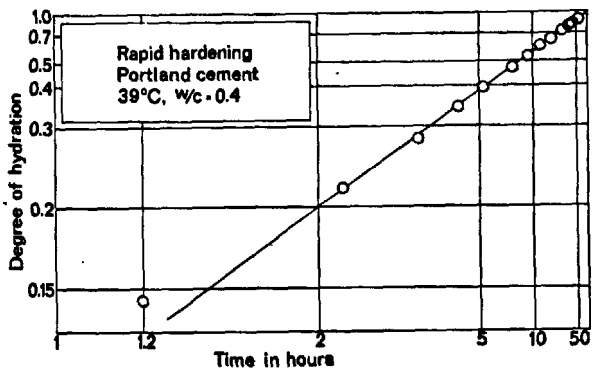

Fig.6. Degree of hydration from calorimetric measurements (ref.(9)) plotted versus time in a double reciprocal diagram. Line is representing eq.(24).

Calculating values of α and rewriting eq.(23) we get:

$$\frac{\alpha_1}{1-\alpha_1} = \frac{t_M}{t_{1/2}} - \frac{t_0}{t_{1/2}} \qquad (25)$$

Thus a plot of $\alpha/(1-\alpha)$ against t_M gives a straight line, and the extrapolation to $\alpha = 0$ will give t_0. $t_{1/2}$ can be found by employing either eq.(24) or eq.(25).

Considering again the results in Fig.5, it should be mentioned, that water/cement ratios for some of these experiments were as low as 0.4. This seems to imply, that the independent particle model of reaction is not seriously violated at these low water/cement ratios.

CONCLUSION

We have examined the role played by the particle size distribution in the development of hydration of Portland cement.

Systems treated were restricted by the following requirements:

a) Particles react independently

b) and need only be classified according to their size.

With the further restriction, that:

c) Particle kinetics obey eq.(5)

we derived the convolution theorem connecting the degree of reaction of the total particulate system to the degree of reaction of the single particles and the particle size distribution. This theorem was useful since it provided an understanding of why the hydration curve of a material with a broad particle size distribution, as in Portland cement, is insensitive to details in the particle kinetics. This point was further elucidated by a numerical example.

Ordinary Portland cement was found to have a:

d) particle size distribution conformal with eq.(1)

and when this further restriction was introduced we derived the Laplace transformation formulation stating, that the Laplace transform of the reaction curve for the single particle yields the reaction curve for the total system.

By means of the Laplace transformation formulation we derived an equation which fitted experimental hydration data for Portland cement quite accurately:

$$\alpha_1(t_R) = \frac{1}{1+t_R^{-1}}$$

where t_R is Bkt, k a reaction constant, B a constant depending on particle size distribution, and t reaction time measured from the end of the dormant period. This showed ordinary Portland cement to react according to linear kinetics.

REFERENCES

1. F.W. Locher, S. Sprung, P. Korf: "Der Einfluss der Korngrössenverteilung auf die Festigkeit von Portlandzement". Zement-Kalk-Gips 62 (1973) 349.

2. G. Frigione, S. Marra: "Relationship between particle size Distribution and compressive strength in Portland Cement". Cement and Concrete Research 6 (1976) 113.

3. I.H. Taplin: "On the Hydration Kinetics of Hydraulic Cements". Proceedings of the 5th International Symposium on the Chemistry of Cement, Tokyo, 1968, Vol. II, p. 337.

4. I.H. Taplin: ibid. p. 249 and p. 421.

5. G. Fagerholt: "Particle Size Distribution of Products ground in Tube Mill". Dissertation, G.E.C. Gads Publ. Copenhagen 1945.

6. P. Rosin, E. Rammler, Sperling: "Korngrössenprobleme des Kohlenstaubes und Ihre Bedeutung für die Vermahlung". Ber. der Reichkohlenrates Ber. C. 52 Berlin, 1933.

7. F. Gille: "Näherungsfunktionen von Kornlinien und Oberfläche des Mahlgutes". Zement 3 (1942) 331.

8. I.H. Taplin: "The temperature Coefficient of the rate of Hydration of β-Dicalcium Silicate". Proceedings of the 4th International Symposium on Chemistry of Cement, Washington, 1960, Vol. I p. 263.

9. P. Freisleben Hansen, D. Lorentzen and T. Nielsen: "E. Calvet mikrokalorimeter". Aalborg Portland Cement Factories, BFL internal report No. 283.

10. Bkf-centralen: "Egenskabsudvikling", diagramblad Nr. B.7, Bkf-centralen 1978.

Influence des basaltes sur la clinkerisation et les propriétés des ciments

Basalt influence on the clinker formation processes and cement properties

A. PACHTCHENKO, membre-correspondant de l'Académie des Sciences d'Ukraine, chef de Chaire des Ciments à l'Institut Polytechnique de Kiev,
G. BAKLANOV, docteur ès sciences techniques, U.R.S.S.

RESUME: L'utilisation de la roche volcanique la plus répandue - du basalte à titrede composant du mélange cru pour le ciment portland contribue à l'apparition d'eutectiques fusibles, ce qui augmente l'activité chimique des constituants et rend possible l'achèvement de la clinkérisation aux températures 1350 - 1420°C.

On a étudié les processus de la décarbonatation et les réactions en phase solide dans les mélanges de basaltes et de carbonates, le mode de distribution des oxydes alcalins dans les phases du clinker et les particularités physico-chimiques de la formation des minéraux du clinker dans les mélanges contenant du basalte en fonction du degré de saturation en chaux.

On a examiné l'aptitude de ces ciments à s'hydrater et la composition de phase.

SUMMARY: Utilization of the vast volcanic - basalt - as a component of the raw portland-cement mixture provides formation of easily meltable eutectics which positively influence upon the raw mixture reactivity and favour clinker forming completion in the temperature range 1350 - 1420°C.

Decarbonizing processes and solid phase reactions in basalt - carbonaceous mixtures has been explored. Alkali oxides distribution nature according to clinker phases and physical-chemical peculiarities of the main clinker minerals formation in the raw basalt mixture depending on the lime saturate has been established.

Hydrolicity of basalt cement, hydrated phase composition and their lifetime stability has been investigated.

Une méthode intéressante d'intensification du processus de cuisson du klinker de ciment portland pourrait être conçue, si on trouvait certains composants du mélange de matières premières agissant de manière que la phase liquide fasse son apparition en quantité élevée et aux températures plus basses, que dans le cas des matières premères traditionnelles. L'utilisation du basalte dans ce but donne une nouvelle solution à ce problème. Le basalte est une des roches effusives les plus répandues de l'écorce terrestre. Il constitue plus de 20 % des roches magmatiques. Par la teneur en silice et autres oxydes, les basaltes correspondent aux roches basiques. Ce qui est très caractéristique, c'est la constance de leur composition chimique et minéralogique, surtout dans un même gisement, ce qui assure la stabilité des procédés technologiques et des propriétés du produit fini. Les variations de composition chimique sont présentées dans le tableau I (1). Pour un même gisement ces variations sont encore moins prononcées.

TABLEAU I

Variations de compositions chimique des basaltes

Teneur en oxydes (en poids, %)					
SiO_2	Al_2O_3	Fe_2O_3	CaO	MgO	Na_2O
45,41- 55,90	14,60- 21,80	8,96- 16,55	4,50- 13,05	1,60- 11,80	2,18- 5,60

Une particularité caractéristique des basaltes est la présence des oxydes de titane, vanadium, barium, ainsi que d'autres microéléments. Le fer est présent sous forme d'oxydes ferrique et ferreux. Selon la composition minéralogique, les basaltes sont des roches polyminérales, contenant des plagioclases, des minéraux mélanocrates, du verre volcanique, des minéraux accessoires (magnétite, ilménite, apatite). Etant une roche effusive, le basalte contient beaucoup de phase vitreuse. En général, les basaltes se distinguent des matières premières traditionnelles. Ils sont facilement fusibles. La fusion s'opère à une température inférieure à 1250°C. Au moment de l'apparition de la phase liquide dans le mélange des matières premières ordinaires du ciment portland tout le basalte serait à l'état fondu. La viscosité du basalte fondu dépend dans une grande mesure de la composition chimique. A la température de 1250°C elle peut varier entre 8,9 et 81 kg/m·s. Lors de l'échauffement ultérieur la viscosité diminue sensiblement et à la température de 1400°C constitue 5,1 - 9,1 kg/m·s (2,3). Les températures de la limite supérieure de cristallisation des basaltes fondus se situent entre 1215° C et 1250°C (3). La dévitrification du basalte, analogue à celle du laitier, décrite par les auteurs (4), doit s'accompagner d'échauffements locaux par suite du dégagement de chaleur de cristallisation, ce qui peut contribuer à la diminution de la viscosité.

Le facteur le plus important déterminant les propriétés technologiques des matières soumises à la cuisson ainsi que la vitesse des processus physico-chimiques est la quantité de phase liquide qui détermine le domaine de réaction, son type et, en fin de compte, la cinétique des transitions de phases et des transferts de masse. La quantité de phase liquide, évaluée (d'après F.M. LEA et T.W. PARKER) dans le clinker, obtenu d'un mélange binaire de basalte et de calcaire, correspondant au coefficient de saturation 0,98, dépasse 31 %, ce qui est bien suffisant pour la formation des silicates hautement basiques. La viscosité de la phase liquide du clinker est faible et s'abaisse linéairement avec le module alumino-ferrique, atteignant 0,168 kg/m·s pour la valeur 0,81 de celui-ci à la température de 1400°C.

Les particularités de la clinkérisation ont été étudiées sur 18 mélanges, préparés à base de basaltes de différente composition. A titre d'exemple nous citons le mélange ayant un coefficient de saturation en chaux

égal à 0,93 (5). On a montré que la fixation intense de chaux dans les mélanges pulvérulents à base de basaltes a eu lieu par réaction en phase solide (figure 1).

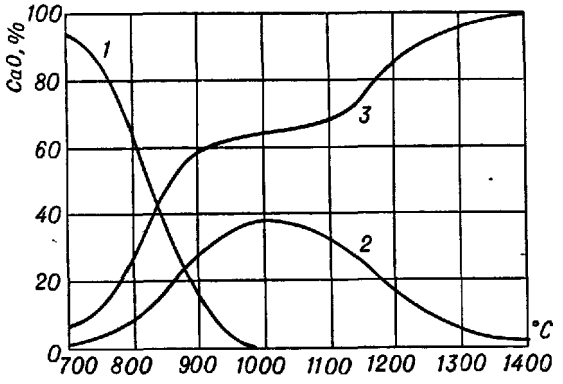

Fig. 1 - Variations de teneur en chaux carbonatée(1), libre(2) et combinée(3) dans le mélange basalte-calcaire.

La vitesse de cette réaction est assez grande. A la température de 1200°C la chaux est fixée à 70 - 98 % selon la composition du basalte utilisé. Lors de l'augmentation ultérieure de la température les oxydes de magnésium et de fer contribuent à l'apparition d'une phase liquide peu visqueuse, ce qui accélère considérablement le processus de formation des minéraux de clinker. Il faut dire que la présence d'ions Na^+, K^+, Mg^{2+} dans la phase liquide aboutit à l'affaiblissement de l'armature anionique, à la diminution du frottement interne et à la fixation plus rapide de la chaux libre. L'analyse aux rayons X montre (figure 2), qu'au cours de la cuisson du mélange le bélite fait son apparition aux températures assez basses, cependant l'intensité de ses raies est faible. L'augmentation de la température de cuisson contribue à une cristallisation plus prononcée des silicates de calcium. A la température de 1200°C on constate l'apparition des raies de l'alite. Leur intensité croît avec la température de cuisson.

La cristallisation des minéraux dans le clinker ainsi obtenu est nette dans tous

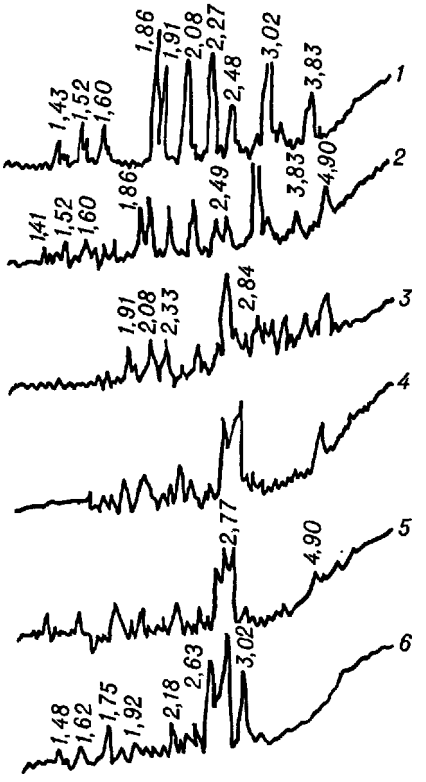

Fig. 2 - Diagrammes X du mélange basalte - calcaire cru (courbe 1) et cuit aux températures 800, 1000, 1200, 1300 et 1400°C (courbes 2 - 6 respectivement)

les cas. La répartition des cristaux est régulière. L'alite se présente généralement sous forme de prismes hexagonaux et tabulaires. Le bélite apparaît sous forme de cristaux arrondis. La substance intermédiaire est constituée par les aluminoferrites de calcium de diverse composition: (C_6A_2F, C_4AF, C_6AF_2) ainsi que par une faible quantité d'aluminate tricalcique, de ferrite bicalcique et de verre enrichi en oxyde de fer. Les études par microsonde et analyse chimique ont mis en évidence la présence du fer principalement dans la phase aluminoferrique et en très faible quantité dans les silicates. Les résultats de l'étude de la répartition des alcalis dans les phases du clinker sont donnés dans le tableau II.

TABLEAU II

Repartition des alcalis dans les phases du clinker

Teneur en K_2O				Teneur en Na_2O			
extrait							
par l'acide boracique	par solution de sucre	par l'acide chlorhydrique	au total	par l'acide boracique	par solution de sucre	par l'acide chlorhydrique	au total
0,04 / 8,33	0,39 / 75,00	0,09 / 16,67	0,52 / 100,00	0,48 / 55,0	0,22 / 25,0	0,17 / 20,0	0,87 / 100,0

Remarque. Au numérateur - la teneur en alcalis en % pondéraux du clinker, au dénominateur,- la teneur en alcalis dans la phase considérée, en % de leur teneur totale dans le clinker.

L'oxyde de potassium fait partie de la phase constituée d'aluminates, forme des solutions solides avec le silicate bicalcique et peut se trouver dans les aluminoferrites de calcium ainsi que dans la phase vitreuse du clinker. L'oxyde de sodium fait partie de toutes les phases principales du clinker. L'oxyde de magnésium forme de préférence des solutions solides avec les phases principales du clinker. Ce n'est qu'une partie insignifiante du MgO qui cristallise sous forme de périclase (à peu près 20 % de la quantité totale), qui n'a pas d'influence sur la stabilité de volume et d'autres propriétés des ciments.

A partir des mélanges basalte-calcaire nous avons préparé les ciments de trois compositions: bélitique(1), moyennement saturé(2) et alitique(3) (tableauIII). L'une des particularités de la composition minéralogique des ciments portlands basaltiques est la proportion élevée d'aluminoferrites de calcium. L'étude de l'hydratation permet de constater, que lorsque ces ciments sont mis au contact de l'eau il y a d'abord une période dite d'induction. Lors de cette période ce sont essentiellement les phases anhydres (2,60; 2,74; 2,77 A°) que mettent en évidence les diagrammes de diffraction des rayons X, l'intensité des raies des hydrates demeurant relativement faible (2,63; 4,92A°). Avec le temps le processus de durcissement se développe assez vite et l'intensité des raies des hydrates croît rapidement. On peut constater l'accumulation dans le système d'hydrosilicates proches de la tobermorite, qui confèrent la résistance mécanique.

Lors de l'hydratation des ciments durant le délai compris entre 3 jours et 2 ans, on constate sur les courbes d' ATD les inflections endothermiques aux températures 190 - 210°C (figure 3, le cas du ciment avec CS= 0,92), caractérisant plusieurs processus, à savoir: le départ de l'eau libre et de l'eau liée dans les hydrosilicates du type de la tobermorite, le début de la déshydratation de l'aluminate de calcium hydraté hexagonal et cubique, de l'hydroferrite de composition analogue, ou de la solution solide $C_3(A,F)H_6$, de l'hydrosulfoaluminate et du sulfoferrite ou de leur solution solide, ainsi que la déshydratation de la fraction

TABLEAU III

Composition minéralogique et propriétés du clinker

Composition	Température de cuisson, °C	CaO libre, en poids, %	Densité, Kg/m^3	Coef. de saturation en chaux (CS)	Module silicique	Module alumino-ferrique	Teneur en % pondéraux de:			
							C_3S	C_2S	C_3A	C_4AF
1	1300	0,18	3,220	0,70	1,98	1,12	10,26	58,43	4,79	22,13
2	1340	0,21	3,170	0,81	1,89	0,94	37,23	35,05	4,75	18,27
3	1380	0,30	3,170	0,92	1,91	0,95	59,55	14,39	4,58	16,96

gélatineuse contenant les hydroxydes d'aluminium, de fer et le gel de l'acide silicique.

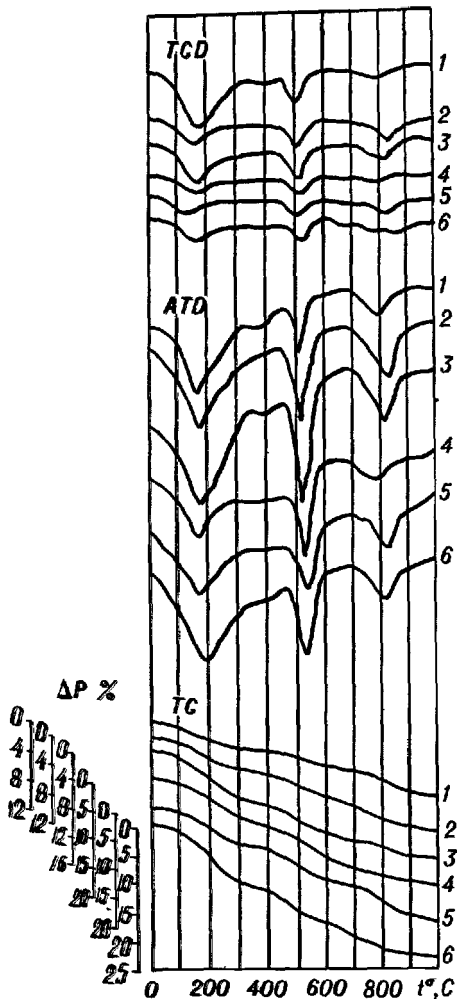

Fig. 3 - Dérivatogrammes du ciment durcissant dans les conditions normales pendant 3, 7, 28, 180, 360, 720 jours (courbes 1-6)

De faibles inflexions sur les courbes d'ATD de toutes les compositions aux températures 380°-410°C caractérisent les transformations des produits gélatineux en cristallins, ainsi que la déshydratation de C_3AH_6.

L'effet endothermique aux températures 500-530°C correspond à la décomposition de l'hydroxyde de calcium, qui se forme lors de l'hydratation des minéraux du clinker. C'est dans ce même intervalle de températures qu'a lieu la déshydratation ultérieure des hydroaluminates ou hydroaluminoferrites mentionnés. Cependant l'intensité de ce pic réflète essentiellement la quantité d'hydroxyde de calcium dans la pierre de ciment.

L'effet endothermique aux températures 800-830°C correspond à la décomposition du carbonate de calcium dû à la carbonatation atmosphérique. Mais la dépendance de la grandeur de cet effet de la composition minéralogique du ciment et de la durée de durcissement rend possible de le rapporter à la présence de l'hydrosilicate de calcium.

A la température de 800°C c'est la déshydratation de l'hydrosulfoaluminate de calcium à basse teneur en sulfate qui a lieu. A 830 - 840°C a lieu le départ de l'eau de constitution des hydrosilicates du type de la tobermorite, de C_2SH_2, ainsi que de l'hydrosilicate $C_2S \cdot Aq$.

L'étude des résultats de l'analyse thermique différentielle ainsi que des diagrammes aux rayons X montre que le processus de durcissement des ciments en question ne diffère pas de façon tangible de celui des ciments portlands courants.

Les propriétés mécaniques des ciments ba-

TABLEAU IV

Essais physico-chimiques des éprouvettes normales

Composition	Consistance normale %	Prise		Résistance à la rupture par compression/ flexion, en 10^{-1} N/mm^2							
		début	fin	3j	7j	28j	90j	180j	1an	2 ans	3 ans
1	24,5	2h55	4h05	50/18	91/20	208/44	276/61	579/67	578/74	616/77	650/89
2	23,82	2h45	5h00	186/33	305/58	411/60	437/68	555/68	562/70	638/79	669/90
3	23,17	1h00	6h00	206/50	306/55	512/67	560/68	630/71	635/73	685/86	730/92

saltiques (tableau IV) sont en bon accord avec les données de l'analyse physico-chimique. On constate la période d'induction et celle de l'acroissement progressif de la résistance mécanique. Il faut souligner, que ces ciments atteignent la résistance à la rupture par compression de 5000 N/mm^2 à 28 jours. Ultérieurement la résistance croît toujours de façon régulière. A trois ans elle dépasse 6500 N/mm^2 dans tous les cas.

Les ciments basaltiques sont caractérisés par une résistance élevée à la flexion. Cette propriété s'explique par le développement d'hydrates fibreux.

On peut citer encore quelques propriétés intéressantes de ces ciments, à savoir: faible dégagement de chaleur, faible retrait et expansion, haute stabilité lors des variations d'humidité.

La stabilité au gel est assez forte. Les éprouvettes ont subi 200 cycles de congélation et de dégel alternés sans destructions visibles et sans baisse de résistance supérieure à 25 %.

L'étude de l'action d'une solution corrosive contenant 5 % Na_2SO_4, 0,2 % $CaSO_4$, 1 % $MgSO_4$ (eau de mer) sur ces ciments a montré leur haute résistance à la corrosion. Pratiquement le coefficient de stabilité dépasse 0,8 pour n'importe quelle durée de conservation ce qui permet de les recommander en qualité de ciments résistant aux sulfates.

Les essais standardisés démontrent que ces ciments peuvent êtreutilisés à titre de ciment pour puits de pétrole. Pour les puits "froids" ils conviennent par leur teneur élevée en silicates ce qui leur confère une activité hydraulique élevée sans accélerer la prise. Pour les puits "chauds" ils conviennent par suite de la teneure faible en aluminate tricalcique et élevée en aluminoferrite de calcium.

CONCLUSIONS

Les ciments basaltiques peuvent être utilisés comme liants usuels et comme liants spéciaux résistant aux sulfates et pour puits de pétrole.

BIBLIOGRAPHIE

1.- A.A. MIASNIKOV, M.S. ASLANOVA (1971) "Utilisation des roches effusives basiques pour la confection de fibres aptes à la lixiviation", Matériaux fibreux à base de basaltes d'Ukraine, pp. 37-41 (en russe).

2.- A.A. PACHTCHENKO (1977) "Chimie physique des silicates", pp. 325-331 (en russe)

3.- V.A. DOUBROVSKY, M.F. MAKHOVA, V.A. RYTCHKO (1971) "Propriétés des roches magmatiques basiques à l'état fondu et des fibres qu'elle donnent", Matériaux fibreux à base des basaltes d'Ukraine, pp. 5-13 (en russe).

4.- N.P. KOGANE, O.P. MCHEDLOV-PETROSSIAN (1978) "Intensification du processus d'obtention de ciment par cuisson de mélanges de constituants de systèmes physico-chimiques indépendants", Comptes rendus de l'Académie des Sciences de l'URSS, Vol. 238, n°2, pp. 408-410 (en russe).

5.- A.A. PACHTCHENKO (1978) "Nouveaux ciments" (en russe).

Raw material effect on clinker quality

L'influence de matières premières sur la qualité du clinker

B. WERYNSKI, Doctor of Engineering, Research Director, Institute for Building Industry Cementing Materials, Opole, Poland.

A. WERYNSKA, Master of Engineering, Institute for Building Industry Cementing Materials, Opole, Poland.

RESUME : La production de ciments a haute résistance se base sur différentes méthodes qui conduisent a la formation de clinker ayant une teneur élevée en silicates calciques, ceux-ci ayant leur structure cristalline propre. On connait des moyens d'augmenter la résistance de ciments par l'introduction au mélange cru de petites quantités d'additifs étrangers.
Dans l'ouvrage presenté on a utilisé l'influence d'oxydes MgO, Na_2O, K_2O et SO_3 se trouvant dans les matieres brutes naturelles, telles que le "muschelkalk" d'origine triasique et une argile keuperique, sur l'activité hydraulique de clinker. A l'aide de diverses méthodes d'analyse, telles que radiocrystallographie, thermogravimétrie et microscopie on a conduisé des analyses structurales et a constaté, que les porteurs d'oxyde de magnésium et d'oxydes de métaux alcalins sont les chlorites, les micas et les caolinites, qui se trouvent dans les argiles et - en petites quantités - dans le calcaire.

En mélangeant ces matieres premieres, on a obtenu des farines crues de compositions chimiques differentes. Les clinkers obtenus par la cuisson de ces crus differaient par leurs facteurs de saturation de 0.90 a 0.94 et par leurs modules siliciques - de 2.27 a 2.72. L'examen des résistances des pates de ciment preparées a partir de ces clinkers a prouvé, que le clinker ayant le module de saturation 0.93 et le module silicique 2.52, apres avoir été broyé jusqu'a obtenir une surface spécifique Blaine de 350 m^2/kg environ, répondait aux exigences du ciment portland 550, apres 28 jours de durcissement. L'augmentation de la surface specifique de ce ciment a 460 m^2/kg enviror , permetait l'obtension du ciment de résistance 18.2 MN/m^2 apres 1 jour et de 74.0 MN/m^2 apres 28 jours de durcissement. Un important accroissement de la résistance du clinker a été obtenu grace a la haute teneur en silicates calciques (C_3S - 72 %, C_2S - 8.1 %) et a la modification de leur structure cristalline due a l'influence de l'oxyde de magnésium et des oxydes de métaux alcalins. MgO, Na_2O, K_2O et SO_3 ont joué le role de mineralisateurs dans la cuisson du cru et de stabilisateurs des variétés polymorphes de silicates calciques, en créant avec ces silicates des solutions solides d'une activité hydraulique élevée.

SUMMARY : The manufacture of rapid-hardening cements is based on various methods leading to the creation of clinker of a high total contens of calcium silicates, those having an adequate crystal structure. There are ways of increasing the strength of cements by introduction of little amounts of foreign additives to the raw mix.

In the work presented the influence has been utilised of oxides MgO, Na_2O, K_2O and SO_3 present in natural raw materials such as shelly limestone of Triassic origin and Keuperous clays, over the hydraulic activity of clinker. By means of various methods like x-ray diffractometry, thermogravimetry and optical microscopy a structural analysis of these raw materials has been made and it's been found out that the carriers of magnesium oxide and of alkali metals oxides are chlorites, micas and kaolinites occuring in clays and - in small quantities - in limestone.

Raw mixes of different chemical composition have been composed of these raw materials. The clinkers obtained by burning these raw mixes differed one from the other in their lime saturation factor - from 0.90 to 0.94 and in their silica ratio - from 2.27 to 2.72.

The examinations of the cement pastes made out of the clinkers showed that the clinker of a lime saturation factor of 0.93 and a silica ratio of 2.52, composed of natural raw materials, after being ground to a fineness of ca. 350 m^2/kg (Blaine), meets requirements for portland cement grade 550 after 28 days of hardening. Increasing the fineness of this cement to ca. 460 m^2/kg enables to obtain a cement of a strength of 18.2 MN/m^2 after 1 day, and that of a strength of 74.0 MN/m^2 after 28 days of hardening. A high increase in the strength of clinker has been obtained thanks to its high contens of calcium silicates (C_3S - 72 %, C_2S - 8.1 %) and thanks to the adequate modifications of the crystal structure of these minerals, resulting from the influence of both magnesium oxide and of oxides of alcali metals.

MgO, Na_2O, K_2O and SO_3 were playing the role of both mineralisers during the burning of raw mix and stabilisers of the polymorphic modifications of calcium silicates, forming with these silicates solid solutions of an increased hydraulic activity.

The developement of science in cement chemistry and of research methods enabled to rich present knowledge concerning the relations occuring between physico-chemical properties of initial raw material and raw mix and the processes of clinker minerals forming.

It is known that the hydraulic activity of cements deciding about their strengths is influenced by many agents related to each other, which is a research problem in many countries.

The main components of portland clinker are following: tricalcium silicate C_3S, dicalcium silicate C_2S, tricalcium aluminate C_3A, and tetracalcium aluminoferrite C_4AF. Their form is a function of their internal structure which consequently de - pends on chemical composition, mineralogical composition, degree of fineness of raw mix, the conditions of clinker burning and cooling, and first of all the reactions performing as a result of diffusion in liquid phase.
Thus, to obtain clinker of high hydraulic activity raw mix should be characterized by: homogeneity of chemical composition and high chemical activity during burning process.

The effect of raw material origin on clinker minerals forming kinetics should be regarded from the following view points:
- mineralogical form under which its main oxides (CaO, SiO_2, Al_2O_3, Fe_2O_3) appear in raw materials;
- mineral origin (natural from mineral deposits or artificial e.g. waste products);
- the effect of the degree of hydration of minerals on reaction kinetics;
- the role of isomorphous admixtures in reaction performance in solid phase.

The optimal set of raw materials for clinker production is formed by limestones containing fine-crystalline calcium carbonate and clays formed of hydrated silicates and aluminosilicates of a high specific surface.
Phase composition and petrographical structure and texture of minerals included in raw mix have a great effect on the process of formation of minerals in clinker.
CaO appears in limestones as calcite, dolomite, rarely as aragonite, gypsum, phosphate, feldspar and also in the form of isomorphous admixtures as adsorbed cation Ca^{2+} in clay components (1).

SiO_2 appears in raw mix first of all as quartz, chalcedony, seldom as cristobalite and opal. Besides, silica is a component of different clay minerals, of kaolinite, montmorillonite, hydromica, chlorites groups and other similar minerals. Al_2O_3 and iron oxides are in calcereous and clay raw materials as hydrargillites, diaspores, boehmites, hydrohematites , lepidocrocites etc.
Thus the reactivity of raw mix is influenced by dissociation process, dehydration process and destruction of crystal lattice of minerals, performing at higher temperatures.
The most reactive CaO is formed at higher temperatures from thermal dissociation of fine-crystalline calcite (aragonite) and dolomite.
Active silica can appear in clinkerization process at the temperatures 773 - 1373 K during dehydration process of clay components.

The grain size and specific surface of reagents have a great effect on reaction time in solid phase.

Quartz and chalcedony grains in raw mix should have sizes not bigger than 30 microns, and for production of high-strength and fast-hardening cements - 15 microns (2).

The time of clinkerization process depends upon the size of CaO and its activity, which makes it diffuse in crystal lattice of SiO_2 thus forming dicalcium silicate and then tricalcium.

According to Krawczenko (3) the time of diffusion of CaO in SiO_2 lattice is 4 - 5 times shorter than diffusion of SiO_2 in CaO.

The presence of different modifications of iron oxides in raw mix influences considerably its reactivity, which increases; especially important is the presence of FeO, which as active mineralizer accelerates the dissociation of $CaCO_3$.

The fineness of raw mix and its increased specific surface influence the amount of minerals in clinker and the amount of free CaO. The other factor influencing the reaction time in clinkerization process is the share of water separated during clay and some not clay minerals burning.

Depending upon the kind of minerals dehydration performs within a large range of temperatures: 473 K - 1273 K, i.e. the temperatures at which raw mix reactions perform first of all in solid phase.
The role of reaction mineralizers in solid phase is played also by isomorphous admixtures occuring in small amounts in natural raw materials. These mineralizers are following: MgO, SO_3, K_2O, Na_2O, P_2O_5, TiO_2, SrO, BaO, Cr_2O_3 (4).

The possitive effect of isomorphous components appears in the change of physico-chamical properties and in the increase of chemical activity of the liquid phase during clinkerization process as well as in the increase of hydraulic activity of clinker, resulting from stabilization of polymorphic modification of calcium silicates (5).

The presence of Al_2O_3, Fe_2O_3, MgO in raw mix decreases the temperature of dissociation of calcium carbonates, which starts already at 723 K. In the range of temperatures 973 - 1273 K, hydrated aluminosilicates disintegrate, forming unstable products, which react with CaO "in statu nascendi". The reactions between the components take place as a result of ion diffusion in solid solutions. The amount of liquid phase depends upon temperature and also upon the presence of mineralizers decreasing the eutectic point of solutions.

The effect of various agents on liquid phase properties has compound character and depends upon their chemical origin and concentration. The kinetics of reactions taking place in the liquid phase are influenced by the physical forces as: viscosity, surface tension and ions mobility in solution (6).

The effect of various chemical compounds on a liquid phase viscosity is shown in Figure 1 (according to Butt, Timaszev, Osokin).

At the presence of Na_2O and K_2O the increase of liquid phase viscosity is observed. The addition of about 1.5 - 2.0 % of MgO decreases the liquid phase viscosity proportionally to its concentration.

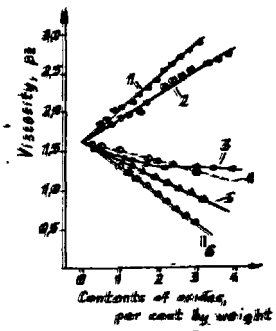

Fig.1. Isothermes (1723 K) of viscosity of the solution saturated at 1723 K in presence of :
1 - K_2O, 2 - Na_2O, 3 - MgO, 4 - K_2SO_4, 5 - Na_2SO_4, 6 - SO_3

Figure 2 shows the effect of compounds on surface tension of liquid phase.

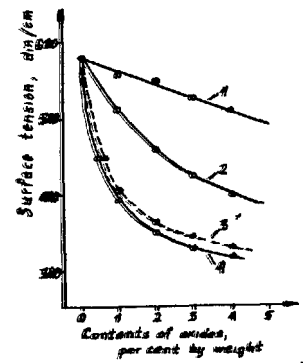

Fig.2. Isothermes (1723 K) of surface tension of the solution composed of CaO, SiO_2, Al_2O_3, Fe_2O_3 in presence of :
1 - MgO, 2 - Na_2O, 3 - SO_3, 4 - K_2O

At presence of MgO, Na_2O, K_2O, and SO_3 the surface tension of liquid phase decreases. In the liquid phase of clinker, the mobility of ions Na^+ and K^+ is overcoming considerably the displacement speed of silicoxide anions; thus their presence causes intensification of solution process of belite in liquid phase. The introduction of MgO into the alkalic solution of liquid phase enables to accelerate the reaction of disintegration of dicalcium silicate, 2 or 3 times. The greatest intensity of tricalcium silicate formation is observed at reactive grains of CaO interaction with liquid phase characterized by high surface tension and minimal viscosity. The presence of SO_3 in liquid phase results in acceleration of contact layers corrosion and acceleration of ions diffusion into the crystal lattice of silicates.

The knowledge of dependence between both viscosity and surface tension of the liquid phase and the concentration oxide in this phase enables to modify certain physical and chemical parameters of liquid phase solution, and consequently the structure of minerals formed in it.
Solid solutions of basic clinker minerals including magnesium, potassium and other compounds are formed from polymineral liquid phase with isomorphic substances.

Woerman and others (7) proved that up to 2 % of MgO and ca. 1 % Al_2O_3 are included in solid solution in tricalcium silicate. Alite with the admixtures Al^{3+} and Mg^{2+} is defined as a solid solution of 54 CaO· 16· SiO_2· Al_2O_3· MgO, where Al_2O_3 and MgO are stabilizers. In the system CaO - MgO + Al_2O_3 - Fe_2O_3 - SiO_2 the role of alien ions essential for the stabilization of polymorphic modifications of tricalcium silicate is not so important when other stabilizing components e.g. Cr_2O_3, SrO, P_2O_5, TiO_2, BaO are introduced.

The research conducted by many authors and concerning accessorical components effect on hydraulic activity of clinker showed that there can be determined proper concentrations of these components causing the optimal activity increase effect e.g. P_2O_5 - 0.2 - 0.3 %, Cr_2O_3 - 0.5 %, SO_3 - 0.5 %, TiO_2 - 2 - 3 %, B_2O_3 - 0.5 %, SrO - 2.4 %, BaO - 0.1 % (8, 9, 10).

Basing upon discussed literature the thesis can be put that applying natural calcareous raw materials and clays including in their composition hydrated magnesium silicate and micas and illits, it is possible to obtain clinkers of right phase composition, which ground with addition of gypsum can give high quality cements.

Results and discussion

The examination of effect of accessorical components included in raw material on cement quality was conducted basing on four clinkers.
Shell limestone of trias origin and keuperous clays were used as raw materials for clinker production. The basic raw materials were chosen basing on geological documentation and wide examination of deposits, applying condensed prospection drill grid. To examine chamical composition of calcareous and clay deposits, x-ray fluorescence analysis was applied. Moreover, trace elements were determined by absorption spectrometry method. The chemical composition of raw materials was presented in Table I.

TABLE I

Chemical composition	Limestone %	Clay %
L.O.I.	40,3	10,7
SiO_2	5,6	54.9
Fe_2O_3	0.7	6.0
Al_2O_3	2.0	14.0
CaO	50.2	7.5
MgO	0,6	3.4
SO_3	0,1	0,3
Na_2O	0.03	0.29
K_2O	0.024	2.90

Table II shows trace elements content in raw materials.

TABLE I I

Chemical composition	Lime %	Clay %
ZnO	0.006	0.014
CuO	0.0017	0.0031
V_2O_5	0.005	0.036
MnO_2	0.027	0.226
Cr_2O_3	0.0039	0.0136
PbO	0.007	0.007
NiO	0.004	0.007

The mineral composition of raw materials was examined by thermogravimetry and x-ray radiography.

Figure 3 presents the diagrams of differential thermal analysis.

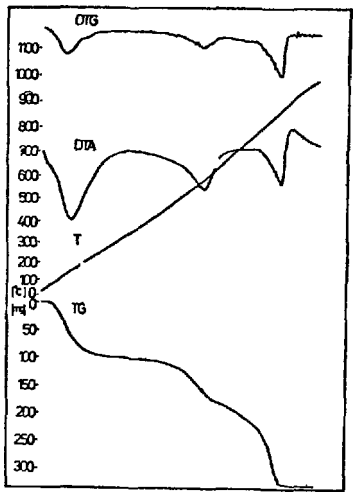

Fig.3. DTA curves for clays

Three characteristic endothermic peaks can be seen on the diagram. At temperature 423K endothermic peak says about lattice water removal from clay minerals. At the temperature 853K we can observe dehydration of illit and kaolinite and also disintegration of crystal lattice of laminar minerals. At the temperature 823 - 973K there is a characteristic endothermic peak for chlorites. At that temperature the loss amounting 75 % of groups OH^- of brucite layer is observed. Endothermic peak at the temperature 1133K indicates the thermal disintegration of $CaCO_3$ and dolomite and also endothermal reaction of lattice destruction of chlorites.(11).

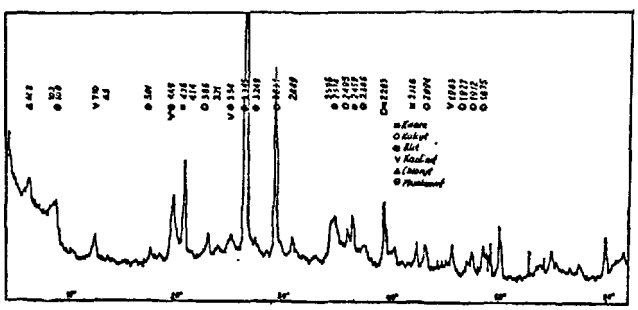

Fig.4. Diffractogram for clays

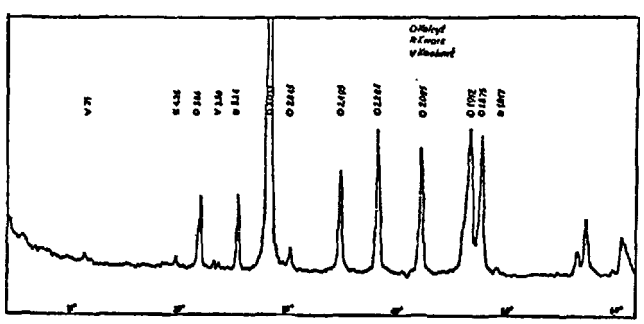

Fig.5. Diffractogram for limestones

Figure 4 and 5 show diffractogram for clays and limestones. As a result of complex examination it was stated that shell limestone of trias origin is composed mainly of calcite more than 91 %,quartz and some small amounts of clay minerals as illit and chlorite.

The clays include first of all aluminosilicates i.e. chlorites (d = 14 Å), micas, illits, muscovites,biotites and caolinites and among them dickit, nacrite, halloysite.

In clay and in limestone samples the presence of small quantities of SiO_2 in form of quartz was observed, but most of silica is included in minerals of caolinite, mica and chlorites group.

In clay examination about 3 % of potassium oxides (K_2O, Na_2O) was observed.

The sinterability of limestones and clays was examined by hightemperature microscope and it was states that sintering temperature for both raw materials is at the same range 1425K - 1523K.

The raw mix was composed with dried limestones and clay, ground before to a great degree of fineness. At all samples the content of fraction < 5 microns was over 20 %, but fraction 5 - 30 microns between 41 - 55 % and fraction > 88 microns about 10 %. Four clinkers of different chemical and mineral composition were burned with the raw mix described above. It is shown in Table III.

TABLE III

CHEMICAL AND MINERAL COMPOSITION OF CEMENT CLINKERS

(See page I - 187)

All clinkers are characterized by SF amounting 0.90 - 0.94. Silica ratio (SR) for clinkers on level between 2.27 - 2.72. The value of alumina ratio (AR) for all samples is similar and is in the range of 2.0 - 2.34. The phase respectively composition of clinker was calculated basing on microscopic examinations. Microscopic examinations for clinkers I to IV are presented in Figures 6,7,8,9.

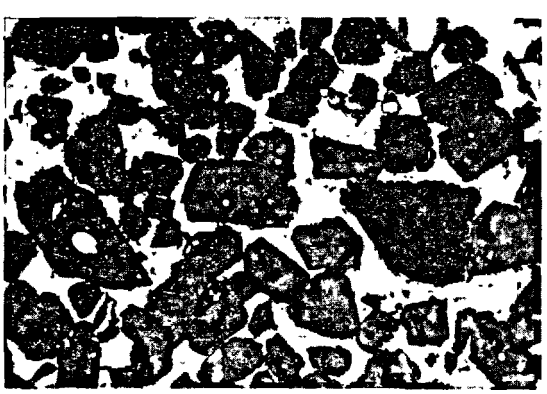

Fig.6. Clinker I (x 800)

Fig.7. Clinker II (x800)

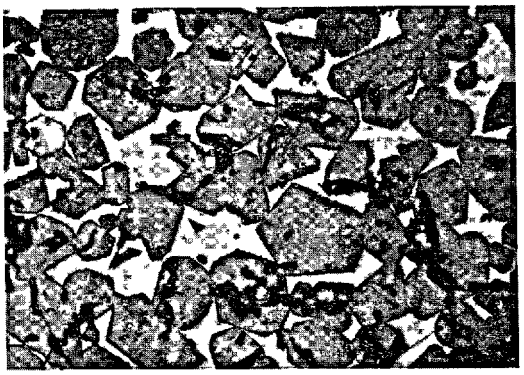

Fig.8. Clinker III (x800)

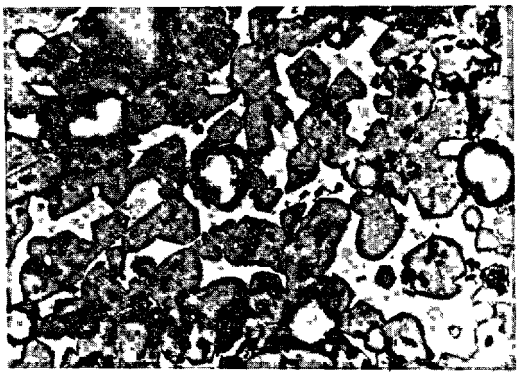

Fig.9. Clinker IV (x800)

The microsection has been etched with the 1 % solution of HNO_3 in alcohol.

Figure 6 presents clinker I of lime saturation factor SF - 0.90, SR - 2.27, AR - 2.0. It is alite-belite clinker of contens: C_3S - 68.4 %, C_2S - 10.5 %.

The conglomerations of alite crystal of irregular cross-section are visible. There are also alite grains of elongated cross-section with corroded edges and on their surface belite inclusion can be seen. Grains of irregular shapes can be observed in the structure of this clinker; it is due to progressive deposition of crystals at the presence of alumina and in the form of solid solutions and due to variation of liquid state composition during crystallization process.

Figure 7 shows clinker II of SF - 0.92, SR-2.54, AR-2.30. It is alite clinker, C_3S-70.2 %, C_2S-8.3 % of fine-crystalline structure (the alite grain diameter - 30 microns). Most of them are alite crystals of hexagonal cross-section with edges corroded by liquid phase and visible enclaves and occlusions of C_2S.

Figure 8 shows clinker III of SF - 0.93, SR-2.49, AR-2.33. It is high alite clinker C_3S - 72.0 %. Alite crystals of hexagonal cross-section are distributed uniformly in aluminate-ferrite filling substance. This clinker is characterized by very clear alite crystals crystallization of axis ratio 1.4:1 and 5 : 1. In alite crystals there are observed quite often irregular and slot micropores and enclaves.

Microscopic picture (Figure 9) shows clinker IV of SF - 0.94. Alite crystals of irregular and polygonal cross-section of average diameter about 40 microns have on their edges and surfaces numerous inclusions, free grains of CaO are also seen.

X-ray examination of clinkers confirmed the presence of tricalcium silicate and in smaller amounts dicalcium silicate and tricalcium aluminate and also some tetracalcium aluminoferrite. As example, the diffractogram of clinker III was shown (Figure 10).

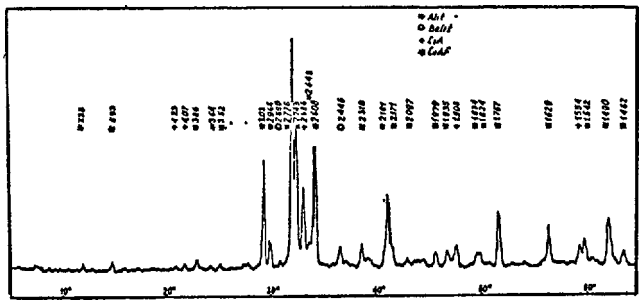

Fig.10. Diffractogram for clinkers III

All clinkers were ground with the addition of the same quantity of gypsum (5 %) to four different specific surfaces amounting 230 m^2/kg - 470 m^2/kg. As a result it was obtained 16 cement samples which were examined concerning physical and strength properties. The results were compilated in Table IV.

Analyzing the results of cements obtained from trias limestones and keuperous clays, very considerable effect of these raw materials origin on strength properties of cements especially after 28 days can be observed.

Complex examination of mineral composition of limestone proved that it is composed with fine-crystallic calcite and similar clay minerals; it can be seen on x-ray and microscopic photographes and on thermograms. As it results from x-ray radiography and thermogravi metry, keuperous clays are composed with aluminosilicates i.e. chlorites, mica, kaolinites, quartz and quartz silica. Chlorites, as laminar silica, introduce magnesium compounds with clays to raw mix (3.4% of MgO was confirmed analitically) but mica and clay - potassium compounds (K_2O - 2.9% and Na_2O - 0.29%).

The presence of minerals characterized by highly developed specific surface in raw mix causes the decrease of eutectic point and enables sintering of this mix.

TABLE III - CHEMICAL AND MINERAL COMPOSITION OF CEMENT CLINKERS

CLINKER NO.	CHEMICAL COMPOSITION (PERCENTAGE BY WEIGHT)										MODULI			MINERAL COMPOSITION*			
	L.O.I.	SiO_2	Fe_2O_3	Al_2O_3	CaO	MgO	SO_3	Free CaO	Na_2O	K_2O	SF	SR	AR	C_3S	C_2S	C_3A	C_4AF
CLINKER I	.2	21.8	3.2	6.4	67.1	1.1	.1	.2	.025	.045	.90	2.27	2.0	68.4	10.5	12.8	4.2
CLINKER II	.2	21.9	2.6	6.0	67.7	1.2	.1	.4	.025	.035	.92	2.54	2.30	70.2	8.3	14.2	4.5
CLINKER III	.1	21.7	2.6	6.1	67.9	1.3	.1	.1	.031	.072	.93	2.49	2.34	72.0	8.1	14.2	4.5
CLINKER IV	.1	21.8	2.9	5.6	68.7	1.2	.1	1.5	.023	.029	.94	2.72	2.33	69.5	7.9	15.2	4.3

*/ - MINERAL COMPOSITION DETERMINED BY OPTICAL MICROSCOPY

The examination of raw materials sinterability confirmed that the range of temperatures for limestone and clays softening is the same, thus active CaO will react with silicaluminates in state"in statu nascendi" when raw mix shows the highest chemical activity. From microstructure of formed clinker minerals it can be concluded about sintering conditions of raw mix at the presence of sintering process intensifiers i.e. magnesium, sodium, potassium compounds and other accessoric components. Complex examination of clinker mineral composition presented on x-ray photography confirms the presence of calcium orthosilicate i.e. alite and some belite and filling substance, composed mainly with tricalcium aluminate and mixture of aluminates and calcium ferrites appearing as tetracalcium aluminoferrite.

The microscopic examinations shown in Figures 6, 7, 8 and 9 enable to determine crystalline structure of minerals.

Clinkers of different lime saturation factor varying between 0.90 - 0.94 have different increase of strength in time, which is presented in Figure 11.

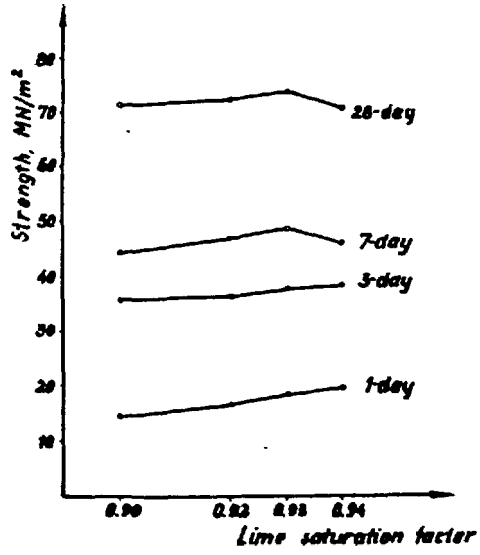

Fig.11. Influence of the lime saturation factor on mortar strengths after 28 days of hardening

At increasing SF the systematic increase of strength after 1 and 3 days of hardening is observed. The highest strength i.e. 19.6 MN/m^2 after 1-day hardening is obtained for clinker IV of SF amounting 0.94. This clinker has the highest value of alumina phase C_3A - 15.2 % and free CaO - 1.5 % and silica ratio 2.72. It is presumed that the increase of strength at the initial phase was possitively influenced by free Ca included in clinker (1.5 %), which after hydration became a center of crystal nucleuses for hydrated silicates and calcium aluminates.

The minimal decrease of strength of this clinker after 7 and 28 days compared to other samples was probably caused by the content decrease of C_3S and by a little different crystalline structure.

High lime saturation factor and increased silica ratio caused the formation of small, irregular alite crystals (12) which can be seen in Figure 9. The highest strengths after 7 days i.e. 48.5 MN/m^2 and after 28 days i.e. 74.2 MN/m^2 and at specific surface amounting 468 m^2/kg are obtained by clinker III of lime saturation factor 0.93 and silica ratio 2.52. This clinker has the highest total content of oxides MgO, Na_2O, K_2O equaling 1.403 %. As Woerman and others (7) make known, the presence of these oxides in mineral synthesis process caused the crystallization of alite characterized by better symetry and higher hydraulic activity.

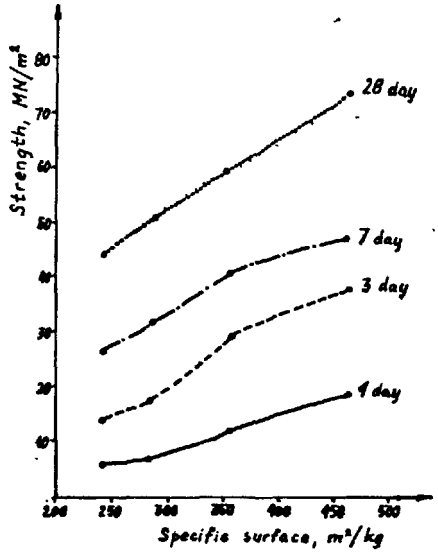

Fig.12. Influence of the cement fineness on the strengths of cement pastes of a different mineralogical composition

Solution of MgO in alite and belite crystal lattice gives solid solutions of defected lattice and also fine-crystalline structure of this clinker (20-40 microns) resulted in higher hydraulic activity of this clinker and higher strengths.

Figure 12 shows cement specific surface effect on its strength, clinker III given as an example.

The clinker grinding to specific surface about 350 m^2/kg let us obtain cement mark 550 of 28 days strength amounting 59.4 MN/m^2. The increase of specific surface up to about 450 m^2/kg gives cement of high strength parameters i.e.after 1 day - 18.2 MN/m^2, after 3 days - 37.1 MN/m^2 and after 28 days - 74.0 MN/m^2, which meets requirements for fast hardening and high strength cements.

Basing on quated above examinations it can be said that there is a considerable effect of raw materials on the quality of clinker produced.

The clinkers of high strengths and high mark cements (after grinding with gypsum addition) i.e. 550 and higher (examined according to ISO) can be obtained with raw materials containing magnesium compounds in the form of chlorides and potassium oxides contained in mica and illites.

REFERENCE LIST

1.- S.D. MAKASHEW (1976) "Effect of Raw Material Physico-Chemical Properties on Reactivity of Raw Mix and on clinker Minerogenesis Processes", VI I.S.C.C.- Moskwa 1974, Promstroizdat Moskwa 1976, Vol. I, p. 156 - 161.

2.- S.M. ROJAK (1949) "Works of the Research Institute of Cement in Moscow, 2nd ed., Promstroizdat.

11.- L. STOCH (1974) "Clay minerals", Wydawnictwa Geologiczne, Warszawa, p. 318 - 323.

12.- J. GRZYMEK (1959) "Applied chemistry", Journal of the Committee of Chemical Sciences of the Polish Academy of Sciences, Vol. III, No. 2, p. 225 - 246.

3.- I.V. KRAWČENKO (1976) "Rapid-Hardening and high strength portland cement", VI I.S.C.C. Moskva 1974, Promstroizdat Moskwa 1976, Vol. I, p. 6 - 19.

4.- Ju.M. BUTT, V.V. TIMASHEW (1965) "Portland clinkers of a required crystal structure and cements of a high quality obtained on their base", Journal of the Mendeleiev National Chemical Association in Moscow, No. 5.

5.- M. REGOURD, A. GUINIER (1976) "The Crystal Chemistry and Crystalochemistry of Cement Minerals, VI I.S.C.C. Moskva, Vol. I, p. 25 - 48.

6.- Ju.M. BUTT, V.V. TIMASHEW, A.P. OSOKIN (1976)"Mechanism of Clinker Formation Processes and the Modification of the Structure' VI I.S.C.C. Moskva, Vol. I, p. 132 - 151.

7.- E. WOERMAN, W. EYSEL, Th. HAHN "Chemical and Structural Inwestigations on the Solid Solutions of Tricalcium Silicate", Zement-Kalk-Gips, Vol. 9, p.414 - 422, 1969.

8.- M.M. SYCEV, B.J. KORNIEJEW (1967) "Technology and properties of special cements", Moscow, p. 201 - 211.

9.- P. APPENDINO, M. MONTORSI (1971) "II Cemento 68", Vol. 3, p. 89 - 98.

10.-W. KURDOWSKI (1976) "Influence of Minor Components on Hydraulic Activity of Portland Cement Clinker", VI I.S.C.C. Moskva, Vol. I, p. 203 - 206.

TABLE IV - PHYSICAL AND STRENGTH PROPERTIES OF CEMENTS

SAMPLE NO.	CEMENT	CEMENT PASTE				MORTARS									
	SPECIFIC SURFACE m^2/kg	PROPER H_2O CONTENTS, %	SETTING TIME BEGINNING hrs.	SETTING TIME END hrs.	LE CHATELIER TEST, mm	STRENGTH, MN/m^2 BENDING 1-DAY	BENDING 3-DAY	BENDING 7-DAY	BENDING 28-DAY	BENDING 90-DAY	COMPRESSIVE 1-DAY	COMPRESSIVE 3-DAY	COMPRESSIVE 7-DAY	COMPRESSIVE 28-DAY	COMPRESSIVE 90-DAY
KI/0	230	27.0	2.50	4.00	1	1.4	4.1	5.8	7.8	7.2	5.3	14.5	26.0	43.8	47.9
KII/0	230	28.0	3.05	5.10	0	1.4	3.2	5.3	7.3	7.3	5.3	13.6	25.7	42.0	49.3
KIII/0	240	27.5	3.00	4.50	0	1.4	3.6	5.3	7.8	7.7	5.6	13.8	26.2	44.2	51.0
KIV/0	240	29.0	3.20	5.00	0	1.4	3.0	4.8	7.3	7.2	5.3	13.2	22.0	39.2	50.8
KI/1	285	30.0	3.20	5.00	0	1.6	4.6	6.2	7.5	8.3	6.2	18.6	31.0	46.9	55.0
KII/1	290	28.0	2.40	4.10	0	2.1	4.2	6.1	7.9	8.7	8.3	18.4	30.9	47.5	55.8
KIII/1	285	27.0	3.25	5.10	0	1.5	4.3	6.1	8.8	7.6	6.0	17.3	30.8	50.3	54.9
KIV/1	290	29.0	2.40	4.10	0	2.1	4.4	6.5	8.0	7.7	8.1	18.5	31.3	49.1	56.0
KI/2	360	30.5	1.45	4.15	0	2.2	5.6	7.6	7.9	8.4	8.3	27.9	39.9	52.6	61.2
KII/2	350	29.0	2.40	4.30	0	2.5	4.9	6.8	7.6	8.4	9.8	22.8	35.6	53.4	68.7
KIII/2	355	28.0	2.30	4.00	0	3.6	6.2	7.4	8.9	8.7	11.9	28.8	40.6	59.4	69.3
KIV/2	360	28.5	2.25	3.50	0	3.0	5.5	7.2	8.9	8.3	12.2	26.7	40.0	57.3	66.2
KI/3	460	29.5	1.30	2.50	1	3.3	6.8	7.7	9.3	8.8	14.7	35.5	44.7	71.7	74.1
KII/3	466	30.0	1.25	2.55	0	3.4	7.1	8.3	8.9	8.8	16.2	36.7	46.8	72.2	74.6
KIII/3	468	28.5	1.20	3.00	0	4.4	7.1	7.7	9.0	8.8	18.2	37.1	48.5	74.0	77.7
KIV/3	455	28.5	0.45	1.40	0	4.1	7.3	7.9	8.4	8.9	19.7	38.1	46.3	70.3	74.1

Reactivity of belite stabilized by $Ca_5(PO_4)_3OH$

Réactivité de la bélite stabilisée avec $Ca_5(PO_4)_3OH$

B. MATKOVIC, "Rudjer Boskovic" Institute, Zagreb,
V. CARIN, T. GACESA, R. HALLE, Research Department of Jucema, Zagreb, Yougoslavie.

RESUME : L'hydraulicité de la bélite activée avec de l'apatite a été étudiée sur des échantillons préparés à partir de produits chimiques purs et à partir d'un mélange de calcaire et sable quartzeux. La modification qui se formait dans le clinker (β-,α-C_2S ou leur mélange)dépendait de la quantité de stabilisant dans le cru. Les clinkers et leurs produits d'hydratation furent caractérisés par des analyses chimiques et thermiques, la diffraction des rayons X la miscroscopie optique et la microscopie électronique à balayage. Les essais de résistance prouvaient que la forme α' seule ou combinée avec la forme β avait des résistances plus élevées que βC_2S.

Pour évaluer l'effet stabilisant de l'apatite, les auteurs comparaient les résistances à la compression des clinkers de bélite activée avec $Ca_5(PO_4)_3OH$ à celles des clinkers stabilisés avec $BaSO_4$. Les résultats obtenus indiquent qu'en présence d'apatite les résistances sont considérablement plus basses pendant le premier mois d'hydratation, les différences étant moins prononcées aux âges ultérieurs, sur tout pour la modification α'.

SUMMARY: Hydraulic activity of belite doped by phosphate was investigated on samples prepared from pure chemicals and on those from limestone and quartz sand. Depending on the stabilizer level in the raw mix there was either β-C_2S or α'-modification or a mixture of the two polymorphs found in clinker. Clinkers and their hydration products were examined by chemical and thermal analyses, X-ray diffraction, optical and scanning electron microscopy. Strength testings disclosed that α'-form alone or in combination with β-polymorph had better strengths than β-C_2S.

To estimate the stabilizing effect of $Ca_5(PO_4)_3OH$ the compressive strengths were compared with those on clinkers doped by $BaSO_4$ where they were considerably higher during the first month of hydration, although the differences diminished at later ages, especially for the α'-modification.

I. INTRODUCTION

Several tetrahedral groups (phosphates, borates, vanadates, sulphates) can substitute the silicate groups in C_2S solid solutions. It is well known (1,2, 3,4,5) that phosphates are efficient for the formation of β-, α'- and α-C_2S. When $Ca_2P_2O_7$ is used as stabilizer the β-form has ample hydraulic properties, α'-modification has some, but α-polymorph has none (2). In C_2S solid solutions stabilized by B_2O_3 (6) and V_2O_5 (7) higher strength development was observed on α'-C_2S than on β-C_2S. Notwithstanding the fact that numerous data are available on this subject it is hard to predict the effect of a certain minor element on the hydraulicity of belite clinkers prepared from different raw materials under different burning conditions. The present paper deals with the effects which different levels of apatite in the raw mix can have on the stabilization of dicalcium silicate phases and their hydraulic activity.

II. EXPERIMENTAL DATA

(1) Preparation of specimens

Chemicals used for the preparation of belites were analytical grade $CaCO_3$ and SiO_2 and pure grade $Ca_5(PO_4)_3OH$.

The initial mix was homogenized, calcined at 1000°C, pressed into pellets and sintered at 1450°C for 90 minutes, then reground, compacted and resintered under identical conditions. The product was air--quenched and ground to the specific surface of 3600±100 cm^2/g (Blaine).

TABLE I

Raw materials for belite clinkers (w.%)		
Components	Limestone	Quartz
SiO_2	0.10	97.20
Al_2O_3	-	0.97
Fe_2O_3	0.07	0.30
CaO	55.90	0.63
Ign.loss	43.88	0.43
MgO, SO_3, Na_2O and K_2O not detected		

The raw materials used for belite clinkers are listed in Table I.

The components for belite clinkers were ground to the respective fineness (no residue on 200 μm m. h sieve and less than 10% on 90 μm), homogenized, calcined at 1000°C, pressed into pellets and fired at 1450°C for 90 minutes, air-quenched and ground to the specific surface of 3600±100 cm^2/g.

Polished samples etched with 1% HNO_3-alcohol solution were studied by optical microscopy in reflected light, while SEM observations were made on fracture surfaces coated with a layer of gold.

The water/cement ratio for all cement pastes was 0.28. Samples were compacted in 1x1x4 cm moulds on vibrating table.

Mortar specimens were prepared according to the Yugoslav standard (based on RILEM-CEMBUREAU method and ISO Recommendation 679). The mix ratio was cement:graded sand 1:3 and the w/c ratio 0.5 constant. Mortars were mixed mechanically, then compacted in 4x4x16 cm moulds on vibrating table.

Paste and mortar specimens were stored 24 hours at 20±2°C and relative humidity of minimum 90%. Moulds were removed after 24 hours, and specimens stored in water at 20 ± 2°C.

Samples for hydration study were ground, washed in acetone, dried in vacuum and conserved in desiccator above KOH.

(2) Investigation methods

X-ray diffraction, wet chemical methods, optical and scanning electron microscopy and thermal analysis served to examine the prepared samples. X-ray diffraction, thermal analysis and microscopic examinations were used to determine the C_2S modifications and to study the process of hydration. The peak temperature of $\alpha' \xrightarrow{H} \alpha$-$C_2S$ conversion in doped samples was determined by differential thermal analysis and the morphology of specimens studied by scanning electron microscopy. Compressive strength testings on paste and mortar samples were repeated three times to obtain mean values.

III. RESULTS AND DISCUSSION

In preliminary investigations belites were synthetized from pure chemicals with the stabilizer added at different levels. Their hydraulic activity was determined by testing strengths on cement pastes. Since very high levels of stabilizer are needed to stabilize α-C_2S, this modification has not been

included into the present work.

Raw mix compositions and phases detected in belites are listed in Table II.

TABLE II

Sample	Raw mix comp. (w.%)			Phases detected by *XD			OM		
	CaO	SiO_2	$Ca_5(PO_4)_3OH$	$\alpha'_{(L)}$	β	γ	α	α'	β
1	64.35	34.46	1.18		++++	-	-	-	++++
2	62.86	33.68	3.46	+	+++	-		+	+++
3	62.12	33.28	4.60	++	++	-		+	+++
4	61.40	32.90	5.70	++	++	-		+	+++
5	57.92	31.03	11.05	+++	(+)	-	(+)	+++	(+)
6	54.66	29.28	16.06	+++	-	-	+	+++	-

(+) small amount

* XD = X-ray diffraction; OM = optical microscopy

β-C_2S was the reaction product in sample 1, while samples with higher levels of P_2O_5 had β- and α'-modifications coexisting, with the content of α'-polymorph increasing proportionally to the increase of the stabilizer level and attaining its maximum in sample 5 where α-modification started to form. Samples where α'-form coexisted with β-modification or where it was the main reaction product had better strengths than those where β-C_2S prevailed.

In literature (3,8,9) it is generally accepted that in C_2S stabilized by phosphates the α-modification is hydraulically inert while α'-modification develops lower strengths than β-polymorph. These results, however, were obtained with a specific stabilizer and under specific experimental conditions (2).

Since our initial investigation of strength development in pastes revealed that β-C_2S stabilized by phosphates was less reactive than α'-C_2S, belite clinkers were synthetized from raw materials listed in Table I and their strength development determined not only on pastes but also on mortars, this being more indicative for the quality of cement (3).

It was also of considerable interest to study the hydraulic activity of α'- and β-C_2S prepared from specific industrial raw materials doped by $Ca_5(PO_4)_3OH$ because natural raw materials contain some minor elements which can incorporate into the crystal lattice of C_2S together with phosphates and thus modify its hydraulic activity.

The chemical composition and phases detected in belite clinkers prepared from limestone, quartz sand and different amounts of $Ca_5(PO_4)_3OH$ are presented in Table III.

TABLE III

Chemical compositions (w.%) and phases detected in belite clinkers		P 1	P 2	P 3	P 4
SiO_2		33.24	33.21	32.88	31.24
Al_2O_3		0.64	0.64	0.27	0.46
Fe_2O_3		0.14	0.20	0.31	0.10
CaO		64.04	63.02	63.80	64.05
P_2O_5		0.78	1.42	2.27	4.02
Insol.		0.90	1.40	-	-
β-C_2S	micr.	++++	++++	+++	+
	X-ray	++++	++++	+++	+
α'-C_2S	micr.		(+)	(+)	+++
	X-ray			(+)	+++

Limestone and quartz of high purity were hence selected to avoid elevated contents of tricalcium aluminate and ferrite phase. The prepared clinkers had only one crystalline phase, i.e. belite, no free CaO and less than 6% amorphous phase as determined by optical microscopy in reflected light which also revealed a few grains of alite in sample P 4. The fact that α'-C_2S develops strength more rapidly than β-C_2S was again confirmed by compressive strengths measured on pastes of belite clinkers, although the obtained values were lower than in case of belites prepared from pure chemicals.

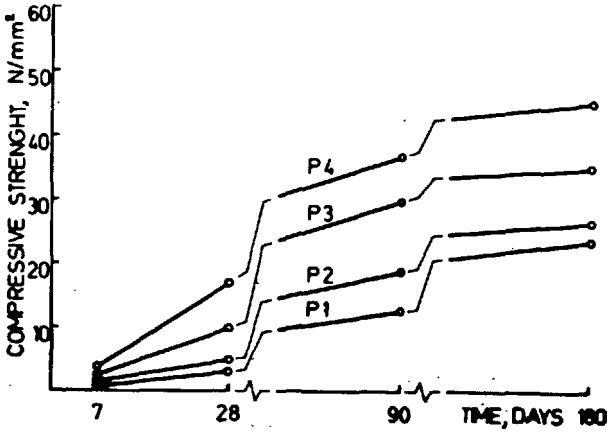

Fig.1 - Compressive strengths on mortars of belite clinkers stabilized by phosphate

The strength of sample P 4 with predominantly α'-C_2S is obviously higher than that in other samples where β-C_2S coexists with α'-form or where it is the main reaction product like in sample P 1 which was doped with the smallest amount of stabilizer.

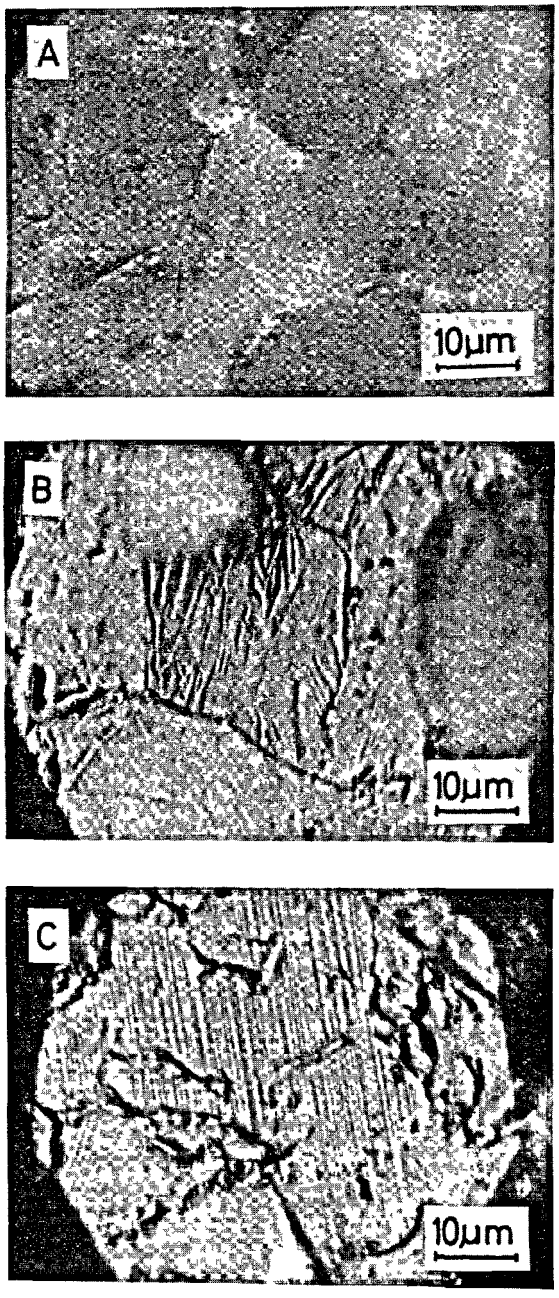

Fig.2 - Reflected light microscopic photographs of belites stabilized by phosphate: (A) α-C_2S; (B) α'-C_2S and (C) β-C_2S

The polymorphic modifications of dicalcium silicate were determined by X-ray diffraction and optical microscopy. Fig.2 illustrates the features typical for particular C_2S polymorphs. The C_2S crystal grains without lamellae Fig.2 (A) are those of α-C_2S; (B) shows α'-grains recognizable by skeleton structure, while (C) illustrates the β-form; complete grain exhibits only polysynthetic lamellae formed by phase transition of α'-C_2S into β-form.

Differential thermal analysis showed that the stabilizer had completely passed into C_2S solid solution during synthesis. The method proceeds from the fact that the decrease in phase conversion temperature depends on the level of stabilizer dissolved in C_2S. Peak temperatures of the endothermic $\alpha'_H \longrightarrow \alpha$-$C_2S$ phase transformation plotted as a function of P_2O_5 percentage in the raw mix are presented in Fig.3.

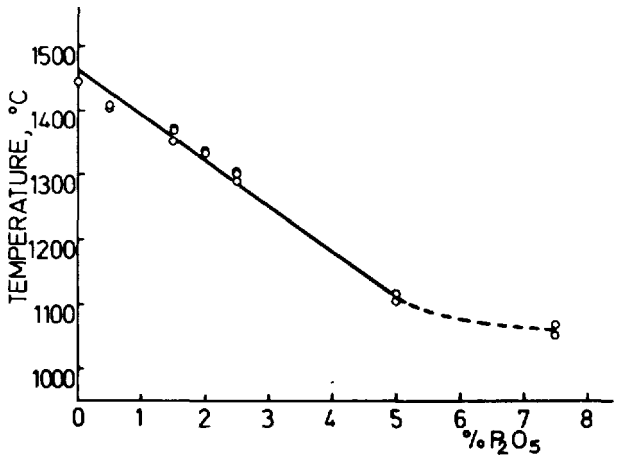

Fig.3 - Effect of P_2O_5 concentrations on the $\alpha'_H \longrightarrow \alpha$-$C_2S$ transition temperature

Scanning electron microscopy studies were made on samples doped with phosphates or barium sulphate (10) for comparison. It is obvious (Fig.4) that the shape and size of grains depend more on the content than on the kind of stabilizer. β-C_2S crystals vary in size between 2 and 10 µm, Fig. 4 (A) and (B), those of α'-C_2S between 10 and 20 µm (C) and (D).

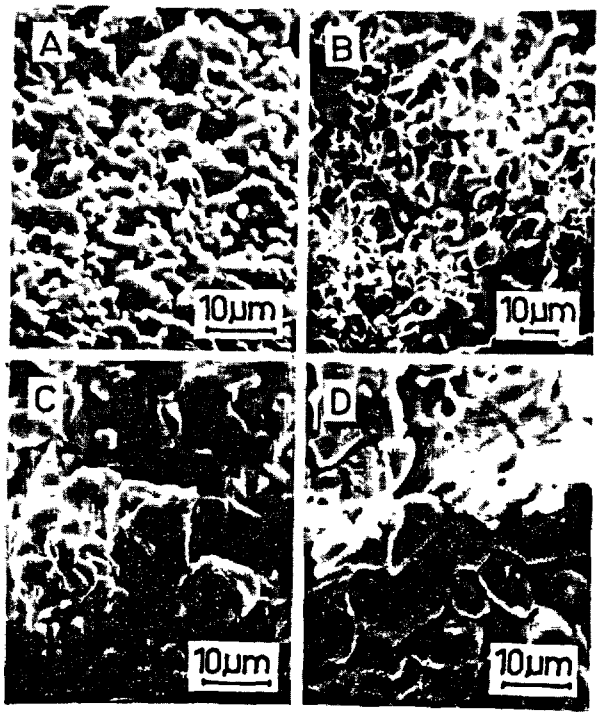

Fig.4 - SEM characteristic morphologies of belites with 1.47% P_2O_5 (A); 6.66% $BaSO_4$ (B); 4.70% P_2O_5 (C) and 12.71% $BaSO_4$ (D) in the raw mix

The hydration process was studied by thermal and X-ray analyses which confirmed that strengths develop with the advancement of hydration.

Fig. 5 presents the water content in C-S-H gel determined in the temperature range from 100 to 350°C by TG and DTG.

Belites from pure chemicals (samples 1-6) have a higher content of C-S-H gel than belite clinkers (samples P1-P4). In both groups the content of gel increases with higher levels of stabilizer and is higher in samples with α'-form than in those with β-C_2S. The gain of the gel formation is most expressed up to 28 days.

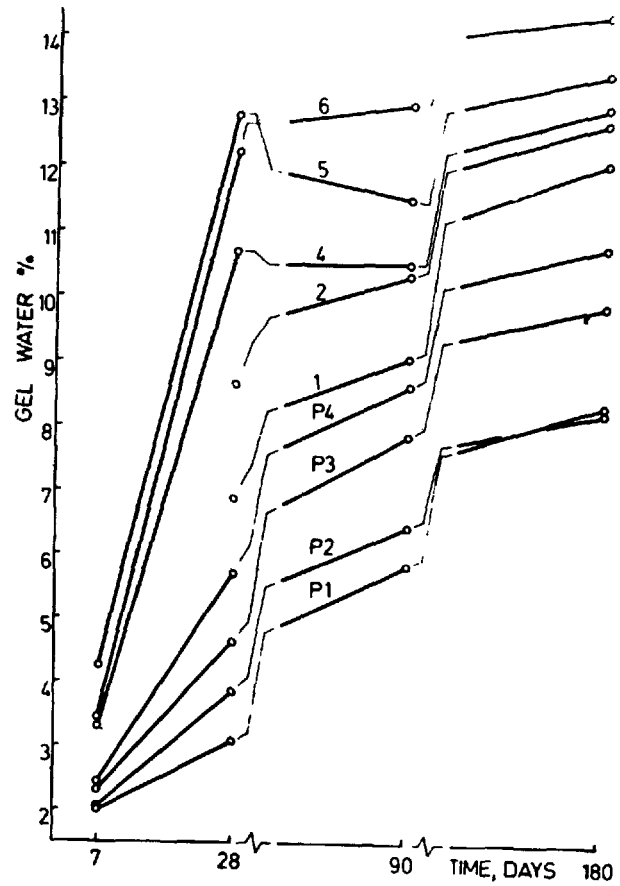

Fig.5 - Water content in hydrated samples as function of hydration time

To estimate the effect of $Ca_5(PO_4)_3OH$ as stabilizer belite clinkers doped with $BaSO_4$ (10) were sintered from the same raw materials, ground to the same specific surface and tested on mortars in the same way as belite clinkers stabilized by phosphates. For comparison with the present data the chemical composition and phases detected in $BaSO_4$ doped belite clinkers are presented in Table IV and their compressive strengths in Fig.6 (10). In the first month of hydration belite clinkers stabilized by phosphate had a remarkably lower strength but after 180 days the differences were less obvious, especially for the α'-modification.

TABLE IV

Chemical composition (w.%) and phases detected in belite clinkers stabilized by $BaSO_4$

		B 1	B 2	B 3
SiO_2		32.68	30.87	28.24
Al_2O_3		0.32	0.31	0.27
Fe_2O_3		0.10	0.09	0.09
CaO		61.04	57.62	55.58
BaO		4.39	8.47	12.02
SO_3		1.21	2.35	3.44
β-C_2S	micr.	++++	+++	++
	X-ray	++++	++	++
α'-C_2S	micr.		+	+
	X-ray		++	++
α-C_2S	micr.			+

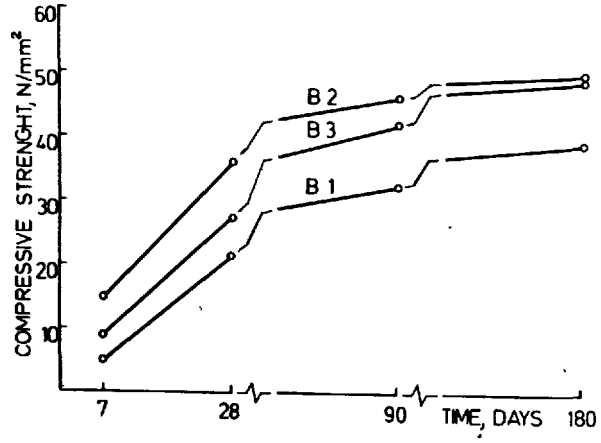

Fig.6 - Compressive strength of mortars from belite clinkers stabilized by $BaSO_4$

The results obtained for $Ca_5(PO_4)_3OH$ stabilized C_2S are in agreement with the findings for belites stabilized by B_2O_3 (6), V_2O_5 (7), $BaSO_4$ (10) and Ba_2SiO_4 (11) but opposed to the statement that the hydraulic activity of α'-C_2S stabilized by phosphates is lower than that of the respective β-C_2S (2,3, 8,9).

IV. CONCLUSIONS

The kind and level of the stabilizer together with the preparation conditions have a strong effect on the hydraulic activity of C_2S solid solution. Like other phosphates (2,4,5) $Ca_5(PO_4)_3OH$ is a good stabilizing agent for β- or α'-C_2S modifications. Stabilized by this compound under described conditions α'-modification or a mixture of α'- and β-C_2S develop higher strengths than β-C_2S.

Acknowledgement. The investigation was supported by U.S. Department of Transportation and by the Selfmanaging Community for Scientific Research of Croatia. SEM examinations were made at the University of Illinois, Urbana, Ill. 61801, U.S.A.

REFERENCES

1. - R.W.NURSE et al. (1959), "High temperature phase equilibria in the system dicalcium silicate - tricalcium phosphate", J.Chem.Soc. 1077-1083.

2. - J.H.WELCH, W.GUTT (1962), "The effect of minor components on the hydraulicity of the calcium silicates", Proc. 4th ISCC, Washington , 1960, Vol. I, pp.59-68(U.S. Dept. of Commerce)

3. - F.M.LEA (1970), "The chemistry of cement and concrete", pp. 80, 155 and 388 (E.Arnold Ltd. 3rd ed. Glasgow)

4. - H.SALFELD (1971), "Kristallchemische Untersuchungen im System Ca_2SiO_4-$Ca_3(PO_4)_2$. Z.Kristallogr. 133, 396-404.

5. - I.M.PRITTS, K.E.DAUGHERTY (1976), "The effect of stabilizing agents on the hydration rate of β-C_2S", Cem.Concr.Res. 6 (6) 783-796.

6. - I.JELENIĆ et al. (1978), "Hydration of B_2O_3--stabilized α'- and β-modifications of dicalcium silicate", Cem.Concr.Res. 8 (2) 173-178.

7. - M.LUIĆ et al. (1979), "Dicalcium silicate stabilized by V_2O_5" in Croat., Cement/Zagreb/ 21 (2) in press

8. - W.GUTT, E.F.OSBORN (1970),"The effect of potassium on the hydraulicity of C_2S", Cem.Technol. 1 (4) 121-125.

9. - M.REGOURD, A.GUINIER (1976), "The crystal chemistry of the constituents of Portland cement clinker", Proc. 6th ISCC, Moscow, 1974, Vol. I, pp.25-51 (Stroyizdat, Moscow, Russ. ed.)

10. - B.MATKOVIĆ et al. (1979), "Influence of $BaSO_4$ on the formation and hydraulic properties of belite clinkers", 81st An.Meet., ACS, Cincinnati, Ohio

11. - M.Ya.BIKBAU (1976), "On hydration activity of silicates", Proc. 6th ISCC, Moscow, 1974, Vol. II (1) pp. 28-31 (Stroyizdat, Moscow, Russ. ed.)

Mineralizers and fluxes in the clinkering process. I. Phase equilibria in the $CaO-Al_2O_3-Fe_2O_3-SiO_2$ system with calcium fluosilicate

Minéralisateurs et fondants dans la formation des clinkers. I. Equilibre des phases dans le système CAFS avec du fluosilicate de calcium

ASOK K. SARKAR, Research Associate,
DELLA M. ROY, Professor of Materials Science,
RODERICK M. SMART, Research Associate, Materials Research Laboratory,
The Pennsylvania State University, University Park, PA 16802, U.S.A.

RESUME : Ceci est le premier d'une série de trois (5,6) comptes rendus sur les effets des fondants et des minéraliseurs utilisés pour accroître l'efficacité du procédé de clinkérisation du ciment. On a étudié les effets de fondants minéraliseurs tels que fluosilicates et fluorures sur l'équilibre des phases dans le système CAFS ainsi que dans ses sous-systèmes C-A-F et C-A-S. Dans ces deux derniers sous-systèmes, les températures d'apparition de la phase liquide sont relativement abaissées, les surfaces des champs primaires de la solution solide $C_{12}A_7$ sont plus étendues, les champs primaires de C_3A sont réduits de beaucoup et dans le système C-A-S une ligne d'Alkemade semble être formée entre la solution solide $C_{12}A_7$ et C_3S , ce qui a pour conséquence de rendre C_3S stable dans des limites de composition plus vastes que celles du système C-A-S pur. Il en résulte aussi la formation de nouveaux points invariants. De plus, la réaction de formation du C_3S est accélérée; sa formation se produit à des températures inférieures à la limite de stabilité apparente indiquée dans le système C-S pur, et l'aire de son champ primaire est agrandie. On a étudié des portions du système CAFS avec un fluosilicate. La solution solide $C_{12}A_7$ reste la phase dominante, même avec l'ajout de 5 à 20 % de Fe_2O_3 au système C-A-S($CaSiF_6$). Certaines des limites de phase des systèmes CAF et CAS contenant du fluosilicate peuvent logiquement être extrapolées au système complexe CAFS + fluosilicate. Ceci a été observé expérimentalement. Les effets sur les relations entre les phases et les phénomènes cinétiques qui s'y rattachent apparaissent être favorables à la fabrication du clinker, ce qui a pour conséquence d'augmenter l'efficacité du four.

SUMMARY: This is the first of a three-part series (5,6) studying the effects of fluxes and mineralizers to increase efficiency of the cement clinkering processes. The effects of flux mineralizers, primarily fluosilicates and fluorides upon phase equilibria in the system $CaO-Al_2O_3-Fe_2O_3-SiO_2$ (C-A-F-S) and its subsystems C-A-F and C-A-S have been investigated. In both the latter subsystems the temperatures for first liquid formation are lowered substantially, the primary phase field areas of $C_{12}A_7$ solid solution are vastly expanded, the field areas of C_3A are much diminished, and in the C-A-S system an Alkemade line appears to be formed between $C_{12}A_7$ solid solution and C_3S, resulting in the stable existence of C_3S over a broader composition range than in the pure C-A-S system. This also results in the formation of new invariant points. Furthermore, reaction to form C_3S is accelerated; its formation takes place at temperatures below the apparent lower stability limit in the pure C-S system; and its primary phase field area is increased in size. Portions of the C-A-F-S system with fluosilicate were studied. When Fe_2O_3 was added to the C-A-S ($CaSiF_6$) system in amounts from five to twenty percent, $C_{12}A_7$ solid solution was still found to be the dominant phase. Some of the phase boundaries determined from the C-A-F and C-A-S systems with fluosilicate, logically can be extrapolated into the complex C-A-F-S system + fluosilicate and are experimentally observed. The effects upon phase relations and related kinetic phenomena appear to be favorable to the cement clinker manufacturing process; resulting in greater kiln efficiency.

INTRODUCTION

The efficiency of cement clinker production can be increased by the addition of minor amounts of other components classified as fluxes and mineralizers (1-6). However, these additions are likely to affect the final equilibrium phase relationships of the end products formed in the basic cement system, $CaO-Al_2O_3-Fe_2O_3-SiO_2$ (C-A-F-S).* The primary goal of this study was to understand the equilibrium relationships in the above basic system with the addition of calcium fluosilicate, and their effect on the clinkering process.

Studies of the effects of fluxes and mineralizers on the kinetics of alite formation (5) and upon the burnability of raw mixes (6) are described in separate parallel papers.

The fluosilicates can be classified as both fluxes and mineralizers because of their abilities to both lower the melting temperatures and to accelerate the reaction kinetics.

The importance of systematic studies to determine the phase equilibrium relationships in the system C-A-F-S with added fluxes (especially fluoride fluxes) has been discussed previously (2-4). Relevant previous studies in these systems or subsystems have also been reported earlier (1-4). Most previous studies used CaF_2 as the flux component, but little systematic work had been done to ascertain the effect of CaF_2 on the ultimate equilibrium phase products starting from a wide range of compositions. The published studies involved various subsystems of the major C-A-S system or the subsolidus phase relationships with CaF_2 as one of the components. Since the cement manufacturing process involves an essential liquid formation step, for efficient flux utilization an accurate knowledge of the phase equilibrium relationships of the actual system including its liquidus surface is highly desired.

Before proceeding to determine the effects of fluxes on the complex system C-A-F-S (7), first the effects upon the two ternary systems, C-A-F (3) and C-A-S (4) were studied. The first system was studied adding 5 wt % $CaSiF_6 \cdot 2H_2O$ (1.85 wt % CaF_2), whereas the latter system was studied adding 5 wt % $CaSiF_6$ (2.2 wt % CaF_2). [Five percent $CaSiF_6$ represents about 1.1 wt % F in the original starting material--cements with ~1.5 wt % F have been prepared commercially (8,9).]

Once the equilibrium relationships were established in the C-A-S system then the equilibrium relationships were studied with incremental additions of Fe_2O_3. The results summarized here include the effect of fluoride additions to both C-A-F and C-A-S systems, together with some observations of the effects of adding up to 20 wt % Fe_2O_3 in the C-A-S system with 5 wt % $CaSiF_6$. (Typical cements contain ~5 wt % Fe_2O_3.) The compositions chosen in the C-A-F-S system lie mainly close to the CaO apex of the C-A-F-S tetrahedron (7), and encompass the important invariant points, phase boundaries, and pseudo-Alkemade lines.**

*Abbreviations: C = CaO, A = Al_2O_3, F = Fe_2O_3, S = SiO_2.

**Pseudo because the systems are quaternary or more complex, though usually containing minor amounts of the added component.

EXPERIMENTAL

The starting mixtures were usually made in batches of 2-3 gm using reagent grade chemicals: $CaCO_3$, silicic acid, Al_2O_3, Fe_2O_3, and $CaSiF_6 \cdot 2H_2O$. The $CaCO_3$, Al_2O_3 and Fe_2O_3 were first dried before weighing, but the silicic acid and the $CaSiF_6 \cdot 2H_2O$ were used as received with weight losses quantified. The mixtures were first moistened with acetone and then blended thoroughly by grinding in an agate mortar. These mixtures were air dried, transferred to a covered Pt-crucible and then fired in an electrically heated pot furnace in air atmospehre at a temperature of 925-950°C (a temperature well below initial liquid formation) for one hour, to decompose the carbonate and the silicic acid. At this temperature, $CaSiF_6 \cdot 2H_2O$ decomposes losing most of its SiF_4, and for all practical purposes behaves as CaF_2. In order to simulate the fluxing action in an actual clinkering process, this way of preparing the mixtures was found to have practical bearing allowing thorough mixing and better fluxing action. The sintered cake after firing was cooled, crushed and ground thoroughly in an agate mortar to assure proper homogeneity of the starting mixtures for the equilibration runs.

All the equilibration runs were made in sealed Pt tubes by suspending them in a controlled temperature quench furnace. At the conclusion of the runs, the samples were quenched in carbon tetrachloride. It was found that, for most of the mixtures, the quenching done either by quickly withdrawing the samples and then quenching in the liquid or by the conventional quenching (wire burn-out method) gave identical results. The identifications of the phases were mostly made by x-ray powder diffraction, supplemented by optical microscopy. In some cases, the presence of the quench phase could not be prevented even by the conventional quenching techniques. It should also be mentioned that some of the compositions studied were hard to quench to form glass, basically because many are not chemically in the glass-forming range. Additionally, maximum convenient furnace temperature operation limits, in combination with the presence of non-quenchable liquids, plus slow subsolidus reaction, sometimes made it difficult to make correct inferences. Difficulty was encountered in positively identifying the C_2S and C_3S in instances when they were both present, with either one only in small amount.

The temperatures were measured by a Pt/Pt90-Rh10 thermocouple and read through a digital thermometer (Doric Series 400 A Digital Trendicator). The thermocouple/digital thermometer was calibrated against the boiling point of tap water (98°C), the melting point of gold (1063°C), and diopside (1392°C), respectively. The temperatures reported here are reliable to ±2°C taking into consideration both the furnace temperature fluctuations (controller error) and the thermometer error.

RESULTS

C-A-F System Plus Fluoride: The subsolidus phase relationships in the normal ternary system at 1145°C is shown in Figure 1 (10). Characteristic of this system is the formation of extensive ranges of solid solutions. The major one of interest is that which is collectively called calcium aluminoferrite solid solution (C_4AF_{ss}, or F_{ss}). All calcium aluminates can incorporate iron (Fe^{3+} ions replacing Al^{3+} ions) in their crystal structures. This type of substitution gives rise to the formation of a ternary phase T,

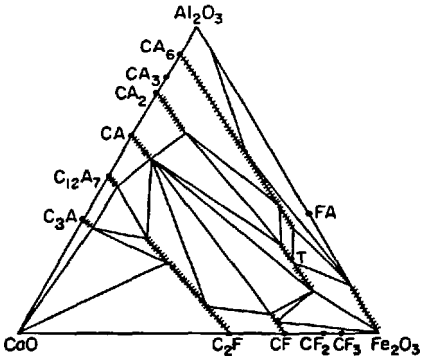

Figure 1. Subsolidus Relations in the Ternary CaO-Fe_2O_3-Al_2O_3 System (10).

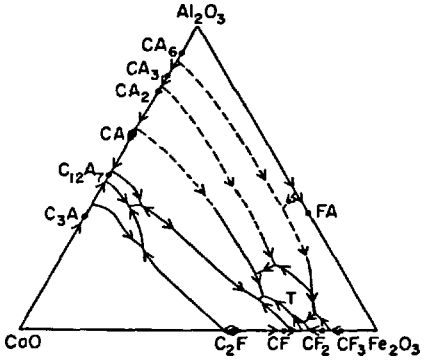

Figure 2. Liquidus Relations in the Ternary CaO-Fe_2O_3-Al_2O_3 System (10).

lying on the join of two imaginary compounds CA_3 and CF_3 between 12 and 28 wt % Al_2O_3 in the C-A-F triangle. The polythermal projection of the liquidus surface of this system is shown in Figure 2 (10). This figure shows the relative sizes of the primary phase field areas of all compounds including that of the ternary T-phase.

The changes to this system, upon the addition of fluosilicate, are shown in Figure 3. The solid lines show the newly-formed phase boundaries and the dashed lines show the "pure" system, plus sequences showing the postulated sequence of change of boundaries with increasing fluoride content.

When compared with the original C-A-F system, the addition of fluosilicate (fluoride) flux depresses the invariant temperatures which now become piercing points through a plane in the quaternary system. Also, the phase boundary positions are shifted substantially. This causes an expansion of the $C_{12}A_7$ss field, as a result of which two new invariant points are established. At the 5 wt % $CaSiF_6 \cdot 2H_2O$ level, the C_3A phase field completely disappears at lower temperatures (solidus to subsolidus temperatures).

Similarly, the expansion of the T-phase field area reduced the area of the CA and CA_2 fields ultimately eliminating the CA-CF boundary curve present in the original system.

C-A-S System Plus Fluoride: A portion of the ternary C-A-S diagram is shown in Figure 4 (11). This portion

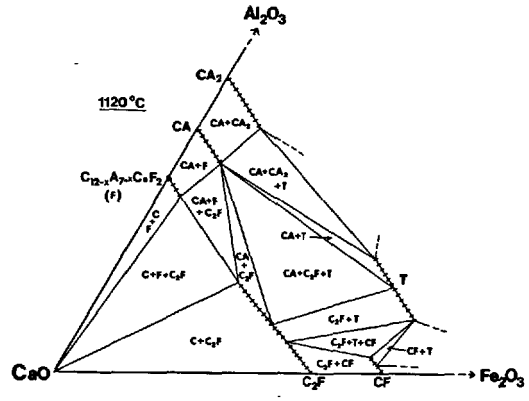

(a) Subsolidus Phase Relationships.

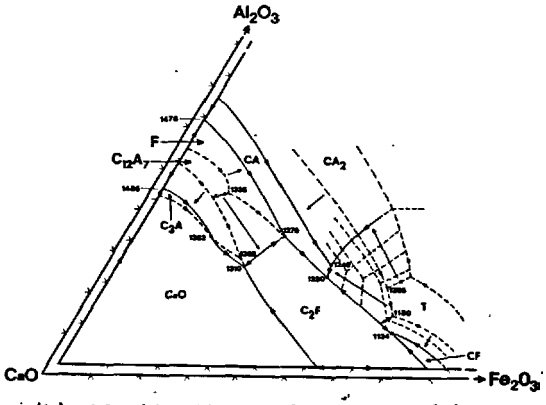

(b) Liquidus Phase Relationships (3).

Figure 3. Phase Diagram of the System CaO-Al_2O_3-Fe_2O_3 Modified by Addition of 5 wt % $CaSiF_6 \cdot 2H_2O$.

of the diagram is of interest to the cement chemist since most of the portland cement compositions are approximated by compositions within the C_3S-C_2S-C_3A triangle. The lowest melting temperature (eutectic) for any compositional mixtures within the C_3S-C_2S-C_3A triangle is 1455°C. This diagram also shows the pertinent phase field areas of the major compounds of interest in cement chemistry, other invariant points and Alkemade lines also.

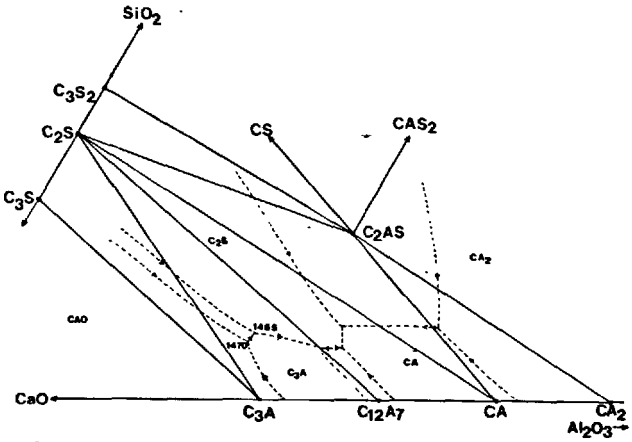

Figure 4. Phase Equilibria in the Ternary System CaO-Al_2O_3-SiO_2 (11).

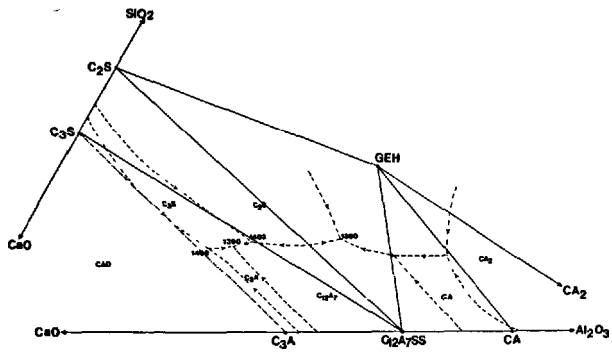

Figure 5. Apparent Phase Equilibria in the System $CaO-Al_2O_3-SiO_2$ with Addition of 5 wt % $CaSiF_6$ (4b).

When fluosilicate is added to this system, the experimental data combined with existing data on this system can be best represented by the liquidus diagram shown in Figure 5 (4b). This figure is actually a polythermal projection of 5 wt % $CaSiF_6$ section through the tetrahedron of the pseudoquaternary system $CaO-Al_2O_3-SiO_2-CaSiF_6$.* A comparison of Figures 4 and 5 shows the notable differences. The primary phase field areas of C_3S, C_3A and $C_{12}A_7$ss are vastly changed. Two new pseudo-Alkemade lines are formed, one joining C_3S and $C_{12}A_7$ss and the other joining $C_{12}A_7$ss and gehlenite. This gives rise to the formation of two new invariant points. Also, the temperatures of the invariant points among 3-phase assemblages from the original ternary system are lowered when fluosilicate is added to the original C-A-S system. C_3A was not detected in any quenching runs below ~1400°C.

C-A-F-S System with Added Fluoride Flux: Fe_2O_3 was added in amounts of 5, 10, and 25 wt % to some selected compositions in the C-A-S system along with 5 wt % $CaSiF_6$. These compositions were chosen at appropriate positions within the compatibility triangles presented in Figure 5. The data obtained to date are insufficient to construct the full quaternary system (plus the fifth component, fluoride flux); thus, it was attempted to observe the effect of adding a constant wt % Fe_2O_3 to the C-A-S (+ fluoride) system keeping the compositions studied in a range relevant to those providing information about potential cement phase compositions. Also, since portland cements commonly have in the vicinity of $\leq$5 wt % of Fe_2O_3 in their chemical compositions the 5 wt % level was selected first. However, compositions using higher Fe_2O_3 contents were studied as well in order to better identify the Fe_2O_3-containing phases.

The results of the quench runs of the compositions studied are listed in Table 1. A careful examination of this table will show that some of the observed phases were not exactly as would be expected. In most cases crystalline "C_4AF" was not found, except at ~1209°C (was not present at 1307°C), and probably was quenched from the liquid phase, to form a glass, even with compositions containing 10 wt % Fe_2O_3. However, in general, the addition of 5 wt % Fe_2O_3 was found to lower the temperature of liquid formation significantly over those of C-A-S system. Though not the "cement" invariant point, the lowest melting temperature in the original C-A-F-S system is at 1280°C among C_2S, C_3A, $C_{12}A_7$ and C_4AF phases (7). The invariant points involving C_3S are also lowered and, due to the addition of fluoride flux, C_3S can be formed at temperatures as low as 1200°C, while it was unstable below 1250°C in the original C-S diagram.

Some of the equilibria established in the fluoride-modified C-A-S and C-A-F systems may be projected, into the C-A-F-S system. Equilibrium sets of three solid phases in the "ternary" system when projected into the "quaternary" system add a fourth phase, liquid. Some of the same features were observed experimentally in the C-A-F-S system. $C_{12}A_7$ss is still dominant in the C-A-F-S system. Though phase compatibilities have been determined (12,13), the only previous detailed equilibrium phase relationship study published on this system is by Uchikawa and Matuzaki (8) in an attempt to understand the process of making jet cement. They studied the C-A-S system with 1 wt % Fe_2O_3 at 2 wt % and 5 wt % CaF_2 level only. Although some of the basic results of their studies agree with the present observations, there are some differences in the temperatures of comparable invariant points. Since the compositions studied were not identical (i.e., 1 vs. 5 wt % Fe_2O_3) this is not surprising. The invariant temperatures in the present study with 5 wt % $CaSiF_6$ (2.2 wt % CaF_2) even in the C-A-S system are lower than the former workers' values for the C-A-S system with 1 wt % Fe_2O_3 at the 5 wt % CaF_2 level. They also observed (8) that fluorine was not lost from the system. The contrast suggests that fluosilicate is an even better flux than CaF_2 itself. Since the first emphasis of the present study was to understand the phase behaviors, no detailed characterization of the extent or compositional ranges of the solid solutions formed among the phases has yet been carried out.

DISCUSSION AND CONCLUSION

The studies on both C-A-F and C-A-S systems with the fluoride flux show some common features. Apart from lowering the liquidus temperatures, the most significant feature in both systems is the formation of the solid solution phase $C_{12-x}A_{7-x}CaF_2$, which greatly increases the primary phase field area of $C_{12}A_7$ss. As a result of this expansion, the C_3A primary phase field area is reduced. At the level of fluosilicate addition studied, no C_3A was detected below solidus temperatures. Also, the increased area of $C_{12}A_7$ss primary field causes the development of new invariant points in the lime-rich regions of both the C-A-F and C-A-S systems. The temperature of the "eutectic" or "peritectic" points are not necessarily the temperatures of first liquid formation, but are piercing points of the quaternary univariant curve proceeding toward an invariant point. At the temperature of the true invariant point the onset of fluxing action occurs through the formation of a very small amount of liquid. It is also noted in the C-A-S (+ flux) system (Figure 5) that the C_3S primary phase field area is enlarged considerably. This is in agreement with the published results for $C-C_2S-CaF_2$ system (14). Similarly, the existence of new pseudo-Alkemade line joining C_3S and $C_{12}A_7$ss in Figure 5 means that C_3S can be formed from

*Actually as discussed earlier, much SiF_4 is lost.

compositions for which it was previously impossible in the original system. Furthermore, the temperature of the quaternary invariant point, 1338°C among C_3S, C_2S, C_3A and C_4AF+L phases (7), which is most relevant to portland cement chemistry is further lowered by the addition of 5 wt % $CaSiF_6$, at a level of 5 wt % Fe_2O_3. Liquid is formed at temperature of ∿1300°C. However, the compatible phases are apparently C_2S + C_3S + $C_{12}A_7$ + C_4AF + L. With increasing percent of Fe_2O_3, the amounts of liquids at these temperatures were further increased. Formation of C_4AF in the quench runs was clearly observed by x-ray diffraction at compositions with 20 wt % Fe_2O_3. In some quench runs, unidentified peaks were observed in the x-ray diffraction patterns. They have been listed as unknown in the table. These were observed with compositions generally low in SiO_2 content and when C_3S was expected as an equilibrium phase. Continued efforts in progress will attempt to characterize such phase or phases in greater detail.

It is noted in conclusion that from the standpoint of phase equilibria, compositions apparently favorable for cements may lie near mixture #15 (Table 1) at 5 wt % levels of Fe_2O_3 and $CaSiF_6$. From such a composition liquid formation takes place at a much lower temperature than without flux, and reaction kinetics are accelerated. The latter factors are discussed in the partial papers by Christensen and Johansen (5), and by Klemm and Jawed (6).

ACKNOWLEDGEMENTS

The support for this research came from National Science Foundation Grant ENG7617217. The authors would like to thank J. Weigner for his assistance.

See Table II

p. I-200

REFERENCES

1. KLEMM, W.A. and SKALNY, J., Cements Research Progress-1976, 259-291, publ. by Amer. Cer. Soc., Columbus, OH (1977).

2. SARKAR, A.K., SMART, R.M., and ROY, D.M., Amer. Cer. Soc. Bull. 57 (3), 323 (1978).

3. SMART, R.M. and ROY, D.M., Cem. Concr. Res. 9, 269-274 (1979).

4. (a) SARKAR, A.K. and ROY, D.M., Amer. Cer. Soc. Bull. 58 (3), 354 (1979).
   (b) ROY, D.M. and SARKAR, A.K., Proc. Eng. Fnd. Conf., Rindge, NH, June (1979).

5. CHRISTENSEN, N.H. and JOHANSEN, V., Part II of three-paper series entitled "Mineralizers and Fluxes in the Clinkering Process," Proc. VIIth Intl. Congress Chem. Cem., Paris (1980).

6. KLEMM, W.A. and JAWED, I., Part III of three-paper series entitled "Mineralizers and Fluxes in the Clinkering Process," Proc. VIIth Intl. Congress Chem. Cem., Paris (1980).

7. LEA, F.M., The Chemistry of Cement, 3rd Edn., Edward Arnold, Glasgow (1970).

8. UCHIKAWA, H. and MATUZAKI, Y., Ceramics Japan 7 (4), 249-261 (1972).

9. GREENING, N.R., COPELAND, L.E., and VERBECK, G.J., Modified Portland Cement and Process, U.S. Patent 3,628,973, Dec. 21 (1971).

10. DAYAL, P.R. and GLASSER, F.P., Science of Ceramics, Vol. 3, Academic Press, London (1967).

11. OSBORN, E.F. and MUAN, A., Plate 1, The System $CaO-Al_2O_3-SiO_2$, publ. by Amer. Cer. Soc., Columbus, OH (1960).

12. MASSAZZA, F. and PEZZUOLI, M., Rev. Mater. Constr. Trav. Publics (642), 81-86 (1969).

13. MASSAZZA, F., PEZZUOLI, M. and GILIOLI, C., Rev. Mater. Constr. Trav. Publics (663), 357-663 (1970).

14. GUTT, W. and OSBORNE, G.J., Trans. Brit. Cer. Soc. 69 (3), 125-130 (1970).

Table 1. Results of Quench Experiments

Composition (wt %)				Temperature (°C) and the phases present
CaO	SiO_2	Al_2O_3	Fe_2O_3	
(1)52.25	16.15	26.60	5.00	1376, L+$C_2S(\beta+\gamma)$+$C_{12}A_7$+C_2AS; 1275, L(?) +$C_2S(\beta+\gamma)$+$C_{12}A_7$+C_2AS.
(2)50.83	7.60	36.57	5.00	1376, L+$C_{12}A_7$+β-C_2S; 1275, L+$C_{12}A_7$ +$C_2S(\beta+\gamma)$.
(3)62.05	16.65	16.30	5.00	1376, L+$C_2S(\beta+\gamma)$+$C_{12}A_7$+C_3S*; 1275, L(?) +$C_{12}A_7$+$C_2S(\beta+\gamma)$+C_3S.
(4)55.00	10.00	30.00	5.00	1357, L+$C_{12}A_7$+β-C_2S.
(5)57.00	4.00	34.00	5.00	1357, L+$C_{12}A_7$+Unknown; 1202, $C_{12}A_7$+C_3S +CaO.
(6)57.60	8.00	28.50	5.00	1357, L+$C_{12}A_7$+C_3S*+Unknown; 1202, $C_{12}A_7$ +C_3S.
(7)57.95	2.85	34.20	5.00	1357, L+CaO+$C_{12}A_7$+Unknown; 1202, CaO+ $C_{12}A_7$+ C_3S.
(8)40.85	15.20	38.95	5.00	1337, L+C_2AS+Unknown.
(9)44.17	11.40	39.43	5.00	1337, L+C_2AS+$C_{12}A_7$.
(10)56.52	11.88	26.60	5.00	1337, L+$C_{12}A_7$+$C_2S(\beta+\gamma)$.
(11)59.85	9.50	25.65	5.00	1337, L+C_3S+Unknown.
(12)40.85	3.80	50.35	5.00	1341, L+$C_{12}A_7$+CA_2+C_2AS*.
(13)66.50	9.50	19.00	5.00	1341, L+CaO+C_3A+C_3S.
(14)39.43	2.85	52.73	5.00	1341, L+$C_{12}A_7$+C_2AS+CA(?).
(15)66.40	16.66	11.95	5.00	1341, L+C_3S.
(16)56.61	22.09	16.30	5.00	1341, L+$C_2S(\gamma)$+C_2AS(?).
(17)40.38	44.65	9.97	5.00	1341, L+C_2AS.
(18)47.74	10.93	36.34	5.00	1341, L+$C_{12}A_7$+C_2AS+C_2S(?).
(19)42.75	7.13	45.13	5.00	1341, L+$C_{12}A_7$+C_2AS+CA_2*.
(20)44.65	8.08	42.27	5.00	1340, L+$C_{12}A_7$+C_2AS.
(21)59.85	2.85	32.30	5.00	1340, L+CaO+$C_{12}A_7$+Unknown.
(22)61.75	8.55	24.70	5.00	1340, L+$C_{12}A_7$+Unknown (C_3S?).
(23)59.85	12.35	22.80	5.00	1340, L+$C_{12}A_7$+Unknown (C_3S?).
(24)62.23	11.88	20.90	5.00	1334, L+$C_{12}A_7$+C_3S(?).
(25)60.80	13.30	20.90	5.00	1334, L+$C_2S(\beta+\gamma)$+$C_{12}A_7$+C_3S*.
(26)53.20	12.35	29.45	5.00	1334, L+$C_2S(\gamma)$+$C_{12}A_7$.
(27)49.40	12.35	33.25	5.00	1334, L+C_2AS+$C_{12}A_7$+β-C_2S.
(28)57.00	6.65	31.35	5.00	1338, L+$C_{12}A_7$+C_3S.
(29)50.35	14.25	30.40	5.00	1338, L+$C_2S(\beta+\gamma)$+C_2AS+$C_{12}A_7$.
(30)69.84	11.84	11.75	6.57	1300, L*+CaO+C_3S+C_3A(?); 1200, CaO+C_3S +$C_{12}A_7$.
(31)62.69	13.16	17.58	6.57	1300, L*+C_3S+$C_{12}A_7$;1200, C_3S+$C_{12}A_7$.
(32)62.23	21.85	9.35	6.57	1300, γ-C_2S+$C_{12}A_7$; 1200, γ-C_2S+$C_{12}A_7$.
(33)63.00	9.00	18.00	10.00	1336, L+CaO+C_3S+C_3A; 1325, L+CaO+C_3S +C_3A; 1307, L+CaO+C_3S+$C_{12}A_7$+Unknown; 1209, CaO+C_3S+$C_{12}A_7$+C_4AF+Unknown.
(34)56.70	11.70	21.60	10.00	1336, L+$C_{12}A_7$+γ-C_2S; 1325, L+$C_{12}A_7$+C_2S $(\beta+\gamma)$+C_3S*; 1307, L+$C_2S(\beta+\gamma)$+$C_{12}A_7$+C_3S; 1209, $C_{12}A_7$+C_4AF+C_3S+$C_2S(\beta+\gamma)$*+Unknown.
(35)53.55	11.25	25.20	10.00	1307, L+$C_{12}A_7$+$C_2S(\beta+\gamma)$+C_3S.
(36)54.00	6.30	29.70	10.00	1307, L+$C_{12}A_7$+$C_2S(\beta+\gamma)$+C_3S.
(37)54.00	15.30	20.70	10.00	1337, L+$C_{12}A_7$+γ-C_2S; 1325, L+$C_{12}A_7$+ $C_2S(\beta+\gamma)$.
(38)49.50	15.30	25.20	10.00	1336, L+C_2AS+γ-C_2S; 1325, L+C_2AS+$C_{12}A_7$ +γ-C_2S*; 1243, L+C_2AS+$C_{12}A_7$+γ-C_2S.
(39)41.85	10.80	37.35	10.00	1324, L+C_2AS+$C_{12}A_7$.
(40)40.00	33.60	6.40	20.00	1300, L+$C_{12}A_7$+C_2AS; 1200, $C_{12}A_7$+C_2AS.
(41)52.40	10.00	17.60	20.00	1200, $C_{12}A_7$+C_4AF+γ-C_2S; 1100, $C_{12}A_7$+C_4AF +Unknown.

*May be very little.
Mix numbers are given within parenthesis before each composition.

Mineral formation and Reactive Capacity of Portland Cement Raw Mixtures

Influence de la composition du cru sur la clinkérisation et la réactivité du ciment

P.V. ZOZULJA, Can.T.Sc. Leningrad Technological Institute, Leningrad, U.S.S.R.
E.A. RODIONOV, Engineer Department of Chemical Technology of Binding Materials.

RESUME : Les particularités du processus de cuisson ont été observées, en continu, par examen diffractométrique des différentes phases qui se forment et disparaissent, au cours d'un traitement thermique bien programmé. Cette méthode permet de déceler les différences, dans la clinkérisation, dues à la composition minéralogique du cru. On a pu ainsi classer les crus, en fonction de leur comportement au cours de la cuisson. On peut aussi en déduire l'efficacité de l'action des composants minéralisateurs et établir des règles sûres, quant à l'effet de variation de la composition du cru, sur sa réactivité.

SUMMARY: The peculiarities of diffractometric study of sintering processes technique are considered. The technique is based on the principle of continuous registering the changes of the analytical line of the phase which appears or disappears in heat treatment of the raw mixture sample according to the predetermined temperature condition. The suggested technique permits to discover the differences in the process of sintering raw mixture charges which are due to the mineralogy of the raw material, enables to classify the raw mixtures according to their behaviour in heating, allows to reveal and to estimate the effect of mineralizing components and is a safe foundation for the comparative estimation of the charge reactivity when its chemical and component composition is changed.

The change of the nature of raw mixture components influences considerably the progress of mineral forming processes both at the stage of hard-phase reactions [1,2] and at the final, liquid-phase stage of clinker formation.

To characterize differenses in the behaviour of raw mixtures during burning, several terms almost equal in their meaning are used in the chemistry and technology of clinker: sinterability, burnability, reactive capacity. Lately, a number of investigations has been carried out the authors of which try to depart from purely descriptive terminology and to work out the methods of obtaining criterial estimations of raw mixture thermal properties on the physico-chemical basis. The methods suggested for solving this task may be conditionally divided into three groups:

Methods of estimating reactive capacity on the basis of the properties of the original condition of raw mixtures and their separate components (reactivity [3], dispercity [4] etc.) may be included into the first group.

Methods based on the characteristics of the sintering process estimating the pequilarities of raw mixture thermal behaviour (according to the degree and the rate of free CaO assimilation by the thermogravimetric method [5], by the intensity of shrinkage deformations [6], by determining the heat of solution [7] and the changes of the heat content of the material in the course of burning, etc. are included into the second group.

Methods based on the calculated determination of the criteria regarding the role of the most important clinker formation parameters (viscosity, the melt amount, the ratio of minerals - silicates, dispercity, the role of admixture components, etc.) are included into the third group.

A great number of the methods suggested does not allow to reproduce and to compare the data obtained in different laboratories for estimating the reactive capacity. The direct measurement of the material heat content in the process of burning by means of high temperature differential microcalorimetry should be considered one of the prospective methods.

Nevertheless, the principal and most widely used method applied in most countries at present is the method of determining sinterability according to dinamics of changing the amount of free CaO. The combination of calculated and experimental approaches gives positive results [8], however the expenditures to the preliminary experimental study in this case are too great and the method itself does not exclude the possibility of mistakes as a result of the influence of unknown factors (for instance, the mineralogy of the raw material).

The task of stabilizing raw mixture compositions by employing new kinds of raw materials in the sphere of production and the usage of commercial wastes, the reduction of heat expenses, intensification and stabilization of the burning schedule, working out of the systems of automation control and the control of automatized technological processes require further development of the methods of rapid and reliable estimation of raw mixture behaviour in the process of burning and the estimation of the changes in their reactive capacity.

For the purpose of obtaining continuous information about the progress of mineral formation in the course of burning raw cement mix and for the reduction of time-consuming character of experiments determining the changes in the reactive capacity of raw mixtures the apparatus was elaborated at the department of chemical technology of binding materials, at the Leningrad Lensoviet Technological Institute. Also, the possibilities were studied to apply the method of Kinetic X-Ray-Phase Analysis (KRA) for the purpose mentioned. The method is based on the principle of continuous recording analytical X-ray diffraction intensity of the phase, appearing or disappearing in heating the investigated sample according to the predetermined schedule.

The realization of this method has become possible with the appearance of difractometers [9], lately this method has acquired wide application in studying the changes in the phase state as a result of various chemical and thermal processes taking place.

Let us consider the possibilities and the pequiliarities of applying the KRA method for studying the progress of mineral formation and the estimation of reactive capacity of cement raw materials. One may obtain valuable information or sintering process by continuous recording the dependance $I_{CaO_{free}} = f(t)$, where I_{CaO} is the diffraction line intensity of the phase CaO/ d/n - 2.405 in pulses per sec. and t - varying sample temperature. Since the diffraction line intensity is influenced by many factors the effect of which is difficult to control (the variation of the size, shape and the number of particles taking place in the diffraction, the influence of admixtures upon the recrystallization rate, variations in the kinetics of the processes taking place in the surface or inside the sample, etc.) the curves in the first approximation give information of the purely qualitative character. If it is necessary, however, they may be supplemented with chemical determination of CaO_{free} in various points of the curve that gives opportunity to compare quantitatively the data for different kinds of raw mixtures. The application of the difractometric method for the description of the curve CaO - f(t) allows to increase the informative character of these curves, gives the identical results, enables to consider the influence of the gas atmosphere (by changing the medium composition in heating the sample), decreases labour-

consuming character and reduces the time of the experiment and it also forms the basis for automatic calculation and for the treatment of the results.

The installation for the KRA includes diffractometer URS-50 IM with modified system of recording on the basis of scintillation detector, high temperature kiln which may reach temperatures up to 1500°C and has heaters made of platino-rhodium alloy containing 30 per cent of rhodium, a program unit with an electronic temperature controller, limiters of goniometer angular rotation, XY type two-coordinate recording potentiometer and temperature control potentiometer with temperature transducer. Block diagram of the apparatus is shown in Fig.1.

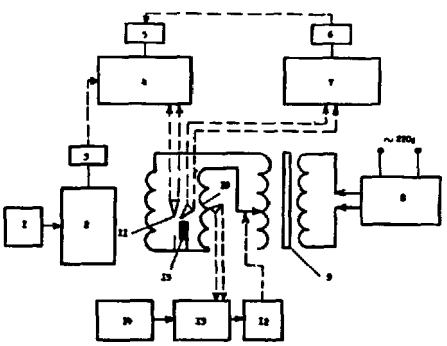

Fig.1. Block Diagram of the installation for Kinetic X-ray Phase Analysis.
1 - Revercing switch, 2 - goniometr, 3 - blocks of signal amplification and conversion, 4 - recording potentiometer, 5 - temperature register, 6 - photoelectric reley, 7 - control potentiometer, 8 - constant voltage regulator, 9 - voltage regulator, 10 - Platino-Rhodium heater, 11 - couples, 12 - Actuating Mechanism, 13 - Electronic controller, 14 - Program control point adjustment.

To obtain the KRA curves the powdery sample is pressed in the platino-rhodium cuvette having the size 8x15 mm. which is placed in the corundum holder of the high temperature kiln. In the course of heating according to the predetermined temperature schedule (usually rate of heating was 10 deg. per min.) recording is made of the shape of the analytical line of the chosen phase. It is made in the fixed range of angular reciprocal rotation of the counter (in this case diffraction intensity of CaO_{free} (d/n - 2.405 is registered). The rate of goniometer angular rotation amounts to 1-2 deg. per min. Time constant of the counting system is 5 sec. Integral curve of $I_{CaO_{free}} - f(t)$ is obtained by outlining the peaks of diffraction lines.

Over fifty samples of commercial raw mixtures from cement factories of the Soviet Union and raw mixture samples made in laboratory were investigated. Some typical examples of the curves are given in Fig.2. The cheking of the shape of KRA curves according to the method of titration of the samples heated according to the same schedule and sharply cooled in fixed points showed good agreement of the results.

It should be noted that in literature [6] the authors met rather detailed curves drawn according to the method of chemical titration of CaO_{free} which remind in their character the ones obtained by the KRA method. The data obtained by the authors allow to explain the shape of the curves from the point of view of raw material mineralogy influence and of a special course of mineral forming processes depending upon the reaction capacity of raw mixtures that is the basis of their composition optimization. The KRA curves give a rather visual evidence of the raw mixture reaction capacity and allow to classify them depending upon the character of mineral formation with considerably less time to obtain the necessary information than in the traditional method of obtaining the sinterability information by measuring the CaO_{free} content according to the method of successively burned samples.

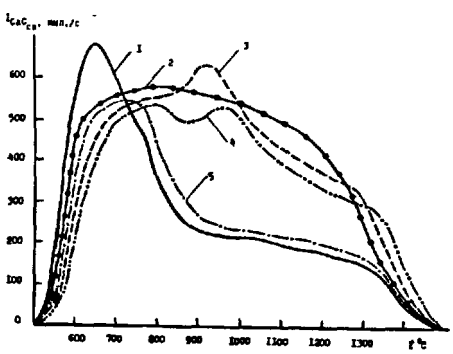

Fig.2. The Curves of Kinetic X-Ray Phase Analysis (KRA) for Various CaO_{free} Types of Raw Mixtures According to their Binding Kinetics. The explanation of the figures 1, 2,3,4,5 are given in the text.

Thus, for instance, Curve 1 shown in Fig.2 is characteristic for the cases when there is an effective mineralizer in the raw mixture. The mineralizing effect manifests itself in the change of temperature when the peak of CaO_{free} first appears, in the increase of the curve incidence and in the appearance of sharp peak, showing that, on the one hand, the speed of evolving CaO_{free} phase leaves behind its assimilation process and recrystallization and, on the other hand, the shape of the curve indicates to the rapid recrystallization and binding CaO with the rize of temperature. Curve 2 indicates to the high rate of dissociation of the carbonate component of the raw mix (in this case it is chalk) and, at the same time, to the retarded course of the mineralizing processes (and recrystallization) that shows

the low reaction capacity of the raw mixture.

Curves 3 and 4 are typical for the raw mixtures with low reaction capacity of the carbonate component (marble, hard limestone). Such type of the curves is characterised by shifting the intensity maximum of CaO_{free} peak to the area of higher temperatures (up to 900°C) and by the hampered binding of CaO into clinker minerals.

Curve 5 shows the made of binding CaO for the case when raw mixture contains considerable quantities of admixture oxides, such as R_2O, SO_3, MgO. Comparatively gently sloping part of the curve in the zone of higher temperatures indicates to the mineralizing effect of admixture components at the stage of hard-phase reactions and to the retardation of clinker-formation in the region of higher temperatures.

Considerable advantage of the KRA method is its continuity that allows to reveal some pequliarities of mineral formation which could be hardly found out, were the method of separate sample titration used. There is a depression in the curves of CaO assimilation when the intermediate compound, spurrite is formed in the range of temperatures in which hard-phase reactions take place. The depression appears as a result of binding carbonate component into a complex silico-carbonate phase spurrite, stable in air up to 940 - 950°C. The dissociation of this compound results in rapid evolution of new portions of CaO_{free} at high temperatures. In general, the formation of spurrite phase in raw mixtures seems to produce negative effect on the conditions of preparing raw mixtures for burning since the dissociation of spurrite takes place with great absorption of heat (50 k.kal/mole) and shifts the zone of material preparation to the range of higher temperatures promoting quick recrystallization and passivation of CaO_{free}. As to the commercial raw mixture samples, the formation of spurrite was characteristic for the cases when the loam component was represented by illite loams. Further experiments made with artificial mixtures of various carbonate rocks and silica components differing in their activity and dispersity (quarts, silicic acid, silica gel) in combination with other methods of analysis (petrography, DTA, dilatometry, high temperature X-Ray phase analysis) allowed to make a conclusion that combination of two factors promotes the formation of spurrite: low reaction capacity of carbonate component and high activity of silica one. Fig.3 shows the action of mineralizer Na_2SiF_6 when F content varies from 0 to 1 per cent.* The curves are reduced to the same scale by chemical determination of CaO_{free} in five points of the curve. Such an approach makes possible to determine exactly the effective concentration of mineralizer

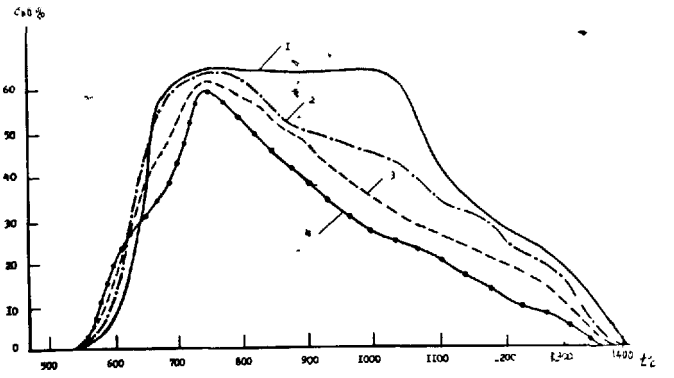

Fig.3. The Effect of Concentration of Mineralizer upon the Change of CaO_{free} Binding Character.
1 - 0%, 2 - 0,25%, 3 - 0,5%, 4 - 1% Na_2SiF_6.

in the raw mixture. The changes in the KRA curves with the increase of mineralizing addition content are characteristic and typical ones and allow to make a qualitative estimation and classification of the raw mixture components in the first approximation, these components being used in practice as the intensifiers of the burning process (for example, various complex commercial wastes, rocks, etc.). Varying heating conditions one can obtain KRA curves in the same scale irrespective of the heating rate (recording in coordinates $I_{CaO_{free}} - f(t)$ that gives opportunity to obtain CaO_{free} easily comparable data on the influence of thermal treatment conditions upon the course of mineral formation. Such a technique may be used for obtaining the optimum burning schedule.

Thus, the curves of the kinetic X-Ray phase analysis (KRA) are the basis for the classification of raw mixtures depending upon the mineralogy and with regard to their reactive capacity, they make possible to obtain important information on the progress of mineral formation, allow to determine the effective action of mineralizing additions and to take into consideration the influence of variations in raw mixture chemical composition upon sinterability.

BIBLIOGRAPHIE

1. Ur.M.Butt, V.V.Timashev (1967), Porland Crment Clinker, Moscow (rus.) pp.97-109.

2. S.D.Makhashev (1976). "The Influence of Pisico-Cemical Raw Material Properties upon the Reactive Capacity of Raw Mixtures and upon the Processes of Clincer Mineral Formation". Proc. of the Sixth Intern. Congr. on the Chem. of Cement, Moscow (rus.) vol.I, pp.156-161.

3. E.Jirku (1947). "Determination of Cement Raw Material Reactive Capacity", Stavivo Check.) p.451.

* The results and the treatment of the experimental data for this part of the work were done by Dolbilova I.B.

4. Zalama I.Z. (1973. "Free Silica in Raw Mixture Portland Cement Materials". Cemento-Hormigon (sp), vol.VXLIV, n°649, pp.295-302; 307-313.

5. P.Longe (1968). "Application of Thermogravimetric Method of Analysis in the Chemistry of Cement" (Supplementary Report). Proc. of the Fifth Intern.Congr. on the Chem. of Cement, Tokyo,Moscow (rus.), vol.i, pp.81-82.

6. E.Sulikovskii (1968). "The Ability of Raw Mixtures to Burning" (Supplementary Report). Proc. of the Fifth Intern.Congr. on the Chem. of Cement, Tokyo, Moscow, 1973, (rus.), vol.1, pp.47-49.

7. M.V.Kougia, A.A.Gnedina (1977) "On the Methods of Cement Raw Mixtures Estimation". Inst.Nil Cement Moscow. vol.42, pp. 3-15.

8. H.Koch, G.Rey, F.Bekker (1968). "Statistical Model for the Determination of the Suitability of Raw Mixtures for Producing the Clincer." Proc. of the Sixth Intern. Congr. on the Chem. of Cement, Tokyo, Moscow 1973 (rus.), vol.1, pp.154-156.

9. A.Guinier (1961). Crystal Radiography. Moscow (rus.), pp.190.

Microscopical estimation of burning condition and quality of clinker

Estimation microscopique de la résistance du ciment

Y. ONO, Dr. Engineering, Senior Research Chemist, Central Research Laboratory of Onoda Cement, Japon.

RESUME : Le clinker pulvérisé ou le ciment est immergé dans l'huile et observé au microscope. Les dimensions et la birefringence des cristaux d'alite, les dimensions et la couleur des cristaux de bélite sont fonction des conditions de cuisson, du mode de chauffage, de la température maximale, de la durée du temps de chauffage et du mode de refroidissement. La résistance à la compression du ciment à l'âge de 28 jours peut être estimée d'après ces caractéristiques cristallines. La contribution de la température maximale et celle du mode de refroidissement sont les plus importantes.

L'erreur de l'estimation microscopique, écart quadratique moyen, est 17 kg/cm^2 par JIS. En comparaison de l'erreur de la mesure actuelle de la résistance (10 kg/cm^2 environ ou plus) et de l'erreur de l'estimation du module hydraulique, de la chaux libre, de la surface spécifique Blaine et de la résistance à l'âge de 7 jours (27 kg/cm^2), la précision de l'estimation microscopique est raisonnable.

SUMMARY : The pulverized clinker or cement is immersed in an oil and observed by polarizing microscope. Crystal size of alite and birefringence of alite, crystal size of belite and color of belite, change corresponding with the change of burning condition, heating rate, maximum temperature, burning time and cooling rate, respectively. From the above terms, the compressive strength at 28-day can be estimated. The contribution of maximum temperature and cooling rate is the most important.

The estimation error, root of mean square variance, is 17 kg/cm^2, JIS. Comparing with the error of actual strength test, about 10 kg/cm^2 or more, and the estimation error from HM, free lime, Blaine and 7-day strength, 27 kg/cm^2, the microscopical estimation error is reasonable.

INTRODUCTION

Microscopical observation is the most handy method to check the quality of cement. Cement or clinker powder is immersed in an oil, and observed by a polarlizing microscope. The observation time is 5 or 10 minutes. The popular checking terms are fineness of cement, freshness of cement, free lime content, admixtures and so on. Moreover, the microscopical characters of clinker minerals show the burning condition of clinker and the hydraulic activity.

The microscopical method has been successfully used on the quality control in Onoda Cement plants for more than 15 years. Recently, the method has been used in many plants in Japan, the USA and Canada.

BURNING CONDITION AND QUALITY OF CLINKER

The burning conditions are simplified as Fig. 1, and shown with the four terms: burning rate, maximum temperature, burning time and cooling rate.

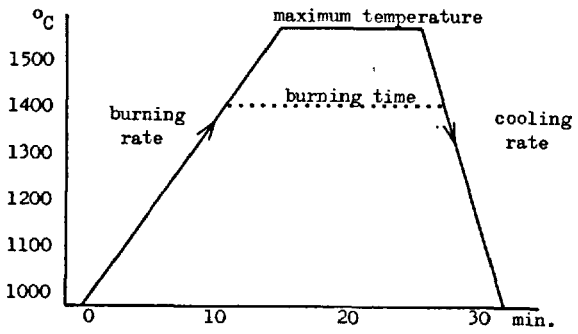

Fig. 1. Schematic temperature-time relation of clinker burning.

The relations between the burning conditions and the microscopical characters of clinker minerals are rather simple, and we have many experimental and thecretical knowledges.

The relations between the hydraulic activity and the microscopical characters are complicated. There are many factors, which are closely related with activity, but can not be detected by microscope. However, the principal parts of the factors can be derived from the burning conditions, which can be detected by microscope. And so, the 28 days strength can be predicted by microscopical observation.

The early strength, at 1, 3 and 7 days, is strongly influenced by the particle size distribution of cement, the contents of alkali and sulfates, C_3A solid solution and probably many other unknown factors. Therefore, the early strength can not be predicted by microscopical observation.

The strength of cement principally depends on the activity of clinker minerals and the contents, and the fineness of cement. Usually the chemical composition, the content of free lime and fineness of cement are controlled in a narrow region. The detection of the activity of the clinker minerals in the cement is the most important factor for the estimation of the cement strength.

The activity of alite and belite changes according to the change of the temperature modifications, the content of impurities and the crystallinity. The kind of the temperature modifications can be detected from the optics and the inversion textures. The contents of impurities and the crystallinity can be deduced from the estimated burning conditions.

In principle, a high temperature form is unstable at room temperature, and is more active than the low temperature forms. The high temperature form stabillized completely in a solid solution is inactive.

In order to obtain the high temperature forms of alite and belite at room temperature, alite and belite must contain a large amount of impurities at burning temperatures. The solubilities are large at high temperatures, and small at low temperatures. The time at low temperatures, pre-ignition zone, must be possibly short. Possibly large amount of alite and belite must crystallize or recrystallize at high temperatures. The rate of diffusion of impurities in alite and belite is small.

Table 1. The relation between the burning condition, hydraulic activity and microscopical characters of alite and belite.

Hydraulic activity:	Excellent(+)	Good(vv)	Average(v)	Poor(-)
Burning rate	Quick	.....		Slow
Size of alite (μ)	15-20	20-30	(25)30-40	40-60(120)
Maximum temperature	High	.....		Low
Birefringence of alite	0.010-0.008	0.007-0.006	0.006-0.005	0.005-0.002
Burning time	Long	.....		Short
Size of belite (μ)	(20)25-40(60)	(15)20-25	(10)15-20	5-10
Cooling rate	Quick	.....		Slow
Color of belite	Clear(C)	faint Yellow(fY)	Yellow(Y)	Amber(A)

High crystallinity of alite and belite at high temperatures and quick cooling are also favorable. In order to attain the high crystallinity, clinker must be burnt at high temperatures for an adequate time. The disorder due to thermal vibration and rotation seems to be the center of inversion. Quick cooling from the lower limits of the stable temperature region of the high temperature form is favorable. However, it is not so easy to attain the ideal cooling curve in actual kiln operation, slow cooling from maximum temperature to the lower limit temperature and quick cooling.

The favorable burning conditions are "quick burning", "high maximum temperature", "long burning time" and "quick cooling".

BURNING CONDITION AND MICROSCOPICAL CHARACTER

Size of Alite

The size of alite principally depends on the burning rate and the crystallization rate.

If clinker is burnt quickly by short flame, a small part of alite crystallizes at low temperatures, and large part of alite crystallizes at high temperatures. The first crystallization at low temperature occurs by direct contact of CaO and C_2S. The crystallization rate is quick, and the crystal size is small. The crystallization rate at high temperatures is also quick, and the crystal size is small.

If clinker is burnt slowly by long flame, large part of alite crystallizes at low temperatures. In this case, CaO and C_2S recrystallizes into large crystal, and the crystallization rate of alite becomes slow, except at the first crystallization stage, and the crystal size of alite is large.

The crystal growth of alite by recrystallization with cannibalism is slow and negligible.

The size of alite in poor burnt clinker is small. This fact does not show that the size of alite depends on the burning temperature and burning time. In this case, low temperature raw material is near the discharge end of kiln, and temperature jumps, for example, from 1100°C up to 1450 °C, and the crystallization rate is quick. In the clinker of 1000 ton per day kiln, less than 15 microm alite shows danger of poor burning. In the clinker of 4000 ton per day kiln, less than 20 microm is danger.

Birefringence of Alite

The birefringence of alite principally depends on the burning temperatures and the kind of temperature modifications. The highest temperature form, R-form, has the highest birefringence, 0.007 to 0.010. The disordered M-I form having remains of R-form, or M-III form after I. Maki,[3] has the next high birefringence, 0.005-0.007. Ordered M-I form has moderate birefringence, 0.004-0.005. Low temperature form, T-II, has low birefringence, less than 0.004.

D. H. Campbell shows a list of birefringences of alite reported by many workers. He pointed out that alite birefringences determined by powder mount and thin section are different. In addition, birefringences given for alite by several other workers show wide differences.

S. Chromy[2] studied the birefringence of alite by high temperature microscope. He found that R-form has a low birefringence at high temperature, and high birefringence at low temperatures, in the stable temperature region of R-form. The birefringence of M-form is the same as R-form at low temperature, and the birefringence of T-form is very low.

The low birefringence of R-form at high temperatures may be due to the thermal vibration and rotation, and R-form with low birefringence can not be quenched to room temperature.

Alite crystallized at low temperature, near the lower limit of the stable region, which is 1250°C for pure C_3S, contains a small amount of impurities, and inverts into low temperature forms through the cooling process. Alite crystallized at high temperatures contains a large amount of impurities, and R-form or disordered M-form with high birefringence is cooled to room temperature. Practically, birefringence of alite changes continuously according to the burning temperatures.

The birefringence of alite crystals occurring in a clinker nodule is not the same each other. Small alite crystal occurring near the cluster of free lime has low birefringence. Large or middle size alite crystal near the cluster of belite has high birefringence. Isolated alite, which may be blown and burnt in the high temperature flame, has very high birefringence.

I. Maki[5] found that alite in the clinker containing MgO higher than 1.5% is M-III form with high birefringence, and alite in the clinker less than 1.5% MgO is M-I form with low birefringence. In Japanese cements, the MgO content is usually controlled from 1.5 to 1.8 %. If MgO content is less than 1.5%, serpentine or olivine is added to the raw mixture. Therefore, alite in Japanese cement seems usually M-III form. The author has not sufficient data on the clinkers, which contain MgO higher than 1.8% and lower than 1.5%. However, alite in high MgO clinker has high birefringence, about 0.001 higher than normal clinker shown in Table 1, and alite in low MgO clinker has low birefringence, about 0.001 lower than Table 1.

Alite is weak against mechanical grinding and chemical attack of moisture, and the birefringence strikingly decreases.

Size of Belite

At low temperatures, 1100-1200°C, belite crystallizes in a minute crystal of alpha prime form, and the crystal growth by cannibalism is slow. At about 1400°C, alpha prime form changes into alpha form. Crystal growth of alpha form is quick. Therefore, the crystal size of belite corresponds with the time maintained above 1400°C.

The crystal growth of belite differs according to the temperatures and circumstances. Feldspar melt reacts with CaO, and coarse alpha belite crystallizes from the melt. This belite is rich in alkali and colorless. Minute belite occurs from iron rich slags. The crystal growth is slow.

Color of Belite

At the highest temperature of clinker burning, belite is alpha form, except very poor burnt clinker. The solubility of Al_2O_3, Fe_2O_3 and Na_2O in alpha form is about 2%, 2% and 3%, respectively. [2] The change of solubility in the temperature range of clinker burning is small. The solubilities of the above elements in alpha prime form are nearly zero, less than 0.5%.

At the highest temperature, alpha belite is satulated with Al_2O_3 and Fe_2O_3, and contains an equilibrium amount of alkalis. Through the cooling process, alpha form changes into alpha prime form, and next into disordered beta form. The impurities in solid solution are satulated in alpha prime form and exsolved in colloidal dispersion state in belite. The color of belite changes from colorless to faint yellow, yellow and amber, according to the slow down of cooling rate.

If clinker is cooled quickly, about 40% alpha phase remains between the fine lamellas of disordered beta form, and exsolution of impurities does not occur. The belite is colorless.

If clinker is slowly cooled in the temperature range of 1400°C to 1300°C, alpha to alpha prime inversion takes place on the surface of belite through the melt of interstitial materials. The lamellas of alpha prime elongate into the interstitial melt, and the surface of belite becomes rough. The depressed cavities are filled with iron bearing phases, an the grain of belite cluster in cement shows deep amber color. The color is not the color of belite itself.

ESTIMATION OF 28 DAYS STRENGTH

The author and his staff[9] studied hydraulic activity of clinker minerals and strength of cement for more than 20 years. In 1965, the author and Y. Soda reported the survey of cement in Japanese market, and showed the change of activity of alite and belite is more important than the change of chemical composition, free lime and fineness of cement for the estimation of 28 days strength. In 1975, K. T. Mau, Vice President of Cyprus Hawaiian Cement Corporation, promoted a private seminar in Hawaii, Microscope Analysis Work Seminar. After the seminar, the author prepared a table on the relation between 28 day strength and burning condition, for the request of K. T. Mau and the participants.

Recently, K. Ogawa and S. Hanehara, staff of the author, statistically analized the data of Japanese cement reported in 1965, and calculated linier multi regression equation, between 7 and 28 days actual mortar strength and several available, using IBM 370-135 computer. From the equation, they made a new table on the relation between the 28 days strength and burning conditions. The difference between the table prepared in 1975 and the new table is less than 20 kg/cm^2, except very weak cement.

Table 2. Data of Japanese cement, reported in 1965

Cement Samples:

46 ordinary cements in Japanese market, 1962 and 1963.

Notation of Terms, Used for Calculation:

Hydraulic Modulus: HM, free lime %: FL,
Blain's specific surface cm^2/gr: BL,
Size of alite: AS, Birefringence of alite: AB,
Size of belite: BS, Color of belite: BC,
7 and 28 days strength kg/cm^2 in JIS: 7d and 28d,

The grade of AS, AB, BS and BC are written in points, after the notation of J. Prout[6] as follows.
Excellent: 4, Good: 3, Average: 2, Poor: 1.

Terms of Cement Samples: Mean, Maximum, Minimum and Standard Deviation:

	HM	FL	BL	AS	AB	BS	BC	7d	28d
Mean	2.08	0.71	3244	2.19	2.39	3.12	2.50	206	386
Max.	2.21	2.0	3610	3.5	4	4	4	256	455
Min.	2.00	0.2	3010	1.5	1.5	2	0.5	165	298
S.D.	0.04	0.30	131	0.52	0.60	0.74	1.38	24	40

The standard deviation of equation 1 and 4 in Table 3, estimation of 7 and 28 days strength from HM, free lime and Blain, is 23.6 kg/cm^2 for 7 days strength, and 37.8 kg/cm^2 for 28 days strength. The standard deviations, estimation errors, are practically equal to the standard deviations of cement strength, strength distribution, shown in Table 2, 24 kg/cm^2 for 7 days and 40 kg/cm^2 for 28 days. Equation 1 and 4 have no meaning of estimation.

Table 3. Multi regresive equations for estimation of 7 days and 28 days strength, standard deviation and regresive coefficient

		R.C.	S.D.
1)	7d = 83 + 52(HM) − 21(FL) + 0.009(BL)	0.29	23.6
2)	7d = 167 + 1.2(AS) + 18.8(AB) − 10.3(BS) + 9.5(BC)	0.74	16.7
3)	7d = 96 + 61(HM) − 18(FL) − 0.012(BL) + 2.9(AS) + 19.9(AB) − 13.1(BS) + 8.4(BC)	0.77	16.5
4)	28d = 228 + 51(HM) − 54(FL) + 0.028(BL)	0.42	37.8
5)	28d = 133 − 8(HM) − 29(FL) + 0.017(BL) + 1.1(7d)	0.77	26.8
6)	28d = 253 + 6.4(AS) + 21.9(AB) + 4.0(BS) + 21.5(BC)	0.91	17.1
7)	28d = 67 + 109(HM) − 22(FL) − 0.005(BL) + 7.7(AS) + 22.3(AB) + 0.6(BS) + 20.7(BC)	0.93	16.1
8)	28d = 175 + 0.5(7d) + 5.8(AS) + 13.1(AB) + 8.9(BS) + 17.0(BC)	0.93	15.4
9)	28d = 31 + 86(HM) − 15(FL) − 0.000(BL) + 0.4(7d) + 6.6(AS) 14.8(AB) + 5.5(BS) + 17.6(BC)	0.94	15.1

The regresive coefficients of equation 2 and 3, estimation of 7 days strength from microscopical data and adding HM, free lime and Blain, are 0.74 and 0.77. The regresive coefficients show that the correlation between 7 days strength and microscopical data is strong. However, the accuracy of estimation is unsatisfactory.

When 7 days strength is known, 28 days strength can be estimated from HM, free lime, Blain and 7 days strength, using equation 5. However, the estimation accuracy, 26.8 kg/cm^2, is less than microscopical estimation, 17.1 kg/cm^2, of equation 6. The accuracy of microscopical estimation can be improved adding HM, free lime, Blain and 7 days strength, up to 15.1 kg/cm^2 of equation 9. However the improvement from 17.1 kg/cm^2 to 15.1 kg/cm^2 is not so large.

K. T. Mau[5] wrote me that the Study of the Uniformity of Cement Strength conducted by the joint PCA/NRMCA Technical Liaison Committee was held from 1976 to 1977, and 120 grab samples were tested. The standard deviation of the microscopical estimation of 28 days strength was 220 lb/in^2 in ASTM, which was 16.3 kg/cm^2 in JIS.

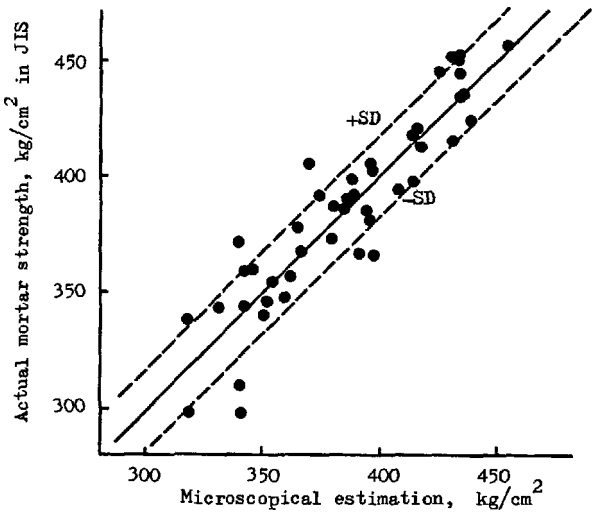

Fig. 2. Microscopical estimation of 28 days strength, calculated from equation 6. SD = 17.1 kg/cm^2.

Table 4. Effect of burning condition on 28 days strength, kg/cm^2 in JIS.
+: excellent, vv: good, v: average, -: poor, refer to Table 1.

Max. Temp.		+				vv				v				-			
Burn Time		+	vv	v	-	+	vv	v	-	+	vv	v	-	+	vv	v	-
Rate of Burn	Cool																
+	+	470	465	460	455	445	440	440	435	425	420	415	410	405	400	395	390
	vv	445	445*	440*	435	425	420*	415*	415	405	400	395*	390	380	375	375	370
	v	425	420	415	415	405	400	395	390	380	375	375*	370	360	355	350	350
	-	405	400	395	390	380	380	375	370	360	355	350	350	340	335	330	325
vv	+	460	460	455	450	440	435	430	430	420	415	410	405	395	390	390	385
	vv	440	435*	430*	430	420	415*	410*	405	395	395	390*	385	375	370	365	365
	v	420	415	410	405	395	395	390	385	375	370	365*	365	355	350	345	340
	-	395	395	390	385	375	370	365	365	355	350	345	340	330	330	325	320
v	+	455	450	445	445	435	430	425	420	410	410	405	400	390	385	380	380
	vv	435*	430*	425	420	410*	410*	405*	400	390	385*	380*	380	370	365	360	355
	v	410	410*	405	400	390*	385*	385*	380	370	365*	360*	355	345	345	340	335
	-	390	385	385	380	370	365	360	355	345	345	340	335	325	320	315	315
-	+	450*	445	440	435	425	425	420	415	405	400	395	395	385	380	375	370
	vv	430*	425*	420	415	405*	400	400	395	385	380	375	370	360	360	355	350
	v	405	400	400	395	385*	380	375	370	360	360	355	350	340	335	330	330
	-	385	380	375	375	365	360	355	350	340	335	335	330	320	315	310	305

Note:
Underline: Japanese cement in 1962-1963, 500-700 t/d kilns.
Asterisk(*): Japanese cements in 1975-1979, 3000-8000 t/d kilns.

Recent 10 years, rotary kilns in Japan have been changed from old type of 500-700 t/d to modern SP kiln with precalcination burner of 3000-8000 t/d. Enviromental pollution with SOx and NOx are prohibited by law Fuel oil is going to be changed to coal and others. Nowadays, the burning conditions are floating, looking for the best conditions. The flame changed from short to long, and the burning zone was deeper, 20-40 m from the discharge end.

The burning conditions are shown as follows in order, / burning rate, maximum temperature, burning time, cooling rate /, after the notation of Table 1. For example, the burning condition,/ burning rate is average(v), maximum temperature is good(vv), burning time is excellent(+), cooling rate is good(vv)/, is shown as (v, vv, +, vv). The 28 days strength is 410 kg/cm^2, after Table 4.

DISCUSSION

The microscopical analysis of clinker, shown in this paper, was prepared for the purpose of kiln site daily test. The terms of microscopical observation and the relation between the schematic burning conditions and the 28 days strength are possibly simplified. This method has been used in the plants of Onoda Cement as the most reliable guidance for the control of kiln operation. However, this microscopical method is never complete.

J.Prout of St. Mary's Cement Company, Ontario,[6] pointed out that very small alite is indicative of under burn, and optimum belite size range will depend on flame conditions. His comments are absolutely correct. Although, Table 1 shows that quick burning and small alite is better than slow burning and large alite, and long burning time and large belite is better than short burning time and small belite. Excessive quick burning and excessive long time burning result in failure. For example, the clinkers asterisked, shown in Table 4 as excellent burning rate, (+,+,vv,vv)=445, (+,+,v,vv) =440, (+,vv,vv,vv)=420, (+,vv,v,vv)=415; contain free lime 1.0-2.0 %, and the actual mortar strengths are lower than the tables. The clinkers were burnt by RSP kilns of 5200 t/d. The limit of alite size must be determined comparing with actual test. After the settlement of SP kiln operation, Table 1 and 4 will be rewritten.

E.Fundal of F.L.Smidth, Kopenhagen,[7] precisely measured the size of alite and the birefringence of alite. The terms of microscopical observation have wide distributions, and the precise measurements are troublesome. Although, precise measurements are important on basic studies. The merit of microscopy is overall sensitive observation and not in precise measurement.

B.Osbaek of Kopenhagen[8] shows that the effect of alkali on the 28-day strength is around -10 MPa per 1 % soluble alkali expressed in K_2O equivalents, and the estimation error is 2.7 MPa, which is about 20 kg/cm^2 in JIS. The estimation error may be the smallest in estimation from chemical analysis. The author has several data showing close relation between alkali content and strength of cement. The combination of alkali and microscopy will be hopeful to increase the accuracy of strength estimation. However, SP clinker contains all alkali of raw materials without expulsion, and alkali content of clinker does not change by burning conditions.

REFERENCES

1) D.H.Campbell. "Comparative microscopy of foreign and North American clinker, a preliminary study". Portland Cement Association, USA, June 1979
2) S.Chromy. "High-temperature microscopical investigation of tricalcium silicate and dicalcium silicate phase in portland cement clinker". J.Am.Ceram.Soc., Vol.50, No.12, 677-681 (1967)
3) I.Maki and S.Chromy. "Microscopic study on the polymorphism of Ca_3SiO_5". Cement and Concrete Research, Vol.8, 407-414 (1978)
4) I.Maki and S.Chromy. "Characterization of the alite phase in portland cement clinker by microscopy". Il Cemento, Vol.75, July-September, 247-252 (1978)
5) K.T.Mau. "Application and experience in the use of Dr.Y.Ono's microscopic analysis".Advanced Microscopy Seminar, held in Skokie, Illinois (PCA) on October 24-25, 1979.
6) J.Prout. "Summary of interpretation of data from the ONO test". Short Course of Microscopy of Clinker and Cement, PCA, Skokie, Illinois, November 7-11, 1977.
7) E.Fundal. "Microscopic analysis of clinker, comments on the method developed by Y.Ono". Private communication, February 1, 1978.
8) B.Osbaek. "Der Einfluss von Alkalien auf die Festigkeitseigenschaften von Portlandzement". Z-K-G.,32 J., Nr.2, 72-77 (1979)
9) Y.Ono and Y.Soda. "Effect of the crystallographic properties of alite and belite on the strength of cement". Semento Gijutsu Nenpo (Technical Meeting of Japan Cement Association), Vol.17, 93-103 (1965)

Anomalies de cuisson - Structures microscopiques Propriétés des clinkers et ciments

Burning anomalies - Microscopic structures Clinkers and cements properties

E. DEMOULIAN - P. GOURDIN - F. HAWTHORN - C. VERNET, Société des Ciments Français
CEREG, France.

RESUME

Ce texte est une synthèse de nombreuses études de clinkers et ciments effectuées au CEREG par microscopie optique avec le support d'autres techniques d'analyses telles que la fluorescence et la diffraction des rayons X.

Le thème retenu est l'étude du domaine de stabilité de l'alite et des paramètres industriels qui peuvent le réduire.

La vitesse de refroidissement des clinkers, l'atmosphère réductrice dans les fours sont des paramètres qui ont été étudiés par différents chercheurs.

La présence de matières combustibles naturelles ou ajoutées avec ou sans fluor dans les crus de cimenteries, les fortes teneurs en anhydride sulfurique et les faibles teneurs en alcalins dans les clinkers peuvent avoir des effets identiques. Les anomalies constatées sont mises en relation avec les propriétés des clinkers et ciments dans chaque cas considéré.

Des conditions et des matériels de fabrication doivent être modifiés pour éviter les inconvénients mis en évidence.

SUMMARY

This paper is a synthesis of several clinker and cement studies carried out at the CEREG by optical microscopy and other technical analysis such as X ray fluorescence and diffraction.

The subject chosen is the study of alite stability and industrial parameters which could reduce it.

Cooling time and reducing atmosphere in the kiln have been studied by many authors. The presence of burnable materials with or without fluorine in raw materials, heavy percentages of SO_3 and low percentages of alkalis in clinkers have the same effects. The observed anomalies are related to clinker characteristics and cement performances in each case.

Conditions and manufacturing equipment should be modified to avoid the disadvantages described.

INTRODUCTION

Dans le cadre des économies d'énergie, plusieurs usines de la SOCIETE des CIMENTS FRANCAIS consomment des matières à bas pouvoirs calorifiques telles que résidus charbonneux, schistes houillers, cendres volantes, scories, déchets industriels divers inutilisables dans d'autres types de fours. L'introduction de ces matières combustibles dans les crus, l'utilisation de poussières ferrugineuses, de fluorine qui permettent des économies substantielles d'énergie noble, nous ont donné l'occasion de mettre en évidence des processus de rétrogradation de l'alite qui n'étaient pas apparus auparavant (1)(2)(3)(4). Le mécanisme d'oxydation des matières combustibles contenues dans les crus est différent dans chaque procédé de fabrication, ce qui a posé à notre Société, divers problèmes technologiques à résoudre pour éviter les anomalies de cuisson. Les différents processus de rétrogradation de l'alite rencontrés au cours de nos examens au microscope optique sont décrits dans cette étude.

1/ CUISSON PROLONGEE, REFROIDISSEMENT LENT

Les examens de trois boules de clinkers qui ont longuement séjourné dans la zone de clinkérisation montrent les différences de caractéristiques suivantes par rapport au clinker normal (Photographies 1 à 10) : la porosité diminue fortement, les cristaux d'alite se soudent entre eux, les inclusions de divers minéraux dans les cristaux d'alite disparaissent, les aluminates n'existent plus en tant que phase interstitielle, mais en petites plages à l'intérieur des cristaux d'alite qui se sont anormalement développés par cannibalisme et phagocytose, les cristaux de bélite ont aussi de fortes dimensions. Au coeur des boules de clinker, les plages de C_3A sont consTellées d'exsolutions de bélite secondaire et certains cristaux d'alite ont subi une rétrogradation partielle en chaux libre et bélite secondaires. Les taux d'alite et de bélite augmentent alors que la quantité de phase interstitielle diminue fortement. Le C_3A cubique disparait plus rapidement que le C_3A tétragonal.

Les examens par diffraction X montrent que l'alite M_{Ib} s'est transformée en alite T_3 par exsudation d'éléments en solution solide (figure 10 bis). La bélite α présente dans le clinker normal a disparu.

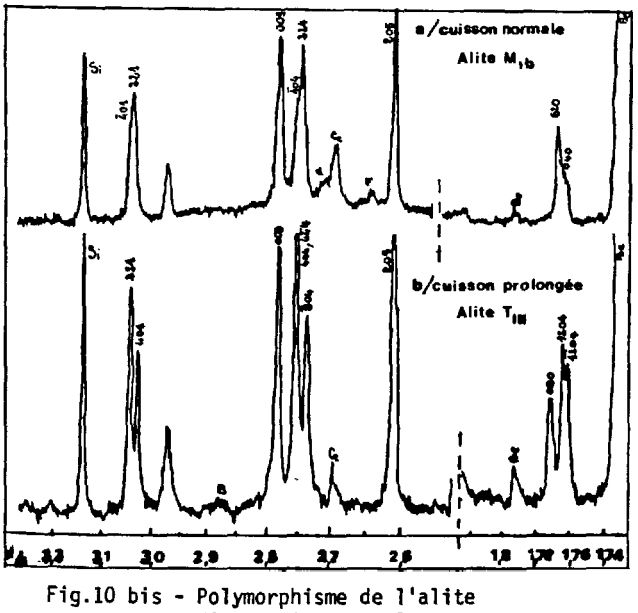

Fig.10 bis - Polymorphisme de l'alite par suite d'une cuisson prolongée.

Les modifications des propriétés physiques et mécaniques sont les suivantes : la broyabilité du clinker diminue de 10 à 20 %, les temps de prise des CPA augmentent d'une heure, leurs résistances en compression baissent de 50 % à 8 heures, 30 % à 24 heures, 20 % à 2 jours, 10 % à 28 jours. Les variations enregistrées sont dues aux faibles taux de C_3A, à la croissance exagérée des cristaux de silicates concomittante avec leur épuration et la transformation allotropique de l'alite M_{Ib} en alite T_3, moins réactive à court terme.

2/ ATMOSPHERES REDUCTRICES DANS LES FOURS

Les clinkers cuits en atmosphère localement réductrice ont une écorce grise sur une épaisseur variable et un noyau beige à roux. L'écorce est grise par oxydation dans la zone terminale du four et dans le refroidisseur. Dans le clinker beige à roux, l'alite est partiellement rétrogradée.

Quand le clinker a été refroidi très rapidement, le C_3A et le C_4AF sont enchevêtrés, il est alors possible de diagnostiquer une rétrogradation due à une atmosphère réductrice, sinon, le C_3A et le C_4AF coexistent en plages séparées, le C_3A et l'alite présentent les mêmes caractéristiques qu'au cours d'un refroidissement lent, il est alors difficile de préciser la cause des rétrogradations observées. Les descriptions précédentes sur les différences de couleur entre zones internes et externes des grains de clinker sont beaucoup plus spécifiques d'une rétrogradation par atmosphère réductrice que par refroidissement lent ; d'autre part avec les refroidisseurs modernes, les anomalies de rétrogradation par refroidissement lent sont très rares, seuls les très gros morceaux de clinker peuvent en présenter. Les conséquences sur les propriétés des clinkers et ciments sont les suivantes : la densité du clinker augmente et sa broyabilité diminue. La teinte des ciments est plus claire : dans l'échelle des W*C.I.E., l'augmentation peut atteindre 2 à 3 points ; la maniabilité des ciments diminue : l'augmentation du pourcentage d'eau de gâchage peut être cause de fissuration : les baisses de résistances peuvent atteindre 10 % à 2 et 7 jours et 20 % à 28 jours : elles sont compensées par broyage plus poussé des ciments.

3/ MATIERES COMBUSTIBLES DANS LES CRUS DE CIMENTERIES

Les matières combustibles présentes dans les crus ont des actions différentes suivant le procédé de cuisson considéré.

3.1 - Fours à voie humide

Les produits charbonneux pulvérulents s'agglomèrent en petits amas qui se mélangent mal avec les autres constituants de la pâte. Après son introduction dans le four, deux cas extrêmes peuvent être envisagés. Dans le premier cas, la pâte est totalement sèche avant sa sortie des chaînes dont les derniers rangs servent de broyeur. Il en sort un produit pulvérulent dans lequel les matières combustibles brûlent avant la zone de clinkérisation et ne perturbent pas la formation des minéraux. Dans le second cas, qui est souhaitable sans combustible dans le cru, la pâte contient encore 6 à 7 % d'eau, les derniers rangs de chaînes granulent ce produit ; les granules brûlent avec défaut d'oxygène jusqu'à la sortie du four. Pendant la clinkérisation les surchauffes locales dues à la présence d'agglomérats de combustible donnent au clinker un aspect localement scorifié avec pour effet une augmentation ponctuelle de la porosité alvéolaire (photographies 11 et 12). Dans ces plages, l'alite du clinker est aciculaire et elle est plus ou moins rétrogradée. L'intensité des rétrogradations est inversement proportionnelle à la porosité des grains de clinker (photographies 13, 14 et 15). On note aussi la présence de périclase dans les clinkers sui contiennent

environ 1 % de magnésie (photographie 16).
Les conséquences sont les suivantes : la broyabilité des clinkers diminue de 10 à 15 %, les baisses de résistances des ciments sont les mêmes que dans le cas précédent et peuvent aussi être compensées par des finesses un peu plus importantes, des gonflements retardés sont à craindre comme le montre la photographie 17. Quand des produits charbonneux pulvérulents ou des goudrons sont injectés par une tuyère latérale, les risques de formations d'anneaux sont fortement accentués et le clinker produit contient aussi de l'alite rétrogradée.

3.2 - Fours voies semi-sèche et semi-humide

Les matières combustibles séquestrées à l'intérieur des granules se comportent comme dans le deuxième cas précédent, sauf dans les fours longs, équipés de croisillons qui peuvent émietter les granules.

3.3 - Fours voie sèche intégrale

Le cru est introduit sous forme pulvérulente, les matières combustibles brûlent avant d'arriver dans la zone de clinkérisation du four, mais quand l'argile est remplacée par des cendres volantes on constate des anomalies sur les retours d'électrofiltre : les cendres volantes subissent des séparations sélectives dans les cyclones et les électrofiltres, ces ségrégations ont pour conséquence la formation d'agglomérats enrichis en carbone et sesquioxyde de fer ou en silice et alumine. Les charges électrostatiques de ces agglomérats leurs donnent une cohésion suffisante pour résister aux contraintes mécaniques jusqu'à leur retour dans le four où ils favorisent la formation de petites boules de clinker très dures enrichies en phase interstitielle, que l'on retrouve de ce fait dans les refus de broyeurs. Cette anomalie est supprimée par adjonction d'un sélecteur sur les retours d'électrofiltre.

4/ PRESENCE SIMULTANEE DE FLUOR ET DE MATIERES COMBUSTIBLES

L'usine concernée est équipée de deux fours voie semi-sèche de 1200 et 1700 T/jour. Dans le cadre des économies d'énergie, l'aptitude à la cuisson du cru a été améliorée par l'utilisation de 4 % de schiste houiller d'un pouvoir calorifique de 1500 Th/T et de 0,5 % de fluorine. Les gains de thermies dus à ces deux ajouts sont additifs et varient entre 100 et 120 Th/T de clinker produit, soit une économie annuelle de 10.000 tonnes de fuel pour les deux fours. L'inconvénient est que le milieu réducteur créé par le schiste entraîne, en présence de fluorine, un allongement des temps de prise, qui passent de 2 h en moyenne à 5 h.

Analyses chimiques
Les bilans effectués montrent que 95 à 97 % du fluor introduit avec le cru sort avec le clinker. L'influence fortement retardatrice des fluorures alcalins est connue : les retards peuvent facilement atteindre 4 h avec 0,5 % de NaF, mais par une méthode mise au point à cette occasion, nous avons montré que le fluor contenu dans ces ciments n'était pas sous forme de fluorures alcalins très rapidement solubles dans l'eau de gâchage.

Examens au microscope optique
Ces examens ont montré que les temps de prise étaient d'autant plus longs que les clinkers étaient plus réduits et les cristaux d'alite plus rétrogradés. Parallèlement, la quantité de périclase et de chaux libre secondaire augmente dans les mêmes conditions (photographies 18 à 24).

Analyses par diffraction des rayons X
Dans les clinkers réduits, les analyses montrent l'augmentation des taux de bélite et de C_3A au détriment de l'alite et de C_4AF, l'augmentation de la chaux libre et du périclase, la disparition du $C_{11}A_7CaF_2$.

Interprétation
Les résultats fournis par les trois méthodes amènent à conclure que le $C_{11}A_7CaF_2$ n'est pas stable en atmosphère réductrice (5)(6). dans un milieu apprauvri en oxygène, la tendance des ions F^- à remplacer les ions O^{2-} dans les minéraux des clinkers semble très fortement augmentée. Les ions F^- libérés au cours de l'hydratation des ciments semblent avoir la même action que les ions F^- des fluorures alcalins solubilisés pendant le gâchage.

5 - RAPPORTS MOLAIRES ALCALINS/ANHYDRIDE SULFURIQUE

Les teneurs respectives en alcalins et en anhydride sulfurique dans les clinkers ont des incidences sur leur porosité, fragilité, granulométrie et sur la morphologie de leurs silicates.

5.1 - Influence sur la granularité et la fragilité

Les clinkers dont le rapport alcalins/SO_3 est voisin ou supérieur à 1 se caractérisent par les porosités montrées sur les photographies 25 et 26 : la zone corticale des grains est compacte et solide. La granularité des clinkers dépend essentiellement de leur composition chimique et minéralogique, du système de préparation et de cuisson du cru, du temps de cuisson à des températures supérieures à 1300°C, de la température maximale de cuisson.
Les clinkers dont le rapport alcalins/SO_3 est nettement inférieur à 1 se caractérisent par les porosités montrées sur les photographies 27 et 28 : la cohésion est beaucoup moins importante, la zone corticale est très fragile, les clinkers contiennent 30 à 50 % d'éléments inférieurs au mm (Photographies 29 et 30).

5.2 - Influence sur la morphologie des silicates

Les cristaux d'alite et de bélite ont des dimensions d'autant plus importantes que le rapport alcalins/SO_3 est plus faible et le taux de SO_3 plus fort (Photographie 31 et 32). Nous constatons aussi la présence de deux sortes de cristaux d'alite : les uns à bordures nettes comme sur la photographie 31, les autres à bordures plus ou moins corrodées sur une épaisseur variable (photographies 33 à 35). Ce type de rétrogradation qui débute par la bordure des cristaux ne ressemble à aucun des cas cités auparavant. La raison de ces rétrogradations semble être fournie par les minéraux intermédiaires qui se forment pendant la fabrication de ces clinkers.

5.3 - Interprétations
Influence sur la granulométrie.
Le rapport alcalins/SO_3 a une incidence directe sur la formation de certains minéraux intermédiaires dans les fours. Quand il est voisin ou supérieur à 1, le principal composé sulfaté mis en évidence au-dessus de 1300°C est K_2SO_4, quand il est nettement inférieur à 1, les composés intermédiaires mis en évidence sont $(CaO.Al_2O_3)_3.CaSO_4$ et $CaSO_4$.
Le sulfate de potassium dont les points de fusion et d'ébullition sont respectivement 1069°C et 1689°C distille progressivement jusqu'à la sortie du four et même dans le refroidisseur où il se condense ensuite en surface et dans les pores des grains du clinker. Leur cohésion n'est pas perturbée par cette distillation lente et elle est même renforcée par la condensation. Au contraire, la décomposition rapide de $(CaO.Al_2O_3)_3.CaSO_4$ et de $CaSO_4$ au-dessus de 1300°C

perturbe fortement la structure interne et superficielle des grains de clinker. La fragilité de la zone corticale est accentuée par le recyclage et la réagglomération tardive de poussières en provenance du refroidisseur.

Influence sur la taille des cristaux de silicates.
Le pouvoir minéralisateur des sulfates calciques est fortement accentué dans les fours industriels car ils y provoquent des recyclages beaucoup plus importants que les sulfates alcalins.

Influence sur la rétrogradation de l'alite.
L'aluminate de calcium sulfaté se décompose tardivement dans les fours en donnant C_3A et SO_4^{2-} qui est alors disponible pour entrer en solution solide dans le réseau de l'alite qui devient rhomboédrique (7).
La réaction suivante peut être envisagée :
$(CaO.Al_2O_3)_3.CaSO_4 + 5\ CaO + O^{2-} \rightarrow 3(3CaO.Al_2O_3) + SO_4^{2-}$
Pour que cette réaction puisse se produire, il faut de fortes teneurs en chaux libre au voisinage de l'aluminate de calcium sulfaté. Si cette chaux libre est disponible, les cristaux d'alite ne sont pas rétrogradés (photographie 31). Si la chaux libre n'est pas disponible elle est apparemment prélevée sur l'alite (photographies 33 à 35) quand les temps de réaction sont suffisants.
Il est donc très important pour la production de ces types de clinkers que le cru soit très homogène, qu'il soit fortement saturé en chaux, que le temps de cuisson entre 1300°C et 1450-1500°C soit suffisamment long pour permettre la transformation complète de $(CaO.Al_2O_3)_3.CaSO_4$ en C_3A. Si cette transformation n'est pas complète on risque de retrouver du $(CaO.Al_2O_3)_3.CaSO_4$ dans le produit fini avec pour conséquences des temps de prise courts et des gonflements anormaux même avec peu de chaux libre dans le clinker (8).

CONCLUSIONS

Au cours de cette étude, nous avons tenté de montrer une des facettes de l'apport de la microscopie optique à la compréhension de quelques unes des très nombreuses mutations dans les fours de cimenteries qui transforment les minéraux naturels des crus en minéraux artificiels des clinkers.
Cette recherche était principalement basée sur le domaine de stabilité de l'alite et sur les paramètres industriels qui peuvent le réduire.
Les économies notables d'énergie réalisées en introduisant des matières combustibles dans les crus de cimenteries ont des incidences sur la stabilité de l'alite et sur les propriétés des clinkers et ciments.
Nous avons montré différents processus de dégradation de l'alite influencés par les procédés de cuisson et par la présence d'éléments mineurs tels que fluor, soufre, alcalins. Le polymorphisme de l'alite a aussi été mis en cause à deux reprises.
Pour pallier les inconvénients cités, les ingénieurs des usines ont dû modifier des conditions et des matériels de fabrication.

REMERCIEMENTS

Les auteurs remercient MM. BERTIN et MAES pour les travaux effectués au CEREG en microscopie et en diffraction X.

BIBLIOGRAPHIE

1. - E. PADILLA - Variazoni nella costituzione mineralogica di clinker e agglomerati di cemento rimasti a lungo in zona di cottura (1953).
2. - K.AKATSU, K.HIGUCHI - On the strength and color of the portland cement clinker burned under reduction atmosphere - Tokyo (1957).
3. - Contribution from the Haupt Laboratorium Portland Cementwerke Heidelberg A.G. - Fourth International Symposium of the Chemistry of Cement - Washington D.C. (1960).
4. - E.WOERMANN - Decomposition of alite in technical cement clinker - Nordic Cement Colloquium - Copenhagen (1972).
5. - F.MASSAZZA et M.PEZZUOLI - Equilibre à l'état solide dans le système quaternaire CaO - Al_2O_3 - SiO_2 - CaF_2 - R.M.C. n° 642 (1969).
6. - F.MASSAZZA, M.PEZZUOLI, G.GILIOLI - Relations d'équilibre dans le système quaternaire CaO - Al_2O_3 - Fe_2O_3 - CaF_2 - R.M.C. n° 663 (1970).
7. - P.GOURDIN, E.DEMOULIAN, F.HAWTHORN, C.VERNET - Polymorphisme de l'alite et du C_3A. Statistiques.
8. - Ciment expansif - Brevet Poliet et Chausson n° 813977 (1936).

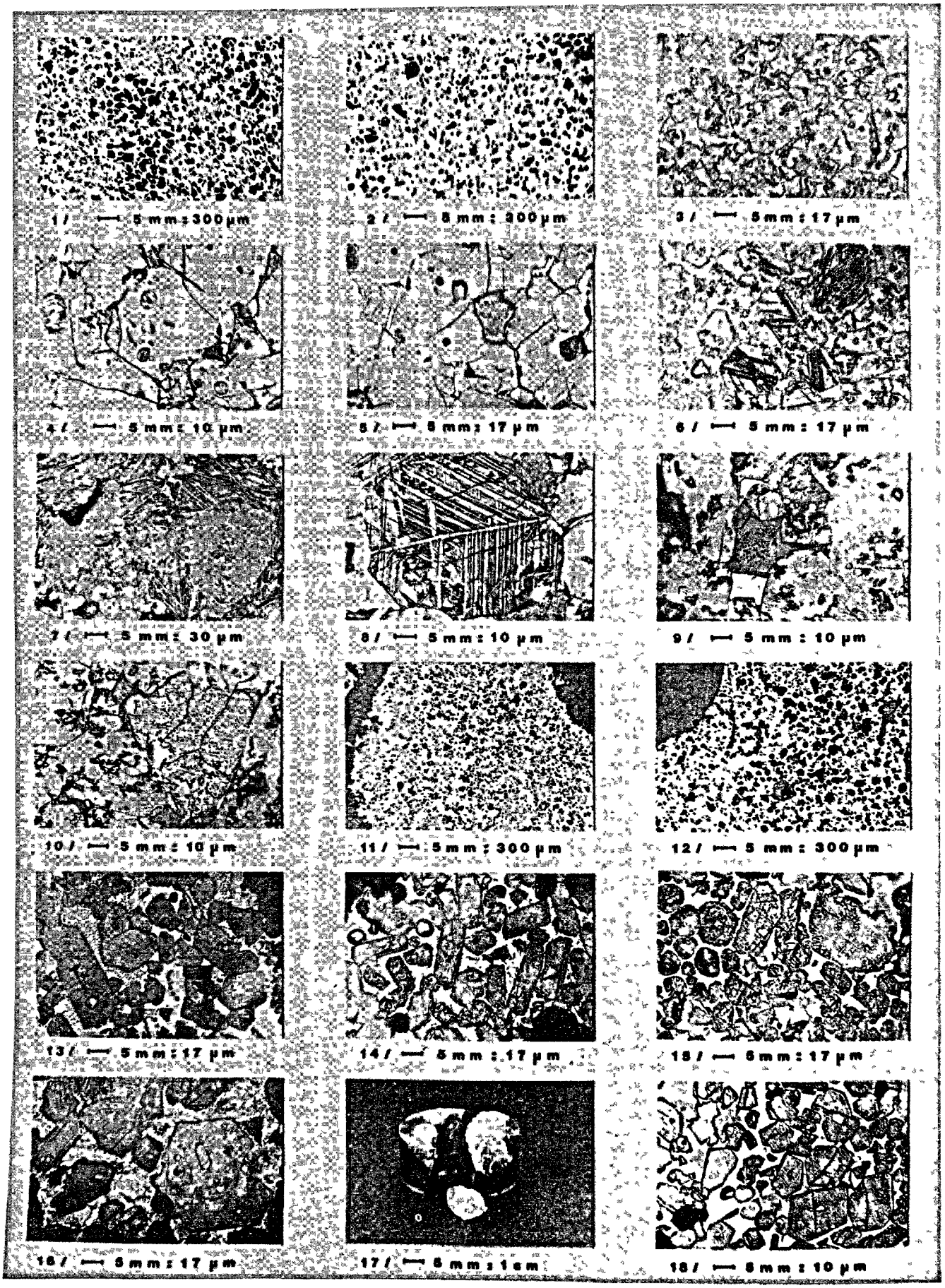
1 / — 5 mm : 300 µm
2 / — 5 mm : 300 µm
3 / — 5 mm : 17 µm
4 / — 5 mm : 10 µm
5 / — 5 mm : 17 µm
6 / — 5 mm : 17 µm
7 / — 5 mm : 30 µm
8 / — 5 mm : 10 µm
9 / — 5 mm : 10 µm
10 / — 5 mm : 10 µm
11 / — 5 mm : 300 µm
12 / — 5 mm : 300 µm
13 / — 5 mm : 17 µm
14 / — 5 mm : 17 µm
15 / — 5 mm : 17 µm
16 / — 5 mm : 17 µm
17 / — 5 mm : 1 cm
18 / — 5 mm : 10 µm

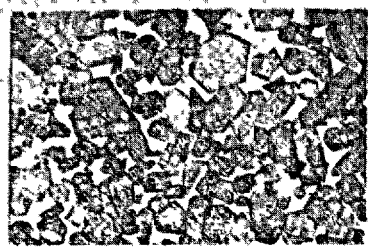

19/ ⟷ 5 mm : 17 µm

20/ ⟷ 5 mm : 17 µm

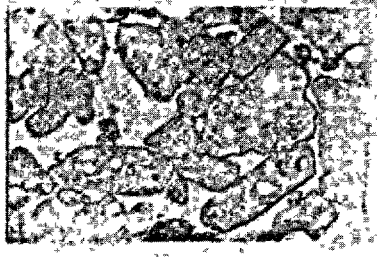

21/ ⟷ 5 mm : 10 µm

22/ ⟷ 5 mm : 17 µm

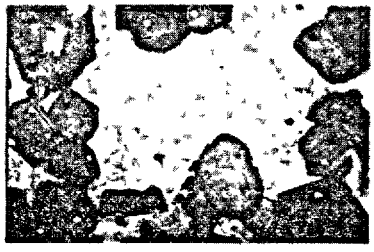

23/ ⟷ 5 mm : 17 µm

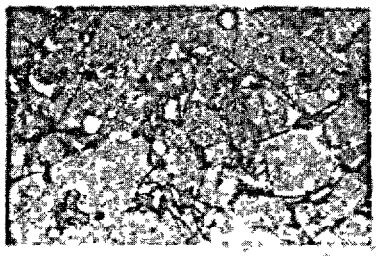

24/ ⟷ 5 mm : 10 µm

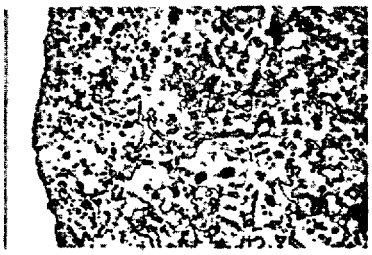

25/ ⟷ 5 mm : 300 µm

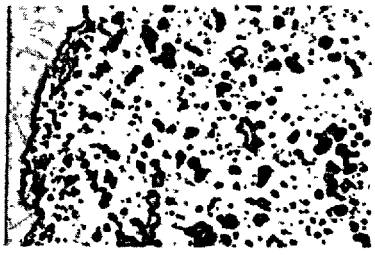

26/ ⟷ 5 mm : 300 µm

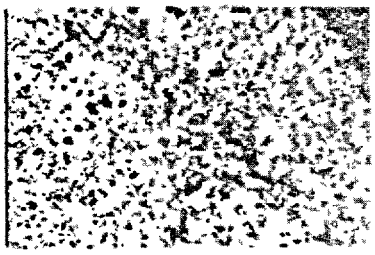

27/ ⟷ 5 mm : 300 µm

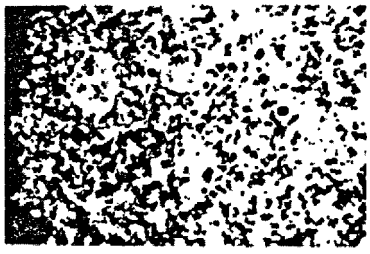

28/ ⟷ 5 mm : 300 µm

29/ ⟷ 5 mm : 8 mm

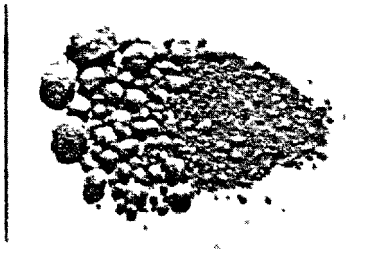

30/ ⟷ 5 mm : 15 mm

31/ ⟷ 5 mm : 17 µm

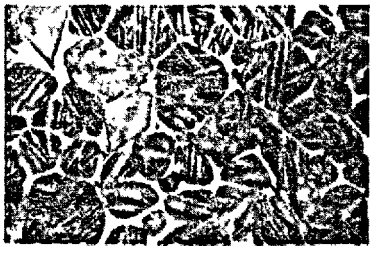

32/ ⟷ 5 mm : 17 µm

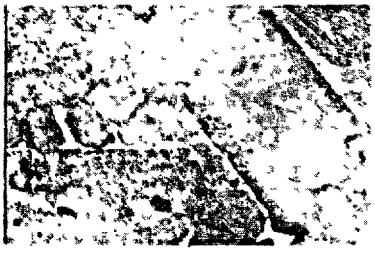

33/ ⟷ 5 mm : 17 µm

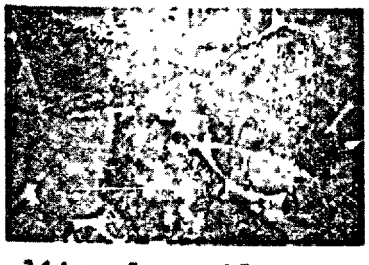

34/ ⟷ 5 mm : 17 µm.

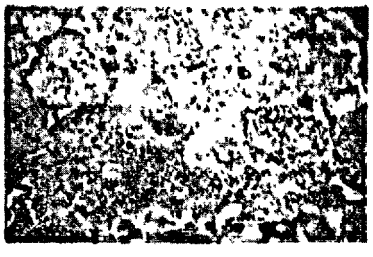

35/ ⟷ 5 mm : 30 µm

36/ ⟷ 5 mm : 5 µm

La célite dans les ciments portland obtenus par fusion

Celite phase in portland cements from molten products

J. MOISSET, B. COTTIN, A. PETIT - Lafarge S.A.,
A. ROUANET, Laboratoire des Ultra-Réfractaires, C.N.R.S., France.

RESUME : Un cru de ciment Portland est traité au four solaire à des températures supérieures à la température de solidification dans l'air ou sous atmosphère réductrice pendant des temps très courts (quelques secondes). La vitesse de refroidissement peut être modérée (10^2 deg. sec^{-1}) ou rapide (10^5 deg.sec^{-1}). L'examen par diffraction X des produits traités met en évidence la cristallinité de toutes les phases ainsi que la réduction partielle ou totale du fer intervenue dans la phase liquide et son incidence sur la nature des phases. On note enbparticulier une destruction de la phase aluminoferrite de calcium qui induit la libération d'une fraction de la chaux et la formation d'aluminate tricalcique.

SUMMARY : Raw materials of Portland cement composition have been melted by means of a solar furnace at T >Tsolidification in air or reducing atmosphere for a short time (few seconds). The cooling rate may be medium (10^{-2} deg.sec^{-1}) or high (10^5 deg.sec^{-1}). X-ray diffraction analysis showed crystalized phases and on another hand the phenomenon of a partially or wholy reduction of iron involved at the liquid state. Characteristics of the molten products due to this reduction are : the desappearing of calcium aluminoferrite and, inductively, the formation of a quantity of lime and the growth of tricalcium aluminate.

A. INTRODUCTION.

Dans les clinkers obtenus dans les conditions habituelles de fabrication industrielle par frittage (de cru de ciment Portland au four rotatif), on obtient principalement de l'alite et un peu de bélite. La phase interstitielle entre la bélite et l'alite contient de la chaux, de l'alumine et des oxydes de fer. Elle a été identifiée par plusieurs auteurs comme étant une solution solide C_4AF - C_6A_2F nommée célite. La composition exacte de cette phase interstitielle est controversée. Certains auteurs considèrent que C_6A_2F est lui-même une solution entre C_2F et un hypothètique C_2A. Mais le C_2A ne peut-il pas être considéré comme une solution solide de $C_{12}A_7$ et de C_3A ? Le diagramme C - A - Fe_2O_3 a été étudié par plusieurs auteurs et Newkirh et Thwaite ont établi le détail d'une portion du diagramme C - CA - C_2F avec les zones de solution solide représentées par des hachures.

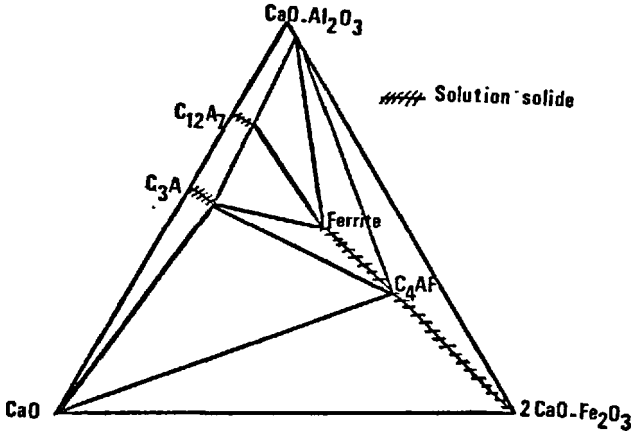

System : $CaO-CaO.Al_2O_3-2CaO.Fe_2O_3$

Dans cette étude nous avons essayé de connaître en première approche, le comportement du fer dans le clinker à partir d'une phase liquide supposée homogène obtenue par fusion totale d'un cru industriel de ciment Portland. Cette solution subit un refroidissement jusqu'à la température ordinaire pour donner un "clinker fondu" dans lequel le fer apparaîtra dans la phase interstitielle sous formes Fe°,Fe^{++}, Fe^{+++}.

Il est important semble-t-il de prendre en considération les quatre paramètres fondamentaux qui influencent l'état du système au cours du traitement thermique :

- la concentration des constituants
- la température T du système au proche voisinage de l'équilibre thermodynamique,
- les pression et nature du gaz,
- le temps t intervenant au cours du refroidissement ($\Delta T/\Delta t$ vitesse moyenne estimée du refroidissement).

Ces quatre paramètres peuvent conjointement jouer sur :

a) les phénomènes physiques :

- ségrégation entre phases comprises entre les liquidus et solidus,
- cristallisation des phases,
- vaporisation sélective d'une ou plusieurs espèces.

b) les phénomènes chimiques :

- réduction totale ou partielle du fer,
- réduction à l'état solide entre phases au cours du refroidissement.

B. EXPERIMENTATION.

Le traitement des matériaux à partir de l'état liquide est effectué au foyer d'un four à concentration de rayonnement solaire équipé pour opérer dans l'air ou sous atmosphère réductrice. Un dispositif de trempe rapide de type splat cooling permet d'atteindre des vitesses de refroidissement élevées.

On a envisagé quatre cas de figures pour les traitements thermiques :

- (C_1) et (C_2) : traitement dans l'air avec refroidissement normal (par simple rayonnement du produit traité après occultation du rayonnement solaire) et hypertrempe,
- (C_3) et (C_4) : traitement sous atmosphère réductrice (Argon + Hydrogène) avec refroidissement normal et hypertrempe.

1) Fusion du cru dans l'air.

Nous avons utilisé des petits fours solaires de 1,5 à 2 kW dits à axe vertical. Ils sont essentiellement constitués par un grand miroir plan (héliostat) de 4,5 m sur 6,5 m qui renvoie le rayonnement solaire sous forme de faisceau parallèle sur un miroir parabolique, ce dernier concentrant le rayonnement reçu en son foyer (Fig. 1).

La tache focale obtenue mesure environ 1 cm^2 et la température peut atteindre jusqu'à 3000°C. Dès que l'on s'écarte du foyer, celle-ci diminue de façon notable. Si l'on s'élève (ou descend) dans le cône de lumière, la vitesse de refroidissement sera plus faible que si l'on s'écarte horizontalement du foyer.

Ces petits fours solaires présentent deux avantages :

- énergie chimiquement pure éliminant tout risque de contamination du matériau avec l'élément chauffant,
- énergie dirigée permettant de chauffer l'échantillon sur un support réfrigéré sans interaction chimique entre ce dernier et le produit traité.

La fusion classique consiste à placer le produit à traiter sur un support en cuivre réfrigéré et à l'amener au foyer à l'aide d'un chariot. La fusion est extrêmement rapide et le produit fondu se présente sous la forme d'un globule de 1 cm de diamètre environ. Le retrait de la pla-

tine (support) du foyer provoque un refroidissement de quelques centaines de degrés/sec.

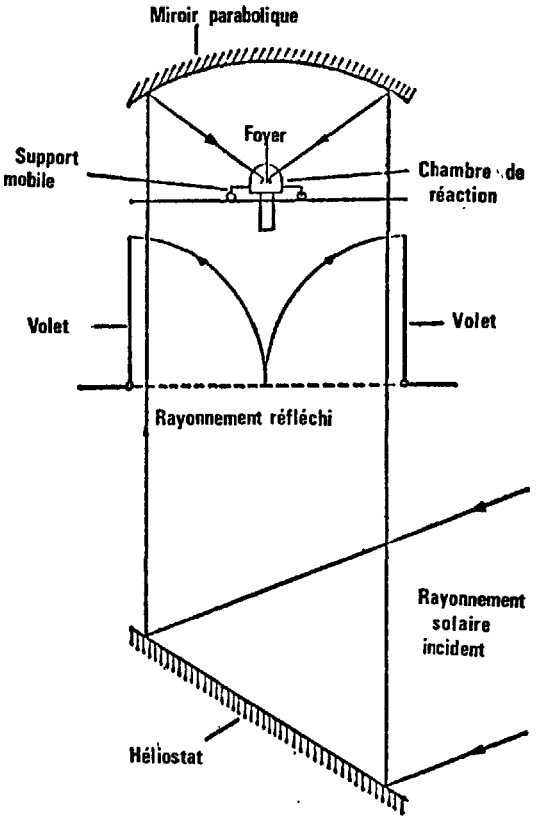

Fig. 1 - Schéma de principe d'une installation à axe vertical.

On peut également obtenir des produits hypertrempés à l'aide d'un montage du type "marteau-enclume", par écrasement du globule fondu (Fig. 2).

Le marteau est une masse de cuivre légèrement convexe qui vient s'ajuster dans la platine réfrigérée ayant la forme d'un creuset. Dès que la fusion s'établit, on laisse tomber le marteau sur le globule et on obtient alors des feuillets très fins de l'ordre de quelques dizaines de microns. La vitesse de refroidissement est estimée à 10^5°C/s.

2) Fusion du cru solaire sous atmosphère réductrice.

Ce montage permet de travailler sous atmosphère contrôlée et de refroidir le produit fondu soit naturellement par retrait du foyer, soit en l'hypertrempant par écrasement de l'échantillon entre deux surfaces métalliques amenées brutalement en contact.

Le shéma de l'appareillage est représenté Figure 3. La masse de produit (∿ 0,5 g) préalablement fondue sous forme de globule, est portée à l'état liquide au foyer du four solaire. Le marteau coulissant sur des roues de guidage est soumis à une force mécanique variable par un ressort. Il peut ainsi être maintenu en position tension par un électro-aimant ou libéré brusquement sur l'échantillon fondu avec une vitesse variable (10 m/s au maximum). L'énergie de l'ensemble marteau-enclume, après la trempe du produit est absorbée par un amortisseur hydraulique.

Le profil des pièces d'écrasement a été conçu de manière à ne tremper que la partie liquide du globule fondu. L'occultation du rayonnement solaire n'intervient que dans la phase finale du processus. On évite ainsi un refroidissement du matériau avant le début de la trempe. L'ensemble de l'appareil est disposé à l'intérieur d'une capacité étanche permettant d'introduire un gaz quelconque sous une pression inférieure ou égale à la pression atmosphérique. Il est

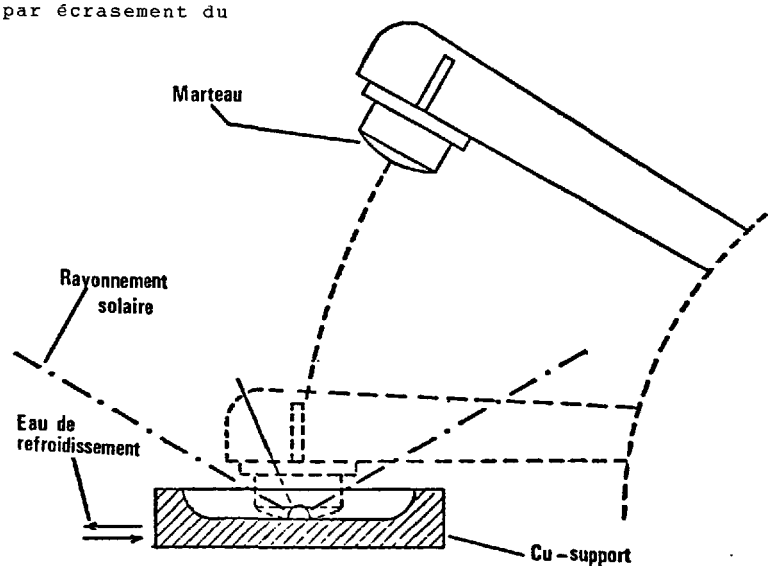

Fig. 2 - Appareil d'hypertrempe associé à un four solaire à axe vertical.

également possible d'établir un courant gazeux permanent. Le rayonnement solaire pénètre au travers d'une coupole hémisphérique transparente de faible absorption. Les échantillons obtenus par hypertrempe se présentent sous forme de feuillets d'épaisseur comprise entre 10 et 50 µ selon la nature du produit. La vitesse de trempe est estimée à environ 10^4°C par seconde.

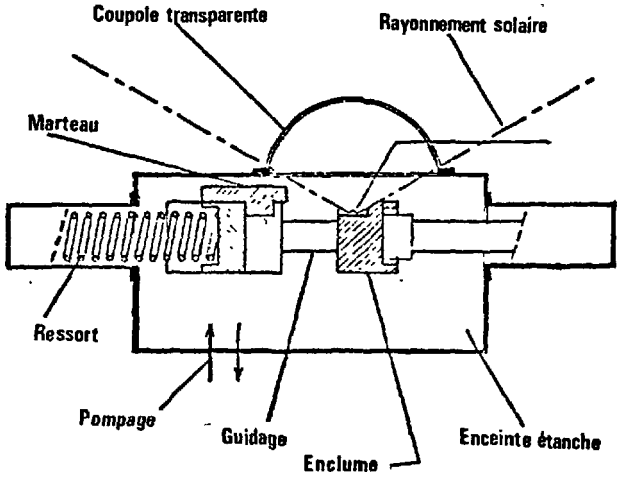

Fig. 3 - Dispositif d'hypertrempe en atmosphère contrôlée, associé à un four solaire : schéma de principe.

C. RESULTATS.

1) Les différentes phases après traitements thermiques sont observées par diffraction X (on a utilisé la radiation CuKα).

Ainsi (Figures 4 et 5) :

- Dans le cas du clinker (C_1) le pic du C_3A ($2\theta = 33°.4$) est faible. Il est même dans ce cas inférieur à celui que l'on obtient dans le clinker industriel fabriqué à partir du même cru. Celui de l'alumino-ferrite (2θ : 33°.7) atteint une dimension arbitraire de 76. La chaux n'apparaît pas et les pics correspondants au C_3S et C_2S sont normaux.

- Dans le cas du clinker (C_2), hypertrempé la phase C_3A s'est considérablement accrue et l'aluminoferrite disparaît. La teneur en chaux libre n'est pas nulle bien que non évaluable par diffraction X. Un recuit de 24 h à 900°C redonne le spectre de diffraction X du produit C_1.

- Dans les cas de clinkers (C_3) et (C_4) traités sous atmosphère réductrice on ne note aucun changement sensible des phases C_2S et C_3S. La phase C_3A par contre évolue très nettement, l'aluminoferrite a disparu et on note dans les deux cas l'existence de chaux résiduelle. De plus, l'étude de ces produits par microscopie optique permet de mettre en évidence la présence de fer métallique. Enfin un recuit de 1 h à 1300°C dans l'air de ces clinkers obtenus sous atmosphère réductrice, ne modifie en aucune façon le spectre de diffraction X initial. Ceci est à rapprocher de la fusion de C_4AF pur sous hydrogène qui donne du C_3A, de la CaO libre et du fer métallique visible à l'oeil nu sous forme de billes.

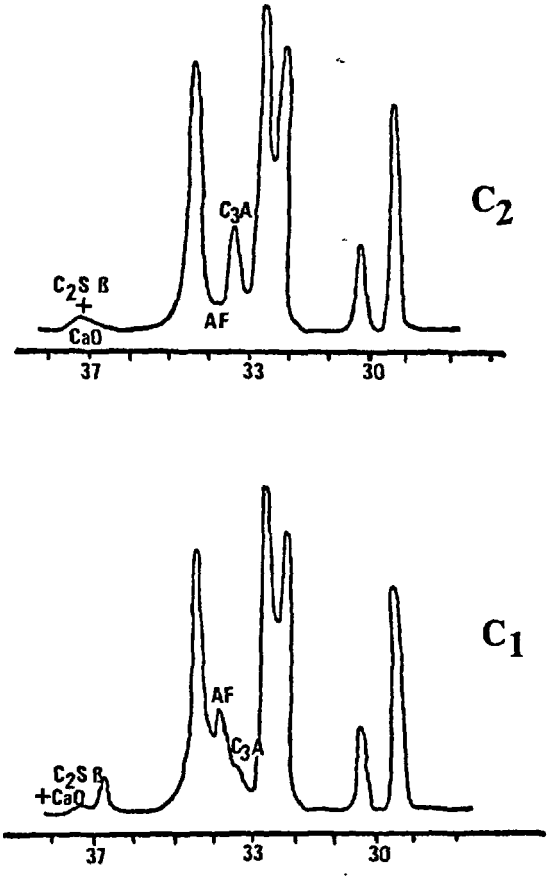

Fig. 4 - Spectres de diffraction X des clinkers C_1 et C_2.

2) D'un point de vue physique on notera que :

- les phénomènes de ségrégation de phases pouvant se produire entre liquidus et solidus au moment du refroidissement n'interviennent pas dans la solidification des phases du clinker compte tenu du caractère stoechiométrique des silicates et aluminates de calcium,

- dans le cas de clinkers refroidis par hypertrempe, le C_3S se présente sous forme de petits cristaux allongés,

- la vaporisation sélective des oxydes de fer dans le mélange liquide, bien qu'ayant été observée par ailleurs, n'intervient pas non plus dans nos essais compte tenu de la rapidité de traitement thermique à la fusion (durée moyenne du traitement de l'ordre de quelques secondes),

- la vitrification des phases

aluminate et aluminoferrite n'a pas été observée après solidification même très rapide du "clinker fondu". A noter que dans ce cas là le comportement du C_3A est totalement différent de celui observé par ailleurs sur du C_3A pur dont la tendance à se vitrifier est d'autant plus élevée que la vitesse de refroidissement est plus grande.

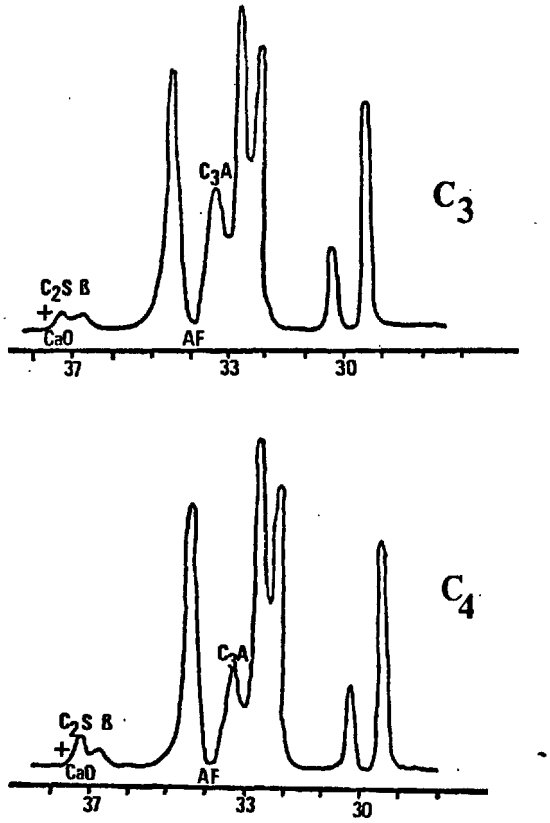

Fig. 5 - Spectres de diffraction X des clinkers C_3 et C_4.

D. CONCLUSION.

Tous ces résultats amènent à penser que :

- dans l'air le Fe^{3+} subit une réduction partielle à la température du liquide [$T_{liq} = T_{fusion} + (200 \sim 300°C)$ avec $T_{fusion} = 1935°C$] et l'on note la destruction de la phase aluminoferrite. Le refroidissement rapide ($\Delta T/\Delta t \sim 10^5$ deg.sec^{-1}) freine alors la réoxydation du fer et bloque la reformation de l'aluminoferrite. Il s'en-suit un enrichissement du C_3A par recombinaison partielle de la chaux libre avec l'alumine en excés.

Le refroidissement normal du liquide ($\Delta T/\Delta t \sim 10^2$ deg.sec^{-1}) permet d'amorcer le processus inverse de la réoxydation du fer tel qu'on l'observe après un recuit du fondu dans l'air à 900 ∿ 1100°C.

Le processus de réoxydation pourrait se schématiser selon :

$$2C_3A + F \rightarrow (2C_2A + C_2F) \sim C_6A_2F$$

ou $$C_3A + C + F \rightarrow (C_2A + C_2F) \sim C_4AF$$

- lorsque l'on procède à une fusion sous atmosphère réductrice, le Fe^{3+} subit une réduction totale jusqu'à l'état de fer métallique. Il semblerait que dans les conditions d'expérimentation utilisées (recuit 1 h à l'air à 1300°C), la réoxydation du fer ne soit pas suffisante pour redonner l'aluminoferrite.

Polymorphisme de l'alite et du C_3A. Statistiques

Alite and C_3A polymorphism. Statistics

P. GOURDIN, E. DEMOULIAN, F. HAWTHORN, C. VERNET - Société des Ciments Français - CEREG, France.

RESUME :

A l'aide d'une population de 60 clinkers, issus de 24 crus clinkérisés dans 32 fours rotatifs différents, les auteurs ont dégagé les relations statistiques entre la minéralogie du cru (teneur en quartz, présence d'argile illite ou kaolinite), les procédés de fabrication (voie humide, voie sèche, type de four), la composition chimique du clinker d'une part et les formes allotropiques de l'alite (monoclinique, trigonale) et du C_3A (cubique, tétragonal) d'autre part.

En complément a été dégagée l'incidence de ce polymorphisme de l'alite et du C_3A sur les résistances à la compression moyenne des ciments portland correspondants, de granulométrie comparable.

Il ressort de ce travail que les éléments mineurs comme MgO, SO_3, K_2O et P_2O_5 des clinkers industriels ont une influence importante sur les résistances à la compression des ciments portland correspondants. Il confirme la meilleure hydraulicité de l'alite trigonale et du C_3A cubique dans les clinkers industriels.

SUMMARY :

Sixty industrial clinker samples from twenty-four raw mixes, burned in thirty-two rotary kilns were analysed in order to find the statistical relations between raw mix mineralogy (quartz, illite or kaolinite clays), clinkering processes (wet or dry processes, kiln), chemical composition of the clinker, in one hand, and the allotropic forms of alite (monoclinic or trigonal alite) and C_3A (cubic or tetragonal C_3A) on the other hand.

In addition, the consequences on the mean compressive strengths of corresponding portland cement with similar granulometry, have been studied.

This paper shows that the minor elements, such as MgO, SO_3, K_2O and P_2O_5 in industrial clinkers have an important influence on the alite and C_3A polymorphism and then on the compressive strengths of the corresponding portland cements. The best hydraulicity of trigonal alite and cubic C_3A, in the industrial clinkers, is confirmed.

INTRODUCTION

En 1969 et 1970, nous avions établi des relations entre la composition minéralogique et granulométrique des ciments portland et leurs performances (1) et (2). Les progrès réalisés dans la connaissance du polymorphisme du C_3S et du C_3A ont posé la question de l'influence de la structure de l'alite et de l'aluminate sur les propriétés des ciments. Des recherches effectuées à l'aide de clinkers de laboratoire et rapportées par GUINIER et REGOURD, en 1968 (3), ont montré que toutes les formes cristallines du C_3S présentent une réactivité comparable mais que les oxydes entrés en solution solide dans le réseau du C_3S induisent des variations d'activité hydraulique et de résistance mécanique dans les alites de synthèse, variations dues surtout aux imperfections cristallines. On a précisé que, en général, les ions de diamètre inférieur au diamètre de Ca^{2+} augmentent l'instabilité des alites, donc leur hydraulicité (4). En 1972, Mme.REGOURD a publié les résultats de trois analyses de clinkers industriels et étudié les propriétés des minéraux (5) ; en 1974, elle a publié les résultats de huit analyses (6) et, en 1978, étudié le polymorphisme du C_3A dans douze clinkers industriels (7).

Dans le présent travail nous recherchons s'il y a des relations entre les matières premières, les conditions de fabrication, la composition chimique des clinkers d'une part et le polymorphisme des phases cristallines, alite et C_3A d'autre part, sur un grand nombres d'échantillons, représentatifs de la production de la SOCIETE des CIMENTS FRANCAIS, en 1978. Nous verrons l'influence importante des éléments mineurs. En complément, nous avons analysé les conséquences de la structure de l'alite et du C_3A sur les résistances à la compression des ciments portland correspondants.

METHODE D'ETUDE

Nous avons constitué une population de 60 clinkers issus de 24 crus de cimenterie, clinkérisés dans 32 fours rotatifs différents, répartis en 21 usines. Ces échantillons de mélanges crus et de clinkers ont été analysés de la façon suivante.

1 - Polymorphisme de l'alite et du C_3A

Nous avons déterminé avec certitude la présence des différentes formes cristallines de l'alite par examen de la raie 1,76 Å qui est double (620 et 040) dans le cas de l'alite monoclinique M_I, dissymétrique dans le cas de l'alite M_{II} et simple (220) dans le cas de l'alite trigonale ou rhomboédrique R. Les formes cristallines du C_3A ont été déterminées par examen des raies 2,69 Å du C_3A cubique et 2,69 Å - 2,71 Å du C_3A tétragonal sur l'insoluble dans l'acide salicylique.

2 - Paramètres considérés

Mélanges crus :
Nous avons dosé quantitativement le quartz à l'aide des raies 4,25 Å - 3,34 Å et 1,82 Å par rapport aux raies 3,14 Å et 1,92 Å du silicium pris comme étalon interne et par la méthode des ajouts dosés ; nous avons ensuite déterminé la présence et les intensités relatives des raies 10 Å et 7 Å des argiles de type illite et kaolinite, ainsi que les raies des feldspaths et de l'hématite, sur l'insoluble dans l'acide nitrique, en pH contrôlé (donc après élimination des carbonates), avant et après traitement à 550°C et au glycol, traitement qui permet de faire disparaître ou déplacer les raies de certains minéraux phyllitiques opale etc...

Procédés de fabrication :
Nous avons examiné les relations entre le polymorphisme de l'alite et du C_3A et le mode de fabrication (voie humide, voie sèche), la nature du combustible et l'influence du four rotatif (par comparaison avec le four de laboratoire).

Clinkers :
Nous avons considéré la composition chimique CaO libre Al_2O_3, Fe_2O_3, TiO_2, MnO, MgO, excès SO_3 (après saturation de K_2O en K_2SO_4), excès de K_2O (après saturation de SO_3 en K_2SO_4), Na_2O, P_2O_5, donc avec une attention particulière aux éléments mineurs.

3 - Dépendance statistique

Pour dégager les relations entre le polymorphisme de l'alite et du C_3A et les différents paramètres industriels, nous avons dressé des tables de fréquences d'apparition des formes allotropiques (caractère A) en fonction de la minéralogie du cru, du procédé de fabrication, ou de la composition chimique (caractère B). Dans le cas de la composition chimique, nous avons distingué, pour chaque élément, deux sous-populations, l'une constituée de clinkers riches en cet élément, l'autre par des clinkers pauvres de cet élément.
Nous avons calculé, pour chaque relation, à partir des tables, la valeur χ^2 du test de Pearson qui permet de dire si la dépendance entre les deux caractères étudiés est significative au seuil de 5 % (8).

RESULTATS OBTENUS

1 - Répartition des formes allotropiques dans les 60 clinkers

Utilisant la nomenclature proposée par Mme.REGOURD (9) nous avons mis en évidence les formes suivantes dans les 60 clinkers industriels examinés :

ALITE	C_3A			TOTAL
	Cubique	Les 2 formes	Tétragonal	
R	11	0	0	11 (18%)
$M_{II}b$	11	9	1	21 (35%)
M_Ib	7	17	4	28 (47%)
T	0	0	0	0
Total	29 (48%)	26 (43 %)	5 (9 %)	60 (100%)

Nous avons observé 2 fois le C_3A orthorhombique (raies 624 et 264) associé au C_3A cubique, mais jamais l'alite triclinique (sauf la forme T_{III} dans un clinker "pathologique" décrit dans une autre communication (10)

2 - Associations de formes allotropiques

Le tableau précédent fait apparaître des associations fréquentes dans ce lot de 60 clinkers industriels :
- alite R et C_3A cubique ;
- alite M_Ib et C_3A tétragonal (avec ou sans (cubique).

On n'a pas vu une seule fois l'association entre alite R et C_3A tétragonal, comme s'il y avait une incompatibilité entre ces deux formes. Le test de Pearson donne $\chi^2 = 21,4 > 9,5$ au seuil de 5 % ce qui veut dire que ces deux caractères (forme de l'alite et forme du C_3A) sont dépendants.

FACTEURS DU POLYMORPHISME DE L'ALITE ET DU C_3A

Nous donnons maintenant tous les tableaux de fréquence des formes allotropiques d'alite et de C_3A, en fonction des paramètres définis plus haut, afin d'en dégager les relations les plus étroites.

1 - Minéralogie du cru

QUARTZ	ALITE		
	$M_I b$	$M_{II} b$	R
Quartz > 8 %	5 (38 %)	3 (24 %)	5 (38 %)
Quartz < 8 %	6 (50 %)	5 (42 %)	1 (8 %)
25 échantillons	11 (44 %)	8 (32 %)	6 (24 %)
	C_3A		
	C	C+T	T
Quartz > 8 %	9 (69 %)	3 (23 %)	1 (8 %)
Quartz < 8 %	5 (42 %)	6 (50 %)	1 (8 %)
25 échantillons	14 (56 %)	9 (36 %)	2 (8 %)

ILLITE-KAOLINITE	ALITE		
	$M_I b$	$M_{II} b$	R
10 Å > 0,27	10 (71 %)	4 (29 %)	0 (0 %)
7 Å > 0,07	4 (36 %)	4 (36 %)	3 (28 %)
26 échantillons	11 (41 %)	10 (37 %)	6 (21 %)
	C_3A		
	C	C+T	T
10 Å > 0,27	5 (36 %)	8 (57 %)	1 (7 %)
7 Å > 0,07	6 (55 %)	5 (45 %)	0 (0 %)
26 échantillons	16 (59 %)	9 (33 %)	2 (18 %)

(Nous n'avons pas fait figurer les sous-populations 10 Å < 0,27 et 7 Å < 0,07).

2 - Procédé de fabrication

PROCEDES de FABRICATION	ALITE		
	$M_I b$	$M_{II} b$	R
Voie humide	7 (39 %)	5 (38 %)	6 (33 %)
Voie semi-sèche	6 (26 %)	14 (61 %)	3 (13 %)
Voie sèche	15 (79 %)	2 (11 %)	2 (10 %)
60 clinkers	28 (47 %)	21 (35 %)	11 (18 %)
	C_3A		
	C	C+T	T
Voie humide	6 (33 %)	9 (50 %)	3 (17 %)
Voie semi-sèche	15 (65 %)	8 (35 %)	0 (0 %)
Voie sèche	8 (42 %)	9 (47 %)	2 (11 %)
60 clinkers	29 (48 %)	26 (43 %)	5 (9 %)

COMBUSTIBLES	ALITE		
	$M_I b$	$M_{II} b$	R
Charbon	3 (42 %)	2 (29 %)	2 (27 %)
Fuel ordinaire	7 (33 %)	9 (43 %)	5 (24 %)
Fuel Ord. + BTS	4 (40 %)	5 (50 %)	1 (10 %)
Fuel Ord. + Gaz	11 (58 %)	5 (26 %)	3 (16 %)
Gaz	3 (100 %)	0 (0 %)	0 (0 %)
60 clinkers	28 (47 %)	21 (35 %)	11 (18 %)
	C_3A		
	C	C+T	T
Charbon	6 (86 %)	1 (14 %)	0 (0 %)
Fuel ordinaire	10 (48 %)	10 (48 %)	1 (4 %)
Fuel + BTS	5 (50 %)	3 (30 %)	2 (20 %)
Fuel + Gaz	8 (42 %)	9 (47 %)	2 (11 %)
Gaz	0 (0 %)	3 (100 %)	0 (0 %)
60 clinkers	29 (48 %)	26 (43 %)	5 (9 %)

Influence du four rotatif :
Pour faire ressortir l'influence du procédé de fabrication industrielle sur le polymorphisme de l'alite et du C_3A, nous avons comparé les clinkers issus des mêmes 19 crus préparés dans un four de laboratoire d'une part et fabriqués à l'usine d'autre part. Voici le tableau de répartition :

CUISSON	ALITE		
	$M_I b$	$M_{II} b$	R
Au laboratoire	7	5	7
A l'usine	7	8	4
	C_3A		
	C	C+T	T
Au laboratoire	10	9	0
A l'usine	6	12	1

En réalité, l'influence de la fabrication industrielle est plus compliquée que le montre le tableau précédent. Nous l'avons mise en relation avec les variations de SO_3 et de K_2O qui sont, en moyenne :

19 échantillons	SO_3	K_2O	soit excès SO_3
Clinkers laboratoire	0,66	0,18	0,51
Clinkers usine	0,84	0,81	0,15

Ces tableaux montrent que c'est l'influence des teneurs en SO_3 et K_2O dans le traitement industriel qui conditionne la répartition des phases. Nous reviendrons sur ce point.

On peut ajouter que les 19 clinkers industriels ici examinés montrent une relation remarquable entre le rapport SO_3/K_2O (en poids) et le polymorphisme de l'alite.

3 - Composition chimique

	ALITE		
	$M_I b$	$M_{II} b$	R
CaO libre > 1,5	10 (37 %)	13 (48 %)	4 (15 %)
Al_2O_3 > 5,21	14 (47 %)	11 (37 %)	5 (11 %)
Fe_2O_3 > 2,7	14 (47 %)	11 (37 %)	5 (16 %)
TiO_2 > 0,21	13 (41 %)	15 (47 %)	4 (12 %)
MnO > 0,03	11 (42 %)	12 (46 %)	3 (12 %)
MgO > 1,45	16 (84 %)	3 (16 %)	0 (0 %)
P_2O_5 > 0,12	15 (54 %)	12 (43 %)	1 (3 %)
Excès SO_3	12 (32 %)	15 (39 %)	11 (29 %)
Excès K_2O	14 (70 %)	6 (30 %)	0 (0 %)
60 clinkers	28 (47 %)	21 (35 %)	11 (18 %)

	C_3A		
	C	C+T	T
CaO libre > 1,5	13 (48 %)	13 (48 %)	1 (4 %)
Al_2O_3 > 5,21	13 (43 %)	16 (53 %)	1 (4 %)
Fe_2O_3 > 2,7	14 (47 %)	12 (40 %)	4 (13 %)
TiO_2 > 0,21	16 (50 %)	15 (47 %)	1 (3 %)
MnO > 0,03	9 (35 %)	15 (58 %)	2 (7 %)
MgO > 1,45	6 (35 %)	11 (58 %)	2 (10 %)
P_2O_5 > 0,12	9 (32 %)	16 (57 %)	3 (11 %)
Excès SO_3	26 (68 %)	10 (26 %)	2 (6 %)
Excès K_2O	3 (15 %)	14 (70 %)	3 (15 %)
60 clinkers	29 (48 %)	26 (43 %)	5 (9 %)

	ALITE		
	$M_I b$	$M_{II} b$	R
Na_2O > 0,19	8 (73 %)	2 (18 %)	1 (9 %)
Na_2O < 0,19	4 (33 %)	6 (50 %)	2 (17 %)
23 clinkers	12 (52 %)	8 (35 %)	3 (13 %)
	C_3A		
	C	C+T	T
Na_2O > 0,19	3 (27 %)	6 (55 %)	2 (18 %)
Na_2O < 0,19	3 (25 %)	9 (75 %)	0 (0 %)
23 clinkers	6 (26 %)	15 (65 %)	2 (9 %)

Dans les deux premiers tableaux ci-dessus, nous n'avons pas fait figurer les sous-populations CaO libre <1,5, Al_2O_3 < 5,21 etc... pour simplifier les tableaux.

CONSEQUENCE DU POLYMORPHISME DE L'ALITE ET DU C_3A SUR LES RESISTANCES A LA COMPRESSION

Quelles sont les formes cristallines de l'alite et du C_3A qui donnent les meilleures résistances à la compression des ciments portland ? Pour répondre à cette question, nous avons calculé les fréquences d'apparition des différentes formes dans les 60 clinkers industriels correspondant aux ciments portland développant les meilleures résistances à la compression à 2, 7 et 28 jours (c'est-à-dire supérieures à la moyenne de tous les échantillons essayés en 1978). On obtient le tableau suivant :

RESISTANCES à la COMPRESSION	ALITE		
	$M_I b$	$M_{II} b$	R
R_c 2j > 26 MPa	7 (28 %)	14 (56 %)	4 (16 %)
R_c 7j > 43 MPa	6 (29 %)	9 (42 %)	6 (29 %)
R_c 28j > 58 MPa	4 (21 %)	7 (37 %)	8 (42 %)
	20 (40 %)	21 (42 %)	9 (18 %)
	C_3A		
	C	C+T	T
R_c 2j > 26 MPa	13 (52 %)	11 (44 %)	1 (4 %)
R_c 7j > 43 MPa	12 (57 %)	7 (33 %)	2 (10 %)
R_c 28j > 58 MPa	13 (68 %)	4 (21 %)	2 (11 %)
	23 (46 %)	22 (44 %)	5 (10 %)

Le test du χ^2 montre que la dépendance entre polymorphisme et résistances à la compression est ici significative puisque le calcul donne $\chi^2 = 18,7$ (la dépendance étant significative pour $\chi = 9,5$ avec 4 degrés de liberté).

DISCUSSION

Les observations tirées de cette étude s'appliquent évidemment à la population de 60 clinkers industriels représentatifs de la production de la SOCIETE des CIMENTS FRANCAIS en 1978.

Les tableaux, ou tables de contingence, que nous avons donnés font apparaître que la dépendance statistique entre les deux caractères examinés (polymorphisme et chacun des paramètres considérés) est plus ou moins étroite. Le test de Pearson comparant les groupes de fréquences observés aux groupes de fréquences théoriques, permet de dire si la dépendance est significative ou ne l'est pas. Voici les résultats :

	ALITE		C_3A	
	χ^2	seuil 5 %	χ^2	seuil 5 %
Assoc. allotr.	18,7	significatif	18,7	significatif
Procédés	17,7	"	6,5	non signif.
MgO	16,3	"	3,2	non signif.
Illite	13,7	"	7,6	significatif
R_c 28 j	13,0	"	7,1	non signif.
SO_3/K_2O	10,3	"	15,0	significatif
P_2O_5	7,7	"	5,4	non signif.
Combustibles	7,5	peu signif.	10,8	significatif
TiO_2	4,6	non signif.	2,6	non signif.
R_c 2j	4,3	"	1,9	non signif.
CaO libre	3,7	"	1,5	non signif.
Na_2O	3,6	"	2,8	non signif.
R_c 7j	3,4	"	1,9	non signif.
Quartz	3,3	"	2,1	non signif.
MnO	3,0	"	3,9	non signif.
Kaolinite	0,3	"	2,2	non signif.
Al_2O_3-Fe_2O_3	0,1	"	3,5 - 2,0	non s.

Nous limitant aux caractères significatifs définis par le test de Pearson, nous rassemblons ici les fréquences d'apparition des principales formes allotropiques de l'alite et du C_3A en fonction de ces caractères et dans l'ordre décroissant des fréquences, de façon à faire ressortir le degré de dépendance. Nous figurons aussi les résistances à la compression.

Fréquences d'apparition des formes allotropiques

ALITE $M_I b$		C_3A C+T		C_3A T	
Voie sèche	79%	Exc.K_2O	70%	V.humide	17%
Illite	71%	Illité	57%	Exc.K_2O	15%
Exc.K_2O	70%	P_2O_5	57%	P_2O_5	11%
P_2O_5	54%	V.humide	50%	V.sèche	11%
60 clinkers	47%	V.sèche	47%	R_c28j	11%
V.humide	39%	R_c2j	44%	R_c7j	10%
Exc.SO_3	32%	60 clinkers	43%	60 clinkers	9%
R_c7j	29%	V.s.sèche	35%	Illite	7%
R_c2j	28%	R_c7j	33%	Exc.SO_3	6%
V.s.sèche	26%	Exc.SO3	26%	R_c2j	4%
R_c28j	21%	R_c28j	21%	V.s.sèche	0%

L'alite $M_I b$ est plus fréquente dans les clinkers provenant de crus riches en argiles de type illite, caractérisés par des teneurs en MgO et alcalis supérieures aux teneurs moyennes. Ces clinkers conduisent à des ciments portland dont les résistances à la compression sont inférieures à la moyenne, à granulométries comparables. Le C_3A tétragonal, souvent associé au C3A cubique et à l'alite $M_I b$, se voit fréquemment dans les clinkers riches en alcalins, Na_2O surtout, et est très favorable aux résistances à long terme.

Les alcalis provenant de crus argileux (illite) ne sont pas entièrement saturés par le SO_3 des fumées provenant des combustibles et entrent en solution solide dans le réseau du C_3S et du C_3A, stabilisant, à la température ambiante, les formes $M_I b$ du C_3S et tétragonal du C_3A. Notre observation confirme les 3 analyses au M.E.B. de Mme.REGOURD (6) :

	ALITE			C_3A		
	$M_I b$	$M_{II} b$	R	C	C+O	T
MgO	1,0	1,3	0,6	1,5	1,9	0,9
SO_3		0,06	0,2	0,2	0,2	0,2
K_2O	0,2	0,1	0,1	0,7	0,8	3,1
Na_2O	0,2	0,2	0,02	0,4	2,4	0,9

D'après MAKI et CHROMY, les fortes teneurs en MgO stabilisent $M_{II} b$ et même R (11) mais KRISTMANN a constaté que les faibles teneurs en MgO correspondent à l'alite trigonale (12). Enfin, d'apres BENSTED (4) la presence de K^+, de diamètre supérieur à Ca^{2+}, dans le réseau du C_3S, réduit l'hydraulicité de l'alite, ce que confirment nos observations.

Pour les autres formes, on a de même :

ALITE $M_{II} b$		ALITE R		C_3A cubique	
Voie s.sèche	61%	R_c28j	42%	R_c28j	68%
R_c 2j	56%	V.humide	33%	Excès SO_3	68%
P_2O_5	43%	R_c7j	29%	V.s.sèche	65%
R_c7 j	42%	Excès SO3	29%	R_c7j	57%
Exc.SO_3	39%	60 clink.	18%	R_c2j	52%
V. humide	38%	R_c2j	16%	60 clink.	48%
R_c28j	37%	V.s.sèche	13%	V.sèche	42%
60 clink.	35%	V.sèche	10%	MgO	35%
Exc.K_2O	30%	P_2O_5	3%	V.humide	33%
MgO	16%	Excès K_2O	0%	P_2O_5	32%
V.sèche	11%	MgO	0%	Excès K_2O	15%

L'alite trigonale R et le C_3A cubique sont fréquents dans les clinkers issus de crus "quartzeux", pauvres en MgO et alcalis et caractérisés par un excès de SO_3 par rapport à K_2O, donnant des ciments portland à résistances à la compression à 7 et 28 jours supérieurs à la moyenne. Ces observations faites sur 60 clinkers industriels infirment le fait, signalé par les auteurs (13), que la présence de SO_4^{2-} en solution solide diminue l'hydraulicité de l'alite car nous ne voyons cette diminution qu'à 2 jours seulement. Nous confirmons aussi les conclusions de HARADA, OHTA et TAKAGI d'après lesquels la vitesse d'hydratation initiale croit dans l'ordre pour les formes monoclinique et rhomboédrique (14).

Nous avons dégagé une dépendance entre le procédé de fabrication et le polymorphisme : si l'alite $M_I b$ est plus fréquente dans les clinkers voie sèche, l'alite R dans les clinkers voie humide (il y a des exceptions), cette observation est probablement fortuite, sauf si les matières premières aptes à la voie sèche sont riches en MgO et alcalis.

REMERCIEMENTS

Les auteurs remercient M.Paul MAES de sa collaboration pour les nombreuses analyses de clinker qui sont à l'origine de ce travail.

CONCLUSION

L'influence des procédés de fabrication sur le polymorphisme de l'alite et du C_3A est ressentie au travers des éléments mineurs tels que MgO, P_2O_5 et de la balance entre K_2O venu de l'argile et SO_3 venu en partie du combustible ; cela ressort des tables de dépendance statistique que nous avons dressées et du test de Pearson que nous avons calculé, sur une population de 60 clinkers industriels, issus de 24 crus, dans 32 fours rotatifs.

Nous n'avons pas mis en évidence le rôle d'autres caractères comme teneurs en Al_2O_3, Fe_2O_3, TiO_2, probablement parce que les teneurs en TiO_2 de nos clinkers industriels sont trop faibles pour reproduire les effets observés au laboratoire (15).

Nous avons montré, en complément, que l'alite monoclinique $M_I b$ et le C_3A tétragonal des clinkers provenant de crus "argileux" sont moins hydrauliques que l'alite monoclinique $M_{II} b$ et surtout que l'alite trigonale ou rhomboédrique et le C_3A cubique provenant de crus clinkérisés avec des combustibles riches en soufre.

BIBLIOGRAPHIE

1. - P.GOURDIN (1969) - Composition minéralogique et propriétés des clinkers portland, Revue des Matériaux de construction n° 650-651, 354-363, 411-421.
2. - M.Von EUW et P.GOURDIN (1970) - Le calcul prévisionnel des résistances des ciments portland, Matériaux et Constructions n° 17, vol. 3, 290-311
3. - A.GUINIER et M.REGOURD (1969) - Structure des minéraux du ciment portland. V^e Symposium Intern. Chim.Ciment - Tokyo, 6-12
4. - J.BENSTED (1978) - The hydraulic calcium silicates. Il cemento n°3, 129 - 135.
5. - M.REGOURD (1972) - Mineralogy of portland cement 2 nordic cement coll., Copenhagen, 11-39.
6. - M.REGOURD et A.GUINIER (1974) - Cristallochimie des constituants du clinker de ciment portland. VI^e Congrès Int.Chim.Ciment, Moscou - Revue des matériaux de construction, n°695, 201-215.
7. - M.REGOURD (1978) - Cristallisation et réactivité de l'aluminate tricalcique dans les ciments portland. Il cemento n° 3, 323-336.
8. - A.VESSEREAU (1972) - La statistique Paris, PUF.
9. - M.REGOURD (1979) - Polymorphisme du silicate tricalcique. Nouvelles données de la diffraction des rayons X - C.R. Acad.Sci.Paris - t 289.
10. - E.DEMOULIAN, P.GOURDIN, F.HAWTHORN, C.VERNET (1980) - Anomalies de cuisson - Structures microscopiques - Propriétés des clinkers et des ciments. VII^e Congrès Intern.Chim.Ciment, Paris.
11. - I.MAKI et S.CHROMY (1978) Characterization of the alite phase in portland cementclinker by microscopy. Il cemento n°3, 247-252.
12. - M. KRISTMANN (1977) - Portland cement clinker, Mineralogical and chemical investigations, Cem. Concr. Res. n° 7, 649 ; n° 8, 93.
13. - W.GUTT et M.A.SMITH (1968) - Studies of the role of calcium sulphate in the manufacture of portland cement clinker. Trans.Brit.Ceram.Soc.67, 487.
14. - T.HARADA, M.OHTA et S.TAKAGI (1977) - Effect of polymorphism of tricalcium silicate on structure and strength characteristics of hardened paste - C.A.J. Review, Tokyo, 31-32.
15. - R.KONDO et K.YOSHIDA (1968) - Miscibilities of special element in tricalcium silicates and alite and the hydratation proporties of C_3S solid solutions - V^e Symp. Intern. Chim.Ciment, Tokyo, 262.

Influence de la température d'apparition des bains fondus eutectiques et des particularités de la structure cristalline des phases réagissantes sur la structure et les propriétés du clinker

Influence of melt eutectic temperature and peculiarities of crystalline structure of reacting phases on structure and properties of clinker

I.V. KRAVTCHENKO, professeur, docteur ès sciences techniques,
A.M. DMITRIEV, candidat ès sciences techniques,
I.E. KOVALEVA, candidat ès sciences techniques,
NIITzement, Moscou, U.R.S.S.

RESUME : On a étudié les processus physico-chimiques qui se produisent dans un four rotatif alimenté en parallèle par deux flux distincts de matières crues, de composition chimique, granulométrique et de phase différente. Le deuxième flux (complémentaire) introduisait directement, dans les zones préparatoires du four, deux types de matières appropriées :

- des matières participant activement aux réactions de clinkérisation, dès l'apparition du liquidus (bélite fondue) dans la masse,
- des matières (laitiers de hauts fourneaux, laitier électrophosphoreux, cendres volantes), qui entrent elles-mêmes en fusion avant l'apparition normale du liquidus.

L'action activante des matières de ce deuxième flux, dans la cuisson du cru, est susceptinle d'accroître fortement (de 20) 25 %) la capacité de production du four rotatif et de réduire la consommation de combustible, tout en conservant les propriétés chimiques, physiques et mécaniques du clinker obtenu, et parfois même, en les améliorant.

SUMMARY: The physical and chemical processes taking place in a furnace being fed by two parallel flows of raw materials with different chemical, phase and granulometric compositions have been investigated. Used as the second (additional) flow introduced directly to the preparatory zones of the furnace are technogenic materials of two types:

- the materials which take an active part in the clinker formation reactions after the basic mass of the clinker melt appears in the raw charge (belite slime);
- the materials (blast furnace and electrothermophosphorus slags, fly ashes) which form the melt before it appears in the bulk of the charge.

The intensifying effect of technogenic materials in the calcination process has enabled to increase drastically (by 20-25%) the capacity of clinker calcination rotary furnaces and decrease specific consumption of fuel for calcination within the same range with preservation, and, on some occasions even improving, the phisico-chemical and phisico-mechanical properties of the clinker obtained.

On a élaboré en U.R.S.S. un procédé d'intensification du processus de clinkérisation, permettant d'accroître sensiblement (de 15-30%) le rendement des fours rotatifs de clinkérisation et de diminuer (de 12-25%) la consommation spécifique de combustibles pour la cuisson.

Ce procédé consiste en alimentation parallèle du four par deux flux de matières brutes de composition chimique, de phase et granulométrique différente. Le premier flux (principal) - les mélanges crus de constituants classiques ordinaires qu'on prépare et introduit dans le four de façon traditionnelle. Le deuxième flux (complémentaire) - les matières technogènes (rejets industriels) ayant subi le traitement thermique préalable en vue de la formation des silicates faiblement basiques, des alumosilicates, des aluminates, des alumoferrites de calcium. De tels composés apparaissent également dans le clinker-portland aux premiers stades de cuisson. Comme il est connu, leur synthèse est précédée par des dépenses de chaleur importantes.

On a étudié et proposé pour l'utilisation dans les cimenteries les sous-produits des branches métallurgique, chimique et énergétique de l'économie nationale (boues de néphéline, cendres et mélanges laitier-cendres des centrales thermiques, laitiers de haut fourneau, laitiers électrothermophosphoriques, etc.).

Les matériaux du deuxième flux sont introduits dans les fours rotatifs directement par leurs zones préparatoires du côté froid.

L'alimentation complémentaire des fours en matières technogènes prévoit la substitution partielle par ces dernières des constituants carbonaté et alumosilicique du flux principal. Ceci change notablement le rapport des constituants crus dans la composition du système de cuisson et par conséquent la cinétique de la clinkérisation et les propriétés des produits de la cuisson. Le degré et le caractère de l'influence des matières utilisées pour l'alimentation complémentaire des fours sur la synthèse du clinker de ciment se déterminent par leurs paramètres physico-chimiques et la quantité de ces matières introduite dans le four.

Dans cette communication on considère deux groupes de matières du deuxième flux:

- (I) matières qui entrent activement en réactions de clinkérisation après l'apparition dans la charge crue de la masse principale du clinker fondu. La boue de néphéline (de bélite) représente ce type de matière technogène;

- (II) matières qui forment le bain fondu avant son apparition dans la charge crue principale. Ce sont des laitiers de haut fourneau, laitiers électrothermophosphoriques, cendres.

L'interaction de la boue de néphéline, introduite complémentairement et représentée principalement par le silicate bicalcique sous forme β , avec la charge crue à excès du composant carbonique, commence principalement à se produire lorsque le clinker fondu apparaît dans le système de cuisson. Comme il est connu (1), dans ces conditions la réaction de formation des alites est limitée par la vitesse de dissolution dans la phase liquide de l'oxyde de calcium et de la bélite et dépend de leur habitus. Il importe de noter que les grains de bélite de la boue de néphéline forment des agrégats et se transforment en cristallites au cours du traitement thermique successif (la vitesse d'élévation de la température dans le four étant de 600°C/heure). Indépendamment de la dispersité initiale de la boue de néphéline, au moment de formation intense des alites leur dimension est de 20 μm, ce qui n'entrave pas le stade final de cuisson.

De plus, la présence dans le système de cuisson des centres de cristallisation formés (β - C_2S) contribue à l'accélération de la synthèse des minéraux faiblement basiques dans la charge crue mélangée déjà au premier stade de cuisson. Ceci est confirmé par les données de l'analyse des phases aux rayons X à haute température (fig.1a), fixant dans le mélange 2 avec 25% de la boue de néphéline l'assimilation plus intense de la silice que dans la charge sans additions 1 (d = 3,40 Å) et l'accroissement des constantes de la vitesse d'assimilation de la chaux dans le mélange 2 dans l'intervalle de température de 900 à 1000°C.

La composition de la phase intermédiaire de la boue de néphéline, contenant jusqu'à 1-1,5% d'oxydes alcalins, est un facteur complémentaire qui contribue à l'accélération de la synthèse de l'alite. D'après les résultats des recherches (3), la présence dans le bain fondu des cations très mobiles Na^+ et K^+ intensifie notablement la réaction de dissolution de la bélite grâce à la formation dans les limites de la couche superficielle de C_2S des eutectiques facilement fusibles. Cet effet de l'influence intensifiante des ions alcalins se manifeste même dans la charge à deux constituants 3 (matériau carbonaté - boue de néphéline) malgré sa teneur limitée en phase liquide (17%) en comparaison des charges à plusieurs constituants.

L'étude des particularités de la clinkérisation en présence des matières technogènes du deuxième groupe a montré que l'action intensifiante de ces additions est due à leur fusion autonome précoce (les bains fondus du laitier de haut fourneau, du laitier électrothermophosphorique et des cendres apparaissent aux températures de 1260-1280°C, 1180-1220°C, 1240°C respectivement) et à l'interaction des bains fondus de laitiers et de cendres avec les constituants de la charge crue. Les observations effectuées à l'aide du microscope optique ont permis de déterminer le mécanisme de pénétration des matières du deuxième groupe, qui se trouvent à l'état fondu liquide, à l'intérieur des volumes microscopiques de la charge crue, en fixant les zones

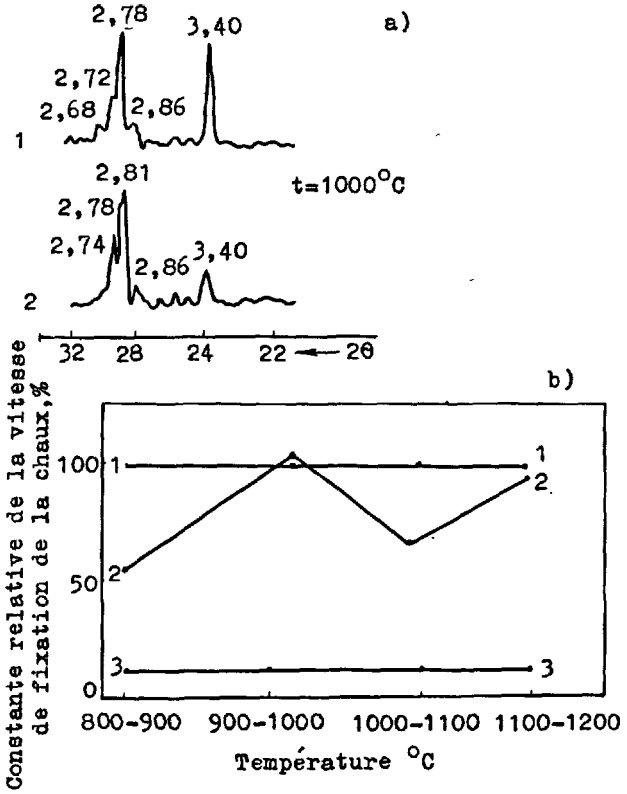

Fig.1. Influence de la boue de néphéline sur le processus de cuisson dans l'intervalle de température de 800 à 1200°C. 1, 2, 3 sont respectivement les parts de la boue de néphéline dans le mélange cru. 0%, 25%, 76% (à deux constituants).

suivantes (fig.2): A - le latier ayant subi le traitement thermique; B - la zone d'interaction du laitier avec la charge principale; C - la charge crue; D - la zone occupée autrefois par le laitier. La présence de cette dernière contribuera à la diminution de la résistibilité au broyage des clinkers obtenus.

Notant le mécanisme général d'interaction des matières de ce groupe avec les constituants de la charge principale, remarquons que chacun d'entre eux apporte des traits spécifiques dans la cinétique de la clinkérisation.

Lorsqu'on utilise en qualité de flux complémentaire le laitier granulé de haut fourneau, son action intensifiante initiale sur la cuisson est notée dans l'intervalle de température de 800 à 1000°C, ce qui corres-

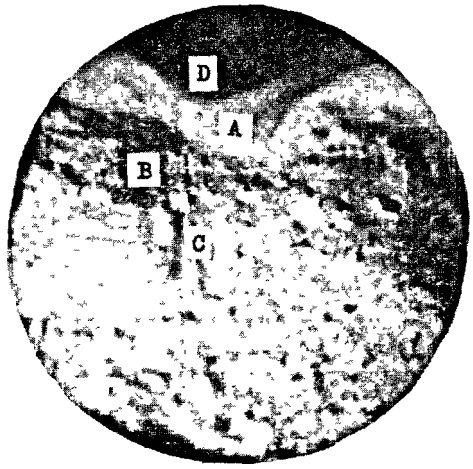

Fig.2 Interaction du laitier avec la charge.

pond à la dévitrification active du laitier et à l'interaction des produits de sa cristallisation avec CaO de la charge principale avec formation du silicate bicalcique. Il convient de noter que les cristaux de C_2S, formés à partir de la mélilite (phase prédominante du laitier de haut fourneau), se caractérisent, d'après les données des recherches(2) , par une structure cristalline plus fine que les cristaux de bélite formés à partir du quartz. Ceci influe de façon favorable sur la vitesse de dissolution de C_2S dans le bain fondu. Quant au silicate bicalcique formé à partir des minéraux de laitier, il joue le rôle de germe cristallin, contribuant à l'accélération de la synthèse de la bélite dans la masse totale du mélange à plusieurs constituants.

On observe l'action intensifiante principale du laitier sur le processus de cuisson dans le système mixte lors de l'apparition dans ce dernier de la phase liquide. La quantité totale de cette phase croît en présence de laitier, facilitant la formation de l'alite. L'accroissement des vitesses d'assimilation de la chaux aux températures correspondant à l'état fondu liquide du laitier, qui est notable en comparaison de la charge sans laitier, en témoigne (fig.3) et s'accorde avec les recherches antérieures (4).

Lors des expériences avec additions du laitier de haut fourneau dans les matières brutes à réactivité différente, on a établi que son action intensifiante se manifeste au plus haut degré lorsqu'on utilise les matières brutes avec le constituant alumosiliceux de basse réactivité et au moindre degré, avec le constituant de haute réactivité. Quant au dosage optimal du laitier de haut fourneau introduit complémentairement dans le système de cuisson, les modifications des paramètres chimiques de la charge qui s'ensuivent ne doivent pas di-

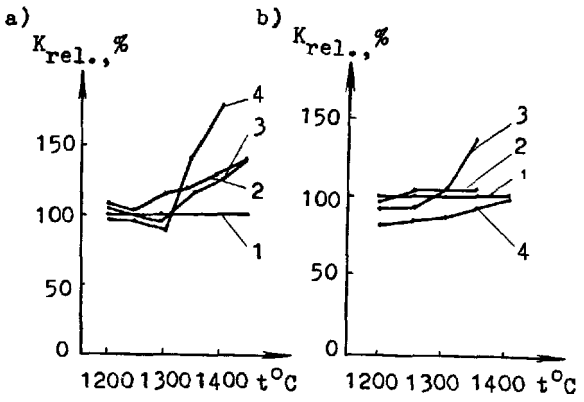

Fig.3. Réactivité des charges crues avec additions du laitier granulé de haut fourneau. Comme matière alumosilicique de base on a utilisé: a - argile sableuse, 1, 2, 3, 4 - charges comportant respectivement 0%, 10%, 14%, 22% de laitier; b- marne, 1, 2, 3, 4 - charges contenant respectivement 0%, 10%, 16%, 24% de laitier.

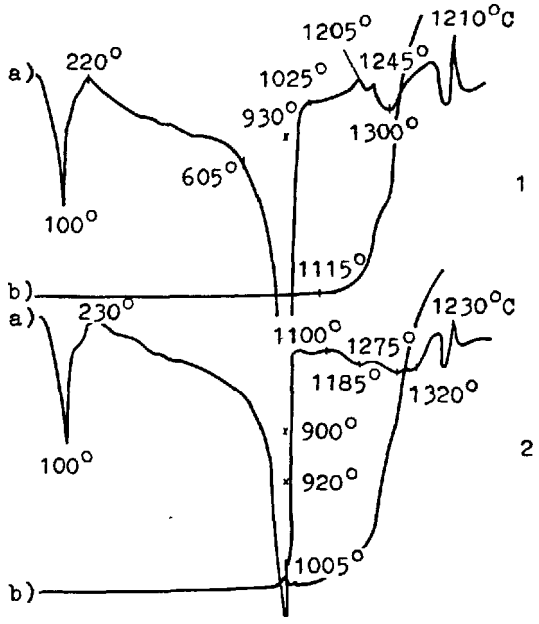

Fig. 4. Thermogrammes des charges 1, 2 contenant respectivement 0% et 25% du laitier électrothermophosphorique calculés pour la matière calcinée: a) courbe différentielle; b) courbe de conductibilité électrique.

minuer sa réactivité et compliquer la clinkérisation. C'est donc le module silicique de la charge sommaire qui en servira de critère.

La substitution partielle dans les charges crues des constituants carbonaté et alumosilicique par du laitier électrothermophosphorique, contenant des éléments modifiants et minéralisants (F,P), exerce une influence spécifique, en comparaison du laitier de haut fourneau, sur le déroulement de la cuisson. D'après les données de l'analyse thermique différentielle (Fig.4) on peut constater entre autres le déplacement de la décarbonisation vers la zone des basses températures, l'apparition sur son effet du pic endothermique double ainsi que de la phase liquide, qui s'exprime par une brusque augmentation de la conductibilité électrique du mélange en cuisson. L'effet double de décarbonisation caractérise un "faux équilibre", il est dû à la formation de l'eutectique de basse température contribuant à l'accélération de l'interaction de CaO avec la silice de la charge principale, les minéraux faiblement basiques du laitier électrothermophosphorique qui se caractérisent par une grande activité à l'étape donnée de la cuisson (cette étape coïncide avec la dévitrification du laitier). La diminution de la concentration de l'oxyde de calcium dans la sphère de réaction crée des conditions favorables à un nouvel accroissement de la décarbonisation (deuxième effet endothermique). Les processus s'accompagnant de l'absorption des ions Ca^{+2} - porteurs de courant principaux - dans le réseau des silicates de calcium, sont à l'origine de la diminution de la conductibilité électrique. Dans ce cas le maximum de la bélite formée dans le mélange avec le laitier apparaît à 100°C plus bas que dans le mélange sans additions. L'apparition des effets endothermiques à des températures correspondant au ramollissement (1180°C) et à la fusion (1220°C) du laitier électrothermophosphorique répond évidemment à la dissolution des phases halogénées initiales des silicates de calcium et de la bélite dans la phase liquide avec formation de l'alite. Dans ce cas les effets endothermiques dans le domaine des températures de 1275°C et 1325°C sont moins forts que dans la charge sans laitier, car dans les mélanges avec le laitier électrothermophosphorique la plus grande partie des matières a déjà passé dans la phase liquide avec formation d'une grande quantité d'alite. On a déterminé que dans les mélanges contenant 20% et plus de laitier, la quantité d'alite formée à 1200-1250°C était de 75 à 95% (relatifs) contre 65% dans le mélange sans laitier. L'accroissement des constantes relatives de la vitesse d'assimilation de la chaux dans les charges contenant du laitier jusqu'à 1300°C confirme tout ce qui a été dit précédemment.

L'introduction complémentaire dans le four rotatif des cendres qui se caractérisent

par la composition acide (contenant par exemple Al_2O_3 - 20%, Fe_2O_3 - 15%, y compris FeO - 7%) accélère notablement l'agglomération en phase liquide. Dans ce cas, la diminution, en présence des cendres, du module silicique dans les charges en cuisson (de2,65 dans le mélange témoin jusqu'à 1,7 dans la charge contenant 24% de cendres) communique au bain fondu du clinker des propriétés facilitant la synthèse de l'alite. Toutefois, la quantité de cendres du type donné introduite dans le lit de fusion est limitée à 8-10% (pour la substance calcinée), car une diminution excessive du module silicique entraîne la diminution des minéraux-silicates de calcium dans le clinker, par suite de quoi on pourrait obtenir un ciment à propriétés peu satisfaisantes. On peut élargir les limites d'introduction des cendres dans la charge crue par sa purification avec une matière, par exemple le laitier électrothermophosphorique, capable d'introduire dans le système de cuisson une quantité complémentaire des silicates de calcium et de normaliser de cette façon la composition chimique du clinker obtenu.

Comme il découle des résultats cités, les matières technogènes, en vertu de leur genèse, ne participent que faiblement aux processus en phase solide exigeant une surface spécifique développée et entrent en interaction avec la charge crue principalement au stade des réactions avec participation de la phase liquide. Dans ce cas, le degré de broyage des matières du deuxième flux ne jouera pas le rôle décisif en clinkérisation, qui est le sien dans l'achèvement du processus de cuisson dans la charge crue principale. Lors de la vérification de cette hypothèse on a noté que la vitesse d'assimilation de la chaux diminue naturellement avec l'accroissement du grain du constituant complémentaire. On a déterminé la dimension limite du grain pour les matières technogènes du deuxième groupe, en particulier pour le laitier granulé de haut fourneau, égale à 5-7 mm. Au-dessus de cette dimension la vitesse d'assimilation de la chaux diminue de façon inadmissible.

En ce qui concerne les grains solides de la boue de néphéline, sa granulométrie initiale plus fine en comparaison des laitiers granulés et le degré de basicité plus élevé assurent l'achèvement du processus de cuisson lorsqu'on introduit dans la charge crue une quantité complémentaire de boue de néphéline non broyée. Les données des analyses au microscope électronique ont permis de représenter plus nettement l'interaction de ses grains avec l'oxyde de calcium de la charge crue principale en démontrant que la pénétration du clinker fondu le long des limites des blocs cristallins de la bélite conditionne sa dissolution rapide.

Les résultats des études théoriques susmentionnées concernant l'efficacité de l'utilisation des matériaux technogènes lors de la synthèse du clinker de ciment trouvent leur confirmation et leur application dans les conditions industrielles aux usines utilisant des fours de dimensions différentes. Le tableau I donne les résultats des essais industriels des fours avec alimentation complémentaire en matières technogènes. Il faut noter que l'introduction séparée mais synchronisée dans le four de deux flux exige un mélange de basicité élevée dont la valeur serait fonction de la quantité du matériau technogène introduit dans le four.

Tableau I

Caractéristique du fonctionnement du four et qualité du clinker

Dénomination des caractéristiques	Dimension relativement au régime de cuisson ordinaire	Alimentation complémentaire des fours de dimension, m			
		3,3x3,6/70m avec les concentrateurs de la boue		4/150 m	4,5 x 170m
		en boue de néphéline	en laitier de haut fourneau	en laitier électrothermophosphorique	en laitier électrothermophosphorique et cendres (1:1)
Accroissement du rendement du four	%	22	25	20	15
Economie du combustible moyen	%	15	20	16	20
Température des gaz perdus	±°C	+20	+10	+15	+20
Basicité de la boue crue (facteur de saturation)	1,0	1,0	1,09	1,18	1,19
Teneur du clinker, en C_3S,%	-	55	70	62	61
Variation d'activité du clinker	± kgf/cm^2	+10	+150	+40	+35

Le fait de mélanger deux flux directement dans le four joue un role important dans la cuisson. Les recherches dans les conditions industrielles ont montre que dans le four de 70 metres on obtient une homogeneisation satisfaisante des materiaux introduits separement et assurant la fabrication du clinker de qualite.

Ainsi, en utilisant les matériaux technogenes pour l'alimentation complementaire des fours, on augmente leur rendement et diminue les depenses specifiques de chaleur pour la cuisson du clinker.

BIBLIOGRAPHIE

I.- Н.А.ТОРОПОВ, П.Ф.РУМЯНЦЕВ (I965) "О кинетике физико-химических процессов образования цементного клинкера" ЖПХ № 3,5,7,8,9, (en russe).

2.- Р.КОНДО (I964) "Скорость реакций при образовании портландцементного клинкера" IУ Международный конгресс по химии цемента", (en russe).

3.- Ю.М.БУТТ, В.В.ТИМАШЕВ, А.П.ОСОКИН (I976) "Механизм процессов образования клинкера и модифицирование его структуры", УI Международный конгресс по химии цемента, (en russe).

4.- Е.И.ЦИВИЛЕВА (I967) "К вопросу о дополнительной подаче шлака в печи в распыленном состоянии со стороны их головок", Труды Гипроцемента, выпуск XXXIII, стр. 39-50, (en russe).

Effect of Raw Materials on Cement Process, and Properties

Influence des matières premières sur la fabrication du ciment et ses propriétés

G.R. GOUDA, Ph.D. Manager, Cement Technology, Fuller Company, Bethlehem, Pennsylvania, U.S.A.

RESUME : Deux crus différents ont été choisis, correspondant aux extrêmes maximum et minimum de la fabrication du ciment. Le cru n° 1 est caractérisé par des matières premières :

A - molles

B - faciles à broyer,

C - faciles à cuire,

Le cru n° 2 est caractérisé par des matières premières :

A - dures,

B - difficiles à broyer,

C - difficiles à cuire.

Des expérimentations ont permis des comparaisons complètes, notamment sur la préparation des crus (concassage et broyage), le processus de cuisson, les propriétés du ciment, l'importance des matériels nécessaires et la consommation d'énergie. La microstructure des deux clinkers produits a été examinée au microscope électronique à balayage.

SUMMARY: Two different raw mixes were selected to represent the minimum and the maximum extremes of the cement manufacturing process. Raw Mix No. 1 is characterized by:

A. Soft raw materials

B. An easily ground mix

C. An easily burned mix

While Raw Mix No. 2 is characterized by:

A. Hard raw materials

B. A hard grinding raw mix

C. A hard burning mix

A complete comparison, including the raw materials preparation (crushing and grinding), burning process, clinker grinding, cement properties, equipment sizing, and energy and power consumption of these two mixes has been studied. A scanning electron microscope was used to characterize the microstructure of the clinker produced from both raw mixes.

INTRODUCTION

The raw materials used in the cement industry are formed naturally and thus vary widely from one place to another (1). The economy of any cement plant is affected by the different properties of the raw materials, which are the key considerations and the principal factors in designing the cement plant (2). These raw materials have considerable effect on the manufacturing process, clinker structure, and the properties of the cement. Two raw mixes were selected which represent the minimum and the maximum extremes of the cement industry. Each mix is characterized by its raw material resources which are completely different from the other. Both mixes were produced by the dry process using a suspension preheater. Each plant, due to its dissimilarities in raw materials, behaves completely differently from the other, as verified by the following information.

RAW MATERIALS

The raw material used for raw mix 1 is soft limestone with compressive strength of about 200 kg/cm^2. X-ray diffraction shows that it contains mainly calcite. Argillaceous materials--clay which is mainly Kaolinite--is used in preparing the raw mix, with about 56% SiO_2. The raw material used for the second raw mix is hard limestone with a compressive strength of about 650 kg/cm^2. No other raw materials are available in the vicinity of the second plant except shale, which consists primarily of quartz and calcite. Small amounts of illite and ankerite are also found in the shale. The limestones from both plants were studied by scanning electron microscopy (SEM). The grains of the limestone of the first plant are small and have pointed edges, Figure 1. The grains of the second limestone are larger and more or less flat, Figure 2. The second limestone appears denser than the first one.

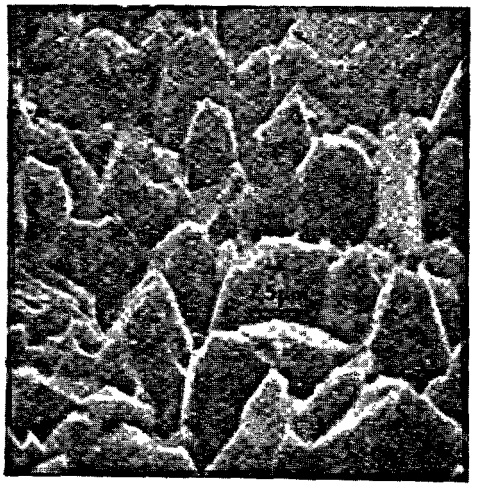

Fig. 1 - The microstructure of the limestone of the first plant showing small grains

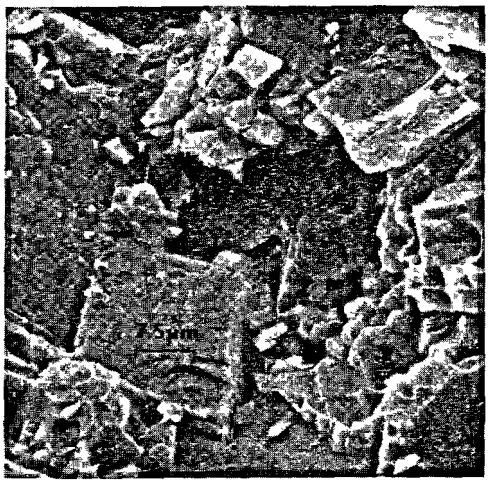

Fig. 2 - The microstructure of the limestone of the second plant showing large and flat grains

CRUSHING AND GRINDING PROCESSES

Both processes are different in each plant, and each plant's equipment is adapted according to the raw materials' properties. A single hammermill is used in the first plant, while a specially designed impactor hammer is used in the second one. The wear in the crushing area of the second plant is much more than that of the first one, primarily because of the quartz in the raw materials.

The residence time in the grinding process of the first plant is about 1/3 that of the second plant, even though the grinding systems are essentially the same. The grinding medium has normal hardness in the first mill, while in the second mill the medium has high hardness. The grinding medium wear in the second plant is more than triple that of the first plant.

RAW MIX PROPERTIES

Both raw mixes are chemically and physically different from each other. Mix 1 is considered the ideal mix for cement manufacture while mix 2 is abnormal. Free silica in mix 1 is 2.82 while that of mix 2 is 12.35. The silica modulus in mix 2 is more than double that in mix 1. A.M. is within the reasonable limits in mix 1, but in mix 2 is high. For these reasons, mix 2 is ground very finely (3.6% residue on 170 mesh) in contrast to mix 1, which is ground to a residue of 14.6% on 170 mesh.

The cements produced from both plants is sold as ordinary Portland cement, although the cement of the second plant complies too with the requirements of moderate sulfate resistance or moderate heat of hydration cement.

BURNING PROCESS

Sintering and the behavior of each raw mix in the rotary kiln is completely different. The first mix performs well in the kiln and forms a good coating. No precaution was taken in the equipment sizing.

In the case of the second mix, kiln size is larger than normal; the sintering process is difficult, and does not form a coating on the kiln bricks. The flame shape is long, the kiln rotates slowly, and the kiln is usually dusty. The clinker is smaller than that of the first mix. Comparative consumption is quite different; about 795 kcal/kg clinker is required to sinter the first mix, while about 915 kcal/kg is required for the second mix. The sintering temperature for the second mix is about 220°C higher than for the first one. The liquid phase of the first clinker is 25.50%, while that of the second mix is 17.20%, as calculated by the Lea and Parker formula. The preheater gas volume in the first plant is about 1.5 NM^3/kg clinker; in the second plant, it is about 1.7 NM^3/kg.

Table I shows the properties of the raw materials, raw mix components, grinding process, mix analysis, burning process and the fuel consumption of each plant.

CLINKER MICROSTRUCTURE

Scanning electron microscopy was used to study the microstructure of both clinkers. Clinker produced from the first raw mix is shown in Figures 3 to 5. In general, the structure is opened with a porosity of about 15%. Polygonal, well developed, compact prismatic alite crystals with a size of about 25 μm were observed, Figures 3 and 4. Small amounts of belite crystals with sizes smaller than the alite can be seen in Figure 4. Formations of C_3S from C_2S and CaO (from the surroundings) are shown in the same figure. The interstitial phases (aluminate and ferrite) are shown clearly in Figure 5, as well as a fracture of a calcium silicate grain (occurred during sample preparation for SEM).

TABLE I

THE PROPERTIES OF THE RAW MATERIALS AND THE BURNING PROCESS

	First Plant		Second Plant
Raw Materials:	Limestone (Calcite - Major) Clay (Kaolinite - Major)		Limestone (Calcite - Major) Shale (Quartz - Major, Calcite - Dominant, Illite & Ankerite - Minor)
Raw Mix Component:	80:20		82:18
Raw Mix Grindability:	11.0	Kwh/MT	23.6
Process:		Dry-Closed Circuit Raw Mill	
Grinding Media Wear:	0.15	Lb/MT	0.53
Raw Mix Properties:			
a. Chemical*: SiO_2	14.00		17.62
Al_2O_3	3.47		2.26
Fe_2O_3	2.02		0.89
CaO	42.70		43.29
MgO	1.82		2.55
SO_3	0.50		0.42
Na_2O	0.20		0.12
K_2O	0.30		0.23
L.O.I.	35.05		32.66
Total	100.06		100.04
Free Silica	2.82		12.35
Cl	0.01		0.01
S.M.	2.55		5.59
A.M.	1.72		2.54
H.M.	2.19		2.08
CaO/SiO_2	3.05		2.46
L.S.F.	0.96		0.82
b. Physical:	14.6 gm %	Residue on 170 Mesh	3.6 gm %
	2.2 gm %	Residue on 72 Mesh	0.2 gm %
Burning Process:		Suspension Preheater System	
Sintering Temperature:	1360°C		1580°C
Fuel-Kind:	Oil		Oil
Consumption:	795 kcal/kg clinker		915 kcal/kg clinker

*: % By Weight

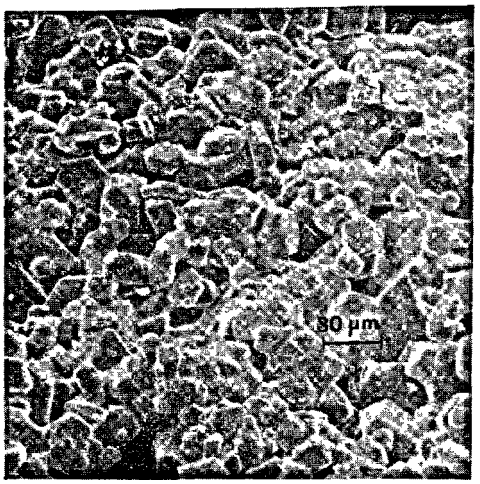

Fig. 3 - Microstructure of the first clinker showing well-developed alite crystals

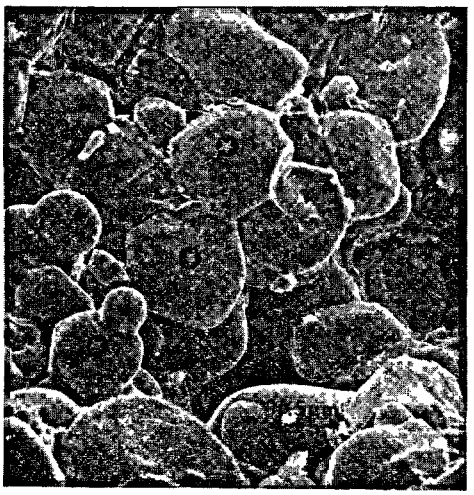

Fig. 4 - Small belite crystals (★) and large alite crystals (✪)

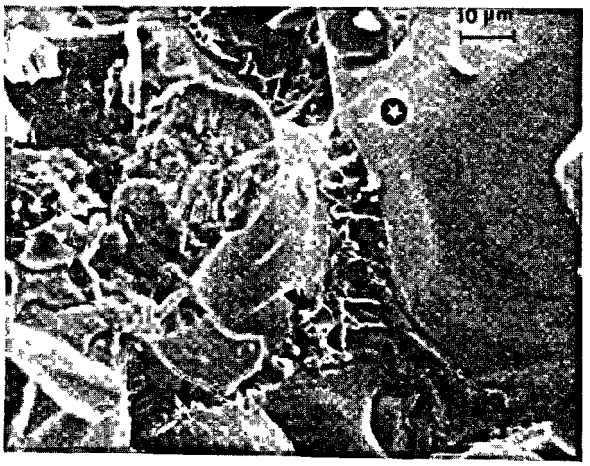

Fig. 5 - Clear interstitial phases (✦) surrounding the calcium silicate grains (✪).

The microstructure of the clinker produced from mix 2 is shown in Figures 6 to 8. It is dense in comparison to the other clinker; its C_3S crystals are small in comparison to the C_2S crystals which are abnormally large, Figure 6. This is because such a raw mix remains in the higher sintering temperature range too long, during which the C_2S becomes coarser (1); also, the L.S.F. is low, and there is insufficient CaO for C_3S formation. Belite shows coarseness and secondary crystallization, Figure 7, which is probably due to excessive heat and SiO_2 (3). A complex inner-belite crystal is shown in Figure 8, which may be due to the inversion into β-form while α-form remains. No clear interstitial phases were observed in this clinker.

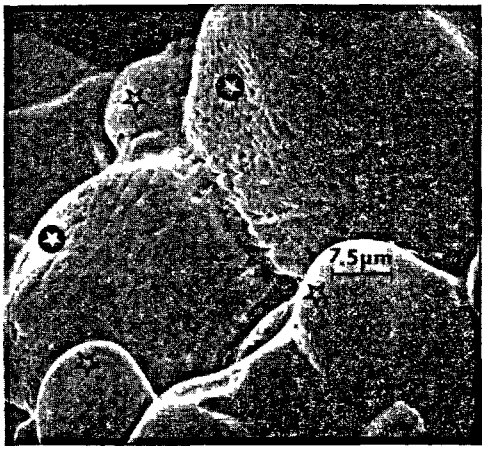

Fig. 6 - Microstructure of the second clinker, which is characterized by abnormally large belite (✪) and small alite (✲) crystals

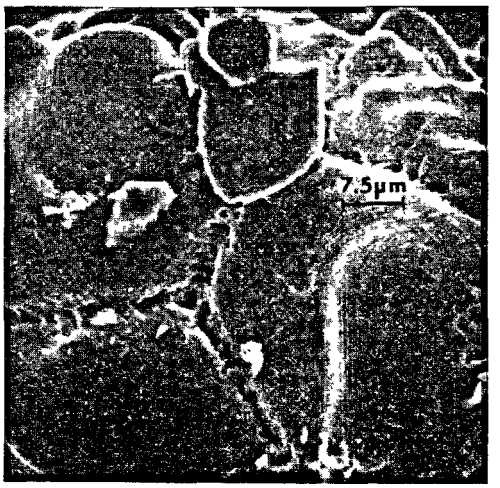

Fig. 7 - Coarseness and secondary crystallization of the belite grains of the second clinker

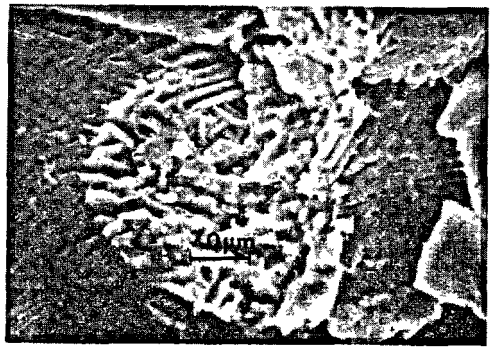

Fig. 8 - A complex inner-belite crystals of the second clinker

CLINKER GRINDING

The clinker produced from the second mix fractures easily and is more brittle in the first compartment, but its residence time in the second compartment is much longer in comparison to the clinker produced from the first mix. The grinding medium in the cement mill of each plant is different. This is because clinker 2 contains a large amount of SiO_2 and C_2S, and is ground to a fine product. The cement mill of the second mix requires more air and water for cooling the cement mill system. Because mix 2 represents the maximum extreme, its clinker is ground even more finely than the clinker produced from the first mix to attain an acceptable property. Specific surface of the cement, measured by Blaine apparatus, is about 2850 cm^2/gm for the second clinker. The clinker properties and grinding are shown in Table II.

TABLE II

THE PROPERTIES OF THE CLINKER AND THE CEMENT

First Plant				Second Plant
Clinker Properties				
a. Chemical*:	SiO_2	21.55		25.80
	Al_2O_3	5.30		3.39
	Fe_2O_3	2.95		1.32
	CaO	65.95		64.03
	MgO	2.63		3.94
	SO_3	0.92		0.76
	Na_2O	0.28		0.15
	K_2O	0.42		0.22
	L.O.I.	0.05		0.30
	Total	100.05		99.91
Insoluble Residue		0.15		0.62
Free Lime		0.70		0.30
S.M.		2.61		5.48
A.M.		1.80		2.57
H.M.		2.21		2.10
CaO/SiO_2		3.06		2.48
L.S.F.		0.96		0.83
C_3S		62.20		37.70
C_2S		14.80		45.50
C_3A		9.10		6.80
C_4AF		9.00		4.00
Liquid Phase %		25.50		17.20
b. Physical:	1180 gm/litre		Clinker litre weight	1310 gm/litre
Clinker Grinding:				
Process			Closed Circuit Cement Mill	
Fineness	7.6 gm %		Residue on 170 Mesh	3.2 gm %
	1.8 gm %		Residue on 72 Mesh	0.5 gm %
	2850.0		Blaine cm^2/gm	4600
Cement Properties:				
a. W/C Ratio		0.26		0.28
b. Setting Time		150 Min.	Initial	125 Min.
		3 Hrs. + 10 Min.	Final	2 Hrs. + 50 Min.
c. Expansion		1 mm	LeChatelier	2.5 mm
		0.03	Autoclave %	0.31
d. Compressive Strength kg/cm^2		115	1 Day	86
		140	3 Days	115
		217	7 Days	185
		320	28 Days	312

*: % By Weight

CEMENT PROPERTIES

The cement produced from the first plant is darker than that of the second one. Although the cement produced from the second plant is ground more finely, its strength is lower than that of the cement produced from the first plant. In the early ages (after one day) the strength of the second cement is less than that of the first cement by about 25%; this can be attributed to low C_3S. After twenty-eight days, the strength of both cement mixes is about the same.

The properties of the ground cement are shown in Table II.

TOTAL POWER CONSUMPTION

The total power consumption of both plants is shown in Table III; the second plant uses about 52% more power than the first plant. The raw materials and cement finish grinding processes are responsible for most of the increase in power consumption.

TABLE III

POWER CONSUMPTION

	First Plant		Second Plant
Raw Materials Preparation	12	Kwh/MT	21
Raw Mix Preparation	23	Kwh/MT	38
Clinker Grinding	41	Kwh/MT	67
Other Equipment	22	Kwh/MT	23
Total	98		149

CONCLUSIONS

The raw materials of any cement plant affect the manufacturing process, the burning process, the fuel consumption, and the economy of the plant. It is economical to work with raw materials which are easier to grind and which form an easy-burning raw mix than those which form a hard-burning raw mix (4). If a wide variety of raw materials are available in the vicinity of a cement plant, it is advisable to choose and work with the most economic material.

BIBLIOGRAPHY

1.- G. R. GOUDA (1979), "Cement raw mix: key for a successful and economical cement plant operation" Cement Technology, Vol.

2.- G. R. GOUDA (1977), "Cement raw materials: their effect on fuel consumption", Rock Products, Vol. 80, No. 10.

3.- G. R. GOUDA (1979), "Clinker Characterization by SEM", Scanning Electron Microscopy/1979, pp. 387-398.

4.- A. K. CHATTERJEE (1979), "Cement raw materials and raw mixes", Pit and Quarry, Vol. 72, No. 3 and 4.

Sur le mécanisme de la cristallogenèse dans les microzones des grains de clinker

Mechanism and kinetics of crystall formation in the microvolumes of clinker grains

V.V. TIMACHEV, membre correspondant de l'Académie des Sciences de l'U.R.S.S., professeur à l'Institut Chimico-Technique Mendéléev,
A.P. OSSOKINE, candidat ès sciences techniques,
E.N. POTAPOVA, ingénieur, Moscou, U.R.S.S.

RESUME : On a étudié le mécanisme et la cinétique des processus de dissolution de CaO et de C_2S dans l'excès de la matière fondue, et de cristallisation de C_2S et de C_3S respectivement dans les systèmes C_2S - matière fondue et CaO - C_2S - matière fondue.

Les réactions de dissolution des minéraux sont contrôlées par la diffusion et leur vitesse dépend de la structure de la phase solide et de la composition de la matière fondue. Dans le système CaO - C_2S - matière fondue, le processus de dissolution devient plus intense grâce à la cristallisation simultanée du silicate tricalcique.

Le volume des cristaux de C_3S qui se forment lors du frittage isotherme du clinker est proportionnel au volume des cristaux de bélite dissous et cette correspondance s'observe jusqu'à l'obtention de l'état équilibré.

Les phénomènes de liquation ayant lieu dans le bain fondu modifient le mécanisme et la cinétique de la dissolution des minéraux, ce qui provoque à son tour la modification du stade de limitation du processus de formation de l'alite dans le grain de clinker en fonction de l'hétérogénéité locale de sa composition.

SUMMARY : Mechanism and kinetics of solution processes of CaO and C_2S in melt excess and crystallization of C_2S and C_3S in the systems of C_2S - melt and CaO - C_2S - melt, respectively, have been studied.
Mineral solution reactions are controlled by diffusion while their rate depends on solid phase structure and melt composition. In the system CaO - C_2S - melt the solution process intensified due to simultaneous crustallization of tricalcium silicate.
The volume of C_3S crystalls formed in isothermal clinker sintering is proportional to the volume of the belite crystalls dissolved and this conformity is observaed up to the state of equilibrium.
Liquation phenomena in the melt changes the mechanism and kinetics of mineral solution. Therefore, limiting stage of alite formation process is changed in clinker grain depending on local heterogeneity of its composition.

En généralisant les résultats des travaux (1 à 5) et d'autres études, on peut représenter le processus de synthèse de C_3S comme un ensemble de transformations physico-chimiques successives et parallèles dont les principales sont les suivantes :

1) formation des matières fondues microscopiques non équilibrées ayant des propriétés acido-basiques différentes en fonction de la composition de la phase solide de contact (CaO, SiO_2, C_2S, etc.) ;

2) dissolution dans le bain fondu de composés intermédiaires, qui s'accompagne d'une variation de sa composition et de sa quantité ;

3) migration de la matière fondue dans les grains d'oxyde de calcium et de bélite ;

4) dissolution des zones de contact des macroparticules, leur dispersion en blocs séparés ;

5) dissolution par diffusion des microcristaux de CaO et de C_2S dispersés et formés par recristallisation ;

6) diffusion des ions Ca^{2+}, O^{2-}, $Si_xO_y^{z-}$ depuis les faces des particules qui se dissolvent vers les zones de croissance des cristaux de C_3S ;

7) formation des centres de cristallisation dans les zones sursaturées ;

8) croissance des cristaux de C_3S. On croît que les étapes les plus lentes limitant la cinétique de la formation de l'alite sont les réactions de dissolution des particules de départ de CaO ou de C_2S (N.A. Toropov, P.V. Roumiantsev, N.F. Vassiliéva, R. Kondo, S. Tchoï, etc.) et la diffusion des ions vers les cristaux croissants de C_3S (P.P. Boudnikov, I.V. Kravtchenko, B.E. Youdovitch, V. Iohansen).

Pour élucider les régularités de la synthèse de C_3S et déterminer le stade de contrôle, on a étudié les processus de dissolution de CaO et de C_2S dans l'excès de matière fondue et lors de la cristallisation du silicate tricalcique dans les microzones du grain de clinker.

DISSOLUTION DE CAO ET DE C_2S

Le processus de dissolution fut étudié dans les conditions de convection naturelle et forcée. Dans les conditions statiques, on procédait à la dissolution des éprouvettes obtenues par décarbonisation du marbre à des températures de 1100 à 1400 °C. Elles se composaient de cristaux arrondis de CaO de 5 à 10 µm de dimension qui se sont agrégés aux points de contact. La porosité des agglomérés variait de 44,76 (1100 °C) à 27,33 % (1400 °C) ; la dimension des pores était de (0,4 à 1,0)d des cristaux.

Dans les conditions dynamiques, on dissolvait les agglomérés de C_2S et de CaO dont la porosité était inférieure à 5 % et qui furent obtenus par compression des poudres correspondantes ayant les particules de dimension jusqu'à 60 µm à 200 MPa, suivie d'un frittage isotherme à 1800-2000 °C pendant deux heures. La dimension des pores dans les éprouvettes variait dans les limites de 180 à 5000 Å en diminuant avec l'élévation de la température de cuisson. Après la cuisson, les éprouvettes de 10^{-2}m de diamètre et de $3\cdot10^{-2}$ m de longueur furent mises en rotation dans le bain fondu à la vitesse de 10 à 20 s^{-1}. Pour les mesures on a préparé une installation spéciale (6) dont la conception permettait de réaliser le processus dans les conditions oxydantes à 1500 °C l'intensité de rotation des éprouvettes étant élevée et leur écart par rapport à l'axe de rotation étant minimale.

L'utilisation du disque tournant en tant que surface de réaction permet de régler l'épaisseur de la couche hydrodynamique et par là même l'épaisseur de la couche frontière de diffusion limitant la vitesse de la réaction se déroulant dans le domaine de diffusion. Dans ce cas le processus se décrit approximativement par l'équation

$$I = 0{,}61\cdot K\cdot D^{2/3}\nu^{-1/6}W^{1/2}\Delta C, \qquad (1)$$

où I est la vitesse de dissolution, m/s ; D le coefficient de diffusion, m^2/s ; ν la viscosité cinématique, m^2/s ; W la vitesse de rotation angulaire, rad/s ; K le coefficient ; ΔC le paramètre de concentration égale à

$$\Delta C = \frac{C_i - C_\infty}{1 - \bar{V}C_i} ;$$

C_i la concentration de saturation, fractions volumétriques ; C_∞ la concentration dans le volume de la matière fondue, fractions volumétriques ; $\bar{V}$ le volume partiel du corps dissous égale à $\bar{V} = \rho_m/\rho_{mf}$; ρ_m la densité du minéral dissous, kg/m^3 ; ρ_{mf} la densité de la matière fondue, kg/m^3.

Conformément à l'équation (1), le mécanisme du processus étant diffusif, sa vitesse est proportionnelle à $W^{1/2}$, ce qui s'observe pour des agglomérés compacts de CaO et de C_2S (fig. 1). Si l'intensité de rotation des éprouvettes de C_2S varie dans les limites de 10 à 20 s^{-1}, la vitesse de dissolution (I) croît dans la gamme $(0{,}8 \text{ à } 1{,}25)\cdot10^{-8}$ m/s, et pour CaO elle était pratiquement d'un ordre de grandeur plus élevée-$(2\text{-}3)\cdot10^{-7}$ m/s. Cette différence est due à une mobilité plus élevée des ions Ca^{2+} devant SiO_4^{4-} (2).

Les valeurs des coefficients de diffusion des ions les moins mobiles qui sont Ca^{2+} pour CaO et SiO_4 pour C_2S, calculées d'après l'équation (1), ne dépendent pas de l'intensité de convection du bain fondu et sont égales à : $D_{Ca^{2+}} = 1{,}45\cdot10^{-9}$ m^2/s ; $D_{SiO_4^{4-}} = 1\cdot10^{-10}$ m^2/s. Ces valeurs sont en accord satisfaisant avec les résultats de la détermination de D des ions correspondants par la méthode capillaire (2), ce qui témoigne également du caractère diffusif du processus.

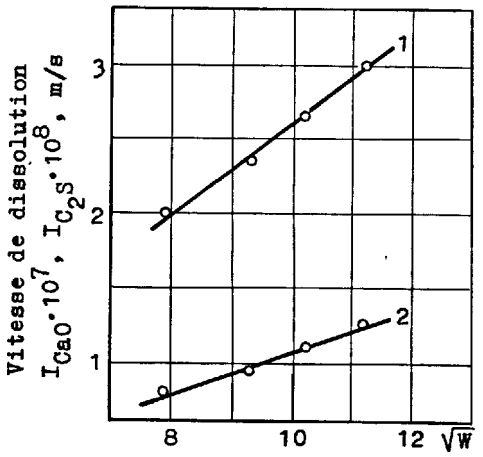

Fig. 1 - Influence de l'intensité de rotation (W) des agglomérés de CaO (1) et de C_2S (2) sur la cinétique de leur dissolution dans le bain fondu eutectique.

Lors de la dissolution de CaO dans les conditions de convection naturelle, au premier moment d'interaction la matière fondue migre intensément dans le volume du grain par son système capillaire à la vitesse de $(1\text{-}2)\cdot10^{-3}$ m/s. Les processus de dissolution moléculaires se déroulant dans le volume et sur la surface de l'éprouvette ainsi que l'action de coinçage de minces films de la phase liquide conduisent à ce que les petits cristaux séparés de CaO se trouvent entourés par la matière fondue.

La vitesse du processus de dissolution dépend dans une grande mesure de la densité des particules et la profondeur de la corrosion est proportionnelle à $\tau^{1/2}$ (fig.2).

Le caractère rectiligne de la fonction $\Delta d - \tau^{1/2}$ témoigne du fait suivant. Bien que par suite de la migration de la matière fondue et de la dissolution des zones de contact ait lieu le processus de dispersion des particules polydispersées en petits cristaux séparés, la vitesse générale de dissolution se détermine, également dans les conditions statiques, surtout par le transfert de masse des particules dissoutes quis s'effectue de la surface extérieure de l'éprouvette dans le volume de la matière fondue. Ceci permet d'utiliser l'équation (2) pour calculer le coefficient de diffusion effectif des ions Ca^{2+} :

$$D_{eff} = 0{,}15 \cdot K \cdot \left(\frac{\nu_i}{\Delta\rho}\right)^{1/3} \cdot \left[\frac{I}{\Delta C^*} \exp \cdot \left(-\frac{\delta^*}{R + \frac{\delta^*}{4}}\right)\right]^{4/3}, \qquad (2)$$

où D_{eff} est le coefficient de diffusion effectif, m^2/s;

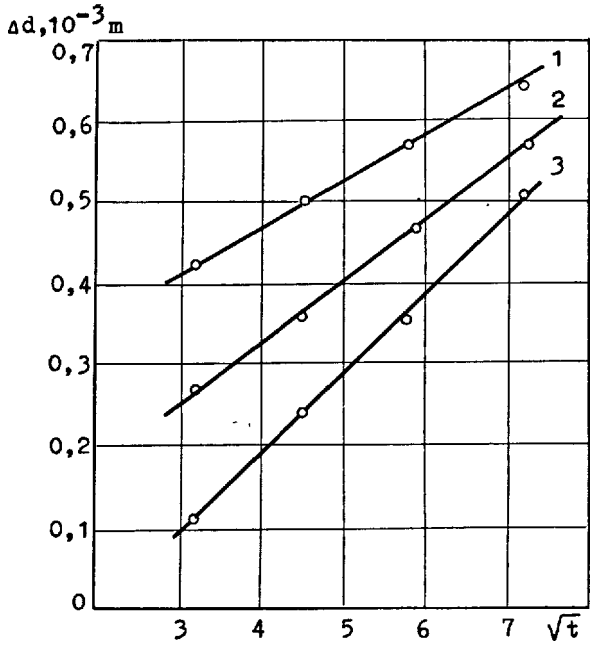

Fig. 2 - Influence de la densité des éprouvettes de CaO sur leur vitesse de dissolution (1 - densité 2060 ; 2 - 2350 ; 3 - 2500 kg/cm^3)

ν_i la viscosité cinématique, m^2/s ;

$\Delta\rho = \frac{\rho_i - \rho_\infty}{\rho_\infty}$ la différence frantionnaire de densité ; $I = DR/d\tau$ la vitesse de dissolution, m/s ; R le rayon de l'éprouvette, m ; $\delta^* = (C_i - C_o)$ l'épaisseur effective de la couche de diffusion ; $\frac{dC}{dy}$ le gradient de concentration sur la surface de séparation.

Avec l'augmentation de la densité des éprouvettes les valeurs de D_{eff} diminuaient (fig. 3) : ainsi pour $\rho = 2060\ kg/m^3$ la valeur moyenne de D_{eff}, au cours des dix premières minutes de la dissolution, était de $19{,}2\cdot10^{-7}$ m/s et pour $\rho = 2350\ kg/m^3$, de $11{,}2\cdot10^{-7}$ m/s. Cette différence traduit le caractère compliqué du mécanisme de la dissolution des agglomérés de CaO, qui est dû de toute évidence au passage dans le bain fondu tant des ions séparés Ca^{2+} que des groupements polyioniques. Les dimensions de ces groupements (particules) dépendent de la structure des cristaux de la phase solide et d'après les données de (1) la grandeur des blocs peut être de 1 μm.

RECRISTALLISATION DANS LE SYSTEME C_2S - MATIERE FONDUE

Les processus de dissolution de CaO et de C_2S et de cristallisation de C_3S dans le grain de clinker dans lequel, à 1450 °C, il se forme près de 30 à 40 % seulement

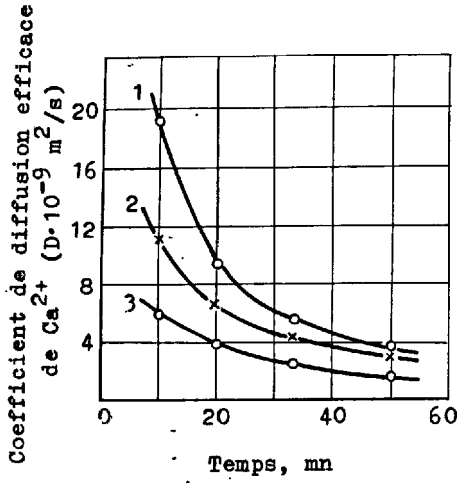

Fig. 3 - Variation des valeurs du coefficient de diffusion effectif de Ca^{2+} en fonction de la structure des éprouvettes de CaO en cours de dissolution et du temps de dissolution. Densité des éprouvettes de CaO (kg/m^3) : 1 - 2060 ; 2 - 2350 ; 3 - 2500

de la matière fondue sont pratiquement simultanés, ce qui rend difficile leur étude. La cinétique de la recristallisation de C_2S fut étudiée dans le clinker bélitique contenant 30 % de matière fondue et 70 % de silicate dicalcique avec les particules de dimension de 60 à 90 et de 160 à 200 μm. Les particules de C_2S étaient mélangées avec des charges préalablement refondues calculées pour l'obtention de la composition eutectique (CaO - 54,8 ; SiO_2 - 6,0 ; Al_2O_3 - 22,7 ; Fe_2O_3 - 16,5 % en masse) ayant la température de fusion de 1338 °C (n° 1) et de la matière fondue qui se forme dans le clinker à 1450 °C (CaO - 57,0 ; SiO_2 - 7,5 ; Al_2O_3 - 22,6 ; Fe_2O_3 - 12,9 % en masse) (bain fondu n° 2). A partir des mélanges obtenus on a formé sous pression de 200 MPa des tablettes de 10 mm de diamètre et de 0,7 g de poids. Les tablettes étaient soumises au frittage isotherme à 1450 °C dans un four vertical en platine-rhodium, suivi d'une trempe dans le milieu aqueux. Pour éprouvette étalon on a pris un aggloméré cuit pendant 1 mn. Sa structure cristalline traduisait tous les changements survenus dans la composition dispersée de C_2S et dus à la compression de la masse et à la désintégration thermique.

On déterminait la cinétique de la dissolution des grains d'après le changement d'aire des sections fixées sur les photos. On a déterminé trois grandeurs : concentration volumique des particules de C_2S en cours de dissolution (%) ; concentration volumique des cristaux de C_2S se dégageant de la matière fondue (%) ; concentration volumique de toute la phase solide (%).

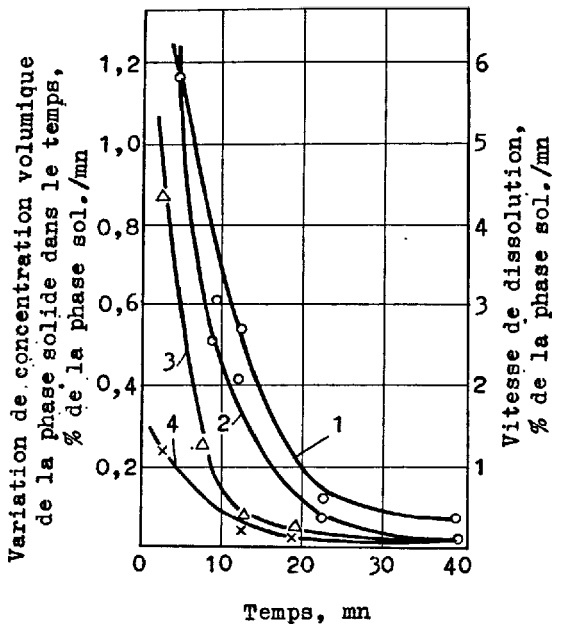

Fig. 4 - Variation des concentrations volumiques de la phase solide (1, 2) dans le système "bain fondu saturé (30 %) - C_2S (70 %)" et de la vitesse de dissolution de C_2S dans les bains fondus eutectique (3) et saturé (4). 1 - particules de C_2S de départ ; 2 - cristaux dégagés du bain fondu par recristallisation

La vitesse de dissolution des particules de C_2S dans les bains fondus eutectique et saturé au cours des premières 5 à 7 minutes est sensiblement différente (fig. 4), ce qui s'explique par la non-saturation du bain fondu eutectique en calcium et en silice à la température de l'expérience de 1450 °C. Toutefois, après la saturation du bain fondu n° 1 les vitesses de dissolution des particules de C_2S restant dans les deux systèmes deviennent pratiquement identiques. Les variations ultérieures des concentrations volumiques des grains en cours de dissolution et des cristaux de C_2S se dégageant des bains fondus saturés sont interdépendantes (fig. 4).

La dispersion des grains de départ est le stade initiale du processus de dissolution de C_2S dans le clinker fondu saturé. Ensuite, on assiste à la dissolution de petites particules et à la redéposition de la matière de la phase solide sur des monocristaux plus gros ou sur leurs agrégats avec formation d'une frange de C_2S secondaire cristallisé. Il est caractéristique qu'avec l'accroissement de l'épaisseur de ce film la vitesse de dissolution diminue, atteignant au bout de 10 mn 0,36 % de la phase sol./mn.

Après environ 10 à 15 mn, sous l'action de

la matière fondue qui migre continûment à travers le film vers la surface de la particule la liaison entre les restes du grain de départ et les cristaux nouvellement dégagés qui constituent le film enveloppant devient plus faible : il en résulte que les particules de ce dernier sont arrachées, par les courants de convection de la matière fondue, à la surface de la phase de départ et se déplacent dans l'espace intergranulaire.

La variation de concentration volumique des grains en cours de dissolution est décrite par l'équation exponentielle

$$U = e^{a-bt}, \qquad (3)$$

où $a = \ln U_0$, U_0 est la teneur initiale du système en C_2S, t le temps, b le facteur dépendant des dimensions des particules de départ : pour 160 à 200 m b = 0,0047, pour 60 à 90 m b = 0,003. Alors la vitesse de dissolution sera

$$I = be^{a-bt}, \qquad (4)$$

où $b = \frac{I_0}{U_0}$, I_0 est la vitesse de dissolution au moment d'interaction initial. L'équation (4) peut s'écrire sous la forme

$$I = I_0 e^{-\frac{I_0}{U_0}t}. \qquad (5)$$

Compte tenu du mécanisme diffusif du processus de dissolution de C_2S et en se servant de l'équation de Nernst on peut écrire

$$I_0 = D\frac{\Delta C}{\delta} \cdot S_0. \qquad (6)$$

Les grandeurs D, ΔC, $\delta = f(\Delta C, D)$ ne varient pas dans le temps et on a

$$I_0 = KS_0. \qquad (7)$$

En portant cette valeur dans l'équation (5) on obtient

$$I = K \cdot S_0 \cdot e^{-\frac{KS_0}{U_0}}. \qquad (8)$$

Il découle de l'expression (8) que la vitesse de dissolution des grains de C_2S dans le bain fondu est fonction de leur concentration de départ et de la surface d'interaction initiale. Il convient de noter que bien que le processus de dissolution se décrive de façon assez satisfaisante par l'équation (8), toutefois par suite de la dispersion périodique des particules de départ on observait à certains instants une accélération importante de la réaction, ce qui conditionne probablement le caractère périodique du processus de formation du clinker, établi également dans les travaux de I.V. Kravtchenko, M.T. Vlassova, B.E. Youdovitch, W. Kurdowski, etc.

FORMATION DE L'ALITE DANS LE SYSTEME CaO - C_2S - MATIERE FONDUE

La méthodologie des études était la même que dans le cas précédent à cette différence près que le système comprenait encore des grains denses de CaO de dimension moins de 60 mm en quantité assurant, après l'achèvement des réactions, la formation de 50 % (en volume) de C_3S.

Dans le clinker contenant C_2S et CaO les processus de dissolution des grains des deux minéraux dans le bain fondu se déroulent à une vitesse plus élevée que dans le cas où une des phases fait défaut. En effet, selon les données de la figure 5 la vitesse de dissolution de C_2S dans le clinker avec le coefficient de saturation de 0,89 était de 7,02 % de la phase sol./mn, alors que dans le système "C_2S - bain fondu saturé" la valeur absolue de la vitesse de dissolution de C_2S dans les mêmes conditions de température et de temps était 6 fois moindre et dans le système "C_2S - bain fondu eutectique" 1,5 fois moindre. Par conséquent, l'élimination constante des ions Ca^{2+} et SiO_4^{4-} du bain fondu intensifie brusquement le processus de dissolution.

Durant les premières 5 mn, la vitesse de dégagement de C_3S était de 6,9 % de la phase sol./mn et correspondait pratiquement à la cinétique de la dissolution de C_2S (fig. 5).

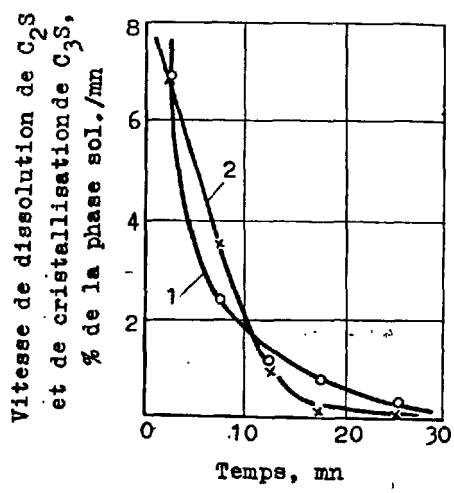

Fig. 5 - Variation des vitesses de dissolution de C_2S (1) et de cristallisation de C_3S (2) en fonction du temps de frittage à 1450 °C du clinker avec KS = 0,89

Et cette correspondance n'était pas perturbée par augmentation de la durée du traitement isotherme jusqu'à l'obtention de l'état équilibré. Ce fait témoigne d'une absorption pratiquement instantanée des ions passés dans la matière fondue par des cristaux croissants.

La plupart des cristaux de C_3S croissent sur la surface des particules de départ du bélite et de telle sorte que l'axe long soit dirigé perpendiculairement à la tengente à la surface de C_2S au point de for-

mation de C_3S.

Au fur et à mesure de la formation sur toute la surface du grain de départ du bélite du film monomoléculaire des germes quasi bidimensionnels de C_3S, l'éventualité de l'apparition de ces germes sur la surface du support diminue et le processus de cristallogenèse se poursuit grâce à la croissance des germes de l'alite susmentionnés. La frange formée par des monocristaux n'a pas de structure cristalline parfaite. Sur la surface du support il y a également des défauts (par exemple les microfissures). Il peut en résulter l'extension de la surface du support et la compression de la surface des nouvelles formations à leur point de contact, conduisant à la limite au détachement des particules de la frange à partir du support.

Les phénomènes de liquation ayant lieu dans le clinker fondu (2) peuvent modifier notablement la cinétique des processus de dissolution et de cristallisation. Dans les bains fondus salins qui se forment sur la base de Na, K, F, Cl, la vitesse de dissolution du bélite croît de 3 à 10 fois, atteignant I de CaO. Avec l'accroissement de basicité de la phase liquide en présence des ions Na, K, Ba, Sr I_{CaO} diminue de 2 à 4 fois pour la concentration des oxydes de 3 ou 4 %. Dans les bains fondus acides l'oxyde de calcium se dissout 1,5 à 2 fois plus intensément que dans le clinker fondu. La microliquation métastable due à la solubilité de SiO_2, de C_2S, de CaO et la mobilité des anions silikooxygenes et de Ca^{2+} différentes conduit a ce que dans les domaines plus acides (bélitiques) la cinétique de la formation de l'alite est contrôlée par la dissolution de C_2S et la diffusion des ions Ca^{2+}. Dans ce cas les cristaux d'alite croissent dans le sens des zones bélitiques en les supprimant. Dans les domaines avec une concentration élevée des ions Ca^{2+} et surtout Na^+ et K^+, le bélite corrode intensément (2) et le processus de synthèse de C_3S se détermine par la vitesse de dissolution de l'oxyde de calcium. Ainsi, le stade de limitation du processus de formation de l'alite peut varier dans le grain de clinker en fonction de l'hétérogénéité locale de sa composition et de la nature des ions étrangers.

BIBLIOGRAPHIE

1.- Н.А.Торопов,А.И.Бойкова,П.Ф.Румянцев (1967)"Структурные превращения и условия образования минералов клинкера",Тёхнология и свойства специальных цементов,М.,Стройиздат,33-50

2.- Ю.М.Бутт,В.В.Тимашев,А.П.Осокин(1976) "Механизм процессов образования клинкера и модифицирование его структуры",Труды VI Международного конгресса по химии цемента,М., Стройиздат,Т.I,I32-I52

3.- R. KONDO, S. CHOI (1970), "The Reaction of Portland Cement clinker Formation", Yogyo-Kyokai-Shi, 78, № 1, 8-13.(en anglais).

4.- V.IOHANSEN (1973), "Model for Reaction Between CaO Particles and Portland Cement Clinker", I. Amer. Ceram. Soc., 56, № 9, 450-454 (en anglais).

5.- И.В.Кравченко,Т.М.Власова,Б.Э.Юдович (I97I),"Высокопрочные и быстротвердеющие цементы",М.,Стройиздат,(en russe).

6.В.В.Тимашев,А.П.Осокин,А.В.Беляков(I973) "Установка для определения скорости растворения методом равнодоступной поверхности", Труды МХТИ им.Д.И.Менделеева:вып.76,II3-II7 (en russe).

Caractéristique de la matière adhérente causant des troubles de fonctionnement et leur élimination

Characterisation and Elimination of Adherent Layers Causing Operational Troubles

M. KOVACS, Dr. Research Scientist, Veszprem University of Chemical Engineering, Dept. Silicate Chemistry, Veszprém - Hungary,
K. BENYEI, Dr., Dept. Leader, Beremend Cement Works, Beremend, Hungary.

RESUME : On a étudié les composés volatils qui circulent dans les fours à voie sèche, et spécialement la relation entre l'enrichissement des composés alcalins et la formation de croûtes adhérentes.

On a constaté que des masses adhérentes se produisaient dans les cyclones des échangeurs de chaleur des fours Humboldt; on a constaté aussi, au moyen des analyses de phases, que ces produits étaient identiques à ceux produits en laboratoire et que la fusion des composés alcalins (notamment des chlorures alcalins) jouait un rôle important, en facilitant la formation de la spurite et des matières adhérentes.

L'addition de phosphate de chaux compense cet effet nocif des chlorures, des carbonates et des sulfates alcalins; toutefois P_2O_5 empêche à la formation de la spurite et celle de l'alite. La présence simultanée dans le clinker de composés alcalins et de P_2O_5 réduit la résistance du ciment, même si P_2O_5 ne dépasse pas la proportion de 0,8 %.

SUMMARY: The results of research on the effect of alkaline circulating compounds on adherent layer formation are presented in this paper.

The phase composition of adherent layers formed in cyclone heat exchangers of the Humboldt clinker burning system, and of similar laboratory samples was examined. The alkali content (in particular, alkali chloride) acts not only as a flux but at the same time also promotes spurrite formation.

Although this latter effect can be succesfully retarded by the addition of phosphates their use is not recommended, as phosphates retard alite formation too, which in turn deteriorates cement quality. The strength of cement is decreased considerably in the joint presence of alkalies and P_2O_5, even if P_2O_5 concentration is as low as 0,8%.

INTRODUCTION

La circulation des alcalins et du soufre se manifestant lors du cuisson à sec du clinker cause beaucoup de problèmes. En étudiant le principe concernant la formation des anneaux de matière ou des masses adhérentes conduisant aux engorgements des systèmes préchauffeurs, beaucoup de travaux ont réussi à montrer le rôle de l'enrichissement des composant volatils [1,2,3,4,5,6].

L'étude de la masse adhérentes se formant aux cyclones du système KHD de production du clinker à Beremend (Hongrie) nous a conduit aux constatations pareilles. Cette publication contient les résultats de ces études ainsi que ceux de nos expériences de laboratoire ayant le but suivant:

a/ étudier la formation de la composition de phase caractéristique de la masse adhérente à un pourcentage d'alcalin élevé.

b/ empêcher la formation de cette composition de phase à l'aide des additifs de P_2O_5.

Etude de la masse adhérente forme au systeme préchauffeur Humboldt

Cette étude a nécessité des prélèvements systématiques des masses adhérentes se formant dans tous les cyclones et toutes les chambres d'admission à regime continu. Les essais chimiques ainsi que les essais de diffraction X, de thermique et de microscopie électronique nous a aidé à déterminer les compositions chimique et de phase de ces échantillons.

Cette publication contient un exemple de ces essais, tout en présentant le diagramme de diffraction X de poudre (figure 1), les diagrammes DTA, TGA, DTGA (figure 2), ainsi que la prise de microscopie électronique de deux parties d'un échantillon obtenu de la masse adhérente du cyclone IV (figures 3, 4). Le pourcentage d'alcalins de cet échantillon déterminé lors de l'analyse chimique est de 16% de poids en K_2O équivalent.

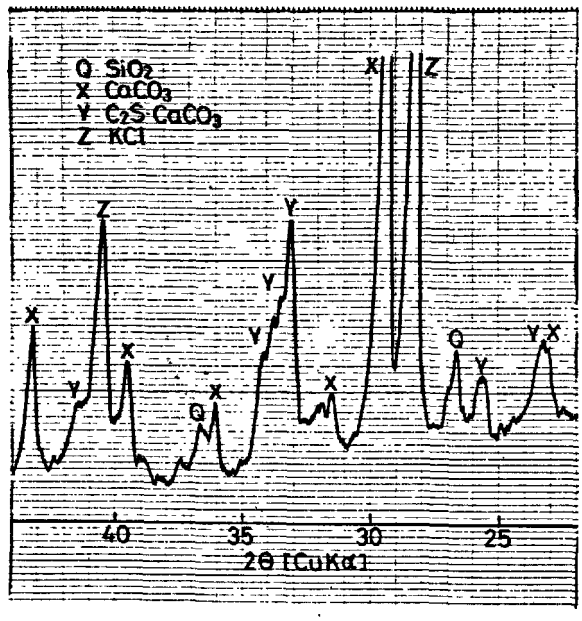

Fig. 1 - Détail de la prise de diffraction X de poudre de l'échantillon adhérent obtenu du cyclone IV.

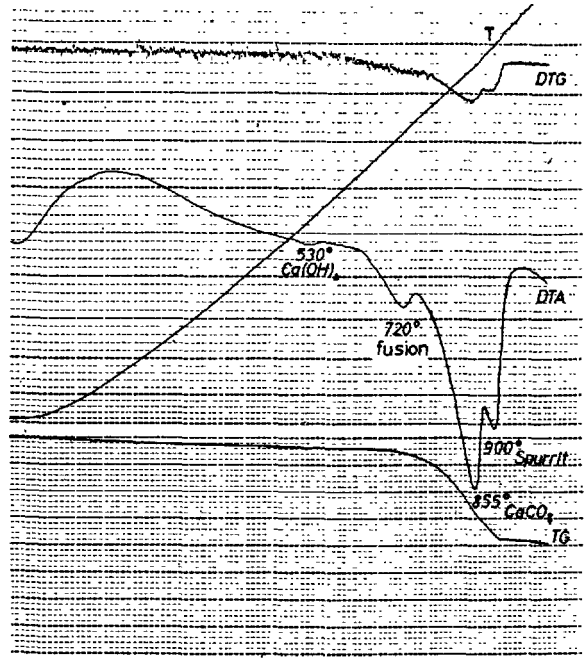

Fig. 2 - Diagramme DTA, DTGA, TGA de l'échantillon adhérent obtenu du cyclone IV.

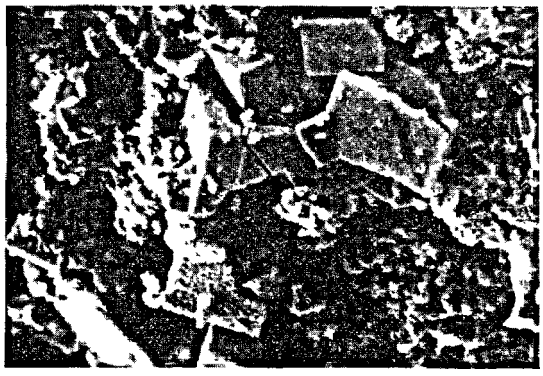

Fig.3 - Cristaux de KCl dans les échantillons adhérents obtenus du cyclone IV. Microscope électronique a balayage (grossissement: 300x)

Fig. 4 - Cristaux de spurrite et de calcite dans les échantillons adhérents obtenus du cyclon IV. Microscope électronique a balayage (grossissement: 5500x)

Le pourcentage élevé de potassium (K_2O > 10% en poids) caractérise en général les échantillons obtenus de la masse adhérente du cyclone IV. Normalement ce potassium s'enrichit au cyclone IV en forme de chloride (fig.1, 3).

(Il faut noter que le pourcentage de chloride de la farine brute de Beremend n'atteint pas 0,015 % en poids, il est donc superflu d' y utiliser le by-pass.)

Les masses adhérentes du cyclone IV et des autres niveaux du système préchauffeur ne contiennent pas de sulfates alcalins et de sulfates alcalins de calcium. Le soufre introduit au système s'enrichit essentiellement en forme d'anhydrite ($CaSO_4$) dans la masse adhérente du cyclone II.

Le tableau I contient les compositions de phase caractérisant les masses adhérentes des cyclones et de la chambre d'admission en se basant sur les résultats des essais ci-dessus de 70 échantillons.

TABLEAU I

Composition de phase caractéristique de la matière adhérente se produisant aux étapes du système préchauffeur (% en poids)

Endroit du prélevement	Calcite $CaCO_3$	Anhydrite $CaSO_4$	Spurrite $2C_2S \cdot CaCO_3$	Portlandite $Ca(OH)_2$	Chaux libre CaO	Phases déterminées qualitativement
Cyclone I.	72,5	2,4	-	-	traces	Quartz
Cyclone II.	16,6	50,0	traces	3,3	traces	Quartz
Cyclone III.	48,3	3,8	traces	10,8	4,5	Mineraux de clinker et quartz
Cyclone IV.	26,6	2,4	22,5	3,2	4,3	Mineraux de clinker et quartz
Entre le cyclone IV. et le four	10,5	-	6,2	12,8	15,0	Mineraux de clinker
Chambre d'admission	19,7	traces	17,1	22,0	7,2	Mineraux de clinker

Expérience de laboratoire

Le problème principal de l'usine de Beremend consiste dans la masse adhérente à pourcentage élevé d'alcalins et de spurrite du cyclone IV. Outre l'effet de P_2O_5 empêchant la formation de spurrite, une relation entre la formation du spurrite caractérisant la composition de phase de la matière adhérente et les composés alcalins a été étudiée lors des expériences de laboratoire.

Les matières utilisées au cours des expériences sont les suivantes: farine brute d'usine, K_2CO_3, Na_2CO_3, KCl, NaCl, K_2SO_4, Na_2SO_4 et $Ca_3(PO_4)_2$.

Le mode de préparation des échantillons est le suivant:

a) On mélange un composé alcalin d'une quantité équivalente à 1,2 % en poids de K_2O et de la farine brute. Un échantillon correspond à un seul composé alcalin.

b) On mélange un composé alcalin et une quantité de $Ca_3(PO_4)_2$ correspondant à 0,8 ou à 1,6 % en poids de P_2O_5 selon la méthode de a). (Le pourcentage de P_2O_5 concerne le clinker.)

A partir des mélanges préparés selon les méthodes a) et b) et de la farine brute sans additifs nous avons aggloméré des pastilles que nous avons cuit pendant deux heures dans un four électrique à température de 750 °C, 840 °C, 970 °C et 1400 °C.

La détermination de la composition chimique et de phase des échantillons ainsi préparés s'est effectuée par les essais chimiques, thermiques et de diffraction X.

Les composants de la farine brute d'usine et sans additifs ne montre pas la formation du spurrite aux températures d'essais.

On peut constater la formation la plus élevée dans les échantillons contenant des composés alcalins et cuits à 840 °C (figure 5).

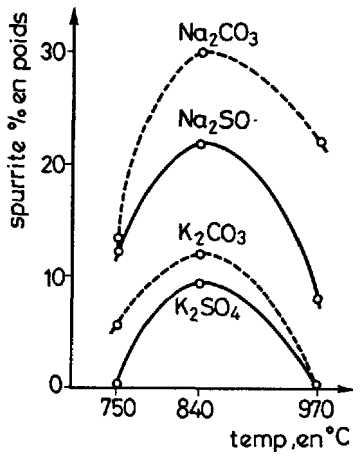

Fig. 5 - Teneur de spurrite en fonction de la température de cuisson.

Tous les composés utilisés dans nos essais aident la formation de spurrite, mais c'est d'une facon différente: la présence des chlorides donne la formation la plus intensive, l'effet des carbonates est moins accentué, les sulfates montrent une efficacité bien réduite (figure 5).

$Ca_3(PO_4)_2$ empêche la formation de spurrite. Cet effet inverse s'augmente avec la quantite de P_2O_5 (figure 6).

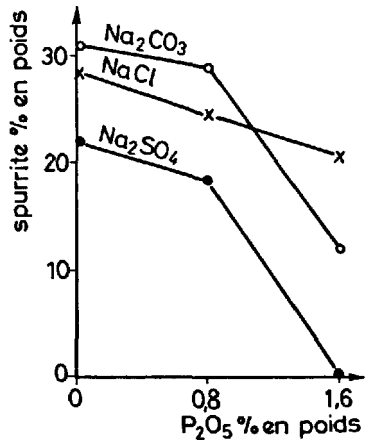

Fig. 6 - Teneur de spurrite des échantillons cuits à 840 °C en fonction de P_2O_5.

Nous avons enfin compensé les compositions de phase des échantillons cuits à la temperature de 1450 °C. Malheureusement il faut constater que les échantillons contenant des composés alcalins et P_2O_5 montrent une formation d'alyte bien réduite. Le pourcentage de 0,8% en poids de P_2O_5 calculé sur clinker empêche déjà la formation d'alyte et les échantillons de P_2O_5 contiennent outre le derivé β du silicate dicalcique beaucoup de derivés α'.

Ces résultats contredisent nombreux données anterieures, par exemple que la présence de P_2O_5 augmente la durée du durcissement en cas d'une matière première à pourcentage d'alcalin élevé, mais augmente aussi la résistance à la compression de 28 jours [7] que le C_3S et la solution solide de C_3S à pourcentage de P_2O_5 réduit ne montre qu'une différence presque négligeable, en ce qui concerne l'hydraulicite [8] et enfin qu'un clinker dont le pourcentage de P_2O_5 ne dépassant pas 1% en poids donne des ciments d'une résistance à la compression bien élevée et cet effet ne dépend pas de l'âge des echantillons [9].

Le résultat de notre analyse de phase montre un pourcentage d'alyte et de β silicate dicalcique moins élevé dans les échantillons de teneur de P_2O_5 que dans ceux sans P_2O_5, ce qui est prouvé par des essais de résistance. La présence de P_2O_5 dans les échantillons augmente la durée du durcissement et ces échantillons peuvent être caractérisés par une résistance moins élevée même de 28 jours que dans caux sans P_2O_5.

CONCLUSION

L'additif de phosfate de calcium peut compenser l'effet des composés alcalins facilitant la formation de spurrite, mais la présence de P_2O_5 empêche à la fois la formation de spurrite et d'alyte même en cas d'un clinker ou le pourcentage de P_2O_5 ne dépassant pas 0,8% en poids. Les additifs de P_2O_5 empêchent donc la formation de spurrite, c'est-a-dire celle de la matière adhérente, mais c'est au détriment de la qualite du clinker.

BIBLIOGRAPHIE

1.- LOCHER, F.W., SPRUNG, S. und OPITZ, D. (1972), "Reaktionen im Bereich der Ofengase", Zement-Kalk-Gips, 25, 1-12, en allemand.

2.- SYLLA, H.-M. (1974), "Untersuchungen zur Bildung von Ansatzringen in Zementdrehöfen", Zement-Kalk-Gips, 27, 499-508, en allemand.

3.- SYLLA, H.-M. (1977), "Ansatzbildung durch Salzschmelzen", Zement-Kalk-Gips, 30, 487-494, en allemand.

4.- MUSSGNUG, G. (1962), "Beitrag zur Alkalifrage in Schwebegaswärmetauscheröfen", Zement-Kalk-Gips, 15, 197-204, en allemand.

5.- DANOWSKI, W. und KIESER, J. (1973), "Zum Verhalten von Alkalien beim Zementbrand nach dem Trockenverfahren mit Schachtvorwärmern", XI. Conference on the silicate Industry, Siliconf, Budapest, 279-287, en allemand.

6.- AMAFUJI, M. and TSUMAGARI, A. (1969), "Formation of the double salt in cement burning", Proc. V. Intern. Symp. Chem. Cem., Tokyo 1968, Vol. I; Chemistry of cement clinker, 136-156, en anglais.

7.- TIMASHEV, V.V., GALPERINA, T.Ya., BYKOVA, S.N., SEBOSTIANOVA, L.I., YANKOV, N.F. (1979), "Effect of Phosphorus on Phase Composition and Properties of Cement Produced of High-Alkali Raw Materials", Cement, n° 3, 6-7, en russie.

8.- GUTT, W. (1963), "High temperature phase equilibria in the system $2CaO \cdot SiO_2$ - $3CaO \cdot P_2O_5$ - CaO", Nature, 197, 142-143, en anglais.

9.- SALGE, H. und THORMANN, P. (1973), "Über den Einfluss von P_2O_5 auf die Konstitution von Portlandzementklinker", Zement-Kalk-Gips, 26, 532-539, en allemand.

Influence du mode de broyage du clinker et des constituants secondaires sur la réactivité des ciments et sur la rhéologie

Clinker Grinding method and secondary components Their effect upon cement reactivity and rheology

Y. LE JEAN, C.E.R.I.L.H., France.

RESUME

Comparaison entre le broyeur à boulets et le broyeur à projection sous le double aspect de l'activation des produits et des caractéristiques rhéologiques des pâtes. On démontre que le broyeur à projection permet d'optimiser la courbe granulométrique pour obtenir des résistances très élevées à court terme. Cette augmentation s'accompagne toutefois d'une modification de la rhéologie des pâtes.

Le broyage sélectif des constituants secondaires du ciment, s'il est effectué suivant des règles prévues, permet d'augmenter le dosage de ses constituants sans pénaliser les résistances à court terme. Ces différences de comportement peuvent être expliquées par des paramètres physiques liés au mode de broyage.

SUMMARY

Comparaison between ball mill and jet-mill, from the double point of view of activation of the products and of the rheological characteristics of pastes. A clear indication is given that the jet-mill allows to obtain the best granulometric properties and, thus, very high strengths at early age. Nevertheless, this increase of strength comes with a change of the rheology of the pastes.

The selective grinding of secondary components of cement, when accomplished under the specified conditions, permits to increase the amont of its components without disadvantage for early age strengths. These differences of the behaviour can be explained by the physical parameters binded with the grinding method.

1. LE BROYAGE PAR PROJECTION

Le rendement du broyeur à boulets chute très rapidement dès que l'on essaie d'obtenir des finesses supérieures à 2500 cm^2/g ; ceci est à attribuer à l'effet d'écran que les grains fins exercent au bénéfice des grains les plus gros et aussi au phénomène d'agglomération des fines particules. Si l'on veut éviter d'avoir des grains très gros dans la poudre, il faut consentir une quantité importante de grains fins qui, dans la plupart des applications, se révèlent inutiles.

Avec le broyage par projection sous vide une telle agglomération est impossible puisque le grain éclate sous sa propre énergie cinétique. Tous les grains ayant une même vitesse et n'étant pas freinés aérodynamiquement, les petits grains sont animés d'une énergie cinétique infiniment moins importante que les grains les plus gros et se trouvent moins sollicités à l'impact sur les cibles : d'où sélectivité du broyage par projection sous vide et obtention de courbes granulaires resserrées des matériaux broyés.

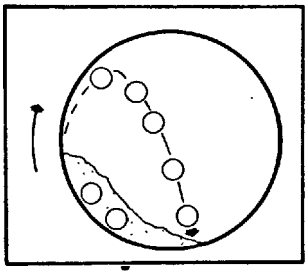

Figure 1 - Broyeur à boulets (percussion)

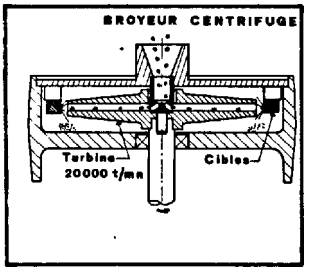

Figure 2 - Broyeur à projection

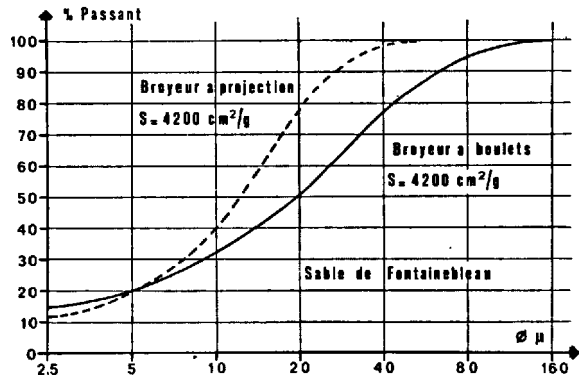

Figure 3

La figure 3 illustre les différences de spectre granulométrique d'un sable de Fontainebleau broyé au broyeur à boulets et du même sable broyé au broyeur à projection sous vide. Ces deux poudres ont sensiblement la même surface spécifique mais le broyeur à projection a fourni que peu de grains supérieurs à 20 microns et aucun à 40 microns, ce qui constitue un avantage considérable sur le broyeur à boulets qui a produit 27 % de grains supérieurs à 40 microns.

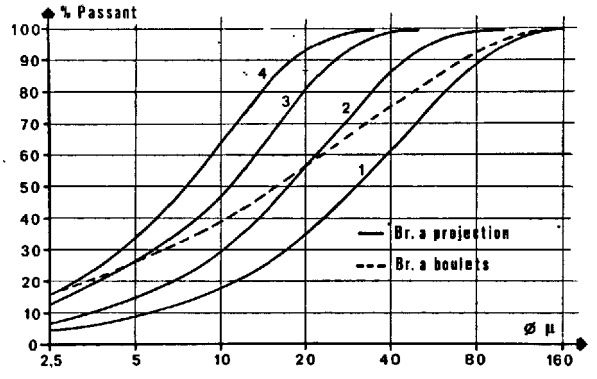

Figure 4

La figure 4 illustre les différents spectres granulométriques d'un clinker de cimenterie broyé au broyeur à boulets et au broyeur à projection. L'avantage du broyeur à projection réside dans la facilité d'obtenir la finesse désirée. Le processus d'éclatement ne dépend que de la vitesse d'impact lorsque le grain ne comporte pas d'inhomogénéité. Le réglage du broyage s'effectue en ajustant la vitesse de rotation du rotor.

Les mesures granulométriques montrent que la surface spécifique en cm^2/g est devenue un paramètre insuffisant pour caractériser des poudres broyées par des procédés différents puisqu'à surface spécifique sensiblement égale on peut avoir des répartitions granulaires très différentes.

Tableau I

Matériaux	Dureté Vickers	Echelle de Mohs
Gypse	70	2
Calcite	110	3
Clinker	450 à 700	
Feldspath	720	6
Quartz	1280	7

	Broyabilité cm^2/Joule
Gypse	200
Clinker	70

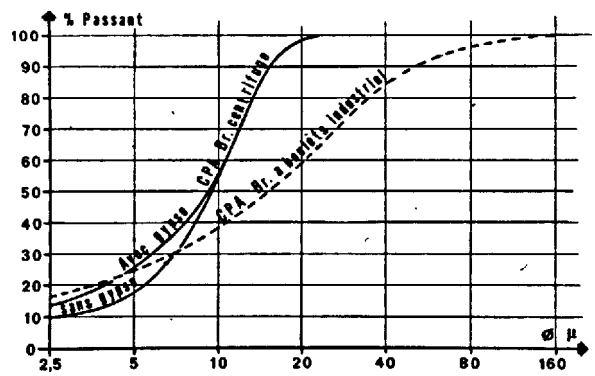

Figure 5

Le tableau I et la figure 5 montrent l'influence de la broyabilité des différents composants du ciment. Le gypse est un élément tendre qui apporte les éléments fins et influence fortement la surface spécifique du mélange et le caractère rhéologique des pâtes, mortiers et bétons au cours de leur préparation et de leur mise en œuvre.

Le clinker étant de plus faible broyabilité, la sélectivité du broyage par projection donne une courbe granulaire particulièrement resserrée, proche de la courbe idéale recherchée pour tirer le meilleur parti du potentiel chimique du clinker.

2. INFLUENCE DE LA GRANULOMETRIE SUR LES RESISTANCES MECANIQUES

Tous les essais se réfèrent à un seul gypse témoin et trois clinkers (G), (R) et (A), chacun d'eux étant broyé avec gypse et sans gypse pour délimiter l'influence de celui-ci, soit avec un broyeur à boulets (BB), soit avec un broyeur à projection (BP).

Tableau II et III

Analyses chimiques des clinkers et CPA

	Caractéristiques des clinkers témoins				
	Usine G		Usine A		Usine R
	clinker	CPA 50	clinker	CPA 50	clinker
pf	0,40	1,51	0,44	1,36	0,45
SiO_2	21,82	20,29	21,90	21,01	21,94
Al_2O_3	6,3	5,89	3,82	3,49	5,03
Fe_2O_3	2,52	2,30	4,50	4,16	3,01
CaO	66,23	64,95	67,00	64,58	65,19
MgO	1,00	0,80	0,50	0,60	1,05
Na_2O	0,20	0,18	0,08	0,06	
K_2O	0,17	0,20	0,53	0,74	1,29
SO_3	0,81	3,44	0,51	3,53	1,57
Insol.	0,17				
CaO libre	0,28				
	Compositions potentielles en %				
SO_4Ca	1,4		0,87		
AFC_4	7,7		13,74		9,15
AC_3	12,5		2,49		8,24
SC_3	54,6		66,44		62,11
SC_2	21,7		13,05		15,54

2.1 Influence du gypsage

a) Granulométrie (fig. 6)

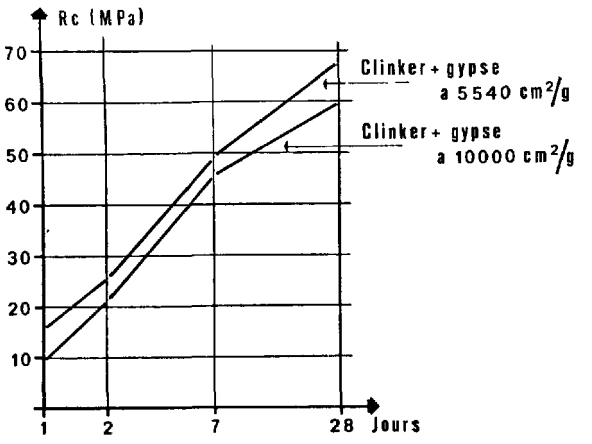

Figure 6

Le clinker (G) et le gypse sont broyés séparément au broyeur à boulets. La surface spécifique du clinker est de 2950 cm^2/g ; le gypse a été broyé à 5540 cm^2/g et 10 000 cm^2/g. Les ciments ont été gypsés à 5 % SO_3.

A quantité égale de gypse, le ciment (A) donne de meilleures résistances que le ciment (B).

b) Influence du pourcentage de gypse (fig. 7)

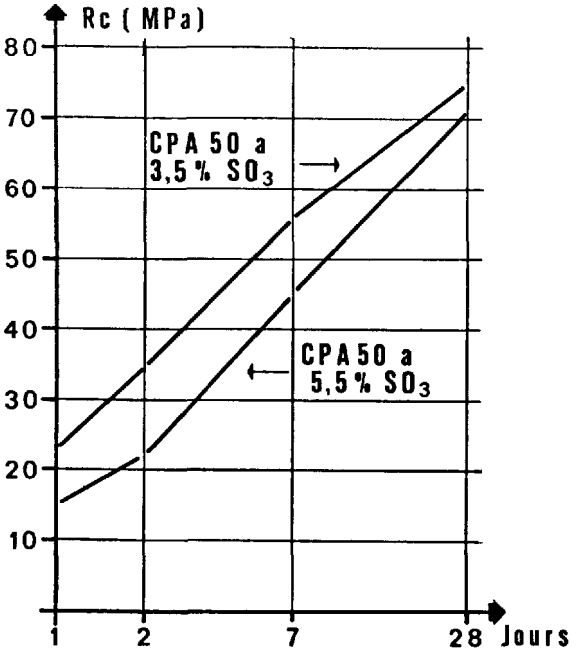

Figure 7

Clinker (G) et gypse sont broyés ensemble au broyeur à boulets. Les résistances mécaniques sont influencées par le pourcentage de gypse.

c) Influence du mode de broyage

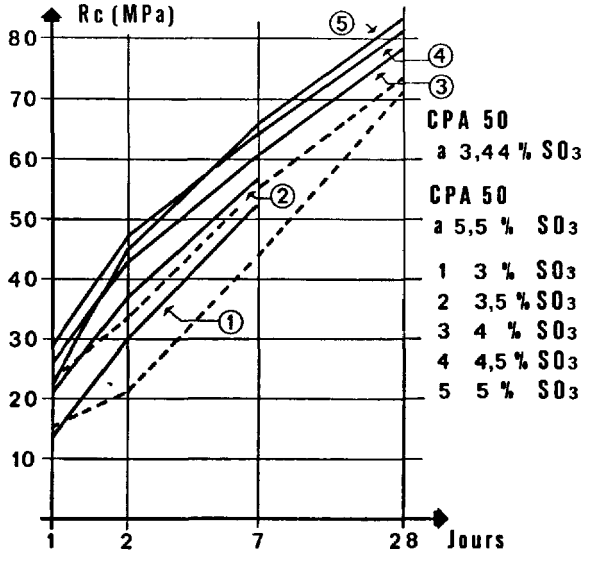

Figure 8

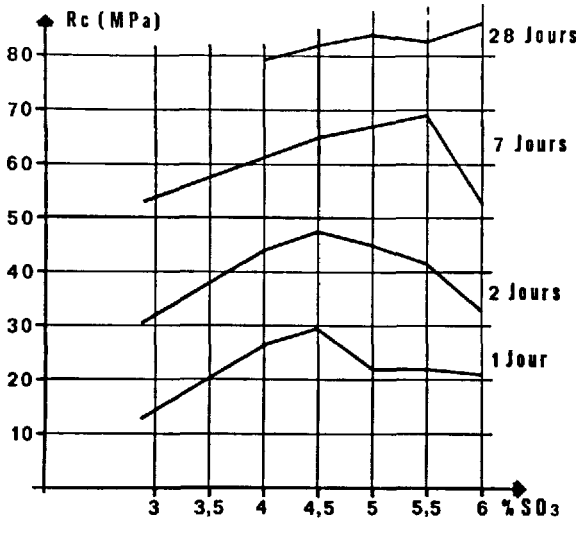

Figure 9

Le résultat des essais montre que le ciment broyé au broyeur à projection permet, par l'optimisation du gypsage, d'obtenir un important gain des résistances mécaniques, et tout en améliorant d'autres caractéristiques telles que le gonflement et la fissuration.

La photo n° 10 prise au microscope optique montre que les gains de clinker restent polycristallins après un broyage au broyeur à bouelts industriel. Par contre, le broyage fin par projection donne des grains monocristallins plus particulièrement par la libération de l'alite et du C_3A, photo n° 11. Le procédé de broyage par projection permet d'augmenter sensiblement le gypsage sans inconvénient.

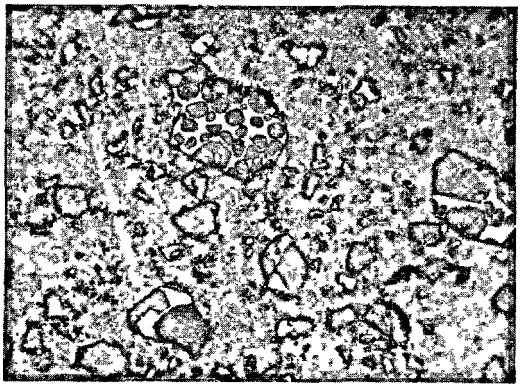

Figure 10

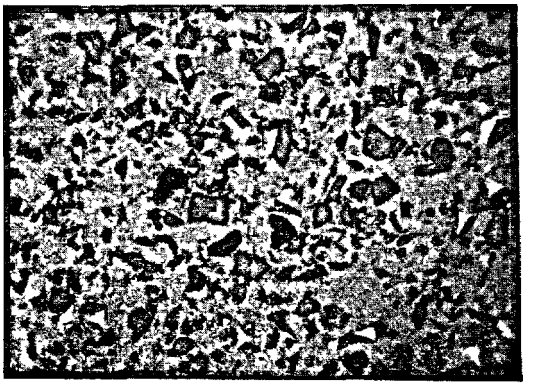

Figure 11

2.2 Ajouts inertes

La structure monodimensionnelle du ciment obtenu par le broyage sélectif favorise l'incorporation de fillers inertes qui, au lieu de diluer le produit comme c'est le cas pour un ciment broyé au broyeur à boulets, jouent le rôle actif d'ajout de remplissage granulométrique.

La figure 12 montre qu'avec 30 % d'ajout inactif (FC) et 70 % de clinker gypsé, broyé au broyeur à projection, on obtient les performances d'un CPA 50. De la même manière, avec 40 % d'ajout inactif, on obtient les performances d'un CPA 40 et avec 50 %, celles d'un CPJ 35 . Une étude récente du Laboratoire Central des Ponts et Chaussées, consacrée aux ciments de broyeurs à boulets, et les essais témoins effectués au CERILH montrent que les résistances mécaniques décroissent rapidement lorsque la teneur en ajout inerte croît, et qu'elles suivent approximativement la loi de FERET.

La figure 13 révèle qu'un même mélange [clinker (G) + gypse] broyé au broyeur à projection donne des résistances mécaniques ne suivant plus la loi de FERET. Les écarts, par rapport à cette loi, se traduisent par un gain important pouvant atteindre 50 % à 100 %.

A performances identiques, la teneur d'ajouts inertes est environ 30 % supérieure au taux d'ajout dans le cas où le clinker + gypse sont broyés au broyeur à projection (BP).

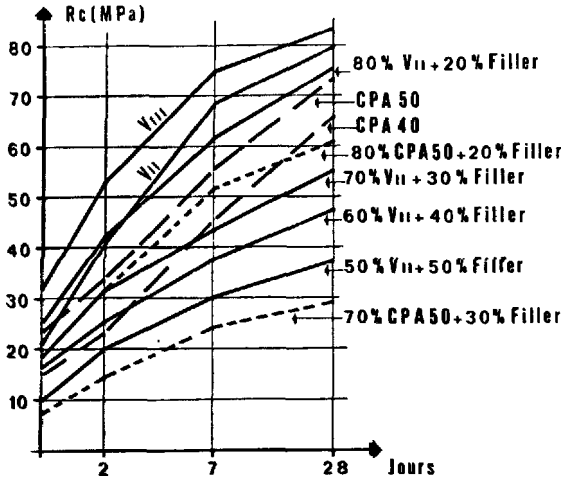

Figure 12

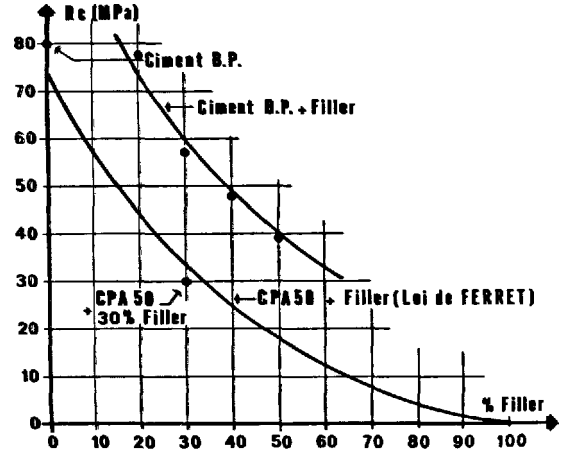

Figure 13

2.3 Ajouts actifs

Dans une moindre mesure que le clinker, les laitiers, les cendres volantes et les pouzzolanes sont des ajouts actifs connus et utilisés pour la fabrication de ciments normalisés. Leur action surtout pouzzolanique est sensible à moyen terme mais leur activité à court terme peut être augmentée par le broyeur à projection.

La figure 14 montre les résistances mécaniques obtenues avec le clinker (R), broyé avec ajout actif au broyeur à projection, pour un béton COPLA à 350 kg (granulat Béton Armé). Sur la même figure sont reportés deux ciments témoins de broyeur à boulets industriel [clinker (R)]. Bien que les ciments de broyeur à projection demandent un rapport E/C plus important, ceux-ci font apparaître leurs avantages en résistances mécaniques.

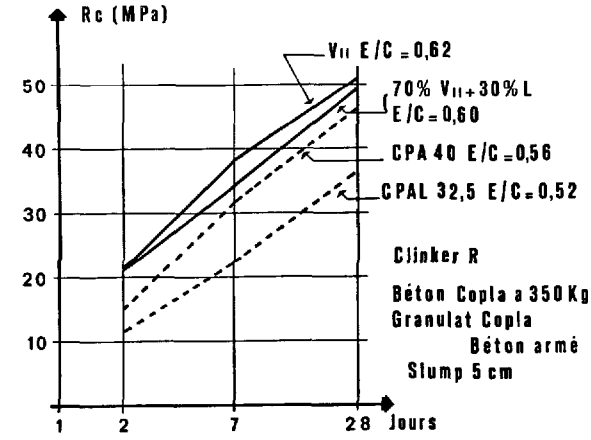

Figure 14

3. RHEOLOGIE ET RESISTANCES MECANIQUES DES MORTIERS ET BETONS

Les mortiers et bétons confectionnés avec un ciment broyé au broyeur à projection sont caractérisés par une mauvaise rhéologie ne favorisant pas une bonne mise en place et un bon serrage dans les moules à éprouvettes. Néanmoins, les résistances mécaniques obtenues avec ou sans ajout sont très largement supérieures à celles obtenues avec un ciment de même composition broyé au broyeur à boulets. Tous les essais d'étalement sur mortier ont, pour référence, la Norme américaine FLOW-TEST C124-39.

3.1 Influence de la granulométrie

a) L'influence de la granulométrie de chaque constituant du ciment est considérable sur la finalité des caractéristiques mécaniques d'un mortier et d'un béton. La cinétique d'hydratation est bouleversée par la séparation des phases du clinker dont la granulométrie se trouve resserrée (Photos 15 et 16). Les études de J.P. BERNARD, M. REGOURD et J.P. MERIC démontrent que les paramètres granulométriques ont une influence déterminante sur la cinétique d'hydratation des constituants du ciment.

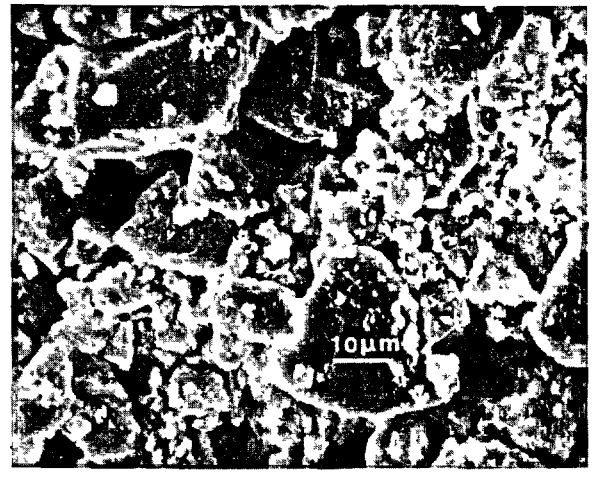

Figure 15 (BB)

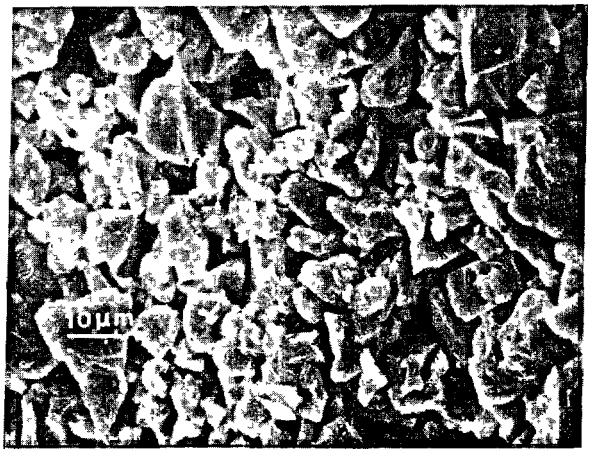

Figure 16

Un grain de 1 micron s'hydrate au cours du gâchage et ne contribue plus aux résistances du béton
" " de 2 microns est hydraté à 100% en 1 h 1/2
" " de 20 microns est hydraté à 69% en volume au bout de 7 jours
" " de 30 microns est hydraté à 52% en volume au bout de 7 jours
" " de 70 microns est hydraté à 70% en volume au bout de plusieurs mois et se comporte comme un granulat.

b) Influence de la granulométrie des agrégats et du ciment

Tous les mortiers témoins ont été confectionnés suivant la Norme AFNOR en vigueur NF P15-403, sans tenir compte de la granulométrie des ciments de broyeur à projection pauvres en éléments fins et en grains supérieurs à 20 microns, c'est-à-dire avec discontinuité granulométrique entre ciment et sable normalisé. L'optimum de remplissage granulométrique correspondant à une distribution privilégiée de particules d'ajouts inertes ou actifs, ou les deux à la fois, a été recherché à partir des formules de FULLER-BOLLOMEY et de JOISEL, pour obtenir une meilleure rhéologie des mortiers et, à rhéologie égale, réduire le rapport eau/ciment.

3.2 Influence de la forme des grains de ciment et ajouts

a) Clinker

Les photos 17 et 18 montrent les différences importantes entre un grain de clinker (G), broyé au broyeur à boulets, et un grain de clinker broyé au broyeur à projection. Celui-ci donne des fragments à angles vifs et à surface lisse et les grains sont souvent monocristallins. Les différences d'aspect et de géométrie peuvent expliquer la mauvaise mobilité des grains au cours du gâchage et de la mise en place des mortiers et bétons dans les moules.

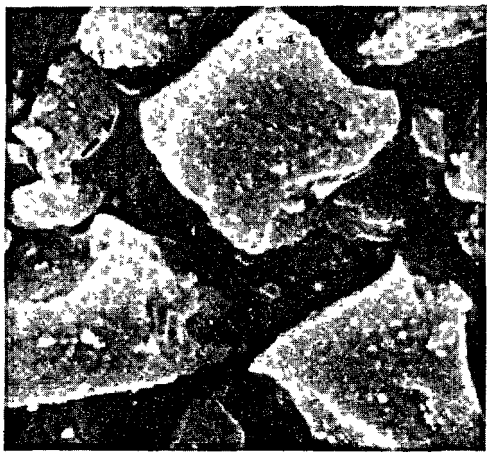

Figure 17

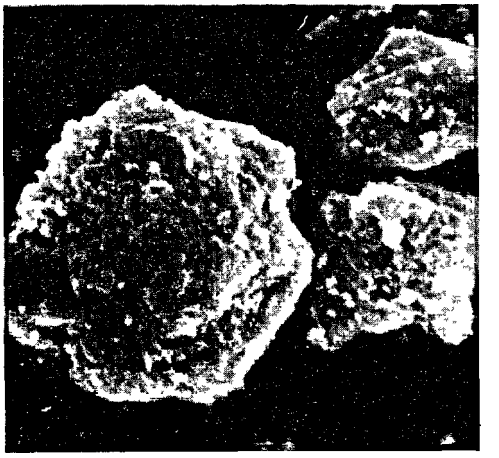

Figure 18

b) Ajouts

Les ciments aux cendres volantes ont généralement la propriété de donner des mortiers et bétons à bonne rhéologie. Cependant, une quantité importante d'essais montrent que les cendres volantes, composées essentiellement de micro-billes, pouvaient aussi bien améliorer que réduire la rhéologie des mélanges, (figure 19).

La granulométrie et la quantité de gypse ont une influence importante sur les résistances mécaniques des mortiers et bétons confectionnés, soit avec un clinker de broyeur à boulets, soit avec un clinker de broyeur à projection. Il y a lieu d'ajouter l'influence rhéologique du gypsage en fonction de la composition potentielle du clinker, (figure 20). Pour mémoire, les CPA 50 de broyeur à boulets industriel donnent généralement des étalements compris entre 65 % et 75 % pour un rapport E/C = 0,5.

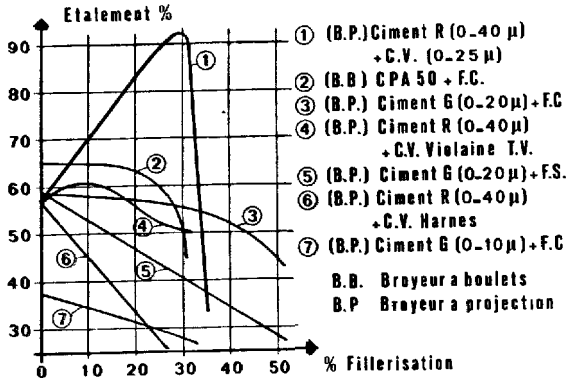

Figure 19

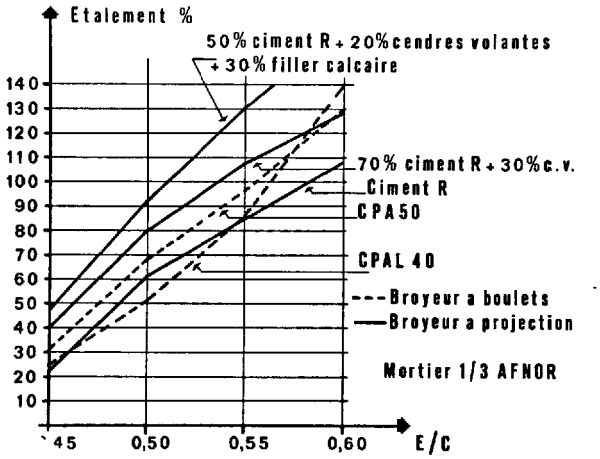

Figure 21

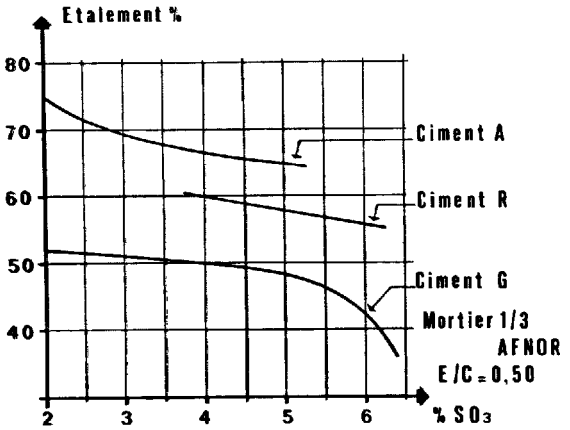

Figure 20

c) Rapport Eau/Ciment

A caractéristiques rhéologiques égales, l'exigence en eau est plus élevée pour les ciments de broyeur à projection.

La figure 21 montre les écarts importants de E/C entre les ciments témoins CPA 50 et CPAL 40 de broyeur à bouletset les ciments de broyeur à projection avec ajouts. L'addition de cendres volantes et de filler calcaire montre l'effet bénéfique de ces ajouts et les possibilités de réduction du rapport Eau/Ciment.
A rhéologie égale, le rapport Eau/Ciment est fonction :

1) du remplissage granulométrique (mouillage par insertion),

2) de la surface spécifique globale des particules (mouillage par adsorption),

3) de la nature minéralogique de chaque composant (mouillage par absorption) porosité ouverte,

4) de la forme géométrique de chaque composant (mobilité),

5) des charges électriques de surface (mobilité).

BIBLIOGRAPHIE

- J.P. BERNARD (1978) : Contribution à l'étude des relations entre les paramètres granulométriques et les propriétés des ciments Portland. Thèse Université de Paris VI.
- F.W. LOCHER, S. SPRUNG, P. KORF (1973) : Der Einflu der Korngrössenverteilung auf die Festigkeit von Portland Zement. Zement-Kalk-Gips, N° 8, 348-355.
- J.P. MERIC (1978) : Le Broyage. Annales des Mines, novembre 1978.
- R.R. KEIENBURG (1977) : Kornverteilung und Normfestigkeit von Portland Zement. Düsseldorf : Béton-Verlag. (Schriftenrei der Zementindustrie, H 42).
- M. RITZMANN (1968) : Uber Beziehungen zwischen der Kornverteilung und der Festigkeit von Portland Zement. Zement-Kalk-Gips, N° 9, 390-396.

Abrévations :

G :	Usine G	BB :	Broyeur à Boulets
R :	Usine R	BP :	Broyeur à Projection
A :	Usine A	C :	Cendres volantes
L :	Laitier	FC :	Filler calcaire
FS :	Filler siliceux	E/C :	Eau/Ciment.

Neutralisation des additions indésirables dans la matière première

Neutralisation of undesirable admixtures in raw materials

I. LUGININA, docteur ès sciences techniques, Belgorod, U.R.S.S.

RESUME : La production du ciment, à partir de matières crues brutes, pose des problèmes de plus en plus aigus, du fait de l'épuisement des gisements de calcaires purs, et de l'emploi, de plus en plus fréquent, de déchets industriels pour la confection des crus. Ces problèmes peuvent être résolus par la neutralisation réciproque des additions.

La composition des composés intermédiaires qui se forment est connue, lorsque le cru contient des oxydes de magnésium, des alcalis ou du phosphore. On a trouvé des interactions chimiques permettant de neutraliser ces corps. Cet effet neutralisant s'accompagne d'ailleurs d'un abaissement de la température de décarbonatation et de la température de formation du liquidus.

L'addition de calcaires dolomitiques aux crus alcalins, accroît la résistance du ciment, et empêche la formation, pendant la cuisson, de silicates magnéso-alcalins. Ces derniers étant en contact avec les principaux silicates du clinker, ne se décomposent pas jusqu'à formation de périclase, comme dans le magnésium octaédrique.

SUMMARY : The cement production from nonconditional raw material is a very important problem in accordance with limiting of pure limestones and with the more wider use of industrial wastes in cement technology. This problem may be solved by mutual neutralisation of admixtures.

The composition of variable intermediate components is known. These compunds are formed when the raw material components include oxides of magnesium, of alkalies, of phosphorus. Chemical interactions, prosiding neutralisation of the given oxides are defined. The neutralised effect is accompained by decreasing of the temperature of decarbonisation and melting.

The addition of dolomit limestones into batches containing alkali, improve the strength of cement and leads to the formation of alkali-magnesium silicates by firing. The latter being in contact with the main climer silicate minerals do mot decompose until selecting of periclase as magnesium is in the fourth octahedronal coordination.

La quantité de molécules de la matière se trouvant sur la surface s'élève considérablement à la mouture fine des corps cristallisés. Les couches superficieles et les phénomènes déterminent les propriétés de la matière dans l'état de poudre. A la mouture fine de quelques matières prises ensemble commencent les réactions mécanochimiques dont la valeur est proportionnelle à la grandeur de la surface des composants. On a découvert quelques sels doubles en étudiant des processus chimiques passant sous l'influence des cataliseurs dans le mélange des matières premières de ciment. Les sels doubles sont des composés complexes, c'est pourquoi les régularités de la formation des complexes doivent se répandre sur les composés apparaissant dans la matière première agglomérant dans des fours rotatoires. Dans ce travail on sousentend sous le terme de "la formation des complexes" la capacité des sels de donner des sels doubles et des composés plus compliqués. Les réactions pareilles avec la formation des sels doubles entre le carbonate de calcium et les sels alcalins commencent à la température 300-400°C.

Un facteur déterminant la formation des complexes sous le chauffage des systèmes de sel est une présence du cation dans le mélange avec une grande action de polarisation en comparaison avec les autres. L'action polarisant du cation Mg^{2+} est presque 2 fois plus fort que de celui de calcium(3,3 pour Mg^{2+} et 1,8 pour Ca^{2+}). En se basant sur les certaines régularités établies par les chimistes soviétiques et sur les travaux du groupe de technologues soviétiques commencés dans les années 30 par Jouravliev V.F. une supposition était fait que: premièrement- certains mélanges en état d'oxydes considérant indésirables peuvent entrer dans un constituant de nouveaux composés complexes; deuxiemement- de nouvelles formations peuvent avoir des propriétés visqueuses et leur apparition ne provoquera pas l'altération des propriétés du ciment. Enfin on peut supposer que de nouveaux composants amelioreront un pouvoir agglomérant du mélange de matière première.

La teneur limitée en additions(cataliseurs) et les températures relativement basses du commencement des intéractions entre les constituants du mélange de matière première de ciment et l'addition ont prédéterminé la tendance d'assurer le contact des réagents le plus étroit au moyen de leur mouture commune. Le réagent le plus probable est un carbonate de calcium, c'est pourquoi le contact le plus étroit est assuré à la mouture justement avec lui. Les essais pareils était avec l'addition des cataliseurs dans les mélanges de matières premières: fluorure de calcium, silicofluorure de sodium et phosphore de platre. On étudiait l'influence du contact initial du cataliseur à la mouture avec de différents composants des mélanges de matières premières. Avec cela la durée totale de mouture restait constante, il n' y a que le composant du mélange de matière première qui était en contact avec le cataliseur aux premiers stades du broyage changeait.

On préparait les mélanges de différents constituants minéralogiques calculés pour l'obtention du ciment d'alite de celui durcissant vite, blanc et stable aux sulfates. Il est établi que dans d'autres conditions de l'introduction du cataliseur les constituants minéralogiques clinkers, la concentration de nouvelles formations intermédiaires, le retrait et la solidité des granules agglomérant, la quantité de clinker fondu changeait. Ayant examiné tous les mélanges on a établi une régularité commune: il convient d'assurer une mouture commune du cataliseur avec du calcaire pour l'obtention de la plus grande solidité du ciment préparé.

L'influence des conditions de la mouture du cataliseur avec de certains constituants du mélange de matière première est représentée partiellement. Un tableaux 1 représente les résultats obtenus aux usines après l'application du procédé de mouture avec des résidus des pyrites qui était moins réussi et les résultats de la mouture optimale avec du calcaire. Il est à noter qu'il avait toute une série de changements dans le matériel agglomérant, mais pourtant en dépit de ces diversités toutes les compositions ont montré les plus grandes valeurs de solidité du ciment à la mouture des cataliseurs avec du calcaire. Le clinker du ciment blanc n'était pas une exception bien que le ciment de la plus grande blancheur fût obtenu à la mouture du kaolin avec le cataliseur.

L'élévation de l'activité de ciment à la mouture des fluorures avec du calcaire est expliquée par la formation de fluorure de silicium de calcium-$Ca_{12}Si_4O_{19}F_2$(1). Le composé se fait pour toutes les variantes du mélange à condition qu'on ajoute le fluorure de calcium. Pourtant en faisant la mouture du cataliseur avec du calcaire on constate que sa teneur est maxima. La formation du carbonate de fluorure intermédiaire de la composition supposée($4CaCO_3.7CaO.CaF_2$) précède l'apparition du silicate de fluorure. Un carbonate de fluorure du calcium est fondu à la température 975°C avec la décomposition postérieure en dégageant un gaz carbonique. Si le mélange contient la silice, dans ce cas se forme un silicate de fluorure qui en se décomposant provoque l'apparition de l'alite et de la fusion à la température 1200°C.

L'élévation de l'activité de ciment obtenu du lit de fusion "cataliseur-calcaire" est expliquée par la teneur minimale des additions dans l'alite, par la microstructure optimale du clinker, par l'absence de l'aluminate tricalcique. Le composant facilement fusible du clinker de ces agglomérations est C_6A_2F. Il est à noter que la concentration max. de l'alite dans les clinkers étudiés ne garantissait pas la plus grande solidité du ciment après l'hydratation.

TABLEAU I

L'influence des conditions de la mouture du cataliseur avec les composants du mélange de matière première.

Clinker	Mouture commune du cataliseur	Composition minéralogique du clinker, %			Limite de solidité sous pression MPa à l'âge (jours)		Blancheur en comparaison avec $BaSO_4$, %
		Alite	Béalite	Substance intermédiaire	3	28	
D'alite	Résidus des pyrites et fluorure de calcium	70	6	24	37,1	53,1	On ne déterminait pas
	Calcaire et fluorure	60	22	18	42,0	56,2	-"-
Stable aux sulfates	Résidus et fluorure	63	22	15	21,4	44,5	-"-
	Calcaire et fluorure	60	24	16	26,0	47,4	
Vite durcissant	Résidus et fluorure	78	10	12	35,6	42,7	-"-
	Calcaire et fluorure	65	20	15	38,9	51,0	
Blanc	Kaolin et fluorure	59	30	11	on ne déterminait pas	38,2	74,5
	Calcaire et fluorure	65	20	15		41,2	69,0

Les conditions du contact initial du cataliseur exercent une influence fort importante à la composition et à la teneur en minéraux-flux aussi bien qu'à la teneur en alite.

La mise en application du procédé proposé aux usines de ciment a assuré l'élévation stable de l'activité de ciment à 5 ou 7% avec le décollage admissible du régime technologique du travail des fours; a amélioré la granulation du clinker; a éliminé la formation de la poussière de clinker.

En cherchant les procédés permettant neutraliser des additions indésirables dans le mélange de matière première de ciment, on a réussi à déterminer quelques nouveaux composants qui apparaissent à la clinkérisation. On peut diviser ces composés en deux groupes: 1- conservé dans le clinker prêt et changeant sa composition minéralogique et les propriétés du ciment: K_2MgSiO_4, Na_2MgSiO_4, K_2SO_4; 2- composé se formant à la période précédente à la clinkérisation qui influencent à la formation de certains minéraux de clinker et élèvent la partie de leur solutions solides: $K_2Ca(CO_3)_2$, $Na_2Ca(CO_3)_2$, $K_2Ca_2(SO_4)_3$, $K_2Mg(CO_3)_2$, $K_3Na(SO_4)_2$, $Ca_7Mg_2P_6O_{24}$, $Ca_{12}Si_4O_{19}F_2$, $Ca_5Si_2CO_{11}$, $Ca_5Si_2SO_{12}$.

Les composés cités ci-dessus sont nommés intermédiaires. A notre avis il convient de les nommer variables. Le terme "intermédiaire" se rapporte aux minéraux- flux et au verre de clinker qui remplissent en effet des espaces entre des minéraux- silicates dans le clinker. De nouvelles formations citées ci-dessus sont stables dans l'intervalle limité des températures, retiennent des atomes et des ions des constituants volatifs dans la solution solide; leur constituant change au chauffage et ils se décomposent facilement en sels et en oxydes.

En règle, toutes les nouvelles formations favorisent l'apparition des microfusions aux températures fort basses et accélèrent catalytiquement tout le procédé de l'agglomération. La commande consciente de ces interactions permet d'assurer la neutralisation complète des additions indésirables. Le dernier est réussi si les oxydes indésirables en réagissant donnent des composés stables. Donc, les interactions activent la clinkérisation, car la température de la formation de la fusion diminue et par consequent le débit de chaleure pour le grillage sans provoquer le changement des indices qualitatifs du ciment. L'effect de neutralisation de la magnésie sur les lits de fusion alcalins est déjà connu. L'addition qui contient

le magnésium accélère une sublimation des oxydes alcalins (Figure 1).

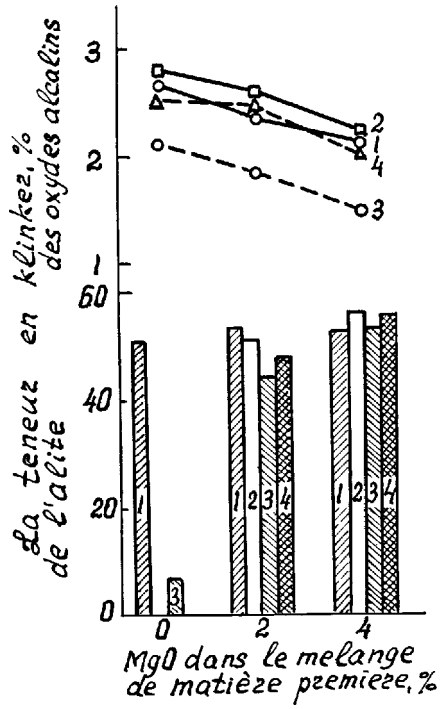

Fig. 1 - Influence de l'oxyde de magnésium à la teneur en alcalin et en alite dans le clinker (CS=0,89).
1,2 - avec les sulfates de potassium et de sodium; 3,4 - avec les carbonates de potassium et de sodium.

Un phosphate de calcium et de magnésium ($7CaO2MgO3P_2O_5$) apparait à l'agglomération des mélanges de matière première de ciment à haute concentration des oxydes de magnésium et de phosphore. L'influence réciproque de la neutralisation des oxydes se voit bien en envisageant les données du tableaux II.

Le premier groupe de composés formant des minéraux indépendants est moins nombreux mais ils diminuent aussi la température de l'agglomération. En prévoyant leur formation il est nécéssaire de changer la composition du mélange de matière première, car une partie d'oxyde se dépense pour de nouveaux composants. De nouvelles formations influent sur les propriétés du ciment, par exemple, les silicates alcalino-magnésiques stimulent l'indurcissement des mâchefers et les oxydes de magnésium et de phosphore se trouvant en même temps dans le ciment élèvent une stabilité aux sulfates.

Les composés contenant le phosphore influent sur les lits de fusion de matière première de ciment alcalins. Voir les données du tableaux III.

TABLEAU II

Influence des oxydes de phosphore et de magnésium à la solidité

CS; n= 2,5; p= 1,2	Teneur en additions, %		Oxyde de calcium disponible dans le clinker, %	Solidité des ciments sous pression, MPa à l'âge (jours)		
	P_2O_5	MgO		1	7	28
0,85	0	0	0	8,9	20,7	33,1
-"-	3	0	5,1	sont détruits		
-"-	3	4,5	0	4,1	14,9	26,9
0,90	0	0	0,2	9,9	23,3	33,4
-"-	3	0	7,2	sont détruits		
-"-	3	4,5	0,8	5,9	21,1	35,9
0,95	0	0	1,5	10,8	20,1	36,1
-"-	3	0	9,9	sont détruits		
-"-	3	4,5	3,5	4,3	16,1	25,3

TABLEAU III

Influence des additions de sulfate de potassium et de concentrat d'apatite à la solidité

Mélange de matière première CS=0,91; n=2,6; p=1,4 avec l'addition(%) en clinker	Solidité sous préssion à l'âge (jours), MPa		
	3	7	28
Sans addition	14,8	19,4	30,2
Sulfate de potassium (5)	14,4	16,1	18,3
Pentoxyde de phosphore (0,5)	14,0	16,3	19,1
Sulfate de potassium (5) et pentoxyde de phosphore (0,5)	14,9	19,2	28,2

Ainsi l'influence négative de certains oxydes peut être compensée au moyen de leur neutralisation réciproque. Un schéma simplifié de la compensation est présenté au dessous:

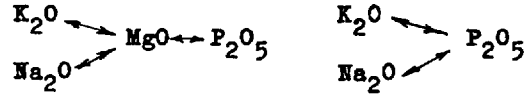

La compensation de l'influence indésirable d'oxydes de magnésium est basée sur la réaction suivante:

$K_2CO_3+MgCO_3+SiO_2=K_2Mg(CO_3)_2+SiO_2=K_2MgSiO_4+2CO_2$ (1)

Les réactions (1) vont jusqu'au commencement de la décarbonisation du magnésium carbonique. Si le sel alcalin ne se formera pas en silicate, il aura la possibilité de réagir avec le carbonate de calcium que provoquera une saturation postérieure des silicates de clinker par les oxydes alcalins. Donc l'addition du carbonate de magnésium dans les lits de fusion alcalins détourne la réaction suivante:

$K_2CO_3+CaCO_3+SiO_2= K_2Ca(CO_3)_2+SiO_2=K_2CaSiO_4+2CO_2$ (2)

La réaction (1) freine aussi le dégagement du périclase à gros cristaux. Avec cela CaO est conservé pour la formation des minéraux silicates et assure l'obtetion du clinker d'alite. On a été découvert avec cela des silicates alcalino-magnésiques K_2MgSiO_4 et Na_2MgSiO_4. Il ya des renseignements que les silicates alcalino-magnésiques ne sont pas assez stables à haute température. C'est pourquoi on a fait les observations des changements des silicates alcalino-magnésiques en contact avec des minéraux de clinker dans un microscope chauffant. Il est établi au moyen de l'analyse de la composition de phase qu'en règle les silicates alcalino-magnésiques ne provoque pas la formation du périclase dans le clinker. L'absence du périclase est expliquée par le changement du nombre de coordination du magnésium, qui peut diminuer dans les compositions alcalines jusqu'à 4 (au lieu de 6). Les tétraedres MgO_4 apparaissent au lieu des octaèdres MgO_6. L'étude des conditions de la formation des silicates alcalino-magnésiques montre que les derniers se forment facilement sur la base des silicates de magnésium naturels. Un grillage rapide est le plus favorable.

Une dépendance établie ne s'étend pas au mélange de l'aluminate tricalcique avec les silicates sodico-magnésiques dans lequel passe l'interaction suivant sous l'action de l'agglomération:

$3(3CaO\cdot Al_2O_3)+Na_2O\cdot MgO\cdot SiO_2=Na_2O\cdot 8CaO\cdot 3Al_2O_3+CaO+MgO+CaO\cdot MgO\cdot 2SiO_2$

Une partie d'oxyde de magnésium se dégage en état du périclase et reste dans la composition du silicate de calcium magnésique. La porosité de la masse agglomérant s'élève à la sublimation de l'oxyde alcalin. La neutralisation réciproque des oxydes de magnésium et de phosphore est accompagnée par l'apparition d'un composé intermédiaire $C_7M_2P_3$ qui se décompose à l'élévation de la température et en présence de l'oxyde du calcium suivant le schéma:

$7CaO\cdot 2MgO\cdot 3P_2O_5+10CaO+7SiO_2 \xrightarrow{1200°C} 3(5CaO\cdot P_2O_5\cdot SiO_2)+2(CaO\cdot MgO\cdot 2SiO_2)$ (4)

D'autres interactions sont aussi possibles, par exemple, avec la participation de la wollastonite. Pourtant le but essentiel du technologue est d'assurer une liaison immanquable de l'oxyde de magnésium et de détourner la formation du périclase. En présence des alcalis et de phosphore l'oxyde de magnésium est fixé à la température 1200°C en silicates de calcium magnésique (diopside) et en autres qui se saturent de l'oxyde de calcium à l'élévation de la température et donnent une formule remplaçant le magnésium α'_L-C_2S (2,3). Suivant les données de l'analyse du roentgen de phase des produits du grillage interrompu aux températures 1200 et 1250°C, α'_L-C_2S dissoud dans un bain fondu du clinker. Un silicate bicalcique peu soluble dans un bain fondu, stabilisé par le phosphore, apparait dans les agglomérés ne contenant pas d'importantes additions de l'oxyde de magnésium. C'est pourquoi une quantité importante de l'oxyde de calcium est non assimilée et il n'y a pas d'alite dans l'aggloméré.

CONCLUSIONS

En préparant des mélanges de matiére première, il convient de prévoir les interactions possibles chimiques entre les additions indésirables et d'assurer leur neutralisation. Il y a le constituant des composés et les interactions chimiques allant à la période précédente à la clinkérisation qui assurent la neutralisation des additions alcalines, magnésiques et celles contenant le phosphore. On a proposé le terme des composants variables dans le mélange agglomérant de matière première à la différence des minéraux intermédiaires du clinker de ciment.

BIBLIOGRAPHIE

1.- M. TANACA, G. SUDO et CH. ACAIVA (1973), "Nouveaux composé $Ca_{12}SiO_4O_{19}F_2$ dans le système $CaO-SiO_2-CaF_2$ et le rôle du CaF_2 dans le processus du grillage du clinker de ciment", Le cinquième congrès international de chimie de ciment, M. Stroiizdat, 52-54.

2.- M. REGOURD, M. BIGARE, J. PORREST et A. GUINIER (1965), "Synthesis and crystallographic investigations of some belistes". Communication supplémentaire n° 1-10.

3.- X. MIDJLEI (1976), "Polyphormisme de l'orthosilicate de calcium". Le cinquième congrès international de chimie de ciment, M. Stroiizdat, Vol.I, 63-68.

Problems of the simultaneous and separate grinding at the production of blast furnace slag cement

Problèmes du broyage simultané ou séparé dans la production des ciments de laitier

L. OPOCZKY, Head of Sci. Res. Group, Ph.D. Central Research and Design Institute for the Silicate Industry, Budapest, Hungary,
T.K. MRAKOVICS, Sci. Officer, Central Research and Design Institute for Silicate Industry, Budapest, Hungary.

RESUME : Le clinker et le laitier, lorsqu'ils sont broyés ensemble, exercent une influence mutuelle l'un sur l'autre. Cet effet peut aider ou retarder le broyage, selon la dureté et la tendance à la réagglomération des composants. On peut caractériser cet effet par un indice d'uniformité n et par l'écart type de la distribution granulométrique du produit broyé.

Ces facteurs permettent de choisir, lorsque l'on doit broyer un ciment de laitier en circuit ouvert, s'il y a lieu d'adopter le broyage séparé ou le broyage simultané. Si le broyage s'effectue en circuit fermé, le broyage simultané semble être le plus favorable à la qualité du ciment.

SUMMARY: The cement clinker and blast furnace slag ground together generally affect one another. This effect may aid but as well retard the grinding process depending on the hardness and tending to aggregation of the components. This latter one can be characterized by the uniformity index /n/ and the standard deviation,resp, of the particle size distribution of the ground product.
When grinding blast furnace slag cement in open circuit system the choosing between simultaneous and separate grinding is determined by the above factors. In a closed circuit system the simultaneous grinding seems to be more favourable in view of cement quality.

INTRODUCTION

In the cement industry, both at raw meal- and cement grinding mixtures of two or more components are produced.

When making blended cements one can choose of two possibilities: the one is the post-mixing of the separately ground components, the other being the simultaneous grinding.

The choosing of the proper method is jointedly determined by the energy consumption and the most favourable developing of the properties of the final product.

The literature of the problematics is very wide /1-5/, in this field Bombled /6/ has dealt with the special problems of the cement industry in details.

In our experiments the character of the simultaneous and separate grinding processes of cement clinker and blast furnace slag were studied in laboratory grinding equipments modelling the open and closed circuit grinding.

MATERIALS AND METHODS

In order to present the results two kinds of industrial clinkers
/K_1: C_3S = 48,76%; C_2S = 26,24%; C_3A =10,41% C_4AF = 7,14% and
K_2: C_3S = 45,04%; C_2S = 28,24%; C_3A =11,42% C_4AF = 9,45% /,
and three kinds of granulated blast furnace slag /H_1, H_2 and H_3/ were choosen. The materials were prepared by a hammer crusher to < 3,4 mm grain size.

In our experiments we tried to modellize the open and closed circuit grinding processes. In the first case our experimental equipment was a 5000 cm³, 68 rpm iron-jacketed mill filled with 8 kg of 20 x 20 mm steel cylpebses.

In the second case experiments were carried out in a Bond-type grindability testing mill /7/. To characterize the dispersity of the ground products the specific surface determined by permeability measurement /S_{Blaine}/ and the granulometric composition /to 3 /um/ determined by sedimentation in alcohol were used. At the evaluation of the particle size distribution two constants of the Rosin-Rammler-Sperling-Bennett /RRSB/ distribution were applied: the particle size /$\bar{x}$/ that belongs to the 36,8 % sieve residue and the uniformity index /n/ of the ground product. This latter is proportional to the reciprocal of the standard deviation of the distribution if calculated by the logarithms of the particle size thus being calculable by mathematical-statistical method /8/. The value of $\bar{x}$ can be read from the RRSB diagram.

The studying of the morphology of the grinding products and powder samples, resp., was made using an ISM-35 type scanning electronic microscope while the identification of the individual particles and components was carried out with the use of a LINK-290 type microprobe. The identification of alite and belite was made on the base of the relation of the Si-Ca peaks while that of the interstitial phase and blast furnace slag particles was made on the base of the Al- and Fe as well as Mg and S peaks, respectively.

DESCRIPTION OF THE EXPERIMENTAL RESULTS

The experimental materials were different in their grindability properties. Discussing the grindability properties we think of the grindability of the material /which is characterized by the surface produced per time unit: $w = S/\tau$ $m^2g^{-1}min^{-1}$/ and of the tendency to interaction, aggregation of the particles of the material. It has been stated in former experiments that the uniformity index /n/ of the ground product is a characteristic of the material's tendency to aggregation. Grinding products of small uniformity index i.e. of diffuse granulometric composition /e.g. limestone/ are generally more tending to aggregation than those ones of big uniformity index i.e. of more uniform granulometric composition /e.g. quartz//9/.

According to this characterization the clinker K_1 in easier grindable and tending more to aggregation /$w = 44.10^{-4}$ $m^2g^{-1}min^{-1}$; n=1,35; $\bar{x}$ = 34 /um/. Among the three blast furnace slags the most difficultly grindable and less tending to aggregation was that marked H_3/ $w = 22.10^{-4}$ $m^2g^{-1}min^{-1}$; n = 1,26; $\bar{x}$ =33um/. The slag H_2 is medium grindable and has a medium tendency to aggregation /$w = 27.10^{-4}$ $m^2g^{-1}min^{-1}$; n = 0,95; $\bar{x}$ = 32 /um/. H_1 is between the above two in this respect /$w = 27.10^{-4}$ $m^2g^{-1}min^{-1}$; n = 1,18; $\bar{x}$ = 28 /um/. The values of n and $\bar{x}$ belong to a grinding time of 75 minutes.

The different grindability properties of the experimental materials are related to the differences in the chemical-mineralogical composition as well as in the macro- and microstructure influenced by the production technology but this problematics will not be dealt with here.

The simultaneous and separate grinding experiments were carried out with three kinds of binary mixtures as follows:

- Mixture K_1-H_1 - Mixture of an easily grindable /K_1/ component tending to aggregation and a more difficultly grindable one/H_1/ less tending to aggregation
- Mixture K_1-H_2- Mixture of an easily /K_1/ and a medium grindable/H_2/ material. Both componefits are tending to aggregation
- Mixture K_2-H_3- Both components are difficultly grindable and not tending to aggregation

Within these three and four, resp., mixing ratios were investigated.

GRINDING EXPERIMENTS IN OPEN CIRCUIT SYSTEM

Fig.1. shows the change of the grindability /w/ of the experimental mixtures as well as that of the uniformity index /n/ at grinding in open circuit system. Dotted line

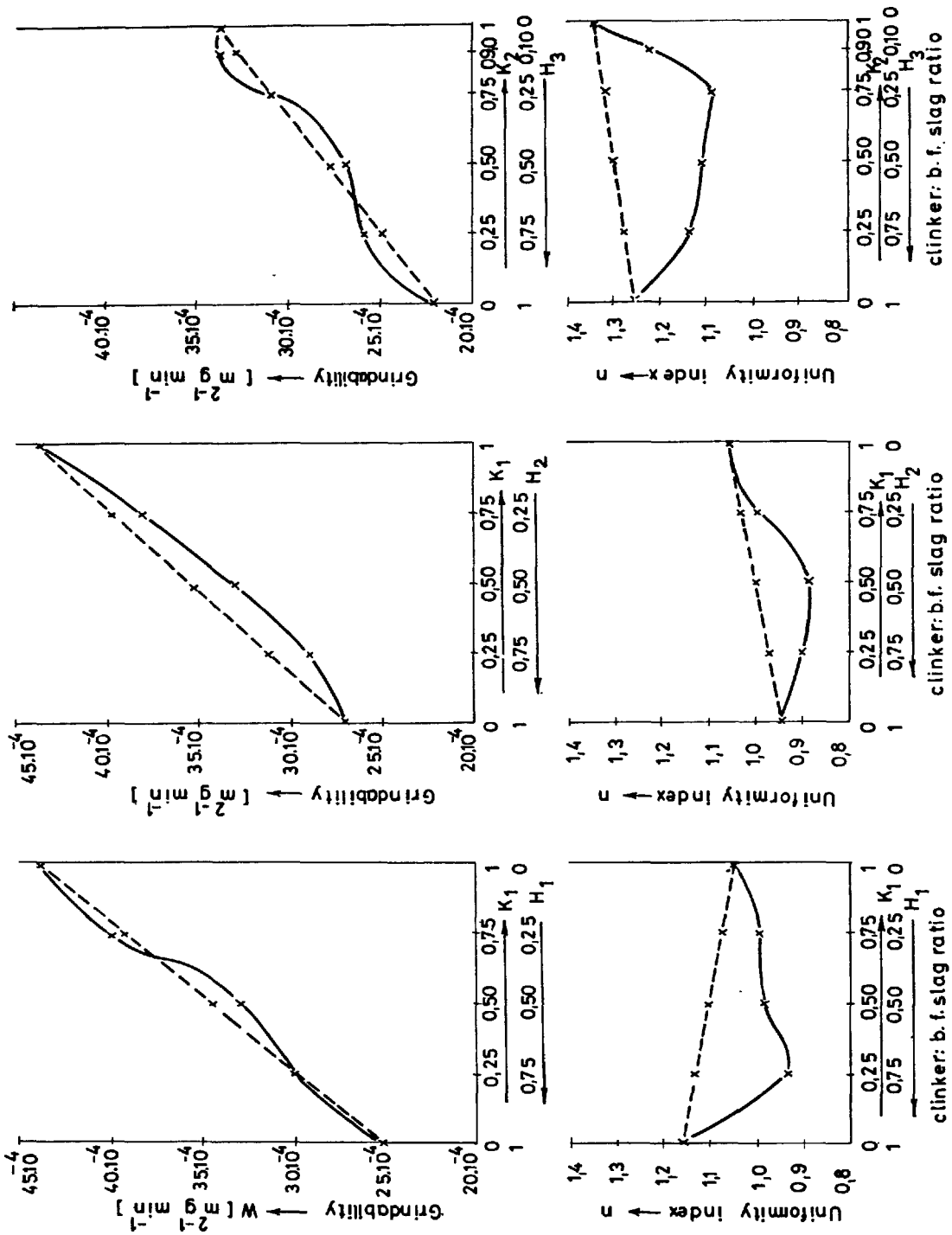

Fig.1. - Simultaneous and separate grinding in open circuit grinding equipment
-------- separate grinding
———— simultaneous grinding

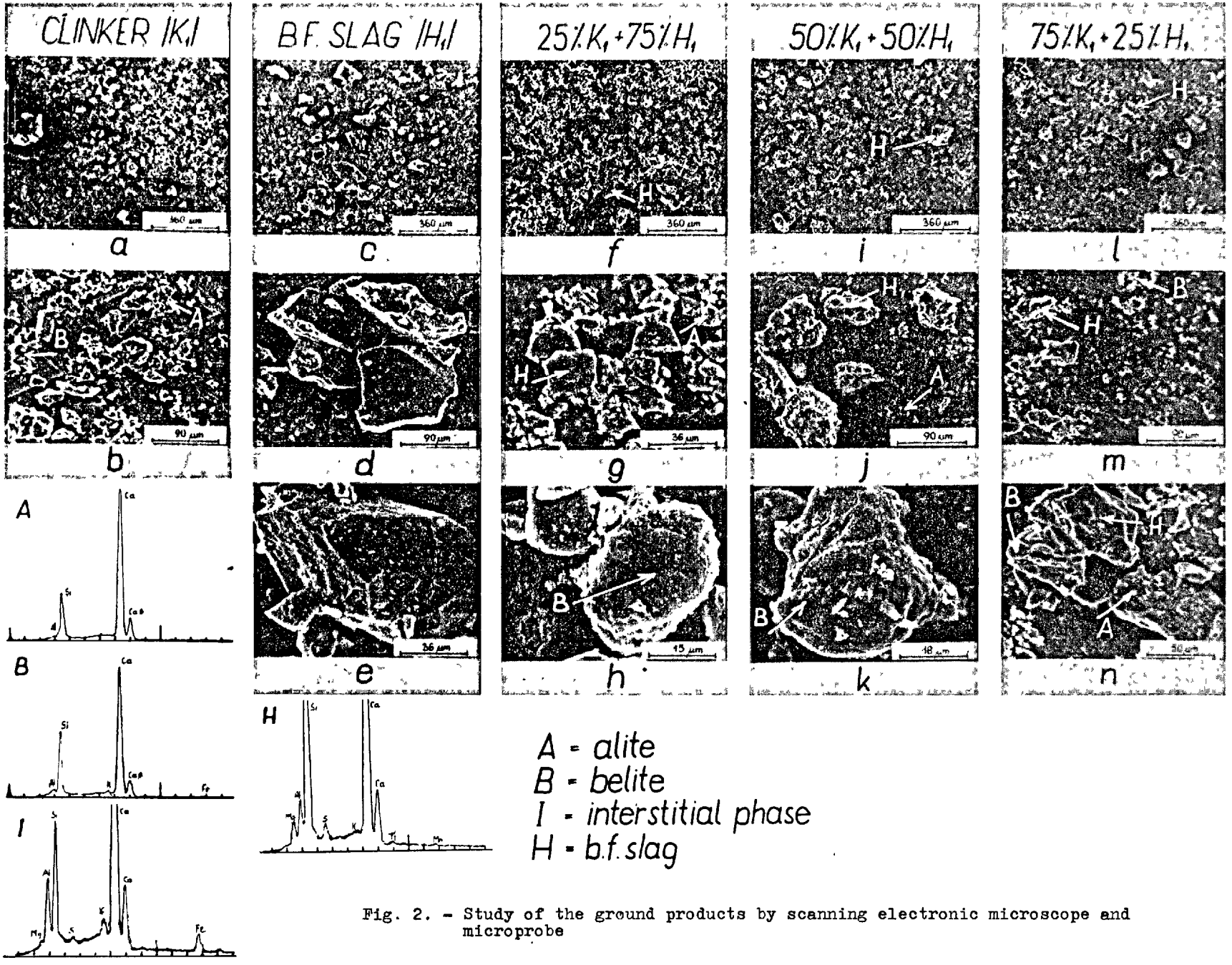

Fig. 2. - Study of the ground products by scanning electronic microscope and microprobe

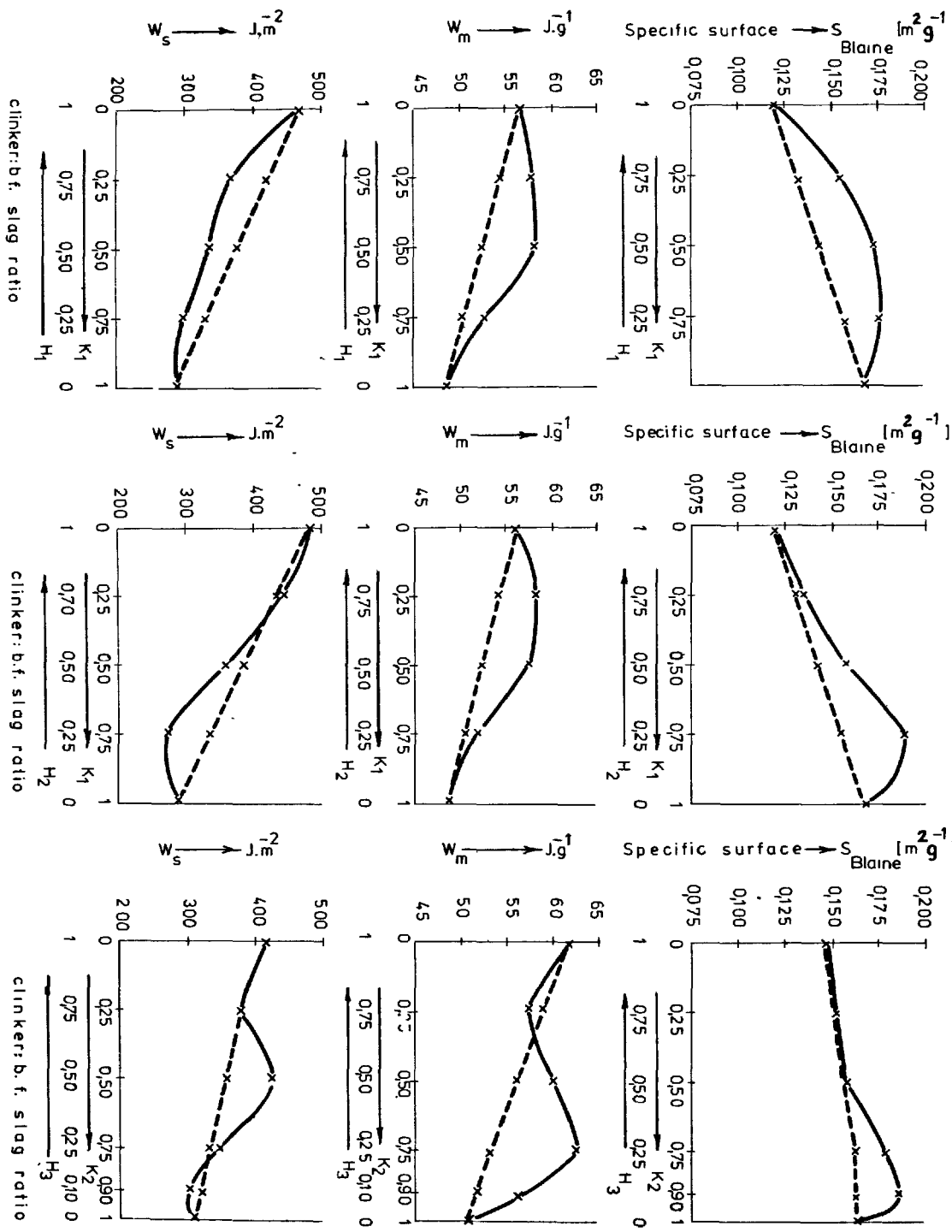

Fig.3. - Simultaneous and separate grinding in a closed circuit grinding equipment
- - - - separate grinding
——— simultaneous grinding

shows the separate while the continuous one the simultaneous grinding.

It may be staed that in general the standard deviation of the distribution according to particle size is always higher /the value of n is smaller/ at simultaneously ground mixtures than at the separately ground ones. This shows that the clinker and blast furnace slag are infuencing the grindability of one another at simultaneous grinding.

At the separate grinding of the mixture K_1--H_1 the value of n decreases with the increase of the clinker quota. At simultaneous grinding n comes to a minimum at 25 % clinker content then increases with the increasing clinker quota. Regarding grindability, according to Bond's method, in the range 25 % < K_1 < 75 % the simultaneous grinding gives a less favourable work index than separate grinding. Since grindability is characterized by the surface formed during time unit and since the formation of surface is first of all due to the smaller size clinker particles, the increase of n accompanied by the increase of the work index suggests that at the simultaneous grinding of the 50 % K_1 - 50 % H_1 mixture the clinker is ground somewhat coarser, the slag somewhat finer than at separate grinding. In the other mixing ranges simultaneous and separate grinding are practically the same the former one being slightly more favourable. At the separate grinding of the mixture K_1-H_2 n increases with the increase of the clinker quota. At simultaneous grinding however, the value of n begins to increase only then if the clinker quota exceeds 50%. The change of n shows that in this mixture probably an interaction of particles takes place during simultaneous grinding since otherwise upon increasing clinker quota the value of n ought to have increased, too. Regarding the grindability and work index, resp., separate grinding is more favourable at this mixture.

At the separate grinding of mixture K_2-H_3 n increases with increasing clinker quota. At simultaneous grinding, in the range 25% ≤ K_2 ≤ 75% n remains practically unchanged; then increases if the clinker quota exceeds 75%. In the change of the n-value this mixture shows the biggest difference between simultaneous and separate grinding.

On the base of grindability and work index both at smaller /< 25%/ and bigger /> 75%/ clinker quota simultaneous grinding is more favourable while in the medium range the separate one is better. The change of the energy index and the n-value of the grinding products suggests that in case of 25% < H_3 < 75% slag content the clinker is coarser and the slag is some finer ground than at separate grinding.
Supplementary informations were received about the change of simultaneous grinding by the investigation carried out with scanning electronic microscope and microprobe made on ground products and powder samples. Fig.2. shows some exposures and spectra, resp., made on samples of the mixture K_1-H_1 produced by millings for 75 minutes.

In Fig.2, a nd b show clinker /K_1/ grinding products while c, d, e show those ones of slag /H_1/.

The granulometric composition of the clinker /K_1/ grinding product is diffuse, besides the larger size grains there are a lot of smaller ones, too. The size of alite /A/ particles identified by microprobe is generally 5-6 /um and that of belite /B/ ones is 15-20 /um. In the clinker grinding product the sticking of the smaller particles to the bigger ones or to one another /i.e. aggregation/ can be observed.

The blast furnace slag /H_1/ has a more uniform granulometric composition but it is in the coarser range of fineness. The main mass of particles is of 30-80 /um size but a lot of 150-200 /um ones can also be found. The particles are angular having "craters" in some places.
In Fig.2, f, g and h show the mixture 25%K_1--75%H_1. The size of slag particles changes from 20 to 120 /um that is the slag particles are some finer here than at separate grinding. The characteristic size of belite /B/ particles is 30 /um and that of alite /A/ ones is 10 - 15 /um. The granulometric composition of the grinding product is diffuse, besides the larger and smaller slag particles a lot of fine and medium size clinker particles can be found. The sticking of the finer clinker particles on the coarser slag ones can also be observed.

In Fig.2, exposures i, j and k show the 50%K_1 - 50%H_1 mixture. Average size of slag /H/ particles is 70-80 /um while that of belite /B/ and alite /A/ ones amounts to 15 - 40 /um and 10 - 15 /um, respectively. This means that compared with the former mixture and separate grinding here the slag particles are finer and the clinker ones are a bit coarser. The granulometric composition is more uniform but it is in a coarser range of fineness. The interaction of particles is not considerable.

In Fig.2, exposures l, m, n show the mixture 75%K_1 - 25%H_1. The size of slag particles/H/ is 60-100 /um while that of belite /B/ and alite /A/ ones amounts to 10 - 15 /um and 3 - 5 /um, respectively. In this case both the slag and the clinker were more finely ground than at separate grinding. The ratio of clinker particles determining the specific surface is big and the fine clinker particles are adhered not to one another but rather to the surface of slag grains. In this case blast furnace slag prevents the aggregation of clinker particles.

GRINDING EXPERIMENTS CARRIED OUT IN CLOSED CIRCUIT SYSTEM

Fig.3 shows the experimental results of closed circuit grinding. The dotted line refers to the separate and the continuous one to simultaneous grinding. Since in this case the grinding takes place in a relatively coarse range /S_B = 0,12 - 0,19 m^2g^{-1}/ the interaction of particles, i.e. aggregation is

of no importance. The specific surface /S_B/ always increases with the increasing of clinker quota at separate grinding.

At the simultaneous grinding of mixture K_1-H_1 the surface is always bigger than at separate grinding i.e. the clinker is always ground finer in this case.

At the mixture K_1-H_2 in case of small clinker quota /up to ccá 25% K_1/ practically there is no difference between the two ways of grinding. Upon increasing the clinker quota the surface of the simultaneously ground product increases, reaching a maximum at 75%.

At the simultaneous grinding of mixture K_1-H_3 the curve S_B has a similar shape. Upon increasing the clinker quota the surface is increasing also in this case reaching a maximum at 90% clinker quota.

The specific energy consumption /w_m/ referred to mass unit is decreasing with the increase of clinker quota at separate grinding. At simultaneous grinding, the values of the energy index are generally less favourable. At mixtures K_1-H_1 and K_1-H_2 the w_m curves have similar shape. The energy consumption increases up to about 50 % clinker content then decreases with the further increase of the clinker quota.
At mixture K_2-H_3 the simultaneous grinding is some more favourable up to 25 % clinker quota but with the further increasing of the clinker content the energy consumption increases rapidly.

The nergy consumption /w_S/ referred to unit surface changes in a different way since according to this characteristic the simultaneous grinding is more favourable. The w_S curve of mixture K_1-H_1 is almost the mirror image of the w_m-curve and a similar case can be found at mixture K_1-H_2. At mixture K_2-H_3 the change of the curve w_S depends on the mixing ratio of the two components. At simultaneous grinding in case of low and high slag content the value of w_S is more favourable than in case of medium slag content.

CONCLUSIONS

Different production technologies often need the preparation of mixture of ground products of various materials. The natural raw materials but also the artificial products/e.g. cement clinker/ may be composed of more minerals and behave as mixtures during grinding.
At simultaneous grinding the interaction of the components cannot be neglected in most cases. This interaction depends on the hardness /hard-hard, hard-soft, soft-soft/ of the partners forming the binary system as well as on their tending to aggregation which latter one can be characterized by the uniformity index /n/ and the standard deviation of the particle size distribution, resp., of the ground product.
To characterize the interaction of the simultaneously ground components we have differentiated the so called "direct" and "indirect" effects. The direct effect means the superficial adhesion of particles of the ground components and the aggregation, resp., which can aid the grinding process /in case if only one partner is tending to aggregation/ but mostly being harmful. Furthermore, the direct effect means the "abrading" effect of the one, generally harder, component affecting the other one. The "indirect" effect means an effect resulting from the excess of the one component thus being positive or negative depending on the mixing ratio.
Cement clinker and blast furnace slag can principally be considered a hard-hard system but within this the slag is more or less harder. Their tending to aggregation is also different.
If both the clinker and slag are tending to aggregation, then in open circuit grinding aggregation - negatively influencing teh prâcess - may occur /e.g.:mixture K_1-H_2/. In this case the separate grinding is more convénient.
If only the clinker is tending to aggregation then providing certain mixing ratios simultaneous grinding is more favourable since the slag prevents the adhesion of the clinker particles to one another thus promoting the size reduction of the clinker particles/e.g. mixture K_1-H_1, at 25 % slag content/. If neither the clinker nor the slag is tending to aggregation and if the slag is very hard, then in case of certain mixing ratios simultaneous grinding is more favourable which can be explained by the "abrading" effect of the slag and thus the more effective size reduction of the clinker being present in excess /mixture K_2-H_2/.
At the simultaneous grinding of clinker and blast furnace slag in a closed circuit system - where the interaction of particles can not prevail - the clinker particles are generally more finely ground than at separate grinding and this is probably due to the "abrading" effect of the slag. In spite of the larger energy consumption the simultaneous grinding in closed circuit system seems to be better from the point of view of the quality of blast furnace slag Portland cement.

LITERATURE

1.- D.W.FUERSTANAU/1963/,"Cinetique de la fragmentation",6éme Cong.Int.de la Prép. des Minerals, Cannes, pp.39-50

2.- D.OCEPEK/1964/,"Grinding of binary mixtures",Rudarsko-Metalurski Zbornik,1,p157

3.- R.PLANIOL/1967/,"Enrichessements comparés de trois magnétites naturelles",Dechema Monographien,No.993-1026,Verl.Chemie, Weinheim,VDI-Verlag Düsseldf.p.835-845

4.- J;A.HOLMES-S.W.PATCHING "A preliminary investigation of differential grinding of quartz-limestone mixtures" Trans.of the Inst.of Chemical Eng.,35.,pp 111-24

5.- K.REMÉNYI/1960/ "Investigation on grindability of limestone and rock-salt mixture in a Hardgrove mill", Acta Technica Acad.Hung. Tomus 56./1-2/., pp.75-90.

6.- J.P.BOMBLED/1965/,"Etude du broyage de mélanges clinker-laitier,Rev.Mat.593.p61

7.- KANNEWURF,A.S./1957/"Research pushes grindability guesses into the background" Rock Products, May, p.66.

8.- BEKE,B./1970/"Die Gleichmässigkeitszahl der Kornverteilung des Mahlgutes",Zement Kalk-Gips, 23., pp.401-406

9.- L.OPOCZKY/1977/"Fine Grinding and Agglomeration of Silicates", Powder Technology, 17., pp.1-7

10.- K.T.MRÁKOVICS/1973/"Problems of the simultaneous and separate grinding in the cement industry", SZIKKTI-Report,No.1-19 pp.1-55 /in Hungarian/

Corrélation de la cinétique des réactions de clinkérisation à l'état solide avec les constituants minéraux et les conditions du traitement thermique

Correlation between kinetics of solid-phase reactions of clinker formation and mineral composition and thermal treatment conditions

O.P. MTCHEDLOV - PETROSSIAN, professeur, docteur ès sciences techniques,
T.Y. CHTCHETKINA, candidat ès sciences chimiques,
N.I. SAPOJNIKOVA, ingénieur, "Youjguiprotzement", U.R.S.S.,
I. TALABER, professeur, docteur ès sciences,
K. BOSCI, docteur ès sciences, Institut des Matériaux de Construction (Hongrie).

RESUME : Les auteurs du présent exposé traitent des données concernant l'effet du milieu gazeux, des catalyseurs ainsi que de la structure de divers carbonates de calcium (calcaires, craies) sur les paramètres cinétiques de leur dissociation.

On a étudié le mécanisme et la cinétique des réactions à l'état solide dans les mélanges de $CaCO_3$ avec divers silicoaluminates : kaolinite, montmorillonite, gehlénite, pseudowollastonite, ainsi que dans les mélanges de $CaCO_3$ avec l'argile, les laitiers mélilitique et pseudowollastonique ou avec leurs combinaisons.

On a établi une corrélation entre les énergies d'activation lors de la formation de bélite dans les réactions à l'état solide et les énergies d'activation lors de la formation d'alite ou de ses modifications dans des mélanges minéraux.

SUMMARY : Data on the influence of the composition of gas medium, catalysts and structure of different calcium carbonates (limestone, chalk) on the kinetic parameters of their dissociation are presented.

The results of investigations of the mechanism and kinetics of solid-phase reactions in the $CaCO_3$ mixtures with different alumosilicate minerals (kaolinite, montmorillonite, gehlenite, pseudowollastonite) as well in the $CaCO_3$ mixtures with clays, melilite and pseudowollastonite slags and their combinations are discussed.

Interrelation between the activation energy of belite formation in solid-phase reactions and activation energy of formation of alite and its modifications in the mineral composition mixture has been found out.

Les recherches sur la réaction de dissociation de $CaCO_3$ (à des fins purement analytiques), de calcite faisant partie de divers carbonates naturels (craies, calcaires) et de mélanges crus à base de ces carbonates ont montré, grâce à la méthode dite analyse thermique différentielle - thermogravimétrie différentielle (ATD-TGD) et à la spectroscopie infrarouge, que ce processus peut être exprimé par les équations cinétiques comme suit:

$$\sqrt[3]{1-\alpha} = 1 - kt \qquad (1)$$

ou bien

$$\sqrt[3]{1-\alpha} = 1 - k\ln t \qquad (2)$$

où t -temps de décomposition de $CaCO_3$, α - degré de dissociation, k - constante de la vitesse.

Lorsqu'il s'agit des matières polydispersées, la constante de la vitesse dans l'équation (1) comprend également l'effet de la granulométrie, de la température et de la pression partielle de CO_2. Au cas où les expérimentations s'effectuent dans la couche mince de la substance réagissante, ce qui assure une évacuation rapide de CO_2, la cinétique de la réaction s'exprime par l'équation (2). Ici, on le sait, la constante de la vitesse est calculée compte tenu de la nature du constituant de carbonate (structure de la calcite, propriétés de minéraux accompagnateurs).

Grâce à la méthode de la spectroscopie IR, on a réussi à définir les constantes de la vitesse de dissociation de toute une série de calcaires et de craies provenant de différents gisements en territoire de l'URSS. Ces données ont permis de calculer les valeurs empiriques d'énergies d'activation de la dissociation (E_a). La valeur E_a des calcaires étudiés varie entre 85 et 250/kJ/moles en fonction de la composition chimique et minérale ou des propriétés physico-mécaniques des carbonates.

On a constaté qu'à mesure que la fréquence des oscillations valentielles du groupe CO_3^{2-} augmente dans les spectres IR de divers calcaires et craies, la valeur empirique d'énergie d'activation de la dissociation du carbonate de calcium et la valeur de microdureté de ces cristaux s'accroissent.

La basse de la valeur E_a de la dissociation des calcaires qui contiennent plus de six pour cent d'impuretés argileuses et de silices amorphes (en comparaison de E_a - $CaCO_3$ - à des fins purement analytiques - qui est de 173 kJ/moles) s'explique par l'action catalytique des impuretés.

Lors du réchauffement, ces impuretés forment des surfaces actives de séparation avec calcite. Celles-ci accélèrent l'évacuation de CO_2 de la zone de la réaction. Ainsi, l'activité chimique de la calcite au moment de la dissociation se détermine, dans une mesure égale, par la solidité des liaisons chimiques du réseau cristallin et par l'action catalytique des phases d'impuretés.

La comparaison des vitesses de dissociation de $CaCO_3$ dans les mélanges crus aux modules et à la granulométrie égaux a montré que, dans le cas où les dépenses énergétiques sont aussi égales, l'addition pendant le broyage de 0,5 pour cent de la masse du nitrate de calcium $Ca(NO_3)_2 \cdot 4H_2O$ fait notablement accélérer la réaction. Par ailleurs, les courbes cinétiques sont pratiquement exemptes de zones de "saturation". L'addition de la même quantité de CaF_2 à un mélange pendant le broyage accélère le processus au stade initial et le ralentit sensiblement au stade final. L'usage en même proportion du phosphate d'aluminium en tant qu'additif rend la vitesse de dissociation de $CaCO_3$ plus lente. Quant aux résultats concernant les recherches sur l'effet des sels sur la cinétique de la dissociation, ceux-ci ont été obtenus dans des conditions isothermiques et non isothermiques.

On sait que la pression partielle de CO_2, plus la composition du milieu gazeux dans la zone de la réaction de dissociation de $CaCO_3$, exercent un effet sensible sur la cinétique du processus (1).

Le tableau I présente les résultats des recherches sur la cinétique de dissociation de $CaCO_3$ dans un même mélange cru - ce n'était que le milieu gazeux qui variait (méthode gravimétrique) - où ΔT - intervalle des températures de décomposition rapide, $\Delta\alpha$ - intervalle α de décomposition rapide de $CaCO_3$, k - constante de la vitesse de la réaction.

A en juger d'après les données du tableau I, au début, la zone de décomposition rapide dans le milieu N_2 se manifeste dans les mêmes conditions que dans l'air ordinaire. Dans le milieu N_2+CO_2, cette zone apparaît à une température plus haute, et dans le milieu CO_2, à des températures encore beaucoup plus considérables.

Tableau I

Milieu gazeux	K, min^{-1}	ΔT, °C	$\Delta\alpha$
Air	0,1060	860-930	0,6
N_2	0,0809	860-960	0,5
90 p.c. de N_2 plus 10 p.c. de CO_2	0,1234	880-950	0,5
CO_2	0,1399	950-1050	0,3

Dans le flux d'azote, la zone de décomposition rapide de ce calcaire se déplace vers le domaine des températures plus basses.

On a étudié l'effet de la vitesse d'évacuation de CO_2 depuis la zone de réaction sur la cinétique de décomposition de $CaCO_3$ (des mesures de CO_2 ainsi dégagée ont été faites par la méthode de la spectroscopie IR). Ces études ont montré que la valeur E_a de dissociation répond à l'équation (2):

$$E_a = E_{a_2} \pm \lambda + mQ \frac{P_s^m}{P_o^m - P^m}$$

où E_{a_2} - énergie d'activation de la réaction inverse; λ - chaleur d'adsorption de CO_2; Q - effet thermique de la réaction; P_{CO_2} - pression équilibrée de CO_2; pm - pression effective de CO_2; m - constante.

Le déroulement de la synthèse des produits de clinkérisation est fonction de l'état physique et des propriétés chimiques des constituants de base et détermine les dépenses énergétiques nécessaires pour la formation des minéraux de clinker (3).

La cinétique des réactions à l'état solide a été étudiée sur des mélanges $CaCO_3$ (à des fins d'analyse uniquement) avec kaolin (gisement de Prossianaya), gehlenite synthétique et α - pseudowollastonite (poudre polycristalline), pris dans des proportions différentes; les réactions se déroulaient dans les conditions de réchauffement rapide à des températures de 900 à 1.200°C. Les résultats de ces recherches sont présentés dans le tableau II. L'évaluation des valeurs de la densité optique des bandes d'absorption de $CaCO_3$, β - C_2S, CS, C_2AS et C_3A a permis d'obtenir des courbes cinétiques de variation des concentrations molaires de ces composés dans les produits de cuisson.

Pour décrire mathématiquement la cinétique des réactions de synthèse, on a fait recours à des équations pseudo-topocinétiques généralisées:

$$kt = -\frac{1}{\alpha^m} \cdot \frac{1-(1-\alpha)^{1-m}}{1-m} \qquad (3)$$

$$kt = -\frac{1}{\alpha^{1-m}} \cdot \ln \frac{1-\alpha}{1+\alpha} \qquad (4)$$

où m - facteur d'hétérogénéité. La variation m de 0 à 1 correspond au passage de la réaction depuis le domaine de diffusion vers le domaine cinétique.

Le tableau II montre la relation entre la composition de phases des produits de cuisson et le rapport des constituants de base.

On y voit également le rapport entre les paramètres cinétiques de la réaction de dissociation de $CaCO_3$, d'une part, et les paramètres cinétiques de la synthèse de C_2AS, C_3A et β - C_2S, d'autre part.

Les calculs thermodinamiques ont montré que les réactions $CaCO_3$ - kaolin, gehlenite et pseudowollastonite sont réalisables à des températures plus basses par rapport à la température de dissociation de $CaCO_3$ (900°C). La baisse de Ea de dissociation de $CaCO_3$, dans des mélanges constitués de divers alumosilicates, s'explique par une réaction triphasée avec carbonate qui aboutit à la formation du bélite, des aluminates et de CaO, exerçant une action catalytique sur le processus de dissociation. La réalisation de ces réactions est facilitée grâce aux transformations, de phase et chimique, des silicates d'alumine, à savoir le passage du kaolin en métakaolinite, la stabilisation du réseau cristallin α - CS et C_2AS.

Les données obtenus pendant les expérimentations témoignent que la formation du la bélite dans les mélanges chaux - argile peut être réalisée par différentes voies.

Les mélanges ayant un rapport stoechiométrique de $CaCO_3$ à kaolin (soit 3,5 à 1), forment de la gehlenite et de α - CS, dont l'interaction avec $CaCO_3$ et CaO fournit la bélite et C_3A. Le surplus de $CaCO_3$ (rapport 9 à 1) contribue à la formation de β - C_2S et C_3A à partir, semble-t-il, de métakaolinite et CaO; CS ou C_2AS ne sont pas observés lors de l'usage de ces constituants. La formation de la gehlenite s'opère dans le domaine chimique (m = 0,98). C_3A se crée à base de gehlenite et de $CaCO_3$, avec une plus basse Ea et des rapports plus faibles de constituants de base; le mécanisme de la réaction est chimique (m = 0,98).

Pendant le réchauffement du mélange de $CaCO_3$ et de kaolinite, se produisent des signaux de la résonance électronique paramagnétique avec g = 2,00, dont le pic d'intensité coïncide de façon satisfaisante avec le domaine des vitesses maximales des réactions de synthèse β - C_2S et C_3A.

Les résultats obtenus permettent d'expliquer la différence de réactivité des mélanges de base constitués par divers minéraux. La baisse de l'énergie d'activation de la dissociation des carbonates est fonction des possibilités de réaliser les réactions à l'état solide de $CaCO_3$ avec alumosilicates avant la dissociation proprement dite. On a étudié la corrélation des paramètres cinétiques de la formation de bélite en phase solide et d'alite dans les mélanges $CaCO_3$, d'une part, et diverses combinaisons de minéraux argileux et de laitiers constitués par mélilites et pseudowollastonites;

En se basant sur les données expérimentales obtenues, on peut conclure que la valeur énergétique d'activation de la formation du bélite en phase solide constitue un critère lors du choix des conditions optimales pour la fabrication du clinker.

Ainsi, l'énergie d'activation (Ea) de la formation du bélite en phase solide étant supérieure à 180 kJ/moles ($CaCO_3$ avec kaolin et montmorillonite), la formation d'alite est caractérisée par la valeur Ea allant de 150 à 170 kJ/moles et contrôlée totalement par la diffusion Ca^{2+} en bélite.

Au cas où la valeur Ea de la formation du bélite en phase solide est faible, c'est-à-dire au-dessous de 150 kJ/moles ($CaCO_3$ avec laitiers de mélilite et de pseudowollastonite), juste avant la formation du clinker fondu on voit apparaître des cristaux du

Tableau II

Constituants	Rapport des constituants (en poids)	Paramètres cinétiques des réactions						
		Dissociation de $CaCO_3$	Synthèse en phase solide					
			C_2AS		β- C_2S		C_3A	
		E_a	m	E_a	m	E_a	m	E_a
$CaCO_3$ + kaolin	3,5:1	143,8	0,98	83,8	-	-	-	-
	6:1	149,7	-	-	0,02	257,7	0,02	599,4
	9:1	174,1	néant		0,02	178,3	0,02	362,4
$CaCO_3$ + C_2AS	1,5:1	127,1	-	-	0,98	105,0	0,98	148,4
	4:1	113,8	-	-	0,02	153,4	0,02	416,8
$CaCO_3$ + α - CS	1:1	97,6	néant		0,02	226,3	néant	
	3:1	111,9	néant		0,02	99,3	néant	

bélite résistants à la résorption. Dans ce cas, la valeur Ea de la formation d'alite constitue 200 à 400 kJ/moles, et c'est alors que le processus ne se limite pas que par la diffusion de Ca^{2+} en bélite, mais aussi par la vitesse de dissolution de la bélite.

Ainsi donc, la constitution minérale d'alumosilicate et la nature de carbonate définissent la cinétique de la formation et de la transformation des cristaux d'alite.

A partir des mélanges de $CaCO_3$ avec kaolin, montmorillonite et leurs combinaisons, se forme une alite en modification essentiellement rhomboédrique. A partir des mélanges de $CaCO_3$ avec hydro-mica et laitier de pseudowollastoniteon a obtenu, dans les mêmes conditions une alite en modification monoclinique; avec laitiers de mélilite on obtient une alite en modification triclinique.

BIBLIOGRAPHIE

1.- Б.ДЕЛЬМОН (1972) Кинетика гетерогенных реакций, 556 с., рус. (en russe).

2.- Е.А.ПРОДАН, М.М.ПАВЛЮЧЕНКО, С.А.ПРОДАН (1976) Закономерности топохимических реакций, 300 с., рус. (en russe).

3.- С.Д.МАКАШЕВ (1976) Влияние физико-химических свойств сырья на реакционную способность сырьевой смеси и процессы минералообразования клинкера. VI Международный конгресс по химии цемента, т.1, с.207-211, рус. (en russe).

4.- О.П.МЧЕДЛОВ-ПЕТРОСЯН, Н.И.САПОЖНИКОВА, Т.Ю.ЩЕТКИНА (1975) Термодинамические методы исследования реакционной способности сырьевых смесей и цементов, "Цемент", № 10, с.17-19, рус. (en russe).

Fissuration et broyabilité du clinker

Cracking and grindability of clinker

H. HORNAIN, ingénieur C.N.A.M. - C.E.R.I.L.H., Paris France,
M. REGOURD, docteur ès sciences physiques - C.E.R.I.L.H., Paris, France.

RESUME

Le clinker est un matériau fragile auquel peuvent être appliqués les concepts de la mécanique de la rupture. Des mesures d'énergie spécifique de rupture γ_F ont été effectuées sur des prismes de clinker compactés et recuits à 1450 °C, par la méthode de l'éprouvette entaillée soumise en flexion simple à déformation imposée. Un indice de fragilité caractérisant l'aptitude à la déformation et à la fracture des différents minéraux du clinker a été mesuré par une méthode d'indentation utilisant le microduromètre VICKERS. La plus grande fragilité de C_3S, qui concentre les contraintes, explique le comportement du clinker au choc thermique. Deux types de fissuration dépendant de l'intensité du choc thermique ont été mis en évidence : fissuration macroscopique des granules et fissuration microscopique de C_3S. Des tests réalisés en laboratoire ont permis de relier la broyabilité du clinker au taux de fissuration de C_3S.

SUMMARY

Clinker is a brittle material to which concepts of fracture mechanics can be applied. Measurements of fracture surface energy γ_F have been made on clinker prisms compacted and reburnt at 1450 °C, by the method of notched bending specimen in imposed deflection conditions. A brittleness index characterizing the aptitude to deformation and to fracture of the different clinker minerals has been measured by an indentation method using VICKERS microindenter. The greater brittleness of C_3S which concentrates the stresses, explains the comportment of the clinker to thermal shock. Two types of cracks depending on thermal shock intensity have been observed : macroscopic cracking of the granules and microscopic cracking of C_3S. Laboratory tests have permitted us to relate grindability of clinker to the rate of C_3S cracking.

1. INTRODUCTION

Le broyage du clinker entraîne une consommation d'énergie moyenne de 38 $kWh.t^{-1}$ (1). Le coût énergétique élevé de cette opération justifie les recherches destinées à améliorer son rendement : mise au point de matériel nouveau (1, 2), étude du comportement du matériau à la fragmentation en relation avec sa composition minéralogique (3, 4), sa texture, son traitement thermique (5). Nous nous proposons, ici, d'appliquer à la fragmentation du clinker les critères relatifs à la propagation des fissures et à la rupture des matériaux, critères déjà largement utilisés par l'Industrie Céramique, notamment dans les problèmes de choc thermique dont nous verrons l'influence sur la fissuration et la broyabilité du clinker.

2. PROBLEMES GENERAUX DE LA FRAGMENTATION DU CLINKER

Le clinker est un matériau fragile auquel peuvent être appliqués les concepts de la mécanique linéaire de la rupture dus à GRIFFITH (6). La théorie de GRIFFITH, complétée depuis par de nombreux travaux, admet la préexistence de microfissures dont la progression stable (contrôlée) ou instable (non contrôlée), dans des conditions données de sollicitations, est déterminée par deux paramètres intrinsèques au matériau (7) : l'énergie spécifique de rupture γ_F, et la taille relative(a)des microfissures préexistantes. Les premières mesures de γ_F effectuées sur des éprouvettes entaillées, soumises en flexion simple à déformation imposée (8), indiquent des valeurs de l'ordre de 12 à 22 $J.m^{-2}$ pour des clinkers compactés sous forme de prismes 80 x 32 x 7 mm, recuits 2 heures à 1450°C, de masse volumique apparente $\sim 3 g.cm^{-3}$, et de module de YOUNG $E \simeq 10^5$ MPa. Ces résultats sont vraisemblablement un peu plus élevés que ceux que l'on obtiendrait sur les granules de clinkers industriels généralement moins denses. Le tableau I regroupe quelques valeurs comparatives de γ_F pour divers matériaux. Il montre que l'énergie spécifique de rupture du clinker est assez élevée, mais que celle des monocristaux est beaucoup plus faible que celle des matériaux polycristallins correspondants. Dans ces derniers, une partie de l'énergie servant à la propagation des fissures est diffusée au niveau des discontinuités telles que les joints de grains, les pores, les inclusions ; la conséquence fréquente est l'arrêt de la fissure à la limite du cristal dans lequel elle avait été amorcée. C'est ce qui est observé dans le clinker où les microfissures dans C_3S sont souvent arrêtées au niveau de la phase interstitielle.

Tableau I : Energie spécifique de rupture de quelques matériaux.

Matériaux polycristallins		Références
MgO	γ_F = 20 à 40 $J.m^{-2}$	(9)
Al_2O_3	18 à 46 "	"
Granit	31 "	(7)
Clinker	12 à 22 "	ce travail
Monocristaux		
MgO	γ_o = 1,2 à 1,5 $J.m^{-2}$	(9) , (10)
Al_2O_3 (11$\bar{2}$3)	24 "	(9)
Al_2O_3 (10$\bar{1}$1)	6 "	"
$CaCO_3$	0,3 "	(10)
C_3S	$\sim$ 1,0 "	estimée
C_3A	$\sim$ 1,4 "	"
Verre	4	(7)

Les relations entre γ_F et la composition minéralogique, les dimensions des cristaux, la porosité n'ont pas encore été établies pour le clinker. γ_F, énergie superficielle, constitue une mesure de la résistance à la fracture des solides. Pour le clinker, une valeur moyenne de γ_F de 17 $J.m^{-2}$ signifie qu'une finesse de 3500 $cm^2.g^{-1}$ exige théoriquement une énergie égale à 1,65 $kWh.t^{-1}$ au lieu de 38 $kWh.t^{-1}$, valeur habituelle. Les concepts de la mécanique de la rupture appliqués au broyage par HUET (7) peuvent fournir une explication à cet écart important : dans les broyeurs à boulets usuels, les conditions sont proches de la déformation imposée où il y a progression instable pour les faibles tailles relatives de microfissures et progression stable pour les tailles relatives élevées. Au début du broyage du clinker, la taille des fissures, du même ordre que celle des cristaux de C_3S, est petite devant celle des grains : la progression des fissures est instable avec rupture complète des grains ; l'énergie dépensée n'est pas très supérieure à l'énergie théorique. Par contre, aux stades plus avancés du broyage, la taille des microfissures devient grande relativement à celle des grains : on se trouve dans le cas de la rupture contrôlée où la progression des fissures ne peut être obtenue que par la répétition du choc. Une part importante de l'énergie est ainsi perdue et dissipée par les frottements entre grains et les déformations plastiques notables pour les petits grains (11). La complexité du phénomène s'accroît si l'on considère qu'au début du broyage la rupture est commandée par l'énergie spécifique de rupture de l'agrégat polycristallin mais qu'en fin de broyage la rupture dépend davantage de γ_o des cristaux proprement dits.

Le comportement du clinker à la rupture dépend également des propriétés de ses minéraux constitutifs, C_3S, C_2S, C_3A, C_4AF. Ces minéraux, qui ont des structures essentiellement ioniques, ont tous un comportement fragile. La fragilité, que l'on peut définir schématiquement comme le rapport entre l'aptitude à la déformation et l'aptitude à la fracture, n'est pas la même pour tous ces composés. Un indice de fragilité a pu être déterminé par une méthode d'indentation utilisant la pyramide du microduromètre VICKERS (12). Le principe consiste à mesurer d'une part les dimensions de l'empreinte et d'autre part la longueur des microfissures qui apparaissent dans le prolongement de l'empreinte lorsque la charge dépasse une certaine valeur critique. La mesure des diagonales de l'empreinte permet de calculer la microdureté H qui représente l'aptitude à la déformation du cristal. L'évaluation de la longueur des microfissures conduit au calcul de la "ténacité" K_c [identique au facteur intensité de contrainte, utilisé en mécanique de la rupture (7)], qui représente l'aptitude à la fracture du cristal. Le rapport H/K_c donne un indice de fragilité. Les valeurs moyennes approchées, trouvées pour les minéraux du clinker ainsi que quelques valeurs tirées de la littérature sont portées dans le tableau II.

C_3S est le minéral le plus fragile. Sa fragilité est en relation avec l'existence d'une direction de clivage privilégiée, qui entraîne une fissuration facile des cristaux (fig. 1). C_2S est beaucoup plus déformable que C_3S et l'essai d'indentation avec les charges utilisées (20 g ou 50 g) ne donne pas toujours des fissures visibles (fig. 2). L'aluminate tricalcique et l'aluminoferrite sont les composés les plus durs, c'est-à-dire les moins déformables. Dans les conditions

de nos essais et pour les clinkers testés, contenant respectivement 15 % de C_3A cubique et 13 % de C_4AF, la phase C_3A (fig. 3) apparaît plus fragile que la phase C_4AF, plus déformable, qui fissure très peu sous les charges utilisées.

Les propriétés globales du clinker, matériau polycristallin, ainsi que celles de ses minéraux constitutifs, expliquent son comportement à la fragmentation qui a lieu suivant un processus à la fois de libération fissurale et de libération minérale : les fissures progressent respectivement à travers les cristaux, en particulier les cristaux de C_3S préfissurés, et le long des limites de phases (fig. 4). Les fissures de C_3S sont le plus souvent bloquées ou déteurnées au niveau de la phase interstitielle, généralement peu fissurée, (fig. 5). Les cristaux ou amas de C_2S sont contournés par les fissures jusqu'à un stade avancé de la fragmentation. Ces cristaux, de forme arrondie, relativement déformables et ayant une certaine "mobilité" (13) par rapport à la phase interstitielle (fig. 6) donnent lieu à une libération minérale type : des individus cristallins sont fréquemment retrouvés intacts en fin de broyage.

Tableau II : Dureté (H), Ténacité (K_c), Fragilité (H/K_c) des minéraux du clinker.

Phase	H (GPa)	K_c ($MPa.m^{1/2}$)	H/K_c ($\mu m^{-1/2}$)
C_3S	7,5	1,7	4,7
C_3A	9,0	3,1	2,9
C_2S	6,7	3,7	1,8
C_4AF	9,0	n.d.	$\sim$ 2 (estimée)
Acier (12)	5	50	0,1
Al_2O_3 "	12	4	3
MgO "	9,2	1,2	8

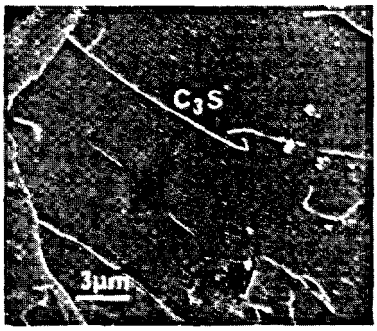

Fig. 1 : Essai d'indentation. Fissuration de C_3S (MEB).

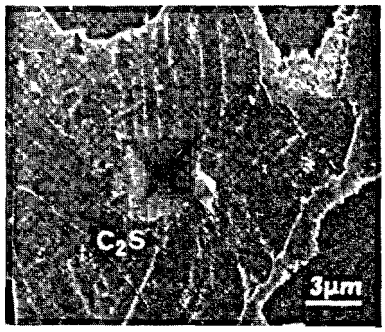

Fig. 2 : Indentation dans C_2S déformable (MEB).

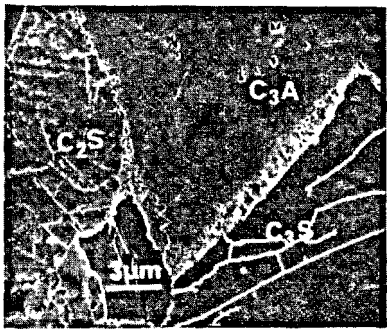

Fig. 3 : Indentation dans C_3A assez fragile, fissuré (MEB).

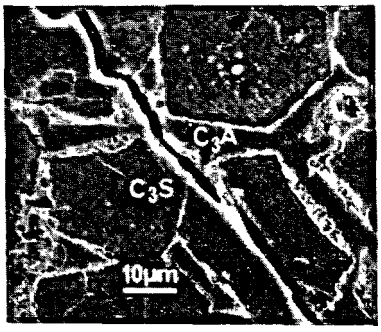

Fig. 4 : Cheminement d'une fissure (MEB).

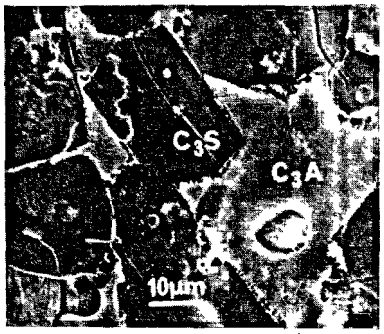

Fig. 5 : Arrêt des fissures de C_3S au niveau de C_3A (MEB).

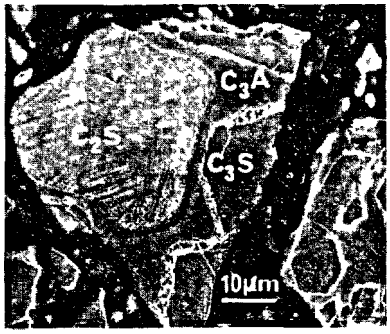

Fig. 6 : Décollement partiel des cristaux de C_2S (MEB).

3. FISSURATION ET RUPTURE PAR CHOC THERMIQUE

Le choc thermique provoque des contraintes susceptibles d'entraîner la fissuration et la rupture des granules de clinker. Les contraintes sont dues au gradient de température, à l'anisotropie des contractions, aux transformations polymorphiques, aux différences de coefficient de dilatation entre phases. Le refroidissement plus ou moins brutal induit, dans le matériau, une énergie thermo-élastique qui se dissipe sous forme d'énergie spécifique de rupture γ_F.

Si l'énergie thermo-élastique dissipée par le champ de contrainte autour d'une microfissure préexistante est supérieure à γ_F, la fissure progresse et peut entraîner la rupture. Le caractère stable ou instable de la progression est déterminé par la taille de la fissure.

Pour les matériaux céramiques, HASSELMAN (14) a montré, à partir d'un modèle idéal représentant les conditions les plus favorables à la rupture, que le domaine d'instabilité était limité par deux valeurs critiques de la taille des fissures : la différence de

température critique provoquant la propagation en fonction de la taille des fissures passe par un minimum. L'application à un clinker donne la courbe de la figure 7. A partir des hypothèses suivantes applicables aux conditions industrielles :

- $\Delta T \simeq 800 - 900$ °C,
- 1 fissure par cristal de C_3S, soit $N \simeq 10^7$ fissures par cm^3,
- longueur des fissures ≃ 30 à 50 µm,

on voit que les courbes obtenues sont proches des courbes de stabilité au-delà desquelles la différence de température ΔT n'est plus suffisante pour amorcer la propagation des fissures. Donc à moins de répéter le choc thermique, la rupture des granules aura peu de chance de se produire. C'est ce qui est généralement observé : les granules sont plus ou moins microfissurés mais non rompus. Pour les petites fissures amorcées dans le domaine d'instabilité, le taux d'énergie élastique dissipée est supérieur à l'énergie spécifique de rupture. Lorsque ces fissures atteignent les longueurs correspondant aux courbes en traits pleins, elles possèdent encore de l'énergie cinétique et progressent jusqu'à une taille limite donnée par les courbes en pointillés, calculées d'après (14). La figure 7 montre qu'il y aurait probablement intérêt à avoir des clinkers à petits cristaux : l'énergie spécifique de rupture serait plus faible et les microfissures plus petites, se trouveraient dans la zone de progression instable.

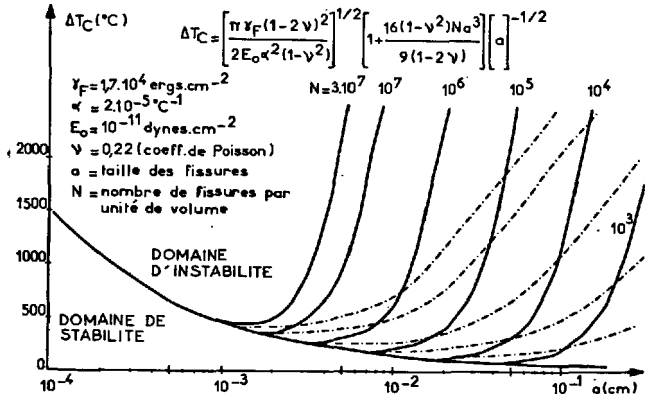

Fig. 7 : Différence critique de température ΔT_c amorçant la propagation des fissures en fonction de la taille des microfissures (courbes en traits pleins). En pointillés, limites de propagation des petites fissures instables [calculées d'après (14)].

4. RELATION ENTRE L'INTENSITE DU CHOC THERMIQUE, LA FISSURATION ET LA BROYABILITE DU CLINKER.

Des granules de clinker de 1 cm de diamètre ont été fabriqués à partir de deux crus industriels, par cuisson au four électrique à 1450 °C, pendant 2 heures. La composition minéralogique moyenne des clinkers, référencés A et B, analysés par diffraction des rayons X, est donnée dans le tableau III.

Tableau III : Composition minéralogique moyenne des clinkers testés (refroidissement lent).

	C_3S	C_2S	C_3A	C_4AF
Clinker A	62 %	17 %	15,5 %	5,5 %
Clinker B	65 %	18 %	3,0 %	13,0 %

Les clinkers ont subi les refroidissements suivants :

- refroidissement lent (300 °C.h^{-1}),
- trempe dans l'eau à 20 °C à partir de 1450 °C,
- trempe dans l'eau à 20 °C à partir de 1250 °C.

L'état de fissuration en fonction de l'intensité du choc thermique a été observé au microscope optique sur section polie, attaquée à l'aide d'une solution de borax à 2 % dans l'eau. Deux types de fissuration ont été observés (15) : d'une part une fissuration macroscopique avec des fissures larges, radiales, traversant le granule et provoquant parfois sa rupture ; d'autre part, une fissuration microscopique qui se développe essentiellement dans les cristaux de C_3S et beaucoup plus rarement dans la phase interstitielle. La fissuration macroscopique est d'autant plus importante que le choc thermique est intense. Mais paradoxalement, la fissuration microscopique est d'autant plus faible. Ainsi dans les clinkers trempés à 1450 °C, la fissuration macroscopique est maximale, mais la fissuration microscopique y est minimale (fig. 8 et 9) ; les granules du clinker A, riche en C_3A, étaient fréquemment rompus en plusieurs fragments tandis que les granules du clinker B, riche en C_4AF, avaient mieux résisté au choc thermique vraisemblablement en raison du comportement moins fragile de la phase ferritique.

La trempe à l'eau à partir de 1250 °C provoque une fissuration macroscopique faible, les granules sont entiers. Par contre, ce mode de refroidissement entraîne la fissuration microscopique la plus forte (fig. 10).

Le refroidissement lent ne provoque pas de fissuration macroscopique et la fissuration microscopique est intermédiaire.

Ce comportement du clinker au choc thermique est en relation avec les propriétés particulières de C_3S, notamment avec son indice de fragilité relativement élevé. Les fissures qui s'y produisent sont dues aux différences entre son coefficient de dilatation et celui de la phase interstitielle, et à l'anisotropie de ses contractions. Le tableau IV donne les coefficients de dilatation thermique de C_3A et C_3S, déduits des données cristallographiques (16,17).

Tableau IV : Coefficients de dilatation thermique mesurés de C_3S et de C_3A (10^{-6}.°C^{-1}).

C_3S Triclinique 20-980 °C	C_3S Trigonal 1050-1100 °C	C_3A Cubique 20-1000 °C	C_3A Orthorh. 500-1000 °C
α_a 10,2 α_b 7,0 α_c 13,9	α_b 8,7 α_c 49	α 8	α_{ab} 9,7 α_c 13,2

Fig. 8 : Clinker A - Trempe à 1450 °C. Fissuration macroscopique forte.

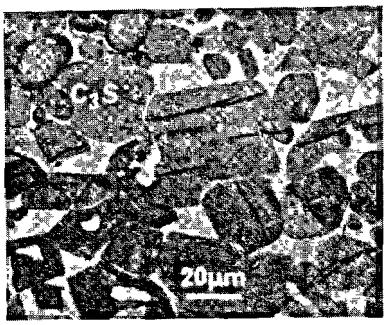

Fig. 9 : Clinker A - Trempe à 1450 °C. Fissuration microscopique faible.

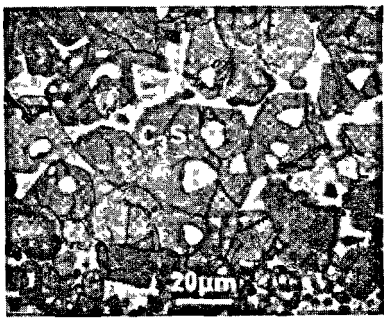

Fig. 10 : Clinker A - Trempe à 1250 °C. Fissuration microscopique forte.

Quand la trempe intervient à 1450 °C, la phase interstitielle se solidifie sous forme d'un verre. Les variations de volume et les différences de coefficient de dilatation entre le verre et C_3S sont plus faibles. Il en est de même pour les contraintes subies par le silicate qui se fissure moins. En outre, une partie de l'énergie élastique, qui dépend entre autre du module de YOUNG E (plus faible aux températures élevées), se dissipe en raison du comportement viscoplastique du matériau avant sa solidification complète. Par ailleurs, la présence d'un verre vraisemblablement plus fragile, associée à une énergie thermo-élastique néanmoins élevée, entraîne la propagation instable très rapide des fissures, jusqu'à la rupture des granules. L'excès d'énergie est dissipé sous forme d'énergie cinétique et d'énergie acoustique. L'énergie théorique, consommée par la rupture des granules et la fissuration des cristaux dans les conditions de l'essai, est alors de l'ordre de 1 Joule, l'énergie théorique disponible étant d'environ 3 à 4 Joule.

Lorsque la trempe a lieu vers 1250 °C, température à laquelle la phase interstitielle est déjà cristallisée, les contraintes subies par C_3S sont maximales. L'énergie thermo-élastique disponible n'est plus suffisante pour provoquer la rupture complète des granules. L'énergie théorique consommée par la fissuration des cristaux de C_3S est du même ordre de grandeur que l'énergie thermo-élastique disponible. Les cristaux de C_3S, très fragiles, constituent des points d'amorçage de fissures privilégiés qui absorbent une grande partie de l'énergie. Les possibilités de fissuration de la phase interstitielle et la rupture des grains de clinkers sont ainsi limitées. C_3S joue le rôle de concentrateur de contraintes ; sa microfissuration empêche la propagation lointaine des fissures, l'énergie thermo-élastique étant diffusée dans toute la masse du granule.

Les tests de broyabilité, effectués à l'aide d'un microbroyeur à résonnance DANGOUMAU sur les deux clinkers A et B et pour les trois modes de refroidissement, indiquent que les clinkers les plus microfissurés sont les plus broyables. Les résultats sont illustrés par la figure 11 qui montre l'évolution de la surface spécifique Blaine en fonction du temps de broyage. Dans tous les cas, les clinkers trempés à partir de 1250 °C possèdent la meilleure broyabilité. L'effet est le plus marqué sur le clinker A riche en C_3A, minéral relativement plus fragile et plus sensible au choc thermique que C_4AF abondant dans le clinker B. Les différences de broyabilité entre les clinkers trempés à partir de 1450 °C et les clinkers refroidis lentement sont peu importantes.

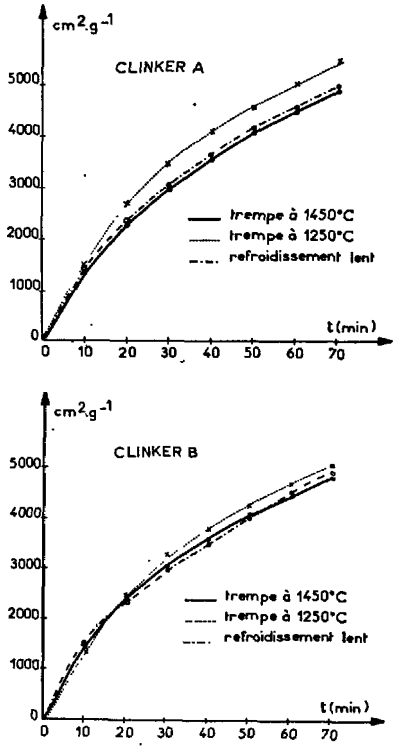

Fig. 11 : Finesse Blaine des clinkers A et B, en fonction du temps de broyage.

Ces essais montrent qu'il doit exister pour chaque clinker une température optimale de trempe, qui entraîne une microfissuration maximale de la phase C_3S avec augmentation corrélative de la broyabilité. Cette température est voisine de la température de solidification de la phase liquide. Les chocs thermiques à très haute température ne semblent pas apporter d'amélioration notable de la broyabilité dans les conditions de nos essais.

5. CONCLUSIONS

Le comportement du clinker à la rupture est déterminé par deux paramètres intrinsèques au matériau :

- l'énergie spécifique de rupture γ_F (environ 12 à 22 $J.m^{-2}$),
- la taille des microfissures préexistantes, du même ordre de grandeur que celle des cristaux de C_3S.

La connaissance de ces paramètres et leur utilisation dans le cadre de la mécanique de la rupture peuvent fournir une explication au mauvais rendement du broyeur à boulets aux stades avancés du broyage.

Le comportement du clinker à la rupture dépend aussi des propriétés particulières de ses minéraux constitutifs. Leurs γ_F sont dix à vingt fois plus faibles que celles de l'agrégat polycristallin. Leurs indices de fragilité mesurés sont : 4,7 pour C_3S ; 2,9 pour C_3A et environ 2 pour C_2S et C_4AF.

La grande fragilité de C_3S explique le comportement du clinker au choc thermique. La trempe à 1450 °C, lorsque le clinker est pâteux, induit une microfissuration faible de C_3S. Elle provoque l'apparition de fissures macroscopiques et la rupture des granules. La trempe à 1250 °C donne une microfissuration importante de C_3S, qui concentre une grande partie des contraintes empêchant la rupture des granules. Cela se traduit par une augmentation de la broyabilité alors que la trempe à 1450 °C n'apporte pas d'amélioration sensible.

Les essais et résultats rapportés ici ne sont qu'une première tentative d'interprétation, à l'aide de la mécanique de la rupture, du comportement du clinker à la fragmentation. Ils devront être largement complétés et précisés par la suite.

Remerciements : Nous adressons nos plus vifs remerciements au Prof. C. HUET et à M. VALAKOON qui nous ont permis de réaliser les premières mesures d'énergie spécifique de rupture du clinker.

Nous remercions également Catherine PEYRE et Françoise MOINE pour leur participation à ce travail.

(The english version of this paper is available. Please write to the authors for a copy : C.E.R.I.L.H. - 23, rue de Cronstadt 75015 PARIS.)

BIBLIOGRAPHIE

1.- J.P. MERIC (1978) : "Le broyage", Rev. Mater. Constr. (CBPC), n° 715, pp. 329-33.

2.- R. PLANIOL (1962) : "Les broyeurs centrifuges et le vide", Symp. Zerkleinern. Verlag Chemie Weinkein, VDI Verlag, Düsseldorf.

3.- M. REGOURD, H. HORNAIN, B. MORTUREUX (1978) : "Influence de la granularité des ciments sur leur cinétique d'hydratation", Rev. Mater. Constr. (CBPC), n° 712, pp. 137-40.

4.- G.R. GOUDA (1979) : "Effect of clinker composition on grindability", Cem. Concr. Res., vol. 9, pp. 209-18.

5.- J.M. BUTT, V.M. KOLBASOV, G.A. MELNICKIJ (1974) : "Zur Wechselbeziehung zwischen der Porenstruktur und Mahlbarkeit von Klinkern aus verschiedenen Brenn und Abkühlungsverfahren", Z.K.G., n° 1, pp. 27-32.

6.- A.A. GRIFFITH (1920) : "The phenomenon of rupture and flow in solids", Phil. Trans. Roy. Soc. (Londres), A221[4], pp. 163-98.

7.- C. HUET (1978) : "Concepts de la mécanique de la rupture", Collège International des Sciences de la Construction, UTI, Séminaire Fragmentation, St Rémy-les-Chevreuse, 12-14 déc.

8.- C. HUET (1973-1974) : "Méthode de détermination de l'énergie spécifique de rupture et application aux céramiques et à divers matériaux minéraux", Industrie Minérale, nov. 1973, pp. 128-142, sept. 1974, pp. 164-176.

9.- S.M. WIEDERHORN (1969) : "Crack propagation in polycristalline ceramics", Proceedings of XVth Sagamore Army Materials Research Conference on fine-grained ceramics. Edité par J.J. BURKE et al, Syracuse Univers. Press, Syracuse, N.Y., pp. 317-38.

10.- J.J. GILMAN (1960) : "Direct measurements of the surface energies of crystals", J. Appl. Phys., 31 [12], pp. 2208-18.

11.- H. RUMPF (1973) : "Physikalische Aspekte des Zerkleinerns, Ähnlichkeitsgesetz der Bruchmechanik und die Energieausnutzung der Einzelkornzerkleinerung", Aufbereitungs-Techn., n° 2, pp. 59-71.

12.- B.R. LAWN, D.B. MARSHALL (1978) : "Hardness, toughness and brittleness : an indentation analysis", J.A.C.S., vol. 62, n° 7-8, pp. 347-50.

13.- B. BEKE (1970) : "Le coefficient d'uniformité de la répartition des grains des matériaux broyés", Z.K.G., n° 9, 401-6.

14.- D.P.H. HASSELMAN (1969) : "Unified theory of thermal shock fracture initiation and crack propagation in brittle ceramics", J.A.C.S., vol. 52, n° 11, pp. 600-4.

15.- M. REGOURD (1979) : "The crystal chemistry of Portland cement minerals. New data", Engineering Fondation Conference on cement production and use, Rindge (U.S.A.), à paraître.

16.- A. GUINIER, M. REGOURD (1968) : "Structure of Portland cement minerals", Ve Symp. Internat. sur la chimie du ciment, Tokyo, vol. 1, pp. 1-32.

17.- M. REGOURD, A. GUINIER (1974) : "The crystal chemistry of constituents of Portland cement clinker", VIe Symp. Internat. sur la chimie du ciment, Moscou, Papier principal.

The effect of Al_2O_3, BaO and B_2O_3 admixtures on C_3S structure

L'effet des additions Al_2O_3, BaO et B_2O_3 sur la structure du C_3S

W. KURDOWSKI, Research Center of the Industry of Binding Materials, Krakow,
M. HANDKE, G. SIEMINSKA, School of Mining and Metallurgy, Institute of Materials Science, Krakow, Poland.

RESUME : On a étudié, à l'aide des rayons X, transformée de Fourier et IR, des échantillons de silicate tricalcique avec une petite addition de Al_2O_3, BaO et B_2O_3.
Les études ont été exécutées sur les échantillons avec l'addition d'un seul oxyde, ainsi qu'avec la combinaison de deux oxydes : Al_2O_3 + BaO et Al_2O_3 + B_2O_3, dans des proportions variées.
On a trouvé que dans la solution solide C_3S-Al_2O_3 ce n'est que l'aluminium en coordination tétraédrale qui peut stabiliser la forme T_{II} et que l'introduction du cation Ba dans la solution solide provoque une transformation des octaèdres $[AlO_6]$ en tétraèdres $[AlO_4]$.
Le cation Ba remplace dans le réseau C_3S seulement le cation Ca qui n'est pas coordonné par les tétraèdres $[SiO_4]$. De très petites quantités de l'addition de B_2O_3 décomposent C_3S en β -C_2S et CaO, et en solution solide C_3S-Al_2O_3.

**SUMMARY : The tricalcium silicate samples with small admixtures of Al_2O_3, BaO and B_2O_3 were investigated by X-ray diffractometry and Fourier Transform IR spectroscopy.
The studies were performed on samples with single oxide admixture and also with double : Al_2O_3+BaO and Al_2O_3+B_2O_3 in different ratio. It was found that in C_3S-Al_2O_3 solid solution only tetrahedral coordinated aluminum can stabilize T_{II} form, and when Ba cations are introduced into solid solution, $[AlO_6]$ octaedra are transformed into $[AlO_4]$ tetrahedra.
The Ba cation replaces only the Ca cation noncoordinated by $[SiO_4]$ tetrahedra in C_3S lattice.
Very small quantity of B_2O_3 admixture decomposes C_3S into β -C_2S and CaO as well as C_3S--Al_2O_3 solid solution.**

INTRODUCTION

The production technology of rapid hardening high strength cements requires some modifications in the classical methods of clinker production. One of the directions in which changes should go, consists in using admixed metal oxides introduced into charge during clinker production. The effect of these admixtures has been studied by many authors /1,2,3,4/. They have confirmed the real effect of the admixtures on different properties, for example on clinker hydraulic activity. Presence of the admixtures in the clinker changes structure and texture i.e. defects of clinker phase crystals, modification of crystal habit and size, stabilization of defined polymorphs of di- and tri-calcium silicate, appearance of new phases including admixtures. The action mechanism of admixtures, and especially the correlation between the character of the component and clinker properties, have not been satisfactorily investigated as yet.

The barium oxide is one of the additions advantageously modificating clinker properties, as has been shown by Kurdowski /5/. The purpose of our work was to investigate the effect of the BaO and B_2O_3 admixtures on the C_3S structure as well as on the C_3S-Al_2O_3 solid solutions. The Portland clinker is a species of very complicated mineral composition. In order to simplify the studies, we have investigated only one but, in our opinion, the most important one of clinker components, which is C_3S.

The infrared absorption spectroscopy has been used as a main method. This method, as opposed to diffraction method, allows to infer about short range order. X-ray diffraction was used as the phase identification method and as the confirmation of some conclusions resulting from the infrared absorption spectra.

EXPERIMENTAL

Two sample series were prepared. The first was pure C_3S with admixed 0,037 - 2,5 mole % BaO and 0,034 - 0,625 mole % B_2O_3. The second was C_3S including 0,25 , 1 and 5 weight % Al_2O_3 to which different quantities of BaO or B_2O_3 were introduced. The samples of the first series have been prepared as follows : to the stoichiometric mixture of the $CaCO_3$ and SiO_2 the corresponding quantity of the water solution of $Ba(NO_3)_2$ or H_3BO_3 has been added. These water suspensions were dried at 100°C and then in the platinum crucible were decalcinated at 1000°C and next heated several times at 1550°C. The samples of second series have been prepared similarly. The additions of the BaO and B_2O_3 were introduced to previously prepared C_3S-Al_2O_3 solid solution. Syntheses were controlled using X-ray patterns and infrared spectra of the synthesized samples.

Infrared absorption spectra were obtained through application of Fourier Transform Spectrometer FTS-14 Digilab. The application of optimum measurement parameters and double precision of the spectra calculations from the interferograms resulted in a very high signal to noise ratio in measurements. This allows to interprete the very small changes of the spectra.

RESULTS AND DISCUSSION

Figure 1 and 2 show the medium and far infrared spectra of the C_3S including Ba /fig.1/ and B /fig.2/ admixtures. The admixture concentration is given in mole percentage; 1 mole corresponds to the 0,04 mole of BaO or 0,02 mole of B_2O_3 for 1 mole of $3CaO \cdot SiO_2$.

One can notice in these spectra that the increase of the admixture concentration causes the change of the intensity and half-bandwidth of some bands. At first the intensity of the 815 cm^{-1} band which is characteristic for symmetric stretch vibration of

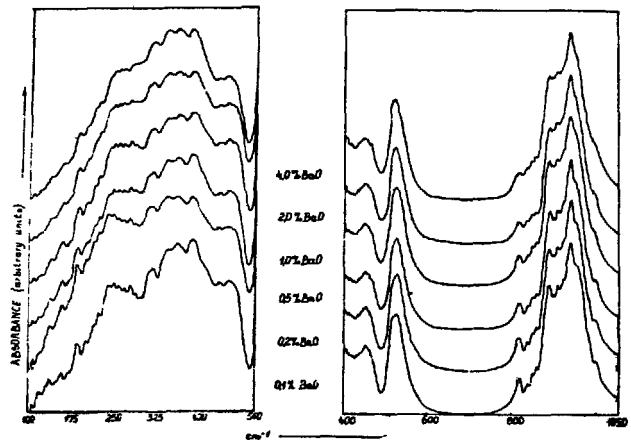

Fig.1. FIR and MIR spectra of the C_3S samples with BaO admixtures

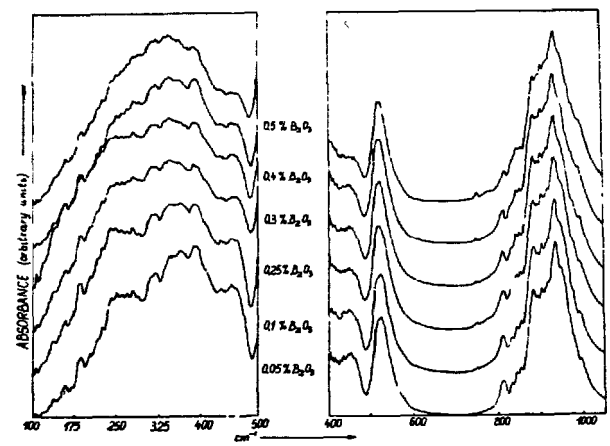

Fig.2. FIR and MIR spectra of the C_3S samples with B_2O_3 admixtures

the Si - O bond in C_3S is changed. This intensity changes from 2,45 to 1,15 /relative units/ for the samples with B_2O_3 admixture and 2,9 to 1,2 with BaO. In the case of B_2O_3 series simultaneous increase of the 847 cm^{-1} band intensity is observed. This band is very intense in the β-C_2S and α'-C_2S spectra. Intensity of this band increase from 62 to 79 /relative units/. For the BaO series intensity of this band is the same within the limits of error.

The different role of both BaO and B_2O_3 admixtures is illustrated on the figure 3 which shows the dependence of the

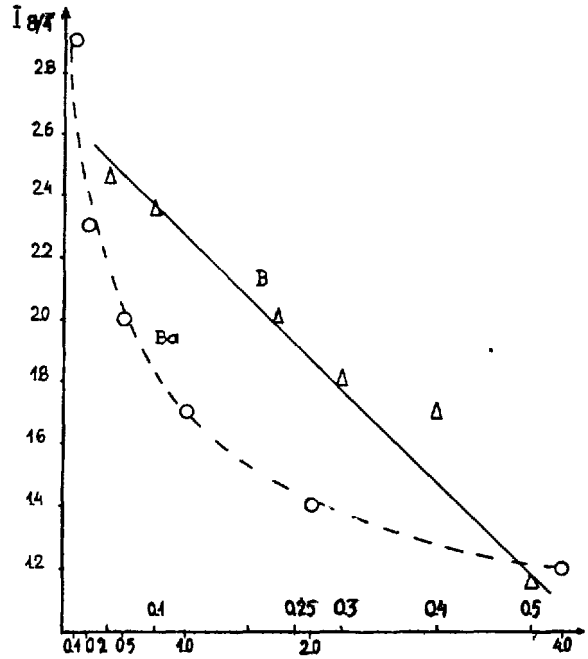

Fig.3. The correlation between 815 cm^{-1} band intensities and admixture concentrations

815 cm^{-1} band intensity on the concentration of barium and boron admixtures in the C_3S. For boron these changes are rectilinear and for barium hiperbolic.
As the 815 cm^{-1} band is characteristic only for C_3S, therefore from figure 3 the conclusion can be drawn that barium ions are introduced partially in the C_3S structure and any presence of the boron ions decomposes this structure on C_2S /847 cm^{-1} band/ and CaO. This conclusion is confirmed by the X-ray patterns and agrees with the findings of other authors. The comparison of the half-bandwidths in the medium infrared, therefore the bands resulting from $[SiO_4]$ tetrahedra vibrations /6/, allows to confirm that it changes only in the case of B_2O_3 admixture. This fact shows that barium ions introduced in the C_3S lattice do not disturb essentially the crystal structure and the position of the $[SiO_4]$ tetrahedra.

The analysis of the far infrared spectra, and therefore the range characteris-

tics for the lattice vibrations indicates that the increase of the Ba ions concentration in the C_3S, does not cause the change of the band intensities but the width of the bands below 300 cm^{-1} changes. According to the assignment of these bands /6/ the change of their shape indicates that barium ions substitute the calcium ions. As the substitution of barium ions does not change the $[SiO_4]$ band width we can conclude that the barium cations substitute mainly these calcium cations which are not coordinated with the $[SiO_4]$ tetrahedra oxygens.

The far infrared spectra of the samples with B_2O_3 confirm completely the previous conclusion that the presence of the B_2O_3 decomposes the C_3S structure. At the higher concentrations of the B_2O_3, the spectrum is only a superposition of the C_3S and α'-C_2S spectra what results from the computer substraction of the spectra. This conclusion is in accordance with Mircea /7/.

The problem of the Al_2O_3 dissolution in the C_3S structure and the influence of this admixture on the structure and properties of the C_3S is very important from the cement chemistry point of view because Al_2O_3 is always present in allite phase in the Portland cement clinker. This was studied by many authors and for example Bigare et al. /8/ has confirmed that in the C_3S structure up to 1,2 weight % Al_2O_3 is dissolved, and at the concentration above 0,4 weight % this admixture stabilizes T_{II} form of C_3S. Further concentration increase of Al_2O_3 decreases the C_3S polymorphic transition temperatures what was shown by Hahn, Rysel and Wooreman /9/. Butt, Timashev and Kaushanskij /10/ have confirmed that up to 0,3 weight % of Al_2O_3, aluminum cations substitute only the calcium ions and they have the coordination number of 6; at the higher concentration, aluminum cations with the coordination number of 4 substitute silicon cations. The introduction of aluminum ions causes defects of the C_3S lattice and, in consequence, the increase of its hydraulic activation.

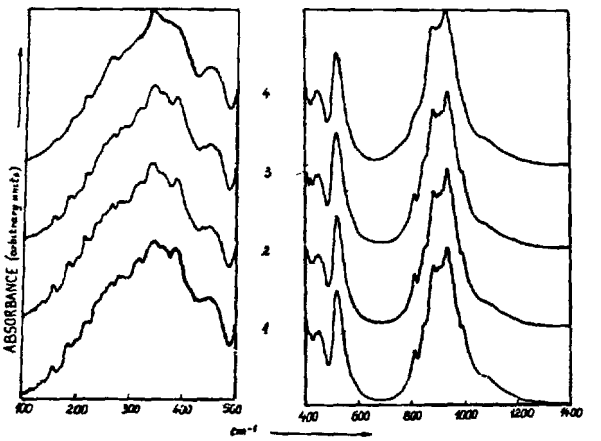

Fig.4. FIR and MIR spectra of the C_3S samples with Al_2O_3 admixtures : 1.-0,25 ; 2.- 0,5 ; 3.- 1 and 4.- 5 mole % of Al_2O_3

On the figure 4 the medium and far infrared spectra of the C_3S - Al_2O_3 solid solutions are shown. It is easy to see that up to 1 mole % /0,45 weight %/ no great changes in the spectra appear. Exceeding this value results in a sharp change of the spectra connected with the stabilization of the T_{II} form. By comparing the spectra of the T_{II} form stabilized by another addition /MgO, ZnO/, it is possible to notice that both the mechanism of the Al_2O_3 stabilizing action differs, and the structure of this form is slightly different, the stabilizing properties being shown by the aluminum ions with tetrahedral coordination.

The purpose of the next step of our investigations was to learn how the double admixtures Al_2O_3+BaO and Al_2O_3+B_2O_3 act upon the structure of C_3S. Figure 5a,b,c and 6a,b,c show the medium and far infrared spectra of the samples containing different quantities of the Al_2O_3 and BaO. In the series with 0,25 mole % of the Al_2O_3 no great changes of the spectra accompanying the increase of BaO concentration, are observed /compare fig.5a and 6a/. The only observed change is the broadening of bands indicating the increase of the defecting of the C_3S crystal lattice. In the spectra of the

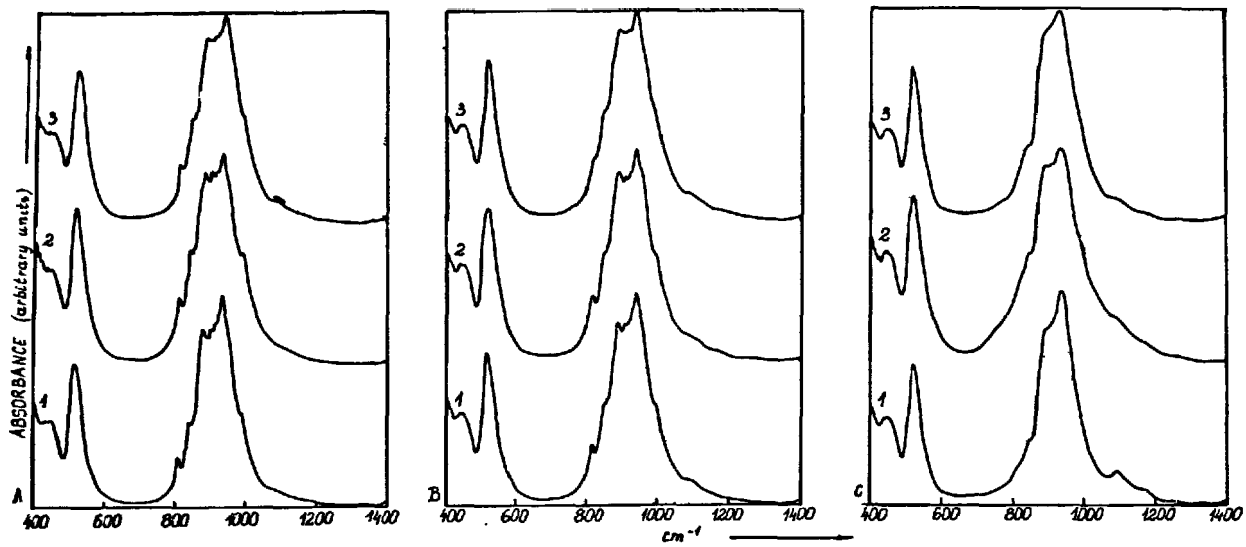

Fig.5. MIR spectra of C_3S-Al_2O_3 solid solutions with BaO admixtures. A-0,25 mole% Al_2O_3+: 1 - 0,5 weight %, 2 - 1 weight %, 3 - 4 weight % of BaO. B - 1 mole % Al_2O_3 + : 1 - 0,5 w.%, 2 - 1 w.%, 3 - 4 w.% of BaO. C - 5 mole % Al_2O_3 + : 1 - 0,5 w.%, 2 - 1 w.%, 3 - 4 w.% of BaO.

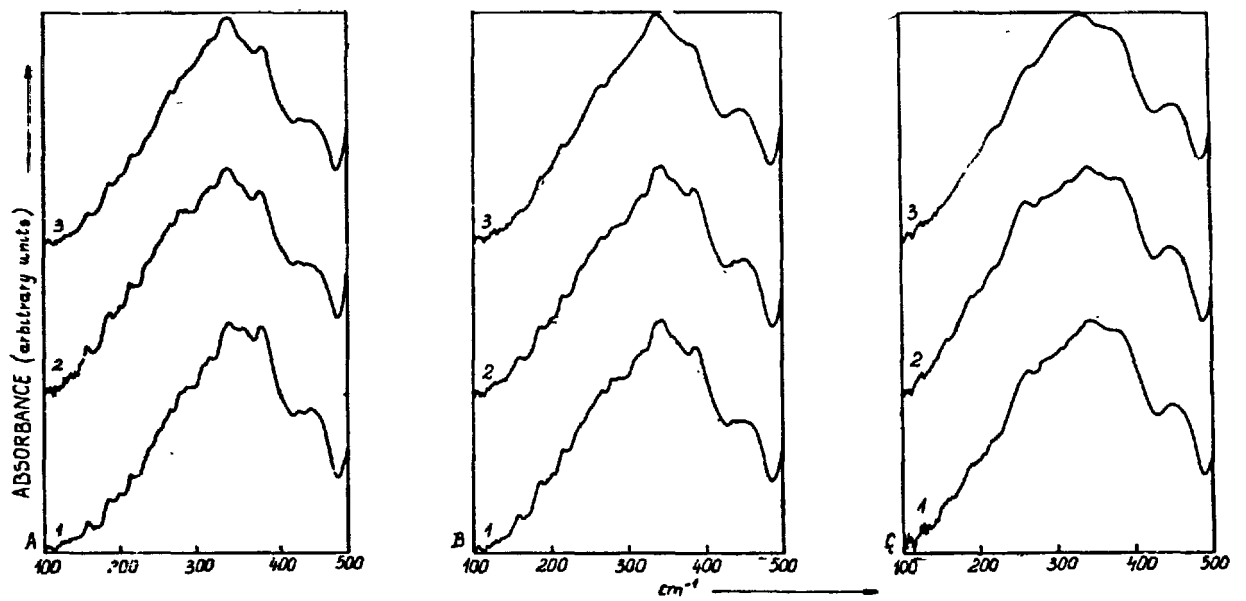

Fig.6. FIR spectra of C_3S-Al_2O_3 solid solutions with BaO admixtures. The concentrations as on figure 5.

next series /compare fig.5b and 6b/ with the increase of the BaO concentration we can observe important changes and for example in the case of the 4 weight % BaO the spectra are identical with the ones of the T_{II} form, in spite of the fact that the quantity of the single Al_2O_3 and BaO in the sample was insufficient for stabilization of this form. In this case cooperation of both admixtures is observed. The mechanism of this cooperation can be explained by dislodging the aluminum ions by the barium ions from the calcium sublattice to the $[SiO_4]$ tetrahedra one. Due to this the quantity of the tetrahedral aluminum ions in the crystal increases up to the level suffi-

cient to the stabilization of the T_{II} form, because only the aluminum in the tetrahedral coordination has got stabilizing properties. In the case of 5 mole % Al_2O_3 series, barium ions have been introduced to the C_3S lattice of the T_{II} form, not of T_I form /compare fig.5c and 6c/. In the spectra of these samples the disappearance of some bands is observed with the increase of BaO concentration, which means the increase of crystal symmetry of these solid solutions. By comparing the sample spectra of the 5 mole % Al_2O_3 and 2,5 mole % BaO with the spectra of different polymorphs of C_3S it can be concluded that we have got now the spectrum of M_I form, which cannot be obtained by the stabilization of Al_2O_3 admixture only. The cooperation of both Al_2O_3 and BaO stabilizing admixtures here appeared. These conclusions have been confirmed by the X-ray patterns.

The same investigations were carried out on the effect of B_2O_3 admixture / the same mole percentage as BaO / on the C_3S - $-Al_2O_3$ solid solutions. These investigations have shown that B_2O_3 does not dissolve in the C_3S - Al_2O_3 solid solutions, nor does it dissolve in the lattice of the pure C_3S, and similarly decomposes C_3S.

REFERENCES

1. R.W.NURSE, Proc.7th Conf.on Silicate Ind., Budapest, /1963/.
2. G.W.KUKOLEW,M.T.MIELNIK,Cement,1,/1956/, 16.
3. J.H.WELCH,W.GUTT,Proc.4th Int.Symp.Chem. of Cement,Washington, /1960/;Nat.Bur.of Standards,1,/1962/,59.
4. M.M.SYTCHEW,Proc.5th Int.Symp.Chem.of Cement,1,/1968/,158.
5. W.KURDOWSKI,Pr.Kom.Ceram.PAN O/Kraków, Ceramika,18 /1972/.
6. M.HANDKE,M.E.JURKIEWICH,Ann.Chem.Fr.,4, /1979/,145.
7. S.MIRCEA,Silikaty,1,/1965/,34.
8. M.BIGARE,A.GUINIER,CH.MAZIERS,M.REGOURD, N.YANNAQUIS,W.EYSEL,TH.HAHN,H.WOREMANN, J.Am.Ceram.Soc.,50,/1967/,609.
9. TH.HAHN,W.EYSEL,H.WOREMANN,Proc.5th Int. Symp.Chem.of Cement,1,/1969/,61.
10. Y.M.BUTT,W.W.TIMASHEW,W.E.KAUSHANSKIJ, Nautsh.Soob.N.I.I.Cementa,20,/1965/,45.

Formation of syngenite during cement grinding

Formation de la syngénite au cours de broyage du ciment

W. KURDOWSKI, Professor, Research Centre of the Industry of Binding Materials,
Z. WELISZEK, Engineer, Research Centre of the Industry of Binding Materials, Pologne.

RESUME : On a observé la grande instabilité de la qualité du ciment obtenu dans un broyeur finisseur fonctionnant en circuit ouvert. Les variations des propriétés du ciment se manifestaient surtout par manque d'augmentation des résistances pour un accroissement de la surface spécifique de 3000 à 4500 cm^2/g, ou même plus.

On a trouvé que cette instabilité résultait de la formation de syngénite au cours de la fragmentation du ciment dans le broyeur finisseur. La phase de syngénite se forme assez facilement dans le processus de broyage des clinkers riches en K_2SO_4, à la température de 80° - 160°C, en présence de la vapeur d'eau injectée dans le broyeur.

Les recherches effectuées donnent des conclusions permettant d'éviter la formation gênante de la syngénite.

SUMMARY : Well - marked instability of the quality of a cement obtained in the finish mill, operating in open circuit, has been observed. The variations of cement properties find expression chiefly in the lack of the increase in strengths with the growth of the specific surface of the cement from 3000 to 4300 cm^2/g or even more.

It has been found, that this instability results from the formation of the syngenite during cement grinding in the finish mill. The syngenite phase forms rather easily in the grinding process of clinker with high K_2SO_4 content, at the temperature of 80° - 160°C, in the presence of water vapour, originating from water injection into the mill.

Carried out investigations give the conclusions allowing to avoid the harmful formation of syngenite.

INTRODUCTION

As is well known, in the modern, dry method of cement production a clinker with higher alkali content is obtained. In European raw mixes the content of potassium surpasses about three times the sodium content. The potassium content, mainly in the form of K_2SO_4, exceeds for the most part 1%, reaching sometimes 1.5%.

The manufacturing of cement from the clinker with such an amount of this component causes a number of problems. Through the strengths after 1 day of hardening increase, nevertheless the strengths after 28-days are lowered /1/. Furthermore the cement obtained from such a clinker is susceptible of syngenite formation during the storage of the cement in the silos, as was noticed by Nielsen /2/.

High early strengths of manufactured cements require rather high dispersion of the product. The installation Minipebs, designed by F.L. Smidth /Fig. 1/, makes a modern solution of the problem of cement grinding to high fineness.

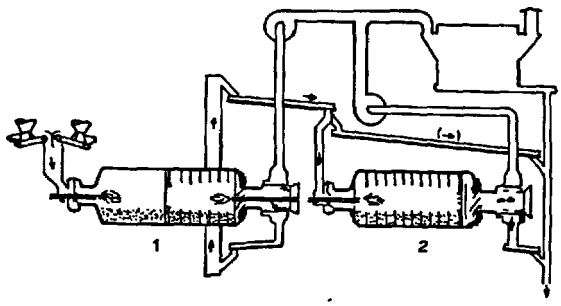

Fig. 1 - Grinding system with the Minipebs mill. 1 - Unidan mill, 2 - Minipebs mill

This high capacity installation is equipped with a primary mill Unidan, which gives a cement having Blaine specific surface 3000--3200 cm^2/g and with a finish grinding mill Minipebs, allowing to grind the cement to a specific surface as high as 6000 cm^2/g.

With all unquestionable advantages of this grinding system, in the case of grinding the clinker with high K_2SO_4 content large variations in the properties of obtained cement have been stated. The strength of mortars do not appear to increase or even is reduced with the growth of the specific surface of cement. This phenomenon is not observed when the cement is ground in a laboratory mill.

The results of examination of cements obtained from the same clinker in an industrial mill and a laboratory mill, are given in Table I. It should be noted, that the granulometric compositions of these two cements, one from the Minipebs mill and other from the laboratory mill, were similar /Table II/.

TABLE I

Mill	Blaine specific surface, cm^2/g	Compressive strengths after 1 day, N/mm^2
Unidan	3400	13.5
Minipebs	4700	13.8
Laboratory	4700	20.2

TABLE II

Particle size μm	Percentage by weigth in the cement from mill	
	Minipebs	Laboratory
above 200	0.04	0.6
200 - 30	14.46	21.4
30 - 20	15.0	16.2
20 - 5	46.9	43.0
below 5	23.6	18.8

The examination of these cements has been carried out with DTA /Fig. 2/.

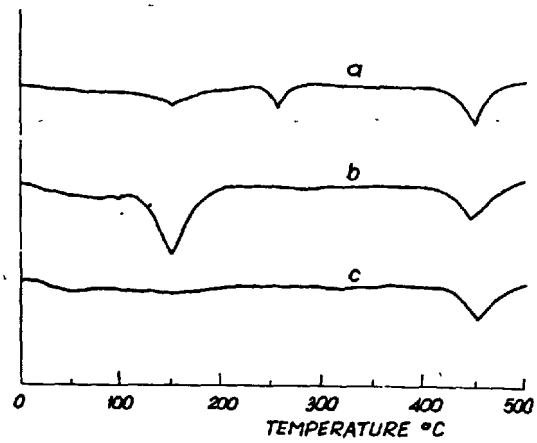

Fig. 2 - DTA curves. a/ cement from Minipebs mill, b/ laboratory cement, c/ cement with anhydrite

It has been found, that in a cement from Minipebs mill the calcium sulphate disappears with simultaneous appearance of the syngenite, which is characterized by an endothermic effect at the temperature 250° - 260°C, connected with removing of water molecule. In the case of the cement ground in a laboratory mill this effect is not observed.

This fact stimulated us to carry out adequate investigations tending towards better knowledge of this problem.

LABORATORY INVESTIGATIONS

In conditions modelling the cement mill atmosphere the studies were carried out to determine the field of formation of the syngenite in a cement with increased K_2O content.

For these studies a cement ground in laboratory mill to a specific surface of about 4500 cm^2/g, from a clinker with chemical and phase composition and modular characteristics given in Table III.

TABLE III

Chemical composition		Phase composition[1/]	
Content of the component in weight-percent			
Ign. loss	0.56	Free CaO	0.7
SiO_2	22.44	C_3S	58
Al_2O_3	4.96	C_2S	10
Fe_2O_3	2.90	C_3A	8
CaO	64.77	C_4AF	9
MgO	1.82	$KC_{23}S_{12}$	12
SO_3	0.72	NC_8A_3	0.1
K_2O	1.23	Na_2SO_4	0.3
Na_2O	0.15	K_2SO_4	1.2
Lime saturation factor		0.86	
Silica ratio		2.85	
A : F ratio		1.71	

1/ Potential phase composition calculated with Newkirk formulas with the content of silicates modified by MgO /3/

Also a further cement was prepared, which contained - instead of calcium sulphate dihydrate - the hemihydrate. SO_3 content in both cements was the same, 3.3%.

These cements were next exposed to the action of the air, the temperature of which varied in the range of 80° to 160°C and with water vapour content of 100 to 1200 g/Nm^3. The presence of the syngenite was determined by DTA.

In this way the field of existence of the syngenite in given temperature range and humidity, reflecting the atmosphere which occurs in cement mill, was determined. This field is presented in Fig. 2.

It has been stated, that the syngenite exists in whole studied temperature range ; at the same time it has been found that the syngenite forms more easily in a cement containing calcium sulphate hemihydrate. Obviously the formation of the syngenite requires at least partial dehydratation of the gypsum. Therefore at the temperature below 70° - 75°C the formation of this compound is not observed, even in the case of very high humidity of the air.

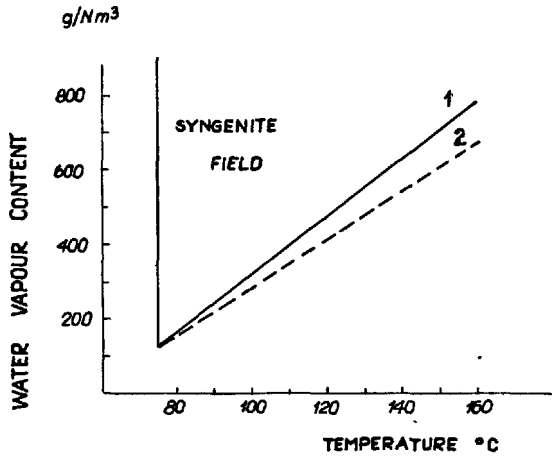

Fig. 3 - Syngenite formation in cement depending on the temperature and water vapour content in the air. 1 - cement with calcium sulphate dihydrate, 2 - cement with calcium sulphate hemihydrate

With the increase of the temperature in the mill larger and larger amounts of gypsum are dehydrated. At the temperature of the order of 120° - 160°C, despite of appreciable dehydratation of the gypsum, at low humidity of the vent air, the syngenite will not form, because of too lower water vapour pressure. This is why at higher temperatures a larger content of water vapour in the air is necessary for originating this compound.

Similar conditions will occur in the mill during hot clinker grinding, as in this case an injection of considerable amounts of water for cement cooling is required.

On the ground of a heat balance of the mill system the diagrams for both mills are drawn /Fig. 3/ of the function

$$t_c = f\,/m,\ t_n/$$

where:

t_c - the temperature of material leaving the mill,

m - the amount of injected water,

t_n - the temperature of feed material.

In the diagram prepared in such a way the field of existence of the syngenite has been plotted. In practice, the range of operation of the mill in dependence of given factors without deterioration of the quality of the product, makes a region between maximum permissible temperature of the cement leaving the mill, viz. 110°C , the range of the syngenite occurence and dew-point, below which the water vapour will condense. In this last case, apart from syngenite, aluminate hydrates can be formed.

The temperature 110°C should be accepted as highest permissible temperature of the cement, as its surpassing will cause a false set of the cement during subsequent

storage. According to Nielsen /2/, as low temperature as 90°C influences negatively the properties of the cement during its storage.

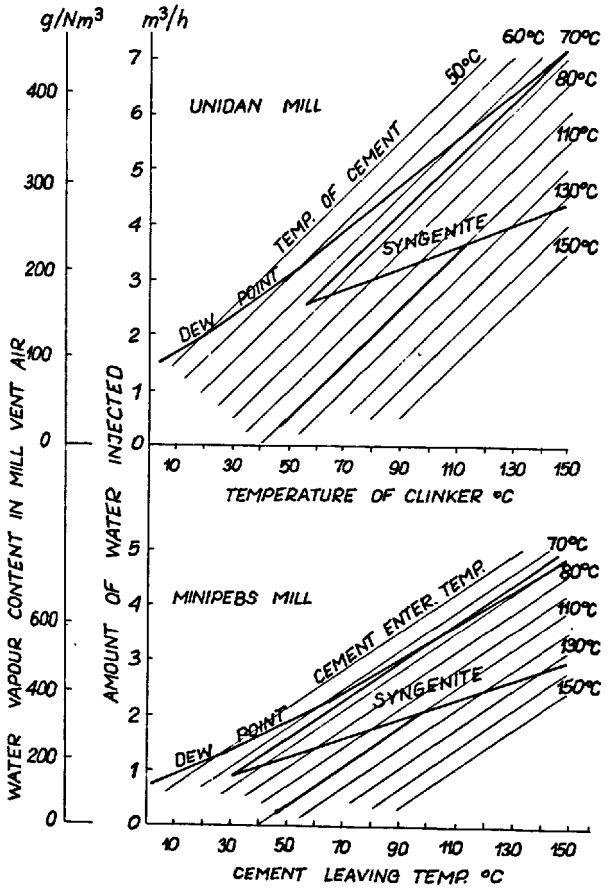

Fig. 4 - Operating conditions of grinding system with Minipebs mill

CONCLUSIONS

It is evident from presented diagram, that for a temperature of cement leaving the Minipebs mill ranging from 90° to 100°C it is necessary to maintain the temperature of the feed 50° - 70°C. As during conveying the cement from the Unidan mill to the Minipebs mill it is hardly to expect the lowering of its temperature, that's just the temperature which should have the cement leaving the mill Unidan. In practice it can be obtained, when the temperature of clinker do not surpass 60°C.

In the case, when the clinker leaving the kiln is cooled in planetary coolers and there is no possibility to cool the clinker to such a temperature, it is necessary to install a cement cooler between the mills. Then the temperature of the clinker can be as high as 100°C.

The second solution of this problem consists in the intensification of ventilation of the Minipebs mill. For example a doubling of the amount of ventilation air increases the permissible temperature of the material entering the Minipebs mill to 90°C; this allows then to introduce to the Unidan mill a clinker 70° - 80°C /Fig. 5/.

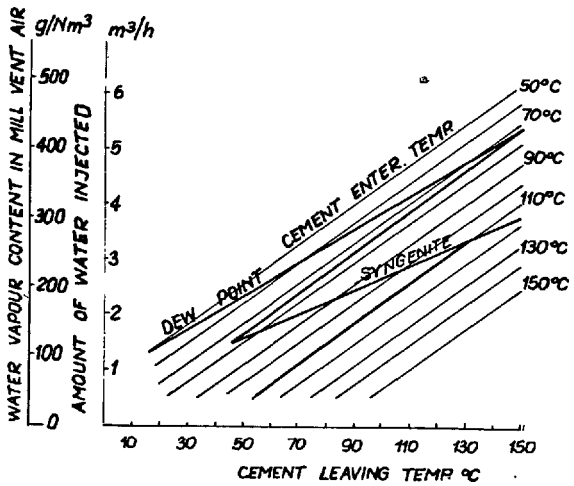

Fig. 5 - Operating conditions of Minipebs mill with doubled amount of vent air

Another preventive measure consists in replacing of part of gypsum addition with the natural anhydrite. In this case the conditions for syngenite formation are missing. This was confirmed by DTA examination of the cement with addition of anhydrite /curve "c" in Fig. 2/, obtained in conditions, for which in the case of cement added with gypsum the syngenite forms easily.

BIBLIOGRAPHY

1.- J. SVENDSEN / 1976 /, "Alkaliarmer Zement aus Hochalkali-Rohstoffen mit energiewirtschaftlich günstiger Verfahrenstechnik", Zement - Kalk - Gips, No 6, 281.

2.- H.C.A. NIELSEN / 1974 /, "How to avoid lumping of cement in silos", Rock Products, Vol. 77, No 2, 72.

3.- J. GAILLARD, R. MAGNAN and C. VIBERT / 1973 /, "Les compositions minéralogiques des clinkers de Portland", Revue des Materiaux de Construction, No 680, 24.

Processing characterization on the industrial scale cement production

Prévision de la qualité d'un ciment, en production industrielle

S. TAKAGI, Doctor, Sc in Eng. Senior research chemist, Central research laboratory of Sumitomo Cement C°, Ltd.,
A. KAWASHIMA, Research chemist. Central research laboratory of Sumitomo Cement C°, Ltd.

RESUME : Le but de l'étude entreprise était de confirmer les bases de la prévision des qualités d'un ciment en précisant les relations entre d'une part les propriétés physiques et mécaniques du ciment, dans des conditions diverses, et d'autre part la composition du clinker et les conditions de cuisson de ce clinker. Il est bien connu que l'action des composants du clinker dépend du processus de la clinkérisation, principalement du gradient de température du four et de la vitesse d'échauffement des matières premières. A ce point de vue, une première étude des modifications intervenues dans la phase d'équilibre et dans la structure du clinker, a été faite.

Selon ces vues, il a été établi que l'on pouvait prévoir à l'avance, les propriétés physiques et mécaniques d'un ciment, en se basant notamment sur le processus de la clinkérisation et sur l'histoire thermique du matériau.

SUMMARY : The object of this experiment is to comfirm the root of characterization by clarifing the corrlation between the physical behaviour and burning condition of clinker from characterization of principal compounds in clinker at various cases of conditions.

It is well known that, the stational logic of principal compounds in clinker was depending upon clinkering process of rawmixes, mainly heating rate and temperature gradient in kiln. From this point of view, opening discussion of this character shift for the phase equibrium and structural phenomenon in clinker was able to be developed under those resultes.

According to this consideration, the physical properties of cement in the future were able to be estimated by judging characterized phenomenon of clinker owing to operating condition in burning and the thermal history in clinkering rawmixes.

In this report the relation between the good quality of products depending upon operating conditions of kiln and shifting grade of character of principal compounds in clinker was discussed.

Introduction.

In the cement industry, the most important property of portland cement is the mechanical behaviour that has been frequently controlled by chemical composition, volume weight, uncombined CaO content of clinker and others.

But it is certain that these indications are not related to the character of clinker such as composition and structure in a broad sense.

In this study, the strength behaviour of cement was discussed about existence of character shift from the state of principal compounds of clinker depending upon manufac-turing conditions.

Consequently the improvement of the clinker burning and the estimation of quality of cement was possible on the basis of those described character data.

The results will contribute to the establishment of economical product of cement industry.

Analysis of character.

The term "material characterization" means to make widely clear the composition, structure, and other described data of material in the system analysis.

Since the existence of a particular material is described as its character, its property will be shown by the characters.

In such consideration, the character of materials will show the property in past to futuer corresponding to the dimensions through the time and other facters.

There fore, if it is possible to analyse the character of material, several properties of material will be estimated by means of character analysis.

In cement industry, according to characterization of clinker from this point of view, the production of controlled quality of clinker was possible to perform by consideration of the range setting with burning techniques.

From the fact that the character setting of clinker is closely correlated to different conditions in burning, the following three steps were considerated in this approach.

First step was consideration of burning rate of clinkering process as maximum temperature, temperature gradent and temperature distribution in kiln.

The indicative character of clinker mainly consists of characteristic structure of each phase, degree of growth of crystallite phase such as habit, size and irregularity of silicate crystal with structural stoichiometry due to conditions of nucleation, reaction kinetics and solid solubility limits without burnability of used raw mixes.

The second step was consideration of cooling rate of clinker for outlet from maximum temperature zone of kiln.

In this case, it was found that the character shifting of principal compounds in clinker was closely connected with cooling history in kiln, phase transition phenomena by shifting of phase equilibrium, exsolution by solid solubility limit and others.

Third step was consideration of effect of rapid quenching for AQC outlet from kiln outlet.

The character shifting was expressed by comparision of change of character among each step.

The good processing of cement making was possible to controll according to the described character by characterization of clinker in clinkering process depending upon various kiln operating conditions, such as rotating velocity and scale of kiln, type and setting position of burner, quantity of fuel, temperature and pressure of oil, primary air condition and secondary air temperature, draft of kiln, O_2 content of kiln inlet, kiln bedding of raw mixes, operating conditions of AQC and others.

Figure-I shows the relation between the macro characters of principal compounds in clinker and those effective parameters.

Character of Principal Compounds		Making Condition of Clinker: Kiln Speed	Coating of Burning Zone	Burning Zone Temp.	Flame Length	Burning Zone Length	Temp. Gradient	Cooling Rate	Atomosphere
Alite	Size	○	○		●		●		
	Optics			●					
	Zoning	●	○		○	○			
	Fringing			○				●	
	Habit	○	○		●		●		
	Crystal form		●				○		
Belite	Size	○	○		○	●	○		
	Optics			○	○		●	●	○
	Morphology and Texture			○			●	○	
	Recrystallization	●	●	○			○		
	Gel appter Exclusion of Impunity							●	
								●	○
Interstitial	Size				○			●	
	Optics							○	●

○ :effective, ● :very effective

Figure-I Characteristic character shifting under various making conditions of clinker.

The relationship between characters and properties in the principal compounds of clinker.

In unique properties of material, the source of property is divided into two media present derived from described character comprised of the statistical mean and the deviation from statistical mean in the composition and structure of materials (I).

Even if cement should be consisted of same components of the principal compounds, the compressive registance may be ranged about 280 to 430 Kg/cm^2 at four weeks.

Recentry the chemistry of cement has been advanced through the characterization of clinker (2)(3)(4)(5)(6) and its hydration products. (7)(8)(9).

In the relation of clinker character to property, П.П. СУПАКАС et al reported that if the habit of alite phase involved in clinker is more distinct, higher strength may be expected (IO).

Furthermore, H.M.Sylla et al (11) showed that the higher strength was possible for the clinker quenched below temperature at 1200°C.
Each report made very important suggestion of the character of clinker to property of cement.
Figure-2 shows that the strength property related to the macro character of principal compounds of clinker obtained from several points of view on the characterization.

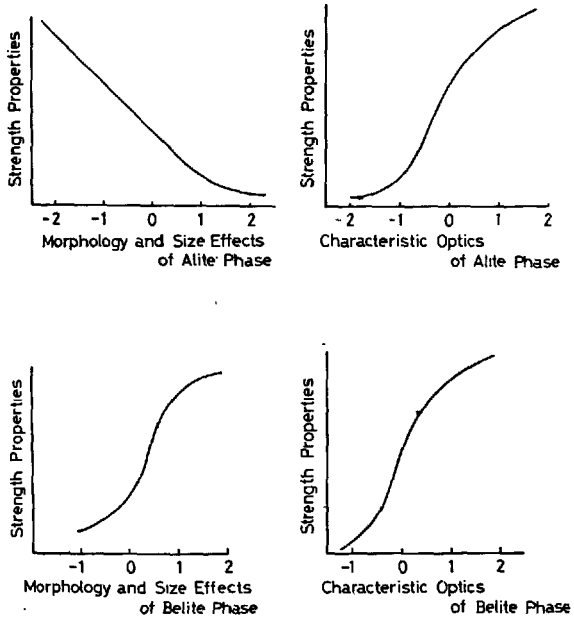

Figure-2 Correlation between the strengh behaviour and character shifting of principal compound in clinker.

In the expression of the characters, they are divisible into two media about the type of description such as "value" and "pattern" in the composition and structure of clinker with which are difficult to deal.
For the latter, recongnition by pattern was essential because of difficulty to express it by using the numerical value as shown in figure-2.
That is, by appling a graphical solution, the relationship of the distribution of each facters to the average value is able to be made clear.
The relation between the summation of des - cribed character and the strength properties of four weeks on the cement produced by conventional type of kiln and NSP is shown in the corresponding part of sigmoidal curve of figure-3.

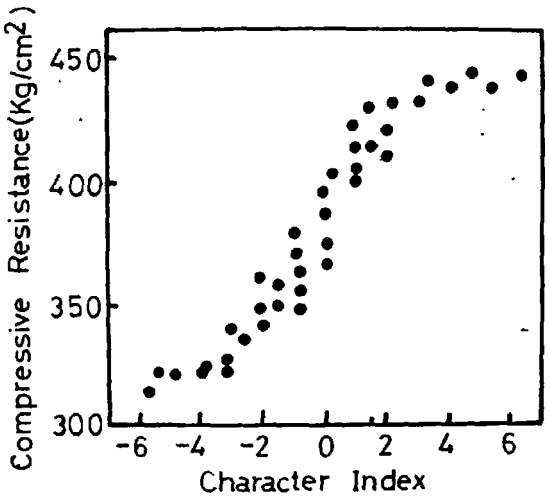

Figure-3 Correlation between the compressive strength of four weeks and its summation of character in clinker.

From these results, economical efficiency will be able to be higher when the best condition for clinker making in which the resulting clinker has a constant level of character is established.

Conclusion
In this wark, the relationship between characters and properties of cement under the processing of burning were shown. It was made up that the burning of clinkers with a high grade constant is possible to perform by controlling a number of operating conditions depending upon such characters of the clinker as composition, structure and other characters appeared in clinkering process.
It may be sure that, the burning technique on a base of such analysis by characterization contributes to the establishment of the operating condition.

References
1 - S.Takagi (1979) "Functional Materials, wet ceramics-opening point of view on the character and properties relation of cement, ceramics JAPAN 14(11) 401-409.
2 - G.Yamaguchi and S.Takagi (1968) " The analysis of portland cement clinker", proc, 5th Intern. Sympo. Chem. of cement I 181-218.
3 - G.Yamaguchi and S.Takagi (1974) "Present-day methods of investigation of the clinker formation mechanism and clinker phase composition". proc.6th Intern.Sympo.Chem. of cement. I 231-251
4 - Y.Ono,S.Kawamura and Y.Soda (1968) "Microscopic observations of alite and belite and hydraulic strength of cement." proc,5th Intern,Sympo, Chem of cement I 275-284.

5 - Y.Ono (1978) "Estimation of the strength in cement by means of microscopic observation." 35th symposium on the cement manufacturing in Japan. 74-83

6 - F.A.DeLisle (1976)"Microscopic analysis of clinker and cement" cement technology. May/June 93-99.

7 - S.Takagi, G.Yamaguchi and M.Saito (1974) "The texture of hydrated products of cement component compounds and cement. Cement Gijutsu Nenpo XXVIII 45-49.

8 - S.Takagi, G.Yamaguchi and M.Saito (1975) "Hydration and carbonation of cement minerals in solid-gas reaction and their texture. Cement Gijutsu Nenpo XXIX 53-57.

9 - T.Harada, M.Ohta and S.Takagi (1978) "Effects of polymorphism of tricalcium silicate on Hydration and structural characteristics of hardened paste. Yogyo-Kyokai-Shi 86 (5) 196-202.

10 - П.Р.Сулакас. В.В Моцартов. М. В. Логинова О.П. Мошкин. (1978) TSement(4) 18~19.

11 - H.M.Sylla (1978) "Einfluss der Ofenatomosphäre beim brennen von zementklinker. Zement-Kalk-Gips 31 (6) 291-293

THÈME II

Hydratation des ciments portland sans constituants secondaires

Hydration of pure Portland Cements

Président : M. LOCHER (R.F.A.)

Early hydration behaviour of sulphate-resisting and white Portland cement

Comportement initial, lors de l'hydratation des ciments Portland à haute résistance aux sulfates et des ciments blancs

JOHN BENSTED, Principal Scientist, Head of Materials Section,
Blue Circle Industries Ltd. Research Division. England.

RESUME : La chimie de l'hydratation du ciment portland à haute résistance aux sulfates et du ciment portland blanc, a été examinée jusqu'à deux heures d'âge à l'aide de plusieurs techniques instrumentales. Les comparaisons avec la chimie du ciment portland ordinaire ont été effectuées. Les différences qui sont observées sont discutées.

SUMMARY :The hydration chemistry of sulphate-resisting and white Portland cements up to two hours has been examined with the aid of a variety of instrumental techniques. Comparisons have been made with the chemistry of ordinary portland cement. Differences occurring are discussed.

INTRODUCTION

Less is known about the hydration behaviour of sulphate-resisting Portland cement (SRPC) and white Portland cement (OPC) than that of ordinary Portland cement (OPC). In comparison with the latter SRPC contains very small quantities of C_3A (less than 3% generally) and WPC has very little iron-containing material (ferrite phase normally less than 1.5%). Such changes as have taken place in major constituents of these cements might well be expected to have distinctive effects upon early hydration behaviour.

SRPC clinker is made by burning calcareous and argillaceous raw material with iron oxide, and sometimes sand as well to give a satisfactory silica ratio. WPC clinker is produced from calcareous material and china clay (low in iron); because of the lack of sufficient iron containing material, which normally acts as a flux during burning, combination of the raw materials is more difficult. Higher burning temperatures than usual ($\sim$1550-1600^{o}C) are often necessary to achieve clinkering. As a result, WPC clinker frequently has a very low alkali content, caused by alkali loss through volatilisation, and higher free lime values than comparable OPC clinkers. Both SRPC and WPC clinkers are ground with gypsum to produce the finished cements. The general properties of these cements have been extensively described. (1,2,3).

In the present study, a number of production SRPC's, WPC's and OPC's have been hydrated for up to two hours and compared.

EXPERIMENTAL

The SRPC's, WPC's and OPC's were each hydrated at a water:cement ratio of 0.5 (10g cement: 5 ml water) at ambient temperature in a glove box under nitrogen for reasons previously discussed (4,5). Samples of each cement were respectively hydrated for 5, 10, 15, 30, 60, 90 and 120 minutes. At the end of the alloted hydration period each sample was dried by quickly washing with AnalaR acetone thrice under suction, followed by storage in a vacuum desiccator over silica gel.

These hydrated cement samples together with specimens of the anhydrous cements were studied by differential thermal analysis (DTA) and infrared spectroscopy (IR). DTA was carried out by employment of simple conventional equipment that had chromel-alumel thermocouples attached to a Kent potentiometric recorder (6). Heating rates of 20^{o}C per minute were utilised. Since ettringite was the most reliable hydration compound to quantify, it was determined quantitatively (6). IR was performed on a Unicam SP1200 infra-red spectrophotometer over the wavenumber range 4000-400cm^{-1} using potassium bromide disc and Nujol mull media. Extensive band overlap precluded quantitative determination of major hydration components like ettringite. Some of these hydrated specimens were also examined by scanning electron microscopy (SEM) on a Cambridge Stereoscan instrument. The SRPC's were subjected to quantitative X-ray diffraction (QXRD) on a Philips instrument, primarily to elucidate the nature of the ferrite phase.

In addition, hydration of one of each of the SRPC's, WPC's and OPC's was investigated by conduction calorimetry (7). Samples were mixed externally with water at water:cement ratio 0.4 (15g cement in 6ml water) and the heat liberated during hydration was measured up to 45 hours.

Water consistency and setting time determinations of the cements were carried out by the British Standards method (8) and surface area measurements by the Rigden modification of the Lea Nurse procedure.

RESULTS

The DTA and IR data showed that less ettringite was formed at up to two hours hydration for the SRPC's and WPC's than for the OPC's examined. SEM revealed insufficient structure in the micrographs to make any definite conclusions. The quantitative DTA data is given in Table 1 and typical differential thermograms at two hours hydration are illustrated in Figure 1. Physical and chemical data for all twelve cements examined is depicted in Tables 2 and 3. The QXRD results for the SRPC's are shown in Table 4. Some useful solubility data has been quoted in Table 5. The results of the conduction calorimetric examination are illustrated for three cements (one of each type investigated) in Figure 2 and the data tabulated in Table 6.

DISCUSSION

a) SRPC's

The observation that the SRPC's reacted to form significant quantities of ettringite when their C_3A contents were very low, indicated that substantial quantities of ettringite were being formed from the ferrite phase by its reaction with lime and calcium sulphate. It was not known precisely how much of the ferrite phase had reacted at up to two hours, since XRD, whilst being able to identify the presence of ettringite, is not per se sufficiently reliable to determine accurately small changes in the quantities of the anhydrous clinker phases present at these early hydration times. Also, iron (III) substituted ettringite gives similar DTA,IR and XRD data to pure ettringite with which it readily undergoes solid solution. It is thus not possible at present to quantify independently ettringite arising from C_3A and ettringite formed from the ferrite phase. Further evidence for the involvement of the ferrite phase in early hydration is afforded by the greater quantities of ettringite formed by cements A and B in comparison with C and D together with changes in the hydralime contents. The former have higher free lime contents than the latter, which presumably gave a greater propensity for the ferrite phase to react. Cement A has a higher specific surface area and water soluble $K_2O + Na_2O$ content than cements B, C and D, which might account for A giving the highest levels of ettringite of these SRPC's, even more than B.

A comparison of the hydration behaviour of cements B and C clearly points to the involvement of the ferrite phase in early cement hydration. These two cements (from the same Works) differ appreciably in free lime content, but have fairly similar values for SO_3, total and water soluble alkalis, C_3A and specific surface area. Significantly more ettringite was produced at all times from five minutes to two hours for cement B (free lime 1.9%) than for cement C (free lime 0.8%).

From the solubility data (Table 5) it might be thought that a higher free lime content should favour less ettringite being formed, because a high lime solubility coincides with low alkali and sulphate ion solubilities and vice versa. The presence of sulphate ions in solution should favour ettringite formation by being able to readily approach the surfaces of the aluminate material. However, for the ferrite phase to react to form ettringite, there must be adequate quantities of lime available, since, what might be considered as an iron (III) substituted C_2A system needs to react with lime to produce a C_3A aq hydrated system such as ettringite, when sulphate ions are present in the hydrating medium.

QXRD for these SRPC's (Table 4) gave higher C_3A values than the Bogue calculation method did.[3] Even allowing for the approximations contained in the latter, one reason for this is shown by evaluation of the % C_2F values from the ferrite present. In these cements the ferrite phase is not simply C_4AF but lies within the range C_4AF - C_6AF_2. Thus there is a lower aluminate content in the ferrite phase than if its composition were to have been C_4AF, and hence the true C_3A value is higher than that calculated by the simply Bogue approach.

b) WPC's

Consider now the WPC's E, F, G and H. These contain very little iron, hence the ferrite phase is negligible (0.8 - 1.4% for these cements according to the simple Bogue calculation in Table 4). All have low alkali (especially water soluble alkali) contents and relatively high free lime values as mentioned earlier.

Despite the fact that cements E and F had higher SO_3 contents (2.6, 2.8% respectively) than the SRPC's (2.1 - 2.3%), this did not lead to more ettringite being formed. The low alkali levels of the WPC's meant that the solubility of lime increased whilst that of sulphate decreased (Table 5). Thus, less sulphate ions were available for reacting with C_3A and there was insufficient ferrite phase present to react with the lime and afford at least some degree of compensation for the effect of the lower sulphate ion solubility. Although the specific surface areas of these cements were very high, particularly for G and H, in no instance did the level of ettringite formation approach, let alone exceed, that for the OPC's I, J, K and L. This could only be attributed to the aforementioned effect of the lower water soluble alkali contents.

c) OPC's

For the OPC's I, J, K and L the effect of marked changes in C_3A and SO_3 content were noticeable, but changes in free lime appeared to be less influential for ettringite formation than with the SRPC's and WPC's. Most ettringite was formed by cement I, which had highish SO_3 and K_2O levels and a high C_3A content. Least ettringite was produced by cement L, which had a moderate C_3A content and low SO_3, water soluble (K_2O + Na_2O) and free lime. Cement K formed slightly more ettringite than L at all ages examined; the SO_3 and free lime were significantly higher, but the water soluble (K_2O + Na_2O) and C_3A were more comparable. Cement J produced even more ettringite than K, but the only significantly different factor noted was the higher Na_2O content.

The greater levels of ettringite formed from the OPC's on the one hand compared with the SRPC's and WPC's on the other appear to be due principally to the combined effects of higher C_3A and/or alkali (particularly water soluble) contents. The higher the quantities of water soluble alkali are, the lower the solubility of lime and the higher the solubility of sulphate ions is. Thus more sulphate is readily available to react with C_3A and in consequence more ettringite is formed.

As previously observed (5,10) no direct correlation was apparent between degree of ettringite formed at these early hydration times and setting behaviour. This applied not only to the OPC's but to the SRPC's and WPC's as well.

CONDUCTION CALORIMETRY

All three cements types (SRPC, WPC, OPC) revealed an initial rapid heat evaluation. Such heat evolution has been generally attributed to arise from heat of wetting and free lime hydration, but recent work (11) had indicated that there is not in general a significant overall hydration of free lime immediately upon mixing Portland cements of different types with water. The major contribution to this peak appears to be hemihydrate to gypsum, hydration, the hemihydrate arising from gypsum decomposition during grinding of clinker with gypsum, although heat of wetting must also be a factor here.

The supplementary peaks, where present, (e.g for the WPC E) are indicative of delayed reaction ensuing significantly after initial mixing has taken place. They are likely to be due to either extended heat of solution effects, or significant hydration of interstitial material (C_3A/ferrite) after initial mixing, or both.

The second major heat peak, which arises outside the early hydration period, but is included here for completeness, appears to be due largely to alite hydration (7, 11) and the points corresponding to the setting times can be observed near the base of the initial slope of this heat peak. For cement C a slight split was apparent in the second heat peak, which might well be due to the formation of significant quantities of C-S-H of a slightly different type, such as a higher polymer, at this stage of hydration.

No third major heat peaks were observed here, because the C_3A contents of the three cements were not high enough (not $\sim$12% or more) to be independently observed under the experimental conditions employed.

Conduction calorimetry has thus been shown to be of use in assisting hydration studies of these three cement types.

CONCLUSION

Examination of the early hydration behaviour of a

number of commercial SRPC's and WPC's in relation to OPC's showed that less ettringite was formed at all stages with the SRPC's and WPC's investigated. This was related to the alkali levels, especially the water soluble alkalis, C_3A, ferrite and free lime quantities. Specific surface area per se did not appear to have a great influence upon ettringite formation with these SRPC's and WPC's.

ACKNOWLEDGEMENT

I wish to thank Dr. S.P. Varma for providing the QXRD data, Mr. M.J. Coole for the conduction calorimetric measurements and Mr. C. Zaris for experimental assistance.

BIBLIOGRAPHY

1. - F.M. LEA (1970) "The chemistry of cement and concrete". 3rd Edition. Edward Arnold (Publishers) Ltd., London.

2. - F. KEIL (1971) Zement-Herstellung und Eigenschaften, Springer-Verlag, Berlin, Heidelberg, New York.

3. - G. TOGNON and A. CAVALLIERI (1964) Italbianco. Italcementi S.p.A., Bergamo

4. - J. BENSTED (1976) A discussion of the paper "Carbonation of the hydration products of tricalcium silicate" by P.A. Slegers and P.G. Rouxhet. Cement and Concrete Research 6 (6), 817-818.

5. - J. BENSTED (1978) "Early hydration behaviour of Portland cement in water, calcium chloride and calcium formate solutions". Part 1. General aspects Silicate Industriels 43 (6), 117-122.

6. - J. BENSTED and G.C. BYE (1976) "The applications of DTA in a study of the formation of ettringite in cement hydration". Proceedings of the First European Symposium on Thermal Analysis, University of Salford, U.K., 2-24 September 1976 (Editor: D. DOLLIMORE). pp 371-373. Heyden & Son Ltd., London, New York, Rheine.

7. - J.A. FORRESTER (1970) "A conduction calorimeter for the study of cement hydration". Cement Technology 1 (3), 95-99.

8. - BRITISH STANDARDS INSTITUTION (1971) "B.S. 12 Ordinary and Rapid-Hardening Portland Cement. Part 2. Metric Units.

9. - J. BENSTED and S.P. VARMA (1971) "Studies of ettringite and its derivatives". Cement Technology 2 (3), 73-76, 100.

10.- J. BENSTED "An investigation of the setting of Portland cement". Silicates Industriels (in press).

11.- J. BENSTED - Unpublished work.

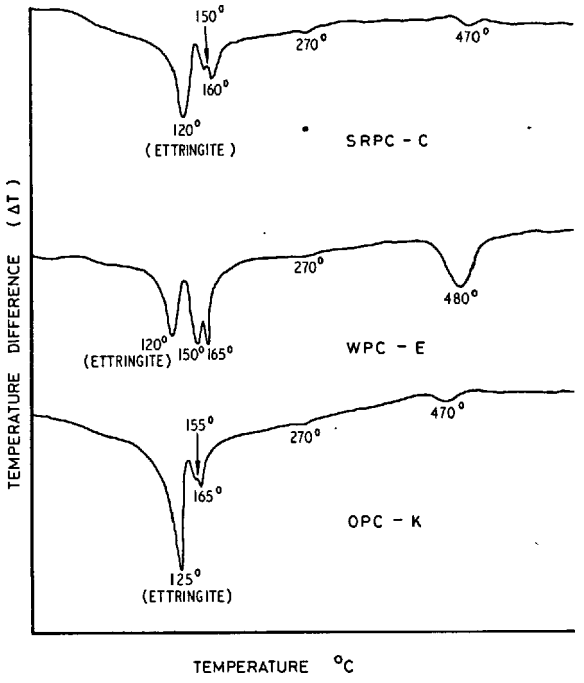

Fig 1 - Differential thermograms at 2 hours hydration

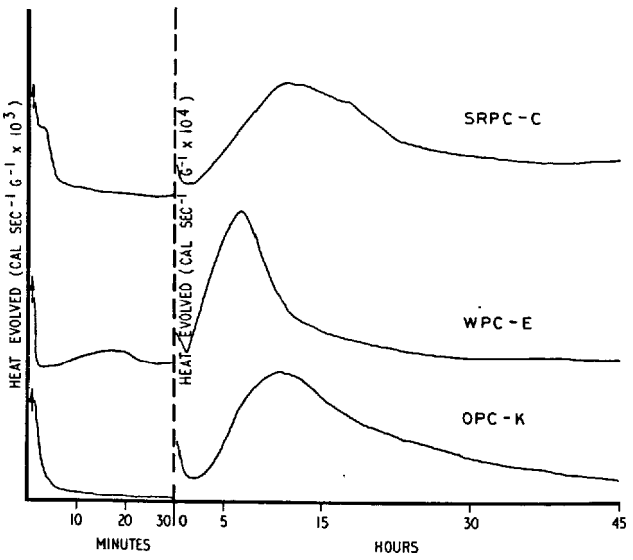

Fig 2 - Conduction calorimetry curves

TABLE 1 - % Ettringite Formed (w/c 0.5)

Hydration Time (min.)		0	5	10	15	30	60	90	120
Cement	Type								
A	SRPC	-	1.35	1.59	1.68	1.73	1.86	1.98	2.13
B	SRPC	-	1.33	1.52	1.59	1.64	1.77	1.89	2.05
C	SRPC		0.81	0.99	1.25	1.39	1.41	1.66	1.67
D	SRPC	-	1.21	1.22	1.41	1.63	1.65	1.68	1.71
E	WPC	-	1.28	1.38	1.39	1.42	1.48	1.63	1.70
F	WPC		0.90	1.02	1.14	1.32	1.69	1.83	1.91
G	WPC		1.13	1.35	1.35	1.42	1.77	1.94	2.19
H	WPC	-	0.73	0.80	0.88	0.97	1.13	1.21	1.22
I	OPC	-	2.27	2.47	2.80	2.90	3.09	3.11	3.52
J	OPC		1.65	1.71	1.98	2.37	2.54	2.67	2.79
K	OPC		1.36	1.39	1.76	2.02	2.17	2.35	2.41
L	OPC		1.34	1.38	1.69	1.94	2.09	2.26	2.35

SRPC = sulphate-resisting Portland cement, WPC = white Portland cement, OPC = ordinary Portland cement.

TABLE 2 Physical Data

Cement	Surface Area m^2Kg^{-1}	Water Consistency %	Initial Set min.	Final Set min.
A	401	24.5	185	225
B	354	25.0	230	275
C	343	24.5	265	325
D	347	24.0	210	255
E	393	26.5	120	165
F	426	27.5	120	150
G	496	30.5	170	200
H	489	28.5	140	185
I	335	25.0	170	230
J	328	26.25	185	235
K	325	25.25	175	220
L	323	25.75	190	245

TABLE 3 - Chemical Analysis

Cement	SO_3 %	Free Lime %	K_2O Total %	K_2O w/s %	Na_2O Total %	Na_2O w/s %	Simple Bogue Composition C_3S %	C_2S %	C_3A %	C_4AF %
A	2.3	2.4	0.47	0.28	0.26	0.08	56.8	13.9	1.7	16.5
B	2.1	1.9	0.16	0.09	0.47	0.11	61.1	11.9	0.5	16.7
C	2.2	0.8	0.15	0.06	0.40	0.07	57.1	15.8	0.3	17.2
D	2.1	0.8	0.29	0.12	0.17	0.03	61.7	10.9	1.2	17.0
E	2.6	2.5	0.19	0.03	0.14	0.04	46.4	33.6	9 7	1.1
F	2.8	2.9	0.22	0.03	0.14	0.04	38.1	40.8	10.4	0.8
G	2.3	2.6	0.11	0.03	0.09	0.02	67.1	12.5	8.5	1.4
H	1.8	2.5	0.17	0.05	0.07	0.02	63.6	22.9	4.7	0.9
I	2.7	2.1	0.60	0.39	0.19	0.03	62.5	13.8	15.1	4.9
J	2.4	1.1	0.51	0.18	0.29	0.13	53.2	18.6	9.5	7.3
K	2.6	1.2	0.51	0.23	0.22	0.06	53.3	23.9	10.4	7.6
L	2.1	0.6	0.58	0.25	0.23	0.04	56.1	16.5	9 8	7.2

w/s = water soluble

TABLE 4 - X-Ray Diffraction Data

Cement	C_3A %	Ferrite %	C_2F %
A	2.0	14.3	58
B	1.6	14.4	61
C	1.4	16.2	61
D	1.5	14.5	59

TABLE 5 Solubilities in Lime Solutions at 25°C(g/1) (ref. (1))

CaO Concentration	0.1	1.0
$CaSO_4$	2.2	1.6
KOH	20.0	0.4
NaOH	10.0	0.4

TABLE 6 -Conduction Calorimetry Data

Cement	1st Heat Peak Time min	1st Heat Peak Heat Evolved $cal.sec^{-1}g^{-1}x10^4$	Supplementary Peak Time min	Supplementary Peak Heat Evolved $cal.sec^{-1}g^{-1}x10^4$	2nd Heat Peak Time hr	2nd Heat Peak Heat Evolved $cal.sec^{-1}g^{-1}x10^4$
SRPC-C	¼	176	2sh	56	12	5.0
					18sh	4.3
WPC-E	¼	535	17	18	6	8 3
OPC-K	¼	520	-	-	11	6.5

sh = shoulder

A study on the evaporation products of the liquid phase of a cement paste

Etude du produit de l'évaporation de la phase liquide d'une pâte de ciment

P. KITTL, Researcher, Department of Materials (IDIEM), Chile,
A. GOLDSCHMIDT, Researcher, Microanalyse Laboratory, Geology Department, University of Santiago, Chile,
C.T.A. SUCHICITAL, Assistant Professor, Department of Materials Engineering, Federal University of São Carlos, S.P. Brazil.

RESUME : Les phases liquides de deux pâtes; l'une du ciment Portland commercial (CPC) et l'autre du C_3S ont été obtenues par pressage. La cristallisation de la phase liquide a été obtenue par séchage lent et étudiée par Microscopie Optique, Microscopie Electronique à Balayage et Microsonde Electronique. CH, $C\bar{S}H_2$, KH, NH et des petites quantités de $C_4A\bar{S}H_{12}$ C_4ASH_{12} et $C_6AS_3H_{31}$ ont été trouvés dans la phase solide résiduelle cristallisée provenant du ciment (CPC); de la même façon, du CH et du S ont été trouvés lorsque la phase solide résiduelle cristallisée provenait du C_3S. Nous supposons que C_3S se dissout, et que S par action pouzzolanique se transforme en $C\bar{H}S$ qui précipite avec le CH résiduel. Ainsi, le mécanisme d'hydratation du C_3S semble être principalement une dissolution-précipitation; il se produit dans l'hydratation du ciment CPC un mécanisme topochimique dont il résulte que la phase hydratée se développe directement à partir du clinker.

SUMMARY : The liquid phase of two pastes, one of a commercial Portland cement (CPC) and the other of C_3S, was extracted by pressing. Crystallization of the liquid phase was produced by slow-drying, and it was studied by Optical Microscopy, Scanning Electron Microscopy and Microprobe. CH, $C\bar{S}H_2$, KH, NH and small quantities of $C_4A\bar{S}H_{12}$, C_4ASH_{12} and $C_6AS_3H_{31}$ were found in the remaining crystallized solid phase arising from CPC, the presence of $C\bar{H}S$ was not detected; similarly, CH and S were found when the remaining crystallized solid was originated from C_3S. It is believed that C_3S becomes dissolved, and S, through a pozzolanic action transform in to $C\bar{H}S$, which precipitates with the remaining CH. Thus the hydration mechanism in C_3S seems to be mainly a dissolution-precipitation, and in CPC it is the topochemical mechanism, which means that the hydrated phase grows directly from the clinker.

INTRODUCTION

The contradictions among the two main theories for the hydration mechanism of a clinker - the Le Chatelier theory[1] defended mainly by Williamson [2] and by Dron et al[3], and the Topochemical theory defend mainly by Kapranov[4,5] motivated the present study on the composition of the evaporation products of the liquid phase of a cement paste.

The hydration mechanism proposed by Le Chatelier implies a constant dissolution and precipitation, of the hydration products from a supersaturated solution. The Williamson idea is that this fact is due to anincrease in temperature, since the hydration is an exothermic reaction. This mechanism requires that all the mass involved in the process of hydration, must dissolve and latter to precipitate. But, as it has been observed[2], the hydration products are formed around the clinker particles, and this hydrated layer would inmediately inhibit that hydration proceeds. Then, it becomes necessary to consider an incoming flux of water to the clinker-hydrated material interface, and an out-going flux from the dissolved clinker to the sourrounding media (Fig. 1,1). The growth process would then take place in the water-hydrated material interface.

The topochemical mechanism sustains that hydration of the clinker particles is due to the penetration of the water molecules into the solid structure, through the already mentioned hydrated layer, and a dissolution of the soluble parts, leaving a silica structure. After reacting with CH this structure transforms into tobermorite (CHS), see figure 1,2. Even though the C, H and S proportions in tobermorite of the hydrated cement are variable, here it will be considered as CHS. The topochemical mechanism is then characterized by a chemical reaction leaving a silicate structure which then forms the insoluble, or very little soluble structure of the hydrated cement; this is also the phase which has the highest mechanical resistance.

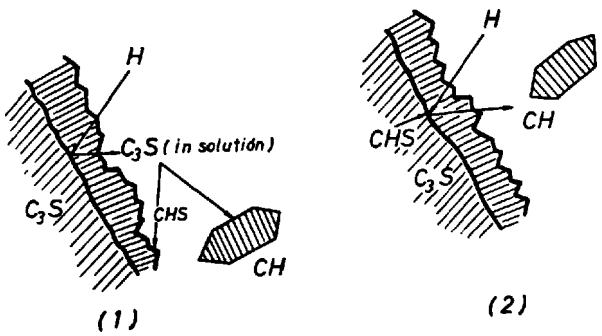

Fig.1. Mechanism of clinker hydration: (1) Le Chatelier model, (2) Topochemical model.

The present work is a study on the solid phases obtained by evaporation of the liquid phase of cement pastes extracted by pressure, and the identification to the differente associations present in such solid phases. The objective is to increase the learning understanding existing at present on the hydration mechanism of clinker.

MATERIALS AND METHODS

The chemical analysis of the comercial Portland cement used is given in Table listed below.

TABLE

Chemical Analysis of the Comercial Portland Cement

Compound	%	Compound	%
CaO	63.27	K_2O	1.01
SiO_2	19.26	TiO_2	0.65
Al_2O_3	5.55	Na_2O	0.61
Fe_2O_3	2.88	MnO_2	0.17
SO_3	2.86	P_2O_3	0.10
MgO	1.97		

This cement was miexed with water, in ratio w/c=0.5, for 3 minutes and left to age 7 minutes and 24 hours. The liquid phase was extracted by pressing the mixture in a steel mold, collected, filtered and stored. For all these operations a plastic equipment was used.

As a comparison material practically pure C_3S was used, employing the same preparation procedure as in CPC to obtain the liquid phase.

The samples were prepared by depositing an amount of the stored liquid in a scanning electron microscope sample holder, which was covered with platinum or with plastic. Such samples were then placed in a thightly clossed desiccator to be dried. The evaporation residues, thus obtained

were then covered with a deposited layer of gold or graphite.

All the sample features were then analysed in a optical microscope (OM), scanning electron microscope (SEM) and with an electron microprobe (EM) following the usual techniques in each case.

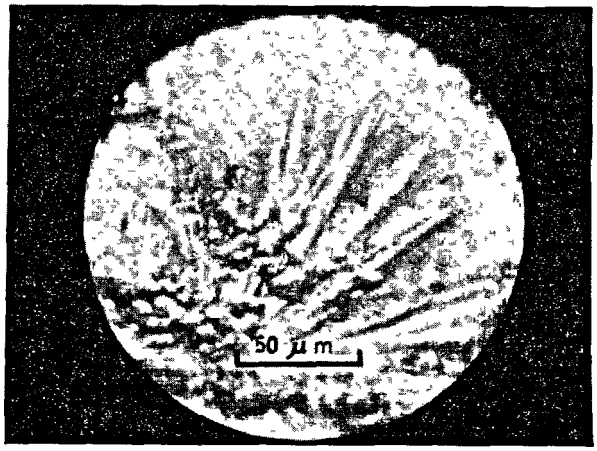

Fig. 2. OM of the solid phase obtained by evaporation of the liquid phase of a CPC paste. The general background and the crystalline agglomerates can be observed.

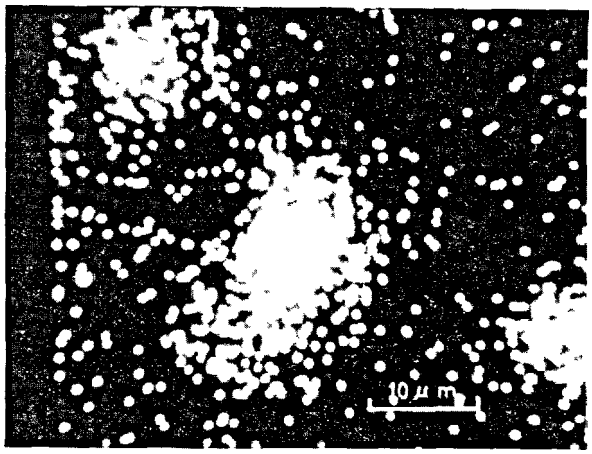

Fig. 3. EM of the solid phase obtained by evaporation of the liquid phase of a CPC paste. The presence of Si can be noticed.

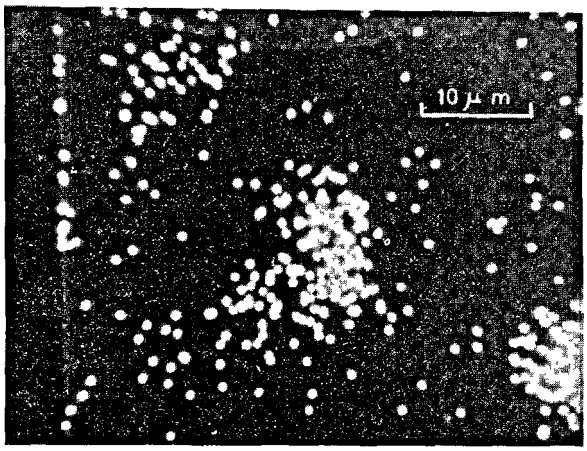

Fig. 4. EM of the solid phase obtained by evaporation of the liquid phase of a CPC paste. The presence of Al, in the same region as in Fig. 3, is distinguished.

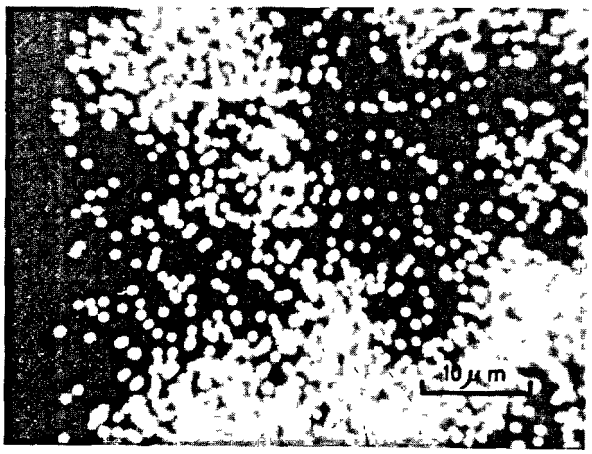

Fig. 5. EM of the solid phase obtained by evaporation of the liquid phase of a CPC paste. If can be seen the presence of Ca in the same region as Fig.3 and 4.

RESULTS

In gneral, the samples from the CPC liquid phase, observed under the OM presented uniform background with some crystalline agglomerates (Fig.2) having in general, a needle or globular like appearance. Analysis the samples under the EM, the background shows an uniform and abundant distribution of

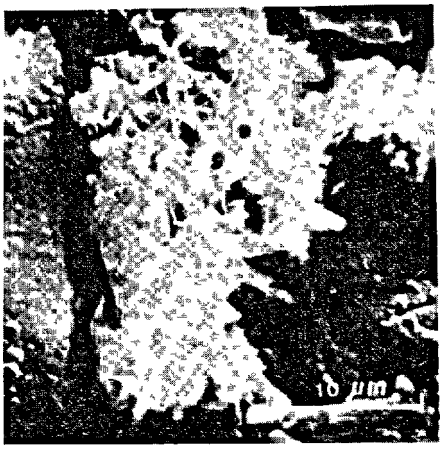

Fig.6. SEM of the solid phase obtained by evaporation of the liquid phase of a CPC paste. Needle like agglomerates, probably of $C_6AS_3H_{31}$ or C_4ASH_{12} can be noticed.

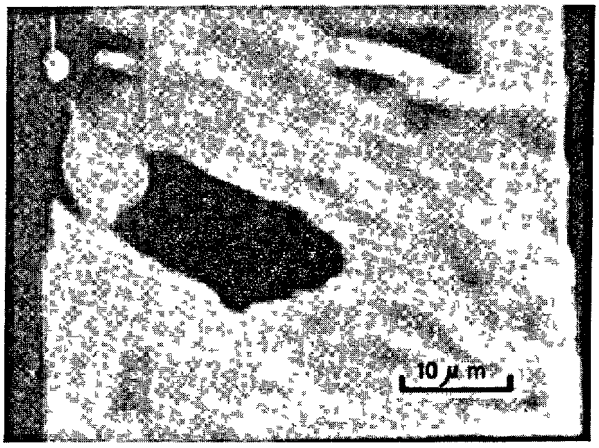

Fig. 8. An $S(SiO_2)$particle in a C(CaO) background. EM Electron Absortion.

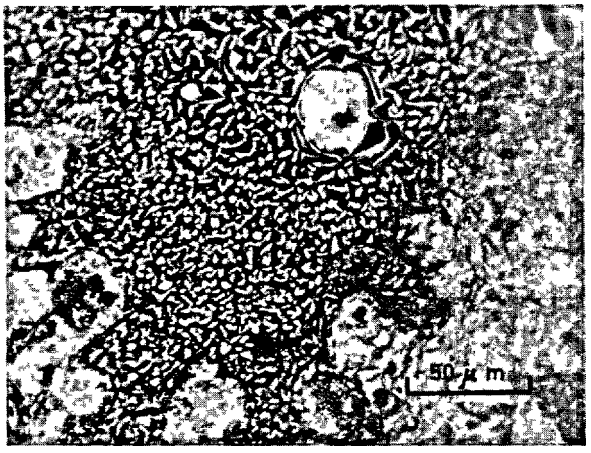

Fig. 7. OM of the solid phase obtained by evaporation of the liquid phase of a C_3S paste. There it is shown large C deposits and a cracked media of Ca-Si.

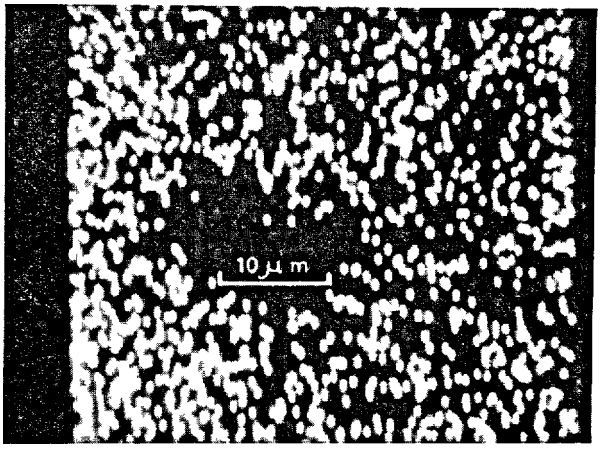

Fig. 9. EM of the solid phase obtained by evaporation of the liquid phase of a C_3S paste. The presence of Ca appears in the same region as in Fig. 8.

K, Na, Ca and S, corresponding to KH, NH, CH and $\overline{S}CH_{0.5}$ which are soluble, being K the most abundant one. These observations are in agreement with results already reported[5]. On the other hand, the agglomerates shows the associations Ca-S, Ca-Si-Al, Ca-Al (Fig. 3, 4, 5), some of them with superposition of K and Na, the Ca-Si association was nowhere seen. The crystalline formations were identified, as reported before[5], being gypsum ($\overline{S}CH_2$) with some K and Na on them. Other precipitates containing S and Ca were found. Zones of needle like formation which presented the associations Ca-Al-S and Ca-Al-Si, which correspod probably to $C_4A\overline{S}H_{12}$, C_4ASH_{12} or $C_6AS_3H_{31}$ (Fig. 6) also appeared.

For the samples obtained by evaporation of the liquid phase from C_3S, it was observed a cracked background and agglomerates of crystalline formations

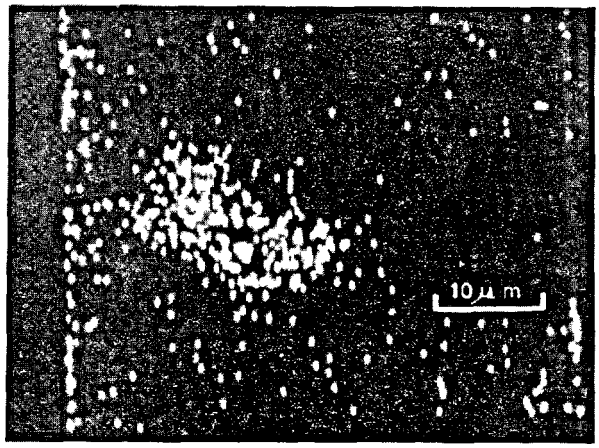

Fig. 10. EM of the solid phase obtained by evaporation of the liquid phase of a C_3S paste. It can be seen the presence of Si in the same region as in Figs. 8 and 9.

(Fig.7). An Em analysis revealed a background made up mostly of Si and C, and large agglomerante of C. In this bacground the Si appears in the form of particles, as can be seen by Electron Absortion Analysis (Fig. 8). In figures 9 and 10 can be seen that Si and Ca are not combined.

DISCUSSION

The basic hypothesis of this work is that if precipitation takes place during the hydration process of clinker, it will be reproduced during the slow evaporation of the liquid phase.

Regarding to the evaporation products arising from the liquid phase of the CPC paste, it is important to notice that the presence of the Ca-Si association which must correspond to tobermorite, was no detected. The lack of this CHS formations in the evaporation products indicates that the hydration process of CPC is the topochemical one, which means that the hydrated phase grows directly from the clinker.

Correspondingly, the evaporation products arising from the liquid phase of pure C_3S show the presence of isolated S and C. If the theory of Tadros et al[6] is right, this fact indicates that an ulterior formation of SCH through the action of C on S will occurs. Thus C_3S hydration involves dissolutions precipitation and a puzzolanization process. Latter on, the SCH inhibits dissolution and the topochemical process is them followed[6]. This mechanism has been confirmed through the morfology of the hydrated C_3S[7], and it is quite probable that the hydration of C_2S[8] will be governed by the same above mechanism.

BIBLIOGRAPHY

1) LE CHATELIER (1961), Comp. Red. 94, 13 (1881); cited by Brunauer, S., "Some Aspects of the Physics and Chemestry of Cements", Jour.Port. Cem. Ass. Res. Develop Lab., 3, 47-56.
2) WILLIAMSON, R.B. (1972), "Solidication of Portland Cement", Progress in Materials Science, 15 189-285.
3) DRON, R., HORNAIN, H. and PETIT, P. (1975), "Localisation du Sicicate de Calcium Hidraté dans les Patés de Laitier Granulé", C.R. Acad. Sc., 280, 187, Paris.
4) KAPRANOV, W.W. (1975), "Solidification of Hydraulic Cement", Cement and Concrete Research, 5, 15-24.
5) KITTL, P. and GOLDSCHMIDT A. (1977), "Sobre la Constitución Química del Agua de Amasado y las Teorías de la Hidratación del Cemento", Inst. Eduardo Torrojas, Materiales de Construcción, N° 168, 21=25, Spain.
6) TADROS, M.E., SKALNY, J. and KALYONCU, R.S. (1976), "Early Hydration of Tricalcium Silicate", Jour. Amer. Cer. Soc., 59, 344-347.
7) GOTO, S., DAIMON, M., KOSAKA, G. and KONDO, R. (1976), "Composition and Morphology of Hydrated Tricalcium Silicate", Jour. Amer. Cer. Soc., 59, 281-284.
8) FUJII, K. and KONDO, W. (1979), "Rate ande Mechanism of Hydration of - β Dicalcium Silicate", Jour. Amer. Cer. Soc., 62, 161-167.

On physicochemical foundations of hydration and setting of binding systems

Bases physico-chimiques de l'hydratation et de la prise des liants hydrauliques

I.P. VYRODOV, Professor of Physics, Dr. of Chemistry, Head of Physics Department of the Krasnodar Polytechnical Institute.

RESUME : La formation topochimique de particules très dispersées, thermodynamiquement instables, et provoquant une sursaturation dans les pâtes de ciment, est l'idée principale de la théorie développée par l'auteur. Le processus, thermodynamiquement stable, de formation de nouveaux cristaux hydratés, s'effectue à la fois par une "distillation" à partir des phases homogènes anhydres, et par la coalescence de nouveaux composés, moins stables thermodynamiquement, qui se produisent à la surface des constituants en cours d'hydratation.

L'effet de destruction de ces croûtes de coalescence, qui retarde le processus topochimique, se manifeste statistiquement avec force dans la période initiale de la prise.

On estime que la formation de liaisons interparticulaires est commandée par le mécanisme de cristallisation de nouveaux composés et par l'action de forces auto-cohésives. On propose alors une méthode universelle d'évaluation de l'activité hydraulique d'un clinker, basée sur une loi exponentielle simple de l'hydratation des liants hydrauliques.

On a constaté une bonne corrélation entre l'activité hydraulique ainsi mesurée et la classification réglementaire des ciments.

SUMMARY : There has been developed a theory the main point thereof relates to a topochemical formation of high dispersive thermodynamically unstable particles causing oversaturation of cement mortars. Thermodynamically stable process of recrystallization of new formations is accomplished both by "distillation" through the homogenous phase and by coalescence of thermodynamically less stable new formations which occur on the surface of hydration.

Cooperative destruction effect of coalescent crusts which retard the topochemical process statistically occurs with strength drop at an early stage of the binding system hardening.

It is estimated that the formation of interparticle contacts is defined by the recrystallization mechanism of new formations and by action of autohesive-cohesive forces.

There has been offered a universal method of hydraulic activity evaluation, which is based on a common exponential law of binding systems hydration process. Correlation between the cement mark (grade) and its hydraulic activity has been determined.

The topochemical theory has mainly been discussed in detail by the author in his works / 1-8 /. According to the diagram primary hydration products formed as a result of said topochemical reactions are being dissociated due to their thermodynamic unstability.

Upon reaching the saturation level of mortar relative to greater particles, the so-called critical particles (nuclei), the latter become also thermodynamically unstable. Process of further particle dissociation goes on and results in oversaturation towards more and more growing particles. It proceeds until thermodynamically stable nuclei are originated in the mortar by fluctuation. The nuclea growth promotes oversaturation relaxation and size increasing of critical nuclei. During the first stage of distillation there takes place degradation of particles with a poor crystal structure, while during the second

stage when the particles are distilled through the homogenous phase of the mortar, they are recrystallized with a proper atomic structure.

Evolution of oversaturated states has been complicated with processes of crust formation and of continuous fluctuating particle origination during the whole period of these oversaturated states. As to the intersecting processes of dissociation and coalescence of contacting particles they are taking place on the surface of reactions on the initial period of hydration. Coalescent formation of crust stimulates a quick saturation relaxation and establishment of the inductive period. Taking into account all peculiarities mentioned above the whole process before the absolute oversaturation relaxation is described by using a system of equations for the distribution function f(R, t) as well as oversaturation $\Delta = C - C_\infty = \Delta C + \alpha/R$ /I/:

$$\Delta C = C - C_H = C - C_R = C - (C_\infty + \alpha/R)$$

$$\frac{\partial f}{\partial t} + \mathrm{div}_R\,(fR) = \varphi = \left(\frac{\partial f}{\partial t}\right)_{\text{topochem.}} + \left(\frac{\partial f}{\partial t}\right)_{\text{fluct.}} \quad (1)$$

$$R = \frac{D}{Rd_k}\left(\Delta - \frac{\alpha}{R}\right), \quad (2)$$

where

D- ion diffusivity in the mortar,

α_k- density of particles being crystallized, $\alpha = \frac{\sigma}{KT} V C_\infty$,

σ - specific interphase energy

V - atomic volume

k - Boltzman constant

T - absolute temperature

Function f (R, t) is a fundamental property of the binding system evolution. According to its asymptotical behaviour it is possible to build up a theory concerning the binding system strength at the end of its hardening.It is possible to establish a strength drop moment t^* with the help of f (R, t), although in practice specialists take interest in strength drop in connection with the technological conditions. This problem has already been solved with allowance for the size distribution function for the initial assumed particles of the binding system /6/. It is of importance to increase dispersity of the solid component as well as hydraulic activity of the binding system to stimulate

a strength (drop) when tycsotropnoreversible macroproperties are being developed, i.e. during that period which is considered to be not dangerous for building up the strength. Oversaturation (t) is known to be of no less importance. Its behaviour has been thoroughly studied both theoretically /2,8/ and experimentally /9/. Formation of the coalescent crust which retards or sometimes (while breaking blockade) accelerates formation of oversaturated states / 8,10 / results in exhibiting periodical properties with a period depending upon crust porosity, hydraulic activity, ultimate watersaturation value of the topochemical surface as well as phenomenological coefficients / 6 /, see also / 3 /, vol.II, book 2, p.108.

While analyzing influence of f (R, t) upon strength formation / 6, II / one can prove the exponential law of strength increment / 6 /:

$$\Delta R\ (t) = R_M - R\ (t) = R_M \exp\ (-Kt^n), \qquad (3)$$

where

R_M - mark value of strength

K - conversion constant, and as a rule n=1. Introducing the actual water-cement ratio X = W/C / 11,13 /into this formula one can get the general formula of strength:

$$R = \eta_1^* X\ (\alpha + X)\ (\eta_2 + X)^{-2}\ (I - \exp\ (-Kt), \qquad (4)$$

where value of parameters α , η are revealed in the works / 12-14 /.
The semiphenomenological consideration of other strength characteristics such as porosity introduced into the formulae like /4/ provides the proper coincidence both experimental and theoretical data / 2,15,16 /.

As yet no structure of pores and anisodesmicity of the particles shape has been considered by us. It is possible to build up a quantitative theory for such systems by way of introducing the divergent item into / 3 / which takes into account the particle growth along the fibres as well as an extra equation like / 2 / to show direction of the particle growth.

Cohesive and autohesive-cohesive links of the fibres to be inosculated develop strength not only by direct inosculation but also by-side reactions namely by reinforcement of the residual solid mass of the cement stone. While these two functions of fibres are being atrophyed, the stone strength characteristics are transferred to the continuum wherein a relict function of crack fibre extinguishing is realized with a number of cracks decreased; the latter are developed in the continuum of the cement mortar and are come out along direction of the fibre localization / 11 / either by conveying energy of cracks to the place of fibre accumulation, or by formation (and coalescence) of cavities in this region. Brittle destruction common to the continuum is thus transformed into viscous at the expence of the static distribution of fibre accumulations.

Let us concern one more molecular-kinetic aspect of the theory - physicochemical foundations of the concrete thermal processing. It has already been noted in our work / 17 / that the most intensive energy transformation of autohesion of quartz fibres occurs in the temperature range of 20-40°C, its saturation point is at 90°C. This value

is valid for all or nearly all interparticle interactions in the cement stone and concrete. Therefore thermal conditions of concrete processing should provide the permissible quantity of the mass that failed to react. This quantity by the moment when the maximum temperature of concrete is achieved can result in allowable decrease of strength by partial destruction of formed contacts being highly saturated due to autohesis energy $W_a = W[T(t), t]$.

As far as the experimental data are approximated by exponential functions $W_t(T) \sim T^m$, $W_T(t) \sim t^n$ one can find a link between optimum time of concrete thermal treatment t_o at upper $T=T_M$ and physicochemical parameters-factors of concrete strength / 17 / by way of converting energy variation of autohesis into zero: $\delta W_a = 0$. The given results

are in accordance with those presented by M.Venua / 18 / at VI Congress, they refer to dependence of concrete compression strength upon steaming temperature.

Experimental data on hydration processes and setting of binding systems show that the quantity of reacting component mass m(t) and hydration rate are linked by ratio:

$$1 - \beta(t) = \frac{m(t)}{m_o} = \exp(-kt^n) \qquad (5)$$

Conversion constant in ratios /3-5/ reflects the system activity, it can therefore be chosen as a base upon standardization (unification) of a notion concerning hydraulic activity γ. For this purpose time of relaxation τ is introduced. After this period $\frac{m(\tau)}{m_o} = e^{-1}$. Hence, $\beta(\tau) = 1 - e^{-1} = 0.632$ and $K = \tau^{-n}$. Thus we approach the definition of hydraulic activity $\gamma = K$ according to the formula:

$$\gamma = K = \tau^{-n} \qquad (6)$$

Thus taking time τ which characterizes hydration rate of the system $\beta = 0.632$, one can find the numerical value of hydraulic activity γ. This value can also be estimated either by kinetic data forming direct relationships in $\ln \frac{m(\Delta t)}{m_o}$ from Δt or by using $R(\tau) = 0.632 R_M$. Hence, the cement grade being determined by value R_M is directly linked with its hydraulic activity ($\gamma = \tau^{-1}$). If

$$\frac{\Delta R}{R_M} = e^{-K_R t} \approx e^{-K_m t} = 1 - \beta(t) \qquad (7)$$

it is easy to get $R(\tau) = (1 - e^{-K_R/K_m}) R_m$. It points to the correlation of the given values. Correlation between values of K_R and K_m is indicated by the fact that the binding system belongs to one of three groups / 5 /. These groups and the definition of the binding system / 5,8 / reflect the fundamental properties of heterogenous systems which involve required and sufficient conditions for exhibiting adhesive properties of the system. All this taken into account will reveal perspectives of the general systematics and prediction of the binding systems.

LITERATURE CITED

1. VYRODOV I.P. On Same Main Aspects of Theory of Solydification and Strength Formation of Cement Stone and Concrete V-ISCC,Suppl. Tokyo (1968),p.111-115; 100-118.E
2. Выродов И.П. О некоторых основных аспектах теории гидратации минеральных вяжущих веществ и формирования прочности цементного камня. Дисс. на соиск. учен. степ. д-ра хим. наук /рукопись/,Л.,1970.
3. Выродов И.П. О некоторых основных аспектах теории гидратации и гидратационного твердения вяжущих веществ. Шестой Международный конгресс по химии цемента. Доп. докл., Москва, 1976, т.II,кн.I,стр.68-73; стр.40,187; т.2I,кн.2,стр.108.
4. Выродов И.П. Исследование процессов гидратации минеральных вяжущих веществ. "Твердение цемента", Уфа,1974, стр.41-47.
5. Выродов И.П. Журн.прикл.химии, т.49,(1976), №2, стр.309.
6. Выродов И.П. Физико-химические основы процессов гидратации и формирования прочности в вяжущих системах и перспективы развития теории. "Гидратация и твердение вяжущих", Уфа,1978, стр.204-213.
7. Выродов И.П. Об основных аспектах развития теории по физико-химическим основам процессов гидратации и формирования физико- механических свойств в вяжущих системах. Краткие тезисы докладов на V Всесоюзном научно-техническом совещании по химии и технологии цемента. М.,1978,стр.88./Русск/.
8. Выродов И.П. Перспективы развития физико-химических основ процессов гидратации и формирования физико-механических свойств минеральных вяжущих систем. "Физико-химические основы процессов гидратации и гидратационного твердения вяжущих систем". Краснодар, 1979, стр.3-27./Русск/.
9. Выродов И.П., Маштаков А.Ф., Осюшкин П.А. О механизме электропроводности и низкочастотной диэлектрической проницаемости в вяжущих системах. Там же./Русск/.
10. Выродов И.П., Вакалов И.А., Маштаков А.Ф. Влияние дисперсности, Т, и pH затворяющей среды на процесс гидратации и прочностные свойства гипса. Деп. ВИНИТИ, №3983-77 Деп. /Русск./.
11. Выродов И.П. Элементы теории прочности цементного камня. Труды Кубанского СХИ; II/39/, Краснодар, 1963, стр.40-49; 13/41/, Краснодар, 1968, стр.252. /Русск./.
12. Выродов И.П., Падалкина Г.Н. Известия СКНЦ ВШ, серия "Технические науки", (1977), №3, стр.105./Русск./.
13. Выродов И.П., Падалкина Г.П. Об уточнении зависимости прочности бетона и цементного камня от различных факторов-показателей прочности."Физико-химические основы процессов гидратации и гидратационного твердения вяжущих систем", Краснодар, 1979. /Русск/.
14. Выродов И.П., Падалкина Г.П. Основные формулы прочности цементного камня и бетона. VII МКХЦ, Париж,1980

15. WYRODOV I.P. Uber die Berechnung des Porositätsfaktors bei der Bildung der Zementstein-und Betonfestigkeit, I. Banstoffindustrie (1970),N°8, 269.

16. WYRODOV I.P. Uberdie Berechnung des Porositatsfaktors bei der Bildung der Zementstein - und Betonfestigkeit, II. Baustoffindustrie (1972),N°1, 14.

I7. Выродов И.П. Известия СКНЦ ВШ, серия "Технические науки",)I978), №I,/Русск./.

I8. Венюа М. Влияние повышенных температур и давлений на гидратацию и твердение цемента. Шестой Международный конгресс по химии цемента. Осн.доклад. Москва, I976,т.II,кн.2, стр.I09-I28./Русск./.

Some applications of infrared spectroscopy in the fields of cement and concrete

Quelques applications de la spectroscopie infrarouge dans les domaines du ciment et du béton

Surendra Nath GHOSH, Ph. D. Cement Research Institute of India.

RESUME :L'étude passe en revue des travaux que l'auteur et ses collègues ont faits dans le domaine des applications de la spectroscopie infrarouge (IR) au ciment et au béton. La technique IR a été employée avec succès pour identifier et caractériser des roches, des minerais et des produits qui s'y rapportent. On y traite des méthodes de détermination de la magnésie dans les calcaires et du quartz α dans les briques siliceuses cuites. A l'aide de l'IR, l'on peut évaluer qualitativement l'aptitude d'un cru à la fabrication de ciment Portland. Le spectre IR d'un cru étant caractéristique, le mode d'emploi éventuel de l'IR pour déterminer la proportion relative des silicates est indiqué. En employant cette technique, le processus de l'hydratation du ciment "Porsal" a été étudié. Des applications aux domaines des bétons de polymères à la corrosion du béton, à l'appréciation des granulats et à la carbonatation et à l'hydratation du ciment sont relatées. En outre, sont indiquées les possibilités d'application de l'IR à l'analyse des gaz du four et à l'étude des problèmes concernant les spectres d'états solides.

SUMMARY : The paper reviews the work done by the author and his colleagues in the field of applications of IR spectroscopy in cement and concrete. The IR technique has been used successfully in the identification and characterization of rocks, minerals and products which are related. Methods for estimation of dolomite in limestone and α-quartz in fired silica bricks have been discussed. The burning of an OPC raw meal can be evaluated qualitatively by IR. The IR spectrum of an OPC is characteristic and the possible use of ascertaining the relative proportion of silicate phases has been given. The hydration behavior of "Porsal" cement has been studied by this technique. Applications to the areas of polymer-concrete, concrete-corrosion, aggregate-evaluation, carbonation and hydration of cement, etc. have been referred. Finally, the problems in dealing with solid state spectra have been touched besides indicating the possible application of IR in the analysis of kiln gas.

INTRODUCTION

This paper reviews the work done by the author and his colleagues in the field of applications of Infra-red spectroscopy (IR) in cement and concrete since 1973. The IR technique is a powerful one and is being used in different fields for quite some time. There has been considerable interest for applying this technique by cement chemists during the last several years. The technique, though being versatile, has its limitations but there is ample evidence to apply this technique singularly or in conjunction with other techniques. In our attempts we have tried to explore the possibilities in areas, such as (i) characterization of rocks, minerals, products, etc., and estimation of these materials; (ii) formation characteristics of ordinary Portland cement (OPC) from raw meal; (iii) identification of OPC phases, OPC and other cements and their hydration-characteristics; and (iv) polymerization process in polymer-mortar, concrete - detereoration, and water-proofing compounds, etc.

Both absorption and attenuated total reflection (ATR) spectral studies were conducted in solid and liquid phases and details of experimental procedures can be obtained from references listed at the end.

SPECTRAL INVESTIGATIONS

The results of our spectral investigations are described in short giving the advantages and limitations of the method and suggestions for further improvements where applicable. The spectral regions and limited to 1600-400 cm-1 and the hydroxyl - stretching region.

ROCKS, MINERALS AND PRODUCTS

IR studies on 49 rocks, minerals and products were conducted (1) with a view to finding simple laboratory methods for rapid identification, estimation and correlation with reactivity, etc-, of these materials. The spectra of calcite, aragonite, magnesite and dolomite are presented in Fig.1. Each spectrum of these rocks has characteristic IR bands in the 700 cm-1 region, ie. 711 (Calcite), 727 (dolomite), 748 (magnesite) and 700 and 1083 cm-1 (aragonite). These bands are very sharp in most rock samples studied and it is possible to estimate the relative percentages of these materials from the spectrum of a composite rock sample. Quantitative estimation of dolomite in limestone was developed (2) by simply correlating the intensity of the 727 cm-1 band of dolomite to its concentration (Absolute method) or by the intensity ratio of 727 cm-1 and 711 cm-1 bands in dolomitic limestone rocks to the concentration of dolomite (Relative method). Some of the early results are shown in Table I. Correlation diagrams (straight lines) were obtained using standard mixes with known percentage of dolomite in calcite.

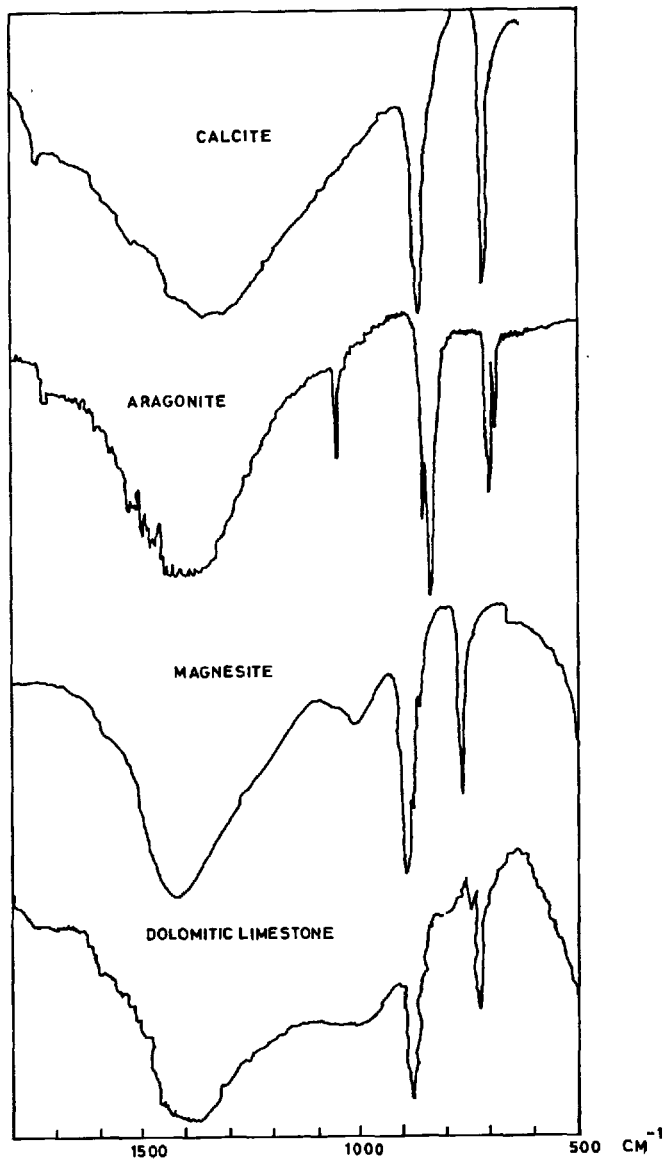

Fig. 1 - Spectra of rocks used in the manufacture of cement.

It was observed that for certain dolomitic lime - stones the relative method was found to give better results than the absolute method. This method is quite rapid and reliable. Qualitative information about the nature of limestone rocks associated with silica, jaspar, phosphate, etc, can be quickly obtained from their IR spectra. The spectrum of a coral limestone sample shows very little silica

while that of a limestone sample containing high percentage of jaspar indicates intense lines in the 1000 cm^{-1} and in the 800 cm^{-1} regions.

TABLE I

Sample Nos.	Chemically determined		Dolomite percentage recalculated from MgO %	Dolomite Content %	
	CaO	MgO		IR	DTG
RS 727	41.10	10.17	46.53	42.5	41.4
BMLS 8	34.63	5.0	22.88	20.5	17.4
RM 353	49.65	3.43	15.78	14.8	15.8

The spectra of orthoclase, feldspar, silica and jaspar are distinctive though the spectra of the first two and last two are nearly equivalent. Crystallinity or degree of disorder in certain local clay samples was studied in conjunction with the pure minerals, kaolin, etc. The spectra of these local clay samples were poorly resolved and the bands are generally broad. It is not difficult to distinguish kyanite, tourmaline, topaz and talc from one another. The important micas can be differentiated rapidly from their spectra. Though the spectrum of crysoltile asbestos can be accounted for partly by tremolite. The spectral investigat - ions were also undertaken to analyse apatite rocks (3). The spectrum of a complex apatite rock containing calcite, dolomite and silica is shown in Fig.2

The spectra of industrial products, such as sillmanite brick, high alumina brick and red clay bricks are rather not distinctive while the spectra of by-products, such as slags are characteristic (1). The conversion of crystalline blast furnace slag to glassy slag appears to be difficult to be determined from the IR spectrum because of overlapping spectra. The spectrum of a ferro-chrome slag is made up of mostly $\gamma - C_2S$ while the crystalline blast-furnace slag contains melilite.

The problem of estimating quartz in fired-silica bricks was referred to us for quality control purposes. It was observed during the course of the investigation that the tridymite line overlaps with the strongest x-ray line for quartz at 3.34 A°(4). The IR spectrum of fired silica bricks consisting of quartz, tridymite, crystobalite, etc, was found to be useful in the low-frequency region because the 690 cm^{-1} quartz peak is quite sharp and not overlapped. However, the detection limit of quartz is normally 4-5% by this method (Fig.3) Attempts were made to correlate the impact strength of aggregates by studying the mineral assemblages of rocks with IR techniques (5). Though no direct correlation can possibly be made out of this, it was observed that rocks, such as calcite, quartzite, granite, etc, were higher quality aggregates when impurities, such as silica in glassy state existing in calcite rocks or the material had some part in glassy state.

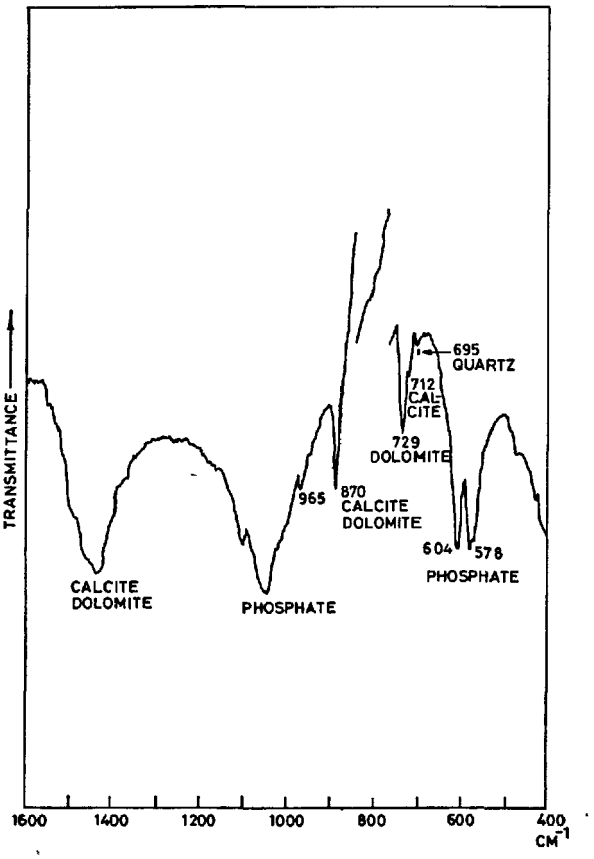

Fig.2 - Spectrum of a complex apatite rock sample.

SPECTRA OF OPC AND OTHER CEMENTS

The absorption and ATR spectra of OPC and its phases have been reported (6,7). The OPC phases have distinctive spectra but the spectrum of OPC is the resultant of these phases and is predominantly of the silicate phases which contribute about 80% of OPC. In our studies on synthetic cements with varying proportions of the silicate phases, the 900 cm^{-1} region strongband (Si-O stretch) was found to alter in shape and splittings (8). An attempt was made to correlate this spectral behaviour with qualitative estimation of the silicate phases as brought out in an institutional manual (9). In general, it was seen that with the increase in belite content, the splitting in the 845 cm^{-1} region band was pronounced and a possible criterion for a first-hand quality control of cement has been indicated (9) as shown in Fig.4. The controversy over the coordination number of Al in C_3A has been mentioned (6) but it appears that no definite information on it can be obtained.

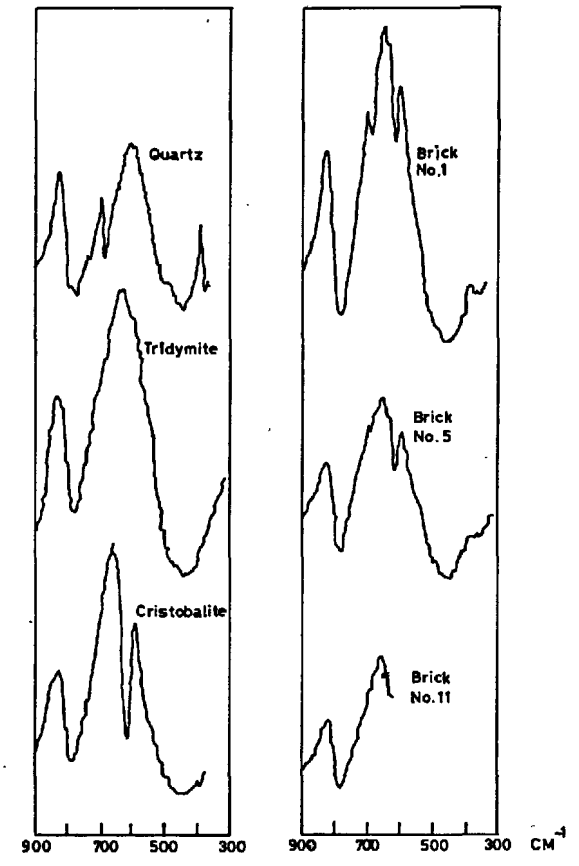

Fig.3 - Estimation of α - quartz by IR.

The ATR spectra of certain standard cements are quite interesting since the systematic appearance of bands (TABLE-II) with changes in intensity,etc., can be made use of for further study in the estimation of the quality of a particular cement.

The author feels that there is a potential scope for using these data in a computer towards quality control of cement.

The transformations of OPC raw meal in a vertical shaft kiln plant were studied by IR as well as XRD. The IR spectral data were published (10). The spectra registered transformations, such as the decomposition of clay (shifting of 1000 cm^{-1} band, etc.) the formation of β - C_2S with some undecomposed calcite and the gradual formation of alite up to the sintering temperature which can be seen in Fig.5. The information thus obtained are admittedly qualitative but pictorial.

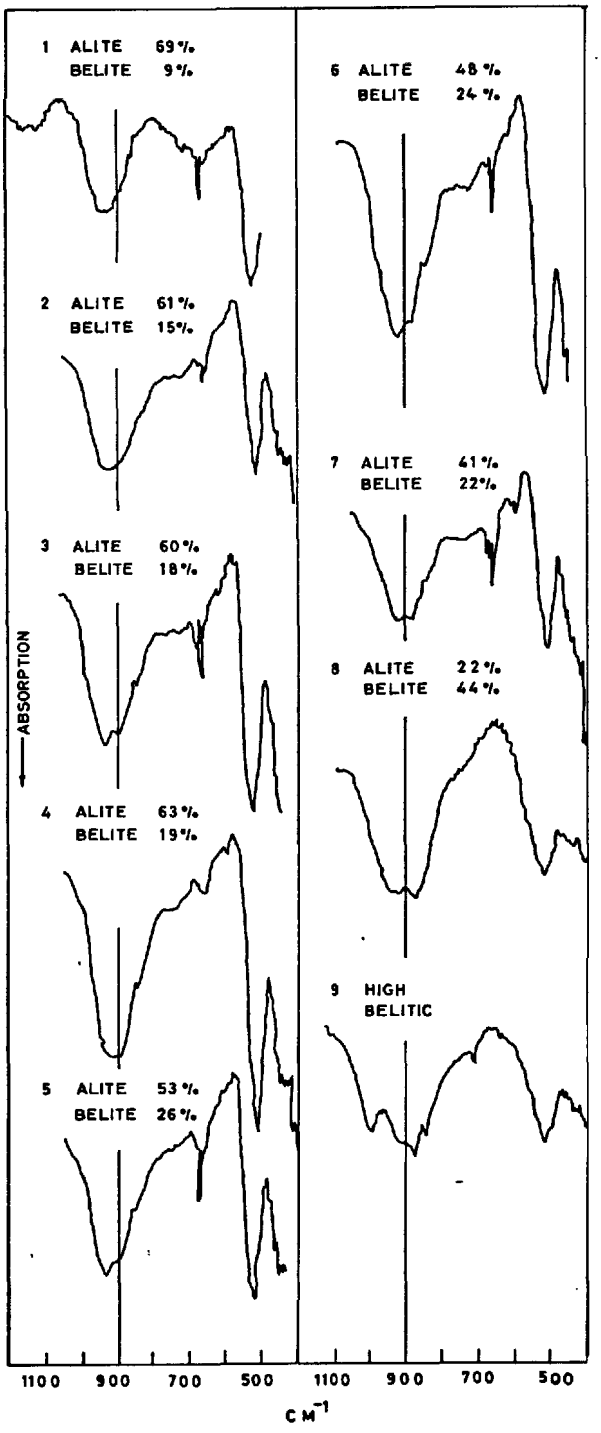

Fig. 4 - Spectra of cements with variable composition.

TABLE II

NBS Standard Cements	IR Bands (ATR Spectra)								
NBS-633	930s	898sh	850sh	730w	620w	600w	533sh	524s	520s
NBS-635	923s	890s	846sh	750w	617w	602w	533sh	524sh	517s
NBS-636	930s	910sh	845sh	750w	620w	603w	533sh	527sh	521s
NBS-637	912s	892s	847sh	760w	618w	600w	-	527sh	515s
NBS-638	923s	892s	847sh	750w	618w	601w	-	525sh	519s
NBS-1016	920s		850sh	748w		603w	532sh	527sh	520sh

S : Strong, Sh: Shoulder, W : Weak

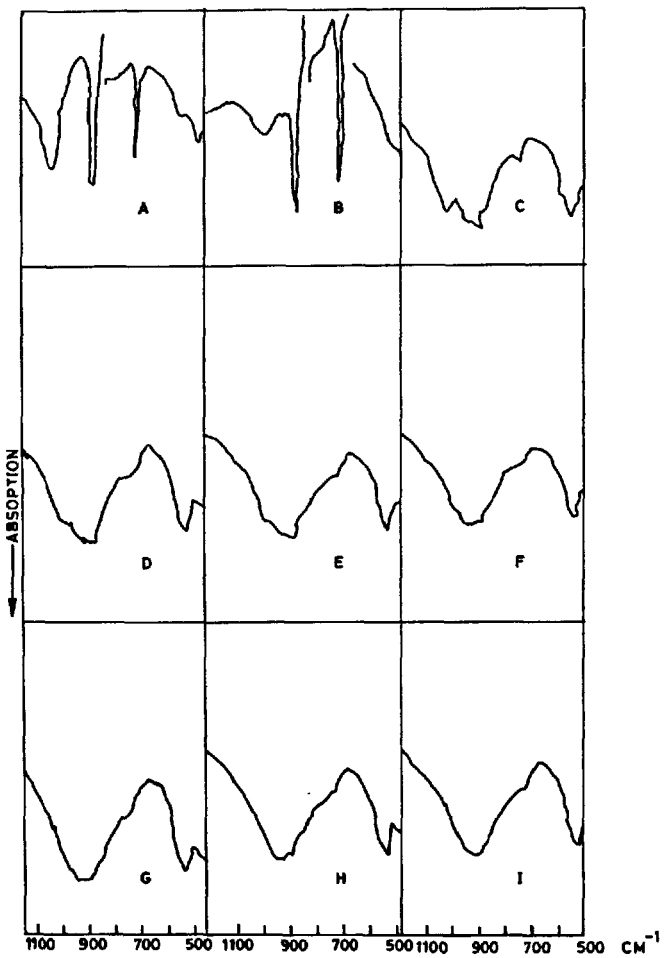

Fig.5 - Spectra of a cement raw mix at different stages of heating up to the sintering temperature.

Studies made on ring-samples showed that the IR spectra did indicate the presence of carbonate (calcite) and sulphate complexes along with β-C_2S but no definite compound compositions could be found (10). The IR spectra appear to be quite powerful in identifying slight hydration (3600 cm^{-1} region band) and carbonation (1400 cm^{-1} band) in standard cement samples exposed once to atmosphere.

During the investigation of a new cement "Porsal" (11), the IR spectral runs of the anhydrous and hydrated cement were taken. The anhydrous cement spectrum truly represents the broad composition of the cement, for example, the high percentage β-C_2S phase and aluminate phases (sharp lines) as shown in Fig.6. The spectrum of 1-day hydrated cement is washed off of the aluminate phases. The broadening of IR bands (silicate) in the spectra of 7-day and 28-day samples is noticeable.

The conversion of monomer methyl methacrylate to polymer methyl methacrylate in mortar-matrix was studied by IR but quantitative conversion was not studied. The spectrum of the in-situ polymerised polymer is similar to that obtained normally (8).

The IR technique was found to rapidly decipher the decomposition products of concrete exposed to sewage environment (12). The spectra of the samples taken from the inner surface indicated high amounts of calcite and sulphate besides silica. The technique was also applied in deciphering a water-proofing compound (8). The spectrum of the water-proofing compound indicated the presence of calcite, sodium stearate and calcium hydroixde (3650 cm^{-1} band).

The selection rules for solid state spectra are different from those for gas or liquid spectra. Factor group analysis of C_3S showed that 29 bands should be expected in its spectrum but actually we observed about 8 bands in the region upto 400 cm^{-1}. The space group for C_3S is C_3V5 (R3m) with 9 molecules per unit cell. The total number of internal modes is $15A_1+2A_2+14E$, where A1 and E modes are IR active. In the case of β-C_2S of

space group $C_2\ h^5$ (P_{21}/n) with 4 molecules per unit cell, the expected IR active internal modes are 12 Au + 12 Bu and we observed about 7 bands (6). The reason is poor resulution, overlapping, etc.

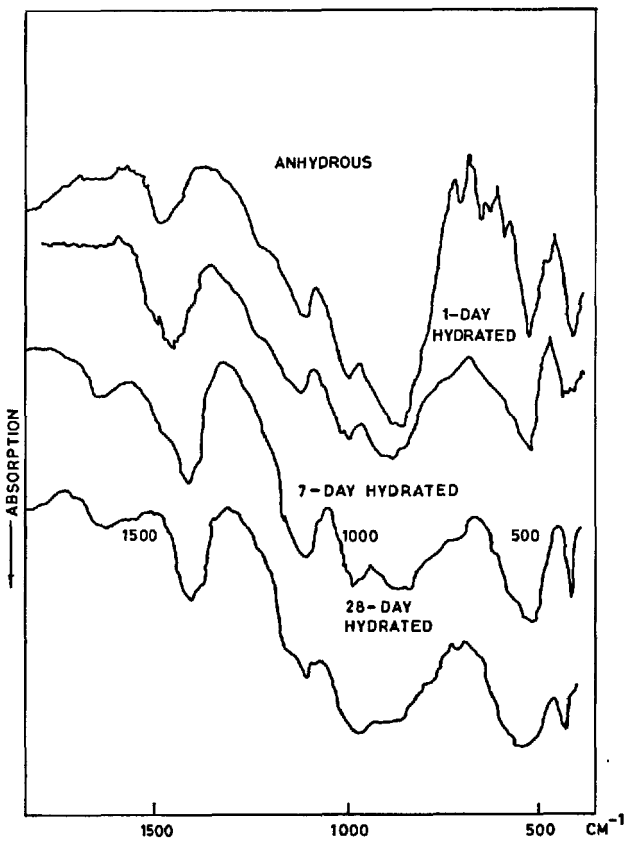

Fig.6 - Spectra of Porsal Cement.

The appearance of an extra band and shifting of bands were observed in the spectrum of a gypsum sample heated to 600°C. The mineral gypsum shows at 669 and 605 cm^{-1} while the heated sample shows three bands in this region at 675, 618 and 599 cm^{-1} in their spectra as shown in Fig,7. This is due to the lifting of degenerecy of the bending mode (SO_4) and this may happen due to substitution resulting in lowering of site-symmetry of a molecule in a crystal lattice.

The presence of impurities, polymorphic forms, glassy phase, etc, may alter drastically the spectrum of a substance in solid state and accordingly precaution may be taken against these when analysing a spectrum of a substance in solid state. There are cases of changes due to reactions taking place while pelleting (KBr) of a solid sample. We observed (6) the appearance of 565 cm^{-1} band in the spectrum of β-C_2S in KBr-pellet while this band is absent in the paraffin-mull of β-C_2S. γ-C_2S has this band both in KBr or paraffin-mull spectrum.

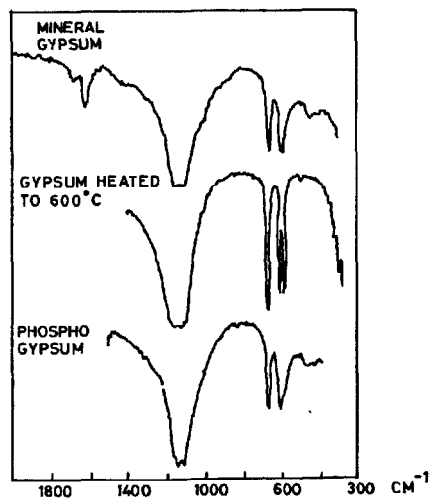

Fig.7 - Spectra of a gypsum sample.

The IR technique is quite powerful in the analysis of gas. The author feels that this technique may be of some value with very little of further development in the analysis of kiln gases.

Table III gives the detection limits of some gases (courtesy - Perkin Elmer Co, USA).

TABLE III

Gas	Detection Limit (PPM)	cm^{-1} range
CO	12.5	2250-2050
CO_2	0.7	2500-2200
SO_2	1.0	1250-1000

CONCLUSION

The applications of IR techniques in the fields of cement and concrete are to some extent qualitative; however much useful information can be obtained quite rapidly. The technique's value can be improved further by attaching a computer to the spectrometer. The ATR method appears to be promising in the study of surface-hydration, curing-process, etc.

REFERENCES

1. - S N GHOSH (1978), "Infra-red spectra of some selected minerals, rocks and products" J. Mater, Sci. 13 1877-1887.

2. - S N GHOSH, V N VISWANATHAN AND A K CHATTERJEE (1976), "Estimation of dolomite mineral in limestone by infra-red spectroscopy," ibid, 11, 1167-1170.

3. - S N GHOSH and S P GHOSH (1977), "Investigation of Indian phasphatic rocks by infra-red spectroscopy "Fertilizer Technology (India), 14, 269-271.

4. - S J RAINA, S N GHOSH and V N VISWANATHAN (1978), "Estimation of quartz in silica bricks by infra-red spectra, "J. Mater. Sci. 13, 913-914.

5. - S N GHOSH and S DAS (1978), "Infra-red spectroscopic analysis of cement and concrete-making rocks, "Ind. Conc. J.52, 241-245.

6. - S N GHOSH and A K CHATTERJEE (1974), "Absorption and reflection infra-red spectra of major cement minerals, clinkers and cement," J. Mater. Sci. 9, 1577-1584.

7. - Idem (1975), "Attenuated total reflectance infra-red spectra of Portland cement," ibid, 10, 1454-1456.

8. - S N GHOSH, V V SUBBARAO, A K CHATTERJEE and P.B. RAO (1976), "Infra-red spectroscopy for characterization and evaluation of cements and related materials, "Cement Research Institute monograph, RB-6-76.

9. - S N GHOSH, P B RAO, V N VISWANATHAN AND R N SHARMA, (1978) "Rapid quality control of of Portland cement/clinker by infra-red spectroscopy," Cement Research Institute, MS-2.

10. - S N GHOSH and A K CHATTERJEE (1978), "Infra-red spectroscopy in cement manufacture, "Trans. Ind. Ceram. Soc. XXXVII, 18-27.

11. - S J RAINA, V N VISWANATHAN and A K CHATTERJEE (1978)," Early hydration characteristics of Porsal cement" Zem - Kalk-Gips, 31, 516-18.

12. - S J RAINA, S N GHOSH and V N VISWANATHAN (1978), "Instrumental techniques for investigations of damaged concrete," Ind. Conc. J.52, 147-149.

Hydration of C_4AF + gypsum : study of various factors

L'hydratation du C_4AF + gypse : étude de divers facteurs

V.S. RAMACHANDRAN (Senior Research Officer) and J.J. BEAUDOIN (Associate Research Officer)
Division of Building Research, National Research Council of Canada, Ottawa, Ontario
K1A OR6 Canada.

RESUME: Les auteurs hydratent de l'aluminoferrite tétracalcique (C_4AF) contenant du gypse dans des proportions de 0, 5, 10, 20 et 30% à 25 ou 80°C soit sous forme de disques (précomprimés à des pressions de 140 et de 690 MPa), soit sous forme de poudre pour des rapports eau/ciment de 0.5 et de 1.0. Ils identifient et quantifient les produits d'hydratation pour des périodes variant de quelques minutes à sept jours au moyen de la méthode thermique différentielle. La séquence de formation des hydrates, c'est-à-dire l'hydrate hexagonal, l'hydrate cubique, l'ettringite, l'hydrate à basse teneur en sulfoaluminates et la solution solide, de même que leurs interconversions dépendent principalement de la température, de la teneur en gypse et du rapport initial eau/solide. Les auteurs montrent que l'ettringite n'est pas nécessairement un précurseur de la formation d'un hydrate à basse teneur en sulfoaluminates lorsque l'hydratation se fait à un très faible rapport eau/solide et à 80°C.

SUMMARY: Tetracalcium aluminoferrite (C_4AF) mixed with gypsum in amounts of 0, 5, 10, 20 and 30% was hydrated at 25 or 80°C either as discs (pre-compacted at pressures of 140 and 690 MPa) or in powder form at water/cement ratios of 0.5 and 1.0. Hydration products formed at periods ranging from a few minutes to seven days were identified and estimated by the Differential Thermal Technique. The sequence of formation of hydrates - viz, hexagonal hydrate, cubic hydrate, ettringite, low sulphoaluminate and solid solution - and their interconversions were primarily dependent on gypsum content, temperature and initial water/solid ratio. The study indicated that ettringite need not necessarily be a precursor of the formation of low sulphoaluminate hydrate when hydration is carried out at a very low w/s ratio and 80°C.

INTRODUCTION

The ferrite phase comprising 8 to 12% of an average portland cement has received very little attention with respect to its hydration and physico-mechanical characteristics. This may be ascribed partly to the assumption that the ferrite and C_3A phases in cement behave in a similar manner. There is evidence, however, that in the presence of gypsum significant differences exist in the hydration behaviour of C_3A and C_4AF, and there is no unanimous opinion on the sequence of hydration and types of hydration products formed under different conditions.

In an earlier investigation (1) of the effect of temperature on the physico-mechanical characteristics of hydrating C_4AF at very low w/c ratios, several new observations were made. This work has been extended to a sequential examination of the hydration products formed in the system C_4AF-$CaSO_4 \cdot 2H_2O$-H_2O (using varying w/s ratios) hydrated for different periods at 25 or 80°C.

EXPERIMENTAL

Tetracalcium aluminoferrite (C_4AF) used in this investigation had the following chemical analysis: Al_2O_3 = 20.43%, Fe_2O_3 = 32.65%, CaO = 45.82% and free CaO <0.5% and loss on ignition 0.37%; the surface area was 3300-3400 cm^2g^{-1} (Blaine).

Eight groups of starting materials, the temperature of hydration, and the periods at which the thermograms were obtained are described in Table I.

The samples were analysed semi-quantitatively by the DSC (Differential Scanning Calorimetric) technique using the DuPont 900 thermal analysis system. Details of these measurements have been described (1). X-ray powder photographs were obtained with a Philips Camera using a CuKα source; length changes were measured by a modified Tuckerman gauge extensometer (2); and rate of heat development during hydration was determined by a conduction calorimeter (1).

RESULTS AND DISCUSSION

Different types of hydration products are formed in the C_4AF-$CaSO_4 \cdot 2H_2O$-H_2O system, depending on initial proportions of materials, temperature and time of hydration. The compounds that may be present at a particular time of hydration may consist of unreacted C_4AF, $CaSO_4 \cdot 2H_2O$ and H_2O and the hydrated products $C_4(A,F)H_{13}$ (hexagonal phase), $C_3(A,F)H_6$ (cubic phase), $C_3(A,F)3\bar{C}S \cdot H_{32}$ (ettringite), $C_3(A,F)\bar{C}S \cdot H_{12}$ (low sulphoaluminate) and a solid solution of the low sulphoaluminate with $C_4(A,F)H_{13}$. In this paper, the solid solution is also referred to as low sulphoaluminate. In each mole of the hydrated product containing x mole of Fe and y mole of A, $x + y = 1$.

Tetracalcium aluminoferrite (C_4AF) does not show any thermal effect in the temperature range studied. Gypsum indicates two endothermal effects with peaks in the range 150 to 200°C, representing the stepwise removal of water. At low concentrations of gypsum the two peaks may merge in a single endothermal peak at about 150 to 160°C. Free water is indicated by an endothermal effect at about 100°C. The hexagonal phase exhibits an endothermal peak at about 160 to 175°C, the cubic form at about 300 to 325°C. Ettringite is identified by an endothermic peak at about 110 to 125°C and the low sulphoaluminate phase by an endothermal effect at about 200 to 210°C. Another of lower intensity is exhibited at about 300°C. The solid solution of low sulphoaluminate with $C_4(A,F)H_{13}$ has thermal effects similar to those of low sulphoaluminate. Small variations in the characteristic peak temperatures may occur, but because products of hydration are examined sequentially at different intervals these variations do not pose any problems for identification.

Thermal curves of C_4AF-gypsum mixtures formed at 140 MPa and hydrated for different lengths of time at 25°C are shown in Figure 1. Figure 1A represents the thermograms of C_4AF hydrated for different periods. The first endothermal effect occurring at about 100°C is due to desorbed water, the second at 170 to 180°C represents the dehydration of the hexagonal phase, and that at about 300 to 320°C is caused by the partial dehydration of the cubic phase. At 1 h both hexagonal and cubic phases are present. As hydration progresses, increased amounts of the cubic phase are formed by the conversion of the hexagonal phase, which is also formed continuously. Even at 7 days there is no complete conversion of the hexagonal to the cubic phase.

TABLE I - Materials Examined by the Differential Thermal Technique

Series	Sample	Compacting Pressure (MPa)	w/s Ratio	Temperature (°C)	Time* of Hydration
I	C_4AF + 0,5,10,20 or 30% gypsum	140	-	25	1,3,5,7 h; 1,3,7 d
II	C_4AF + 0,5,10,20 or 30% gypsum	140	-	80	15 m; 1,3,7 h; 1,2,7 d
III	C_4AF + 5,10,20 or 30% gypsum	690	-	25	4 h, 16 h; 2 d, 7 d
IV	C_4AF + 5,10,20 or 30% gypsum	690	-	80	4 h, 16 h; 2 d, 7 d
V	C_4AF + 5,10,20 or 30% gypsum	-	0.5	25	2 d
VI	C_4AF + 5,10,20 or 30% gypsum	-	0.5	80	2 d
VII	C_4AF + 5,10,20 or 30% gypsum	-	1.0	25	2 d
VIII	C_4AF + 5,10,20 or 30% gypsum	-	1.0	80	2 d

* (m = min, h = hr, d = day)

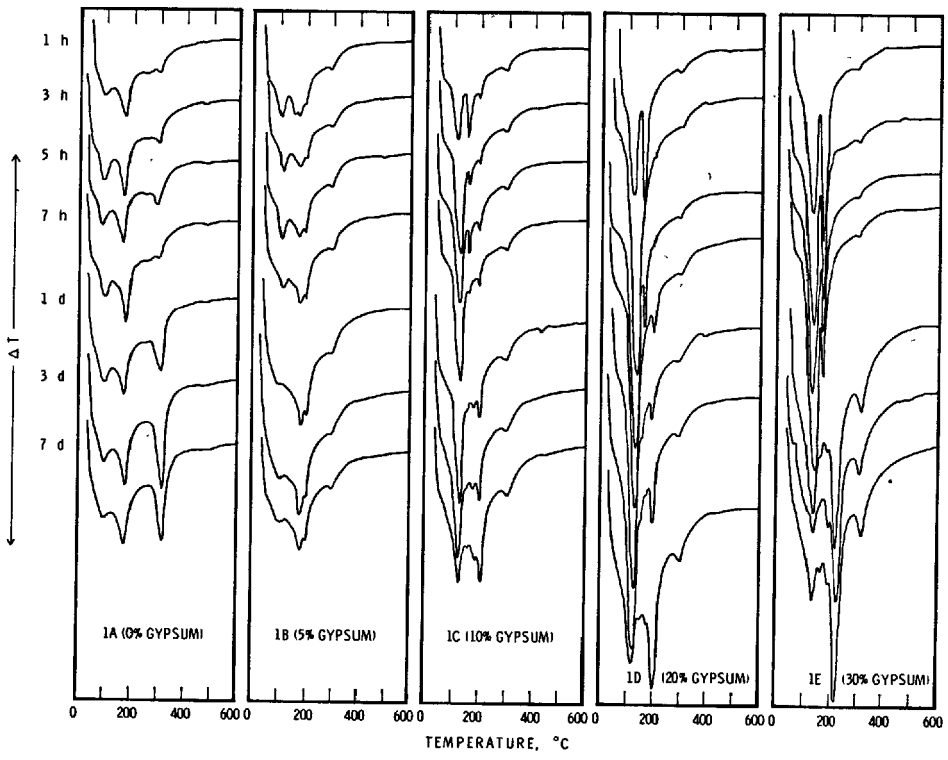

Fig. 1 - Differential thermal behaviour of C_4AF + gypsum (140 MPa) hydrated to different periods at 25°C

Formation of the hexagonal phase and its conversion to the cubic phase proceeds much faster in the C_3A-H_2O system than in the C_4AF-H_2O system (3). Whereas C_3A forms hexagonal plates within a few minutes of contact with H_2O, the C_4AF phase hydrated to the same extent may not develop a well-defined morphology (4). It appears that a higher surface area product enveloping the unhydrated C_4AF grains impedes the diffusion of water molecules more efficiently than the crystalline product formed on the C_3A grains.

Addition of 5% gypsum alters the hydration behaviour of C_4AF (Figure 1B). In the first hour of hydration gypsum (peaks in the range 150 to 170°C), the hexagonal phase (peak at about 180°C), and ettringite (peak at about 105 to 110°C) are present. As hydration progresses the intensity of the peak due to ettringite decreases. Low sulphoaluminate formed from the conversion of ettringite can be identified by a peak at about 200°C. At 7 days the major phases present in the system are the low sulphoaluminate and the hexagonal form. The absence of an intense endothermal peak at 300°C suggests that at 5% gypsum the conversion of the hexagonal to the cubic phase is retarded.

Similar observations were reported on the inter-conversion reactions in the C_3A-H_2O-gypsum system (5). It was suggested that sorption of even small amounts of SO_4^{--} are capable of retarding the conversion of hexagonal to cubic phase. As the amount of gypsum in the mixture is increased from 5 to 30%, larger amounts of ettringite are formed within minutes of contact with water (Figure 1 (C to E)). The commencement of conversion of ettringite to low sulphoaluminate is delayed as the concentration of gypsum is increased in the mixture. Almost complete inhibition of the formation of the hexagonal phase also occurs. In most samples both ettringite and monosulphate co-exist at periods of hydration from a few hours to several days.

The relative amounts of unreacted gypsum and high and low sulphoaluminate contained in samples at different times at 25°C are shown in Figure 2. Calculations suggest that within 1 h relatively more gypsum has reacted to form ettringite in mixtures containing larger amounts of gypsum (Figure 2B). Conduction calorimetric data also indicate that in the first 30 min larger amounts of heat are developed in mixtures containing greater amounts of gypsum. Although almost all gypsum has reacted at 7 h in samples containing 5 to 20% gypsum, substantial amounts are still present in the mixture prepared with 30% gypsum (Figure 2A). All samples show a general decrease in the amount of ettringite after 3 to 7 h of hydration and an increase in the amount of the low sulphoaluminate phase. It is generally believed that ettringite begins to convert to low sulphoaluminate after all gypsum has been consumed. In mixtures containing low amounts of gypsum this may be valid; but at 30% gypsum, although there is a decrease in the amount of ettringite and an increase in the amount of low sulphoaluminate, there is still a substantial amount of unreacted gypsum at 7 h. It appears that after this length of time the reaction between ettringite and C_4AF to form low sulphoaluminate progresses at a faster rate than the reaction between C_4AF and gypsum to form ettringite. A higher rate of decrease in the amount of ettringite in the sample containing 30% gypsum after 7 h indicates that the

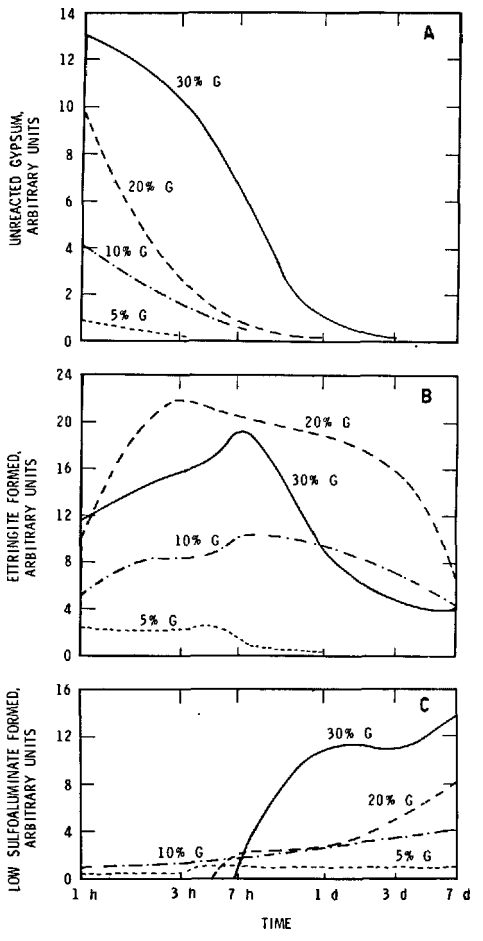

Fig. 2 - Relative amounts of various phases present in the C_4AF-$CaSO_4 \cdot 2H_2O$ (140 MPa) system hydrated at 25°C for different periods. (G: per cent gypsum with respect to C_4AF)

C_4AF surface becomes more easily accessible for the formation of ettringite and its conversion to monosulphates after this period (Figure 2B). Length change measurements reveal that the mixture containing 30% gypsum shows as high an expansion as 10.8% at 7 h, compared to only 2.9% for that containing 20% gypsum. A higher expansion may result in a higher porosity and better availability of the C_4AF surface for reactions.

Differential thermal characteristics of C_4AF-gypsum mixtures containing 0, 5, 10, 20 and 30% gypsum (pressed at 140 MPa) and hydrated at 80°C to different periods are shown in Figure 3. The C_4AF sample forms a large amount of the cubic phase within 15 min (Figure 3A). Hydration occurs at a faster rate at 80°C than at 25°C, as evidenced by an almost complete absence of the hexagonal phase after about one day. At 80°C there is a possibility of direct conversion of the C_4AF to the cubic form without the formation of a metastable phase (6). At an addition of 5% gypsum, low sulphoaluminate is formed even at 15 min (Figure 3B). A concurrent formation of the cubic phase is also evident, increasing as hydration progresses. At a dosage of 5% gypsum, the formation of the cubic form is retarded more efficiently at 25 than at 80°C (Figure 1B). As the percentage of gypsum is increased from 5 to 30%, lower amounts of cubic phase are formed owing to the preferential reaction of C_4AF with gypsum to form sulphoaluminate. The rate of consumption of gypsum and formation of low sulphoaluminate are shown in Figure 4. The low sulphoaluminate form evident at 15 min increases as hydration progresses (Figure 4B); the ettringite phase, if present at all, is formed in small amounts. It is generally suggested that the initial product of hydration of C_3A or C_4AF in the presence of gypsum is ettringite. The non-existence of ettringite in C_4AF-gypsum mixtures formed at 140 MPa and hydrated at 80°C suggests that in a low porosity system, in which the particles of gypsum and C_4AF are in intimate contact with each other, the mobility of ions is restricted, and at this temperature a direct formation of low sulphoaluminate may be favoured. The other possibility is that ettringite formed initially converts to low sulphoaluminate at an extremely fast rate. Further work is in progress to resolve the question of the mechanism involved in the direct formation of low sulphoaluminate in low porosity systems.

Figure 5 compares the thermal characteristics of hydrated products prepared from C_4AF-gypsum mixtures (pressed at 690 MPa) containing 5, 10, 20 and 30% gypsum and hydrated to different periods at 25°C. Generally, gypsum is consumed at a slower rate in this mixture and the rate of ettringite formation and its conversion to low sulphoaluminate is retarded to a greater extent than in one formed at 140 MPa (Figure 1B to E). At a pressure of 690 MPa the particles in the sample are in much more intimate contact with each other and the effective porosity is much lower than in that prepared at 140 MPa.

The mobility of ions is restricted in samples made at a higher pressure, facilitating the formation of products at the original sites of the starting materials. Hydration and interconversions may be impeded, therefore, in samples formed at 690 MPa.

The thermograms of C_4AF-gypsum mixtures formed at 690 MPa and hydrated at 80°C for different periods are shown in Figure 6. There is evidence of simultaneous formation of both ettringite and low sulphoaluminate as a consequence of high temperature and low porosity.

Figure 7 represents the thermal curves of C_4AF-$CaSO_4 \cdot 2H_2O$ mixtures hydrated at w/s = 0.5 or 1.0 for two days at 25 or 80°C. Most samples hydrated for two days at 25°C contain mainly low sulphoaluminate. The interconversions seem to occur at a faster rate at higher w/s ratios. At 80°C and low gypsum content, C_4AF hydrates to form the cubic form. The conversion of ettringite to monosulphate also occurs at a faster rate. A combination of higher w/s ratio and higher temperature is conducive to faster hydration and interconversions.

Most samples were also subjected to XRD studies. In many, especially at earlier times of hydration, though thermal peaks indicated the formation of various products of hydration, XRD did not. Either the amounts of hydration products were low or they were not well crystallized for identification purposes by XRD technique.

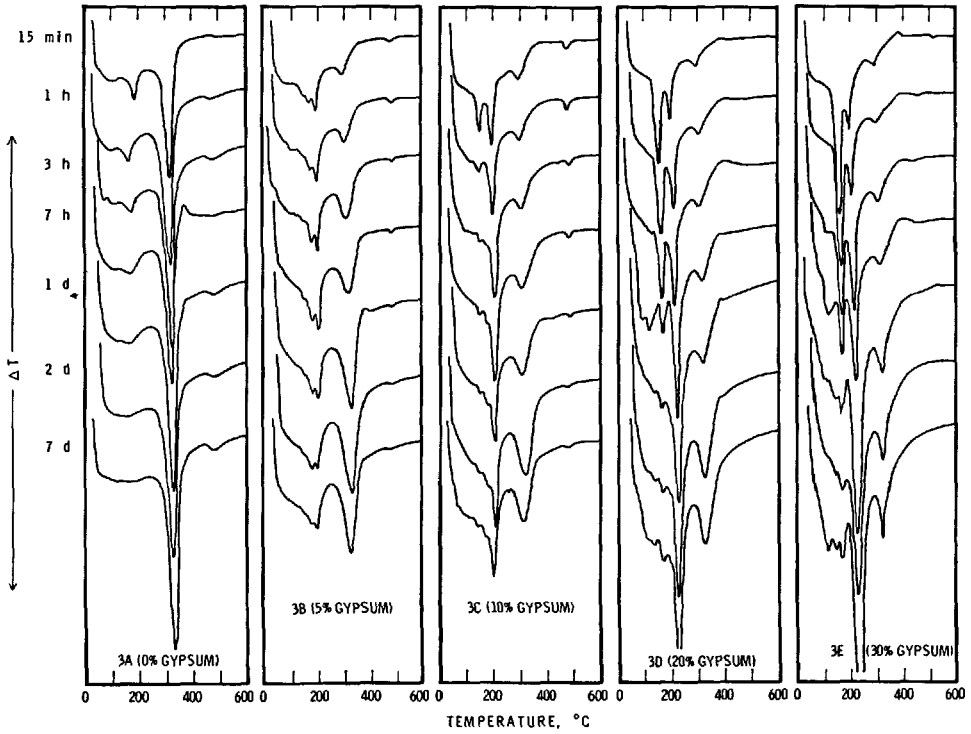

Fig. 3 - Differential thermal behaviour of C_4AF+gypsum (140 MPa) hydrated to different periods at 80°C

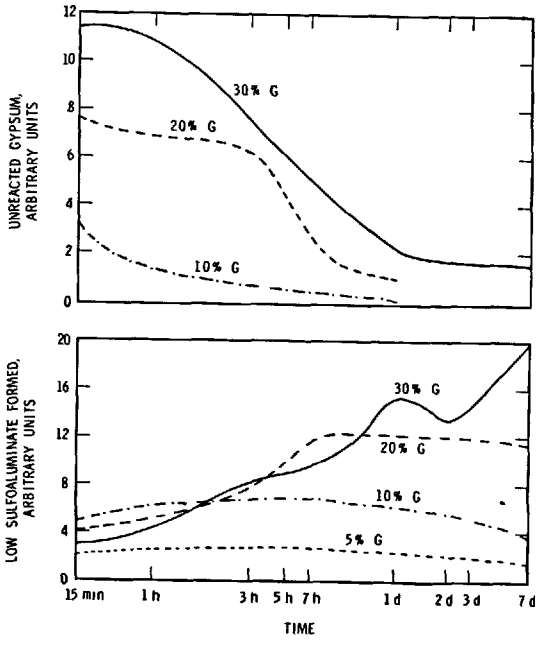

Fig. 4 - Relative amounts of gypsum and low sulphoaluminate present in the C_4AF-$CaSO_4 \cdot 2H_2O$ (140 MPa) system hydrated at 80°C for different periods. (G: per cent gypsum with respect to C_4AF)

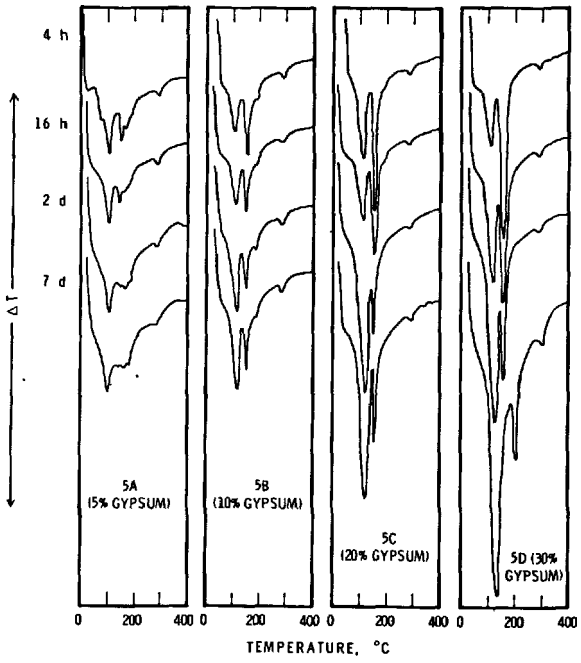

Fig. 5 - Differential thermal behaviour of C_4AF+gypsum (690 MPa) hydrated to different periods at 25°C

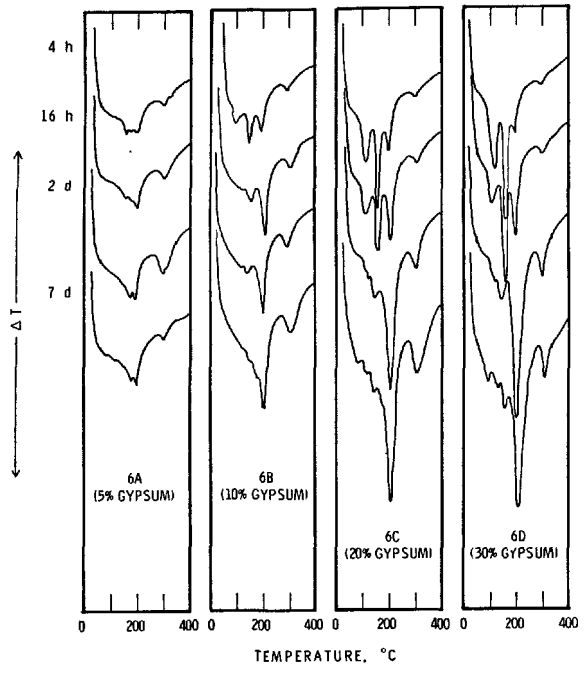

Fig. 6 - Differential thermal behaviour of C_4AF+gypsum (690 MPa) hydrated to different periods at 80°C

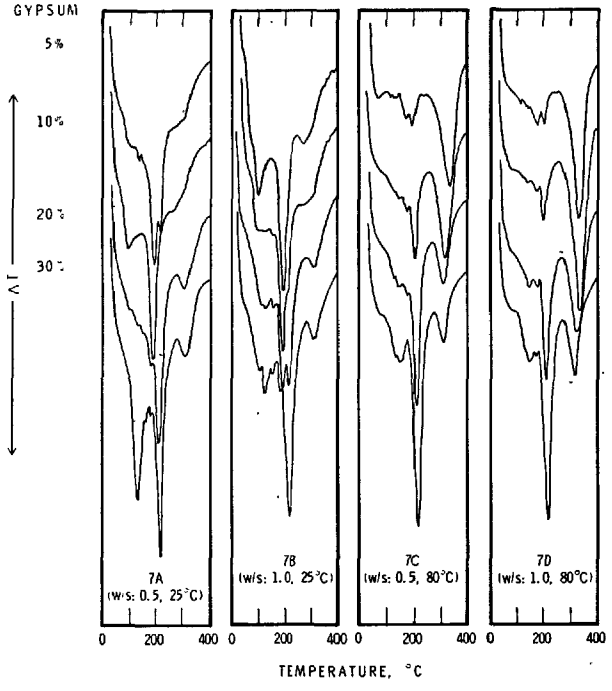

Fig. 7 - Differential thermal behaviour of C_4AF-gypsum (w/s 0.5 or 1.0) hydrated for 2 days at 25°C or 80°C

CONCLUSIONS

1. The sequence of reactions and interconversions in the C_4AF-$CaSO_4 \cdot 2H_2O$-H_2O system at low w/s ratios and high temperatures is different from those occurring at normal w/s ratios.

2. In this low porosity system there is evidence at the original sites of the reactants of formation of cubic hydrate, low sulphoaluminate and ettringite.

3. At very low w/s ratios and higher temperatures low sulphoaluminate need not result from the conversion reaction involving ettringite.

4. Contrary to general belief, conversion of ettringite to low sulphoaluminate can occur even in the presence of gypsum.

5. The Differential Thermal Technique is more sensitive than XRD for identifying and estimating various hydration products in the C_4AF-$CaSO_4 \cdot 2H_2O$-H_2O system.

REFERENCES

1.- V.S. RAMACHANDRAN and J.J. BEAUDOIN (1976), "Significance of water:solid ratio and temperature on the physico-mechanical characteristics of hydrating $4CaO \cdot Al_2O_3 \cdot Fe_2O_3$," Journal of Material Science, Vol. 11, 1893-1910.

2.- R.F. FELDMAN, P.J. SEREDA and V.S. RAMACHANDRAN (1964), "A study of length changes of compacts of portland cement on exposure to H_2O," Highway Research Record, No. 62, 106-118.

3.- R.F. FELDMAN and V.S. RAMACHANDRAN (1966), "Character of hydration of $3CaO \cdot Al_2O_3$," Journal of the American Ceramic Society, Vol. 49, 268-272.

4.- I. JAWED, S. GOTO and R. KONDO (1976), "Hydration of tetracalcium aluminoferrite in presence of lime and sulfates," Cement and Concrete Research, Vol. 6, 441-454.

5.- R.F. FELDMAN and V.S. RAMACHANDRAN (1967), "The influence of $CaSO_4 \cdot 2H_2O$ upon the hydration character of $3CaO \cdot Al_2O_3$," Magazine of Concrete Research, Vol. 18, 185-196.

6.- V.S. RAMACHANDRAN and R.F. FELDMAN (1973), "Significance of low water/solid ratio and temperature on the physico-mechanical characteristics of hydrates of tricalcium aluminate," Journal of Applied Chemistry and Biotechnology, Vol. 23, 625-633.

Study of the Structure and Crystallization properties of Tricalcium Silicate (C_3S) and dicalcium Silicate β (β - C^2S) Hydrate, and the new Calcium Silicate Hydrate (C-S-H (III) C-S-H (I^1) and C-S-H (II^2)

Etude de la structure et de la cristallographie du Silicate tricalcique (C_3S), du silicate bicalcique β(β-C_2S) et des silicates calciques hydratés : C-S-H (III), C-S-H (I^1) et C-S-H (II^2)

F. HANNAWAYYA, Dr. of Chemical Technology, Department of Inorganic Chemistry The Royal Institute of Technology (Kunglia Tekniska Högskolan, KTH) S-100 44 Stockholm, Sweden.

RESUME:L'hydratation d'un mélange de C_3S et de β-C_2S, dans un bocal maintenu à la température ambiante, produit un même type de silicate hydraté (C-S-H) et diverses quantités de chaux hydratée. Les propriétés de $Ca(OH)_2$, la phase aqueuse, la composition, le mécanisme de la réaction avec l'eau et la structure des cristaux formés ont été examinés en détail.

Dès l'origine Hannawayya a donné le nom de C-S-H(I^1), de C-S-H(II^2) et de C-S-H(III) aux divers silicates de calcium hydratés, qui sont formés par l'hydratation des mélanges de β C_2S et de C_3S, selon les proportions respectives de ces deux constituants. Les limites supérieures et inférieures du rapport moléculaire CaO/SiO_2 sont 1,56 et 1,88 pour la production du C-S-H(II) et 2,25 et 2,90 pour la production du C-S-H(III).

La présente recherche concernant le C-S-H a été effectuée lorsque l'équilibre de l'action des divers constituants a été atteint. Le rapport C/S dans la phase anhydre était choisi, de façon à atteindre les divers équilibres déterminés par la théorie. Les produits hydratés formés constituent une série de combinaisons de compositions variées. Leurs structures cristallines ont été examinées au microscope électronique à transparence et à l'appareil de diffraction X.

SUMMARY :The concentration of C_3S and β C_2S by bottle hydration at room temperature produced a similar type of calcium silicate hydrate (C-S-H) and different amount of calcium hydroxide. The properties of $Ca(OH)_2$, the aqueous phase, the composition, the mechanism of the reaction with water, and the structure of the crystalline compounds formed in C-S-H system are discussed in details.

Hannawayya originally gave the name (C-S-H(I^1), C-S-H(II^2) and C-S-H(III) to the calcium silicate hydrate which is produced by bottle hydration of β-C_2S and C_3S hydrate respectively. The lower and upper limits of CaO/SiO_2 mole ratio of C-S-H(II^2) are 1.56 and 1.88 respectively, and of C-S-H(III) are 2.25 and 2.90 respectively.

The present research dealswith the system $CaO-SiO_2-H_2O$ (C-S-H), in which equilibrium is reached through interaction between the components. The ratio of CaO/SiO_2 was determined in the solid phases under condition of hypothetical equilibrium in solution, in which the CaO concentration was varied. The products formed are a series of compounds, whose composition varies. Their crystal structure are illustrated by scanning electron microscopy and X-ray diffraction.

INTRODUCTION AND GENERAL DISCUSSION

A study of the hydration of individual phases (C_3S and β-C_2S) is essential for a basic understanding of the hydration of portland cement and has important bearing on the phenomenon of setting, development of strength, durability, etc.

This investigation was based on the determination of calcium silicate hydrates (C-S-H(I^1), C-S-H(II^2)) and (C-S-H(III)) and calcium hydroxide formed by bottle hydration of C_3S and β-C_2S respectively. Bottle hydration of C_3S and β-C_2S have the potential to form metastable products (C-S-H system) which transform slowly. Final equilibrium is approached by the interaction of the components and takes several months. Bottle hydration is a method in which the anhydrous phase is mixed with an excess of water (usually more than 10 times its own weight) and placed in a rotating wheel. The progress of the present investigation shows for the first time metastable equilibrium curves of C_3S (HANNAWAYYA, fig.5) and its calcium silicate hydrate(III) (C-S-H(III) and of β-C_2S (HANNAWAYYA, fig.5) and its two calcium silicate hydrate (C-S-H(I^1) and C-S-H(II^2)). The product C-S-H(II^2) was studied extensively, its X-ray and electron diffraction data are presented elsewhere [1].

Gibbs Phase Rule is applied in this research to determine whether true metastable equilibrium in the reaction between the components could occur in a certain period of time during bottle hydration of C_3S and β-C_2S. The use of the phase rule is basic for an understanding of the reaction which gives rise to silicates or portland cement clinker and for knowledge of the chemical nature of the product.

HANNAWAYYA [2] investigated C_3S in an excess amount of water (bottle hydration). LEDUE [3] showed that dicalcium silicate was the essential hydraulic material of portland cement. The hardening of the cement was explained as being due entirely to the hydration of the $2CaO.SiO_2$, the fine needles of the $CaO.SiO_2.aq.$ becoming interlaced and penetrating the gel of the same composition. The products formed at room temperature in the system $CaO.SiO_2.H_2O$ has been studied by KALOUSEK [4] using the method of differential thermal analysis. Various mixture of calcium hydroxide and silica gel were prepared and aged for 28 days. The products led KALOUSEK to postulate a continuous series of compounds having the end composition of $C_4S_5H_x$ and $C_4S_3H_x$. Some investigators [5-7] have studied the structure and morphology of C-S-H (calcium-silicate-hydrate) and have presented evidence for the semi-crystalline fibrous forms of the hydration products. Others [8-10] have discussed the fibrous particles which appear as bundles and aggregates, and (sometimes) as sheets having an interlacing structure oriented in 3 directions at an angle of about 60^o. The author emphasizes that the hydration of calcium silicates is an important reaction. Moreover, the β-C_2S compound is vital in several fields of silicate science, especially, different kinds of cement, refractories, and slag.

Many authors have estimated or measured C/S mole ratio of C-S-H which is produced from C_3S hydrate. DIAMOND [11] reported a ratio between 1.9 ±0.2 by Spot EDXA determination. GRUTZECK and ROY [12] used Electron Probe Microanalysis (EPMA), for direct measurement on a single C_3S paste hydrated for 24 weeks. They obtained an average value of 1.7 ± 0.1 LOCHER [13] found ratio between 1.5 and 1.75 by thermogravimetry. KANTRO et al [14] reported ratio between 1.4 and 2.0 TAYLOR $C_2SH(II)$ [8] first reported ratio close to 2.0 and later he estimated it to be 1.75. LEA [15] reported ratio of completely-hydrated-silicate, about 1.4-1.6.

Hydrated C_3S and β-C_2S should yield a fixed maximum of C/S mole ratio. The author took evidence from the hydration of C_3S and β-C_2S to deduce 2 formulae which fix the values of C/S mole ratio thus providing the missing link. The author suggests that the upper limit of the CaO/SiO_2 ratio of C-S-H(III) should be 2.90. This value never reaches 3.0 (see equation 1) and the upper limit of CaO/SiO_2 ratio of C-S-H(II^2) should be 1.88. This value never reaches 2.0 (see equation 2).

MATERIALS AND METHODS

The initial material used in this investigation, tricalcium silicate (C_3S, is composed as follows: 75.6844 wt.% CaO, 26.3156 wt.% SiO_2, and beta-dicalcium silicate (β-C_2S), is composed as follows: 66.2440 wt. % CaO, 33.6575 wt.% SiO_2, and 1.0985 wt.% Al_2O_3. The shaking apparatus shown in figure 1 was employed. By shaking different amounts of tricalcium silicate of beta-dicalcium silicate with a fixed amount of distilled water, a change in concentration occurs on reaction. The amounts of C_3S are calculated from equation 1 and those of β-C_2S calculated from equation 2.

$$\frac{(3 - C/S)W_o}{228} = \frac{[CaO]}{1000} \qquad \text{---------- (1)}$$

$$\frac{(2 - C/S)W_o}{172} = \frac{[CaO]}{1000} \qquad \text{---------- (2)}$$

where W_o (g/litre) is the starting weight of C_3S or β-C_2S, C/S refers to the CaO/SiO_2 ratio, and [CaO] to the millimole concentration in the solution.

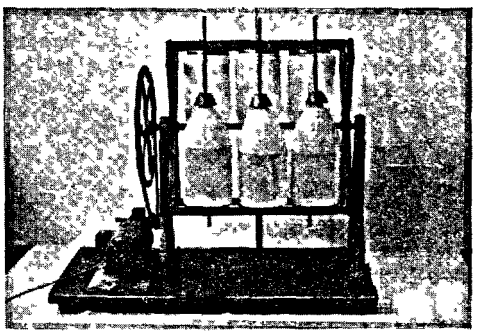

Fig.1. Shaking apparatus.

Samples of different concentration, e.g. 0.3, 0.5, 2.0, 3.0, 4.5, 8.0, 9.72, 15.50, 31.92, 40.47 and 82.88 gm of C_3S, and/or e.g. 0.5, 1.5, 2.25, 7.88 and 35.0 gm of β-C_2S in 1000 ml. of distilled water, were shaken at room temperature in the shaking apparatus. The use of glass bottles was found to be undesirable whenever prolonged treatment with aqueous solutions was required due to the effect of the high alkalinity (above PH 11) of aqueous phase (see tables 1 and 2). Shaking took place for varying lengths of time, and once a week the concentration of CaO in the solution was estimated by titration to determine when the reaction had almost ceased (fig. 2 of C_3S: curve I, 0.3 gm; curve II, 0.5 gm; curve III, 2.0 gm; curve IV, 3.0 gm; curve V, 4.5 gm; curve VI, 8.0 gm; curve VII, 9.72 gm; curve VIII, 15.50 gm; curve IX, 31.92 gm; curve X, 40.47 gm; curve XII, 82.88 gm. and/or fig. 3 of β-C_2S: curve I, 0.5 gm; curve II, 1.0 gm; curve III, 1.5 gm; curve IV, 2.25 gm; curve V 7.88 gm; curve VI, 35.0 gm).

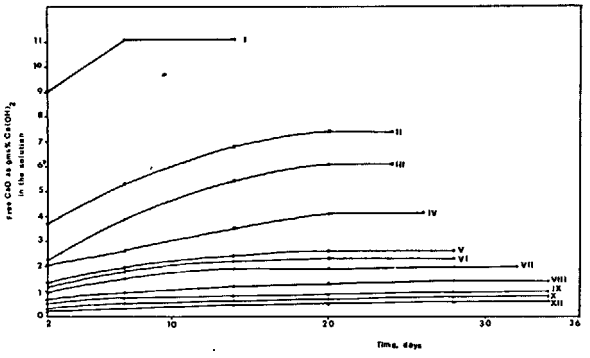

Fig.2. Variation of the $Ca(OH)_2$ content of bottle hydrated C_3S with time of shaking.

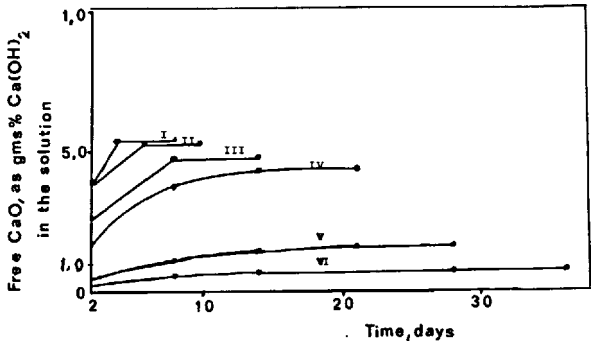

Fig.3. Variation of the $Ca(OH)_2$ content of bottle hydrated β-C_2S with time of shaking.

The contents of the bottle were then filtered and the precipitate dried. Using e.g. eqns 1 and 2, an arbitrary weight of C_3S and β-C_2S, respectively, was chosen and added to the bottle which were then inserted into the rotating shaking apparatus (fig.1). The shaking period was varied as described above, until the reaction had almost ceased.

Immediately after filtration, as shown in fig. 4, the PH of the clear filtrate was measured by means of a high-alkali glass electrode.The calcium concentration of the filtrate was determined by titration, 50 ml. being titrated with HCL using phenolphthalein as indicator. One ml. of HCL is equivalent to 0.03705 gm.of $Ca(OH)_2$. The precipitate on the glass filter was placed in a vacuum desiccator for one hour The precipitate was then brushed into a weighed crucible and dried under vacuum at 105°C to constant weight. After drying, the precipitate was quantitatively analysed by X-ray diffraction 16 to determine the uncombined calcium oxide as calcium hydroxide. The results of the calculation are given in tables 1 and 2. Scanning electron microscopy was used for the morphological study.

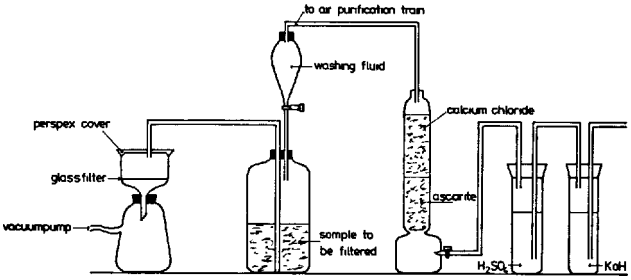

Fig.4. Apparatus for filtration of contents of a polyethylene bottle or other vessel under CO_2-free condition.

Table 1. Composition of hydrated C_3S

C_3S g/litre	PH	CaO/SiO_2 mole ratio	CaO m.mole	H_2O/SiO_2 mole ratio	Composition of C-S-H
0.3	11.1	0.98	2.66	0.69	$C_{0.98}{}^{SH}{}_{0.69}$
0.5	11.3	1.209	3.94	0.93	$C_{1.22}{}^{SH}{}_{0.93}$
2.0	11.9	1.28	15.00	0.99	$C_{1.28}{}^{SH}{}_{0.99}$
3.0	12.5	1.49	19.67	1.27	$C_{1.49}{}^{SH}{}_{1.27}$
4.5	12.6	1.90	21.71	1.71	$C_{1.90}{}^{SH}{}_{1.71}$
8.0	12.7	2.17	29.12	2.15	$C_{2.17}{}^{SH}{}_{2.15}$
9.72	12.72	2.25	32.00	2.20	$C_{2.25}{}^{SH}{}_{2.20}$
15.50	12.735	2.50	34.00	2.25	$C_{2.50}{}^{SH}{}_{2.25}$
31.92	12.74	2.75	35.00	2.35	$C_{2.75}{}^{SH}{}_{2.35}$
40.472	12.75	2.80	35.50	2.40	$C_{2.80}{}^{SH}{}_{2.40}$
82.88	12.76	2.90	36.00	2.45	$C_{2.90}{}^{SH}{}_{2.45}$

Table 2. Composition of hydrated β-C_2S

β-C_2S g/litre	PH	CaO/SiO_2 mole ratio	CaO m.mole	H_2O/SiO_2 mole ratio	Composition of C-S-H
0.5	11.88	0.20	5.22	0.10	$C_{0.20}{}^{SH}{}_{0.10}$
1.0	12.21	0.45	9.01	0.22	$C_{0.45}{}^{SH}{}_{0.22}$
1.5	12.37	0.50	12.85	0.32	$C_{0.50}{}^{SH}{}_{0.32}$
2.25	12.51	0.62	18.00	0.45	$C_{0.62}{}^{SH}{}_{0.45}$
7.88	12.56	1.56	20.10	0.92	$C_{1.56}{}^{SH}{}_{0.92}$
35.00	12.64	1.88	23.80	1.66	$C_{1.88}{}^{SH}{}_{1.66}$

RESULTS AND DISCUSSION

The reactions that cause setting and hardenin of Portland cement are collectively describe as hydration reactions, i.e. the combinatio of ions in aqueous solution with one or mor molecules of water by the formation of coordinate links. β-dicalcium silicate (β-C_2S) i the essential hydraulic material of Portlan cement together with C_3S. This is due to th reactivities of anhydrous silicates (β-C_2S, and C_3S) towards water at ordinary tempefa-ture and the characteristic of their hydration products.The hydration products of β-C_2 and C_3S are calcium hydroxide(CH) and calciu -silicate-hydrate (C-S-H), which grow into space lattice, filling the spaces between th grains so that the entire product forms one single mass.

The mechanism of bottle hydration of β-C_2 hydrate and scanning electron microscopy an X-ray diffraction of β-C_2S paste hydration after 1 day up to 36 days is described in detail by [16].

(i) PHASE EQUILIBRIUM THROUGH INTERACTION OF COMPONENTS

The present investigation concerns system CaO -SiO_2-H_2O (from bottle hydration of β-C_2S and C_3S) in which equilibrium was approached through interaction of the components. The progress of the reaction has ordinarily been observed by determining the CaO/SiO_2 ratio in the solid phase under conditions of hypothetical equilibrium in a solution in which the CaO concentration was varied.

The solution of this problem is complicated and interesting. The differences between the investigations are indicated in various details of the curves and their interpretation. Most of the differences are probably due to a failure to obtain equilibrium between the solution and the colloidal hydrate; other investigators ascribed these differences to variations in the size of the colloidal particles resulting from the different conditions in the test procedure.

This paper presents the typical curves for C_3S and β-C_2S (HANNAWAYYA, fig.5) showing the CaO/SiO_2 molar ratio in the solid phase plotted against the CaO concentration of the solution at assumed equilibrium. The investigation concludes that the value of the CaO/SiO_2 ratio depends somewhat on the state of hydration and also on drying at sufficient temperature.

HANNAWAYYA called the hydrate from β-C_2S with a CaO/SiO_2 mole ratio which varied from 0.20 to 0.62, calcium-silicate-hydrate (I^1) or C-S-H(I^1). When the CaO/SiO_2 ratio was increased at lime saturation and varied from 1.56 to 1.88, HANNAWAYYA called it calcium-silicate-hydrate(II^2) or C-S-H(II^2). HANNAWAYYA also called the hydrate from C_3S with a CaO/SiO_2 ratio which varied from 2.25 to 2.90, calcium-silicate-hydrate(III) or C-S-H(III) this occurs at lime saturation.The quantity of water in the structure associated with C-S-H(III) and C-S-H(II^2) seemed to be larger than that with C-S-H(I^1). The H_2O/SiO_2 ratio depending on the degree to which

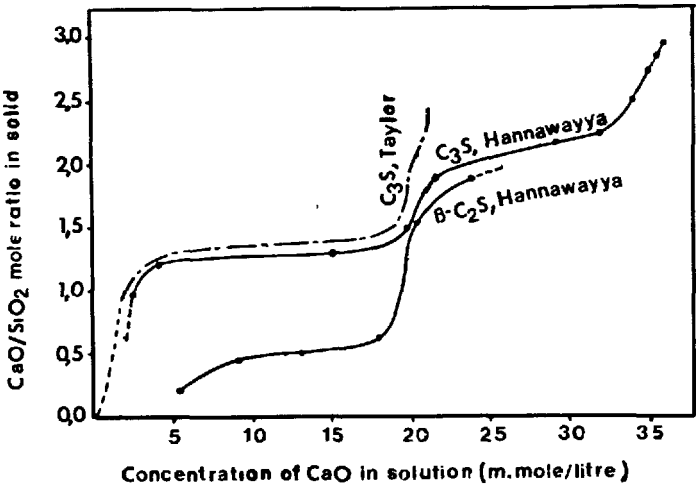

Fig.5. Equilibrium curve showing the relation between the CaO/SiO_2 mole ratio and the concentration of CaO in solution at room temperature.

it was dried and substantially independent of CaO/SiO_2 ratio. Fig.5 shows that the result of the experiments differed depending on the shaking time, due to different concentrations of C_3S or β-C_2S/litre. TAYLOR's curve [17] is included for comparison. Many explanations e.g. (18, 19, 20, etc.) concern the slope of the curve rises gradually to a CaO concentration.

The author explains that the change from a gradual to a nearly vertical rise in the curve occurs because $Ca(OH)_2$ begins to precipitate at lime saturation, causing a rapid rise when the saturation point is passed. It seems that it is difficult to decide upon a fixed value for CaO concentration but in practice, a close approximation can be obtained. It appears that the gradual rise of the slope of the curve, represented by a CaO/SiO_2 ratio from 0.45 to 0.62 of β-C_2S and 1.209 to 1.49 of C_3S, occurs in places where the concentration of $Ca(OH)_2$ (or CH) increases in the solution. The molecules of $Ca(OH)_2$ would be attached to the surface of the hydrosilicate by adsorption up to the lime saturation point, and $(CH)_{n+1}CSH$ would be produced by adsorption, and this is reversible according to the following equation:

$$(CH)_nCSH + CH \longrightarrow (CH)_{n+1}CSH \quad \text{----- (3)}$$

Here, Gibbs phase rule is valid because it is a true equilibrium. The author suggests that the upper limit of the CaO/SiO_2 ratio of β-C_2S should be 1.88 for C-S-H(II^2), and of C_3S should be 2.90 for C-S-H(III). These values never reached 2.0 in β-C_2S nor 3.0 in C_3S.

(ii) SCANNING ELECTRON MICROSCOPY

(a) Morphology of C-S-H(I^1) and C-S-H(II^2) were clearly discussed in 16 .

(b) Morphology of C-S-H(III)

The morphology, shown by scanning electron microscopy, of C-S-H(III) of CaO/SiO_2 mole ratio varying between 2.25 to 2.90 is described by the author as mass crystals of high solidity, and a net of crystals development folded into the shape of a cigar. Under microscopy this crystal is transparent like glass. See Figures 6 and 7, magnified 5000 times. Figure 8 presents the morphology of the C-S-H(II[2]) from β-C_2S included for comparison with the cigar shape of C-S-H(III) from C_3S.

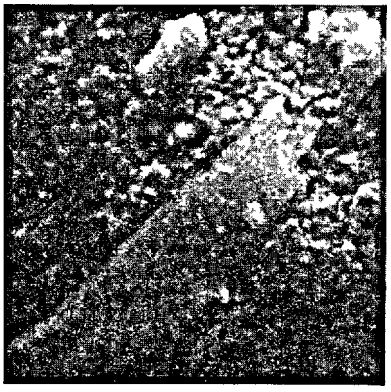

Fig.6. C-S-H(III), The shape of cigar.

Fig.7. C-S-H(III), shows the crystal like glass.

(iii) X-RAY DIFFRACTION DIAGRAMS

(a) X-ray diffraction diagrams of C-S-H(I[1]) and C-S-H(II[2]). Their diagrams were clearly discussed in [16].

(b) X-ray diffraction diagram of C-S-H(III). The X-ray diagram of samples in which the CaO/SiO_2 ratio were 2.50, 2.75, 2.80, and 2.90 contained a strong CH pattern together with a weak pattern of unreacted C_3S, and

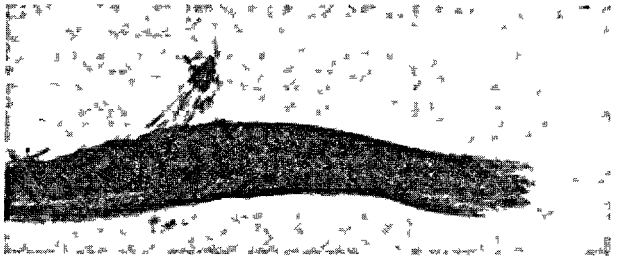

Fig.8. C-S-H(II[2]). (X400). Its crystal has also the shape of cigar.

a pattern of C-S-H(III) at 3.038Å(v. very strong), 1.929 Å (very strong), 2.455, 5.471 Å (strong), 9.654 Å (weak). (see fig. 9).

CONCLUSIONS

The present paper reviews present-day knowledge of the bottle hydration reaction of C_3S and β-C_2S compounds, generally considered to be chiefly responsible for the hydraulic properties of Portland cement.

ACKNOWLEDGEMENTS

Tha author is deeply grateful to Professor INGMAR GRENTHE who is the head of the Institute of Inorganic Chemistry, the Royal Institute of Technology (Kungliga Tekniska Högskolan, KTH) who made this research possible by putting his department facilities at the author's disposal. Thanks are also due to members of the Institute of Inorganic Chemistry for their help in various directions.

REFERENCES

1.- F. HANNAWAYYA, (1977), "Study of the Microstructure of calcium-silicate-hydrate by Electronography", STU report 76-5598, Department of Chemical Technology (Kungl. Tekniska Högskolan) S-100 44 Stockholm, Sweden, No. 83.

2.- F. HANNAWAYYA, (1975) "Study of Hydrated Tricalcium Silicate (C_3S)", Swedish Cement and Concrete Research Institute No. 3:75, Stockholm, Sweden.

3.- E. LEDUE, (1902), Internatial Assoc. Testing Material.

4.- G.L. KALOUSEK, (1952), "Application of Differential Thermal Analysis in a Study of the System Lime-Silica-Water", Proceding Symposium Chemistry of Cement London, Discussion to paper No 0.

5.- S. BRUNAUER AND S.A. GREENBERG, (1962), Proceding 4th. International Symposium Chemistry of Cement, Washington, D.C. NBC Monograph 45, p. 135

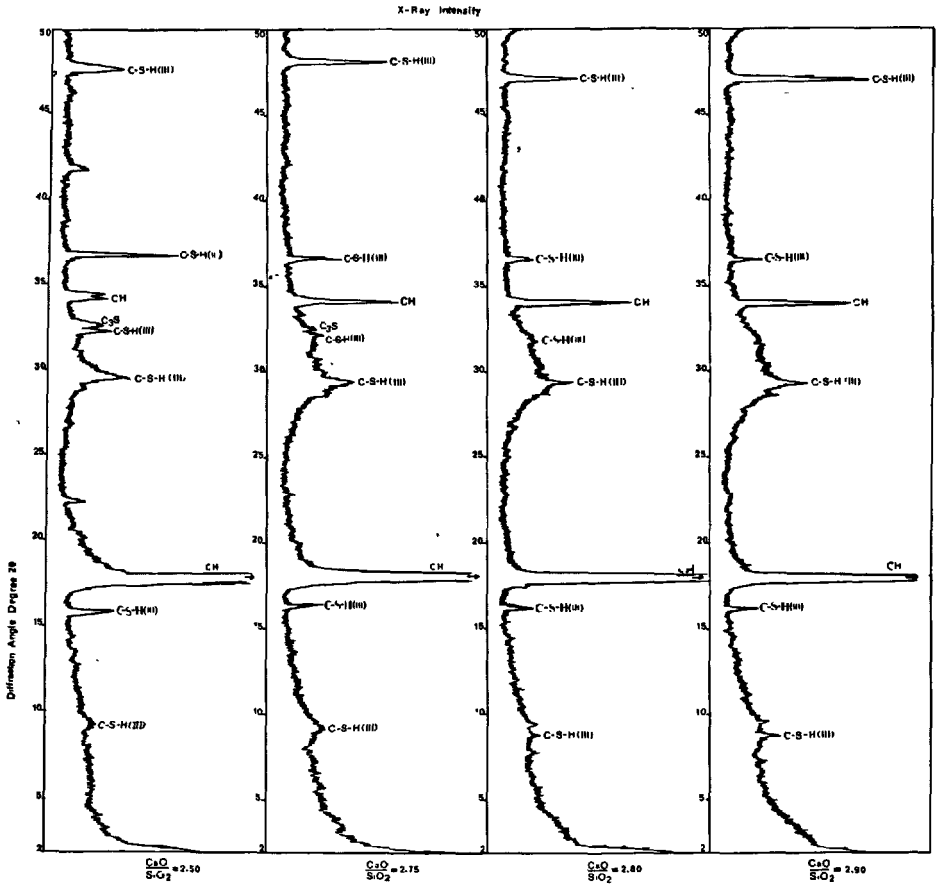

Fig.9. X-ray diffraction diagrams of C-S-H(III).

6.- S. BRUNAUER, (1966), Proceeding 8th Conference Silicates Industry, Budapest.

7.- L.E. COPELAND AND D.L. KANTRO, (1968), 5th International Symposium Chemistry of Cement Tokyo, 11, p. 387.

8.- H.F.W.TAYLOR, (1950), "Hydrated Calcium Silicate I, Compound Formation at Ordinary Temperature", Journal Chemical Society, pp. 3682-3690.

9.- H.F.W. TAYLOR, (1968), 5th International Symposium Chemistry of Cement, Tokyo, 11, p. 1.

10.- L.E. COPELAND AND P. G. SHULK, (1962), Journal Research Development Laboratory Portland Cement, Ass., 4, p. 2.

11.- S. DIAMOND, (1976), "C/S Mole Ratio of C-S-H Gel in a Nature C_3S Paste As Determined by EDXA", Cement and Concrete Research Journal Vol. 6, pp. 413-416, Printed in the United States.

12.- M.W. GRUTZECK AND D.M. ROY, (1969), Nature 223, p. 492.

13.- P.W. LOCHER, (1966), Special Report 90, Highway Research Budapest, Washington D.C., 300.

14.- D.L. KANTRO, C.H. WEISE AND S. BRUNAUER, (1966), Special Report 90, highway Research Budapest, Washington, D.C. 309.

15.- F.M. LEA, (1970), "The Chemistry of Cement and Concrete", Edward Arnold, London St. Martin's Press Inc., New York.

16.- F. HANNWAYYA, (1978), "Study of the Structure and Crystallization Properties of β-dicalcium Silicate (β-C_2S) Hydrate", Materials Science and Engineering, 34, pp. 183-197. Elsevier Sequoia S.A. Lausanne, Printed in the Netherlands. Or Department of Chemical Technology, the Royal Institute of Technology (Kungliga Tekniska Högskolan), S-100 44 Stockholm, Sweden.

17.- H.F.W. TAYLOR, (1951), "Hydrated Calcium Silicate II, Compound Formation at Ordinary Temp." J. Chem. Soc. p. 2397.

18.- W.M. SHOW AND W.H. MACINTIRE, (1930), Soil Science, 29, p. 429.

19.- J.R. BAYLIS, (1928), J. Phys. Chem. 72, p. 1936.

20.- G.E. BESSEY, (1938), Proceeding Symposium Chemistry of Cement, Stockholm, Sweden. Discussion, p. 189.

The effects of several heavy metal oxides on the hydration and the microstructure of hardened mortar of C_3S

Effets de quelques oxydes de métaux lourds sur l'hydratation du C_3S et sur la structure fine des corps durcis

C. TASHIRO, Asst. Professor, Yamaguchi University, Faculty of Engineering, Ube, Japan.

RESUME : Les effets de quelques oxydes ou hydroxydes de métaux lourds sur l'hydratation du C_3S sont déjà bien connus. Cr_2O_3, Fe_2O_3, NiO, $Cu(OH)_2$, ZnO, ou PbO ont été employés comme additifs au C_3S afin d'étudier l'effet produit sur l'hydratation de ce dernier, et le comportement des corps durcis, la structure fine, la résistance à la compression, le taux d'hydratation et la quantité de chaleur dégagée au premier stade d'hydratation.

Cr_2O_3, Fe_2O_3, NiO, $Cu(OH)_2$, ZnO et PbO produisent des effets sur le degré d'hydratation du C_3S, les caractères des hydrates, la structure fine, ainsi que la résistance à la compression, $Cu(OH)_2$, ZnO, et PbO retardent le premier stade d'hydratation et y exercent des effets particulièrement remarquables.

SUMMARY: The effects of heavy metal oxides or hydroxides on the hydration of C_3S have not been clarified. In the present study, Cr_2O_3, Fe_2O_3, NiO, $Cu(OH)_2$, ZnO or PbO was added as an additive, and the effects of such compounds on the hydration of C_3S were examined on the hardened hydrates and their microstructure, compressive strength, degree of hydration reaction and heat liberation in early hydration.

Cr_2O_3, Fe_2O_3, NiO, $Cu(OH)_2$, ZnO and PbO affect the degree of hydration of C_3S, properties of hydrates and microstructure and compressive strength of hardened mortars. $Cu(OH)_2$, ZnO and PbO retard the early hydration of C_3S, produce particularly pronounced effects.

INTRODUCTION

A study was conducted on the hydration of C_3S and the effects of addition of Cr_2O_3, Fe_2O_3, NiO, $Cu(OH)_2$, ZnO or PbO on the fine structure of the hardened C_3S mortar as part of a series of studies on the effects of heavy metal oxides on the hydration of cement, characterization of hydrated and properties of hardened hydrates(1-3).

The hydration of C_3S was investigated by measuring the heat of early hydration, ignition loss and compressive strength while the fine structure was examined by observation under a scanning electron microscope and determinations of powder x-ray analysis and pore size distribution.

EXPERIMENTAL

The experimental C_3S was synthesized from reagents at 1,500°C and was found to have a specific surface area (Blaine method) of 2,700 + 200 cm^2/g. The mortar was prepared by mixing C_3S and Toyoura standard sand at a ratio of 1 : 2 with Water/C_3S = 0.65. The additive such as Cr_2O_3, Fe_2O_3, NiO, $Cu(OH)_2$, ZnO and PbO is a reagent grade material and is added to 5 mol% of the total inclusive of such additive.

Removal of the mortar from the mold is undertaken one day after mixing in principle and curing was carried out in moist air. The test specimen has a dimension of 1X1X4 cm. The compressive strength reported here is the average of two speciments. The ignition loss was computed from the loss in weight produced by heating the specimen at 1,000°C for one hour.

EXPERIMENTAL RESULTS AND DISCUSSION

Compressive strength

The compressive strength is shown in Fig.1. Development of strength in the early period is strongly hindered by $Cu(OH)_2$, ZnO and PbO. In particular, the hindering effect of $Cu(OH)_2$ is very pronounced not only in the early period but also at an age of 28 days. On the other hand, Cr_2O_3, Fe_2O_3 and NiO exert no significant influence or slightly promote development of the strength at an age of 3 days.

Ignition loss

The ignition loss of the mortar is presented in Fig.2. It seems that $Cu(OH)_2$, ZnO and PbO yield smaller ignition losses. In particular, $Cu(OH)_2$ reduces the ignition loss to about 1/4 of the value obtainable without addition of $Cu(OH)_2$ at an age of 28 days. On the other hand, Cr_2O_3, Fe_2O_3 and NiO exert a small influence.

Heat liberation in early period

The results of differential calorimetric analysis between C_3S without and with heavy metal oxides are shown in Fig.3. The acceleration of heat liberation shows the acceleration of hydration reaction, heat of adsorption or heat of formation of an complex and all, which occurred by additives.

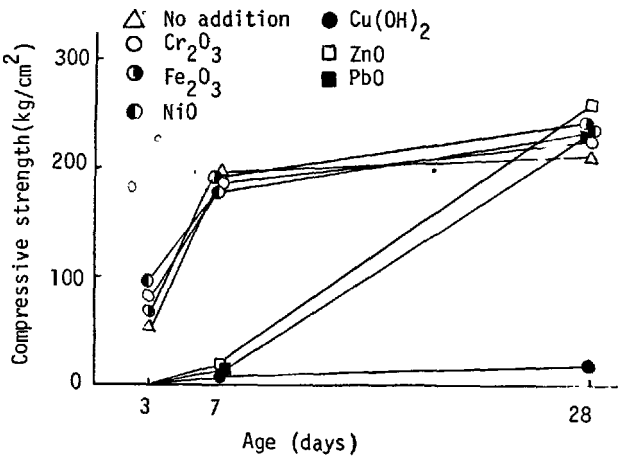

Fig.1 - Compressive strngth of C_3S mortars without and with heavy metal oxides or hydroxide.

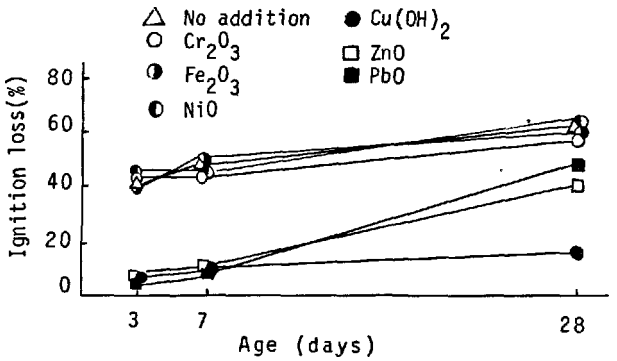

Fig.2 - Ignition loss of C_3S mortars without and with heavy metal oxides or hydroxide.

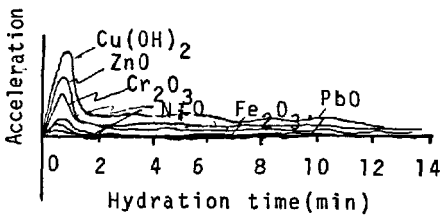

Fig.3 - Differential calorimetric analysis of C_3S without and with heavy metal oxides or hydroxide.

Powder x-ray analysis

The powder x-ray diffraction patterns are shown in Fig.4. As is apparent from figures, $Ca(OH)_2$ in hydrate in C_3S adding $Cu(OH)_2$ is negligible. And that in C_3S adding ZnO or PbO is a slight amount.

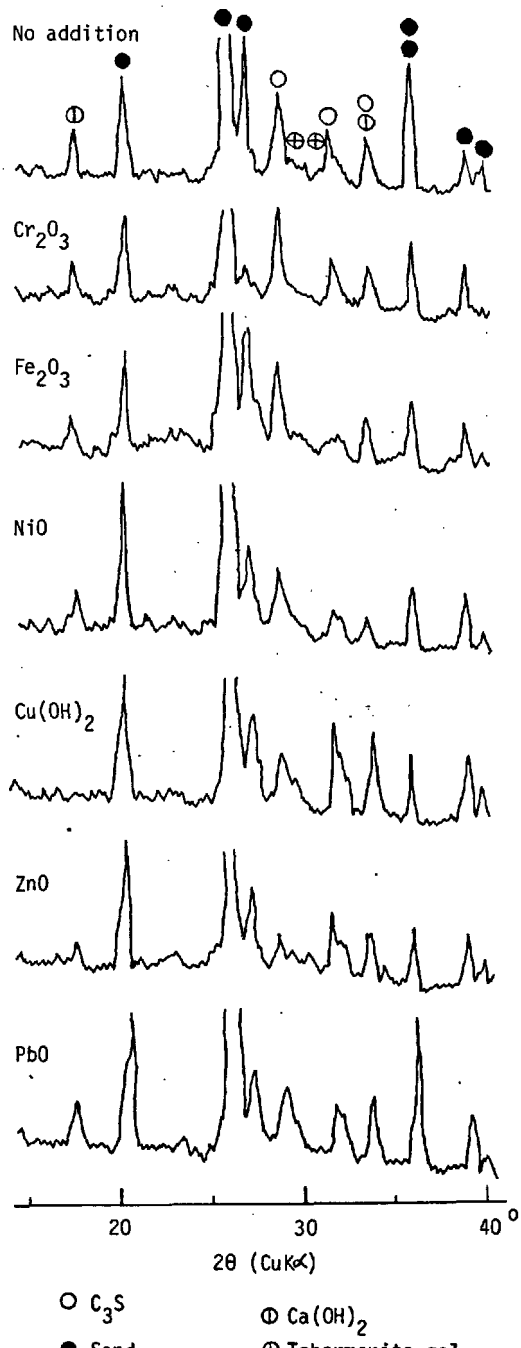

Fig.4 - X-ray powder diffraction patterns of C_3S mortars with addition of 5mol% heavy metal oxides.

Observation under scanning electron Microscope

The scanning electron micrographs are shown in Fig.5 and 6. At an age of 3 days, $Cu(OH)_2$, ZnO and PbO distinctly produce a retarding effect on the hydration. At an age of 28 days, there are observed retardation of the hydration by $Cu(OH)_2$ and some effects of ZnO and PbO on formation of hydrates. Powder x-ray diffractometry indicated that the hydrates are tobermorite in gel and slaked lime. On the other hand, Cr_2O_3, Fe_2O_3 and NiO did not produce any significant effect.

Pore size distribution

The pore size distribution of a 28-day old specimen is shown in Fig. 7. The additives produced changes in pore size distribution and $Cu(OH)_2$ increases the total pore volume and ZnO in particular increased the number of pores greater than 27,000 Å.

Hydration and Microstructure

As is apparent from above figures, the additives can be divided into three groups with respect to their characteristic effects on the relation among compressive strength, ignition loss, heat liberation, X-ray analysis and observation under scanning electron microscope : (a) no additive, Cr_2O_3, Fe_2O_3 and NiO; (b) ZnO and PbO; and (c) $Cu(OH)_2$. The group of ZnO and PbO yields a smaller ignition loss but develops a roughly equal strength compared with the group of no additive, Cr_2O_3, Fe_2O_3 and NiO at 28-day specimen.

On the other hand, the presence of a correlation betweem hydration and pore size distribution is not clearly demonstrated. It is generally stated that reduction of the total pore volume and shift of pore size distribution towards smaller pore are connected with an increases in hydration or strength (4). However, as is apparent from Fig.1 and 7, considerable differences exist in pore size distribution and pore volume for a given strength. This suggests that the additives affect the hydrates not only in structure but also in compositions.

The mechanism of this hindering effect on the strength or retardation of hydration is not clear, but it is thought that surface of C_3S grain is coated by metal ion or complex; invasion of water to inner parts is hindered. The coating action may be correlated to ionic potential of metal ions. Namely, ionic potential of Ca^{2+} is 0.50, Cr^{3+}: 0.23, Fe^{3+}: 0.21 , Ni^{2+}:0.34, and Zn^{2+}:0.37, Cu^{2+}: 0.36, Pb^{2+}: 0.62, consequently, metal ions of ionic potential similar to Ca^{2+} give the hindering effect.

When added $Cu(OH)_2$, concentration of CaO in bottle hydration is larger than that of no addition in early hydration. It shows the acceleration of hydration as illustrated by Fig 3 And Cu^{2+} is no detectable amount

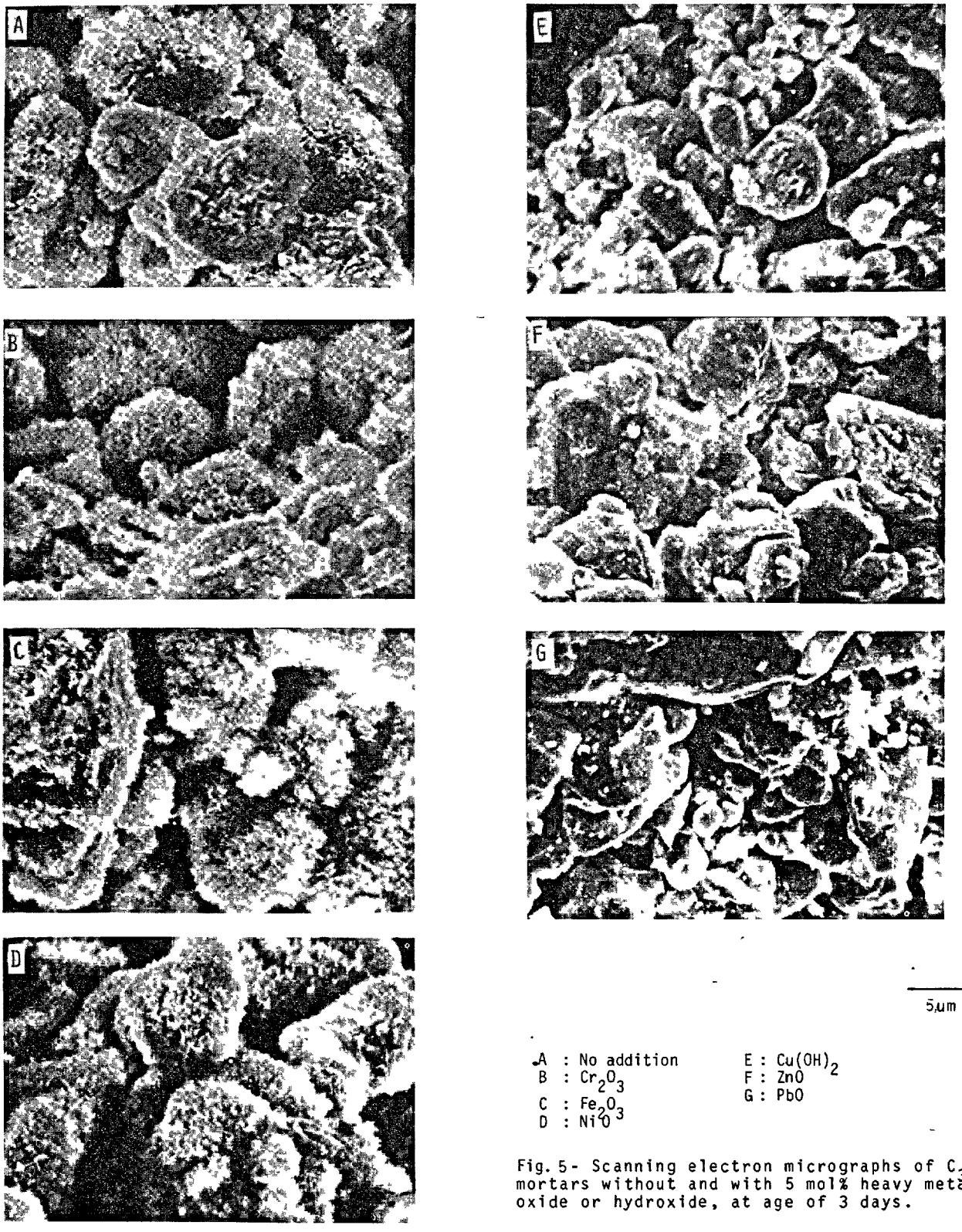

A : No addition
B : Cr_2O_3
C : Fe_2O_3
D : NiO
E : $Cu(OH)_2$
F : ZnO
G : PbO

Fig. 5- Scanning electron micrographs of C_3S mortars without and with 5 mol% heavy metal oxide or hydroxide, at age of 3 days.

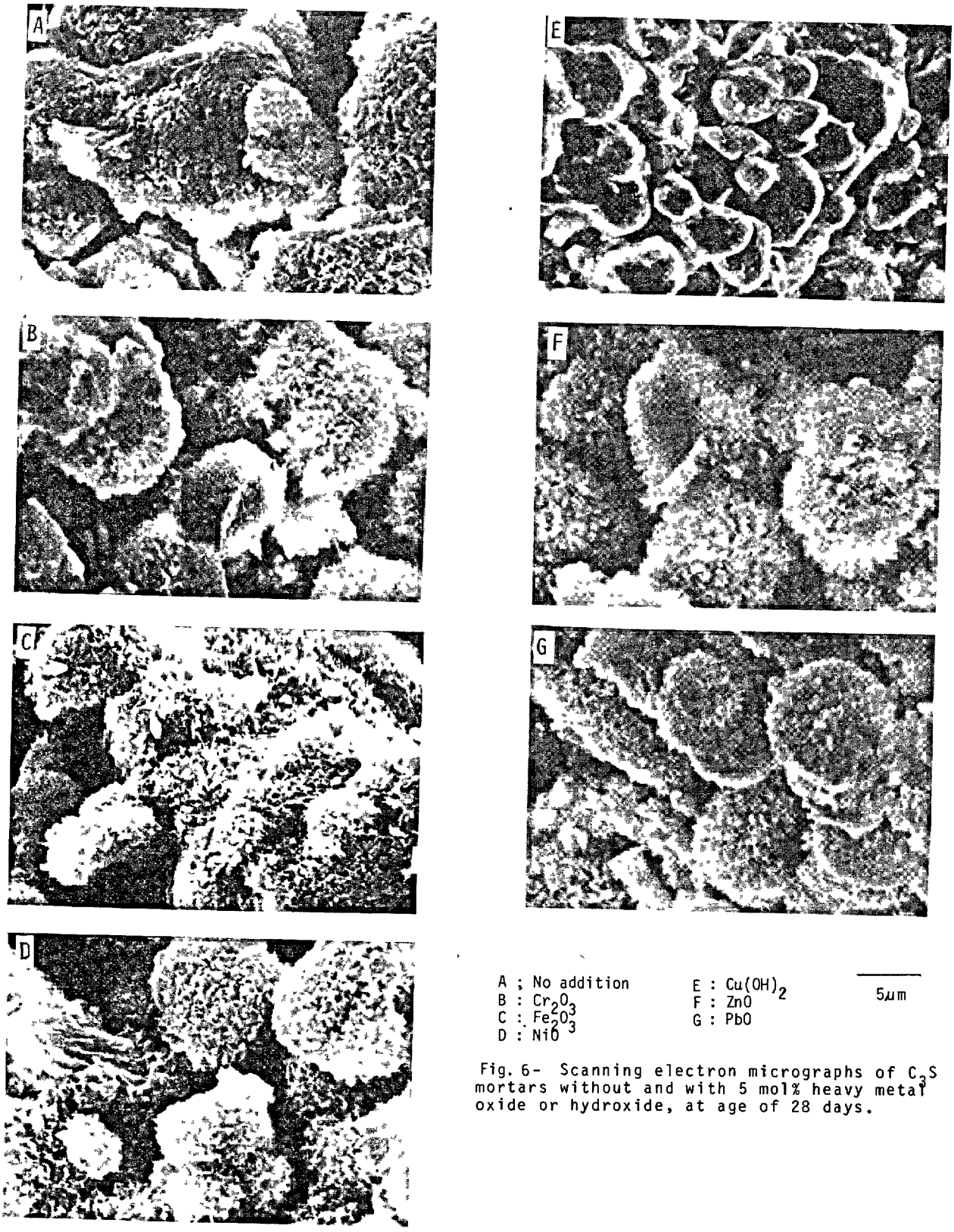

Fig. 6- Scanning electron micrographs of C_3S mortars without and with 5 mol% heavy metal oxide or hydroxide, at age of 28 days.

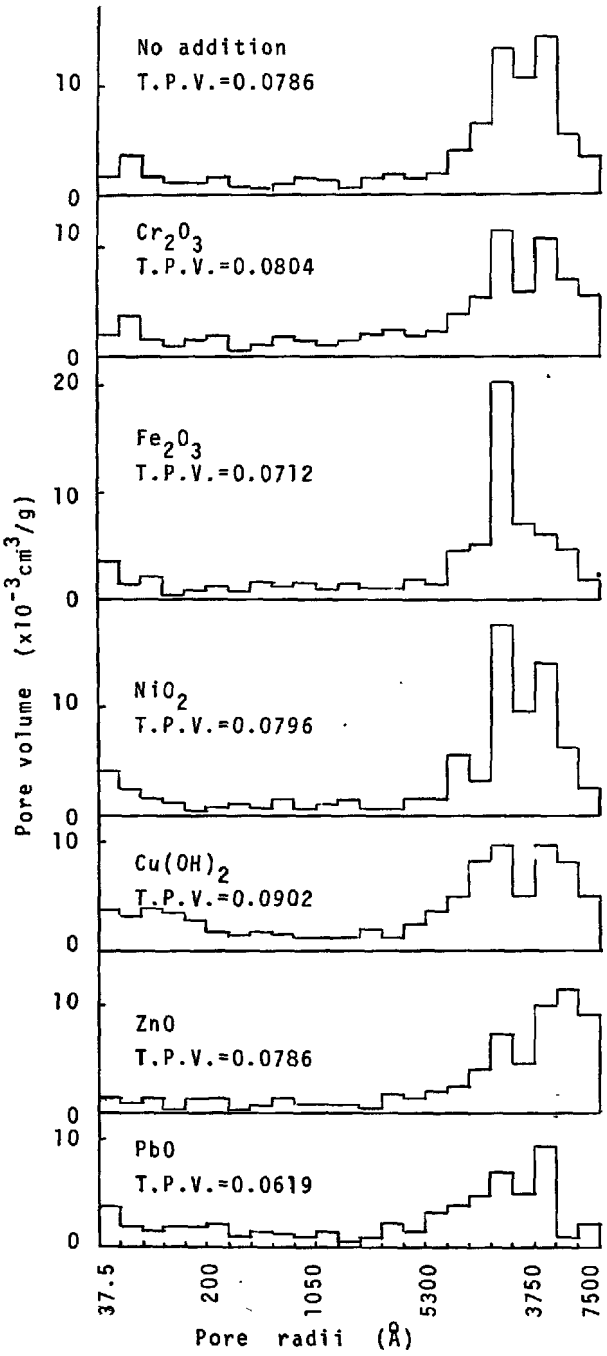

Fig.7- Pore size distribution of 28 days mortars without and with additives.

CONCLUSION

Cr_2O_3, Fe_2O_3, NiO $Cu(OH)_2$, ZnO and PbO affect the degree of hydration of C_3S, properties of the hydrates and the compressive strength and fine structure of the hardened hydrates and $Cu(OH)_2$, ZnO and PbO produce particularly pronounced effects.

The mechanism of this effects is not clear, but it seems due to similarity of ionic potential.

The author wishes to thank K. Okuni for help of experiment.

BIBLIOGRAPHIE

1.- C. Tashiro, H. Takahashi, et al.,(1979) "Hardening property of cement mortar adding heavy metal compound and solubility of heavy metal from hardened mortar", Cement and Concrete Research, 7,283-290.

2.- C. Tashiro and J. Oba,(1979) "The effects of Cr_2O_3, $Cu(OH)_2$, ZnO and PbO on the compressive strength and the hydrates of the hardened C_3A paste", Cement and Concrete Research,9, 253-258.

3.- C. Tashiro,J.Oba et al.,(1979)," The effects of several heavy metal oxides on the formation of ettringite and the microstructure of hardened ettringite", Cement and Concrete Research, 9, 303-308.

4.- E. Kamata(1977), "Experiments of compressive strength and pore distribution of concrete", Cement Gijutsu Nenpo,31, 256-259.

A thermoanalytical method for the determination of the amount of calcium hydroxide in systems containing hydrated Portland cement

Une méthode de l'analyse thermique pour la détermination quantitative de l'hydroxyde de calcium dans des systèmes contenant du ciment portland hydraté

F.G. BUTTLER, Dr., and S.R. MORGAN, Chemistry Department, Teesside Polytechnic, Middlesbrough, England.

RESUME : On décrit une méthode d'analyse pour la détermination quantitative de l'hydroxyde de calcium dans des systèmes contenant du ciment portland hydraté. Cette méthode utilise du dioxyde de carbone gazeux pour convertir l'hydroxyde de calcium en carbonate; celui-ci est décomposé ensuite à une température élevée. La quantité résultante de carbonate de calcium est proportionnelle à l'hydroxyde de calcium présent dans les échantillons, à condition que ceux-ci soient chauffés à 200°C avant d'être exposés au dioxyde de carbone gazeux. De cette façon on empêche la carbonatation des silicates et des aluminates hydratés de calcium. Il est possible d'employer cette méthode pour des échantillons de mortiers récemment prélevés, sans autre traitement avant l'analyse thermique. On donne une comparaison de cette méthode avec d'autres, actuellement utilisées pour la détermination de l'hydroxyde de calcium dans les ciments hydratés.

ABSTRACT: A method of analysis is described for the determination of the amount of calcium hydroxide present in systems containing hydrated Portland cement. The method involves the conversion of $Ca(OH)_2$ to $CaCO_3$ using gaseous CO_2, followed by the high temperature decomposition of the $CaCO_3$ formed. The amount of $CaCO_3$ formed is proportional to the amount of $Ca(OH)_2$ present in the samples provided that the samples are heated to 200°C before exposure to gaseous CO_2. In this way the carbonation of hydrated calcium silicates and aluminates is prevented. The method can be used on freshly drilled samples of mortars without any pre-treatment before thermal analysis. A comparison of the method with others available for estimating $Ca(OH)_2$ in hydrated cements is given.

INTRODUCTION

A number of methods involving the estimation of the amount of $Ca(OH)_2$ present have been used to study the reactions occurring between water and the compounds present in Portland cement. These methods include quantitative X-ray diffraction, thermal analysis and the extraction of the calcium hydroxide with solvents (1). Another method for studying these systems is that of trimethylsilylation. With this technique, information is obtained with respect to the silicates produced during hydration (2).

The methods used to estimate the amount of calcium hydroxide present tend to give widely differing results. Quantitative X-ray powder diffraction only measures the amount of crystalline material present, and amorphous $Ca(OH)_2$, will not be detected. Solvent extraction suffers from the disadvantage that the amount of $Ca(OH)_2$ removed is dependent on the time of extraction, and, in addition, calcium ions may also be removed from other compounds present. Thermogravimetry is usually carried out by monitoring the loss of water from the hydrated compounds with respect to temperature and time. The interpretation of results can be difficult due to the overlap of the step corresponding to the loss of water from calcium hydroxide with the steps due to loss of water from other hydrated compounds present. This is particularly true when the technique is applied to set Portland cements. Similar problems arise with differential thermal analysis and the measurement of areas of overlapping peaks. A comparison of results using these techniques on a sample of set Portland cement has already been made (3).

THEORY

The analytical method is based on the fact that, as it dehydroxylates, calcium hydroxide reacts rapidly with gaseous carbon dioxide to form calcium carbonate, and provided there is sufficient time of exposure of the calcium hydroxide to the carbon dioxide, the reaction can be used quantitatively. The amount of calcium hydroxide originally present can then be determined by using the high temperature decomposition of the calcium carbonate formed. Provided the bulk of the water present in the samples is removed at low temperatures and before they are exposed to carbon dioxide, it is thought that there is little or no carbonation of other compounds arising from the hydration of Portland cement. This procedure overcomes the problem associated with the concurrent loss of water from hydrated calcium silicates and aluminates and from the calcium hydroxide, since all the water has been removed at lower temperatures than that observed for the decomposition of calcium carbonate.

EXPERIMENTAL

Because the calcium hydroxide generally contained some calcium carbonate most experiments started with calcium oxide prepared by ignition of 'Analar' calcium carbonate. Suitable portions of the calcium oxide and finely divided quartz were weighed into the crucibles to be used for the thermal analysis and the calcium oxide converted into calcium hydroxide by adding slightly more than the required amount of carbon dioxide free distilled water immediately before analysis.

A series of mortars were prepared as 5.0 cm cubes and stored at 20°C. These mortars ranged from 1:3 mixtures of Portland cement:British standard sand with a water:cement ratio of 0.45 to similar mixtures in which up to 60% of the cement was replaced by fly ash, the water content of the mortars remaining the same. The samples for analysis were prepared by drilling, and were analysed without any further treatment.

The TG experiments were carried out using Stanton Automatic thermo-recording balances, models HT5 and TR1. The samples were contained in conical fused alumina crucibles and the weight changes determined with dynamic atmospheres of nitrogen and mixtures of nitrogen and carbon dioxide with flow rates of 100 cm^3/min over the samples. Various heating rates and sample and crucible sizes were used (see Table 1).

RESULTS

Fig. 1 shows the results obtained when a laboratory sample of $Ca(OH)_2$ containing 10.2% $CaCO_3$ was heated in atmospheres of nitrogen and in a mixture of 80% nitrogen and 20% carbon dioxide. After the initial loss of free water, the loss between 350 and 550°C in nitrogen corresponded to the loss of water from the $Ca(OH)_2$ and the final loss to the decomposition of the $CaCO_3$ present in the sample. In the nitrogen/carbon dioxide atmosphere there was little carbonation below 300°C but the reaction became rapid as the water was lost from the $Ca(OH)_2$. The final step in an atmosphere of nitrogen and carbon dioxide was due to the decomposition of the $CaCO_3$ formed from the $Ca(OH)_2$ and to the $CaCO_3$ originally present. The higher temperature of decomposition was a consequence of the presence of carbon dioxide in the gas stream. Calculation from these results showed that 93% of the $Ca(OH)_2$ had been converted into $CaCO_3$.

The results obtained from the carbonation of the $Ca(OH)_2$ produced from CaO are shown in Table 1. These were obtained by heating the samples in nitrogen with a flow rate of 100 cm^3/min, and then holding the temperature at 200°C until the evolution of water was negligible. The temperature of the samples was then raised again at the recorded heating rates but the atmosphere was changed to 80% nitrogen and 20% carbon dioxide. At about 700°C, after the carbonation reactions were complete, the purging gas was changed again to nitrogen in order to allow the $CaCO_3$ formed to decompose easily. Changes in the poise of the balances due to changes in the purging gas were found to be very small. The shapes of the TG curves obtained were very similar to that shown in Fig. 1 except that they had an additional loss due to the free water present.

Finely divided quartz of about 75μ diameter was used as diluent for the CaO, and therefore of the $Ca(OH)_2$, in order to represent the drilled aggregate from mortar and concretes.

The results show that, using a variety of heating rates, sample and crucible sizes, and differing concentrations of $Ca(OH)_2$ in the samples, over 90% of the $Ca(OH)_2$ present was converted into $CaCO_3$. A heating rate of 3°C/min was selected in order [3]that the exposure time of the $Ca(OH)_2$ to carbon dioxide should be as long as possible within a normal working day.

The results obtained using the Portland cement:sand mortars are shown in Fig.2. The samples were prepared by drilling holes to the centre of the cubes and were analysed immediately without any further treatment. The thermo-analytical conditions were the same as those described above. Fly ash was used as a replacement for some of the Portland cement in the mortars since it was known that over short periods of time at 20°C there was no noticeable reaction between the calcium hydroxide formed on hydration of the cement with this particular fly ash (4). There was an additional advantage in that the particle size distribution of the fly ash was similar to that of the cement which it was replacing.

All of the results shown in Fig.2 were obtained on 11 day old mortars and have been corrected for the loss on ignition arising from the fly ash. They show that the amount of $Ca(OH)_2$ found was directly proportional to the Portland cement content of the mortars, and that the carbonation method is suitable for monitoring such systems.

DISCUSSIONS AND CONCLUSIONS

Although the results using pure $Ca(OH)_2$ have not shown 100% carbonation, no attempt has been made to multiply the amount of $Ca(OH)_2$ found in hydrated Portland cements by an appropriate factor. It is felt that the particle size distribution and surface area of the $Ca(OH)_2$ present in hydrated cements is likely to be different, and probably much smaller, than that produced in the experiments starting with CaO. It is therefore probable that the percentage carbonation of the $Ca(OH)_2$ in hydrated cements will be greater. However, even if this should be proved to be not so, the method offers a way of estimating more than 90% of the $Ca(OH)_2$ present, and, moreover, one in which a mass change is involved and one where no pre-treatment of the samples is necessary. The method should be compared with the others that are available, with their inherent difficulties, as described in the introduction. Estimation, by the ethylene glycol extraction method, of the amount of $Ca(OH)_2$ present in the mortar samples always gave variable results which were much higher than those obtained by this carbonation method as soon as the extraction time exceeded one hour.

It should be noted that this method relies on the unreactivity of hydrated calcium silicates and aluminates to gaseous carbon dioxide under the experimental conditions used. It was found during the development of the method that the results with freshly drilled pastes and mortars were not as reliable if the carbon dioxide were added before most of the water was removed. The results using the technique described imply that the amount of reaction of the hydrated calcium silicates and aluminates is very small. Further work on this aspect is in progress. However, whatever is the outcome of these experiments, the carbonation method gives a ready way of following the changes that occur in systems containing hydrated Portland cement over periods of time and temperature (4).

REFERENCES

1.- F.M. LEA (1970), "The chemistry of cement and concrete", Edward Arnold, London, p.108-111.

2.- E.E. LACHOWSKI, (1979), Cement concr., Res. 9, 111.

3.- H.G. MIDGLEY, (1979), Cement Concr., Res. 9, 77.

4.- F.G. BUTTLER and P.L. OWENS, in press.

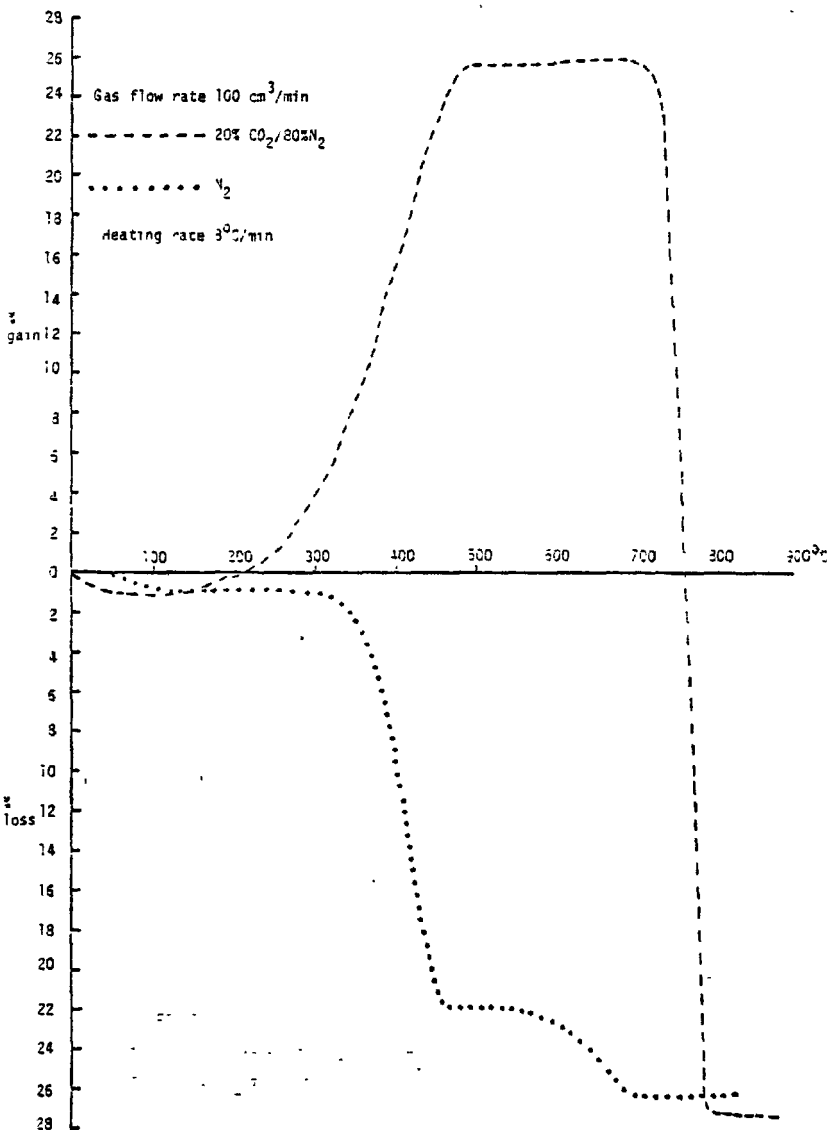

Fig. 1 - The decomposition of $Ca(OH)_2$ in N_2 and in CO_2/N_2 atmospheres

TABLE 1

Results obtained from the carbonation of $Ca(OH)_2$

Heating rate °C/min	Crucible	Wt. of CaO,g	Wt. of SiO_2,g	Wt. of H_2O,g	Wt. of $Ca(OH)_2$ calculated from wt. of CaO g	Final loss g	Wt. of $Ca(OH)_2$ calculated from final loss g	% carbonation of $Ca(OH)_2$
1.25	A	0.4378		0.3371	0.5785	0.327	0.5505	95.2
1.25	B	0.0869	0.0996	0.1176	0.1148	0.0632	0.1064	92.7
3	A	0.4241	0.4380	0.5592	0.5604	0.314	0.5287	94.3
3	B	0.0781	0.1533	0.1153	0.1032	0.0557	0.0938	90.9
3	A	0.3843	1.1760	0.5181	0.5078	0.277	0.4664	91.8
3	B	0.0788	0.4937	0.2901	0.1041	0.0583	0.0982	94.3
4.5	A	0.3988	0.4434	0.4297	0.5270	0.279	0.4697	89.1

Internal dimensions	Crucible Type A	Crucible Type B
height	23 mm	18 mm
diameter of base	14 mm	10 mm
diameter of top	19 mm	14 mm

FIG. 2. $Ca(OH)_2$ present in cement:sand mortars after 11 days at 20°C

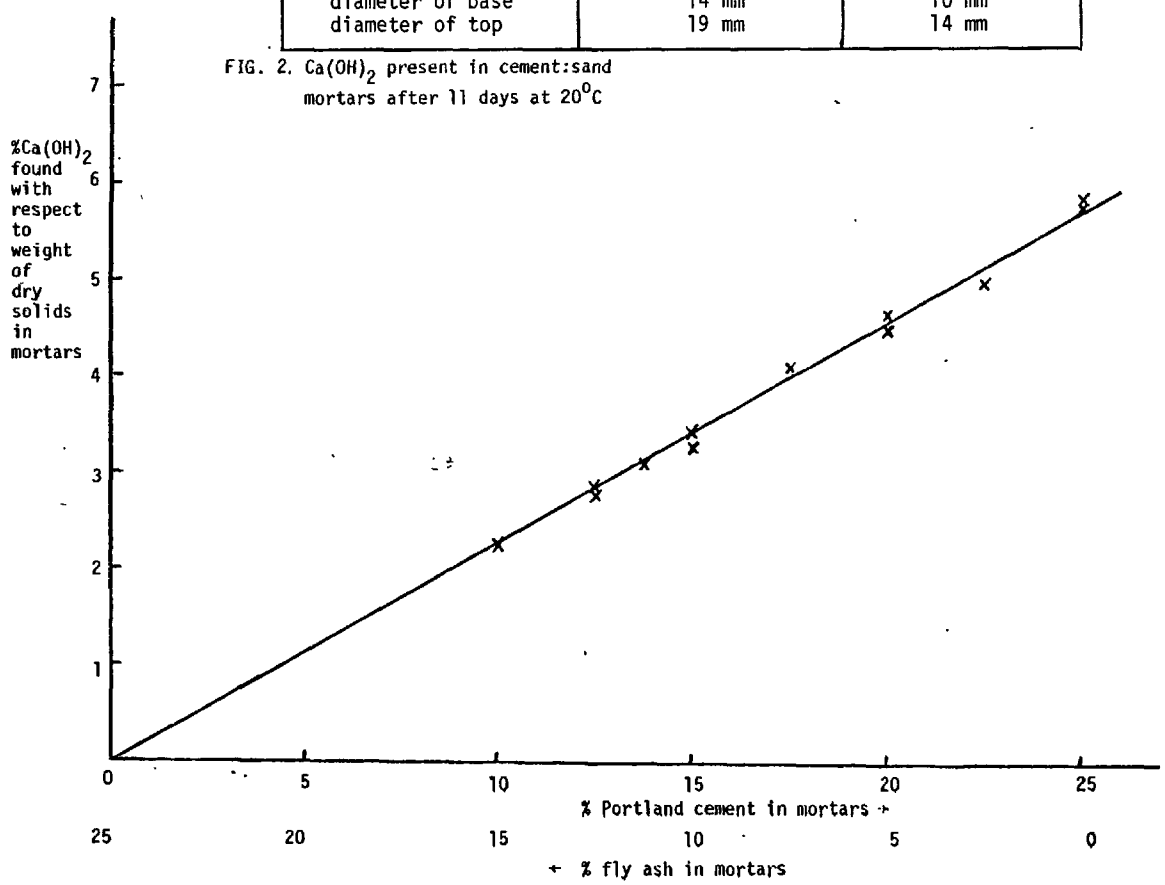

Hydration and strength of α-, α'- and β- dicalcium silicates stabilized with Na-Al, K-Al, Na-Fe and K-Fe

Hydratation et résistance de α-, α'- et β- dicalcium silicates stabilisés par Na-Al, K-Al, Na-Fe et K-Fe

Kazutaka SUZUKI, Dr. Professor, Department of Inorganic Materials, Nagoya Institute of Technology, Suketoshi Ito, Sumio Shibata and Namitsugu Fugii, Japon.

RESUME : L'étude a porté sur l'hydratation et la résistance à la compression des diverses formes cristallines du C_2S, stabilisées à l'aide de Na et Al(Na-Al), K et Al(K-Al), Na et Fe (Na-Fe) et K et Fe (K-Fe).

Dans les séries comportant la substitution Na-Fe et K-Fe, les phases α et β cristallisent séparément, mais la phase α' est accompagnée de la phaseα . Dans les séries comportant la substitution Na-Al et K-Al, seules les phases α' et β se sont formées.

Généralement lors de l'hydratation de ces phases polymorphiques, de petites quantités de $Ca(OH)_2$ se forment en même temps que des feuillets de silicate monocalcique hydraté (C-S-H). Dans les phases comportant la substitution alcali-Al, il se forme beaucoup moins de $Ca(OH)_2$ et de C-S-H.

La résistance des mortiers préparés avec les phases comportant la substitution K-Fe est supérieure à celle comportant la substitution Na-Fe. La phase α stabilisée avec K-Fe a une résistance notablement plus grande que celle des phases α' etβ et qui s'approche de celle des ciments portland.

Dans les séries comportant la substitution alcali-Al, on n'a pas obtenu de résistances très élevées. On a mesuré les variations en fonction du degré d'hydratation, de la résistance à la compression de la phase α cuite à 1360, 1440 et 1520°C. Les points sont pratiquement alignés sur une même droite, ce qui montre que ces phases ont le même processus d'hydratation. Cependant, les points correspondant à la phase α avec substitution K-Fe, et cuits à 1360 et 1440°C, et ceux correspondant à la substitution Na-Fe cuite à 1360°C sont situés hors de cette ligne. Ceci montre que l'hydratation de ces produits suit un processus différent.

Lors du frittage à 1360 ou 1440°C, le matériau intersticiel qui se forme autour des cristaux de C_2S est instable. Les ions Ca^{2+} et les ions alcalins, de cette phase, se dissolvent rapidement dans l'eau et donnent une haute résistance dès le début de l'hydratation.

SUMMARY : The hydration of dicalcium silicate polymorphs stabilized with Na and Al (Na-Al), K and Al (K-Al), Na and Fe (Na-Fe), K and Fe (K-Fe), and their compressive strength were investigated.
In the Na-Fe, K-Fe substituted series, the α and β phases were crystallized as a single phase but α'-phase accompanied α-phase. In the Na-Al, K-Al substituted series, only α' and β-phase were formed.
Generally in the hydration of these polymorphs, small amounts of $Ca(OH)_2$ were formed, together with foil like calcium silicate hydrate (C-S-H). In the alkali-Al substituted modifications, far less of $Ca(OH)_2$ and C-S-H were formed.
The strengths of mortars prepared with the K-Fe substituted phases surpassed those of the corresponding Na-Fe substituted phases. The α-phase stabilized with K-Fe exhibited compressive strength markedly higher than those of α' and β-phases and approached those of portland cement mortars. In the alkali-Al substituted series the effective compressive strength was not expected.
Compressive strengths versus hydration ratios were plotted in a figure for the α-phase burned at 1360, 1440 and 1520 °C. Almost the all of the plotted points formed a straight line and this showed that these phases had the same hydraulic process. But the plots of K-Fe substituted α-phase burned at 1360 and 1440 °C and of Na-Fe substituted α-phase burned at 1360 °C stood off this line. This shows that these phases hydrate with different process. In the sintering process at 1360 °C or 1440 °C, the interstitial material was formed in unstable around the C_2S crystal. Ca^{2+} or alkali ion dissolved in water quickly from this phase and gave high strength in the early hydration time.

INTRODUCTION

Dicalcium silicate (C_2S) hydrates via the same mechanism as Ca_3SiO_5. However, it is thought that the higher temperature polymorphs exhibit greater hydraulicity than the lower temperature polymorphs because their free energies are larger. The influence of polymorphs on hydraulic activity and strength has been discussed in several papers. Boikova et al. (1) investigated the effect of P_2O_5; α'-C_2S containing 14 % $3CaO \cdot P_2O_5$ was found to have greater hydraulicity than β-C_2S. Gutt and Osborn (2), who studied the strength of α'- and β-C_2S stabilized with K_2O, found that the strength of α'-C_2S containing 3.6% K_2O surpassed that of β-C_2S containing 2.1% K_2O. Bikbau (3) investigated the hydraulicity and strength of α-, α'- and β-C_2S in which Ba was substituted for Ca; the α-phase exhibited the greatest compressive strength. Jelenic et al. (4) reported that the degree of hydration and compressive strength of B_2O_3-substituted α'-C_2S were greater than those of β-C_2S when alit was contained. In these studies however, the additional stabilizer was limited to only one component. The authors studied the hydration and compressive strength of cements composed of α-, α'- and β-C_2S stabilized with Na and Fe (Na-Fe), K and Fe (K-Fe), Na-Al (Na-Al), K and Al (K-Al).

EXPERIMENTAL PROCEDURE

Assuming that Na or K is substituted for Ca, and Fe or Al for Si, the crystal chemical substitution of each atom was carried out, and the ratio of Ca + Na or K : Si + Fe or Al was always fixed to 2:1.

The mixtures were prepared from crushed quartz (99.9%), $CaCO_3$ (99.9%) and the additives (Na_2CO_3, K_2CO_3, Al_2O_3 and Fe_2O_3), and pressed into small cylinders (20mm diameter × 20mm height), burned at 1360, 1440 and 1520°C for 30 min. in a SiC furnace and quenched in air. The clinkers were crushed and powdered to a fineness and other compounds were examined by X-ray diffraction.

One part was used to make pastes having a water cement ratio of 0.36, another was mixed with silica sand to make 1:2 mortars, kneaded with water and shaped into rectangles 2×2×8 cm in size. The quantity of added water to mortars necessary to have identical flow was decided by a improved way that followed the standard method using Vicat Tester. In this way the water cement ratio was fixed between 0.62 and 0.65. The compressive strengths were measured at suitable intervals of curing. Each ten pieces of mortar were tested and averaged their data. Simultaneously the hydration products of pastes and their microstructural characteristics were also examined by X-ray diffraction and scanning electron microscopy. The dispersion of additives into interstitial material or C_2S crystals was examined by X-ray micro analysis.

To investigate the hydration process of the C_2S polymorphs, the mixtures of each phase with 10% of quartz were blended, and moulded into 2×2×8 cm with water cement ratio of 0.36. These test pieces were cured for one day at 90% relative humidity and thereafter in water at 20°C. The quantitative X-ray diffraction was tested at the ages of 7, 14 and 28 days. The degree of hydration was determined by applying

$$\frac{I_t / I_{qt}}{I_0 / I_{qo}} = 1 - \alpha_t$$

I_0, I_t Intensity of analytical diffraction of C_2S in the original and after hydration time t. The diffraction 400, 130 and 110 lines were used for α-, α'- and β-phase respectively.

I_{qo}, I_{qt} Intensity of 101 diffraction of quartz in the original and after hydration time t.

α_t Degree of hydration of C_2S at hydration time t.

RESULTS

Synthesized Products The ranges where each polymorph is stable are shown in Fig. 1. In the Na-Fe, K-Fe substituted series, the α-phase was easily crystallized as a single phase in an extensive substituted amount of Na or K and Fe by quenching from above 1360 °C. The α'-phase was formed at above 1440°C, always accompanied by α-phase. The β-phase was formed in smaller substitution range at above 1440°C, and in the composition in which Na or K was substituted above 0.13 mole, $K_2O \cdot 23CaO \cdot 12SiO_2$ or $Na_2O \cdot 3CaO \cdot 2SiO_2$ was crystallized, in the composition in which only Fe was substituted, γ-phase was formed and after that $CaFeO_4$ was formed with Fe increasing.

In Na-Al and K-Al substitution, the α-phase did not form in any burning temperature, but α'- and β-phase were crystallized at above 1440°C, accompanied by a small quantity of $3CaO \cdot Al_2O_3$. In Na-Al series, $Na_2O \cdot 8CaO \cdot 3Al_2O_3$ was formed in the composition where larger Na was contained.

The samples for the experiment were adopted from these ranges as shown in Table 1.

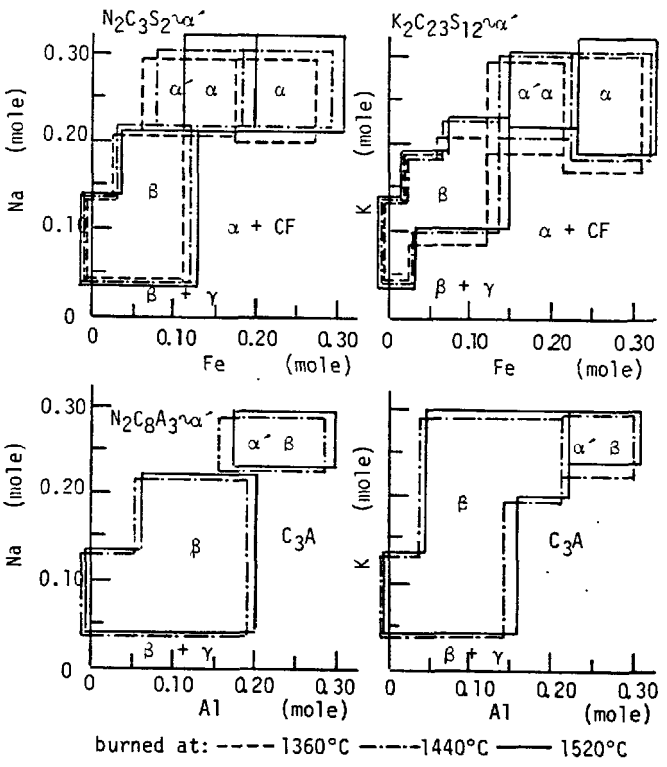

Fig. 1 - Substituted range of Na or K and Fe or Al to stabilize α-, α'- and β-phase. Symbol was used as follows:- $N_2C_3S_2$: $Na_2O \cdot 3CaO \cdot 2SiO_2$, $K_2C_{23}S_{12}$: $K_2O \cdot 23CaO \cdot 12SiO_2$, $N_2C_8A_3$: $Na_2O \cdot 8CaO \cdot 3Al_2O_3$, CF: $CaFeO_4$, and C_3A: $3CaO \cdot Al_2O_3$.

Table 1 - Compositions of mixtures

Sample designation	Composition	Phases formed	Heating temperature(°C)
Na-Fe-α	$Ca_{1.75}Na_{0.25}Si_{0.75}Fe_{0.25}O_4$	α	1520
		α	1440
		α	1360
Na-Fe-αα´	$Ca_{1.75}Na_{0.25}Si_{0.85}Fe_{0.15}O_4$	α, α´	1520
		α, α´	1440
Na-Fe-β	$Ca_{1.85}Na_{0.15}Si_{0.90}Fe_{0.10}O_4$	β	1520
		β	1440
K -Fe-α	$Ca_{1.75}K_{0.25}Si_{0.75}Fe_{0.25}O_4$	α	1520
		α	1440
		α	1360
K -Fe-αα´	$Ca_{1.75}K_{0.25}Si_{0.85}Fe_{0.15}O_4$	α, α´	1520
		α, α´	1440
K -Fe-β	$Ca_{1.85}K_{0.15}Si_{0.90}Fe_{0.10}O_4$	β	1520
		β	1440
Na-Al-α´β	$Ca_{1.75}Na_{0.25}Si_{0.75}Al_{0.25}O_4$	α´,β	1520
		α´,β	1440
Na-Al-β	$Ca_{1.85}Na_{0.15}Si_{0.85}Al_{0.15}O_4$	β	1520
		β	1440
K -Al-α´β	$Ca_{1.75}K_{0.25}Si_{0.75}Al_{0.25}O_4$	α´,β	1520
		α´,β	1440
K -Al-β	$Ca_{1.85}K_{0.15}Si_{0.85}Al_{0.15}O_4$	β	1520
		β	1440

Hydration Products Characteristically, early hydration of portland cement results in crystallization of fairly large amount of $Ca(OH)_2$, together with a small amount of calcium silicate hydrate (C-S-H). In the hydration of C_2S, however, only small amount of $Ca(OH)_2$ was formed. The hydration ratio was shown in Fig. 2.

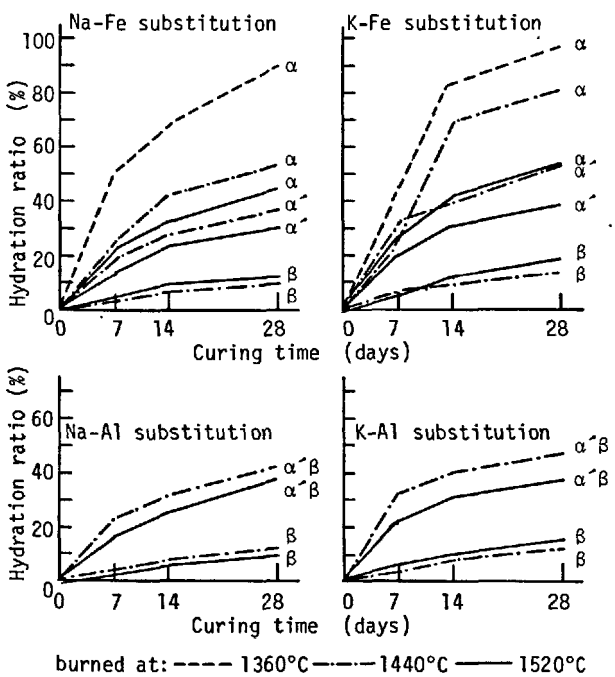

Fig. 2 - Change in hydration ratio of the polymorphs by their burning temperature.

In the Na-Fe and K-Fe substitution, the hydration ratio of α-phase was greatly changed by burning temperature, and the lower the burning temperature was, the more rapidly the hydration proceeded forming much $Ca(OH)_2$ and foil like C-S-H. The hydration ratios of Na-Al and K-Al substituted series, were generally low and far less amount of C-S-H was formed.

Compressive Strength The 1 : 2 mortars were prepared in accordance with the Japanese Industrial Standard, and their compressive strengths were tested. The results were shown in Fig. 3.

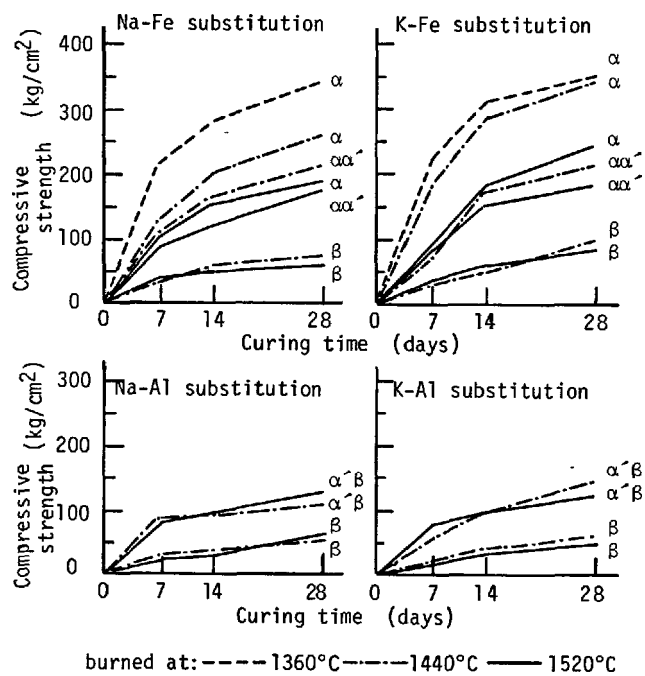

Fig. 3 - Changes in compressive strength of each phase with curing time.

The α-phase exhibited compressive strength markedly higher than those of α´ and β-phase. Also, the strength of it stabilized with K and Fe surpassed that of the corresponding Na-Fe substituted phase. The effects of burning temperature on the strength were clearly characterized as the better development of strength in the lower temperature burning. But the Na-Fe substituted phase burned at 1440 and 1520 °C showed especially slow hardening corresponding to the low strength development. In the Al substituted series, effective compressive strengths were not expected, as will be discussed later.

Compressive strengths versus hydration ratios were plotted for Na-Fe and K-Fe substituted α-phases as shown in Fig. 4. Two lines were formed with different inclinations. The α-phases burned at lower temperature exhibited a rapid development of early strength within 7 days, while the other α-phases showed a slow hardening and low strength in this period. Their different hydration ratios will probably be caused by their phase structure as will be discussed later.

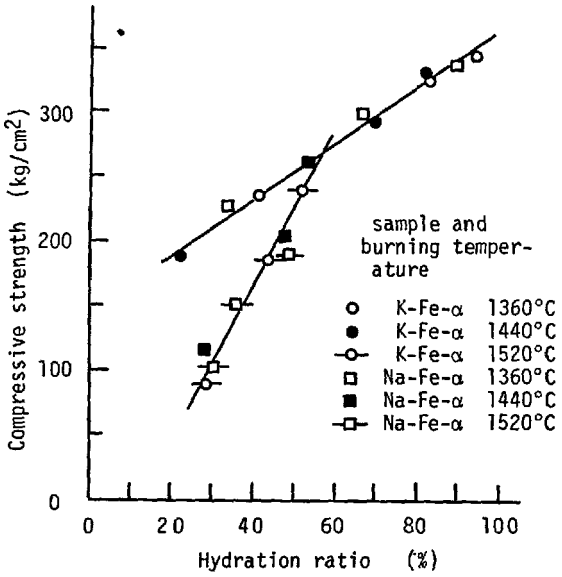

Fig. 4 - Compressive strengths versus hydration ratio for α-phases.

DISCUSSION

As was shown in Fig. 1, the α-phases were crystallized when about the same molecules of alkali and Fe were substituted for Ca and Si respectively. We could not get α′ as a single phase, it accompanied α when comparatively much of alkali was substituted. It is supposed that this phase has a continuous solubility with $K_2O \cdot 23CaO \cdot 12SiO_2$ or $Na_2O \cdot 3CaO \cdot 2SiO_2$, but we need more investigation hereafter. The β-phase crystallized at the range where far less quantity of alkali or Fe was contained and also where only alkali was substituted to Ca (∿0.13 mole). When only Fe or Al was substituted for Si in low quantity, β and γ-phase were formed. But in high quantity of Fe, α-phase and $CaFeO_4$ were produced, and in high quantity of Al, β-phase and $3CaO \cdot Al_2O_3$ were produced.

The components that composed C_2S crystal were quantitatively analyzed with the technique of X-ray micro analysis. Consequently each component was uniformly distributed in Na-Fe and K-Fe substituted series. Table III shows the results on the samples burned at 1360 °C.

Table III. - Compositions of each phase calculated from the analyzed data by X-ray micro analysis. The oxygen was added assuming (Ca, Na or K)O/(Si, Fe)O_2 = 2.

Phase produced	Composition
α	$Ca_{1.80}Na_{0.18}Si_{0.82}Fe_{0.17}O_4$
α, α′	$Ca_{1.81}Na_{0.21}Si_{0.89}Fe_{0.12}O_4$
β	$Ca_{1.87}Na_{0.11}Si_{0.95}Fe_{0.06}O_4$
α	$Ca_{1.80}K_{0.19}Si_{0.87}Fe_{0.18}O_4$
α, α′	$Ca_{1.79}K_{0.22}Si_{0.88}Fe_{0.11}O_4$
β	$Ca_{1.88}K_{0.12}Si_{0.94}Fe_{0.06}O_4$

Comparatively great decreases of alkali and Fe were observed in α or α′-phase. Some of them moved into the liquid that was formed around C_2S crystal as an interstitial phase and other alkalis vaporized in the burning process. On the vaporization of alkalis, we will investigate hereafter in relation to the manufacturing procedure.

In the Na-Al and K-Al substituted series, none of the α-phase was formed and α′-phase was always accompanied by β. The distributions of alkalis and Al in α′ and β-crystal were not constant and we could not determine the composition.

Lattice lengths of α-C_2S were measured by X-ray diffraction as shown in Fig. 5. In the Na-Fe substitution a and c axis increased as Na and Fe were substituted, but in the K-Fe substitution only a axis increased by substituting K for Ca. The c axes of Na-Fe substituted α were larger than those of K-Fe substituted, not corresponding to the ion size of Na and K. This must be studied hereafter from the point of crystal chemical investigation.

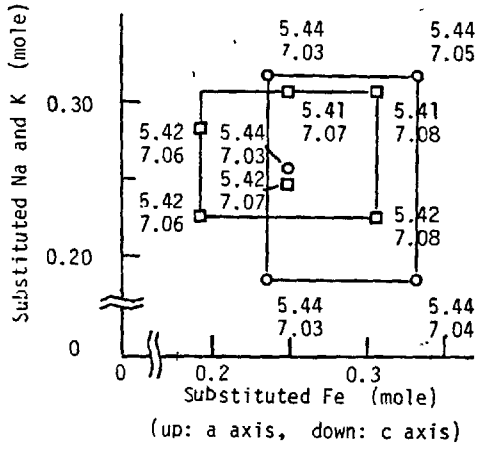

Fig. 5 - Change in lattice lengths of α-phases with the substitution range. Samples were burned at 1360°C.

Any change in the lattice lengths was not observed when the burning temperature was changed. This fact means that the substituted quantity of additives will not change by burning temperature, then the lattice strains of them are the same. The lattice strain was investigated from the line broadening as shown in Fig. 6. Four reflection of 102, 110, 201 and 202 were used for the calculation, and the change of $\beta \cdot \cos\theta/\lambda \times 10^{-3}$ with $\sin\theta/\lambda$ was plotted for α-phases burned at 1360, 1440 and 1520°C. The lattice strains of K-Fe-α are slightly larger, however, no great changes of their strains by burning were observed.

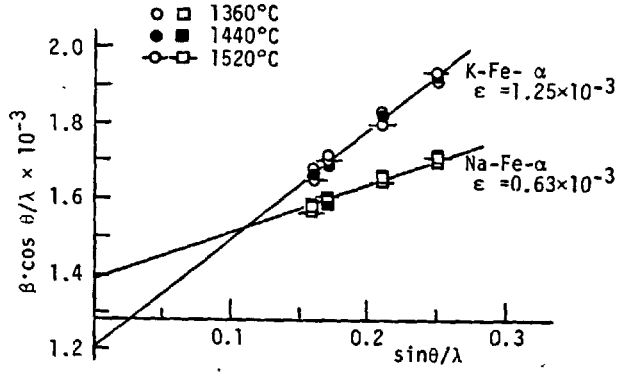

Fig. 6 - Lattice strain profile of Na-Fe and K-Fe substituted α-crystal. ε:lattice strain, θ:reflection

angle, λ:wave length, β:breadth of diffraction profile.

From these investigation, it is clear that the hydration and the strength were greatly affected by the hydraulicity or solubility of interstitial phase. When K-Fe and Na-Fe substituted α-phase were crystallized at low temperature (for the former, at 1360 and 1440 °C, and for the latter, at 1360 °C), the liquid phase coagulated around these crystals in unstable and the dissolution of Ca, SiO_2 and other components into water takes place immediately after contacting with water as shown in Table IV. The analysis of Ca and SiO_2 dissolved in water was proceeded as follows. The dispersed solution was obtained by stirring 2g of C_2S with 10 ml of water. After continuing the stirring for 5 and 20 minutes, the filtered solution was analyzed. Ca ion concentrations were determined by titrating with ethylene diamine tetraacetic acid (EDTA). Soluble SiO_2 was estimated colorimetrically, using reduced silico-molybdic acid.

Table IV - Ca and SiO_2 dissolved in water from α-C_2S pastes

Sample designation	Burning temperature(°C)	Dispersed time (min)	Ca mmole/g	SiO_2 mmole/g $\times 10^{-1}$	Ca/SiO_2
K-Fe -α	1360	5	5.86	0.67	88
		20	2.61	1.00	26
	1440	5	3.46	0.78	44
		20	1.45	1.33	11
	1520	5	2.71	1.67	16
		20	0.80	1.34	6.0
Na-Fe -α	1360	5	1.40	1.34	10
		20	0.95	1.34	7.0
	1440	5	1.05	1.67	6.3
		20	0.80	1.64	4.8
	1520	5	1.05	2.45	4.3
		20	0.70	2.22	3.2

The hydration of α crystal and the hardening were accelerated by their dissolution and affects the high development of strength. This is also clearly understood from Fig. 4.
The hydration products were observed by electron microscopy. In the all of this series the foil like crystal was observed, and its quantity corresponds approximately to their compressive strengths.

CONCLUSION

In the Na-Fe and K-Fe substitution, the α-phase could be stabilized easily, but in the Na-Al and K-Al substitution, only α′ and β phases were crystallized.. The α-phase exhibited high compressive strength and hydraulicity, and the strength of K-Fe substituted α-phase surpassed others as shown in Fig. 3 and the effects of their burning temperature were characterized as the better development of strength and hydraulicity in the lower temperature burning.

BIBLIOGRAPHY

1. - A. I. BOIKOVA, M. G. DEGEN and V. A. PARAMONOVA (1974) "Defect state of solid solutions of dicalcium silicate", Supplementary paper, 1-3. The 6th International Congress on the Chemistry of Cement. Moscow
2. - W. GUTT, G. J. OSBORN (1970) Cem. Tehn. 1. 121
3. - M. Y. BIKBAU (1974) "On hydration activity of silicates", Supplementary paper, II -6. The 6th International Congress on the Chemistry of Cement Moscow.
4. - I. JELENIC, A. BEZJAK and M. BUJAN (1978) "Hydration of B_2O_3-stabilized α′ and β-modifications of dicalcium silicate", Vol. 8, pp. 173-180, Cement and Concrete Research.

Durcissement du ciment à des températures au dessous de zéro

Cement hardening under below zero temperature

S.A. MIRONOV, professeur, docteur de sciences techniques, chef du laboratoire,
I.I. KOURBATOVA, candidat de sciences chimiques, collaborateur scientifique supérieur,
O.S. IVANOVA, candidat de sciences techniques, collaborateur scientifique supérieur,
S.A. VYSSOTSKY, candidat de sciences techniques, collaborateur scientifique supérieur,
Institut des Recherches Scientifiques du Béton et du Béton Armé (NIIZhB), Gosstroy, URSS.

RESUME : Par un ensemble de méthodes d'analyse physico-chimique, y compris la détermination de la composition de la phase liquide, sont étudiées : les caractéristiques de l'hydratation du ciment, la composition et la cinétique de cristallisation des formations nouvelles, les transformations de phase de l'eau et le durcissement à des températures au-dessous de zéro. On peut noter une influence favorable sur les propriétés du ciment durci, d'une cure préalable à des températures au-dessus de zéro, avant la congélation.

L'introduction d'adjuvants-électrolytes représentant la combinaison de deux ou trois sels, est un procédé efficace de l'intensification du durcissement des ciments sous les températures au-dessous de zéro. Non seulement ils réduisent la quantité de glace, mais par le changement de la composition, du pH et de la force ionique de la phase liquide, ils accélèrent l'hydratation des composants siliceux du clinker. Ils assurent aussi une cristallisation intensive de l'ettringite dans les états initiaux et protègent contre le développement des processus destructifs pendant le durcissement ultérieur.

SUMMARY: Peculiarities of cement hydration, composition and kinetics of crystallization in new formations, phase water transformation and hardening under below zero temperature have been studied by complex of methods for physicochemical analysis, including investigations of liquid phase composition. Favourable effects of cement stone precuring under above zero temperature before freezing on its properties have been noted.

Effective method of cement hardening intensification under below zero temperatures is the introduction of electrolyte admixtures, representing combination of two or three salts. They do not only decrease the quantity of ice but accelerate hydration of silikate component of clinker, changing composition, pH and ionic force of liquid phase as well as they ensure intensive crystalization of ettringite on early stages that prevents development of destructive processes in forther hardening.

Les problèmes concernant le durcissement du béton soumis à des températures au-dessous de zéro, sont très actuels et signifiants pour la construction durant toute l'année /I,2/. Nous avons étudié l'hydratation conétique du ciment et les transformations de l'eau en phases, de même que le durcissement du ciment et du béton avec ou sans les différents anti-gel, pour les basses températures. Ces recherches avaient pour but d'étudier le changement cinétique dans la composition de la phase liquide et la capacité de silicate tricalcique à se hydrater - tout cela est par la méthode analytique aux rayons X, de même que la teneur en eau d'hydratation et en éttringite - par les méthodes chimiques.

Le décroissement de la température provoque une réduction de la capacité d'hydratation du ciment. L'hydratation et le durcissement du ciment à des températures au-dessous de zéro sont les fonctions directes de sa teneur en eau non-congélée. A des basses températures au-dessous de zéro et proches à 0°C, l'hydratation du ciment est ralentie. A l'âge de 28 jours, lorsque la température reste an même niveau (-2°C), les 28% de silicate tricalcique se trouvent déjà hydratés. L'abaissement ultérieur de la température jusqu'à -5°C provoque un brusque décroissement du degré d'hydratation de C_3A (et cette valeur n'est égale qu'à 7,6%). Pour les températures entre -I0°C et -20°C toute la quantité de silicate tricalcique reste pratiquement non-hydratée (Tableau I).

TABLEAU I

Hydratation du ciment portland à des températures au-dessous de zéro

Durée d'exposition à +20°C avant la congélation (conditions normales)	t°C	Degré d'hydratation de C_3A, en %	Teneur en eau d'hydratation, %
0	-2	26	4,05
0	-5	7,6	I,48
0	-I0	2	I,63
0	-20	2	0,64
3	-20	3	0,60
6	-20	7	0,99
I2	-20	2I,5	3,35
24	-20	30	4,63
72	-20	42	6,49

Remarque: Eprouvettes exposées au gel jusqu'à 28 jours d'âge et essayées immediatement avant le dégel.

L'exposition préalable de la pièrre de ciment à des températures au-dessus de zéro étant favorable pour l'hydratation subséquente, toutefois celle-ci ne permet pas d'intensifier essentiellement ce processus.

Une amélioration qualificative peut y être obtenue par addition des anti-gel dans le béton, dont le rôle pour l'abaissement de la température de congélation d'eau dans les pores est bien connu. A titre de ces anti-gel, comme le clorure et le nitrate de calcium, le nitrite de sodium et autres adjuvants, sont de plus en plus répandus les compositions qui comprennent un certain nombre de sels à savoir: le nitrite-nitrate de calcium (NNK, ici et ailleurs - abréviation russe), le nitrite-nitrate-clorure de calcium (NNKhK) et d'autres. Le clorure, le nitrate et le nitrite de calcium, aussi bien que les adjuvants complexes, fabriqués sur leur base (NNK et NNKhK), sont les adjuvants à l'effet polyvalent, dont l'action consiste non seulement à abaisser la température de congélation de la phase liquide dans les pores, mais à favoriser l'accélération d'hydratation du ciment, influençant sur les composants du clinker, tels comme les silicates, les aluminates et les alumoférrites. Avec ces derniers, ils forment les compositions de type de sels doubles /3-5/. Leur influence sur la composante de silicate, se manifestant en sa plus parfaite solubilité, en accélération de vitésse d'hydratation, en transformation de la morphologie et du dégré de polymerisation d'hydrosilicates /6-7/, est conditionnée, en premier lieu, par le changement de valeur de pH et de force ionique dans la phase liquide. La présence des sels modifie la composition de la phase liquide et la valeur de saturation supérflue par rapport à des phase initiales d'hydratation, ce qui même, reciproquement, a un changement de la cinétique de formation de leurs cristaux et d'ettringite tout d'abord.

L'addition du NNKhK en quantité de 3% du poids du ciment à +20°C provoque un abaissement de pH et une ogmentation, pour un ordre de valeurs, de la force ionique dans la phase liquide, par rapport au système sans ledit adjuvant. Ou observe l'hydratation accrue du ciment, ce qui peut être confirmé par le caractere même des courbes cinétiques $C_{Ca^{2+}}(\tau)$ et $C_R + (\tau)$ - fig. I.

La montée brusque de la courbe cinétique $C_R + (\tau)$ témoigne que la dissolution des grains de clinker passe plus activement, de même que le décroissement rapide de la courbe $C_{Ca^{2+}}(\tau)$, ainsi que l'absence de points d'extrémum sur la courbe caractérisant le ciment portland, témoignent la formation intense des cristaux dans les phases contenant le calcium /3/. Les courbes analogues, caractérisant la pâte avec addition du NNKhK, durcie à -5°C, sont moins inclinées.

Cette allure de courbes cinétiques, tout aussi comme les renseignements sur la cinétique de contenance d'eau liée, dont la teneur angmente continuelement avec le temps, allant jusqu'à 9% dans I2 heures, témoigne que l'hydratation passe suffisamment vite à des températures au-dessous de zéro.

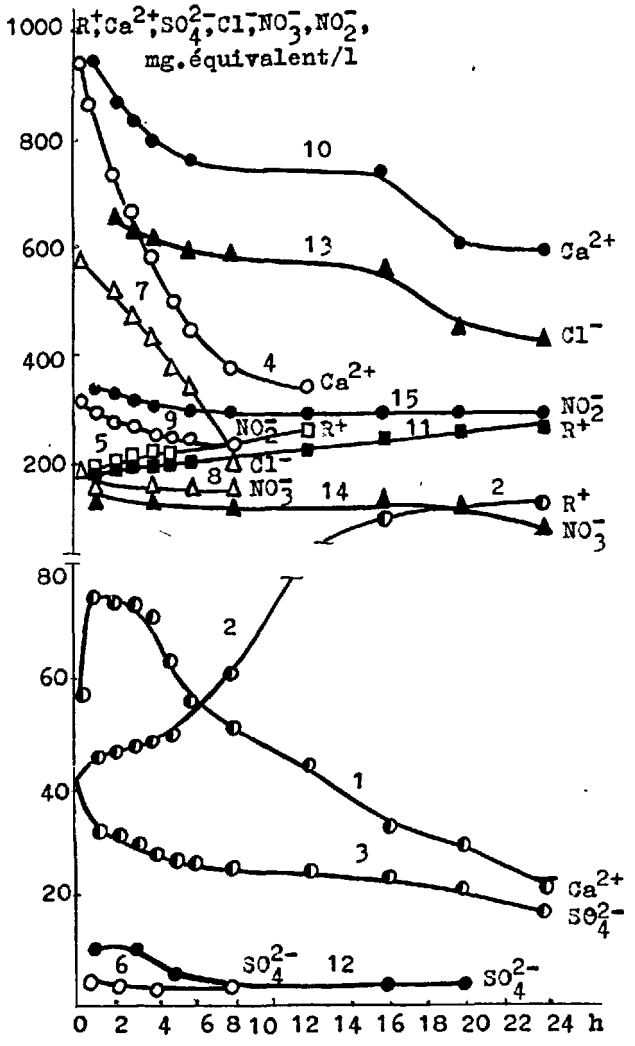

Fig. I - Modification en composition de la phase liquide pandant l'hydratation du ciment à +20°C et à -5°C.

I,2 et 3 - sans adjuvant, à 20°C;
4,5,6,7,8 et 9 - avec adjuvant de NNKhK à 20°C;
I0,II,I2,I3,I4 et I5 - avec adjuvant de NNKhK à -5°C.

L'addition du NNKhK influe sur la formation cinétique des cristaux doubles à des températures au-dessus aussi bien qu'au-dessous de zéro. La présence de chlorures, des nitrates et de nitrites de calcium inténcifie la formation d'ettringite ($C_6A\bar{S}_3H_{32}$) au moment initial. Dans I0 min aprés le gachage à +20°C, à peu prés de 75% de gypse se trouvent liés en $C_6A\bar{S}_3H_{32}$. La formation des cristaux d'ettringite se termine pratiquement vers 2 h, lorsqu'il reçoit 83% de gypse, en même temps que la formation de 6,85% de $C_6A\bar{S}_3H_{32}$ a eu lieu. Pour la même période on peut voir que la courbe cinétique $C_{SO_4^{2-}}(\tau)$ présente une allure de chute correspondant à la disparition du gypse de la phase solide. Comme on a déjà mentionné ci-dessus, le caractère brusque de la courbe $C_{Ca^{2+}}(\tau)$ dépend de la formation abondante des cristaux d'ettringite. Dans la suite, la teneur en $C_6A\bar{S}_3H_{32}$ ne s'augmente point mais présente même une tendance à se diminner (4% dans 24 h et 2,78% dans 7 jours). Pandant l'hydratation du ciment portland exempt du NNKhK la teneur d'ettringite croit continuellement et dans 2,6 et 24 h correspond à 3,6; 5,5 et 8,5%.

La formation d'ettringite dans la pâte avec addition de $CaCl_2$, $Ca(NO_2)_2$ et de NNKhK, dont le durcissement a lieu à la température de -5°C, touche à sa fin pendant les premiers heures après le gachage. La teneur en ettringite dans ce cas pratiquement ne change pas avec le temps, ce qui assure le non-développement des processus déstructifs pour le compte de la cristallisation d'ettringite secondaire. L'addition de nitrite de sodium n'accélére pas l'hydratation et n'intensifie pas la formation d'ettringite au période initial (Tableau II).

TABLEAU II

Quantité d'ettringite pendant l'hydratation du ciment avec adjuvants: $CaCl_2$ - 5%, $Ca(NO_2)_2$ - 5%, NNKhK - 3%, $NaNO_2$ - 5% à T = -5°C

Temps, h	Pourcentage d'ettringite correspondant á l'adjuvant de			
	$CaCl_2$	$Ca(NO_2)_2$	NNKhK	$NaNO_2$
I	4,I	6,0	6,2	2,4
2	3,8	6,2	6,2	2,4
4	3,8	6,3	5,8	3,3
6	3,8	6,0	5,8	3,I
8	3,I	5,9	5,9	4,0
I2	3,I	6,3	6,0	4,0
I6	3,0	6,3	5,7	4,2
24	3,5	6,4	5,3	4,4

Les chlorures, les nitrates et les nitrites de calcium non seulement n'accélérent la formation des cristaux d'ettringite, mais aussi participent eux-mêmes dans la formation des sels doubles, qui sont les éléments de baze pour la formation de la structure lors de durcissement, ce qui est confirmé par la concentration décroissante des iones corréspondants dans la phase liquide, ainsi que par leur présence dans la phase solide. Le plus fort décroissement de cette concentration conforme à une phase liquide de chlorures, tandis que le décroissement moins prononcé correspond aux nitrates et finalement - aux nitrites, lorsque celui devient presque nul. Dans 24 h, en tenant compte de la température, de 40 à 60% de chlorures peuvent passer en phase solide. L'éloigne-

ment de telle grande quantité d'ions de calcium et de chlorures horsde cette phase ne se trouvant point undemnisé par son enrichissement, pandant l'hydratation, à l'égard des ions de métaux alcalins et d' hydroxil, la température de cougélation de la phase liquide montre une hausse; toutefois celle-ci ne meme pas à des conséquences graves et néfastes, parce que, dans le béton frais, additionné de tels produits, il éxiste déjà vers le moment donne la pierre de ciment, caractériseé par une structure capillaire, suffisamment compacte et fine, ce qui favorise le décroissement de la température de congélation de la phase liquide.

Cette température, dans le cas d'addition de nitrite de sodium, reste pratiquement sur le même niveau, la concentration de celui-ci restant inchangable. L'éloiguement des nitrites hors de la phase liquide,lorsqu'ils sont lies aux sels doubles, sera compensé par leur concentration toujours croissante, tout cela pour le compte de la volume décroissante de la phase liquide pendant l'hydratation. Ainsi, l'effet favorable du $NaNO_2$, utilisé comme adjuvant dans le ciment et dans le béton durcissants, est-il confitionné généralement par un abaissement de la température de congélation de la phase liquide, assurant l'effet d'hydratation au gel d'un côté et les des destructions moins prononceés de la structure de l'autre, celles-ci étant conditionnées par la transformation d'une partie de l'eau en glace. Quant à la formation de la structure avec les sels doubles sur baze du $NaNO_2$, leur rôle reste secondaire.

Les études des transformations à phases de l'eau pendant la congélation du béton, réalisées par la méthode analytique de calométrie, ont démontré que l'utilisation des anti-gel favorise la réduction considérable en quantité et en qualité de la glace dans le béton et participe aussi à une modification de la vitesse de congélation. Comme les courbes I et 4 le montre (fig. 2), les bétons et la pâte de ciment exémpts d'adjuvant NNKhK et sonmis à l'action de gelée immédiatement après la confection, se caractérisent par la congélation pratiquement complète de la liquide dans les pores, lorsque la température est an-déssous de -4°C.

La teneur en glace dans les éprouvettes de béton avec addition de 3% de NNKhK du poids de ciment, sonmis a l'action de gelée immédiatement après la confection (courbe 2), est égale à 72%. L'éxposition préalable du béton à des températures auxdessus de zéro provoque une diminution supplémentaire de la quantité de glace. Ainse, apres 24 h de l'exposition avan la congélation des épronvettes (courbe 3), la teneur en glace u'était-elle égale qu'à 27%.

L'addition du NNKhK est capable à influencer essentiellement sur la modification cinétique de teneur en glace dans le béton. Si pendant l'exposition an gel de la pête de ciment on du beton exempts d'adjuvants,

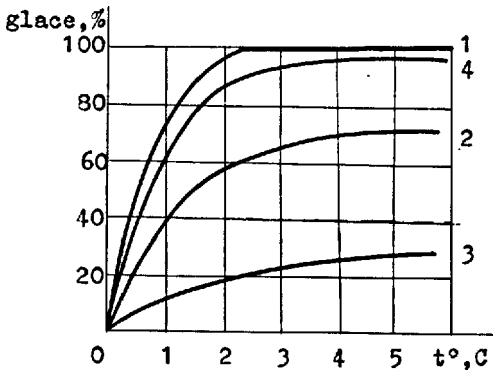

Fig. 2 - Quantité de glace dans le béton aprés 28 jours de congélation à T = -5°C.

I - béton saus adjuvant; 2 - béton avec 3% du NNKhK; 3 - idem, congélé dans 24 h; 4 - pâte normale, sans adjuvant, congélation immédiate.

la teneur en glace ordinairement est augmentée, l'addition du NNKhK fait une sensible réduction de glace avec le temps. De même, la teneur en glace dans le béton saus adjuvants, sonmis à température de -2°C etait egale a 87% dans 24 h et a 98% a l'âge de 28 jours. Les résultats de l'ingénieur N.DOMACHEVSKY montrent, qu'avec addition du NNKhK l'augmentation considérable de teneur en glace ne pent avoir lieu que durant les premiers jours de durcissement au gel, après quoi la vitesse de ce phénomène se trouve sendiblement réduite et dans 28 jours cette teneur diminue de 22% (fig.3, courbe 3).

On pent voir la chose à la température de -5°C, mais dans ce cas la diminution de la teneur en glace y était égale à I2%. Ces renseignements témoiguent que l'hydratation du ciment avec adjuvant passe d'une manière intense, de même que les phénomènes déstructifs, causés par la transformation de l'eau à phases, sont moins prononcés, ce qui assure, en somme, le durcissement plus intense du béton par temps froid.

Les recherches présentés ici et ayant pour but d'étudier le problème de durcissement du béton avec on sans adjuvants anti-gel soumis à des températures an-dessous de zéro, ont confirmé les résultats obtenus. Ces études ont été effectuees avec le béton de classe "300", congelé immédiatement apres la confection on dans 24 h de conservation normale, jusqu'à 90 jours de mise en froid dans une chambre souterraine, en contact avec le sol toujours congelé a température de -3°C.

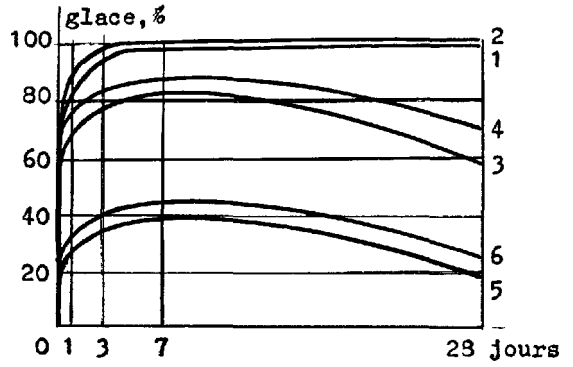

Fig. 3 - Influence du NNKhK sur la quantité de glace dans le béton

I÷4 - béton congelé immediatement aprés la conféction; 5 - dans 24 h de consérvation normale.
I - béton sans adjuvant, T = -2°C; 2 - idem, à T = -5°C; 3 - 3% de NNKhK, T = -2°C; 4 - 3% de NNKhK, T = -5°C; 5 - 3% de NNKhK, T = -2°C; 6 - 3% de NNKhK, T = -5°C.

La conservation pendant 24 h suivant la caractéristique de température correspond à des conditions récles de congélation du béton dans les ouvrages, p.ex. dans les fondations sur pilotis. La fig. 4 donne un exemple de courbes qui montrent une augmentation de la résistance du béton avec addition de 3% de $NaNO_2$ + 0,2% de sulfolevure (SDB, abréviation russe). Comme on peut voir, le béton sans adjuvants, mis directement sur terre congelée, vers 90 jours n'a augmenté sa résistance que de 20% par rapport à celle de 28 jours. Après le durcissement normal de 24 heures la résistance du béton de même âge était égale à 56%. L'addition de susdit sel en quantité de 3% du poids de ciment fait augmenter la resistance du béton, car, pour la même période, ce dernier est capable d'obtenir la valeur (classe) de résistance de 28 jours on environ (dans le cas de son éxposition au gel immédiatement après la confection). La susdite méthode du bétonnage en hiver a été utilisée en particulier pour le coulage des fondations de la cheminée en béton armé, de 180 m d'hauteur, à Norylsk, an lien du bétonnage par chauffage électrique, utilisé auparavant, plus coûteux et compliqué.

Pour faire une estimation de l'efficacité d'utilisation de différents produits antigels enfluent sur le durcissement du béton an gel jusqu'à -10°C, ou a entrepris les essais spéciaux. Ces expériments se rapportent à des bétons ayant la classe de resistance "400". Les dosages des additions etaient: 3% - à T = 0 ÷ -2°C; 5% - à T =

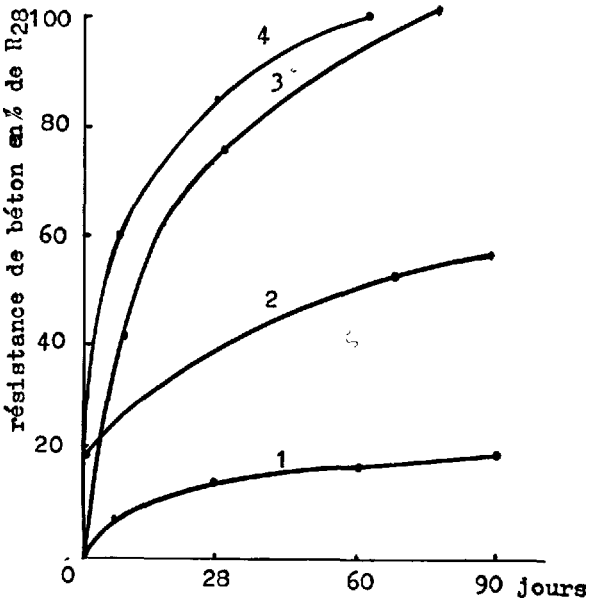

Fig. 4 - Augmentation de la résistance du béton à T = -3°C.

I - sans adjuvants chimiques, béton congelé immédiatement; 2 - sans adjuvants chimiques, béton congelé dans 24 h de consérvation normale; 3 - avec addition de 3% de $NaNO_2$ + 0,2% de SDB, congélation immédiate; 4 - idem, congélation dans 24 h de conservation normale.

-5°C et 7,5% - à T = -10°C. On n'utilisait que le nitrite de sodium, le nitrate de sodium, le nitrite de sodium en pourcentages égaux avec le chlorure de calcium et le NNKhK en proportion égale entre les composants. L'analyse de résultats obtenus (tableau III) montre que lorsqu'on ajonte les produits chimiques dans le béton, il est possible d'obtenir la résistance demandée du béton au gel dans 90 jours, qui sera égale à 75÷100% de la résistance à 90 jours de cousérvation dans les conditions normales, on 60÷84% de la même valeur de résistance dans 28 jours.

Ces essais ont confirmé l'efficacité d'utilisation des adjuvants compléxes, ayant, dans leur composition, l'accélérateur de durcissement ($CaCl_2$), surtout à l'âge jeune.

En Union Soviétique, plus de 25 aus, on utilise avec efficacité et sur une large échelle les différents anti-gel pour le bétonnage par temps froid des structures massives de bâtiments et des ouvrages. Pour

élargir l'efficacité d'utilisation de la capacité d'hydratation et des propriétés structurelles du ciment, enfluant sur la formation de la structure optimale du beton, ce derniers temps, on a commencé a pratiquer l'utilisation des anti-gel avec les produits à action superficielle. Donc, dans les standarts, il est admix d'utiliser ces adjuvants à des temperatures de dehors jusqu'a -25°C.

Pour les conditions climatiques plus dures, aussi que pour l'approchement des délais de decoffrage te,de mise en charge des structures achevées, cette méthode est utilisée en combinaison avec celle du thermos on avec le traitement thermique. Pour compléter les standarts officiels, les manuels de recommandations et les instructions ont été créés et publiées /8/.

TABLEAU III

Influence des anti-gel sur le durcissement du béton a des temperatures au-dessous de zéro

Adjuvant	Age du beton	Résistance du béton en % de R_{28} à temperature, °C			
		+20	0+-2	-5	-I0
Sans adjuvant	7	-	I2	-	-
	28	I00	45	5	I,5
	90	-	57	I0	6
$NaNO_2$	7	-	23	20	I7
	28	I04	65	76	60
	90	-	82	8I	70
$NaNO_3$	7	-	56	32	28
	28	III	84	82	66
	90	-	89	88	9I
$NaNO_2$ + $CaCl_2$	7	-	42	47	4I
	28	II2	84	83	84
	90	-	98	97	I02
NNKhK	7	-	45	32	27
	28	I27	70	75	70
	90	-	8I	85	75

CONCLUSIONS

L'hydratation du ciment et le durcissement du béton a des températures au-dessous de zéro, sont considérablement retardés a moins qu'ils n'en se stoppent pas tatolement. Pour intensifier ces processus il est utile d'y ajouter les differents anti-gel, qui engendrent le decroissement de la température de congélation de la phase liquide, accélérent l'hydratation du ciment, modifient en quantite et en qualité la vitesse de formation de glace dans le beton, ce qui provoque finalement le durcissement accéléré fu ciment et du béton. Le procédé le plus efficace consiste a utiliser les adjuvants complexes. L'addition de tels produits antigels et le traitement plus prolonge du béton avant sa congélation assurent la possibilité du bétonnage a des températures au-dessous de zero.

BIBLIOGRAPHIE

I. - S.A.MIRONOV (I975) "La theorie et les methodes du betonnage par temps froid" Ed. "Stroiyzdate".

2. - S.A.MIRONOV (I976) "L'hydratation et le durcissement du ciment au gel", VI-eme congres international sur la chimie du ciment, Ed. "Stroiyzdate", vol. II, partie I, p. I82-I85.

3. - I.I.KOURBATOVA (I977) "La chimie d'hydratation du Portland", Ed. "Stroiyzdate".

4. - V.B.RATINOV et T.I.ROSENBERG (I973): "Les adjuvants pour le beton", Ed. "Stroiyzdate".

5. - F.VAVRGINE (I976) "L'enfluence des additions chimiques sur les processus d'hydratation et de durcissement du ciment", VI-eme congres international sur la chimie du ciment", Ed. "Stroiyzdate", vol. II, partie 2, p. 6-II.

6. - I.I.KOURBATOVA et V.G.ABRAMKINA (I976) "La cristallisation cinetique des nouvelles formations dans les pates de ciment avec addition de clorure de calcium", Magazine "Chimie appliquee", XLIX, p. I020-I023.

7. - A.RIO (I976) "Approchement a la description macromoleculaire de processus d'hydratation du silicate tricalcique", VI-eme congres international sur la chimie du ciment", Ed. "Stroiyzdate", vol. II, partie I, p. I45-I57.

8. - "Manuel d'utilisation des betons avec les anti-gel" (I978). Ed. "Stroiyzdate", Moscou.

The effects of $Cu(OH)_2$ on the hydration of C_3A

Action du $Cu(OH)_2$ sur l'hydratation du C_3A

C. TASHIRO, Asst. Professor, Yamaguchi University, Faculty of Engineering, Ube, Japan,
J. OBA, Master of Engineering.

RESUME : Plusieurs études ont déjà été faites, par divers chercheurs, sur l'action d'additifs sur l'hydratation du C_3A. Mais le cas dex oxydes ou des hydroxydes de métaux lourds a été peu exploré. Dans la présente étude, $Cu(OH)_2$ est ajouté à C_3A, et on a observé, pendant la période d'hydratation, la concentration en CaO et Al_2O_3 de la phase liquide, la quantité de chaleur dégagée et la nature des hydrates.

$Cu(OH)_2$ retarde, à ses débuts, l'hydratation du C_3A, abaisse la concentration de CaO, augmente celle d'Al_2O_3 et empêche la formation de cristaux de C_3AH_6, dans la phase liquide. Dans le même temps, les cristaux hexagonaux d'aluminate de calcium se forment progressivement. La vitesse d'hydratation obéit à la loi suivante :

$(1 - \sqrt[3]{1-\alpha})^n = kt.$

SUMMARY : The effects of additives on the hydration of C_3A have been investigated by a number of researchers. However, the very little knowledge has been gained on how heavy metal oxides or hydroxides affect the hydration of C_3A. Therefore, in the present study, $Cu(OH)_2$ was added to C_3A, and CaO or Al_2O_3 concentration of liquid phase under hydration, heat liberation in early hydration reaction, characterization of hydration products and rate of hydration were examined.

$Cu(OH)_2$ retards the early hydration, tends to decrease the solubility of CaO and increases the solubility of Al_2O_3 in liquid phases under hydration, and so hinders the formation of C_3AH_6. In the meantime, hexagonal calcium aluminate hydrates grow with the passage of curing time, and rate of hydration in second stage follows $(1-\sqrt[3]{1-\alpha})^n=kt$.

INTRODUCTION

The effects of gypsum on the hydration of C_3A have been investigated by a large number of researchers(1-3). However, the effects of heavy metal oxides have not been published to data. The studies present an fundamental data of hydration of Portland cement clinker. On the other hand, the studies are under way in recent years on disposal of industrial wastes containing heavy metals through solidification of such wastes by cement(4-6).

For these reasons, heavy metal oxides are added to C_3A and the effects on the hydration were examined(7). It has become apparent that $Cu(OH)_2$ and ZnO strongly retard the early hydration of C_3A.

Therefore, in the present study, in order to clarify the mechanism of the retardation, $Cu(OH)_2$ was added to C_3A and effects on the bottle hydration of C_3A were examined on Cu^{2+}, CaO and Al_2O_3 concentration in liquid phase and on the characterization of hydrates.

EXPERIMENTAL

$CaCO_3$ and Al_2O_3 were mixed to a composition of C_3A and the mixture was calcined twice, each time at 1350°C for 5 hours. The calcined material was then ground to a Blaine value of about 3500 cm^2/g. $Cu(OH)_2$ is commercially available as reagent.

$Cu(OH)_2$ was added as $0.8C_3A + 0.2Cu(OH)_2$ mol. The hydration was carried out in water with 20water/C_3A, at 20°C for 3 days under vibrating condition with 120 time/min.

The hydrates were filtered off, washed with acetone, and dried in vacuum. The solution separated from the bottle hydration was analysed by EDTA titration or spectrophotometer with CaO, Al_2O_3 and Cu^{2+}.

The hydrates were observed and identified by a polarization microscope, powder x-ray diffractometry, differential thermal analysis, and a scanning electronic microscope.

The hydration rate was calculated from C_3A in hydrates which was heating at 650°C for 3 hours. And the quantities of C_3A were measured by X-ray scanning techniques with α- Al_2O_3 as an internal standard.

EXPERIMENTAL RESULTS AND DISCUSSION

Hydrates

Without $Cu(OH)_2$: The powder x-ray diffraction, differential thermal analysis and scanning electron micrographs of hydrates obtained from hydration reaction are shown in Fig. 1, 2 and 3 respectively. As is apparent from the X-ray differential analysis, after 10 minutes from water mixing, C_3AH_6 forms in a considerable amounts and hexagonal hydrates is slight amount. But the scanning micrographs indicated that platy and needle like crystals grow and characteristic crystal of C_3AH_6 is not observed. This is believed to be due to the very small grain and high crystallization of C_3AH_6. With the passage of hydration time, new formation of hexagonal hydrates increase as the amount of unhydrated C_3A decrease, and after one day, hexagonal hydrates decompose and transfer to C_3AH_6. Then, the hexagonal hydrates are chiefly C_4AH_{13}.

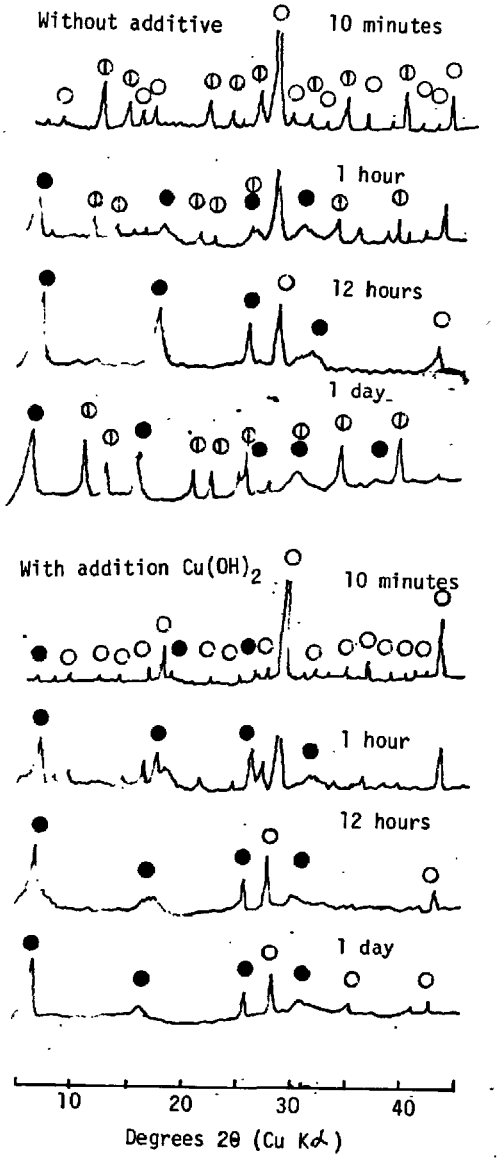

Fig.1-X-ray powder diffraction patterns of C_3A hydrated without and with addition $Cu(OH)_2$.

○ C_3S ● Hexagonal hydrates (C_4AH_{13})
Φ C_3AH_6

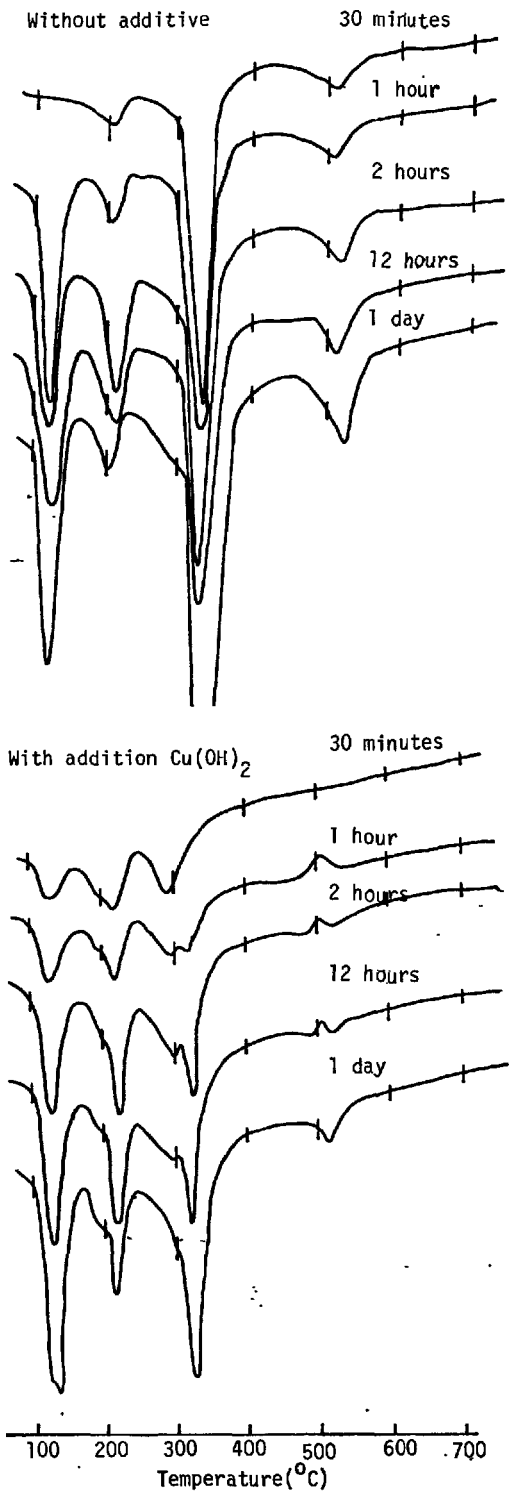

Fig.2 - DTA curves of C_3A hydrates without and with addition $Cu(OH)_2$.

With addition $Cu(OH)_2$: After 10 minutes from water mixing, C_3AH_6 hardly appears and fine platy crystal grows on the C_3A. With the passage of hydration time, hexagonal hydrates grows. After 3 days, it indicated that the hydrates formed are mostly hexagonal phases. From one day, formation of C_2AH_8 is observed.

The ratio of quantity between C_3AH_6 and hexagonal hydrates is shown by ratio of an endthermic peak area of differential thermal analysis at about 330 vs 120 and 220°C as shown in Fig.2 and4. Its illustration explains well the formation of hydrates.

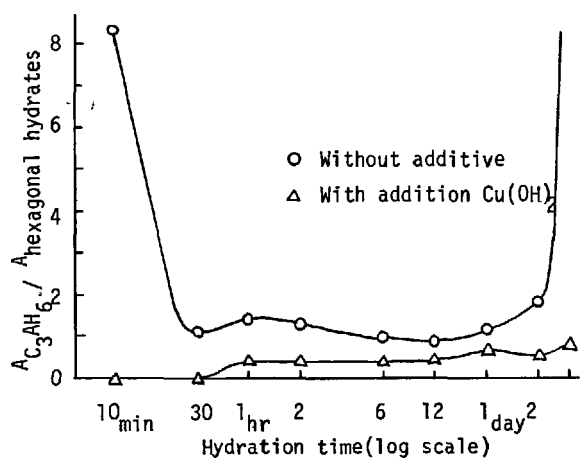

Fig.4 - Relation between DTA peak area of C_3AH_6 and hexagonal phases.

CaO and Al_2O_3 concentration in liquid phase

The concentration of CaO and Al_2O_3 in liquid of bottle hydration without and with addition $Cu(OH)_2$ is shown in Fig. 5.

After 30 seconds from water mixing, CaO concentration becomes 551 ppm without additive, and 497 ppm with addition $Cu(OH)_2$. At about 1.5 hours, CaO concentration temporarily increases because of the C_4AH_{13} transfer to C_3AH_6. Namely, excess CaO component solves in liquid.

On the other hand, Al_2O_3 concentration is 272 ppm without additive, and 325 ppm with addition $Cu(OH)_2$. Al_2O_3 concentration is gradualy decreases until one hour from water mixing, and subsequent concentration is kept at about 100 ppm.

CaO/Al_2O_3 mol ratio in liquid phase without and with addition $Cu(OH)_2$ is 7 to 8, which is higher than that of C_3A.[2] This data similar to report of Kondo(8),[3] but the relation between concentration and hydration time differs because of difference of water/C_3A and finess of C_3A. CaO/Al_2O_3 mol ratio with addition $Cu(OH)_2$ is lower than that of case of no addition. On the contrary, CaO/Al_2O_3 ratio of hydrates certainly higher. Namely, C_4AH_8 trend to be formed than C_3AH_6.

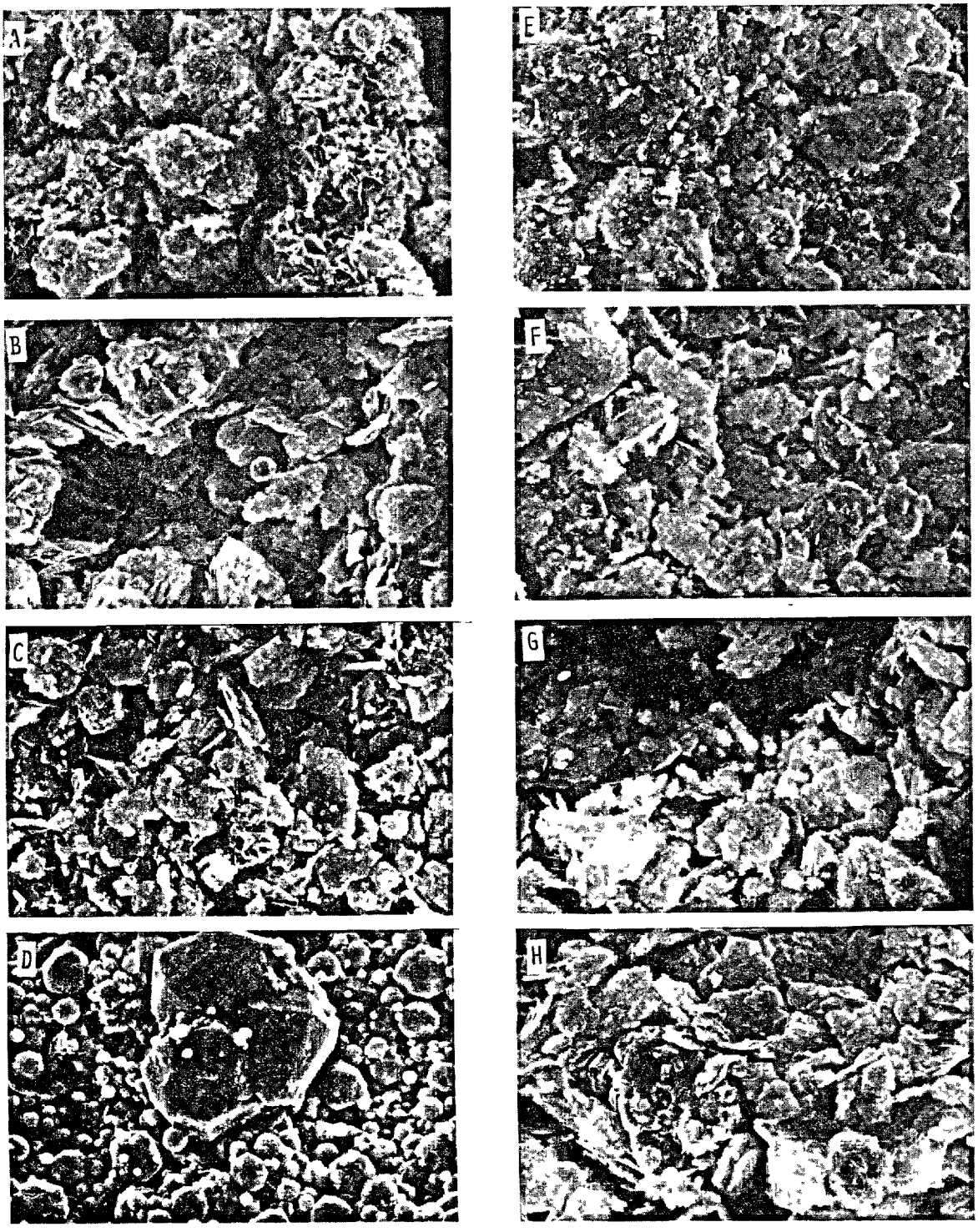

Fig.3 - Scanning electron micrographs of C_3A hydrated without and with addition $Cu(OH)_2$.

A : Without additive after 10 minutes.
B : Without additive after 2 hours.
C : Without additive after 6 hours.
D : Without additive after 3 days.
E : With addition $Cu(OH)_2$ after 10 minutes.
F : With addition $Cu(OH)_2$ after 2 hours.
G : With addition $Cu(OH)_2$ after 6 hours.
H : With addition $Cu(OH)_2$ after 3 days.

5µm

Cu^{2+} concentration in liquid phase

Cu^{2+} concentration is shown in Fig. 5. After 30 seconds from water mixing, Cu^{2+} is 1.75 ppm, and after 10 minutes, becomes 3 ppm, and decreases to 0.8 ppm at 1 hour. This shows that, Cu^{2+} is soluble with increase of pH, after 10 minutes, reached to maximum 10 ppm, for this period, Cu^{2+} is adsorbed on the C_3A or hydrates and subsequently, adsorption of Cu^{2+} is accelerated with increasing hydration. C_3A adsorbed by Cu^{2+} is apt to be developt the hexagonal hydrates. Because of addition $Cu(OH)_2$, solubility of CaO from C_3A decreases and that of Al_2O_3 increases, and calcium aluminate containing saturated CaO is formed as hexagonal hydrates. Then, Cu represents as $[Cu(OH_2)_4]^{2+}$ (9) or $Ca_2[Cu(OH)_4]$ in solution.

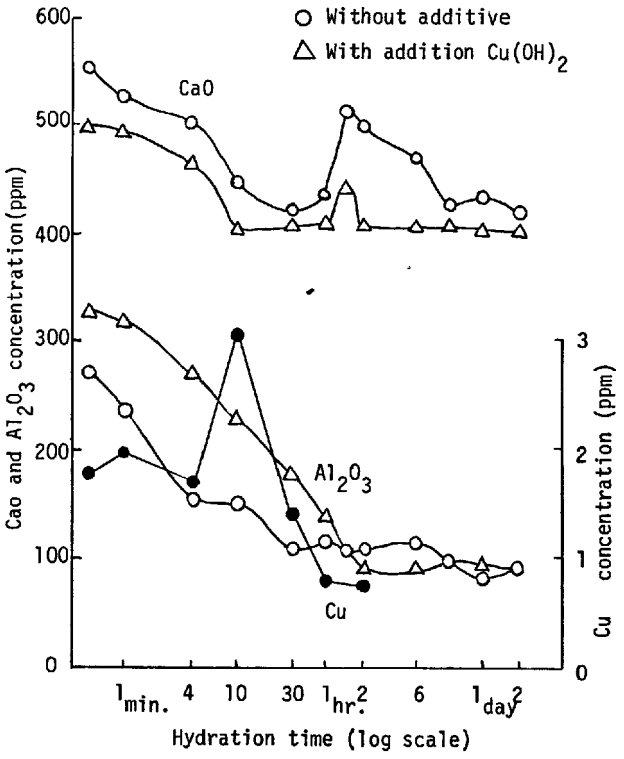

Fig.5 - The concentrations of CaO, Al_2O_3 and Cu in liquid phase.

Rate of hydration

The rates of hydration of C_3A without and with addition $Cu(OH)_2$ are shown in FiG. 6. As is apparent from this illustration, hydration of C_3A is divided into two stages. In the case of C_3A without additive, first stage is an early stage for 10 minutes from water mixing. When $Cu(OH)_2$ added, this first stage hydration is retarded and the stage is prolonged up to 1 hour.

The second stages of hydration without and with additive satisfy the hydration formula(8)

$$(1 - \sqrt[3]{1-\alpha})^n = kt$$

where α is hydration rate, t hydration time and n,k constant. The rate of hydration in second stage is slower than the first stage. In the case of no additive, $k = 1.05 \times 10^{-2}$, $n = 3.82$ and with addition $Cu(OH)_2$, $k = 3.9 \times 10^{-3}$, $n = 3.72$. The order of the hydration reaction is really stage known as diffusion rate-determinig stage. And first stage during the first 10 minutes is concordant with the results of Buikova(10).

The retardation of hydration in early stage is measured by differential calorimetric analysis as shown in Fig.7. The difference in heat of hydration is about - 21.8 kcal/mol.

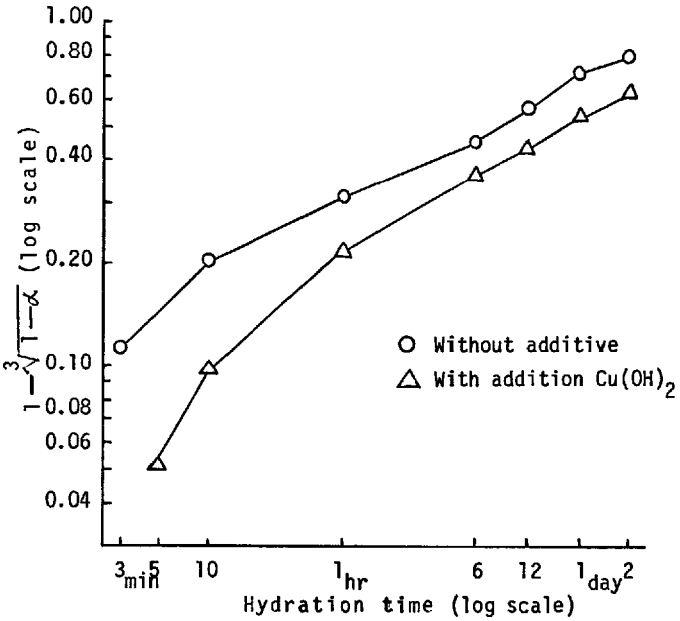

Fig. 6 - Rate of hydration of C_3A without and with addition $Cu(OH)_2$.

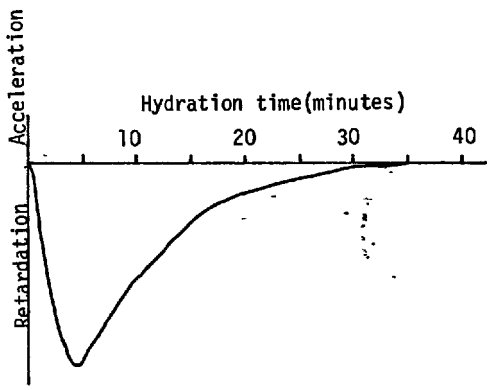

Fig.7 - Differential calorimetric curve on the initial hydration of C_3A with addition $Cu(OH)_2$.

Effects of addition $Cu(OH)_2$

As the above descriptions, in the early stage of hydration, $Cu(OH)_2$ is solved and adsorpted by C_3A or hydrates, and consequently, hydration is retarded, concentration of CaO in liquid phase decreases and Al_2O_3 increases and hexagonal hydrate is formed.

The mechanism of retardation of hydration is no clear but it seems that surface of C_3A or hydrates is coated by Cu^{2+} and invasion of water to inner parts is prevented, and this effect is responsible for similarity of ionic potential and crystal structure F.C.C. between Ca^{2+} and Cu^{2+}.

CONCLUSION

To examine the effects of $Cu(OH)_2$ on the hydration of C_3A, experiments on bottle hydration were carried out and the effects on the hydrates, their microstructure, concentration of CaO, Al_2O_3 or Cu^{2+}, and rate of hydration were studies .

The results are as follow.

$Cu(OH)_2$ strongly retards the early hydration of C_3A, and hinders the formation of C_3AH_6. In the meantime, hexagonal hydrates grow with the passage of hydration time. And $Cu(OH)_2$ affects the CaO and Al_2O_3 concentration of liquid phase. CaO/Al_2O_3 mol ratio in liquid phase is lower than that of case of no addition.

The hydration of C_3A is distinguished between first stage and second stage. Without additive, the first stage is an early stage for 10 minutes, and with addition, this is prolonged up to 1 hour. The both second stages of hydration without and with $Cu(OH)_2$ addition satisfy the hydration forumla $(1-\sqrt[3]{1-\alpha})^n = kt$.

It seems that the mechanism of retardation of hydration is owing to coating or adsorption on the C_3A with Cu^{2+}. This action is responsible for similarity of ionic potential and crystal structure between Ca^{2+} and Cu^{2+}.

REFERENCES

1.- R.F. FELDMAN (1966) "The influence of $CaSO_4 \cdot 2H_2O$ upon the hydration character of C_3A", Mag. concr. Res., 18, 185-196.

2.- A.TRAETTEBERD et al.(1975), "Hydration of C_3A, gypsum with and without $CaCl_2$", J. Am. Ceram. Soc., 58, 221-227.

3.- P. GUPTA (1970), " Studies of the effects of various additives on the hydration reaction of tricalcium aluminate", Cement Tech. ,1, 59-66.

4.- C.TASHIRO et al.(1979),"Hardening property of cement mortar adding heavy metal compound and solubility of heavy metal from hardened mortar", Cement and Concrete Research, 7, 283-290.

5.- C. TASHIRO et al.(1979),"The effects of several heavy metal oxides on the formation of ettringite and the microstructure of hardened ettringite", Cement and Concrete Research, 9, 303-308.

6.- C.TASHIRO and M.FUKUYAMA (1975),"The hydration of C_3A in $CaCrO_4$ solution", Cement Gijutsu Nenpo,29, 50-52.

7.- C. TASHIRO and J.OBA (1979),"The effects of Cr_2O_3, $Cu(OH)_2$, ZnO and PbO on the compressive strength and the hydrates of the hardened C_3A paste", Cement and Concrete Research, 9, 253-258.

8.- R. KONDO and S.UEDA (1969), Kinetics and mechanisms of the hydration of cements" Proc. 5th Int. Symp. Chem. cement, Tokyo, Vol. II, 203-248.

9.- A.J.BARD(1975),"Chemical equilibrium", Harper & Row Publishers, New york.,P70.

10- A.I.Boikova et al.(1977),"The influence of Na_2O on the structure and properties of $3CaO \cdot Al_2O_3$", Cement and Concrete Research, 7, 483-492.

The composition of CSH phase(s) in hydrated C_3S paste

Composition des phases HSC dans la pâte hydratée de C_3S

D.L. RAYMENT and A.J. MAJUMDAR, Building Research Establishment, Garston, Grande-Bretagne.

RESUME : La microsonde électronique Microscan 9 a été utilisée pour déterminer les compositions des phases d'hydrate de silicate de calcium (HSC) dans les pâtes de silicate tricalcique hydrate (rapport eau/solide 0,6) à l'âge d'un mois et d'un an. Les analyses faites sur divers éléments de microstructure considérés comme étant des phases de HSC, à des voltages électroniques accélérés de 6 à 25 kV montrent que les coefficients C/S mesurés sont influencés par le voltage du faisceau électronique utilisé, dépendant vraisemblablement du volume des régions particulières analysées. Par exemple, les grains qui offrent des caractéristiques morphologiques semblables donnent des valeurs C/S de 1.44 ± 0.08 et 1.62 ± 0.06 à des voltages de faisceau de 6 et de 15 kV respectivement. Au contraire, les grains non-hydrates de C_3S qui sont présents dans les échantillons de pâte donnent 3.09 ± 0.09 et 3.06 ± 0.04, car les coefficients C/S à ces voltages et les échantillons de tobermorite naturelle provenant de plusieurs sources ne montrent pas d'effet important des variations de voltage dans leurs analyses.

L'étendue des variations observées dans les coefficients C/S des divers éléments de microstructure de la pâte avec le voltage du faisceau sera discutée. Ces variations ne sont pas considérées comme étant dues à la détérioration du faisceau.

SUMMARY: The electronprobe microanalyser Microscan 9 has been used to determine the compositions of the calcium silicate hydrate phase(s) in hydrated tricalcium silicate pastes (water/solid ratio 0.6) at the age of one month and one year. Analyses carried out on various microstructural elements considered to be CSH phase(s) at electron accelerating voltages in the range 6-25 KV show that the measured C/S ratios are influenced by the beam voltage used, presumably depending on the volume of individual regions analysed. For instance, particles displaying similar morphological features gave C/S values of 1.44 ± 0.08 and 1.62 ± 0.06 at 6 and 15 KV beam voltages respectively. By contrast, unhydrated C_3S grains present in the paste samples gave 3.02 ± 0.09 and 3.06 ± 0.04 as the C/S ratios at these two voltages and natural tobermorite samples from several sources did not show any significant effect of voltage variations on their analyses.

The extent of the variations observed in the C/S ratios of the various microstructural elements in the paste with beam voltage will be discussed. These variations are not considered to be due to beam damage.

INTRODUCTION

The importance of calcium silicate hydrate (CSH) phases as the principal cementing agent in concrete is well recognised. These phases are very poorly crystalline and occur as aggregates of very small particles often intermixed with other products of cement hydration. The application of electron microscopy, particularly the scanning electron microscope (SEM), in recent years has been very useful in the characterisation of the CSH phases, enabling Diamond(1) to classify them into several microstructure-types.

The composition(s) of the CSH phase(s) in hydrated cements are, however, more difficult to determine. Using the SEM in conjunction with an energy-dispersive X-ray microanalysis (EDAX) system, a comprehensive study of the elemental composition of the gel phase in hydrated Portland cement was made in this laboratory a few years ago(2). It was pointed out that the task of isolating the CSH phase(s) free of other hydration products within the volume of X-ray excitation in an SEM is a formidable one and only a statistical assessment of the results was possible. Recognising these difficulties Dent Glasser et al(3) have recently attempted X-ray microanalysis of dispersed CSH particles produced by the hydration of tricalcium silicate (C_3S) using a transmission electron microscope (TEM). For isolating the CSH phase(s), this method of analysis is undoubtedly superior but as the authors have remarked hydrate phases that are strongly attached to the unhydrated grains can sometimes escape dislodgement and, therefore, are not analysed. Moreover, there is at present a prevalent view that in hydrated C_3S the composition of the CSH phase(s) varies with its distance from the unhydrated core and indeed such variations form an important part of the interesting speculations(3-5) that are currently being made about the mechanisms of cement hydration. In an electron-optical study of a dispersed cement paste sample, information on the progressive nature of the microstructure development in CSH is likely to be, at least, partially lost and from this point of view X-ray microanalyses carried out with an SEM or an electron probe microanalyser (EPMA) have merits of their own.

Some aspects of the microanalysis of CSH phase(s) in hydrated C_3S by EPMA, particularly the effect of electron beam voltage on the analysis are described in this paper.

EXPERIMENTAL

Two samples of C_3S paste were examined in this study. One was a 30-day material prepared using a water/solid ratio of 0.6 and previously described by Stucke and Majumdar(6) and the other represented the same sample hydrated for a further period of 11 months. For the second sample, which was hydrated for a total period of one year hydration had been temporarily arrested at one month to obtain the specimens for the earlier study(6). From the point of view of assessing the effect of electron accelerating voltage on the C/S ratio of CSH, this interruption in the hydration processes is considered not very important. Two specimens of naturally occuring tobermorite from two different localities were also analysed.

The specimens examined by EPMA were polished sections of samples impregnated in resin, the final polishing having been done with 0.25 μm diamond paste. The mineral wollastonite was used as the standard for Ca and Si. After polishing the C_3S paste specimens were lightly etched by immersing them in ethanol containing 1% HNO_3 for 3 seconds. These and the standard specimen were vacuum coated with~30 nm of carbon in the same operation. SEM examinations were carried out on freshly fractured surfaces which were sputter coated with 20 nm of gold.

The instrument used in the analysis was a Microscan 9, a computer controlled EPMA having a take-off angle of 75° manufactured by the Cambridge Instrument Company. The SEM used was a 'Stereoscan IIA' from the same Company. Initially, the EPMA analysis of the 30-day sample was carried out at 15 KV to obtain comparisons with the previous SEM/EDAX results(6). The analysis was then repeated at 10 KV when it was observed that there were systematic differences between the results obtained at the two voltages. This was confirmed by analyses carried out on the one year old sample and it was felt that an experimental assessment of the voltage effect on CSH phase analysis was warranted. Analyses were, therefore, carried out at different voltages in the range 6-25 KV.

It is well known that materials such as CSH are likely to suffer from beam damage during analysis in an EPMA. To reduce this effect a probe current of 1 nA was used throughout. At the lower accelerating voltages the count rates were consequently low (for example, ∿24 c/sec for CaKα and SiKα on wollastonite at 6 KV) and the counting times were increased at the lower accelerating voltages to reduce the statistical error. The analysis times on the standard and unknowns were kept the same at each accelerating voltage to ensure that the level of carbon contamination (due to cracking of pump oil) on the specimens were similar.

The primary standard wollastonite was analysed each day prior to the analysis of the hydrated C_3S samples. The Ca and SiKα count rates were measured from 6 or more positions on the standard, 20 μm apart, and an average taken. A new set of positions were chosen each time the standard was analysed and only those sets of analyses that gave coefficients of variation less than 2.0% were accepted. During the first measurements on the standard a peak searching routine was performed by the spectrometers. At low count rates this took 3-4 minutes and during this period the electron probe remained focussed on the specimen. This sometimes led to inconsistent results which were rejected. During subsequent analyses this problem did not arise as the probe was blanked off from the specimen at all times except when emergent X-rays were counted. For all analyses the background count rates were measured at a distance of $1^{o}\theta$ from the centroid of the peak on the side of the increasing Bragg angle.

With the hydrated C_3S samples, the regions to be analysed were selected on the basis of morphological features seen in their back-scattered electron images. In the initial work at 10 and 15 KV analyses were carried out on one spot only once and between 5 and 20 positions were analysed. Where unhydrated C_3S grains were present, they served as internal

standards. The stability of the instrument could be judged by performing analysis on them periodically. As a further check, analysis of the woolastonite standard was carried out from time to time.

In the study concerned with the effect of beam voltage on the C/S ratios of CSH phase(s) measurements were first made at an accelerating voltage of 6 KV. The voltage was then increased to a predetermined level and the appropriate analysis carried out. The voltage was then reduced to 6 KV and the C/S ratio re-determined. If there was no significant difference between this figure and the previous one, both measured at 6 KV, the voltage was increased to the next higher value. This procedure was repeated until the highest selected voltage (ie 25 KV) was reached. When the analysis from successive 6 KV measurements showed a significant difference, the spot position was moved ∿2 μm along the centre line of the region analysed. For each selected voltage at least seven spot analyses were obtained and the average taken.

RESULTS AND DISCUSSION

(a) Microstructure of C_3S pastes

The microstructure of one month old C_3S paste has been described previously in some detail(6). Figure 1 is a low-magnification SEM photograph showing fibrous CSH (Type I after Diamond(1)) and large $Ca(OH)_2$ crystals. Figure 2 is a corresponding EPMA photograph taken on the polished sample. In this micrograph the fibrous detail is missing and it is thought that vacuum impregnation of the sample with resin employed in the preparation of polished specimens is responsible for the covering up of this detail.

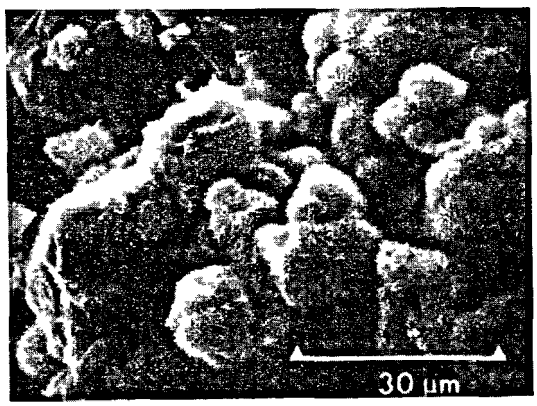

Fig 1 SEM photo showing fibrous CSH in one month old C_3S paste

Higher magnification SEM and EPMA photographs of the C_3S/CSH interface are shown in Figures 3 and 4. The rim surrounding the unhydrated C_3S core, described in the earlier paper(6) as 'inner product' represent Type IV CSH in Diamond's(1) classification. The dark region in the EPMA photographs (Figures 2 and 4) is a mixture of the embedding resin and CSH, probably of the Type I variety. Between this and the inner product layer there is seen (Figure 4) a dense but granular structure.

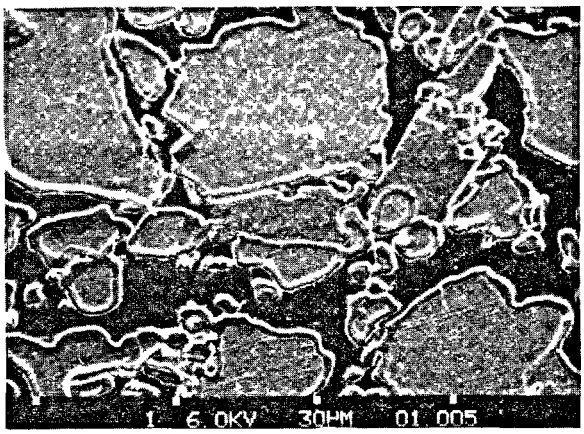

Fig 2 Backscattered EPMA photo corresponding to Fig 1

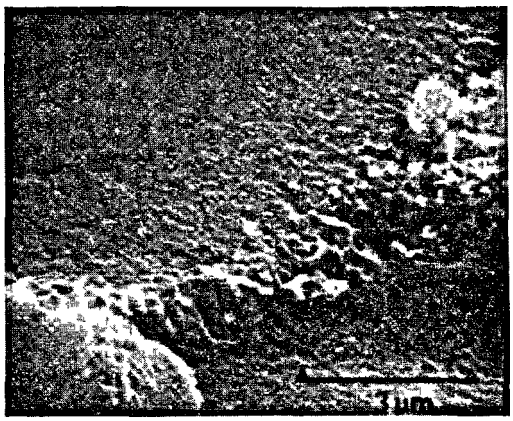

Fig 3 C_3S/CSH interface, SEM photo of one month old C_3S paste

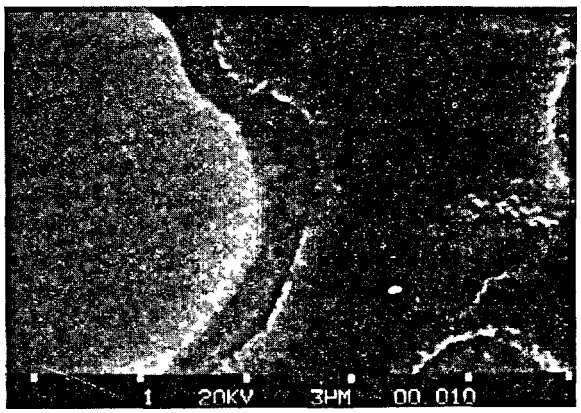

Fig 4 C_3S/CSH interface, EPMA photo corresponding to FIg 3.

Low magnification SEM and EPMA micrographs of the one year old C_3S paste are shown in Figures 5 and 6. It can be seen that in comparison with the 30-day sample the hydration rim is wider here and the proportion of hydrated material greater. In this Type IV CSH rim that surrounds the C_3S core, a discontinuity was often seen. Analysis of C/S ratios of hydrate regions on either side of the

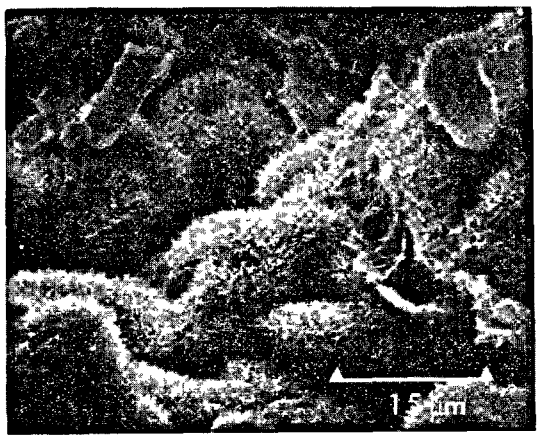

Fig 5 SEM photo of one year old C_3S paste

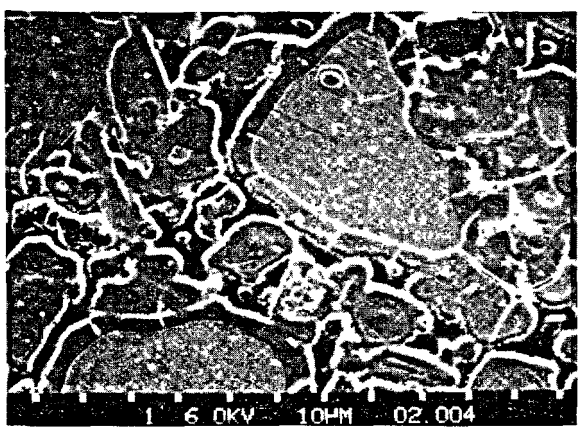

Fig 6 EPMA photo of one year old C_3S paste

discountinuity gave virtually the same results (1.7 ± 0.15 for 6 measurements and 1.63 ± 0.05 for 11 measurements, all at 15 KV). It can only be assumed that this discontinuity was caused by the arrest in the hydration process in the sample at one month as mentioned in a previous section. In other respects the microstructure of the one year sample was essentially the same as that of the one month old sample and the CSH exhibited Type I and IV morphologies. In some EPMA photographs the fibrous Type I CSH was clearly discernible forming the outermost hydration layer.

(b) C/S ratios in CSH phase(s)

The C/S ratios of unhydrated C_3S grains, Type IV CSH and Type I CSH obtained by microanalysis at 10 and 15 KV are listed in Table I. It is clearly seen that for immature C_3S, the effect of increasing the beam voltage was to increase the C/S ratios of both CSH IV and CSH I phases in a significant way. This trend was also observed for CSH phase(s) present in the one year old sample albeit to a lower extent. No such trend was found in the analyses performed on hydrated C_3S cores. The other noteworthy observation was that the Type I CSH in the pastes showed a much wider scatter in the Ca and Si count rates from spot to spot although the scatter in the C/S ratios was significantly lower than that observed for Type IV CSH in the 30-day old sample.

TABLE I ANALYSIS OF PASTE HYDRATED C_3S

SAMPLE	ACCELERATING VOLTAGE (KV)	C/S	NO. OF ANALYSIS	95% CONFIDENCE INTERVAL
A. One month old water/solid = 0,6				
C_3S	10	3.02	13	± 0.07
	15	3.05	6	± 0.09
CSH Type IV	10	1.60	5	± 0.16
	15	1.82	9	± 0.22
CSH Type I	10	1.52	6	± 0.05
	15	1.74	5	± 0.05
B. One year old water/solid = 0,6				
C_3S	10	3.04	7	± 0.03
	15	3.00	6	± 0.06
CSH Type IV	10	1.60	20	± 0.07
	15	1.66	17	± 0.05
CSH Type I	10	1.60	6	± 0.10
	15	1.65	11	± 0.12

(c) Effect of beam voltage on C/S ratios of CSH

The variations in the C/S ratios of the Type IV CSH phase with beam voltage observed with both one month and one year old C_3S pastes are shown in Figure 7. The variations shown for each voltage represent at least six different spot analyses. The hydrate rims analysed rarely exceeded 1.5 µm for the one month sample but they were approximately 5 µm wide in the one year old sample. It is seen that the voltage effect is more pronounced for the one month old sample where the CSH phase consists of smaller and thinner particles. It is also evident from Figure 7 that unhydrated C_3S grains do not show this voltage effect and neither does the tobermorite sample from Portree which has a dense, featureless microstructure (Figure 8). The other tobermorite specimen, from Zacatecus in Mexico has a platy microstructure intermixed with FeS_2 (Figure 9) and a slight dependence of its C/S ratio on the beam voltage has been recorded.

In order to explain the observed voltage effect on CSH phase analysis it is necessary to consider the effective ranges of the electron in the hydrate as this would be the limiting distance up to which the electrons are still capable of exciting characteristic X-radiation. Many workers have studied this problem, both theoretically and experimentally and a summary is given in the review by Beaman and Isasi(7). Calculations based on some of the relationships tabulated in reference 7 show that for a material of composition $C_3S_2H_3$(8) having a density of 2.7 the electron penetration for calcium X-ray generation increases from ∿0.3 µm at 6 KV to ∿5-6 µm at 25 KV. For lateral spread of electrons the radius

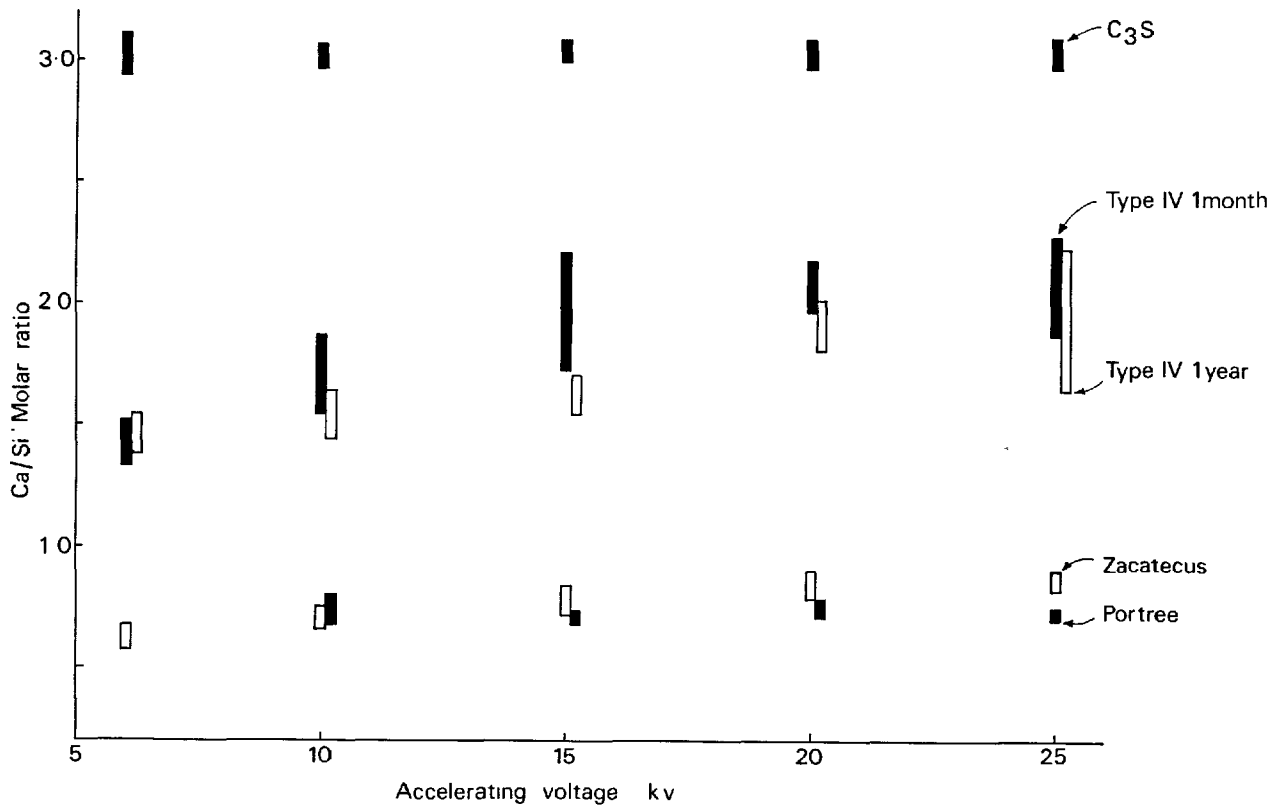

Fig 7 Variation of C/S ratio with accelerating voltage.

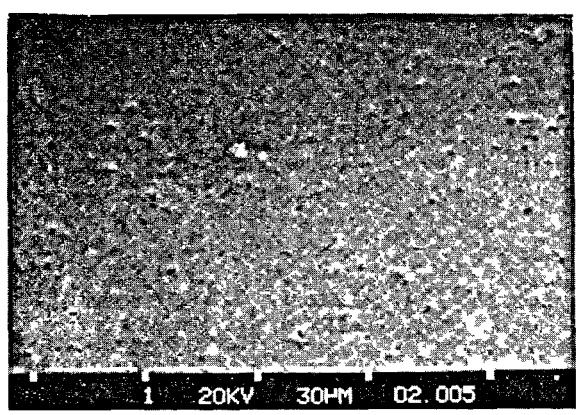

Fig 8 Tobermorite from Portree, EPMA photo

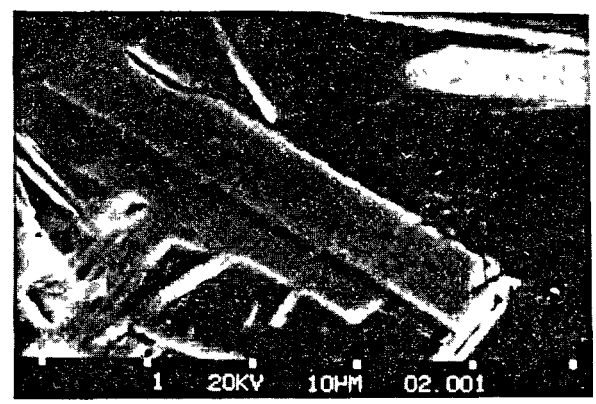

Fig 9 Tobermorite from Mexico, EPMA photo

of the probe diameter, typically 0.14 and 0.08 μm at 6 and 25 KV respectively for the instrument used, has to be added to these values. Of all the studies cited by Beaman and Isasi(7), the work of Andersen(9) who measured the penetration and spread of the volume of X-ray excitation with a Si/SiO_2 combination is perhaps the most relevant to the present study. The values of electron penetration and spread for C_3S and $C_3S_2H_3$ calculated from the expressions given by Andersen are shown schematically in Figure 10 for different electron accelerating voltages.

Calculation of the quantitative X-ray resolution as defined by Reed(10) were also made without the correction due to Duncumb. The results obtained gave values that were higher than Andersen's spread values by up to 18% in the range 6-25 KV. The estimates illustrated in Figure 10 leave no doubt that high electron accelerating potentials have a very pronounced effect on the size of X-ray excitation volume in CSH and allied materials. In the present

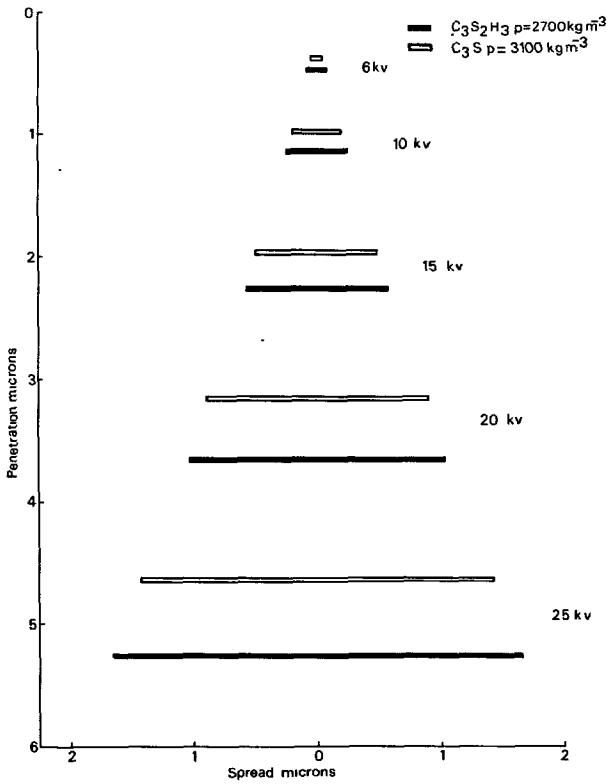

Fig 10 Effective electron penetration and spread for C_3S and $C_3S_2H_3$

work polished specimens of C_3S pastes have been subjected to microanalysis by the EPMA. In these specimens the location of the cutting plane through any hydrated C_3S particle is difficult to establish without definite knowledge of the size and shape of the particles concerned. As the electron ranges increase appreciably with accelerating potential, at high KV's say, 15-25 KV, the analysis of the CSH phase is likely to include a contribution from the underlying material which could either be unhydrated C_3S or $Ca(OH)_2$ or both. In each case the estimated C/S ratio will increase, and the effect will be more pronounced in the thinner and smaller hydrate particles analysed. Results shown in Figure 7 supports this view. That the lowest scatter in the observed C/S ratios of the hydrates correspond to analyses carried out at the lowest beam voltage is also in agreement with the above argument. Judged from this point of view, the most accurate estimate of CSH phase(s) in hydrated C_3S samples from EPMA is likely to be obtained if the analysis is carried out at the lowest possible beam voltage that is compatible with a reasonable count rate. Present work would indicate that Type IV CSH in C_3S pastes has a C/S ratio of 1.44 $\pm$ 0.08.

Because the fibrous, Type I hydrate appeared only as a mixture with the resin the amount of hydrate in any analysis volume was variable. This is reflected in the high variation in the Ca and Si weight percent results and the low variation in the C/S ratios. The analyses of this hydrate also showed a reduction in the C/S ratio with decreasing accelerating voltage. This reduction was most significant for the thirty day old sample where the proportion of unhydrated C_3S would be greatest. The volume analysed by the probe is expected to be similar in both the Type IV and the Type I/resin materials.

The CaO and SiO_2 analyses obtained at 6 KV for the Type IV hydrate was used to calculate the formula of the hydrate. It was assumed that remainder of the hydrate was chemically combined water. The molar proportions obtained were 3 $\pm$ 0.3, 2.07 $\pm$ 0.16, 3.6 $\pm$ 0.62 for CaO, SiO_2 and H_2O respectively for the one year sample and 3 $\pm$ 0.3, 2.1 $\pm$ 0.17 and 3.0 $\pm$ 1.0 for the thirty day sample.

These observations need to be confirmed by other workers but they strongly suggest that the stoichiometry of the different types of CSH phase(s) in mature C_3S pastes may not be far removed from the ideal formulae $3CaO.2SiO_2.3H_2O$ put forward by Brunauer et al many years ago(8).

(d) Beam Damage

In some instances beam damage has been observed on CSH particles on prolonged electron bombardment. Typical examples are shown in Figure 11. While studying the effect of beam voltage on Type IV CSH phase analysis it has been observed that as a consequence of increasing the voltage from 6 KV to 25 KV in stages as described, the final spot analysis at 6 KV (ie after 9 analyses altogether on the spot requiring a total analysis time of 7-8 minutes) can show a depletion in the calcium content of up to ~35%. The silicon content remains relatively unaffected. The instability of calcium bearing minerals due to electron bombardment has been reported in the literature(11). In the analysis of small and thin CSH particles particular attention needs to be paid to this aspect.

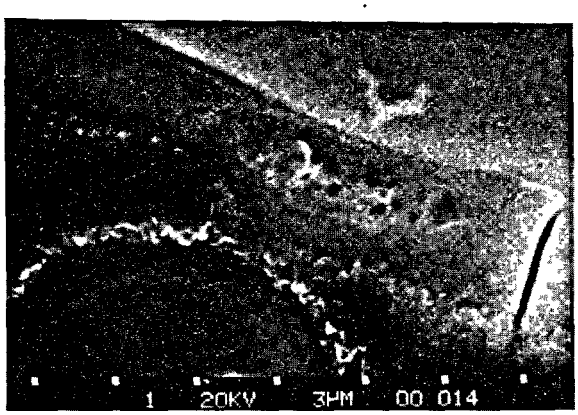

Fig 11 Electron beam damage in CSH

CONCLUSIONS

1 The C/S ratios of Type IV and Type I CSH phase(s) present in immature C_3S pastes as determined by EPMA were found to be 1.82 $\pm$ 0.22 and 1.74 $\pm$ 0.05 respectively at 15 KV. Previous SEM/EDAX analyses on the same sample gave 1.9 $\pm$ 0.1 and 1.6 $\pm$ 0.1 at the same voltage. The agreement between the two sets of results is considered to be good.

2 The C/S ratios of Type IV and Type I CSH phase(s) present in one year old C_3S pastes as determined

by EPMA were 1.66 ± 0.05 and 1.65 ± 0.12 at 15 KV. A similar study by Grutzeck and Roy(12) on the hydration rim around C_3S in a 24-week old paste gave a C/S ratio of 1.7 ± 0.1, also at 15 KV.

3 The C/S ratios of CSH phase(s) obtained by EPMA were dependent on the beam voltage used. At the lowest beam voltage used (ie 6 KV) where the analysis is least affected by the penetration and lateral spread of the electron beam, the C/S ratio obtained for Type IV CSH was found to be 1.44 ± 0.08.

4 The present work suggest that the stoichiometry of CSH phase(s) in mature C_3S pastes is not far removed from the ideal formula $3CaO.2SiO_2.3H_2O$. It is not impossible that CSH phases exhibit different morphologies but their equilibrium compositions are very similar.

ACKNOWLEDGEMENT

The work described has been carried out as part of the research programme of the Building Research Establishment of the Department of the Environment and this paper is published by permission of the Director.

REFERENCES

1 Diamond S (1976). Cement paste microstructure - an overview at several levels. Hydraulic cement pastes: their structure and properties. Proceedings of Conference at University of Sheffield, Cement and Concrete Association, 2-30.

2 Stucke M S, Majumdar A J (1976). The composition of the gel phase in Portland Cement. Hydraulic cement pastes: their structure and properties. Proceedings of Conference at University of Sheffield, Cement and Concrete Association, 31-51.

3 Dent Glasser L S, Lachowski E E, Mohan K, Taylor H F W (1978). A multi-method study of C_3S hydration. Cement and Concrete Research, 8, 733-740.

4 Double D D, Hellawell A, Perry S J (1978). The hydration of Portland Cement. Proc R Soc Lond A, 359, 435-451.

5 Birchall J D, Howard A J, Bailey J E (1978). On the hydration of Portland Cement. Proc R Soc Lond A, 360, 445-453.

6 Stucke M S, Majumdar A J (1977). The morphology and composition of an immature C_3S paste. Cement and Concrete Research, 7, 711, 718.

7 Beaman and Isasis (1971). Electron beam microanalysis. Parts I and II. Materials Research & Standards, Vols 11 and 12.

8 Brunauer S, Kantro D L, Copeland L E (1958). The stoichiometry of the hydration of β-dicalcium silicate and tricalcium silicate at room temperature. J Am Chem Soc, 80, 4, 761-767.

9 Andersen C A (1966). Electron probe of thin layers and small particles with emphasis on light element determinations. The Electron Microprobe, T D McKinley, K F J Heinrich, D B Wittry, Eds., Wiley, New York.

10 Reed S J B (1966). Spatial resolution in electron probe microanalysis. X-ray Optics, Microanalysis, IV, International Congress, Orsay, R Castaing, P Descamps, J Philibert, Herman, Paris.

11 Sweatman T R, Long J V P (1969). Quantitative electron probe microanalysis of rock-forming minerals. Journal of Petrology, JPTGA, Vol 10, Part 2, p342.

12 Grutzeck M W, Roy D M (1969). Electron microprobe studies of the hydration of $3CaO.SiO_2$. Nature 223, 492-494.

Caractéristiques thermochimiques du ciment et accélération de durcissement du béton

Thermochemical characteristics of cement and acceleration of concrete setting

I.B. ZACEDATELEV, professeur, chef de laboratoire, VNIPI Teploproekte, Moscou, U.R.S.S.

RESUME : Les recherches calorimétriques d'hydratation du ciment permettent non seulement d'obtenir des informations complètes sur la cinétique du processus en fonction de la composition minéralogique et granulométrique du ciment, mais aussi d'évaluer, sans perturbation du cours naturel du processus, l'influence spécifique des effets thermiques, chimiques et mécaniques.

Le présent rapport a pour objet l'étude de l'ensemble des facteurs cinétiques, thermodynamiques et énergétiques sur l'hydratation du ciment dans des conditions de durcissement accéléré par un traitement thermique.

Des recherches expérimentales effectuées à l'aide d'un dispositif calorimétrique automatisé ont permis, non seulement de déterminer l'influence de la température sur la vitesse d'hydratation, mais aussi de mettre en évidence l'influence de cette température en fonction du degré d'achèvement du processus d'hydratation. Elles ont montré ainsi l'action différente de la température à quatre étapes distinctes du processus d'hydratation, dans des conditions isothermes.
On a observé que l'augmentation, avec la température, du dégagement de chaleur de l'hydratation du ciment était inévitable, à chaque étape du processus d'hydratation, surtout quand le degré d'hydratation était compris entre 0 et 0,8. Ceci met en opposition les caractéristiques cinétiques et thermodynamiques de l'hydratation.

Les résultats ont montré qu'une dérogation au principe thermodynamique de Le Chatelier n'avait pas d'influence nocive sur l'hydratation. Donc l'indépendance, vis à vis de la chaleur dégagée par l'hydratation, d'une action thermique extérieure, tant en durée qu'en intensité, est bien fondée. On en a déduit une méthode d'optimisation du traitement thermique des structures en béton, pour obtenir un durcissement accéléré et utiliser au mieux la chaleur d'hydratation.

SUMMARY: Calorimetrical investigation of cement hydration gives full information about kinetics of process not only depending on mineralogical and grain composition of cement but allows without breaking natural course of process to estimate specifical influence on it of thermal, chemical and mechanical kinds of action.

The present paper accented combined consideration of kinetic, thermodynamical and power factors of cement hydration process at accelerated hardening of concrete at application of thermal action.

Experimental investigation of kinetic characteristics of process (carried out on automated calorimetrical device) allowed to determine not only dependence of damped influence of temperature factor (with increase of temperature level) on hydration rate but also revealed influence of temperature factor in relation to degree of completness of hydration process. Also non-equivalence of temperature function at four different stages of hydration process at isothermal temperature regimes is showed.

Inevitability of intensification of heat liberation of cement at application of thermal action at any stage of completness of hydration process, especialy in limits up 0 to 0.8, is revealed. It causes contradiction between kinetic and thermodynamical characteristics of process.

Results of accomplished physicochemical investigation do not reveal negative influence of infrigement of thermodynamical principle of Le Chatelier. Thus freedom of choice of time of application and intensity of outer thermal influence on hardening system "cement-Water" is substantiated without dependence of action of inner source of heat. Considered ways of optimization of thermal regimes of accelerated setting of cement predetermine more full usage of cement hydration heat in kinetics of heating of products and structures.

L'étude des caractéristiques thermochimiques du ciment à l'aide des dispositifs calorimétriques automatisés à large gamme de conditions limites (1) a permis d'obtenir de nouvelles données sur l'influence des paramètres du régime sur les processus d'hydratation. Pour évaluer l'influence de la température sur la cinétique d'hydratation, il est nécessaire d'adopter une méthode plus stricte de détermination de la fonction de température du processus f_t. L'analyse des données expérimentales obtenues sur base du principe des dégagements calorifiques égaux démontre la nécessité de leur comparaison non pas à choix arbitraire des états équivalents des systèmes durcissants à températures différentes, mais aux états précisement fixés, définis par le degré d'hydratation L:

$$L = \frac{Q_3^x}{Q_3}$$

où: Q_3^x - représente le dégagement calorifique au moment X, Q_3 - représente le dégagement calorifique total.

En vue de simplifier l'expériment, la valeur de Q peut être limitée par la valeur totale du dégagement calorifique à l'âge de 28 jours Q_3^{28}, car à cet âge le degré d'hydratation d'un système (pâte de ciment, mortier de ciment ou béton) à des températures différentes tend à une même valeur (2). On a trouvé expérimentalement les rapports de vitesse V et durée τ pour les températures de 313, 333 et 353°K relatifs à la température normale de durcissement (293°K) pour chaque valeur relative du degré d'hydratation L, déterminée aux intervalles de 10%:

$$\frac{V_t}{V_{20}} = \frac{\tau_{20}}{\tau_t}$$

Ce qu'il y a de particulier, c'est que, en comparant l'intensité du dégagement calorifique $(\partial Q_3/\partial \tau)$ de telle manière, les valeurs maximales ce concentrent dans une même zone à toutes les températures de conservation isotherme (fig.1). Ce fait démontre la justesse de tel approche à la détermination de la fonction de température d'hydratation et confirme, du point de vue de thermochimie du ciment, l'identité du mécanisme d'hydratation à différentes températures.

Telle méthode d'évaluation de l'influence de température sur l'hydratation et le dégagement calorifique du ciment a permis de déceler certaines particularités de leur apparition à différentes étapes du processus. On a remarqué que, tout d'abord, à l'étape d'hydratation L = 0 ÷ 0,3, l'influence de la température sur l'intensification du dégagement calorifique des ciments de tous types était maximale. Ce fait est contribué par la rupture des métastables gaines-protectrices entourant les grains de ciment, ainsi que par l'activation du transfert par diffusion et par convection des

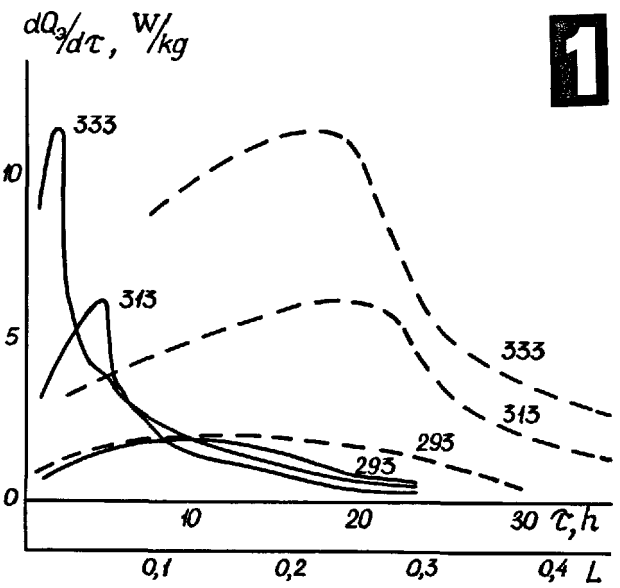

Fig. 1. Intensité de dégagement calorifique en fonction de température aux différentes durées et aux différents degrés d'hydratation du ciment: ——— au temps absolu; — — — — au degré d'hydratation (L) relatif

produits d'hydratation dans le système durcissant. Ayant atteint les valeurs maximales, la fonction de température diminue aux étapes plus avancées à cause d'accroissement de la densité des gaines qui protectent les grains du liant.

Pourtant, on a remarqué que, aux valeurs L = 0,45 ÷ 0,5, pour un certain nombre de ciments, la température intensifie derechef le processus d'hydratation. A notre avis, ce fait est dû à la teneur élevée du ciment initial en fractions grosses (40-60 μ).

Après l'étape d'hydratation active de ces fractions on a observé derechef la diminution des valeurs de la fonction de température du processus. Donc, pour évaluer les processus cinétiques d'hydratation et de dégagement calorifique sous l'influence de température dans des conditions isothermes de durcissement, il faut prendre en considération la composition granulométrique du liant.

En examinant l'influence des caractéristiques thermochimiques du ciment sur durcissement accéléré du béton, il faut faire attention tout d'abord aux régimes thermiques de ces processus. La plupart des problèmes concernant l'utilisation pratique des données de la cinétique d'hydratation et de dégagement calorifique des ciments doivent être résolus pour les régimes thermiques non-stationnaires. Le durcissement accéléré du béton est en général effectué dans des conditions de programme thermique compliqué,

y compris l'irrégulier chauffage et refroidissement.

Jusqu'à présent, de nombreux travaux se rapportant à l'hydratation du ciment ne concernaient essentiellement que l'influence de la température dans des conditions isothermes; aussi la plupart des recommandations d'utilisation des propriétés thermochimiques du ciment avait-elles été données à base de régularités du régime isotherme d'hydratation du ciment et ne représentaient pas toute la complexité des processus réels. Donc, il est nécessaire d'effectuer expérimentalement des recherches de la cinétique de dégagement calorifique dans des conditions de température non-stationnaires. Les recherches de l'influence des températures variables sur l'intensité de dégagement calorifique du ciment sont effectuées d'après une méthode spéciale. Cette méthode consiste à agir sur le mortier de ciment dans le vase du calorimètre différentiel automatisé à température 293°K aux étapes différentes d'hydratation par une impulsion thermique, la valeur de cette impulsion étant choisie de telle sorte que la température du matériel à étudier soit élevée à vitesse de 5, 10 et 15°C/h. Les régularités obtenues de variation de vitesse de dégagement calorifique en fonction de la durée de conservation préalable ont montré que l'action thermique sur le ciment durcissant conduit inévitablement à l'intensification du dégagement calorifique, pratiquement indépendamment du degré d'hydratation (fig. 2). Il est à noter que l'intensité maximale de dégagement calorifique est atteinte au moment final d'élévation de température, et que la valeur absolue de dégagement calorifique dépend de la durée de l'action thermique.

On a constaté l'abaissement monotone de l'intensité du dégagement calorifique en fonction du degré d'achèvement du processus d'hydratation dans les limites L = 0,1÷0,8. Cependant, même si le maximum de dégagement calorifique est atteint au cours de conservation préalable (t = 293°K, τ = 15h, L = = 0,2-0,28), le chauffage extérieur du système durcissant à vitesse 15°C/h provoque une intensité de dégagement calorifique 2,5 fois plus grande que celle de la période maximale.

Les résultats obtenus ont montré l'inévitabilité d'intensification des réactions exothermiques d'hydratation du ciment sous l'action thermique à n'importe quelle étape de durcissement actif du béton. Donc, au cours de durcissement accéléré du béton, il est impossible d'assurer le principe thermodynamique de Le Chatelier qui consiste à la séparation des périodes d'action des sources thermiques intérieures et extérieures en vue d'obtenir des conditions de maximale plénitude des réactions chimiques. Quelles sont les consequences de telle contradiction insoluble entre les conditions thermodynamiques de réalisation de la maximale plénitude du processus d'hydratation et les conditions cinétiques de développement de la vitesse maximale de ce processus? Pour répondre à

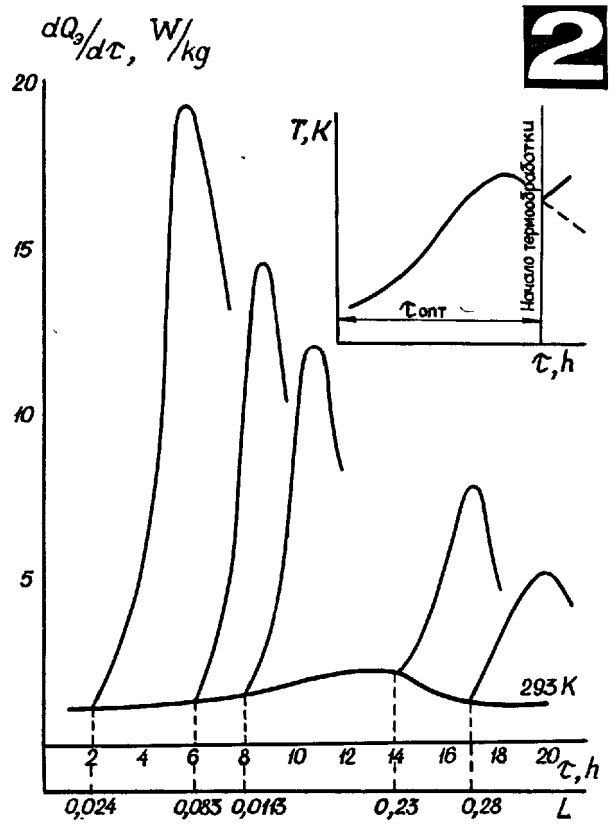

Fig. 2. Intensité de dégagement calorifique aux différentes étapes de traitement thermique (t' = 15°K/h): a) valeurs réelles de "rejaillissement" de l'intensité; b) le schéma recommandé de point de vue thermodynamique d'application de traitement thermique.

cette question on a exécuté des recherches physico-chimiques* de l'influence de différentes formes de conjugaison des caractéristiques cinétiques et thermodynamiques du processus d'hydratation sur les propriétés finales de la pierre de ciment.

On a examiné la cinétique d'hydratation et de formation de structure de la pierre de ciment à quatre régimes thermiques (fig. 3), ensuite le durcissement se poursuivait dans des conditions d'humidité normale pendant une durée de 28 jours. Dans les deux premiers régimes, on a simulé les conditions favorables (régime 1) et défavorable (régime 2) relativement à l'observation du principe de Le Chatelier à la période initiale d'hy-

* Les collaborateurs suivants ont pris part à ces recherches: D.D. Cotelnicoff, S.A. Chifrine, E.E.Coulago, V.P. Poddoubenco

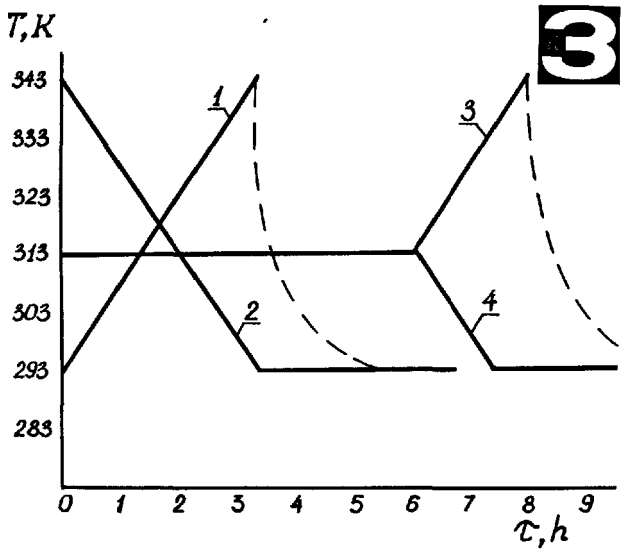

Fig. 3. Régimes thermiques de différentes conjugaisons des caractéristiques cinétiques et thermodynamiques d'hydratation du ciment.

dratation, dans les régimes 3 et 4 - la même chose au moment de dégagement calorifique propre maximal. La détermination de l'eau de constitution et de la chaleur d'hydratation du ciment, l'analyse quantitative et qualitative aux rayons X, les recherches à l'aide du microscope électronique, ainsi que la détermination de résistance à la compression ont démontré qu'il n'y avait pas de différence considérable entre les caractéristiques des systèmes durcissant dans des conditions favorables (refroidissement) et défavorables (chauffage).

Il y avait un devancement d'hydratation aux régimes 1 et 3, ce qui démontre l'influence prédominante des caractéristiques cinétiques. Ces régimes se caractérisent aussi par une plus grande valeur de résistance finale des échantillons à l'âge de 28 jours. En même temps, l'étude de la structure poreuse aux rayons des pores de 0,05 à 25 a montré son identité pour les échantillons qui avaient durci selon les régimes 2 et 4 et ceux qui avaient durci dans des conditions d'humidité normale. Les échantillons qui avaient durci selon les régimes 1 et 3 contenaient plus de pores à rayons 0,6-8 en comparaison aux ceux qui avaient durci dans des conditions d'humidité normale.

Ainsi, les données obtenues permettent de conclure que la combinaison de l'action thermique extérieure (à l'intensité de 15°C/h) avec le dégagement thermique intérieur n'influence d'aucune manière la cinétique et le degré d'hydratation, cette dernière étant un processus physico-chimique irréversible.

Donc, il est possible de choisir une durée d'application et d'intensité de l'action thermique extérieure au béton dans un intervalle plus large. La liberté de choix du temps de début de traitement thermique et de l'intensité d'apport calorifique au béton est d'une grande importance énergétique. En effet, la consommation d'énergie extérieure pour chauffage des articles et structures en béton doit être envisagée en totalité avec les caractéristiques thermochimiques des ciments, ainsi qu'avec la possibilité de maximale utilisation de dégagement calorifique intérieur dans le béton durcissant.

Au cours d'accélération de durcissement du béton sous l'action thermique - à l'usine ainsi qu'à la construction de structures monolithes - l'étape d'élévation de température du béton est critique au point de vue de détermination de puissance de la source énergétique extérieure. Donc, la participation de la source calorifique intérieure en rapport avec le potentiel thermochimique du ciment doit être assurée tout d'abord à cette étape de traitement thermique du béton. Il apparaît que la plus raisonnable solution de ce problème consiste à l'utilisation des régimes étendus ("doux") de traitement thermique, quand la vitesse d'élévation de température du béton peut être comparée au degré d'intensification de chaleur d'hydratation du ciment.

La participation de la source calorifique intérieure au chauffage du béton dépend nonlinéairement de l'intensité du traitement thermique extérieur. Si on dimunue la vitesse d'élévation de température, l'influence de l'effet thermochimique d'hydratation du ciment sur le chauffage du béton accroît sensiblement (fig. 4).

Outre l'intensité de traitement thermique extérieur, la participation du dégagement calorifique intérieur au chauffage du béton est influencée par la durée de ce traitement. En diminuant la période de conservation préalable on peut observer une tendance d'accroissement de participation du dégagement calorifique au chauffage du béton, aux régimes "doux" d'élévation de température (3-5°K/h) qui suivent. Dans des conditions de traitement thermique plus intense, la durée de conservation préalable du béton influence moins la participation du dégagement calorifique au chauffage du béton. Il est à noter que, outre l'économie d'énergie thermique de 40 à 60%, les régimes "doux" de traitement thermique du béton permettent de réduire les processus physiques de destruction dans le béton. Les caractéristiques physico-mécaniques et structurales finales du béton chauffé dans des régimes "doux" sont identiques à celles du béton durci dans des conditions d'humidité normale.

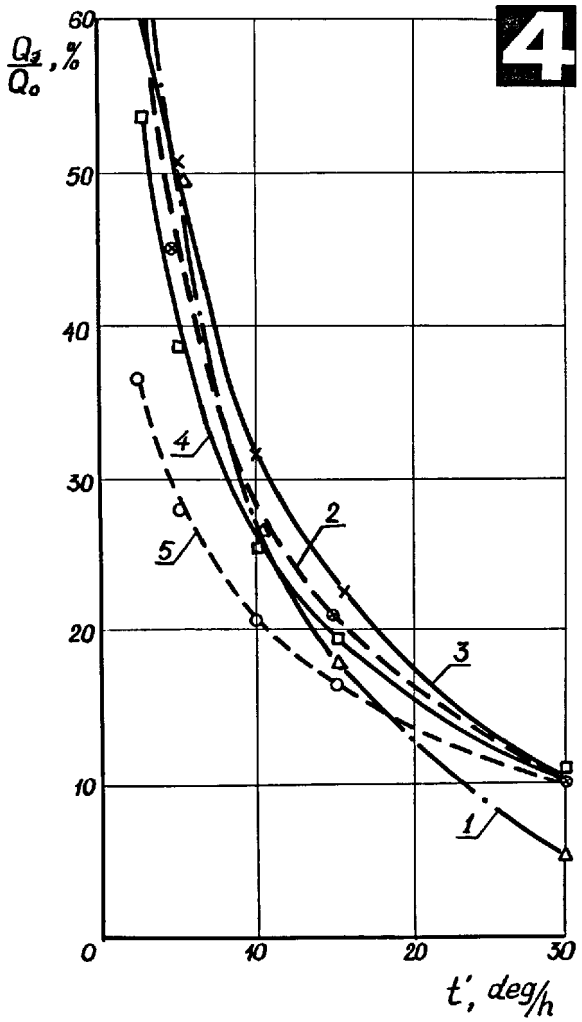

Fig. 4. Degré de participation de la chaleur d'hydratation du ciment (Q_3) à la consommation totale d'énergie thermique (P) pour chauffage du béton à la durée de conservation préalable: 1-0h; 2-2h; 3-6h; 4-10h; 5-24h

CONCLUSIONS

Pour évaluer les processus cinétiques d'hydratation et de dégagement calorifique du ciment, il faut déterminer l'influence du facteur de température aux degrés équivalents d'achèvement des processus d'hydratation (L) dans des conditions isothermes à températures différentes.

On a mis en évidence l'inévitabilité d'intensification de dégagement calorifique au traitement thermique à quelconque étape d'hydratation du ciment (L = 0 ÷ 0,8), ce qui provoque une contradiction entre les caractéristiques thermodynamiques et cinétiques du processus.

Il est démontré par les résultats des recherches physico-chimiques que la dérogation du principe thermodynamique de Le Chatelier n'a pas d'effet nocif sur la cinétique et le degré d'hydratation du ciment.

L'optimisation de la durée et de l'intensité de l'action thermique extérieure permet de recommander des régimes économes de durcissement accéléré du béton diminuant la consommation d'énergie de 40 à 60%.

BIBLIOGRAPHIE

1. - I.B. ZACEDATELEV (1976) "Fonction de température de la chaleur d'hydratation des ciments". 6e Congrès International de la Chimie des Ciments, Moscou, Stroiizdat, v.II, I, 34-38 (russe).

2. - L.E. COPELAND, D.L. CANTRO (1973) "Hydratation du ciment portland". 5e Congrès International de la Chimie des Ciments, Moscou, Stroiizdat, russe.

Les variations de phase et les propriétés du ciment durci

Phase change and properties of hardened cement paste

Z.M. LARIONOVA, candidat de sciences techniques, chef du laboratoire,
L.P. KOURASSOVA, candidat de sciences techniques, collaborateur scientifique supérieur,
Institut des Recherches Scientifiques du Béton et du Béton Armé (NIIZhB), Gosstroy, U.R.S.S.

RESUME : Est étudié le comportement des minéraux principaux du ciment portland durci tels que: hydrosilicate, hydroaluminate et oxyde du calcium hydraté sous différents régimes de traitement thermique à la vapeur ou à sec. Est établi le rapport direct entre la stabilité thermique des formations nouvelles et les propriétés de déformabilité et de résistance du ciment durci.

Est déterminée l'influence de l'adjuvant hydraulico-actif provenant d'un agrégat poreux finement moulu (kéramsite) sur les propriétés du ciment durci. Cet adjuvant exerce une action plastifiante qui dépend de sa composition en grains et en minéraux. Sont mises en évidence les formations dans les zones de contact, et l'évolution de la microstructure du ciment étuvé, qui améliore sa compacité et son durcissement.

SUMMARY: Behaviour under different regimes of moist steam curing and dry heating for main minerals of portland cement hardened paste - hydrosilicate, hydroaluminate, hydrate calcium oxide has been studied. A direct dependence between thermal stability of new formations and deformative and strength properties of hardened cement paste has been given.

There has been determined the influence of hydraulicly active admixture from fine-ground porous aggregate-ceramsite on properties of hardened cement paste. The admixture produces a plasticizing action, which depends on its grain and substance fineness. Regularities of forming of contact zone and microstructure of steam-cured hardened cement paste, resulting in its compaction and strengthening, has been revealed.

Les caractéristiques techniques du ciment durci et du béton sont dans une mesure considérable conditionnées par la stabilité de leures composantes minérales et de leures structures. Pendant le durcissement du ciment la composition de la phase liquide change et cela entraîne les changements, de phase dans certaines nouvelles formations d'hydrates. D'autre part, dans les conditions d'exploitation du béton (par exemple, sous le chauffage) les changements des minéraux du ciment durci et la reconstruction de la microstructure ont lieu aussi.

Dans la pierre de ciment portland sans adjuvants un hydroaluminate de calcium à haute basicité, C_4AH_{13}, se cristallise. L'examination radiographique a montré que dans les conditions de haute saturation de la phase liquide par les ions de calcium (dans le ciment d'alite-aluminate) une transformation d' α - C_4AH_{13} dans β- forme a lieu. Cela n'exerce pas de grande influence sur la résistance du ciment durci /5/.

Pendant un long durcissement dans les conditions normales ou sous le traitement thermique la transformation de C_4AH_{13} hexagonal dans C_3AH_6 cubique a lieu et cela abaisse la résistance du ciment durci. Si la température dépasse 150°C l'hydroaluminate cubique de calcium se décompose en $C_4A_3H_3$ et $Ca(OH)_2$. Sous l'élévation ultérieure de la température on peut observer la déshydratation de $Ca(OH)_2$ (t° = 450 - 520°C) et la décomposition postérieure de $C_4A_3H_3$ (t° = 620°C) /3-5/.

Dans la pierre de ciment portland additionnée de gypse et sous la température normale hydrosulfoaluminate de calcium $C_3A \cdot 3CaSO_4 \cdot H_{31}$ est la nouvelle formation essentielle contenant l'aluminate (ettringite) dont la stabilité est déterminée par la composition minérale du ciment de base (Fig.1). Dans les ciments d'alite-aluminate

Fig. 1 - Les custaux d'ettringite $C_3A \cdot 3CaSO_4 \cdot H_{31}$ sous la température normale. Une réplique platino-carbonique, x 10000

et d'alumoferrite c'est l'ettringite qui est une nouvelle formation stable. Il paraît que ses cristaux aciculaires "renforcent" le ciment durci et le font par cela plus consolidé. Dans le ciment de bélite-aluminate après la fixation complète du gypse a lieu la transformation d'ettringite dans monosulfoaluminate de calcium, $C_3A \cdot CaSO_4 \cdot H_{12}$. L'augmentation de la résistance des éprouvettes dans cette période est ralentie /4/.

Le traitement par le chauffage dans la vapeur contribue aussi à la transformation partielle d'ettringite dans monosulfoaluminate de calcium. Au cours de chauffage à sec sous la température 100°C l'ettringite perd $20H_2O$ et commence à se décomposer en dégageant le gypse bi-hydraté et le gypse semi-hydeaté. A la Fig.2 sont présentée les clichés radiographiques d'ettringite chauffé gamme des températures etant 20-800°C. Est montré que sous la t° = 100°C les lignes principales d'ettringite (d = 9,8; 5,7; 3,86; 3,48; 2,57; 2,2 Å) diminuent brusquement; une ligne à partir de d = 7,6 Å appartenante au gypse.

Sous le chauffage jusqu à la température 200°C $6H_2O$ reste dans l'ettringite; un dérèglement dans la structure cristalline du minéral a lieu; le changement de ses propriétés optiques et les résultats de l'analyse radiographique le témoigne. On peut observer la disparition des lignes principales d'ettringite.

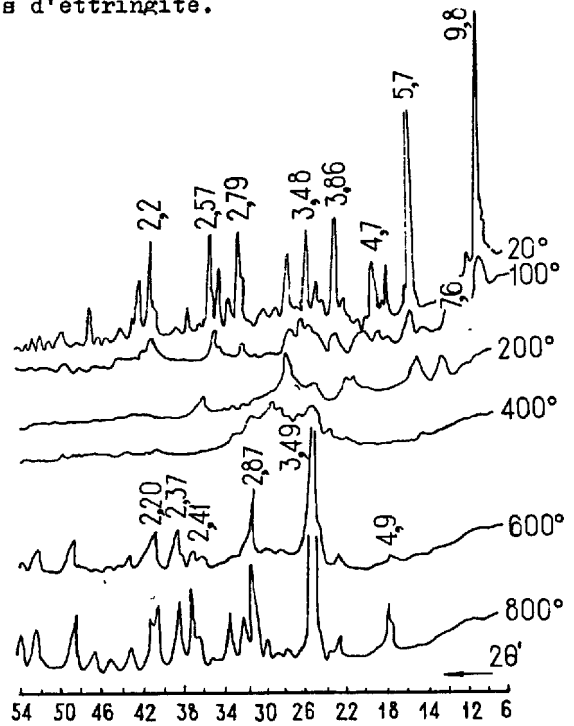

Fig. 2 - Les radiographiques d'ettringite chauffé des températures 20, 100, 200, 400, 600, 800°C

Le chauffage jusqu à la température 400° et 600°C amène à la décomposition d'ettringite en CaO, $C_{12}A_7$ et $CaSO_4$. Une ligne faible d'anhydrite a partir de d = 3,49 Å paraît sous la t° = 400°C. Sous la température 600°C on peut voir les lignes CaO (d =

2,41 Å), $C_{12}A_7$ (d = 4,9 Å) et $CaSO_4$ (d = 3,49; 2,87; 2,32; 2,2 Å) à la Fig.2. Après le chauffage sous la température 800°C une décomposition complète a lieu /5/. A la place de lui (d'ettringite) sur les clichés radiographiques (Fig.2) sont marquées des lignes nettes des produits de décomposition cités plus haut. Fig.2 les clichés radiograhiques d'ettringite sous les températures telles que: 20, 100, 200, 400, 600, 800°C.

La composition de hydrosilicate de calcium dans le ciment hydraté varie de C_2SH_2 au CSH(B) /3-5/. Au cours de durcissement du ciment durci dans les conditions normales la composition de hydrosilicates de calcium pratiquement ne change pas mais ses cristaux s'agrandissent un peu (Fig.3). Au cours de traitement autoclave, surtout si on y additionne de silice, la composition de hydrosilicate change vers CSH(B). Avec cela on peut observer sa cristallisation nette qui amène à l'augmentation de la résistance des éprouvettes (Fig.4). Un traitement autoclave de longue durée contribue à la formation dans le ciment durci de gros cristaux de tobermorite $C_4S_5H_5$ (Fig.5).

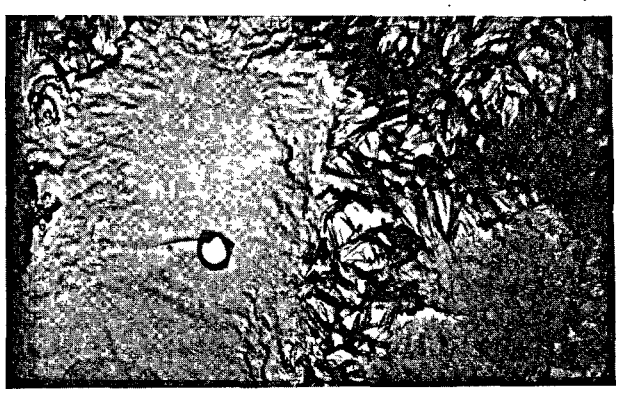

Fig. 3 - Les cristaux de hydrosilicate de calcium C_2SH_2 sous la température normale. Une réplique platino-carbonique, x 10000

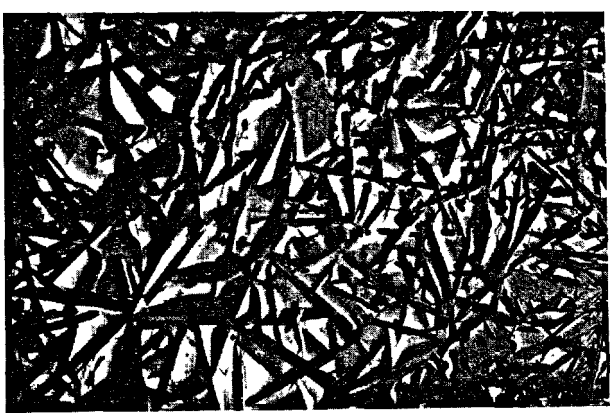

Fig. 4 - Les cristaux de hydrosilicate de calcium CSH(B) après le traitement autoclave.
Une réplique platino-carbonique, x 10000

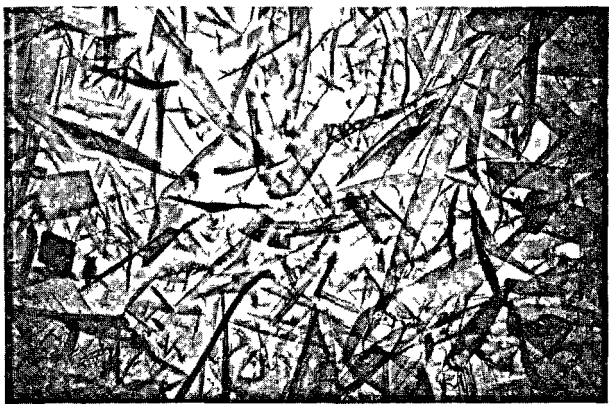

Fig. 5 - Les cristaux de tobermorite $C_4S_5H_5$ après le traitement autoclave de longue durée.
Une réplique platino-carbonique, x 10000

Sous le chauffage du ciment durci dans le milieu sec à l'air une déshydratation progressive des nouvelles formations hydrosiliciques a lieu. On peut en juger d'après la réduction de la quantité de l'eau hydratée, d'après l'accroissement de la masse spécifique des éprouvettes ainsi que d'après la diminution de grandeur des ligne CSH(B) sur les clichés radiographiques. La déshydratation du ciment durci est accompagnée par la diminution de volume de la phase solide, par l'augmentation de la porosité, par l'affaiblissement de la résistance (par rapport aux éprouvettes de durcissement normal).

L'hydrate d'oxyde de calcium $Ca(OH)_2$ (portlandite) se forme pendant l'hydratation de C_3S et se dégage dans le ciment durci, en général, en état d'agglomérations microgranulées. Dans les zones inétanches et sur les parois des pores se forment les cristaux plus gros de portlandite. Sous le chauffage au-dessus de température 500°C la déshydratation de $Ca(OH)_2$ a lieu, avec cela les grains de CaO se forment dans le ciment durci. Dans les conditions de durcissement sec à l'air dans le ciment durci a lieu une facile carbonatation de portlandite qui se transforme dans la calcite. La calcite est une composante stable du ciment durci et contribue au compactage et à la consolidation de ce dernier. L'aragonite et le vaterite sont les variétés de la calcite. La décomposition thermique de la calcite a lieu sous la température 780-820°C /4,5/.

Les résultats des études complexes ont témoigné un rapport direct entre la stabilité thermique des nouvelles formations et les propriétés techniques du ciment durci.

Les changements importants du composé de phase et de microstructure du ciment de portland durci se produisent en présence des particules des agrégats poreux hydrauliquement actives et à dispersion fine (pulvérulentes). Par la réalisation des essais spéciaux on a détermine l'influence de ces particules sur les caractéristiques

rhéologiques et sur les caractéristiques de résistance du ciment durci.

En qualité d'agrégat poreux de base on a utilizé le kéramsite dont le grain a une structure zonaire (zone extérieure et zone intérieure) et dont la composition chimico-minéralogique, la structure et les propriétes physiques pour chaque zone sont inégales. Il est présenté par la phase de verre (≈70%) d'une composition alumosiliceux. Quartz est le minéral principal, de la phase cristallique (≈20%), les minéraux de second ordre sont tels que: feldspath, spinelle, hematite et d'autres - 10% au total.

On a effectué les études du ciment durci et des mortiers de ciment - sable avec du sable quartzeux et addittionnés de particules pulvérulentes des zones extérieure (P.e.) et intérieure (P.i.) du granule de kéramsite en quantité de 5-20%; ses particules remplacent la partie de masse du ciment. Le nombre maximum des particules répondait au teneur en ces particules dans le béton de kéramsite réel. La surface spécifique, Ssp., de particules soit correspondait à celle du ciment de base, Ssp. = 3000 cm^2/g, soit en était considérablement supérieure, Ssp. = 7000 cm^2/g. Le ciment de portland alitique a été à faible teneur en aluminates. On a étuvé les éprouvettes sous la température 85°C avec la régime 3+6+3, après cela avant la réalisation des essais (pendant 28 jours et plus) on les a conservé dans la chambre du durcissement normal. On a réalisé la comparaison avec des compositions sans particules (composition-temoin) avec Ɛau/Liant = const. et Ɛau/Liant ≠ const.

Indépendamment de la composition minéralogique et de la composition en grains des particules pulverulentes, à Ɛau/Liant = const., a eu lieu l'épaississement de la pâte de ciment; ce processus devient de plus en plus intensif à mesure de l'augmentation de leur nombre et de leure dispersité. Plasticité de mélanges des mortiers se change en fonction de la dispersite et de la composition minéralogique des particules

La résistance du ciment durci et du mortier composé de ciment et de sable (avec Ɛau/Liant = const. et avec Ɛau/Liant ≠ const.) à l'age de 1; 28 et 360 jours change d'une façon identique en fonction de la quantité et du type des particules. A la Fig.6 sont représentés les diagrammes du changement rélatif de la résistance des mortiers composés de ciment et de sables. Sont présentés les résultats des essais pour les mélanges des mortiers a consistance uniforme à l'age de 28 jours.

La présence des particules de la zone extérieure du granule de kéramsite en quantité jusqu'aux 10% et avec Ssp. = 2700 cm^2/g et jusqu'aux 20% avec Ssp. = 7000 cm^2/g n'abaisse pas la résistance. Le plus grand dépassement de la résistance de 10% dans le premier cas et de 20% - dans le deuxième cas est caractéristique pour les compositions contenants 3-5% et 10% des particules.

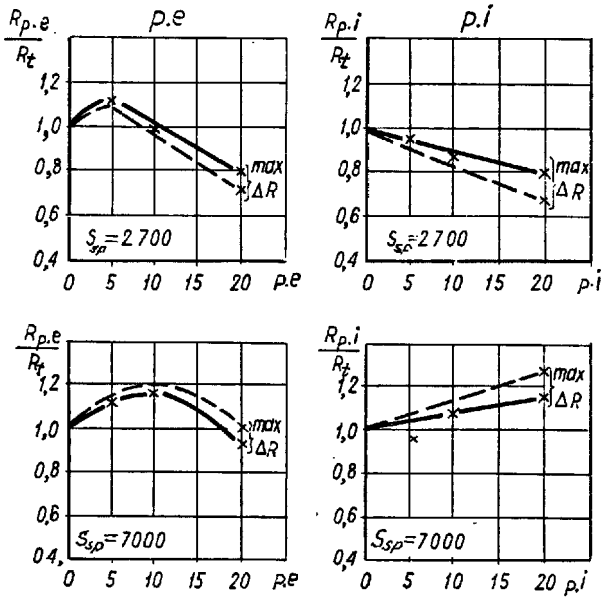

Fig. 6 - Le changement de la résistance rélatives R_p/R_t des mortiers selon la quantité des particules (en %) avec Ssp. = 2700 et 7000 cm^2/g
Rpe. - la résistance des mortiers avec des particules de la zone extérieure de kéramsite, Rpi. - la résistance des mortiers avec des particules de la zone intérieure de kéramsite, R_t - la résistance des mortiers sans particules (composition témoin)
——— compositions avec Ɛau/Liant = const;
----- compositions à consistances égales (Ɛau/Liant ≠ const.).

L'introduction des particules extraites de la zone intérieure du granula de kéramsite avec Ssp. = 2700 cm^2/g abaisse la résistance à mesure de l'augmentation de leur nombre; avec Ssp. = 7000 cm^2/g on peut constater l'augmentation de la résistance de 20% accompagné par l'accroissement de la masse volumétrique proportionnellement à la teneur en adjuvant; dans le même temps dans d'autres cas la masse volumétrique diminue un peu /2/.

On a déterminé que les particules de la zone extérieure du granule de kéramsite se distinguent de celles des particules de la zone intérieure du granule par leure composition chimico-minéralogique, par une plus grande activité hydraulique, par des plus petites masses spécifique et volumétrique. Elles ont une structure imbriquée, stratifiée et aux pores fins (aux pores <1 mkm). Les particules de la zone intérieure du granule ont une surface régulière et vitreuse, les pores y sont rarement situés et ont le diamètre de ≈10 mkm (Fig.7). C'est pourquoi a mesure de diminution de grains la porosité des particules de la zone extérieure du

granule presque ne change pas; et la structure des particules de la zone intérieure du granule change brusquement jusqu'à devenir compacte-dans les particules < 15 mkm.

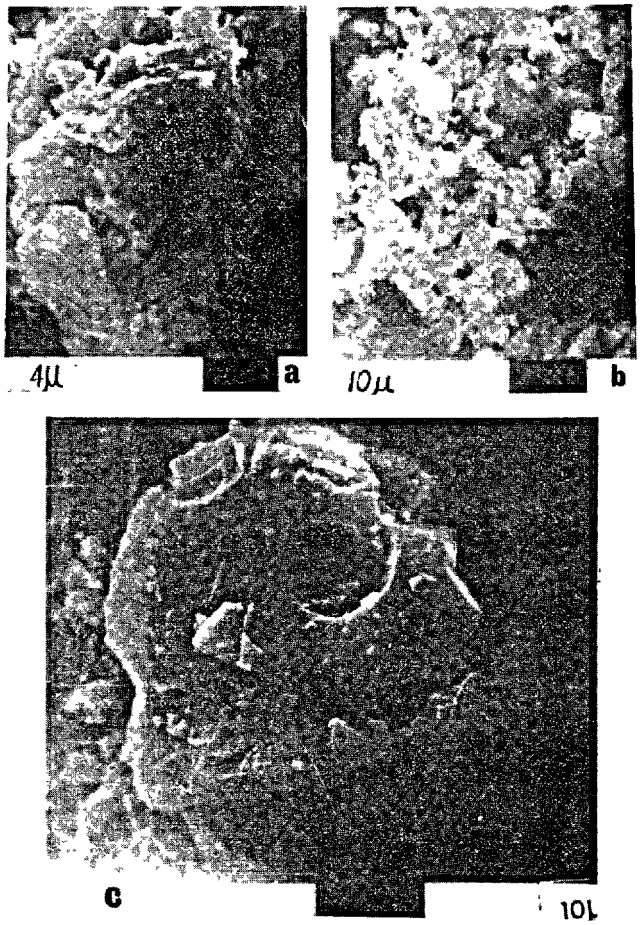

Fig. 7 - Les particules d'écorce (a,b) et celles de noyau (c) du kéramsite, SEM.

Par la méthode de radio-phase et par la méthode microscopique on a détermine, que 5-10% des particules de la zone extérieure du granule intensifient l'hydratation du ciment (jusqu'aux 10%), et avec cela cette intensification est plus grande pour la surface spécifique 7000 cm^2/g que pour la Ssp. = 2700 cm^2/g. Les particules de la zone intérieure du granule ralentissent quelque peu l'hydratation à mesure de l'accroissement de leur nombre et de leure dispersion. Le ciment durci avec les particules de kéramsite indépendamment de leur type se distingue de ciment de base par la diminution de quantite de portlandite et par une accroissement considérable de la teneur en hydrosilicates de calcium à faible basicité, CSH(I) (partiellement Al - substitués) qui y sont la phase principale de gelatinisation.

Dans le ciment durci à la limite avec les particules de kéramsite il y a des couches consolidées de 20-30 mkm de largeur (avec des particules de la zone extérieure du granule) et de 10-15 mkm de largeur (avec des particules de la zone interieure du granule) qui se distinguent par la couleur dans un microscope polarisant (exceptionnellement en lumière réfléchie) /2/. Ces couches se caractérisent par une microdureté élévée qui abaisse à la mesure de leures éloignement de contact et dont la valeur approche à celle de microdureté du ciment durci en volume /1,2/. La microdureté et le volume des couches entourant des particules de la zone extérieure du granule sont plus grands que ceux entourant les particules de la zone intérieure du granule. Par un complexe des méthodes physico-chimiques on a déterminé que c'est une couche intermédiaire entre la partie centrale de particule de l'agrégat et le ciment durci non-changé qui contient des nouvelles formations ainsi que les moindres (≤1-2 mkm) incorporations de l'agrégats. Donc, autour les moindres particules de kéramsite qui ont une grande microdureté se forme un microvolume du ciment durci (avec un durcissement 5 fois plus grand) dont le diamètre dépasse de 7-10 fois les dimensions de la particule. Avec une teneur considérable en telles particules ces couches se rapprochent et s'entre-croisent et forment un nouveau type du ciment durci compacté d'une résistance élevée.

CONCLUSIONS

Le traitement par le chauffage dans la vapeur du ciment durci contribue à l'élévation du dégré d'hydratation des minéraux de clinker et a une cristallisation plus nette de nouvelles formations des hydrates. Le chauffage à sec sous la température 100°C ne provoque pas de changements sensibles dans la composition minérale de phase et de dérèglements dans la structure; les propriétés du ciment durci sont maintenues. Sous 200°C une déshydratation partielle et un dérèglement de la structure cristalline ont lieu; cela amène à l'augmentation des déformations de retrait et à l'affaiblissement de la résistance du ciment durci. Une postérieure conservation humide des éprouvettes chauffées contribue à la reconstitution de la microstructure du ciment durci à la diminution des déformations et à l'augmentation de la résistance. Le chauffage sous la température 100°C et au-dessus provoque une décomposition thèrmique des compositions des dérèglements irréversibles de la microstructure du ciment durci et des pertes de ses propriétés.

Dans le ciment durci contenant les particules pulverulantes de kéramsite une élèvation du dégré d'hydratation (jusqu'aux 15%) et une diminution de la teneur en portlandite ont lieu. Sous l'effet de l'interaction chimique de particules avec la solution de $Ca(OH)_2$ du ciment durci dans le dernier augmente la teneur en hydrosilicates à basse basicité et se forme la structure aux

pores fins. Outre cela, dans la zone de contact se forment des couches chimiquement changées du ciment durci qui sont d'une microdureté élèvée. Les résultats obtenus, contrôlés pendant la production des bétons réels nous permettent de considérer les particules de kéramsite (de la zone extérieure du granule $\leq$ 60 mkm, de la zone intérieure du granule $\leq$ 20 mkm) comme des composantes pour la formation de gel et les considérer comme une partie du ciment.

BIBLIOGRAPHIE

1. - L.P.KOURASSOVA (1972) "Méthodologie de la mesure de microdureté du ciment durci et du béton". Ouvrages de NIIZhB, publ.7, "Les études physico-chimiques du ciment durci et du béton". Stroyizdat, M. (russe)

2. - L.P.KOURASSOVA, L.A.MAKEEVA (1977), "L'influence de microstructure sur les propriétés de résistance du béton de kéramsite". L'information d'analyse, TsINIS, Serie VII, publ.10. (russe)

3. - Z.M.LARIONOVA (1972) "La formation de la structure du ciment durci et du béton". Stroyizdat, M. (russe)

4. - Z.M.LARIONOVA, B.N.VINOGRADOV (1974) "La pétrographie des ciments et des bétons". Stroyizdat, M. (russe)

5. - Z.M.LARIONOVA, L.V.NIKITINA, V.R.GARACHINE (1977) "La composition de phase, la microstructure et la résistance du ciment durci et du béton". Stroyizdat, M. (russe)

On ettringite and modification of slag cement

Sur l'ettringite et l'amélioration des ciments de laitier

Zonghan LOU, Associate Professor, Xianyu Xu, Lecturer, and Ren Han, Lecturer, Chekiang University, Chine Populaire.

RESUME : En examinant la formation, la morphologie, la transformation, la stabilité et l'expansibilité de l'ettringite ($3\ CaO.Al_2O_3.3CaSO_4.31H_2O$) dans les ciments formés de gypse et de laitier et dans les ciments de laitier, et en étudiant le mécanisme de l'activation du laitier granulé, les auteurs ont abouti aux règles qui permettraient de fabriquer un ciment sans retrait, ou légèrement expansif, en mélangeant du clinker de ciment portland, du gypse et du laitier. Ce nouveau ciment aurait plus de clinker et moins de gypse que les ciments "laitier-gypse" et moins de clinker et plus de gypse que les ciments de hauts-fourneaux, de façon à mieux utiliser les propriétés de l'ettringite.

Quand l'hydratation de ce nouveau ciment atteint un certain stade, les phases cristallines de $Ca(OH)_2$ et de $CaSO_4.2\ H_2O$ disparaissent, laissant C-S-H (B) et l'ettringite comme produits principaux de l'hydratation. Au début de l'hydratation, lorsque la phase aqueuse est saturée en chaux, l'ettringite forme sur les grains d'aluminate des sortes de hérissons. Lorsque l'hydratation progresse, CaO s'épuise graduellement, et l'ettringite s'étend à toute la solution en grains distincts. Ce ciment a une résistance élevée, surtout à la traction. Il augmente légèrement de volume lors de la prise; il est stable ensuite. Il présente une bonne résistance aux sulfates et une faible chaleur d'hydratation. Et ce qui est encore plus important, il produit moins de poussière que le ciment "laitier-gypse".

SUMMARY: From the comparison made on formation, morphology, transformation, stability and expansibility of Ettringite ($3CaO.Al_2O_3.3CaSO_4.31H_2O$) in gypsum slag cement and portland blastfurnace slag cement, the authors have brought forward, in connection with the discussion on the mechanism of the activation of granulated blastfurnace slag, a proportioning principle of preparing a non-shrinking or slightly expansive cement from portland cement clinker, slag and gypsum. The new cement is designed to have a larger clinker content and a smaller gypsum content as compared with the usual gypsum slag cement, and at the same time a smaller clinker content and a larger gypsum content as compared with the portland blastfurnace slag cement, so as to bring out all the positive factors of the Ettringite.
As the reactions of hydration of this new cement reach a certain stage, the crystalline phases of $Ca(OH)_2$ and $CaSO_4.2H_2O$ will disappear, leaving CSH(B) and the Ettringite as its main products. Dufing the early stage of hydration, when the hydrating solution is saturated with CaO, the Ettringite builds up on the aluminate particles in hedgehoglike form. As hydration proceeds, however, the CaO gradually depletes, and the Ettringite is formed in the entire solution in discrete particles. The cement proves to have high strength, especially high tensile strength. It expands slightly on hardening, but it is volume-stable otherwise. It has good sulfate resistance and comparatively low heat of hydration. Most important of all, it does not cause dusting trouble like the gypsum slag cement.

INTRODUCTION

It becomes more and more clear that ettringite ($3\,CaO \cdot Al_2O_3 \cdot 3CaSO_4 \cdot 31H_2O$ --E-salt for short) plays an important role in the hydration and hardening of different kinds of cement. Along with the progress of researches in this field, it is obvious that ettringite has not brought the positive effects into full play in the hydration and hardening of the principal varieties of slag cement, i.e., slag Portland cement(SPC) and gypsum slag cement (GSC). Taking account of the relation of chemical interaction and restriction between common Portland cement clinker(K), granulated blastfurnace slag (S) and anhydrous gypsum(G), our studies were to find out certain appropriate proportions between them, in order that certain reasonable physico-chemical conditions can be created to enable the quantity, growing rate, morphology, transformation, stability and expansion of the newly formed ettringite, to develop in the direction we expected, offering the principal theoretical basis for the preparation of a special kind of slightly expansive slag cement. Our studies were just an attempt to bring forth both the advantage of ettringite and the benefit of slag into full play.

ON THE FORMATION OF ETTRINGITE AND ITS EFFECTS AND LIMITATION IN SLAG CEMENTS

The formation, the development and the transformation of ettringite play an important role in the hydration and hardening of these two kinds of slag cement, i.e., SPC and GSC. In earlier days the authors(1)(2) and other researchers(3) had noticed the difference in appearance of ettringite in these slag cements in SPC ettringite was observed, Under polerized microscope as crystals distributing in an aggregate manner backed up with a solid phase, whereas in GSC, ettringite was observed as needle crystals distributing individually. Both of these different crystals were found through X-ray examination and DTA to be the same constitution -- ettringite. On the other hand, the crystalline phase of $Ca(OH)_2$ appeared obviously in set cement of SPC, but not in GSC, and the concentration of $Ca(OH)_2$ in the liquid phase rapidly approached a very low value. It is due to the fact that the admixture of clinker to SPC generally consists of 50-60%, but to GSC only of 3-5%. So the morphology of ettringite in these two kinds of cement must be the direct result caused by differen alkaline conditions hydration and hardening of cement. In order to testify this concept, experiments were carried out as follows: blend synthesized pure mineral of $3CaO \cdot Al_2O_3$ (C_3A) and dihydrous gypsum according to the chemical compositions of ettringite, put this blend in $Ca(OH)_2$ solutions containing 0.15, 0.30, 0.50, 0.80 and 1.10g/l CaO respectively; sealing them on microscopy slides; and observe them microscopically. The results were shown as below.

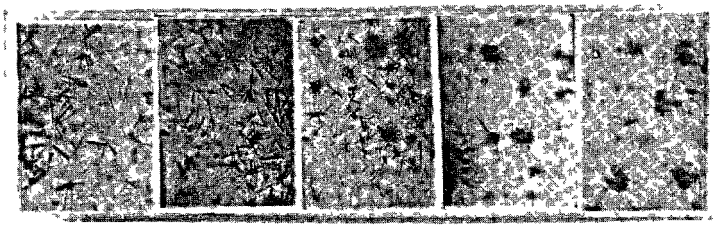

0.15g/l 0.30g/l 0.50g/l 0.80g/l 1.10g/l

Figure I. The relations between the morphology of ettringite and the concentration of CaO.

The same result was obtained with pure minerals $12CaO \cdot 7Al_2O_3$ ($C_{12}A_7$) and $CaO \cdot Al_2O_3$ (CA). The morphology of ettringite in these experiments agreed with those of these slag cements.

The morphology of ettringite is a reflection of the behaviour and the kinetics in the formation of ettringite. It is obvious that from the phase diagrams of systems of $CaO-Al_2O_3-H_2O$ and $CaO-CaSO_4-H_2O$(6), the solubilities of gypsum, especially those of calcium aluminates, are seriously inhibitted in solutions saturated or nearly saturated with CaO. Nevertheless, Cao and gypsum are comparatively soluble materials, so the liquid phase of set cement always contains more Ca^{++} and $SO_4^{=}$ but less AlO_2^-. Inevitably, the ions Ca^{++}, $SO_4^{=}$ and AlO_2^- form precipitates of ettringite crystals almost at once. As a result, AlO_2^- is released from aluminates in solid phase and a concentration gradient is established around the solid particles. Consequently, ettringite grows step by step as crystals distributing in aggregate manner backed up with solid particles containing aluminates. Whereas, when the concentration of CaO in solution is low, the solubility of gypsum and aluminates becomes much larger, thereupon, ettringite forms in solution as needle crystals distributing individually in a random way. Therefore, these two different configurations of ettringite are closely related to their formation processes. Substantially it is a subject of kinetics.

The intrinsic impedance of the formation of ettringite is its expansion. Theoretical calculation shows that during the formation of ettringite the expansion of the total volume of solid phases increased more than doubled. Ettringite crystals were distributing in aggregate manner backed up with solid particles; they might grow in certain directions and bring crystal-growing pressure to bear upon the circumferential matrices. As a result, the volume expansion of crystalline phase together with the crystal growing pressure makes possible the bulk expansion of set cement. Ettringite in SPC is just such a case we consider. It is necessary to control accurately the gypsum content in cement blend, so as to restrict

the quantity of ettringite formed. The formation of ettringite would end essentially when the cement paste is still in its plastic state in order to avoid the disintegration due to the expansion of ettringite.

On the other hand the needle shaped ettringite crystals were distributing singularly, they might grow freely on both ends. This growth bring forth low or even no crystal growing pressure, and few effects in the bulk change of set cement. In this case, the force making possible the bulk expansion of set cement mainly depends on the volume expansion of crystalline phase. Ettringite in GSC just belongs to this type. Even though ettringite forms in large amounts, the volume change on setting still remains contractive, the contraction being small with the interior structure becoming more compact.

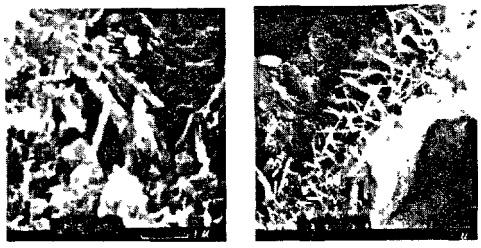

GSC SPC

Fig.2 Ettringite formation in slag cements.

It is clear from the ablove expositions that different clinker contents in cement bring about different alkaline conditions of hydration, that ettringite forms in different configurations, and that different forces were made possible in the bulk expansion of set cement. In fact it is a problem related to the chemical interaction and restriction between K, S and G.

Another important problem, we should pay attention to, is the long-term stability of ettringite in these two slag cements. $3\,CaO.Al_2O_3.CaSO_4.12H_2O$ (abbreviated as L-salt) was found in set cement of SPC by X-ray examination. When $CaO.Al_2O_3$ is introduced into SPC, L-salt becomes more pronounced. This L-salt must be transformed from ettringite.

We have verified further these experiments, that in the case of high CaO concentration and low $CaSO_4$ concentration, e.g., $CaSO_4/Al_2O_3 \leq 1$, ettringite could transform into L-salt. Just because of this, ettringite is not stable in SPC from a long-term viewpoint(5).

But GSC is not the case. After the hydration and hardening of GSC, gypsum is in excces and solubility of CaO approaches a very low value. Therefore, ettringite would exist stably forever in GSC. This was confirmed by the experimental results of the long-cured set cement of GSC.

The following experiments were carried out with synthesized E-salt and L-salt.

E-salt + $CaSO_4$ —— E-salt

L-salt + $CaSO_4$ —— E-salt

This confirms that ettringite exists stably in GSC(5).

But ettringite can not stand the action of carbon dioxide in atmosphere. We put synthesized pure ettringite in moist CO_2 for seven days and found that it was completely decomposed into aragonite $CaCO_3$ and dihydrous gypsum as shown by X-ray examination.

This is because of the neutralization of $Ca^{++} + CO_3^{=} \rightarrow CaCO_3\downarrow$, which depresses the CaO concentration in the liquid phase, causing the decomposition of ettringite by disturbing its concentration in equiliubrium. GSC is a cement of low alkalinity and it produces insufficient CSH(B) to shield ettringite against the action of CO_2. As a result, ettringite in GSC might be destroyed or decomposed by CO_2 in atmosphere, and it is known as "dusting", the formation of a spongy layer on the surface of set cement.

The instability of ettringite in GSC and SPC under different conditions is also a substantial problem relating to the chemical interaction and restriction between K, S and G. The physico-chemical conditions of the hydration and hardening of these two slag cements have inhibited the positive effect of ettringite.

ETTRINGITE AND THE MODIFICATION OF SLAG CEMENT

According to our study on ettringite in both gypsum slag cement and slag Portland cement, and for the purpose in developing all the positive factors of the ettringite, we revised the ratio between clinker, slag and gypsum to certain appropriate components to bring about a new kind of slightly expansive slag cement. Portland cement clinker produced by general cement plants and granulated blastfurnace slag produced by steel mills are adaptable; As with gypsum, anhydrous or calcined gypsum meet the needs. Thus, the new cement is designed to have greater clinker and less gypsum portion as comparing with the usual gypsum slag cement, on the other hand to have less clinker and greater gypsum portion as comparing with slag portland cement.

This new kind of slightly expansive cement is a mixture of clinker, slag and gypsum. After concocting with water, it gets into the colloided state, in which clinker hydrates rapidly, separating out $Ca(OH)_2$ that will dissolve in water together with gypsum, while the powder of slag is soaking into the solutions. Hence a series of physical, chemical and physico-chemical changes occur among the clinker, slag and gypsum, resulting in the set cement becomes as hard as natural stone. This kind of cement has both the main characterstics of main characterstics of slight expansion and lower heat of hydration.

After hydration of this cement, a large quantity of ettringite exists which may be found through XRD and TDA:

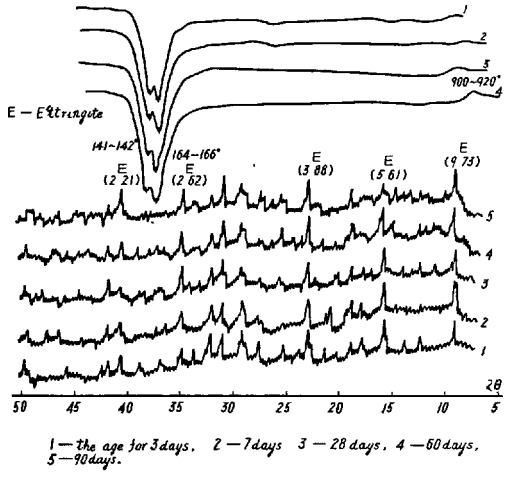

1—the age for 3 days, 2—7 days 3—28 days, 4—60 days, 5—90 days.

Fig.3 XRD and TDA of slightly expansive slag cement

It proves that the presence of ettringite in slightly expansive slag cement is an obvious fact.

The formation of ettringite absorbs quite a quantity of CaO. From XRD and DTA it is clear that the crystalline phase of $Ca(OH)_2$ does not appear in the set cement. It will be entirely different if we remove gypsum from this cement blend, so that ettringite will certainly not come into existence and the crystalline phase of $Ca(OH)_2$ will be obviously found in XRD and DTA curves, shown as follows.

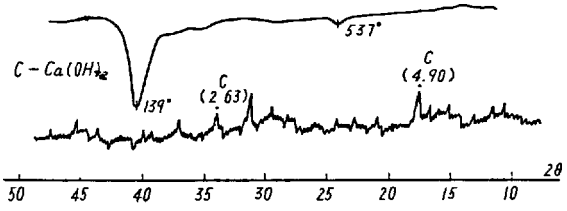

Fig.4 XRA and DTA of slightly expansive slag cement (with gypsum removed)

These experiments suggest that the formation of ettringite is a process which continuously absorbs CaO and lowers the basicity. This can be shown from the change (decrease) of CaO content in aqueous solution during hydration.

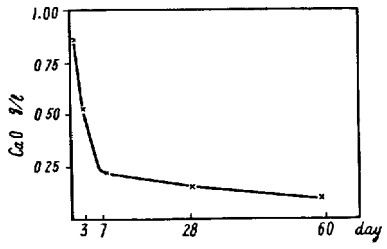

Fig.5 The decreasing of CaO content during hardening of slightly expansive slag cement.

Therefore, at the beginning of the hydration of cement, with CaO nearly saturated in the hydrating solution, ettringite forms crystals in aggregate manner, backed up with a solid phase, and then with the decreasing of CaO content in hydrating solution, it forms needle-like crystals distributing individually. Both of them form successively but exist simultaneously. As stated above, the ettringite crystals are distributing in aggregate manner, the volume expansion of crystalline phase combined with crystal growing pressure makes possible the bulk expansion of set cement. Whereas the ettringite crystals are distributing individually, so they bring about seldom or never crystal growing pressure, and have less effect on bulk expansion of set cement which is mainly caused by volume expansion of crystalline phase. Therefore, this cement differs both from GSC and from SPC in having appropriate expansion. Our experiments which will be stated later would prove that the formation of ettringite is completed within 7 days. Other experiments confirm that the expansion of set cement reaches the limit within 7 days, moreover the expansion of this cement is much more stable than others.

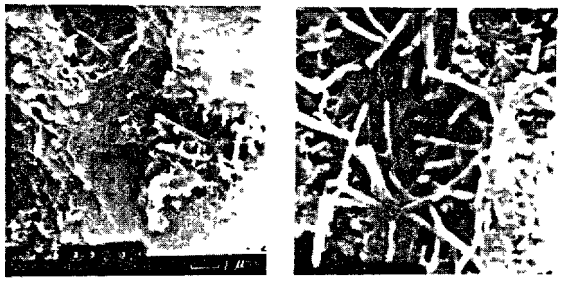

Fig.6 Ettringite formation in slightly expansive slag cement.

While the ettringite is produced in large amount, hydrated calcium silicate is formed massively too. According to 140°C heat-absorbing valley and the 920°C heat-diffusing peak on TDA curve, and through analysis in combination with the phase equilibrium in system $CaO-SiO_2-H_2O$, it is obvious that in this case hydrated calcium silicate formed must be $(0.8-1.5)CaO\cdot SiO_2\cdot(0.5-2.5)H_2O$, i.e. CSH(B), but must not be $(1.7-2.0)CaO\cdot SiO_2\cdot(2-4)H_2O$, i.e. C_2SH_2. CSH(B) plays more important role in the strength and other properties of this cement.

Granulated blastfurnace slag accounts for a great part. In connection with the mechanism of the activation of this slag, we would know, clinker in these cement components offers CaO for activation of slag and at the same time the minerals in it hydrate and harden independently, among them C_3A and

C_4AF combine with gypsum and form a crystalline phase of ettringite. Thus the clinker acts both as the independent cementing component and as the alkaline activator. On the other hand, gypsum acts as sulphate activator. Both of them activate the slag. Slag is the unstable glass in the system $CaO-Al_2O_3-SiO_2$. The alkaline stimulation brings about the formation of CSH(B) and partial disintegration of granulated slag glass, thus furnishes the prerequisite to the sulphate stimulation. Meanwhile the sulphate stimulation brings about the formation of ettringite which upsets certain established equilibrium and promotes the alkaline stimulation. Therefore, the development of the strength of set cement is based on the cementation of clinker and the multiply repeated promotion between these two stimulations. This cement has high strength.

In hydration of different slag cements, the alkaline stimulation plays an important role in SPC which consists of much more clinker and less gypsum, whereas the sulphate stimulation develops fully in GSC with less clinker and excessive gypsum. Both are considered as the basic weak points which are unreasonable for the under-development of the reactions of slag. We keep the proper ratio between clinker and gypsum used in this slightly expansive slag cement, thus both the alkaline and sulphate stimulations would develop more fully and the slag would react more effectively. As mentioned above, we know, in slightly expansive slag cement, one of the principal hydrated products is CSH(B) in which the ratio between CaO and SiO_2 approaches to 1, and the unacted slag in large quantity remained. Thereby, the concertrations of both CaO and $CaSO_4$ tend to decrease to low values, finally approaching equilibrium concentrations of both hydrated products, ettringite and CSH(B), as the limit. This state of the slightly expansive slag cement ensures the long time stable existence of ettringite, and prevents the latter from transforming into L-salt. It also has the ability of resistance to sulphate corrosion, though this cement contains a large quantity of unacted slag which offers the active Al_2O_3, but without the necessary condition of basicity, therefore can not react with $SO_4^=$ in water to form ettringite. Besides, even if some ettringite forms, it will be the crystals distributing individually, and is unlikely to disintegrate the set cement due to its expansion.

The constancy of volume and soundness is another problem we should pay greater attention too. Compared with SPC, this cement contains excessive gypsum, and compared with GSC, it contains much more clinker. From the tranditional viewpoint about cement compositions, both cases are impermissible. Thus an important problem is put before us, in order to answer this problem related with the long-time safety of construction, which has been deeply concerned, the following experiments were carried out in two aspects.

1) Pure ettringite ($3CaO\cdot Al_2O_3\cdot 3CaSO_4\cdot 31H_2O$) and pure L-salt ($3CaO\cdot Al_2O_3\cdot CaSO_4\cdot 12H_2O$) were sythesized and their solubilities in aqueous solution in equilibrium with crystals were determined respectively. The solubility products calculated are 1.1×10^{-40} for ettringite and 1.7×10^{-28} for L-salt in which the former being much less than the latter(5). At the beginning of the hydration of cement, the concentration of $CaSO_4$ in liquid phase is enough, but that of Al_2O_3 is comparatively too low. This condition absolutely benefits the formation of ettringite and not of L-salt. Large amount of X-ray diffraction patterns of set cement for ages of 1,2,3,7,14,28,90,360days and 4 years show that ettringite persists in large quantity but L-salt only appears once in trace after long time. Therefore, it is confirmed both theoretically and practically that in no case can L-salt form in large amount at the beginning of the hydration and then changes into ettringite which causes expansive disintegration(6).

2) It was verified that the formation of ettringite finished within 7 days by comparing the relative intensities on the X-ray diffration patterns of set cement of the expansive slag cement, prepared with dihydrous gypsum for ages of 3 and 7 days, and of set cement powder for age of 60 days with addition of 0.5% and 1% dihydrous gypsum. (In fact this expansive slag cement is prepared with anhydrous or calcinated gypsum. But it is difficult to resolve $CaSO_4$ from ettringite and the main mineral C_2AS in slag, for their main relative intensities on X-ray differaction patterns are duplicate and covered each other.) The remaining amount of unreacting gypsum in set cement can be detected. It was confirmed that the left-over gypsum was very few after 3 days and only trace after 7 days, as compared with that obtained with the specimen with addition of 0.5% and 1% dihydrous gypsum.

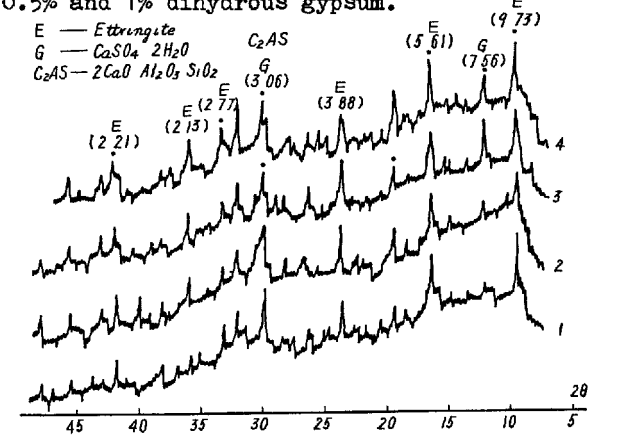

1 — the age for 3 days, 3 — 60 days, with addition of 1% $CaSO_4$ $2H_2O$
2 — 7 days. 4 — 60 days, with addition of 0.5% $CaSO_4$ $2H_2O$

Fig.7 The X-ray examination of set cement specimens

Meanwhile, according to the X-ray examination on cement specimens prepared with calcinated gypsum at ages of 3,7,28,60 and 90 days, the main spectra of ettringite,i.e.,

d=9.73Å(100), 5.61Å(80), 3.88Å(50), 2.77Å(40) principally reached maximum within 7 days. This also meant that the formation of ettringite approximately finished within 7 days. Since gypsum will disappear and the formation of ettringite will finish within a short time, so the constancy of volume would be good and there will be no danger of to get disintegration caused by further formation of ettringite.

Another powerful evidence of the constancy of volume and soundness is the fact that we built a small dam, 32m long and 15m height with this slightly expansive slag cement in 1975, and until now no cracks, chaps or local swellings are found in it any where and its surface is still compact and smooth.

SOME CONCLUSIONS

1) On the basis of our studies on ettringite in both slag cements, SPC and GSC, the proportioning ratio between K, S and G can be revised to suit a reasonable physico-chemical condition of hydration and hardening of cement, thus bringing about a new slightly expansive slag cement which is characterized by fully developing the advantage of ettringite. This slightly expansive slag cement can be prepared from granulated blastfurnace slag, common portland cement clinker and anhydrous gypsum with simple common cement production process, though it may conserve slightly more power to get better pulverization. This cement is characterized by slight expansion and low heat of hydration. The strength developed by this cement using plastic mortar (Chinese National Standards GB177-77) is as follows for example: compressive strength (kg/cm^2): 3days-131; 7days-320; 28days-437; bending strength (kg/cm^2): 3days-30.2, 7days-76.5, 28days-88.7. ratio of linear expansion when neat cement tested 0.2%, heat of hydration less than 40 Kcal/kg within 7days. So this cement is applicable to the mass concrete building of water conservancy that it would bring about some basic changes in the construction of the mass concrete building(11).
2) On the other hand, this slightly expansive slag cement might be a basic reform of GSC. Through this reform, the main defects of GSC, such as poor constancy of quality, poor resistance to weathering in storage of cement and dusting on setting, etc, would be all overcome. Therefore it is reasonable to produce this slightly expansive cement instead of GSC, and any GSC plant can be easily transferred to produce this slightly expansive cement without changing its raw materials and technological processes but only modifying the K-S-G ratio in proportioning of cement, though the GSC might sometimes have a higher strength.

The long-period production and application of slag cements have accumulated a wealth of practical knowledge on ettringite. Our study is an attempt to make fully effective use of ettringite in cement industry. The development of this slightly expansive slag cement is the natural result of the deepening of the comprehension of ettringite.

References

1. Lou Zonghan, Xu Xianyu, Zhou Zhichao, Zhang Feipeng: Study on Alkaline Condition of the Formation of Ettringite and the hydration and Hardening of Cement. Transactions of Chekiang University. No.1 1964
2. Lou Zonghan: Study on the Alkality of Gypsum Slag Cement. Symposium on Researches in Ceramic Science 1959. Science Publishing House, NoV. 1962
3. Cheng Xibi, Miao Jisheng: Study on the Formation of Calcium Sulphoaluminate Hydrates in Gypsum Slag Cement. Journal of the Chinese Silicate Society, No. 4, 1962
4. Xue Jungan et al: On Sulphate Expansion of set Cement and also the Behaviour of Calcium Sulphoaluminate Hydrates in Liquid Phase not Saturated with CaO. Journal of the Chinese Silicate Society No. 1, 1979.
5. Zhang Feipeng, Zhou Zhifa, Lou Zonghan: Solubility product and stability of ettringite. Candidate for the Seventh International Conference on Cement Chemistry 1979.10.
6. F. M. Lea, The Chemistry of Cement and Concrete. 1970
7. p.p Budnikov, I.L Znachko-Yovorskii, Granulated Blastfurnace Slag and Slag Cement 1953
8. P. K. Mehta, Scanning Electron Microscaphic Studies of Ettringite Formation. Cement and concrete Research. Vo16, No.2 March 1976
9. P. K. Mehta, Effect of Lime on Hydration of Pastes Containing Gypsum and Calcium Aluminates or Calcium Sulfoaluminate. J.A.C.S. Vol. 56, No.6, 1973
10. Julie C. Yang, Chemistry of Slag-Rich Cements Sym, Tokyo 1968
11. Rapid Construction of Concrete Dams California 1970

Solubility product and stability of ettringite

La stabilité de l'ettringite et le "produit de solubilité"

Feipeng ZHANG, Lecturer, Zhifa ZHOU, Lecturer, and Zonghan LOU, Associate Professor,
Chekiang University, Chine Populaire.

RESUME : La formation, le développement et la transformation de l'ettringite jouent un rôle capital dans l'hydratation, le durcissement et le processus de corrosion des divers ciments, notamment les ciments de laitier et les ciments expansifs. Du fait que l'ettringite est un membre de la série des composés complexes du type 3 $CaO.Al_2O_3.mCa$ (X et /ou Y_2).nH_2O, les auteurs envisagèrent la possibilité de prévoir la formation et la stabilité de l'ettringite, en même temps que sa transformation entre les membres de la série. Des expériences ont été faites en tenant compte de ces composés complexes apparentés.
Les résultats obtenus,et indiqués ci-dessous, confirment les vues des auteurs :

$C_3A.CaCl_2.10H_2O + CaSO_4 \rightarrow C_3A.3CaSO_4.31\ H_2O$
$C_3A.3CaSO_4.31H_2O + CaCl_2 \rightarrow C_3A.CaCl_2.10H_2O$
$C_3A.CaCO_3.11H_2O + CaSO_4 \rightarrow C_3A.3CaSO_4.31H_2O$
$C_3A.3CaSO_4.31H_2O + CaCO_3 \rightarrow C_3A.CaCO_3.11H_2O$
$C_3A.CaSO_4.12H_2O + CaSO_4 \rightarrow C_3A.3CaSO_4.31H_2O$
$C_3A.CaCl_2.10H_2O + CaCO_3 \rightarrow C_3A.CaCO_3.11H_2O$

Le concept de "produit de solubilité" peut aussi éclairer d'une manière satisfaisante le mécanisme de l'hydratation, du durcissement et de la corrosion des ciments divers, compte tenu de l'ettringite.

SUMMARY:The formation, develpment and transformation of Ettringite play a decisive role in the hydration, hardening and corrosion processes of various cements, especially the slag cement and the expansive cement. In view of the fact that Ettringite is a member of the series of complex compoundsof the type $3CaO.Al_2O_3.mCa$(X and/or Y_2).nH_2O, the authors envisaged the possibility of predicting the formation and stability of Ettringite as well as the mutual transformation among the membersof the series. Experiments, therefore, have been carried out with respect to some of the related complex compounds. The results as illustrated below prove to support the authors' views.

$C_3A.CaCl_2.10H_2O + CaSO_4 \rightarrow C_3A.3CaSO_4.31H_2O$
$C_3A.3CaSO_4.31H_2O + CaCl_2 \rightarrow C_3A.CaCl_2.10H_2O$
$C_3A.\ CaCO_3.11H_2O + CaSO_4 \rightarrow C_3A.3CaSO_4.31H_2O$
$C_3A.3CaSO_4.31H_2O + CaCO_3 \rightarrow C_3A.CaCO_3.11H_2O$
$C_3A.CaSO_4.12H_2O + CaSO_4 \rightarrow C_3A.3CaSO_4.31H_2O$
$C_3A.CaCl_2.10H_2O + CaCO_3 \rightarrow C_3A.CaCO_3.11H_2O$

The conception with reference to the solubility product may also satisfactorily explain the mechanism of hydration, hardening and corrosion processes of various cements related to Ettringite.

INTRODUCTION

The formation, the development and the transformation of ettringite play an important role in the hydration, hardening and corrosion processes of different kinds of cement on their strength development, constancy of volume and soundness, sulphate-resisting ability and so forth. Ettringite is one of the main hydration products in gypsum slag cement and also the expansive element in expansive cement. But ettringite is just one of the compounds in a series of complex compounds of the type $3CaO \cdot Al_2O_3 \cdot mCa(X \text{ and/or } Y_2) \cdot nH_2O$, with $X = SO_4^=$, $CO_3^=$, and $Y = Cl^-$, Br^-, I^-, OH^-, NO_3^- or BrO_3^-: that is to say, there are quite a number of related complex compounds.

Different kinds of cement differ in compositions and display their respective hydration and hardening behavious. The change of the concentration of Ca^{++}, AlO_2^- and $SO_4^=$ ions in liquid phase of set cement behaves in complex ways. Cements are also used with addition of blastfurnace slag, pozzolanas blending and differents additives, such as $CaSO_4$, $CaCl_2$, NaCl, $CaCO_3$, etc, which being in Ca^{++}, Na^+, $SO_4^=$, Cl^-, $CO_3^=$ or other ions. Set cement in concrete construction might be acted by different active ions over a long period of time. When used in sea or salt lake, the concrete will be acted upon by different ions, such as Cl^-, $SO_4^=$ etc; whereas in spring water it might be acted upon by HCO_3^- ion: for underground construction in saline alkali soil area, it will be corroded by Cl^-, $SO_4^=$, $CO_3^=$, etc; and even in air, it will be also acted upon by CO_2 and water vapor and so on. So the stability of ettringite in every possible case must be throughly examined.

There are many academic papers on the comprehensive study, discussion and comments on $3CaO \cdot Al_2O_3 \cdot mCa(X \text{ and/or } Y_2) \cdot nH_2O$ [1][2][3][4][5][6][7][8]. In this paper, it is our purpose to try to explain the stability of ettringite by applying "the rule of solubility product", though it is only an attempt.

EXPERIMENTS

The hydration products of cement consist of gelatineous portion and crystalline portion. Ettringite and related complex compounds are of crystalline phases which are rarely soluble electrolytes and are under the rule of solubility product.

We have synthesized the following complex compounds which are of practical importance.

$3CaO \cdot Al_2O_3 \cdot 3CaSO_4 \cdot 31H_2O$ abbreviated as E-salt;

$3CaO \cdot Al_2O_3 \cdot CaSO_4 \cdot 12H_2O$ abbreviated as L-salt

$3CaO \cdot Al_2O_3 \cdot CaCO_3 \cdot 11H_2O$ abbreviated as C-salt

$3CaO \cdot Al_2O_3 \cdot CaCl_2 \cdot 10H_2O$ abbreviated as Cl-salt

$3CaO \cdot Al_2O_3 \cdot Ca(OH)_2 \cdot nH_2O$ abbreviated as A-salt

For determination of the concentration in equilibrium with crystals in aqueous solution, complex compounds were synthesized, with chemically pure reagents checked by chemical analysis as raw materials: E-salt with $Ca(OH)_2$ and $Al_2(SO_4)_3 \cdot 18H_2O$, Cl-salt with $Ca(OH)_2$ and $AlCl_3 \cdot 6H_2O$, L-salt with $Ca(OH)_2$, $Al_2(SO_4)_3 \cdot 18H_2O$ and $CaO \cdot Al_2O_3$, and C-salt with $Ca(OH)_2$, $CaO \cdot Al_2O_3$ and $CaCO_3$. Syntheses were carried out between solutions, except $CaO \cdot Al_2O_3$ and $CaCO_3$, which should be pulverized, then added into the solutions to react with other reagents. In solutions the concentration of the starting materials were usually limited below 0.05N. The concentration of some ions were increased to make the precipitation complete (usually applying nearly saturated $Ca(OH)_2$ solution,) and distilled water reboiled to be free of CO_2. In order to get rid of the effect of CO_2, all the synthesizing operations, such as filtration, should be done as fast as possible and the products must be kept in desicators with decarbonating agent "alkali-lime".

After the X-ray examinations about their purity, in which C-salt was not quite pure, containing some $CaCO_3$, their solubilities in mg/l in aqueous solution at 25°C were determined respectively by volumetric analysis as

follows:

The Concentrations in equilibrium (mg/l)

table I.

Compound	E-salt	L-salt	Cl-salt	C-salt
Duration of Equilibrium	3 days	4 days	3 days	11days
CaO	68.5	168.0	180.0	78.6
$CaSO_4$	177.5	44.8	$CaCl_2$ 73.6	$CaCO_3$ 70.2
Al_2O_3	36.4	93.8	61.2	65.3

According to the above-mentioned value of concentrations in equilibrium with their crystalline phases, we converted them into concentrations in mg-mole per liter and molar ratios composition as follows:

The concentrations in my mole per liter and molar ratios of composition

table II.

Compound	E-salt		L-salt		Cl-salt		C-salt	
Soln / Comp	mg-mole per liter	molar ratio	mg-mole per liter	molar ratio	mg-mole per liter	molar ratio	mg-mole per liter	molar ratio
CaO	1.223	3.42	2.977	3.23	3.206	5.32	1.403	2.21
$CaSO_4$	1.303	3.65	0.330	0.36	$CaCl_2$ 0.664	1.11	$CaCO_3$ 0.702	1.11
Al_2O_3	0.358	1	0.920	1	0.601	1	0.634	1

The constants of solubility product were calculated in accordance with the following dissociation reactions of these complex compounds.

E-Salt: $3CaO \cdot Al_2O_3 \cdot 3CaSO_4 \cdot 31H_2O = 6Ca^{++} + 2AlO_3^- + 3SO_4^= + 40H^- + 29H_2O$

$K^E_{s.p} = (Ca^{++})^6 \cdot (AlO_3^-)^2 \cdot (SO_4^=)^3 \cdot (OH^-)^4$

L-Salt: $3CaO \cdot Al_2O_3 \cdot CaSO_4 \cdot 12H_2O = 4Ca^{++} + 2AlO_2^- + SO_4^= + 40H^- + 10H_2O$

$K^L_{s.p} = (Ca^{++})^4 \cdot (AlO_3^-)^2 \cdot (SO_4^=)^1 \cdot (OH^-)^4$

Cl-Salt: $3CaO \cdot Al_2O_3 \cdot CaCl_3 \cdot 10H_2O = 4Ca^{++} + 2AlO_3^- + 2Cl^- + 40h^- + 8H_2O$

$K^{cl}_{s.p} = (Ca^{++})^4 \cdot (AlO_2^-)^2 \cdot (Cl^-)^2 \cdot (OH^-)^4$

C-Salt: $3CaO \cdot Al_2O_3 \cdot CaCO_3 \cdot 11H_2O = 4Ca^{++} + 2AlO_2^- + CO_3^= + 40H^- + 9H_2O$

$K^c_{s.p} = (Ca^{++})^4 \cdot (AlO_2^-)^2 \cdot (CO_3^=)^1 \cdot (OH^-)^4$

The solubility products were calculated from the dissociation reactions, gaving E-salt as an example:

We take, $(Ca^{++}) = (CaO) + (CaSO_4)$

$(OH) = 2 \times (CaO)$

$(AlO_2^-) = 2 \times (Al_2O_3)$

$(SO_4) = (CaSO_4)$

then,

$$K^E_{s.p} = (1.223 \times 10^{-3} + 1.303 \times 10^{-3})^6 \cdot (2 \times 0.3575 \times 10^{-3})^2 \cdot (1.303 \times 10^{-3})^3 \cdot (2 \times 1.223 \times 10^{-3})^4 = 1.1 \times 10^{-40}$$

The rest may be inferred by analogy. Thereby, the following values of solubility product were obtained.

Compound	E-salt	L-salt	Cl-salt	C-salt
SP	1.1×10^{-40}	1.7×10^{-28}	1.0×10^{-30}	1.4×10^{-30}

Furthermore, the solubility product values of Cl-salt and C-salt are quite close, the experiment was carried out to confirm the sequence: The mixture of 1gm Cl-salt+ ½gm$Ca(OH)_2$+1gm$CaCO_3$, which had been cured in moist state for 3 years, was examined, still as Cl-salt and $CaCO_3$ in stable state. Thereby, it is confirmed that the solubility product of Cl-salt is smaller than that of C-salt.

Generally speaking, these solubility data are adaptable though our determinations were not quite precise. According to these determinations the sequence of the solubility product values, which we expected, is as follow:

E-salt < Cl-salt < C-salt < L-salt

From the above sequence of solubility product values, according to the rule of solubility product, the conclusion is: The general tendency of equilibrium between these complex compounds is that E-salt is the first to form and the most stable to exist over a long period of time.

We have also performed some experiments dealing with the transformations among the complex compounds, such as:

A-salt+$CaSO_4$ → E-salt

L-salt+$CaSO_4$ → E-salt

E-salt+NaCl → Cl-salt

(1gm E-salt in 1 liter water with 1gm NaCl added.)

E-salt + $CaCO_3$ — C-salt (but aragonite $CaCO_3$+E-salt)
(in one liter water 1.71gm $Al_2(SO_4)_3 \cdot 18H_2O$, 2.50gm $Ca(OH)_2$ and 0.25gm $CaCO_3$ added)

Specimens blended with water, and cured in moist state for 3 years, were examined under X-ray, the results are as follows:

5gm E-salt+H_2O — E-salt (no change)
5gm E-salt+1gm$CaCO_3$ — E-salt (no change)
5gm E-salt+1gm$CaCO_3$+1gm$Ca(OH)_2$ — E-salt (no change)
1gmCl-salt+1gm$CaSO_4$+½gm$Ca(OH)_2$ → Cl-salt (changed)

In addition, further results are as follows:

L-salt+$CaCl_2$ — E-salt+Cl-salt
L-salt+$CaCO_3$ — E-salt+C-salt

These experimental results mentioned above are all ruled by the sequence of solubility product values.

But in special case the E-salt would sometimes transform into L-salt, such as:

E-salt + $CaO \cdot Al_2O_3$ — L-salt
(1gm E-salt in 800mlH_2O, 0.4gm$CaO \cdot Al_2O_3$ and 0.3gm CaO added)

It is not ruled by the sequence of solubility product values.

DISCUSSION AND CONCLUSION

1. The gypsum slag cement and some expansive cement were designed to have more gypsum which would partially remain in the hardening cement pastes, thus:

E-salt + $CaSO_4$ — E-salt,
L-salt + $CaSO_4$ — E-salt,

According to the rule of solubility product, because of excessive gypsum, Ettringite would not be able to transform into L-salt and would exist stably for a long period of time.

Besides, The slightly expansive slag cement which we studies[10] would keep that the concentrations of both CaO and $CaSO_4$ in hydrating solution tend to decrease to low values, finally approaching equilibrium concentrations of the hydrated products, ettringite and CSH(B), as the limit. The state of this cement insures the long time stable existence of ettringite too.

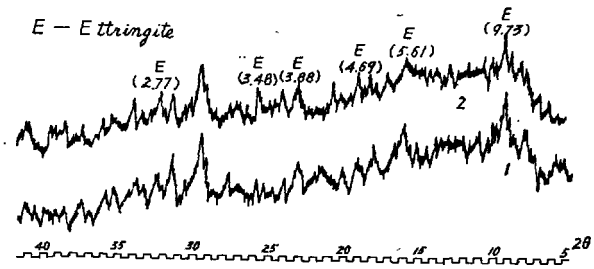

Fig. XRD of two set cement specimens of the slightly expansive slag cement for age of 4 years.

2. Our experiment showed that equal mole mixture of C_3A and $CaCO_3$, or C_4AH_x and $CaCO_3$, or $2Ca(OH)_2+CaO \cdot Al_2O_3+CaCO_3$ form C-salt easily in the presence of water. In the aqueous solution the equilibrium concentration of $CaCO_3$ is less than that of C-salt. On the contrary, the solubility product of $CaCO_3$ 8.7×10^{-9} is greater than that of C-salt 1.4×10^{-30}, in active Al_2O_3-containing solution saturated with $Ca(OH)_2$, $CaCO_3$ will be converted into C-salt. It is an inevitable outcome. To certain cement, such as portland slag cement, when blended with insufficient gypsum, it is feasible to add some $CaCO_3$ powder (pulverized limestone) to decrease the concentrations of active Al_2O_3 and CaO in liquid phase in set cement in order to prevent the transformation of E-salt to L-salt, and the C-salt is contained in set cement, thus the long-time stable existence of E-salt is insured.

3. It has been several decades since $CaCl_2$ was used as an accelerator. It was confirmed that after the addition of $CaCl_2$ to cement paste, Cl-salt will form immediately with soluble Al_2O_3 and CaO in paste.

We believe the very fact that is the substantial essence of the mechanism of the accelaration of hydration was due to the addition of $CaCl_2$. In comparison with $CaCl_2$, $CaSO_4$ is much less soluble in water. The solubility of $CaSO_4$ is only about 2 gm/l at room temperature and is further restricted by the concentration of $Ca(OH)_2$ obviously as shown in $CaO-CaSO_4-H_2O$ phase diagram(9).

Whereas $CaCl_2$ has chemical affinity for water, its solubility is 745 gm per liter(7), usually the water -- cement ratio is 0.5, when we add only 1% of $CaCl_2$ to the cement, the concentration of $CaCl_2$ in liquid phase of set cement will be 20gm/l. Therefore at the beginning of the hydration of cement paste containing certain amount of active Al_2O_3 and CaO, Cl-salt should form immediately and rapidly. The solubility product of Cl-salt 1.1×10^{-30}, is greater than that of E-salt 1.1×10^{-40}, thus greatly accelarating the transformation of Cl-salt to E-salt. This is the very reason why we are able to explain the mechanism of accelarating the formation of E-salt by $CaCl_2$ as confirmed earlier by Nemat Tenoutasse(4). In our experiments, X-ray and other examinations, Cl-salt appeared obviously, Synthesized Cl-salt looks like fibres which possess tensile force somewhat like the asbestos fibres in the prefabricated asbestos-cement articles. Cl-salt distinctly strengthens the set cement as rib lath in concrete. It is clear that the long time stable existence of E-salt is insured due to the, Cl-salt contained in the set cement.

4. When excessive active Al_2O_3 and CaO exist, E-salt can transform into L-salt, which by itself is usually unstable. This fact is difficult to be explained with the rule of solubility product. Therefore, we once inclined to agree with the hypothesis about the existence of solid solution between $C_3A \cdot 3CaSO_4 \cdot 32H_2O$ and $C_3A \cdot Ca(OH)_2 \cdot nH_2O$; but the latest studies denied this possibility because they are different in crystal structure. Some people suspected, though generally recognized, the existence of solid solution between $C_3A \cdot CaSO_4 \cdot 12H_2O$ and $C_3A \cdot Ca(OH)_2 \cdot nH_2O$ (2).

It is hard to synthesize pure L-salt, whereas pure E-salt is rather easy to prepare. Once we kept a large amount of sythesized pure L-salt in a sealed ground glass stoppened bottle; after several months (moisture 3-5%), L-salt all transformed into E-salt and C_4AHx, as examined by X-ray.L-salt is a metastable compound; its formation and stable existence require high basicity (CaO) and low concentration of $CaSO_4$, maintaining the molar ratio $CaSO_4/Al_2O_3 \leq 1$. In portland cement and Portland slag cement, L-salt may be transformed from E-salt which is formed at the beginning of hydration;(8) Deducing from the system of $CaO-Al_2O_3-CaSO_4-H_2O$, we can reach the same conelusions(10). The above mentioned transformation requires us to continue this study more thoroughly.

With the increase of varieties of cement, the extensive adaption of different admixture and additives, and the increasing development of the steam cured silicate materials of fly ash and slag. The type of complex compounds $C_3A \cdot mCa(X \text{and/or } Y_2) \cdot nH_2O$ would play an even more important role.

Many research workers made thorough and extensive studies on these complex compounds, and acquired a vast amount of knowledge and experimental data in this field. But it is an urgent need to sum up all these accomplishments so as to raise the general theoretical level. Our present research is just one of the attempts along this line

References

1. Paul Seligmann and Nathan R. Greening. "Phase Equilibrim of Cement-Water". Proc. Fifth. Inte'l. Symp, on the Chemistry of Cements, Tokyo, 1968, Part.2 pp.180-183
2. Melville H.Roberts, "Calcium Aluminate Hydrates and Related Basic Salt solid Solutions"
   Sym. Tokyo, 1968 Part. 2 pp. 114-115
   111-113
3. W. Dosch, H. Keller and H. Zur Strassen, "Discussion on Hans E. Schwiete and Udo Ludwig's Paper on Crystal Structures and Properties of Cement Hydration Products".
   Sym. Tokyo 1968 pp. 72-75
4. Nemat Tenoutasse, "The Hydration Mechanism of C_3A and C_3S in the Presence of Calcium Chloride and Calcium Sulphate".

Sym. Tokyo 1968 Part.2 pp.372-278

5. Walter L. De Keyser and Nemat Tenoutasse, "The Hydration of the Ferrite Phase of Cements"
   Sym. Tokyo 1968 Part.2 pp.379-386
6. L. E Copeland and D. L. Kantro, "Hydration of Portland Cements".
   Sym. Tokyo 1968 Part. 2 pp. 408-414
7. J. Bensted, "Chloroaluminates and the role of calcium chloride in accelerated hardening of Portland cement."
   World Cement Technology Vol.8 No.5 Sept/Oct. 1977
8. J. Bensted and S. Prakash Varma, "The Lowsulphate form of Calcium sulphoaluminate (Monosulphate)"
   Cement Technology Vol.4 No.3 May/June 1973
9. F.M. Lea, The Chemistry of Cement and Concrete.
   London 1970
10. Lou Zonghan, Xu Xianyu, Han Ren: On Ettringite and Modification of Slag Cement.
    Candidate for the Seventh International Conference on Cement Chemistry.1979.10.

Effect of $Ca(OH)_2$ on alkali-silica reaction

Effet de $Ca(OH)_2$ sur l'alcali-réaction

Associate Professor Tang MING-SHU and Lecturer Han SU-FEN, Department of Silicate Engineering, Nanjing Institute of Chemical Technology, Chine Populaire.

RESUME : L'action sur l'opale de solutions de pH différents a été étudiée. Les résultats montrent que la quantité de SiO_2 dissous croît rapidement quand les solutions ont des pH supérieurs à 12 à 12.5. Des recherches comparatives des réactions alcalis-silice dans le ciment portland, le ciment alumineux, le ciment métallurgique sursulfaté et le ciment sulfaté de boue rouge ont été faites.

Les réactions alcalis-silice dans le ciment portland sont les plus importantes, quoique leur teneur en alcalis soit à peu près la même que celle des autres ciments. Ceci peut être expliqué par le fait que la concentration en ions OH^- du liquide intersticiel de la pâte du ciment portland est forte, et en même temps le pH est toujours supérieur à 12.5, alors même que la teneur en alcalis n'est pas grande.

Ce n'est pas le cas pour les autres ciments. Le mécanisme de l'inhibition de la réaction alcalis-silice par des matériaux pouzzolaniques peut être expliqué rationnellement, en prenant l'action de $Ca(OH)_2$ en considération, et vérifié expérimentalement. La suggestion est faite que la réaction alcalis-silice causée par des alcalis, qui viennent des sources autres que du ciment, peut être empêchée en utilisant du ciment contenant peu ou pas de $Ca(OH)_2$.

Summary: The action on opal by solutions of different pH values has been investigated. Results show that the amount of SiO_2 dissolved increases rapidly when the solutions have pH values greater than 12-12.5. Comparative studies of the alkali-silica reaction in portland, aluminous, supersulphated and red mud-sulphated cements respectively were then carried out. Alkali-silica reaction in the portland cement is the most noted though the alkali content is about the same as in the other cements. This might be explained by the fact that the OH^- ions concentration of pore solutions in portland cement paste is rather high, as the pH value is always greater than 12.5 even though the alkali content is low. It is not the case with other cements. The mechanism of inhibiting alkali-silica reaction by the pozzolanic materials may be resonably explained by taking the effect of $Ca(OH)_2$ into consideration and has been verified experimentally. Suggestion is made that the alkali-silica reaction caused by alkali came from sources other than cement can be prevented by using cements containing little or no $Ca(OH)_2$.

I. Introduction

Stanton[1] discovered in 1940 the destructive action on concrete of the alkali-silica reaction. Since then, extensive investigations have been made in many countries and several comprehensive review papers have been reported[2,3,4,5]. Certain reactive aggregates, such as flint, rhyolite and andesite, have been found in the dam structures built in China. In addition, many cement factories in China are still producing a large amount of cement with high alkali content. Consequently, field observations and laboratory experiments to disclose the intrinsic nature of the alkali-silica reaction are urgently needed.

The role of $Ca(OH)_2$ in alkali-silica reaction has been studied by many authors. Powers[6] concluded that the diffusion rates of alkali versus calcium ions would be an important factor. The alkali-silica complex formed would cause expansion, but the lime-alkali-silica complex formed would not do so. This is known as competitive reaction theory[7].

Hansen[8] suggested that the migration of Ca^{2+} ions into opal would also induce expansion, because the volume occupied by calcium silicate thus formed would be larger than that of the opal itself. Moskvin[4] reported that both alkali and $Ca(OH)_2$ would take part in reaction, but at the same time the latter would regenerate the alkali ions to make the reaction going further. In addition, the semipermeable membrane which develops osmotic pressure would be formed by the reaction of $Ca(OH)_2$ with reactive aggregate.

Experimental work done previously by the present author[9] confirmed that the $Ca(OH)_2$ would increase the expansion caused by alkali-silica reaction. The objective of the present work is to investigate the effect of $Ca(OH)_2$ on alkali-silica reaction by considering as the most influential factor the relation of $Ca(OH)_2$ to the CH^- ions concentrations of pore solutions in the cement pastes.

II. Experimental results and discussion.

1. Effect of solutions with different pH values on opal.

The great importance of CH^- ions concentrations to alkali-silica reaction was well recognized by many investigators. In order to illustrate quantitatively the action of various pH solutions on opal, buffer solutions with different pH values were prepared by mixing 0.1 mol glycocoll and NaCl solution with 0.1 mol NaOH solution, according to the predetermined volume ratios. Buffer solution was used to make the CH^- ions concentration drop comparatively small during the reaction.

Experiments were carried out by putting 2 grams of opal (0.25 - 0.75 mm) in each plastic container with 70 ml. of buffer solution, then sealing them to prevent carbonization. After keeping it at room temperature($\sim 22^{\circ}C$) for 24 days, the dissolved silica was determined by photoelectric colorimeter. The aim of these experiments was to examine the corrosion on opal by solutions which have different CH^- ions concentrations but the same R^+ ions concentrations. Experimental results are shown in Fig.1. It can be clearly seen that only a

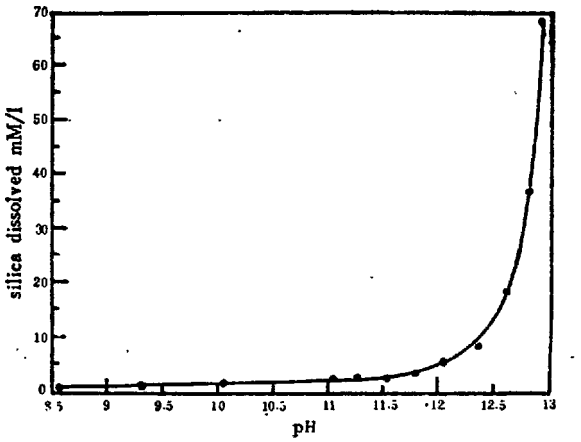

Fig. 1. Silica dissolved in different pH buffer solutions

little silica is dissolved when the pH value of the solution is less than 12.0 - 12.5, but beyond these values, the amount of silica dissolved increases rapidly. These results can be utilized to explain the different behavior of alkali-silica reactions in various types of cement.

2. Alkali-silica reactions in different types of cement.

Mortar bars containing 6% (by weight of sand) of opal (0.15 - 0.30 mm) were made of different cements. Expansion after ageing was determined by measuring the length changes. The results are given in Table I. It shows that the expansion of portland cement is much greater than the others when their alkali contents are almost the same. This is supposed to be due to the difference of OH^- ions concentrations in the pore solutions. To verify this, the ions concentrations were determined by using the method proposed by Schwiete[10] but modified by the present author. Cement paste with W/C = 0.65 was prepared. After keeping the sample at room temperature ($\sim 25^0C$) for 18 days, the liquid was expelled out of the cement paste by a pressure of 45 N/mm^2 instead of centrifugation. The OH^- ions concentrations of pore solutions thus obtained were then determined. The results are shown in Table II.

Table I Expansion of mortar bars containing opal

No.	Type of cement	Mix of cement	Alkali content expressed as equiv. Na_2O(%)	Age	Expansion (%)	Condition of mortar bars
1	Portland		1.22	2 years	1.275	Cracked
2	Aluminous		1.17	3 years	0.054*	Good
3	Supersulphated	blast-furnace slag:gypsum: clinker=81:15:4	1.61	2 years	0.112*	Good
			2.61	2 years	0.160*	Good
			3.01	2 years	0.389	Cracked
4	Red mud-sulphated	red mud:clinker. gypsum:blast-furnace slag =40:10:15:30	1.27	4 months	0	Good
			1.77	4 months	0.001	Good

① The original alkali contents of No.1,2,3,4 are 0.52%,0.17%,0.31% and 1.27% respectively(calculated as equiv.Na_2O),the alkali make-up is added when mixed;
② Red mud is the waste slag from alumina factory, containing 75% CaO. Its alkali content is calculated as equiv. Na_2O to be 2.61%;
③*means the expansion value is same as that with no opal

Table II

Ions concentrations of pore solutions in cement pastes

Type of cement	Alkali content expressed as equiv. Na_2O (%)		Ions concentrations (mM/l)	
	original	total*	$R^+(Na^+ + K^+)$	OH^-
Portland	0.43	1.2	359.3	434.7
Aluminous	0.06	1.2	414.3	pH=12.97 (detd. by pH-meter)
Supersulphated	0.60	1.79	445.7	31.3

*The alkalis other than original are added when mixed.

Comparison of the results shows clearly that the OH^- ions concentration of portland cement is much greater than that of supersulphated cement, but the difference of R^+ ions concentrations is small. As mentioned above, the opal would be attacked more seriously as the concentrations of OH^- ions are much higher. This is also confirmed by microscopic observations. Nearly all of the opal in portland cement paste (Na_2O = 1.72%) was attacked and cracks were distributed over the whole surface, while the opal in the supersulphated cement (Na_2O = 1.61%) maintained its original contour (Fig. 2).

With respect to aluminous cement, though the OH^- ions concentration is lower than that of portland cement, but it is much higher than that of supersulphated cement. Consequently the opal is still attacked seriously. The OH^- ions concentrations of red mud-sulphated cement paste however determined with a W/C value higher than 0.65, is the smallest one among all the cements tested. Obviously, the opal in the paste of this cement would be reacted upon only slightly.

(a) (b)

Fig. 2. Opal in cement pastes of (a) portland cement and (b) supersulphated cement, aged for the same period of 75 days.

The higher OH^- ions concentration of pore solutions in portland cement paste is related to the presence of solid $Ca(OH)_2$ in the paste. According to Maiquori,[11] the total OH^- ions concentration of $Ca(OH)_2$ + NaOH solution is always higher than that of NaOH present alone (Fig. 3).

It must be pointed out that the $Ca(OH)_2$ present may keep the pH of pore solutions greater than 12.5 even if the alkali content is very low. As mentioned above, opal is reacted upon severely under such pH value conditions. Therefore, the alkali-silica

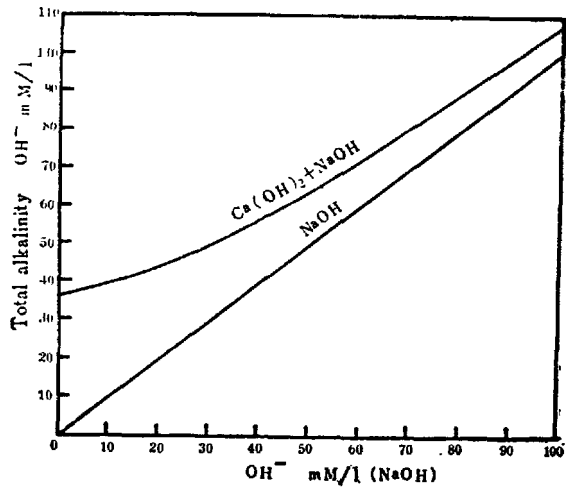

Fig. 3. The total alkalinity of NaOH and ($NaOH + Ca(OH)_2$) solutions

reaction may go on in portland cement though the alkali content is low, or even though a great part of alkali has been used up. Thus, D.O. Woolf[12] did report the expansion produced by the small amount of reactive aggregate in a low alkali cement.

It is very interesting that Diamond[5] interpreted the alkali-silica reaction by emphasizing the effect of the ions concentrations in the pore solutions. The present work suggests that the different behavior of alkali-silica reaction in different types of cement as above described are just due to their different concentrations of OH^- ions in pore solutions.

3. Mechanism of inhibiting alkali-silica reaction by additives.

Additives such as pozzolana and slag were proved by many investigators to be very effective to inhibit the alkali-silica reactions. The mechanism, however, as both Lea[13] and Malquori[11] stated, is yet to be elucidated.

Three questions might be put forward for discussion: (a) In order to reduce expansion, why should a large quantity of additives be always needed, as the alkali content of the cement amounts to approximately 1% only? (b) Why do certain additives cause expansion when a little amount of them is used? (c) Certain high alkali pozzolanas, in reacting with $Ca(OH)_2$, may release most part of the alkali contained, can these pozzolanas be used to inhibit the alkali-silica reaction? Presumably, these questions can be answered by taking the effect of $Ca(OH)_2$ into consideration.

The pozzolana in pozzolanic cement reacts not only with alkali but also with $Ca(OH)_2$, both of them are released by portland cement clinkers during the process of hydration. The large amount of $Ca(OH)_2$ present in the hydrated cement may regenerate the alkali absorbed by pozzolanic materials. Furthermore, the alkali contained in pozzolanas can also be released by ion exchange with $Ca(OH)_2$. Therefore, to inhibit an alkali-silica reaction, it is necessary to add a large amount of pozzolanic materials until there is enough to reduce the $Ca(OH)_2$ to such an extent that it will release or regenerate only a little alkali. It needs not, however, to take away all the $Ca(OH)_2$ because the last remaining $Ca(OH)_2$ would be embedded in the hydrated parts. In practice, the alkali-silica reaction can be inhibited only when the pozzolanic materials added amount to more than 25 - 30%. If a small amount ($\sim$10%) of high alkali pozzolanic materials such as fly ash or pozzolana is added, the R^+ and OH^- ions concentrations of pore solutions would increase instead of the reverse. Thus the alkali-silica reaction will be accelerated. The high alkali pozzolanas, however, might have an inhibiting effect, if the amount added is sufficiently high. This has been proved in the laboratory and with field constructions. For example, in Italy,[11] pozzolanic cements made from high alkali pozzolanas were mixed with reactive aggregates, but no trouble was found thenceforth.

Two experiments were done with a portland cement (Na_2O = 1.2%) to which 25% of fly ash and 45% of calcined clay were used respectively. The alkali-silica reaction in both samples was found to be inhibited. For the purpose of illustrating the role of $Ca(OH)_2$, extra 10% of low temperature calcined lime

was added in both samples. Expansion of mortar bar increased evidently with time (Fig. 4).

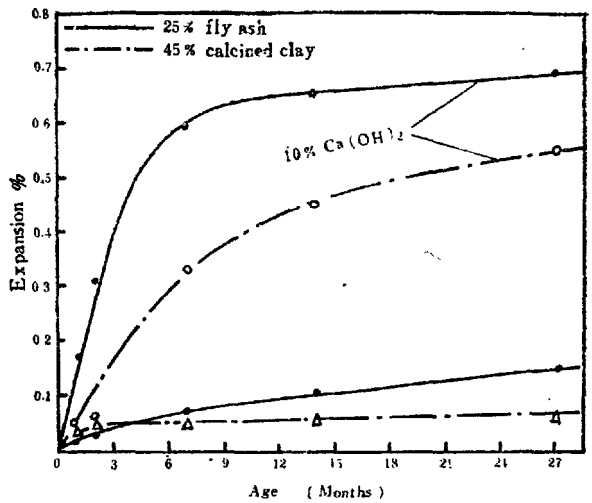

Fig. 4. Expansion of mortar bars made from pozzolanic cement with opal added.

It was thus proved that additives must absorb enough $Ca(OH)_2$ in order to inhibit the alkali-silica reaction. In general, the inhibiting ability of blastfurnace slag is inferior to pozzolana, because the $Ca(OH)_2$ absorbed by blastfurnace slag is less than by pozzolana.

It is highly likely that the mechanism of inhibition by pozzolanic materials would be not only to reduce the alkali-silica reaction but also related to the structure of the cement paste. Further work of investigation is to be planned.

4. Prevention of alkali-silica reaction caused by alkali from sources other than cement.

Bredsdorff[2] had call attention to the fact "that in cases where alkalies may be contained in the mixing water, in the aggregate or in the surroundings of concrete, special precautions, besides the use of low alkali cement, are called for." According to the discussion mentioned above, it would be expected that supersulphated cement may not cause severe alkali-silica reaction even if the surrounding water contains alkali salts. On this account, mortar bars containing opal were kept in alkali salt solutions and their length changes were measured. The results are shown in Table III.

Table III

Expansion of mortas bars kept in solutions of alkali salts

Type of cement	Alkali content expressed by equiv. Na_2O(%)	Opal, % replacement of sand by weight	Solutions	Period of ageing(months)			
				1	4	9	13
Portland	0.52	0	5% Na_2SO_4	0.036	0.035	0.063	0.109
	0.52	6	5% Na_2SO_4	0.032	0.067	0.68	1.41
Supersulphated	0.61	0	5% Na_2SO_4	0.045	0.040	0.055	0.057
	0.61	6	5% Na_2SO_4	0.058	0.059	0.058	0.065
	0.61	0	5% NaOH	0.069	0.068	—	0.074
	0.61	6	5% NaOH	0.061	0.060	0.076	0.088
	1.31	0	5% Na_2SO_4	0.129	0.121	0.123	0.127
	1.31	6	5% Na_2SO_4	0.128	0.126	0.128	0.132

Results showed that the mortar bars made from low alkali portland cement and being kept in 5% Na_2SO_4 solution expanded 1,41% and cracked after 13 months. But those made from supersulphated cement and being kept either in 5% Na_2SO_4 solution or in 5% NaOH solution expanded only slightly. In particular, these expansions were almost the same as those of the mortar bars, which, with no opal in them, had been kept under the same conditions. Hence, it can be expected that by using such cements as supersulphated or portland cement, with the sufficient amount of pozzolana or slag being added, the alkali-silica reaction caused by the alkali from sources other than cement could be prevented, since hydration of these cements will produce little or no $Ca(OH)_2$.

Discussions so far are concerning mainly the effect of OH^- ions on alkali-silica reaction. Mention may be made on the migration of Ca^{2+} ions. By using EDAX technique, it is discovered that the Ca^{2+} is concentrated on the surface of the larger opal particles (1 cm) (Fig. 5a, the shadows show the elements on surface and the points show the elements in center). But it is verified by repeated tests that with the smaller opal particles (0.25 - 0.75 mm), a large amount of Ca^{2+} ions is concentrated in the center of opal (Fig. 5b). It seems that the Ca^{2+} ions also take part in and promote the alkali-silica reaction.

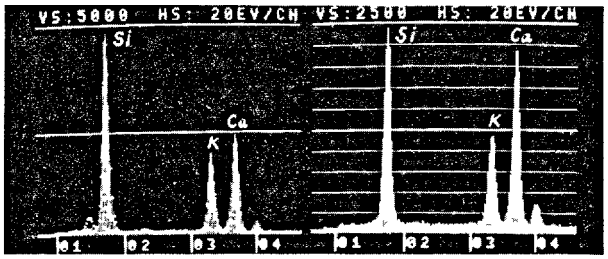

(a) (b)

Fig. 5. EDAX of opal in cement pastes
(a) Opal size, ~1 cm;
(b) Opal size, 0.25 - 0.75 mm.

III. Conclusion.

1. Alkali-silica reaction is actually a base-acid neutralization reaction. Hence, when the concentrations of R^+ ions is fixed, the more concentrated the OH^- ions solution is, the more vigorous is the reaction.

2. The differences of expansion caused by alkali-silica reaction in different types of cement are mainly due to the difference of OH^- ions concentrations in the pore solutions of cement pastes.

3. The alkali-silica reaction may be effectively inhibited, if a sufficient amount of pozzolanic materials is added to the cement. A large part of $Ca(OH)_2$ would be vanished in reaction and the last remained $Ca(OH)_2$ could be embedded by the hydrated products.

4. The alkali-silica reaction caused by alkali from sources other than cement can be prevented by the use of supersulphated cement or cement with additive such as pozzolana or blastfurnace slag.

References:

1. T. E. Stanton, ASSCE Proceedings 66, 1781 (1940).

2. P. Bredsdorff, G. M. Idorn, N. M. Plum, Chemistry of Cement, Proc. 4th. Int. Symp., NBS Monograph 43, V. II, 749 (1963).

3. U. Ludwig, G. Wolff, D. Hirche, Die Alkali-Kieselsäurereaktion, Westdeutscher Verlag, 1974.

4. V. M. Moskvin, G. S. Royak, Corrosion of Concrete by The Action of Alkali of Cement on The Silica of Aggregates, Moscow, 1962.

5. S. Diamond, Cement and Concrete Research, 5 (4) 329 - 347 (1975); 6 (4) 549 - 561 (1976).

6. T. C. Powers and H. H. Steinour, ACI Journal, Proc. 51, 497 (1955); 51, 585 (1955).

7. G. Verbeck, Proc. ASTM, 55, 1110 (1955).

8. W. C. Hansen, Chemistry of Cement, Proc. 4th. Int. Symp., NBS Monograph 43, V. II, 784 (1963).

9. Tang Ming-shu, Xue Wan-rong, Journal of The Chinese Silicate Society, 1 (1) 20-30 (1962); 2 (2) 110-117 (1963).

10. H. E. Schwiete, TIZ-Zbl, 18, 86 (1962).

11. G. Malquori, Chemistry of Cement, Proc. 4th. Int. Symp., NBS Monograph 43, V. II, 983 (1963).

12. D. O. Woolf, Public Roads, 27 (3), 50 (1952).

13. F. M. Lea, The Chemistry of Cement and Concrete, third edition, 575 (1970).

Effect of glucose on the hydration of portland cement

Action du glucose sur l'hydratation du ciment portland

N.B. SINGH and P.N. OJHA, Department of Chemistry, Gorakhpur University, Gorakhpur (U.P.), India.

RESUME : L'action du glucose, à diverses concentrations, sur l'hydratation du ciment Portland a été étudiée en utilisant la calorimétrie, l'analyse thermique différentielle et la diffraction X. On a mesuré la quantité de chaux libérée par l'hydratation du ciment, et la résistance à la compression de ciments additionnés ou non de glucose. Le potentiel Zéta de ces ciments, additionnés ou non de glucose, a été déterminé par électrophorèse. Ce potentiel Zéta du ciment anhydre ou hydraté pendant 24 heures, ou encore hydraté pendant 24 heures en présence de $2,0 \times 10^{-2}$ M de glucose a été trouvé égal respectivement à + 14,6 mv, -8.4 mv et + 4.5mv. Les résultats montrent qu'en présence de glucose, la vitesse de réaction entre le C_3A et le gypse est augmentée, et dépend de la concentration en glucose; ainsi, une concentration plus grande en glucose provoque une vitesse de réaction plus élevée. L'effet global du glucose est de retarder l'hydratation. Ces résultats ont été exprimés en fonction du potentiel Zéta.

SUMMARY: Effect of different concentration of glucose on the hydration of portland cement have been studied. Calorimetric, DTA and X-ray diffraction techniques were used for the hydration studies. Percent free lime of the hydrated cement and the compressive strength of the hardened cement in the presence and absence of glucose were determined. Zeta potential of the cement hydrated in the presence and absence of glucose have also been calculated by determining the electrophoretic velocity. The zeta potential values of unhydrated cement, hydrated for 24 h and hydrated for 24 h in the presence of 2.0×10^{-2} M glucose were found to be + 14.6 mv, -8.4 mv and + 4.5 mv respectively. Results indicate that in the presence of glucose, the rate of reaction between C_3A and gypsum is increased and this depends on the concentration of glucose i.e. greater is the concentration, faster is the rate of reaction. The overall effect of glucose is the retardation of hydration. The results have been explained in terms of zeta potential value.

INTRODUCTION

Effect of admixtures, both accelerators and retarders, on the hydration of cements have been studied extensively. The saccharide compounds (or sugars as they are commonly called) are one of the effective retarders and have been studied by various research workers[1-7]. Suzuki and Nishd studied the retarding effect of saccharides on the hydration of cements and they explained their results in terms of adsorption theory. Breuer[2] also explained the retarding action of sugars in terms of adsorption theory. During the action of polysaccharides on the hydration of cement pastes, Young[1] found that in the presence of alkalies, the degradation of saccharides take place and the degradated products are more effective retarders. Milestone[8] also supports the Young's observation and he found that the sugar acids of glucose are atleast ten times more effective in retarding the hydration of C_3A than glucose. Previte[9] found that the retarding power of saccharides are related to the molecular size and conformation. Mariampol'skii et al[10] studied the retarding action of saccharic, aldonic and uronic acids and their salts on the hydration of cements and explained their results in terms of chelation between organic compounds and the Ca^{2+} ions. Singh[11] on the other hand believes that the gluconates retard the hydration of portland cement by poisoning certain growing nucleis.

Recently Singh[12,13] studied the effect of glucose on the hydration of portland cement and found that it accelerates the reaction between tricalcium aluminate and gypsum.

The survey of the literature shows that although the effects of organic additives such as sugars on the hydration of cements have been studied extensively, there are still significant disagreements regarding the mechanism of their action.

The purpose of this article is to study the mechanism of the action of glucose on the hydration of portland cements. The results have been interpreted in terms of zeta potential ( ).

EXPERIMENTAL

Material: Portland cement(ACC) was used for the hydration studies. Glucose (G. Merck) was used as an admixture.

Method: Heat of hydration were determined by a microcalorimeter. The details of the method are described elsewhere[14]. The experiments were performed at 30°C at W/c = 0.5.

Hydration of the cement (W/c = 0.5) in the presence and absence of glucose was stopped at various intervals of time by absolute ethyl alcohol. 0.5×10^{-2}M, 1.0×10^{-2}M, 1.5×10^{-2}M and 2×10^{-2}M glucose solutions were used for the study.

Measurement of electrophoretic velocity

For the measurement of electrophoretic velocity, a similar method as adopted by Kastogi et al[15] was used. The apparatus used is shown in Fig. 1. The cement particles were homogenized mechanically and dispersed in isopropyl alcohol. The experimental cell was fixed in a vertical

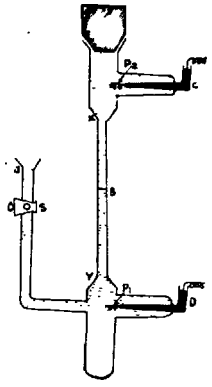

Fig. 1. Apparatus for measurement of electrophoretic velocity.

position and the suspension was introduced into the experimental cell through J till half of the tube was filled. The stopcock, S, was now closed and pure isopropyl alcohol was gently filled in the remainder of the tube, XY, so that distinctly sharp boundary B was formed. The internal diameter of XY was 0.33 Cm. A potential difference was applied through coiled platinum electrodes, P_1 and P_2, 12.7 Cm. apart with an electronically operated power supply in such a way that movement of the boundary occured in the downward direction. The position of the boundary at various time intervals was noted and the rate of movement of boundary or the electrophoretic velocity was thus determined. Corrections were made for the downward movement due to the action of gravitational forces. From the electrophoretic velocity, potential was calculated. The experiments were performed at 35°C and for anhydrous cement, and cement hydrated for 24 h in the presence and absence of 2.0×10^{-2} M glucose solution.

X-ray diffraction patterns of the hydrated samples were taken with a x-ray diffractograph using CuK_α radiations. The following x-ray lines are used for the analysis.

Phase	d(A°)
C_3S	2,776, 3.02
C_3A	2.70

$Ca(OH)_2$	4.90
$CaSO_4 \cdot 2H_2O$	7.56
$C_3A \cdot 3CaSO_4 \cdot 31H_2O$	9.70

DTA of the hydrated samples were made with a manual differential thermal analyser. Caliberation curve by using different concentration of gypsum in alumina were also made.

Free lime content was determined by the extraction method[16]. The samples were extracted for one hour with a mixture of iso-propyl alcohol and acetoacetic ester at boiling temperature, after which the suspensions were cooled down and filtered. The extracted lime were determined by titrating against 0.1N HCl.

Compressive strength of the samples in the form of 4"x4"x16" bricks were measured at different intervals of time in the presence and absence of glucose.

RESULTS

Heat of hydration

The heat of hydration of cement in the presence and absence of glucose with different hydration times are given in Fig. 2. From the figure it is clear that as soon as the cement comes in contact to water rapid heat evolution takes place and after which the reaction slows down.

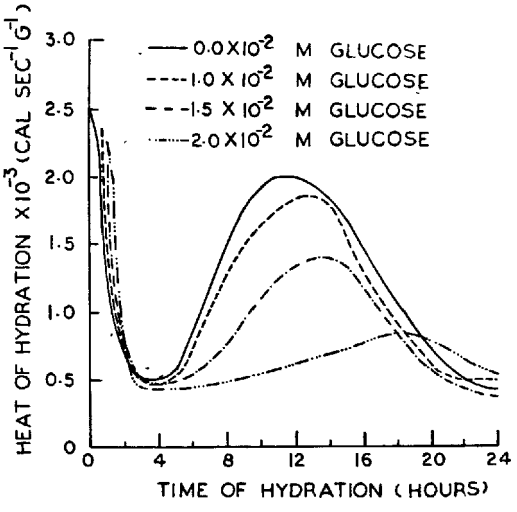

Fig. 2. Effect of glucose on the heat evolution of cement.

This early heat liberation may be due to cement wetting, dissolution of alkalies, hydration of hemihydrate, free lime and C_3A. The hydration reaction is very slow during the induction period which continues approximately upto 5 hrs. After the induction period is over the reaction accelerates with time, and reaches a maximum value at around 10 hrs. and after which deacceleration of the reaction starts and ultimately it becomes very slow. During this period mainly the hydration of C_3S phase takes place. In the presence of different concentration of glucose (1.0×10^{-2} M, 1.5×10^{-2} M and 2.0×10^{-2} M) the rate of heat evolution is decreased and the time for maximum heat evolution is increased. The overall effect is that by increasing the concentration of glucose the hydration of cement is decreased.

X-ray Studies

The variation of concentration of C_3S, C_3A and gypsum in the solid samples hydrated at different intervals of times, as represented in terms of x-ray intensities, are shown in Fig. 3. From the figure it appears that in the absence of glucose, the concentration of C_3S phase is constant upto approximately 10 hrs and after which it starts decreasing.

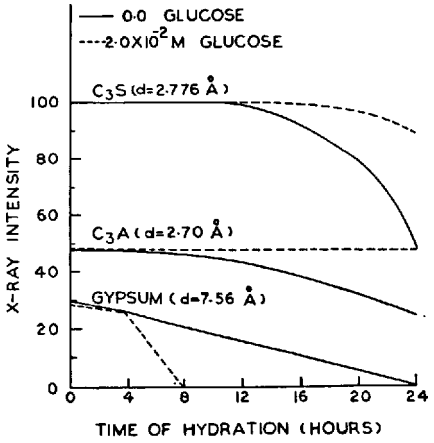

Fig. 3. Variation in X-ray intensity for the different phases of cement during hydration.

In calorimetric curve, also a maximum comes at about 10 h of hydration. After this time the x-ray intensity starts decreasing and reaches to 50% at 24 hr. This shows that only nearly 50% of C_3S is hydrated at 24 h. On the otherhand in the presence of 2.0×10^{-2} M glucose solution, the x-ray intensity remains constant upto nearly 18 h and then starts decreasing and reaches to 90 at 24 h. Here also a maximum appears at around 18 h. A decrease of only 10 in the x-ray intensity simply indicates that in the presence of glucose the hydration of C_3S phase is practically negligible.

In the absence of glucose, the x-ray intensities of the C_3A phase are constant upto nearly 10 h and then start decreasing whereas in the presence of 2.0×10^{-2} M glucose, there is not much variation in the x-ray intensity of the C_3A phase (Fig. 3). In other words the concentration of C_3A is roughly constant during the time of experiment in the presence of glucose.

As indicated by the x-ray intensity, in the absence of glucose, the gypsum is consumed between 18 and 24 hr. Whereas in the presence of 2.0×10^{-2} M glucose solution, it is consumed in between 4-8 hr. (Fig. 3). This is supported by DTA experiment also. The consumption of gypsum is as a result of the reaction between C_3A and gypsum with the formation of ettringite. This reaction is accelerated in the presence of glucose and hence gypsum is consumed quickly. Since only a small amount of C_3A is involved in the reaction, its concentration is not effected much.

In the absence of glucose, the presence of calcium hydroxide is indicated only after 4 h whereas in the presence of 2.0×10^{-2} M glucose, it does not come even upto 24 h.

ξ Potential

The electrophoretic velocity is given from double layer theory as

$$(V_e)_{g=0} = D\xi g/f\pi\eta \quad \ldots.(1)$$

where, η = viscosity of the medium, D = its dielectric constant, ξ = zeta potential of the interface, g is the gravitational field per unit mass and f is between 4 and 6. According to regorous theory of Debye and Hiickel, it is 6, when the electrophoretic drag due to double layer is also considered[17]. In equation (1); $E = \Delta\phi/\ell$, where $\Delta\phi$ is the potential difference and ℓ is the distance between the two electrodes. Thus, on substituting the value of E in equation (1).

$$V_e = D\xi\phi/\ell f\pi\eta \quad \ldots.(2)$$

A plot of V_e against $\Delta\phi$ (Fig. 4) would give a straight line. The slope of the curve will be equal to D

$$\text{Thus,} \quad \xi = \frac{\ell f \pi \eta}{D} \text{ slope} \quad \ldots(3)$$

The zeta potential for pure cement, and cement hydrated for 24 h in the presence and absence of 2.0×10^{-2} M glucose solution were calculated by using eq.(3)

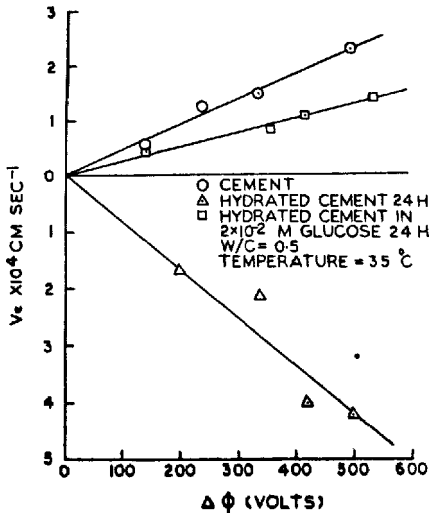

Fig. 4. Variation of electrophoretic velocity with the applied voltage

and are given in table I. From the table it is clear that the zeta potential is positive and maximum for unhydrated cement whereas it is decreased considerably for other samples. In the cement hydrated in the absence of glucose, the zeta potential even becomes negative.

Table I

Zeta Potential (ξ)
Temperature = 35°C

Sample	Zeta Potential (mV)
Cement	+ 14.6
Cement hydrated for 24 h	- 8.4
Cement hydrated for 24 h in 2.0×10^{-2} M glucose	+ 4.5

Free lime content

The variation of percent free lime with hydration lime is shown in Fig.5. In the absence of glucose, the percent free lime is roughly constant upto 5 hr($\simeq$1%) and after which increases rapidly and then becomes slow after 18 h. In the calorimetric experiment also, the induction

period is upto 5 h and hence the free lime determination shows that the hydration is very slow upto 5 h and it increases only after the induction period is over. In the presence of glucose, the percent free lime is very low(< 1%) and is nearly constant during the course of experiment. This simply shows that in the presence of glucose the hydration is decreased considerably.

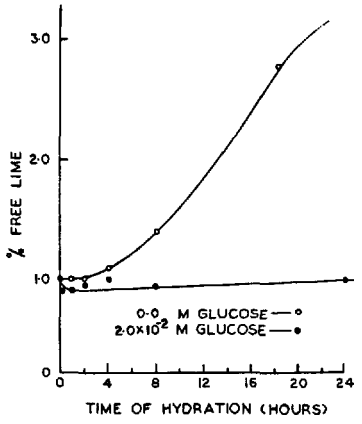

Fig. 5. Variation of free lime content with the hydration time.

Compressive Strength

The variation of compressive strength with hydration time in the presence of different concentration of glucose solution is given in Fig. 6. From the figure it is

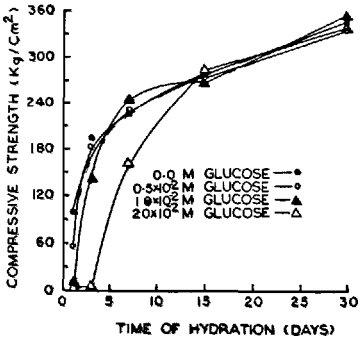

Fig. 6. Effect of glucose on the compressive strength of cement.

clear that in the presence of glucose the strength is lower at early stages of hydration but becomes nearly equal to that hydrated in the absence of glucose at latter stages of hydration. The decrease of compressive strength and the time of equalization of the two strengths (in the presence and absence of glucose) increases with the increase in glucose concentration.

DISCUSSION

Results indicate that in the presence of glucose, the overall hydration of the cement is retarded and the gypsum is consumed quickly. A positive value of zeta potential indicates that the overall charge on the cement grains are positive. The development of charge on the cement grains may be due to the non-stoichiometry present in the constituent compounds of the cement. The cement grains with a positive surface when comes in contact to water, a dipole, dipolar interaction starts. As a result of this dipole-dipole interaction, the reaction proceeds and various hydrates are formed, at the surface of the cement grains. These hydrates may take some time for reorientation of charges, which causes the induction period of the hydration reaction. Once the reorientation of the charges is over, the reaction will accelerate with time and hydrates thus formed are probably rich in OH^- groups and because of this the overall charge on the hydrated cement grains become negative and accordingly the zeta potential. On the other hand the zeta potential of the cement hydrated in the presence of glucose is decreased. This decrease in zeta potential can be explained as: As soon as cement grains come in contact to glucose solution, glucose molecules are adsorbed on the cement grains. Since the glucose molecules are neutral and bulky, they act as a screen. As a result of this the magnitude of the effective charge on the cement grains are decreased. Because of the lower effective charge, the dipole-dipole interaction between water and glucose adsorbed cement grains are decreased and the overall magnitude of charge on the hydrated cement in presence of glucose is decreased. This causes a retardation of hydration and a decrease in the zeta potential of the hydrated sample in the presence of glucose. The decrease in zeta potential can be explained with the help of following equation

$$\zeta = \frac{4\pi\sigma d}{D} \qquad \ldots(4)$$

where d is the double layer thickness, σ is the charge density and D is the dielectric constant of the medium. Thus keeping D as constant, ζ will depend mainly on σ.

However it is difficult to explain the accelerating action of glucose on the reaction of gypsum with C_3A on the basis of zeta potential unless a seperate experiment with C_3A alone is performed.

The decrease in free lime and strength in the presence of glucose is mainly due to lower degree of hydration.

CONCLUSION

From our results the following conclusions can be made.

1. Calorimetric experiments indicate that the hydration of cement is retarded in the presence of glucose.By increasing the concentration of glucose, the induction period and the time for maximum heat evolution is increased whereas the total amount of heat evolved is decreased.
2. X-ray diffraction and differential thermal studies indicate that in the presence of glucose,the reaction between C_3A and gypsum is accelerated. This is indicated by early consumption of gypsum in the presence of glucose.
3. The zeta potential of unhydrated cement was found to be +14.6 mv, whereas the zeta potential of the cement hydrated in the presence of absence of 2.0×10^{-2} M glucose for 24 h were found to be -8.4 mv and +4.5 mv respectively.
4. The positive value of zeta potential of the unhydrated cement indicates a positive charge on the cement and this may be due to the nonstoichiometric compounds present in the cement. The hydration reaction is considered as a dipolar interaction between positively charged cement grains and water dipoles.
5. The negative value of the zeta potential indicates a negative charge on the hydrated cement which may be due to more OH^- groups on the surface of the hydrated cement. A decrease in zeta potential in the presence of glucose is explained as a result of adsorption.
6. The compressive strength of the cement in the presence of glucose is decreased in the early days of hydration whereas after longer time it becomes nearly equal.
7. In the presence of glucose, the percent free lime is less than one and remains constant upto 24 h, whereas in the absence of glucose it is nearly one upto 5 h and after than it increases rapidly.

ACKNOWLEDGMENTS

The authors are thankful to Dr.P.Rastogi, Dr. I. Das and Mr. V.N. Srivastava for giving help during the course of experiment.

REFERENCES

1. J.F. Young, Proc. Vth Int. Sym. Chem. Cem. Tokyo, (1968).
2. G.M. Breuer, Nature, 212, 502, (1966).
3. K. Ashworth, Proc. Inst. Civ.Eng. 31, 129 (1965).
4. L.H. Tuthill, R.F. Aams and J.M.Hemme, ASTM Spec. Tech. Publ. No. 266, 97, (1960).
5. S. Suzuki and S. Nishi, Semento Gijutsh, Nenpo, 13, 160 (1959).
6. G. BabaChew and V. Velkov, Stroitelstov, 20(4), 1(1973), Chem. Abs. 80, 111941, (1974).
7. F. Vavrin, Moscow Congress 1974.
8. N.B. Milestone, Cem. Concr. Res., 7(1), 45, (1977).
9. R.W. Previte, Ibid, 1,301 (1971).
10. N.A. Mariampol'skii, A.I. Pen'hov and Yu. A. Shavachkiu, Nebt. Khoz, (10) 27 (1974), Chem. Abst. 82,89549 (1975).
11. N.B. Singh, Cem. Concr. Res., 6, 455 (1976).
12. N.B. Singh, Ind. J. Tech., (Published) 1978.
13. N.B. Singh, Tond. Ztg., 1, 6 (1978).
14. N.B. Singh, Cem. Concr. Res., 5,454 (1975).
15. E.S. Presslev, S. Brunauer, D.L.Kantro, and C.H. Weise, Anal. Chem., 33, 877 (1961).
16. R.P. Rastogi, K. Singh and J.Singh, J. Phys. Chem., 79, 2574 (1975).
17. R.P. Rastogi and B.M. Misra, Trans. Faraday Soc., 63, 584 (1967).

Conditions of the Hydroxyl Ellestadite Formation in Mixtures containing Calcium Sulphate

Les conditions de la formation de l'hydroxyle-ellestadite dans les mélanges comprenant du sulphate de calcium

Z. SAUMAN, Professor, Research Institute of Building Materials, Brno,
F. VAVRIN, Professor, Technical University, Brno, CSSR, Tchécoslovaquie.

RESUME : Au cours du traitement hydrothermique des mélanges de sable quartzeux et de chaux avec addition de plâtre, l'hydroxyle-ellestadite se forme /$Ca_{10}(SiO_4)_3(SO_4)_3(OH)_2$/. Dans le cas d'une teneur très accentuée, celui-ci cause la détérioration des caractéristiques mécaniques et physiques des produits autoclavés. Dans les mélanges de CaO et de quartz à granulométries différentes, et avec plâtre, on a constaté qu'au cours du processus hydrothermique, la quantité de la phase susmentionnée formée est maximum pour une dimension des particules de quartz comprise entre 60 et 90 µm.

Avec du quartz de granulométrie inférieure à 10 µm, l'hydroxyle-ellestadite se forme au commencement de la réaction et se décompose immédiatement en phase tobermoritique et en sulphate de calcium. L'augmentation de la grandeur des particules de quartz prolonge cette décomposition dans le temps. Dès le remplacement partiel de la chaux par le C_3S ou par le ciment, ce composant se forme, mais seulement pour des teneurs en plâtre plus élevées (> 10 %).

SUMMARY : During the hydrothermal processing of mixtures of quartz sand with lime and a gypsum rock admixture is formed hydroxyl ellestadite /$Ca_{10}(SiO_4)_3(SO_4)_3(OH)_2$/ which in a more pronounced quantity causes the deterioration of the physical and mechanical properties of autoclaved products. It was found in mixtures of CaO with quartz of a different granulometry and gypsum rock that in the course of the hydrothermal process is formed the maximum quantity of the above phase when employing quartz with particle size within 60 to 90 µm.

When quartz of granulometry under 10 µm is employed, hydroxyl ellestadite is formed at the beginning of the reaction, but it is immediately decomposed into tobermoritic phase and calcium sulphate. With growing quartz particle sizes, the decomposition period of the latter is prolonged. Already through the partial replacement of lime by C_3S or cement there occurs the formation of this component only at higher gypsum rock content (>10%).

INTRODUCTION

Studies of SO_4^{2-} ions influence onto the $CaO-SiO_2-H_2O$ system under hydrothermal conditions have shown that the transformation of CSH gel into 11 Å tobermorite is accelerated by the relatively low additions of $CaSO_4.2H_2O$ (1-3).

As soon as, however the content of the added $CaSO_4.2H_2O$ in the starting mixture above 3-4% is increased, the formation of hydroxyl ellestadite/$Ca_{10}(SiO_4)_3(SO_4)_3(OH)_2$/ could be noted. At the same time it was found that increasing sulphate additions lead to a proportional increase in the contents of the formed hydroxyl ellestadite (further only : HXEL).

With regard to the fact that the experimental part of this work was aimed at the formation of HXEL under production technology conditions of autoclaved building materials on the basis of quartz sand, lime and cement, also their physical and mechanical properties were studied.

It was proved that an increasing content of sulphate ions in the above system causes the reduction of strengths after the hydrothermal processing of the investigated mixtures, proportionaly to the quantity of the formed HXEL. This fact follows from the actual particles morphology of the above phase (4).

The formation of HXEL and the effect of gypsum rock in mixtures of cement and quartz sand, respectively, onto the actual mechanism of the reactions, were studied also by Takemoto and Kato (5) and Djabarov and Slatanov (6).

EXPERIMENTAL

Starting raw material components and method of their preparation.

For the experimental work there was employed α-quartz (low) having following chemical composition (%) :

Moisture content - 0,09; ignition loss - 0,11; SiO_2 - 99,75; Al_2O_3 - traces; Fe_2O_3 - 0,06; TiO_2 - 0,01; CaO - traces; MgO - traces; K_2O - traces; Na_2O - traces.

CaO was obtained by igniting $CaCO_3$ (Merck, anal. grade) at 1050°C, 4 h.

As the sulphate component $CaSO_4.2H_2O$ (anal. grade) was employed. Quartz, employing laboratory air classifier and suitable sieves was separated into following fractions (/um) : < 5, 5-10, 20-30, 30-40, 40-60, 60-90, 90-100, 100-150, 150-200, 200-300, 300-400, 400-500 and 500-600.

Furthermore there was employed portland cement clinker with following phase compostition (%) : C_3S - 69,1; β-C_2S - 13,2; C_3A - 6,2; $C_6A_xF_y$ - 6,9, from which also cement was obtained by grinding with 4% $CaSO_4.2H_2O$ to the fineness of 3200 $cm^2.g^{-1}$ (Blaine).

RESULTS AND THEIR DISCUSSION

Formation and stability of HXEL in relation to quartz granulometry and length of the hydrothermal process.

Quartz fraction mixtures were homogenized with CaO in a mass ratio of 80:20 simultaneously with 10% $CaSO_4.2H_2O$ (converted to a lime-quartz mixture) and processed in the form of a paste or suspension (solid phase : H_2O = 1 : 10) hydrothermally in small pressure vessels at 193°C, isothermal holding period 5 h. From the prepared X-ray diagrams there was employed the height of the 2,83 Å diffraction line (corresponding to HXEL) for plotting the graphical relationship between the relative quantity of the above phase and the quartz granulometry.

It follows from Fig.1 that a larger HXEL quantity is formed in the paste, whereas in mixtures with fine quartz fractions (<40 /um) this component could not be positively identified. In both series the highest HXEL quantity was determined in samples that contained quartz with the granulometry of 60-90 /um.

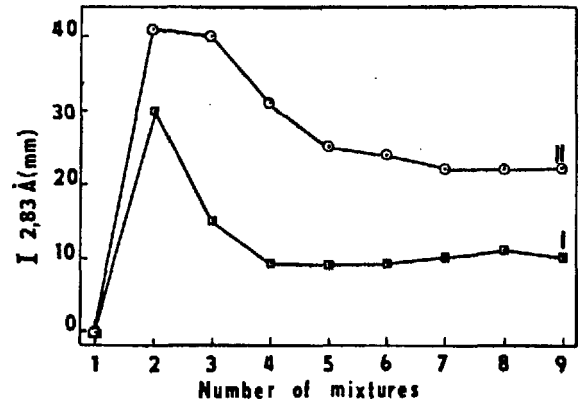

Fig. 1 - Formation of HXEL in relation to the quartz granulometry.

I. Suspensions		II. Pastes	
No.	/um	No.	/um
1	30 - 40	6	200 - 300
2	60 - 90	7	300 - 400
3	90 - 100	8	400 - 500
4	100 - 150	9	500 - 600
5	150 - 200		

Fig. 2 shows the morphology of the HXEL crystals prepared synthetically and finally Fig. 3 represents the microstructure of the No. 2 mixture.

HXEL crystals are characterized by a columnar shape which predetermines the low binding properties of this component.

Fig. 4 indicates the existence of HXEL in relation to the isothermal holding period (0, 1, 2, 3, 4 and 5 h) and the quartz granulometry.

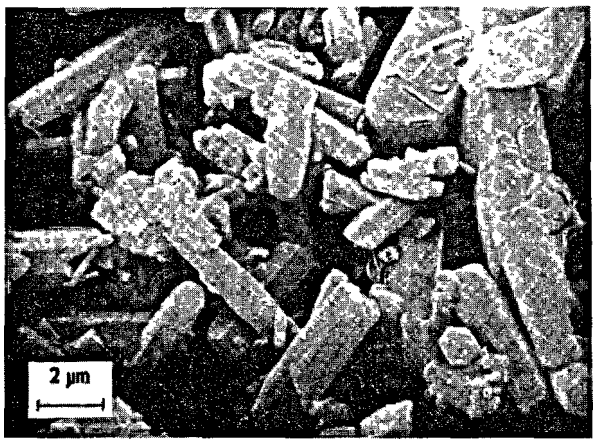

Fig. 2 - SEM of synthetically prepared HXEL

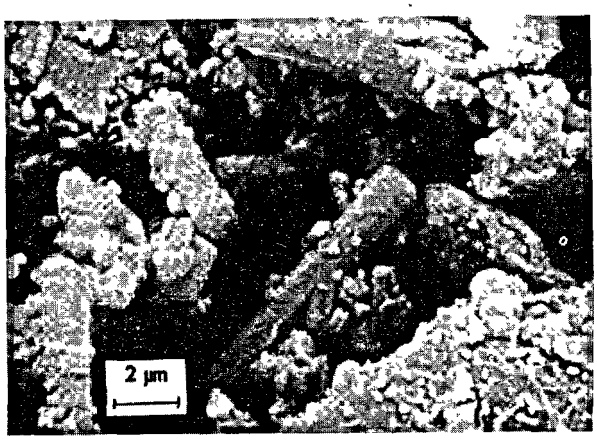

Fig. 3 - SEM of sample No.2 suspension.

Even though in mixtures with the finest quartz fractions (< 5 and 5-10 µm) HXEL is formed at the beginning of the reaction, it is subsequently decomposed into tobermorite and calcium sulphate.

In the following mixtures the HXEL quantity is markedly higher at the beginning of the reaction and its decomposition is shifted with the growing quartz particle size towards the longer periods of time. When employing the 40-60 µm granulometry, then only after a 4 hour period it was possible to prove a very slight decrease in HXEL contents. It was also found that HXEL formed in a mixture with quartz of 60-90 µm granulometry does not decompose even within 5-10 hours (193°C).

Definition of temperature and $3CaO.SiO_2$ influence onto the HXEL formation.

With regard to the employement of cement as one of the starting raw material components in the production of autoclaved building materials, it appeared expedient to give precision to the above mentioned influence onto the formation of HXEL, in two different types of mixture processing : steam curing at 100°C (8 h) and autoclaving at two temperatures : 175°C and 193°C (5 h).

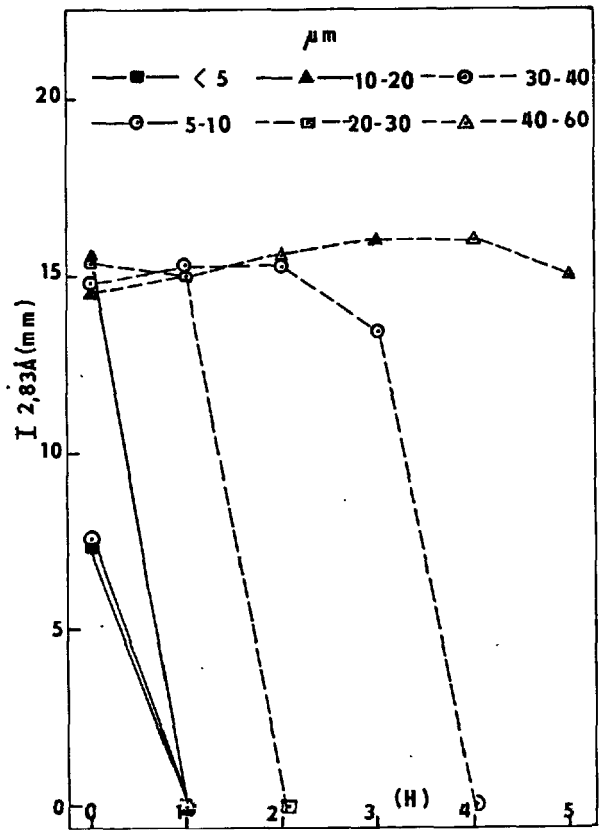

Fig. 4 - Formation and existence of HXEL in relation to the quartz granulometry and the reaction period (193°C).

The composition of the investigated mixtures is shown in Table I.

TABLE I

Mix. design.	Quartz (60-90 µm) (%)	$3CaO.SiO_2$ (%)	CaO (%)	$CaSO_4.2H_2O$ (%)
1	80,0	20,0	-	-
2	80,0	20,0	-	10,0
3	80,0	19,0	1,0	10,0
4	80,0	15,0	5,0	10,0
5	80,0	10,0	10,0	10,0
6	80,0	5,0	15,0	10,0
7	80,0	-	20,-	10,0

As can clearly be seen from the characteristic angular region of the X-ray diagrams (Fig. 5), the lowest HXEL quantity was formed at 100°C. The last two mixtures, processed at 175°C, exhibit a somewhat larger proportion of this component; at the same time in sample "7" it is no longer possible to identify the presence of 11 Å-tobermorite, since the major newly formed phase is HXEL.

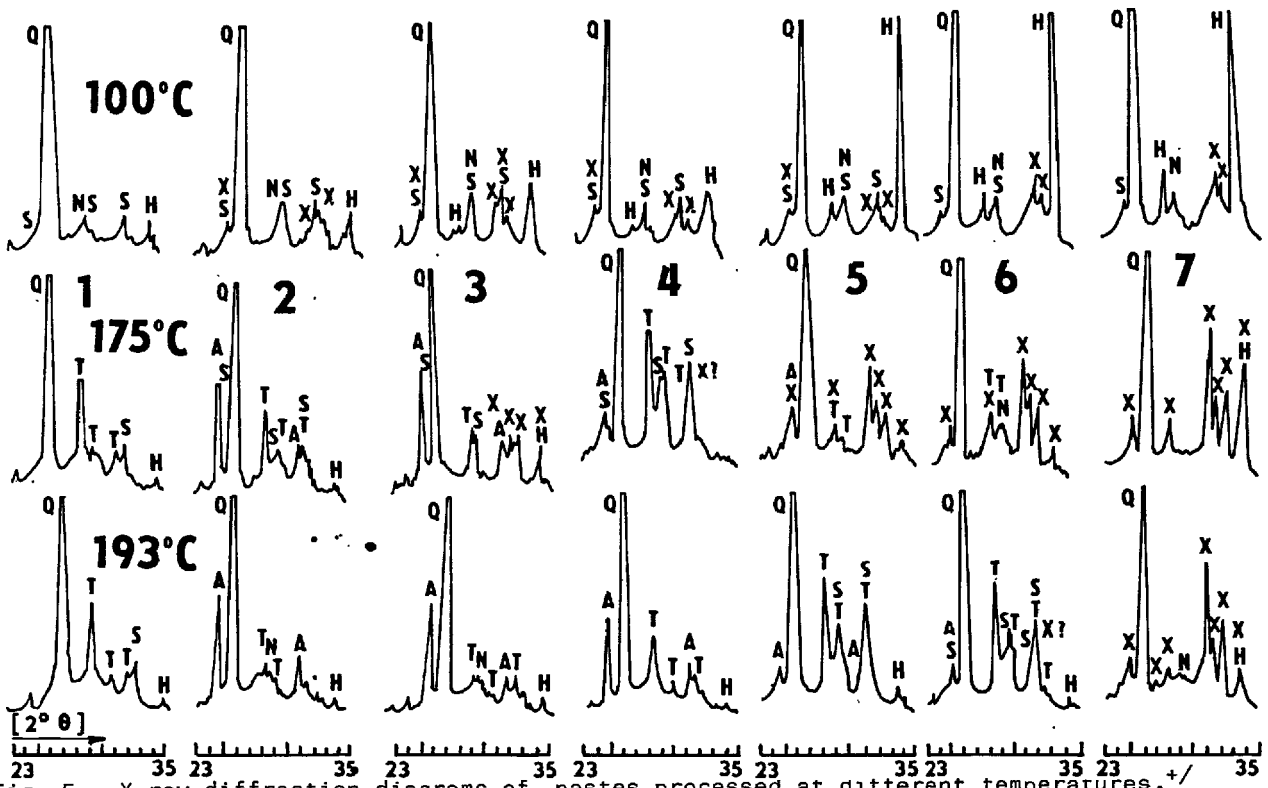

Fig. 5 - X-ray diffraction diagrams of pastes processed at different temperatures.+/

As long as the temperature of 193°C was used, there was formed a pronounced HXEL quantity only in mixture "7", in mixture "6" its presence appears to be controversial.

Influence of a graded sulphate addition onto the formation of HXEL.

It was proved by orientated experiments that the bottom limiting contents of clinker (cement) in the investigated quartz--CaO mixtures which suppress the formation of HXEL, correspond to the value of 7-10%. In order to clarify the influence of $CaSO_4.2H_2O$ onto the formation of HXEL there were selected mixtures containing 80% quartz, 12,5% CaO, 7,5% portland cement clinker and a graded gypsum rock fraction (0-20%).

In mixtures in the form of paste processed at 193°C/5 h with a growing addition of $CaSO_4.2H_2O$, the quantity of anhydrite increases. Starting with 15% gypsum rock there occurs a pronounced decrease of the anhydrite and 11 Å-tobermorite in connection with the formation of HXEL (Fig. 6).

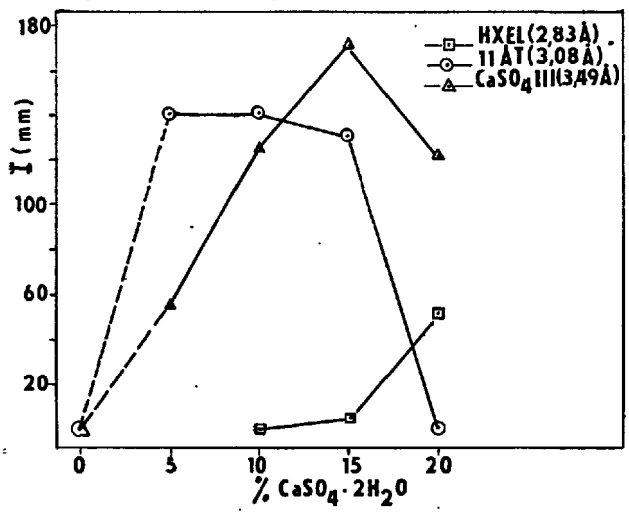

Fig. 6 - Formation of main phases related to gypsum rock additive(quartz 60-90 µm, 193°C/5 h).

CONCLUSIONS

The highest quantity of hydroxyl ellestadite in quartz mixtures of varying granulometry with CaO and gypsum rock subjected to hydrothermal processing was noted, when using particles of 60-90 µm in size. Even though in the case of very fine quartz (< 10 µm), HXEL is formed at the beginning of the reaction, it is immediately decomposed with the formation of 11 Å-tobermorite and calcium sulphate.

+/ Used symbols :

A - $CaSO_4$(III); H - $Ca(OH)_2$; N - CSH_n; Q - quartz; S - $CaSO_4.1/2H_2O$; T - 11 Å-tobermorite; X - hydroxyl ellestadite.

With quartz particles growing in size, the stability period of HXEL is prolonged. If the lime is fully or partly replaced by cement, the above mentioned phase is formed only after a considerable addition of gypsum rock.

REFERENCES

1.- Z. ŠAUMAN (1973, "Study of Gypsum Rock Effect on the Reaction Mechanism of Quartz or Fly Ash-$Ca(OH)_2$ under Hydrothermal conditions", Proc.Third Intern.Symp.Calc.Silic.Build.Prod., Paper 2.4, (Utrecht).

2.- Z. ŠAUMAN (1973), "Bedingungen der Entstehung von Hauptbindephasen in autoklavbehandelten Produkten", Silikattechnik 34, 272-278.

3.- Z. ŠAUMAN and O. HOFFMANN (1978), "Study of Autoclaved Building Materials Binder Systems". Research Report of Research Institute of Building Materials Brno (in Czech).

4.- Z. ŠAUMAN (1978), "Die Hydroxyl-Ellestadit-Bildung/$Ca_{10}(SiO_4)_3(SO_4)_3(OH)_2$/-unter den Bedingungen des Hydrothermalprozesses", Referat Nr.12, Intern.Symp. über Bezieh.zw.Eigensch.KS-Prod. und Bindemittelaufbau (Karlsruhe).

5.- T. TAKEMOTO and H. KATO (1968), "Hydroxyl Ellestadite Produced by Hydrothermal Reaction Containing Calcium Sulphate", Proc.Fifth Intern.Symp. Chem.Cem., Vol.III., pp.563-569.

6.- N. DJABAROV and W. SLATANOV (1963), "Die Wirkung des Gipses auf die Festigkeit der Kalksanderzeugnisse", Zement-Kalk-Gips 16, 104-107.

A Kinetic Study of Alite Hydration

Etude cinétique de l'hydratation de l'alite

A. BEZJAK, Faculty of Pharmacy and Biochemistry, University of Zagreb,
I. JELENIC, V. MLAKAR and A. PANOVIC, Association of Yugoslav Cement Producers, Yougoslavie.

RESUME : Les auteurs ont étudié la cinétique de l'hydratation de l'alite dans le système pur minéral-eau, dans le mélange alite-C_3A-plâtre et dans les pâtes du ciment portland, en appliquant un procédé qui tient compte des effets des interactions des processus, déterminants pour la vitesse de la réaction. Les échantillons étaient hydratés à un rapport eau-solide de 0.5 à 20°C et en présence ou absence des sulfates alcalins. Les degrés d'hydratation de l'alite à des âges allant de 4h. à 2 mois furent déterminés par la diffraction des rayons X. L'équation d'Avrami-Erofeev et les équations de la cinétique linéaire ou quadratique servaient à calculer les paramètres. Pour une distribution des tailles des particules donnée, on calculait les degrés d'hydratation en supposant des contributions différentes de chaque processus déterminant la vitesse de réaction. La comparaison des degrés d'hydratation calculés et observés a fourni une relation linéaire entre le temps d'hydratation t (α-observé) et le temps réduit τ (α-calculé/ α-observé) et a donné le paramètre nécessaire pour calculer les constantes de la vitesse de réaction. Les degrés d'hydratation calculés correspondant aux degrés d'hydratation observés, montrent la contribution des mécanismes à chaque étape d'hydratation de l'alite. Les valeurs des constantes de vitesse de germination et de croissance des produits d'hydratation sont de l'ordre de $11.0.10^{-2}$ à $2.2.10^{-2}$ h^{-1} et celles de l'interaction à l'interface à $6.7.10^{-2}$ à $25\cdot10^{-2}$ $\mu m\ h^{-1}$. Le processus de la diffusion contrôlée montre l'existence de deux ou trois étapes, avec des constantes de vitesse nettement plus grandes pour la première étape que pour la deuxième ou la troisième, surtout pour les systèmes qui contiennent des sulfates alcalins. Les très grandes vitesses observées pour la première étape de diffusion sont essentiellement responsables de l'effet accélérateur des sulfates alcalins.

SUMMARY : The kinetics of alite hydration in pure mineral-water system, in the alite-C_3A-gypsum mixture and in Portland cement pastes with high and with low C_3A content was studied by applying a procedure that takes into account the effects of simultaneous action of different rate-determining processes. Specimens were hydrated at 0.5 water-to-solid ratio at 20°C, in presence and in absence of alkali sulphates. The degrees of alite hydration at various ages ranging from 4 hours to 2 months were determined by quantitative X-ray diffraction. Avrami and Erofeevs's expression and linear and quadratic rate equations were used to calculate the parameters required.. The degrees of hydration for a given particle size distribution were calculated presuming different contributions of particular rate-determining processes. The comparison of the observed and the calculated degrees of hydration providing linear relationship between hydration time t (α-observed) and relative time τ (α-calculated = α-observed) yields the parameter required for the calculation of actual rate constants. Computed contributions to the calculated degrees of hydration, corresponding to the observed ones, show the distribution of the rate-determining mechanisms at particular stages of alite hydration. The obtained values of the rate constants for nucleation and growth of hydration products range between $11.0\cdot10^{-2}$ and $2.2\cdot10^{-2}h^{-1}$, and those for phase-boundary interaction between $6.7\cdot10^{-2}$ and $25\cdot10^{-2}\mu m\ h^{-1}$. The diffusion-controlled process proved to be two- or three-stage in nature, with the rate constants for the first stage being considerably higher than for the second or the third one. This applies especially to the systems containing alkali sulphates, and the extraordinarily high rate constants of the first-stage diffusion are most responsible for the observed acceleratory effect of the readily soluble alkalies.

INTRODUCTION

The hydration kinetics of C_3S has been extensively studied on pure mineral-water systems (1-8). Numerous data obtained by several investigators indicate that the rate of hydration process during the acceleratory stage is controlled either by nucleation and growth of hydration products or by phase-boundary interaction. The C-S-H phases that form at this stage influence the course of the subsequent, diffusion-controlled reaction.

In a complex cement-water system the rate of alite hydration depends on a number of parameters, and so does the development of C-S-H binding material. It seems that the course of this development can be decisive for the final properties of Portland cement pastes, since there is evidence that the rate of hardening per se influences the ultimate strength of mortars, with the cause of the rate change from one sample to another being secondary (9). In an attempt to explain the observed correlation between the rate of hardening and the final strength as exactly as possible, the kinetics of alite hydration in Portland cement pastes should be considered first. When seeking to evaluate the most reliable rate constants for the hydration process in such a complex polysize system, the effects of simultaneous action of different rate-determining mechanisms should be taken into account. By applying a procedure which includes this item (10) we investigated the influence of alkali sulphates on the kinetics of alite hydration in various Portland cement pastes, and in some simpler systems as well.

MATHEMATICAL SOLUTIONS FOR THE EVALUATION OF KINETIC PARAMETERS

As already mentioned in the introductory part, different rate-determining processes follow after one another in the course of alite hydration, which implies that within a given polysize system they can act simultaneously. The fractions hydrated according to different laws at the same time are decided by both the rate constants and the particle size distribution. In accordance with the present state of knowledge on the hydration kinetics of alite, it can be assumed that the process of nucleation and growth, followed by eventual impingement of growth products, is the slowest step at early ages. In the subsequent period it is either the phase-boundary interaction or the diffusion process that becomes the slowest step, the latter being definitely the rate-determining one at high degrees of hydration. The described course of the hydration process can be represented for a single particle j by the following series of basic equations:

$$G_1(\alpha_j) = k_1 t \tag{1}$$

$$G_2(\alpha_j) - G_2(\alpha_{1j}) = k_2(t-t_{1j})/R_j \tag{2}$$

$$G_3(\alpha_j) - G_3(\alpha_{2j}) = k_3(t-t_{2j})/R_j^2 \tag{3}$$

where α_j degree of hydration of particle j at time t

t_{1j} time when G_2 process has become the rate-determining one

α_{1j} degree of hydration of particle j at time t_{1j}

t_{2j} time when G_3 process has become the rate-determining one

α_{2j} degree of hydration of particle j at time t_{2j}

k_1, k_2, k_3 rate constants

R_j original radius of particle j

$G_1(\alpha)$, $G_2(\alpha)$ and $G_3(\alpha)$ functions denote the process of nucleation and growth of hydration products, of phase-boundary interaction and of diffusion respectively. Their explicit forms are usually the following:

$$G_1(\alpha) = \left[-\ln(1-\alpha)\right]^{1/n} \tag{4}$$

$$G_2(\alpha) = 1-(1-\alpha)^{1/3} \tag{5}$$

$$G_3(\alpha) = \left[1-(1-\alpha)^{1/3}\right]^2 \tag{6}$$

When one rate-determining process substitutes the other, their rates ($d\alpha/dt$) have to be equal. For different R_j values the exchange of the rate-determining processes will take place at different α_{1j} and α_{2j}, since the apparent rate constants for both the phase-boundary interaction and the diffusion process depend upon R_j. If the hydration of a particle with the original radius R_L has become controlled by the phase-boundary interaction at time t_0 (i.e. when the maximum rate of nucleation and growth has been achieved), and if the hydration of a particle with radius R_D has become diffusion-controlled at the same time, then Eqs. 1, 2 and 3, combined with Eqs. 4, 5 and 6, can be transformed into:

$$\left[-\ln(1-\alpha)\right]^{1/n} = A\tau \tag{7}$$

$$\left[1-(1-\alpha_j)^{1/3}\right] - \left[1-(1-\alpha_{1j})^{1/3}\right] = B(\tau-\tau_{1j})R_L/R_j \tag{8}$$

$$\left[1-(1-\alpha_j)^{1/3}\right]^2 - \left[1-(1-\alpha_{2j})^{1/3}\right]^2 = C(\tau-\tau_{2j})R_D^2/R_j^2 \tag{9}$$

where $A = \left(\frac{n-1}{n}\right)^{1/n}$

$$B = \frac{n}{3}\left(\frac{n-1}{n}\right)\exp\left(-\frac{n-1}{3n}\right)$$

$$C = 2B\left[1-\exp\left(-\frac{n-1}{3n}\right)\right]$$

and $\tau = t/t_0$ (10)

If α_{1j}, α_{2j} and τ_{1j}, τ_{2j} values have been determined by using the conditions of equal rates at the exhange points of the rate-determining mechanisms, the expressions 7, 8 and 9 can be applied to compute the α_j-τ relationship for a given set of R_L, R_D and n values. The total calculated degree of hydration $\bar{\alpha}_{calc.}$ for the relative time τ is then

$$\bar{\alpha}_{calc.}(\tau) = \sum_j \alpha_j w_j \tag{11}$$

where $\bar{\alpha}$ total degree of hydration

w_i R_i weight fraction of particles with original radius

Calculations have to be made for different sets of R_L, R_D and n values. When the set has been correctly assumed, a linear relationship is obtained between t(α-observed) and τ(α-calculated = α-observed). In other words, a plot of t-s for experimentally determined α-values versus τ-s belonging to adequate α-values, calculated according to Eq. 11, gives a straight line provided that R_L, R_D and n have been assumed correctly. It is obvious from relation 10 that the slope of this line corresponds to t_0-value. By using graphically determined t_0 the most reliable values of actual rate constants are obtained, since

$$k_1 = A/t_0 \quad (12)$$

$$k_2 = R_L B/t_0 \quad (13)$$

$$k_3 = R_D^2 C/t_0 \quad (14)$$

If the actual rate constants change after a certain period of hydration, the t_0 slope will change as well. For the time interval in which the linear relationship is not preserved, calculations should be repeated with new sets of tentative R_L, R_D and n values, until linear relationship with a new t_0 slope has been achieved.

EXPERIMENTAL PROCEDURE

Two industrial clinkers, C-1 and C-2, similar in alite content but different in aluminate content, were used for the kinetic study of alite hydration in Portland cement pastes. Their phase compositions as determined by X-ray diffraction and calculated after chemical analysis, are shown in Table I, and their alkali and sulphate contents are presented in Table II.

TABLE I
Phase Composition of Clinker Samples

Phase	C-1		C-2	
	XD	Calc.	XD	Calc.
C_3S	65	63.4	65	58.2
C_2S	12	16.0	12	19.9
C_3A	3	6.0	9	9.8
F.f.	7	11.1	4	8.6

The clinkers were ground in a laboratory ball mill, and the particle size distribution of the obtained samples was determined by the Coulter-Counter method (Table III). In order to obtain cements with higher contents of readily soluble alkalies, C-1 and C-2 samples were blended with 1 and 2% K_3NS_4 ($3K_2SO_4 \cdot Na_2SO_4$) respectively, giving two additional samples marked C-1' and C-2'. For the sake of comparison of the kinetic parameters of alite hydration in cement pastes with the kinetic parameters of alite hydration in somewhat simpler systems, a sample of pure alite (A) and a mixture (M) containing 90% alite and 10% C_3A were also prepared. Monoclinic alite stabilized by MgO and Al_2O_3, and cubic C_3A were synthesized from

TABLE II
Total and Readily Soluble Alkalies and Sulphates (%) in Clinker Samples

Sample	SO_3	Na_2O	K_2O
C-1	0.59	0.30	0.36
	0.48*	0.14*	0.25*
C-2	0.25	0.19	0.23
	0.01*	0.02*	0.04*

* readily soluble

analytical grade chemicals at 1450°C. After double refiring satisfactory products were obtained, as confirmed by X-ray diffraction analysis. The pure phases were ball-milled and thereafter gently homogenized in order to obtain mixture M. Simple systems containing alkali sulphates, i.e. A' and M' mixtures were prepared by adding 2% K_3NS_4 to each A and M sample. The particle size distribution of pure alite A, which was used for the preparation of all the mixtures, is also given in table III.

TABLE III
Particle Size Distribution

Particle Size, d /µm	Weight Fraction		
	C-1	C-2	A
2.00	0.035	0.063	0.045
4.50	0.035	0.045	0.035
5.70	0.050	0.058	0.048
7.20	0.065	0.064	0.068
9.05	0.080	0.070	0.096
11.40	0.085	0.097	0.156
14.30	0.100	0.116	0.171
18.10	0.135	0.130	0.174
22.80	0.120	0.141	0.078
28.70	0.110	0.108	0.064
36.20	0.100	0.054	0.035
40.00	0.090	0.054	0.030

Prior to hydration 5% analytical grade gypsum was admixed to each C-1, C-1', M and M' sample, and 6% to each C-2 and C-2' sample. All samples were paste-hydrated at 0.5 water-to-solid ratio, cast into cylinders 15 mm in diameter and cured for 24 hours at 100% rh. After 24 hours they were unmolded and stored separately in tightly closed polyethylene vessels containing saturated $Ca(OH)_2$ solution. Casting and curing was done at 20°C. After various ages ranging from 4 hours to 2 months the specimens were ground, washed with acetone, dried in vacuum and examined by X-ray diffraction. For quantitative analysis the samples were further ground and simultaneously homogenized with 10% quartz which was taken as an internal standard. To determine the degree of alite hydration the intensity of the 620-400 reflection group of alite and the intensity of the 10.1 reflection of quartz were used. The scan rate was 1/4°/min, and the ratio of alite to quartz peak areas of the mean from five samples served for calculating the degree of hydration.

RESULTS AND DISCUSSION

The data on the observed degrees of alite hydration at different ages are given in Table IV and linear relationships between t(α-observed) and τ (α-calculated = α-observed) in Fig. 1. The relationships are calculated for the 240-hour interval and shown for the 80-hour interval. The R_L and R_D values used to compute the corresponding $\bar{\alpha}_{calc.}$ - τ interdependence are quoted in the respective diagrams. All the represented t-τ relationships are obtained with n = 3.

TABLE IV
Degree of Alite Hydration (%)

Time (h)	Sample A	A'	M	M'	C-1	C-1'	C-2	C-2'
4		7				10		
6	3	14	5	4	4	13		7
8	8	22	8	14	7	16		10
10	15	31	13	23	12	20	2	13
12	20	37	18	30	19	24	8	27
14	23	43	25	35	24	29	16	38
16	25	47	30	40	28	33	25	44
18	26	50	35	44	32	38	32	46
20	28	53	37	46	35	44	35	49
24	29	58	40	51	37	53	38	53
32	33	64	45	56	42	56	42	55
40	35	68	49	60	45	59	46	56
48	38	71	53	63	49	61	50	57
56	40	71	56	65	52	62	54	58
64	42	75	59	67	54	63	57	59
72	44	76	62	69	55	65	59	61
96	47	78	69	74	60	68	65	63
120	49	79	74	77	63	70	68	66
144	53	81	77	79	66	72	71	68
168	56	82	79	80	69	74	74	69
240	65	84	83	84	73	79	77	73

As seen from Fig. 1 a unique slope t_0 was obtained in not one case, which proves that the hydration rate constants of particular rate-determining processes change after a certain period of time, even for the pure alite specimen. An inspection of the composed α_i contributions (Eqs. 7, 8, 9) to $\bar{\alpha}$-values reveals that different rate--determining mechanisms act simultaneously indeed, especially during the first t_0 interval, and sometimes also during the second one. The distribution of rate-determining processes for alite hydration in various samples are illustrated in Fig. 2 where the diagrams show the percentages of particles reacting according to Eq. 7, 8 and 9 respectively, at various degrees of alite hydration. *Intervals with different t_0-values are separated by* vertical lines.

The rate constants were calculated according to Eqs. 12, 13 and 14 using t_0-s given in Fig. 1. The obtained values are listed in Table V for each sample and each t_0--interval. The consecutive intervals are marked I, II and III respectively. To facilitate the discussion on the obtained k-values two rows are added at the bottom of Table V. They contain the time of transition from one

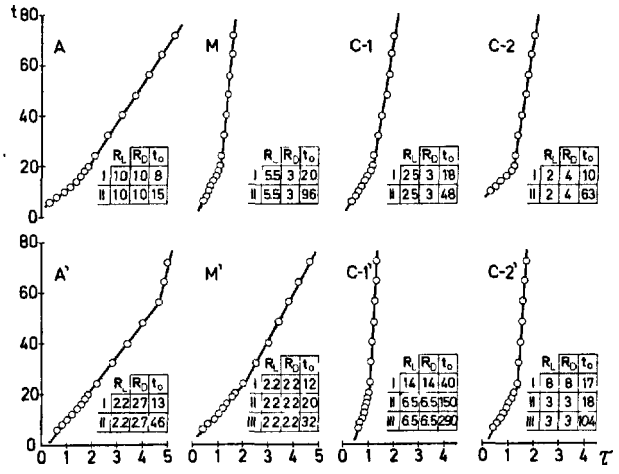

Fig. 1 - t-τ relationships

t_0-interval to the other, with the belonging degrees of hydration given in parentheses. As quoted in Table V, the obtained value of the rate constant for nucleation and growth process in pure alite paste amounts to 11.0 $10^{-2}h^{-1}$ *this being consistent with the value obtained by Tenoutasse* and De Donder (4) who followed the kinetics of alite

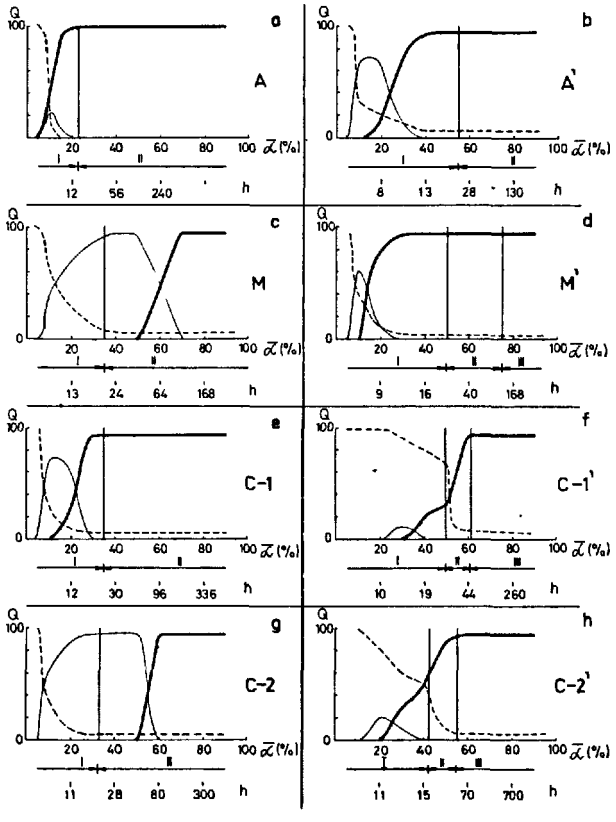

Fig. 2 - Percentages of particles (Q) that react according to Eq. 7 (dotted line), Eq. 8 (thin line) and Eq. 9 (full line) at various $\bar{\alpha}$.

TABLE V
Rate Constants for Alite Hydration in Simple Systems and in Cement Pastes

Interval		Value of Rate Constant for Alite Hydration in Sample: A	A'	M	M'	C-1	C-1'	C-2	C-2'
I	$k_1(h^{-1})$	0.110	0.067	0.044	0.073	0.048	0.022	0.087	0.052
	$k_2(\mu m h^{-1})$	0.067	0.092	0.080	0.110	0.074	0.190	0.110	0.250
	$k_3(\mu m^2 h^{-1})$	0.026	0.120	0.31	0.110	0.100	1.	-	0.82
II	k_2	-	-	0.016	-	-	-	0.017	-
	k_3	0.014	0.035	0.059	0.067	0.040	0.056	0.054	0.110
III	k_3	-	-	-	0.042	-	0.031	-	0.018
I → II	$t_I(\alpha_I)$	14(23)	24(55)	20(37)	24(51)	20(35)	22(50)	19(33)	15(42)
II → III	$t_{II}(\alpha_{II})$				105(75)		48(61)		24(53)

hydration by using monosize specimens. However, in our sample the nucleation and growth process is the major rate-determining mechanism only at very low degrees of hydration (Fig. 2a). It is already in the first t_0-interval that the rate of hydration is diffusion-controlled for a high percentage of particles. The transfer from the process controlled by nucleation and growth to the process controlled by diffusion includes a short period in which the phase-boundary interaction is the rate-determining mechanism. The phase-boundary interaction is detectable as the slowest step of reaction for a small fraction of particles between 6 and 9 hours. After the degree of hydration has reached 20%, the second period will start during which all particles react according to Eq. 9, with the k_3-value diminished (Table V). It is interesting to note that the observed change in the rate constant for the diffusion-controlled reaction occurs at the same degree of hydration at which significant structural changes in C-S-H were ascertained (11).

When pure alite hydrates in the presence of alkali sulphates (sample A'), the rate-determining processes that act simultaneously are distributed in a different way (Fig. 2b). In that case the phase-boundary interaction is the rate-determining mechanism for a considerably higher percentage of particles and for a considerably longer period of time, the main reason therefor being the larger rate constant of the diffusion process which takes place during the first t_0-interval.

The high value of the diffusion-rate constant can be explained by the higher permeability of the hydration coating formed in the presence of alkali sulphates and by the Ca^{2+}-concentration gradient existing between the alite grain boundary and the bulk of the liquid phase. After approximately 24 hours, once the degree of hydration has reached about 55%, the second period starts in which the rate of hydration is governed by the diffusion process only, with its rate constant significantly diminished in comparison with the previous one (Table V).

In sample M containing 10% C_3A and 5% gypsum the hydration process of alite is accelerated as well, though only after 12 hours (Table IV). The first-stage diffusion across the layer of hydration product is also in this case very fast, and it is not the rate-determining process until ~50% hydration has been reached (Fig. 2c). At the time of transition from the first to the following t_0-interval the majority of particles hydrate according to linear kinetics (Eq. 8), but the rate constant of the rate-determining phase-boundary interaction is much smaller in the second t_0-interval (Table V). It amounts to $1.6 \cdot 10^{-2} \mu m\ h^{-1}$, and a similar value for the linear rate constant is given in reference 2. The cause of the decrease of k_2-value for sample M is evident from the diagram showing the courses of both alite and C_3A hydration in sample M (Fig. 3a). As indicated in the diagram the onset of the second t_0-interval characterized by the low k_2 coincides with the renewed C_3A hydration, which means that it starts when the sulphate ions have been depleted from the liquid phase. Such a slow phase-boundary interaction was not detected as the rate-determining mechanism for alite hydration in sample M' containing besides gypsum also alkali sulphates, which is due to the fact that the renewed C_3A hydration in sample M' is shifted to later ages (Fig. 3b) when the rate constant of the diffusion-controlled alite hydration is already much lower than during the first t_0-interval. The onset of the second t_0-interval for sample M' does not coincide with any significant change in the course of C_3A hydration. However, it occurs at the same degree of alite hydration as observed in sample A' (Table V), indicating that the changes of the diffusion-rate constants are in both cases very likely associated with the incorporation of SO_3 in C-S-H.

The kinetic parameters obtained for alite hydration in Portland cement pastes are less reliable than those obtained in simple systems, because individual cement particles are not always monophase grains. Nevertheless, they exhibit the diverse features of the kinetic behaviour of alite in cements with and without alkali sulphates. The observations gained on cement pastes are in general agreement with the observations on simple systems. The rate constants calculated

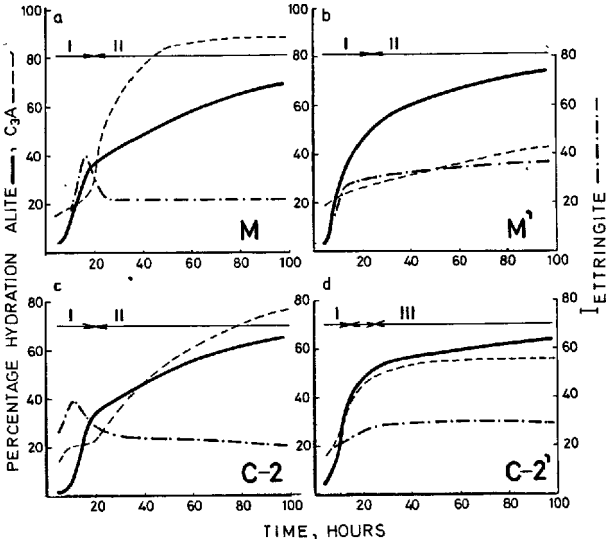

Fig. 3 - Courses of alite and C_3A hydration and standardized intensities of 10.1 reflection of ettringite for samples M (a), M' (b), C-2 (c) and C-2' (d)

from t_0-values (Fig. 1) show that the rate of phase--boundary interaction is considerably enhanced by the addition of alkali sulphates, which is even more pronounced than in the case of simple systems. That is the reason why the hydration of alite in cements containing alkali sulphates is controlled by the nucleation and growth mechanism for the majority of particles in the first t_0--interval (Figs. 2f and h), the more so as the rate constants for the diffusion process in this interval are very high. The very slow phase-boundary interaction observed for alite hydration in sample M is also detectable during the second t_0-interval in the C-2 paste containing high C_3A and low alkalies. The course of C_3A hydration in sample C-2 (Fig. 3c) allows the same explanation for the decreased k_2-value as has been offered for alite hydration in sample M. Similarly to the simple system containing alkali sulphates, a slow phase-boundary interaction was not detected as the rate-determining step of alite hydration in sample C-2', because sulphates are still present in the liquid phase during the t_0 (I) and t_0 (II) intervals in which the diffusion process is fast. The presence of sulphates in the liquid phase is confirmed by the continuous ettringite formation in the two t_0-intervals (Fig. 3d). For the alite hydration in sample C-2' the differences between k_3--constants are found to be the greatest, but to fully elucidate the factors influencing these differences further work is needed.

The described approach to the kinetic study of alite hydration can be improved by introducing some modified expressions for the $G_1(\alpha)$, $G_2(\alpha)$ and $G_3(\alpha)$ functions into the calculation procedure. Structural investigations of C-S-H for particular t_0-intervals, accompanied by monitoring the changes in the liquid phase at the transition points between two adjacent intervals, will certainly also contribute to better understanding of the kinetic behaviour of alite in the course of the hydration process.

CONCLUSIONS

The determination of reaction-rate constants by taking into consideration the effects of simultaneous action of different rate-determining mechanisms provides better insight into the kinetic behaviour of alite during its hydration process in various cement pastes.

The diffusion-controlled reaction is shown to be two- or three-stage in nature. The very high rate constants of the first-stage diffusion are predominantly responsible for the acceleratory effect observed in the systems containing alkali sulphates.

REFERENCES

1.- R. KONDO and S. UEDA (1968), "Kinetics and Mechanisms of the Hydration of Cements", Proceedings of the Fifth International Symposium on the Chemistry of Cements, Tokyo, Vol. II, 203-255.

2.- J.H. TAPLIN (1968), "On the Hydration Kinetics of Hydraulic Cements", Proceedings of the Fifth International Symposium on the Chemistry of Cements, Tokyo, Vol. II, 337-348.

3.- R. KONDO and M. DAIMON (1969), "Early Hydration of Tricalcium Silicate: A Solid Reaction with Induction and Acceleration Periods", J. Am. Ceram. Soc., 52, No. 9, 503-508.

4.- N. TENOUTASSE et A. DE DONDER (1970), "La cinétique et la méchanisme de l'hydration du silicate tricalcique", Silicates Industriels, Belg. 35, No. 12, 301-307.

5.- R. SIERRA (1974), "Contribution to the Kinetic Study of Hydration of Tricalcium Silicate", The VI International Congress on the Chemistry of Cements, Moscow, Supplementary paper, Section II, II-2.

6.- J. DESCAMPES, P. FIERENS and J.P. VERHAEGEN (1974), "Chemical Defects and Hydration of Doped Tricalcium Silicates", The VI International Congress on the Chemistry of Cements, Moscow, Supplementary paper, Section II, II-2.

7.- A.V. USHEROV-MARSHAK and A.M. URZHENKO (1974), "Thermokinetic Analysis of Early Stages of Binder Hydration", The VI International Congress on the Chemistry of Cements, Moscow, Supplementary paper, Section II, I-6, II-2.

8.- K. FUJI and W. KONDO (1974), "Kinetics of Hydration of Tricalcium Silicate", J. Am. Ceram. Soc., 57, No. 11, 492-497.

9.- S. POPOVICH (1976), "Phenomenological Approach to the Role of C_3A in the Hardening of Portland Cement Pastes", Cem. Concr. Res., 6, No. 3, 343-350.

10.- A. BEZJAK and I. JELENIĆ, "On the Determination of Rate Constants for Hydration Processes in Cement Pastes", in preparation.

11.- L.S. DENT GLASSER, E.E. LACHOWSKI, K. MOHAN and H.F.W. TAYLOR (1978), "A Multi-Method Study of C_3S Hydration", Cem. Concr. Res., 8, No. 12, 733-740.

Formation de la structure des ciments avec fausse prise

Structure formation of cements with false setting

Z.B. ENTINE, candidat ès sciences techniques, L.S. KLIOUEVA, ingénieur,
Ou. I. PAPIACHVILI, candidat ès sciences techniques, NIITzement, Moscou, U.R.S.S.

RESUME : En opérant sur des modèles de ciment, on a révélé le rôle particulier des formes de gypse dans le phénomène de la fausse prise, sans toutefois épuiser toutes les particularités des systèmes ciment-eau pour lesquels on ne doit pas oublier l'importance des propriétés du clinker, et tout particulièrement de sa teneur en alcalis. Les ciments à prise normale et fausse, au moment du développement de la fausse prise, se caractérisent par une bonne corrélation entre la teneur de la phase liquide en SO_3 et en alcalis, de même qu'entre la conductibilité électrique dans la phase liquide et sa teneur en alcalis, la conductibilité électrique et la teneur en SO_3. La différence en composition de la phase liquide des ciments à prise normale et fausse sa manifeste au moment qui précède le développement de la fausse prise, quand dans la phase liquide des ciments à fausse prise se dégage un précipité de gypse dihydraté et d'ettringite. Avec le passage de la prise normale à la fausse, la composition ionique de la phase liquide se caractérise par une élévation de la teneur en ions Ca^{2+} et SO_4^{2-}, du fait de la dissolubilité élevée du semi-hydrate devant le dihydrate, et par la diminution du déficit en anions, de la valeur du pH et de la conductibilité électrique de la phase liquide.

Les résultats de l'étude ont permis de formuler, en la soutenant par des expériences, une théorie concernant le mécanisme de la fausse prise.

SUMMARY: Investigations of model cements have revealed a specific part played by gypsum forms in the false setting phenomenon which, however, does not exhaust all the peculiarities of the cement-water systems wherein properties of clinker, especially alkali content, are also very essential. The moment of origination of false setting for normal and false setting cements is characterised by good correlation between the content of SO_3 and alkalis in the liquid phase, as well as the electrical conductivity of the liquid phase and the content of alkalis, the electrical conductivity and the content of SO_3. The differences in the composition of the liquid phase of the normal and false setting cements occur only at the moment preceding origination of the false setting, when a deposit comprising dihydrate gypsum and ettringite precipitates from the liquid phase of the false setting cements. The ion composition of the liquid phase at the transfer from normal setting to false one is characterised by increased content of Ca^{2+} and SO_4^{2-} ions owing to increased solubility of hemihydrate as compared with bihydrate; decrease of anion deficite, hence the pH value and electrical conductivity of the liquid phase.

The investigation results have been used as grounds for putting forward and supporting experimentally a hypothesis of the false setting mechanism.

La variation anomale des propriétés rhéologiques de la pâte de ciment aux stades initiaux de durcissement connue sous la dénomination de fausse prise vu sa nature temporaire ne constitue pas un défaut insurmontable du ciment mais elle influe négativement sur l'utilisation efficace du ciment dans le béton. Les causes de la fausse prise sont assez variées: déshydratation du gypse au cours de la mouture du ciment, déshydratation du gypse suivie d'hydratation superficielle du ciment au cours de l'aération dans les silos, présence dans le ciment des sulfates et carbonates alcalins, introduction de certains agents tensio-actifs (1, 2, 3, 4), etc. D'où la variété d'hypothèses proposées pour expliquer le mécanisme de la fausse prise reliant ce phénomène soit à la cristallisation du gypse (2, 3, 4), soit à l'influence d'hydroxydes alcalins sur la précipitation topochimique de l'ettringite (5), soit à la formation de pellicule d'hydrocarbo-aluminate de calcium sur les particules C_3A et abaissement du pouvoir réacteur de l'ion SO_4^{2-} dans la solution (6), soit à la cristallisation de composés alcalins complexes du type de syngénite (7), soit à l'apparition de charge de signe opposé sur les différentes phases du clinker (8).

Malgré la diversité des causes de la fausse prise dans tous les cas on est en présence d'une manifestation externe identique ce qui permet, lors de l'étude de la fausse prise de rechercher un mécanisme unique de fausse prise qui décrirait de façon satisfaisante ce phénomène malgré la variété des causes l'ayant provoqué. A son tour cela permet de choisir en qualité de modèle une "variante gypseuse" de fausse prise qui peut être facilement reproduite, se construit par des procédés élémentaires et facilite l'étude de divers modes de prise sur des matériaux notoirement identiques.

Les modèles de ciment destinés à l'étude de la fausse prise étaient préparés à partir des clinkers industriels dont la constitution minéralogique théorique est donnée au tableau I pour les variantes suivantes:

1.- ciment ordinaire moulu en laboratoire (ciment normal);

2.- idem après chauffage à la température de 150°C durant 3 h;

3.- ciment moulu en laboratoire avec gypse préalablement déshydraté jusqu'à obtenir une modification hémihydratée;

4.- ciment moulu en laboratoire fabriqué du clinker rechauffé préalablement à 150°C durant 3 h et broyé en grenaille;

5.- ciment moulu en laboratoire avec chauffage préalable du gypse et du clinker en grenaille à la température de 150°C durant 3 h.

Les particularités de la formation de la structure des modèles de ciment ont été suivies en fonction des variations de la résistance plastique (P,mm) et de la conductibilité électrique (x, $ohm^{-1} \cdot cm^{-1}$)du système en voie de durcissement (respectivement du mortier de ciment-sable et de la pâte de ciment).

Tableau I

Dénominations	Constitution, %				
	C_3S	C_2S	C_3A	C_4AF	R_2O
De Briansk	60	17	4	15	0,36
De Nikolaev	44	27	10	13	0,85

Le processus de formation de la structure au cas de gâchage du ciment par l'eau est décrit par diverses courbes de résistance plastique et des courbes corrélatives de la conductibilité électrique (fig.1).

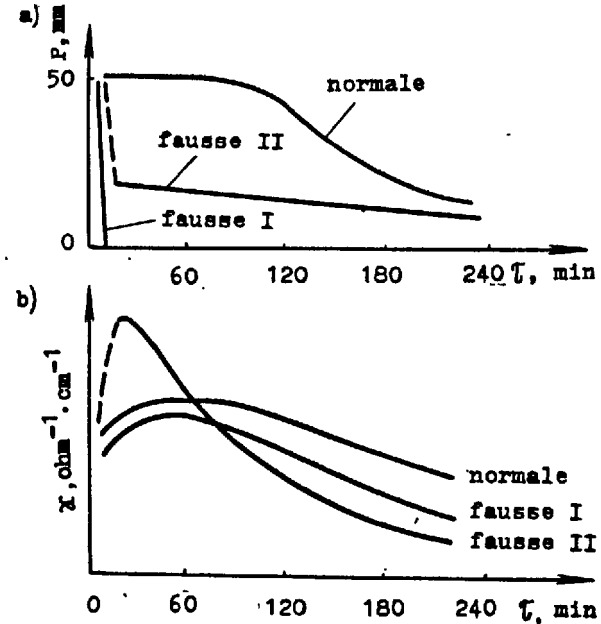

Fig.1 Variation de la résistance plastique (a) et de la conductibilité électrique (b) en fonction du mode de prise.

D'après la forme des courbes de formation de la structure on est en mesure de distinguer deux types de fausse prise du ciment: le 1-er type se caractérise par une perte totale de la plasticité et le II-ème par une perte partielle de la plasticité à la fin du processus de malaxage. L'étude d'un grand nombre de ciments de fabrication industrielle et au laboratoire a montré qu'à chaque ciment correspond l'une des paires de courbes de formation de la structure mentionnée. Des études plus poussées de modèles de ciment ont établi qu'entre les deux modes de fausse prise il n'y a pas de frontière insurmontable - il est possible d'obtenir pour un même ciment l'un et l'autre mode de prise suivant le degré de déshydratation du gypse laquelle à son tour est fonction du régime de traitement thermique du ciment.

Le rôle des deux composants du ciment, le clinker et le gypse, dans le phénomène de fausse prise est illustré par les courbes de résistance plastique de la figure 2 établies pour des variantes diverses du modèle de ciment donné.

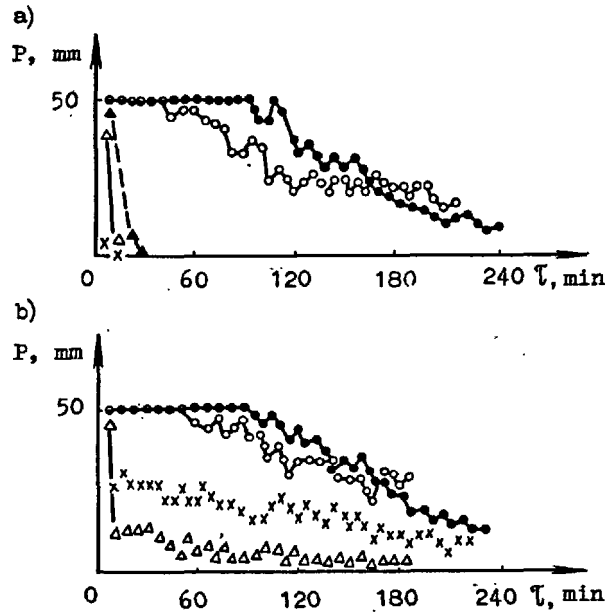

Fig.2 Variation de la résistance plastique pour les différentes variantes du modèle de ciment fabriqué à partir du clinker de Briansk (a) et de Nikolaev (b)

(Variantes de modèle: 1—●— , 2 —×— , 3 —△— , 4 —○— , 5 —▲—)

L'analyse des particularités et des formes de manifestation de la fausse prise sur les modèles de ciment établit le rôle important des formes déshydratées du gypse dans le phénomène de fausse prise: dans tous les cas la déshydratation du gypse entraîne la fausse prise du ciment et cela indépendamment du fait que le gypse s'est déshydraté durant le chauffage du ciment ou a subi une déshydratation préalable. Le traitement thermique du clinker seul n'entraîne pas de fausse prise si en même temps le gypse n'a pas été déshydraté.

Toutefois les variations observées dans la nature du processus de formation de la structure des ciments à gypse déshydraté ne peuvent être expliquées par l'acquisition par le gypse d'une structure propre du fait d'une réhydratation du semi-hydrate lors du gâchage du ciment par l'eau. Ce phénomène est confirmé par les différences dans le degré de manifestation de la fausse prise dans des ciments fabriqués avec des clinkers divers, mais possédant une teneur identique en gypse de même que par la confrontation de courbes de formation de la structure de ciments ayant des courbes semblables pour le mélange moulu (normal et rechauffé à 150°C) de sable quartzeux et de gypse (fig.3).

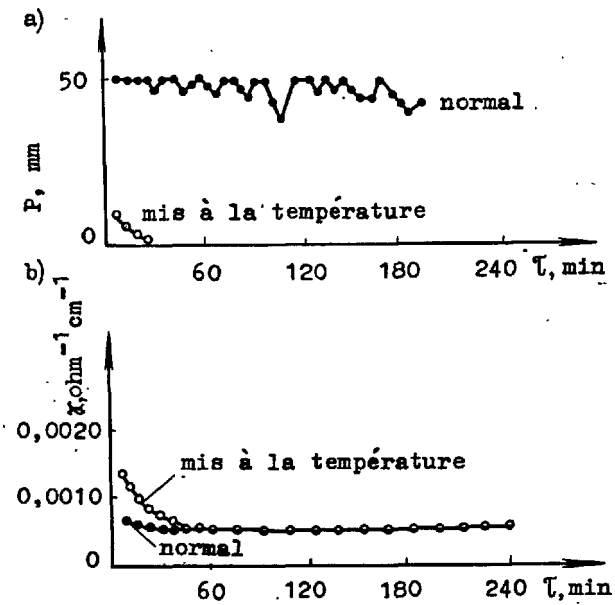

Fig.3 Variation de la résistance plastique (a) et de la conductibilité électrique (b) au cours du gâchage du mélange moulu de sable quartzeux et de gypse.

Pour éclaircir le mécanisme des processus exerçant une influence sur la variation du mode de prise on a étudié la composition des phases liquide et solide de la pâte de ciment aux stades initiaux de l'hydratation. La phase liquide était prélevée 2 et 10 minutes après le gâchage du ciment (E/C 0,25) sous pression de 150 MPa.

Pour la phase liquide prélevée 10 minutes après le gâchage des ciments présentant une prise normale et fausse on observait une corrélation étroite entre la teneur en oxydes alcalins et en d'autres composants de même qu'avec sa conductibilité électrique. Les coefficients de corrélation correspondants sont indiqués au tableau II, tandis que la figure 4 offre un exemple de dépendance entre la teneur en SO_3 et R_2O dans la phase liquide, de même qu'entre la conductibilité électrique de la phase liquide et la teneur en alcalis.

On n'a pas décelé de différences notables dans la composition ionique de la phase liquide des ciments à prise normale et fausse au moment du développement de la fausse prise (c'est-à-dire, 10 minutes après le gâchage). Dans tous les cas la composition ionique de la phase liquide présente un déficit d'anions, c'est-à-dire, l'insuffisance d'anions déterminés par rapport à la somme de cations existants ($\Sigma C - \Sigma A$). Le déficit stable d'anions dans la phase liquide est conditionnée par la fixation par ions du calcium de l'anion HCO_3 introduit dans la phase liquide avec les carbonates alcalins du clinker. Le déficit d'anions est quelque peu inférieur au cas de ciments à fausse prise et, partant, plus faible est la quantité

d'ions OH^- compensant ce déficit ce qui se traduit par un abaissement de la valeur du pH et de la conductibilité électrique de la phase liquide des ciments à fausse prise.

Tableau II

Temps écoulé depuis le gâchage	Rapports de corrélation				
	SO_3-R_2O	CaO-R_2O	χ-R_2O	χ-SO_3	χ-CaO
2 min	0,848	-0,138[x]	0,992	0,886	manque
10 min	0,978	-0,826	0,932	0,976	-0,648

[x] au-dessous du niveau de signification

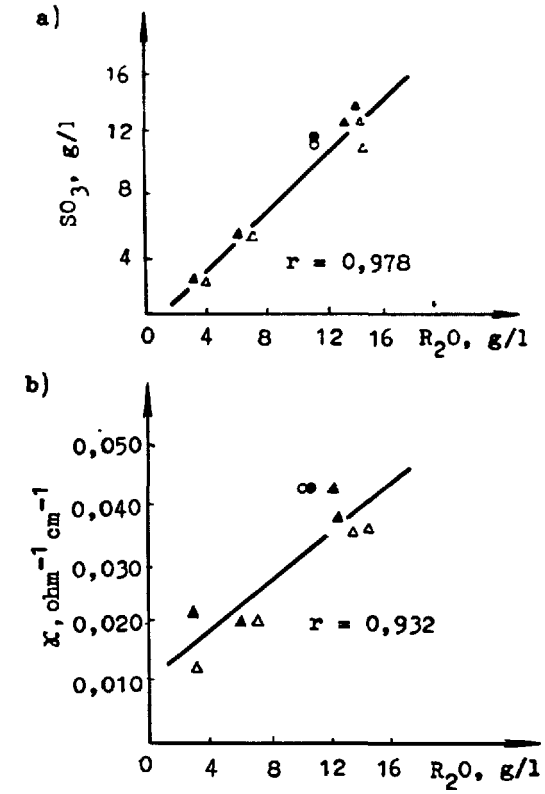

Fig.4. Rapports entre SO_3 et R_2O, χ et R_2O dans la phase liquide prélevée 10 minutes après le gâchage du ciment moulu en laboratoire à prise normale (▲) et fausse (△) et du ciment industriel à prise fausse après un malaxage initial (o) et répété (●).

Les rapports propres à la composition et à la conductibilité électrique de la phase liquide prélevée 10 minutes après le gâchage sont communs aux ciments de fabrication industrielle et en laboratoire indépendamment de leur composition chimique et minéralogique. La figure 4 indique les points obtenus expérimentalement de la composition et de la conductibilité électrique de la phase liquide du ciment industriel à fausse prise, lesdits points se superposant sur la ligne de régression calculée pour les ciments moulus en laboratoire ce qui confirme la nature commune des résultats obtenus.

La phase liquide des ciments à fausse prise 2 minutes après le gâchage (c'est-à-dire au stade précédant le développement de la fausse prise) se caractérise par un si haut degré de sursaturation, qu'une fois prélevée elle donne lieu à une sédimentation qui se compose, selon les analyses aux rayons X et chimique, de gypse dihydraté et d'ettringite. 2 minutes après le gâchage dans la composition ionique de la phase liquide passant de la prise normale à la fausse, on observe un accroissement caractéristique d'ions Ca^{2+} et SO_4^{2-} du fait de l'élévation de la dissolubilité des semi-hydrates devant les dihydrates: il y a également un abaissement du déficit d'anions, de la valeur du pH et de la conductibilité électrique de la phase liquide (fig.5).

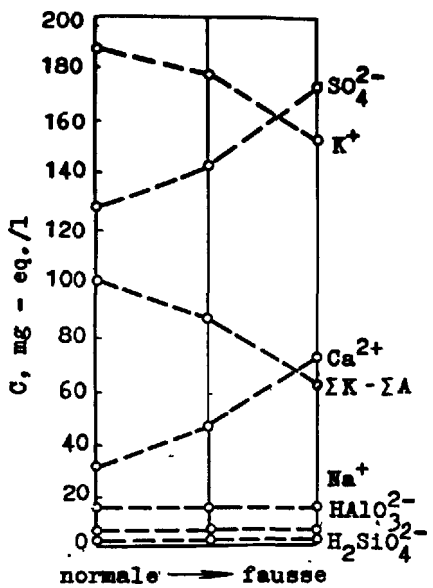

Fig.5. Variation de la composition de la phase liquide 2 minutes après le gâchage au cours du passage de la prise normale à la fausse.

Cependant, comme il découle du tableau II, il se maintient dans ce cas également un rapport assez étroit entre la teneur dans la phase liquide en ions alcalins et en ions de sulfates. Cela signifie que la teneur en ion SO_4^{2-} dans la phase liquide est conditionnée non seulement par la présence du semi-

hydrate et sa dissolubilité élevée mais également par la force ionique de la phase liquide régie essentiellement par la teneur en alcalis. La force ionique de la phase liquide exerce à son tour une action sensible sur la vitesse de formation et de croissance des germes d'hydrates cristallins.

On peut donc, sur la base des résultats de l'étude de la composition et des propriétés de la phase liquide, formuler l'hypothèse sur le mécanisme de la fausse prise. La fausse prise du ciment est en rapport avec la formation de la structure primaire gypse-ettringite dont la condition nécessaire de formation est la sursaturation de la phase liquide en ion SO_4^{2-}. L'intensité de formation de la structure primaire gypse-ettringite, autrement dit le degré de manifestation de la fausse prise, est conditionnée par la force ionique de la phase liquide.

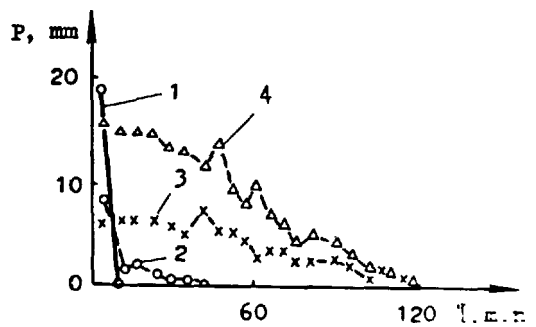

Fig.6. Variation du mode de prise en fonction de la variation de la force ionique de la phase liquide (1 - gâchage par l'eau; 2, 3, 4 - gâchage par la solution Na_2SO_4 à concentration 10, 20 et 30 g/l de Na_2O).

Au cas de sursaturation de la phase liquide en ion SO_4^{2-} et de force ionique réduite de la phase liquide, c'est-à-dire au cas de ciments à faible teneur en alcalis, il est le plus probable qu'il se formera une quantité limitée de germes d'hydrates cristallins qui se développent de façon intense. Le développement d'une structure gypse-ettringite rigide conditionne la perte totale par le système de la plasticité une fois le malaxage achevé, c'est-à-dire la fausse prise du type I.

L'élévation de la force ionique de la phase liquide avec l'accroissement de la teneur en alcalis et la sursaturation de la phase liquide en ion SO_4^{2-} entraînera la formation d'une quantité beaucoup plus grande de germes d'hydrates cristallins dont la croissance est par contre moins rapide, ce qui influe sur le mode de prise dont le type est intermédiaire entre la prise normale et la prise nettement fausse, c'est-à-dire on est en

a) Désagrégation des parcelles initiales du ciment

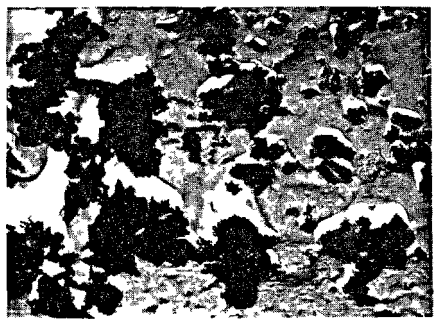

b) Formation autour des grains initiaux de cristaux aciculaires des produits d'hyratation

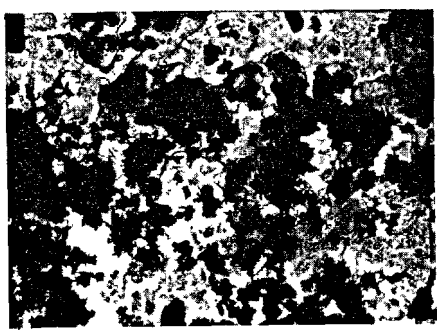

c) Stade initial de formation de produits d'hydratation à la forme allongée

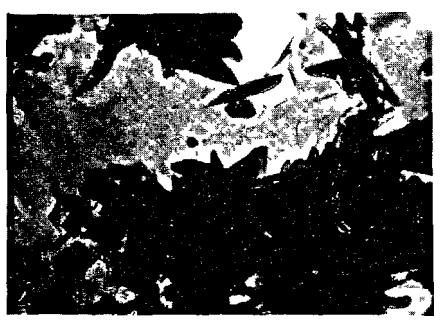

d) Enchevêtrement des cristaux en forme de tiges

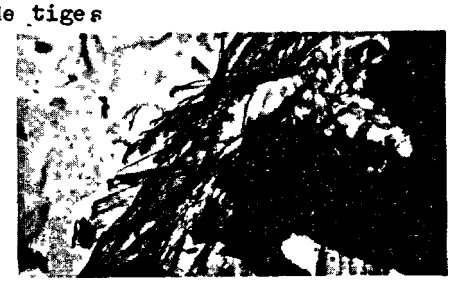

Fig.7.Microphotographies électroniques (10 000 x) du ciment à prise normale(a,b) et fausse(c,d) après 5 minutes d'hydratation.

présence de la fausse prise du type II.

Cette hypothèse a été soumise à l'expérience par variation contrôlée du mode de prise avec introduction proportionnelle d'ions alcalins et d'ions de sulfates (fig.6). Comme le montre la figure 6, avec l'élévation de la force ionique de la phase liquide, on observe un passage régulier de la courbe caractéristique de la fausse prise du type I aux courbes caractéristiques de la fausse prise du type II.

Cette hypothèse sur le mécanisme de la fausse prise est également confirmée par les microphotographies électroniques du ciment hydraté à base du clinker à faible teneur en alcalis (0,49 R_2O) de l'usine "Bolchevik".

Pour un ciment à prise normale après 5 minutes d'hydratation, on observe une désagrégation de parcelles initiales avec formation autour d'elles de cristaux aciculaires produits par l'hydratation (fig.7 a,b). Par contre, au cas de la fausse prise, on observe une formation intense de la structure gypse-ettringite, ainsi qu'un ralentissement de l'hydratation du clinker, par suite du blocage de la surface des grains du clinker avec des constituants nouveaux (fig.7 c, d). La formation de la structure gypse-ettringite s'accompagne de la fixation d'une grande quantité d'eau aussi bien chimiquement que par adsorption à la suite du développement de la surface des constituants nouveaux et conditionne la perte temporaire de plasticité du système en voie de durcissement.

Au cas où il est possible de détruire la structure gypse-ettringite par un nouveau malaxage, les propriétés rhéologiques de la pâte de ciment se rétablissent complètement, phénomène observé généralement dans la pratique lorsqu'on utilise les ciments à fausse prise. Toutefois le développement et la consolidation de la structure gypse-ettringite peuvent être si poussés que le malaxage répété est incapable d'arrêter l'épaississement précoce et, dans ce cas, la fausse prise peut devenir une prise rapide.

BIBLIOGRAPHIE

1.- Г.Л.КАЛОУСЕК (1976) "Процессы гидратации на ранних стадиях твердения цемента", В сб. трудов VI Международного конгресса по химии цемента, т.II, кн.2, 65-81, (en russe).

2.- А.КУНЦЕ, П.ХАВКИНС (1973) В сб. трудов V Международного конгресса по химии цемента, 474-476, (en russe).

3.- Б.Г.СКРАМТАЕВ, Л.И.ПАНФИЛОВА, Б.Д.ТРИНКЕР (1966) "О мерах борьбы с ложным схватыванием цемента", "Цемент", 2 , 12-13, (en russe).

4.- М.Ф.ЧЕБУКОВ, В.А.ПЬЯЧЕВ, Т.Г.ЯКОВЛЕВА, Г.Е.ПЬЯЧЕВА, В.К.НОВОСАДОВ (1977) "Влияние сульфатов кальция на свойства портландцемента", "Цемент", 7 , 15 - 16 , (en russe).

5.- Z.T.JUGOVIC, J.L.GILLAM (1968) "Early hydration of abnormal setting cement", "Journal of Materials", vol. 3, 3 , 517-537, (en anglais).

6.- Л.Е.КОУПЛЕНД, Д.Л.КАНТРО (1969) "Химия гидратации портландцемента при обычной температуре", в сб. "Химия цементов", 233-276, (en russe).

7.- F.M.LOCHER (1973) "Erstarren und Anfangstectigkeit von Zement","Zement-Kalk-Gips", 26, 2 , 53-62 , (en allemand).

8.- G.L.KALOUSEK, Z.T.JUGOVIC, J.L.GILLAM (1967) "A new factor in abnormal setting of portland cement", "Am. Ceram. Soc. Bull.", vol. 46, 3, 270 - 274 , (en anglais).

X-Ray Photoelectron spectrometry investigation of the early stages of C_3S Hydration-the role of NaF admixture

Etude par la spectrométrie de photoelectrons XPS des stades initiaux de l'hydratation de C_3S-rôle de l'adjuvant NaF

M. REGOURD, Département Microstructures - C.E.R.I.L.H., Paris, France,
J.H. THOMASSIN, P. BAILLIF et J.C. TOURAY - Université d'Orléans, France.

RESUME

La spectrométrie de photoélectrons XPS est une méthode sensible et reproductible pour l'étude de l'hydratation initiale de C_3S. Elle révèle des transformations à la surface des grains du silicate dès les premiers instants de leur contact avec l'eau dans des pâtes de rapport eau/C_3S = 0,5. Ces modifications ont été mises en évidence par un changement dans l'environnement des atomes de Si et une variation du rapport Ca/Si. La surface de C_3S est, entre cinq secondes et une minute, un site d'échanges continuels entre le solide et la solution. Ce stade correspond à la précipitation d'un hydrate primaire de rapport C/S $\ll$ 3. Au-delà de la première minute se forme un hydrate secondaire de rapport C/S $\simeq$ 2 qui subsiste jusqu'à la fin de la période dormante.

Le fluorure de sodium dissous dans l'eau de gâchage jouerait son rôle de retardateur en supprimant la formation de l'hydrate primaire. L'épaisseur du premier hydrate formé, de rapport C/S $\simeq$ 2, atteindrait 60 Å à 3 minutes.

SUMMARY

X-ray Photoelectron Spectrometry is a sensitive and reproducible method for the study of the early hydration of C_3S. XPS reveals surface transformations of silicate grains from the first few seconds of their contact with water in pastes (water/C_3S = 0,5). These modifications have been evidenced by a change of the environment of Si atoms and a variation of the Ca/Si ratio. The C_3S surface, between five seconds and on minute, is a site of continuous exchange between the solid and the solution. This stage corresponds to the precipitation of a primary hydrate with a ratio C/S $\ll$ 3. After one minute, a secondary hydrate with a ratio C/S $\simeq$ 2 is formed and it subsists up to the end of the dormant period.

Calcium fluoride dissolved in mixing water would play its retarder effect in leaving out the formation of the primary hydrate. The thickness of the first hydrate formed with a ratio C/S $\simeq$ 2 would attain 60 Å at 3 minutes.

1. INTRODUCTION

The initial hydration of C_3S has not yet been completely clarified because of the complexity of the physico-chemical changes occuring during the dormant period at the surface of grains. SKALNY et al (1) have recalled the results of numerous studies of C_3S hydration and their interpretation related to the theory of a protective layer or a delayed nucleation.

In previous works (2, 3), we have shown the importance of the first five minutes from the contact between C_3S and H_2O . In this paper, we develop the results of our studies by XPS on the evolution of the surface C_3S crystals under normal conditions of hydration and with dissolved NaF as admixture.

2. X-RAY PHOTOELECTRON SPECTROMETRY XPS

X-ray Photoelectron Spectrometry XPS, also called ESCA (Electron Spectroscopy for Chemical Analysis) is a technique for measuring the kinetics energy of electrons photoejected from a solid surface using soft X-rays. The kinetic energy E_K of the photoelectrons can be related to the binding energy E_B which these electrons had originally in the solid (4).

XPS is a rather new technique in the cement field. In the study of silicate materials, this method has been used for determining the surface composition of materials from the intensity of the peaks of different chemical elements (5, 6 et 7).

For a conducting sample, the relation between the kinetic energy of photoelectrons and the binding energy is :

$$E_K = h\nu - E_B - \Phi_S$$

$h\nu$: energy of impinging photons,

Φ_S : work function of the material of the spectrometer.

In the case of an insulator sample, the same relation must be corrected by a factor due to the surface charging effects of the sample. Nevertheless, it is possible to determine the binding energy of the electrons by means of an external standard. Using the carbon C_{1s} peak of the contamination layer and assuming that the charging shift is the same for the sample and for the contamination layer, the expression of the binding energy becomes :

$$E_B = E_K(C_{1s}) + E_B(C_{1s}) - E_K$$

In our experiments the value of $E_B(C_{1s})$ is assumed equal to 285.0 eV.

2.1 Characteristics of the X-ray photoelectron spectrometry

[a] The depth of investigation : This depth into the oxides and silicates varies from 50 to 100 Å. It has been chosen to 3 λ (λ is the mean free path of the ejected electrons). It corresponds to 95 % of the analyzed electrons. The other 5 % come from deeper zones (8). It is sufficient to provide data in volume while still allowing surface analysis.

[b] The qualitative aspect : It is possible to determine chemical elements on the surface of solid samples. For most of the elements (hydrogen excepted), a minimum atomic concentration is required to detect, it is generally about 1 %. The variation of the binding energy (chemical shift) is significant of a change in the atomic surrounding.

[c] The quantitative aspect : In fact, it is a quantitative method providing it can be standardized on fresh fracture surfaces of homogeneous materials of known composition.

[d] The fiability of the measures : Measurements of the intensity of peaks are easily reproduced and are usually of a quality superior to ± 10 %, providing that a ratio of concentrations in a homogeneous material is determined.

[e] The facility of sampling : The samples do not require any particular preparation. Cleavage surfaces, grains, powders and fibers may be analyzed in the same way.

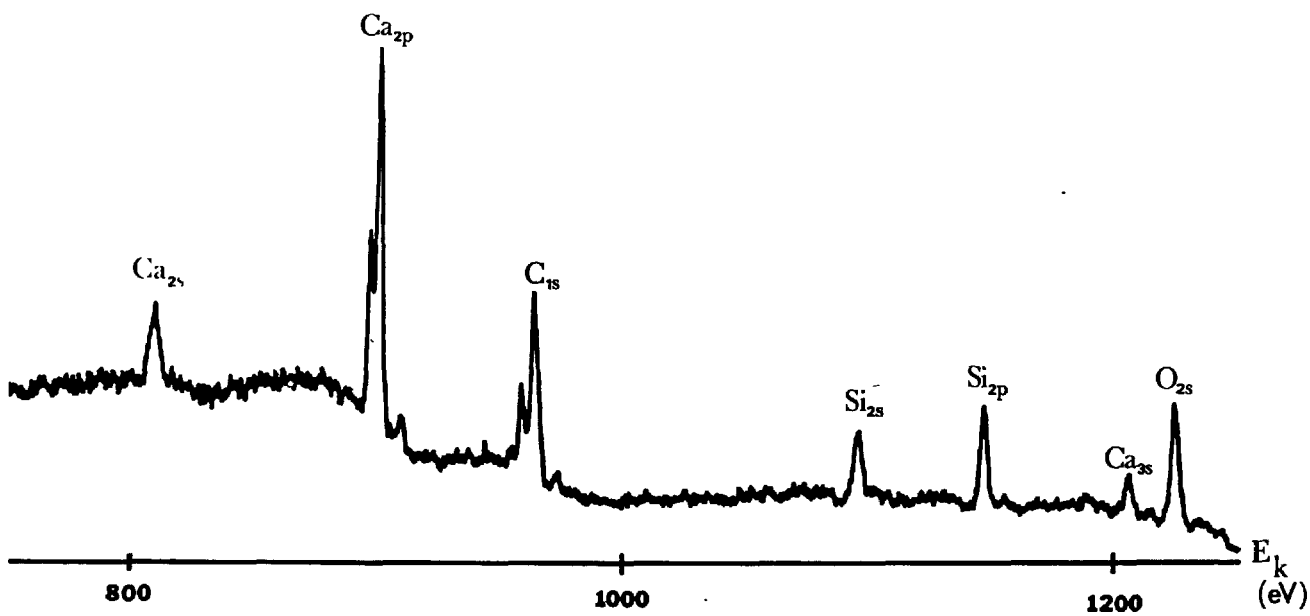

Fig. 1 : XPS spectrum of C_3S.

2.2 The apparatus

The apparatus utilized was an AEI ES 200 Photoelectron Spectrometer fitted with a magnesium anode (MgKα = 1253.6 eV) under an irradiation power of 240 W. The XPS peaks studied were : Ca_{2p} 3/2 (E_B = 346.9 eV), Si_{2p} (E_B = 101.2 eV), O_{1s} (E_B = 530.9 eV) and C_{1s} (E_B = 285.0 eV). The samples were fixed on adhesive conducting tape. The analyzed area was about 25 mm^2.

A typical spectrum of C_3S is shown in the figure 1. The XPS peaks correspond to the inner shell electrons of calcium, oxygen and silicium of the sample. The carbon C_{1s} peak is due to the contamination by oil vapor from the diffusion pumps.

2.3 The calibration curve

In order to determine the Ca/Si ratios in hydrated silicates, a standard curve was drawn (2). The ratio of the area of the XPS peaks (Ca_{2p}/Si_{2p}) was compared to the atomic ratios Ca/Si in materials of a well determined composition : synthetic glasses (Na_2O - CaO - MgO - SiO_2 system) kindly furnished by SAINT-GOBAIN Industries, natural wollastonite $Ca_3Si_3O_9$, dicalcium silicate Ca_2SiO_4 and tricalcium silicate Ca_3SiO_5. The variation of the XPS results determined on several samples of the same anhydrous Ca_3SiO_5 preparation is less than 5 %.

3. C_3S HYDRATION

3.1 Material

The tricalcium silicate was synthetized at 1600°C by solid state reaction of a mixture of amorphous silica and reagant grade/calcium carbonate in a closed platinum crucible. The product of this synthesis was air quenched and analyzed by X-ray diffraction, atomic absorption and electron probe microanalysis.

After grinding to a specific surface of 3000 $cm^2.g^{-1}$, a series of pastes was prepared with distilled water (water/solid = 0.5). At selected intervals, between 5 seconds and 4 hours, the hydration was stopped by the addition of acetone.

3.2 Results

The results of the photoelectron spectrometry are presented in the form of a kinetic curve (fig. 2) and a table giving the position of the XPS peaks Ca_{2p} 3/2, Si_{2p}, O_{1s} (Table I).

The variation of the Ca_{2p}/Si_{2p} ratio (fig. 2) from approximately 5 seconds to 5 minutes proves the importance of the perturbations on the surface of the grains. These results show that the value of the Ca_{2p}/Si_{2p} ratio is always lower in hydrated samples than in C_3S, but the binding energy and the shape of the Si_{2p} peak show that the surface of the hydrated particles begins to differ significantly from that of the anhydrous C_3S within a very short period. In particular, it is noticed that the differences of the binding energies Ca_{2p} 3/2 - O_{1s} tend toward the constant while those relative to Ca_{2p} 3/2 - Si_{2p} and Si_{2p} - O_{1s} vary significantly between the anhydrous sample and the hydrated samples. These last results demonstrate a variation in the binding energy of the Si_{2p} electrons from 5 seconds on.

3.3 Interpretation

The XPS data relating to C_3S can be interpreted in the framework of a model suggested by the XPS studies of the glass/water solutions interactions (9). With this model, it would be possible to explain the form of the XPS kinetic curve of Ca_3SiO_5 hydration, the evolution of the dissolution of calcium and silicate ions, the existence of a dormant period and the setting of the paste.

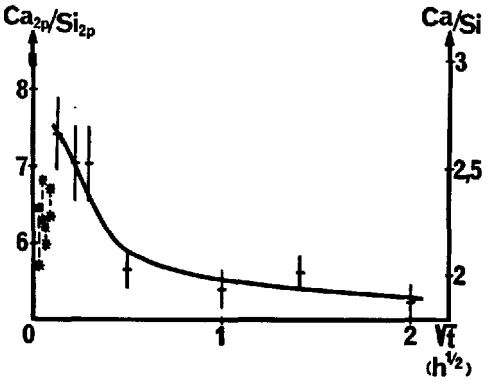

Fig. 2 : Kinetic curve of hydration of C_3S

Table I : Difference between the binding energies of the XPS peaks, Ca_{2p} 3/2, Si_{2p}, O_{1s} and width at mid-height of the Si_{2p} peak.

Time	δ (Ca_{2p} 3/2 - Si_{2p}) eV ± 0.2	δ (Si_{2p} - O_{1s}) eV ± 0.2	δ (Ca_{2p} 3/2 - O_{1s}) eV ± 0.2	Width at mid-height of the Si_{2p} peak eV ± 0.1
0	245.7	429.7	184.1	2.5
5, 10, 15, 30 sec 1, 3, 5, 15 min 1, 2 hours	245.1	429.3	184.2	2.8
4 hours	245.1	429.1	184.0	2.4

[1] At the beginning of the C_3S-H_2O reaction and after protonation of silicate and oxygen ions, a congruent dissolution of Ca_3SiO_5 is assumed (10,11). We emphasize in this regard, that in an open medium with a high rate of percolation, the interaction can limit itself to this first stage because of the lack of accumulation of the dissolution products.

[2] The second stage detectable in the first few seconds (5 seconds on the curve fig. 2) corresponds to the formation of a Primary Hydrate with a ratio C/S << 3 on the grains of the anhydrous silicate. The cloud of points show that the surface, between 5 seconds and 1 minute, is a site of continous exchange and not in a state of equilibrium.

The quantitative interpretation of the XPS data has been carried out in a previous paper (5). The computed thickness of the Primary Hydrate is 8 Å. It should be noted that this thickness is comparable to the thickness of the layer of C_3S dissolved after one minute in the experiments of FUJI and KONDO (10). This value is 7 Å for a w/s = 0.7 and a specific surface of 3800 $cm^2.g^{-1}$.

[3] The third stage manifests itself by an increase of the I_{Ca}/I_{Si} ratio in which the maximum is attained at the end of one minute of hydration. This situation can be explained by the formation of a Secondary Hydrate having a Ca/Si ratio higher that of the Primary Hydrate but lower than the observed maximum value of 2.7 because the latter includes a contribution of the underlying C_3S. This reaction is compatible with a dual origin of Ca^{2+} : the solution (process a) and the inner part of the grain (process b). These latter ions are a part of the ions released by the solid during the advancement of the interface hydrate-C_3S.

In this regard, the values of the intermediate Ca/Si, between 2 and 2.7 (fig. 2), would confirm the hypothesis of the chemisorption of Ca^{2+} ions on a surface enriched in silicon, hypothesis deduced from the measures of the ζ potential, giving a positive charge to the Ca_3SiO_5 particles in the first minutes of hydration (12). That the values of the Ca/Si ratios are superior to 2 is explained by the contribution to the XPS signal of the subjacent anhydrous C_3S, the amount of the Secondary Hydrate still being very low.

Finally, the proposed model assumes that a layer of the Secondary Hydrate with C/S ≃ 2 grows on a substratum of C_3S. This assumption is strongly suggested by the value C/S ≃ 2 obtained when this layer is thicker than 60 Å at t > 15 minutes.

Subsequently, the Ca/Si ratio indicated on the kinetic curve slowly decreases and tends asymptotically towards a value close to 2 in about 15 minutes. At this moment, the thickness of the layer of the Secondary Hydrate has sufficiently increased (via the process b also) so that the contribution of the C_3S to the XPS signal is negligible. This thickness is equal to 3 times the mean free path of the Ca_{2p} and Si_{2p} electrons, that is to say approximately 60 Å.

The formation of the Secondary Hydrate could also be partly explained by the precipitation from solution. This mechanism explains why silica concentrations in solutions drop drastically after some minutes of hydration (10, 11). In our model, this process cannot be distinghished from the process a and probably occurs simultaneously. The Secondary Hydrate develops and persists through the dormant period up to the supersaturation of the solution.

In slowing down the transfers between the solution and the reactional interface, we could consider that the Secondary Hydrate plays the role of a barrier which accounts for the low activity of the induction period revealed by the calorimetric curves. However the rate of C_3S hydration and the nucleation of hydrates are governed by the concentration of Ca^{2+} and OH^- in the solution. This was shown by BARRET et al (13), YOUNG et al (14) : either removal of Ca^{2+} and OH^- from the solution reactivated the hydration of C_3S or, on the contrary, a supersaturated solution used as mixing water strongly delayed the dissolution of C_3S crystals.

[4] After four hours, important reorganizations take place in the interior of the Secondary Hydrate as evidenced by the change in the shape of the Si_{2p} peak. Apparently, this modification indicated the end of the dormant period.

The end of the dormant period manifests itself by the brutal nucleation of $Ca(OH)_2$ and the Tertiary Hydrate (C-H-S Type I) with dimeric silicate ions $(Si_2O_7)^{6-}$.

One hypothesis to explain this new stage is that of the existence of a not very permeable, superficial barrier that slows down the exchanges between the solution and the solid. In this case, the end of the dormant period corresponds to a brutal increasing in the porosity of that barrier, by the formation of cracks, for example at the grain boundaries or at dislocations emergency. In this hypothesis the reorganizations observed in the Secondary Hydrate are the cause of the brutal increase in its porosity. This schema shows that the C_3S, protected till that moment, can be placed in contact with a very alkaline solution susceptible of leading to a large congruent dissolution. The silica, thusly liberated, precipitates at the same time in the form of the Tertiary Hydrate.

3.4 The role of aging

In order to test the effect of aging on the kinetics of hydration, we placed about 500 mg of C_3S in a chamber at 20 °C, with uncontrolled conditions of humidity and atmospheric CO_2.

After five and eight days, several samples were analyzed by XPS. The aging was characterized by an increase in the Ca_{2p}/Si_{2p} ratio and an enhancement of the C_{1s} peak related to the carbon of CO_3^{2-} ions. Slight modifications were observed on the Si_{2p} peak. A kinetic curve of the hydration of a carbonated sample has been drawn on fig. 3. Qualitatively, the shape of this curve is the same as for uncarbonated C_3S. Nevertheless because of the presence of the calcium carbonate, it is not possible to relate the XPS ratio to the atomic ratio Ca/Si.

After heating this last sample at 1500 °C during one hour, the aspect of the hydration curve (fig. 4)is a little different, probably by a modification occured on the surface of the grains during the heating. This curve retains the same tendency as that of the carbonated sample (fig. 3) but remains different from that of the fresh sample (fig. 2) with higher Ca/Si ratios and delayed formation of the Secondary Hydrate.

Carbonation has a retarder effect on C_3S hydration and the composition of hydrates has not been determined.

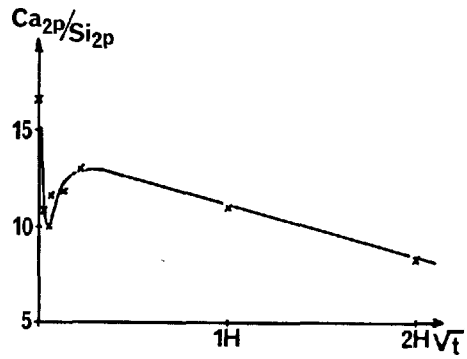

Fig. 3 : Kinetic curve of hydration of a carbonated C_3S sample.

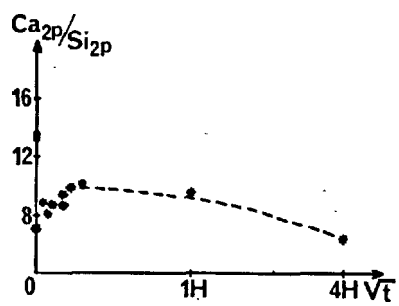

Fig. 4 : Kinetic hydration curve of the carbonated C_3S sample after heating at 1500 °C.

4. THE ROLE OF NaF ADMIXTURE

4.1 Sample preparation

The pastes were prepared in the same manner as above with a solution containing 1 % NaF.

The XPS peaks studied were Ca_{2p}, Si_{2p}, O_{1s}, C_{1s}, Na_{2s} (E_B = 63.0 eV) and F_{1s} (E_B = 683.6 eV).

4.2 Results

The results are reported in the form of a kinetic curve (fig. 5) and a table (Table II) giving the position of the XPS peaks.

The variations of the binding energy and the shape of the Si_{2p} peak are the same as for C_3S hydration in pure water.

The kinetic curve decreases regularly up to 3 minutes and the value of the Ca/Si ratio is close to 2 all over the dormant period. The third stage observed in the system C_3S-H_2O which manifests itself by an increase in the Ca/Si ratio does not exit in the system $C_3S - H_2O + 1$ % NaF.

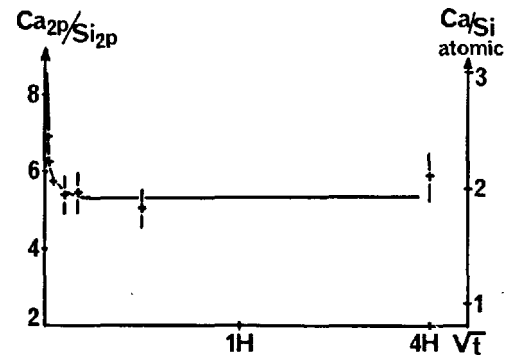

Fig. 5 : Kinetic curve of hydration of C_3S with 1 % NaF admixture.

Table II

Hydration of C_3S + 1 % NaF : Evolution of the binding energies of the XPS peaks $Ca_{2p}^{3/2}$ and Si_{2p}, and width at mid-height of the Si_{2p} peak.

Time of hydration	δ Ca_{2p} 3/2 - Si_{2p} eV ± 0.2	width of the Si_{2p} peak at mid-height eV ± 0.2
0	245.6	2.4
10, 30 seconds 1,3, 5, 15 minutes 4 hours	244.9	2.8

4.3 Discussion

The interpretation of the kinetic XPS curve is not univocal. A possible interpretation could be a lack of precipitation of the Primary metastable Hydrate and the direct formation of the Secondary Hydrate. This formation combinated perhaps with CaF_2 precipitation would explain the important drop in the calcium concentration in the solution noticed by YOUNG et al (14) in comparison with hydration in pure water. The value of the ratio Ca_{2p}/Si_{2p} at the plateau strongly suggests that the thickness of the layer of the hydrate is higher than the depth of investigation of the method i.e. superior to 60 Å at about 3 minutes.

In this interpretation, the difference between the length of the dormant period for hydration in pure water and in NaF solutions could be related to a "memory effect" in the texture of the hydrate. Such effects would determine the behaviour of the hydrated layer around anhydrous C_3S grains over long periods : reactivity with Na and/or F and recrystallisation.

The same interpretation could be available for 4 °C experiments of MENETRIER et al (15). Low temperatures are well known to delay the setting of the cement pastes.

5. CONCLUSION

The XPS method seems well adapted to the study of the early interactions between C_3S and water. It could allow, with the utilisation of other techniques (SEM, STEM, chemical analysis of solutions) the understanding of the mechanisms which occur during the hydration of C_3S. However, due to the carbonation, it underlines the difficulty in obtaining a good sample for the quantitative surface analysis.

Our data suggest the existence of at least two intermediate hydrates during the dormant period. For hydration with dissolved NaF admixture, the formation of the Primary Hydrate would not take place and the formation of the Secondary Hydrate would be predominant.

La version française de cette communication est disponible aux adresses suivantes :

- *Madame M. REGOURD*
  Département Microstructures
  C.E.R.I.L.H.
  23, rue de Cronstadt
  75015 PARIS (FRANCE)
- *Messieurs J.H. THOMASSIN, P. BAILLIF, J.C. TOURAY*
  Géologie appliquée - Institut de Recherches RMM
  UNIVERSITE d'ORLEANS
  45045 ORLEANS CEDEX (FRANCE)

REFERENCES

1.- J. SKALNY, I. JAWED and H.F.W. TAYLOR (1978) : "Studies on hydration of cement. Recent developments". World Cement Technology, 9, 183.

2.- J.H. THOMASSIN, M. REGOURD, P. BAILLIF et J.C. TOURAY (1979) : "Etude de l'hydratation initiale du silicate tricalcique par spectrométrie de photo-électrons". C.R. Acad. Sci. Ser. C, t. 288, 93.

3.- M. REGOURD, J.H. THOMASSIN, P. BAILLIF and J.C. TOURAY (1980) : "Study of the early hydration of Ca_3SiO_5 by X-ray Photoelectron Spectrometry", To appear in Cement Concrete Res., vol. 10, n° 2.

4.- H. SIEGBAHN, C. NORDLING, A. FAHLMAN, R. NORDBERG, K. KAMRIN, J. HEDMAN, G. JOHANSSON, T. BERGMARK, S.E. KARLSSON, I. LINDGREN, B. LINDBERG (1967) : ESCA Nova Acta Reg. Soc. Sci. Upsaliensis, Ser 4, vol. 20, 282 p.

5.- R. PETROVIC, R.A. BERNER, M.B. GOLDHABER (1976) : "Rate control in dissolution of alkali feldspars. I. Geochimica and Cosmochimica Acta, 40, 537.

6.- J.H. THOMASSIN (1977) : "Apport de la spectrométrie de photo-électrons XPS à la cinétique géochimique. Etude de la dissolution de quelques silicates magnésiens", Thèse de 3ème cycle, Spécialité Géochimie, Orléans.

7.- J.H. THOMASSIN, J. GONI, P. BAILLIF, J.C. TOURAY M.C. JAURAND (1977) : "An XPS Study of the Dissolution Kinetics of Chrysotile in 0.1 N Oxalic Acid at Different Temperatures." Phys. Chem. Minerals, 1, 385-398.

8.- L. COLOMBIN (1979) : "Analyse physico-chimique des zones superficielles du verre plat. Evaluation critique de diverses spectroscopies", Thèse Namur (Belgique).

9.- J.H. THOMASSIN, S. SCHERRER, P. BAILLIF, J.C. TOURAY and F. NAUDIN : "Etude du comportement de l'aluminium lors de l'interaction H_2O-verre : apport de la spectrométrie XPS et de la sonde ionique", Bull. Soc. Fc. Miner. Crist., 102, 319 (1979).

10.- K. FUJIIand W. KONDO (1975) : "Rate and Mechanism of Hydration of Tricalcium Silicate in an early Stage", Yogyo, Kyokai shi, 83, 214.

11.- P. BARRET (1978) : "Les mécanismes d'hydratation et de durcissement des ciments", Conférence Société Encouragement pour l'Industrie Nationale, L'Industrie Nationale, n° 1, 3-41.

12.- M. TADROS, J. SKALNY and R. KALYONCU (1976) : "Kinetics of calcium hydroxide crystal growth from solution", J. Colloid. Interface, Sci., 55, 20.

13.- P. BARR: , D. MENETRIER, D. BERTRANDIE (1977): Cinétiq d'hydratation des aluminates et silicates de .ium en relation avec les mécanismes du durciss .t dans les ciments. Rev. Int. Htes Temp. et fract., t 14, 127-133.

14.- J.F. YOUNG, H.S. TONG and R.L. BERGER (1977) : "Compositions of solutions in contact with hydrating tricalcium silicate pastes", J. Amer. Ceram. Soc., 59, 344.

15.- D. MENETRIER, I. JAWED, T.S. SUN and J. SKALNY (1979) : "ESCA and SEM studies on early C_3S hydration", Cem. Concr. Res., vol. 9, n° 4, 473-482.

Condensation properties of dispersed products of portland cement hydration and rehydration

Propriétés agglomérantes des composants dispersés du ciment, après leur hydratation ou leur réhydratation

V.D. GLUKHOVSKY, Prof. Dr. Technical Sciences,
P.V. KRIVENKO, Cand. Technical Sciences,
R.F. RUNOVA, Cand. Technical Sciences, Institute of Civil Engineering, Kiev, U.R.S.S.

RESUME : On a étudié les propriétés agglomérantes du ciment portland et du β C_2S hydratés puis broyés et comprimés, en fonction de leur degré de rehydratation et de leur composition. On a montré que, bien que cette dernière ait une influence sur la résistance finale obtenue, elle ne détermine pas les propriétés agglomérantes du produit. Ces propriétés sont déterminées par l'état physique du produit hydraté et broyé. L'hydratation du ciment à des températures comprises entre 400 et 1000° entraîne la formation de produits amorphes ou de cristaux instables, qui ont un effet déterminant sur la capacité de réagglomération.

Il a été trouvé que ces propriétés agglomérantes ne dépendent pas de l'eau combinée ou adsorbée; et ,e dépendent pas seulement des produits d'hydratation. Ces propriétés ont été observées dans des ciments ou du βC_2S complètement hydratés.

On a montré que cette réagglomération dégageait de l'énergie et que les propriétés agglomérantes étaient fonction de l'énergie dégagée. La transformation de l'énergie interne en énergie thermique accompagne la solidification du matériau et se produit dès que la compression met les particules en contact.

SUMMARY : The dependence of condensation properties of dispersed products of hydration and rehydration of Portland cement clinker and βC_2S on the degree of their rehydration and substance composition has been observed. It is shown that, although the latter has an influence on the relative strength of the stone being synthesized, it does not determine the condensation capacity of the binder. This capacity is determined by the physical state of the dispersed substance. The rehydration of hydrates within the temperature range of from 400 to 1000°C is accompanied by formation of amorphous and unstable crystalline structure phases, this determining their capacity for both the contact and hydration hardening.

It has been found that the condensation capacity of dispersed substances under examination does not depend on the presence in the system of chemically combined and physically bound gravitation water, it being displayed not only by the hydration products. These properties are also found in the products of complete rehydration, as well as in ground Portland cement clinker and β-C_2S.
The estimation of these phases is given from the point of view of availability in them of excessive free energy. It is shown that this energy determines the capacity for condensation. The transformation of such energy into thermal energy, its release accompanying the synthesis of the stone from dispersions at the moment of contact forming between the particles has been recorded.

INTRODUCTION: The capacity of mineral systems to reveal binding properties is linked with the nature of their interaction with water. The possibility of revealing hydration binding properties is assumed only for the substances of slow and limited solubility (1). It led to the discovery of binding properties in the compounds of alkaline-earth metals (2) and to the development of their hardening theories the basis of which underlie the regularities of transition of anhydrous dispersed substances into aqueous formations.

The discovery of contact hardening (3) and the ability to such hardening of anhydrous binding substances and dispersed products of their hydration, partial or complete rehydration (4) permits a further step in generalizing the regularities of this process and an inference that neither physically nor chemically combined water is the determining factor in the condensation of dispersed systems into a water-resistant stone. According to these generalizations, the capacity of mineral systems to reveal the binding properties is determined by their energy potential, this being a function of the physical state of the substance by which they are represented.

The synthesis of a water-resistant stone can be realized at the moment of contact forming between both the aqueous and anhydrous dispersed mineral particles in the event of them being in a mutable (amorphous or unstable) crystalline state. The process of contact as well as of hydration condensation is accompanied by intensive release of thermal energy. The release of the latter continues even after the petrification of the dispersed system due to a gradual transition of the binder particle substance into a stable state, the particles comprising the concrete stone. This permits to draw a conclusion that the condensation properties of the products of hydration and rehydration of Portland cement and its separate minerals are manifested as the effect of structure ordering in these substances (5).

Using the principles of this effect, a series of experiments was conducted on the investigation of condensation properties of the dispersed products hydration, partial or incomplete rehydration of Portland cement and β-C_2S aimed at the extension of the ideas about the causes of Portland cement condensation into stone-like formations.

EXPERIMENTAL METHODS: Portland cement clinker and β-C_2S crushed to a specific surface of 3500 cm^2/g, the products of their hydration as well as of partial and complete rehydration have been employed as the investigation objects. The hydrates were obtained by wet grinding process at B/T=5 with subsequent autoclaving at constant stirring at Pgauge = 0.8 MPa of suspensions of initial substances, as well as of mixtures of β-C_2S with additions of CaO and SiO_2 in quantities ensuring the synthesis of high-base and low-base calcium hydrosilicates, respectively. The autoclaving was conducted up to the full hydration of anhydrous minerals. Following that they were dried at a temperature of 100±5°C up to a powdery state. The synthesized products were rehydrated at 400, 600, 800 and 1000°C by heat treatment followed by rapid cooling.

To determine the properties of dispersions under investigation at contact hardening, sample cylinders were made of them under pressure at specific load of 400 and 200 kgf/cm^2 applied for 1 min. The samples were pressed without water addition. They were tested immediately after pressing, as well as after 14, 28 and 120 days of storage in water and under dry-air conditions. The samples were placed into water immediately after pressing.

To determine their capacity to hydration hardening, the powders were mixed with water to the consistency of a normal-density paste from which sample cubes were prepared.

Structural changes in the substances were studied by X-ray diffractometric, electron-microscopic, infra-red spectroscopic, and differential-thermal analyses. The presence of excessive free energy in the systems under investigation was estimated by the results of thermobarographic analysis the essence of which underlies the recording of thermal effects springing up during condensation of dispersed substances in the process of their pressing.

KNOWN CONDENSATION PROPERTIES OF HYDRATE SUBSTANCES: In our paper (1) has been shown that, in contrast to natural hydrates of stable crystalline structure, the dispersed hydration products of Portland cement and its component minerals, while being in the metastable state, reveal for a long time the capacity of forming stone-like bodies at the moment of particles approach without the supply of thermal energy, these bodies retaining their shape and strength in water; they manifest also the ability of forming in them water-resistant structural bonds capable of restoration after mechanical dispersion due to iterative approach of particles or bonds strengthened due to distance reduction between them; the condensation of such dispersions into a water-resistant stone is the result of the reciprocal attraction forces inherent in the hydrate particles of unstable structure and is manifested as the effect of their structure ordering since these forces decrease in the process of substance transformation from the amorphous into the unstable crystalline state and disappear as their crystalline structure becomes stabilized; the condensation capacity of the hydrated dispersions is the function of the state of their structure only, whereas the strength of the cement stone is at the same time the function of their substance composition as well; the hydrate dispersions represented by unstable-structure substances should be regarded as independent hydraulic

binding substances of contact hardening.

Condensation capacity of dispersed products of rehydration is characterized by the fact that the powdery products of partial or complete rehydration of hydrates obtained by autoclaving dispersed Portland cement, β-C_2S and its mixes with Cao and SiO_2, like the hydrates proper, reveal the capacity for contact hardening during a long period of time since they are condensed into stone-like formations acquiring strength and water-resistance at the moment of contact appearance between the particles of these dispersions (Table I).

Table I

Strength of samples immediately after dry pressing at a pressure of 400 kgf/cm^2 and in-water storage

Hydrate designation	Hydrated substance composition	Compression strength, kgf/cm^2, of autoclaved dispersion samples rehydrated at temperature, °C, after pressing (following 14 days of in-water storage)				
		100	400	600	800	1000
A	$2.5CaO \cdot SiO_2 \cdot nH_2O$	110/152	115/167	120/380	125/350	120/290
B	$2CaO \cdot SiO_2 \cdot nH_2O$	105/137	110/160	100/320	100/240	120/250
C	$CaO \cdot SiO_2 \cdot nH_2O$	72/112	75/90	90/190	57/80	40/75
K	Hydrated Portland cement clinker	95/125	105/170	115/300	120/310	120/350

The obtained data permit an assertion that the condensation capacity is revealed independent of the presence of gravitation, chemically and physically combined water in the system.

This conclusion can be made from the fact that the samples moulded without water from dry powders of substances analysed gain strength with the passage of time when stored under dry-air conditions and do not decompose in water immediately after pressing and acquire strength in hot water. Ground Portland cement clinker and β-C_2S also reveal the ability for contact hardening.

In contrast to the hydrates, the rehydration products like the Portland cement clinker and β-C_2S, when mixed with water, manifest the capacity for hydration hardening revealed to a greater extent with the increase of the degree of substance rehydration.

Estimating the condensation capacity of the investigated substances by the strength of samples immediately after their pressure-moulding and prolonged dry-air and in-water storage (Table II), it can be noted that it depends on the chemical composition of the dispersed substances and their rehydration temperature.

Table II

Strength changes in samples dry-pressed at a pressure of 400 kgf/cm^2

Hydrate designation	Compression strength, kgf/cm^2, of samples press-moulded from autoclaved dispersions rehydrated at temperature, °C, stored in open air/water, days									
	100		400		600		800		1000	
	28	120	28	120	28	120	28	120	28	120
A	200/190	230/220	260/310	320/412	240/390	310/480	410/470	505/590	230/310	250/360
B	187/165	245/260	195/210	255/270	260/410	310/490	190/245	235/310	240/280	260/350
C	115/217	145/270	120/180	160/205	172/230	204/280	70/90	86/105	60/95	70/115
K	175/157	240/182	180/206	200/250	300/350	320/380	370/400	400/450	300/360	350/400

The strength increases with the increase of their basicity, independent of petrification conditions, hydration or contact hardening, higher strength is characteristic of samples obtained from hydration and rehydration products formed on the basis of the mix of β-C_2S and calcium oxide ($2.5CaO \cdot SiO_2 \cdot nH_2O$); it increases correspondingly in hydration products of β-C_2S ($2CaO \cdot SiO_2 \cdot nH_2O$) and its mix with SiO_2 ($CaO\ SiO_2\ nH_2O$). Similar dependence has been revealed in the studies of substances having similar composition and synthesized by autoclaving from chemically pure oxides.

It should be noted that the samples moulded from damp powders also retain their strength in water right after the pressure-moulding. In this case introduction of water into the system somewhat reduces the initial strength of the stone body synthesized from dispersed hydrates and enhances the strength of samples made of partially or fully rehydrated dispersed substances.

The increase of the moulding pressure in all instances results in the rise of the initial stone strength. So, at the moulding pressure of 2000 kgf/cm its strength immediately after pressure-moulding reaches 500-600 kgf/cm^2. However, the degree of the moulding pressure effect decreases with the rise of the basicity and the degree of dispersed substance rehydration. But here a positive effect on the strength of a stone body synthesized from dry powders increases with its impregnation with water right after the moulding.

The physical state of the hydrates varied in the course of their rehydration. The study of the changes in the physical state of dispersed substances obtained in the systems under consideration, with their partial and complete rehydration, was aimed at the determination of its effect on the condensation capacity.

The initial hydrates were represented by gel-like and submicrocrystalline calcium hydrosilicates whose clear identification is hampered by their structure irregularity. Calcium oxide added to β-C_2S during the synthesis of hydrate A had considerably reacted with it at autoclaving which enabled the obtaining of a hydrate of utmost basicity. This is signified by the presence of relicts with d=2.28; 2.49; 2.74; 3.03Å on the X-ray photograph and of endoeffects on the DTA line at 180, 380 and 480°C characteristic of $C_2SH(B)$. The addition of silica to β-C_2S in the synthesis of hydrate B promoted the drop of basicity in the hydrosilicates being formed: phase (A) is identified on the X-ray photograph by lines with d=2.71; 2.76; 3.01; 3.04Å, and on the thermograph - by the exoeffect of wollastonite crystallization at 820°C.

The presence of unstable-structure hydrate phases in the products obtained by autoclaving β-C_2S and mixes on its basis is also confirmed by the way of water removal during thermographic examinations: it occurs at temperatures up to 850°C with the highest intensity within the temperature ranges of from 100-300 and 500-700°C; a highly intensive exoeffect of amorphous hydrosilicates crystallization has been recorded within the temperature range of 300-500°C.

The initial rehydration stage of the hydrates being examined is accompanied at 400°C by the removal of zeolitic and adsorption water, this having no effect on the strength characteristics of samples from dispersed products of rehydration. The rehydration at 600°C results in the development of substance amorphism. At this temperature the structures of high-basicity calcium hydroxides are subject to a greater degree of destruction, this being reflected by the weakening of lines of the corresponding hydrates on the X-ray photographs. This process is even more intensified at 800°C, when parallel to it commences the crystallization of anhydrous calcium silicates it being signified by rudimentary relicts on X-ray photographs with d=2.18; 2.70; 2.80 Å pertaining to wollastonite. The presence in rehydration products at this temperature of residual hydrosilicates is signified by low-intensity endoeffects at 200 and 780°C as well as by the presence of valent oscillations in the OH-group within the band range of 3600 cm^{-1} on the spectrogram; the presence of silica gel is indicated by the absorption band 960-1000 cm^{-1} and the presence of anhydrous crystalline substances is confirmed by the endoeffect at 780°C connected with their recrystallization and being the most intensive for the hydrate $2.5CaO \cdot SiO_2 \cdot nH_2O$. The identity of the rehydration process at 600°C and 800°C is signified by close strength characteristics of samples right after their pressure moulding, the samples having been obtained from rehydration products at these temperatures. However, their strength rises in the course of time under dry-air and water conditions to a greater extent in samples of more amorphous dispersions (600°C), this being due to the process of substance structure ordering. The rehydration at 1000°C is accompanied by the crystallization of unstable anhydrous silicate phases.

These formations rehydrated within the temperature range of from 600-1000°C display a tendency both to the contact and the hydration hardening.

The rehydration processes of Portland cement clinker products are more complex on account of the polymineral substance composition, although the changes in the physical state of the substance occur in the same succession, i.e. through the crystallization of hydrates, their amorphization up to the formation of unstable anhydrous crystalline phases.

The above investigations show that the dispersed hydrosilicates and their rehydration products, while in the metastable state, reveal the capacity of condensing into wa-

ter-resistant bodies at the moment of contact forming between them irrespective of their substance composition. As can be seen from the data of Table III, this capacity is not connected with the presence of chemically combined water in the substance.

Table III

Content of chemically combined water in hydrates and their rehydration products

Rehydration temperature, °C	Specific surface, cm^2/g			Loss of ignition, %		
	Designation of hydrates					
	A	B	C	A	B	C
100	7400	6500	6400	23.00	21.60	16.70
400	7100	5900	6350	15.30	12.20	8.20
600	8000	6100	6000	10.81	9.67	5.23
800	8100	6800	7100	2.63	4.40	0.32
1000	4000	3560	5600	0	0	0

The ability thus established is explained by that all the investigated substances, while in the unstable state, have surplus free energy which becomes apparent during the condensation of these substances in the form of reciprocal attraction forces directed at the structure ordering, i.e. at the displacement of microparticles in a macrosystem aimed at its compaction and further order establishment. This energy has to be transformed into thermal energy and be emitted as a thermal flux when the particles approach.

Such thermal energy liberation has been recorded by Yu.A.Shepljakov by differential thermobarographic analysis which enables the recording of the thermal effect at the moment the pressure-moulding load acts upon the standard and examined dispersions. When standard and examined dispersed substances of stable crystalline structure are pressure-moulded, no energy is liberated throughout the entire interval of the moulding pressure increase. Due to this the differential thermobarogram appears as a straight line. In the studies of ground clinker and β-C_2S, their hydration products, as well as products of their partial and complete rehydration, i.e. substances of unstable structure, the thermobarograms have recorded exothermic effects. This can be explained by the transformation of kinetic energy, spent on structure ordering, into thermal energy and confirms the above assumptions.

The reciprocal attraction forces of unstable structure macroparticles, like gravitational ones, are incapable of saturation. They allow attraction of a considerable number of other particles due to which they cannot be explained by chemical bonds which, as is generally known, can be saturated. These forces surpass considerably the gravitational ones, but have an insignificant radius of action and because of that can be referred to as electromagnetic surfaces forces.

CONCLUSIONS

Ground cement clinker and β-C_2S, as well as the dispersed products of their hydration, partial and complete rehydration are capable of instant condensation into water-resistant stone during their pressure moulding both in dry and wet state. In this connection all of them can be regarded as hydraulic binders of contact hardening.

The formation processes of constructional and technological properties of the concrete stone on the basis of such binders and hydration hardening binders are accompanied by liberation of thermal energy. Their resulting quality and direction depend on the kinetics of the internal energy changes in the stone, which can be determined as a sum total of rest energies of particles it has been condensed from; the kinetic energies of these particles moving in a certain manner in a resting body and of potential energies of fields accomplishing the interaction between the particles, or potential energies of attraction forces between them.

The control of the rate at which the internal energy of the stone is changing opens possibilities of controlling the process of its structure and properties formation. So, in the pressure-moulding of Portland cement and β-C_2S powders, as well as of completely rehydrated products of their hydration, both dry and wet, water-resistant stone is condensed which has an initial strength. However, this strength and its growth in the course of time depend on the presence of water in the system.

This follows from the fact that the initial strength of the stone obtained from dry powders often proves to be lower than the strength of a stone pressure-moulded from the mixes of these powder with water. The higher is the basicity of the powders, the greater is the water effect. It is explained by that the internal energy of bodies condensed from dry powders represented by substances capable of chemical hydration by

water proves to be higher and its decrease is slower than in bodies condensed from mixes of these powders and water. The process of internal energy changes in such anhydrous systems can be speeded up by impregnating the anhydrous stone with water. In the latter case the rate of the stone strength growth and the strength itself considerably exceed these parameters in a stone obtained from wet powders. When powders of aqueous mineral systems are used, such as the hydration products of the aforementioned anhydrous formations and their partial rehydration, the structure stabilization, strength growth in the course of time and the decrease of the internal energy of a concrete stone synthesized from dry powders runs faster than in a stone made of the mixes of these powders with water.

This permits an assertion that water, while being not a determining factor in the condensation of binding systems into a water-resistant concrete stone, in a number of cases can serve as one of the control factors in the rate of changing its constructional and technological properties. It must be noted that the degree of water effect is determined not only by the mere fact of its presence in the system but depends on the time of its introduction - before or after the moulding of the stone.

The binders and concretes of the contact hardening make it possible to extend the nomenclature of hydraulic binders and to diversify their production technique; to obtain structures fully water-resistant and having their design strength immediately after their pressure-moulding; to bring the production technology of the concrete structures as close as possible to the metal-working technology and to develop principally new highly productive technological methods not used in this field hitherto.

Although some of the above possibilities seem at first sight quite hypothetical, they signify that we have reached the stage when the prospects for the development of the artificial stone production on the basis of the principles of the structure ordering effect are far beyond those limits which are considered conceivable [illegible] generalized form they reveal one o[illegible] w tendencies in the world's devel[illegible] of the building materials producti[illegible]

REFERENCES

БИБЛИОГРАФИЯ

1. Мощанский Н.А. Труды совещания по химии цемента, М.,1956,стр.114-125.
2. Журавлев В.Д. Химия вяжущих веществ.Л., 1952, стр.12-18.
3. Боженов П.И.,Глуховский В.Д.,Рунова Р.Ф. Труды конференции ЛИСИ, Л.,1973г.,стр.7.
4. Щелочные и щелочно-щелочноземельные гидравлические вяжущие и бетоны. Под редакцией проф.Глуховского В.Д.,К.,"Вища школа",1979г.,стр.15-50, 180-220.
5. Глуховский В.Д.,Рунова Р.Ф. Труды VI Международного конгресса по химии цемента, т.II, М., 1977,стр.116-118.

The Influence of the Content and Distribution of Alkalies on the Hydration Properties of Portland Cement

Influence du contenu et de la répartition des alcalis sur les propriétés d'hydratation du ciment Portland

B. OSBAECK, F.L. Smidth & Co. A/S Vigerslev Alle 77,
E.S. JONS, DK-2500 Valby, Copenhagen, Denmark.

RESUME : Les alcalis contenus dans le clinker de ciment Portland se trouvent, en partie, sous la forme de sulfates solubles, et en partie sous la forme de composants des minéraux de clinker. L'effet des alcalis sur l'évolution des résistances du ciment peut être attribué à des modifications de la composition de la phase liquide causées par les sulfates alcalins, ou à des modifications des propriétés hydrauliques des minéraux de clinker causées par les alcalis dans leurs réseaux cristallins.

Pour pouvoir évaluer l'importance de la répartition des alcalis, il a été cuit en laboratoire une série de clinkers qui ne se différencient les uns des autres que par leur teneur en alcalis et la répartition de ceux-ci. A partir de ces clinkers, on a produit des ciments d'une teneur en gypse variable.

Les propriétés de résistance des ciments ont été étudiées en mesurant les résistances du mortier à la compression. Pour des ciments choisis, le degré d'hydratation du C_3S, C_3A et C_4AF a été emsuré à différents intervalles.

L'effet général obtenu par le déplacement des alcalis des minéraux de clinker dans les phases de sulfates par augmentation du contenu de SO_3 dans les clinkers a été une augmentation des résistances initiales et une diminution des résistances ultérieures. Des teneurs élevées de gypse dans les ciments semblent amoindrir ces effets.

Sur la base des mesures du degré d'hydratation sont discutées les causes possibles des effets observés sur les résistances.

SUMMARY: The alkalies in Portland cement clinker are found partly as soluble sulphates and partly as constituents of the clinker minerals. The effects of alkalies on the strength development properties of hydrating cement can be attributed to changes in the composition of the liquid phase mainly caused by the alkali sulphates, or to changes in the hydraulic properties of the clinker minerals caused by the presence of alkalies in their lattice structure.

In order to evaluate the importance of the distribution of the alkalies, a series of laboratory-burned clinker, differing only in content and distribution of alkalies, have been prepared, and have been ground to cement fineness at various gypsum addition levels.

The strength-producing properties of these cements have been investigated by measuring their mortar compressive strength. Selected cements were subjected to determinations of degree of hydration of C_3S, C_3A, and C_4AF at various ages.

Transferring alkalies from the clinker minerals to sulphate phases, achieved by increasing the SO_3-content in the clinker, generally resulted in an increase in early strength and a decrease in late strengths. High gypsum contents in the cements tended to weaken the effects.

Based on results of the degree of hydration measurements, possible causes of the observed effects on strength are discussed.

INTRODUCTION

Industrially manufactured Portland cement clinker normally contain 0-2% of alkalies. Despite these low levels, however, alkalies have been shown to have a strong influence on many of the properties of Portland cement (1). Furthermore, recent investigations have indicated that the variations in strength-producing properties of industrially manufactured Portland cement clinker may be due largely to variations in their alkali content (2,3).

The alkalies in Portland cement clinker are present partly as easily soluble sulphates and partly as constituents of the clinker minerals (4). The investigations mentioned above have indicated that it is the soluble alkalies that affect strength. Moreover, additions of alkali salts to a cement have been shown to affect its strength development in fundamentally the same way (2,5-7). On the other hand, several authors have demonstrated that incorporation of alkalies into the structure of the clinker minerals may change their hydraulic properties (8-10); thus changes in strength properties of clinker due to such effects should also be considered.

In order to evaluate the importance of the distribution of alkalies, a series of laboratory-burned clinker, differing only in content and distribution of alkalies, have been prepared, and their strength-producing properties have been investigated in cements containing varying amounts of gypsum.

EXPERIMENTAL

Clinker: A raw mixture was prepared from naturally occurring materials of low alkali- and SO_3-content. The desired alkali- and SO_3-contents were obtained by adjusting this raw mixture with additions of K_2SO_4, K_2CO_3, Na_2SO_4, Na_2CO_3, and $CaSO_4$ sufficient to allow for volatilization during the burn.

A clinker burning was carried out according to the following procedure: 300 g of the raw mix, ground to <90µ, is packed loosely in a platinum crucible and calcined at 950°C. Then the crucible is covered and placed in an electric furnace at 1450°C. After 40 minutes the furnace is switched off. When the temperature has decreased to 1300°C, (in about 30 minutes) the crucible is removed from the furnace and permitted to cool further in laboratory surroundings.

Each clinker was composed of 3-5 batches of clinker prepared as described above; the composition was checked by full chemical analyses, including determinations of soluble alkalies (ASTM C-114).

Cement: Cements of varying SO_3-content were prepared by grinding the clinker with different amounts of a 1:1-mixture of gypsum and hemihydrate. After each cement had been ground for 15 minutes in a ball mill, its SO_3-content, specific surface (Blaine) and grain size distribution (LASER-granulometry) were checked.

TABLE I

Chemical Composition of Clinker

Clinker:		K-2	K-4	K-5	K-6	K-7	K-8	K-9
Chemical analyses	SiO_2	22.92	22.81	22.87	22.32	22.11	22.53	22.17
	Al_2O_3	5.36	5.36	5.33	5.20	5.33	5.30	5.51
	Fe_2O_3	2.98	3.09	3.14	3.02	2.86	2.99	2.83
	CaO	65.77	65.37	65.24	64.82	64.35	63.78	62.86
	MgO	1.25	1.23	1.22	1.20	1.28	1.26	1.20
	K_2O	0.35	0.75	0.76	0.76	1.20	1.19	1.26
	Na_2O	0.26	0.55	0.53	0.54	0.74	0.79	0.71
	SO_3	0.34	0.34	0.68	1.20	0.53	1.00	1.96
	L.o.i.	0.82	0.63	0.46	0.54	0.79	0.37	0.52
	free CaO	0.53	0.63	0.69	0.56	0.57	0.55	0.49
	$(K_2O)_S$	0.15	0.33	0.49	0.60	0.59	0.83	1.03
	$(Na_2O)_S$	0.09	0.14	0.18	0.25	0.14	0.25	0.42
Bogue-calc.	C_3S	51.0	49.7	48.6	52.0	51.6	46.2	43.2
	C_2S	27.3	28.0	29.0	24.8	24.5	29.8	31.1
	C_3A	9.2	9.0	8.8	8.7	9.3	9.0	9.8
	C_4AF	9.1	9.4	9.5	9.2	8.7	9.1	8.6
Alkali-distr.	K_{tot}	0.75	1.59	1.57	1.58	2.32	2.39	2.34
	MSO_3	0.54	0.25	0.51	0.89	0.27	0.49	0.99
	K_S^{II}	0.29	0.54	0.76	0.98	0.80	1.21	1.67
	K_{-S}^{II}	0.46	1.05	0.81	0.60	1.53	1.18	0.67

Mortar: The strength development of the cements prepared was tested using a "small prism" method similar to the ISO-RILEM-method: From a mortar mix of 3 parts of standard sand, 1 part of cement, and 0.5 parts of water, 4 small prisms (2 x 2 x 15 cm) are cast. Since each prism is cut into 3 pieces (2 x 2 x 5 cm), each casting yields 12 pieces for compressive strength testing. In the present investigation, the following number of specimens were broken at each age: 1 day (2) - 3 days (3) - 7 days (2) - 28 days (3), and 90 days (2). The strength results obtained using this method are about 25% higher than those obtained by the ISO-RILEM-method. The bulk density of the prisms was measured after 1 day of hardening.

Paste: The degree of hydration of the clinker minerals after 1, 3, and 28 days of paste-hardening (w/c = 0.44) was measured in selected cements by means of X-ray diffraction with 10% CaF_2 as internal standard. The C_3S-content was established from the peaks at 30.1° and 51.7° 2θ (Cu - Kα). The contents of C_3A and C_4AF were measured after extraction of the silicate-phases with a solution of salicylic acid in methanol. A reliable measure ment on C_2S could not be achieved.

Prior to their use for determination of the degree of hydration, the paste samples, in the form of small, 1 cm^3 cylinders, were tested for compressive strength. The results were in good agreement with the results from the mortar specimens, but the reproducibility lower.

TABLE II

	Cement: Composition & Fineness						Mortar: Density & Compr.Strength					
	$C\bar{S}H_x$ %	$\bar{S}_{tot}$ %	n	R_{20} %	Blaine m^2/kg	B(4%) m^2/kg	γ_1 kg/m^3	σ_1 MPa	σ_3 MPa	σ_7 MPa	σ_{28} MPa	σ_{90} MPa
C-2.1	1.4	1.00	0.83	31.7	328	355	2293	4	25	45	82	94
C-2.2	4.0	2.28	0.82	32.7	366	366	2306	15	36	54	86	100
C-2.3	7.2	3.76	0.81	33.0	408	376	2285	17	40	56	83	94
C-2.4	10.3	5.29	0.86	32.7	430	367	2298	15	30	44	81	
C-4.1	4.0	2.26	0.83	40.2	319	319	2282	13	31	48	77	85
C-4.2	7.6	4.03	0.87	37.5	384	348	2275	17	39	56	76	83
C-4.3	10.2	5.38	0.79	36.9	399	337	2276	15	35	52	75	85
C-4.4	12.2	6.35	0.84	32.3	465	383	2273	16	32	39	67	
C-5.1	4.0	2.65	0.86	37.2	323	323	2287	15	33	17	70	83
C-5.2	6.9	3.95	0.86	37.8	359	331	2259	15	36	48	66	79
C-5.3	9.5	5.36	0.87	35.8	404	349	2273	17	35	53	76	92
C-6.1	2.5	2.50	0.89	38.6	330	344	2247	15	27	41	63	71
C-6.2	4.0	3.26	0.89	37.0	356	356	2251	20	33	45	64	75
C-6.3	5.9	4.19	0.88	39.0	357	338	2251	17	35	48	65	74
C-6.4	8.1	4.86	0.87	35.6	400	360	2258	16	38	54	72	83
C-6.5	10.3	6.16	0.92	31.4	415	352	2255	14	25	34	54	
C-7.1	4.0	2.54	0.80	39.4	316	316	2245	11	27	41	61	70
C-7.2	7.0	4.00	0.78	38.3	371	341	2266	18	38	52	69	76
C-7.3	9.6	5.17	0.79	37.0	396	340	2264	14	44	59	71	82
C-7.4	11.7	6.11	0.78	39.3	383	306	2255	12	26	33	52	72
C-8.1	3.0	2.54	0.81	38.4	322	332	2265	14	30	45	63	71
C-8.2	4.0	3.02	0.81	38.7	332	332	2257	15	30	41	58	66
C-8.3	6.0	3.87	0.82	41.6	349	329	2248	17	32	43	58	68
C-8.4	8.7	5.24	0.79	41.3	352	305	2245	11	29	44	61	77
C-9.1	1.0	2.47	0.97	43.3	255	285	2232	12	22	30	45	54
C-9.2	4.0	3.75	0.80	39.8	331	331	2291	20	35	42	57	68
C-9.3	6.7	5.10	0.78	41.3	340	313	2285	14	36	40	61	77
C-9.4	8.9	6.21	0.80	40.1	359	310	2288	12	25	36	63	82

RESULTS

The chemical compositions of the clinker are given in table I, which also includes the calculated potential mineralogical compositions. The alkali contents and distributions are characterized by the following terms: The total alkali content, expressed as $\%K_2O$-equivalent ($\bar{\bar{K}}_{tot} = K_2O + 1{,}52 \times Na_2O$), the molar ratio of sulphur to alkali ($MSO_3 = SO_3/(0{,}85 \times \bar{\bar{K}}_{tot})$), and the content of soluble ($\bar{\bar{K}}_s$) and insoluble ($\bar{\bar{K}}_{-s}$) alkalies, also expressed as $\%K_2O$-equivalent. As can be seen from the table, three levels of total alkali contents are represented (0,8, 1,6 and 2,4% $\bar{\bar{K}}_{tot}$). For the two highest levels, three different distributions of alkalies are obtained, corresponding to three different MSO_3-values.

Data describing the cements, as well as their performance in mortar, are collected in table II. The grain size distributions of the cements were well described by a Rosin-Rammler-expression; thus they are characterized by just two parameters: the steepness (n) and the 20µ-residue ($R_{20\mu}$). As expected, the directly measured Blaine values of the cements were strongly dependent on the content of gypsum. A specific contribution of about 10 m^2/kg per 1% of gypsum was evaluated by means of regression analysis on the available data. This value was used to calculate the equivalent Blaine values for cements containing 4% gypsum (B(4%)). These corrected Blaine values are assumed to give a better description of fineness variations for the clinker part of the cements.

The mortars are characterized by their 1-day bulk density and compressive strengths as measured. Differences in these strength results can be attributed to differences in clinker composition (content of alkalies and SO_3), content of gypsum, fineness and mortar density. In order to isolate the effects of clinker composition and gypsum content, the strengths were corrected for the influence of fineness and mortar density.

To eliminate the influence of fineness, equivalent strengths of cements with B(4%)= 300 m^2/kg were calculated using the following empirical values of the effect of an increase of fineness of 10 m^2/kg: + 0,9 MPa for σ_3, σ_7 and σ_{28} and + 0,45 MPa for σ_1 and σ_{90}.

The calculated bulk density of a mortar free from air is 2300 kg/m^3. Consequently the prepared mortars all contain more or less air (cf. table II). An attempt to eliminate this effect on strength consists of calculating all strength values back to the same mortar density (γ_o = 2300 kg/m^3) using the following formula:

$$\frac{\sigma_o - \sigma}{\sigma_o} = 5 \times \left(\frac{\gamma_o - \gamma}{\gamma_o}\right)$$

This is infact the commonly used rule saying that introduction of 1% air causes a 5% reduction in strength.

Fig.1 shows the 1-, 3- and 28-day strengths, corrected for differences in cement fineness and mortar density (σ"), plotted as a function of the total SO_3-content at various levels of $\bar{\bar{K}}_{total}$ and MSO_3. The results show a marked effect of the total SO_3-content on early strength. Increasing clinker MSO_3 results in higher 1-day strengths for total-SO_3-contents up to about 4%. All cements of higher SO_3-content seem to yield equal 1-day strengths.

For cements with 4% gypsum (framed points in fig. 1) a clear positive effect of increasing MSO_3 is found. However, the effect could be interpreted as a combined effect of increasing the total SO_3-content in the cement and increasing the fraction of soluble alkalies. After 3 days of hardening the initial advantage of a high MSO_3 has disappeared, and later on a negative effect becomes dominant. It is clear from fig. 1 that increasing $\bar{\bar{K}}_{total}$ or MSO_3 at constant $\bar{\bar{K}}_{total}$ brings about a decrease in 28 days strength. Apparently, this negative effect is diminished when the total SO_3-content in the cement is increased up to the optimum level regarding 28-days strengths.

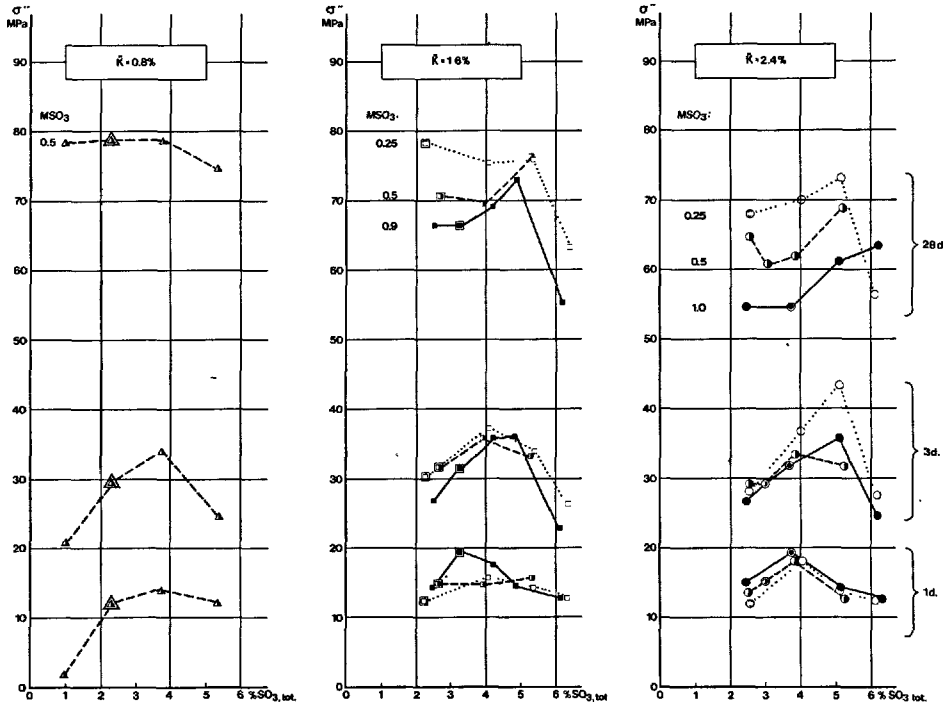

Figure 1:
Mortar compressive strength (corrected to same clinker fineness and mortar density) versus total SO_3-content of cement. Shown for three different total-alkali levels ($\bar{\bar{K}}$) and three different clinker SO_3-to-alkali mole ratios (MSO_3).

DISCUSSION

A previous statistical investigation on strength properties of plant-produced clinker showed that the content of soluble alkalies was the parameter correlating most strongly to strength (2). That it is the soluble part of the alkalies which are most important for strength properties has been verified in the present work.

Fig. 2 shows the close connection between 28-day strength and content of soluble alkalies in clinker. The previously found quantitative effect of - 10 MPa per 1% increase in $\bar{\bar{K}}_S$ is verified here recalling that 10 MPa in ISO-RILEM-strength corresponds to 12,5 MPa in the method used here.

The previous findings were based on cements containing 4% gypsum. The present investigation indicates that the negative effect can be somewhat counteracted by adding more gypsum, but in these cases the SO_3-contents of the cement will exceed the limits of 3-4% SO_3 presently specified in cement standards. The side effects of such high SO_3-contents could be expansion problems and, as indicated here, reduced early strengths (fig. 1). Too much gypsum may be detrimental to strength development even up to 28-days (fig. 1 and 2).

Strength results in fig. 1 and 2 are corrected for differences in cement fineness and mortar density. It could be argued whether the latter correction is relevant, as there seems to be a correlation between mortar densities obtained and content of soluble alkalies (Table II). It is assumed that the presence of soluble alkalies causes entrainment of air in mortar during mixing by promoting premature structure formation in the paste (precipitation of gypsum, syngenite or ettringite). Such an indirect effect of alkalies will introduce a general reduction of strength at all ages, but most pronounced at late ages.

As this air-entraining effect presumably is strongly dependent on the mix properties and mixing procedure, we have chosen in this presentation to evaluate the effects of alkalies on strength after applying corrections for density differences.

Apart from a potential density effect, alkalies may affect strength development in the following ways:

- By changing the rate of hydration of one or more of the clinker minerals

or

- by changing the strength producing quality of the products of hydration.

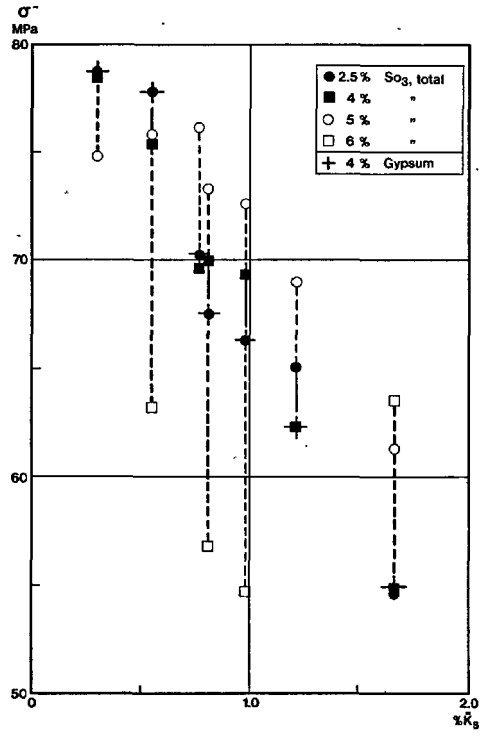

Figure 2: 28-days compressive strength of mortar versus content of soluble alkalies in clinker.

In the present study the degree of hydration of C_3S, C_3A and C_4AF after 1, 3 and 28 days has been measured in cements containing 4% gypsum. These measurements indicate an accelerating effect of soluble alkalies on hydration of all three phases (table III), which is in good agreement with their effect on 1-day strength.

It could be debated whether this accelerating effect is achieved because of more alkali in the liquid phase or because of less alkali in the clinker minerals. However, the close resemblance between the hydration and strength behavior of clinker K-5 ($\bar{K}_S$ = 0,76, $\bar{K}_{-S}$ = 0,81) and clinker K-7 ($\bar{K}_S$ = 0,80, $\bar{K}_{-S}$ = 1,52) supports the belief that alkalies influence the hydration and strength development primarily by changing the composition of the liquid phase.

The marked negative effect of soluble alkalies on the 28-days strength does not seem to be clearly linked to a corresponding effect on the degree of hydration of the clinker minerals, even though the data might give some suggestions in that direction. More data are needed to clarify such effects, and, furthermore, knowledge of the behaviour of belite in this respect is necessary to get a complete picture.

TABLE III

Cement	Degree of hydration								
	C_3S			C_3A			C_4AF		
	1d	3d	28d	1d	3d	28d	1d	3d	28d
C-2.2	0.26	0.57	0.84	0.18	0.43	0.76	0.04	0.18	0.50
C-4.1	0.37	0.54	0.75	0.18	0.40	0.70	0.00	0.14	0.41
C-5.1	0.39	0.53	0.75	0.18	0.39	0.66	0.02	0.20	0.47
C-6.2	0.44	0.63	—	0.12	0.41	—	0.00	0.20	—
C-7.1	0.33	0.60	0.73	0.14	0.49	0.66	0.02	0.25	0.43
C-8.2	0.39	0.62	0.70	0.25	0.57	0.65	0.04	0.26	0.37
C-9.2	0.56	0.69	0.74	0.27	0.56	0.62	0.11	0.32	0.43

However, the fact that soluble alkalies enhance strength only for the first three days' hydration, and inhibit its development thereafter, could be interpreted as indicating that the quality of the hydration products may be an important factor in the strength decline.

The favourable influence of high gypsum-contents on late strengths of cements rich in soluble alkalies is in good agreement with earlier findings (12-14). This effect could be due to the fact that more gypsum is necessary to counteract the faster removal of gypsum from the system caused by the alkalies. Thus the presence of gypsum to control the composition of the liquid phase is believed to be favorable for the hydration of C_3S. However, too much gypsum will be detrimental to strength development even after 28 days. This could be due to a prolonged retardation of the C_3A- and C_4AF-phases and thus a reduced contribution from these phases to the total hydrate formation.

A more profound understanding of the influence of alkalies on the strength development properties of cement must, in our opinion, be based on an understanding of the changes induced by alkalies to the complex interactions between C_3S, C_3A and gypsum. It is our hope that the present, primarily empirical investigation may serve as a source of inspiration to the investigation of such considerations.

CONCLUSIONS

The influence on cement strength of the content of alkalies in clinker is dependent on the content of SO_3 in clinker as well as the content of gypsum in the cement.

Increased SO_3 levels in clinker of the same alkali content imply that a greater fraction of the alkalies will be in a easily soluble form. The effect of this transfer of alkalies will generally be an increase of early strength and a decrease in late strengths.

However, the effects are modified by the content of gypsum in the cements. Thus the effect on early strength seems to be absent when gypsum content is higher than the optimum content. By analogy high gypsum contents tends to diminish the negative effect of alkalies on late strengths.

While the positive effect of soluble alkalies on early strength seem to be associated with a faster hydration of the clinker minerals (C_3S, C_3A, C_4AF) it is less clear whether the strength decline at later ages is due to diminutions in degree of hydration or to adverse effects on the quality of the hydrates.

An additional negative effect due to air entrainment with increasing amounts of soluble alkalies was found.

ACKNOWLEDGEMENTS

The efficient technical assistance of Kenn Svanlundh and Margrethe Møller is gratefully acknowledged. F. MacGregor Miller's critical remarks helped to clarify linguistic and conceptual difficulties.

REFERENCES

1.- I. JAWED and J. SKALNY (1978), "Alkalies in Cement: A Review. II. Effects of Alkalies on Hydration and Performance of Portland Cement", Cem. Concr. Res. 8 1, 37-51.

2.- B. OSBÆCK (1979), "Der Einfluss von Alkalien auf die Festigkeitseigenschaften von Portland Zement", Zement-Kalk-Gips 32, 2, 72-77.

3.- J. GEBAUER and M. KRISTMANN (1979), "The Influence of the Composition of Industrial Clinker on Cement and Concrete Properties", World Cem. Techn., March 1979, 46-51.

4.- H.W.W. POLLITT and A.W. BROWN (1968), "The Distribution of Alkalies in Portland Cement Clinker". Proc. of the Fifth Int. Symp. on the Chemistry of Cement, Tokyo 1968, I - 126, 322-333.

5.- K.M. ALEXANDER and C.E.S. DAVIES (1960), "Effect of Alkali on the Strength of Portland Cement Paste", Austr. J. Appl. Sci. II, 1, 146-156.

6.- E.M.M.G. NIËL (1968), "The Influence of Alkali-Carbonate on the Hydration of Cement", Proc. of the Fifth Int. Symp. on the Chemistry of Cement, Tokyo 1968, II - 117, 472-486.

7.- L.D. ERSHOV and A.S. TIMOFEEVA (1972), "Effect of Alkalies on the Hydration Process and Strength of Portland Cement", Tsement 10, 17-18.

8.- M. REGOURD and B. MORTUREUX (1977), "Tricalcium Aluminate in Synthetic Solid Solutions and in Cement", Summaries of Contributions to a Seminar at the University of Technology, Eindhoven, The Netherlands, April 13-14, 1977.

9.- A.I. BOIKOVA, A.I. DOMANSKY, V.A. PARAMONOVA, G.P. STAVITSKAJA and V.M. NIKUSHCHENKO (1977), "The Influence of Na_2O on the Structure and Properties of $3CaO \cdot Al_2O_3$", Cem. Concr. Res. 7, 5, 483-92.

10.- YOSHIO ONO, TOSHINORI HIDAKA and MASARU SHIRASAKA (1969), "On the Influence of Na_2O, K_2O and MgO on the Development of Strength of Portland Cement Mortar", The CAJ Review 1969, 61-65.

11.- H. MORI, G. SUDOH, K. MINEGISHI, T. OHTA, (1974), "Some Properties of C-S-H Gel formed by C_3S Hydration in the Presence of Alkali". The VI Int. Congress on the Chemistry of Cement, Moscow 1974, Suppl. paper, section II.

12.- J.D.S. MORJARIA (1976), "A Study of the Effects of Gypsum on the Properties of Alkali Containing Portland Cements", A Thesis subm. to The University of Trondheim 1976.

13.- I. JELENIC, A. PANOVIC, R. HALLE and T. GACESA (1977), "Effect of Gypsum on the Hydration and Strength Development of Commercial Portland Cement Containing Alkali Sulphates", Cem. Concr. Res. 7, 3, 239-46.

14.- W. LERCH (1946), "The Influence of Gypsum on the Hydration and Properties of Portland Cement Pastes", PCA Bull. 12 (1946).
(Also: Proc.Am.Soc.Test.Mat.Vol. 46).

On the reactions leading to calcium silicate hydrate, calcium hydroxide and ettringite during the hydration of cement

A propos des réactions produisant le silicate de calcium hydraté, l'hydroxyde de calcium et l'ettringite pendant l'hydratation du ciment

H.M. JENNINGS, Lecturer, and P.L. PRATT, Professor in the Department of Metallurgy and Materials Science, Imperial College of Science and Technology, London, SW 7, England.

RESUME : La première partie de cette communication examine certains aspects phénoménologiques de l'hydratation du ciment de Portland (PC), ainsi que de son constituant pur : le silicate tricalcique (C_3S). Les deux systèmes comportent une phase initiale, d'une durée d'à peu près quatre heures, pendant laquelle il y a très peu de réaction. Pendant cette période, il paraît se produire dans le ciment Portland une sorte de membrane qui crée la prise initiale du ciment. Au contraire, le C_3S paraît seulement former une couche légère d'hydrate qui se délite lentement. Pendant toute cette période, les ions de calcium et aussi l'hydroxyde se dissolvent. A la fin, l'hydroxyde de calcium est précipité d'une solution sursaturée et une réaction rapide s'amorce, produisant un gel de C-S-H. Avec le PC, des aiguilles d'ettringite sont produites après la phase initiale.

Les produits courants qui se forment dans le PC peuvent être distingués, soit par leur composition, soit par leur morphologie. Par contre, si la composition de la phase aqueuse varie, la composition des produits qui se forment peut changer dans une gamme beaucoup plus large. Les produits peuvent alors comporter une plus grande variation que celle que l'on rencontre normalement. Ce fait, et d'autres résultats qui indiquent que la formation de l'hydrate de calcium et de l'ettringite résulte d'un mécanisme de réaction en solution, conduisent à penser que le C-S-H est produit par une réaction "quasi solide".

Une théorie du mécanisme des réactions mettant en jeu C_3S, ou C_3S + C_3A et le gypse est esquissée. Dans tous les cas une enveloppe inhibitive se forme autour des grains pendant la période initiale.

Avec le C_3S pur, cette membrane est fragile et se délite rapidement; une nouvelle enveloppe se forme immédiatement dès que la solution aqueuse augmente de pH. Avec le ciment Portland, cette enveloppe est plus robuste. Pendant la période initiale, l'eau pénètre dans les grains, et dès que la réaction s'amorce, un gel de C-S-H se forme, dont l'inhibition diminue avec le développement de la réaction, ce qui termine la phase initiale. La couche pauvre en calcium réagit rapidement, ensuite une réaction, modérée par la diffusion de l'eau vers le centre des grains, se poursuit dans les couches non encore hydratées. Dans le ciment Portland, des aiguilles d'ettringite se forment alors, probablement par osmose.

SUMMARY : The first part of this paper explores some phenomenological features of both the hydration of portland cement (PC) and the pure constituent of tri-calcium silicate (C_3S). Both systems exhibit an induction period lasting about four hours where very little reaction takes place. During the induction period the PC system appears to form a membrane which is responsible for the initial "set" of cement. C_3S, on the other hand, appears to have only a delicate hydrate layer which slowly exfoliates. Throughout this period both calcium and hydroxide ions enter solution. At the end, calcium hydroxide precipitates from a supersaturated solution and rapid reaction takes place forming a C-S-H gel. In PC ettringite needles form during the post induction period.

The usual products which form in PC can be separated both compositionally and morphologically. In a system where compositions of the aqueous phase are altered however, the composition of products formed can be varied throughout a much wider range. The products, therefore, can tolerate greater variation than is normally seen. This, coupled with other results indicating that both calcium hydroxide and ettringite form by essentially through solution reaction mechanisms suggests that C-S-H forms by a reaction taking place in the "quasi solid" state.

An overall mechanism for the reaction of C_3S, and of C_3S with C_3A and gypsum, is outlined. Both cases form an inhibitive envelope around the particles during the initial stages. For pure C_3S, the delicate membrane exfoliates and a new one immediately forms as the unreacted surface is exposed to high pH aqueous phase. For PC the envelope is much more robust. Throughout the induction period water is imbibed into the "solid" and when finally a reaction takes place a C-S-H gel product forms which no longer inhibits further reaction, thus ending the induction period. The calcium-depleted layer quickly reacts followed by diffusion-controlled reaction of the unaffected core. In PC ettringite needles then form, possibly by an osmotic mechanism.

INTRODUCTION

Of the several early products formed during the hydration of Portland cement (PC), by far the most important are calcium silicate hydrate (C-S-H), calcium hydroxide (CH) and ettringite ($C_3A.3\bar{C}S\bar{H}_{32}$) and related phases referred to as AFt.[3] In addition to detailed study of many aspects, both chemical and physical, of the overall reaction, each constituent has been studied in detail by first simplifying the system to the pure reactants. This paper combines some results of a microscopic investigation of the hydration of both PC and the pure constituent C_3S, with some other experimental observations obtained both in our laboratory and reported in the literature. The purpose is to attempt to produce a self consistent model for the mechanisms of important hydration reactions.

REACTIONS OCCURRING IN PORTLAND CEMENT

The products which form by the end of the first few days of reaction at W/C ratios of 0.5 are chemically and physically very distinct. Although the exact compositions are not critical to this paper the following suggests average impurities typically (1) found in the principle phases in PC. For C-S-H impurities in ratios Si:Al, Si:Fe and Si:S of 11, 43 and 15 respectively occur. AFt has roughly the composition of ettringite but may contain Si and may have some sulphate replaced by hydroxide. CH is usually quite pure but may contain small amounts of silicate. Figure 1 is an electron micrograph of a five day old specimen which has been kept moist (2) during observation; a number of phases are shown growing into an open pore. Although the morphology changes somewhat during drying (2), analytical microscopy has established that the square-ended bundles of needles compositionally are consistent with ettringite; it should be noted that all needle-like morphologies observed in PC contain various amounts of the appropriate elements of AFt. The thin transparent membranes around and between the needles are almost certainly C-S-H because when dried and placed in an analytical microscope Ca and Si can be detected almost exclusively. Underneath this detached surface layer of C-S-H and making up the major fraction of C-S-H in hydrated PC, is a finer, less structured product. Here, significant quantities of impurities may be present, as reported by Lachowski et al (1). Small crystals of CH form throughout the surface products, as seen near the base of the needles, and with the passage of time they can often grow forming large well-faceted crystals.

Ettringite formed in PC is crystalline while C-S-H is amorphous, and although both are non-stoichiometric materials they can be separated compositionally. It is interesting to note that the highest substitution of impurities seems to occur in fine grain completely hydrated specimens (3). Under contrived conditions (4), however, the compositional distinction between AFt phases and C-S-H can become blurred. For example, in fibres, Figure 2, grown by the "dilution technique" (4) and containing various amounts of Al, S and K, the Si count can vary from 0-80% of the total depending on the details of the dilution; the other elements can exhibit great variation as well. $Ca(OH)_2$ on the other hand, exhibits almost no compositional variation. In spite of the great compositional variation that can be tolerated in products in the PC system the fact that relatively pure C-S-H and AFt form simultaneously, particularly in the early stages and in intimate proximity with one another demands that they have separate formation reactions in the hydrating PC system.

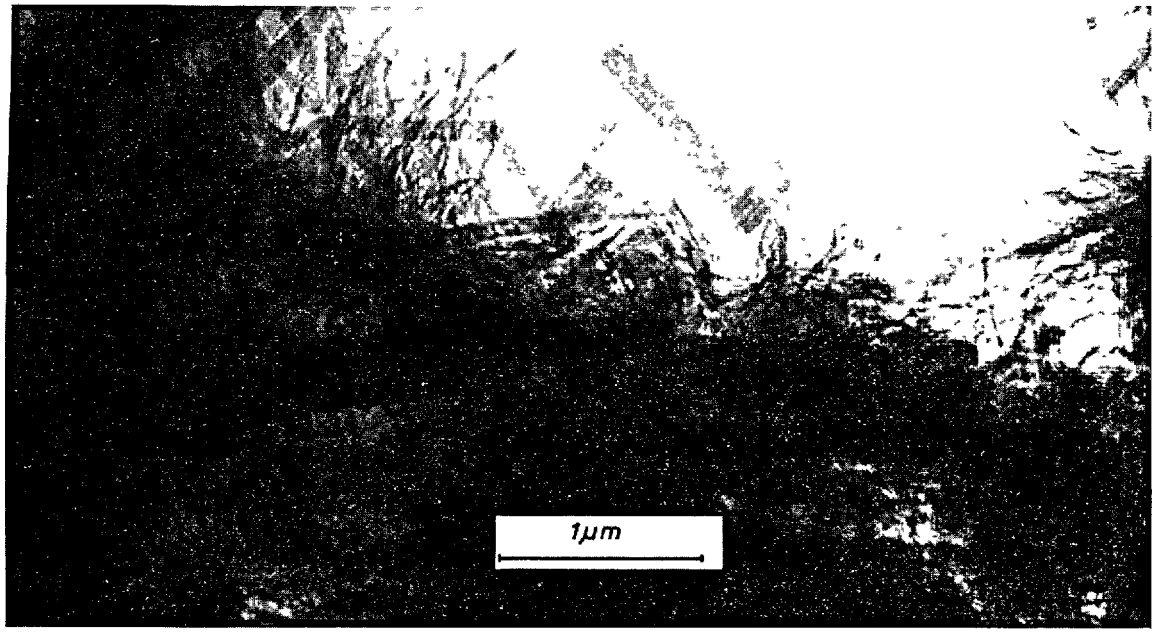

Fig. 1 - H.V.E.M. and wet cell micrograph of 5 day old, W/C = .5, specimen. Square-ended needles contain Al, S and Ca whereas thin foils contain Ca and Si exclusively.

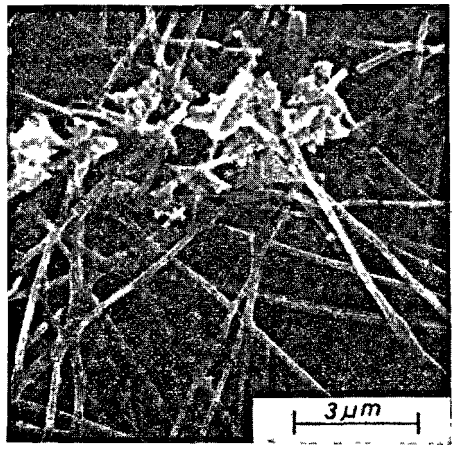

Fig. 2 - SEM of fibres, containing variable amounts of Al, S, K, Si and Ca grown by dilution technique.

In describing the various reactions which take place, it is important to define the location of the reaction site. When a grain of cement is placed in water certain elements dissolve and water may start entering the boundaries of the grain. As water continues to enter the grain a layer near the surface may lose some of its solid properties, becoming a quasi-solid. Thus, this paper will refer to solution reactions, quasi-solid reactions and reactions that take place on the surface between the two. There is, of course, an unreacted core where no reaction has yet taken place.

Although in PC there is a tendency for the smaller particles to be rich in Al phases most particles are polymineralic. Thus, on average, any one particle contains the elements required for all products.

Formation of Calcium Hydroxide:

CH appears to form from solution by a process of precipitation. The concentration of calcium ions is known to become supersaturated with respect to calcium hydroxide very soon after mixing with water and towards the end (or at the end) of the induction period nucleation takes place throughout the solution. In spite of the fact that many elements and ions are in solution it seems that bonding requirements and a rather inflexible structure hinder the incorporation of foreign atoms into CH. It is interesting to note (5) that the precipitation of CH in the presence of excess silicon ions is retarded and this could be related to structural intolerance of impurities.

Formation of Ettringite and related AFt:

There is evidence to suggest (6,7) that ettringite also forms via a solution mechanism. Although there may be a tendency for crystalline square-ended ettringite needles to form preferentially on C_3A grains the evidence is that, like Portlandite, AFt phases also precipitate throughout the solution on the surface of the particles. For example, some experiments (4) show evidence for a membrane covering the particles of PC, but only when they exist in an aqueous solution containing the relevant elements for at least a matter of 15 minutes. If placed in large quantities of distilled water a distinct membrane never forms, suggesting that at least some of the constituents must dissolve reaching a certain concentration before they can precipitate. When the membrane has formed, hollow needles can be grown by adjusting concentrations so as to encourage an osmotic mechanism as in Figure 2. Since similar needles, are found in ordinary PC systems growing into pores, Figure 3, we suggest that some of the ingredients are pumped down the centre of the needle to the end where reaction takes place causing further growth. Although data on the solubility of Al is scarce it may be that only very small quantities of Al are in solution, particularly in the presence of sulphates, and this may account for the slow reaction of C_3A in the early stages of hydration. In fact the formation of a membrane may involve the transportation of all ingredients except Al through solution, while Al is transported to the reaction site through the solid where it either reacts or dissolves and reacts and precipitates. At some time after the membrane forms, needles start to grow.

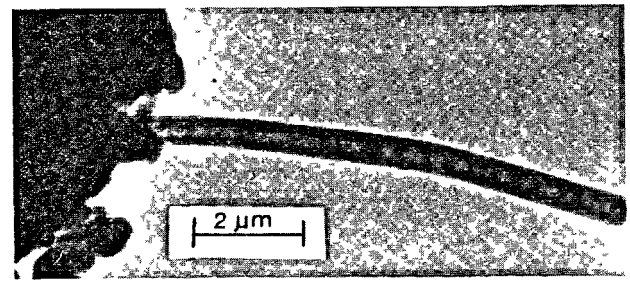

Fig. 3 - H.V.E.M. and wet cell micrograph of 6 day old P.C., W/C = 5. Fluid in needle shot out just before photo was taken.

Here, Al rich material may be transported down the centre of the needles whereupon it reacts with other elements that are in solution. More generalized dissolution-precipitation throughout the solution may account for a variety of morphologies, but we feel that the AFt forms via a solution mechanism and the composition of the product is related to the composition of the aqueous solution. The lack of Si in solution is the main reason why only small amounts of Si are present in AFt.

Formation of C-S-H:

Measurable quantities of silicates are found in solution only during the first few minutes (8,9) after mixing cement with water. We believe that as the pH rises the silicates precipitate out of solution forming the thin transparent membrane around all the particles present. In the PC system the dissolution of Al is suppressed in the early stages by the presence of sulphates. Thus if the product forms on C_3S substrate, the composition of this membrane appears to be largely C-S-H. If the product forms on C_3A it may contain AFt phases. After this early rapid reaction, AFt slowly forms underneath the exfoliating thin transparent C-S-H membrane.

Unlike many silicates found in nature, the C-S-H formed after the induction period is best described as an amorphous gel of colloidal dimensions and variable stoichiometry. Thus, we have considered three points regarding the formation of C-S-H in PC after the induction period: (1) it forms in a system in which there are essentially no silicates in solution, (2) it forms by a reaction which must be physically separated from other reactions taking place in PC and (3) it forms in circumstances which restrict its ability to order. Taken together a quasi-solid state reaction is suggested.

THE REACTION OF PURE C_3S

Hydrating pure C_3S exhibits an induction period, lasting about four hours, similar to that observed in PC. In the case of pure C_3S however, the "dilution technique", used previously (4) on PC systems, was unable to establish the existence of any well defined membrane.

Nevertheless, during the first few hours, we have observed C-S-H products "peeling" away from the surface, figure 4, an observation similar to that reported by Ménétrier et al (10). Our observations were made while the grains were kept moist. If the specimens are dried in air, the thin membranes formed during the induction period can become detached, figure 5, forming a morphology sometimes referred to as "cigar" shaped. Analysis shows them to have a very high calcium content with C/S = 2.5 - 3.5

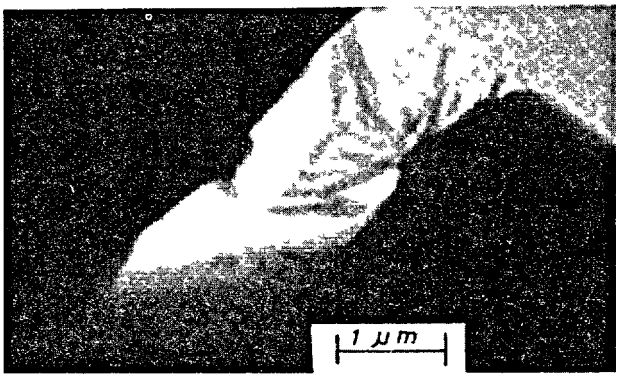

Fig. 4 - H.V.E.M. and wet cell micrograph of 3 hr hydration of C_3S, W/C = .5.

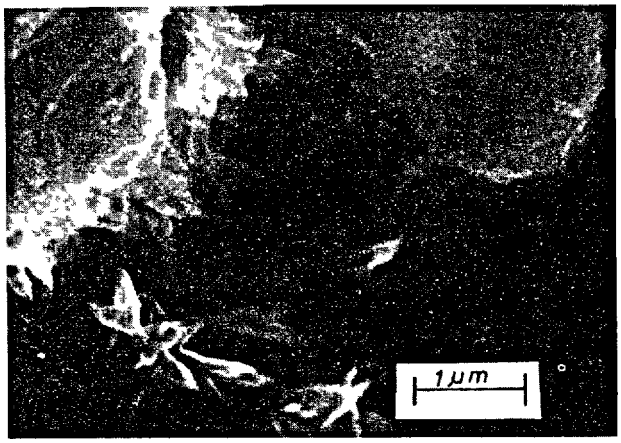

Fig. 5 - TEMSCAN of C_3S hydrated for ½ hr, W/C = .5. Thin foils are readily peeling away from surface.

At the end of the induction period a reaction occurs rapidly, forming a colloidal gelatinous layer around the particle as seen in figure 6. It should be noted that the needle morphology is absent (so long as the specimen is kept moist) and the quasi-solid region, where the C-S-H product is now forming, is in contact with the particles, where water enters the solid. As this reaction continues the bonding becomes stronger and the process of separating the particles, during preparation of thin specimens (1), can pull the gelatinous layer into the drawn out root-like morphology seen in figure 7. Thus, the often seen C-S-H needles are artefacts formed either by rolling up thin membranes or by drawing out the gelatinous product, but they are not a naturally occurring morphology.

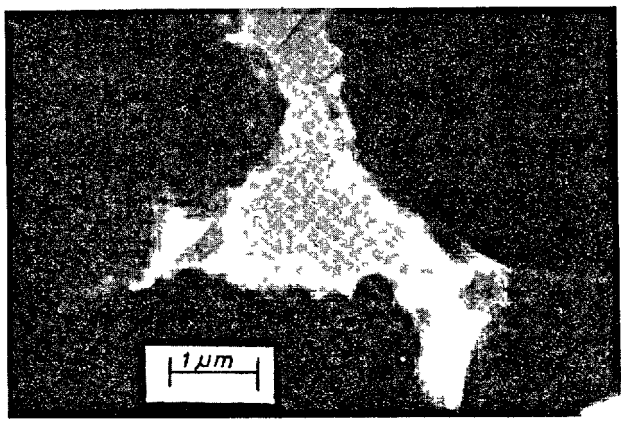

Fig. 6 - H.V.E.M. wet cell of C_3S hydrated for 6 hrs. W/C = .5.

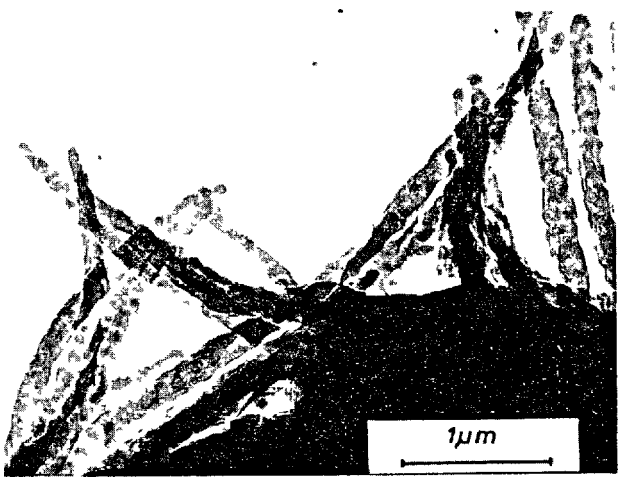

Fig. 7 - TEMSCAN micrograph of 4 day C_3S W/C = .5 showing gelatinous layer being pulled away from surface.

A MECHANISTIC MODEL FOR THE REACTION OF C_3 WITH AND WITHOUT C_3A AND GYPSUM.

This section will outline some of the important feature of our proposed reaction mechanism for PC when mixed with water. As already discussed we believe the overall reaction to be the sum of separate mechanisms which, although possibly interconnected when taken together, can lead to distinct and well-defined separate products. Figure 8 is a schematic representation of (a) pure C_3S hydration, and (b) C_3S and C_3A hydrating together.

Initial Reaction:

When either C_3S or PC is placed in water both calcium and, to a lesser extent, silica (9,11) dissolve during the first seconds. The pH quickly rises to about 12.5, (8,12) and in both cases the silica

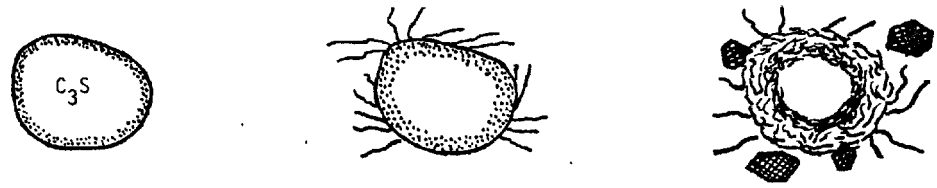

Initial Reaction Forming C-S-H coating Ca^{++} and OH^- into solution

Induction Period Exfoliating C-S-H membrane and formation of new membrane

End of Induction Period Formation of C-S-H Gel and CH.

a) Reaction of C_3S

b) Reaction of C_3S + C_3A + Gypsum

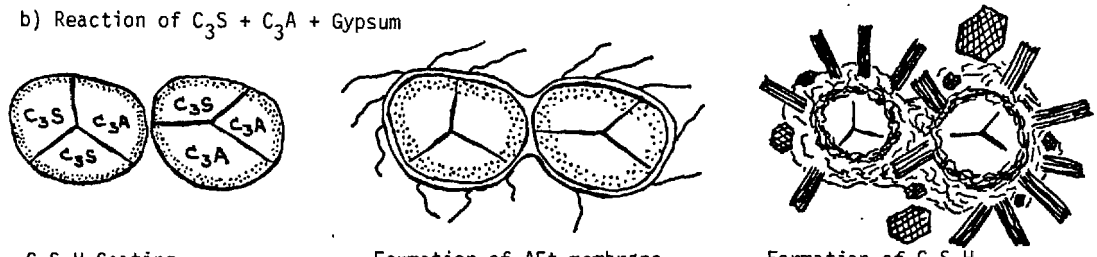

C-S-H Coating Ca^{++} and OH^- S + K into solution

Formation of AFt membrane causing particles to agglomerate

Formation of C-S-H Gel, CH and AFt needles.

Fig. 8 - Simplified schematic of reaction sequence of pure C_3S and C_3S + C_3A + gypsum.

concentration in solution quickly drops (9,11) to an almost unmeasurable level. Now Birchall, Howard and Bailey (8) have pointed out that, in the cement system, SiO is almost insoluble in the pH range of 11.0-13.5. We think, therefore, that as the pH reaches a value of about 11 a layer of hydrate with high C/S ratio precipitates from solution. For C_3S this dissolution and consequent reduction in surface calcium, followed almost immediately by precipitation of high C/S product, accounts for the fall and subsequent rise in the C/S ratio as observed on the surface by ESCA techniques (10). For PC, the initial layer of hydrate may contain small amounts of elements such as S, and possibly Al if it forms on C_3A.

Induction Period:

During the induction period calcium (and in the case of PC, S, K and possibly to a lesser extent Al) continue to dissolve and water is imbibed into the silica-enriched zone as discussed by Dent-Glasser (13). For C_3S the boundary between liquid and solid undergoes continual change and at first the thin delicate precipitated membrane peels off, exposing the underlying area to water of high pH which causes an immediate reaction forming another layer of C-S-H. In the case of PC, the initial C-S-H is slowly replaced by a membrane probably with composition approaching AFt which can form only as Al becomes available, and whose composition may change with time. Here (as opposed to pure C_3S) the continued formation of the membrane, a through-solution process which does not depend on soluble silicates, accounts for the agglomeration or "set" of PC during the early stages by enveloping and tying the particles together. Both the rheology of the mix as well as the long term course of the reaction can thus be profoundly affected by such things as the introduction of sulphates (discouraging the dissolution of Al), or artificial buffering of the pH. In both cases water continues to be imbibed slowly into an ever-thickening layer rich in silicate-species, and the membrane should be considered more enveloping and possibly inhibiting, than protective.

End of Induction Period:

In spite of the fact that all the ingredients necessary to form C-S-H are present in the "quasi-solid", the reaction does not proceed rapidly during the induction period, possibly because of the small amount of H_2O and/or because the local "pH" is not high enough. This situation is gradually overcome with the passage of time and the continued imbibing of water into the "quasi-solid". When finally the conditions become favourable for the formation of C-S-H, the induction period comes to an end and a quasi-solid state reaction takes place. Unlike the surface reaction which continually (and slowly) heals the rupturing membrane, this reaction forms a colloidal gel which is much less effective at slowing the transportation of water to the interior. At first the reaction is rapid as water flows into the volume already depleted in calcium but very quickly it becomes diffusion-controlled. As the reaction proceeds inwards fresh reaction product pushes the early product into the volume of original void space. This diffusion-controlled interior product is formed under much more constrained conditions and is therefore denser, as has been observed (14), than the product formed at the end of the induction period. There is, however, no real distinction between "inner" and "outer" product, the distinction is really between early and late product.

The end of the induction period is also signalled by the precipitation of CH. In the case of PC the wholesale destruction of the membrane, which may be considered as an envelope (behaving as an inhibiting membrane) may be encouraged by CH precipitation.

In either case the calcium-depleted layer reacts rapidly to form C-S-H without the necessity of expelling calcium. The later product, however, requires the removal of calcium before C-S-H can form. The thickness of the calcium-depleted zone before the end of the induction period can be affected by many variables that determine the amount of calcium taken into solution; this thickness can control the morphology and density of the early product as well as the distribution and morphology of the CH formed throughout.

During this renewed reaction ettringite needles, and needles whose composition resembles AFt, form in PC, possibly by local osmotic mechanisms where the now depleted calcium in solution (caused by CH formation) causes water to pump into the inside of a membrane still surrounding the particles. Micrographs showing a bulging membrane have already been reported (15).

In several respects this overall mechanism is a combination of both delayed nucleation and protective membrane theories. The nucleation of C-S-H is delayed by the membrane which in the case of C_3S is very thin and is continually rupturing and rehealing. When, however, the gel finally starts to form under the membrane it forms a product which is no longer protective and a renewed reaction starts. Because the early product remains this model is different from the proposal that an early protective product slowly transforms into a non-protective product.

CONCLUSIONS

1. The reactions forming C-S-H and ettringite and AFt are separate in the PC system. C-S-H forms by a quasi-solid state reaction and ettringite and AFt form from solution.

2. In the pure C_3S system C-S-H forms from solution only during the first few minutes of reaction. This forms a thin inhibitive membrane (slowing the transportation of water) which is repaired by a surface reaction. When a reaction takes place in the quasi-solid state the product is gelatinous and no longer has inhibitive properties.

3. Portlandite forms from solution but its structure tolerates less impurities than other phases present.

REFERENCES

1. - E.E. LACHOWSKI, K. MOHAN, H.F.W. TAYLOR and A.E. MOORE, "Analytical Electron Microscopy of Cement Pastes" submitted to J. Am. Ceram. Soc.

2. - H.M. JENNINGS and P.L. PRATT (1980) "The Use of a High Voltage Electron Microscope and Gas Reaction Cell for the Microstructural Investigation of Wet Portland Cement" J. Mater. Sci. 15, in press.

3. - A.E. MOORE, Personal Communication.

4. - H.M. JENNINGS and P.L. PRATT (1979) "An Experimental Argument for the Existence of a Protective Membrane Surrounding Portland Cement During the Induction Period", Cement and Concrete Research, 9, 501-506.

5. - M.E. TADROS, J. SKALNY and R.S. KALYONCU (1976) "Kinetics of Calcium Hydroxide Crystal Growth from Solution" J. Col. Interf. Sci. 55, 20-24.

6. - P.K. MEHTA (1976) "Scanning Electron Microscope Studies of Ettringite Formation" Cement and Concrete Research 6, 169-182.

7. - M. COLLEPARDI, M. CORRADI, G. BALDINI and M. PAURI (1978) "Tricalcium Aluminate Hydration in the Presence of Lime, Gypsum or Sodium Sulphate" Cement and Concrete Research, 8, 571-580.

8. - J.D. BIRCHALL, A.J. HOWARD and J.E. BAILEY (1978) "On the Hydration of Portland Cement", Proc. Roy. Soc. Lond. A360, 445-453.

9. - C.D. LAWRENCE (1966) Special Report 90, Highways Research Board, Washington, 378-391.

10.- D. MENETRIER, I. JAWED, T.S. GUN and J. SKALNY (1979) "ESCA and SEM Studies of Early C_3S Hydration" Cement and Concrete Research, 9, 473-482.

11.- J.F. YOUNG, H.S. TONG and R.L. BERGER (1977) "Compositions of Solutions in Contact with Hydrating Tricalcium Silicate Pastes", J. Am. Ceram. Soc. 60, 193-193.

12.- J. SKALNY and J.N. MAYCOCK (1975) "Mechanisms of Acceleration by Calcium Chloride: A Review", J. Test Evaluation, 3, 303-311.

13.- L.W. DENT GLASSER (1979) "Osmotic Pressure and the Swelling of Gels" Cement and Concrete Research, 9, 515-517.

14.- T.N. TIEGS (1973) "Investigation of Ion-Thinned Tricalcium Silicate Pastes by Transmission Electron Microscopy" M.Sc. Thesis, U. Illinois, Urbana, U.S.A.

15.- H.M. JENNINGS and P.L. PRATT (1979) "On the Hydration of Portland Cement" Proc. of Brit. Ceram Soc. Ed. D. Taylor and P.S. Rogers No. 28, June, 179-193.

16.- J. SKALNY, I. JAWED and H.F.W. TAYLOR (1978) "Studies on Hydration of Cement - Recent Developments", World Cement Technology, Sept. 183-195.

ACKNOWLEDGEMENTS

We are happy to acknowledge the assistance we have received from continuing discussions with Professor H. Taylor and Dr. A. Moore, from J.E.O.L. for the use of TEMSCAN and from the Marine Technology Directorate of S.R.C. for financial support.

Propriétés électrocinétiques à la surface des minéraux du ciment Portland

Electrokinetic surface properties of Portland cement minerals

A. ZELWER, Ing. C.N.A.M. - C.E.R.I.L.H., Paris, France.

RESUME

Nous limitons les propriétés des surfaces solides apportées par les ciments en cours d'hydratation aux premières heures en excluant le début de la prise, les résultats étant destinés à améliorer l'action des adjuvants en relation avec le comportement rhéologique des bétons frais.

Le potentiel ZETA (PZ) ne rend compte des charges électriques et des énergies d'interaction coulombiennes entre particules que pour des surfaces solides en équilibre ioniques stables et au repos. Toute perturbation mécanique (agitation, malaxage) entraîne un réarrangement ionique conduisant à un PZ complètement différent, non mesurable.

Les suspensions et les pâtes de ciment sont des systèmes "dynamiques" : l'apparition, la transformation de nouvelles phases solides hydratées et l'évolution ionique de la phase liquide maintiennent hors d'équilibre une interface composite car cinq phases minérales, au moins, contribuent à l'hétérogénéité de la surface des grains : C_3S, C_2S, C_3A, C_4AF et le gypse. Pour un tel système le concept de PZ n'a pas de signification et doit être remplacé par celui de "PZ dynamique" (PZD).

La simulation d'un système "dynamique" à partir d'une suspension stable (QUARTZ-EAU) montre que les variations relatives de PZD en fonction du temps sont mesurables à condition de les relier au pH et à la force ionique de la solution en réalisant un traitement automatique instantané du mouvement électrophorétique (calculateur et anémométrie laser doppler - ALD).

En pâte concentré on ne peut pas atteindre directement les objectifs fixés : la forte sursaturation d'un volume limité de phase liquide interstitielle masque un PZD "global" ne tenant pas compte des hétérogénéités de surface.

En suspension diluée, une analyse statistique très fine des mouvements électrophorétiques rend beaucoup mieux compte des hétérogénéités de surface.

Les suspensions de C_3S et de ciment portland ont un PZD négatif (celui du C_3S est le plus faible). Le C_3A paraît avoir un PZD très fortement positif.

D'autres essais sont encore nécessaires pour confirmer ces résultats et les étendre à tous les minéraux purs du ciment.

SUMMARY

We limit our study of the properties of the solid surfaces developped by the cements during their hydration to the first hours, excluding the beginning of the set, the results are intended to put in practice a better knowledge of the action of the admixture in relationship with the rheological behaviour of fresh concrete.

The ZETA Potentiel (ZP) expresses the electrical charges and the Coulombian interaction energies between particles only for solid surfaces in a stable ionic equilibrium and in a motionless state. Every mechanical perturbation (agitation, mixing) causes an ionic rearrangement leading to a completely different immeasurable ZP.

Cement suspension and pastes are "dynamic" systems : the apparition, the transformation of new hydrated solid phases and the ionic evolution of the liquid phase, keep out of equilibrium a composite interface, since at least five mineral phases contribute to the heterogeneity of the surface of the grains : C_3S, C_2S, C_3A, C_4AF and gypsum. For such a system, the concept of ZP is meaningless and must be replaced by that of "dynamic ZP" (DZP).

The simulation of a "dynamic" system from a stable suspension (QUARTZ-WATER) shows that the relative variations of DZP in function of the time are measurable provided that they are related to the pH and to the ionic force of the solution by realizing an instantaneous automatic treatment of the electrophoretic movement (calculator and doppler laser anemometry - DLA).

In a concentrated paste it is not possible to reach directly the defined objectives : the strong over saturation of a limited volume of interstitial liquid phase conceals a "global" DZP, since it does not reflect the surface heterogeneity.

In a diluted suspension, a very minute statiscal analysis of the electrophoretic movement give a much better picture of the surface heterogeneity.

C_3S and cement suspension have a negative DZP (that of C_3S is the weakest). C_3A seems to have a very strongly positive DZP.

Other tests are still necessary to confirm these resulsts and to extend them to all pure minerals of the cement.

I. INTRODUCTION

Compte tenu de la surface spécifique élevée des minéraux du ciment en cours d'hydratation, il est intéressant de prêter une attention particulière au rôle des charges électriques de surface, à l'origine d'interactions coulombiennes entre particules, qui influencent les comportements rhéologiques des bétons frais. De leurs connaissances on peut espérer une maîtrise plus efficace de l'emploi des adjuvants spécifiques des modifications de plasticité, maniabilité, teneur en eau, etc... Pour cette raison nous nous limiterons aux premières heures de l'hydratation, à l'exclusion du début de la prise.

Mais nous allons voir que les suspensions et les pâtes de ciment en cours d'hydratation sont assimilables à des systèmes colloïdaux évolutifs, hors d'équilibre auxquels le concept habituel de potentiel électrocinétique ZETA n'est pas applicable.

Le cas des systèmes quasi-hydratés et complètement durcis, où les interfaces sont en équilibre est mieux connu et de nombreux travaux concernent des phase minérales pures (1,2,3 et 4).

Dans cette communication préliminaire nous proposons d'établir une distinction entre les systèmes "statiques" constitués par les minéraux inertes en équilibre et les systèmes "dynamiques" en adoptant pour ces derniers le concept de "PZ dynamique" (PZD).

Enfin une bonne approche expérimentale de l'étude de l'interface dynamique passe par les suspensions diluées de minéraux inertes pour les systèmes statiques (par exemple QUARTZ-EAU) et des minéraux purs du Ciment Portland pour les systèmes dynamiques.

II. POSITION DU PROBLEME

Dans le cas des surfaces solides en équilibre ionique stable (systèmes statiques) les phénomènes électrocinétiques sont bien connus. Ils font l'objet de nombreuses théories développées depuis 1910 et sans cesse affinées par l'introduction de nouveaux paramètres (5,6,7,8 et 9).

Dans un souci de simplification extrême, on rappellera que les charges électriques proviennent de l'ionisation de groupes hydratés, d'adsorption spécifique et aussi d'imperfections et lacunes du réseau cristallin ; elles constituent une couche rigide (de STERN) compensées dans la phase liquide par un environnement ionique perturbé (couche mobile diffuse) Une telle structure schématique de la double couche ionique (FIGURE N° 1 A) permet de retenir que le PZ est une différence de potentiel (en mV) entre le plan de cisaillement et la phase liquide non perturbée. En d'autres termes, c'est aussi une grandeur numérique qui intègre la quantité de charges électriques et l'énergie électrostatique de répulsion entre les surfaces solides chargées de mêmes signes. Mais ces énergies d'intéraction sont en réalité les bilans d'une composante répulsive et d'une composante de force de Van der Waols (d'attraction) qui peut l'emporter pour des distances entre solides assez petites.

Ainsi un PZ élevé caractérise un système colloïdal bien dispersé, l'état floculé correspondant à un PZ faible ou nul.

A partir d'une telle structure ionique de la double couche, tous les phénomènes électrocinétiques des systèmes colloïdaux n'ont pour origine que les déplacements relatifs de la phase solide et de la couche diffuse entraînés par la phase liquide. Il en résulte une dissymétrie statistique de la répartition des charges anioniques et cationiques. (FIGURE N° 1 B)

L'application d'un champ électrique provoque une mobilité électrophorétique des particules solides ou un déplacement électroosmotique du liquide interstitiel.

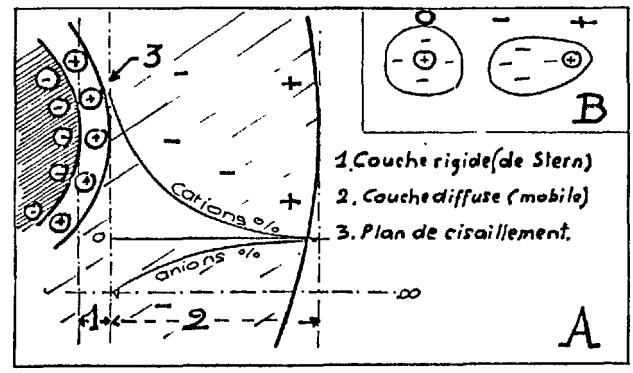

FIGURE 1 - STRUCTURE DE LA DOUBLE COUCHE IONIQUE

Par ailleurs, le déplacement forcé de cette dernière, sous l'action d'une contrainte physique (pression), donne naissance à des potentiels de filtration, d'écoulement, et même de sédimentation.

Par conséquent, un système colloïdal de type statique appelle déjà trois remarques importantes :

1°) La structure ionique d'une interface résulte d'un processus d'adsorption ionique très lent.

2°) Les paramètres utilisés pour calculer le PZ n'ont aucune signification tant que les conditions d'équilibre ioniques ne sont pas respectées.

3°) Le PZ est très sensible aux perturbations d'origine mécaniques en raison de la redistribution statistiques des ions de compensation.

Cela signifie que le concept PZ ne peut pas être appliqué sans discernement aux interfaces du type dynamique (ciments en cours d'hydratation), ceci pour plusieurs raisons :

- l'interface est toujours hors d'équilibre ionique,
- la force ionique de la phase liquide évolue durant l'hydratation,
- la transformation de phases hydratées nouvelles complique l'hétérogénéité des phases solides,
- en raison de la structure polyphasée des grains de ciment portland, au moins cinq minéraux sont présents à la surface : C_3S, C_2S, C_3A, C_4AF et le gypse.

Enfin, parmi les facteurs et paramètres importants (mis à part les effets de la température sur les isothermes d'adsorption et les vitesses d'hydratation), l'influence du pH sur le PZ est la conséquence de l'adsorption spécifique des ions OH^- qui participent à la structure de la double couche. Par ailleurs cette dernière est comprimée par tout accroissement de la force ionique, ce qui entraîne un abaissement du PZ.

III. SIGNIFICATION DU POTENTIEL ZETA DYNAMIQUE (PZD)

En pâte concentrée les variations de concentrations ioniques, dans la phase liquide (E/c = 0,3 à 0,5) suivent en fonction de l'hydratation une loi bien connue et bien située par rapport aux échéances cruciales des limites de saturation et de sursaturation en $Ca(OH)_2$, quand on considère l'hydratation du C_3S pur (10). Un équilibre très stable subsiste entre les hydrates intermédiaires et la solution tant que la limite de saturation n'est pas atteinte. La sursaturation est une condition nécessaire et suffisante de la rupture de cet équilibre, et de l'évolution exothermique des hydrates précédents accompagnant la prise. En présence des minéraux du ciment portland, on retrouve sensiblement cette même loi malgré le recul de l'équilibre de concentration en ion Ca^+ et OH^- en présence

des quantités d'ions alcalins Na_2O et K_2O (11). On a une bonne représentation, d'après les variations de conductivités λ, des variations relatives de concentration ioniques globales, en fonction de l'avancement de l'hydratation. (FIGURE N° 2 A).

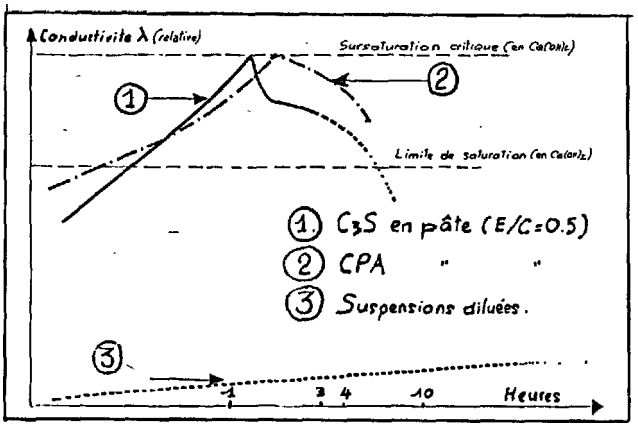

FIGURE 2 - EVOLUTION IONIQUE DES PHASES LIQUIDES INTERSTITIELLES

Il est évident que les conditions d'hydratation sont très différentes en suspension diluée (très grand excès d'eau) : la saturation n'est jamais atteinte, ce qui privilégie les phases solides hydratées intermédiaires, moins représentatives de celles des bétons frais avant prise. (FIGURE N° 2 B).

Il en résulte que pour caractériser une interface hors d'équilibre dans ces systèmes dynamiques, il faut à chaque instant relever simultanément TROIS GRANDEURS en fonction du TEMPS D'HYDRATATION :

1°) Les variations relatives, continues, du potentiel ZETA dynamique (PZD),
2°) Le pH (indication spécifique de la concentration (OH^-),
3°) La conductivité (λ) indication de la concentration globale.

Nota :

Il va de soi que l'analyse élémentaire de la phase liquide devra être également suivie si l'on veut, en présence des adjuvants, faire le bilan des ions qui participent à la structure de la double couche.

Les mesures et les calculs du PZD appliquées à de tels systèmes colloïdaux nous placent devant un problème très difficile de choix et d'accessibilité des paramètres expérimentaux vis à vis des pâtes consistantes ou des suspensions diluées. (TABLEAU I).

En pâte, la phase solide est bloquée et la seule detection électrocinétique possible est liée au déplacement de la phase liquide. Ce dernier nécessairement global, ne tient pas compte de l'hétérogénéité de la surface solide en rapport avec les différents composants minéraux présents. De surcroît, le faible volume de liquide interstitiel favorise une sursaturation trop rapide par rapport aux moyens de détection électrocinétiques et la "conductivité de surface" apportée par les solides devient une composante non négligeable et difficile à estimer. S'agissant d'une localisation de l'action spécifique des adjuvants toute spéculation sur le PZD "global" est alors hasardeuse.

TABLEAU I

PARAMETRES		MOYENS DE CONTROLES	INCIDENCES SUR L'HYDRATATION	REMARQUES
TEMPERATURE θ		Contrôle thermostatique des suspensions et de la cellule de mesure.	Vitesse d'hydratation et d'hydrolise	Action sur : viscosité - Constante diélectrique - Mobilité-déplacement des phases liquides
TEMPS D'HYDRATATION		STOCKAGE CONTINU DES DONNEES EXPERIMENTALES EN FONCTION DU TEMPS (PZD - pH - λ)	- Degré de transformation des hydrates - Degré de sursaturation - Force ionique(pH,λ)	Evolution continu de : - PZD et charges électriques - Forces d'intéractions inter-particulaires.
E/c	SUSPENSIONS DILUEES	- Temps d'hydratation écoulé. - Force ionique (pH,λ). - Analyse élémentaire des ions en solution (en fonction du temps)	- Phase liquide très diluée (force ionique faible)	Transformation incomplète des hydrates intermédiaires sur les surfaces solides
	PATES CONCENTREES	Force ionique	Phase liquide	FORCE IONIQUE ELEVEE (Compression DC et abaissement PZA).
PERTURBATIONS MECANIQUES MALAXAGE				PZD modifié non mesurable

En raison de ce qui précède et malgré des conditions d'hydratation différentes, il nous a paru beaucoup plus intéressant de nous orienter vers les suspensions diluées. Les différences de déplacements électrophorétiques des particules solides fournissent notamment des informations beaucoup plus sélectives quant à l'influence des composants minéraux.

Ce sont les variations relatives du PZD qui sont importantes (non leurs valeurs absolues) : il est impératif de réaliser des essais à la fois comparatifs et parfaitement normalisés. Les résultats expérimentaux présentés dans cette communication préliminaire sont limités, dans un premier temps, uniquement aux suspensions diluées.

IV. FACTEURS ET METHODES

Il n'est pas possible de suivre en continu les changements apportés au niveau de l'interface par le passage des suspensions dilués aux pâtes consistantes, ni de relier directement les systèmes statiques et dynamiques. Les principales techniques électrocinétiques connues, qui sont rappelées dans le TABLEAU II, sont complémentaires, mais leurs domaines d'utilisation se recouvrent peu.

Dans le cas de la microélectrophorèse des particules en suspension diluée sous un champ électrique horizontal et uniforme H, nous rappelons ci-après les facteurs et paramètres fondamentaux :

TABLEAU II

TECHNIQUE EXPERIMENTALE	DOMAINE D'UTILISATION	TAILLE DES PARTICULES	CONTRAINTE APPLIQUEE	PHASE MOBILE	MODE DE DETECTION	REMARQUES
MICROELECTROPHORESE	SUSPENSIONS DILUEES	0-2 µm 0-15 µm	Champ électrique H (V stabilisé)	Particules solides	M.O.M. et A.L.D.	Couche stationnaire cylindrique Sédimentation possible dans le plan stationnaire
TRANSFERT DE MASSE	SUSPENSIONS CONCENTREES	0-50 µm	Champ électrique H (I stabilisé)	Particules solides	Concentration relative des particules	Inutilisable en système "dynamique" et force ionique élevée
ELECTROOSMOSE	PATES SUSPENSIONS FLOCULEES	400 µm à 1000 µm	Champ électrique H Contrainte physique	Phase Liquide	M.O.M.. A.L.D. Potentiel électrique	Erreurs par courants de "surface" conductivités des surfaces solides élevées
POTENTIEL DE FILTRATION						

M.O.M. : Microscopie Optique Manuelle
A.L.D. : Anémométrie Doppler Laser

IV.1 Influence statistique du comptage électrophorétique sur les calculs de PZ et dimension des particules.

Au départ l'application d'un champ électrique uniforme H sur UNE particule solide entraîne un mouvement électrophorétique à la vitesse V_e (µm/s), sur

une trajectoire horizontale en direction de l'électrode de signe contraire (dans un milieu liquide immobile ou $V_L = 0$).

La mobilité électrophorétique a la dimension d'une vitesse par unité de champ H :

$M_e = V_e/H$ µm/s/V/cm

Tant que la force ionique du milieu dispersant reste inférieure à 10^{-3}M, on calcule le PZ à partir de l'équation de HENRY (I) uniquement sur les particules inférieures à 0,1 µm (F est le facteur de HENRY). En milieu plus concentré et au-dessus de 0,1 µm, seule l'équation d'HELMOLTZ - SCHMOLUKOVSKI (II) est utilisable.

$$(I)\ PZ_{mV} = \frac{6\pi\eta}{D(1+F)} M_e \qquad (II)\ PZ_{mV} = \frac{4\pi\eta}{D} M_e$$

L'influence multiple de la température se retrouve ici au niveau des coefficients de viscosité (η) et de la constante diélectrique (D) du milieu dispersant.

Mais, la mobilité M_e doit être UNE MOYENNE statistique de 50 à 100 particules pour une suspension statique ce qui est insuffisant pour un système dynamique hétérogène. Or avec un champ H de 5 à 20 V/cm et des durées d'électrophorèse de 5 à 30 S, le temps de comptage ΔT de 25 particules consomme déjà 15 à 30 minutes au cours de l'enregistrement, point par point, du PZD en fonction du temps.

L'influence de la taille des particules a lieu à deux niveaux :

1°) Sur l'épaisseur relative de la double couche ionique à travers le facteur de HENRY utilisé dans l'équation I, ci-dessus,

2°) Avec la combinaison à l'électrophorèse, d'un mouvement vertical, lié à la sédimentation, notable à partir de 5 µm.

IV.2 Parabole de l'électroendosmose :

En considérant les mouvements des particules, à travers l'épaisseur totale de suspension, il est bien connu que la vitesse apparente V_e de chacune d'elles est une fonction parabolique de leur distance à la paroi latérale [12]. Les parois des cellules de mesures fermées sont toujours également chargées et il y a un double courant liquide superposé à l'électrophorèse (déplacement au voisinage de la paroi compensé par un retour au centre de la veine liquide).

Si les particules sont détectées uniquement dans le plan focal optique et si ce dernier coïncide exactement avec la couche stationnaire située dans le plan de cisaillement séparant les deux courants liquides contraires, le déplacement liquide est nul et les vitesses électrophorétiques mesurées sont les vitesses vraies, mais seulement dans ce plan.

Aucun moyen ne permet de vérifier si le plan stationnaire est respecté : il doit être calculé et localisé avec un très grand soin.

V. MATERIEL EXPERIMENTAL

Son développement a été conditionné par deux objectifs prioritaires : combiner l'électrophorèse avec la sédimentation et traiter automatiquement les données expérimentales :

1°) Le fait d'accepter la composante verticale des déplacements permet de travailler sur une étendue granulométrique plus importante, donc plus représentative : il suffit de remplacer la veine liquide cylindrique par une cellule de mesure plane à parois verticales:la couche stationnaire concentrique devient un plan stationnaire ververtical (le plan de KOMAGATA [12]. FIGURE N° 3 A et B. Pendant l'électrophorèse, les mouvements des particules sont des bilans des composantes verticales et horizontales. Ces dernières c'est-à-dire V_e) ne sont pas sensiblement modifiées pour des composantes de sédimentation relativement faibles.

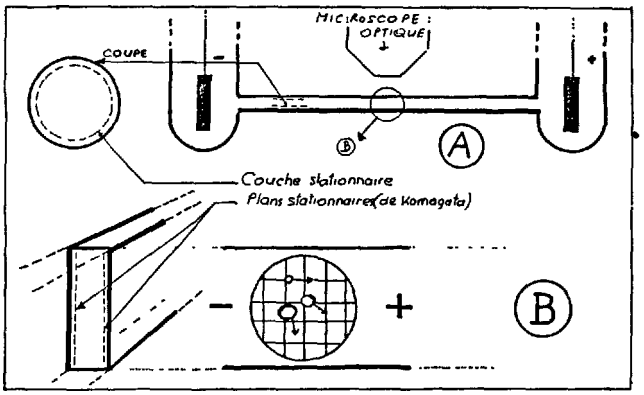

FIGURE 3 - COMBINAISON DE L'ELECTROPHORESE ET DE LA SEDIMENTATION DES GRAINS SUPERIEURS A 5 µm

2°) Pour arriver à réduire au minimum la durée de comptage ΔT il est impératif de réaliser un stockage très rapide et de traiter automatiquement les données expérimentales suivantes : V_e, H, pH, λ, temps d'hydratation.

Pour y arriver, nous avons adopté comme élément de base un appareil de microélectrophorèse classique de RANK BROS (Type MK II) spécialement aménagé pour suivre en continu l'hydratation des suspensions de ciment sans une enceinte thermostatique. Une réserve de suspension-mère permet de renouveler la cellule de mesure de suivre le pH et la conductivité sans apporter de perturbation.

Remarque :

Un autre mode de traitement électrophorétique automatique est en cours de développement : il s'agit de l'anémométrie laser doppler (ALD), qui procède d'une exploitation électronique de la lumière laser diffusée par les suspensions. Avantages : ΔT négligeable ; double application possible à l'électrophorèse et à l'électroosmose (détection du mouvement liquide interstitiel).

VI. RESULTATS EXPERIMENTAUX

Nous avions d'abord vérifié sur des suspensions statiques et homogènes (QUARTZ-EAU) l'influence du temps sur l'équilibre ionique et des écarts de pH sur la dérive du PZ, lorsque l'interface est maintenue hors d'équilibre. La durée de stabilisation du PZ correspondant à l'équilibre dépasse fréquemment 25 à 45 heures et l'écart type est inférieur à 5 $_{mV}$.

Par ailleurs, lorsque l'on fait varier très rapidement le pH;les écarts de potentiels obtenus peuvent atteindre du 15 à 20 $_{mV}$. (FIGURE N° 4).

Nous avons étudié l'hydratation des surfaces solides à partir de différentes suspensions de ciments et de minéraux purs. Dans chaque cas les évolutions d PZD, pH, conductivité ont été établies en fonction de la durée de l'hydratation à 25 °C (FIGURES N° 5, 6, 7 8 et 9).

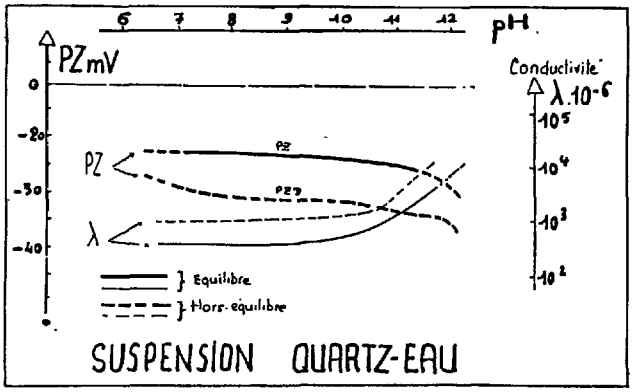

FIGURE 4 - SIMULATION D'INTERFACE DYNAMIQUE ET DERIVE DU PZD PAR RAPPORT AU PZ.

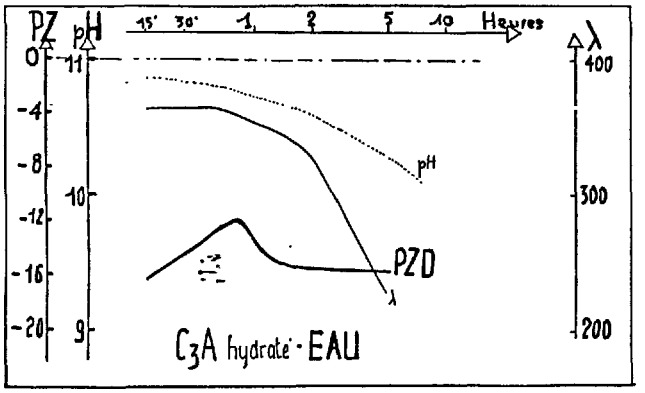

FIGURE 7 - SUSPENSION DE C_3A DEJA HYDRATE 1 MOIS

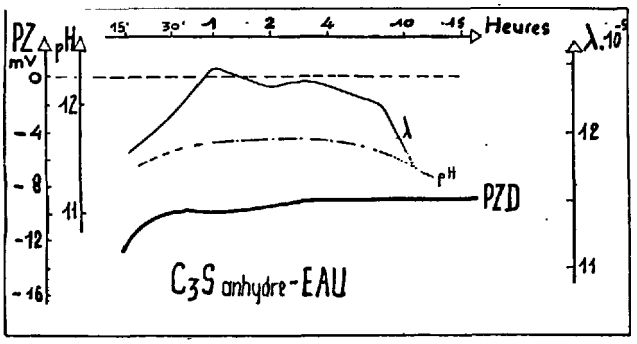

FIGURE 5 - HYDRATATION DU C_3S

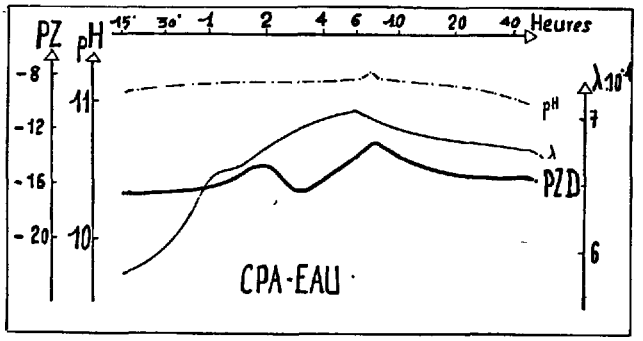

FIGURE 8 - HYDRATATION DU CPA 55 (EX CPA 400)

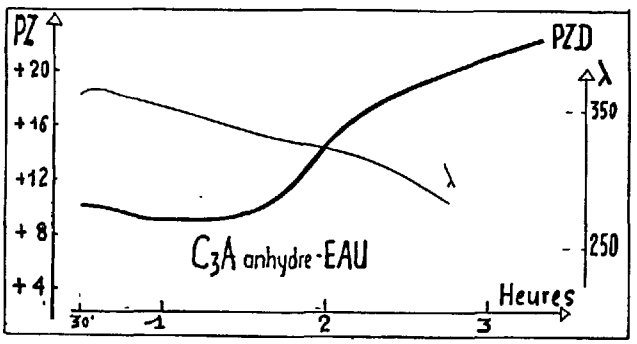

FIGURE 6 - HYDRATATION DU C_3A

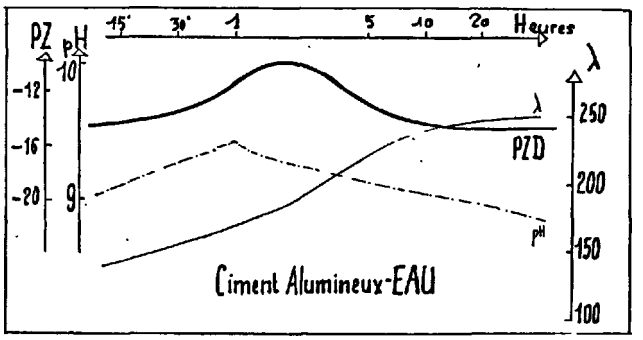

FIGURE 9 - HYDRATATION DU CIMENT ALUMINEUX FONDU

La conductivité (λ) est un moyen commode de capter le sens des variations relatives de la force ionique du milieu dispersant alors que le pH permet de spécifier celui des seuls ions OH. Les augmentations de pH et de conductivité partant de force ionique, vont généralement dans le sens d'un abaissement (en valeur absolue) du PZD en raison d'une diminution (par "compression") de l'épaisseur de la double couche.

La corrélation systématique des minima de PZD avec les pics de conductivité traduit bien plus l'influence ionique du milieu dispersant qu'une modification brutale des propriétés électrocinétiques des surfaces solides.

Les suspensions de C_3A sont très difficiles à étudier en raison de leur floculation immédiate. Le signe du PZD paraît nettement positif alors que la suspension d'un produit déjà préalablement hydraté (FIGURE N° 7) donne une surface négative. Ceci confirme bien la prudente distinction qu'il faut faire avec les différents degrés d'hydratation intermédiaire.

Les valeurs retenues pour les PZD des suspensions étudiées sont résumées dans le TABLEAU III suivant :

TABLEAU III

QUARTZ	KCl 10^{-3}M(pH = 5,5) PZ = -40mV ± 5
ALUMINE	KCl 10^{-3}M(pH = 8,0) PZ = - 20mV ± 5
C_2S	De 0 à 24 H : PZD= ~ 9 à - 11 mV
C_3A * anhydre ** hydrate	De 0 à 5 h PZD = +9 à + 22mV * PZD = -12 à ~ 20mV **
CPA 400	De 0 à 24 H : PZD = -14 à -17 mV
CIMENT ALUMINEUX	De 0 à 24 H : PZD = -10 à -15 mV

La valeur statistique des moyennes effectuées sur les temps d'électrophorèse (V_e) doit être considéré avec une très grande prudence : les histogrammes sont des polygônes de fréquence assymétriques et aléatoires dans le temps qui traduisent bien l'existence simultanée de plusieurs types de particules chargées (et des surfaces de signes contraires) et l'apparition incessante de nouvelles phases hydratées. Cependant malgré cela l'écart entre les moyennes arithmétiques et statistiques ne dépasse pas 2_{mV} mais l'écart type est beaucoup plus étendu (3 à 5_{mV}).

VII. CONCLUSIONS

Au cours de l'hydratation du ciment portland au moins cinq phases minérales sont présentes à la surface : C_3S, C_2S, C_3A, C_4AF et le gypse.

Le cas des suspensions diluées correspond à une hydratation en présence d'un très grand excès d'eau et les hydrates intermédiaires présents à la surface ont un PZD négatif, celui du C_3S étant le plus faible.

Le C_3A, au contraire, semble présenter un PZD très fortement positif suivant les conditions initiales de contact avec l'eau.

Compte tenu de l'inévitable hétérogénéité des surfaces solides apportées par les ciments et de la contribution des différentes phases minéralogiques, l'expression globale du PZD apporte des informations sans doute intéressantes quant à la résulatnte des intéractions particulaires, mais reste sans signification au niveau des corrections spécifiques recherchées à partir des adjuvants pour la mise en oeuvre des bétons frais. Il nous parait indispensable de mieux connaître l'évolution du PZD de chacune des phases minérales les plus importantes ainsi que les ions qui participent à la structure des interfaces correspondante. A cet égard la suspension diluée n'est qu'une première étape, mais essentielle.

De très nombreuses expériences sont encore nécessaires pour confirmer ces premiers résultats et les perspectives offertes par informatisation des données électrophorétiques avec, si possible, l'anémométrie laser (ALD) permettent d'espérer une exploration beaucoup plus rapide des suspensions de minéraux purs et en mélange.

VIII. BIBLIOGRAPHIE

1. H.N. STEIN : Surfaces charges on calcium silicates and calcium silicates hydrates. J. COLLOID Interface. Sci U.S.A. (1968) 28 N° 2 - p. 203.
2. C.A.M. SISKENS-H.N. STEIN-J.M. STEVELS : Surface of silicate in aqueous alkaline solutions. I. J. COLLOID Interface Sci U.S.A. (1975) 52 N° 2 pp 244-50.
3. M.E. TADROS-W.Y. JACKSON-J. SKALNY : Study of dissolution and electrokinetic behaviours of C3A J.COLLOID Interface U.S.A. (1976) 4 - pp 211-223.
4. M.E. TADROS-J. SKALNY-R.S. KALYONCU : Early hydration of C_3S. J. AMER Ceram.Soe(1976) 59 N°7.8 p. 344..
5. G. KORTUM : Treatise on electrochemistry. Elsevier (1965).
6. T.M. RIDDICK - Control colloid stability through ZETA Potential. LIVINGSTONE (1968).
7. J. FRIPPIAT-J.CHAUSSIDON-A.JELLI : Chimie physique des phénomènes de surface. MASSON (1971).
8. P. SENNET-J.P. OLIVIER : Colloid dispersions Electrokinetics effects and the concept of ZP. Indust. and Engng. Chem. U.S.A. (1965) 57 N° 8 pp 32-50.
9. S.ROSS-R.F. LONG : Electrophoresis as method of investigating electric double layer. Ind. Engng. Chem. U.S.A. (1969) 61 N° 10,pp58-71.
10. A. ZELWER : Conductrimétrie du C_3S en pâte pure. R.M.C.N° 681; CERILH juin-juillet 1973.
11. P. LONGUET-L. BURGLEN-A.ZELWER : la phase liquide du ciment hydraté - R.M.C. N° 219 - CERILH jan 1973
12. E. DELATOUR-M. HANSS : Apparatus for alternating field microelectrophoresis. Rev.Sci Instrum. U.S.A. (1976) 47 N° 12 p 1531-35

Study of kinetics of industrial cements hydration

Vitesse d'hydratation des ciments industriels

R. KRSTULOVIC, T. FERIC, P. KROLO, Split, Yougoslavie.

RESUME : Ce travail a comporté l'application des connaissances théoriques et expérimentales les plus récentes concernant la cinétique de l'hydratation des clinkers à l'hydratation des ciments industriels.

On s'est attaché spécialement à suivre la cinétique de l'hydratation par des méthodes thermo et électrocinétiques. L'hydratation d'échantillons de divers ciments industriels a été étudiée au moyen de ces méthodes. La méthodologie choisie s'est avérée être très utile à des fins pratiques.

La cinétique de l'hydratation appliquée à des échantillons variés de ciments industriels est parfaitement adaptée au processus de ka théorie générale de l'hydratation des composants minéraux du clinker pur et du ciment. Certaines hypothèses théoriques sur les caractères et les processus d'hydratation ont été contrôlées expérimentalement.

SUMMARY : The aim of our work has been to apply up to date theoretical and experimental knowledge about kinetics of pure clinker minerals hydration to hydration of industrial cements.

Special attention has been paid when following the kinetics of hydration by thermo and electrokinetic methods. Hydration of samples of various industrial cements has been investigated by means of these methods. The methodology chosen has proved to be very useful for practical purposes.

The kinetics of hydration for various samples of industrial cements fits the general theory of hydration processes for pure clinker mineral systems and cement very well. Some theoretical hypotheses have been proved by means of criterion theory as applied in research into character and type of hydration process.

INTRODUCTION

The study of the kinetics and the mechanisms of reactions in the cement hydration process has led to many new conclusions that have explained in a more exact way the already classical theory of hydration, setting and hardening of cement. These data and results apply to the study of pure clinker mineral systems. Abundant experimental methods and equipment indicate a wide range of approach to the hydration of binding materials in order to adjust this process to the needs of the builders. In short, the science has already explained much about the phenomena in the cement hydration and their mechanisms and has calculated these processes mathematically /1, 2/. But what and how much of this can apply to the study of the industrial cements hydration? The examinations should be simple in their methodology and the equipment used but exact in measurements, and they should not differ much from the tests carried out according to the cement certificates.

EXPERIMENTAL

Investigations were carried out in order to have a systematical study of the hydration processes in various types and qualities of industrial cements with simple instruments, equipment and testing methods. At the same time the results obtained were coordinated to the laws and phenomena in hydration reactions in pure clinker minerals and cement in general.

The samples were: portland cement of varying quality with additives, the metallurgical cement, the asbestos cement. The cements were taken from the factory. An alite sample and the synthetic cement clinker made of pure components of clinker minerals were used in comparison.

Method of work: calorimetrical and electrochemical measurements and chemical analyses.

Equipment and measuring instruments: Hydration heat was determined with a thermos bottle calorimeter. The tests were carried out according to the JUS standard B.C8.027 1975 with automatic temperature and time reader. The electromotor force (EMF) i.e. pH was measured with the pH-meter Radiometar M22. The cement pastes were examined continuously with metal indicator electrodes (Mo, Bi) at isothermic conditions (20°C) with a referent saturated calomel electrode /3/. Setting time was measured with the Pb-Cu electrode system in isothermic conditions (20°C) by means of the Radiometar M22. The Vicat apparatus was used in comparison. The water-cement ratio was the same in both measurements: W/C = 0.30. Conductivity (L_s) was measured discontinuously in suspensions (W/C = = 4) with a conductometer type Iskra Kranj MA 5960.

RESULTS

As the measurements showed equal reproducibility and applicability the results obtained for the most characteristic samples will be given here.

The experiments were to examine quantitatively and qualitatively the cement hydration process. The portland cement PC-550, the clinker mineral alite and the synthetic cement clinker of approximately identical phase composition as the PC-550 (73% C_3S, 13.8% C_2S, 6.4% C_3A, 6.3% C_4AF, 0.5% CaO) were chosen. Calorimetrical and electrochemical methods were used in measurements. The results are shown graphically in the Fig.1 (a = PC-550, b = synthetic cement clinker, c = alite).

The curves in Fig.1 can give us the following information on the hydration process in the function of time: the thermokinetic curves give qualitative and quantitative data on the rate and intensity of the hydration process. Three main processes are clearly discernible, corresponding to those described by Lerch and other authors using this method of examination of the kinetics and mechanisms of the hydration process. EMF measurements show the change in OH^- ions.

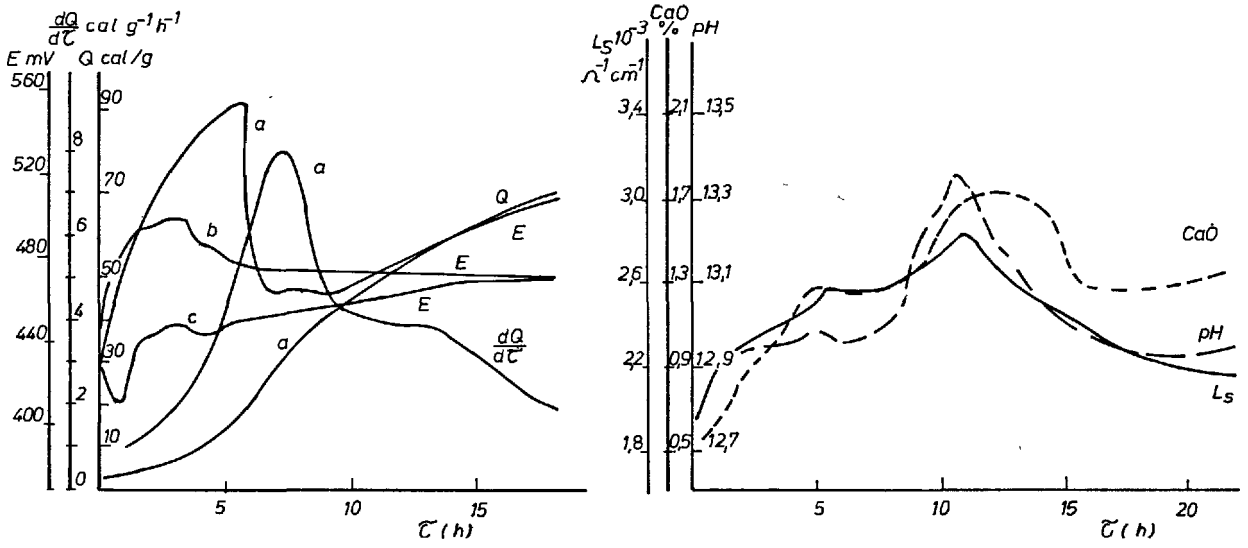

Fig.1 Comparison of methods for examination of the cement hydration kinetics in A) paste, B) suspension

concentration as a consequence of hydration of main components of the cement clinker C_3S and C_2S /3, 12/. A good choice of the metal indicator electrode is very important in obtaining clear and sharp changes in potential with time. In the case on Fig.1 the peaks of the calorimetrical and electrochemical curves (EMF_m) are coordinated well. The comparative results of EMF measurements in industrial cement, synthetic cement clinker and alite show that the difference in the change of EMF with time indicates verying degree of quality of the samples, i.e. their reactivity and thus the characteristics of the hydration process development. Conductivity (L_S) measurements and determination of pH and CaO concentration were carried out on the filtrates of the suspension as shown in Fig.1B. CaO was determined in a complexometrical chemical analysis.

A very good agreement was noticed in our work with suspensions with regard to the difference in the methods for determination of the hydration development.

Calorimetric and electrochemical methods are very useful in examination of the hydration kinetics when testing the influence of the additives on the acceleration or retardation of the hydration process and setting of the cement. Fig.2 shows these phenomena in the same cement samples as those in the previous experiment. The comparative measurements were carried out with Bi and Mo electrodes and various types and quantities of additives. The results are shown in Fig.2 (a = PC-550, b = PC-550 + additive plastificator /0.3%/, c = PC-550 + additive retarder /0.6%/).

The curves in Fig.2 indicate the similarity and correlation of the calorimetric and electrochemical examinations. Both methods record the changes in the hydration process very well, i.e. they clearly outline the acceleration or retardation of the process in time. Fig.2 also shows the individual stages of the hydration process equal to those in cements without additives. The EMF curves, obtained with Mo and Bi electrodes follow one another very well, i.e. the typical changes in the potential take place at the same time in both cases, although the changes in EMF are clearer when the Mo electrode is used. The measurements show that the change in the potential i.e. pH is very rapid at the beginning of the hydration process. The potential increases rapidly, reaches its peak value and then decreases and rises again to its final values. The sudden changes of the potential at the beginning of

the process indicate the intensity of the hydration reactions and formation of new structures.

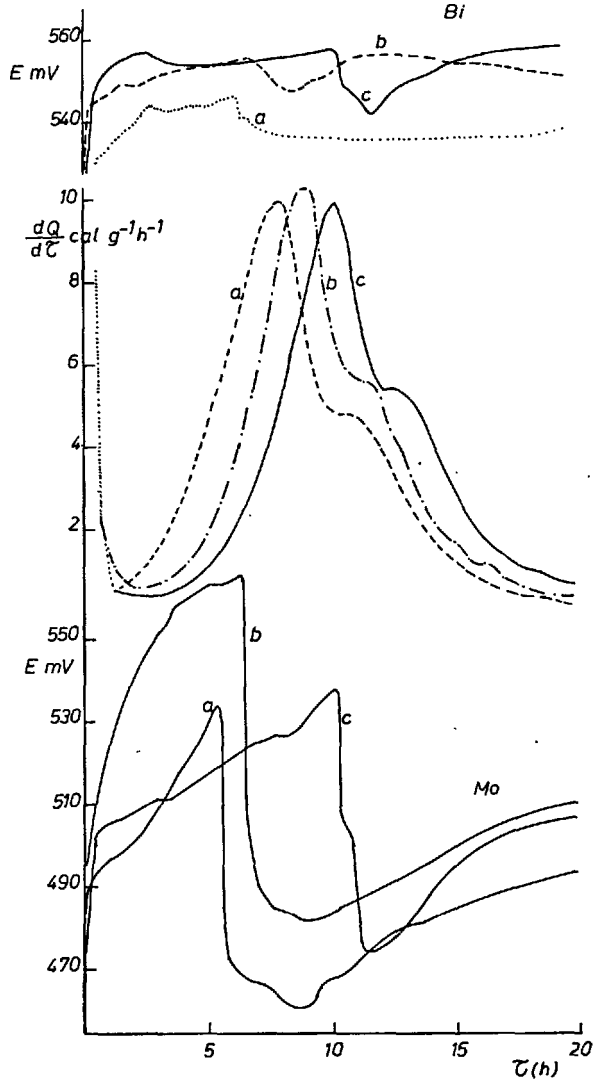

Fig.2 Comparative measurements of the influence of the additives on the cement hydration process, PC-550 W/C = 0.30 T = 20°C

The Pb-Cu electrode system was used to determine the beginning and the end of setting. The results were compared to those obtained by the Vicat method. Fig.3 shows comparative measurements of the PC-550 cement with and without additives. The marks in Fig.3 correspond to those in Fig.2. The shaded areas correspond to the measurement with the Vicat needle.

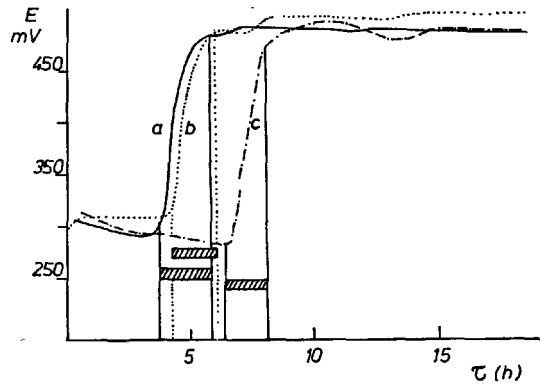

Fig.3 Comparative setting measurements carried out with electrochemical and Vicat methods

The above measuring methods are important in the control of the cement production process. The calorimetrical method in particular, can determine well the influence of production factors on the quality of the same cement type at different times. Fig.4 shows the difference in quality in cements produced at different times. In the case "a" the thermokinetic curves apply to various samples of asbestos cement produced from PC-450 + 20% slag, and the asbestos added in the laboratory. Sample 1 is pure PC-450 + 20% slag. The "b" series of samples is metallurgical cement with addition of 50% of slag.

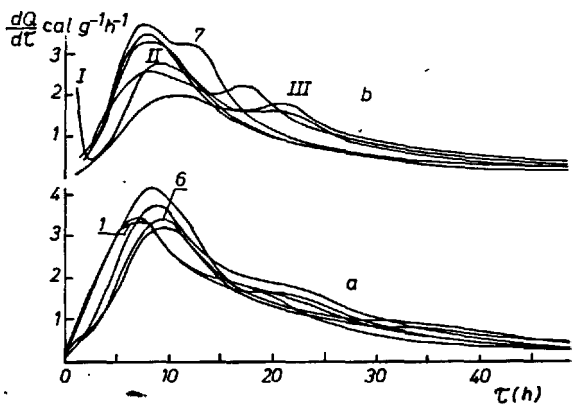

Fig.4

ANALYSIS OF THE MEASURED DATA

The value for the hydration degree transformation (α) was calculated from the calorimetrical data and used for calculation of the hydration process rate constant /4, 5/.

Table I shows the results of these calculations carried out with the samples of asbestos and metallurgical cemets.

(h)	SAMPLE 6 α	$k_1 x10^{-2}$ (h^{-1})	$k_2 x10^{-2}$	SAMPLE 7 α	$k_1 x10^{-2}$ (h^{-1})	$k_2 x10^{-2}$
5	0.0523	0.895	3.86	0.1374	2.46	6.41
11	0.3169	3.17	5.14	0.4526	5.02	6.46
17	0.5030	3.88	4.64	0.6820	6.36	5.94
23	0.6147	3.97	4.06	0.7856	6.41	5.17
29	0.6983	3.99	3.64	0.8474	6.26	4.57
35	0.7702	4.08	3.36	0.8880	6.08	4.93
41	0.8312	4.23	3.17	0.9165	5.91	3.75
47	0.8800	4.41	3.03	0.9387	5.86	3.48
53	0.9182	4.63	2.93	0.9567	5.81	3.28
59	0.9491	4.96	2.87	0.9722	5.97	3.15
65	0.9748	5.57	2.90	0.9859	6.45	3.12

Table I - Hydration degree (α) and rate constants (k_1, k_2) in asbestos and metallurgical cements in the function of time

The data on the hydration degree and rate constants make it possible to assume quantitatively the factors influencing the development of the hydration process.

Calorimetrical measurements have made possible the mathematical approach to the determination of the number of individual processes in the first stages of the cement hydration. The possible number of typical processes is calculated by means of the criterion theory for determination of the number of phases in a multiphase system./6, 7/. Final values of these calculations expressed by means of the reliability factor ($\bar{R}$, $\Delta\bar{R}$) have shown that during hydration three or four basic individual (isolated) processes take place, these processes being responsible for the speed and the mechanisms of the total hydration process /6, 7/. Table II shows the calculated values for the reliability factor for the PC 450 + 20% slag sample.

Number of combinations	$\bar{R}$	$\Delta\bar{R}$	Number of combinations	$\bar{R}$	$\Delta\bar{R}$
123	17.85	29.911	245	0.02	0.003
124	0.02	0.008	345	27.40	45.958
125	0.04	0.012	1234	0.01	0.008
134	0.12	0.061	1235	0.03	0.021
135	0.04	0.021	1245	0.01	0.002
145	0.03	0.006	1345	0.03	0.014
234	0.09	0.043	2345	0.02	0.008
235	0.02	0.008	12345	0.01	0.004

Table II - Reliability factors in determination of the number of processes during hydration of PC-450 + 20% slag

In these measurements, the necessary number of samples (always one more than the assumed number of processes) was prepared by varying the additive content in the cement. The tests resulted in the hypothesis of the four process system.

In examination of the process kinetics, the influence of the temperature on the hydration heat releasing process was observed and the temperature difference i.e. temperature coefficient (ε) was calculated. In order to calculate the temperature factor a corrected Arhenins' temperature function was used./8, 9/. Table III shows the measured data and values for the temperature coefficient in observed temperature intervals for the sample of metallurgical cement with 50% slag.

Q cal/g	Equivalent time (h) at the temperature (°C)				ε in intervals of time		
	20°C	30°C	35°C	40°C	20-30	30-35	30-40°C
4	5	2.8	2.0	-	11.95	10.3	-
22	13	9.1	7.7	6.2	19.43	20.7	18.1
41	25	14.9	12.8	10.2	13.39	22.8	18.3
48	32	17.4	14.5	11.9	11.38	19.0	18.2
53	40	19.0	15.7	13.0	9.31	18.1	18.3
56	46	20.2	16.5	13.6	8.42	17.1	17.5
69	-	26.0	20.8	16.2	-	15.5	14.7

Table III - Temperature coefficient (ε) for the metallurgical cement

The results obtained for the temperature coefficient indicate a deviation from the Rustrup's relation /10/ which has adjusted Arhenins' equation for the cement hydration process. At higher temperatures increases for more than 10°C. So, the value of the temperature factor depends on the time as well. Its value changes in the various stages of the process. It becomes monotonously reduced in the indicated temperature areas./9/.

CONCLUSIONS

The above presented experimental data and measurements make it possible to connect the theory and the practice. The standardized procedure for determination of the hydration heat with the thermos bottle method gives valuable results which may serve as a basis for more exact explanations and remarks on the hydration process development. The differential curves contain individual stages describing the whole process from the beginning of the contact of cement with water, i.e. from the hydration, setting and hardenning reactions.

The transformation hydration degree and the rate of the reaction constants, describing individual change phases in the differential curves, can be calculated from the calorimetrical data. This is a simple approach and can be applied well in everyday practice. The description of the hydration process kinetics and mechanisms can be coordinated well with examinations carried out on clinker minerals and cement systems.

The number of individual processes in the whole cement hydration process, determined by means of the basic equation of the criterion theory, serves as a basis for calculating the reliability factors which should be

lower than 0.05. This confirms mathematically the munber of individual processes described in the differential curves. In a two-process system, the reliability factor is much higher than that allowed, while in a three-phase system it ranges from 0.01 to 0.03. In a four-process system, R decreases to 0.01, which means that the measurements showed 3 i.e. 4 individual processes in the cement hydration, analogous to the graphic representations of the kinetics. The explanation of individual processes agrees with those found in literature /1/.

The temperature coefficient varied and differed from 10 in the examined temperature intervals up to 40°C in metallurgical cements.

The differential curves for the metallurgical cements (Fig.1) show a third peak which is not caused by a later hydration of C_3A. When compared to the data found in literature, the same explanation was reached: the hydration mechanism in the metallurgical cements is caused by other phenomena and reactions, different from those in portland cement./11/.

The calorimetrical results, processes in a computer, prove this method to be appropriate for scientific research, as well as for quick practical information on the influence of various factors on the initial phases of the cement hydration process.

To obtain comparative measurements, the electrochemical method which showed good agreement with calorimetrical results was used. The electrochemical measurements are simple in their methodology and equipment. The change in the potential of the metal indicator electrodes depend linearly on the change in the pH of the environment, which is caused by cement components hydration. The potential varies with the type of addition and additive to the cement, so that pH measurements indicate well their influence on the process of setting and hardening of cement.

The measurements of the electrical conductivity on the cement suspension filtrates show the conductivity to be changing quickly at the beginning of the hydration process. The changes are most intensive in the very area where the most intensive changes in pH and the total CaO concentration occur /12/.

Thermo- and electrokinetic measurements indicate the peaks of differential and electrokinetic curves (EMF) to take place at the same time, while the conductivity curves, due to the fact that the examinations were carried out on the suspension filtrates, show certain deviations, i.e. shifts of the peak in time in recording the effects described.

REFERENCES

/1/ R.Kondo, S.Ueda: Kinetics and mechanisms of the Hydration of Cements, Proceedings of the Fifth International Symposium on the Chemistry of Cement, Tokyo,1968. Hydration of Cements, Vol.2

/2/ The VI International Congress on the Chemistry of Cement, Moscow, Sept.1974 (Hydration and Hardening of Cement)

/3/ R.Krstulović, P.Krolo, J.Vujnović Hydration Process of Cement Examined by Electrochemical Methods, Cement N°1, pp 6-9, 1977-78

/4/ C.Ostrowski, Z.Kowalczyk: Hydratations kinetik des Zementes, Baustoftindustrie A.4(July) pp4-6, 1975

/5/ N.Tenoutasse, A.de Donder: La cinétique et le mécanisme de l'hydratation du silicate tricaleique, Silicates Industriels, 35.N°12 pp.301-307, 1970

/6/ R.Krstulović, A.Bezjak: Study on Determination and Heat Evolution of Cement Hydration, Hemijska industrija N° 10, pp 449-458, 1975.

/7/ R.Krstulović: The Cement Hydration Process by Means of Criterion Method Theory Siliconf, Budapest, pp513-525, 1977

/8/ J.B.Zasedatelev: On the Temperature Heat Function of Hydratation of Cements (I-6, II-I) The VI International Congress on the Chemistry of Cement, Moscow, Sept, 1974

/9/ J.B.Zasedatelev, V.G.Petrov-Denisov: Heat and Mass Transmission on Concrete for Special Industrial Constructions, p.73, Moscow, 1973

/10/ D.B.Milinčić: The Heat of Hydration and Methods of Testing, Cement N°1, pp.15-31, 1966

/11/ J.G.M.de Jong: Le mécanisme de reaction de l'hydratation des cements métalurgiques, Silicates Industriels, pp.5-11, 1977 -1

/12/ R.Sierra: Contribution to the Kinetic Study of Tricalcium Silicate (II-2), The VI International Congress on the Chemistry of Cement, Moscow, Sept.1974

Influence of Water-Soluble Melamine Formaldehyde Resin on Hydration of C_3S, $C_3A+CaSO_4.2H_2O$ Mixes and cement pastes

L'influence de la résine hydrosoluble de mélamine-formaldehyde sur l'hydratation des pâtes préparées de C_3S, du mélange de $C_3A+CaSO_4.2H_2O$ et des pâtes de ciment

SLANICKA Stefan - Tchécoslovaquie.

RESUME : A l'aide de l'analyse par les rayons X et de l'analyse thermique différentielle, l'auteur a découvert l'effet retardateur de la résine hydrosoluble sulfonnée de mélamine-formaldéhyde sur le dévéloppement de l'ettringite et sur sa transformation en monosulfate. Ce phénomène correspond aussi à une teneur élevée de C_3A non encore transformé. L'influence retardatrice de la résine est plus importante si sa dose s'élève à 4 % que si elle n'est que de 1 %. Dans les pâtes contenant 1 % de résine, cet effet est très prononcé au cours des premières 24 heures; plus tard il disparaît; au contraire, une légère accélération de l'hydratation est constatée. Ce phénomène se traduit par un retard du processus d'hydratation des pâtes de ciment, par le ralentissement du dégagement de la chaleur d'hydratation et par l'augmentation de la durée de prise; celle-ci est d'autant plus grande que la dose de l'agent et le rapport eau/ciment sont plus élevés.
L'influence retardatrice de la résine sur les premières étapes de l'hydratation des pâtes mentionnées ci-dessus contribue à l'intensification de son effet plastifiant.

SUMMARY : In the case of C_3A and $CaSO_4.2H_2O$ mix a spectacular retardation effect of the water-soluble sulphonated melamine formaldehyde resin on the development of ettringite and its transformation to monosulphate was disclosed by the X-ray phase analysis and differential thermal analysis. To this phenomenon correspondes also the higher contents of non-reacted C_3A. The retardation influence of the resin is substantially higher if the dose amounts to 4 % than for the 1 % dose. In C_3S pastes with 1 % resin the retardation effect is clearly apparent during the first 24 hours, later on it disappears, on the contrary a slight acceleration of the hydration takes place. To this correspond the indications of the retardation of the cement pastes hydration process such as the retardation of the development of the hydration heat and prolongation of the setting period which are the more spectacular the higher the admixture dose and the w/c ratio. The retardation effect of the melamine formaldehyde resin on the first stages of the hydration process of the above mentioned pastes obviously contributes to the intensification of the plastification effetc.

The water-soluble sulphonated melamine formaldehyde resins with plastification effects may be used for acceleration of concrete hardening, if their plastification effect is utilized for the reduction of the quality of mixing water and this applies also for heat treated concrete /3/. In spite of the reduction of the quantity of mixing water the acceleration effect is not achieved immediately but only after a certain time. For this reason it is advisable to contribute to the clarification of the influence of the water-soluble sulphonated melamine formaldehyde resins on the hydration of clinker minerals and portland cement.

Used materials:

The following materials were used for the tests:

- tricalcium silicate with specific surface of 3 148 cm^2/g,
- tricalcium aluminate with specific surface of 4 452 cm^2/g,
- gypsum with 46,3 % of SO_3 and with specific surface of 4 501 cm^2/g,
- distilled water,
- water-soluble sulphonated melamine formaldehyde resin in the form of 20 % solution[x] /further on it will be referred to only as melamine formaldehyde resin/ with molecular weight of 2.10^4 /1/.

Preparation of specimens

For the tests the specimens were made of a mix of C_3A and $CaSO_4.2H_2O$ with molecular ratio 4 : 3. For a contents of 11 % of C_3A in the portland cement this ratio corresponds to the contents of 2,34 % of SO_3. After a homogenization of the dry components 0,8 part by weight of distilled water was added to 1 part by weight of the mix. To the pastes containing the melamine formaldehyde resin its solution was added. The water contained in the solution of the resin was reckoned with as a part of the mixing water. The paste was wrapped in plastic foils to prevent both evaporation of water and influence of atmospheric CO_2. This storage allows, at the same time, to change mechanically the orientation of the specimens until their perfect hardening to prevent bleeding of the mix.

The following pastes were manufactured for the tests:

- reference paste with water alone,
- paste including 1 % of dry substance of the melamine formaldehyde resin by weight of $C_3A + CaSO_4.2H_2O$
- paste including 4 % of dry substance of the melamine formaldehyde resin by weight of $C_3A + CaSO_4.2H_2O$.

The samples of the pastes were taken after 2, 4, 6, 24 and 48 hours, dried by washing in acetone and by subsequent washing in ether.

Furthermore, the following C_3S pastes were made for the tests:

- paste containing 1 part by weight of C_3S and 0,7 part by weight of water,
- paste containing 1 part by weight of C_3S, 0,7 part by weight of water and 0,32 % of dry substance of the resin by weight of C_3S,
- paste containing 1 part by weight of C_3S, 0,7 part of water and 1 % of dry substance of the resin.

The pastes were sampled after 1, 3, 7 and 28 days, they were also dried by washing in acetone and ether.

Test results

The X-ray diffraction analysis was made with the Mikrometa 2 apparatus manufactured by Chirana, Czechoslovakia. The X-radiation was monochromatized by an Ni filter.

Figs 1 to 3 show the results obtained by testing pastes of $C_3A + CaSO_4.2H_2O$ mix.

Table II shows the results obtained by tests of C_3S pastes.

The complex thermal analysis was made using the apparatus Derivatograph made by the firm MOM, Budapest.

The results are tabulated. When evaluating the pastes made of the $C_3A + CaSO_4.2H_2O$ mix the endotherm used for evaluation was according to Midgley and Rosaman /2/ at about 150° C characteristic of ettringite and about

[x] marketed under the name Melment L 10, a product of Süddeutsche Kalkstickstoffwerke, Trostberg, German Federal Republic.

250° C characteristic of monosulphate.

Evaluation of results and their discussion.

Paste made of $C_3A + CaSO_4.2H_2O$ mix.

As early as after 2 hours of hydration of the paste without resin admixture the gypsum is practically absorbed by the formation of ettringite on the detriment of the initial components C_3A and the gypsum. The process goes on under intensive development of monosulphate so that successively after 24 hours and 48 hours C_3A is practically absorbed and similarly the ettringite contents has dropped whereas the monosulphate contents has increased /Fig. 1/.

As little as 1 % of dry substance of the resin retards the hydration /Fig. 2/, it is, however, not so spectacular as if the resin dose amounts to 4 % of the dry substance /Fig. 3/.

In this case the retardation of the monosulphate development is clearly visible; all over the period of 48 hours its contents varies only little. A pronounced retardation is visible as late as after 28 days.To this

Fig. 1 Paste $C_3A + CaSO_4.2H_2O + H_2O$

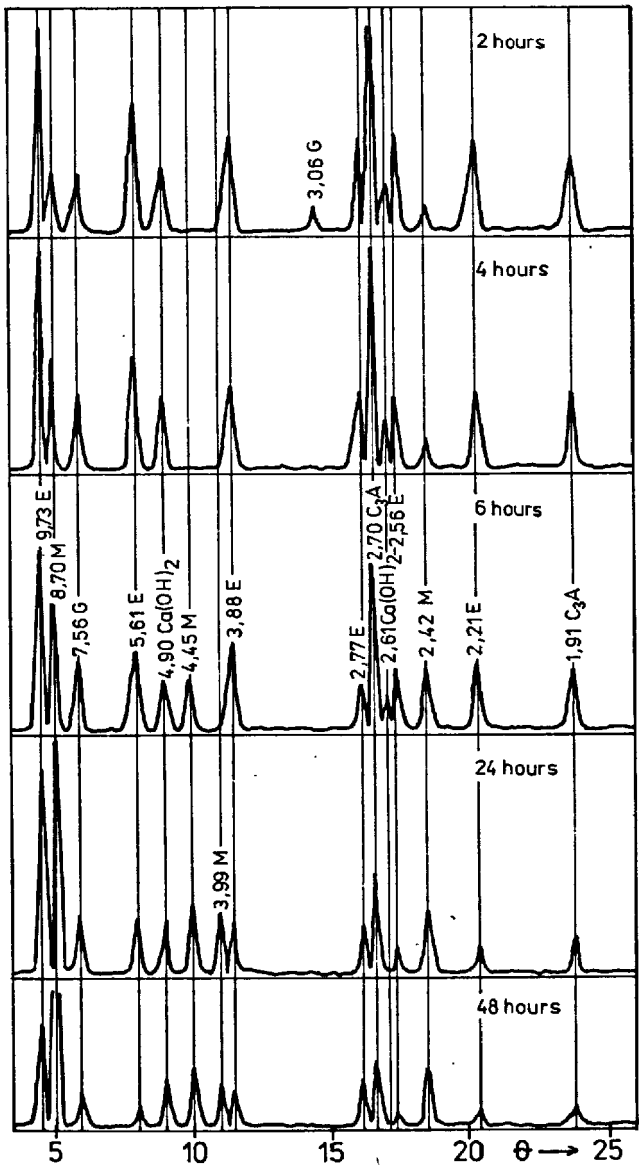

Fig. 2 Paste $C_3A + CaSO_4.2H_2O + H_2O$ + 1 % melamine resin

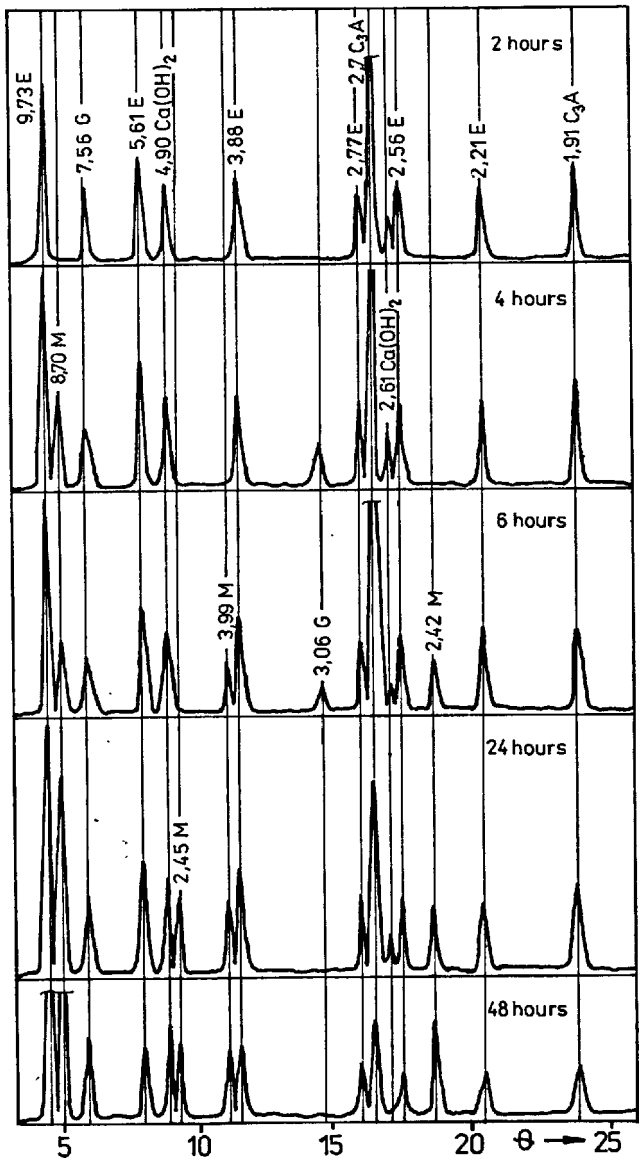

Table I.

Comparison of results of thermal analysis of pastes of C_3A and $CaSO_4.2H_2O$ mix.

temperature area	loss of % by weight after a period of					
	reference paste				paste containing 4 % resin	
	2 h	6 h	24 h	48 h	6 h	48 h
ettringite 150° C	28,3	17,6	12,3	10	24,4	18
250° C monosulphate	0	5,5	13,2	15	3,5	9,9

Fig. 3 Paste $C_3A + CaSO_4.2H_2O + H_2O$ + 4 % melamine resin

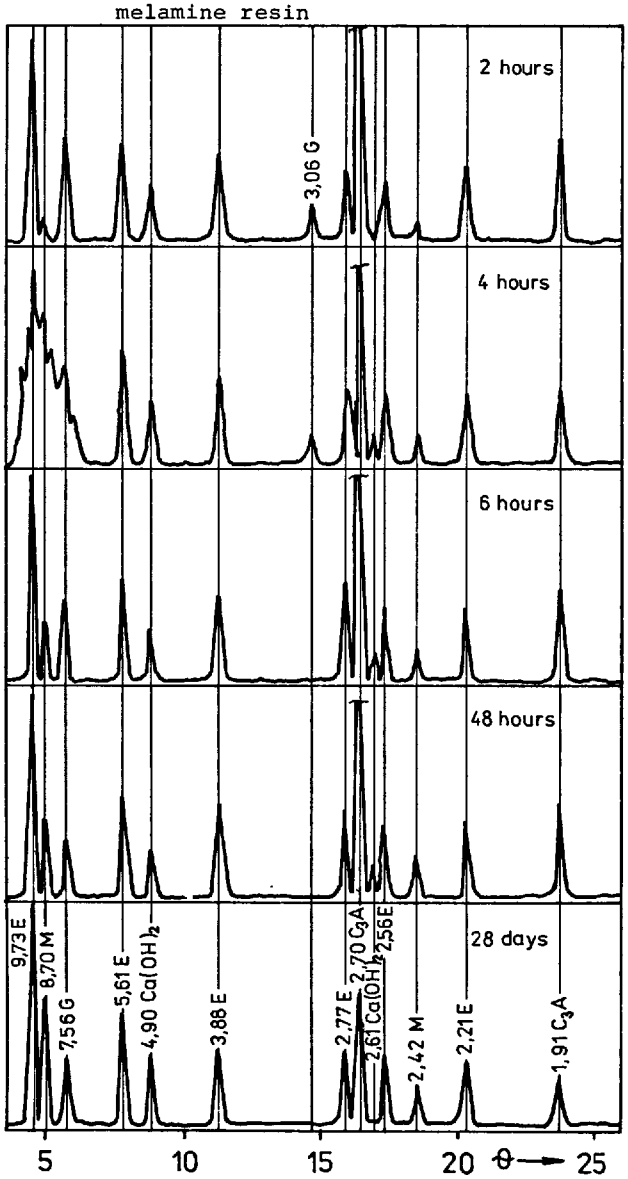

Table II.

Comparison of results of X-ray diffraction analysis of C_3S paste.

contents of m.f. resin	compound	d_{hkl}	The relative height of the peaks after days			
			1	3	7	28
without	$Ca/OH/_2$	4,90	27	35	50	80
	C_3S	2,19	34	31	29	20
0,32 %	$Ca/OH/_2$	4,90	6	40	60	80
	C_3S	2,19	56	32	28	24
1 %	$Ca/OH/_2$	4,90	7	40	60	80
	C_3S	2,19	50	32	28	19

Table III.

$Ca/OH/_2$ contents in C_3S pastes according to thermal analysis results

Time /day/	$Ca/OH/_2$ contents in % by weight of paste		
	reference paste	paste containing resin admixture	
		0,32 %	1 %
1	13,0	11,0	1,4
3	16,5	17,2	17,2
7	19,9	21,0	20,9
28	21,9	22,0	22,3

fact corresponds the higher contents of the non-reacted C_3A in comparison with the preceding pastes. The melamine formaldehyde resin retards the hydration of the paste of C_3A + $CaSO_4.2H_2O$ mix as well as the ettringite to monosulphate transformation.

A comparison of Figs 1, 2 and 3 shows clearly that the retardation influence of the resin on the hydration process increases with increasing dose of the resin. The results of the thermal analysis /Tab. I/ roughly confirm the results of the X-ray analyses.

C_3S paste

The admixture of 1 % of dry substance of the resin slows down the initial course of hydration of the C_3S pastes. The retardation effect of the melamine formaldehyde resin is accompanied with pronounced plastification effects on the fresh nonhardened paste. The retardation of the hydration of paste containing 1 % of the resin is spectacular during the first 24 hours which is also shown by the X-ray analyses /Tab. II/ as well as by the thermal analysis /Tab.III/.

Later, during the subsequent days,this retardation effect vanishes and in the case of pastes containing the resin certain marks of hydration acceleration in comparison with the pastes without resin admixture appear. The retardation effect of the resin on the hydration of the C_3S pastes depending on the admixture of the resin is, however, visible and if the doses of the resin amount to 0,32 % the results of the thermal analyses exhibit only an insignificant retardation after the first 24 hours.

Comparison with tests of cement pastes

Supplementary tests of initial set of two thirds of the portland cement pastes have shown that:

- if the w/c ratio is low /corresponding to normal density of the cement paste/ and if the plastification effect of the resin on the reduction of the quantity of the mixing water is used, the doses of the dry substance of the resin up to 1 % do not cause any changes in the initial set and the period of setting,
- if the w/c ratio of the reference pastes and the pastes containing the resin is kept constant, the increasing resin dose and the increasing w/c ratio causes prolongation of the initial set and of the period of setting of cement pastes.

The supplementary tests have also shown that the admixture of the melamine formaldehyde resin slows down the development of the hydration heat of the cement.

The results obtained with the cement pastes correspond to the results obtained with C_3S and mixes of C_3A + $CaSO_4.2H_2O$ pastes.

Conclusion

The melamine formaldehyde resin slows down distinctly the hydration of pastes consisting of C_3A + $CaSO_4.2H_2O$ mix particularly the transformation of ettringite to monosulphate.

If the dose is higher /4 % of the dry substance of the resin/ this influence is substantially more spectacular than if the dose is lower /1 %/. The melamine formaldehyde resin slows down for a dose of 1 % the hydration of a paste of C_3S even after 24 hours, whereas during the subsequent days this retardation effect vanishes away and even certain indications of hydration acceleration appear.

If the admixture of the resin amounts to 0,32 % of the dry substance only, the retardation effect is hardly noticeable.

At the same time, a distinct plastification effect of the resin on fresh pastes has been recorded.

The retardation effect of the resin on the first hydration stages of the C_3S pastes and the C_3A + $CaSO_4.2H_2O$ mix contributes to the improvement of the plastification effect.

The above mentioned results agree with the results obtained during the investigation of the development of hydration heat and the process of setting of cement pastes.

Literature:

1. Aignesberger A., Schrämli W., /1969/, Elektronenmikroskopische Studien der Erhärtungsvorgänge von Zement mit Zusätzen von Melaminharzen, Zement-Kalk-Gips /22/, 297-305 p., in German.
2. Midgley H.G., Rosaman D., /1960/, Paper III-S2, IV-th Int. Symp. Chem. Cement, Washington.
3. Slanička Š., /1979, Anwendung von Ver - flüssigungsmitteln zweks Beschleunigung der Betonhärtung, Vortrag Nr. 1.2.2, 7. Internationale Baustoff- und Silikattagung, Weimar, in German.

Agglutination (bridging) of Particles during Hydration Hardening and the Effect of Surface Active Additives

Agglutination des particules pendant l'hydratation et le durcissement des ciments. Influence des Ajouts tensio-actifs

E.D. SHCHUKIN, Professor, Colloid Chemistry Dept. Moscow State University, USSR, The Institute of Physical Chemistry Acad. Sci. USSR,
E.A. AMELINA, Associate Professor, Colloid Chemistry Sept., Moscow State University,
E.P. ANDREEVA, Doctor of Chemical Sciences, Coll. Chem. Dept. MSU,
S.I. KONTOROVICH, Doctor of Chem. Sciences, Inst. of Phys. Chemistry Acad. Sci., USSR.

RESUME : La prise d'un liant minéral implique l'agglutination des particules individuelles. On a mesuré la force de cohésion entre ces particules (gypse, quartz, calcite ou silicate) dans diverses conditions de phase (amorphe ou cristallisée) dans des solutions sursaturées. On a observé une relation étroite entre la probabilité d'agglutination de particules semblables ou différentes et les paramètres physico-chimiques de base, responsables de la prise et du durcissement du ciment.

Le mécanisme de l'effet plastifiant des carbohydrates, au cours de l'hydratation des ciments Portland a été étudiée. On a observé que cet effet provient de l'adsorption des carbohydrates à la surface des grains anhydres et des nouveaux hydrates formés. On suggère que le mécanisme de l'adsorption du saccharose et du tregalose est commandé par leur capacité d'adsorption et leur effet plastifiant, compte tenu des nouveaux hydrates formés.

SUMMARY : The hydration hardening (setting) of mineral binding agents involves agglutination of individual particles. The force of cohesion between such particles (gypsum dihydrate, quartz, calcite and silica) was measured under the conditions of new phase (crystalline and amorphous) formation in supersaturated solutions. The results reveal the dependence of probability of agglutination of similar and different particles on the basic physico-chemical parametres responsible for the conditions of hardening.

The mechanism of the plastisizing effect of carbohydrates in hydration hardening of Portland cement constituents was studied. The effect was found to arise from the adsorption of carbohydrates on the surface of the anhydrous solid phase and newly formed hydrates. The suggested mechanism of adsorption of saccharose and tregalose accounts for their different adsorption capacity and plastisizing effect with respect to newly formed hydrates of various composition.

1. Experimental Study on Agglutination of Individual Particles.

Current physico-chemical theories of hardening attribute the formation of strong disperse structures (artificial stone) in plastic suspensions of mineral binding agents to the appearance of contacts, sometimes called bridging or agglutination, between particles of the newly formed phase (1). Thus the formation of individual contacts between particles during the emerging of a new phase attracts special interest. The corresponding studies should apparently be based on the ideas of the new phase formation put forward in the classical works of Gibbs and Volmer. A stage-by-stage theoretical description of the process of hardening has been given in (2).

This section of our paper deals with experimental investigations of elementary acts of agglutination of individual particles (crystalline and amorphous), i.e. the formation of primary contact bridges between them, under a variety of conditions depending on such parametres as supersaturation, the duration of contacting, the nature of particles and the presence of surfactants.

The instrument used was described elsewhere (3). It permits direct measurements of cohesion force in the individual contacts between particles over the range as wide as from 10^{-3} to 10^{2} dynes. The materials included 5x5x0.5 mm gypsum dihydrate crystals cleaved out of single crystals and particles of amorphous silica which were deposited onto the surface of fused quartz threads about 2 mm in diametre by means of precipitation from freshly prepared silicic acid sols. During the experiments two samples (gypsum crystals or silica-covered quartz threads) were brought into contact in the corresponding supersaturated solutions (of calcium sulphate or silicic acid) and were allowed to stay in a fixed position for a certain period. Measured was the force necessary to separate the samples. We shall call this force, which is equal to the cohesion force in the contact, the contact strength . Gypsum crystals were brought into contact by edges of certain crystallographic symbols (one edge normally to the other); silica-covered threads in the contact were mutually perpendicular.

Since the strength of contacts appearing under identical conditions is scattered over a wide range, it appeared necessary to carry out the statistical analysis of the results and to consider the corresponding distributions. Fig.1 presents some of our data in the form of histograms, i.e. the dependences of the differential function of distribution on the logarithm of strength (and are the current and the total number of measurements respectively). The analysis of the histograms shows that crystalline and amorphous particles alike form contacts of two types with sharply different strengths. These are "weak" contacts with 10^{-2} dyne which correspond to the case when the particles merely touch one another and "strong" ones with 10^{-1} dyne which correspond to agglutination (bridging) of the particles. The strength of the latter contacts arises from the short-range forces of cohesion acting on the area considerably exceeding that of a unit cell. The weak-to-strong contacts transition occurs in a jump-like manner and manifests as the second (right-hand) maximum in the histograms and the absence of contacts with strength from 10^{-2} to 10^{-1} dynes. The sharpness of the transition makes it possible to notice the fact of agglutination and thus study the probability of agglutination as a function of various physico-chemical factors. Such results may provide for deeper insight into the intimate mechanisms of agglutination (bridging), by probability of which we mean the ratio of the number of experimentally observed cases when it had taken place to the total number of experiments on bringing particles into contact and separating them under the given conditions,

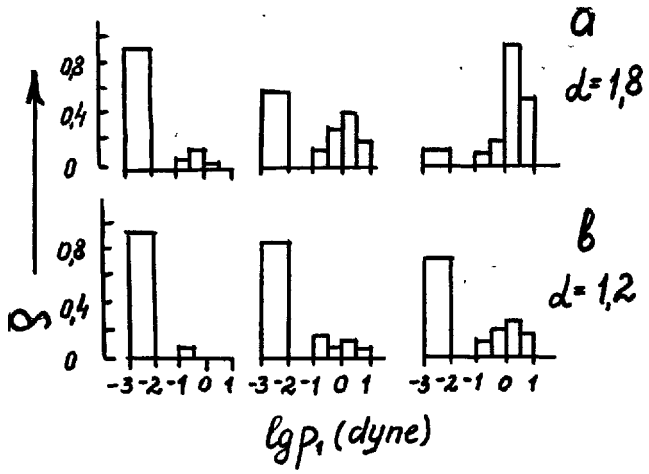

Fig.1. Differential histograms of strength.

As is seen from Fig.1, the probability of agglutination increases with the time the particles are staying in contact . Table 1 indicates that increases also with supersaturation of the solution (, where and are the concentrations of the solutions supersaturated and saturated respectively with respect to gypsum and silica).

TABLE 1.

Probability of agglutination of particles , %, at different supersaturations

Particles	1.2	1.4	1.5	1.8	3.0
Gypsum	17	-	24	49	83
SiO_2	16	52	-	68	81

Such a dependence makes it possible to relate the elementary act of agglutination with the fluctuation formation of a nucleus-contact critical for the given supersaturation. The rapid growth of the nucleus-contact is the main process responsible for the jump-like change of the contact strength or, in other words, for the sharp transition to a different

type of contact.

We should note that in such experiments it is hardly possible to measure the strength due to the nucleus-contact itself (the primary contact bridge). Since the critical nucleus--contact is in mobile equilibrium with the supersaturated solution, a minor increase in its size results in spontaneous crystallization in the contact zone and in rapid growth of the contact strength. And the very fact of agglutination is well detectable from the sharp transition from "weak" contacts to the "strong" ones.

The analysis of experimental data on the basis of corresponding mathematical processing (3) has shown their qualitative agreement with the fundamentals of the fluctuation theory of new phase formation (4). This enabled us to estimate such energetical and geometrical parametres of the agglutination process as the work of formation ( ) and the size of the nucleus-contact and to establish the dependence of the probability of agglutination on the variable parametres of the experiments (3). Table 2 presents the values of calculated from the experimental data; also given are the values of the work of formation for gypsum two-dimensional (surface) nuclei calculated according to (2).

TABLE 2.

Agglutination of gypsum and silica particles: the works of nucleus-contact formation.

Particles	1.2	1.4	1.5	1.8	3.0
Silica	2.8	1.5	-	-	0.5
Gypsum	6.7	-	5.9	5.3	4.3
	45	-	22.5	15	8.5

Table 2 shows that the values of obtained are quite reasonable from the standpoint of the fluctuation theory of new phase formation. In particular, they are, as predicted by the theory, lower than the values of . The linear dimensions of the critical nucleus--contact in both systems at all the supersaturations studied were estimated as 4--9 Å.

Our results thus indicate that the formation of bridge contacts in supersaturated solutions obeys one and the same mechanism for both crystalline and amorphous particles.

Similar experiments were also performed for the case when different crystals were contacting (gypsum and calcite, fluorite or quartz), and when two quartz crystals were brought into contact in supersaturated calcium sulphate solutions. It was shown (3) that all these experiments involved agglutination of crystals and, as its first stage, the fluctuation formation of a nucleus-contact. These results suggest that the so-called inert fillers may actually behave as active structure--building elements taking part in the contact formation according to the contact bridge mechanism.

The process of hardening and the strength of the appearing structures are often controlled with the help of surfactants. Their effects are usually attributed to the influence on the dissolution kinetics, the level of supersaturation and the morphology of the newly formed crystals. In terms of contact formation, the role of surfactants may amount to changing the conditions of agglutination via chemical modification of the surface of the particles and affecting the properties of the solution. In our study the chemical modification of the surface was carried out so that the properties of the solution were virtually unchanged. It was shown that the process of agglutination may be hindered by octadecylamine and gelatine. For instance, the modification of gypsum crystals by octadecylamine and gelatine adsorption from aqueous solutions decreases the probability of agglutination from 67% (at =1.8 and t=1000 sec) to 36% and 29% respectively. A similar effect is observed in agglutination of gypsum crystals with crystals of quartz previously hydrophobized by gaseous dimethyldichlorosilane, and in gypsum agglutination with quartz in the presence of octadecylamine and gelatine (3).

2. The Adsorption Effect of Plastisizing Carbohydrate Additives.

Owing to their capacity of affecting structure formation processes of mineral binding agents, surfactants are widely used in building industry. Carbohydrates belong to the surfactants exerting pronounced plastisizing effects, tregalose being a weaker decelerator than saccharose (5,6). In order to investigate the mechanism of the carbohydrate effects we have studied the processes of tregalose and saccharose adsorption in hydrating suspensions of individual binding agents such as tricalcium silicate $3CaO.SiO_2$ (C_3S), tricalcium aluminate (C_3A), tetracalcium alumoferrite (C_4AF) and monocalcium aluminate (CA).

Data on the kinetics of concentration changes in the liquid phase of hydrating suspensions of various minerals indicate that the adsorption capacities of saccharose and tregalose may be either sharply different or virtually identical. As is seen from Fig.2, in suspensions of C_3S and C_3A the decrease in saccharose concentration with time due to adsorption is far more pronounced than that of tregalose. In C_4AF suspensions, however, the adsorption of tregalose on the appearing hydrates is almost as high as that of saccharose. During the initial three hours of monocalcium aluminate hydration in solutions of either carbohydrate the adsorption is insignificant. In 24 hours the adsorption of saccharose (the decrease in concentration) comes to exceed that of tregalose.

Comparison of our data on the adsorption of carbohydrates with the information on hydration products in the systems studied (7,8) shows that the adsorption of tregalose in CA and C_4AF suspensions is likely to be so high (almost reaching the value of saccharose adsorption) because these systems contain $Al(OH)_3$ and $Fe(OH)_3$ hydrogels respectively. In cont-

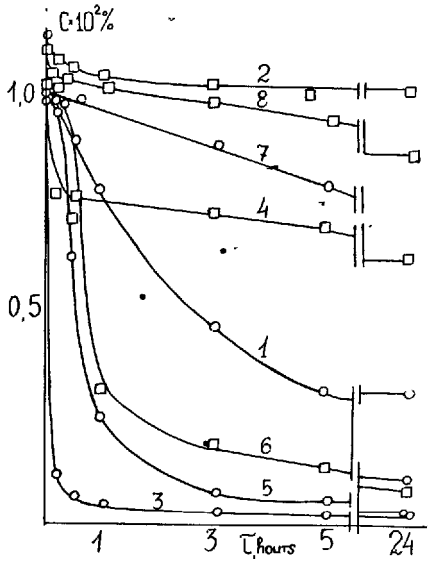

Fig.2. The decrease in concentration of saccharose (o) and tregalose (□) in hydrating suspensions of binding agents C_3S (1,2), C_3A (3.4), C_4AF (5,6), CA (7.8). Initial carbohydrate concentration 0.01%. Composition of suspensions 2 g mineral in 100 ml carbohydrate solution.

rast to this, calcium-containing hydrates adsorb saccharose much more intensely than tregalose. To explain these facts let us consider the structure of the adsorbing molecules. The structural formulas of the two carbohydrates are rather similar, but the fructose ring in the saccharose molecule makes it asymmetrical, while tregalose has a symmetrical molecule. Adsorption on hydrophilic surfaces is markedly dependent on the hydroxy-groups of both molecules, which are capable of forming hydrogen bonds or even, if dissociation is involved, ionic bonds with the adsorbent surface (9,10). In the saccharose molecule the hydroxy-group in the vicinity of two oxygen atoms is very active and readily yields a proton. The tregalose molecule contains no group of similar activity. The evident consequence is the different capacity of forming ionic bonds with the adsorbent surface. Dissolved carbohydrate molecules may take different conformations. As they are approaching the surface, however, the conformation is determined by the orientation of the molecule and by the conditions of adsorption. In principle, a carbohydrate molecule may be oriented towards the surface of the adsorbent in either a "plane" or an "edge" manner (Figs.3a and 3b). The "edge" orientation does not require any essential conformation changes, while the "plane" orientation is energetically favourable only provided the molecule takes a certain conformation. Namely, the pyranose ring should change its "chair" conformation, which is more favourable for the free molecule, for the "bath" conformation. Fig.3a shows that in the "plane" orientation saccharose and tregalose face the ad-

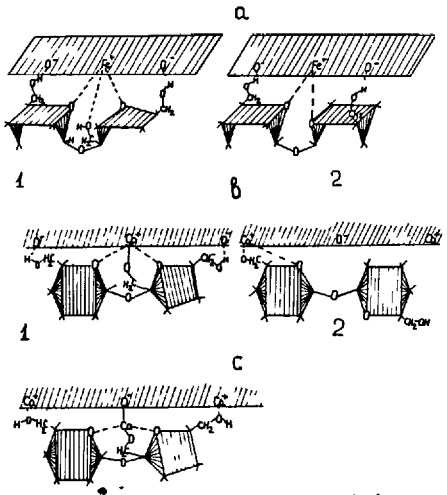

Fig.3. Schematic of saccharose (1) and tregalose (2) adsorption. (a) "Plane" orientation of the carbohydrate molecules towards the adsorbent surface, (b) "edge" orientation, (c) the adsorption of saccharate-cation $CaC_{12}H_{21}O_{11}^{+}$ on a calcium-containing surface.

sorbent surface with approximately the same number of adsorption-active groups (hydroxy--groups and the oxygen atoms of the nuclei). In this orientation the carbohydrates considered should therefore manifest approximately the same adsorption capacity. It appears that the adsorption on hydrogel surfaces involves namely this orientation. In alkaline environment the negative surface charge of hydrogels promotes the formation of hydrogen bonds between the OH-groups of the carbohydrates and the oxygen atoms of the adsorbent. Apart from hydrogen bonds, coordination bonds are formed between the carbohydrate oxygen atoms and the metal atoms of the surface (Fig.3a). The carbohydrate adsorption is the higher the greater is the complex formation capacity of the metal, i.e. adsorption on the $Fe(OH)_3$ gel (in C_4AF suspensions) is greater than on $Al(OH)_3$ (in CA suspensions). In the "edge" orientation the strength of saccharose bonds with the mineral surface is quite different from that of tregalose bonds (Fig.3b). The above--mentioned asymmetricity of saccharose and the presence of a particularly dissociable OH-group in its molecule promotes formation of ionic and hydrogen bonds with the host surface. Tregalose in this orientation can not form such strong bonds.

It seems likely that the adsorption of carbohydrates on the surface of calcium hydroaluminates and hydrosilicates requires the "edge" orientation in which the adsorbing active groups better fit the metal atoms of the lattice and the saccharose hydroxy-group may easier form a bond with the lattice calcium. The probability of formation of ionic bonds between the carbohydrate and the surface grows with the number of calcium atoms on the surface and with pH, since at higher pH the surface acquires a negative charge which favours saccharose dissociation as an acid.

In hydrating suspensions of mineral binding agents the pH is high and the liquid phase contains, along with neutral carbohydrate molecules, saccharate anions and calcium saccharates. Of these, only the $CaC_{12}H_{21}O_{11}^{+}$ cation can compete with neutral saccharose molecules in active adsorption on the mineral surface. At the same pH tregalose, which contains no hydroxy--group as active as that of saccharose, is far less likely to form a similar cation. The adsorption of $CaC_{12}H_{21}O_{11}^{+}$ on the surface of calcium-containing hydrates leads to the neutralization of the surface charge by virtue of formation of ionic bonds between calcium and the lattice oxygen (Fig.3c). The adsorption of these cations vs. that of neutral molecules is thus enhanced by electrostatic attraction. Therefore at high concentrations of $CaC_{12}H_{21}O_{11}^{+}$ (as by hydration of minerals in saccharose solutions saturated by $Ca(OH)_2$) its adsorption would somewhat suppress the adsorption of the neutral molecules. Bruere (5) suggested that tregalose is less effective than saccharose as a decelerator of Portland cement setting because of its higher stability in alkaline environment. He believes that the adsorption capacity of carbohydrates is determined by the presence of the *HO-C-C=O* group. In these terms any monosaccharide must be more active as an adsorbate than saccharose. Our results, however, indicate that glucose in hydrating suspensions of C_3S is less active than saccharose. Moreover, we have found that inversion of saccharose even in saturated $Ca(OH)_2$ solutions is low and the resulting minor amounts of glucose and fructose can not play any active part in adsorption.

Carbohydrates adsorb not only on the surface of hydrate phases, which causes their comminution and prevents recrystallization of metastable hydrates into stable ones, but also on the surface of anhydrous minerals. This is evidenced by our results on the adsorption of carbohydrates from alcohol solutions. The adsorption isotherms for saccharose are S-shaped and reversible; for tregalose they are of Z--shape. The adsorption of saccharose from alcohol solutions exceeds that of tregalose.

The carbohydrate-induced deceleration of dissolution of anhydrous hydrolyzable minerals may cause changes in the ionic composition of metastable solutions resulting from hydration and thus affect the chemical composition of the newly formed hydrates.

CONCLUSIONS

Analytical processing of the results of direct measurements of cohesion forces between individual particles (crystalline and amorphous) in supersaturated solutions supplies evidence that the initial stage of agglutination, i.e. the formation of the first bridge-contact, obeys the fluctuation mechanism. The dimensions of the nucleus-contact and the work of its formation have been estimated. The effect of surfactants on agglutination of gypsum dihydrate crystals has been studied.

The plastisizing effect of carbohydrates, which consists in deceleration of dissolution of the anhydrous binding agent and the crystallization of newly formed hydrates, arises from the formation of screening layers from small crystals of newly formed hydrates and the adsorption layers of carbohydrates. The adsorption capacity of disaccharides (saccharose and tregalose) depends on the chemical nature of the adsorbent, on the orientation of the carbohydrate towards the surface (in a "plane" or "edge" manner) and on the capacity of yielding ions in alkaline media, which are capable of increased adsorption due to electrostatic attraction.

REFERENCES

1.- E.E.SEGALOVA and P.A.REHBINDER (1962) in "Novoye v Khimii i Tekhnologii Tsementa", Gosstroyizdat, Moscow, 202.

2.- A.F.POLACK (1966) "Hardening of Mineral Binding Agents", Stroyizdat, Moscow.

3.- E.D.SHCHUKIN and E.A.AMELINA (1979) "Cohesion of Particles in Disperse Systems", Adv.Coll.Interf.Sci., 11, 235-287.

4.- M.VOLMER (1939) "Kinetik der Phasenbildung", Dresden-Leipzig.

5.- G.M.BRUERE (1966) "Carbohydrate Retardation of Portland Cement Setting", Nature, 212, No.5061, 502-504.

6.- J.F.YOUNG (1973) "The Effect of Carbohydrates on Hydration of Tricalcium Aluminates", Proc.V Intern.Symp. on the Chemistry of Cement, Tokyo, 1968; Moscow, Stroyizdat, 209-210.

7.- R.TURRICIANI (1969) "Calcium Hydroaluminate and Related Compounds", The Chemistry of Cements, ed. by F.W.Taylor, Moscow, Stroyizdat, 167-190.

8.- S.BRUNAUER and D.L.QUANTREAU (1969) "Hydration of Tricalcium Silicate and -Dicalcium Silicate in the Temperature Range from 5 to 50 C", ibid, 214-232.

9.- W.S.HANSEN (1959), in "Symposium on Effect of Water-Reducing Admixtures and Set-Retarding Admixtures on Properties of Concrete", Amer.Soc.Test.Mater.Spec.Techn. Publ. No.266, 3-25, 35-37.

10.- H.M.STEINOUR, discussion of Ref.8, 25-33.

The stiffening of mortar accompanied with the early hydration of cement

Le raidissement du mortier accompagnant l'hydratation initiale du ciment

M. ONO, Senior Research Engineer, Research and Development Laboratory,
M. NAGASHIMA, Senior Research Engineer, Mitsubishi Mining and Cement Co., Ltd.,
M. SAITO, Research Engineer, Tokyo, Japan.

RESUME : Le raidissement, c'est à dire la diminution de plasticité du mortier frais, a été déterminé par l'essai de la pénétration, et on a étudié sa relation avec l'hydratation initiale du ciment.

La résistance à la pénétration, déterminée dans des conditions appropriée, est adoptée comme mesure du raidissement initial du ciment.

Les expériences ont été menées sur des mortiers et des pâtes préparées à partir des ciments de Portland, selon divers mélanges réalisés à partir des clinkers cuits dans les fours électriques du laboratoire.

Le raidissement du mortier est en corrélation avec la quantité d'eau de combinaison dans le ciment hydraté, c'est à dire le degré d'hydratation du ciment.
Dans le cas du ciment sans alcali, la formation d'ettringite augmente principalement la quantité d'eau de combinaison.

K_2O dans le ciment augmente la quantité d'ettringite, réduit sa dimension cristalline, et, par conséquent, provoque l'augmentation du raidissement.

Summary : Stiffening, i.e. decrease in plasticity of fresh mortar was determined with a penetration test and its dependence on the early hydration of cement was investigated.
The penetration resistance determined under the appropriate condition is adopted as a measure of the stiffening accompanied with the early hydration of cement.
Experiments were carried out on the mortars and pastes prepared from portland cements with various composition which made of clinkers burned in the laboratory electric furnace.
The stiffening of the mortar correlates with the amount of the combined water of hydrating cement, i. e. the degree of hydration of cement.
In the case of alkali free cements, the combined water in the hydrated cement arises mainly from ettringite.
K_2O in cement increases the amount of ettringite, reduces its crystal size and consequently brings about increasing the stiffening of the fresh mortar.

INTRODUCTION

Fresh mortar or concrete stiffen gradually losing its plasticity. The decrease in plasticity is small quantity in the early hydration stage and it is rather difficult to detect its change in the short time. The modified penetration test of mortar was deviced and the stiffening, i.e. the decrease in plasticity up to about an hour after the mixing of mortar was measured. The results were related to the early hydration of cement.

THE MEASUREMENT OF THE STIFFENING

The plasticity of mortar was determined by the penetration resistance test.
The cylindrical plunger with the hemispherical bottom is caused to penetrate the mortar placed in the cylindrical container with a certain speed and the resistance is measured employing the load cell.
The ratio of the cross section of the plunger to that of the container is 1/3.
In a certain range of the penetration depth, the increase in the resistance is almost constant. When the resistance is determined at a definite depth under this condition, the ratio of the resistance, R, at any time up to about one hour to that, R_0, immediately after the mixing is dependent on cement used for mortar and usually almost independent of the mix proportion of mortar or the grading of sand.
Therefore, this resistance ratio is adopted as a measure of the stiffening accompanied with the hydration of cement. The resistance at 5 minutes after the gauging was used as R_0 and that at 70 minutes as R, and the ratio of R/R_0 was regarded as the measure of the stiffening.

EXPERIMENT

Preliminary experiments carried out using cements with various composition which were made of clinkers burned in the laboratory electric furnace revealed that the C_3A and K_2O content of cement might influence the stiffening. Hence, the dependence of the stiffening on the hydration of cement was investigated using cements with various C_3A and the K_2O content prepared in similar manner as above. Three experimental series are as follows.
Series A : The C_3A content of clinkers varies from 5% to 14% and alkali is free.
Series B : The C_3A content of clinkers is similar to that in series A and clinkers contain about 0.7% Na_2O and about 0.9% K_2O.
Series C : The K_2O content of clinkers varies from 0.4% to 1.1% and the Na_2O and C_3A content are respectively about 0.7% and 9%.
The mixture of the reagents were burned in the laboratory electric furnace and then clinkers were ground with 4.3 % gypsum to the Blaine value of 3000 cm^2/g. The mortars were made of Japanese sand for the strength test of cement. S/C and W/C of the mortars are respectively 1.0 and 0.35-0.40.
In addition to the mortars, cement pastes with W/C of 0.4 were prepared for the determination of the amount of combined water and ettringite in hydrating cement. The hydration was stopped at 5 and 70 minutes after the gauging.
The combined water was measured by the loss on ignition at 1000°C. The amount of ettringite was determined by quantitative XRD employing the X-ray diffractometer with a strong X-ray tube which has a rotating target. The calibration curve was made using the mixtures of a unhydrated cement and the ettringite which was prepared from C_3A and gypsum. The notation W_d and E_d will be used to designate the increment of the combined water and the ettringite from 5 to 70 minutes.

RESULTS

The results of experiments on the resistance ratio of the mortar and the amount of the combined water (W_d) in the cement paste are summarized in Fig. 1. As a whole the stiffening increases with the combined water. In both series A and B, the stiffening depends on the C_3A content and

alkali presence.

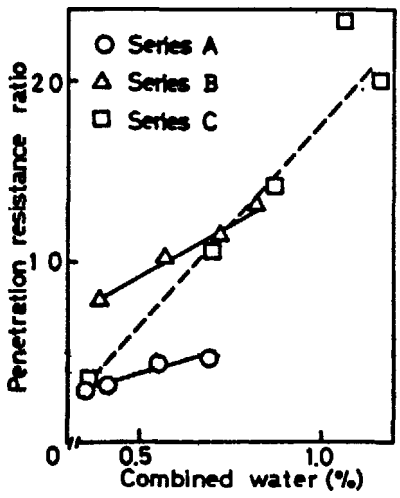

Fig. 1 Relationship between the ratio of penetration resistance and the amount of combined water

In series A, the stiffening increases with the C_3A content showing minimum at about 9 % C_3A, but in series B decreases linearly. Fig. 2 shows the relationship between the amount of ettringite (E_d) and the amount of the combined water (W_d) in the paste. A dotted line represents the combined water upon ettringite. In series A where the cements contain no alkali, the amount of the combined water is directly proportional to that of the ettringite and line vicinity of the dotted line in Fig. 2. Therefore, the increase of the stiffening is mainly attributed to the formation of ettringite in the case of alkali free cement. However, the amount of ettringite scarcely varies in series B where the cements contain alkali, although the amount of the combined water varies considerably. Since both effect of alkali and C_3A exists in series B, the effect of alkali should be obtained in series C.

Fig. 3 shows the relationship between the amount of combined water (W_d) in the paste and the K_2O content of clinker in series C. The combined water increases with the K_2O content. Since the combined water is composed of that upon ettringite and that upon hydrate except ettringite, they are plotted separately in Fig. 3.

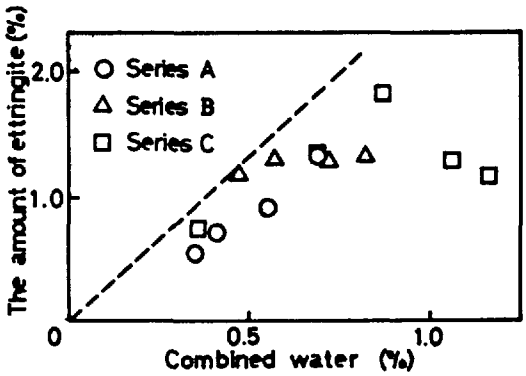

Fig. 2 The amount of ettringite against combined water

It is shown that K_2O increases mainly the combined water upon ettringite up to about 0.8 % K_2O and increases the combined water upon hydrate other than ettringite above about 0.8 % K_2O.

Because the stiffening increases with the combined water as shown in Fig. 1, it is suggested that K_2O in cements may increase the stiffening by the acceleration of the formation of ettringite and the other hydrate. As mentioned above, the resistance ratio increases with the amount of the combined water which varies with the C_3A content or the K_2O content in clinker.

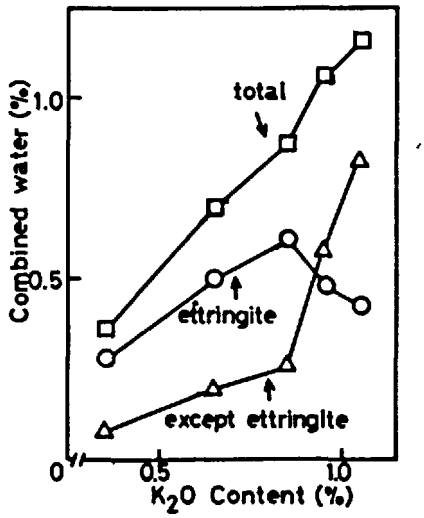

Fig. 3 Relationship between the amount of combined water and K_2O content of clinker

As shown in Fig.1, the K_2O content of cements affects strongly on the relation

between the resistance ratio of mortars and the combined water. From the observation of the hydrated cement by SEM, it is shown that K_2O more than 0.5 % makes ettringite very fine. It is supposed from this fact that the increase in the surface area of the ettringite may make the mortar to stiffen.

CONCLUSION

The stiffening of the mortar up to about one hour after the mixing correlate with the increase in the combined water. Therefore, the stiffening arises from the hydration of cement. In the case of the alkali free cement, this hydration reaction is mainly the formation of ettringite. K_2O in cement increases the combined water upon ettringite and that upon the hydrate other than ettringite and reduces the crystal size of ettringite. As the result of these effects, K_2O in cement increases the stiffening of the mortar.

On the mechanism of Hydration Hardening of Portland Cement Ferrite Phase

Mécanisme de l'hydratation et du durcissement de la phase ferritique des ciments Portland

R. SANZHAASUREN, Professor, Ulan-Bator State University, Mongolia,
E.P. ANDREEVA, Doctor of Chemical Science, Moscow State University, USSR,
N. STUKALOVA, Candidate of Chemical Sciences, Moscow State University, USSR.

RESUME : Le processus de la formation d'une structure et les réactions chimiques dans les pâtes de C_4AF ont été étudiés à 5, 25 et 50°C. On a examiné l'action de l'hydroxyde de calcium, du gypse et du chlorure de calcium sur ce processus.

On a observé que C_4AF subit une hydratation rapide, suivie d'un lent durcissement dû à la recristallisation de l'hydroaluminoferrite tétracalcique $C_4A_xF_{1-x}H_{13}$, dans la solution en alumino ferrite tricalcique $C_3A_xF_{1-x}H_6$. La résistance de cette structure, d'apparence dispersée, dépend des facteurs affectant l'hydratation du C_4AF et de la cristallisation des hydrates (température, dispersion du C_4AF ...).

Le gypse et le chlorure de calcium modifient la composition chimique des hydrates et leur effet est alors commandé par la cinétique du développement des structures dispersées, à base d'hydrosulfo ou d'hydrochloroaluminate ferritique de calcium. L'hydroxyde de calcium ralentit l'hydratation du C_4AF et les hydrates qui se forment successivement font la transition entre le métastable et le stable. Les résultats obtenus permettent de prévoir le comportement de la phase ferritique du ciment Portland, à divers âges d'hydratation, dans l'eau, et dans des solutions aqueuses de chaux, de gypse, et de chlorure de calcium.

SUMMARY : The structure formation processes and chemical interactions in tetracalcium alumoferrite (C_4F) pastes at 5, 25 and 50 C have been studied. The effect of calcium hydroxide, gypsum and calcium chloride on these processes has been investigated.

It was found that C_4AF undergoes rapid hydration followed by slow hardening due to the recrystallization of tetracalcium hydroaldemoferrite $C_4A_xF_{1-x}H_{13}$ through the solution into tricalcium alumoferrite $C_3A_xF_{1-x}H_6$. The strength of the appearing disperse structures depends on the factors affecting the hydration of C_4AF and the crystallization of hydrate phases (temperature, dispersity of C_4AF, etc.).

Gypsum and calcium chloride change the chemical composition of the hydrates and their effect is thus determined by the kinetics of development of disperse structures based upon calcium hydrosulpho- or hydrochloroalumoferrites. Calcium hydroxide decelerates the hydration of C_4AF and the metastable-to-stable transition of newly formed hydrates. The results obtained make it possible to predict the behaviour of Portland cement ferrite phase at various stages of hydration in water and in aqueous solutions of calcium hydroxide, gypsum and calcium chloride.

The chemical processes involved in hydration of C_4AF have been extensively investigated by Carlson (1), Schwiete (2), Malquori and Cirilli (3) and other workers. However essential, their information yet does not suffice for the explanation of the very process of hardening. To develop a quantitative theory of hardening of mineral binding agents one has to know, as suggested in pioneer works by Rehbinder and Segalova (4), the mechanism of disperse structure formation from newly formed hydrate phases. Thus our studies concerned with both structure formation and chemical interactions involved in C_4AF hydration under various conditions depending on the dispersity of C_4AF and on temperature.

According to our X-ray analysis and thermographic data the first product of C_4AF hydration in water at 5, 25 and 50 C is hexagonal tetracalcium hydroalumoferrite which in due course recrystallizes into cubic tricalcium hydroalumoferrite. Carbonate fillers do not stop the recrystallization as reported in (4) but rather decelerate it due to the epitaxional effect of calcite which stabilizes the hexagonal phase.

The $Fe_2O_3/Fe_2O_3+Al_2O_3$ ratio in the mixed crystals of cubic hydroalumoferrite decreases as the temperature is raised from 5 to 50 C (Table 1).

T°C	5		20		50		$S_1 \times 10^{-3}$
Time hydration (months)	0.3	6	0.3	6	0.3	6	cm^2/r
a_o, A°	12.63	12.61	12.60	12.60	12.58	12.58	1.9
$\frac{F}{A+F}$	0.40	0.37	0.30	0.30	0.19	0.19	
a_o, A°	12.61	12.63	-	12.58	12.57	12.56	8.0
$\frac{F}{A+F}$	0.37	0.4	-	0.19	0.12	0.05	

TABLE 1. Unit cell parametres and mole ratios $Fe_2O_3/Fe_2O_3+Al_2O_3$ in cubic tricalcium hydroalumoferrite resulting from the hydration of C_4AF.

This effect arises from the shift of the equilibrium $FeO_2^- + 2H_2O \quad Fe(OH)_3 + OH^-$ to the right-hand side and the corresponding increase in FeO_2^- concentration in the liquid phase. On addition of calcium hydroxide to C_4AF pastes the F/A+F ratio in hexagonal and in cubic calcium hydroalumoferrite increases. This is due to the fact that the solubility of iron in its anionic form grows with pH (according to (5), $HFeO_2^- / OH^- = 2.5 \times 10^{-5}$).

Hexagonal tetracalcium alumoferrite which crystallizes in C_4AF suspensions with the molar ratio $Ca(OH)_2/C_4AF = 2$ at 5 C has the parametre $a = 5.82 \pm 0.02$ Å. According to (5) this value of a corresponds to the F/A+F molar ratio 0.48-0.52 (0.5 on the average). During the hydration process this ratio was constant over the range of C_4AF dispersities from 1.9×10^3 to 8.0×10^3 cm^2/g (Table 2).

Calcium hydroxide decelerates the hydration of C_4AF and the phase transitions of newly formed hydrates. By analogy with the $CaO-Al_2O_3-H_2O$ system (6) it seems likely that the higher is the concentration of calcium hydroxide, the smaller is the difference between the solubilities of hexagonal and cubic hydroalumoferrites. Therefore the dissolution of the hexagonal phase brings about lower supersaturations with respect to the cubic hydrate thus decelerating its crystallization and phase transitions. In saturated $Ca(OH)_2$ solutions at temperatures below 50 C $C_4A_{0.5}F_{0.5}H_{13}$ displays long-term stability and at 5 C no recrystallization into $C_3A_{0.5}F_{0.5}H_{13}$ was observed for 8 months.

The process of C_4AF hydration involves the development of crystallization disperse structures of hardening (Fig.1a, b and c).

T°C	20			50			$S_1 \times 10^{-3}$
Time hydration (months)	0.5	1	4	0.5	1	3	cm^2/r
a_o, A°	12.66	12.67	12.67	12.62	12.63	12.63	1.9
$\frac{F}{A+F}$	0.60	0.63	0.63	0.40	0.45	0.45	
a_o, A°	12.67	12.67	12.68	12.63	12.64	12.63	8.0
$\frac{F}{A+F}$	0.63	0.63	0.64	0.45	0.50	0.45	

Table 2. Unit cell parametres and F/A+F mole ratios of cubic tricalcium hydroalumoferrite resulting from C_4AF hydration in the presence of $Ca(OH)_2$. Mole ratio $Ca(OH)_2/C_4AF = 2$.

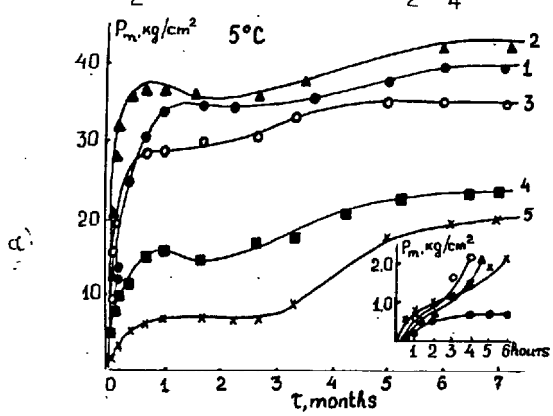

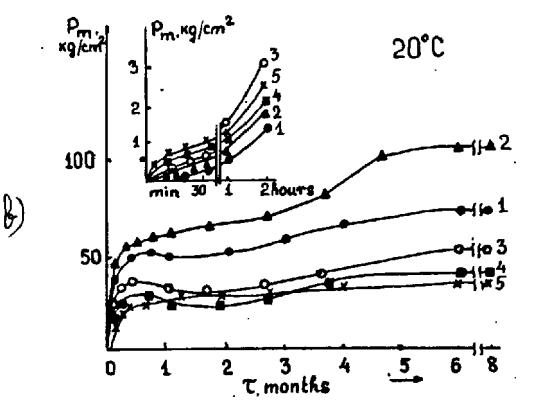

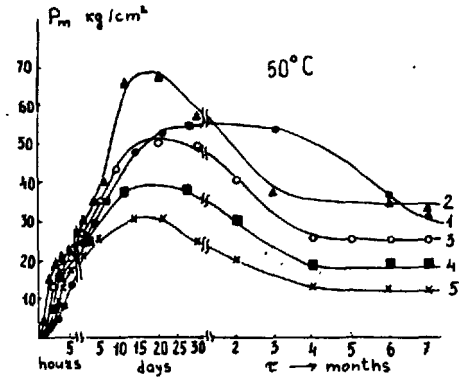

Fig.1. Structure formation in 5% C_4AF pastes of various dispersity + 95% fine calcite powder + 28 ml H_2O at various temperatures. a - 5 C, b - 20 C, c - 50 C. The curves correspond to 1 - 1.1×10^3, 2 - 1.9×10^3, 3 - 2.7×10^3, 4 - 5.5×10^3, 5 - 8.0×10^3 cm^2/g dispersity. P_m is strength as measured by conical plastometer (16), $P_m \sim R_{compr.}$

The increase in strength due to the phase transitions of newly formed hydrates is uneven and continues when the hydration of anhydrous C_4AF is over. Depending on the temperature and on the dispersity of the binding agent C_4AF hydration in water takes from 1 to 15 days. The processes of post-hydration structure formation last for several months. During the post-hydration strength increase the role of the initial binding agent is played by the metastable hexagonal phase crystallized during the hydration of C_4AF. This is evidenced by the fact that destruction of C_4AF hardening suspensions after the hydration is over does not prevent the crystallization structure from further development. Moreover, such destruction increases the final strength of the system, apparently on account of partial relaxation of internal stresses emerging during hydration. Over the temperature range from 5 to 50 C not only the kinetics of strength development but also the final strength of the system based upon cubic and hexagonal calcium alumoferrites are strongly affected by the dispersity of the initial C_4AF. The final strength vs. dispersity curve has a maximum whose position and shape are markedly dependent on active supersaturation in the liquid phase during and after the C_4AF hydration period. Our studies have shown that C_4AF belongs to the type of binding agents which display no metastable solubility during hydration (7). The supersaturation provided by such binding agents increases with the initial active surface. In C_4AF suspensions the increase in supersaturation leads to an increase in the specific surface of the crystallizing hexagonal phase and, accordingly, in the active supersaturation during the hexagonal-to-cubic phase recrystallization in the post-hydration period.

Supersaturation with respect to newly formed hydrates is responsible for the probability that the growing crystals agglutinate to form a disperse structure. On the other hand, high supersaturations increase internal destructive stresses which result from the crystallization pressure of growing agglutinated crystals. Owing to this ambivalent effect of supersaturation there exists an optimum dispersity of C_4AF (1900 cm^2/g) which provides for the highest strength of the structures formed by metastable and stable phases.

During the initial period of hardening the strength growth rate increases with temperature, as does the hydration rate. Thus the strength of the structures of hardening is the greatest when they are formed at 20 C. The low final strength at 50 C results from the after-hydration strength drop which appears to be due to the increase in cubic hydroalumoferrite solubility with temperature and, accordingly, to the dissolution of thermodynamically unstable crystallization contacts. Our results indicate that the hydration hardening of C_4AF is basically similar to that of tricalcium aluminate (4). Due to recrystallization of metastable hexagonal newly formed hydrates into stable cubic hydrates the strength in C_4AF systems grows unevenly and also has a maximum at a certain dispersity of the binding agent. In contrast to C_3A, however, the absolute values of C_4AF final strength are considerably higher and the phase transitions of newly formed hydrates do not involve such sharp strength drops as in the case of C_3A. This difference evidently arises from the formation of highly disperse hydroxides of iron and aluminium during C_4AF hydration. The hydroxides decrease the number of agglutination contacts between crystals and relax internal stresses thus promoting the formation of stronger structures.

In saturated $Ca(OH)_2$ solution the crystallization of tetracalcium hydroalumoferrite and its recrystallization into tricalcium hydroalumoferrite also involves formation of disperse structures of hardening (8). In the light of current concepts of hardening of mineral binding agents this fact implies that the hexagonal-to-cubic recrystallization occurs via the liquid phase. Over the range of temperatures studied (from 5 to 50 C) the strength of the structures of hardening based on the hexagonal phase was a maximum when they had been formed at 5 C ($Ca(OH)_2$ was added in an amount sufficient for binding all the initial C_4AF into $C_4A_xF_{1-x}.aq$). The strength growth rate and the final strength of hexagonal phase structures were growing as the dispersity of C_4AF was increased from 1×10^3 to 8×10^3 cm^2/g. The final strength of this structures decreased as the temperature was raised from 5 to 20 and further to 50 C. This effect appears to arise from the decrease in active supersaturation with respect to $Ca(OH)_2$ which, in its turn, is brought about by the decrease in equilibrium solubility of $Ca(OH)_2$.

The recrystallization of the hexagonal phase into the cubic phase at 20 and at 50 C leads to the increase in the strength of the system. In mixed structures based on the hexagonal and on the cubic phase the strength is a maximum when S=5500 cm^2/g at 20 C and S=1900 cm^2/g at

50 C (the initial mole ratio $Ca(OH)_2/C_4AF$ was equal to 5). Thus the strength growth kinetics and the final strength of the structures resulting from C_4AF hydration in the presence of $Ca(OH)_2$ depend on the phase composition of newly formed hydrates, on the ratio between them in the system, the temperature and dispersity of C_4AF.

X-ray phase and thermographic investigations of C_4AF hydration in the presence of gypsum performed in our laboratory (9) have shown, in agreement with (10,11) that the composition of newly formed hydrates is dependent on n, the initial molar ratio between gypsum and C_4AF. At n 4 the trisulphate form of calcium hydroaluminoferrite ($C_3A_{0.74}F_{0.36}Cs_3.31H_2O$) crystallizes over the entire hydration period. The F/A ratio in this compound was inferred from X-ray analysis data with the help of the dependence of unit cell parametres a and b on this ratio reported by Bobrov (11). As long as free gypsum is present in the system, the only newly formed hydrate is the trisulphate. If the amount of gypsum added does not suffice to transfer all C_4AF into the trisulphate, a monosulphate form of calcium hydrosulphoaluminoferrite starts to crystallize after all the gypsum is bound. The monosulphate may crystallize only provided simultaneous dissolution of the trisulphate and anhydrous C_4AF occurs: C_4AF supplies the necessary Al_2O_3 while the trisulphate is a source of gypsum. As C_4AF dissolves more rapidly than the trisulphate, the initial C_4AF partially undergoes hydration and forms tetracalcium hydroaluminoferrite which is isomorphic to the monosulphate form of calcium hydrosulphoaluminoferrite and forms a solid solution with it as a result of simultaneous crystallization. Namely this solid solution and tetracalcium hydroaluminoferrite are the products of crystallization of C_4AF+gypsum suspensions with n 4 after all the gypsum is bound. The content of either component in the solid solution depends on the ratio between the hydration rates of the trisulphate form of calcium hydrosulphoaluminoferrite and C_4AF. The solid solution, whose general formula is $3CaO.xAl_2O_3.(1-x)Fe_2O_3.yCaSO_4.(1-y)Ca(OH)_2.12H_2O$ contains the more monosulphate the greater is the amount of the trisulphate resulting from the initial crystallization and, accordingly, the overall dissolution rate of the trisulphate. At n=1 y=0.92, at n=0.5 y=0.82. The composition of the crystallizing solid solution was evaluated on the grounds of comparing its unit cell parametre c with the corresponding parametre of various solid solutions of the monosulphate form of calcium hydroaluminoferrite with tetracalcium hydroaluminoferrite reported by Schwiete (10). No recrystallization of the monosulphate, of tetracalcium hydroaluminoferrite or of their solid solution into tricalcium cubic hydroaluminoferrite was observed in course of six months. In the simultaneous presence of gypsum and $Ca(OH)_2$ the composition of the metastable and stable phases and the sequence of their crystallization during C_4AF hydration were the same as if only gypsum were present in the system (12). This fact becomes clear when one considers C_4AF hysration at low n, when the relative rate of gypsum binding is high. At n=0.25 and 0.5 in the presence of $Ca(OH)_2$ the first reaction product to crystallize is the trisulphate form of calcium hydroaluminoferrite which in due course undergoes complete transformation into the monosulphate form (or its solid solution with $C_4A_xF_{1-x}H_{13}$) and tetracalcium hydroaluminoferrite.

The deceleration of C_4AF hydration and gypsum binding by $Ca(OH)_2$, in its turn, brings about the deceleration of phase transitions of the trisulphate into the monosulphate (or its solid solution with $C_4A_xF_{1-x}H_{13}$). In the presence of $Ca(OH)_2$ at n=1 this process takes as long as two years (vs. four months without $Ca(OH)_2$). At the same time the joint effect of $Ca(OH)_2$ and gypsum consists in sharp deceleration of C_4AF hydration. For instance, at n=6 and n=3 the endothermic effects characteristic of gypsum dihydrate are present in the thermograms of the samples after two years of hydration, while in the absence of $Ca(OH)_2$ these effects disappear in the thermograms in one month at n=3 and in half a year at n=6.

In the presence of gypsum the hydration and hardening of C_4AF are dependent on the processes of formation of disperse structures from the trisulphate form of calcium hydroaluminoferrite, tetracalcium hydroaluminoferrite and its solid solution with the monosulphate form. They are also dependent on the phase transitions accompanying the decomposition of the trisulphate (Fig.2 a and b).

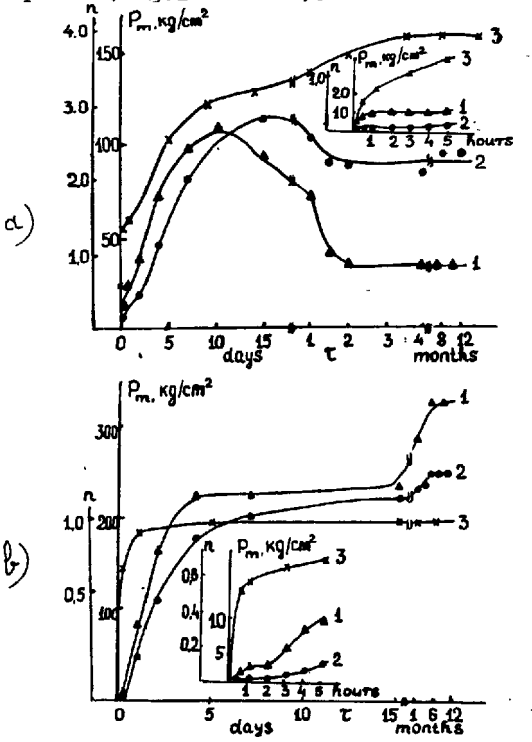

Fig.2. Time dependences of strength (1,2) and n, the amount of bound gypsum (3) in C_4AF pastes with gypsum, calcite and water. The initial gypsum/C_4AF mole ratio m=4 (Fig.2a) and m= (Fig.2b). The water/solid ratio w/s=0.18 (curve 1) and 0.22 (curve 2).

The formation of disperse structures of hardening from the trisulphate involves the development of appreciable internal stresses revealed by the strength "drops" observed until the C_4AF hydration is finished and increasing as the water/solid ratio decreases. In the beginning of C_4AF crystallization, when the supersaturation in the liquid phase is high, the trisulphate structure of hardening is formed by very small crystals connected by numerous contacts. Being thus relatively weak, it undergoes destruction under the effect of the internal stresses. At n 4 the initial crystallization of the trisulphate also does not lead to any appreciable strength increase. The strength grows primarily during the period of phase transitions involved in the decomposition of the trisulphate crystals in the course of C_4AF further hydration, when the solution yields the monosulphate form of calcium hydrosulphoalumoferrite, its solid solution with $C_4A_xF_y$ and $C_4A_xF_y$ itself. The final structure of the hardened C_4AF+gypsum suspensions is determined by the phase composition of newly formed hydrates, their ratio in the mixture and the conditions of crystallization.

On addition of $Ca(OH)_2$ the general crystallization and hardening behavior of the structures based on the trisulphate form of calcium hydrosulphoalumoferrite, the monosulphate form and its solid solution or mixture with $C_4A_1F_1$. aq does not essentially change (13). However, on formation of sulphate-rich films on the C_4AF surface its hydration sharply decelerates, as does the phase transition associated with decomposition of the complex salt. Thus the low strength period in the system becomes considerably longer.

In C_4AF suspensions containing gypsum the addition of $Ca(OH)_2$ is not so detrimental to final strength as in C_3A suspensions. One may think in this case that the weakening effect of internal stresses which increase with active supersaturation with respect to $Ca(OH)_2$ is counterbalanced by the increase in the amount of hydrate phases resulting from the reaction between $Ca(OH)_2$ and Al_2O_3.aq (Fe_2O_3. .aq), the hydroxides being the product of the initial stage of C_4AF hydration.

It is widely believed that ettringite may be formed either by crystallization from the solution or by solid phase reactions. In the former case ettringite is thought to crystallize in the pores of the structure at early stages of hydration and to contribute to the strength of the system, while in the latter case a destructive effect is assumed. Our data, however, contradict to these ideas by indicating that at early stages of hydration ettringite is incapable of forming disperse structures of hardening.

In C_4AF pastes containing gypsum calcium chloride accelerates the crystallization of the trisulphate form of calcium hydrosulphoalumoferrite (n 4) and therefore causes a strength increase at early stages of hydration. On the other hand, in the presence of $CaCl_2$ the supersaturation with respect to the binary salt increases. The result is the increase in internal stresses and the decrease in final strength. At m=$CaSO_4/C_4AF$ 4 the first product of hydration in the presence of $CaCl_2$ is $C_3A_xF_{1-x}Cs_3H_{32}$. In the course of C_4AF further hydration this salt decomposes to yield calcium hydrochloroalumoferrite, the compound which is rosponsible for the basic increase in strength (like in the case of C_4AF hydration in $CaCl_2$ solutions (14,15).

CONCLUSION.

The information obtained in this study and concerning with the processes of structure formation, i.e. with the development of disperse structures of hardening based upon newly formed C_4AF newly formed hydrates crystallizing in water and in the solutions of calcium hydroxide, gypsum and calcium chloride, is in line with the theory presenting hydration hardening of mineral binding agents as a process consisting of consequent stages, namely the dissolution of the binding agent, the formation of solutions supersaturated with respect to the newly formed hydrates and the crystallization of the hydrates resulting in a crystalline agglomerate. The strength of disperse structures based on C_4AF (the ferrite phase of Portland cement) may be controlled by changing the conditions of C_4AF hydration and of crystallization of hydrate phases, as well as by changing the chemical composition of the hydrates.

REFERENCES

1.- T.CARLSON (1966) "Some Properties of the Calcium Alumoferrite Hydrates", U.S.A. Dept. of Commerce, Building Research Division, Institute for Applied Technology, NBS. Wash., Building Science, 6, 1-11.

2.- H.E.SCHWIETE and T.IWAIS (1964) "The Behaviour of the Ferritic Phase in Cement during Hydration", Zement-Kalk-Gips, 17, 379-386.

3.- G.MALQUORI and V.CIRILLI (1943) "The Hydrated Calcium Ferrites and the Complexes which Originate from Tricalcium Ferrite by Association with Different Salts of Calcium" (Note 4), Ric.Sci., 14, 78-84.

4.- E.E.SEGALOVA and P.A.REHBINDER (1962), in "Novoe v Khimii i Tekhnologii Tsementa", Gosstroyizdat, Moscow, 20?-213.

5.- B.N.KABANOV and D.LEIKIS (1946) "Aktivny Gladky Zhelezny Elektrod", Zh.Fiz.Khimii, 20, No.9, 995-1003.

6.- F.E.JONES and M.H.ROBERTS (1962) "The System CaO-Al_2O_3-H_2O at 25 C", Bldg.Research Current Papers, Research Series 1, Dept. of Sci.& Industr.Research, London.

7.- E.P.ANDREEVA, R.SANZHAASUREN and R.A.ZALETSKAYA (1972) "On the Physical Chemistry of Supersaturated Solutions in Tetracalcium Alumoferrite Suspensions", Zhurn. Prikl.Khimii, XLV, 1413-1419 (in Russian).

8. - E.P.ANDREEVA and R.SANZHAASUREN (1977) "On the Structure Formation Processes in Aqueous Pastes of Tetracalcium Alumoferrite in the Presence of Calcium Hydroxide", Kolloidn.Zh.,39, No.4, 738-741 (in Russian).

9.- E.P.ANDREEVA and R.SANZHAASUREN (1977) "Chemical Interactions in Tetracalcium Alumoferrite Aqueous Suspensions in the Presence of Gypsum Dihydrate", ibid, 39, No.2, 227-233 (in Russian).

10.- G.E.SCHWIETE and U.LUDWIG (1973) "Calcium Hydroaluminates and Hydroferrites", Proc. V Intern.Symp. on the Chemistry of Cement, Tokyo, 1968; Stroyizdat, Moscow, 130-152.

11.- B.S.BOBROV and M.B.EPELBAUM (1969) "Hydration of Calcium Alumoferrites in the Presence of Gypsum", in "Gidratatsiya i Tverdenie Tsementov, Chelyabinsk, 11-21 (in Russian).

12.- R.SANZHAASUREN and E.P.ANDREEVA (1978) "Chemical Interactions in Tetracalcium Alumoferrite Aqueous Suspensions in the Presence of Calcium Hydroxide and Gypsum", Vestnik MGU, ser.khim., 19, No.1, 60-64 (in Russian).

13.- R.SANZHAASUREN and E.P.ANDREEVA (1978) "Structure Formation Processes in Tetracalcium Alumoferrite Aqueous Suspensions in the Presence of Calcium Hydroxide and Gypsum", ibid, No.2, 160-164 (in Russian).

14.- N.P.STUKALOVA and E.P.ANDREEVA (1977) "Study on the Structure Formation and Chemical Interaction Processes in Tetracalcium Alumoferrite Aqueous Suspensions in the Presence of Calcium Chloride and Gypsum", Kolloidn.Zh., 39, No.4, 718-724 (in Russian).

15.- N.P.STUKALOVA and E.P.ANDREEVA (1977) "Study on the Structure Formation and Chemical Interaction Processes in Aqueous Suspensions of Tetracalcium Alumoferrite in the Presence of Calcium Chloride", ibid, 39, No.3, 508-512 (in Russian).

16.- E.E.SEGALOVA, P.A.REHBINDER and O.I.LYUBIMOVA (1954) "Physico-Chemical Investigation of Structure Formation in Cement Suspensions", Vestnik MGU, ser.khim., No.2, 17-32 (in Russian).

Early hydration of calcium silicates: surface phenomena

L'hydratation initiale des silicates de calcium : phénomènes de surface

I. JAWED, D. MENETRIER and J. SKALNY Martin Marietta Laboratories, Baltimore, Maryland, U.S.A.

RESUME: Le mécanisme de l'hydratation initiale des silicates de calcium hydrauliques n'est pas encore bien élucidé. On tente d'interpréter des résultats expérimentaux obtenus par spectroscopie de photoélectrons (ESCA) et par microscopie électronique à haute résolution (STEM).

Les résultats montrent qu'il se forme une couche riche en silice à la surface des grains de β-C_2S et C_3S au cours des premiers instants de l'hydratation. Rien n'indique que cette couche est uniforme, par contre, on observe que la dissolution et la formation des hydrates sont localisées.

SUMMARY: The mechanism of the initial hydration of hydraulic calcium silicates is still inadequately understood. An attempt is made to interpret experimental data obtained by electron spectroscopy for chemical analysis (ESCA) and high-resolution electron microscopy (STEM, scanning mode).

The data show that in the very early stages of hydration, a Si-rich surface is obtained for both β-C_2S and C_3S. No evidence was found for the existence of a uniform layer of surface hydrate, but there was evidence of localized dissolution and formation of hydration products.

INTRODUCTION

Performance of portland cement in concrete depends to a large degree on the interaction of calcium silicates with water because they constitute approximately 80 percent of the cement clinker. Although they react with water at very different rates, the mechanisms of their dissolution and the subsequent formation of hydration products are believed to be similar.

The cementing action of clinker minerals results from the products of their hydrolysis being less water-soluble and having a larger volume than the anhydrous phases. Thus, for calcium silicates, the hydration products, C-S-H and calcium hydroxide, precipitate into the water-filled space and consequently decrease the porosity of the system.

Details of the initial interaction of calcium silicates with water are complex and only partially understood. Several mechanisms have been proposed to explain these phenomena. They may be classified as protective hydrate theories (1,2), lattice defect theories (3,4), nucleation theories (5-7), and osmotic pressure theories (8, 9). They differ in the interpretation of the dissolution phenomena, the reasons for the existence and termination of the induction period, and the sequence of formation and composition of hydration products. An attempt has been made recently by Taylor (10) to unify the various views.

The mechanism of the early stages of hydration clearly depends on the processes occurring on the solid-liquid interface and, thus, can be studied by appropriate physico-chemical techniques. The purpose of this paper is to interpret ESCA and high-resolution SEM results in view of the available data on the early hydration of C_3S and β-C_2S.

EXPERIMENTAL

For spectroscopic studies, we used a Physical Electronics Model 548 Auger/ESCA spectrometer, featuring a double-pass cylindrical mirror analyzer, an ultra-high vacuum system, and a magnesium-anode X-ray source. The surface morphology was studied with a JEOL JEM-100 CX Scanning Transmission Electron Microscope (STEM), that has bright and dark fields, and microprobe and electron diffraction capabilities. In the present study, we used the SEM mode with 30 Å resolution. Other papers (11,12) give details of the C_3S and β-C_2S sample preparation, use of instrumentation, and data interpretation.

Whenever possible, the same samples were used for both the spectroscopic and electron optical experiments. To eliminate errors in interpretation due to sample preparation, we took precautions to avoid carbonation and to assure the reproducibility and accuracy of data.

RESULTS AND DISCUSSION

Morphological Studies

It has been shown (11,12) that the surfaces of C_3S and β-C_2S prior to contact with water contain no impurities. Upon contact with water, minute hydration products (approximately 200-400 Å) form on the surface: with time, these particles grow in amount but not in size. In C_3S hydration, the particles cover — although not continuously — the whole surface, whereas their formation on β-C_2S surfaces seems to be more localized, both at room temperature and at 50°C (Fig. 1). Simultaneously, etching or corrosion of the surfaces becomes visible. This is more pronounced for C_3S, most probably because of its easy dissolution in water (Fig. 2).

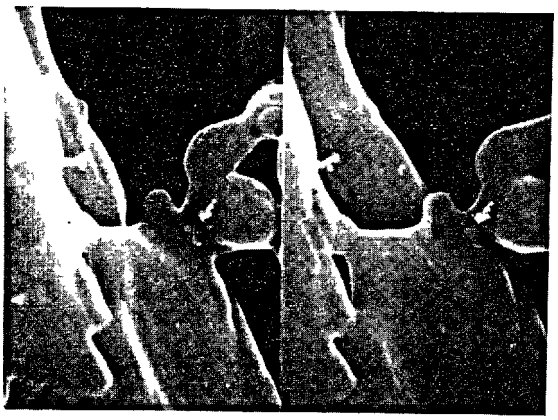

Fig. 1. β-C_2S hydrated at 25°C for 15 seconds. Magnification: x20,000 (stereo).

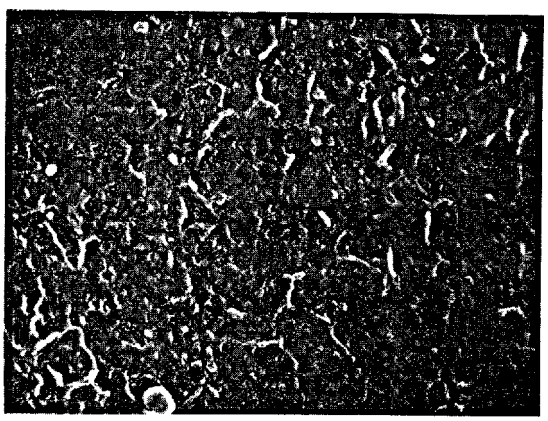

Fig. 2. C_3S hydrated at 25°C for 15 minutes. Note the beginning of formation of Type II C-S-H and etching of surface. Magnification: x20,000.

β-C_2S reacts at a lower rate — this is clearly shown by the much easier detectability

of the various surface phenomena. The minute hydration products are already visible after 15 seconds of hydration and are formed mostly, but not exclusively, at grain boundaries that became exposed by preferential dissolution. Only selected surface localities are covered by hydration products, and dissolution of the surface is not uniform. Some grains or their parts dissolve faster than others. At no time did we detect the existence of a uniform protective surface layer that has been claimed to be responsible for the induction period of β-C_2S and C_3S hydration (1,2).

As the hydration progresses, the surfaces of the two hydraulic calcium silicates become more etched, and hydration products resembling Type II C-S-H form (13). This happens for C_3S at 25°C after about 30 minutes (Fig. 3), for β-C_2S at 25°C after a few days, and for β-C_2S at 50°C at about 18-24 hours (Fig. 4). These hydrates are not unlike the gel formed at initial stages of C_3A hydration, as reported by Breval (14).

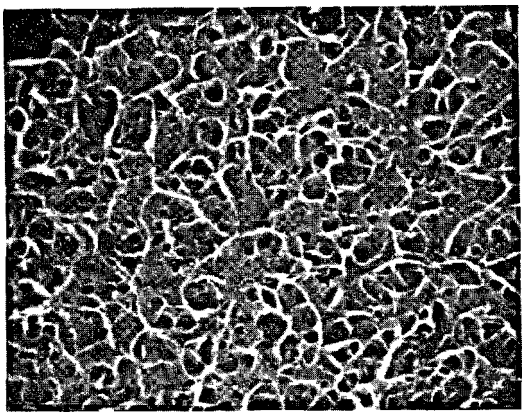

Fig. 3. Surface of C_3S, hydrated at 25°C for 30 minutes, covered by Type II C-S-H. Magnification: x 20,000.

Fig. 4. β-C_2S hydrated at 50°C for 24 hours. Magnification: x 30,000.

ESCA Studies

ESCA scans of calcium silicates give peaks for oxygen, calcium, and silicon (Fig. 5).

Changes in the position, shape, and intensities of these peaks would indicate changes on the surface due to hydration. ESCA spectra show definite changes on the C_3S and β-C_2S surfaces as soon as they come in contact with water. This is most clearly indicated by changes in the position and shape of the O_{1s} peak and the intensities of the Ca_{2p} and Si_{2p} peaks.

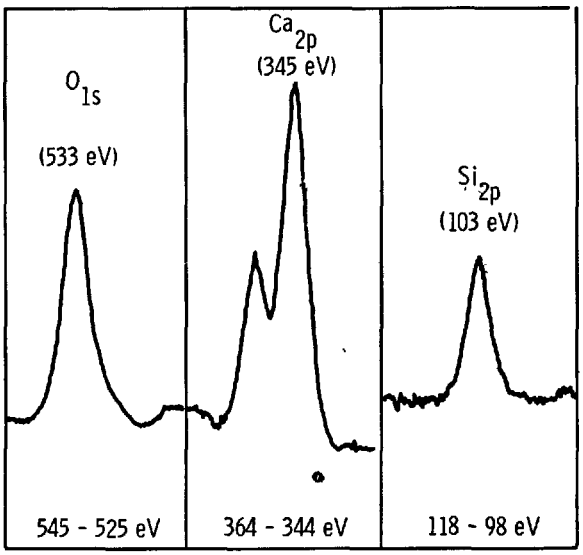

Fig. 5. ESCA spectrum of C_3S.

In unhydrated and sputtered C_3S samples, the O_{1s} peak at 532±0.2 eV is symmetric and 2.7 eV wide, whereas in unsputtered samples, it is broader (3.2 eV) and slightly asymmetric. In hydrated samples, the O_{1s} peak becomes broader, and its maximum shifts toward higher binding energy values. After about 10 minutes of hydration it becomes symmetrical and 3.5 eV wide, and its maximum shifts to 533.5±0.2 eV. Afterwards, up to 3 hours, the shape and position of the peak remain unchanged. For β-C_2S, the O_{1s} peak shows the same trend as for C_3S (Fig. 6). The broadening of the O_{1s} peak and the shift in its binding energy is the manifestation of the initiation of hydration of calcium silicates. These changes indicate that there are, at that point, more than one oxygen-containing species on the hydrated surface. Also, the new oxygen-containing species has higher binding energy, presumably due to the O-H bond since the oxygen in the O-H bond has a higher binding energy than in O-Ca and O-Si bonds.

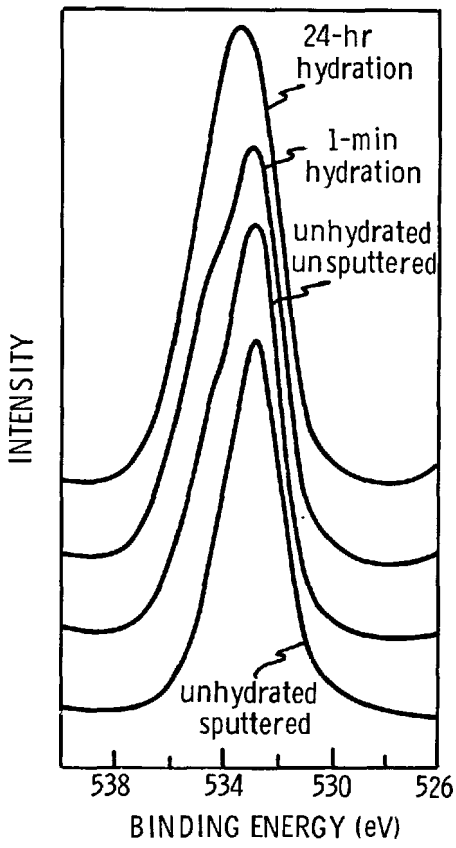

Fig. 6. Changes in the O_{1s} peak of β-C_2S as a result of hydration.

Tricalcium Silicate: Figure 7 gives typical results for an experiment that shows the change in the Ca/Si ratio on the C_3S surface as a function of hydration time.

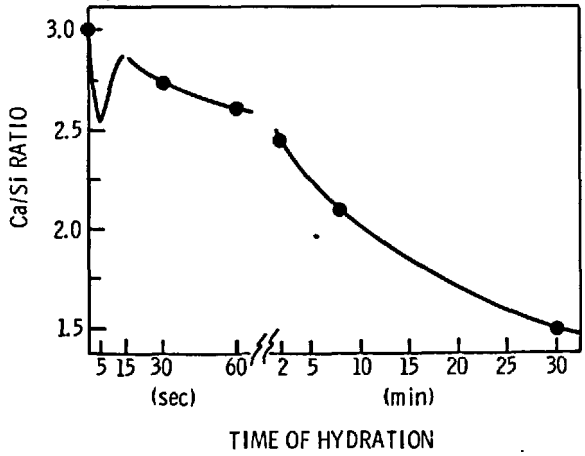

Fig. 7. Ca/Si ratio on the C_3S surface as a function of hydration time.

As can be seen, the Ca/Si ratio drops to about 2.6 - 2.7 with only 2 seconds of hydration. It then passes through a minimum at about 2.5 and a maximum at about 2.8. From then on, it gradually decreases to a value of about 2.0 in 10 minutes, and 1.5 in 30 minutes. Afterwards, there is very little change, even up to 3 hours. It should be pointed out that the times when minima and maxima in the Ca/Si curves appeared were not exactly reproducible and probably depend on the fineness and thermal history of the C_3S.

The departure of the Ca/Si ratio from a value of 3.0 on the C_3S surface in the very early seconds of hydration shows that the first hydrates on the C_3S surface do not have a Ca/Si ratio of 3.0 as was believed previously. The probing depth of ESCA is about 20 Å. The hydrated layer in the early seconds of hydration is probably less than 20 Å but, in spite of this, a Ca/Si ratio close to 3.0 is not obtained. Thus, it may be concluded that the C_3S surface in the early stages of hydration is rich in Si (5-7). The significance of the minimum and maximum in the Ca/Si curves is not entirely clear. If we assume that the minimum represents a hydrated surface rich in Si, then the maximum may represent a surface on which Ca^{2+} ions have chemisorbed, supporting the views of Tadros et al. (7).

Dicalcium Silicate: It was found that both pure and stabilized C_2S gave very similar ESCA spectra and Ca/Si ratios. Variation in the Ca/Si ratio on the β-C_2S surface is a function of hydration time, as shown in Fig. 8. Because of the very slow β-C_2S hydration, samples were hydrated up to 24 hours, both at 25° and 50°C.

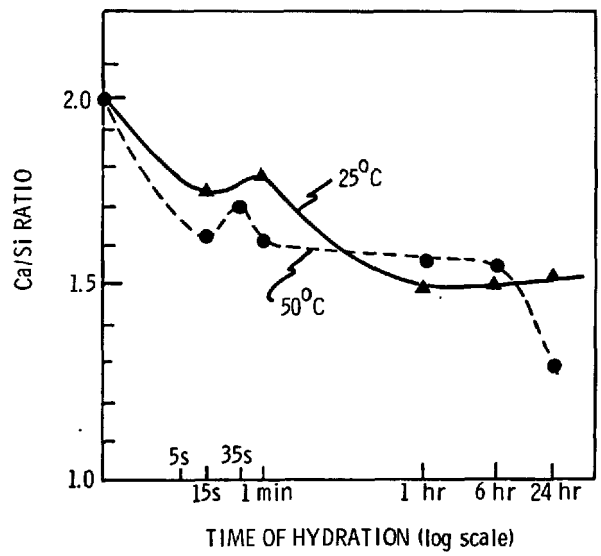

Fig. 8. Variation with time of the Ca/Si ratio for β-C_2S hydrated at 25° and 50°C.

The shape of the Ca/Si-vs-hydration time curves is similar to those obtained for C_3S: a minimum is followed by a maximum in the very early stages of hydration. However, the fluctuations are less pronounced and appear somewhat later than for C_3S. They also appear earlier in samples hydrated at 50°C than in those hydrated at 25°C. These differences may be attributed to the higher hydration rate of C_3S and to the acceleration of β-C_2S hydration due to increased temperature.

The Ca/Si ratio for 50°C hydration reaches a value of about 1.6 in one minute, and then remains practically unchanged up to 6 hours. After 24 hours, it has decreased to about 1.3. At 25°C, the Ca/Si ratio reaches a value of about 1.5 in an hour, and from then on remains practically unchanged (1.50-1.55) up to 24 hours. The difference in the starting times of the plateaus in these Ca/Si curves is presumably due to the different hydration rates of β-C_2S at the two temperatures. The duration of these plateaus may have something to do with the induction period. If this is the case, then it also implies that the Ca/Si ratio on the surface hydrates does not change significantly during the induction period.

Although the probing depth of ESCA is only about 20 Å, bulk analyses can be obtained by sputtering the surface. Sputtering provides the possibility of estimating the thickness of the hydrated layer. Measurements were made on β-C_2S hydrated both at 25° and 50°C. For unhydrated β-C_2S, sputtering did not change the Ca/Si ratio from a value of 2.0 (Fig. 9). For samples hydrated at 50°C for 24 hours, sputtering up to a depth of 150 Å did not change the Ca/Si ratio from 1.3. For other samples, the Ca/Si ratio eventually reached a value of 2.0 as a result of sputtering, but required deeper sputtering with increased hydration time or temperature. From these data, the depth of the hydrated layer for the 25°C samples is on the order of 50 Å after 15 seconds and about 100 Å after 6 hours.

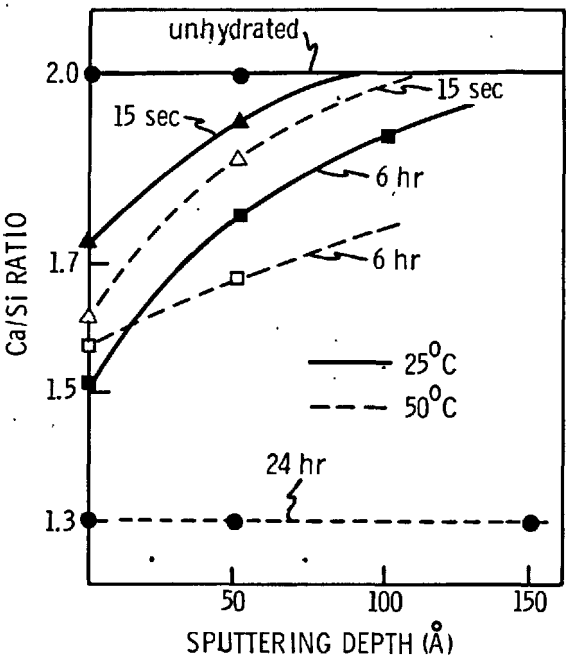

Fig. 9. Ca/Si profile as a function of sputtering depth for hydrated β-C_2S.

Another interesting observation was made regarding the Ca/Si ratio of β-C_2S samples hydrated at 50°C. The surface Ca/Si ratios, after one minute and 6 hours of hydration, are 1.56 and 1.57, respectively. Sputtering to a depth of 50 Å changes these ratios to 1.80 and 1.68. The lower Ca/Si ratio beneath a depth of 50 Å for the 6-hour sample shows that hydration continues progressively beneath the surface, although it may not be noticeable at the surface during the induction period.

In addition to the information provided by the changes in the O_{1s} peak, some interesting conclusions can be drawn from the differences in the binding energies of Ca_{2p} and Si_{2p}. A decrease of 0.6 eV is observed for β-C_2S hydrated for 24 hours at 50°C. This is due to a shift of either Ca_{2p} towards lower, or Si_{2p} towards higher binding energies. The latter case is more probable, since the binding energy of Si_{2p} increases as the material goes from silicate to silica gel (15). Our results would then indicate that the monomer form of SiO_2 in unhydrated β-C_2S is progressively transformed into dimeric or possibly higher polymeric forms upon hydration.

CONCLUSIONS

The present study clearly shows the usefulness of ESCA and high-resolution SEM in elucidating the mechanisms of early hydration of calcium silicates.

New information on the surface morphology of the hydrated calcium silicates has been obtained. Immediately upon contact with water, minute hydration products form on the surface. Simultaneously, dissolution or corrosion of the surface becomes visible. Both the dissolution of β-C_2S and C_3S, and the deposition of the hydrates are nonuniform, and are preferentially localized at grain boundaries. With the progress of hydration, what is believed to be honeycomb Type II C-S-H forms on the surface.

Surface analysis by ESCA revealed changes in the average Ca/Si ratio as a result of hydration. Immediately upon contact with water, the Ca/Si ratios drop for both of the calcium silicates and, following a maximum, continuously decrease. The data indicate the formation of a silica-rich hydrated surface in the early stages of hydration. Chemisorption of Ca^{2+} takes place on this surface. Sputtering of the hydrated surface enabled estimation of its depth as a function of hydration time.

ACKNOWLEDGMENTS

The authors gratefully acknowledge the support of this work through a grant by the U.S. Army Research Office.

REFERENCES

1) H.N. STEIN, (1977) "The initial stages of hydration of C_3S," Il Cemento, 74, 3.

2) J.G.M. De JONG, H.N. STEIN and J.M. STEVELS (1967) "Hydration of tricalcium silicate", J. Appl. Chem., 17, 246.

3) P. FIERENS and J. VERHAEGEN, (1977) "Microcathodoluminescence of C_3S", Il Cemento, 73, 39.

4) P. FIERENS and J. VERHAEGEN, (1974) "Thermoluminescence applied to the kinetic study of the chemisorption of water by tricalcium silicate", Silicates Industriels, 39, 125.

5) J.F. YOUNG, (1972) "A review of the mechanisms of set retardation in portland cement pastes containing organic admixtures", Cem. Concr. Res., 2, 415.

6) J.F. YOUNG, H.S. TONG and R.L. BERGER, (1977) "Compositions of solutions in contact with hydrating tricalcium silicate pastes, J. Amer. Ceram. Soc., 60, 193.

7) M.E. TADROS, J. SKALNY and R.S. KALYONCU, (1976) "Early hydration of C_3S", J. Amer. Ceram. Soc., 59, 344.

8) D.D. DOUBLE and A. HELLAWELL, (1976) "The hydration of portland cement", Nature (London), 261, 486.

9) D.D. DOUBLE, A. HELLAWELL and J.S. PERRY, (1978) "The hydration of portland cement", Proc. Roy. Soc. (London), A359, 435.

10) H.F.W. TAYLOR, (1979) "Cement hydration reactions: The silicate phases", in Proceedings of a conference on cement production and use, held at Franklin Pierce College, New Hampshire, on 24-29 June, in press.

11) D. MÉNÉTRIER, I. JAWED, T.S. SUN and J. SKALNY, (1979) "ESCA and SEM studies on early C_3S hydration", Cem. Concr. Res., 9, 473.

12) D. MÉNÉTRIER, D. McNAMARA, I. JAWED and J. SKALNY, "Early hydration of β-C_2S: Surface morphology", Cem. Concr. Res. in press.

13) S. DIAMOND, (1976) "Cement paste microstructure - an overview at several levels", in Hydraulic Cement Pastes: Their Structure and Properties, p. 2, Cem. Concr. Assoc., London.

14) E. BREVAL, (1977) "Gas-phase and liquid-phase hydration of C_3A", Cem. Concr. Res., 7, 297.

15) C.D. WAGNER, W.M. RIGGS, L.E. DAVIS and J.F. MOULDER, and G.E. MUILENBERG (1979) in Handbook of X-ray photoelectron spectroscopy, p. 52, Perkin-Elmer Corp., U.S.A.

Materials from the Synthetic Tobermorite

Matériaux comportant de la tobermorite de synthèse

T. CIACH, J. DYCZEK, M. PETRI, L. WESTFAL, Stanislaw Staszic Academy of Mining and Metallurgy, Cracow, Poland.

RESUME : La tobermorite de 11 Å, obtenue par traitement à l'autoclave de chaux et de silice en suspension aqueuse, se présente sous la forme de cristaux agglomérés en grains sphériques. La dimension moyenne des grains peut varier selon les particularités du traitement.

L'étude détaillée de la porosité des produits polycristallins obtenus par ce procédé de synthèse, avec diverses formes de granulats, a montré que la porosité totale et la distribution des pores pouvaient être très variés.

Nous avons étudié l'influence des propriétés d'agrégation de la tobermorite de 11 Å sur les propriétés mécaniques, la porosité totale et la distribution des pores des produits obtenus.

SUMMARY : 11 Å tobermorite obteined in a hydrothermal processing of an aqueous solution of lime and silica has the shape of a spherical aggregats of cristallites.
The average size of adjacent grains in particular synthesis may be different.
The detailed study of porosity of polycristalline products made of synthetic tobermorite /with different shapes of aggregates/, indicate the total porosity, although there is a very different pore size distribution to be observed.
In this study we are trying explain the origin aggregate forming, the interactions of pore shapes and their influence on the observed porosity structure as well as mecanical factors of products made of 11 Å tobermorite.

INTRODUCTION

Tobermorite is the main product of reaction derived during the course of autoclavisation of building materials such as: silicate bricks, autoclaved concrete and other materials. The optimal reception of these materials is often empiriely treated. On the other hand as the main product of the reaction, tobermorite is responsible for the utilitarian properties of the product /1,2,3,4/. Established methods syntheses of 11Å tobermorite was observed on the 50's /5,6,7/, but not untill recently were they applied to production, in particular to attractive products such as wollastonite, highly porous materials, insulation materials and so forth.

A particulary attractive method of obtaining calcium silicate hydrates in this and tobermorite is the hydrotermal treatment of quartz -lime water suspension.
It is easy to obtain a water suspension of tobermorite, and after removing water from it /pressing/ obtein light polycrystalline materials. They give evidence of their sufficient mechanical and insulative properties. A mixture of 11 Å tobermorite and CSH phase in the water suspension are usually products of lime and quartz hydrothermic syntheses, by wchich the quantitive ratio of the phase and stage of crystalisation of tobermorite differ in conditions of syntheses.
SEM microscopic observations proved the following:

1-inthe water suspension appear aggregates composed of the tobermorite crystals cemented together by a CSH phase,
2-a dimension of these aggregates are different depending on the conditions of syntheses.

The following experimental description was carried out in the hope of explaning the influence of the aggregates dimensions on the formconnditions and mechanical properties of the polycrystalline materials from synthetic 11 Å tobermorite.

EXPERIMENTAL

The syntheses of tobermorite was carried out with CaO /analytical grade/ and SiO_2 in quartz form of specific surface area 160000m^2/kg in 0,01 m^3 volume of an autoclave with the agotator /120 rpm/ in the temperature of 448°K in saturated steam pressure. The molar ratio of CaO to SiO_2 was 0,87.
The amount of Al_2O_3 present as kaolinite was 0,2 % on the weight of total solids..
In the order of syntheses the change in time of the autoclavisation and the water do dry substance ratio /w:s/, in this cases was as following:

	w:s	time
syntheses A	10:1	10 hrs
syntheses B	7:1	7 hrs

X-ray diffraction showed than the product of syntheses A was 11 Å tobermorite and a small amount of CSH phase, the presence wchich resulted in a slightly raised background in the region of reflex /220/ /fig. 1/.

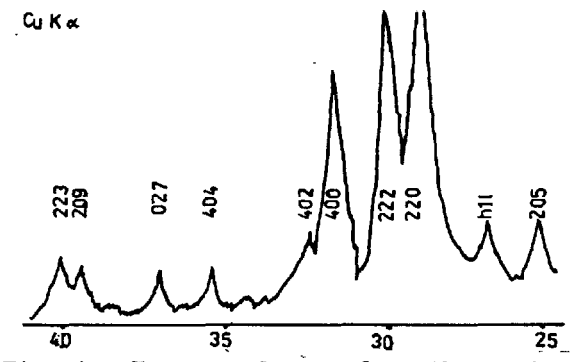

Fig. 1 - X-ray analyses of syntheses A

SEM mocroscopic observation allowed to state that tobermorite appeared in a sphericalag aggregate form of dimension $1 \div 6 \cdot 10^{-6}$m.

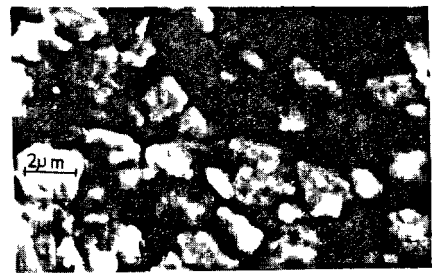

Fig. 2 - The aggregates of tobermorite A

X-ray analyses of syntheses B products showed olso the presence of 11 Å tobermorite but less crystalline. It was stated also that in B material was a greater quantity of CSH phase /fig. 3/.

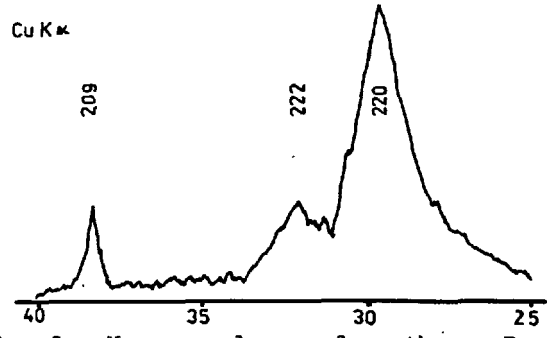

Fig. 3 - X-ray analyses of syntheses B

The aggregates observed on SEM microgcope showed greater dimensions /$20 \div 40 \cdot 10^{-6}$m/ than in material A /fig. 4/.

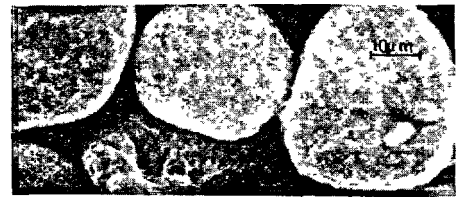

Fig. 4 - The aggregates of tobermorite B

Samples of materials from both syntheses were heated to 673°K and X-ray diffraction showed a characteristic peak of 9,3 Å tobermorite. We may certify the obteined tobermorite as a "normal" variation at 11,3 Å tobermorite /8/.

Samples of $10x20x60 \cdot 10^{-3}$m dimensions were formed from water suspensions of tobermorite by pressing, the top and bottom removing the water from it. The pressing conditions are in Table I. They wery dried by superheated water steam a temperature of 393°C.

Dynamical Young's modulus E_d and Poisson's ratio ϑ were determined by measouring the speed of transmition of ultrasonic wave. An ultrasonic generator was used with frequency of 11 Hz. Precision of measurment were 0,1 s.

$$E_d = C_L^2 \varrho \frac{/1+\vartheta//1-2\vartheta/}{1-\vartheta}$$

C_L - speed wave
ϱ - bulk density

Values of crck initiation energy γ_I and crack propagation energy γ_F were determinated by the "across bending bar with a notch" method /3,10,11,12,13/,
The bars were deformed in three point bending at $4 \cdot 10^{-2}$m span.
The samples of $a=10^{-2}$m, $b=6 \cdot 10^{-2}$m, $d=2 \cdot 10^{-2}$m dimension were nothed to depth c.
c/d ratio was as follows: 0,5; 0,6; 0,7; 0,8.
Load deflection curves were recorded on an INSTRON machine operating at crosshed speeds of $5 \cdot 10^{-5}$m/min.

Using the following formules were determinated the values of γ_I /12/,and γ_F :

$$\gamma_I = \frac{9/1-\vartheta^2/P_F L^2 f/c/d/}{8Eb^2/d-c/^3}$$

P_F - fracture Load
$f/c/d/$ - values are in /12/

$$\gamma_F = \frac{U}{2b/d-c/}$$

U - fracture's total work

γ_F is a function of c/d, decreasing with increasing notch depth. The true γ_F value are given by extrapolating the results to c/d = 1 /10/.
The values of Young's static modulus E ,and bending strength σ_F, were determinated by deforming the bars without notch under the meantioned conditions.
Compressive strength σ_K, was determinated on the cubic samples.

The value of critical defect C, was calculated from Griffith's equation /11/.

$$\sigma_F = \left[\frac{2\gamma}{\pi C}\right]^{1/2}$$

Data of the specimens: ϑ, E_d, E, σ_F, σ_K, γ_I, γ_F, C are sumarized in Table I.

Pores and pores size distibution were determinated in 75 000 ÷ 37,5 Å range, and were carried out by using mercury porosimeter /fig. 5 and 6/.
Total porosity was calculated. The results are tabulated in Table I.

Table I

	Material A	Material B
Pressing conditions $N/m^2 \cdot 10^6$	20,89	15,94
Bulk density ϱ $kg/m^3 \cdot 10^{-3}$	0,600	0,600
Total porosity $m^3/kg \cdot 10^{-3}$	1,4166	1,4166
Mercury porosity $m^3/kg \cdot 10^{-3}$	1,1135	1,1445
Poisson's ratio ϑ	0,05	0,05
E_d $N/m^2 \cdot 10^9$ $\perp$	1,524	1,934
E_d $N/m^2 \cdot 10^9$ $\parallel$	2,052	2,005
E $N/m^2 \cdot 10^8$	4,562	3,544
σ_F $N/m^2 \cdot 10^6$	3,42	2,97
σ_K $N/m^2 \cdot 10^6$	10,86	9,21
γ_I I/m^2	4,02	7,04
γ_F I/m^2	0,41	0,092
C $m \cdot 10^{-4}$	1,000	1,794

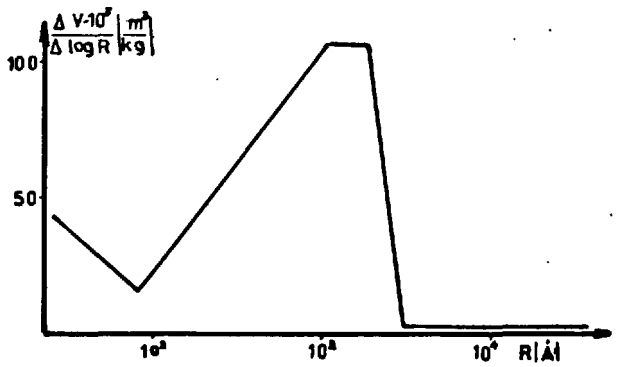

Fig. 5 - Pores size distribution material A

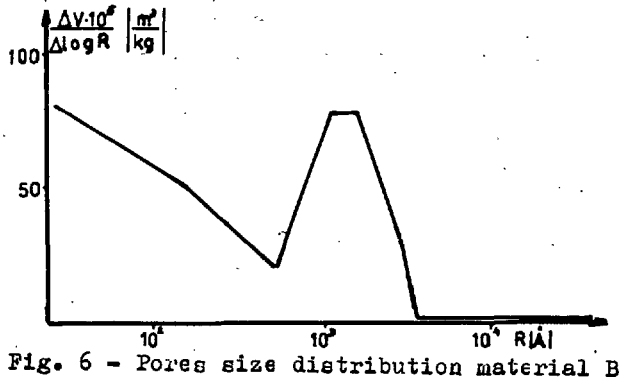

Fig. 6 - Pores size distribution material B

RESULTS

The mechanical properties of materials A and B show significent difference.
Material A has higher values of compressive strength σ_K, bending strength σ_F, and Youngs static modulus E.
In both materials the values of compresive strength are much higher than of the bending strength. It is typical for brittle materials.
Measurment of Young's Dynamic modulus E_d, was determined vertically and horizontally with respect to the forming directions.
The value differenses of E_d depending on the direction of measurment indicate an anisotropic efect of the tested material.
If we can say that material B is isotropic, to the same ettent material A showed significant anisotropic mechanical properties.

Material A was formed from a tobermorite water suspension with a small quantity of CSH concentrated in the aggregates having small dimensions.
For both materials it was found that the value of γ_I was greater than γ_F. So we use more energy for crack initiation than for crack propagation for the fracture of the material. It means that there is possibility of a cathastrophic course of fracture process, in this case when a high deflection force is used. Material A was better, becouse it showed a higher resistance to fracture/ e.g. γ_F for A is greater than that for B/.
A pore determination allowed to say, that the total mercury porosity of both examined materials in range of 75 000 ÷ 37,5 Å was almost identical. We have observed a difference in the pore size distribution. Material B was formed from a water suspention containing tobermorite aggregates with a larger quontity of CSH than material A, thus it can be said that material B has greater amount of small pores with radius less than 500 Å.

CONCLUSIONS

/i/ Obtaining tobermorite in a water suspension creates aggregates of 11 Å tobermorite cemented by the CSH phase. The stage of tobermorite crystalization and quantity of CSH combining has an influence on the eatent of these aggregates and machanical properties of the obteined products by pressing.

ii The obteined materials from the tobermorite water suspension of smalle aggregate dimensions and with smaller amaunts of CSH phase showed better mechanical properties. However, to obtein such a suspension and form from these materials requires more energy for autoclavisation and formation.

iii When examining the mechanism of fracture on the samples it was stated that the amount of energy required for crack initiation is many times greater than energy necessery for fracture propagation. The practical results of this are, that the products from synthetic tobermorite aught to have a much smoother surface /with out cracks or notches/ and that the addition of reinforcing materials will fortify this tobermorite material.

REFERENCES

1.- G.L. KALOUSEK /1954/, "Studies of the Cementitions Phases of Autoclaved Concrete Products Made of Different Raw Materials", J.Amer.Conc.Inst.,50, 365.

2.- L.D. SANDERS, W.J. SMOTHERS /1957/, "Effect to Tobermorite on the Machanical Strength of Autoclaved Portland Cement-Silica Mixtures", J.Amer.Conc.Inst., 54, 1929.

3.- S. MINDESS /1970/, "Relation between the Compresive Stregth and Porosity of Autoclaved Calcium Silicate Hydrates", J.Amer.Ceramic.Soc., 53, 621.

4.- J.M. CRENNAN, J.R. DYCZEK, H.F.W. TAYLOR /1972/, "Quantitive Phase Compositions o of Autoclaved Cement-Quartz Cubes", Cement and Conc.Res., 2, 277.

5.- L. HELLER, H.F.W. TAYLOR /1951/,"Hydrated Calcium Silicates", J.Chem.Soc.,531, 2397.

6.- G.L. KALOUSEK /1955/,"Tobermorite and Related Phase in the System CaO-SiO_2-H_2O" J.Amer.Conc.Inst., 51, 989.

7.- G.L. KALOUSEK /1957/,"Crystal Chemistry of the Hydrous Calcium Silicates".I. J.Amer.Ceramic.Soc., 40, 124.

8.- T. MITSUDA, H.F.W. TAYLOR /1974/,"Normal and Anomalous Tobermorites", Proc.VI Int Cong.of Cement. Moscow.

9.- K. KONSZTOWICZ /1976/,"Breaking Energy of the Ceramic Materials", Szkło i ceramika, Poland, 27,n°7, 184.

10.- R. DAVIDGE, G. TAPPIN /1968/,"The Effective Surface Energy of Brittle Materials", J.Mater.Sci.,3, 165.

11.- A.A. GRIFFITH /1920/,"Phenomena of Rupture and Flow in Solids", Phil.Trans.Roy. Soc. London. Ser.A. 221, 163.

12.- H.G. TATTERSALL, H. TAPPIN /1966/, Mater.Sci., 1, 296, acc./10/.

13.- J. NAKAYAMA /1965/, J.Amer.Cer.Soc., 48, 583, acc./10/.

Hydration and strength of normal portland cement admixed with anhydrous calcium sulfate

Hydratation et résistance du ciment portland normal additionné d'anhydrite

K. NAKAGAWA, Senior Research Manager, Denki kagaku Kogyo Co., Ltd. R & D Department,
K. ISOZAKI, Research Chemist, of Omi-Plant, Japan,
Y. WATANABE, Research Chemist.

RESUME : Des recherches ont été entreprises sur l'hydratation et le durcissement de ciments composés de ciment portland normal et de sulfate de calcium anhydre du type II ou de silice activée; il s'agissait notamment de connaître l'influence des conditions de cure et des agents réducteurs d'eau.

L'addition d'une quantité appropriée de II $CaSO_4$ retarde le début de l'hydratation du C_3S, mais plus tard augmente son taux d'hydratation. A température plus élevée, l'effet de cette addition d'anhydrite est augmenté. L'addition d'un agent réducteur d'eau (condensat de formol et de sulfonate β naphtalénique de sodium) retarde l'hydratation du C_3S aux premiers âges, mais accélère la formation de l'ettringite.

L'addition d'une quantité optimale de II $CaSO_4$ accélère l'hydratation du C_3S et la formation de l'ettringite, augmente la proportion d'eau non évaporable dans la pâte, et contribue ainsi à améliorer la structure de la pâte durcie. A température plus élevée, la cure est améliorée lorsque la proportion d'anhydrite ajoutée augmente; l'addition de silice activée peut alors compenser les inconvénients de l'anhydrite et améliorer la résistance à long terme et la stabilité.

SUMMARY: Investigations were made on the hydration process and the mechanism of strength development of cements composed of normal portland cement and Type II anhydrous calcium sulphate or further admixed with active silica to know the influences of the curing condition and the water reducing agent affecting thereon.

When an optimum quantity of II-$CaSO_4$ is added to normal portland cement, the early hydration of C_3S is retarded but the degree of hydration at the later age is increased. The effect of the admixture is noticeable so far at a high temperature. The addition of a water reducing agent (formalin condensates of β-naphthalene sodium sulfonate) promotes the retardation of C_3S hydration at the early stage, but accelerates the ettringite forming reaction.

The addition of an optimum quantity of II-$CaSO_4$ accelerates the hydration of C_3S and the formation of ettringite and the increase in non-evaporable water with attendant improvement of paste structure and strength development. It is considered that a high temperature curing is effective if the added quantity of II-$CaSO_4$ is large, and that the further addition of active silica compensates the disadvantage of II-$CaSO_4$ and contributes to the long-period strength and the stability.

I. INTRODUCTION

Addition of gypsum to normal portland cement (NPC) is limited from the viewpoint of preventing the flash setting and the abnormal expansion (1). Important factors producing effects on these phenomena are the content of C_3A, the alkali content and the fineness of the cement. It has been known that the strength may be considerably increased by adding an optimum quantity of gypsum (1) (2), but it is supposed that if an excess quantity of gypsum is added to the cement, the unreacted SO_3 and SO_3 contained in the CSH gel will react with the aluminate components to accelerate the formation of ettringite or the growth of crystal, whereby the stability of the cement stone has been eventually lost for a long period of time (1) (3) (4).

On the other hand, regulated set cement and expansive cement etc. contain large amounts of calcium aluminate and gypsum and/or anhydrite (II-$C\bar{S}$), In view of these background facts, this article reports the investigation which have been made on hydrate structure and mechanism of strength development of the cement admixed with II-$C\bar{S}$ to know the fundamental facts including the influences of curing conditions and water reducing agent.

II. EXPERIMENTAL

Table I shows the mineral compositions of the admixtures, and Table II shows the chemical composition of NPC. In Table III, there are shown the curing methods. The high temperature curing was effected at 65°C for 6 hours by steam curing after pre-curing at 20°C, 80%rh and then left standing for spontaneous cooling.

TABLE I

Mineral composition of admixtures (wt%)

Name of admixture	II-$CaSO_4$	Activated SiO_2
$C\bar{S}$	100	0
$C\bar{S}$+S	85	15

TABLE II

Chemical composition of normal portland cement(NPC) (wt%)

ig.loss	insol.	SiO_2	Al_2O_3	Fe_2O_3	CaO
0.7	0.3	22.0	4.7	3.2	64.8

MgO	SO_3	Na_2O	K_2O	f-CaO	blaine(cm^2/g)
1.2	2.0	0.40	0.43	0.8	3090

TABLE III

Curing method

No.1	Initial curing	After one day
NPC	20°C,80%rh	20°C,80%rh 20°C(in water)
NPC+$C\bar{S}$	"	"
NPC+$C\bar{S}$+S	"	"

No.2	Pre-curing	Steam curing cycle
NPC	4hrs	65°C,6hrs 20°C 80%rh / 20°C/hr natural cooling
NPC+$C\bar{S}$	6hrs	
NPC+$C\bar{S}$+S	5hrs	
	After one day	20°C,80%rh 20°C(in water)

The water to cement ratio was 0.3 and 0.5% of the water reducing agent (formalin condensates of β-naphthalene sodium sulfonate) was added to cement (substituted for water).

Each of the paste specimens (4x4x16 cm beam) at the predetermined age was subjected to strength test. The crushed specimen was divided into a first group having the size of 5.0mm to 2.5mm and a second group having the size of less than 1.7mm. The former group was D-dried (for 48 hours) and used as samples for determining the evaporable water, the non-evaporable water, and the pore volume (measured by using mercury pressure porosimeter) and observing the morphology of hydrates by scanning electron microscope, whereas the latter group was washed with ethanol and subjected to X-ray diffraction analysis.

III. RESULTS AND DISCUSSION

III-1. HYDRATION OF C_3S AND FORMATION OF ETTRINGITE

The differences in hydration degree of C_3S between the curing at 20°C and 65°C at the curing age of 24 hrs, were found about 10% for the NPC system wherein the admixture was not added, about 15% for the $C\bar{S}$ system wherein 10% of II-$C\bar{S}$ was added, and about 18% for the $C\bar{S}$+S system wherein 10% of II-$C\bar{S}$ and activated silica were added. These results show that the effect of high temperature curing is remarkably promoted by the addition of the admixtures. (Fig. 1 (a) (b) (c))

The hydration of C_3S is accelerated by the admixtures. The difference in hydration degree of C_3S at the 24 hour age between the NPC and the systems of the admixtures added is increased by 5 to 10% when the curing is effected at 20°C and about 10% when the curing at 65°C.

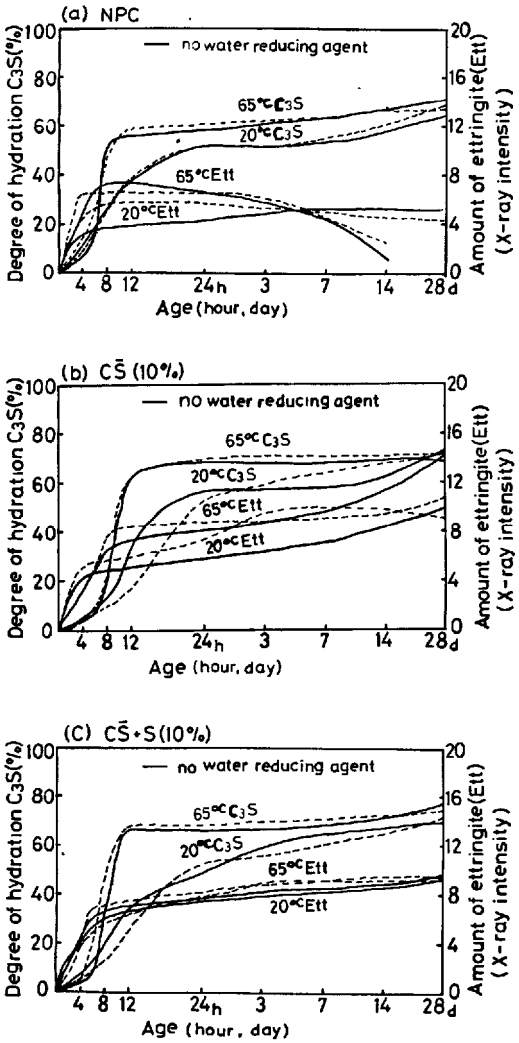

Fig.1 Hydration process by X-ray analysis (Water curing after one day).

However, the difference has been lessened at the 28 day age. In both of the $C\bar{S}$ and $C\bar{S}$+S systems, when the added amounts of the admixtures are decreased to respectively 5% and 7.5%, the hydrations of C_3S are more effectively accelerated as compared to the system wherein the added amount is 10%, whereas there is found tendency that the acceleration effect is decreased when the added amount is increased in excess of 10%.

The water reducing agent apparently retards the initial hydration of C_3S in both of the $C\bar{S}$ and $C\bar{S}$+S systems, but does slightly accelerate the hydration at the curing age of later than 24 hrs.

Although it had been recognized that the degree of super saturation of Ca^{2+} in the liquid phase was promoted by adding gypsum to pure C_3S alone to accelerate the initial hydration of it (5), the hydration of C_3S contained in the cement was found to be retarded. This is considered as related to the ettringite formation reaction which is activated by the addition of II-$C\bar{S}$ and in this activated period the nucleation for enterring into the acceleration period of hydration of C_3S becomes small. The added water reducing agent is adsorbed onto the surfaces of cement particles to facilitate this phenomenon. If the curing is effected at the high temperature of 65°C, this phenomenon is ceased and the hydration of C_3S takes place actively concurrent with the formation of ettringite.

The formation of ettringite is appreciably affected by the action of the water reducing agent. The cement admixed with II-$C\bar{S}$ is particulary affected thereby, but similar actions are observed in the system of NPC alone and other systems referred to above irrespective of the curing temperature. As the mechanism attributing to this phenomenon, it may be assumed that the water reducing agent is partially adsorbed onto the surfaces of the calcium aluminate particles to render the organization of protective film, at which the ettringite is formed at the initial stage of hydration, to be coarse to facilitate the dissolution of Ca, Al ions.

In the $C\bar{S}$+S system, at both of the early and later curing ages, the difference in ettringite formation due to the curing temperature is small. Whereas in the $C\bar{S}$ system, the amount of formed ettringite is relatively increased when the curing is effected at 65°C, and gradually increased further with the lapse of time. It is shown that active silica acts to form a large amount of ettringite at the early stage of curing. (Fig. 1(c))

III-2 MORPHOLOGY OF HYDRATION PRODUCTS

At the early age of curing at 20°C, the hydration does not proceed so far and the cement particles have the sizes of several to several tens microns and are dispersed to form a coarse matrix. Although no acicular or needle-like ettringite is visually confirmed at this stage, a relatively amount of ettringite has been found by X-ray analysis. It is, therefore, considered that the crystals of ettringite are not grown to have appreciable sizes and they form minute organizations adhering to the surfaces of calcium aluminate particles. (Fig. 2)

When the curing is effected at 65°C, a large numbers of needle-like ettringites are found in the voids of cement matrix at the 24 hour age, the diameter of such needle-like crystals being 0.2 to 0.4 μ and the length being several μ, and the crystals are grown to have diameters of 0.4 to 0.6 μ, but the lengths are not changed. The shapes of ettringite are characterized by the needle-like crystal and the hexagonal cross-section of prismatic crystal.

The hydrated particles form continuous gel as the hydration proceeds, and the matrix of 24 hrs age cured at 65°C shows the substan-

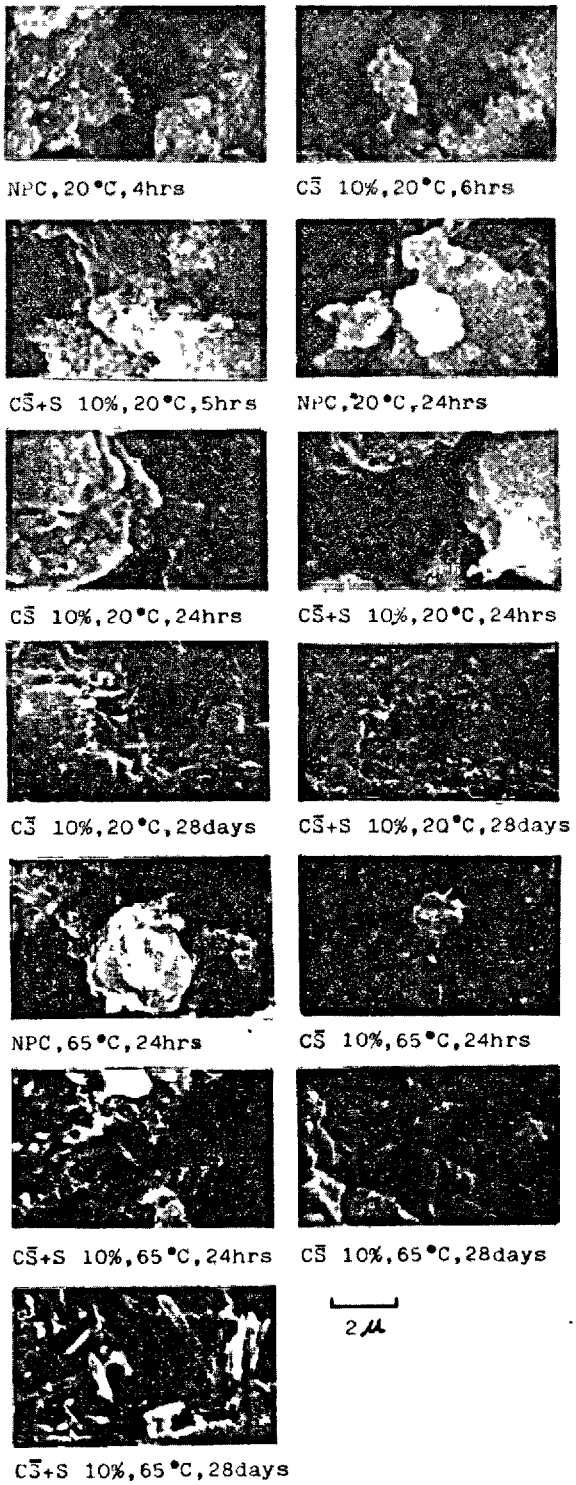

Fig.2 Observation of hydrates by scanning electron microscope. (water curing after one day.)

tially same state as that of the matrix of about the one month age at 20°C. It has been observed that ettringite crystals grow into the liquid phase presented in the voids of the gel from the surfaces of calcium aluminate particles.

III-3 STRENGTH DEVELOPMENT AND HYDRATION DEGREE

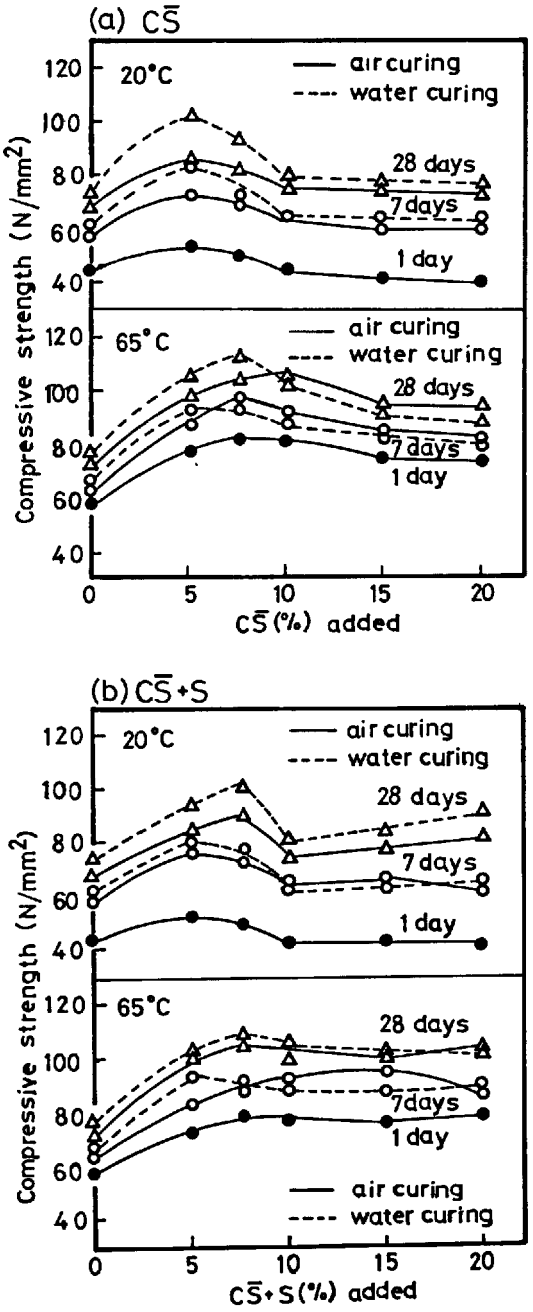

Fig.3 Relation between compressive strength and admixture content.

In the $C\bar{S}$ system cured at 20°C, the cement admixed with 5% of $C\bar{S}$ has the highest strength throughout the curing ages of 1 to 28 days, and the strength at the curing age of 28 days of the cement admixed with 5% of $C\bar{S}$ is about 1.4 times as high as that of the NPC. Those admixed with more than 5% of $C\bar{S}$ have the strengths approximately equal to or slightly lower than that of the NPC. If the curing is effected at 65°C, the cement admixed with 7.5% of $C\bar{S}$ has the maximum strength. The strengths of the cement admixed with larger amounts of $C\bar{S}$ are somewhat different from the strengths of similar cement cured at 20°C so that the strengths of the cements cured at 65°C are increased by 10 to 20% as high as that of the NPC and inter alia the strengths in air curing are particularly improved (6). (Fig. 3(a))

In the $C\bar{S}$+S system cured at 20°C, the cement admixed with 5% of $C\bar{S}$+S has the maximum strength at the curing ages of 1 to 7 day, and the cement admixed with 7.5% of $C\bar{S}$+S has the maximum strength at the 28 day age. Although the strengths of the cements of the $C\bar{S}$ system admixed with larger amount of $C\bar{S}$ are not increased as compared to that of the NPC, the strengths of the cements admixed with larger amounts of $C\bar{S}$+S are increased by 10 to 15% as high as that of the NPC at the 28 day age. When the curing is effected at 65°C, the cement admixed with 7.5% of $C\bar{S}$+S has the maximun strength at the curing age of 28 days. No appreciable difference has been found between the strengths of the cements admixed with 5 to 20% of $C\bar{S}$+S, respectively, and the functional effect of the activated silica become obvious so that the developed strengths of the cements are approximately 1.4 times as high as that of the NPC. (Fig.3(b))

If an optimum quantity (5-7.5%) of II-$C\bar{S}$ is added, unreacted II-$C\bar{S}$ being scarcely present at an early age, the strength development is facilitated futher effectively.

The rate of increase in strength in terms of the increase in non-evaporable water in each cement is obviously different in every system. In the NPC cured at 20°C, the strength is developed relatively rapidly with small increase in the quantity of non-evaporable water until it reaches to 50 N/mm^2 but the rate of increase in strength at the later age is small. On the contrary, in the $C\bar{S}$ and $C\bar{S}$+S systems, the rates of increase in strength are larger, and this tendency is more remarkable in the $C\bar{S}$+S system. When the curing is effected at 65°C, slightly difference is found between the rate of increase in strength of the $C\bar{S}$ system and that of the NPC, whereas the rate of increase in strength of the $C\bar{S}$+S system is prominent. It is considered that the addition of activated silica serves to strengthen the matrix.(Fig.4(a)(b))

When the curing is effected at 20°C, the interrelation between the total pore volume and the strength may be plotted on a substantially straight line in either of the NPC and $C\bar{S}$ and $C\bar{S}$+S systems irrespective of the

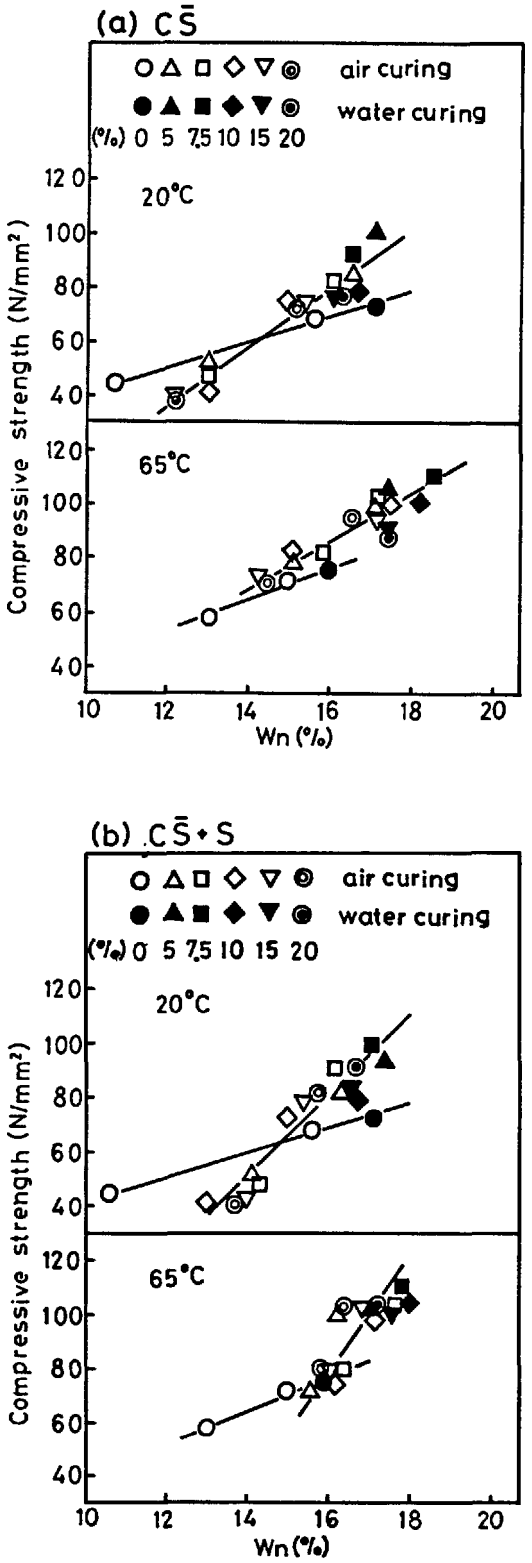

Fig.4 Relation between compressive strength and non-evaporable water (Wn).

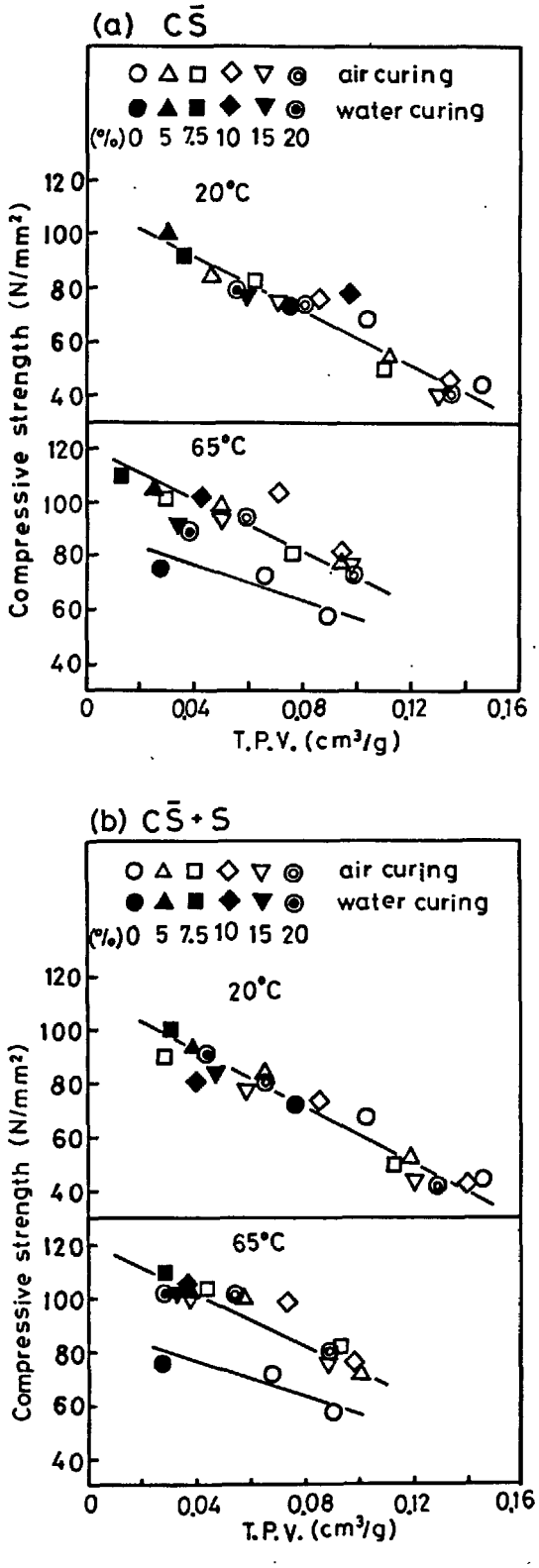

Fig.5 Relation between compressive strength and total pore volume (75-75000 Å).

quantities of the admixtures. However, when the curing is effected at 65 °C, the cements admixed with admixtures have higher strengths as that of the NPC having the same total pore volume, and inter alia the strength in air curing are improved rather than the strengths in water. Different from the rate of increase in strength in terms of the increase in non-evaporable water, the rate of increase in strength in terms of the decrease in pore volume is not distinguishable between the $C\bar{S}$ system and the $C\bar{S}$+S system. (Fig. 5 (a)(b)) This aspect requires further investigation.

IV. CONCLUSION

When an optimum quantity of II-$C\bar{S}$ (5-5.7%) is added to normal portland cement, the hydration of C_3S is retarded at the early stage but after aged for one day it is accelerated.

The addition of a water reducing agent (formalin condensates of β-naphthalene sodium sulfonate) promotes the retardation of C_3S hydration at the early stage, but accelerates the ettringite formation reaction.

The addition of an optimum quantity of II-$C\bar{S}$ facilitates the hydration of silicate phase and increases the formation of ettringite thereby to increase the amount of non-evaporable water and to strengthen the paste structure.

A higher temperature curing becomes effective with the increase in amount of II-$C\bar{S}$.

The activated silica serves to strengthen the paste structure and improve on the stability for a long period of time due to the promotive effect on ettringite formation at the early stage and the suppressive effect on it at the later age.

REFERENCE

1.- W. LERCH (1946), "The influence of gypsum on the hydration and properties of portland cement pastes", Proceed. Am. Soc. Test. Mater., 46, 1252-1292.

2.- M. VENUAT (1974), "Effect of elevated temperatures and pressures on the hydration and hardening of cement", The VI Inter. Symp. Chem. of Cement, Moscow, Principal Paper.

3.- I. JELENIĆ, A. PANOVIĆ, R. HALLE and T. GAĆEŠA (1977), "Effect of gypsum on the hydration and strength development of commercial portland cements containing alkali sulfates" Cement and Concrete Research, 7, 239-246.

4.- R.S. AL-RAWI (1977), "Gypsum content of cements used in concrete cured by accelerated methods", J. Test. Eval., 5, No. 3., 231-237.

5.- N. KAWADA and A. NEMOTO (1967), "Hydration process of calcium silicates during first 24 hrs", CAJ Review of the 21th general Meeting, 58-62.

6.- K. ISOZAKI, K. NAKAGAWA and Y. WATANABE (1978), "Studies on the strength of high ettringitic cement stones steam cured at normal pressure", CAJ Review of the 32th General Meeting, 42-43.

Le rôle des aluminates et des sulfoaluminates de calcium dans l'élaboration de propriétés de la pierre de ciment

Part played by aluminates and calcium sulfoaluminate in formation of properties of cement stone

T.V. KOUZNETSOVA, candidat ès sciences techniques,
I.V. KRAVTCHENKO, docteur ès sciences techniques, NIITzement, Moscou, U.R.S.S.

RESUME : On a étudié le phénomène d'hydratation du sulfoaluminate de calcium ainsi que de ses mélanges avec les silicates et les aluminates de calcium. On a démontré que la morphologie des cristaux formés ainsi que leur microstructure présentent des traits physiques propres au ciment hydraté. On a constaté que suivant le rapport quantitatif entre l'ettringite et les hydroaluminates de calcium dans la pierre de ciment en voie de durcissement il s'y forme soit une structure d'hydratation stable, soit des conditions favorables à son extension. La formation de structure d'hydratation, sa solidité, son extension et son autotension sont régies par la quantité d'aluminates et de sulfoaluminates de calcium contenue dans le ciment.

SUMMARY : Hydration of calcium sulfoaluminate and its mixtures with calcium silicates and aluminates has been investigated. It is shown that the morphology of novel formation cristalls and microstructure charactérise physical properties of hydrated cement. It has been found out that depending on the ratio in the amounts of ettringite and calcium hydroaluminates, a strong hydration structure is formed in the hardening cement stone, or conditions for its spreading are provided. Formation of the hydration structure, its strength, expanding and self-stressing are controlled by the amounts of aluminates and calcium sulfoaluminate in cement.

Les aluminates et les sulfoaluminates de calcium constituent justement les phases de clinker qui attirent l'attention lorsqu'on étudie les différents types de ciment : ciment portland, ciment alumineux à teneur élevée en alumine, ciment expansif. La cinétique de l'hydratation, la constitution des composés hydratés, la stabilité au cours d'un long durcissement, l'influence exercée sur la formation de la structure d'hydratation de la pierre de ciment sont l'objet de nombreuses études entreprises sur ces ciments.

L'analyse de données publiées sur la composition des hydroaluminates de calcium montre que le rapport entre CaO et Al_2O_3 dans les composés hydratés est fonction de la composition des aluminates de calcium déshydratés (1-3), de la température et de la durée d'hydratation (4, 5), de la présence ou de l'absence de $Ca(OH)_2$ dans le milieu d'hydratation (6, 7). L'hydratation des aluminates de calcium en présence du gypse s'accompagne de la formation de l'hydrosulfoaluminate de calcium dont la composition dépend de la quantité de sulfate de calcium contenue dans la phase liquide du mortier (8, 9).

L'hydratation du sulfoaluminate de calcium entraîne la formation de la variante monosulfate de l'hydrosulfoaluminate de calcium et, en présence du gypse - de l'ettringite et de l'alumine hydratée (10).

La cinétique de l'hydratation d'aluminates et de sulfoaluminates de calcium est régie par de nombreux facteurs en conditionnant les particularités morphologiques des composés hydratés ainsi que la structure de la pâte de ciment qui durcit (11). La morphologie des produits d'hydratation et la microstructure de la pierre de ciment en voie de durcissement ainsi que ses interdépendances avec les propriétés physiques de la pâte de ciment ont été étudiées par de nombreux chercheurs. Cependant le nombre important de facteurs à actions réciproques sur la vitesse d'hydratation et la formation de la structure d'hydratation nécessite une étude détaillée de tous les stades d'hydratation du ciment et de durcissement de la pâte de ciment.

L'objet des recherches a été l'étude de l'hydratation du sulfoaluminate de calcium et de ses mélanges avec les aluminates, les silicates de calcium et le gypse ainsi que de l'influence réciproque des réactions d'hydratation sur la résistance et le gonflement du ciment en voie de durcissement.

L'étude du processus d'hydratation a été conduite par deux méthodes :
- par agitation de la charge d'éprouvette dans l'eau pour un rapport S/L = 1/50 durant 1, 7 heures, 1 à 28 jours ;
- en éprouvettes de pâte de ciment dont le rapport E/C est égal à 0,4.

Par la première méthode étaient préparées les suspensions de sulfoaluminates de calcium qu'on conservait dans des ballons étanches. Le malaxage de la suspension était conduit continûment durant 3 jours, puis trois fois par jour pendant une heure. Les délais prescrits écoulés les suspensions étaient filtrés et on déterminait la composition chimique de la phase liquide, tandis que le résidu de filtrage était soumis à l'analyse aux rayons X et à l'analyse thermique différentielle.

Tableau I

Composition de la phase liquide au cours de l'hydratation du sulfoaluminate de calcium

Délais de l'hydratation, jours	Concentration, mg/l		
	CaO	Al_2O_3	SO_3
0,04	851	1105	132
0,29	608	1053	74
1	600	1038	38
3	218	242	36
7	187	195	13
28	125	111	15

Comme il ressort des données figurant dans le tableau I la dissolution du sulfoaluminate de calcium s'effectue de façon non congruente. Une heure après sa mise en interaction avec l'eau, le rapport molaire d'oxydes dans la phase liquide ne correspond plus à la composition initiale du sulfoaluminate de calcium. Le rapport de CaO à Al_2O_3 est voisin de l'unité durant les deux premiers jours d'hydratation. La solution est métastable et avec l'hydratation subséquente du sulfoaluminate de calcium le rapport CaO/Al_2O_3 s'accroît jusqu'à 1,8-2.

Les études aux rayons X des phases solides après filtrage des suspensions ont montré qu'après une heure d'hydratation on détectait dans la composition des produits formés l'hydrosulfoaluminate de calcium des variantes tri- et monosulfate. Le jour suivant l'hydratation se poursuivant, on observa sur le radiogramme, à côté de ces composés des raies de diffraction caractéristiques de l'aluminate de calcium de formule $2CaO \cdot Al_2O_3 \cdot 8H_2O$.

D'après les données fournies par l'analyse aux rayons X et l'analyse thermique différentielle l'hydratation du sulfoaluminate de calcium s'effectue de façon intense et, au bout de 28 jours, tout le $3CaO \cdot 3Al_2O_3 \cdot CaSO_4$ est pratiquement hydraté.

Dans la seconde méthode l'étude de l'hydratation du sulfoaluminate de calcium avec une quantité restreinte d'eau a montré que dans ce cas l'hydratation se ralentit et après 28 jours, le degré d'hydratation du sulfoaluminate ne constitue que 71 % de la masse initiale. L'analyse aux rayons X et l'analyse thermique différentielle ont établi que la composition des produits d'hydratation contenait : l'alumine hydraté, l'ettringite, l'hydroaluminate de cal-

cium, hydromonosulfoaluminate de calcium (après trois jours de durcissement) et les hydrocarboaluminates de calcium (à 28 jours et plus de durcissement).

Les essais physiques et mécaniques d'éprouvettes ont montré (fig. 1) que l'hydratation du sulfoaluminate de calcium s'accompagne de la formation d'une structure d'hydratation solide qui en un jour de durcissement atteint une résistance de 337 kgf/cm^2. Durant les temps de durcissement suivants l'accroissement de la résistance de la structure se ralentit et au bout de 28 jours la pierre de ciment acquiert une résistance de 500 kgf/cm^2.

L'extension des éprouvettes est peu sensible de l'ordre de 0,05 à 0,08 %.

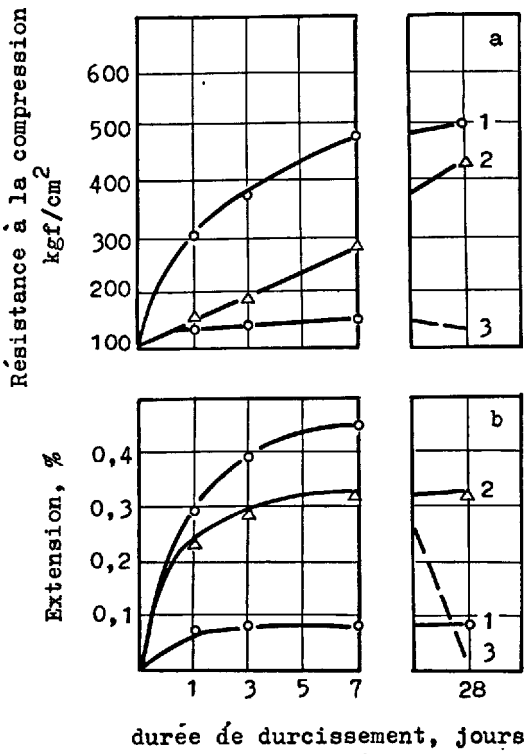

Fig. 1 - Résistance (a) et extension (b) d'éprouvettes durant le durcissement s'étendant sur 1 à 28 jours. 1 - du sulfoaluminate de calcium, 2 - idem avec addition de 10 % de gypse, 3 - idem avec addition de 36 % de gypse. On a montré en pointillé la désagrégation de l'éprouvette.

L'étude de l'hydratation du sulfoaluminate de calcium en présence de gypse a permis d'établir que la composition des produits d'hydratation est fonction de la quantité de gypse introduit. Pour de petites additions de gypse (10 % de la masse du mélange avec le sulfoaluminate de calcium) la quantité d'ettringite monte quelque peu (fig. 2) par rapport à sa quantité obtenue avec l'hydratation sans gypse. A côté de l'ettringite on rencontre dans la composition des produits d'hydratation des aluminates hydratés et des hydrocarboaluminates de calcium. Les premiers jours du durcissement la résistance des éprouvettes est beaucoup inférieure à celle de la pierre de ciment obtenue par hydratation du sulfoaluminate de calcium pur.

Avec l'adjonction au sulfoaluminate de calcium du gypse en quantité dosée pour la fixation complète du sulfoaluminate de calcium en ettringite, la résistance de la structure d'hydratation chute brusquement, et, après 7 jours de durcissement, les éprouvettes se désagrègent, par suite d'importantes contraintes au sein de la structure engendrées par la formation d'une grande quantité d'ettringite (sa quantité augmentant du double devant celle formée avec l'hydratation de $3CaO \cdot 3Al_2O_3 CaSO_4$ en absence de gypse). Cela engendre une forte dilatation des éprouvettes et un abaissement de la résistance de la structure qui ne peut être maintenue devant les contraintes développées. Même une limitation de la dilatation (par armaturage biaxiale des éprouvettes) ne peut s'opposer aux efforts engendrés par la formation d'une grande quantité d'ettringite dans la pierre de ciment qui durcit.

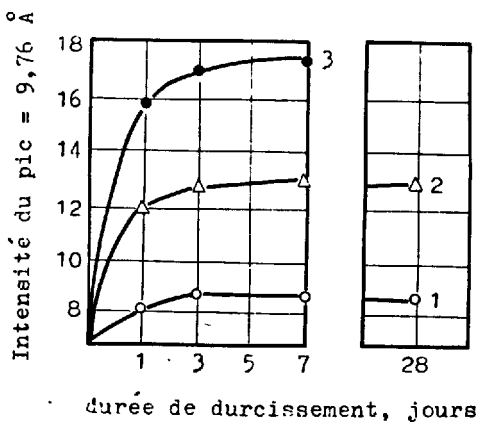

Fig. 2 - Hauteurs des pics de diffraction de l'ettringite sur les diagrammes radiographiques d'éprouvettes dont le durcissement s'étale sur 1 à 28 jours. 1 - du sulfoaluminate de calcium, 2 - idem avec 10 % de gypse, 3 - idem avec 36 % de gypse.

Les études microscopiques d'éprouvettes par diffraction des électrons ont montré qu'avec l'hydratation du sulfoaluminate de calcium, à l'expiration d'un jour, il apparaît à côté de l'ettringite des cristaux lamellaires d'aluminate de calcium hydraté et du monosulfoaluminate de calcium hydra-

té. Les dimensions des cristaux d'ettringite s'accroissent au bout de 28 jours de durcissement. L'éprouvette manifeste une compacité élevée.

L'hydratation du sulfoaluminate de calcium avec l'addition de 10 % de gypse, un jour après, fait acquérir à l'éprouvette une nette structure cristalline de fins cristaux lamellaires d'aluminates de calcium hydratés et de gros cristaux d'ettringite de dimension atteignant 6 μm. La quantité d'ettringite et la dimension de ses cristaux augmentent durant 7 jours de durcissement. Les cristaux d'ettringite en s'allongeant repoussent les cristaux lamellaires voisins en engendrant des pores entre ces derniers. Au cours de l'hydratation ultérieure du mélange de sulfoaluminate de calcium et de gypse, la quantité d'ettringite et la dimension de ses cristaux demeurent invariables, les pores et les vides entre les cristaux d'ettringite se remplissant de cristaux lamellaires et de masse informe ; la compacité des éprouvettes durant cette période augmente.

La confrontation des résultats d'études physico-chimiques et des données d'essais physiques et mécaniques d'éprouvettes montre que suivant le rapport entre la quantité d'ettringite et d'aluminate de calcium hydraté dans le système en voie de durcissement il est possible soit d'augmenter la résistance, soit de provoquer l'expansion et l'autotension de la pierre de ciment. C'est ainsi que la pierre de ciment au cours de l'hydratation du sulfoaluminate de calcium possède une autotension de 14 kgf/cm^2, tandis qu'en présence de gypse elle s'élève à 38 kgf/cm^2.

Les études ont montré que pour obtenir des ciments à contraindre il est utile de combiner l'aluminate tricalcique au sulfoaluminate de calcium. Le tableau 2 nous fournit les résultats d'essais de ciments obtenus par broyage simultané du clinker-portland et du sulfoaluminate de calcium. Dans cette opération l'éprouvette 1 contenait 2 % de C_3A, tandis que l'éprouvette 2 - 7 % ; l'éprouvette 3 contenait 10 % de C_3A.

Tableau II

Résultats d'essais de ciment à contraindre

n^{os} d'éprouvettes	Résistance, kgf/cm^2	Expansion, %	Autotension, kgf/cm^2
1	552	0,7	31
2	530	1,05	46
3	452	1,5	51

D'après les données fournies au tableau 2 on voit que l'augmentation de la quantité d'aluminate tricalcique dans le clinker-protland permet d'obtenir un ciment à autotension élevée. Comme il a été déjà mentionné (12) l'autotension de la pierre de ciment est le résultat de deux processus se déroulant au cours de l'hydratation du ciment : le compactage et le durcissement avec l'accentuation du degré d'hydratation du ciment et le gonflement dû à l'augmentation de la quantité et de la vitesse de formation de l'ettringite. Pour engendrer et conserver l'autotension au sein de la pierre de ciment, il faut que la résistance de la structure d'hydratation soit supérieure à l'effort créé par les cristaux d'ettringite en croissance. Il a été établi que la période de cristallisation spontanée de l'ettringite s'accompagne d'une extension maximale et de l'apparition de grandes contraintes au sein de la structure de la pierre de ciment qui conditionnent l'accroissement spontané des cristaux filiformes de l'ettringite renforçant la pierre de ciment. Mais l'auto-renforcement et la consolidation ne sont assurés qu'au cas d'un excès de la phase d'hydroaluminate devant celle nécessaire à la formation de l'ettringite. Cette condition est garantie par un rapport correspondant entre les aluminates et le sulfoaluminate de calcium dans le ciment.

Au cours de l'hydratation du mélange de sulfoaluminate de calcium et de gypse en présence du silicate tricalcique, le gypse est fixé dès le premier jour avec formation d'ettringite à côté duquel on observe dans l'éprouvette une importante quantité d'aluminates de calcium hydratés. Il a été établi que l'hydratation de C_3S en présence du sulfoaluminate de calcium s'accélère. Dans ce cas le degré d'hydratation de C_3S est au bout de 28 jours de 80 %, tandis qu'en absence de sulfoaluminate de calcium il est de 60 %. En qualité de corollaire on observe une élévation de résistance de la structure d'hydratation. Dans le premier cas la pierre de ciment se caractérise par une résistance de 550 kgf/cm^2, et dans le second de 465 kgf/cm^2.

L'hydratation du silicate bicalcique, du sulfoaluminate de calcium et du gypse s'accompagne de la formation de l'ettringite, d'hydrosilicates fibreux et d'aluminates de calcium hydratés en forme de lamelles écailleuses. Le degré d'hydratation de C_2S mélangé au sulfoaluminate de calcium et au gypse est supérieur à celui de l'hydratation de C_2S pur au cours de tous les stades de durcissement des éprouvettes. Il a été constaté qu'au cours de l'hydratation du mélange mentionné il s'établit une structure très résistante de beaucoup supérieure à celle de la pierre de ciment obtenu lors du durcissement de C_2S pur. On a utilisé cet effet pour la mise au point du ciment de sulfoaluminatobélite. Dans des conditions de production industrielle on a obtenu un clinker de sulfoaluminate composé de sulfoaluminate de calcium, d'aluminate de calcium de formule $12CaO \cdot 7Al_2O_3$ et de silicate bicalcique (fig. 3).

Le clinker moulu avec et sans gypse a permis d'obtenir des ciments qui soumis aux

essais ont donné les résultats groupés au tableau 3.

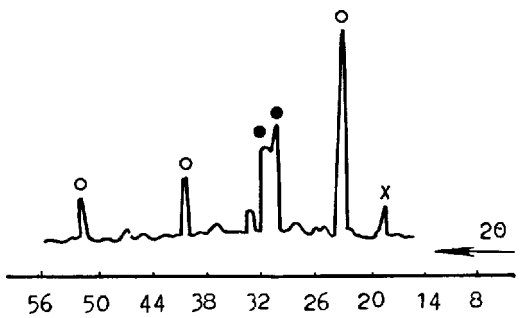

Fig. 3 - Diagramme radiographique du clinker de sulfoaluminate. o - $C_3A_3\overline{C}\overline{S}$, x - $C_{12}A_7$, • - C_2S

Les études montrèrent que l'hydratation des phases de sulfoaluminates et de silicates s'effectue simultanement. Comme au cas d'études d'éprouvettes en laboratoire on a établi qu'au cours de l'hydratation du ciment de sulfoaluminatobélite il se forme des cristaux allonges d'ettringite, des hydrosilicates et des aluminates de calcium hydrates de forme fibreuse et lamellaire. La grande resistance de la pierre de ciment d'une telle microstructure a été notée maintes fois par V.V. Timachev et O.P. Mtchedlov-Petrossian.

Tableau III

Désignation du ciment	Surface specifique, cm^2/g	Résistance à la compression, kgf/cm^2 à		
		1 j.	3 j.	28 j.
De sulfoaluminatobelite	4000	352	400	620
Idem avec addition de gypse	4000	382	425	642

Mélangé au clinker-portland et au gypse le clinker de sulfoaluminate garantit une production de ciments expansifs et à contrainte se caractérisant par une extension égale à 0,1-1,0 % et une autotension de l'ordre de 20 à 38 kgf/cm^2 suivant le rapport entre les composants.

Donc la grande résistance ainsi que l'extension et l'autotension de la pierre de ciment sont des effets de la grande vitesse et du degre d'hydratation du ciment qui régissent la rapide formation de l'ettringite et d'aluminates de calcium hydratés dès le premier jour de durcissement et, les jours suivants, d'hydrosilicates de calcium. Le rapport optimal entre la quantité d'ettringite et d'aluminates de calcium hydratés varie en fonction des besoins d'obtenir soit un ciment a haute resistance, soit un ciment expansif.

BIBLIOGRAPHIE

I. - У. ЛЮДВИГ (I976) Исследование механизма гидратации клинкерных минералов. УI Международный Конгресс по химии цемента, М., Стройиздат, (en russe).

2. - Г.Е. ШВИГЛЕ, У. ЛЮДВИГ (I973) Гидроалюминаты и гидроферриты кальция. У Международный Конгресс по химии цемента, М., Стройиздат, (en russe).

3. - И.В. КРАВЧЕНКО (I960) Глиноземистый цемент, М., Госстройиздат,(en russe).

4. - F.E. JONES, M.H. ROBERTS (1959), "The system $CaO-Al_2O_3-H_2O$ at 25 °C", DSJR, Bulding Research Station, NE 965, HMSO, London (en anglais).

5. - F. CREPTER, S. CHATTERJI, J.W.JEFFERY (1973), "Studies of the Effect of different additives on the Hydration Reaction of Tricalcium Aluminate", Part. 5, Cement Technology (en anglais).

6. - T.D. ROBSON (1966) "Some Principles Covering the Performance of refractory concreate", Materials Technology in Steam Reforming Processes, London (en anglais).

7. - Ю.М. БУТТ, В.В. ТИМАШЕВ, Портландцемент, М., Стройиздат, (en russe).

8. - И.В. КРАВЧЕНКО, Т.В. КУЗНЕЦОВА, М.Т. ВЛАСОВА, Б.Э. ЮДОВИЧ (I979) Химия и технология специальных цементов, М., Стройиздат, (en russe).

9. - О.П. МЧЕДЛОВ-ПЕТРОСЯН, Л.Г. ФИЛАТОВ (I965) Расширяющиеся составы на основе портландцемента, М., Стройиздат, (en russe).

IO.- Н. ФУКУДА (I973) Фундаментальное исследование расширяющегося цемента Лосье. У Международный Конгресс по химии цемента. М., Стройиздат, (en russe).

II.- Р. ХЕДИН (I973) Прочность и структура из смесей гидравлических компонентов. УI Международный Конгресс по химии цемента. М., Стройиздат, (en russe).

I2.- Т.В. КУЗНЕЦОВА (I979) Химия и технология расширяющихся и напрягающихся цементов, "Цемент", № 2, (en russe).

Very early hydration of tricalcium silicate

L'hydratation aux premiers âges du silicate tricalcique

E. SAKAI, Dr. Research Associate, M. DAIMON, Dr. Associate Professor and R. KONDO, Dr. Professor, Dept of Inorg. Materials, Faculty of Eng. Tokyo Institute of Technology, Japan.

RESUME : On a étudié l'hydratation aux premiers âges du silicate tricalcique anhydre, broyé à des finesses variées. Les propriétés du silicate tricalcique anhydre ont été déterminées par IR, par analyse aux rayons X, par Kr-adsorption, et par la mesure de la chaux libre. Le dégagement de chaleur de l'hydratation a été mesuré au moyen d'un calorimètre "isopéribol", à deux cellules associées dans un montage différentiel. D'autre part, on a recherché l'influence de $Ca(OH)_2$ et de sulfonates aromatiques de soude ayant des structures moléculaires variées, sur la composition de la phase liquide. L'hydratation, aux tous premiers âges, du silicate tricalcique peut être divisée en deux phases: la première correspond à la libération immédiate d'ions Ca^{2+}, et la seconde, qui suit la première, correspond à la libération plus lente d'autres ions Ca^{2+}. Les résultats expérimentaux peuvent être expliqués par la théorie topochimique conventionnelle.

Après la première phase de l'hydratation, le sulfonate aromatique de soude ayant une longue chaîne hydrophobe, est adsorbé par le silicate tricalcique et ses premiers hydrates. Il s'ensuit que la seconde phase du dégagement de chaleur est retardée, de même que la poursuite de l'hydratation du silicate tricalcique.

SUMMARY : Very early hydration of tricalcium silicate was studied using samples with various grinding times. Properties of unhydrated tricalcium silicate was determined by IR, X-ray diffraction, Kr-adsorption and free lime analysis. Heat liberation of hydration was measured by means of twin isoperibol calorimeter. Furthermore, influence of $Ca(OH)_2$ and sodium aromatic sulfonates, with different molecular structures, were investigated in connection with the composition of liquid phase. The very early hydration of tricalcium silicate could be divided into two steps. The first corresponded to the immediate liberation of Ca^{2+} ion and the second following slower liberation of Ca^{2+} ion respectively. The experimental results could be explained by conventional topochemical theory.

After the first step of hydration, sodium aromatic sulfonate, having a long hydrophobic chain was adsorbed on tricalcium silicate or the first hydrates. Then the second step of heat liberation was retarded, and the further hydration of tricalcium silicate was retarded.

INTRODUCTION

It has long been discussed whether the hydration of tricalcium silicate (C_3S) takes place through solution or topochemically. A principle paper entitled "Phase composition of hardened cement paste" was contributed at the previous congress, and dealt with the mechanisms of cement hydration and the phase composition (1). However, the mechanisms of C_3S hydration have not been well known, and especially, the studies on the very early stages are insufficient.

Authors have investigated the kinetics and the mechanisms of hydration of C_3S using samples with narrow particle size distribution, and five stages were introduced as follows (2). In the S_I stage, the reaction took place immediately on contact with water. In the S_{II} stage, nucleation of C-S-H having low CaO/SiO_2 (C/S) ratio with slow liberation of Ca^{2+} ion. In the S_{III} stage, the reaction took place very actively and was accelerated with time. In the S_{IV} stage, the rate of hydration decreased gradually, S_{IV} and S_V were the decay period. According to de Jong et al. (3), calcium silicate hydrate (C-S-H) coatings having high C/S ratio were formed on C_3S particles surface, thus prevented any further hydration of C_3S. With the passage of time, when C/S ratio of C-S-H decreased and the first hydrates converted into the second hydrates which were more permeable, the hydration of C_3S was accelerated. And Stein summarized the conventional studies of the mechanism of C_3S hydration and reconfirmed the validity of topochemical reaction theory (4).

Young et al., on the other hand, suggested that the induction period was controlled by the nucleation of calcium hydroxide (CH), and that the second peak of rate of heat liberation was controlled by the growth of CH (5). Fujii and Kondo (6) reported that when the maximum supersaturation of solution with calcium ions was attained, then the induction period would terminate and the reaction would proceed rapidly, probably as the result of propagative surface nucleation-growth of C-S-H(II). Maycock et al., who proposed the schematic model of C_3S hydration suggested that the induction period corresponded to nucleation of CH and the second hydrates (7). According to Tadros et al., calcium ions adsorbed on the Si-rich surface of C_3S particles, greatly reducing their further dissolution, thus initiating the induction period (8). Dent Glasser et al., recently, have studied the hydration of C_3S by means of analytical electron microscopy and trimetyl silylation, and they have postulated that initial protonic attack gave a surface layer of high C/S ratio and calcium ions was then lost and silicate tetrahedra condense gave dimer (9).

Very early hydration of C_3S had to be studied by considering the mechanochemical effect such as lattice defect or surface activity. Relations between surface activity, lattice defect and the reactivity of cement were discussed (7,10,11). But the investigation of the correlation between the mechanochemical effect and the very early hydration of C_3S was scarce.

In this study, the mechanisms of the very early hydration of C_3S are investigated using samples which were ground for 15h, 30h, 48h, exposed to 100%RH for 1h, and the CH saturated solution or sodium aromatic sulfonates with different molecular structures were added. This study is also very important in considering the retarding mechanisms of organic compounds on the hydration of cement.

EXPERIMENTAL

Materials

C_3S was sythesized based on the composition as shown in Table I (12). The synthesized C_3S was the so-called M phase or alite from the X-ray diffraction patterns.

Table I Chemical composition (%)

SiO_2	Al_2O_3	CaO	MgO	Total
25.8	1.2	72.0	1.0	100.0

The synthesized C_3S was crushed in an alumina mortar and was ground for 15, 30, 48h respectively. The properties of ground C_3S were analyzed as follows. $B\cos\theta/B^\circ\cos\theta$ was measured using (009) of X-ray diffraction patterns. Specific surface area of ground C_3S was measured by Blaine's method and Kr adsorption. Particle size distribution of C_3S was measured by the photo-extination method. The infrared spectrum of ground C_3S was observed by means of KBr disk method. The amount of free-CaO was measured by glycerol-alchol method.

In the study of effect of sodium aromatic sulfonates, a large amount of C_3S was synthesized and was ground for 20h in order to study the effect of various organic compounds.

Additives, used in this study were sodium benzenesulfonate (BS) and sodium p-dodecylbenzenesulfonate (12N) made by TOKYO KASEI KOGYO CO. (Japan), and sodium salts of formaldehyde high condensate β-naphthalenesulfonate (HCNS). The degree of polymerization of the latter was about 10, it was Mighty-150 made by KAO SOAP CO. (Japan). Table II shows the formulas of sodium aromatic sulfonates used in this study. BS has a hydrophilic group ($-SO_3Na$) at an end of the molecule and a short hydrophobic group. 12N has a hydrophilic group at an end of the molecule and a long hydrophobic group. HCNS has many hydrophilic groups in the long molecule.

Table II Used sodium aromatic sulfonates

Sodium benzenesulfonate (BS)

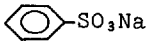

Sodium p-dodecylbenzenesulfonate (12N)

Sodium salts of formaldehyde high condensate of β-naphthalenesulfonate (HCNS)

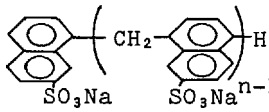

n≒10

Condition

The water to solid ratio was 10 and hydration temperature was 20°C. The amount of additives was 0.5% by weight of C_3S.

Calorimetry

Conduction calorimetry was highly suitable for measuring the heat liberation of cement hydration and was used by many investigators, but it is unsuitable for measuring the rapid change of heat. Therefore the twin isoperibol calorimeter (TOKYO RIKO CO., Japan) as shown in Fig.1 was used in this study.

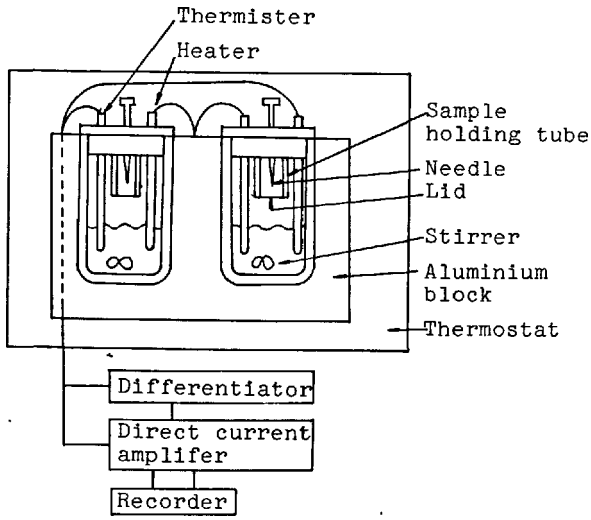

Fig.1 - The twin type of isoperibol calorimeter

Analysis of liquid phase

After C_3S was hydrated using the apparatus as shown in Fig.2, liquid phase was extracted by filtration. After adding Sr^{2+} ion as releaser, Ca^{2+} ion of liquid phase was analyzed by atomic absorption spectrophotometry. And pH changes of liquid phase were recorded continuously.

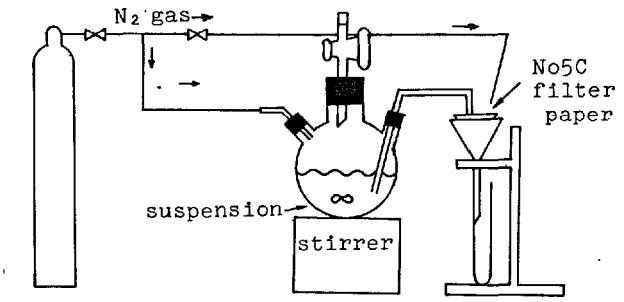

Fig.2 - The reaction apparatus

RESULTS

Properties of ground C_3S

The specific surface area of C_3S increases with grinding time as shown in Fig.3. The results of Kr adsorption do not agree well with and are larger than those of Blaine's method. Particle size distribution of C_3S is shown in Fig.4. The amount of C_3S having fine particle diameter increases with grinding time. The properties of ground C_3S are summarized in Table III. Free-CaO and $B\cot\theta/B°\cot\theta$ increases with grinding time. IR spectra become broader with grinding time, and adsorption band of C_3S ground for 48h shifts to longer wave lengths (Absorption of $930cm^{-1}$ shifts to $940cm^{-1}$). Specific surface area of C_3S sample, used in the study of the effect of sodium aromatic sulfonates, as measured by Kr adsorption and Blaine's method are $0.54m^2/g$ or $0.41m^2/g$ respectively. In this case , free-CaO is 0.02% and IR spectrum indicates the same results with 15h ground sample in Fig.3.

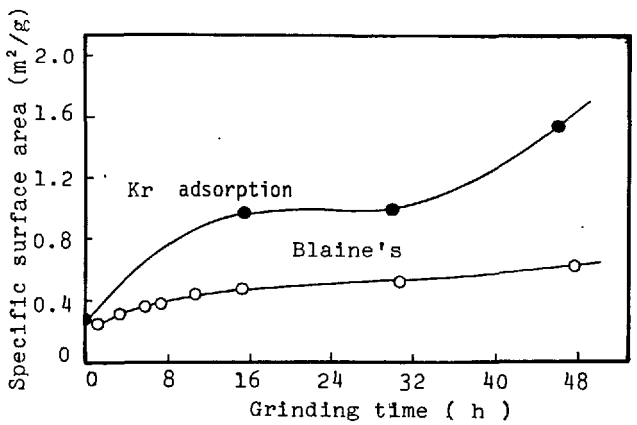

Fig.3 - Relation between grinding time and specific surface area

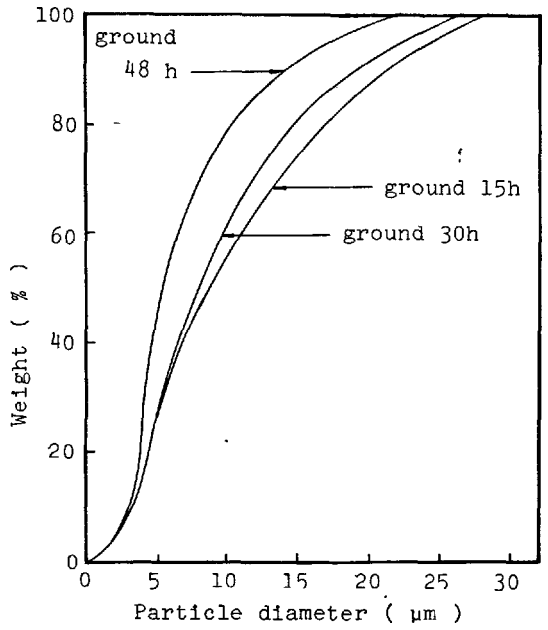

Fig.4 - Relationship between particle size distribution of C_3S and grinding time

Table III The properties of ground C_3S

Grinding time (h)	Bcotθ/B°cotθ	Free-CaO (%)
0	1	0.019
15	1.025	0.027
30	1.058	0.049
48	1.064	0.055

Suspension hydration of C_3S

Heat liberation of very early hydration of C_3S is shown in Fig.5. These heat liberation curves calculated from experimental data using equation (1).

$$\Delta Tad = \Delta Tex + \alpha \quad \cdots\cdots\cdots (1)$$

$$\Delta Tex = T_2 - T_1$$
$$\alpha = \Delta Tex \cdot \exp(t/\tau)$$

where ΔTad is the adiabatic rise of temperature and ΔTex is experimental value. T_2 and T_1 is experimental data of temperature. t is the time from T_1 to T_2, τ is the time constant of the calorimeter (in this case, 60 min.).

The very early hydration of C_3S takes place by two steps. With the increase of grinding time, heat liberation in the first step (Q_1) is increased and the appearance of the second step of heat liberation (Q_2) is accelerated.

In 0h-ground sample, which is crushed in alumina mortar, it is not clear whether the reaction takes place by two steps. When C_3S hydrates in $Ca(OH)_2$ saturated solution, the second step of heat liberation does not take place. The heat liberation of the first step decreases when C_3S sample is exposed to 100%RH for 1h.

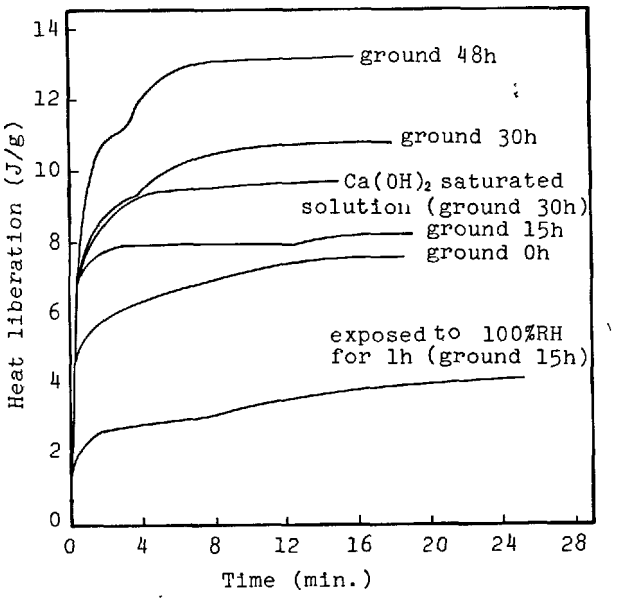

Fig.5 - Heat liberation of C_3S hydration

Influence of sodium aromatic sulfonates on the very early hydration of C_3S

The heat liberation owing to C_3S hydration with sodium aromatic sulfonates is shown in Fig.6. BS does not retard the very early hydration of C_3S. In the presence of 12N, Q_1 is smaller than no addition case, and Q_2 is not detected. The second step of very early hydration is found to be retarded by the addition of HCNS, and the main hydration of C_3S may be overlapped by the second step. The changes of Ca^{2+} concentration in liquid phase are shown in Fig.7. As soon as C_3S contacts with water , Ca^{2+}ion of liquid phase increases rapidly, and thereafter, it increases gradually with processing time. In the case of 12N and HCNS addition, Ca^{2+}ion of liquid phase increases rapidly, but does not increase in the second step. The results of pH measurements show the parallel tendency with those of Ca^{2+}ion.

DISCUSSION

Mechanisms of the very early hydration of C_3S

Authors have reported that the very early hydration of C_3S using narrow particle size distribution, took place by two steps (2), the two-step reaction does not depend on the particle size distribution.

Q_1 and Q_2 are larger than the heat of immersion of SiO_2, TiO_2, and SnO_2 which are about 0.59J/m^2. Thus, it may be considered that the heat liberation depends on the

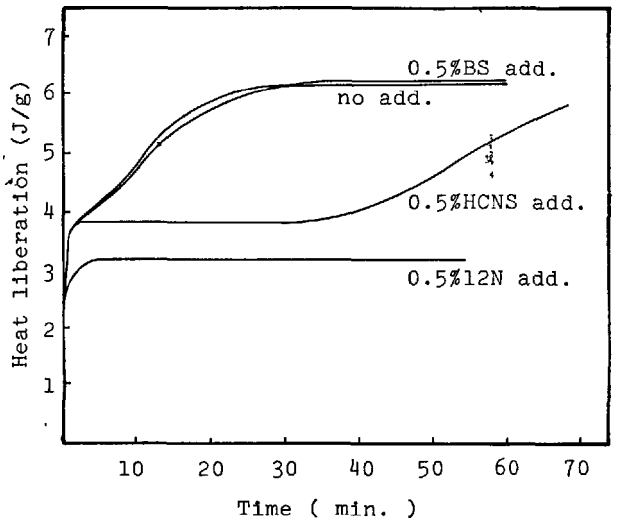

Fig.6 - Influence of sodium aromatic sulfonates on the very early hydration of C_3S

chemical reaction. Q_1 increases with the increasing specific surface area and surface activity of C_3S, which increases with grinding time. The values of $B\cot\theta/B^{\circ}\cot\theta$, shown in Table III, are affected by crystallite size as well as lattice defects. But it is supposed to be true that surface activity of C_3S becomes higher with grinding time, because IR spectra become broad and free-CaO increases.

The hydration of C_3S has been discussed based on topochemical theory. Q_1 may be corresponded to the formation of the first hydrates with rapid release of Ca^{2+}ion. When C_3S is exposed to 100%RH for 1h, Q_1 decreases as the first hydrates are already formed.

In the case of C_3S, hydrated in CH saturated solution, Q_2 is not observed for liquid phase is saturated with CH, and main hydration of C_3S was retarded (2). Q_2 should correspond to the nucleation of hydrates having low C/S ratio, that is, the formation of the second hydrates with release of Ca^{2+}ion. The mechanisms of C_3S hydration are illustrated in Fig.8.

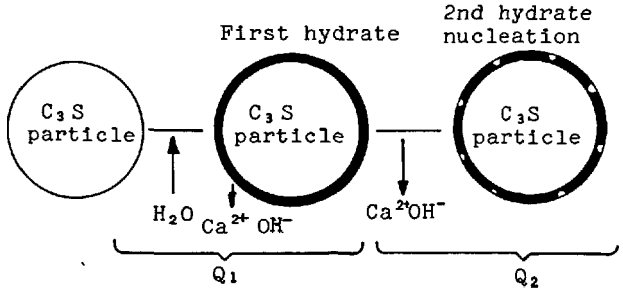

Fig.8 - Illustration of C_3S very early hydration

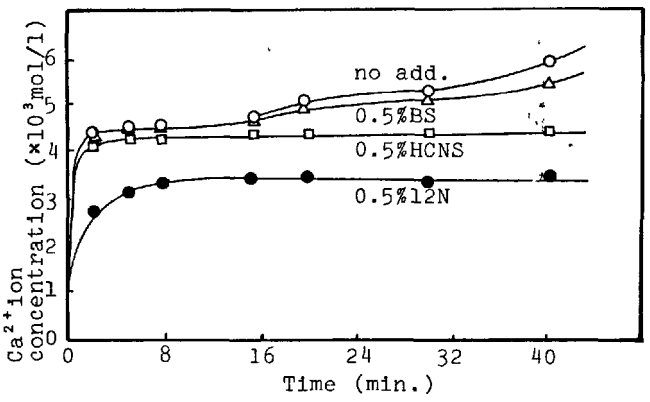

Fig.7 - The concentration of Ca^{2+}ion of a hydrating C_3S suspension with or without additives.

Retarding mechanisms

The influence of sodium aromatic sulfonates having different molecular structures on the main hydration of C_3S and portland cement has been reported in connection with the amount of adsorption (13). A certain type of surfactants having a long hydrophobic group and a hydrophilic group at the end of the molecule such as 12N, shows a critical amount of addition. The hydration of cement is significantly retarded only when the dosage exceeds a critical amount. 12N is, then, closely adsorbed on cement. HCNS gradually retards the hydration with the amount of addition. The retarding effect of BS having a short hydrophobic chain is low because the amount of adsorption is small, even if the concentration is high.

In all cases, Q_1 takes place, but with the addition of 12N, Q_1 is smaller than others. Q_2 is retarded by the addition of 12N and HCNS. In the first step of very early hydration, the concentration of Ca^{2+}ion approximately reaches the point of zero charge range acoording to Stein's study of surface charge of calcium silicates and calcium silicate hydrates (14). Tadros et al. have suggested that calcium ions are adsorbed on Si-rich surface of C_3S particles (8).

Therefore, when the first step of very early hydration occurs, the surface charges of C_3S or the first hydrates become positive. Because anionic additives having a long hydrophobic chain is adsorbed on positive surface, the slow release of Ca^{2+}ion is prevented, and the formation of the second hydrates are prevented. Then the second step is retarded, and therefore the further hydration of C_3S is also retarded.

CONCLUSION

Very early hydration of C_3S takes place by two steps. The heat liberation in the first step increases, and the appearence of the second step of heat liberation is accelerated with grinding time. The heat liberation of the first step decreases when C_3S was exposed to 100%RH for 1h before hydration. When C_3S hydrates in CH saturated solution, the second step of heat liberation (Q_2) was not detected. The first step may be corresponded to the formation of the first hydrates with rapid release of Ca^{2+}ion, and the second step to the nucleation of hydrates having low C/S ratio, with slow release of Ca^{2+}ion.

Sodium aromatic sulfonates having a long hydrophobic chain are adsorbed onto the first hydrates of C_3S. Then the second step of very early hydration is retarded, and therefore the further hydration of C_3S is also retarded.

REFERENCES

1.- R. KONDO and M. DAIMON (1976), "Phase composition of hardened cement paste", (in Russian), Proceeding of sixth International Congress on the Chemistry of Cement, Moscow, 1974, vol.II book 1, 244-257.

2.- R. KONDO and M. DAIMON (1969), "Early hydration of tricalcium silicate: A solid reaction with induction and acceleration periods", J. Amer. Ceram. Soc., 52, 503-508.

3.- J.G.M. de JONG, H.N. STEIN and J.M. STEVELS (1967), "Hydration of tricalcium silicates", J. appl. Chem., 17, 246-250.

4.- H.N. STEIN (1977),"The initial stages of the hydration of C_3S", il cemento, 74, n° 1, 3-13.

5.- J.F. YOUNG, H.S. TONG and R.L. BERGER (1977), "Compositions of solutions in contact with hydrating tricalcium silicate paste", J. Amer. Ceram. Soc., 60, 193-198.

6.- K. FUJII and W. KONDO (1974), "Kinetics of the hydration of tricalcium silicate", J. Amer. Ceram. Soc., 57, 492-497.

7.- J.N. MAYCOCK, J. SKALNY and R.S. KALYONCU (1974), "Crystal defects and hydration: 1. Influence of lattice defects", Cement & Concrete Res., 4, 835-847.

8.- M.E. TADROS, J.SKALNY and R.S. KALONCU (1976), "Early hydration of tricalcium silicate", J. Amer. Ceram. Soc., 59, 344-347.

9.- L.S. Dent GLASSER, E.E. LACHOWSKI, K. MOHAN and H.F.W. TAYLOR (1978), " A multi-method study of C_3S hydration", Cement & Concrete Res., 8, 733-740.

10.- Y. ONO and M. SHIRASAKA (1971)," Mechano-chemical study of grinding of cement", (in Japanese), Semento Gijutsu Nenpo, 25, 64-68.

11.- S.SUDO, T. AKIBA, K. ARAI and S. Nawata, (1973), " The correlation between surface activity and hydraulic quality in C_3S", (in Japanese), Semento Gijutsu Nenpo, 27, 33-36.

12.- G. YAMAGUCHI and S. TAKAGI (1969), "The analysis of portland cement clinker", Proceedings of the fifth International Symposium on the Chemistry of Cement, Tokyo, 1968, vol.1, 181-218.

13.- E. SAKAI, S. YAMANAKA, M. DAIMON and R. KONDO (1977), "Influence of sodium aromatic sulfonates on the early hydration of cement", (in Japanese), Nippon Kagaku Kaishi, 208-213.

14.- H.N. STEIN (1968), "Surface charges of calcium silicates and calcium silicate hydrates", J. Colloid & Interface Sci., 28, n° 2, 203-213.

Eventement et raidissement des ciments

Air aging and stiffening of Portland cements

A. BONIN, ingénieur de recherche, laboratoire de recherche générale, Lafarge S.A., France.

RESUME : L'étude a été réalisée sur un CPA 55 R industriel ne présentant, en conservation prolongée à l'abri de l'air, aucun phénomène de raidissement lors de l'utilisation en pâtes ou mortiers.

Dans un premier temps, on a montré que des éventements contrôlés du ciment à 20°C et 50 ou 80 % d'hygrométrie relative entrainaient des modifications néfastes plus ou moins marquées du comportement rhéologique. On a ensuite déterminé dans chaque cas de conservation la nature et la cinétique d'apparition, après gâchage, des premiers hydrates. Une corrélation entre ces cinétiques et l'effet passivateur de la vapeur d'eau sur la phase alumineuse du ciment a permis d'expliquer les anomalies d'écoulement observées dans le cas des ciments éventés.

SUMMARY : For this study a high early strength industrial Portland cement was used, which did not show any sign of stiffening, even after prolonged aging under dry air.

First, it was established that checked air agings of the cement at 50 or 80 % R.H. and 20°C result in more or less pernicious modifications of the rheological behaviour.

Then the nature and kinetics of formation of hydrates were determined in all cases of conservation. The surprising types of flow observed with pastes or mortars of wet air exposed cements are explained by comparing the kinetics of hydrates formation and the passivation effect of water vapour on aluminous phases.

INTRODUCTION

L'éventement ou exposition à l'air plus ou moins humide d'un ciment Portland ne présentant aucun phénomène de fausse prise, peut modifier de diverses manières le comportement rhéologique des pâtes, mortiers ou bétons dans les premières minutes de l'hydratation.

Nous écarterons d'office le cas bien connu de la fausse prise carbonate due à la carbonatation des alcalins pendant l'éventement. Les carbonates alcalins qui en résultent réagissent au gâchage avec la chaux et précipitent de la calcite ; ce mécanisme est générateur de raidissement.

Dans le cas d'un clinker broyé non gypsé, tous les auteurs admettent que c'est l'hydratation immédiate du C_3A qui entraine la prise rapide. La présence de gypse suffit à ralentir, et même à bloquer, l'hydratation de cette phase supprimant ainsi tout raidissement.

L'interprétation de l'action retardatrice du gypse ne fait par contre pas encore l'unanimité :

SKALNY (1) pense que la dissolution du C_3A est incongruente. Avec un rapport C/A dans la solution supérieur à trois, il se formerait au contact du C_3A une couche riche en alumine sur laquelle s'adsorberaient les ions calcium. Cette pellicule alors chargée positivement attirerait les ions SO_4^{--} et formerait ainsi une barrière à la diffusion de l'eau vers le C_3A.

FELDMAN et RAMACHANDRAN (2) font intervenir la cinétique de dissolution du C_3A qui serait contrôlée par la présence et le mouvement des dislocations cristallines, lesquelles seraient bloquées par l'adsorption superficielle des ions SO_4^{--} ralentissant ainsi la mise en solution.

GUPTA (3) envisage la formation d'une pellicule imperméable de C_4AH_x en présence de $Ca(OH)_2$ et de $SO_4Ca\ 2\ H_2O$ stable tant que la concentration en $Ca(OH)_2$ reste assez élevée. Il n'exclut pas la formation de petites quantités d'ettringite, mais pense qu'elle précipite par réaction entre le C_4AH_x et le gypse avec libération de chaux hydratée qui renforcerait alors la stabilité du C_4AH_x.

Enfin STEINOUR (4), STEIN (5), COTTIN (6), COLLEPARDI (7) admettent la formation directe d'une coquille d'ettringite par réaction C_3A - gypse. Cette capsule de trisulfoaluminate plus ou moins bien cristallisée serait assez imperméable à l'eau et aux ions SO_4^{--} pour isoler mécaniquement le C_3A du reste de la solution de gâchage.

En ce qui nous concerne, nous admettons cette interprétation et c'est avec ce modèle que nous expliquerons les comportements des ciments éventés.

Dans cette hypothèse, pour que le blocage du C_3A soit efficace, il faut que la coquille d'ettringite se forme rapidement sur les surfaces de C_3A. Son épaisseur minimale nécessaire sera de plus fonction de l'imperméabilité de la couche d'hydrate, donc de sa structure. Tout ce qui pourra dans le système C_3A - gypse - eau modifier la cinétique de formation et la structure de la couche d'ettringite, aura une influence certaine sur le comportement rhéologique des pâtes.

Dans cette optique, il faut citer les considérations de LOCHER (8) qui fait intervenir les réactivités relatives des deux phases principales que sont le C_3A et le sulfate. Par exemple, si le C_3A est plus actif que le sulfate (gypsage à l'anhydrite), il y aura possibilité de précipitation de C_4AH_x et de formation différée d'ettringite plus éloignée des surfaces de C_3A et par ce fait moins protectrice. Si par contre c'est le sulfate qui est plus actif (présence de semihydrate ou d'anhydrite soluble) la formation ralentie d'ettringite laisse la possibilité de précipitation de gypse entrainant le raidissement de type sulfate.

Enfin, si en présence de semi hydrate on a un C_3A super actif, la précipitation rapide d'ettringite consomme très vite tout le semi hydrate et élimine le risque de précipitation du gypse, tout en bloquant énergiquement le C_3A.

Ayant mis en évidence des comportements rhéologiques inhabituels d'un ciment industriel selon son mode de conservation, nous avons émis l'hypothèse que l'éventement modifiait suffisamment la réactivité du C_3A pour provoquer des changements de fluidité. C'est pourquoi nous avons réalisé l'étude expérimentale de tels phénomènes.

REALISATION DES ESSAIS

Choix du ciment

Nous avons choisi le CPA 55 R qui avait posé industriellement des problèmes de conservation. Le clinker a pour composition potentielle :

C_3S = 66,3 %, C_2S = 15,4 %, C_3A = 0,5 %, C_4AF = 14,5%

Chaux libre : 1,55 %

K_2O est le seul alcalin présent (0,25 %) entièrement combiné sous forme sulfate. Le ciment est obtenu par broyage industriel avec du gypse (SO_3 = 2,25 %) à la finesse de 4575 cm^2/g. On a vérifié qu'il ne contenait pas de semi hydrate en proportion décelable.

On peut remarquer la forte teneur en C_4AF et la quasi absence de C_3A dans ce ciment mais nous savons par ailleurs que ce composé a dans le cas présent une très forte activité et que le ciment non gypsé raidit aussi fortement qu'un ciment contenant une proportion prépondérante de C_3A. Par ailleurs, en accord avec COLLEPARDI (9), nous savons que C_4AF en présence de gypse et de chaux (cas d'un ciment) a le même comportement que C_3A dans la première demi-heure d'hydratation (formation d'ettringite avec la même cinétique).

Eventement du ciment

Le ciment a été éventé pendant 24 heures, à 20°, en couche mince soit à 50 % d'hygrométrie relative, soit à 80 %. L'atmosphère n'étant pas exempte de CO_2, nous avons vérifié que les produits éventés ne contenaient pas de carbonates alcalins de manière décelable et susceptibles de provoquer une fausse prise carbonate. Dans les deux cas, quelques essais de durée d'éventement différente ont été réalisés pour juger de la cinétique de passivation de l'aluminate de calcium.

Comportement rhéologique en présence d'eau

On a testé le comportement rhéologique après gâchage de deux manières :

- En pâte pure par la méthode de raidissement au bol : on gâche à la spatule dans un récipient appelé bol une certaine quantité de pâte qui ensuite est transvasée dans le moule troncônique des essais de consistance normalisés (NF P 15-414). La mesure consiste ensuite à déterminer à des temps fixés : 2 - 5 - 10 - 15 et 30 minutes, le refus d'enfoncement de la sonde de Vicat (Φ = 1 cm). Le E/C d'obtention de la pâte dite normale est ajusté pour obtenir immédiatement après gâchage un refus de 4 à 5 mm. La hauteur du moule normalisé étant de 40 mm, le refus de la sonde ne

peut évidemment pas dépasser cette valeur.

- En mortier normalisé (norme NF P 15-403) par la technique du maniabilimètre LCPC où l'on mesure après 30 minutes de repos du mortier mis en place dans l'appareil, un temps d'écoulement sous vibration, dans des conditions standardisées (10).

Détermination des cinétiques d'hydratation

La cinétique d'hydratation a été suivie de deux manières :

- Par enregistrement à 20° de la chaleur d'hydratation avec un calorimètre à conduction. Le dégagement calorifique est mesuré dès le contact eau-ciment. Il n'y a pas de gâchage mécanique mais simple mouillage de la poudre par capillarité, l'eau étant introduite par une seringue.

- Par dosages en analyse thermique différentielle. A cet effet, on gâche des pâtes pures manuellement pendant une minute puis aux échéances de 0 - 2 - 5 - 10 - 15 minutes (décomptées immédiatement après la fin du gâchage) on prélève des échantillons dont on stoppe l'hydratation par lavage acétone-éther. L'examen de ces produits par ATD permet l'identification des hydrates et leur dosage quantitatif (moyennant un étalonnage préalable (11)). Quand la teneur en hydrate est suffisante, on peut confirmer par diffraction des rayons X leur nature minéralogique.

RESULTATS OBTENUS

Comportement rhéologique

Ciment	Ecoulement au maniabilimètre LCPC		Essai de raidissement au bol						
	E/C	Temps après 30' de repos	E/C	Refus d'enfoncement de la sonde aux échéances de (mn)					
				0	2	5	10	15	30
Témoin	0,50	17 s.	0,275	6	22	26	27	27	28
24 h. à 50 % HR	0,50	168 s.	0,280	5	40	40	40	40	40
24 h. à 80 % HR	0,50	23 s.	0,306	7	15	20	21	25	30

TABLEAU N° 1 : Comportement Rhéologique des ciments.

Le tableau n° 1 montre que, par rapport au ciment témoin, celui éventé à 50 % d'hygrométrie relative accuse un très fort raidissement, alors que celui éventé à 80 % n'a pas vu ses caractéristiques rhéologiques sensiblement modifiées.

On note toutefois que le E/C nécessaire à l'obtention d'une pâte normale inchangé pour le produit éventé à 50 % HR augmente significativement pour celui éventé à 80 % HR.

On a aussi remarqué qu'en remalaxant la pâte ou le mortier après cinq minutes de repos, on détruit le raidissement du produit éventé à 50 % HR et celui-ci ne se régénère plus par la suite.

Ces mesures de raidissement après éventement sur un ciment à forte teneur en C_4AF ont été reproduites de nombreuses fois sur des ciments à fortes teneurs comparées en C_3A et conduisent toujours au même comportement rhéologique des pâtes.

Nature et cinétique de formation des premiers hydrates

Les examens en analyse thermique différentielle et en diffraction des rayons X ont montré que l'ettringite était le seul hydrate présent pendant la première demi-heure d'hydratation. Le tableau n° 2 et le graphique n° 1 donnent les résultats de dosage de l'ettringite en fonction des temps d'hydratation.

Ciment	% d'ettringite aux échéances de (mn)							anhydre	
	dans l'anhydre	0	2	5	10	15	30	% perte au feu à 1000°	% CO_2
Témoin	0	2,4	2,7	3,0	2,9	2,2	3,2	2,00	0,33
24 h. à 50 % HR	0	0,4	1,7	2,4	3,2	3,4	3,5	2,06	0,35
24 h. à 80 % HR	1,4	1,8	1,7	1,6	1,7	1,7	1,5	4,70	1,70

TABLEAU N° 2 : Dosage de l'ettringite en fonction du temps d'hydratation.

On remarque que :

- Au niveau du ciment anhydre le témoin et celui éventé 24h à 50 % HR sont très semblables : absence d'ettringite, même perte au feu à 1000° et même teneur en CO_2.

- En ce qui concerne les cinétiques d'hydratation en ettringite de ces deux ciments, on note une grande différence. D'une part, la quantité globale de trisulfoaluminate atteinte à l'équilibre est inférieure pour le témoin et d'autre part elle se forme à des moments différents. En effet, sur les 3,0 % d'ettringite du témoin, 80 % se forment au gâchage et seulement 20 % dans la période de repos qui suit. Le phénomène est inversé pour le ciment éventé 24 heures à 50 % HR puisque sur les 3,5 % d'hydrate formé à 15 minutes, 10 % seulement apparaissent au gâchage et les 90 % durant la période de repos.

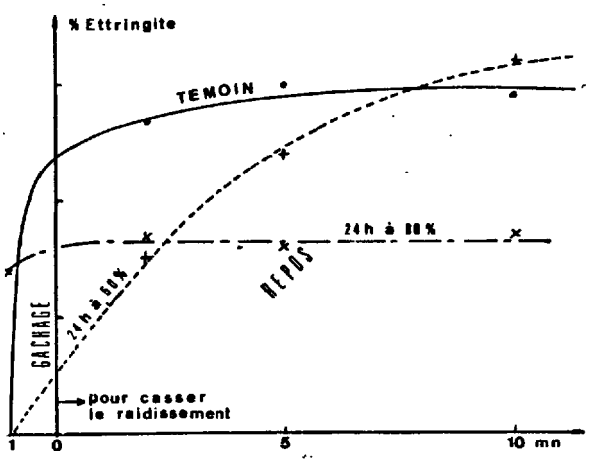

GRAPHIQUE N° 1 : Cinétique de formation de l'ettringite

- Pour le ciment éventé 24 heures à 80 % HR, on voit que l'ettringite en quantité moindre (1,4 %) est déjà formée pendent l'éventement et qu'au contact de l'eau de gâchage cette teneur évolue très peu. La formation d'ettringite est confirmée par l'accroissement de la perte au feu à 1000°. En tenant compte du CO_2, on trouve un accroissement de l'eau liée de 1,33 % exprimé par rapport à l'anhydre alors que la perte au feu à 1000°, due à l'ettringite, et exprimée dans les mêmes conditions est de 1,20 % pour 1,4 % ettringite. L'augmentation du CO_2 est vraisemblablement due à la carbonatation de la chaux libre et en tout cas sans aucun effet sur le raidissement.

- Les courbes calorimétriques données par le graphique n° 2, sont en accord avec les résultats précédents à savoir un retard de dégagement de chaleur par rapport au témoin du ciment éventé à 50 % HR et une quasi absence de réaction pour celui éventé à 80 % HR.

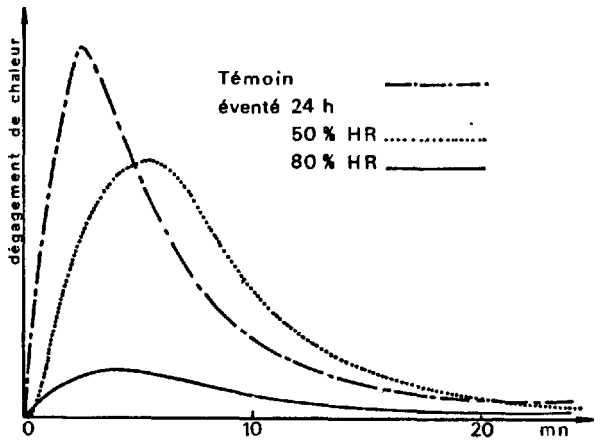

GRAPHIQUE N° 2 : Microcalorimétrie des ciments

En faisant varier les temps d'éventement, les courbes calorimétriques montrent que :

- à 50 % HR, il faut maintenir l'exposition au moins pendant 8 heures pour avoir un effet mesurable. A partir de 24 heures, les cinétiques de formation d'ettringite sont semblables, seule augmente la quantité finale d'ettringite globale.

- à 80 % HR, l'action est visible dès les premières heures d'exposition à l'air humide et se poursuit jusqu'à 16 heures, en restant stable par la suite.

INTERPRETATION DES RESULTATS

Nous avons mis en évidence que le seul hydrate présent pendant les premières minutes de contact avec l'eau était l'ettringite. De plus, on note de grandes différences de cinétique de formation selon les modes de conservation du ciment. C'est donc là qu'il faut chercher les causes des anomalies du comportement rhéologique constatées.

Lors de l'utilisation d'un ciment, il y a trois périodes importantes

- Son gâchage en présence de granulats plus ou moins gros

- Une période d'attente plus ou moins longue avant l'emploi

- La prise et le durcissement après la mise en place.

L'ettringite est susceptible, nous l'avons vu, de se former à n'importe lequel de ces moments : pendant le gâchage, nous l'appellerons ettringite de gâchage, et durant la période d'attente : ettringite de repos.

En admettant le modèle de protection de l'aluminate de calcium anhydre par une pellicule d'ettringite, il est clair que si deux grains de ciment se trouvent en contact au niveau de la matière interstitielle, les coquilles d'ettringite à cet endroit, auront une partie commune. Cette mise en commun de matière va assurer une liaison augmentant ainsi la rigidité de la pâte. Le raidissement sera d'autant plus intense que ces contacts seront plus nombreux et mieux consolidés. Lors du gâchage, où toutes les particules sont en mouvement, la probabilité pour que deux surfaces de matière interstitielle soient suffisamment longtemps en contact pour mettre leurs coquilles d'ettringite en commun, est relativement faible. Il s'ensuit un petit nombre de liaisons. De plus celles qui ont pu s'établir, ne sont pas très fortes et sont en quasi totalité détruites par l'énergie de malaxage. En d'autres termes, l'ettringite de gâchage tout en assurant son rôle bloquant de l'aluminate de calcium, n'est pas préjudiciable à la fluidité de la pâte.

Par contre, au repos, ces mises en commun de coquilles ont tout le temps de s'établir et de se consolider sans que rien ne vienne les briser. Il s'ensuit un raidissement important de la pâte que l'énergie des moyens de mise en place ne peut briser. L'ettringite de repos apparait donc particulièrement néfaste pour la fluidité bien qu'elle remplisse encore son rôle bloquant.

En revenant au cas concret du ciment étudié, on voit que :

- Le témoin a 80 % de son ettringite totale sour forme d'ettringite de gâchage non néfaste, et effectivement, il ne présente aucun raidissement.

- Le ciment éventé à 50 % HR a par contre 90 % de son ettringite sous forme d'ettringite de repos très néfaste et il présente bien un fort raidissement. Il est possible de transformer une grande partie de l'ettringite de repos en ettringite de gâchage. Il suffit pour cela, à l'échéance de 5 mn, de remalaxer la pâte ou le mortier. Nous sommes alors ramenés au cas du témoin et observons bien une fluidité normale retrouvée et stable.

- Le comportement du ciment éventé à 80 % HR est un peu plus particulier. Il ne présente ni ettringite de gâchage, ni de repos. Tout se passe comme si, dans cette atmosphère proche de la saturation, l'ettringite était capable de se former en surface de l'aluminate de calcium, l'encapsulant avant le gâchage. Il faut remarquer que l'imperméabilité de cette couche parait excellente puisque 1,4 % d'ettringite suffisent pour passiver le C_3A. L'eau de la pâte n'arrivant plus au contact de ces surfaces, il est normal de ne pas observer de raidissement.

Nous avons constaté que pour les ciments éventés à 80 % HR, il fallait, pour obtenir la fluidité normalisée, augmenter l'eau de gâchage de 10 % en pâte pure et qu'il n'était pas nécessaire de modifier celle du mortier.

Nous pouvons expliquer cette variation d'eau de gâchage si on considère que :

- L'éventement à 80 % HR est susceptible de souder des grains entre eux par l'intermédiaire de l'ettringite.

- Dans la poudre de ciment, la distance moyenne des grains est très élevée (densité apparente inférieure à 1) comparée à celle obtenue dans les pâtes normales.

L'action du gâchage qui apparait comme le moyen de permet-

tre aux grains de se distribuer pour rapprocher leurs centres au maximum dans un empilement le plus compact possible sera plus aisée pour des grains libres que pour des grains soudés entre eux.

Si donc, pour le ciment éventé, le gâchage est peu énergique (cas des pâtes pures obtenues à la spatule), l'assemblage sera moins compact donc plus riche en eau. Par contre, en présence de granulats et au malaxeur mécanique, l'énergie est suffisante pour séparer les grains et permet d'obtenir la même compacité que pour le ciment non éventé.

En ce qui concerne les temps d'éventement autres que 24 heures :

- à 50 % HR quand on poursuit jusqu'à 15 jours, on augmente de quelques points la teneur en ettringite de repos accentuant le raidissement. La cinétique de formation de l'ettringite étant inchangée, il faut croire que la coquille d'ettringite est moins imperméable (peut-être mieux cristallisée) et nécessite pour bloquer l'aluminate,des épaisseurs, donc des teneurs plus élevées.

- à 80 % HR, dès 16 heures, la coquille protectrice est formée et elle n'évolue plus par la suite. Elle protège donc l'aluminate anhydre aussi efficacement de la vapeur d'eau que de l'eau liquide du gâchage.

CONCLUSION

Nous venons de montrer l'existence d'un nouveau type de raidissement des pâtes, mortiers et bétons. Ce raidissement, dû à une altération de la réactivité de l'aluminate de calcium de la matière interstitielle, n'est pas la conséquence de modification des réactions chimiques de cette dernière avec le gypse mais est induit par un changement de la cinétique de formation de l'ettringite permettant au repos, la formation d'un squelette rigide d'hydrate.

Accessoirement, le fait d'avoir pu expliquer simplement les comportements rhéologiques des ciments éventés à l'aide du modèle d'une coquille d'ettringite bloquant le C_3A, ne contredit pas cette hypothèse.

BIBLIOGRAPHIE

1. SKALNY J., TADROS M.E., Journal American Ceramic Society. 60, 174-75 (1977).

2. FELDMAN R.F., RAMACHANDRAN S.V., Mag. Concr. Res. 18, 185-96 (1966).

3. GUPTA P., CHATTERJI S., JEFFERY J., Cement Technology. 4, 1-4 (1973).

4. STEINOUR H.H., "Setting of Portland Cement : A Review of Theory, Performance and Control". Res. Lab., Portland Cement Assoc. Dept Bull. N. 98, 124 (1958).

5. STEIN H.N., Silicates Ind. 28 (3), 141-45 (1963).

6. COTTIN B., Hydratation et expansion des ciments. Ann. Chim. Fr., 1979, 4 pp. 139-144.

7. COLLEPARDI H., CORRADI M., BALDINI G., PAURI M., Meccanismo d'azione del gesso sull'idratazione dell'alluminato tricalcico. Il Cemento - 75ème Anniversario 169, 176.

8. LOCHER F.W., RICHARTZ W. and PRUNG S., "Setting of cement. Part 1. Reaction and development of structure". Zem. Kalk Gips, 29 (10), 435-442 (1976).

9. COLLEPARDI M., MONOSI S., MORICONI G., CORRADI H., Tetracalcium aluminoferrite hydration in the presence of lime and gypsum. Cem. Con. Res. Vol. 9, N° 4, 431-437, 1979.

10. BARON J., LESAGE R., Réalisation d'un maniabilimètre à mortier. Bulletin des Laboratoires des Ponts et chaussées. N° 30 - Mars/Avril 1968.

11. CONJEAUD M., American Ceramic Society, 79th Annual Meeting, Chicago (1977).

Réactivité de l'aluminate monocalcique vis-à-vis de l'eau

Reactivity of monocalcium aluminate

P. GALTIER et B. GUILHOT, Ecole Nationale Supérieure des Mines de Saint-Etienne, Laboratoire deChimie-Physique,

M. MURAT, Institut National des Sciences Appliquées de Lyon, Département de Génie Energétique, Laboratoire de Chimie Appliquée,

A. BACHIORRINI et A. NEGRO, Politecnico di Torino, Istituto de Chimica Generale ed Applicata, France.

RESUME : Dans le cadre d'un programme de travail interlaboratoire sur la réactivité des liants calciques, les auteurs ont étudié l'hydratation d'une préparation d'aluminate monocalcique synthétisé par réaction solide-solide à haute température (1360°C). En se basant sur les échéances d'hydratation mises en évidence par la courbe de calorimétrie, les prises d'essai ont été mélangées avec de l'eau (rapport eau/solide = 1), hydratées à 25°C, de 30 mn à 15 heures et analysées par différentes techniques (diffraction des R.X., spectroscopie I.R., thermoluminescence, analyse thermique différentielle et microscopie électronique à balayage). Il apparaît qu'une hydratation locale commence dans la "période de latence", mais ce phénomène semble grandement influencé par des hétérogénéités locales de composition (probablement inclusions de $C_{12}A_7$) de l'aluminate anhydre et par le procédé employé pour stopper la réaction d'hydratation. La manifestation macroscopique du phénomène de croissance apparaît après 7 heures d'hydratation : l'hydrate formé de manière prédominante est C_2AH_8, mais il est accompagné de CAH_{10} et contaminé par du carboaluminate.

SUMMARY : Within the framework of an interlaboratory programme about reactivity of hydraulic binders, the authors have studied the hydration of a monocalcium aluminate sample prepared by solid state reaction at high temperature (1360°C). Basing on the calorimetric hydration curve, the sample was mixed with water (Water/solid ratio = 1) cured at 25°C from 30 minutes to 15 hours, and investigated by different techniques (X-ray diffraction, I.R. spectroscopy, thermoluminescence, differential thermal analysis and scanning electron microscopy). It was pointed our that local hydration begins during the "latent period" but it appears that this phenomenon may be largely influenced by local composition heterogeneities (probably $C_{12}A_7$ inclusions) in the anhydrous aluminate and by the process employed to stop the hydration reaction. Macroscopically, after a curing of 7 hours, C_2AH_8 is the predominent hydrated formed but it is accompagnied by some CAH_{10} and contamined by carboaluminate.

I - INTRODUCTION

L'hydratation de l'aluminate monocalcique CA est un phénomène relativement complexe : à basse température il se forme CAH_{10} (θ < 20°C) ; à température plus élevée (θ > 35°C) on obtient C_2AH_8 et de la gibbsite ; à l'ambiante (20-25°C) se forment simultanément CAH_{10} et C_2AH_8. Ces deux hydrates hexagonaux se transforment ensuite lentement en C_3AH_6 cubique (1 à 3).

Compte tenu de cette complexité, une approche systématique de la réaction d'hydratation, en mettant en oeuvre sur une même préparation un maximum de techniques d'investigation, a été entreprise dans le cadre d'un programme interlaboratoire sur la réactivité des liants hydrauliques.

II - PREPARATION ET CARACTERISATION DE L'ALUMINATE MONOCALCIQUE

II-1 - L'aluminate monocalcique est préparé à partir d'alumine Al_2O_3 et de carbonate de calcium $CaCO_3$ (réactifs purs Carlo Erba pour analyse).

Les deux réactifs sont mélangés dans le rapport stoechiométrique Ca/Al = 0,5 pendant 24 heures dans un mélangeur rotatif à billes. Le mélange pulvérulent, légèrement tassé, est cuit pendant 6 h à l'air à 1360°C, température légèrement inférieure à celle de l'eutectique (4). Après cuisson, l'échantillon est broyé à $\emptyset$ < 75 µ puis repassé au mélangeur pendant 24 h et recuit pendant 6 h à 1360°C. L'opération est répétée encore une 3è fois.

Le produit final est broyé à $\emptyset$ < 75 µ puis tamisé dans un appareil Alpine (5) qui permet d'obtenir deux fractions granulométriques : 40 < $\emptyset$ < 75 µ et $\emptyset$ < 40 µ. Les essais ultérieurs seront essentiellement effectués sur la fraction 40 < $\emptyset$ < 75 µ.

II-2 - Caractérisation par diffraction X

La technique de diffraction a été utilisée pour caractériser les produits de cuisson obtenus selon le protocole de préparation décrit précédemment.

La première cuisson pendant 6 h conduit à un produit constitué d'aluminate monocalcique CA et d'aluminates $C_{12}A_7$ et CA_2. On observe la présence d'alumine Al_2O_3 et de chaux CaO résiduelles.

La seconde cuisson met en évidence la présence de $C_{12}A_7$ résiduel. La troisième montre que le produit final (CA) contient encore des traces de $C_{12}A_7$.

II-3 - Caractérisation par microscopie électronique à balayage et spectrométrie X.

Les clichés de microscopie électronique à balayage mettent en évidence une structure sphérolitique sans zone présentant des faciès cristallins nettement définis (Fig. 4, cliché 1). Une évaluation, par comptage, du rapport Ca/Al met en évidence des valeurs anormalement élevées de ce rapport (2 à 5 fois supérieur à celui de CA pur) sur de très rares zones microcristallisées à faciès cubique.

II-4 - Caractérisation par spectrographie I.R.

Les spectres d'absorption I.R. réalisés sur les produits de cuisson à 6h, 12h et 18h mettent en évidence une évolution vers un état de cristallisation marqué du produit final.

II-5 - Caractérisation par thermoluminescence

Le composé préparé présente une thermoluminescence artificielle sous forme d'un pic intense dont le maximum apparaît à la température de 284 K (Fig. 1). Le pic qui apparaît aux très basses températures est dû à l'interaction solide-éthanol, l'éthanol étant utilisé pour étaler la poudre d'aluminate sur le porte-échantillon.

II-6 - Surface spécifique

Les valeurs des surfaces spécifiques, déterminées par la méthode B.E.T., sont respectivement de 0,1 $m^2 . g^{-1}$ pour les fractions 40/75 µ et < 40 µ.

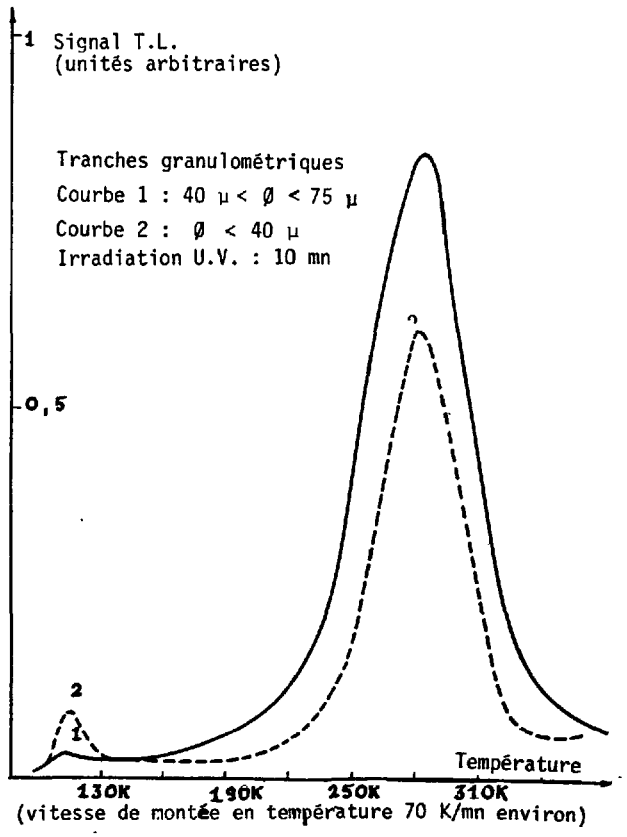

FIG. 1 - Caractérisation de l'aluminate monocalcique par thermoluminescence.

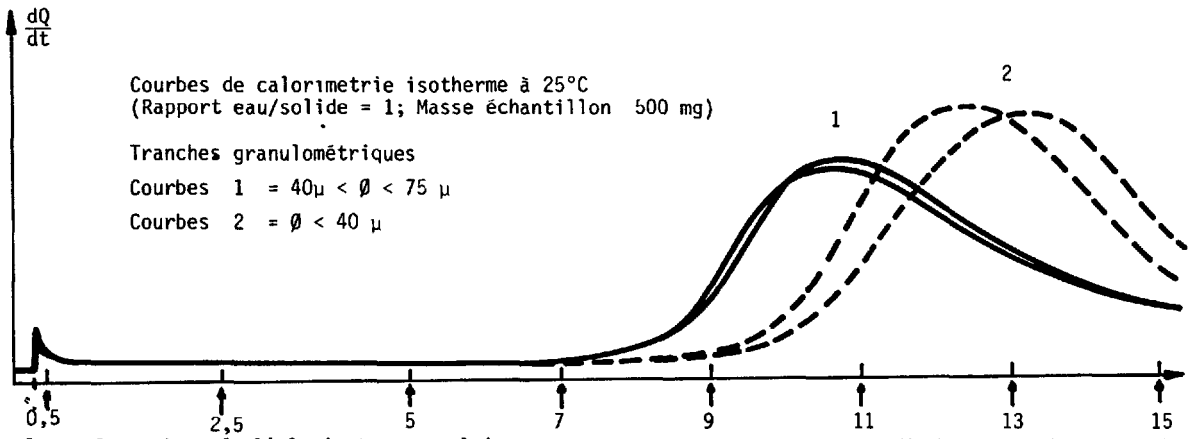

FIG. 2 - Hydratation de l'aluminate monocalcique.

III - ETUDE DE L'HYDRATATION

III-1 - Etude cinétique par calorimétrie isotherme à 25°C

On observe généralement (6) une assez grande dispersion dans les courbes calorimétriques des aluminates monocalciques si on ne travaille pas sur un produit de granulométrie bien définie, dans des conditions de température et d'hydratation bien déterminées (7). Dans le cas considéré ici aussi, avec la fraction 40/75 µ (Fig. 2) qui ont servi de base aux investigations ultérieures. Par contre, les fines (Ø < 40 µ) donnent des courbes calorimétriques très dispersées.

Par ailleurs, comme cela a été observé par d'autres auteurs (8-9), une élévation de la température d'hydratation (dans la gamme de 19°C à 26°C explorée) se traduit par un ralentissement de la cinétique d'hydratation.

III-2 - Etude des produits d'hydratation à différentes échéances à 25°C

La courbe calorimétrique de la fraction 40/75 µ à 25°C permet de définir les échéances auxquelles va être stoppée l'hydratation, à savoir : 30 min. ; 2 h 30 mn ; 5 h ; 7 h ; 9 h ; 11 h ; 13 h ; et 15 h. Les poudres ont dont été conservées en présence d'eau (E/S = 1) à 25°C et la réaction d'hydratation a été stoppée de la façon suivante : l'eau est aspirée à la seringue à l'échéance choisie. Le solide est ensuite dispersé d'abord dans de l'éthanol et on élimine le solvant par aspiration à la seringue. L'opération est répétée trois fois avec l'éthanol puis trois fois à nouveau avec un mélange 1/1 éthanol-éther. Le produit est ensuite séché - soit par passage à l'étuve sous air pendant 6 heures à 40°C (mode A), - soit par vide primaire dynamique pendant 2 heures dans un dessicateur (mode B).

Les produits d'hydratation sont ensuite examinés par différentes techniques.

III-2-1 - Résultats des analyses par diffraction X et analyse thermique différentielle.

Une certaine incertitude a concerné l'échéance d'apparition des premières traces d'hydrate (en l'occurrence C_2AH_8 hexagonal caractérisé par sa raie la plus intense (0001) à d = 10,5 Å) : si le séchage est réalisé selon le mode B, cet hydrate est à la limite de la détection par diffractométrie X dès l'échéance 2 h 30. La disparition aux échéances de 5 h et de 7 h de la raie d = 4,89 Å de $C_{12}A_7$ résiduel peut lever cette incertitude et confirmer la formation de petites quantités de C_2AH_8 aux échéances faibles.

Les produits d'hydratation apparaissent très nettement au-delà de l'échéance de 7 h : à 9 h on observe la raie principale de C_2AH_8 et plus faiblement celle de CAH_{10}. L'échantillon hydraté est cependant, comme tous ceux examinés aux échéances supérieures, contaminé par le monocarboaluminate. L'intensité de la raie la plus intense de C_2AH_8 croît avec la durée de l'hydratation tandis que l'intensité des raies caractéristiques de CAH_{10} et du monocarboaluminate reste constante. A l'échéance de 9 h on décèle la présence de gibbsite.

L'analyse thermique différentielle confirme les résultats de diffraction X. Elle permet en outre, dans le cas du séchage selon le mode B, de mettre en évidence par son pic endothermique à 80°C (12), l'apparition de gel d'alumine dès l'échéance de 2 h 30, ce qui n'est pas détectable par diffraction X et par spectrographie I.R.

Ce petit pic, présent dès les premières minutes du séchage sous vide, ne peut être attribué ici (10) à une hydratation ultérieure par de"l'eau résiduelle non éliminée par le séchage".

III-2-2 - Résultats de spectrographie I.R.

Les spectres d'absorption I.R. ont été réalisés sur pastilles d'iodure de potassium avec un rapport massique échantillon/iodure de potassium de 1/100. L'observation des spectres d'absorption a permis de tirer les conclusions suivantes :

- l'hydratation de l'aluminate monocalcique ne devient significative qu'à l'échéance de 9 h.

- une résolution suffisante des spectres des produits hydratés n'est obtenu que pour les échantillons hydratés 11 heures, échéance à partir de laquelle l'hydratation concerne la masse interne du

produit de départ.

- les bandes d'absorption entre 1500 et 1350 cm^{-1} mettent en évidence de façon incontestable la formation de carboaluminate et ce, à partir de 9 h d'hydratation (11).

III-2-3 - Résultats de thermoluminescence

La thermoluminescence met en évidence trois signaux (Fig. 3) :

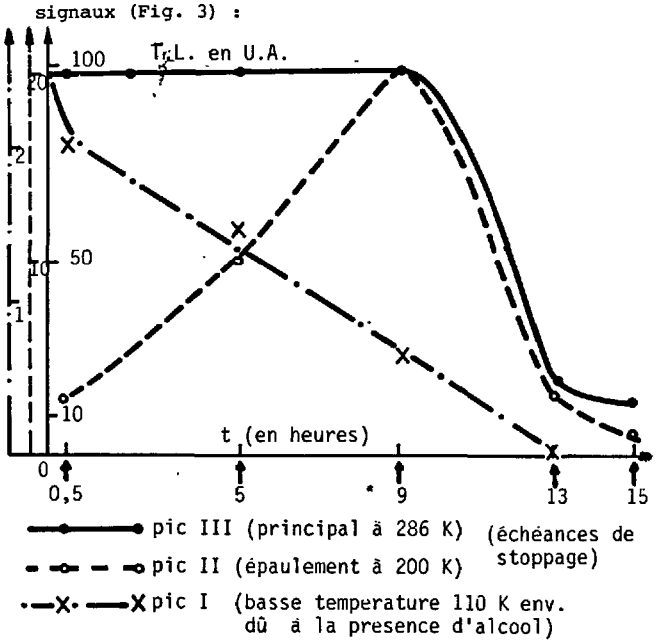

FIG. 3 - Etude des produits d'hydratation par thermoluminescence.

- un pic principal dont le maximum se situe à 186 K (pic III)

- un épaulement sur le pic principal à 200 K (pic II)

- un pic de faible intensité lié à la présence d'éthanol lors du dépôt du composé sur le porte-échantillon (pic I).

L'évolution du pic III semble liée à la teneur en CA. Ce pic diminue à partir de l'échéance 9 h.

L'intensité du pic II passe par un maximum pour la même échéance. Le pic I lié à l'adsorption de l'éthanol sur le CA décroît régulièrement en fonction du temps d'hydratation.

L'évolution de l'intensité de ces pics marque bien la différence de part et d'autre de l'échéance 9 h qui correspond à la manifestation macroscopique du phénomène de croissance cristalline des hydrates. Dans la période dite "de latence" on peut penser que la thermoluminescence puisse apporter des informations toutes nouvelles sur les phénomènes de germination, mais ce point nécessite une expérimentation plus poussée avant de proposer une interprétation des résultats.

III-2-4 - Résultats de microscopie électronique à balayage

Le fait le plus marquant de l'observation des échantillons par microscopie électronique à balayage est que même dans les conditions de séchage selon le mode A, une faible partie de l'aluminate de départ s'est déjà hydraté à l'échéance 5 h (fig. 4, cliché 2). Ce résultat n'est pas en désaccord avec les observations de spectrométrie X (existence locale de composés à rapport Ca/Al bien supérieur à celui de CA dans le solide de départ), de diffraction X (disparition du $C_{12}A_7$ résiduel avant l'échéance 5 h), d'analyse thermique différentielle (apparition de gel d'alumine dès l'échéance 2 h 30) et de thermoluminescence.

IV - CONCLUSION

Ce travail met en évidence la nécessité de définir de manière rigoureuse les conditions de préparation (synthèse, broyage, tamisage ...) et d'hydratation de l'aluminate monocalcique, tout au moins pour obtenir des échéances d'hydratation reproductibles et comparables entre différents laboratoires.

-La détection de produit hydraté dans la période de "latence" semble dépendre, de manière très sensible, du protocole adopté pour le stoppage de la réaction en cours d'hydratation.

-On peut également s'interroger sur le rôle que peuvent jouer les microhétérogénéités de composition sur la manifestation de ces phénomènes.

Ces différents problèmes font l'objet d'études complémentaires.

BIBLIOGRAPHIE

(1) V.S. RAMACHANDRAN et R.F. FELDMAN : "Hydration characteristics of monocalcium aluminate at low water/solid ratio" - Cement and Concrete Research 1973, 3, pp. 729-750

(2) A. NEVILLE : "High-Alumina Cement. A Current Review" - Il Cemento, 1978, (3), pp. 291-302.

(3) B. COTTIN : "Etude au microscope électronique des pâtes de ciment alumineux hydratées en C_2AH_8 et CAH_{10}, I et II" - Cement and Concrete Research, Vol. 1, pp. 177-186 et pp. 273-284, 1971.

(4) J.H. WELCH : "Phase equilibria and high-temperature chemistry in the $CaO-Al_2O_3-SiO_2$ and related systems" in H.F.W. TAYLOR "The chemistry of Cements", Academic Press, London and New-York, 1964, vol. 1, p. 55.

(5) V.M. MALHOTRA : "The alpine air jet sieve : a new method for determining the fineness of Cement" - Indian Concrete Journal, pp. 305-309, August 1967.

(6) P. LONGUET : Communication au XXIVè Congrès International de Chimie Industrielle.

(7) P. GALTIER et al. (à paraître)

(8) BOBROV B.S., ZALDAT G.I. : "Action de la température sur l'hydratation de l'aluminate monocalcique" - Izvest akad. Nauk. SSSR Neorg. Mater 1973, 9, 11, 1986/9.

(9) K. MISHIMA : "Relation between the hydration of alumina cement mortars and their strengh in the early stages" - Proc. V Int. Symp. on the chemistry of cement, vol. III, p. 167, Tokyo (1969).

(10) R. MAGNAN, B. COTTIN, J.J. GARDET : "Initial stages in the hydraulic activity of sulphate, aluminate and silicate compounds of calcium" - Proc. VI Int. Congress on the chemistry of cement, Moscow, 1974.

(11) T. VASQUEZ, F. TRIVINO et A. RUIZ DE CAUNA : Revista materiales de construccion, 1975, (159), pp. 1-29.

(12) H.G. MIDGLEY : "The mineralogy of set high-alumina cement" - Trans. Brit. Ceram. Soc., vol. 66, p. 161, 1967.

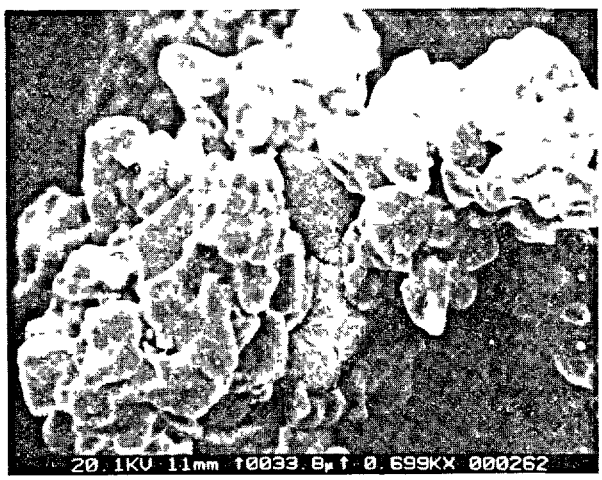

Cliché 1 - CA (40 < Ø < 75 µ
Produit hydraté 5 h à 25°C
Grossissement 2100
(au centre) zone de formation d'hydrate

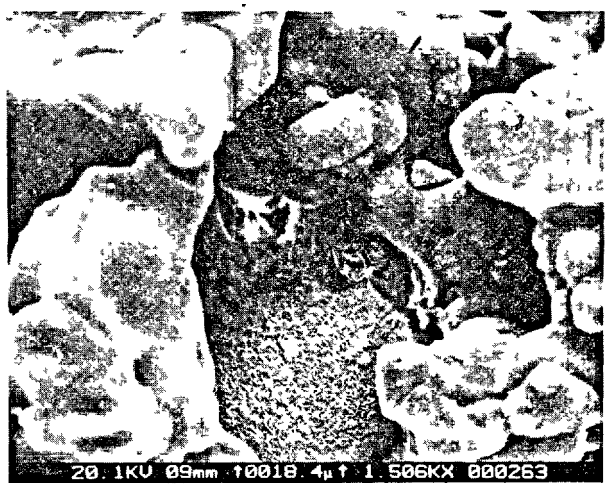

Cliché 2 - CA (40 < Ø < 75 µ)
Produit hydraté 5 h à 25°C
Grossissement 4500

Cliché 3 - CA (40 < Ø < 75 µ)
Produit hydraté 13 h à 25°C
Grossissement 1080

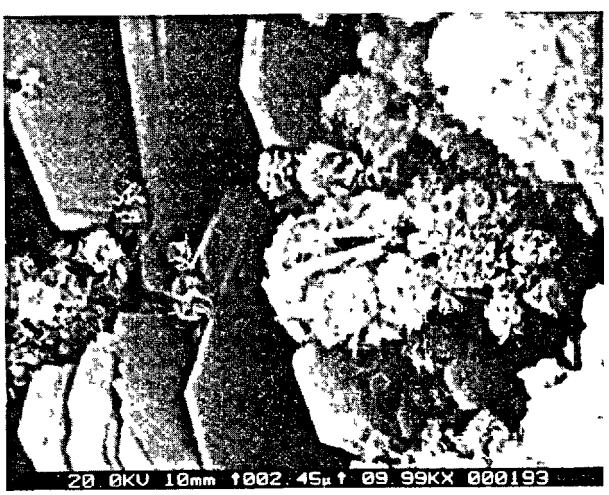

Cliché 4 - C_2AH_8 standard
Grossissement 10000

FIGURE 4 - Observation en microscope électronique à balayage

Cinétique de l'hydratation du ciment Portland

Hydration kinetics of Portland cement

C. VERNET, E. DEMOULIAN, P. GOURDIN, F. HAWTHORN, Société des Ciments Français, CEREG, France.

RESUME

Les auteurs ont étudié la séquence et la cinétique de l'hydratation de 7 clinkers industriels et des ciments portland correspondants à l'aide d'un appareillage permettant des mesures ioniques en continu, des analyses chimiques et physico-chimiques séquentielles, sur des suspensions de rapport (eau/ciment) E/C = 4. Cette étude montre l'interdépendance des vitesses de réaction des phases du clinker, par l'intermédiaire de couplages thermiques et chimiques, ainsi que les différences de comportement des ciments en fonction de leurs particularités (type de C_3A, quantité de sulfates alcalins). La séquence de l'hydratation reste la même à E/C = 4 qu'en pâte pure mais l'échelle des temps est modifiée car, en suspension, l'influence de la diffusion sur la diminution de vitesse de réaction est moindre. Les mécanismes d'influence du K_2SO_4 sur les vitesses de réaction de C_3A et C_3S sont étudiés dans le cadre des mécanismes généraux de dissolution-cristallisation.

La méthode aboutit à l'étude directe de la cinétique d'hydratation des ciments industriels, des ajouts et des adjuvants.

SUMMARY

The authors have studied the sequence and kinetics of the hydration of 7 clinkers and the corresponding portland cements, on suspensions of water/cement ratio (W/C) = 4, using an apparatus which measures continuously the ions contents, and sequential physico-chemical analysis.

This study points out the interdependance of the reaction speeds of the clinker phases, through thermic and physic couplings and the different behaviours of the cements according to their particularities such as C_3A type and alkali-sulphates contents.

The sequence of hydration for W/C = 4 is the same as in cement pastes, but the time scale is modified because in a suspension, the influence of the diffusion on the slowing down of the reaction speed is less than in the cement pastes.

The mechanism of K_2SO_4 influence on C_3A and C_3S reactions are developped, according to general dissolution-crystallization mechanisms.

The method leads to a direct study of the kinetics of industrial cements, adds and admixtures.

INTRODUCTION

Nous avons montré dans une étude des mécanismes réactionnels de l'hydratation (1) que les phénomènes de dissolution-précipitation, envisagés par LE CHATELIER (2) dès 1887, sont prépondérants pendant la prise. Ceci implique une correspondance permanente entre la composition de la solution au contact, l'apparition ou la disparition des phases solides, l'ensemble des vitesses de dissolution des anhydres et de précipitation des hydrates. A chaque instant, les concentrations ioniques résultent de la différence de ces vitesses et les hydrates formés ne sont pas en équilibre thermodynamique : cet équilibre n'étant atteint que lorsque leur vitesse de précipitation tend vers zéro. L'énergie libérable par les anhydres est donc utilisée à maintenir en permanence un certain taux de sursaturation, moteur de la cristallisation et de l'évolution des résistances. Nous avons introduit le concept de distance de précipitation, qui permet une interprétation cinétique du mode particulier de cristallisation du CSH et de ses variations de structure. Il est donc théoriquement possible de mesurer indirectement les vitesses de réaction des phases à partir des mesures de concentrations ioniques. Nous tentons ici de mettre cette théorie en pratique : pour cela, nous avons conçu et réalisé un appareillage original permettant :
- de mesurer en CONTINU la composition ionique de la solution, par des méthodes chimiques et électrochimiques ;
- d'effectuer séquentiellement des dosages simultanés des anhydres et hydrates, pendant une durée suffisante pour observer l'ensemble des réactions ;
- d'effectuer des mesures thermiques simultanées.
Pour des raisons pratiques, ces mesures ne pouvant être effectuées facilement sur des pâtes de ciment, on est amené à utiliser des suspensions agitées. Nous avons choisi un rapport eau/ciment (E/C) égal à 4, ce qui constitue un minimum compatible avec le bon déroulement des essais et des dosages. D'autre part, cette valeur du E/C permet d'accélérer considérablement les réactions finales, qui dans les pâtes, sont limitées par la diffusion à travers les hydrates. A la fin de chaque essai nous pouvons alors tracer un diagramme de l'évolution chimique du système solide-solution, montrant la séquence de l'hydratation de la manière la plus complète possible.

1/ METHODOLOGIE

1.1 - Méthodes d'analyse et appareillage :
Nous ne pouvons décrire ici dans le détail l'ensemble des méthodes d'analyse utilisées. Ceci fait l'objet d'une communication séparée (3). L'appareillage (fig.1) comprend les éléments suivants :
• un réacteur étanche en acier inoxydable d'une contenance de 5 l, comportant un système d'agitation et un système de filtration en continu ;
• une double enveloppe thermostatique à circulation d'eau, entourant complètement le réacteur ;
• un système de recyclage du filtrat, le long duquel on place un certain nombre de capteurs électrochimiques (conductance, pH, pK^+, pNa^+ ...) ;
• un système de prélèvement de suspension pour analyses séquentielles ;
• des capteurs de température et de température différentielle ;
• un thermostat à circulation ;
• une batterie d'appareils de mesure, renvoyant les informations issues des capteurs vers un enregistreur à 12 voies.

Un essai se déroule de la manière suivante :
1) étalonnage des capteurs à l'aide de solution étalon ;
2) remplissage du réacteur par le volume d'eau distillée;
3) mise en température du réacteur (25°C) ;
4) introduction rapide de la masse m du ciment (V/m=4) au temps t_0. L'évolution ionique et thermique se traduit alors par les courbes sur l'enregistreur ;
5) à des échéances t_1, t_2 ... t_n variables selon les vitesses de réactions observées, prélèvements de petites quantités en suspension ;
6) filtration des aliquotes prélevées, analyse chimique du filtrat. Analyse cristallographique des phases solides (diffraction X, ATG, ATD).

Nous avons également effectué des essais complémentaires dans un autre réacteur pour des mesures particulières comme celle de la viscosité dynamique de la suspension en fonction du temps.

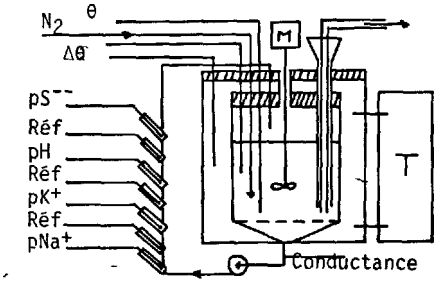

Fig. 1 - Schéma du réacteur filtrant

Les précautions suivantes ont été prises pour obtenir des analyses représentatives :
1) Prélèvements et analyses séquentielles :
- essais entièrement conduits en atmosphère d'azote,
- forte agitation de manière à obtenir une suspension homogène et des prélèvements instantanés représentatifs
- filtration ultra rapide des prélèvements de suspension, lyophilisation rapide d'une petite partie du gâteau de filtration, rinçage du reste du gâteau au méthanol immédiatement après récupération du filtrat aqueux, qui est filtré une deuxième fois sur filtre micropore à l'abri de l'air.
2) Circuit d'analyse automatique :
- volume du filtrat circulant à l'extérieur du réacteur négligeable par rapport au volume total,
- étalonnage périodique des électrodes par analyse chimique séquentielle du filtrat,
- suppression des interférences entre capteurs par cellules à circulation spéciales.
L'appareillage et les méthodes utilisées ici permettent donc de ne laisser échapper aucun phénomène rapide ou transitoire, grâce à l'analyse en continu, dont le principal défaut, à savoir le manque de fiabilité dans le temps est corrigé par les analyses ponctuelles.

2/ CHOIX DES ECHANTILLONS

Nous avons sélectionné parmi un lot plus important de clinkers de la SOCIETE des CIMENTS FRANCAIS, un groupe de 7 clinkers choisis pour leur composition minéralogique et leurs propriétés hydrauliques différentes, de manière à obtenir l'éventail le plus large possible des comportements des clinkers industriels. Pour chaque clinker, un ciment portland à 3,2 % de SO_3 a été réalisé et nous avons effectué les mesures, d'une part sur le clinker et d'autre part sur le ciment. Les clinkers sélectionnés ont la composition suivante (tableau 1), (analyse élémentaire par fluorescence X-Analyse cristallographique par diffraction X) :

TABLEAU I

		C_1	C_2	C_3	C_4	C_5	C_6	C_7
Analyse Fluorescence X	CaO lib.	1,90	1,48	1,29	2,35	2,16	2,52	2,35
	P.F.	2,46	0,99	0,65	0,98	0,55	1,95	0,61
	SiO_2	23,31	21,87	22,97	20,50	20,61	21,46	23,47
	Al_2O_3	4,92	6,19	3,48	6,87	5,83	4,93	3,58
	Fe_2O_3	0,33	2,11	3,22	2,56	3,19	4,22	3,77
	TiO_2	0,17	0,26	0,20	0,24	0,26	0,20	0,16
	MnO	0,00	0,00	0,07	0,04	0,03	0,15	0,00
	CaO	67,40	66,53	67,76	65,64	64,57	63,77	65,90
	MgO	0,36	0,49	0,43	1,01	2,00	1,24	1,03
	SO_3	0,57	1,14	0,22	0,67	1,42	0,88	0,83
	K_2O	0,34	0,42	0,29	1,39	1,66	0,70	0,50
	Na_2O	0,08	0,22	0,35	0,26	0,14	0,14	0,22
	P_2O_5	0,11	0,15	0,22	0,18	0,17	0,14	0,11
Diffraction X	Alite	68,40	61,40	73,50	65,50	65,90	57,80	65,20
	Bélite	26,20	20,80	14,70	11,10	12,70	22,20	20,60
	C_3A cub	2,5	12,5		1,2	5,1	1,9	0,9
	C_3A tét	0,0	1,7	5,6	15,8	3,1	1,4	1,2
	C_4AF	0,0	4,6	8,5	5,1	10,9	15,6	10,2
	K_2SO_4	0,0	0,0	0,0	0,8	2,3	0,6	0,0
	MgO(per)	0,0	0,0	0,0	0,0	0,8	0,3	0,1

3/ RESULTATS

La même séquence de l'hydratation se répète pour tous les clinkers d'une part et pour tous les CPA d'autre part. Nous nous proposons donc de décrire cette séquence pour un clinker et pour le CPA correspondant, à titre d'exemple. L'interprétation des courbes obtenues sera donnée pour chaque étape de l'hydratation. Nous décrirons simultanément les différences observées pour les autres échantillons en fonction de la minéralogie et de la teneur en éléments mineurs solubles (CaO libre, sulfates alcalins).

3.1 - Suspensions de clinkers (fig.2)

1ère étape : dissolution rapide exothermique (durée 10 à 20 minutes). On observe une augmentation rapide des concentrations en Ca^{++} et OH^- et une dissolution quasi instantanée des sulfates alcalins, se traduisant par un palier des concentrations en K^+ et Na^+. La concentration en SiO_2 passe en 15 minutes d'une valeur élevée à moins de 30 micromoles/l.

Pour les clinkers contenant K_2SO_4, le sulfate réagit très rapidement dans les premières minutes, pour former de l'ettringite. La vitesse de réaction semble liée au rapport E/C et à la quantité de sulfate du clinker, ainsi qu'à des facteurs modifiant la diffusion comme l'agitation et la température : la réaction ralentit jusqu'à une vitesse très faible, du fait de l'intervention d'un effet de barrière. Le sulfate disparait alors au bout d'un temps croissant avec la teneur initiale (plusieurs heures pour C5, 20 minutes pour C6). Pendant toute cette période, K^+ est supérieur à la valeur correspondant à la solubilisation totale de K_2SO_4, ce qui montre que C_3A a réagi très rapidement au départ, en libérant le potassium contenu dans son réseau. L'alumine devient presque instantanément indosable dans la solution en présence de sulfates. En leur absence, on peut encore en trouver quelques micromoles/l au bout de 10 minutes : ceci est dû à la solubilité de l'ettringite beaucoup plus faible que celle des aluminates hydratés. La chaux libre est consommée par formation de CSH_I et d'ettringite en présence de sulfates.

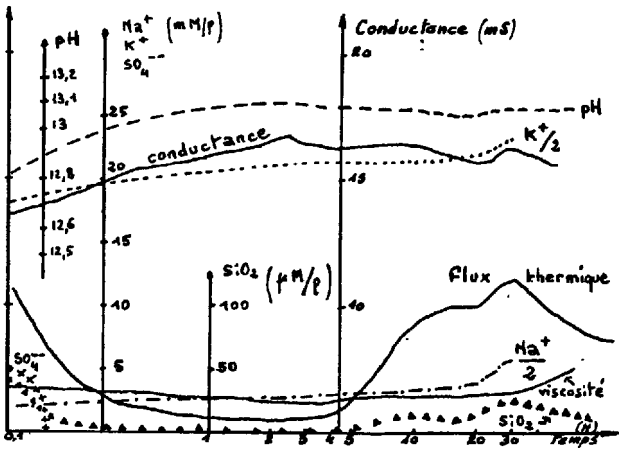

Fig. 2 - Diagramme d'hydratation du clinker C4

2ème étape : Sursaturation en chaux, "période dormante"

En présence de K_2SO_4, après consommation du calcium de la chaux libre, la formation d'ettringite ne peut se poursuivre que par consommation du calcium libéré par l'alite selon :

$$C_3A + 3Ca^{++} + 6OH^- + 6K^+ + 3SO_4^{--} + 31\ H_2O \longrightarrow$$
$$Ca_6[Al(OH)_6]_2\ (SO_4)_3(H_2O)_{25} + 6K^+ + 6\ OH^-$$

On observe effectivement des teneurs en calcium d'autant plus basses au départ que la teneur en K_2SO_4 est élevée. La réaction ci-dessus déplace la solubilité de l'alite et le taux de réaction est alors inhabituellement élevé durant la période dormante. Dans le cas des mortiers, l'alite ainsi consommée ne peut évidemment plus servir à produire de la portlandite et du CSH_{II} dans les périodes suivantes : ce facteur s'ajoute à la modification de structure du CSH_{II} et contribue à un manque de résistance à long terme.
Le flux thermique et la concentration en SiO_2 restent très faibles. OH^- et Ca^{++} augmentent ensemble et l'on atteint des sursaturations en chaux de 1,4 à 1,6 lorsqu'on parvient au maximum de conductance.

Comme nous l'avons montré par ailleurs (1) pendant cette 2ème période on observe un ralentissement des vitesses de dissolution de l'alite et de précipitation du CSH et l'on tend vers un état stationnaire caractérisé par une croissance quasi-linéaire de la concentration en chaux. La germination de la portlandite est ralentie par un inhibiteur qui pourrait être l'ion silicate (4)(5). La vitesse de sursaturation mesurée par la pente de la courbe de conductance est fonction de l'alcalinité, de la forme et de la quantité d'alite. Les flux instantanés de dissolution de l'alite s'échelonnent entre 2,76 et 0,14 $\mu M \cdot m^{-2} \cdot s^{-1}$ (calcul d'après le modèle mathématique que nous avons établi par ailleurs) (1).
La fin de la "période dormante" se produit à l'apparition de la portlandite, très peu de temps avant le maximum de conductance. Malgré les teneurs extrêmement variables en alcalis des clinkers et donc les basicités très variables en début de période, cette précipitation se produit à un pH sensiblement constant pour tous les clinkers (pH 12,9 ± 0,2).

3ème étape : Au bout de quelques heures, la précipitation de la portlandite, très rapide au départ, puis stationnaire, produit une violente reprise de la dissolution de l'alite : le flux de dissolution varie

alors, d'après notre estimation, entre 5 et 50 $\mu M.m^{-2}s^{-1}$ selon les cas. Le flux thermique augmente rapidement et une déformation du pic indique l'effet endothermique de précipitation de $Ca(OH)_2$. On observe une légère augmentation de la teneur en SiO_2, due à un écart plus grand entre vitesses de dissolution de l'alite et de précipitation du CSH, ce que nous avons montré par ailleurs (1). Après le palier de concentration en chaux caractérisant l'état stationnaire, on observe un maximum de teneur en SiO_2, correspondant au maximum de flux thermique. Il se produit alors une reprise de l'hydratation du C_3A détectable grâce à l'augmentation du pH, des teneurs en K^+ et Na^+ et de la conductance (effet particulièrement visible avec C_3A tétragonal). Cette réaction n'est pas nécessairement la même pour tous les clinkers : la séquence de réaction des aluminates dépend en effet du rapport molaire SO_3/C_3A au départ (fig.3) qui conditionne le nombre de transformations des sulfoaluminates pour arriver à l'état stable final.

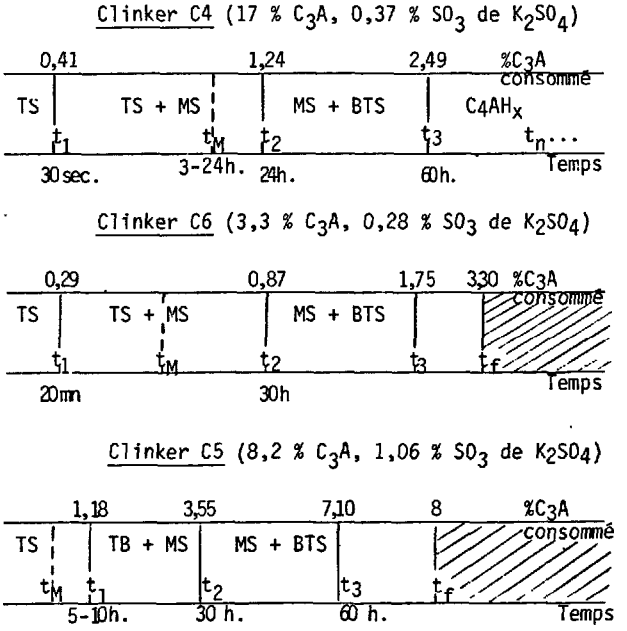

Fig. 3 - Schémas de transformations des sulfoaluminates pour 3 rapports K_2SO_4 / C_3A.

TS : ettringite
MS : *monosulfoaluminate*
BTS : solution solide à 0,5 mole $CaSO_4$
t_1 : disparition du sulfate en solution, fin de la formation d'ettringite, début de formation de monosulfoaluminate
t_2 : disparition de l'ettringite, fin de la formation de monosulfoaluminate
t_3 : disparition du monosulfoaluminate
t_M : 2ème pic de flux de chaleur d'hydratation
t_f : fin de réaction

Les % C_3A consommé indiqués sur les échelles correspondent aux quantités stoechiométriques (calculées d'après le SO_3) de chaque sulfoaluminate.
L'échelle des temps correspond aux mesures expérimentales des temps de réaction.

Le flux thermique fourni par l'alite augmente les vitesses de ces réactions qui sont toutes lentes.

On voit que lorsque SO_4^{--} n'est pas consommé pendant les premières minutes, il faut alors attendre le 2ème pic de flux thermique pour observer la formation de monosulfoaluminate. Dans le cas contraire, c'est la réaction MS → BTS qui se produit avec retard. Par son effet thermique l'hydratation de C_3A relance l'hydratation de l'alite. Pour les clinkers riches en K_2SO_4, la teneur en calcium étant systématiquement plus faible pendant la période d'hydratation du C_3A, la distance de précipitation (1) augmente et le CSH aura donc tendance à prendre une structure d'autant plus cristalline. Au bout de 50 à 70 heures, le système évolue de plus en plus lentement sans que l'on puisse détecter de nouveaux changements de composition de la phase solide : les hydrates obtenus alors sont essentiellement constitués du CSH_{II} et soit de C_3A hydraté (C_4AH_x) soit de sulfoaluminates dans les clinkers contenant du K_2SO_4. Les taux d'hydratation atteignent des valeurs très élevées après 100 heures pour l'alite et le C_3A. Le C_4AF et la bélite sont peu hydratés. La solution reste sursaturée par rapport à tous les hydrates. Les trajets des points figuratifs des solutions dans les diagrammes ($CaO - SiO_2 - H_2O$) ($CaO - SO_3 - H_2O$) ($Ca^{++} - OH^-$) sont du même type :
Après une période de sursaturation rapide, le point figuratif atteint un point de rebroussement et longe la courbe d'équilibre en suivant un trajet sensiblement parallèle. Le mécanisme est donc du même type que pour l'alite (dissolution-précipitation).

3.2 - Suspensions de ciments portland (Fig.4 et 5)

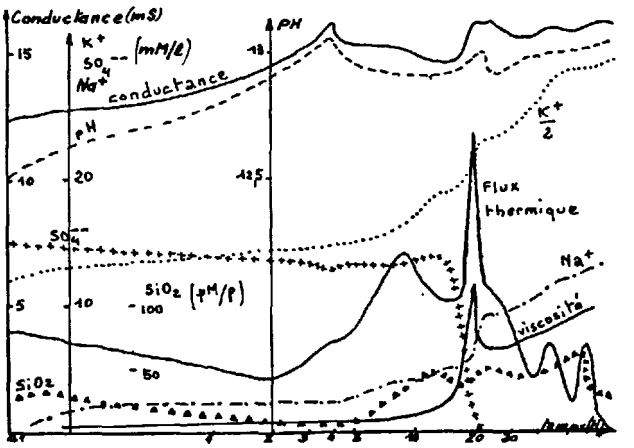

Fig.4 - Mesures ionométriques et thermiques (ciment C4)

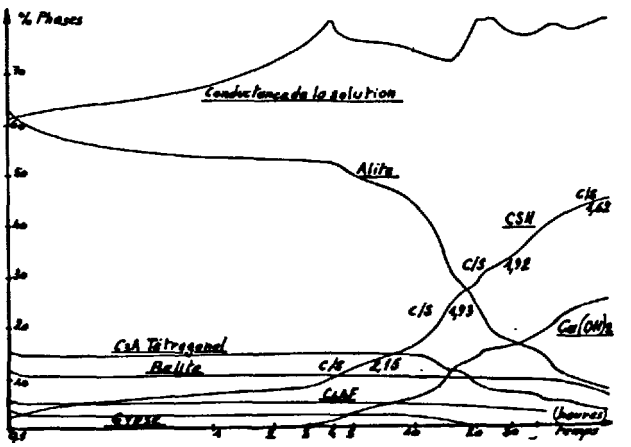

Fig.5 - Allure de composition du solide (ciment C4)

La figure 4 représente l'évolution chimique de la solution et la figure 5 montre les variations correspondantes des phases (périodes 2, 3 et 4).
La présence de gypse produit ici la formation systématique d'ettringite aux premiers instants.
La séquence de l'hydratation de l'alite n'est pas modifiée.

Pendant la 1ère période
Nous n'avons pas observé la formation de syngénite pour les clinkers riches en K_2SO_4 (le produit de solubilité de ce sel n'est pas atteint dans nos conditions opératoires).
Le gypse bloque beaucoup plus rapidement l'hydratation du C_3A, que le K_2SO_4 : la teneur en aluminium de la solution est beaucoup plus faible dès le départ, de même que le flux de chaleur.

Pendant la 2ème période, comme le montre la fig. 4, on n'observe pas de modifications sensibles des réactions. Comme pour les clinkers, la solution se sursature progressivement en chaux, les teneurs en alcalins restent sensiblement constantes et la teneur en silice décroît jusqu'à des valeurs très faibles, difficilement dosables sans concentration du filtrat ou extraction.
La teneur en sulfate n'évolue pratiquement pas (légère diminution avec l'augmentation du calcium) le flux thermique est faible, mais jamais nul. Les taux de réaction sont tous faibles. Les vitesses de sursaturation sont systématiquement plus élevées pour les CPA que pour les clinkers correspondants, en fin de période dormante et plus faibles au début, ce qui aboutit souvent à des échéances très voisines pour l'apparition de $Ca(OH)_2$ dans les deux cas. Ceci est en parfait accord avec nos mesures faites par ailleurs en système ouvert (1) et montrant qu'en présence de solutions de chaux + gypse, la dissolution de l'alite est ralentie par le calcium. On précipite ensuite des CSH beaucoup moins solubles, ce qui augmente la vitesse de dissolution. L'influence accélératrice du gypse sur l'hydratation de l'alite ne se manifeste donc qu'en fin de période dormante et ne doit pas modifier beaucoup le temps de prise rhéologique.

Pendant la 3ème période, la fig. 4 montre une augmentation simultanée du flux thermique et de la teneur en SiO_2 en solution, la chute de conductance accompagnant la précipitation de $Ca(OH)_2$ est plus élevée que pour les clinkers : la formation de CSH moins solubles en présence de gypse augmente leur vitesse de précipitation et déplace la solubilité de l'alite dans le sens d'une dissolution plus rapide. A la fin de la période quasi-stationnaire de précipitation rapide de la portlandite, la conductance diminue et le flux thermique commence à décroître : la dissolution de l'alite se ralentit. On aboutit alors à un minimum de conductance suivi peu après d'un second maximum. Pendant cette courte remontée de conductance, les concentrations en Ca^{++}, OH^-, SiO_2, Na^+, K^+ augmentent (fig.4). Le flux thermique et la viscosité de la suspension forment un pic pointu pour les fortes teneurs en C_3A. La concentration en SO_4^{--} chute brutalement et parvient à une valeur très faible. La teneur en C_3A diminue rapidement (fig.5) et il y a reprise de l'hydratation de l'alite. L'ensemble de ces phénomènes montre de manière remarquable l'interdépendance des vitesses de réaction, à la fois par des effets de couplage thermique (la chaleur de réaction de l'alite augmente la vitesse de formation de l'ettringite, puis la chaleur de réaction de C_3A produit une reprise de l'hydratation de l'alite) et par des effets de couplage chimique : l'épuisement du gypse et la chute de SO_4^{--} provoquent la transformation ettringite → monosulfate et la reprise de l'hydratation de C_3A.
Comme dans le cas des clinkers, la séquence de l'hydratation de C_3A dépend du rapport initial C_3A/SO_3. La transition ettringite - monosulfate ne peut donc avoir lieu que si la quantité de C_3A est suffisante. Or, pour les 2 ciments contenant très peu d'aluminates, nous observons vers 30-40h la disparition de SO_4^{--} (qui devrait rester en excès) et les hydrates obtenus à 100 h sont l'ettringite et le monosulfoaluminate. Bien que C_4AF réagisse simultanément, son taux de réaction reste beaucoup trop faible pour expliquer cette anomalie. Nous sommes donc amenés à conclure à l'entrée de l'ion SO_4^{--} en solution solide dans le CSH_{II} : ceci contribue à l'épuisement rapide du gypse pendant la période d'hydratation intense de l'alite.
Pour les ciments à forte teneur en C_3A, les transformations successives des sulfoaluminates en des formes de teneur de plus en plus faible en sulfate peuvent être détectées par notre appareillage, à condition que la teneur en alcalins du C_3A soit suffisante. Ces transformations se produisent en général vers 50 heures puis vers 70 heures et sont accompagnées de petites reprises de l'hydratation et de petits pics exothermiques.

Comparaison des vitesses de réaction des différentes formes de C_3A. Nos essais montrent bien que, dans le milieu complexe du ciment industriel, la réactivité intrinsèque du C_3A n'est que l'un des nombreux facteurs influençant sa vitesse d'hydratation. Il faut en effet tenir compte également du rapport gypse/C_3A, de la chaleur d'hydratation de l'alite, du sulfate entrant dans le CSH, de la quantité d'alite, de la quantité de C_3A, de sa chaleur d'hydratation, et de la quantité d'alcalins qui modifient le pH et les vitesses de précipitation. Au cours de nos essais, nous avons observé des temps de disparition du gypse variant de 9h à 20h pour C4. Ces temps varient fortement avec la température et la vitesse d'agitation : ceci montre qu'il existe un mécanisme diffusionnel empêchant la dissolution du C_3A en présence de gypse.
D'une manière générale, on peut dire que la disparition du sulfate est d'autant plus tardive que :
- la chaleur d'hydratation, la teneur en C_3A et la teneur en sulfate alcalins sont faibles et que la teneur en alcalins du C_3A est élevée.
Ces facteurs influencent de la même manière, par le biais d'effets thermiques, les temps de prise rhéologique et les durées des périodes dormantes définies par les courbes de conductance. C'est ainsi que le ciment C3, qui contient 5,6 % de C_3A tétragonal a une vitesse de montée en résistance faible, le temps de prise et les temps de réaction les plus longs en suspension : apparition de la portlandite à 6h, disparition du gypse à 40 h. Ceci ne l'empêche pas à 6 mois de montrer d'excellentes performances mécaniques, bien meilleures que celles de C2 et C4, qui sont riches en C_3A. Lorsque l'on vise des résistances élevées à long terme, on peut donc tenter de reculer au maximum la transformation de l'ettringite de manière que les contraintes mécaniques qu'elle provoque puissent être absorbées par le CSH suffisamment résistant. Par contre, si l'on repousse trop loin ou si l'on supprime cette transformation, on perd alors le bénéfice de la reprise thermique de l'hydratation de l'alite. Il faut trouver un compromis : l'optimum de gypse sera toujours un peu supérieur à la quantité nécessaire à la transformation totale du C_3A en ettringite, du fait de la consommation de sulfate par le CSH. Cet optimum sera variable selon la pente de montée de résistances désirée. Un rapport gypse/C_3A élevé favorisera les résistances à long terme. Inversement, un rapport faible augmentera plutôt les résistances initiales, aux

dépens des résistances finales.
Les diagrammes d'évolution chimique montrent pour les ciments C4 (15,8 % C_3A_T) et C2 (12,5 % C_3A_C) des temps d'épuisement du gypse de 10 h pour C2 et 13 à 20h pour C4 selon la vitesse d'agitation. Ceci montre que le K_2SO_4 du ciment C4 (0,8 %) accélère notablement l'hydratation du C_3A tétragonal (6) et lui permet presque de rattraper la vitesse de C2 : ce qui est parfaitement logique car nous avons vu que K_2SO_4 agit par couplage chimique, en déplaçant par formation d'ettringite la dissolution de l'alite qui à son tour accélère l'hydratation de C_3A.

4/ CONSEQUENCES

Lien avec les réactions à faible E/C

Ayant montré que la séquence de l'hydratation reste la même en suspension à E/C = 4 qu'en pâte pure, on en vient à rechercher des correspondances de temps de réaction entre ces deux cas. Compte tenu des connaissances actuelles sur les réactions en pâte pure, on peut remarquer que les paramètres qui différencient les réactions en pâte pure et à E/C = 4, sont principalement : l'intervention de la diffusion à travers les hydrates qui est considérablement facilitée à E/C = 4 sous forte agitation et les effets thermiques qui sont plus faibles à E/C = 4 qu'en pâte pure (mais ils seraient du même ordre en mortier normal). On peut donc s'attendre à une liaison entre échelles des temps du type parabolique : nous obtenons effectivement à 100 h, à E/C = 4 des taux de réaction équivalents à 1 an en pâte pure.
L'effet de barrière intense de l'ettringite a tendance à annuler l'influence de l'agitation et du E/C élevé sur les temps de réaction, tant que cette influence n'est pas suffisante pour briser ou diminuer la couche d'hydrates. On doit donc observer un décalage du temps plus faible pour les aluminates que pour les silicates.
Le temps mis pour parvenir au maximum de sursaturation en chaux (1er pic de conductance) est en relation étroite avec le début de prise. Les véritables réactions de la prise commencent en effet avec la précipitation de la portlandite, peu avant ce maximum. Nous trouvons à E/C = 4 des temps à peu près doubles des temps de prise mesurés sur pâte pure, les écarts étant liés à des effets thermiques et rhéologiques des aluminates. A ce titre, le temps de sursaturation limite mérite bien le nom de "début de prise chimique", par opposition au début de prise "rhéologique", lié à la consommation rapide de l'eau libre. En pâte pure, le maximum de conductance signalant la précipitation de la portlandite a lieu avant cet effet rhéologique, alors que la pâte est encore plastique : il ne faut donc pas confondre début de prise "rhéologique" et précipitation de la portlandite.
L'influence des éléments mineurs comme K_2SO_4 sera encore plus grande à E/C = 0,3 qu'à E/C = 4. En toute rigueur, il faut donc essayer de reproduire à E/C = 4 les concentrations de la solution de départ que l'on obtiendrait à E/C = 0,30. Mais ce faisant, on modifierait énormément les quantités par rapport au clinker : il faut donc rechercher un compromis.

CONCLUSIONS

L'ensemble des phénomènes que nous décrivons montre que, par l'intermédiaire des couplages de vitesse de réaction, chaque ciment portland forme un système particulier où chaque constituant intervient sur la dynamique de l'ensemble. Les mêmes mécanismes s'appliquent à tous indifféremment. Parmi ceux-ci, le mécanisme de dissolution-cristallisation tient une place très importante.
Notre démarche d'étude simultanée de toutes les réactions est à ce titre parfaitement bien adaptée, car elle permet l'examen direct de l'influence d'un paramètre sur l'ensemble du comportement. En particulier nous avons dégagé ici le mécanisme de l'action simultanée des sulfates alcalins sur la vitesse de réaction de C_3A et sur l'hydratation de l'alite. Ce mécanisme aboutit dans ses conséquences, aux effets bien connus sur l'évolution des résistances et sur la structure des hydrates.
La même méthode peut permettre de déterminer l'influence des caractéristiques propres du clinker et d'éventuelles anomalies sur la cinétique de l'hydratation. Le mécanisme d'action d'un grand nombre d'ajouts et d'adjuvants peut également être mis en évidence. Ces études peuvent être faites de manière rationnelle et rapide en utilisant des méthodes d'analyse chimique automatique combinées aux méthodes classiques d'analyse cristallographique.

BIBLIOGRAPHIE

1. - C.VERNET, E.DEMOULIAN, P.GOURDIN, F.HAWTHORN
Mécanismes réactionnels de l'hydratation -
VII[e] Symp. Int. Chimie des Ciments - Paris 1980.

2. - H.LE CHATELIER - Recherches expérimentales sur la constitution des mortiers hydrauliques -
Thèse Paris 1887.

3. - C. VERNET
Cinétique de l'hydratation du ciment Portland-
Aspects méthodologiques
VII[e] Symp. Int. chim. des ciments - Paris 1980
(Affiche commentée).

4. - R. SIERRA - Thèse Univ. Rennes (Fév. 1974).

5. - M.E. TADROS, J. SKALNY, R.S. KALYONCU
"Early hydration of tricalcium silicate"
Journal of the Americ. Ceram. Soc. Vol.5 - n°7-8
pp 344 - 347.

6. - M.REGOURG - Cristallisation et réactivité de l'aluminate tricalcique dans les ciments Portland
"Il cemento" Vol. 75 July - Sept 78 pp 323-336

Influence of pretreatment on the microstructure of calcium silicate hydrate gels

Influence du prétraitement sur la microstructure des gels de silicate de calcium hydraté

F.G.R. GIMBLETT, Lecturer in Chemistry,
Z. MOHD. AMIN, Research Student and K.S.W. SING, Professor of Chemistry, School of Chemistry, Brunel University, Uxbridge, England.

RESUME : Le gel de silicate de calcium hydraté est l'un des principaux composés intervenant dans l'hydratation des ciments. Des échantillons de gel, préparés par réaction à l'hydroxyde de calcium sur le métasilicate de sodium, dans un rapport molaire de 1:1, en solution aqueuse à un pH de 12,5, ont été étudiés par porosimétrie au mercure, adsorption d'azote et de vapeur d'eau, complétées par l'étude de la diffraction des rayons X et la microscopie électronique à balayage.

L'adsorption d'azote et d'eau par les gels dépend du prétraitement; la microstructure du matériau étant conditionnée par la méthode de séchage et par le (ou les) solvant organique utilisé dans la procédure de séchage par déplacement de l'eau par un solvant.

L'adsorption d'azote à -196°C est reversible jusqu'à une pression relative de 0,45, alors que l'adsorption d'eau est caractérisée par une hystérésis s'étendant jusqu'à des faibles valeurs de pression relative. En général, les aires spécifiques B.E.T. obtenues à partir de l'adsorption d'azote sont bien inférieures à celles obtenues avec l'eau, bien que, sous certaines conditions, il soit possible d'obtenir des valeurs ayant le même ordre de grandeur.

L'influence du séchage, et d'autres facteurs, sur la porosité et l'aire spécifique du matériau sont discutés ; une explication de la spécificité de l'eau est proposée, basée sur son interaction avec les sphères de coordination des ions calcium de la structure.

SUMMARY: Calcium silicate hydrate gel is one of the major products in the hydration of cement. Samples of the gel, prepared by the interaction of calcium hydroxide and sodium metasilicate at 1:1 molar ratio in aqueous solution at pH 12.5, have been studied by mercury porosimetry and nitrogen and water vapour sorption supplemented by X-ray diffraction and scanning electron microscopy studies.

The adsorption of nitrogen or water by the gel is very dependent on its pretreatment, the microstructure of the material being influenced both by the method of drying and by the organic solvent(s) used in the solvent displacement drying procedure.

Nitrogen adsorption at -196°C is reversible up to a relative pressure of 0.45, whereas water sorption is characterised by open hysteresis loops down to low relative pressures. In general, the BET surface areas for nitrogen adsorption are substantially less than those obtained with water, although under certain special conditions it is possible to obtain values of approximately similar magnitude.

The influence of drying, and other factors, on the porosity and surface area of the material is discussed, and an explanation advanced for the high specificity of water based on its interaction with the coordination spheres of the calcium ions in the structure.

INTRODUCTION

Extensive studies have been made of the adsorption of nitrogen and water vapour on cement pastes and related calcium silicates (1). However, in most cases, both the pore volumes (2) and the BET surface areas (3,4) computed from the water sorption isotherms have proved to be much higher than those calculated from the nitrogen isotherm (5-8). Two principal explanations have been advanced for these differences: the presence in the samples of "ink-bottle" pores, i.e. pores with wide bodies and constricted entrances, accessible to water but not to nitrogen (6,8), or the possibility that nitrogen measures the surface area and porosity correctly while the increased values with water are a consequence of the penetration of water vapour into the layer structure of the calcium silicate hydrate gel common in these hydrated systems (9,10).

Recently, Litvan (11) has demonstrated that these differences are removed, certainly as far as cement pastes are concerned, if special techniques are employed for drying the samples. The main features of such methods were the use of a solvent displacement method during the washing procedure and the use of vacuum distillation to remove final traces of the solvent from the sample. Using methyl alcohol as the solvent, Litvan obtained a value of approximately 200 $m^2 g^{-1}$ for both the nitrogen and water surface areas of his specially dried cement pastes.

One of the problems associated with the study of cement pastes is the degree of inhomogeneity, both chemical and physical, frequently encountered in these materials. Since the surface characteristics of such pastes are controlled by the calcium silicate hydrate gel they contain, the present systematic study was undertaken on samples of calcium silicate hydrate gel prepared in a manner to ensure, as far as possible, chemical and physical uniformity.

EXPERIMENTAL

Materials

Polythene containers were used throughout to eliminate any stray contamination arising from the use of glass vessels, and all experiments were conducted in a nitrogen-flushed glove box to avoid, as far as possible, interference from atmospheric carbon dioxide.

Aqueous solutions of sodium metasilicate were prepared by dissolving AR sodium hydroxide in conductivity water and slowly adding, with constant stirring, an appropriate amount of silica gel (Merck kiesel gel 60HR). The resulting solution was further diluted and stored in a well-stoppered vessel to exclude carbon dioxide. The silicate content of the final solution was analysed using methods described by Vogel (12).

Calcium hydroxide solution was prepared by dissolving the AR grade solid in conductivity water. The calcium content was determined by EDTA titration using Eriochrome Black T as an indicator (13).

Calcium silicate hydrate gel (CSH(I)) was prepared by adding an aqueous solution of calcium hydroxide (18 mmol dm^{-3}) to a sodium metasilicate solution of the same concentration. Constant stirring was employed throughout to avoid flucuations of pH, the latter being continuously monitored as 12.5. The resulting gel ($CaO:SiO_2$ = 1:1) was stored for various lengths of time in the mother liquor before being transferred to a stoppered stainless steel vessel, frozen overnight at -196°C and then allowed to thaw to room temperature. The sample was centrifuged, the mother liquor decanted and the solid gel shaken for 5 min with 50 cm^3 of a given organic solvent. Decantation of the organic solvent was followed by similar treatment with the same volume of acetone and the washed sample was then initially dried by brief suction over a laboratory pump. Further drying was effected through the use of various drying agents (see below) and the final samples were stored in tightly capped bottles sealed with paraffin wax contained in a vacuum desiccator.

Conductivity water was prepared by passage of distilled water through a mixed-bed ion-exchange column, and all the organic solvents were of AR purity as were the solid desiccants employed.

Methods

The CSH(I) samples were dried before examination by a variety of methods. When solid desiccants were employed, drying was effected by storage of the sample for various lengths of time over the desiccant in a vacuum desiccator. Alternatively, reduction of the ambient water vapour pressure of samples to a constant value of 5 x 10^{-4} Torr (the so-called method of D-drying) was achieved through the use of a conventional vacuum line, involving a liquid nitrogen trap in conjunction with a rotary oil pump and a mercury diffusion pump, the pressure being continuously monitored by a Pirani gauge.

The volumetric apparatus used to study the adsorption of nitrogen at -196°C was similar to that described by Harris and Sing (14). Nitrogen gas of 99.9% purity was employed, being first dried by slow passage through a cold trap. Outgassing of the solid under investigation was carefully controlled at 2 x 10^{-4} Torr, a slightly lower pressure than that achieved during D-drying but chosen to compensate for the possible small uptake of moisture by the sample during its introduction into the apparatus. Where the solid was heated before adsorption of nitrogen, this was only commenced after the attainment of the above pressure to eliminate any possible contamination of the sample by residual gas or vapour in the system. Equilibrium gas pressures were measured with a pressure-sensitive transducer gauge and a mercury manometer (to $\pm$0.001 cm). An oxygen vapour pressure thermometer was used to measure the adsorbent temperature.

Water sorption was measured gravimetrically using a quartz spring balance of the McBain-Bakr type (15), whose operation has been described by Carruthers et al. (16). Care was again taken regarding ourgassing the sample and, where necessary, its heating. Water vapour was admitted slowly into the apparatus to reach the solid at the desired relative pressure, sorption being allowed to proceed until the pressure reached a steady value and no further extension of the quartz spring had occurred over a period of 30 min. The time necessary to attain this condition varied with the solid employed and the relative pressure in the system.

Mercury porosimetry measurements were made with a Carlo Erba 225 Pressure Porosimeter. Gel samples were outgassed for 30 min at room temperature to a pressure less than 10^{-2} Torr and the mercury pressure increased

from 1 atm to 2000 kg cm^{-2} at a fairly constant rate over a period of 1-2 h.

RESULTS

Coding of samples

The narrative has been simplified by coding the samples to provide a complete summary of their pretreatment prior to surface investigation. For the particular sample CSH/18/IA/D(8)/100, reading from left to right tells us that this is a sample of CSH(I) gel (information before the first solidus), stored for 18 days in the mother liquor before filtration (information between first and second solidi), washed with propan-2-ol (I) followed by acetone (A) (information between second and third solidi), dried to a constant water vapour pressure of 5×10^{-4} Torr (D-drying) for 8 days (information between third and fourth solidi) and heated to 100°C before being investigated either by nitrogen or water vapour sorption. Variants of this code refer mainly to organic solvents used in the solvent displacement method (M = methanol; E = ethanol) and to the various desiccants employed (Ca = calcium chloride; Mg = magnesium perchlorate; P = phosphorus pentoxide) or water vapour pressure attained (D or D*). In the last case the symbol D*(8) indicates that the sample was initially dried for 4 days at a water vapour pressure of 2×10^{-2} Torr followed by a further 4 days at 5×10^{-4} Torr, making a total of 8 days drying in all.

Description of isotherms

Typical examples of nitrogen and water vapour sorption isotherms are illustrated in Figure 1(a) and (b), respectively. Nitrogen adsorption at -196°C is reversible to a relative pressure of 0.45, while water sorption is characterised by open loops down to low relative pressures. The isotherms illustrated were obtained using samples washed with propan-2-ol and acetone and outgassed at 25°C prior to investigation, but similar results were obtained for samples prewashed with other organic solvents and outgassed at higher temperatures.

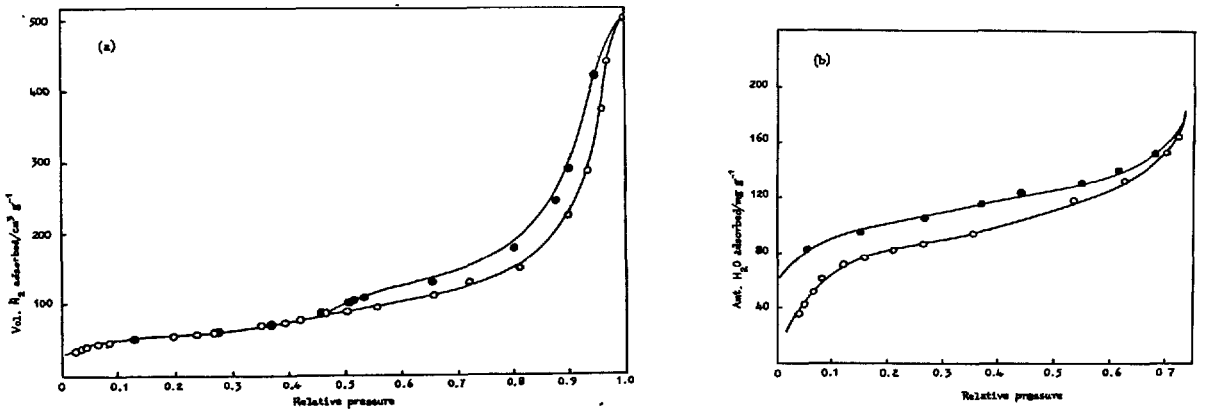

Fig. 1 - Typical isotherms for CSH(I) gels: (a) nitrogen adsorption; (b) water sorption. O - adsorption; ● - desorption branch.

Influence of drying conditions

Preliminary experiments were conducted to investigate the effect of the drying conditions on the surface properties of prepared CSH(I) gels. The results obtained from porosimetry are illustrated in Figure 2, while the nitrogen and water surface areas for some of the same samples, as well as those computed from the porosimetry data are listed in Table I.

From the table is will be seen that a wide variety of drying conditions and methods of pretreatment were employed during the preparation of the samples.

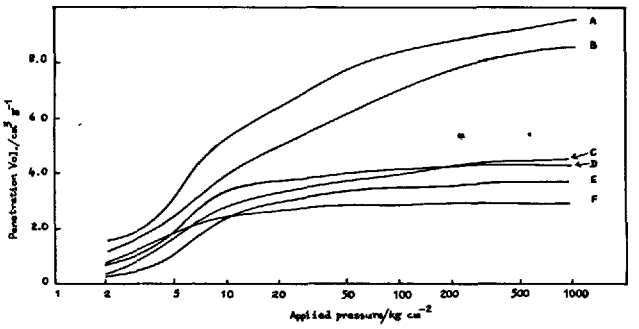

Fig. 2 - Influence of drying agent on porosity of CSH(I) gels. A - CSH/18/IA/D(8)/25; B - CSH/30/A/D(8)/25; C - CSH/2/A/P(3)/25; D - CSH/7/A/Ca(8)/25; E - CSH/2/A/Ca(8)/25; F - CSH/2/A/Mg(3)/25.

Of the results quoted, those relating to the use of solid desiccants show the widest variation in surface area (nitrogen and water) but the least variation in porosity with change of conditions. Thus the porosimetry results show that pores with the smallest radii are generated by storage over phosphorus pentoxide, with calcium chloride being the next most efficient drying agent, and magnesium perchlorate the least efficient in this particular sequence. Increasing the storage time in the mother liquor before drying seems to increase the percentage of smaller pores in the sample although, as the results discussed below indicate, this is by no means clear-cut.

All of the solid desiccants studied suffer from a major defect in that their efficiency is drastically reduced on prolonged exposure to water vapour. As a result, samples "dried" in the presence of phosphorus pentoxide, calcium chloride or magnesium perchlorate are not really dry, but contain traces of moisture capable of catalysing ageing processes when the samples are stored for prolonged lengths of time. Such ageing processes lead to considerable decreases in the

TABLE I

Influence of drying conditions on the surface areas of CSH(I) gels

Sample No.	Drying agent	$S^{N}_{BET}/m^2\ g^{-1}$	$S^{H_2O}_{BET}/m^2\ g^{-1}$	$S_{Hg}/m^2\ g^{-1}$
CSH/2/A/Ca(8)/25	$CaCl_2$	72 (7 d)[a]	150 (757 d)	66
CSH/7/A/Ca(8)/25	$CaCl_2$	56 (18 d)	90[b] (766 d)	48
CSH/2/A/P(3)/25	P_2O_5	35 (323 d)	195 (295 d)	36
CSH/2/A/D(8)/25	D-dried	174 (112 d)	220 (245 d)	162
CSH/4/IA/D(8)/25	D-dried	203 (52 d)	231 (68 d)	201

[a] Length of storage time after drying and before outgassing prior to examination given in parentheses.
[b] Low value attributed to carbonation before examination, as demonstrated by X-ray diffraction and scanning electron microscopy studies.

in the nitrogen surface areas of samples (cf. the S^{N}_{BET} values in Table I for CSH/2/A/Ca(8)/25 and CSH/2/A/P (3)/25 stored for seven and 323 days, respectively) but have little effect on the water surface areas (cf. the $S^{H_2O}_{BET}$ values for the same samples stored for 757 and 295 days, respectively). The $S^{H_2O}_{BET}$ value recorded for CSH/7/A/Ca(8)/25 is anomalous and is attributed to interaction between the sample and atmospheric carbon dioxide before examination as shown by X-ray diffraction data, which clearly indicate the presence of calcite in the sample, and scanning electron microscopy, which shows that on storage the surface of the sample changed from an open porous form to one consisting of close-packed spherical nodules.

Because of the deficiencies of powdered solid desiccants, all systematic studies of the influence of various conditions have been made on samples whose ambient water vapour pressure had been reduced to a constant value (2×10^{-2} Torr and/or 5×10^{-4} Torr) during drying. The latter pressure is that attained by the so-called D-drying method and this term is used here. Typical results obtained for D-dried samples are illustrated in Figure 2 and listed in Table I as CSH/2/A/D(8)/25 and CSH/4/IA/D(8)/25, respectively. Figure 2 shows that D-drying induces a much higher proportion of smaller pores while Table I indicates that the nitrogen surface areas are much higher for D-dried samples than for those exposed to solid desiccants. What is also important is that samples dried by this method show none of the instabilities and inconsistencies in surface area mentioned above for samples dried over phosphorus pentoxide, calcium chloride and magnesium perchlorate. Thus D-dried samples have surface areas which appear to be independent of the length of storage time between drying and experimental examination, i.e. they are free from ageing processes, and as has been demonstrated on numerous occasions in this laboratory, using the same method of preparation and pretreatment always leads to a constant value for the surface area (to within $\pm 5\%$) for a given adsorbent.

Influence of solvent displacement

The curves for samples CSH/2/A/D(8)/25 and CSH/4/IA/D (8)/25 illustrated in Figure 2 indicate that the inclusion of propan-2-ol as a solvent for the displacement of water prior to D-drying appreciably influences the porosity of the final sample, while the results tabulated in Table I show that the nitrogen and water surface areas for such a sample approach each other in the manner described by Litvan (11) for methanol-treated cement pastes.

To see whether such changes may be related to the nature of the organic solvent, studies have been made on a series of samples prepared in an exactly similar manner except that different alcohols have been employed for solvent displacement prior to D-drying. The mercury porosimetry results obtained for such samples are illustrated in Figure 3, while Table II lists their corresponding S^{N}_{BET}, $S^{H_2O}_{BET}$ and S_{Hg} values.

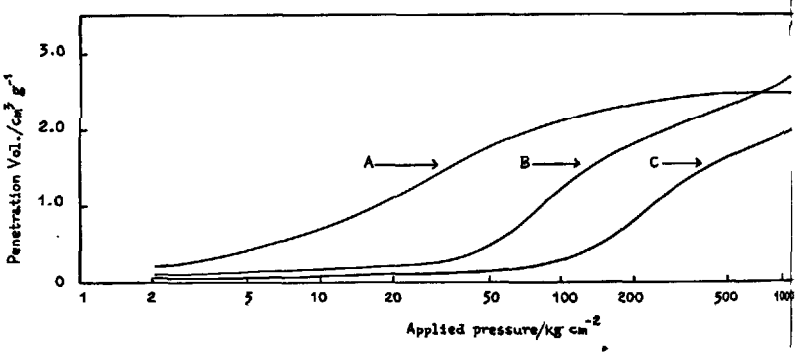

Fig. 3 - Influence of solvent on porosity of CSH(I) gels. A - CSH/10/EA/D*(8)/25; B - CSH/10/MA/D*(8)/25; and C - CSH/10/IA/D*(8)/25.

Of the three alcohols studied, propan-2-ol yields samples with the highest percentage of smaller pores as well as nitrogen surface areas substantially closer to those measured by water sorption. However, it is interesting to note that both the porosity and nitrogen surface area of the propan-2-ol washed sample listed in Table II are appreciably different from those recorded in Figure 2 and Table I for a similar sample washed with the same solvent. These differences may be attributed to the variation in the length of storage of the two samples in the mother liquor before filtration and to the different mode of drying employed in the two cases. These points are pursued in greater detail below.

In contrast to the nitrogen surface areas, those measured with water are approximately constant for the three samples listed in Table II, being apparently independent of the alcohol used in the solvent displacement procedure and of the length of storage time prior to examination. The surface area determined by mercury porosimetry appears to be more closely related to the value for nitrogen than for water, as far as the results recorded in Tables I and II are

TABLE II

Influence of solvent on the surface areas of CSH(I) gels

Sample No.	Solvent	$S^{N}_{BET}/m^2\ g^{-1}$	$S^{H_2O}_{BET}/m^2\ g^{-1}$	$S_{Hg}/m^2\ g^{-1}$
CSH/10/EA/D*(8)/25	Ethanol	111 (243 d)[a]	210 (180 d)	65
CSH/10/MA/D*(8)/25	Methanol	155 (275 d)	223 (296 d)	188
CSH/10/IA/D*(8)/25	Propan-2-ol	174 (283 d)	233 (312 d)	201

[a]Length of storage time after drying and before outgassing prior to examination given in parentheses.

TABLE III

Storage in mother liquor and its influence on the subsequent surface areas of CSH(I) gels

Sample No.	Length of storage/d	$S^{N}_{BET}/m^2\ g^{-1}$	$S^{H_2O}_{BET}/m^2\ g^{-1}$
CSH/4/IA/D(8)/25	4	203 (52 d)[a]	231 (68 d)
CSH/10/IA/D(8)/25	10	184 (283 d)	235 (312 d)
CSH/18/IA/D(8)/25	18	163 (243 d)	223 (247 d)
CSH/30/IA/D(8)/25	30	98 (360 d)	-

[a]Length of storage time after drying and before outgassing prior to examination given in parentheses.

TABLE IV

The influence of outgassing temperature on the subsequent surface areas of CSH(I) gels

Sample No.	Outgassing temperature/°C	$S^{N}_{BET}/m^2\ g^{-1}$	$S^{H_2O}_{BET}/m^2\ g^{-1}$
CSH/10/EA/D(8)/25	25	115 (243 d)[a]	221 (180 d)
CSH/10/EA/D(8)/40	40	-	229 (180 d)
CSH/10/EA/D(8)/80	80	109 (246 d)	-
CSH/10/EA/D(8)/100	100	103 (243 d)	127 (180 d)
CSH/10/EA/D(8)/200	200	114 (243 d)	57 (180 d)

[a]Length of storage time after drying and before outgassing prior to examination given in parentheses.

concerned, in agreement with observations reported for macroporous alumina gels (17).

Influence of storage of mother liquor

Mention has been made above of the apparent influence of the length of storage in the mother liquor before drying on the porosity and nitrogen surface areas of both propan-2-ol/acetone- and acetone-washed samples. For this reason, studies have been made of the porosity and surface areas of a number of samples where the only difference in pretreatment before drying was in their storage time in the mother liquor.

No simple relationship seems to exist between the porosity of the samples and their length of storage, and this could possibly be attributed to the increasing crystallinity of the samples on storage, as demonstrated by the sharpening of lines observed in the X-ray diffraction patterns of these solids. Such crystallinity would lead to increasing inhomogeneity as crystalline regions grow at the expense of amorphous areas, and affect the porosity of the materials in an erratic manner.

In contrast, the nitrogen and water surface areas of the samples listed in Table III follow a regular pattern, with the water surface area being substantially unchanged while the nitrogen surface area shows a steady decline until after 30 days storage it is less than one-half of that recorded after 4 days of the same treatment.

Influence of outgassing temperature

In all the work discussed above, outgassing of the samples immediately before the commencement of nitrogen and water vapour sorption was always undertaken at 25°C. As the results recorded in Table IV show, increasing the outgassing temperature to 200°C makes little difference to the nitrogen surface area of the samples, the value remaining virtually unchanged within experimental error. However, over the same temperature range, the water surface area is drastically reduced until at 200°C it is only one-quarter of the value attained at 25°C.

Influence of outgassing pressure

Although most of the systematic work recorded in this report has been undertaken on D-dried samples, some results (recorded in Table II) have been obtained on samples which although ultimately outgassed at 5×10^{-4} Torr have attained this pressure in stages rather than in one progressive process. This raises the question as to whether the outgassing pressure has any significant effect on the surface properties of the resulting solid, similar to that observed for the rate of drying on the surface area of cement pastes (18).

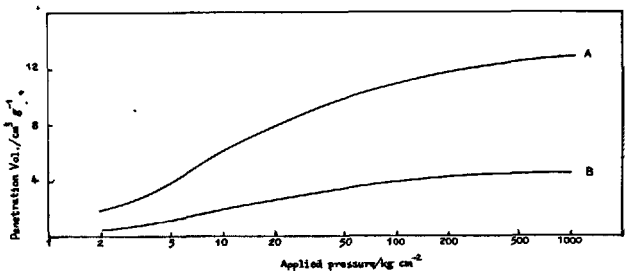

Fig. 4 - Influence of outgassing pressure on porosity of CSH(I) gels. Sample CSH/4/IA/ - /25 outgassed (A) at 5×10^{-4} Torr and (B) at 1×10^{-2} Torr.

The porosimetry results depicted in Figure 4 indicate that decreasing the outgassing pressure from 1×10^{-2} Torr to 5×10^{-4} Torr increases the porosity of the sample, with a much higher precentage of smaller pores being generated at lower pressure - an observation supported by scanning electron microscopy. Whether the surface area is affected to the same extent is doubtful however. Certainly, outgassing in stages rather than continuously down to 5×10^{-4} Torr has little effect on the surface area of the final sample when measured by nitrogen or water sorption, as shown by a comparison of the results listed for samples CSH/10/EA/D*(8)/25, CSH/10/EA/D(8)/25, CSH/10/IA/D*(8)/25 and CSH/10/IA/D(8)/25 in Tables II, III and IV. In this respect, the behaviour of CSH(I) gel appears to differ from that of cement pastes, although it must be stressed that the pressure range studied was rather small and the rate of drying was far from rapid.

DISCUSSION

The results reported here clearly show that the surface characteristics of CSH(I) gels are very dependent on their pretreatment before examination. Thus, five principal factors: method of drying; treatment with organic solvents; storage in mother liquor; heating; and outgassing pressure, have been identified in this work, with two other factors, viz. the influence of atmospheric carbon dioxide and the ageing of samples containing traces of moisture, noted but not studied in any great detail.

The existence of so many factors calls into question the value of much of the previous work on the surface chemistry of CSH(I) gels and also, by implication, of cement pastes. Too often work in this field has been characterised by the use of poorly defined materials whose pretreatment has been largely ignored - certainly as far as published accounts are concerned - and subjected to a variety of drying procedures including an arbitrary selection of organic solvents. Under these circumstances it is little wonder that widely divergent results have been obtained by different groups of workers.

However, despite these divergencies, there has always been general agreement between workers that surface areas measured by nitrogen adsorption are much less than those determined through the use of water on the same samples. This observation is sustained by the work described here, where it has been shown that it is only a coincidence of factors which leads to the nitrogen and water surface areas being approximately equal. These are short storage in mother liquor, washing with propan-2-ol followed by acetone, D-drying and outgassing at elevated temperatures (ca 100°C) prior to examination.

Like other workers in this field, we have been tempted to speculate on the reason(s) for the normally observed differences between the nitrogen and water surface areas. The results obtained point to the enhanced specificity of water and suggest that a more accurate estimate of surface area is obtained from nitrogen adsorption. The decrease in the nitrogen surface area observed for CSH/2/A/P(3)/25 on storage for 323 days, which has been attributed to ageing processes catalysed by traces of moisture, indicates that water interacts with the material of the gel, and the general shape of the water isotherm (Figure 1(b)) with its open hysteresis loop down to low relative pressures shows that water is trapped and retained in the sample on desorption.

As mentioned above, other workers have suggested that trapping of water occurs in "ink-bottle" pores (6,8) or through penetration into the layer structure of CSH(I) gel (9,10). We would like to advance a third suggestion involving the assumption that the structure of CSH(I) gel consists of a silicate framework whose intrinsic negative charge is balanced by the presence of an appropriate number of ancillary calcium counterions. Drying the gel at low ambient water vapour pressure (D-drying) removes bulk water from the silicate framework (a process which is enhanced by the use of an appropriate solvent) as well as some water from the coordination spheres of the calcium ions in the system. This leaves pores in the silicate framework accessible to both nitrogen and water, and vacancies in coordination spheres accessible only to water where the adsorbate is retained.

Provided that relatively mild drying conditions are employed, there is no danger of collapsing the coordination spheres; hence, reducing the outgassing pressure from 1×10^{-2} Torr to 5×10^{-4} Torr in stages, although increasing the porosity of the overall material, has little effect on either its nitrogen or water surface areas. However, increasing the length of storage in the mother liquor increases the crystallinity of the sample; this, in turn, introduces a measure of order into the silicate framework thus reducing the number of pores accessible to nitrogen in the bulk material, although penetration of water into the framework remains unchanged. The nitrogen surface area of the material is correspondingly reduced but the water surface area remains unchanged since the water content of the coordination spheres is unaltered by crystallisation, being determined solely by the drying process employed.

Heating the samples to elevated temperatures has a drastic effect on coordinated water, and leads to the successive collapse of coordination spheres as the temperature is raised. This process is irreversible and causes a decrease in the water surface area as well as a change in the shape of the desorption branch of the isotherm, indicating an approach to a closed loop at sufficiently high temperatures (19). In contrast, the nitrogen surface area remains virtually constant as the temperature is raised indicating that the number of pores accessible to nitrogen in the silicate framework is much less affected by heating (certainly in the range to 200°C) than the coordination spheres of the calcium ions.

REFERENCES

1. - For a review of this work see T.C. HANSEN., F. RADJY and E.J. SELLEVOLD (1973), Ann. Rev. Mater. Sci. 3, 233.

2. - J. SKALNY (1972), Cement & Concrete Research 2, 387.

3. - T.C. POWERS and T.L. BROWNYARD (1947), J. Am. Conc. Inst. Proc. 43, 469.

4. - J. HAGYMASSY, Jr., T. ODLER M. YUDENFREUND, J. SKALNY and S. BRUNAUER (1972), J. Coll. Interface Sci. 38, 20.

5. - R.L. BLAINE and H.G. VALIS (1949), J. Res. Nat. Bur. Standards 42, 257.

6. - R.Sh. MIKHAIL, L.E. COPELAND and S. BRUNAUER (1964), Can. J. Chem. 42, 426.

7. - C.M. HUNT (1966), Highway Research Board Spec. Rep. No. 90 112.

8. - E.E. BODOR, J. SKALNY, S. BRUNAUER, J. HAGYMASSY, Jr. and M. YUDENFREUND (1970), J. Coll. Interface Sci. 34, 560.

9. - R.F. FELDMAN and P.J. SERADA (1968), Materiaux et Constructions 1, 509.

10. - R.F. FELDMAN (1968), "5th International Symposium on the Chemistry of Cement" Paper No.III-23 (preprint), Tokyo.

11. - G.G. LITVAN (1976), Cement & Concrete Research 6, 139.

12. - A.I. VOGEL (1961), "A Text-book of Quantitative Inorganic Analysis", 3rd edn., Longmans, London, p. 582.

13. - Reference 12, p. 436.

14. - M.R. HARRIS and K.S.W. SING (1955), J. Appl. Chem. 5, 223.

15. - J.W. MCBAIN and A.M. BAKR (1926), J. Am. Chem. Soc. 48, 690.

16. - J.D. CARRUTHERS, D.A. PAYNE, K.S.W. SING and L.J. STRYKER (1971), J. Coll. Interface Sci. 36, 205.

17. - B. CORMACK, J.J. FREEMAN and K.S.W. SING, J. Chem. Tech. Biotechnol. manuscript submitted for publication.

18. - C.D. LAWRENCE, F.G.R. GIMBLETT and K.S.W. SING, paper to be presented, "7th International Congress on the Chemistry of Cement", Paris, 1980.

19. - F.G.R. GIMBLETT, Z. MOHD-AMIN and K.S.W. SING, unpublished results.

Etude analytique des C-S-H obtenus par action de la chaux sur la silice

Analytical study of C-S-H obtained by the action of lime on silica

D. MENETRIER, docteur ès sciences, attachée de recherches CNRS (L.A. 23), Faculté des Sciences de Dijon,

B. COTTIN, ingénieur de l'Ecole Centrale, Société des Ciments Lafarge, Centre de Recherches de Trappes,

P. BARRET, professeur à l'Université de Dijon, directeur du L.A. 23 (Réactivité des Solides), France.

RESUME : L'étude cinétique de la réaction à 21°C de l'eau de chaux de diverses concentrations initiales (0 à 35.10^{-3} mol.kg^{-1}) avec la silice amorphe (aérosil) a été faite systématiquement pour établir les courbes d'évolution en fonction du temps des concentrations en chaux et silice. Les produits solides de réaction ont été analysés aux instants successifs ainsi qu'à l'état d'équilibre final par diffraction X et spectrométrie de vibration IR. Il a été établi que le dosage de la silice solide résiduelle pouvait être effectué quantitativement par cette dernière méthode et la possibilité d'un dosage simultané du CSH global a été précisée.

Les résultats mettent en évidence la rapide diminution initiale de la concentration en chaux due à la fixation superficielle d'ions Ca^{2+} par les groupes silanols, suivie, après passage par un minimum, de la remontée de concentration des ions Ca^{2+} vraisemblablement sous l'influence de l'enrichissement simultané de la solution en silice totale (H_4SiO_4, $H_3SiO_4^-$, $H_2SiO_4^{2-}$).

Un maximum de concentration des ions Ca^{2+} est alors atteint. Il est le point de départ d'une décroissance régulière jusqu'à l'équilibre en raison de la précipitation des hydrosilicates dont la composition stoechiométrique pour C/S = 0,5 et plus encore pour C/S = 1 reçoit l'appui d'arguments expérimentaux à condition d'admettre simultanément l'existence d'une solution solide avec la chaux s'étendant au moins jusqu'à C/S = 2.

Le report sur le diagramme chaux-silice-eau des variations de composition des solutions accompagnant l'évolution des systèmes étudiés montre que les chemins cinétiques se développent parallèlement aux courbes d'équilibre de solubilité.

SUMMARY : The kinetic study of the reaction, at 21°C, of lime water with various initial concentrations (0 to 35.10^{-3} mol.kg^{-1}) with amorphous silica (aerosil) was carried out to establish the evolution curves versus time of lime and silica concentration. The solid products of the reaction were analysed at successive times as well as at final equilibrium state by X-diffraction and IR vibration spectrometry. It was established that dosing residual solid silica could be quantitatively performed by the latter method and the possibility of a simultaneous titration of the bulk CSH was clarified.

The results show the rapid diminution of initial lime concentration due to the surface fixation of Ca^{2+} ions by the silanol groups, followed, after passing through a minimum, by the concentration increase of Ca^{2+} ions probably under the influence of the simultaneous enrichment of the solution in total silica (H_4SiO_4, $H_3SiO_4^-$, $H_2SiO_4^{2-}$).

A concentration maximum of Ca^{2+} ions is then reached. It is the starting point of a regular decrease until equilibrium due to the precipitation of hydrosilicates whose stoichiometric composition for C/S = 0.5 and even more for C/S = 1 is validated by experimental arguments providing it is simultaneously assumed that there is a solid solution with lime extending to at least C/S = 2.

Reporting the compositions changes in the solutions accompanying the evolution of the systems investigated on the lime-silica-water diagram shows that kinetic paths develop in parallel to the solubility equilibrium curves.

INTRODUCTION

La compréhension des processus de prise et de durcissement du ciment Portland suppose une bonne connaissance des diagrammes d'équilibre de solubilité qui permettent de relier la composition des hydrates à celle des solutions. Les variations de composition que subissent celles-ci en fonction du temps par suite de la dissolution des phases solides anhydres et de la précipitation des hydrates peuvent être représentées par une construction graphique simple (1) sur les diagrammes d'équilibre, aussi bien dans le cas des silicates de calcium que dans celui des aluminates. Or, les deux diagrammes du système $CaO-SiO_2-H_2O$ publiés antérieurement (2, 3) offrent entre eux de notables différences. L'un des objectifs de ce travail a été de préparer des C-S-H purs et de développer des techniques d'analyse pour mieux les caractériser.

Steinour a fait, dès 1947, une synthèse des travaux déjà publiés sur le système $CaO-SiO_2-H_2O$ (4). Beaucoup d'entre eux démontrent l'existence d'une relation entre le rapport molaire global $[C/S]_s$ des phases solides et la concentration en chaux des solutions avec lesquelles elles sont en équilibre ; cette courbe $[C/S]_s = f\,[CaO]_\ell$ traduit toutefois les résultats de façon incomplète - elle ne tient pas compte de la concentration en silice des solutions - et cela a été une source de désaccords entre les auteurs : le rapport $[C/S]_s$ est un rapport global ; il peut donc être interprété soit par l'existence de deux hydrates, C-S-H (I) et C-S-H (II) de composition variable dans un large domaine (5), soit par le mélange dans des proportions différentes de plusieurs hydrates de composition définie (3).

Dans deux articles seulement, ceux de Flint et Wells (2) et de Greenberg (3) les données sur la composition des solutions en chaux et en silice sont suffisantes pour établir le diagramme d'équilibre du système $CaO-SiO_2-H_2O$. Récemment, Dron (6) a calculé le diagramme théorique et a conclu à la validité de l'hypothèse de Greenberg sur l'existence d'un hydrate $CaH_2SiO_4.nH_2O$.

Malgré les nombreuses recherches faites à leur sujet, la nature de ces hydrates n'est pas bien élucidée et ils sont toujours écrits dans la forme C-S-H pour montrer qu'ils n'ont pas de composition définie. Les méthodes classiques d'analyse apportent peu de renseignements dans le cas de ces produits de faible cristallinité ; il faut cependant mentionner que le développement récent de la méthode de triméthylsilylation a permis de progresser dans la distinction des anions silicates (7). Nous avons essayé de tirer parti de la spectrométrie de vibration infrarouge.

Méthodes expérimentales :

A l'instant initial, 1.000 g de silice amorphe (Aérosil 200) est mélangé avec 1 litre de solution de chaux dont la concentration est différente à chaque essai (colonne 2 - tableau I). Les solutions sursaturées de chaux sont obtenues soit par filtration de suspensions de C_3S dans l'eau, soit à l'aide de résines échangeuses d'ions (essais n, o, p, q). Pour les essais r, s, t, de la chaux vive fraîchement décarbonatée est ajoutée à des solutions de chaux saturées.

Le flacon est placé dans un bain thermorégulé à 21°C et le mélange est agité à vitesse constante, sous courant d'azote. Des échantillons sont prélevés à intervalles de temps réguliers. La concentration en chaux et en silice des filtrats est déterminée par

TABLEAU I

N° essai	Solution (10^{+3}.mol.kg^{-1})			Solide rapport molaire
	$[C]_i$	$[C]_f$	$[S]_f$	$[C/S]_s$
a	2,17	0,97	3,00	0,08
b	2,39	1,39	3,90	0,07
c	3,22	1,50	3,95	0,14
d	3,80	1,55	3,96	0,20
e	4,45	1,49	3,91	0,23
f	5,25	1,12	3,30	0,31
g	6,12	1,20	3,50	0,38
h	10,40	1,35	3,71	0,70
i	11,30	1,40	2,85	0,72
j	12,50	1,23	2,55	0,80
k	14,10	1,13	2,38	0,91
l	17,70	2,25	0,25	0,94
m	20,45	3,72	0,09	1,01
n	23,10	5,00	0,10	1,09
o	28,10	8,35	0,04	1,19
p	31,60	10,32	0,03	1,24
q	37,40	14,95	0,03	1,35
r	20,65 10,25	9,85	0,03	1,26
s	23,45 17,47	15,47	0	1,53
t	21,50 35,30	20,30	0	2,19
u	22,10 0,500g SiO_2	11,50	0,03	1,27

spectrophotométrie d'absorption atomique ; la fraction solide est d'abord séchée (acétone puis éther) avant d'être soumise à une série d'examens, diffraction des rayons X, microscopie électronique à balayage, spectroscopie infrarouge en particulier. En vue de l'utilisation de cette dernière technique, les échantillons sont pastillés avec KBr dans la proportion de 1,20 mg pour 500 mg de KBr ; trois pastilles de 100 mg sont préparées chaque fois, afin d'assurer une bonne reproductibilité des résultats.

Résultats expérimentaux - Discussion :

Il est impossible de rapporter ici les résultats détaillés de tous les essais ; ils sont explicités dans une thèse (8).

Etude des solutions : Nous avons sélectionné quelques courbes pour montrer l'évolution en fonction du temps des concentrations en chaux notée [C] et en silice notée [S] des solutions. (Figure 1).

Au cours des premières minutes, [C] baisse de 2 à 4 millimoles en raison, probablement, d'une fixation d'ions Ca^{++} sur les groupes silanols de la surface de la silice ; chaque Ca^{++} doit réagir avec 2 groupes silanols. Nos résultats sont en bon accord avec ceux de Fripiat et col. (9) qui ont montré que l'aérosil 200 contenait $2{,}90.10^{-3}$ mol de groupes silanols par gramme de silice. Dans les essais r, s, t, où de la chaux solide a été ajoutée, ce phénomène, s'il existe, est masqué par le passage d'un peu de chaux dans la phase liquide tendant à donner des solutions saturées. L'augmentation de [C] souvent observée

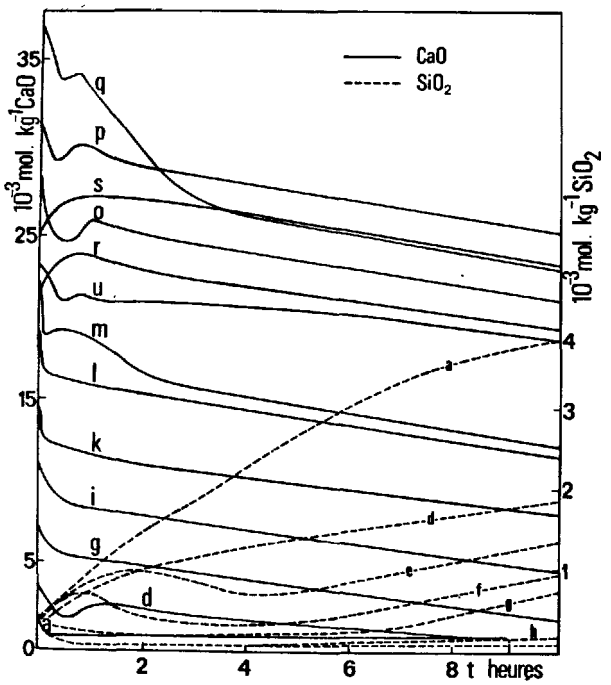

Fig. 1 - Evolution en fonction du temps des concentrations en chaux et silice des solutions.

ultérieurement, peut s'expliquer par le passage en solution, sous l'influence de changements dans le milieu réactionnel : modification de pH, dissolution de silice ...), d'une partie des ions Ca^{2+} chimisorbés.

Dans la période suivante, les courbes [C] sont parallèles (la longueur et les limites de cette période dépendent du titre initial de la solution de chaux). La vitesse moyenne de consommation est de 0,0125 $\mu mol.kg^{-1}.sec^{-1}$. L'essai a est exclus : [C] ne varie plus. La courbe de l'essai u, réalisé à partir de 0,5 gramme de silice n'est pas parallèle à celle des autres essais, tous effectués avec 1 gramme : la pente de la courbe est moins forte et la vitesse de consommation de la chaux est réduite de moitié environ. La vitesse de précipitation des C-S-H est indépendante de la concentration initiale de la solution de chaux, elle est directement proportionnelle à la quantité de silice présente, donc à la surface de la silice.

A l'opposé des courbes [C] qui présentent une évolution générale commune, celles de la silice se divisent en plusieurs groupes. La courbe (a) peut être utilisée comme base de comparaison ; en effet, après quelques minutes, [C] ne varie plus et il y a seulement une dissolution de silice sous forme H_4SiO_4, accompagnée d'une transformation partielle de l'acide monosilicique H_4SiO_4 en $H_3SiO_4^-$, $H_2SiO_4^{2-}$. La courbe de l'essai (d) a la même forme que celle de (a) mais les valeurs de [S] sont inférieures à celles obtenues lors de l'essai (a), pour des temps identiques. Une nouvelle forme de courbe apparaît dans les essais (e) et (f) : après avoir suivi le même trajet qu'en (a) et (d), (40 min.), les courbes se séparent: [S] décroît puis réaugmente soit rapidement comme dans (e), soit après quelques heures, comme dans (f). Ceci reste valable pour l'essai (g), mais, les deux premières périodes de la courbe d'évolution durent très peu de temps. Pour (h) et (i), [S] conserve une valeur faible (environ $0,1.10^{-3}$ $mol.kg^{-1}$) pendant de nombreuses heures, puis croît brusquement au bout de 18 h dans le cas de l'essai (h) et de 20 h dans celui de (i), alors que dans les deux cas, [C] passe par la valeur 2.10^{-3} $mol.kg^{-1}$.

De la comparaison des résultats obtenus pour [C] et [S], il est possible de tirer des conclusions importantes quant au mécanisme de formation des C-S-H. La décroissance continue de [C], et la forme des courbes [S] suggère l'existence d'une compétition entre le passage en solution de la silice et la précipitation des C-S-H à partir des ions de la phase liquide. Dans l'essai (d), la vitesse de précipitation des hydrates reste faible ; par suite, [S] ne s'arrête pas de croître ; en revanche, à partir de l'essai (l), la vitesse de précipitation des hydrates croît rapidement par rapport à la vitesse de dissolution de la silice ce qui permet d'expliquer les deux premières parties de la courbe : apparition de SiO_2 en solution puis sa diminution. Pour les essais (g), (h), (i), la vitesse de précipitation des C-S-H est grande depuis le début ; la concentration de la silice en solution reste faible car la dissolution de la silice est l'étape déterminante de la cinétique de la réaction. On peut penser, sans toutefois en apporter de preuve formelle, que le même mécanisme reste valable lors des essais effectués avec des solutions sursaturées de chaux. On retrouve là l'un des problèmes majeurs posés par l'hydratation de C_3S. La formation des C-S-H a-t-elle lieu par précipitation à partir des ions en solution ou bien est-elle de nature topochimique en entendant par là la fixation directe des molécules d'eau dans la phase solide et la transformation structurale aboutissant à C-S-H.

Au bout de plusieurs mois d'évolution, chaque système atteint un état d'équilibre métastable, caractérisé partiellement par sa concentration en chaux et en silice en solution (colonnes 3 et 4 du tableau I) et par le rapport global $[C/S]_s$ des phases solides (colonne 5). Chaque couple de valeurs $[C]_f$, $[S]_f$, définit un point d'une courbe de solubilité des C-S-H, ce qui nous a permis de reconstruire le diagramme d'équilibre du système $CaO-SiO_2-H_2O$ (8). Il est particulièrement instructif de reporter sur ce diagramme les variations de composition des solutions accompagnant l'évolution des systèmes : on remarque alors que ces "chemins cinétiques" se développent parallèlement aux courbes d'équilibre de solubilité. La conséquence intéressante qui en découle est qu'il suffit de connaître les concentrations initiale $[C]_i$ et finale $[C]_f$ en chaux de la solution pour savoir qu'elle sera l'évolution de [S] tout au long d'un essai.

Etude des phases solides : Les spectres de diffraction X d'échantillons prélevés pendant les essais (a), (b), (c), (d) ne montrent guère qu'une bosse de diffusion due au gel de silice ; la première raie de C-S-H (I) à 3,07Å apparaît sur le spectre final de l'essai (d), mais elle est très large et peu intense ; un épaulement à 2,83 Å [2ème raie de C-S-H(I)] apparaît sur celui de (e). Si l'on déshydrate ces produits finals à 1000°C, on obtient le spectre du quartz pour (a), (b), (c), celui du quartz et de la parawollastonite pour (d),(e) et (h). Les trois raies principales sont présentes sur le spectre final de (h), mais seule la raie à 3,07 Å est fine. Les trois raies deviennent fines quand $[C/S]_s$ atteint l'unité (essai m); le fond continu que donnait la silice a alors complètement disparu.

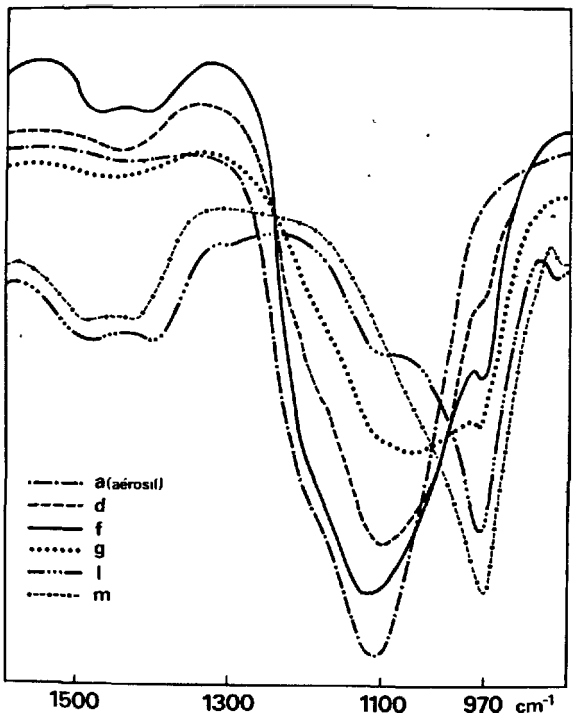

Fig. 2 - Spectres d'absorption infrarouge dans le domaine des vibrations de valence Si-O des phases solides obtenues à l'équilibre.

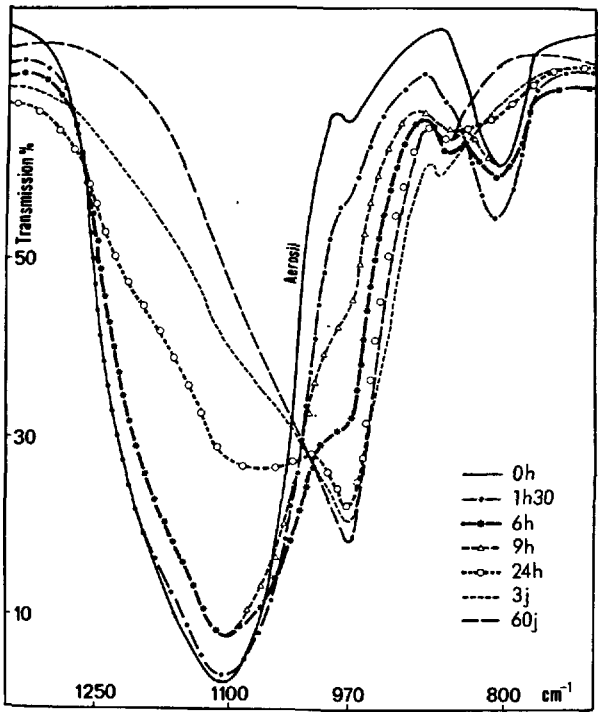

Fig. 3 - Etude cinétique par spectroscopie infrarouge de la transformation des phases solides (essai m).

La spectroscopie infrarouge confirme ces premiers résultats et apporte des informations supplémentaires. Nous ne donnerons ici que les résultats relatifs au domaine 1200 cm^{-1} - 400 cm^{-1}. La silice amorphe y présente des bandes caractéristiques à 1100 cm^{-1}, 805 cm^{-1} et 468 cm^{-1} ; elles sont respectivement attribuées aux vibrations de valence des liaisons Si-O et Si et à la vibration de déformation asymétrique des liaisons Si-O (10). Les C-S-H sont caractérisés essentiellement par une bande large et intense à 970 cm^{-1} et par une bande à 450 cm^{-1} ; l'intensité de la bande à 805 cm^{-1} est beaucoup plus faible. Les spectres des produits finals de quelques essais ont été tracés sur une même figure pour comparaison (figure 2). Le spectre de (a) est identique à celui de l'aérosil ; ceux des échantillons (b), (c), (d) (C/S < 0,20) présentent un élargissement progressif de la bande à 1100 cm^{-1} vers les nombres d'onde inférieurs. Un épaulement à 970 cm^{-1} apparaît sur le spectre de (d) ; la bande n'apparaît vraiment que sur le spectre de l'échantillon (e), mais la bande à 1100 cm^{-1} de la silice reste la plus intense. La présence de la silice est encore décelable sur le spectre du produit se caractérisant par $[C/S]_S$ = 0,94 (essai l), mais elle a complètement disparu du spectre de (m), pour lequel $[C/S]_S$ = 1,0 ; ceci est donc un argument en faveur de l'existence d'un hydrate défini, de rapport $[C/S]_S$ = 1. En revanche, on n'observe pas de modifications sur les spectres IR et X de tous les échantillons pour lesquels $1,0 \leq [C/S]_S \leq 1,50$. Il faut donc reconnaître que l'hydrate précédent est capable de fixer un excès important de calcium dans son réseau.

Dans les essais où de la chaux solide a été ajoutée (r), (s), (t), un précipité de $Ca(OH)_2$ accompagne au début la précipitation des C-S-H. Ses raies apparaissent sur les spectres de rayons X et infrarouge ; leurs intensités s'affaiblissent progressivement alors que celles des raies de C-S-H augmentent. $Ca(OH)_2$ n'est plus détecté dans les échantillons finals (r) et (s) (C/S = 1,26 et 1,53), mais il est présent à côté de C S-H (I) dans le produit (t) pour lequel C/S = 2,19.

Des analogies radiocristallographiques et infrarouges des phases solides, jointes à celles des solutions apportent les résultats suivants :

1/ Rapport $[C/S]_S$ global des phases solides $\leq 0,23$:

Ces phases sont de la silice amorphe et de petites quantités de C-S-H ; elles sont en équilibre avec des solutions dont la concentration en chaux demeure faible ($1 - 1,50.10^{-3}$ $mol.kg^{-1}$) alors que la concentration en silice va en croissant à cause de la formation d'ions $H_3SiO_4^-$ quand le pH augmente.

2/ $0,20 \leq [C/S]_S \leq 1,00$:

Il s'agit d'un mélange de silice et de C-S-H (I) dans des proportions croissantes. La concentration en chaux des solutions varie peu mais celle de la silice décroît jusqu'à la valeur $0,1.10^{-3}$ $mol.kg^{-1}$ [essais (f) à (m)].

3/ $1,00 \leq [C/S]_S \leq 1,50$:

La chaux excédentaire se répartit entre le solide (sans qu'il y ait apparition d'une nouvelle phase) et la solution ; $[C]_f$ atteint $15,47.10^{-3}$ $mol.kg^{-1}$ quand $[C/S]_S$ = 1,53, alors que $[C]_f$ = $3,70.10^{-3}$ $mol.kg^{-1}$ seulement pour $[C/S]_S$ = 1,01.

4/ $[C/S]_s > 1,50$: l'hydroxyde de calcium précipite en même temps que C-S-H qui a fixé une partie de la chaux excédentaire. Ces phases solides sont en équilibre avec une solution saturée de chaux.

Là encore, il est intéressant de remarquer les analogies dans les résultats que donne l'ensemble des systèmes à l'équilibre (figure 2) et ceux que donne un système particulier en cours d'évolution. On a choisi comme exemple l'essai (m) et rassemblé sur la figure 3 quelques spectres d'échantillons représentatifs de l'évolution du système. Au cours des premières heures, la bande à 1100 cm^{-1} se déforme progressivement vers les nombres d'ondes plus petits et son intensité diminue légèrement (1h30) ; un épaulement à 970 cm^{-1} apparaît au bout de 6 heures puis s'accentue (9h), la séparation en deux bandes distinctes se produit vers 12 heures et on note la variation en sens inverse des deux bandes à 1100 et 970 cm^{-1}, ce qui permet d'envisager un dosage quantitatif des C-S-H.

CONCLUSIONS

Dans cette étude des réactions entre silice amorphe et solutions de chaux, la méthode adoptée a été l'analyse simultanée des phases solides et des solutions en contact avec elles, au cours de l'étude cinétique aussi bien que de celle des états d'équilibre. Il a ainsi été mis en évidence que les C-S-H précipitent à partir des ions en solution et que l'étape qui gouverne la cinétique globale des réactions est celle du passage en solution de la silice. On a également construit les courbes de solubilité du système CaO,SiO_2,H_2O et associé, à chaque point définissant la composition des solutions, le rapport $|C/S|_s$ des phases solides avec lesquelles elles sont en équilibre. La spectroscopie infrarouge a apporté des informations nouvelles en permettant de différencier les produits finals des réactions et de suivre la cinétique de formation des hydrosilicates de calcium.

D'autre part, l'étude du système $CaO-SiO_2-H_2O$ sous deux aspects généralement étudiés séparément - cinétique et états d'équilibre -, a montré qu'ils sont en fait étroitement liés : les chemins cinétiques représentant la variation de composition des solutions au cours de leur évolution se développent parallèlement aux courbes d'équilibre de solubilité.

BIBLIOGRAPHIE

1. - P. BARRET (1979),"Les mécanismes d'hydratation et de durcissement des ciments", l'Industrie Nationale, ISSN 00 19-9133, 1, 1-41.
2. - E.P. FLINT, L.S. WELLS (1934), "Study of the system $CaO-SiO_2-H_2O$ at 30°C and of the reaction of water on the anhydrous calcium silicates", J. Res. Nat. Bur. Standarts, research paper, 687, 12, 751-783.
3. - S.A. GREENBERG and T.N. CHANG (1965), "Solubility relationships in the calcium oxide-silica-water system at 25°C", J. Phys. Chem., 69, n° 1, 182-188.
4. - H.H. STEINOUR (1947), "The system $CaO-SiO_2-H_2O$ and the hydration of the calcium silicate", Chem. Rev., 40, 391-460.
5. - H.F.W. TAYLOR (1968), "The calcium silicate hydrates",principal paper, proc. 5th Int. Symp. Chem. Cement, Tokyo, Vol. II, 15-17.
6. - R. DRON (1973), "Mécanisme de la prise du laitier sous activation alcaline", Université de Paris VI, 42-58.
7. - E.E. LACHOWSKI (1979), "Trimethylsilylation as a tool for the study of cement pastes", Cem. Concr. Res., 9, 337-342.
8. - D. MENETRIER (1977), "Contribution à l'étude cinétique de la période initiale d'hydratation de C_3S, constituant principal du ciment Portland", Thèse d'Etat, Université de Dijon, 1-74.
9. - J. UYTTERHOEVEN, M. SLEEX, J.J. FRIPIAT (1965), Bull. Soc. Chim. France, 6, 1801.
10. - E.R. LIPPINCOTT, A. an VALKENBURG, Ch. WEIR, E. BUNTING (1958), J. Res. Nat. Bur. Standarts, 61, 1.

Calorimétrie des liants

Calorimetry of binders

A.V. OUCHEROV-MARCHAK, collaborateur scientifique, candidat ès sciences techniques,
KhICI, A.M. OURJENKO, collaborateur scientifique,
O.P. MTCHEDLOV-PETROSSIAN, professeur, docteur ès sciences techniques, U.R.S.S.

RESUME : Cet exposé constitue un examen des objectifs concernant l'application de l'analyse calorimétrique à la chimie et à la technologie du ciment. Il fait état de la mise au point d'une méthode de microcalorimétrie isotherme différentielle. Les études portent sur la suppression des erreurs qui ont pour cause des interactions hétérogènes et la correction dynamique de l'inertie des instruments de mesure, ainsi que le dépouillement automatique des données finales et l'interprétation cinétique des relations obtenues pour des liants modèles monominéraux. Les auteurs mettent en évidence l'apport, dans l'effet thermique général, de la chaleur des processus élémentaires de durcissement : adsorption, dissolution et cristallisation. On y trouve également des données concernant les possibilités de régulation technologique et l'obtention de ciments aux propriétés voulues sur la base des données de l'analyse calorimétrique. Celle-ci englobent la composition chimique et minéralogique, la granulométrie, l'addition d'adjuvants et de germes cristallins, les conditions de durcissement et d'exploitation.

SUMMARY : The problems of using calorimetric analysis in the chemistry and technology of cement are considered. The results of development of the isothermic differential microcalorimetry method are presented. The developments comprise elimination of errors connected with the heterogeneous nature of interaction and dynamic correction of the time-lag of the instruments, as well as automatic processing of results and kinetic interpretation of the relationships obtained for model monomineral binders. Contributions of the elementary hardening processes (adsorption, dissolving and crystallization) in the total thermal effect are established. The possibility of technological control and preparation of cement with required properties on the basis of the calorimetric data is discussed. The data cover the chemical and mineral composition, granulometry, introduction of additives and crystal seeds, conditions of hardening and of exploitation.

Le dégagement calorifique est un des plus importants phénomènes qui accompagnent le durcissement des ciments. Ses caractéristiques sont utiles pour les recherches sur le mécanisme et la cinétique d'hydratation, on y fait recours lors du choix et de la prescription des paramètres dans la technologie des ciments et des bétons. La calorimétrie joue un rôle toujours croissant dans l'ensemble des méthodes chimiques et physiques de la recherche sur la chimie des ciments. Ceci s'explique par une grande capacité d'information de la méthode. Les données sur l'effet thermique global Q, la vitesse de dégagement thermique $dQ/d\tau = f(\tau)$ lors de la réaction d'hydratation, permettent, dans le cas de leur interprétation à l'aide de l'appareil cinétique des processus hétérogènes, d'obtenir des renseignements quantitatifs sur le degré α et la vitesse $d\alpha/d\tau$ de transformation des liants. En dépit de certaines contradictions, on connaît fort bien les possibilités de l'analyse calorimétrique à laquelle on fait recours pendant les investigations des voies de régulation technologique et des modalités de conférer au ciment des propriétés nécessaires par une modification de la capacité de dispersion et de la granulométrie, de la composition de phase et chimique, et l'addition d'adjuvants et de germes chimiques.

A des fins scientifiques et pratiques, on utilise la calométrie de dissolution, les méthodes adiabatique et isothermique, ou bien leurs variétés. La calorimétrie isothermique différentielle permet d'enregistrer de faibles variations de la puissance thermique d'un système en état de durcissement dès le contact avec de l'eau, ce qui est important pour les études sur des stades initiaux de durcissement, puisqu'en cette période le degré d'hydratation est minime, alors que la vitesse d'hydratation est grande.

On a plus d'une fois attiré, dans des ouvrages scientifiques, l'attention sur la nécessité de franchir des obstacles, sur le plan méthodologique, créés par la spécificité de l'interaction hétérogène dans les systèmes dispersés en voie de durcissement, ainsi que sur la nécessité de surmonter les difficultés d'interprétation quantitative des résultats de mesures, dues à la disproportion des vitesses de dégagement calorifique et d'hydratation aux divers stades de durcissement.

L'évolution de la technique des expérimentations a permis d'assurer la suppression de toute une série d'erreurs. Nous utilisons pendant nos travaux des calorimètres munis d'un dispositif d'introduction automatique des liants en poudre dans la cellule de la réaction et d'un malaxage des réagents par vibration lors de leur combinaison. On a envisagé la suppression de l'effet de la température sur la poudre du liant et sur l'eau. Ces dispositifs réduisent au minimum les erreurs qui ont lieu à cause de l'hydratation préliminaire des liants dans les vapeurs d'eau, de l'évaporation des liquides et de l'homogénéité insuffisante d'un mélange. On applique également un dispositif électronique de correction dynamique de l'inertie de la partie mesurage du calorimètre. Le microcalorimètre isothermique différentiel est muni d'un potentiomètre d'enregistrement des rapports $dQ/d\tau = f(\tau)$, d'un intégrateur de leur transformation en rapport $Q - \Phi(\tau)$ et d'un potentiomètre à double orientation d'enregistrement des courbes $dQ/d\tau = F(Q)$. La sensibilité du potentiomètre est de 10^{-5}W, la constante du temps, de 120 sec. La construction automatique des rapports modèles et le dépouillement des résultats d'expérimentation à l'aide d'un ordinateur facilitent dans une grande mesure l'interprétation des données d'analyse calorimétrique. L'objet des recherches calorimétriques quantitatives sont essentiellement des liants monominéraux $3CaO \cdot Al_2O_3$ et $CaSO_4 \cdot 0,5H_2O$. Pendant des recherches sur l'hydratation du silicate tricalcique, R.Kondo, M.Daimon (1) P.Longuet (2) et N.Stein (3) se sont heurtés à des difficultés quant à l'utilisation des données calorimétriques à cause de la disproportion des indices $dQ/d\tau$ et $d\alpha/d\tau$, de la différence de précision lors de l'évaluation de la vitesse d'hydratation par les méthodes chimique, radiologique et calorimétrique. Cependant, Stein (3) estime l'utilisation des résultats d'analyse possible lorsque la composition d'un hydrosilicate au cours du processus reste invariable ou bien quand on observe le rapport constant entre les hydrosilicates de haute et basse basicité. D'une façon générale, on a su mettre en évidence et décrire certains stades du processus, évaluer le rôle de la formation des noyaux et de la pellicule, la possibilité d'application des équations cinétiques essentielles, de la règle de Van't Hoff lors des variations de température, de l'introduction des additifs, etc. Les recherches sur le gypse semi-hydraté en tant que modèle d'un liant sont plus avantagées, puisque le gypse est hydraté sans former des produits intermédiaires et la valeur Q/α demeure constante au cours du processus. Par ailleurs, la chaleur d'adsorption d'eau par des produits cristallins d'hydratation du gypse est incomparablement plus basse que celle par des hydrosilicates.

Nous avons étudié certaines équations cinétiques utilisées pour décrire le phénomène d'hydratation (4). La figure 1 présente les rapports $d\alpha/d\tau = f(\alpha)$ pour les équations Kolmogorov - Avrami - Eroféev

$$d\alpha/d\tau = (1-\alpha)\left[-\ln(1-\alpha)^{3/4}\right] \quad (1)$$

Reedje $$d\alpha/d\tau = \alpha(1-\alpha)^{2/3} \quad (2)$$

Comb et d'autres $$d\alpha/d\tau = 3(1-\alpha)\ln(1-\alpha)^{1/3} \quad (3)$$

Les valeurs calculées du degré de transformation α_{max} où la vitesse du processus atteint son maximum constituent respectivement 0,52; 0,60 et 0,28. En même temps, pour

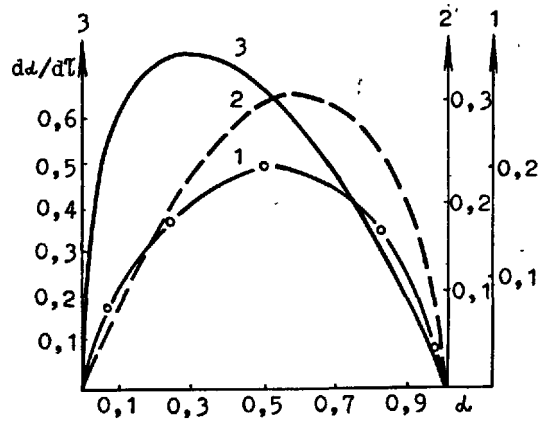

Fig. 1. Rapports théoriques entre la vitesse et le degré de transformation calculés sur les équations (1), (2) et (3).

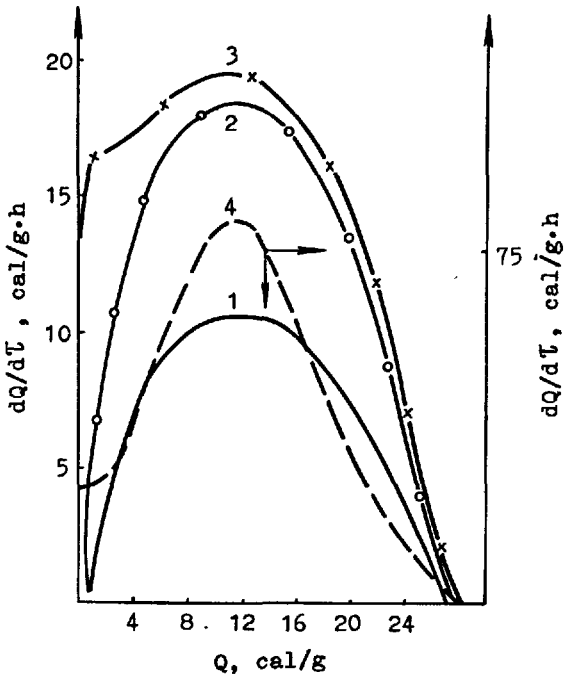

Fig.2. Rapport entre le dégagement calorifique et la chaleur d'hydratation de α - forme (1,2,3) et β - forme du gypse semi-hydraté (4).

l'équation (1) n = 4.

Les calculs de α_{max} d'après les résultats d'analyse calorimétrique pour α - forme et β - forme du semi-hydrate (Fig.2) montrent que sa valeur de l'ordre de 0,4 est bien au-dessous des prévisions théoriques. La meilleure concordance des données théoriques et expérimentales doit être observée quand la valeur α_{max} est plus basse ce qui peut être expliqué par le fait que les germes d'hydrate adoptés pour les équations (1) et (2) sont de forme lamellaire ou aciculaire, et non sphérique tridimensionnelle. La meilleure explication des données des expérimentations offrent les équations qui tiennent compte de deux constantes cinétiques (vitesse de dissolution et cristallisation) puisque la vitesse maximale du processus doit varier en fonction des variations du rapport de ces constantes.

La conclusion essentielle de cette analyse tient à ce que la relation linéaire de $d\alpha/d\tau = k\alpha$ même si la valeur α_{max} est minime, n'est pas observé et la formation et l'accroissement d'une phase nouvelle sont régis plutôt par la fonction puissance et non par la fonction exponentielle ce qui est propre pour la plupart des réactions hétérogènes. Par ailleurs, pour expliquer le caractère des courbes cinétiques pendant la période de ralentissement de la vitesse d'hydratation (rapport 2, Fig.2), il conviendrait d'adopter, dans l'équation du type $d\alpha/d\tau = k(1-\alpha)^m$, la valeur de $m \gg 2/3$ et d'expliquer le phénomène par une large distribution de particules selon les dimensions.

Les recherches calorimétriques ont permis d'élucider toute une série de questions concernant le mécanisme et la cinétique d'interaction entre les additifs chimiques et, notamment, les amorces et les minéraux de clinker (5). On a découvert une différence d'action des amorces pendant le durcissement de divers minéraux (Fig.3).

On enregistre sur les courbes thermocinétiques d'hydratation de $3CaO \cdot SiO_2$ (Fig.3,A) un accroissement de la valeur du premier exo-effet dans les éprouvettes avec amorces dû à la chaleur d'adsorption d'eau par la surface bien développée d'hydrosilicates de calcium similaires à des tobermorites. La différence calculée en valeurs de l'effet thermique pour une éprouvette de contrôle et des mélanges avec amorce constitue 7,79 Joules; le taux de chaleur étant de 97,13 J pour un gramme de $3CaO \cdot SiO_2$, ce qui est bien conforme au taux de chaleur d'adsorption par le gel tobermorite.

Lors de l'introduction des amorces, il est nécessaire de créer un contact intime avec liant.

Ceci est obtenu pendant nos expérimentations grâce à la trituration du mélange pendant 1 ou 2 minutes. Dans ce cas, la période d'hydratation essentielle évaluée sur la va-

leur du deuxième exo-effet se réalise plus amplement. Cela se produit, paraît-il, pour le compte de l'augmentation de la réactivité par activation mécano-chimique, puisqu'on dispose de données sur l'effet insignifiant de $4CaO \cdot 5SO_2 \cdot 5H_2O$ sur la cinétique de durcissement du silicate tricalcique. Un résultat analogue a été obtenu pendant les recherches sur l'influence de l'amorce d'afwillite sur l'hydratation et le développement de la résistance du silicate tricalcique (6).

La nature de l'hydratation de $3CaO \cdot Al_2O_3$ (Fig.3,B), appartenant à la catégorie des liants qui durcissent rapidement, reste invariable à l'usage d'une amorce d'aluminate hydraté Ca, quoique son action sur le dégagement calorifique est très efficace, surtout lorsqu'elle est introduite par la méthode de trituration. L'accélération de la vitesse de durcissement dès le gâchage provoque la réduction de la période, pour l'essentiel à cause de l'effet écran de l'enveloppe d'hydrate.

L'action d'activation des amorces la plus efficace se manifeste pendant l'hydratation de $4CaO \cdot Al_2O \cdot FeO_3$ (Fig. 3,C). La courbe thermocinétique du durcissement de ce minéral enregistre la présence d'une période d'induction de la cristallisation. L'introduction de l'amorce (produit d'hydratation de $4CaO \cdot Al_2O_3 \cdot Fe_2O_3$) réduit la période d'induction de 6 à 2 heures pendant le malaxage ordinaire et jusqu'à une heure quand on assure un contact serré du minéral et de l'amorce.

L'analyse thermique différentielle, l'analyse des phases au rayons X ainsi qu'au microscope électronique ont confirmé la différence qui existe dans la constitution et la structure de nouvelles formations, cependant les données de l'analyse calorimétrique sont particulièrement appréciables vu l'existence des informations concernant l'effet des amorces sur le mécanisme et la cinétique de l'hydratation au stade initial. L'interprétation quantitative des données de l'analyse thermocinétique pour des poudres polyminérales et polydispersées des ciments est limitée, bien que, on l'a noté ci-dessus, leur importance pour la régulation technologique soit grande.

Une importance particulière est attribuée aux recherches sur la cinétique d'hydratation d'une série de ciments modèles spéciaux.

Ainsi, par exemple, les investigations dans le domaine du dégagement thermique des systèmes de dilatation à base de $3CaO \cdot Al_2O_3$ et $CaO \cdot Al_2O_3$, du gypse et de la chaux, ont montré que la haute sensibilité de la méthode permettait d'enregistrer des variations thermiques insignifiantes qui accompagnent la formation et les transformations des aluminates hydratés et des hydrosulfoaluminates. On a établi des différences principales quant à l'influence du gypse et de la chaux sur la cinétique d'hydratation des aluminates .

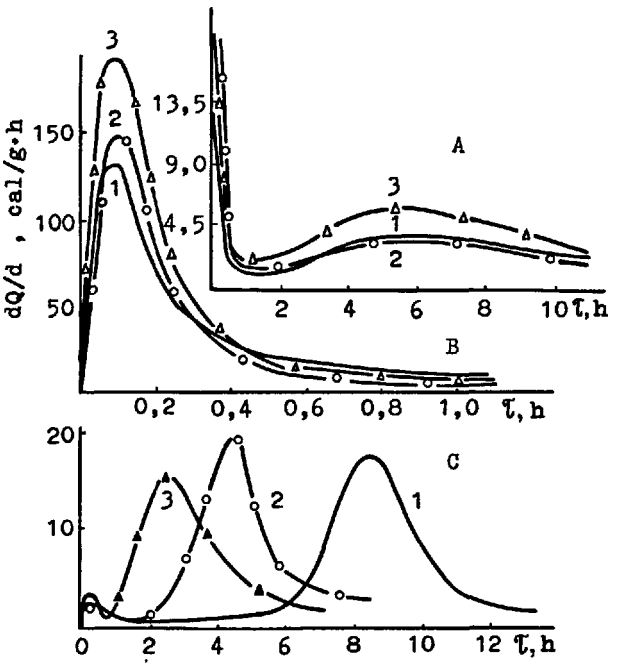

Fig.3. Intensité du dégagement calorifique pour $3CaO \cdot SiO_2$(A), $3CaO \cdot Al_2O_3$ (B) et $4CaO \cdot Al_2O_3 \cdot Fe_2O_3$(C). 1 - matière de base, 2 - mélange avec amorce introduite par malaxage, 3 - mélange avec amorce introduite par trituration.

Lors de l'introduction du gypse dans C_3A, on relève une baisse de 2 fois de la valeur absolue du premier exo-effet, une extension de la période d'induction et une extinction de la vitesse du dégagement calorifique, ce qui s'explique par un effet atténuant des enveloppes d'hydrosulfoaluminate de calcium. L'addition de $Ca(OH)_2$ freine davantage l'action thermocinétique du système.

Tout comme H.Mori et K.Minegishi (7), nous avons enregistré la fission du deuxième exo-effet et sa transformation en doublet, ce qui est lié à la formation du monosulfate et sa transformation en solution solide et C_4AH_{13}.

Par contre, l'hydratation et le dégagement calorifique des systèmes à base de $CaO \cdot Al_2O_3$ se déroulent d'une autre façon. A l'interaction de CA avec gypse qui s'effectue dans les conditions d'une sursaturation plus faible, il se produit une cristallisation rapide de l'ettringite qui s'achève au bout de 14-16 heures.

A ce moment près, la valeur $dQ/d\tau$ devient minimale et s'approche d'une manière asymptotique du zéro. L'addition du gypse accélère l'hydratation de CA. La valeur des deux exo-effets s'accroît avec augmentation de la teneur en gypse, l'effet thermique total augmente, le degré d'hydratation s'élève. La présence de la chaux accélère la

cristallisation de l'ettringite, et l'augmentation de sa teneur provoque une augmentation de l'effet thermique total. Il est claire que dans les ciments expansifs à base de $CaO \cdot Al_2O_3$ il est assuré une synchronisation des indices de vitesse des réactions chimiques et de la formation des structures, alors que l'expansion, au stade initial est compensée par une plus profonde hydratation et par une consolidation de la structure du matériau.

Jusqu'ici nous avons examiné les aspects d'application des données de l'analyse calorimétrique au stade de la préparation des liants. Des résultats fort appréciables ont été obtenus également lors de l'application de la calorimétrie à la fabrication des pièces et constructions préfabriquées. Dans ce cas, c'est le principe de la conformité de l'ensemble des caractéristiques du liant (technologiques, cinétiques, thermodynamiques et d'autres) aux paramètres des effets appliqués lors du durcissement pour recevoir un matériau à composition de phases et à structure désirées. Ce principe est formulé par O.P.Mtchedlov-Petrossian. La durée, l'intensité et le moment d'application d'un de ces effets (thermique, mécanique, chimique ou de leurs combinaisons) doivent être choisis compte tenu de l'utilisation optimale des propriétés potentielles des ciments.

Les questions de l'influence de la température sur le dégagement thermique et de la prise en considération du dégagement thermique lors du choix des régimes de traitement thermique ont été examinées dans une communication, faite au séminaire "D" du présent Congrès.

On sait que les caractéristiques technologiques des liants, telles que la composition chimique et minéralogique, la dispersité, etc., sont liées étroitement à l'utilisation très répandue de l'effet chimique sur des mélanges en voie de durcissement au moyen de l'introduction d'additifs différents. Nous avons analysé l'influence de divers adjuvants - accélérateurs, retardateurs, porophores, plastificateurs - sur la cinétique du dégagement calorifique des minéraux de clinker et des ciments.

Auparavant (8), on a confirmé le fait de l'effet sélectif des additions sur les processus élémentaires d'hydratation et de durcissement - adsorption, hydrolyse, cristallisation - que nous avons appelé EFFET LE SELECTIVITE CINETIQUE de l'activité des composés chimiques. Utilisant les données sur la constante de la vitesse et l'énergie d'activation on a établi les séries d'activité des additions minérales les plus répandues avec anion commun SO_4^{2-}, Cl^-, NO_3^-, OH^- et avec cation commun Ca^{2+}, Mg^{2+} et d'autres. Cette conception a permis d'étayer d'une façon quantitative des séries d'additions chimiques complexes qui sont utilisées avec succès dans le bâtiment. Ces derniers temps, sont en cours de réalisation toute une série de travaux de recherche sur la cinétique du dégagement calorifique des ciments avec addition de plastificateurs de forte action.

On a analysé l'effet de l'additif "Melment" et de certaines modifications des lignosulfonates. Une relation a été établie entre l'efficacité de l'action plastifiante et la modification successive de la vitesse d'hydratation qui se traduit par la baisse d'intensité du dégagement calorifique. Ainsi donc, les résultats des recherches sur les processus de durcissement, obtenus par la méthode de la microcalorimétrie isothermique différentielle, permettent, au stade de la préparation et de l'utilisation des liants, d'approfondir les connaissances sur le mécanisme et la cinétique d'hydratation, d'étudier, d'une façon rationnelle, sur la base expérimentale et théorique, les modalités de perfectionnement de la technologie des liants et des bétons.

BIBLIOGRAPHIE

1. R.Kondo, M.Daimon (1969) "Early hydration of tricalcium silicate. A solid reaction with induction and acceleration periods". I.Am.Ceram. Soc, 52, N°9, p.503-508 (en anglais)

2. P.Longuet (1968) "Written disc." Proc. V symp. of Chem on the Cem., v.2, p. 30-32 (en anglais)

3. H.N.Stein (1977) "The initial stages of the hydration of C_3S". Cemento, 1, p.3-14 (en italien)

4. M.Murat, E.Karmazsin (1977) "The kinetics of hydration of calcium sulphate hemihydrate". Colloque Int. RILEM, Saint-Rémi (en anglais)

5. О.П.МЧЕДЛОВ-ПЕТРОСЯН, А.Н.УРЖЕНКО, А.В. УШЕРОВ-МАРШАК (1977) "Калориметрическое исследование кристаллохимической активации процессов твердения". Доклады АН СССР, 233, № 3, 439-441 (en russe)

6. R.DAVIS, I.Yong (1975) "Hydration and strength development in tricalcium silicate pastes with Afwillite", J.Am.Ceram Soc., 58, N1-2, p.67-70 (en anglais)

7. H.Mori, K.Minegishi (1968) "Effect of the Temperature on the Early Hydration of the System $3CaO \cdot Al_2O_3 - CaSO_4 \cdot 2H_2O - Ca(OH)_2 - H_2O$". Proc.V Symp. of Chem. on the cem., Tokyo, p.349-361, vol.II (en anglais)

8. А.В.УШЕРОВ-МАРШАК, А.М.УРЖЕНКО (1973) "Кинетика гидратации $3CaO \cdot SiO_2$ в растворах сульфатов" Журн.физ.химии, 47, 8, 2078-2080 (en russe)

Effects of Admixtures upon Electrokinetic Phenomena During Hydration of C_3S, C_3A and Cement

Effets des adjuvants sur les phénomènes électrocinétiques au cours de l'hydratation de C_3S, C_3A et du ciment

D.M. ROY, Professor, Materials Research Laboratory, The Pennsylvania State University,
M. DAIMON, Associate Professor, and K. ASAGA, Research Associate, Dept. of Inorganic Materials, Tokyo Institute of Technology, U.S.A.

RESUME : On a étudié le rôle des adjuvants superplastifiants utilisés pour réduire l'eau de gâchage des ciments dans des applications spéciales. Pour comprendre leur action, on a étudié les phénomènes provoqués par l'hydratation du C_3S(alite) et du C_3A de divers ciments (type I, type V, classe C et classe H), lorsque ces ciments sont malaxés avec de l'eau contenant des proportions variées de ces superplastifiants ainsi que divers ions. Les techniques d'électrofiltration et d'électrophorèse ont été utilisés pour déterminer le potentiel zêta, produit à l'interface liquide-solide. Par la suite l'électrophorèse a été utilisée de préférence. La peptisation des grains de ciment, sous l'action de superplastifiants constitués par des condensats de formaldéhyde de naphtalène sulfoné et de formaldéhyde de mélamine sulfoné, semble due à la formation d'un potentiel zêta fortement négatif à la surface des cristaux d'alite et de C_3A. D'autres ions peuvent modifier ces effets, mais le phénomène reste le même en général, bien que son intensité puisse varier. Les variations systématiques du potentiel zêta ont été mesurées en fonction de la concentration en ajouts et en fonction du temps; ces variations sont importantes, notamment pour le C_3A. Ces variations semblent dues à l'adsorption des adjuvants à la surface des grains du ciment et du granulat. Il suffit de concentrations plus faibles en adjuvants pour créer ce potentiel zêta, si le ciment contient des cendres volantes. Ont aussi été examinées les relations entre ces phénomènes et d'autres facteurs physiques, comme la rhéologie du mortier et l'adsorption isotherme.

SUMMARY: The actions of superplasticizing admixtures, utilized for reducing the required water contents of cementitious mixes for special applications, have been investigated. To understand their effects, electrokinetic phenomena have been investigated for C_3S (alite), C_3A and cement particles (Type I, Type V, Class C and Class H) in contact with water containing different concentrations of superplasticizing admixtures and other ions. Streaming potential and electrophoresis techniques were explored to determine the zeta potential generated at the liquid-solid interface. Subsequently the electrophoresis technique was used primarily for measurements. The dispersion of cement particles through use of superplasticizing admixtures of the sulfonated naphthalene formaldehyde condensate and sulfonated melmamine formaldehyde condensate families is apparently related to the generation of a strongly negative zeta potential at the surfaces of both alite and C_3A particles. Other ions in solution modify the effects, but the phenomena generally remain similar, though having differing magnitudes. Systematic changes in the magnitude of the zeta potential with concentration of admixture and time have been determined, and are significant, particularly with C_3A. The changes observed are related to adsorption of the admixture species upon the surfaces of the individual cement compounds and their admixtures. Smaller concentrations of admixtures are required to generate strong negative zeta potentials with flyash particles in similar suspension. Relations to other measurements such as mortar flow, viscosity and adsorption isotherms are also discussed.

INTRODUCTION

The achievement of optimally dense very low permeability hardened cement composites is important for applications requiring high performances, such as plugging, because such materials have superior mechanical properties, and potential for chemical stability. Admixtures such as superplasticizers are employed for the purpose of decreasing the water-to-cement ratio, without decreasing the fluidity of the mixture. Zeta-potentials of cements in suspension have been studied (1), and the surface generated forces thus quantified were used to explain some of the effects of the superplasticizers upon the rheological properties of pastes and slurries. Recently, studies have been made of the related viscometric properties as well (2-4). The use of so-called superplasticizers or super-water-reducers have recently attracted the attention of concrete engineers (5) and for predictability, it is important to understand the mechanisms of their benavior. Significant attractive forces exist between cement particles in cement-water suspensions, and in time the particles link together to build rigid networks. Water reducing admixtures are effective in breaking the cement particle networks and dispersing them (6), preventing premature agglomeration minimizing the amount of water required to suspend the particles and render the mix workable for the required period of time. The admixtures control the forces between particles and increase fluidity of the mix (1).

Until recently (1), very little experimental work was carried out to apply zeta potential measurements to calcium silicates or cement (7,8). Ernsberger and France (9) studied the effect of calcium lignosulfonate, concluding that cement suspension viscosity reduction took place due to an electrostatic repulsion between cement particles in the presence of surface-adsorbed surfactant molecules. Petrie (6) reported that the attractive charge on cement particle surfaces was neutralized by adsorption (onto active sites), when an anionic surfactant based on certain naphthalenesulfonic acid condensates was present. Hattori (10) recently showed results fundamentally similar to those of Ernsberger and France, on one kind of superplasticizer.

Following the suggestion that potentially more than one mechanism may be applicable for generating a stable colloid (11) preliminary capillary rise experiments (1a) demonstrated that solid-liquid affinity played little role in the action of typical superplasticizers; the zeta potential was shown to have a dominant role; but the additional effect of steric hindrance could not be entirely discounted (1).

EXPERIMENTAL

Two techniques were utilized at first for determination of zeta potential: streaming potential* and electrophoresis (1). After preliminary experiments by both methods, primarily the electrophoretic method was utilized (1a).

The electrophoresis technique involved measurement of the velocity of a charged particle moving through a fluid under the influence of an electric field. According to Akers (13) the electrophoretic mobility of a particle suspended in an electrolyte is given (in $\mu m.cm.sec^{-1}.v^{-1}$) by

$$\nu_e = \frac{\Delta W \lambda}{tI\phi(1-\phi)(\rho_s-\rho_L)},$$

where ΔW is the change in weight of particles, λ is specific conductance of the dispersion, t = time, I = current, ϕ = volume fraction of dispersed solid, ρ_s = density of solid, ρ_L = density of electrolyte. Henry (in ref. 13) related the zeta potential to the electrophoretic mobility (ν_e) from which the zeta potential is calculated as follows:

$$\zeta = \frac{\nu_e \eta \pi}{f\epsilon}$$

where η is the viscosity of the electrolyte, and f depends on the value of the product $k\alpha$ where k is the Debye-Huckel double layer reciprocal thickness and α is the radius of the spherical particles. The admixtures used are listed in Table I.

Table 1 - Superplasticizers

designation	form	density (g/ml)	concentration (wt % solid)
A9[x]	sulfonated napthalene formaldehyde condensate	--	100.0
M1*	sulfonated melamine formaldehyde condensate	1.125	20.0
A3[+]	sulfonated naphthalene formaldehyde condensate	1.21	43.0
A4	sulfonated napthalene plus retarder		45.4
A14	sulfonated melamine formaldehyde condensate	1.11	24.8
A28	sulfonated naphthalene formaldehyde condensate	-	

x #3 in Table I ref. (1a)

* #1 in Table I ref. (1a)

\+ #2 in Table I ref. (1a)

** Where liquids were used in mixture preparations concentrations were expressed as vol. % liquid, as received (except in Fig. 1). Thus, the effective component concentration is higher in A3 and A4 than in M1 and A14.

ZETA POTENTIAL RESULTS

Cements. The negative zeta potential generated on the cement particle surfaces is illustrated in Fig. 1, using the naphthalene-based admixture A3 in deionized water. Slightly lower magnitudes of negative zeta potentials were found with tap water than deionized water (1b). A general decrease in the

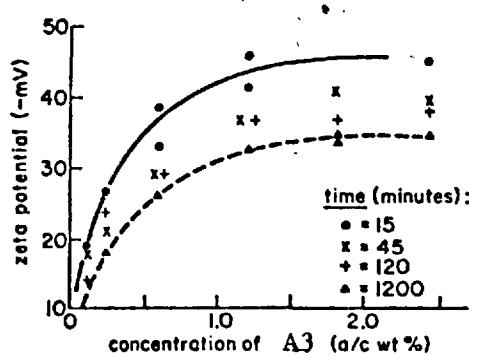

Fig. 1 - Change in zeta potential of Type I cement with concentration of A3.

*In apparatus constructed by N. Macmillan

magnitude of the negative potential is shown with time, but it remains strong even after 1200 minutes. Similar though not identical behaviors have been shown with admixtures A1 and A2 as well (1).

Zeta potential measurements have been continued comparing the results with a napthalene-based admixture containing a retarder (A4) to that without a retarder (A3). The maximum negative zeta potential similarly was reached at ∿ 1% admixture concentration upon the same cement (14). Measurements for additional comparisons have been continued with a class C (HSR) cement [Fig. 2], a type V (HSR) [Fig. 3] and a class H (MSR) cement [Fig. 4]. Though the results were in general similar in all, some differences were found. The presence of the retarder in A4 allowed a smaller change in the zeta potential as a function of time, with the HSR class C and V cements; and a smaller magnitude of zeta potential for the type V cement. Further measurements were made using a newer melamine-based admixture (A14) with the Type I cement as shown in Fig. 5. These show less change with time in the magnitude of zeta potential than in previous measurements with M1 [Fig. 4 in Ref 1(b)]. The higher concentration of admixture (2%) is more effective than the 1% concentration, after 2 hours time. Similarly, with class H cement (Fig. 6) admixture A14 appears to require higher concentrations, at least 2% for greatest effectivenes. One additional naphthalene-based admixture A28 was studied in combination with the Class H cement [Fig. 7], showing a slightly different relationship than that shown in Fig. 4 for admixture A4.

Effect of Mixing Water. Since the mixing water in a cement slurry is saturated with $Ca(OH)_2$ early in the cement hydration process, the behavior of admixtures in a saturated solution of $Ca(OH)_2$ was also investigated (15). In addition, the specific conductance of the binary system of a saturated $Ca(OH)_2$ solution with both a 10 percent and 1 percent admixture A4 was measured. The specific conductance of 0.2 normal solution of NaCl with 10 percent of admixture A4 was also measured (15). The specific conductance of the saturated $Ca(OH)_2$ solution was 7375 μmho/cm, larger than any specific conductance measured thus far. The liquid phase in which the cement zeta potentials were measured could not have been saturated with $Ca(OH)_2$; because of the lower conductances reflecting the large w/c ratios.

$Ca(OH)_2$. The zeta potential of $Ca(OH)_2$ crystals was measured in a saturated solution to be +33.5 mv. (15) In the presence of admixtures A3 or A4 the zeta potential of $Ca(OH)_2$ crystals changed from plus to a minus; indicating that the admixture is adsorbed on the surface of $Ca(OH)_2$ particles. However, the exact amount could not be determined because water decomposition began to take place at the high specific conductivity values.

Alite and C_3A. The zeta potentials of alite and C_3A were measured with admixtures A3 and A4 (Figs. 8 and 9). C_3A developed higher negative zeta potentials, which in general showed greater concentration dependence. The presence of retarder A4 caused an increase in the magnitude of alite's zeta potential with increasing time, in contrast to the behavior of A3 in alite, or in type I cement (1b). The effects with C_3A were similar with and without retarder, diminishing with time, in both instances. Further measurements were made in a saturated vs a non-saturated solution of $Ca(OH)_2$, and compared. In the saturated solution the zeta potential had a smaller negative value compared with that of the non-saturated solution for both the A3 and the A4 admixtures. Additionally, there appears to be a reaction between the admixtures and Ca^{++} ions which varies directly with the concentration of $Ca(OH)_2$, especially at higher concentrations. Specific conductance measurements of mixed solutions of varying concentrations in liquids, of admixture vs NaCl and admixture vs saturated $Ca(OH)_2$ revealed departures from theoretical linearity (15), in the latter case, correlating with the same phenomenon.

Fly Ash. The zeta potential of a fly ash (B15) which is used for partial replacement of cement was measured in a naphthalene-based admixture, A-28 as shown in Fig. 10. It is noted that a smaller magnitude zeta potential (-16 mv) is generated in tap water, vs -22 mv in deionized water, for the pure fly ash. A highly negative zeta potential was generated with a very small admixture addition, 0.05%, indicating that some superplasticizer is adsorbed on the fly ash surface, but that a saturation effect is reached with very low levels.

DISCUSSION AND CONCLUSIONS

The effectiveness of superplasticizing admixtures in their fluidifying cement-based mixes has been investigated by a combination of methods, including studying their adsorption characteristics on cement particle surfaces, the flow characteristics of mortars (1), the zeta potentials generated at the cement-liquid interface, and quantitative viscometric measurements (2-4). From the overall results to date it is apparent that the water reducing effect of the superplasticizers investigated (both of the sulfonated melamine and naphthalene formaldehyde condensate types) is caused mainly by their dispersion abilities which are in general correlated with a change in zeta potential as a function of surfactant adsorption onto the cement particle surfaces. C_3S (alite), C_3A, mixed cements and even $Ca(OH)_2$ are subject to generation of high magnitude (-30 mv to -50 mv) negative zeta potentials in the presence of increasing admixture concentration, generally reaching a saturation value at 1-2%. The ionic content of the mix solutions (including degree of $Ca(OH)_2$ saturation) affects their specific conductivities and the magnitude of the zeta potentials, though within the range of usual mixing waters, the general phenomena observed are similar. The fly ash studied required much smaller quantities of superplasticizer to generate a very negative zeta potential. Thus, the latter may be largely neglected when calculating amounts of superplasticizer required for a mix. The adsorption characteristics and the zeta potentials generated in cement-water-superplasticizer suspensions are among their most important characteristics, reflecting the generation of strong repulsive forces, causing dispersion. Additional and detailed viscometric studies are in progress to further elaborate these characteristics, and provide more adequate prediction of the flow properties of slurries containing superplasticizers.

ACKNOWLEDGEMENT

This research was performed under an R&D subcontract with Union Carbide Corp. (OWI), Nuclear Division, and

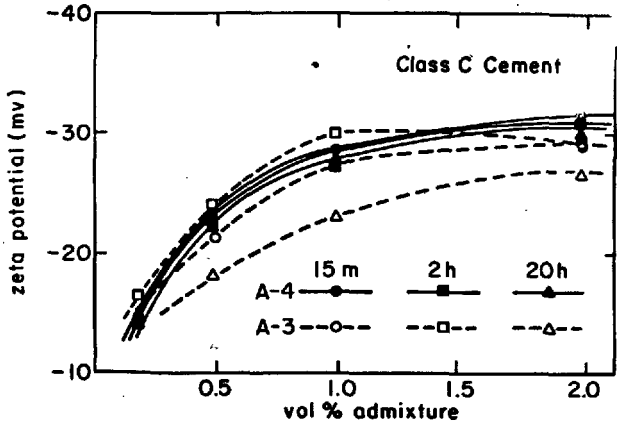

Fig. 2 Zeta potential of C-2 cement vs. admixture concentration

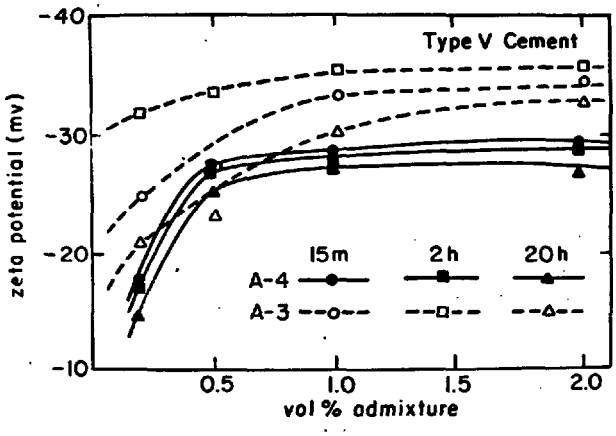

Fig. 3. Zeta potential of V-1 cement vs. admixture concentration

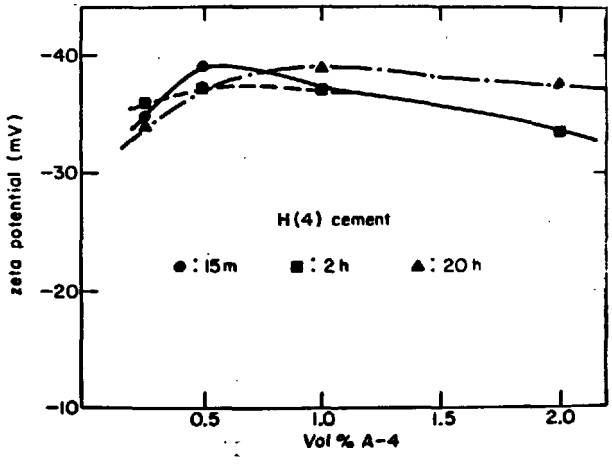

Fig. 4. Zeta potential vs. A4 concentration

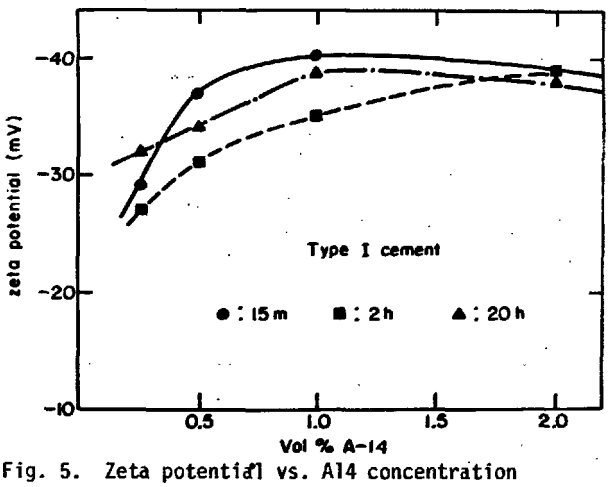

Fig. 5. Zeta potential vs. A14 concentration

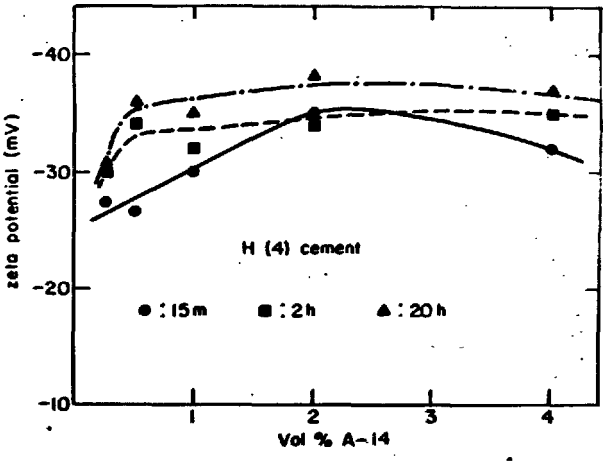

Fig. 6. Zeta potential change with A14 concentration.

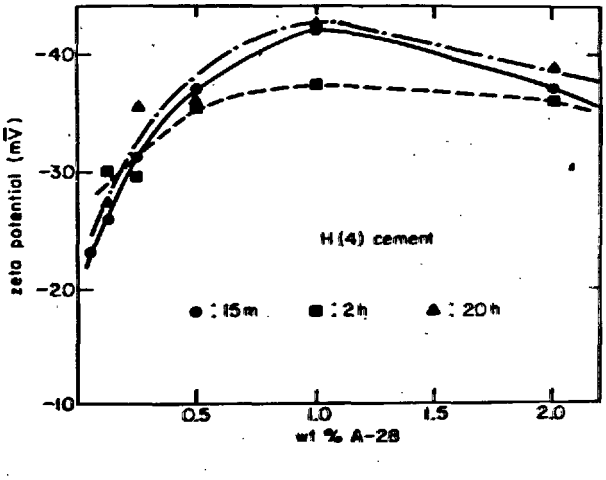

Fig. 7. Zeta potential change with A28 concentration.

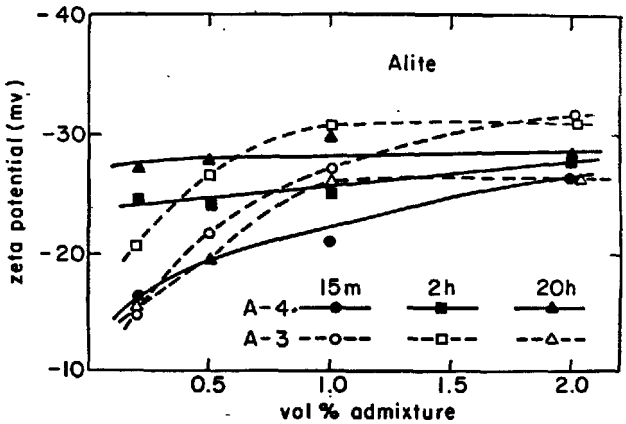

Fig. 8. Zeta potential of alite vs. admixture.

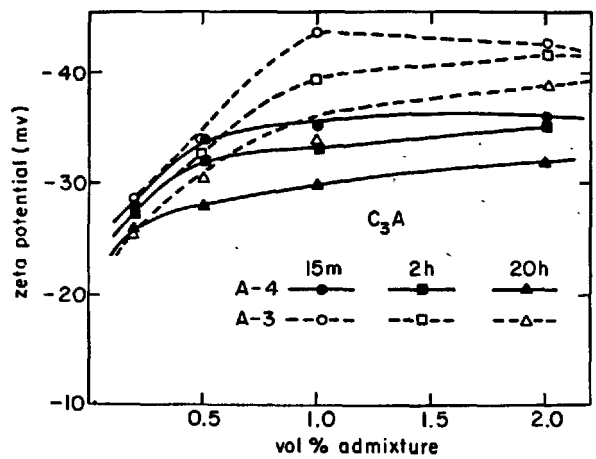

Fig. 9. Zeta potential of C_3A vs. admixture.

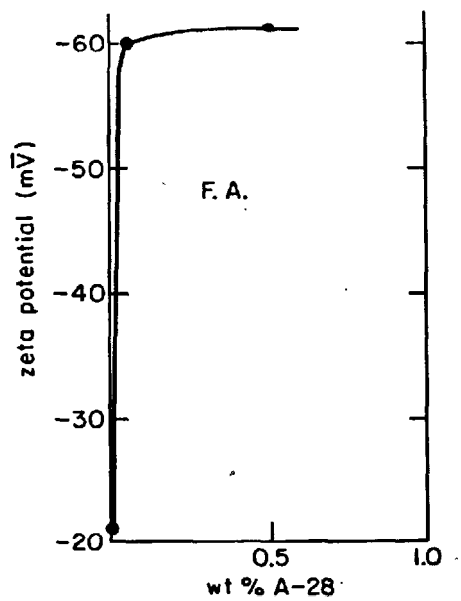

Fig. 10. Zeta potential of fly ash (B15) vs. A28.

Battelle Memorial Institute, ONWI, under contract with the U.S. Department of Energy. The advice of Dr. N. Macmillan and the assistance of colleagues including Dr. E.L. White is gratefully acknowledged.

REFERENCES

1. M. DAIMON and D.M. ROY, (a) (1978) Cem. Concr. Res. 8, 753-764; (b) (1979) Cem. Concr. Res. 9, 103-110.

2. D.M. ROY, M. DAIMON, B.E. SCHEETZ, D. WOLFE-CONFER, and K. ASAGE (1978), in Scientific Basis for Nuclear Waste Management, Vol. I, Proceedings of the Symposium on "Science Underlying Radioactive Waste Management," pp. 461-467. Materials Research Society Annual Meeting, Boston, MA, November 28-December 1.

3. D.M. ROY and K. ASAGA (1979). Cem. Concr. Res. 9(6), 731-40.

4. D.M. ROY, K. ASAGA and E.L. WHITE, in "Energy and Resources Conservation in Concrete Technology," U.S.-Japan Cooperative Science Program Seminar Proceedings, San Francisco, CA Sept. 10-13, 1979.

5. (a) (1978) Proc. Intl, Symp. Superplasticizers in Concrete, pp. 801, Dept. Energy, Mines and Resources, Ottawa; (b) (1976) Joint Working Party, Cem. Admixtures Asso. and Cem. and Concr. Assn., Superplasticizers in Concrete, Cem. Concr. Assn. Wexham Springs, U.K.

6. E.M. PETRIE (1976), Ind. Eng. Chem., Prod. Res. Devel. 15, 242-249.

7. H.N. STEIN (1960), J. Coll. Sci. 15, 578-584.

8. H.N. STEIN (1968), J. Coll. Sci. 28, 203-213.

9. F. ERNSBERGER and W.G. FRANCE (1945), Ind. Eng. Chem. 37, 298-500.

10. K. HATTORI, Experiences with Mighty Superplasticizers in Japan (in ref. 5a).

11. T.M. RIDDICK (1968), Control of Collid Stability through Zeta Potential, pp. 372, Zeta-Meter, Inc., NY

12. P. SOMASUNDARAN and R.D. KULKARNI, J. Coll. Interface Sci. 45, 591-600.

13. R.J. AKERS (June 1972) American Laboratory (9 pp.)

14. D.M. ROY, B.E. SCHEETZ, E.L. WHITE, and M. DAIMON, (1978), Borehole Cement and Rock Properties Studies, ONWI-5 (Part A).

15. D.M. ROY, P.H. LICASTRO, M.W. GRUTZECK, K. ASAGA and E.L. WHITE, (1978), Borehole Cement and Rock Properties Studies, ONWI/SUB/98/E512-00500-1 (Task I) December 29.

Modifications of Structure and Properties of Cement Stone

La modification de la structure et propriétés des ciments hydratés

V.M. KOLBASOV, Doctor of technology, Assistant professor, MCTI n.a. Mendeleev, Miusskaja sq., 9 Moscow, USSR,
N.A. KOZYREVA, Doctor of Technology, Head of the Laboratory MCTI n.a. Mendeleev, U.R.S.S.

RESUME : Cette communication montre que la formation des structures du ciment et le durcissement de ce dernier dépendent du développement des processus initiaux de la cristallisation des hydrates. Ce processus est déterminé par le milieu où il a lieu.

Les formes initiales de la croissance cristallographique des nouvelles formations des hydrates sont liées à la composition de la phase liquide dans le système durcissant "ciment-eau" et dans une grande mesure influent sur le processus postérieur de l'hydratation de la formation des structures ainsi que sur les propriétés du ciment hydraté.

En agissant sur les processus initiaux d'hydratation du ciment, il est possible de diriger efficacement la formation des structures du ciment hydraté et ses propriétés techniques. En particulier cela peut être réalisé au moyen d'additions solubles dans l'eau.

SUMMARY: The interdependence of structure forming and cement hardening with the development of initial stages of hydrates crystallization is traced. The initial process of crystallization is determined by the medium in which it is carried out.

The initial crystallographic forms of hydrates new formations growth are connected with the composition of the liquid phase in the hardening system "cement-water" and influence sufficiently the further process of hydration, structure and properties of formation of cement stone.

The directed influence on the initial processes of interaction of cement with water gives an opportunity of effective ruling of processes of structure forming on cement stome and its industrial properties. For instance it may be done by means of chemical additives soluble in water.

The process of crystal formation during the initial period of cement hydration which in many respectes determines further stages of its character, is not thoroughly studied [1] .

The process of initial mass growth of crystal hydrates which helps us to form full understanding of their ontogenese, formation mechanism and their interdependence with the hydration system medium is also studied not carefully.

In order to find out the interdependence of structure formation and cement hardening with the initial processes of crystal formation in MCTI named after Mendeleev were carried out some experiments in "cement-water" systems and some systems modelling these processes [2] .

These experiments were carried out by means of transmission and scanning microscoping including micro-diffraction and other methods of phase analysis. The works were made using the electronic microscopes VEMHv and JSM-50-A.

The investigations of the very initial stage of phase formation (when Portland cement and its components hydration is taking place) helps us to detalize some aspects of the process of the initial processes of hydration in "cement-water system and to imagine the beginning of these processes in the following way.

After cement and water interaction just at the moment of coming into contact of water molecules and the most active parts of the surface of clinker minerals (dislocations, outlets, picks and edges of crystals and so on) takes place their solving and the transfer of hydrated ions into the adjoining layer of the liquid phase. And in the local volumes of the system in the layer less than 0.1 mmc thick momentary conditions are created. They are favourable for the formation of new phases and the crystallysation from the surface of basic grainses which form the separating line for hydrate formation.

The formation of hydrates is seen a second later and that's why it is evident that the mechanism of initial crystallization of cement hardening is in action.

Phase composition of new formations, their morphology and characters of their growth depend directly on the qualities of the liquid phase which is formed in the local volumes of the system.

Depending on the concrete conditions which are created in the layer of the liquid phase adjoining the basic particle,certain hydration phases are formed. They have the form of filamentous, prismatic, skeleton and anti-skeleton crystals, hexagonal plates and round particles of irregular form with dimentions of hydrates from 5 mc to 1 mmc.

New formations which include ions of SO_4^{2-} and $Al(OH)_6^{3-}$ are formed near the grains of any clinker mineral. Hydrate phases are seen not all over the surface of the basic clinker grains.Analysis of a number of electrono-diffraction photographs of the surface of grains of Portland cement clinker made in the following time intervals 1,5,15 seconds and one minute, which have reflections of about 8.06; 5.27; 4.54; 4.17; 3.38--3.22; 3-23-3.07; 2.98; 2.84-2.78; 2.78--2.70; 2.22; 2.08-2.04; 2.00; 1.96-1.76; 1-67-1,64; 1.59; 1.49; 1.43-1.41; 1.39--1.37 Å support the fact that there is a variety of phases and crystals of hydrate phases.

The reflections mentioned above are typical for hydrocilicates and hydroaluminates of calcium of different composition, attringitt, calcium monosulphoaluminate, hydrogematite, portlandite and aluminium hydroxide.

The process of two-water gypsum grains solving dominates the process of hydrate phases formation near them at the first moments of interaction. A high diffusion coefficient let the ions of Ca^{2+} and SO_4^{-} diffuse easily into liquid phase of the system and thus creates favourable conditions for newformations crystallization in actively growing forms [3] .

Initial crystallographic forms of new formations influence greately the process of hydration. Crystalhydrates formed in actively growing crystallographic forms-filamentous, skeleton and anti-skeleton - favour rapid decrease of solving products in the adjoining layer of the liquid phase thus stimulating the processes of further solving of the basic adhesive and the recrystallization of meta-stable (under certain conditions) new formations into stable ones.

Phase composition of new formations of Portland cement clinker in hydration period (up to 24 hours) is rather various with the domination of the formation of calcium hydrocilicates CSH(B) and $C_2SH(A)$.

The connection between different clinker particles is carried out by means of prismatic, filamentous and fine-filamentous mass of hydrates consisting of round particles of irregular form and also by means of filling of spaces between the newformations of poorly crystallized hydrates.

The analyses revealed the dependence of cement structure formation and cement hardening on the development of initial process of crystal-formation. And the initial process of crystal formation in turn depends on the initial conditions of the medium.

The action directed of the initial processes of cement and water interaction (for instance on the initial conditions) determines the efficiency of ruling the processes of cement stone structure formation and its industrial properties.

A well-known method of influencing the medium (beginning with the moment of cement and water interaction) is the use of chemical additives soluble in water.

As a result of this use the additives change meta-stable solubility of Portland cement clinker ralating to CaO (mainly alite); ba-

lance concentration and consequently the extent of oversaturation of the liquid phase by different ions.

Additives influence the solubility of the basic adhesive and the products of its hydration, change and interaction of ions of the solution and the extent of initial oversaturation of the system which determines the crystallization nucleus, the rate of formation, morphology, dispersion, the extent crystallization of hydrates, the rate and their capacity of grow.

The medium of the system "cement-water" is originally connected with the physical processes of crystallization of hydrates which in turn influence the processes of solving of the basic clinker that is the kinetics of cement hydration. For instance it is shown that the formation on hydrates having filamentous, skeleton, dendrite-like crystals which is connected with the ion composition and oversaturation of the liquid phase intensifies the solving of basic grains of cement and its components, fastens the process of crystallization of "primary" hydrates which are formed at the first moment of cement and liquid phase of the system contacting and, on the contrary, slowers the process of mass crystallization of the "secondary" hydrates, especially in the poorly crystallized forms thus favouring the increase of general amount of hydrates and improving the conditions of grows of crystal hydrates.

All this in turn determines the development of constructive processes of formation of optimal micropore cement stone structure which is more or less strengthened by the filamentous hydrosilicates arming the structure. Or, on the contrary, it may initiate the destructive processes lying in the basis of stressed hardening structure, formed as a result of initial stressed crystallization of hydrated phases. The initial stress of structure is emphasized by further processes of hydrates recrystallization and by growth of crystallization pressure.

Chemical additives added to water for its mixing with cement give an opportunity from the very beginning of the process of hydration to exercise directed influence on the formation of the structure of hardening cement anticipating its quality, structural density and durability of cement stone.

Thus for example chemical additives in common use $CaCl_2$ and $NaNO_2$ added with water for mixing increase the meta-stable solubility of clinker phases of Portland cement CaO concentration in the liquid phase in the presence of these additives is higher than in cement hydration in clear water. But if to take into consideration balance concentrations of this oxide in water (1.13g/l CaO at 20°C) and its corresponding concentrations in the solutions of $CaCl_2$ and $NaNO_2$ (1.06 g/l CaO in 4% solution of $CaCl_2$ and 1.7 g/l CaO in 4% solution of $NaNO_2$ at 20°C) one can see that the adding of $CaCl_2$ increases the oversaturation of the liquid phase relating to CaO from 1.49 to 1.79 and $NaNO_2$ on the contrary decreases the oversaturation in such conditions to 1.28.

Thus changing the properties of the liquid phase these additives create quite different conditions for the crystallization of new formations and the formation of structures of cement hardening.

Illustrations 1,2,3 demonstrate the structure of the surface of grains C_3S after 5 sec of hydration in 4% solutions of $CaCl_2$ and $NaNO_2$, and the illustration 3 - C_3S acted by water.

Fig.1. The surface of grains C_3S after 5 sec of hydration in the system C_3S-H_2O (x12000).

It is known that is the presence of $CaCl_2$ newformations in cement stone are represented by well crystallized hydrated phases. It is supposed that quick and time-consuming active cement hydration in the presence of $CaCl_2$ leads to the formation of hydrates in the forms tending to recrystallization processes and this is accompanied by the development of sufficient internal pressures. Illustration 4 depicts the structure of grains C_3S which had been hydrated in the paste for 6 hours (the mixing was carried out by a corresponding solution $CaCl_2$).

One can see a substantial amount of skeleton crystals tending to the processes of recrystallization in case of the decrease of the number of constructive particles in the liquid phase. It reaffirmes that the liquid phase of the system is highly oversaturated even after 6 hours of hydration.

The results reflecting durability comparison given in the Table I are in full accordance with all said above i.e. various levels of oversaturation of the liquid phase relating CaO favour the formation of structures differing in durability.

Cement stone with $CaCl_2$ additive has a higher level of durability under pressure, but it renders small resistance to following pressures; as to the resistance of cement stone with $NaNO_2$ additive it is greater. It proves that the structure in this case can endure even higher folding pressures and actually cement stone structure

Fig.2. The surface of grins C_3S after 5 sec of hydration in 4% solutions of $CaCl_2$ (x 40 000).

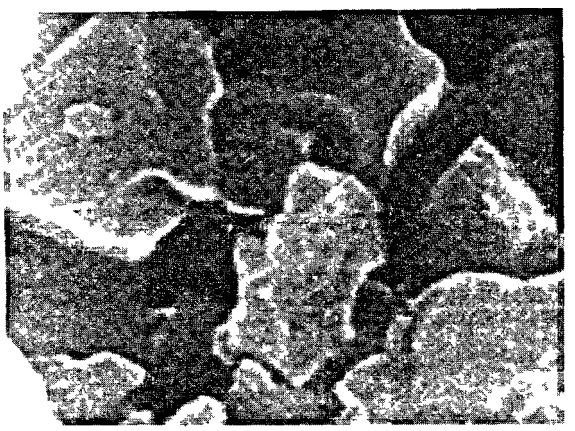

Fig.3. The surface of grains C_3S after 5 sec of hydration in 4% solutions of $NaNO_2$ (x45000).

Fig.4. The surface of grains C_3S after 6 hours of hydration in the paste in 4% solutions of $CaCl_2$ (x 20 000).

Fig.5. The surface of grains C_3S after 6 hours of hydration in the paste in 4% solutions of $NaNO_2$ (x 35 000).

given at the illustration 5 after 6 hours of hydration is the evidence of this fact. And the presence of large amount of pin - - like hydrates makes the system stronger this particularly referes to folding pressures.

Table I

The Influence of $CaCl_2$ and $NaNO_2$ Additives on the Strength Properties of Cement Stone

Additives	Strength parameters MPa	Sample age, hours				
		24	72	168	672	8640
$CaCl_2$	R_{com}	21.9	50.0	40.0	51.1	47.0
	R_{bend}	3.6	4.5	3.7	4.2	5.1
$NaNO_2$	R_{com}	13.3	37.5	41.0	47.5	48.0
	R_{bend}	2.9	4.3	5.2	5.8	7.0

The possibility of substantial increase of strength of cement stone (concerning bending pressures) due to chemical additives influencing the hardening structure formation in a necessary direction is of great importance. It is known that the rising of quality of cement on one grade (R_{pr} to 10 MPa which is reached at cement producing factories by means of great efforts gives only insignificant increase of strength level concerning bending pressure). (0.5-1.0 MPa). Even more with the improving of cement grade ratio R_{fold}/R_{pres} decreases (see Table 2). So we may say that the further increase of cement grades doesn't ensure desirable growth of cement strength (folding pressures).

That is why the rising of R_{bend} of cement stone by other ways including the directed structure formation when hardening is the most important problem. The solution of this problem is available using chemical additives - structure modifications.

Table II

The Standard Properties of Cements

Cement type	R_{comp} 672 hours: MPa	R_{bend} 672 hours: MPa	R_{bend}/R_{comp} in %
300	30.0	4.5	15.0
400	40.0	5.5	14.0
500	50.0	6.0	12.0
550	55.0	6.2	11.0
600	60.0	6.5	11.0

Cement stone investigation with the application of scanning electronic microscoping revealed substantial differences in the morphology of hydration phases, which are formed under the influence of $CaCl_2$ and $NaNO_2$. Sample without additives had a large-pore structure and poorly expressed crystallization of newformations.

In the pores of cement stone hydration without additives one can trace the hydrates which have the form of round irregular particles with dimensions 0.1-0.5 mmc with $CaCl_2$ additive. Calcium hydrosilicates are crystallized in the form of the plates with dimensions up to 3 mmc (and with the $NaNO_2$ additive crystals of filamentous structure dominate).

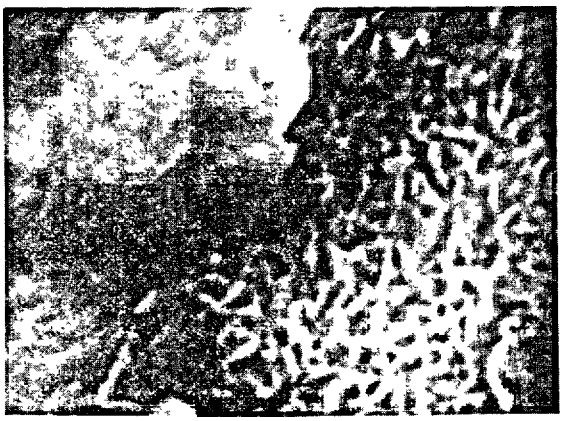

Fig.6. The surface of grains C_3S after 6 hours of hydration in the paste when mixing (x 45 000).

Table III gives the data, characterising micropore structure of cement stone with $CaCl_2$ and $NaNO_2$ additives. As one can see from the data given above in the pressence of the mentioned additives are formed some structures of hardening. They differ from the structure of cement stone which doesn't contain additives from the very moment of cement and water interaction.

Table III

The influence of $CaCl_2$ and $NaNO_2$ on the Quantitative and Qualitative Pore Structure of the Hardened Cement

Additions	The total porosity kg/m^3	Distribution of pore size in radii 10^3nm:	10^3- 10^2nm:	10^2-10nm:	10-1 nm
H_2O	122.0	3.0	1.6	3.4	2.0
$CaCal_2$	94.0	2.6	2.3	3.8	1.4
$NaNO_2$	113.0	1.6	1.9	4.5	2.0

CONCLUSION The experiments carried out revealed a certain dependence of the initial processes of crystalformation of hydrates on the medium of cement and water interaction, and the influence of initial crystallographic forms of "primary" hydrates on the further process of structure formation and cement hardening.

Crystallohydrates found in the actively growing forms (pin-like, skeleton, dendrite-like and anti-skeleton) favours rapid thinning of the adjoining layer of the liquid phase by solution products, stimulating the process of the further, solving of basic clinker and recrystallization of unstable newformations, thus favouring the formation of the most stable and durable hardening structures of cement stone.

REFERENCES

1. G.L.KALOUSEK (1976) "Processes of Hydration at Early Stages of Cement Hardening", Proceeding of the VI-th International Congress on Cement Chemistry, v.5, b.2, 65-81 (Russian).

2. J.M.BUTT, V.M.KOLBASOV, N.A.KOZYREVA (1975) "Phase Formation on the Early Stages of Portland Cement Hydration", Proc. of MCTI n.a. D.I.Mendeleev, ed.57, 48-52 (Russian).

3. N.A.KOZYREVA, J.M.BUTT, V.M.KOLBASOV (1971) "The Studies of Crystalgrowth Kinetics of C_3A during Hydration of C_3A in C_3S- C_2S-C_3A-C_4AF-$CaSO_4.2H_2O$-H_2O", Proc. of MCTI n.a. Mendeleev, ed. 58, 197-201 (Russian).

Comportement de l'aluminate tricalcique en milieu glycol - comparaison avec l'hydratation

Tricalcium aluminate behaviour in glycol - comparison with water

P. LONGUET, G. BELLINA - C.E.R.I.L.H. Paris, France.

RESUME

La base O^{2-} de C_3A réagit avec le glycol en formant deux particules distinctes:

$$(CH_2OH)_2 + O^{2-} \rightarrow (CH_2O)_2^{2-} + H_2O$$

tandis qu'avec l'eau, dans l'hydratation classique, on forme deux particules identiques:

$$O^{2-} + H_2O \rightleftarrows 2\ OH^-$$

Cette particularité liée à la formation de molécules H_2O dans le milieu initial glycol anhydre permet de suivre la cinétique des réactions et de mettre en évidence le mode de formation et la nature des produits solvatés.

SUMMARY

The base O^{2-} of C_3A is reacting with glycol to create two different particles:

$$(CH_2OH)_2 + O^{2-} \rightarrow (CH_2O)_2^{2-} + H_2O$$

whereas with water, for usual hydration, two identical particles are created:

$$O^{2-} + H_2O \rightleftarrows 2\ OH^-$$

This particularity relied on the creation of molecules of water from the anhydrous glycol initial medium allows us to follow the speed of these reactions and to clear up the way of formation and the kind of solvated products.

INTRODUCTION

L'espèce chimique OH^- présente dans les phases du système eau-ciment, à un moment donné de son évolution, provient:

- soit de la dissociation du solvant $H_2O \rightleftarrows H^+ + OH^-$
- soit de la réaction du proton avec la base oxygène O^{2-} des constituants anhydres initiaux $O^{2-} + H^+ \rightleftarrows OH^-$.

Cette particularité caractéristique de l'eau limite beaucoup l'interprétation des bilans réactionnels relatifs à l'hydratation.

Des études antérieures nous ont montré que des réactions comparables à celles mises en jeu dans l'hydratation des ciments pouvaient se développer en milieu glycol (1) (2). Dans ce cas, la dissociation ionique globale du solvant:

$$(CH_2OH)_2 \rightleftarrows (CH_2O)_2^{2-} + 2H^+$$

libère la base glycol $(CH_2O)_2^{2-}$ différente de celle provenant de la réaction du proton avec la base oxygène.

Cette caractéristique du glycol doit permettre de lever l'incertitude apportée par l'eau dans l'étude des mécanismes de l'hydratation des liants hydrauliques.

Dans cet exposé nous examinerons uniquement le cas de l'aluminate tricalcique $Al_2O_6Ca_3$ (C_3A) en milieu glycol. Après un rappel de l'essentiel des résultats déjà obtenus (1) (2) nous proposerons une interprétation dégageant des hypothèses sur le mécanisme de la solvatation dans ce milieu non aqueux.

DONNEES EXPERIMENTALES

Le glycol est un dialcool (éthane diol 1,2). C'est un solvant polaire, sa constante diélectrique est environ la moitié de celle de l'eau. Il donne lieu à des équilibres de dissociation acido-basiques du même type que ceux de l'eau (solvant amphiprotonique). Son produit ionique est de 10^{-11} à 20°C. Il dissout les substances minérales polaires.

Dans nos études seul l'équilibre d'ionisation global suivant a été pris en considération:

$$(CH_2OH)_2 \rightleftarrows (CH_2O)_2^{2-} + 2H^+$$

Avec CaO le glycol réagit selon l'équation:

$$CaO + (CH_2OH)_2 \rightarrow (CH_2O)_2^{2-} + Ca^{2+} + H_2O$$

La solvolyse de la base oxygène O^{2-} de l'oxyde de calcium par le glycol est pratiquement complète

$$O^{2-} + (CH_2OH)_2 \rightarrow (CH_2O)_2^{2-} + H_2O$$

A chaque mole O^{2-} solvolysée correspond une mole de base glycol et une mole d'eau.

La solution obtenue conduit le courant électrique.

Le dosage acidimétrique de la base $(CH_2O)_2^{2-}$ est facilement réalisé avec un acide titré en repérant le point équivalent par conductimétrie.

L'eau provenant de la solvolyse peut être déterminée selon la méthode de KARL FISHER.

Ces deux dosages permettent de suivre les cinétiques de solvolyse et d'établir les bilans réactionnels.

L'aluminate tricalcique $Al_2O_6Ca_3$ (C_3A) réagit avec le glycol. D'ailleurs c'est l'observation expérimentale de la prise et du durcissement d'une pâte de C_3A dans le glycol qui est à la base de tous nos travaux dans ce domaine.

Deux séries générales d'essais ont été réalisées. L'une sur des suspensions dans le glycol à 1,5 g pour cent environ de C_3A à 25 et 70°C dans le cadre du dosage de la chaux libre, l'autre sur des pâtes de rapport solvant/solide de 0,3 environ pour vérifier la généralisation des conclusions déduites de l'étude sur les suspensions.

Une suspension de C_3A dans le glycol conduit le courant électrique et son évolution en fonction du temps peut-être suivie par un conductimètre enregistreur.

Sur la solution au contact du solide les teneurs en H_2O, Ca^{2+}, Al^{3+} et la basicité ont été déterminées à différents moments de l'évolution de la suspension.

Ces valeurs mettent en évidence la formation au sein de la suspension de nouvelles phases solides qui ne peuvent prendre naissance qu'avec consommation de base glycol $(CH_2O)_2^{2-}$. Pour vérifier cette hypothèse nous avons séparé le solide présent dans la suspension après un long contact (24 heures), puis nous avons extrait le C_3A n'ayant pas réagi avec une adaptation de la méthode de TAKASHIMA (2) et analysé le précipité solvaté restant [Al^{3+}, Ca^{2+}, carbone, hydrogène et oxygène (par différence)]. A partir de ces dosages nous avons pu calculer une composition molaire moyenne du type (Al, Ca, C_6, H_{13}, O_6) aux erreurs expérimentales près. Ces valeurs complétées par l'analyse thermopondérale permettent de calculer la formule suivante:

$$[2Al,\ 5\ (CH_2O)_2,\ (CH_2OH)_2]Ca_2$$

Le composé solvaté obtenu est cristallisé, la diffraction X montre des raies nettes dont aucune ne correspond aux raies connues des aluminates de calcium hydratés.

La formule proposée est évidemment hypothétique, elle ne traduit que des bilans réactionnels et ne représente aucunement la structure du composé. Elle montre essentiellement que le composé solvaté se forme à partir de la base $(CH_2O)_2^{2-}$ présente dans la phase liquide au contact du solide. Cette remarque importante est d'ailleurs complétée par l'étude acidimétrique de cette phase liquide qui permet de mettre en évidence l'existence d'ions organominéraux en solution comme:

$[Al,\ 2(CH_2O)_2]^-$

$[2Al,\ 3(CH_2O)_2]^0$ composé comparable à l'hydroxyde $Al(OH)_3$ en milieu aqueux.

et même:

$[2Al,\ 2(CH_2O)_2]^{2+}$ qui met en évidence l'importance de l'affinité entre l'ion aluminium Al^{3+} et la base glycol $(CH_2O)_2^{2-}$.

Notons encore que les produits solvatés qui précipitent au cours de l'évolution de la suspension ont un rapport $(CH_2O)_2^{2-}/2Al$ qui croît régulièrement d'environ 3 à la valeur 5 (valeur correspondant à la formule proposée plus haut) et que d'autre part la cinétique de l'évolution de la suspension enregistrée par conductimétrie indique une augmentation de la vitesse de réaction aux environs du début de la précipitation du composé solvaté.

Les résultats précédents obtenus sur des suspensions prennent tout leur intérêt si on peut les transposer aux pâtes.

Les essais ont été réalisés à 25°C sur microéprouvettes de 1 cm^3 en pâte pure de rapport $glycol/Al_2O_6Ca_3 = 0,3$. On obtient ainsi:

- à l'échéance 2 jours une éprouvette subissant une forte déformation plastique avant de se rompre aux environs de 450 bar.

- à 7 jours on observe une rupture plus franche vers 550 bar.

- à 28 jours c'est une rupture classique à 650 bar.

Les éprouvettes à 28 jours ont été reprises après rupture et dispersées par broyage dans du méthanol anhydre. La suspension a été filtrée. Le filtrat et le précipité séparé ont été analysés comme nous l'avons indiqué pour les suspensions. Les résultats obtenus sont tout à fait comparables à ceux obtenus sur les suspensions et conduisent aux mêmes conclusions.

INTERPRETATION DES DONNEES EXPERIMENTALES

Il convient d'abord de rappeler brièvement les conceptions actuelles sur la formation des solutions. Le passage en solution d'un solide dans un solvant suppose que des particules se séparent de la masse du solide pour venir s'insérer parmi les molécules du solvant. Cette première étape définit la dissolution.

Dans le cas d'un solvant polaire et d'un solide possédant des liaisons ioniques la dissolution s'accompagne d'une dissociation électrolytique, les particules en solution sont alors des ions. Ces ions s'entourent par attraction électrostatique d'un cortège de molécules du solvant polaire qui assure la stabilité de la dissolution. C'est le phénomène de solvatation. Cette solvation s'accompagne d'intéractions plus ou moins importantes entre les ions et les molécules du solvant. La gamme des actions possibles peut s'étendre d'attractions électrostatiques pratiquement négligeables (le solvant joue alors un rôle d'espace) jusqu'à des liaisons chimiques définies, on parle alors de solvolyse. Il apparaît alors dans le milieu de nouvelles espèces chimiques renfermant une ou plusieurs particules provenant du solvant. Il est alors possible que les nouvelles espèces formées puissent donner lieu à de nouvelles réactions, par exemple à des précipitations si l'évolution du système amène à des concentrations correspondant au produit de solubilité d'un composé peu soluble.

Compte tenu de ces conceptions nos études peuvent s'interpréter de la manière suivante. Pour le système CaO-glycol la dissolution provoque la formation des ions Ca^{2+} et O^{2-}. La solvatation de ces ions se fait sans solvolyse pour Ca^{2+} et avec solvolyse pour O^{2-} soit:

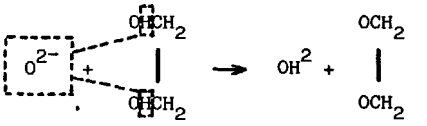

Les teneurs en eau et en base glycol du milieu sont proportionnelles à la quantité de CaO passée en solution.

Pour $Al_2O_6Ca_3$ un raisonnement analogue conduit à la formation d'ions solvatés avec Al^{3+}, Ca^{2+} et O^{2-}. O^{2-} se solvolyse comme précédemment, la concentration en base glycol $(CH_2O)_2^{2-}$ augmente en fonction de cette solvolyse.

L'ion Al^{3+} donne en général des complexes hexacoordonnés par exemple:

$$\left[2\,Al,\ 6(CH_2OH)_2\right]^{6+}$$

Cet ion solvaté peut se dissocier dans le milieu basique en perdant successivement tous les protons disponibles de ses molécules de glycol en fonction de la concentration en $(CH_2O)_2^{2-}$ en formant des anions. Citons:

$$\left[2\,Al,\ 3(CH_2OH)_2\ 3(CH_2O)_2\right]^{0}$$

$$\left[2\,Al,\ 2(CH_2OH)_2\ 4(CH_2O)_2\right]^{2-}$$

$$\left[2\,Al,\ (CH_2OH)_2\ 5(CH_2O)_2\right]^{4-}$$

qui sont, à la solvation près, ceux mis en évidence dans nos études.

Le milieu s'enrichit aussi par ailleurs en ions calcium solvatés. Si un composé insoluble est susceptible de se former il précipite lorsque les concentrations des différents ions présents dans le milieu vérifient le produit de solubilité du composé peu soluble. Dans notre cas il s'agit vraisemblablement de l'aluminate bicalcique pour lequel nous avons proposé la formule:

$$\left[2\,Al,\ 5(CH_2O)_2,\ (CH_2OH)_2\right]\ Ca_2$$

Cette précipitation rompt l'équilibre ionique du milieu et permet la poursuite de l'évolution du système vers son état final.

Bien que cette interprétation soit présentée sous une forme simplifiée (bien des facteurs ne sont pas pris en considération: concentrations au lieu d'activités, condensation ou polymérisation possibles des anions, influence des liaisons hydrogène, dissociations successives du solvant, viscosité, utilisation d'autres solvants polaires de constantes diélectriques ou de dissociations différentes...).

Il est intéressant de constater que les hypothèses ainsi avancées s'accordent et viennent compléter la théorie de Le CHATELIER sur l'hydratation des liants hydrauliques. Elles permettent de plus une généralisation des mécanismes de "l'hydraulicité": la réactivité d'un composé hydraulique apparaît liée à sa teneur en O^{2-} solvolysable par les protons d'un solvant polaire amphiprotonique. Cette solvolyse

libère la base du solvant et permet la formation d'anions avec les ions amphotères présents (Al^{3+}, Si^{4+} ...). Ces anions en précipitant des sels de calcium insolubles assurent la prise et le durcissement.

CONCLUSION

Nous souhaitons d'abord que le lecteur ne nous tienne pas trop rigueur de cet exposé spécialisé assez inhabituel dans la chimie des ciments.

L'étude du système C_3A-glycol permet de proposer une généralisation des phénomènes particuliers à l'hydraulicité et fournit une version actualisée de la théorie de Le CHATELIER. Il est évident que nos études apportent une modeste et bien incomplète contribution à cette chimie des ciments en milieu non aqueux; nous espérons cependant en avoir montré l'intérêt sur le plan fondamental et sur le plan technologique.

BIBLIOGRAPHIE

(1) P. LONGUET, L. BURGLEN, G. BELLINA
Rev. Mat. Constr. janv. fév. 1970 n° 652-653
p.1 à 19.
L'extraction au moyen du glycol et le dosage de la chaux libre dans la chimie du ciment.

(2) P. LONGUET, G. BELLINA
Rev. Mat. Constr. janv. fév. 1974 n° 686
p.45-51.
Processus physicochimiques liés à l'hydraulicité.

The Hydration of Portland Cement. Evidence for an Osmotic Mechanism

L'hydratation des ciments Portland. Intervention évidente d'un processus osmotique

D.D. DOUBLE, N.L. THOMAS and D.A. JAMESON, Grande-Bretagne.

RESUME : Il est proposé d'expliquer l'hydratation des ciments Portland par l'intervention évidente d'un processus osmotique. Ce modèle osmotique permet de prévoir, avec un plein succès, les valeurs calorimétriques et la composition chimique des produits en solution; il est confirmé par des études faites sur des matériaux synthétiques analogues. La microscopie électronique apporte la preuve des similitudes qui existent entre les gels synthétiques de C.S.H. et les produits d'hydratation du ciment; et les caractéristiques osmotiques de tels gels peuvent être mises en évidence par le phénomène des "jardins chimiques".

Abstract

An osmotic mechanism of Portland cement hydration has been proposed, and evidence for the model is reviewed. The model successfully accounts for observed calorimetric and solution chemistry data, and is reinforced by studies of analogous synthetic systems. Electron microscopy provides collaborative evidence of similarities between synthetic C-S-H gels and cement hydration products, while the osmotic characteristics of such gels can be demonstrated by the phenomenon of "chemical gardens".

1. Introduction

Almost 20 years ago, Powers put forward the suggestion that osmotic effects might play an important role in the hydration of Portland cement (1). For reasons that are not clear, this proposal was not developed further - until recently, when two groups of researchers published articles reinforcing the original idea and elaborating on it further to provide a viable model explaining the mechanism of hydration of cement (2-4). This osmotic/membrane model has been the subject of some discussion in the literature (5-8) and it seems an appropriate time to review the points in its favour and to consider its wider implications.

2. Colloidal Membranes

The feature that makes the hydration of Portland cement rather different from a simple dissolution and crystallisation process (i.e. a 'through solution' mechanism such as has been proposed for the hydration of Plaster of Paris, for example) is that the main reaction product is a colloidal gel and it is precipitated by local reaction at the surfaces of the cement grains. In a hydrated cement paste there are crystalline hydration products (viz. $Ca(OH)_2$ and various complex aluminate hydrates) but the main constituent of the hydrated matrix responsible for the strength development is the calcium-silicate-hydrate (C-S-H) gel phase. Diamond (9) in a recent review of cement hydration refers to "the unusual compositional flexibility and quasi-amorphous character" of the gel. Only very poorly defined and diffuse peaks are obtained by X-ray/electron diffraction observations compatible with a colloidal microstructure in which the unit particle sizes are extremely small (of the order 100Å).

In general, when metal ion silicates are precipitated from aqueous solution at ordinary temperatures, an amorphous colloidal solid is usually the result. Crystalline silicates may be obtained through slow growth from dilute solution or after prolonged aging, particularly at elevated temperatures. The reason lies in the stereochemical difficulty that the molecular silicate units (generally in varying degrees of polymerisation) have in arranging themselves into a repeatable three-dimensional lattice. As is noted by Iler (10), essentially the process is one of mutual coagulation of the hydroxides of the metal ion and the silica. These principles should apply equally to the C-S-H gel in cement, (compare figures 1(a) and (b)).

Figure 1(a): Colloidal C-S-H gel in hydrated Portland cement.
Transmission electron micrographs.

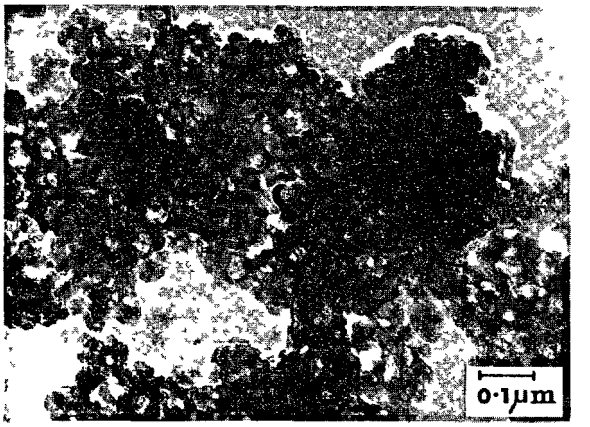

Figure 1(b): C-S-H gel obtained by precipitation between aqueous solutions of calcium chloride and sodium silicate.

An important property of silicate gels is that, when precipitated as a continuous membrane between two solutions of different compositions, they can display osmotic phenomena. A good example of this occurs in so-called 'silicate gardens', obtained when metal ion salt crystals are immersed in dilute aqueous sodium silicate solution (figure 2). Double et al. (2,3) and Birchall et al. (4) have drawn attention to the striking visual analogy between the growth sequence in silicate gardens and the morphological developments occuring during the hydration of Portland cement. The point of this analogy was to illustrate that:

(a) osmotic pressure effects can be generated across metal-silicate gel membranes (including C-S-H gel membranes) by virtue of their selective permeability to ions in aqueous solution,
(b) the osmotic properties derive mainly from the colloidal gel character of the membrane. The effect is not restricted to silicates but also occurs for gel membranes formed from ferrocyanides (refer to Pfeffer's experiments for example (11)), large oxyanion species such as aluminates/borates/zincates, and even oxalates and carbonates (12,13).

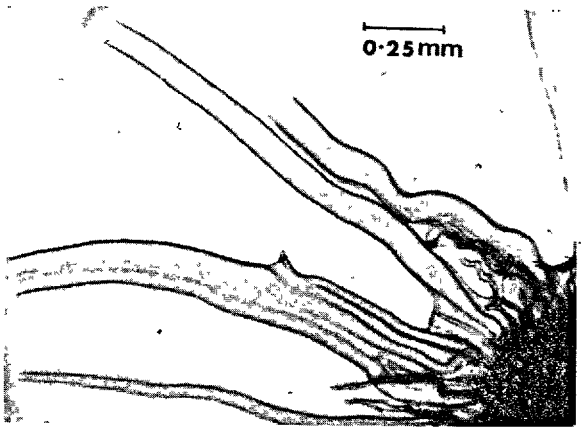

Figure 2: Tubular fibre growth from a 'silicate garden' obtained from a crystal of cobalt nitrate immersed in dilute aqueous sodium silicate solution. Optical micrograph.

Clearly, there are some points of difference between the growth of silicate gardens and the hydration of Portland cement. The analogy is not exact but the fundamental features (i.e. the preferential diffusion of species through a colloidal gel membrane) are essentially the same. This inevitably leads one to the conclusion that osmotic effects ought to play a significant part during the hydration of cement.

3. The Mechanism of Hydration of Portland Cement

In the osmotic model of cement hydration, one visualises the sequence of events illustrated diagrammatically in figure 3.

Initial reaction. There is ample evidence to show that gelatinous coatings (possibly involving both silicate and aluminate) are formed on the surface of cement grains very soon after contact with water. The development of these coatings has been directly observed in 'in situ' experiments in the environmental cell in the high voltage electron microscope (3,6). It has been postulated that the formation of the coatings is responsible for the onset of the induction pericd following the initial rapid hydrolysis of the anhydrous clinker (1,14). Essentially, a membrane is formed which inhibits access of water to the reactive cement constituents. Some insight into the way that these membranes are formed has been provided by recent SEM/ESCA studies by Ménétrier et al. (15) of the composition of surface hydrates on C_3S grains exposed to water for short time intervals. These showed a sharp initial decrease in the Ca/Si ratio followed by a rapid rise, reaching a maximum within 15 seconds. At the same time, fine-grained reaction products were observed to oover the surface. This behaviour is consistent with (i) an initial leaching of lime from the C_3S structure by hydrolysis, followed by (ii) recombination between the calcium ions released into solution and the hydrosilicate residue left on the surface of the cement grains to precipitate a C-S-H gel membrane.

Induction period. Calorimetric measurements of the rate of heat evolution during the induction period suggest that little is happening at this stage of hydration. However the situation is not quiescent because, as studies by various workers have shown (16,17), the concentration of the bulk aqueous phase is rapidly rising with respect to dissolved Ca^{++} and OH^- ions - and indeed exceeds the saturation level for the precipitation of $Ca(OH)_2$ by a factor of 1.5 - 2.0. Significantly, the silicate concentration in solution remains negligibly small (less than 5 ppm). These observations would imply (i) that hydrolysis of the clinker is still continuing and (ii) that there is preferential diffusion through the membrane coating (ingress of water and egress of Ca^{++} and OH^- ions). The inability of the hydrolysed silicate to diffuse out through the membrane is reconcilable with its large molecular size, particularly because of its tendency to polymerise into configurations larger than the basic SiO_4^{4-} unit. This preferential diffusion process is precisely the situation that will lead to the development of an osmotic pressure within the membrane coating around the cement grains. Powers cited these pressure effects as being responsible for the transient dilation that occurs in cement pastes at early stages of hydration (1).

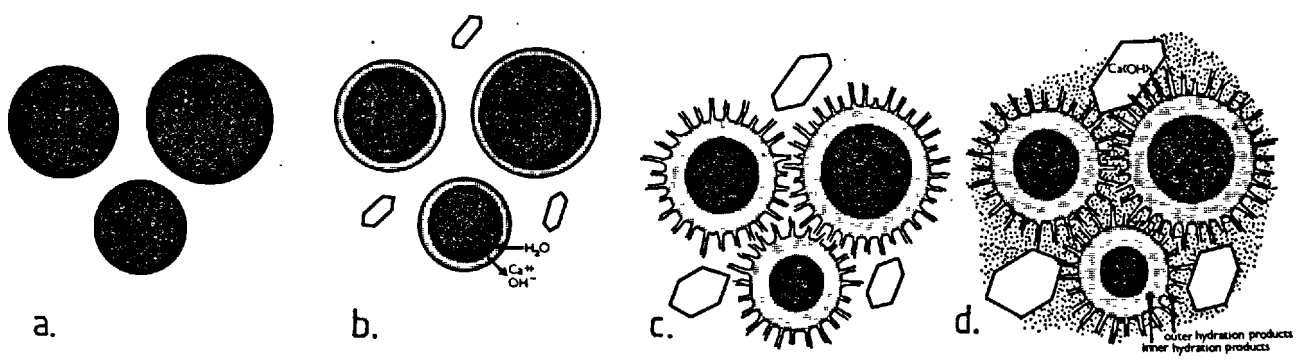

Figure 3: Diagrammatic representation of the sequence of hydration of cement. (a) Cement grains in water, (b) initial gel coatings around cement grains, (c) secondary growth of C-S-H gel after osmotic rupture of gel coatings and (d) long term infilling and consolidation of microstructure.

Post-induction period. The end of the induction period is considered to occur when the gel coatings around the cement grains rupture because of osmotic pressure effects. Hydrosilicate material is extruded through the ruptured membrane and combines with the calcium ions in solution to precipitate C-S-H gel as excrescences on the surfaces of the cement grains. These growths constitute the secondary hydration products. In this way, one accounts for the drop in the calcium ion concentration in the bulk aqueous solution that is observed to occur at the end of the induction period (6,17).

By analogy with silicate gardens, these excrescences may be expected to develop a tubular morphology. Indeed, observations by several workers have shown that the fibrillar gel growths on the surface of cement grains have a hollow structure (3,6,8). Pratt and Jennings (6) have observed enhanced growth of tubular fibres when partially hydrated cement pastes were subsequently immersed in distilled water. This effect can readily be understood in terms of an osmotic process in which the driving force for secondary growth (the difference in chemical potential between the dissolved species on either side of gel membrane) is promoted by sudden dilution of the aqueous phase.

Tubular morphologies are by no means the only type of secondary growths to be expected. Since the hydrosilicate material is forced out through a ruptured membrane, the form assumed by the outer precipitate will be governed by the local conditions under which the combination between the calcium and the silicate occurs. The extrusion process could easily give rise to hollow or solid fibres, and even sheet and foil-like structures - as has been observed (figure 4). In any case, it is possible to reconcile the variety of morphologies of the hydrated cement gel with an osmotically driven hydration process such as has been described.

While one visualises that osmotic effects are important in the early stages of hydration, it seems likely that as the gel coatings thicken and become increasingly difficult to rupture, other precipitation processes become more important in the progressive infilling and consolidation of the cement microstructure.

4. Conclusions

A model has been proposed to explain the mechanism at early stages of the hydration of Portland cement. This is based on osmotic effects associated with the colloidal C-S-H membrane formed around the cement grains. The evidence for this model is circumstantial but it has the advantage of explaining the following facts:

(a) It gives a reason for the onset and eventual termination of the induction period.
(b) It explains the morphology of growth of the outer C-S-H products - tubular fibres and other forms.
(c) It is compatible with the variations that occur in the composition of the bulk aqueous phase during hydration.
(d) It provides a transport mechanism for the silicate material from the anhydrous cement core to the outer hydration products - without having to postulate diffusion through the bulk aqueous solution, where its concentration is known to be extremely low.

By emphasising the colloidal nature of the C-S-H gel and its inherent properties, the model provides a different insight into the hydration mechanism as opposed to other theories which invoke conventional nucleation and growth processes.

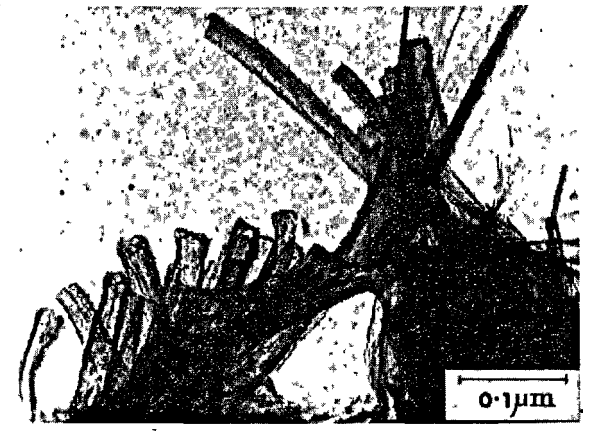

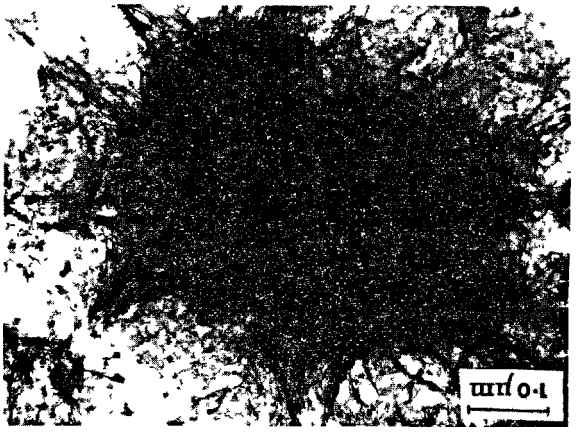

Figure 4: Variety of morphologies observed in the secondary gel hydrates on the surface of cement grains.
Transmission electron micrographs.

Acknowledgements

The authors acknowledge the financial support of the Science Research Council and Imperial Chemical Industries in the furtherance of this research. They also express appreciation to Professor Sir Peter Hirsch FRS for the provision of laboratory facilities and to the personnel at I.C.I. Mond Division (Runcorn, Cheshire) for helpful discussion of the results of this work.

References

1. T.C. Powers, J.Portland Cement Assn., Res.Dev.Labs., 3, p.47 (1961).
2. D.D. Double and A. Hellawell, Nature, 261, p.486 (1976).
3. D.D. Double, A. Hellawell and S.J. Perry, Proc.Roy.Soc. (London), A 359, p.435 (1978).
4. J.D. Birchall, A.J. Howard and A.J. Bailey, Proc.Roy.Soc. (London), A 360, p.445 (1978).
5. J. Skalny, I. Jawed and H.F.W. Taylor, World Cement Technol., p.183, Sept. (1978).
6. H.M. Jennings and P.L. Pratt, Cem. & Concr.Res., 9, p.501 (1979).
7. L. Dent Glasser, Cem. & Concr. Res., 9, p.515 (1979).
8. J.E. Bailey and D. Chescoe, Proc.Brit.Ceram.Soc. (London), in press (1978).
9. S. Diamond, Proc.Conf. "Hydraulic Cement Pastes; their Structure and Properties", Sheffield (1976) (Cement & Concrete Assn. publication No.15.121, p.2).
10. R.K. Iler, "The Chemistry of Silica", Wiley Interscience, p.161 (1979).
11. W. Pfeffer in "Treatise on Physical Chemistry", Ed. H.S. Taylor, 2nd edn. Van Norstrand, p.370 (1931).
12. W.J. Clunies Ross, J.Proc.Roy.Soc. (NS Wales), 44, p.583 (1910).
13. T.H. Hazlehurst, J.Chem. Education, 18, p.286 (1941).;
14. De Jong, H.N. Stein and J. Stevals, J.Appl.Chem., 17, p.246 (1967) and 18, p.9 (1968).
15. D. Ménétrier, I. Jawed, T.S. Sun and J. Skalny, Cem. & Concr.Res., 9, p.473 (1979).
16. R. Kondo and S. Ueda, Proc. 5th Int.Symp.Chem.Cem., Tokyo, 2, p.203 (1968).
17. J.F. Young, H.S. Tong and R.L. Berger, J.Amer.Ceram.Soc., 60, p.193 (1977).

Etude comparée de la formation de C-S-H à partir de solutions sursaturées et de mélanges C_3S-solution

Comparative study of C-S-H formation from supersaturated solutions and C_3S solution mixtures

P. BARRET, professeur, directeur du Laboratoire de Recherches sur la Réactivité des Solides (L.A. 23) Université de Dijon (France),
D. BERTRANDIE, docteur de l'Université de Dijon, CNRS (L.A. 23),
D. MENETRIER, docteur ès sciences physiques, attaché de recherches (L.A. 23), France.

RESUME : En système fermé, l'évolution de mélanges hétérogènes (C_3S-eau ou solutions aqueuses de composition initiale donnée) a été comparée à celle des milieux homogènes obtenus par filtration ou par mélange initial de deux solutions et sursaturés par rapport au C-S-H. Des données complémentaires ont été fournies par l'étude en système ouvert de la composition initiale et de l'évolution de filtrats obtenus par flux d'une solution de chaux et de silice à travers une couche de C_3S sur filtre et par mélange de deux solutions de chaux et de silice de compositions appropriées, sur filtre. Le report sur le diagramme chaux-silice-eau (C,S,H) des variations de composition en CaO et SiO_2 (chemins cinétiques), accompagnant l'évolution de ces différents systèmes, a permis de constater qu'il n'y avait pas de différence, au point de vue cinétique, entre la vitesse de précipitation de C-S-H à partir de milieux homogènes sursaturés et la vitesse de formation du C-S-H à partir de mélanges hétérogènes C_3S-eau ou C_3S-solution. Ces chemins cinétiques sont tous situés dans le domaine sursaturé délimité supérieurement par la courbe de supersolubilité du C-S-H construite par les auteurs (2) et qui correspond à une nucléation immédiate, inférieurement par la courbe d'équilibre de solubilité de C-S-H. On peut donc conclure que le C-S-H formé à partir de mélanges hétérogènes C_3S-eau ou solution tire également son origine d'un processus de précipitation. Des constructions graphiques fondées sur les expressions du bilan analytique permettent de rendre compte de la forme de ces "chemins cinétiques" dans le cas des milieux homogènes aussi bien que dans celui des mélanges hétérogènes et pour ces derniers, par la mise en œuvre de la dissolution congruente de C_3S superficiellement hydroxylé, suivie de la précipitation de C-S-H de rapport $[C/S]_S$ variables suivant la concentration en chaux du milieu.

SUMMARY : The evolution of heterogeneous mixtures (C_3S water or aqueous solutions with a given initial composition) was compared in a closed system with that of homogeneous media obtained by filtration or initial mixture of two solutions supersaturated with respect to C-S-H. The open system study yielded further data on the initial composition and evolution of filtrates obtained by pouring a silica and lime solution through a C_3S layer on a filter and by mixing on filter two solutions of lime and silica of appropriate compositions. Reporting the CaO and SiO_2 composition variations (kinetic path), on the lime-water-silica diagram (C,S,H), and accompanying the evolution of these different systems allowed to note that there was no difference, from the kinetic viewpoint, between the C-S-H precipitation rate from supersaturated homogeneous media and the formation rate of C-S-H from heterogeneous C_3S water or C_3S solution mixtures. These kinetic paths are all in the supersaturated domain delineated in its upper part by the C-S-H supersolubility curve plotted by the authors (2) and corresponding to immediate nucleation, and in its lower part by the C-S-H solubility equilibrium curve. It may thus be concluded that the C-S-H formed from heterogeneous C_3S water or solution mixtures also derives from a process of precipitation. Plots resulting from the expressions of the analytical balance allow to account for the profile of these "kinetic paths" in the case of homogeneous and heterogeneous media as well, and for the latter by performing congruent dissolution of superficially hydroxylated C_3S followed by the precipitation of C-S-H with variable $[C/S]_S$ ratios depending on the lime concentration in the medium.

INTRODUCTION

Nous postulons une analogie fondamentale entre le mécanisme de formation des hydrosilicates de calcium et celui des hydroaluminates (1), pensant que, dans un cas comme dans l'autre, ces hydrates résultent d'un processus de précipitation à partir d'une solution sursaturée (processus du type Le Chatelier). Notre position est donc défavorable à l'idée d'une formation "topochimique" de ces hydrates (2). Encore convient-il de définir avec précision ce que l'on entend par ce terme.

En revanche, nous posons comme principe qu'*il ne faut pas confondre hydratation et précipitation.* En effet, nous considérons que tout ou partie de l'hydratation des phases anhydres qui interviennent comme constituants des ciments se produit au cours d'étapes cinétiques élémentaires, consistant en l'hydroxylation des ions négatifs superficiels par interaction directe de la surface du solide anhydre avec les molécules d'eau (3,4). Ce processus d'hydroxylation, par protonation dans le cas de C_3S, par addition dans celui de CA, est une étape nécessaire pour permettre le passage en solution de ces ions. Ainsi, à notre point de vue, cette étape d'hydroxylation est suivie d'étapes de transfert en solution des anions hydroxylés et des cations. La précipitation des C-S-H, comme celle des aluminates hydratés, introduit seulement une fraction d'eau supplémentaire, ou pas du tout.

Ce que nous entendons par "formation topochimique des hydrates" consisterait en une accumulation des défauts superficiels que constituent, dans la structure de la phase anhydre, les ions hydroxylés, suivie d'une réorganisation structurale directe de ceux-ci, en l'édifice des différents hydrates, sans passage par la phase liquide. Il s'agirait d'une transformation solide-solide, qui à aucun moment, ne mettrait en jeu la phase liquide pour se réaliser. Notre opinion est que ce processus n'intervient pas ou que, s'il intervient, il est beaucoup moins rapide que le processus de dissolution-précipitation avec lequel il est en compétition.

Pour étayer ce point de vue, nous avons procédé à un ensemble d'expériences. Celles que nous rapporterons ici sont fondées sur la comparaison de la cinétique d'évolution en système fermé, d'une part de mélanges phase solide anhydre-solution, d'autre part de phases liquides, soit séparées par filtration du solide anhydre et des hydrates, soit résultant, à l'instant initial, du mélange de deux solutions. Pour faciliter la rédaction, les expériences du premier type seront désignées par la lettre W et celles du second, par la lettre B. En outre, nos idées sont fondées sur un ensemble de considérations thermodynamiques et cinétiques.

Dans des travaux antérieurs, (5) la comparaison des courbes d'évolution de mélanges solides-solutions et de solutions pures nous avait amenés à conclure au caractère non hétérogène de la nucléation des phases hydratées, la période d'induction précédant la précipitation des aluminates de calcium hydratés à partir de CA étant du même ordre de grandeur (une vingtaine d'heures) dans les deux cas. Il semble en être de même dans la précipitation à partir de C_3S de $Ca(OH)_2$ dont la période d'induction n'est pas sensiblement plus courte en présence des grains de C_3S qu'à partir d'une solution sursaturée pure (6).

ETUDE EXPERIMENTALE

Pour bien situer les expériences plus particulièrement concernées dans cet article par rapport à notre approche expérimentale du problème des mécanismes d'hydratation, on se reportera au tableau I où l'on distingue les expériences de type W et B :

TABLEAU I

Bilans analytiques

- syst. fermé
  - s + ℓ
    - eau initiale
      - stagnant
      - agité (W)
    - solution initiale
      - stagnant
      - agité (W)
  - ℓ (filtrat)(B); ℓ+ℓ initial puis B.
- syst. ouvert
  - s/f + ℓ
    - eau
      - bref
        - versé
        - pulvérisé
      - solution
        - bref
        - pulvérisé
      - long
        - versé
        - pulvérisé
  - (ℓ + ℓ)/f + B (fermé)

Le principe de ces expériences est de suivre la cinétique en faisant un bilan analytique aussi complet que possible, portant à la fois sur les phases solides et sur les solutions. Les essais en système fermé sont ceux où aucun constituant n'est ajouté ni retranché au cours d'une expérience. Dans les essais de type W où une phase solide s est agitée dans une phase liquide ℓ qu'il s'agisse initialement d'eau ou d'une solution de composition déterminée, le mélange de rapport pondéral ℓ/s est placé dans un ballon sous atmosphère d'azote décarbonaté et à une température maintenue constante grâce à un thermostat. Dans les essais de type B, les conditions sont les mêmes mis à part le fait qu'initialement, le système est homogène : filtrat ℓ ou mélange de deux solutions ℓ+ℓ. La cinétique d'évolution est suivie par prélèvements, filtration et analyse du filtrat et des constituants solides au moyen de la spectrométrie d'absorption atomique, de la diffraction X et éventuellement de méthodes complémentaires : analyse colorimétrique de la silice par réduction du complexe silico-molybdique, microscopie électronique à balayage et sonde à dispersion X, spectrométrie IR. Naturellement, tous ces essais sont effectués sans que les solutions ne soient jamais au contact du verre ou d'un matériau susceptible de libérer de la silice.

Les essais en système ouvert sont ceux durant lesquels un ou plusieurs constituants sont ajoutés ou retranchés au cours d'une expérience. La lettre f indique que l'essai est effectué sur filtre. Initialement, un solide s (constituant anhydre d'un ciment) peut être étalé en couche mince sur le filtre et le réactif liquide ℓ peut le traverser pendant une durée soit très brève soit longue, auquel cas le système évolue en régime stationnaire. Le liquide peut être, ou versé sur le filtre, ou finement pulvérisé. Dans des expériences d'un autre type, c'est un mélange initialement homogène qui est réalisé sur filtre en versant simultanément deux liquides ; le précipité qu'ils sont susceptibles de donner par réaction est retenu sur le filtre et le filtrat est éventuellement soumis à une expérience de type B, en système fermé, afin de suivre la cinétique de précipitation. Les variations de composition entraînées par cette précipitation sont reportées systématiquement sur les diagrammes d'équilibre correspondant : chaux-alumine-eau ou chaux-silice-eau. Dans cet article, l'attention sera principalement attirée sur la

cinétique d'évolution en système fermé de mélanges de C_3S agité soit dans l'eau, soit comparativement, dans une solution préparée indépendamment et de concentrations données en silice [S] et en chaux [C] avec plusieurs valeurs du rapport ℓ/s initial.

RESULTATS

La première série d'expériences (8) avait pour but de comparer la cinétique d'évolution en système fermé des systèmes définis par les conditions initiales suivantes :

Exp. 1) s + ℓ (tableau I); avec s : 1g de C_3S T_1 (triclinique T_1) ; ℓ : 1000 g d'eau (ℓ/s = 1000). Courbes W_C : [C] = f(t) et W_S : [S] = g(t) Figure 1.

Exp. 2) s + ℓ avec : s = 1g de C_3S, ℓ = 1000 g de solution contenant : $[C]^o = 3,95.10^{-3}$ mol.kg^{-1} ; $[S]^o = 1,19.10^{-3}$ mol.kg^{-1} ; $[C/S]_\ell = 3,32$; courbe W' (figure 2).

Exp. 3) ℓ (tableau I) avec : $[C]^o = 3,95.10^{-3}$mol.kg^{-1} $[S]^o = 1,19.10^{-3}$ mol.kg^{-1}. Courbes B : [C]= f(t) ; [S] = g(t) (figure 1).

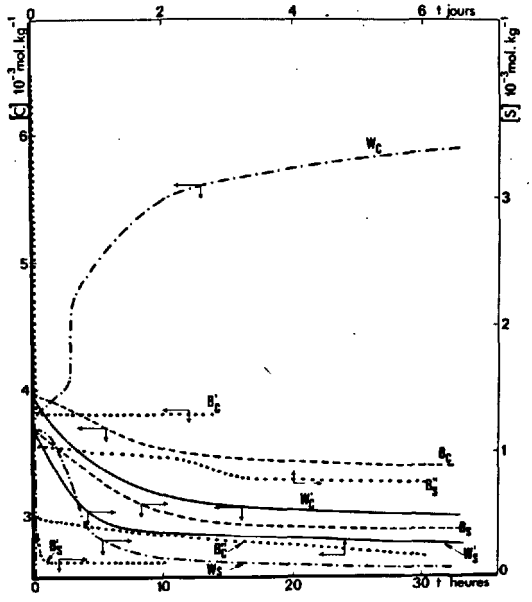

Fig. 1 - Evolutions comparées en fonction du temps -·-·-, courbes W_C et W_S (exp. 1) ; —— courbes W'_C et W_S (exp. 2); - - - courbes B_C et B_S (exp. 3). ..... courbes B'_C et B'_S , B''_C et B''_S après ℓ + ℓ (exp.8,9) avec, respectivement de fortes ou de faibles concentrations dans le mélange initial.

Il convient de souligner la grande différence entre les courbes W et W' et la similitude entre les courbes W' et B.

Des expériences du même type : s + ℓ (courbe W), ont été faites dans un rapport ℓ/s = 10 avec comme conditions initiales :

Exp. 4) s : 10 g de C_3S ; ℓ : 1000 g d'eau. La figure 2 donne les courbes W_C et W_S obtenues dans deux expériences différentes en dosant les faibles concentrations [S] par la méthode de réduction du complexe silico-molybdique. En effet, par spectrométrie d'absorption atomique, on ne peut espérer doser la silice avec une incertitude inférieure à $0,1.10^{-3}$ mol.kg^{-1}. C'est pourquoi la courbe de la silice n'est généralement pas tracée et certains auteurs croient même pouvoir affirmer qu'à ℓ/s = 10, il n'y a pas de silice en solution sauf dans la période initiale, ce qui est une erreur. Une courbe de variation de [S] à ℓ/s = 10 a été établie également par J.F. Young et col. (7). Mais il semble que les valeurs trouvées soient entachées d'une erreur par excès.

Exp. 5) s : 10 g de C_3S ; ℓ : 1000 g de solution préparée indépendamment par agitation pendant 75h de silice (aérosil) dans l'eau de chaux diluée. Après filtration, la composition de cette solution était : $[C]^o = 1,75.10^{-3}$ mol.kg^{-1}, $[S]^o = 4,70.10^{-3}$ mol.kg^{-1}. Les courbes obtenues W'_C et W'_S ont été reportées sur la figure 2 en même temps que les courbes W_C et W_S. Il est remarquable de constater que, dans sa partie initiale, la courbe W'_C est décroissante, [C] passant de $3,65.10^{-3}$ mol.kg^{-1} à t = 1mn à $1,85.10^{-3}$ mol.kg^{-1} à t = 15mn, ce qui est pratiquement $[C]^o$. Après ce minimum, W'_C amorce une remontée, d'abord lente ([C] passe de 1,85 à $2,20.10^{-3}$ mol.kg^{-1} à 15 et 25 mn), puis plus rapide ([C] prend les valeurs 5,40 et $11,12.10^{-3}$ mol.kg^{-1} à 30 et 45 mn). Simultanément, [S] décroît, passant de 3,83 à $0,38.10^{-3}$ mol.kg^{-1} quand t passe de 1 à 30 mn ; cette décroissance est moins rapide dans la seconde demi-heure, mais au bout d'une heure, la courbe W'_S rejoint la courbe W_S à [S]= $0,063.10^{-3}$ mol.kg^{-1} et par la suite, les deux courbes coïncident. On peut donc dire que toute la silice présente à l'origine dans le solvant a été éliminée. [S] continue à décroître lentement avec des valeurs telles que 0,020, 0,0175 , $0,0130\ 10^{-3}$ mol.kg^{-1} respectivement pour t = 4h30, 7h30, 24h.

Si l'on revient à la branche ascendante de la courbe W'_C, on constate qu'elle reste décalée par rapport à celle de W_C et qu'il en est de même pour la branche descendante, le début de la chute de concentration en CaO intervenant avec un retard de 1h environ.

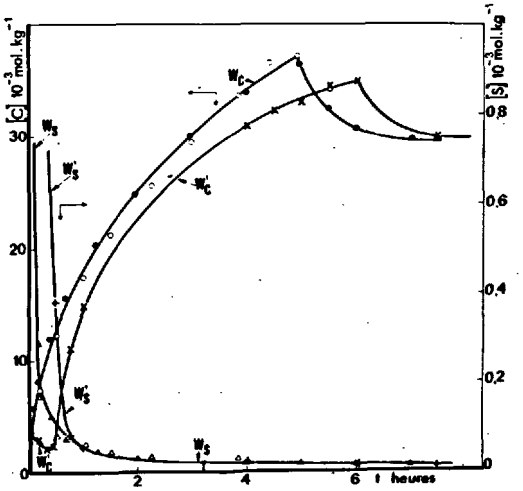

Fig. 2 - Courbes d'évolution de mélanges C_3S + eau (ℓ/s = 10). • Courbe W_C : [C] = f(t), ▲ courbe W_S : [S] = g(t) (D. Bertrandie, Réactivité des Solides, Dijon) ; o courbe W_C, Δ courbe W_S (D. Ménétrier, Martin Marietta Laboratories, Baltimore). Courbes d'évolution de mélanges C_3S + solution de composition $[C]^o$ = $1,75.10^{-3}$ mol.kg^{-1}, $[S]^o = 4,70.10^{-3}$ mol.kg^{-1}. x courbe W'_C ; + courbe W'_S (D. Bertrandie, Dijon).

De cette dernière expérience, est à rapprocher un essai effectué également avec un rapport $\ell/s = 10$, mais dans les conditions initiales suivantes (8) :

Exp. 6) $[C]^o = 34.10^{-3}$ mol.kg^{-1}, $[S]^o = 0{,}012.10^{-3}$ mol.kg^{-1}, c'est-à-dire en utilisant comme solvant le filtrat prélevé peu avant le maximum de W_c d'un essai antérieur à $\ell/s = 10$ avec de l'eau comme solvant.

La figure 3 présente la courbe W_c' obtenue comparée à la courbe W_c normale (avec l'eau) ainsi que, en pointillé, les courbes de variation concomitante du pourcentage d'eau liée déterminée par perte au feu.

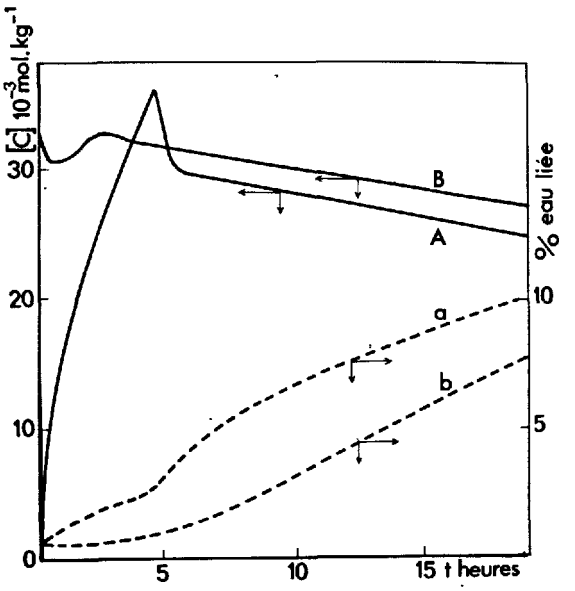

Fig. 3 - —— A et B : Courbes d'évolution W_c à $\ell/s = 10$ avec comme solvant ℓ : (exp. 4) de l'eau, (exp. 6) une solution à $[C]^o = 34.10^{-3}$ mol.kg^{-1}. - - - a) et b) Courbes de pourcentage d'eau liée correspondantes.

Il convient de noter une baisse initiale de [C] d'une amplitude de 2.10^{-3} mol.kg^{-1} environ, au début de la courbe W_c', puis à $t \simeq 30$ mn, une remontée ramenant [C] approximativement à sa valeur primitive, suivie à $t \simeq 4$h30 d'une décroissance continue.

La baisse initiale de [C] représente un retrait de 120 mg de CaO pour 100 g de C_3S. Quant au pourcentage d'eau liée, il est clair qu'il est très amoindri pendant les 4 ou 5 premières heures du cas b par rapport à la même période du cas a ; la masse d'eau liée est au maximum de 500 à 700 mg dans le cas b contre au moins 2000 mg dans le cas a et l'on doit constater que ce décalage se maintient dans la suite de l'évolution. La présence de C-S-H reconnaissables à leur morphologie en nid d'abeilles est facilement détectée par microscopie électronique à balayage durant cette période, au bout d'une heure par exemple dans le cas a, mais non dans le cas b.

Des expériences du type $s/f + \ell$ en système ouvert, $\ell + \ell$ initial + B en système fermé et $(\ell + \ell)/f$ + B en système fermé apportent des résultats complémentaires très intéressants (8). Les essais du premier type (exp. 7) consistent à faire passer à travers une couche de 20 g de C_3S étalée sur filtre, 14 l d'une solution de composition : $[C]^o = 3{,}80.10^{-3}$ mol.kg^{-1}, $[S]^o = 1{,}17.10^{-3}$ mol.kg^{-1} avec un débit de 1 l.mn^{-1}.

La composition du filtrat est : $[C] = 4{,}03.10^{-3}$ mol.kg^{-1}, $[S] = 1{,}11.10^{-3}$ mol.kg^{-1} et le pourcentage d'eau liée 0,88 (figure 4) :

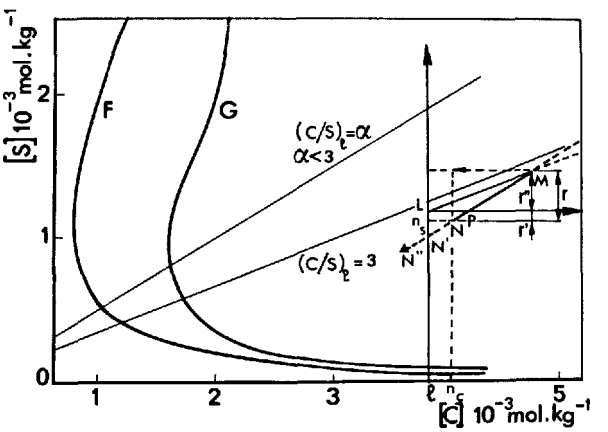

Fig. 4 - L point du diagramme C,S,H correspondant à la composition de la solution versée sur filtre à débit constant à travers une couche de C_3S. N : composition du filtrat. La construction graphique montre que la quantité de chaux et de silice transformées en C-S-H sont données par les projections du vecteur $\vec{NM}$; soit r la silice engagée dans le C-S-H : la partie $r' = -\Delta q$ provient de la silice préexistant en solution ; la partie r" de la silice provenant de C_3S. Une partie de la chaux complémentaire $(3 - \alpha)$ est utilisée entre P et N. Elle le serait totalement si N était en N' et de la chaux préexistante serait consommée si N était en N" (exp. 2 et 5).

Les essais du second type ont pour but d'étudier la cinétique d'évolution du mélange de deux solutions dont le titre était calculé de façon que la composition initiale du mélange appartienne soit au domaine s'étendant au-dessus et à droite de la courbe (I) (figure 5) dont la construction expérimentale est décrite dans de précédentes publications (8, 9, 10), par exemple (exp. 8) : $[C]^o = 6{,}47.10^{-3}$ mol.kg^{-1}, $[S]^o = 2{,}20.10^{-3}$ mol.kg^{-1}, soit à celui situé au-dessous et à gauche de cette courbe, par exemple (exp.9): $[C]^o = 3{,}0.10^{-3}$ mol.kg^{-1}, $[S]^o = 1{,}05.10^{-3}$ mol.kg^{-1}. Les courbes de variation de ces concentrations en fonction du temps sont reportées sur la figure 1 et les changements de composition correspondants sur le diagramme C,S,H (figure 5).

Sur cette dernière figure, ont été portés également les résultats des essais du 3ème type en système ouvert (exp. 10) : le mélange des deux solutions sur filtre a la composition théorique suivante : $[C]^o = 7{,}02.10^{-3}$ mol.kg^{-1}, $[S]^o = 2{,}20.10^{-3}$ mol.kg^{-1}, $[C/S]_\ell = 3{,}62$; celle du filtrat est : $[C] = 5{,}31.10^{-3}$ mol.kg^{-1}, $[S] = 1{,}47.10^{-3}$ mol.kg^{-1}, $[C/S]_\ell = 3{,}62$.

DISCUSSION

Pour faire apparaître les conséquences intéressantes de l'ensemble des résultats, il est utile, lorsque l'évolution en fonction du temps du système fermé est accompagnée d'un changement de composition de la phase liquide, de reporter sur le diagramme C,S,H les trajectoires du point représentatif de la composition. A chaque point de ces "chemins cinétiques", correspond une valeur du degré de sursaturation du

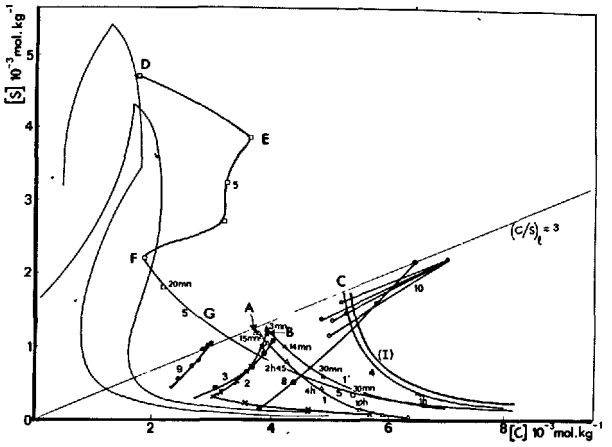

Fig. 5 - Report sur le diagramme C,S,H des changements de composition accompagnant l'évolution en fonction du temps dans les expériences 1, 2, 3, 4, 5, 8, 9, 10. Les trajectoires obtenues portent le même numéro que les expériences citées. (1' : W à $\ell/s = 100$).

milieu calculable, ou tout au moins évaluable, par rapport aux courbes d'équilibre de solubilité des C-S-H. Des indications peuvent également être tirées de la pente en chaque point de ces courbes.

Ainsi, sur le diagramme de la figure 5 la courbe 1) relie les valeurs au même instant de $[C]$ et $[S]$ des courbes W_C et W_S de l'expérience 1 à $\ell/s = 1000$. Avec cette dilution, la sursaturation en $Ca(OH)_2$ n'est jamais atteinte puisque 1 g de C_3S représente $4,30.10^{-3}$ mol.kg^{-1} soit 13.10^{-3} mol.kg^{-1} en CaO si tout passait en solution. Alors que $[C]$ est constamment croissante, $[S]$ passe par un maximum au bout de 15 mn ($[S] = 1,19.10^{-3}$ mol.kg^{-1}, $[C/S]_\ell = 3,12$) et commence à décroître au-delà de la 31ème minute. Du 13ème au 25ème jour, $[C]$ et $[S]$ se sont stabilisées respectivement à 6,32 et $0,040.10^{-3}$ mol.kg^{-1} sur la courbe d'équilibre de C-S-H. La formule du bilan (8, 9, 2) exprimant que toute la chaux (en solution et à l'état solide) est dans le même rapport avec toute la silice (en solution et à l'état solide) que dans C_3S, permet de calculer le nombre de millimoles r de silice engagées dans un C-S-H de rapport $[C/S]_S = \alpha$:

$$r = \frac{\beta q - 3q}{3 - \alpha} \qquad (1)$$

Dans cette relation, β est la valeur du rapport $[C/S]_\ell$ et q celle de la concentration $[S]$ de la silice en solution. En admettant que la totalité de C_3S ait été transformée, cela donnerait : $r = 4,35.10^{-3}$ mol. et compte tenu des valeurs ci-dessus de βq et q, la valeur moyenne de α serait : $\alpha = 1,57$.

En fait le C-S-H commence à être aisément détecté en microscopie électronique à balayage par son aspect en nid d'abeilles, au bout de 2 h (8,9). Il est remarquable de constater que la trajectoire sur le diagramme C,S,H est constituée du segment de la droite $[C/S] = 3$ allant de l'origine au point A et de la courbe (1) approximativement parallèle à la courbe (I) que nous avons définie expérimentalement (8, 9, 2) comme la limite entre la cinétique rapide et la cinétique lente de nucléation des C-S-H. A titre indicatif, la courbe 1'), obtenue avec $\ell/s = 100$ est légèrement décalée en direction de (I) donc, dans un domaine un peu plus sursaturé.

Si à la trajectoire 1), nous comparons la trajectoire 2) (exp. 2), la partie OA ne doit pas être prise en compte puisque la solution a, au départ, la composition correspondant au point B. Ce qui prévaut, c'est la décroissance de $[C]$ en même temps que celle de $[S]$, à peu près parallèlement à $[C/S]_\ell = 1$, jusqu'à t = 20h; au-delà, $[C]$ commence à croître pour atteindre $5,7.10^{-3}$ mol.kg^{-1} au 20ème jour alors que $[S]$ continue à décroître jusqu'à $0,07.10^{-3}$ mol.kg^{-1}. Le début de la courbe 2) rappelle ainsi les courbes telles que 3) 8) 9) 10) qui sont des trajectoires correspondant aux courbes de type B des expériences de même numéro d'ordre, c'est-à dire de solutions de rapport $[C/S]^0 = \beta^0$ dont S et C consommées ne sont pas renouvelées par dissolution de C_3S. En outre, leur tangente en chaque point est parallèle à la droite de $[C/S]_S = \alpha$ du C-S-H précipité. Dans le cas de l'expérience 2) en présence de C_3S, celui-ci peut bien se dissoudre pour renouveler C et S, mais l'expérience montre que le C-S-H qui se forme consomme non seulement toute cette silice et la chaux correspondante dans le rapport α, mais aussi la chaux complémentaire $(3 - \alpha)$, plus une partie de la chaux préexistante, (figure 4) puisque $[C] \leq [C]^0$. *Cela implique que le processus de précipitation est au moins aussi rapide que tout autre processus de formation du C-S-H, notamment topochimique, qui pourrait intervenir avec C_3S.*

Considérons à présent les expériences 4 et 5 à $\ell/s = 10$. Il apparaît une très grande simulitude avec les expériences 1 et 2 à $\ell/s = 1000$ lorsque l'on considère les trajectoires correspondantes sur le diagramme C,S,H (figure 5). Avec l'eau comme solvant (exp. 4), la branche OC est initialement parcourue, puis la branche 4) se développe aussi parallèlement à la courbe (I) mais beaucoup plus près d'elle, dans un domaine plus fortement sursaturé que pour la courbe 1). Cela est explicable par la plus grande densité de grains dans le liquide permettant une compensation plus rapide de S et C consommées. La seule différence avec le cas à $\ell/s = 1000$ est qu'ici le rapport ℓ/s est assez petit pour que la sursaturation en chaux soit possible. Lorsque celle-ci est suffisante pour que s'amorce la nucléation de $Ca(OH)_2$, l'accumulation de ce constituant en solution cesse et un état quasi stationnaire du système entre dissolution et précipitation permet à $[C]$ de ne décroître que très lentement vers la saturation.

La détermination expérimentale de $[S]$ que nous avons faite montre que même à la plus forte sursaturation en chaux, la silice reste dosable, avec $[S] \geq 0,018.10^{-3}$ mol.kg^{-1}. Il convient de remarquer que la formule du bilan (1) permet de calculer de façon simplifiée dès lors que $q << \beta q$ le nombre r de millimoles de silice transformée en CSH de rapport $[C/S]_S = \alpha$. A α constant, r est donc proportionnel à βq, par exemple si $\alpha = 2$, $r = \beta q$ et la branche ascendante de W_C (figure 2) représente aussi l'accroissement en fonction du temps du nombre de millimoles de silice transformées en CSH. La tangente en un point de cette courbe renseigne donc sur la vitesse au temps t de formation des C-S-H. Ceci n'est plus valable naturellement après le maximum de W_C lorsque la précipitation de portlandite s'est amorcée. On voit que la vitesse de formation de CSH diminue, mais pas considérablement, lorsque $[C]$ croît.

En ce qui concerne l'expérience 5, elle diffère de l'expérience 2, hormis la valeur de ℓ/s, par la forte valeur de $[S]^0$ par rapport à $[C]^0$, de sorte que la trajectoire sur le diagramme C,S,H (figure 5) ne comporte pas de branche OC, mais commence en D qui est

pratiquement sur la courbe d'équilibre. Il n'est donc pas étonnant que, dans un premier stade (branche DE) le processus de dissolution de C_3S avec formation de CSH soit le plus rapide et contribue à accroître [C] et à abaisser [S]. Mais de ce fait, le degré de sursaturation créé incite à précipiter en C-S-H, avec la silice préexistante, non seulement le reliquat de chaux (3 - α) non engagé dans un C-S-H, provenant de la dissolution de C_3S, mais aussi une fraction de la chaux préexistante et accumulée. Il est donc manifeste que ce processus est plus rapide que la formation de CSH aux dépens de C_3S quel que soit son mécanisme (topochimique ou non) et ramène le point figuratif vers la courbe d'équilibre en F ce qui correspond au minimum de W'_C (figure 2) et à l'élimination de pratiquement toute la silice préexistante. On observe alors une discontinuité des vitesses avec une brusque remontée de [C] suivant une branche W'_C parallèle à W_C alors que W'_S rejoint W_S et se confond avec elle. Il en résulte une situation de la branche FG de la trajectoire sur le diagramme C,S,H (figure 5) dans la partie beaucoup moins sursaturée du domaine à gauche de (I). Au cours de la partie DEF de la trajectoire, 16/(3 - α) millimoles de silice dont les 4,39 millimoles préexistantes sont rentrées dans le C-S-H et comme cela ramène au début de la branche ascendante W'_C, cet excédent se conserve aux instants ultérieurs par rapport à la courbe normale W_C. Comme dans l'expérience 2, *il est donc manifeste que le processus de précipitation de C-S-H à partir de l'excédent de silice en solution est au moins aussi rapide que la formation de C-S-H à partir de C_3S et qu'il ne laisse pas plus de silice dans la phase liquide.*

La conclusion la plus simple que l'on peut en tirer est *que les deux processus sont identiques c'est-à-dire que la formation de C-S-H à partir de C_3S est aussi le résultat d'un processus de précipitation.*

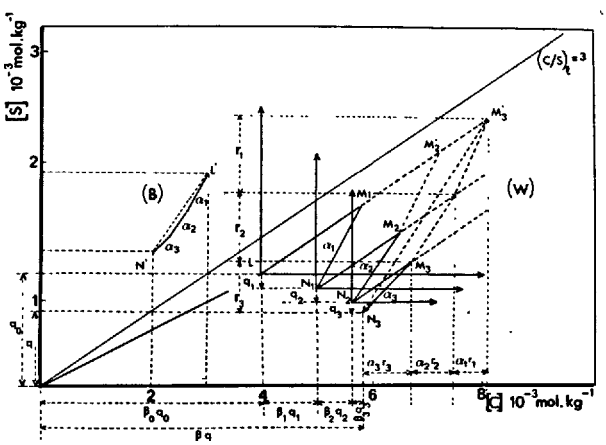

Fig. 6 - Constructions graphiques illustrant dans le cas B et le cas W, les formules de bilan (2) et (3) correspondantes et rendant compte des "chemins cinétiques" sur le diagramme C-S-H.

Les trajectoires du point N représentatif de la composition sur le diagramme C,S,H peuvent être analysées à l'aide de constructions qui transcrivent graphiquement les formules de bilan dans les cas B et W.

La composition initiale de la solution est dans les deux cas : $[C]^o = \beta_o q_o$, $[S]^o = q_o$ (points L et L") ; $[C] = \beta q$, $[S] = q$ est la composition finale dans le cas B (point N') et la composition au temps t de la solution agitée avec C_3S dans le cas W ; α_1, α_2..α_i sont les $[C/S]_S$ du C-S-H, r_i les quantités correspondantes de silice fixées dans le C-S-H ; les coordonnées $\beta_i q_i$, sont exprimées par rapport aux axes d'origines L, N_1, N_2 .., N_i.., (figure 6). Les expressions du bilan s'écrivent alors :

Cas B : (relation 2)

$$\frac{\beta q + \sum_i \alpha_i r_i}{q + \sum_i r_i} = \beta_o$$

Cas W : (relation 3)

$$\frac{\sum_i \beta_i q_i + \sum_i \alpha_i r_i}{\sum_i q_i + \sum_i r_i} = 3$$

avec : $\sum_i \beta_i q_i = \beta q - \beta_o q_o$ et $\sum_i q_i = q - q_o$

CONCLUSIONS

Les "chemins cinétiques" tracés sur le diagramme C,S,H à partir des essais de types B et W sont instructifs, du fait qu'ils se situent tous dans le domaine sursaturé compris entre la courbe I dont l'origine cinétique (nucléation très rapide des C-S-H) est bien illustrée par la comparaison des expériences 8) et 10) et la courbe de solubilité du C-S-H. Cela suggère l'unicité du mécanisme : la formation du C-S-H par précipitation.

Remerciements

Ces travaux ont été faits en coopération avec la Société Lafarge à laquelle nous exprimons notre gratitude.

BIBLIOGRAPHIE

1.- P. BARRET, D. MENETRIER et D. BERTRANDIE (1977), "Cinétique d'hydratation des aluminates et silicates de calcium", Rev. int. Htes Temp. et Réfract., t 14, 127-133.

2.- P. BARRET and D. MENETRIER (1980), "Filter dissolution of C_3S as a function of the lime concentration", Cem. and Concr. Res. (à paraître).

3.- P. BARRET et Ph. DUFOUR (1978), "Sur l'existence d'un stade d'hydratation superficielle dans le processus de dissolution de CA", C.R. Acad. Sc. Paris, t 286, C, 569-571.

4.- P. BARRET (1979), "Sur l'existence d'un stade d'hydroxylation superficielle dans le processus de dissolution de C_3S", C.R. Acad. Sc. Paris, t 288, C, 461-464.

5.- P. BARRET, D. MENETRIER et D. BERTRANDIE (1974), "Contribution of the study of the kinetic mechanism of aluminous cement setting", Cem. and Concr. Res., vol. 4, 545-556.

6.- A. ZELWER (1973), "Etude électrochimique de la phase aqueuse interstitielle au cours de l'hydratation de C_3S", Rev. Mat. Constr., n° 681.

7.- J.F. YOUNG, H.S. TONG and R.L. BERGER (1977), "Composition of solutions in contact with hydrating C_3S pastes", J. Am. Ceram. Soc., 60, n° 5-6, 193-198.

8.- D. MENETRIER (1977), "Contribution à l'étude cinétique de la période initiale d'hydratation de C_3S", Thèse Doct. d'Etat, Univ. de Dijon (France).

9.- P. BARRET (1979), "Les mécanismes d'hydratation et de durcissement des ciments", l'Industrie Nationale, n° 1, 3-41.

Mécanismes réactionnels de l'hydratation

Mechanisms of hydration reactions

C. VERNET, E. DEMOULIAN, P. GOURDIN, F. HAWTHORN, Société des Ciments Français, CEREG, France.

RESUME

Dans le but de comparer les vitesses de réaction des ciments dans des conditions standard, les auteurs ont réalisé un appareillage permettant de mesurer en continu les flux ioniques pendant l'hydratation. Les courbes obtenues démontrent l'existence d'un mécanisme de dissolution-cristallisation du type proposé par LE CHATELIER.
Pour évaluer la contribution de ce mécanisme relativement à tout autre susceptible d'agir simultanément, ils ont réalisé des mesures de vitesse de précipitation des CSH, dont les résultats montrent la prépondérance du mécanisme de LE CHATELIER.

Ils décrivent ensuite les différentes étapes de l'hydratation, en montrant que, dans ses conséquences, le mécanisme de LE CHATELIER n'est pas en contradiction avec l'ensemble des observations connues.

Ils présentent enfin un modèle mathématique de la cinétique d'hydratation, basé sur ce mécanisme et permettant d'expliquer les influences observables des autres réactions chimiques sur la vitesse de l'hydratation. Les applications pratiques de ce modèle s'étendront à l'étude de l'influence des adjuvants et des ajouts du ciment, ainsi qu'à la mesure physique de l'hydraulicité des clinkers.

SUMMARY

In order to compare the reaction speeds of the cements in standard conditions, the authors have constructed an apparatus which measures continuously the ionic fluxes during the hydration. The curves obtained show the existence of a dissolution-crystallization mechanism as proposed by LE CHATELIER.

For estimating the rôle of this mechanism in hydration, the authors have determined the CSH precipitation speed. The results demonstrate the preponderance of the LE CHATELIER mechanism over all the others put forward.

They also describe four hydration periods and show the agreement of the proposed mechanism with all the known data.

Finally on the basis of this mechanism, they give a mathematical model of the hydration kinetics, which can be applied successfully in the presence of other chemical reactions during hydration. In practice, this model will be used for the study of admixtures and adds in cement, and also for the physical evaluation of clinker hydraulicity.

INTRODUCTION

Pendant l'hydratation de l'alite on distingue quatre périodes :
- 1ère période : réaction rapide et exothermique, débutant par une chimisorption d'eau (1) ;
- 2ème période dite "période dormante" : lente, presque athermique, avec sursaturation progressive en chaux de la solution, sans modifications rhéologiques ;
- 3ème période caractérisée par la précipitation de la portlandite, l'accélaration brutale des réactions, l'augmentation du flux thermique ;
- 4ème période : ralentissement progressif des réactions. Dans le cas des ciments portland, les réactions secondaires des aluminates, aluminoferrites et du gypse se produisent, sans modifier la séquence ci-dessus.

Malgré de très nombreuses publications, les mécanismes réactionnels des ciments portland restent mal connus : on trouve dans la bibliographie des théories différentes, que l'on peut classer en 3 groupes :
- théories du type "LE CHATELIER" basées sur l'hypothèse de la dissolution congruente de l'alite et la cristallisation d'hydrates, de rapports CaO/SiO_2 (C/S) plus faibles (7) ;
-théories du type "topochimique" basées sur l'action directe de l'eau entrant dans le réseau de l'alite, avec formation d'hydrates in situ, par réorganisation structurale et libération de la chaux excédentaire par diffusion ;
- théories mixtes, combinant les deux précédentes en leur attribuant plus ou moins d'importance.

Du point de vue cinétique, l'approche des phénomènes est différente selon l'hypothèse de départ :
. dans l'hypothèse "topochimique", le flux de chaux libérée dépend de l'énergie libérable par l'alite et de la stoechiométrie des CSH. Il ne peut exister aucun flux de silice vers la solution. La concentration en SiO_2 est alors régie par la solubilité de l'hydrate le plus externe, la mesure du flux de CaO et du C/S du CSH permet d'accéder directement à la vitesse d'hydrolyse de l'alite ;
. dans l'hypothèse de LE CHATELIER, le flux de silice libérée est la différence des flux de dissolution et de précipitation et la solution est d'autant plus sursaturée que cette différence est grande. Pour obtenir la vitesse de réaction de l'alite, il faut donc mesurer par ailleurs la vitesse de précipitation, en calculer le flux, pour le déduire du flux mesuré : on obtient ainsi la vitesse de dissolution.

Sans préjuger de la validité de telle ou telle hypothèse, nous avons effectué des mesures précises de flux ioniques, afin de comparer les vitesses de réaction des ciments dans des conditions standard et de rechercher des éclaircissements sur les mécanismes réactionnels. Nos essais ont été effectués : d'une part à l'aide d'un appareillage de lixiviation spécialement étudié, permettant d'extraire en permanence une partie des ions libérés par le système ciment-eau, ce qui rend possible la mesure du flux de silice (système ouvert) d'autre part, en vase clos (système fermé) pour étudier la cinétique de précipitation des CSH.

1 - MESURES EN SYSTEME OUVERT

1.1 - Appareillage (fig.1)

Principe : Une suspension de ciment dans une solution à choisir est agitée dans le réacteur (R) dans lequel circule la solution de lixiviation, pompée à travers le filtre micropore en téflon (F), puis injectée dans un circuit comportant une série de capteurs ioniques. Le filtrat est, soit recyclé, soit recueilli et dosé séquentiellement. Ce montage, réalisé au début de 1977 diffère de celui qu'ont publié BARRET et MENETRIER en 1978, par son degré poussé d'automatisme et l'utilisation de capteurs électrochimiques, dans le but de mesurer en continu les flux ioniques et non pas de faire des bilans en fin d'essai.

Equations de fonctionnement du réacteur : Soient
m : la masse de ciment en suspension,
s : la surface spécifique du ciment (m^2/g),
S : la surface totale du ciment (m^2), S' = dS/dt
Q_Λ : la quantité en mMoles d'un ion libéré,
Φ_Λ : le flux résultant (en mM/m^2),
I_Λ : Intensité résultante de libération (en mM/mn),
Δ_Λ : flux instantané (en $mM/m^2.mn$), = $d\phi_\Lambda/dt$
C_ℓ : concentration du réactif de lixiviation (mM/l),
C : concentration à la sortie du réacteur (en mM/l),
h : débit de lixiviation (ml/mn),
V : volume total du filtrat (en ml),
v : volume du réacteur (en ml).

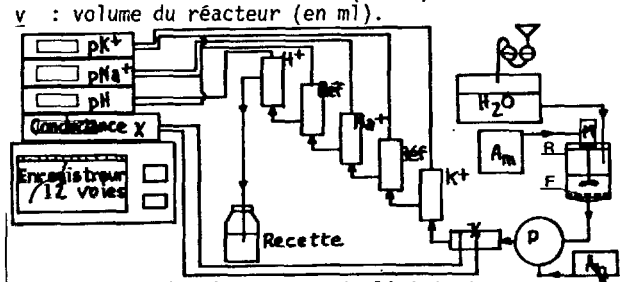

Fig. 1- Montage de lixiviation avec capteurs électrochimiques.

L'équation générale du réacteur s'écrit :

$$10^3 I_\Lambda = v\frac{dC}{dt} + h(C - C_\ell) \quad [I]$$

or $I_\Lambda = \frac{Sd\phi}{dt} + \phi\frac{dS}{dt} = S\Delta_\Lambda + \phi S'$

d'où le flux résultant :

$$\Delta_\Lambda = \frac{10^{-3}}{S} v\frac{dC}{dt} + h(C - C_\ell) - \phi\frac{S'}{S} \quad [II]$$

Dans le cas particulier d'une lixiviation par l'eau avec une surface sensiblement constante s_o:

$$10^3 I_\Lambda = v\frac{dC}{dt} + hC = 10^3 m_o s_o \Delta_\Lambda \quad [III]$$

Dans le cas de la dissolution-précipitation, le flux de dissolution sera obtenu en faisant la différence :
$a\Delta_d = \Delta_\Lambda - b\Delta_p$ (où a et b sont des coefficients stoechiométriques de C_3S et CSH),
des flux résultant et de précipitation.
Si dX/dt est la vitesse de précipitation (en mM/l.mn)

$$b\Delta_p = \frac{bv}{1000}\frac{1}{S}\frac{dX}{dt}$$

La formule III se ramène alors à :

$$10^3 a\Delta_d = \frac{v}{m_o s_o}\left(\frac{dC}{dt} - b\frac{dX}{dt}\right) + \frac{h}{m_o s_o} C \quad [IV]$$

Le terme $v\frac{dC}{dt}$ traduit l'existence d'une constante de temps du montage : on prendra donc le volume v du réacteur suffisamment faible si l'on veut rendre la concentration C proportionnelle à l'intensité I_Λ.
Dans le cas d'un flux Δ constant, on voit que l'expression de C sera très simple :

$$C(t) = \frac{m}{v}\Delta s_o\, 10^3 (1 - \exp.-\frac{ht}{v}) \quad [V]$$

$t \to +\infty \quad C \to c_\infty = 10^3 \frac{m}{h} s_o$

$t \to 0 \quad \frac{dC}{dt} \to 10^3 \frac{m}{v}\Delta s_o$

ce qui montre bien l'influence des rapports $\frac{m}{v}$ et $\frac{h}{v}$ sur la concentration C.
La constante de temps est ici $\frac{v}{h}$ (mn)
Pour h = 0, c'est-à-dire en système fermé,

$$I_\Lambda = 10^{-3} v\frac{dC}{dt} \quad [VI]$$

le flux peut alors être obtenu par dérivation de la courbe de concentration.

1.2 - Mesures

Les précautions suivantes ont été prises pour que nos mesures soient significatives :
- asservissement électronique du débit de lixiviation,
- commande électronique de l'agitation,
- contrôle de la réponse des capteurs par analyse chimique séquentielle du filtrat,
- dans le domaine des traces, prise en compte uniquement des résultats d'analyse supérieurs au triple de l'incertitude,
- thermostatisation à 25°C.

Vingt-deux essais ont été réalisés dans diverses conditions opératoires (rapport m/v, débit, agitation) pour une alite de synthèse et un clinker industriel. Le réactif de lixiviation étant, soit de l'eau, soit de la chaux saturée, soit un mélange chaux + gypse, ce qui permet de se placer dans des conditions très proches de l'hydratation des pâtes de ciment.

Nous avons tracé les courbes d'évolution des concentrations et calculé les flux ioniques correspondants, à l'aide des formules du réacteur.

En reportant les valeurs des concentrations instantanées dans le diagramme d'équilibre CaO, SiO_2, H_2O, nous avons tracé le trajet du point figuratif (F) de la solution, pendant la réaction. Peu de chercheurs ayant calculé la courbe de solubilité des CSH en tenant compte à la fois des équilibres entre $H_2SiO_4^{--}$, $H_3SiO_4^-$, Ca^{++} et $CaOH^+$ et de la force ionique, nous avons donc calculé un nouvel abaque donnant une série de courbes d'équilibre avec OH^- comme paramètre.

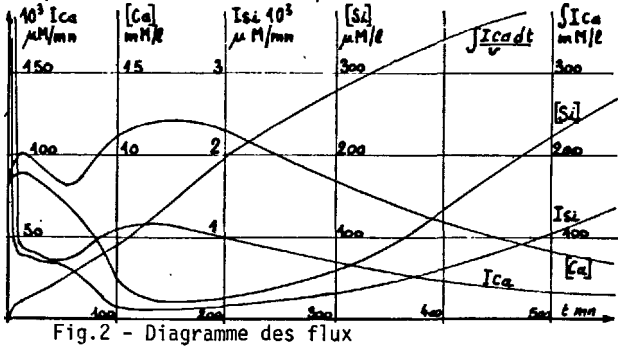

Fig.2 - Diagramme des flux

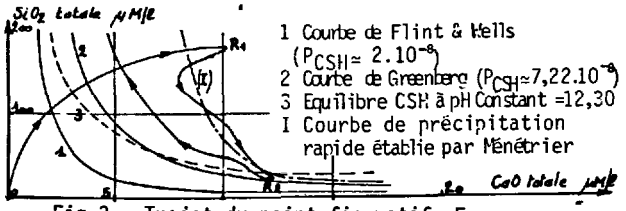

Fig.3 - Trajet du point figuratif F

1.3 - Résultats - Description des phénomènes

L'ensemble des essais donne des courbes analogues à celles de l'exemple (fig.2 et 3). On distingue toujours 3 étapes dans le mécanisme, chacune comportant une cinétique particulière :

1ère étape : (Trajet OR_1 sur le diagramme)
Le point figuratif F se déplace très rapidement et entre dans le domaine sursaturé. Pour les ciments, le C/S de départ est très supérieur à 3 (présence des phases mineures solubles). Pour l'alite, le point F s'éloigne rapidement de l'axe C/S = 3, dont il est d'autant plus proche au départ que le débit et le rapport v/m sont élevés.
En quelques minutes, F atteint donc le point de rebroussement R_1, où le taux de sursaturation prend sa valeur maximum. Simultanément, les flux de silice et de calcium atteignent une valeur très basse.

2ème étape : (Trajet R_1R_2 sur le diagramme)
Le trajet de F s'incurve de manière à s'approcher tangentiellement de la courbe (1) établie par MENETRIER par une méthode différente (2). Le flux de calcium augmente jusqu'à un maximum et le flux de silice diminue jusqu'à un minimum lorsque F atteint le point R_2, proche de la courbe d'équilibre.

3ème étape :
Le point F remonte selon une courbe voisine de la courbe d'équilibre, située dans le domaine sursaturé. Pendant tout le trajet, on observe alors l'existence d'un "produit de solubilité apparent" $P_{CSH} = a_{Ca^{++}}.aH_2SiO_4^{--}$ traduisant un taux de sursaturation pratiquement constant. Dans un seul cas sur 22, où le débit de lixiviation et le rapport v/m étaient élevés, le trajet de F passe dans le sous-saturé, au cours de cette 3ème étape. Dans tous les autres cas, au bout d'un temps suffisamment long, P_{CSH} tend vers une limite commune à chaque essai, un peu supérieure à la valeur d'équilibre pour le CSH précipité ($1{,}3.10^{-7}$) au lieu de ($7{,}22.10^{-8}$).
Ce schéma se répète également lorsqu'on utilise des solutions de chaux ou chaux + gypse : les étapes sont alors parcourues plus rapidement et les flux ioniques plus faibles qu'avec l'eau. Le point R_2 est situé plus bas, ce qui indique une solubilité plus faible des hydrates. Les dosages de SiO_2 deviennent rapidement difficiles. Dans la 3ème étape, la concentration en chaux tend vers celle de la solution de lixiviation.

1.4 - Interprétations

Le niveau de sursaturation en CSH, maintenu malgré la dilution permanente par l'eau de lixiviation, la chute brutale, dès le départ, des flux de silice et de calcium, dans l'étape 1, le trajet suivi par le point F le long de la courbe (1), entre R_1 et R_2, tout cela ne peut s'expliquer selon le mécanisme topochimique seul. Il faut donc admettre qu'il y a une contribution du mécanisme de LE CHATELIER à la réaction. Le trajet R_1R_2 soit, en moyenne, la courbe I, apparait alors comme la résultante d'une famille de trajets instantanés que l'on peut représenter vectoriellement sur le diagramme chaux-silice-eau (fig.4).

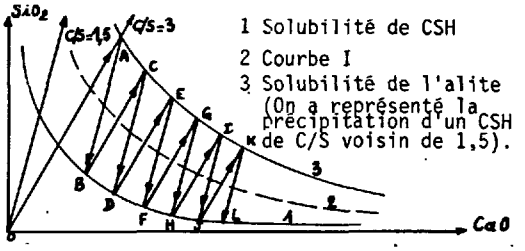

Fig.4 - Diagramme chaux-silice-eau

Vecteurs OA, BS, DE, FG ... dissolution congruente
Vecteurs AB, CD, EF, GH, IJ ... précipitation de CSH.
La forme de ce trajet implique l'existence pour l'alite d'un produit de solubilité, ce que BARRET (3) a montré par des considérations thermodynamiques.
La diminution du flux de calcium dans la 3ème étape peut s'expliquer par l'évolution de la surface spécifique (état stationnaire final avec concentration proportionnelle à la surface S). L'allure nettement diffusionnelle observée nous a cependant conduit à étudier la vitesse de précipitation des CSH et leur composition afin d'évaluer la part d'un éventuel mécanisme topochimique coexistant avec le mécanisme de LE CHATELIER (§2.1)

1.5 - Phénomènes secondaires - Réactions entre phases

Ayant observé des taux de réaction anormalement bas pour le C_3A lors des lixiviations par l'eau, nous avons dosé l'aluminium dans les filtrats pour plusieurs essais : l'hydratation du C_3A, dont la période rapide se traduit par une augmentation du flux d'ions AlO_2^-, ne commence que lorsque la concentration en SiO_2 a atteint une valeur suffisamment basse, en fin de 1ère étape de l'hydratation de l'alite. Ceci est en parfaite concordance avec l'existence de silico-aluminates mis en évidence par Mme.REGOURD (4) autour des grains de C_3A, et empêchant son hydratation.

2 - MESURES EN SYSTEME FERME

2.1 - Cinétique de précipitation des CSH

Ayant confirmé l'existence réelle du mécanisme de LE CHATELIER, il reste à voir son importance par rapport à un éventuel 2ème mécanisme simultané : nous avons donc cherché à mesurer la vitesse de précipitation des CSH dans divers domaines de sursaturation. En utilisant des solutions pures de chaux et de silice, nous avons effectué 15 essais en plusieurs étapes permettant de suivre l'évolution de la composition chimique de la solution et du CSH précipité. L'ensemble des opérations a été conduit sous atmosphère d'azote. Les précipités de CSH ont été lyophilisés. Les vitesses de précipitation initiales ont été mesurées par conductimétrie et analyse chimique.

Résultats

Les vitesses observées sont très élevées. Elles augmentent avec les concentrations initiales en chaux et en silice, en suivant approximativement la relation :

$$-\left(\frac{dC}{dt}\right)_i = k\,(C_i)^{1,5}\,(S_i)$$

Les vitesses initiales sont donc proportionnelles au taux de sursaturation.

La courbe (I) correspondrait, d'après nos essais à des vitesses initiales de précipitation voisines de 4 mM/l.mn.

Ce chiffre nous donne un flux de précipitation extrêmement voisin du flux de dissolution, d'où la faiblesse de la concentration en SiO_2 en solution. La contribution du mécanisme de LE CHATELIER est donc très importante par rapport à tout autre mécanisme.

L'application de la formule IV du § 2.1 nous conduit à un flux maximum de dissolution de 58 $\mu M/m^2.mn$, au maximum de l'exemple, résultat extrêmement voisin de celui de MENETRIER (2) obtenu par des méthodes différentes (60 $\mu M/m^2.mn$).

Aux alentours de la courbe (I), la précipitation est limitée par la diffusion et on vérifie avec une bonne approximation la relation :

$$-\frac{d(SiO_2)}{dt} = 3,5\,[(SiO_2) - (SiO_2)^*]$$

où SiO_2^* est la teneur à la saturation.

Cette relation permet de calculer la loi de variation de la distance d parcourue par les ions silicate, depuis l'interface réactionnelle jusqu'au site de précipitation. On obtient :

$$d = \frac{v}{3,5}\,\mathrm{Ln}\,\frac{(X_0 - X^*)}{(X_d - X^*)}$$

où v = volume de solution ; X_d = concentration en SiO_2 à la distance d ; X^* = concentration à la saturation ; X_0 = concentration à l'interface

Le rapport $\pi = \frac{X_d - X^*}{X_0 - X^*}$ représente la fraction non précipitée à la distance d, la précipitation étant totale lorsque $X_d = X^*$. La fraction précipitée est donc $(1 - \pi)$, fonction que nous avons représentée (fig.5) pour les conditions opératoires utilisées.

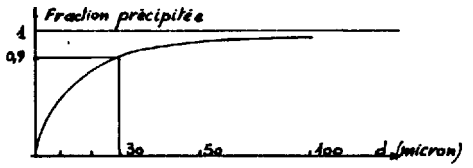

Fig.5 - Relation (1-r) = f(d)

En conclusion, la vitesse de précipitation est suffisamment grande pour que la majeure partie des CSH se forme à une très faible distance des grains, de l'ordre de l'épaisseur de la couche de diffusion, une faible proportion d'hydrates peut cependant se former à distance plus grande, à une vitesse plus faible, là où la solution est moins sursaturée.

On peut s'attendre à une différence de structure et de composition entre ces hydrates, formés dans des zones où les concentrations sont très différentes. En effet, nos résultats montrent bien la croissance du C/S avec les concentrations (le C/S varie linéairement entre 1,25 et 2 lorsque la teneur en chaux passe de 5 à 20 mM/l).

2.2 - Courbes de WELLS - Relation avec les courbes de lixiviation

Les courbes d'évolution ionique des suspensions de ciment en fonction du temps sont souvent appelées courbes de WELLS. Elles présentent des points remarquables bien connus (fig.6).

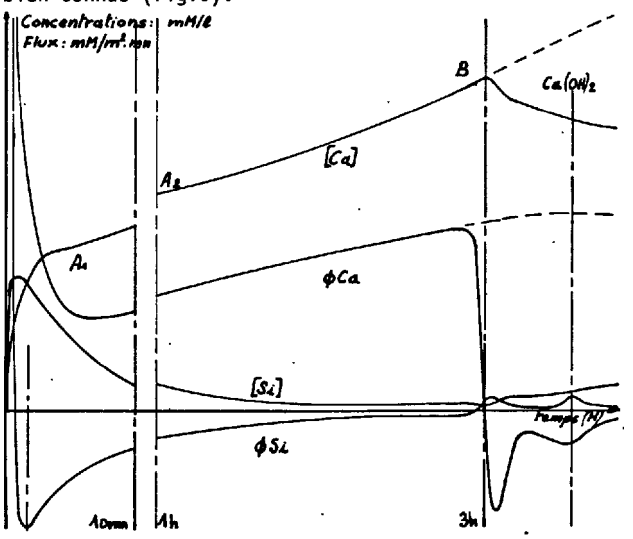

Fig.6 - Diagramme des flux en système fermé

A_1 = fin de dissolution rapide
A_1A_2 = faible flux de calcium
A_2B = "période dormante"
B = maximum de saturation (36 mM/l Ca) début de précipitation de $Ca(OH)_2$

B_c = période de réaction rapide donnant lieu à la prise lorsque E/C est suffisamment bas.

Dans le cas des ciments, des points singuliers s'ajoutent à chaque apparition ou disparition d'une phase. Nous les avons étudiés par ailleurs (5).

Pendant la réaction en système fermé, le point figuratif F décrit un trajet parallèle à la courbe (I) à une distance dépendant du rapport v/m.

Lorsque l'on compare les diagrammes en système fermé et en système ouvert, on constate que la courbe inté-

grale du flux de calcium (système ouvert) redonne bien une courbe homologue de la courbe de concentration en système fermé, à la différence près, qu'en système fermé, la précipitation de la portlandite interrompt l' augmentation de la teneur en chaux. Par contre, l'intégrale du flux de silice donne une courbe différente de celle du système fermé, où le flux de silice prend une valeur négative dès les premières secondes : cette allure, obtenue aussi pour les faibles débits de lixiviation, indique une vitesse de précipitation supérieure à la vitesse de dissolution. Pendant la période dormante, c'est donc la lenteur de la dissolution de l'alite qui freine la réaction : la vitesse de dissolution diminue avec la sursaturation en chaux tandis que la vitesse de précipitation n'évolue plus au bout de quelques minutes : on se rapproche donc de plus en plus de l'équilibre. Le taux de sursaturation en CSH diminue et si rien ne vient perturber le quasi-équilibre obtenu, le taux d'hydratation restera faible.

3 - CONSEQUENCES = MODE DE CROISSANCE DES CSH

L'ensemble de nos observations nous amène à décrire le mode de développement des CSH au cours de chaque étape de l'hydratation de la manière suivante :

1) Hydroxylation superficielle de l'alite. Dissolution congruente rapide et formation des premiers germes de CSH au voisinage des défauts de réseau, où la vitesse de dissolution est maximum. La distance de précipitation passe par un minimum ; la croissance de CSH est surtout superficielle.

2) La vitesse de précipitation diminue. La vitesse de dissolution diminue beaucoup plus vite. La croissance des CSH est de plus en plus verticale au fur et à mesure que la silice en solution diminue ($SiO_2 \rightarrow SiO_2^{\ddot{}}$). Le taux de réaction n'augmente pratiquement plus : c'est la "période dormante". Pendant cette période, les défauts de réseau ont fait place à des fissures d'où s'échappent les flux d'ions et les CSH, formés lentement, sont assez bien cristallisés. Leur C/S est relativement faible, car ils ont cristallisés dans une zone assez éloignée de l'interface, zone où la teneur en chaux est moins élevée.

3) La portlandite précipite, ce qui produit une brutale reprise de la dissolution de l'alite. La vitesse de précipitation de $Ca(OH)_2$ est plus faible que celle de CSH : elle cristallise en gros cristaux loin de l'interface. Le CSH est plus mal cristallisé et précipite plus vite et plus près de l'interface que précédemment : son C/S est plus élevé. Les fissures de l'alite s'agrandissent et forment des pores ouverts où le CSH cristallise. D'autres fissures les remplacent et fournissent des flux d'ions intenses : peu à peu la surface initiale est totalement remplacée par le CSH.

4) La réaction ralentit à nouveau, suite au recouvrement complet des grains d'alite par le CSH, laissant encore passer un faible flux d'ions. La vitesse de précipitation de $Ca(OH)_2$ diminue considérablement. La sursaturation en CSH diminue et la distance de précipitation augmente. La croissance du CSH se poursuit de plus en plus lentement selon un arrangement de type "corallien". Le C/S de ce CSH "externe" devient plus faible, sa structure est plus cristalline et il tend à combler les pores et à produire des ponts entre les grains, tandis que le mécanisme se poursuit (fig.7).

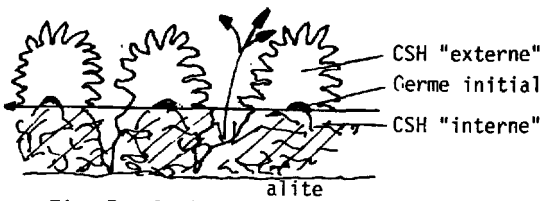

Fig. 7 - Croissance du CSH

4 - RECHERCHE D'UN MODELE MATHEMATIQUE DE LA CINETIQUE D'HYDRATATION

Après en avoir précisé les mécanismes, nous sommes maintenant en mesure de construire un modèle mathématique dont la forme sera adaptée à chaque étape de la réaction.

1ère étape : Dissolution congruente de l'alite avant le début de précipitation du CSH.
La précipitation du CSH ne peut intervenir qu'au moment où son produit de solubilité est atteint : le point figuratif de la solution se trouve alors à l'intersection de l'axe C/S = 3 et de la courbe de solubilité du CSH. L'alite va se dissoudre selon :

$$C_3S + 4H_2O \rightleftharpoons 3Ca^{++} + 5OH^- + H_3SiO_4^- \quad (pH < 12,7).$$

La vitesse de dissolution sera limitée seulement par la diffusion, selon une loi du type :

$$k_d = \frac{Dd}{e_d}(X_d^{\ddot{}} - X) = \frac{\Delta}{v} = \frac{1}{S}\cdot\frac{dX}{dt} \qquad IX$$

où k_d = vitesse de dissolution spécifique ($Ml^{-1}mn^{-1}m^{-2}$)
D_d = coefficient de diffusion de l'ion X($mn^{-1}m^{-1}$)
e_d = épaisseur de la zone de diffusion (m)
$X_d^{\ddot{}}$ = valeur de X à la saturation (M/l)
X = concentration de l'ion (M/l)
(Δ, S et v sont définis précédemment).
L'équation [IX] associée aux équations liant les concentrations permet de tirer

$$X = [B(1 - e^{-9At})]^{1/9} [X]$$

avec $A \# S\frac{Dd}{e_d} \simeq 4,2\ mn^{-1}$ $\quad B \# 9,61.10^{-21} = \frac{3P_{C_3S}}{5^5}$

on constate que la saturation en CSH, qui est obtenue au point F_1 du diagramme, où (CaO) = 1,88 mM/l, SiO_2 = 0,627 mM/l est atteinte quasi-instantanément ($t < 10^{-3}s$). Au delà de ce point, le rapport C/S de la solution sera alors de plus en plus supérieur à 3 (système fermé).

2ème étape : Au mécanisme de dissolution s'ajoute maintenant la précipitation dont la vitesse sera également limitée par la diffusion et suivra une loi du type

$$k_p = \frac{Dp}{e_p}(X - X_p) = \frac{1}{S'}\cdot\frac{dX}{dt}$$

(même terminologie que IX . Indices p et surface S' pour CSH).
La quantité dn_d d'alite dissoute pendant le temps dt va produire dn_p moles de CSH et dn_S moles de SiO_2 en solution. Posons X = (SiO_2) totale en solution
C = chaux totale et α = C/S du CSH.

$$dn_S = dn_d - dn_p = \frac{v}{1000}\frac{dX}{dt}$$

$$\frac{dX}{dt} = \frac{1000}{v}(dn_d - dn_p) = Sk_d - S'k_p$$

$$\frac{dX}{dt} = S\frac{D_d}{e_d}(X_d - X) - S'\frac{Dp}{e_p}(X - X_p) \qquad [XI]$$

De même que pour la chaux :

$$\frac{dC}{dt} = 3S\frac{D_d}{e_d}(X_d - X) - S'\alpha\frac{D_d}{e_p}(X - X_p) \qquad [XII]$$

En posant $A = S\frac{D_d}{e_d}$ $\quad B = S'\frac{D_p'}{e_p}$, on peut écrire l'équation [XI] sous la forme :

$$X = \frac{\frac{A}{B} X_d + X_p - \frac{1}{A+B} \cdot \frac{dX}{dt}}{\frac{A}{B} + 1}$$

qui montre bien que lorsque $A/B \to 0$ $X \to X_p$ et $A/B \to \infty$ $X \to X_d$
A/B étant le rapport des constantes de vitesse de dissolution et de précipitation.
On aura également :

$$\frac{dC}{dt} = 3 S \frac{D'_d}{e'_d} (C_d - C) - S'\alpha \frac{D'_d}{e'_d} (C - C_p) \quad [XIII]$$

où $D'_d D'_p$ sont les coefficients de diffusion pour Ca^{++}.
Pour chacune de ces relations différentielles, les conditions initiales sont définies par : $C_o = 3 X_o$, $X_o = X_p$. Théoriquement, X_p et X_d sont données par les lois des équilibres de CSH et C_3S, liant les constantes thermodynamiques et les concentrations :

$$X_d = \frac{P_{C_3S} \left(1 + \frac{KB}{(OH^-)}\right) \left(1 + \frac{(OH^-)}{K_3}\right)^3}{C^3 (OH^-)^5} \quad [XIV]$$

$$X_p = \frac{P_{CSH} [K_3 + (OH^-)] [K_B + (OH^-)]}{K_3 C (OH^-)} \quad [XV]$$

En pratique, on ne pourra définir un produit de solubilité théorique pour le CSH dont la composition est variable. On utilisera plutôt des relations expérimentales comme $X_p . C^{1,68} \# 10^{-7,69}$, obtenue avec une très bonne approximation. Ainsi, connaissant l'équation approchée du trajet du point figuratif : pour la courbe (I) $X.C^{4,62} \# 10^{-13,36}$, on débouche sur l'utilisation pratique du modèle (les valeurs de C_d et X_d peuvent être mesurées directement en fonction du pH).
Les formules ci-dessus montrent que toute réaction chimique consommant les ions calcium et OH^- va permettre d'augmenter la solubilité de l'alite : formation de complexes, que nous avons étudié par ailleurs (8) précipitations, dont le meilleur exemple est la précipitation de la portlandite.

3ème étape : Bien que manquant de données expérimentales sur la cinétique de précipitation de la portlandite permettant de compléter le modèle, on peut voir d'après les relations XIV et XV que la diminution de teneur en Ca^{++} et OH^- va augmenter plus rapidement X_d que X_p. Le système sera donc déplacé vers un nouvel état beaucoup plus sursaturé en CSH, où la vitesse de dissolution de l'alite est plus grande.
De même, en présence d'ajouts comme le laitier qui consomment de la chaux durant cette étape, l'équilibre de solubilité de l'alite sera déplacé, ce que nous avons étudié par ailleurs (6).

4ème étape : Pendant cette étape, les vitesses sont fortement diminuées par la diffusion à travers les hydrates et le calcium en solution est peu à peu remplacé par des alcalins, ce qui augmente le pH et freine encore la dissolution de l'alite (X_d diminue). Pour utiliser les relations précédentes, il reste à déterminer X_d, X_p et C, dans des milieux de composition chimique voisine.

CONCLUSION GENERALE

La méthode expérimentale indirecte par laquelle nous avons abordé le mécanisme de l'hydratation s'est révélée très fructueuse : les résultats obtenus démontrent la prépondérance du mécanisme de dissolution-cristallisation imaginé par LE CHATELIER.
Seul ce mécanisme permet en effet d'expliquer le comportement des concentrations pendant la réaction. Il explique également l'existence de la "période dormante" des ciments et les phénomènes de couplages chimiques entre les réactions d'hydratation des constituants des ciments, que nous avons observé ici, et étudié en détail par ailleurs (5). A ce titre, la précipitation de la portlandite apparait comme indispensable à la reprise de l'hydratation produisant la prise et permettant l'évolution des résistances. D'autre part, nos mesures montrent que la vitesse de précipitation est très élevée et qu'en conséquence, le CSH cristallise au voisinage immédiat de l'interface, à une distance variable selon le taux de sursaturation. Cette observation permet d'expliquer le mode de croissance particulier du CSH, selon une progression "corallienne".
Disposant d'une théorie globale cohérente reliant le comportement cinétique des ciments en système ouvert à celui en système fermé et en parfait accord avec toutes les observations connues, nous en avons tiré un modèle mathématique théorique possédant une véritable signification physique. L'application pratique de ce modèle permet actuellement de prévoir l'action de certaines variables chimiques sur la vitesse d'hydratation et d'expliquer ainsi, de manière qualitative, l'influence des constituants mineurs solubles,des adjuvants,et des anomalies de l'eau de gâchage.
Après avoir précisé par des mesures expérimentales les constantes de vitesse et les relations entre paramètres, cette théorie doit nous permettre de déterminer les caractéristiques intrinsèques de solubilité des ciments, dans des conditions à choisir. Ces caractéristiques, définissant de manière précise le terme d'hydraulicité pourront être reliées à des caractéristiques de structure et de forme allotropique des phases, établissant ainsi un lien entre l'histoire thermique du produit au cours de la cuisson et son histoire cinétique au cours de l'hydratation.

REMERCIEMENTS

Les auteurs remercient M. MAES, technicien au CEREG, pour sa contribution importante à l'étude, en ce qui concerne les analyses quantitatives en diffraction X.

BIBLIOGRAPHIE

1. - P.FIERENS, J.P.VERHAEGEN, Ind.Chim.Belge 39 - 363 (1974)
2. - D.MENETRIER - Thèse Univ. Dijon 1977/42
3. - P.BARRET, D.MENETRIER, D.BERTRANDIE - Rev. int. Htes. Temp. et Réfract. 1977, t 14, pp 127-133
4. - M.REGOURD, H. HORNAIN, B.MORTUREUX - Rev. Mat. Const. n° 687 -MArs-Avril 1974, pp.69-79
5. - C.VERNET, E.DEMOULIAN, P.GOURDIN, F.HAWTHORN - Cinétique de l'hydratation des ciments Portland VII^e Symp. Int. Chim. des ciments - Paris 1980
6. - C.VERNET, E.DEMOULIAN, P.GOURDIN, F.HAWTHORN Cinétique de l'hydratation des ciments de laitier VII^e Symp.Int.Chim.Ciments - Paris 1980
7. - H.LE CHATELIER - Recherches expérimentales sur la constitution des mortiers hydrauliques - Thèse Paris 1887
8. - E.DEMOULIAN, C.VERNET, F.HAWTHORN, P.GOURDIN - Détermination de la teneur en laitier dans les ciments par dissolutions sélectives - VII^e Symp. Int. Chim. des Ciments - Paris 1980

La régularité et la théorie d'hydratation des liants

Regularity and theory of binder hydration

V.V. KAPRANOV, docteur, chef de la chaire de la Construction, l'Institut Polytechnique de Tchéliabinsk, av. Lénine, 76, 454080, U.R.S.S.

RESUME: Cette communication est consacrée à l'étude de la nouvelle voie scientifique dans la recherche des processus d'hydratation. L'auteur a essayé de mettre en évidence la régularité et de donner la théorie mathématique d'hydratation se basant principalement sur la recherche des forces motrices intérieures et sur la direction énergétique des stades à part du processus. On développe les modèles physiques et mathématiques des stades à part du processus d'hydratation, on déduit les relations pour l'étude de l'interaction des particules des phases liquides et solides compte tenu de la structure, des tailles, des charges des ions et des autres propriétés physico-chimiques de la substances. La régularité de chaque processus élémentaire reflète la liaison des phénomènes d'hydratation avec les propriétés des substances avec l'abaissement ininterrompu du niveau de libre énérgie du système. La théorie d'hydratation permet de révéler le mécanisme du processus et de déterminer les traits particuliers du processus et les voies d'influence sur lui en changeant les paramètres du système. La théorie proposée montre les voies de perfectionnement de la technologie du ciment et du béton, la création des substances dont la structure est donnée avant. La coïncidence des caractéristiques de calcul du processus avec l'expérience confirme la régularité révélée.

Comme il est impossible de donner les calculs précis du système étudié, l'auteur propose de considérer les résultats obtenus comme la première approximation, dont la précision revendique la création des méthodes de calcul plus précises et l'obtention des données supplémentaires suivant la structure des substances, la distribution de la densité électronique etc.

SUMMARY : The paper is devoted to development of a new scientific trend dealing with research into hydration processes. An attempt has been made to reveal objective laws governing hydration and to elaborate a mathematic theory of the latter on a completely new basis - that of research into internal motive forces and power directivity of some phases of the process.

There have been worked out physical analogs and mathematical models of the hydration process. Formulas have been derived for investigation of interaction of liquid and solid particles in view of their structure, size, ionic charges, and other physical-and-chemical properties of substances.

Objective laws governing each elementary process reflect the connection between the phenomena occuring through hydration and basic properties of reacting substances as well as constant decrease in the free energy level of the system.

The elaborated hydration theory makes it possible not only to reveal the process mechanism but also to theoretically determine the process characteristics as well as the ways of influencing the process by change of specific parameters. The theory shows the means of improving cement and concrete technology as well as of creating materials with a preset structure. Good coincidence of the process design characteristics with experimental data proves the objectivity of the revealed laws and a sufficient reliability of the theory.

Accurate calculations for a very complex system under investigation being impossible, the results obtained should be regarded as the first approximation. To make it more accurate more perfect methods of calculation should be elaborated and additional data on the structure of substances, electronic density distribution and others should be obtained.

Il est à noter que le 7^{e} Congrès International sur la Chimie des Ciments se passe à Paris, où il y a cent ans Le Chatelier publia ses premiers travaux concernant la théorie de durcissement. (1,2). Il écrit: "Cette théorie peut encore expliquer la prise de tous les autres ciments et mastics, dont le durcissement ne résulte plus d'une simple hydratation, mais de la combinaison des différents corps déjà plus ou moins hydratés" (2,p.1056).

Dans la communication présente on donne les résultats des études sur le développement et le perfectionnement de la théorie de Le Chatelier et des travaux théoriques des autres savants (Brunauer, Mchedlov-Petrosyan, Sytchov, Polak etc). On se base sur les revendications modernes prévoyantsla direction de la réaction, sa régularité essentielle, la structure du liant et les voies d'influence sur le processus.

L'hydratation - c'est le processus de la liaison d'eau par des agents chimiques. En somme, la marche de n'importe quel processus chimique est causée par les interactions électromagnétiques entre les particules du système (les ions, les molécules).

Ainsi, la base méthodologique des études est la détermination théorique des forces motrices intérieures du processus et sa directions énergétique sur toutes les étapes: de l'adsorption à la formation de la structure.

La série des relations d'énergie d'interaction entre les particules du système était exposée au 6-e Congrès (3) et plus tard (4).

Au temps dernier on a réussi à calculer le processus d'hydratation du plâtre semi-hydraté et mettre en évidence sa régularité particulière, déduire la relation de la résistance théorique de la pâte de ciment etc. On donne ci-après les relations essentielles de calcul à l'aide desquelles on peut étudier le processus élémentaire d'hydratation des liants, la régularité et le mécanisme des stades à part.

L'adsorption des particules des phases liquides sur la surface du liant est le premier processus élémentaire d'hydratation. Pour calculer l'énergie d'interaction de l'ion (H^+, OH^-, les ions du soluté) avec le cristal on peut utiliser la relation déduite dans le travail (3) basée sur la méthode quantique.

Mais la relation

$$U = - \frac{q^2(\varepsilon_2 - \varepsilon_1)}{8\pi \varepsilon_o \varepsilon_1 (\varepsilon_2 + \varepsilon_1)\, r}, \quad (1)$$

est aussi valable, où

ε_o, ε_1 u ε_2 - constante diélectrique du vide par rapport à l'eau et au cristal, q - charge des ions de la phase liquide, r - distance entre le cristal et l'ion. On utilise également la relation déduite sur la base de l'équation de Borne

$$U = - \frac{0{,}728\, q_1 q_2}{4\pi \varepsilon_o \varepsilon_2} \sum \frac{N_i}{r_i}, \quad (2)$$

où N_i - quantité des ions du cristal (compte tenu de signe) disposés à la distance r_i de l'ion de la phase liquide. On a obtenu les relations analogiques pour le système molécule cristal-dipôle H_2O, de la molécule PAV.

L'analyse des relations montre que l'énergie de l'adsorption monte avec l'augmentation de la charge d'ion ou avec le moment dipôle de la molécule, de la constante diélectrique du cristal et avec la diminution de la constante diélectrique de l'eau. L'énergie d'adsorption d'ion dépasse celle-ci de la molécule. A partir de cette régularité le processus active d'adsorption sera la dissociation électrolytique de l'eau. L'effet d'écran PAV accroît avec l'augmentation du moment dipôle et avec la diminution des tailles des molécules PAV. Le calcul théorique de l'épaisseur de la couche diffusante aux limites de laquelles les particules de la phase liquide possèdent l'énergie de liaison avec le cristal pas moins que KT, c'est-à-dire de l'énergie thermique moyenne de la molécule, est conduit à la valeur de 10-12A ce qui s'accorde bien avec l'expérience.

LA DISSOLUTION DES LIANTS

Dans les différentes théories de durcissement ce processus ainsi que ceux de la surface se discute beaucoup, mais en même temps il est peu étudié. La régularité révélée des processus sur la surface des cristaux ioniques (les liants sont les représentants) lors de l'interaction avec l'eau montre l'inévitablité d'hydratation superficielle. Le fait le plus important est celui que l'interaction des ions O^{2-} (ou SO_4^{2-}) et Ca^{2+} avec l'eau conduit au dégagement de l'énergie dépassant celle des liaisons ioniques avec le cristal. Ce n'est que cela qui détermine la possibilité d'arrachage d'ion du cristal et leur passage à la phase liquide c'est-à-dire - la dissolution. La condition générale de la dissolution est le dépassement d'énergie d'hydratation superficielle sur celle de la liaison de la particule avec le cristal: $U_{h.s.} > U_l$. Ceci est montré par des calculs pour les cristaux ioniques du type sodium chloreux dont le trait particulier est le dégagement des paires ioniques dans la phase liquide. Pour le plâtre les calculs montraient que la dissolution passe les étapes suivantes:

- l'adsorption de l'eau sur la surface du cristal avec le dégagement d'énergie 122kJ/Mol (ici et plus loin on donne les effets moyens énergétiques) obtenu lors de la déduction des relations (1) ou (2);
- les processus sur la surface avec le dégagement d'énergie en quantité de 587 kJ/Mol suivant la méthode expliquée dans (4) (la formation des liaisons chimiques, la dissociation de la molécule d'eau $H_2O \rightarrow H^+ + OH^-$, le passage des électrons des ions SO_4^{2-} de la surface aux ions H^+ de la phase liquide et des ions OH^- aux ions Ca^{2+} de la surface;
- l'arrachage des produits de la réaction du cristal sous l'influence d'énergie dégagée en excès (l'énergie de liaison des molécules

$CaSO_4$ avec le cristal) obtenu par le calcul électrostatique du réseau suivant la relation (2) est égale à 697kJ/Mol;
- le dégagement des produits moléculaires de la réaction dans le volume de la phase liquide.

Ce mécanisme de la dissolution est plus avantageux et conduit au dégagement d'énergie en quantité de 122 + 587 - 697 = 12 kJ/Mol ce qui est proche à l'expérience (19,2kJ/Mol). Les calculs ont montré que pour CaO se passe la rupture de liaison Ca - O dans les produits de la réaction sur la surface et le dégagement des ions $CaOH^+$ et OH^- dans le volume de la phase liquide. Le dégagement général d'énergie - 56kJ/Mol (suivant l'expérience 54 ÷ 65 kJ/Mol). L'excès d'énergie favorise l'arrachage et la transition des produits de la réaction dans le volume de la phase liquide. Suivant la relation d'énergie de transistion on déduit cette voie:

$$A=E_n=\int_{r_1}^{r_2} F\,dr=\frac{q_1 q_{cond}}{4\pi\varepsilon_o\varepsilon_1}\left(\frac{1}{r_1}-\frac{1}{r_2}\right), \qquad (3)$$

où $q_{cond.}$ - charge conditionnée superficielle du cristal (déduite suivant la relation (1) où on suppose que : q_1 - charge d'ion arraché, U - énergie calculée de liaison, $q_2 = q_{cond.}$; E_n - énergie dégagée lors de la réaction; r_2 - rayon d'ion superficiel arraché. La voie de déplacement de la surface ($r_1 - r_2$) est égale 3-15Å, après quoi le mouvement est conditionné par les lois de diffusion.

Comme au ciment les restes du groupes d'ions (outre CaO) s'hydratent pratiquement sans dégagement d'énergie, leur dissolution du clinker ne se passe qu'après l'élimination des ions, Ca^{2+} et O^{2-}, étant la combinaison. Leur déplacement du grain du ciment est négligeable. Ainsi, nous voyons que les tetraèdres SiO_4 restent sur la surface ou près d'elle et se polymérisent (5,6). Les calculs théoriques montrent pourquoi dans la phase liquide du ciment durcissant le contenu des ions Ca dépasse à 10-100 celui de la silice. Avec ce caractère de la dissolution du ciment la surface de la réaction se déplace à l'intérieur du grain. Le passage de la phase liquide à cette surface et l'élimination des produits de la réaction se passe dans les conditions de la diffusion en solide. Pour cette dissolution incongruente des liants (le ciment et le monominéral) la relation de la cinétique d'hydratation est déduite

$$C = C_o\left[1 - \frac{4\sin\xi}{\pi\xi}\exp\left(-\frac{t}{\tau}\right)\right], \qquad (4)$$

où C = Concentration des molécules d'eau dans la couche du grain du ciment, C_o - concentration des molécules au dehors de la particule (qu'elle soit égale à 1), $\xi = r/R$ - rayon adimentionnele de la particule, $\tau = R^2/D$ - paramètre temporaire de la relaxation du processus. (R- rayon de particule, D - coefficient de diffusion), t - temps. Pour les liants dissolutifs d'une manière congruente (plâtre, chaux, monominéraux aux conditions déterminées) on déduit la relation de cinéti ue d'hydratation:

$$N_t = N_o\sqrt{\frac{t}{\tau}}\exp\frac{R^2}{4D}\left(\frac{1}{\tau}-\frac{1}{t}\right), \quad 0<t<\tau, \qquad (5)$$

où N_t - nombre des ions diffusés vers le liquide; N_o - nombre des ions dans le grain, $\tau = R^2/4D$ - paramètre temporaire de la relaxation du processus.

Les calculs suivant des relations (4) et (5) montrent le processus d'hydratation. Ils dónnent la possibilité de faire la courbe de la cinétique d'hydratation et de déterminer le temps d'hydratation. Pour les particules du ciment de 10^{-5} à 10^{-7} m. il se change de quelques heures à une année. Pour le plâtre le temps d'hydratation est de quel ues secondes à la dizaine de minutes. Les résultats obtenus correspondent à ceux de l'expérience.

IA FORMATION DE LA SOLUTION SATUREE

L'étude énergétique montre que la condition limitée inférieure de la formation de solution saturée est l'égalité d'énergie d'interaction des ions dissous et de la moyenne thermique : U = KT. Suivant cette condition de la relation

$$r = \frac{q_1 q_2}{4\pi\varepsilon_o\varepsilon_1^m U} \qquad (6)$$

on peut déterminer la distance entre les ions de la solution saturée et de cette manière sa concentration. La condition U=KT se garde aux distances de 21, 30 et 40Å pour l'interaction ionique des homocharges, homocharges avec bicharges et bicharges. Ayant appris les charges des ions et les distances entre eux il est facile de déterminer la concentration de la solution saturée. Pour le plâtre et l'oxyde de calcium elle est 12,7 et 5 g/l (suivant l'expérience 8-11 et 3,6 - 7,2 g/l respectivement).

LA GERMINATION CRISTALLINE

La relation déduite

$$R_{g.c} = \frac{\dfrac{(\varepsilon_2-\varepsilon_1)\,q^2}{4\pi(\varepsilon_2+1{,}5\varepsilon_1)\varepsilon_o\varepsilon_1}}{\dfrac{(\varepsilon_2-\varepsilon_1)\,q^2}{8\pi(\varepsilon_2+1{,}5\varepsilon_1)\varepsilon_o\varepsilon_1\,r} - U}, \qquad (7)$$

donne la grosseur du germe cristallin, où q - charge d'ion décantant sur le germe (sur la surface du petit cristal dans le cas général); r - distance entre le germe et l'ion; U - énergie d'interaction entre les mêmes composants, égale à l'énergie de la liaison intermoléculaire de la structure de l'eau $U_{l.i.}$ si, pendant la cristallisation les ions ne se dégagent pas de l'enveloppe hydratée, ou égale à l'énergie d'interaction des ions avec la molécule dipôle de l'eau $U_{ion-dipôle}$ si les ions se dégagent de l'en-

veloppe hydratée.Dans ces conditions la valeur des rayons du germe critique compose quelques angstroems (5-16).

Le résultat le plus important est celui qui permet de déterminer suivant (7) la sphère d'attraction r des ions par les cristaux de tailles différentes. La sphère d'attraction c'est la distance de la surface du cristal vers lequel tous les ions dissous s'attirent. Il est évident qu'avec la taille du cristal la sphère d'attraction s'accroît. La régularité découverte de la germination montre que la diminution de la rayon du germe critique est possible lors de l'augmentation des charges des ions de la substance cristallisante, lors de l'augmentation de sa constante diélectrique mais aussi lors de la diminution de cette dernière du solvant. Ce phénomène est lié à la sursaturation suivant la relation de Tomson et diminue avec l'augmentation de la sursaturation, mais ce phénomène montre encore des autres voies: l'introduction des additions chimiques - les électrolytes, l'action des champs électriques et magnétiques.

LA PERIODE D'INDUCTION DU DURCISSEMENT

Se basant sur les connaissances énergétiques la periode inductive est conditionnée par le mécanisme de la germination des cristaux, pendant lequel se passe non seulement la cristallisation, mais encore la dissolution des cristaux, n'ayant pas de tailles critiques. Ceci se confirme: aux conditions que $U = U_{l.i}$ on peut trouver le volume et la masse des germes dont la quantité est

$$N = \frac{1}{(2R_{g.c.} + l)^3}, \qquad (8)$$

où $R_{g.c.}$ - rayon du germe critique; l - épaisseur de la couche d'eau entre les surfaces des germes, déduite suivant la relation (6) $l = r - (R_1 + R_2)$ où R_1 et R_2 - rayons des ions de la surface des germes. Pour les ciment la masse des germes est 5-7% de tout le liant ce qui s'accorde bien avec l'expérience d'hydratation, correspondante à la fin de la prise du ciment et au commencement du deuxième pic exothermique du dégagement de chaleur.

LA CROISSANCE DES CRISTAUX DE L'HYDRATE

est conditionnée par le fait que, outre le gradient de concentration, la force motrice pour les ions des substances dissoutes est le dépassement d'énergie d'attraction vers les cristaux des hydrates pqr rapport au grain du liant jusqu'à 50%, déduit suivant la relation (7), lors de l'augmentation simultanée de la sphère d'attraction jusqu'à 150%. Ceci explique que la constante diélectrique des hydrates est supérieure de celle-ci du liant initial et compose 10,6 contre 7,47 pour le ciment.

Il est naturel que la régularité de croissance des cristaux est évident après la formation des germes de tailles critiques et notamment après que la couche d'eau entre le grain du liant et les hydrates cristallins est devenue moins que les deux sphères d'attraction des particules; déduite suivant la relation (7) par rapport à r. Suivant la croissance des particules des hydrates cristallins, l'énergie de liaison ionique de la substance dissoute grandit ce qui provoque l'accélération du mouvement et l'augmentation du volume de la substance du ciment initial par rapport aux particules hydratées. Les calculs énergétiques confirment le caractère sigmatique de la courbe cinétique de l'hydratation. Dans la période initiale on n'observe pas leur croissance quand la distance entre les germes cristallins de l'hydrate est grande. Mais à mesure que la distance entre les particules différentes et la structure diminue, apparaissent les conditions pour la croissance prépondérante des cristaux ayant la grande valeur de la distance diélectrique. Par exemple, les hydrocilicates du Ca (C-S-H) dans le rapport CaO/SiO étant 2, 1,5 et 0,83 ont la constante diélectrique atteignant 13, 14,2, 19 respectivement. Donc, la diminution de la basicité des hydrosilicates pendant l'hydratation conforme à la régularité, ce qui correspond à l'expérience.

LE CHANGEMENT D'ETAT DE LA PHASE LIQUIDE

Le fait essentiel, déterminant l'énergie d'attraction des particules dissoutes, causant la dissolution, la germination et le durcissement est la constante diélectrique du solvant: Se basant sur la théorie du changement de la constante diélectrique de l'eau ε_1 tout près d'ion, proposée par Debye (7), on a révélé l'expression de la constante diélectrique moyenne de l'eau entre les ions:

$$\varepsilon_1^m = \frac{2}{r}\int_0^{r/2} f(r)\,dr, \qquad (9)$$

où f(r) - fonction ε_1 de r suivant la théorie de Debye, r - distance entre les ions On a déduit les valeurs ε_1^m pour les ions dont la distance est différente (tableau1) On ne prêtait aucune attention au changement d'état de la phase liquide, outre les travaux de M.Sychev (8) , bien que cet état influe sur le mécanisme d'hydratation.

TABLEAU 1

r,Å	0	2	6	10	20	40	50
ε_1^m	1	1,8	2,2	6,3	24,5	57	78

La particularité de l'eau changer la constante diélectrique près d'ion et de la surface ionique est la base pour la dissolution. Ceci est bien prouvé par les calculs énergétiques refutant l'opinion que le pouvoir dissolvant de l'eau est conditionné par la haute constante diélectrique. Il s'est trouvé que l'eau d'un côté assure la bonne dissolution des substances en diminuant la constante diélectrique dans la zone du contact avec le cristal jusqu'à 1. D'un autre côté l'eau assure la conservation du

SOLvant aux grandes distances entre les ions, puisque la constante diélectrique de l'eau augmente (à 80) ce qui diminue l'énergie d'attraction entre les ions dissous. Le changement du contenu ionique H^+ et OH^- a la grande importance puisqu'il détermine le mécanisme d'hydratation, surtout pour les substances difficile à dissoudre. Il est montré que l'influence des températures sentent à travers l'augmentation de la dissociation électrolytique mais non pas à travers l'augmentation du contenu des molécules actives déduites suivant la loi de distribution de Bolzman. Il est prouvé que le coefficient d'accélération de réaction est correlatif avec celui d'augmentation de la concentration des ions H^+ et OH^-. Suivant la relation $f = C_x/C_o$ on déduit le coefficient de température d'accélération de réaction, où C_x et C_o - concentrations des ions H^+ respectivement aux températures T_x et T_o.

LA RECRISTALLISATION AU DURCISSEMENT est bien montré dans le travail (6) mais ses calculs théoriques sont vagues. L'analyse énergétique montre qu'elle est causée par le changement d'énergie d'attraction entre les ions des substances dissoutes et les particules des hydrates cristallins dont les tailles et la constante diélectrique sont différentes. Lors de la superposition des sphères d'attraction des particules de l'hydrate cristallins dont la constante diélectrique est différente (par exemple $Ca(OH)_2$, $\varepsilon_2 = 5,39$ et C-S-H $\varepsilon_2 = 14,2$) les ions de la substance dissoute ne s'orientent que vers le cristal C-S-H dont l'énergie d'interaction avec ion est plus forte. Le cristal C-S-H grandit plus vite ce qui augmente plus l'énergie d'attraction entre le cristal et les ions. Enfin le moment viendra quand la sphère d'attraction dépasse celle du cristal $Ca(OH)_2$ et tous les ions ne s'orientent que vers le grain C-S-H (on peut calculer précisement ce schéma). La sortie des ions de substance de la couche diffusée du cristal $Ca(OH)_2$ conditionnera sa dissolution lors de la croissance ultérieure du cristal C-S-H. Cette régularité conditionne la diminution de la basicité des hydrosilicates lors de la recristallisation et la croissance des gros cristaux en compte de la dissolution des petits.

LA FORMATION DE LA STRUCTURE DU DURCISSEMENT

Suivant la croissance des cristaux de l'hydrate la distance entre eux diminue. Ceci conduit à la décroissance de la constante diélectrique d'eau dans l'espace entre les cristaux et à la croissance des forces d'attraction entre eux. Ayant formé à l'intérieur du mortier des germes de tailles critiques quand l'énergie d'attraction entre eux dépasse l'énergie de liaisons intermoléculaires dans la structure d'eau, on note l'augmentation sensible de la solidité structurale du système. A cette période la structure se compose des particules de tailles colloïdales. On peut étudier le processus de raprochement des particules solides de l'hydrate suivant les relations d'énergie d'interaction données ci-dessus. Lors de la diminution de la couche et de la constante diélectrique d'eau les forces de liaison entre les cristaux augmentent et peuvent être calculées suivant la relation, basant sur la loi de Koulon

$$F_{i-i} = \frac{q_1 q_2}{4\pi \varepsilon_o \varepsilon_1 r^2}, \qquad (11)$$

où q_1 et q_2 - charges des ions superficiels de ces particules, car on a montré que l'interaction entre les ions peut être représentée comme l'interaction de deux ions proches de la surface de ces particules.

Les lois révélées de la formation de la structure du durcissement donnèrent la possibilité de déterminer la structure linéaire de la molécule $Ca(OH)_2$ et la texture feuilletée du plâtre. La même régularité permit d'expliquer la basse solidité de la structure de la chaux, l'extension du composé additionnée par le plâtre et la chaux, les propriétés universelles du ciment.

Analysant les lois énergétiques on déduit la relation de solidité de la structure de pâte de ciment et de la pierre.

$$R_c = \frac{q_1 q_2 N}{4\pi \varepsilon_o \varepsilon_1^m \left[\frac{2(V_g - V_{l.ch}) V_1}{k S_{s.s}} + R_1 + R_2\right]^2}, \qquad (12)$$

où N - nombre des particules et des contacts à l'unité de la surface de section (voir par exemple (8)), V_g et $V_{l.ch}$ - volumes d'eau: de gâchage et liée chimiquement, V_1 - volume relatif de la couche sphérique d'eau entre les particules de l'hydrate (vers la fin de l'hydratation égal à 0,2-0,3), K - coefficient de la sphéricité (environ 1,02-1,1); $S_{s.s.}$ - surface spécifique des particules de l'hydrate, R_1 et R_2 - rayons des ions des particules.

Se basant sur la relation (12) on peut prédire la solidité théorique maximale de la structure de la pierre. La solidité sera plus forte si dans la zone du contact des particules de l'hydrate il n'y a pas de couche d'eau. ($l = 2(V_g - V_{l.ch.}) V_1 / K S_{s.s} = 0$). Si les tailles des particules sont 95Å (9) la résistance à la traction sera 64,6 MePa. Notons que la résistance maximale de la pierre obtenue par D.Roy et G.Gouda (10) est égale à 60,3 MePa. La relation donne de bons résultats suivant la cinétique d'augmentation de la résistivité dépandant du contenu d'eau libre. ($V_g - V_{l.ch.}$) L'écart moyen compose 2% par rapport aux données expérimentales révélées ci-dessus par les auteurs (10) Ainsi, La relation reflète la cinétique du changement de la solidité de la structure, montre la liaison de la solidité dépendant de l'hydratation (à travers $V_{l.ch.}$) et donne des voies pour augmenter la solidité de la pierre cimentée: l'augmentation q, N et $S_{s.s.}$ la diminution ($V_g - V_{l.ch.}$) et ε_1^{moyen}.

CONCLUSION

La méthode de la recherche théorique de la direction énergétique des stades à part du processus d'hydratation avec la mise en évidence des forces motrices intéreures permet de révéler la régularité objective et le mécanisme du processus.

Les relation déduites donnent la possibilité de déterminer les caractéristiques du processus (effet énergétique des stades, concentration de la solution saturée, la durée de la période d'influence et d'hydratation etc. et même la solidité de la pâte de ciment et de la pierre). Notons qu'apparait la possibilité d'influer sur le processus en changeant les paramètres du système contenus dans les formuls de calcul, la prévision de la structure des hydrates obtenus et plus tard - la création des substances dont la structure et les propriétés sont données auparavant.

L'avantage de la méthode proposée pose le problème d'approfondir les connaissances sur la structure (compte tenu d'électronique) de la substance initiale sur les propriétés physico-chimiques afin de donner les calculs précis pour les monominéraux du clinker ciminté et du ciment.

BIBLIOGRAPHIE

1.H. LE CHATELIER (1883), "Sur le mécanisme de la prise du plâtre", Comptes Rendus p.p. 94,715-718.

2.H.LE CHATELIER (1883), "Application des phénomènes de sursaturation à la théorie du durcissement de quelques ciments et mastics", Comptes Rendus, t.94pp.1056-1059.

3.V.V.KAPRANOV (1976), "Interaction des phases liquides et solides pendant le processus d'hydratation du ciment", 7 Congrès International sur la Chimie des Ciments, v.6 l.1 pp.80-84, (russe).

4.V.V.KAPRANOV (1976),"Durcissement des liants et des produits sur leurs bases",(rus.)

5.Yu.S.CHERKINSKY (1967), "La chimie des liants polymères inorganiques", (russe).

6.Yu.S.MALININ (1968), "Sur l'hydratation et sur le durcissement du ciment Portland", Les oeuvres de RILEM, (russe).

7.P.DEBYE (1931), "Les molécules polaires", (traduit de l'allemand), (russe).

8.M.M.SYTCHEV (1974), "Le durcissement des liants", (russe).

9.T.C.POWERS (1964), "Les propriétés physiques de la pâte de ciment et de la pierre", 4 Congrès International sur la Chimie des Ciments", (traduit de l'anglais) pp.402-438, (russe).

10.D.M.ROY, G.R. GOUDA (1976), "L'optimisation de la solidité de la pâte de ciment", 6 Congrès International sur la Chimie des Ciments, v.2,l.1, pp.310-315, (russe).

Aspects thermodynamiques et cinétiques du passage en solution de C_3S et de la formation de C-S-H

Thermodynamic and kinetic aspects of C_3S passage in solution and C-S-H formation

P. BARRET, professeur à l'Université de Dijon, directeur du Laboratoire de Recherches sur la Réactivité des Solides associé au C.N.R.S. (L.A. 23),
D. MENETRIER, docteur ès sciences, attaché de recherches au C.N.R.S. (L.A. 23), Dijon,
D. BERTRANDIE, docteur de l'Université de Dijon, C.N.R.S. (L.A. 23), Dijon.
M. REGOURD, docteur ès sciences, chef de Service CERILH, maître de conférences à l'Ecole Nationale Supérieure des Ponts et Chaussées, Paris, France.

RESUME : Plusieurs problèmes fondamentaux sont étudiés : celui de la congruence de la dissolution de C_3S ; il est suggéré d'abord d'après les données thermodynamiques qu'il ne convient de parler non pas de la dissolution de C_3S, mais de celle de son état superficiellement hydroxylé (C_3S_{sh}) par pronotation interfaciale directe. Les espèces ainsi constamment renouvelées après leur passage en solution sont les vecteurs de l'hydratation, mais la prise et le durcissement résultent de la précipitation de C-S-H de rapport $[C/S]_S < 3$. La vérification de la congruence est obtenue expérimentalement aussi bien dans l'eau de chaux que dans l'eau distillée à l'état dynamique stationnaire réalisé par passage du solvant à flux élevé à travers une couche mince de C_3S sur filtre dans des conditions telles que les concentrations en chaux [C] et en silice [S] ne pénètrent pas trop dans le domaine sursaturé à nucléation rapide de C-S-H. C'est ce qui se produit en doublant l'épaisseur de la couche de C_3S et qui donne $[\Delta C/\Delta S]_\ell > 3$ en raison de la précipitation de C-S-H. Un modèle d'écriture des étapes élémentaires est proposé et celle du transfert en solution des ions Ca^{2+} superficiels est utilisée pour établir une loi théorique de diminution de la vitesse en fonction de l'augmentation de [C]. Cette loi est bien vérifiée par la branche ascendante des courbes d'évolution de C_3S agité dans l'eau dans un rapport pondéral solide/liquide (ℓ/s) de 10. En ce qui concerne la variation de composition de C-S-H en fonction de la concentration en chaux dans la phase liquide, la comparaison des résultats obtenus d'une part par fixation ou perte de chaux au contact d'eau de chaux ou d'eau distillée d'un C-S-H préparé avec un $[C/S]_S$ donné, d'autre part, par formation de C-S-H à partir de C_3S sur filtre sous courant d'eau distillée, conduit à supposer que la fixation de chaux accompagne la précipitation du C-S-H, mais des expériences actuellement en cours avec les techniques utilisées permettront d'apporter une vérification directe. Enfin, des expériences par passage à travers une couche de C_3S sur filtre, d'eau et d'eau de chaux pulvérisées, réalisant un ℓ/s comparable à celui d'une pâte, donnent des résultats analogues à ceux obtenus par flux de liquide, ce qui est en faveur de l'unicité du mécanisme à (ℓ/s) grand ou petit.

SUMMARY : Several basic problems are studied : that of the congruence of the C_3S dissolution ; first it is suggested, from thermodynamic data, that we should not talk about C_3S dissolution but talk about the dissolution of its superficially hydroxylated state (C_3S_{sh}) by direct interface protonation. Thus the constantly renewed species after passing in solution are the hydration vectors but setting and hardening result from the precipitation of C-S-H with a ratio $[C/S]_S < 3$. Congruence is experimentally verified both with lime water and distilled water in the stationary dynamic state achieved by passing the high flow solvent through a their layer of C_3S, on filter under conditions such that the lime [C] and silica [S] concentrations do not penetrate too much in the supersaturated domain of C-S-H rapid nucleation. This is what happens by doubling the thickness of C_3S and gives $[\Delta C/\Delta S]_\ell > 3$ due to the precipitation of C-S-H. A model describing the early stages is proposed and the expression of the transfer in solution of surface Ca^{2+} ions is used to establish a theoretical law about the rate decrease as a function of the increase of [C]. This law is verified by the ascending part of the evolution curves of C_3S stirred in water with a solid/liquid weight ratio (ℓ/s) equal to 10. As for the composition variation of C-S-H versus lime concentration in the liquid phase the comparison of results obtained on the one hand by fixation or lime loss on contact with the lime or distilled water of a C-S-H prepared with a given $[C/S]_S$ and on the other hand by formation of C-S-H from filter C_3S under distilled water flow leads to assume that lime fixation accompanies C-S-H precipitation but experiments that are being made with the techniques used will allow a direct verification. Finally experiments consisting in passing sprayed water and lime water through a C_3S layer with an ℓ/s ratio comparable to that of a paste give results that are similar to those obtained with liquide flow, which favours the unicity of the mechanism with a high or low (ℓ/s).

INTRODUCTION

La dissolution congruente de C_3S est encore contestée par certains auteurs (1). A notre sens, il convient d'ailleurs de parler non pas de la dissolution de C_3S anhydre, mais de celle de C_3S_{sh} (superficiellement hydroxylé) (2). En outre, c'est un état dynamique du système et non un état statique qui doit être considéré. Pour éclaircir ces notions, nous apportons un certain nombre de résultats expérimentaux et de considérations théoriques, d'ordre thermodynamique et cinétique.

Quelles peuvent alors être les causes de l'écart apparent à la congruence qui se manifeste par un rapport chaux/silice (C/S) > 3 ? Notre point de vue est que ces causes sont : 1) La précipitation de C-S-H de rapport $[C/S]_s < 3$, 2) L'enrichissement qui en résulte par complément à 3 de la phase liquide en chaux. Or, l'expérience nous a permis d'établir ce fait remarquable du maintien de la dissolution congruente de C_3S_{sh} dans un milieu enrichi en chaux.

Le ralentissement de la dissolution de C_3S_{sh} est-il un effet de "couche protectrice" ou un effet cinétique normal ? Nous apportons une réponse en faveur de la seconde interprétation.

Les mécanismes que nous proposons ne sont-ils valables que quand C_3S se trouve dispersé dans un volume important de solution [(ℓ/s) grand] ? Nos expériences d'hydratation de C_3S par de l'eau et de l'eau de chaux pulvérisées sur filtre suggèrent que les mécanismes sont les mêmes à ℓ/s grand ou petit.

En ce qui concerne enfin le changement de composition de C-S-H avec la concentration [C] en chaux dans la phase liquide, il semble que la précipitation de C-S-H dans un milieu plus ou moins riche en chaux et la fixation ou la perte de chaux par un C-S-H déjà, synthétisé avec un $[C/S]_s$ donné, lorsqu'il est plongé dans un milieu plus riche ou moins concentré en chaux, ne soient pas exactement superposables. Mais les protocoles expérimentaux que nous avons mis au point et qui permettent en principe d'obtenir un C-S-H pur au contact d'une phase liquide de concentration stationnaire en chaux et silice seront susceptibles d'apporter une réponse plus précise à cette question.

METHODE EXPERIMENTALE

Nous avons donné, dans une autre communication (3), une classification des techniques que nous avons utilisées. Ici, il s'agira essentiellement d'études en système ouvert du type s/f + ℓ, consistant à faire passer à travers une couche de solide pulvérulent sur filtre un liquide soit versé soit pulvérisé. Dans une autre publication (4), certains d'entre nous avaient donné les résultats obtenus grâce à des essais du même type mais de courte durée (quelques secondes). Ces essais avaient permis notamment de construire sur le diagramme chaux-silice-eau (C,S,H) une courbe I délimitant le domaine sursaturé à nucléation de C-S-H rapide de celui à nucléation lente ; appliqués à C-S-H, ils avaient également permis d'établir que la dissolution de cet hydrate dans l'eau et l'eau de chaux ne conduisait pas à des compositions appartenant au domaine sursaturé et que le C-S-H était capable de fixer de la chaux aux dépens de la phase liquide. Dans cette publication, nous avions en outre défini les notions de temps de contact θ concernant le liquide et de temps de passage τ, concernant le solide sur filtre. Nous nous sommes efforcés, dans les expériences décrites ici, de réaliser des temps de contact très brefs et pour cela une couche de C_3S d'épaisseur h est uniformément étalée sur un disque de papier filtre d'aire a = 102 cm^2, maintenu par un support en polyéthylène poreux dans un appareil à filtration sous pression millipore. L'échantillon est recouvert d'une seconde feuille de papier filtre et maintenu en place par un disque en matériau poreux élastique lui-même comprimé dans le logement cylindrique de l'appareil par un second disque analogue au support poreux du filtre. L'appareil est relié par une canalisation souple à une pompe péristaltique capable de développer jusqu'à une pression de 0,5 $N.mm^{-2}$. Le débit maximum obtenu à travers l'échantillon est de l'ordre de 250 $l.h^{-1}$. Divers essais ont été effectués différant l'un de l'autre par la masse de l'échantillon et donc l'épaisseur de couche h et par la composition de la phase liquide : eau, eau de chaux, solution de concentrations en chaux [C] et en silice [S] données.

Le débit $\dot{q}$ est maintenu constant pendant une durée Δt au cours de laquelle il passe un volume V de liquide ; le temps de contact $\theta = ah/\dot{q}$ est celui pendant lequel un plan du liquide traverse la couche d'épaisseur h. La difficulté de l'expérience, étant donné l'importance du flux, est de maintenir l'épaisseur de la couche uniforme. Au débit maximum, avec h = 0,07 cm, $\theta \simeq 0{,}11$ s. Cela signifie que le liquide recueilli n'est resté à l'état stationnaire que 0,11 s au contact de C_3S c'est-à-dire pendant une durée beaucoup plus faible que les temps de contact réalisés à l'instant initial dans des expériences récentes (5, 6). L'expérience montre que des temps de contact aussi brefs et des vitesses linéaires d'un plan du liquide à travers la couche : $dz/dt \simeq 0{,}6\ cm.s^{-1}$ aussi petites sont nécessaires pour que, d'une part [C] et [S] n'excèdent pas de beaucoup la saturation par rapport à C-S-H, d'autre part que ces valeurs soient proches de celles atteintes dans la couche limite au contact immédiat des grains et non des valeurs très inférieures obtenues par diffusion. Si ces conditions sont bien réalisées et qu'en particulier la dilution due à des filets liquides qui ne rencontreraient pas de grains est de faible importance, en doublant l'épaisseur de la couche à débit constant, la vitesse linéaire n'est pas changée mais le temps de contact double de sorte que [C] et [S] peuvent pénétrer dans le domaine sursaturé où la nucléation de C-S-H devient rapide. Le fait que le flux du liquide à travers la couche soit grand a de plus l'avantage de rendre négligeable la rétrodiffusion en amont de la couche de sorte que le rapport (ℓ/s) effectif est pratiquement limité par la porosité intergranulaire du lit solide pulvérulent.

Néanmoins, nous avons complété ces expériences par des essais de même principe, mais en utilisant une phase liquide pulvérisée au moyen d'un pulvérisateur de spectrométrie d'absorption atomique qui donne un aérosol exempt de grosses gouttelettes. Un filtre millipore est utilisé et le jet est diaphragmé pour éviter le rassemblement de gouttelettes sur le bord du support du filtre. L'aspiration par la trompe à eau est suffisante pour qu'aucune accumulation de liquide n'ait lieu de sorte que le rapport ℓ/s soit comparable à celui qui règne dans une pâte.

En ce qui concerne les études relatives au changement de composition de C-S-H en fonction de la concentration en chaux dans le milieu, nous avons fait appel à plusieurs techniques : 1) Passage à travers une couche de C-S-H sur filtre d'une solution de chaux de diverses concentrations. 2) Agitation en système fermé de C-S-H préparé indépendamment, dans de l'eau de chaux saturée ; dosage de la chaux et de la silice

dans le C-S-H après dissolution dans HF , puis essai de réversibilité de la transformation par agitation dans un grand volume d'eau du C-S-H ayant fixé de la chaux. 3) Evaluation par les équations du bilan analytique de la composition du C-S-H obtenu par un flux d'eau de longue durée à travers une couche de C_3S sur filtre. 4) Mise en œuvre de notre technique de filtration rapide ci-dessus décrite pour obtenir, dans des conditions de composition stationnaire de la phase liquide, un C-S-H comme seul résidu solide sur filtre. La composition de celui-ci pourra alors être étudiée avec précision en fonction de la composition du milieu dans lequel il aura été formé et l'état de condensation de la silice dans les ions silicates déterminée par la technique de triméthylsilylation. Ce type d'étude est en cours.

RESULTATS

Les résultats des essais de filtration à grand débit à travers une couche de C_3S sont consignés dans le tableau (I). Ils font clairement apparaître les conditions dans lesquelles la dissolution congruente est observée : faible épaisseur de la couche de C_3S et flux de l'ordre de 2,5 $l.h^{-1}.cm^{-2}$. Avec l'eau pure comme solvant, on pourrait objecter qu'en cas de formation de C-S-H, une partie de celui-ci aurait pu être redissous. Mais en partant d'une solution de composition $[C] = 1{,}20.10^{-3}$ mol.kg^{-1}, $[S] = 0{,}40.10^{-3}$ mol.kg^{-1}, $[(C/S)_\ell = 3]$, correspondant à la saturation de C-S-H, cette objection n'a plus de valeur et, dans les mêmes conditions de flux et d'épaisseur de couche, on trouve encore un $\Delta C/\Delta S \simeq 3$ ce qui laisse supposer que le domaine de forte sursaturation n'a pas été atteint. De la même façon, avec une solution de chaux de $[C]^o = 3.10^{-3}$ mol.kg^{-1}, $\Delta C/S$ très peu supérieur à 3.

TABLEAU I

Solvant $[C]^o, [S]^o$ 10^{-3} mol.kg^{-1}	h cm	τ mn	θ s	$\frac{dz}{dt}$ cm.s^{-1}	$\Delta[C]$, $\Delta[S]$ 10^{-3} mol.kg^{-1}		$\left[\frac{\Delta C}{\Delta S}\right]_\ell$
eau	0,07	2	0,11	0,64	2,45	0,82	2,99
	0,07	10	0,14	0,50	2,24	0,76	2,96
	0,05	18	0,11	0,45	2,10	0,69	3,04
	0,14		0,21	0,67	3,07	0,90	3,42
eau de chaux $[C]^o = 3{,}0$	0,07	5	0,11	0,64	1,30	0,42	3,10
	0,07	10	0,13	0,54	1,41	0,45	3,15
	0,05	20	0,14	0,36	1,27	0,40	3,18
	0,15	5	0,22		2,35	0,61	3,88
	0,15	10	0,26		2,41	0,63	3,83
Solution $[C]^o = 1{,}20$ $[S]^o = 0{,}40$	0,07	10	0,11	0,64	1,41	0,46	3,05
	0,06	20	0,12	0,50	1,38	0,45	3,07
	0,15	1	0,23	0,65	1,85	0,54	3,43
	0,15	5	0,26	0,58	1,69	0,49	3,45
	0,14	10	0,26	0,54	1,59	0,47	3,35
eau pulvérisée sur T_I	0,03	10			3,60	1,10	3,27
	"	10			3,72	1,12	3,32
	"	10			3,70	1,14	3,24
	"	11			3,80	1,15	3,29
eau de chaux pulvérisée $[C]^o = 3{,}95$	"	12			1,40	0,42	3,33
	"	12			1,41	0,40	3,53
	"	9			1,20	0,40	3,22

Il est donc remarquable que la congruence de la dissolution se conserve avec comme solvant, non seulement une phase liquide déjà saturée par rapport à C-S-H, mais aussi de l'eau de chaux. En revanche, lorsque l'épaisseur de la couche de C_3S est doublée, on obtient $[C] > 3.10^{-3}$ mol.kg^{-1} et $\left[\Delta C/\Delta S\right]_\ell > 3$ ce qui s'explique simplement par la précipitation d'un C-S-H de rapport $[C/S]_s < 3$.

En effet, alors que dans les essais où $\left[\Delta C/\Delta S\right]_\ell$ reste très voisin de 3, la fixation d'eau déterminée par perte au feu est négligeable, même pour des temps de passage de 30 à 45 mn, elle devient importante dès lors que $\left[\Delta C/\Delta S\right]_\ell > 3$. Par exemple, dans l'expérience sur une couche de 0,15 cm de C_3S (T_{II}) avec une solution de concentrations initiales $[C]^o = 1{,}20.10^{-3}$ mol.kg^{-1} et $[S]^o = 0{,}40.10^{-3}$ mol.kg^{-1} (Tableau I), l'essai de perte au feu donne après un temps de passage $\tau = 40$ mn sur une masse résiduelle de 8g (masse initiale 20 g) : 9,7 %, ce qui représente une masse d'eau liée de 0,76 g, correspondant à une masse de C-S-H de 3 à 5 g selon le taux d'hydratation et le rapport $[C/S]_s$. La microscopie électronique à balayage met en évidence des amas floconneux qui pourront être complètement caractérisés en poussant ce type d'expériences, suivant le protocole 4) ci-dessus défini, jusqu'à la disparition complète de C_3S ce qui nécessite des échantillons T_I purs. De tels essais sont en cours de réalisation. Un autre résultat remarquable apparaissant aussi dans le tableau I est l'extension des mêmes conclusions aux essais dans lesquels le solvant (eau ou eau de chaux) est pulvérisé et où le rapport ℓ/s est très comparable à celui d'une pâte.

En attendant les résultats des essais de type 4, ceux de nos expériences sur la variation du rapport $[C/S]_s$ du C-S-H avec $[C]$ dans la phase liquide suivant les protocoles 1) 2) et 3) ci-dessus décrits (méthode expérimentale) tendent à montrer : 1°) que la composition d'un C-S-H de rapport $[C/S]_s$ donné varie dans des limites assez étroites et avec une cinétique lente lorsqu'il est maintenu dans l'eau de chaux saturée ou dans l'eau pure (Tableau II), 2°) qu'un C-S-H obtenu par filtration continue avec une composition stationnaire du filtrat $[C] = 4{,}17.10^{-3}$ mol.kg^{-1}, $[S] = 1{,}25.10^{-3}$ mol.kg^{-1}, a un rapport $[C/S]_s \simeq 2$. Ces derniers résultats, portés également dans le tableau II, ont été obtenus à partir de données analytiques comportant l'analyse quantitative par diffraction X de C_3S résiduel. Les équations établies par certains d'entre nous (7, 8) pour calculer le nombre de moles et la composition du C-S-H, c'est-à-dire: r et αr, respectivement les nombres de moles de silice et de chaux et γ le nombre de moles d'eau, à partir des données analytiques, sont, en posant :

$$B = [n_c^o - \Delta(\beta q)]M_C + (n_S^o - \Delta q)M_S ,$$

$$r = n_S^o - \Delta q - \frac{pB}{100M_{C_3S}}\left(1 + \frac{a}{100}\right) \qquad (1)$$

$$\alpha r = n_c^o - \Delta(\beta q) - \frac{3pB}{100M_{C_3S}}\left(1 + \frac{a}{100}\right) \qquad (2)$$

$$\gamma = \frac{Ba}{100M_H r} \qquad (3)$$

M_{C_3S}, M_C, M_S, M_H : masses molaires de C_3S, CaO, SiO_2, H_2O ; n_c^o et n_S^o , nombre de moles de CaO et SiO_2 dans C_3S initial ; $\Delta(\beta q) = \beta q - \beta_0 q_0$ et $q = q - q_0$ différences entre le nombre de moles respectivement de chaux et de silice dans le volume V de la solution finale et du solvant ; p : pourcentage en masse de C_3S résiduel par rapport à la masse m de solide restant

sur filtre ; a, pourcentage en masse d'eau liée par rapport à la masse déshydratée de solide restant sur filtre.

TABLEAU II

	$[C/S]_s$ init. ou interméd.	eau de chaux [C] 10^{-3} mol. kg^{-1}	Durée mn	α $[C/S]_s$	γ $[H/S]_s$
Agitation de 2,5 g de C-S-H préparé par silicate de Na+CaO, dans 1 l de liquide (successivement eau de chaux et eau)	1,05	21,6	330	1,25	2,93
	1,25	0	15	1,11	2,41
	1,11	21,8	90	1,21	2,53
	1,21	0	90	1,18	3,23
	1,18	20,0	1020	1,22	2,58
C-S-H préparé par SiO_2 + eau de chaux, 50 mg sur filtre	0,83	6,78	0,75	0,94	
Passage d'eau distillée sur 10g de C_3S T_I étalé sur verre fritté n° 4 diamètre 90mm, débit ∿ 1 l/mn		0	18	1,84	3
		"	20	1,94	2,08
		"	16	2,10	1,76
		"	15	1,70	2,54

DISCUSSION

Etapes élémentaires et cinétique de dissolution-précipitation :

Ces étapes ont été formulées par certains d'entre nous (9) en éléments de structure avec l'écriture de Kröger et Vink (10).

1) Hydroxylation par protonation des ions superficiels de C_3S :

$$O_O + H_2O_\ell \rightleftarrows OH_O^{\cdot} + (OH_{ad}^-)'$$

$$SiO_4^{n\cdot}_{SiO_4} + H_2O_\ell \rightleftarrows H_{(n+1)}SiO_4^{(n+1)\cdot}_{SiO_4} + (OH_{ad}^-)'$$

(n = 0, 1, 2, 3)

2) Transfert interfacial du solide dans la phase liquide

$$(OH_{ad})' \rightleftarrows OH_{aq}^-$$

$$OH_O^{\cdot} \rightleftarrows V_O^{\cdot\cdot} + OH_{aq}^-$$

$$H_{(n+1)}SiO_4^{(n+1)\cdot}_{SiO_4} \rightleftarrows V_{SiO_4}^{\cdot\cdot\cdot\cdot} + H_{(n+1)}SiO_{4\,aq}^{(4-n-1)}$$

$$Ca_{Ca} \rightleftarrows V_{Ca}'' + Ca_{aq}^{2+}$$

3) Diffusion des ions de l'espèce i de concentration C_i de l'interface vers l'intérieur de la solution dans des conditions d'agitation données ou en milieu stagnant :

$$\text{div } D_i \vec{\text{grad}}\, C_i = \frac{\partial C_i}{\partial t}$$

4) Nucléation et croissance de germes de C-S-H : Etant donné la variation de composition du C-S-H en fonction de [C] dans la phase liquide, probablement due à l'existence d'une solution solide avec $Ca(OH)_2$, C-S-H peut être représenté par une formule telle que: $Ca_\alpha(OH)_{(2\alpha-1)}H_3SiO_4$ ou pour $\alpha \geq 1$, $Ca_\alpha OH_{(2\alpha-2)}H_2SiO_4$.

S'il se produit une condensation des ions silicates, la première de ces formules peut être remplacée par $Ca_{2\alpha}\ OH_{2(2\alpha-1)}\ H_4Si_2O_7$.

5) Lorsque la solution est sursaturée par rapport à $Ca(OH)_2$, nucléation et croissance de germes de portlandite.

Ces étapes élémentaires peuvent être regroupées en trois ou seulement en deux réactions stœchiométriquement simples selon que l'on considère ou non l'état d'hydroxylation superficielle comme un état intermédiaire observable. Or, il paraît logique d'admettre qu'il en est bien ainsi étant donné, d'une part l'importance de l'affinité chimique d'une telle réaction, que nous tenterons d'évaluer, d'autre part, les fréquences des chocs des molécules d'eau à l'interface.

Dès qu'un ion superficiel hydroxylé est passé en solution, un autre doit être immédiatement reconstitué sur le site laissé découvert. La répétition de ce même processus jusqu'au passage complet en solution de la totalité de la masse initiale de C_3S réalise la majeure partie, sinon l'intégralité de l'hydratation de cette phase anhydre.

Cette équation stœchiométriquement simple peut être écrite :

$$\text{I)}\quad 3CaO,SiO_2 + 4H_2O_\ell \rightleftarrows 3Ca_{Ca} + OH_O^{\cdot} + H_3SiO_{4\,SiO_4}^{\cdot\cdot} + 4(OH_{ad}^-)'$$

Elle entraîne l'écriture d'une autre réaction stœchiométriquement simple, celle de la dissolution de cet état superficiellement hydroxylé noté C_3S_{sh}:

$$\text{II)}\quad 3Ca_{Ca} + OH_O^{\cdot} + H_3SiO_{4\,SiO_4}^{\cdot\cdot} + 4(OH_{ad}^-)' \rightleftarrows 3Ca_{aq}^{2+} + 5\,OH_{aq}^- + H_3SiO_{4\,aq}^-$$

Cette écriture suppose la dissolution congruente, alors que les étapes élémentaires du groupe 2 (transfert interfacial) sont des réactions parallèles. Elles pourraient avoir des vitesses propres indépendantes et non pas statistiquement égales entre elles comme l'exige la congruence. Mais, l'expérience montre, qu'à condition que le flux de solvant (eau, eau de chaux) soit suffisamment rapide et l'épaisseur du lit solide assez faible, le passage des ions de l'interface à la solution a bien lieu statistiquement dans les proportions stœchiométriques $[C/S]_\ell = 3$. Il faut croire que les effets compensateurs des champs électriques résultant d'accumulations locales de charges, assurent une autorégulation.

Enfin, dans l'état actuel des connaissances, il est difficile de dire si la nucléation donne, dans un premier stade, un C-S-H stœchiométrique (par exemple de $[C/S]_s = 1$), suivi d'un second stade au cours duquel celui-ci fixe ou libère de la chaux pour se mettre en équilibre avec la phase liquide, ou si elle aboutit directement à un composé de formule $Ca_\alpha OH_{(2\alpha-1)}H_3SiO_4$ par exemple. Par raison de simplicité, nous adopterons le second point de vue se traduisant par une équation du type :

$$\text{III)}\quad \alpha Ca_{aq}^{2+} + (2\alpha-1)OH_{aq}^- + H_3SiO_{4\,aq}^- \rightleftarrows Ca_\alpha OH_{(2\alpha-1)}H_3SiO_4\downarrow$$

Quant à la nucléation de l'hydroxyde de calcium, elle répond à l'équation classique :

$$\text{IV)}\quad Ca_{aq}^{2+} + 2\,OH_{aq}^- \rightleftarrows Ca(OH)_2\downarrow$$

Si l'on admet ce regroupement des étapes élémentaires en ces quelques réactions stœchiométriquement sim-

ples, il est alors possible de décrire schématiquement le réseau de telles réactions simultanées (8) comme on l'a fait dans le schéma (figure 1) :

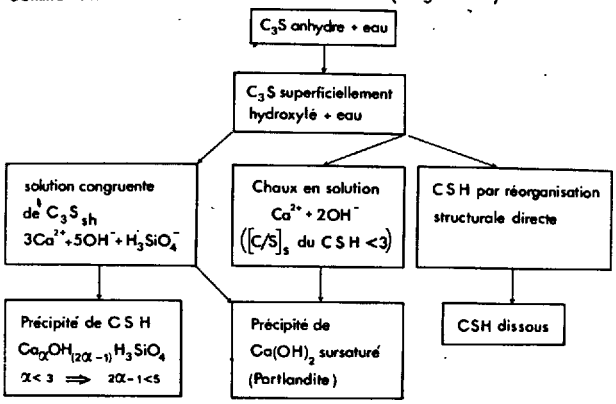

Fig. 1 - Réseau de réactions mises en jeu pour la formation de C-S-H et d'hydroxyde de calcium précipité à partir de C_3S.

On a fait figurer à droite, en compétition avec le processus de dissolution de C_3S_{sh} - précipitation de C-S-H, le processus hypothétique de réorganisation structurale de C_3S_{sh} en C-S-H sans passage par la solution (hypothèse topochimique). Si, comme cela paraît vraisemblable, le rapport stœchiométrique 3 de C_3S est conservé dans son hydroxylation superficielle, une telle étape de réorganisation structurale en un C-S-H de $[C/S]_s < 3$ devrait être accompagnée du passage de chaux en solution conformément au schéma réactionnel suivant avec $[C/S]_s = 2$ par exemple :

1) Création de lacunes de calcium superficielles :

$$3Ca_{Ca} + OH_O^{\cdot} + H_3SiO_4^{\cdot\cdot} + 4(OH^-_{ad})' \rightleftarrows 2Ca_{Ca} + V''_{Ca} + OH_O^{\cdot} + H_3SiO_4^{\cdot\cdot} + 2(OH^-_{ad})' + Ca^{2+}_{aq} + 2\,OH^-_{aq}$$

(SiO_4 au-dessus de $H_3SiO_4^{\cdot\cdot}$; SiO_4 au-dessus de $H_3SiO_4^{\cdot\cdot}$)

2) Réorganisation structurale :

$$2Ca_{Ca} + V''_{Ca} + OH_O^{\cdot} + H_3SiO_4^{\cdot\cdot} + 2(OH^-_{ad})' \rightleftarrows 2Ca_{Ca} + 3\,OH_{OH} + H_3SiO_4$$

(SiO_4 au-dessus de $H_3SiO_4^{\cdot\cdot}$; H_3SiO_4 au-dessus de H_3SiO_4)

Certains d'entre nous ont procédé, dans d'autres publications (4, 7, 8, 9) à une comparaison approfondie d'un tel processus avec le processus de dissolution-précipitation, notamment par une construction graphique sur le diagramme C,S,H.

Il est utile de rappeler que le processus de réorganisation structurale, s'il permet de rendre compte du passage en solution de la chaux, n'autorise pas, en revanche, celui de la silice, du moins, avec une concentration supérieure à la solubilité du C-S-H, de sorte qu'il est nécessaire d'admettre que les états sursaturés de $[C/S]_\ell$ de peu supérieurs à 3 (3,3 ; 3,4) observés expérimentalement proviennent de la dissolution de C_3S_{sh} suivie de la précipitation d'un C-S-H de rapport $[C/S]_s < 3$.

En outre, nos expériences de dissolution sur filtre à grand débit montrent que la vitesse de transfert interfacial des ions de la surface hydroxylée est très grande puisqu'il faut un temps de passage très court ($\theta < 0{,}11$s) pour obtenir le rapport exact de congruence $[C/S]_\ell = 3$ et cela sans que la composition n'atteigne le domaine de nucléation rapide. Cette vitesse diminue en fonction de la concentration en chaux dans le solvant, non seulement dans les expériences d'évolution en système fermé, mais aussi dans celles de dissolution sur filtre à grand débit, ce qui montre que ce n'est pas seulement un problème de diffusion, mais que le transfert interfacial est concerné. La vitesse de la dernière étape du groupe 2) peut s'écrire en effet :

$$\frac{d[C]}{dt} = k - k' \frac{c_\ell}{c_r}[C] \qquad (4)$$

où c_ℓ et c_r sont respectivement les concentrations superficielles en lacunes de Ca^{2+} et en sites normaux d'ions Ca^{2+}. Si pour simplifier, on fait rentrer la probabilité de présence d'une lacune d'ion Ca^{2+}, $W = c_\ell/c_r$ dans la constante K d'équilibre, l'expression (4) devient :

$$\frac{d[C]}{dt} = k\left(1 - \frac{[C]}{K}\right) \qquad (5)$$

Cette équation (5) s'intègre facilement et donne :

$$\mathrm{Log}_e\left[1 - \frac{[C]}{K}\right] = -\frac{k}{K}t \qquad (6)$$

Or, si l'on considère par exemple, à partir des résultats d'expériences d'évolution de C_3S agité dans l'eau avec $\ell/s = 10$, les valeurs de $[C]$ aux instants successifs le long de la branche ascendante de la courbe de variation de la concentration en CaO en fonction du temps (voir par exemple les courbes construites indépendamment par D. Bertrandie et D. Ménétrier dans une autre de nos communications (3)) ; ces valeurs de $[C]$ donnent bien des droites lorsqu'on les porte dans l'expression (6) en prenant arbitrairement K = 40. Toutefois, comme le montre la figure (2) ces droites ne passent pas tout à fait par l'origine alors que la droite théorique devrait y passer. Comme les phénomènes sont complexes dans de telles expériences puisqu'il y a formation de C-S-H dont le rapport $[C/S]_s$ peut varier, le résultat obtenu paraît assez satisfaisant. *Il montre en tout cas qu'il n'est nul besoin de faire appel à la constitution d'une couche protectrice autour des grains pour expliquer le ralentissement de la dissolution.*

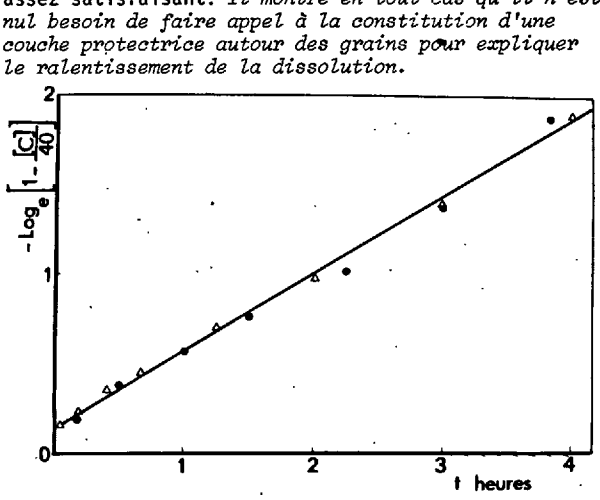

Fig. 2 - Transformée linéaire par la loi de vitesse de transfert des ions Ca^{2+} en solution en fonction de $[C]$ de la branche ascendante de la courbe d'évolution de C_3S agité dans l'eau à $\ell/s = 10$, d'après les résultats expérimentaux de : Δ D. Bertrandie (Dijon), o D. Ménétrier (Baltimore).

Mais il attire une autre remarque importante, c'est que, la concentration en silice $[S]$ diminuant simul-

tanément dans le milieu conformément à la courbe de solubilité de C-S-H, la vitesse de transfert interfacial en solution des ions silicates devrait avoir tendance à augmenter ; en effet les vitesses des étapes correspondantes du groupe 2) conduiraient à des lois semblables à l'équation (4). On devrait donc s'attendre à une distorsion de la dissolution congruente en faveur de la silice par rapport à la chaux. Or, nos expériences montrent qu'il n'en est rien et que le rapport $[\Delta C/\Delta S]_{\ell}$ reste égal ou légèrement supérieur à 3 (en raison de la précipitation de C-S-H) comme dans l'eau. Cela donne une idée des forces de compensation engendrées par les écarts à la stoechiométrie pour imposer l'alignement des vitesses de transfert en solution des différents ions et assurer la congruence de la dissolution. Il se peut que, dans un milieu stagnant, l'uniformité de composition de la solution au voisinage de l'interface soit perturbée par des processus d'adsorption et par une distribution particulière des charges sous l'influence d'un potentiel de surface. Mais cela ne doit pas conduire, en régime dynamique, à une accumulation indéfinie d'un des types d'ions et compromettre à terme la congruence de la dissolution.

Etat superficiellement hydroxylé :

La variation d'enthalpie libre $\Delta G'$ accompagnant l'hydroxylation superficielle est évidemment d'autant plus importante que C_3S_{sh} est moins soluble. Sa solubilité doit être suffisante pour expliquer la sursaturation de la solution par rapport au C-S-H. Faute de données expérimentales, du fait de l'absence de période d'induction avant nucléation de C-S-H, on ne peut faire qu'une évaluation reposant sur une valeur hypothétique de la solubilité de C_3S_{sh} dans l'eau.

Dans une note précédente (2), l'un de nous avait proposé un mode de calcul en admettant comme résultat d'une dissolution congruente de C_3S_{sh} à saturation, une valeur double, $[C] = 9{,}78.10^{-3}$ mol.kg^{-1} de celle que l'on obtient expérimentalement en faisant passer de l'eau à travers une couche mince ($\sim$ 1 mm) de C_3S sur filtre millipore (7,8). Dans ces conditions c'est, non pas une solution saturée de C_3S_{sh} qui est obtenue, mais un filtrat dont les germes de C-S-H ont été éliminés et qui, de ce fait, correspond à un domaine de plus faible sursaturation par rapport à C-S-H où la vitesse de nucléation de cet hydrate est petite.

Si l'on considère l'équation globale de passage en solution de C_3S :

$$3CaO,SiO_2 + 4H_2O \rightleftharpoons 3Ca^{2+}_{aq} + 5\ OH^-_{aq} + H_3SiO^-_{4\,aq}$$

le calcul de la solubilité à l'aide des ΔG^0_{298} de formation des différentes espèces conduit à une valeur de la solubilité théorique de C_3S très élevée (11) et qui paraît aberrante. L'hypothèse que nous avons formulée est précisément que l'étape cinétique d'hydroxylation superficielle consomme une grande partie de cette enthalpie libre et que ce sont les ions qui en résultent qui passent en solution réversiblement. Le calcul que nous avons proposé avec l'estimation indiquée ci-dessus de la composition de la solution saturée avec C_3S_{sh} conduit aux valeurs suivantes :

Passage de C_3S anhydre à C_3S_{sh} en équilibre avec sa solution : $\Delta G' = -75{,}2$ KJ.mol^{-1}.
Passage de C_3S_{sh} à la solution en équilibre avec C-S-H : $\Delta G'' = -15{,}38$ KJ.mol^{-1}.
On trouverait une valeur analogue pour $\Delta G''$ en calculant l'enthalpie libre de précipitation du C-S-H à partir de la solution en équilibre avec C_3S_{sh}.

Ces résultats illustrent l'importance de l'abaissement d'enthalpie libre consécutif à la formation de l'état superficiellement hydroxylé par rapport à celui qui accompagne la précipitation de C-S-H.

CONCLUSIONS

Le processus de dissolution congruente des espèces ioniques de l'état superficiellement hydroxylé ayant déjà emmagasiné pratiquement toute l'eau d'hydratation est un stade qui paraît bien établi à la fois expérimentalement et d'un point de vue thermodynamique, dans l'évolution de C_3S au contact non seulement de l'eau, mais de l'eau de chaux et quel que soit le rapport (ℓ/s). Ce processus rapide conduit, préférentiellement au voisinage immédiat de l'interface, à une sursaturation provoquant une nucléation immédiate de C-S-H de $[C/S]_s < 3$ dépendant de $[C]$ locale. Le ralentissement du transfert ionique interfacial en solution en fonction de $[C]$ paraît pouvoir s'expliquer par un effet cinétique normalement prévisible sans nécessiter l'intervention d'une couche plus ou moins perméable.

BIBLIOGRAPHIE

1.- M.E. TADROS, J. SKALNY et R.S. KALYONCU (1976), "Early hydration of C_3S", J. Am. Ceram. Soc., 59, n° 7-8, 344-347.

2.- P. BARRET (1979), "Sur l'existence d'un stade d'hydroxylation superficiel dans le processus de dissolution de C_3S", C.R. Acad. Sc. Paris, t 288, C, 461-464.

3.- P. BARRET, D. BERTRANDIE et D. MENETRIER (1980), "Comparative study of C-S-H formation from supersaturated solutions and C_3S solution mixtures", 7ème congrès international de la chimie des ciments, Paris.

4.- P. BARRET et D. MENETRIER (1980), "Filter dissolution of C_3S as a function of lime concentration", Cem. and Concr. Res. (à l'impression).

5.- J.H. THOMASSIN, M. REGOURD, P. BAILLIF et J.C. TOURAY (1979), "Etude de l'hydratation initiale de C_3S par spectrométrie de photoélectrons", C.R. Acad. Sc. Paris, t 288, C, 93.

6.- D. MENETRIER, I. JAWED, T.S. SUN et J. SKALNY (1979), "ESCA and SEM studies on early C_3S hydration", Cem. and Concr. Res., vol. 9, 473-482.

7.- D. MENETRIER (1977), "Contribution à l'étude cinétique de la période initiale d'hydratation de C_3S", Thèse Docteur d'Etat, Univ. de Dijon (France).

8.- P. BARRET (1979), "Les mécanismes d'hydratation et de durcissement des ciments", l'Industrie Nationale, n° 1, 3-41.

9.- P. BARRET, D. MENETRIER et D. BERTRANDIE (1977), "Cinétique d'hydratation des aluminates et silicates de calcium", Rev. int. Htes Temp. et Réfract., t 14, 127-133.

10.- R.A. KRÖGER (1964), "The chemistry of imperfect crystals", North-Holland Publishing Company, 208.

11.- H. N. STEIN (1972), "Thermodynamic considerations on the hydration mecanisms of C_3S and C_3A", Cem. and Concr. Res., vol. 2, 167-177.

Nous exprimons notre gratitude à la Société Lafarge pour sa coopération.

THÈME III

Structure des laitiers et hydratation des ciments de laitier

Structure of slags and hydration of slag cements

Président : M. VON EUW (France)

Hardened slag-cement pastes of low porosity

Pâtes durcies de ciment de laitier, à faible porosité

S.A. ABO-EL-ENEIN, Chemistry Department Qatar University Doha State of Qatar,

R.I. ABD-EL-MALEK and R.Sh. MIKHAIL, Department of Chemistry, Faculty of Science, Ain Shams University, Abbasia, Cairo, Egypte.

RESUME : Deux mélanges secs de ciment ont été préparés, contenant un poids égal de laitier et de clinker, broyés, l'un à la finesse de 5.000 cm2/g ± 100, l'autre à la finesse de 3.000 cm^2/g ± 100.

Pour obtenir des pâtes à faible porosité, trois méthodes ont été employées :

i. Pâtes normales malaxées à une teneur en eau, par rapport au ciment, de 0,20

ii. Pâtes préparées comme ci-dessus, puis comprimées, après mouillage, à des pressions variant entre 10 et 500 kg/cm2.

iii. Pâtes comprimées, avant hydratation, à des pressions variant entre 100 et 1000 kg/cm2, puis hydratées.

Pendant trois ans, on a mesuré l'évolution de la chaux libre, du laitier libre, de l'eau combinée, de la densité et de la résistance à la compression, de ces diverses pâtes. On a observé ainsi la cinétique de l'hydratation des ciments riches en laitier, et montré l'influence de la compression aux premiers âges. Pendant ces premiers âges, la chaux libérée par l'hydratation du clinker, accélère l'hydratation du laitier, et provoque la réaction topochimique. L'augmentation de la pression accélère cette hydratation, grâce à la réduction des trajets de diffusion de la chaux libre entre les grains de clinker et les grains de laitier.

La réactivité du laitier diminue quand la finesse de broyage diminue.

SUMMARY: Two dry cement mixtures were prepared from equal weights of slag and clinker having the same fineness of 6000 or 3000 cm^2/g, ± 100. Low-porosity pastes were prepared by three different methods: (i) normal pastes of initial water/cement ratio of 0.20; (ii) post-hydration compressed pastes prepared by compressing the pastes after mixing the cement with water at a ratio of 0.20, and by applying pressures ranging between 10 and 500 Kg/cm^2; and (iii) pre-hydration compressed pastes prepared by comparing the dry cement at pressures ranging between 100 and 1000 Kg/cm^2 before mixing with water.

Free lime, free slag, combined (non-evaporable) water content, bulk density and compressive strength were determined for pastes cured up to three years. Hydration kinetics could reveal the mechanism of hydration of the slag-rich cement pastes under investigation, and could show the effect of compression on the hydration mechanism especially during the early stages of hydration. During the early stages the calcium hydroxide released in the hydration of clinker activates the hydration of slag and the reaction proceeds topochemically. Increasing the compaction pressure increases the rate of hydration due to a decrease in the spaces located in between clinker and slag particles leading to a decrease in the diffusion path in which the free lime is proceeding to react with the slag grains.

With increasing particle size of cement constituents, the results obtained indicates the lower hydraulic reactivity of the granulated blastfurnace slag when ground to lower Blaine area.

INTRODUCTION

Several techniques were used and interesting conclusions have been advanced concerning the production of low-porosity compacted cement pastes. Kamio et al.(1), for example, showed that partially hydrated cement sets instantaniously on pressing to give high compressive strength. Hara et al (2) were able to obtain light weight building materials, having high strength and good fire-resistance, by mixing blastfurnace slag with lime, gypsum and fibrous materials, heating this mixture at 45°C in water, compression moulding at 30 kg/cm^2, curing and hardening. Grudemo (3) found that there is a relationship between strength of the cement and the volume of the solid phase of specimens prepared from crushed and compressed high alkali and high Al cement stone. In addition Yoshimoto et al (4) reported that by pulverizing hardened mortar, then placing it in a vessel and pressing, a remoulded compact of high strength is obtained through adhesion binding; the various factors affecting the compressive strength of the compacted remoulded specimens were also discussed.

On the other hand, Auskern et al (5) studied the effect of different curing conditions, including hot-pressing, on the capillary porosity of hardened Portland cement pastes using mercury porosimetry; they showed that hot-pressed pastes had essentially no porosity accessible to mercury. Usually high-strength cement pastes, prepared by hot pressing techniques, were investigated at various temperatures, hot pressing times and periods of hydration after hot pressing (6,7). Mikhail, Abo-El-Enein and Oweimreen (8) investigated the low-porosity Portland cement pastes prepared either by reducing the water/cement ratio to 0.20, or by the pre-hydration compression of the dry cement, followed by hydration under water; the changes in degrees of hydration, surface areas and pore structure are reflected on the compressive strength values of the various pastes.

In an earlier investigation (9), kinetics and mechanism of hydration of low-porosity slag-lime pastes were reported and the developed strength was significantly related to the chemical composition and/or the physical state of the formed hydrates. Under hydrothermal conditions, however, the reactivity of granulated slag was also reported (10).

The optimum composition of blastfurnace slag cement made from slag-clinker mixture was specified in order to get more favourable cementing materials (11). By studying the main characteristics of the system as well as the structure of the formed hydrates; the specified composition, obtained for the slag cement produced in Egypt, consists of equal weights of slag and clinker (12).

EXPERIMENTAL

The granulated blastfurnace slag used in this study has the following oxide composition: CaO, 46.00%; SiO_2, 35.04%; Al_2O_3, 14.58%; MgO, 2.97%; Fe_2O_3, 0.52% and SO_3, 0.14%. The phase composition of the Portland cement clinker used was: C_3S, 41.81%; β-C_2S, 27.65%; C_3A, 15.83% and C_4AF, 8.51%.

Two dry cement mixtures were prepared from slag and clinker having the same fineness of 6000 or 3000 cm^2/gm, ± 100. Equal weights of slag and clinker, having the same Blaine area, were first mixed in ethanol for one hour; then, ethanol was evaporated completely.

Three methods for the development of low-porosity slag cement pastes were used. These are (i) normal low-porosity pastes prepared with an initial water/cement ratio of 0.20, (ii) post-hydration compressed low-porosity pastes prepared by the compression of the freshly prepared paste, after mixing the cement with water (W/C = 0.20), by the application of various pressures of 10, 20, 50, 100 and 500 kg/cm^2 in cylindrical moulds to produce specimens of 3.14 cm^2 cross-section and 1 cm in height, and (iii) pre-hydration compressed low-porosity pastes prepared by the compression of the dry cement at various pressures of 115, 230, 460 and 1030 kg/cm^2 before hydration under water. The normal low-porosity pastes will receive the notations HN and LN for the high Blaine and low Blaine cement samples, respectively; the post-hydration compressed pastes were designated as H10, H20, H50, H100 and H500 for the high Blaine area cement, and L10, L50 and L100 for the low Blaine area cement according to the pressure used in compression; the pre-hydration compressed specimens will receive the notations H115p, H230p, H460p and H1030p for the high Blaine area cement, and L115p, L230p, L460p and L1030p for the low Blaine area cement, respectively.

The pastes were hydrated under water for ages of 0.25, 1,3,7,28,90,180,365, and 1095 days for the normal and post-hydration compressed pastes; and 1,3,6,9,12 and 36 months for the pre-hydration compressed specimens, respectively. At the end of each time interval, the fresh specimens were tested for compressive strength, bulk density, and the resulting crushed samples were then dried at 105°C for 24 hours to determine the evaporable water content. The free lime, free slag and combined (non-evaporable) water contents were determined in the crushed dried samples according to the methods described in an earlier publication (9).

RESULTS AND DISCUSSIONS

1. HYDRATION KINETICS AND MECHANISM

The results in Fig. 1 show that for the post-hydration and the pre-hydration compressed specimens, the non-evaporable (combined) water content increases with curing age and that the hydration of these slag cement specimens follows a consecutive reaction as

a result of an indirect activation of the blastfurnace slag with cement clinker.

During the early stages of hydration the combined water content increases with increasing the pressure of compaction (decreasing the initial porosity) after mixing the cement with water. This result is unexpected, since during the hydration of portland cement or slag cement with a lower slag content the increase in the initial porosity of the paste is associated with an increase in the combined water content (degree of hydration) mainly because more spaces are available for hydration products to deposit. However, in the hydration of the present pastes, which contain large amounts of blastfurnace slag (50% by weight), the hydration reaction starts with clinker to give hydration products composed mainly of calcium silicate hydrates and free calcium hydroxide. The free calcium hydroxide released during clinker hydration activates the hydration of granulated blastfurnace slag. Therefore, the slag grains react topochemically with the free calcium hydroxide solution located in the originally water-filled spaces, and consequently, by decreasing the spaces between clinker and slag particles (decreasing the porosity with increasing pressure of compression), the free lime will find a shorter diffusion path to react with slag grains leading to an increase in the rate of hydration of slag during the early stages of hydration. This stage ends after 3-7 days at room temperature for the post-hydration compressed pastes and after 2-3 months for the pre-hydration compressed specimens.

In the later stages of hydration, however, the normal expected behaviour predominates, namely the rate of hydration increases with increasing the porosity (decreasing the pressure of compaction) of the specimen. Higher porosity pastes can accomodate larger amounts of hydration products in their pore system than lower porosity pastes. Nevertheless, in the pre-hydration compressed specimens, the rate of diffusion of water through the partly hydrated sheath of the specimens into the unhydrated middle parts seems to be the rate controlling step in the final stages of hydration; the rate of hydration in the final stages increases with decreasing the compaction pressure used in the preparation of the specimens as a result of the increase in the rate of diffusion.

With increasing particle size of cement constituents, the differences in hydration kinetics diminishes during the early stages of hydration of the post-hydration compressed pastes; this result is associated with the lower hydraulic reactivity of the granulated blastfurnace slag when ground to a lower Blaine area. However, in the pre-hydration compressed specimens, the degree of compaction of coarse cement particles becomes less than that of fine cement particles when compressed at the same pressure leading to higher degree of hydration in the former pastes, especially during the early stages of hydration.

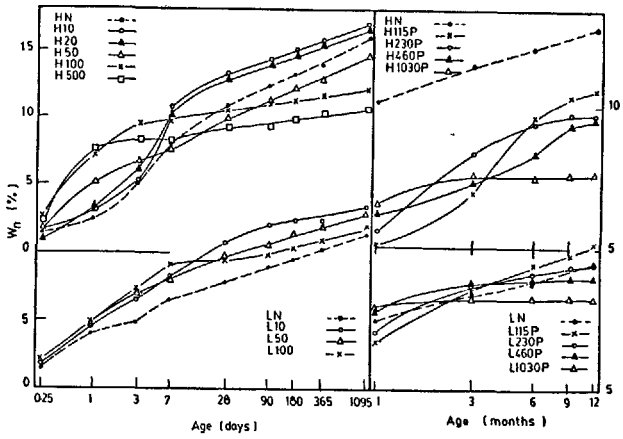

Fig. 1 - Combined water contents as a function of curing age

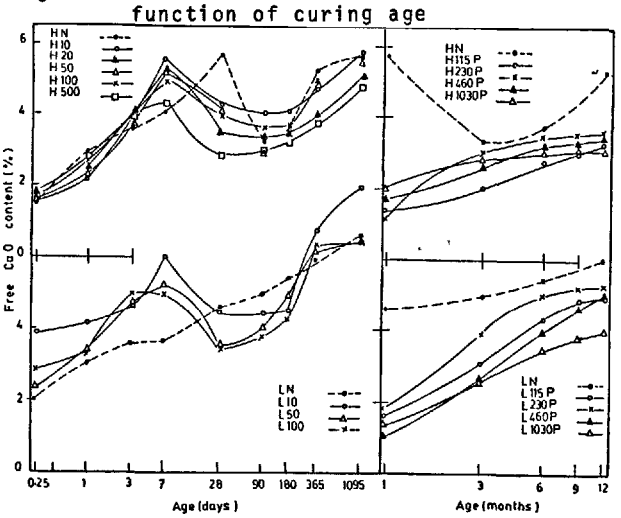

Fig. 2 - Free lime contents as a function of curing age

The results in Fig. 2 indicate that, for the post-hydration compressed pastes, the free lime content increases during the early stages of hydration up to 7 days. This result is mainly attributed to the fact that the amount of free lime released during clinker hydration exceeds that consumed by slag hydration at the early stages; therefore there appeared a net initial increase in the free lime contents of the specimens. After 7 days, however, the free lime content decreases as a result of its consumption by slag hydration; the acceleration period during slag hydration is then initiated leading to an increased rate of consumption of free lime by slag hydration as compared with the rate of release of free lime by clinker hydration. In the final stages of hydration, the major fraction of slag was already hydrated and a consequent increase in the free lime content was obtained. These results indicate that the rate of hydration of slag during the final stages, which is diffusion controlled, is very small

as compared with the rate of hydration of portland cement clinker.

In the hydration of the normal low-porosity pastes, prepared with an initial water/cement ratio of 0.20, there appeared a continuous increase in the free lime content of the pastes, prepared from the finer cement (Blaine area = 6000 cm^2/g), up to 28 days hydration; this result is due to the high initial porosity of the normal low-porosity pastes leading to a higher rate of clinker hydration for a longer period as compared with the rate of hydration of slag. By increasing the particle size of the slag and clinker grains, however, the free lime content shows a continuous increase at the various ages of hydration due to the decreased hydraulic reactivity of blast-furnace slag with increasing particle size.

The variations of the free lime contents with duration of hydration of the pre-hydration compressed specimens are similar to those obtained during the hydration of the post-hydration compressed pastes beyond one month hydration. This result indicates that the mechanism of hydration of the pre-hydration compressed specimens is almost similar to that of the post-hydration compressed pastes; the only difference is the diffusion of water into the compacted cement grains in the former specimens.

From free slag determination, the reaction ratio of slag could be derived and the values obtained are shown in Fig. 3.

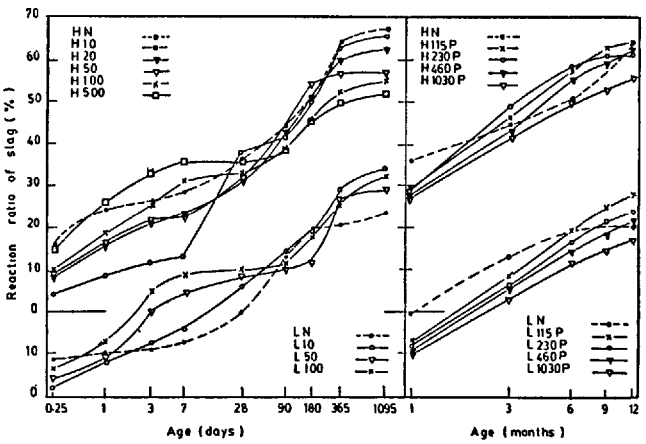

Fig. 3 - Reaction ratio of slag as a function of curing age

The results in Fig. 3 show that in the post-hydration compressed slag cement pastes, the hydraulic reactivity of granulated blast-furnace slag increases with increasing the pressure used in compression (decreasing the initial porosity) during the early stages of hydration, indicating that the hydration reaction is governed by the rate of dissolution of free lime released by the clinker grains and its subsequent diffusion to activate the slag grains. Apparantly, the hydration of granulated blastfurnace slag during the early stages of hydration is not under normal equilibrium conditions of saturation of the water-filled spaces by calcium hydroxide which needs longer times to attain this condition. Therefore, the early hydration of slag takes place in an unsaturated free lime solution and this leads to an increased rate of hydration with decreasing the distance of contact between clinker and slag grains. In the final stages of hydration, however, the hydration of slag proceeds under equilibrium conditions in the saturated lime solution when most of the clinker grains are consumed by hydration, leading to the accumulation of free lime; this effect leads to an increase in the rate of hydration of slag with decreasing pressure of compression (increasing initial porosity). In addition, higher porosity pastes could accomodate larger amounts of hydration products than the denser low-porosity pastes.

Evidently, the rate of slag hydration in the normal low-porosity pastes, prepared with water/cement ratio of 0.20 without compression, is found to be different than that in the compressed pastes indicating a difference in the mechanism of hydration.

In the pre-hydration compressed specimens, beyond the first month of hydration, the rate of hydration of slag increases with increasing the initial porosity of the specimen (decreasing the compaction pressure). Therefore, the rate of diffusion of water through the porous system of the unhydrous compacted specimens is not the rate controlling step, and the paste which is capable to accomodate larger amounts of hydration products in its pore system should have a higher rate of hydration.

In all pastes investigated, the hydraulic reactivity of the granulated blastfurnace slag was found to diminish markedly by decreasing the Blaine area of slag.

2. TOTAL POROSITY

The total porosity of the hardened cement paste could be calculated according to the relation : $\varepsilon = W_e/V_p$; where W_e is the weight of evaporable-water per one gram of the paste, and V_p is the volume of one gram of the paste.

The results shown in Fig. 4 clearly indicate that for the post-hydration compressed pastes, the total porosity decreases with increasing time of hydration; the fall in the total porosity is sharp during the early stages of hydration and is gradual during the later stages of the hydration process. In addition, the pastes compressed at higher pressures were found to have lower porosities than the pastes compressed at lower pressures when hydrated for the same age. Furthermore there appeared a sharper decrease in the total porosity of the denser (low initial porosity) pastes than that of the lean samples (compressed at lower pressure); this result might be partly attributed to the

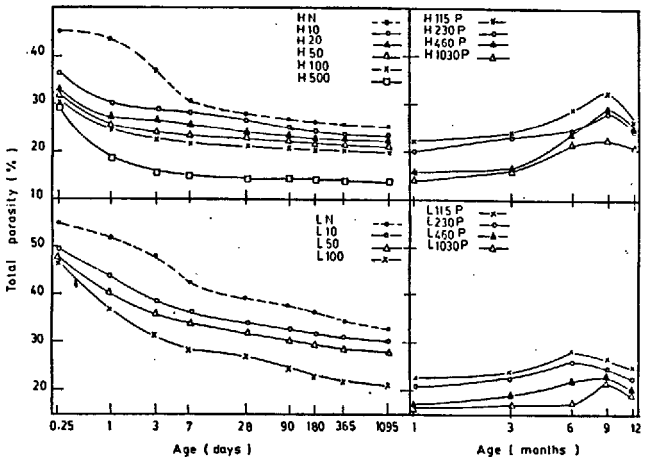

Fig. 4 - Total porosity as a function of curing age

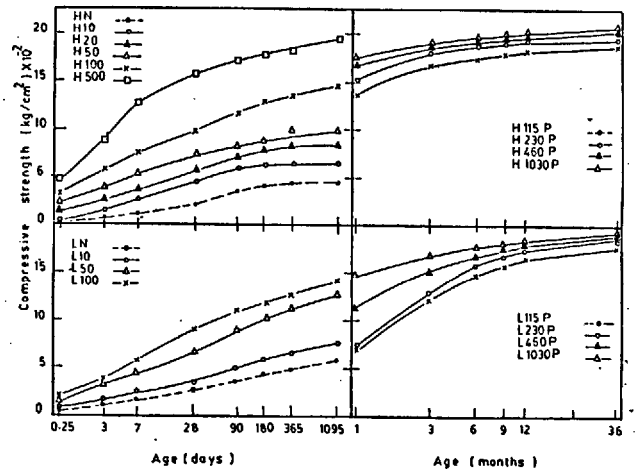

Fig. 5 - Compressive strength as a function of curing age

initial porosity as controlled by the pressure of compression, and partly due to the increased hydraulic reactivity of slag with clinker with increase of compression pressure (decreasing initial porosity) of the paste.

The total porosities of the hardened pastes prepared from the coarser slag cement were found to be higher than those of the pastes prepared from the finer cement, a result which is mainly due to the increased degree of compaction in the finely ground cement than in the case of the coarser cement; the hydraulic reactivity of the granulated slag is also diminishing with increasing particle size.

Actually, the total porosity of the pre-hydration compressed specimens could not be derived from the evaporable water contents due to the continuous diffusion of water through the compressed dry specimens.

3. COMPRESSIVE STRENGTH

The results in Fig. 5 clearly indicate that the strength of every cement paste increases with increasing age of hydration; this behavior is similar to that reported earlier, and which is normally correlated with the total porosity and degree of hydration. In addition, the compressive strength values are higher for the pastes prepared from the finely ground cement as compared with the values obtained using the coarser cement; this result might be attributed partly to the increased degree of compaction and partly to the increased hydraulic reactivity of the blastfurnace slag with decreasing particle size.

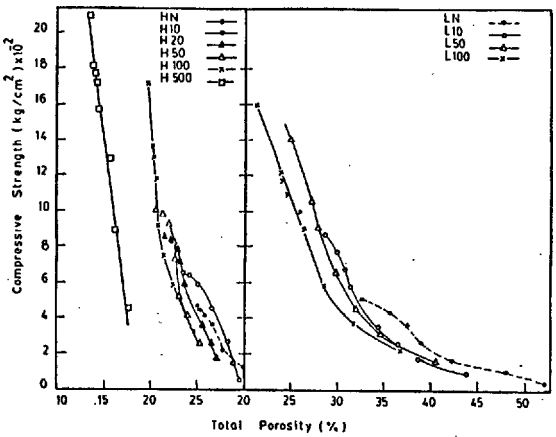

Fig. 6 - Compressive strength versus total porosity of the post-hydration compressed pastes

The relation between compressive strength and total porosity is shown in Fig. 6 for the post-hydration compressed pastes. There appeared a gradual and slight increase in the strength with decreasing porosity at relatively higher porosity values, where the amounts of hydration products deposited in the pores contribute slightly to the strength development. At intermediate total porosities, a distinguishable increase in the compressive strength with decreasing porosity was observed; such notable increase in strength was obtained below a certain porosity value characteristic of the initial porosity of the compressed paste as controlled by the pressure used during the compression. In this range of total porosity, the precipitation of the hydration products within the pore system has a distinct contribution to the strength of the hardened pastes. At lower values of toal porosity (longer time of hydration) only a slight increase in strength with decreasing porosity was observed for the pastes compressed at relatively low pressures (10-50 kg/cm^2); this result might be associated with the nature of the hydration products to undergo some sort of partial crystallization as a result of the available empty spaces provided by the initial porosity of the paste. At

relatively higher compression, however, (pressures of 100 and 500 kg/cm^2), the lower porosity values cause a sharp increase in the strength of the paste, and this is mainly attributed to the highly amorphous (ill-crystalline) state of the hydration products as controlled by the extremely limited initial porosity.

BIBLIOGRAPHY

1.- T. KAMIO, O. MATSUDA and H. NAKANO (1975) "Instantaneous hardening by pressing of hydrated cement", Cemento Gijutsu Nenpo, 29, 452-5.

2.- N. HARA, N. INOUE, MIYAMOTO and M. INOUE (1977) "Lightweight building material from blastfurnace slag", Japan Kakai, 77, 222, 23 Feb. 1977, Apl. 19 Aug. 1975.

3.- A. GRUDEMO (1976) "Strength of cement stone in relation to its structure", Gidratatsiya Tverd. Tsem., 2, pt. 1, 302-6.

4.- I.A. YOSHIMOTO, C. TASHIRO and H. SHIRAGAMI (1978) "Remolding of hardened mortar", Cement Concr. Res., 8, 87.

5.- A.B. AUSKERN and W.H. HORN (1976) "Effect of curing conditions on the capillary porosity of hardened portland cement pastes", J. Am. Ceram. Soc., 59, 29-33.

6.- G.R. GOUDA and D.M. ROY, (1975) "Properties of hot-pressed calcium aluminate cements", Cement Concr. Res., 5, 551-564, and references cited there.

7.- S.O. OYEFESOBI and D.M. ROY (1977) "Effect of admixtures on hot-pressed cements", Cement Concr. Res., 7, 165-72.

8.- R.Sh. MIKHAIL, S.A. ABO-EL-ENEIN and G.A. OWEIMREEN (1973) "Surface area and pore structure of low-porosity cement pastes" in "Recent Advances In Science And Technology Of Materials", ed. A. BISHAY, Plenum Press, Vol. 1, p. 337.

9.- S.A. ABO-EL-ENEIN, M. DAIMON, S. OHSAWA and R. KONDO (1974) "Hydration of low porosity slag-lime pastes", Cement Concr. Res., 4, 299-312.

10.- R. KONDO, S.A. ABO-EL-ENEIN and M. DAIMON (1975) "Kinetics and mechanisms of hydrothermal reaction of granulated blastfurnace slag", Bull. Chem. Soc. Japan, 48, 222-6.

11.- S.A. MIRONOV, S.A. VYSOTSKU and M.V. SMIRNOVA (1976) "Hardening of cement-based concretes containing different amounts of blastfurnace slags", Tsement, 7, 6-7.

12.- R.Sh. MIKHAIL, S.A. ABO-EL-ENEIN and M.A. SHATER (1977) "Investigation on the early hydration of some specified Egyptian slag cements", Egyptian Journal of Chemistry, 20(5).

L'hydratation hydrothermale des laitiers

The hydrothermal hydration of slags

A.A. GOVOROV, Institut de chimie colloïdale et de chimie de l'eau, Kiev, U.R.S.S.

RESUME : L'on a étudié l'hydratation et le durcissement des coulis de laitiers vitreux synthétiques du système $CaO-MgO-Al_2O_3-SiO_2$ dans des bombes hydrothermales dont on élevait progressivement la température à la vitesse de 150°C/h jusqu'à 285°C.

La diminution du rapport $CaO:SiO_2$ dans la composition des laitiers entraîne une réduction de la vitesse du passage en solution de la silice, mais aussi un accroissement des teneurs maximales de silice dissoute ainsi que des températures auxquelles ces maxima sont atteints pour la première fois. Cela peut s'expliquer d'une part par un plus haut degré de condensation des tétraèdres siliciques dans la structure des laitiers, et d'autre part par le déficit croissant en CaO.

L'apparition d'hydrosilicates de calcium ainsi que le début du durcissement des coulis succèdent au premier maximum de teneur de silice en solution, et correspondent à un accroissement de leur résistance électrique. Les ajouts de CaO, dans certaines proportions, ont pour effet d'abaisser les températures auxquelles ces maxima sont atteints, et font apparaître à des températures moins élevées un accroissement préliminaire de résistance électrique, qui met en évidence un stade plus avancé dans la formation des hydrosilicates de calcium. Il semble qu'à ce stade la part des réactions topochimiques soit importante.

SUMMARY : The author investigated the hydration and hardening processes of finely ground synthetic vitreous slags in the system $CaO-MgO-Al_2O_3-SiO_2$, which were heated in hydrothermal bombs to 285°C at the rate of 150°C/h.

It was found that a decrease of the $CaO:SiO_2$ ratio in the slag compositions is slowing down the early dissolution of silica, but at the same time it increases its maximal concentrations in solution, as well as the temperatures they are reached at first. This may be explained by a higher degree of condensation of the SiO_4 tetrahedra in the structure of the slags, and by the increasing lack of CaO.

The appearance of the calcium silicate hydrates, as well as the beginning of hardening are coming next to the first maximum of silica in solution, and correspond to an increase in the electrical resistance of the slag suspensions. Additions of CaO, made in certain proportions, lower the temperatures at which this maximum occurs, and cause a preliminary increase in the electrical resistance, indicates an earlier step of formation of the calcium silicate hydrate phase. The role of the topochemical processes seems to be important at this stage.

Le durcissement des liants hydrauliques résulte de la destruction hydrolytique plus ou moins profonde de leurs constituants anhydres et de la formation de phases hydratées en particules extrêmement fines, pratiquement insolubles dans l'eau. La cinétique de cette destruction, ainsi que celle de la formation des produits hydratés joue un rôle de premier plan.

L'intensification de ces réactions en milieu hydrothermal a pour effet de conférer une activité hydraulique et des propriétés liantes à certains matériaux inertes à la température ambiante, tels en particulier les laitiers métallurgiques finement moulus. Du fait de l'accroissement du degré de dissociation de l'eau et de la mobilité des ions H^+ et OH^- avec la température, ainsi que du nombre de liaisons Si-O-Si rompues (1,2), le passage en solution de la silice se trouve facilité. Cela a pour effet d'intensifier la genèse des phases hydratées, ainsi que le durcissement des pâtes, mais aussi la croissance des cristaux et leurs transformations éventuelles, ce qui peut nuire au durcissement.

L'une des applications intéressantes de l'aptitude au durcissement des suspensions de laitiers en milieu hydrothermal est leur emploi pour la consolidation des puits de pétrole et de gaz naturel profonds. Dans les conditions de température et pression élevées qui y régnent les liants à base de laitiers présentent des avantages incontestables sur ceux à base de ciment portland (3,4), en particulier une meilleure résistance mécanique et à la corrosion, ainsi qu'un prix de revient moindre.

La structure des constituants anhydres des liants hydrauliques est un facteur primordial de leur activité. Dans le cas des liants à base de laitiers son importance est encore accrue du fait de la diversité de composition et de structure des laitiers industriels.

Le problème de la structure de la phase vitreuse des laitiers granulés et du verre en général n'est pas encore résolu. Il est cependant acquis que leur structure contient des éléments ordonnés, dont la forme et les dimensions restent toutefois hypothétiques. Selon (5) la phase vitreuse des laitiers granulés contiendrait des groupements d'ions dénommés "phases quasi cristallines", pouvant être des structures du type Zachariasen, des structures cristallitiques ou de tout autre nature. Selon ces auteurs ces groupements dépendent des sous-systèmes de paragenèse de phases, où la phase primaire joue probablement un rôle prépondérant.

L'on sait d'autre part que les groupements possibles de tétraèdres siliciques SiO_4 dépendent dans leur forme et leurs dimensions de la proportion relative d'atomes de silicium et d'oxygène se trouvant dans le verre. Ainsi dans le cas où Si:O est inférieur à 0,286 les tétraèdres siliciques ne peuvent théoriquement se grouper que par deux ou qu'être isolés les uns des autres; lorsque Si:O est compris entre 0,286 et 0,333 ces tétraèdres peuvent se grouper par deux ainsi qu'en anneaux ou chaînes séparés; lorsque Si:O est compris entre 0,333 et 0,400 ces groupements de tétraèdres peuvent se réunir dans le plan et dans l'espace par l'intermédiaire de tétraèdres communs; lorsque Si:O est compris entre 0,400 et 0,500 il ne peut plus y avoir de groupements séparés, tous les tétraèdres étant nécéssairement réunis par au moins trois des sommets (atomes d'oxygène) en un réseau, dont la densité devient maximale lorsque Si:O atteint la valeur 0,500.

L'existence de tels groupements de tétraèdres siliciques, ainsi que leur accroissement avec la teneur en silice sont confirmés par les études au moyen de spectres infrarouges (6,7,8). Cependant leur interprétation dans le cas des laitiers vitreux est compliquée par la présence de tétraèdres AlO_4 et de liaisons Si-O-Al en proportions difficiles à déterminer avec précision.

D'après nos résultats de recherches (9,10) effectuées sur des laitiers vitreux synthétiques $CaO-MgO-Al_2O_3-SiO_2$ avec 0 et 5% MgO il semble que l'on puisse distinguer: les laitiers orthosilicatiques, donnant une bande d'absorbtion IR ayant deux à trois faibles maxima dans l'intervalle 860-950 cm^{-1}; les laitiers alumineux, donnant une bande avec deux maxima 760-780 et 950-980 cm^{-1}, le premier étant le plus intense; les laitiers mélilitiques, donnant les bandes 700-730 et 950-990 cm^{-1}; les laitiers wollastonitiques donnant les bandes 720-810 et 1000-1050 cm^{-1}; les laitiers anorthitiques donnant les bandes 790-800 et 940-1110 cm^{-1}, cette dernière étant la plus intense et comportant deux maxima à 940-980 et 1090-1110 cm^{-1}.

Compte tenu de la disposition des points figuratifs de ces laitiers sur le diagramme du système $CaO-MgO-Al_2O_3-SiO_2$ à 5% MgO, et de l'intérprétation structurale (6,7,8) des spectres IR des silicates et alumosilicates, l'on peut admettre l'existence de tétraèdres isolés dans les laitiers orthosilicatiques, de groupements limités et séparés de tétraèdres dans les laitiers mélilitiques, de groupements illimités pouvant être réunis par des tétraèdres communs dans les laitiers wollastonitiques, d'un réseau de tétraèdres tous réunis entre eux dans les laitiers anorthitiques.

Au traitement hydrothermal à 200-250°C les laitiers mélilitiques donnent essentiellement des hydrogrenats, et les laitiers wollastonitiques - de la tobermorite (10-11). Ainsi la disparition des groupements limités et séparés de tétraèdres au profit de leurs groupements polymères illimités dans la structure du laitier correspond à un changement analogue dans celle de leurs produits d'hydratation au cours du traitement hydrothermal.

Le coulis de ciment introduit dans les puits de forage est soumis, au cours de sa descente jusqu'au niveau nécessaire, à un accroissement considérable de température et de pression, et ne doit pas faire prise ni durcir pendant sa mise en place, qui dure en moyenne de une à deux heures et demi. Aussi l'étude de l'hydratation et du durcissement des ciments au cours d'une élévation progressive de température en milieu hydrothermal présente-t-elle un intêret pratique pour cette application.

De telles recherches ont été effectuées en notre laboratoire sur des coulis de laitiers vitreux synthétiques, moulus jusqu'à la finesse de 3500-4000 cm^2/g. La pâte à 50% d'eau était introduite dans des moules cylindriques que l'on immergeait aussitôt dans des bombes hydrothermales remplies d'eau distillée à 80% de leur volume intérieur. Celles-ci étaient alors chauffées à la vitesse de 150°/h jusqu'à diverses températures, puis rapidement refroidies par de l'eau froide.

L' on déterminait alors, par la méthode du complexe silicomolybdique, la fraction de silice du laitier se trouvant en solution, exprimée en pourcentage pondéral. Le durcissement de la pâte était exprimé par la résistance à la pénétration d'un cône de duromètre, calculée en N/mm^2. Par ailleurs l'on enregistrait, dans un autoclave spécialement conçu (10), les variations de résistance électrique du coulis en cours de montée en température.

Les laitiers synthétiques étudiés étaient obtenus par fusion à 1600-1700°C et refroidissement brusque à l'eau froide, de deux séries de mélanges d'oxydes purs, contenant respectivement 5 et 20% en poids de Al_2O_3 pour 5% de MgO, avec $CaO:SiO_2$ variable.

TABLEAU DES COMPOSITIONS

	Teneurs, moles %				C/S	Type de laitier
	CaO	MgO	Al_2O_3	SiO_2		
A	51,6	7,2	2,8	38,4	1,34	orthosil.
B	41,5	7,2	2,9	48,4	0,85	wollast.
C	31,4	7,2	2,9	58,5	0,53	wollast.
D	21,0	7,3	2,9	68,8	0,31	anorth.
E	44,2	7,7	12,1	36,0	1,22	mélilit.
F	33,3	7,7	12,2	46,7	0,72	wollast.
G	22,4	7,8	12,3	57,5	0,39	anorth.
H	11,3	7,8	12,4	68,5	0,17	anorth.

L'on voit sur la fig.1 que la fraction de silice des laitiers qui se trouve en solution croît différemment selon leur composition et leur type. Avec la diminution du rapport CaO/SiO_2 l'on observe: a/ un ralentissement du passage en solution de la silice, b/ un accroissement de la fraction de la silice du laitier se trouvant en solution aux teneurs maximales, c/ un décalage de ces maxima vers les températures plus élevées. L'accroissement des teneurs en alumine des laitiers jusqu'à 20% a pour effet d'intensifier légèrement le passage de la silice en solution aux basses températures, mais aussi de réduire ses teneurs maximales en solution.

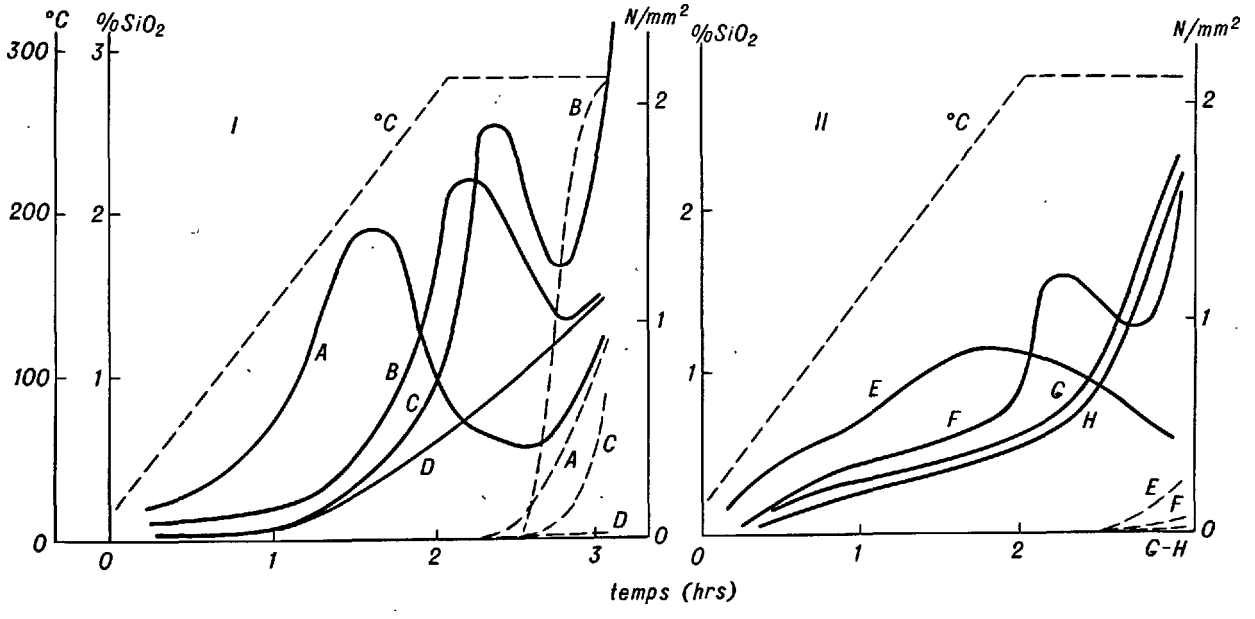

Fig. 1 - Les variations des teneurs de silice en solution (trait plein) et le durcissement des coulis (pointillé) des laitiers contenant 5% (I) et 20% (II) d'alumine (voir tableau ci-dessus).

Les considérations sur la structure des laitiers vitreux exposées au début de cette communication permettent d'expliquer la lenteur initiale du passage en solution de la silice des laitiers acides par le degré de condensation élevé de leurs tétraèdres SiO_4. La légère accélération initiale observée dans le cas des laitiers plus riches en alumine pourrait être due à l'introduction de tétraèdres AlO_4 parmi les tétraèdres siliciques, entraînant une certaine diminution du degré de condensation de ceux-ci, à teneurs en silice égales (en moles %).

Une contribution intéressante à l'interprétation des maxima de teneurs de silice en solution est fournie par les mesures de résistance électrique des coulis au cours de leur traitement hydrothermal. Afin de mettre en évidence l'influence propre du laitier sur la résistance électrique de l'eau, et d'exclure l'effet de l'échauffement, nous avons comparé les variations de résistance R_e de l'eau distillée avec celles des coulis de laitiers R_s, et considéré le rapport $(R_e-R_s):R_e$ exprimé en % aux différetes températures.

La fig. 2 montre les variations de ce rapport en fonction de la température dans le cas de trois laitiers synthétiques à 5% d'alumine. L'on voit que l'abaissement de résistance électrique de l'eau par le laitier (ou plus exactement par le passage en solution de ses constituants) croît d'abord avec

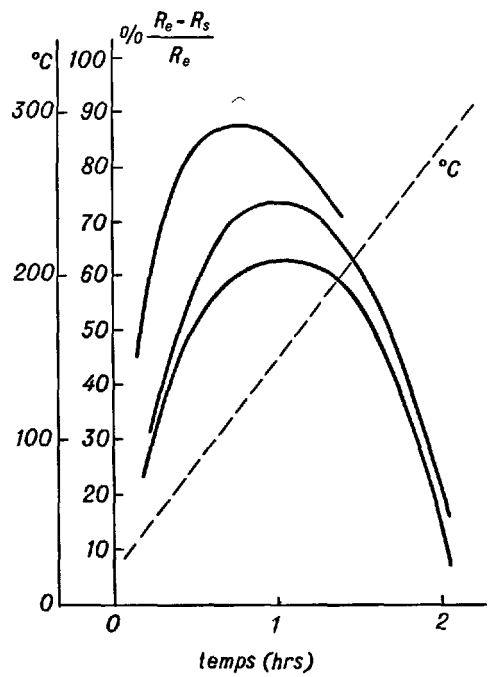

Fig. 2 - L'abaissement relatif de la résistance électrique de l'eau par les laitiers A, B, C, au cours de la montée en température hydrothermale des coulis.

la température, passe par un maximum entre 120 et 160°C, puis décroît. La valeur de ce maximum diminue avec le rapport $CaO:SiO_2$ du laitier, tandis que la température correspondante augmente. Cela semble indiquer que ces courbes réflètent essentiellement les variations de teneur de CaO en solution.

La comparaison des fig. 1 et 2 permet alors de constater que ces maxima de teneur de CaO en solution surviennent en même temps qu'une accélération du passage de la silice du laitier en solution. Ainsi est mise en évidence la recombinaison de la chaux, préalablement lixiviée du laitier, avec la silice passée en solution, avec pour résultat la formation de silicates de calcium hydratés. Des diagrammes de rayons X ont en effet montré l'apparition des raies principales de la tobermorite dès 280°C dans le cas du laitier B dans ces conditions de traitement.

L'accroissement de la teneur maximale de silice en solution avec sa teneur dans les laitiers s'explique par le déficit croissant en CaO nécessaire à sa recombinaison en silicates de calcium hydratés, ce qui se confirmera plus loin. La diminution de la teneur maximale de silice en solution dans le cas des laitiers plus riches en alumine correspond à la formation d'une quantité moindre d'hydrosilicate. Nous avons de même observé une réduction de cette teneur maximale dans le cas d'un remplacement partiel de CaO par MgO dans la composition des laitiers.

Ainsi qu'on le voit sur la fig. 1, la teneur maximale de silice en solution n'est pas atteinte dans le cas des laitiers D, G, H, du type anorthitique. Il est intéressant de constater que si l'on admet qu'en moyenne 2/3 des atomes d'aluminium se trouvent en coordination tétraèdrique dans les laitiers vitreux, le degré de condensation des tétraèdres SiO_4 et AlO_4 donné par le rapport $(Si+2/3Al):O$, sera respectivement égal à 0,394 , 0,405 , 0,439 pour les laitiers D, G, H, c'est à dire sera pratiquement égal ou supérieur à 0,400. Ainsi la limite entre les domaines de composition des laitiers wollastonitiques et anorthitiques, basée sur les données des spectres IR semble s'accorder avec celle basée sur le calcul du degré de condensation des tétraèdres si l'on admet que 2/3 des atomes d'aluminium sont tétracoordonnés.

La teneur de silice en solution passe par une série de nouveaux maxima lorsqu'on maintient constante pendant quelques heures la température à 285°C, leur amplitude étant la plus élevée dans le cas des laitiers wollastonitiques. La teneur moyenne de silice en solution se stabilise alors pour quelque temps à des niveaux d'autant plus élevés que le degré de condensation des tétraèdres siliciques est plus grand. Cette stabilisation survient dès avant 100°C dans le cas des laitiers orthosilicatiques et entre 150 et 250° pour les laitiers mélilitiques.

On a vu sur la fig.1 que les coulis commen-

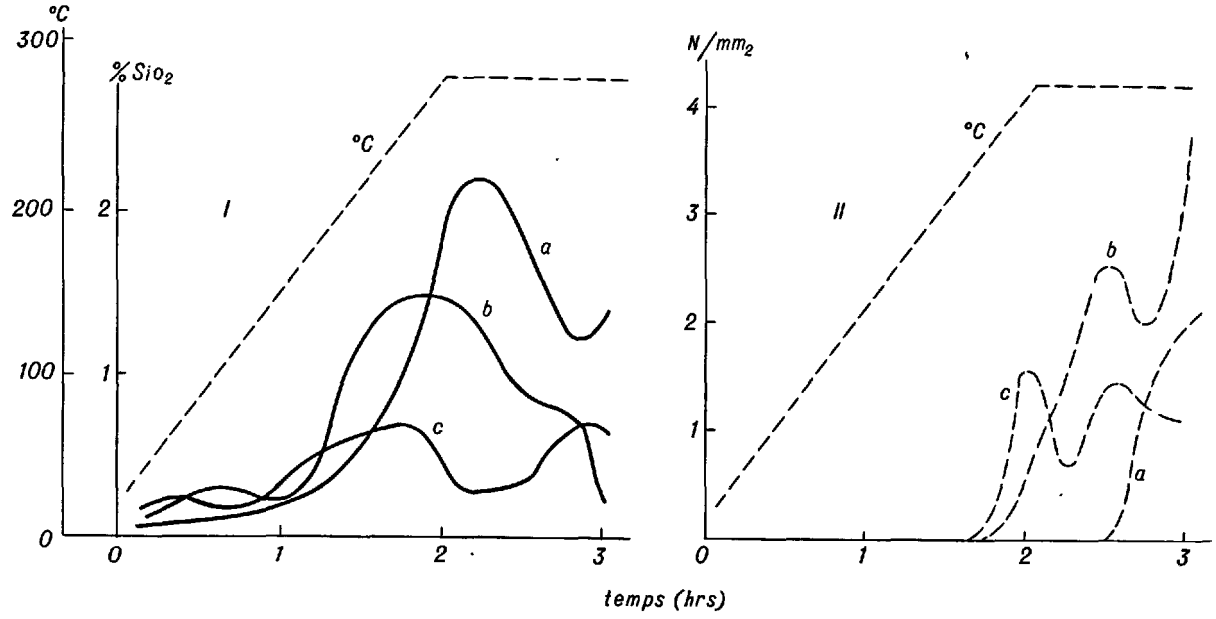

Fig. 3 - Les variations des teneurs de silice en solution (I) et le durcissement des coulis de laitier B (II), sans ajout (a) et avec ajout de 0,3% CaO (b), et de 3% CaO (c).

cent à durcir lorsque la teneur de silice en solution baisse après avoir atteint sa valeur maximale. Le durcissement le plus intense s'observe dans le cas du laitier B du type wollastonitique, ayant donné de la tobermorite dans ces conditions. Au cours d'un traitement hydrothermal de 48 h à 250°C ce sont également les laitiers wollastonitiques qui donnent les résistances mécaniques les plus élevées (10,11).

L'addition de CaO aux laitiers a pour effet (fig.3) d'abaisser les teneurs maximales de SiO_2 en solution, ainsi que les températures auxquelles elles sont atteintes. En même temps le passage de la silice en solution est sensiblement intensifié aux basses températures. Ainsi la chaux accélère aussi bien le passage de la silice en solution que sa recombinaison en hydrosilicates de calcium. Cela a pour effet d'avancer le début du durcissement, ainsi que le montre la fig.3, cependant le gain de résistance mécanique initiale qui en résulte diminue lorsque la quantité de CaO ajoutée dépasse un certain optimum, en l'occurrence 0,3-0,8%.

Cela se répercute également sur l'allure des courbes de résistance électrique des coulis (fig.4). Dans le cas du laitier B sans ajout la baisse initiale de résistance, due à l'échauffement et au passage en solution des constituants du laitier, se ralentit entre 150 et 170°C, ce qui correspond au maximum de la fig.2, ainsi qu'au début du passage en solution accéléré de la silice (fig.1). L'accroissement ultérieur de la résistance électrique correspond à la baisse de teneur de silice en solution, ainsi qu'au début du durcissement du coulis.

En présence d'ajout de CaO la résistance électrique initiale du coulis se trouve considérablement réduite, mais elle augmente brusquement avant que la température ait atteint 100°C. L'intensité de cet accroissement croît avec la quantité de CaO ajoutée, mais diminue lorsqu'elle dépasse 0,3-0,8%, c'est à dire la quantité qui s'est révélée optimale pour l'intensification du durcissement initial.

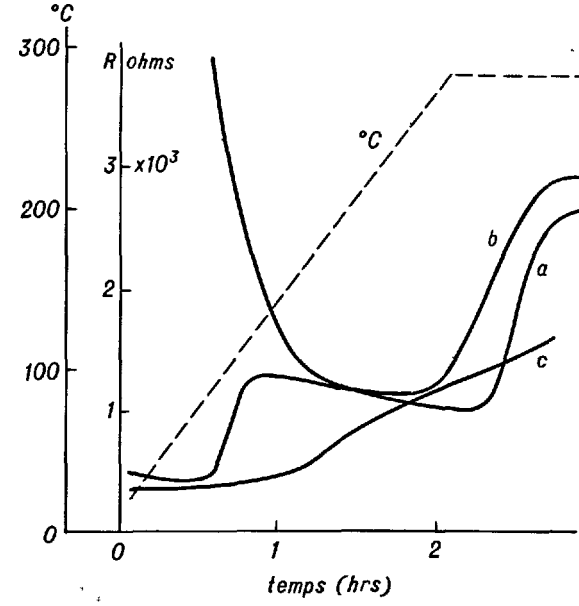

Fig.4 - Les variations de résistance électrique du coulis de laitier B sans ajout (a), et avec ajout de 0,3% CaO (b), et 3% CaO (c).

Il est intéressant de constater que cet accroissement de résistance électrique ramène sa valeur à celle du coulis sans ajout, et compense sa chute initiale due à la chaux. En outre cet accroissement de résistance correspond à l'apparition de produits d'hydratation et à un épaississement du coulis.

Etant donné que l'intensification par CaO du passage de la silice en solution aux basses températures est beaucoup plus faible que l'accroissement de résistance électrique mentionné, l'on est amené à admettre que les réactions topochimiques jouent un rôle important à ce stade avancé.

L'on a également étudié le comportement des laitiers réels de haut-fourneau dans les mêmes conditions de traitement hydrothermal, et obtenu des résultats analogues, quant aux variations de teneur en silice en solution et au durcissement des coulis. Les laitiers de haut-fourneau se rapportant au type mélilitique de notre classification, des ajouts de sable siliceux permettent d'obtenir des mélanges correspondant à des valeurs moins élevées du rapport $CaO:SiO_2$ et équivalents aux laitiers du type wollastonitique. De tels mélanges sont utilisés avec succès dans les puits de forage profonds (4).

CONCLUSIONS

Au cours de l'hydratation, en milieu hydrothermal à température et pression progressivement croissantes, des laitiers granulés moulus, la teneur de silice en solution croît différemment selon leur composition et le degré de condensation des tétraèdres siliciques dans leur structure.

Il existe un lien entre les premiers maxima de teneur de silice en solution, les variations de résistance électrique des coulis au cours de leur échauffement hydrothermal, l'apparition des produits d'hydratation et le début du durcissement des coulis.

Des ajouts de CaO en certaines proportions abaissent considérablement les températures auxquelles la silice en solution atteint les teneurs maximales, ainsi que ces teneurs elles-mêmes, et accélèrent le durcissement des coulis. Les réactions topochimiques semblent jouer un rôle important au premier stade de l'action du CaO.

Les résultats de ces recherches peuvent contribuer à l'utilisation rationnelle des divers laitiers métallurgiques dans la fabrication des ciments destinés à durcir en milieu hydrothermal, en particulier dans les puits de forage profonds.

L'auteur tient à exprimer sa reconnaissance à ses collaborateurs E.V.Djouss, N.V.Bakouchina et L.I.Khokhlova pour leur participation dans la partie expérimentale de ces recherches.

BIBLIOGRAPHIE

1.- E.D. LACY (1967), "Etude de la vitesse des réactions métamorphiques", dans "La nature du métamorphisme" (en russe), éd. "Mir", Moscou, pp.147-160.

2.- J. WYART (1964), "Le mécanisme de l'action de l'eau dans les conditions de température et pression élevées lors de la synthèse et des transformations des silicates", dans "La chimie de l'écorce terrestre" (en russe), éd. "Naouka", Moscou, pp.156-168.

3.- A.I. BOULATOV (1964), "La consolidation des puits de forage profonds" (en russe), éd. "Nédra", Moscou.

4.- A.I. BOULATOV, D.F. NOVOKHATSKY (1974), "Oil-well cements for high-temperature bore wells", The VI International Congress on the Chemistry of cement, Moscow, Suppl. paper, Section III-6, III-7.

5.- S. SOLACOLU, P. BALTA (1964), "Les propriétés hydrauliques des laitiers de haut-fourneau du système $MgO-CaO-Al_2O_3-SiO_2$ contenant du manganèse et du soufre" Revue des matériaux de construction et des travaux publics, n°583, pp.95-110.

6.- V.S. FARMER (1964), "Infra-red Spectroscopy of Silicates and Related Compounds", in "The Chemistry of Cements", ed. H.F.W. Taylor, "Academic Press", London - New York, vol.2, pp.289-309.

7.- A.N. LAZAREV (1968), "Les spectres de vibration et la structure des silicates" (en russe), éd. "Naouka", Léningrad.

8.- P. TARTE (1967), "Infra-red spectra of inorganic aluminates and characteristic vibrational frequences of AlO_4 tetrahedra and AlO_6 octahedra", Spectrochimica Acta, vol.23A, pp.2127-2143.

9.- A.A. GOVOROV (1974), "Hydrothermal hardening of Slag glasses dispersions", The VI International Congress on the Chemistry of Cement, Moscow, Suppl. paper, Section III-2.

10.-A.A.GOVOROV (1976), "Le durcissement hydrothermal des suspensions de laitiers" (en russe), éd. "Naoukova doumka", Kiev.

11.-A.A.GOVOROV, E.V.DJOUSS, N.A.OVRAMENKO (1973), "La cinétique du durcissement hydrothermal des suspensions de verres $CaO-MgO-Al_2O_3-SiO_2$", dans "La mécanique physico-chimique et la lyophilie des systèmes dispersés" (en russe), éd. "Naoukova doumka", Kiev, n°5, pp.116-119.

Composition, Morphology, Hydration and Bond Characteristics of some Granulated Slags

Composition, Morphologie, Hydratation et Propriétés adhésives de quelques laitiers granulés

H. ROPER, Senior Lecturer, Department of Civil Engineering, The University of Sydney, Australia.

RESUME : La technologie de la fabrication du ciment dépend du mode de production du laitier. Une étude de la morphologie d'une série de laitiers granulés a été faite afin d'étudier l'influence de leur composition et de leur mode de trempage. Il est suggéré que certains laitiers ont tendance à présenter les caractéristiques des liquides de Stuart, c'est à dire une grande facilité de formation de particules aciculaires ou en forme d'aiguilles.

Certains résultats d'essais de compression et de traction et des observations au microscope électronique suggèrent que l'adhérence entre la surface des particules de laitier et les produits de l'hydratation du ciment de Portland est inférieure à celle du sable quartzeux. Ceci mène à la suggestion que les surfaces de certains laitiers tendent à être de caractère hydrophobe.

SUMMARY : Different methods of producing granulated slags are influencing the technology of cement binder production. A study has been made of the morphology of a series of granulated slags in order to study the influence of composition and quench methods used in their production. It is suggested that certain of the slags tend to show the characteristic of Stuart liquids, viz great ease of acicular or needle-like particle formation.

Some data on compressive and tensile testing combined with electron microscopy suggest that the bond between a slag particle surface and portland cement hydration products is lower than that for quartz sand. This has led to the suggestion that the surfaces of certain slags tend to be hydrophobic in character.

INTRODUCTION

In Australia, research interest in slags for use in hydraulic cements dates back to 1966, when production of blended cements consisting of an interground mixture of granulated slag and portland cement clinker commenced. The developmental work was described by Ryan (1), who, for the locally produced slag, noted in particular, the retardation of initial set when concrete was cast at low ambient temperatures, and its high susceptibility to the adverse effects of improper curing. Since then such blended cements have been produced from Port Kembla slags in New South Wales where up to 100,000 tonne of granulate is used annually, and, more recently, from Kwinana in Western Australia, where a blended cement containing 30% ground granulated slag is being produced by two companies leading to the use of 50,000 tonne per annum of granulate.

METHODS OF GRANULATION

In the past slag cements were exclusively produced from high-glass, water quenched granulates. One of the more interesting recent developments in granulated slag technology has been the introduction in several countries of a variety of quenching processes. Kister et al (2) have described a new system for the production of granulated blast furnace slag with a high content of glass and a low content of residual moisture. Special attention was paid to the spray box design in order to break up the slag stream at high flow rates, and to guarantee an effective contact between water and fluid slag and hence the production of a high glass content in the product.

Margesson et al (3) patented a process for air pelletizing of slag. Cotsworth (4) describes the use of such pelletized slag in concrete masonry units and notes that the structure of such pelletized slag is primarily a glass, and that if ground to a size finer than 75 μm the resulting product is cementitious, hydrating in a manner similar to portland cement.

Alderete et al (5) have patented a portland blast-furnace slag cement containing up to 25% air-cooled blast-furnace slag. Unlike granulated slag, the air-cooled slag is generally more than 50% crystalline, representing a marked departure from usual practice where only glassy slags are used. A typical cement composition containing 10% air-cooled slag and 5% gypsum developed compressive strengths of 7.85, 21.2, 25.9 and 36.7 MPa as compared to 7.6, 20.2, 24.0 and 34.0 MPa, respectively, for a normal Type I portland cement.

Although not strictly a slag cement, the production in Japan of granulated slag sand for use as fine aggregate is of considerable interest. Recent work has been described by Fujimoto (6). The slag sand is formed in a similar manner to granulated slag, but cooling water is under a higher pressure than conventionally employed. Slag sand production is being studied in Australia; Ryan et al (7) have disucssed the use of such a material in a test road pavement.

MATERIALS

In order to study how the composition and preparation methods influence the morphology of granulates, eight slags were selected for study. Two were produced by Australian Iron and Steel at Port Kembla, Australia, the first being a low MgO product, and the second a slag having a somewhat higher percentage of MgO. Both of these products were quenched using sea water. A South African slag produced by I.S.C.O.R. was water quenched as were three European slags from Hoogovens, Ymuiden Plant, Holland; Voest A.G., Linz, Austria; and Hoesch-Westfalenhutte, Dortmund, Germany. Special slags included in the study were a Canadian slag produced by air quenching and a Japanese slag sand.

CHEMICAL COMPOSITION

The chemical composition of quenched slags can vary in at least three ways, first, bulk differences due to changes in the composition of the tapped slag secondly, differences between individual particles developed as the quenching occurs, and thirdly by the development of different silicate phases within the glass. In order to assess the bulk variations over a period of six months (January to June 1978), twenty-four samples taken from approximately 12,000 tonne of granulated slag from Port Kembla were analysed by usual silicate analysis techniques. The averages of the analyses together with the ranges, standard deviations and coefficients of variation of the data are given in Table I.

TABLE I

Uniformity of Composition of Granulated Slag

January - June 1978

	Ave	Range	Standard Deviation	Coefficient of Variation
SiO_2	35.3	34.3 - 36.3	0.55	1.56
CaO	40.3	39.4 - 41.4	0.66	1.64
Al_2O_3	17.6	17.2 - 18.4	0.26	1.48
MgO	3.2	2.9 - 3.7	0.21	6.57
S	0.60	0.54 - 0.66	0.03	5.00
Fe_2O_3	0.36	0.32 - 0.43	0.03	8.33
MnO	0.99	0.84 - 1.1	0.07	7.07
Cr_2O_3	0.005	0.003 - 0.007	0.001	20.00
TiO_2	0.98	0.47 - 2.1	0.56	57.14
Na_2O	0.37	0.24 - 0.50	0.07	18.92
K_2O	0.43	0.1 - 0.7	0.09	20.93

It is concluded from the data that in a steel works subject to strict quality control, variations over a considerable period of time in the bulk composition of granulated slag, may be held within limits accepted by cement producers. The coefficients of variation of SiO_2, CaO and Al_2O_3, are all below 2.0%. The value rises to 6.57% for MgO and to about 20% for the minor elements such as NaO and K_2O. Even higher variations are noted for trace elements. As yet it has not been fully established how such variations, particularly those of NaO and K_2O influence the rate of hydration of the ground granulated products, but judging from high-alkali portland cement clinkers such influences are probably significant.

Grains of granulated slag produced from the Port Kembla

plant were mounted in resin and the chemical composition of a series of grains was determined, this time using an electron probe. Care was taken to vary the position of the scanned area within any single grain so that any possible zonal variation was taken into account. Obvious crystalline materials were avoided in the scans, particularly metallic inclusions but no attempt was made to limit scans to any areas of possible heterogenity within the glass itself. This procedure was also conducted on all the other slags discussed above, however in the case of the Japanese material, crystalline material could not be avoided. The data obtained for all the slags are presented in Table II.

It must be concluded, since the samples are all from stockpiles and not specifically selected materials, that certain processes lead to glass particles which vary in composition to a greater degree than results from others. It may be concluded from the Canadian slag that air quenching may increase the variability from grain to grain, perhaps due to incipient crystallization. The heterogenity of the slag glasses in the micro-range by separation of liquid phases has been described by Schröder (8). It is possible that such development of different solid glass phases is reduced in the slags having low coefficients of variation.

TABLE II

MEAN COMPOSITION AND COEFFICIENT OF VARIATION FOR PARTICLES OF GRANULATED SLAG

	Australian		Australian (high MgO)		German		Austrian		South African		Dutch		Japanese		Canadian	
	Mean	C.V.	Mean	C.V.	Mean	C.V.	Mean	C.V.	Mean	C.V.	Mean	C.V.	Mean	C.V.	Mean	C.V.
SiO_2	35.83	0.92	34.21	1.05	33.95	0.59	35.74	1.71	34.18	3.45	31.47	4.35	31.23	1.67	35.63	3.65
CaO	41.05	0.51	40.11	1.15	35.85	0.84	33.89	0.65	39.40	5.13	36.84	3.23	37.36	2.86	38.76	2.37
Al_2O_3	16.19	1.42	16.87	2.61	13.06	1.38	10.66	2.15	10.35	3.78	16.01	7.37	16.24	8.19	7.76	5.15
MgO	2.65	4.91	5.27	2.66	12.26	1.71	11.56	3.36	11.62	5.65	10.08	4.17	8.46	11.58	11.52	6.51
SO_3	1.52	4.60	1.53	5.23	2.59	5.02	2.77	6.14	2.09	5.26	2.36	3.39	3.03	19.14	4.36	11.01
FeO	-	-	0.07	28.57	-	-	-	-	-	-	-	-	0.05	40.00	0.11	36.36
MnO	1.33	12.03	0.87	10.34	0.55	12.73	2.76	11.96	1.26	25.40	0.47	21.28	0.65	23.07	0.60	34.62
Cr_2O_3	-	-	-	-	-	-	-	-	-	-	-	-	0.01	-	0.01	-
TiO_2	-	-	-	-	0.55	9.09	0.43	11.63	0.39	12.82	1.08	9.26	1.95	13.33	0.27	29.63
Na_2O	-	-	0.17	35.29	0.57	8.77	0.47	8.51	0.25	26.09	0.90	35.56	0.64	31.25	0.27	36.11
K_2O	1.43	11.19	0.92	16.30	0.62	6.45	1.70	14.71	0.50	36.00	0.77	18.18	0.47	14.89	0.43	39.53

Consider firstly the results for the grains of Australian low MgO slag. Although from Port Kembla, they are not strictly of the set used to assess the bulk variability of slag over the six month period, since they are a more recent product and certain of the mean values lie outside the ranges already given for slags from that plant. Nevertheless, the coefficient of variation of all the oxides except MnO are lower for the different grains than for changes in the bulk product over the six month period. These results indicate that a very uniform glass is being produced during granulation at this plant.

Comparable coefficients of variation to those of this Australian slag are noted for the high MgO Australian slag, the German and Austrian products. In all of the other slags at least three coefficients of variation are greater than twice the highest of the above four materials for the compounds in question. For example, the Japanese coefficients of variation are relatively high for CaO, Al_2O_3, MgO and SO_3. The explanation for this is that the Japanese material is in fact crystalline and it would be anticipated that specific points on different grains would have different compositions (figure 1). This does not explain the high values of coefficient of variation for the other materials, in particular for the CaO and SiO_2 of the South African and Canadian slags.

Figure 1 Japanese Slag showing Crystalline Nature (Polished Section)

MORPHOLOGY

Stereo-microscopic examination of the slags indicated significant differences in their morphology. Rather than describing in detail each slag the important

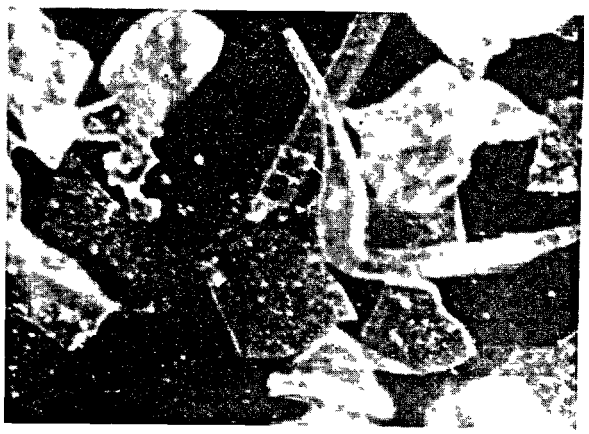

Figure 2 Straight and Bent Acicular Particles - Australian Slag

similarities and differences will be discussed. The first important difference between certain of the slags and others is the tendency to form acicular particles. The South African product is a dark buff coloured slag with marked vesicular characteristics. Needle-like particles can be seen macroscopically, and under the microscope it is noted that the finer fractions are almost all made up of either straight or bent acicular particles. The Australian materials (figure 2) show a smaller proportion of acicular particles, the quantity being less in the high MgO Australian slag. The Dutch slag is greyish-buff and is formed of equant grains with relatively few acicular particles, but a fair proportion of material smaller than 330 μm is present. The granulated slag from Austria is dense and either black or brown in colour. The finer fraction appears to be made up of an abundance of shards. A few very long (>20mm) fine individual fibres are present, but there is no significant amount of needle-like particles in the finer fractions. Acicular particles are absent from the Japanese and Canadian slag (figure 3).

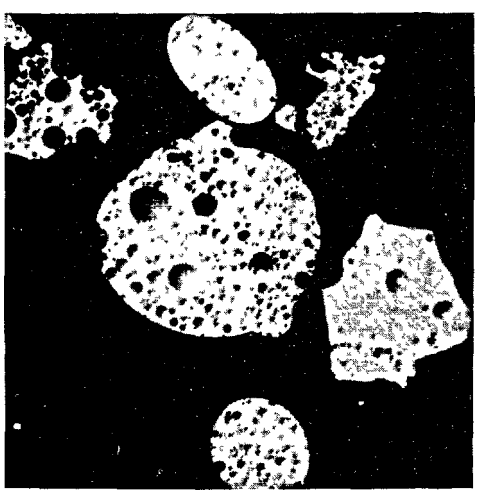

Figure 3 Air Quenched Canadian Slag (Polished Section)

There are two possible explanations of the tendency of certain slags to form such acicular particles. The first is that they are formed by the purely mechanical process of high-speed attenuation of steam jets, converging at a small included angle upon the stream of molten glass. This process may not be smooth, such as to form long uniform fibres of the type developed in fibre glass manufacture, but the melt may be drawn out turbulently in many directions to produce short, fine often bent fibres, together with some small glass particles or shot.

The other possibility is that the glasses which form such acicular products are Stuart liquids, consisting of elongated polymer chains. Schröder (8) suggests that slag melts rich in basic oxides cannot be blown into fibres without increasing their proportion of Stuart liquid by the addition to the melt of fine quartz sand, and this would suggest that the melts should be considered Frenkel liquids. It is tentatively suggested that, under conditions such as that associated with the formation of granulated slags using water-quench spraying techniques, the structural elements of the Frenkel liquid are forced into elongated chain structures by the mechanism of rapid flow. This would explain the development of fibres in certain of the slags and not in others, and for the fact that experiments done on non-mobile melts would indicate that they are essentially Frenkel liquids.

ASPECTS OF HYDRATION OF GRANULATE PARTICLES

In order to study some aspects of hydration of slag in the presence of cement paste, a series of 25 mm cube specimens were cast using unground, low MgO, Australian slag mortar, quartz sand mortar and cement paste, all having a water-cement ratio of 0.5. Half of the specimens were cured over water at 21°C; the others were subject to a continuous moist curing regime at 80°C from six hours after casting. The cubes were tested at 21°C in compression at the times indicated in figure 4, care being taken to minimise the effects of thermal shock by slow cooling of the specimens cured at 80°C.

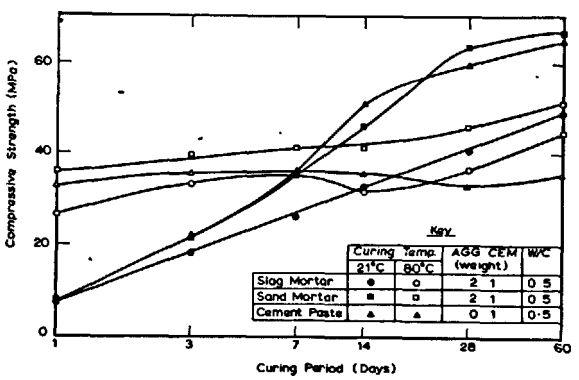

Figure 4 Compressive Strength vs Curing Period

For the normally cured specimens the curves of the paste and sand mortar follow one another closely. The curve for the slag mortar is almost linear on a log-time plot. This mortar appears to continue gaining strength at this rate even between 28 and 60 days, during which period strength gain of the other two materials is increasing at a somewhat lower rate. The strength of the slag mortar is always lower than that of the sand mortar up to an age of 60 days. The two

mortars were designed with the same proportions by weight, even though there is a slight difference in specific gravity between the fine aggregates; the difference in strengths is not however due to this fact.

Elevated temperature curing leads to rapid strength gain in all the specimens, but increments at later ages are low. The sand mortar strengths are again higher than the slag mortar values at all ages.

Mortar bars (500 x 40.5 x 68.5 mm, 2:1 Agg:cement, 0.5 W:C) were subjected to flexural four-point loading in order to determine the tensile strength characteristics of slag and sand mixes. The data obtained are summarised in figure 5.

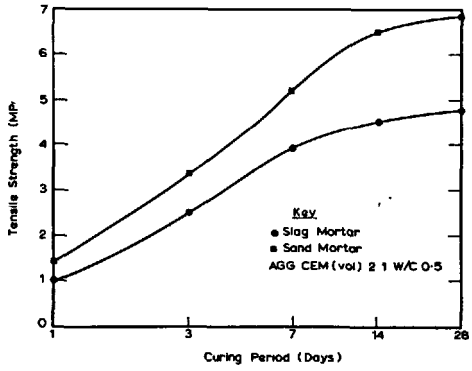

Figure 5 Tensile Strength vs Curing Period

At all ages the slag mortar has a lower strength than a comparable sand mortar. The ratio of slag mortar strength to sand mortar strength is fairly constant (0.7) at all ages between 1 and 28 days. If figures 4 and 5 are compared it is noted that the linear increment of slag-mortar strength with log-time is true only for the compressive strength; the rate of tensile strength increment with time is always less for slag mortar than for sand mortar.

It can be concluded from electron microscopy conducted on specimens which had been failed by compressive loading, that bonding between the granulated slag and the cement is less well developed than bond between quartz particles and cement. Failure invariably occurred at the aggregate-paste interfaces in slag mortars (figure 6a and b), despite the fact that the high temperature curing allowed hydration to proceed into the slag particles as evidenced by reaction rims (figures 7a and b).

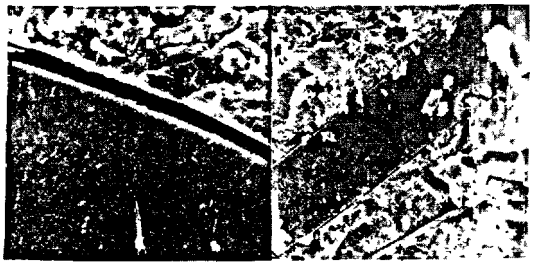

Figures 6a and 6b Paste-Aggregate Interface Failure (21°C, Compressive Strength Specimen)

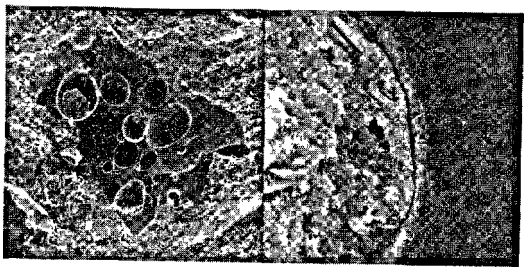

Figures 7a and 7b Reaction Rims and Failure Plane on Slag Cured at 80°C

In the case of sand aggregate, cracks through sand particles and through the cement matrix were often in evidence. The failures at the cement-slag interfaces were also manifest by the existence of casts left in the paste matrix.

These results suggest the anomaly that although for very fine slag particles hydration reactions do occur and reaction rims do form under high temperature curing, yet bonding of the cement paste hydrates to the slag surfaces appears to be weak. Consideration was given to the possibility that granulated slag may be somewhat hydrophobic. A study was therefore made of the interaction of slag particles with water.

In the presence of air, the contact angles between water and the three solids, slag, cement clinker and quartz sand were measured by placing a water droplet on a clean ground surface of the individual materials and measuring the angle by means of an ocular fitted with cross hairs in a rotatable microscope barrel. The higher contact angle (average 50°) for the slag, as opposed to that of sand and cement clinker (average angle for both being 46°) indicates that the adhesion of water to sand and unground clinker is greater than the adhesion of water to slag. The particular slag therefore shows a reduced affinity for water when compared with sand or portland clinker. This factor could in part lead to the phenomena noted previously in terms of the mechanical strength. The fact that granulated slag generally drains rapidly and has been used for this purpose in road construction projects may also be explained by this lack of affinity between its surface and water.

Whether the somewhat hydrophic nature of slag is still operative after grinding has not yet been determined, but it may possibly explain some of the observed differences in properties both between slags, and between slag and portland cement behaviour.

CONCLUSIONS

Some important granulation techniques have been mentioned which will influence products and procedures in cement use and manufacture. An attempt has been made to assess chemical variability of some slags which have been differently treated under conditions of practice. The morphology of slags treated in such different ways varies significantly. It is believed that certain slag melts show a propensity towards being Stuart liquids under dynamic water quenching and that some may show an hydrophobic tendency which should be further studied.

ACKNOWLEDGEMENT

Mr. R. Williams of Australian Iron and Steel Pty Ltd was responsible for the procurement of the slags; both he and D. Campbell-Allen, Professor of Civil Engineering at the University of Sydney are thanked for their interest in this work.

BIBLIOGRAPHIE

1.-W.G.J. RYAN (1969), "The Use of Fine Granulated Blast Furnace Slag in Concrete", Trans. of Instn of Engrs Australia, Vol.CEII No.1 88-96.

2.-H. KISTER and WYSOCKI (1978), "A New System for the Production of Granulated Blast Furnace Slag with a High Content of Glass and a Low Content of Residual Moisture", Zement Kalk Gips Nr.6/1978, 297-299.

3.-R.D. MARGESSON and W.G. ENGLAND (1971), "Processes for the Pelletization of Metallurgical Slag", U.S. Patent 3, 594, 142, July 20, 1971.

4.-R.P. COTSWORTH (1978), "Use of Pelletized Slag in Concrete Masonry Units", J. of Testing and Evaluation, Vol.6 No.2, March, 148-152.

5.-W.E. ALDERETE, J.P. BOYER, K.E. DAUGHERTY and D.L. JOHNSON (1977), "Cement Composition", U.S. Patent 4 047, 961 Sept.13, 1977.

6.-Y. FUJIMOTO (1979), "Co-operative Studies in Japan on Granulated Slag Sands for Concrete", Symp. on Utilisation of Steelplant Slags, Australian Inst. of Mining and Metallurgy, Illawarra Branch 65-74.

7.-W.G. RYAN, R.T. WILLIAMS and R.L. MUNN (1977), "The Durability of Concrete Containing Various Cementitious Materials in an Experimental Concrete Road Pavement", Concrete Engineering Symp., Instn of Engrs Australia, Brisbane, August, 29-34.

8.-F. Schröder (1978), "Principal Paper - Blastfurnace Slags and Slag Cements", Fifth International Symposium on the Chemistry of Cement, Tokyo, Part IV, 149-199.

Research on the Main Mineral Phase and Its cementituous Properties of Oxygen Converter Slag (O.C.S.)

Etude des principales phases minérales des laitiers de fours à oxygène et de leur activité

WANG YU-JI, Lecturer, Department of Construction Materials Engineering, Tong Ji University,
XIE GONG-XIN, Engineer, Jiang You Cement Research Institute, China.

RESUME : Ce rapport décrit spécialement certaines notions importantes sur la fabrication de ciment en employant les laitiers provenant de fours à oxygène. A l'aide de l'analyse chimique et thermodifférentielle, de la technique pétrographique et des essais de diffraction par rayons X, on a réussi à déterminer les compositions chimiques des laitiers, de leurs composants minéraux et leurs propriétés d'hydratation. En outre, on a élaboré une méthode théorique de calcul des principaux éléments des laitiers et de leurs propriétés physiques et mécaniques.

Les éléments principaux de laitiers à four rotatif à oxygène sont : le silicate tricalcique, le silicate bicalcique et sa solution solide contenant du phosphore, la ferrite bicalcique, la phase RO et la chaux libre. En outre, il y existe aussi, en faible quantité, de l'aluminate, de l'aluminoferrite, de l'apatite, de la fluorine, du métal ferreux etc...

Les qualités de laitiers des fours à oxygène peuvent être déterminées approximativement par les teneurs en silicate tricalcique et chaux libre. D'où leur classement en catégories pour la facilité du contrôle et leur utilisation. Les laitiers contenant plus de 40 % de silicate tricalcique et moins de 3 % de chaux libre sont souvent utilisés pour fabriquer le ciment de laitier, en ajoutant une certaine quantité de plâtre pendant la mouture. Les laitiers contenant 50 à 55 % de silicate tricalcique, ont une résistance à la compression à 28 jours de 50 à 60 N/mm2; pour une teneur en C_3S de 46 à 50 %, une résistance à la compression égale à 40-50 N/mm2; et pour une teneur de 40 à 46 %, 30 à 40 N/mm2.

SUMMARY: This article describes mainly about some problems in the experimental works for making of cement with O.C.S. The chemical composition, mineral component and the properties of hydration of the steel slag were investigated by chemical analysis, petrographic technique, XRD and DTA. Theoretical calculations for chief minerals were carried out and physico-mechanical properties of the steel slag cement were tested.

The main minerals of the O.C.S. are tricalcium silicate, dicalcium silicate and its solid solution containing phosphorous, dicalcium ferrite, RO-phase, free lime and some amount of aluminate, aluminoferrite, fluor apatite, fluorspar, metallic iron and etc.

The quality of O.C.S. can be approximately discriminated by the content of tricalcium silicate and free lime, so that the slags can be graded accordingly and utilized appropriately. When a steel slag has a content of tricalcium silicate>40% and that of free lime <3%, it can be milled together with a definite amount of gypsum to produce qualified steel slag cement. As the content of tricalcium silicate amounts to 50-55%, the cement made from it will have a compressive strength of 50-60 N/mm^2 at 28 days; a content of C_3S of 46-50%, a compressive strength of 40-50 N/mm^2; a content of 40-46%, 30-40 N/mm^2.

The Mineral Components and Morphological Structure of O.C.S.

As we all know steel slag is the by-product of steel making, sometimes it was considered as a kind of waste. In fact, it is a cumulative product of many kinds of minerals. During a certain period of time we collected about 30 sample slags from different converters that were producing various kinds of steel and investigated them. We found that the main minerals presented in those slags are tricalcium silicate, dicalcium silicate and its solid solution containing phosphorous, dicalcium ferrite containg some small amount of Al_2O_3, RO-phase (the solid solution of Fe, Mg and Mn, mainly of FeO), free lime, solid solution containing Fe and in addition, some small amount of fluor apatite, fluorspar, metallic iron and etc.

Under the direct lighting of a microscope the C_3S in the slags appears to be colorless or unevenly and slightly tinted with yellow-green transparent crystals. According to morphology they have different forms. In the thin section of the sample, they are usually observed to be hexagonal in shape (Fig.1),

Fig.1 Hexagonal section of C_3S
Direct lighting 100 x

but most of their crystals are columnar, tabular or acicular, their grain size are bigger and they are always encrusted by many cladding substances. Usually we can see RO-phase that grows along the bands of C_3S with definite orientation (Fig.2), and sometimes we can see also granular C_2S and fluor apatite co-existing with C_3S in the notch at the boundary of C_3S crystal.

C_3S has a refractive index n = 1.720-1.725, low colour interference, it appears to be first grade grey to greyish white, parallel extinction, positive elongation.

The phosphorous in O.C.S. mostly dissolves into C_2S in solid state to form solid solution. Due to the differences in the content of phosphorous, alkalinity and metallurgical

Fig.2 RO-phase grown along the bands of C_3S with definite orientation
Parallel poloriyed light 250 x

process of various kinds of steel, the contents of phosphorous in the solid solution of C_2S of different slags are different. The slags in which the phosphorous is stabilized to form fluor apatite contain β-C_2S.

The solid solution containing phosphorous is usually cladded by C_3S and appears to be round granular, irregularly granular, cnidoblastic or finger like and other forms. Their optical property is similar to that described by Agrell [1] about the metamorphism of C_2S containing phosphorous. In the slags with low alkalinity we found what was described by Agrell, the clear rhombic crystal of C_2S which was grown out from the contaminated type of C_2S (Fig.3), its optical property is the same as C_2S. We found: refractive index n = 1.75-1.735, a colour inter-

Fig.3 Rhombic crystal of C_2S
Direct lighting 250 x

ference of first grade yellow to bright yellow, inclined extinction, section of parallel extinction has negative elongation, +2v greater.

O.C.S. are the slags produced with the addition of fluorspar during the metallurgical process, but their phosphorous contents are not always stabilized to form fluor apatite

and more often they dissolve into C_2S in solid state. We carried out petrographic analysis for 22 slag samples picked up during the year of 1973 and 1975. The result of the analysis shows that only one sample contains slender needle shaped fluor apatite. In samples which contain more phosphorous and at the same time the phosphorous is not stabilized to form fluor apatite, in such case even if its alkalinity is very high, it can not be saturated with all the silica it contains to form C_3S, a part of the silica will form the solid solution of C_2S containing phosphorous.

Usually we can find solid solution of C_2F containing a small amount of Al_2O_3 in solid state in the slags. Under the direct lighting of a microscope it appears to be reddish black, no polychromatic property, and under crossed polarized light, to be deep red in colour. Its crystals may be columnar, irregularly columnar, granular or ball like, usually intergrowing with RO-phase and sometimes being cladded by C_3S. It is characterized by biaxial crystal, parallel extinction with negative elongation and having cracks and incomplete cleavages at the base.

The RO-phases are isotropic homogeneous mass. They are opaque and dark or black in colour and in myrmekitic, granular, dropwise,stripy, hackly or other forms (Fig.2). They are usually cladded by C_3S, and coexist with the solid solution of C_2F.

There are two kinds of free lime in the slags, the purer one and the solid solution (Fig.4). The former is f-CaO and the latter is CaO+x% FeO ($0<x\leq10\%$). They can be easily distinguished in the XRD patterns, f-CaO has d=2.41± and F-CaO in solid solution state has d = 2.38±.

A Study of the Cementituous Properties of O.C.S.

1. Chemical Composition of O.C.S.
From table I, we can see that O.C.S. are alkalinic slags. They are characterized by its high c/s ratio and low aluminium and high iron contents.

2. The cementituous Properties of O.C.S.
We tried to add different amount of gypsum to prepare several steel slag cements and the physico-mechanical properties of their pastes were tested. The results are shown in Fig.5. O.C.S. is such a material of having certain hydraulic property. In case,without adding of any additive so long as it has a fineness same as ordinary cement, its 28 days strength is quite high, although its early strength is rather low. The addition

Fig.4 The solid solution of granular f-CaO having dark brown fringe & cross cleavage Direct lighting 100 x

Table I. Average chemical composition of the sample slags of Shanghai Steel Plant

	Chemical composition					
year	SiO_2	CaO	Al_2O_3	Fe_2O_3	FeO	P_2O_5
1970-1972	12.35	56.80	1.24	6.86	12.69	3.67
1972-1973	14.30	50.80	1.18	6.54	17.70	1.73
May 1973	11.29	50.80	1.20	7.23	14.80	3.00
1975	10.50	44.98	2.67	8.93	26.10	1.05

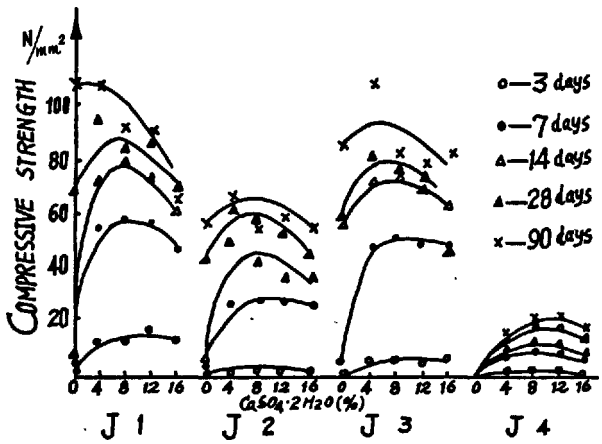

Fig.5 The influence of gypsum content to the compressive strength of cement prepared with O.C.S.

of gypsum do increase its early strength greatly, but it gives little contribution to the strength at later days. If the gypsum is in excess the strength will tend to decrease. According to the above principle we selected 8% gypsum content to prepare 64 sets of steel slag cement samples with various kinds of slag, and their properties were examined.We obtained an average 28 days compressive strength of 34.9 N/mm^2 and higher ones reached 50 N/mm^2, but the fluctuation in quality

appeared evident, the coefficient of variation was 40%. The results of soundness tests also varied in a wide range. Now we put forward several problems and try to discuss them in the following sections.

Discussion on Problems for Making Cements from O.C.S.

1. Factors affecting the fluctuation on the strength of steel slag cement.

As slags are the products which have passed through melting at high temperature and then cooled down gradually, the course of their formation may be regarded as an equilibrium process in physical chemistry.

To 64 sets of slag cement samples, basing upon their chemical composition, we carried out theoretical calculations to the amounts of their component minerals. Though such kind of calculation could hardly to be strictly accurate because of the complexities of the states of solid solutions in the slags, yet the components of slags can be generally estimated, thus their cementituous properties can be evaluated.

On the basis of primary investigation on the structures of main mineral constituents in slags, they are divided into two major groups: the one is the type of fluor apatite and the other, solid solution of C_2S containg phosphorous. The former has $p/s < 0.1$ and the latter has $p/s > 0.1$. [2]

From the calculated results, the correlation between each content of mineral component in slags and the 28 days strength of slag cements were analized by Computor, through progressive regression analysis, we found that the correlation between the theoretical content of C_3S and the 28 days compressive strength was the best one. Thus we took the average values of C_3S of m samples with ΔC_3S = 0-1% and their corresponding 28 days compressive strength to make a correlogram as shown in Fig. 6.

From Fig.6 we can see the correlation curve starts gently; when C_3S content < 20%, the 28 days compressive strength < 10 N/mm^2; after C_3S > 20%, the effect of C_3S content to the compressive strength increases appreciably; when C_3S > 40%, without any exception, all the 28 days compressive strengths exceed 30 N/mm^2; when C_3S > 46%, the 28 days compressive strength reaches 40 N/mm^2; when C_3S > 50%, the 28 days compressive strength reaches 50 N/mm^2.

Certainly, the factors affecting the strength of hardened cement paste are numerous. In addition to the C_3S content, there are also the effect of crystalline structure, the

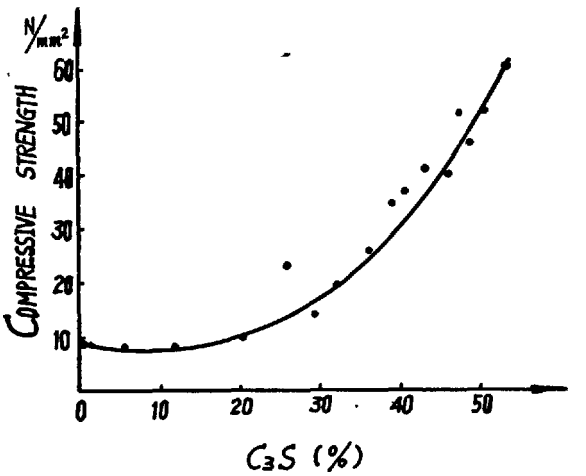

Fig.6 The correlation of 28 days compressive strength of slag cement to its theoretical content of C_3S.

effect of other minerals, as well as the degree of weathering of the slags, fineness of cement, water cement ratio, and curing conditions, etc.

The early strength of slag cements are generally rather low. The 7 days compressive strength in comparison with that of 28 days is only about 40%; but in later stage, the strength increases more quickly, the 90 days compressive strength will reach 125-140% of 28 days compressive strength. This can be explained by two main reasons: the lack of minerals of aluminates in slag and the C_3S crystals formed in the melting state are dense and hydrate slowly.

2. Hydration of steel slag cement

We choose two typical samples J_3 and J_4 for analytical study. The chemical constituents and mineral components of the samples are listed in Table II.

Table II. The Chemical Constituents and Mineral Components of Slags J_3 and J_4

sample	Chemical Constituents (%)					
	CaO	SiO_2	Al_2O_3	Fe_2O_3	FeO	P_2O_5
J_3	52.0	12.05	1.33	6.01	13.78	3.04
J_4	48.3	7.33	0.82	8.55	19.60	2.39

sample	Mineral Components (%)				
	C_3S	C_2S	C_3A	C_2F	f-CaO
J_3	46	0	1.3	12	3.9
J_4	20	11	0.8	16	16.0

The slags are milled to the fineness of ordinary cement, and the products are the pure

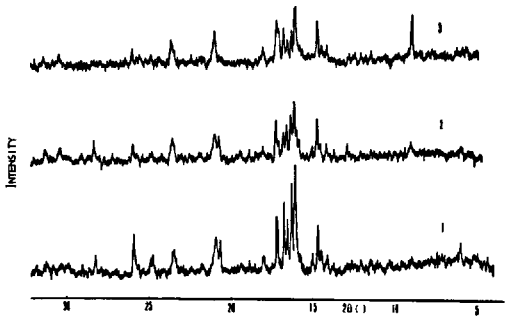

Fig.7-1a XRD patterns for J_{3-0} at different stages of hydration. Paste composition: slag 100%, water cement ratio 0.2. 1-3 days, 2-14 days, 3-28 days.

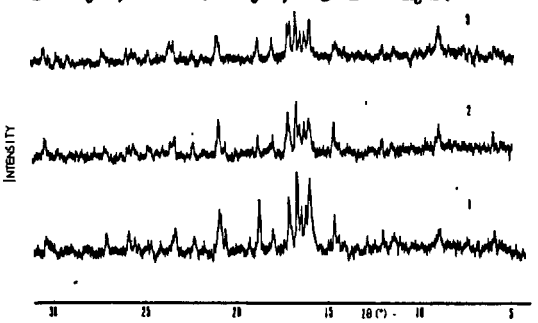

Fig.7-1b XRD patterns for J_{4-0} at different stages of hydration. 1, 2, 3, same as above.

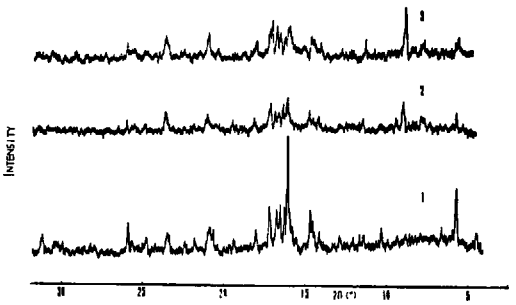

Fig.7-2a XRD patterns for J_{3-8} at different stages of hydration. Paste composition: slag 92%, gypsum 8%, water cement ratio 0.20. 1-3 days, 2-14 days, 3-28 days.

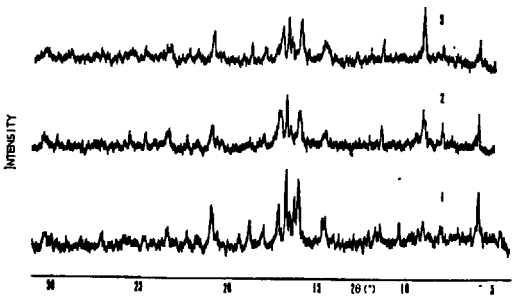

Fig.7-2b XRD patterns for J_{4-8} at different stages of hydration. 1, 2, 3, same as above.

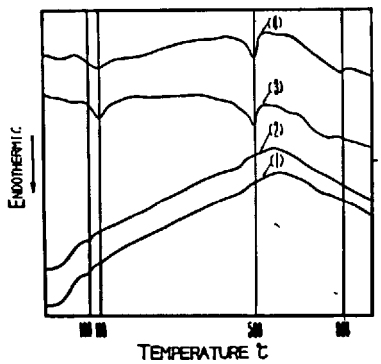

Fig.7-3a DTA curves for J_{3-0} at different stages of hydration (1)-3 days, (2)-7 days, (3)-28 days, (4)-90 days.

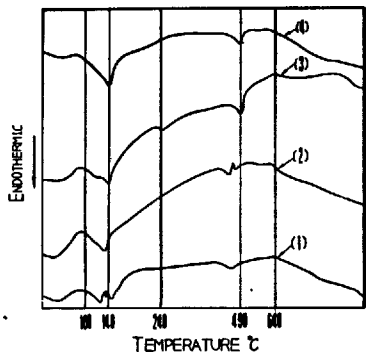

Fig.7-4a DTA curves for J_{3-8} at different stages of hydration (1)-3 days, (2)-7 days, (3)-28 days, (4)-90 days.

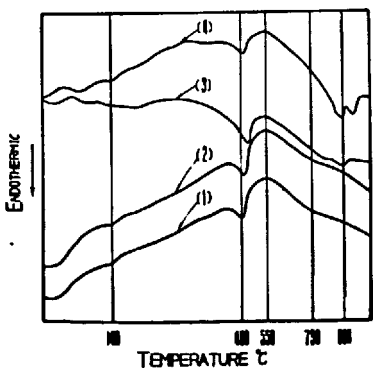

Fig.7-3b DTA curves for J_{4-0} at different stages of hydration. (1),(2),(3), (4), same as above.

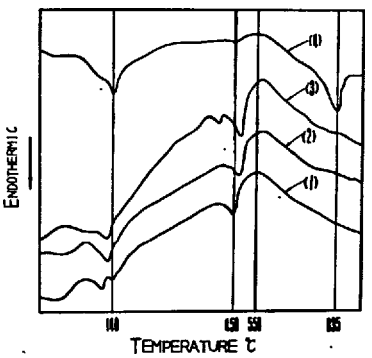

Fig.7-4b DTA curves for J_{4-8} at different stages of hydration. (1),(2),(3), (4), same as above.

Fig.7 Patterns of XRD and DTA for slag cements at different stages of hydration.

slag cements labeled by J_{3-0} and J_{4-0}, when with the addition of 8% gypsum, by J_{3-8} and J_{4-8}. The results of XRD and DTA investigations at different stage of hydration are shown in Fig. 7.

From the analysis to the results of the experiment, we concluded:
(a) solid solution of C_2S and solid solution of C_2F are minerals of poor hydration activity or of very low cementituous property. RO-phase, fluor apatite, fluorspar etc. are minerals with very poor hydration activity or without cementituous property.
(b) minerals containg aluminates and aluminoferrites have good hydrating property, and when gypsum is added, their hydration products are ettringite.
(c) C_3S in slags provide good cementituous property, they are the main minerals for the hardened cement paste to gain strength. With slags of high lime content (J_{4-0} and J_{4-8}), their hydration products are mainly C_2SH. When their lime content are relatively low (J_{3-0} and J_{3-8}), the main hydration products are C-S-H. In the absence of gypsum the hydration process begins to be evident after 14 days. In the presence of gypsum, the hydration process is greatly accelerated.
(d) Free lime, especially their solid solutions, hydrates slowly, its hydration products are $Ca(OH)_2$.
(e) By adding with gypsum, it changes the hydrates from aluminates and aluminoferrites into needlelike polyhydro-complex of polysulfo-aluminates, more over, it accelerates the hydration of C_3S at the early stage, increases the early strength, but has no distinct effect on the setting time and the soundness of the cements. [3]

3. Factors affecting the volumetric soundness of slag cements

Excessive free lime, especially in presence of solid solution with small amount of FeO, is the primary cause of volumtric unsoundness of steel slag cement. When free lime content is above 4%, all samples fail to meet the general requirements; when the contents are above 3%, most of the samples are disqualified, the free lime in the remainder qualified samples (such as J_3) was determined to be in relatively pure state. Thus we can see, for the cause of unsoundness in slag cements, both the content and the state of free lime have to be concerned.

CONCLUSIONS

O.C.S. is a kind of material with certain cementituous property. Its hydralic activity depends primarily upon the C_3S content. Although the minerals of aluminates and aluminoferrites are of high hydraulic activity, yet their contents in O.C.S. are too low, and the rest minerals are considered to be less active.

In the slags, the presence of excessive free lime, especially in the presence of its solid solutions with rather slow hydraulic activity, is the main cause of unsoundness. They could be milled directly into slag cements only when their free lime contents lie below 3%.

The slags with theoretical amount of C_3S above 40% and free lime below 3%, by blending with 5-8% of gypsum, can be milled to obtain slag cement. These cements have qualified soundness and normal setting time although early strength are rather low, but increases more rapidly in the later stage, they are also fairly abrasion proof and impermeabiable.

ACKNOWLEDGEMENTS

The authors would like to acknowledge comrades FANG QIU-QIN, LING DA-LI and WENG WEI-SONG, Dept. of Construction Materials Engineering, Tong Ji University, for their participating the experimental works for this article.

BIBLIOGRAPHY

1.- S.O. AGRELL, "Mineral Observations on some Basic Openhearth Slags" Journal of Iron and Steel Institute, No.152, 19-55 (1945).
2.- "Experimental Studies on Some Problems about Preparation of Cements from Converter Slags in Shanghai Steel Plant", page 31-36, edit. and published by Information Service of Science and Technology of Tong Ji University (Shanghai), 1976 (in Chinese).
3.- G.HOSAKA, M. DAIMON, S.GOTO, R. KONDO "Early Strength of Hardend Alite Mortar with C_3A and $CaSO_4 \cdot 2H_2O$" "Gypsum and lime", No. 122, 1973 (in Japanese).

Effect of MgO in steel slag on soundness of cement

Influence du MgO contenu dans les laitiers sur la stabilité du ciment

Luo SHOUSUN, Engineer, Cement Research Institute, Chine Populaire.

RESUME : Des études ont été faites sur l'influence de la forme et de la teneur en MgO sur la stabilité à long terme des ciments de laitier. En général, les MgO se présentant en état de combinaison chimique dans les monticellites etc. n'exercent pas d'influence sur la stabilité du ciment. Mais quand les MgO sont libres, c'est à dire en forme de périclase, le ciment sera instable. La stabilité du ciment dépend du rapport MgO/FeO+MnO lorsque les MgO sont en solution solide dans la phase RO. Le ciment est stable quand ce rapport est < 1 et le ciment est instable quand ce rapport est $\geqslant 1$.

On peut obtenir la stabilité à long terme du ciment de gypse et de laitier, c'est à dire la prévention de l'hydratation du périclase dans le ciment, en prenant une des trois mesures ci-dessous :

1) Addition d'un peu de sels de magnésium, par exemple $MgSO_4 \cdot 7H_2O$;
2) Addition convenable de laitier expansé ou de matières siliceuses telles que des cendres volantes;
3) Carbonisation du ciment hydraté.

SUMMARY: The relationship between the form and content of MgO in steel slag and the long-term soundness of steel slag cement has been studied. When MgO is in the form of combined state, e.g. in monticellite, etc. The cement is usually sound. Whereas if MgO is in free state, i.e. periclase, the cement is liable to be unsound. In the case of RO phase in which the MgO is formed in solid solution, the soundness of the cement depends upon the ratic of MgO/FeO+MnO. The cement is sound when the ratio is < 1, whereas the cement is unsound, when the ratio is ≥ 1.

The long-terme soundness of gypsum-steel slag cement or otherwise the prevention of the hydration of periclase in cement have been successfully achieved by one of the three methods, i.e.:

1) By adding a small amount of magnesium salt, e.g. $MgSO_4 \cdot 7H_2O$;
2) By mixing a pertinent amount of granulated blast furnace slag or siliceous material such as fly ash;
3) By carbonization of the hydrated cement products.

INTRODUCTION

In recent years, the use of steel slag to make cement has aroused interest because of the nuisance created by the volume of the stock-pile and also in view of energy economy. Up to this date, there has been no report outside this country about the production of steel slag cement. Since the early years of the seventies, China has achieved in utilizing steel slag to produce gypsum steel slag cement and carbonized steel slag products with satisfactory result in the construction work (1,2).

THE PHYSICOCHEMICAL STATE OF MgO

Steel slag of different varieties have been investigated, e.g., the early slag, the refining slag and the tapping slag from open hearth furnace, the oxidizing slag and the reducing slag from electric arc furnace and the Thomas slag from converter. The chemical compositions, ratios of CaO/SiO_2 and of MgO/FeO+MnO of the slags investigated are as shown in table I. The minerals of the slags have been identified by means of XRD (fig. 1) and optical microscope (fig. 2)

Table I Chemical Compositions of Steel Slags (%)

No.	Types of Furnace	Kinds of slags	SiO_2	Al_2O_3	Fe_2O_3	CaO	FeO	MnO	MgO	$\frac{CaO}{SiO}$	$\frac{MgO}{FeO+MnO}$
1	Open Hearth	Early	12.14	4.35	5.38	50.46	9.33	4.52	6.56	4.16	0.47
2	"	Refining	9.48	4.11	21.18	33.54	10.35	3.11	14.77	3.53	1.10
3	"	Tapping	13.65	4.88	7.44	39.94	11.12	0.62	14.65	2.92	1.25
4	Electric arc furnace	Oxidizing	25.89	4.00	1.36	28.52	15.68	3.44	18.34	1.10	0.95
5	"	Reducing	19.68	13.05	1.04	47.64	-	1.84	14.97	2.42	8.13
6	Converter	Thomas(5)	17.68	2.70	4.75	48.25	12.97	1.46	9.08	2.70	0.63

In the steel refining process, the use of dolomite as flux and the corrosion of magnesia refractory lining often result in the slag to contain MgO exceeding the limit of 6% normally set on portland cement. Question therefore arises, what about the long term soundness of cement and its products that are made from steel slag? J.J.Emery (3) and H. Kondo (4) have recently reported about the undue expansion that might arise from MgO in steel slag. With the view to utilize steel slag with benefit in the making of cement, we have made investigations on the physicochemical states and the relative quantities of MgO in the steel slags in relation to the long term soundness of cement.

MgO in steel slag of basic furnace exists in three states, i.e., chemically combined state, uncombined or free state and solid solution. As it can be seen from fig. 1 and 2, the chemically combined form monticellite is found in the oxidizing slag from the electric arc furnace, the free form periclase is found in the reducing slag also from electric arc furnace and MgO in solid solution form or the RO phase, as named by Mason (6), is found in all slags except the rrducing slag.

The RO phase is a solid solution of MgO-FeO-MnO series. When the slag has a high content of CaO, e.g., CaO= 52.30%, the RO phase may also contain a small portion of CaO in the solid solution. This

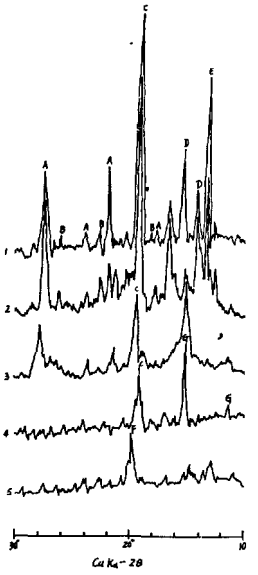

Fig. 1. XRD Diagrams of Open Hearth And Electric Arc Furnace Slags

A: Alite (1.437, 1.78, 1.927, 2.336 Å)

B: Belite (1.61, 1.88, 2.29 Å)

C: RO phase (2.116-2.166 Å)

D: Merwinite (2.66, 2.84 Å)

E: CaF_2 (3.16 Å) F: Periclase (2.106 Å)

G: Monticellite (2.67, 3.64 Å)

Note: The numerical notations in the diagrams are identical with table I

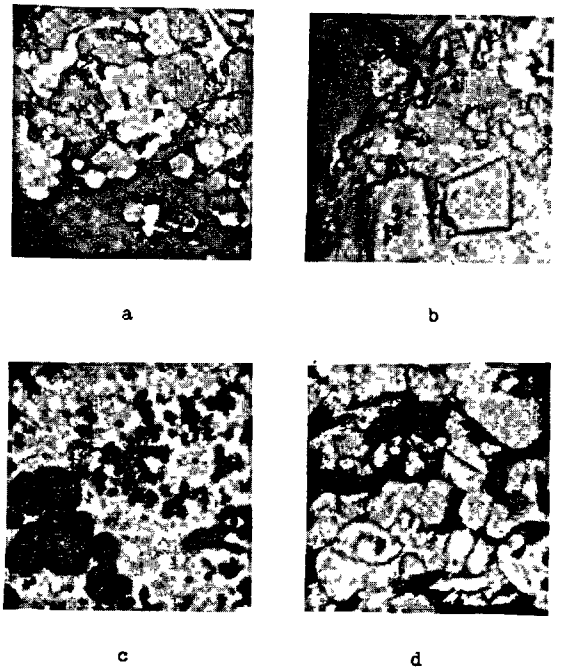

Fig. 2. Steel Slags Under Optical Microscope

a. RO phase in Thomas slag
Reflected light, 400x

b. Periclase in the reducing slag
Reflected light, 640x

c. Monticellite (white, prismatic) and Mg-Wustite (black, spherical) in oxidizing slag; Transmitted light 200x

d. Ferrous periclase (brown, spherical) in refining slag
Transmitted light, 200x

has been verified with electron probe micro-analysis by Beijing Building Materials Institute in the study of Thomas slag (7). As the divalent oxides of RO phase are all of regular system, their cell dimensions, lattice spacings and cationic radii are quite approximate (see table II), so that the

Table II Crystallinic Characteristics of the Divalent Oxides in RO phases (8)

Names of Minerals	Molecular formulae	Crystal Systems	Cell dimensions (Å)	Lattice spacings (Å)	Cationic radii (Å)
Periclase	MgO	Regular	4.2	2.106	0.78
Wustite	FeO	"	4.3	2.153	0.83
Manganous oxide	MnO	"	4.35	2.200	0.91

cations are interreplaceable to form solid solution. When Fe and/or Mn cations of larger radii enter into solid solution with periclase crystal, the cell dimension and the lattice spacing become larger; whereas if Mg cations of smaller radius enter into the solid solution with wustite or manganous oxide, the cell dimension and the lattice spacing become smaller. In other words, the variations in cell dimensions and the lattice spacings are related with the compositions of the solid solutions.

As it may be seen from table III, the smaller is the MgO/FeO+MnO ratio, the larger are the cell dimensions and the lattice spacings. When the ratio is ≥1, RO phase is of periclase or ferrous periclase type, the cement made from which is unsound after autoclave treatment. On the contrary, when the ratio is <1, the RO phase is of wustite, Mg-wustite or Mg-Mn-wustite type, the cement made from which is sound after autoclave treatment.

When MgO is in chemically combined state such as it is in monticellite or in merwinite, it is usually nonreactive. So it is not necessary to set limit on its content. The MgO in the oxidizing slag is either contained in monticellite or in Mg-wustite phase so the cement is sound under sutoclave treatment, whereas the cement made from the reducing slag, because of the high content of periclase in the slag, collapses under autoclave treatment. Therefore due measures have to be taken in the use of reducing slag.

MEASURES TO IMPROVE THE LONG TERM SOUNDNESS OF STEEL SLAGS

Investigations have been carried out to improve the long term soundness of cement made from the

Table III Characteristics of Steel Slags And Their Properties

Kinds of Slags	Reducing	Tapping	Refining	Oxidizing	Thomas (5)	Early
MgO/FeO+MnO	8.13	1.25	1.10	0.95	0.63	0.47
CaO/SiO_2	2.42	2.92	3.53	1.10	2.70	4.16
Types of RO phase	periclase	Fe-periclase	Fe-periclase	Mg-wustite	-	Mg-Mn-wustite
Cell dimensions of RO phase (Å)	4.215	4.235	4.254	4.266	-	4.317
Lattice spacings of RO phase (Å)	2.106	2.116	2.128	2.135	-	2.166
Deepest color under microscope	deep yellow	yellowish brown	brown	black	red	reddish black
Proportion of cement: Steel slag	88	50	30	92	88	30
gypsum	12	5	5	8	12	5
P.C. clinker	-	45	65	-	-	65
Specific surface of cement (cm^2/g)	3990	3500	3100	3480	3500	3320
Compressive strengths (N/mm^2) 7 days	26.9	29.5	42.3	2.4	24.3(7)	35.9
28 days	31.8	45.3	51.1	3.0	44.0(7)	55.0
Autoclave pre.(atm.)	8	20	20	20	127	20
time (hr.)	4	3	3	3	7	3
Result	collapsed	cracked	cracked	sound	sound	sound

reducing steel slag. The slag that has been studied has the following chemical aspects, i.e., CaO/SiO_2= 3.3, MgO=10.60%, FeO=0.59%, MnO=0.37%. Experiment shown that the gypsum steel slag cement made from the above reducing slag with slag to gypsum ratio= 92:8 is unsound when it is subjected to autoclave treatment. But when a pertinent amount of any of the following ingredients is incorporated with the slag, e.g., granulated blast furnace slag, siliceous materials or $MgSO_4 \cdot 7H_2O$, the long term soundness of the cement is improved as proved by autotoclave testings (See table IV). Our experiments further shows (See table V) that the reducing slag products having 0.2% syrup added as retarder but with no addition of gypsum, if carbonizied prior to autoclave treatment, could be also sound.

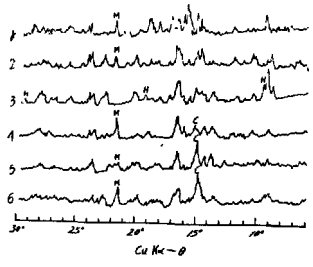

Fig. 3. XRD Diagrams of Reducing Steel Slag And Its Hardened Cement Pastes

1 Reducing Steel slag
2 Hardened paste of (reducing steel slag + gypsum) cement
3 The above paste after autoclave treatment
4 Reducing steel slag paste after carbonation autoclave treated
5 Reducing steel slag + 5% $MgSO_4$ autoclave treated after carbonation
6 Reducing steel slag + 45% fly ash, autoclave treated after carbonization

M Periclase (2.10-2.11 Å)
H Brucite (4.77, 2.17, 1.58 Å)
C Calcium carbonate (3.04 Å)

Table IV Improvement of Soundness of Slag Cement (Reducing Slag + Gypsum) by Additives

Additives	None	5 % $MgSO_4$*	30% Diatomeceous earth	30% Quzrtz	30% Fly Ash	45% Blast furnace slag
Autoclave Testings						
Pressure (atm.)	8	8	8	20	20	20
Time (hr.)	4	4	4	3	3	3
Result	Collapsed	Sound	Sound	Sound	Sound	Sound

* Adding $MgSO_4 \cdot 7H_2O$ calculated to $MgSO_4$

Table V Effect of Carbonization on Soundness of Steel Slag (reducing) products

Autoclave Testings (20 atm. x 4 hrs.)	Without carbonization	Carbonizing for 24 hrs., % Fly ash							
		0	15	25	35	45	55	65	75
Result	collapsed	ALL SOUND							

The effect of the additives is shown in fig. 3. In XRD spectra 1 and 2 respectively of the reducing slag and its hardened paste, periclase can be recognized by its peak at d=2.10-2.11 Å. In spectrum 3 of the autoclave treated specimen which collapsed, the peak of periclase vanished while there appeared instead peaks of prucite at d=4.77, 2.7 and 1.58 Å, which fact implies that the collapse of the specimen was due to the hydration of periclase (MgO) to brucite ($Mg(OH)_2$) which results in destructive expansion. Spectrum 4 represents carbonized paste after autoclave treatment that

has remained intact. There can be seen peak of periclase but none of brucite which implies that carbonation can protect periclase from hydration even under autoclave treatment, thereby keep the specimen sound. The specimen with addition of $MgSO_4 \cdot 7H_2O$ which has also remained intact after autoclave treatment is shown in spectrum 5. In spite of the fact that the height of the peak of periclase has appreciably decreased which could imply that at least part of the periclase has undergone hydrolysis, yet it does not result in undue expansion. The reason thereof might be that the formation of some complex salt like $mMgO \cdot MgSO_4 \cdot nH_2O$ as suggested by Butt(9) accelerated the hydration of periclase before the specimen was subjected to autoclave testing. The specimen that has been incorporated with fly ash but without gypsum and carbonized prior to autoclave treatment has also remained intact. Its XRD spectrum 6 indicates the presence of periclase and calcium carbonate. Likewise it implies that periclase has been protected from hydration. Our experiment has further verified that the incorporation of quartz also helps to improve the soundness of steel slag cement. We notice that similar result has been obtained by Gaze and Smith with high magnesia portland cement (10).

CONCLUSION

The long term soundness of steel slag as assessed from results of autoclave testings is related with the form or state of MgO and its content relative to other divalent oxides present as RO phase. The chemically combined MgO has not but the free MgO or periclase has harmful effect. The effect of MgO in form of solid solution on soundness is determined by MgO/FeO+MnO ratio. It can be detrimental when the ratio exceeds 1 and vice versa. The long term soundness of the reducing steel slag can be favorably improved by additive of magnesium sulphate, incorporation of siliceous materials or granulated blased furnace slag as well as carbonization treatment.

BIBLIOGRAPHIES

1.- Utilization of steel slag in making cement, Cement Technology, No. 2 pp. 13-22, Jiangyou, Cement Techical Research 1973 (Chinese).

2.- On Carbonization of Steel Slag and Its Application in Manufacturing Steel Slag Building Elements, Cement Research Institute 1978 (Chinese).

3.- J.J. Emery, Silicates Industries, 42 (4-5), pp. 209-218, 1977.

4.- R. Kondo, Gypsum and Lime No. 147, pp. 13-22, 1977 (Japanese).

5.- Relation Between The Form of MgO And Soundness of Steel Slag Cement, Nanjing Chemical Engineering Institute, 1979 (Chinese).

6.- B. Mason, The Constitution of Some Open Hearth Slags, Journal of Iron and Steel Institute (11) 69-80, 1944.

7.- On Improvement of Strength and Soundness of Steel Slag Cement, Beijing Building Materials Institute 1977 (Chinese).

8.- Inorganic File to The Power Diffraction File, 1972.

9.-U.M. Butt, Binding Material Technology, pp. 470, 1952 (Russian).

10.- M.E. Gaze, M.A. Smith, High Magnesia Cements (part II), Cement Technology Vol. 5, No. 1 pp. 291-295, 1974.

Cements along the join $C_4A_3\bar{S}$—C_2S

Ciments en fonction de l'ensemble $C_4A_3\bar{S}$—C_2S

K. IKEDA, Doctor of Science, Department of Mining and Mineral Engineering, Yamaguchi University, Ube, Japan.

RESUME : Une série de nouveaux ciments, utilisant principalement du laitier de haut-fourneau et du plâtre comme matière première, a été étudiée en fonction de l'ensemble $C_4A_3\bar{S}$ —C_2S. Deux sortes de clinkers ont été préparés à 1200 et 1300°C. Les constituants de ces clinkers ont été identifiés : ce sont principalement $C_4A_4\bar{S}$ et α'-C_2S, avec une proportion appréciable de CA et une petite quantité de $C\bar{S}$. La présence de verres a été décelée dans les clinkers fabriqués à 1300°. Ces clinkers sont très fragiles et se broient très facilement.

Les résistances des pâtes hydratées à E/C = 0,40 ont été mesurées sur micro-éprouvettes à 28 jours. L'alumine augmente les résistances, surtout aux premiers âges. Par exemple, pour des clinkers fabriqués à 1200°C, les résistances étaient respectivement de 16,1, 27,2, 30,9 MPa à un jour, et 34,2, 58,0 et 60,2 MPa à 28 jours, quand la proportion d'alumine croissait.

Bien que le durcissement des ciments fabriqués à 1300°C soit retardé par la présence du verre, de fortes résistances à la compression ont été obtenues à 3 jours. Cette rapide augmentation semble due à l'action des ions calcium provenant de la dissociation du silicate bicalcique; ces ions activent la précipitation de l'ettringite en solution solide, par suite d'un effet de surface entre $C_4A_3\bar{S}$ et C_2S dans la solution.

On a observé une baisse de la résistance à la flexion dans certains de ces ciments; mais cette résistance restait au moins égale à celle du ciment Portland; il n'en résultait donc pas en pratique d'inconvénient. Cette baisse de résistance à la flexion peut être combattue par addition de plâtre ou de gypse dans les ciments, de façon à empêcher la transformation du trisulfate en monosulfate.

SUMMARY : A series of newly developed cements called "supersulphated alumina-belite cements" has been studied along the join $C_4A_3\bar{S}$ - C_2S, using blast furnace slag and gypsum as main raw materials. Limestone and bauxite are needed in the production, but they are replaced by the chemicals of calcium carbonate and alumina in the present experiments. Two series of clinker were prepared at 1200°C and 1300°C. The main constituent minerals were identified to be $C_4A_3\bar{S}$ and α'-C_2S, associated with considerable amounts of CA and $C\bar{S}$. In the 1300°C series presence of glassy phases was noticed. The raw mixtures gave so soft clinkering that no hard grinding was required to make cements.
Hydration strength was examined in pastes with W/C 0.40, using small scale test pieces up to 28-day age. With increasing alumina content, compressive strength as well as early strength was increased. For several 1200°C series, for instance, the strength of 16.1, 27.2 and 30.9 MPa at 1-day age increases to 34.2, 58.0 and 60.2 MPa at 28-day age, respectively, when alumina content is increased. Although the hardening of 1300°C series was retarded due to the "coating effect" of glassy phases present, high compressive strength was also reached in 3-day age. This rapid developement of hardening may be attributed to the catalizer action of calcium ions derived from the C_2S in solutions, i.e., the calcium ions stimulate the precipitation of ettringite solid solutions by the "cooperative effect" between the $C_4A_3\bar{S}$ and the C_2S.
Some depression of bending strength was observed in several cements, but the strength after depression is nearly equal to that of Portland cements. Therefore, there will be no trouble in practical use of it. The depression may be improved by admixing gypsum or anhydrite, Since the trisulphate-monosulphate conversion estimated to occur in later age would be the cause of the depression.

INTRODUCTION

Portland cements mainly consist of four principal clinker minerals, C_3S, C_2S, C_3A and C_4AF. The latter two minerals are present in small amounts and are of minor importance for the strength. Therefore, for simplification, Portland cements may be regarded to be composed of two principal minerals, C_3S and C_2S. On the other hand the compound of $C_4A_3\overline{S}$, identical with naturally occurring mineral "haüyne" in structure (1), is known to be hydraulic and its hydration strength was tested by Budnikow et al. (2). The compressive strength observed is 18.9 MPa at best at 28-day age. The resulting strength is not so high as that of C_3S, which is generally 49 MPa at 28-day age. Therefore, replacement of C_3S with $C_4A_3\overline{S}$ seems to be disadvantageous in Portland cements and its application has been limited in the field of expansive cements. However, utilization of $C_4A_3\overline{S}$ replacing C_3S in Portland cement system will result in saving of energies for burning, since $C_4A_3\overline{S}$ requires lower temperature for its formation.
From this viewpoint "supersulphated alumina-belite cements" burnt along the join $C_4A_3\overline{S}$ - C_2S, utilizing blast furnace slag and gypsum as main sources of raw materials have been investigated in the present study.

EXPERIMENTAL

Raw materials and mineralogical setting

A water quenched powdered blast furnace slag, "Esment" commercially sold by Shin-nittetsu Chemicals Co. was used as one of the main sources, although both gradually cooled slags and low grade clays will also do for the present purpose. Specifications of the slag are given in Table I. Chemicals of JIS first grade $CaSO_4.2H_2O$, Al_2O_3 (α-alumina) and $CaCO_3$ were used for present investigation in place of industrially used "gypsum", "bauxite" and "limestone" for the ease of treatment. As the measure of mixing the raw materials A/S wt ratios, 0.4, 1.0, 2.0 and 3.0 were set instead of the mineral ratio $C_4A_3\overline{S}/C_2S$, which represents four points of the join $C_4A_3\overline{S}$-C_2S, because of the complexity of chemical compositions of the slag. Several test burnings were performed first at 1200°C for 1 hour on the mix 0.4 in order to adjust calculated compositions to get maximum amount of $C_4A_3\overline{S}$ with varying $C\overline{S}$ and C components in small amount. Thus, best fitted chemical compositions were determined on the mix 0.4. The other mixes were also prepared on the basis of the mix 0.4, simply blending the chemicals for the formation of $C_4A_3\overline{S}$ (Tables II and III).

Burning of cements

Prior to the burning of cements the solidus of present system was determined on the mix 0.4 to be 1268°C. Above this temperature the amount of $C_4A_3\overline{S}$ begins to decrease abruptly by the formation of liquid and C_2AS begins to appear as a stable phase as well as C_2S in α'-form. Therefore, cements in the present system should be burnt below this temperature. Thus, the burning was made at 1200°C for 1200 °C series, using an electric resistance furnace and a 20-cc platinum crusible. A 20-minute burning is enough for small amount of charges and longer one for large amount of charges is necessary to avoid unburnt corns in the center of the charges. After 30-minute burning an intermediate grinding was done, followed by 30-minute heating for 1200°C series. Clinkers were also prepared by 30-minute burning at 1300°C without intermediate grinding for 1300°C series. Clinkers thus prepared were ground softly to serve as cements with nearly natural fineness, indicating that cement powders can be made without hard grinding. In the present study, therefore, the cements with nearly natural fineness were used in order to save grinding energies in the practical applications, although the fineness is rather coarse as given in Table VII.

X-ray quantitative analyses

Burnt clinkers were analized quantitatively by X-ray for each clinker mineral, following the method described by Viswanathan et al. (3) with synthetic minerals, C_2AS, CA and $C\overline{S}$ as internal standards. Quantities of $C_4A_3\overline{S}$ and C_2S were recalculated on the basis of the chemical compositions represented in Table III, taking the ratios of the three clinker minerals into account. Small amount of liquid phases estimated to be present in 1300°C series was neglected in the calculation owing to the difficulty of detection.

Hydration strength of pastes and hydration

Small scale test pieces of 1 x 1 x 4 cm dimention were used to examine the hydration strength of the cements in the pastes at W/C 0.40. After cured in humid air for the first day, the test pieces were demoulded and cured in water at 20°C. Laboratory scale setting

TABLE I (wt %)

SiO_2	Al_2O_3	CaO	MgO	SO_3	Fe_2O_3	MnO	TiO_2	Total
32.90	13.45	43.05	6.51	2.37	0.65	0.31	1.02	100.26

Fineness 3950 cm^2/g, Blaine, S.G. 3.26, Glassy

Chemical and physical specifications of the slag. S is expressed as SO_3.

TABLE II

A/S	Slag	Gypsum	Alumina	Ca-carbonate
0.4	80.13	6.12(4.84)	-	26.83(15.03)
1.0	61.16	11.36(8.98)	11.87	32.13(18.00)
2.0	43.67	16.18(12.79)	22.81	37.02(20.74)
3.0	33.96	18.84(14.90)	28.88	39.72(22.26)

Mixing proportions of raw materials in weight. Weights after heating are shown in brackets to make total 100.

TABLE III (wt %)

A/S	SiO_2	Al_2O_3	CaO	MgO	SO_3	Fe_2O_3	MnO	TiO_2
0.4	26.30	10.75	51.43	5.20	4.74	0.52	0.25	0.81
1.0	20.07	20.07	47.96	3.97	6.73	0.40	0.19	0.61
2.0	14.33	28.67	44.76	2.83	8.55	0.28	0.13	0.45
3.0	11.15	33.44	42.98	2.20	9.56	0.22	0.10	0.35

Representative chemical compositions of the raw mixes.

times were measured by using small scale testing pastes of 10 gram at W/C 0.40 in plastic vesseles of 4.5 ø x 1.3 cm dimension with wetty covers at 20°C. This is an alteration of the standard method used for Portland cements. Hydrates which appeared during curing were studied by the X-ray powder diffraction technique.

RESULTS AND DISCUSSION

Clinkers and clinker minerals

An example of X-ray powder pattern of the present cements is shown in Fig. 1 and the results of designed mineral compositions and resulting mineral compositions are given in Tables IV, V and VI, respectively. In both series the main clinker minerals are $C_4A_3\overline{S}$ and α'-C_2S. The α'-C_2S may be stabilized mainly by the incorporation of $\overline{S}$ component as studied by Sakurai et al. (4), although the effect of other impurities cannot be disregarded. In 1200°C series generally, considerable amount of CA is noticed in addition to the two kinds of clinker minerals. Consequently small amount of $C\overline{S}$ component remains and probably some of this may be incorporated to the α'-C_2S as $\overline{S}$ component. Nakamura et al. (5), in their study of silica-rich expansive cements, reported that the volatilization of $\overline{S}$ was negligibly small in amount below 1250°C. According to Pliego-Cuervo and Glasser (6), one of the ternary stable assemblages in the system C-A-S-$\overline{S}$ is $C_4A_3\overline{S}$, C_2S and CA. Accordingly, most of the CA encountered in the present study may be stable due to the effect of impurities other than C, A, S and $\overline{S}$, included in the slag. Occasionally very small amount of $C_5S_2\overline{S}$ was detected. The metastable formation of C_2AS is suspected, but this was not clearly identified in the product. In 1300°C series anhydrite is present only in trace because of the formation of liquids in small amount that accelerates the clinker formation. Formation of gehlenite is trace and also $C_5S_2\overline{S}$ was not detected due to its dissociation into C_2S and $C\overline{S}$ at this temperature (5). Gutt (7) found that the maximum solubility of magnesia in α'-C_2S is 3.7 wt percent as M_2S in the join C_2S - C_3MS_2. The join C_2S - CMS studied by Schlaudt and Roy (8) indicates that the maximum solubility of M_2S in α'-C_2S at 1400°C is about 2.5 wt percent. From these studies it is evident that the solubility of magnesia is very small, i.e., 1.4-2.1 wt percent as MgO. Considering that present raw mixes have 2.20-5.20 wt percent of magnesia, some of the magnesia should be also dissolved in the clinker minerals other than α'-C_2S. Present clinkers can be easily pulverized because of soft sintering due to considerably high vapour pressure of SO_3 as well as rather low temperature burning. This feature is remarkable in saving energies for pulverization as well as low temperature required in the practical apprications.

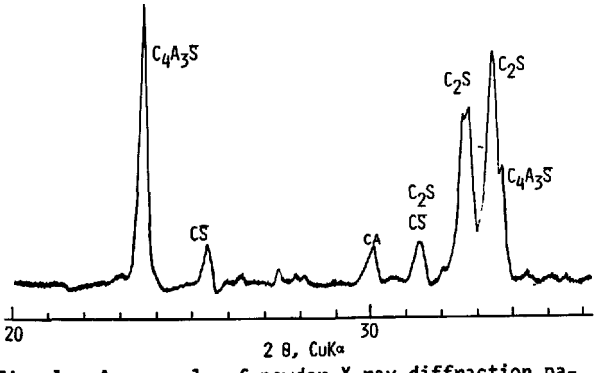

Fig. 1. An example of powder X-ray diffraction pattern of the present cement. Mix 1.0 burnt at 1200°C. Only characteristic peaks are labelled. The C_2S is in α'-form, bredigite.

Hydration strength

Both compressive and bending strengths of the present cements are summarized in Figs. 2 - 5 for 1200°C and 1300°C series, respectively. At first sight compressive strength is increasing with increasing A/S ratio for each cement series and markedly high strength is attained by the mixes of 2.0 and 3.0. Development of hydration strength for 1300°C series is extremely retarded owing to the probable presence of glassy phase which has coating effect on clinker minerals. However, the strength of this series gradually increases with prolonged curing time until it exceeds the strength of 1200°C series except for the mix 0.4. It is noted that depression of bending strength of some mixes, especially those of 1300°C series, occurs at later age. It is

TABLE IV (mole %)

A/S	Clinker minerals $C_4A_3\overline{S}$	Clinker minerals C_2S	Mineralizers $C\overline{S}$	Mineralizers Others
0.4	17.8	74.2	4.1	3.9
1.0	34.7	58.9	3.2	3.2
2.0	51.5	43.6	2.4	2.5
3.0	61.6	35.0	1.9	1.5

Clinker minerals designed common to both 1200°C series and 1300°C series. MgO is included in CaO. CA.1/3$C\overline{S}$ is used for a unit molecule of $C_4A_3\overline{S}$.

TABLE V (mole %)

A/S	Clinker minerals $C_4A_3\overline{S}$	C_2S	CA	$C\overline{S}$	Mineralizers $C\overline{S}$	Others
0.4	17.8	74.2	tr.	1.2	2.9	3.9
1.0	20.1	56.3	13.0	1.7	5.8	3.1
2.0	28.8	40.8	20.0	1.2	7.5	1.7
3.0	38.7	32.8	19.0	0.7	7.4	1.4

Clinker minerals resulted from 1200°C series.

TABLE VI (mole %)

A/S	Clinker minerals $C_4A_3\overline{S}$	C_2S	CA	$C\overline{S}$	Mineralizers $C\overline{S}$	Others
0.4	17.8	74.2	tr.	tr.	4.1	3.9
1.0	25.6	57.3	8.2	tr.	5.8	3.1
2.0	44.1	42.6	6.3	tr.	4.5	2.5
3.0	54.3	34.2	6.1	tr.	3.9	1.5

Clinker minerals resulted from 1300°C series. Small amounts of glassy phases are disregarded.

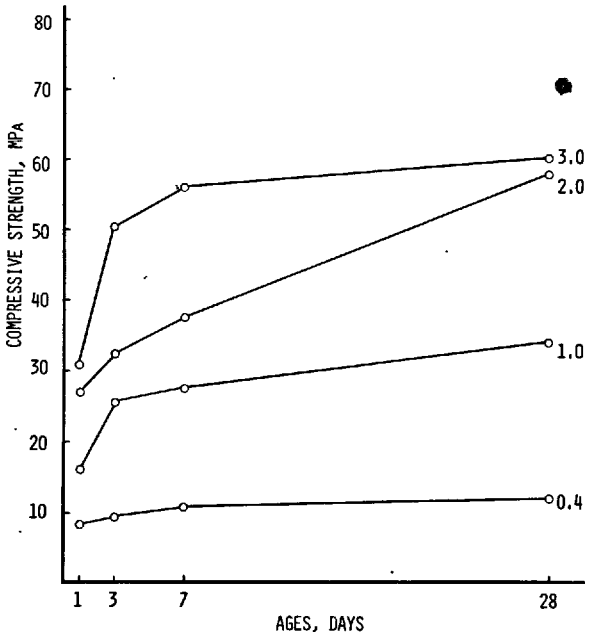

Fig. 2. Compressive strength of the cements in hardened paste for 1200°C series. W/C 0.40.

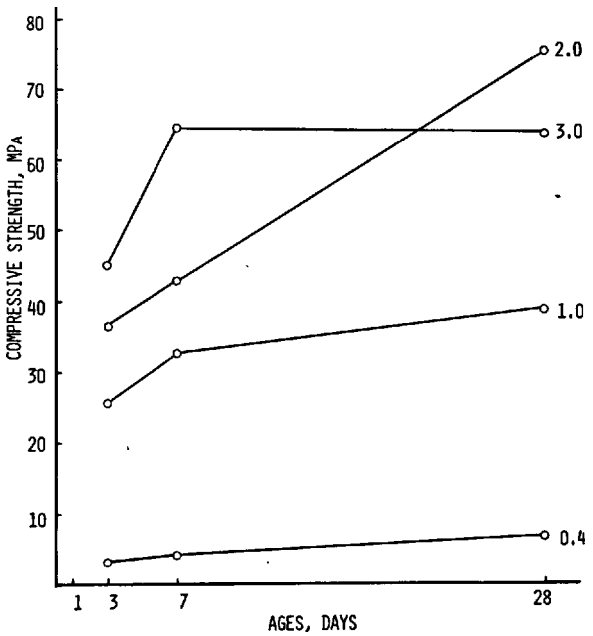

Fig. 3. Compressive strength of the cements in hardened paste for 1300°C series. W/C 0.40.

estimated that the depression may be due to the gradual formation of monosulphate hydrates as will be mentioned later. Cements of mixes 0.4, 1.0 and 3.0 in 1200°C series and that of mix 1.0 in 1300°C series have excellent characters both in compressive and bending strengths with no or little depression of bending strength up to about 28-day curing. Generally the present cements have higher bending strength than that of Portland cements because of the formation of ettringite solid solutions as generally seen in high sulphated slag cements. Even after depression the bending strength is nearly equal to that of Portland cements. Besides the depression would be improved by admixing some gypsum or anhydrite in the cements to prevent the trisulphate - monosulphate conversion, which probably occurred during the hydration of the present cements. The bending strength with no depression is nearly twice that of Portland cements.

Hydration

Hydration of the present cements seems not so simple. The hydration process is discussed from the observation of X-ray powder diffraction patterns. The hydration of the present cements is different in the 1200°C series without glassy phase and the 1300°C series with glassy phase. In both cases the hydration process is initiated by the hydration of $C_4A_3\bar{S}$ to form ettringite solid solutions accompanied by gibbsite gels, and followed by the formation of hypothetical hydrates given in the dashed box in Fig. 6. These hydrates are estimated to be C_6AH_{32}, CAH_{10}, C_4AH_{13}, C_2AH_8, C_3AH_6 and so on, including all calcium aluminate hydrates which exist in the solution. It seems likely that the hydration of $C_4A_3\bar{S}$ is accelerated by the action of calcium ions derived from the coexisting α'-C_2S as will be mentioned in the following section. The ettringite solid solution would contain more C_6AH_{32} component that is formed by the reaction between portlandite component from the hydration of the C_2S and the gibbsite gel from $C_4A_3\bar{S}$. The CA forms CAH_{10}, which may be also incorporated to the ettringite solid

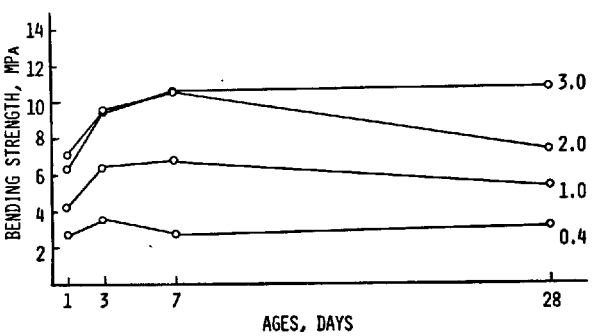

Fig. 4. Bending strength of cements in hardened paste for 1200°C series. W/C 0.40.

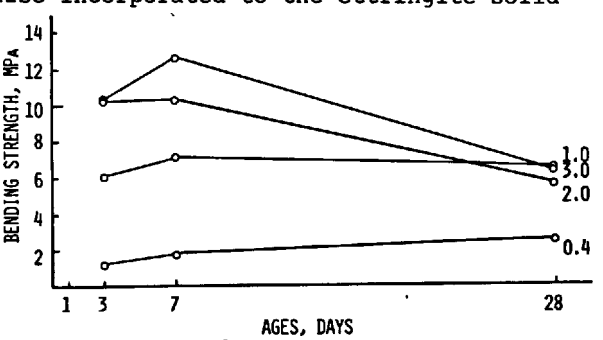

Fig. 5. Bending strength of cements in hardened paste for 1300°C series. W/C 0.40.

solutions in the form of C_6AH_{32} as calcium ions increase in solutions in accordance with the sluggish hydration of the α'-C_2S. At later age small amount of monosulphate solid solutions appears owing to the reaction between the ettringite solid solution and the C_6AH_{32} component, when the solid solution limit of the ettringite is reached, since C_6AH_{32} component cannot survive alone (9). This may cause the marked depression of bending strength observed in the cements possessing moderate amount of C_2S and $C_4A_3\bar{S}$ in 1200°C series, i.e., the trisulphate - monosulphate conversion may require more calcium ions. In the mix 3.0, for instance, the content of C_2S is lower and the conversion may not easily occur. Since the content of C_2S is high, supplying abundant calcium ions in the mix 0.4, the depression takes place earlier or the conversion effect would be slight because of lower content of $C_4A_3\bar{S}$ in this mix. Thus, this conversion phenomenon may be marked in the intermediate mixes 1.0 and 2.0. The hydrate CAH_{10} is also produced by the hydration of the glassy phase present in 1300°C series cements. Consequently the depression may occur more easily in the cements of this series than in the cements of 1200°C series. The depression, however, may be improved as mentioned in the preceding section. Final hydrates produced comprise ettringite solid solution, gibbsite, monosulphate hydrate solid solution, CAH_{10} and C-S-H at 28-day age. Monosulphate hydrate solid solution and CAH_{10} are not always found in the cements and their presence depends on chemical potentials in solutions as described above. At the begining of initial hydration CAH_{10}, C_2AH_8 and monosulphate hydrate appear metastably owing to the presence of CA and $C\bar{S}$, and then disappear soon, incorporated to ettringite solid solution with the progress of hydration. Some $C_4A_3\bar{S}$ remains unhydrated at least up to 7-day age or even more than 28-day age in accordance with the initial content of this mineral in the cements. Zakharov (10) stated that no conversion of CAH_{10} to C_3AH_6 would occur in his "alumina-belite cement" because of low concentration of calcium ions in the solution. The same would be true

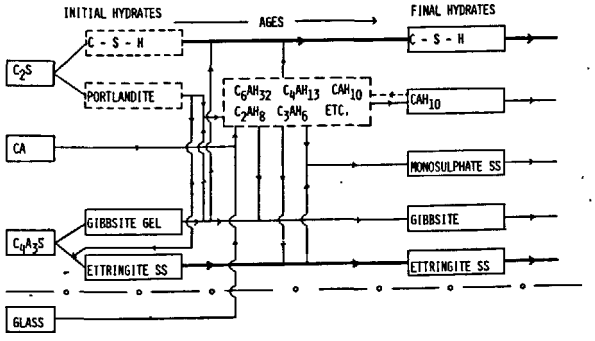

Fig. 6. Schematic hydration courses drawn on the basis of XRD. Thick lines, main hydration courses. Fine lines, subordinate ones. Hydrates outlined by dashed lines are considered to be in solutions, but not as precipitates. Slight C_2ASH_8 was sometimes encountered in later age, but not always.

in the present cements. However, it is considered that a reversible reaction would take place for the CAH_{10} phase in the present cements as illustrated in Fig. 6. This would prevent the conversion of the CAH_{10} into C_3AH_6, forming ettringite solid solutions or monosulphate hydrate solid solutions. Mehta (11) also stated that no conversion was noticed in his high alumina cements added with $C_4A_3\bar{S}$ at 38°C curing.

Setting times

Setting times of the laboratory scale are given in Table VII. They depend on the content of $C_4A_3\bar{S}$ in the cements. Initial setting times for 1200°C series are quite fast — quick setting, but they are not so fast as the setting time of regulated set cements with no retarders — flash setting. Final setting times are also relatively short especially in the mixes 0.4 and 1.0. Initial setting times of 1300°C series are generally prolonged due to the glass coating effect on clinker minerals, and it is extremely retarded when the mixing ratio reaches 3.0. Final setting times are also delayed with increasing alumina contents in the cements. The clinker mineral $C_4A_3\bar{S}$ itself shows not so fast hydration. According to Fukuda (12) the initial setting time is 3 hours, and the final one is 3 hours and 35 minutes at W/C 0.40 for this compound. Judging from the hydration nature of $C_4A_3\bar{S}$ and C_2S, it is quite surprising that present cements set so fast, especially in 1200°C series and some 1300°C series. The mechanism of the faster hardening may be ascribed to relatively high initial concentration of calcium ions dissolved from the α'-C_2S, though the absolute concentration may be low. It is considered that ettringite solid solutions can be precipitated quickly by this catalyzer action of the calcium ions in solutions, resulting in the fast setting times. The precipitation of ettringite solid solutions may accelerate the formation of calcium ions from the α'-C_2S, as a consequence of which, hydration of present cements may proceed in this "cooperative mechanism" between the α'-C_2S and the $C_4A_3\bar{S}$. Near the termination of this cooperation low C/S C-S-H may precipitate. This interpretation is supported by Fukuda's observation (12) that 10 percent blending of portlandite to $C_4A_3\bar{S}$ makes flash setting, i.e., 4 minutes and 10 minutes for initial and final setting times, respectively, at W/C 0.45.

Comparison with cements previously reported

In 1974 Zakharov (10) reported a new type of cement called "alumina-belite cement" which has peculiar features of rather high early strength, high later strength and high resistance to aggressive media. Desired burning temperature is no higher than 1250-1300°C and the main chemical composition of the new cement is located in the system C_2S-CA-$C_{12}A_7$ with small amount of $C_4A_3\bar{S}$, i.e., between Portland cement and aluminous cement compositions. Some gypsum and other mineralizers were added to stabilize belite as β-form and excess $C\bar{S}$ component forms $C_4A_3\bar{S}$ and $C_5S_2\bar{S}$. Viswanathan et al. (3) also made cements similar to that of Zakharov at 1300°C from Indian raw materials containing "anorthosites"

TABLE VII

A/S	Setting times Initial	Final	Fineness cm^2/g, Blaine	S.G.
0.4	0 h 17 min	0 h 28 min	2440	3.44
1.0	0 18	0 31	2300	3.34
2.0	0 23	2 12	2290	3.18
3.0	0 27	1 56	2340	3.11
0.4	0 h 19 min	0 h 36 min	2460	3.42
1.0	0 30	3 55	2230	3.35
2.0	1 58	5 28	1900	3.28
3.0	6 23	12 20	1670	3.16

Setting times and relevant specifications of the present cements. Above for 1200°C series. Below for 1300 °C series. See the text for the laboratory scale test.

prevailing in India. Their cements are called "Porsal cement". The present cements are different from thses two kinds of cement, since they have more $\bar{S}$ component and the main compositional system is located along the join $C_4A_3\bar{S}$ - C_2S. The author wishes to call the present cements "supersulphated alumina-belite cements"

CONCLUSION

From the present experiments the author has a confidence that a series of supersulphated alumina-belite cement can be manufactured from blast furnace slag and gypsum with addition of bauxite and limestone. He also showed that various cements having different strength can be produced, by changing mixing proportions of alumina and silica along the join $C_4A_3\bar{S}$ - C_2S. If we intend to obtain superior cements possessing early strength, clinkers should be burnt below the solidus temperature of 1268°C in the present cement system. If liquid forms, initial hydration of cements is retarded more or less, depending on the amount of glassy phases generated. Some depression of bending strength was noticed in several hardened cements in later age of curing. This may be caused by the conversion of ettringite solid solution into monosulphate hydrate solid solution or the trisulphate - monosulphate conversion that occurs gradually in the later age, when cements have moderate amount of $C_4A_3\bar{S}$ and C_2S. This phenomenon becomes clear, when glassy phases are present in the cements. The depression, however, would be no troublesome, because bending strength after depression is nearly equal to the strength of Portland cements. This means that present cements have higher bending strength in early age. Hardened cements with no depression of bending strength give nearly twice the strength of Portland cements as generally seen in high sulphated slag cements owing to the formation of ettringite solid solution, except for alumina-poor cements whose strength does not develop so high at room temperature in the present cement system. The depression phenomenon of bending strength would be improved by admixing some gypsum or anhydrite in the cements. It is very important, however, to study the effect of ferric component replacing alumina in order to use low grade bauxite containing considerable amount of ferric iron. It is noteworthy that the only one cement ready to be used among the present cements is the one with 0.4 A/S mixing ratio, burnt at 1200°C. This cement requires no bauxite and has relatively high strength that permits demoulding. Further grinding of the clinker into finer powder will increase the initial strength of this mix; recent study shows 12 MPa at 1-day age at 3000 cm^2/g, and steam curing, autoclaving and reinforcement with fibre glass will bring practical utilization as prefabricated materials. Thus, the present cement system is expected to widen the utilization of "blast furnace slags", "gypsums" of byproduct and low grade "bauxites" with high silica and iron contents, which do not deserve exploitation at present. Strength characteristics of present cements in older ages will be reported elsewhere.

Acknowledgement: The author wishes to express his thanks to Prof. S. Ogino for the facilities of testing apparatus and regulated room.

REFERENCES

1.- R. Kondo (1965) The synthesis and crystallography of a group of new compounds belonging to the hauyne type structure, Yogyo-Kyokai-Shi, 73, 1-8.

2.- P.P. Budnikow, I.P. Kusnezowa and W.G. Saweljew (1965) Eigenschaften von $3CaO.3Al_2O_3.CaSO_4$ und sein Einfluss auf die Festigkeit von Klinkermineralien und Zement, Silikattechnik, 16, 414-417.

3.- V.N. Viswanathan, S.J. Raina and A.K. Chatterjee (1978) An exploratory investigation on Porsal cement, World Cement Technology, 9, 109-118.

4.- T. Sakurai, T. Ueda, K. Sato, M. Fukunaga and T. Matsu (1964) Influence of minor components on Portland cement clinker minerals, Cemento Gijutsu Nenpo, 18, 26-32.

5.- T. Nakamura, G. Sudoh and S. Akaiwa (1968) Mineralogical composition of expansive cement clinker rich in SiO_2 and its expansibility, Proc. 5th Inter. Sympo. Chem. Cem., Tokyo, 4, 351-356.

6.- Y.B. Pliego-Cuervo and F.P. Glasser (1979) The role of sulphates in cement clinkering: subsolidus phase relations in the system $CaO-Al_2O_3-SiO_2-SO_3$, Cem. Concr. Res., 9, 51-55.

7.- W. Gutt (1965) The system dicalcium silicate-merwinite, Nature, 207, 184-185.

8.- C.M. Schlaudt and D.M. Roy (1966) The join Ca_2SiO_4-$CaMgSiO_4$, J. Amer. Ceram. Soc., 49, 430-432.

9.- H.F.W. Taylor (1972) The chemistry of cement, vol. 1, p.272-273, pp.460, Academic Press, London.

10.- L.A. Zakharov (1974) Alumina-belite cement, Proc. 6th Inter. Sympo. Chem. Cem., Moscow, 3, 1-11,(English edition).

11.- P.K. Mehta (1968) Successful prevention of loss of strength in concrete made with high-alumina cement, Proc. 5th Inter. Sympo. Chem. Cem.,Tokyo,2,148-151.

12.- N. Fukuda (1968) Fundamental studies on the expansive cement. Ibid.,4, 341-350.

The study of a non traditional Pozzolan : Copper Slags

Etude d'une Pouzzolane non traditionnelle : Laitier de Cuivre

J.R. BARAGANO, Dr. Chem. Sc, Asland S.A., Villaluenga de la Sagra (Toledo) Espagne,
P. Rey, Dr. Chem. Sc., Asland S.A., Villaluenga de la Sagra (Toledo) Espagne.

RESUME

Dans la métallurgie du cuivre, on obtient un laitier compact, dur, abrasif et à grains fins, se composant essentiellement, dans sa phase cristallisée, de fayalite (Fe_2SiO_4) et d'oxydes de fer.

Différentes méthodes d'essai démontrent que ce laitier a des propriétés de pouzzolane.

La formation de S-C-H fin et mal cristallisé, à structure alvéolaire et "vermiculée", et l'existence possible d'une ferrite de calcium hydratée, du type C_4FHx, dans sa réaction avec l'hydroxyde de calcium, $Ca(OH)_2$, ont été mises en évidence par l'application des techniques de D.R.X., A.T.D. et M.E.B.

Les ciments préparés avec ce laitier ont des caractéristiques similaires à celles des ciments portland et à la pouzzolane, avec des avantages sous l'angle de la maniabilité.

Les courbes de durcissement indiquent une certaine inertie dans l'augmentation des résistances au jeune âge, avec à la fin un gain très considérable, mais elles réagissent bien avec une activation aux sulfates alcalins.

Il faut en souligner le comportement face aux agents atmosphériques, aux cycles de gel-dégel et aux réactions alcali-silice.

Dans la protection des charpentes, quand les mortiers ne contiennent aucun adjuvant chimique, les ciments de laitier se comportent plus ou moins comme les superciments portland (P-450) qu'ils dépassent en cas de présence de $CaCl_2$ avec des aciers normaux, spécialement celui fabriqué avec 45% de laitier.

Lors des essais de durabilité face à des solutions de $CaSO_4\ 2H_2O$, $Mg\ SO_4$ et Na_2SO_4, ils donnent des resultats supérieurs à ceux qu'on obtient avec des portland purs et à la pouzzolane. Il faut faire remarquer leur grande stabilité face à l'eau de mer.

C'est pourquoi le laitier de cuivre convient très bien pour fabriquer des ciments à ajouts ., à la pouzzolane ou spéciaux résistant aux agents extérieurs.

L'expérience acquise avec les ciments industriels et les bétons obtenus avec eux le confirme.

SUMMARY

The slags obtained in copper metallurgy are vitreous, hard, compact, abrasive, of fine granulometry and are principally composed of fayalite (Fe_2SiO_4) and iron oxides in their crystallized phase.

Different assay methods show that the slags possess pozzolanic properties.

The formation of fine, deficiently crystallized S-C-H with alveolar and vermiculate structure and the possible existence of a C_4FHx type of hydrated calcium ferrite when reacted with calcium hydroxide, $Ca(OH)_2$, was shown in X-R.D., D.T.A. and S.E.M. techniques.

Cements prepared with these slags have similar characteristics to those of Portland and pozzolanic cements with advantages in workability.

The hardening curves show certain inertia in the increase in strength over short periods but with considerable later advantage, though the initial strengths improve well due to activation by alkaline sulphates.

Their behaviour in the presence of atmospheric agents, freezing-thawing cycles, and in alkali-silica reactions is noteworthy.

In the protection of reinforcements, when the mortars do not contain any chemical additives, the behaviour of the slag cements is similar to that of Portland super-cements (P-450) and is superior to these when $CaCl_2$ is present with normal steels, especially when 45% slags are used in their manufacture.

The durability tests with solutions of $MgSO_4$, $CaSO_4.2H_2O$, and Na_2SO_4 give results which are better than those obtained with pure Portland and pozzolanic cements. They are particularly stable to sea water.

Thus, copper slags are especially suitable for the manufacture of addition and pozzolanic cements and those which are resistant to external agents.

Experience with industrial cements and concrete manufactured with them supports this statement.

I. INTRODUCTION

There has been an increase in the production of cements based on active constituents to palliate somewhat the high cost of the continuing energy crisis to the cement industry.

Spanish manufacturers have striven to locate traditional additives backed by experience and to study other products which had not previously been used for this purpose.

One such product is copper slag which is produced in copper metallurgy.

II. PHYSICAL PROPERTIES OF COPPER SLAGS

On removal from the kiln, the slags in their fluid state are subjected to brusque water cooling, vitrifying in relatively fine and compact granulometry.

The shining black slags which are compact and irregular in shape have a humidity of less than 5% when immersed in water.

The specific weight varies from 3,72 to 3,98.

II.1. Granulometry

Sieve(mm)	4,76	2,38	1,19	0,59	0,297	0,149	Less
%Retained	0,5	9,3	34,5	32,3	18,2	3,7	1,5

II.2. Grindability test

The test were carried out using F.C. Bond's method. The work index was 24 Kwh/Tm equivalent to a theoretical grindability of 40 Kwh/Tm. In identical conditions, clinkers give a value of 23, pozzolan 32 and blast furnace slags 34 Kwh/Tm.

II.3. Resistance to abrasion utilising the Los Angeles machine(ASTM-C-535-75 modified)

In view of the high abrasion values of vitreous materials, the Los Angeles test was used for calculation ; an abrasion coefficient of 1% being obtained, compared with 10% for clinkers from Lépol kilns, 4% for natural pozzolan and 3% for blast furnace slags.These products were previously ground to correspond with the granulometry of the copper slags.

III. CHEMICAL AND MINERALOGICAL PROPERTIES

III.1. Chemical composition

The chemical composition varies within the range which is usual for this type of subproducts. The limit values found for each element are as follows:

SiO_2: 30,7-35,9 Al_2O_3:2,4-3,4 FeO: 49,7-54,0 Fe_2O_3: 0,3-3,6 CaO:1,1-2,8 Mn_2O_3:0,05-0,10 SO_3: 0,01-0,08 $S^=$: 0,14-0,50 K_2O: 0,28-0,64 Na_2O: 0,27-0,83 TiO_2: 0,11-0,30 MgO: 1,8-3,1 Cr_2O_3: 0,03-0,07 CuO:0,50-1,25 ZnO:1,21-3,87 Cl^-<0,02 Pb:Indicios, IR:2,8-8,9 LI:(+4)-(+7), SiO_2 soluble (s/Florentin): 12,1-15,9.

III.2. Mineralogical composition

III.2.1. Microscopy

The presence of crystalline structures in the form of tubular fayalite needles (Photo nº 1) was detected in the samples attacked by HF using the reflected light technique. This was confirmed by electronic transmission microscopy (TEM) (Photo nº 2).

Bands of iron oxides which accompany fayalite crystals with small inclusions of metallic iron spherolites also to be found.

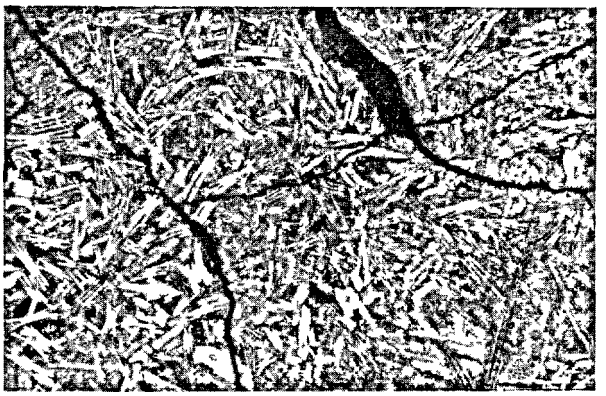

Photo nº 1: Tubular needles of fayalite

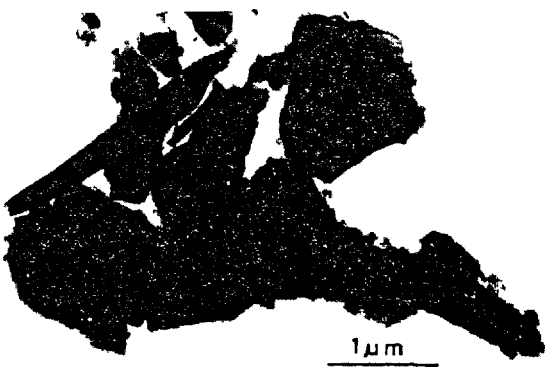

Photo nº 2: Partial aspect of the slags(TEM)

III.2.2. X-Ray diffraction

An X-ray tube with molybdenum anticathode (λ:0,71A) and zirconium filter was used.

And increase in background noise was observed between 11º and 19º due to the vitreous state and the principal crystallized component, fayalite (Fe_2SiO_4) of the olivine family.

When the slags were treated in an oxidising atmosphere for 1 hour at 800ºC and allowed to cool very slowly to force the crystallization of the glass, the formation of hematites (Fe_2O_3) and magnetite (Fe_3O_4) was observed. When the experiment was repeated at 1200ºC, crystobalite was observed together with the above mentioned components. In both cases the vitreous phase decreased with the temperature.

III.2.3. Differential thermic analysis

A domeshaped exothermic band was observed in an air atmosphere above 400ºC, indicating the oxidation of the fayalite.

An exothermic peak, attributed to devitrification was observed in a nitrogen atmosphere at 580ºC when the sample was mixed with 50% chemically unreactive periclase to avoid adhesion to the thermocouple.

IV. POZZOLANITY TESTS

Due to its chemical composition, this product is considered to belong to the pozzolan family rather than to the hydraulic slags obtained from blast furnaces. Thus, this possible property was tested by various methods.

IV.1. $Ca(OH)_2$-Copper slag mixtures

IV.1.1. Accelerated comparative method

A conglomerate of three parts by weight of the pozzolan (20%>45μ) and one part of hydrated lime (>95% in $Ca(OH)_2$) was prepared.

This mixture was used to make a (1:3) mortar with standardized Spanish sand and W/C=0,5 in 4x4x16 cm specimens.

After remaining at 21ºC for 48 hours, these specimens were placed in a container at 50ºC with saturated humidity for 72 hours.

As resistances were not specifically defined in the methods, a comparison was made with a natural pozzolan of proved characteristics, and standard quartz sand was used as inert matter. The following values were obtained.

Copper slags	Natural pozzolan	Standard sand
17-58 Kp/cm²	39-116 Kp/cm²	4-10 Kp/cm²

IV.1.2. DIN 51.043

In this case a minimun of 50Kp/cm² compression after 28 days was required.

Copper slags	Natural pozzolan	Standard sand
30-56 Kp/cm²	25-82 Kp/cm²	5-6 Kp/cm²

IV.1.3. Portuguese Method

The method consisted in preparing a paste with 25% $Ca(OH)_2$ and 75% pozzolan which was kept in 4x4x16 cm moulds in a humid chamber for three days and then in water at 21ºC until breakage date, after 7 and 28 days.

For Type I: 10-20 Kp/cm² was required at 7 days and 20-60Kp/cm² at 28 days.

For Type II: 10-30 Kp/cm² was required at 28 days.

TABLE I

DAYS	Cu SLAG H_2O – 26 % Kp/cm²	POZZOLAN H_2O – 35 % Kp/cm²	SAND H_2O – 36 % Kp/cm²
7	SOFT	19-62 (100-100)	SOFT
28	11-33 (50-29)	22-112 (100-100)	4-4 (18-4)
60	31-142 (107-93)	29-153 (100-100)	5-9 (17-6)
90	35-192 (117-107)	30-179 (100-100)	7-11 (23-6)
180	37-217 (116-107)	32-202 (100-100)	13-23 (41-11)
270	39-234 (108-113)	36-207 (100-100)	18-33 (50-16)
365	42-252 (111-118)	38-214 (100-100)	21-43 (55-20)

Different analytical techniques such as DTA, X-Ray diffraction, electronic transmission microscopy (TEM) and electronic scanning microscopy (SEM) fitted with a dispersive energy spectrometer were used to study the different components formed in samples of these three types of mixtures (25% $Ca(OH)_2$ and 75% additives) after a minimun of 28 days.

In the case of the sand, the mixture remained porous and brittle and hydrated lime crystals adhering to the quartz grains but without forming any type of silicate were observed. X-R.D showed a proportion of 23% $Ca(OH)_2$ and a certain amount of $CaCO_3$ due to partial carbonation of the sample.

GTA and X-R.D. $Ca(OH)_2$ determinations showed no decrease in the course of time, during a period of 300 days.

The natural pozzolan reacted well with the lime, and relatively compact and only slightly brittle hydrated compounds, identified as hydrated calcium silicates, formed after 28 days. These compounds were fine and deficiently crystallized with an alveolar aspect and the exact C/S ratio could not be determined. At this stage, X-R.D. determination showed 11% unreacted $Ca(OH)_2$.

As time passed a better crystallized higher S-C-H content was observed and the presence of hydrated calcium aluminates (C_4AH_{13}) and hexagonal carbonated calcium aluminate crystals ($C_3A.CaCO_3.12H_2O$) were identified by SEM, DTA and X-R.D.

4% of unreacted $Ca(OH)_2$ remained after 300days.

After 28 days the copper slag samples showed a hydrated mixture which appeared to be compact and not very brittle but the microporosity was greater than that of the natural pozzolan.

Fine poorly crystallized alveolar and vermiculate C-S-H (Photos nº 3 and 4) which was similar to natural pozzolan was detected and there was 13% non combined $Ca(OH)_2$. This value agrees with the mechanical resistances at the above mentioned age.

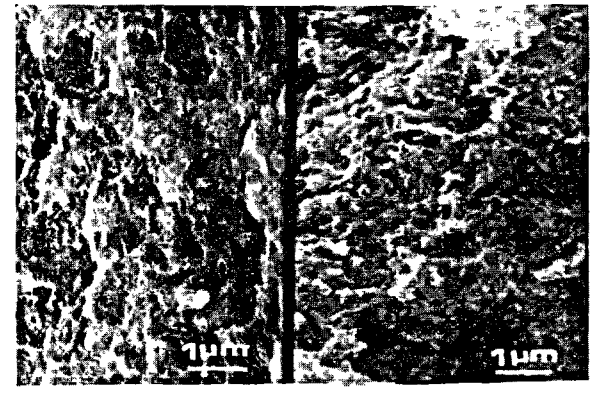

Photo nº 3: C-S-H Deposits. Alveolar-vermiculate.

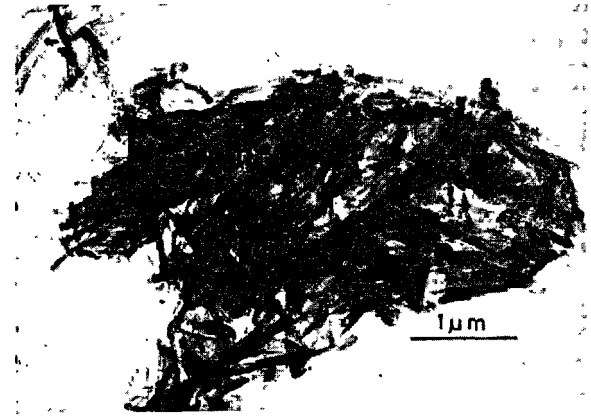

Photo nº 4: C-S-H. Texture examined by TEM

However, after 300 days the non combined $Ca(OH)_2$ is 4%, which is equal to that of the natural pozzolan. The presence of a (C_4FHx) type hydrated calcium ferrite is also probable. This could be interpreted as corresponding to the C_4AH_{13}, detected after 28 days in the pozzolan, and could explain the higher resistance of the copper slag mortars after a period of 90 days.

IV.2. Portland cement-Copper slag mixtures

IV.2.1. English method

The method consists in keeping a series of samples at 18ºC for 7 days, another series at 18ºC for 5 days and the other two at 50ºC. The greatest difference between the two resistances is used to evaluate the pozzolanity of the products studied.

TABLE II

	MOIST ROOM 18°C Kp/cm²	WATER BATH 50°C Kp/cm²	DIFFERENCE (50°C-18°C) Kp/cm²
S.S.BLAINE - 3500 cm²/gr			
65%CEMENT+35% SLAG	49-193	58-288	9-95
65%CEMENT+35%POZZOLAN	51-248	64-371	13-123
65%CEMENT+35%SAND	46-230	58-260	12-30
S.S.BLAINE 4500 cm²/gr			
65%CEMENT+35% SLAG	52-268	64-341	12-73
65%CEMENT+35%POZZOLAN	55-298	72-398	17-100
65% CEMENT+35% SAND	54-258	58-267	4-9

IV.2.2. TGL 28 101/03 East Germany

Cements were manufactured at 3500 and 4500 cm²/gr in proportions of 70% pure cement and 30% copper slags and standardized sand, and others with only 30% cement and 70% additives. They were compared with pure cements.

TABLE III

DAYS	CEMENT PORTLAND(A) Kp/cm²	70%CEMENT 30%SLAG(B) Kp/cm²	70%CEMENT 30% SAND(C) Kp/cm²	30%CEMENT 70%SLAG(D) Kp/cm²	30%CEMENT 70% SAND(E) Kp/cm²
S.S.BLAINE 3500 cm²/gr					
7	73-406	52-267	51-272	16-47	19-70
28	80-450	61-355	60-312	44-153	25-83
	[(B-C):(A-C)]x100 = 31,2 (>30)		[(D-E):(A-E)]x100 = 19,0 (>10)		
S.S.BLAINE 4500 cm²/gr					
7	75-424	54-297	56-320	16-59	18-70
28	85-501	75-399	62-350	43-176	25-102
	[(B-C):(A-C)]x100 = 37,4 (>30)		[(D-E):(A-E)]x100 = 18,5 (>10)		

IV.2.3. ASTM C-618-73

The specimens were kept at 21º for 1 day and at 39º for 27 days. The resistances should be above 75% of the standard cement.

TABLE IV

	CEMENT PORTLAND (A)	65%CEMENT+35%SLAG (B)
W/C	0,58	0,54
FLOW%	105	105
28 DAYS	56-370 Kp/cm²	44-285 Kp/cm²
(B:A) 100 = 79-77 (>75%)		

IV.2.4. N. Fratini

Cements with a total of 3,0% SO_3 and Blaine S.S. of 2500, 3500 and 4500 cm²/gr were manufactured with the same clinker and gypsum. In each series 25-35 and 45% of this was substituted by ground copper slag, rejecting 20% above 45 m.

The 9 cements prepared were tested after 7, 15 and 28 days (Table V).

TABLE V

S.S.BLAINE	2500 cm²/gr			3500 cm²/gr			4500 cm²/gr	
millimoles CaO per litre solution / millimoles OH⁻ per litre solution								
DAYS	7	15	28	7	15	28	7	15
75%CEMENT 25% SLAG	10,7/58 (-)	8,9/56,7 (-)	7,4/54,8 (+)	10,3/58,7 (-)	8,9/56,4 (-)	7,4/55,5 (+)	9,8/58,7 (-)	7,9/55,5 (+)
65%CEMENT 35% SLAG	9,3/51,4 (+)			9,3/52,4 (+)			8,7/52,0 (+)	
55%CEMENT 45% SLAG	7,4/43,4 (+)			7,2/44,4 (+)			7,1/44,4 (+)	

It may be deduced from the assays described that copper slags show pozzolanic qualities which are appreciable over a short period but superior to a good quality natural pozzolan over a longer period.

V. PHYSICAL TESTS

V.1. Setting and rheology

A pure cement of 3500 cm²/gr were taken as a standard and 5-10-25-35 and 45% ground copper slags at 20% rejection above 45 m were substituted. There cements were used for setting determinations in an automatic penetrometer, and the rheological properties of the pastes were measured in CERILH coaxial cylinder viscometer (Table VI). Flow tests (ASTM C-109-77) and bleeding (ASTM C-243-75) in mortars (Table VII) were also performed. The results were as follows:

TABLE VI

		Time of setting		Coaxial-Cylinder Viscosimeter		
	%H_2O	INITIAL	FINAL	W/C	Dinas/cm²	POISES
PORTLAND CEMENT(P.C.)	25	1h05'	2h05'	0,5	142,0	3,3
95%(P.C.)+5% SLAG	25	1h10'	2h10'	0,5	135,7	3,1
90%(P.C.)+10% SLAG	24,5	1h 20'	2h20'	0,5	116,7	2,7
75%(P.C.)+25% SLAG	23,5	1h 30'	2h35'	0,5	96,1	1,9
65%(P.C.)+35% SLAG	22,5	1h 40'	3h00'	0,5	76,6	1,7
55%(P.C.)+45% SLAG	22	1h 50'	3h15'	0,5	71,6	1,2

TABLE VII

	MORTAR (1:3)			MORTAR (1:2,5)		
	W/C K	FLOW%	BLEEDING	W/C	FLOW%	BLEEDING
PORTLAND CEMENT(PC)	0,5	27,3	0,7	0,54	112,8	3,9
95%(P.C)+5% SLAG	0,5	34,5	0,7	0,53	110,3	3,2
90%(P.C.)+10% SLAG	0,5	45,7	1,2	0,52	106,8	3,3
75%(P.C.)+25% SLAG	0,5	53,4	2,1	0,51	106,5	3,0
65%(P.C.)+35% SLAG	0,5	58,0	2,5	0,51	106,8	5,8
55%(P.C.)+45% SLAG	0,5	60,5	2,7	0,49	108,3	5,2

There is a substantial increase in plasticity with greater slag addition, and less water is needed than in pure cements.

V.2. Hydration heat (ASTM C-186-78)

The results obtained are shown and it may be observed that the presence of 25% slags in the cements complies amply with type IV ASTM.

TABLE VIII

	7 DAYS (cal/gr)	28 DAYS (cal/gr)
CEMENT PORTLAND(PC)	75	94
95%(P.C)+5% SLAG	72	83
90%(P.C)+10%SLAG	63	73
75%(P.C)+25%SLAG	52	64
65%(P.C)+35%SLAG	47	56
55%(P.C)+45%SLAG	40	48

V.3. Mechanical resistances. Influence of alkalis in the first stages.

A conglomerate of 65% pure ground cement

(3500 cm^2/gr), type P-450 and 35% slags with rejection of 20% above 45µm was prepared to compare the increase in resistances of the slag cement as a function of time. The same test conditions were used for the P-450 cement and for the cement which contained 35% ground quartz sand in substitution, at identical rejection with the slags.

Percentages with respect to the pure cement are given in brackets (Table IX)

TABLE IX

DAYS	CEMENT P-450	(P-450:SLAG) (65:35)	(P-450:SAND)(65:35)
3	63 - 350	41-194 (65-55)	43-221 (68-63)
7	72 - 417	48-239(67-57)	50-262 (69-63)
28	77 - 494	61-365(79-74)	52-320 (67-65)
60	82 - 524	71-422(87-81)	59-349 (72-67)
90	84 - 535	74-434(88-81)	62-351 (74-66)
180	85 - 537	76-445(89-83)	64-353(75-66)
365	87 - 542	78-462(90-85)	65-355(75 - 65)
450	87 - 545	79-470(91-86)	65-360(75 - 66)

The cement containing sand showed similar resistances at all ages to the pure cement content (65%), thus demonstrating the inert nature of the sand used.

Low values were obtained after 3 and 7 days for the cements prepared with copper slags. However the difference from the inert standard was evident after 28 days, and values were closer to those obtained for pure cement as time increased (≃90% at 450 days), showing its pozzolanic character.

Althougt the low initial resistances may be useful in many aspects, higher values are required for others, and thus the contribution of alkali, in the form of precipitator dust, acting as an activator, improving resistances, was compared.

The chemical composition of the powder was as follows:

I.L. 11,3% SiO_2 15,5% Al_2O_3 3,9% Fe_2O_3 2,1% CaO 46,0% MgO 2,4% TiO_2 0,13% SO_3 11,9% K_2O 5,2% Na_2O 0,65% $S^=$ traces.
Soluble salts: SO_3 5,1% K_2O 4,6% Na_2O 0,44%

An industrial P-350 with 35% of its weigt substituted by sand and copper slags ground in the same conditions as above, was used.

It is assumed that the slag cement (nº 3) contains additions of 5 and 10% power (95:5) and (90:10), (cements nº 6 and 7) or that for the same pure cement content (61,75 and 58,50) (cements 4 and 5), the copper slags are partially substituted by electrostatic powder (Table X). Cement nº 8 and 9 are equivalent to nº 6 and 7 but contain standardized sand and serve as standard.

It may be observed that for equal percentages of pure cement, nº 6 and 7, containing electrostatic powder, give higher resistances in the first 7 days when compared with those not containing the powder (4 and 5). The increase is 25%, and there was a decrease in those which contained sand as a substitution, particularly after 3 days (cements 8 and 9).

All the values were similar after 28 days.

The beneficial effet of alkaline sulphates during the first ages of the mortars is obvious, and thus this factor will not be a problem, even if high percentages of slags are used. A lower slag addition and/or a greater Blaine S.S. will give PUZ-350 type cements, IP of ASTM or similar types.

VI. RESISTANCE TO EXTERNAL AGENTS

VI.1. Protection of reinforcements against corrosion

Three cements numbered 2, 3 and 4 containing increasing quantities of slags(25, 35 and 45%) were used to study the protective capacity by means of electrochemical techniques and the results were compared with those obtained for pure Portland, P-450(nº 1) and PUZ-350(nº 5).

It was necessary to know: a) the response of steel on incorporation in a cement without additives, and b) the regenerating capacity of the passive layer of the said cement when the metal was subjected to a corrosion process with depasivating ions, in order to carry out this study.

A mortar without additives was used to study a) and a mortar with 2% $CaCl_2$ was prepared to study b).

The progress of corrosion was observed during 28 days which provided approximate criteria on the future behaviour of each steel.

Two types of steel were used for reinforcements: type N of natural hardness and type F, cold twisted, both of 6 mm ∅.

The following measurements were taken:

1) The corrosion rate was followed by determination of polarization resistence Rp and later calculation of the weight loss using Stern's formula: Icorr=B/Rp and the integration of the Icorr-time curves.

2) Gravimetric determination of the weight loss.

3) Electrochemical determination of potential of pitting by the galvanostatic method.

TABLE X

Nº	CEMENT	SAND	SLAG	POWDER	900	4900	10.000	S.S.B.	H_2O	INITIAL	FINAL	3 DAYS	7 DAYS	28 DAYS	60 DAYS	90 DAYS
1	100	—	—	—	0,8	4,1	12,0	3670	25	1h 05'	2h 05'	58-301	64-355	74-438	74-493	78 - 488
2	65	35	—	—	1,6	2,6	8,7	4365	26	1h 25'	2h 45'	41-190	53-240	57-297	60-315	59 - 310
3	65	—	35	—	0,6	3,0	8,5	3380	23	1h 50'	3h 20'	42-160	48-220	64-339	73-382	69 - 407
4	61,75	—	38,25	—	0,2	2,8	9,0	3367	22,5	2h 40'	4h 10'	39-151(100-100)	45-189(100-100)	61-295(100-100)	67-355	64 - 396
5	58,50	—	41,50	—	0,2	2,8	10,4	3340	22,5	2h 50'	4h 15'	36-139(100-100)	43-181(100-100)	62-307(100-100)	67-349	70 - 386
6	61,75	—	33,25	5	1,0	4,4	10,8	3653	23	1h 50'	3h 20'	49-188(126-125)	53-231(118-122)	67-311(110-105)	71-354	75 - 371
7	58,50	—	31,50	10	1,4	5,4	12,3	3883	24	1h 40'	3h 30'	45-182(125-131)	51-223(119-123)	65-302(105-98)	77-350	76 - 344
8	61,75	5	33,25	—	1,2	4,2	11,0	3478	23,5	2h 05'	3h 50'	36-137(92-91)	46-198(102-105)	61-303(100-103)	67-353	71 - 376
9	58,50	10	31,50	—	1,5	5,4	12,1	3422	23,5	2h 10'	3h 45'	34-118(94-85)	42-178(98-98)	57-289(92-94)	67-354	66 - 346

The results obtained show the five cements tested give similar protection to the two types of steel if the mortar is made without additives.

In presence of $CaCl_2$ the classifications of measurements in decreasing order of protection are:

TABLE XI

STEEL	TYPE OF MEASUREMENT	CLASSIFICATION
N	Weight loss gravimetric	3>4>2>1>5
	Weight loss electrochemical	3>4≥2>5>1
	Breaking potencial	4>1>3>5>2
F	Weight loss gravimetric	1>4>5≥3≥2
	Weight loss electrochemical	1>4>5≥3≥2
	Breaking potencial	1>4≥5>2≥3

In the case of F, cement nº 4 was more protective than nº 5 (PUZ-350) and less than nº 1 (P-450).

In the case of steel N, the Icorr show better behaviour of cements 2, 3 and 4 and indicating the favourable response of rupture potentials of nº 4, and partially nº 3 against the attack of depasivating ions.

VI.2. Aggressive action of calcium, magnesium and sodium sulphate solutions and sea water

The accelerated Koch-Steinegger method was used, which defines that a cement is resistant to the action of sulphates when the corrosion coefficient or the ratio between the resistance to flexure of the samples submerged in the potentially aggressive solutions and submerged in filtered tap water is equal to or greater than 0,70 at 56 days.

Four types of cement were used, nº 1 or pure Portland, nº 2 with 35% copper slags, nº 3 with 35% silica sand and nº 4 with 35% natural pozzolan.

The slag cement showed greatest resistance to the three sulphates and was the only one which resisted the attack of sea water (Table XII). This property may be attributed to the formation of iron oxide gels which act as impermeabilizers and resist aggression.

TABLE XII

AGGRESSIVES	DAYS	COEFFICIENT OF CORROSION — CEMENTS 1	2	3	4
$CaSO_4 \cdot 2H_2O$	28	1,19	1,13	1,11	1,17
	56	1,04	1,31	1,24	1,16
	90	1,09	1,28	1,17	1,24
Na_2SO_4	28	1,23	1,10	1,11	1,07
	56	1,00	1,24	1,06	1,12
	90	0,96	1,17	0,97	1,13
$MgSO_4$	28	1,21	1,11	1,06	1,01
	56	1,00	1,22	1,14	1,22
	90	1,08	1,23	1,11	1,26
SEA WATER (A.S.T.M.)	28	0,78	0,87	0,38	0,61
	56	0,50	0,75	0,14*	0,53
	90	0,27*	0,64	0,18	0,57

* DESINTEGRATION

VI.3. Alkali-silica reactivity

An accelerated method consisting in preparing a mortar using Pyrex nº 7740,30 to 50 mesh, as aggregate was used, and W/C ratio of 0,4 and aggregate/cement ratio of 0,75, kept at 43ºC for 14 days and 75 days.

The initial clinker gave a total value of K_2O=0,88% and Na_2O=0,32%, equivalent to 0,89% in total Na_2O. Soluble K_2O and Na_2O were 0,62% and 0,10% respectively.

TABLE XIII

CEMENT	% EXPANSION 7 DAYS	14 DAYS	75 DAYS	ASPECT
PORTLAND CEMENT(P.C.)	0,12	0,30	0,47	WARPED
65%(P.C.) + 35% SLAG	0,02	0,05	0,06	GOOD
65%(P.C.)+35%POZZOLAN	0,01	0,02	0,03	GOOD

The mean value of three samples indicates good behaviour of the cements containing slags and pozzolan and deficient behaviour in the pure Portland cement.

VI.4. Behaviour in freezing-thawing cycles

4x4x16 cm mortar prisms were used for this experiment and they were subjected to three hour cycle.

The samples began the first cycle after 7 days in a wet chamber at 21ºC and 95% R.H.

The values obtained and your aspect show that they are exceptionally useful for these purposes.

TABLE XIV

CEMENT	7 DAYS Kp/cm²	75 CYCLES Kp/cm²	µ/m	Δ Kp/cm²	125 CYCLES Kp/cm²	µ/m	Δ Kp/cm²
P-350(P.C.)	70-347	77-480	213	7-133	73-517	381	3-170
65%(P.C.)+35% SLAG	54-211	63-338	344	9-127	59-346	781	5-135
65%(P.C.)+35% POZZ	57-284	71-403	238	14-119	69-409	650	12-125

VI.5. Effect of atmospheric agents in a warm climate

Similarly, tests were carried out keeping 4x4x16 cm prisms for 16 hours in water and 8 hours in an oven at 40ºC and the characteristics were determined after 50 cycles.

TABLE XV

CEMENT	7 DAYS Kp/cm²	50 CYCLES Kp/cm²	Δ Kp/cm²	ASPECT
P-350(P.C.)	70 - 347	73 - 424	3 - 77	GOOD
65%(P.C.) + 35% SLAG	54 - 211	58 - 297	4 - 88	GOOD
65%(P.C.) + 35%POZZOLAN	57 - 284	70 - 410	13 - 126	GOOD

The results obtained confirm the excelent qualities of the cement studied.

VII. EXPERIENCE INDUSTRIAL

The industrial cements obtained as yet, and the concretes made with them, support the validity of the stated parameters.

.....

ASLAND RESEARCH AND DEVELOPMENT CENTRE
VILLALUENGA (TOLEDO) - SPAIN

Pelletized slag cement : autoclave reactivity

Ciment à base de laitier pelletisé : réactivité à l'autoclave

R.D. HOOTON, Graduate Student, and J.J. EMERY, Associate Professor, Department of Civil Engineering and Engineering Mechanics, McMaster University, Hamilton, Ontario, Canada, L8S 4L7.

RESUME : La pelletisation est un procédé qui a été mis au point récemment pour remplacer la granulation des laitiers de hauts fourneaux. Il communique des propriétés hydrauliques latentes au laitier de haut fourneau, mais les facteurs physico-chimiques influençant ces propriétés n'ont jamais été étudiés en détail. Des ciments à base de différents types de laitier pelletisé provenant de plusieurs pays, dont le Canada, ont été préparés de telle sorte que de grandes variétés de compositions chimiques et de degrés de vitrification et de finesse de broyage soient obtenues. Ces ciments ont été ajoutés comme liants dans des pâtes autoclavées à haute température (185°C).

La résistance, la porosité et la composition (sous la forme hydratée) de ces liants (laitier-ciment portland-silice) ont été déterminées dans le but de trouver des relations entre les propriétés physico-chimiques des ciments et celles des pâtes hydratées. La principale phase hydratée pour la plupart des liants de différentes compositions consiste en de la tobermorite (11.3 A). Lors de l'analyse quantitative à l'aide d'un diffractomètre à rayons X, des courbes d'étalonnage ont été construites.

Ce travail de recherche est particulièrement orienté vers l'augmentation des résistances et l'étude de l'hydratation des produits formés à partir d'un système à trois composantes (ciment à base de laitier, ciment portland et poudre de silice), traité à l'autoclave.

SUMMARY: Pelletizing, a recently developed processing and product alternative to both foaming and granulating, imparts latent hydraulic properties to iron blast furnace slag, but the physical and chemical factors influencing these properties have not been previously studied in detail. Pelletized slag cement from both Canadian and foreign sources, covering a wide range of chemical compositions, degrees of vitrification (i.e. glass contents) and fineness of grinding have been incorporated as the major binder component in high temperature (185°C) autoclaved pastes. The strengths, porosities and hydrated compositions of these slag-Portland cement-silica binders have been determined, and it is intended to establish relationships between the physical and chemical properties of the original slag cements and the hydrated pastes established. Over a wide range of proportions, 11.3 Å Tobermorite has been found to be the major hydrated phase and XRD calibration curves were developed for its quantitative analysis. This contribution is primarily concerned with strength development and the hydration products formed in the ternary system of autoclaved, pelletized slag/Portland cement/silica flour.

EXPERIMENTAL

Materials: Chemical and mineralogical compositions as well as physical properties of the pelletized slag (1,2), Portland cement and silica flour are shown in Table I. The sand used in the mortar cubes was standard ASTM C109 Ottawa quartz sand.

The estimate of the glass content of the slag depends on the method employed. By individual, optical particle analysis under crossed polars (3), the glass content was estimated at 69%. The percent of emission at 590 nano meters, compared to a glass standard on a UV spectrophotofluorometer was found to be >100%. The XRD value of 95% glass shown in Table I, was obtained by comparison of peak intensity ratios of the CaF_2 internal standard to the mellilite and merwinite peaks in relation to those found for synthetic materials. This method was thought to be the most reliable.

Methods: Pastes: After sieving all materials through a 150 μm sieve, and mixing at W/C = 0.32, pastes were vibrated into cylinder molds. After autoclaving, three of the 30mm diameter by 50 mm cylinders were capped and tested in compression and two were subjected to splitting tension.

Mortars: Three 51 mm mortar cubes were prepared according to ASTM C109 and C305 (constant workability rather than a constant W/C) and were tested in compression after autoclaving.

Curing: After mixing, both pastes and mortars were stored for 16 - 18 h at 23°C and 100% RH in order to develop green (initial) strength. Specimens were demolded then placed in a Cenco laboratory autoclave. The maximum temperature of 185°C (1.03 N/mm^2 steam pressure) was reached in 1h, held for 4h, then the pressure was released slowly over 1.5h. The specimens were left in the autoclave for a further 16 - 18 h before removal.

X-Ray Diffraction (XRD): A Norelco diffractometer and monochromatic CuKα radiation (30 KeV, 16 mA) were used for the most part at a scanning speed of 1°2θ/minute over the range 6 to 70°2θ. Several repeat scans were made to verify the presence of weak peaks and to enable the averaging of intensities. 10% by weight of CaF_2 was added as an internal standard.

Differential thermal Analysis (DTA): Samples were heated in air at 12°C/minute using a Dupont 900 analyser at a sensitivity of $\Delta T = 0.6°C/cm$.

Non-Evaporable Water: While initially gaining weight during ignition at 1050°C, the slag was found to lose weight during continued ignition periods. After 20 to 30h ignition, the weight changes became consistent and levelled off (often at a net loss in weight) parallel to the rate of weight change of the pastes. Therefore the method of Copeland and Hayes (4) for determining non-evaporable water content in pastes was modified to include the three binder components and was based on ignition times of 20 and 30 h.

OBSERVATIONS

Mortars: Mortar cubes were made at 10% intervals over most of the range of the ternary system and compressive strengths are shown in Figure 1. It can be seen that at

MATERIAL	OXIDE CHEMISTRY - By XRF except as noted											SG (g/cc)	BLAINE (m^2/g)	MINERALOGY
	CaO	SiO_2	Al_2O_3	MgO	K_2O	Na_2O	S	Fe	Mn	TiO_2	LOI -			
PELLETIZED BLAST FURNACE SLAG	39.75	36.75	8.87	11.37	0.44	-	2.06	0.58	0.51	-	Varies: 0.10 at 20h 0.63 at 30h	2.94	409	95% glass of mellilite (C_2MS_2 - C_2AS) composition. 4% C_3MS_2 crystals 1% mellilite crystals
PORTLAND CEMENT	61.77 CaO (free) = 0.24 *	20.27	5.81	2.56	1.25	0.21	3.32 (SO_3)	2.11 (Fe_2O_3)	-	-	1.55	3.11	343	Bogue Calculation: C_3S = 46.9% C_2S = 23.7% C_3A = 11.5% C_4AF = 6.4 % $CaSO_4$ = 5.5 % $CaCO_3$ = 3.3 %
SILICA FLOUR	0.12	95.83 **	2.34	0.06	0.62	0.08	-	(Fe_2O_3)	-	0.12	0.45	2.68	274	93.1% quartz 6.1 % sericite mica ($KA_3S_6H_2$) - non reactive

*: by ethylene glycol-methonal extraction. **: obtained by difference.

TABLE I: PROPERTIES OF BINDER MATERIALS

20% silica flour contents, high strengths were obtained over the whole range of slag cement/Portland cement. Maximum strengths were obtained at high slag contents (60% slag cement/20% Portland cement/20% silica flour, 70%/20%/10%, and 75%/15%/10%).

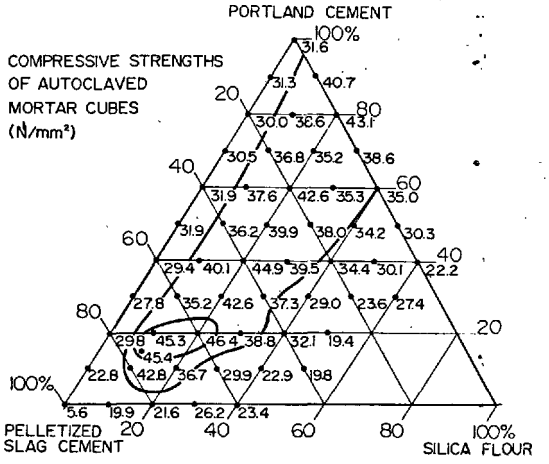

Fig. 1 - Compressive strengths of autoclaved mortar cubes (N/mm^2)

Pastes: The compressive strengths of paste cylinders, made at 20% intervals in the ternary system, are shown in Figure 2. Comparison of these values with the mortar cube strengths in Figure 1, shows that the region of optimum strengths has shifted over to about 40% silica flour. This would seem to indicate that some of the coarse quartz sand (150-600 μm) in the mortars reacted to form hydration products. Even though pastes initially containing 20% silica flour, had large quantities of unreacted silica (detected by XRD), their strengths were less than the pastes containing 40% silica flour. This hydrothermal reaction of coarse quartz sand is supported by Menzel (5) who noted the reaction of 0.3 to 0.58 mm sand at 177°C.

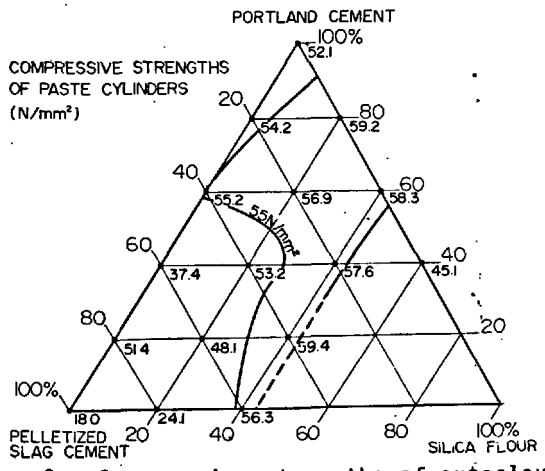

Fig. 2 - Compressive strengths of autoclaved paste cylinders (N/mm^2)

Non-Portland Cement Combinations: one important observation was that without Portland cement, the silica flour reacted hydrothermally with the slag cement in both mortars and pastes resulting in higher strengths than that obtained by slag cement alone. A further point of interest is observed from Figure 3, which gives tensile to compressive strength ratios for the ternary combinations of pastes. While ratios for binders including any proportion of Portland cement did not exceed 0.15, ratios for slag cement and slag cement/silica flour combinations were at least 0.50. Along the slag cement/silica binary, the maximum compressive (56.3 N/mm^2) and tensile (31.4 N/mm^2) strengths occurred using 60% slag cement and 40% silica flour. From analysis by XRD, it was found that well crystallized 11.3 Å tobermorite was the only hydrated phase formed at this combination.

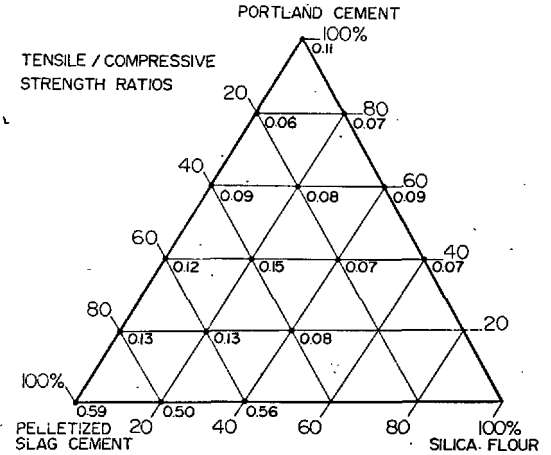

Fig. 3 - Ratios of tensile to compressive strengths of pastes

The small quantity of free lime liberated by the slag is unlikely to have produced 11.3 Å tobermorite to the extent it was found. Therefore reactions, as yet unaccounted for, must have occurred between the slag minerals and the silica flour. The mechanism of these reactions must certainly be different than the commonly accepted theory of alkali activation, originally proposed by D'Ans and Eick (6). Although not considering autoclave temperatures, they proposed that hydration-inhibiting, acidic gels initially coated the surfaces of the slag grains and could only be penetrated by a sufficient concentration of externally supplied alkali.

The practicality of these non-Portland cement binders was questioned due to low green strengths obtained in the pastes. However, in a related industrial application study, full scale 200 mm masonry blocks were successfully produced, with a binder of 67% slag cement (285 m^2/g Blaine fineness) and 33% silica flour (7).

Unreacted Materials: While Figure 4, shows the molar CaO/SiO_2 ratio of the starting materials for each binder composition, these values would be different than the C/S ratios of the hydrates due to the presence of unreacted portions of all three materials. Unreacted silica flour could be easily detected, by XRD, at any binder composition having it as a component. The presence of unreacted slag glass was assumed to be responsible for the amorphous halo (hump) in the diffraction traces. Unreacted Portland cement (mainly alite) was found in many of the pastes as shown in Figure 5.

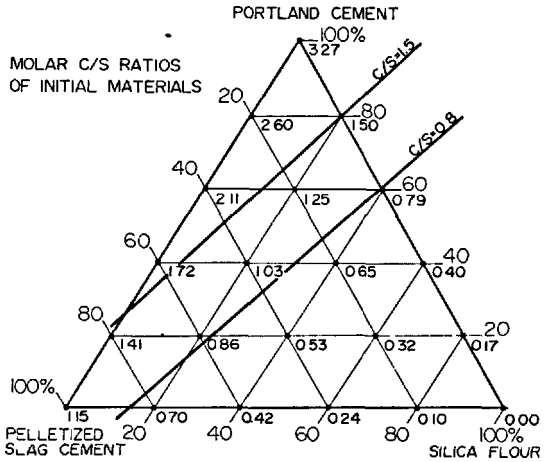

Fig. 4 - Molar C/S ratios of initial paste materials

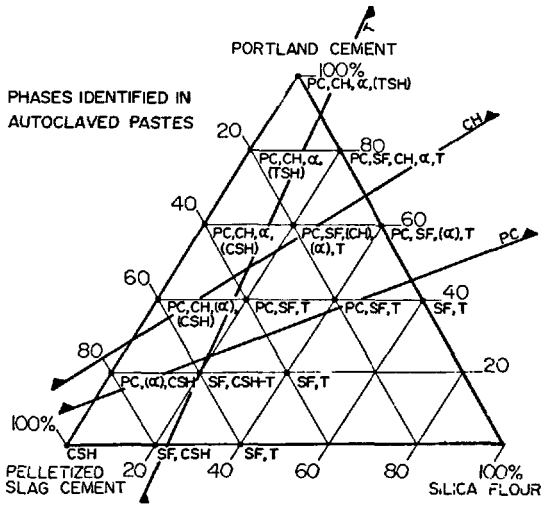

Fig. 5 - Phase identified in autoclaved pastes PC= unreacted Portland cement, SF = unreacted silica flour, CH = $Ca(OH)_2$, α = αC_2SH, TSH = C_3SH_2, T = tobermorite with 11.3 Å peak, CSH = poorly crystalline tobermorite, ( ) = only trace of phase detected.

Hydration Products: The hydration products detected by XRD and DTA are also shown in Figure 5. 11.3 Å tobermorite, in various degrees of crystallinity, was found to be the main hydrated phase in all binders containing silica flour, and for 100% slag cement. Poorly crystalline tobermorite was also found in autoclaved (188°C) slag glass by Midgley and Chopra (8). Using an XRD calibration curve for synthetic 11.3 Å tobermorite (not detailed here), the maximum content of tobermorite (about 10 to 15% by weight) was found along the line of binders containing 40% silica flour, coincident with high strengths.

αC_2SH was detected in all combinations of slag and Portland cement not containing silica flour and silica combinations with at least 60% Portland cement, some of which exhibited high strengths as well. αC_2SH was not detected readily by XRD but the DTA endotherm at 475°C was easily distinguished. Tricalcium silicate hydrate was only found in small quantities in the 100% Portland cement paste and at 20%/80%/0%. The presence of the 3.03 Å peak of either calcite or scawtite was detected in some pastes but was not included in Figure 5, since it was not known if this phase was formed during autoclaving or if it was due to carbonation during storage afterwards.

Free Lime: From Figure 5, it can also be seen that slag and silica flour each consume the free lime liberated by Portland cement, during hydration.

Non-Evaporable Water: In Figure 6, estimates of the non-evaporable water, uncorrected for any carbonation of the hydrates, are given. The non-evaporable water content generally increased with increasing Portland cement content, which would seem to indicate more complete hydration of pastes containing large quantities of Portland cement after 4h autoclaving at 185°C. However, the presence of increasing quantities of $Ca(OH)_2$ with increasing Portland cement content would account for some of this phenomenon.

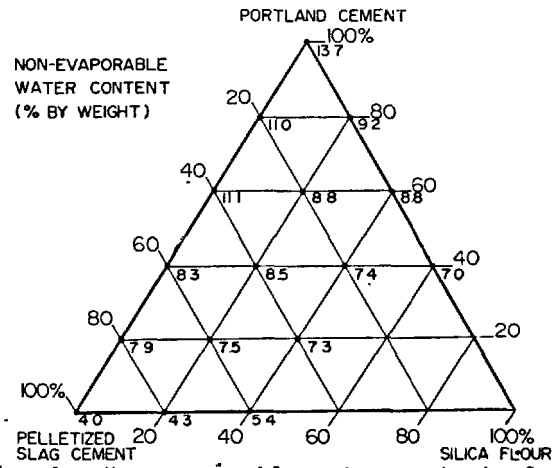

Fig. 6 - Non-evaporable water content of pastes (% by weight)

Effect of Slag Variables: While the analysis of this work is still in progress, a short summary is in order. Paste prisms containing 18 different industrial and synthetic slags were prepared at W/C = 0.28, 0.32 and 0.40, composed of 60% slag cement/20% Portland cement/20% silica flour. The strength and porosity data obtained were used to extrapolate to zero-porosity strengths from least squares line fits, following the methods of Beaudoin and Feldman (9). Realizing the importance of variations in porosity on strengths, the zero-porosity strength was used to eliminate this effect for comparison of strengths to slag properties. The quantity of hydration products was also found to vary with W/C. The higher the water/cement ratio, the larger was the quantity of hydration products.

From preliminary analysis, the changes in glass contents and chemistry between different pelletized slags,whether from the same blast furnace or not, show no trend with respect to either the non-evaporable water contents, strengths at a constant W/C, or zero-porosity strengths. Of the available empirically derived chemical moduli, commonly found in slag studies (10) and slag cement specifications (e.g., Canada CSA:A363, West Germany - DIN:1164), no correlation has been found with reactivity. As mentioned earlier, different techniques of measuring the degree of vitrification in slags exist and these are being evaluated in relation to reactivity and strength development. In summary, none of the commonly accepted methods of assessing slag quality has proved satisfactory.

CONCLUSIONS

For autoclaved mortars, higher strengths were obtained with pelletized slag cement as the principal constituent in the ternary system than with any non-slag cement combination.

Paste combinations giving high strengths generally contained more silica flour than in mortars.

Pelletized slag cement was activated by silica flour, forming 11.3 Å tobermorite and resulted in high strengths without the use of Portland cement. These slag-silica binders also showed very high tensile to compressive strength ratios.

Most of the pastes having high strengths also had 11.3 Å tobermorite as the major hydration product. Some pastes also containing αC_2SH exhibited high strengths, but αC_2SH was only detected either in pastes not containing silica flour or pastes having greater than 60% Portland cement.

Preliminary investigations into the effect of chemistry and glass content on the hydrothermal reactivity of pelletized slag have shown no definite trends..

REFERENCES

1.- R.D. MARGESSON and W.G. ENGLAND (1971), "Processes for the pelletization of metallurgical slag", United States Patent 3,594,142, 20 July.

2.- J.J. EMERY (1978), "Slags as industrial minerals", Proceedings, Third Industrial Minerals Congress, Paris, 127-142.

3.- J.J. EMERY, C.S. KIM, and R.P. COTSWORTH (1976), "Base stabilization using pelletized blast furnace slag", Journal of Testing and Evaluation, 4(1), 94-100.

4.- L.E. COPELAND, and J.C. HAYES (1953), "The determination of non-evaporable water in hardened portland cement paste", Portland Cement Association Research Bulletin 47, 1-9.

5.- C.A. MENZEL (1934), "Strength and volume change of steam-cured portland cement mortar and concrete", Journal of the American Concrete Institute, 31, 125-149 (Nov. - Dec.).

6.- J. D'ANS and H. EICK (1954), "Investigations on the setting process of hydraulic blast furnace slag", (in German), Zement-kalk-Gips, 7, 449-459.

7.- J.J. EMERY and R.D. HOOTON (1978), "Ground pelletized slag autoclaved blocks", Proceedings, International Conference on the Use of By-products and Wastes in Civil Engineering, Paris, 2, 303-307.

8.- H.G. MIDGLEY and S.K. CHOPRA (1960), "Hydrothermal reaction between lime and aggregate fines", Magazine of Concrete Research, Vol. 12 (35), 73-82.

9.- J.J. BEAUDOIN and R.F. FELDMAN (1975), "A study of mechanical properties of autoclaved calcium silicate systems", Cement and Concrete Research, 5, 103-118.

10.- F.M. LEA (1971), The Chemistry of Cement and Concrete, Chemical Publishing Company Inc., New York, 463-464.

ACKNOWLEDGEMENTS

The authors would like to acknowledge the technical assistance provided by the following people: L.P. MacDonald, L. Zimmerman, St. Lawrence Cement; H. Chen, Canada Cement Lafarge; R. Doelle, Dominion Foundries and Steel; R. Warren, W. Berry, Standard Slag Cement; J.R. Foster, Dravo Lime; G. Gerrites, J. Cartwright, Indusmin.

The authors also wish to thank R.H. Mills, University of Toronto, for reviewing this paper.

High Manganese High Alumina Slag for Cement Manufacture

L'utilisation des laitiers alumineux à forte teneur en manganèse, dans la fabrication des ciments

C.A. TANEJA, S.P. TEHRI and MANJEET SINGH, Scientists, Central Building Research Institute, Roorkee (U.P.) India.

RESUME : Le laitier de Rourkela a pour caractéristique d'avoir une teneur en MnO supérieure à 6,75 %. Des études antérieures ont montré l'effet défavorable de cette forte teneur en MnO sur l'hydraulicité de ce laitier. Cependant le laitier de Rourkela diffère des laitiers étrangers par sa plus forte teneur en Al_2O_3 et un plus faible rapport CaO/SiO_2, bien qu'ayant une forte teneur en MnO. L'activation du clinker par des verres synthétiques de même composition (CaO, Al_2O_3, SiO_2, MnO) que le laitier de Rourkela, ont montré que MnO pouvait avoir, dans les conditions optimales, un effet favorable. Cependant ces verres synthétiques ne pourraient avoir, au broyage, la même granulométrie que le laitier. En outre, des recherches ont été entreprises sur des échantillons commerciaux de laitier à haute teneur en manganèse.

Des ciments PBFS ont été préparés par mélange de laitier, de clinker et de gypse. Ils ont été essayés. On a trouvé que les proportions optimales de laitier et de clinker étaient de 50x50 avec addition de 4 % de gypse. Ces ciments PBFS sont conformes aux normes. Le laitier à haute teneur en manganèse est recommandé pour la fabrication du ciment PBFS.

SUMMARY: Rourkela slag is characterised by having MnO content upto 6.75 per cent. Studies abroad have shown adverse effects of MnO in slag on its hydraulicity. However, Rourkela slag is different from foreign slags in having higher Al_2O_3 and lower CaO/SiO_2 besides having high MnO. Clinker activation of synthesized $CaO-Al_2O_3-SiO_2-MnO$ glasses corresponding to composition of Rourkela slags showed favourable effects of MnO under optimum conditions. However, quenching of synthetic glass composition does not simulate conditions of granulation. Therefore, commercial samples of high manganese slag were investigated.

PBFS cements were prepared by intergrinding slag, clinker and mineral gypsum and tested. Optimum proportions of slag and clinker were found to be 50:50 with 4 per cent of gypsum. PBFS cements were found to comply with the standard requirements. High manganese slag is recommended for manufacture of PBFS cement.

Indian slags are characterised by low lime and high alumina contents. The slag from the blast furnaces of Rourkela Steel Plant, Rourkela (Orissa) which employs L.D. process for steel making and makes addition of pyrolusite in the furnace burden, is different from other slags in having comparatively high MnO content (3.1 to 6.75 per cent). Doubts were expressed about the suitability of this slag for cement manufacture. Laboratory investigations were carried out to study the effect of increasing amount of MnO in water-quenched synthetic slag glasses corresponding to chemical composition of Indian slags on their hydraulic behaviour on activation with portland cement clinker. Results showed that MnO content upto 2.5 per cent in slags was beneficial but a higher content affected the early strength adversely though the late strengths at 28 days and beyond improved appreciably (1). However, quenching of molten synthetic slag compositions does not simulte the conditions of commercial granulation method. Therefore, it was considered desirable to study the hydraulic properties of commercially produced high manganese granulated slags on clinker activation.

EXPERIMENTAL

Raw Materials

a) Granulated Slags:

Chemical Composition:

Four samples of commercial granulated blast furnace slag were received from Rourkela Steel Plant. Their chemical composition is reported in Table 1.

Table 1

Chemical Composition of Slags

Constituents	Composition Percent Sample No.			
	1	2	3	4
SiO_2	34.46	34.50	34.00	33.80
Al_2O_3	23.35	24.10	24.00	23.30
FeO	0.42	0.30	0.56	0.37
CaO	31.40	30.90	29.90	28.60
MgO	6.00	5.60	5.30	6.00
MnO	3.10	4.00	5.10	6.75
S	0.60	0.65	0.52	0.52
Total	99.30	100.05	99.38	99.34

Hydraulic index employed for evaluating the hydraulicity of high manganese slagsas recommended by Keil (2) and computed from chemical composition is reported in Table II.

Table II

Hydraulic Indices of Slags

Formula	Slag samples			
	1	2	3	4
$\frac{CaO+CaS+\frac{1}{2}MgO+Al_2O_3}{SiO_2 + MnO}$	1.55	1.51	1.45	1.36

According to Keil (2) slags of index more than 1.5 (samples 1 and 2) are of good hydraulic property whereas those of less than 1.5 (samples 3 and 4) are of moderate hydraulicity. These indices are, however, recommendatory only. Hydraulicity is known to depend more on the conditions of granulation of slags.

Sulphur in slags is known to have greater affinity for Manganese forming Manganese sulphide than for calcium or iron. The amount of MnS formed computed from sulphur content in slags and the balance of MnO percent in glassy phase are reported in Table III.

Table III

Form of Manganese in Slags

Constituent	Slag Samples			
	1	2	3	4
MnS	1.63	1.77	1.41	1.41
MnO	1.77	2.61	3.95	5.60

Physical Properties

Representative samples of slags were oven dried at 105°C and examined for their bulk density, glass content and refractive index. Results are reported in Table IV

Table IV

Physical Properties of Slags

Sample No.	Bulk Density (kg/m^3)	Refractive Index	Glass Content (%)
1	1480	1.64	90
2	1240	1.62	95
3	1360	1.64	90
4	1320	1.60	91

Data on bulk density shows that the slag is of medium to hard grindability (3) and is expected to be harder to grind than cement clinker: Glass content is more than the minimum specified limit of 90 per cent.

Table V

Analysis of Rajgangpur Clinker and Gypsum

Constituents	Clinker Percent	Gypsum Percent
SiO_2	23.68	18.20
Al_2O_3	5.18	3.92
Fe_2O_3	2.46	
CaO	64.40	27.18
MgO	3.95	2.21
SO_3	tr	31.13
Loss on Ignition	1.18	18.00
	100.85	100.64

b) Portland cement clinker was obtained from Orissa Cement Works, Rajgangpur. Chemical Composition is reported in Table V.

c) Gypsum was obtained from the above source. Its chemical composition is reported in Table V.

Preparation of Portland Blast Furnace Slag Cement

The four samples of slag were interground with cement clinker in the proportions of 40:60, 50:50 and 60:40 with 4 per cent of gypsum to fineness of about 4000 sq.cm/gm(Blains). As a control sample, the cement clinker was ground with 4 per cent of gypsum to fineness of about 3200 sq.cm/gm (Blains).

Results

Portland blast furnace slag cements and portland cement thus produced were tested for physical properties as per Indian standard 4031-1968. Results are reported in Table VI.

Table VI

Physical Properties of Slag Cements

Slag Sample No.	MnO Percent	Slag Cement composition S : C : G	Surface Area cm^2/g (Blains)	Setting Time (minutes) Initial	Final	Compressive strength (N/mm^2) 3days	7days	28days	90days
1	3.1	40 : 60 : 4	4141	250	300	30.2	41.4	57.2	61.4
		50 : 50 : 4	4100	275	315	24.1	33.0	49.2	60.0
		60 : 40 : 4	4040	295	340	21.0	28.4	43.7	57.1
2	4.0	40 : 60 : 4	4020	250	300	29.0	41.2	56.9	68.6
		50 : 50 : 4	4261	275	310	27.8	40.4	50.0	60.8
		60 : 40 : 4	4140	275	310	20.2	33.7	43.7	58.8
3	5.0	40 : 60 : 4	4020	270	310	27.8	39.2	58.2	65.3
		50 : 50 : 4	4140	260	300	24.5	35.7	54.1	61.3
		60 : 40 : 4	4040	260	300	20.0	27.4	39.2	54.0
4	6.75	40 : 60 : 4	4100	260	305	29.0	39.6	58.8	70.2
		50 : 50 : 4	4020	265	305	26.0	34.5	51.6	64.5
		60 : 40 : 4	4020	270	310	19.0	27.2	38.4	52.9
Portland Cement		0 : 100 : 4	3230	285	335	34.5	45.3	52.1	64.7
		IS 269-1976	2250	30	600	15.7	21.6		

Discussion

Manganese sulphide content in samples of slag is much below the maximum prescribed limit of 5 per cent reported by Solacolu and Balta (4) to affect the hydraulic activity adversely and hence is not likely to cause deleterious effect.

Since the slag cements produced by intergrinding of granulated slag and clinker in the ratios of 40:60, 50:50 and 60:40 pass the standard specifications, these slags can be recommended for manufacture of cements. However, 3 and 7 days strengths of slag cements are much lower than those of control portland cement. Lowering of strength does not bear any correlation with MnO or CaO or CaO+MgO. It appears that apart from chemical composition, the condition of granulation namely temperature and speed, play an important role in deciphering quality of slag.

Conclusion

PBFS cements produced by intergrinding granulated slag containing MnO as high as 6.75 per cent and portland cement clinker with 4 per cent gypsum comply with the requirements of standard specifications and hence slags are suitable for manufacture of cement.

References

1. C.A.TANEJA (1973) 'Role of Alumina Magnesia and Manganese oxides on the hydration and hardening of slag glasses. Trans.Ind.Cer.Soc.32(5) 109-124.
2. F.KEIL (1952) 'Slag Cements' Chemistry of Cement, Proc. Third Int. Sym. London Published by Cement & Concrete Association London pp 549-550.
3. Ibid, 560
4. S.SOLACOLU et P.BALTA (1964) 'Hydraulic properties of blast furnace slags in the $MgO-CaO-Al_2O_3-SiO_2$ system containing manganese and sulphur, Revue des Materiaux de construction et de Travaux publics 583, 98-110.

The Hardening of Nickel Slags

Le durcissement des laitiers de nickel

J. LANEUVILLE, Director of Research and Development, St. Lawrence Cement Company, Mississauga, Ontario, Canada.

SUMMARY: The chemical composition of non-ferrous slags produced in Canada from nickel and copper smelters contains mostly iron oxide and silica, with minor amounts of calcium oxide. This composition is quite distinct from steel blast furnace slags normally used in blended cements.

The Pozzolanic properties of finely ground nickel slags have been investigated in comparison with fly ash and ground quartz by means of the Pozzolanic Activity Test ASTM C 595. A good relationship exists between the lime mortar strengths of the materials investigated and their HCl-soluble SiO_2 plus Al_2O_3 contents after 7 days curing. The granulated slag showed the highest pozzolanic activity.

The hardening properties of granulated nickel slag, in blends of slag and cement, have been investigated in ASTM C 109 modified mortars, cured at 23°C for periods extending to 1 year or autoclaved at 2 MPa. The contribution of slag to strength is negligible at early ages, but is equivalent to that of cement at later ages, say 90 days to 1 year, provided the slag content of binder does not exceed 45%.

On mortars made with various slag/cement ratios, hydrated for 7, 28 and 90 days at 23°C and dried at 105°C, the combined water was calculated from thermogravimetric curves and loss at 1000°C. A fair relationship was found between the mortar strengths and the combined water contents. The proportions and nature of hydration products was found to vary with slag/cement ratios.

Comparative micrographs of cement paste and cement-slag paste, hydrated for 2 months, have been obtained with a scanning electron microscope and analyses of selected areas made with an X-ray energy dispersive spectrometer.

RESUME: La composition chimique des laitiers non-ferreux produits au Canada par les fonderies de nickel et de cuivre contient principalement de l'oxyde de fer et de la silice avec des quantités mineures de chaux. Cette composition diffère fortement de celle des laitiers de haut fourneau qui sont normalement employés dans les ciments métallurgiques.

On a étudié les propriétés pouzzolaniques des laitiers de nickel finement broyés en comparaison de cendres volantes et de quartz moulu en suivant l'essai de pouzzolanicité ASTM C595. Une bonne relation existe entre les résistances mécaniques des divers mortiers et les teneurs en silice et alumine solubles dans HCl après 7 jours de durcissement.

On a aussi suivi l'évolution du durcissement d'un laitier de nickel granulé, mélangé au ciment en diverses proportions, en mortiers modifiés ASTM C109, maintenus à 23°C, pendant des périodes s'étendant jusqu'à 1 an ou autoclavés à 2 MPa. La contribution du laitier à la résistance à la compression est négligeable à de jeunes âges, mais elle équivaut à celle du ciment entre 90 jours et 1 an, pourvu que la teneur en laitier du liant ne dépasse pas 45%.

A partir de courbes thermogravimétriques et de la perte à 1000°C, on a calculé la teneur en eau combinée de mortiers de divers rapports laitier/ciment, hydratés pendant des périodes de 7, 28 et 90 jours et séchés à 105°C. On a trouvé une bonne relation entre la teneur en eau combinée des mortiers et leur résistance à la compression. On a trouvé que le rapport laitier/ciment influe sur les proportions et la nature des produits d'hydratation.

A l'aide d'un microscope électronique à balayage, on a pris des photos d'une pâte de ciment et d'une pâte de ciment-laitier durcies pendant 2 mois. Sur des microzones choisies, on a fait l'analyse à l'aide d'un spectromètre en dispersion d'énergie.

INTRODUCTION

Annual production of non-ferrous slags in Canada is estimated to be 8 million tons and is mostly produced from copper, nickel, zinc or lead smelters (1). These slags contain mainly iron oxide and silica (2).

Recently, research on the cementitious properties of non-ferrous slags have been the subject of a few publications. E. G. Thomas (3,4) studied the influence of ground copper reverberatory furnace slag, dezinced lead smelter slag, copper converter slag and lead blast furnace slag on the hardening properties of cemented hydraulic fill. He found that all these slags when used in a quenched, glassy state and ground to a specific surface of about 300 m^2/kg act as pozzolans providing glassy silica, which reacts with lime and water to produce stable, cementitious hydrated calcium silicates. Thomas pointed out that the pozzolanic nature of the reaction between cement and slags is verified by the fact that addition of these ground slags to a fixed cement content produces increased strength over long periods.

The present author (5) studied the hardening properties of copper and nickel slags produced in Canadian smelters. Experiments were made in order to study the rate of hardening, over the period of one year, of mortars made with binders containing various proportions of cement and ground slag or cement and ground quartz. In the main series of experiments, the Blaine fineness of cement, slag and quartz was 400 m^2/kg. The mortars were prepared and tested according to ASTM C109-64, the mass of cement plus slag used for preparing the mortar cubes being the same as the mass of cement prescribed in the test method.

The contribution of the granulated nickel slag to mortar strength compared to Portland Cement was very small at 7 days, but it showed increases with longer curing periods attaining that of the cement at 1 year, at slag/cement ratio less than one. For higher slag to cement ratio, the strength decreased more rapidly at the later ages.

Basic knowledge on the hydration characteristics of nickel slag is still very scanty. The present paper makes an endeavour to narrow this gap.

MATERIALS

The composition of the materials used is shown in Table I. The quartz sample contained 96.4% SiO_2. Total iron and sulphur have been calculated as Fe_2O_3 and SO_3, although they are predominantly found in a reduced state in slags.

Slag A was an air-cooled nickel slag and slag B a granulated nickel slag. Their crystallinity were qualitatively checked by X-ray diffraction in 1970. The main constituent in both slags was a glass phase of low crystallinity, the glass phase being more abundant in slag B. Both slags also contained fayalite, more abundantly in slag A than in slag B, but of higher crystallinity. Both slags contained magnetite as a minor constituent.

TABLE I-Percentage composition of materials

	Cement	Fly Ash	Slag A	Slag B
SiO_2	20.65	49.24	36.77	37.96
Al_2O_3	5.81	24.84	5.21	6.30
Fe_2O_3	2.14	22.50	53.80	50.89
CaO	62.91	1.84	2.84	3.10
MgO	2.80	0.72	2.32	3.10
K_2O	1.26	-	0.61	0.71
Na_2O	0.21	-	-	-
SO_3	2.78	0.77	3.71	2.83
L.O.I.	1.44	-	-	-

POZZOLANICITY OF SLAGS

Experimental procedure. Samples of slag A, slag B and quartzite were ground in the dry state in a laboratory ball mill. The Blaine specific surface areas of cement, fly ash, quartz, slag A and slag B were respectively 350, 310, 400, 400 and 380 m^2/kg.

The pozzolanicity of these materials was studied in lime mortars according to the procedures set out for the Pozzolanic Activity Test in Standard ASTM C595.

The HCl-soluble SiO_2, Al_2O_3 and Fe_2O_3 content of the lime-slag, lime-fly ash, lime quartz mortar specimens was determined immediately before and after the 7-day curing period prescribed in the ASTM Pozzolanic Activity Test. The mortar specimens were dried and ground for 2 minutes in a Shatter Box disc grinder. To 1 g of sample, 100 ml of cold HCl (d=1.12) were added and stirred for 10 minutes with a magnetic stirrer. The solution was filtered and the SiO_2, Al_2O_3 and Fe_2O_3 content was determined in the filtrate, using standard gravimetric methods for SiO_2 and Al_2O_3, and titration with $K_2Cr_2O_7$ for Fe_2O_3. The loss on ignition was also determined and the amounts of soluble SiO_2, Al_2O_3 and Fe_2O_3 calculated as percent of the original mass of slag, fly ash and quartz.

Results: the amounts of HCl-soluble SiO_2, Al_2O_3 and Fe_2O_3 extracted from the mortar specimens, before and at the end of the curing period are shown in Table II and expressed as percent of the original mass of the tested materials.

The soluble SiO_2 and Al_2O_3 contents of lime-slag mortars increased during the curing period, whereas the Fe_2O_3 content showed no definite trend.

TABLE II-HCl-soluble SiO_2, Al_2O_3 and Fe_2O_3, as percent of original mass of materials.

Materials	SiO_2		Al_2O_3		Fe_2O_3	
	1*	2*	1*	2*	1*	2*
Slag A	13.89	18.37	2.30	3.05	43.96	39.70
Slag B	17.96	22.99	3.63	5.79	46.57	42.51
Fly Ash	0.63	9.68	1.82	4.44	1.59	6.78
Quartz	0.94	4.37	1.51	0.36	1.04	4.52

1* and 2* refer to extractions from mortar before and after the curing period (Pozzolanic Activity Test).

No relationship could be established between the compressive strength of the mortars and the increase in soluble SiO_2 and Al_2O_3 during the curing period. However, as shown in Fig.1 a relationship exists between the compressive strength of all lime mortars and their soluble SiO_2+Al_2O_3 contents after 7 days curing. This confirms the pozzolanicity of the two nickel slags, the granulated slag B being more reactive than the air-cooled slag A.

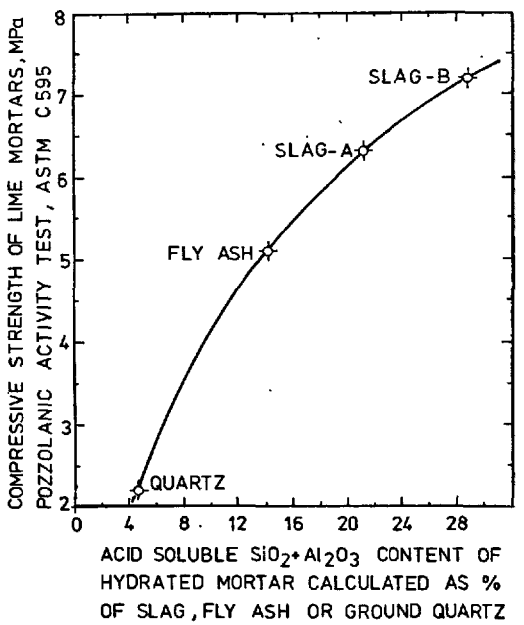

Fig. 1 - Factor related to pozzolanicity

HARDENING RATE OF CEMENT-SLAG MORTARS

The hardening rate of mortars made with granulated slag B (400 m^2/kg) and a Portland cement (400 m^2/kg) has been previously reported (5). The series presently reported made in 1973 deals with the hardening rate of mortars made with the same slag B (380 m^2/kg) with a coarser cement (350 m^2/kg). Experimental procedure: Mortars were prepared according to Standard ASTM C109-64, except that it will be understood that when references are made to the "cement", they will in this case, be to the binders as described in Table III.

TABLE III - Proportions of constituents of binders, in part per mass.

Binders	Cement	Slag B
A	100	Nil
B	70	30
C	55	45
D	25	75

The amount of mixing water was determined with the flow-table. The water-cement ratio was 0.485 for cement mortar and 0.48 to 0.45 for mortars made with slag containing binders, the ratio showing a tendency to decrease with increasing slag content.

A series of 50-mm mortar cubes were prepared by the same procedure and autoclaved at 2 MPa according to the Standard ASTM C151.

Results: as in the previous series (5), the strength producing properties of granulated slag B (Fig.2) is illustrated by a negligible contribution at early ages and a progressively greater contribution at later ages. The strength of the slag binders is approximately equivalent to that of cement at later ages such as 90 days to 1 year, provided the slag content of binders does not exceed 45%. The slightly higher one year strength of binder B mortar over that of Binder A mortar could be ascribed to the effect of a slight difference in water "cement" ratio, as determined by means of the flow-table. The rapid decrease in mortar strength corresponding to slag content of binders exceeding 45% may be ascribed to a deficiency in lime in this composition range.

These results seem contradictory to the results obtained by E.G. Thomas (4) who proved that mixes of tailings, cement and slag can gain additional strength when the slag content is many times that of the cement. In such a case, when progressively larger amounts of slag are added to a fixed cement content, the water-cementitious material ratio decreases. This could explain the apparent discrepancies between the two sets of results.

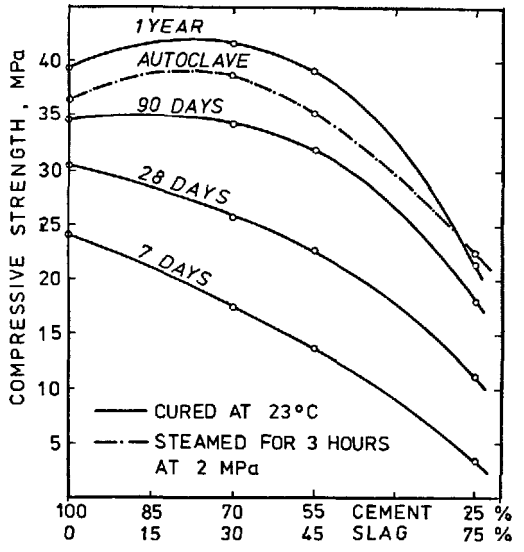

Fig.2 - Effect of slag content of binders on the compressive strength of ASTM C109 mortars cubes.

WATER IN SET MORTARS

The combined water in hydrated cement mortars and cement-slag mortars was determined by two test methods. The following samples were used: slag B ground to a Blaine surface area of 390 m^2/kg and a Normal Portland cement (350 m^2/kg) similar in composition to cement of Table I.

Experimental procedure: with these materials, binders A, B, C, D were prepared in the proportions shown in Table III. Each of the binders was blended with graded standard sand (ASTM-C778), the proportions being 1 part of binder to 2.75 parts of graded standard sand by mass. Mortars were mixed, using a fixed water to binder ratio of 0.50. Immediately after mixing, the mortars were placed in air-tight plastic capsules and held at 23°C in a moist closet. At test ages of 7, 28 and 90 days, the hardened mortars were crushed, dried at 105°C, ground for 90 seconds in a Shatter Box disc grinder and dried again at 105°C, avoiding prolonged exposure to air.

Results: Thermogravimetric analysis 5°C/min. from 20°C to 1000°C provided the basic data for calculating the combined water of the following samples: cement and slag (TG, DTG), dry mortar blends (L.O.I.) and each of the 12 hardened mortars (TG, DTG and L.O.I.).

The total TG loss for cement and slag amounted respectively to 1.54% and - 5.6% of the original material. The L.O.I. values from muffle furnace tests were 0.51%, -0.04%, -0.33% and -0.86% respectively for the dry mortar blends A, B, C and D.

The total combined water was calculated by two methods: a) from the total TG loss minus corrections for CO_2 and oxidation of slag in TG curves, and b) from muffle furnace values, minus corrections for L.O.I. on dry mortar blends. Table IV is the average calculated by the two methods.

TABLE IV - Percent combined water in set mortars.

Mortars	7 days	28 days	90 days
A	3.71	4.32	5.17
B	3.25	3.64	4.34
C	2.87	3.26	3.97
D	1.69	2.06	2.75

As the main features of the derivative thermograms of set mortars, one sharp peak at 453°C was ascribed to loss of water from Ca $(OH)_2$ and a broad peak at 630°C ascribed to the loss of CO_2. No peak was perceptible at 453°C on the 90 day-D mortar thermogram.

Curves showing the decrease of combined water per unit mass of binders in mortars made with binders of increasing slag content are shown in Fig. 3.

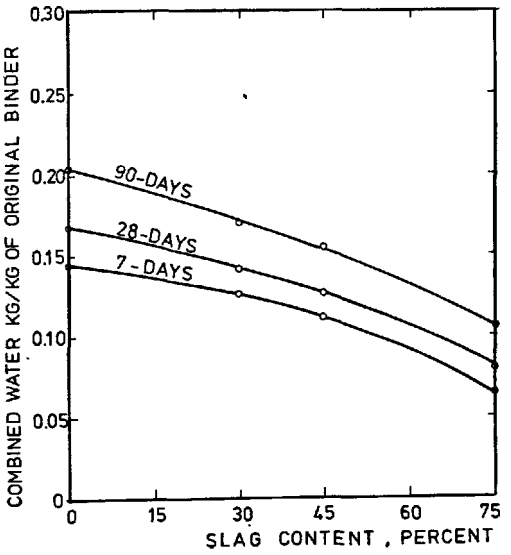

Fig.3 - Combined water as a function of slag content of binders in mortars of W/binder ratio of 0.5 by mass.

In comparison with Fig.2, one could have expected that points corresponding to 90 day mortars B and C (30% and 45% slag) be located higher on Fig.3. The slag has recently been re-checked by X-ray diffraction and no basic change in crystallinity seemed to have occured over the last 9 years. In another experiment, water was expelled from mortars A and C, hydrated for 90 days, by raising the temperature at a constant rate of 5°C/minute between 20°C and 800°C, the water vapour being swept by dry nitrogen into a Beckman Trace Moisture Analyzer. This apparatus works on the principle described by Forrester (6): absorption of water in P_2O_5 and electrolysis of water, the d.c. current used being proportional to the amount of electrolysed water.

Water evolution curves of these two hydrated mortars showed major discrepancies. Both curves showed a broad peak between 100° and 300°C mainly ascribed to the evolution of water from calcium silicates and a much smaller peak between 430 and 480°C ascribed to the evolution of water from calcium hydroxide. The ratio of the latter peak over the former peak was 3.3 times smaller for mortar C comparatively to mortar A, thus showing that the proportions of hydration products were different in the two mortars.

In spite of this, by plotting combined water values calculated from Table IV against compressive strength values of mortars (Fig.2), a fairly good linear relation is obtained in Fig.4.

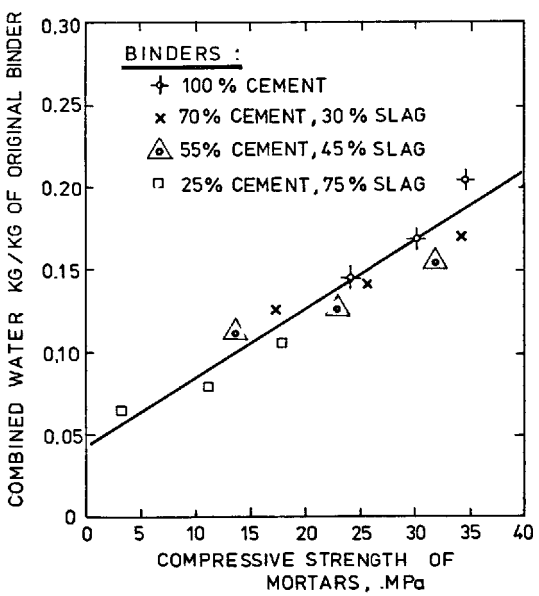

Fig.4 - Relation between combined water and compressive strength.

SEM AND KEVEX ANALYSIS

In order to compare some physical and chemical features of hydrated cement with hydrated cement-slag, pastes of cement and binder C (55% cement plus 45% slag B), W/binder = 0.50, were cured for 2 months at 23°C, in plastic capsules. Surfaces of the broken specimens were examined (Fig.5A and B) with an electron scanning microscope (Cambridge S4-10) and plots of analysis of selected areas were obtained (Fig.6) with a Kevex 5100 X-ray energy spectrometer.

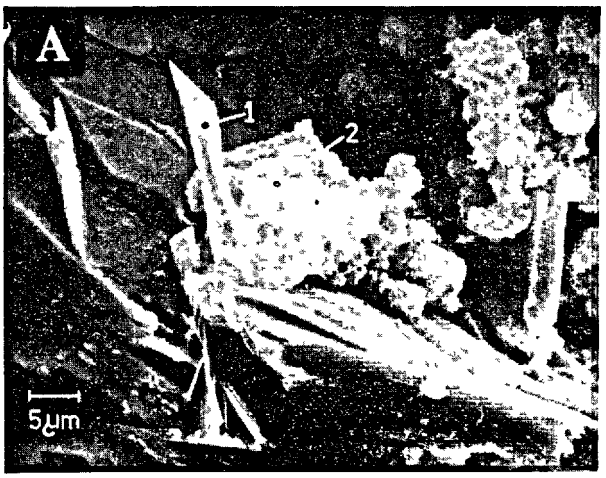

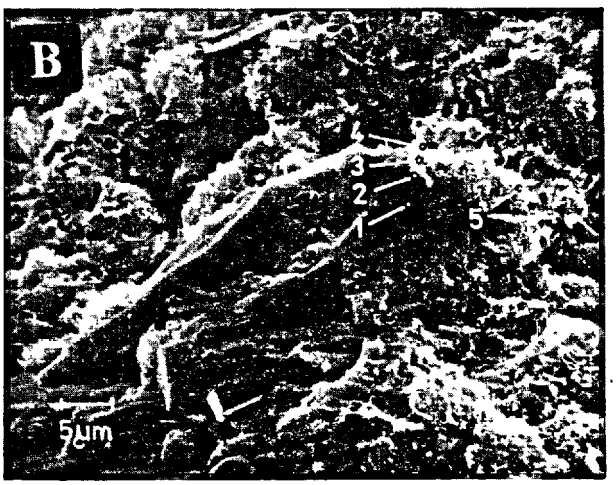

Fig.5 - Scanning electron micrographs of pastes hydrated for 2 months, W/binder = 0.50, A (cement), B (cement 55% / slag 45%)

Characteristic features of hydrated cement paste include the presence of $Ca(OH)_2$ shown in A_1, in agreement with plot A_1, and hydrated calcium silicates in A_2, as indicated in plot A_2.

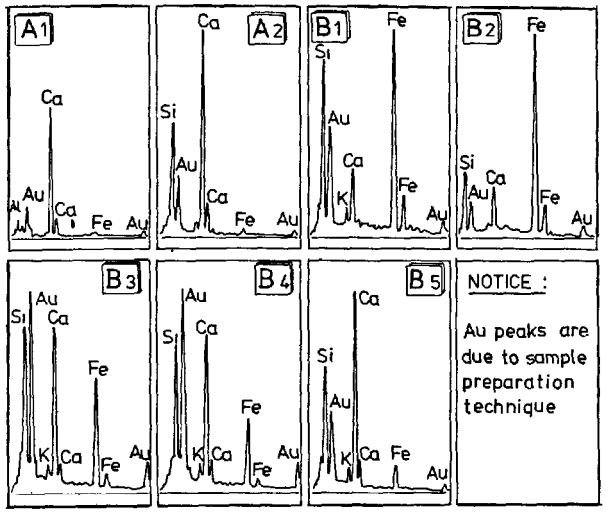

Fig.6 - Plots of X-ray energy analysis of selected areas of Fig.5.

Hydration of cement-slag paste is more complex: areas of unreacted slag with typical slag analysis is shown in B_1 and likely magnetite inclusion in slag as indicated in plot B_2; calcium silicate hydrates possibly with inclusion of iron compound may have been formed by an attack of lime on the slag particle in B_3 and B_4; slightly farther away from the slag particle, calcium silicate hydrates appear at B_5. Analysis at B3 and B_4 may also reveal a mixture of C-S-H produced by cement plus some very fine slag particles.

CONCLUSIONS

When tested in lime mortar, ground granulated nickel slag has been shown to possess significant pozzolanic properties. In cement-slag mortar, the contribution of slag to strength is negligible at early ages, but is equivalent to that of cement at later ages, say 90 days to 1 year, provided the slag content of binder does not exceed 45%.

A fair relationship exists between the compressive strength of mortars made with various slag/cement ratios and the combined water content.

Differences found in water evolution patterns upon heating hydrated cement and cement-slag mortars suggest that the proportions of combined water and likely the nature of some hydration products vary with the composition of binders and the hydration period. This points out the need to investigate more thoroughly the most appropriate method for drying the hydrated cement-slag mixes. Compared to hydrated cement mixes, the hydrated cement-slag mixes may contain larger amounts of hydrated products which lose water below 105°C.

ACKNOWLEDGEMENTS

The author is indebted to L.P. MacDonald and his staff, St. Lawrence Cement Company, Theo Rey, Holderbank Technical Centre and R.B. Bruce, Ontario Research Foundation for their invaluable help.

REFERENCES

1. - R.K. Collings (1978), "Mineral Waste Resources of Canada", Can. Mining and Metallurgical Bulletin, Vol 71, No. 798, 80-86.
2. - J.R. Boldt (1967), "The Winning of Nickel", Longmans Canada Limited, Toronto.
3. - E.G. Thomas (1971), "Cemented Fill Practice and Research at Mount Isa", Australian Institute of Min. and Metall. Proceedings, No. 240, pp 33-51.
4. - E.G. Thomas (1973), "A Review of Cemented Agents for Hydraulic Fill", Austral. Inst. Mine, Metall. Jubilee Symposium on Mine Filling, Mount Isa, pp 65-75.
5. - Jean Laneuville, "Portland Cement - Slag Binders", Canadian Patent No. 963482, filed June 14, 1972, issued February 25,1975, granted to St. Lawrence Cement Company.
6. - J.A. Forrester (1969), Chem. and Ind., 1244.

MgO-bearing phases in the hydration products of slag cement

Action de composés magnésiens sur l'hydratation des ciments de laitier

G. MASCOLO and O. MARINO, Istituto di Chimica Applicata, Facolta d'Ingegneria, Universita di Napoli, Italy.

RESUME : Des hydroxydes doubles de Mg et de Al, carbonatés ou non, ont été fabriqués synthétiquement à la température ambiante, à partir de gels. Ces composés ont aussi été fabriqués dans une solution saturée de chaux. On a constaté qu'ils étaient semblables à ceux qui se forment au cours de l'hydratation des ciments de laitier, et qu'ils présentaient une bonne résistance aux sulfates.

La présence de composés de MgO, autres que $Mg(OH)_2$, explique la stabilité volumétrique des ciments de laitier à haute teneur en MgO.

SUMMARY: Synthetic Mg-Al double hydroxides and corresponding carbonated phases were synthetized from gels at room temperature. These compounds were also synthetized in presence of lime satured solution and are very similar to those found in the hydration products of slag cements.

They also turned out to be resistant to sulfate attack.

The presence of MgO-bearing hydration products different from $Mg(OH)_2$ explains the volume stability of slag cements having high MgO content.

INTRODUCTION

The volume stability of blast-furnace cements made up with slags having a high MgO content, may be explained by the formation of MgO-bearing phases different from $Mg(OH)_2$(1). There is some debate in the literature on the nature of the hydration products containing MgO. In fact, Schwiete et al.(2), by hydrating suspensions of vitreous gehlenite and/or akermanite, have found at least two hydration products, consisting of MgO intercalated into both CSH^ and C_2ASH_8.

Kühle and Ludwig (3) have found in the hydration products of cements made with slags having a high MgO content, the compound $Mg_6Al_2CO_3(OH)_{16}\cdot 4H_2O$, similar to hydrotalcite. One of us (1), besides, has found a phase near to M_4AH_x, by hydration of synthetic vitreous slags in lime suspension. The latter phase was later identified by Taneja (4) among the hydration products of blast furnace slag cement made from slags with a high MgO and Al_2O_3 content.

Recently, the synthesis of pure Mg-Al double hydroxides $[Mg_{1-x}Al_x(OH)_2]^{+x}[xOH\cdot(0.81-x)H_2O]^{-x}$ with $0.23\leq x\leq 0.33$, has been reported (5). Their X-ray patterns are very similar to that of M_4AH_x previously identified in lime-slag suspensions (1).

On the basis of these results it was felt worthwhile preparing Mg-Al hydroxides in presence of lime satured solutions. This has two purposes: firstly, to investigate on the possibility that some Ca enters in the Mg-Al hydroxides lattice, secondly to verify the resistance of Mg-Al compounds to sulfate attack.

EXPERIMENTAL

Alumina gel, MgO and CaO from decomposition of magnesium basic carbonate and calcium carbonate, respectively, were employed as raw materials. The Al/(Mg+Al) molar ratio (x_{Al}) in the prepared mixtures ranged between 0 and 1. For each x_{Al} value, different mixtures containing increasing quantities of CaO were prepared. The different suspensions, using distilled and boiled water, were kept in sealed teflon containers, rotated for two weeks at room temperature. After filtration under CO_2-free conditions the products were dried over silica gel and characterized.

MgO, Al_2O_3 and CaO were determined using atomic absorption spectroscopy after dissolution of the solid in diluted nitric acid. The sulfate was determined as $BaSO_4$.

The reaction products were characterized by X-ray powder diffraction analysis using CuKα radiation and a Guinier de Wolff camera. Accurate d-spacing of selected reflections from specimens were measured by scanning 1/8°(2θ) per minute using a spacing standard.

Some samples were submitted to sulfate attack using a solution of $MgSO_4$ 0.5M. Every now and then the contact solution was replaced and the height of the sedimented powder measured.

RESULTS AND DISCUSSION

Fig.1 summarizes the crystalline phases formed in the whole range of the initial compositions (x_{Al} versus percent by weight of CaO in the $CaO-MgO-Al_2O_3$ mixture).

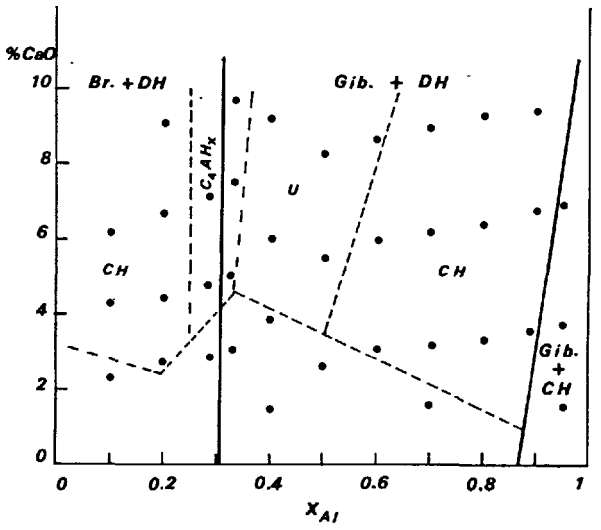

Fig. 1 - Crystallization field in the $CaO-MgO-Al_2O_3-H_2O$ system. U=unidentified phase.

The full lines divide three main crystallization fields; Brucite (Br) and Mg-Al hydroxides (DH) at low values of x_{Al}, Gibbsite (Gib) and DH by increasing Mg content in the magma and Gib and $Ca(OH)_2$ (CH) at highest x_{Al} values. The dashed lines represent the boundaries between zones containing a third phase besides those of the above main crystallization fields. The third indicated phase, time by time in the various zones, generally appears at higher CaO content. A wide zone without CH appears in correspondence

^The following common abbreviations currently used in the chemistry of cement have been adopted: S = SiO_2; C = CaO; A = Al_2O_3; M = MgO; H = H_2O.

with the compositions favorable to the DH formation ($0.23 \leq x_{Al} \leq 0.33$). This indicates the presence of some calcium in DH lattice; in fact, the c-axial length of DH phases increases with the CaO-doping in correspondence with each x_{Al} value, as shown in fig.2. The highest c value in correspondence with each x_{Al} has been measured throughout the range of the starting compositions. This appears

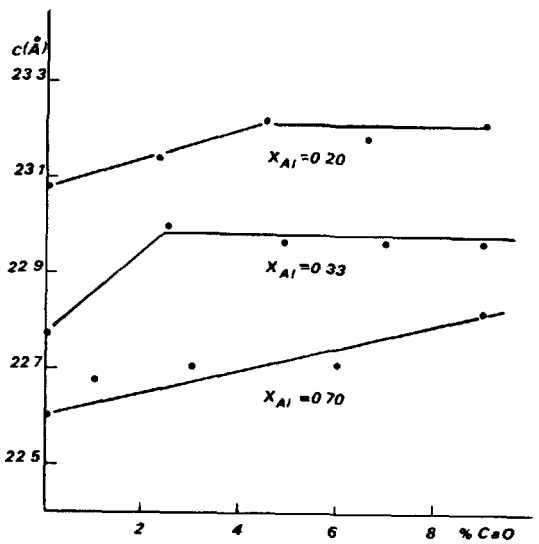

Fig. 2 - Ca-doping effect on the c-lattice parameter of DH samples, obtained with different x_{Al} compositions.

in the upper curve (b) of fig.3; in the same figure the c values of undoped x_{Al} compositions are also reported. On the other hand,

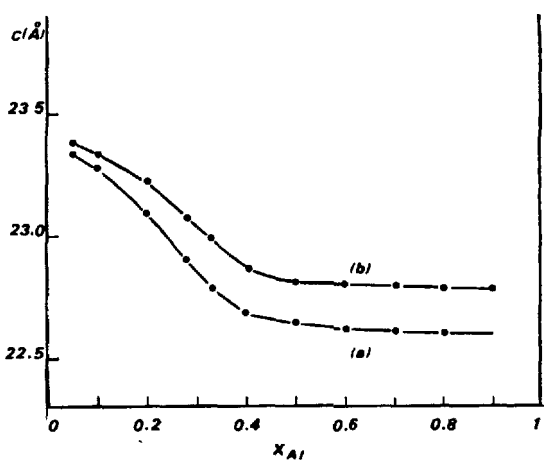

Fig. 3 - c lattice parameter of Ca-doped (b) and pure DH sample (a), as a function of x_{Al} composition.

slow diffractometric scanning showed a marked broadening of the reflections of Ca-doped phases for $x_{Al}<0.8$, while for $x_{Al}>0.8$ a contrary effect was observed. The former effect is showen in fig.4 in which it is possible to compare the trace of the (002) reflections of two specimens, corresponding to the same x_{Al} value (0.33), undoped (a) and Ca-doped (b). The Ca-doping of DH phases promotes

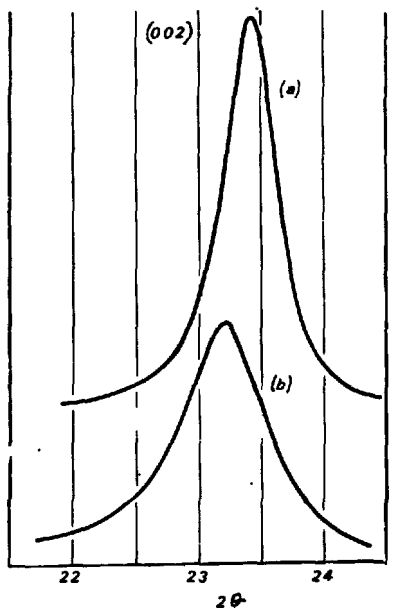

Fig. 4 - Traces of (002) reflections of undoped (a) and Ca-doped (b) DH samples with $x_{Al} = 0.33$.

strains and distortions in the lattice with consequent line broadening.

The contrary effect at $x_{Al}>0.8$ between doped and undoped samples might be attributed to a possible ordering in the structure of DH phases, as Taylor (6) suggested for some analogous Mg, Fe-compounds.

As the c parameter of pure DH phases was found to vary linearly (5) in the composition range (curve (a) in fig.5), supposing an analogous behaviour for the Ca-doped samples, the corresponding c parameters were estimated: 22.80 Å for Al-rich and 23.45 for Al-poor phases, respectively (curve (b) in fig.5).

The X-ray patterns of DH phases, doped or not, are very similar to those previously found in lime-slag suspensions (1), that is why there is an obvious analogy between the formation of DH from gels and from vitreous

slags. As the magnesium aluminate hydrate forms in presence of free $Ca(OH)_2$, the upper curve (b) might be utilized as a calibration curve to determine the composition of magnesium aluminate hydrate in the hydration products of slag cements.

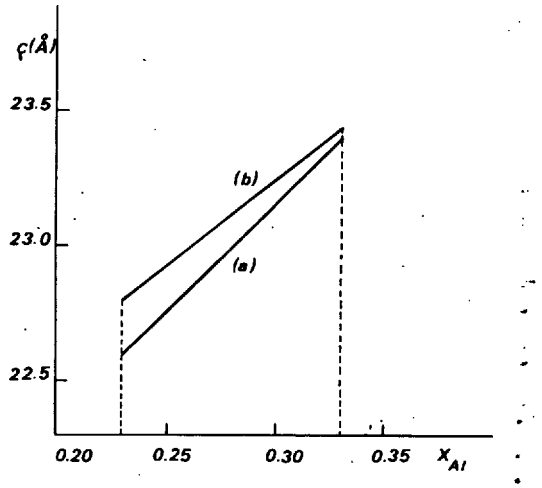

Fig. 5 - c lattice parameter of undoped (a) and Ca-doped (b) Mg-Al hydroxides, as a function of x_{Al} composition.

The CaO content of DH phases in specimens containing two or more phases can obviously only be estimated at about 4-5% by weight.

Two significant samples with $x_{Al} = 0.23$ and $x_{Al} = 0.29$ were submitted to the sulfate attack test. After three months in contact with a $MgSO_4$ solution the samples showed no volume expansion, as happens for C_4AH_x used as reference.

The X-ray diffraction analysis on the products of the sulfate attack showed some additional broad d spacings, together those less intense of DH and those more intense of $Mg(OH)_2$. The significant extra d values observed were: 10.6, 9.2, 5.38, 4.61 and 3.63Å. These reflections have been attributed to two sulfate-containing phases. The first (10.6, 5.38 and 3.63 Å) phase has the same pattern as a compound prepared by Cole and Hueber (7), by reacting potassium aluminate and magnesium sulfate. To this compound was assigned the probable formula: $4MgO \cdot 2Al_2O_3 \cdot MgSO_4 \cdot xH_2O$.

The second phase (9.2 and 4.61 Å) has a pattern very similar to that of the first phase with a lowering of the values of the d spacings.

It must be stressed that the Mg-Al hydroxides (DH) show ability for anionic exchange, due to exchangeable OH^- in the interlayer sheet (8). The Mg-Al hydroxides quickly trap CO_2 giving rise to the corresponding carbonated phases: $[Mg_{1-x}Al_x(OH)_2]^{+x}\ [x/2CO_3(0.81-3/2x)H_2O]^{-x}$, according to the CO_3^{-2} for $2OH^- + H_2O$ substitution. In this case X-ray analysis showed no significant variation between Mg-Al hydroxides and related carbonate phases (8).

The fact that, in the products of the sulfate attack, phases characterized by a higher c axial value are found, indicates the exchange of OH^- for SO_4^{-2} in the DH phase, as also confirmed by the chemical analyses and by the increased $Mg(OH)_2$ content.

The explanation of the different behaviour of CO_3^{-2} and SO_4^{-2} on the c-axial value of the layer structure lattice of DH must be attributed to the planar conformation of CO_3^{-2} which enters in the structure without strains, while the exchange with SO_4^{-2}, having a tetrahedral conformation, promotes strains, consequently a low exchange rate and a noticeable variation in the c-axial value of the resulting exchanged phases.

CONCLUSION

The results indicate that Mg-Al hydroxides, synthetically prepared in presence of $Ca(OH)_2$ take up some CaO (∿5%) as shown by the increase in their c-parameters, if compared to those of pure Mg-Al compounds. Being the powder patterns of these compounds and related carbonated phases similar to those of magnesium aluminate hydrate found in lime-slag suspensions (1), and keeping in mind the Ca-doping, a calibration curve, using the c axial lenght v.s.: $[Mg_{1-x}Al_x(OH)_2]^{+x}\ [(xOH(0.81-x)H_2O]^{-x}$ composition with x_{Al} ranging from 0.23 to 0.33, is available to determine the composition of MgO-bearing phase. Under CO_2-conditions the corresponding compositions must be employed: $[Mg_{1-x}Al_x(OH)_2]^{+x}\ [x/2CO_3(0.81-3/2x)H_2O]^{-x}$

The MgO bearing phases showed a volume stability after sulfate attack, although sulfate bearing phases have been found. These phases show a low formation rate, depending on the difficulty of the tetrahedral SO_4^{-2} entering in the layer structure lattice of Mg, Al compounds.

REFERENCES

1.- G. MASCOLO (1973), "Hydration products of synthetic glasses similar to blast furna-

ce slags", Cement and Concrete Research 3, 207.

2.- H.E. SCHWIETE, U. LUDWIG, K.E. WÜRTH and G. GRIESHAMMER (1969), "Neubildungen bei der Hydration von Hochofenschlacken", Zement-Kalk-Gips 4, 154.

3.- K. KÜHLE and L. LUDWIG (1972), Über die Verwendung MgO-reicher Huttensande in Hochfenzementen", Sprechsaal für Keramik glas email Silikate 10, 421.

4.- C.A. TANEJA (1974), "Role of magnesia on hydration of high alumina slags", VI Congress on the Chemistry of cement,Moscow.

5.- G. MASCOLO and O. MARINO (1979), "A new synthesis and characterization of magnesium-aluminium hydroxides, Mineralogical Magazine (in press.).

6.- H.F.W. TAYLOR (1969), "Segregation and cation ordering in sjogrenite and pyroaurite", Mineralogical Magazine 37, 338.

7.- W.F. COLE and H.V. HUEBER (1957), "Hydrated magnesium silicates and aluminates formed synthetically and by the action of sea water on concrete", Silicates Industriels 2, 75.

8.- G. MASCOLO and O. MARINO (1979), "Discrimination between synthetic Mg-Al double hydroxides and related carbonate phases", Thermochimica Acta (in press.).

Microstructure and properties of hydrated cements with different slag content

Microstructure et propriétés de ciments hydratés à différentes teneurs en laitier

R. SERSALE, Professore, B. MARCHESE, Professore, Istituto di Chimica Applicata, Facolta di Ingegneria, Universita di Napoli,

G. FRIGIONE, Direttore Laboratorio Ricerca e Controllo, Cementir-Cementerie del Tirreno, Napoli, Italie.

RESUME : Les auteurs rapportent les résultats d'une recherche expérimentale accomplie dans le but d'approfondir nos connaissances sur le comportement des liants à haute teneur en laitier de haut fourneau.

L'ensemble des données recueillies montre une évolution des pâtes préparées avec ces liants vers des textures de plus en plus compactes, au fur et à mesure que la chaux libre disparaît. Aux longs âges, d'environ 120 jours, on a relevé le même degré de compacité aussi bien pour les pâtes en portland, que pour celles préparées avec le ciment de haut fourneau, toutes modalités égales; et on a confirmé ce résultat à l'aide des essais de résistance mécanique sur mortier. Ces essais ont parfois indiqué des valeurs franchement plus hautes pour les mortiers préparés avec les liants de haut fourneau.

L'augmentation du rapport Ca/Si des phases de type C-S-H, qui proviennent de la fraction laitier en vertu d'une adsorption d'ions Ca^{++} semble exalter le degré de cohésion entre les granules et se révéler donc décisive pour une texture plus compacte. Cette dernière est favorisée aussi bien par une finesse de mouture plus poussée du liant, que par une maturation à plus haute température.

SUMMARY: Results are given of experiments aimed at contributing to knowledge of the behaviour of cements with a high blast-furnace slag content. In all, the data obtained indicate that pastes made from such cements develop an increasingly more compact texture, with a simultaneous disappearance of free calcium hydroxide. For conveniently long curings, at 120 days, a similarity in compactness has been found for both portland and blast furnace cement pastes, under the same operating conditions, as confirmed by the mechanical strengths of the mortars. Indeed these values are sometimes higher for blast-furnace cements. Increase of the Ca/Si ratio in the C-S-H type of phases, produced by the slag fraction, owing to the absorption of Ca^{++} ions, seems to promote adhesion between the grains and is thus a determining factor in obtaining a more compact texture. This result is further favored by a finer initial grinding and curing at higher temperatures.

INTRODUCTION

The factors favoring an increase in blastfurnace cement production are essentially two: the market demand for cements more and more able to satisfy the multiple requirements of building techniques; and the energy crisis dating from October 1973 (1). In fact it is known that cements made from blast-furnace slags give pastes which, compared to those made from Portland, have: a lower hydration heat; greater resistance to sulfate attack; less expansive due to alkali-aggregate reaction effect; lower permeability; in general, greater mechanical strength after long curing (2).

The experiments referred to in this paper aim at widening our understanding of the part played by basic, granular blast-furnace, within the clinker, so as to enable us to forecast the operational behaviour of high slag content cements and, consequently, to select them suitably for the work to be undertaken. Such research presupposes the identifying of the newly-formed compounds in hydrated and hardened pastes; their quantitative evaluation in relation to the slag/clinker mixture and curing time; systematic observation of the evolution of the microstructure of the pastes and its correlation to the physical and mechanical properties of the mortars, starting from our present knowledge. As regards the nature of the phases, reliable opinion (3) holds that the initial hydration stage of the slag reveals new-formed sulfate phases, such as ettringite, which may later evolve into monosulfate, to give solid solutions with tetracalcium aluminate. The appearance of calcium hydroxide, produced by hydration of clinker silicates, would then favor considerable formation of C-S-H type hydrate masses containing significant quantities of Mg and Al, and play a decisive part in determining the paste texture. It is also true that C-S-H type phases may be conditioned by the presence of electrolytes in the aqueous solution in contact with the slag, and that the presence of gypsum stabilizes ettringite and aluminium hydroxide. The formation of hydrate gehlenite would be precluded, since CH would be consumed in forming C-S-H phases with Ca/Si ratio close to that characterizing those of the clinker (4). The microstructure plays a well known decisive role in the physical and mechanical properties and is influenced by changes in the morphology of newly formed products during the consolidation of hydrating masses (5).

EXPERIMENTAL

Four industrial cements, one of Portland cement, and three obtained from the same batch of clinker blended by gypsum and different

TABLE I

Composition (wt%) and physical properties of Portland and blast furnace cements

	slag	clinker		
	chemical	chemical	Bogue composition	
CaO	44.60	66.19	C_3S	60
SiO_2	35.01	21.65	C_2S	17
Al_2O_3	10.39	4.77	C_3A	6.9
Fe_2O_3	1.39	3.38	C_4AF	10.3
Mn_2O_3	0.60	-		
MgO	4.44	1.10		
Na_2O	0.66	0.50		
K_2O	0.69	1.01		
SO_3	-	1.20		
S(sulphide)	0.81	-		
Loss on ignition	0.46	0.17		
CaO free	-	1.07		

Sample no.	1	2	3	4
Clinker	96	71	28	28
Slag	-	25	69.5	69.5
Gypsum	4	4	1.5	1.5
Specific surface Blaine	3550	3880	3000	4000
Tensile Strength (N/mm^2)				
1 day	3.5	2.5	1.0	1.8
2 days	4.6	3.9	2.1	2.8
3 "	5.3	4.8	3.0	3.7
7 "	6.5	6.6	5.0	6.4
14 "	7.9	8.1	7.0	8.1
28 "	8.4	8.6	7.7	8.8
90 "	8.5	8.7	8.2	9.2
365 "	8.6	8.8	8.6	9.6
Compressive strength (N/mm^2)				
1 day	16.5	10.0	3.5	5.1
2 days	22.9	15.2	8.0	8.9
3 "	29.0	22.5	12.1	14.2
7 "	37.3	33.5	21.0	27.4
14 "	44.1	40.0	32.6	43.0
28 "	46.0	45.3	37.5	50.2
90 "	54.0	49.6	47.4	57.7
365 "	55.0	55.2	55.0	66.1

of slag were investigated. Their characteristics are reported in Table I.

Specimens 1x1x6 cm were made from pure pastes obtained by hand mixing with a water:solid ratio of 0.33 and cured for 24 hrs in 100% RH atmosphere and then in water for 3.7,28 and 120 days. The steam curing cycle was: 2h at room temperature, 2 h from 20° to 80°, 6h at 80°, 6h from 80° to 20° and then in water at 20°C. Slices were cut from each specimen, wet-ground in acetone and held over silica gel for 24 hrs.

Different fractions of the dried samples were submitted to thermogravimetric (TG), thermodifferential (DTA) and X-ray diffractometric (XRD) analysis, as described previously (6).

XRD was performed on the anhydrous specimens and on the mature pastes, before and after TG, using TiO_2 (anatase, 5%) as an internal standard. The intensities of the diffraction lines at 3.52 Å (25.28 °2θ), at 2.85 Å (31.4 °2θ) and at 4.90 Å (18.08 °2θ) for TiO_2, for CH and for crystalline slag respectively were utilized for obtaining an approximate percentage of both CH and uncombined slag (7).

The matching surfaces of the two halves obtained by a single fracture operation, "twin"

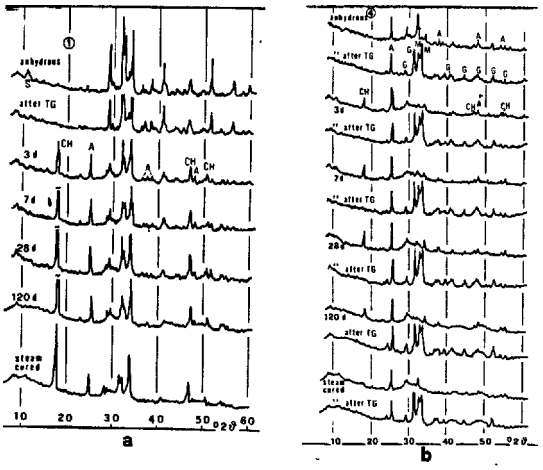

Fig.1-XRD patterns of the samples no.1 (fig. 1a) and no.4 (fig.1b). CH=$Ca(OH)_2$, Cc=$CaCO_3$, A=Anatase, M=Merwinite, G=Gehlenite, d=days.

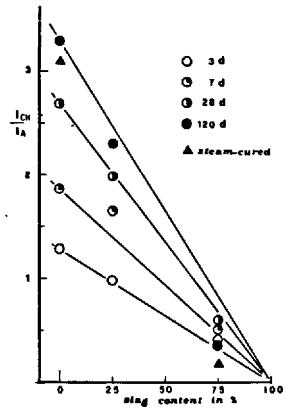

Fig.2-XRD quantitative determination of CH in the samples no.1,2,4.

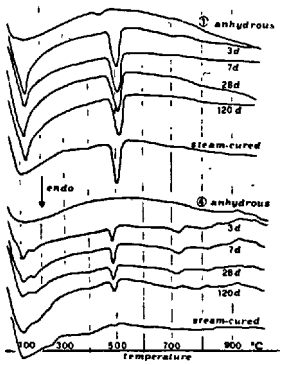

Fig.3-DTA traces for the no.1 and no.4 samples pastes.

surfaces, were examined with a Scanning Electron Microscope (SEM) (6).
Mechanical strenghts were determined on mortars (ISO-Rilem).

RESULTS

Most of the results reported refer to samples 1 and 4, since sample 2 an intermediate behavior. Sample 3, moreover, has the same composition as 4, but a lower Blaine specific surface.
Fig.1 shows the original XRD patterns for both anhydrous and hydrate samples. The addition of anatase as internal standard makes it possible to measure the relative amount of the crystalline phases present, with the hydration time. It is seen that the quantity of CH in sample 1, Fig.1a, increases with the hydration time, and more so when steam curing is adopted. For slag pastes, Fig.1b, the hydroxide increases slightly at early ages, decreases considerably at 120 days, and disappears after steam-curing.
The paste fractions, after TG analysis show the disappearance of reflections of all the hydrate phases, as well as of the wide band at 26-36°2θ, characteristic of the vitreous structure, Fig.1b. Instead, merwinite and gehlenite reflections appear; so indicating devitrification. Moreover, there is an increase of reflections of the anhydrous phases, which is attributable to greater concentration, due to dishydration, and probably, to partial reconstitution of poorly hydrated layers toward the original structure.
The data obtained from the TG and XRD, and also from DTA, of the various saples, have been related to the slag content. Comparison may be considered almost quantitative, given the similarity of the experimental treatments. Fig.2 shows that the CH content of sample 4 is not only lower, at 28 days, than that corresponding to the initial clinker fraction, but is notably lower after 120 days and even lower after steam-curing.
Fig.3 gives the DTA curves for anhydrous samples 1 and 4 and their relative pastes cured for differing times. The traces of the anhydrous samples show two very weak endothermic peaks, attributable to slight, incipient hydration. For samples 2, 3 and 4 only, the

TABLE II

Weight losses (%) for the hydrated pastes from TG traces (d=days)

sample		weight in mg initial W	weight in mg final $W_{900°}$	partial weight loss = $\frac{\Delta w}{W_{900°}} \cdot 100$ 50-350	350-440	440-560	560-800	800-900°C
1	3d	300	252.8	11.7	1.0	3.7	1.7	0.5
	7d	300	252.0	11.1	1.3	4.2	1.9	0.5
	28d	300	248.0	13.0	1.5	4.4	1.8	0.5
	120d	300	244.2	13.8	2.1	4.6	1.8	0.5
	steam-cured	300	252.2	8.5	1.9	5.1	2.5	0.9
2	3d	300	257.5	10.2	8.9	2.5	2.5	0.3
	7d	300	252.2	11.8	1.0	3.1	2.3	0.3
	28d	300	249.0	13.1	1.4	3.1	2.3	0.5
	120d	300	242.2	15.5	2.1	3.4	2.3	0.4
3	3d	300	271.2	5.7	0.6	0.4	3.8	-
	7d	300	267.3	7.2	0.6	0.9	3.4	-
	28d	300	265.0	7.8	0.8	0.8	3.8	-
	120d	300	261.0	9.3	1.0	0.7	3.7	-
4	3d	300	275.0	5.9	0.7	0.8	1.6	-
	7d	300	269.0	7.7	1.0	1.0	1.7	-
	28d	300	260.0	11.2	1.1	1.1	1.8	0.2
	120d	300	258.4	11.3	1.4	1.5	1.5	0.1
	steam-cured	300	267.8	6.9	2.2	1.5	1.4	-

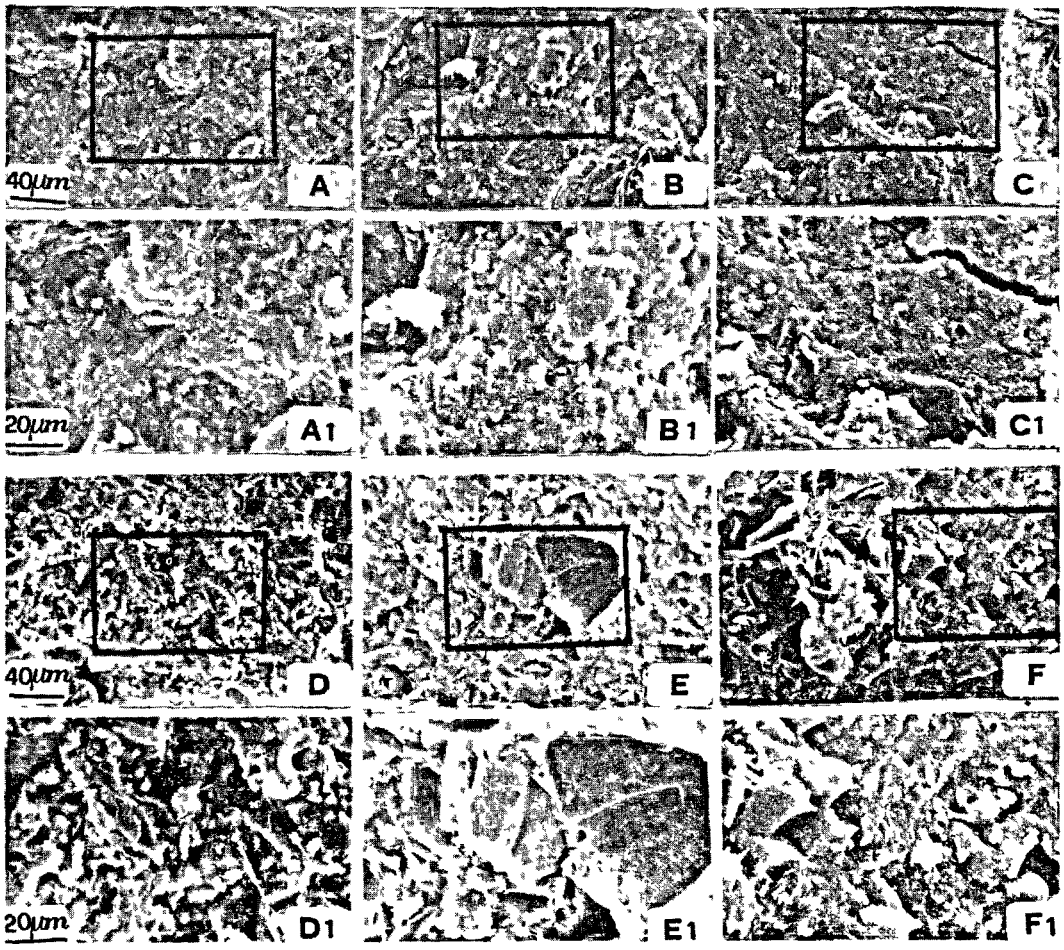

Fig.4-SEM's micrographs of fracture surfaces of pastes of samples (no.1 and 4) hydrated at 3 (A and D), 7 (B and E), and 28 days (C and F, respectively).
A1, B1, C1, D1, E1 and F1 are enlargements of areas marked in A,B, C, D, E and F.

exothermic peaks at 860°-900°C may be attributed to the devitrification process of the slag fraction. Their intensity diminishes with the hydration time. The endothermic peak attributable to the C-S-H fractio, around 130°C, is common to all the traces. Its intensity increases with the course of hydration, while its base widens notably for steam-cured paste. The endothermic peak attributable to CH, at maximum around 500°C is also common to all. The traces of samples containing slag shows further endothermic peaks at 170°C and 400°C; and steam cured ones at 237°C, too. These may be attributed to hydrated aluminates (8) Moreover, pastes containing slag seem to have greater carbonation also.

Table II gives analytical data from the TG profiles of the four paste samples. The values for each sample are referred to their final weight at 900°C. This was found to be greater for samples with a higher slag content and diminishes during the hydration time. The highest partial losses recorded are those in the 50-300°C range, and are mainly attributable to decomposition of the C-S-H phases. Losses in the 350-440°C range, characterized by a constantly inclined profile may also be attributed to C-S-H phases and eventual aluminates. Decomposition of CH and Calcium carbonate is indicated by losses in the 440-550°C and 550-800°C ranges, respectively. A slight increase in weight after 900°C in pastes containing slag disappears after 120 days' hydration.

The SEM images of the fracture surfaces of the hydrated pastes, at 3,7,28 and 120 days, for samples 1 and 4, are given in Figs.4 and 5. Both samples clearly show a mass consolidation which intensifies with the hydration time. Minor compactness is found in slag cement pastes, for early hardening times, Fig. 4D and 4E. This difference tends to disappear when the hardening time is more than 28 days (fig.4F and 5I).

Resistance to water attack is more or less the same for the two pastes cured for 120 days (fig.5G and 5I). A high degree of compactness is achievable for steam cured pastes, as may be seen by comparing the "twin" fracture surfaces (fig.5H and 5L).

In steam-cured concrete, too, the mechanical strength of sample 4, after 28 days, is

Fig.5-SEM's micrographs of "twin" fracture surfaces of sample no.1 (G,G' and H,H') and no.4 (I,I' and L,L'). The areas in G' and I' were etched with water for 30s. H and L represent fracture areas of steam-cured pastes. G1, H1, I1 and L1 are magnifications of areas marked in G, H, I and L.

higher than that of sample 1.

TABLE III

Compressive strengths (N/mm^2)of concretes

sample	curing at 20°C		steam-curing (6h at 80°C)	
	1d	28d	1d	28d
1	10	37	25	34
4	4	39	24	40

DISCUSSION

The results obtained from thermal and XRD analyses all indicate that slag, in the presence of clinker, manifests a hydraulic activity even at early reaction times. It is true that the hydration of clinker grains occurs before that for slag grains, the former having phases of different chemical nature. This means that the most rapidly formed new phases are of the C-S-H type, and calcium hydroxide; so that Ca^{++} ion concentration abounds in solution. Calcium hydroxide plays a particularly important role in stabilizing the hydrate phase; a role determined by its crystallinity and solubility characteristics. One part is devoted to stabilizing C-S-H phases, originating from the clinker; another, initially smaller, is absorbed by the C-S-H type phases of the slag grains.

With the hydration age, particularly for higher slag content cements, there is a considerably decreasing hydroxide content; so much so that, as may be seen in Fig.2, after 120 days the crystalline calcium hydroxide is very much reduced. With such pastes (Fig.5I and 5L), however, the length and type of curing favor the forming of a compact texture, very similar that for portland cement pastes, as observation of the fracture surfaces shows. Steam curing accelerates hydroxide consumption by the hydration products of the slag (Fig. 1b, 3 and Table III). The amount and constitution of the C-S-H type phases, thus, have a determining effect on the cementing action. These phases, as has bean stated, originate both from hydration of the clinker grains and from hydration of the slag grains.

In the case of clinker grain hydration, the rapid appearance of hydroxide involves its necessary coexistance with larger volumes of C-S-H phase, and so a more difficult steric accomodation, which only in part improves later. This explains the higher mechanical strengths at early ages and smaller increases at later ones, as well as the lower flexion strengths in portland cement pastes in comparison with cements containing slag.

In the latter case, Ca^{++} ion absorption occurs slowly, so that a more compact texture is obtained, due to the more gradual incorporation into the mass. This gives initially lower mechanical strengths, but increased ones with ageing.

In slag cements tecture compactness is reached only after a long period of curing, because of the greater quantity of C-S-H produced. High degree of compactness is obtainable earlier, however, both by suitable steam-curing and by finer grinding.

ACKNOWLEDGEMENTS: The writers gratefully thank Mr.A.Annetta and Mrs.M.Palumbo Piccioli for technical assistance. Two of writers (R.S. and B.M.) received financial support from the Consiglio Nazionale delle Ricerche, Italia.

REFERENCES

1.- J.P.BOMBLED (1978) "Activation des ciments a forte teneur en constituants secondaires", Publ. CERILH.

2.- R.DRON,J.-C.VAUTRIN,F.VERHEE (1978), "Les différents liants hydrauliques et pouzzolaniques", Bull. Liaison. Labo.P. et Ch. 94 73-83.

3.- J.G.M. de JONG (1977), "Le mécanisme de réaction de l'hydratation des ciments métallurgiques" Silic.Industriels 42 5-11.

4.- I.A.VOINOVITCH, R.DRON (1976), "Action des differents activants sur l'hydratation du laitier granulè", Silicates Industriels 41 209-212.

5.- M.REGOURD, H.HORNAIN, B.MORTUREUX (1976), "Microstructure des ciments de laitier" Rev.Mater.Constr. n°699, 83-86.

6.- B.MARCHESE, (1977) "SEM Topography of Twin Fracture Surfaces of Alite Pastes 3 Years Old", Cem.Concr.Res. 7 9-18.

7.- JCPDS file, card 4-0681 for Akermanite (melilite) and card 21-1272 for Anatase.

8.- H.G.SMOLCZYK (1965) "Die Hydratations produkte hütttensandreicher Zemente" Zement-Kalk-Gips 18 238-248.

Intensification des processus de durcissement du ciment portland de laitier et perfectionnement de la structure du ciment durci

Intensification of process of slag portland cement hardening and improvement of cement stone structure

V.I. SATARINE, professeur, docteur ès sciences techniques,
S.V. CHESTOPEROV, professeur, docteur ès sciences techniques,
Y.M. SYRKINE, candidat ès sciences techniques,
A.I. ZDOROV, candidat ès sciences techniques,
B.G. CHOKOTOVA, candidat ès sciences techniques,
L.A. FEDNER, candidat ès sciences techniques, Youjguiprotzement,
MADI, U.R.S.S.

RESUME : L'exposé traite des résultats de l'élaboration de nouvelles compositions efficaces des ciments portlands de laitier ayant une teneur élevée en laitier granulé de haut fourneau, de l'étude des particularités des processus de durcissement de ces ciments, conditionnant un accroissement intense de la résistance et la formation de la structure du ciment durci avec les caractéristiques mécaniques et les propriétés de construction techniques élevées.

Les paramètres du ciment portland de laitier à faible teneur en clinker assurent, après l'étuvage, une activité qui est supérieure de 20 à 25 % à celle du ciment portland du type 500.

En introduisant, lors du broyage, une addition spéciale, on arrive à élaborer un ciment portland de laitier dont la résistance précoce est élevée et croît intensément au cours du durcissement dans les conditions normales et après le traitement à la chaleur humide, lorsqu'on utilise des clinkers de composition variée et des laitiers de basicité différente.

SUMMARY : The results of development of new and efficient compositions of slag portland cement with increased content of granulated blast furnace slag, and of study of specific features of hardening of the said cements which ensure intensive increase of strength and formation of cement stone structure with high mechanical and construction-technological characteristics are presented.

The parameters of the developed low-clinker slag portland cement ensure activity after steaming which is 20-25 % as higher than of portland cement, grade 500.

By introduction of a special additive during grinding a slag portland cement with improved early strength and intensive strength increase in the course of hardening under normal conditions and after hydrothermal treatment when using clinkers of different compositions and slags of different basicity, was obtained.

Nombre d'études et l'utilisation du ciment portland de laitier dans l'industrie de construction ont permis d'établir son efficacité élevée en comparaison du ciment portland : résistance chimique plus élevée, exothermicité plus basse, coefficient d'utilisation et d'accroissement d'activité élevé à l'aide du traitement à la chaleur humide ainsi que consommation d'énergie et de chaleur moindre pour la production.

Dans notre rapport et des communications au VI-ième Congrès sur la chimie du ciment, on a déjà parlé des propriétés du ciment portland de laitier (1, 2), de l'introduction dans la production de ciments portlands de laitier à durcissement rapide et très rapide (2). En ce qui concerne la cinétique du durcissement dans les conditions normales et les indices de résistance, ces ciments sont équivalents au ciment portland des types 400, 500 et 600.

A l'heure actuelle, un grand accroissement de la production du béton et du béton armé pose devant les constructeurs et les technologues le problème d'élévation notable de la qualité du béton pour la création des pièces et ouvrages d'une longue durée en béton et en béton armé. Pour résoudre ce problème on a besoin de ciments de haute qualité et rentables, car seul le choix des régimes optimaux du traitement à la chaleur humide des pièces en ciments portlands n'assure pas l'obtention des produits à propriétés voulues.

Après le VI-ième Congrès sur la chimie du ciment on a continué les études visant à améliorer les propriétés techniques du ciment portland de laitier et menées dans deux directions :

1. Changement de la cinétique du durcissement du ciment portland de laitier lors du traitement à la chaleur humide, par variation du rapport entre clinker et laitier dans la composition, de la finesse de leur broyage, et du régime de durcissement des produits lors du traitement à la chaleur humide.

2. Variation de la cinétique du durcissement du ciment portland de laitier à l'aide d'additions - accélérateurs de durcissement.

Pour la production des pièces en béton armé soumises au traitement à la chaleur humide, on a mis au point et essayé une variété du ciment portland de laitier dont la teneur en laitier granulé de haut fourneau est de l'ordre de 70 %. Après le traitement à la chaleur humide ce ciment se caractérisait par une activité supérieure de 20 à 25 % à celle du ciment portland du type 500. Au cours du durcissement prolongé le ciment portland à teneur élevée en laitier granulé de haut fourneau continue à acquérir intensément de la résistance. Dans un régime d'étuvage déterminé, les paramètres choisis de broyage du ciment portland de laitier à faible teneur en clinker avec dosage optimal du gypse augmentent le degré d'hydratation du laitier. Ceci entraîne l'accroissement de la quantité de hydrosilicates de calcium faiblement basiques de structure submicroscopique qui augmentent la densité de la composante en gel. Les fissures et les pores qui se forment au cours d'étuvage sont remplis d'une masse gélatineuse à grains fins des nouvelles formations (produits d'hydratation du ciment portland de laitier). C'est pourquoi il se forme une texture plus finement poreuse de la pierre de ciment, des bétons et des mortiers en comparaison de la texture du ciment durci dans les bétons étuvés au ciment portland. La pierre de ciment étuvée à partir du ciment portland de laitier à faible teneur en clinker se caractérise par la réduction du volume des macrocapillaires et l'augmentation du volume des pores de dimension de $5 \cdot 10^{-7}$ cm à $1 \cdot 10^{-5}$ cm.

Il est établi qu'au cours du durcissement, la chaux, qui se dégage lors de l'hydratation accélérée et de l'hydrolyse de C_3S, est continûment fixée par le laitier. Ceci assure le monolithisme de la pierre de ciment qui procure de hautes propriétés techniques aux bétons et détermine une grande résistance au gel et la stabilité dans un milieu agressif. Les données comparatives sur les propriétés techniques principales du ciment portland et du ciment portland de laitier à peu de clinker sont représentées dans le tableau ci-dessous.

Une autre propriété positive du ciment portland de laitier devant le ciment portland est le rapport entre la résistance à la compression et la tension par flexion. Du point de vue de la construction, l'indice de résistance à la flexion a une grande importance. C'est pourquoi on peut supposer que, sur ce point également, le béton au ciment portland de laitier de cette composition aura un grand avantage devant le béton préparé à base de ciment portland.

Les particularités notées de la structure du ciment durci en combinaison avec la capacité du ciment soumis à l'étuvage d'acquérir de façon intense de la résistance au cours du durcissement prolongé permettent d'augmenter la longévité du béton armé préfabriqué. La création des conditions optimales de durcissement avec l'utilisation maximale de l'effet de contraction (fig. 1) prédétermine une grande résistance au gel de la pierre de ciment dans le béton et rend possible une large application des adjuvants plastifiants et entraîneurs d'air.

La méthode de variation de la cinétique du durcissement du ciment à l'aide des additions (accélérateurs du durcissement) n'est pas nouvelle (3, 4). Toutefois cette méthode est étudiée à un moindre degré pour le ciment portland de laitier et nous étions les premiers à étudier sous cet angle le ciment portland de laitier à teneur élevée en laitier.

Sur la base des données expérimentales on a établi la composition d'une addition qui élève la résistance initiale du ciment portland de laitier et intensifie son accroissement au cours de durcissement pro-

TABLEAU

Propriétés techniques principales des ciments étuvés de composition différente

Teneur en laitier, %	Résistance, %			Coefficient de résistance au gel après 100 cycles de gel et de dégel	Coefficient de stabilité dans la solution à 5 % de Na_2SO_4 après 6 mois
	après l'étuvage	par unité de clinker	après 6 mois par rapport à la résistance à l'âge de 28 jours		
-	100	100	126	0,41	0,76
70	120	400	130	1,12	0,82

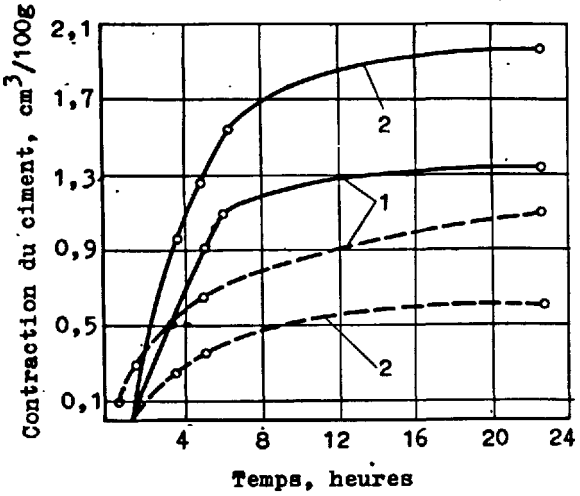

Fig. 1 - Influence des conditions de durcissement et du type du ciment sur la valeur de contraction : ———— étuvage ; - - - - - - durcissement normal ; 1 - ciment portland ; 2 - ciment portland de laitier à 70 % de laitier granulé de haut fourneau.

longé. Il s'agit de l'addition polyminérale sulfoalumosiliceuse (SAS). Une combinaison favorable des constituants minéraux de l'addition contribue à la réduction du temps de prise et, avant tout, accélère la prise initiale, augmente la résistance dans les délais précoces (1 à 3 jours) et, à la différence d'une série d'additions connues, à l'âge de 28 jours. L'action accélératrice de l'addition sur les processus de prise et la cinétique de l'accroissement de résistance du ciment portland à teneur en laitier de 60 % est établie lors de l'utilisation des clinkers à teneurs différentes en C_3S et C_3A et des laitiers basiques, acides et électrothermophosphorique. Le gain de résistance dû à l'introduction de l'addition dépend de la composition et des propriétés des constituants du ciment portland de laitier.

Le gain maximal de résistance à l'âge de 28 jours est obtenu grâce à l'introduction d'une quantité optimale d'addition. C'est pourquoi en fonction de la composition et des propriétés des constituants du ciment portland de laitier, on établit expérimentalement la composition de la charge composée de clinker et de laitier à base de l'addition SAS, qui assure l'élaboration d'un ciment à hauts indices de résistance et à temps de prise normaux. A l'aide de l'addition SAS, en faisant varier la teneur de la charge en clinker de 30 à 60 % sans augmentation de la finesse de broyage du ciment (résidu sur le tamis n° 008 est de 7 ± 1 %), on peut élaborer un ciment dont l'activité va jusqu'à 50 MPa lors de durcissement dans les conditions normales (fig. 2).

La capacité du ciment portland de laitier avec addition SAS d'acquérir intensément de la résistance se conserve également dans le cas de traitement à la chaleur humide (fig. 3). L'utilisation d'un tel ciment dans la production des pièces en béton et en béton armé permet de réduire la durée de la mise à la température isotherme de 2 ou 3 h.

L'accélération du durcissement initial et l'accroissement de l'activité du ciment à l'âge de 28 jours suivi d'augmentation de la résistance au cours de durcissement prolongé en présence, dans le ciment, de l'addition SAS sont dus à la capacité de l'addition d'accélérer les processus d'hydratation des constituants du ciment portland de laitier et de prendre part aux réactions de durcissement aux stades les plus précoces.

A la différence du ciment portland de laitier ordinaire, dans le ciment portland de laitier hydraté avec addition SAS à l'âge de 1 à 28 jours, on observe une diminution intense des maximums de diffraction des constituants de clinker et en premier lieu

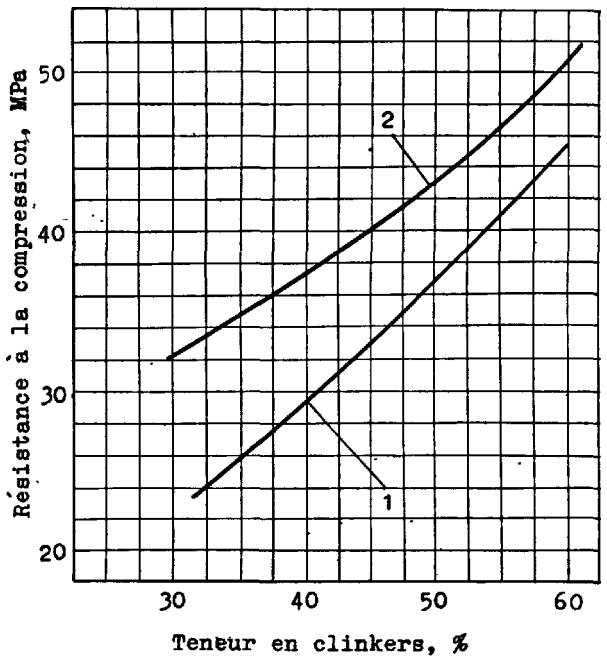

Fig. 2 - Influence de l'addition SAS sur les indices de résistance du ciment portland de laitier ; 1 - ciment portland de laitier ordinaire ; 2 - ciment portland de laitier avec addition SAS

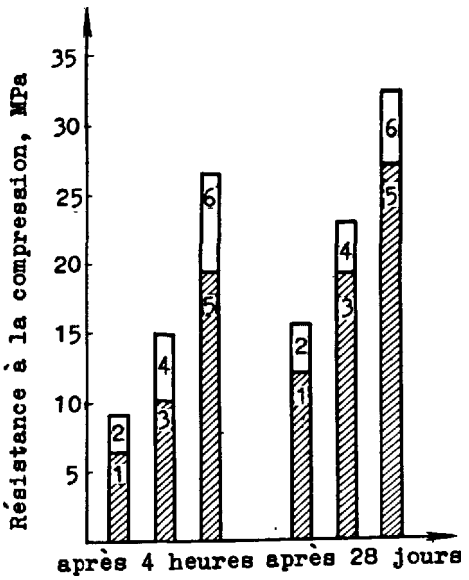

Fig. 3. Influence de l'addition SAS sur les indices de résistance du béton après l'étuvage : 1 - béton du type 100 ; 3 - béton du type 200 ; 5 - béton du type 300 au ciment portland de laitier ordinaire ; 2, 4 et 6 - idem, au ciment portland de laitier avec addition SAS. Teneur du ciment en laitier, 60 %.

de l'alite (d = 1,76 Å), l'accroissement de l'intensité des réflexions à 3,03 Å et 9,8 Å avec diminution simultanée de l'intensité des maximums de diffraction correspondant à la formation de l'hydroxyde de calcium (d = 4,91 Å ; 2,63 Å).

En procédant aux études physico-chimiques complexes *), on a établi qu'en présence d'addition la quantité d'hydrates varie grâce à la formation de quantités complémentaires d'ettringite, d'hydrosilicates de calcium et d'alumogel à partir des constituants de l'addition. On a établi ce fait en procédant à l'étude séparée de l'influence de l'addition SAS sur les produits de durcissement du constituant de clinker représenté par C_2S et C_3A synthétisés et sur le laitier granulé de haut fourneau. L'accroissement de la quantité d'hydrates lors de l'introduction dans le ciment de l'addition SAS est confirmé également par les données sur la variation de la concentration de volume des nouvelles formations avec l'accroissement de la quantité d'addition.

L'addition contribue à l'accélération des processus d'hydratation des constituants du ciment portland de laitier, à la fixation de la chaux dégagée par Al_2O_3 et SO_3 hydrosolubles additionnés et par la silice active avec la formation des hydrates. Ceci détermine la formation, dès l'âge de un jour, d'une carcasse d'ettringite remplie d'hydrosilicates de calcium en quantité beaucoup plus grande que dans le ciment portland de laitier ordinaire. Les hydrosilicates de calcium formés se distinguent par leur structure et leurs propriétés des hydrosilicates de calcium dans le ciment portland de laitier ordinaire.

Une activité élevée de l'addition donnée envers l'hydroxyde de calcium, sa capacité de participer aux réactions de durcissement ont conditionné des différences notables dans les processus de durcissement du ciment portland de laitier avec addition SAS. Ces différences consistent également dans la formation de l'alumogel du type de la boehmite et de la gibbsite, la diminution de la quantité de $Ca(OH)_2$ cristallin et des hydroaluminates de calcium, la formation, à un stade plus précoce de durcissement, des hydrosilicates de calcium de structure secondaire (ecaillieux), qui se distinguent des hydrosilicates de calcium fibreux par une densité et une résistance plus élevées.

*) Avec la participation de T.Y. Chtchetkina, L.N. Skrynnik, V.F. Gribko.

Tout cela avait pour résultat la réduction des périodes principales de formation de la structure, conduisant à l'accélération de la prise, à un accroissement intense de la résistance au cours de durcissement prolongé, à la formation d'une structure plus homogène et plus dense avec un autre rapport, entre l'agrégat cristallin et la composante en gel que dans le ciment portland de laitier ordinaire. Ceci a assuré l'accroissement de la résistance du ciment durci, de la résistance au gel, surtout après le durcissement normal, de la stabilité dans des milieux agressifs et la diminution de déformations de retrait de 1,5 à 2 fois.

CONCLUSIONS

1. On a déterminé les paramètres de production du ciment portland de laitier contenant jusqu'à 70 % de laitier granulé de haut fourneau et ayant, après le traitement à la chaleur humide, une structure dense et homogène, des indices élevés de résistance et un accroissement intense de la résistance au cours de durcissement de longue durée.

On a étudié le processus de durcissement de ce ciment et les causes de l'accroissement de la densité du ciment durci.

Le ciment portland de laitier à teneur élevée en laitier granulé de haut fourneau est efficace lors de la fabrication des produits en béton armé soumis au traitement à la chaleur humide.

2. En introduisant, lors du broyage du ciment, l'addition SAS on a élaboré un ciment portland de laitier à résistance précoces élevée, qui se caractérise par un accroissement intense des indices de résistance au cours du durcissement dans les conditions normales et après l'étuvage et qui possède des propriétés techniques et de construction améliorées. Ceci est obtenu sans changement du schéma technologique et de la finesse du broyage, lorsqu'on utilise un clinker de composition minéralogique non normalisée et de différents laitiers.

Les études physico-chimiques ont établi les particularités des processus de durcissement, l'ordre de formation des phases, leurs propriétés et élucidé le processus de formation de la structure du ciment durci.

BIBLIOGRAPHIE

I.- Х. СМОЛЬЧИК (I976) Шлакопортландцементы и реагирующие со щелочами заполнители. Шестой международный Конгресс по химии цемента. М., Стройиздат, т.Ш, с. 57-63, (en russe).

2.- В. САТАРИН (I976), Шлакопортландцемент. Шестой международный Конгресс по химии цемента. М., Стройиздат, т.Ш, с.45-55, (en russe).

3.- Ф. ВАВРЖИН (I976) Влияние химических добавок на процессы гидратации и твердения цемента. Шестой международный Конгресс по химии цемента. М., Стройиздат, т.П, кн.2, с.6-II, (en russe).

4.- В. РАТИНОВ (I976), Классификация добавок по механизму их действия на цемент. Шестой международный Конгресс по химии цемента. М., Стройиздат, т.П, кн.2 , с.I8-2I, (en russe).

Influence des particularités physiques et chimiques des laitiers de haut fourneau sur leur activité hydraulique

Influence of physical and chemical features of blast furnace slags on their hydraulic activity

S.M. ROIAK, professeur, chaire de la Technologie des Matériaux Liants et des Bétons de "Vzisi",
J.Ch. CHKOLNIK, candidat ès sciences techniques, chef de laboratoire de "Ouralniitchermet", U.R.S.S.

RESUME : En utilisant la résonance paramagnétique électronique, la spectroscopie infrarouge ainsi que d'autres méthodes on montre que l'activité du laitier est fonction du degré de dépolymérisation des complexes ion-oxygène dans le verre de laitier. Un role important est joué par la liaison simple Me-O du cation-dépolymérisateur ainsi que sa coordinance. On étudie la fonction de l'aluminium et du magnésium dans la structure de formation du verre de laitier démuni, en particulier, de périclase; on a établi la teneur admissible en oxyde de magnésium par rapport avec l'alumine présente.

On détermine la teneur en Ti^{4+} dans le laitier de haut fourneau titanifère, de même qu'en Ti^{3+} pour des coordinances différentes.

On constate que suivant la teneur en magnésium, en aluminium et en titane dans le laitier de haut fourneau il se produit dans le verre des modifications de coordinance, de plus, l'accroissement de l'indice de coordination du cation contribue à l'augmentation de l'activité hydraulique du laitier.

On a étudié de même l'opportunité de la présence dans la structure du laitier d'une petite quantité de phases cristallines présentant une activité hydraulique.

SUMMARY : It has been proved by the use of the EPR (electronic paramagnetic resonance), IRS (infra-red spectrography) and other methods that activity of slag depends on the degree of depolymerization of ion-oxygen complexes in the slag glass. The energy of the Me-O cation-depolymerizer single bond and its coordination state is of primary importance. The part played by aluminium and magnesium in the structure of periclase-free slag glass formation has been considered; the permissible rational content of magnesium oxide in accordance with presence of alumina has been found out. Content of Ti^{4+} in the titanium-containing blast furnace slag and content of Ti^{3+} in various coordination states have been determined.

It has been detected that depending on aluminum, magnesium and titanium content in the blast furnace slag, their coordination in the glass varies, with increase of the cation coordonation number providing for increase of hydraulic activity of slag.

The problem of expediency of introducing small amounts of hydraulically active crystal phases into the slag structure has been considered.

Selon la théorie actuellement admise les laitiers ont une structure ionique, c'est-à-dire que le laitier liquide constitue des fusions microhétérogènes composées de cations simples, d'anions, d'oxygène et de soufre de meme que d'anions complexes dont la dimension et la stabilité sont fonction de la nature du cation.

L'expérience de plusieurs années a montré que l'activité du laitier de haut fourneau granulé est fonction de paramètres physico-chimiques des phases vitreuse et cristalline.

Avec un rapide refroidissement il s'établit dans le laitier des groupements structuraux de la fusion. Suivant la température de granulation de la fusion de laitier, à coté de la phase vitreuse, il peut se développer une cristallisation de minéraux du laitier, présents dans la fusion avant le début de la granulation; si, par contre, le refroidissement est rapide, on aboutit à une structure vitreuse du laitier.

La similitude entre les structures des silicates cristallins et vitreux réside, selon A.A.Appen, dans la présence dans les deux états d'un squelette en Si-O continu et dans l'existence du principe de coordination dans l'arrangement mutuel des ions. C'est sous cet angle qu'on peut parler d'une chimie structurale du verre, et de ranger parmi les facteurs régissant les propriétés du verre la coordinance et la valence des cations (1).

Certains métaux entrant dans la structure du verre de silice sont considérés non seulement comme des modificateurs mais aussi comme des formateurs du verre, la position des cations Me étant déterminée par son indice de coordination dont l'accroissement augmente l'apport modificateur du cation. Dans ce cas il se place entre les ions sans pont des complexes Si-O.

On peut considérer que la différence dans l'arrangement des cations dans le verre doit constituer un des facteurs essentiels déterminant l'activité du laitier, vu que les dépenses en énergie de rupture de la laison Me-O doivent varier avec la position du cation.

Si l'on tient compte de la nature iono-covalente de la liaison entre les ions dans les silicates, on peut, de façon conventionnelle, représenter l'énergie de rupture de la liaison Me-O comme le travail développé pour la rupture de la partie ionique (X) et de la partie covalente (I - X) de la liaison. L'énergie de rupture de la liaison ionique dépend de la constante diélectrique du milieu (en cas d'hydratation, de l'eau), de l'énergie de la liaison simple Me-O et de la coordinance du cation à l'égard de l'oxygène. Au cas où l'énergie de la liaison affaibli (du fait de la constante diélectrique de l'eau) est de l'ordre de grandeur de l'énergie cinétique des molécules de l'eau, il se crée des conditions favorables au passage du cation dans la solution. On peut donc admettre, qu'au cours de l'interaction du verre de laitier avec l'eau, c'est, en premier lieu, les cations modificateurs qui passent dans la solution, car, par suite du grand indice de coordination, l'énergie de la liaison simple Me-O est relativement plus faible. Il en résulte un déséquilibre du système et pour maintenir l'électroneutralité les cations de coordinance inférieure tendent à occuper la place tenue par les cations modificateurs transférés dans la solution. Cela entrainera la perturbation de stabilité de la structure et de mobilité d'ions $Si_xO_y^{2-}$.

Le passage de ces derniers dans la solution facilité par l'accroissement de la valeur de pH du milieu, par suite de la présence dans ce dernier de cations hydratés, aboutit à la formation d'hydrosilicates de métaux correspondants.

Selon les conceptions actuelles le début du processus d'hydratation est la dissolution du liant, la réaction chimique à la surface du grain s'accompagnant d'un échange ionique entre les ions se trouvant dans le liquide de gâchage et les ions composant la structure du silicate (2).

La nature différente de l'interaction des minéraux et des verres ayant la même composition avec l'eau au cours de l'hydratation s'explique par la modification de la structure du minéral avec son passage à l'état vitreux.

A la différence du cristal, où l'orientation mutuelle d'éléments structuraux est constante et régulière, dans les verres elle est perturbée, ce qui appliqué aux silicates peut entrainer une modification de la symétrie des groupements métal-oxygène.

L'étude par la résonance paramagnétique électronique de la variation de la structure, en particulier, de l'okermanite et de la gehlenite, au cours de leur passage à l'état vitreux, a montré que dans les minéraux cristallins on n'observe pas de centres électroniques paramagnétiques sur les tétraèdres (SiO_4), tandis que dans les minéraux vitreux ces centres apparaissent.

L'absence de centres paramagnétiques sur les tétraèdres SiO_4 dans les minéraux cristallins peut signifier un haut degré de liaison des tétraèdres Si-O à l'aide des tétraèdres (MgO_4) et (AlO_4) respectivement dans l'okermanite et la gehlenite.

Dans les minéraux vitreux le degré de liaison des tétraèdres(SiO_4) s'abaisse sous l'effet du passage d'une partie de l'aluminium (de la gehlenite) et du magnésium (de l'okermanite) de la structure anionique, constituant le minéral, à la structure cationique. Evidemment, on peut considérer que le passage du minéral de l'état cristallin à l'état vitreux entraine un abaissement de la symétrie des groupements anioniques Me-O jouant le role de formateurs du verre, mais, par contre, ce passage accroit la symétrie des groupements cationiques Me-O dont les atomes centraux jouent au sein du verre le role de modificateurs.

Les cations de grande énergie de liaison avec l'oxygène, par exemple Si, Al, Ti en se séparant de la surface sous forme de complexes anioniques compliqués demeurent dans

le contour entourant le grain. Au moment du détachement de la surface de la graine les complexes constituent des restes d'ions-radicaux chargés positivement et négativement. On peut admettre qu'avec la perturbation de la coordinance du silicium il se produit dans ce cas une hydratation superficielle des radicaux par adjonction d'ions OH^- et formation de la liaison Si-OH ainsi qu'une compensation de l'oxygène chargé négativement par le proton H^+.

Par suite de la dimension différente des radicaux déterminée par la composition chimique du laitier, essentiellement par le rapport O/Si, on voit se former des composés du type Si x (OH)y. La présence dans la solution d'ions OH^-, formés en surplus suivant la réaction $O^{2-} + H_2O \longrightarrow 2OH^-$ sous l'effet de la rupture de la liaison Me-O, contribue à la polymérisation des radicaux hydratés; l'indice de coordination du silicium monte dans ce cas jusqu'à 6, tandis que dans les composés déshydratés il est en général égal à 4.

Le phénomène de polymérisation contribue à la formation de particules gélifiantes dont la dimension est fonction des complexes initiaux et de la cinétique de polymérisation. A coté des processus de polymérisation des radicaux hydratés, il s'effectue à leur surface une adsorption secondaire d'hydrates de cations de métaux alcalinoterreux déjà passés dans la solution avec formation d'hydrosilicates de métaux correspondants. Etant donné que la mobilité des radicaux hydratés est faible, vu leurs grandes dimensions, ces derniers restent au sein du contour du grain de laitier.

Le mécanisme exposé de la formation de phases hydrosilicacées gélifiantes et calciques, de basicité élévée devant celle du laitier de base, permet d'admettre qu'entre la partie non hydratée du verre de laitier et les produits d'hydratation, par exemple, entre les hydrosilicates du calcium, il existe une couche gélifiante intermédiaire de basse basicité, c'est-à-dire que la basicité du grain hydraté peut être représentée sous forme d'une courbe présentant un minimum.

C'est probablement la raison de la présence dans les substances liantes hydratées de produits d'hydratation extérieurs et intérieurs dont la basicité est différente (3).

Nos études du rôle de différents éléments dans la formation de la structure des laitiers établissent que Al, Mg, Ti sont susceptibles dans des conditions déterminées de changer leur role structural en influençant fortement le processus d'hydratation.

C'est ainsi que dans les spectres de résonance paramagnétique électronique obtenus au cours de l'étude (4) du role structural de l'aluminium dans les verres de laitier à teneur constante en CaO = 50%, la variation de Al_2O_3 dans les limites de 10 à 40% entraîne l'apparition de l'étroite raie à facteur-g 2,007 ± 0,001 engendrée par les groupements (AlO_6). Avec l'accroissement de la teneur en Al_2O_3 dans le verre l'intensité de la raie croit d'abord et atteint un maximum pour une teneur en Al_2O_3 de 20%, puis elle chute. Les spectres infrarouge, en particulier, permettent de fixer le groupement triplet aux nombres d'ondes ν = = 470, 460 et 446 cm^{-1} qui sont caractéristiques pour les oscillations du groupement (AlO_6).

La confrontation de données sur la variation de la coordinance de l'aluminium avec les propriétés liantes des laitiers en fonction de la teneur en Al_2O_3 a permis d'établir que le maximum d'activité des laitiers contenant 18 à 20% d'Al_2O_3 coincide avec la teneur maximale en complexe (AlO_6) dans le laitier surfondu.

La teneur quantitative en Al_2O_3 dans le laitier est étroitement liée au role structural joué par Mg dans le laitier.

Les études qu'on a mené des propriétés hydratantes des laitiers de synthèse du système $CaO-MgO-SiO_2-Al_2O_3$ ont montré que la substitution admissible de MgO à CaO est conditionnée par leur teneur en alumine, avec l'accroissement duquel la teneur tolérée de l'oxyde de magnésium augmente.

L'analyse des spectres infrarouges a permis d'observer des variations engendrées par le fait que pour une teneur en Al_2O_3 de 15% la quantité d'aluminium octacoordonné augmente avec la pénétration d'une partie de magnésium dans le squelette anionique du verre. Pour la teneur en alumine de 17%, la teneur tolérée d'oxyde de magnésium dans le laitier n'abaissant pas son activité est également de 17%.

Dans un système à quatre composants ces laitiers ne sont pas soumis à la cristallisation nuisible aux propriétés liantes du periclase et se trouvent dans le domaine où la phase primaire de cristallisation ne concerne que la monticellite et la spinelle.

La teneur en titane de certains laitiers de haut fourneau a conditionnée l'étude à la résonance paramagnétique électronique des particularités de sa pénétration dans la structure du laitier.

Pour la détermination de la coordinance on a utilisé la méthode consistant à un bombardement préalable du verre par des particules gamma.

On a établi que dans le laitier contenant jusqu'à 11% de titane calculé en TiO_2, on observe vu la nature réductrice du processus de haut fourneau, également du Ti_2O_3, où le titane occupe des positions tétraédriques dans la structure en élevant la polymérie du verre. La formation de complexes compliqués Si-Ti-O ainsi que la diminution de la longueur de la liaison Ti-O avec le passage du titane à la coordinance 4(la teneur en TiO_2 est de 4%) conduisent selon les données des mesures de relaxation spin-

réseau et spin-spin de protons d'hydrogène à la diminution de l'adsorption de molecules d'eau par la surface du grain de laitier.

Peut-être c'est la conséquence du fait que l'ion Ti^{4+} est un meilleur sorbant de l'eau que les ions de métaux alcalino-terreux de plus, pour de petites teneurs en TiO_2, ce dernier est partiellement hexacoordiné; la distance Ti-O étant suffisamment grande ce qui permet aux molecules d'eau d'interagir directement avec l'ion Ti^{4+}.

Avec l'accroissement de la quantité de TiO_2 le titane acquiert la coordinance 4 et la distance Ti-O diminue. Cela aboutit à ce que l'adsorption de l'eau par les ions Ti^{4+} devient moins probable à cause de l'ecran d'oxygene par rapport au titan.

On a indiqué plus haut que le facteur déterminant de la structure des laitiers de haut fourneau, ayant rapport à leur activite, est le degré de polymerisation des complexes Si-O, qui à son tour est fonction de la concentration en anions d'oxygène du laitier.

Aussi a-t-on émis l'idée que les propriétes hydratantes du laitier peuvent être elevées par introduction d'adjuvants facilitant la destruction du reseau Si-Ti-O. Nous l'avons montre sur l'exemple des laitiers contenant du titane.

Les études de ces dernières années ont permis d'établir que l'existence de la phase vitreuse ne constitue pas par elle-même un facteur déterminant de l'élevation de l'activité des laitiers. Certains estiment même que les proprietes liantes les plus elevées sont propres aux laitiers dont la teneur en phases cristallines varie entre 5 et 20%.

A notre égard le problème de l'opportunité d'un laitier partiellement cristallisé (5) doit se resoudre dans chaque cas particulier compte tenu de la composition chimique du laitier et, en premier lieu, de sa basicite, car cette dernière determine l'ordre de précipitation des phases cristallines lors du refroidissement du laitier au-dessous de la temperature du liquide (Tl). La granulation des laitiers basiques (Mo > 1) à la temperature inferieure à Tl contribue à la fixation de la structure dans laquelle, à côté du verre, est présente la phase mineralogique $2CaO\ SiO_2$, très active sur le rapport des propriétés liantes, et dont l'activite est superieure a celle du verre.

Avec le refroidissement des laitiers acides (Mo < 1) au-dessous de Tl c'est le mélilite qui cristallise le premier et pour certains laitiers speciaux (titanifères), le pérowskite et le baïkovite dont les proprietes liantes sont denuées d'activite. Aussi la granulation des laitiers acides au-dessous de Tl doit-elle abaisser leurs proprietes liantes.

CONCLUSION

En se fondant sur la théorie de la structure ionique des laitiers de haut fourneau on a étudié les problèmes de l'interdépendance de leur structure et de l'activité hydraulique; les conceptions répandues sur la similitude entre les structures des laitiers cristallins et vitreux ainsi que de l'influence de l'arrangement des cations dans le verre de laitier sur son activite.

On a analysé l'explication de la possibilité d'apparition dans les laitiers de haut fourneau hydrates de produits d'hydratation exterieurs et interieurs différant entre eux par leur basicite.

On a étudié le rôle de l'aluminium, du magnesium et du titane dans la formation de la structure du laitier de haut fourneau et établi la capacité de variation de leur coordinance, phenomene agissant fortement sur le mecanisme de l'hydratation.

On a passé en revue les problèmes de l'opportunité de la regulation de la granulation du laitier de haut fourneau en rapport avec sa basicite chimique, vu l'influence positive sur l'activité du laitier d'une faible teneur en phases cristallines à activité hydraulique dans sa structure.

BIBLIOGRAPHIE

1.- А.А.АШПЕН (1970) Химия стекла, М.,"Химия", (en russe).

2.- Ю.М.БУТТ, В.В.ТИМАШЕВ (1974) Портландцемент, М., Стройиздат, (en russe).

3.- Р.КОНДО (1961) Труды пятого Международного конгресса по химии цемента, Токио, (en russe).

4.- С.М.РОЯК, Я.Ш.ШКОЛЬНИК, В.В.ОРЛОВ и др. (1973) Журнал прикладной химии, том 46, № 1, (en russe).

5.- С.М.РОЯК, Я.Ш.ШКОЛЬНИК, В.В.ОРЛОВ и др. (1975) Журнал прикладной химии, том 48, № 5, (en russe).

Utilisation d'un laitier de magnésium comme liant alumineux

Using magnesium slag as aluminous cement

A. CARLES-GIBERGUES, Département de Génie Civil de l'Institut National des Sciences Appliquées de Toulouse,
B. THENOZ, Institut de Géotechnique de l'Université Paul Sabatier de Toulouse,
A. VAQUIER, Institut de Géotechnique de l'Université Paul Sabatier de Toulouse, France.

RESUME : La fabrication du magnésium à partir de dolomites décarbonatées puis réduites par le silicium conduit à la formation d'un laitier récupéré sous deux formes distinctes : un matériau pulvérulent refroidi à l'air et un matériau granulé par trempe à l'eau ; le premier est essentiellement formé de $C_2S\beta$ et de petites quantités de $C_{12}A_7$; le second renferme d'importantes proportions de $C_2S\beta$ enrobés dans une matrice hétérogène où l'on distingue une phase vitreuse, et du C_3AH_6.

Gâché avec de l'eau, chacun des deux constituants fait prise spontanément sans l'aide d'activant. Dans les deux cas, les phases hydratées responsables du durcissement sont associées à de la gehlénite hydratée et des aluminates de calcium.

Par contre, d'importantes différences existent dans les vitesses de formation de ces hydrates : rapide pour le laitier fusant, lente pour le laitier granulé. Corrélativement, on note la même disparité dans l'accroissement des résistances mécaniques. Il est donc intéressant d'utiliser ces deux matériaux conjointement.

Les meilleurs résultats, dans une perspective d'emploi comme liant économique de granulats routiers, sont enregistrés avec des dosages de 40 % de laitier granulé broyé et 60 % de laitier fusant.

En technique routière classique des graves laitiers où les deux matériaux sont employés simultanément sans broyage préalable, de bonnes performances mécaniques ont aussi été atteintes.

Les deux composés peuvent également être utilisés séparement ; ainsi, le laitier fusant peut servir à la confection à froid de matériaux cellulaires par simple ajout de poudre d'aluminium, alors que l'autoclavage du laitier granulé broyé donne des matériaux très résistants.

SUMMARY : The fabrication of magnesium from dolomite, by eliminating carbonate, and then reduced by silicium results the formation of slag in two distincted forms : the powdered material by cooling in the air and the granulated material by soaking with water. This primary is essentially formed $C_2S\beta$ and a little quantity of $C_{12}A_7$. The latter mostly consists of $C_2S\beta$ covered in the heterogeneous matrix in which we distinguish by the vitreous phase and C_3AH_6.

By mixing with water, each of these two constituents will set immediately without the aid of active agent. In both cases, the hydrated phases, responsible for hardening, are associated with hydrated gehlenite and aluminated calcium.

Nevertheless, the velocity of hydrated formation is greatly different ; it is quick for powdered slag, slow for granulated slag. Similarly, we observed that the growth of mechanical resistance is different in the same manner. It is therefore interested to use both forms of slags combining together.

Better results, in view of using economic slag as road aggregate, are obtained by proportioning 40 % of crushing granulated slag with 60 % of melted slag.

For graved slag road, the use of the two materials together, without previous crushing, allowed us to obtain the mechanical performances.

The two compositions can also be used separately as followed : the melted slag can serve as the cold production of cellular materials by adding aluminium powder while the autoclave of the crushing granulated slag yields high resistance material.

I - INTRODUCTION

La récupération des sous-produits industriels est à l'ordre du jour dans le double souci d'économie d'énergie et d'aménagement du cadre de vie menacé par l'entassement anarchique des rebuts.

L'expérience acquise permet de penser que les tonnages importants de laitiers de hauts-fourneaux recyclés dans le génie civil tendent vers une limite difficile à reculer.

Mais les déchets inutilisés des autres branches de l'industrie métallurgique (pour nous en tenir à ce seul domaine de l'activité industrielle) n'ont pas fait -et loin de là- l'objet d'études systématiques de remploi. Sans doute, parce que les quantités en jeu dans chaque unité de production ne sont pas aussi considérables que dans le cas de la production de fonte et d'acier. Il n'empêche que des réutilisations techniquement et économiquement intéressantes sont possibles.

Cette note a précisément pour objet l'étude de la valorisation d'un laitier de fabrication du magnésium.

La première partie du travail a trait à l'identification précise des phases constitutives du laitier : pouvait-on, a priori, entrevoir une utilisation analogue à celle des laitiers de hauts-fourneaux avec ou sans traitement physico-chimique complémentaire ?

La réponse ayant été franchement positive : présence de certains des constituants classiques des ciments, il convenait, dans une deuxième partie, de confirmer l'aptitude à la prise hydraulique par l'étude du comportement en présence d'eau.

Des possibilités de prise se manifestant effectivement, il restait à examiner dans une troisième partie les différents emplois possibles en génie civil.

II - CONSTITUTION DU PRODUIT DE RECUPERATION

II.1 - Propriétés physico-chimiques

La nature et la structure du laitier que libère la fabrication du magnésium dépendent évidemment de la composition des matières premières et du processus de fabrication. Dans le procédé "Magnetherm", en usage à l'usine de Marignac (Haute-Garonne), d'où provient le laitier étudié (1), on réduit, après décarbonatation de la dolomite, l'oxyde de magnésium par le silicium suivant la réaction théorique

$$2(MgO, CaO) + Si \xrightarrow{1600°C} SiO_2, 2CaO + Mg \uparrow$$

Le magnésium se dégage à l'état de vapeur, puis le four est retourné au-dessus d'une fosse pleine d'eau. La partie du bain liquide qui s'en écoule est ainsi transformée en laitier granulé qui se présente sous l'aspect de granulés poreux et friables de granulométrie comprise entre 0,2 et 10 mm. La masse volumique apparente (tous vides compris) est 1,070 T/m^3. La masse volumique mesurée sur poudre inférieure à 50 µm et dans un liquide est de 3,00 T/m^3.

D'autre part, une fraction moins importante du bain (environ le tiers) reste collée aux parois du four et se refroidit lentement à l'air en se délitant en une poudre fine qui constitue le laitier dit fusant.

Cette poudre a une surface spécifique de 1 800 cm^2/g BLAINE. Sa masse volumique est, soit de 0,950 T/m^3 (vides entre grains inclus), soit de 2,960 T/m^3 (vide entre grains exclus).

La composition chimique moyenne ne dépend évidemment que de la composition du bain et non du mode de refroidissement : elle est la même pour les 2 fractions, granulée et fusante, conformément au tableau ci-après.

SiO_2	25,0
Al_2O_3	14,0
CaO	54,2
MgO	3,9
Na_2O	0,2
SO_3	1,3

On constate que ce laitier est plus riche en chaux et plus pauvre en silice que les laitiers de fonte de hauts-fourneaux.

La connaissance de la seule composition chimique n'est pas suffisante pour identifier les espèces cristallines susceptibles de prise hydraulique, d'où la nécessité d'une diagnose minéralogique.

II.2 - Constitution minéralogique

Le laitier granulé diffère considérablement, par sa structure, des laitiers de fonte ; il est largement cristallisé. Ce fait est, selon toute vraisemblance, explicable par son très fort indice de basicité CaO/SiO_2 = 2,16.

Les cristaux, pour leur quasi-totalité, sont des silicates bicalciques. Ils constituent 50 % du laitier granulé. Leur étude par diffractométrie X -radiation $K\alpha_1$ du cobalt, détection par compteur linéaire- montre la présence des deux variétés α' et β et, probablement de α.

Ils s'individualisent en constituants arrondis, d'environ 30 à 80 µm au sein d'une matière interstitielle presque exclusivement vitreuse.

Les examens à la microsonde électronique (figure 1) confirment que le rapport molaire CaO/SiO_2 est très voisin de 2, et que les remplacements du silicium par l'aluminium et du calcium par le magnésium y sont rares : 1,1 % d'Al_2O_3 et 1,3 % de MgO.

La matière interstitielle est hétérogène. Dans sa masse, elle se définit par un rapport $[CaO+MgO]/[SiO_2+Al_2O_3]$ très proche de 2, l'aluminium jouant cette fois un rôle important (environ 11 Al pour 2 Si) : ainsi, ont pu se différencier en petites quantités des cristaux d'aluminate de calcium que la trempe a hydratés directement en C_3AH_6.

Au contact des silicates bicalciques, existent des zones riches en magnésium. Certaines correspondent à des cristaux de périclase, dont l'existence est bien visible sur les diffractogrammes X ; d'autres, à rapport molaire MgO/SiO_2, voisin de 2, sont constitués de forsterite $Mg_2.SiO_4$, minéral plusieurs fois trouvé dans des laitiers (2).

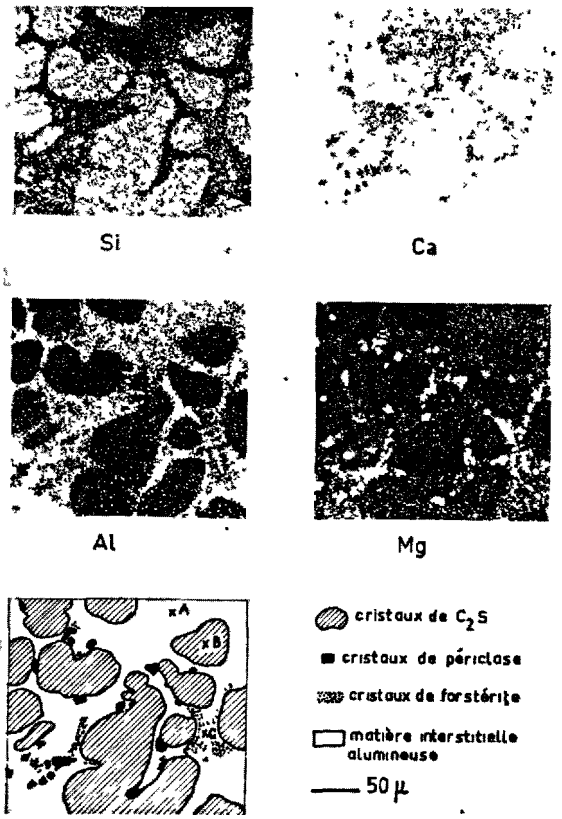

FIGURE 1 : Grain de laitier granulé

Le laitier fusant est largement cristallisé, le constituant majeur étant la variété γ du silicate bicalcique (calcio-olivine).

Le refroidissement lent à l'air conduit, vers 500°C, à la transformation de $C_2S\beta$ en $C_2S\gamma$, avec un accroissement de volume d'environ 13 %, ce qui provoque la pulvérisation spontanée du laitier.

A côté de ce silicate, existent de petites quantités de périclase et d'aluminate de calcium $C_{12}A_7$ qui, comme le montre la figure 2, se concentrent dans les fractions les plus fines.

III - COMPORTEMENT EN PRESENCE D'EAU ET IDENTIFICATION DES PHASES HYDRATEES

La mise en évidence de constituants connus pour leurs propriétés hydrauliques conduit naturellement à étudier le comportement du laitier en présence d'eau, sous ses deux formes, soit prises séparément, soit associées.

III.1 - Comportement dans l'eau pure des constituants séparés

III.1.1 - Fraction fusante

La solution se sature rapidement en chaux, puis sa concentration diminue régulièrement avec le temps (figure 3). On note également la présence en faible quantité du sodium et de l'aluminium. Par contre, pratiquement pas de silice et pas du tout de magnésie. Les premiers composés hydratés sont décelables par diffractométrie X, moins de deux heures après le gâchage. L'aluminate C_2AH_8 est le premier à apparaître et constitue, pendant les trois premiers jours, l'essentiel de la phase hydratée. On décèle également de petites quantités de CAH_{10} et de C_4AH_{13}. De la gehlénite hydratée C_2ASH_8 se forme quand la concentration en chaux de la solution diminue (3) et, encore plus tardivement, apparaît l'aluminate C_3AH_6.

III.1.2 - Fraction granulée

Ce matériau, préalablement broyé à la même finesse que le laitier fusant a une nettement moindre réactivité : les diffractogrammes X ne montrent, en effet, l'apparition des permiers hydrates qu'au bout de 1 jour ; il s'agit d'aluminates de calcium et de gehlenite hydratés. On constate simultanément une dissolution beaucoup plus lente du calcium dont la concentration atteint un palier au bout d'une dizaine de jours. Les solutions renferment initialement des concentrations non négligeables de silice dont la teneur s'amenuise ensuite régulièrement avec le temps (figure 3).

III.2 - Comportement des constituants associés

Les courbes de mise en solution du mélange de 1/3 de la forme fusante et 2/3 de laitier granulé résultent de la superposition des courbes correspondant à chaque forme prise isolément. Les diffractogrammes montrent la formation des mêmes espèces hydratées. Par contre, C_2AH_8 a une existence très courte ; C_4AH_{13} et C_2ASH_8 se développent à même vitesse.

On peut penser que la libération lente des ions Ca, Al, Si, à partir de la matière vitreuse de la forme granulée devrait favoriser la formation de quantités croissantes de gehlenite et de silicates de calcium hydratés. Pour confirmer cette hypothèse, nous avons étudié la prise (figure 4) et le durcissement (figure 5) de pâtes pures de mélanges en proportions variables des 2 formes granulée et fusante (amenées à la même finesse), gâchées avec des quantités d'eau ajustées pour que la maniabilité reste constante.

On note qu'il-y a réaction mutuelle des deux formes, traduite par la forme en cloche des courbes de la résistance mécanique. Le maximum d'activation correspond à une proportion 40-60 de granulée-fusante.

IV - LES EMPLOIS POSSIBLES

Ainsi, l'étude de la réactivité à l'eau du laitier de magnésium montre qu'il se comporte, sous sa forme fusante (et à un degré moindre, sous sa forme granulée), comme un liant hydraulique à la différence des laitiers de hauts-fourneaux qui ont besoin d'un activant ou d'un catalyseur pour stimuler une hydraulicité latente.

Ce point étant acquis, il restait à étudier les utilisations effectivement possibles du laitier sous ses deux formes combinées, ou sous chacune d'elles séparément. Nous avons retenu les 4 exemples ci-après.

IV.1 - Mélange utilisé comme liant

Les résultats de l'étude du comportement en présence

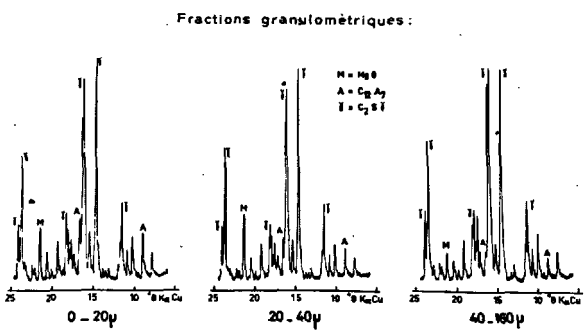

FIGURE 2 : Diffractogrammes X du laitier fusant

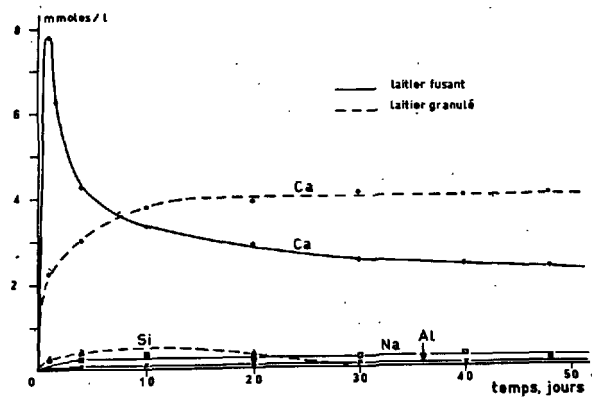

FIGURE 3 : Dissolution du laitier dans l'eau pure

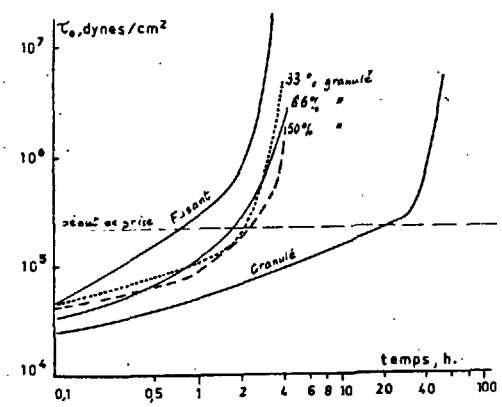

FIGURE 4 : Influence de la composition des mélanges sur leur vitesse de prise

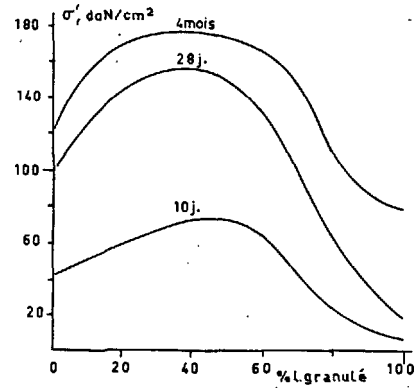

FIGURE 5 : Influence de la composition des mélanges sur leur résistance à la compression simple

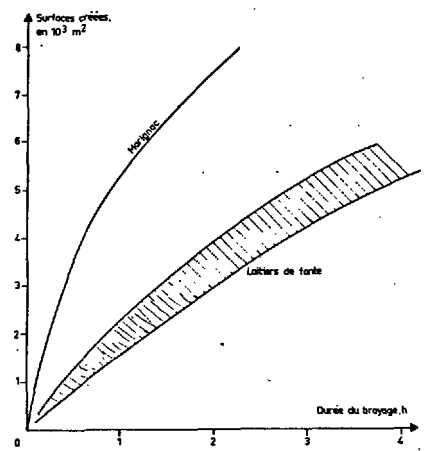

FIGURE 6 : Broyabilité du laitier granulé

d'eau conduisent à essayer un liant formé de 1/3 de forme fusante et de 2/3 de forme granulée, préalablement broyée jusqu'à une finesse comparable à celle de la forme fusante, ce qui est économiquement possible dans un broyeur à barres, comme le montre la figure 6 qui met en évidence une broyabilité bien supérieure à celle de laitiers sidérurgiques variés.

Les performances obtenues sont loin d'être négligeables et autorisent toute une gamme d'emplois.

IV.2 - Mélange utilisé directement sans broyage préalable, en technique routière

L'addition de 10 à 15 % du mélange optimum à une grave siliceuse de granulométrie continue permet de fabriquer des éprouvettes de résistance à la compression simple voisine de 7,2 mPa, soit de l'ordre de grandeur des résistances habituellement admises en technique routière.

IV.3 - Matériaux cellulaires à partir de la forme fusante

Le laitier fusant étant un véritable ciment alumineux, on peut l'utiliser pour préparer à froid des matériaux cellulaires en ajoutant seulement de la poudre d'aluminium : on a ainsi obtenu des masses volumiques de 0,850 T/m^3 et des résistances de 6 mPa.

IV.4 - Matériaux autoclavés à partir de la forme granulée

L'autoclavage du laitier granulé plus ou moins broyé entraîne son activation par l'hydratation des silicates bicalciques et donne des matériaux très résistants : on a obtenu des résistances atteignant 78 mPa (4).

V - CONCLUSION

Nous nous étions proposés de rechercher les conditions de valorisation d'un laitier jusqu'ici mal utilisé. Nous avons constaté qu'il contenait des composés hydrauliques en quantité suffisante pour justifier une utilisation pratique, soit directement sous sa forme fusante, soit en mélangeant (dans les proportions de leur production) les formes fusante et granulée (après éventuellement un simple broyage de cette dernière), soit, enfin, en activant la forme granulée par autoclavage. Ce cas particulier illustre tout l'intérêt écologique et énergétique d'études systématiques complètes de matériaux dont les propriétés hydrauliques étaient, jusqu'ici, méconnues.

BIBLIOGRAPHIE

(1) R. SEVIN (1973) "L'usine de magnésium silicothermique de la Société Française d'Electrométallurgie à Marignac" Journal du Four Electrique, n° 5 (Français)

(2) F. M. LEA (1970) "The chemistry of cement and concrete" 3ème édition, Arnold Publisher (Anglais)

(3) R. DRON (1974) "Mécanisme de la prise du laitier sous activation alcaline" Rapport de recherche du Laboratoire Central des Ponts et Chaussées, n° 38 (Français)

(4) A. MARTINELLI (1979) "Influence de divers traitements physiques sur les propriétés mécaniques des déchets industriels" D. E. A. de Génie Civil, Université Paul Sabatier de TOULOUSE (Français).

Expérience et fondements physico-chimiques de l'utilisation des sous-produits dans l'industrie du ciment

Experience and physico-chemical bases of using secondary raw materials in cement industry

A.S. BOLDYREV, Ministère de matériaux de construction de l'U.R.S.S.,
Z.B. ENTINE, candidat ès sciences techniques, NIITzement, Moscou,
A.I. ZDOROV, candidat ès sciences techniques, Youjguiprotzement, Kharkov,
A.V. KISSELEV, candidat ès sciences techniques, collaborateur scientifique, Guiprotzement, Léningrad,
S.D. MAKACHEV, NIITzement, U.R.S.S.

RESUME : L'utilisation dans l'industrie du ciment de sous-produits permet d'économiser le combustible, d'abaisser les frais de production et d'établissement, de mettre en valeur les résidus industriels, de contribuer à l'amélioration de l'équilibre écologique.

On utilise chaque année en U.R.S.S. 25 à 27 millions de tonnes de sous-produits dont le rôle d'adjuvant minéral actif est fonction de son interaction acido-basique avec la solution aqueuse de chaux hydratée et formation de sels de calcium hydratés difficiles à dissoudre. Une telle interaction est propre aux laitiers ferro-siliceux composés pour l'essentiel de verre alumoferrosiliceux et de fayalite.

A des fins de contrôle de la prise du ciment on se sert de gypses chimiques aux compositions variées en phases, dont la solubilité est proche de celle du gypse naturel bihydraté.

Les sous-produits et, notamment, les cendres des centrales thermiques sont efficacement utilisés en qualité de constituant de base pour l'obtention du clinker.

SUMMARY : Utilization of the secondary raw materials in the cement industry ensures economy of fuel, reduction of production and capital costs, utilization of waste products, improvement of ecology balance.

From 25 to 27 million tons of the secondary raw materials are used in the USSR annually. The suitability of the secondary raw materials for use as an active mineral additive is determined by its ability for acid-base interaction with an aqueous solution of hydrated lime with formation of difficultly soluble hydrates of calcium salts. The ability for such a reaction is offered by ferrosilicate slags consisting mainly of alumoferrosilicate glass and fayalite.

To control the setting time of the cement, use is made of chemical gypsum of different phase compositions whose solubility approaches that of the natural gypsum dihydrate.

The secondary raw materials, especially fly ash of the power plants is also advantageously used as an ingredient of raw mix in the production of ciment clinker.

L'utilisation des résidus industriels est un des plus efficaces moyens d'abaisser les besoins en énergie et en investissement d'établissement de cimenteries et d'améliorer le bilan écologique de ces derniers. Dans nombre de pays on observe une tendance permanente à l'accroissement de la mise en oeuvre de matériaux tels que les laitiers de haut fourneau, les cendres de centrales thermiques, les boues bélitiques (2-6).

En Union Soviétique une grande expérience a été accumulée dans le domaine de l'utilisation en cimenterie de produits technogènes (résidus des productions techniques). Le volume total mis en oeuvre atteint 25 à 27 millions de tonnes par an, ce qui dépasse de beaucoup leur emploi dans les autres pays. Dans le rapport de V.I.Satarine, présenté au VI-ième Congrès International de chimie du ciment tenu à Moscou, ont été exposées les conclusions de l'expérience d'utilisation des laitiers granulés de haut fourneau (7).

Dans la présente communication une tentative est faite d'analyser les fondements physico-chimiques de l'élargissement de l'assortiment de produits technogènes utilisés dans la production du ciment, de même que l'expérience acquise dans ces applications.

EXPLOITATION DE L'EFFET D'ADJUVANTS MINERAUX ACTIFS DES PRODUITS TECHNOGENES SECONDAIRES. Les normes soviétiques autorisent à utiliser en qualité d'adjuvants minéraux actifs des matériaux à effet soit hydraulique, soit, le plus souvent, pouzzolanique.

Le trait commun de ces matériaux est leur aptitude à l'interaction acido-basique dans des solutions aqueuses de l'oxyde calcique hydraté avec formation d'hydrates difficilement solubles.

Selon les conceptions développées pour la première fois par Bernstade l'interaction acido-basique se réduit au transfert du proton de l'acide-donneur à la base-acceptteuse. La force thermodynamique active du phénomène est engendrée par la diminution de l'enthropie de la substance de basicité intermédiaire par rapport à la somme d'enthropies de l'acide et de la base initiaux. Dans les solutions aqueuses de $Ca(OH)_2$ le rôle d'acide peut être joué par toute substance capable de transmettre le proton à l'ion hydroxyle. Si le produit des solubilités du composé de la réaction s'avère dans ce cas inférieur au produit des solubilités des substances de base, les cristeux hydratés formés seront alors stables et inattaquables par l'hydrolyse, tandis que la concentration de $Ca(OH)_2$ dans la phase liquide du système sera inférieure à celle d'équilibre de la solution pour la température et le pH donnés. Ce dernier phénomène est un indice de la possession par la matière de propriétés pouzzolaniques.

La silice active et le verre alumosiliceux sont des pouzzolanes manifestes. Les donneurs de proton sont dans ce cas les surfaces hydroxylées de particules de ces matières. L'aptitude à l'hydroxylation et aux manifestations de propriétés acides est également propre au verre alumoferrosiliceux de même qu'aux matériaux de composition essentiellement ferrosiliceuse à teneur importante en FeO. Pour une dispersion très fine de ces matériaux, l'oxyde ferreux qu'ils contiennent est oxydé en présence d'alcali jusqu'à l'oxyde ferrique par l'oxygène dissous dans la phase liquide du ciment en voie de durcissement et s'avère capable de s'hydroxyler avec formation subséquente d'hydroferrites ou d'hydroaluminoferrites calciques de formule générale $C_4(A_x, F_{1-x})H_{13}$ $(0 < x < 1)$, et à des conditions déterminées également d'hydrogrenats.

En guise d'exemple examinons les résultats d'études réalisées par I.G. Boun, A.S.Sventsitzki et Z.B. Entine des propriétés des ciments aux laitiers ferrosiliceux dont la composition chimique et la teneur en phases sont communes à de nombreux résidus de la métallurgie de métaux non ferreux. La composition des matières étudiées est donnée au tableau I.

TABLEAU I

Composition chimique des laitiers et du clinker, %

Dénomination de la matière	SiO_2	Al_2O_3	Fe_2O_3	FeO	CaO	R_2O
Clinker	21,6	4,20	4,32	-	64,6	1,08
Laitier granulé	31,82	6,31	6,95	40,70	5,97	2,47
Laitier non granulé	32,96	5,94	7,88	39,98	7,15	2,42

Une partie des éprouvettes de laitier était granulée, tandis que l'autre était progressivement refroidie à l'air. Les deux types d'éprouvettes se conformaient aux normes soviétiques établies pour les adjuvants minéraux actifs quant aux délais de prise et à la résistance à l'eau, une fois mélangés à de la chaux blanche. La concentration de $Ca(OH)_2$ dans la phase liquide du ciment s'est avérée inférieure à celle d'équilibre pour la température donnée. Elle a été pour les laitiers granulés et lentement refroidis respectivement de 2,6 et 6,3 mmole/litre, tandis que celle d'équilibre s'élevait à 8,2 mmole/litre.

Les analyses pétrographique et aux rayons X ont établi que les laitiers se composent pour l'essentiel de fayalite (45 à 55 %), de verre alumoferrosiliceux (35 à 40 %) et de magnétite (12 à 15 %). La teneur en verre était quelque peu élevée dans les laitiers granulés, toutefois cela n'exerçait pas d'influence sensible sur la résistance ainsi que sur les autres caractéristiques des ciments.

La figure 1 représente l'influence de l'addition de laitiers sur la résistance des ciments.

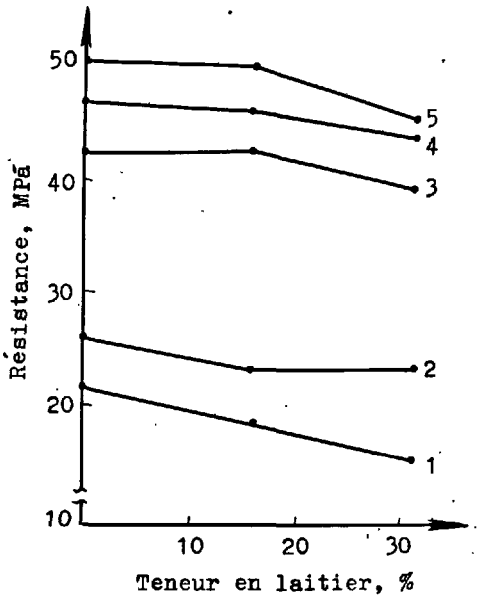

Fig. 1 - Influence des laitiers ferrosiliceux sur la résistance des ciments (laitier granulé) : 1 - à 3 jours ; 2 - à 7 jours ; 3 - à 28 jours ; 4 - à 90 jours ; 5 - à 180 jours

Avec l'addition de laitiers la résistance du ciment diminue au début, toutefois au bout de 28 jours et plus les ciments contenant 15 % de laitier ne cèdent en rien aux ciments de contrôle sans constituants secondaires. L'addition du laitier pour 30% abaisse la résistance de 10 %, par rapport au ciment de contrôle, également à des délais avancés, mais même dans ce cas l'effet pouzzolanique de l'adjuvant se manifeste de façon évidente. Des résultats similaires ont également été obtenus après étuvage des éprouvettes.

L'étude de la composition en phases de la pierre de ciment durcie a montré qu'il y a fixation de nouvelles formations identifiables sous forme d'hydroferrite de calcium aux cristallisations peu prononcées.

La résistance des ciments aux laitiers aux agents atmosphériques et aux sulfates était supérieure à celle des ciments de contrôle. L'efficacité de l'utilisation des ciments aux laitiers dans les bétons était estimée par comparaison du taux de consommation de contrôle, exigé pour l'obtention du béton de même résistance, non pas du ciment naturel mais du clinker qui y est contenu (8). L'addition de 15 et de 30 % de laitier se solde ainsi par un gain en clinker respectivement de 10-12 et de 20-25 %.

Les résultats obtenus confirment la validité des principes généraux du choix d'adjuvants minéraux actifs à additionner aux ciments et permettent d'élargir l'assortiment de matériaux utilisés à cette fin.

GYPSES CHIMIQUES. Les résidus de nombreuses branches de l'industrie chimique : production de superphosphate , d'acides phosphorique et borique, etc., constituent des matériaux composés pour 60 à 95 % de modifications variées du sulfate de calcium. L'intérêt pour l'exploitation des gypses chimiques en tant que régulateurs de prise du ciment se manifeste dans de nombreux pays. Les résultats obtenus sont encourageants, mais l'utilisation de ces matières demeure toujours assez limitée (9, 10).

Parmi les résidus se présentant en grande masse il faut nommer le phosphogypse contenant pour 95-98 % de gypse bihydraté. Le taux de phosphore calculé en P_2O_5 est de 1,0 à 1,5 %, celui de fluor, jusqu'à 0,3 %.

Le borogypse qui est un résidu de fabrication de l'acide borique contient pour 60 à 70 % de sulfate de calcium. L'impureté principale est la silice qui s'y trouve en quantité allant de 20 à 25 %. La teneur résiduelle en B_2O_3 est de 0,5 à 1,5 %, dont 0,5-1,0 % d'acide orthoborique. Les autres impuretés constituent en masse près de 5 %. D'après les données d'analyses pétrographique et aux rayons X le sulfate de calcium s'y trouve sous forme de gypse hydraté (40-55 %) et d'anhydrite (20-35 %). La silice se présente en une structure dendritique amorphe (11).

Le fluorogypse contient pour 80 à 95 % de sulfate de calcium. En qualité d'impureté on y trouve de la fluorine (0,5-5,0 %) et de la silice (1,5-4,0 %). Les autres impuretés ne dépassent pas au total 3 à 5 %. Le sulfate de calcium se présente pour l'essentiel sous forme d'anhydrite et de gypse semi-hydraté en étroites coalescences. La quantité de gypse bihydraté est moindre. Vu la présence dans les gypses chimiques d'impuretés sous forme de phosphore, de fluor, de bore, etc., ainsi que de différentes variétés de gypse il s'est avéré intéressant de procéder à l'étude du rôle de ces facteurs dans les délais de prise, la résistance et les caractéristiques techniques de construction du ciment.

L'essentiel de l'action de réglage du gypse sur les délais de prise réside dans son aptitude de former avec C_3A et C_4AF des hydrosulfoaluminates et des hydrosulfoferrites de calcium. La forme stable de l'hydrosulfoaluminate de calcium est celle du trisulfate qui en cas de teneur insuffisante en gypse dans la solution et un excès d'autres ions, formant le sel complexe, devient un monosulfate. En outre, la concentration d'ions SO_4^{2-} dans la phase liquide est un des facteurs essentiels impliquant l'aptitude des ciments à engendrer des réactions de fausse prise (12). Aussi la cinétique de la dissolution des gypses chimiques en phase liquide est-elle

un des principaux facteurs déterminant les possibilités de leur exploitation en qualité d'accélérateurs-retardateurs de prise. Le problème ne se pose pas au cas où le gypse des résidus se trouve sous la forme de sel bihydrique, situation ne se présentant toutefois que pour le phosphogypse.

La figure 2 fournit les données sur la variation de la composition en phases d'une éprouvette industrielle de gypse chimique (fluorogypse) maintenue en contact avec l'eau durant 7 jours. L'anhydrite soluble se transforme progressivement en gypse hemihydraté, tandis que la teneur en gypse bihydraté s'accroît de façon relativement lente (13). La coexistence prolongée de sels bihydraté et hemihydraté implique que la présence du fluor s'oppose à la transformation du gypse hemihydraté en gypse bihydraté, la dissolubilité des deux formes du gypse étant presque la même. A 20 °C la dissolubilité du fluorogypse est de 1,5-1,9 g/l $CaSO_4$, ce qui est quelque peu inférieur à celle du gypse bihydraté, mais dépasse de beaucoup celle de l'anhydrite.

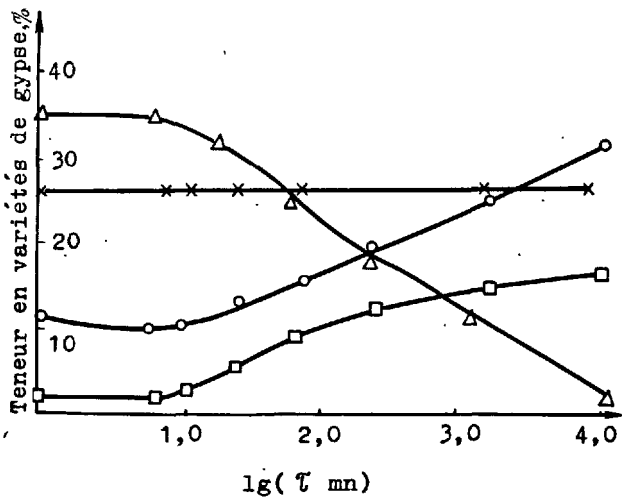

Fig. 2 - Variation de la composition en phases du fluorogypse au contact de l'eau ; △ - anhydrite ; o - gypse hemihydraté ; □ - gypse bihydraté ; x - anhydrite insoluble.

Tous les gypses étudiés garantissent des délais de prise du ciment fixés par les normes pour des dosages à peu près les mêmes que le gypse naturel.

La présence de l'anhydrite dans les gypses chimiques soulevait des doutes que cette forme difficile à rehydrater du sulfate de calcium entraîne la destruction de la pierre de ciment déjà durcie par formation à des délais plus avancés de l'hydrosulfoaluminate de calcium (destruction gypseuse). Pourtant, des études spéciales ont montré que déjà après trois jours de durcissement tout le sulfate de calcium y compris l'anhydrite s'avérait fixé dans l'hydrosulfoaluminate de calcium, et on ne décelait pas de gypse libre dans la pierre de ciment.

L'étude de l'influence des gypses chimiques sur la résistance des ciments a établi que le remplacement du gypse par l'une quelconque des formes du gypse chimique ne se répercute pratiquement pas sur la résistance du ciment à tous les délais d'essais (11, 13).

Une autre application efficace des gypses chimiques est l'exploitation de leurs qualités minéralisatrices pendant la cuisson du clinker.

L'efficacité du phosphogypse dont l'utilisation par les cimenteries en qualité de minéralisateur date déjà de plusieurs années, est bien connue. Son emploi permet d'améliorer le rendement des fours et d'obtenir un clinker à alite mieux cristallisé et de meilleure qualité (14).

L'utilisation à des fins identiques du fluorogypse se révèle également rentable. La figure 3 montre l'influence du fluorogypse sur la cinétique de la fixation de la chaux dans le mélange cuit comparée à celle du phosphogypse et du gypse naturel (15).

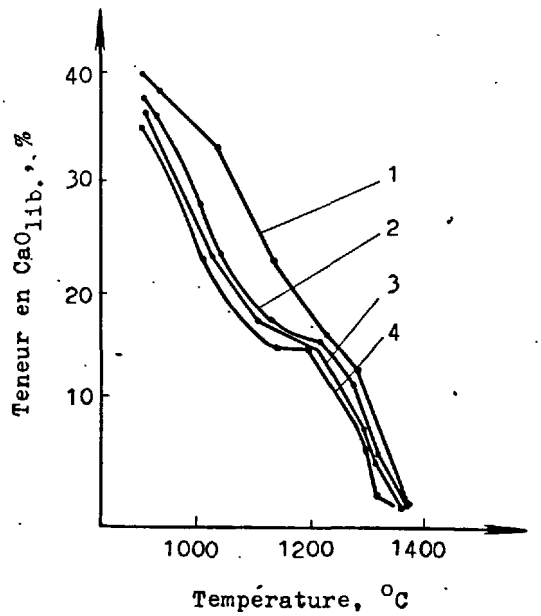

Fig. 3 - Influence des gypses sur la fixation de l'oxyde de calcium dans les mélanges bruts soumis à la cuisson : 1 - sans minéralisateur ; 2 - avec addition de gypse naturel ; 3 - avec addition de phosphogypse ; 4 - avec addition de fluorogypse

Toutes les variétés de gypse accusent un effet minéralisateur sensible dans l'in-

TABLEAU II

Teneur en CaO_{lib} et C_3S dans les éprouvettes cuites à des températures variées, %

Composition du mélange brut	1280 °C		1300 °C		1320 °C		1340 °C		1360 °C	
	CaO_{lib}	C_3S	CaO_{lib}	C_3S	CaO_{lib}	C_3S	CaO_{lib}	C_3S	CaO_{lib}	C_3S
Mélange avec cendre basique	12,36	n.d.	7,52	17,5	5,05	32,7	2,82	47,9	0,65	62,8
Mélange avec cendre acide	20,99	n.d.	10,24	3,1	5,20	24,4	1,91	55,0	1,03	60,2
Mélange avec argile	12,62	n.d.	10,64	3,0	6,93	25,2	4,01	55,6	0,74	65,5

tervalle de températures allant de 900 à 1300 °C, l'action du fluorogypse se manifestant de façon un peu plus forte dans l'intervalle de 1200 à 1300 °C. Dans les éprouvettes cuites, obtenues avec tous les minéralisateurs essayés, on a observé une quantité élevée de sulfates alcalins. On n'y a pas décelé de phases alcalines siliceuses et alumineuses, quant à la microstructure des éprouvettes elle s'est avérée meilleure. Les essais à l'échelle industrielle du fluorogypse en qualité d'agent minéralisateur de la cuisson du clinker ont montré que son efficacité ne cède en rien à celle du spath fluor (fluorine).

Enfin il existe encore une application possible des gypses chimiques et, surtout, du phosphogypse, celle consistant à obtenir sur sa base de l'acide sulfurique et du ciment.

Sous ce rapport, les nouvelles orientations se concentrent sur l'obtention, en partant du phosphogypse non pas du ciment portland de composition ordinaire, mais du ciment à sulfoalumosilicates, dont le clinker contient une sensible quantité de sulfoaluminate de calcium anhydre $3(CA)\ CaSO_4$ (16).

SCHLAMM ROUGE. Lors de la production de l'alumine à partir des bauxites on obtient pour chaque tonne de produit fini jusqu'à 2 tonnes de résidus sous forme de schlamm rouge. Les schlamms rouges sont des poudres finement dispersées, où plus de 90 % de particules ont des dimensions inférieures à 10 µm. Leur composition chimique varie dans les limites suivantes : SiO_2 - de 9 à 11 %, Al_2O_3 - de 17 à 19 %, Fe_2O_3 - de 39 à 43 %, TiO_2 - de 4 à 6 %, CaO - de 7 à 10 %, Na_2O - de 6 à 7 %.

La composition chimique du schlamm rouge autorise son emploi en qualité d'addition complexe ferroalumineuse de correction, ce qui s'avère très important au cas de la nécessité d'obtenir un clinker à partir de matières brutes très siliceuses. Les calculs établis d'après le diagramme d'état C-A-F-S montrent que pour chaque pour cent de schlamm rouge additionné au mélange brut et dosé en fonction de la substance calcinée la teneur en phase liquide dans la matière cuite s'accroît à la température de 1350 °C de 1,3 % et à la température de 1450 °C de 1,5 %. De manière correspondante s'accroît la réactivité du mélange brut.

La réactivité rélevée des mélanges bruts à schlamm rouge s'observe déjà à partir de 360-375 °C. A 900-1000 °C les constituants du schlamm sont aptes à former des bains fondus intermédiaires qui disparaissent ensuite par interaction avec d'autres constituants du mélange brut. Le processus de fixation de la chaux s'intensifie donc sur une large gamme de températures. Toutefois, le facteur essentiel demeure l'influence de l'addition de schlamm sur la quantité et les propriétés de la phase liquide.

UTILISATION DE PRODUITS TECHNOGENES EN QUALITE DE CONSTITUANTS DE BASE DU MELANGE BRUT. L'application de sous-produits en qualité de constituants de base du mélange brut s'est révelée très intéressante dans l'optique de l'emploi massif des résidus industriels ainsi que de possibilités s'ouvrant pour des économies en énergie et en combustible de même qu'en investissement d'établissement.

C'est ainsi que l'utilisation des cendres acides de centrales thermiques permet de réduire les frais de séchage et de mouture de la matière première, quant à l'utilisation des cendres basiques elle se solde par un gain résultant de l'élévation du rendement des fours et de l'abaissement des dépenses en combustible brulé pendant la cuisson.

L'étude de la réactivité des mélanges bruts où les cendres volantes ont remplacé l'argile a été réalisée par G.G. Lepechenkova et Z.B. Entine.

Le tableau II fournit des données sur la cinétique de la fixation de la chaux dans les mélanges bruts à cendres. Les mélanges bruts contenant des cendres et de l'argile étaient amendés jusqu'à une composition

chimique presque identique.

Comme il s'ensuit des données fournies, les cendres des centrales thermiques possèdent une réactivité non inférieure à celles des argiles à montmorillonites dont la réactivité est très grande.

Il est également très intéressant d'utiliser en qualité de matière première les boues bélitiques et les schlamms γ , les résidus de wollastonite ainsi que d'autres sous-produits. Il s'ensuit de l'exposé que l'assortiment de résidus industriels utilisés en cimenterie peut être sensiblement élargi.

BIBLIOGRAPHIE

I.- В.С.КАРЕЛИН, Г.Ю.ВАСИЛИК, И.А.ФРИДМАН (I978) Состояние и перспективы экономии топлива, электроэнергии и материалов в цементной промышленности. Краткие тезисы докладов на У Всесоюзном совещании по химии и технологии цемента. Москва, 26-29 сентября I978 г. НИИЦемент-ВНИИЭСМ, (en russe).

2.- Dutron P. L'Economie d'energie par les ajouts au ciment . Доклад на УI коллоквиуме директоров и специалистов испанских цементных заводов,(en français)

3.- I.BASSI (1978) Industrial wastes are potential cement "Rock Products", 78, N 8, 72-75, (en anglais).

4.- W.GUTT, M.A.SMITH (1976) Utilisation of waste materials in building and construction in Great Britain"Silicate industr", 41, N 12, 521-533, (en anglais).

5.- А.С.БОЛДЫРЕВ (I979) Второй продукт, "Социалистическая индустрия", № I68, (I978) Слово об отходах, "Химия и жизнь", № 2, (en russe).

6.- В.Е.ОРЛОВ (I978) Резервы народного хозяйства в использовании отходов производства. "Финансы СССР", № 3, II-I5 , (en russe).

7.- В.И.САТАРИН (I976) Шлакопортландцемент. УI Международный конгресс по химии цемента. т.2, часть I , Москва, Стройиздат, (en russe).

8.- З.Б.ЭНТИН, Е.Т.ЯШИНА, Н.З.РЯЗАНЦЕВА (I975) Строительно-технические свойства цементов. ВНИИЭСМ, Москва, (en russe).

9.- D.R.LANKARD, W.A.HEDDEN (1976) Industr applications for processed gypsum "Rock Products",76,N 6, 72-76, (en anglais).

I0.- M.NAGY, R.KOVACS (1976) Akemiai gipsz cementipari felhasznalhatosaganak wizgelata "Epitöanyag, 28, N 8, 297-302, (en hongrois).

II.- А.В.КИСЕЛЕВ, Т.Я.ГАЛЬПЕРИНА, А.А.ЛУКАЦКИЙ, Г.В.КОЖЕМЯКИН, В.Ф.СУХАНОВ (I977) Регулирование сроков схватывания цемента с помощью гранулированного борогипса. "Цемент", № 4, I5-I6, (en russe).

I2.- З.Б.ЭНТИН, Л.С.КЛЮЕВА, У.И.ПАПИАШВИЛИ (I979) Исследование особенностей процесса структурообразования цементов с ложным схватыванием. ДАН СССР, 246, № 6, I439-I44I, (en russe).

I3.- В.К.НОВОСАДОВ, В.Е.АГЕЕНКО, А.В.КИСЕЛЕВ, Т.Я.ГАЛЬПЕРИНА (I978) Гранулированный фторгипс- регулятор сроков схватывания цемента. "Цемент", № 6, I5-I6, (en russe).

I4.- Е.З.ОГНЯНОВА, И.Л.КРАМЕР (I964) Фосфогипс как минерализатор при обжиге цементного клинкера. "Цемент", № 3, (en russe).

I5.- Л.Я.ГОЛЬДШТЕЙН, Е.В.РЕБРИК (I978) Фторангидрит-интенсификатор обжига сырьевой смеси. "Цемент", № 6, I6-I7, (en russe).

I6.- Комплексные методы переработки фосфогипса. Сборник. Труды Ташкентского политехн. инст. № 200 (I977), (en russe).

Influence de la composition chimique et de la texture des laitiers sur leur hydraulicité

Influence of slags chemical composition and texture on their hydraulicity

E. DEMOULIAN, P. GOURDIN, F. HAWTHORN, C. VERNET, Société des Ciments Français, CEREG, France.

RESUME

L'étude commentée dans ce texte porte actuellement sur 27 laitiers de haut fourneau représentatifs des productions françaises et luxembourgeoises.

L'analyse complète de ces laitiers de type hématite ou lorrain, granulés ou bouletés, est effectuée par des méthodes physico-chimiques très précises. La reconnaissance des cristaux en microscopie optique a nécessité le concours du microscope électronique à balayage, de la microsonde électronique de Castaing et de la diffraction des rayons X.

Les taux de cristaux sont mesurés par microscopie optique et par diffraction des rayons X.

Les caractéristiques ainsi mesurées sont corrélées avec les résultats d'essais mécaniques sur mortiers ISO ou sur mortiers activés à la soude. Les auteurs montrent que les éléments mineurs des laitiers ont une grande influence sur leur hydraulicité et que les corrélations les plus fortes sont celles qui tiennent compte des compositions chimiques complètes et des taux de cristallinité.

Ils montrent aussi qu'à composition chimique identique, une vitrification parfaite n'est pas le critère d'une réactivité maximale.

SUMMARY

The study described here considers 27 blast furnace slags representative of the french and luxemburg productions.

A complete analysis of these slags of hematite or lorrain type, granulated or pelletized, has been done with very accurate methods. The recognition of crystals by optical microscopy needed the scanning electron microscopy, the X ray microprobe analysis and X ray diffraction. The percentages of crystals have been measured by optical microscopy and X ray diffraction.

These measured characteristics are correlated with compression strength on ISO mortar or with mortar activated by sodium hydroxide. The authors show that minor elements of the slags have a very important influence on their hydraulicity and the best correlations are the ones which considers the total chemical analysis and the percentage of crystals.

They also show that for the same composition, a perfect vitrification is not the criterion of an optimal reactivity.

INTRODUCTION

Depuis que TETMAJER a défini les conditions de l'hydraulicité des laitiers par les rapports CaO/SiO_2 et Al_2O_3/SiO_2, de nombreux indices chimiques destinés à prévoir leur valeur hydraulique, après activation à la soude, à la chaux ou au clinker, ont été proposés par de nombreux chercheurs que nous ne pouvons tous citer dans la bibliographie restreinte de cette courte communication (références 1 à 7). Parmi les travaux les plus récents, la recherche qui s'apparente le plus à celle qui est développée dans ce texte est celle de SMOLCZYK qui montre, entre autres, l'influence non négligeable des éléments mineurs tels que P_2O_5, MnO, Na_2O et K_2O sur l'évaluation de l'hydraulicité des laitiers (référence 8).

Les études effectuées depuis de nombreuses années, au CEREG, sur plusieurs centaines de laitiers de provenances diverses ont confirmé la valeur de certains indices chimiques.

Une recherche plus récente a montré que la composition minéralogique potentielle des laitiers vitrifiés, qui fait une distinction entre les structures en chaines et les structures en doubles ou simples tétraèdres, permettait une bonne appréciation de leur valeur hydraulique.

Dans une troisième étape, les auteurs montrent que la composition chimique complète des laitiers vitrifiés et leur taux de cristallisation sont les paramètres prépondérants de leur réactivité.

1/ CARACTERISTIQUES DES LAITIERS

1.1 - Compositions chimiques et potentielles

Les compositions chimiques et les compositions potentielles sont mentionnées sur le tableau I qui donne les valeurs moyennes, minimales, maximales et les écarts types.

Tableau I : Compositions des laitiers analysés

Comp. chimiques	Moyenne	Minimum	Maximum	Ec. type
Perte au feu	0,42	0,00	1,04	0,28
Insoluble	0,41	0,00	1,32	0,30
Silice totale	33,48	31,96	37,29	1,36
Al_2O_3	13,29	10,26	16,01	1,68
FeO	1,24	0,29	9,32	1,73
TiO_2	0,55	0,49	0,65	0,05
MnO	0,64	0,34	1,31	0,21
CaO	42,24	37,92	44,38	1,71
MgO	5,99	3,63	8,66	2,14
K_2O	0,70	0,44	0,98	0,17
Na_2O	0,39	0,25	0,50	0,08
P_2O_5	0,13	0,00	0,34	0,13
SO_3	0,04	0,00	0,19	0,04
S^{--}	0,94	0,68	1,25	0,25
F^-	0,16	0,06	0,31	0,10
Cl^-	0,019	0,003	0,050	0,019
Comp. potentielles	**Moyenne**	**Minimum**	**Maximum**	**Ec. type**
Merwinite C_3MS_2	1,74	0,00	20,2	4,83
Gehlénite C_2AS	35,74	27,6	43,05	4,52
Akermanite C_2MS_2	40,17	24,50	55,30	10,96
Rankinite C_3S_2	10,28	0,00	29,50	9,79
Pseudowollast. CS	3,46	0,00	14,60	5,33
Silicate bical. C_2S	3,32	0,00	20,63	4,08
Diopside CMS_2	0,48	0,00	12,90	2,44

1.2 - Cristallinité des laitiers

Analyses qualitatives. A l'échelle du microscope optique, aucun des laitiers analysés n'est totalement exempt de cristaux. Leur distribution ainsi que celle des gaz occlus est d'une hétérogénéité remarquable. Dans les laitiers qui contiennent de fortes teneurs en cristaux, il subsiste des quantités variables de grains totalement vitreux (photographies 1, 2, 3).

Les aspects des cristaux de merwinite et de mélilite sont visualisés sur les photographies 4 à 10. Pour les cristaux de quelques microns, la distinction entre merwinite et mélilite est parfois difficile.

Les cryptocristaux contiennent des quantités variables de merwinite et de mélilite, qui ne peuvent être différenciées en microscopie optique et même électronique (photographie 11). La diffraction X peut alors donner les renseignements souhaités. Le fer métallique se présente sous la forme de nodules très réfléchissants comme sur la photographie 12 : il est absent dans 70 % des laitiers, mais présent en quantités parfois importantes dans les autres.

Les photographies au microscope électronique à balayage (MEB) montrent des aspects de cristaux de merwinite et de mélilite. Les images en électrons absorbés visualisent la distribution des éléments : ces images montrent par exemple que le potassium et le soufre sont principalement localisés dans le verre, que la distribution de l'aluminium et du magnésium est différente dans le verre et dans les cristaux (photographies 13 à 23). A l'échelle de la microsonde électronique de Castaing (MEC), les cristaux de mélilite contiennent des proportions variables de gehlénite et d'akermanite. Au centre des gros cristaux, la solution solide C_2AS-C_2MS_2 est plus proche du terme C_2MS_2 qu'en bordure. Dans les dendrites, la composition est plus proche de la gehlénite.

Les minéraux accessoires sont des phases riches en titane, en soufre et potassium, des composés de type spinelle : ces phases sont très localisées et rares. Les photographies 24 à 32 montrent des aspects d'hétérogénéités mises en évidence par microscopie électronique.

Analyses quantitatives. En diffraction X, l'étalonnage a été réalisé par fusion et recristallisation complète de mélanges synthétiques qui avaient la composition des minéraux à analyser. Les mesures comparatives des hauteurs de pics ont été faites en prenant le silicium comme étalon interne. En microscopie optique, les taux de cristaux sont mesurés par comptages de points sur des échantillons enrobés dans de la résine. Les deux méthodes donnent des résultats identiques mais avec des limites de détection différentes. En diffraction X, les limites sont de 1 % à 100 % pour la gehlénite et de 2 % à 100 % pour la merwinite alors que la microscopie optique permet de déceler des traces de cristallisation mais n'est plus précise au-delà de 50 % de cristaux. Dans les laitiers examinés, les taux de cristaux varient entre 0,01 % et 35 % pour une moyenne de 5,5 % et un écart type de 9,0 %. Les taux de merwinite varient dans les mêmes proportions mais 5 laitiers contiennent aussi 0,01 % à 3 % de mélilite.

1.3 - Essais mécaniques

Pour les essais à la soude, les laitiers sont broyés à refus constant de 10 % au tamis de 40 µm, mélangés avec 3 parties de sable ISO, gâchés à S/L = 0,5, S est une solution qui contient 200 g de soude et 1 litre d'eau. Les éprouvettes 4 x 4 x 16 cm sont conservées en armoire humide. Les essais en compression sont ef-

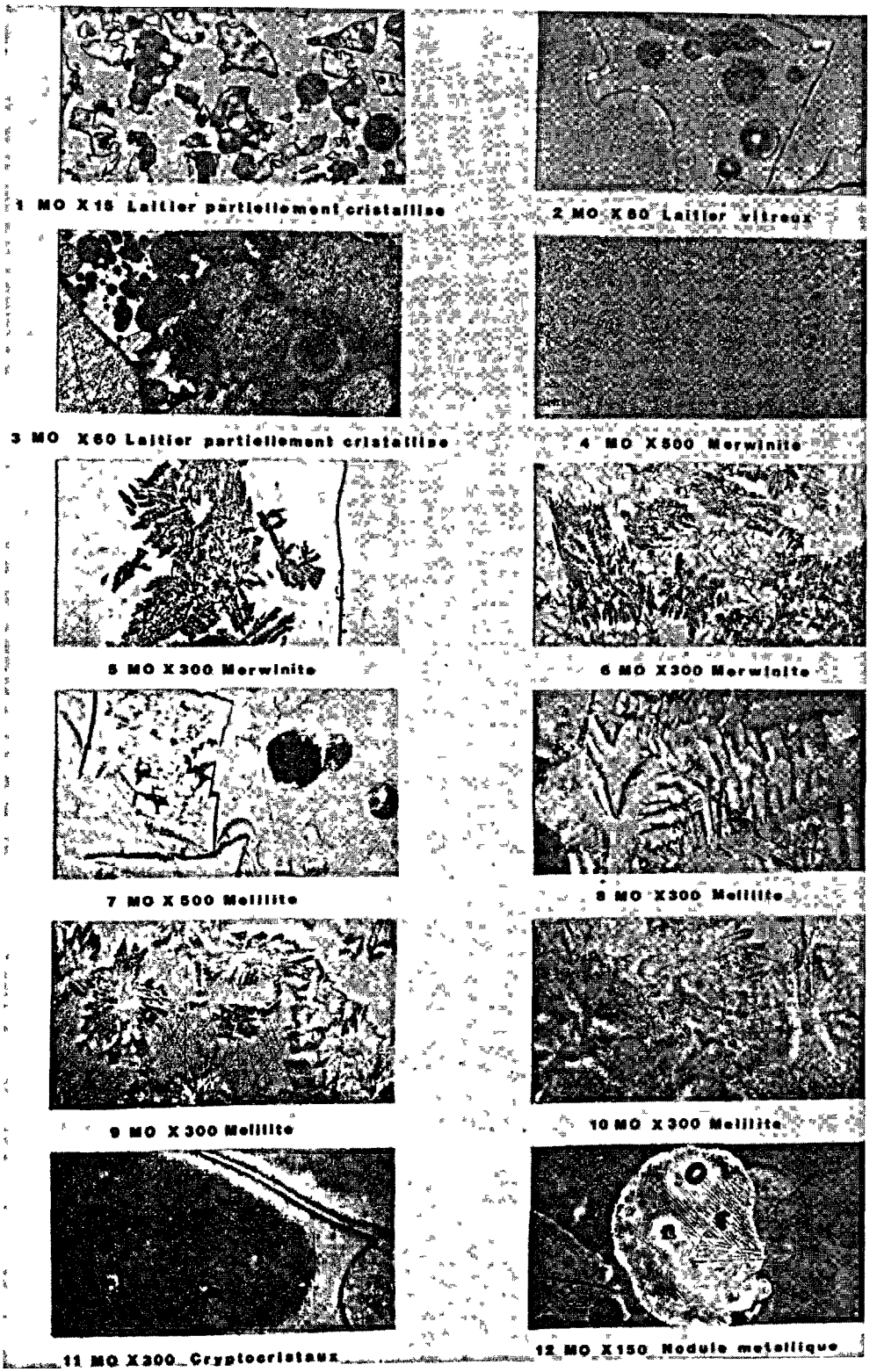

1 MO X 15 Laitier partiellement cristallise

2 MO X 80 Laitier vitreux

3 MO X 60 Laitier partiellement cristallise

4 MO X 500 Merwinite

5 MO X 300 Merwinite

6 MO X 300 Merwinite

7 MO X 500 Melilite

8 MO X 300 Melilite

9 MO X 300 Melilite

10 MO X 300 Melilite

11 MO X 300 Cryptocristaux

12 MO X 150 Nodule metallique

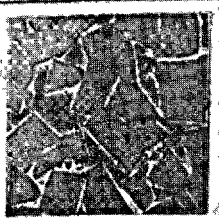

13:1.Melilite ; 2. Verre

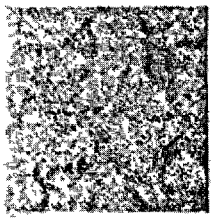

14 - Image X: Al

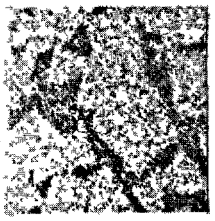

15 Image X : Mg

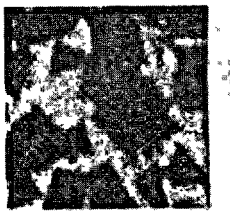

16 Image X : S

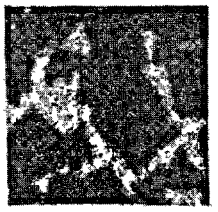

17 Image X : K

13,14,15,16,17 : MEC X 350

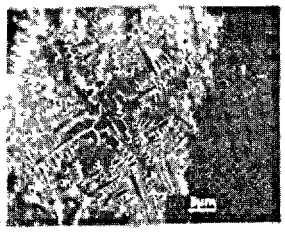

18 MEB X 1200 1.Verre ; 2.Melilite

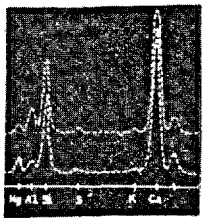

19 Spectres

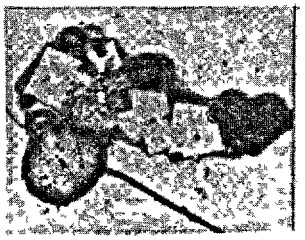

20 MO X175 1.Melilite ; 2.Merwinite;3.Verre

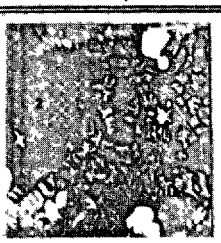

21,22,23:MEC X 350

21: 1. Merwinite ; 2. Verre

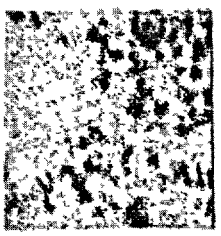

22 Image X : Al

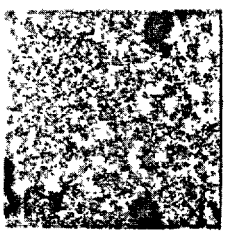

23 Image X : Mg

24 MEB X 350 1.Verre ; 2. Phase riche en MgO et Al_2O_3 ; 3. Phase riche en TiO_2

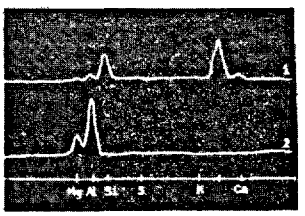

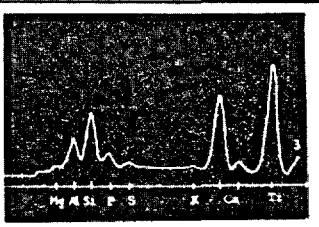

25, 26 : Spectres en dispersion d'energie

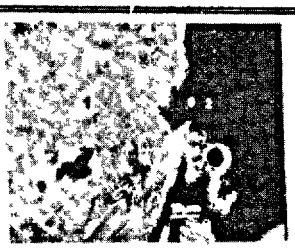

27 MEB X 350 1.Melilite ; 2.Verre

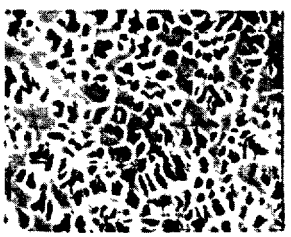

28 MEB X 3500 Detail de la photo 27

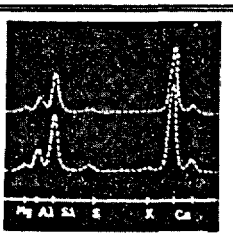

29 Spectres

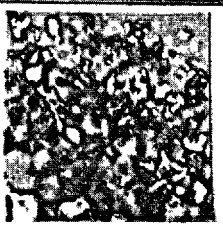

30,31,32:MEC X 350

30 Sulfures de fer(noirs);Melilite;Merwinite

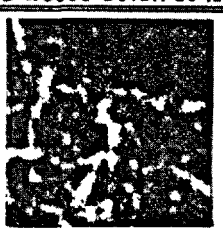

31 Image X : Fe

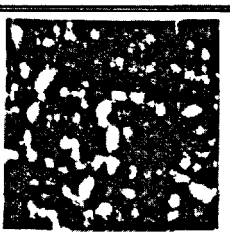

32 Image X : S

MO: Microscope optique ; MEB: Mic. electronique a balayage; MEC: Microsonde electronique de Castaing

fectués après 6 h et 24 h de durcissement. Pour les laitiers étudiés, les résistances varient de 2,7 à 8,4 MPa à 6 h et de 6,3 à 14,4 MPa à 24 h avec des écarts types respectifs de 1,5 et 3,0 MPa.

Pour les essais en mortier ISO, les laitiers sont mélangés avec du clinker et du gypse dans les proportions : 76 % de laitier, 19 % de clinker, 5 % de gypse. Pour ces essais, nous utilisons toujours le même clinker et le même gypse et les mélanges sont broyés à refus de 10 % au tamis de 40 µm. Pour les laitiers étudiés, les résistances varient de 3,0 à 13,2 MPa à 2 jours ; 17,3 à 32,4 MPa à 7 jours ; 31,7 à 49,1 MPa à 28 jours avec des écarts types respectifs de 1,8 ; 2,9 ; 2,9 MPa. Les étendues et les écarts types sont suffisamment importants pour que les corrélations calculées ultérieurement soient généralisables pour les types de laitiers étudiés.

2/ CORRELATIONS SIMPLES

2.1 - Indices d'activité et résistances mécaniques

Les indices d'activité proposés par les chercheurs peuvent être classés en trois groupes. Le premier tient seulement compte des éléments majeurs et place l'alumine soit au numérateur, soit au dénominateur. Le second tient aussi compte des éléments majeurs mais donne un rôle amphotère à l'alumine comme formateur ou modificateur de réseau avec des coefficients variables pour les deux rôles. Le troisième tient aussi compte de certains éléments mineurs.

Pour les laitiers étudiés, 15 indices ont été calculés et corrélés avec les résistances en compression des mortiers ISO (tableau II). Les meilleurs indices sont: $(C + M + A/S) - (20 + C + A + 0,5\,M - 2\,S) - (C + 0,56\,A + 1,4\,M/S) - (C + M + 0,66\,A/S + 0,33\,A)$, viennent ensuite le C/S des sidérurgistes qui est mis en relation avec d'autres caractéristiques que l'activité hydraulique (5) (6) et l'indice $C + A + 0,5\,M + Ca\ S/S + Mn$. Cette classification est en bon accord avec les résultats de différentes recherches.

Nous constatons que les relations qui accordent trop d'importance au rôle formateur de réseau de l'alumine sont les plus mauvaises.

Tableau II : Corrélations simples

Relation	Coefficients		
	R 2 j	R 7 j	R 28 j
S/A	0,76	0,65	0,75
C/S	0,85	0,78	0,80
C/A	0,56	0,43	0,58
(C + M)/S	0,82	0,79	0,72
(C + M + A)/S	0,91	0,82	0,84
(C + 0,56 A + 1,4 M)/S	0,85	0,81	0,77
20 + C + A + 0,5 M - 2 S	0,88	0,79	0,83
(C + M)/(S + A)	0,09	0,09	0,07
(C + A - 10)/(S + 10)	0,82	0,72	0,78
(C + M + 0,33 A)/(S + 0,66 A)	0,37	0,40	0,20
(C + M + 0,66 A)/(S + 0,33 A)	0,86	0,81	0,76
S/(A + F + T + Mn)	0,57	0,50	0,60
(C + A + 0,5 M + Ca S)/(S + Mn)	0,85	0,77	0,80
(C + A + 0,5 M)/(S + FeO + MnO)	0,79	0,69	0,73
$\frac{C + A - 10 + CaS + Na_2O + K_2O}{S + 10 + M + MnO}$	0,72	0,63	0,72

2.2 - Activations à la soude et au clinker

Les essais à la soude donnent de meilleurs corrélations à 6 h qu'à 24 h. A 6 h, tout en restant significatives aux trois périodes, la corrélation est meilleure à 2 jours (r2 = 0,73 - r7 = 0,53 - r28 = 0,59).

A 24 h, seule la corrélation à 2 jours est significative au seuil de 0,05 (r2 = 0,55 - r7 = 0,39 - r28 = 0,39).

2.3 - Relations entre essais mécaniques et taux de cristallisation des laitiers

Le graphique de la figure 33 montre que les relations entre résistances en compression et taux de cristaux des laitiers d'une même provenance ne sont pas linéaires. Les pentes des courbes sont positives entre 0 % et 5 % et négatives entre 5 % et 35 % de cristaux. Les pentes sont d'autant plus négatives que les temps de durcissement sont plus longs.

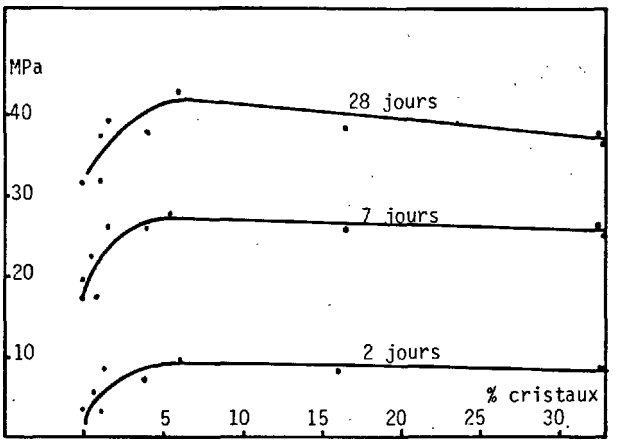

Fig. 33 : Influence du taux de cristaux dans les laitiers

Pour les laitiers qui contiennent 5 à 35 % de cristaux, les baisses de résistances ne sont pas proportionnelles aux taux de cristallisation : dans ce domaine, les courbes peuvent être assimilées à des droites et leurs pentes sont nettement inférieures à l'unité. Les pentes nettement inférieures à 1 pour ces laitiers peuvent être expliquées par des compositions chimiques des verres différentes des compositions chimiques moyennes des laitiers. L'exemple donné sur le tableau III pour un laitier qui contient 35 % de merwinite montre ces différences : le verre est enrichi en alumine et en éléments mineurs. Les photographies 16-17-22-23 confirment ces différences. Les corrélations simples ou multiples confirment aussi que la composition moyenne du verre est plus réactive que la composition moyenne du laitier.

Tableau III : Composition du laitier et du verre qu'il contient

	SiO_2	Al_2O_3	FeO	MnO	TiO_2	CaO
Laitier	33,6	11,1	0,89	0,64	0,55	42,1
Verre	32,0	17,0	1,37	0,98	0,85	37,2
	MgO	Na_2O	K_2O	S^{--}	F^-	Cl^-
Laitier	8,7	0,38	0,81	1,10	0,09	0,044
Verre	6,7	0,58	1,25	1,69	0,14	0,068

Les performances accrues des laitiers qui cristallisent jusqu'à 5 % de merwinite ne sont pas expliquées. En microscopie optique, nous observons des attaques préférentielles par les acides suivant une multitude de lignes qui s'élargissent par des attaques plus prononcées. Ces attaques préférentielles mettent en évidence des hétérogénéités submicroscopiques qui peuvent être dues à des germes de cristallisation, à des compositions chimiques différentes, à des tensions internes plus élevées dans les verres qui contiennent des cristaux ...

3/ CORRELATIONS MULTIPLES

Les indices de réactivité donnés par les chercheurs négligent partiellement ou totalement l'influence des éléments mineurs qui entrent dans la composition des laitiers industriels. Nous avons calculé plusieurs séries de corrélations multiples linéaires qui tiennent compte de l'analyse chimique complète des laitiers, des variations dans le temps de l'influence des différents éléments, des compositions potentielles, des pourcentages de verre, des résistances en mortiers ISO. Les corrélations multiples qui donnent les coefficients r les plus élevés sont celles qui prennent en compte les compositions chimiques complètes et les pourcentages de verre.

Tableau IV : Calculs prévisionnels de résistances

Variables	Coefficients		
	2 jours	7 jours	28 jours
Perte au feu	- 0,646	- 2,450	+ 0,029
SiO_2	- 1,401	- 1,766	- 3,392
Al_2O_3	+ 0,158	- 0,578	- 1,479
FeO	- 0,233	- 0,320	- 1,011
TiO_2	- 10,40	- 25,58	- 16,53
MnO	- 1,206	- 3,308	+ 3,005
CaO	+ 0,117	+ 0,242	- 0,059
MgO	+ 0,375	+ 0,857	+ 0,243
SO_3	- 1,263	- 1,673	- 1,454
S^{--}	- 3,649	- 0,754	- 0,167
K_2O	+ 3,948	+ 1,120	- 2,294
Na_2O	- 0,500	+ 11,87	+ 9,411
P_2O_5	+ 1,887	+ 12,24	+ 5,632
F^-	+ 0,501	+ 1,739	+ 13,04
Cl^-	+ 62,29	+ 126,7	+ 110,5
Insoluble	- 1,145	- 3,922	- 4,173
% Verre	+ 0,041	+ 0,131	+ 0,279
Constante	+ 48,75	+ 74,17	+ 149,92
r	0,974	0,944	0,934
r2	0,949	0,891	0,872

Ces coefficients r sont respectivement 0,97 - 0,94 - 0,93 à 2, 7, 28 jours. Les meilleures corrélations simples obtenues avec l'indice (C + M + A)/S étaient 0,91 - 0,82 - 0,84 pour les mêmes périodes. Ces différences montrent l'influence importante des éléments mineurs.

Les corrélations multiples mentionnées affectent des coefficients élevés à différents éléments mineurs tels que TiO_2, Na_2O, F^-, Cl^-. Ces corrélations ne sont que des formulations mathématiques, mais elles paraissent tout de même mettre l'accentuation sur l'action de différents éléments. Le rôle du titane comme agent nucléant, le rôle du fluor sur la vitesse de cristallisation, les actions différentes de Na^+ et de K^+ sont connus des verriers (9). L'influence accélératrice du chlorure de sodium est utilisée par les cimentiers.

Dans ces corrélations, le rôle des cristaux n'est pas suffisamment mis en valeur car le nombre d'échantillons de chaque provenance est insuffisant pour en tenir compte autrement qu'en relations linéaires. Ces corrélations seront améliorées ultérieurement lorsque notre étude comprendra un nombre d'échantillons plus important.

CONCLUSIONS

Au cours de cette recherche sur des laitiers de types hématite et lorrain, granulés ou bouletés, nous avons mis en évidence que le procédé de trempe n'était pas un facteur déterminant de leur réactivité. Les facteurs principaux sont la composition chimique compte tenu de tous les éléments mineurs et le taux de cristallinité. La composition chimique qui induit beaucoup d'autres propriétés telles que viscosité, fusibilité, hétérogénéités microscopiques et submicroscopiques donne de ce fait de très fortes corrélations avec les résistances mécaniques des ciments dans lesquels la quantité de laitier est prépondérante.

Pour des laitiers qui dévitrifient principalement de la merwinite au cours de trempes industrielles, nous avons aussi montré qu'une vitrification totale n'est pas souhaitable pour obtenir une réactivité maximale : la présence de 3 à 5 % de cristaux augmente leurs performances. Pour des taux de cristaux supérieurs, leur précipitation enrichit le verre restant en alumine et en éléments mineurs, ceci améliore leur réactivité, d'où en pourcentages, des baisses de résistances nettement inférieures aux taux de cristaux.

REMERCIEMENTS

Les auteurs remercient MM. BERTIN, MAES et le personnel du département ECPM pour les travaux effectués au CEREG, en microscopie, diffraction X et essais physiques et mécaniques.

NOTA

Les analyses au microscope électronique à balayage et à la sonde électronique de Castaing ont été effectuées au CERILH sous la direction de Mme REGOURD par Mme MOINE, M. HORNAIN du CERILH et M. BERTIN du CEREG.

BIBLIOGRAPHIE

1 - L. Von TETMAJER - Ciments de laitiers - Compte-rendu en français dans Nouvelles Annales de la Construction (1886).

2 - CLERET DE LANGAVANT - Considérations théoriques sur la nature du laitier de cimenterie - Tentative de synthèse de nos connaissances actuelles. R.M.C (1949).

3 - L. BLONDIAU - Du contrôle des laitiers granulés utilisés en cimenterie - R.M.C (1951).

4 - F. KEIL - Ciments de laitier - Symp. Intern. Chim. Ciment - Proceedings 530 - 580 - Londres (1952).

5 - J. ROQUEJOFFRE - La valeur hydraulique du laitier d'après l'allure de marche du haut fourneau - R.M.C n° 512 (1958).

6 - M. KUNICKI - Contribution à l'étude physique de l'influence de la composition chimique et des conditions de trempe sur les propriétés hydrauliques des laitiers vitrifiés de haut fourneau de fonte Thomas - Soutenance de thèse d'ingénieur CNAM (1968).

7 - M. CHERON, C. LARDINOIS - Le rôle de la magnésie et de l'alumine dans les propriétés hydrauliques des laitiers granulés de haut fourneau - 5ème Symp. Intern. Chim. Ciment - Tokyo (1968).

8 - H. - G. SMOLCZYK - Duisburg - Rheinhausen - L'influence de la chimie du laitier sur les résistances des ciments de haut fourneau - Zement Kalk Gips n° 6 (1978).

9 - M. SCHOLZE - Le verre - Nature, Structure et Propriétés - Traduit par J. le DU - Institut du Verre - Paris (1974).

The hydration of blast furnace slag cement

L'hydratation du ciment de laitier de haut fourneau

Y. TOTANI, Y. SAITO, M. KAGEYAMA and H. TANAKA, Japon.

RESUME : Pour étudier l'activité de divers laitiers granulés, sous-produits de l'industrie métallurgique, on a mesuré, à l'aide d'un calorimètre à conduction, le dégagement de chaleur, lors de leur hydratation, de ciments de laitier fabriqués avec ces laitiers. Il existe de grandes différences entre le mode de dégagement de chaleur des ciments portland et des ciments de laitier; la teneur en laitier et la nature de celui-ci ont une grande influence sur ce dégagement de chaleur.

On a observé, en essayant trois sortes de laitiers industriels, que malgré des basicités et des teneurs en verre très voisines, les dégagements de chaleur pouvaient être très différents

Pour les ciments à faible teneur en laitier, le dégagement de chaleur cumulé est plus faible, initialement, que celui du ciment Portland de même clinker, mais peut être bien plus élevé en fin d'hydratation. Si le dégagement de chaleur du ciment Portland est bien ralenti, dans la deuxième partie de l'hydratation, il n'en est pas de même du ciment de laitier.

Les phénomènes observés peuvent s'expliquer ainsi :

1. Dans l'hydratation du ciment de laitier, une partie inconnue du dégagement de chaleur provient de l'hydratation du laitier lui-même.
2. Puisque le laitier granulé absorbe le $Ca(OH)_2$ dégagé par l'hydratation du clinker, l'hydratation du laitier est accélérée par la baisse de concentration, qui en résulte, de $Ca(OH)_2$ dans la phase aqueuse.
3. Pour un même clinker du ciment de laitier, puisque le rapport E/C doit augmenter avec la proportion de laitier, il doit en résulter une augmentation plus importante de la chaleur dégagée.

SUMMARY :To study the activity of slag on the hydration of slag cement with granulated blast-furnace slag by-produced from iron and steel industry, the heat liberation process was measured by conduction calorimeter.

There are essentially large differences between the heat liberation process on the hydration of slag cement and that of portland cement; the content and the kind of slag affect considerably on the difference.
Moreover, it was revealed that, in spite that there aren't appreciable difference in the basicity and the glass content of three kinds of industrial slag used, their undetectable properties give a large effect on the heat liberation process of each slag cement.

The accumulated heat liberation of the slag cement with relatively lower content of slag is slightly less than that of original portland cement during early stage, however in later stage, exceeds. Because, though the rate of heat liberation of original portland cement considerably slow down after middle stage, that of the slag cement doesn't so much.

The abovementioned phenomena would be explained as follows;
1) In the hydration of slag cement, an ignorable portion of the heat liberation is occupied by that of hydration reaction of the slag itself.
2) Since the granulated slag acts as a consumer for $Ca(OH)_2$ which is liberated from portland cement during the hydration, the hydration of clinker portion in the slag cement is accelerated by lowering $Ca(OH)_2$ concentration in the aqueous phase.
3) Referred to the clinker portion in slag cement, since the w/c-value increases as the slag content increases, the heat liberation becomes propotionally larger.

INTRODUCTION

The hydration of slag cement is depended largely on the hydration property of clinker and the hydration activity, finess, content of slag, etc.

Alégrel) showed that the heat of hydration of slag cement linearly decreases as the content of slag increases. On the other hand, Schröder2) reported that the linear relation between the heat of hydration and the content of slag is not always existed, but the heat of hydration of the slag cement with less content of slag is essentially analogous to that of portland cement and that of the slag cement decreases as the slag content increases.

In many studies, it has been considered that the heat of hydration of slag cement is mainly originated from the hydration of clinker portion.

The authors, in present paper, have shown that the heat of hydration of slag cement is consisted of those of clinker and slag portion, respectively, and beside complex interaction exists between both portions in the hydration.

EXPERIMENTAL (Materials and Methods)

Three kinds of industrial granulated blast-furnace slag and a comercial portland cement were used. The chemical composition, the basidity and the glass content of the materials used are shown in Table 1. The three slags have similar basidity and glass content and in any of them the existence of crystalline materials is not detected by XRD. After they were pulberized with gypsum (SO_3 2%) to Blaine 4000 + 50 cm^2/g, mixed with portland cement in definite proportions (slag content 30, 60 and 80%).

Table 1. The chemical composition, basidity and glass content of industrial slag and portland cement.

	Ig.Loss	SiO_2	Al_2O_3	Fe_2O_3	CaO	MgO	SO_3	Na_2O	K_2O	MnO	S	$\frac{CaO+MgO+Al_2O_3}{SiO_2}$	glass cont. %
slag A	0.1	33.8	15.6	0.5	42.9	5.7	—	0.2	0.5	0.5	0.8	1.89	96
slag B	-0.2	34.2	15.3	0.6	43.6	4.8	—	0.3	0.5	0.6	1.1	1.86	98
slag C	-0.4	34.8	15.6	0.5	41.9	5.7	—	0.2	0.3	0.5	0.9	1.82	97
portland cement	0.8	21.6	5.5	3.2	63.7	1.5	2.2	0.5	0.9	—	—	—	—

In measurement of heat of hydration of slag, powdered $Ca(OH)_2$ is used as an activator and for examining the effect of w/c, reagent grade powdered ZrO_2 is used in stead of slag .

A conduction calorimeter with six cells is used for measuring the heat of hydration and each slag cement sample is mixed with water outside the calorimeter, then put into the calorimeter. Therefore, the exact recording of heat liberation is not taken place for one hour after the water added.

The heat liberation for this one hour is corrected by data gotten by other method.

RESULTS AND DISCUSSIONS

The heat of hydration of the slag cement

Fig. 1, 2 and 3 shows the heat of hydration of the slag cement with each of three slags (A , B and C) at 30C.

The heat of hydration of slag cement with 30% and 60% slag A contents and 30% slag B content are slightly less than that of only portland cement in early stage, however exceed in later stage.

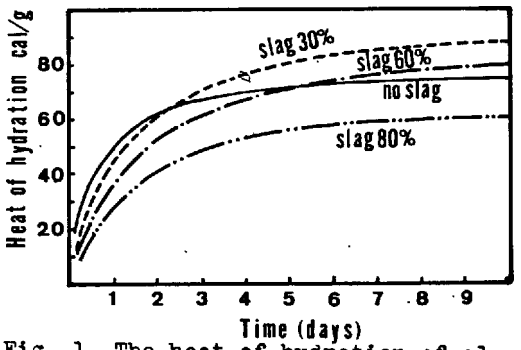

Fig. 1 The heat of hydration of slag cement with slag A at 30C. w/c = 0.5 cement paste.

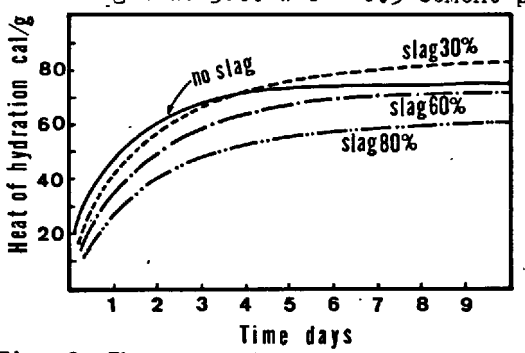

Fig. 2 The heat of hydration of slag cement with slag B at 30C. w/c = 0.5 cement paste.

On the contrary, the heat of hydration of the slag cement with slag C decreases linearly as the content of slag increases.

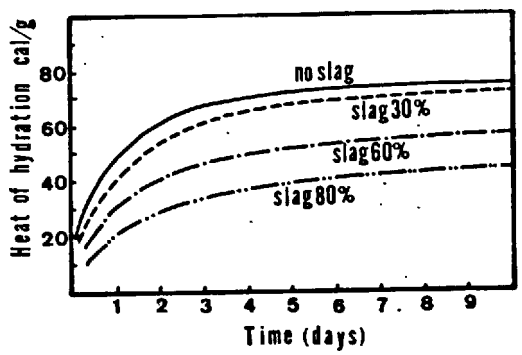

Fig. 3 The heat of hydration of slag cement with slag C at 30C. w/c = 0.5 cement paste.

From above-mentioned, it is apparent that, although there aren't detectable differences among each basidity and glass content of three slag A , B and C, there are unignorble differences among the hydration heat of slag cement with each of them, which hydrate at same temperature.

The heat of hydration of slag in presence of $Ca(OH)_2$

As shown in Fig.4, the hydration tendency of slag A, B and C is similar to that of slag cement and their activities in the hydration would be in order of A B C.

There is a large difference in the heat of hydration between slag A and B and slag C; in the former about 40 cal/g after 7 days, in the later about 25 cal/g.

The heat which is liberated from the slag-H_2O system in the presence of $Ca(OH)_2$ added as an activator can be regarded as the heat of hydration originated from slag predominantly.

Since it is possible to consider that the slag in slag cement hydrates also by activation of $Ca(OH)_2$ produced from the hydration of clinker portion, the portion occupied by the hydration of slag in the hydration heat of slag cement is so large that it could hardly ignore.

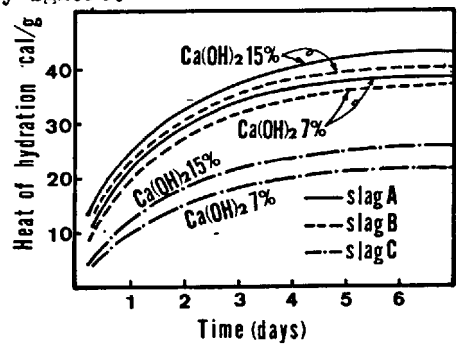

Fig. 4 The heat of hydration of slag in presence of $Ca(OH)_2$ at 30C. w/(slag + $Ca(OH)_2$) = 0.5.

The hydration heat of slag increases as the added $Ca(OH)_2$ increases.

Furthermore, it was revealed that the hydration heat of slag linearly increases in less addition of $Ca(OH)_2$ than 7% and also gradually in the addition from 7% to 15%.

The heat of hydration of portland cement with ZrO_2 in stead of slag

It has been estimated that referring to clinker portion of slag cement, the W/C-value increases than that of slag cement as the content of slag increases, because the hydration of slag would be generally slower than that of clinker.

To check the effect of W/C to the hydration of clinker portion, the heat of hydration of portland cement with various content of powdered ZrO_2 was meaured (ZrO_2 content 30 , 60 and 80%).

The powdered ZrO_2 was used for examining the effect of only the W/C-value, because it doesn't has any inter-reaction to clinker.

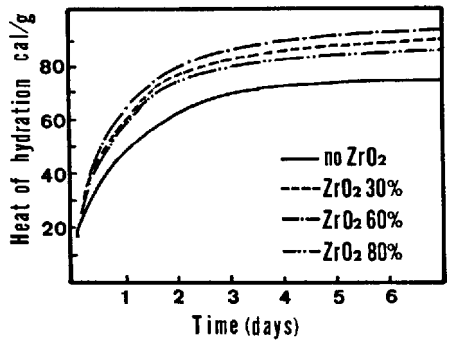

Fig. 5 The heat of hydration of portland cement with and without ZrO_2 at 30C. w/(portland cement ZrO_2) = 0.5.

The heat of hydration shown in Fig.5 isgiven as per gram of portland cement, not per portland cement which mixed ZrO_2. The heat of hydration of clinker portion was larger, though being irregular relation, in all the portland cement mixed with ZrO_2 than that of portland cement without ZrO_2.

It can be suggested that the W/C effect as shown in Fig.5 exists also in the hydration of slag cement. However, it is not apparent how much the W/C effect would be realized in the hydration of slag cement, because there is a great difference in the activity between ZrO_2 and slag.

The rate of hydration of alite and slag

The rate of hydration of slag and alite in the slag cement with slag B were estimated from the heat of crystallization by means of DTA in the former and the pattern of XRD in the latter. As shown Fig.6, the hydration of alite in the slag cement is faster than that of alite of portland cement without slag, as the content of slag increases.

In the slag cement, the acceleration of alite hydration would be caused by lowering $Ca(OH)_2$ concentration in the aqueous solution phase, which is also attributed to consumption of $Ca(OH)_2$ liberated from the clinker portion by pozzolanic reaction with slag.

It should seem that the w/c-effect abovementioned also plays the role of the acceleration of alite hydration.

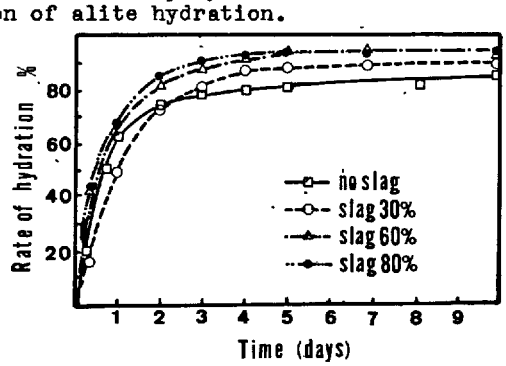

Fig. 6 The rate of hydration of alite in the slag cement at 30C.w/c = 0.5 cement paste.

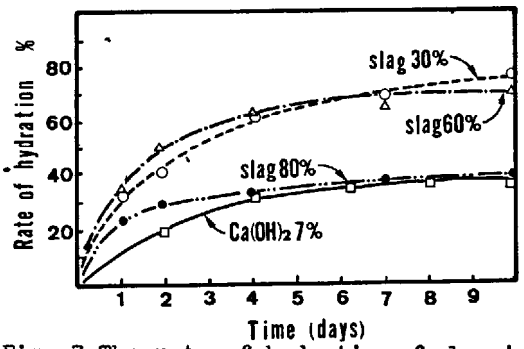

Fig. 7 The rate of hydration of slag in the slag cement at 30°C. w/c = 0.5 cement paste.

On the other hand, the rates of slag hydration in the slag cement with 30% and 60% slag B contents are apporoximately same.

Being over 80% slag B content, the rate of slag hydration decreases, because $Ca(OH)_2$ liberated from the clinker portion becomes less and then, consequently, can not accelerate strongly the hydration.

Fig. 7 shows not only the rate of slag hydration in slag cement, but also that of slag hydration in system of slag B-$Ca(OH)_2$-H_2O.

The latter's curve is similar to that of slag cement with 80% slag B.

From these results, it can be suggested that the hydration heat of slag portion of slag cement with slag B 80% is analogous to that of the slag with $Ca(OH)_2$ 7% shown in Fig. 4. It can be approximately calculated, by using the hydration heat of slag portion, that the about 70% of the hydration heat of slag cement with slag B 80% is occupied by that of the slag portion.

Thus, it should be considered that the heat of hydration of slag cement consists of that of the clinker portion and the slag portion, respectively.

The interesting fact obtained from present work is that the slag cement with the slag which has a high activity often shows larger heat of hydration than that of portland cement in later stage.

The slag cement with slag B 30% has larger hydration heat than portland cement, because the rate of hydration of the slag portion is larger and the hydration of the clinker portion is accelerated by the presence of slag.

On the other hand, the slag cement with slag C which has lower hydration heat doesn't show larger hydration heat than portland cement.

CONCLUSION

The results obtained as follows;

1) The studies on the hydration heat of slag portion, the W/C-effect and the rate of hydration of slag portion and alite phase of clinker portion in the hydration of slag cement show that the slag cement with the slag which has a high activity often shows larger heat of hydration than portland cement.

2) In spite that there aren't appreciable differences in the basidity and the glass content of three kinds of industrial slag used, the heat liberation processes of the slag cement show that there are large differences among their hydration activities.

The authors, at present time, suggest that the difference is hardly revealed by the present conventional method for defining the hydration activity of slag. Speaking additionally, the definition of glassy state of slag paticle would be impossible by the conventional method with optical microscope.

Because the glassy state from the melt to the crystalline widely spreads. Besides, the difference in the glassy state effects largely the hydration activity.

Therefore, in order to know the exact characteristics of the hydration of the slag cement, include the definition of glassy state should be established.

References

1) R.Alégre, (1961) Rev.Mater.Constr. 544-549
2) F.Schröder,(1968)"Slag and Slag Cement" Pro. of the 5th Inter. Symp. on the chemistry of cement. Tokyo. 180

Hydrated phases in slag-water-activator systems

Phases hydratées dans les systèmes laitier-eau-activateur

I. TEOREANU, Professor Dr.Doc., Polytechnical Institute Bucarest,
M. GEORGESCU, Lecturer Dr., Polytechnical Institute Bucarest,
A. PURI, Lecturer, Polytechnical Institute Bucarest, Roumanie.

RESUME: Les processus de durcissement et la nature des phases hydratées formées dans les systèmes laitier-activateur-eau sont influencés par beaucoup de facteurs, parmi lesquels les plus importants sont: la nature du laitier et de l'activateur, leurs proportions relatives et les conditions de durcissement.

Cette ouvrage est une analyse de la nature des phases hydratées formées pendant le durcissement des systèmes laitier-chaux-gypse-eau et laitier-chaux-silicate de sodium - eau, dans conditions normales et par traitement à la vapeur, à 60° et 95°C.

L'analyse thermique differentielle, la diffractometrie et la microsocpie électronique nous ont montré que dans les systèmes mentionés, les plus importantes phases hydratées sont des hydrosilicates de calcium de type tobermoritique; auprès d'eux sont decelés, dans certaines conditions, l'ettringite (pour les systèmes que contiennent du gypse) et des hydrosilicates où le Ca^{2+} est partiellement remplacé par le Na^{+} (pour les systèmes activées à $Na_2O.nSiO_2$).

SUMMARY: The hardening processes and the nature of the hydrated phases formed in slag-water-activator systems are influenced by some factors, as: the nature of the slag and of the activator, the relative amounts of these substances in the system, and the conditions under wich the hardening process take place.

The present work deals with a study of the hydrated phases formed in the hardening process of the slag-lime-gypsum-water and slag-lime-sodium silicate-water systems, under normal conditions and steam-cured at 60° and 95°C, respectively.

The DTA curves and the results of the diffractometry and electronic microscopy (EM) analysis revealed that in the above mentioned systems, the main hydrated phases are tobermorite-type calcium hydrosilicates, there are also noted, under certain conditions, hydrated gehlenite, ettringite (in the case of the systems containing gypsum) and hydrosilicates in wich Ca^{2+} is partly replaced by Na^{+} (in the case of the systems activated by $Na_2O.nSiO_2$).

An increased use of slags as binders requires a deeper investigation of their behaviour in the hardening processes, especially in complex systems, as, e.g., slag-water-activator. This investigation is primarily aimed at discovering new means for the decrease of the amount of portland cement clinker in hydraulic binders exhibiting satisfactory qualities.

EXPERIMENTAL

In order to get informations concerning the nature of the new hydrated phases, two classes of systems were examined: slag-lime-gypsum-water and slag-lime-sodium silicate-water. The characteristics of the used slags are given in table I. Considering the main oxidic components, the slags belong to the $CS-C_3S_2$-mellilite subsystem.

TABLE I

Type of slag	CaO	SiO_2	Al_2O_3	MgO	Fe_2O_3	Mn_3O_4	TiO_2	R_2O	sulfides	loss on ignition
Galaţi, type G	43,49	34,31	8,48	5,2o	o,6o	o,61	o,24	o,88	1,45	o,39
Hunedoara, type H	44,25	38,o3	7,24	5,39	o,5o	1,12	o,26	1,o6	1,23	o,15

The X-ray analysis of the slags (figure 1) shows a nonequilibrium composition, as expected, and a low degree of crystallisation. The crystalline phases identified are the high-temperature forms of the dicalciumsilicate (interferences at 2,7o-2,74 Å, 2,21 Å, 2,o3 Å), merwinite (2,65-2,66 Å, 2,86 Å, 2,7o-2,74 Å, 2,25-2,28 Å, 2,17 Å, 1,91-1,92 Å) and mellilite (2,86 Å, 2,o3 Å, 2,5o Å, 1,91-1,92 Å).

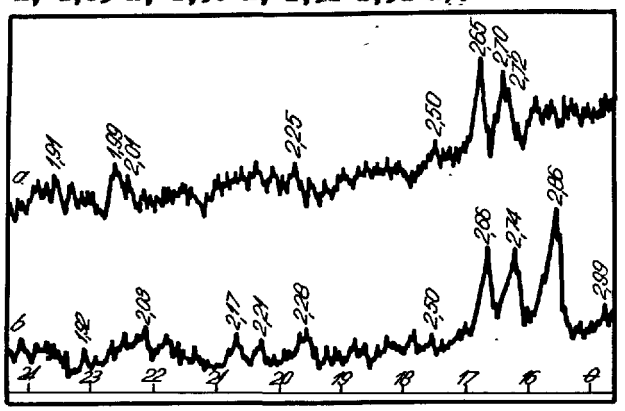

Fig.1 - X-ray patterns of the anhydrous slags:
a - G-type slag; b - H-type slag.

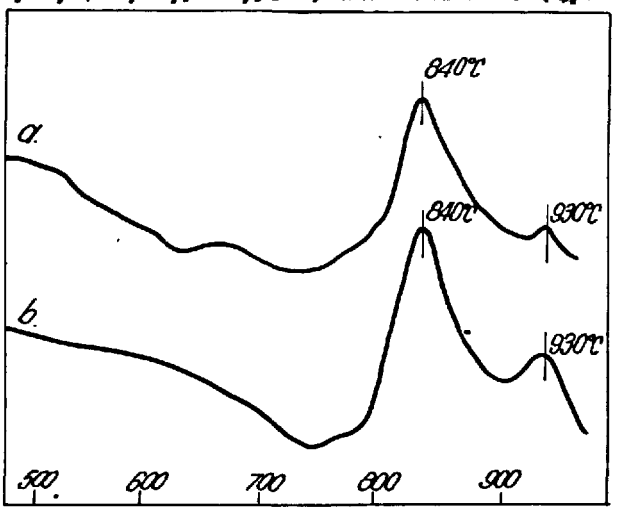

Fig.2 - DTA curves of the anhydrous slags:
a - G-type slag; b - H-type slag.

The DTA curves show specific crystallization effects (1), thus indicating the presence of a mellilite-type solid solution, mainly gehlenitic (effects at 930°C, in figure 2) and of a vitreous component, containing mainly calcium metasilicate (effects at 840°C).

The active CaO amount in the lime used was of 90-94 wt% and the $CaSO_4.2H_2O$ amount in gypsum was of 98 wt%. There were used two types of sodium silicate ($Na_2O.nSiO_2$), namely n=1,5 - type L and n=2,6 - type C.

The water/binder ratio of the investigated pastes was 0,4.

HYDRATED PHASES IN SLAG-LIME-GYPSUM-WATER SYSTEMS

There were investigated masses with slag/lime ratios of 90/10 and 95/5, respectively, and containing 3-5 wt% gypsum, hardened in a water-saturated atmosphere, working both at ambient (20-22°C) and higher (90-95°C) temperatures.

The diffraction patterns in figure 3 show that in slag-lime-gypsum-water systems, hardened under normal conditions, the main products are calcium silicates of the tobermorite type (interferences at 3-3,o4 Å, 2,9-2,98 Å, 2,83-2,87 Å, 3,33-3,38 Å, 3,7o-3,78 Å). The low intensity of the characteristic peaks, mainly for samples hardened for 7 days only, indicates a relatively weak hydration of the slags and a low degree of crystallinity of the resulting compounds. The increase in the intensity of the X-ray peaks after 28 days of hardening signifies a more complete hydration and a higher degree of crystallinity of the formed hydrosilicates. The progress in the hydration degree is also pointed out by the DTA curves given in figure 4. There are noted an increase on the endothermal peak at 140-150°C (prior to the measurement the samples were dried at 110°C), corresponding to the decomposition of the calcium hydrosilicates, and a lowering of the free $Ca(OH)_2$ amount in the system because it is bound by hydrocompounds (the endothermal peaks at 480°C consecvently decrease).

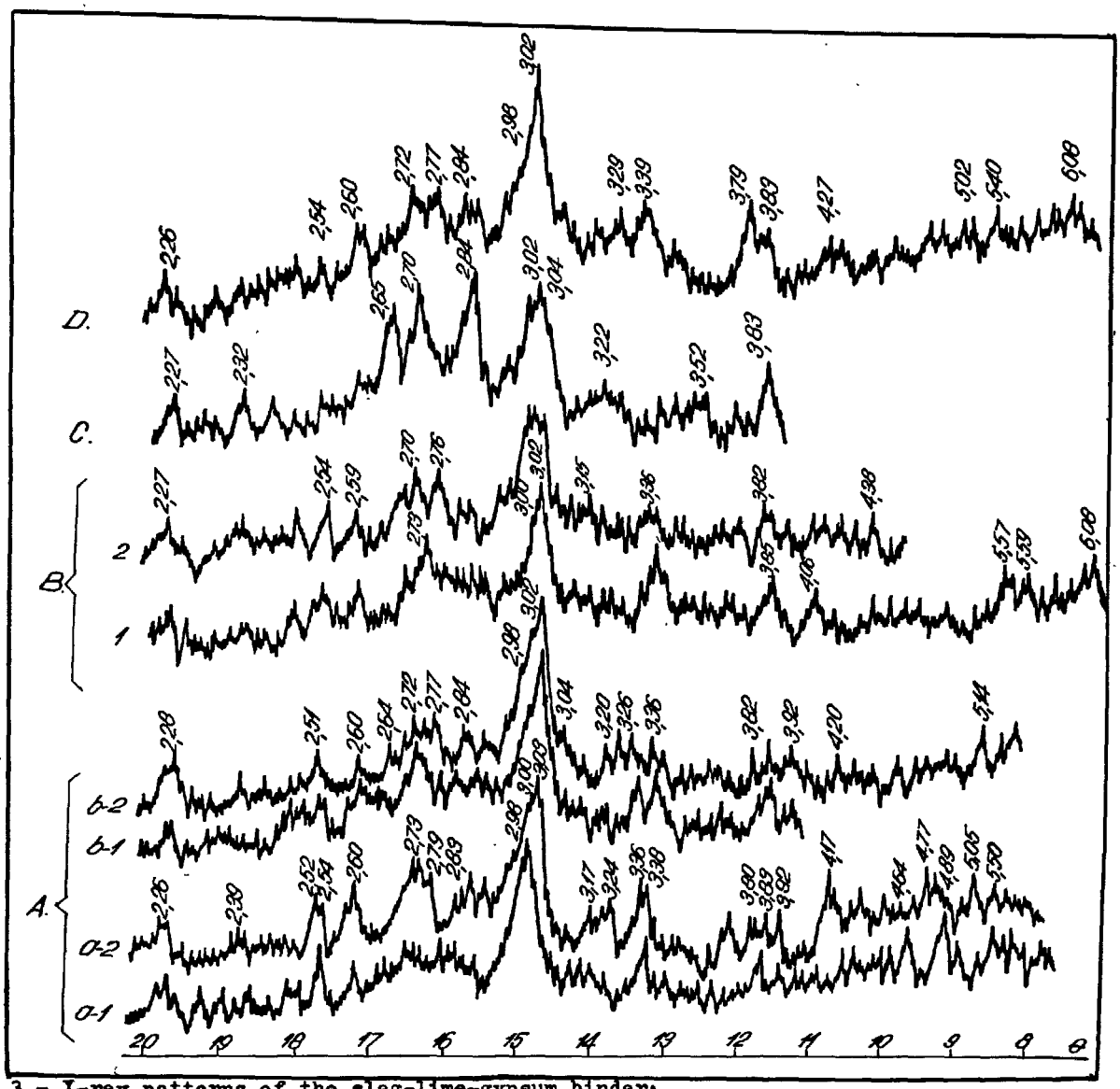

Fig.3 - X-ray patterns of the slag-lime-gypsum binder:
A - G-type slag/lime ratio = 90/10, hardened under normal conditions; B - G-type slag/lime ratio = 95/5, hardened under normal conditions; C - H-type slag/lime ratio = 90/10, 3 wt% gypsum, hardened for 28 days under normal conditions; D - G-type slag/lime ratio = 90/10, 5 wt% gypsum, steam-cured at 95°C for 8 hours;
a - 5 wt% gypsum; b - 3 wt% gypsum; 1 - hardened for 7 days; 2 - hardened for 28 days.

The presence of ettringite is noted by the X-ray interferences at 5,4-5,5 Å, 3,83-3,89 Å, 2,54 Å, 3,24-3,29 Å, even after 7 days of hardening. On the thermal analysis curves, the presence of ettringite is mainly seen on the DTG curves, wich show overlapped weight losses up to 300°C, resulting from the decomposition of some hydrocompounds; in the 160-270°C temperature range, ettringite undergoes a complete dehydration (2-4).

The interferences at 4,17-4,3 Å, 3,o Å, 6-6,o8 Å, 2,59-2,62 Å (figure 3) indicate that, after 7 days of hardening, there might be present a gehlenite hydrate (C_2ASH_8). For longer hardening periods, there is possible that this low-stability compound (5-6) undergoes a gradual transformation into compounds in the hydrogarnets series. This supposition is supported by the X-ray analysis: there are seen interferences specific to hydrogarnets (at 5,o2-5,14 Å, 3,17-3,19 Å); there is noted that the intensity of the interferences at 2,7o-2,78 Å, characteristic both of the dicalcium silicate and of the $C_3A(SH_2)_3$-type hydrogarnets (2) increases, in the case of the samples hardened for 28 days as compared to the anhydrous slag or the systems hardened for 7 days only (figure 3).

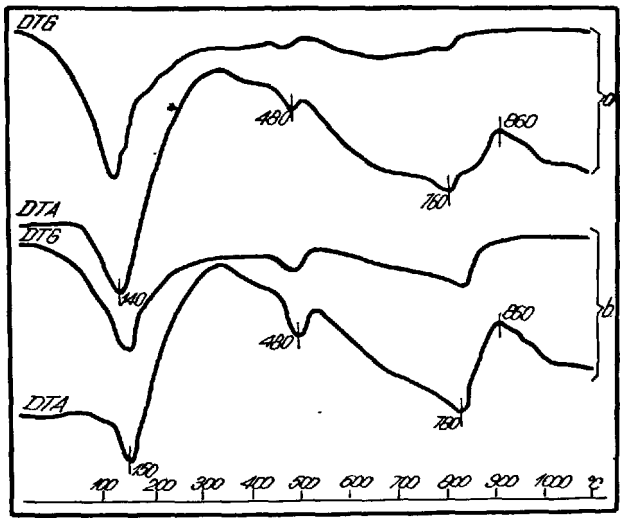

Fig.4 - Thermal analysis of the binder with a G-type slag/lime ratio of 90/10, gypsum 5 wt%, hardened under normal conditions:
a - after 7 days; b - after 28 days.

The increase in the amount of lime in the composition of the studied binders determines an intensification of the hydration processes, rendered visible by the somewhat greater intensity of the X-ray peaks characteristic to the hydrocompounds. The increase in the gypsum amount from 3 wt% to 5 wt% exerts no influence on the nature of the hydrated phases; the only effect recorded was a somewhat greater intensity of the interferences of ettringite in 5 wt% gypsum samples (figure 3).

During the hardening process of the slag-lime-gypsum-water samples steam-cured at 95°C for 8 hours, there is noted a visible increase in the intensities of the interferences characteristic to the hydration products, their nature remaining unchanged (figure 3). The greater intensity of the interferences signifies that the hydration -hydrolysis processes and the crystallization of the hydrated products are more intense. This is confirmed by the values of the mechanical properties of the samples hardened under these conditions.

HYDRATED PHASES IN SLAG - LIME - SODIUM SILICATE - WATER SYSTEMS

The nature of the hydration products in G-type slag-lime-sodium silicate-water systems hardened under normal conditions and steam-cured at 60° and 95°C, respectively, was investigated. The slag/lime ratio in the studied masses was 95/5 and the sodium silicate amount was 8 wt% (calculated as solid material).

The X-ray patterns taken on the masses hardened under normal conditions show interferences characteristic to the anhydrous slag even after 28 days; their intensity decreases gradually, as the hydration proceeds (see interferences at 2,65 Å and 2,71 Å in figure 5). They are suggesting a low participation in the hydration-hydrolysis processes of the crystalline phases in slag: this is supported by the EM images of the hardened masses, wich show the hydrated products and the contours of some crystalline products, namely anhydrous slag (figure 6).

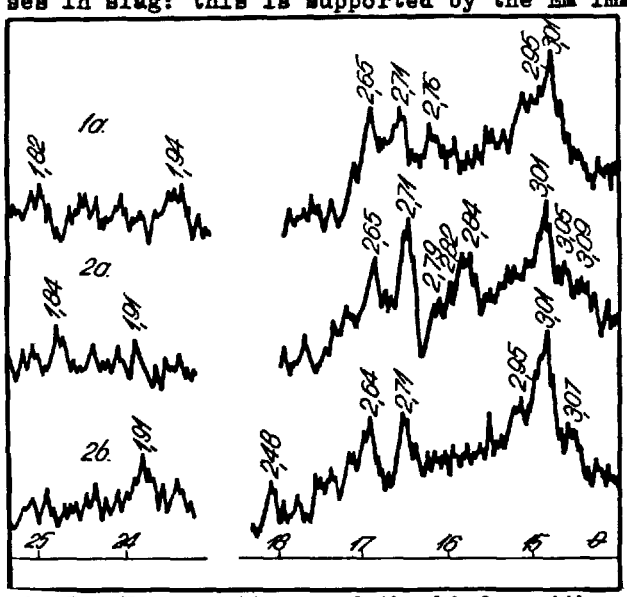

Fig.5 - X-ray patterns of the binder with a G-type slag/lime ratio of 95/5, with 8 wt% sodium silicate, hardened under normal conditions:
a - after 1 day; b - after 28 days;
1 - C-type sodium silicate;
2 - L-type sodium silicate.

Fig.6 - EM pattern (x5000) of the binder with a G-type slag/lime ratio of 95/5, with 8 wt% C-type sodium silicate, hardened under normal conditions for 28 days

The hydration products identified even after keeping the samples for 24 hours in a water-saturated atmosphere, are tobermorite -type calcium hydrosilicates, whose basicity and degree of crystallinity increase as

the modulus of the sodium silicate decreases and the hydration proceeds. Thus, in the mass containing C-type sodium silicate there is identified a tobermorite gel (the interferences at 3,01 Å, 2,76 Å, 1,82 Å) while in the mass with L-type sodium silicate there are found more basic hydrosilicates of the CSH(II)-type (3,09 Å, 2,80 Å, 2,84 Å, 1,84 Å - figure 5).

The EM images of the masses hardened under normal conditions for 28 days and steam-cured (figure 6 and 7) show that the surfaces of the slag grains are corroded because hydration products are formed at the interface, determining a cementation of the slag grains; this process is more advanced in the case of the masses with L-type sodium silicate and of the steam-cured masses.

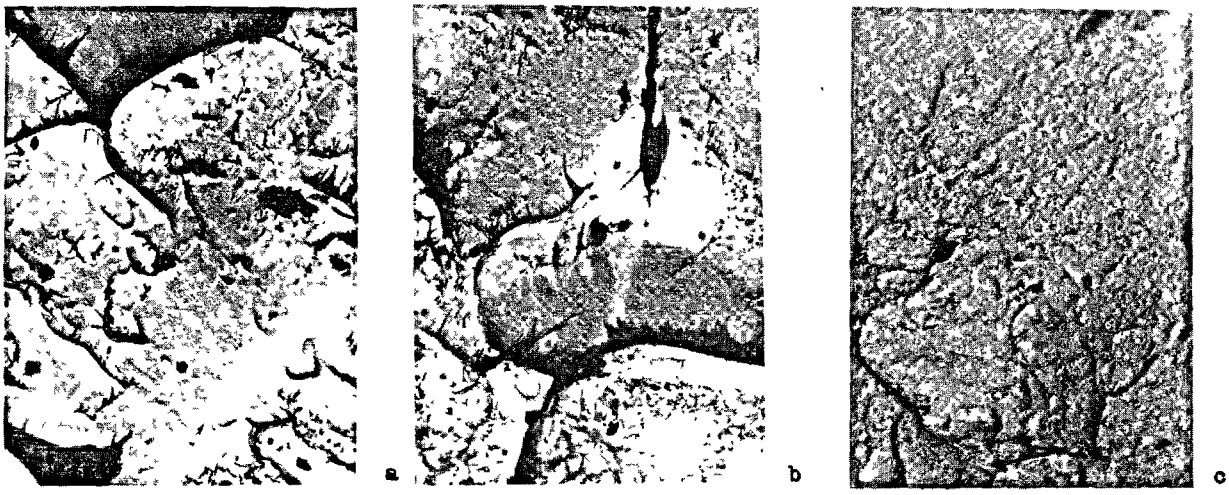

Fig.7 - EM pattern (x5000) of the binder with a G-type slag/lime ratio = 95/5:
a - with 8 wt% L-type sodium silicate, hardened under normal conditions for 28 days;
b - with 8 wt% L-type sodium silicate, steam-cured at 95°C for 6 hours;
c - with 8 wt% C-type sodium silicate, steam-cured at 95°C for 6 hours.

The steam-curing determines a remarkable acceleration of the formation and crystallisation processes of the hydration products. On the X-ray pattern of the sample with C-type sodium silicate, steam-cured at 60°C for 2 hours, the interferences characteristic to the weakly basic calcium hydrosilicates of the CSH(I)-type (3,01 Å, 2,78 Å, 2,40 Å, 2,06 Å, 1,80-1,82 Å) are clearly visible. A longer thermal treatment intensifies the hydration-hydrolysis processes and leads to an increase of the degree of crystallinity of the hydrocompounds, without modifying their nature (see figure 8).

Fig.8 - X-ray patterns of the binder with a G-type slag/lime ratio = 95/5, with 8 wt% C-type sodium silicate, steam-cured at 60°C: a - after 2 hours; b - after 6 hours.

In the masses with L-type sodium silicate, steam-cured at 60°C, there are formed more basic hydrosilicates, whose degree of crystallinity markedly increases as the thermal treatment period gets longer; after 6 hours of steam-curing, some crystalline tobermorite appear (at 3,85 Å, 3,33 Å, 3,02 Å, 2,90 Å, 2,80 Å, 1,82 Å - see figure 9); the peaks at 4,27 Å, 3,0 Å, 2,64 Å, 2,57 Å, 2,26 Å might show that gehlenite hydrate is formed (this was also reported by (7) for an alkaline activated slag). The increase of the steam-curing temperature to 95°C determines the intensification of the crystallization processes of the hydrocompounds; after only two hours of steam-curing there are identified crystalline tobermorite and well-crystallized CSH(II); after 6 hours, the interferences of tobermorite became more intense and gehlenite hydrat formation is noted (see figure 9).

In this study no crystalline alkaline hydroaluminiumsilicates were identified, even in the case of the masses with L-type sodium silicate. It is still possible that such compounds (reported by Constantinov and Puzhanov (8), may result as gels, their identification by X-ray techniques being impossible. It is possible, too, that in the crystalline hydrocompounds identified, a fraction of the Ca^{2+} ions might be replaced by Na^{+} ions, but this replacement does not determine changes in the lattice parameters. This affirmation is supported by the exothermal effect at 750-780°C, recorded on the DTA curves (figure 10), wich might be generated by the crystallisation of some hydrosilicates in whose composition the Ca^{2+} ions might

be replaced by Na^+ ions. This might determine a certain labillization of the lattice of these hydrosilicates and might explain the decrease of the temperature of the exothermal effect characterising the crystallization of the weakly basic hydrosilicates, from 800-850°C to 750-780°C (9).

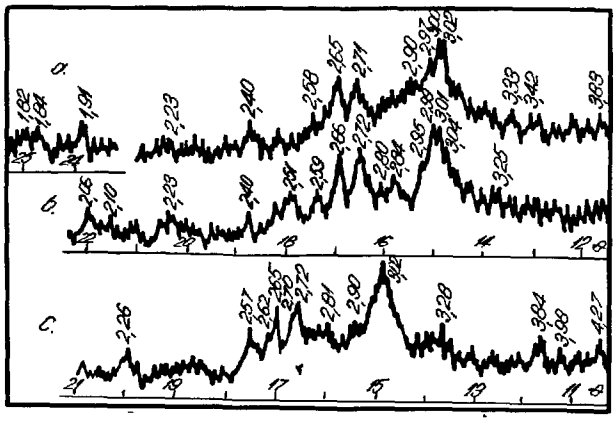

Fig.9 - X-ray patterns of the binder with a G-type slag/lime ratio = 95/5, with 8 wt% L-type sodium silicate, steam-cured: a - at 60°C, after 6 hours; b - at 95°C, after 2 hours; c - at 95°C, after 6 hours.

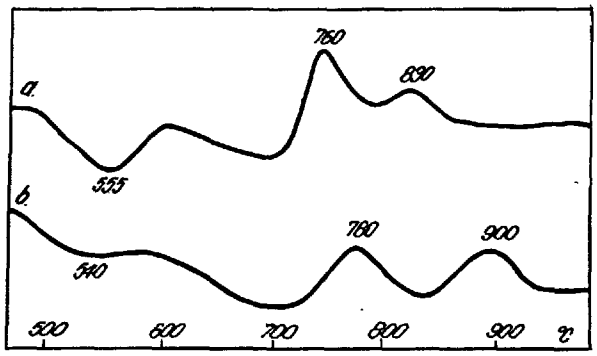

Fig.10 - DTA curves of the binder with a G-type slag/lime ratio = 95/5, with 8 wt% L-type sodium silicate, steam-cured for 6 hours, at: a - 60°C; b - 95°C.

CONCLUSIONS

In the investigated systems, the most important hydrocompounds are tobermorite-type calcium hydrosilicates. Under given hardening conditions, the amount and nature of the activator may modify the amount of the hydrosilicates formed and their basicity and crystallinity.

In both investigated systems there was noted the formation of the gehlenite hydrate, wich may eventually transform into hydrogarnets.

In the system slag-lime-gypsum-water there is also noted the formation of ettringite, while in the system slag-lime-sodium silicate-water it is suggested that solid solutions of calcium and sodium hydrosilicates, wich might have an important role in cementing the binder system, are formed.

BIBLIOGRAPHY

1. - M. Georgescu (1972), "Procese fizico-chimice la întărirea zgurelor de furnal înalt", Thesis, Polytechnical Institute Bucarest

2. - P.P.Budnikov, V.S.Gorschkov (1957), "Fiziko-himitscheskie prozessi tverdenie zementa v prisutstvie gipsu", Zhurnal Prikladnoi Himii, 30, nr.1, 21.

3. - P.P.Budnikov, V.S.Gorschkov (1957), "Obrazovanie etringita na ghidratazii zementa", Dokladi Akad. Nauk SSSR 113, nr.6, 1272.

4. - I.Teoreanu, M.Moldovan, M.Georgescu, M.Muntean, A.Puri (1972), "Bazele fizico-chimice ale întăririi lianţilor anorganici", EDP Bucarest.

5. - G.Schippa (1966), La Ricerca Scientifica 36, nr.4, 311.

6. - H. Zur Strassen (1958), "Die chemischen Reaktionen bei der Zementerhärtung", Zement-Kalk-Gips 11, nr.3, 137.

7. - I.A.Voinovich, R.Dron -(1976), Laboratoires des ponts et chaussées, 83, 55.

8 .- V.V.Constantinov, G.I.Puzhanov -(1960), "Bistrotverdenie viazhuschtschie veschtschestva iz granulirovanie schlaka i rastvorimoe stekla", Stroitelnie materiali nr.8, 33.

9. - I.Teoreanu, A.Puri (1975), "Über die Anregung der Hochofenschlacken mit Natriumsilikat", Silikattechnik 26, nr.6, 209.

Caractérisation et activation thermique des ciments au laitier

Characterization and thermal activation of slag cements

M. REGOURD, B. MORTUREUX, E. GAUTIER, H. HORNAIN, J. VOLANT, Département Microstructures, C.E.R.I.L.H. - Paris, France.

RESUME :

Sept laitiers industriels ont été caractérisés à l'aide de la microsonde électronique, de la diffraction des rayons X, de la microscopie électronique à balayage et de l'analyse thermique différentielle dans le but de relier leur hydraulicité à leur composition chimique élémentaire, à leur composition de phases (phase vitreuse et phases cristallisées) et à la constitution de leurs mélilites de recristallisation.

L'hydratation des laitiers dans des ciments de haut fourneau (66,5 % laitier, 28,5 % clinker, 5 % gypse) a été suivie :

- à la température ambiante, par la méthode de dissolution sélective et par diffraction des rayons X,
- à 20, 40, 50 et 80 °C par calorimétrie à conduction et mesure des résistances mécaniques en compression.

La méthode la plus rapide d'évaluation de la réactivité hydraulique d'un laitier dans un ciment est la mesure de la chaleur d'hydratation en pâte pure à 40 °C.

L'énergie d'activation d'un ciment au laitier peut être déterminée au moyen de courbes d'évolution isotherme, soit de chaleur d'hydratation, soit de résistances mécaniques en compression. Elle permet de prévoir la cinétique du durcissement lorsque la température varie au cours de l'hydratation. Des essais de courte durée permettraient ainsi d'estimer la résistance mécanique du ciment au jeune âge et à long terme.

SUMMARY :

Seven industrial slags have been characterized with the aid of electron microprobe, X-ray diffraction, scanning electron microscopy and differential thermal analysis in order to link their hydraulicity to their elemental chemical composition, their phases composition (glassy phase and crystalline phases) and the constitution of their recrystallized melilites.

The slag hydration in blastfurnace cement (66,5 % slag, 28,5 % clinker, 5 % gypsum) was followed :

- at room temperature by selective extraction analysis and X-ray diffraction,
- at 20, 40, 50 and 80 °C by conduction calorimetry and measures of mechanical compressive strengths.

The quickest method to evaluate the hydraulic reactivity of the slag in a cement is the measure of the heat of hydration in pure paste at 40 °C.

The activation energy of a slag cement can be determined by using isothermal evolution curves either of the heat of hydration or of the mechanical compressive strengths. It permits the prediction of the hardening kinetics when the temperature varies during the course of hydration. Thus, short term tests could permit to estimate the mechanical strength of a cement at early age and at long term.

1. INTRODUCTION

Il n'est pas aisé de relier la réactivité hydraulique des laitiers granulés à des paramètres tels que l'état de vitrification et la composition chimique (1). Deux laitiers vitreux de même composition chimique peuvent présenter des propriétés hydrauliques différentes (2).

Dans ce travail, nous avons cherché à différencier sept laitiers industriels, à l'état anhydre et au cours de leur hydratation à 20 et 80 °C, à l'aide de plusieurs méthodes d'analyse : microsonde électronique (MSE), diffraction des rayons X (DRX), analyse thermique différentielle (ATD), microscopie électronique à balayage (MEB), calorimétrie à conduction.

2. CARACTERISATION DES LAITIERS ANHYDRES

2.1 Analyse élémentaire

L'analyse élémentaire des sept laitiers granulés, obtenue grâce à la MSE, est reportée dans le Tableau I.

Tableau I : Composition chimique des sept laitiers

Laitier	1	2	3	4	5	6	7
MgO	4,7	8,4	8,2	9,6	8,6	5,5	4,3
Al_2O_3	14,6	12,2	11,9	14,6	13,3	16,4	14,8
SiO_2	33,9	33,6	35,1	35,8	38,8	32,0	33,1
CaO	44,5	42,5	42,8	34,3	32,2	41,6	44,4
Na2O	0,24	0,26	0,30	0,17	0,22	0,68	0,40
S	0,33	1,7	0,37	0,94	0,86	0,89	0,83
K_2O	0,62	0,45	0,61	2,4	3,6	1,49	0,86
TiO_2	0,69	0,49	0,59	0,68	0,48	0,67	0,57
MnO	0,66	0,55	0,37	1,50	1,79	0,58	0,62
FeO	<0,1	0,12	0,09	0,05	0,11	0,19	0,15

La composition élémentaire est assez homogène d'un grain de laitier à l'autre. Toutefois, certaines hétérogénéités peuvent exister localement, notamment sous forme de sulfures et de sulfates.

Les points figuratifs des compositions chimiques du Tableau I, dans le diagramme ternaire $CaO-Al_2O_3-SiO_2$ (fig. 1) sont relativement proches les uns des autres ; les laitiers 4 et 5 sont les plus acides. Trois indices d'hydraulicité ont été calculés (Tableau II). Ils montrent, pour les deux premiers et pour les laitiers 4 et 5, des valeurs plus faibles qui devraient correspondre à une moindre réactivité.

Tableau II : Indices d'hydraulicité des 7 laitiers

Laitier	1	2	3	4	5	6	7
$C+M/(S+\frac{1}{2}A)$	1,19	1,28	1,24	1,02	0,90	1,17	1,20
$\frac{C+M+\frac{2}{3}A}{S+\frac{1}{3}A}$	1,52	1,57	1,51	1,32	1,15	1,55	1,41
A/S	0,43	0,36	0,34	0,41	0,34	0,51	0,45

2.2 Analyse de phases

• D'après la DRX, les sept laitiers, vitreux, sont caractérisés par un "anneau" centré à 3,0 Å qui définit la distance moyenne entre atomes plus proches voisins (fig. 2). Un enregistrement pas-à-pas n'a révélé aucune différence significative quant à la position et au profil du halo. La position du second anneau (1,9 Å) varie légèrement d'un laitier à l'autre mais ces faibles variations ne semblent pas pouvoir caractériser aisément un produit industriel. A l'anneau principal se superposent, dans certains cas, des raies de phases cristallisées : merwinite pour les laitiers 2 et 3, mélilite pour les laitiers 3,4 et 6. Avec 5 % de merwinite, le laitier 2 apparaît le plus cristallisé de la série (fig. 2).

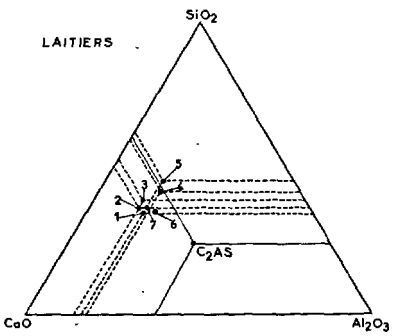

Fig. 1 : Position des sept laitiers dans le diagramme ternaire chaux-silice-alumine.

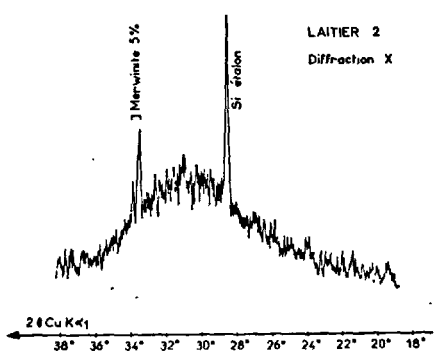

Fig. 2 : Le laitier 2 est caractérisé par un anneau de corps amorphe et par les raies de la merwinite cristallisée (5 %).

Après un recuit d'une heure à 850 °C, on trouve une mélilite plus ou moins bien cristallisée dans tous les laitiers et de la merwinite dans les laitiers 2, 3 et 6. Toutes les cinétiques étudiées ont montré qu'au cours du recuit, la merwinite cristallise d'abord, puis décroît et peut même disparaître (laitier 1 traité à 1000 °C). Les laitiers 4 et 5 se comportent différemment des autres : le diopside CMS_2 apparaît dans le laitier 4 et la mélilite recristallisée, détectée dans le laitier 5, est proche de l'akermanite.

Les mélilites de recristallisation diffèrent par leurs paramètres cristallins, intermédiaires entre ceux de la gehlénite et de l'akermanite (fig. 3) et par la largeur de leurs raies DRX que l'on peut considérer comme un paramètre d'ordre. Les laitiers 1,4 ,5 et 7 donnent par recuit une mélilite très bien cristallisée. Au contraire, la mélilite des laitiers 2 et 3 présente des raies larges.

• En ATD, la dévitrification du laitier se manifeste par un ou plusieurs signaux exothermiques, entre 800 et 1000 °C. Ces pics, plus ou moins complexes, sont, en général, précédés d'un pic endothermique dû à une

certaine réorganisation du verre (3).

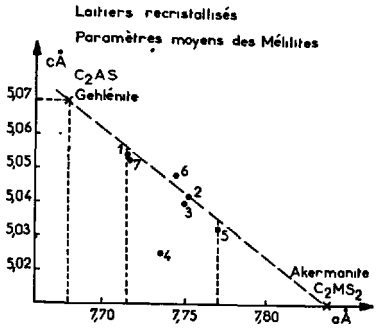

Fig. 3 : Paramètres cristallins a et c de la mélilite après recuit des 7 laitiers.

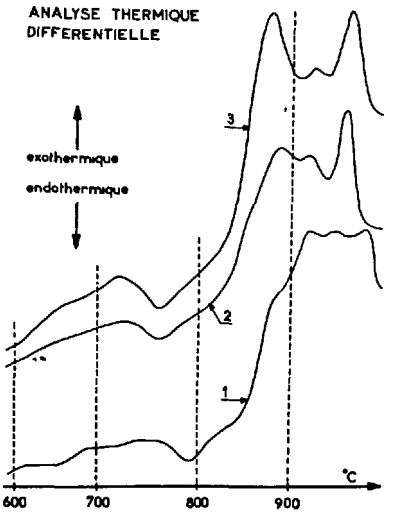

Fig. 4 : Thermogrammes des laitiers 1, 2 et 3 (sonde semi-micro).

La figure 4 montre les thermogrammes comparés des laitiers 1, 2 et 3. Les laitiers 2 et 3 ont un comportement assez proche : deux signaux respectivement à 870 et 940 °C et un pic intermédiaire vers 900 °C. Des diagrammes DRX, effectués après trempe du produit à différentes températures, ont confirmé que le premier pic doit être attribué à la merwinite (4). L'effet thermique, vers 950 °C, serait le pic de cristallisation de la mélilite bien cristallisée mais la formation de cette phase commence, dans tous les cas, vers 800 °C. La merwinite, apparue au cours du recuit, est très importante dans les laitiers 3 et 6, elle l'est moins dans le laitier 2 et elle est très faible dans les laitiers 1 et 7 où la cristallisation de la mélilite s'étale sur une grande plage de température.

• Au MEB, l'examen de sections polies montre que certains grains contiennent des domaines orientés de microcristaux, le plus souvent sous forme dendritique (fig. 5). Ces domaines correspondent à un stade précoce de cristallisation. Leur analyse élémentaire ponctuelle n'est pas aisée en raison de leurs très faibles dimensions. Des dosages répétés ont montré que les zones dévitrifiées étaient systématiquement plus riches en MgO mais plus pauvres en Al_2O_3 que le verre environnant : dans cet échantillon (laitier 2), seule la merwinite C_3MS_2 avait été détectée par DRX.

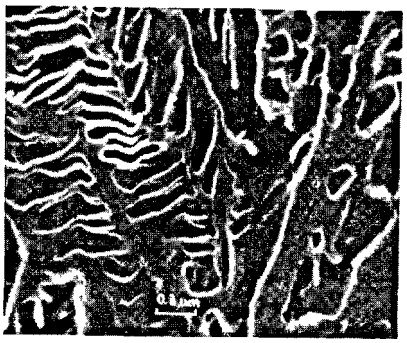

Fig. 5 (MEB) : Cristallisation denditrique de la merwinite (M) dans le laitier vitreux (V) n° 2 (section polie attaquée par NH_4Cl).

3. HYDRATATION DES CIMENTS AU LAITIER

Les laitiers broyés à une surface spécifique Blaine de 3500 $cm^2.g^{-1}$ ont été ajoutés à un clinker de ciment Portland (63 % C_3S, 17 % C_2S, 14,5 % C_3A, 4,5 % C_4AF) dans les proportions 66,5 % laitier, 28,5 % clinker, 5 % gypse. Les éprouvettes de pâte pure de ce ciment de haut fourneau CHF, (e/c = 0,4, cubes 2 x 2 x 2 cm) ont été conservées 1, 3, 6 et 12 mois dans l'eau à 20 °C. A chaque échéance, le degré d'hydratation du laitier a été mesuré et la microstructure du matériau durci, examinée au MEB.

3.1 Mesure du degré d'hydratation des laitiers

Le degré d'hydratation du laitier a été déterminé par dissolution des constituants hydratés et du ciment Portland anhydre dans une solution d'acide salicylique dans le méthanol et l'acétone (5). L'analyse quantitative par DRX (méthode de l'étalon interne silicium) a permis de suivre les variations de la concentration en $Ca(OH)_2$ et la diminution de l'intensité de l'anneau d'amorphe du laitier anhydre.

Les résultats obtenus par ces deux méthodes font nettement apparaître, dès la première échéance (28 jours), des différences de réactivité entre les laitiers étudiés (fig. 6).

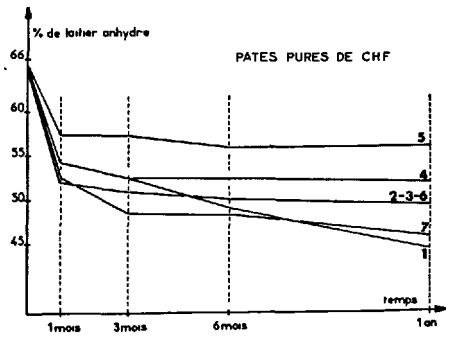

Fig. 6 : Décroissance du laitier anhydre, en fonction du temps, dans les CHF- (méthode de dissolution KONDO- OHSAWA).

A 3 mois, la quantité de $Ca(OH)_2$, présente dans les pâtes, varie du simple au double entre les laitiers 1 et 3 par exemple. On note, par ailleurs, une nette diminution de l'anneau des laitiers 1 et 7, entre 28 jours et 3 mois. A 6 mois, les CHF 1 et 3 se différencient de la même manière qu'à 28 jours, en ce qui concerne le taux de $Ca(OH)_2$.

La fraction de laitier n'ayant pas encore réagi, déterminée par la méthode de dissolution, a été reliée à la composition de la mélilite cristallisée au cours du recuit (Tableau III), composition estimée à partir des paramètres cristallins représentés sur la figure 3.

Tableau III : Pourcentage de laitier n'ayant pas encore réagi à 6 mois dans les CHF et composition minéralogique de la mélilite recristallisée.

Laitier	1	2	3	4	5	6	7
résidu (%)	48	51	51	52	56	50	48
gehlénite (%)	80	59	59		42	68	80
akermanite (%)	20	41	41		58	32	20

Les résultats du Tableau III montrent que la réactivité d'un laitier pourrait être reliée à la teneur en gehlénite (ou en akermanite) de la mélilite recristallisée. Les laitiers 1 et 7 ont le mieux réagi, leur mélilite était formée de 80 % de gehlénite et de 20 % d'akermanite. Le laitier 5 est le moins réactif, sa mélilite contenait 58 % d'akermanite. Le laitier 4 est une exception, la composition de sa mélilite ne correspondait pas à une solution solide gehlénite-akermanite mais à une phase plus complexe contenant des éléments mineurs, du potassium en particulier.

L'autre caractéristique des mélilites, à savoir le degré d'ordre de la solution solide (raies DRX élargies), ne semble pas pouvoir être corrélée à la réactivité du laitier.

A un an, les CHF 1, 2 et 3 contiennent sensiblement la même quantité de $Ca(OH)_2$ mais les fractions hydratées, déterminées par voie chimique, ne sont pas égales. Le taux de chaux donne donc une indication de la réactivité d'un laitier mais cette estimation ne peut être suffisante car l'activation calcique n'est pas seule en cause. Il s'y ajoute l'activation sulfatique due au gypse du ciment Portland et une autoactivation par les sulfates provenant de l'oxydation des sulfures présents dans les laitiers. Le laitier 2 contient le pourcentage le plus élevé de l'élément S (1,79 %), presque cinq fois plus que celui des laitiers 1 et 3 (Tableau I). D'après les résultats à 1 an, le laitier 3 a réagi plus lentement que les laitiers 1 et 2 ; les essais mécaniques sur mortier confirment cette observation.

Dans nos conditions expérimentales, les laitiers les plus réactifs ne se sont pas hydratés à plus de 30 % à un an, en pâte pure. Des taux d'hydratation plus élevés ont été atteints avec une mouture très fine du laitier (6).

3.2 Mesure de la chaleur d'hydratation

La réactivité des laitiers 6 et 7 étant respectivement proche de celle des laitiers 3 et 1, la mesure du dégagement de chaleur au cours de l'hydratation des CHF en pâte pure a été effectuée sur les cinq premiers ciments de haut fourneau, à 40 °C, à l'aide d'un calorimètre à conduction. Les courbes de flux de chaleur mettent en évidence, avant 24 heures, des différences très importantes entre les laitiers (fig. 7). Le maximum du flux est retardé dans le temps et nettement moins intense avec les laitiers 2 et 3 qu'avec le laitier 1, plus encore avec les laitiers 4 et 5.

Ces observations sont à rapprocher des estimations du taux d'hydratation par voie chimique.

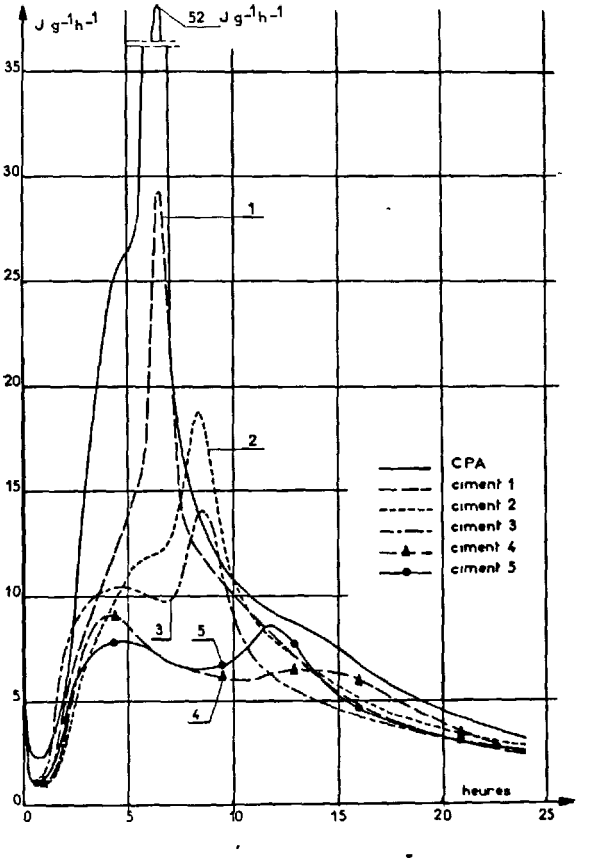

Fig. 7 : Chaleur d'hydratation à 40 °C du CPA et des cinq premiers CHF.

L'interprétation des courbes de chaleur d'hydratation paraît plus délicate que la comparaison des flux de chaleur.

L'étude au MEB et par DRX du CHF n° 1, avant et après le pic le plus intense (fig. 7) montre que :

1) l'hydratation des silicates du clinker est déjà commencée avant la partie ascendante du pic : présence de $Ca(OH)_2$ et diminution de C_3S. Le gypse a très peu réagi.

2) au-delà du pic, le gypse est entièrement consommé. L'ettringite, abondante, n'a pu se former qu'avec l'alumine du laitier, compte tenu de la faible teneur en C_3A du CHF. La concentration en C-S-H a nettement augmenté. Il s'agit donc bien d'une activation du laitier par la chaux et le sulfate.

Par ailleurs, pour un laitier très réactif tel que le laitier 1, le pic survient au même moment que celui du CPA témoin et le rapport entre l'énergie libérée par le CHF et celle libérée par le CPA est très supérieur à la proportion de clinker (28,5 %). Ces résultats (Tableau IV) prouvent la participation du laitier au dégagement de chaleur.

Dans la comparaison de la réactivité des laitiers, la calorimétrie se révèle donc une méthode très sensible.

Tableau IV : Valeur de l'énergie totale libérée à 40 °C par les 5 CHF et le CPA à 108 heures.

CHF	1	2	3	4	5	CPA
$J.g^{-1}$	241	242	223	174	180	341

3.3 Mesure des résistances mécaniques des mortiers ISO

Les résistances mécaniques ont été mesurées sur les mortiers ISO de CHF 1, 2 et 3 et comparées à celles du CPA. La variation de la résistance à la compression en fonction du temps sépare bien les quatre ciments dès les brèves échéances (fig. 8) et la distinction est particulièrement nette à 7 jours. A 90 jours, le CHF contenant le laitier le plus réactif est aussi résistant que le CPA entrant dans sa composition. Le développement des résistances mécaniques est lié à l'hydratation des constituants du ciment. La différenciation des laitiers est plus nette dans le cas de la mesure des résistances mécaniques sur mortier que lors de l'estimation du degré d'hydratation en pâte pure par la méthode de dissolution. Elle reste toutefois moins rapide que le classement des CHF par la calorimétrie à conduction à 40 °C.

Les différences sont plus marquées dans les mortiers que dans les pâtes pures de ciment. A 14 et 28 jours, les mortiers de CHF contiennent beaucoup moins de $Ca(OH)_2$ en plaquettes massives mais plus de sulfoaluminates que le CPA. Le monosulfoaluminate est plus abondant, dès 14 jours, dans le CHF 1 que dans les CHF 2 et 3 qui, par contre, contiennent plus d'ettringite.

4. ETUVAGE DES CIMENTS AU LAITIER

A l'activation alcaline et sulfatique des laitiers peut s'ajouter une activation thermique lors d'un étuvage. Nous avons étudié l'évolution des chaleurs d'hydratation et des résistances mécaniques au cours de différents traitements thermiques.

4.1 Chaleurs d'hydratation et résistances mécaniques

Les mesures de chaleur d'hydratation ont été effectuées sur pâte pure (e/c = 0,40) à 20, 40 et 80 °C (Tableau V). La variation du dégagement de chaleur en fonction du temps (fig. 11) montre que l'évolution du phénomène est la même à 20 et 40 °C. L'élévation de température de 20 °C accélère les réactions d'hydratation mais les hydrates formés sont les mêmes qu'à température ambiante, d'où l'intérêt de classer les laitiers par leurs courbes calorimétriques à 40 °C (fig.7).

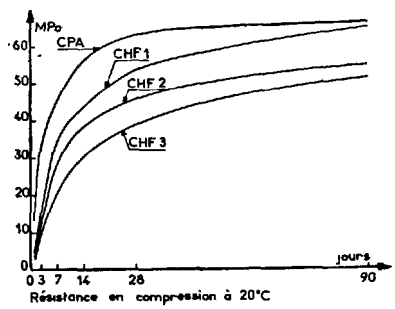

Fig. 8 : Evolution des R_c en fonction du temps.

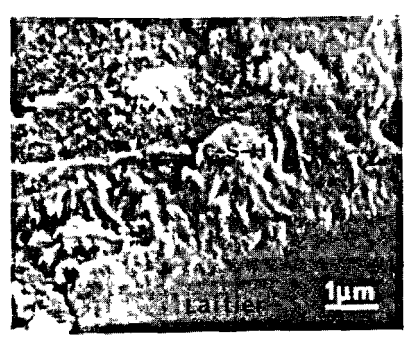

Fig. 9 : Grains de laitier entourés de C-S-H.

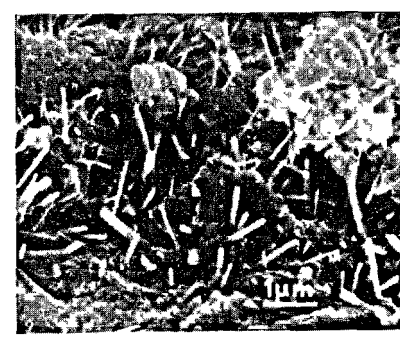

Fig. 10 : Cristallisation de l'ettringite en fines aiguilles disséminées.

3.4 Examen de la microstructure des pâtes et mortiers

L'examen au MEB de sections polies et de surfaces de fracture d'éprouvettes de pâte pure révèle que le clinker s'hydrate en premier. Les grains de laitier couverts par le C-S-H du clinker s'entourent ensuite d'une zone hydratée qui devient très compacte à un an (fig. 9). L'analyse élémentaire ponctuelle montre que le C-S-H est plus riche en MgO et Al_2O_3 que celui du clinker, mais il est moins calcique. A ce C-S-H se mêlent des aiguilles d'ettringite, plus courtes et plus fines que celles données par le clinker (fig. 10). L'ettringite est encore détectée par DRX à un an, elle coexiste alors avec le monosulfoaluminate, elle est probablement due à l'auto-activation sulfatique du laitier.

Il est difficile d'apprécier par ces examens une différence de réactivité entre plusieurs laitiers. Tout au plus peut-on séparer les laitiers 1 et 3 par exemple, les zones hydratées autour des grains de laitier étant à 28 jours plus larges dans le premier échantillon que dans le second.

Les résistances mécaniques ont été mesurées sur des mortiers ISO conservés en moules métalliques dans l'eau jusqu'à leur rupture. Le cycle d'étuvage n'a débuté que 4 heures après le gâchage. La vitesse d'échauffement était de 20 °C.h^{-1}, celle du refroidissement de 30 °C.h^{-1}. Afin d'englober la majeure partie de la période d'accroissement des résistances, les mesures ont été poursuivies jusqu'à 180 jours à 20 °C, 21 jours à 50 °C et 6 jours à 80 °C (Tableau V). Après un cycle d'étuvage, certaines éprouvettes ont été replacées dans l'eau à 20 °C jusqu'à ce que la durée totale d'hydratation atteigne 28 et 90 jours.

Pour chaque ciment étudié, les courbes d'évolution des résistances mécaniques en fonction du temps, à 50 et 80 °C, croisent plus ou moins rapidement la courbe d'évolution à 20 °C (fig. 12 et 13). Si l'on exclut du durcissement les réactions initiales d'hydratation jusqu'à la fin de la période dormante et si l'on donne à α, degré d'avancement, la valeur 1 quand la résistance ne varie plus de manière significative (variation

Tableau V : Chaleur d'hydratation des pâtes pures de CPA et des CHF à 20, 40, 80 °C ($J.g^{-1}$)

T (°C)	20 °C							40 °C							80 °C						
t (h)	3	9	18	48	120	336	504	1	5	10	18	108	168	408	1	2	3	6	15	44	240
CPA	19	51	119	219	314	365		13	72	193	287	341			35	126	182	246	306	335	
CHF 1	7	20	53	130	194	238	247	5	37	116	167	241	253	277	12	63	135	174	193	217	253
CHF 2	5	19	50	129	190	228		4	29	97	150	242	252	278	9	49	113	172	204	233	
CHF 3	7	24	50	112	166	209		4	36	87	128	223	243	276	16	69	112	158	188	215	260
CHF 4								4	30	64	112	174	182								
CHF 5								5	28	63	112	180	187								

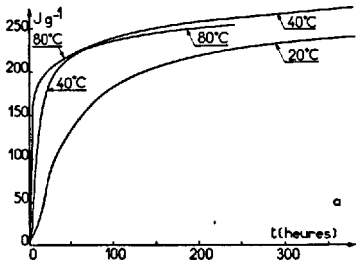

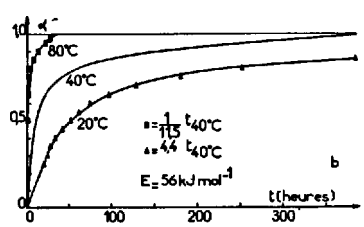

Fig. 11 - CHF 1 - a : Chaleur d'hydratation. b : Courbes relatives affines.

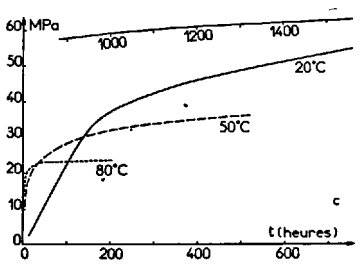

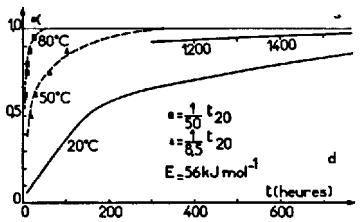

Fig. 12 - CHF 1 - c : Résistances d : Courbes relatives affines.

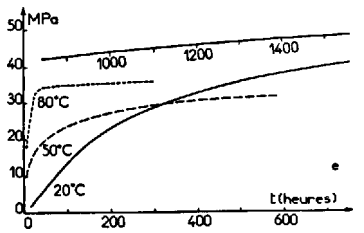

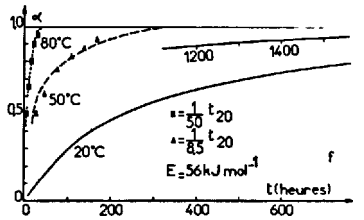

Fig. 13 - CHF 3 - e : Résistances f : Courbes relatives affines.

Tableau VI : Résistances mécaniques en compression des mortiers étuvés (MPa) (coefficient de variation 3 %)

T (°C)	20 °C							50 °C			50 °C 20 °C	50 °C 20 °C	80 °C				80 °C 20 °C	80 °C 20 °C
t (h)	24	72	168	336	672	2160	4320	24	65	504	65 + 607	65 + 2095	7	13	40	134	7 + 655	13 + 659
CPA	13	36	46	56	63	66	68	34	40	49	50	57	30	31	35	38	47	
CHF 1	5	16	34	43	53	65	69	22	26	36	26	37	21	22	24	25	27	27
CHF 2	3	13	26	38	46	54	60	20	23	34	29	35	26	29	33	34	37	37
CHF 3	3	10	20	30	39	51	56	17	21	31	27	32	22	27	34	35	36	37

inférieure à 5 % quand le temps double), les courbes d'évolution du phénomène, pour chaque température, sont affines. Les rapports d'affinité suivent la relation d'ARRHENIUS :

$$\gamma = \exp.\left[\frac{E}{R}\frac{T_2 - T_1}{T_1 T_2}\right] = \frac{t_1}{t_2}$$

t_1, t_2 = temps d'hydratation, T_1, T_2 = température en °K.

Les essais à 20, 50 et 80 °C permettent ainsi de déterminer une valeur moyenne de l'énergie d'activation E du ciment pendant la durée du durcissement considérée. Les valeurs finales sont supposées correspondre à des systèmes de même nature et de même degré d'avancement.

L'énergie d'activation E déterminée dans ces conditions est pour les trois premiers CHF étudiés de 56 $kJ.mol^{-1}$. La même valeur est obtenue à partir des mesures de dégagement de chaleur. Les rapports d'affinité entre la courbe à 20 °C et les courbes à 40, 50 et 80 °C sont respectivement de 4,4, 8,5 et 50. L'énergie E du CPA entrant dans la composition des CHF est de 42 $kJ.mol^{-1}$ et les rapports d'affinité respectivement de 3, 5 et 19 à 40, 50 et 80 °C. La température a donc un effet plus important sur les CHF que sur le CPA.

Dans nos conditions expérimentales à 50 et 80 °C, les formules de NURSE-SAUL, ou leurs variantes, ne peuvent pas représenter la cinétique du durcissement au-delà des premières heures d'étuvage. En effet, dans ces formules, le rapport des temps d'hydratation t_1/t_2, pour deux températures différentes θ_1 et θ_2, reste constant quelles que soient les valeurs de t_1 et t_2. Or nos courbes d'évolution des résistances à 50 et 80 °C coupent la courbe à 20 °C (fig. 12 et 13).

Les courbes de l'évolution isotherme à 50 et 80 °C (fig. 11, 12 et 13) tendent vers des valeurs asymptotiques plus faibles que celles des courbes à 20 °C. Un traitement thermique prolongé réduit donc l'accroissement de la résistance (Tableau VII).

Tableau VII : Coefficients d'amortissement

Mortier	R_c		Q
	50 °C/20 °C	80 °C/20 °C	80 °C/40 °C
CPA	0,75	0,60	0,90
CHF 1	0,50	0,40	0,70
CHF 2	0,60	0,60	0,80
CHF 3	0,60	0,75	0,75

L'affaiblissement de la valeur asymptotique de la chaleur d'hydratation Q à 80 °C est moindre que celui des résistances R_c. Il peut être négligé au-dessous de 40 °C.

Par ailleurs, l'accroissement de la résistance des éprouvettes étuvées puis conservées à 20 °C pendant 28 et 90 jours (Tableau VI) suit, après étuvage, la courbe d'évolution relative du ciment à 20 °C.

A partir de ces observations, l'influence de la température sur le durcissement d'un ciment peut être caractérisée par l'énergie d'activation et l'amortissement. Le durcissement peut alors être considéré comme un système à variables séparées : température et temps. Son évolution à température variable dans le temps est déduite d'essais isothermes.

4.2 Comportement des CHF à l'étuvage

L'étuvage est très favorable aux ciments peu réactifs comme les CHF 4 et 5 ou réagissant lentement comme le CHF 3. Après un traitement à 80 °C, tous trois acquièrent des propriétés mécaniques voisines de celles du CHF 2. Les grains de laitier et de sable s'entourent d'une épaisse couche hydratée, preuve que le laitier a beaucoup plus réagi qu'à la température ambiante (fig. 14).

Des cinq ciments, le CHF 1 est celui qui se comporte le moins bien à l'étuvage. Ses résistances n'atteignent que la moitié de leur valeur après 7 heures à 80 °C puis 28 jours à 20 °C (Tableau VI). A 80 °C, leur amortissement est de 40 % par rapport à 20 °C (Tableau VII). Après 7 heures à 80 °C, des amas de monosulfoaluminate en cristaux massifs forment une texture hétérogène peu favorable à la cohésion du mortier (fig. 15).

Fig. 14 : CHF 5 (13 h à 80 °C). Larges zones de C-S-H (x) autour des grains de laitier (L).

Fig. 15 : CHF 1 (7 h à 80 °C). Monosulfoaluminate (M) en cristaux massifs.

5. CONCLUSION

L'analyse, par différentes méthodes, de sept laitiers industriels à l'état anhydre et en cours d'hydratation a permis de confirmer et de préciser certains points tels que :

1) L'insuffisance des indices d'hydraulicité ne tenant compte que des éléments principaux Ca, Si, Al, Mg.

2) L'importance du degré de vitrification du laitier, de la composition minéralogique des mélilites de recristallisation, de la teneur en merwinite.

3) L'intérêt de la méthode de dissolution de KONDO et OHSAWA pour apprécier l'hydratation du laitier dans un ciment.

4) La facilité de classement des ciments au laitier par la mesure de leurs résistances mécaniques en compression sur mortier ISO.

La méthode la plus rapide d'évaluation de la réactivité hydraulique d'un laitier, dans un ciment, nous semble la mesure de la chaleur d'hydratation en pâte pure à 40 °C. Cette réactivité est révélée en quelques heures. Toutefois, au-delà de 40 °C, Les comportements peuvent être différents de ceux observés à 20 °C (formation importante de monosulfoaluminates à 80 °C).

Dans un large domaine de température, la cinétique d'hydratation et les résistances mécaniques des ciments au laitier peuvent être connues après détermination de leur énergie d'activation et de leur coefficient d'amortissement. Des essais de courte durée devraient ainsi permettre d'estimer la résistance mécanique du ciment au jeune âge et à long terme.

Remerciements : Nous remercions vivement de leur participation à cette étude Martine BADEYAN, Félix SAINZ, Claude TISSIER et Eddy ZWIANZEK.

6. BIBLIOGRAPHIE

1.- P. TERRIER (1973), "Recherche sur l'hydraulicité des laitiers granulés de haut fourneau", CILAM-Inform. n° 8, 9 et 10.

2.- H.G. SMOLCZYK (1978), "L'influence de la composition chimique du laitier sur les résistances des ciments au laitier de haut fourneau", Zement-Kalk-Gips, 31, 6, 294-6.

3.- P. GIORDANO-ORSINI, A. BURI and A. MAROTTA (1975), "Devitrification of glasses in the åkermanite-gehlénite system", J. amer. Ceram. Soc., 58, 7-8, 306-11.

4.- W. VAN LOO (1977), "Factors determining the hydraulicity of granulated blastfurnace slag", Seminar CEMBUREAU on "Reaction of aluminates during the setting of cements". Univ. Technol. Eindhoven, 13-14 April.

5.- R. KONDO and S. OHSAWA (1968), "Studies on a method to determine the amount of granulated blastfurnace slag and the rate of hydration of slag in cement", Proceedings VISCC, Tokyo, vol IV, 255-62.

6.- M. REGOURD (1980), "Structure et comportement des hydrates des ciments au laitier", Rapport principal, III-2, Congrès de Paris.

Nouveaux aspects de l'hydratation de laitiers industriels

New aspects of industrial slags hydration

P. FIERENS et P. POSWICK, Université de Mons (Belgique).

RESUME : L'hydratation d'un laitier vitreux industriel a été étudiée par exoémission électronique et thermogravimétrie. Les résultats obtenus permettent de penser que, comme pour la géhlénite et des laitiers synthétiques, la vitesse d'hydratation est liée notamment aux caractéristiques de centres correspondant à des défauts de structure de l'état vitreux et le mécanisme semble comporter au moins deux étapes : germination croissance autoinhibée et diffusion.

Il est également montré que, pour différentes durées d'hydratation, la résistance à la compression de microéprouvettes standard est d'autant plus grande que le nombre d'exoélectrons émis par le laitier non hydraté est élevé.

Enfin, il n'existe pas de relation simple entre la résistance à la compression et le degré d'hydratation d'un laitier industriel donné trempé dans différents milieux.

SUMMARY : Hydration of a glassy industrial slag has been studied by electronic exoemission and thermogravimetry. The results show that as in the case of gehlenite and synthetic slags, the hydration velocity depends among others on characteristics of centres corresponding to structure defects of the glassy state and the mechanism seems to include at least two steps : autoinhibated nucleation and diffusion controlled processes.

It is also showed that, for different hydration durations, the highest the number of exoelectrons emitted by the unhydrated slag, the highest the compressive strength of the hydrated one.

At last, there is no single relationship between compressive strength and degree of hydration of a given industrial slag quenched into different media.

1. Introduction

Une étude (1) de l'hydratation de la géhlénite et de laitiers synthétiques vitreux en présence d'hydroxyde de sodium a permis les conclusions suivantes.

Le mécanisme de la réaction comporte au moins deux étapes. L'hydratation commence au niveau des centres actifs de la surface du matériau selon un processus de germination autoinhibé ; lorsque les grains sont recouverts d'une couche continue d'hydrates, l'hydratation est cinétiquement contrôlée par un processus de diffusion jusqu'à la fin de la réaction.

La "qualité" de l'état vitreux de la géhlénite et des laitiers synthétiques est caractérisée par la probabilité p de sortie d'électrons piégés mesurée par thermoluminescence ou par le nombre n d'exoélectrons émis par le matériau dans des conditions standard. Il a été montré expérimentalement (1) que pour un matériau donné ces deux grandeurs sont liées par une relation linéaire log n/log p.

La probabilité p et le nombre d'exoélectrons n sont en rapport, l'une et l'autre, avec les défauts de structure de l'état vitreux du matériau et dépendent notamment des conditions de trempe du matériau fondu.

Le présent travail constitue l'extension de cette étude au domaine des laitiers industriels.

2. Préparation et caractérisation des échantillons

Le laitier industriel utilisé dans cette recherche provient de la Société Métallurgique Hainaut-Sambre (Belgique) et présente la composition chimique élémentaire donnée dans le tableau I.

TABLEAU I

Composition chimique élémentaire du laitier industriel étudié (poids %)

SiO_2	= 35,57 %	TiO_2	= 1,10 %
CaO^2	= 39,74 %	MnO^2	= 1,09 %
Al_2O_3	= 12,39 %	Cr_2O_3	= 0,10 %
MgO	= 6,20 %	SrO	= 0,11 %
FeO	= 0,17 %	SO_3	= 0,23 %
Na_2O	= 0,64 %	Sulfures	= 0,79 %
K_2O	= 1,30 %	P_2O_5	= 0,15 %

Total = 99,58 %

Résidu insoluble dans les acides : 0,35 %

Le laitier fondu s'écoulant du haut fourneau a été trempé dans quatre milieux différents comme l'indique le tableau II.

TABLEAU II

Mode de trempe

Echantillon n°	Milieux de trempe
1	Azote liquide (-192°C)
2	Méthanol fondant (-80°C)
3	Eau glacée (8°C)
4	Air ambiant (20°C)

Les quatre échantillons ont été broyés et leur surface spécifique BET a été déterminée (Tableau III).

TABLEAU III

Surface spécifique BET

Echantillon	Surface spécifique (m^2/g)
1	0.60
2	0.72
3	0.82
4	0.75

Les quatre échantillons sont entièrement vitreux : leur pic de dévitrification ATD s'est révélé identique.

Une tentative de les différencier par thermoluminescence a échoué. En effet, le laitier industriel contient des éléments mineurs tels que le fer, le manganèse, le chrome qui absorbent la lumière émise et rendent la mesure inopérante.

Les échantillons ont été caractérisés par exoémission électronique photostimulée.

Le tableau IV donne le nombre n d'exoélectrons émis dans des conditions standard.

TABLEAU IV

Exoémission électronique photostimulée (n = nombre d'exoélectrons)

Echantillon	n
1	202.10^3
2	738.10^3
3	481.10^3
4	595.10^3

Les quatre échantillons, de même composition chimique, présentent donc des différences de défauts de structure de l'état vitreux dues aux conditions de trempes.

De plus,on observe la séquence décroissante du nombre d'exoélectrons émis :

2 > 4 > 3 > 1

3. Cinétique de l'hydratation

Les quatre échantillons du laitier industriel ont été hydratés à 20°C par une solution aqueuse molaire d'hydroxyde de sodium, dans les mêmes conditions que la géhlénite et les laitiers synthétiques des travaux précédents.

La cinétique de la réaction a été suivie par thermogravimétrie. La perte d'eau chimiquement liée a été déterminée en fonction de la durée du contact laitier - solution d'hydroxyde de sodium.

Nos observations font l'objet du tableau V. On y trouve la perte d'eau observée et, en regard, la perte d'eau corrigée tenant compte de la surface spécifique de chaque échantillon.

Voir Tableau V

p.III - 11 6

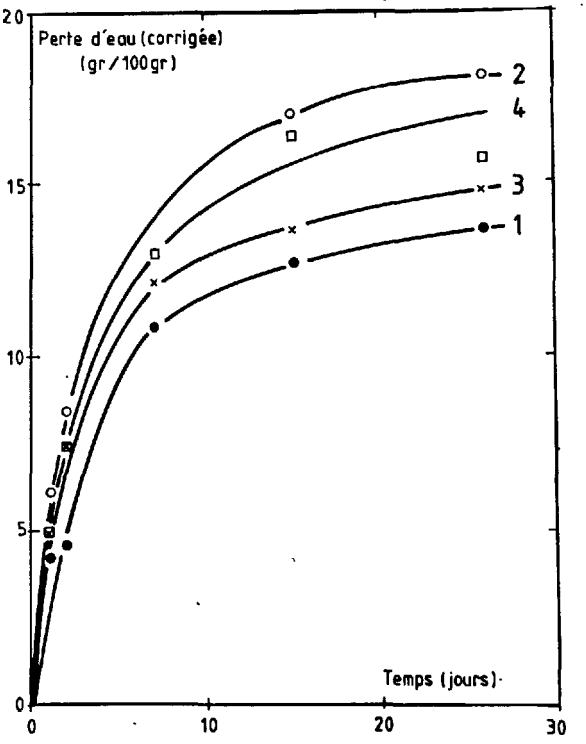

Fig. 1 : Perte d'eau chimiquement liée en fonction du temps : thermogravimétrie (gr. par 100 gr. de laitier)

La figure 1 illustre l'évolution des pertes de poids corrigées en fonction de la durée de l'hydratation.

La forme de ces courbes est analogue à celles obtenues, dans les mêmes conditions, avec la géhlénite et des laitiers synthétiques pour lesquels il a été montré qu'elles correspondaient sur le plan cinétique à un processus de diffusion. Cette conclusion paraît pouvoir être étendue au cas présent.

On observe que la vitesse d'hydratation des échantillons contrôlée par ce processus de diffusion suit la séquence :

2 > 4 > 3 > 1

C'est la même que celle des nombres d'exoélectrons émis par les laitiers non hydratés.

Il semble donc bien que pour le laitier industriel étudié, les défauts de structure de l'état vitreux aient une nette influence sur la vitesse de l'étape "diffusion" de l'hydratation, comme on peut l'observer dans le cas de la géhlénite et de laitiers synthétiques.

4. Résistance à la compression

Dans le but de réaliser une meilleur approche de la pratique, nous avons mesuré la résistance à la compression sur microéprouvettes. Celles-ci ont été fabriquées en gâchant 2,25 gr de laitier anhydre avec 0,25 gr d'une solution aqueuse d'hydroxyde de sodium normale (E/C = 0.11). Avec ce mélange, pétri pendant 3 minutes, on confectionne des microéprouvettes selon le procédé bien connu.

Les résultats des résistances à la compression après 3, 7, 15 et 28 jours sont donnés dans le tableau VI et la figure 2.

Les résultats montrent que, pour les quatre échantillons, la vitesse de croissance de la résistance à la compression suit la séquence :

2 > 4 > 3 > 1

c'est-à-dire la même que celle observée dans les mesures d'exoémission électronique photostimulée et de thermogravimétrie.

TABLEAU VI

Résistance à la compression (MPa)

Durée (jours)	Echantillon			
	1	2	3	4
3	16	33	20	21
7	24	59	36	41
15	26	71	37	47
28	34	77	43	57

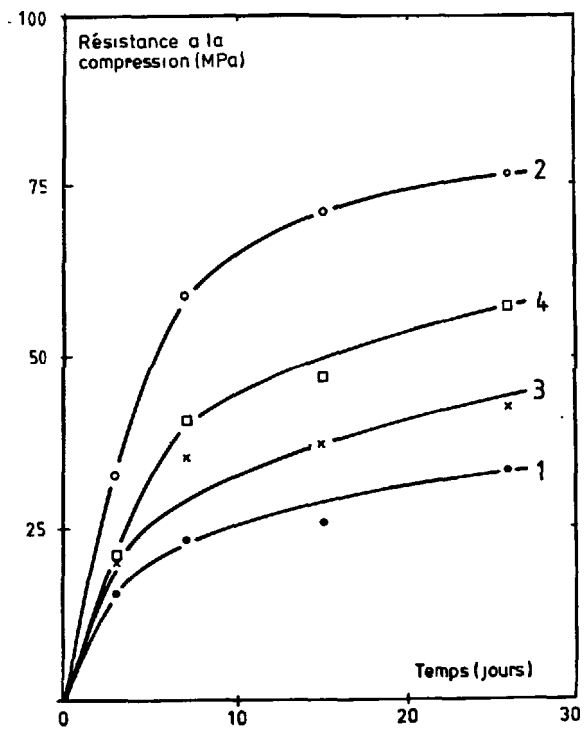

Fig. 2 : Résistance à la compression (MPa)

5. Résistance à la compression et degré d'hydratation

Dans le graphique de la figure 3, nous avons indiqué la perte en eau chimiquement liée non corrigée (c'est-à-dire une expression du degré d'hydratation) en regard de la valeur correspondante, pour une même durée, de la résistance à la compression.

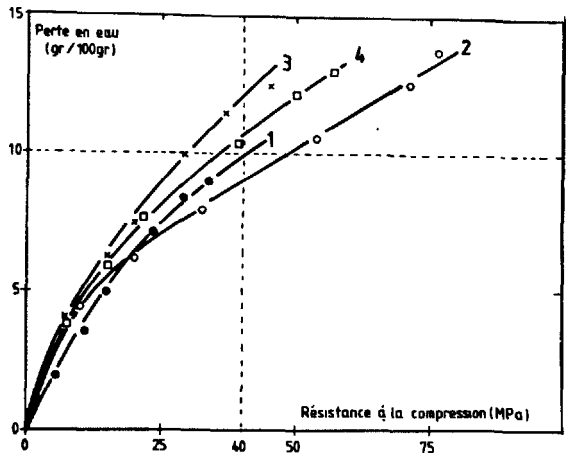

Fig. 3 : Relation entre le degré d'hydratation et la résistance à la compression.

Pour chaque échantillon, on observe une courbe distincte.

Cela signifie que, pour l'ensemble des quatre échantillons, il n'existe pas de relation simple entre la résistance à la compression et le degré d'hydratation du laitier, en dépit du fait que la composition chimique de celui-ci est constante.

L'examen du graphique montre qu'un degré d'hydratation déterminé (par exemple représenté par 10 gr/100 gr) correspond à différentes valeurs de la résistance à la compression d'un échantillon à l'autre :

échantillon		
	2	50 MPa
	1	41 MPa
	4	35 MPa
	3	29 MPa

La séquence décroissante est :

2 > 1 > 4 > 3

De plus, pour développer une résistance à la compression donnée (par exemple 40 MPa) il faut atteindre des degrés d'hydratation différents, obtenus d'ailleurs après des durées de conservation très variées :

échantillon	2	perte 9.0gr/100g	après 4 j.
	1	perte 9.8gr/100g	" 28 j.
	4	" 10.7gr/100g	" 7 j.
	3	" 11.8gr/100g	" 18 j.

Ici la séquence décroissante est :

3 > 4 > 1 > 2

Ce résultat montre que la relation entre la résistance à la compression et le degré d'hydratation est complexe même pour un

laitier de composition chimique déterminé.

Les défauts de structure jouent un rôle à côté d'autres facteurs comme la texture des hydrates formés.

Cette conclusion est probablement valable également pour le ciment Portland et les ciments de laitier, systèmes pour lesquels il est beaucoup plus difficile de la mettre en évidence par l'expérience.

6. Bibliographie

1.- P. FIERENS et P. POSWICK (résultats inédits à paraître dans Cement and Concrete Research).

TABLEAU V

Perte d'eau chimiquement liée en fonction du temps : thermogravimétrie (gr. par 100 gr. de laitier)

Temps	1		2		3		4	
	Perte	Perte corrigée	Perte	Perte corrigée	Perte	Perte corrigée	Perte	Perte corrigée
1 jour	2,76	4,20	4,46	6,07	4,25	5,02	3,93	4,95
2 jours	2,97	4,51	6,22	8,46	6,32	7,46	5,89	7,42
7 jours	7,17	10,90	9,59	13,04	10,30	12,15	10,31	12,99
15 jours	8,39	12,75	12,60	17,14	11,66	13,76	13,07	16,47
28 jours	9,01	13,70	13,28	18,06	12,53	14,79	12,38	15,60

Etude des Gaz des laitiers granulés de haut fourneau

Gazes study of granulated blastfurnace slags

B. COURTAULT - C.E.R.I.L.H. - Paris, France.

Les gaz des laitiers sont extraits par broyage sous vide. Ils sont identifiés et dosés par spectrométrie de masse quadripolaire.

Après une description du dispositif de broyage, les résultats obtenus avec huit laitiers sont présentés, les gaz rencontrés sont par ordre décroissant : H_2, N_2, CO, H_2O, A, CO_2. Une dépendance est observée entre la broyabilité du laitier et la quantité d'hydrogène libéré.

The gases are extracted by grinding under vacuum. They are identified and determined by means quadrupole mass spectrometry. After a description of griding device, the results obtained with eight slags are presented, the gases found are by decreasing order : H_2, N_2, CO, H_2O, A, CO_2. A dependence is observed between the slag grindability and the quantity of the released hydrogen.

1. INTRODUCTION

La présence de gaz occlus et dissous intéresse à divers titres les silicates naturels et artificiels. Certaines laves basaltiques présentent des teneurs pondérales en gaz de 0,5 % à 1 % et voient leur dynamique d'éjection en dépendre largement. Des teneurs beaucoup plus faibles (<0.1 %) sont rencontrées dans les verres industriels et affectent leur propriétés.

La présence de gaz dissous dans les laitiers fondus de haut fourneau a retenu l'attention sur deux points : le rôle possible sur l'expansion du laitier solidifié de la désorption durant le refroidissement, l'influence de la vapeur d'eau solubilisée sur la teneur en hydrogène de l'acier.

Les teneurs en gaz généralement faibles des silicates conditionnent le choix des méthodes analytiques qui distinguent les gaz dissous et les inclusions gazeuses. Les premiers sont extraits par fusion sous vide et analysés en combinant les techniques de condensation fractionnée, de combustion, d'absorption et de micromanométrie ou plus directement de chromatographie. Les gaz des bulles du verre sont recueillis par bris de l'échantillon sous vide ou par fonction de la paroi. Enfin, il faut signaler l'emploi possible, en relation avec la morphologie du matériau, de méthodes microanalytiques non destructives utilisant les réactions nucléaires de basse énergie pour doser les gaz dissous et la microthermométrie ou la microsonde MOLE à effet Raman pour étudier les inclusions fluides des minéraux.

Le présent travail concerne l'étude des gaz des laitiers granulés de haut fourneau et fait appel à la spectrométrie de masse.

2. METHODES EXPERIMENTALES

2.1 Principe

Le laitier granulé, pris dans son état originel, est broyé sous vide jusqu'à différents stades de fragmentation, caractérisés par une courbe de distribution granulométrique, et les gaz libérés analysés par spectrométrie de masse.

2.2 Caractéristiques des matériaux étudiés

Un ensemble de huit laitiers de provenance française est examiné dont les analyses chimiques, limitées aux quatre constituants principaux sont données dans le TABLEAU I.

L'analyse radiocristallographique révèle pour deux laitiers (n° 3 et 7) l'absence de phases cristallines, le diagramme de diffraction X présente seulement un halo large et diffus de corps amorphe entre 0,1 et 0,2 en sin θ/λ . La présence de faibles quantités de merwinite est observée dans les autres laitiers qui présentent tous un rapport molaire Al_2O_3 / Al_2O_3 + MgO inférieur à 0,42 (1).

TABLEAU I

	SiO_2	Al_2O_3	CaO	MgO
1	32,61	12,20	42,91	7,70
2	34,82	12,17	42,35	7,00
3	32,62	14,70	45,00	4,33
4	32,95	11,96	43,28	7,39
5	33,09	11,35	38,94	7,11
6	32,54	11,97	41,76	7,85
7	35,71	10,10	39,45	7,50
8	33,69	11,98	41,38	8,09

2.2 Appareillage

Le pot broyeur étanche est un cylindre de 35 mm de diamètre intérieur et 65 mm de longueur, muni d'une vanne latérale, dont les extrémités sont obturées par des plaquettes appuyées sur des joints toriques par des bouchons vissés.(Fig. 1)

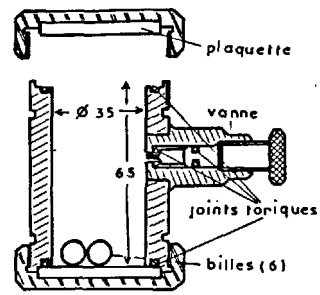

Fig. 1 : Pot de broyage sous vide

La mise sous vide du pot est réalisée dans une enceinte annexe permettant successivement le dégazage dans de bonnes conditions de "conductance" - bouchon supérieur non vissé - puis la mise en place de ce dernier. Une pompe turbomoléculaire produisant un vide très propre, exempt d'hydrocarbures, est utilisée. Le dégazage, contrôlé par jauge de Penning et jugé satifaisant à pression inférieure à 10^{-2} Pa, nécessite, en absence ou non d'échantillon de laitier (15g.), des temps respectifs de 20 et 90 minutes. Le broyage est réalisé au moyen d'un dispositif d'agitation du pot provoquant un mouvement violent, à trois composantes orthogonales,se répétant 1200 fois par minute (Mixer Mill 8000 SPEX).

Après broyage, le pot est mis en communication, par l'intermédiaire de sa vanne, avec une réserve de volume connu dans laquelle l'atmosphère gazeuse est détendue avant l'introduction, en régime moléculaire, dans le spectromètre de masse quadripolaire Q M M 1.7 RIBER, dont les procédés d'étalonnage ont été indiqués (2).

Le choix du matériau constitutif du pot broyeur, conduisant à un dégazage minimum en fonctionnement, est d'une importance primordiale. Dans la forme actuelle, le pot et les plaquettes sont usinés dans un acier élaboré sous vide E 40 CDV 20 AFNOR, contenant moins de 5 ppm de gaz résiduels. Les billes de broyage de 10 mm, au nombre de six; sont constituées d'un alliage chrome, tungstène, cobalt ... (Alacrite 505). Le dégagement gazeux par minute de broyage est le suivant : hydrogène 1 $10^{-3}cm^3$, méthane 0,3 $10^{-3}cm^3$ TNP (l'utilisation d'un acier inoxydable austénitique Z 2 CN 18-10 conduit à un dégagement global dix fois plus important, comportant des hydrocarbures à nombre de carbone plus élevé, accentué encore par l'emploi de carbure de tungstène.

3. RESULTATS EXPERIMENTAUX

Les gaz libérés d'échantillons de laitier (15g.) broyés respectivement 30 secondes, 1, 2 et 3 minutes sont caractérisés par leur spectre ionique et dosés par étalonnage de l'analyseur quadripolaire pour chaque constituant. Dans tous les laitiers, les gaz observés sont par ordre de décroissance en volume : H_2, N_2, CO, H_2O, A, CO_2. Les rapports masse/charge identiques des pics moléculaires N_2 et CO - 28 - conduisent à tenir compte, pour l'analyse ,

de la contribution différente des ions N^+ et CO^{++} à la masse 14.

Les distributions granulométriques déterminées par tamisage et au moyen du granulomètre à laser permettent de calculer les surfaces spécifiques des échantillons broyés. La relation entre celles-ci et le temps de broyage caractérise la broyabilité du laitier (Fig. 2).

La Fig. 3 présente l'évolution des dégagements gazeux du laitier N° 1.

La concentration en volume du gaz, supposée uniforme, c, dans le laitier est déduite du dégagement gazeux au moyen du modèle suivant. Le volume de gaz extractible d'un échantillon de masse M, constitué de grains de rayon r pour lesquels l'épaisseurde la couche d'extraction est y, est donné par :

$$v = \frac{M}{\rho}\left[1 - \frac{(r-y)^3}{r^3}\right] c \quad (1)$$ avec ρ masse volumique

ou, en appelant S la surface totale de l'échantillon et V son volume :

$$v = V\left[3\frac{S\rho y}{3M} - 3\left(\frac{S\rho y}{3M}\right)^2 + \left(\frac{S\rho y}{3M}\right)^3\right] c \quad (2)$$

qui permet d'écrire en première approximation :

$$\left[1 - \frac{v}{V}\right] \approx \exp\left[-\frac{S\rho y}{M} c\right] \quad (3)$$

et $$\mathrm{Ln}\left[1 - \frac{v}{V}\right] \approx -\frac{Syc}{V} \quad (4)$$

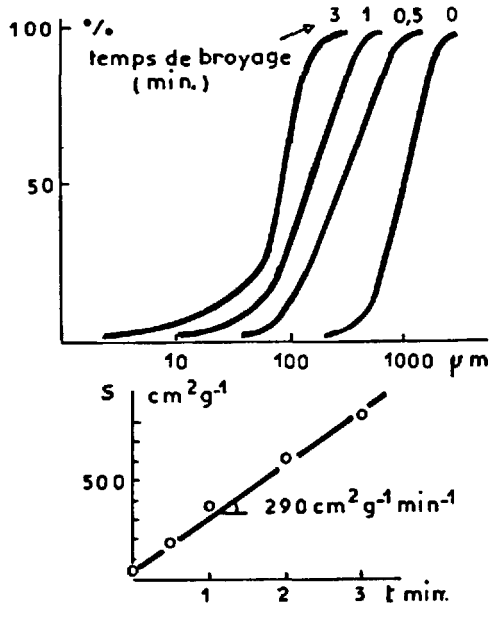

Fig. 2 : Distributions granulométriques et broyabilité (laitier N° 1)

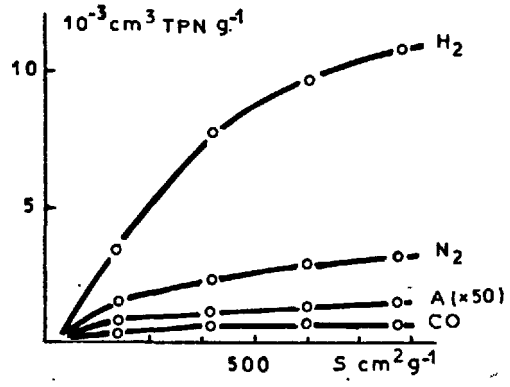

Fig. 3 : Dégagements gazeux (laitier N° 1)

La relation (4) fournit une valeur de yc, par ailleurs une expression de $c\sqrt{y}$ est obtenue par le tracé de v (relation (2)) en fonction de $\sqrt{S}$.

Les concentrations en volume ainsi calculées sont converties et rapportées à la masse de laitier, elles sont indiquées Ci - Concentration interne - dans le TABLEAU II. Le premier dégagement gazeux, observé après 30 secondes de broyage, est exprimé séparément en Concentration superficielle - Cs - par suite de l'application délicate du modèle à la morphologie d'origine des laitiers. Les profondeurs d'extraction, y, trouvées dans les différents cas sont de l'ordre de grandeur du micron.

TABLEAU II

Laitiers		1	2	3	4	5	6	7	8
Broyabilité $cm^2\,g^{-1}\,min^{-1}$		290	200	270	125	175	260	284	250
Concentrations $10^{-3}cm^3$ TPN g^{-1}	H_2 Cs	3,2	9,6	2,1	4,3	5,0	4,5	1,3	5,5
	H_2 Ci	20,7	18,6	5,6	3,0	3,2	7,6	9,7	13,5
	N_2 Cs	1,6	1,4	0,9	1,3	2,0	2,5	0,6	2,1
	N_2 Ci	6,3	2,0	2,6	2,5	2,6	2,4	1,8	-
	CO Cs	0,29	0,53	0,14	0,34	0,67	0,39	0,11	0,48
	Ci	1,13	0,75	0,39	0,58	0,44	0,36	0,34	-
	H_2O Cs	0,07	0,23	0,10	0,12	0,20	0,11	0,07	0,14
A/N_2 I		1,06	0,96	0,96	0,93	0,88	0,92	0,93	0,93

Ces résultats appellent les remarques générales suivantes :

- Les quantités totales de gaz des laitiers granulés (10 à 35 $10^{-3}cm^3$ TPN g^{-1}) sont inférieures d'un facteur 10 environ à celles mentionnées pour les laitiers fondus [3]. Le dégazage lors de la trempe peut en être la cause ainsi que l'absence de réactions secondaires dans le procédé utilisé, contrairement à la méthode thermique d'extraction.
- L'oxygène n'est jamais rencontré contrairement à certaines données [4], de même le CO_2 est présent en quantités limitées, toujours inférieures à $3\ 10^{-6}cm^3$ TPN g^{-1} ($6\ 10^{-3}$ppm).
- L'hydrogène sulfuré est absent des laitiers granulés, alors qu'il est présent dans les laitiers cristallisés ainsi que de petites quantités d'hydrazine (N_2H_4).

Par ailleurs, les concentrations des différents gaz conduisent aux observations suivantes :

- Le rapport CO/N_2 est très variable - 0,15 à 0,37- et toujours inférieur à celui de l'atmosphère du haut fourneau - 0,4 environ -. Pour un laitier donné, il est identique dans la couche superficielle et dans la masse, cette homogénéité semble indiquer l'absence d'occlusion d'air durant la trempe.
- Le rapport A/N_2, voisin de celui de l'air atmosphérique, paraît résulter d'une dissolution physique de l'air dans le laitier fondu, avec absorption de l'oxygène. Les concentrations en azote, voisines de la solubilité physique dans les verres (5) présentent une décroissance avec l'augmentation de la viscosité du laitier fondu (Fig. 4) et, partant, la diminution de la basicité qui va à l'encontre des observations pour les verres. Toutefois la solubilité chimique qui est considérée pour ces derniers et la solubilité physique peuvent présenter une complémentarité (6)

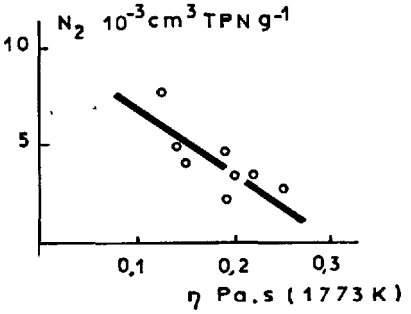

Fig. 4 : Concentration en azote et viscosité du laitier fondu (valeur calculée)

- La présence d'hydrogène mérite une attention particulière. Sa solubilité dans les laitiers industriels et synthétiques est faible, 4-7 ppm (45-78 $10^{-3}cm^3$ TPN g^{-1}) (7), mais néanmoins supérieure aux concentrations observées. Sa présence, dans les gaz extraits par voie thermique des verres et des laitiers est due à la solubilité de la vapeur d'eau dans les silicates fondus où elle s'incorpore suivant des mécanismes variables avec la basicité du milieu (8).

$$\gtrless Si\text{-}O\text{-}Si \lessgtr + H_2O \rightarrow \gtrless Si\text{-}OH + HO\text{-}Si \lessgtr \quad (1)$$

$$2(Si\text{-}O^-) + H_2O \rightarrow 2\,OH^- + \gtrless Si\text{-}O\text{-}Si \lessgtr \quad (2)$$

Devant cette conjoncture, la possibilité de dégagement d'hydrogène par broyage d'un matériau hydroxylé, est examinée avec deux échantillons de verre de silice présentant une granulométrie originelle analogue aux laitiers et des teneurs en ions OH respectives de 950 et 100 ppm environ, déterminées par absorption du rayonnement infrarouge à 2,72 µm.

Le comportement des verres de silice est plus complexe que celui des laitiers puisque, parallèlement à sa libération, l'hydrogène est adsorbé sur le matériau broyé. Deux modes de broyage et d'extraction permettent de départager les deux processus : un broyage continu avec extraction finale du gaz, un broyage discontinu avec extraction intermédiaire du gaz et accumulation Fig. 5. Ces deux types de données permettent, tenant compte d'une adsorption dans le modèle de Langmuir, avec dissociation de la molécule d'hydrogène et occupation de deux sites, de calculer le dégagement réel de gaz à chaque stade.

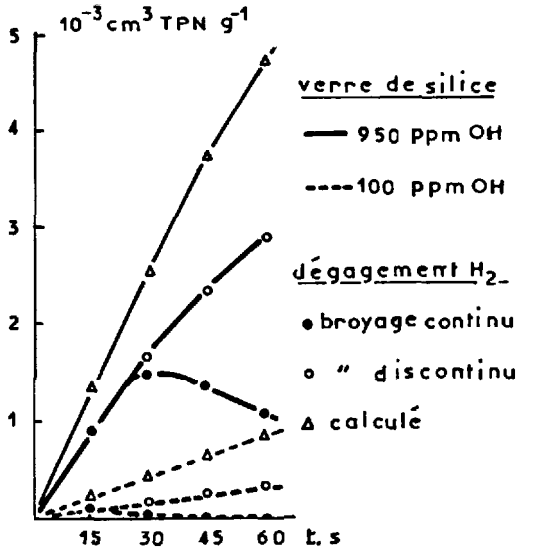

Fig. 5 : Dégagements d'hydrogène des verres de silice en fonction du temps de broyage

L'application à ce dernier du modèle analytique déjà présenté conduit aux concentrations. Les concentrations apparentes en hydrogène ainsi déterminées et les concentrations réelles sous forme d'ions OH sont données dans le TABLEAU III.

TABLEAU III

Verre de silice ppm OH	950	100
Concentrations H_2		
(a) apparente $10^{-3}cm^3$ TPN g^{-1}	8,31	1,41
(b) réelle $10^{-1}cm^3$ TPN g^{-1}	6,26	0,66
a/b %	1,3	2,1

Le rapport moyen des concentrations apparentes et réelles en hydrogène des verres de silice (1,7 %) conduit, par transposition aux laitiers, à des concentrations réelles en hydrogène allant de 0,18 à 1,22 cm^3 TPN g^{-1} (270-1836 ppm OH). Celles-ci sont parfaitement compatibles avec les données sur la solubilité de la vapeur d'eau dans les silicates fondus, dans le domaine pratique de température de la granulation industrielle (9).

L'intérêt que suscite cette solubilitisation apparait plus certain, dans la mesure où la broyabilité du laitier semble en dépendre (Fig. 6).

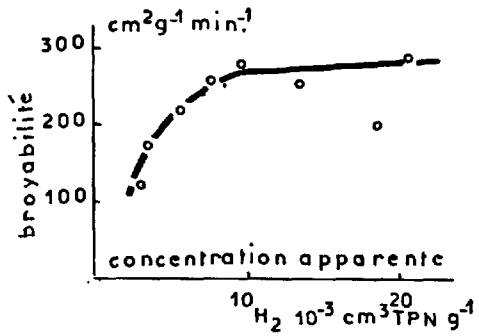

Fig. 6 : Broyabilité des laitiers en fonction de la concentration en hydrogène

L'augmentation de la fragilisation avec l'incorporation d'ions OH ne peut dans le cas des laitiers, compte tenu de leur composition, s'expliquer par une rupture du réseau silicique comme l'indique la réaction (1) . On peut toutefois penser que la réaction (2) concoure à cette action. En effet, la teneur importante en ions modificateurs permet de considérer les laitiers comme des verres inversés au sens donné par TRAP et SEVELS, c'est-à-dire possédant un réseau très fragmenté et une cohésion assurée de façon non négligeable par les liaisons cation-oxygène autres que Si-O.

4. CONCLUSION

Le broyage sous vide du laitier permet d'extraire les gaz dissous physiquement et pour certains chimiquement. Les gaz rencontrés dans les laitiers granulés - H_2, N_2, CO, H_2O, A, CO_2 - sont en concentration relativement faible (0,1 à 25 $10^{-3}cm^3$ TPN g^{-1}) eu égard aux teneurs mentionnées pour les laitiers liquides au sortir du haut fourneau.

La spectrométrie de masse est bien adaptée à la mesure de ces faibles quantités et conduit à des seuils de détection très faibles, de l'ordre de 10^{-3}ppm.

La broyabilité apparaît en relation avec le dégagement d'hydrogène, lié à la solubilisation de la vapeur d'eau dans le laitier fondu ; une fragilisation du matériau par incorporation d'ions OH pourrait en être la cause.

5. REFERENCES

(1) COURTAULT.B.(1977). Journées de calorimétrie et d'analyse thermique, Orsay, 2-71 (français).

(2) COURTAULT B.(1978). Colloque "Analyse des gaz", Soc. Chim. Ind., Saint Etienne, K-1 (français).

(3) ZILBER M.K., ZJATKOVA L.R.,(1962). Izvestija Akademii Nauk SSSR, 5,66, (russe).

(4) ZJATKOVA L.R., CERNJAVSKIJ I., (1968). Izvestija Akademii Nauk SSSR, Metally, 4, 38 (russe).

(5) MULFINGER H.O. (1966). Journal of the American Ceramic Society, 49, 462 (anglais).

(6) DEBRAS G., PIERET M, VAN CANGH L., DECONNINCK G. (1979). Silicates Industriels, 3, 59 (français).

(7) WALSH J.H., CHIPMAN J., KING T.B., GRANT N.J. (1956). Journal of Metals, 8, 1568 (anglais).

(8) UYS J.M., KING T.B. (1963). Transactions of the Metallurgical Society of AIME, 227, 492 (anglais).

(9) DAVIES M.W., SPASSOV A. (1967). Journal of the Iron and Steel Institute, 10, 1031. (anglais).

Ciment de laitier granulé sans clinker

Slag cement without clinker

I. VOINOVITCH, chef du Service de Chimie,
M. RAVERDY, chef du Groupe des Liants Hydrauliques, Département Bétons et Métaux,
R DRON, chargé de recherche, Service de Chimie,
Laboratoire Central des Ponts et Chaussées, France.

RESUME : On a étudié la possibilité de réaliser un nouveau ciment à faible coût énergétique, composé de laitier granulé broyé, additionné de métasilicates alcalins qui jouent le rôle d'activants de prise. Le maximum de simplicité et de sécurité d'emploi est obtenu par incorporation de l'activant en poudre sous sa forme hydratée. La bonne maniabilité des mortiers obtenus avec ces ciments permet une réduction appréciable du rapport E/C. On a pu montrer également que l'addition de gypse, y compris sous forme de phosphogypse, améliore les résistances et permet de réduire à des teneurs économiquement valables les additions de métasilicate. Les résistances en compression et en flexion des mortiers et des bétons, classiques et allégés, sont comparables à celles obtenues avec des ciments Portland.

SUMMARY : The possibility of realizing a new cement, at a low energetic cost, composed of crushed granulated slag with addition of alkaline metasilicates as setting activators has been studied.

The best simplicity and utilization safety has been reached by incorporation of the activator under the powder hydrated form. The good workability of mortars obtained with these cements allows the ratio W/C to be greatly reduced. We have been able to point out that the addition of gypsum and also phosphogypsum (industrial waste) improves the strength and allows to cut down metasilicate additions : this procedure is the most economic. Compression and flexion resistances of mortars and concretes with standard and light aggregates are similar to those obtained with Portland cements.

INTRODUCTION

Les études en vue de réaliser un nouveau liant par association du "verre liquide" (jidkoïé steklo) et du laitier granulé de hauts fourneaux remontent aux années 1950 et sont à mettre à l'actif de P.P. Boudnikov et al. (1).

Ces chercheurs ont mis à profit l'observation faite en 1939 par A.I. Jilin (2) selon laquelle "le laitier granulé ajouté au "verre liquide" en tant que charge inerte accélèrait le durcissement du silicate de soude". V.I. Outkin (3), puis G.T. Poujanov (4) ont développé ces études dans les années 1955-1960 en examinant plus en détail différents paramètres tels que : - la finesse de broyage du laitier, - le module silicique du silicate de sodium, - les rapports de ces deux constituants, - la température.

Ces auteurs se sont également penchés sur l'aspect théorique du durcissement du liant ainsi activé. En bref, ils aboutissaient à la conclusion que cette prise était très accélérée par les activants alcalins (soude, silicate de sodium) ou sulfatiques (gypse) et l'élévation de la température du traitement hydrothermal (autoclavage).

En ce qui concerne le mécanisme d'action du silicate de sodium, ils retenaient l'hypothèse formulée par L.M. Rosenfeld (5) suivant laquelle l'action de l'eau sur le laitier commence par la dissolution et l'hydrolyse du sulfure de calcium avec transformation de ce dernier en $CaSO_4$ et formation en fin de réaction de silicate de calcium hydraté (CSH) à partir d'autres formes de calcium et de silicium passant en solution. Ils estimaient également, en accord avec P.P. Boudnikov (6) que la prise des laitiers granulés pouvait être due à la formation de silicates, aluminates et sulfoaluminates hydratés. Procédant plutôt par déduction que par mise en évidence expérimentale, ces chercheurs ont eu le mérite d'adopter la théorie de Le Chatelier de : dissolution - cristallisation des hydrates et de faciliter ainsi les recherches ultérieures.

En se basant sur ces travaux, dans la période 1964-1966, V.I. Outkin (7), M.A. Matveev et G.T. Poujanov (8) ont développé les études sur la préparation des bétons à partir de tels liants à base de laitiers activés.

Conscients du rôle joué par l'eau dans la prise du laitier granulé, nous avons étudié ce facteur dans la période 1968-1970 en tenant compte des travaux de J. D'Ans et H. Eick (9), de G. Malquori et al. (10) et de Schwiete et al. (11), en aboutissant à la conclusion que l'eau a un double rôle

- elle dissout les éléments du laitier, à partir de la surface des grains, et c'est au sein de la phase aqueuse que prennent naissance les composés très peu solubles qui cristallisent ensuite. Le pouvoir dissolvant de l'eau est modifié par une élévation de pH qui assure le passage en solution de l'alumine;

- elle participe à la réaction de la prise, les composés qui prennent naissance étant des hydrates.

Le rôle de l'activant a été partiellement élucidé : il agit de façon certaine sur la solubilisation de la chaux, de la silice et surtout de l'alumine par élévation du pH. Ainsi, l'hydroxyde d'aluminium précipite en milieu ammoniacal (pH 11,5), mais il se redissout vers pH 12,5 par formation de l'ion $Al(OH)_4$. Cette valeur est atteinte avec la chaux (pH 12,6) et a fortiori avec la soude ou le métasilicate de sodium. Cela explique, sans doute, que l'activation puisse se faire indifféremment avec la soude, la chaux ou un silicate alcalin à la dose requise (pH du milieu > 12,6). Leur présence permet de passer d'un état métastable (phase vitreuse + eau) à un état stable (phase cristalline hydratée), par l'intermédiaire de l'état dissout, sans être obligatoirement consommé par la réaction. Enfin, toute action hydrophobante exercée au niveau des grains de laitier granulé inhibe la réactivité de ce dernier (12).

Les travaux approfondis que nous avons entamés en 1970 sur l'étude de la cohésion dans une pâte de laitier granulé (13) et le mécanisme de la prise du laitier granulé sous activation alcaline (14) nous ont permis d'aboutir à un procédé de préparation de ce type de ciment au laitier exempt de clinker pour lequel des brevets français ont été déposés en 1970 et 1971 (15, 16), antérieurement à un brevet japonais (17).

1 - PARTIE EXPERIMENTALE

Dans ce qui suit, nous relaterons brièvement les études effectuées sur pâtes pures de laitier granulé activé par différents silicates alcalins, puis sur des mortiers de différentes compositions, enfin sur deux types de béton, l'un à base de granulats classiques et le second avec des granulats allégés.

1.1 Essais sur pâtes pures

Ces essais préliminaires avaient pour but d'examiner sur un type de laitier granulé donné, broyé à une finesse voisine de 3 500 Blaine, les paramètres suivants :

- le module silicique (environ : 2,0 - 2,8 et 3,8) du silicate de sodium,

- les dosages en silicate, ajouté à l'eau de gâchage,

- les teneurs en eau,

- la température

et leur influence sur les caractéristiques telles que :

- l'allure de la prise (début et fin de prise),

- la maniabilité,

- les résistances mécaniques.

Le début et la fin de prise étaient suivis par l'aiguille Vicat, la maniabilité des pâtes sur le maniabilimètre Lesage-L.C.L., enfin les essais en flexion et en compression ont été effectués sur trois éprouvettes 4 x 4 x 16 cm à : 1, 2, 7, 28 et 90 jours.

Il ressort de ces essais :

- que le module silicique voisin de 2,0 conduit aux meilleurs résultats, à dosage égal, ce qui recoupe les observations faites par plusieurs auteurs (6, 7, 17),

- qu'en variant le dosage en silicate de sodium, au module silicique cité, de 2 à 10 % par rapport au poids du laitier on modulait la vitesse de la prise. Ainsi, pour des teneurs extrêmes (> à 9 %) on observait une véritable prise en masse de la pâte au bout de 5 minutes de malaxage ...,

- que le début et la fin de la prise (testés à l'aiguille de Vicat) étaient fonction de l'activant employé. Ainsi, pour un dosage moyen de 4 à 6 %, ces caractéristiques sont voisines de celles observées avec le témoin,

- que la maniabilité était très améliorée, même pour des faibles dosages en activant, par rapport aux témoins (CPA 400). Les pâtes obtenues ont une consistance d'une "crème onctueuse". Les mesures faites au maniabilimètre Lesage-L.C.L. donnent des valeurs de 30 à 50 % supérieures à celles des témoins à mêmes teneurs en eau. On peut évoquer à cet égard les phénomènes de thixotropie pour expliquer ce comportement des pâtes : laitier - silicates de sodium à bas module silicique,

- que les teneurs en eau pour des dosages moyens en activant (4 à 6 %) peuvent être réduites de 12 à 15 % par rapport aux essais témoins effectués avec le ciment Portland, CPA 400 dans l'ancienne nomenclature française, par augmentation de la maniabilité des pâtes de laitier activé au silicate de sodium,

- que les retraits, par contre, étaient très supérieurs à ceux des témoins, de l'ordre de 15 à 20 %,

- qu'aux températures de + 5, 20 ± 1 et 70 °C le comportement des pâtes de laitier variaient en fonction du dosage en activant. Ainsi, pour un dosage élevé (8 %), le durcissement à + 5 °C était plus rapide que celui des témoins. Pour une température élevée (70 °C) et un dosage moyen en activant (4 - 5 %) les forces obtenues sont similaires à celles des témoins. Si l'on tient compte qu'une élévation de + 10 °C double grosso modo la vitesse de prise, on peut moduler cette dernière par des dosages appropriés d'activant en fonction des forces que l'on désire obtenir.

1.2 Essais sur mortiers

De nombreux essais ont été effectués en vue de cerner la formulation optimale pour la confection ultérieure des bétons. On travaillait dans ce cas également sur des séries de 3 éprouvettes de 4 x 4 x 16, soumises aux essais de flexion (3) et compression (6).

En plus des paramètres et caractéristiques étudiés sur pâtes pures (1.1), on a examiné sur des mortiers du type Afnor (sable 1350 g, liant 450 g, eau 225 ml pour le témoin CPA 400) l'influence de :

- la nature du laitier (Hématite et Thomas),

- la finesse des laitiers (environ 3000 et 4000 cm^2/g Blaine),

- la nature des silicates, à modules siliciques voisins, et leur forme : liquide, anhydre ou cristallisé,

- l'ajout des fillers : calcaires et siliceux.

Il ressort de ces essais que :

- La différence est à peine significative (5 % environ), lorsque l'on passe d'un laitier Thomas à un laitier Hématite,

- La finesse de broyage accroît nettement les performances, aussi bien en compression qu'en flexion. Une série d'essais effectuée avec du laitier granulé ultra fin (> à 5000 cm^2/g) a permis d'obtenir des performances de l'ordre de 20 % supérieures à celles obtenues avec les témoins (CPA 400), en ajustant les quantités d'eau compte tenu de la grande surface spécifique du laitier ultra fin.

- La nature chimique des silicates (de sodium ou de potassium) ou du silicate de potassium plastifié par une macromolécule

organique (brevet Rhône Poulenc), influe moins sur les performances mécaniques, surtout aux jeunes âges, que le module silicique de ces mêmes molécules, dont l'optimum se place également entre 1,9 et 2,2 dans cette série d'essais. Toutefois, des essais ultérieurs effectués avec du métasilicate de sodium au module voisin de 1,0 ayant donné les meilleurs résultats, c'est ce rapport que l'on a retenu pour les formulations des bétons.

De plus, le métasilicate de sodium anhydre (difficile à manipuler), ou cristallisé (hydrate à 5 H_2O) peuvent être utilisés par simple incorporation dans le laitier en cours de malaxage.

- L'ajout de fillers à raison de 15 à 20 % en substitution au sable peut conférer des résistances améliorées. C'est le filler calcaire micronisé à grande surface spécifique qui se place en tête de ces essais.

Les caractéristiques étudiées en 1.1. : teneurs en eau et maniabilité sont confirmées sur les mortiers et celles ayant trait aux retraits paraîssent atténuées dans ce cas.

1.3 Essais sur bétons

Les études systématiques effectuées sur les mortiers (1.2) ont permis d'établir des formules de bétons avec du métasilicate de sodium utilisé à des concentrations de 4,5 à 9 % par rapport au poids du laitier broyé à la finesse de 3 000 cm^2/g Blaine seulement. En plus du granulat classique, on a fait des essais avec des granulats légers. Dans ce dernier cas, on a pu réduire les quantités d'eau de gâchage (20 % environ) par rapport aux témoins (CPA). A 1 et à 5 ans d'âge les résistances sont, dans certains cas, légèrement supérieures à celles des témoins.

Dans ces essais sur béton avec des granulats légers, on a tenté également une activation mixte en ajoutant à du métasilicate de sodium (5,5 %), du gypse (4,5 %) employé sous forme de phosphogypse (déchet industriel). L'expérience montre que ce procédé est très valable puisqu'on trouve encore des résistances très voisines de celle des témoins (CPA). En outre, ce dernier procédé est plus économique.

Nous donnons, à titre d'exemple, la composition des formules employées ainsi que les résistances obtenues à : 7, 28, 90 jours et à 1, 3 et 5 ans.

Dans tous les cas, le métasilicate et le gypse exprimés en % sont rapportés au total "liant" (laitier + métasilicate + gypse).

2 - DISCUSSION DES RESULTATS

La plupart de nos mesures étaient déjà faites sur mortiers et bétons, y compris celles à 5 ans lorsque nous avons eu connaissance en 1977 des travaux similaires effectués en Pologne par A. Derdacka et J. Malolepszy (18). Ces auteurs activent le laitier par le carbonate de sodium, la soude ou le silicate de sodium au module silicique de 1,5. Ils constatent comme nous : "que la surface spécifique (S.sp) du laitier et la nature de l'activant utilisé ont une influence déterminante sur la résistance du liant. Si l'activant est la soude, avec une S.sp du laitier de 3 200 cm^2/g, on obtient un liant dont la résistance est de 32 à 38 M Pa à 28 jours. Par contre, une élévation de la S.sp jusqu'à 4 200 cm^2/g entraîne un accroissement de la résistance jusqu'à 44 M Pa. En utilisant comme activant du silicate de sodium, on obtient avec des degrés de broyage analogue du laitier, des résistances de l'ordre de 60 à 70 M Pa. Ces résultats ont été obtenus après traitement des mortiers par la vapeur à basse pression". Les résultats obtenus par les auteurs polonais recoupent les nôtres, à cette différence près qu'à la finesse > à 5 000 Blaine, on atteint à la température ambiante ce qu'ils obtiennent par autoclavage.

En ce qui concerne le mécanisme d'action, ils estiment, rejoignant en cela nos observations (12, 13, 14), que sous l'effet des activants alcalins cités, il y a passage en solution des oxydes donateurs de cristaux, tels que la gehlénite hydratée, l'aluminate tétracalcique et le silicate de calcium faiblement basique (CSH). Il y a tout lieu de croire que l'activation mixte employée dans nos essais sur bétons conduit en outre à la formation de l'ettringite qui contribue à une meilleure structuration de l'édifice. Enfin, un récent travail japonais fait mention de l'emploi du silicate de lithium dont l'efficacité serait supérieure à celle du silicate de sodium pour de telles activations, ce qui montre que cette voie continue à être explorée.

RESISTANCE A LA COMPRESSION (C) ET A LA TRACTION PAR FENDAGE (F)

SILICOCIMENT avec et sans gypse sur béton de granulats légers

	7 jours		28 jours		90 jours		1 an		3 ans	
	C	F	C	F	C	F	C	F	C	F
5,5 % métasilicate 0 gypse	15,6	2,0	25,4	2,9	35,9	3,2	40,0	3,0	39,5	2,8
5,5 % métasilicate 4,5 % gypse	21,7	2,2	34,1	2,9	41,3	3,4	46,8	3,6	48,0	2,9
Témoin CPA 400	27,2	3,1	41,3	3,7	41,3	4,0	45,4	4,2	50,0	3,9

SILICOCIMENT sans gypse sur béton routier

	7 jours		28 jours		90 jours		1 an		5 ans
	C	F	C	F	C	F	C	F	C
laitier hématite 9 % métasilicate	29,7	3,0	38,6	4,2	48,9	4,7	54,1	5,0	57,9
laitier Thomas 9 % métasilicate	29,7	3,1	37,6	3,7	48,8	4,3	47,6	4,5	53,1
laitier hématite 4,5 % métasilicate	12,7	1,7	21,6	2,9	37,4	3,6	33,1	4,0	43,0
laitier Thomas 4,5 % métasilicate	9,9	1,6	15,3	2,2	19,8	3,0	29,4	3,6	37,4
Témoin CPA 400	30,9	3,0	37,9	3,5	42,9	3,8	53,4	4,6	56,0

Nota : Toutes les valeurs sont exprimées en méga Pascal (M Pa).

Formules

1
Béton Routier

Granulat 4/20	134 kg
Sable 0/4	96 kg
Laitier ou ciment	43,75 kg
eau	19,35 l pour 4,5 % métasilicate 21,90 l pour 9 % métasilicate et témoin

2
Béton de granulat léger

Granulat léger	130 kg
Sable 0/5	163 kg
Laitier ou ciment	100 kg
eau	37,6 l (témoin) 49,5 l

CONCLUSIONS

L'étude sur pâtes pures et mortiers de ciments de laitiers activés aux silicates alcalins à différents modules siliciques a permis d'établir que les meilleurs résultats sont obtenus avec le métasilicate de sodium (module silicique 1,0).

Cet activant augmente la maniabilité des pâtes de sorte que le rapport : E/C peut être réduit. Son emploi est compatible avec une augmentation de la finesse du laitier, qui améliore considérablement les propriétés mécaniques.

A partir de ces données, on a préparé des bétons (classiques et allégés) dont le liant était constitué par du laitier broyé à 3 000 cm^2/g, additionné de métasilicate pentahydraté à des doses variant de 5 à 9 % par rapport au laitier. Les mesures de résistance à la compression et à la traction par fendage montrent que ces bétons sont comparables à ceux à base de ciment Portland. Un gypsage modéré, par le phosphogypse, améliore les résistances et permet de réduire les doses de métasilicate.

Ce liant, à faible coût énergétique, pourrait être utilisé en construction routière et pour la production d'éléments préfabriqués.

BIBLIOGRAPHIE

1.- P.P. BOUDNIKOV, I.L. ZNATKO-JAVORSKI, (1953), Laitiers granulés de hauts fourneaux et ciments aux laitiers, Promstroïzdat, Ed. Moscou.

2.- A.I. JILIN, (1939), Le verre liquide, ses propriétés et utilisations, Gonti-NKTP, URSS, Sverdlovsk-Moscou.

3.- V.I. OUTKIN, (1959), Sur la théorie du durcissement du liant de laitier vitrifié, C.R. Filiale Moldave de l'Acad. Sc. de l'URSS, n° 12, 66, 79-85.

4.- G.T. POUJANOV, (1960), Propriétés physico-mécaniques de matériaux de construction à base de laitier et de verre liquide, Recueil des travaux de la Filiale de Khazakstan de l'Acad. Sc. de l'URSS, n° 2/4.

5.- L.M. ROSENFELD, (1958), Laitier expansé autoclavé, Gosstroïzdat Ed.

6.- P.P. BOUDNIKOV, V.L. PANKRATOV, E.P. KEVES, (1962), A propos de la réactivité et de l'activité du laitier hydraulique vitrifié, Dok. Akad. Nauk., URSS, 146, n° 2, 415-417.

7.- V.I. OUTKIN, (1961), Bétons à base de liants en laitier vitrifié, C.R. Filiale Moldave de l'Acad. Sc. de l'URSS, n° 6, 84, 84-91.

8.- M.A. MATVEEV, G.T. POUJANOV, (1964), Interaction en phase liquide du laitier de hauts fourneaux et de ses constituants avec le silicate alcalin, Recueil des travaux du NIISM de Alma-Ata, n° 6/8.

9.- J. D'ANS, H. EICK, (1954), Recherches sur la prise des laitiers de hauts fourneaux, Zement-Kalk-Gibs, 12, 449-459.

10.- G. MALQUORI, R. SERSALE, E. GREGORIO, (1951), L'appréciation de la valeur hydraulique des laitiers de hauts fourneaux, Indus. Ital. Cemento, 10-11, 232-237.

11.- H.E. SCHWIETE, V. LUDWIG, K.E. WURTH, G. GRIESHAMMER, (1959), Formations nouvelles en cours d'hydratation du laitier de hauts fourneaux, Zement-Kalk-Gibs, 4, 154-160.

12.- I.A. VOINOVITCH, R. DRON, (1970), le rôle de l'eau dans la prise du laitier granulé, Bull. Liaison Labo. Routiers P. et Ch., n° spécial "Les laitiers de hauts fourneaux en construction routière", 87-94.

13.- Ph. PETIT, (1973), Contribution à l'étude de la cohésion dans une pâte de laitier granulé, Rapport de recherche n° 27, LPC, 94 pages.

14.- R. DRON, (1974), Mécanisme de la prise du laitier granulé sous activation alcaline, Rapport de recherche n° 38, LPC, 128 pages.

15.- Brevet français des Labo. Ponts et Chaussées (24.9.1970), Procédé d'amélioration des mélanges de graves et de laitier granulé au moyen de silicates alcalins, n° de dépôt 70.34.691.

16.- Brevet français du Labo. Central des Ponts et Chaussées (24.12.1971), R. DRON, I. VOINOVITCH, Nouvel additif pour ciments, n° de dépôt 71.46.535 et Additif du 3.8.1973, n° 73.28.527.

17.- MORI ZENJI, 17.11.1971, Additives for concrete and concrete blocks, Japon, n° 72.39.120 (Brevet).

18.- A. DERDACKA, J. MALOLEPSZY, (1975), Le laitier granulé de hauts fourneaux pour la préparation de liants hydrauliques sans clinker, Cement-Wapno-Gibs, n° 10, 291-295.

Cinetique de l'hydratation des ciments au laitier

Kinetics of slag cements hydration

C. VERNET, E. DEMOULIAN, P. GOURDIN, F. HAWTHORN, Société des Ciments Français, CEREG, France.

RESUME :

Après avoir étudié par ailleurs les mécanismes et la cinétique de l'hydratation des ciments portland, les auteurs appliquent ici la même méthode globale d'étude des suspensions concentrées, à l'analyse des phénomènes particuliers aux ciments à haute teneur en laitier.

Après une description rapide de la méthodologie et du choix des échantillons, ils montrent pour chaque étape réactionnelle, les particularités cinétiques des ciments considérés en fonction des différences minéralogiques et chimiques des clinkers et des laitiers utilisés.

L'interprétation des phénomènes est donnée dans le contexte des mécanismes généraux de dissolution-cristallisation, en utilisant les concepts de couplage chimique et de distance de précipitation. Les variations de S^{--} en solution laissent supposer la présence d'hydrates sulfurés. De même, l'observation des courbes de concentration en Cl^- permet d'étudier la séquence de précipitation des chloroaluminates.

Enfin, une comparaison est établie entre les réactions en suspension et en pâte pure, liant la cinétique aux résistances mécaniques et à l'évolution de la microstructure.

SUMMARY :

Following another study of the mechanism and kinetics of portland cement hydration in concentrated suspension, the authors apply here the same method to the cements with high content of blast-furnace slag.

The method and the samples are shortly described. They show for each reaction period the differences observed between portland and slag cement according to chemical and mineralogical composition of clinkers and slags.

The phenomena are explained in relation with the general dissolution-crystallization mechanisms and using the concept of chemical couplings and precipitation distance. The evolution of S^{--} concentration let suppose the presence of sulphide hydrates. In the same way, the Cl^- evolution allows the study of chloroaluminates precipitation.

Then a comparison is established between suspension and cement pastes which connect kinetics with compressive strengths and microstructure developments.

INTRODUCTION

Cette communication vise à étudier la cinétique de l'hydratation des ciments de laitier, avec la même méthode que celle appliquée à l'étude du CPA (3). Nous avons montré par des mesures cinétiques que pendant l'hydratation des clinkers, les mécanismes réactionnels sont essentiellement du type dissolution-cristallisation, selon l'hypothèse formulée dès 1887 par LE CHATELIER (1).

La composition ionique de la solution résulte donc à chaque instant de la différence entre vitesse de dissolution de l'anhydre et vitesse de précipitation de l'hydrate correspondant. L'énergie libérable par les anhydres permet de maintenir en permanence la sursaturation de la solution, produisant un déséquilibre thermodynamique, moteur de l'avancement des réactions.

Introduisant le concept de distance de précipitation des hydrates, nous avons expliqué le mode particulier de cristallisation du CSH et proposé une explication cinétique de ses changements de structure (2).

A l'aide d'un appareillage original, nous avons ensuite mis en pratique la mesure indirecte de la cinétique et de la séquence de l'hydratation des suspensions de ciments portland, avec un rapport eau/ciment (E/C) de 4. Cette étude (3) montre que K^+ et surtout Na^+, sont d'excellents traceurs de l'hydratation du C_3A et que l'on peut repérer à l'aide des courbes de conductance, de pH et d'évolution ionique de la solution toutes les étapes de l'hydratation. Ceci nous a permis de mettre en évidence l'interdépendance étroite entre vitesses de réaction des constituants du ciment, causée par des couplages de nature thermique et chimique. D'autre part, les conditions opératoires à E/C = 4 conservent la séquence de l'hydratation par rapport aux mortiers, par contre l'échelle des temps est modifiée de manière telle qu'on obtient en une semaine des taux de réaction correspondant à plusieurs mois sur mortier. Ceci constitue un avantage précieux, lorsqu'on cherche à mesurer la vitesse d'hydratation du laitier, activé par le clinker, les réactions des laitiers étant toujours très lentes (5). Nous avons donc appliqué notre méthode à des suspensions de ciments au laitier, fabriquées à partir des clinkers étudiés précédemment (3) et de 3 laitiers représentatifs de la production française.

1/ METHODOLOGIE

1.1 - Choix des échantillons

Les 7 clinkers utilisés ont des compositions minéralogiques différentes (tableau I), aussi bien par la forme de l'alite que par la forme et la quantité de C_3A et par la teneur en sulfates alcalins. Leur comportement hydraulique en CPA (évolution de résistances en fonction du temps) est très variable.

Les 3 laitiers sont de provenances différentes et montrent des comportements hydrauliques différents, que nous avons étudiés par ailleurs (6).
Leurs compositions chimiques, ainsi que les données minéralogiques et de structure que nous avons réunies, figurent aux tableaux II et III.

A l'aide des clinkers C1 à C7, broyés à 3500 cm^2/g et des laitiers A, B et C, nous avons préparé deux séries de ciments au laitier dont nous avons étudié par ailleurs l'évolution des résistances mécaniques (6) ; une première série de caractéristiques suivantes :

- rapport laitier/clinker L/C = 4
- surface spécifique du laitier : 3500 cm^2/g
- gypsage : 3 % en SO_3

et une deuxième série avec broyage séparé du laitier :

- L/C = 4
- surface spécifique du laitier : 6000 cm^2/g
- gypsage : 5 % en SO_3.

Tableau I : Minéralogie des clinkers (analyse diffractométrique quantitative)

% Phases	C1	C2	C3	C4	C5	C6	C7
Alite	68,4	61,4	73,5	65,4	65,9	57,8	65,2
sous forme	(R)	(R)	($M_I b$)	($M_I b$)	($M_I b$)	($M_{II} b$)	($M_I b$
bélite	26,2	20,8	14,7	11,1	12,7	22,2	20,6
C_3A cub.	2,5	12,5	0,0	1,2	5,1	1,9	0,9
C_3A tétrag.	0,0	1,7	5,6	15,8	3,1	1,4	1,2
C_4AF	0,0	4,6	8,5	5,1	10,9	15,6	10,2
K_2SO_4	0,0	0,0	0,0	0,8	2,3	0,6	ε
$CaCO_3$	1,5	0,5	0,0	0,0	0,0	0,0	0,0
MgO péric.	0,0	0,0	0,0	0,0	0,8	0,3	0,1
CaO libre	1,9	1,5	0,0	2,3	2,2	2,5	2,4

Tableau II : Composition des laitiers

Composition chimique %	A	B	C
Perte au feu	0,39	0,42	0,85
Silice totale	32,91	33,03	34,78
Al_2O_3	14,95	12,33	12,11
FeO	0,54	1,74	0,61
TiO_2	0,51	0,52	0,59
MnO	0,34	0,69	0,61
CaO	43,74	40,88	41,04
MgO	4,53	7,64	7,97
SO_3	0,05	0,04	0,05
S^{--}	0,88	1,12	0,92
K_2O	0,57	0,44	0,53
Na_2O	0,26	0,34	0,30
P_2O_5	0,09	0,03	0,02
F^-	0,23	0,09	0,13
Cl^- (ppm)	<35	284	<35
Rapport C/S	1,33	1,24	1,18

Tableau III : Données minéralogiques

Laitiers	A	B	C	Méthode
% Merwinite	< 2	2,5	3	Diffraction X
% Géhlénite	< 1	< 1	< 1	Diffraction X
% Cristaux	0,01	5,9	4,1	Microscopie
Diamètre moyen des cristallites (Å)	300	900	800	Diffusion X Petits angles

1.2 - Méthodes

Nous décrivons par ailleurs la méthodologie complète des mesures cinétiques (4). Son originalité réside dans l'utilisation du maximum de capteurs électrochimiques, de manière à ne laisser échapper aucun phénomène transitoire dans l'évolution ionique de la suspension. Des dosages chimiques séquentiels permettent de réétalonner périodiquement les capteurs, et de compléter l'investigation lorsqu'on ne dispose pas de capteur pour un ion donné (SO_4^{--}, $H_2SiO_4^{--}$). Des dosages de phases sont effectués par des méthodes physiques classiques (diffraction X, ATG, ATD) sur des fractions de solide, prélevées en cours de réaction. Des mesures thermiques sont réalisées simultanément et permettent ainsi d'obtenir une description complète des paramètres cinétiques, sous forme d'un diagramme d'évolution de la phase liquide, de la phase solide, et du flux thermique. Dans le cas présent, nous avons utilisé les capteurs électrochimiques suivants : conductance, pH, pK^+, pNa^+, pS^{--}, pCl^-.

Les dosages chimiques séquentiels ont porté sur les ions Ca^{++}, SO_4^{--}, $H_2SiO_4^{--}$, OH^-, S^{--}, Na^+, K^+, Cl^-.

Aux dosages de phases classiques, nous avons ajouté ici le dosage chimique du laitier résiduel non hydraté. par notre nouvelle méthode de séparation sélective (7).

1.3 - Mesures

De grandes précautions ont été prises pour assurer la validité des dosages : travail sous atmosphère d'azote, essais répétés, prélèvements et filtration par 2 méthodes de séchage (lyophilisation et lavage au méthanol), circuit d'analyse automatique de faible volume mort et exempt d'interférences entre capteurs.

Trois séries d'essais ont été effectuées :

- mélanges à 3500 cm^2/g avec laitier A et chacun des 7 clinkers
- mélanges à 3500 cm^2/g avec clinker C7 et chacun des 3 laitiers
- et 5 mélanges avec laitier à 6000 cm^2/g soit 16 au total.

2/ RESULTATS

En comparant les diagrammes des 16 ciments au laitier et des CPA correcpondants, nous avons constaté une différence beaucoup plus importante entre les CPA et les ciments au laitier, qu'entre ces derniers. Cependant l'examen des courbes fait apparaître dans tous les cas l'existence de 4 périodes au cours de l'hydratation.

A titre d'exemple, nous avons choisi ici 3 diagrammes, dont le premier rappelle l'allure obtenue pour les CPA (fig. 1) et les suivants montrent les particularités de deux ciments au laitier (fig. 2 et 3). En s'aidant de ces diagrammes, nous nous proposons maintenant d'étudier successivement chacune des périodes.

1ère période : (temps 0 à t_1)

Nos observations nous conduisent à penser que le laitier participe aux réactions dès les premiers instants. Ces réactions sont initialement rapides, puis très vite ralenties, ce qui conduit à un taux de réaction très faible :

. la chute de SiO_2 en solution montre la précipitation de CSH ;
. l'aspect de la courbe des sulfures, en relation avec des mesures faites par ailleurs sur les laitiers seuls en suspension dans l'eau où dans une solution de chaux + gypse, peut être expliquée par une légère réaction du laitier. Cette dernière est cependant suffisante pour modifier les concentrations en Ca^{++} en fin de période. En effet, au bout de 10 minutes on observe pour un même clinker, (C7) et 3 laitiers différents, les concentrations suivantes (à 3500 cm^2/g)

C7 + Laitier	A	B	C	CPA C7
(Ca^{++}) mM/l t = 10 mn.	14	9	6	17

Ces valeurs varient comme le C/S du laitier : nous pensons que les différences observées sont dues à la fois aux variations de composition chimique et aux variations de vitesse de réaction de chaque laitier.

Pendant la 2ème période dite "période dormante", (temps t_1 à t_2),

. la concentration en S^{--} reste constante et très faible, de même que le taux de réaction du laitier, inférieur à 2 % en fin de période ;
. le flux thermique est faible, mais, rapporté à la quantité de clinker, plus élevé que le CPA corres-

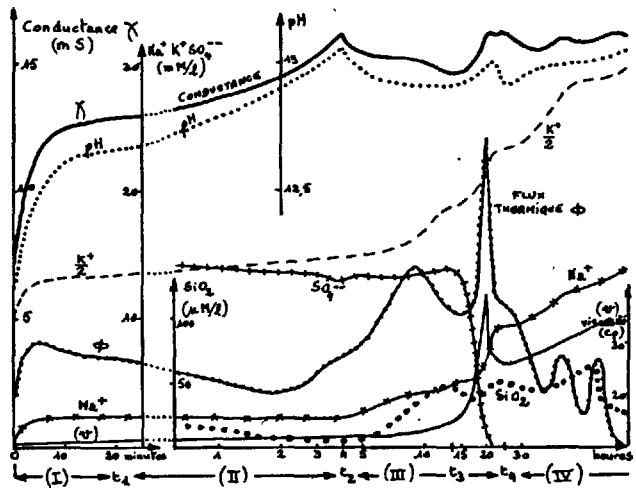

Fig. 1 : CPA C4

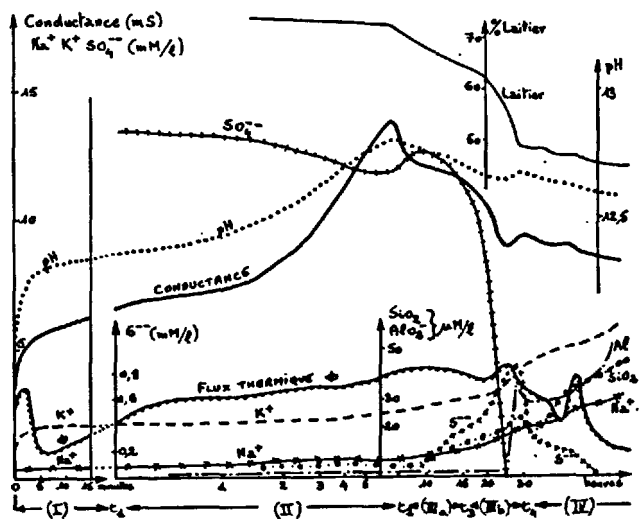

Fig. 2 : Ciment au laitier (A + C6)

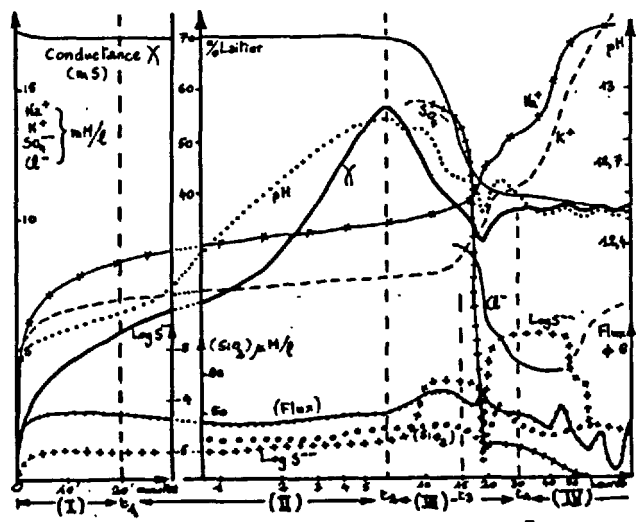

Fig. 3 : Ciment au laitier (A + C4) + Cl^-

pondant ;
les pentes des courbes de conductance sont plus élevées. Pour un même laitier, les différences d'allure des courbes de divers clinkers sont atténuées et ce, d'autant plus que le laitier est finement broyé.
Le tableau IV donne, pour un même clinker, les valeurs des pentes des courbes de teneur en chaux, calculées à partir des courbes de conductance au temps $t_2/2$.

Tableau IV : Vitesses de sursaturation en chaux

$\frac{dC}{dt}$ (t/2) en $mM.l^{-1}.mn^{-1}$ Mélanges AC7, BC7, CC7

Laitiers		A	B	C
3500 cm^2/g	dCa/dt	4.10^{-2}	8.10^{-2}	9.10^{-2}
	(Ca^{++})temps t_1	14 mM/l	9 mM/l	6 mM/l
6000 cm^2/g	dCa/dt	7.10^{-2}		8.10^{-2}
	(Ca^{++})temps t_1	9 mM/l		6 mM/l
C/S laitiers		1,33	1,24	1,18

On remarque les variations en sens inverse de dC/dt et de $(Ca^{++})t_1$.

A partir des teneurs en Ca^{++} variables au temps t_1, l'alite des 7 clinkers parvient donc, par une adaptation de sa vitesse de réaction, à créer au temps t_2 un état de sursaturation en chaux du même ordre de grandeur que pour les CPA. Ceci nécessite une vitesse de réaction plus élevée du clinker pendant cette période, qui se traduit par un flux thermique plus élevé. Ce comportement s'interprète bien par le mécanisme de dissolution précipitation : la dissolution de l'alite est ici déplacée et accélérée par la réaction initiale du laitier, et par le rapport eau/clinker élevé conduisant à des concentrations en chaux plus faibles au temps t_1. La faible réaction du laitier entre t_1 et t_2 peut éventuellement participer à cette accélération.

3ème période (temps t_2 à t_4)

Nous avons divisé cette période en deux étapes :

1ère étape (temps t_2 à t_3)

De même que pour les CPA, nous remarquons au temps t_2 une chute de sursaturation en chaux, accompagnant la précipitation de la portlandite, mais nous n'observons plus ici de palier de concentration en chaux. La teneur en chaux diminue d'autant plus vite que la finesse du laitier est grande et pour un même clinker la pente est plus forte avec le laitier A qu'avec B et C. Le taux de réaction du laitier augmente significativement, de même que la teneur en S^{--}. Cependant, cette teneur ne correspond qu'au dixième de la quantité calculable d'après la consommation de laitier. Simultanément, les réactions des clinkers s'accélèrent. Le flux thermique augmente, de même que les concentrations en K^+ et Na^+, indiquant la réaction du C_3A.

La 2ème étape (temps t_3 à t_4) se caractérise par la chute de concentration en SO_4^{--} qui fait suite à la disparition du gypse. A l'épuisement de SO_4^{--} succède la transformation ettringite - monosulfate, que nous avons observée en diffraction X, et qui s'accompagne d'une augmentation significative du flux thermique et des teneurs en Al_2O_3 et SiO_2 en solution.
C'est pendant cette deuxième étape que nous observons la réaction la plus rapide du laitier. De même, dans le CPA, on observe à ce moment, un maximum de vitesse d'hydratation des aluminates, suivi d'une reprise de l'hydratation de l'alite.
A ces remarques de caractère général s'ajoutent les particularités suivantes :

- le mélange A + C2 montre une chute de concentration en SO_4^{--} en deux étapes rapprochées, ce qui peut signifier que le C_3A cubique de C2 est totalement consommé avant la disparition complète de SO_4^{--}, qui est alors achevée par la réaction du laitier ;
- pour un certain nombre de mélanges, la solution passe dans le domaine sous-saturé en chaux, ce qui produit la dissolution de la portlandite, en particulier dans le cas des laitiers broyés à 6000 cm^2/g ;
- les courbes d'évolution de S^{--} sont différentes selon le clinker et le laitier, mais nous observons pour tous les mélanges des variations brutales de la pente de ces courbes, indiquant une discontinuité des réactions produisant la disparition du sulfure. Parmi ces réactions, la formation d'hydrates analogues aux sulfoaluminates nous ayant semblé probable, nous avons tenté d'en faire la synthèse à partir de produits purs. Par réaction directe du C_3A avec un sulfure de sodium dans le rapport molaire :

$$\frac{S^{--}}{C_3A} = 3$$

en milieu tamponné à pH 12,55 par de la chaux saturée sous atmosphère d'azote, nous avons observé une diminution du sulfure en solution d'un tiers et la précipitation d'un composé de couleur verdâtre. Le diagramme de diffraction X du composé synthétisé est très proche de celui du C_4AHx et les raies du C_3A ont presque totalement disparu. D'après la littérature, x peut varier de 7 à 19 et dans les conditions opératoires, l'examen de la raie principale à 8,05 Å fait penser que le composé hydraté est proche de C_4AH_8. Compte tenu de la disparition d'un tiers des sulfures, on peut penser à la formation d'un hydrate qui fixe S^{--}.

Une recherche ultérieure sera consacrée à l'étude de la précipitation des aluminates hydratés en présence de SO_4^{--} et de S^{--} car nous pensons que la rétention des sulfures est due à un composé de type sulfuroaluminate hydraté.

Pendant la quatrième période (temps t_4 à t_5), les réactions sont ralenties par la diffusion à travers les hydrates. La teneur en chaux de la solution diminue progressivement et passe en général au-dessous de la saturation en fin d'essai (≃ 100 h). Lorsque la vitesse de réaction a été suffisante dans les étapes précédentes, on peut observer une ou plusieurs transformations successives des sulfoaluminates, décelables par les variations simultanées du % de laitier, de la conductance, des teneurs en K^+, Na^+ et S^{--}, et de petits pics de flux thermique.

Influence de Cl^-

De faibles quantités de chlorures (0,2 % NaCl) modifient la cinétique de l'hydratation des ciments de laitier : l'évolution des résistances mécaniques est significativement plus rapide aux premiers âges.

En suspension à E/C = 4, nous observons les particularités suivantes des courbes d'évolution (fig. 3).

- La chute plus brutale de SO_4^{--}, annonçant l'épuisement du gypse en fin de 3ème période (t_3-t_4) aboutit non plus à une valeur presque nulle de la concentration, mais à un palier intermédiaire voisin de 1 mM/l.
- La teneur en Cl^- varie très peu jusqu'en fin de 3e période.
- La chute de (Cl^-), annonçant la formation bien connue de chloroaluminate, intervient aussitôt après la chute de SO_4^{--}. (Cl^-) ne s'annule pas complètement et atteint un palier au bout de quelques dizaines d'heures. A ce moment (SO_4^{--}) diminue à nouveau jusqu'à une valeur très faible, (Cl^-) augmente, (S^{--}) chute très rapidement, (Na^+) et (K^+) augmentant, chacune des variations brutales de concentration étant accompagnée d'un pic thermique. Ceci montre un mécanisme complexe où coexistent des effets antagonistes de solubilité et de vitesse de précipitation des chloro, sulfo et sulfuroaluminates, qu'il faudrait étudier plus en détail.

3/ INTERPRETATION - COMPARAISON AVEC LES OBSERVATIONS SUR MORTIERS

3.1 - Correspondance entre cinétique et microstructure des hydrates

Mme.REGOURD (5) a montré que dans les ciments au laitier, le CSH peut se déposer loin des grains de clinker : par exemple sur les grains de laitier ou sur une lame porte-objet. Ses observations faites au MEB s'interprètent parfaitement dans le modèle cinétique théorique basé sur le mécanisme du type LE CHATELIER. Les variations de la taille des particules de CSH en fonction du temps correspondent bien aux distances de précipitation que nous avons définies : peu après la prise, la solution reste suffisamment sursaturée et l'on obtient des fibres courtes, puis, la teneur en calcium diminuant, la distance de précipitation augmente et les CSH forment alors une texture alvéolaire, en cristallisant loin de l'interface, en reliant les CSH précédents et en comblant peu à peu les pores.

La cristallisation des "CSH du laitier" dans une zone compacte autour des grains de laitier s'explique par la formation d'une partie des CSH, de composition très différente, dans la zone de diffusion entourant le grain.

D'autres CSH se forment simultanément dans les pores lointains et leur formation contribue d'ailleurs à la corrosion de la portlandite.

Nous n'observons pas systématiquement la disparition de la portlandite : à 3500 cm^2/g, seul le mélange C1A parvient dans le domaine sous-saturé (à 18 h). Les autres montrent une très faible teneur en portlandite. Par contre, avec les laitiers broyés à 6000 cm^2/g, tous les mélanges passent dans le domaine sous-saturé en chaux lorsqu'ils approchent du minimum de conductance signalant la chute de SO_4^{--} (entre 15 et 30 h selon le cas) et la reprise des réactions du laitier. D'après les observations de Mme. REGOURD, on peut donc faire la correspondance des échelles des temps pour cette période : 28 jours en pâte pure correspondent à environ 20 h en suspension : l'ettringite atteint alors sa teneur maximum. Nous situons de même la période de fortes teneurs en monosulfoaluminates à 50 - 60 h en suspension et à 3 mois - 6 mois en pâte pure.

3.2 - Cinétique et évolution des résistances

Dans l'hypothèse de dissolution-cristallisation, les taux de réaction obtenus après le maximum de sursaturation sont reliés à la vitesse de chute de la teneur en calcium en solution. Nous avons donc cherché à mettre en relation la chute de conductance correspondante, directement mesurable sur l'enregistrement, avec les résistances mécaniques mesurées sur mortiers. Pour le laitier A, associé à divers clinkers, on constate une corrélation assez bonne, entre le rapport X_m/X_M des conductances au minimum et au maximum de la courbe, et les résistances sur mortier ISO à 7j, 28j, 3 mois et 6 mois. Les écarts par rapport aux droites de régression s'expliquent bien en tenant compte dans la corrélation des variables supplémentaires C_3A tétragonal et K_2SO_4, dont les alcalins perturbent à la fois la conductance et les résistances.
C'est ainsi par exemple qu'à 3500 cm^2/g, à l'échéance de 6 mois :

- 93 % des variations de R sont expliquées par la chute de conductance seule,
- 96,6 % des variations sont expliquées par la chute de conductance et le C_3A tétragonal,
- 98 % des variations sont expliquées par la chute de conductance, le C_3A tétragonal et la teneur en K_2SO_4.

De même, pour la série à laitier variable et clinker C7, on obtient une variation de résistance sensiblement linéaire en fonction de Xm/XM.

Il n'est évidemment pas question d'utiliser de telles relations pour faire des prévisions de résistance : le nombre d'essais n'est pas assez élevé ici pour que l'on puisse généraliser les relations obtenues. Mais ces relations montrent que lorsqu'on opère dans des conditions standardisées, on peut mettre en évidence l'influence de la cinétique chimique sur les résistances : les paramètres de porosité et de mise en oeuvre étant rendus sensiblement constants.

Par ailleurs, les coefficients obtenus dans la relation résistances = $A + B\,(Xm/XM) + C(K_2SO_4) + D(C_3AT)$ nous fournissent des indications sur les influences de chacune des variables.

Le coefficient D est positif et faible par rapport à B. Effectivement, le rôle bénéfique de C_3A tétragonal n'apparaît pas clairement dans nos mesures cinétiques. Tout au plus peut-on supposer que les alcalins libérés au cours de son hydratation contribuent à diminuer la solubilité de la portlandite, en élevant le pH. Ceci peut diminuer la vitesse de redissolution de la portlandite lorsqu'on atteint le domaine de sous-saturation en chaux.

Le coefficient C est faible par rapport à B et négatif à long terme. L'action de K_2SO_4 du clinker n'est en effet pas évidente, dans des mélanges où le clinker est dilué par 4 parties de laitier. Dans les CPA, nous avons dégagé les mécanismes accélérateurs de l'hydratation de C_3A par K_2SO_4 : celui-ci déplace au départ les réactions de l'alite en consommant le calcium pour former de l'ettringite. Il en résulte une accélaration de la dissolution de l'alite, et par couplage thermique, une accélaration de l'hydratation du C_3A (2). D'autre part, K_2SO_4 agit sur la structure des CSH, ce qui peut s'expliquer en utilisant le concept de distance de précipitation : l'abaissement de la concentration en chaux ci-dessus diminue la sursaturation en CSH et sa vitesse de précipitation : il cristallise plus loin de l'interface, ce qui retentit sur les résistances.

On conçoit donc que, dans les ciments au laitier, K_2SO_4 puisse avoir deux effets antagonistes sur les résistances, l'ettringite y étant au départ relativement abondante par rapport au CSH.

3.3 - Correspondance des échelles des temps sur mortier et en suspension

Ne disposant actuellement que de peu de renseignements sur les taux de réaction du laitier des ciments en pâte ou mortier, nous pouvons faire les remarques suivantes :

- dans l'établissement de la correspondance des temps, il faut prendre comme origine commune le "début de prise chimique" situé sur mortier peu avant le temps de "prise rhéologique" mesuré à la soude de VICAT.
- les observations du paragraphe 3.1 confirment l'hypothèse faite par ailleurs pour les CPA (3), d'une loi non linéaire de correspondance.

CONCLUSION

Notre méthode d'étude globale des suspensions concentrées est donc riche d'informations.

Elle permet de montrer qu'au cours de l'hydratation des ciments au laitier, il existe des périodes caractéristiques où laitier et aluminates réagissent simultanément mais à des vitesses différentes. La séquence de l'hydratation des ciments au laitier est donc la même que celle des CPA. Ce comportement commun est lié à l'existance de phénomènes de couplage chimique et thermique des vitesses de réaction que nous avons mis en évidence.

La présence de sulfures solubles dans les laitiers, et l'intervention d'un mécanisme de dissolution-précipitation associant le laitier et des hydrates sulfurés, ajoutent quelques particularités au comportement des ciments au laitier. Ces phénomènes rendent difficile l'utilisation directe de S^{--} comme traceur de l'hydratation du laitier. Les variations brutales de S^{--} sont cependant liées à la séquence des réactions et peuvent servir de points de repère.

Nous montrons également que le laitier, par sa consommation de chaux, augmente la vitesse de dissolution de l'alite pendant toute l'hydratation, ce qui conduit en général à une sous-saturation et une consommation de la portlandite dans l'étape finale.

L'influence des éléments mineurs et des aluminates du clinker est fortement atténuée dans les mélanges riches en laitier. Par contre, des adjuvants comme Cl^-, en faible teneur, en formant des hydrates intermédiaires parviennent à modifier la séquence et les vitesses des réactions, ce qui produit des effets importants relativement à leur quantité.

Enfin, nous avons relié les échelles des temps en suspension et en pâte pure, la cinétique aux résistances mécaniques et à l'évolution de la microstructure. Cette évolution est en parfait accord avec les mécanismes de dissolution-précipitation, dont l'importance pendant l'hydratation devient évidente.

REMERCIEMENTS

Les auteurs tiennent à remercier Mme CAULLIER et M. MAES, techniciens au CEREG, pour les nombreux dosages chimiques et diffractométriques effectués.

BIBLIOGRAPHIE

1 - H. LE CHATELIER - Recherches expérimentales sur la constitution des mortiers hydrauliques - Thèse, Paris, 1887.

2 - C. VERNET, E. DEMOULIAN, P. GOURDIN, F. HAWTHORN - Mécanismes rationnels de l'hydratation - VIIème Symp. Int. Chim. des Ciments, Paris, 1980.

3 - C. VERNET, E. DEMOULIAN, P. GOURDIN, F. HAWTHORN - Cinétique de l'hydratation du ciment portland - VIIème Symp. Int. Chim. des Ciments, Paris, 1980.

4 - C. VERNET - Cinétique de l'hydratation du ciment portland - Aspects méthodologiques - VIIème Symp. Int. Chim. des Ciments, Paris, 1980 - Affiche commentée.

5 - M. REGOURD, H. HORNAIN, B. MORTUREUX - Microstructure des ciments de laitier - Rev. des Mat. Const. n° 699 - Mars-Avril 1976 pp. 83-86.

6 - F. HAWTHORN, E. DEMOULIAN, P. GOURDIN, C. VERNET Laitiers et clinkers - Influences réciproques - VIIème Symp. Int. Chim. des Ciments, Paris, 1980.

7 - C. VERNET, E. DEMOULIAN, P. GOURDIN, F. HAWTHORN - Détermination de la teneur en laitier dans les ciments par dissolutions sélectives - VIIème Symp. Int. Chim. des Ciments, Paris, 1980.

Approche du problème de la réactivité du laitier granulé

Approach to the problem of the reactivity of granulated slag

R. DRON, docteur-ingénieur,
F. BRIVOT, chimiste,
Laboratoire Central des Ponts et Chaussées, Service de Chimie, France.

RESUME : Les rapports des flux de dissolution des éléments du laitier (Ca, Al, Si) dans une liqueur de soude à pH 12,6 sont constants dans l'étape qui précède l'apparition de la sursaturation par rapport au C-S-H. Ils tendent ensuite vers les valeurs correspondant à la dissolution congruente du laitier.

Pour un élément donné, la concentration instantanée varie comme le logarithme du produit *temps x surface spécifique x rapport laitier/eau*.

En fixant ces trois facteurs à des valeurs arbitraires choisies de façon à rester dans le domaine de dissolution pure, c'est-à-dire avant toute précipitation d'hydrates, on peut caractériser de façon comparative la réactivité des différents laitiers par simple détermination des concentrations des éléments en solution.

SUMMARY : The ratio of the dissolution fluxes of the elements of slag (Ca, Al, Si) in a soda liquor with a pH of 12.6 are constant at the stage which precedes the onset of supersaturation with respect to C-S-H. They then tend to move towards the values corresponding to the congruent dissolution of the slag.

For a given element, instant concentration is a logarithmic function of the product time x specific area x slag/water ratio.

By fixing these three factors arbitrarily so as to remain in the pure dissolution area, that is, before precipitation of hydrates takes place, the comparative reactivity of various slags can be characterized simply by determining the concentrations of the elements in solution.

Par contact prolongé avec une solution alcaline, le laitier granulé donne naissance à des composés hydratés qui sont à l'origine des phénomènes de prise et de durcissement. Nous avons montré (1, 2) que le nombre et la nature de ces phases hydratées sont conformes aux conclusions d'ordre thermodynamique tirées de l'étude des équilibres hétérogènes qui régissent le système CaO, Al_2O_3, SiO_2, H_2O, le laitier anhydre restant hors équilibre. Ces conclusions tendent à prouver que les échanges de matière se font par l'intermédiaire de la solution, selon le schéma de Le Chatelier.

La nature des hydrates étant indépendante du laitier d'origine, leur précipitation ne dépend que de facteurs extérieurs à celui-ci et seule l'étape initiale de dissolution peut être mise en relation avec la réactivité intrinsèque du laitier.

Des informations sur la réactivité peuvent donc être recueillies par l'étude de l'évolution de la solution. Le problème a été abordé par Kondo (3) qui a étudié la solubilisation par l'eau pure et par l'eau de chaux de verres ayant la composition de la gehlenite. Il a montré que par des extractions répétées par l'eau pure, on dissout des quantités décroissantes de chaux, de silice et d'alumine dans des rapports qui restent voisins de 6, 2 et 1. En mettant ce verre en présence d'eau de chaux, il a constaté que les concentrations en alumine ou en silice de la solution croissent et passent par un maximum au bout de 24 heures environ, et que la chaux suit une évolution inverse. Seule la seconde expérimentation est à l'image de ce qui se passe dans la réalité. Il est toutefois difficile d'en tirer des enseignements sur le plan de la réactivité car la décroissance de la concentration en chaux, puis en silice et en alumine, ne peut s'expliquer que par des précipitations. Cet écueil est lié au haut niveau initial de la concentration en calcium, qui fait que le produit de solubilité des hydrates est atteint pratiquement dès le début de l'expérience.

Pour surmonter la difficulté, nous avons remplacé l'eau de chaux par une solution de soude de même pH et nous avons cherché des conditions opératoires permettant d'explorer l'étape précédant la précipitation des premiers hydrates. Il faut pour cela utiliser un échantillon de faible surface spécifique et adopter un rapport de masse eau/laitier maximal.

METHODOLOGIE ET APPAREILLAGE

L'étude comparative de différents laitiers exige que l'on fixe avec précision la surface de contact. On y parvient en travaillant sur un échantillon constitué par des grains isodimensionnels, obtenus par calibrage entre deux tamis consécutifs (80 et 100 µ) et rebroyage du refus jusqu'à épuisement de la fraction supérieure à 100 µ.

Le contact statique de cet échantillon avec l'eau intergranulaire confinerait le rapport des masses au dessous de l'unité. Or des essais préliminaires nous ont montré que pour étaler suffisamment la phase initiale de dissolution pure, il convenait de porter ce rapport à des valeurs de l'ordre de 100.

Ayant exclu la mise en suspension par brassage, qui provoque une attrition des grains se traduisant par une augmentation considérable de la surface spécifique, nous avons été amenés à retenir le principe de la lixiviation en circuit fermé.

On utilise le montage de la figure 1.

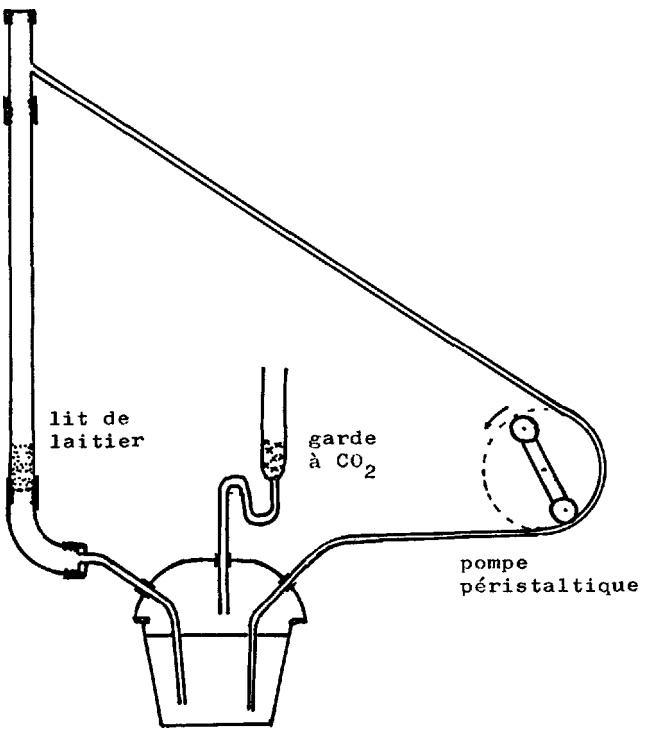

Figure 1 - Appareil de lixiviation en circuit fermé.

La solution est forcée par une pompe péristaltique à travers un lit de 2 g de grains contenus dans une colonne de verre de 13 mm de diamètre intérieur. La hauteur du lit est de 17 mm, le volume de la solution de 260 ml et le débit de 360 m/min. Le temps de rotation de la solution est donc de : 260/360 = 0,72 minutes, soit 43 secondes. Le rapport massique eau/laitier est égal à 130.

Nous avons vérifié que la solubilisation de la verrerie était négligeable.

EXPERIMENTATION

Nous avons utilisé trois laitiers caractéristiques de la production française :

Laitier n° 1 : laitier de fonte Thomas, granulation ordinaire.

Laitier n° 2 : laitier de fonte hématite, granulation ordinaire.

Laitier n° 3 : laitier de fonte hématite, granulation spéciale, dit "bouleté" ou "pellétisé".

Les compositions chimiques sont les suivantes :

	CaO	Al_2O_3	SiO_2	MgO
n° 1	43,7	14,8	33,0	4,4
n° 2	40,5	12,5	34,8	7,7
n° 3	41,0	12,1	34,7	7,0

La solution est préparée par dissolution de 1,6 g de soude pure dans 1 litre d'eau distillée fraîchement bouillie et refroidie à l'abri du CO_2 atmosphérique.

On remplit la colonne avec la solution et on introduit le laitier de façon à ce qu'il sédimente en un lit homogène. On établit alors la circulation de la solution pendant le laps de temps voulu, au terme duquel on soutire la liqueur et on la soumet à l'analyse. Chaque essai est répété 6 fois pour les temps courts et 2 fois seulement pour les temps longs. Chaque série correspondant à un temps donné est faite sur le même échantillon de laitier, après deux cycles de 20 minutes, destinés au nettoyage de la surface, et qui ne sont pas pris en compte.

La silice est dosée par colorimétrie du complexe silico molybdique bleu, l'alumine par compléxométrie à l'EDTA et le calcium par compléxométrie à l'EGTA.

RESULTATS ET COMMENTAIRES

Le tableau I donne les concentrations exprimées en mg/l de SiO_2, Al_2O_3 et CaO des liqueurs d'extraction après des cycles de différentes durées.

Le résultat le plus frappant est la forte diminution de la vitesse de solubilisation au fur et à mesure que la solution se charge ce qui rend caduc notre espoir de caractériser la réactivité par le flux de dissolution, puisque ce dernier n'est pas constant. On voit toutefois que pour des temps égaux, les quantités dissoutes sont significativement supérieures d'environ 30 % dans le cas du laitier n° 1, par rapport aux deux autres, qui donnent des valeurs sensiblement voisines.

TABLEAU I

temps (minutes)	10	20	40	80
laitier n° 1				
SiO_2	8,4	13,6	18,2	23,4
Al_2O_3	4,4	7,1	9,6	11,6
CaO	13,8	21,1	30,0	37,0
laiter n° 2				
SiO_2	6,9	10,3	13,4	16,2
Al_2O_3	3,0	4,4	5,9	7,2
CaO	10,7	16,3	21,5	26,8
laitier n° 3				
SiO_2	6,0	9,0	14,7	17,9
Al_2O_3	2,5	3,8	6,1	7,2
CaO	9,2	14,2	20,7	27,2

Un examen plus attentif des chiffres trouvés révèle un fait assez remarquable : la constance aux écarts analytiques près, des rapports des concentrations en silice, alumine et chaux (tableau II).

TABLEAU II

temps (minutes)	10	20	40	80	laitier d'origine
laitier n° 1					
CaO/SiO_2	1,65	1,55	1,64	1,58	1,32
Al_2O_3/SiO_2	0,527	0,523	0,526	0,498	0,45
CaO/Al_2O_3	3,12	3,19	3,12	3,17	2,95
laitier n° 2					
CaO/SiO_2	1,55	1,58	1,60	1,65	1,16
Al_2O_3/SiO_2	0,43	0,43	0,44	0,44	0,36
CaO/Al_2O_3	3,56	3,68	3,63	3,75	3,24
laitier n° 3					
CaO/SiO_2	1,53	1,58	1,40	1,52	1,18
Al_2O_3/SiO_2	0,42	0,42	0,413	0,402	0,35
CaO/Al_2O_3	3,68	3,63	3,55	3,77	3,39

Le rapport CaO/SiO_2 est sensiblement le même pour les trois laitiers et voisin de 1,6. Par contre, le rapport Al_2O_3/SiO_2 est significativement différent dans le cas du laitier n° 1 (0,52) comparativement aux laitiers n° 2 (0,44) et n° 3 (0,41).

Les valeurs de ce rapport sont à rapprocher des rapports correspondants dans les laitiers eux-mêmes (dernière colonne du tableau II). La comparaison montre que le laitier ne se dissout pas de façon globale : parmi les éléments structuraux de la phase vitreuse, ce sont les plus riches en calcium et en aluminium qui passent préférentiellement en solution.

SIGNIFICATION STRUCTURALE DES RAPPORTS CONSTANTS

Il résulte de la théorie statistique que nous avons proposée (4), en généralisant la théorie thermodynamique de Masson (5), que les verres à moyenne teneur en silice sont formés de chaînes silicatées droites et ramifiées (fig. 2). La longueur de ces chaînes n'est pas uniforme comme dans un cristal mais elle est distribuée suivant une progression géométrique.

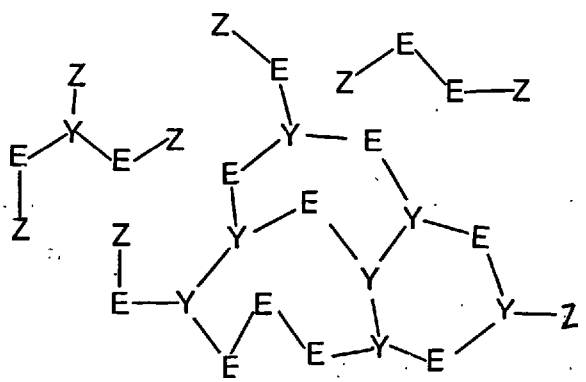

Figure 2 - Structure des verres à moyenne teneur en silice.

Par ailleurs, les éléments structuraux :

$$Y = SiO^{-}_{2,5} \qquad E = SiO^{2-}_{3}$$

et $Z = SiO^{3-}_{3,5}$

sont distribués de part et d'autre de la basicité moyenne suivant une loi binomiale. Cela signifie qu'un verre contient des éléments structuraux plus basiques et des éléments structuraux moins basiques que le cristal de même composition.

Les rapports trouvés sont assez proches des rapports théoriques $CaO/SiO_2 = 1,633$ et $Al_2O_3/SiO_2 = 0,425$ qui correspondraient au composé fictif C_7S_4A, ou encore $2C_3S_2$, CA. On peut donc interpréter la solubilisation initiale du laitier comme le passage sélectif en solution des éléments structuraux de la rankinite, soit $SiO^{3-}_{3,5}$ et de l'aluminate monocalcique, soit AlO^{-}_{2}.

L'écriture des réactions d'hydratation de ces éléments :

$$2SiO^{3-}_{3,5} + 3H_2O \rightarrow 2SiO_4H^{2-}_2 + 2OH^-$$

et

$$AlO^-_2 + 2H_2O \rightarrow AlO_4H^-_4$$

montre que l'ion OH^- n'intervient pas dans le premier membre que par conséquent l'attaque est hydrolytique et non hydroxylique. La première des deux réactions montre même que des ions hydroxyle sont formés au cours de ce processus, ce qui explique la réaction alcaline du laitier.

La mobilisation de ces éléments "hydrauliques" doit laisser en place un squelette spongieux formé par les éléments moins basiques (SiO^{2-}_3) et acides ($SiO^{-}_{2,5}$) qui restent disponibles pour une mobilisation du type pouzzolanique, mais sur lequel, entre temps, des fixations topochimiques (d'ion Ca^{2+} et OH^-) ne sont pas à exclure.

EXPERIMENTATION COMPLEMENTAIRE

Par suite du ralentissement progressif du flux de dissolution, il est difficile, dans les conditions opératoires décrites plus haut, d'explorer l'étape de sursaturation, dont la mise en évidence est fondamentale dans la démonstration du processus dissolution précipitation, et à plus forte raison, l'étape de précipitation des hydrates. L'avancement de la réaction variant approximativement comme le logarithme du produit tSm/e, l'étude de ces étapes n'est possible, dans des temps compatibles avec l'expérimentation qu'en augmentant le rapport laitier/solution (m/e) ou la surface spécifique S. Dans les essais à 80 minutes, le produit tSm/e atteint la valeur de 160 minutes.cm^2. Il est possible, sur le même montage, de travailler sur 50 g de grains calibrés de même surface spécifique (250 cm^2/g), de sorte que pour 60 minutes, le produit tSm/e est de l'ordre de 3 000.

On obtient alors les résultats suivants sur le laitier n° 1 :

SiO_2	33,5 mg/l	C/S	= 1,50
Al_2O_3	16,5 "	A/S	= 0,49
CaO	50,0 "	C/A	= 3,03

On constate que les rapports commencent à s'infléchir pour se rapprocher de ceux du laitier.

A ce stade, la solution est déjà sursaturée par rapport au C-S-H. En effet, d'après Greenberg et al. (6), le produit de solubilité de C-S-H est de 10^{-7}, c'est-à-dire que :

$$|Ca^{2+}| \quad |SiO_4H_2^{2-}| = 10^{-7}$$

Le pK de la deuxième acidité de SiO_4H_4 étant voisin de 12,6, à pH 12,6, qui est précisément celui des solutions que nous employons, la moitié de la silice est sous forme $SiO_4H_2^{2-}$, l'autre moitié étant sous forme $SiO_4H_2^{-}$.

Le produit des concentrations en chaux et silice, exprimées en g/l, est donc :

$$CaO \times SiO_2 = 2.10^{-7} . 56.60 = 672.10^{-6}$$

soit 672 si elles sont exprimées en mg/l.

Nos propres déterminations nous conduisent à une valeur plus élevée, de l'ordre de 1 000 à 1 200. En tout état de cause, pour 33,5 mg/l de silice et 50 mg/l de chaux, le produit est égal à 1 675 et dépasse nettement le produit de solubilité. Nous sommes bien dans le domaine de sursaturation, ce que confirme la précipitation de ces solutions lorsqu'on les conserve 24 heures.

L'étape de précipitation du C-S-H peut être atteinte par mise en contact prolongé de laitier broyé à 3 000 cm^2/g, avec un rapport m/e = 0,1. Le procédé de lixiviation n'est plus utilisable et on se contente d'une simple mise en suspension par brassage. Au bout de 7 jours, sur le laitier n° 1, on obtient les résultats suivants :

SiO_2	6 mg/l
CaO	203 mg/l
Al_2O_3	55 mg/l

Le produit SiO_2, CaO a alors pour valeur 1 218, ce qui montre que l'équilibre dynamique est atteint. L'accumulation de la chaux en solution montre que l'on précipite un C-S-H dont le rapport C/S est inférieur à celui des fractions du laitier qui se dissolve.

Une dernière série d'essais, dont les conditions opératoires pourraient servir de base à la définition d'un essai de réactivité, montre que l'on passe, avant le début de la précipitation du C-S-H, par un stade de dissolution quasi congruente. On opère avec 2,5 g de laitier broyé à 3 000 cm^2/g, mis en suspension pendant 10 minutes avec 250 ml de solution de soude à 1,60 g/l. On laisse décanter 5 minutes, on filtre sur millipore et on dose les trois éléments. Les résultats sont les suivants :

TABLEAU III

			Solution	Laitier
Laitier n° 1				
SiO_2	35 mg/l	C/S	1,34	1,32
Al_2O_3	16 "	A/S	0,46	0,45
CaO	47 "	C/A	2,94	2,95
Laitier n° 2				
SiO_2	29 mg/l	C/S	1,38	1,16
Al_2O_3	10 "	A/S	0,36	0,36
CaO	40 "	C/A	3,81	3,24
Laitier n° 3				
SiO_2	26 mg/l	C/S	1,31	1,18
Al_2O_3	10 "	A/S	0,38	0,35
CaO	34 "	C/A	3,40	3,39

CONCLUSION

La réactivité des laitiers peut être définie comme le taux de dissolution dans une solution sodique de même pH que l'eau de chaux, pour une surface spécifique, un rapport e/c et un temps standardisés, avant que n'interviennent les précipitations d'hydrates.

Notre expérimentation montre que les réactivités se classent de la même façon que l'on opère au stade initial de dissolution non congruente ou au stade plus tardif de dissolution quasi congruente.

La réactivité semble être en relation directe avec la richesse du laitier en éléments structuraux silicatés basiques SiO_2^{3-}, (et donc avec la basicité) d'une part et avec celle des éléments alumineux AlO_2^- (et donc avec la teneur en alumine) d'autre part, ce que confirme l'expérience pratique.

.../...

BIBLIOGRAPHIE

1.- R. DRON, (1973), Mécanisme de la prise du laitier granulé sous activation alcaline, Thèse Univ. Paris VI, Rapport de recherche n° 38, LPC.

2.- R. DRON, (1974), Experimental and theoritical study of the CaO - Al_2O_3 - SiO_2 - H_2O system, VI Int. Cong. on the Chem. of Cem., Moscou.

3.- R. KONDO, (1958), Thèse de doctorat, Institut de Technologie de Tokyo.

4.- R. DRON, (1980), Théorie statistique des silicates fondus à forte et moyenne teneurs en silice, C.R. Acad. Sc. Paris, série C, t. 290.

5.- C.R. MASSON, (1968), Ionic equilibria in liquid silicates, J. of the Am. Ceram. Soc., 51, 3, 134-143.

6.- S.A. GREENBERG, T.N. CHANG, E. ANDERSON, (1960), Investigation of colloidal hydrated calcium siiicate, solubility products, J. Phys. Chem., 64, 1151-1156.

Valorization of basic oxygen steel slags

Valorisation des scories d'acieries BOP

C.M. GEORGE, Technical Manager, Lafarge Fondu International,
F.P. SORRENTINO, Research, Scientist, Lafarge S.A., France.

RESUME : Les problèmes posés par les scories d'acieries BOP,

- instabilité dimensionnelle dûe à une teneur en chaux libre, haute et variable,

- manque d'activité hydraulique

ont pu être résolus par l'utilisation en cours d'affinage de la fonte, d'un nouveau fondant synthétique à base de CaO, MgO, Al_2O_3 et oxyde de fer. Les nouvelles scories ainsi produites présentent une activité hydraulique intéressante avec une teneur en chaux libre basse tout en permettant l'élaboration d'acier de qualité choisie.

La préparation de telles scories est brièvement évoquée dans cette communication, suivie de la présentation de l'étude sur leurs propriétés minéralogiques et hydrauliques.

SUMMARY : The problems of dimensional instability due to a high and variable free lime content in BOP slags as well as their lack of hydraulic activity have been overcome by the use of a new slag forming agent. This synthetic material, combining CaO, MgO, Al_2O_3 and iron oxide in specific proportions when added to the converter during refining leads to final slags with a consistently low free lime content and useful hydraulic properties, without prejudice to the conversion of iron into steel.

This paper deals briefly with the preparation of such slags and then reports the study of their mineralogy and hydraulic behaviour.

INTRODUCTION

An important method of reducing energy consumption in the production of cement consists of adding to the clinker, natural pozzolanes, fly ash, etc., Blast Furnace Slags in particular, principally in granulated or pelletised form are now quite widely used. By contrast, steel making slags arising from the BOP find little application, (1).

The potential interest in BOP (or LD) slags stems from the large quantities arising (50 M tonnes per year, world wide) and their chemical and mineralogical composition which is similar to that of cement, (Table I).

Amongst many attempts to find outlets for steel slag in the construction industry may be cited :
- use as an aggregate, for road foundations and in road surfaces (2, 3, 4, 5) ; the high density and free lime content of the slag hinders this application ;
- use as an addition to Portland cement in a manner analogous to that of Blast Furnace Slag. For this purpose it is necessary to eliminate reactive free lime in steel slags chemically (carbonation) or by long term weathering (5, 6) which is neither cheap nor convenient ;
- use as a raw material for manufacture of Portland cement clinker, as a source of lime and silica (7) ; this offers little if any savings in energy.

The use of steel slags is thus limited by the following main technical factors :
- heterogeneity,
- free lime content,
- absence of hydraulic activity.

The first two factors result from incomplete reaction during the simultaneous production of steel and slag in the refining process - a method of overcoming this should thus open uses for such slags while also improving the refining of iron into steel.

The research and development described in this paper provide a method of achieving this result, producing homogeneous low free lime slags and also imparting hydraulic activity without prejudice to the manufacture of good quality steel by the conventional BOP route.

PRINCIPLE FOR THE PRODUCTION OF HYDRAULIC STEEL SLAG FOR THE CEMENT INDUSTRY

This development is based on introducing into the BOP converter at the beginning of the refining process a prefired flux (*) of chosen composition : $CaO - Al_2O_3 - MgO - Fe_2O_3$. The effect on the physico-chemical interactions between metal and slag which result have been described previously (8, 9, 10). The resulting steel making process compares with traditional practice as follows :

	Classical process	Modified process
Raw materials	Iron + Scrap	Iron + Scrap
	Oxygen	Oxygen
	Iron oxide	Iron oxide
	CaO - MgO	CaO
	Flux (fluorspar)	Prefired flux (CAMFlux) { $\underline{CaO}$; $\underline{Al_2O_3}$; $\underline{MgO}$; $\underline{Fe_2O_3}$

(*) In cement technology, CaO, Al_2O_3, MgO, Fe_2O_3 is abbreviated to C, A, M, F. Hence the name CAMFlux has been chosen for this new material.

Table I : Compositions of slags, fly ash and cements %

Chemical Composition	Blast Furnace Slag	BOP steel slag	Fly ash		Portland cement	Aluminous cement
CaO	45	47	3.5	45	64	40
SiO_2	33	13	54	18	20	5
Al_2O_3	15	1	30	12	6	40
Iron oxide	1-2	25	10	7	2	15
MgO	5	6	2.0	1.8	2	
MnO	0.5	5			0	
P_2O_5		2			0	
$S^{=} + SO_3$	1.0	0.1	0.5	6	2.5	0.1
Mineralogical Composition						
	glass	C_2F	glass	glass	C_3S	glass
	C_2AS - CS	C_2S	AS	C_2AS	C_2S	CA
			S		C_4AF	C_4AF
	C_2S	(Mn.Mg.Fe.Ca)O			C_3A	C_2S

Products	Steel Classical slag	Steel Modified slag
CaO	40 - 50	40 - 50
SiO_2	8 - 20	8 - 20
FeO	20 - 30	15 - 20
MgO	2 - 12	2 - 12
Al_2O_3	0 - 2	5 - 15
MnO	3 - 6	3 - 6
P_2O_5	1 - 2.5	1 - 2.5
Free CaO	5 - 15	1 - 5

The new slag thus differs from classical BOP slag in having a higher alumina content and a lower iron oxide content.

STUDY OF NEW HYDRAULIC STEEL SLAG

Preparation

Semi-industrial trials, in a 5 tonne converter were carried out to produce two types of slag, one based on conventional materials, the other obtained with the aluminous flux (CAMFlux), of average composition: CaO = 50 %, Al_2O_3 = 25 %, MgO = 5 %, FeO + Fe_2O_3 = 15 %, SiO_2 = 5 %.

Table II shows the typical compositions of the slags obtained.

Table II

	Classical Slag	Aluminous Slag
SiO_2	9.61	9.0
CaO	44.1	45.8
Al_2O_3	0.9	11.4
MgO	10.4	7.2
MnO	4.4	3.8
P_2O_5	2.4	2.2
Fe^{++}	19.7	12.6
Fe^{+++}	8.6	8.7
Free CaO	10.8	3.8

Mineralogy

The calculated phase compositions of the standard and modified slags, assuming the alumino-ferrite phase to have the formula C_4AF, are shown in table III.

Table III : Calculated phase compositions of slags

	Classical Slag	New Slag
Solid solution C_2S - C_3P	31 - 6	22 - 5
Ferrite phase	16	32
(Mn-Mg-Fe-Ca)O solid solution	36	20
Free CaO	11	4
C_3A	0	17

The actual phase compositions were studied by X-ray diffraction, optical microscopy and electron microprobe analysis.

X-ray diffraction and optical microscopy confirmed the presence of C_2S - C_3P, calcium ferrite or calcium alumino-ferrite and the (Mn, Mg, Fe, Ca)O solid solution. C_3A could not be positively identified however and this implies that the calcium alumino-ferrite has an A/F ratio greater than unity. This was confirmed by the microprobe which showed the presence of the following phases :

Classical slag :

- Periclase, average composition
  $Mg_{0.7}\ Ca_{0.03}\ Mn_{0.03}\ Fe_{0.2}\ O$
  The composition varied widely from the centre of grains to their surfaces.

- Magnesio wustite, solid solution
  $Mg_x\ Ca_y\ Mn_{0.11}\ Fe_{0.6}\ O$
  with $0.12 < x < 0.21$ and $0 < y < 0.14$

- Lime solid solution
  $Ca_{0.83}\ Mg_{0.08}\ Mn_{0.04}\ Fe_{0.05}\ O$

- Dicalcium silicate
  $Ca_2\ Si_{0.91}\ P_{0.1}\ Fe_{0.01}\ O_4$

- Calcium alumino-ferrite, average
  $Ca_{2.2}\ Si_{0.03}\ Al_{0.4}\ Fe^{II}_{1.4}\ O_5$
  with variable composition within grains suggesting that equilibrium had not been reached.

New slag :

- Magnesio wustite, solid solution
  $Mg_{0.47}\ Ca_{0.05}\ Mn_{0.07}\ Fe^{II}_{0.45}\ O$

- Dicalcium silicate
  $Ca_2\ Si_{0.89}\ P_{0.1}\ Al_{0.02}\ Fe_{0.01}\ O_4$

- Calcium alumino-ferrite
  $(Ca_{1.8}\ Fe^{II}_{0.2})\ Al_{1.32}\ Fe^{III}_{0.59}\ O_5$
  all of very homogeneous composition.

Hydraulic activity

This aspect of the study is concerned with three points :

- the hydraulic activity of the phases formed in the new aluminous slags,
- the durability of cements containing these slags as a function of their free lime and magnesia contents,
- the influence of the MnO and P_2O_5 contents of these slags on their suitability for cementitious applications (a factor for which very little information has yet been reported).

Samples of the slags, ground to cement fineness (3600 $cm^2\ g^{-1}$, Blaine) were made into neat pastes with a water/slag ratio of 1. The hydration kinetics were followed by calorimetry and measurement of bound water, free water being eliminated at each age of measurement, by washing with acetone and drying with ether.

Reaction with water appears to take place in 2 stages as shown in figure 1.

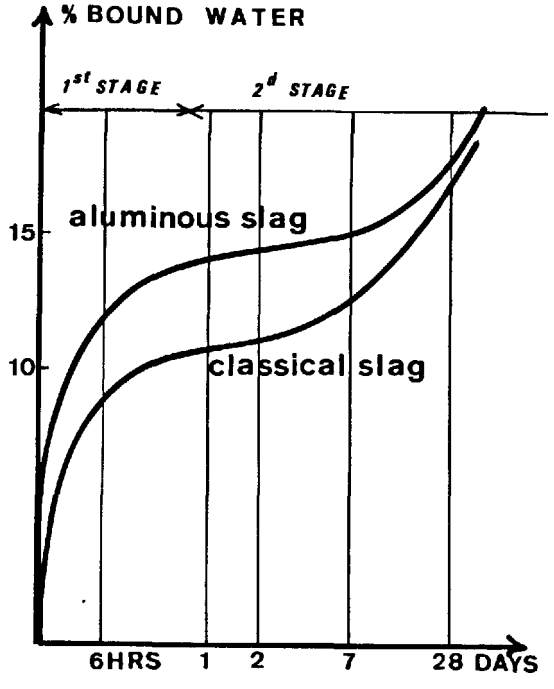

Fig. 1 - Hydration of classical and aluminous slags measured as bound water

Short term hydration rates increased with the alumina content of the slags due to reaction of the calcium alumino-ferrite phase. Very little hydration occured with the classical slag in which the ferrite phase contained only minor quantities of alumina. Quite a significant degree of early hydration occured with the new, alumina-rich slags. This result is in agreement with the work of Carlson (11) on pure alumino-ferrites.

A second, later hydration, common to both slag types, corresponds to the reaction of dicalcium silicate.

X-ray diffraction of the reacted slags showed that the product of ferrite hydration in the classical slag was $C_4(A,F)H_x$ whereas that of calcium alumino-ferrite hydration in the new slag was $C_3(A,F)H_6$. In both cases these hydrates are transformed into mono carbo calcium alumino-ferrite hydrate, in contact with air.

Neither slag is sufficiently hydraulic to be used alone as a cementitious alternative to normal Portland cement, so that studies of strength development were made by mixing them with Portland cement. Mortars were prepared with the composition, in parts by weight :

Sand, 6 ; Slag, 1 ; Portland cement, 1 ; Water, 1.

The chemical composition of the slag/cement portion of the mix were thus :

Table IV

	Portland cement + classical slag	Portland cement + aluminous slag
CaO	54.9	54.4
SiO_2	15.3	16.4
Al_2O_3	2.62	7.30
MgO	5.6	3.3
Fe oxide	15.6	15.0
Free CaO	6.1	2.8
MnO	2.2	1.6
P_2O_5	1.2	1.05

The quantities of free lime and magnesia in the mix based on classical slag are high and the test specimens disintegrated by cracking after a few days storage under water. The specimens containing the new aluminous slag remained intact. Some compressive strength test results are given in table V.

Table V : Compressive strengths (MPa) of slag - Portland cement - Sand mortars (AFNOR P 15-403)

Age (days)	2	7	28	90
Portland cement + classical LD slag	7	19	disintegration by cracking	
Portland cement + aluminous LD slag	12	25	42	49
Portland cement + Blast Furnace Slag	16	30	45	53

In order to check on later age effects due to free MgO, similar mortar specimens based on the new aluminous lags, were subjected to the standard autoclave test (ASTM C 151) with fully satisfactory results.

CONCLUSIONS

1. A slag forming flux based on a prereacted composition containing $CaO-Al_2O_3-MgO-Fe_2O_3$ has been developed for use in BOP steel making converters.

2. This flux produces an end slag which is alumina rich by comparison with traditional BOF-slags.

3. The fluxing action of this new material (CAMFlux) leads to a more homogeneous end slag and hence a low free lime content.

4. The alumina in the flux is retained in the end slag as calcium alumino-ferrite, which induces early hydraulic activity not displayed by conventional slags. This enables such slags to be added to Portland cement with results at least as beneficial as those normally achieved with good quality Blast Furnace Slags.

5. The hydraulic activity of calcium alumino-ferrite in BOP slags increases with alumina content, in agreement with previous observations on pure materials.

6. The MnO and P_2O_5 contents (normal) of the aluminous slag do not inhibit its hydraulic activity.

7. The low free lime and free MgO contents of the new slags containing alumina results in freedom from cracking or long term swelling when these slags are used in concrete mixed with Portland cement.

8. Use of the new flux does not affect steel quality and provides for the first time a viable route to the utilisation of BOP steel slags in the construction industry. Since very little of the large quantities of steel slags of conventional composition are utilisable at present, this development offers consider potential savings in energy.

REFERENCES

1. C.M. GEORGE, F.P. SORRENTINO, "Nouvelle méthode de valorisation des scories d'affinage BOP", Colloque international sur l'utilisation des sous-produits et déchets dans le Génie Civil, Paris 28-29 Novembre 1978.

2. M.J. PIRET, "Valorisation de la scorie LD : aspects généraux du problème et réalisations dans le domaine de la construction routière", 6th International Steelmaking Day, Paris 13 Octobre 1977.

3. M.I. PANFILOV, (1978) "Valorisation totale des laitiers sidérurgiques", Ed. Metallurgi.

4. J.J. EMERY, (Dec. 1975), "New uses of metallurgical slags", Canadian mining and met. bull. "Steelmaking slag utilization in canadian highway construction",6th International Steelmaking Day, Paris 13 October, 1977.

5. G.H. THOMAS, "U.K. experience in the use of BOS slag as roadstones", 6th International Steelmaking Day, Paris 13 October, 1977.

6. CRM, "Procédé pour valoriser les scories métallurgiques", Brevets belges N° 856.711 - 11 Juillet 1977, 839.899 - 22 Mars 1976, 839.989 - 22 Mars 1976, 839.753 - 18 Mars 1976

7. R. KONDO, M. DAIMON, N. ASAKAWA, T. ITO (1976) "Iron cement made from Blast Furnace and converter slag", C.A.J. N° 16 - pp 66-67

8. J. WHITE (1976), "Slag control in basic steelmaking process : an examination of the possibility of eliminating fluorspar", Iron and Steelmaking N° 2 - 115.

9. H. GAYE, C.M. GEORGE, P. RIBOUD, F.P. SORRENTINO, J. WHITE, "A new aluminous product for BOP steelmaking and slag utilization", International Conference on the Physical chemistry of iron and steelmaking, Versailles, France October 23-25, 1978.

10. J. WHITE, "Process for steelmaking by oxygen refining of iron", US Patent N° 4.010. 027 - March 1, 1977, British Patent N° 1 508 024 - May 15, 1976.

11. CARLSON (Sept. Oct. 1964), "Action de l'eau sur les alumino-ferrites de calcium", J. Res. Nat. Bur. Stand. - A. Physics and Chemistry - USA, Vol. 68 A - 453-63.

Laitiers et clinkers - influences réciproques

Blast-Furnace slags and clinkers - mutual influences

F. HAWTHORN, E. DEMOULIAN, P.GOURDIN, C. VERNET, Société des Ciments Français, CEREG, France.

RESUME

Les auteurs ont étudié des mélanges à 80 % de laitier vitrifié de haut fourneau et 20 % de clinker avec ajout de gypse réalisés à partir des combinaisons deux à deux de 7 clinkers et 3 laitiers broyés à deux finesses différentes, représentatifs de la production française. Ils ont montré par analyse de la variance, la prépondérance de la qualité et de la finesse du laitier sur les performances de ce type de ciment.

La minéralogie des clinkers a plus d'influence quand les laitiers sont broyés normalement que quand ils sont surbroyés.

La courbe d'évolution des résistances de ces mélanges est très différente de celle des ciments portland réalisés avec les mêmes clinkers. L'influence de la teneur en sulfate de calcium et d'une faible augmentation de la teneur en clinker ont aussi été étudiées.

SUMMARY

The authors have studied mixes containing 80 % blast-furnace vitrified slag and 20 % clinker with an add of gypsum, prepared with combinations two by two of 7 clinkers and 3 blast-furnace slags ground to two different degrees of fineness, representative of french production. They showed, with the help of the analysis of variance the preponderance of type and fineness of slags in the performances of these cements.

The clinker mineralogy has more influence with the normaly ground than with the finely ground slag.

The evolution curve of compressive strength of these mixes is generally different from that of portland cement made with the same clinkers. They also studied the influence of the sulphate content and of a slight increase in clinker.

INTRODUCTION

Quand on fabrique des ciments qui contiennent 80 % de laitier, 20 % de clinker et du gypse, la qualité principale recherchée est la résistance chimique des bétons à l'eau de mer et aux eaux séléniteuses. Dans le passé, ces ciments développaient des résistances moyennes jusqu'à 28 jours et fortes à long terme.

Depuis quelques années, on demande à ce type de ciments des performances mécaniques plus importantes. Industriellement, il est connu que la qualité du laitier a un rôle important sur les performances mécaniques, mais l'influence du type de clinker n'a pas été aussi clairement mise en évidence.

Nous présentons ici les résultats d'une étude où nous avons utilisé 7 clinkers de compositions minéralogiques différentes et 3 types de laitier. Nous avons déterminé l'influence, sur les résistances, de la minéralogie du clinker, en relation avec la finesse et le type du laitier, et, sur quelques exemples, celle du taux de sulfate et de petites augmentations de la proportion de clinker.

ECHANTILLONS ETUDIES - RESULTATS

Nous avons sélectionné trois laitiers français représentatifs de trois types de production dont la composition chimique et le procédé de vitrification diffèrent, ainsi que sept clinkers de la SOCIETE DES CIMENTS FRANCAIS dont les compositions minéralogiques couvrent l'ensemble des valeurs habituellement rencontrées.

Les caractéristiques des laitiers sont données au tableau I.

Dans celui-ci, Φ représente le diamètre moyen des hétérogénéités de densité, déterminé par diffusion centrale des rayons X.

Tableau I : Composition chimique des laitiers

		A	B	C
Perte au feu	%	0,39	0,42	0,85
SiO_2	%	32,91	33,03	34,78
Al_2O_3	%	14,95	12,33	12,11
FeO	%	0,54	1,74	0,61
TiO_2	%	0,51	0,52	0,59
MnO	%	0,34	0,69	0,61
CaO	%	43,74	40,88	41,04
MgO	%	4,53	7,63	7,97
SO_3	%	0,05	0,04	0,05
$S^=$	%	0,88	1,12	0,92
K_2O	%	0,57	0,44	0,53
Na_2O	%	0,26	0,34	0,30
F^-	%	0,23	0,09	0,13
Cl^-	%	<0,0035	0,0284	<0,0035
Φ diff. cent.	A°	300 Å	900 Å	800 Å
CaO/SiO_2		1,33	1,24	1,18

Les compositions minéralogiques des clinkers que nous avons déterminées quantitativement par diffraction des rayons X sont données au tableau II :

Tableau II : Compositions minéralogiques des clinkers

	C1	C2	C3	C4	C5	C6	C7
Alite forme	R	R	MIb	MIb	MIb	MIIb	MIb
Alite %	68,4	61,4	73,5	65,5	65,9	57,8	65,2
Bélite	26,2	20,8	14,7	11,1	12,7	22,2	20,6
C_3A cubique	2,5	12,5	0,0	1,2	5,1	1,9	0,9
C_3A tétrag.	0,0	1,7	5,6	15,8	3,1	1,4	1,2
C_4AF	0,0	4,6	8,5	5,1	10,9	15,6	10,2
K_2SO_4	0,0	0,0	0,0	0,8	2,3	0,6	0,0

Nous avons broyé séparément les clinkers à 3500 cm^2/g, les laitiers à 3500 et 6000 cm^2/g (Blaine) et le gypse à 0 % de refus au tamis de 40 µm. Nous avons ensuite effectué 42 mélanges à 80 % de laitier et 20 % de clinker en réalisant tous les couples laitier-clinker possibles. Le gypse a été ajouté à raison de SO_3 = 3 % pour les laitiers à 3500 cm^2/g et SO_3 = 5 % pour les laitiers à 6000 cm^2/g. Les résistances à la compression à 1, 2, 7, 28, 90, 180 et 360 jours ont été déterminées et les résultats figurent au tableau III.

Tableau III : Résistances à la compression en MPa des 42 mélanges

CLINKER	C 1			C 2			C 3			C 4			C 5			C 6			C 7		
LAITIER 3500	A	B	C	A	B	C	A	B	C	A	B	C	A	B	C	A	B	C	A	B	C
R2	9,1	6,7	3,9	8,2	6,4	3,7	8,5	4,3	2,9	9,0	5,8	4,7	8,0	5,4	3,0	7,4	3,4	2,7	6,6	3,8	3,4
R7	22,2	21,9	17,2	19,7	19,5	14,2	18,7	19,8	16,3	23,4	21,1	16,6	20,4	18,8	18,4	17,8	17,8	16,9	17,8	18,5	17,3
R28	32,2	33,1	28,0	30,5	30,6	26,6	33,5	31,8	26,9	36,8	32,5	30,1	31,7	31,7	27,2	27,6	28,4	26,7	28,2	29,1	27,7
R90	41,7	39,9	36,5	42,1	37,7	32,4	44,3	39,1	34,4	47,9	40,7	38,5	44,0	36,6	38,1	36,9	33,1	32,8	38,6	35,2	34,9
R180	47,3	43,8	40,5	46,0	39,7	35,5	47,4	41,7	38,4	51,3	44,0	43,2	45,4	40,3	41,7	40,0	36,6	37,1	41,6	37,0	37,9
R360	51,7	47,8	43,5	49,2	45,7	40,7	53,4	46,0	39,5	54,2	47,4	47,4	49,8	45,6	42,3	43,3	41,8	38,6	45,1	41,9	40,4
LAITIER 6000	A	B	C	A	B	C	A	B	C	A	B	C	A	B	C	A	B	C	A	B	C
R1	9,0	5,5	2,9	9,7	5,2	2,9	5,9	3,7	2,2	6,9	4,4	2,8	5,9	3,3	2,5	6,5	3,9	2,2	5,4	3,7	2,3
R2	23,4	20,0	13,2	21,0	19,1	13,5	21,3	16,5	10,6	21,2	18,4	12,1	20,2	14,7	10,5	19,4	15,9	10,4	20,5	15,0	9,5
R7	30,2	30,8	31,2	29,5	28,0	27,9	31,6	31,9	29,5	33,8	29,6	31,5	30,8	25,6	32,3	29,9	26,1	29,6	30,5	27,9	29,6
R28	42,0	37,8	37,9	38,6	36,2	36,4	46,8	41,9	41,1	45,4	39,1	40,3	42,0	33,4	38,3	37,9	35,4	36,6	43,1	37,7	38,7
R90	45,2	43,9	45,0	44,0	38,9	41,2	49,8	45,0	45,1	51,0	41,6	48,6	46,1	37,1	47,8	41,9	37,8	44,2	47,4	40,6	45,7
R180	48,3	46,1	47,9	46,8	42,3	43,8	52,1	49,9	47,9	53,4	46,7	51,2	50,0	41,3	50,3	44,7	42,3	47,2	50,8	44,4	48,5
R360	56,0	50,3	52,4	53,0	48,1	47,7	61,2	52,6	52,7	59,8	48,9	53,5	54,8	42,0	50,9	50,9	47,2	48,9	56,2	50,3	49,7

INFLUENCE DU CLINKER ET DU LAITIER

Nous avons testé l'influence du clinker sur les résistances de ce type de mélange d'une part, et d'autre part, l'existence de couples, type de laitier-type de clinker, conduisant à des résistances significativement différentes de celles des autres couples. Pour cela, nous avons préalablement dépouillé les résultats par analyse de la variance, nous les avons ensuite mis en relation avec les caractéristiques des laitiers et des clinkers, puis nous avons recherché les associations laitier-clinker favorables ou défavorables.

1 - Etude par analyse de la variance de l'influence du laitier, du clinker et de la finesse

L'analyse de la variance est une technique statistique qui permet, grâce à un plan d'expérience, d'étudier avec un minimum de mesures, l'influence sur une grandeur de plusieurs facteurs variant simultanément. L'analyse des résultats permet de conclure à l'influence ou non d'un paramètre ou d'un couple de paramètres. Les paramètres sont, dans notre cas, le type de laitier, la finesse du laitier et le type de clinker, les variables sont les résistances aux différentes périodes de durcissement.

1.1 - Analyse à 2 dimensions

Pour étudier l'influence du clinker et du laitier, nous avons préalablement effectué des calculs d'analyse de la variance à deux dimensions.

Nous posons symboliquement :
V = variance ; L = laitier ; C = clinker ; F = finesse
R = résiduelle.
Pour une même finesse de laitier, nous obtenons les résultats suivants :

Tableau IV		V_L/V_R	V_C/V_R
Laitier 3500	R_2	24,57	1,39
	R_{28}	15,56	5,09
Laitier 6000	R_1	68,3	4,68
	R_2	243	10,36
	R_{28}	23,5	9,81

L'influence du paramètre étant significative au seuil de 1 %, si $V_L/V_R > 6,93$ ou si $V_C/V_R > 4,82$ et au seuil de 5 % si $V_L/V_R > 3,88$ ou si $V_C/V_R > 3,00$, on remarque que l'influence du type de laitier est prépondérante dans tous les cas. A 3500 cm²/g, l'influence du type de clinker n'est pas significative à 2 jours, elle l'est à 28 jours. A 6000 cm²/g, elle est à peine significative à un jour, le devient à 2 jours et à 28 jours. On observe que les caractéristiques propres des clinkers interviennent plus rapidement lorsque la finesse du laitier augmente.

1.2 - Analyse à 3 dimensions

Pour étudier ensuite l'existence de couples laitier-clinker, nous avons effectué des analyses à trois dimensions : laitier-clinker-finesse du laitier. Nous avons porté au tableau V les quotients des rapports des variances par la valeur F du test de SNEDECOR au seuil de 5 % par le nombre de degrés de liberté de chaque rapport. Une valeur supérieure à 1 permet de conclure que la valeur est significative au seuil de 5 %.

Tableau V	$\frac{1}{F}\frac{V_L}{V_R}$	$\frac{1}{F}\frac{V_F}{V_R}$	$\frac{1}{F}\frac{V_C}{V_R}$	$\frac{1}{F}\frac{V_L.F}{V_R}$	$\frac{1}{F}\frac{V_F.C}{V_R}$	$\frac{1}{F}\frac{V_L.C}{V_R}$
R_2	2,1	12,2	0,1	0,3	0,02	0,01
R_7	3,2	274,3	3,1	4,9	0,40	1,38
R_{28}	9,7	130,7	5,2	3,9	1,18	0,60
R_{180}	24,2	71,1	11,6	7,2	2,29	2,06
R_{360}	20,8	39,2	5,3	3,3	1,43	0,93

L'examen de ce tableau montre qu'à 2 jours, la finesse et le type de laitier sont prépondérants, le type de clinker n'a pas d'influence significative. A 7 jours et au-delà, l'influence du type de clinker est significative ainsi que le terme $V_F.C/V_R$: le type de clinker a donc une influence qui est fonction de la finesse du laitier. Par contre, l'interaction type de laitier-type de clinker n'est pratiquement pas significative. On remarque aussi que l'influence relative de la finesse du laitier décroît avec le temps.

2 - Influence de la minéralogie des clinkers

Pour expliquer et quantifier l'influence du type de clinker, nous avons caractérisé les clinkers par leurs compositions minéralogiques et les laitiers, soit par leur rapport CaO/SiO_2, soit par le diamètre en Å des microhétérogénéités déterminé par diffusion centrale des rayons X. On peut penser que ce diamètre est une résultante de la composition chimique et de l'histoire thermique du laitier car il représente une estimation du volume moyen des particules organisées du laitier, il peut donc être utilisé comme variable caractéristique. D'autres paramètres de caractérisation des laitiers que nous décrivons par ailleurs (1), comme par exemple (C + M + A)/S ont été testés. Ils sont nécessaires pour déterminer l'influence de la qualité propre d'un laitier mais, dans le cas présent, nous utilisons trois laitiers représentatifs de trois productions différentes et les paramètres simples que nous avons choisis devraient être suffisants pour la caractérisation de chaque laitier.

Nous avons testé un grand nombre de corrélations multiples entre les résistances des mélanges à divers âges prises comme fonction et, comme variable, les différents paramètres ci-dessus définis. Pour les laitiers à 3500 cm²/g, les meilleurs résultats sont obtenus en définissant le laitier par le rapport CaO/SiO_2 et les clinkers par C_3S, C_3A cubique, C_3A tétragonal, C_4AF et K_2SO_4. A finesse élevée, nous utilisons pour les laitiers le rapport CaO/SiO_2 à 1 et 2 jours et le diamètre Φ à plus long terme : nous conservons les mêmes paramètres pour les clinkers.
Les tableaux VI et VII donnent les coefficients des équations obtenues et r de la corrélation multiple.

Tableau VI : Coefficient des équations de régression multiple pour les laitiers broyés à 3500 cm²/g

	R2	R7	R28	R90	R180
Constante	-35,3	- 1,36	-11,2	-33,2	-30,76
C/S	+30,6	+18,8	+24,2	+48,3	+43,5
C_3S	+ 0,023	- 0,037	+ 0,138	+ 0,177	+ 0,223
C_3A cubique	+ 0,123	- 0,112	+ 0,099	+ 0,017	+ 0,185
C_3A tétrag.	+ 0,117	+ 0,064	- 0,293	+ 0,253	+ 0,447
C_4AF	- 0,019	- 0,188	- 0,021	- 0,027	- 0,007
K_2SO_4	+ 0,055	+ 0,799	+ 0,348	+ 1,238	+ 0,805
Coef.corr. multiple r	0,97	0,77	0,86	0,94	0,93

Tableau VII: Coefficient des équations de régression multiple pour les laitiers broyés à 6000 cm²/g

	R1	R2	R7	R28	R90	R180
Constante	-32,67	-69,16	+25,7	+25,8	+47,27	+49,68
C/S	+28,35	+61,84	-	-	-	-
Φ en Å	-	-	-0,0032	-0,008	-0,008	-0,007
C_3S	-0,002	+0,072	+0,109	+0,308	+0,114	+0,113
C_3A cubique	+0,218	+0,334	-0,107	-0,177	-0,443	-0,474
C_3A tétrag.	+0,111	+0,244	+0,099	+0,133	+0,003	+0,0004
C_4AF	+0,080	+0,157	-0,131	-0,067	-0,421	-0,414
K_2SO_4	-0,47	-0,83	+0,221	-0,704	+0,510	+0,655
Coeff.corr. multiple r	0,96	0,97	0,74	0,95	0,79	0,83

La corrélation multiple est très significative à 2 jours, comme le laissait prévoir l'analyse de la variance, en effet, la corrélation simple avec le seul paramètre du laitier est déjà égale à 0,90, l'introduction des paramètres du clinker n'améliore pas sensiblement la corrélation : la faible plage de variation des clinkers industriels et l'incertitude relative sur les résistances à 2 jours ne permettent pas de quantifier l'influence du clinker avec les méthodes statistiques utilisées. A 7 jours, les corrélations sont les moins significatives pour les 2 finesses. A partir de 28 jours, les effets positifs de l'alite et du C_3A tétragonal et négatifs du C_4AF deviennent plus importants. Le K_2SO_4 a toujours une influence positive sur les laitiers broyés à 3500 cm^2/g mais dans le cas des laitiers à 6000 cm^2/g, l'action est moins nette et l'incertitude de connaissance du coefficient est importante. L'élimination de ce paramètre modifie très peu le coefficient de corrélation multiple.

L'ensemble de ces corrélations nous permet donc de définir les paramètres principaux d'action des clinkers : taux d'alite et C_3A tétragonal élevé, taux de C_4AF faible. A 6000 cm^2/g, la diminution du coefficient de l'alite après 28 jours, contrairement au cas à 3500 cm^2/g, peut être mis en correspondance avec la désaturation en chaux de la solution (2). L'activation devenant alors plus alcaline que calcique.

Nous allons maintenant étudier l'interaction clinker-laitier en fonction de la finesse du laitier.

3 - Recherche des associations laitier-clinker

Pour mettre en évidence les associations favorables laitier- clinker, nous classons à chaque échéance et pour chaque type de laitier les mélanges par ordre décroissant de résistance et, à titre de comparaison, les ciments portland obtenus avec les mêmes clinkers. S'il n'y a pas d'associations préférentielles laitier-clinker, le classement sera indépendant du type de laitier. Bien entendu, nous avons pris en compte la précision des mesures pour examiner ces classements. Les résultats pour les laitiers à 6000 cm^2/g sont présentés au tableau VIII.

Ce tableau nous montre qu'à 1 jour, le classement n'est significatif que pour le laitier A ; pour le laitier C, les écarts sont de l'ordre de la précision des mesures. Le laitier A, qui est très réactif, différencie mieux les clinkers que les autres laitiers, ce phénomène disparaît avec le temps. A 1 et 2 jours, le classement des CPA est différent de ceux des mélanges à base de laitier, particulièrement dans le cas du clinker C5 très riche en K_2SO_4. Les ciments les plus performants sans K_2SO_4 donnent sensiblement les meilleurs mélanges mais les clinkers très riches en K_2SO_4 s'associent moins bien aux laitiers. La comparaison des laitiers A et C à 1 jour nous montre que le laitier A réagit très rapidement car les résistances se développent beaucoup plus vite que si le laitier est remplacé par un inerte ; dans le cas du laitier C, le taux de réaction est très faible à 24 heures et les résistances sont pratiquement identiques avec tous les clinkers. A 2 jours, ce n'est plus le cas, le laitier C participe plus activement au développement des résistances.

Nous en déduisons que le laitier réagit aux premiers temps de l'hydratation, dès que l'alite libère de la chaux et, très vite, les résistances ne sont pas seulement dues aux hydrates des clinkers car, dans ce cas, les classements devraient être les mêmes pour les CPA et les ciments au laitier.

Nous avons, par ailleurs, examiné les mélanges à 20 % de clinker et 80 %, soit de laitier entièrement cristallisé, soit de sable de Fontainebleau broyé en présence de gypse, à une granulométrie équivalente, les résistances sont mentionnées au tableau IX.

Tableau VIII: Classement par résistance décroissante des mélanges pour les laitiers à 6000 cm^2/g

	Laitier A		Laitier B		Laitier C		CPA	
1 jour	C2	9,7	C1	5,5	C1	2,9	C5	20,6
	C1	9,0	C2	5,2	C2	2,9	C4	17,6
	C4	6,9	C4	4,4	C4	2,8	C2	17,4
	C6	6,5	C6	3,9	C5	2,5	C1	14,2
	C3	5,9	C3	3,7	C7	2,3	C7	13,6
	C5	5,9	C7	3,7	C3	2,2	C3	10,8
	C7	5,4	C5	3,3	C6	2,2	C6	10,1
2 jours	C1	23,4	C1	20,0	C2	13,5	C5	32,2
	C3	21,3	C2	19,1	C1	13,2	C2	31,5
	C4	21,2	C4	18,4	C4	12,1	C4	31,2
	C2	21,0	C3	16,5	C3	10,6	C1	28,8
	C7	20,5	C6	15,9	C5	10,5	C3	26,1
	C5	20,2	C7	15,0	C6	10,4	C7	25,7
	C6	19,4	C5	14,7	C7	9,5	C6	20,2
28 jours	C3	46,8	C3	41,9	C3	41,1	C1	66,2
	C4	45,4	C4	39,1	C4	40,3	C3	65,2
	C7	43,1	C1	37,8	C7	38,7	C2	61,1
	C5	42,0	C7	37,7	C5	38,3	C7	59,3
	C1	42,0	C2	36,2	C1	37,9	C4	50,8
	C2	38,6	C6	35,4	C6	36,6	C5	50,5
	C6	37,9	C5	33,4	C2	36,4	C6	46,5
360 jours	C3	61,2	C3	52,6	C4	53,5	C3	76,5
	C4	59,8	C1	50,3	C3	52,7	C1	76,3
	C7	56,2	C7	50,3	C1	52,4	C7	76,2
	C1	56,0	C4	48,9	C5	50,9	C2	68,6
	C5	54,8	C2	48,1	C7	49,7	C6	68,5
	C2	53,0	C6	47,2	C6	48,9	C5	56,0
	C6	50,9	C5	42,0	C2	47,7	C4	53,1

Tableau IX : Résistances en MPa

	R_2	R_7	R_{28}
Clinker + Laitier cristallisé	1,5	2,3	3,5
Clinker + Sable	1,5	2,0	2,2

Ceci, associé avec nos études de l'hydraulicité des ciments à haute teneur en laitier (3) nous confirme que le laitier réagit dès les premiers âges et que les résistances observées sont bien dues à l'association laitier-clinker.

Nous constatons aussi que les différences entre les classements CPA et mélanges croissent avec le temps. Nous n'avons remarqué qu'un seul couple laitier-clinker singulier : C5 + Laitier B à 28 et 360 jours.

Si l'on tient compte des faibles différences entre les résistances, on peut dire que dans le cas des laitiers broyés très finement, il n'existe pas d'associations laitier-clinker préférentielles dans ce type de mélanges à très forte teneur en laitier.

Etudions maintenant les classements établis dans le cas des laitiers broyés à 3500 cm^2/g et décrits au tableau X.

Tableau X : Classement par résistances décroissante des mélanges pour les laitiers à 3500 cm^2/g

	Laitier A		Laitier B		Laitier C		CPA	
2 jours	C1	9,1	C1	6,7	C4	4,7	C5	32,2
	C4	9,0	C2	6,4	C1	3,9	C2	31,5
	C3	8,5	C4	5,8	C2	3,7	C4	31,2
	C2	8,2	C5	5,4	C7	3,4	C1	28,8
	C5	8,0	C3	4,3	C5	3,0	C3	26,1
	C6	7,4	C7	3,8	C3	2,9	C7	25,7
	C7	6,6	C6	3,4	C6	2,7	C6	20,2
28 jours	C4	36,8	C1	33,1	C4	30,1	C1	66,2
	C3	33,5	C4	32,5	C1	28,0	C3	65,2
	C1	32,2	C3	31,8	C7	27,7	C2	61,1
	C5	31,7	C5	31,7	C5	27,2	C7	59,3
	C2	30,5	C2	30,6	C3	26,9	C4	50,8
	C7	28,2	C7	29,1	C6	26,7	C5	50,5
	C6	27,6	C6	28,4	C2	26,6	C6	46,5
360 jours	C4	54,2	C1	47,8	C4	47,4	C3	76,5
	C3	53,4	C4	47,4	C1	43,5	C1	76,3
	C1	51,7	C3	46,0	C5	42,3	C7	76,2
	C5	49,8	C2	45,7	C2	40,7	C2	68,6
	C2	49,2	C5	45,6	C7	40,4	C6	68,5
	C7	45,1	C7	41,9	C3	39,5	C5	56,0
	C6	43,3	C6	41,8	C6	38,6	C4	53,1

Comme à finesse élevée, on constate que le laitier A réagit très vite alors que le laitier C commence à peine à réagir à 2 jours, les phénomènes sont identiques mais avec un décalage dans le temps. A toutes les périodes, le clinker C3 riche en alite et à faible teneur en K_2SO_4 et C_3A tétragonal se situe parmi les meilleurs clinkers avec le laitier A, est moyen avec le laitier B et parmi les moins bons avec le laitier C. Le clinker C7, de composition chimique voisine, mais moins riche en alite et en C_3A est un des moins bons activants des trois laitiers de 28 à 360 jours. Les clinkers à fort taux d'alite activeront donc très bien à long terme les laitiers de C/S élevés de type fonte Thomas et moins bien les laitiers de type hématite. D'autre part, l'examen des résultats avec le clinker C4 nous montre que les clinkers à teneur en alite moyenne mais à fort taux de C_3A tétragonal seront parmi les meilleurs, quel que soit le type de laitier.

On peut donc conclure que dans le cas de nos mélanges à très haute teneur en laitier, le rendement de l'association laitier-clinker est une fonction de la finesse du laitier. L'activité des clinkers sera équivalente vis-à-vis de tous les laitiers très finement broyés. Par contre, l'action des clinkers à fort taux d'alite ou à fort C_3A tétragonal sera différente suivant le type de laitier dans le cas des finesses peu poussées. Pour obtenir les mêmes résistances mécaniques, les laitiers hématite devront être broyés finement avec des clinkers riches en alite et faibles en C_3A qu'avec des clinkers à fort taux de C_3A tétragonal.

A l'aide des tableaux VI et VIII, nous avons déterminé les rapports $R_{360\ jours}/R_{28\ jours}$ pour tous les mélanges. On remarque que pour les laitiers à 3500 cm^2/g, il est en moyenne de 1,51, indépendant du clinker utilisé et varie de 1,46 à 1,57 selon le laitier. Par contre, pour les laitiers à 6000 cm^2/g, il est de 1,31 en moyenne, indépendant du laitier, et varie légèrement de 1,28 à 1,35 avec le type de clinker.

Ce rapport est donc principalement une fonction de la finesse du laitier.

INFLUENCE DE LA TENEUR EN SULFATE ET DE LA FINESSE DU CLINKER

Dans une série d'expériences complémentaires, nous avons fait varier la teneur en sulfate pour des mélanges réalisés avec le laitier A et les clinkers C4 et C6 qui conduisent aux résistances les plus différentes au tableau III.

Nous avons obtenu les résultats suivants portés au tableau XI.

Tableau XI : Influence de la teneur en sulfate et de la finesse du clinker sur le laitier A

Finesses	SO_3 %	R_1		R_2		R_7		R_{28}	
		C4	C6	C4	C6	C4	C6	C4	C6
L : 3500 C : 3500	0,5	1,5	1,6	4,9	5	26,9	25,3	46,0	46,5
	1	2,0	1,9	6,2	6,1	27,1	26,0	44,5	43,7
	2	2,2	2,7	8,8	7,2	29,6	22,6	45,2	38,2
	4	1,7	2,0	4,2	5,6	25,7	20,1	39	32,2
	6	1,6	1,8	3,5	4,2	6,0	8,2	32,7	20,3
L : 6000 C : 3500	0,5	2,9	2,9	10,1	9,6	37,8	33,7	53,3	47,6
	1	3,5	3,9	11,6	11,0	38,1	33,5	51,0	48,8
	2	5,5	4,8	13,6	11,9	36,2	30,9	51,5	43,7
	4	7,5	7,2	15,9	14,4	35,2	28,5	48,8	39,0
	6	6,1	5,1	9,6	15,7	32,6	28,5	45,6	36,6
C : 6000 L : 3500	2	2,2		10,1		27,1		41,7	
	4	2,8		11,0		24,0		35,7	
	6	3,1		7,5		22,9		35,9	
C : 6000 L : 6000	2	6,1		14,5		34,0		48,0	
	4	10,3		17,2		31,1		43,2	
	6	6,9		21,8		34,9		45,3	

L'examen de ce tableau montre que les résistances à tous les âges sont influencées par la teneur en SO_3. La teneur optimum varie avec la période et la finesse du laitier.

A 1 et 2 jours, l'optimum se situe vers 2 % pour une finesse de 3500 cm^2/g et 4 % à 6000 cm^2/g. A 7 jours, on remarque qu'une teneur élevée en SO_3 (6 %) perturbe le développement des résistances et avec le laitier à 3500 cm^2/g, elles sont diminuées d'un facteur 5. Par contre, à 6000 cm^2/g, le laitier tolère une teneur en SO_3 élevée du fait de la dissolution plus importante d'ions Al. A 28 jours, les résistances sont inversement proportionnelles à la teneur en sulfate. On pourrait se demander s'il ne s'agit pas d'un simple effet de dilution. Avec le laitier à 6000 cm^2/g, pour le clinker C4, très riche en aluminate, la baisse est proportionnelle à la dilution, mais plus forte que la dilution dans le cas du clinker C6 à faible teneur en aluminate. Tout ceci montre que, malgré la faible teneur en laitier, la teneur en C_3A du clinker doit être considérée pour déterminer l'optimum en SO_3.

On constate aussi qu'une plus grande finesse du clinker permet d'élever les résistances à court terme, mais les diminue à long terme. Il faut donc adapter la finesse du clinker pour qu'il active le laitier au moment où il en a besoin pour développer les résistances maximales à long terme.

INFLUENCE D'UNE PETITE AUGMENTATION DE LA TENEUR EN CLINKER

Cet essai a été réalisé avec le clinker C4 à différentes finesses et teneurs en sulfates. Le mélange A est à 75 % de laitier et 25 % de clinker et le mélange B à 80 % de laitier et 20 % de clinker.

Tableau XII : Influence de la teneur en clinker

Finesses	SO_3 %	R_1		R_2		R_7		R_{28}	
		A	B	A	B	A	B	A	B
C : 3500	2	5,6	5,5	18,2	13,6	46,1	36,2	60,8	51,5
	4	8,8	7,5	24,2	15,9	44,5	35,2	61,7	48,8
L : 6000	6	6,6	6,1	22,2	9,6	42,2	32,6	55,3	45,6
C : 6000	2	7,3	6,1	23,9	14,5	44,6	34,0	56,3	48,0
	4	10,3	10,3	25,2	17,2	44,4	31,1	54,9	43,2
L : 6000	6	10,0	6,9	28,3	21,8	42,5	34,9	55,1	45,3

L'augmentation de la teneur en clinker de 5 % a peu d'influence à 1 jour, mais elle se fait très fortement sentir à 2 jours, dès que le laitier réagit rapidement, pour atteindre environ 10 MPa à 28 jours. Si le seul but était les performances mécaniques maximales, on aurait intérêt à augmenter légèrement la teneur en clinker. L'augmentation de la quantité de chaux disponible permettrait de maintenir une sursaturation constante de la solution interstitielle : ce qui ne serait pas favorable à la résistance des bétons aux attaques chimiques.

Cet essai nous montre aussi les limites des conclusions de cette étude sur l'influence du clinker qui n'a été testée que sur les mélanges de rapport laitier/clinker = 4, soit plus de 76 % de laitier dans des ciments où SO_3 = 3 %. Nous sommes à une limite imposée par la résistance chimique. Une faible augmentation de la teneur en clinker peut faire passer dans une autre catégorie de ciments et les conclusions sur l'influence du clinker seraient différentes.

CONCLUSIONS

Nous précisons que l'objet de cette étude était de comparer divers types de laitiers et de clinkers de compositions minéralogiques différentes et non pas d'étudier les variations de qualité d'un même laitier. Dans cette étude de laboratoire, nous n'avons pas pris en compte la broyabilité relative du clinker et du laitier, puisque nous avons broyé séparément chaque constituant à une finesse prédéterminée.

L'ensemble des essais réalisés avec 42 mélanges de clinker et de laitier nous permet de tirer les conclusions suivantes.

Contrairement aux idées reçues, les résistances à 1 jour des ciments à très haute teneur en laitier (laitier > 76 % dans le ciment) sont principalement fonction de la qualité du laitier. Il réagit dès les premiers instants et les résistances mesurées aux premiers âges sont celles de l'association laitier- clinker et non pas celles du clinker seul. La qualité du clinker ainsi qu'une légère augmentation de sa teneur n'ont pas d'influence notable avant deux jours. Les meilleures résistances à 28 jours sont obtenues avec les clinkers riches en alite et en C_3A tétragonal. L'influence de ces deux minéraux sur les résistances est équivalente vis-à-vis de tous les laitiers broyés très finement, mais dans le cas des laitiers à 3500 cm^2/g, l'action des clinkers à fort C_3A tétragonal est indépendante du type de laitier alors que les clinkers riches en alite et à faible C_3A activent mieux les laitiers les plus basiques. On constate aussi qu'il existe un rapport entre les résistances à 1 an et celles à 28 jours qui est principalement fonction de la finesse du laitier.

Les courbes d'évolution des résistances dépendent principalement de la qualité du laitier. Le clinker n'intervient qu'au deuxième ordre et les classements résistances ciment portland et résistances des mélanges étudiés sont différentes.

L'influence du sulfate de calcium est modulée par deux facteurs : le temps et la teneur en C_3A du clinker. Comme dans le cas des ciments portland, il existe une teneur optimale en sulfate de calcium variable en fonction de l'objectif recherché mais toujours relativement faible. La contribution de l'activation calcique est donc plus importante pour le développement des performances mécaniques que celle de l'activation sulfatique. Par ailleurs, dans le cas des laitiers à 6000 cm^2/g, nous avons montré l'influence de l'activation alcaline à long terme.

En définitive, dans le cas que nous avons étudié, tous les laitiers ne permettent pas d'obtenir des ciments à hautes performances mécaniques. Par contre, une faible augmentation de la teneur en clinker et une optimisation de la finesse et du taux de sulfate de calcium permettent d'améliorer significativement les résistances mécaniques.

REMERCIEMENTS

Les auteurs remercient le personnel des départements ECPM et ECPC du CEREG qui a effectué l'ensemble des broyages, des mélanges et des essais mécaniques des produits.

AVERTISSEMENT

Les analyses par diffusion centrale des rayons X ont été réalisées par M. LACHAUD au CEBTP à SAINT-REMY-LES-CHEVREUSE.

BIBLIOGRAPHIE

1 - E. DEMOULIAN, P. GOURDIN, F. HAWTHORN, C. VERNET
Influence de la composition chimique et de la texture des laitiers sur leur hydraulicité - VIIème Symp. Int. Chim. des Ciments, Paris, 1980.

2 - C. VERNET, E. DEMOULIAN, P. GOURDIN, F. HAWTHORN
Cinétique de l'hydratation des ciments au laitier VIIème Symp. Int. Chim. des Ciments, Paris, 1980.

Détermination de la teneur en laitier dans les ciments par dissolutions sélectives

Slag content determination in cements by selective dissolutions

E. DEMOULIAN, C. VERNET, F. HAWTHORN, P. GOURDIN, Société des Ciments Français, CEREG, France.

RESUME :

L'étude des différences de pH et de vitesses de dissolution des constituants des ciments à l'aide d'un titrateur automatique a conduit à la mise au point d'une méthode de séparation chimique quantitative du laitier.

Dans des conditions opératoires bien déterminées, une solution qui contient de l'EDTA, de la triéthanolamine et de la soude dissout totalement, à pH 11,5, les minéraux du clinker et le sulfate de calcium sans attaque notable du laitier. La soude évite la précipitation de la silice et des hydroxydes.

Dans les ciments hydratés, la méthode permet de déterminer la quantité de laitier qui n'a pas réagi. Pour les ciments ternaires, elle doit être complétée par les méthodes préalablement mises au point pour doser les cendres volantes et les pouzzolanes.

SUMMARY

The study of pH and dissolution speeds of cement constituents with an automatic titrator had led to a quantitative chemical method for the separation of the slag in cements.

In well determined operational conditions, an EDTA, triethanolamine and sodium hydroxide solution, dissolves the clinker minerals and calcium sulphate, at pH 11,5, without a notable dissolution of the slag. The silica and hydroxides precipitating is avoided by sodium hydroxide.

In the hydrated cements, the method allows the quantitative determination of the non hydrated slag. In the case of ternary cements, it can be completed by supplementary methods, already perfected for determining fly ashes and pozzolanas contents.

INTRODUCTION

Depuis plusieurs années, nous étudions au CEREG la dissolution sélective des phases anhydres ou hydratées des clinkers et ciments. Nous avons expérimenté de nombreux réactifs en milieu aqueux ou organique. Ces recherches ont abouti à la mise au point de deux méthodes de détermination des teneurs en cendres et en pouzzolanes dans les ciments. Ces méthodes, mises à l'épreuve par les nombreux participants du CEN GT 4 TC 51 ont été testées avec succès et proposées comme méthodes de référence en projets de normes européennes (1)(2). Le problème de la séparation sélective du laitier restait à résoudre.

L'apparition d'appareillages très élaborés de titration automatique qui permettent des ajouts incrémentiels du réactif, asservis soit aux dérivées du signal, soit à l'écart par rapport à un point de consigne, nous a permis d'étudier les cinétiques de dissolution des laitiers et des phases des clinkers dans différents milieux.

A la suite de cette étude, nous avons mis au point une attaque sélective rapide du clinker et du gypse qui permet de séparer quantitativement le laitier et les autres ajouts que l'on peut identifier par un examen complémentaire de l'insoluble.

1/ CINETIQUE DE DISSOLUTION DES MINERAUX ANHYDRES OU HYDRATES DES CIMENTS

L'étude des différences de vitesses et de pH de dissolution des clinkers et ciments a été réalisée à l'aide du titrateur automatique représenté sur la photographie n° 1.

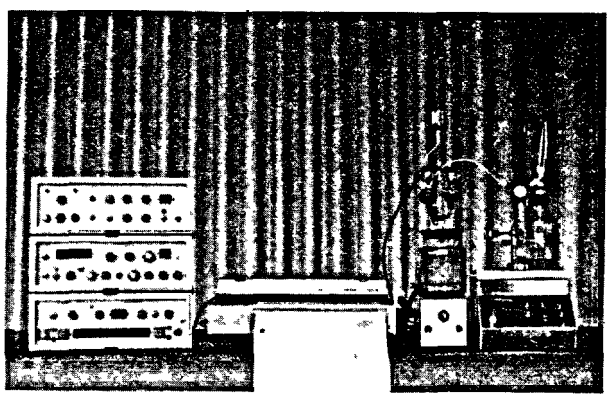

Photographie n° 1 - Ensemble de titrage automatique

Les fonctions d'asservissement du titrateur ont été utilisées pour ajouter le réactif, par incréments, à une vitesse continuellement égale à la vitesse de réaction de la phase étudiée, qui peut ainsi être mesurée. Nous avons choisi le pH comme variable indicatrice.

Le mode opératoire suivant a permis d'étudier les phases anhydres et hydratées des ciments : alites, bélites, C_3A cubique et tétragonal, C_4AF, silicates hydratés, ettringite, monosulfate de calcium et différents laitiers.

Dans une cellule thermostatée à 20°C contenant 500 ml d'eau, on introduit 200 mg de la phase à étudier. Un acide 0,2 N est ajouté par incréments de 100 microlitres. L'asservissement obéit aux principes suivants :

1) l'ajout d'un incrément supplémentaire est déclenché lorsque la vitesse de variation du signal (pH) est inférieure à une valeur seuil (en mV/minute) correspondant à la fin de réaction de l'incrément précédent ;

2) pour prendre en compte le temps de réponse du capteur, un délai supplémentaire constant mais ajustable, fixé ici à 20 secondes, est imposé par le titrateur.

Les courbes obtenues pour les phases étudiées sont représentées sur les figures 2 à 12.

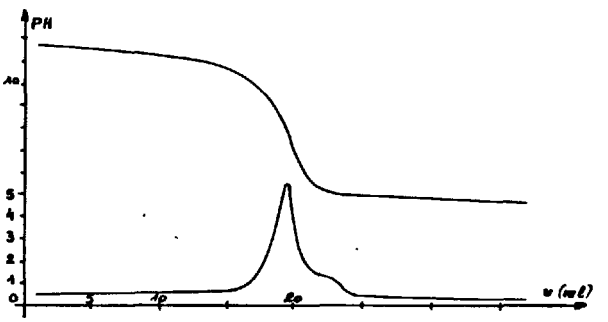

Fig. 2 - ALITE

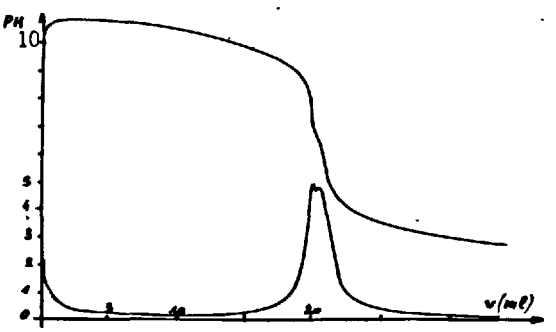

Fig. 3 - BELITE

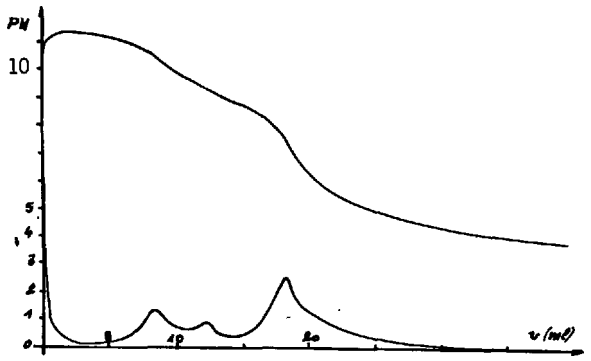

Fig. 4 - C_3A cubique

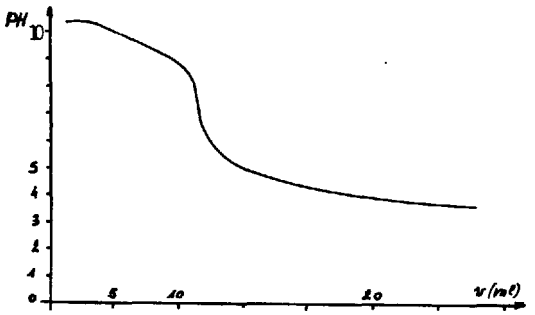

Fig. 7 - CSH

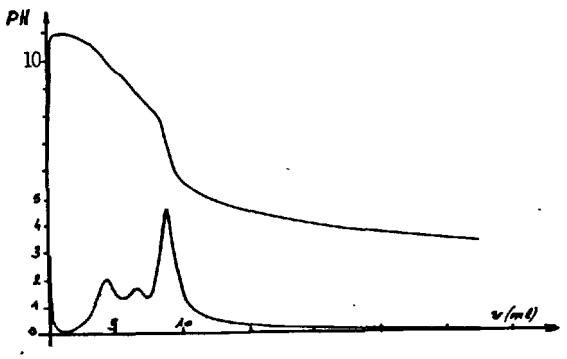

Fig. 5 - C_4AF

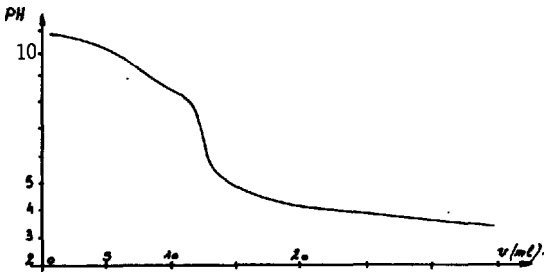

Fig. 8 - ALITE HYDRATEE [CSH + $Ca(OH)_2$]

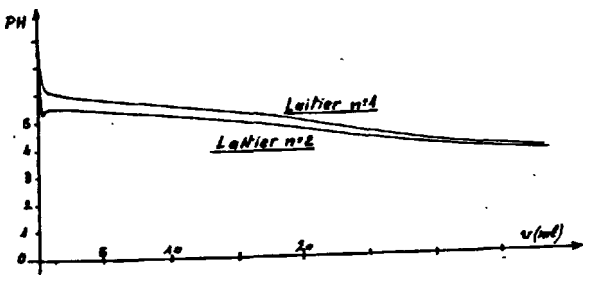

Fig. 6 - LAITIERS

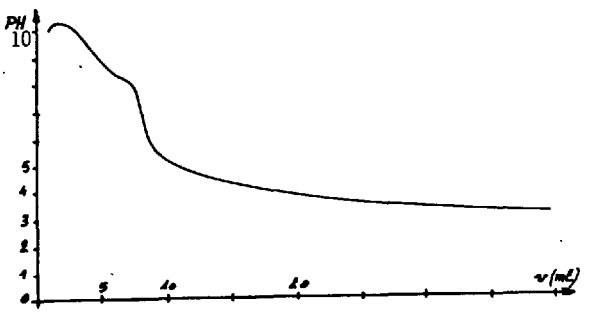

Fig. 9 - ETTRINGITE

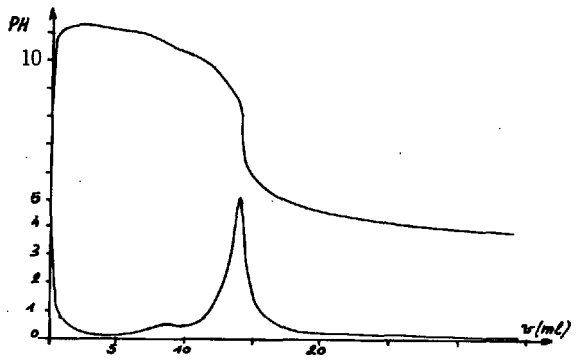

Fig. 10 - CPA

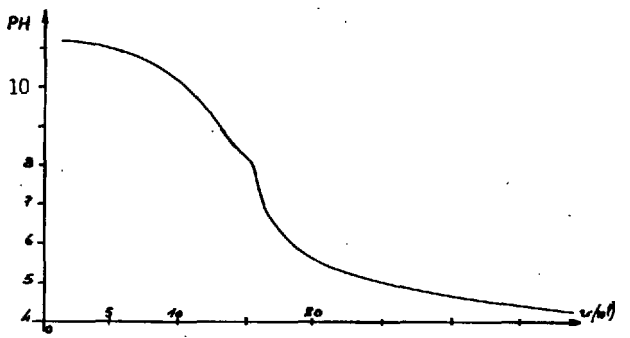

Fig. 11 - CPA HYDRATE

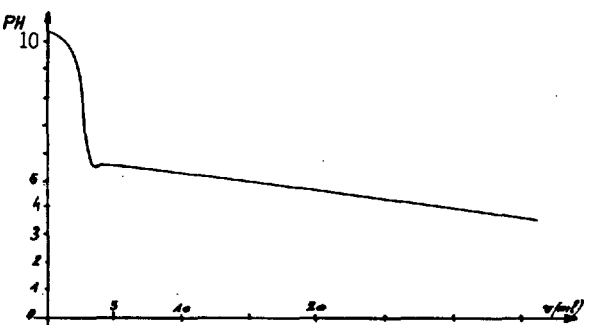

Fig. 12 - Courbe de dissolution d'un mélange laitier + clinker

Elles montrent les différences de vitesses et de pH de dissolution ainsi que l'existence de plusieurs étapes dans le mécanisme de dissolution. Pour les minéraux anhydres ou hydratés, les pH de fin de réaction sont compris entre 7 et 8, dans cet intervalle le laitier n'a pas réagi de manière significative. Lorsque l'acide utilisé est un acide fort comme HCl, la dissolution des aluminates et même des silicates est fortement ralentie, soit par précipitation d'hydroxydes d'aluminium et de fer, soit par précipitation de silice et les dissolutions sont incomplètes à pH7. A ce pH, l'utilisation d'un acide complexant tel que l'acide citrique, comme pour les exemples des figures 2 à 12, n'évite que partiellement ces précipitations, les aluminates du clinker ne sont pas totalement dissous, de la silice reprécipite. Les séparations ne sont pas quantitatives, ce qui a été confirmé sur des mélanges de laitier, de clinker et de gypse en différentes proportions.

Cependant, les différences de vitesses et de pH de dissolution mises en évidence doivent permettre une séparation quantitative du laitier en utilisant des réactifs formant des complexes solubles plus stables que les hydroxydes d'aluminium et de fer. Pour éviter la précipitation de la silice, il faudra opérer à un pH plus élevé, ce qui aura pour inconvénient de diminuer les vitesses de dissolution. Il faudra donc les accélérer en déplaçant les équilibres par complexation du calcium.

2/ METHODE DE DOSAGE RAPIDE DE LA TENEUR EN LAITIER DANS LES CIMENTS

Compte tenu des études et observations précédentes, nous avons mis au point une méthode rapide de séparation quantitative du laitier qui ne nécessite que l'utilisation d'un appareillage courant. L'acide citrique ne convenant pas pour séparer sélectivement le laitier du clinker à pH7, après de nombreux essais, nous avons utilisé le sel disodique de l'acide éthylènediaminetétraacétique ou EDTA de formule :

$$\begin{matrix} CH_3COOH \\ CH_3COONa \end{matrix} > N - CH_2 - CH_2 - N < \begin{matrix} CH_3COOH \\ CH_3COONa \end{matrix}$$

et la triéthanolamine $(CH_2OHCH_2)_3\ N$ comme complexants du calcium, de l'aluminium, du fer et l'hydroxyde de sodium pour éviter la précipitation de la silice entre pH 11,0 et 12,0.

2.1 - Etude de la méthode

Influence du pH du réactif : Sur un mélange constitué de 50 % de laitier, 45 % de clinker, 5 % de gypse, l'influence du pH de dissolution a été mise en évidence par différentes solubilisations à des pH prédéterminés entre 11,0 et 12,0.

Les résultats mentionnés sur le tableau I montrent que la quantité d'insoluble est pratiquement identique entre pH 11,4 et 11,8. La moyenne de 48,6 ± 0,2 met en évidence une faible solubilisation du laitier. Cet effet est un peu plus important aux pH 11,0 et 12,0. Pour les autres vérifications et pour la méthode définitive, le pH de solubilisation du clinker et du sulfate de calcium sera fixé à pH 11,6 ± 0,1.

Tableau I : Influence du pH du réactif

pH	11,0	11,4	11,5	11,6	11,7	11,8	12,0
Insoluble %	47,5	48,5	48,8	48,5	48,6	48,4	47,5

Analyse de l'insoluble séparé : Nous avons reporté sur le tableau II, la composition chimique du laitier et celle de l'insoluble séparé à pH 11,6 ± 0,1. Ces résultats montrent que les compositions chimiques sont très voisines et que l'insoluble séparé est principalement constitué de laitier.

L'absence de sulfate montre que le gypse a été totalement dissous. La solubilisation du clinker semble quantitative. Nous notons toutefois un très léger enrichissement en silice et en FeO.

Tableau II : Composition chimique du laitier et de l'insoluble séparé à pH 11,6 ± 0,1

	SiO_2	Al_2O_3	FeO	CaO	MgO	SO_3	S^{--}
Laitier	32,91	14,95	0,54	43,74	4,53	0,04	0,88
Insoluble	33,40	14,77	0,70	43,74	4,60	0,00	0,89

Examen de l'insoluble au microscope optique : Après enrobage dans de la résine, l'insoluble obtenu à pH 11,6 ± 0,1 a été examiné au microscope optique. Cet examen a confirmé la solubilisation complète du clinker et du gypse. D'autre part, les grains de laitier à angles vifs ne semblent pas avoir été corrodés par le réactif au cours de l'attaque sélective (photographie n° 13).

Photographie n° 13 - Aspect de l'insoluble séparé à pH 11,6 ± 0,1

Essais de répétabilité : Ces essais ont aussi été effectués sur le mélange à 50 % de laitier.

Pour 20 essais effectués par un même opérateur, la quantité d'insoluble varie entre 47,8 % et 50,6 % avec une moyenne de 48,8 % et un écart type de 0,7 %.

Les résultats obtenus sont mentionnés sur le tableau III.

Tableau III : Essais de répétabilité sur un mélange constitué de 50 % de laitier, 45 % de clinker, 5 % de gypse

N° Essai	1	2	3	4	5	6	7
Insoluble %	48,6	48,1	48,1	48,5	48,7	48,6	49,9
N° Essai	8	9	10	11	12	13	14
Insoluble %	49,5	49,1	49,1	48,7	48,4	47,8	50,0
N° Essai	15	16	17	18	19	20	
Insoluble %	48,6	48,2	48,3	48,4	49,2	50,6	

Etalonnage de la méthode : Les essais de répétabilité ayant montré une solubilisation non négligeable du laitier, l'exactitude de la méthode préconisée peut être améliorée par un étalonnage préalable.

L'étalonnage a été réalisé sur des mélanges synthétiques qui contiennent 5 % de gypse et des proportions variables de 3 laitiers référencés A, B, C et de 2 clinkers C2 et C4, comme dans une autre de nos communications qui donne leurs compositions chimiques et minéralogiques (3).

Les laitiers sont des laitiers vitrifiés de fontes hématite et de fonte Thomas représentatifs de la production française, les clinkers ont été choisis pour leurs grandes différences minéralogiques.

Les résultats obtenus, mentionnés sur le tableau IV, conduisent à la relation : $y = 1,024\ x - 0,05$, où x est le pourcentage d'insoluble, y le pourcentage de laitier calculé et dans laquelle, l'ordonnée à l'origine peut être négligée.

L'application de la relation $y = 1,024\ x$ au pourcentage moyen d'insoluble trouvé au cours des essais de répétabilité donne 49,97 % de laitier pour un mélange qui en contient 50 %. Ceci montre la validité de l'étalonnage dans le cas des laitiers considérés.

Tableau IV : Etalonnage avec des mélanges synthétiques

Pourcentage de laitier dans le mélange	Pourcentage d'insoluble
0	0,0 - 0,8
20	19,6 - 18,0
35	34,0 - 33,0 - 35,0 - 35,2
45	44,9 - 44,2
50	48,4
55	53,3
65	64,6 - 62,4
75	73,1 - 75,4 - 73,8 - 73,1
85	82,4 - 82,7
95	92,2 - 92,6

2.2 - Mode opératoire préconisé

Dans un bécher de 600 ml, introduire successivement :

- 250 ml d'une solution d'EDTA 0,05 M dans de la soude 0,1 N,
- 25 ml de triéthanolamine à dilution 1-1 avec de l'eau distillée,
- ajuster à pH 11,6 $\pm$ 0,1 avec NaOH N,
- après broyage à refus nul au tamis de 40 µm, ajouter progressivement pendant l'agitation de la solution 500 mg (P1) du ciment à doser (l'ajout doit être progressif pendant l'agitation pour éviter la formation d'amas difficilement délayables),
- continuer l'agitation pendant 20 minutes,
- filtrer sur verre fritté n° 4 préalablement taré (P2),
- rincer 7 fois à l'eau distillée,
- rincer 3 fois à l'alcool éthylique,
- sécher à l'étuve à 105°C pendant 30 minutes,
- laisser refroidir en dessicateur et peser (P3).

Pourcentage de laitier :

$$\% L = \frac{P3 - P2}{P1} \times 100 \times K \qquad (I)$$

K est le coefficient obtenu par étalonnage, il est destiné à tenir compte de la faible dissolution du laitier. Il est de 1,024 dans le cas présent.

3/ CONCLUSIONS

Cette recherche nous a conduit à mettre au point une méthode applicable aux ciments contenant du laitier vitrifié. Elle peut, avantageusement, remplacer les méthodes de séparation par liqueurs denses et les mesures par microscopie optique, qui sont des méthodes à temps de réponse longs et de mises en oeuvre délicates.

Elle permet, de plus, l'étude des produits hydratés des ciments qui contiennent du laitier.

Pour déterminer les quantités de chaque ajout, dans les ciments ternaires, elle peut être complétée par les méthodes de détermination des teneurs en cendres et en pouzzolanes dans les ciments (1) (2).

REMERCIEMENTS

Les auteurs remercient Mme CAULLIER, technicienne au CEREG, qui a effectué les très nombreux essais de mise au point de la méthode.

BIBLIOGRAPHIE

1 - Méthode proposée au CEN GT4 TC 51 pour la détermination de la teneur en cendres volantes dans les ciments.

2 - Méthode proposée au CEN GT4 TC 51 pour la détermination de la teneur en pouzzolanes dans les ciments.

3 - C. VERNET, E. DEMOULIAN, P. GOURDIN, F. HAWTHORN - Cinétique de l'hydratation des ciments au laitier VIIème Symp. Int. Chim. des Ciments, Paris, 1980.

7e Congrès International de la Chimie des Ciments

7th International Congress on the Chemistry of Cement

VOLUME III

COMMUNICATIONS
(suite)

PARIS 1980

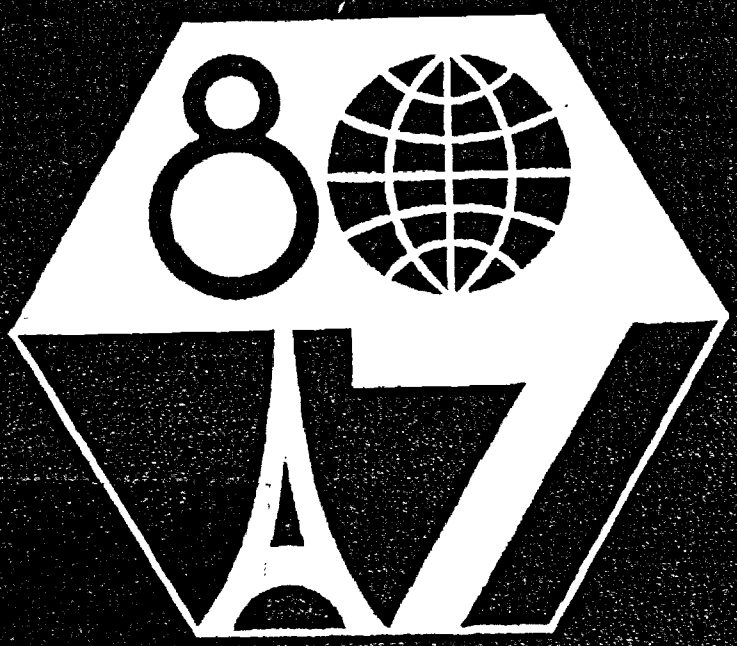

7e Congrès International de la Chimie des Ciments

7th International Congress on the Chemistry of Cement

VOLUME III

COMMUNICATIONS
(suite)

PARIS 1980 [June 30 - July 4]

EDITIONS SEPTIMA - 14, rue Falguière,
75015 PARIS (France).

Imprimé en France - 1980.

TABLE DES MATIERES
CONTENTS

* La pagination comporte tout d'abord un chiffre romain correspondant au numéro du thème, suivi d'un numéro de page à l'intérieur du thème. Dans chaque thème, les communications ont été publiées dans l'ordre où elles sont parvenues au Secrétariat Général du Congrès pour permettre une publication plus rapide.
The pagination consists of a roman numeral corresponding to the theme number, followed by a page number in the interior of the theme. In each theme the communications have been published in the order they reached the General Secrétariat of the Congress, in order to accelerate the publication.

IV-104	R. Kovacs (Hongrie)	The influence of the production technology of fly ash cements upon their hydration and hardening. L'influence de la technologie sur l'hydratation et sur le durcissement des ciments de cendre volante.
IV-110	B. Mortureux, H. Hornain E. Gautier, M. Regourd (France)	Comparaison de la réactivité de différentes pouzzolanes. Comparison of the reactivity of different pozzolana.
IV-116	A. Verhasselt (Belgique)	Caractérisation de la pouzzolanicité de cendres volantes. Characterization of the pozzolanicity of fly ash.
V-0	**THEME V – Ciments spéciaux.** Special cements.	
V-1	V. Moldovan, N. Butucescu (Roumanie)	Sur le mécanisme de l'expansion des ciments expansifs. Expansion Mechanisms of Expansive Cements.
V-6	P.K. Mehta, D. Pirtz, G.J. Komandant (USA)	Magnesium oxide additive for producing selfstress in mass concrete. Oxyde de magésium, additif producteur d'autocontrainte dans la masse du béton.
V-10	P. Kittl (Chili) J.H.C. Castro, L.C. Pompeu (Brésil)	Microstructure and hydration of high alumina cement clinkers. Microstructure et hydratation des ciments à haute teneur en alumine.
V-15	Y. Efes (RFA)	Investigations on two special cements. Etude de deux ciments spéciaux.
V-21	R. Sh. Mikhail, S. Hanafi (Egypte) S.A. Abo.El.Enein (Qatar)	Post-Hydration Compressed Expansive Clinker Pastes. Pâtes de clinker dilaté compressé après hydratation.
V-27	Wu Chung-wei, Wan Yan-sheng (Chine Populaire)	On alunite expansive cement and concrete. Ciment expansé d'alun et béton précontraint.
V-33	Xue Jun-gan, Chen Wen-hao, Tong Xue-li, Zhao Yu-ping, Xu Ji-Zhi (Chine Populaire)	Expansion of sulfoaluminate under under-saturated CaO. Expansion du sulfoaluminate en solution sous saturée en CaO.
V-39	L.V. Nikitina, K.G. Krassilnikov, A.I. Lapchina (URSS)	La nature physico-chimique des auto-contraintes des ciments expansifs. Physicochemical nature of own stresses in expanding cements.
V-45	T.V. Kouznetsova, V.P. Riasine, V.I. Gousseva, V.A. Vorobiev (URSS)	Composition en phases du clinker de ciment alumineux à teneur d'alumine élevée en fonction de la température et du milieu gazeux de cuisson. Phase composition of clinker of high-alumina cement versus calcination temperature and gas medium.
V-51	P. Bhaskara Rao, V.N. Viswanathan (Inde)	Chemistry of arresting strength retrogression in structural high alumina cements. Les causes chimiques des baisses ou des limitations de résistance dans les structures en ciments alumineux.
V-57	F. Skvara, J. Novotny, K. Kolar, Z. Zadak, Z. Bazantova (Tchécoslovaquie)	The Cement for Use at Low Temperatures. Le ciment pour emploi aux températures basses.
V-62	L. Cussino, A. Negro (Italie)	Hydratation du ciment alumineux en présence d'agrégat siliceux et calcaire. Hydration of aluminous cement in the presence of silice and calcareous aggregate.
V-68	H.G. Midgley (Grande-Bretagne)	The relationship between cement clinker composition and strength recovery of hydrating high alumina cement during conversion. La relation entre la composition du clinker de ciment et la capacité de récupération du ciment alumineux.
V-71	Gunji Shikami, Hirofumi Shimatani, Ryoichi Shikata, Michio Mitsuhashi (Japon)	Property and Application of Thermosetting Cement. Propriétés et applications du ciment thermo-durcissant.
V-75	R. Struillou, M. Arnould (France)	Synthèse vers 750°C et propriétés d'un "β C_2S sulfaté". Synthesis at about 750°C and properties of a "sulphated β C_2S".
V-80	A. Pachtchenko, H. Startchevskaia, V. Serbine, L. Kalita (URSS)	Utilisation du ciment sulfaté dans le béton armé de fibres de verre. Application of sulfating cement in glass fibre reinforced concrete.
V-85	H.G. Midgley (Grande-Bretagne)	The chemical resistance of high alumina cement concrete. La résistance chimique du béton de ciment alumineux.
V-88	N.B. Djabarov, Y.T. Simeonov, (Bulgarie)	Ciment expansé composé d'un ciment normal et d'un ajout complexe. Expansive cement conceived on the basis of normal cement and a complex admixture.

V-94	K. Karibayev, K. Bekishev, D. Aldiyarov, V. Lysenko (URSS)	The structure and characteristics of bleached clinker. Structure et propriétés des clinkers de ciment blanc.
V-98	V. Valkov, A. Deneva D. Stavrakeva (Bulgarie)	Recherches sur les phases de ferrites de baryum dans la zone fortement basique du système $BaO-Fe_2O_3$. Research studies of the barium ferrites in the upper base part of the system $BaO-Fe_2O_3$.
V-102	J. Calleja (Espagne)	Calculation of hypothetically possible potential composition of high-alumina cements. Calcul des compositions potentielles théoriquement possibles des ciments alumineux.
V-108	I. Teoreanu, N. Ciocea (Roumanie)	Ciments réfractaires alumineux dans le pseudosystème $BaO.Al_2O_3-CaO.Al_2O_3-MgO-Al_2O_3-BaO.6Al_2O_3-CaO.6Al_2O_3$. Refractory aluminous cements in the $BaO.Al_2O_3-CaO.Al_2O_3-MgO-Al_2O_3-BaO.6Al_2O_3-CaO.6Al_2O_3$ pseudosystem.
V-113	B.F. Cottin (France)	Hydratation des mélanges silicates-aluminates de calcium. Hydration of calcium silicates and aluminates mixes.
V-119	T. Goto, A. Matzubara, K. Nakano (Japon)	Properties of Super Low Heat Cement concrete. Propriétés des bétons de ciment à très faible dégagement de chaleur.
V-124	P. Barret, Ph. Dufour (France)	Solubilité dans l'eau de CA et CAH_{10} partiellement déshydraté. Solubility of CA and partially dehydrated CAH_{10} in water.
V-130	Y. T. Simeonov, N. B. Djabarov, (Bulgarie)	Méthode de modification des caractéristiques des ciments au moyen des adjuvants. Method for characteristics modification of cements by means of admixtures.
V-134	P. Barret, D. Bertrandie (France)	Courbe d'instabilité minimale dans une solution métastable de CA. Minimum instability curve in a metastable solution of CA.
V-140	B. Guilhot, J.-F. Hugo, A. Mathieu, A. Petit (France)	Influence des conditions de synthèse de l'alumine sur sa réactivité vis-à-vis de la chaux. Influence of the alumina preparation conditions on the reactivity with the calcium oxyde.
V-145	C. A. Langton, E. L. White M.W. Grutzeck, D.M. Roy, (USA)	High temperature cements with goethermal applications. Ciments pour applications géothermiques.
V-152	G. Sudoh, T. Ohta, H. Harada (Japon)	High strength cement in the $CaO-Al_2O_3-SiO_2-SO_3$ system and its application. Ciments à haute résistance, du système $CaO-Al_2O_3-SiO_2-SO_3$; leurs applications.
V-158	A. Bonin, G. Cariou (France)	Système aluminate de calcium - gypse - chaux - eau. On the calcium aluminate - gypsum - lime system.
V-164	V.D. Glukhovsky, G.S. Rostovskaja, G.V. Rumyna (URSS)	High strength slag-alkaline cements. Ciments de laitier alcalin, à haute résistance.
V-169	B. Noudelman, M. Bikbaou, V. Iliukhine A. Sventsitski (URSS)	Structure et propriétés de l'alynite et du ciment d'alynite. Structure and properties of alinite and alinite cements.
V-175	P. Barret, C. Benes D. Bertrandie, J. Moisset (France)	Comportement de divers phosphates avec des constituants des ciments. Behaviour of various phosphates with constituents of cements.
V-181	P. Bojenov, B. Grigoriev (URSS)	Problème de l'utilisation des sous-produits minéraux dans la production des liants. Use of mineral sub-products in binder manufacturing.
V-186	V.I. Akounov, A.M. Dmitriev, S.D. Makachev, G.P. Litvinov, V.I. Jarko, G.V. Zavadski, B.E. Youdovitch (URSS)	Activation mécano-chimique du silicate dicalcique technogène. Mechanochemical activation of technogenic bicalcium silicate.
V-191	J. Talaber, K. Dolezsai (Hongrie)	The development of the structure of CA and CA_2 type high alumina cement clinkers and the properties of cements. Formation des clinkers des ciments alumineux des types CA et CA_2 ; propriétés de ces ciments.
V-197	Bojenov P.I., Grigoriev B.A. Ovtcharenco G. (URSS)	Possibilités de l'intensification des propriétés liantes des matériaux à la base du C_2S. Possibilities of increasing the binding properties of materials rich in C_2S.
V-202	V.S. Bakchoutov, KH.Al-Vardi, Tchjao Pin-Khouan, M.K. Nikolaeva (URSS)	Analyse de la composition granulométrique des ciments de forages pétroliers. Study of the grain composition of oil-well cements.
V-208	V.V. Ilioukhine, V.S. Backchoutov, A.N. Lioussov, M.K. Nikolaeva (URSS)	Aspect cristallochimique du durcissement des ciments pour forages pétroliers. Crystallochemical aspect of hardening of oil - well cements.
V-214	K. Isozaki, S. Sakamaki, K. Nakagawa (Japon)	Application of activated calcium aluminate clinker to quick hardening cement. Utilisation d'une pouzzolane artificielle alumino-calcique dans la fabrication d'un ciment à durcissement rapide.
V-220	U. Yamazaki, H. Kamiaka, S. Kobayashi (Japon)	Role of Expansive additive CaO in expansive cement. Rôle d'une addition de CaO expansive dans les ciments expansifs.

---

* This communication constitutes the principal report of sub-theme VI-0 which was received too late to be published in the volume I ofl principal reports.

** Cet exposé constitue le rapport principal du sous-thème VI-0 qui, parvenu trop tardivement n'a pu être publié dans le volume I réservé aux *rapports principaux.*

VI-93	K. Goriainov, A. Stchastnii (URSS)	La structure de pierre de ciment de nouveaux types de béton. A structure of the cement stone of the new types of concrete.
VI-97	A.E. Moore (Grande-Bretagne)	Structure and composition of compounds in some fully hydrated cement pastes. Structure et composition de certaines pâtes de ciment totalement hydratées.
VI-103	Ya. Ivanov, S. Zacharieva (Bulgarie)	Influence of fly-ash on the rheology of cement pastes. L'influence de la cendre volante sur la rhéologie des pâtes de ciment.
VI-108	A.Ph. Polak, V.V Babkov (URSS)	L'effet des propriétés physico-chimiques du ciment sur la structure et la résistance du ciment hydraté. The Effect of Physico-Chemical Properties of Cement on Structure and Strength of Cement Stone.
VI-114	Sidney Diamond, Sidney Mindess (USA)	Scanning Electron Microscopic Observations of Cracking in Portland Cement Paste. Observations des fissures de pâtes de ciment au microscope électronique.
VI-120	S. Nagataki, S. Kawano (Japon)	Analysis on fluidity of cement paste and mortar. Recherches sur la fluidité de la pâte et du mortier de ciment.
VI-125	Y.S. Malinine, V.P. Riazine, L.S. Batoutina, N.D. Klichanis, B.E. Youdovitch (URSS)	Préhydratation superficielle des ciments et son influence sur le processus de durcissement. Surface pre-hydration of cements and its influence on hardening process.
VI-131	L.J. Parrott (Grande-Bretagne)	Structure and thermal creep of cement paste. Structure et fluage thermique de la pâte de ciment.
VI-135	R. Lapasin, V. Longo, S. Rajgelj (Italie)	The effect of the water reducer addition on the rheology properties of cement pastes. L'influence de l'addition de fluidifiants sur le comportement rhéologique de pâtes de ciment.
VI-141	C.D. Lawrence, F.G.R. Gimblett, K.S.W. Sing (Grande-Bretagne)	Sorption of N_2 and n-C_4H_{10} on hydrated cements. Etude porométrique de ciments hydratés par adsorption de N_2 et n-C_4H_{10}
VI-147	I.F. Ponomarev, I.A. Kryjanovskaia A.G. Kholodnyi (URSS)	Réglage de la formation de la structure et des propriétés du ciment. Control of structure formation and properties of cement.
VI-153	G.M. Tarnaroutski, N.V. Gribanova, G.M. Telycheva, V.N. Sergueeva (URSS)	Influence de la composition chimique des lignosulfonates sur l'hydratation et la plastification des ciments. Influence of chemical structure of lignosulfonates on hydration and plastification of cements.
VI-158	Dr. M. Maultzsch U. Meinhold (RFA)	Testing methods for the set of pastes and mortars. Méthodes de détermination de la prise des pâtes et mortiers.
VI-164	J.P. Bombled (France)	Influence des sulfates sur les comportements rhéologiques des pâtes de ciment et sur leur évolution. Influence of sulfates on the rheological behavior of cement pastes and on their evolution.
VI-170	B.E. Scheetz, E.L. White, D. Wolfe-Confer, D.M. Roy (U.S.A.)	Effect of mix rheology, admixtures and salts upon physical and mechanical properties of hardened cement pastes. Action combinée des adjuvants et des additions de sel sur les propriétés physiques et mécaniques des pâtes de ciment durcies.
VI-176	Yu. Zaitsev (URSS)	Influence of structure on facture mechanism of hardened cement paste. L'influence de la structure sur le mécanisme de rupture des pâtes de ciment durcies.
VI-181	B.K. Nyame, J.M. Illston (Grande-Bretagne)	Capillary pore structure and permeability of hardened cement paste. Structure des pores capillaires et perméabilité des pâtes durcies de ciment.
VI-186	A.M. Paillere, Ph. Briquet (France)	Influence des résines de synthèse fluidifiantes sur la rhéologie et la déformation des pâtes de ciment avant et en cours de prise. Influence of fluidifying synthetic resins on the rheology and deformation of cement pastes before and during the setting.
VI-192	L.N. Popov (URSS)	Effect on micro-additives on properties of concretes. Influence des micro-additifs sur les propriétés des bétons.
VI-195	M. Pommersheim, R. Clifton G. Frohnsdorff (USA)	Conceptual and mathematical models for tricalcium silicate hydration. Modèles qualitatifs et quantitatifs pour l'hydratation du silicate tricalcique.
VI-201	R. Sierra (France)	Répartition des différentes formes d'eau dans la structure des pâtes pures des C_3S et de ciment Portland. Distribution of different forms of water in the structure of pure slurries of C_3S and Portland Cement.

VII-0 **THEME VII – Réactions aux interfaces entre ciment et granulat dans les bétons et mortiers.**
Interface reactions between cement and aggregate in concrete and mortar.

L'index des auteurs se trouve en fin du volume III
The author index is at the end of the volume III

THÈME IV

Structure des pouzzolanes et des cendres volantes et hydratation des ciments aux pouzzolanes et aux cendres volantes

Structure of pozzolana and fly-ash and the hydration of pozzolanic and fly-ash cements

Président : M. MASSAZZA (Italie)

Utilization of Pozzolanic and Cenospheric Ashes,

L'utilisation des cendres volantes pouzzolaniques et cénosphériques

E. RAASK, Senior Research Officer, Fuel Ash Sciences, Central Electricity Research Laboratories, Leatherhead, U.K.

RESUME : Les cendres volantes sont largement utilisées comme additifs des mortiers et bétons, mais présentent une capacité variable de remplacement du ciment Portland. Il est donc important de disposer d'un test permettant d'évaluer rapidement leur pouvoir pouzzolanique. Le laboratoire du CEGB a mis au point une méthode de détermination de l'activité pouzzolanique des cendres volantes dans laquelle le taux de dissolution de la silice des particules de cendre est mesuré dans une solution d'acide fluorhydrique à 0.1 mole. Le taux d'extraction de la silice suit une loi logarithmique; la constante représente l'indice d'activité pouzzolanique de la cendre.

L'addition de cendres présentant une activité aux mélanges pour béton peut améliorer la stabilité thermique et chimique de la structure en béton. C'est ainsi que la réaction entre la fraction $MgCO_3$ d'un agrégat de calcaire dolomitique et le $Ca(OH)_2$ formé lors de l'hydratation du ciment Portland peut être évitée par l'addition de cendres volantes. La réaction du $Ca(OH)_2$ se faisant de préférence avec la silice des cendres, l'agrégat n'est pas affecté.

Une caractéristique intéressante des cendres volantes est constituée par la présence d'une certaine quantité de micro-sphères creuses, d'un diamètre de 25 à 250µm. Ces cénosphères sont formées par le dégagement de gaz au sein des particules de silicate à demi-fondues, à une température d'environ 1400°C. Les cendres légères sont récupérées dans les décharges de cendres, et sont maintenant disponibles en Grande Bretagne pour livraison en vrac (cendres non calibrées) ou en quantités moindres, mais calibrées selon des tailles spécifiées. Les cénosphères de cendres sont utilisées dans les ciments hydrauliques et les liants à résine organique pour la fabrication de matériaux composites pour l'isolation thermique, et celle de matériaux imperméables pour constructions nouvelles.

SUMMARY: P.f ash is widely used as a cement-extender in concretes and groutings, but the ash can vary in its ability to replace Portland cement. It is important therefore to have a rapid test of this pozzolanic quality. A method has been developed at the Central Electricity Research Laboratories where the pozzolanic activity of p.f. ash is determined by measuring the rate of dissolution of silica from the ash particles dispersed in 0.1 molar hydrofluoric acid. The rate of extraction of silica follows a logarithmic law and the rate constant is an index of the pozzolanic activity of the ash.

Addition of the pozzolanic quality p.f. ash to concrete mixes can enhance the chemical and thermal stability of the concrete structures. For example, the reaction between the $MgCO_3$ fraction of a dolomitic limestone aggregate and $Ca(OH)_2$ formed on hydration of Portland cement can be prevented by addition of p.f. ash. Preferential reaction of $Ca(OH)_2$ with silica in ash leaves the aggregate unscathed.

An interesting feature of p.f. ash is that it contains a proportion of hollow micro-spheres, 25 to 250 µm in diameter. The cenospheres are formed by the evolution of gases inside the semi-molten silicate particles at about 1400°C. The lightweight ash material is being recovered from the ash disposal lagoons and it is now available in Britain for delivery in bulk as ungraded material or in smaller quantities of specified size ranges. The ash cenospheres are used with hydraulic cements and organic resin binders to manufacture heat insulating composites and non-absorbent buoyancy materials.

INTRODUCTION

For the next two or three decades coal is likely to remain the most important primary fuel for electricity generation in this country and also in many other countries. The Central Electricity Generating Board (C.E.G.B.) in Britain utilizes at present about 70 million tonnes of coal a year. The fuel contains on average between 16 and 18 per cent by weight of uncombustible mineral matter, therefore the total ash products from the C.E.G.B. power stations boilers amount to about 12 million tonnes a year.

At present the majority of large coal-fired boilers in operation and to be constructed, are based on the system of pulverized fuel firing. This mode of firing produces between 15 to 25 per cent ash clinker which is discharged from the bottom of the combustion chamber in the form of crushed pieces of sintered or fused ash, usually 2 to 20 mm in size. The bulk of the incombustible material in a pulverized-coal fired boiler is transported through the combustion chamber and heat exchange ducts and it is captured in the electrical precipitators. The catching efficiency of the modern ash collectors is high, so that only 0.5 per cent weight or less fraction of the total solids escapes the ash collecting system.

The ash captured in the electrical precipitators is known in Britain as pulverized fuel ash, or p.f. ash, or PFA. Historically the term "pulverized fuel ash" was chosen to include the ash residue from pulverized coke. In the U.S.A. and in some other countries it is known as fly ash. This paper describes some of the research work on p.f. ash carried out at the Central Electricity Research Laboratories.

Raask (1) has shown that an interesting feature of p.f. ash is that it contains a proportion of hollow microspheres (or cenospheres) which are formed by internal evolution of gases at about 1400°C. This paper describes the properties of ash cenospheres and some of the lightweight composite materials made with hydraulic cements and resin binders.

POZZOLANIC ACTIVITY

Lea and Desch (2) have stated that for a material to be pozzolanic it should be capable of combining with calcium hydroxide liberated on hydration of Portland cement to form calcium silicates at room temperature. The definition implies that a pozzolanic material or pozzolana contains a "reactive" form of silica which is capable of reacting with calcium hydroxide at significant rates relative to the rate of hydration of cement. Volcanic ashes and some diatomitic deposits to varying degrees are pozzolanic in behaviour; so is p.f. ash as discussed by Turriziani (3). The ash acquires the pozzolanic activity by the high temperature when the particulate mineral matter of the coal is dispersed in the coal flame.

P.f. ash is being increasingly used in concrete and grouting mixes for partial replacement of Portland cement as described by Barber et al. (4). There is a need for a rapid method of assessing the extent of pozzolanic activity of a given supply of ash. A search was made for a method for the determination of pozzolanic activity based on previous work on the formation and properties of p.f. ash by Raask (5).

The "classical" method of assessing pozzolanic materials is that proposed by Fratini (6) and modified by Rio (7). A mixture of the test material and Portland cement is kept in water at 40°C for eight days and the amount of soluble calcium hydroxide left in the solution determined. A low Ca^{++}-ion concentration is a qualitative sign of a reactive material. The method is slow and errors can be introduced by variations in the quality of cement used.

Engineers designing concrete mixes with p.f. ash prefer to use the cementing efficiency factor (κ) of the ash proposed by Smith (8). He suggested that the weight of p.f. ash (W) in a concrete could be considered as equivalent to a weight κW of cement in its contribution to the strength of the mix. Usually, the κ values are obtained from the strength measurements of ash, cement and water mixes after 28 days. A value of 0.15 or higher indicates an ash with a useful pozzolanic activity. The method has the same shortcomings as the chemical test of Fratini and Rio, but it is more readily acceptable and in this work it has been used as a standard for comparison.

A rapid test of pozzolanic property was proposed by Jambour (9). In his method the rate of heat evolution is measured when a pozzolana dissolves in a solution of hydrofluoric and nitric acid in a calorimeter. The test takes one hour to complete. Peck (10) applied the method to a selection of ashes but found a poor correlation with the method of Smith (8). The solvent medium, a mixture of 2 molar nitric acid (HNO_3) and 0.6 molar hydrofluoric acid (HF) was too aggressive, and masked differences in the reactivity of the ashes. By omitting HNO_3, the HF-solution reacts more selectively with silica and the reaction, results in an increase in H^+-ion concentration of the solution. HF is largely associated in water, whereas the reaction product, hydrofluosilicilic acid is dissociated in water as shown by Palmer (11)

$$6HF + SiO_2 = 2H^+ + SiF_6^{--} + 2H_2O \qquad \ldots (1)$$

This suggests the possibility of following the reaction by measurement of the electrical conductance of the solution. A conductivity cell was constructed from PTFE which is resistant to chemical attack by hydrofluoric acid, as described by Raask and Bhaskar (12)

The conductance measurements were made at 27°C by an a.c. bridge, and the cell was calibrated with pure silica in the form of condensed fume. This material reacts rapidly and quantitatively with 0.1 molar hydrofluoric acid because of its very small particle size (0.01 μm to 0.15 μm) as described by Raask and Wilkins (13). The conductance of the solution was found to be proportional to the amount of silica dissolved according to equation (1).

Ash samples of known cementing efficient (κ-values as defined by Smith (8)) were used in these experiments. The ash dispersion in HF-solution contained one milligramme of solid per one cubic centimetre of acid, and the increase in conductance was monitored over a period of two hours.

The plots in Fig. 1 show the results for an initial reaction period between 15 minutes and one hour. The results fitted an exponential decay equation of the form,

$$W_r = W_o(1 - b\, e^{-ct}) \qquad \ldots (2)$$

where W_r is the amount of silica reacted at time t and W_o is the initial amount of silica; b is a numerical constant and c can be defined as the reaction constant.

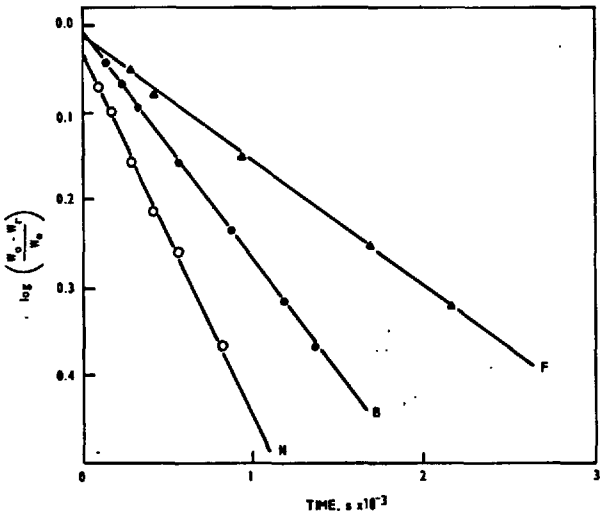

Fig. 1 - Dissolution of Silica of P.F. Ash in 0.1 Molar Hydrofluoric Acid.

The rate of silica dissolution deviates (it slows down) from the diffusion law prediction after about 50 per cent of the total silica in ash has been dissolved. Kiss et al. (14) have shown that the majority of ash particles are made up from an inhomogeneous mixture of glassy material and crystalline species. The latter are resistant to acid attack and the dissolution rate of SiO_2 will decrease. The inhomogeneity characteristics of p.f. ash particles are evident in Fig. 2 which shows the acid dissolution residue on the surface of ash particles after HF-treatment.

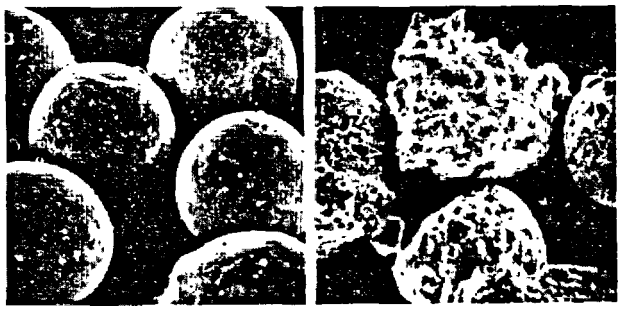

Fig. 2 - P.F. Ash Particles, Left - before the HF-Treatment, Right - after the Treatment.

The c-values for different ashes obtained by computer iteration were between 0.4×10^{-3} s^{-1} and 1.25×10^{-3} s^{-1}. The pozzolanic index (P_z) is defined in units of reciprocal kiloseconds, i.e.

$$P_z = 1000\, C \qquad \ldots (3)$$

The plot on Fig. 3 shows that there was a reasonably good correlation between the pozzolanic index (the acid dissolution test) and the cementing efficiency (crushing strength of p.f. ash mortars).

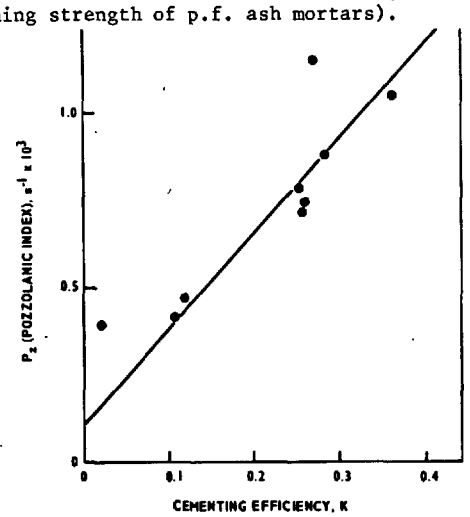

Fig. 3 - The Relationship Between the Pozzolanic Index (P_z) and Cementing Efficiency (κ).

Of the ten samples tested seven passed the pozzolanity tests and three failed. That is, the ashes which have a pozzolanic index value, as defined by equations (2) and (3), below 0.5 should not be used as a pozzolanic material in concrete or grouting mixtures. A simplified method of HF-dissolution test can be applied for routine checks of the pozzolanic quality of p.f. ashes as described by Raask and Bhaskar (12).

UTILIZATION OF POZZOLANIC P.F. ASH

The majority of limestone aggregates are stable in concretes at room temperature. However, in the U.S.A. and Canada there have been occurrences of aggregate failure caused by chemical attack as described by Hadley (15), and by Swenson and Gillott (16).

The thermal stability of a concrete made with Portland cement is influenced by the type of aggregate used in the mix. Hannant (17) and Imlach and Taylor (18) have shown that concretes made with limestones lost strength to a much greater degree than those made with siliceous aggregates. The strength loss could be caused by chemical reations between limestone and the calcium hydroxide, $Ca(OH)_2$, liberated on hydration of Portland cement. Limestones quarried for use as aggregates in concretes contain some magnesium carbonate, $MgCO_3$, which would be the species first to be attacked in the alkaline media of hydrated cement paste.

The rate of decomposition of the $MgCO_3$ fraction of dolomitic limestone in a calcium hydroxide solution can be determined by measuring the electrical conductance of the solution. After the solubility limit of $Mg(OH)_2$ is reached, the amount of $MgCO_3$ reacted is proportional to the decrease in conductance due to the removal of OH^- and Ca^{++} ions from the solution,

$$Ca^{++} + 2[OH] + MgCO_3 \rightarrow Mg(OH)_2 + Ca\,CO_3$$

Experimental results suggest that the rate of conversion of $MgCO_3$ fraction limestone to $Mg(OH)_2$ in

$Ca(OH)_2$ solution is governed by diffusion inside the solid particle. Glover and Raask (19) have suggested that a test for a diffusion-controlled mechanism is to plot the rate of change of conductivity $\left(\frac{d\Omega}{dt}\right)$ against the inverse of the square root of time as in Fig. 4. The rate of dissolution of the $MgCO_3$ expressed as $\frac{dw}{dt}$ is given by

$$\frac{dw}{dt} = 3 w_o \left(\frac{D}{a^2} - \frac{D^{\frac{1}{2}}}{\pi^{\frac{1}{2}} a t^{\frac{1}{2}}}\right) \quad \ldots (4)$$

where w_o is the original molar fraction of $MgCO_3$ in the sample and w that at times t, a is the radius of particles, D is the diffusion constant. Since the conductivity change $\left(\frac{d\Omega}{dt}\right)$ is proportional to the amount of $MgCO_3$ reacted, equation (14) can be changed to,

$$\frac{d\Omega}{dt} = 3 \Omega_o \left(\frac{D}{a^2} - \frac{D^{\frac{1}{2}}}{\pi^{\frac{1}{2}} a t^{\frac{1}{2}}}\right) \quad \ldots (5)$$

The above results fit the above diffusion equation as shown on Fig. 4 where the values of $\frac{d\Omega}{dt}$ are plotted against $t^{-\frac{1}{2}}$ values.

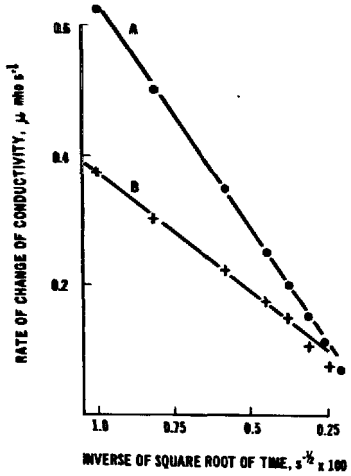

Fig. 4 - Conductance Changes of $Ca(OH)_2$/Dolomitic Limestone Dispersion (A) Particle size <53 μm (B) Particle size 53 μm to 76 μm.

In order to demonstrate the beneficial effect of p.f. ash in stabilizing the dolomitic limestone aggregate in concretes the mortar specimens were made with and without the ash. The test mortars were cured at room temperature for six months, followed by another six months in the autoclave at 150°C.

The results of the differential thermal analysis (DTA) in Fig. 5 show that the preferential reaction of $Ca(OH)_2$ in the hydrated cement mortar with ash leaves the aggregate unscathed.

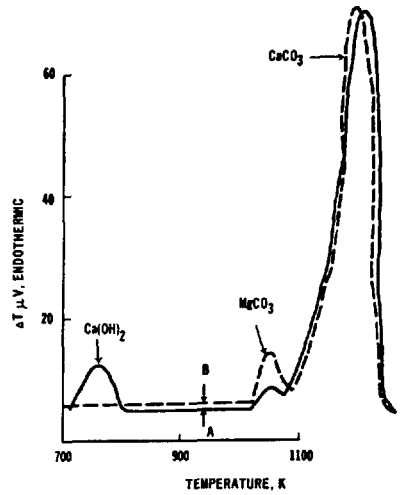

Fig. 5 - Stabilizing Effect of P.F. Ash on Dolomitic Limestone Concrete (A) Limestone concrete (B) Limestone concrete with p.f. ash.

Fig. 6 shows that the spherical particles of p.f. ash were well embedded in the cement matrix. The interface between the surface of the ash particles and the hydrated cement paste was diffused and no microcracking was observed in this locality.

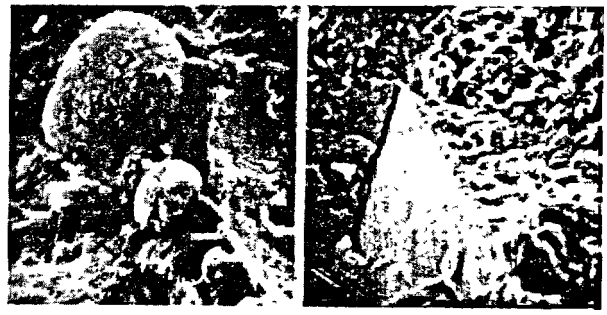

Fig. 6 - Embedded P.F. Ash Particles in Hydrated Cement Paste (Left) - Crack Propagation at Limestone Aggregate/Cement Paste Interface (Right).

On the other hand, the sharp-edged particles of crushed limestone were less intimately bonded in the cement matrix. On drying the cement paste had shrunk away from one of the faces of the aggregate particles, thus initiating a crack propagation in the cement paste matrix. It was therefore concluded by Raask (20) that addition of p.f. ash to the concrete mixes with certain aggregates can enhance the chemical, thermal and mechanical stability of the concrete structures.

FORMATION AND PROPERTIES OF ASH CENOSPHERES

The large boilers at modern power stations burn coal in the form of powder of particle size about 1 to 100 μm. During the process of milling, the minerals in coal are also ground approximately to the same fineness. In the flame the mineral particles fuse as discrete entities and the irregular shapes are changed to spherical forms by the force of surface tension as described by Raask (5). At the same time gases are generated inside those mineral particles which contain some carbonaceous matter, thus internal combustion takes place on the micro-scale. A vigorous

evolution of gas explodes the particles but a steady rate of expansion followed by a rapid cooling results in the formation of a stable cenosphere.

Raask (1) has found that the process of gas evolution is catalysed by iron oxides present in the molten glass. The formation of the ash cenospheres is governed also by the viscosity and surface tension of fused silicate glass. In view of the complexity of the formation process, and since the boiler furnace is not designed to produce "freak" ash, it is not surprising that the number of cenospheres produced in the flame is small - a few particles in every hundred. However, a number of large stations each produce several thousands of tons of the cenospheres each year.

The unique property of the cenospheres follows from the enclosed single void in each particle which is much larger than that of the shell. Low apparent density and the impervious shell permit the particles to separate from the dense ash in the disposal lagoons. This incidental separation process is fortunate, otherwise the recovery of the material would be uneconomical.

When the particles are viewed under the Stereoscan electron microscope the striking feature (Fig. 7) is that they are almost perfect spheres although there are a few particles with surface blemishes.

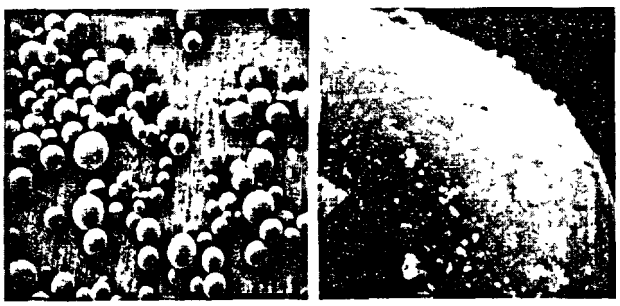

Fig. 7 - Ash Cenospheres and Close-up of a Particle

The characteristic properties of a typical sample of ash cenospheres are summarized in Table 1.

Table 1 - Properties of Ash Cenospheres

Particle size	-	20 to 300 μm
Apparent density	-	500 kg m^{-3}
Bulk density	-	300 kg m^{-3}
Thermal conductivity	-	0.1 W m^{-1} °C
Thermal stability limit	-	1300°C

LIGHTWEIGHT COMPOSITES MADE WITH ASH CENOSPHERES

Composite lightweight materials can be made with the cenospheres using a variety of binders. The choice of binders and the amount used depends on the strength, density and working temperature requirements as shown in Table 2. Further data on the properties of ash cenospheres and on the composites can be found in the previous work of Raask (21 to 23).

Table 2 - Properties of Cenosphere Composites

Binder	Binder to Ash ratio Vol:Vol	Density kg m^{-3}	Crushing Strength MN m^{-2}
Portland Cement	1:8	470	2.4
Ciment Fondu	1:8	440	2.5
Polyester resin	1:12	380	2.6
Phenol Formaldehyde	1:12	400	3.1

The above experiments were made with the view of using a minimum of binder to give a product of crushing strength above 2 MN m^{-2}. These composites have sufficient strength for use as heat insulation materials.

An alternative to the approach of using a minimum of binder is to dispense the lightweight ash particles in a continuous matrix of the binder. The correct ratio of binder, including the fine clay for lightweight bricks, can be calculated from the density values given in Table 1. The bulk density of the fired product (870 kg m^{-3}) is about the same as that of Moler bricks made of diatomaceous earth. As the thermal conductivity of lightweight materials is proportional to the bulk density the cenospheres/clay brick should have approximately the same heat insulating properties as that of Moler brick of equal density. However, the advantages of the experimental material are that it has a higher crushing strength than that of the Moler brick, and a low absorptive capacity for liquids. In fact, the amount of H_2SO_4 absorbed was found to be less than that taken up by a dense acid resistant brick. This makes it possible to use the material for lining chimneys and ducts where condensation of water or acids may take place.

Lightweight materials, impervious to liquids, can be made from ash cenospheres bound by resins. For example, the specimens made with phenol formaldehyde absorbed less than 0.1% by volume of water.

The lightweight cenosphere ash is now available in Britain for the home market and the material is shipped to a number of overseas countries. The lightweight ash is supplied in bulk as an ungraded material for the manufacture of heat insulating materials of a low liquid absorption capacity. These are usually made with high alumina cements or with sodium and potassium silicate cements. For the manufacture of high quality epoxy resin composites the graded and cleaned material is supplied. The epoxy composites are used as buoyant materials and in other marine applications.

ACKNOWLEDGEMENT

The work was carried out at the Central Electricity Research Laboratories and the paper is published by permission of the Central Electricity Generating Board.

REFERENCES

1.- E. RAASK (1968), "Cenospheres in pulverized fuel ash", Jour. Inst. Fuel 43, 339.

2.- F.M. LEA and C.H. DESCH (1956), "The chemistry of cement and concrete, Arnold, London.

3.- R. Turriziani (1964), "The Chemistry of Cements" (Ed. H.F.W. Taylor), Acad. Press, London.

4.- E.G. BARBER, G.T. JONES, P.G.K. KNIGHT and M.H. MILES (1972), "PFA untilization", C.E.G.B. Publication, Newgate Street, London.

5.- E. RAASK (1969), "Fusion of silicate particles in coal flames", Fuel, 48, 366.

6.- N. FRANTI (1949) "Hydrolysis in cements - I", Ann. Chim. (Rome) 39, 41.

7.- A. RIO (1952), "Pozzolanic cements - II", Ann. Chim. (Rome) 42, 526.

8.- I.A. SMITH (1967), "The design of fly-ash concrete", Proc. Inst. Civil Eng. 36, 6982.

9.- J. JAMBOUR (1962), "Une novelle methode de determination de l'activite pouzzolanique", Rev. Mat. Constr. Trav. Pub. No. 504, 240.

10.- J.R. PECK, Private communication.

11.- W.G. PALMER (1930), "Action of aqueous hydrofluoric acid on silica", Jour. Chem. Soc., p 1656.

12.- E. RAASK and M.C. BHASKAR (1975), Pozzolanic activity of pulverized fuel ash, Cement and Concrete Research, 5, 363.

13.- E. RAASK and D.M. WILKINS (1965), "Volatilization of silica in gasification and combustion processes", Jour. Inst. Fuel 38, 255.

14.- L.T. KISS, B. LLOYD and E. RAASK, (1972), "The use of copper oxy-chloride to alleviate boiler slagging", Journ. Inst. Fuel 43, 213.

15.- D.W. HADLEY (1964), U.S.A. Highway Research Board Symp. on alkali-carbonate reaction, page 1.

16.- E.G. SWENSON and J.E. GILLOTT (1964), U.S.A. Highway Research Board Symp. on alkali-carbonate reaction, page 21.

17.- D.J. HANNANT (1967), "Effect on the strength of various concretes of sustained temperatures near 100°C", Civ. Eng. and Pub. Works Reg. 62, 665.

18.- B.V. IMLACH and H.F.W. TAYLOR (1972), "Prolonged Hydrothermal Treatment of Cement Mixes", Trans. Brit. Ceram. Soc., 71 , No. 3.

19.- G.M. GLOVER and E. RAASK (1972), "Water diffusion and microstructure of hydrated cement pastes", Materials and Structures 5, 315.

20.- E. RAASK (1974) "The thermal and chemical stability of limestone aggregates", Materials and Structures 7, 387.

21.- E. RAASK (1970), "A Lightweight Material", Brit. Chem. Eng. 15, 1165.

22.- E. RAASK and A.W. STANNETT (1971), "Lightweight electrical insulation using ash cenospheres", Electrical Times, 12 March.

23.- E. RAASK (1973), "Ash Cenospheres as a Basis for Industrial Chimney Linings", 1st Chimney Design Symp., Edinburgh.

Composition and hydration of high calcium fly ash

Composition et hydratation de cendres volantes à haute teneur en calcium

LIU HUAKUN, Engineer. LU ZHONGYAI Engineer and LIN SHENGJIE, Engineer Cement Research Institute. Chine Populaire.

RESUME : Les cendres volantes à haute teneur en calcium, provenant de charbons pulvérisés à haute teneur en calcium ont une bonne hydraulicité et par des traitements simples peuvent devenir un ciment. Il y a dix ans que ce ciment est produit et utilisé en Chine, à petite échelle.

On a fait des études générales sur la composition des phases et sur l'hydraulicité de ces cendres volantes par diffraction à rayons X, microscopie à balayage, ATD, etc. Ces études montrent que les cendres volantes à haute teneir en calcium se composent principalement de verre, d'un peu de cristaux de β-C_2S et de $CaSO_4$ et de beaucoup d'oxydes de calcium libres. Durcies, elles comportent essentiellement des gels de tobermorite incrustés de cristaux à haute teneur en alumino-sulfate de calcium. Ainsi les cendres volantes à haute teneur en calcium étant différentes des cendres volantes ordinaires, possèdent une bonne hydraulicité.

Les oxydes de calcium libres dans ces cendres volantes sont formés presqu'instantanément; leurs cristaux sont très petits et souvent ils adhèrent sur les surfaces des grains de verre. L'hydratation et la formation d'hydrates s'accélèrent mutuellement. Les oxydes de calcium libres n'ayant pas d'influence défavorable sur la stabilité, sont d'importants composants actifs dans les cendres volantes à haute teneur en calcium.

SUMMARY: The high calcium fly ash produced from the pulverized coal boiler possesses good hydraulicity. By simple treatment, it can be made into cement which has been manufactured and used in small scale in China for ten years.

The phase compositions of the ash and the hardened cement paste have been investigated by means of optical microscope, X-ray diffraction, scanning electron microscope and differential thermal analysis. The high calcium fly ash mainly consists of high calcium glass and a small amount of crystals -- β-C_2S, $CaSO_4$, etc. Besides, it contains a considerable amount of free lime. The hardened cement paste consists of ettringite and other crystals embedded in tobermorite gel. So the high calcium fly ash is different from ordinary fly ash. It possesses hydraulic property by itself. The free lime contained in the high calcium fly ash is formed almost instaneously, its crystal size being very small. It usually adheres on the surface of the glass. The slaking of lime and the forming of hydration products work out to mutual advantage. The free lime in the high calcium fly ash does no harm to soundness and is rather an useful ingredient of the ash.

INTRODUCTION

The pulverized coal, which contains a relatively high content of lime that is inherent in coal itself as in the case of lignite or is deliberately added to the coal either to improve the hydraulicity of fly ash or for sulphur removal, is transformed into high calcium fly ash (HCFA) when the coal dust burns away in the boiler. The phase composition of HCFA and so also its properties are different from those of ordinary fly ash which contains lime no more than 5%. HCFA possesses hydraulicity by itself. After grinding and mixing with a few per cent of salt (NaCl) or gypsum etc., HCFA can be made into cement with 28 days compressive strength (mortar) of 30-50 N/mm^2. It expands slightly during hardening, but otherwise has similar performance characteristics as slag cement. It has been made and used in small scale in China for some ten years.

CONSTITUTION OF HCFA

When pulverized coal is injected into the boiler, it burns at a rate of 10^6°C/min, and is heated up to over 1200°C in 0.05 sec. (1). Due to the impact of the high temperature, the immediate product of fly ash essentially becomes glass embedded with 10-25% of crystalline minerals.

In the case with ordinary fly ash, the major crystals are quartz and mullite, while in the case with HCFA, the crystalline substances are usually β-C_2S, $C_{12}A_7$, C_2F, $CaSO_4$, free CaO etc., the content of free CaO can be as high as 5-15%. The X-ray diffraction patterns of some of the HCFA investigated are illustrated in figure 1. Their chemical compositions are given in Table I. As indicated, the constitutions of the crystalline substances of the HCFA are almost alike.

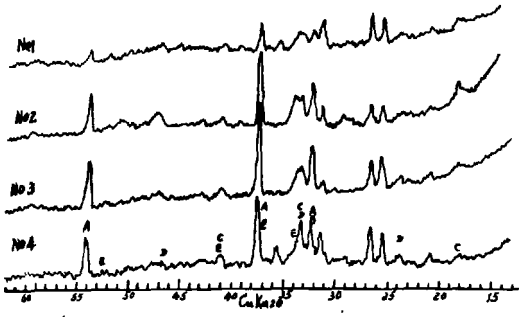

Fig. 1 XRD of HCFA
A=CaO B=β-C_2S C=$C_{12}A_7$ D=C_2F E=$CaSO_4$

The circumstances of formation of HCFA are quite different from those of portland cement clinker though both are products of high temperature. The high calcium coal dust burns in suspension state at very high temperature rising rate in an extremely short period and is then rapidly quenched. So the crystals are poor in form and very small in size. The minute crystals appear to disperse in the glasses or adhere to the surface of the glasses as

TABLE I

NO.	Ig.loss	SiO_2	Al_2O_3	Fe_2O_3	CaO	MgO	SO_3	Free Lime	Total
1	1.66	26.76	16.22	11.42	33.11	5.21	3.11	6.42	97.49
2	2.12	21.07	10.87	10.01	47.08	5.88	1.90	9.51	98.93
3	0.92	13.61	9.79	8.75	55.29	4.77	2.95	13.08	96.48
4	2.54	25.15	14.46	8.99	39.72	2.76	5.54		98.76
5	4.90	25.49	13.94	6.59	36.31	4.15	3.48	10.30	94.96

discrete particles. The spherical particles of free lime adhering to the surface of glass are illustrated in figure 2. Their sizes are 1-5 μ or even smaller. The electron microprobe shows that a small amount of ferrous oxide can be dissolved in the free lime, which can be also discerned by the small shift of the 2.41 Å d value ($2\theta = 37.31^\circ$) of CaO.

Investigation of the glass components have been made by means of polarizing microscope. They may be differentiated by their optical properties as according to H.A. Popov and E.A. Ivanov (2) (see figure 3):

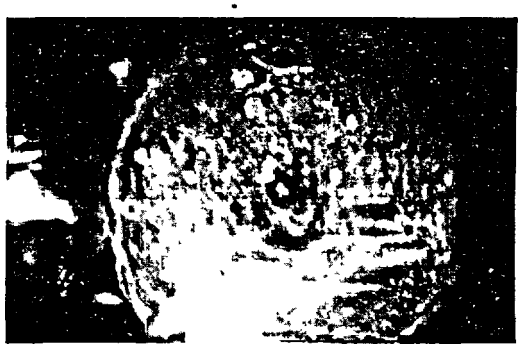

Fig. 2 Free lime adhering to glass
SEM 1000X

Fig. 3 Types of glasses in HCFA,
polarizing microscope, 430X

1. Pink or greenish transparent glass, with refractive indices 1.620-1.640. They can be glassy melilite or gehlenite.
2. Yellow or yellowish brown translucent glass, with refractive indices 1.670-1.720. They are probably related to system C-F-S.
3. Brown or brownish black translucent glass, with refractive indices 1.720-1.735. They can be high calcium glasses.
4. Black opaque glass, their refractive indices being very high, often appear in chain form due to their mutual attraction. They are glassy magnetite.
5. Agglomerates of fused particles, mostly spherical, the larger particles can be porous. Some of the smaller spherical particles adhere to the surface of the larger particles or enter into the latter's cavities as shown in figure 4.

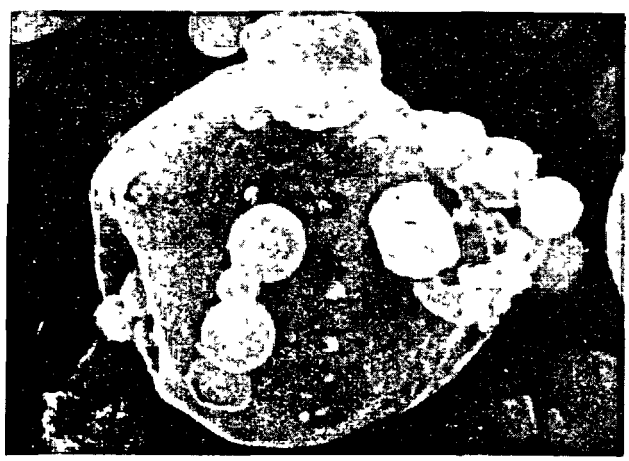

Fig. 4 Agglomerates of glass
SEM 2600X

As can be seen from the electron microprobe, the compositions of different spherical particles could be quite different. This is because the compositions of coal dust particles of different sizes are different, and the frequencies of collision between particles of argillaceous materials and the

CaO particles are also different. The interreaction during collision of the particles results in the formation of eutectic mixtures which tend to contract into spherical particles due to surface tension.

In the mean time, particles that are less liable to melt become porous when the combustibles burn away. In comparison with ordinary fly ash, there are in HCFA much more glasses of types 2 and 3 which possess good hydraulicity. the higher the content of CaO, the more are the types 2 and 3 and the less glass of type 5 in HCFA. Up to the limit of 45%, the higher the content of total CaO in HCFA, the higher is the strength of the HCFA mortar, whereas the strength of the mortar decreases when the CaO content exceeds 45% because the free CaO then also becomes too high. The reason, that HCFA possesses hydraulicity by itself in comparing with slag that has as high content of CaO, lies in the fact that the free CaO in HCFA acts as activator of hydration. When HCFA is reheated to a temperature of 1350-1450 °C and then rapidly cooled, it loses its hydraulic property because all the free lime become absorbed, so is the constitution of the product also changed. This has been confirmed by our experiments.

HYDRAULIC PROPERTY

When HCFA is mixed with water, it starts hydration almost instantly. Free lime slakes to form $Ca(OH)_2$ which together with $CaSO_4$ dissolves in water. They act as activators in the hydration of glasses, β-C_2S and some of the other minerals also hydrate. The final hydration product of the hardened paste then consists essentially of calcium trisulphoaluminate embedded in tobermorite gel.

Gypsum, salt (NaCl) and other additives improve the strength of the hardened paste as shown in table II. the HCFA cement used for the test has its composition marked NO. 5 in table I.

If 6% of gypsum were mixed with HCFA, the content of SO_3 in the mixture as calculated increases to 5.44%, from which considerable amount of ettringite could have been formed in the hardened paste. If, instead, 2% salt were mixed with HCFA, in addition to calcium trisulphoaluminate and CSH, there would be also calcium chloroaluminate in the hydration product. The X-ray diffraction patterns of the hydrating pastes at different ages are illustrated in figure V. Ettringite forms largely during the first day of hydration, the height of its peaks

TABLE II

Weight proportion HCFA : Additivies	Specific surface cm^2/g	Initial set hr. min.	Final set hr. min.	Tensile strength N/mm^2 7 days	Tensile strength N/mm^2 28 days	Compressive strength N/mm^2 7 days	Compressive strength N/mm^2 28 days
100 : 0	6250	0 36	1 40	2.8	2.9	29.6	33.4
94 : 6 (gypsum)	6620	0 58	2 58	2.8	2.7	33.4	44.8
98 : 2 (salt)	6100	0 35	1 39	3.1	3.7	44.0	56.4

Note: Tests made on 1:3 mortar (GB 177-62)

rises no longer from the second day of hydration, but, instead, calcium chloroaluminate is being formed. This is analogous to the experimental result by Nemat Tenoutasse (3). He described that when C_3A is hydrated in the presence of $CaCl_2$ and $CaSO_4 \cdot 2H_2O$, the SO_4" ions react first to give trisulphoaluminate, the formation of monochloroaluminate begins only after the SO_4" ions have been depleted. As reaction proceeds further, C_4AH_{19}

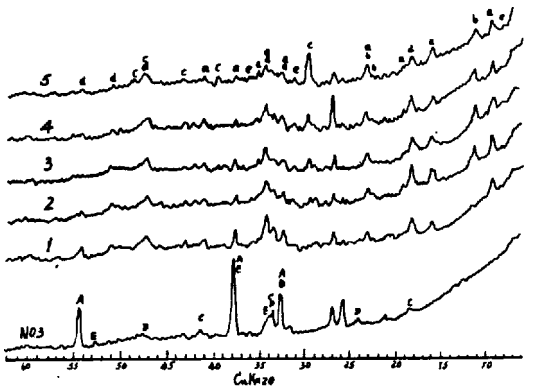

Fig. 5 XRD of hydration pastes of HCFA with addition of 2% salt

a=$C_3A \cdot 3CaSO_4 \cdot 32H_2O$ b=$C_3A \cdot CaCl_2 \cdot 10H_2O$

c=$CaCO_3$ d=$Ca(OH)_2$ e=C_4AH_{19}

A=CaO B=β-C_2S C=$C_{12}A_7$

D=C_2F E=$CaSO_4$

1.2.3.4.5-- 1 day, 2.3.7.28 days respectively

The DTA curve of the hardened HCFA cement paste steam cured at 100°C for 4 hours after 7 days wet curing is illustrated in figure 6. The 130°C and 170°C endothermic peaks correspond to the dehydration of CSH and ettringite respectively, the 465°C exothermic peak indicates the combustion of the residual carbon in HCFA, the 830°C endothermic peak indicates the decarbonization of $CaCO_3$ and lastly 890°C exothermic peak indicates the formation of β-CS from dehydrated CSH.

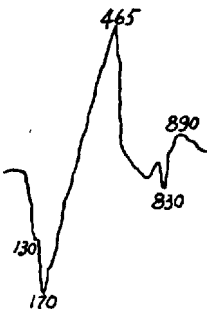

Fig. 6 DTA curve of the hardened HCFA cement paste

The addition of salt accelerates the hydration of free lime and the formation of calcium aluminate hydrate (4) while it depresses the pH value of the hydrating solution, so that the rate of hydration of the silicate is also accelerated (5). This can be verified by the increase of heat of hydration at early ages as is shown in table III. It should be pointed out, so is it well known, that salt promotes corrosion of the reinforcing steel.

TABLE III

Common salt %	heat of hydration Cal/g		
	1 day	2 days	3 days
0	58.2	62.6	69.7
1.5	68.1	73.3	79.4

The morphology of HCFA hydration products is shown in figure 7.

Fig. 7 Morphology of HCFA cement (added with 2% salt) hydration products. SEM 2100X

Unlike the dead burned free lime in portland cement clinker, the free lime in HCFA serves only as an alkaline activator of hydration and causes no undue expansion after hardening of the paste, even though its content could be sometimes as high as 15%. This can be readily understood from the circumstance of formation of HCFA which has already been described. As it is shown in Fig. 5, from the second day of hydration, the peaks of CaO decrease appreciably and after the seventh day, no CaO can be detected any more. The coefficient of expansion of the testing prism is less than 0.8% for HCFA neat paste steam cured at 100°C for 4 hours after 7 days wet curing. There has not been record to this day unsoundness of concrete made from HCFA cement since its first use some ten years ago.

CONCLUSIONS

1. High calcium fly ash is composed of 15-25% of crystalline substances i.e., β-C_2S, $C_{12}A_7$, C_2F, $CaSO_4$, free CaO, etc. and heterogeneous glasses of different varieties.

2. The hydration products of HCFA without additive essentially consist of calcium trisulphoaluminate embedded in tobermorite gel.

3. The free CaO acts as an important activator in the hydration of HCFA and causes no harmful effect on the soundness of mortar or concrete inspite of its high content.

4. Common salt (NaCl) as an additive, accelerates the hydration of free lime, the formation of calcium sulphoaluminate and silicate, and reacts with excess hydrous aluminate to form calcium chloroaluminate.

5. The utilization of HCFA does not only contribute to the betterment of the environment in removal of SO_2 from the exit gases of coal fired boilers, but also provides cement as a by-product of power plants.

REFERENCES

1.- "The Testing Methods and Adjustment of Combustion of Coal Fired Boilers", (in Chinese), Xian Heat Engineering Institute and Department of Technology Improvement of the Northeastern Bureau of Electric Power, (1974), p.465.

2.- H.A. Popov and E.A. Ivanov, "The Utilization of Fly Ash of Power Plants", Building Materials, Vol. 8, pp. 5-8, (1963), (in Russian).

3.- Nemat, Tenoutasse, "The Hydration Mechanism of C_3A and C_3S in the Presence of Calcium Chloride and Calcium Sulphate", Proc. of the 5th Intern. Symp. on the Chem. of Cement, Tokyo, (1968), Vol. II, pp. 372-377.

4.- Wilhelm Eitel, "Silicate Science", Vol. V -- Ceramics and Hydraulic Binders, Academic Press, New-York, London, (1966), p. 477.

5.- H.F. Vivian, "Some Chemical Additiors and Admixtures in Cement Paste and Concrete" Proc. of the 4th Intern. Symp. On the Chem. of Cement, Washington, (1960), Vol. 2, p. 913.

Formation of 10 Å and 14 Å tobermorite from pozzolanic glassy silica

Les tobermorites de 10 Å à 14 Å formés à partir de pouzzolane siliceuse vitreuse

N. HARA and N. INOUE, Government Industrial Research Institute, Kyushu, Japon.

RESUME : On a étudié la réactivité hydrothermique, en présence de chaux, de deux sortes de pouzzolanes siliceuses vitreuses :
1) le verre volcanique (perte au rouge 2.7, SiO_2 74.3, Al_2O_3 12.7, Fe_2O_3 1.3, CaO 1.5, MgO 0.2, Na_2O 4.4, K_2O 3.0 %; 5,950 et 3,460 cm^2/g) d'une sorte déposée au midi de Kyushu; et
2) la silice vitreuse de quartz fondu (SiO_2 99.97 %; 1,550 cm^2/g)

Dans le premier cas le rapport Ca/Si est de 0.6 à 0.9, et eau/solide 20 en poids. Les expériences ont été réalisées à des températures de 70 à 100°C, avec une durée de réaction de 2 à 120 jours.

A partir du verre volcanique, la tobermorite 10 Å est formée par une réaction à 80°C d'une durée de 20 à 30 jours. Les cristaux sont constitués de plaquettes ou de fibres allongées parallèlement à b avec clivage (100). La tobermorite 10 Å est remplacée par la tobermorite 11 Å si la réaction dure plus de 40 jours.

La tobermorite 14 Å est formée directement à partir de la silice vitreuse. Par chauffage dans l'air, celui-ci se convertit en tobermorite 11 Å à 60-400°C. Cependant celui-ci ne se transforme pas en tobermorite 9 Å par chauffage jusqu'au 800°C, contrairement à ce qui se passe avec la tobermorite naturelle.

La longueur des mailles de la tobermorite 14 Å est diminuée par l'addition de Al_2O_3. L'addition de Al_2O_3 0.5.5% mélangée de silice vitreuse et de CaO a réalisé des longueurs de maille de 14 Å et 12 Å, 2 % 11 Å et 5 % 10 Å. L'addition de Al_2O_3 2 % et de NaOH 0.5 % donnait la longueur de 10 Å . L'addition de NaOH seule à 0.5 à 1 % pourrait améliorer la cristallisation de la tobermorite 14 Å.

Ces résultats permettent de comprendre le mécanisme de synthèse des tobermorites de longueurs de maille diverses ainsi que la similitude des tobermorites aux C-S-H (I) pour des rapports Ca/Si variés.

SUMMARY : Hydrothermal reactivities with lime of two kinds of pozzolanic glassy silica ; i) volcanic glass (ig loss 2.7, SiO_2 74.3, Al_2O_3 12.7, Fe_2O_3 1.3, CaO 1.5, MgO 0.2, Na_2O 4.4, K_2O 3.0% ; 5,950 and 3,460cm^2/g), a kind of pozzolana deposited in South Kyushu, and ii) silica glass made from fused quartz (SiO_2 99.97% ; 1,550cm^2/g), were studied at starting Ca/Si mole ratios of 0.6-0.9 and water/solid ratio of 20 by weight under various combinations between reaction temperatures (70-100°C) and periods of reaction time (2-120days).

From volcanic glass, 10Å tobermorite formed by the reaction at 80°C for 20-30days. The crystals were lath-like or fibrous elongated parallel to *b* with (100) cleavage. The 10Å tobermorite was replaced by 11Å tobermorite for more than 40days' reaction.

From silica glass, 14Å tobermorite formed reproducibly. By heating in the air it transformed into 11Å tobermorite at 60-400°C. But this 11Å tobermorite did not transform into 9Å tobermorite during heating up to 800°C in contrast to natural 14Å tobermorites.

The basal spacing of 14Å tobermorite decreased by addition of Al_2O_3. Addition of 0.5-1.5% of Al_2O_3 to the mixture of silica glass and CaO gave the basal spacings of 14Å and 12Å, 2% 11Å, and 5% 10Å. Addition of 2% of Al_2O_3 and 0.5% of NaOH gave that of 10Å. Addition of 0.5-1% of NaOH improved the crystallinity of 14Å tobermorite.

These results suggest well how to synthesise tobermorites of different basal spacings, and similarities of these tobermorites to C-S-H(I) of different Ca/Si mole ratios.

INTRODUCTION

Reactions of pozzolanas with lime at ordinary temperatures have been well investigated due to the practical standpoint, where hydration products are usually poorly crystalline. When autoclaving is applied, the hydration products become well crystalline but are very often dominated by the formation of 11Å tobermorite.

By applying the temperatures of steam curing to the reactions of pozzolanas, the present authors (1, 2, 3) could synthesise 10Å and 14Å tobermorites reproducibly. There have been many reports on synthetic 11Å tobermorite, but very few or none on synthetic 10Å and 14Å tobermorites. These 10Å and 14Å tobermorites showed not only some interesting characteristics which have not been reported so far, but also close relationships to C-S-H(I) of various Ca/Si. Besides, effects of Al and Na ions investigated in the syntheses at around these temperatures seem to give some clues to clarify how various tobermorites of different basal spacings could occur including 12Å tobermorite and tacharanite.

These results are reported in this paper.

METHODS

Two kinds of pozzolanic glassy silica were chosen as a starting material, i.e. i) volcanic glass (ig loss 2.7, SiO_2 74.3, Al_2O_3 12.7, Fe_2O_3 1.3, CaO 1.5, MgO 0.2, Na_2O 4.4, K_2O 3.0% ; 5,950 and 3,460cm^2/g), separated hydraulically from volcanic ash deposited abundantly in South Kyushu, and ii) silica glass (SiO_2 99.97% ; 1,550cm^2/g), made from fused quartz. CaO was obtained by calcining precipitated $CaCO_3$ at 1,000-1,100°C.

Each siliceous material was mixed with CaO at starting Ca/Si of 0.6-0.9 and with water at water/solids ratio by weight of 20. For some preparations, 0.5-5% of γ-Al_2O_3(<0.05μm) or 0.5-1% of NaOH were added to the mixture of silica glass and CaO by weight. Each mixture was kept in a stoppered polyethylene bottle and cured at 70-90°C for 2-120days. For reactions at 100°C a stainless autoclave with a stirrer was used instead of the polyethylene bottle.

At intervals of 3-10days, a portion of preparation was pipetted from the bottle, filtered and dried in a vacuum desiccator at room temperature.
All the preparations were examined by x-ray powder diffractometry and DTA-TG. Besides, some of them were examined by electron microscopy, energy dispersive x-ray microanalysis, selected area electron diffraction (SED) and chemical analysis of unreacted siliceous material. Changes of the basal spacing on heating in the air from 60°C to 900°C for 20hrs at each temperature were measured by x-ray powder diffractometry to identify a type of tobermorite according to its thermal behaviour.

RESULTS

1. Reaction of Volcanic Glass

Hydration products obtained by starting from volcanic glass are summarised in Table I. 10Å tobermorite formed at 80°C for 20-30days.

TABLE I

Reaction temp. 80°C					100°C	
Days	Starting Ca/Si 0.6	0.7	0.8	0.8*	Days	Ca/Si 0.8
10	C-S-H CH	C-S-H CH	C-S-H CH	C-S-H CH	1	C-S-H A,CH
20	9.9T	9.9T	9.9T	9.9T CH	2	C-S-H CH
30	10.0& 11.9T	10.0T	10.0T	10.0T	3	C-S-H CH
40	11.8& 10.0T	10.0& 11.9T	11.8& 10.0T	10.0T	4	C-S-H
50	11.8& 10.0T	11.8& 10.0T	11.8& 10.0T	10.0T	5	C-S-H
60	11.8& 10.0T	11.8& 10.0T	11.8& 10.0T	10.0T	6	11.8T
70	11.8& 10.0T	11.8& 10.0T	11.8T	10.0& 12.3-13T	7	11.8T

Hydration products from volcanic glass.
C-S-H : C-S-H and C-S-H(I). CH : $Ca(OH)_2$.
T : Tobermorite. Numerals in front of 'T' show the basal spacing (Å) of the tobermorite.
A : $C_3A \cdot CaCO_3 \cdot 12H_2O$.
* : Volcanic glass of 3,460cm^2/g was used in this preparation. That of 5,950cm^2/g was used in the other preparations.
Hydrogarnet, C_3ASH_4, formed in most of the run, but was excluded from the table.

TABLE II

hkl	Natural* d(Å)	I/I_{002}	Synthetic** d(Å)	I/I_{002}
002	10.0	100	9.94	100
			8.93	12
			5.40	7
202	4.92	50	5.04	10
204	3.78	50	3.80	7
			3.63	10
006	3.34	50	3.29	44
220	3.05	100	3.06	95
206	2.93	80	2.96	65
			2.92_s	21
400	2.80	80	2.83	24
			2.70	28
			2.60	21
008	2.53	30	2.529	17
?	2.44	20	2.442	9
208	2.31	50	-	-
?	2.21	30	2.201	8
00·10	2.05	50	2.058	9
040	1.83	70	1.838	23
?	1.72	30	1.746	8
620	1.67	40	1.672	5
606	1.62	40	1.629	6
440	1.53	30	1.526	4
00·14	1.44	20	1.439	3
800	1.40	40	1.404	4

X-ray diffraction data of 10Å tobermorite.
* : ASTM diffraction data card 6-0020.
** : Starting Ca/Si=0.7, 80°C, 30days.
s : This line was detected as a shoulder on 2.96Å peak.

X-ray powder diffraction data of the synthetic 10Å tobermorite which showed the highest crystallinity among the preparations are listed in Table II compared with those of a natural specimen from Crestmore. The lattice parameters of the synthetic 10Å tobermorite computed by the least square method from the indexed data in Table 2 are a_o=11.24Å, b_o=7.31Å and c_o=20.26Å. These agreed well with those of Crestmore specimen, i.e. a_o=11.2Å, b_o=7.3Å and c_o=20.5Å.

The crystals of 10Å tobermorite were lath-like [A] or fibrous [B] elongated parallel to *b* with (100) cleavage (figure 1, A & B).
In the SED pattern of a lath-like crystal lying on (100), diffraction spots were indexed to *0kl* where *k* and *l* were even (figure 2). When *k* was odd, reflections became continuous streaks parallel to *c** due to disorder.
Some of the fibrous crystals showed a similar pattern to figure 2, but the diffraction spots disappeared very often during observation, and others gave diffraction rings similar to those of C-S-H(I). These results suggest that the lath-like crystals were the higher in crystallinity than the fibrous ones.
Figure 3 is a high resolution electron micrograph of the synthetic 10Å tobermorite lying on (100). Lattice planes 10Å apart are resolved.

On prolonging the reaction time, 10Å tobermorite was gradually replaced by 11Å tobermorite, but a trace of 10Å tobermorite was detected even after 60-70days. The basal spacing of these 11Å tobermorite was 11.8Å, a little longer compared with 11.3Å of ordinary ones. This is characteristic of Al-bearing 11Å tobermorite (4, 5).
The crystals of 11Å tobermorite were platy elongated parallel to *b* with (001) cleavage.

11Å tobermorite formed also by the reaction at 100°C for more than six days.

Moreover in almost all the runs, the formation of hydrogarnet, C_3ASH_4, was observed. Its yield was higher at 100°C than 80°C.
$C_3A \cdot CaCO_3 \cdot 12H_2O$ was also obtained at 100°C for one day.

Chemical compositions were determined by energy dispersive x-ray microanalysis on each crystal of 10Å and 11Å tobermorites using β-wollastonite and kaolinite for calibration (Table III). 10Å tobermorite gave the higher Ca/Si and Ca/(Si+Al) than 11Å tobermorite.

On heating in the air, 10Å tobermorite deteriorated to an amorphous form at around 300°C, which transformed into β-wollastonite at 800°C. 11Å tobermorite proved to be an anomalous type since it kept the basal spacing at about 11Å until the transformation into β-wollastonite occurred at 800-900°C.

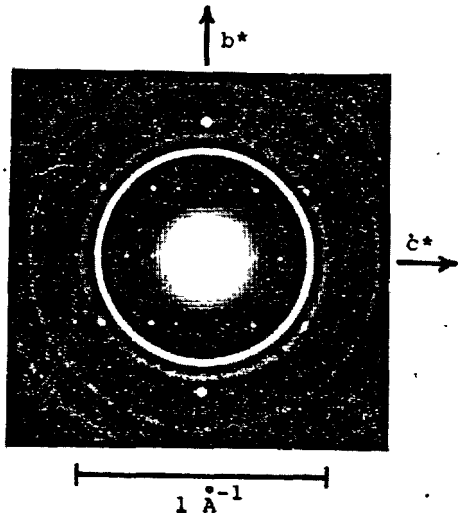

Fig. 2 - SED pattern of 10Å tobermorite with Au ring for calibration.

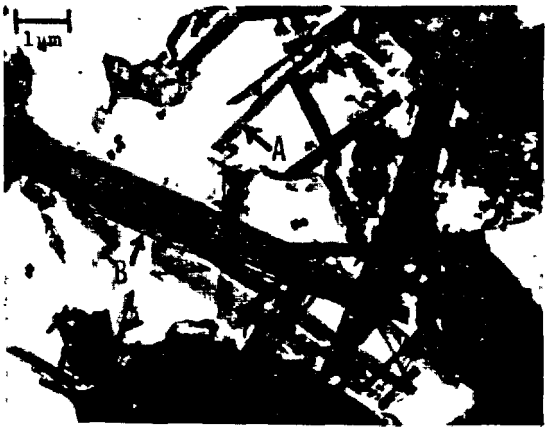

Fig. 1 - Electron micrograph of 10Å tobermorite.

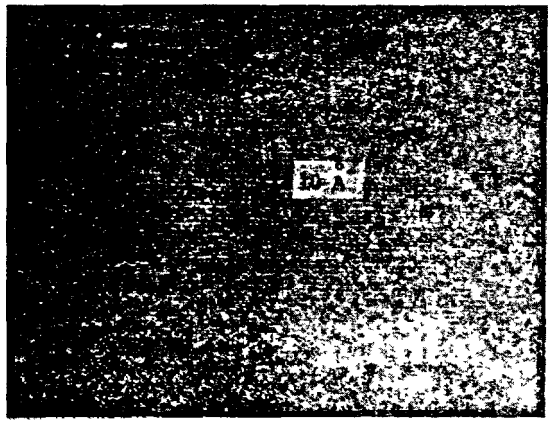

Fig. 3 - High resolution electron micrograph of 10Å tobermorite.
Lattice planes 10Å apart are resolved.

TABLE III

Tobermorite	10Å		11Å		
Days	20	30	20	30	40
Ca/Si	1.38†	1.15	1.75*	0.94**	0.93
Ca/(Si+Al)	1.13	0.95	1.46	0.78	0.79
Al/(Si+Al)	0.18	0.17	0.17	0.17	0.16

Chemical compositions of tobermorites prepared from silica glass (5,950cm^2/g ; starting Ca/Si=0.8, 80°C).
† : Fibre bundle, precursor of 10Å tobermorite.
* : Crumpled foil
** : Thin plate
} precursor of 11Å tobermorite.

2. Reaction of Silica Glass

14Å tobermorite was reproducibly obtained from mixtures of silica glass and CaO over a wide range of temperatures from 70°C to 100°C (Table IV). The lower the reaction temperature and the higher the starting Ca/Si were, the longer the period of reaction time was necessary to obtain 14Å tobermorite. At the reaction temperatures less than 80°C 14Å tobermorite was stable, but a tendency was observed that it might transform to 11Å tobermorite at temperatures higher than 90°C. X-ray powder diffraction data of the synthetic 14Å tobermorite agreed well with those of a natural specimen from Crestmore (6). Lattice parameters of the synthetic 14Å tobermorite were a_o=11.26Å, b_o=7.33Å and c_o=27.88Å.

The crystals of 14Å tobermorite were lath-like or platy elongated parallel to *b* with (001) cleavage (figure 4). In the SED pattern of the lath-like crystal lying on (001), diffraction spots were indexed to *hk0* where *h* and *k* were even (figure 5). When *h* and *k* were odd, streaks parallel to *a** were observed, which show the presence of disorder.

Ca/Si and H_2O/Si of 14Å tobermorite prepared at 80°C determined by chemical analysis converged to 0.74-0.82 and 1.35-1.42 respectively for more than 40days. Ca/Si of the crystals determined by energy dispersive x-ray microanalysis are summarised in Table V.

On heating in the air, the synthetic 14Å tobermorite transformed to 11Å tobermorite at 60-400°C. These kept their basal spacing at about 11Å or reduced it to about 10Å during heating up to temperatures where the transformation to β-wollastonite occurred. The former should be designated as an anomalous type and the latter a mixed type (= an intermidiate of normal and anomalous types) in the same way as shown in the classification of 11Å tobermorite (7).

Effects of addition of γ-Al_2O_3 and NaOH are summarised in Table VI as the hydration products prepared at 80°C.

Addition of alumina decreased the basal spacing and finally gave Al-substituted 11Å tobermorite.

TABLE IV

Temperature, °C	Days	Starting Ca/Si 0.6	0.7	0.8	0.9
70	5	C-S-H CH	C-S-H CH	C-S-H CH	C-S-H CH
	10	C-S-H	C-S-H	C-S-H	C-S-H
	20	14.0T	14.0T	C-S-H	C-S-H
	30	14.0T	14.0T	14.0T	13.6T
	40	14.0T	14.0T	14.0T	14.0T
80	2	C-S-H CH	C-S-H CH	C-S-H CH	C-S-H CH
	5	C-S-H	C-S-H	C-S-H	C-S-H
	10	14.0T	14.0T	C-S-H	C-S-H
	20	14.0T	14.0T	14.0T	14.0T
	30	14.0T	14.0T	14.0T	14.0T
	40	14.0T	14.0T	14.0T	14.0T
	70	14.0T	14.0T	14.0T	14.0T
	120	14.0T	14.0T	14.0T	Δ
90	5	14.0T	14.0T	C-S-H	C-S-H
	10	14.0T	14.0T	14.0& 12.6_sT	14.0T
	20	14.0T	14.0T	14.0T	14.0T
	30	14.0T	14.0T	14.0& 12.6_sT	14.0& 12.6_sT
	40	14.0T	14.0T	14.0& 12.1T	14.0& 12.6_sT
	70	14.0T	14.0& 12.2_sT	14.0& 12.6T	14.0& 12.6T
100	2	Δ	14.0T	Δ	Δ
	7	13.8T	14.0T	14.0& 12.4T	11.8& 14.0T

Hydration products from silica glass.
C-S-H : C-S-H and C-S-H(I). CH : $Ca(OH)_2$.
T : Tobermorite. Numerals in front of 'T' show the basal spacing (Å) of the tobermorite.
s : The basal spacing suffixed by 's' was observed at a shoulder of the neighbouring basal reflection in x-ray diffractometry.
Δ : This preparation was omitted.

TABLE V

Tobermorite	14Å				11Å
Days	5	10	20	40	20*
Foil	1.00	0.82	0.70	0.65	1.38
Plate	Δ	0.81	0.78	0.78	0.89

Ca/Si mole ratios of tobermorites prepared from silica glass (Starting Ca/Si=0.7, 80°C).
Foil : C-S-H(I), precursor of each tobermorite.
Plate: Crystalline tobermorite. Δ : Unobserved.
* : 2% of γ-Al_2O_3 to solids by weight was added to this preparation.

Fig. 4 - Electron micrograph of 14Å tobermorite.

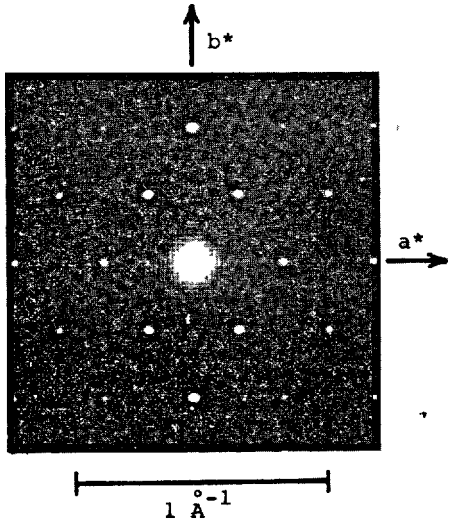

Fig. 5 - SED pattern of 14Å tobermorite.

TABLE VI

	Days	5	10	20	40	70
γ-Al_2O_3	0.5 %	C-S-H	13.4T	14.1& 13.0_sT	14.0& 13.0_sT	14.0& 13.0_sT
	1	C-S-H	C-S-H	12.1T	12.1& 14.0T	12.1& 14.0T
	1.5	C-S-H CH	C-S-H	10.7T	11.9& 14.1T	11.8& 14.0T
	2	C-S-H CH	C-S-H	11.8T	11.6T	11.6T
	5	C-S-H CH	C-S-H CH	10.0T CH	10.2T	11.8T
NaOH	0.5%	C-S-H	14.1T	14.0T	14.0T	14.0T
	1	C-S-H	14.1T	14.1T	14.0T	14.0T
Al_2O_3 2 % NaOH 0.5%		C-S-H CH	C-S-H CH	C-S-H CH	11.8& 10.7T	11.7& 14.0_sT

Hydration products prepared from silica glass with addition of γ-Al_2O_3 and NaOH (Starting Ca/Si=0.7, 80°C).

C-S-H : C-S-H and C-S-H(I). CH : $Ca(OH)_2$.

T : Tobermorite. Numerals in front of 'T' show the basal spacing (Å) of the tobermorite.

s : The basal spacing suffixed by 's' was observed at a shoulder of the neighbouring basal reflection in x-ray diffractometry.

When 2% of alumina to solids by weight was added, 11Å tobermorite formed in all the preparations of starting Ca/Si 0.6-0.9. The 11Å tobermorite was platy with (001) cleavage. Besides, addition of alumina decreased SiO_2 reactivity and H_2O/Si, increased Ca/Si and improved normality in thermal behaviours of 11Å tobermorite.

The results in Table VI may suggest the formation of 12Å tobermorite or tacharanite during a decrease of the basal spacing according to an increase of alumina from 0.5 to 5%.

Addition of 5% of alumina retarded the reaction and gave 10Å tobermorite of poor crystallinity as an intermidiate phase.

The crystallinity of 14Å tobermorite was improved with addition of 0.5-1% of NaOH.

The reaction with addition of alumina and NaOH showed a certain similarity to that of volcanic ash.

DISCUSSION

As crystalline tobermorites, the phases having the basal spacing of 14Å, 12Å, 11Å, 10Å and 9Å are known so far. Since 9Å tobermorite is obtained as a dehydrated form of the other tobermorites, its hydrothermal synthesis at low temperatures seems to be impossible.

14Å tobermorite has been found in several places (8), but its synthesis was only once reported by Kalousek and Roy (9). The synthetic 14Å phase seems to be poorly crystalline judging from their brief description on it. 14Å tobermorite prepared in the present study was well crystalline, and showed different thermal behaviours from the natural specimens. The synthetic ones were an anomalous type or a mixed type. On the other hand; all the natural specimens have been reported to transform to 11Å tobermorite at about 60°C on heating in the air, and then to 9Å tobermorite at about 300°C. Namely, these are a normal type. Anomaly of the synthetic specimens seem to be caused by its low Ca/Si due to high solubility of silica glass (10).

12 Å tobermorite is recently thought to be possibly the same as tacharanite (11). The fact that tacharanite, $Ca_4(Si_6O_{18}H_2)\cdot 2/3Al_2O_3 \cdot 5H_2O$ (12), contains Al ions in its composition may suggest the similarity of the 12Å phase prepared with addition of alumina (Table VI) to tacharanite. 12Å phase was also observed in the preparations without addition of alumina at 90-100°C (Table IV), and during heating the synthetic 14Å tobermorite in the air. Further investigations are still continuing

to clarify relationships among them.

The lowest temperature ever reported where the formation of 11Å tobermorite was possible was 90°C by Mitsuda et al (13)who could succeed by using clinoptilolite, a natural zeolite. The present results suggest the possibility to lower it even below 80°C, when suitable siliceous materials of high solubility are selected and sufficient periods of reaction time are allowed. The presence of alumina was confirmed to function well for this purpose.

The synthesis of 10Å tobermorite has been unknown so far. However, by starting from volcanic glass, or silica glass with addition of 5% of alumina 10Å tobermorite could be obtained reproducibly. A decrease of silica solubility caused by the presence of Al ions may be suitable for the formation of 10Å tobermorite which is thought to be richer in Ca and deficient in Si compared to 11Å tobermorite (11). The synthetic 10Å tobermorite was peculiar in its crystal habit to show (100) cleavage. Almost all tobermorites have been known to be (001) cleavage except 11Å tobermorite from Loch Eynort (14). Further study is still necessary to clarify these reasons.

A rough correlation has been reported on C-S-H(I) between the basal spacing and Ca/Si; the basal spacing falls from 13-14Å for Ca/Si of 0.8, 12-12.5Å for Ca/Si of about 1.0, to about 10Å for Ca/Si of 1.5 (15). In the present study, 14Å tobermorite showed the lowest Ca/Si , 10Å tobermorite the highest Ca/Si and 11Å tobermorite an intermidiate Ca/Si between 14Å and 10Å phases. It seems therefore reasonable to consider that each tobermorite of different basal spacing is a well crystalline form of each C-S-H(I) of different Ca/Si respectively. Temperatures around 80°C are thought to be effective to crystallise these C-S-H(I) especially to semi-stable 14Å tobermorite, or less stable 10Å and 12Å tobermorite.

CONCLUSIONS

Reproducible syntheses of 10Å and 14Å tobermorite were possible by hydrothermal reactions of volcanic glass or silica glass with lime at temperatures about 80°C.

The 10Å tobermorite was lath-like or fibrous elongated parallel to *b* with (100) cleavage. The 14Å tobermorite was stable hydrothermally at temperatures less than 80°C in the absence of Al ions, and was confirmed to be an anomalous or a mixed type in its thermal behaviour.

Addition of alumina to the mixture of silica glass and lime functioned to decrease the basal spacing of tobermorite from 14Å to 11Å, the latter of which was the most stable under the present reaction conditions.
12Å phase, which might be 12Å tobermorite or tacharanite, and 10Å tobermorite formed on the way of crystallisation to 11Å tobermorite with addition of alumina. These were less stable than 11Å or 14Å tobermorite.

It is suggested from these results that each tobermorite of different basal spacing may be a well crystalline form of C-S-H(I) of different Ca/Si.

REFERENCES

1.- N. HARA and N. INOUE (1976), "Formation of 14Å tobermorite from silica glass", Yogyo-Kyokai-Shi, 84, n°4, 181-85 (Jap.).

2.- N. HARA, N. INOUE and O. MATSUDA (1979), "Hydrothermal reaction of volcanic ash (shirasu) with lime at 80° and 100°C", Yogyo-Kyokai-Shi, 87, n°2, 86-94 (Jap.).

3.- N. HARA and N. INOUE (1979),"Hydrothermal reaction of silica glass with lime at 70° -100°C", Yogyo-Kyokai-Shi, 87, n°3, 134-41 (Jap.).

4.- G.L. KALOUSEK (1957), "Substitution of aluminum in lattice of tobermorite", J. Am. Ceram. Soc., 40, n°3, 74-80.

5.- S. DIAMOND, J.L. WHITE and W.L. DOLCH (1966), "Effects of isomorphous substitution in hydrothermally-synthesized tobermorite", Am. Mineral., 51, 388-401.

6.- H.F.W. TAYLOR, ASTM x-ray diffraction data card 6-0005.

7.- H.F.W. TAYLOR (1974), "Crystal chemistry of portland cement hydration products", Preprint, 6th Int. Symp. Chem. Cement, Moscow.

8.- T. MITSUDA and H.F.W. TAYLOR (1978), "Normal and anomalous tobermorites", Mineral. Mag., 42, 229-35.

9.- G.L. KALOUSEK and R. ROY (1957), "Crystal chemistry of hydrous calcium silicates : II, Characterization of interlayer water", J. Am. Ceram. Soc., 40, n°7, 236-39.

10.- N. HARA, N. INOUE, H. HAYABUCHI and H. NAKAO (1974), "Thermal behaviours of 11.3Å tobermorite", Synop. Ann. Meeting of Ceram. Soc. Japan, p.69 (Jap.).

11.- S. DIAMOND (Chairman) (1972), "Guide to compounds of interest in cement and concrete research", U.S. Highway Res. Board Sp. Report 127.

12.- H.F.W. TAYLOR (1979), "Some observations on calcium silicate hydrates", Lecture at Ann. Meeting of Mineral. Soc. Japan, Tokyo.

13.- T. MITSUDA, Y. HIKICHI and M. MURACHI, (1970), "Low-temperature synthesis of Al-tobermorite", Cement Assoc. Japan, Review of 24th General Meeting, pp.43-47.

14.- J.A. GARD and H.F.W. TAYLOR (1957), "A further investigation of tobermorite from Loch Eynort, Scotland", Mineral. Mag., 31, 361-70.

15.- H.F.W. TAYLOR (1964), "The Chemistry of Cements" (Academic Press), Vol.1, pp. 181-203.

Hydration Reactions of C_3A Contained in an Unusual Flyash

Réactions d'hydratation d'une cendre volante particulière contenant du C_3A

SIDNEY DIAMOND, U.S.A.

SUMMARY :

Flyashes produced from certain lignite and sub-bituminous coals have high contents of analytical CaO, presumably derived from limestone within the coal deposits. In the U.S. a special category, "Class C" flyash has been designated for these materials. The mineralogy of the non-glassy portions of some of these flyashes is different from conventional flyashes, and in the material described C_3A, free lime, and anhydrite are all present. The flyash sets rapidly when mixed with water, and produces ettringite and $C_4A\bar{S}H_{12}$. The unique spherical morphology of the flyash grains makes the morphological relationships between the hydration products and the unhydrated material unusually clear. The early reactions are similar to those of C_3A in portland cement, and the ash might serve as a useful model system for the study of the influence of various admixtures and other substances on C_3A reactions and setting behavior. Presumably ettringite and $C_4A\bar{S}H_{12}$ are also produced when flyashes similar to the one studied are incorporated in concrete, and their production should enhance early strength development.

RESUME :

Les cendres volantes produites par certains lignites et par des charbons bitumineux ont une teneur élevée en ions CaO, provenant probablement des calcaires incorporés à ces dépôts géologiques. Aux Etats-Unis, une catégorie spéciale de cendres volantes "la classe C" a été définie pour ces matériaux. La minéralogie des phases vitreuses de quelques unes de ces cendres volantes est différente de celle des cendres volantes habituelles, et dans ces matériaux on trouve du C_3A, de la chaux libre et de l'anhydrite. Ces cendres volantes font prise rapidement lorsque malaxées avec de l'eau; il se produit de l'ettringite et du $C_4A\bar{S}H_{12}$.
La forme, uniquement sphérique, des grains de cendres volantes, rend particulièrement nettes les relations morphologiques entre le matériau anhydre et les produits de son hydratation.
Les réactions initiales sont analogues à celles du C_3A dans le ciment portland, et ces cendres ont pu servir de modèle courant, pour l'étude de l'action de divers additifs et autres substances, sur les réactions du C_3A et le comportement durant la prise. Il est probable que de l'ettringite et du $C_4A\bar{S}H_{12}$ sont aussi produits quand des cendres volantes analogues à celles étudiées ci-dessus sont incorporées au béton; leur utilisation pourrait apporter une augmentation des résistances initiales.

INTRODUCTION

The chemical and mineralogical composition of flyashes largely reflect the nature of the inorganic portions of the coal being burned, and to a lesser degree the burning conditions involved. Most flyashes typically contain glass and such minerals as quartz, mullite, magnetite, hematite, periclase, etc. The reactive component is primarily the glass, and reaction in concrete occurs only slowly.

In recent years lignite and sub-bituminous coals have become major sources of fuel for electric power plants in the western part of the U.S. Many of these coals include significant contents of limestone, thus generating flyashes much richer in CaO than conventional flyashes. With large volumes of such flyashes now available, their use in concrete is becoming widespread. Committee C-9 on Concrete of ASTM now recognizes such flyashes as constituting a special and separate category of admixture, distinguishing them as "Class C" flyashes (1).

The mineralogy of the crystalline portions of Class C flyashes tends to be somewhat different from that of conventional flyashes. In addition to quartz, some of these materials contain significant contents of C_3A. Free CaO is often present, as might be expected. Sometimes some, or most of the limited content of SO_3 present occurs as anhydrite. The major component remains glass, however.

With the presence of C_3A and a source of available sulfate, the obvious expectation is that ettringite and the calcium monosulfate hydrate $C_4\overline{A}S\overline{H}_{12}$ might be produced when such flyashes are mixed with water, especially since free CaO should insure a relatively high pH. Thus responses similar to some of the early hydration reactions occurring in portland cement might take place in flyash-water pastes.

The present work describes such a response with a particular Class C flyash from Muskogee, Oklahoma. This material has a CaO content of approximately 26% and a relatively high SO_3 content, approximately 3%. X-ray diffraction peaks are weak, indicating that glass is the major constituent as expected, but significant contents of quartz, C_3A, anhydrite, and uncombined CaO are detected. In addition, a little calcite (presumably due to secondary carbonation of the free lime), some periclase, and even a trace of $C_4A_3\overline{S}$ appear to be present.

FLYASH MORPHOLOGY

The morphology of this flyash is similar to those of a number of Class C flyashes examined by the writer, and significantly different from many conventional flyashes. Essentially all of the particles seem to be solid spheres, mostly of diameters between 1 and 15 μm. A few larger spheres are occasionally found, but carbonaceous residues and other evidences of incomplete burning and melting are generally absent, as are very coarse particles of any kind. Also almost completely absent are hollow-shell spheres and complex sphere-within-sphere structures so prominent in scanning electron microscope (SEM) photographs of conventional flyashes.

A typical field showing a reasonably representative size distribution for this material is given as Fig. 1. In this figure the largest sphere, in the lower central portion of the field, is approximately 25 μm in diameter.

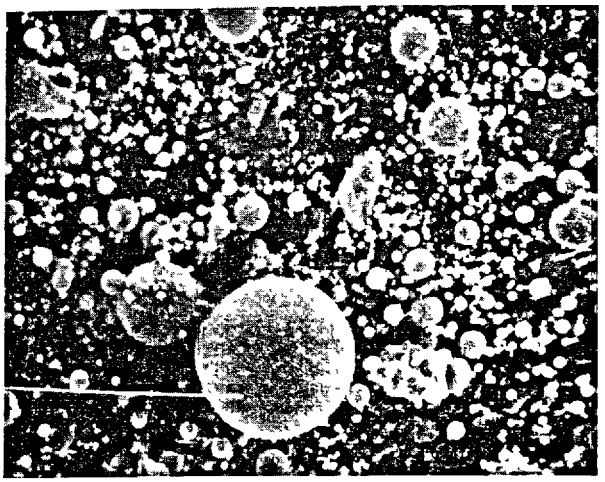

Fig. 1. Morphology and Size Distribution of Flyash Particles. Original Magnification 1,000 x.

REACTIONS WITH WATER

Pastes were prepared by mixing flyash and deionized water and the resulting responses were recorded by various techniques. The water:solids (w:s) ratios used varied from 0.2 to 0.5.

It was noted that there was a distinct but short-lived induction period before any temperature elevation was observed, typically about 15 minutes. Rapid and continuous temperature elevation then took place in the small exposed paste specimens, reaching to as high as 36° C from the initial 22° C laboratory temperature for the w:s 0.2 paste. The temperature rise terminated in about 30 minutes or less after mixing.

Setting, as measured by Vicat needle, took place with exceeding suddenness, at times between 15 minutes for the w:s 0.2 paste and 45 minutes for the w:s 0.5 paste.

X-ray diffraction examination of the hardened pastes immediately after set revealed the presence of significant contents of ettringite.

The pastes were maintained in sealed containers after set, and sampled periodically for x-ray and SEM examination.

After about 4 hours a small peak for calcium monosulfoaluminate hydrate ($C_4\overline{A}S\overline{H}_{12}$) at approximately 9Å was detected in most of the pastes, and this increased somewhat with further curing. In contrast, the ettringite pattern was initially quite strong and a large number of peaks of this compound were recorded, even at the earliest period examined. Both components seemed to be retained indefinitely, without too much apparent change in the relative proportions as judged by XRD.

MICROSTRUCTURE OF REACTED PASTES

Fig. 2 shows a characteristic field taken of the w:s 0.3 paste shortly after set, at approximately ½ hour after initial mixing. It is immediately obvious that in these pastes set is due to formation of ettringite, rod-shaped particles of which are seen to protrude from individual flyash spheres and act as bridges. In the lower right portion of the micrograph a considerable cluster of ettringite rods seems to have developed, presumably from a grain that is rapidly decomposing.

Fig. 2. Flyash Paste, W:S 0.3, ½ Hour, Showing Development of Ettringite Rods.

In Fig. 2 and subsequent figures the scale is indicated by the length of the separated right-hand portion of the white marker bar, which is in all cases 5 μm in length. The gap between the two portions is 0.5 μm wide.

The appearance of the pastes after 4 hours is indicated in Fig. 3, where again the ettringite rods are clearly defined, and the newly-developing $C_4A\bar{S}H_{12}$ plates are visible for the first time. It is apparent how a rigid three dimensional structure developed initially through the growth of ettringite rods can be reinforced through the subsequent development of platy particles of the $C_4A\bar{S}H_{12}$, which tend to build up a characteristic "edge to face" or "cardhouse" structure. This has previously been observed by the present writer to be characteristic of this compound in portland cement pastes as well (2).

Further details of the intimacy of the connection between the flyash spheres giving rise to the ettringite and $C_4A\bar{S}H_{12}$ products and the products themselves can be seen in Fig. 4, which shows the central area observed in Fig. 3 at higher magnification. Attention is called to growth of the large ettringite rods almost perpendicular to the surface of the host sphere in the large sphere in the upper central portion of the figure and in the smaller sphere in the lower right portion; to the bridging action effected by the platy particle cluster between the large sphere previously mentioned and the small sphere at the center of the micrograph, and to the many connections visible between the

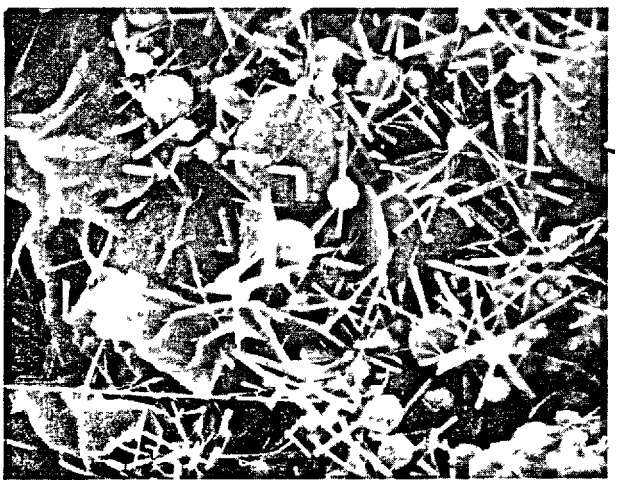

Fig. 3. Flyash Paste, W:S 0.4, 4 Hours, Showing Initial Development of $C_4A\bar{S}H_{12}$ Plate Structure Reinforcing Ettringite.

ettringite rods and the $C_4A\bar{S}H_{12}$ plates, which thus constitute a single, combined, continuous reinforcing system.

Fig. 4. Higher Magnification View of Area of Fig. 3 Showing Details of Connections Between Particles.

Fig. 5 for a paste taken at 8 hours shows at a somewhat reduced scale how such a structure apparently can bridge quite wide gaps between residual flyash spheres and maintain a rigid, reinforced, but not very dense structure. Also, here for the first time in a few areas some nondescript small products which appear to be neither ettringite nor $C_4A\bar{S}H_{12}$ start to appear.

It is noteworthy that the residual flyash spheres in the figures so far displayed mostly do not show any significant change in character of surface texture arising as a result of the reactions. The large sphere in the lower right portion of Fig. 5 is not significantly rougher in surface character than some of the spheres present in the original flyash, even

though it does appear rougher than the large sphere in Fig. 1.

A typical view of the appearance of the pastes after 7 days is shown in Fig. 6. There has been comparatively little change after the first few hours, except that an increasing proportion of nondescript particles seems to be present in many areas. Some of the flyash spheres have lost their earlier almost pristine appearance and are visibly corroding and disintegrating, as can be seen near the left margin and also in the upper left portion of the micrograph.

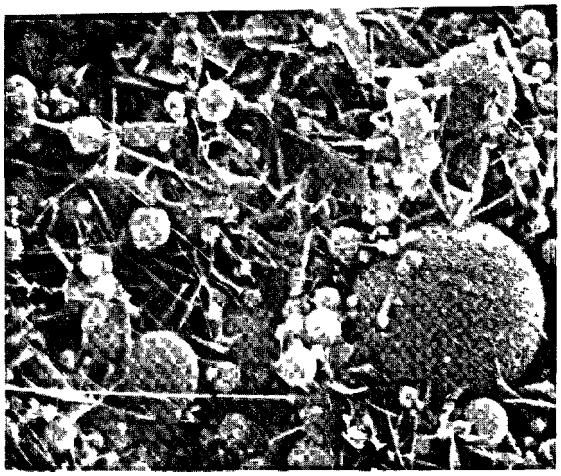

Fig. 5. Flyash Paste, W:S 0.4, 8 Hours, Showing Effects of Reaction Products in Bridging Wide Gaps Between Flyash Spheres.

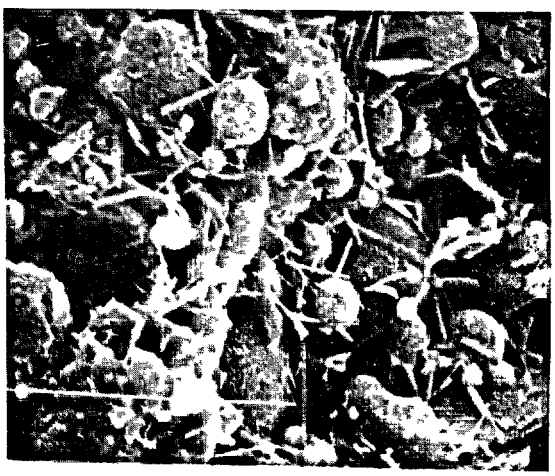

Fig. 6. Flyash Paste, W:S 0.4, 7 Days, Showing Accumulation of Nondescript Particles and Fragments of Decomposing Spheres.

Comparatively little further change takes place in the period between 7 and 28 days. The general appearance remains roughly the same. However, especially at low w:s ratios, here and there one can detect individual particles and occasionally clusters of small rods which the writer takes to be C-S-H gel of the Type I variety (2). The appearance of this material is indicated in Fig. 7. Presumably this represents the product of the reaction of the glassy siliceous component in the flyash with dissolved $Ca(OH)_2$, i.e. the conventional, slow "pozzolanic" reaction. If this interpretation is correct, this system is unusual in that the "pozzolan", that is, the flyash, is supplying its own lime.

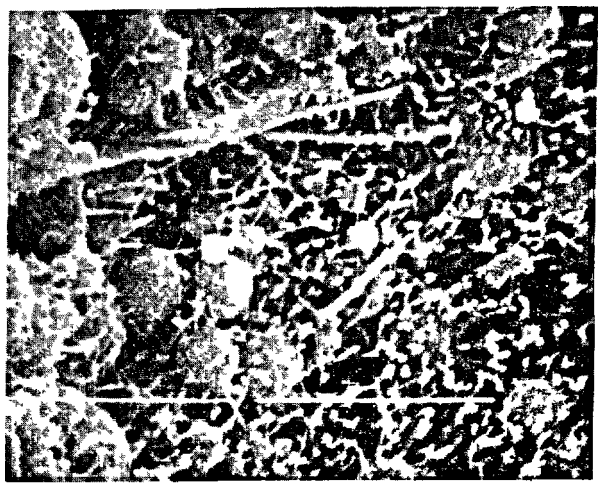

Fig 7. Flyash Paste, W:C 0.2, 28 Days, Showing Late Development of Occasional C-S-H Gel Particles

DISCUSSION

It is apparent from the preceding descriptions that C_3A in the present flyash reacts in a manner entirely analogous to the way it does in portland cement. However, the unique spherical morphology of the flyash particles provides an unusually clear opportunity for visualization of the spatial relationships between the newly formed hydration products and the starting material, and for studying the details of the structure that develops.

Possibly useful information concerning the effects of various parameters, set modifying chemicals, and other influences on the early reactions in concrete can be obtained using such flyash pastes as model systems. Of course due allowance must be made for the differences between flyash pastes and the more complex portland cement pastes in concrete.

Perhaps of more significance, it is clear that the contribution of flyashes like the present one to early strength gain when they are used in concrete stems from formation of additional ettringite and $C_4A\bar{S}H_{12}$ hydration product particles, of the same type as formed from the C_3A within the portland cement. This action is thus completely different in character from the conventional pozzolanic response associated generally with flyashes, and involving the formation of C-S-H gel from reaction of the glassy component. The latter response occurs in the present flyash as well, but at a much different and later time.

ACKNOWLEDGEMENTS

The courtesy of Mr. William F. Scriminger of the Muskogee Environmental Conservation Co. in supplying the flyash and chemical analyses is much appreciated.

REFERENCES

1.- American Society for Testing and Materials, (1979) Annual Book of ASTM Standards, Part 14, Concrete and Mineral Aggregates, Designation C 618-78, pp. 362-365.

2.- S. Diamond (1977), "Cement Paste Microstructure- An Overview at Several Levels", in "Hydraulic Cement Pastes: Their Structure and Properties", C and CA, London, pp. 2-30.

Influence of pozzolana on the hydration of C_3A

Influence de la pouzzolane sur l'hydratation du C_3A

H. UCHIKAWA, Doctor of Engineering, Onoda Cement Co., Ltd. and S. UCHIDA, Onoda Cement Co., Ltd, Japon.

RESUME : Des échantillons primaires de C_3A, de $CaSO_4 \cdot 2H_2O$, de C_3A, $CaSO_4 \cdot 2H_2O$, ou de $Ca(OH)_2$ ont été mélangés à de la pouzzolane (40% pouzzolane en poids). Les mélanges ont alors été hydratés à 20°C (±1°C) dans le rapport eau/solide de 0.6. Cette expérimentation est destinée à étudier l'influence de la pouzzolane sur l'hydratation du C_3A, la réaction "pouzzolanique", et le mécanisme de l'hydratation du système : - pouzzolane-C_3A-$CaSO_4 \cdot 2H_2O$-$Ca(OH)_2$-.

Le taux d'hydratation initial du C_3A est ordinairement accéléré, mais on note un retard en début de réaction. Dans la phase moyenne et finale de la réaction, le taux d'hydratation est quasiment identique à celui observé sans pouzzolane.

Bien qu'il n'y ait pas de différence notable entre les deux sortes d'hydrates formés, avec ou sans pouzzolane dans le début de la réaction, dans les phases myoennes et finales, on observe la formation de C-S-H lorsque de la pouzzolane reche en silicium est utilisée, alors que l'on obtient un comoposé C_3AH_6, par utilisation de pouzzolane alcaline.

Un changement dans la phase liquide lors du début de la réaction conduit à la formation d'ettringite. Contrairement à la pouzzolane placée en milieu aqueux pur, on a pu noter également un changement des concentrations en ions Na^+ et K^+ augmentant avec le temps; Ceci suggère une attaque de la surface des grains de pouzzolane. Cette assertion est confimée par l'observation "MET" et "MES", au microscope électronique à transmission et à balayage.

Le début de la réaction, variable selon de type de pouzzolane utilisé, prend place en 1 à 28 jours.

Malgré la grande différence entre la vitesse de réaction du C_3A avec la pouzzolane observée suivant les cas, la réaction semble avoir lieu par diffusion d'ions Ca^{2+}, d'ions alcalins, ou des deux ensemble - suit un gonflement, puis la déstruction du films superficiel par la pression osmotique; la précipitation en surface de l'hydrate ainsi formé, termine cette réaction. L'alcalinité intrinsèque des pouzzolanes joue un grand rôle non seulement lors de l'hydratation, mais aussi dans la formation de la texture solide de la forme pâteuse durcie; Ce rôle est aussi primordial dans la constitution de l'espace entre les grains de pouzzolane et leur hydrate superficiel.

SUMMARY : The preliminary samples containing C_3A and $CaSO_4 \cdot 2H_2O$ or C_3A, $CaSO_4 \cdot 2H_2O$ and $Ca(OH)_2$ were mixed with 40% by weight of pozzolana and the mixtures were hydrated at 20±1°C with W/S ratio of 0.6 in order to study the influence of pozzolana on the hydration of C_3A, the pozzolanic reaction and the mechanism of the hydration in the system pozzolana-C_3A-$CaSO_4 \cdot 2H_2O$-$Ca(OH)_2$.

The rate of the initial hydration of C_3A was generally accelerated by the addition of pozzolana. But it was depressed in the early stage. The rate of the hydration of C_3A in middle and later stage recovered almost the same level as without pozzolana.

Though there were no remarkable difference of the kinds of hydrates with or without pozzolana in early stage, C-S-H was formed when Si rich pozzolana was used and C_3AH_6 was observed when alkali rich pozzolana was used in middle and later stage.

Compositional change of liquid phase in initial stage corresponded to the change in ettringite formation. The change in Na^+ and K^+ concentration, quite different from the case of pozzolana's immersing in pure water, increased with age which suggests the destruction of the surface structure of pozzolana grain. This speculation was confirmed by TEM and SEM observation.

The staring time of pozzolanic reaction varied with the character of pozzolana from one day to 28 days.

In spite of large difference between the rate of reaction of C_3A and pozzolana, the reaction proceeds through the formation of amorphous surface layer by leaching out of Ca^{2+} and/or alkalies ions, swelling and destruction of surface film by osmotic pressure and precipitation of hydrate on the surface of the film. The alkalies in pozzolana play an important role not only in the hydration reaction but also in the formation of the texture of hardened paste especially the clearance between pozzolana grain and hydrate.

1. PREPARATION OF SAMPLE AND EXPERIMENTAL PROCEDURE

1 mole of synthesized C_3A from stoichiometrical mixture of guaranteed reagent having 3000 cm^2/g of Blaine specific surface area was mixed with 0.5 mol of $CaSO_4 \cdot 2H_2O$ and/or 0.5 mole of $Ca(OH)_2$. Then 40% by weight of pozzolanas and the fly ash were added and blended sufficiently to prepare the samples.

The samples were hydrated at 20±1°C with W/S= 0.6 except for the case of conduction calorimetry (W/S=0.8) and the measurement of liquid phase composition (W/S=10).

Powder X-ray diffraction (XRD) and simultaneous differential thermal analysis (DTA)-differential scanning calorimetry (DSC)-thermogravimetry (TG) under argon atomosphere (1) were used for the identification and quantitative analysis of crystalline phase. Conduction calorimetry was applied to study the initial hydration. Scanning electron microscope (SEM) and high resolution transmission electron microscope (TEM) were used to observe the microfeature and microstructure of pozzolana, C_3A, hydrate and hardened paste.

Mercury penetration porosimetry was used to know the macrostructure of hardened paste and pore size distribution in the paste above 75Å.

To determine the degree of reaction of pozzolana, separation of C_3A, $CaSO_4 \cdot 2H_2O$, $Ca(OH)_2$ and hydrate from hardened paste was effectively performed by 3% HCl-methanol solution.

2. RATE OF HYDRATION OF C_3A IN THE SYSTEM CONTAINING POZZOLANA

Initial hydration of C_3A was pursued by conduction calorimetry. First peak within an hour is the formation of Ca-Al hydrate and ettringite when gypsum is present. The second peak usually appears in a couple of hours after mixing with water corresponds to the formation of monosulfate hydrate.

The effect of $CaSO_4 \cdot 2H_2O$ and $Ca(OH)_2$ on the initial hydration of C_3A was the same as in the case without pozzolana and the effect of pozzolana varied with their own character.

The rate of the hydration of C_3A in the initial stage within one day was the order of C_3A, pozzolana-C_3A, pozzolana-C_3A-$CaSO_4 \cdot 2H_2O$, C_3A-$CaSO_4 \cdot 2H_2O$, pozzolana-C_3A-$CaSO_4 \cdot 2H_2O$-$Ca(OH)_2$ and C_3A-$CaSO_4 \cdot 2H_2O$-$Ca(OH)_2$. Generally speaking, pozzolana accelerate the initial rate of hydration of C_3A in the presence of $CaSO_4 \cdot 2H_2O$ and $Ca(OH)_2$. Among pozzolanas, Kanto loam which has large specific surface area, high content of aluminum and high cation exchange capacity (CEC) value showed the most remarkable acceleration proportional to the added quantity as shown in Fig. 1. This effect is more clearly recognized in the second peak than in the first peak. One exception was observed in the second peak of Furue shirasu mixed sample containing much alkalies.

The degree of hydration estimated by the measurement of unhydrated C_3A with XRD in Fig. 2 shows that C_3A in the sample mixed with Kanto loam attained to about 65% at one day while the others were remained about 25%. The degree of hydration other than Kanto loam at 28 days attained to about 95% but it remained below 90% in Kanto loam mixed sample.

3. CHANGE IN ION CONCENTRATION OF LIQUID PHASE

The change in concentration of several kinds of ions in the liquid phase separated from

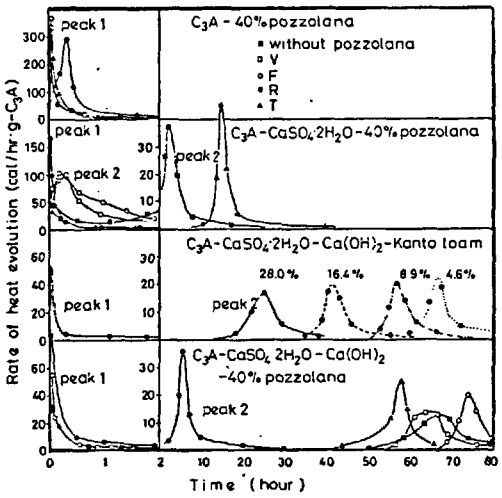

Fig. 1-Heat evolution curve in the hydration in the system containing C_3A

Table I Characters of pozzolanas

Natural and artificial pozzolana	Chemical composition (%) ig.loss*	SiO_2	Al_2O_3	Na_2O (K_2O)	Conc-HCl soluble part (%)	BET specific surface area(m^2/g)	CEC (m mol /100g)	Water soluble part W/S=10, 1min.-1d.** (m mol/l)
Beppu white clay (V)	4.1	87.4	2.4	0.1 (0.1)	15.6	14.7	4	SiO_4^{4+}:0.08-0.20, AlO_2^- and Na^+:nondetective, Ca^{2+}:0.3-0.9, pH:4.0
Furue shirasu (F)	1.9	69.3	14.3	3.0 (2.4)	12.0	3.0	5	SiO_4^{4+}, AlO_2^- and Ca^{2+}:nondetective, Na^+:0.27-0.27, pH:9.2
Kanto loam (R)	12.1	33.0	20.9	0.4 (0.2)	86.4	199	26	SiO_4^{4+}:0.27-0.27, AlO_2^-, Ca^{2+} and Na^+:nondetective, pH:6.8
Takehara fly ash(T)	4.6	49.1	24.4	2.2 (1.3)	47.9	2.3	2	SiO_4^{4+}:0.07-0.07, Ca^{2+}:11.4-14.3, Na^+:4.0-4.0, K^+:0.04-0.10, AlO_2^-:nondetective, ***

Note:

*. 100°C dry base, **. measuring time, ***. pH:12.2

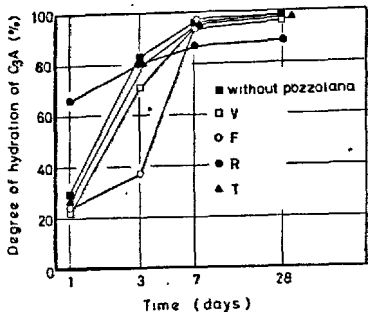

Fig. 2-Degree of hydration of C_3A in the paste [pozzolana-C_3A-$CaSO_4 \cdot 2H_2O$-$Ca(OH)_2$]

the sample of suspension hydration indicates that the degree of hydration of C_3A is closely related to the concentration of Ca^{2+}, AlO_2^- and SO_4^{4-}. In Kanto loam mixed sample Ca^{2+} consumed rapidly by the precipitation of ettringite. High AlO_2^- concentration in initial stage is fabourable to the formation of ettringite. On lowering the concentration of Ca^{2+}, AlO_2^- and SO_4^{4-} by the precipitation of ettringite, C_3A, $CaSO_4 \cdot 2H_2O$ and $Ca(OH)_2$ dissolve into liquid phase which brings high degree of hydration of C_3A. When $CaSO_4 \cdot 2H_2O$ is completely consumed, AlO_2^- begin to increase and the hydration of C_3A is slow downed.

Alkalies were not released from Beppu white clay and Kanto loam in pozzolana-water system. Only from Furue shirasu and fly ash, Alkalies were dissolved into pure water and they show fairly high level from initial and kept constant. On the contrary, in the present system pozzolana-C_3A-$CaSO_4 \cdot 2H_2O$-$Ca(OH)_2$ alkali concentration increased with age. The fact indicates the destuction of the surface structure of pozzolana grain through the leaching out of alkalies by the protonic attack of dissociated water under caustic circumstance.

4. PROCESS OF HYDRATION

Hydrates procuced during the hydration were identified by XRD, DTA and TEM observation as shown in Table II.

Initially formed Ca-Al hydrate and ettringite changed to monosulfate hydrate, hexagonal solid solution of monosulfate hydrate-tetra calcium aluminate hydrate, Ca-Al hydrate with low C/A ratio and C-S-H in later age through monosulfate hydrate. Though there were no remarkable difference of the kind of hydrate with or without pozzolana in early age, C-S-H was formed when Si rich pozzolana was used and C_3AH_6 was observed when alkali rich pozzolana was used in later age. The existence of C_3AH_6 in fairly early age is considered to be responsible to alkali concentration of liquid phase as the stability of hexagonal Ca-Al hydrate decreases under coexistence of alkali (2) (3).

5. MICRO STRUCTURE OF HYDRATE AND HARDENED PASTE

The Al rich amorphous layer caused by the elusion of Ca^{2+} from the surface of C_3A grain and the thin Ca-Al hydrate precipitated on the outer side of amorphous film were observed by

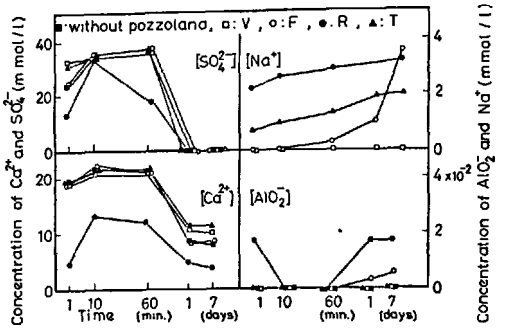

Fig. 3-Composition of liquid phase in the hydration [pozzolana-C_3A-$CaSO_4 \cdot 2H_2O$-$Ca(OH)_2$]

Table II Hydrate comfirmed in the paste [pozzolana-C_3A-$CaSO_4 \cdot 2H_2O$-$Ca(OH)_2$]

Kind of pozzolana	A	B	C	D	E
-	1d	-	3d	-	-
Beppu white clay(V)	1d	-	3d	(3)-7d	-
Furue shirasu(F)	1d	-	7d	(28d)-91d	28d
Kanto loam(R)	<1d	3d	7d	-	91d
Takehara fly ash(T)	1d	-	3d	(3)-7d	(91d)

Note:
A. (Ca-Al hydrate→) ettringite
B. monosulfate hydrate
C. monosulfate hydrate and $C_3A \cdot (CaSO_4, Ca(OH)_2) \cdot H12$
D. C-S-H
E. monosulfate hydrate and C_3AH_6
Prenthesis in Table means uncertainty.

high resolution TEM as shown in Fig. 4. The similar figure of surface layer on pozzolana grain brought by the dissolving-out of alkali ions and Ca^{2+} and precipitated hydrate on the surface of the layer were also recognized by TEM as shown in Fig. 4.

By SEM observation, precipitated hexagonal Ca-Al hydrate, short rod shaped ettringite of the surface of C_3A grain, rectangular ettringite just outside them and large monosulfate hydrate grown towards the capillary space were clearly seen at the neighbour of C_3A grain. While small hexagonal Ca-Al hydrate, rectangular ettringite and type II C-S-H were observed on the surface of pozzolana grain as shown in Fig. 5.

6. POZZOLANIC REACTION

The pore size distribution above 75Å measured by mercury penetration method is shown in Fig. 6. In Beppu white clay mixed sample, pore size distribution shifted towards small radius with age. The densification of hardened paste in this case is considered to be due to the formation of C-S-H. In Kanto loam mixed sample, added $Ca(OH)_2$ was completely consumed to form aluminate hydrate and built paste structure in early age maintained for long time without changing the pore size distribution. Furue shirasu mixed sample showed similar behavior to Takehara fly ash mixed sample in the change of pore size distribution but the densification was delayed owing to the conversion of hexagonal solid solution to C_3AH_6. $Ca(OH)_2$ in hardened paste determin-

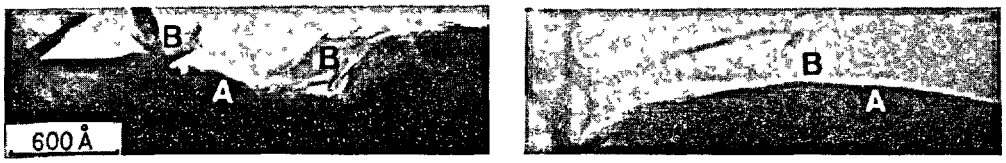

A. amorphous surface layer
B. Ca-Al hydrate

The surface of C_3A grain (2 min. after mixing with water)

The surface of pozzolana grain (F) (3 months' hydration)

Fig. 4-High resolution trasmission electronmicrograph

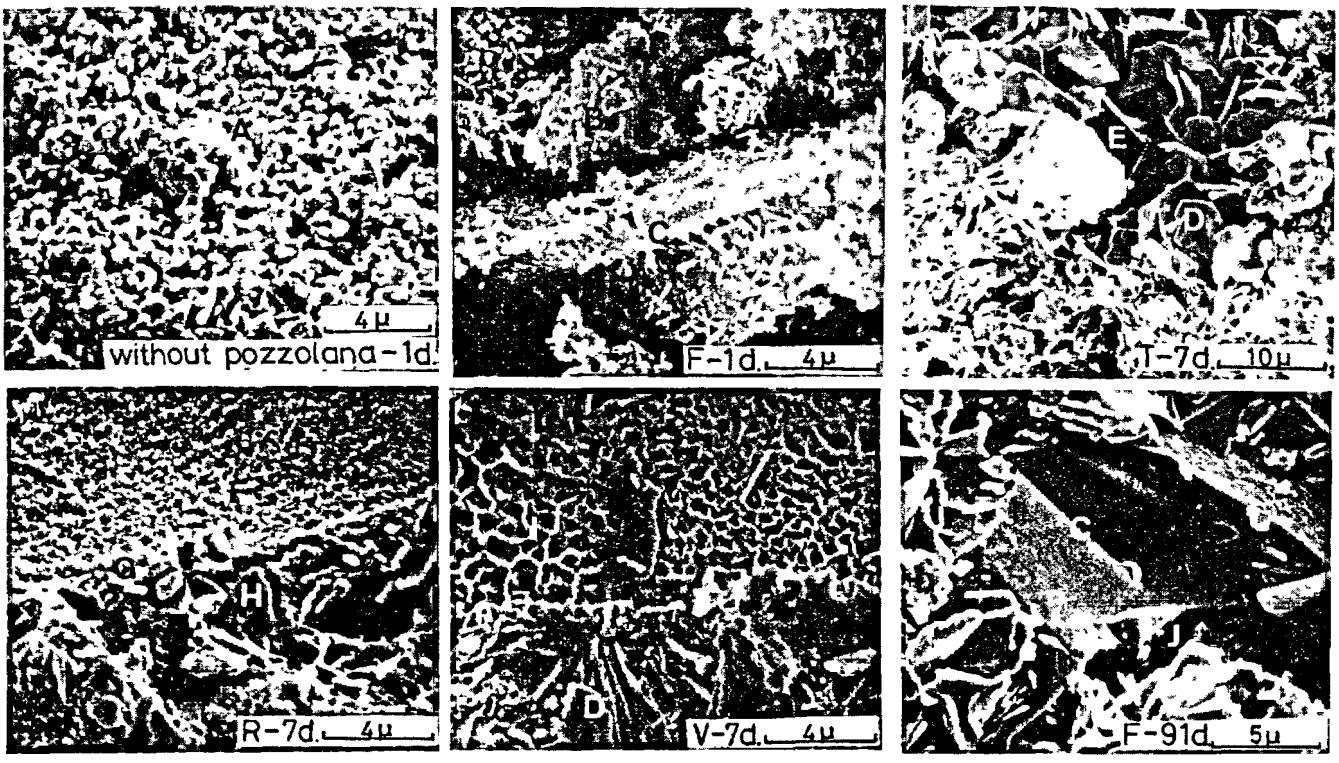

A. short rod shaped ettringite
B. rectangular ettringite
C. pozzolana grain
D. monosulfate hydrate
E. capillary space
F. cast-off trace of pozzolana (R)
G. Ca-Al hydrate
H. hexagonal solid solution of C_3A-($CaSO_4$, $Ca(OH)_2$)·H_{12}
I. type II C-S-H and cast-off trace of pozzolana (V)
J. clearance between pozzolana (F) and hydrates

Fig. 5-Scanning electronmicrograph of fracture surface of hardened pozzolana-C_3A-$CaSO_4$·$2H_2O$-$Ca(OH)_2$ paste

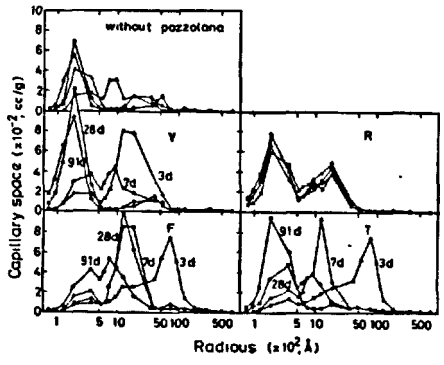

Fig. 6-Pore size distribution curve of hardened paste above 75Å [pozzolana-C_3A-$CaSO_4$·$2H_2O$-$Ca(OH)_2$]

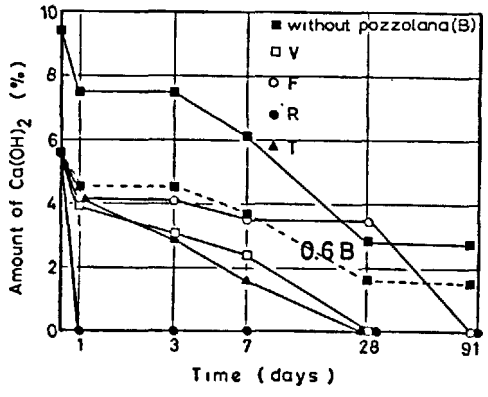

Fig. 7-Amount of $Ca(OH)_2$ in the paste [pozzolana-C_3A-$CaSO_4$·$2H_2O$-$Ca(OH)_2$]

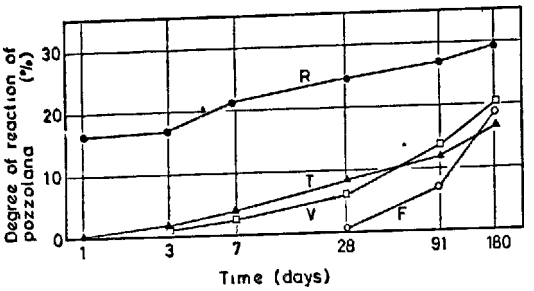

Fig. 8-Degree of reaction of pozzolana in the paste [pozzolana-C_3A-$CaSO_4 \cdot 2H_2O$ -$Ca(OH)_2$]

ed by DSC-TG are shown in Fig. 7. In Kanto loam mixed sample $Ca(OH)_2$ was completely consumed within one day by vigorous formation of ettringite. The degree of reaction of Kanto loam attained to 16% even at one day (Fig. 8.). In the other samples, consumption of $Ca(OH)_2$ attributed to the formation of C_4AH_{13} and solid solution of $C_3A \cdot (CaSO_4, Ca(OH)_2) \cdot H_{12}$. The solid solution tends to decompose to monosulfate hydrate and C_3AH_6 when the concentration of $Ca(OH)_2$ is lowered. In Beppu white clay mixed sample, C-S-H was formed by pozzolanic reaction in fairly early stage and decomposition of hexagonal solid solution to monosulfate hydrate and C_3AH_6 was retarded as it contained much reactive opal and less alkalies. In Furue shirasu mixed sample containing much alkali, conversion of $C_3A \cdot (CaSO_4, Ca(OH)) \cdot H_{12}$ to monosulfate hydrate and C_3AH_6 occured at 28 days in spite of coexisting large amount of $Ca(OH)_2$. The pozzolanic reaction started at 28 days as in Fig. 7., C-S-H, however, was not observed until 91 days.

7. MECHANISM OF THE HYDRATION IN THE SYSTEM POZZOLANA-C_3A-$CaSO_4 \cdot 2H_2O$-$Ca(OH)_2$

Referring the before-mentioned experimental results and the idea of Skalny, Jawed and Taylor (4) on the hydration of C_3A, the mechanism of the hydration in the system pozzolana-C_3A-$CaSO_4 \cdot 2H_2O$-$Ca(OH)_2$ is considered to be as follows:

On contact with water, C_3A is protonially attacked by H_3O^+ formed by the dissociation of water releasing Ca^{2+} and leaving amorphous Al rich layer on C_3A grain surface. Amorphous layer is expanded by osmotic pressure and forms slight clearance between hydrated C_3A grain and itself. This clearance is filled with AlO_2^- rich solution. There exists Ca^{2+}, SO_4^{2-} rich solution near at the outside of the layer brought by the coproceeding dissolution of calcium sulfate and calcium hydroxide. Ca^{2+} is adsorbed on the amorphous Al rich layer on the surface of C_3A. The grain charges positively and the active sites on the surface of C_3A decreases. Therefore, hydration of C_3A is stopped temporarilly. SO_4^{2-} is adsorbed on the surface of positively charged grain and play a part of blocking against protonic attack of hydronium ion. Amorphous Al rich film is brocken at the weakest point by osmotic pressure. From the openings Ca^{2+} and SO_4^{2-} introduced into inner side of film.

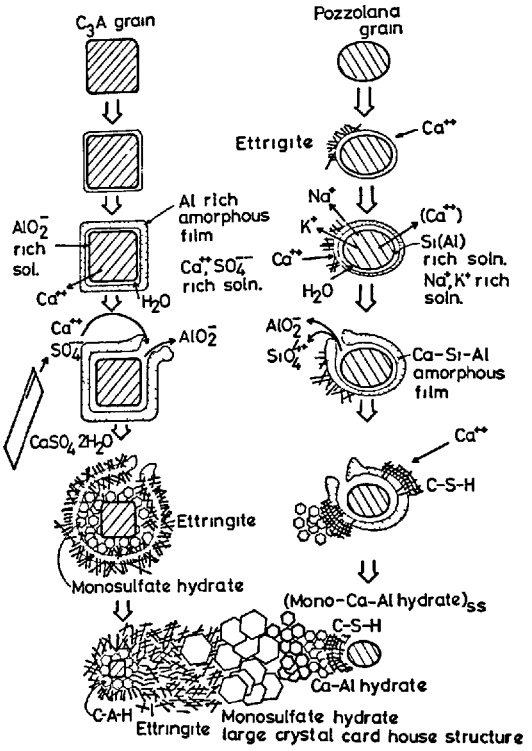

Fig. 9-Schematic explanation of the mechanism of hydration in the system pozzolana-C_3A under the existence of $Ca(OH)_2$ and $CaSO_4 \cdot 2H_2O$

AlO_2^- moves towards outer side of film and ettringite precipitates on both sides of film. On inner side of film, monosulfate hydrate often precipitates as SO_4^{2-} is apt to be in shortage. Monosulfate hydrate on the inner side is generally small in size because of the narrow precipitation space. Precipitated hydrates have high crystallinity, so it is easy for Ca^{2+}, AlO_2^-, SO_4^{2-} etc. to diffuse through the hydrate layer covering on the C_3A grain. The porous ettringite layer is broken by the expansion of itself to make the contact of water to C_3A easy.

Hydration of C_3A proceeds repeating above mentioned process as one cycle. When solid $CaSO_4 \cdot 2H_2O$ consumed completely and concentration of SO_4^{2-} lowers, monosulfate hydrate or solid solution of monosulfate hydrate and C_4AH_{13} precipitates on the outside of film. Void in the paste outside the grain is usually large so hexagonal monosulfate hydrate or its solid solution precipitate as large crystal towards large void to build the well-known card house structure.

Ettringite once formed convert to monosulfate hydrate or its hexagonal solid solution. The time of conversion of hexagonal solid solution to cubic C_3AH_6 depends upon the concentration of alkali ion.

Negatively charged grains of pozzolana, on the other hand, adsorb Ca^{2+} formed by the hydration of C_3A, $CaSO_4 \cdot 2H_2O$ and $Ca(OH)_2$ on its surface. By presenting the sites of precipi-

tation of ettringite formed by the hydration of C_3A, pozzolana accelerates the hydration of C_3A.

Protonic attack of water against pozzolana grain proceeds gradually and Na^+ and K^+ begin to dissolve into water from several minutes to one day after mixing with water. According to the dissolution of Na^+ and K^+ into water, solubility of Ca^{2+} decreases and Ca^{2+} precipitates as $Ca(OH)_2$ to lower OH^- concentration in liquid. As solubility products in liquid are constant, water dissociate to compensate the decrease of OH^- concentration and produce hydronium ion which result in accelerating the protonic attack.

Si and Al rich amorphous layer swell gradually and makes slight clearance between pozzolana grain and itself. The clearance filled with Si, Al and alkalies rich solution. Thereafter the film is broken by the osmotic pressure, SiO_4^{4+} and AlO_2^- in clearance diffuse through the openings. SiO_4^{4-} and AlO_2^- near at the outside of film precip tate as ettringite, monosulfate hydrate, Ca-Al hydrate and C-S-H on the surface film of the outside of pozzolana grain or on the surface hydrate layer of C_3A grains according to the concentration of Ca^{2+} and SO_4^{2-} in the liquid. As the rate of diffusion of SiO_4^{4-} is slow and the concentration of Ca^{2+} is rather high even at the neighbour of pozzolana grain, C-S-H precipitates restrictively on the outside surface of the amorphous film enveloping pozzolana grain. C-S-H is observed in the paste containing negatively charged acidic pozzolana with low alkali and high SiO_2.

Concentration of SO_4^{2-} in the liquid near the pozzolana grain is low, so the nearest hydrate to the pozzolana grain consists mainly of Ca-Al hydrate and towards outside the solid solution of Ca-Al hydrate and monosulfate hydrate and monosulfate hydrate precipitate in this order. Ettringite, precipitated in the early stage of hydration, is not observed in the later stage.

When alkalies do not exist, destruction of amorphous Si, Al rich film enable Ca^{2+} to move into inside of the film from the openings and to precipitate C-S-H, Ca-Al hydrate on pozzolana grain and filled the clearance. Therefore no void is observed between pozzolana grain and hydrates in this case.

Pozzolana is a mixture composed of alkali containing minerals and glasses and those without alkali. In paste hydration, some places become rich in alkali and others are poor. Therefore, the hydrates produced in alkali rich region tend to be stripped off from pozzolana surface and the hydrates produced in alkali poor region attached closely to pozzolana grain. The glass such as in fly ash contains homogeneously much alkali, so the typical stripping off of the hydrates from pozzolana grain is often clearly observed.

8. CONCLUSION

(1) In the system pozzolana-C_3A-$CaSO_4 \cdot 2H_2O$, regardless of the presence of $Ca(OH)_2$, initial hydration of C_3A, formation of ettringite and monosulfate hydrate were accelerated by the addition of pozzolana.

In the system pozzolana-C_3A, initial hydration corresponding to the formation of Ca-Al hydrate was retarded by the addition of pozzolana.

$Ca(OH)_2$ acted as retarder in above-mentioned system.

Pozzolana tend to lower the degree of hydration of C_3A in later age.

(2) Alkalies in liquid phase from pozzolana, quite different from the case of pozzolana-water suspension, increased in concentration with age. Alkalies accelerated the conversion of hexagonal $C_3A \cdot (CaSO_4, Ca(OH)_2) \cdot H_{12}$ to cubic C_3AH_6 by decreasing the stability of hexagonal solid solution.

(3) There were no essential difference of the kind of hydrate and process of hydration with or without pozzolana. Besides Ca-Al hydrate, ettringite, monosulfate hydrate, hexagonal solid solution; type II C-S-H and C_3AH_6 were produced accoding to the composition of used pozzolana.

(4) Structure of hardened paste was more porous than that of pozzolanic cement and pozzolana-C_3S. Formation of C-S-H contributed to the densification of hardened paste, while aluminate hydrates showed less contribution.

(5) TEM and SEM observation give us valuable information to understand the mechanism of the hydration in the system pozzolana-C_3A-$CaSO_4 \cdot 2H_2O$-$Ca(OH)_2$. The hydration of this system proceed through the formation of amorphous surface layer by leaching out of Ca^{2+} and/or alkalies ions, swelling and destruction of surface film by osmotic pressure and precipitation of hydrate on the surface of the film. The alkalies in pozzolana play an important role not only in the hydration reaction but also in the formation of the texture of hardened paste.

REFERENCE

1.- H. UCHIKAWA, S. UCHIDA and Y. MIHARA, In preparation, "Quantitative analysis of $Ca(OH)_2$ and hydrate in cement paste by DSC-TG under argon atomosphere"

2.- G. A. C. M. SPIERINGS and H. N. STEIN (1976), "The influence of Na_2O on the hydration of C_3A. I. paste hydration" Cem. Conc. Res., 6, 265-272.

3.- G. A. C. M. SPIERING and H. N. STEIN (1976), "The influence of Na_2O on the hydration of C_3A. II. suspension hydration" Cem. Conc. Res., 6, 487-496.

4.- J. SKALNY, I. JAWED and H. F. W. TAYLOR (1978), "Studies on hydration of cement-recent developments", World Cement Technology, 2, 183-195.

Long-term experiments on the neutralisation of concrete mixed with fly ash and the corrosion of reinforcement

Experiences à long terme sur la neutralisation du béton avec des cendres volantes, ainsi que sur la corrosion de l'armature.

R. TSUKAYAMA, Dr. Director, Division of Clean Set, Nihon Cement Co., Ltd.
H. ABE, Dr. Head, Concrete Structural Section, Central Research Institute of Electric Power Industry and
S. NAGATAKI, Dr., Associate Professor, Dept. of Civil Eng. Faculty of Eng. Tokyo Institute of Technology, Japon.

RESUME : Il est évident que beaucoup d'avantages peuvent être tirés des cendres volantes quand elles sont employées comme ajouts dans le béton. Cependant, il est aussi signalé que la réaction pouzzolanique des cendres volantes produit une réduction de l'alcalinité et par conséquent accélère la neutralisation du béton et par conséquent la corrosion des armatures du béton.

Cette étude rend compte des résultats des expériences faites depuis 1963 pour confirmer ces phénomènes. Ces expériences ont porté sur le comportement à long terme de bétons confectionnés avec ou sans cendres volantes.

Ces expériences ont été faites en faisant varier les proportions de ciment et de cendres volantes, la nature du ciment, le dosage en eau, la valeur du slump et les conditions de conservation des éprouvettes. Des expériences ont aussi été faites à l'extérieur, dans dix emplacements répartis dans tout le Japon, et même dans des sites marins, ou des sites exposés aux embruns ou aux courants marins.

SUMMARY : It is clear that numerous advatages may be obtained when fly ash is being used as an admixture in concretes. However, it is also pointed out that the pozzolanic reaction of fly ash leads to a reduction in alkalinity and hence accelerates the neutralization of the concrete as well as the corrosion of the reinforcing bar embeded in the concrete.

This paper reports the results of experiments carried out since 1963 to confirm these phenomena of concretes with and without fly ash in the long term.

The experiments were carried out for different mix proportions by changing the cement factor, replacement ratio of fly ash, water-cement ratio and the value of slump and under different conditions of curing indoors and outdoors. The outdoor experiments were performed at 10 selected places over the whole country of Japan including places under the sea and places affected by winds and currents.

INTRODUCTION

Fly ash demonstrates a so-called finely-divided powder effect and a pozzolanic effect to improve workability of concrete, reduce heat of hydration, improve watertightness and increase long-term strength [1], [2], and has a proven record of use as a concrete admixture for approximately 40 years.

While there are many advatages, it has been pointed out on the other hand that when fly ash is used the alkalinity of concrete is lowered due to reduction through pozzolanic reaction of free $Ca(OH)_2$ because of which neutralization of concrete is accelerated and reinforcing steel embedded is corroded [3], [4], [5].

In order to solve this problem, the Committee on Concrete of the Japan Society of Civil Engineers organized a Sub-Committee on Fly Ash and embarked on long-term research and testing in regard to neutralization of concrete mixed with fly ash. It has already been concluded and reported for the intermediate ages of 2 and 5 years that (i) water-cement ratio is the factor predominently governing depth of neutralization, and (ii) a constant relationship exists between 28-days compressive strength and depth of neutralization regardless of whether of not fly ash is added [6], [7]. In the present report, a comprehensive examination is made of the influence of fly ash on neutralization of concrete based on results at the age of ten years.

TEST PROGRAM

Tests were performed divided into the 3 series described below and neutralization depths and rusting of reinforcing bars were measured at the ages of 2 years, 5 years and 10 years.

Series I

Unit cement-fly ash content, slump, fly ash replacement ratio and type of cement were selected as factors and tests in commom were performed at 13 laboratories on the influences of mix proportions. Cement and fly ash used were the same at seven laboratories and at other six laboratories, fly ash were supplied by each six manufactures while cement were the same.

Unit cement-fly ash content	: 250, 290, 330 kg/m³
Slump	: 5, 15 cm
Fly ash replacement ratio	: 0, 15, 30 %
Cement	: normal cement, moderate heat cement

Series II

Series II and III were tests planned with the purpose of supplementing points which could not be clarified with Series I. In Series I, after casting specimens, testing was done with the period of curing in water prior to exposure in air 14 days, but in Series II, curing periods were varied between 1 and 91 days before exposure outdoors and indoors to find the influence of the period of curing in water in neutralization.

Period cured in water	: 1, 7, 28, 91 days
Exposure conditions	: indoors, outdoors
Unit cement-fly ash content	: 250, 290, 330 kg/m³
Fly ash replacement ratio	: 0, 30 %

Series III

In this series, specimens cast at the same place were exposed to outdoor conditions scattered at various locations troughout Japan to examine regional influences on neutralization. At one region, specimens were submerged in seawater and the effects on neutralization and rusting were examined.

Specimens

The specimens for neutralization tests were cylinders of 15-cm diameter by 30 cm height with 3 reinforcing bars of 9-mm diameter embedded at the locations indicated in Fig. 1 for depths of cover of 2, 3 and 5 cm.

Measurement of Neutralization Depth

The cross sections at which neutralization was measured were the transverse cross sections 7 cm and 23 cm from the top surface, and the longitudinal cross section at the diameter of the middle portion obtained as a result of cutting at 7 and 23 cm. The specimens were dried after cutting, immediately sprayed with phenolphthalein, and colored (unneutralized) and neutralized portions were identified. The average neutralization depths at the various cross sections were calculated by the equations below [6], [7].

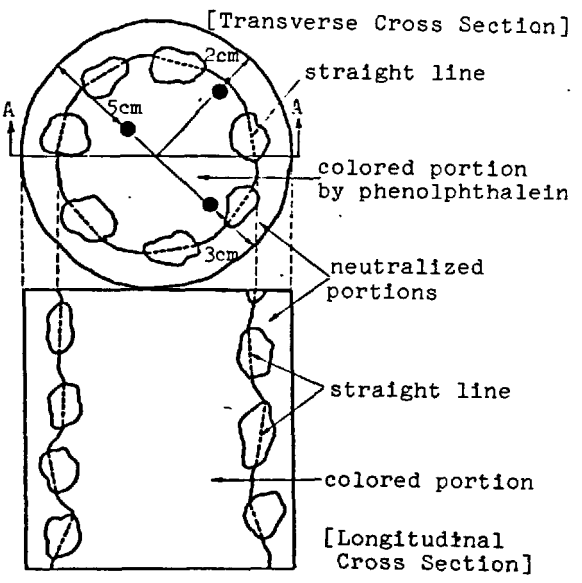

Fig. 1 - Specimen for Neutralization

Transverse Cross Section
Average Neutralization Depth
$= R - \sqrt{B/\pi}$ .....(A)

Longitudinal Cross Section
Average Neutralization Depth
$= (A-B)/2h$ .....(B)

where
B : area of colored portion
A : total cross-sectional area
R : diameter of specimen
h : height of specimen

Reinforcing bars were removed from concrete after measurement of neutralization depth, inspected for rusting, and rusted areas were measured.

TEST RESULTS

The average of the average neutralization depth of the two transverse cross sections determined by Eq. (A) and the neutralization depth determined by Eq. (B) was taken as the average neutralization depth of that specimen, and the examinations made by factor were as described below.

Concrete Mix Proportions

On examination of the relationships of unit cement-fly ash contents and fly ash replacement ration with neutralization depths for the case of 15-cm slump in Series I, the results were as shown in Fig. 2. Depth of neutralization was increased with decreased unit cement-fly ash content and increased fly ash replacement ratio, and especially, in case of such a lean mix as unit cement-fly ash content of 250 kg and replacement ratio 30%, depth of neutralization was large and the progress of neutralization was great at advanced age also. This was due, as previously said [8], to lowerling of the quality of concrete, in effect, the increase in water-cement ratio, and the same thinking may be applied to the influence of slump.

When moderate heat cement was used depths of neutralization were slightly larger or equal compared with normal cement. Other conditions being equal, uint water content is reduced when moderate heat cement is used, but

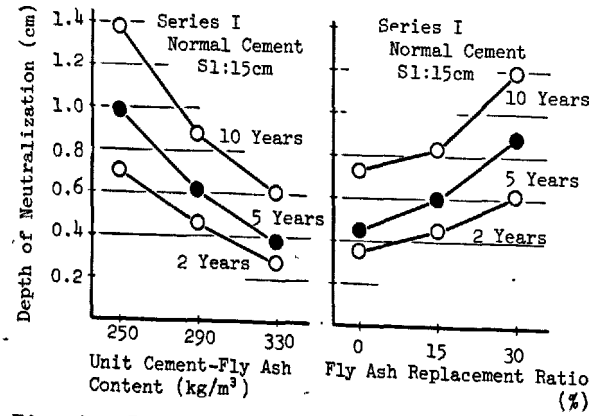

Fig. 2 - Relation between Mix Proportions and Depth of Neutralization

probably, due in part to slower initial strength gain, the result was that neutralization depths were roughtly equal.

Relation Between Water-Cement Ratio and Depth of Neutralization

That depth of neutralization has a correlation with water-cement ratio has been suggested by many researchers [9], and here, determining water-cement ratios from cement contents excluding fly ash and indicating the relationships with depth of neutralization for Series I and II together, the results were as shown in Fig. 3, and linear relationships were recognized. However, similarly to a previous report [6], the relationships were different depending on whether or not fly ash was adimxed. And in case of water-cement ratio of about 0.60 to 0.70, the depth of neutralization of concrete with fly ash was approximately 0.1 cm smaller at the age of two years and approximately 0.3 cm smaller at the age of ten years than that of concrete without fly ash. The main reasons for this probably are the pozzolanic reaction with free $Ca(OH)_2$ of particles of fly ash added resulting in densiflying the constitution and the acceleration of hydration due to the finely-divided powder effect.

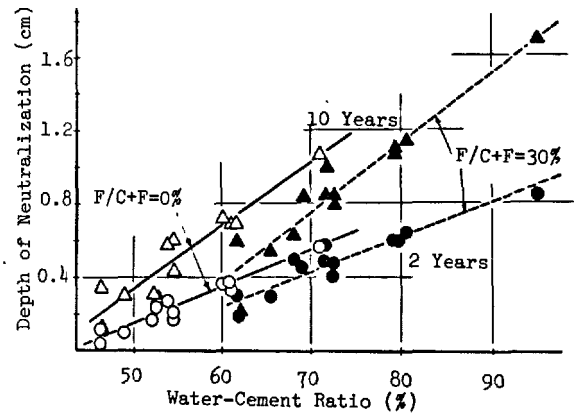

Fig. 3 - Relation between Water-Cement Ratio and Depth of Neutralization

Relation Between Compressive Strength and Depth of Neutralization

Since compressive strength has a correlation with water-cement ratio, and water-cement ratio and depth of neutralization have a linear relationship as described in the preceding section, it is thought the same thinking would apply regarding compressive strength also. Therefore, the depths of neutralization at a certain age were arranged according to the relationship with compressive strength at identical age of specimens cured under identical conditions. An example for 2-year age is shown in Fig. 4. Here, similarly to the case of water-cement ratio, the relationship is expressed by two roughly parallel straight lines with and without fly ash, and at identical compressive strengths the depth

of neutralization is 0.1 to 0.2 cm greater in case of admixture of fly ash. The reasons for this are that alkalinity of concrete is lower and initial strength gain smaller, and the result was the view that much of the neutralization occurs at a comparatively early stage [8] was substantiated.

On expressing depth of neutralization be the relationship with strength gained, as can be seen in the figure, it was possible to arrange the data with the same straight line even in cases of types of cement and exposure conditions being different.

The relationship between compressive strength at 28-day age and depth of neutralization is as shown in Fig. 5, and similarly to the previous report [6] the expression may be made by a straight line irrespective of the admixture of fly ash. However, in the case of using moderate heat cement where quality cannot be evaluated at 28 days, a straight line different from the one for normal cement is indicated, while in the case also of exposure conditions being different the relation cannot be expressed with the same straight line.

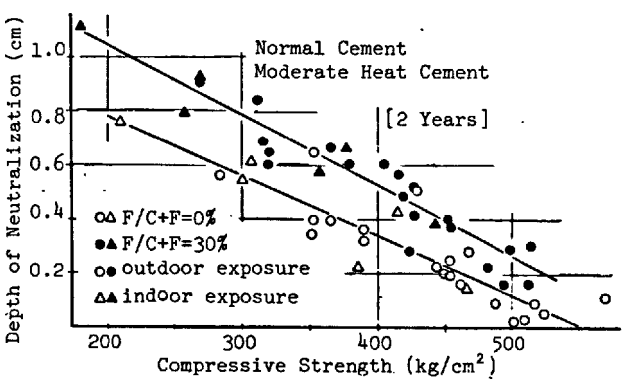

Fig. 4 - Relation between Compressive Strength and Depth of Neutralization

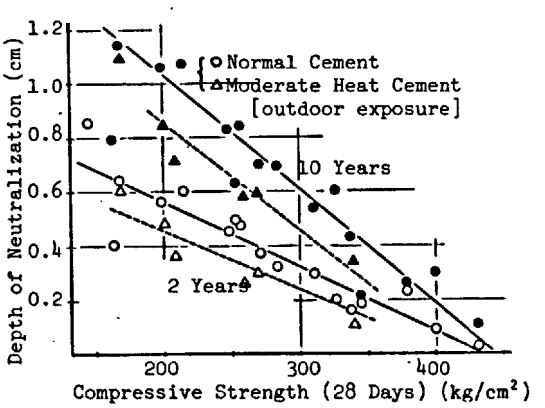

Fig. 5 - Relation between compressive Strength and Depth of Neutralization

Curing Condition

The influences of the period of curing in water on depths of neutralization in outdoor and indoor exposure were as shown in Fig. 6. In outdoor exposure, depth of neutralization was great in the case of curing period of 1 day, while the results for 7 to 91 days were of about the same degree. In effect, it is thought that if curing in warer is performed at the initial stage for about 7 days, there will subsequently be supply of water from rainfall and other sources so that hydration of cement and pozzolanic reaction continue to progress to densify the constitution. However, when curing in water is not performed, it is thought that since the supply of water is insufficient the hydration of cement is slow and neutralization progresses greagly at the initial stage.

In indoor exposure, since there is no supply of water, hydration of cement mainly occurs only during the period of curing in water, and even if some amount of pozzolanic reaction were to occur subsequently, it will be accompanied by reduction in alkalinity, and it is thought that the degree to which the constitution is made dense during the period of curing in water will greatly affect the subsequent progress of neutralization. However, for both outdoor and indoor exposure, the influence on depth of neutralization was seen during the earlier stage of up to 2-year age, with the progress of neutralization after 2 years being constant regardless of the period of curing in water.

Comparing indoor exposure with outdoor depths of neutralization of specimen cured indoor were considerably larger than that of outdoor, because there are many conditions disadvantageous indoor for preventing progress of neutralization such as the moisture condition (humidity) of concrete and concentration of carbon dioxide.

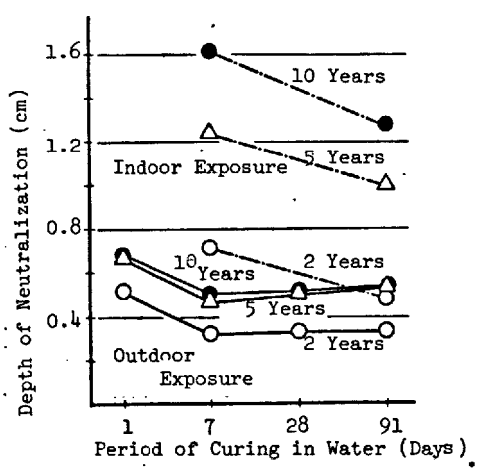

Fig. 6 - Relation between Period of Cruing in Water and Depth of Neutralization

Relation Between Age and Depth of Neutralization

With regard to the influence of age on depth of neutralization, there is a formula proposed that neutralization is proportional to the root of age [10], and a report that neutralization has a linear relation with the logarithm of age [9]. On arranging the depths of neutralization obtained in the present tests based on root of age and water-cement ratio, the equations below were respectively obtained for fly ash replacement ratio of 0% (w/c=0.45-0.6) and replacement ratio of 30% (w/c=0.6-0.95).

$$\text{Neutralization Depth (cm)} = (1.187w/c-0.493)\sqrt{t} \quad ...(F/C+F=0\%)$$

$$\text{Neutralization Depth (cm)} = (1.241w/c-0.597)\sqrt{t} \quad ...(F/C+F=30\%)$$

where

t : age

w/c : water-cement ratio

Regional Influence on Depth of Neutralization

The depths of neutralization of the same concrete exposed outdoors at various locations in Japan at ages of 2, 5 and 10 years shown in the form of a bar graph is Fig. 7. The differences in the climatic conditions of these locations are mainly in temperature and precipitation, and distinct differences according to region were not seen. The results at the one region where specimens were submerged in seawater showed ueutralization to be very small.

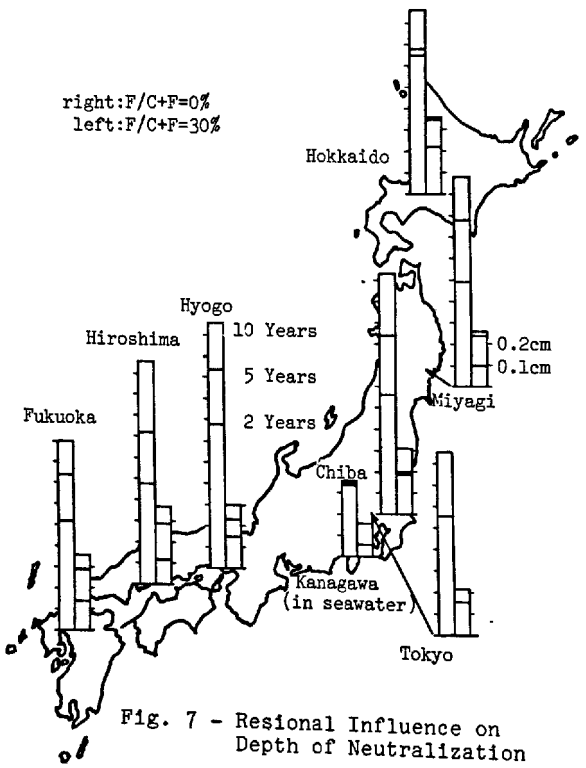

Fig. 7 - Resional Influence on Depth of Neutralization

Rusting of Reinforcing Bars

In outdoor exposure in Series II, at 2-year age there was no rusting of reinforcing bars at all, and rusting was produced at 5 and 10 years when neutralization had progressed. With the proportion of the specimens in which rusting of reinforcing bars occurred to the total number of specimens as the rusting rate the relation with water-cement ratio was found to be as shown in Fig. 8. The relation between degree of cover and rusting was distinct, and whenever neutralization had progressed to the vicinity of a reinforcing bar, rusting occurred in practically all cases.

Rusting of reinforcing bars in the specimens submerged in seawater was peculiar, where even at the age of 2 years when neutralization had hardly progressed, considerable rusting was seen on reinforcing bars with small depth of cover in lean mixes concrete specimen. The rusting was concentrated at the sides toward specimen surfaces in all cases, indicating that rusting of reinforcement is accelerated regardless of neutralization when there is infiltration of chloride ions.

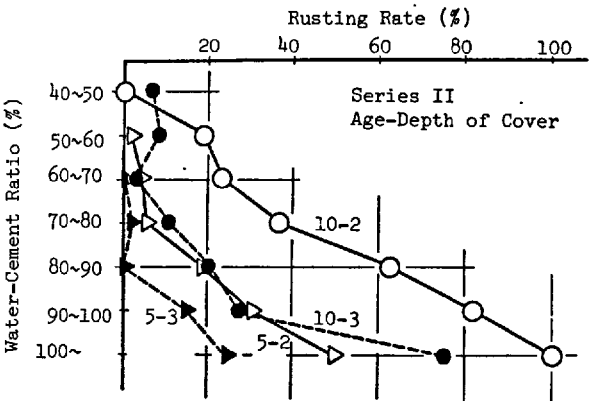

Fig. 8 - Relation between Water-Cement Ratio and Rusting Rate

Scanning Electron Microscope Examination of Fractured Surfaces of Concrete

In Series II, scanning electron microscope examinations were made of fractured surfaces of neutralized and unneutralized portions of concrete exposed for 10 years after curing in water for 91 days. The photographs are of fly ash particles scanned. For cases of exposure both outdoors and indoors, when curing in water had been adequately performed, and at the center portions of specimens where neutralization had not been produced, it may be seen that pozzolanic reaction had occurred between the free $Ca(OH)_2$ and fly ash particles and crystals were formed at the surfaces of the fly ash particles. On the other hand, at neutralized portions at the surface of concrete specimen there are no traces seen of reaction at the surfaces of fly ash particles, and particularly, the tendency for this was seen to be prominent for indoor conditions.

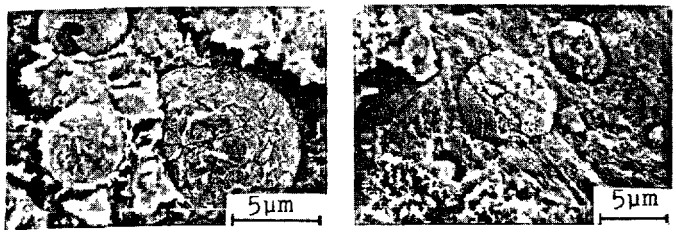

Indoor, Unneutralized. Outdoor, Unnuetralized.

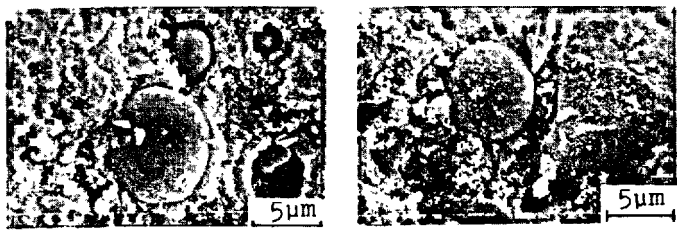

Indoor, Neutralized. Outdoor, Neutralized.

Photo. 1 - Scanning Electron Microscope Examination

CONCLUSIONS

Neutralization tests were carried out under various conditions on concretes containing fly ash as an admixture, and from the results obtained up to 10-year age, the following remarks may be concluded.

(1) Depth of neutralization has a relation with the quality of concrete, and a linear relationship is found to exist with water-cement ratio excluding fly ash. However, at identical water-cement ratio, neutralization is slightly decreased when fly ash is added. Further, it is possible to estimate depth of neutralization by the root of age and water-cement ratio.

(2) There is a given linear relationship between compressive strength at 28-day age and depth of neutralization reagrdless of fly ash addition when type of cement and exposure conditions are identical. On the other hand, there is a constant linear relationship irrespective of other conditions between compressive strength at the time of measurement of neutralization and depth of neutralization for fly ash replacement ratios of 0% and 30%.

(3) The period of curing in water after casting specimens has a great influence in case of indoor exprsure, and neutralization is increased unless adequate curing is perfomed. In the case of outdoor exposure, if curing in water of about one week is performed, this appears to be adequate against neutralization. However, in all cases, the period of curing in water has no influence on the progress of neutralization after 2-year age.

(4) In ordinary outdoor air in Japan, there is little regional difference in the influence on depth of neutralization. There is a distinct cause-and-effect relationship seen between progress of neutralization in air and rusting of reinforcing bars.

ACKONWLEDGEMENTS

These tests were performed under the direction of the Sub-Committee on Fly Ash of the Japan Society of Civil Engineers, and the authors wish to express their deepest gratitude to the Chairman, Dr. Masatane Kokubu, and members of the committee for their untiring guidance during the testing.

REFERENCES

1.- K. Yamazaki, "Fundamental Studies of the Effects of Mineral Fines on the Strength of Concrete", Japan Society of Civil Engineers, No. 85, Sep. 1962 (in Japanese)
2.- N. Kawade and A. Nemoto, "On Early Hydration Phenomenon of Cement as Mixed with Fly Ash", Proc. 22nd General Meeting, Cement Association of Japan, 1968, (in Japanese).
3.- Anon., "Relationship of Fly Ash and Corrosion", LR47-60, ACI Journal, Sept. 1950.
4.- J. P. Ryan, "Relationship of Fly Ash and Corrosion", LR47-60, ACI Journal, Feb. 1951.
5.- M. Hamada, "Neutralization of Concrete and Corrosion of Reinforcing Steel", Fifth International Symposium on the Chemistry of Cement (5th ISCC), Tokyo, 1968.
6.- H. Abe, S. Nagataki and R. Tsukayama, "Written Discussion on Fly Ash and Fly Ash Cement", 5th ISCC, Tokyo, 1968.
7.- Japan Society of Civil Engineers, "Long Term Study on Neutralization and Corrosion of Reinforcing Steel of Concrete with Fly Ash", Concrete Library No. 20, 1960, (in Japanese).
8.- M. Kokubu and S. Nagataki, "Carbonation of Concrete Correlating with the Corrosion of Reinforcement in Fly Ash Concrete", Proc. Symposium on Durability of Concrete, RILEM, Final Report, Part II, 1969.
9.- A. Meyer, "Investigation on the Carbonation of Concrete", Supplementary paper, III-52, 5th ISCC, Tokyo, 1968.
10.-K. Kishitani, " Consideration on Durability of Reinforced Concrete", Transactions of the Architectural Institute of Japan, No. 65, 1960, (in Japanese)
11.-R. Kondo, M. Daimon and T. Akiba, "Mechanisms and Kinetics of Carbonation of Hardened Concrete", Supplementary paper, III-116, 5th ISCC, Tokyo, 1968.
12.-M. Kokubu, "Fly Ash Cement", IV-105, 5th ISCC, Tokyo, 1968.
13.-M. Kokubu and J. Yamada, "Fly Ash Cements", Principal paper, 6th ISCC, moscow, 1974.

Appréciation de l'activité pouzzolanique des constituants secondaires

Appreciation of pozzolanic reactivity of minor components.

M. RAVERDY, Chef de Groupe "Liants" à la Section des Produits Nouveaux au Département des Bétons et Métaux, Laboratoire Central des Ponts et Chaussées, Paris,
F. BRIVOT, Chimiste au L.C.P.C., Paris,
A.M. PAILLERE, Docteur es Sciences, Chef de Section "Produits Nouveaux" L.C.P.C., Paris, et
R. DRON, Docteur Ingénieur, L.C.P.C. Paris, France.

RESUME : Le taux de réaction pouzzolanique peut être déterminé par un essai accéléré consistant en un contact pendant une nuit, au voisinage de l'ébullition, de matière pouzzolanique et de chaux en suspension dans l'eau (essai Chapelle). La dispersion des résultats inhérente à cette méthode est réduite de façon décisive par emploi du chauffage au bain marie et de l'agitation magnétique. Les résultats sont corrélés à la teneur en phase vitreuse.

L'étude approfondie des principales caractéristiques des mortiers confectionnés avec des ciments à la pouzzolane permet de montrer le bien fondé de cette méthode.

SUMMARY : The rate of pozzuolanic reaction can be determined by an accelerated test consisting in having bath pozzuolanic materials and lime suspended in water which is rearly boiling (Chapelle test). The result dispersion inherent in this method is considerably reduced by water-bath heating and magnetic stirring the results are correlated with the ratio of vitreous phase.

The elaborated study of principal characteristics of mortars obtained with cements containing pozzuolanic materials shows that this method is well-founded.

INTRODUCTION

L'existence en France de ciments CPJ composés de Portland et de constituants secondaires, à effet plus ou moins pouzzolanique, dont le dosage peut atteindre jusqu'à 35 % pose le problème de leur réactivité ou propriétés hydrauliques dont va dépendre l'activité réelle du ciment dont ils constituent les ajouts au clinker.

Les matériaux pouzzolaniques français peuvent provenir de trois origines différentes :

- volcanique ou éruptive,
- naturelle,
- artificielle.

Ces matériaux sont désignés généralement par le terme pouzzolane. Terme qui englobe les cendres volantes ou fondues.

Selon la nature et provenance du matériau pouzzolanique les deux caractéristiques essentielles des pouzzolanes qui sont, la fixation de la chaux en présence d'eau et l'aptitude à constituer des produits à propriétés liantes, sont plus ou moins marquées. Il importe donc à l'utilisateur de connaître avec le maximum d'exactitude la réactivité du matériau utilisé afin de déduire les performances que le ciment CPJ, constitué avec lui, pourra atteindre à une échéance donnée.

En effet, le supplément apporté par le matériau pouzzolanique aux qualités hydrauliques du clinker ne survient qu'à des échéances relativement longues 6 mois, 1 an ou plus. Dès lors, il est souhaitable de connaître de la façon la plus certaine possible, et ceci avant utilisation, les possibilités offertes par le ciment à la pouzzolane.

Le problème étant posé au niveau du ciment, il s'agissait de pouvoir déterminer à partir d'un ciment contenant une pouzzolane, au sens français du terme, l'activité pouzzolanique du constituant secondaire introduit dans le ciment CPJ et de trouver la relation existante entre cette"activité" et les caractéristiques à long terme du mortier ou béton hydraulique correspondant.

La recherche a donc été menée d'une part du point de vue analytique sur la mise au point d'une méthode visant à déterminer l'activité pouzzolanique du constituant secondaire présent dans les ciments CPJ et d'autre part du point de vue physique sur l'étude des caractéristiques mécaniques à long terme des mortiers confectionnés avec ces ciments.

Essais chimiques

Parmi les méthodes chimiques proposées pour estimer l'activité des matières pouzzolaniques, celle qui fut imaginée en 1958 par J. CHAPELLE (1) est particulièrement séduisante par son principe et sa rapidité de réponse. Elle permet théoriquement de caractériser une pouzzolane à sa finesse d'utilisation par le taux de réaction de la chaux, au terme d'un temps de contact standardisé (généralement 16 heures), la réaction étant accélérée par élévation de la température (100°C).

On a parfois opposé au principe même de cette détermination l'argument selon lequel les hydrates qui se forment dans ces conditions n'ont ni la même nature, ni la même solubilité que ceux qui se forment à température ordinaire. Cette objection serait valable si la cinétique de la réaction était gouvernée par la précipitation des hydrates. Or, l'étape limitante de la réaction pouzzolanique est en réalité l'attaque hydroxylique de la matière, et le flux de dissolution, c'est-à-dire la quantité d'éléments acides passant en solutions par unité de surface et par unité de temps et le reflet direct de la réactivité de la pouzzolane. L'étape suivante de précipitation des hydrates, quels qu'ils soient, est un processus rapide, qui en tout état de cause ne peut que suivre le rythme de la dissolution.

Le mode opératoire d'origine de la méthode Chapelle est le suivant :

Dans un erlenmeyer contenant 200 ml d'eau distillée débarrassée de CO_2, on met 1 g de matériau présumé à action pouzzolanique, broyé à la finesse du ciment et 1 g de chaux. On porte à ébullition pendant 16 h. Pour éviter que l'eau ne se perde par évaporation, on dispose au dessus de l'erlenmeyer un tube réfrigérant surmonté d'une garde à CO_2, (solution de soude ou chaux sodée). Après refroidissement, on dose la chaux qui n'a pas réagi, en présence de sucre.

Contrastant avec l'élégance du principe, la dispersion des résultats est assez décevante et, dans ces conditions opératoires, ne peut être réduite que par une stantardisation fastidieuse de tous les facteurs : mode de chauffage, règlage de celui-ci, forme et matière du récipient, corrections de blanc, etc...

Les causes de cette variabilité sont de trois ordres:

- L'agitation de la suspension résulte de là seule ébullition et n'est par conséquent pas reproductible. Si elle est trop faible, la matière sédimente. Si elle est trop forte, il se produit des projections qui forment un dépôt en anneau sur les parois situées au dessus de la surface.

- Il existe un gradient de température au niveau de l'interface paroi-suspension, qui provoque la formation d'un tartre, dont la matière est soustraite à la réaction et qu'il est difficile de détacher en fin d'opération.

- On évite difficilement toute carbonatation car au sommet du réfrigérant, l'eau refroidie est totalement décarbonatée et donc avide de CO_2. Malgré la présence d'une garde à CO_2, par suite de l'importance du reflux et l'effet étant cumulatif, au bout de 16 heures la quantité de CO_2 entraîné est loin d'être négligeable. Par ailleurs, l'essai à blanc est majoré en raison d'une légère attaque du verre.

Nous sommes parvenus à réduire de façon radicale la variabilité en agissant sur ces causes de dispersion la première précaution consistant en l'emploi de fioles en inox, qui élimine l'attaque du récipient.

L'artifice principal réside dans le fait que la réaction a lieu dans un récipient hermétiquement fermé, placé dans un bain-marie à ébullition d'eau. Le milieu est donc porté à 100°C mais il ne bout pas. Pour éviter la mise en pression, on porte préalablement la suspension à l'ébullition sur un bec bunzen avec toile métallique, on retire prestement du feu et on ferme aussitôt par un bouchon d'élastomère siliconé. On place alors le récipient lesté dans un bain marie

d'eau à ébullition, conçu de telle façon qu'il permette l'agitation magnétique (l'inox est perméable aux champs magnétiques). Il n'y a de cette façon ni dépôts, ni projection, ni entartrage puisqu'il n'y a pas de gradient de température, ni carbonation puisque le récipient est hermétiquement fermé.

Lorsqu'on arrête la réaction, on refroidit le récipient sous un courant d'eau, sans l'ouvrir. L'intérieur se met donc en dépression et on fait pénétrer l'air en déformant le bouchon.

DIPOSITIF UTILISÉ POUR L'ESSAI CHAPELLE MODIFIÉ.

Figure 1

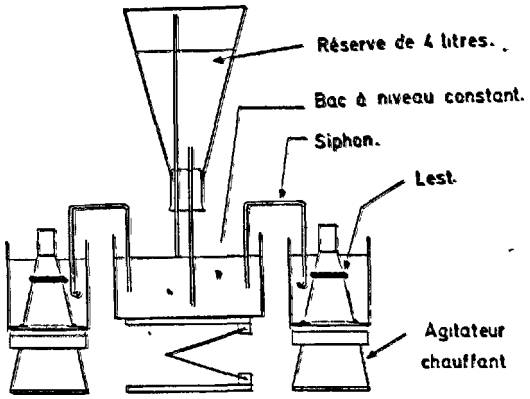

Le montage que nous avons utilisé (Fig. 1) répond aux impératifs requis. Il n'est toutefois pas superflu de signaler que sa réalisation en verre et la mise en oeuvre de masses d'eau bouillante et de récipients chauds requièrent de sévères précautions d'utilisation pour éviter les accidents.

La détermination de l'activité pouzzolanique des constituants présents dans les ciments a été menée en parallèle à l'aide de l'essai Chapelle modifié tel qu'il a été décrit précédemment et par détermination aux rayons X de la phase vitreuse.

La figure 2 donne la relation existant entre la quantité de CaO consommée et le pourcentage de phase vitreuse.

Il apparaît ainsi qu'il existe une bonne corrélation entre les 2 mesures et les deux méthodes utilisées.

Ainsi donc dans le présent exposé, on s'est limité à relier l'activité du constituant secondaire déterminé à partir de la quantité de chaux consommée à diverses caractéristiques des mortiers.

Essais physiques

L'étude a été menée sur 6 ciments industriels CPJ constitués par des pouzzolanes (Z) ou des cendres (C) et sur 5 pouzzolanes (Bizac - Volvic - Dômes - Paugnat Cinérite), une cendre volante et une cendre fondue. Avec ces sept matériaux à effet pouzzolanique, on a confectionné au laboratoire, 63 ciments à partir de trois clinkers différents dont les teneurs en C_3A étaient 1,5 - 9,5 et 14 %. Pour chacun des constituants secondaires, on a utilisé les pourcentages de 10, 20 et 35 % du poids de clinker. Après broyage à la finesse Blaine 9000 cm2/g le constituant secondaire a été mélangé dans les proportions indiquées précédemment à chacun des clinkers broyés à une finesse de 3200 cm^2g.

Figure 2

CaO consommée en fonction des % de phases vitreuses des pouzzolanes utilisées dans les ciments CPJ industriels et CPJ fabriqués en laboratoire

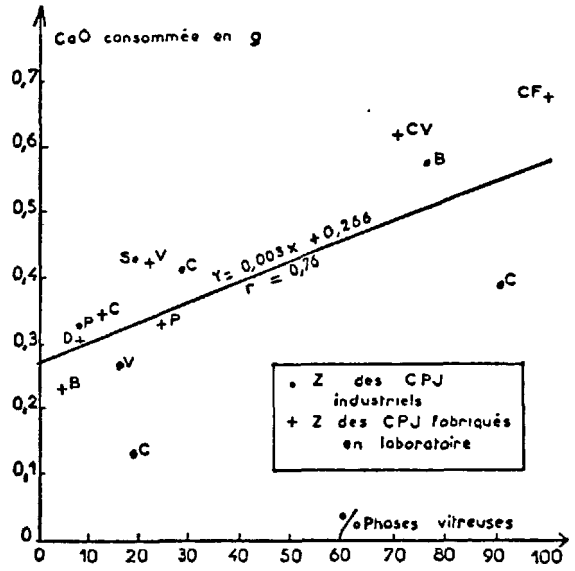

La figure 3a donne la courbe granulométrique des diverses pouzzolanes et cendres après broyage, ainsi que celles des 3 ciments utilisés dans les mélanges.

Figure 3 A — COURBES GRANULOMÉTRIQUES — Figure 3 B

DÉTERMINÉES AU GRANULOMÉTRE A LASER

CLINKERS N°1.2.3 et différentes Pouzzolanes (Z) — CPJ (90 % de Clinker N°1 et 10 % de Z)

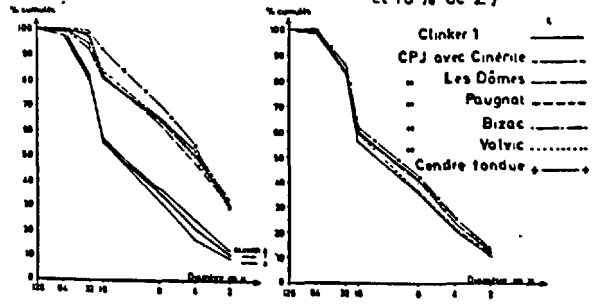

Les figures 3b, 3c et 3d représentent les courbes granulométriques des ciments CPJ constitués avec le clinker n° 1 à 1,5 % de C_3A.

On constate ainsi que pour 10 % d'ajouts il n'y a pratiquement pas de différence granulaire entre le ciment d'origine et le CPJ reconstitué. A partir de 20 %, l'augmentation du pourcentage d'éléments inférieurs à 16 µ croît en fonction du pourcentage de constituants secondaires. Cette remarque s'applique également aux deux autres CPJ à C_3A plus élevé et aux ciments indus-

triels utilisés dans la recherche.

Figure 3 C

CPJ (80% de Clinker N°1 et 20% de Z)

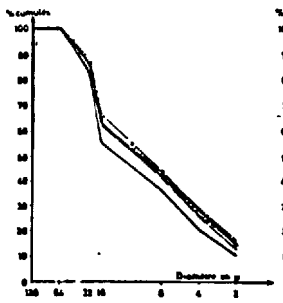

Figure 3 D

CPJ (65% de Clinker N°1 et 35% de Z)

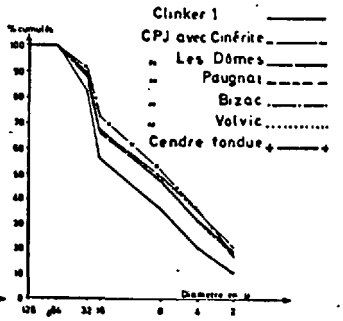

Le pouvoir hydraulique ou liant des constituants secondaires utilisés, se traduisant sur mortier par un accroîssement plus ou moins marqué des résistances, il va de soi que plus une pouzzolane ou cendre est réactive, plus cet accroîssement est élevé et plus son échéance est rapprochée de la date de fabrication.

L'étude comparative des mortiers ISO confectionnés avec des CPA et les mêmes CPA additionnés de 10 à 35% de Z ou de C (CPJ industriels et de laboratoire) montre que quelque soit la quantité de CaO consommée mesurée, aucun ciment CPJ ne conduit avant 28 jours à des résistances du mortier supérieures à celles des témoins CPA. A 28 jours, les cendres volantes et fondues associées à des ciments à teneur en C_3A > à 8 % ont des résistances supérieures à celles du témoin (Fig. 4a, 4b, 4c, 4d - Tableau I).

Résistances à la compression en fonction de l'age et de la CaO consommée mesurée à l'essai Chapelle modifié

CPJ (à base de Z) industriels

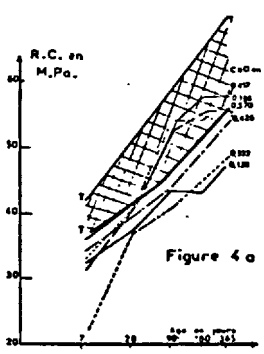

Figure 4 a

CPJ N°1 avec clinker à 15% C_3A et 20% de Z ou C

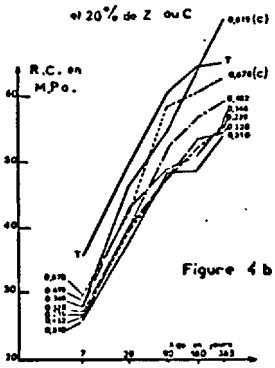

Figure 4 b

Si l'on étudie l'évolution des résistances des ciments à partir de la progression de celles du mortier ISO aux échéances X supérieures à 28 j, on a :

pour les ciments aux pouzzolanes :
$R_Z = R_{ZX} - R_{Z28}$

et pour les ciments CPA :
$R_T = R_{TX} - R_{T28}$.

R = Résistances à la compression du mortier
X = Age du mortier aux échéances de 180 j - 1 an.

La valeur $R_Z - R_T = (R_{ZX} - R_{Z28}) - (R_{TX} - R_{T28})$ renseigne sur la progression du pouvoir hydraulique des pouzzolanes.

CPJ N°2 avec clinker à 9% C_3A et 20% de Z ou C

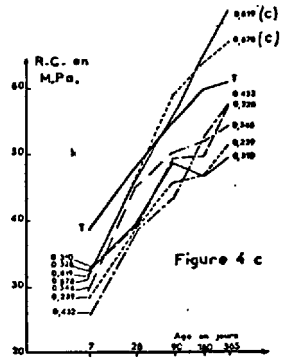

Figure 4 c

CPJ N°3 avec clinker à 14% C_3A et 20% de Z ou C

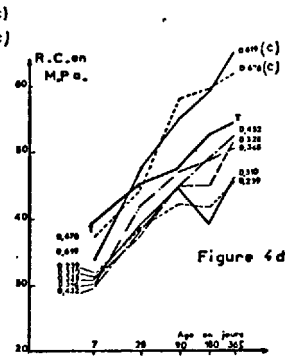

Figure 4 d

TABLEAU N° 1 - RESISTANCES A LA COMPRESSION DES CIMENTS CPJ FAITS EN LABORATOIRE

RESISTANCES A LA COMPRESSION EN M.Pa.	CPJ N° 1					CPJ N° 2					CPJ N° 3				
	7 j	28 j	90 j	180j	1 an	7 j	28 j	90 j	180j	1 an	7 j	28 j	90 j	180j	1 an
TEMOIN	35,4	48,8	60,9	64,6	65,2	38,1	48,1	55,0	59,9	60,9	37,7	45,3	47,7	52,6	54,6
% de Z															
10% Pouzzolane VOLVIC	31,5	43,1	54,5	57,0	59,6	29,0	40,8	49,6	51,9	61,1	34,9	41,4	48,9	49,4	54,9
10% Pouzzolane BIZAC	29,0	41,9	54,5	55,6	57,1	31,9	43,7	50,4	54,1	54,6	31,5	44,1	45,9	51,2	49,4
10% Pouzzolane DOMES	29,5	44,1	56,7	57,3	56,5	31,9	45,0	53,4	53,4	54,4	33,4	43,9	49,1	45,8	51,1
10% Pouzzolane PAUGNAT	29,7	42,8	54,5	55,2	59,2	32,0	43,4	49,2	54,4	59,6	36,0	47,2	47,3	47,1	52,7
10% Cinérite	22,1	41,9	55,1	53,8	58,1	34,7	43,8	45,1	53,7	55,3	28,5	40,4	46,7	46,9	50,0
10% Cendres Volantes	29,7	46,1	57,3	57,8	58,7	36,3	46,4	59,2	63,4	66,1	39,3	46,7	52,6	57,8	64,7
10% Cendres Fondues	27,8	42,0	60,1	62,8	69,3	28,2	48,2	64,0	62,4	67,6	30,8	44,6	53,5	56,6	66,3
20% Pouzzolane VOLVIC	25,7	39,9	51,9	56,5	59,1	25,2	38,3	43,1	52,2	57,2	29,6	38,1	44,9	48,9	52,2
20% Pouzzolane BIZAC	26,2	39,5	46,7	52,2	55,3	28,0	38,6	45,8	46,8	51,5	31,4	38,4	42,0	41,7	45,5
20% Pouzzolane DOMES	25,5	37,9	48,3	48,7	54,0	32,4	39,4	48,5	46,4	49,3	30,6	38,7	44,3	39,0	46,1
20% Pouzzolane PAUGNAT	26,4	39,9	47,6	51,3	58,1	31,2	39,1	49,1	49,5	57,2	30,6	37,3	44,9	44,8	51,5
20% Cinérite	27,7	42,9	48,9	51,2	55,7	30,0	44,9	50,0	51,8	54,1	29,8	41,7	47,5	48,7	50,4
20% Cendres Volantes	27,3	46,1	54,6	64,1	74,2	31,6	45,2	55,3	64,5	72,5	34,3	47,0	54,9	58,4	64,9
20% Cendres Fondues	29,2	42,2	58,2	60,6	62,6	31,1	45,4	58,1	63,4	66,5	37,0	49,1	58,8	59,1	61,9
35% Pouzzolane VOLVIC	18,8	29,3	41,3	44,3	50,8	18,4	30,0	40,1	46,8	49,2	24,7	31,0	38,5	41,3	45,8
35% Pouzzolane BIZAC	20,2	30,1	36,4	38,0	44,7	21,2	30,5	36,7	41,1	40,7	25,9	30,3	36,1	35,7	38,7
35% Pouzzolane DOMES	20,2	30,1	38,7	39,0	42,6	21,2	31,7	39,5	38,0	41,6	26,3	33,1	35,0	35,2	35,4
35% Pouzzolane PAUGNAT	22,1	30,8	42,3	48,5	52,1	22,4	31,2	38,4	45,1	52,0	26,4	32,7	39,9	42,0	47,4
35% Cinérite	21,7	33,5	42,9	44,3	49,2	23,9	35,0	41,0	39,1	45,9	22,2	34,0	37,2	39,5	44,1
35% Cendres Volantes	19,0	32,9	49,9	57,8	62,5	21,7	38,5	49,7	60,2	60,7	29,4	39,5	53,5	58,8	59,8
35% Cendres Fondues	22,6	38,1	54,7	60,0	61,6	26,4	41,5	53,1	56,7	58,2	27,6	41,5	58,4	59,9	59,9

En reliant $R_Z - R_T$ aux valeurs de CaO consommée mesurée dans les divers ciments aux pouzzolanes, on peut connaître à partir du mortier confectionné avec les ciments CPJ la relation qui peut exister entre la progression du pouvoir liant du constituant secondaire et son activité pouzzolanique.

L'étude de la représentation graphique de $R_Z - R_T$ (Fig. 5a - 5b) pour différents âges en fonction de CaO consommée fait apparaître tout d'abord que, à 180 jours, la famille de pouzzolanes dont la CaO consommée est supérieure à 0,33 g a une progression des résistances supérieure à celle des témoins :
$R_Z - R_T$ 0.

A 1 an, les pouzzolanes à faible réactivité commencent à avoir des qualités liantes, certaines dont la CaO consommée est de > 0,25 présentent un $R_Z - R_T \geq 0$. Par contre, toutes choses étant égales par ailleurs, la gamme des valeurs négatives de cette différence se trouve réduite :

$R_Z - R_T$ passe ainsi de (- 6,5 0) à (- 4,0).

Ceci est vérifié autant sur les ciments industriels que sur ceux du laboratoire.

On peut donc estimer que les pouzzolanes à faible réactivité ne présenteront un pouvoir hydraulique qu'à partir d'un an.

Evolution de la relation Rz-RT à 180j et à 1an
en fonction de la CaO consommée.
CPJ industriels et CPJ fabriqués
en laboratoire a 20 et 35% de Z ou C.

Figure 5A

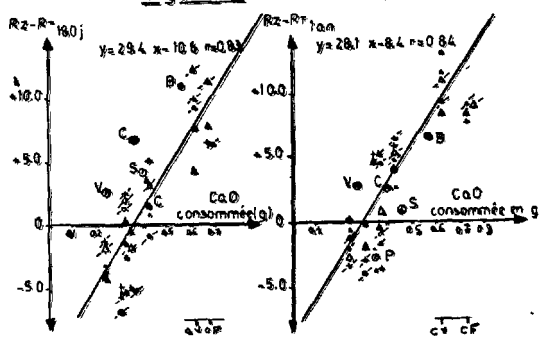

Figure 5B

20.35% Clinker à 1.5% à C_3A
" " 9 % "
" " 14 % "

En ce qui concerne la progression des résistances, on remarque dans le cas des ciments CPJ de laboratoire, une influence très marquée du dosage en C_3A. En effet la progression des résistances à 1 an est accentuée dans les cas ou le clinker utilisé dans le CPJ possède un pourcentage de $C_3A \geqslant 9,5$. Ainsi on constate que pour le clinker à 1,5 % de C_3A on a $R_Z - R_T \geqslant 0$ pour 57 % des CPJ indifféremment dosés en pouzzolane (Z, etc...)(Fig. 6).

Pour le clinker à 9,5 % de C_3A on a $R_Z - R_T \geqslant 0$ pour 71 % de CPJ dosés à 35 % et 20 % de Z et C, 25 % pour ceux dosés à 10 % de Z et C. Pour le clinker à 14 % de C_3A on a $R_Z - R_T \geqslant 0$ pour 57 % de CPJ dosés à 10 et 20 % de Z et C, 71 % des CPJ dosés à 35 % de Z et C.

Cette progression des résistances semble peu sensible au dosage en éléments pouzzolaniques. Il faut toutefois signaler que les Z ou C étaient broyés à une très grande finesse (9000 cm2/g) ce qui leur donnait une surface active très élevée.

D'une façon générale, on peut dire que la mesure de l'effet pouzzolanique à partir de la quantité de CaO consommée se relie de façon très satisfaisante à la progression des résistances exprimées en $R_Z - R_T$ (Fig. 5a - 5b) En effet les coefficients de corrélation sont de 0,83 à 180 j et 0,84 à 1 an. Les équations générales à 180 j et 1 an des droites de régression établies sur les résultats obtenus sur les ciments industriels et de laboratoire mélangés sont très proches et se trouvent dans le même intervalle de confiance (Fig. 5c).

$$\text{A 180 j } (R_Z - R_T) = 29,36\ C_aO - 10,6$$
$$\text{A 1 an } (R_Z - R_T) = 28,12\ C_aO - 8,4$$

Il semble donc possible de déduire à partir de la mesure de la CaO consommée effectuée sur un ciment CPJ, la progression prévisionnelle des résistances sur mortier à partir de 180 j.

La mesure de l'effet pouzzolanique faite à partir de l'essai Chapelle modifié semble donc être bien représentative du pouvoir liant des Z contenus dans un ciment CPJ.

Evolution de la relation Rz Rt à 180j et 1 an
en fonction de la CaO consommée
CPJ industriel et CPJ fabriqué en laboratoire
de 20% et 35% de Z.

Figure N° 5 C

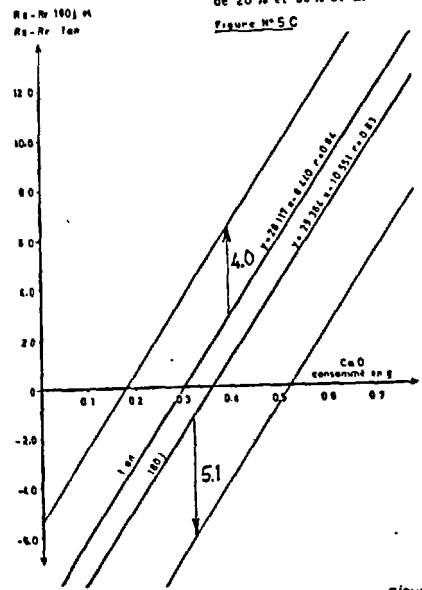

FIGURE 6.
Progression des résistances
en fonction du C_3A et de la CaO consommée par l'essai Chapelle modifié.

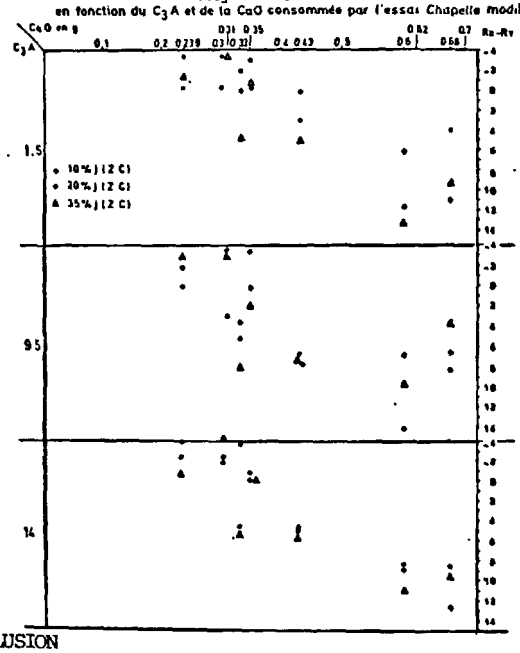

CONCLUSION

Les améliorations apportées à l'essai conçu par J. CHAPELLE pour estimer l'activité des matières pouzzolaniques permettent de déduire la réactivité de la pouzzolane entrant dans la composition d'un ciment.

Les essais sur mortiers confectionnés avec de nombreux ciments contenant des pouzzolanes de provenances très diverses et plus ou moins réactives ont montré qu'il était possible de relier l'accroissement des résis-

tances dans le temps, à l'effet pouzzolanique, du constituant secondaire mesuré à partir du ciment lui-même.

En effet, le pouvoir hydraulique des pouzzolanes mesuré sur mortier est en parfaite corrélation avec la quantité de chaux consommée déterminée à l'aide de l'essai Chapelle modifié.

Dans le cas présent, les matériaux pouzzolaniques les plus actifs sont les cendres associées à des clinkers à forte teneur en C_3A.

BIBLIOGRAPHIE

(1) J. CHAPELLE "Attaque sulfocalcique des laitiers et pouzzolanes" - Revue des Matériaux de Construction 1958 - n° 512 (p. 136-145).

F. MASSAZA "Chimie des additions et ciment pouzzolaniques" 6ème Congrès International de la Chimie des Ciments - Moscou Septembre 1974.

M. VENUAT "Effet de l'addition des cendres volantes sur les propriétés des ciments" Revue Matériaux de Construction n° 565, 566, 567 (1962).

L, GUILLAUME "L'activité pouzzolanique des cendres volantes dans les ciments" Silicates Industriels n°28 (1963).

Structure of the Products of Hydration of Cement with Shale Ash

Structure des produits d'hydratation de ciment additionné de schiste

I. YANEB, Dr. Eng. Scientific Institute for Building Materials,
M. RADENKOVA-YANEVA, Dr. Eng. High Institute for Architecture and Civil Engineering,
I. LAZAROV, E. TCHULEVA, Scientific Institute for Building Materials, U.R.S.S.

RESUME : La présente étude porte sur l'hydratation de ciments composés, dont l'ajout est constitué par le résidu minéral du traitement des schistes bitumineux des gisements bulgares. On a utilisé pour cela deux sortes de clinker (à faible et à forte teneur en alite) et deux sortes de schistes ainsi cuits. L'activité de ces schistes cuits dépend de leur composition minéralogique et de la température atteinte pour leur production. Les éprouvettes ont été étudiées au spectrographe infrarouge et au microscope électronique. On observe une vitesse plus élevée de l'hydrolyse des composants du clinker et un début de réaction entre la chaux dégagée et le schiste cuit, qui conduit à un développement plus grand du C-S-H et de la portlandite au cours de l'hydratation. On observe aussi une absorption du $Ca(OH)_2$ par le schiste cuit, qui forme à la surface des grains des cristaux aciculaires.
On en a déduit le moyen d'accroître au maximum la compacité, à long terme, des pâtes de ces ciments. Une interprétation des propriétés des produits obtenus a pu être faite en se basant sur la composition et la morphologie des schistes cuits.

SUMMARY: Having a knolege of the special features of the cement stone structure and the factors of its determination is of a great theoretical and practical importance. Up to now investigations were carried on with individual clinker minerals and real cements. It might be said thete there is little information about the structure and the properties of the cement stone received during the process of hydration of cements with the mineral residium obtained during thermal treatment of bulgarian shales.

This work deals with the processes of hydration of the cements with such additive and the developing of the cement stone structure. Two kinds of clinker (with high and low amount of alite) and two kinds of mineral residium (shale ash) with different hydraulic activity were used. This different hydraulic activity is determined by the difference in the mineral composition of the shales and the temperature treatment for extracting their organic ingradients. The samples were examined by means of infra-red spectroscopy and scanning electron microscopy. Were established the peculiarities of the processes of hydration - the greater rate of hydrolisis of the clinker minerals, the initial stage of interaction between shale ash and $Ca/OH/_2$, the relative amount of the C-S-H phase and portlandit during the course of hydration. The consumption of $Ca/OH/_2$ for the puzzolanic reaction, formation of the products of interaction on the shale ash grains were established. The view of the new formed phase in the initial stage of the interaction was shown - very fine needle-like crystals. The interaction between the investigated additives and $Ca/OH/_2$ was followed and were expressed some thoughts covcerning the formation of espesially dense cement stone structure in the later periods of hydration. On the base of the view and the morphology of the products of interaction the interpretation of some properties of the investigated cements was done.

Studying the structure of cement stone and the factors of its determination contribute to the clarification of the mechanism of formation of the dense structure of the portland cement stone and enable to control this process in using binders.

Up to now there have been carrying on investigations on the base of the individual clinker minerals (1,2) or real cements (2,3,4). It has been obtained information about the composition and morphology of the hydration products and expressed some thoughts with respect to the mechanism of contact formation between the different phases and their distribution in the hardened binder pastes. There is little information about the structure and properties of cement stone containing different kinds of additives. Mineral residium received from shales during their thermal treatment aiming to extract their organic ingradients is such an additive interesting from theoretical and practical point of view.

We have used the mineral residium received during thermal treatment of bulgarian shales in semi-industrial equipment in temperature interval 823 - 1023°K. It is granular material with grain size less than 2,5 mm. Thermal treatment in above mentioned conditions determines hydraulic activity of the mineral residium (shale ash) and the possibility of its using as additive in cement.

In our previous work (5) was shown the possibility of using the above mentioned shale ash as additive to the grinded clinker. Cements with good physico-mechanical properties were obtained. Having in mind the conditions of the shale thermal treatment and the phase composition of shale ash it was interesting to study its reaction with cement and establish the character of the products of this interaction. Two kinds of portland cement clinker with different content of alite and belite (samples from series "A" with C_3S = 68,86 % and C_2S = 9,18 % and samples from series "B" with C_3S = 40,80 % and C_2S = 28,52 %) and two kinds of shale ash with different hydraulic activity were used. From the above mentioned materials by combined grinding using the corresponding quantity of gypsum were prepared mixtures with 15 and 40 % shale ash and were moulded specimen-prisms (1 x 1 x 3 cm) using water from 24 to 32 % depending on the percentage of shale ash. The samples obtained were kept in water and after certain periods the process of hydration was discontinued by chemical dehydrogenation.

Infra-red spectroscopic measurements were carried out on a UR - 20 Zeiss infra-red spectrophotometer over the wavelength 400 - 4000 cm^{-1} using the Nujol mull or KBr disc as appropriate. On freshly broken surfaces were identified the type and morphology of the reaction products between the grains of shale ash and portland cement clinker. The investigated surfaces were covered with a thin layer of aluminium and by means of scanning electron microscope (type JEOL ISM S - 1) were taken the photos of the typical parts. Some of the taken infra-red spectra and micrographs are shown on the figurs below.

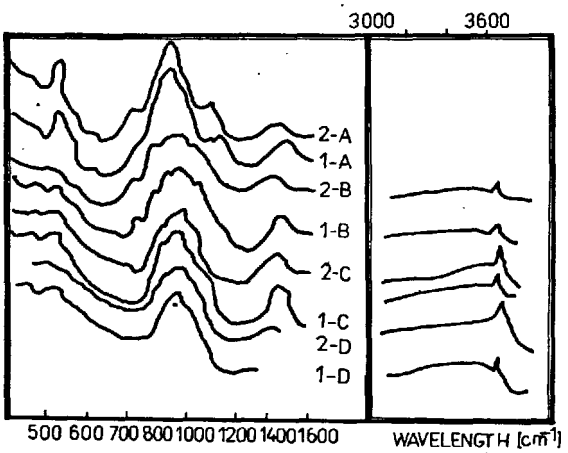

Fig. 1. Infra- red spectra of pure clinker cements. a - 0, b - 3, c - 28 and d - 90 days of hydration.

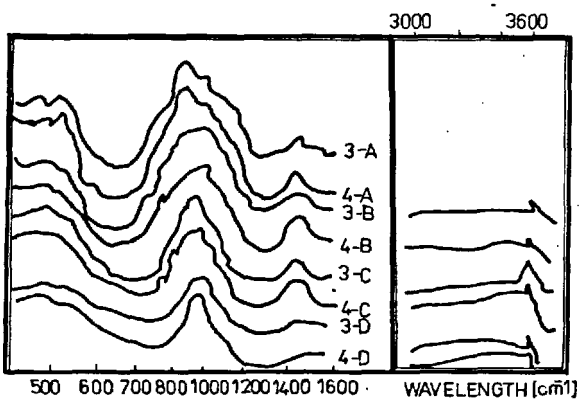

Fig. 2 . Infra-red spectra of cements with clinker from series "A" (3) and series "B" (4) and shale ash (40 %) with high hydraulic activity.

Infra-red spectra of the investigated pure clinker cements (fig.1) contain absorption bands of alite at 895 and 935 cm^{-1} and at 465 and 520 cm^{-1} . Comparing with pure C_3S the bands maxima in the region 850 - 950 cm^{-1} were shifted to the high frequency spectra region. This is due to the incorporation of small quantities of

Na^+, K^+, Mg^{2+}, Ti^{4+}, Fe^{3+}, Al^{3+} and others in crystal lattice of C_3S to form alite. Belite is characterised with absorption bands at 895 and 995 cm^{-1} and at 520 and 545 cm^{-1}. Absorption bands at 415 and 525 cm^{-1} are due to the C_3A. Comparing the form and intensity of alite's and belite's bands one can see what is the relative amount of these two minerals in the cements investigated. The sample 1 contains more alite whereas the sample 2 contains more belite.

In the spectpa of cements with shale ash absorption bands due to the amorphous SiO_2 with maximum at 804 cm^{-1}, calcite with maximum at 435 cm^{-1} and the dublet band for quartz at 804 and 784 cm^{-1} can be seen.

The process of hydration is assosiated with gradually disappearing of the bands due to the clinker minerals and appearing of new absorption bands of the hydration producrs. The principal products established during portland cement hydration are calcium silicate hydrate with absorption bands at 965-975 cm^{-1} and 980-990 cm^{-1} ; $Ca/OH/_2$ giving strong sharp peak at 3640 cm^{-1} and calcium sulphoaluminate most probably monosulphate with absorption maxima at 1170 and 3675 cm^{-1} (6).

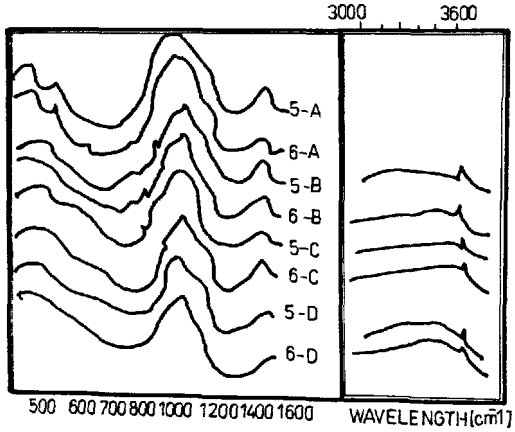

Fig. 3. Infra-red spectra of cements with clinker from series "A" (5) and series "B" (6) and shale ash (40 %) with low hydraulic activity.

In the course of hydration of pure clinker cements (fig.1) the intensity of the bands at 465 and 520 cm^{-1} decreases sharply and in the region 800-1100 cm^{-1} forms a complex band with absorption maxima at 890, 945 and 1080 cm^{-1}. This is connected with decreasing the quantity of alite and relative increasing this of belite. The absorption maxima at 925 cm^{-1} is shifted to the longer wavenumbers up to 940 cm^{-1} due to the formation of C-S-H phase. The bands at 605 and 662 cm^{-1} disappear and the dublet at 1120 and 1150 cm^{-1} changes in shoulder of the band at 1150 cm^{-1}. This is connected with decreasing the quantity of gypsum and formation of calcium sulphoaluminate. At longer hydration was found that the amount of C-S-H phase, monosulphate and $Ca/OH/_2$ has progressively increased.

At hydration of cements with shale ash were observed the same events as at this of pure cements, but undoubtedly was established the interaction between shale ash and $Ca/OH/_2$ obtained during hydration of the clinker minerals. The mentioned interaction causes gradual decreas of the intensity of the $Ca/OH/_2$ bands in the course of hydration (fig. 2-3). Comparing the infra-red spectra for the samples of the two series we can see that the $Ca/OH/_2$ remaining at the end of the process is more in samples containing clinker with higher amount of C_3S. (fig.2). At the same time using the shale ash with lower hydraulic activity the rate of assimilation of $Ca/OH/_2$ is lower and the samples contain a little bit more portlandit (fig.3). Comparing very carefully the intensity of the bands of C-S-H phase we can see that this phase is more in the samples with shale ash.

The regularities established with infra-red spectroscopy were confirmed with scanning microscope study and were observed the view and morphology of the new phases.

According to Copeland (4) the first elements of the cement stone structure were etringit, main constituent of C-S-H gel and needles growing from the clinker grains surfase. After a few hours in the spase filled with water and out of cement grains were formed small crystals of $Ca/OH/_2$. In the case of cements with shale ash this $Ca/OH/_2$ reacts with the hydraulic active phases. The result of this reaction is C-S-H gel, formed very near to the shale ash grains. Therefore the samples with shale ash at different age would show less amount of $Ca/OH/_2$ and more C-S-H phase. It is considered that portlandit crystals act the main role in formation of the initial cement stone strength. Addopting this conception we might explain in a satisfactory way the low initial strength of the investigated samples (5).

At the same time we have to differentiate the C-S-H phase resulting from the process of hydration of the clinker minerals from this one resulting from interaction between shale ash and $Ca/OH/_2$. The first has the possibility to grow in the pores of cement stone, while the second is formed on the grains of shale ash and is characterised with small niddle-like crystals. They are result from interaction with $Ca/OH/_2$ in over-saturated solution and their morphology is according this conditions. Hence the interaction products so formed, are not able to grow continuously in length and the number of contacts between them in the initial moment of interaction is small. This one explains the smaller strength of cements with hydraulic active additives at the beginning of the process of hardening.

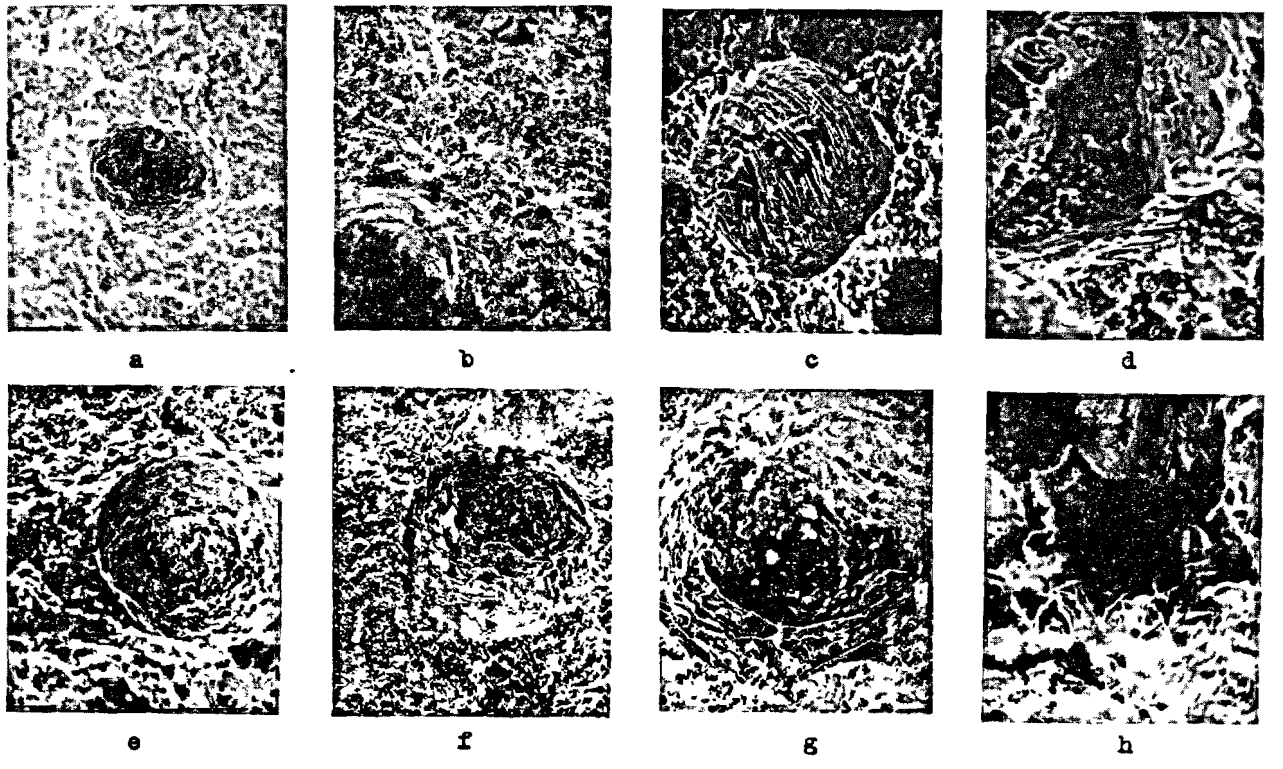

Fig. 4. Micrographs of the samples from clinker with high conteht of C_3S and shale ash with high hydraulic activity. a,b,c,d - 15 % shale ash, e,f,g,h - 40 % shale ash. a,e - 3 , b,f - 7, c,g - 28, d,h - 90 days of hydration.

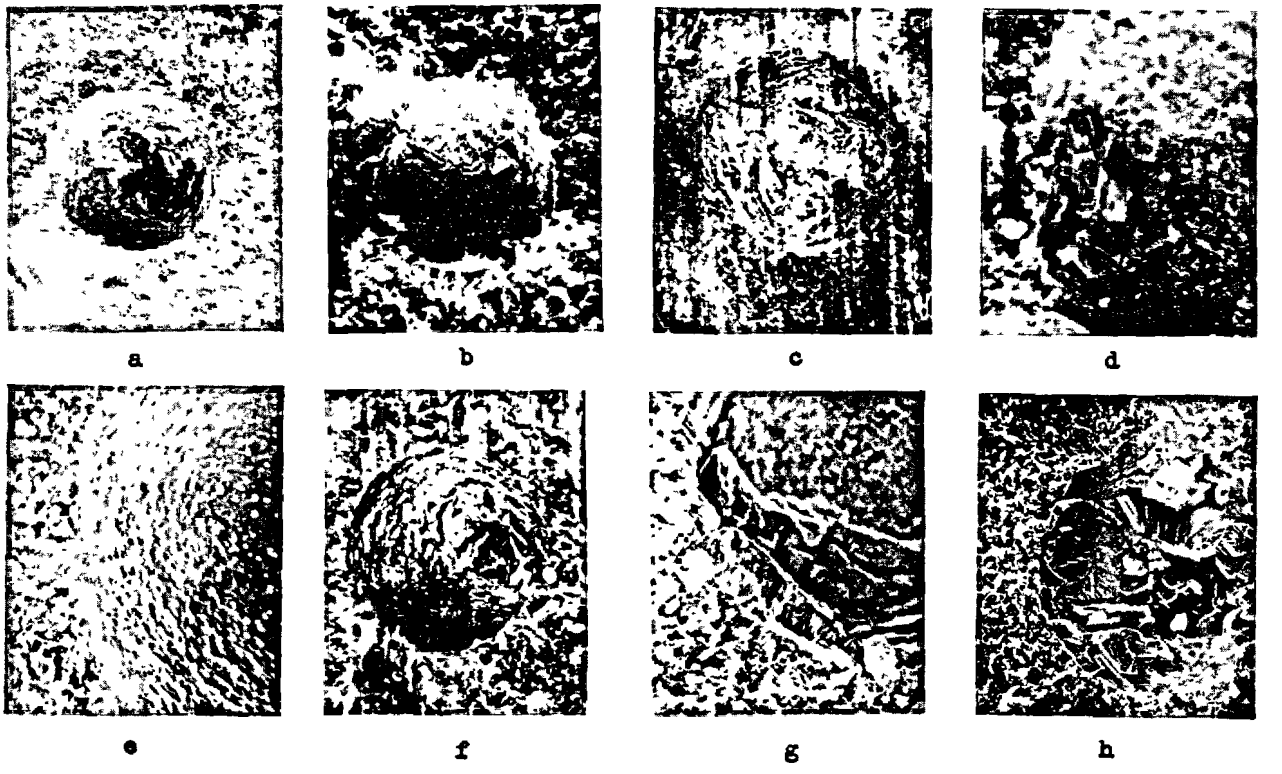

Fig. 5. Micrographs of the samples from clinker with high content of C_3S and shale ash with low hydraulic activity; a,b,c,d - 15 % shale ash, e,f,g,h - 40 % shale ash; a,e - 3, b,f - 7, c,g - 28, d,h - 90 days of hydration.

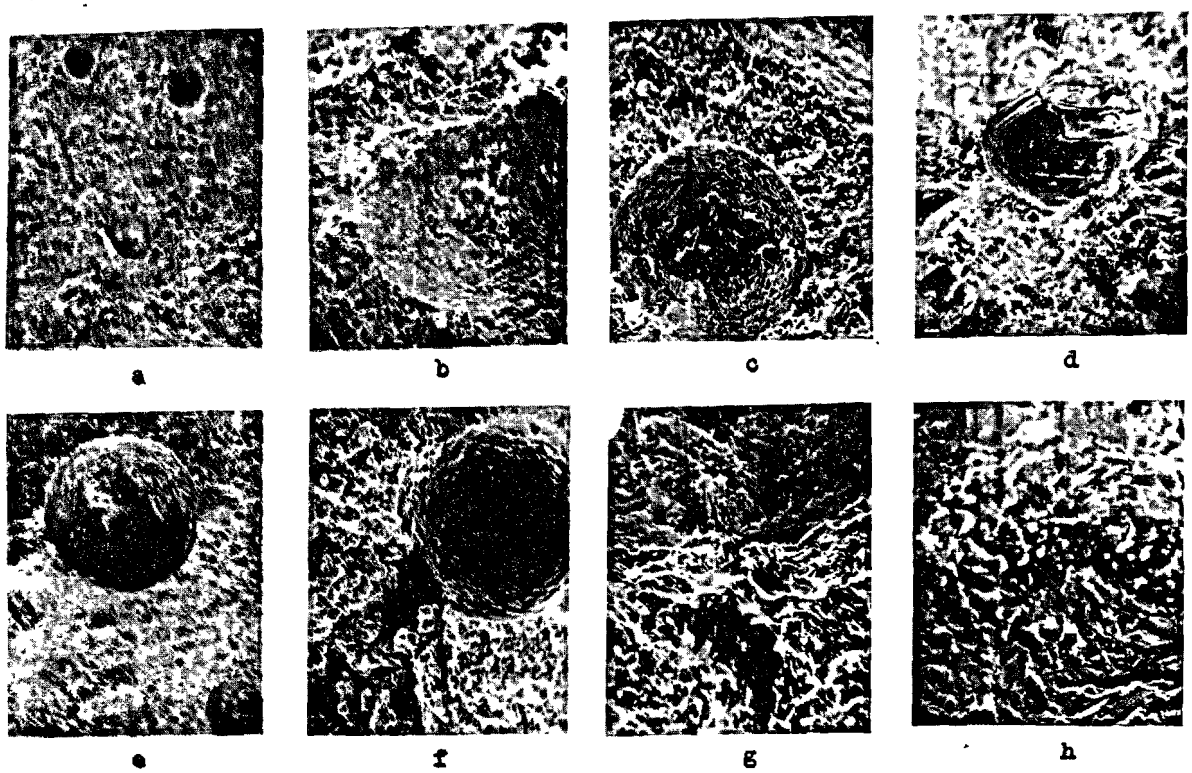

Fig. 6. Micrographs of the samples from clinker with low content of C_3S and shale ash with high hydraulic activity. a,b,c,d - 15 % shale ash, e,f,g,h 40 % shale ash; a,e - 3, b,f - 7, c,g - 28, d,h - 90 days of hydration.

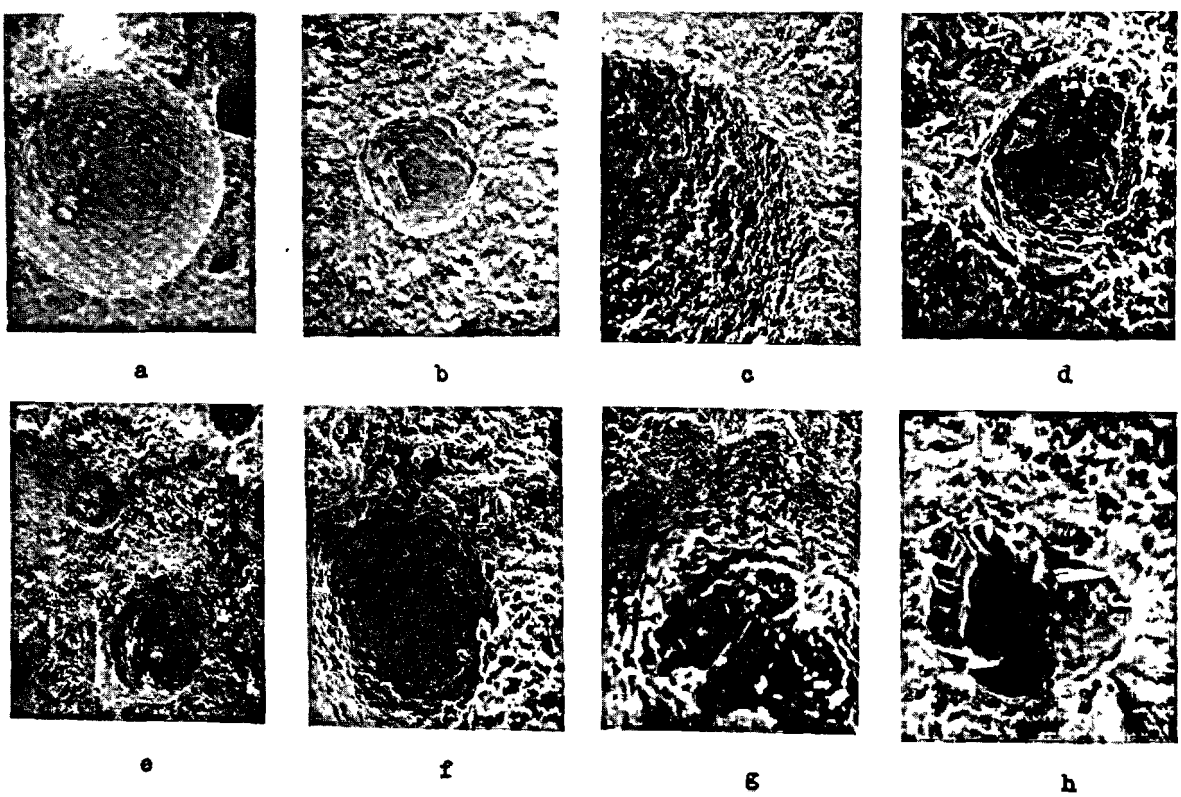

Fig. 7. Micrographs of the samples from clinker with low content of C_3S and shale ash with low hydraulic activity. a,b,c,d - 15 % shale ash, e,f,g,h - 40 % shale ash. a,e - 3, b,f, - 7, c,g - 28, d,g - 90 days of hydration.

On the electron microscope's photographs shown at fig. 4 - 7 it is seen that the srtucture of the investigated cements has a very fine morphology. It is known that (7) cements with hydraulic active additives have a higher rate of hydrolises of silicates. This is second reason because of which the products of C-S-H gel are not able to form long filaments. The greater quantity of calcium silicate hydrates formed for a definite period of time causes formation of many and short filaments. The number of contacts between them is small, and the structure is with the lower physico-mechanical properties. In the course of hydration and hardening the so formed elements of the structure interweave, form a dense skeleton and cement stone increases its strength.

At the same time it might be said that the C-S-H phase formed very near to the shale ash grains hardly has high proportion C/S; $Ca/OH/_2$ is comperatively in smaller amount that the active additive and in the initial moment of reaction would form low-basic calcium silicate hydrates. Therefore it might be said that at hydration of cements with shale ash besides the two phases ("inner" and "outer" C-S-H gel) formed near to the clinker grains, at the boundary surfase of the shale ash grains is formed C-S-H phase with lowest basicity. The morphology of the so formed phase - plates, discs - confirms this (fig. 4,5,6). From another side "The outer" C-S-H phase, which is richer at CaO forms fibrouse new formations. In other words during the later periods of hydration, when the puzzolanic reaction is in its advanced stage the basicity of the calcium silicate hydrates increases and in the samples with lower amount of shale ash is observed fibrouse C-S-H gel (fig. 4,5).
The time is a factor which in a very great degree influences the type of the cement stone structure. Calcium silicate hydrates owing their origin to the reaction between C_2S and water change continuously their composition while those received from C_2S do not so. According to this circumstance is the continuous change of the morpfology of C-S-H phase observed at the photos above.

The received picture allows to follow the intensity of interaction between hydraulic additive and $Ca/OH/_2$. From the most general point of view this interaction might be explained with thermodynamic instability of the system $Ca(OH)_2$ - hydraulic additive - water. It might be said that seven days are enough for beginning of interaction in this system. As it was already said, the low-basic C-S-H gel was formed with very fine particles.The process of interaction is more clearly expressed in the samples prepared from clinker with high amount of alite and s shale ash with high hydraulic activity (fig. 4).In the case of samples of series "B" and shale ash with lower hydraulic activity (fig. 7) at the seventh day was observed only the initial stage of interaction. Very clearly expressed products of puzzolanic reaction were observed in the samples containing clinker with low amount of alite and shale ash with high hydraulic activity (fig.6).

At the longer periods of hydration (28 days) at the every combination between used materials might be seen clearly the interaction between the two components (fig.4-7). But it has to be underlined that depending on the activity of the shale ash used, side by side with the products of interaction were observed and crystals of portlandit. Their relative amount is more in the samples with low hydraulic active shale ash.

The study carried out and the result obtained indicate that the shale ash received from bulgarian shales has hydraulic properties, reacts with $Ca/OH/_2$ in cement stone and influences the type of its structure.It might be said that at the seventh day of hydration the puzzolanic reaction has already begun. But the influence of the new formed C-S-H phase on the physico-mechanical properties of the samples investigated is clearly observed in the later stages of hydration (5). In the structure of cement stone it has to be differentiated from one side "outer" high basic C-S-H phase and "inner" low-basic C-S-H phase formed at the clinker grains, and at the other side, another C-S-H phase with the relatively lowest basicity and formed at the shale ash grains. These three phases during the process of hydration form contacts between them. When the process of interaction between $Ca/OH/_2$ and shale ash is in advanced stage, the conditions are created for decreasing the whole amount of portlandit in cement stone. As the result of the latter the long fibrous new formations of C-S-H phase are formed and grown. Everything mentioned above leads to the creation of espessially dense structure of cement stone and the connected with this properties of shale ash cements.

REFERENCES

1.L.G.SHPYINOVA,V;I.CHIKH,I.I.NIKONETS, (1976),"Formation of β-C_2S and C_3S Stone Microstructure",Proc.Six.Con.Chem.Cem., vol.2,pp.277-281.
2.J.JAMBOR (1976),"Phase Composition Structure and Strength of Hardened Cement Pastes, ibid.,vol. 2, pp. 315-320.
3.S.DIAMOND (1972)"Identification of Hydrated Cement Constituents", Cem. Con. Res., Nr.2, pp.617-632.
4.A.E.COPELAND,G.J.VERBECK (1976),"Structure and Properties of the Hardened Cement Pastes", Proc. Six. Con.Chem.Cem,,vol.2, pp.258-274.
5.I.YANEV,I.LAZAROV,"The Possibility of using the Shale Ash as Additive in Cement,"to be published.
6.J.BONSTED,S.P.VARMA,(1974),"Some Applications of Infra-red and Raman Spectroscory in Cement Chemistry",Cem.Techn.,vol.5, Nr.1 pp.256-261;Nr.4,pp.378-383;Nr.5,pp.440-450
7.F.MASSAZZA (1976),"Chemistry ofPuzzolanic Addition and Mixed Cements", Proc. Six. Con.Chem.Cem.,vol.3, pp.209-221.

An examination of Ordinary Portland cement blended with pulverised-fuel ash

Examen du ciment Portland ordinaire mélangé à des cendres volantes

W.A. GUTTERIDGE, Mr. Cement and Concrete Association, Materials Research Department, Slough, England.

RESUME : Des échantillons de cendres volantes ont été examinés par diffraction X pour mesurer ce que l'on appelle : leur indice de cristallisation. En effectuant des mesures quantitatives par diffraction X sur des ciments contenant des ajouts de cendres volantes, on a montré que les résultats permettaient l'analyse quantitative des constituants minéralogiques de ce ciment composé; ils permettent aussi, si l'on dispose d'un échantillon de ciment Portland pur ayant servi à la fabrication de ce ciment composé, de connaître l'analyse quantitative et les proportions du clinker et des cendres volantes.

SUMMARY : Samples of pulverised fuel ash (ash) have been examined using X-ray powder diffraction and an estimate of a so-called "crystallinity index" obtained. Using quantitative X-ray diffraction it has been shown that Ordinary Portland cement blended with ash can be analysed either in terms of the ash and synthetic cement minerals or equally well when a sample of the Ordinary Portland cement is available, in terms of the cement and the ash.

INTRODUCTION

In general, the values obtained from a quantitative X-ray powder diffraction analysis (QXDA) of either a cement or a clinker are precise but not absolute. They are relative only to the intensity data of the compounds used to provide the basis for the analysis. Every laboratory strives to ensure that these compounds (or their intensity data) are representative. Nevertheless it is still assumed by many that intensity data from say an alite (or alites) used at one laboratory are identical to those obtained at another laboratory. That variability exists is reflected in the results obtained from the international QXDA surveys of 1964 (1) and 1973 (2). In certain circumstances however it is possible to analyse a cementitious mixture not just in terms of compounds thought to represent the mixture but in terms of the actual components. Cement blended with either pulverised-fuel ash or slag is such a mixture. The analysis would be given in terms of the proportions of cement and ash (or slag) used in the blend.

Results are presented here for clinker and cement blended with ash. No attempt has been made to analyse the ash in terms of its individual compounds. A so-called "crystallinity index" has been used to characterise each ash.

The analytical procedure is that used at the Cement and Concrete Association for the analysis of anhydrous Portland cement and clinker, the analysis being given in terms of a set of synthetic cement minerals. This procedure has been tested using mixtures containing between two and eight synthetic cement minerals in several combinations. It has been shown by the author that the method is reliable and will produce an analysis of an acceptable precision. Three such analyses are given in Table I together with appropriate 95 percent confidence limits (95% CL).

standard the intensity I_p can be normalised using the intensity I_s from a selected diffraction of the internal standard (3),(4),(5) to give

$$I_p/I_s = N_p$$

It can be shown (6) that $I_c/I_s = {}_{100}(N_c)_p \cdot w_c$

where ${}_{100}(N_c)_p$ is the normalised intensity at the angle 2-theta of a binary mixture (or primary standard) containing only the particular compound c and the same weight fraction w_s as is contained in the multicomponent mixture; w_c is the weight fraction of compound c in the multicomponent mixture.

The weight fraction w_c of each compound in the multicomponent mixture is obtained by minimising the sum of the squares of the errors for the intensity data collected by step counting at each of the T 2-theta values and solving the resultant normal equations.

A reliability factor R is computed where R is given by

$$R = \sum_{P=1}^{P=T} \left(N_p - \sum_{c=1}^{c=M} {}_{100}(N_c)_p \cdot w_c \right)^2 \Big/ \sum_{P=1}^{P=T} (N_p)^2$$

Finally the weight fraction of each component in the mixture is expressed as a weight percentage and a total w_T obtained.

Both R and w_T are used to assess the reliability of the analysis. It has been found by the author that when w_T is 100 $\pm$ 2 and R is less than 0.02 the analysis is reliable.

Experimental

a) Sample preparation and data collection

A set of X-ray intensity data were collected on punched paper tape, by step counting for 20 seconds at intervals of 0.05 degrees 2-theta from 12 degrees to 45 degrees 2-theta, for each sample of ash (in its as-received condition) using a Philips vertical circle powder diffractometer with pulse height discrimination and copper K-alpha radiation.

Primary standards were prepared using 1g of rutile (TiO_2) as the internal standard and 5g of one of the following, a cement, a clinker and a pulverised-fuel ash. These mixtures were ground for 40 minutes

TABLE I

	Cement mineral				
	Alite	Belite	C_3A	Ferrite	$CaSO_4$
Nominal composition	59.7	24.875	0.5	14.925	nil
1. Analysis	60.25	24.94	0.55	14.26	-
95% CL	0.42	0.46	0.09	0.16	
Nominal composition	65	18	9	6	2
2. Analysis	63.93	18.55	8.64	7.15	1.83
95% CL	0.35	0.06	0.09	0.24	0.09
Nominal composition	55	27	6	9	3
3. Analysis	54.90	27.24	5.71	9.10	3.04
95% CL	0.71	0.89	0.03	0.26	0.31

Analyses obtained from mixtures containing synthetic cement minerals and analysed in terms of the same synthetic minerals using X-ray diffraction (weight percentage)

Procedure

The analytical procedure uses intensity data collected by step-wise counting and the fact that in any powder diffraction pattern obtained from a mixture containing M components, the intensity I_p diffracted at any angular position 2-theta is related to the linear sum of the intensity I_c diffracted by each component at the angle 2-theta. When such a mixture contains a weight fraction w_s of an internal

in an agate ball mill using 10ml of cyclohexane as a grinding aid.

Intensity data were collected, on punched paper tape, from these primary standards by step counting at each interval of 0.05 degrees 2-theta over the range 24.8 to 38.25 degrees 2-theta using a Philips vertical circle powder diffractometer with pulse height discrimination and copper K-alpha radiation. Twelve primary standards were prepared in this way using four Portland cements, a sulphate resisting Portland cement clinker and seven samples of pulverised-fuel ash.

An additional eight mixtures were prepared each containing rutile (having the same weight fraction w_s as used in the primary standards) together with one of the seven samples of ash and either the sulphate resisting Portland cement clinker or one of the Portland cements. These mixtures were to be the subject of the QXDA and were made in exactly the same way as the primary standards. Intensity data were also collected in exactly the same way as was used with the primary standards. Nominal compositions are given in Table II.

TABLE II

Mixture No.	Clinker or Cement		Ash	
	No.	wt%	No.	wt%
1	5	85	7	15
2	1	80	1	20
3	1	80	2	20
4	1	80	3	20
5	2	60	4	40
6	5	50	7	50
7	3	40	5	60
8	4	30	6	70

Nominal composition of the blended mixtures containing pulverised-fuel ash and either a cement or a clinker (weight percent)

b) Data processing

Intensity data obtained from the pulverised-fuel ash in its as-received condition and collected over the angular range 12-45 degrees 2-theta were processed by removing a linear background and then fitting an eighth order polynomial in $\sin^2\theta$ to data comprising the "amorphous halo". The total integrated intensity defined by the polynomial represented the diffracted intensity I_A from the "amorphous halo" in each sample of ash. The ratio

$$\frac{(\text{Total integrated diffracted intensity} - I_A)}{(\text{Total integrated diffracted intensity})} \times 100$$

was used to give a value for the "crystallinity index" of the ash.

The X-ray intensity data collected from the eight mixtures were processed by:-

(i) location and subtraction of background data.

(ii) location of the mid-chord at 80 percent of the peak height (80% PH) of the Rutile (110) diffraction.

(iii) interpolation of the intensity data until the 80% PH of the Rutile (110) diffraction was at 27.475 degrees 2-theta.

(iv) determination of the integrated intensity of the Rutile (110) diffraction.

(v) normalisation of the intensity data.

c) Analysis

Each mixture was analysed in two ways. First in terms of an ash and either a cement or a clinker and second in terms of an ash and a set of synthetic cement minerals. Two sets of seven analyses were obtained from each mixture of cement and ash. For example the QXDA intensity data recorded from mixture number one (which contained only ash No 7 and cement No 5) was first analysed in terms of the primary standard (PS) data for both ash No 7 and cement No 5. Six other results in this set were obtained by substituting (one at a time) the PS data for the remaining six ashes for that of ash No 7. The second set of seven analyses were obtained using PS data from a set of synthetic minerals instead of that for the cement and repeating the procedure outlined above with each ash in turn. Of these fourteen analyses only one is specific to the actual components of the mixture in that pulverised-fuel ash No 7 and cement No 5 were used. The other thirteen analyses indicate the range of results which are obtained when a mixture is analysed in terms of components which are similar to, but not identical with the components in the mixture.

Analyses are given in Table III for the four Portland cements and the SR Portland cement clinker used in this work. These results are based on synthetic cement minerals. The crystallinity indexes obtained from the seven samples of ash are given in Table IV. The analyses obtained from mixtures 2, 3 and 4 are given in Tables V and VI whilst those results obtained from mixture 8 are given in Tables VII and VIII.

TABLE III

Cement	Alite	Belite	C_3A	Ferrite	$CaSO_4$	CaO	R-Factor
1 (Clinker)	62*	19	nil	13(a)	nil	0.7	0.007
2	59*	26	7	5(b)	2.6	0.6	0.032
3	71+	17	2	6(c)	2.4	0.9	0.009
4	67+	13	10	6(b)	3.2	0.4	0.020
5	62*	19	11	5	2.5	0.5	0.029

Analysis of the SR Portland cement clinker and the Portland cements used in the blended mixtures (weight percent by X-ray diffraction)

*denotes a monoclinic alite; +denotes a rhombohedral alite (a) denotes F_{ss} 62:38; (b) denotes F_{ss} 54:46; (c) denotes F_{ss} 50:50

TABLE IV

Sample No.	Index	Sample No.	Index
1	24	5	14
2	54	6	19
3	62	7	16
4	22	-	-

Crystallinity indexes for the seven pulverised-fuel ashes used in the blended mixtures.

TABLE V

Mixture No.	wt % Clinker	wt % ash	Ash used in analysis	R-Factor
2	80.8	19.2	1	0.003*
2	84.5	15.6	2	0.004
2	82.7	17.3	3	0.004
3	78.7	21.3	1	0.006
3	80.0	20.0	2	0.002*
3	79.5	20.5	3	0.004
4	82.5	17.5	1	0.004
4	84.7	15.3	2	0.003
4	83.0	17.0	3	0.003*

Analyses obtained by X-ray diffraction for mixtures containing an S.R. Portland cement clinker and pulverised-fuel ash. Analysed in terms of the clinker and three different ashes. Nominal composition 80 weight percent clinker and 20 weight percent pulverised-fuel ash.

*denotes analysis using the correct reference components

TABLE VI

	Alite[x]	Belite	Ferrite	CaO	Ash	R-Factor	Ash used in analysis
Nominal (d)	53.4	15.5	10.5	0.6	20		
Mixture No.							
2	50.6	15.6	10.0	0.8	23.0	0.008*	1
2	53.5	16.5	10.7	0.8	18.4	0.010	2
2	52.4	15.9	10.2	0.8	20.7	0.008	3
3	49.4	15.2	9.7	0.7	25.0	0.010	1
3	51.0	15.5	10.0	0.7	22.7	0.007*	2
3	50.6	15.2	9.8	0.7	23.7	0.009	3
4	52.7	15.3	9.9	0.6	21.6	0.007	1
4	54.8	15.9	10.3	0.6	18.3	0.007	2
4	53.7	15.3	9.9	0.6	20.5	0.006*	3

Analyses obtained by X-ray diffraction for mixtures containing an S.R. Portland cement clinker and pulverised-fuel ash. Analysed in terms of synthetic cement minerals and three different pulverised-fuel ashes. Nominal composition of each mixture 80 weight percent clinker and 20 weight percent pulverised-fuel ash.

*denotes analysis using the correct reference components; [x]denotes a monoclinic alite (d) denotes data obtained from Table III.

TABLE VII

wt % cement No.4	wt % ash	Ash used in analysis	R-Factor
31.1	68.9	1	0.004
40.0	60.0	2	0.029
34.4	65.6	3	0.017
31.7	68.3	4	0.004
31,5	68.3	5	0.010
30.9	69.1	6	0.004*
30.9	69.1	7	0.004

Analyses obtained by X-ray diffraction for a blended mixture containing an O.P. cement and a pulverised-fuel ash. Nominal composition 30 weight percent cement and 70 weight percent pulverised-fuel ash. (Mixture No 8). Analysed in terms of cement and different pulverised-fuel ashes.

*denotes analysis using the correct reference components.

Discussion

Results given in Table IX show that satisfactory analyses are obtained when the blended mixtures are analysed in terms of their particular components. The agreement between the results in Table IX and the nominal composition given in Table II is good.

By chance the pulverised-fuel ashes used in this work appear to fall into two groups when classified according to their crystallinity index. Samples 1,4, 5,6 and 7 have an index in the range 20 $\pm$ 6 whereas sample 2 and 3 are significantly different in that their index is in the range 58 $\pm$ 4. It would not be surprising therefore to find a similarity in the analyses given by ashes in the same group. This is shown by the results given in Table VII for a mixture containing an ash from group one i.e. having an index in the range 20 $\pm$ 6. Those analyses which have been obtained using other ashes in this group are similar in as far as a mean value of 68.8 (σ= 0.36) is obtained for the ash content of this mixture. This contrasts with the value of 62.8 (σ= 3.96) obtained from the two ashes of group two. The contrast is more marked in the results given in Table VIII where a mean value of 70.1 (σ=1.1) is

TABLE VIII

	+Alite	Belite	C_3A	Ferrite	$CaSO_4$	Ash	R-Factor	Ash used in analysis
Nominal (d)	20.1	3.9	3.0	1.8	1.0	70.0		
	20.5	3.6	3.1	1.8	0.6	72.0	.008	1
	23.0	4.9	3.5	2.3	1.8	55.0	.034	2
	22.0	3.3	2.5	1.7	1.5	63.0	.020	3
	19.8	4.3	3.3	1.8	0.9	69.3	.008	4
	20.8	3.6	2.3	1.7	1.1	69.8	.012	5
	19.7	3.7	2.9	1.5	0.8	69.4	.007	6*
	19.3	4.3	3.1	1.5	0.8	70.1	.008	7

Analyses obtained by X-ray diffraction for a blended mixture containing an O.P. cement and a pulverised-fuel ash. Nominal composition 30 weight percent cement and 70 weight percent pulverised-fuel ash. (Mixture No.8). Analysed in terms of synthetic cement minerals and different pulverised-fuel ashes.

*denotes analysis using the correct reference components; +denotes a rhombohedral alite; (d) denotes data obtained from Table III.

TABLE IX

Mixture	Nominal wt % cement	wt % cement	wt % ash	R-Factor
1	85	83.8	16.2	.003
2	80	80.8	19.2	.003
3	80	80.0	20.0	.002
4	80	83.0	17.0	.003
5	60	61.4	38.6	.004
6	50	52.8	47.2	.003
7	40	40.9	59.1	.005
8	30	30.9	69.1	.004

Analyses obtained by X-ray diffraction for all of the blended mixtures based on the actual components used in the blend.

obtained using ashes in group one and 59 (σ = 5.65) using the two ashes of group two. In general it appears from the results presented here that acceptable analyses are obtained only when the analysis is given in terms of an ash whose crystallinity index is similar to that of the ash used in the blend. This criterion applies when the analysis is in terms of either an ash and a cement or in terms of an ash and synthetic cement minerals.

CONCLUSION

A blended mixture of pulverised-fuel ash and cement can be analysed equally well either in terms of the ash and synthetic mineral or in terms of the ash and the cement used in the blended mixture. There is some evidence that for the analysis to be acceptable the ash used in the calibration should have a similar crystallinity index to that in the unknown blend.

REFERENCES

1. - A.E.MOORE (1964), SCI Monograph 18, 373-390.

2. - L.P. ALRIDGE (1978), International Cement analysis study, Report No. CO 2267, D.S.I.R. (New Zealand) Chemistry Division, 18p.

3. - G.J.C. FROHNSDORFF AND P. HARRIS (1964), "Use of Digital Techniques to Aid in the Phase Analysis of Multicomponent Mixtures by X-ray Diffraction", Developments in Applied Spectroscopy, Vol 3, Plenum Press New York, 58-68.

4. - L.E.COPELAND AND R.H. BRAGG (1958), Anal Chem 30, 196-201.

5. - R.F. KARLAK AND D.S. BURNETT (1966), Anal Chem 38, 1741-1745.

6. - H.P. KLUG AND L.E. ALEXANDER (1974), "X-ray diffraction procedures for polycrystalline and amorphous material". John Wiley and Sons, New York, 531-565.

Mécanisme d'hydratation d'une cendre de lignite calcaire

Hydration mechanism of a fly ash produced from calcareous lignite

A. CARLES-GIBERGUES, Département de Génie Civil de l'Institut National des Sciences Appliquées de Toulouse,
B. THENOZ, Institut de Géotechnique de l'Université Paul Sabatier de Toulouse et
A. VAQUIER, Institut de Géotechnique de l'Université Paul Sabatier de Toulouse, France.

RESUME : Les cendres volantes de GARDANNE (FRANCE) proviennent de la combustion de lignites calcaires. Elles sont utilisées pour leurs propriétés hydrauliques. Elles renferment essentiellement de la chaux vive, de l'anhydrite et de la larnite associées à une phase vitreuse.

Gâchées avec de l'eau à température ordinaire, ces cendres manifestent une forte réactivité : il apparaît rapidement de la Portlandite, responsable de la prise, puis de l'ettringite. Par la suite, C H diminue progressivement, jusqu'à disparaître, en se combinant au silicium, libéré par le verre et par β- C_2S, sous forme d'un C S H ; parallèlement, se forme C_2ASH_8.

La vitesse de cristallisation de C H et, par voie de conséquence, la vitesse de prise des pâtes cendre-eau est accélérée par la diminution de la quantité d'eau de gâchage et par l'accroissement de la température. L'ettringite, par contre, se décompose au-dessus de 60°C.

C'est la pression de cristallisation de l'ettringite dans des espaces intergranulaires trop faibles qui fissure puis ruine précocement les pâtes pures. Par contre, si la cendre est incorporée, en petite quantité, dans un squelette de gros éléments (grave routière, par exemple) il existe des cavités suffisamment grandes pour assurer la libre expansion de l'ettringite. Dans ce cas, l'enchevêtrement des aiguilles de $C_6A\bar{S}_3H_{30}$ vient s'ajouter à l'action liante de C H qui est, plus tardivement, renforcée puis définitivement remplacée par celles de C S H et C_2ASH_8.

SUMMARY : Fly ash of GARDANNE plant are produced from calcareous lignite coal. They have cementitious properties. The major components are crystalline : lime, anhydrite and larnite. Glassy phase represents some 30 percent of fly ash.

The material reacts with water : C H is formed, which causes the set and ettringite appears more slowly. Afterwards, the amount of C H decreases : this mineral combines with silica, released by the glass and C_2S, to form C S H : subsequently C_2ASH_8 appears.

The rate of hydration of C and setting of pastes are much increased by rise in temperatures (from 2°C to 60°C) and decrease of water : fly ash ratio . Crystallisation of ettringite is also accelerated up to 40°C : the mineral decomposes above 60°C.

The crystallisation pressure of the needles of $C_6A\bar{S}_3H_{30}$ growing in too little intergranular spaces, introduces stresses in hardened young pastes and leads to breakdown.

On the other hand, when fly ash is introduced in coarse aggregates (i. e. in road bases) ettringite develop freely in the large voids of the mix : so, an important contribution to strength is made by the filling of these spaces. In final stage of hydration, C S H and C_2ASH_8 are responsible for rise in compressive strength up to 15 MPa at the age of 180 days.

Ces cendres résultent de la combustion des lignites calcaires du bassin de GARDANNE (FRANCE). Les stériles des combustibles sont, pour la majorité, de la calcite, du gypse, de l'illite, du quartz et de la pyrite. Ils donnent naissance à des cendres relativement pauvres en verre et surtout caractérisées par leurs oxyde et sulfate de calcium cristallisés ; elles font prise au contact de l'eau. A ce titre, elles ne sont pas utilisées comme addition pouzzolanique mais bien comme liant de graves routières. Cette communication, suite des travaux exposés dans une précédente publication (1), se propose d'expliquer l'influence des divers paramètres qui commandent l'hydratation du matériau.

1 - CONSTITUTION MINERALOGIQUE DE LA CENDRE

Les variations de teneurs relatives des minéraux des steriles se répercutent sur la composition chimique des cendres. Aussi, indiquons-nous sur le tableau I les limites 1 et 2 à l'intérieur desquelles se sont situés les échantillons que nous avons étudiés.

TABLEAU I - Composition chimique de la cendre

	Cendre totale		Verre
	lim. 1	lim. 2	
SiO_2	24,8	21,0	32,5
Al_2O_3	14,9	14,7	43,2
Fe_2O_3	6,8	6,6	7,6
CaO	42,9	47,2	11,2
MgO	1,8	0,8	2,4
KO	1,0	0,4	1,2
Na_2O	0,8	0,4	1,2
SO_3	7,0	9,1	0

L'étendue de variation est moins grande que celles rapportées par des auteurs étrangers concernant d'autres types de cendres de lignites (2) (3).

De nombreux grains sont sous forme de sphérules vitreuses : elles sont essentiellement silico-alumineuses et renferment parfois du fer qui les teinte alors en rouge. Les autres particules sont cristallisées en chaux vive, anhydrite, hématite, magnétite, quartz et larnite. L'existence de ce dernier minéral, qui a fait l'objet de controverses, a été, d'une part, constatée par J. MILLET (4) et, d'autre part, est clairement montrée par les diffractogrammes X (figure 1) réalisés sur la cendre brute (1a), sur la cendre traitée à l'eau sucrée (1b), sur ce résidu attaqué par l'acide salicylique (1c).

Le bilan quantitatif des diverses phases s'établit aux valeurs suivantes :

chaux vive : 28 %
anhydrite : 15 %
larnite : 14 %
quartz : 5 %
hématite+magnétite : 4 %
verre : 34 %

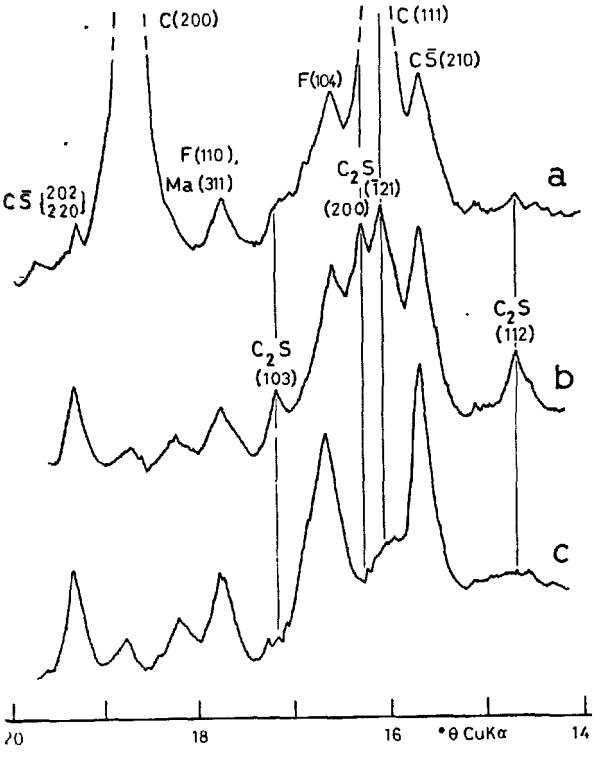

FIGURE 1 - Mise en évidence de $\beta.C_2S$ dans la cendre

Nous avons reporté dans le tableau I la composition chimique -calculée- du verre. Celle-ci s'applique à l'ensemble de la phase vitreuse : elle varie très largement d'une sphérule à l'autre, comme l'ont montré de nombreux auteurs, travaillant sur des cendres de houille, dont B. ALPERN a été l'un des premiers (5).

La répartition de ces constituants varie considérablement avec la granulométrie : c'est ainsi que l'anhydrite se concentre dans la partie la plus fine et que la chaux s'y raréfie.

La masse volumique absolue du matériau avoisine 28 kg/dm^3 ; sa surface spécifique (Blaine) varie entre 2 500 et 3 200cm^2/g et sa granulométrie s'étale, en pratique, de 0,5 à 100μ m.

2 - HYDRATATION DE LA CENDRE

Nous avons mené deux séries d'expériences.

Tout d'abord, et en vue de préciser les mécanismes exacts qui commandent la prise de la cendre, nous avons déterminé les éléments susceptibles de passer en solution. Pour ce faire, comme le conseille COTTIN (6), nous avons jugé préférable d'éviter aussi bien les suspensions très diluées que les rapports solide/liquide élevés et avons choisi la valeur eau/solide, E/S = 10.

Nous avons ensuite cherché à approcher les conditions réelles d'hydratation de la cendre utilisée comme liant en Travaux Publics ; nous avons donc étudié le comportement de pâtes gâchées avec peu d'eau, au rapport E/S = 0,20.

2.1 - Cendre placée dans un excès d'eau

La cendre de GARDANNE agitée dans dix fois son poids d'eau, à température ordinaire (19 à 21°C), subit une dissolution extrêmement rapide et fort importante puisque la perte de poids atteint 3 % après 1 heure, 6 % à 2 heures et se fixe à 9 % au bout de 4 jours. Dans les mêmes conditions, pour une cendre de houille silico-alumineuse, on note respectivement, 0,6 % - 0,9 % et 1,2 %.

Comme il fallait s'y attendre, la cendre relâche surtout de la chaux et des sulfates (figure 2). Le passage en solution de la chaux est extrêmement rapide et important ; il précède celui des sulfates.

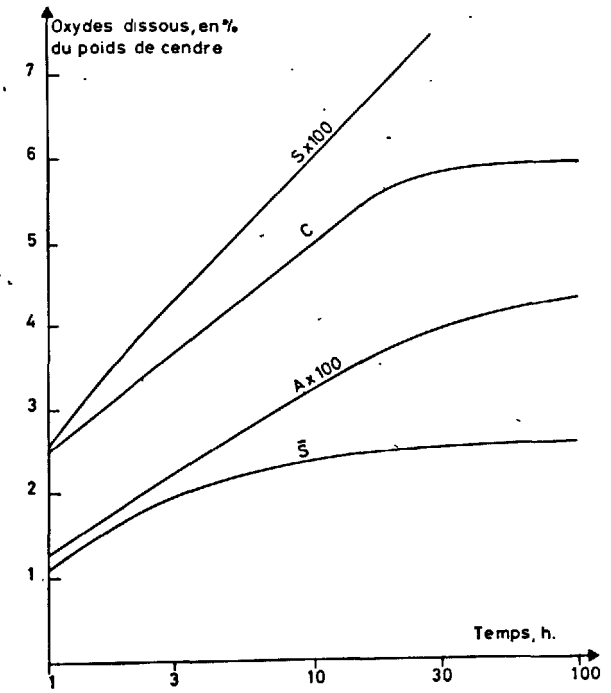

FIGURE 2 - Dissolution de la cendre dans l'eau

La partie vitreuse de la cendre témoigne d'une réactivité non négligeable : silicium et aluminium se retrouvent eux aussi en solution, très vite, mais à des taux évidemment bien inférieurs.

L'étude, par diffractométrie X, montre qu'il s'ensuit des transformations de la constitution minéralogique du matériau. Sur la figure 3, nous avons reporté l'évolution des hauteurs des raies de diffraction, caractéristiques de :

- la chaux, C, plans (200) et (220)
- l'anhydrite, C $\overline{S}$, réflexion $\{^{002}_{020}\}$
- l'association chaux+larnite : plans (111) de C, ($\bar{1}03$), ($\bar{1}21$), et (200) de β - C_2S

rapportées à celle de la réflexion (101) du quartz. L'examen des courbes amène à distinguer deux périodes qui s'articulent approximativement au quinzième jour.

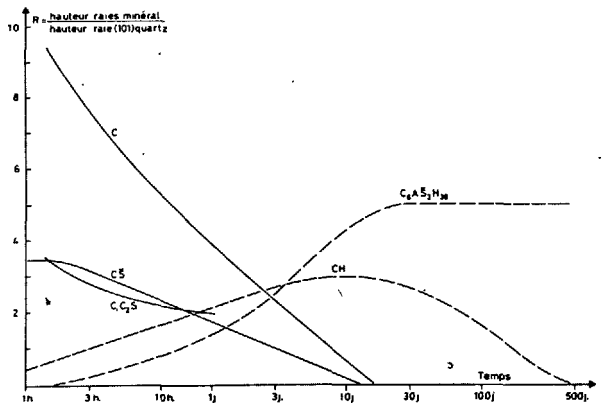

FIGURE 3 - Hydratation de la cendre dans un excès d'eau (E/S = 10)

2.1.1 - Hydratation durant les 15 premiers jours

La chaux vive diminue très rapidement au cours des premières heures, plus lentement ensuite ; elle disparaît pratiquement au bout de quinze jours. La dissolution de l'anhydrite est un peu plus lente à démarrer mais, au bout de quelques heures, elle acquiert une vitesse constante jusqu'à disparition du minéral qui intervient au treizième jour.

La larnite se dissout beaucoup plus lentement que la chaux, comme en témoigne la décroissance, avec le temps, de l'intensité du pic à 2,778 Å ($C + C_2S$), nettement moins rapide que celle de la somme des diffractions de (200) et (220) de CaO.

Simultanément, apparaissent des minéraux hydratés ; au bout d'une heure, de la portlandite, puis, après une heure trente, de l'ettringite.

Ces deux composés sont discernables, tout d'abord, par microscopie électronique à balayage (figure 4), mais aussi, plus tardivement, au microscope optique.

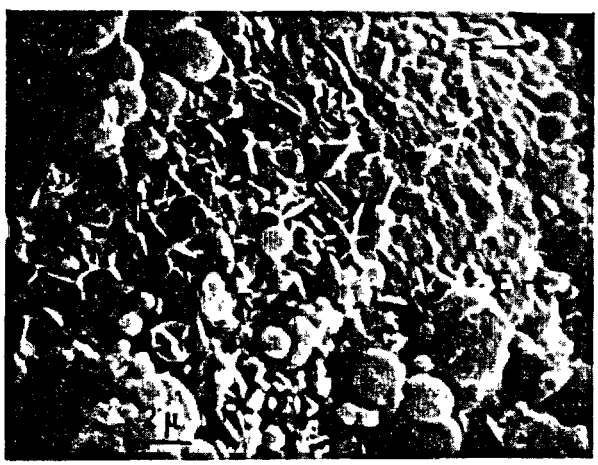

FIGURE 4 - Cendre hydratée 1H30 (E/S = 10)*
(E : ettringite ; P : portlandite)

On se rend compte que les cristaux de portlandite se multiplient et forment un squelette qui rigidifie le matériau. Les cristaux d'ettringite, seulement visibles en petit nombre sur la figure 4 (car l'hydratation n'a duré que 1 heure 30), sous forme de prismes trapus, se développent par la suite surtout perpendiculairement à la surface des grains. Ils reproduisent un arrangement, décrit notamment par A. GRUDEMO (7), caractéristique des structures type-ettringite qui apparaissent dans les jeunes pâtes de ciment. Ces prismes s'allongent avec le temps, écartant progressivement les grains de cendre et détruisant ainsi l'assemblage précédemment réalisé par la soudure des plaquettes de portlandite.

2.1.2 - Hydratation à longue échéance

La consommation de la chaux vive étant achevée au quinzième jour, il ne se forme pratiquement plus de portlandite. Bien au contraire, ce minéral diminue progressivement jusqu'à totale disparition au seizième mois. Ce phénomène est expliqué par la libération continue de silice, à partir de la phase vitreuse et de la larnite qui amène la formation d'un silicate de calcium hydraté, dont les amas de gel spongieux sont bien visibles sur la figure 5.

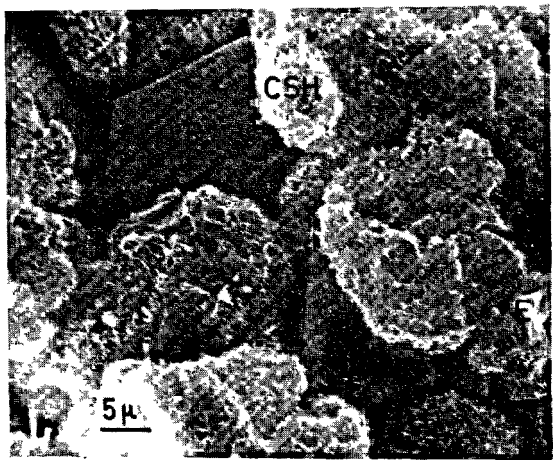

FIGURE 5 - Cendre hydratée 20 mois (E/S = 10)
(E : ettringite, P : portlandite)

La totalité de l'anhydrite ayant disparu au quinzième jour, il n'apparaît pratiquement plus, au-delà de ce terme, d'ettringite supplémentaire : à la longue, elle se convertit partiellement en C_4ASH_{12}. Dans ce milieu où la chaux devient de plus en plus rare et où l'aluminium continue à être libéré par les sphérules vitreuses, on met en évidence, en proportions notables, aux longues échéances, de la gehlénite hydratée C_2ASH_8. Ceci s'accorde bien avec les résultats de LOCHER qui a établi l'instabilité de C_2ASH_8 en présence de chaux (8) et ceux de DRON (9) dans son étude des laitiers.

2.2 - Cendre gâchée en pâte pure

Compte tenu de l'absence d'agitation qui freine le passage des ions en solution, le comportement de la cendre au contact de faibles quantités d'eau (E/S = 0,20), ne diffère pas fondamentalement de celui des suspensions diluées (figure 6).

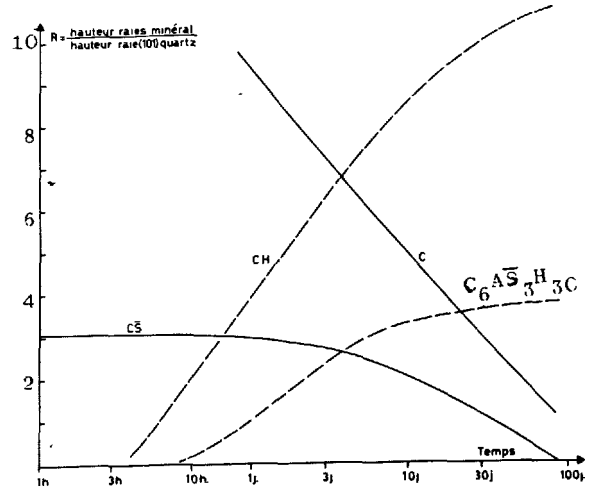

FIGURE 6 - Hydratation de la cendre en pâte pure (E/S = 0,20)

C'est ainsi que la teneur en chaux vive décroît régulièrement pour s'annuler à 6 mois : la portlandite devient décelable au bout de 4 heures. Il faut attendre 7 heures environ pour noter une diminution significative de $C\bar{S}$ conjuguée à l'apparition d'ettringite. Cette dernière atteint pratiquement un palier au bout de 3 mois (épuisement de $C\bar{S}$) et C H y parvient en 6 mois.

3 - FACTEURS PRINCIPAUX COMMANDANT L'HYDRATATION

Nous avons limité notre étude aux deux paramètres qui nous paraissaient devoir jouer un rôle primordial et qui, de surcroît, varient fortement sur un chantier : proportion d'eau de gâchage et température.

3.1 - Influence de la proportion d'eau de gâchage

Celle-ci intervient sur le délai d'apparition des hydrates, puis sur la vitesse de croissance de ceux-ci, mais aussi sur le comportement dimensionnel du matériau hydraté.

3.1.1 - Vitesse de formation des hydrates

Une première indication, globale, susceptible d'intéresser le praticien, est fournie par la vitesse de prise des pâtes pures (mesurée suivant la norme P 15-431). Comme on pouvait s'y attendre, la prise est d'autant plus tardive que E/S est grand. On remarque que c'est spécialement dans le domaine des E/S élevés -qui se rapproche le plus des conditions de chantier- qu'une variation de teneur en eau a les plus fortes répercussions sur le délai de début de prise. C'est ainsi qu'en s'écartant seulement de ± 4 % d'une teneur en eau de 36 %, on fait varier le délai de prise du simple au double. L'examen diffractométrique de pâtes gâchées aux rapports E/S de 0,2 - 0,3 - 0,4, montre que la cristallisation de C H dépend notablement de la teneur en eau (figure 7). Des quantités croissantes d'eau retardent la saturation en C H et, par voie de conséquence, l'apparition de portlandite. Si l'on admet que la rigidification de la pâte est précisément

due à la formation de C H, il y a un bon accord entre vitesse de prise et délai d'apparition de C H. Par la suite, du moins au long des 4 premiers jours où ont été faits nos essais, il n'y a pas de différence significative dans la vitesse de cristallisation de C H lorsque le rapport E/S varie de 0,2 à 0,4.

En ce qui concerne l'ettringite, la précision de la méthode de mesure n'a pas mis en évidence de différence de comportement liée à E/S.

3.1.2 - Comportement dimensionnel du matériau hydraté

Les déformations dues à l'hydratation de la cendre ont été déterminées concurremment par deux méthodes.

a - mesure du volume apparent de la pâte, enfermée dans une membrane très souple et imperméable (par pesée dans un liquide) ;

b - mesure de la longueur d'une plaque, maintenue à température et humidité constantes, au moyen d'un appareil mis au point par C. H. DETRICHE (10).

Sans vouloir entrer dans les controverses qui ont pu naître entre les tenants de ces deux techniques, il est rare que les résultats fournis par ces deux types de procédés coïncident, ainsi que l'on fait remarquer J. BARON et M. BUIL (11). Nos propres essais n'ont pas dérogé à cette règle. Nous avons retenu comme étant les plus significatifs les résultats des essais volumétriques. D'une part, il s'agit d'appréhender le comportement d'un matériau qui sera utilisé en masse et non en couche mince. D'autre part, à cause d'un premier gonflement parasite qui apparaît dans l'essai monodimensionnel, dès que E/S > 0,25, en raison de la trop grande fluidité de la pâte et que nous avons jugé beaucoup plus perturbateur que le très léger frettage exercé par la membrane élastique dans l'essai volumétrique.

Les courbes enregistrées, à 20°C, pour les 4 rapports E/S 0,166 - 0,2 - 0,25 et 0,30 (figure 7), présentent la même allure générale : une première phase de retrait, provoqué par la diminution de volume apparent qui accompagne l'extinction de la chaux vive, précède un gonflement très important, lié à la cristallisation de l'ettringite.

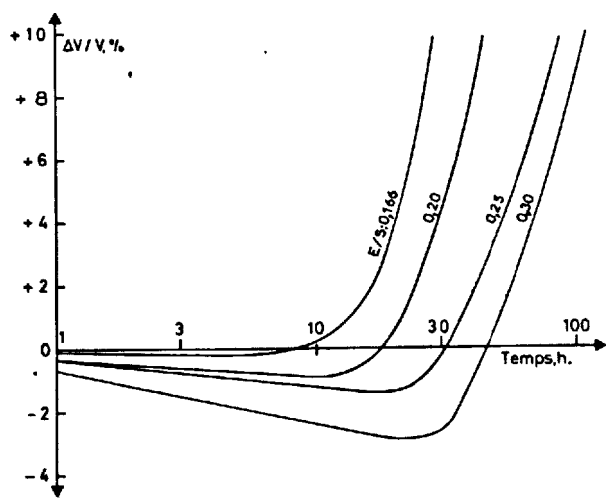

FIGURE 7 - Variations de volume au cours de l'hydratation de la cendre. (température : 20°C)

Le retrait s'effectue suivant une loi en A+B log(temps), A et B étant des constantes dépendant de E/S ; c'est également, dans le même laps de temps, à une loi logarithmique qu'obéit la croissance des réflexions (001) et (101) de C H. Cela établit bien que l'ampleur du retrait initial est liée au degré d'avancement de l'hydratation de C H.

Par la suite, il y a compétition entre ce retrait et l'expansion due à la cristallisation plus tardive de l'ettringite. Bien que la progression de l'hydratation de l'ettringite soit pratiquement indépendante de la teneur en eau, on s'explique toutefois que le délai nécessaire à l'annulation du retrait s'allonge lorsque E/S croît (passant de 4 H. pour E/S = 0,166 à 20 H. pour E/S = 0,30) par la plus grande porosité des pâtes à fort E/S. Dans ce cas, les espaces intergranulaires sont les plus grands, donc les plus longs à combler par les aiguilles d'ettringite.

3.2 - Influence de la température

Elle intervient sur les délais de début de prise, mais aussi sur la vitesse des transformations structurales et sur le niveau des performances mécaniques à long terme.

3.2.1 - Vitesse de prise

Indiquons tout d'abord que la vitesse de prise des pâtes pures est fortement influencée par les variations de température de l'ambiance.

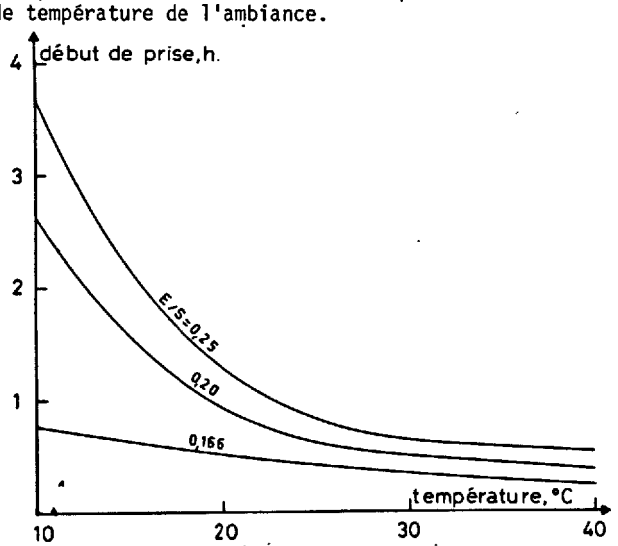

FIGURE 8 - Influence de la température sur le délai de début de prise

La figure 8 l'indique clairement. On ne manquera pas de remarquer que c'est pour les E/S assez élevés (0,30 par exemple) et pour des températures inférieures à 20°C, conditions qui règnent fréquemment dans l'emploi de la cendre en Travaux Publics, que l'action de la température est la plus accentuée ; ainsi, un abaissement de la température ambiante de 18 à 12°C double le délai de début de prise.

3.2.2 - Transformations structurales

Des pâtes gâchées au rapport E/S = 0,25, ont été conservées à des températures de 2°C, 8°C, 20°C, 40°C et 60°C. Nous avons suivi, par diffractométrie X,

l'avancement des modifications structurales en déterminant la vitesse d'extinction de CaO et mesurant la vitesse de formation de l'ettringite.

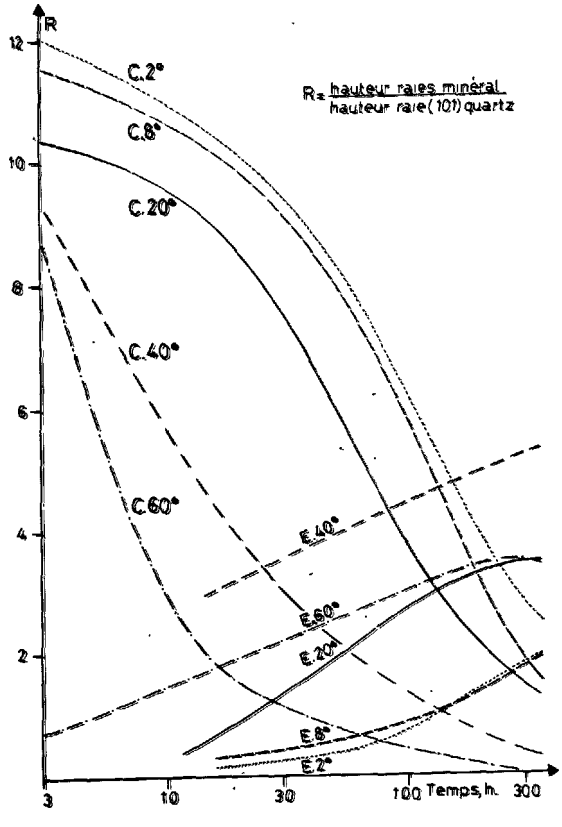

FIGURE 9 - Influence de la température sur l'hydratation de la cendre (E/S = 0,25) (C : CaO ; E : ettringite)

On constate (figure 9) que l'extinction de la chaux est accélérée par la chaleur et ceci dans tout l'intervalle 2°C - 60°C. Par contre, en ce qui concerne $C_6\overline{AS}_3H_{30}$, si sa formation s'accélère bien de 2°C à 40°C, un freinage intervient dès que la température avoisine 60°C. Le minéral devient instable : ceci est confirmé par sa totale disparition des pâtes conservées 7 mois à 60°C.

Par ailleurs, nous avons observé que les pâtes maintenues à basse température manifestent les meilleures résistances mécaniques. Les spécimens conservés à 60°C et 40°C, pendant 7 mois, sont redevenus pulvérulents ; à 20°C, leur cohésion est négligeable ; au-dessous de 8°C, leur structure est encore compacte et leur résistance à la traction (par fendage) atteint 0,7 à 1 MPa.

4 - CONCLUSION

Il convient essentiellement de noter que la cendre de GARDANNE, selon qu'elle est hydratée en pâte pure ou fortement diluée dans un squelette très poreux, et bien que les réactions d'hydratation soient les mêmes, manifeste deux comportements différents.

A court terme et à température ordinaire, apparaît d'abord de la chaux éteinte responsable de la prise, puis de l'ettringite. Si la cendre a été gâchée en pâte pure, par suite de l'exiguïté des vides intergranulaires, la croissance des aiguilles de $C_6\overline{AS}_3H_{30}$ amène rapidement la fissuration, puis la désagrégation du matériau hydraté. Par contre, lorsque cette même cendre est incorporée en faible proportion dans un arrangement de gros granulats (par exemple une grave routière traitée par 3 à 5 % de cendre), il existe une porosité suffisamment grande pour que le développement des cristaux d'ettringite n'écarte pas les éléments déjà soudés par la portlandite. On peut même penser que, par sa cristallisation enchevêtrée, cette ettringite renforce largement la cohésion du matériau hydraté, ce qui s'accorde avec les observations faites notamment par D. CZAMARSKA et al. (12) sur des bétons.

A long terme, la libération d'alumine et de silice par le verre et de silice par C_2S provoque la disparition de C H qui se transforme en un C S H auquel vient s'ajouter, plus tardivement, du C_2ASH_8. Ces deux constituants contribuent, par leurs propriétés hydrauliques marquées, à accroitre les performances mécaniques du matériau durci ; c'est ainsi que les résistances à la rupture par compression monoaxiale de mélanges graves-cendres de GARDANNE dépassent largement 15 MPa.

REFERENCES BIBLIOGRAPHIQUES

(1) A. CARLES-GIBERGUES (1978) "Propriétés hydrauliques des cendres volantes sulfocalciques de GARDANNE" Bulletin de liaison des Laboratoires des Ponts et Chaussées, n° 93, 5-8 (Français)

(2) M. MRAZ (1978) "Utilisation des cendres volantes en Tchécoslovaquie" Compte rendu conférence sous-produits et déchets dans le Génie Civil, Paris, vol. II, pp. 387-391 (Français)

(3) D. L. NICOLESCU (1978) "Influence des cendres volantes de Roumanie sur les propriétés des ciments et bétons" Compte rendu conférence sous-produits et déchets dans le Génie Civil, Paris, vol. II, pp. 393-398, (Français)

(4) J. MILLET(1977) Laboratoire Central des Ponts et Chaussées - Communication orale

(5) B. ALPERN (1965) "Application de la microsonde électronique à l'étude des cendres volantes et des minéraux des charbons" Document intérieur CERCHAR, n° 1562, (Français)

(6) B. COTTIN (1978) "Cinétique d'hydratation du ciment Portland en présence de gypse et de sulfate de potassium" Il Cemento, n° 75, 177-188 (Français)

(7) A. GRUDEMO (1977) "Strength-structure relationships of cement paste materials" CBI forskning research, 83-84, (Anglais)

(8) F. W. LOCHER (1960) "Proceedings fourth international symposium chemistry of cements, Washington

(9) R. DRON (1974) "Mécanisme de la prise du laitier granulé sous activation alcaline" Rapport de recherche du Laboratoire Central des Ponts et Chaussées n° 38, (Français)

(10) C. H. DETRICHE (1977) "Contribution à l'étude des déformations des couches minces de mortiers de liants hydrauliques" Thèse Université Paul Sabatier de Toulouse (Français)

(11) J. BARON, M. BUIL (1979) Remarque à propos de l'article "Mechanical features of chemical shrinkage of cement pastes" par N. SETTER et D. M. ROY, Cement and Concrete Research, vol. 9, pp. 545-547, (Français)

(12) D. CZAMARSKA, St. JAZWINSKI, K. BURACZYNSKI (1972) "Etude de la zone de contact entre le mortier en gypse et le béton à l'aide du microscope à balayage" Comptes rendus Colloque R. I. L. E. M. 1972, Toulouse, vol. I, pp. 18-32 (Français)

The reactions of fly ash and Portland cement with relation to the strength of concrete as a function of time and temperature

Les réactions des cendres volantes sur le ciment portland et leur effet sur la résistance du béton en fonction du temps et de la température

P.L. OWENS, Technical Manager, Pozzolanic Limited, Chester, U.K. and
F.G. BUTTLER, Chemistry Department, Teeside Polytechnic, Middlesbrough, U.K.

RESUME : Quand le béton de ciment Portland subit des élévations de température, dues à la chaleur d'hydratation du ciment, sa résistance à long terme et sa durabilité s'en trouvent affectées. En outre, si ce béton subit de fortes élévations de température (par exemple plus de 60°C) dans son jeune âge, il en résulte un matériau amoindri et de résistance limitée à long terme, bien inférieure à celle du même béton conservé dans l'eau à 20°.

En utilisant un ciment Portland additionné de proportions variables de cendres volantes de qualité contrôlée, et en le soumettant à différentes sortes d'hydratation et de cure, on a établi que la résistance de ce ciment hydraté, aux divers âges, était en relation étroite avec la proportion de $Ca(OH)_2$ présente dans ce ciment hydraté. Il aussi été établi qu'en augmentant la proportion de cendres volantes, non seulement on augmentait les résistances (qui d'ailleurs croissent plus vite quand la température de cure augmente), mais aussi que la proportion de chaux libre diminuait.

SUMMARY : Where Portland cement concrete is subjected to rises in temperature, due to the effect of the heat of hydration of the cement, the long term strength and durability of that concrete is usually adversely affected. Further when Portland cement concrete is subjected at early ages, to excessively large temperature rises i.e. exceeding 60°C, the result is a concrete of restricted and limited strength reached within days, in contrast to that which is expected from the long term storage of concrete in water at 20°C.

By simulating different typical curing regimes to which concrete can be subjected the strength of the hydrate at different ages, with various combinations of Portland cement and controlled quality fly ash, can be related to the quantity of lime, as $Ca(OH)_2$, found in the structure of the hydrate. It was also found that as the proportion of fly ash increased not only was there an improvement in strength, which increased with temperature of curing, but that in the hydrate there was an incidental reduction in the quantity of lime.

Within the range from nil to 75% fly ash as a proportion of the cement content, at about 30% fly ash, a maximum strength was attained at 28 days from curing at 80°C, this coincided with a reduction of about 50% in lime content of the hydrate. However, this amount of lime is more than sufficient to provide adequate protection to embedded steel reinforcement.

1.0 INTRODUCTION

1.1 When concrete made with Portland cement undergoes an early age temperature rise, such as that caused by the heat of hydration of the cement, the strength at 28 days is reduced in proportion to the size of the temperature change (1).

1.2 This reduction of strength can be partly explained by the combination of the impaired bond at the interface of paste and aggregate, known as micro-cracking (2) and by the macro-fracture of the gel structure by the expansion of air and water (3). However, if these phenomenon normally occur in concrete, how can the significant increase of strength be explained that occurs to concrete by the use of a composite cement, such as made of Portland cement and fly ash.

1.3 Research has shown that under comparable high temperature curing conditions, the 28 day strength of Portland cement concrete can be 60% or less of that made with a composite cement (4). This indicates, that whilst concretes made with different types of cement can undergo similar orders of temperature change, during hydration, there could be a significant difference in the chemical structure of the hardened paste.

2.0 EXPERIMENTAL

2.1 For this research to have practical application the test specimens required conditions of curing typical of that known to occur in concrete at early ages (5). The profiles of temperature and time known to be caused as a result of cement hydration are mainly dependant on the quality of cement and the dimensions of the element. Thus both the greater the cement content and/or size of the element, the greater will be the profile of temperature with time.

2.2 Figure 1 illustrates four profiles of temperature and time that are typical for a range of different conditions. Profile A represents for instance the standard curing of test specimens at 20°C, and profile D which could be typical of that within an element that has dimensions exceeding 2.5m x 2.5m x 2.5m, cast with concrete made with 450 kg/m^3 Portland cement.

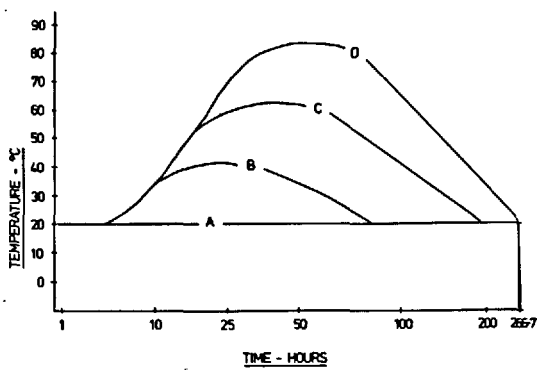

Fig. 1 - Typical temperature/time profiles for concrete.

2.3 The technique for inducing the temperature rise in the test specimens, similar to that of the profiles in Figure 1 was to match by similation the different curing regimes. This was done by having a series of 7 water baths each held at a constant temperature of 20, 30, 40, 50, 60, 70 & 80°C. Then by the transfer of sealed test specimens at various predetermined times the heating and cooling cycles of each profile of temperature could be similated to those shown in Figure 2.

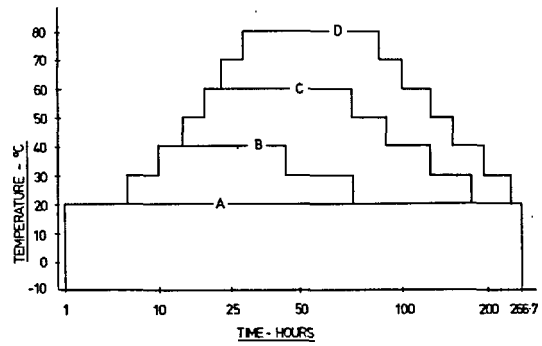

Fig. 2 - Curing cycles simulated to typical temperature/time profiles.

2.4 The authors have also observed from other research

i) Other than under adiabatic conditions the peak temperature experienced in most concrete elements usually occurs within 50 hours after casting.

ii) At 20°C the pozzolanic reaction between Portland cement and fly ash commences usually at about 11 days.

2.5 The means of correlating the effects of the different temperature profiles with both the maturity and the test results of the specimens, was to assume the equivalent period at 20°C was to the base temperature of -10°C (6). Thus the relative maturity of specimens cured by different regimes of temperature could be assessed to approximately 11 days or 8000°C hours (266.67 hours at 20°C.) Then by making the curing regimes conform with convenient factors of maturity i.e. 1.0, 1.125, 1.5 & 2.0, the test results could be correlated to 8000°C.

2.6 In conjunction with the primary test age at 11 days, the test times at 50 hours and 28 days were included so that crushing strength, the more conventional method of assessment, could be related to the different levels of maturity.

3.0 DETAILS of materials, mixes and tests

3.1 The criteria for the Portland cement selected was that it should be from a source with characteristics as close to the mean of that for all UK produced Ordinary Portland cements. Details of the cement used together with the mean and range of variability of 25 UK sources (excluding N. Ireland) are shown in Table 1.

See table I
page IV - 65

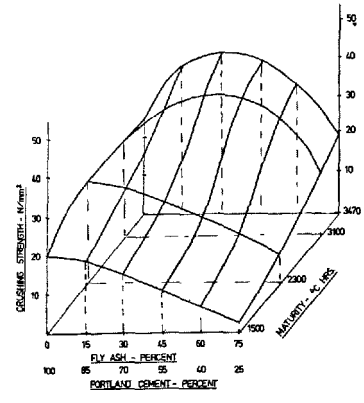

Fig. 3 - Effect of fly ash on the 50 hour strength as affected by maturity.

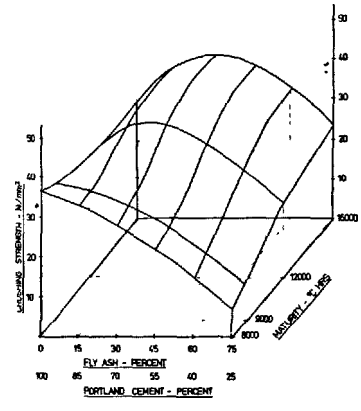

Fig. 4 - Effect of fly ash on the 11 day strength as affected by maturity.

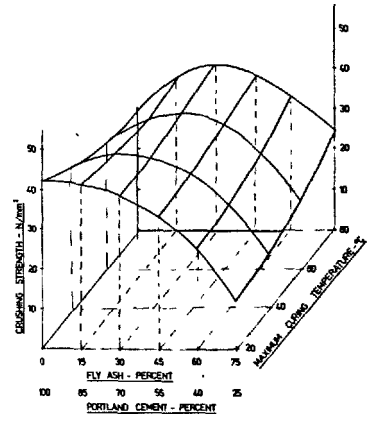

Fig. 5 - Effect of fly ash on the 28 day strength as affected by maximum curing temperature

3.2 The fly ash conformed with UK Agrement Board Certificate ABC 75/283 (7). The results are compared in Table 1 with

i) the typical chemical composition of UK fly ash, calculated to 3.0% loss on ignition, after (8) and

ii) the mean quality of fly ash to ABC 75/283 produced during the period July, 1978 to June, 1979.

3.3 The mix was mortar, based on 1:3; cement:sand, to BS 4550 Part 6 quality. The mortar was machine mixed by a standard procedure, with sufficient water to attain a measured ASTM flow consistency of 100 - 110%. In each mix the fly ash substituted a proportion of the Portland cement in increments from nil to 15, 30, 45, 60 & 75%. In consequence the proportion of gauging water required was reduced relative to the amount of fly ash used from 0.495 for the control mix with no fly ash to 0.465, 0.445, 0.415, 0.40 & 0.39 respectively

3.4 From each mix 18 No. 50 mm cube specimens were made, compacted by vibration in 2 layers, then sealed and stored immediately, still in the mould, in water at 20°C. All specimens were removed from the moulds at 22 hours, sealed in polythene air evacuated envelopes and returned to the respective curing regime. At the appropriate time 3 specimens from each mix were tested for the determination of crushing strength and $Ca(OH)_2$ content.

3.5 The technique used for the determination of $Ca(OH)_2$ content was by the carbonation method of thermal analysis (9). This was effected by drilling to the centre of each of 3 cubes and immediately testing each of the drillings.

4.0 TEST results

4.1 The results of the crushing tests at 50 hours, 11 days and 28 days are shown diagramatically in Figures 3, 4, & 5.

4.2 The results for the amount of $Ca(OH)_2$ present at 11 days are shown diagramatically in Figures 6, 7, & 8.

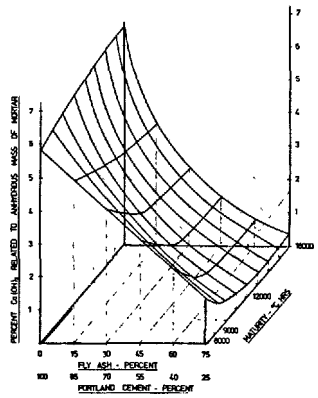

Fig. 6 - Calcium Hydroxide in mortar at 11 days

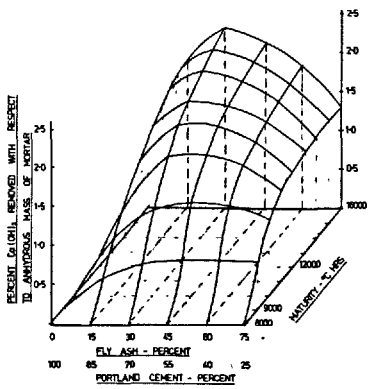

Fig. 7 - Percent Calcium Hydroxide removed in mortar at 11 days.

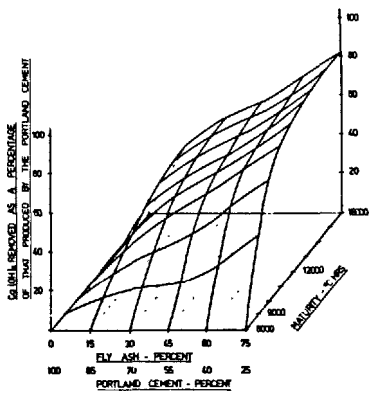

Fig. 8 - Percent Calcium Hydroxide remaining at 11 days.

5.0 DISCUSSION of the results

5.1 The crushing strength of the mortar with no fly ash cured at 20°C at 50 hours, 11 and 28 days was 19.1, 36.3 & 41.8 N/mm² respectively. Although the mortar was different in every respect i.e. mix proportions, size of aggregate and water/cement ratio, very close agreement was obtained to the respective concrete crushing strength shown in Table 1.

5.2 The reduction of 32 percent in 28 day crushing strength of the mortar, with no fly ash, cured at more than 60°C is similar in magnitude to that found by other research (1).

5.3 For comparable curing conditions, at and exceeding 60°C, the 28 day crushing strength of the mortar with no fly ash was less than 70% of that made with 30% fly ash, this follows the effects found in (4).

5.4 Figure 3 shows that

i) The strength at 20°C decreases proportionally with the percentage fly ash.

ii) The increase in strength with maturity of the mortar with no fly ash is not maintained above 2750°C hours, where increased maturity reduces the strength.

iii) Corresponding with increases in both fly ash content and maturity, the strength of the mortar increases. The optimum strength occurs with about 35% fly ash at a maturity of 3470°C hours. This approximates with a 2.64 factorial increase in strength for 2.33 factorial increase in maturity.

5.5 As Figure 4 shows at 11 days the trend is similar to that at 50 hours, in that:

i) The crushing strength at 20°C proportionally decreases with the amount of fly ash, indicating little or no pozzolanic reaction.

ii) The reduction in strength with increasing maturity for the mortar containing no fly ash is in agreement with other research (1).

iii) By doubling the maturity and increasing the fly ash to 50%, twice the strength is obtained. However, the maximum strength obtained corresponds with about 30% fly ash.

5.6 Figure 5 shows the effect of fly ash on the 28 day crushing strength as affected by the early curing regimes and that:

i) The crushing strength at 20°C is no longer proportional to the increase in fly ash, and there is indications of a strong pozzolanic reaction at all percentages of fly ash.

ii) The strength, as affected by the early age curing regime of mortar without fly ash, is decreased, but increased at all percentages of fly ash, particularly at 75% where the 20°C strength is doubled by curing at 80°C.

5.7 Figure 6 shows the percentage $Ca(OH)_2$ plotted with respect to both the percentage fly ash and the maturity in °C hours. The $Ca(OH)_2$ is expressed as a percentage of the anhydrous weight of the sample, as the total loss on ignition of each sample was known from the thermogravimetric analysis.

The surface denoted by the solid lines in Figure 6 shows the amount of $Ca(OH)_2$ found to be present, and the surface denoted by the dashed lines the amount of $Ca(OH)_2$ that would have been present, from the cement, if there had been no reaction with the fly ash.

With each of the curing regimes the amount of $Ca(OH)_2$ present, is proportional to the amount of Portland cement used and, therefore the amount of $Ca(OH)_2$ formed for each concentration of Portland cement was calculated from the results obtained with no fly ash.

5.8 It is apparent from Figure 6 that:

i) For samples cured at 20°C for 11 days there is a straight line relationship between the percent $Ca(OH)_2$ and the percentage fly ash, indicating no pozzolanic reaction, which confirms the strength observations in 5.5.i.

ii) For all other samples, in which both the maximum temperature attained and the period the samples experienced temperatures in excess of 20°C, the linear relationship ceases to exist between the percent $Ca(OH)_2$ and the percentage of fly ash. In every case the fly ash reduced the amount of $Ca(OH)_2$ present when compared with similar samples cured at 20°C.

iii) Where no fly ash was used there was an increase in the percentage of $Ca(OH)_2$ when the curing temperature exceeded 20°C.

5.9 The difference between the two surfaces illustrated in Figure 6, corresponds with the amount of $Ca(OH)_2$ which has been removed by reaction with the amount of fly ash present. This difference is shown in Figure 7 where the percentage $Ca(OH)_2$ removed is plotted with respect to both the amount of fly ash and the maturity at 11 days. Figure 7 also shows that the greatest amount of $Ca(OH)_2$ was removed from specimens containing about 30% fly ash. Since the amount of $Ca(OH)_2$ removed must have reacted with the fly ash, and if it is assumed that such a reaction increases the strength of the mortar, then this result implies that the greatest increase in strength with the curing regimes used, should occur with this amount of fly ash. This conclusion is seen from Figure 4 to be in very good agreement with the strength of the mortars at 11 days.

5.10 Figure 8 shows the amount of $Ca(OH)_2$ that has been removed expressed as a percentage of that available from the cement. It is evident that the quantity removed increases with the percentage of fly ash. With the greatest percentage of fly ash very little free $Ca(OH)_2$ remained in the hydrate. Such evidence is important when considering the necessity of having sufficient $Ca(OH)_2$ present from the cement for good corrosion protection to the steel reinforcement of structural concrete. However, it should be noted that although some 50% percent of the available $Ca(OH)_2$ has been removed when using about 35% fly ash, the amount of $Ca(OH)_2$ remaining is more than sufficient to maintain a pH of about 12.5 with good corrosion protection.

6.0 CONCLUSIONS

6.1 By subjecting mortars to curing temperatures similar to those that can occur in practice the effects on concrete strength can be simulated.

6.2 The adverse effects of high curing temperatures on the strength of Portland cement mortars can be related to the amount of lime in the hydrate.

6.3 If high temperatures are likely to be experienced in practice, gains in strength are likely to occur with cements composed of Portland cement and fly ash.

6.4 The amount of residual lime in the hydrate, even when 75% fly ash was used, is sufficient to afford inhibition of corrosion to embedded steel reinforcement.

REFERENCES

1. - VERBECK, G.J. & HELMUTH, R.H. Structures and physical properties of cement paste. From the proceedings of the 5th International Symposium on the chemistry of cement, Tokyo, 1968, Part 3, Properties of cement paste and concrete.

2. - FORRESTER, J.A., Discussion, Propagation of cracks and their detection under short and long-term loading. The structure of concrete and its behaviour under load, Proceedings of an International Conference, London September, 1965 pp 157 to 160, Cement & Concrete Association, 1968.

3. - ALEXANDERSON, J. Strength losses in heat cured concrete. Swedish Cement and Concrete Research Institute, Stockholm, 1972 pp 135. Handlingar Nr 43.

4. - BAMFORTH, P.B., In-situ measurement of the effect of partial Portland cement replacement using either fly ash or ground granulated blast furnace slag on the early age behaviour of mass concrete. Taylor Woodrow Research Report No. 014J/77/1939, October, 1977(Project on behalf of Building Research Establishment).

5. - HARRISON, T.A., Early-age temperature rises in concrete sections with reference to BS 5337 : 1976. Cement and Concrete Association ITN5, November, 1978.

6. - MALHOTRA, V.M., Maturity concept and the estimation of concrete strength - a review. Department of Energy, mines and Resources (Ottawa, Canada, November, 1971, Catalogue No.M38-3/277.

7. -THE AGRÉMENT BOARD CERTIFICATE No 75/283 "Pozzolan - a selected fly ash for use in concrete".

8. - SMITH, M.A. & HALLIWELL, F., The application of the BS 4550 test for pozzolanic cements to cements containing pulverized-fuel ashes. Department of the Environment, Building Research Establishment. Magazine of Concrete Research, Volume 32, Number 108. September, 1979. Cement and Concrete Association.

9. - BUTTLER, F.G. & MORGAN, S.R., A thermoanalytical method for the determination of the amount of Calcium hydroxide formed by hydration of Portland cement. Contribution to this Congress.

TABLE 1

Details of the chemical and physical properties of the Portland cement and fly ash used compared with the UK typical characteristics for those materials

Property Description	PORTLAND CEMENT			FLY ASH		
	Sample	Typical 1978 UK Ordinary Portland cement to BS 12.		Sample	Typical UK fly ash calculated to 3.0% Loss on ignition	
		mean	Std. Deviation		mean	Std. Deviation
Lime Saturation Factor	0.94	0.96	0.03	-	-	-
Bogue Compound Composition % C_3S	56.4	54.0	5.25			
(assuming nil free lime) C_2S	15.2	18.0	5.56			
C_3A	10.5	9.5	1.92			
C_4AF	7.8	7.7	1.61			
Chemical Composition % Silica as SiO_2	20.13	20.48	0.87	52.5	50.00	2.54
Insoluble residue	0.40	0.44	0.26	-	-	-
Alumina as Al_2O_3	5.60	5.29	0.59	27.5	27.23	2.91
Iron as FeO	-	-	-	-	2.40	0.67
Fe_2O_3	2.56	2.53	0.52	9.50	6.75	2.32
Lime as CaO	63.10	64.26	0.71	1.8	2.52	1.08
Magnesia as MgO	2.25	1.39	0.48	1.9	1.76	0.31
Alkalis as Na_2O	0.18	0.21	0.08	0.9	1.04	0.57
as K_2O	0.78	0.70	0.24	3.8	2.96	1.00
Sulphate as SO_3	2.92	2.57	0.23	0.7	0.84	0.37
				Fly ash to ABC 75/283 (1978 / 79)		
Colour Index	3	3.04	0.73	4.0	3.2	1.50
Loss on Ignition %	1.18	1.52	0.41	3.0	2.7	1.33
45 µm sieve residue %	12.0	12.9	4.0	5.8	6.5	1.97
Specific Surface Area m^2/kg	345	345	31	405	385	97
Density kg/m^3	3225	3180	47	2325	2320	80
Concrete Strength N/mm^2 50 hours	20.1	-	-			
0.60 w/c ratio, 20mm Aggregate 3 days	23.0	23.0	2.60			
310 kg/m^3 Portland cement 11 days	34.7	-	-			
28 days	41.3	43.9	2.46			

Hydration of cements with pozzolanic additions

Hydratation des ciments avec additions pouzzolaniques

J. GRZYMEK, Professor, Stanislaw Staszic Academy Of Mining and Metallurgy in Cracow Poland.,
W. ROSZCZYNIALSKI, Assistant,
K. GUSTAW, Assistant professor.

RESUME : Des recherches ont été faites sur la cinétique de l'hydratation des ciments contenant des ajouts de gaize ou de diatomites. Pour faciliter les comparaisons, on a essayé simultanément les mêmes ciments, additionnés de filler calcaire. Les observations ont duré une année, en utilisant la calorimétrie, l'analyse aux rayons X, l'A.T.D. et la porométrie. Les propriétés physiques fondamentales de ces ciments ont aussi été mesurées.

On a pu ainsi déterminer les variations qualitatives et quantitatives des pâtes hydratées, en fonction de l'ajout pouzzolanique. Une attention particulière a été portée à la composition minéralogique des pâtes pendant l'hydratation. Des relations ont été établies entre le processus d'hydratation de ces ciments et leurs propriétés physiques.

SUMMARY : Investigations concerning the kinetics of pozzolanic cements hydration were carried out for the cements with the additions of diatomite /high silica pozzolana//and lime-gaize /silica-lime pozzolana/. For comparative reasons similar investigations were carried out for the ordinary Portland cement and for cement with the addition of limestone. The processes of hydration was examined from its very beginning over one-year period. The following investigations methods were used: calorimetric analysis of the heat evolved during hydration, as well as X-ray diffraction, DTA and porosimetric analyses of cement pastes. The basic physical properties of cements were also determined.

The results of the investigations allowed to determine various qualitative and quantitative changes which occured in the hydration process under the influence of pozzolanic additions. Special attention was paid to the phase contents of the hydrating pastes. The relations between the hydration processes of the examined cements and their physical properties were also analysed.

INTRODUCTION

The process of hydration of pozzolanic cements is very complicated and difficult to be fully explained because of the fact that it is differently influenced by different pozzolanic addition. The papers published till today dealt mostly with the influence of natural volcanic pozzolanic materials and with such artificial pozzolanic additions as flying ashes /1,2,3,4/. The number of investigations on natural pozzolanic materials of sedimentary origin is however much smaller /5/. Numerous investigations have already thrown some light on the process of hydration of pozzolanic cements, several problems remain however still unsolved.

The present investigations have been carried out in order to determine the influence of diatomites with high silica content and of gaizes containing silica and lime on the hydration of pozzolanic cements. Diatomites are well known and widely used as pozzolanic additions /6/, the suitableness of gaizes has been recently established in the result of our former investigations /7,8/.

The investigations comprised determinations of hydration heat, of phase composition, of porosity and of the specific surface area of pozzolanic cements in the process of binding and hardening. To facilitate the comparison pure Portland cements /without additions/ and cements with limestone additions were parallelly investigated.

MATERIALS USED IN INVESTIGATIONS

Materials used in investigations are characterized in the table I. These materials were mixed together in appropriate proportions

TABLE I

	Diatomite	Gaize	Limestone	Portland clinker	Gypsum
SiO_2 %	72,71	45,58	8,68	21,96	8,38
Al_2O_3 "	8,27	2,73	2,62	4,71	1,53
Fe_2O_3 "	3,69	1,89	1,31	2,99	1,67
CaO "	1,19	25,44	47,86	67,66	30,32
MgO "	0,96	1,04	1,21	1,52	0,92
SO_3 "	-	0,18	0,02	0,35	36,77
Ign.loss "	11,05	21,96	38,04	0,10	20,01
SiO_2 act.%	43,82	14,05	-	-	-
Phase composition	Amorphic silica ~50% Detrital quartz ~15% Glauconite ~15% Illite ~10% Kaolinite~ 5% Hydrogethite, Ilmenite, Oxides of iron, titanium and manganium	Amorphic silica ~15% Detrital quartz ~25% Calcite~45% Glauconite ~10% Muscovite, Feldspars, Oxides and Hydroxides of iron	Calcite~85% Detrital quartz ~ 5% Glauconite, Illite, Muscovite, Oxides and Hydroxides of iron	C_3S = 69,1 % βC_2S = 10,5 " C_3A = 7,4 " C_4AF = 9,1 " CaO_{free} = 0,8 "	$CaSO_4.2H_2O$ ~80% Detrital quartz ~ 5% Calcite ~ 5% Anhydrite, Dolomite, Feldspars, Clay minerals, Oxides of iron
Specific weight G/cm³	2,17	2,56	2,75	3,10	2,41
Spec. surface area according to Blaine cm^2/G 1/	4060	4530	5020	2270	-
Spec. surface area according to BET 1/ cm^2/G	494 000	474 000	426 000	188 000	-

1/ Specific surface area as determined after grinding during 30 min. in a normalized laboratory mill.

and ground to cements with following compositions:

cement 1 - 95% clinker + 5% gypsum

cement 2 - 52% clinker + 3% gypsum + 45% diatomite

cement 3 - 52% clinker + 3% gypsum + 45% gaize

cement 4 - 52% clinker + 3% gypsum + 45% limestone

Investigations were carried out on pastes and mortars obtained from these cements.

DETERMINATION OF THE DEGREE OF HYDRATION

Heat of hydration was determined dynamically in almost adiabatic conditions using a differential calorimeter system. Calorimetric investigations were carried out for mortars containing cement, sand and water in following weight proportions: 167 : 751 : 100. During first three days of hydration the determinations were carried out continuously.

X-ray, DTA and porosimetric determinations were carried out on pastes with W/C = 0,5 after 1, 3, 7, 28, 90 and 365 days of curing in normalized conditions.

CALORIMETRIC ANALYSIS

Curves illustrating the evolution of hydration heat as determined from calorimetric investigations are shown in figure 1.

All additions investigated in this paper i. e. diatomite, gaize and limestone accelerate the apparition of the maximal heat effect. This fact can be explained as follows: pozzolanic additions i.e. diatomite and gaize bind and remove calcium hydroxide from the reaction interface and accelerate the process of hydration owing to the fact that the hydration rate is influenced by the concentration of $Ca/OH/_2$ in the solution. Calcium carbonate contained in the limestone and gaize reacts with C_3A very fast and with a great heat effect to form a hydrated calcium compound of the formula $C_3A.CaCO_3.12H_2O$. All additions under investigation exhibit a remarkable grindability and appear therefore in cement mixtures in form of very fine grains which separate the cement grains and accelerate the reaction between cement and water facilitating the access of water molecules. Micrograins of additions act simultaneously as crystallization nuclei in the first stage of hydration.

X-RAY INVESTIGATIONS

From all results of X-ray investigations diffractograms shown in figure 2 have been chosen to illustrate the phase composition of cements pastes after 90 days of hydration.

X-ray investigations have demonstrated that the additions affect the qualitative phase composition of hydration products in a very small extent. The relative amounts of diffe-

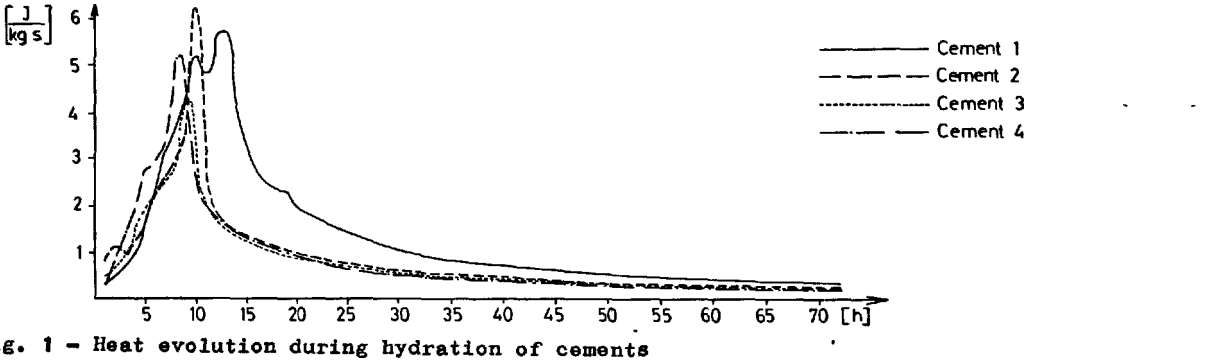

Fig. 1 - Heat evolution during hydration of cements

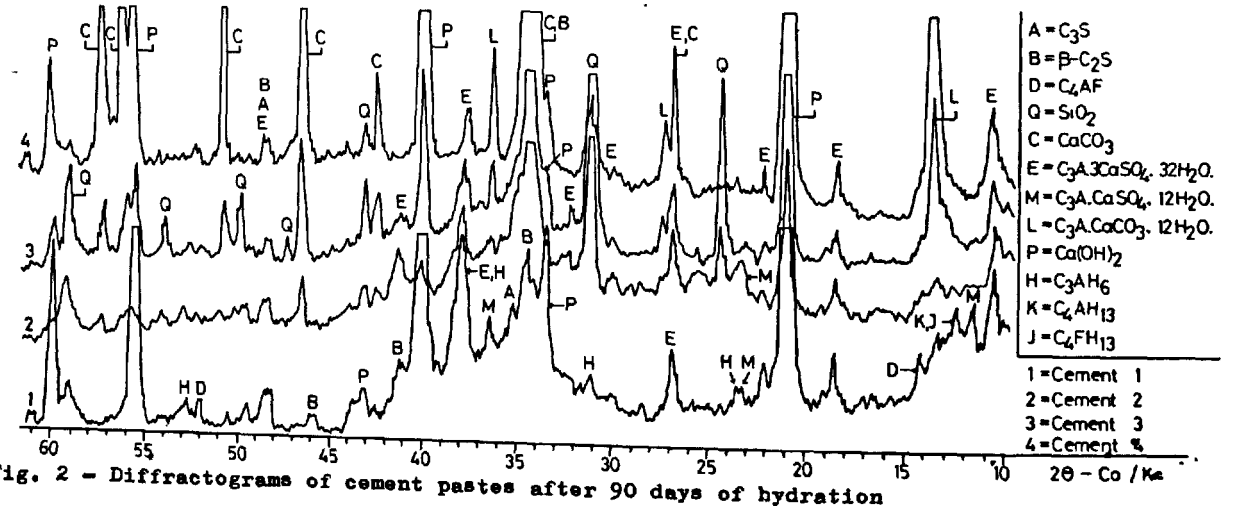

Fig. 2 - Diffractograms of cement pastes after 90 days of hydration

rent products changing in the function of time are however very strongly influenced by the introduced additions. The influence exerted by additions is better observable after longer hydration times; diffractograms taken after 90 days have been therefore selected to be presented in this paper.

Cement pastes with diatomite and gaize additions contain great quantities of CSH especially after longer hydration times. This can be explained by the assumption that active silica contained in these additions reacts with calcium hydroxide formed in the result of hydrolysis from calcium silicates.

X-ray investigations prove - in the case of all examined pastes - that clinker minerals and active additions succesively disappear with increasing hydration time. In the case of cements with additions the hydration of alite occurs faster than in the case of pure Portland cement. This phenomen can be clearly observed in the case of diatomite and gaize additions. Already in the course of some first hours of hydration considerable amounts of ettringite are formed. After three days the ettringite content begins to decrease and the $C_3A.CaSO_4.12H_2O$ - content correspondingly to increase. Gypsum additions can not be detected already after 24 hours of hydration. After longer hydration times /90 and 365 days/ formation of $CaCO_3$ and $C_3A.CaCO_3.12H_2O$ is observed. It must be however emphasized that in the case of cements with limestone and gaize additions great amounts of $C_3A.CaCO_3.12H_2O$ have been observed already in the very first stages of hydration. This can be explained taking into account the activity of $CaCO_3$ contained in limestone and gaize towards C_3A /9/.

DTA INVESTIGATIONS

The DTA method creates the opportunity to determine the amount of water bound in hydration products, type of these products and their content in the paste. The $Ca/OH/_2$ content can be determined with a considerable exactness owing to the fact that the endothermic heat effect which appears at 500°C and corresponds to dehydration of this compound does not coincide - in the majority of cases - with other thermal effects. The calcium hydroxide content in the paste after different hydration times illustrates the influence of additions on the rate of hydration. The amounts of $Ca/OH/_2$ in function of time for pastes containing pozzolanic active additions are shown in figure 3.

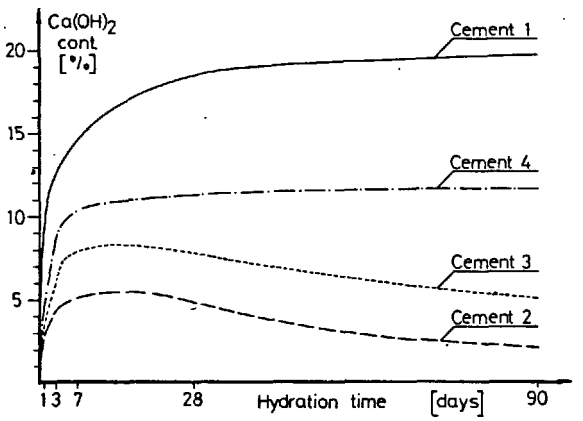

Fig. 3 - $Ca/OH/_2$ content in cements pastes in function of time.

The curves presented in figure 3 prove that with increasing hydration time the $Ca/OH/_2$ content in the case of pure Portland cement pastes increases and amounts to 19,8% after 90 days. The $Ca/OH/_2$ content increases most rapidly in the first stage of hydration. In the case of cements containing limestone additions the shape of this curve is almost the same. Substitution of 45% clinker by limestone results in decreasing the $Ca/OH/_2$ content. In the case of cements with diatomite and gaize additions the maximal $Ca/OH/_2$ content appears between the 7th and 28th day of hydration. After this period the $Ca/OH/_2$ content in pastes begins slowly to decrease and amounts after 90 days to 2,26 for diatomite and to 5,06 for gaize additions. Active silica contained in these additions reacts obviously with $Ca/OH/_2$ formed in the process of hydration, binds it up to hydrated calcium silicates and decreases therefore its content in the paste. The amounts of active SiO_2 in gaizes are smaller than in diatomite; the quantities of $Ca/OH/_2$ bound by gaize are therefore smaller than in the case of diatomite.

DETERMINATIONS OF THE SPECIFIC SURFACE AREA AND OF POROSITY

Specific surface areas determined according to the BET method after different hydration times for cements pastes under investigation are presented in table II.

Specific surface areas increase from the be-

TABLE II

Cement	Specific surface area in m^2/G after different hydration times					
	1 day	3 days	7 days	28 days	90 days	365 days
1	26,3	32,0	38,1	49,7	48,2	35,9
2	42,0	47,3	62,1	64,9	51,9	49,8
3	36,1	42,8	53,4	62,0	54,2	42,3
4	37,2	43,1	53,4	57,4	47,4	38,1

ginning to the 28th - 90th days of hydration, pass a maximum and then slowly decrease. Such changes result from the fact that the porosity of pastes is also changing in the process of hydration. The porosity of pastes decreases - generally taken - with increasing degree of hydration, but simultaneously changes also the size distribution of pores /the number of micropores increases and the number of meso- and macropores decreases/. In the result the specific surface area of hardening pastes firstly increases and then begins to decrease when the decreasing porosity has reached a definite level /usually between the 28th and the 90th day of hydration/

Specific surface area and porosity of cement pastes containing diatomite are greater then those found for gaize and limestone additions. Smallest values of specific surface area and of porosity were observed in the case of pure cement pastes /without additions/.

INFLUENCE OF ADDITIONS ON THE PROPERTIES OF HARDENED PASTES AND MORTARS

Compressive strengths of mortars obtained from investigated cements are shown in figure 4.

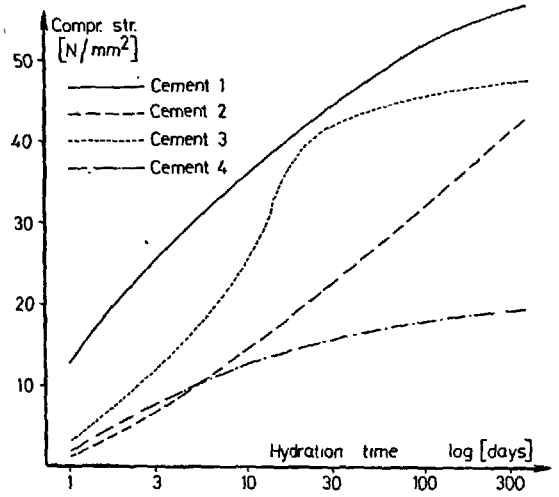

Fig. 4 - Compressive strength of examined cement mortars

In the first stage of hardening the compressive strength of specimens containing addition is smaller than that of mortars obtained from pure Portland cement. This can be easily understood in view of following facts:
1/ 45% of cement have been substituted by materials which do not increase the compressive strength in the first stage of hydration,
2/ all introduced additions increase considerably the porosity of mortars.
After longer hydration times, when the products of reaction between pozzolanic additions and calcium hydroxide begin to be already important, the compressive strength of cements with diatomite and gaize additions considerably increases.

Figure 5 illustrates the relation between porosity of pastes and their compressive strength. The influence of porosity on compressive strength is more pronounced at lower porosities i.e. after longer hardening

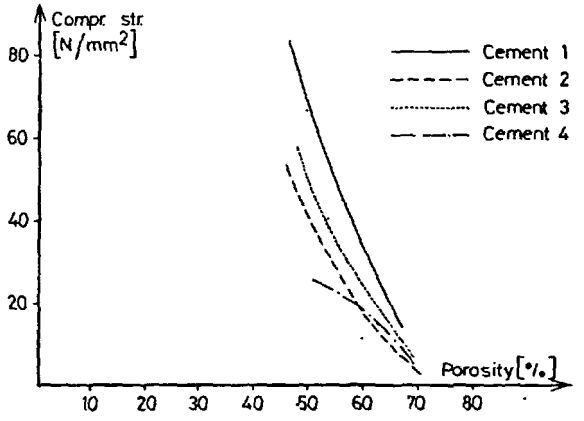

Fig. 5 - Compressive strength in function of porosity of cement pastes

times /28 - 365 days/. As easily seen from figure 5 compressive strengths of different pastes can be different inspite of the fact that the porosities are similar. This is due to the fact that the compressive strength of cement pastes do not depend on their porosity only but also on their qualitative and quantitative phase composition /10/.

TABLE III

Cement	Compressive strength after 3 years storing N/mm²					
	in water		in a 2% Na_2SO_4 solution		in a 2% $MgSO_4$ solution	
	B	C	B	C	B	C
1	10,0	67,2	4,0	38,9	0,2	20,0
2	8,4	42,8	5,3	45,3	3,9	41,6
3	8,8	47,2	6,5	51,4	6,0	44,4
4	4,9	19,5	4,7	31,6	3,2	25,4

B - bending strength C - compressive strength

All investigated additions increase the corrosion resistance of cement mortars to sulphates. The results of determinations are shown in table III.

The positive influence of diatomite is due to pozzolanic reaction which results in binding calcium hydroxide and in formation of low-basic hydrated calcium silicates resistant to corrosion. Decrease of calcium hydroxide content in the mortar prevents formation of greater quantities of gypsum /under the influence of sulphates contained in the solution/ and of ettringite. The resistance improving influence of limestone can be explained by reaction with C_3A and formation of $C_3A.CaCO_3.12H_2O$ which is insoluble in aggressive sulphate solutions. Gaize improves the corrosion resistance owing to pozzolanic reactions and owing to the binding of C_3A by $CaCO_3$ contained in this addition.

Cements containing diatomite and gaize additions are characterized by smaller /57 - 62%/ hydration heats than that observed in pure Portland cement mortars.

CONCLUSIONS

Pozzolanic additions i.e. diatomite and gaize have been proved to exert a considerable influence on the process of hydration of cements. Limestone additions participate also actively in this process. Additions change the properties of cements in which they have been introduced. Owing to their properties the diatomite, gaize and limestone added cements can find use as low-caloric binding materials highly resistant against aggressive sulphate solutions. Cements with gaize additions exhibit especially usefull properties.

BIBLIOGRAPHY

1.- R. TURRIZIANI /1964/, "Aspects of the Chemistry of Pozzolanas", The Chemistry of Cement, Edited by H.F.W. Taylor, Accad. Press, 2, 68 - 86.

2.- R. SERSALE, P.G. ORSINI /1969/, "Hydrated Phases after Reaction of Lime with Pozzolanic Materials or with Blast Furnace Slags", Proc. Fifth Int. Symp. on the Chem. of Cement, Tokyo 1968, The Cement Assoc. of Japan, Tokyo, Part IV, 114 - 121.

3.- P. TERRIER, M. MOREAU /1966/, "Recherche sur le mechanisme de l action pouzzolanique des cendres volantes dans le ciment", Rev. Mater. Construct. Trav. Publics 613, 379 - 396 et 614, 440 - 451.

4.- M. KOKUBU, D. YAMADA /1976/, "Cementy s dobawkoj zoły", Szestoj Miezdunarodnyj Kongress po chimii cementa, Moskwa 1974, T. III Cementy i ich swoistwa, Moskwa, Strojizdat, 83 - 94.

5.- F.Ł. GLEKIEL /1975/, "Fiziko-chimiczeskije osnowy primienienija dobawok k mineralnym wjażuszczim", Izd. FAN Uzbekskoj SSR, Taszkent, 69 - 115.

6.- H. von RIEPERT /1927/, "Zement Industrie", Zementverlag GMBH - Charlottenburg, 3 - 87.

7.- A. DERDACKA, K. GUSTAW, S. KOZŁOWSKI, W. ROSZCZYNIALSKI, K. WYRWICKA /1975/, Symp. "Dziś i jutro wykorz. nauki do zmniejsz. materiałochł. wyrobów z tw. poch. min. lub nieorg.", Sopot, 81 - 89

8.- A. DERDACKA, W. ROSZCZYNIALSKI, K. GUSTAW /1976/, "Der Einfluss von Zusätzen auf die Eigenschaften von Zementen", Baustoffindustrie A - 3, 14 - 16.

9.- E. SPOHN, W. LIEBER /1965/, "Reaktionen zwischen Calciumcarbonat und Portlandzement", Zement Kalk Gips 9, 483 - 485.

10.- J. JAMBOR /1963/, "Relation between phase composition, overall porosity and strength of hardened lime - pozzolana pastes", Mag. Concrete Res. 15, 131 - 142.

Preparation of Fly Ash Cements.

Préparation des ciments aux cendres volantes.

H.C. ALSTED NIELSEN, F.L. Smidth et Co. A/S Vigerslev Alle 77 DK-2500 Valby Copenhagen, Denmark.

RESUME : Il est toujours possible d'utiliser des cendres volantes pour la production de clinker. Elles peuvent être ajoutées au mélange cru destiné aux fours à voie sèche alors que, pour le procédé humide, elles nécessitent certaines modifications.

Les cendres volantes à haute teneur en carbone doivent être insufflées dans la zone de cuisson, ce qui permet de tirer profit de leur pouvoir calorifique.

Seules des cendres volantes de composition uniforme et appropriée et de basse teneur en carbone peuvent être utilisées comme composant dans le ciment fini. Les travaux d'essais et de perfectionnement dont il est fait ici mention, indiquent comment broyer les cendres volantes.

SUMMARY: Fly ash may always be used in the manufacture of clinker. It can be added to the raw mix for dry process kilns, but only with certain modifications for the wet process.

High-carbon fly ash should be insufflated into the burning zone, whereby advantage can be taken of the heat value.

Only fly ash with a consistent, suitable composition and a low carbon content should be used as a constituent of finished cement. The testing and development work reported here indicates how fly ash cement should be milled.

1. INTRODUCTION

Fly ash is, and will be, collected at our power stations in large quantities; one of the areas where this material can be put to use is in the manufacture of cement and concrete.

Technically, fly ash can be utilized in several ways at a cement works; the optimum utilization for any fly ash will be a function of its fineness, chemistry, and homogeneity.

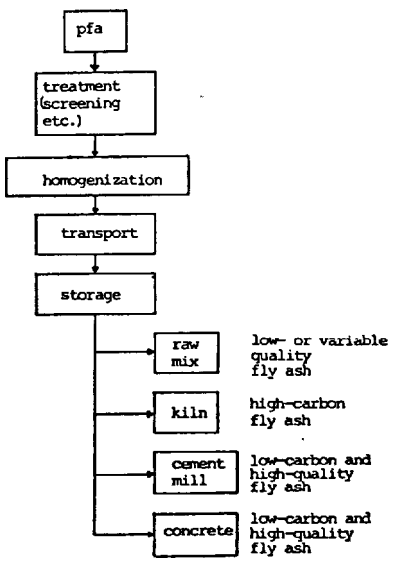

Fig. 1 - Utilization of FLY ASH (PFA)

When of a sufficiently high standard, fly ash may be added directly to concrete. Similarly, cement clinker can be milled together with gypsum and fly ash, yielding either a modified Portland cement or a fly ash cement, depending on the relative amounts of clinker and fly ash. Also in this instance, a consistently high quality of the fly ash is essential.

However, when fly ash either varies in quality or is of low quality as, for example, with respect to colour due to carbon content, special precautions have to be taken; one way is to treat fly ash as a conventional raw material, using it as part of the raw mix - meal or slurry - which is fed to the kiln. In this way fly ash of varying chemical composition can be utilized without impairing the quality of the cement.

When the coal content of fly ash is high, a better method would be to insufflate the fly ash into the burning zone of the rotary kiln. In this manner it is possible to utilize the heat value remaining in the residual carbon of the fly ash.

The method chosen to utilize each fly ash should be decided on its individual merits; a combination of two or more methods can also prove to be the optimum solution.

PFA - pulverized fuel ash or fly ash - can also be upgraded. Stockpiling of ash in a large homogenizing plant or in silos is possible and at times quite desirable, either when fly ash is drawn from different sources, or when coal of various origins is burned.

Residual carbon in PFA is an undesirable constituent, due to its colour as well as to its tendency to absorb concrete additives. Many plants have tried to overcome these difficulties by removing the carbon from the PFA; the coal can be separated off by screening, as the coal particles are concentrated in the coarser fraction of PFA (above 100 microns). Other solutions are to burn off the carbon, or for instance to submit the coal to a flotation process.

The best solution of all, of course, exists when the power plant regards the fly ash as a product; this means using boilers designed for coal combustion, operating them as base load utilities, and burning blended coal.

This procedure must yield a PFA with suitable, consistent chemical and mineralogical composition, and containing less than 2-3% residual coal.

2. CEMENT WITH PFA

Our testing and development work has shown us how to utilize fly ash from different sources and of varying composition.

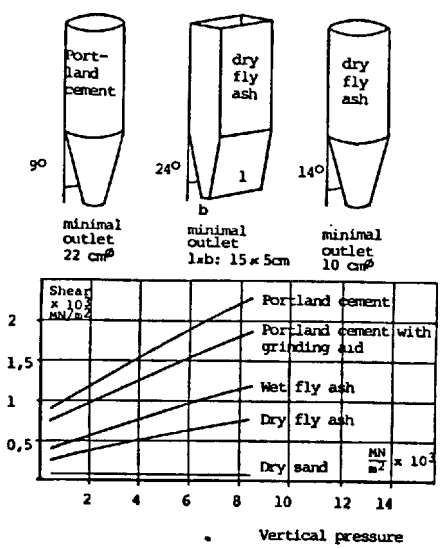

Fig. 2 - Shear testing of PFA and cement and silo dimensions for mass flow.

Inferior grades of PFA should always be used as raw material. At a cement plant operating according to the dry process, fly ash can easily replace part or all of the shale or clay in the raw mix. Certain factors have to be considered when designing the handling facilities for PFA, owing to its easy flowability. Fig. 2 shows the easy flow of a dry fly ash compared to that of a Portland cement.

At a wet process plant, the hydraulic properties of fly ash prove to be a drawback to its use in the kiln slurry, thickening the slurry, raising its viscosity, and increasing the water content required for acceptable flowability. One solution to the problem is to add a retarding agent, but usually the costs involved are too high.

A more economical way is to prepare the slurry within 1-2 hours before usage. Research work at our laboratories has indicated that such a slurry may be handled in a pressure filter, thereby reducing the amount of water evaporated in the rotary kiln.

In both wet and dry process kilns, PFA can be insufflated directly into the burning zone, thus utilizing the heat value. This method is the best solution when dealing with high-carbon fly ash, which may be injected in an amount of up to 8% by weight of clinker.

3. FLY ASH CEMENT

High-quality fly ash can be utilized directly in cement. The desired cement product might be one with a low PFA-content or with up to 30% of PFA. The qualities required are the following:

High fineness
Low carbon content
High glass content
Low alkali content

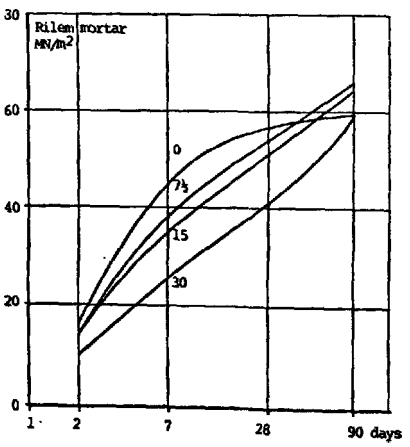

Fig. 3 - Variation in compressive strengths with the PFA content in per cent. Inter-ground cements at 42% residue on 25 μ by air elutriation.

In judging the strength development, however, it can be concluded that an addition of fly ash results in a reduction in early cement strength as shown in Fig. 3.

The figure shows compressive strength obtained with cements of constant fineness. Cement and fine, low-carbon fly ash were ground together in a ball mill. The cement and fly ash compositions are shown in the Table.

TABLE

Analysis	Cement	Fly Ash
SiO_2 %	21.4	46.9
Al_2O_3 -	5.2	23.1
Fe_2O_3 -	3.1	8.7
CaO -	64.6	6.2
MgO -	1.5	4.0
K_2O -	0.56	2.2
Na_2O -	0.38	0.7
Loss on Ign.	1.0	4.2
S -	0.8	0.5
Carbon -	-	3.6
Fineness		
+ 0.25 mm		3
+ 0.09 mm		18
+ 0.063 mm		23
+ 0.045 mm		29
+ 0.02 mm		50
Blaine, cm^2/g		4250
Spec.gravity g/cm^3		2.4

The decrease in compressive strengths can be partly compensated for by finer grinding. For instance, examination of Fig. 4 reveals that increased grinding improves the compressive strength; however, some difference in strength is likely to remain at the higher fly ash substitution levels. Part of this remaining difference could be eliminated by further prolonged grinding, using more energy per ton cement produced.

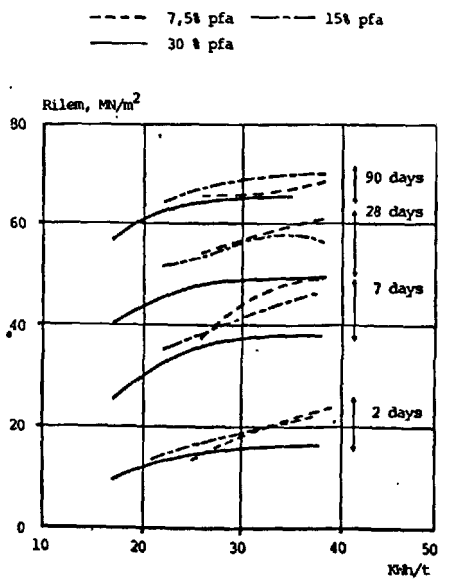

Fig. 4 - Variation in strength with grinding energy and PFA cement.

The milling of cement and fly ash can be carried out in several ways. Clinker, gypsum, and fly ash may be fed to the same mill, grinding either in open or in closed circuit, with an air separator.

Fly ash may also be mixed directly with Portland cement, since the fly ash from some installations is extremely fine.

Fig. 5 shows suggestions for some possible milling circuits.

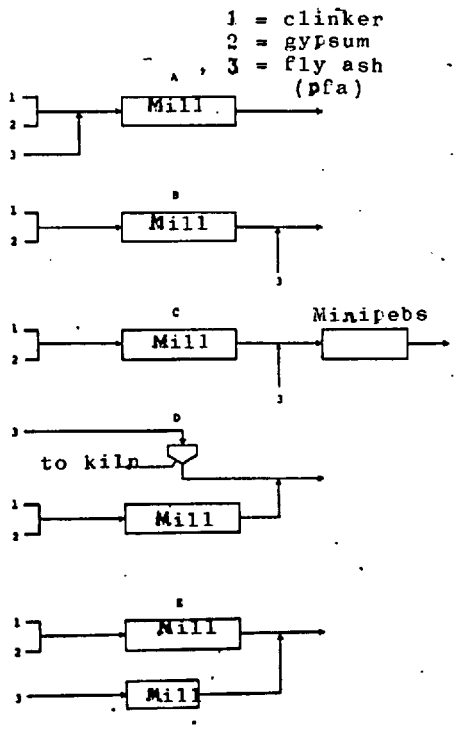

Fig. 5 - Milling circuits.

We have studied these circuits in a large number of test grinds, accurately recording the specific power consumption and measuring the compressive strengths of the resulting cements. One set of results appears on Fig. 6.

Here intergrinding (Circuit A) gives the best overall performance, followed by the circuit in which only the finest part of the fly ash is utilized for mixing into cement (Circuit D).

Using the PFA as received (Circuit B) appears to be a less suitable way of preparing fly ash cement.

Fly ash is fine, and a special mill might be used for its grinding before mixing with Portland cement (Circuit E). Judged on the basis of energy consumed, the final result is better than using PFA as received, but is not so good as when PFA is separated, and only the fine fraction is utilized. The PFA was ground in an ordinary Cylpebs mill to a 5.5% residue on 25 microns and a specific surface of 5000 cm^2/g, according to the Blaine method.

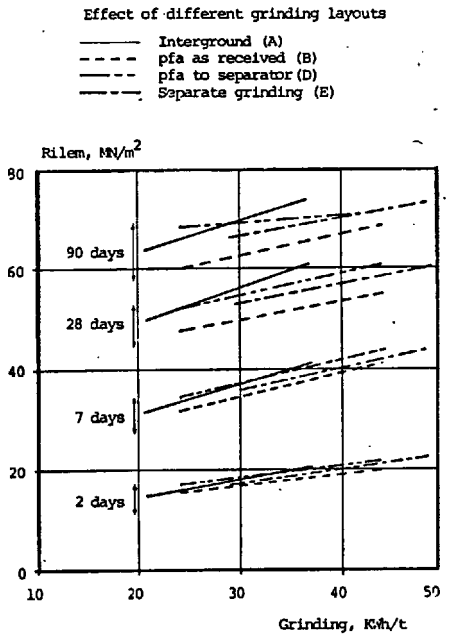

Fig. 6 - 15% PFA cement

In fact, fly ash is so fine that a special mill with quite small grinding media should be employed as for instance the Minipebs mill. In this way a saving in the overall consumption of energy between 5 and 10% can be achieved.

A method combining the advantages of Minipebs grinding and of combined grinding is shown in the layout labled Circuit C.

Although combined grinding appears to be the optimum solution, possibly owing to the mutual abrasion of fly ash and cement, further studies have been made of separate grinding of cement and of fly ash. The reason for this is that, generally, when grinding two materials of different hardness or toughness, a saving in energy is obtained if each material is ground in its own mill.

In our grinding experiments we have carried out three test series:

Series 1 30% PFA, Total 35 kWh/t
Series 2 15% PFA, total 35 kWh/t
Series 3 30% PFA, total 45 kWh/t

With the three series we varied the extent of grinding of fly ash (PFA) and of Portland cement (96% clinker + 4% gypsum). The degree of milling was varied in such a manner that the total energy consumption for grinding the mixture of Portland cement and fly ash added up to either 35 kWh/t or 45 kWh/t.

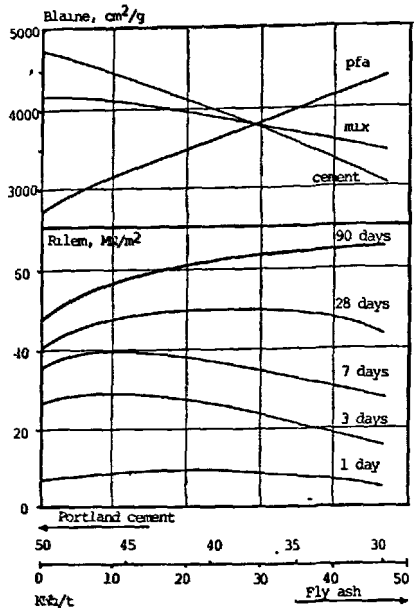

Fig. 7 - PFA cement with 30% PFA. Mixed from separately ground Portland cement and fly ash - power consumption of the mixture equal to 35 kWh/t.

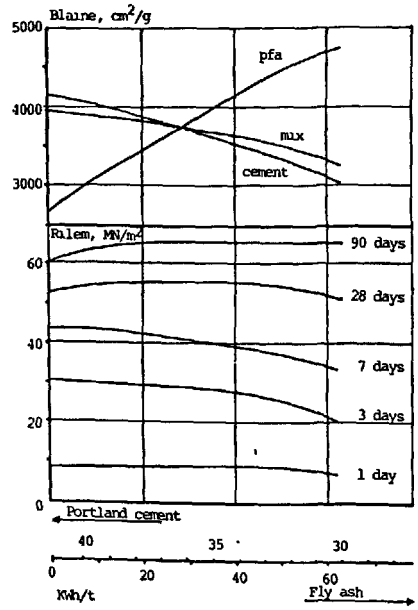

Fig. 8 - Fly ash cement containing 15% fly ash. A total energy consumption of 35 kWh/t has been achieved by mixing separately ground Portland cement with separately ground fly ash.

The results appear in Fig. 7, Fig. 8, and Fig. 9. Each of these figures contains two sets of curves, one for the Blaine surfaces of Portland cement, fly ash, and PFA cement obtained at a given specific energy input, while the second set describes the strength found for the mixtures (PFA cements), also as a function of the distribution of energy between Portland cement and fly ash.

All the results indicate that the long-term strength level (90 days) improves as more of the energy input is used for grinding the fly ash.

Good short-term strengths (3 days) can be obtained, even with a PFA cement containing 30% of fly ash, provided that the Portland cement-part receives proportionally more of the grinding energy than the fly ash. It appears that the finer Portland cement results in an early strength development.

The very early (1 day) strengths are always on the low side. The strengths at intermediate testing ages (7 days, 28 days) tend to be low. The highest 7-day strengths are found when grinding is concentrated on the Portland cement-part, while the optimum 28-day values are achieved at equal milling of cement and fly ash.

In other words, it is possible to design the strength development of a PFA cement to suit the market conditions by concentrating the grinding on either the Portland cement or the fly ash.

CONCLUSION

Fly ash (PFA) may always be used in the manufacture of clinker. It can be added to the raw mix for dry process kilns, but only with certain modifications for the wet process, unless the fly ash is non-hydraulic.

High-carbon fly ash should be insufflated into the burning zone, whereby advantage is taken of the heat value. Fly ash up to 8% of clinker by weight can be injected with air into the burning zone.

Only fly ash with a consistent and suitable composition and a low carbon content should be used for cement grinding.

For production of a PFA cement with a fly ash content of up to 15%, milling can with advantage be carried out by combined grinding of the three materials (clinker, raw gypsum, and fly ash) in one mill.

For higher fly ash contents, separate grinding of fly ash and Portland cement presents some advantages, as it is possible to design the rate of strength development to suit the market requirements.

Up to a certain level increased comminution will be beneficial. When considering separate grinding, more grinding energy results in an equalizing of the optimum grinding values for clinker and fly ash, respectively (Fig. 9).

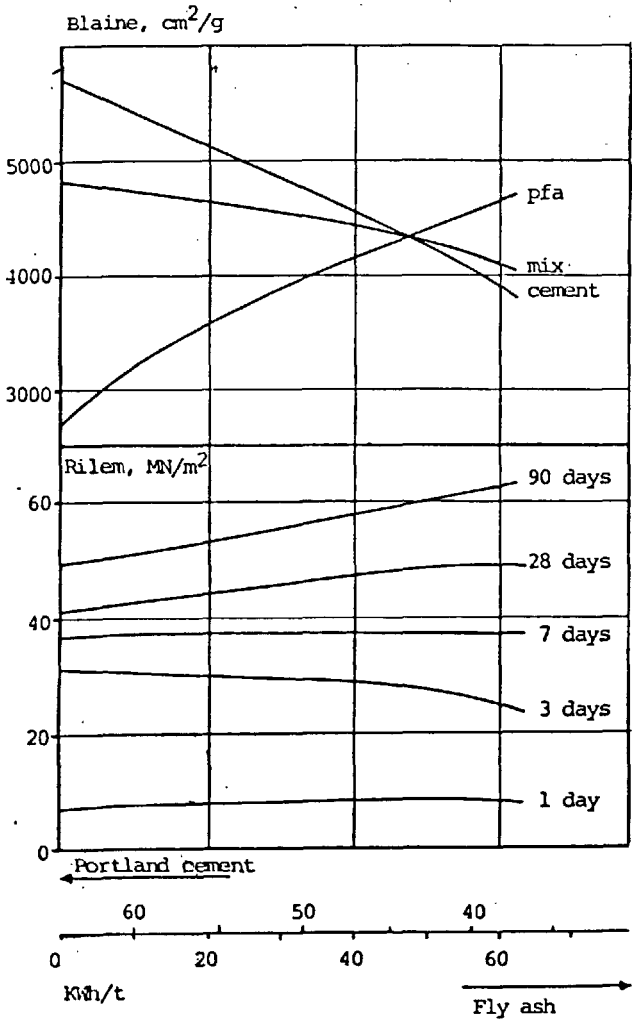

Fig. 9 - Fly ash cement containing 30% PFA.

A total energy consumption of 45 kWh/t has been achieved by mixing separately ground Portland cement and fly ash.

Except after 90 days, a fly ash cement with 30% fly ash will have strength inferior to a Portland cement. The relative strengths for a PFA cement and an ordinary Portland cement, both ground with an energy consumption of 35 kWh/t, are shown in Fig. 10. Combined grinding presents an acceptable solution to the grinding problem. However, separate grinding has the advantage that planned levels of strength are achievable; indeed, either short-term or long-term strengths can be emphasized, (starting with the same clinker and fly ash).

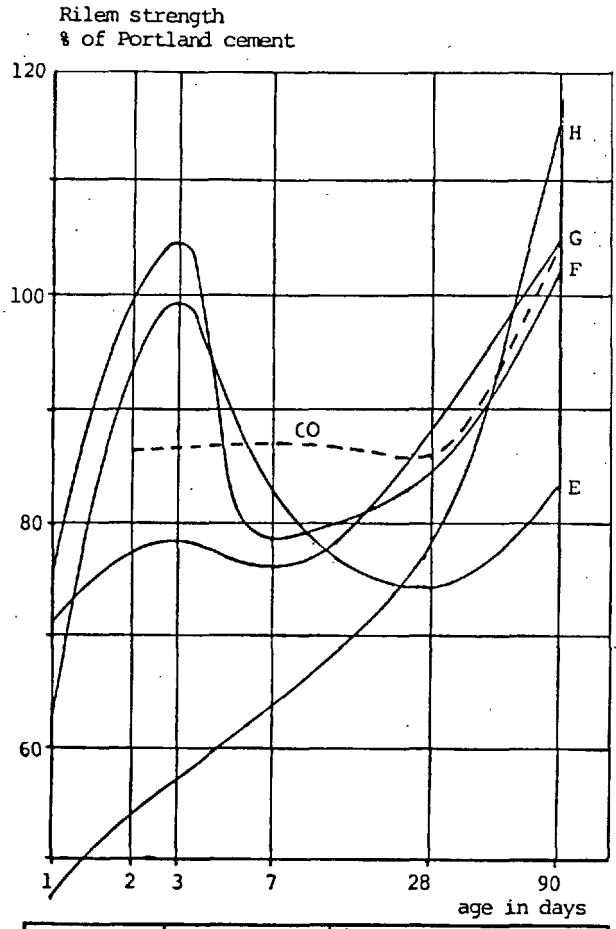

Legend index	ground	energy distribution PC, %	pfa, %
E	separate	100	0
F	—	90	10
G	—	70	30
H	—	60	40
CO	combined		

Fig. 10 - Comparison between interground and separately ground fly ash cements. Total grinding energy 35 kWh/t. 30% fly ash.

Cementitious Fly Ashes - Structural and Hydration Mechanism

Cendres volantes hydrauliques. Mécanisme de l'hydratation et de la formation de la structure

R.C. JOSHI, Associate Professor and M.A. WARD, Professor, Department of Civil Engineering.
The University of Calgary, Calgary, Alberta, Canada.

RESUME : Certaines cendres volantes, provenant du traitement des roches bitumineuses et des lignites du Canada et des Etats-Unis, présentent des propriétés hydrauliques, peu différentes de celles du ciment Portland. La littérature technique et le travail présenté dans cette communication ont montré que ces cendres étaient très dissemblables physiquement et chimiquement, ce qui suggère que leurs propriétés hydrauliques ne résultent pas de leur composition. A l'aide d'un microscope électronique à balayage, complété par l'analyse aux rayons X, on a observé que le calcium réactif ou peu réactif se présentait sous des formes variées. Dans les cendres provenant des roches bitumineuses, les composés du calcium apparaissent comme formant une enveloppe amorphe ou cristalline autour de chaque grain de cendre. Après hydratation, ces composés présentent une morphologie très variée. Les liaisons entre les grains sont principalement dues à ces composés hydratés, qui sont donc à l'origine des propriétés hydrauliques de ces sortes de cendres volantes. Les recherches se poursuivent, afin de bien identifier les composés de ces enveloppes, soit avant, soit après hydratation.

SUMMARY: Some sub-bituminous and lignite fly ashes produced in Western Canada and the United States exhibit cmentitious properties when mixed with water, not unlike portland cement. The literature and work reported here indicates that these ashes are dissimilar both physically and chemically which suggests that the self-hardening property of these ashes is not related to their fundamental composition. Using a scanning electron microscope and probe and complementary x-ray analysis it was determined that calcium is present in the reactive and relatively un-reactive ashes in a variety of forms. In the highly reactive sub-bituminous ashes studied, calcium compounds appear to be present as amorphous and crystalline coatings around the individual ash particles. Upon hydration these compounds produced hydration products with varied morphology. These products are the principal binding agents which give these ashes their unique cementitious properties. Work is continuing in an effort to identify the calcium compounds present in the fly ash and the resulting hydration products.

INTRODUCTION

Sub-bituminous and lignite fly ashes unlike bituminous fly ashes possess self-hardening properties (4). Some sub-bituminous fly ashes when mixed with water hydrate in a similar manner to portland cement (13). It is known that the rate and degree of self-hardening resulting from hydration of these ashes varies significantly despite similarity of chemical and physical properties of different ashes (5).

Until a few years ago the majority of the fly ash produced in Canada and the United States was the result of burning relatively high sulphur bituminous coals. Environmental concerns and increased energy demands forced exploitation of low sulphur sub-bituminous and lignite coal deposits located in the mid-west and on the eastern slopes of the Rockies, far from the principal population and industrial centers (3). Physical, chemical and engineering properties of sub-bituminous fly ashes are significantly different from those of the bituminous ashes (3,4).

Sub-bituminous ashes are generally light cement grey to light cream in color. Bituminous fly ashes on the other hand are light to dark grey. The specific gravity of bituminous fly ashes varies between 1.80 and 2.84 (1). A survey of the data from various sources suggests that sub-bituminous ashes appear to possess higher specific gravities than the bituminous ashes.

The majority of the sub-bituminous fly ashes produced in Great Britian possess self-hardening properties (10,12). Presence of free lime in British fly ashes is suspected to be the source of this self-hardening. However, no test data is available to prove or disprove this hypothesis. The water soluble fraction of some fly ashes has been correlated with the degree of self-hardening (12). However, the solubility of fly ash in water is generally less than 3 percent and it can not be used as a guide for the degree or rate of self-hardening.

The earliest data on North American cementitious fly ashes was reported by Mateos (7). Although the source of self-hardening could not be positively identified, free lime in the fly ash, detected by x-ray analysis, was suspected to be the principal contributing factor in imparting the cementitious value to the fly ash. Due to the preponderance of non-cementitious bituminous fly ashes in the United States in the 1960's Mateo's observations went almost unnoticed.

Polish investigators, from a study of fly ash produced from brown coal, have reported that lime, detected by the heat of reaction between fly ash and dilute hydrochloric acid, is related to the degree of self-hardening (9). However, the same test does not seem to be applicable when used with similar fly ashes produced in Canada and the United States.

This paper presents the results of a study of the self-hardening properties of three Canadian sub-bituminous fly ashes. The hydration of the fly ashes were studied by x-ray analysis and a scanning electron microscope with microprobe. Based on laboratory test data and comparison of these results with data from three different fly ashes from the United States, the hydration mechanism and the self-hardening properties of the sub-bituminous fly ashes are discussed.

SOURCE OF FLY ASHES INVESTIGATED

The majority of the sub-bituminous fly ash collected in Canada is produced in the province of Alberta. Fly ash samples from the Wabemun, Sundance and Forestburg power plants in Alberta were selected for this study. These ashes are derived from burning sub-bituminous coal from Whitewood, Highvale, and Battle River mines in the Wabemun, Sundance and Forestburg power plants, respectively.

Sub-bituminous fly ashes from three different power plants in two different States of the United States were selected for comparative studies. The names of the power plants indicate the states in which they are located. Wyoming I, and Kansas I power plants burn sub-bituminous coal from Campbell County in Wyoming. The second power plant in Kansas burns sub-bituminous coal from Medicine Bow County in Wyoming.

LABORATORY STUDIES

Elemental analysis on different fly ashes was performed. Data on elemental analysis of various fly ashes was also obtained from suppliers or from other sources for comparison and to assess the variability with time for these ashes. Typical elemental analysis of the three Canadian fly ashes are presented in Table 1. Chemical composition of some of the U.S. fly ashes are given in Table 2.

TABLE I

Chemical Constituent	Weight % Forestburg	Sundance	Wabemun
SeO_2	48-57	46-52	56-69
Al_2O_3	19-26	22-28	19-27
Fe_2O_3	5-6	4-5	3-4
CaO	12-13	12-14	11-13
MgO	1.2-1.5	0.9-1.2	0.8-1.5
SO_3	0.2-0.4	0.2-0.8	0.1-0.3
Ng_2O	3.2-5.3	2.1-2.4	0.2-0.5
K_2O	1.0-1.5	0.9-1.1	0.8-1.2
L.O.I.*	0.5-0.8	0.2-0.8	0.5-0.8

*L.O.I. = loss on ignition

TABLE II

Chemical Constituent	Weight % Wyoming I	Kansas I	Kansas II
SiO_2	36	34	38
Al_2O_3	26	19	18
Fe_2O_3	5	6	6
CaO	27	29	18
MgO	2	4	**
SO_3	2	2	**
Na_2O	**	14	**
K_2O	**	14	**

*All figures rounded to nearest integer, **Not determined.

Moisture-density tests were performed to determine the optimum moisture content and maximum density of the fly ashes according to American Society for Testing Materials specification ASTM D-698-70. The results are presented in Table III. Wyoming I and, Kansas I fly ashes produced from Campbell County coal were very reactive and hardened within less than an hour after mixing. These two fly ashes also generated appreciable heat of hydration immediately after mixing with water. The optimum moisture content and maximum dry density of Wyoming I, and Kansas I fly ashes have been estimated. Similar data has been obtained for other highly reactive fly ashes (4,12).

TABLE III

Fly Ash Sources	Color	Average Specific Gravity	Optimum Moisture Content %	Maximum Dry Density kg/m^3
Forestburg	Light Buff Grey	1.95-2.0	18	1350
Sundance	"	2.0-2.43	20	1290
Wabemun	"	1.98-2.2	16	1530
Wyoming I	Light Cream	2.65	12	1840
Kansas I	"	2.61	13	1710
Kansas II	"	2.4-2.44	15	1630

The self-hardening characteristics of the three Canadian fly ashes were determined by conducting unconfined compressive strength tests on compacted fly ash samples moist cured from 1 to 28 days, Table IV. Tests were also conducted to determine if the hardened ash samples would retain strength after saturation or innundation with water. Although data are not presented in Table V, observations and strength tests indicated that generally the samples cured for less than 2 weeks disintegrated when soaked in water. However the samples of Canadian ashes cured for more than 2 weeks did not disintegrate when water saturated and retained 75 to 100 percent of their initial compressive strength. Some of the samples even gained strength on innundation in water.

TABLE IV

Curing Period Days	Unconfined Compressive Strength kN/m^2		
	Forestburg	Sundance	Wabemun
0	111	56	75
1	497	221	335
7	522	190	367
19	847	590	393
28	2408	870	752

NOTE: Average strength obtained from 3 or more samples

TABLE V

Curing Period	Unconfined Compressive Strength kN/m^2		
	Wyoming I	Kansas I	Kansas II
1 hour	2256	-	-
1 day	7700	5940	498
7 days	6303	-	546
14 days			392

NOTE: Average strength obtained from 3 or more samples

Data on self-hardening characteristics of the three U.S. fly ashes are also presented in Table V. All the samples of U.S. fly ashes tested for strength after curing 1 to 28 days, retained their shape on innundation in water.

X-ray and scanning electron microscope (SEM) studies were conducted to observe changes due to hydration in ash particle mineralogy and morphology. Specimens for SEM and x-ray studies were prepared from raw and hydrated fly ashes then stored in sealed containers or vacuum desiccators to avoid contact with moisture or atmospheric carbon dixoide. The fly ash specimens for SEM study were initially coated with gold but such samples exhibited excessive charging under the electron beam. When the specimen was mounted on a carbon stud and coated with carbon no such problem was encountered. Elemental analyses of fly ash particles and hydration products were obtained using an EDAX energy dispersive electron microprobe attachment to the SEM. Micrographs of some raw and hydrated fly ashes are presented in Figure 1 through 8.

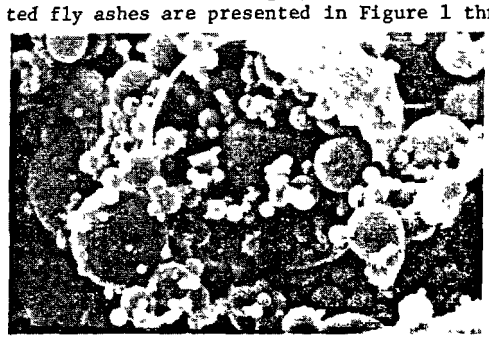

Fig. 1 - Forestburg Fly Ash (2000 x)

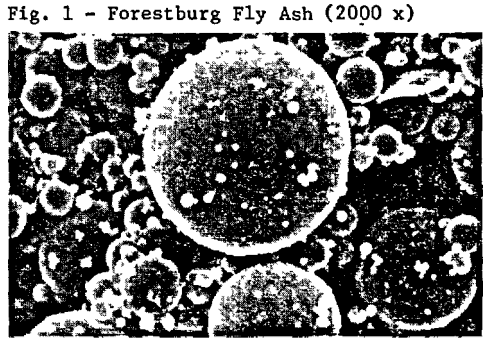

Fig. 2 - Sundance Fly Ash (2000 x)

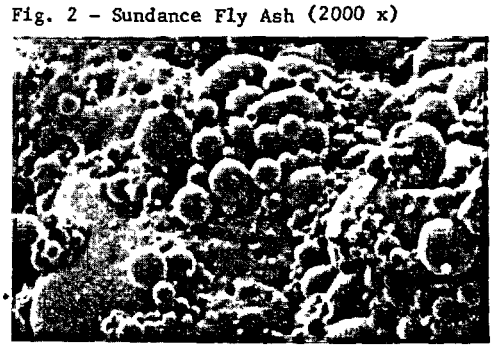

Fig. 3 - Wabemun Fly Ash (2000 x)

Fig. 7 - Fly Ash Hydration Product (28 days) (10,000 x)

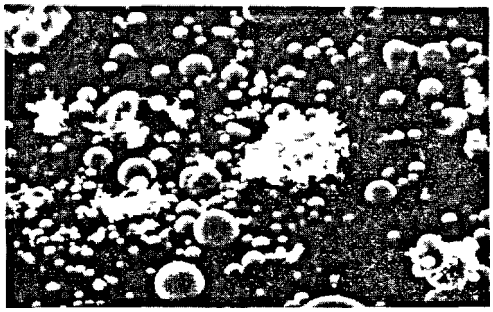

Fig. 4 - Kansas II Fly Ash (1000 x)

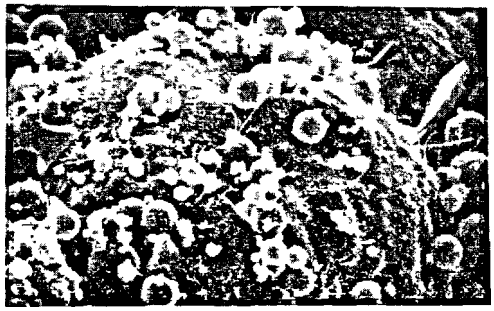

Fig. 5 - Fly Ash Hydration Product (28 days) (2000 x)

Fig. 6 - Fly Ash Hydration Product (28 days) (5000 x)

Fig. 8 - Fly Ash Hydration Product (28 days) (10,000 x)

X-ray diffraction traces using molybdenum radiation were obtained for the raw and hydrated fly ashes. Unfortunately space does not permit reproduction of the diffraction traces. However results of the x-ray studies are considered in the Discussion.

DISCUSSION OF RESULTS

Data in Table IV indicates that the three Canadian sub-bituminous fly ashes exhibit completely different rates and degrees of self-hardening. Forestburg fly ash achieved the highest strength at the end of 28 days. Sundance and Wabemun fly ashes could attain only about one third of the 28 day compressive strength of the Forestburg fly ash even at the end of 4 weeks curing. The chemical composition of the four ashes varies between 11 to 14 percent. The variations in other chemical constituents are also not significant; certainly not significant enough to suggest a reason for the observed variations in the degree of self-hardening.

It is interesting that Wyoming I and Kansas I fly ashes, produced from the same coal and having a similar chemical composition and containing almost the same amount of calcium oxide, also exhibit variations in the degree of self-hardening. One day cured samples of Wyoming I fly ash attained a compressive strength of 7700 kN/m^2 whereas one day cured samples of Kansas I fly ash samples attained a compressive strength of only 5440 kN/m^2. Furthermore, examination of data in Table II and V indicates that Kansas II fly ash containing about 10 percent calcium oxide exhibited very low degree of self-hardening.

Even if free lime in fly ash is assumed to be the source of self-hardening as suggested by various investigators (7,12), then the rate and degree of self-hardening of the fly ash would be controlled by the pozzolanic reactions between free lime and alumino-silicious glassy fly ash particles (2). Such pozzolanic reactions are known to occur at relatively slow rate (2). As a result the rate of self-hardening of the fly ashes due to the presence of free lime will be rather slow. Therefore, rapid rate of the hydration reaction and strength development, in Wyoming I, Kansas I, and other similar fly ashes (4) cannot be attributed to this factor.

Joshi and Rosaure (6), from a study of synthetic fly ashes, observed that adding extra calcium oxide or lime to a fly ash does not increase the reactivity of the ash to the level exhibited by fly ash containing the same amount of calcium oxide formed during the sintering process in the suspension fired furnace. Data on lime-fly ash mixtures reported by various other investigators (2) also indicates that increasing the calcium oxide content by adding lime does not increase the rate of self-hardening to the degree characteristic of the Wyoming I and Kansas I fly ashes.

All these observations suggest that calcium in the fly ashes has to be present in some form other than calcium oxide to cause variations in the rate and degree of self-hardening. The total calcium determined by chemical methods and reported as calcium oxide in the fly ash obviously does not provide any clue to the self-hardening potential of the sub-bituminous fly ashes.

X-ray studies indicated that all the fly ashes contained substantial amounts of amorphous material.

The crystalline material in the fly ashes contained quartz, mullite, hematite, manetite, calcium hydroxide and possibley αC_2S. One strong peak with a d-spacing of 2.29 Å was observed in raw Forestburg fly ash. The 2.29 Å peak was considerably reduced in hydrated paste of the Forestburg fly ash. In addition, medium size peaks in the vicinity of 2.75 Å and 2.78 Å were observed in raw samples of Forestburg fly ash. These peaks possibly belong to some form of calcium silicate or calcium aluminate. However, in the absence of second and third order peaks, none of the strong peaks could be positively identified. Similar but less intense peaks at 2.29 Å, 2.76 Å, and 2.78 Å could be identified in the other two Canadian fly ashes. Minor peaks attributable to calcium oxide and calcium hydroxides were also observed. The intensity of many of these peaks was reduced significantly in the diffraction patterns of the hydrated samples of the fly ash. It would appear that calcium is present in various forms in the raw ashes. If small amounts of calcium are present in the silicate or aluminate forms it may be that these are the components that impart the self-hardening property to the fly ash. It is also hypothesized that the calcium compounds which could not be identified are possibly present in partly amorphous and partly crystalline form. It is known that compounds present in an amorphous form have distorted crystal structures and will tend to be highly reactive (11).

Wyoming I and Kansas I fly ashes had the sharpest defined peaks in the vicinity of 2.74 to 2.78 Å d-spacing. There were various other peaks in these two fly ashes which could not be positively identified. Further work is needed to evaluate the significance of unidentified peaks in relation to self-hardening of the sub-bituminous fly ashes.

An examination of SEM micrographs shown in Figures 1, 2 and 3 indicates that raw Canadian fly ashes generally contained smooth spherical particles. Some of the spherical particles are hollow and are filled with other smaller particles. Very few irregularly shaped particles are observed in any of the three Canadian fly ashes. There was no observable difference in particle size or morphology of the three Canadian ashes.

Kansas II fly ash, which contained about 18 percent calcium oxide, consisted of clusters of irregularly shaped partciles, Figure 4. Elemental analysis of one of these particle clusters indicated a presence of calcium and silicon almost in equal proportion.

Elemental analysis was also performed on raw Canadian fly ashes. A selected field of view was mapped for calcium, aluminium, and silicon. Observations indicated that all the three elements were distributed evenly over the field of view. Elemental analysis of individual fly ash particles on EDAX indicated that, except for irregularly shaped particles, all other particles contained more than one element. The irregularly shaped particles contained mainly silicon. The irregularly shaped particles are possibly quartz particles which become surrounded while passing through the hot zone of the suspension fired furnace. Individual spherical particles contained calcium, silicon, iron, aluminium and occassionally sulfur in various proportions. The spherical particles never showed the presence of less than two elements, and calcium was always one of the elements. It is believed the exterior of all the spherical particles is coated with some calcium compound. It is possibly for this reason that the elemental mapping on the EDAX indicated the presence of calcium uniformly over the field of view.

Micrographs of hydrated Canadian fly ashes, Figures 6 to 8, indicate that the majority of the hydration products were fibrous. Some hexagonal shaped particles were also observed as seen in Figure 9. An examination of Figures 6 and 7 indicates that hydration products were always formed on the surface of spherical particles. Figure 7 indicates that cementitious products have been formed by peeling off the exterior surface of the particles.

Elemental analysis of fibrous particles as well as hexagonal and tubular particles indicated the presence of calcium, silicon and aluminium. The proportion of calcium, silicon and aluminium varied for different hydration products. It should be noted that elemental analysis using the EDAX may be influenced by the presence of other particles close to or under the particle to be analyzed. However, intense calcium and silicon peaks could always be seen whenever any of the new hydration products suspected to be a cementitious compound were analyzed. Fibrous morphology of hydration products containing calcium and silicon suggests the presence of calcium silicate hydrate I.

Based on the explanation given above it can be argued that the majority of the fly ash particles are coated with calcium compounds. The composition and structure of the calcium compounds cannot be positively identified at this time. It is clear however that coating of calcium compounds, around the spherical particles, provides cementation between different particles as seen in Figure 8. Minnick (8) also observed the presence of a reactive amorphous material coating, even on iron rich magnetite particles.

CONCLUSIONS

1. The sub-bituminous Canadian fly ashes investigated possessed varying degrees and rates of self-hardening.
2. The degree and rate of self-hardening is not directly related to the fundamental chemical or physical properties of the ashes.
3. Calcium is present in fly ashes in various forms. In the sub-bituminous fly ashes investigated calcium compounds appear to be present as coatings around the individual particles. These calcium compounds react to provide fibrous hydration products which provide particles with their cementitious properties.
4. Further research is necessary to identify the calcium compounds present and to confirm the suggested hypothesis.

ACKNOWLEDGEMENT

Funds for this research were provided by the National Science and Engineering Research Council of Canada. Fly ash samples and strength test data on some of the fly ashes from the United States were obtained from Woodward Clyde Consultants of Kansas City, Missouri. The Kansas I fly ash sample was furnished by Mr. P. Tansey of Kansas City Power & Light Company Dr. L. N. M. Parti and Mr. D. Lam conducted many of the tests on the Canadian fly ashes.

REFERENCES

1.- E. A. ABDUN NUR (1961), "Fly Ash in Concrete, An Evaulation", Highway Research Board Bulletin 284.

2.- D. T. DAVIDSON, J. B. SHEELER, N. G. DELBRIDGE (1958), "Reactivity of Four Types of Fly Ashes with Lime", Highway Research Board Bulletin 193.

3.- J. H. FABER (1978), "Ash Availability and Uses", Ash Management Conference, Texas A & M University, College Station, Texas, September 25-27, pp. 67-80.

4.- R. C. JOSHI (1978), "Structural Fills Using Fly Ash", Proceedings Ash Management Conference, Texas A & M University, College Station, Texas, September 25-27, pp. 186-213.

5.- R. C. JOSHI, D. M. DUNCAN and H. M. McMASTER (1975), "New and Convetional Uses of Fly Ash", Journal of Transportation Division of ASCE, Vol. 101, No. TE4, 11, pp. 791-806.

6.- R. C. JOSHI and E. A. ROSAUER (1973), "Pozzolanic Activity in Synthetic Fly Ashes" - I & II, American Ceramic Society Bulletin, Vol. 52, No. 5, pp. 456-463.

7.- M. MATEOS (1963), "Stabilization of Soils with Fly Ash Alone", Iowa State University Soils Research Laboratory Contribution, 63:21.

8.- J. J. MINNICK (1968), "The Application of the Rotoflux Magnetic Separator to Pulverize Coal Fuel Ash", American Society of Mechanical Engineers Paper 61-WA-313.

9.- J. PACHOSVSKY et al. (1976), "The Application of Fly Ash From Brown Coal for Road Base Courses", Ministry of Transport, Warsaw, Poland.

10.- S. RAYMOND (1958), "The Utilization of Pulverized Fuel Ash", Civil Engineering and Public Works Review, London, England, September.

11.- F. SINGER and S. S. SINGER (1963), "Industrial Ceramics", New York, New York, Chemical Publishing Company Inc.

12.- P. H. SUTHERLAND, T. W. FINLAY and I. A. CRAM (1968), "Engineering and Related Properties of Pulverized Fuel Ash", Journal of the Institute of Highway Engineers, Vol. 5, No. 6, pp. 19-27.

13.- S. I. THORNTON, D. G. PARKER and D. N. WHITE (1976), "Soil Stabilization Using a Western Coal High Calcium Fly Ash", Proceedings of the 4th International Ash Symposium, St. Louis, Missouri, March 24-25, pp. 170-181.

The influence of pulverized fuel ash on the early and long term strength of concrete

Influence d'une addition de cendres volantes sur la résistance à court terme et à long terme du béton

J.G. CABRERA, Lecturer, Department of Civil Engineering, the University of Leeds, U.K. and
C. PLOWMAN, Scientific Officer, Central Electricity Generating Board, North Eastern Region, Scientific Services Department, Grande-Bretagne.

RESUME : L'étude a porté sur les résistances à court terme et à long terme de bétons préparés en remplaçant une partie du ciment Portland par quatre cendres volantes produites en Grande Bretagne. Les modifications de la résistance à la compression simple sont dues à des réactions qui ont été étudiées grâce à la diffraction X; elles concernent le C_3A et le C_4AF extraits du ciment Portland ordinaire, et hydratés après mélange intime avec la cendre volante et du quartz finement broyé. On a constaté qu'un remplacement du ciment par des cendres volantes jusqu'à 30 % augmentait les résistances à long terme (91 jours) par rapport aux bétons sans cendres volantes. Les cendres volantes conservées à l'état humide ont une plus faible activité. A court terme, l'augmentation des résistances varie avec le pourcentage de cendres volantes. Il est proposé d'expliquer ces augmentations de résistance par deux mécanismes :

a) un effet physique qui résulte de la forme des grains de cendres et de leur surface spécifique,
b) un effet chimique qui résulte lui-même de deux réactions :b1) Un retard à l'hydratation du C_3A et du C_4AF , qui réduit la chaleur dégagée et stimule la formation des silicates hydratés; b2) une réaction véritablement pouzzolanique que l'on a détectée, dès l'âge de trois jours, grâce au microscope électronique à balayage.

ABSTRACT: A study of the early and long term strength of concrete mixes prepared with four British pulverised fuel ashes used as part replacement of ordinary portland cement is presented. The mechanism and reactions responsible for changes in the unconfined compressive strength were studied by XRD of C_3A and C_4AF extracted from the ordinary portland cement and hydrated with PFA and with inert ground quartz. It is shown that with the hopper ashes replacement of cement up to 30% resulted in higher long term (91 days) strengths as compared with the concretes without PFA. The conditioned PFA 2 performed poorly in relation to its cement-concrete counterpart. Hopper ashes gave higher early strengths at varying percent replacements. It is proposed that the mechanism by which strength changes is a two-fold mechanism: a) a physical effect which depends on the shape and specific surface of the PFA and b) a chemical effect consisting of two distinct reactions: 1st. a retardation of the hydration of C_3A and C_4A which effectively reduces the heat of hydration and encourages the formation of silicate hydrates, and 2nd. a proper pozzolanic reaction which was detected as early as three days of age by the use of a Scanning Electron Microscope.

INTRODUCTION

The use of Pulverized Fuel Ash (PFA) as part replacement of portland cement for the manufacture of concrete dates back to 1914 (1), although research on the properties of PFA and PFA-concrete started seriously around 1940 (2). Today the use of PFA in concrete is still very limited, specially in the U.K. where not more than 1% of the total production of PFA is utilized as part replacement of portland cement. By the end of this century coal will play a major role in the production of energy since it comprises about 80% of the world energy reserves, these amount to 70,000 million Tonnes in Western Europe alone (3). It seems clear then that PFA will become an abundant source to be used as pozzolanic material, specially for the replacement of cement which as it is known requires high levels of energy for its production.

Reports in the literature regarding the influence of PFA on the properties of concrete are mostly related to the measurement of physical properties. The mechanism by which PFA alters the engineering properties of concrete are not really clear, hence the contraditions found in the literature.

This paper presents a limited study on the influence of PFA from four power stations on the properties of concrete. Ordinary portland cement was replaced by 15, 30 and 45% of each PFA and unconfined compressive strength measurements were made up to 91 days. The influence of PFA on the process of hydration was studied only with reference to the C_3A and C_4AF hydration process. The methodology used is explained and interpretations are made in the light of the physical and chemical results obtained.

ENGINEERING PROPERTIES OF PFA-CONCRETE

The properties which are of importance for the evaluation of PFA-concretes are: workability, strength, creep and shrinkage and durability. Different authors have reported sometimes contradictory results for the same property. Referring to workability, for example, the majority of reports (e.g. 4,5) agree that PFA improves the workability of concrete when PFA has been properly selected, however there is no agreement as to the properties which should be measured to select a PFA material. Scholtz (5), for example, recommends selection of PFA in terms of specific surface, while some standards (6) recommend the use of particle size. Apparently it is implied that the finer the ash the better the workability of concrete. This concept is by no means proved since it will imply that the finer the ash the higher the strength of the concrete. Some authors have reported that there is no relation between fineness and strength(7,11). Cabrera and Gray (7) showed that high specific surface ashes may not necessarily be fine grained since it is the irregular carbonaceous particles which contribute greatly to the specific surface.

The strength of PFA-concrete has been studied and reported by many investigators. Most reports refer to the long term beneficial effects of PFA, based on the accepted idea that the reaction of PFA with cement is that of a pozzolana, i.e. reaction of soluble silica and alumina from the PFA with calcium hydroxide produced by hydration of the calcium silicates in the cement to form hydrated calcium silicates and aluminates. However, there are still some reports which indicate that PFA-concretes did not reach the strength of their cement-concrete counterparts even at the age of 5 years (9). With reference to short term strength there is still great controversy. Some authors report improved strengths while others report inferior strengths (5,9,10,11,12). Here again the contradictions have their origin in the fact that there is no agreement as to the properties of PFA which should be measured to qualify it as a suitable material. Furthermore, there is no agreement in relation to the actual concrete mix design (10,13,14).

There is general agreement with relation to the influence of PFA on creep and shrinkage properties of concrete. Scholtz (5) indicated that using PFAs with specific surface areas between 1.2 to 1.3 m^2/g, creep and shrinkage were reduced by 20%, while Ryan (15) reported reductions up to 30% of the shrinkage measured in plain concretes.

It is generally accepted that concretes with PFA exhibit lower permeabilities than their portland cement-concrete counterparts, this fact alone has been used to explain the improved resistance of PFA-concrete to sulphate attack. Davis (16) measured the permeability of plain and PFA-concrete where PFA replaced 30% of the cement; the permeability was reduced to 1/5 of the permeability of the plain concrete, thus reducing penetration of potential harmful solutions. Dikeou (17) reported improved resistance of PFA-concrete to sulphate attack and showed that the effectiveness of PFA in improving resistance to sulphate attack increased with the severity of exposure to sulphates.

MECHANISMS OF PFA-CEMENT REACTION

Pozzolanic reactions are the acknowledged mechanism occurring between PFA and cement in the presence of water. Changes in the properties of concrete produced with PFA have invariably been interpreted using the pozzolanic properties of PFA. Minnick (18) and Plowman (19) have summarized some of the possible reactions of PFA-cement-water systems and Jambor (22), Raask and Bhaskar (21), Shikami (22), among others have proposed methods to evaluate the pozzolanic activity of PFA by either measuring release of silica or reduction of calcium hydroxide generated by the hydration of cement. While these methods have given satisfactory results for particular conditions, their general use is not warranted. There are still some questions which have to be answered, for example when does the pozzolanic reaction between PFA and cement take place? Various investigators have attempted to answer this question but the data which have been published are inconsistent. Guillaume, for example, came to the conclusion that the reaction between PFA and cement starts from an age of about 14 days (23), while Venaut (24) stated that pozzolanic reaction is not detected before 28 days.

It is apparent that with regard to the mechanism or mechanisms of reaction more studies are necessary, in particular the chemistry of early reactions which do not seem to exist in the literature, and also the extent of the physical effects of PFA in the composition of the water/solids ratio, as well as the influence of PFA in the morphology of the reactions products.

MATERIALS AND METHODS USED IN THE INVESTIGATION

Pulverized Fuel Ashes from four power stations in the north of England were used. Their properties are given in Tables 1, 2 and 3. PFA 1, PFA 3 and PFA 4 were hopper ashes, while PFA 2 was collected from a disposal stockpile where the ash is conditioned with approximately 12% of water.

Ordinary portland cement and quartzitic coarse and fine aggregates were used for the preparation of the concrete mixes. Cement was replaced by PFA in proportions of 15, 30 and 45%. Cubes of 10 cm side were prepared and cured in water at 18°C for varying periods up to 91 days. The cubes were tested in unconfined compression at the end of each curing period. The reported results are the average of three specimens per point. Immediately after testing, small pieces of the fractured concrete cubes were freeze-dried and stored in sealed containers for later studies of the micromorphology of the reaction products.

The early chemistry of PFA-cement hydration was studied using only PFA 3 and C_3A and C_4AF obtained directly from the ordinary portland cement. Chemical separation of C_3A and C_4AF were carried out by extracting the calcium silicate and calcium oxide phases from the ordinary portland cement with a maleic acid/methanol solution. Calcium sulphate was removed with ammonium chloride solution. These methods have been described in the literature (31). X-ray diffraction of the residue detected only C_3A and C_4AF. Since the maleic acid passivated the residual compounds they were reactivated by ignition at 800°C.

Hydrations were carried out not only with the C_3A and C_4AF but with mixtures in which the dilution effect was studied by replacing the aluminates with 30% of ground quartz (to pass sieve of 45 μ) so as to separate any effect due to dilution occasioned by incorporating 30% PFA 3 in the aluminate residue.

Each hydration process was followed with a Philips APD-10 computer controlled diffractometer, programmed to scan over an angular range of 5° 2θ - 40° 2θ. Cu radiation was used at 45 kV, 35 mA, and the diffractometer was fitted with a graphite manochromator. The scanning rate was 16° 2θ per minute, the programme allowed recycling immediately after each scan. To avoid the possibility of rapid carbonation of calcium aluminate hydrates which may occur in air, each sample was mixed dry; 0.7 ml of distilled, deionised and freshly boiled water was then added and mixed. The wet mixture was immediately placed in the diffractometer which was modified so as to provide a nitrogen atmosphere which eliminated the possibility of carbonation.

In order to detect phase changes at very early ages (from as early as one minute) a fast scanning speed of 16° 2θ/minute was necessary. This resulted in two problems: a) poor peak resolution, b) slightly reduced peak intensity due to the relatively long response time of the chart recorder. Therefore no attempt was made to obtain absolute measurements of the amount of each phase, but it was found to be perfectly feasible to measure the change in intensity of a peak, even in the case of quite severe overlaps.

Ash Source	Ash Code	Specific Gravity	Specific Surface, m^2/g
Ferrybridge 'C'	PFA-1	2.22	1.26
Drax	PFA-2	2.18	2.50
Eggborough	PFA-3	2.40	1.10
Thorpe Marsh	PFA-4	2.09	1.31

Table 1 Specific gravity and specific surface of the ashes used in the investigation

Particle size (μm)	Percentage passing (by weight)			
	PFA-1	PFA-2	PFA-3	PFA-4
75	92.7	76.1	88.5	91.7
63	78.3	69.4	84.8	87.8
45	46.6	50.4	81.9	42.7
30	34.0	18.6	77.2	7.4
10	12.3	3.4	3.2	3.9
4	3.4	1.4	2.8	3.1
<2	2.1	n.d	n.d	n.d

n.d - Not determined

Table 2 Particle size distributions of the ashes

RESULTS AND DISCUSSIONS

Hydration of C_3A and C_4AF

Most studies of the hydration of calcium aluminates and alumino-ferrites, and subsequent reactions with calcium and sulphate, have been carried out with laboratory synthesised calcium aluminates as starting materials. Times quoted by various investigators (27,28,29,30) regarding transformation of ettringite into monosulphate are quite different. Collepardi et al. (27) attributed this to differing experimental procedures and to the type and reactivity of C_4AF; for this reason the experiments reported in this investigation were carried out with starting material separated from an ordinary cement clinker.

The process of hydration for the C_3A and C_4AF is shown in Figure 1. The initial crystalline hydration product is C_2AH_8. Substitution of Al_2O_3 by Fe_2O_3 can occur, forming a solid solution series whose end members are C_2AH_8 and C_2FH_8. No attempt was made to distinguish between substituted products. Similar solid solution series exist for other hydrates. As shown in Figure 1 C_2AH_8 reaches a maximum concentration at about 15 minutes. Both C_3A and C_4AF have reacted to a considerable extent by this time, but no C_4AH_{19} is detectable. It does, however, appear after about one hour, with very low crystallinity. The XRD peaks of C_4AH_{19} gradually narrow down with time, indicating a gradual increase in crystallinity. It is possible, then, that it is present at an earlier age as an amorphous phase. The initial hydration reactions may therefore be:

Ash Code	Percentage by weight										
	Loss on ignition	SiO_2	Al_2O_3	Na_2O	MgO	K_2O	Fe_2O_3	TiO_2	CaO	SO_3	Cl
PFA-1	4.95	48.41	25.43	0.58	1.19	3.64	8.28	0.93	1.52	0.28	0.03
PFA-2	3.11	50.98	26.42	0.77	1.19	3.71	9.45	0.93	1.19	0.16	0.04
PFA-3	3.29	49.01	27.73	0.75	1.30	4.05	8.77	0.96	1.20	0.58	0.01
PFA-4	2.52	52.62	26.45	1.11	1.33	3.90	8.98	0.98	1.49	0.63	0.02

Table 3 Chemical compositions and loss of ignition of the ashes

$$C_4AF + 16H \rightarrow 2C_2(AF)H_8 \quad \ldots\ldots\ldots\ldots\ldots\ldots(1)$$

$$2C_3A + 27H \rightarrow C_2AH_8 + C_4AH_{19} \quad \ldots\ldots\ldots\ldots\ldots\ldots(2)$$

The findings of many workers (31) that C_3A hydrates initially faster than C_4AF are confirmed in the present work. The subsequent reaction of C_2AH_8 appears to be mainly with C_4AF, the product being $C_3(AF)H_6$. This may be:

$$C_4AF + C_2(AF)H_8 + 7H \rightarrow 2C_3(AF)H_6 + (AF)H_3 \ldots(3)$$

The effect of diluting the aluminates by incorporating 30% of inert material (ground quartz) is shown in Figure 2. The rate of reaction is slower in comparison with the undiluted material. Figure 3 shows that 30% substitution by PFA results in much more marked retardation of the initial reaction. Much less C_2AH_8 is produced and the diffraction peaks disappeared significantly faster. Unlike the two previous hydrations, ettringite ($C_3A.3\bar{C}S.31H$) was detected after less than two minutes, reaching a maximum after eleven minutes. After 20 minutes ettringite was no longer detectable, but the monosulphate ($C_3A.\bar{C}S.12H$) was identifiable. The basal spacing of the monosulphate (8.9Å) subsequently reduced to 8.2Å. Consideration of this, and other peaks on the XRD trace leads to an identification of C_4AH_{13}. In view of the precautions taken to exclude carbon dioxide, it is improbable that this compound contained "essential carbonate". However, it is possible that it may contain "essential sulphate", and is likely to be a solid solution as described by several workers (31).

It is well known that gypsum retards the hydration of C_3A and C_4AF by forming a layer of ettringite (27,32). Since studies of the release of ions from British PFAs in neutral and also alkaline solutions (33,34) have shown that calcium and sulphate are released at a very early stage (within 1 to 2 minutes) in sufficient quantity to form a saturated solution with respect to gypsum, it was thought that the mechanism of retardation of the aluminates hydration might be similar to the manner in which gypsum controls the hydration process. Experiments carried out substituting PFA by equivalent sulphate concentrations provided by gypsum reported elsewhere (35) have shown that the retardation with gypsum does not occur to the same extent as with the addition of solid PFA, even when sufficient solid gypsum to replenish the calcium and sulphate in solution is provided. Thus it is clear that PFA is a more effective retarding agent than gypsum. Why this is so will be discussed later on in conjunction with findings related to the physical properties of PFA-concrete.

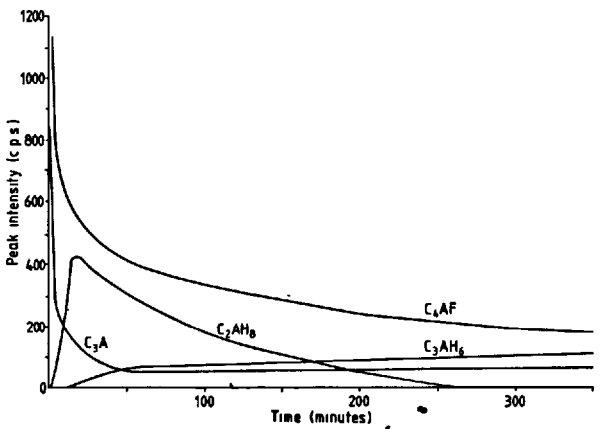

Figure 1 Hydration-time relation for $C_3A + C_4AF$

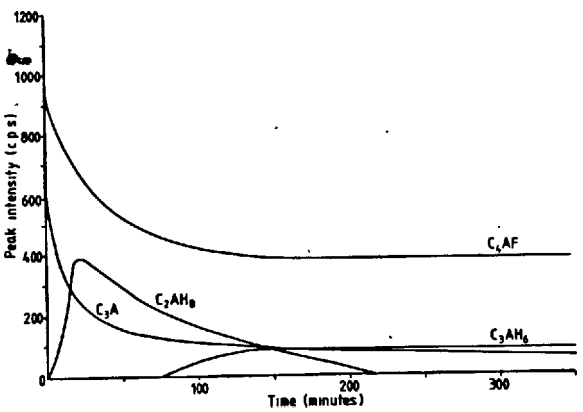

Figure 2 Rate of hydration of a mixture of $C_3A + C_4AF$ + 30% ground quartz

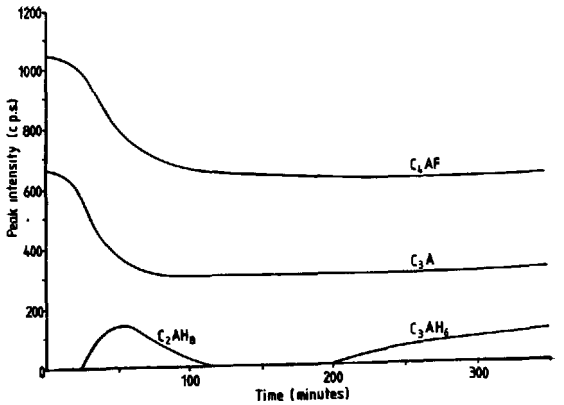

Figure 3 Rate of hydration of a mixture of C_3A + C_4AF + 30% PFA 3

Early and Long Term Strength of PFA-Concretes

Early strength of concrete is a very important property, specially from the point of view of economy and facility of construction procedures. The three day strength chosen as the early strength of the mixes used in this study is presented in Figure 4. For convenience strengths are expressed as a percentage of the control portland cement concrete as a function of percentage of cement replacement. It can be observed that each PFA gives a different strength-replacement relation. The hopper ashes gave greater early strengths for various replacement percentages while the conditioned ash PFA 2 resulted in lower early strengths even at 15% replacement.

The long term strengths are shown in Figure 5 a, b, c, and d. It can be observed that for the hopper ashes replacement up to 30% resulted in considerably increased strengths at 91 days. Replacement at 45% level gave in all cases lower long term strengths. PFA 2 showed the poorest performance at early and long term strength.

Attempts to relate the strength behaviour to the intrinsic properties of the PFAs used were not successful. For example, specific surface values show that PFA 2 should have given the best results in terms of the requirements of specifications (6), but in reality the PFA with the lowest specific surface gave the best results. A number of countries advocate the use of an arbitrary percentage of retention on a 45 μ sieve above which a PFA should not be acceptable, here again observing the results of particle size distribution it can be ascertained that there is no relation between size and strength.

MECHANISM BY WHICH PFA INFLUENCES CONCRETE STRENGTH

From the results of this investigation and the data of other workers it is apparent to the authors of this work that the mechanism by which PFA influences the engineering properties of concrete is a two-fold mechanism:

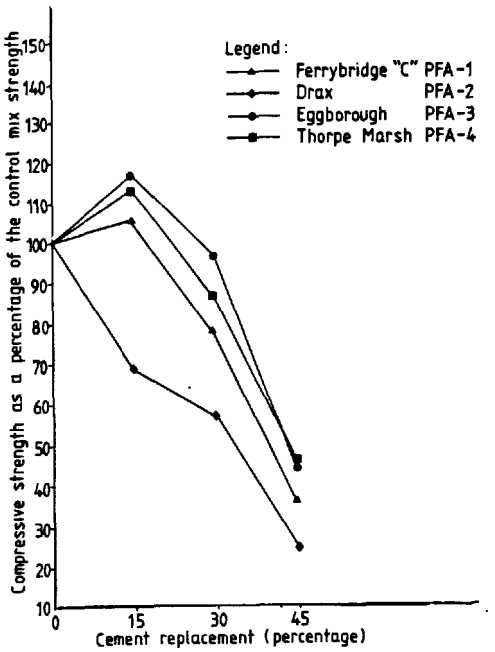

Figure 4 Relation between three day strength and percentage of cement replacement for the ashes used in the study

a) a predominantly physical effect which consists of reducing the water demand without decreasing the workability of the mix and allowing better packing of the hydration products and the unhydrated particles.

During the production of the mixes for this study it was observed that the same water/cement ratio gave increasing values of slump for increasing replacement of cement. Although recognizing that the slump test is too coarse a measure of workability, nevertheless it gives an indication of the effects of PFA on water demand. Other authors have consistently reported very low values of permeability for PFA-concrete mixes, this tends to confirm the idea of better packing properties of a mix containing PFA.

Figure 6 shows schematically the probably behaviour of PFAs. Considering that there is a maximum practical limit of replacement as indicated by the dashed vertical line, a particular PFA will probably show one of the trends indicated, depending on whether the specific surface is relatively low, intermediate or high and/or whether the shape of the particles is 100% round smooth shape or whether there is a significant amount of coarse irregular, and porous particles.

b) a double chemical effect which consists of: 1) retarding the hydration of C_3A and C_4AF. The immediate beneficial consequence is a reduction in the heat of hydration, but most important the retardation of the aluminate's hydration produces

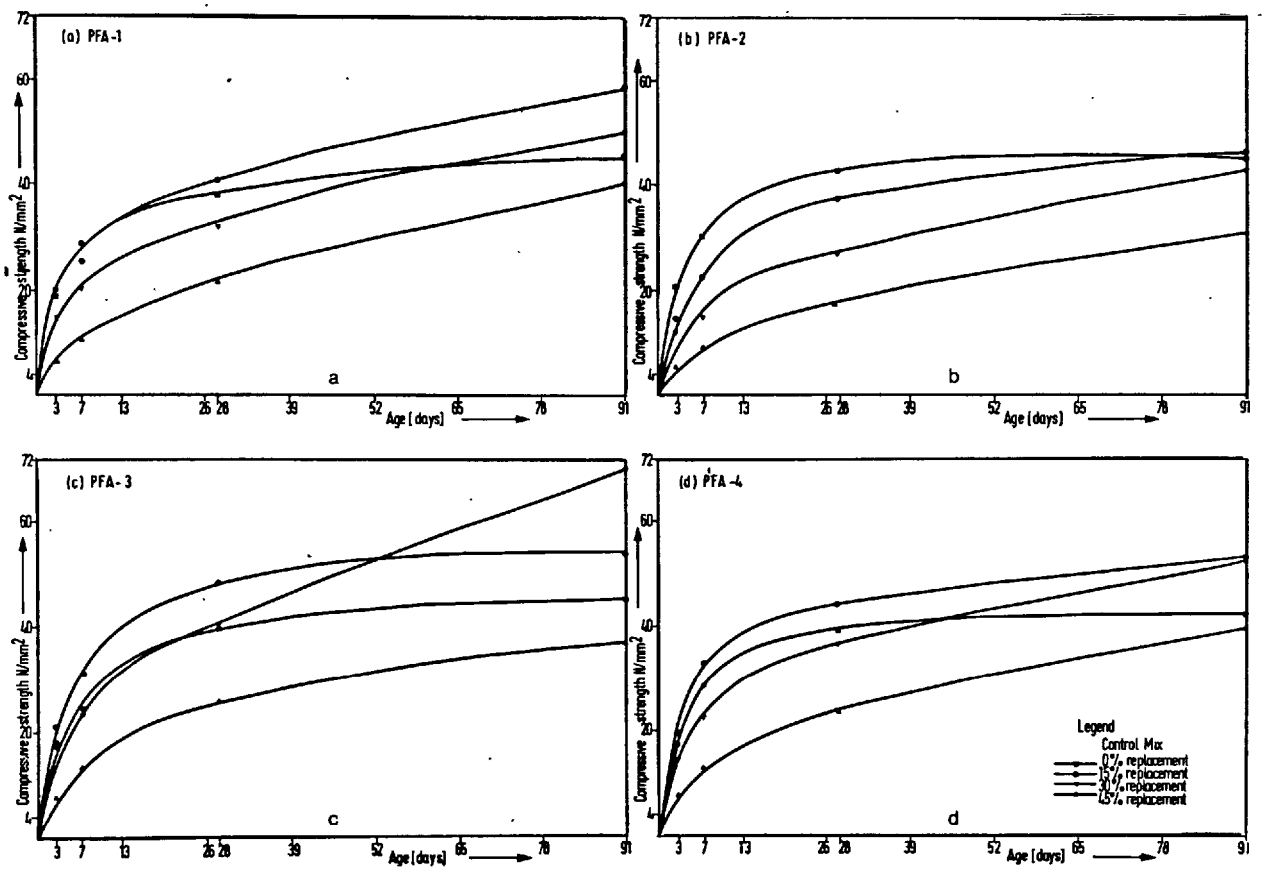

Figure 5 Unconfined compression strength-age relations (a) PFA 1, (b) PFA 2, (c) PFA 3 and (d) PFA 4

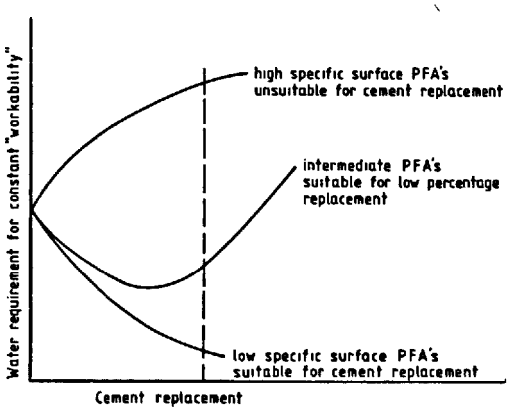

Figure 6 Schematic representation of water requirements for different PFA materials

as a counter-effect the possibility of increasing the volume of calcium silicates, which will undoubtedly result in increased ultimate strengths. Evidence for this proposition has been presented by Jelenic et al. (36). They studied the effect of gypsum on the hydration and strength of various portland cements and showed that at increased percentages of SO_3 there is a reduction of aluminate hydrates and a corresponding increase in the silicate hydrates. They showed, furthermore, that there exists an optimum percentage of SO_3 for maximum increase in strength; 2) a pozzolanic reaction proper between the soluble silica and alumina of the PFA and the calcium hydroxide produced by the hydration of the cement. As it has been indicated in the review of mechanisms of reaction, workers do not agree on the time at which the pozzolanic reaction can be detected.

During this investigation limited use of an SEM (JEOL-35) allowed a study of the early and long term morphology of reaction products. Figure 7 shows evidence of formation of reaction products at the PFA-cement interface and Figure 8 shows poorly crystalline compounds. The age of the specimen was only three days, thus it appears that pozzolanic reaction products may be formed earlier than other investigators have reported. There is some evidence for an early pozzolanic reaction from experiments which are now in progress. These demonstrate a reduction at 3 days in the quantity of $Ca(OH)_2$ present in cement pastes with PFA replacement, compared with controls with no

replacement. Figures 9 and 10 correspond to specimens with long term hydration. It can be clearly seen that the reaction products have a morphology similar to the type I calcium silicates (Figure 8) and type III calcium silicates (Figure 9) (39).

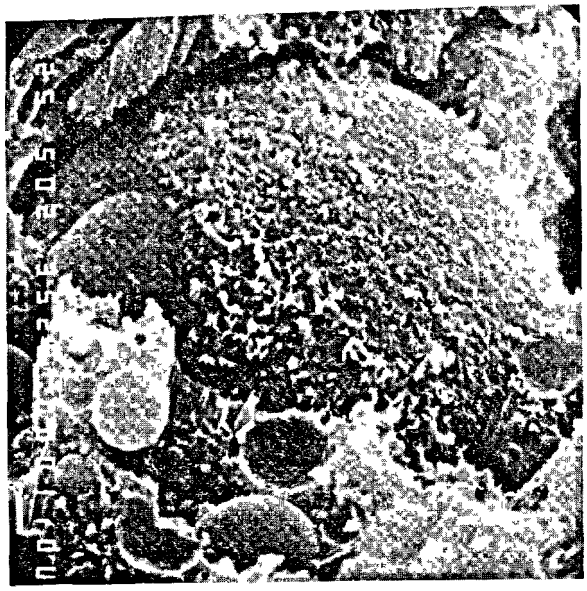

Figure 7 PFA particle surface showing evidence of reaction products. Age of specimen three days.

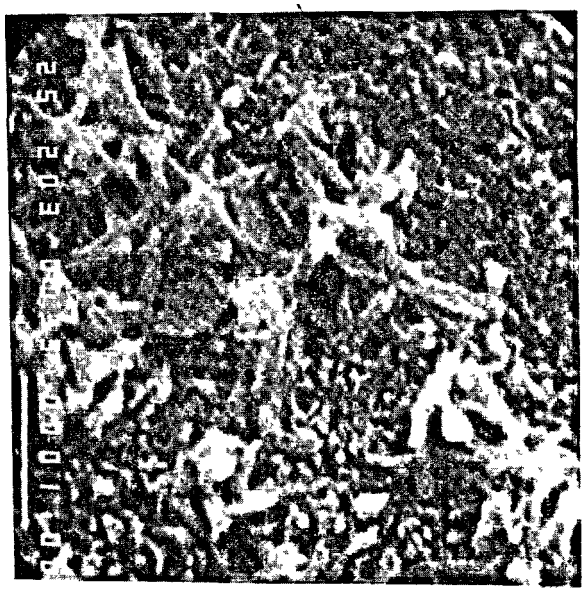

Figure 8 Magnified view of Figure 7 showing the morphology of reaction products at the PFA-cement interphase.

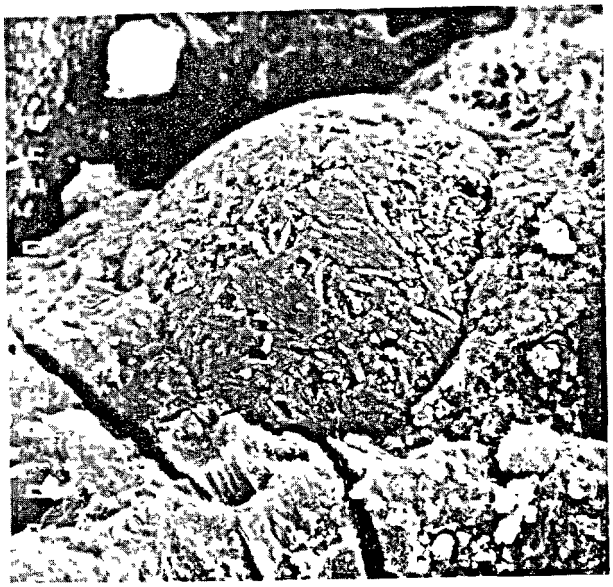

Figure 9 Long term cured specimen showing type I reaction products on the surface of a PFA particle.

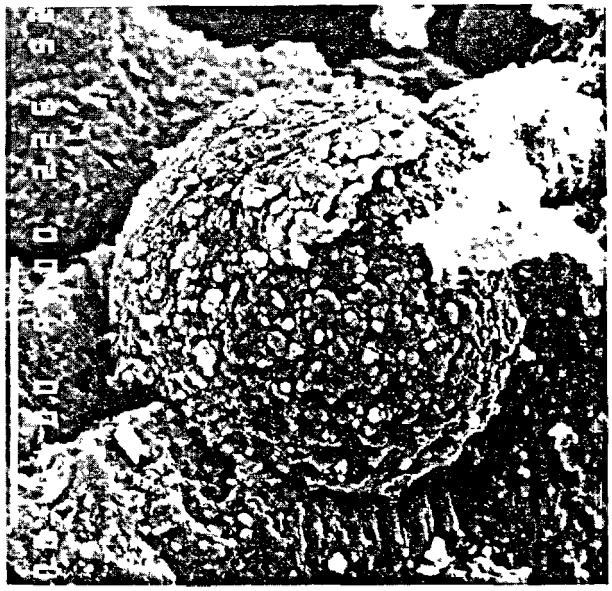

Figure 10 Long term cured specimen showing type III reaction products resulting from the PFA-cement reaction.

Several attempts have been made to relate development of strength to the structure of the reaction products of portland cement. Feldman and Beaudoin (37), for example, studied porosity and particle type in relation to strength development. They indicated that for any given porosity there is an optimum blend of particle types, i.e. at the same porosity the average strength of a composite

particulate material depends on the intrinsic strengths of coarse, dense, crystalline particles and the better bonding properties of finely divided low-density, amorphous material. Their results included a PFA-cement paste which in comparison to a pure cement paste showed higher strength at the same porosity. They believed that the optimum blend of particle types was probably the one corresponding to the PFA-cement paste. Taylor (38), in a recent review of mechanisms and products of cement hydration, has pointed out the fact that strength development of blended cements might not be explained by the chemical reactivity of the PFA alone but also by the effect that unreacted particles of these materials have on the microstructure. This tends to support the idea proposed by the authors of this paper in relation to a mechanism which is a combination of physical and chemical effects.

REFERENCES

1.- ANONYMOUS (1914), "An investigation of the pozzolanic nature in coal ash", Engineering News Record, Vol. 71, No. 24, pp. 1334-1335.

2.- N.W. ELMER (1940), "Profitable fly-ash handling", Steel, Vol. 106, pp. 64-65.

3.- CEPCED (1978), "Energy in Western Europe - vital role of coal", NCB, London.

4.- K. YAMAZAKI (1962), "Fundamental studies of the effects of mineral fines on the strength of concrete", Trans. Japan Society of Civil Eng., Vol. 85, pp. 15-44.

5.- H. SCHOLTZ (1978), "German black coal combustion residues, types and uses", Central Electricity Generating Board, National Ash Assc. (USA), Conference on Ash Technology and Marketing, London.

6.- BRITISH STANDARDS INSTITUTION (1965), BS 3892: 1965, Specifications for pulverized fuel ash for use in concrete, BSI, London.

7.- J.G. CABRERA and M.N GRAY (1973), "Specific surface, pozzolanic activity and composition of pulverized fuel ash", Fuel, Vol. 52.

8.- J.D. WATT and D.J. THORNE (1966), "The composition and pozzolanic properties of pulverized fuel ash", Journal of Applied Chemistry, Vol. 15, pp. 585-604 and Vol. 16, pp. 33-39.

9.- F.E. LEGG (1965), "Experimental fly ash concrete pavement in Michigan", Highway Research Record, No. 73, pp. 1-12.

10.- C.E. LOVEWELL and G.W. WASHA (1958), "Proportioning concrete mixtures using fly-ash", ACI Journal, Proc., Vol. 54, No. 12, pp. 1093-1102.

11.- M. BOGDANOVIC (1978), "The use of PFA in concrete - an assessment of present knowledge and future research", Central Electricity Generating Board, National Ash Assoc. (USA), Conference on Ash Technology and Marketing, London.

12.- K.K. JAIN (1978), "Concrete mix proportioning with coarse fly ash", Central Electricity Generating Board, National Ash Assc. (USA), Conference on Ash Technology and Marketing, London.

13.- S.S. RESHI and S.K. GRAG (1964), "Proportioning concrete mix concrete fly ash", Journal of the Institution of Engineers (India), Vol. 45, Part CII, pp. 68-75.

14.- K.K. JAIN, B.D. NAUTIYAL and O.P. JAIN (1975), "Compressive strength and modulus of elasticity of fly ash concrete", Journal of the Institution of Engineers (India), Vol. 56, Part CII, pp. 32-37, Discussion pp. 201-203.

15.- W. RYAN (1976), "Fly ash utilization and research in Australia", Proc., Fourth International Fly Ash Utilization Symposium.

16.- R.E. DAVIS (1950), "Use of pozzolanas in concrete", Proc., American Concrete Institution, Vol. 46, pp. 377-384.

17.- J.T. DIKEOU (1960), "Fly ash increases resistance of concrete to sulphate attack", Research Report No. 23, U.S. Department of the Interior, Bureau of Reclamation.

18.- L.J. MINNICK (1967), "Pozzolanic properties of fly ash", Proc., First Fly Ash International Utilization Symposium.

19.- C. PLOWMAN (1978), "The chemistry of PFA in concrete - an assessment of present knowledge and future research", Central Electricity Generating Board, National Ash Assc. (USA), Conference on Ash Technology and Marketing, London.

20.- J. JAMBOR (1962), "A new method for determination of pozzolanic activity", Rev. Mater. Constr. Trav. Publics., Vol. 564, pp. 240-256.

21.- E. RAASK and H.C. BHASKAR (1975), "Pozzolanic activity of pulverized fuel ash", Cem. & Concr. Res., Vol. 5, pp. 363-376.

22.- G. SHIKAMI (1956), "On pozzolanic reaction of fly ash", Proc., Japan Cement Engineering Assc., Vol. 10, pp. 221-227.

23.- L. GUILLAUME (1963), "Pozzolanic activity of fly ash in portland cement and slag cement", Silicate Industry, Vol. 28, No. 6, pp. 297-300.

24.- M. VENAUT (1962), "Fly ash cement, influence of the proportion of fly ash on properties of cement", Rev. Mater. Constr. Trav. Publics., Vol. 565, pp. 271-279, Vol. 566, pp. 315-324, Vol. 567, pp. 349-356.

25.- K. MATHER (1971), "X-ray diffraction examination of the phases in expansive cement", Adv. X-ray Anal., Vol. 20, pp. 41-52.

26.- J.E. MANDAR, L.D. ADAMS and E.E. PARKIN (1974), "A method for the determination of some minor compounds in portland cement and clinker by x-ray diffraction", Cem. & Concr. Res., Vol. 4, pp. 533-544.

27.- M. COLLEPARDI, S. MONOSI and G. MORICONI (1979), "Tetracalcium aluminoferrite hydration in the presence of lime and gypsum", Cem. & Concr. Res., Vol. 9, pp. 431-437.

28.- I. JAWED, S. GOTO and R. KONDO (1978), Cem. & Concr. Res., Vol. 8, p. 571.

29.- S. CHATTERJI and J.W. JEFFERY (1962), Jour. Amer. Cer. Soc., Vol. 45, p. 536.

30.- W.L. DE KEYSER and N. TENOUTASSE (1968), Proc., Fifth International Symposium on the Chemistry of Cement, Part II, pp. 379-386.

31.- F.M. LEA (1970), "The chemistry of cement and concrete", 3rd Edition.

32.- M. COLLEPARDI, G. BALDINI, M. PAURI and M. CORRADI (1978), "Tricalcium Aluminate hydration in the presence of lime, gypsum or sodium sulphate", Cem. & Concr. Res., Vol. 8, pp. 571-580.

33.- J.G. CABRERA (In preparation), "The use of PFA for land reclamation".

34.- C. PLOWMAN (1980), "The chemical behaviour of PFA with added water", Central Electricity Generating Board Research Report, NE/R/396.

35.- C. PLOWMAN (In preparation), "X-ray diffraction studies on the C_3A and C_4AF hydration products".

36.- I. JELENIC, A. PANOVIC, R. HALLE and T. GACESA (1977), "Effect of gypsum on the hydration and strength development of commercial portland cements containing alkali sulphates", Cem. & Concr. Res., Vol. 7, pp. 239-246.

37.- R.F. FELDMAN and J.J. BOUDOIN (1976), Cem. & Concr. Res., Vol. 6, pp. 389-400.

38.- H.F.W. TAYLOR (1979), "Mechanism and products of portland cement hydration", Annual meeting of the Japan Cement Assoc.

39.- S. DIAMOND (1972), "Identification of hydrated cement constituents using a scanning electron microscope - energy dispersive X-ray spectrometer combination", Cem. & Concr. Res., Vol. 2, pp. 617-632.

The effect of curing temperature on the development of strength of mortar containing fly ash

L'effet de la température de conservation sur le développement de la résistance du mortier contenant des cendres volantes

J.A. DALZIEL, Mr. Materials Research Department, Cement and Concrete Association, Slough, England.

RESUME : Des prismes de mortier ISO-Rilem ont été faits avec du ciment Portland ordinaire ainsi qu'avec ce même ciment contenant 20 % de cendres volantes. Des comparaisons ont été faites sur le développement de la résistance à la flexion et à la compression de ces mortiers jusqu'à l'âge d'un an après une conservation continue dans l'eau à 20, 35, 50, 65 et 80°C. Pour des températures de conservation inférieures à 50°C, la présence de cendres volantes a augmenté à long terme la résistance à la flexion de 40 % approximativement, et la résistance à la compression de 15 % approximativement. Aux jeunes âges la résistance a augmenté avec l'augmentation de la température de conservation aussi bien pour le mortier pur que pour celui contenant des cendres volantes, mais il a été ensuite plus rapide pour ce dernier à cause de la pouzzolanicité de la cendre qui a fortement contribué à la résistance dès les premiers jours. A 20°C, le mortier avec cendres volantes ne dépasse pas la résistance du mortier pur avant 150 jours, mais cela se produit après 28 jours à 35° et après 6 jours à 50°C. Pour les deux genres de mortier, la résistance à long terme était plus faible pour les éprouvettes conservées à température plus élevée.

SUMMARY : ISO-Rilem mortar prisms were made using ordinary Portland cement and with 20% of the cement replaced by fly-ash. Comparisons are made between the development of flexural and compressive strength of these mortars up to an age of one year after continuous water cure at 20, 35, 50, 65 and 80°C. For curing temperatures up to 50°C, the presence of fly ash increased the long term flexural strength by approximately 40% and the long term compressive strength by approximately 15%. For young specimens, the rate of gain of strength increased as the curing temperature increased for both the plain and fly ash mortars but was more rapid in the latter case due to the ash pozzolanicity contributing effectively to the strength at earlier ages. At 20°C the fly ash mortar did not exceed the strength of the plain mortar before 150 days whereas it exceeded it after 28 days at 35°C and after 6 days at 50°C. With both mortars the long term strength was lower for specimens cured at the higher temperatures.

INTRODUCTION

Raising the curing temperature of mortars and concretes made with Portland cement improves the strengths at early ages but invariably causes a reduction in the strength which is attained in the long term. When a reactive fly ash is incorporated in the mix, an additional contribution is made to the strength due to its pozzolanicity. This contribution is also temperature dependent being negligible at early ages and at low or normal temperatures but becomes increasingly significant as the curing temperature is raised. This effect, which is of great importance in the manufacture of precast products, depends on the age of the mix when the temperature is raised and also on the rate, magnitude and duration of the increase. Kohno, Emura and Kinoshita (1) subjected fly ash concrete to short periods of heating to 65, 80 and 90°C soon after moulding. They found the rate of gain of strength at one day was greatly increased as the temperature increases and that the strength was also improved by delaying the time at which the heating was applied. In all cases, however, the 28 day strengths were less than that of normally cured concrete. Venuat (2) cured specimens normally at 20°C for one or two days before subjecting them to short periods at 80°C and found that, whilst this had little effect on the specimens which did not contain fly ash, it substantially increased not only the short term strength of the fly ash mixes but also improved the long term strength as well. Phat (3) employed longer periods of heating of 1, 3 and 7 days at 5, 20, 40 and 60°C followed by 7 days normal cure and in all cases found that the higher temperatures improved the strength development of specimens containing fly ash. Kokubu, Miura, Takano and Sugiki (4) who mixed and cured concrete at 10, 21 and 30°C found after three months the strength of specimens containing no fly ash were lower the higher the temperature but for fly ash specimens the reverse was true. Nasser and Marzouk (5) have reported the effect of temperatures up to 230°C on the properties of mass concrete containing fly ash.

In this investigation the mortar specimens were cured for 24 hours in a 20°C fog-room before being water cured at elevated temperatures until shortly before testing.

TEST SPECIMENS

40 x 40 x 160 mm mortar prisms were made accordingly to ISO-Rilem recommendation R679 (similar to the French Afnor NP-P 15-451 and the German DIN 1164 standards). These had a water/binder ratio of 0.5 and an aggregate/cement ratio of 3. The specimens were compacted in their moulds by using a jolting table. After demoulding the specimens were weighed in air and water and then placed immediately in water baths at the appropriate temperature. Two hours before testing they were returned to water at 20°C. The physical and chemical analyses of the Portland cement and the fly ash used are given in Table I.

PROGRAMME OF TESTS

Two mortar mixes were employed, one with the Portland cement and the other with 20% by weight of the cement replaced by the fly ash. No adjustment was made to the water content to compensate for the increased workability of the fly ash mix. Specimens of each mix were cured at 20, 35, 50, 65 or 80°C after an initial 24 hour at 20°C, and tested at 3, 7, 28 and 56 days. Specimens cured at 20, 35 and 50°C were also tested after 184 and 365 days. The mean bulk density, flexural strength and compressive strength were determined from three specimens for each condition (from 6 specimens for the 20°C conditions).

TABLE I

	Portland cement	Fly ash
Density (kg/m^3)	3150	2300
Specific surface (m^2/kg)	330	340
Loss on ignition	1.75%	4.92%
45µm residue	-	11%
SiO_2	22.02%	49.92%
CaO	64.60%	-
Al_2O_3	3.99%	24.32%
Fe_2O_3	1.74%	9.76%
MgO	1.20%	-
Alkalies (as Na_2O)	0.53%	-
SO_3	3.36%	-
Free CaO	1.54%	-
Moisture		0.27%
C_3S	51%	-
C_2S	25%	-
C_3A	7.5%	-
C_4AF	5.2%	-
$CaSO_4$	5.7%	-

DENSITY

The bulk density at demoulding was on average 0.6% greater for the fly ash cement mortar specimens than for the plain cement specimens despite the fact that the fly ash had a density 0.7 that of the cement it replaced. This difference, although small, was statistically significant and corresponded to a reduction of 2% in the volume of entrained air of the mix containing fly ash. A reduction in voidage of this magnitude would be expected to increase compressive strength by at least 4%. At later ages the 20 and 35°C cured specimens had increased in density to a greater extent than the specimens cured at higher temperature whilst maintaining the density differential between the two mixes.

COMPRESSIVE STRENGTH

Figure 1 shows the compressive strength of the two mortars as a function of age and curing temperature. The results obtained with the plain cement mortar show that elevated curing temperatures increase early age strength but reduce later age strengths. With the exception of the 80°C cured mortar, which failed to gain strength significantly after 7 days, the temperature-strength inversion occurred at approximately 28 days after which strength was lower the higher the curing temperature.

Increasing the curing temperature had a greater effect on the fly ash cement mortar, accelerating to a considerable extent the development of strength at early ages. Whilst the strength-temperature inversions again occurred, they were generally at much later ages, and the specimens were cured for

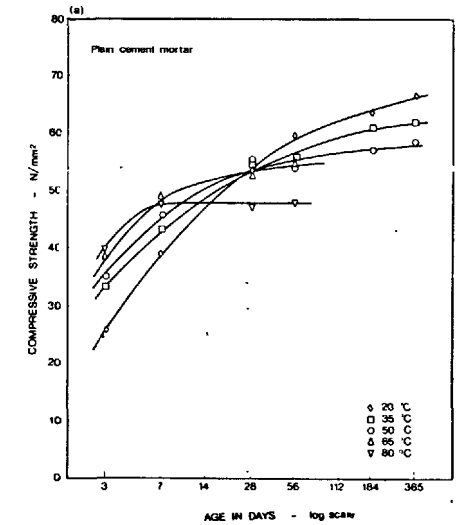

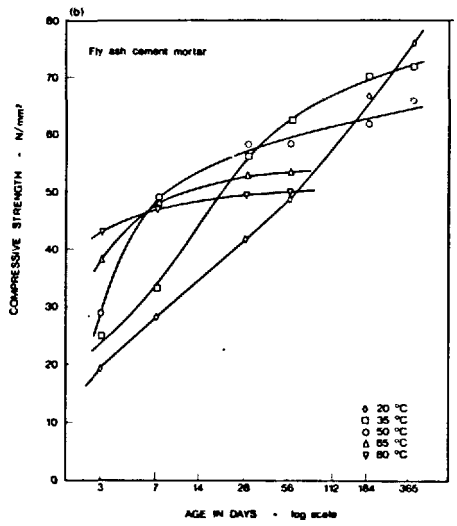

FIGURE 1. Compressive strength as a function of age and curing temperature.

See figures 2 and 3 PAGE 5

one year before the 35°C cured specimens were less strong than the 20°C cured ones. This is broadly in agreement with the results of Kokubu, Miura, Takano and Sugiki (4) discussed earlier. In order to compare the strength development of the two mortars, the ratio of the fly ash cement mortar strength to the plain cement mortar strength at the same age and curing condition is shown as a function of curing age and temperature in Figure 3(a). The fly ash cement mortar was stronger than the equivalent plain cement mortar when this ratio exceeded unity. This did not occur with the 20°C cured specimens until approximately 150 days. For the 35°C cured specimens the age was reduced to approximately 24 days and to only 6 days for the 50°C cured specimens. At 65°C the fly ash cement mortar behaved little differently from the plain cement mortar although at 80°C it was stronger at early ages but the strength ratio decreased with time of curing. Lühr and Efes (6) showed, with similar prisms cured at 20°C, that the age at which fly ash cement mortars exceed the strength of the equivalent plain mortar depended on the relative fineness of the Portland cement and the fly ash. The strength development up to 28 day was shown to be mainly a function of the cement fineness and after 28 day to be also a function of the fineness of the fly ash. Homma and Kikuchi (7), relating the strength development of mortars containing fly ash up to 90 days to Feret's coefficient to avoid the effect of water/cement ratio, found the coefficient exceeded that of plain cement mortar after four weeks at 20°C but after only 7 days at 40°C. From Feret's coefficient, in this investigation, if the fly ash acted as an inert filler the strength ratio would be expected to be 0.75 at all ages. Although the ratio appears to start from this figure, it rises, in the case of the 20, 35 and 50°C cured specimens, to show a strength advantage of approximately 15% after one year for the fly ash cement mortar.

The contribution to strength made by the fly ash alone may be estimated by subtracting 0.75 of the plain mortar strength from that of the equivalent fly ash mortar. If this contribution is plotted against age for the various curing temperatures, curves very similar in shape to those shown in Figure 3 result. After one year the highest pozzolanic contribution from the fly ash was in the specimens cured at 20°C. As the curing temperature increased this contribution decreased. The highest long term strengths for both mixes were for those cured at 20°C. It is interesting to note that Mateos (8) found that sand, lime fly ash mixtures cured at 10, 20, 40, 60 and 120°C showed no temperature-strength inversions up to 28 days.

FLEXURAL STRENGTH

Figure 2 shows the flexural strength of the mortars as a function of age and curing temperature. In contrast to the effect on compressive strength, for the plain cement mortars the effect of moderately increased curing temperature was small except at early ages. Curing at 65 and 80°C was again detrimental to long term strength and again the temperature strength inversion effect occurred.

The effect of increased curing temperature on the strength development of the fly ash cement mortar was striking. After 7 days the effect of raising the temperature from 20 to 50°C was to almost double

the flexural strength and at one year there was still a 26% strength advantage. At all the ages and temperatures tested, there was a significant increase in strength over the 20°C cured specimens although for the 65 and 80°C specimens this increase was reduced.

Again in order to compare the strength development of the two mortars, the ratio of the flexural strength of the fly ash cement mortar to that of the plain cement mortar is shown in Figure 3(b) as a function of age and temperature. For the 20°C cured specimens, the fly ash cement mortar had to be cured for one year before it attained the same flexural strength as the plain cement mortar. For the 35°C cured specimens this age was reduced to 14 days and at one year the fly ash cement mortar was over 30% stronger. Only 3 days curing at 50°C was required to equal the plain mortar strength. The trend of the curves indicate that the fly ash mortars would eventually achieve a flexural strength 30 to 40% higher than the plain cement mortar but for the 20°C cured specimens this would take several years of continuous curing to achieve.

CONCLUSIONS

Although this investigation was undertaken with a single fly ash cement combination and with temperature increases held constant for longer periods than would occur in practice, the conclusions drawn are probably valid for any reactive fly ash used at this level of cement substitution.

1) Raising the curing temperature moderately accelerates the pozzolanic contribution made by the fly ash to strength development more than it does the contribution made by the hydration of Portland cement. This also implies the corollary that low temperatures would adversely affect the strength development of a fly ash mortar to a greater extent than to a Portland cement mortar. In consequence laboratory tests at 20°C will have little relationship to the behaviour of structural concrete containing fly ash in which temperature changes occur due to heat of hydration and changes in ambient temperature.

2) Replacing 20% by weight of a Portland cement by fly ash has the effect of reducing the short term compressive strength when cured at 20°C. A moderate temperature rise during the early stages of strength development, as a result of heat of hydration or heat applied externally, can substantially reduce this early age strength loss. The effect of reduced long term strength potential resulting from such a rise in temperature is compensated for by the effect the fly ash has in actually increasing this potential compared with the equivalent plain Portland cement mix.

3) Including fly ash in a mix can substantially increase the flexural strength of mortar but this improvement may take several years to materialize if the curing takes place at 20°C.

REFERENCES

1. - K.KOHNO, K. EMURA and K. KINOSHITA (1966), "Effect of maximum temperature during steam curing on the compressive strength of concrete". 9th Japan Congress on Testing Materials (Non-metallic materials) 122-124.

2. - M. VENUAT (1973) "L'accélération du durcissement du béton par la chaleur". Annulles de l'Institut Technique du Bâtiment et des Travaux Publics Serie : Beton, No 126.

3. - T.T. PHAT (1973) "La dureté des bétons de ciments aux cendres". Rev. Mat. Const. Trav. Public 676, 10 - 20.

4. - M. KOKUBU, I. MIURA, S. TAKANO and R. SUGIKI (1960), "Effect of temperature and humidity during curing on the strength of concrete containing fly ash". Trans. Japan Soc. of Civil Eng. No 71 Extra papers (4-3) 1 - 10 (in Japanese).

5. - K. NASSER and H. MARZOUK (1979), "Properties of mass concrete containing fly ash at high temperatures". A.C.I. Journ. Vol 76, 537 - 550.

6. - H. LÜHR and Ya EFES (1974), "Influence of the granulometry of fly-ashes with low ignition losses on the strength development of mortar prisms". 6th Intern. Cong. Chem. of Cement, Moscow.

7. - E. HOMMA and Y. KIKUCHI (1968), "On the development of strength in fly-ash cement". Rev. 22nd Gen. Meeting Cement Assoc. of Japan 82 - 84.

8. - M. MATEOS (1964), "Heat-curing of sand-lime-fly-ash mixtures". Mat. Res. and Std. Vol 4 (5) 212 - 217.

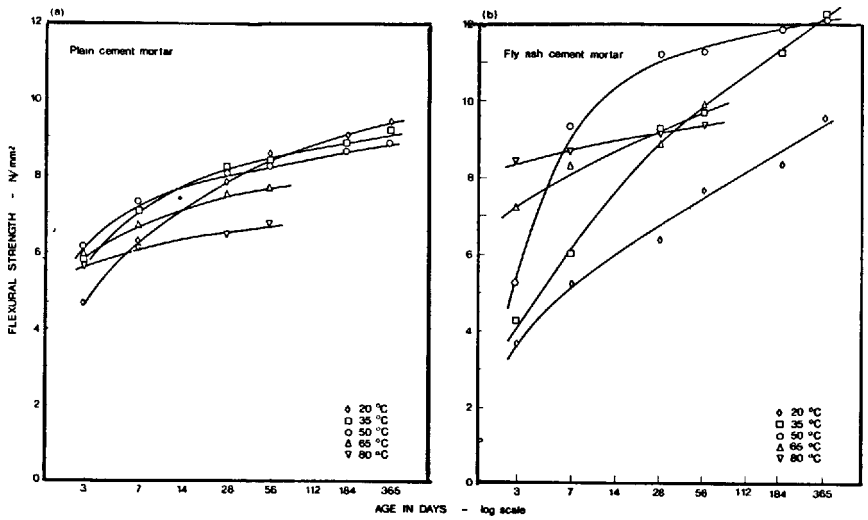

FIGURE 2. Flexural strength as a function of age and temperature.

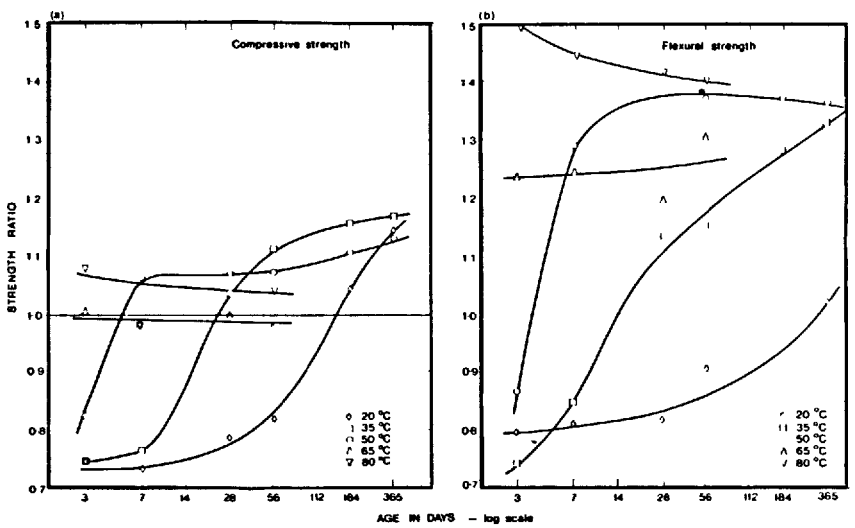

FIGURE 3. Ratio of strength of the fly ash cement mortar to the strength of the plain cement mortar as a function of age and temperature.

Hydratation, morphologie et propriétés des ciments de cendres

Hydration, morphology and properties of ash cements

A.M. DMITRIEV, Candidat ès Sciences Techniques,
Z.B. ENTINE, Candidat ès Sciences Techniques, NIITzement, Moscou,
L.J. GOLDSTEIN, Candidat ès Sciences Techniques, Guiprotzement, Léningrad,
L.P. CHATOKHINA, Candidat ès Sciences Techniques, Youjguiprotzement, Kharkov, U.R.S.S.

RESUME : Les propriétés techniques des ciments à base de cendres se définissent par l'apparition au début de l'hydratation d'un vide sphérique d'une épaisseur de 1 à 3 μm autour du grain de cendre, qui se remplit progressivement de cristaux de portlandite, d'ettringite et, aux stades plus avancés, d'hydrosilicates formés par corrosion superficielle de la particule-cendre. La vitesse de la corrosion est fonction de l'état de la particule.

En fin de durcissement la structure de la pierre du ciment à base de cendres rappelle par sa compacité et ses traits morphologiques celle des ciments sans additions.

On a détecté dans les mâchefers de basicité élevée, également utilisés en qualité d'addition pouzzolanique aux ciments, des cristaux de phases alitiques comportant la "river texture" propre à l'alite. La phase alitique se caractérise par une texture en petits blocs avec un grand nombre de dislocations. L'introduction de modificateurs (CaO, FeO) modifie l'activité des verres de laitier. On peut obtenir des ciments de haute qualité en utilisant non seulement des cendres volantes acides, mais également basiques, à teneur en CaO_{libre} jusqu'à 20 %.

SUMMARY: The technological properties of ash cements are determined by the existence at the initial period of hydration of a 1-3 μm spherical pore, around the ash particle and gradual suturing of it by crystals of portlandite, ettringite and at later stages, by hydrosilicates formed by surface corrosion of the ash particle. The rate of corrosion depends on the state of the particle.

At the late ages of hardening the ash cement stone structure is similar to the structure of additive-free cements as regards the density and morphological properties.

Crystals of alite phases with a characteristic river pattern are detected in high-base fuel slags which are also used as a puzzolanic additive to cements. Alite phases are characterised by fine-block structure with a plurality of dislocations. Introduction of modifiers (CaO, FeO) changes activity of slag glass.

High-quality cements can be obtained when using not only acid but also base fly-ash containing up to 20% CaO_{free}.

Les problèmes d'utilisation des cendres et des mâchefers des centrales thermiques dans la production du ciment ont été depuis longtemps l'objet d'études (1-3), mais, pratiquement, leur mise en oeuvre demeure très limitée. Le tableau I fournit des données sur le volume de production et de consommation de cendres de centrales thermiques pour quelques pays économiquement développés. En 1975 l'industrie du ciment des USA a utilisé pour la production du ciment moins de 0,5 million de tonnes de cendres volantes et 0,4 million de tonnes de mâchefers, de plus, environ 0,6 million de tonnes ont servi à remplacer partiellement le ciment en béton et ceci pour une production totale de cendres de 54 millions de tonnes (4). En U.R.S.S., les cendres des centrales thermiques sont utilisées régulièrement en grand volume dans deux usines de ciment et, à un moindre degré, dans six cimenteries. En 1977 le volume total de cendres consommées a atteint environ 900 mille tonnes (5). En outre une certaine quantité de cendre a servi directement à la préparation du béton.

Tableau I

Production et consommation des cendres et des mâchefers des centrales thermiques (pour les années 1974-1975)

en millions de tonnes/an

Pays	Volume de rejets de centrales thermiques	Utilisé pour la production du ciment
U.R.S.S.	69,0	0,80
USA	54,0	0,90
Grande-Bretagne	11,0	0,14
France		1,00
Japon		0,50
Pologne	12,0	1,00
Hongrie	5,0	0,13
Bulgarie	6,5	0,06
RDA	13,3	0,10

Dans d'autres pays la consommation de cendres ne dépasse également pas un million de tonnes par an.

Une étude plus profonde des processus d'hydratation et des caractéristiques techniques de construction doit contribuer à une plus large utilisation des ciments de cendre.

Les caractéristiques techniques de construction les mieux étudiées sont celles des ciments de cendre avec addition de cendres volantes acides. Ces ciments se caractérisent généralement par un durcissement ralenti aux premiers stades, une aptitude à un long accroissement de la résistance, un abaissement de dégagement de chaleur, une résistance élevée aux actions corrosives (la tenue de l'armature en acier n'y est prise en général en considération), une déformation limitée, due au retrait et au gonflement, un besoin élevé en eau (1,6).

Sont moins connues les propriétés des ciments aux cendres basiques, contenant l'oxyde calcique libre, ainsi qu'aux mâchefers. L'expérience d'emploi de ces matériaux s'est révélée intéressante principalement en U.R.S.S. (7,8).

Comme il a été noté dans (2) les caractéristiques techniques et de construction des ciments aux cendres sont conditionnées par l'existence dans la période initiale d'hydratation et de durcissement d'un pore annulaire épais de 1 à 3 μm autour du grain de cendre rempli de phase liquide. Ce pore se remplit progressivement, d'abord de cristaux aciculaires de portlandite et d'ettringite puis d'hydrosilicates semblables au tobermorite, engendrés par l'interaction dans la zone de contact du portlandite avec le verre alumosilicateux, constituant la surface de la particule de cendre. On fournit plus loin de nouvelles données sur l'hydratation des ciments de cendre. Le processus de remplissement du vide se voit distinctement sur la figure 1 (Dosage des cendres - 15%, durée de durcissement - 28 jours).

Fig.1. Remplissage du pore annulaire autour du grain de cendre par des cristaux de portlandite et d'ettringite (10 000 X, âge - 28 jours).

Le remplissage complet du vide n'a lieu qu'après un délai de 3 à 6 mois (Fig.2), mais, même après ce délai, il subsiste une frontière nette entre la particule de cendre et la pierre de ciment. A la place du vide disparu, on observe une frange de nouvelles formations, tandis que la masse principale de la particule de cendre demeure inchangée. Donc la structure et les propriétés de la pierre de ciment de cendre durcie sont fonction de l'état de la zone de contact et non pas de la quantité de cendres étant entrée en réaction.

Sous cet angle sont d'un grand intérêt les études de la résistance des ciments de cendre à granulométrie différente des cendres,

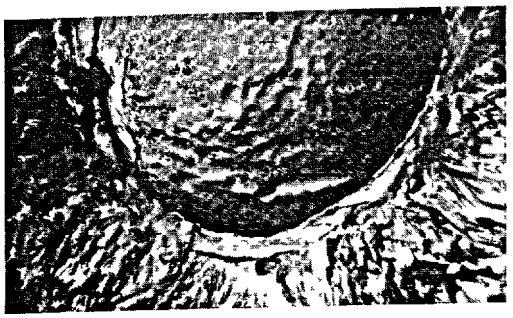

Fig.2. La frange de gel hydrosilicateux ayant remplacé le vide annulaire autour de la particule de cendre (10 000 X, âge - 180 jours).

entreprises au "NIITzement" par G.G.Lepechenkova et Z.B.Entine.

La cendre prélevée à la centrale thermique était dispersée en fraction < 40 μm, de 40 à 80 μm et > 80 μm. On a utilisé dans l'étude les deux premières fractions de chaque cendre. Le rendement par rapport à la masse totale de l'échantillon ainsi que la composition chimique de fractions de cendre sont données au tableau II pour deux centrales thermiques.

Tableau II

Désignation de la cendre	Dimension de la friction, μm	Rendement de la fraction, %	SiO_2	Al_2O_3	Fe_2O_3	CaO
1.1	40-80	49	56,08	28,45	7,15	3,33
1.2	< 40	47	49,22	34,91	6,98	3,47
2.1	40-80	40	61,24	27,92	4,65	1,53
2.2	< 40	57	63,12	27,55	4,44	1,25

L'analyse aux rayons X a montré que la composition en phases des fractions de cendre à éléments gros et fins était à peu près la même. Les deux cendres étaient composées pour l'essentiel de phase vitreuse, quant aux phases cristallines, elles contenaient de quartz α et la sillimanite. A en juger par l'intensité des principales réflexions du quartz -α, la teneur en phases cristallines dans la fraction à éléments fins était supérieure à celle de la fraction à gros éléments, mais ces différences étaient peu sensibles.

La figure 3 a, b montre la résistance des ciments à cendres fine et grosse, tandis que la figure 4 a, b fournit la résistance des mêmes ciments après étuvage.

Comme il s'ensuit des résultats fournis, au début de durcissement jusqu'à 1 à 3 mois, les ciments à cendres fines retardent en résistance sur les ciments aux cendres à gros grains mais, par la suite, rattrapent et dépassent ces derniers.

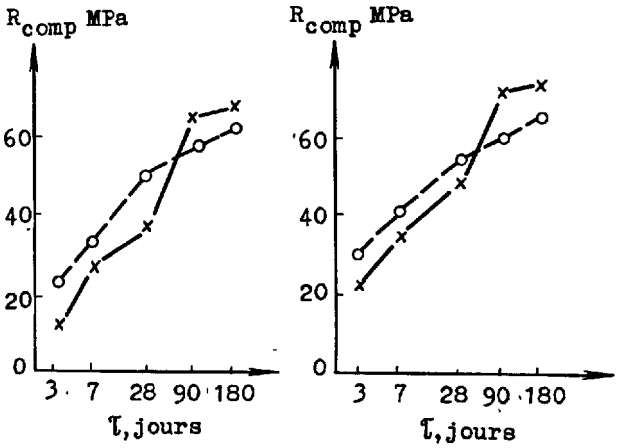

Fig.3 . Résistance des ciments à cendres de fractions fine (x) et grosse (o); a) cendre de la centrale thermique de Troïtsk; b) cendre de la centrale thermique de Chtchekino.

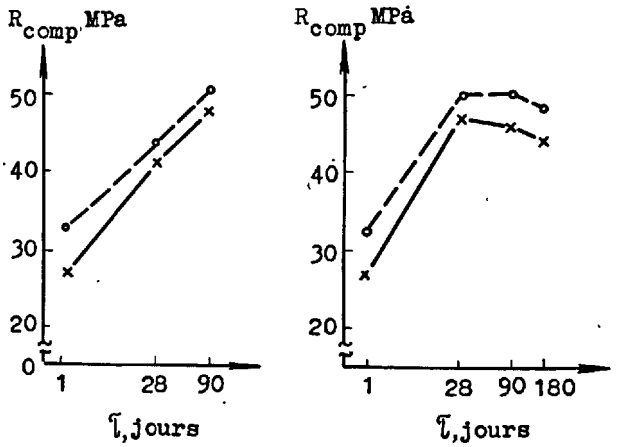

Fig.4. Résistance des ciments à cendres de fractions fine et grosse après étuvage. Les désignations sont les mêmes que sur Fig.3.

Après étuvage, les ciments à cendres de fraction fine continuent à retarder en résistance, même à des délais plus longs, allant jusqu'à six mois.

Ces résultats s'expliquent si l'on tient compte que pour des dosages en masse égaux, la surface totale des particules de cendres de fraction fine est de beaucoup supérieure à celle des cendres de grosse fraction. En conséquence, le volume total des pores annulaires formés au début d'hydratation autour des grains de cendre est plus grand et, partant, leur résistance est plus faible. C'est seulement après le rem-

plissage suffisant des vides par des nouvelles formations que la résistance des ciments à cendre de fraction fine devient plus grande.

Après étuvage, quand les vides se remplissent relativement vite de formations à gros cristaux, la couche de contact demeure affaiblie durant des délais plus longs.

La formation, dans la pierre qui durcit, autour des grains de cendre de vides annulaires remplis de phase liquide, conditionne toutes les propriétés principales des ciments de cendre. L'influence de la formation et du remplissage des vides sur la cinétique de l'augmentation de la résistance ainsi que leur action compensatrice exercée sur les déformations dues au retrait et au gonflement deviennent ainsi immédiatement compréhensibles. La présence de vides saturés d'eau et repartis de façon uniforme entraîne également un abaissement de la résistance au gel des ciments de cendre. Mais en même temps il est évident que les ciments de cendre constituent une pierre de ciment d'une longue durée de vie, de plus la corrosion prolongée des particules de cendre contribue à un meilleur compactage et solidification.

L'accroissement de la masse de cendre étant entrée en réaction n'augmente pas sensiblement la résistance du ciment de cendre. On en obtient la preuve en analysant les données d'essais mécaniques des ciments dont l'un a été obtenu par mélange du ciment avec des cendres volantes et l'autre par mouture simultanée du clinker et des mêmes cendres volantes. Pour un degré de dispersion de la cendre brute de 2800-3000 cm^2/g la résistance des deux ciments était à peu près la même à tous les temps de durcissement. Pourtant l'utilisation dans le béton a révélé d'importants avantages des ciments obtenus par mélange avec des cendres volantes non moulues. Dans ce cas le besoin en eau du béton diminue de 20 à 30 l/m^3, ce qui se traduit, pour une même résistance, par un abaissement de consommation du ciment de 7 à 15%. Le tableau III nous fournit les données correspondantes.

Tableau III

Mode d'obtention du ciment	Consommation du ciment, kg/m^3	Résistance du béton, MPa	
		7 j.	28 j.
Par broyage simultané	240	15,3	25,2
idem	320	25,0	32,3
Par mélangeage	184	14,4	20,6
idem	246	23,5	33,4

Les données fournies montrent que la meilleure méthode d'obtention des ciments de cendre est de mélanger le ciment avec des cendres volantes finement dispersées. Ce mode s'avère également judicieux sous l'angle de gain en énergie électrique. Pourtant certaines centrales thermiques de l'U.R.S.S., en particulier celles de Ladyjeno et de Kourakhovo, produisent des cendres volantes de dispersion très grossière, à surface spécifique de 1800-2000 cm^2/g et contenant des grains moins de 80 μm que pour 50 à 55%. Dans ce cas la mouture simultanée de la cendre avec le clinker est obligatoire et il est recommandé de l'introduire dans la deuxième chambre du moulin à ciment ou dans le séparateur, au cas où la mouture s'effectue en cycle fermé.

Avec l'installation dans les nouvelles centrales de chaudières puissantes à mâchefer liquide il se pose un nouveau problème pour l'utilisation des cendres et des mâchefers de centrales thermiques. Ici on obtient le mâchefer granulé par granulation de la matière fondue au moyen de l'eau.

Le mâchefer est généralement constitué de granules compactes de couleur sombre, qui quelquefois, se présentent sous forme de lamelles ou de fils clairs. La composition chimique varie largement: SiO_2 - de 35 à 65%, Al_2O_3 - de 10 à 25%, CaO - de 1 à 50%, FeO jusqu'à 20%. Le mâchefer peut comporter de sensibles quantités de phases cristallines, mais, en règle générale, ce sont les matières vitreuses qui y dominent. Dans la phase vitreuse on distingue un grand nombre de régions polymérocristallines de composition mullitique (au cas d'une teneur en CaO jusqu'à 10%), mélilitique et même wollastonitique (teneur en CaO - 10 à 40%), parfois gehlenitique (teneur en CaO - 40 à 50%). Dans la phase cristalline on rencontre quelquefois le mullite, le gehlenite, le pseudowollastonite, le $\beta - C_2S$ ainsi que d'autres minéraux (8).

Même avec l'élévation de la teneur totale en CaO le mâchefer est démuni de chaux libre et sa calcination n'implique pas de pertes.

Les études entreprises par "Guiprotzement" (S.D.Okorokov, L.J.Goldstein, V.V.Andreev) de l'activité des mâchefers ont montré qu'avec l'accroissement de la teneur en CaO on assiste à une dépolymérisation de l'ossature alumosilicateuse du verre, ce qui est confirmé par les études des spectres infrarouges. L'affaiblissement de l'ossature implique une augmentation de la teneur en alumine soluble dans les matières vitreuses du mâchefer et, partant, une élévation de l'activité hydraulique de ce dernier. Les données correspondantes sont groupées au tableau IV. L'activité des mâchefers était appréciée d'après la résistance du ciment à centre-mâchefer contenant 29% de clinker, 66% de mâchefer et 5% de gypse.

Toutefois un important accroissement de la teneur en CaO dans le mâchefer et, surtout, l'augmentation du module basique des mâchefers ($M_0 = \frac{CaO+MgO}{SiO_2+Al_2O_3}$) au-dessus de 1,0

entraîne une sensible chute d'activité, car alors le mâchefer est essentiellement composé de phases cristallines.

Tableau IV

CaO,%	Al_2O_3, %		Limite de résistance, Mpa	
	Contenu total	En solution	7 j.	28 j.
2,09	25,45	néant	6,8	14,4
21,07	20,98	1,15	8,3	15,9
29,21	17,30	3,84	10,5	21,5
40,63	12,32	9,13	9,9	23,4

D'après les données fournies par Andreev V.V, Goldstein L.J. et Okorokova S.D., l'accroissement de la teneur en FeO dans les mâchefers basiques jusqu'à 4% ne se répercute pas sur leur activité, mais, si cette proportion est dépassée, la résistance des ciments obtenus avec ces mâchefers diminue de façon sensible (Fig.5). Cela s'explique pour l'essentiel par la variation du contenu en matière vitreuse dans le mâchefer.

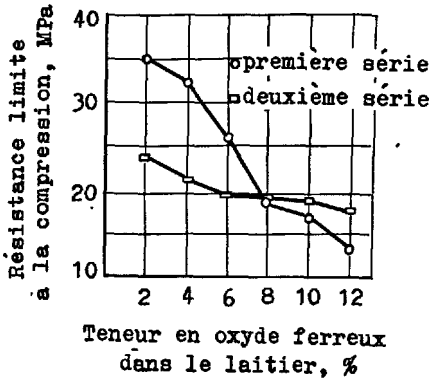

Fig.5. Influence de l'oxyde ferreux sur la résistance des ciments de mâchefer:
o - premier groupe; □ - deuxième groupe.

Cependant dans les cas heureux où la composition du mâchefer se rapproche de celle du clinker, la cristallisation du mâchefer fondu se solde par une augmentation de la résistance limite. C'est ainsi, par exemple, qu'on observe dans les mâchefers cristallisés de certains gisements du bassin houiller de Kansk-Atchinsk une importante quantité d'alite (tableau V).

Il est possible d'obtenir des superciments, ne différant presque pas en résistance et en rythmes de durcissement des ciments sans constituants secondaires, avec une teneur en ces mâchefers allant jusqu'à 60% et plus.

Tableau V

Désignation du produit	Alite, %	Bélite, %	Substance intermédiaire, %
Mâchefer	36	31	33
Clinker	66	11	23

On a étudié au microscope électronique la texture fine de l'alite isolée des mâchefers obtenus dans des conditions semi-industrielles par la méthode de séparation densimétrique des phases minérales. On distingue nettement sur les microfilms (Fig.6) les figures en "river" texture propres à l'alite témoignant de sa texture en fines cellules. Cette texture, comme on le sait, est en rapport avec la densité des dislocations dans l'alite. Ce facteur exerce une grande influence sur la broyabilité des mâchefers et contribue à une meilleure expression de leur activité pendant le broyage.

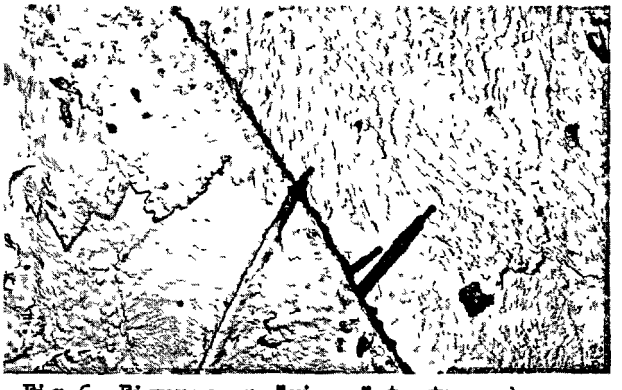

Fig.6. Figures en "river" texture des cristaux de l'alite isolée des mâchefers.

L'emploi des résidus de centrales thermiques se heurte encore au problème de l'utilisation des cendres volantes basiques contenant 7 à 20% de chaux libre. Habituellement ces cendres sont considérées comme inutilisables en qualité d'adjuvant minéral actif au ciment.

Cependant l'expérience acquise en U.R.S.S. dans l'utilisation des cendres basiques montre qu'il est possible d'obtenir à leur base des ciments de haute qualité et qui, de plus, possèdent des propriétés spécifiques fort intéressantes.

C'est ainsi que la cimenterie de Pounane-Kounda produit jusqu'à 350 mille tonnes par an de ciment Portland aux cendres schisteuses. Ce ciment contient pour 20 à 25% de fines cendres schisteuses de la centrale thermique Pribaltiïskaïa, dont la teneur en CaO est de 7-10% (7) et la classe de résistance 500 (d'après la norme sovié-

tique Gost 10178-76). Sous l'angle de la résistance et des rythmes de durcissement, le ciment Portland aux cendres schisteuses est supérieur au ciment sans additifs produit par la même usine. De plus son besoin en eau est plus faible et la résistance après l'étuvage plus grande, ce qui augmente l'intérêt de son utilisation dans la réalisation d'articles préfabriqués en béton armé par traitement à la chaleur humide. On n'utilise pour la fabrication du ciment Portland aux cendres schisteuses que les plus fines fractions de cendres schisteuses dont la surface spécifique est d'environ 4000 cm^2/g. Cependant un intérêt particulier présente l'utilisation de la masse principale des cendres volantes dont la surface spécifique est de l'ordre de 1700 à 2500 cm^2/g et la teneur en CaO_{lib} oscille entre 12 et 20%.

Comme l'ont montré les études au microscope électronique cette cendre est composée d'un mélange de particules sphériques vitrifiées finement dispersées dont la constitution et les propriétés sont analogues à celles des cendres acides, et d'agglomérats cristallins informes composés de chaux libre et d'anhydrite.

Les études ont montré que le CaO_{lib} de la cendre possède une grande activité, grâce à quoi le ciment de cendre supporte les épreuves d'uniformité de variation du volume pour une addition de cendre jusqu'à 20% et une teneur en CaO_{lib} dans le ciment jusqu'à 3,5-4%. Le tableau VI fournit les données sur la résistance des ciments avec constituants secondaires, sous forme de 15-18% de cendres volantes, les plus répandues en U.R.S.S. dans les charbons de Kansk-Atchinsk (1) et les schistes d'Estonie (2). La surface spécifique des ciments est d'environ 3000 cm^2/g.

Les particules acides et basiques de la cendre se comportent différemment lors de la formation de la pierre de ciment.

Autour des bulles vitrifiées de la cendre se forme un vide annulaire qui, par la suite, en se corrodant suit le schéma d'hydratation et de durcissement décrit plus haut pour des ciments à cendres acides.

Tableau VI

Désignation du ciment	Durcissement normal			Etuvage	
	3 j.	7 j.	28 j.	1 j.	28j.
1	20,7	37,0	46,7	29,0	43,0
2	31,2	39,4	51,3	41,1	54,2

Les particules contenant du CaO s'hydratent assez vite. L'hydratation des particules de CaO s'achève déjà au bout de 1-3 jours avec formation de cristaux assez gros de portlandite ce qui entraîne une certaine expansion et un compactage de la pierre de ciment.

Par la suite, la portlandite peut entrer en interaction avec la partie acide de la cendre en accentuant sa corrosion et augmentant ainsi la résistance et la durée de vie de la pierre.

Par un choix optimal de la quantité et de la dispersion de la cendre ainsi que d'autres procédés technologiques, on arrive à contrôler non seulement la résistance mais également les déformations linéaires de la pierre de ciment, ce qui est très important, en particulier, pour l'obtention de bétons à faible perméabilité.

CONCLUSIONS.

L'étude des processes d'hydratation des ciments de cendre permet de dégager dans ces derniers de précieuses qualités pour l'industrie du bâtiment. Dans les conditions de manque aigu d'énergie et de combustible le développement de la production de ciment de cendre s'avère particulièrement efficace. En même temps on contribue à la résolution des problèmes de l'environnement.

BIBLIOGRAPHIE

1.- М.КОКУБУ, Д.ЯМАДА "Цементы с добавкой золы-уноса" УІ Международный конгресс по химии цемента т.Ш, 83-93 Москва, Стройиздат, 1976, (en russe).

2.- З.Б.ЭНТИН, Г.Г.ЛЕПЕШЕНКОВА, Е.Т.ЯШИНА, Н.З.РЯЗАНЦЕВА "О гидратации и твердении цементов с золой-уносом" УІ Международный конгресс по химии цемента т.Ш, 95-98, Москва, Стройиздат, 1976, (en russe).

3.- Р.КОВАЧ "Процессы гидратации и долговечности зольных цементов". УІ Международный конгресс по химии цемента т.Ш, 99-103, Москва, Стройиздат, 1976, (en russe).

4.- Proceedings IV-th. Ash Utilization Simposium, U.S.A., 1976, (en anglais).

5.- А.М.ДМИТРИЕВ, З.Б.ЭНТИН, С.Д.МАКАШЕВ, Г.Г.ЛЕПЕШЕНКОВА "Опыт и перспективы использования золошлаковых отходов ТЭС в цементной промышленности". Комплексное использование минерального сырья № 5 , 1978, (en russe).

6.- Р.КОВАЧ "Использование золы ТЭС в промышленности строительных материалов Венгрии" Венгерский строительный бюллетень, № 1-7-12, 1976. Центр строительной информации, (en russe).

7.- В.Х.КИКАС (1971) Изучение и применение сланцезольных цементов, Таллин, (en russe).

8.- Л.Я.ГОЛЬДШТЕЙН, Н.П.ШТЕЙЕРТ (1977) "Использование топливных зол и шлаков при производстве цемента", Ленинград, Стройиздат, (en russe).

The influence of the production technology of fly ash cements upon their hydration and hardening

L'influence de la technologie sur l'hydratation et sur le durcissement des ciments de cendre volante

R. KOVACS, Ph. D. Deputy Head of Dept. Cement, Central Research and Design Institute for Silicate Industry, Budapest, Hungary.

RESUME : Les propriétés des ciments et leur vitesse d'hydratation dépendent, dans une grande mesure de leur technologie de production. La broyabilité différente du clinker et des cendres volantes rend possible de choisir au point de vue des propriétés désirées des ciments aux cendres volantes, la technologie approchant l'optimum du broyage.

On a examiné les propriétés physiques et l'hydratation des ciments aux cendres volantes à des teneurs différentes en cendres volantes et broyés de manière différente. En partant des résultats obtenus, nous donnons des propositions concernant la technologie optimale du broyage des ciments de cendre volante, qui est appelé "broyage isochrone".

SUMMARY: The properties and the rate of hydration of cements depends considerably on their production technology. The difference between the grindabilities of clinker and fly ash enables to choose a grinding technology which is approximately optimal regarding the desired properties of the fly ash cements.

The physical properties and hydration of fly ash cements ground in different ways and containing various amounts of fly ash were investigated. On the base of the results recommendations were made for the application of the most effective / the so called isochronous / grinding technology in fly ash cement production.

INTRODUCTION

The manufacture of energy-saving products as well as the application of such technologies is gaining more and more ground nowadays. Such type of product are fly ash cements, too, since proportionally to the amount of fly ash added less energy is consumed for the quarrying and drying of raw materials and for clinker burning.

That is why the production of fly ash cements is in Hungary, too, ever widening. The amount of the fly ash used as an admixture is expected to reach 250 thousand tons while that of fly ash cements 2 million tons in 1980. The possibilities, however, are not at all exhausted by this but although further extension of production and utilization is limited by the lower initial strength and higher sensitivity to early freezing of fly ash cements as compared to the Portland cements. /For this reason maximal fly ash content is limited by Hungarian Standard to 20 %/.

It is known that the initial strength of cements depends on a number of production technological factors /mineralogical composition of the clinker, the fineness and granulometric composition of the cement as well as its SO_3-content, etc./. The aim of our research was to determine those technological parameters of fly ash cement production by which the initial strength can be increased in the simplest way and with the least energy consumption.

The literature in this field is rather poor /1-3/ mentioning first of all the positive role of increased C_3S content.

THE RELATIONSHIP BETWEEN THE HYDRATION AND STRENGTH OF FLY ASH CEMENTS

In the course of our former research /4,5/ the hydration processes of fly ash cements were studied in details. It was concluded that the hydration products of fly ash cements were practically the same as those of pure Portland cement, i.e. a gel phase consisting of calcium silicate and calcium-aluminate-hydrates /later partially crystallizing/, calcium hydroxide and -carbonate. The correlation of the amounts of the individual phases, however, is different e.g. in fly ash cement there is more gel phase than in the Portland one but less calcium-hydroxide /portlandite/. The amount of carbonate phase is also somewhat higher.

The deviations in certain properties of fly ash cements as compared to those of the Portland cements can be explained by the differences between the rates of growth and compositions of the hydrate phases.

It was also found that the hydration processes of fly ash cements are exactly expressed by the change of their strength with time. The strength of such cements is lower at the beginning because the amount of the active component /the clinker/ in them is less and their structure is also looser.

Due to the increasing amount of secondary hydrate compounds formed in the reaction of the fly ash and the lime released during hydration of the clinker minerals as well as to the filling up of the pores the density of the cement stone increases and its strength will match or even exceed that of the fly ash-free cement.

From the above mentioned it can be concluded that higher initial strength of fly ash cements can be achieved by increasing the hydration rate. In order to do so experiments were carried out varying the different technological parameters.

INVESTIGATION OF THE ROLE OF VARYING THE CLINKER COMPOSITION

Clinkers of free CaO-contents below 0,1 % were burnt from raw mixes of identical lime saturation factor /0,9/ having different silica /2,0 ÷ 2,4/ and alumina /0,6 ÷ 1,4/ moduli, in a laboratory silite rod furnace at 1400°C. The duration of burning altered between 3-5 hours depending on the moduli.

The 15 different clinkers thus obtained were pre-ground to a cca. 200 m²/g specific surface and after the adding 6 % gypsum on the one hand and 6 % gypsum plus 20 % fly ash on the other they were post-ground in a laboratory Bond-mill for about 35-40 minutes.

The specific surface and the chemical composition of the fly ash used were the following: 530 m²/kg; SiO_2 - 57,46; Al_2O_3 - 17,95; Fe_2O_3 - 8,43; CaO - 7,07; MnO - 2,40 SO_3 - 1,71; loss on ignition - 3,02 %.

Plotting the initial strengths as a function of the moduli of the cements prepared in the described way in a space diagram an increasing tendency towards the corner characterized by AM = 1,4 and SM = 2,4 was observed. That is why the investigations were extended to the contacting clinker composition range /SM = 2,4 ÷ 2,6 and AM = 1,4 ÷ 1,7/

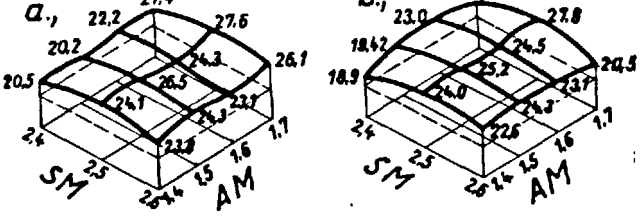

Fig. 1. - Effect of the modular composition of clinker upon the 3 days compression strength /MPa/ of pure /a/ cement and that containing 20 % fly ash /b/

Fig 1. shows the initial strengths of these experimental cements in a space diagram. On the base of this as well as the results of long-term investigations not given here in details it can be concluded that the optimal clinker composition to produce fly ash

cements using the given fly ash /typical for the Hungarian acidic fly ashes/ is characterized by the following moduli: SM about 2,5 and AM = 1,6 - 1,7 /provided the LSF is cca. 0,9/. In the future we wish to extend our investigations to clinkers of a lime saturation factor higher than 0,9 and aluminate moduli higher than 1,7.

INVESTIGATION OF THE ROLE OF THE GYPSUM CONTENT OF CEMENT

It is known that the amount of the gypsum required for the regulation of setting depends on the composition and grinding fineness of cements. Since these characteristics of the fly ash cements differ from those of the Portland cement, we thought it necessary to investigate the gypsum-demand of these cements.

In the course of the research on the one hand the gypsum content of industrial fly ash cements were increased by adding further 1 to 4 % gypsum, on the other hand cements of different fineness were ground from industrial clinkers with various gypsum addition. The optimal gypsum content was determined based on the strength-changes of the cements thus obtained.

Because of the lack of space we cannot give the results in details, only the conclusions are summarized here briefly.

For the cements containing no and 10 % fly ash, resp. the optimal gypsum addition is practically the same and, depending on the grinding fineness, amounts to 4-5 % for cements with a specific surface in the range of 300-350 m²/g and 6-7 % in case of a surface of 400 m²/g and higher, resp.

The optimal gypsum content od cements containing about 20 % fly ash amounts to 5 % for a specific surface of 300-350 m²/kg and 6 % for 400 m²/kg and higher, resp.

It can be stated in general that the gypsum demand of fly ash cements is less modified by the change of its fineness than in case of the pure cement.

These results refer to the mixtures made of usual Portland cement clinker containing about 50 % C_3S, 25 % C_2S, 10 % C_3A and 8 % C_4AF and of the acidic fly ash mentioned above.

INVESTIGATION OF THE ROLE OF THE GRINDING TECHNOLOGY

Two basic technological variants of making fly ash cements are known: blending and inter-grinding.

In the blending technology fly ash is added to the ready-ground cement and the mixture is properly homogenized. Among the sub-versions of this technology the preliminary fine grinding of the fly ash as well as the different points and ways of introducing the fly ash can be mentioned. The advantage of the blending technology lies in its simplicity but as a disadvantage it should be mentioned that it cannot be applied for all types of fly ash and the initial strength of the cements produced this way is generally low.

In the intergrinding technology the fly ash is ground together with the clinker and gypsum in the mill to make cement. According to the terminology suggested by us, complete intergrinding means the simultaneous feed of the fly ash, gypsum and clinker into the mill, while partial intergrinding means that the intergrinding takes place only in the final phase of the grinding process of the clinker.

There are further sub-versions within this, i.e. when the whole amount of the fly ash is fed into the mill or when the fine-fractions of it are previously separated and only the coarse ones let to be interground with the clinker.

During the laboratory, pilot plant and industrial scale experiments carried out by us several versions of the intergrinding technology were studied in details.

In the course of laboratory experiments we used the clinker and fly ash of the above mentioned compositions. To investigate the effect of the duration of intergrinding the following method was applied.

10 and 20 %, resp. of fly ash and 5 % of gypsum were added to the clinker pre-ground to different fineness /specific surface/ and these mixtures were post-ground for different times then the properties of the cements thus obtained were investigated.

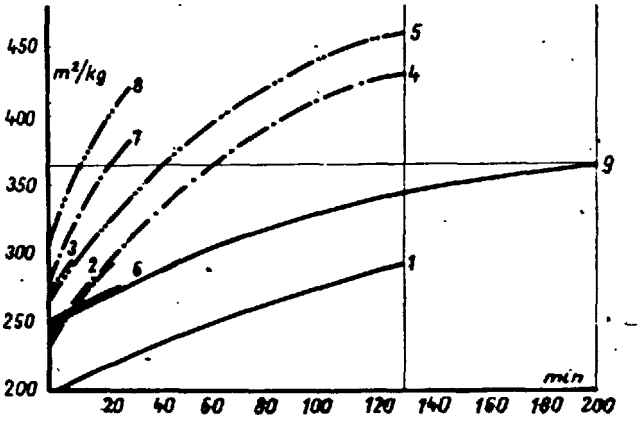

Fig.2 - Change of the specific surface of the pure /——/ cement and those containing 10 % /- . -/ and 20 % /- .. -/ fly ash as a function of grinding time

Fig.2 and Fig.3 show the grinding curves and the compressive strengths, resp., of the cements. It can be seen from these figures that, starting from a clinker with a specific surface of about 200 m²/kg, in order to reach identical specific surface of about 300 m²/kg post-grinding times of 130 minutes for pure cement, 20 and 10 minutes resp., for the cements containing 20 and 10 % fly ash, resp., were necessary /ce-

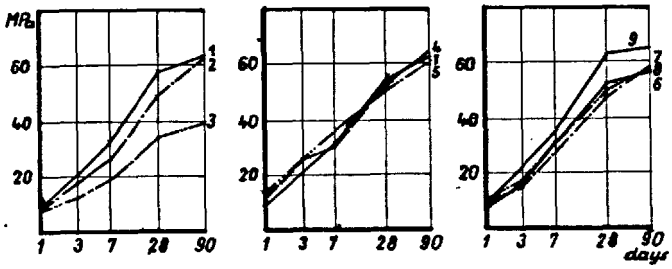

Fig.3 - Effect of the duration of grinding upon the compressive strength of the pure cement /—/ and those containing 10 % /- - -/ and 20 % /— .. —/ fly ash

ments 1,2 and 3/. The hydration of the cements post-ground for short times is poorer its hardening is slower thus their initial strength does not reach that of the pure cement.

The specific surface of the fly ash cements /cements 4 and 5/ post-ground for identical time /according to our terminology: isochronously post-ground/ with the pure cement / cement 1/ is considerably higher showing the effect of fly ash as a grinding aid. At the same time their strength at all ages is identical to or even surpasses that of the pure cement.

The same conclusion can be drawn when comparing the finenesses and strengths of the cements pre-ground to a specific surface of about 250 m²/kg and isochronously post-ground for a shorter time /30 minutes/ /cements 6, 7 and 8/. As an experiment a cement of high initial strength with a specific surface of cca. 350 cm²/kg was also obtained by post-grinding the cement 6 for 170 minutes. It can be stated that the strength characteristics of the fly ash cements obtained by considerably shorter post-grinding i.e. by considerably lesser energy consumption match or exceed those of the pure cement already after 28 days.

Investigating the effect of the pre-grinding fineness similar experiments were carried out with cements made from clinkers pre-ground to a specific surface of about 150, 200 and 250 m²/kg and containing 0, 10 and 20 % fly ash, and 6 % gypsum, post-ground uniformly for 60 minutes. Fig. 4 and Fig.5 show the grinding curves and the compressive strengths of these cements.

From these results it can be concluded that the grindability-improving effect of fly ash manifests itself more obviously in case of the clinkers pre-ground to higher specific surfaces i.e. fly ash admixture helps at that point where otherwise the grindability would show already decreasing tendency.
It can be seen from the figures that the

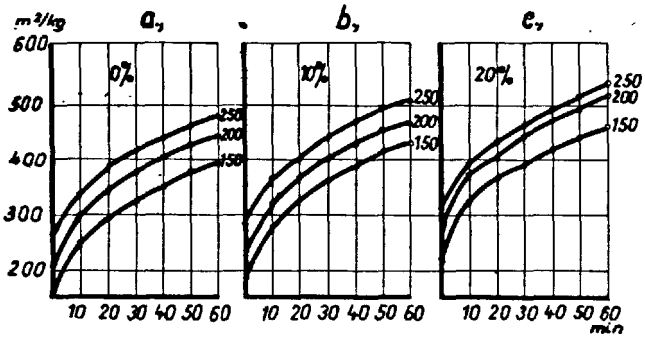

Fig.4 - Change of the specific surface of the cements containing 0. 10 and 20 % fly ash as a function of pre-grinding fineness and duration of grinding

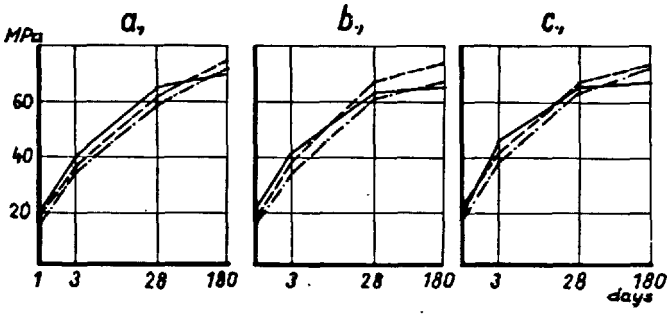

Fig.5. - Effect of the pre-grinding fineness upon the compressive strength of the pure cement /——/ and those containing 10 % /- . - /and 20 % /- .. - / fly ash
Pre-grinding fineness: a - 150,
b - 200 and c - 250 m²/kg

dependence of the 1- and 3-days strength of cements upon the pre-grinding fineness of the clinker is more expressed than that of the 28-days strength.

Investigating the granulometric composition of the cements prepared in laboratory experiments as well as their separated clinker and fly ash fractions obtained using a liquid of a 2,6 kg/m³ density /which was possible due to the different densities of clinker and fly ash being 3,1 and 2,2 kg/m³ resp.,/ interesting conclusions could be drawn.

It was pointed out that when intergrinding clinker and fly ash in the coarse grinding range both components become finer but the clinker only to a smaller extent. In the fine grinding range, however, mainly the

fineness of the fly ash changes only while that of the clinker remains practically unchanged. Due to this the major part of the fine fraction of fly ash cements interground for longer time is represented by the finest fly ash particles and there are much less fine clinker particles in it. That is why the initial hydration of such cements is slower. We suppose this to be one of the main reasons why the initial strength of these cements is lower than that of the pure cement.

Similar results were obtained in the course of the pilot plant experiments not described here in details due to the lack of space.

The industrial scale experiments were carried out on a closed circuit cement mill sized Ø 4 x 12 m equipped with a static air swept classifier /seriesly connected with a grits-separator and two Ø 5,6 m air classifiers with distribution plates/ /Fig.6/. In the course of the experiments the load of the mill, the amount of fly ash and the point of introducing it into the mill as well as the rpm of the air classifier were varied.

Separating in heavy liquid the cement samples taken at different points of the mill system the fly ash content of them and following this the specific surface and granulometric composition of the separated clinker component were determined. Tables I and II give the results in abstracted form.

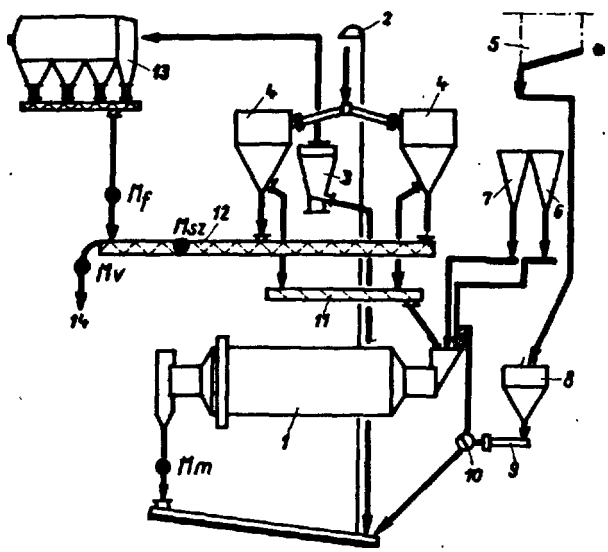

Fig.6 - Technological diagram of the mill system used in industrial scale experiments 1 - mill; 2 - elevator; 3 - grits separator; 4 - air classifier; 5 - fly ash silo; 6 - clinker bin; 7 - gypsum bin; 8 - fly ash feed bin; 9 - screw feeder; 10 - diverting valve; 11 - grits transporter; 12 - cement transporter; 13 - electric precipitator; 14 - to cement storage silos; M - sampling points;

TABLE I

Characteristics of the products at different mill loads /air classifiers rpm. 30 %/

Clinker + gypsum feed, t/h		60	60	70	70	80	80
Fly ash feed, t/h		-	12	-	14	-	16
Fly ash content, %		-	15,60	-	23,63	-	19,57
Granulometric composition, %							
minus 60 µm		90,9	88,4	89,7	91,6	88,3	93,2
minus 30 µm		65,3	70,5	58,3	66,4	55,6	65,9
minus 10 µm		1,9	20,7	1,8	14,3	0,9	13,2
Specific surface m²/kg	cement	291,7	294,5	285,5	291,9	272,0	290,4
	clinker	-	196,8	-	166,0	-	161,5
Compressive strength MPa	1 day	13,0	8,20	13,4	7,6	11,2	8,2
	3 days	21,0	16,5	22,6	16,2	18,3	16,3
	7 days	27,5	22,1	32,2	24,3	26,7	23,3
	28 days	35,9	34,4	42,2	35,6	35,6	35,0
	90 days	44,5	44,8	48,7	46,0	45,2	46,6

As a summary it can be stated from these that when grinding pure cement the highest initial and final strength was observed at a 70 t/hour mill performance. The initial strength of fly ash cements - almost independently from the mill performance /72-96 t/hour/ - is lower in every case than that of the pure cement, after 28 days their strengths are practically identical, while after 90 days the former usually exceeds the latter.

In case of complete intergrinding, when fly ash was fed into the mill together with the clinker, the specific surface of the cement amounted at the different loads to 290-295, while that of the clinker varied only bet-

TABLE II

Effect of the place of introducing the fly ash into the closed circuit system

Place of sampling and its mark	Mill I. Fly ash introduced into the air classifier		Mill II. Fly ash introduced into the mill	
	Fly ash content,%	Specific surface, m²/kg	Fly ash content,%	Specific surface, m²/kg
Mill outlet /M_K/	2,55	203,8	20,48	239,2
Air classifier fine fraction /M_{SZ}/	18,75	268,3	22,17	261,7
Electric precipitator outlet /M_E/	6,64	416,0	29,66	448,2
Final product /M_V/ Mills I and II	20,10	272,5		

ween 161-196 m²/kg. This proves the conclusion drawn for laboratory experiments i.e in this case the major part of the fine fractions is represented by fly ash.

We also tried to introduce fly ash into the air classifier.

The air classifier separated the fine part /about 88 %/ of the fly ash i.e. really it was introduced into the product by simple "blending". Only the coarse fraction /about 12 %/ of the fly ash was interground in the mill thus the positive influence of the fly ash upon grinding couldn't become effective.

The results of the industrial scale experiments proved that by adding fly ash a plus performance of about 20 % can be achieved - at identical energy consumption - but the price of this is the decrease of the initial hydration and initial strength of the cement.

Fly ash cements of high initial strength cannot be produced in the investigated mill system since the optimal technology necessary for it - i.e. the partial intergrinding - cannot be realized in this system. On the base of the experiences of the experiments the possibilities and conditions of optimizing such mill systems for the production of fly ash cements are being investigated in our Institute.

CONCLUSIONS

Summarizing the experiences of the laboratory, pilot plant and industrial scale experiments the following main conclusions can be drawn:

- on the base of the investigations carried out thus far the optimal clinker composition to produce fly ash cements is characterized by a silica module of about 2,5 and alumina module between 1,6-1,7;
- the optimal gypsum content of fly ash cements, depending on the quality of clinker and fly ash, is about 6 %;
- the grindabilities of the clinker and fly ash are different which should be taken into account when the grinding technology is to be chosen and designed;
- an effective method of accelerating the hydration and increasing the initial strength of fly ash cements is the partial intergrinding /the separate pre-grinding of the clinker followed by the simultaneous post-grinding of the clinker and fly ash/;
- the optimal pre-grinding time /and the specific surface to be obtained, resp./ of the clinker depends on the quality of the clinker and fly ash and on the fineness of the latter, resp.. In the case of the materials investigated by us in order to achieve the best initial strength of fly ash cements containing 10-20% fly ash the clinker should be pre-ground to a specific surface of about 200 - 250 m²/kg.

LITERATURE

1.- M. KOKUBU /1968/ V.Int. Symp. Chem. Cem. Tokyo

2.- F. MASSAZZA /1974/ VI. Int. Congr. Chem. Cem. Moscow

3.- KOKUBU - D. YAMADA /1974/ VI. Int. Cong. Chem. Cem. Moscow

4.- R. KOVÁCS /1968/ Proc. 9th Conf. Silic. Industry, Budapest

5.- R. KOVÁCS /1975/ Cement and Concr. Res. 5, pp. 73-82;

Comparaison de la réactivité de différentes pouzzolanes

Comparison of the reactivity of different pozzolane

B. MORTUREUX, H. HORNAIN, E. GAUTIER et M. REGOURD. Département Microstructure C.E.R.I.L.H., Paris, France.

RESUME : La réactivité de six pouzzolanes d'origine et de composition diverses, la microstructure de leurs hydrates ont été étudiées grâce à la diffraction des rayons X et la microscopie électronique à balayage, d'une part dans des pâtes 80 % Pouzzolane + 20 % $Ca(OH)_2$, d'autre part dans des pâtes de ciment Portland à 20 % de Pouzzolane. Le taux de fixation de $Ca(OH)_2$ dans les pâtes de ciment a été comparé aux résistances mécaniques des mortiers ISO.

D'après l'analyse minéralogique, quatre des pouzzolanes sont d'origine volcanique (feldspathique, zéolitique, vitreuse), une autre, siliceuse, d'origine sédimentaire, la dernière une cendre volante de centrale thermique.

L'activité de ces ajouts est fonction de leur composition chimique, leur nature minéralogique, leur surface spécifique. Certaines pouzzolanes telles les cendres volantes qui s'hydratent peu aux brèves échéances, peuvent être activées par étuvage.

SUMMARY : The reactivity of six pozzolana of different origin and composition and the microstructure of their hydrates were studied by X-ray diffraction and scanning electron microscope. Two paste samples series were studied, one containing 80 % pozzolana + 20 % $Ca(OH)_2$ and the other Portland cement + 20 % pozzolana. The combination rate of $Ca(OH)_2$ in the cement pastes was compared to the mechanical resistances of ISO mortars.

According to mineralogical analysis, four of the pozzolana are of volcanic origin (feldspar, zeolitic, vitreous), an other of sedimentary siliceous origin and the last, power station fly ash.

The activity of these additives is in function to their chemical composition, their mineralogical nature and their specific surface. Certain pozzolana, such as fly ash, which hydrate only slightly over short periods can be activated by thermal treatment.

INTRODUCTION

Les pouzzolanes peuvent être définies comme des matériaux ayant une aptitude à réagir avec la chaux en présence d'eau et à former des composés possédant des propriétés liantes (1). Les pouzzolanes naturelles sont d'origine volcanique ou sédimentaire; elles sont soit vitreuses et se présentent comme une ponce contenant des inclusions de silicoaluminates alcalins cristallisés, soit cristallisées, et contiennent des zéolithes (silicoaluminates alcalins hydratés). Les pouzzolanes naturelles d'origine sédimentaire peuvent être des argiles que l'on utilise après torréfaction ou des terres à diatomées constituées de squelettes siliceux : la gaize utilisée en France est une roche sédimentaire. Les pouzzolanes artificielles comme les cendres volantes sont essentiellement vitreuses, elles contiennent en inclusion des silicoaluminates (mullite) et de la magnétite.

Toutes ces pouzzolanes ont en commun une teneur élevée en Al_2O_3 et SiO_2 qui leur confère un caractère acide et une grande affinité pour la chaux; la somme Al_2O_3 + SiO_2 est de l'ordre de 70 % et peut atteindre 80 %.

Les études précédentes (2) ont montré que la quantité de chaux fixée par les pouzzolanes variait avec leurs caractéristiques physiques et chimiques : à court terme l'activité dépendrait surtout de la surface spécifique (BET) et à plus long terme de la teneur en silice et alumine réactives.

ANALYSE des POUZZOLANES

Nous avons dans notre étude de ciments aux pouzzolanes utilisé 6 produits d'origine et de nature différentes : un tuff de Naples, une pouzzolane phlégréenne, un trass du Rhin, une pouzzolane naturelle de Volvic (France), une cendre volante de Violaines (France) et une pouzzolane siliceuse provenant du Maroc. Les trois premières nous ont été aimablement fournies par le Prof. R. SERSALE que nous tenons à remercier ici.

Ces produits ont été caractérisés par analyse chimique et leur composition minéralogique a été précisée par diffraction des rayons X et microscopie optique.

La composition chimique des 6 pouzzolanes est présentée dans le tableau suivant :

TABLEAU 1 : Analyse chimique des pouzzolanes

	Trass	Tuff	Phlégréenne	Volvic	Cendre de Violaines	Opale du Maroc
P.au f.	10.00	12.16	3.40	0.61	1.85	12.15
CaO	3.20	1.80	3.90	6.70	1.50	6.83
SiO_2	55.90	53.60	57.20	54.30	52.50	70.45
Al_2O_3	16.80	16.10	17.90	16.80	28.20	2.35
K_2O	4.70	7.90	8.00	2.60	4.40	0.32
Na_2O	3.19	3.67	3.56	4.47	0.82	0.49

- Le trass du Rhin et le tuff de Naples sont des pouzzolanes à zéolithes. Les minéraux identifiés sont pour le tuff : une zéolithe type herschélite, de l'analcime, des feldpaths potassiques et une phase vitreuse peu importante. Dans le trass, le minéral dominant est la chabasie, on trouve également du quartz (10 à 12 %), de l'analcime et des feldspaths; la phase vitreuse est très peu importante (3).

- Les deux pouzzolanes à phase vitreuse (Volvic et Phlégréenne) donnent par DRX un anneau dont l'intensité permet de déterminer le pourcentage de verre : 50 % pour la phlégréenne et 20 à 25 % pour Volvic (4).

Les minéraux cristallisés identifiés dans la pouzzolane phlégréenne sont des feldspaths (sanidine), de l'analcime et une zéolithe potassique déjà rencontrée dans le tuff de Naples, du quartz, de l'augite et de la dolomite. On remarque la forte concentration en alcalis : 12 % au total.

Dans la pouzzolane de Volvic, le minéral cristallisé principal est l'andésine mais on trouve également du quartz, du diopside et de la magnétite. La perte au feu est particulièrement faible.

- Dans la pouzzolane microcristallisée à haute teneur en silice du Maroc, les minéraux identifiés par DRX sont, outre l'opale, des formes bien cristallisées de silice (quartz et cristobalite) assez rares, de la dolomite et quelques phosphates; les pourcentages d'alcalins sont faibles et il est clair que l'essentiel de la réactivité provient de la silice.

- Dans la cendre volante le verre est très abondant, les quelques minéraux cristallisés sont la mullite, la sillimanite, la magnétite et un peu de quartz.

Ces analyses ont été complétées par quelques observations au microscope optique et électronique à balayage ainsi que par des analyses ponctuelles à la microsonde électronique.

Les pouzzolanes à phase vitreuse (phlégréenne et Volvic) se distinguent par des grains à contours anguleux parfois dévitrifiés qui ne subissent pas de changement d'aspect après attaque acide tandis que les grains de zéolithe sont rapidement attaqués par HNO_3.

Vus au MEB, les grains de Volvic ou de phlégréenne présentent une surface lisse tandis que dans le trass et le tuff on trouve des grains zéolithiques à surface rugueuse, spongieuse. La surface spécifique de tels grains est certainement supérieure à granulométrie égale.

L'opale apparaît comme très finement divisée. L'aspect des grains de cendre volante, sphériques, est bien connu (5, 6, 9).

La finesse des produits utilisés était la suivante (surface Blaine en cm^2/g) :

Cendre	Trass	Tuff	Phlégréenne	Volvic	Opale	Ciment
4300	7300	5300	2900	4300	7200	3920

Un essai complémentaire de pouzzolanicité a, par ailleurs, été effectué à finesse Blaine égale.

ESSAI de POUZZOLANICITE

Les méthodes chimiques habituellement utilisées pour évaluer l'activité pouzzolanique consistent soit à déterminer la quantité de chaux fixée par la pouzzolane après un certain temps de contact, soit à déterminer le taux de silice et d'alumine solubilisées par un traitement approprié (alumine et silice "réactives")

(8, 10, 11,12). Nous avons utilisé la diffraction des rayons X pour déterminer la quantité de chaux fixée aussi bien dans les ciments aux pouzzolanes que dans des pâtes pouzzolane-chaux, cette technique permettant en même temps de caractériser l'évolution des minéraux de la pouzzolane : 4 g de pouzzolane étaient ajoutés à 1 g de $Ca(OH)_2$, la poudre homogénéisée était gâchée à l'eau distillée avec un rapport e/s = 0.6, les éprouvettes démoulées au bout de 48 heures et conservées dans une atmosphère à 100 % d'humidité à l'abri du CO_2.

La chaux $Ca(OH)_2$ restante a été dosée par DRX (méthode de l'étalon interne Si) en utilisant les 3 raies de diffraction X à 4.92, 3,11 et 2.63 Å. Pour 1 g de pouzzolane, les quantités de chaux consommées sont les suivantes à 7 et 21 jours :

	Trass	Tuff	Opale Maroc	Phlégréenne	Volvic	Cendre de Violaines
7 j	0.14 g	0.14	0.13	0.09	0.04	0
21 j	0.18 g	0.19	0.23	0.11	0.08	0.08

On peut voir que l'opale a le mieux réagi puisque la quantité de $Ca(OH)_2$ fixée à 21 j correspond à 90 % de la quantité totale disponible au départ ceci étant probablement en rapport avec la grande division de la silice.

Les produits d'hydratation du type C-S-H sont bien visibles sur le diagramme de diffraction à 21 jours (raie large à 3.05 Å).

Le trass présente une bonne réactivité ainsi que le tuff : ce sont les zéolithes qui ont réagi comme le montre la diminution de leurs raies de diffraction X.

La phlégréenne, de finesse inférieure aux précédentes, montre cependant une bonne réactivité; la pouzzolane de Volvic réagit peu (30 % de la chaux fixée à 21 j).

La cendre de Violaines n'avait pas fixé de chaux d'une manière décelable par DRX à 7 jours; à 21 j le taux de fixation est égal à celui de la pouzzolane de Volvic mais il est certain qu'aux échéances plus longues la réactivité de la cendre serait au moins égale à celle des autres pouzzolanes comme l'a montré l'essai sur ciment.

Ce dosage de la chaux consommée par les pouzzolanes a été complété par l'observation du produit formé au moyen du MEB (échéance 21 jours).

- Sur la cendre volante, la première hydratation donne de l'ettringite et un peu de C-S-H (peu de $Ca(OH)_2$ fixée). La surface des grains ronds paraît corrodée; l'ettringite est en fines aiguilles.

- Sur le trass qui a fixé 70 % de la chaux disponible, le C-S-H semble très dense et recouvre tous les grains, son aspect est parfois feuilleté; d'après le spectre d'émission X, le produit d'hydratation contient beaucoup plus de Ca que le minéral anhydre; la chaux n'est pas entièrement combinée et se retrouve en plaquettes.

- Sur le tuff jaune de Naples le silicate hydraté paraît dense et recouvre les grains; son aspect est assez voisin de celui du trass (2 pouzzolanes de même composition chimique à l'exception des alcalis).

- Sur la pouzzolane phlégréenne nous trouvons un aspect moins compact : beaucoup de grains ont une surface assez peu attaquée et il est visible que la réaction pouzzolanique concerne surtout la fraction fine du produit (fig. 1).

- Sur l'opale du Maroc (fig. 2) on retrouve le maximum de réactivité avec un maximum de compacité de l'éprouvette, on ne distingue plus les grains, le silicate hydraté C-S-H recouvre tout et assure un bon pontage entre les grains. Ce produit d'hydratation sur l'opale nous a paru assez épais pour faire un dosage des éléments Ca et Si à la microsonde électronique. Sur 200 mesures, la valeur moyenne du rapport C/S est 0.85.

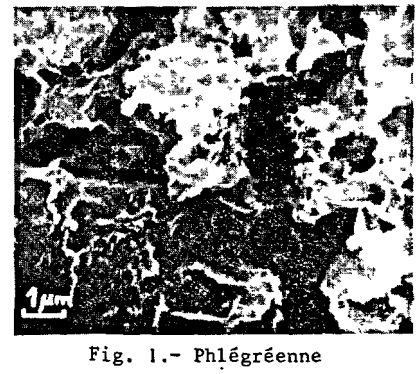

Fig. 1.- Phlégréenne

Fig. 2.- Opale du Maroc

Microstructure des pâtes pouzzolane-chaux hydratées 21 jours.

- Sur la pouzzolane phlégréenne les valeurs de C/S trouvées sont plus dispersées sans doute en raison de microcristaux de $Ca(OH)_2$ non encore fixés par la pouzzolane : les valeurs restent cependant centrées autour de 0.75 mais il faut également tenir compte des alcalis (K_2O). Le dosage moyen donne alors (C+K)/S = 0.8.

La microsonde électronique donne également des images de la répartition des éléments dans la pâte; celles-ci montrent que l'hydratation est très limitée sur des grains massifs, de feldspath par exemple, dans la phlégréenne. Tandis que des grains plus petits ou moins compacts (zéolithes) donnent une meilleure diffusion de Si et Al dans la pâte.

Un deuxième essai de pouzzolanicité a été fait avec les six pouzzolanes broyées à la même finesse Blaine (7000 cm^2/g). Cet essai donne le même classement des six pouzzolanes pour la fixation de chaux (fig. 3 et 4).

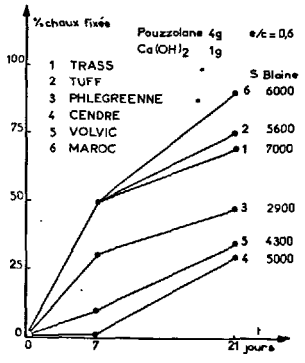

Fig. 3

Fixation de la chaux par les pouzzolanes de surfaces spécifiques différentes

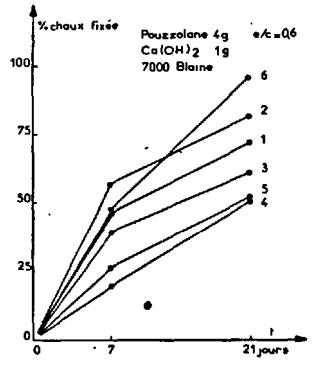

Fig. 4

Fixation de la chaux par les pouzzolanes de surface spécifique égale à 7000 $cm^2.g^{-1}$

Nous retiendrons de cet essai les conclusions suivantes : les pouzzolanes à zéolithes sont très réactives vis-à-vis de la chaux, le tuff de Naples est de ce point de vue légèrement supérieur au trass à finesse égale. La pouzzolane phlégréenne (50 % de verre) fixe moins de chaux que les pouzzolanes à zéolithes (7). L'opale a une excellente réactivité qui dépasse celle des autres pouzzolanes puisque dans notre essai la quasi totalité de la chaux est fixée à 21 jours. La cendre de Violaines réagit lentement et ceci en rapport avec sa finesse : un essai à 3 mois nous a montré une forte fixation de chaux.

La pouzzolane de Volvic a une réactivité très appréciable par rapport aux pouzzolanes italiennes bien que la réaction soit plus lente. La surface spécifique BET des six pouzzolanes broyées à 7000 $cm^2.g^{-1}$ (ss Blaine) est la suivante :

PZ	Trass	Tuff	Phlégréenne	Cendre de Violaines	Volvic	Opale du Maroc
S(m^2/g)	6.6	12.7	3.0	1.6	0.8	36

Le classement des six pouzzolanes par la surface BET est le même que dans l'essai de pouzzolanicité; on remarque la valeur très élevée obtenue avec l'opale du Maroc. Les deux pouzzolanes à zéolithes ont un BET nettement supérieur à celui de la phlégréenne ou de Volvic; pour la cendre volante, la surface BET varie avec le degré de broyage; pour une finesse Blaine de 4500 nous ne trouvons par la méthode BET que 4000 cm^2/g ce qui explique le faible taux de fixation de $Ca(OH)_2$.

CIMENTS aux POUZZOLANES et à la CENDRE VOLANTE

Le ciment utilisé était un CPA; sa composition chimique était la suivante :

CaO libre	SO_3	p.f.	SiO_2	Al_2O_3	Fe_2O_3	CaO	MgO	Na_2O	K_2O
2.00	3.43	4.63	19.12	4.11	2.23	61.77	3.60	0.20	0.73

La composition minéralogique a été déterminée par diffraction des rayons X :

C_3S 60 %; C_2S 15 %; C_3A 8.5 %; C_4AF 5 % ; MgO libre 2 % et sulfate 7 %.

Des microéprouvettes de pâte pure de ciment à 20 % de pouzzolanes ont été préparées avec un rapport e/c = 0.33 et examinées après 28 jours, 3 et 6 mois; 1 et 2 ans de conservation dans l'eau.

Nous avons aussi mesuré la résistance à la compression et à la flexion d'éprouvettes de mortier ISO 2 x 2 x 16 cm conservées en eau douce et en eau de mer. Outre les 6 pouzzolanes, un laitier HF a servi à préparer des éprouvettes dans les mêmes conditions à titre de comparaison.

La microstructure des éprouvettes de pâte pure ou de mortier a été étudiée par DRX, MEB et microsonde électronique.

Il y a progression constante de la fixation de la chaux libérée par le Portland pour toutes les pouzzolanes. La cendre se classe à part ayant peu réagi jusqu'à 6 mois et davantage entre 6 mois et un an.

A 6 mois, pour 1 g de $Ca(OH)_2$ libéré par le ciment et présent dans l'échantillon témoin CPA pur, les quantités de $Ca(OH)_2$ présentes dans les différents CPAZ sont les suivantes :

	Témoin	Cendre	Phlégréenne	Trass	Tuff	Volvic
6 mois	1 g	0.55	0.65	0.60	0.60	0.75
1 an	-	0.35	0.60	0.50	0.55	0.70

Un laitier de référence donne 0.50 g à 1 an. On trouve donc un maximum de CaO fixé par la cendre volante (35 % seulement de la chaux présente dans le témoin pour 20 % d'ajout); viennent ensuite le trass, le tuff, la phlégréenne et la pouzzolane de Volvic. Il y a une bonne corrélation entre la fixation de chaux dans les éprouvettes de pâte pure et les résistances à la compression sur mortier ISO à 6 mois comme à 1 an. Nous n'avons pas fait à 2 ans de mesures de chaux fixée mais noté les résistances des mortiers :

	Témoin	Cendre	Phlégréenne	Trass	Tuff	Volvic	Laitier
6 mois	70 MPa	77.5	54	60	62.5	63	70
1 an	70.5	85	58	76	60	65	75
2 ans	73.7	86	63	69	67.5	67	75

On note une certaine égalisation des résultats entre le tuff et la phlégréenne; le trass reste meilleur, presque à égalité avec le témoin mais seule la cendre volante donne des résultats supérieurs au témoin; la cendre donnait aussi dès 3 mois d'excellentes résistances à la flexion avec des valeurs nettement supérieures à Rf témoin (11.2 MPa contre 9.1 à 6 mois et 12 MPa contre 10 à un an).

Ce critère de la quantité de $Ca(OH)_2$ restant dans les éprouvettes peut paraître insuffisant; on remarque par exemple que les constituants du clinker sont plus hydratés avec la pouzzolane phlégréenne à 1 an comme à 6 mois; il en est de même avec la pouzzolane de Volvic qui donne de bonnes résistances.

Trois ciments aux pouzzolanes (Volvic, Tuff et Phlégréenne) restent riches en $Ca(OH)_2$; leur résistance en eau douce est inférieure à celle du témoin et ils donnent par ailleurs de mauvaises résistances en eau de mer.

Nous avons étudié par diffraction X et MEB la microstructure des hydrates à un an.

Avec la cendre volante les hydrates identifiés par DRX sont l'ettringite, C_4AH_{13}, C-S-H et de la chaux $Ca(OH)_2$ peu abondante. La figure 5 représente un grain couvert d'hydrate; cette hydratation pouvant avoir lieu à la fois à l'intérieur et à l'extérieur du grain; le C-S-H formé est pauvre en chaux (rapport CaO/SiO_2 proche de 1) (9).

Sur la pouzzolane phlégréenne de granulométrie assez grossière, la bordure d'hydrate autour des grains paraît mince, la chaux encore très abondante. Le silicate C-S-H de la pouzzolane est plus pauvre en K et plus riche en Ca que l'anhydre, mais il contient moins de Ca que le reste de la pâte et davantage d'Al (Fig. 6).

Le diagramme de diffraction X du tuff à 1 an est voisin de celui de la phlégréenne : on remarque l'abondance d'aluminate hydraté (ettringite et C_4AH_{13}). Les phases zéolithiques ont pratiquement disparu comme sur le trass, on retrouve de la portlandite en amas dans l'éprouvette (Fig. 7 et 8).

Sur le trass on trouve de faibles zones d'hydratation autour des grains et l'analyse élémentaire montre qu'elles sont plus pauvres en K et Na que l'anhydre et plus riches en Ca (Fig. 9).

Sur l'échantillon Volvic, la proportion d'ettringite est assez élevée à 1 an; cela tient sans doute à la plus grande proportion de sulfates disponibles par rapport au clinker puisque la pouzzolane est peu active. La chaux $Ca(OH)_2$ est moins abondante que sur le CPA témoin mais plus qu'avec les autres ajouts; les raies de diffraction des feldspaths sont peu altérées; comme pour la phlégréenne, le ciment paraît plus hydraté qu'avec les autres ajouts.

Avec l'opale du Maroc l'étude en pâte pure a montré un très fort effet pouzzolanique avec diminution de la chaux dès l'échéance de 3 mois et une atténuation rapide de la bande de diffraction de la silice.

Nous avons par ailleurs utilisé une méthode de détermination accélérée des résistances par étuvage dans l'eau à 80°C d'éprouvettes de mortier. Les échéances choisies étaient à 20 h, 44 h, 146 h, un même degré d'avancement de la réaction étant obtenu dans un temps environ 25 fois plus court qu'à 20°C. La résistance des éprouvettes à 30 % de Volvic ou d'opale du Maroc a été comparée à celle d'éprouvettes témoins de CPA pur d'une part, de CPA additionné de 30 % de quartz d'autre part. La figure 10 montre clairement l'effet pouzzolanique obtenu (zone hachurée) dès l'échéance de 20 h. Le développement des résistances est moins rapide avec Volvic mais la réaction pouzzolanique est cependant nettement visible par rapport à l'inerte dès 20 h (équivalent 28 j).

Un même résultat avait été obtenu avec un ciment à 30 % de cendre volante étuvé 7 j à 80°C (fig.11 & 12).

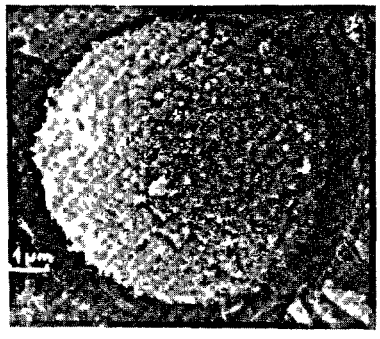

Fig. 5.- Cendre

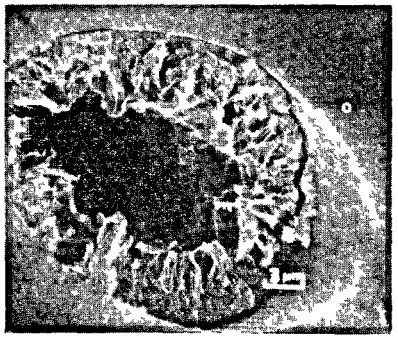

Fig. 6.- Phlégréenne

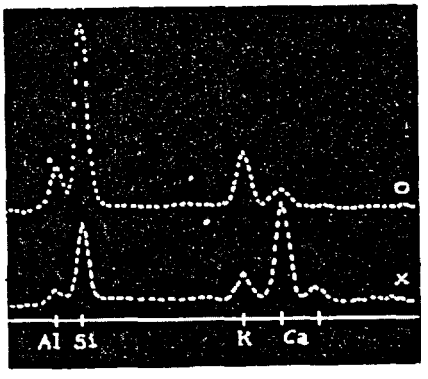

Fig. 6 bis

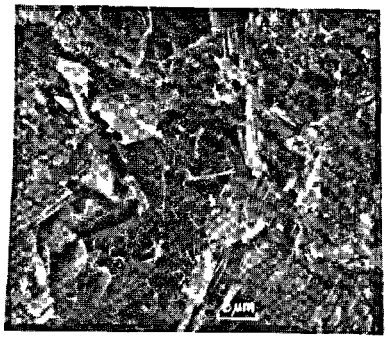

Fig. 7.- Tuff

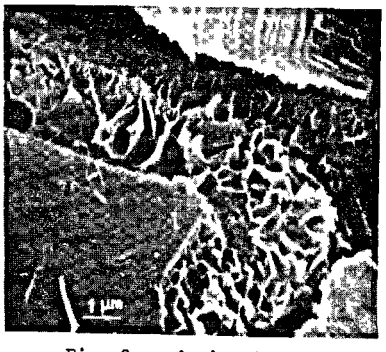

Fig. 8.- Détail fig. 7

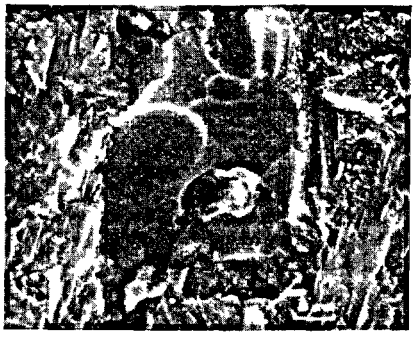

Fig. 9.- Trass

Microstructure des mortiers de ciments à la pouzzolane conservés un an dans l'eau.

CONCLUSION

Nous pensons avoir montré que la valeur pouzzolanique d'un ajout doit être appréciée en fonction de plusieurs éléments tels que la composition chimique, la minéralogie, la finesse du broyage, la surface spécifique BET.

Pour les pouzzolanes à phase vitreuse, plus celle-ci est abondante meilleure est la réactivité mais à finesse égale les pouzzolanes à zéolithes réagissent plus rapidement que les premières. Les cendres volantes peuvent donner d'excellents résultats mais la finesse de broyage joue un grand rôle.

Nous avons montré que la vitesse d'hydratation de la pouzzolane et les résistances obtenues sur mortier étaient en rapport avec la fixation de $Ca(OH)_2$ mais d'autres éléments doivent parfois être pris en compte comme l'interaction ciment-pouzzolane.

L'essai accéléré par étuvage semble un moyen très intéressant d'évaluation rapide d'une pouzzolane.

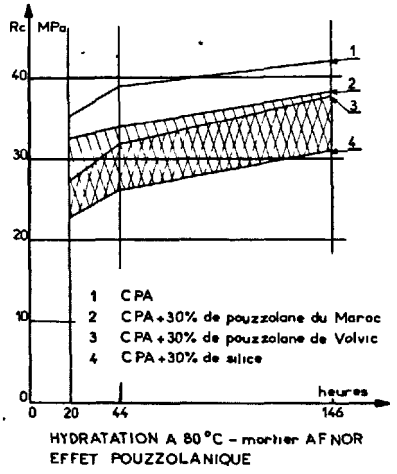

Fig. 10. Résistance à la compression de mortiers AFNOR en fonction du temps d'étuvage. Le traitement thermique est très favorable à la pouzzolane de Volvic.

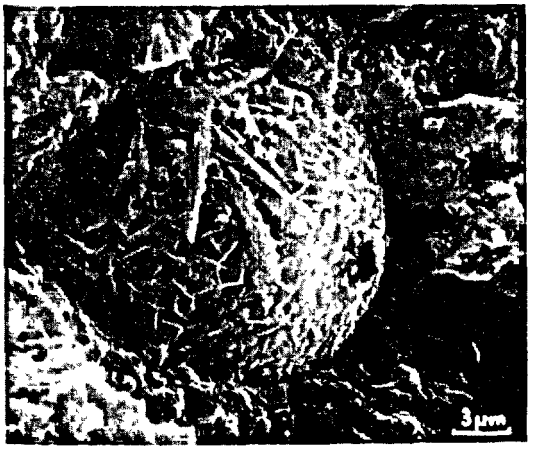

Fig. 11. Grain de cendre couvert de C-S-H et d'aluminates hydratés après un traitement de 110 heures à 80°C.

BIBLIOGRAPHIE

1. F. MASSAZZA (1974). Chemistry of Pozzolanic Additions and Mixed Cements, Principal Paper, 6th Inter. Cong. Chem. Cement, Moscow.
2. U. COSTA, F. MASSAZZA (1974). Factors affecting the reaction with lime of Pozzolonas. Supplementary Paper, 6th Inter. Cong. Chem. Cement, Moscow.
3. R. SERSALE, R. AIELLO (1965). Investigation of genesis, constitution and reactivity of Rhenanian Trass. Silicates Industriels (1), 13-23.
4. J. MILLET, R. HOMMEY, F. BRIVOT (1977). Dosage de la phase vitreuse dans les matériaux pouzzolaniques. Bull. Liaison Lab. P. et Ch., 92, 101-104.
5. M. KOKUBU, J. YAMADA (1974). Fly Ash Cements. Principal Paper, 6th Inter. Cong. Chem. Cement, Moscow.
6. P. TERRIER, M. MOREAU (1960). Mécanisme de l'action pouzzolanique des cendres volantes. Rev. Matér. Constr. , n°613, 379-396, n°614, 440-449.
7. U. LUDWIG, H.E. SCHWIETE (1960). Researches on the hydration of Trass. Cements Proc. 4th. Inter. Symp. Chem. Cement, Washington T 2, 1092-1098.
8. O. BENOIT (1967). Determination de l'activité pouzzolanique par voie chimique. Bull. Liaison Lab. P. & Ch., 26, D 1-D 5.
9. Z.B. ENTIN, E.T. YASHINA, G.G. LEPESHENKOVA, N.Z. RYAZANTSEVA (1974). On the hydration and hardening of cements with fly-ash additions. Supplementary Paper, 6th Inter. Cong. Chem. Cement, Moscow.
10. R. LARGENT (1978). Estimation de l'activité pouzzolanique. Recherche d'un essai. Bull. Liaison Lab. P. & Ch., 93, 61-65.
11. R. DRON (1975). Les pouzzolanes et la pouzzolanicité. Rev. Matér. Constr., n°692, 27-30.
12. ISO (1968) Recommandation R. 863.

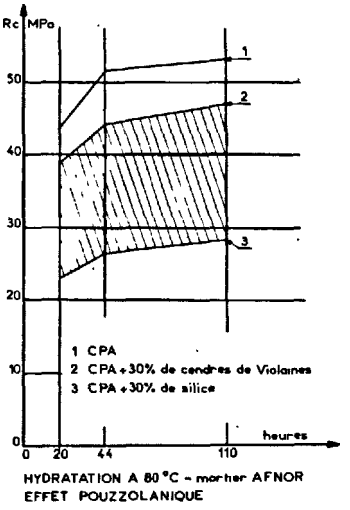

Fig. 12. Résistances à la compression de mortiers AFNOR en fonction du temps d'étuvage. Le traitement thermique est très favorable à la cendre volante de Violaines.

Caractérisation de la pouzzolanicité de cendres volantes

Characterization of the pozzolanicity of fly ash

A. VERHASSELT, Docteur en Sciences, Chercheur, Centre de Recherches Routières, Bruxelles, Belgique.

RESUME : En partant de la description d'un matériau pouzzolanique, quatre grandeurs, qui permettent d'évaluer le niveau de pouzzolanicité à travers les manifestations chimiques et mécaniques de celle-ci, ont été définies : l'activité, la réactivité, l'efficacité pouzzolaniques et l'efficacité pouzzolanique relative.

Avec comme objectif une appréciation valable et non équivoque de la pouzzolanicité d'un matériau à partir de ces grandeurs, une méthode d'essai a été mise au point et testée, son originalité résidant dans la manière de combiner les différents paramètres mécaniques et chimiques mesurés. Cette méthode permet, dans un premier stade, de classifier les matériaux pouzzolaniques par rapport à un produit de référence suivant leur qualité pouzzolanique et la vitesse d'évolution des réactions pouzzolaniques. Dans un second stade, sur base d'un indice de qualité pouzzolanique, chiffre synthétisant l'ensemble des résultats, elle permet de les répartir entre différentes classes pouzzolaniques qui ont pour but d'orienter le matériau examiné vers des utilisations en rapport avec son indice : matériau à traiter (amélioration ou stabilisation), liant pouzzolanique, ajout pour ciment....

Une pouzzolane broyée et quelques cendres volantes étudiées selon la méthode standardisée décrite se sont réparties entre trois classes, mais d'une manière plus fréquente entre les deux auxquelles correspondent les utilisations appropriées du type "liant pouzzolanique" et "ajout pour ciment".

Pour ces échantillons, aucune relation entre les différentes grandeurs pouzzolaniques déterminées et les caractéristiques physico-chimiques mesurées ne s'est dégagée.

SUMMARY : Based on the description of a pozzolanic material four quantities have been defined : pozzolanic activity, reactivity, efficiency and relative pozzolanic efficiency. These quantities enable us to assess the pozzolanic level of a material through the chemical and mechanical signs of its pozzolanicity.

With a view to making a valid and unequivocal assessment of the pozzolanicity of a material upon those quantities, a testing method has been developed and tried; its originality lies in the manner of combining the different measured mechanical and chemical parameters. This method enables us in a first stage to classify pozzolanic materials compared to a reference product according to their pozzolanic quality and to the evolution rate of pozzolanic reactions. In a second stage it allows to divide them into different pozzolanic classes on ground of a pozzolanic quality index that synthesizes the obtained results as a whole. The purpose of those classes is to associate the use of the material investigated to its index : material to be treated (amelioration or stabilization), pozzolanic binder, admixture for cement....

One milled pozzolana and a few flyashes have been studied according to the described standardised method. They spread over three classes, but mainly over those two that correspond to their use as "pozzolanic binder" or "admixture for cement".

For those samples no relation between the different determined pozzolanic quantities and measured physico-chemical properties has emerged.

1. INTRODUCTION

Les cendres volantes, rebut des centrales électriques consommant du charbon, trouvent de plus en plus de débouchés dans la construction routière, dans le génie civil et dans l'industrie cimentière (réf. 1, 2).

Une grande partie des utilisations possibles se basent sur le caractère pouzzolanique plus ou moins prononcé de ces cendres. Si le concept de la pouzzolanicité semble assez bien établi, il n'en va pas de même pour l'appréciation quantitative de celle-ci ou de son niveau (réf. 3, 4): les voies suivies considèrent, en effet, soit l'aspect chimique soit l'aspect mécanique des manifestations de la pouzzolanicité alors que les deux sont intimement liés.

Une méthode de caractérisation globale et non équivoque a été mise au point et appliquée à différents matériaux pouzzolaniques et, entre autres, à différentes cendres volantes. Cette caractérisation permet de proposer des utilisations adéquates en rapport avec le niveau de pouzzolanicité des matériaux.

2. DEFINITIONS

D'une manière générale, une cendre volante est un matériau pouzzolanique, c'est-à-dire un matériau silico-alumineux, généralement pauvre en oxyde de calcium sous forme liée ou disponible (souvent moins de 5%), et dont la solubilisation partielle par l'attaque d'une solution aqueuse d'hydroxyde de calcium conduit à la formation de substances ayant des propriétés liantes analogues à celles d'un liant hydraulique.

D'un point de vue pratique, c'est donc un matériau qui a la faculté de former à la température ordinaire, en présence d'eau et par combinaison avec de la chaux, des composés hydratés et stables, résultat d'une réaction chimique dite pouzzolanique dont un autre résultat est l'obtention d'un mélange durci.

Il résulte de ce qui précède que, pour caractériser d'une manière valable et non équivoque la pouzzolanicité (ou son niveau) d'une cendre volante ou d'un autre matériau pouzzolanique, il est nécessaire de considérer simultanément les aspects chimique et mécanique des manifestations de cette pouzzolanicité. Dans ce but, quatre grandeurs, calculées à partir d'essais effectués dans des conditions standardisées, précisées au § 3, ont été définies :

(1) $\Delta R'_c$ ou ΔS_t : activité pouzzolanique (aspect mécanique) définie conventionnellement comme l'augmentation de résistance à la compression uniaxiale ($\Delta R'_c$) ou à la traction par compression diamétrale (ΔS_t), en MN/m^2;

(2) ΔCaO cons : réactivité pouzzolanique (aspect chimique) définie conventionnellement comme la quantité d'oxyde de calcium consommée, en pourcent en masse de mélange sec décrit au § 3;

(3) EPz (en compression ou en traction) : efficacité pouzzolanique (aspects mécanique et chimique combinés) définie par le rapport

$$\frac{\text{activité pouzzolanique}}{\text{réactivité pouzzolanique}} = \frac{\Delta R'_c \text{ ou } \Delta S_t}{\Delta \text{CaO cons}}$$

qui représente l'augmentation de résistance (R'_c ou S_t) associée à une consommation de un pourcent d'oxyde de calcium, en MN/m^2. % CaOcons.

(4) EPzR : efficacité pouzzolanique relative : rapport de l'efficacité pouzzolanique du matériau étudié à celle de l'hydroxyde d'aluminium, choisi comme matériau pouzzolanique de référence.

Par extension et pour permettre une comparaison avec d'autres essais (l'essai Chapelle, par exemple), on peut généraliser les deux premières grandeurs en les rapportant à la concentration de matériau pouzzolanique dans le mélange sec (18, 75g/100 g pour le mélange utilisé) et définir ainsi une activité et une réactivité pouzzolaniques spécifiques.

3. DESCRIPTION RESUMEE D'UNE METHODE D'APPRECIATION DU NIVEAU DE POUZZOLANICITE D'UN MATERIAU

Les grandeurs définies ci-dessus sont évaluées à partir de mesures (1) de résistance à la compression uniaxiale ou à la traction par compression diamétrale (vitesse :1, 27 mm/min) et (2) de consommation d'oxyde de calcium pour des mélanges constitués de :

- 12 parts de sable normalisé (réf. 5)
- 4 parts de liant pouzzolanique, composé de 3 parts de matériau pouzzolanique à étudier et de 1 part de chaux grasse hydratée (réf. 6, 7)
- et de 1,6 parts d'eau, soit une teneur en eau de 10%.

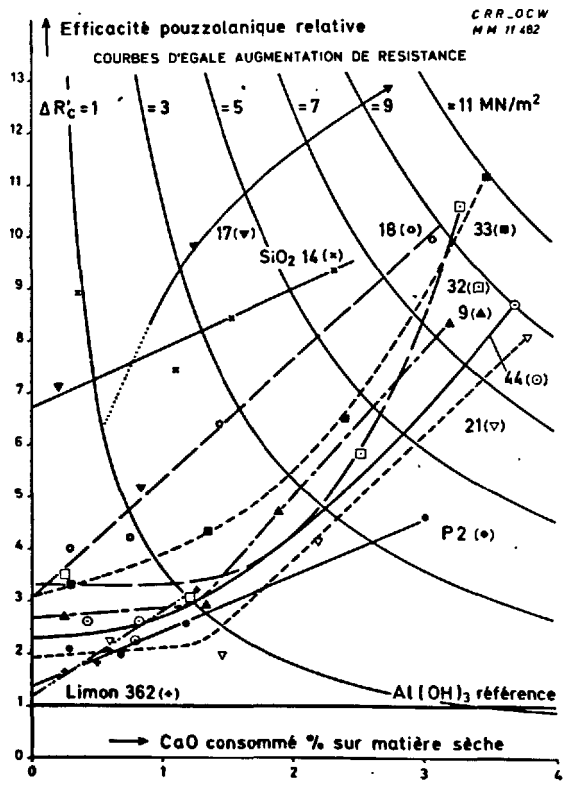

Fig. 1: Efficacité pouzzolanique relative de quelques matériaux (cendres volantes nos 9, 17, 18, 21, 32, 33 et 44, pouzzolane P2, limon n°362 et farine de quartz n°14) en fonction de la consommation de CaO-Essais de R'_c

Les éprouvettes cylindriques de 5 cm de diamètre sur 10 cm de haut après moulage à une masse volumique apparente sèche de 1,85 g/cm³ par compression sur les deux faces, sont conservées à 20°C et 40°C en atmosphère humide saturée. Les essais sont effectués à 0, 7 et 28 jours d'âge, l'essai à 0 jour servant de blanc.

Pour la détermination de l'oxyde de calcium consommé, la méthode est décrite dans la référence 8 : elle repose sur des extractions successives par une solution de saccharose (CaO non fixé) et par une solution de tampon formique (CaO fixé et consommé).

Pour l'interprétation des résultats des quatre essais (7 et 28 jours à 20° et 40°C, l'âge 0 servant de point de départ pour le calcul de $\Delta R'_c$ ou ΔS_t et de $\Delta CaOcons$) trois stades successifs sont envisagés :

1° vue détaillée : mise en diagramme de l'efficacité pouzzolanique relative en fonction de la réactivité pouzzolanique ($\overline{EPzR}$, $\overline{\Delta CaO}$) : le graphique peut se présenter sous forme d'une droite ou d'une courbe dont la concavité peut être tournée vers le haut ou vers le bas (fig. 1). Diverses informations peuvent en être déduites, entre autres : comportement du liant pouzzolanique à court et à long terme, importance de l'effet de la température, résistance que pourrait atteindre le mélange à différents degrés d'avancement de la réaction, vitesse de réaction, estimation de la dose de chaux nécessaire pour atteindre une résistance donnée.

2° caractérisation globale : sur la base du calcul des valeurs moyennes (résultats à 7 et 28 jours, à 20°C et 40°C), d'une part, de l'oxyde de calcium consommé et, d'autre part, de l'efficacité pouzzolanique relative, valeurs moyennes $\overline{\Delta CaOcons}$ et $\overline{EPzR}$ qui sont les coordonnées du "point moyen", on peut situer le matériau dans une grille "qualité du matériau pouzzolanique-évolution des réactions pouzzolaniques", comme il est montré dans la fig.2 . Cette qualité est d'autant meilleure qu'est élevée la valeur de l'efficacité pouzzolanique relative et le durcissement du mélange se déroule à une vitesse d'autant plus grande que l'évolution des réactions pouzzolaniques est rapide.

3°caractérisation globale synthétique : la caractérisation globale de la pouzzolanicité d'un matériau basée ainsi sur la détermination des deux paramètres $\overline{\Delta CaOcons}$ et $\overline{EPzR}$, peut être exprimée plus synthétiquement par le résultat de leur produit, c'est-à-dire par un seul chiffre que l'on propose d'appeler "indice de qualité pouzzolanique (IQPz)" :

$$IQPz = \overline{EPzR} \cdot \overline{\Delta CaOcons} \qquad (1)$$

. Cet indice serait ainsi pour les matériaux pouzzolaniques ce qu'est le coefficient d'activité α pour les laitiers granulés.

. Cet indice permet de caractériser d'une manière simple et globale la pouzzolanicité d'un matériau

TABLEAU I : Exemple de classification des matériaux pouzzolaniques sur base de leur indice de qualité pouzzolanique (en considérant, par exemple, la résistance à la compression uniaxiale)

Classe	Position du point moyen représentatif du matériau (voir figure 2)	Indice de qualité pouzzolanique IQPz (voir figure 3)	Exemples d'utilisations appropriées
0	entre 0 et la courbe $\Delta R'_c = 1$ MN/m²	$0 \leq IQPz < 3,6$	tel quel * ou après traitement à la chaux, au ciment, à la chaux et au ciment ou avec un mélange chaux/gypse
1	entre les courbes $\Delta R'_c = 1$ et $\Delta R'_c = 2$ MN/m²	$3,6 \leq IQPz < 7,15$	- après traitement à la chaux ou au mélange chaux/gypse - comme liant pouzzolanique de qualité médiocre (après mélange avec de la chaux ou avec de la chaux et du gypse)
2	entre les courbes $\Delta R'_c = 2$ et $\Delta R'_c = 3$ MN/m²	$7,15 \leq IQPz < 10,7$	- comme liant pouzzolanique de qualité croissante, le matériau étant utilisé en fonction de sa classe et des buts poursuivis (sous-fondations, fondations, fabrication de blocs....) ou - comme ajout pour ciment ou comme substitut du clinker du ciment (ciments aux cendres volantes ou aux pouzzolanes)
3	entre les courbes $\Delta R'_c = 3$ et $\Delta R'_c = 4$ MN/m²	$10,7 \leq IQPz < 14,3$	
4	entre les courbes $\Delta R'_c = 4$ et $\Delta R'_c = 5$ MN/m²	$14,3 \leq IQPz < 17,9$	
5	au-delà de la courbe $\Delta R'_c = 5$ MN/m²	$17,9 \leq IQPz$	

* si le matériau n'est pas à déclasser sur le plan géotechnique ou sur le plan économique

donné et constitue dès lors un moyen de comparaison facile de différents matériaux pouzzolaniques. On perd toutefois une partie des informations :lors de la comparaison de deux matériaux d'indice de qualité pouzzolanique équivalent, il se peut que pour l'un deux, une efficacité pouzzolanique relative moyenne $\overline{EPzR}$ beaucoup plus petite soit compensée par une évolution des réactions ($\overline{\Delta CaOcons}$) beaucoup plus rapide ; lors de la formulation d'un mélange, il sera nécessaire de tenir compte de ces faits pour les proportions matériau pouzzolanique/chaux.

Les courbes d'égale augmentation de résistance (fig. 2) étant également des courbes d'indice de qualité pouzzolanique constant (EPzR. Δ CaO = constante), elles peuvent servir à délimiter des classes de matériaux pouzzolaniques, classes qui ont pour but d'orienter le matériau examiné vers des utilisations en rapport avec son IQPz. Un exemple de classification est proposé dans le tableau I et la fig. 3 donne l'aspect synthétique ainsi obtenu pour différentes cendres volantes et pour quelques autres matériaux pouzzolaniques.

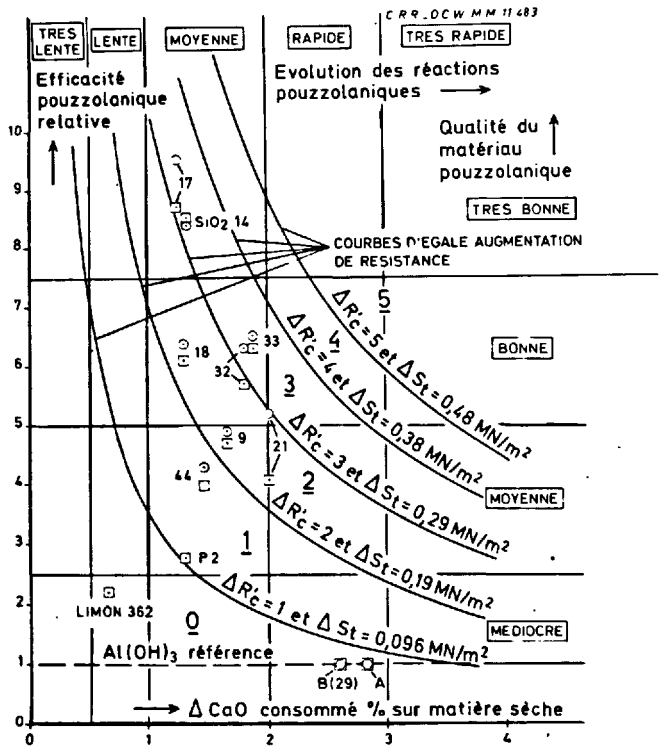

Fig. 2: Caractérisation de la pouzzolanicité de différentes cendres volantes (nos 9, 17, 18, 21, 32, 33 et 44) et de quelques autres matériaux à titre de comparaison (pouzzolane P2, limon n° 362 et farine de quartz SiO_2 n° 14) sur base de la position du "point moyen" :

⊡ = en compression

⊙ = en traction par compression diamétrale

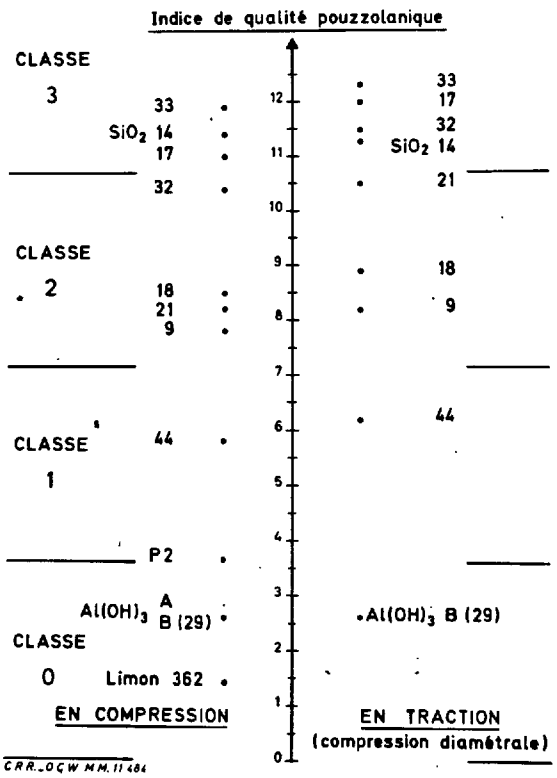

Fig. 3: Classification des cendres volantes étudiées et de quelques autres substances (voir fig. 2) selon leur indice de qualité pouzzolanique (=produit de l'efficacité pouzzolanique relative moyenne et de la consommation moyenne de CaO)

Tableau II : Caractéristiques physico-chimiques et pouzzolaniques des deux échantillons d'hydroxyde d'aluminium

Caractéristique	Unité	Echantillon A	Echantillon B (n°29)
. masse volumique à 25°C	g/cm³	$2,43_8$	$2,44_0$
. masse volumique appar. après sédimentation dans le toluène	g/ml	0,55	0,50
. surface spécifique Blaine	cm²/g	n. d.	5320
. inférieur à 37 µm	%	100	100
. perte au feu (2h à 1000°C)	%	33,9	33,8
Pouzzolanicité			
. réactivité pz moyenne $\overline{\Delta CaOcons}$	%	$2,8_2$	$2,6_0$
. efficacité pz moyenne en compression $\overline{EPz}$	MN/m².%CaO	$0,28_3 \pm 0,02_9$	$0,28_5 \pm 0,03_8$
. efficacité pz moy. en traction $\overline{EPz}$	MN/m².%CaO	n. d.	$0,0274 \pm 0,003_5$

4. DONNEES CONCERNANT LE MATERIAU POUZZOLANIQUE DE REFERENCE, L'HYDROXYDE D'ALUMINIUM

L'hydroxyde d'aluminium $Al(OH)_3$ utilisé est de l'hydrargillite pure en poudre très fine (produit Merck n°1093). Deux échantillons différents, dont les principales caractéristiques figurent au tableau II, ont été étudiés du point de vue de leur pouzzolanicité dans les conditions standardisées décrites au § 3. Les résultats sont donnés dans le même tableau.

Par définition, leur efficacité pouzzolanique relative vaut 1. En conséquence : leur qualité pouzzolanique est médiocre (mais l'évolution des réactions est rapide), leur indice de qualité pouzzolanique vaut 2, 8 et 2, 6 respectivement pour l'échantillon A et B et ils font partie de la classe 0.

Ce type d'hydroxyde d'aluminium convient bien comme matériau pouzzolanique de référence, car son efficacité pouzzolanique ne dépend pas ou peu du degré d'avancement des réactions ni, dans les limites des essais effectués, des caractéristiques physico-chimiques de l'échantillon (mais elles influencent la réactivité pouzzolanique de celui-ci: voir tableau II). Les valeurs adoptées comme référence pour l'efficacité pouzzolanique de l'hydroxyde d'aluminium sont 0, 28 et 0, 027 $MN/m^2 . \%CaOcons$ respectivement pour les essais en compression et pour ceux en traction par compression diamétrale.

Tableau III : Caractéristiques physico-chimiques et appréciation de la pouzzolanicité de cendres volantes et de quelques autres substances à titre de comparaison

Caractéristique	Unité	Farine de quartz n°14	Limon n° 362	Pouzzolane broyée n° P2	CENDRE VOLANTE n°9	n°17	n°18	n°21	n°32	n°33	n°44
Origine		Mol	Hingeon	Mutura (Rwanda)	Les Awirs dépôt	Auvelais dépôt	Auvelais dépôt	Wilhemshaven RFA fraîche	Monceau fraîche	Schelle fraîche	Nijmegen NL fraîche
Masse volumique à 25°C	g/cm^3	$2,64_6$	$2,70_2$	$2,92_2$	$2,24_4$	$2,06_2$	$2,19_8$	$2,41_7$	$2,22_5$	$2,10_0$	$2,38_6$
Masse volumique appar. après sédimentation dans le toluène	g/ml	0, 33	n. d.[e]	0, 83	0, 90	0, 60	0, 69	0, 99	0, 82	0, 78	0, 71
Surface spécifique Blaine	cm^2/g	>10000	n. d.[e]	3.300	2.570	5.410	4.390	2.910	3.050	2.470	4.520
Passant à 45 µm	%	100	90	80	70	81	92	55	85	68	80
Perte au feu (2 h à 1000°C)	%	0, 3	3, 1	0, 6	6, 9	24, 0	13, 1	1, 0	2, 8	3, 9	3, 5
POUZZOLANICITE [a]											
Réactivité pz moyenne $\overline{\Delta CaOcons}$	%	$1,3_4$	$0,6_5$	$1,2_9$	$1,6_7$	$1,2_6$	$1,3_9$	$2,0_1$	$1,8_2$	$1,8_9$	$1,4_4$
Evolution des réactions pz [b]		M	L	M	M	M	M	R	M	M	M
A. En compression											
$\overline{EPzR}$		8, 5	2, 2	2, 8	4, 7	8, 7	6, 1	4, 1	5, 7	6, 3	4, 0
qualité pz [c]		TB	m	M	M	TB	B	M	B	B	M
IQPz		11, 4	1, 4	3, 6	7, 8	11, 0	8, 5	8, 2	10, 4	11, 9	5, 8
classe pz		3	0	1	2	3	2	2	2	3	1
B. En traction [d]											
$\overline{EPzR}$		8, 4	n. d.[e]	n. d.[e]	4, 9	9, 5	6, 4	5, 2	6, 3	6, 5	4, 3
qualité pz [c]		TB	-	-	M	TB	B	B	B	B	M
IQPz		11, 3	-	-	8, 2	12, 0	8, 9	10, 5	11, 5	12, 3	6, 2
classe pz		3	-	-	2	3	2	2	3	3	1

a) voir figures 2 et 3 et tableau I
$\overline{EPzR}$ = efficacité pouzzolanique relative moyenne
IQPz = indice de qualité pouzzolanique (= $\overline{EPzR} . \overline{\Delta CaOcons}$)
pz = pouzzolanique
b) L = lente; M = moyenne; R = rapide
c) m = médiocre; M = moyenne; B = bonne; TB = très bonne
d) par compression diamétrale
e) n. d = non déterminé

5. APPRECIATION DE LA POUZZOLANICITE DE CENDRES VOLANTES

Le niveau de pouzzolanicité de différentes cendres volantes et, à titre de comparaison, de quelques autres matériaux a été évalué suivant la méthode décrite au § 3. Les résultats sont rassemblés dans le tableau III où figurent aussi les principales caractéristiques physico-chimiques de ces matériaux.

Ce tableau ainsi que les figures 1,2 et 3 montrent, pour les matériaux étudiés, que :

- il y a des différences relativement importantes quant à la pouzzolanicité ou à son niveau ;
- en général, l'efficacité pouzzolanique relative moyenne en traction par compression diamétrale est un peu plus grande que celle en compression uniaxiale . La différence dépassant assez rarement 10%, on pourrait donc en pratique se limiter à un seul type de mesure de résistance mécanique, soit par compression simple soit par compression diamétrale (le choix étant fonction de l'équipement du laboratoire et de l'expérience acquise).

En ce qui concerne plus particulièrement les cendres volantes, les constatations sont les suivantes :

- le niveau de pouzzolanicité diffère assez fortement de l'une à l'autre et ceci ne peut pas être mis en relation avec le fait que la cendre provient d'une production récente ou d'un dépôt âgé de plusieurs années ;
- pour ces échantillons, il ne se dégage aucune relation entre le niveau de sa pouzzolanicité (aussi bien à travers la réactivité que l'activité ou l'indice de qualité pouzzolanique) et une des caractéristiques physico-chimiques déterminées : l'IQPz augmente de 3 unités environ à plus de 5 pour des valeurs équivalentes de la masse volumique (cendres n° 9 et 32), de la masse volumique apparente après sédimentation dans le toluène (n°44 et 18), de la surface spécifique Blaine (n°9 et 33), du passant au tamis de 45 µm (n°9 et 33 et n°44 et 17 ou 32) ;
- la cendre volante qui consomme le moins de CaO est celle qui a la plus grande efficacité pouzzolanique relative moyenne (échantillon n°17) et ± inversément pour l'échantillon n°21. Or à l'analyse chimique, la cendre n°17 se révèle comme étant celle contenant la plus haute teneur en imbrûlés. La présence de ce carbone imbrûlé ne semble donc pas être un facteur affectant a priori négativement la pouzzolanicité du matériau.

Les résultats obtenus pour ces échantillons de cendres volantes montrent clairement que, pour exploiter au mieux les propriétés pouzzolaniques d'un matériau, il est nécessaire d'apprécier sa pouzzolanicité en même temps à travers les aspects chimique et mécanique des manifestations de celle-ci.

Le niveau de pouzzolanicité étant fortement lié à la granularité du produit, son appréciation doit se faire sur le matériau dans son état naturel ou après broyage suivant le type d'utilisation prévu.

6. CONCLUSIONS

Les manifestations de la pouzzolanicité d'un matérau ayant en même temps un aspect chimique et mécanique, une appréciation valable et non équivoque du niveau de cette pouzzolanicité doit faire appel simultanément à ces deux aspects.
La méthode d'essai décrite permet, dans des conditions standardisées, de déterminer les paramètres mécaniques et chimiques nécessaires à cette appréciation et de là, in fine, de répartir les matériaux entre différentes classes pouzzolaniques auxquelles correspondent des utilisations appropriées.

Les résultats obtenus pour diverses cendres volantes et une pouzzolane broyée ont montré l'utilité d'une telle méthode, car il ne se dégage aucune relation entre les différents aspects de la pouzzolanicité et une des caractéristiques physico-chimiques mesurées.

Pour six des sept cendres volantes étudiées, les utilisations appropriées sont du type "liant pouzzolanique" ou "ajout pour ciment", la septième cendre ainsi que la pouzzolane broyée, étant plutôt à considérer comme un matériau à utiliser après traitement (amélioration ou stabilisation).

REMERCIEMENTS

L'auteur remercie Monsieur J. Reichert, Directeur, Monsieur J. Verstraeten, Directeur -Adjoint - Chef de la Division Recherches et Monsieur J. Huet, Chef du Service des Méthodes de Mesure du Centre de Recherches Routières sous la direction de qui ce travail a été effectué.

Il remercie également le Pool des Calories pour son aide financière dans la réalisation d'une partie de ces travaux.

BIBLIOGRAPHIE

1. Central Electricity Generating Board (1978) First International Conference on Ash Technology and Marketing London, 22-27 octobre 1978.
2. Ecole Nationale des Ponts et Chaussées et le Laboratoire Central des Ponts et Chaussées(1978) Colloque international sur l'utilisation des sous-produits et déchets dans le génie civil, Paris, volume II, p. 327-410
3. R. LARGENT (1975) "Estimation de l'activité pouzzolanique-Recherche d'un essai" Thèse de doctorat, Université de Paris VI, Paris.
4. R. LARGENT (1978) "Estimation de l'activité pouzzolanique-Recherche d'un essai" Bulletin de Liaison du Laboratoire des Ponts et Chaussées, n°93, p. 61-65.
5. Institut Belge de Normalisation (1966) "Sable normal", Norme NBN 715, Institut Belge de Normalisation, Bruxelles.
6. Institut Belge de Normalisation (1977) "Chaux de Construction-Vocabulaire des Chaux"-Norme NBN-B 13.001, Institut Belge de Normalisation, Bruxelles.
7. F. CHOQUET et J. HUET (1977) Les chaux-Classification et terminologie Revue des Matériaux de Construction, Ciments, Bétons, Plâtres et Chaux, n°706 (3), p. 169-173.
8. A. VERHASSELT (à paraître) Etude des matériaux et des réactions pouzzolaniques par voie chimique.

THÈME V

Ciments spéciaux

Special cements

Président : M. de ASSIS BASILIO (Brésil)

Sur le mécanisme de l'expansion des ciments expansifs

Expansion Mechanisms of Expansive Cements

V. MOLDOVAN, Professeur, ing. dr. Institut de Construction Bucarest, Roumanie,
N. BUTUCESCU, Ingénieur, Institut de Recherche pour Matérjaux de construction Bucarest.

RESUMÉ: La composition des ciments expansifs et les conditions d'utilisation sont étroitement liées au mécanisme d'éxpansion determiné par la formation d'ettringite.

Les recherches effectuées sur quelques ciments:

(a) ciments expansif constitué d'un mélagne de ciment portland + ciment alumineux + + gypse + pouzzolane;

(b) ciment portland (contenant 11% C_3A) + 12% gypse

(c) ciment alumineux (contenant 70% CA) + 12% gypse

permettent de conclure que la formation d'ettringite (mis en evidence par analyse diffractometrique aux rayons X) a determiné une expansion (sur eprouvettes 4x4x16 cm) de 10 mm/m pour le ciment (a), 4 mm/m pour le ciment (b) et sans expansion pour le ciment (c).

La composition chimique de la phase liquide en équilibre avec les ciments étudiés met en évidence la présence d'Al_2O_3 en solution seulement pour le ciment (c). Des recherches électro - microscopiques des pâtes et des suspensions soulignent le fait que la cristallisation d'ettringite dans l'espace intergranulaire ne produit pas une expansion et c'est vrai même pour le ciment expansif dans un excès d'eau. La vraie cause de l'expansion c'est la cristallisation d'ettringite, en l'absence d'Al_2O_3 en solution, à la surface des grains anhydres par voie topochimique; elle contribue à l'accroissement des résistences mécaniques.

SUMMARY: The composition of expansive cements and the conditions of use are closely linked with the expansion mechanism determined by the formation of ettringite.

Research crried on with such cements:

(a) expansive cement made up of a mixture of Portland cement + aluminous + gypsum + + pozzolanas;

(b) portland cement (containing 11% C_3A) + 12% gypsum;

(c) aluminous cement (containing 70% CA) + gypsum,

lead us to the conclusion that the formation of ettringite (evinced by X - ray diffraction) determined an expansion (on prism 4x4x16 cm) of 10 mm/m for cement (a), 4 mm/m for cement (b) and withaut expansion for cement (c).

The chemical composition of the liquid phase in equilibrium with the studied cements evinced existence of Al_2O_3 in solution only for the cement (c). Electronomicroscopical research of pastes and suspensions underlies the fact that the crystalization of ettringite in intergrain space does not produce an expansion, an this is true even for expansive cement E when an exces of water is used. Expansion is in fact determined by crystalisation of ettringite, in the absence of Al_2O_3 in solution, on the surfave of anhydric grains topochemically and contribute to the increase of mechanic strength.

1. GENERALITÉS

De nombreuses recherches pendant les dernières années donnent des explications differentes au mécanisme d'expansion des ciments expansifs dont l'expansion est basée sur la formation d'ettringite. Ainsi l'expansion est attribuée: à la formation d'ettringite sans dissolution des sels anhydres [1], à la transformation du monosulfate hydraté en trisulfate hydraté [2], à la pression osmotique de la solution [3] , à la cristallisation d'ettringite via solution [4] , soit à la structure colloïdale d'ettringite qui gonfle par adserbtion d'eau [5] , Les expansions élevées et les grandes résistences mecaniques dans la periode initial d'hydratations des plusieurs ciments actuelles sont conditionnées par le mécanisme de la formation d'ettringite, par sa structure et ses propriètés.

A l'occasion des travaux d'impermeabilisation du métro de Bucarest nous avons etudié le mécanisme d'expansion du ciment expansif "E" constitué en principal d'un mélange: clinker portland + ciment alumineux + gyps + pouzzolane. La composition chimique des constituents et du ciment "E" est presentée dans le tableau I.

TABLEAU I

Compos. chimique	S_iO_2 + ins%	Al_2O_3 %	Fe_2O_3 %	CaO %	MgO %	SO_3 %	Na_2O+K_2O %	P.c %
clinker portland	21	5,75	5,35	64,5	o,89	o,61	o,84	o,76
ciments aluminieux	6,49	41,6	15	32,3	o,4o	o,1o	o,36	o,9
ciment expansif "E"	28,2	9,53	4,53	45,2	1,49	5,71	1,16	3,49
gyps	92% $CaSO_4.2H_2O$*							

*notations abregées: $C_s=CaSO_4$; $S=S_iO_2$; $C=CaO$; $F=Fe_2O_3$. $A=Al_2O_3$; $H=H_2O$

Pour étudièr le mécanisme d'expansion nous avons préparé deux autres composition en utilisant:

- le clinker portland (ayant 11% C_3A) (tableau I)+ 12% gyps, noté P_e;
- le ciment alumineux, ayant 70% CA, (tableau I)+ 12% gyps, noté A_G.

Nous avons utilisé comme méthodes de recherche: l'analyse diffractometrique aus rayons X, la mesure des variations dimensionelles des eprouvettes, l'analyse chimique de la phase liquide et la microscopie électronique.

2. RESULTATS

2.1. L'analyse diffractometrique a été effectuée sur les mélanges: CA+gyps (1:3) et C_3A+gyps(1:3). Nous avons preparé des pâtes (raport $\frac{eau}{solide}$=1) en solution saturée en chaux ou en utilisant de l'eau distillée. Les résultats obtenus à 1 et 7 jours sont presentés dans le tableau II:

TABLEAU II

Nr.	Mélange analyse	Temps jours	Intensité de la raie caracteristique*)	
			C_sH_2	$C_3A.3C_s.H_{32}$
1.	$CA+C_s+H_2O$	1	145	4o
2.	$CA+C_s+Ca(OH)_2$	1	115	4o
3.	$CA+C_s+H_2O$	7	7o	125
4.	$CA+C_s+Ca(OH)_2$	7	7o	1o8
5.	$C_3A+C_s+H_2O$	1	138	65
6.	$C_3A+C_s+Ca(OH)_2$	1	135	57
7.	$C_3A+C_s+H_2O$	7	45	145
8.	$C_3A+C_s+Ca(OH)_2$	7	28	18o

*) Les determinations pratiques ont été effectués par nos collaborateurs ing.dr. F.Paul et ing. M.Crişan.

Pandant la période 1 à 7 jours la formation d'ettringite est intense pour tous les systemes étudiés au fur et à mesure que la quantité du gypse diminue. Nous n'avons pas constaté la presence d'hydroaluminate de calcium monosulfaté.

2.2. Les variations dimensionelles des pâates ($\frac{eau}{ciment}$= o,35) sur éprouvettes 4x4x16 cm ont été determinées pour les ciments: E (expansif), P_E(portland + 12% gyps) et A_G (alumineux + 12% gyps). Les eprouvettes ont été conservées dans l'eau pendant les 28 premièrs jours, puis à l'humidité de 65% et à la température 20°C jusqu'à 24o jours. Les résultats sont

presentés sur la figure 1.

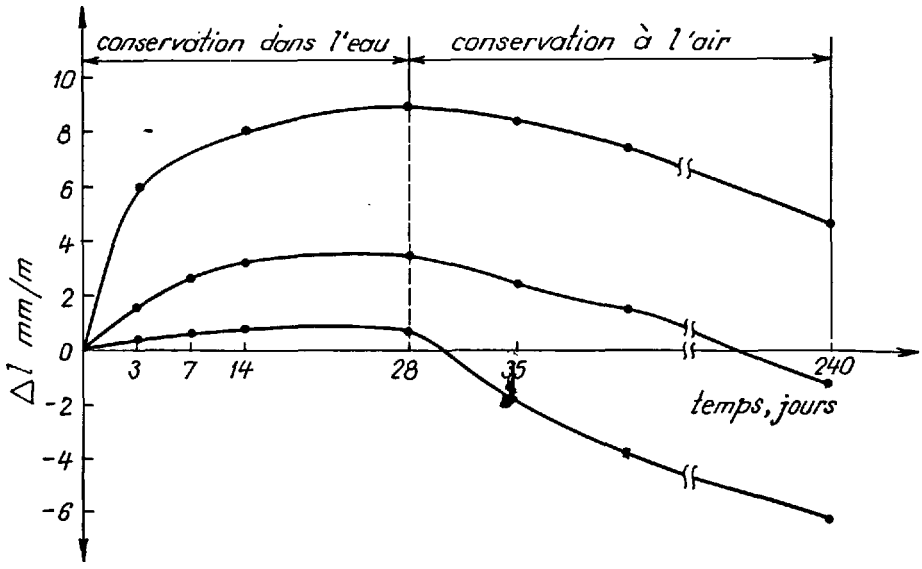

Fig.1. Les variations dimensionelles des eprouvettes pour les ciments E, P_E A_G

Il en résulte des variations dimensionelles résiduelles à 24o jours: + 5 mm/m pour le ciment E, - 1 mm/m pour le ciment P_E et -5 mm/m pour le ciment A_G qui n'est pas un ciment expansif et qui a eu une trés grande contraction.

L'analyse diffractometrique aux rayons X effectuée le trentième jour sur les pâtes durcis, a bien mis en evidence les raies caracteristique de l'ettringite pour tous les ciments étudiés.

2.3. La composition chimique de la phase liquide en equilibre avec les ciments étudiés (E, P_E, A_G) au cours d'hydratation dans les premiers 7 jours effectuée sur le fil - trat (rapport $\frac{\text{eau}}{\text{ciment}}$ =1) est presentée dans le tableau III.

Dans nos conditions de travail (rapport $\frac{\text{eau}}{\text{ciment}}$ =1) la basicité elevée et l'insolubilisation d'Al_2O_3 est assurée pour le ciment E dans les 3 premièrs jours, pour le ciment P_E pendant les premièrs lo heurs et pour le ciment A_G la quantité de CaO n'atteint pas le degré de saturation et diminue après 3 heures ce qui determine la presence d'Al_2O_3 en solution.

Les faits experimentaux (fig.1 et tableau III) mettent en evidence le fait que seulement l'absence d'Al_2O_3 en solution peut determiner des expansions en accord avec la théorie d'Henri Lafuma [1]. Mais la contribution indubitable de l'ettingite à l'accroissement des résistence mecaniques dans la période initiale de durcissement souligne le complexité du phenomène en ce qui concerne la cinetique de la formation d'ettringite. En fonction de la basicité de la solution (influencée par la presence des alcalis), des cristaux d'ettringite peuvent se former dans l'espace intergranulaire ou des cristaux d'ettringite peuvent se former á la surface des grains anhydres et ce le cas des ciments expansifs, comme nous avons constaté par des nombreuses observations electronomicroscopiques presentées ci-dessous.

TABLEAU III

Ciment	Composition de la phase liquide g/l	T E M P S						
		1o min	1 h	3 h	1o h	24 h	3 j	7 j
E	CaO	1,14	1,2$	1,8	1,81	1,83	o,92	o,486
	SO_3	1,25	1,33	1,6	1,76	1,82	o,64	o,345
	Al_2O_3	o,oo16	o,oo16	o,oo18	o,oo2o	o,oo22	o,oo2o	o,oo21
	Na_2O+K_2O	o,8o	1,1o	1,3o	1,56	1,65	2,oo	2,32
	PH	11,5	11,5	11,5	11,5	11,5	11,5	11,5
P_E	CaO	1,46	1,71	1,54	o,98	o,3o	o,29	o,24
	SO_3	1,75	1,63	1,66	1,oo	o,25	o,o22	o,o27
	Al_2O_3	o,oo42	o,o52	o,o43	o,o54	o,o54	o,o83	o,o88
	Na_2O+K_2O	1,75	1,85	1,7o	2,5o	4,1o	4,93	5,75
	PH	11,7	11,8	11,8	11,5	11,7	11,8	11,8
A_G	CaO	o,365	o,776	o,511	-	o,113	o,113	o,o22
	SO_3	o,585	o,932	o,64	o,45	-	o,o48	o,o49
	Al_2O_3	o,4o	o,4o	o,427	o,47	-	o,5o6	o,48o
	Na_2O+K_2O	o,oo3	o,oo3	o,oo2	o,oo3	o,oo5	o,oo5	o,17

2.4. Les recherches electronomicroscopiques effectuées sur pâtes ($\frac{eau}{ciment}$=o,35..1) et sur des suspensions ($\frac{eau}{ciment}$=25...5o) aqueuses dans le 5 premières heures d'hydratation ont mis en evidence quelques faits experimentaux presentés ci-dessous.

l'hydratation du ciment E en pâtes est caractérisée par l'apparition des produits d'hydratation de type ettingite à la surface des grains anhydres (fig.2). Dans la période initiale d'hydratation il n'y a pas des produits d'hydratation dans l'espace intergranulaire.

Fig.2. Produits d'hydratation (ettringite) $\frac{a}{c}$ =o,5o; 3o min,3o.ooo x

Pour un excès d'eau, la majorité des produits d'hydration dans l'intervalle 5 min-1 heure sont apparus dans l'espace intergranulaire (fig.3). Le processus est semblable pur le ciment P_E.

Fig.3. Produits d'hydratation (ettringite) $\frac{a}{c}$ = 25; 15 min.5.ooo x.

Dans le cas du ciment A ce qui caractérise l'hydratation c'est l'apparition des produits d'hydratation via solution dans l'espace intergranulaire.

3. CONSIDERATIONS SUR LE MÉCANISME D'EXPANSION

Les recherches deffractometriques et par l'analyse termodifferentielle (les dernières n'etant pas presentées dans le present article) n'ont pas mis en evidence l'existance du monosulfate hydraté.

La forme exterieure et les dimensions des cristaux d'ettringite sont influencées par les conditions de leur formation. L'apparition d'ettringite par cristallisation dans l'espace intergranulaire, en presence d'Al_2O_3 en solution, ne produit pas une expansion. La vraie cause de l'expansion c'est la formation d'ettringite à la surface des grains anhydres en presence d'une solution saturée en $Ca(OH)_2$ et en l'absence d'Al_2O_3 en solution. Des pressions de cristallisation locales determinent l'augmentation du volume du systeme deformable. Un explication semblable a été donnée dans la recherche [6] . La saturation en CaO de la solution avec l'insolubilisation d'Al_2O_3 est decisive plutôt que la valeur du PH de la solution [7] influencée aussi par la presence des alcalis du ciment. Les faits experimentaux presentés et des calculs thermodynamique [8] sont favorables à la reaction de gypse dissout sur les aluminates solides.

La voie par laquelle les cristaux d'ettringite sont apparus à la surface des grains anhydres c'est l'hydratation sans dissolution des aluminates anhydres en presence du gyps, mécanisme basé sur la grande mobilité du CaO des composants anhydres et hydatés. Des phénomènes de récristallisation d'ettringite pendant l'hydratation on été aussi observés. Les cristaux d'ettringite peuvent s'enchevêtrer entre eux ou avec des autres produits. La valeur élevée de l'expansion et les grandes resistances mécaniques de plusieurs ciments expansifs actuels doivent être liées aux propriétés d'ettringite comme élément de résistance pendant son existance. Dans le cas des produits durcis la formation d'une petite quantité d'ettringite par voie topochimique à la surface des grains anhidres peut provoquer la pulverisation des produits.

BIBLIOGRAPHIE

1. H.LAFUMA (1964) - Liants hydrauliques, pp.35
2. S.CHATTERJI (1968)- The V Intern.Symp. on the Chemistry of Cement, Tokio, III-138.
3. A.E.SEIKIN, [illegible]Iu.[illegible]AKUB (1966)- Ciment sans retrait (en russe) Moscou, pp.17.
4. V.I.KRAV[illegible]NKO (1966) - Ciments expansifs (en russe) Moscou,pp. 6-19.
5. P.MEHTA, M.POLIV[illegible] (1974) - Expansive Cements. The Intern.Congress on the chemistry of Cement Moskow, Princip. paper.pp.12-13.
6. K.G. KRASILNIKOV (1974)- La Physico-chimie des ciments expansifs 7e Congrès intern.de la chimie des ciments (en russe) Moscou. Comunication III-5.
7. H.LUDWIG (1974). Investigations on the hydratation mechanism of clinker minerals. The VI.Int.Congress on the chemistry of cement. Moskow.Principal paper.pp.25-29.
8. V.I.BABUSKIN, G.M.MATVEEV,O.P.PETROSIAN (1965)- La thermodinamique des silicates (en russe). Moscou, pp.249-259.

Magnesium oxide additive for producing selfstress in mass concrete

Oxyde de magnésium, additif producteur d'autocontrainte dans la masse du béton

P.K. MEHTA and D. PIRTZ, Professors, and
G.J. KOMANDANT, Lecturer, Department of Civil Engineering, University of California, Berkeley, California 94720, U.S.A.

SUMMARY: The hydration reaction of MgO was investigated for obtaining expansion in typical mass concretes. The rate of hydration of MgO additive was found to be sensitive not only to the calcination temperature and particle size of MgO, but also to curing temperature of concrete. The additive made by calcination above 970°C was too slow to hydrate, whereas the material calcined below 900°C hydrated too rapidly to be useful for producing self-stress in concrete. Particles > 1180 μm produced large differential expansions in concrete which led to internal distress. Expansive additive for portland cement in the form of 5% MgO calcined at 900-950°C, and sized to 300-1180 μm, hydrated at a rate which was considered adequate with regard to expansion and self-stress necessary for producing crack resistance in typical mass concrete structures exposed to 32-54°C.

RÉSUMÉ: La réaction d'hydratation de MgO a été étudiée afin d'obtenir une expansion dans la masse de bétons typiques. Le taux d'hydratation de MgO e été trouvé sensible non seulement à la température de calcination et à la taille de la particule MgO mais aussi à la temperature de cure du béton. L'additif préparé, par calcination au-dessus de 970°C, s'hydratait trop lentement tandis que le matériau calciné en-dessous de 900°C s'hydratait trop rapidement pour être utile dans la production d'une autocontrainte du béton. Les particules supérieures a 1180 μm ont produit de grandes expansions différentielles dans le béton entrainant des détérioriations internes. L'additif expansif pour le ciment Portland, sous la forme de 5% MgO calciné à 900-950°C et de taille comprise entre 300 et 1180 μm s'est hydraté à un taux qui a été considéré comme adéquat vis-à-vis de l'expansion et de l'autocontrainte nécessaires à la production d'une résistance à la fissuration dans la masse de bétons de structure typiques exposés à 32-54°C.

INTRODUCTION

Mass concrete structures may crack due to thermal tensile stresses unless appropriate measures are taken to control the temperature gradient within the structure. Excessive tensile stresses capable of cracking concrete can occur when concrete under restraint cools from higher temperatures caused by the heat of cement hydration to ambient temperatures.

Currently, the primary measure taken to prevent cracking consists of controling the temperature rise by cooling the concrete. The control of temperatures in hardened concrete is an expensive procedure, at times involving internal cooling by pipe-refrigeration techniques. An alternative or supplemental procedure which needs to be investigated is to reduce the potential tensile stress which may develop on cooling by producing chemical prestress. It is theorized that the compressive stress thus established would tend to offset tensile stresses induced by cooling.

To achieve the maximum benefits in mass concrete from chemical prestressing, the compressive stresses should be formed after the temperature rise has occurred, but prior to any significant cooling of the concrete. Since mass concrete has limited ability of developing and retaining chemical prestress at early ages, the commercially available expansive cements, based on ettringite formation or $Ca(OH)_2$ formation from CaO, are of little benefit because they would undergo expansion before the maximum temperature has been reached in concrete, with the compressive stress relaxed prior to the beginning of cooling. On the other hand, expansive cements deriving their expansion from hydration of MgO to $Mg(OH)_2$ may prove useful here because the hydration-expansion phenomena due to MgO can perhaps be appropriately delayed. Several investigators have reported that the amount of expansion by MgO hydration can be controlled by calcination temperature and grain size of the product. However, in concrete there is little published information correlating the effects of heat treatment and particle size of MgO, and curing conditions, on expansion.

MATERIALS AND PROCEDURE

The MgO used in this investigation was a high-purity pelletized material produced commercially by calcination of magnesite to 900°C. MgO calcined to higher temperatures were produced in the laboratory by further heat treatment of the material in an electrical furnace. Unless otherwise specified, an ASTM Type II portland cement was used for making expansive cements containing MgO as additive.

Curing temperatures in the range 32-54C, which is typical temperature range for uncooled mass concrete, were investigated. Hydration rates at 32°C were studied for MgO alone, and expansion due to MgO hydration was studied both in cement pastes and concrete. Natural sand and gravel were used for making the fineness modulus of sand 150 by 300 mm concrete cylinders containing MgO expansive cements, 2.6, and the maximum aggregate being 38 mm. The mix proportions used were typical of mass concrete in dam construction:

cement = 124 kg/m³ concrete
water = 85 kg/m³ concrete
sand = 571 kg/m³ concrete
gravel = 1594 kg/m³ concrete

EFFECT OF HEAT TREATMENT TEMPERATURE AND PARTICLE SIZE OF MgO ON HYDRATION:

From a preliminary investigation it was established that MgO exposed to >1300° hydrated too slowly, even in <45 μm size fraction. Therefore, studies on hydration rates of MgO at 32°C were limited to the material heat treated for one hour at 900, 1000, 1100, 1200, or 1300°C, and subsequently fractioned into 300-150, 150-75, 75-45, and <45 μm fractions. The theoretical water requirement for complete hydration of MgO to $Mg(OH)_2$ corresponds to 0.45 water-solids ratio by weight. However, pastes were made with 0.6 water-solids ratio, and stored at 32°C in air-tight plastic vials for 90 days. At various intervals, the hydrating material was pulverized, dried at 110°C, and subjected to X-ray diffraction and ignition loss analyses.

For comparison purposes the data from the ignition-loss test are shown in Table 1. It is obvious from the data that, even for the <45 μm size fraction, MgO heated to 1200 and 1300°C hydrated at undesirably slow rates. Also, the 900 and 1000°C material hydrated too rapidly when particles were smaller than 45 μm. It was concluded, therefore, that potentially useful MgO additives should comprise coarse fractions of the material heat treated at < 1200°C.

Table 1 Effect of Calcination Temperature and Particle Size of MgO on Degree of Hydration at 32°C

calcination temperature, °C	particle size, μm	Percent MgO hydrated at age, days:						
		1	3	7	14	21	28	90
900	300-150	46	57	68	76	79	82	98
1000	300-150	0	24	52	60	63	65	78
1100	300-150	0	2	4	33	52	58	68
1200	300-150	0	0	0	1	3	4	40
1300	300-150	0	0	0	0	2	2	18
900	150-75	60	67	76	80	87	90	100
1000	150-75	1	27	68	73	76	77	87
1100	150-75	0	0	2	36	65	67	80
1200	150-75	0	0	0	1	3	u.d.	u.d.
1300	150-75	0	0	0	0	2	u.d.	u.d.
900	75-45	67	85	85	91	96	98	100
1000	75-45	1	79	79	86	89	91	96
1100	75-45	0	4	4	60	77	80	90
1200	75-45	0	0	0	1	2	5	44
1300	75-45	0	0	0	1	2	3	21
900	<45	74	89	89	95	99	100	100
1000	<45	6	81	81	88	91	92	97
1100	<45	0	6	6	66	82	87	95
1200	<45	0	1	1	2	8	u.d.	u.d.
1300	<45	0	0	0	1	2	u.d.	u.d.

u.d.= undetermined

EXPANSION IN CEMENT PASTE PRISMS:

The next phase of study involved direct investigation of free expansion of portland cement prisms containing MgO additives made by heat treatment in the temperature range 900-1150°C. Varying amounts of 45-150 μm additive, made under different conditions of heat treatment were added to the portland cement. The pastes were made with 0.35 water-solids ratio by weight, and cast into 80 by 14 by 3 mm prisms. The prisms were demolded at age 1 day, and then stored in water at 32°C up to age 90 days. The expansion data are shown in Table 2.

Table 2 Expansion in Cement Paste Prisms, cured at 32°C

specimen No.	calcination conditions for MgO		% MgO weight of cement	percent expansion at age, days:					
	temp, °C	hold time, hrs.		7	14	21	28	40	90
1	900	1	5	0.043	0.069	0.079	0.088	0.098	0.171
2	900	1	10	0.085	0.133	0.157	0.181	0.216	0.385
3	900	1	20	0.172	0.262	0.315	0.353	0.406	0.795
4	900	1	30	0.227	0.360	0.427	0.555	0.630	1.230
5	900	4	10	0.011	0.025	0.040	0.050	0.090	0.198
6	925	1	10	0.003	0.020	0.035	0.053	0.075	0.191
7	925	4	10	0	0.008	0.020	0.035	0.063	0.180
8	950	1	10	0	0.004	0.013	0.025	0.040	0.163
9	1000	1	5	0	0	0.002	0.008	0.014	0.045
10	1050	1	5	0	0	0.001	0.003	0.005	0.033
11	1100	1	5	0	0	0	0.001	0.002	0.014
12	1200	1	5	0	0	0	0	0.001	0.003
13	1000	1	10	0	0	0.006	0.018	0.025	0.111
14	1050	1	10	0	0	0.003	0.005	0.015	0.106
15	1100	1	10	0	0	0.001	0.004	0.011	0.066
16	1200	1	10	0	0	0	0.003	0.006	0.036

The expansion data from the cement paste prisms No. 1-4 showed that, generally, the expansion was directly proportional to the amount of the expansive additive present. Correlation between the rates of hydration of pure MgO (Table 1) and the degree of expansion when MgO hydrated as additive present in the portland cement (Table 2), was found to be poor. For instance, at the 32°C curing temperature, both the 45-75 μm and the 75-150 μm fractions of the 900°C MgO were almost completely hydrated in 28 days, however, 5 to 30 percent of the 45-150 μm materials (Specimens 1-4), when added to the portland cement, produced less than 50 percent of the 90-day expansion during the same time period. A probable explanation for this lack of correlation is that MgO hydration in the alkaline medium of hydrated portland cement would be considerably slower than MgO hydration in a neutral environment.

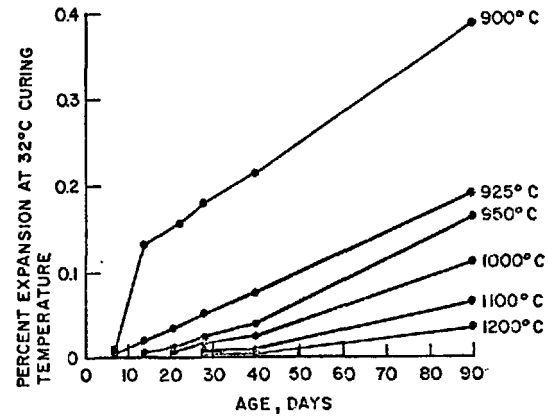

FIG 1. EXPANSION OF CEMENT PASTE PRISMS CONTAINING 10% MgO(45-150 μm)

sion of cement pastes the expansion data of Specimen Nos. 2, 6, 8, 13.15 and 16, which contained 10% MgO additive by weight of cement, are plotted in Fig. 1. As expected, the data showed that in the 900-1200°C range, increasing temperatures of MgO heat treatment produced correspondingly lower expansions in the prisms.

EXPANSION IN CONCRETE CYLINDERS:

Due to the restraining effect of aggregates in concrete the expansions were expected to be much lower than obtained in the corresponding cement paste

Table 3 Expansion in Concrete Cylinders

specimen No.	characteristics of MgO additive		% MgO by weight of cement	concrete curing temp.,C	concrete expansion, microstrain							properties of concrete expressed as percentages of control containing no MgO	
	calcination temp.,°C	particle size, μm			age after casting, days							modulus of elasticity	compressive strength
					7	14	28	40	90	180	360		
A	900	300-150	10	32	60	65	65	65	65	65	65	90	95
B	900	300-150	10	32-43-54	80	170	190	200	200	200	200	90	98
C	920	1180-600	5	32	25	60	65	100	110	125	125	96	91
D	920	1180-600	5	32-43-54	65	390	465	465	465	465	465	86	72
E	920	2360-1180	5	32	0	25	65	75	90	100	140	u.d.	u.d.
F	920	2380-1180	5	32-43-54	40	740	1110	1110	1110	1100	1110	50	67
G	950	300-150	5	32	35	75	110	110	110	110	110	90	86
H	950	600-300	5	32-43-54	20	65	110	125	140	140	140	84	93
I	950	1180-600	5	32-43-54	35	130	275	610	635	635	635	85	89
J	950	2360-1180	5	32-43-54	70	440	960	1015	1030	1030	1030	60	65

In Table 2, comparison of the expansion data between specimen No. 1 and 5, and specimen No. 6 and 7 showed the effect of duration of the heat treatment period on the rate of expansion of the cements containing the MgO additives. In general, the expansion rates were significantly reduced with increase in the calcination time of MgO from 1 to 4 hours. In order to illustrate the effect of calcination temperature of MgO on expansion of cement pastes the expansion data of Specimen Nos. 2, 6, 8, 13.15 and 16, which contained 10% MgO additive by weight of cement, are plotted in Fig. 1. As expected, the data showed that in the 900-1200°C range, increasing temperatures of MgO heat treatment produced correspondingly lower expansions in the prisms. From the data in Table 2, it was obvious that the heat treatment of MgO additive above 950°C would produce very low expansions in concrete within the desired time period. In order to obtain reasonable levels of expansion, it was decided to experiment with coarse fractions of MgO produced in the temperature range 900-950°C. A preliminary investigation showed that expansions were negligible when

MgO particles were less than 150 μm. Some concrete cylinders were cured continuously at 32°C, then at 43°C for the next 7 days, and thereafter for 28 or more at 54°C. The higher curing temperature are presumably attained in mass concrete when concrete making materials are not precooled, and heat of hydration of cement is not dissipated by cold water circulation through concrete.

From the results shown in Table 3, the effect of particle size of MgO, especially of coarse fractions, on concrete expansion was highly pronounced in specimens exposed to warm curing cycle typical of uncooled mass concrete. For instance, Specimen D showed much higher expansions than Specimen C, and Specimen F showed higher expansion than Specimen E. Similarly, for Specimens G-J, the 90-day expansions were correspondingly greater for the 32-43-54°C curing cycle. It may also be noted from the data that potential expansions were stabilized earlier for the 32-43-54°C curing cycle than for the normal or 32°C curing.

CONCLUSION

It is concluded that carefully calcined and sized MgO powders have the potential of being useful as expansive agents for preventing cracks in mass concrete due to thermal stresses. At curing temperatures typical of uncooled mass concrete, 5 percent MgO addition to a portland cement produced a satisfactory rate of expansion provided the heat treatment of the MgO was limited to 900-950°C temperature range and the material was sized to 300-1180 μm particles.

Microstructure and hydration of high alumina cement clinkers

Microstructure et hydratation des ciments à haute teneur en alumine

P. KITTL, Researcher, Department of Materials (IDIEM), University of Chile, Santiago, Chile,
J.H.C. CASTRO, Professor, Department of Materials Engineering, Federal University of Sao Carlos, S.P. Brasil,
L.C. POMPEU, Ceramica Saffran s/A, Betin-M.G., Brazil.

RESUME : La réactivité des ciments à teneur en alumine élevée et variée a été étudiée par des examens microstructurels. Plusieurs compositions ont été essayées, allant de $C_{12}A_7$ à $CA_{3.5}$; les échantillons étaient préparés par fusion, suivis d'un rapide refroidissement (état vitreux). On a observé que les premiers avaient une faible réactivité avec l'eau, et que les derniers avaient par contre une grande capacité d'hydratation.

On a constaté une amélioration de la capacité d'hydratation, par la dévitrification des échantillons vitreux. Le retard à l'hydratation serait provoqué par une couche épitaxique de 5.000 Å d'épaisseur environ, qui se développe sur les surfaces vitrifiées et les protège de l'action de l'eau. Dans les zones dévitrifiées, le mécanisme de l'hydratation est basé sur l'action de H, et la formation en rosette de CAH_{10}.

SUMMARY: The reactivity of high alumina cements of several compositions with water was studied under controled microestructure conditions. Several compositions ranging from $C_{12}A_7$ to $CA_{3.5}$ were prepared by melting followed by fast cooling (vitreous state) while others of them, by sintering. The first group, shows low reactivity with water, meanwhile the last one has high capacity of hydration. By devitrification, the hydration capacity of the glass samples was developed. It was also found that the hydration mechanism in the vitreous state consists in the growth of an epitaxial layer of about 5000 Å which interrups a further hydration process. Instead, in the divitrified state the hydration mechanism is based on defoliation by the action of H and the formation of CAH_{10} rosette shaped.

INTRODUCTION

Mention may here be made of Locher's[1] work in simply composed glasses of the C-A-S system, in which all the hydraulic strengths must be activated by CH products during hydration. A recent work on an industrial aluminous clinker[2] gives evidence that the glass state in a high alumina cement clinker do not present hydraulic strengths without an activation process, even if its composition would be CA, which is the aluminous clinker with the higher hydraulic strength[3]. In consecuence some investigations must be done relating the microestructure of high aluminious clinkers and its hydration, because those reported strengths are concerned to a sintered CA. Obviously high alumina sintered cement clinkers are in the crystalline state. These can be obtained by devitrification[4], with appropiate heat treatments in a glass of the same steicheometric composition.

MATERIALS AND METHODS

The compounds appearing in the binary C-A system are normally given[5] by C_3A, $C_{12}A_7$, CA, CA_2 and CA_6, the portion which is near adjacent to the $C_{12}A_7$ composition have two eutectic points at 1360°C so this is the sinterization temperature. Samples of compacted powder with a composition $C_{12}A_7$ ($C_{1.71}A$), CA, $CA_{1.5}$ were fused in a graphite crucible using an induction furnace and subsequently quenched to room temperature in a steel sheet. In this way a practically transparent material was obtained. Half of the samples were annealed at 1300°C during two hours and then slowly cooled in the furnace. After this treatment the specimens presented a complete opaque yellow colour. This glass of calcium aluminates were mounted in plastic molds and polished until the 0.1µm grade diamont paste with querosene in order to avoid hydration. Thereafter they were etched with H from half a minute up and afterwards, observed in a reflection optical (ROM) and a scanning electron (SEM) microscopes. Back X-ray reflection patterns were taken from some of these samples.

Other compacts of CA, $CA_{1.5}$, CA_2, $CA_{2.5}$, CA_3, $CA_{3.5}$, composition were sintered at 900°C, 1000°C, 1100°C, 1200°C, 1300°C, 1400°C abd 1450°C during two hours and cooled in the furnace. The presence of free lime was detected by mantaining the samples during 30 days in a receptacle at 25°C saturated with water vapour. Those specimens which did not disintegrate by the expantion produced by the free C hydration, were considered totally combined. This fact occured with the samples: $CA_{3.5}$ at 900°C; $CA_{3.5}$ and CA_3 at 1000°C and at1100°C; $CA_{3.5}$, CA_3, $CA_{2.5}$, CA_2 and $CA_{1.5}$ at 1200°C and 1300°C; $CA_{3.5}$, CA_3, $CA_{2.5}$, CA_2, $CA_{1.5}$ and CA at 1400°C and 1450°C. The presence or absence of free lime was tested by X-rays and differential thermal analysis, but the most simple method used for detecting the uncombined C was the exposition to humid air. The material without combined lime was pulverized and mixed with water in a water/clinker relation 0.3 (w/c) in weigth. In order to inquire the material strength, compacted bars were manufactured. The paste thus formed was also observed in the SEM.

RESULTS

The ROM observations of the vitrous material reveal the presence of dendrites. They can be noticed after water etching (Figs. 1, 2 and 3) as intense coloured ones over a less coloured background. All those colours, arise from the interference of the ligth with an epitaxic layer of a thickness corresponding at least to the wave length of the observed color (5000 Å). Normally the epitaxial layers which grow on the dendrites are thicker than those of the sourrondings. Furthermore, these last becomes thinner as the distance from the dendrite increase finally disappearing. As it is evidenced from the SEM observations, it was not possible to detect any surface level difference.

As a consequence of the treatment the samples were devitrified, showing all of them a yellow colour.They became completely brittle and the back reflection X-ray diagrams revealed that the rings changed from continuos to finelly fragmented, which corresponds to the formation of small crystalline grains. Also when they were water etched a very strong surface hydration effect takes place which can be observed better by ROM after metallization[6] (Fig.4). The hydration products were clearly seen by SEM, they preferentially concentrates (Fig.5) in the polishing lines, which means that the mechanical distortions increase the water reactivity of the samples. At higher magnifications it can be detected the devitrified material grains and the hydration process also (Fig.6). Hydration seems to consist (Fig.6) in a defoliation process producing rossete

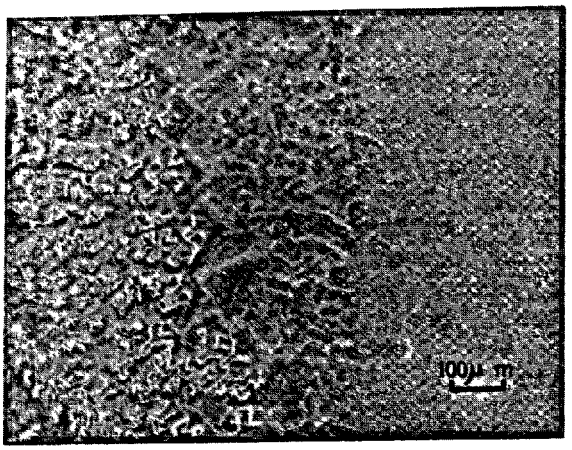

Fig. 1.- $C_{12}A_7$ glass water-etched during 5 minutes. MOR.

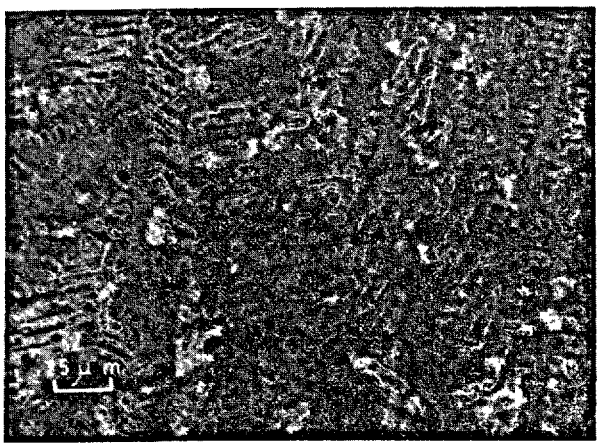

Fig. 3.- $C_{12}A_7$ glass water-etched during 5 minutes. MOR

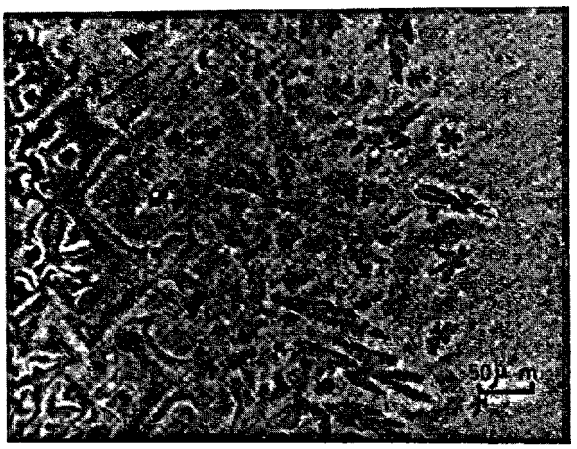

Fig. 2.- $C_{12}A_7$ glass water-etched during 5 minutes. MOR.

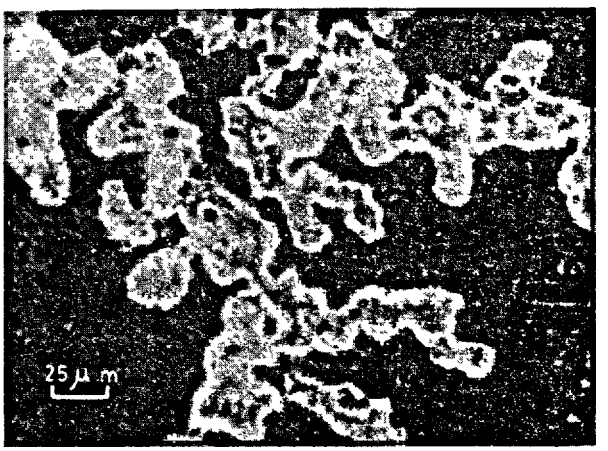

Fig. 4.- Devitrified $C_{12}A_7$ glass annealed at 1300°C for two hours and subsequently hydrated during half a minute. MOR.

shaped leafs (Fig.7). This early hydratation product of the compounds $C_{12}A_7$-CA has the same morphology that the one obtained with identical treatments in the aluminous industrial clinkers[2] and can be identified as CAH_{10}. This phase arise as the hydration product of aluminates with low C content.

In the case of the sintered compounds, all of them show a strong hydraulic strength irrespective of the presence of additives. The paste reveals hexagonal[7] crystals which probably must be C_3AH_6 (Fig.8).

DISCUSSION

In the case of compounds in the vitreous state, which always can be activated with CH in aquous solution, the hydration process was interrupted by the epitaxial layer already observed. The reactivation by CH consist in the disolution of this layer. When the thermal treatment allows crystalline growing hydration occurs by a defoliation mechanism. It is suposed that H penetrates between the crystalline layers raising them as leafs. Therefore two processes occurs: a) in the glass state, thin hydrated epitaxial sheets subsequently disolved (puzolanic reactior)by CH in solution are formed; b) in the crystalline state, the penetration of H between the crystalline layers produces leafs of CAH_{10} which afterwards dissolve precipitating crystals of probably

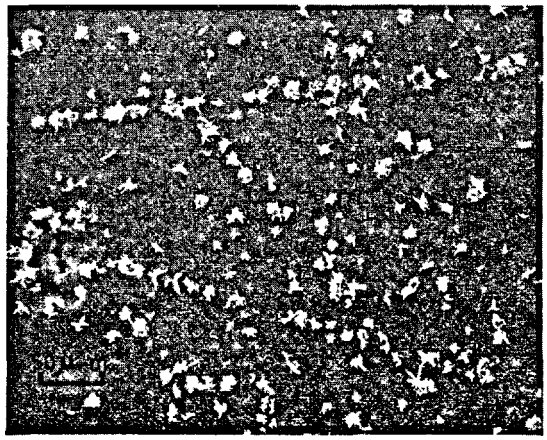

Fig. 5.- Devitrified $C_{12}A_7$ glass annealed at 1300°C for two hours and subsequently hydrated during half a minute. SEM.

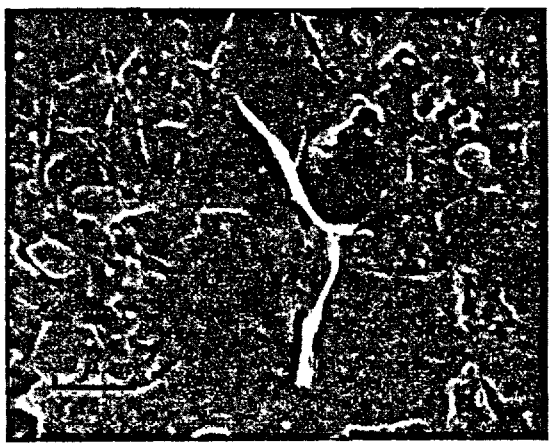

Fig. 6.- Devitrified $C_{12}A_7$ glass annealed at 1300°C for two hours and subsequently hydrated during half a minute. SEM.

Fig. 7.- Devitrified $C_{12}A_7$ glass annealed at 1300°C for two hours and subsequently hydrated during half a minute. SEM.

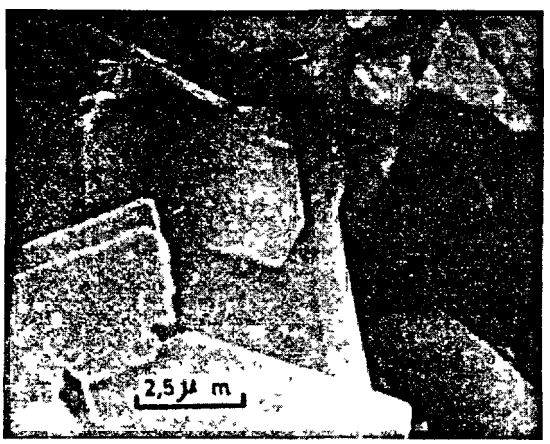

Fig. 8.- Past of sinterized CA (w/c = 0,3). SEM.

C_3AH_6. The second mechanism is the one occuring in the hydratation of the sinterized products. The hydraulic activation produced in the devitrified glasses must be strongly connected with the rearrangement of quenched-in vacancies, which is in turn related with the material brittleness and also with the fragmentation of the X-ray diffraction rings. All of these facts are in agreement with research works entailing lattice deffects with hydratation[8].

ACKNOWLEDGEMENTS

The authors wish to thank Mr. J.C. Ferri, A.D. Oliveira, J. Castral and W.A. Mariano for their help with the experimental work. Also to BID-FINEP (Brazil) and CNPq(Brazil) for is finantial support.

BIBLIOGRAPHY

1.- F.W. LOCHER (1960), "Hydraulic Properties and Hydration of Glasses of the System $CaO-Al_2O_3-SiO_2$", preceedings of the Fourth International Symposium of the Chemistry of Cement, vol. II, pp. 267-277.

2.- P. KITTL, L.C. POMPEU, A. GOLDSCHMIDT and J.H.C. CASTRO (1978), "Etudo de un Clinquer Industrial Aluminoso", Proc. V Interamerican Conference on Materials Technology, Sao Paulo, Brazil, pp. 245-251.

3.- A. JOISEL (1968), "Some Principles in Cement Hydration", Proceedings of the Fifth International Symposium on the Chemistry of Cement, vol. II, pp. 268-277.

4.- G. W. MOREY (1954), "The Properties of Glass", Reinhold Publisching Corporation, New York, pp. 29-68.

5.- T.D. ROBSON (1968), "The Chemistry of Calcium Aluminates and their Relating Compounds", Proceedings of the Fifth International Symposium on the Chemistry of Cement, vol. I, pp. 349-365.

6.- P. KITTL and J.H.C. CASTRO (1976), "Observacao de Fase Hidratada do Clinker Pela Técnica de Metalizacao", Revista Brasileira de Tecnología vol. 7, pp. 367-374.

7.- H.H. STEINOUR (1951), "Aqueous Cementitious Systems Containing Lime and Alumina" Portland Cements Association, Bulletin 34, Chicago.

8.- J.N. MAYCOCK, J. SKALNY and R. KALYONCY (1974), "Cristal Defects and Hidratation. I. Influence of Lattice Defects", Cemente and Concrete Research, vol. 4, pp. 835.

Investigations on two special cements

Etude de deux ciments spéciaux

Y. EFES, Institut für Bauforschung der Rheinisch-Westfälischen Technischen Hochschule Aachen, Federal Republic of Germany.

RESUME : Deux ciments spéciaux - un ciment à durcissement exceptionnellement rapide et un ciment de lave - ont été étudiés pour leur agrément par l'autorité de surveillance de constructions.

Le ciment à durcissement exceptionnellement rapide (CDER) était composé de clinker portland, de ciment alumineux, de produits d'addition et de sulfate de calcium. Mortiers et bétons ont été essayés avec ce ciment. La vitesse de la carbonatation des mortiers de CDER était nettement moins élevée que celle des deux mortiers de ciment normalisés avec à peu près la même résistance à la compression après 7 jours. Les bétons faits avec le CDER atteignaient déjà, après 2 heures, une résistance à la compression comprise entre 3,0 et 6,5 N/mm^2. La résistance à la compression était, après 28 jours, entre 30,2 et 46,6 N/mm^2.

Le ciment de lave était obtenu par broyage d'une gachée de clinker portland, de sable de lave et de sulfate de calcium. Après une évolution des résistances initiales relativement rapide (résistance à la compression du mortier 19,8 N/mm2 après 2 jours), cette évolution, après 7 jours, devenait semblable à celle du ciment de trass de la même classe de résistance. Comparé avec les ciments normalisés (ciment de trass et ciment de haut-fourneau), la carbonatation du mortier de ciment de lave se produisait à une vitesse peu élevée, mais il avait une résistance peu élevée à l'action du gel-dégel.

SUMMARY: Two special cements -one extra rapid hardening cement and one lava cement- have been tested for approval by the construction supervising authority.

The extra rapid hardening cement (ERHC) consisted of portland cement clinker, aluminous cement, additives and calcium sulphate. Mortars and concretes have been tested with this cement. The carbonation rate of the ERHC mortars has been significantly lower than that of the two standard cement mortars with nearly the same compressive strength after 7 days. Concretes with the ERHC obtained a compressive strength between 3.0 and 6.5 N/mm^2 already after 2 hours. The compressive strength was between 30.2 and 46.6 N/mm^2 after 28 days.

The lava cement is made by grinding a mixture of portland cement clinker, lava sand and calcium sulphate. After a relatively quick initial strength development (mortar compressive strength 19.8 N/mm^2 after 2 days), it showed a similar strength progress as a trass cement of the same strength class after 7 days. Compared with standard cements (trass cement and blast-furnace slag cement), mortar of lava cement carbonated at a lower rate, however it showed a somewhat lower resistance to freezing and thawing cycles.

INTRODUCTION

In recent years the building and construction supervising authorities of the Federal Republic of Germany have approved the use of several nonstandard special cements. The Institut für Bauforschung (Institute for Building Research) has carried out some of the investigations on three of these cements in order that their use may be approved. The three cements in question are two extra rapid-hardening cements of different compositions and a lava cement. A report has already been published (1) on the properties of one of the extra rapid-hardening cements, a portland cement modified with the $C_{11}A_7.CaF_2$ phase. The following will describe the results of the investigations on the two remaining special cements.

EXTRA RAPID-HARDENING CEMENT

The Extra Rapid-Hardening Cement (ERHC) tested consisted of a mixture of 82 % by mass portland cement clinker and 18 % by mass aluminous cement to which additives and calcium sulphate were admixed. The additives were to regulate setting and hardening.

As shown in Table I, this cement exhibits a somewhat lower SiO_2, CaO and SO_3 content and a higher Al_2O_3, Fe_2O_3 and Na_2O content, due to the aluminous cement constituent, when compared to portland cement.

Table I - Chemical composition of the ERHC and the Lava Cement examined (percent by mass)

Components	ERHC	Lava Cement
SiO_2	17,55	21,14
Al_2O_3	10,76	6,71
TiO_2	0,58	0,53
Fe_2O_3	4,83	3,19
MnO	0,02	0,09
CaO	59,46	53,30
MgO	0,69	2,07
Na_2O	0,87	0,23
K_2O	0,54	0,98
SO_3	2,71	2,34
Insoluble residue	0,33	5,52
Loss on ignition	1,70	3,95

The ERHC develops a mortar compressive strength (DIN 1164) of approx. 5 N/mm^2 after only 2 hours. During hydration substantially the same hydration products are formed as in a portland cement. An increase in the duration of hydration displays an increase in the production of hydrogarnet and CSH-phases. On the other hand, a reduction in $Ca(OH)_2$, monosulphate hydrate and ettringite may be observed as also is an increase in the formation of hydrogarnet with increasing storage temperatures up to 80 °C (2). Some of the properties of the cement tested according to DIN 1164 are given in Table II.

Table II - Properties of the ERHC and the Lava Cement according to DIN 1164

Properties	ERHC	Lava Cement
Density (kg/dm^3)	3,16	3,04
Finess		
Specific surface (Blaine) (cm^2/g)	5580	4910
Retained on the sieve 0,02 DIN 4188 (% by mass)	0,20	<0,10
Setting times		
Initial setting time (h-min)	0-51	3-00
Final setting time (h-min)	0-54	3-40

In the investigations, mortar and concrete tests were carried out. The strengths, carbonation behaviour of mortars, steel corrosion in mortars, and the compressive strength, carbonation behaviour, time-dependent consistency, static modulus of elasticity, time deformation under load and shrinkage of concretes were tested.

Mortar Tests

The carbonation and corrosion tests were carried out with the following mortar mix proportions by mass:

A) 1.00 cement : 2.16 sand [1] : 0.45 water
B) 1.00 cement : 3.38 sand [1] : 0.60 water
C) 1.00 cement : 4.92 sand [1] : 0.70 water

For purposes of comparison, mortars were produced also according to DIN 1164 with the standard cements PZ 35 F and HOZ 45 L (45 % by mass slag) which exhibited approx. the same 7-day compressive strength (see Table III).

Table III - Compressive strength of the ERHC and the standard cements

Age (d)	Compressive strength (N/mm^2)		
	ERHC	PZ 35 F	HOZ 45 L
2	26,4	24,5	19,5
7	37,9	35,6	37,9
28	44,5	44,9	55,9

The mortars with the ERHC possessed a weaker consistency than those with standard cements. The spread (flow table) measured, e.g. with mixture A, 245 mm whereas with PZ 35 F and HOZ 45 L the measurements were 183 mm and 180 mm respectively.

Four series of prisms (40 mm x 40 mm x 160 mm) were produced from the above mortars according to DIN 1164 and cured as shown in Table IV. The test specimens of the series cured according to regimes III and IV each contained a steel rod, inserted diagonally, 5 mm diameter and 119 mm in length. The rods touched the corners of the test specimens by means of steel pins which were attached to both ends of the rods. The corners of the specimens were sealed

[1] Standard sand according to DIN 1164.

after demoulding with epoxy resin. These experiments were designed to determine a possible influence of the ERHC in the various mortar mixtures on the extent of steel corrosion (rusting) in comparison to the standard cements.

The curing series I (rapid test) and II were examined at different ages for carbonation depth with the aid of the phenolphthalein method. The test results are shown in Fig. 1 a to c. The carbonation depth d_k of the mortar with the ERHC was in both cases the lower compared to those with the standard cements.

Table IV - Curing regimes of the specimens for the carbonation tests

Curing regimes	Pre-curing [1]				Main-curing			
	Time [2] (d)	Med.	Temp. (°C)	R.H. (%)	Time (d)	Med.	Temp (°C)	R.H. (%)
I	7 +7	water air	20 20	- 65	360	air + CO_2 [3]	20	65
II	7 +7	water air	20 20	- 65	360	air	20	65
III	7	water	20	-	360 [4]	air	20	a) 65 b) 95
IV	7	water	40	-	360 [4]	air	20	a) 65 b) 95

1) After demoulding

2) Including the time with mould in moist air (ERHC: 1 h; standard cements: 1 d)

3) 3 % by volume

4) Consisting of cycles of 28 days a) plus 2 days b)

The regression analyses of the results yielded the lines shown in Fig. 1 a to c, which were calculated with the equation $d_k = a + v_k\sqrt{t}$, where t is curing time. The slope of the lines corresponds to the carbonation rate v_k. From the ratio of v_k values of both curing regimes I and II we can determine an acceleration factor of $b_k = v_{k,I}/v_{k,II}$. These results are given an Table V. The acceleration factors of all three cements are similar to each other so that the above comparison of v_k may be used for both curing regimes.

As is known, carbonation generally results in greater strength. After total carbonation of the mortar specimens with the ERHC, the compressive strengths were 99 % and 71 % (w/c = 0.60 and 0.70) respectively higher than after pre-curing. Thereby, a hardening portion due to hydration of approx. 10 % was estimated. The increases in flexural strength were 83 % and 47 % respectively. These increases in strength were greater than with the standard cements.

The carbonation depths of the mortar prisms cured according to regimes III and IV approximated to that of the prisms of regimes I and II. The rust areas appearing on the steel rods inserted in the mortars with the ERHC were generally neither more nor greater than those inserted in the standard cements. Rust formation was limited to the carbonation zones (e.g. see Fig. 2).

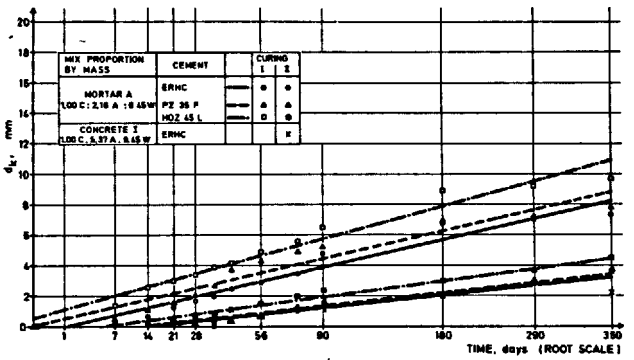

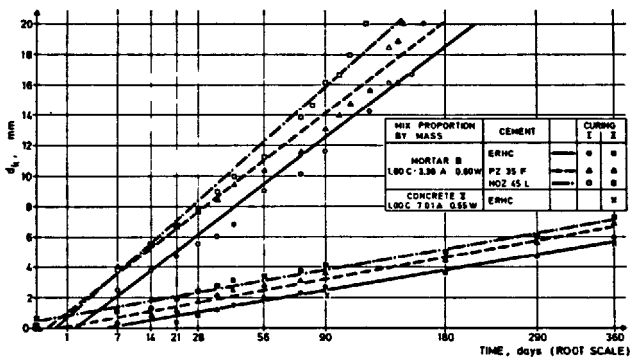

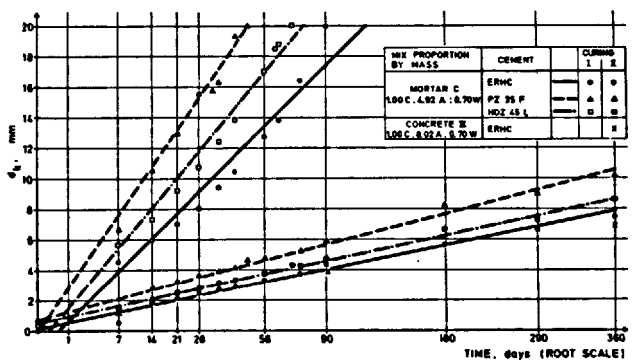

Fig. 1a-c - Mean carbonation depths of the mortar and concrete test specimens d_k dependent on the time of the main curing t_k

Concrete tests

Three concretes with approximately the same consistency (spread [1] = 400 ± 20 mm) were produced for these tests. The mix proportion of the concretes was as follows (by mass):

1) According to DIN 1048.

Table V - Carbonation rate v_k and acceleration factor b_k for the mortars produced from the ERHC and the standard cements (time of curing: up to 360 days)

Mixes	ERHC		PZ 35 F		HOZ 45 L	
	I	II	I	II	I	II
	v_k (mm $d^{-0,5}$)					
A	0,46	0,21	0,46	0,22	0,54	0,27
B	1,51	0,34	1,54	0,37	1,79	0,35
C	1,98	0,40	2,87	0,52	2,38	0,43
	b_k					
A	2,5		2,4		2,3	
B	4,4		4,2		5,1	
C	4,8		5,3		5,5	

I, II: Curing regime according to Table VI

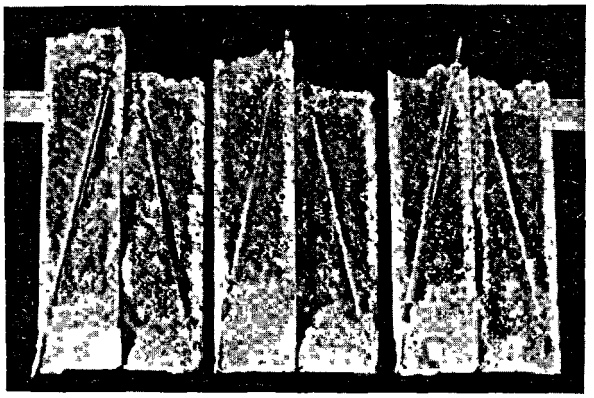

Fig. 2 - Rust formation on the steel rods and carbonation zones in the specimens of the mortar with the ERHC and w/c = 0.70 (curing regime III)

I) 1.00 cement : 5.37 aggregate [1] : 0.45 water
II) 1.00 cement : 7.01 aggregate [1] : 0.55 water
III) 1.00 cement : 8.02 aggregate [1] : 0.70 water

A workability time for the test concretes of approx. 10 min was determined using the spread and compacting factor [2] dependent on the time after the addition of water at 20 °C.

The compressive strength of the 200 mm cubes made of these concretes (produced and cured according to DIN 1048) consisted after only 2 hours of between 3.0 and 6.5 N/mm² (see Fig. 3). The 28-day compressive strength was 30.2 to 46.6 N/mm². At the age of 360 days the compressive strength was roughly 20 % greater.

The carbonation depth of the concretes also given in Fig. 1a to 1c (measured on the cubes for strength tests) was comparable to the results of the mortar tests.

[1] Grading corresponded to B_{32} (concretes I and II) and B_{32}/C_{32} (concrete III) according to DIN 1045.

[2] According to DIN 1048.

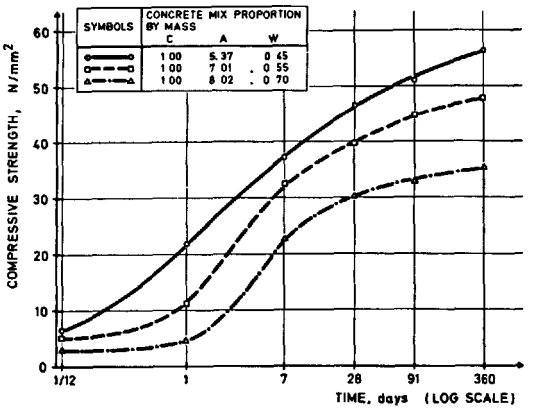

Fig. 3 - Compressive strength of concretes produced with the ERHC

In further concrete tests (curing : 7 d in moist air, then in normal climate 20 °C/65 % R.H.) described in detail in (3), the static modulus of elasticity was determined on cylindrical specimens. At the age of 35 days this was - in the sequence of concretes I to III - 30070, 31500 and 25910 N/mm² respectively, and at the age of 1 year 31660, 31460 and 23450 N/mm². On the concretes I to III a shrinkage of 0.58, 0.47 and 0.77 mm/m respectively, was measured after 1 year. The creep strain of the concrete specimens subjected to a stress of 1/3 of the 7-day compressive strength was measured, at an age of loading of 360 days, 1.05, 0.94 and 1.11 mm/m respectively. Final creep coefficients of 3.55, 4.58 and 5.35 respectively were calculated.

LAVA CEMENT

The Lava Cement in question is a puzzolanic cement of the strength class Z 35 F according to DIN 1164. This cement is produced by grinding of 75 ± 7.5 % by mass portland cement clinker and of 25 ± 7.5 % by mass lava sand of grain size < 4 mm with the addition of calcium sulphate. The chemical composition of the cement tested (Table I) is similar to the mean composition of trass cements in the Federal Republic of Germany (4). The lava used comes from the Eifel area and contains, however, less SiO_2, Al_2O and alkalis (with approx. 39, 12 and 4 % by mass respectively) and more CaO and Fe_2O_3 (with approx. 15, 11.5 % by mass respectively) than the trasses (5). Table II contains some of the physical properties of the Lava Cement according to DIN 1164.

Mortar Tests

The compressive and flexural strengths of the Lava Cement were determined, with reference to DIN 1164, on mortar specimens in comparison to two standard cements, a trass cement Z 35 L and a HOZ 35 L (with 54 % by mass slag). From the results given in Figs. 4a and 4b, it is evident that the early strengths of the Lava Cement are greater than those of the comparison cements. The strength development after a period of 7-days, however, is similar to that of the trass cement. The strengths of the Lava Cement between 28 and

90 days are inferior to those of the portland blast-furnace slag cement which increases more rapidly.

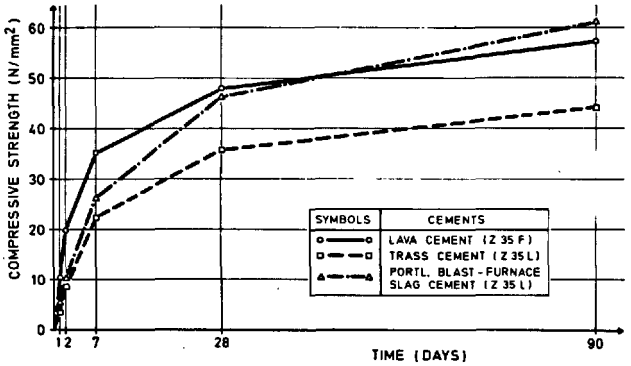

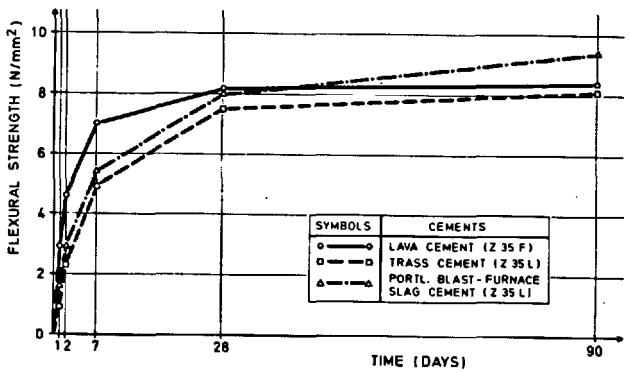

Fig. 4a,b - Mortar compressive and flexural strength of the Lava Cement and the standard cements

Concrete Tests

The carbonation behaviour of Lava Cement in comparison to that of the standard cements was examined using concrete with fine aggregate (maximum size: 8 mm) with a mix proportion by mass of 1.00 cement : 3.00 aggregate [1]: 0.50 water. The prisms produced according to DIN 1164 (40 mm x 40 mm x 160 mm) were cured after demoulding 28 days in water at +20 °C and after this, 7 days in the air at normal climate of 20 °C/65 R.H. Thereafter, one set of test specimens remained stored in the air whilst a second set was cured under the same climatic conditions in air enriched with 10 % by volume CO_2. The carbonation depths were also determined on the concrete test specimens with a mix proportion by mass of 1.00 cement : 7.19 aggregate [2]: 0.60 water with all three cements. The pre-curing period of the specimens in water, later cured in the air, was 35 days. The carbonation rates given in Table VI were lowest for the concretes containing Lava Cement. Most evident were the differences produced by curing in CO_2 enriched air (Fig. 5).

1) Grading A_8/B_8 according to DIN 1045

2) Grading B_{32} according to DIN 1045

Table VI - Carbonation rate v_k and the acceleration factor b_k during carbonation of the produced from the Lava Cement and the standard cements:

Mix proportion by mass of cement:aggregate :water	Lava Cement		Tr Z 35 L		HOZ 35 L	
	CO_2 [1]	Air	CO_2 [1]	Air	CO_2 [1]	Air
	v_k (mm · $d^{-0.5}$)					
1.00:3.00 [2] :0.50	0.15 [4]	0.21 [5]	0.65 [4]	0.30 [5]	0.24 [4]	0.23 [5]
1.00:7.19 [3] :0.60		0.26 [6]		0.35 [6]		0.32 [6]
	b_k					
1.00:3.00 [2] :0.50	0.7		2.2		1.0	

1) CO_2: Main curing in air with 10 % by volume CO_2

2) Maximum size: 8 mm. 3) Maximum size: 32 mm

4) Up to 150 d. 5) Up to 1080 d. 6) Up to 900 d.

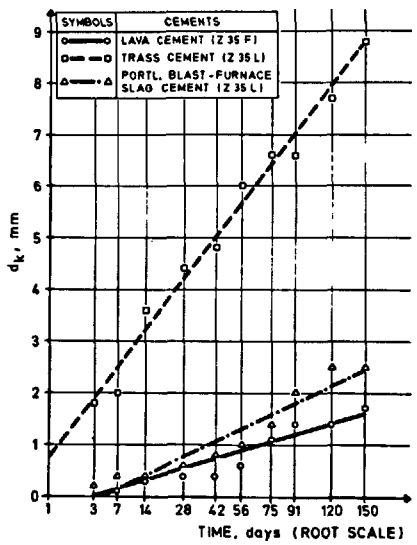

Fig. 5 - Mean carbonation depths of the concrete specimens d_k dependent on the time of the main curing in air with 10 % by volume CO_2.

Freeze-thaw-cycling tests were carried out on prisms of concrete with fine aggregate [3] of the same dimensions. The prisms were precured for 28 days in water at +20 °C. After this they were subjected to an 8-hour freeze-thaw-cycle of between +20 °C and -20 °C. After 150 cycles the compressive strength measured 56 % and the flexural strength 16 % of the strength after pre-curing. The loss in strength after subjection to freeze-thaw-cycles was greater with Lava Cement concretes than whith

3) Grading A_8/B_8 according to DIN 1045

the concretes produced with the two standard cements (trass cement : 93 % and 45 % : portland blast-furnace slag cement : 77 % and 36 % respectively).

The compressive strength of a concrete produced from Lava Cement (mix proportion by mass of 1.00 cement : 6.50 aggregate [1] : 0.55 water) was also determined. The spread (flow test) of the concrete was 370 mm. Production, curing and testing of the test specimens took place according to DIN 1048. At the ages of 7, 28 and 90 days mean compressive strengths of 27.7, 38.5 and 46.0 N/mm^2 respectively were found.

CONCLUSIONS

The ERHC is characterised by very high early strengths in the first few hours and a very short workability period. Because of the positive results from carbonation tests, there can be no doubts as far as this is concerned about its use. Although for the quantity of alumina present the formation of convertible low calcium content calcium aluminate hydrates cannot be expected, losses in strength are possible at high temperatures upwards of approx. 60 °C. The ERHC can not be used for prestressed concrete.

The Lava Cement represents a complement to the existing puzzolan cements and is to a large extent comparable to their properties. Due to the finess of grinding it possesses a greater early strength. Lava Cement is permissible for reinforced concrete but not for prestessed concrete.

REFERENCES

1.- Y. EFES and P. SCHUBERT (1976) "Mörtel- und Betonversuche mit einem Schnellzement", Betonwerk u. Fertigteil-Techn., 49, 541-545, 620-623 (German).

2.- "Institut für Gesteinshüttenkunde" of the Technical University Aachen (1978), Report Nr. GA 934 II (German).

3.- "Institut für Bauforschung" of the Technical University Aachen (1978), Report Nr. A 723 (German).

4.- Verein Deutscher Zementwerke (Ed.) (1976) "Zement Taschenbuch 1976/77", Bauverlag, Wiesbaden-Berlin (German).

5.- U. LUDWIG and H.-E. SCHWIETE (1961) "Das mörteltechnische, das chemische und mineralogische Verhalten von Traßzement- und Traßkalkgemischen", Aachen (German).

[1] Grading A_{32}/B_{32} according to DIN 1045

Post-Hydration Compressed Expansive Clinker Pastes

Pâtes de clinker dilaté compressé après hydratation

R. SH. MIKHAIL and S. HANAFI, Department of Chemistry, Faculty of Science, Ain Shams University, Abbasia, Cairo, Egypt,
S.A. ABO-EL-ENEIN, Chemistry Department Qatar University, Doha, State of Qatar.

RESUME : Le clinker de ciment expansif du type I est préparé à partir de kaolin, de gypse et de carbonate de calcium. Deux méthodes sont utilisées pour confectionner des éprouvettes de pâte de ce ciment : la première, en mélangeant le clinker broyé à l'eau dans un rapport eau sur ciment ($\frac{E}{C}$) égal à 0,25; la seconde, en préparant tout d'abord la pâte comme dans la premlère méthode (toujours avec le rapport $\frac{E}{C}$ = 0,25), mais en comprimant la pâte fraiche à des pressions de 50, 200 et 500 kg/cm2.

Sont exposées, pour ces diverses valeurs de la compression, les conséquences sur la cinétique de l'hydratation, la microstructure et la structure des pores des pâtes durcies. On a observé que l'ettringite était la phase principale aux divers âges de l'hydratation. L'état physique de l'ettringite varie en fonction de l'espace disponible pour sa formation et sa cristallisation; l'ensemble limité des pores, utilisable pour l'hydratation des constituants du ciment, conditionne très strictement la structure des pâtes durcies.

SUMMARY: Type I expansive cement clinker was prepared from kaolin, gypsum and calcium carbonate. Two methods were used for the preparation of expansive clinker pastes; the first involves mixing the unhydrous expansive clinker with a low water/cement (W/C) weight ratio of 0.25, and the second involves using the same W/C ratio of 0.25 followed by compression of the fresh paste at pressures of 50, 200 and 500 Kg/cm^2.

The results of compressive strength, hydration kinetics, microstructure and pore structure of the hardened pastes are presented. Ettringite was found to be the dominant phase prevailing at the various ages of hydration. The physical state of Ettringite was found to vary according to the space available for its formation and crystallization; the limited pore system available for the hydration products affected strongly the microstructure of the hardened pastes.

INTRODUCTION

The development of the expansive cement, which has an expansion that equals or exceeds the shrinkage of portland cement, has in principle made it possible to prevent shrinkage crack of concrete. Several publications concerning the expansion-shrinkage characteristics of expansive cement have been reported in the literature (1-5). Expansive cement also makes it possible to produce prestressed concrete by chemical prestressing (5-7).

The mineral composition and crystal structure of calcium sulpho-aluminous clinker have been examined by various investigators (8-10). The main component of calcium sulphoaluminous clinker and the hydration characteristics have also been investigated (11,12).

For the formation of ettringite ($C_3A.3C\bar{S}.32H_2O$), it is necessary that the cement clinker should contain sufficient amounts of free $CaSO_4$ and CaO. Expansive clinkers containing these two free components have usually been made using bauxite as a raw material, but other investigators have examined the possibility of replacing this by kaolin (13-16).

In the present paper, we present results on hydration kinetics, total porosity, compressive strength, surface properties and microstructures of low porosity expansive clinker pastes prepared by the post-hydration compression technique, as compared with the normal low porosity pastes, made without compression.

EXPERIMENTAL

The expansive cement clinker used in this study was prepared from kaolin (Aswan, Egypt) and chemically pure calcium carbonate and gypsum. The relative amounts required to produce type I expansive clinker were calculated using Nakamura's equations (13) as follows:

Kaolin = 100

Calcium carbonate = $1.78\ |(0.55 + 0.183\ n)\ P + 1.17F + 1.87S|$

Gypsum = $1.13\ |0.445\ (1 + m)\ P + 1.13S|$

where P = (% Al_2O_3 - 0.426% Fe_2O_3) in kaolin,

F = % Fe_2O_3 in kaolin,

S = % SiO_2 in kaolin,

m = molar $CaSO_4/C_4A_3\bar{S}$ ratio in the expansive clinker,

and n = molar $CaO/C_4A_3\bar{S}$ ratio in the expansive clinker.

The molar $C\bar{S}/C_4A_3\bar{S}$ and $C/C_4A_3\bar{S}$ ratios required to produce type I expansive clinker are 8 and 6, respectively.

Type I expansive clinker was made by following the same procedure described in earlier studies (14,15). The three main constituents were ground separately in a porcelain ball mill to pass completely through a 200-mesh B.S. sieve, then mixed in the ball mill with few number of balls for 6 hours, and burned as pellets for two hours at 1150°C. The product was cooled slowly and ground to a Blaine area of 4300 cm^2/g.

The oxide composition of the clinker produced was found to be: SiO_2, 10.74; Al_2O_3, 8.90; Fe_2O_3, 0.70; CaO, 48.23 and SO_3, 31.65, respectively. This corresponds to the phase composition of: $C_4A_3\bar{S}$, 17.06; $2(C_2S).C\bar{S}$, 41.17; C_4AF, 2.13; $C\bar{S}$, 30.44 and C, 9.40, respectively.

Post-hydration compressed pastes were made at pressures of 50, 200 and 500 kg/cm^2; the expansive clinker was mixed with water (W/C = 0.25) for 3 minutes continuously and then compressing at the pressures mentioned above into cylindrical specimens having 2 cm diameter and approximately 2 cm height. The specimens were cured in a moist cabinet for 6 hours and then cured in water at room temperature until the desired time of testing was reached. The times of hydration selected were 1,3,7,28,90 and 180 days. The normal low porosity pastes were prepared by mixing the unhydrous expansive clinker with a water/cement ratio of 0.25 followed by moulding, without any compression, into cylindrical specimens having 2 cm diameter and approximately 2 cm height.

Compressive strength and total water content (W_t) determinations were carried out on the fresh specimens. Hydration was stopped for one representative sample from each specimen by immersion in 50 ml. of acetone-methanol mixture (1:1 by volume) stirred mechanically for one hour. The solid part was separated by filtration through a Gooch crucible, G4, washed with acetone-methanol mixture followed by several washings with ether. The solid was then dried at 50°C for one hour to complete evaporation of the ether. The combined water content (W_n) was determined as the ignition loss of the dried solid.

The total porosity was calculated from the densities using the following expression: $100\ (\rho_T - \rho_B)/\rho_T$ where ρ_T is the true density and ρ_B is the bulk density.

Nitrogen and water vapour adsorptions were carried out on the dried samples. SEM examination was done on freshly fractured specimens, coated with 300-400 Å layer of gold, using a JEOL JSM-25 high resolution scanning electron microscope.

RESULTS AND DISCUSSIONS

1. COMPRESSIVE STRENGTH, TOTAL POROSITY AND HYDRATION KINETICS

The results of compressive strength tests, non-evaporable water contents (W_n) and total porosity of the hardened pastes are shown in Fig. 1, for various ages of hydration. In the pastes investigated, the non-evaporable water content was found to decrease with increasing the pressure used in the compression, and to increase markedly during the early stages of hydration, indicating that the hydration reaction starts with a fast step which is comparable with the "predormant period" in the hydration of normal

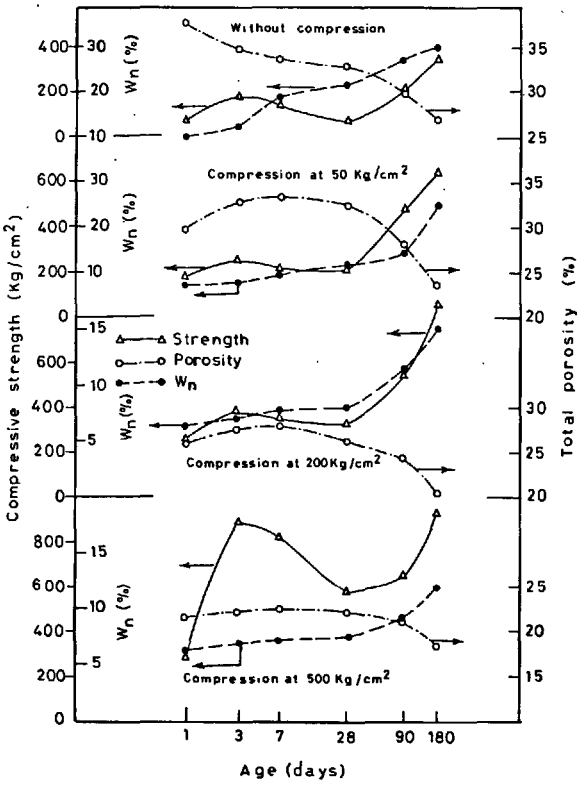

Fig. 1- Non-evaporable water, total porosity and compressive strength of the pastes investigated.

cements (17,18). The duration of this period was found to vary with the initial porosity of these compressed pastes; it ends before one day in the relatively higher porosity pastes, (with no compression or compressed at 50 kg/cm^2), and after 3 days in the lower porosity pastes (compressed at higher pressures). The non-evaporable water content then increased slowly, reflecting a slow step in the hydration; this step is similar to the "dormant period" in cement hydration (17.18). This period is shortened markedly with increase in the initial water/solid ratio (initial porosity as controlled by the pressure used in compression), and it is strongly deminished by suspension hydration in which a large amount of water is normally used (19). Finally the non-evaporable water content increases markedly indicating an "acceleration period" similar to the hydration behaviour of various types of cements (17,20).

The total porosity of the post-hydration compressed expansive clinker pastes showed an initial increase during the first 7 days of hydration, and then it decreased. The earlier increase in the total porosity may be attributed to the instability of the binding centres in the initial hydration products which permits the diffusion of the water of curing in the paste during the recrystallization (stabilization) of the initial hydrates, leading to expansion of the paste. However, when the paste had achieved stability by recrystallization of the initially formed hydrates, the total porosity decreased as a result of the accumulation of the hydrates within the pore system. There appeared to be only small variations due to the limited initial porosity as controlled by the post-hydration compression technique. The expansion characteristics of the hardened expansive cement pastes including this expansive clinker were presented in earlier publications (15,16). In the normal low porosity pastes made without compression, the total porosity decreases continuously with age of hydration. This is due to the easier access of water and the availability of the space to accomodate the hydration products. Their accumulation in the pore system leads to the normal behaviour of a continuous decrease of total porosity with age. In general, the total porosity decreases, as expected, with increase in the compression pressure.

The results of compressive strength tests show an initial increase in the early stage of hydration followed by a decrease during the recrystallization of the initial hydrates. The accumulation of hydrates in the pores causes a development in the strength of the paste during the final stages of hydration (cf. Fig. 1). Compression causes an increase in compressive strength.

The results of X-ray diffraction, DTA and SEM showed that the trisulphate hydrate (ettringite) respresents the dominant hydration product in these expansive clinker pastes. A small amount of the monosulphate hydrate also was present.

It is postulated that the mechanism of hydration and hardening of these expansive clinker pastes is the following: (1) A fast reaction taking place as a result of topochemical interaction between water and the bare surface of the sulphoaluminous clinker ($C_4A_3\bar{S}$), in presence of $CaSO_4$ and CaO in solution, leading to the formation of an almost impervious coating of microcrystalline or gel-like ettringite around the clinker particles (20-22); this is the "pre-dormant" period. (2) The ettringite layer by virtue of its low permeability, causes a retardation of hydration; this leads to a slow "dormant" period. During the dormant period, the initially formed ettringite recrystallizes on the surface of the clinker grains. This recrystallization and grain growth causes gaps between grains, and hence an increased accessibility of water through the crystalline

coat into the unhydrated part of the grains. The result is an increase in the rate of hydration; this is the "acceleration" period. (3) Finally, the hydration reaction is again slowed down as a result of deposition of ettringite within the transport limiting pores of these pastes. As a consequence, the diffusion of water through the dense hydration products into the unhydrated part of clinker grains becomes the rate controlling step. A schematic representation of the mechanism is shown in Plate I.

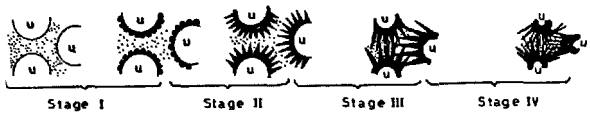

Plate I. Schematic representation of the suggested mechanism

Stage I: "Predormant period" Rapid step which leads to the formation of a thin layer of microcrystalline hydrate on the unhydrated clinker grains (U).

Stage II: "Dormant period" Crystallization of the initial hydrate takes place which is relatively slow step.

Stage III: "Acceleration period" Water becomes again accessible through the crystalline coat into the unhydrated part of grains leading to a fast reaction.

Stage IV: "Diffusion period" Almost all the pore system becomes filled with hydration products and the diffusion of water through the dense structure of hydrates into the unhydrated part of grains becomes the rate controlling step.

2. SURFACE PROPERTIES

Typical adsorption-desorption isotherms of nitrogen at 77.2°K on the hardened expansive clinker pastes are shown in Fig. 2. The isotherms show no hysteresis loops, indicating that the adsorption of nitrogen on these hydrated pastes is completely reversible for all pastes cured for up to 90 days. For the pastes cured for 180 days, small hysteresis loop is obtained.

The V_g-t plots shown in Fig. 3 also indicate that these pastes behave as non-microporous solids. This is evidenced by the linear character of the V_g-t plots, up to relative vapour pressure close to the saturation pressure of the adsorbate. Therefore, although these pastes possess extremely low porosities, their hydration product (ettringite) represents an open-pore system simulating non-porous solids.

Some surface characteristics derived from nitrogen adsorption are shown in Fig. 4; this figure includes the surface area derived from the BET equation, S_{BET} (m^2/g), and the total pore volume calculated from the saturation point of the adsorption isotherm, V_p (ml/g). Evidently, the surface area and the total pore volume show a first increase with curing age up to 3 days hydration followed by a decrease. The early increase in the surface area and the total pore volume is due to the recrystallization of the initially formed ettringite; recrystallization results in an increased accessibility of nitrogen, to measure additional parts of the pore system of the paste. However, the accumulation of ettringite within the limited pore system causes a decrease in the accessibility of nitrogen to measure the total porosity of the paste. The recrystallization of ettringite

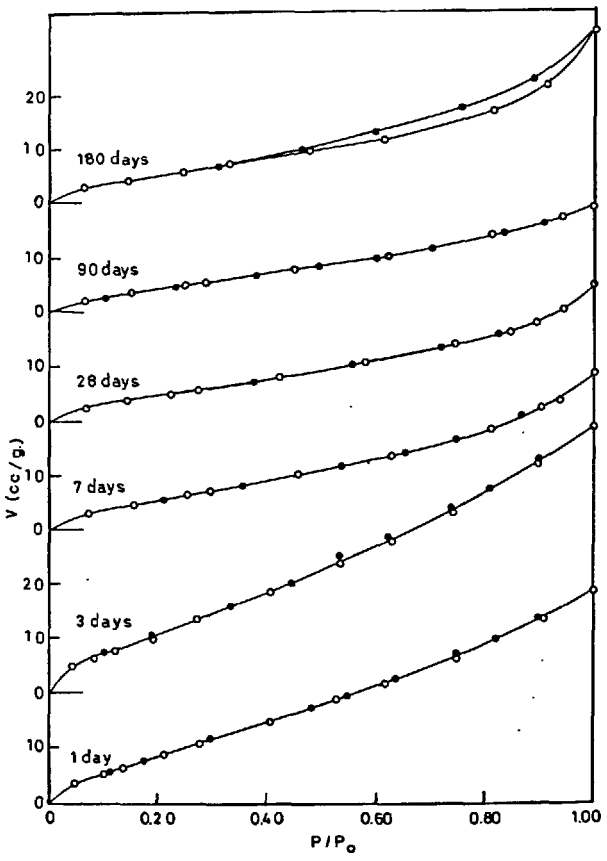

Fig. 2- Adsorption-desorption isotherms of nitrogen on the post-hydration compressed expansive clinker pastes (compressed at 200 kg/cm²).

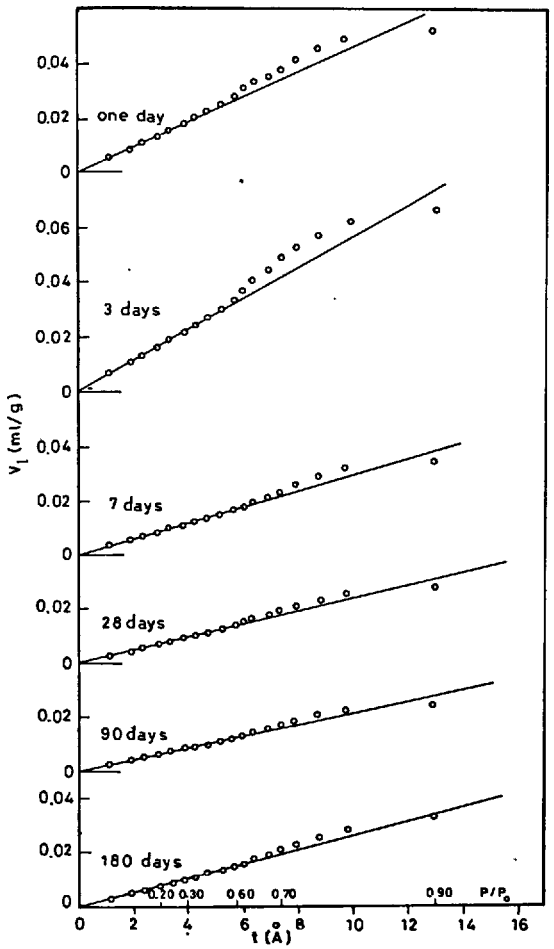

Fig. 3- V_ℓ-t plots of nitrogen on the post-hydration compressed expansive clinker pastes (compressed at 200 kg/cm^2).

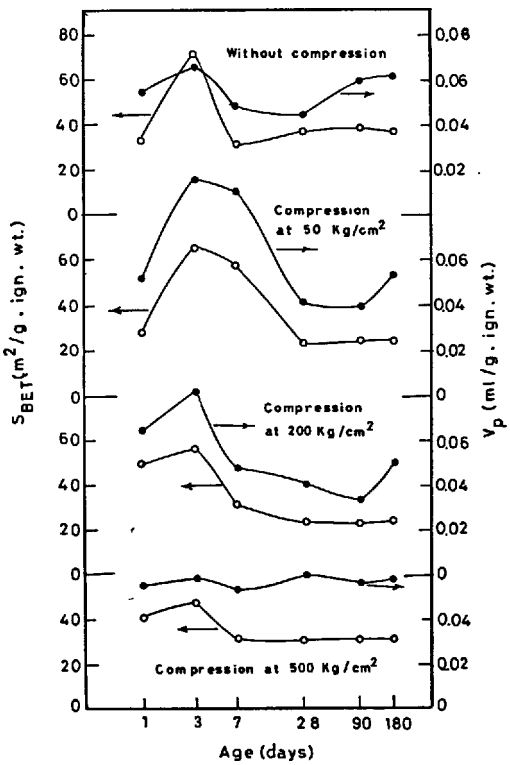

Fig. 4- Variation of the nitrogen surface area and total pore volume with age of hydration of the hardened pastes.

into large rod-like crystals (vide infra) is accompanied by a decrease in its specific surface area.

In the final stages of hydration, the normal low porosity pastes possess high surface area and pore volume as compared with the post-hydration compressed pastes; this is mainly attributed to the relatively higher porosity of these pastes which permits the growth of a large number of crystallites (hydration products). Such increase in the number of these crystallites in the paste leads to high surface area and total pore volume at the final stages of hydration. Post-hydration compressed pastes however, possess a more limited and smaller pore spaces; therefore, the hydration process is controlled by the limited space available in the hardened paste. It is noticed that lower values of surface areas and pore volumes were obtained during the final stages of hydration of the pastes compressed at 50 and 200 kg/cm^2; in these pastes recrystallization and crystal growth of the hydration products within the limited pore system is still possible. However, in the later stages of hydration of the pastes compressed at the highest pressure used (500 kg/cm^2), relatively higher values of surface areas and total pore volumes were obtained. This result is interesting and is probably associated with the microcrystallinity of the hydration products formed within the limited pore system of the paste. The available pore space has reached such a small size which actually hinders the growth of microcrystallites into larger crystals; microcrystallites have larger surface area than large crystals.

3. MORPHOLOGY AND MICROSTRUCTURE

X-ray diffraction of the anhydrous type I clinker showed the presence of $CaSO_4$, CaO, $C_4A_3\bar{S}$ and $2(C_2S).C\bar{S}$ phases.

SEM micrographs were obtained at various ages of hydration, and those for the pastes pressed at 200 kg/cm^2 are typical representatives of the series of micrographs obtained, and which support the above mentioned conclusions.

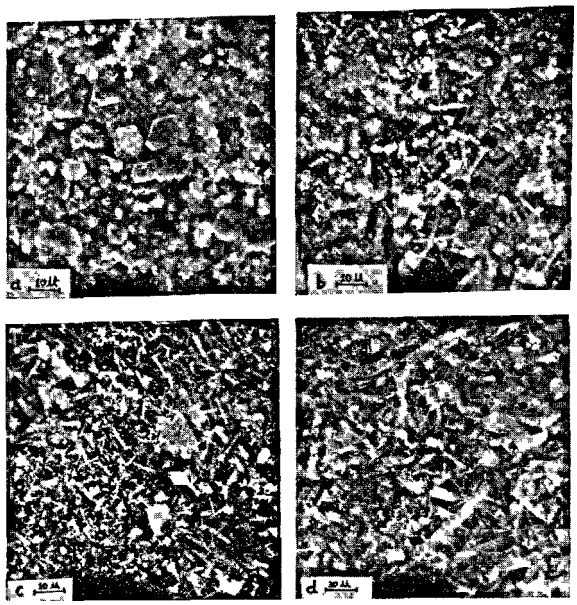

Fig. 5- SEM micrographs of the hardened expansive clinker pastes compressed at 200 kg/cm^2.

a- Cured for one day b- Cured for 3 days
c- Cured for 7 days d- Cured for 28 days

After one day hydration, large crystals of the principal phase, $C_4A_3\bar{S}$, prismatic crystals of 2 $(C_2S).C\bar{S}$. hexagonal crystals of $Ca(OH)_2$ and small round crystals of gypsum were the main phases present together with microcrystalline ettringite as the only hydration product identified (Fig. 5a). The gel-like ettringite recrystallizes after 3 days hydration into rod-like particles in the dense structure of the remaining unhydrated grains (Fig. 5b). The microstructure after 7 and 28 days hydration displayed a dense structure of large rods of fully crystalline ettringite as the dominant hydration product (Fig. 5c and d). At all ages of hydration, $Ca(OH)_2$ crystals were clearly detected. Gypsum is noticed to be consumed after 7 days.

CONCLUSIONS

From the results obtained in this study the following conclusions could be derived:

1. The rate of hydration of expansive clinker is high during the early stage of hydration (pre-dormant period), low in the intermediate stage of hydration (dormant period), and then it increases again indicating an acceleration as a result of recrystallization of the initial hydrates (acceleration period). The final stage in the mechanism of hydration is a very slow diffusion process.
2. An earlier increase in the total porosity was obtained in the post-hydration compressed pastes and this may be attributed to the instability of the binding centres in the initial hydration products. However, when the paste had achieved stability, the porosity decreased as a result of accumulation of the hydrates within the pore system.
3. The results of surface area and pore volume measured by nitrogen confirm the proposed hydration mechanism in terms of the accessibility of nitrogen molecules towards the pore system of the hardened low porosity pastes.
4. X-ray and SEM studies showed that the ettringite phase predominates at all ages of hydration with varying degree of crystallinity.
5. Compressive strength values show an initial increase followed by a decrease during the recrystallization of the initial hydrates. Later, the accumulation of hydrates in the pores causes a noticeable increase in the strength of the paste.

BIBLIOGRAPHY

1.- H. LOSSIER (1948), Mémoires, Société des Ingenieurs Civils de France, 3-4, 189.
2.- H. LAFUMA (1952), Proc. 3rd Int. Symp. Chem.Cem.,587.
3.- M.E. PERRE (1947), Cement and Lime Manufacture,24,75.
4.- V.V. MIKHAILOV (1957), Proc. of The World Conference on Prestressed Concrete, 25.
5.- A. KLEIN and G.E. TROXELL (1958), Proc. of The ASTM, 58, 986.
6.- A. KLEIN, T. KARBY and M. POLIVKA (1961), J. of ACI, 58, 39.
7.- T.Y. LIN and A. KLEIN (1963), J. of ACI, 60, 1187.
8.- N. FUKUDA (1961), J. Ceram. Assoc. Japan, 69, 187.
9.- R. KONDO (1965), J. Ceram. Assoc. Japan, 73, 1.
10.- P.E. HALSTEAD and A.E. MOORE (1962), J. Appl. Chem., 12, 413.
11.- R.K. MEHTA and A. KLEIN (1965), Annual Meeting of The Highway Research Board, 328.
12.- R. KONDO and N. NAWATA (1965), JCEA Review of 19th General Meeting, 19, 52.
13.- N. NAKAMURA, G. SUDOH and S. AKAIWA (1969), 5th Inter. Symp. Chem. Cement, Tokyo 1968, 4, 351.
14.- H. EL-DIDAMONY and O. HENNING (1973), Silikattech., 24, 279.
15.- H. EL-DIDAMONY and M.Z. MOSTAFA (1976), Cement Conc. Res., 6, 707.
16.- H. EL-DIDAMONY, M.Y. HAGGAG and S.A. ABO-EL-ENEIN (1978), Cement Concr. Res., 8, 351.
17.- S.A. ABO-EL-ENEIN, M. DAIMON and R. KONDO (1974), Cement Concr. Res., 4, 299.
18.- S. BRUNAUER, M. YUDENFREUND, I. ODLER and J. SKALNY (1973), Cement Concr. Res., 3, 129.
19.- J. SKALNY and M.E. TADROS (1977), J. Amer. Ceram. Soc., 60, No. 3-4, 174.
20.- R.Sh. MIKHAIL and S.A. ABO-EL-ENEIN (1972), Cement Concr. Res., 2, 401.
21.- L. FORSEN (1938), Proc. Symp. Chem. of Cement, Stockholm, Sweden.
22.- H.H. STEINOUR (1958), Res. Dev. Lab., Portland Cem. Assoc., Res. Dept. Bull., 98, 124.
23.- H.E. SCHWEITE, U. LUDWIG and P. JAEGER (1966), Symp. on Structure of Portland Cement Paste and Concrete, Highway Res. Board, Special Report, 90, 353.

ACKNOWLEDGEMENT

The authors gratefully acknowledge their indebtedness to the National Science Foundation for Grant INT76-18977, which has supported the research described in this paper.

On alunite expansive cement and concrete

Ciment expansé d'alun et béton précontraint

WU CHUNG-WEI, Chief engineer, vice director, Research Institute of Building Materials Professor, Qinghua University,
WANG YAN-SHENG, Engineer, Research Institute of Building Materials, Chine Populaire.

RESUME : Depuis une vingtaine d'années, six types de ciment expansif sont produits en Chine, dont la plupart sont des ciments d'auto-contrainte; leur pouvoir d'auto-contrainte est de 3 à 8 N/mm2. Parmi eux, une grande quantité de ciment d'auto-contrainte de silicate et d'aluminate sont utilisés pour fabriquer des conduites d'eau en béton précontraint; leur production a dépassé 2.000 km/an. Le ciment expansif d'alun (l'alun naturel étant utilisé comme matière première principale), lui, est un ciment à retrait compensé, utilisé avec succès depuis ces dernières années pour les constructions souterraines, les travaux d'étanchéité et la construction de réservoirs.

Cet article montre la possibilité de remplacement d'alun cuit par l'alun naturel; il énumère les avantages du ciment expansif d'alun naturel, en les expliquant par l'action d'hydratation et la microstructure. L'indice d'expansion (ε) proposé par les auteurs, comme rapport entre l'expansion libre et l'expansion contrariée, et les courbes d'évolution de l'expansion avec le temps exposés dans cet article, contribueront à améliorer la propriété du ciment et du béton expansifs, et aboutiront ainsi à une application plus étendue.

SUMMARY: During the past 20 years,six types of expansive cements have been produced in China. Most of them are self-stressing cements with different self-stress levels of 3 to 8 N/mm^2. Some have been widely used to manufacture self-stressing concrete pressure pipes amounting to 2,000 kilometers a year. Alunite (uncalcined) expansive cement as a shrinkage-compensating cement has been used successfully for years in underground and waterproofing structures and tanks and as joint-fillers.

In this paper,the feasibility of uncalcined alunite to replace the calcined and the merits of this alunite cement are explained through hydration and micro-structure studies. The authors propose a new expansion index ε = free expansion (e_1%)/ restrained expansion (e_2%) and a revised time-dependent curve of highly restrained expansion. Both of them may prove useful in further development and wider application of expansive cements and concretes.

INTRODUCTION

During the past 20 years,six types of expansive cements have been investigated and produced in China. They are silicate expansive cement (type M),aluminate expansive cement,sulfo-aluminate expansive cement, alunite expansive cement,low-heat expansive cement and gypso-aluminate cement. They are mostly self-stressing cements with different self-stress levels of 2 to 8 N/mm^2. Silicate expansive cement and aluminate expansive cement have been widely used to manufacture self-stressing concrete pressure pipes,amounting to 2,000 kilometers a year,90% for city water-supply and the rest for gas pipelines,etc. Alunite (uncalcined) expansive cement as a shrinkage-compensating cement has been used successfully for years in underground and waterproofing structures and tanks and as joint-fillers.

ALUNITE EXPANSIVE CEMENT

Our alunite expansive cement consists of natural alunite rock (containing 20-50 % $K_2SO_4 \cdot Al_2(SO_4)_3 \cdot 4Al(OH)_3$),cement clinker,anhydrite and fly-ash or blast furnace slag. The main physical properties of the alunite expansive cement are as follows:

1. Time of setting: Initial 1:30-4:00 hrs
   Final 2:30-6:00 hrs
2. Free expansion (e_1) of cement paste in water (Table 1).

Table 1

Age	1 day	28 days	1 year
e_1(%)	$\geqslant 0.15$	0.5-1.2	$\leqslant 1.2$

3. Mortar strength (1:3 earth-dry mortar method) (Table 2).

Table 2

Age	1 day	7 days	28 days	1 year	3 years
Compressive (N/mm^2)	30-40	40-60	60-80	90	100
Tensile (N/mm^2)	1.3-2.5	1.6-3.0	3.0-4.5	5.0	6.0

In comparison with the alunite expansive cement of other countries as well as some other expansive cements,our cement has the following distinguishing features: first,regular setting,hence no retarder is needed;second,high strength at later age,which guarantees the integrity and structural safety of concrete;and third,the most important,low expansive index ε,newly proposed for the evaluation of expansive cements and concretes. As ε is defined by the ratio of free expansion to restrained expansion at certain degree of restraint,a low ε value means small difference between free and restrained expansion, i.e.,no excessive expansion will occur where there is least or no reinforcement. With low ε,the prevailing worry about scaling of coverage and nonuniformity of concrete quality will prove unnessary. Table 3 shows the ε values of our alunite cement in comparison

Table 3

% of reinforcement (μ)		0.24	0.56	1.08	1.57
ε value	Alunite cement concrete	1.70	3.03	4.50	4.76
	Type "M" cement concrete in China				>15 (μ =1.4)
	Type "M" cement concrete in USSR (1)			7-20 (μ = 1.0)	
	CSA cement concrete in Japan (2)			approx. 5-14 (μ = 1.0)	

with the approximately ε values of some other cements under various percentages of reinforcement.

HYDRATION AND MICRO-STRUCTURE

1. Chemical analysis shows that natural alunite rock dissolves in water at a much lower rate than calcined alunite and supplies SO_3 and Al_2O_3 for ettringite formation. The solution process is accelerated at the presence of CaO and $CaSO_4$.

2. Based on X-ray diffraction analysis data of the alunite cement paste cured in water at different ages, a semi-quantitative diagram was plotted (Fig. 1), by which the hydration kinetics of the cement can be visualized to a certain degree. The continuous but slow formation of ettringite after 7 days is due to the existence of alunite rock.

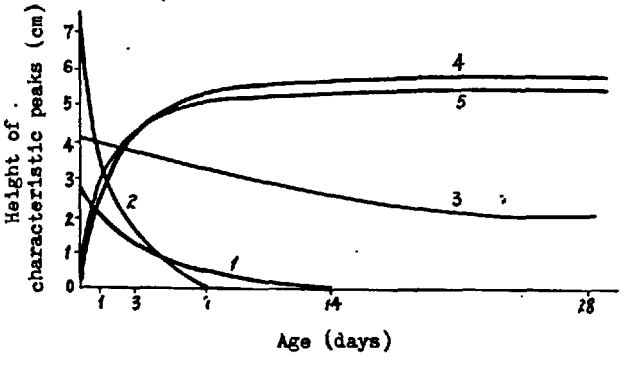

Fig.1 The semi-quantitative diagram of the alunite cement paste.

1 - C_3S , 2 - $CaSO_4$, 3 - natural alunite rock , 4 - ettringite , 5 - $Ca(OH)_2$

3. The formation of ettringite in the liquid phase and the precipitation of ettringite in pores and fissures of mortar and concrete (see SEM micrograph, Fig. 2) are closely related to the characteristics of hardened concrete, including comparatively small free expansion, effective restrained expansion, low expansion index, high strength at later age, impermeability, etc. The data of pore measurement (Table 4) by the mercury penetration method confirm that the accumulation of ettringite in pores and fissures persistently improves the structure of concrete.

Fig. 2 The precipitation of ettringite in pores. 1:1 mortar, W/C = 0.3, 7 day water curing

Table 4

Curing ages	Total porosity (cm^3/g) (pores sizes 55,000-25Å)	Most probable pore radius (Å)
1 day	0.0881	182
7 days	0.0603	159
14 days	0.0595	114
28 days	0.0472	65
1 year	0.0295	41

Notes: 1:1 mortar, W/C = 0.28, water curing before test

4. The C-S-H gel formed at the same time with ettringite has the dual functions of cementing and cushioning. The crystallization of the C-S-H gel at later ages strengthens the hardened cement paste as shown in the TEM micrograph at the age of 10 months (Fig. 3).

5. The addition of fly-ash as stabilizer can also expedite the hydration process at early age.

EXPANSION UNDER RESTRAINT

The prerequisite of self-stressing and shrinkage-compensating is proper restraint. Without restraint there will be no prestress. In fact, nearly all parts of structures and elements made of expansive concrete are under certain restraint functioned by reinforce-

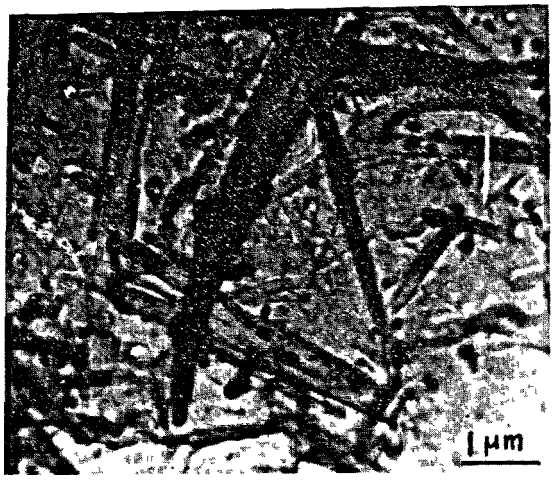

Fig. 3 Alunite cement paste
10 month water curing

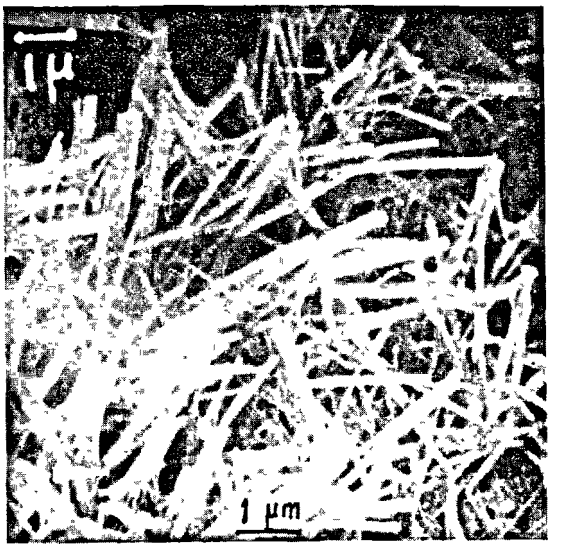

Fig. 4 Ettringite crystals under restraint
1:1 mortar, 7 day water curing

ments, foundations or neighbouring blocks. Self stressing concrete as well as shrinkage-compensating concrete for joint-filling are usually under high restraint. In the investigation of restrained expansion of alunite and other expansive concretes, we found that:

1. By SEM observation, ettringite crystals in alunite expansive cement paste under restraint are usually of smaller size and have closer spacing in comparison with those without restraint. (Fig. 4,5)

Fig. 5 Ettringite crystals without restraint
1:1 mortar, 7 day water curing

2. The alunite expansive cement mortar under restraint has lower porosity and better pore gradation (size distribution). (Fig. 6)

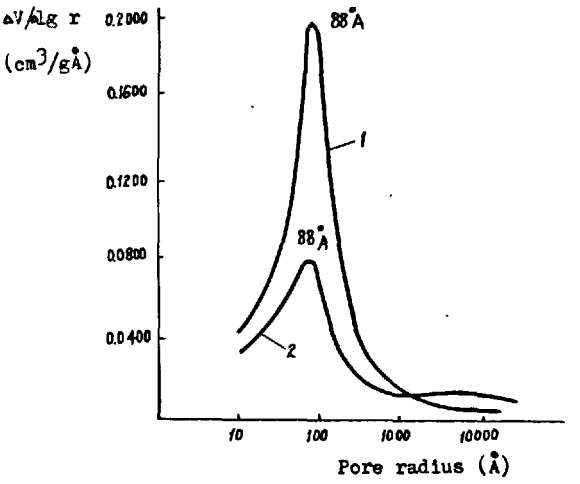

Fig. 6 Pore size distribution of alunite cement mortar

1- Without restraint, 28 day water curing
2- Under restraint, 28 day water curing

3. The boundary fissures around sand grains in alunite cement mortar under restraint are much thinner and are clogged with ettringite crystals. (Fig. 7,8)

As for expansion under high restraint, there have been doubts upon the effectiveness of shrinkage compensa-

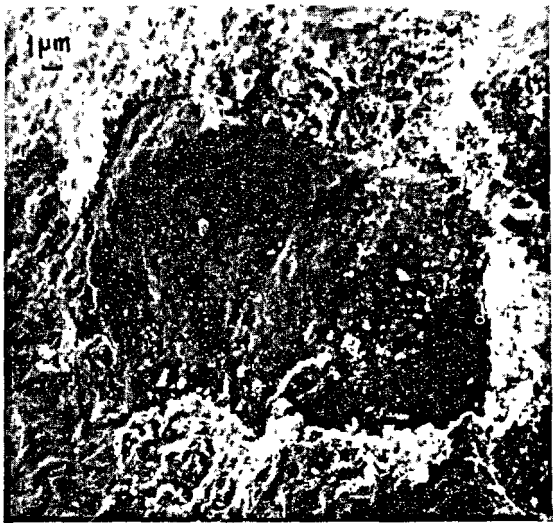

Fig. 7 Boundary fissure

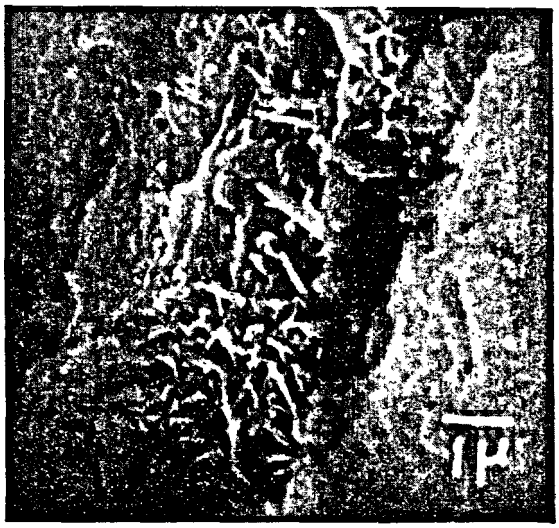

Fig. 8 Crystals clogging in fissures

tion due to the sensitiveness of contraction at drying (3). The conventional time-dependent curve (curve 1 in Fig. 9) of highly restrained expansion supports these doubts. Taking advantage of elastic recovery at drying, we have revised the conventional curve 1 and changed it to curve 2, which shows the delay of cracking from t_1 to t_2. If creep in tension is taken into consideration, the revised curve may be further modified to curve 3 in Fig. 9, and cracking is eliminated. Our successful experiences in utilizing alunite expansion cement concrete to fill a number of very rigid joints justify the above modifications.

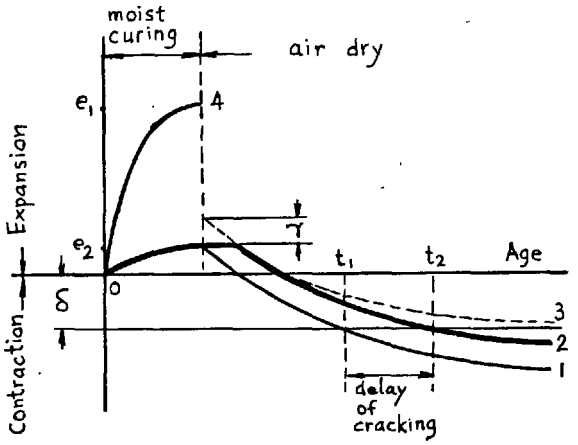

Fig. 9 Time-dependent curves of expansion

1- Conventional curve of highly restrained expansion
2- Revised curve
3- Revised curve further modified by creep in tension
4- Free expansion curve
γ = Elastic recovery after stress-release at drying
δ = Contraction pending cracking

CONCLUSION AND PROSPECT

1. Alunite (uncalcined) expansive cement marked with low expansion index, high strength at later age, impermeability and other merits is one of the effective shrinkage-compensating cements.

2. Proper restraint is necessary not only for the required prestress but also for good quality concrete.

3. The modification of restrained expansion curve gives a good picture of the effectiveness of expansive cements in reduction or even elimination of cracking.

4. Good results may be expected from addition of a small amount of expansive agent to most portland cements in cement factories or to most concretes in mixing plants to improve the general quality of concrete.

ACKNOWLEDGEMENT

The authors wish to thank Messrs. You Bao-kun, Deng Shen-cao and Miss Zhang Gui-qing for their help and cooperation in the whole investigation.

REFERENCES

1. V.V.Mikhailov: "Stressing cement and self-stressed structures in the USSR", Klein Symposium on Expansive Cement Concretes, p. 461 (1972)

2. Masatane Kokusu: "Use of expansive components for concrete in Japan", Klein Symposium on Expansive Cement Concretes, pp. 353-378 (1972)

3. Henry G. Russell: "Design of shrinkage compensating concrete slabs", Klein Symposium on Expansive Cement Concretes, pp. 193-226 (1972)

Expansion of sulfoaluminate under under-saturated CaO

Expansion du sulfoaluminate en solution sous saturée en CaO

XUE JUN-GAN, Engineer, Vice-Director, Cement Research Institute,
CHEN WEN-HAO, TONG XUE-LI, ZHAO YU-PING, Engineers, Cement Research Institute,
XU JI-ZHI, Technician, Cement Research Institute, Chine Populaire.

RESUME : L'étude de l'hydratation, en présence de gypse, de mélanges d'aluminates de chaux de rapports C/A variés (par exemple C_3A, $C_{12}A_7$, CA, et CA_2) et celle de ciments alumineux expansifs du type M, a été faite, en examinant les caractéristiques de l'expansion.

Elle a montré que : 1) l'importance de l'auto-contrainte produite par l'expansion du sulfoaluminate dépend de la morphologie et de la proportion de l'ettringite formée; elle dépend aussi de la résistance du ciment hydraté au moment où se forme l'ettringite et du processus de formation du gel d'ettringite.

2) si la phase aqueuse intersticielle est sous-saturée en chaux, l'ettringite se forme en plus grande quantité, mais est moins expansive dans le gel hydro-alumineux produit; la croissance de la résistance et de l'expansion sont alors compatibles; la microstructure de la pâte hydratée est plus dense, et le taux d'expansion libre du béton plus limité.

Deux types de ciment expansif en ont été déduits, en faisant varier le taux de saturation en chaux; ils ont été utilisés pour construire des conduites de 500 mm de diamètre autocontraint, la précontrainte s'élevant à 8 N/mm2. Ces conduites ont été installées dans des centrales hydro-électriques, dont l'une a une chute de 160 m.

SUMMARY: The effect of hydration products of mixtures of calcium aluminate compounds of various C/A ratio (i.e. C_3A, $C_{12}A_7$, CA and CA_2) with gypsum and of hydration products of aluminate and Type-M expansive cements on the characteristics of expansion have been investigated.

It has been shown that: Firstly, the magnitude of self-stress resulted from sulfoaluminate expansion is affected by the morphology and amount of ettringite being formed; The strength of the hardened cement paste at ettringite formation; and the morphology, amount and mode of the gel phase that is formed simultaneously. And secondly, at the condition of under-saturated CaO concentration, since more ettringite of less expansibility is formed with hydro-alumina gel in the same reaction, and the development of strength and expansion of the hardened paste are mutually compatible, the micro-structure of the paste is therefore denser, and the ratio of free against restraint expansion is relatively small in the concrete. Two kinds of high self-stressing cements which expand at the condition of under-saturated CaO have been developed and concrete pipes of 500 mm diameter with self-stressing value up to 8 N/mm^2 have been produced. These pipes have been used in penstocks of three water power stations with head up to 160 meters.

INTRODUCTION

Since the use of expansion of ettringite to compensate the shrinkage of hardened cement paste by Lossier(1), Mikhailov(2),Klein(3,4),Budnikov(5) and others have successively developed Type-M,Type-K and gypsum-aluminate expansive cements.

According to Mikhailov(2,6),Schwiete(7),Mehta(8,9) and others,only ettringite formed at the condition of saturated CaO expands,while Budnikov and Kravchenko (5) stated to the contrary,that the ettringite formed at under-saturated CaO also expands.

In order to make use of the expansion produced by ettringite to the benefit of the structure of hardened expansive cement paste and to obtain a higher self-stress value,the characteristics of expansion of sulfoaluminate at the condition of under-saturated CaO have been investigated.

THE MORPHOLOGY OF THE ETTRINGITES UNDER VARIED CONCENTRATIONS OF CaO

Optical and electron microscopy have been employed in studying the morphology of ettringites formed in the following systems,i.e.,CA-CaO-$CaSO_4$-H_2O,CA_2-, CA-,$C_{12}A_7$- and C_3A-$CaSO_4$-H_2O,C_2AS glass-CaO-$CaSO_4$-H_2O and CAS_2 glass-CaO-$CaSO_4$-H_2O,as well as those formed in hardened pastes of aluminate self-stressing cement and Type-M expansive cement. The concentrations of the liquid phases of these systems have also been analysed. It has been shown that under the condition of saturated CaO,ettringite of smaller size is formed and it often forms near the surface of the original aluminate phase; but at the condition of under-saturated CaO,larger size ettringite is formed and often at a distance from the surface of the original aluminate phase. The hexa-prismatic ettringite in the hardened paste of the Type-M expansive cement,as an instance of ettringite formed under saturated CaO, exhibits a dimension of 0.1-0.2 x 0.5-1.0 μm (Fig.-1.A),and the ettringite in the paste of the aluminate self-stressing cement,as an instance of ettringite formed under under-saturated CaO,exhibits a dimension of 0.5-1 x 4-6 μm (Fig. 1.B).

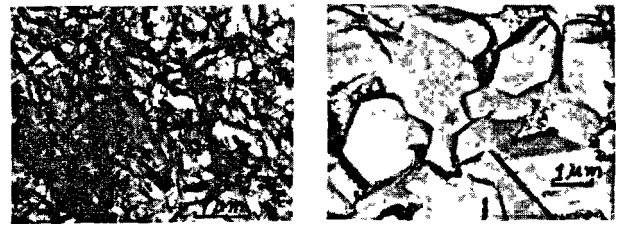

A. Type-M self stressing cement paste B. Aluminate self-stressing cement paste

Fig. 1. The surface replicas of hardened pastes of Type-M and aluminate self-stressing cements

THE QUANTITY OF ETTRINGITE AND GEL PHASE

The physical properties of 1:1 sand mortars made from the mixtures of CA_2,CA,$C_{12}A_7$ and C_3A with gypsum are shown in Table 1. X-ray diffraction and differential thermal analysis have been employed in the study of hydration products of the pastes. Results indicate that ettringite is formed in all the pastes. There are found 9.8 and 5.7 Å peaks in the X-ray diffraction patterns and an endothermic peak at 150°C in the DTA curves. Also formed is AH_3 in pastes of mixtures of CA_2,CA and $C_{12}A_7$ with gypsum with broad humps of 4.83 and 4.35 Å in the diffraction patterns and an endorthermic peak at 290°C in the DTA curves. As shown in Table 2,the amounts of AH_3 gel formed in the various mixtures vary by the following order: $CA_2 > CA > C_{12}A_7$,but there has not been noticed formation of AH_3 in paste made from the mixture of C_3A and gypsum. The shape of AH_3 exhibits equant particles with a dimension up to 0.1 μm in the electron microscope. The chemical analyses of liquid phases of the pastes indicate that in the paste of mixture of C_3A and gypsum,the concentration of CaO is in saturated state during the first seven days,while in other pastes,the concentrations of CaO are in

under-saturated state. The residual gypsums in the pastes were determined by the selective resolution method developed by the authors(10). The quantities of ettringite and gibbsite in the pastes and their ratios are shown in Table 2.

results indicate that: Firstly,for the same mixture the expansion generally increases as the quantity of ettringite increases,irrespective of the CaO concentration being saturated or not in the liquid phases of the pastes. However,the ettringite formed during the early hardening stage contributes only to development of skeleton which imparts strength but not expansion in spite of its quantity. As it can be seen from Table 2,in the specimens of the four aluminates,ettringites formed in one day moist curing as actually determined amount to 10.0 to 81.9% of the theoretical maximum ettringite that can be formed (the latter implies that when the gypsum originally

Table 1

Components %		Setting time hour:minute		Compressive strengths N/mm²					Linear expansions %			
				Moist curing	Water curing				Water curing			
Aluminate	Gypsum	Initial set	Final set	1 day	1 day	3 days	7 days	28 days	1 day	3 days	7 days	28 days
CA_2 60.20	39.80	1:38	2:06	1.0	1.0	1.0	0	0	0.54	2.33	8.52	Failure
CA 47.86	52.14	0:14	0:25	12.0	7.0	7.0	5.0	3.0	1.52	2.94	4.55	5.46
$C_{12}A_7$ 40.20	59.80	0:09	0:17	5.0	0	0	0	0	4.12	5.90	Failure	
C_3A 34.30	65.70	5:44	14:50	0	0	0	0	0	Excessive swelling			

notes: 1. Compressive strengths of 1 x 1 x 1 cm cubes
2. Linear expansions of 1 x 1 x 6 cm prisms
3. Test temperature, 20 ± 2°C

Table 2

Mixtures	Hydration products	Moist curing		Water curing			
		5 hours	1 day	1 day	3 days	7 days	28 days
CA_2 + gypsum	SO_3 in ettringite, % *		10.0	9.5	21.8	28.6	60.5
	Ettringite, mg/g paste		80.8	75.0	169.8	216.5	384.0
	AH_3, mg/g paste		32.0	29.7	67.1	85.6	151.5
	Ettringite / AH_3	Ratio by weight : 2.5,		Ratio by mole : 1 : 3			
CA + gypsum	SO_3 in ettringite, % *	35.4	44.2	45.7	52.0	58.2	74.1
	Ettringite, mg/g paste	316.5	372.5	376.0	411.0	437.0	494.0
	AH_3, mg/g paste	41.8	49.2	49.6	54.2	57.7	65.2
	Ettringite / AH_3	Ratio by weight : 7.5,		Ratio by mole : 1 : 1			
$C_{12}A_7$ + gypsum	SO_3 in ettringite, % *	71.7	81.9	86.3	90.0	87.5	88.4
	Ettringite, mg/g paste	742	810	816	852	787	814
	AH_3, mg/g paste	16.3	17.8	17.9	18.7	17.3	17.9
	Ettringite / AH_3	Ratio by weight : 45.5,		Ratio by mole : 6 : 1			
C_3A + gypsum	SO_3 in ettringite, % *	12.8	15.0	22.4	31.3	69.8	92.5
	Ettringite, mg/g paste	192.3	227.0	332.0	431.0	791	929
	AH_3, mg/g paste	0	0	0	0	0	0
	Ettringite / AH_3	Ratio by weight : ∞		Ratio by mole : ∞			

* Percentage of ettringite actually determined as against the theoretical total amount of ettringite that can be formed if gypsum originally present were all converted to ettringite.

present in the system has all been converted to ettringite). Secondly,under the condition of saturated CaO concentration,the formation of the smaller ettringite exhibits larger expansion; while under the condition of under-saturated CaO concentration,the formation of the large ettringite exhibits smaller expansion. Finally,in order to provide consistency for the development of strength and expansion,there must be presence of a definite amount of gel phase at the time of ettringite formation. As the ratio of ettringite to gel phase in the hardened pastes affects to a great extent the characteristics of strength and expansion of the hardened pastes,so it also affects the value of self-stress.

THE STRENGTH AND SELF-STRESSING VALUE OF HARDENED PASTES

The magnitude of selfstressing value in hardened pastes is affected not only by the quantity and morphology of ettringite but also by the strength of the hardened pastes. Therefore,the relation between self-stressing value calculated as per unit weight ettringite (N/mm^2 / g ettringite) and compressive strength of the aluminate self-stressing cement paste has been investigated,the result of which being shown in Fig. 2. In order to obtain a higher self-stressing value,it is necessary that,on the one hand,the ettringite be formed at the time when the paste has attained a relatively high strength,and on the other hand,a sufficient quantity of gel phase be formed in the mean time.

THE CHARACTERISTICS OF THE EXPANSION OF SULFOALUMINATE AT THE CONDITION OF UNDER-SATURATED CaO

The aluminate self-stressing cement paste has been chosen as the typical example of expansion of sulfoaluminate at the condition of under-saturated CaO, and the Type-M expansive cement paste as that of

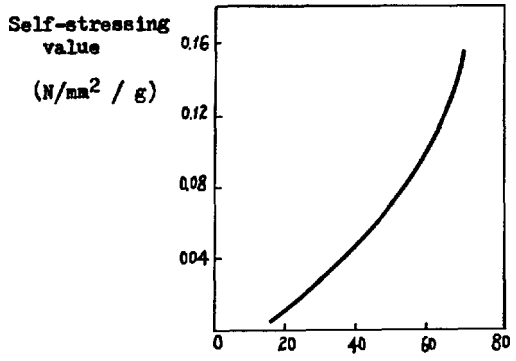

Fig. 2 Relation between self-stressing value calculated as per unit weight ettringite and compressive strength of the aluminate self-stressing cement paste

expansion of sulfoaluminate at the condition of saturated CaO. The following aspects have been investigated and compared in the study,i.e. the CaO concentrations of liquid phases,the formation of hydrates and their consistency,the quantity of ettringite formed at the respective stages of hydration,the structure of cement pastes and the properties of the expansive cements and their concretes. The test results are summarized in Table 3.

As can be seen from Table 3,at the condition of under-saturated CaO concentration,since a large amount of ettringite species of less expansibility is formed with hydroalumina gel in the same equation of chemical reaction,the development of strength and expansion of the hardened paste is compatible. Therefore,the micro-structure of the paste is denser,and the ratio of free against restraint expansion is relatively small in the concrete. The expansive concrete is thus provided with a protecting layer of superior quality. All of the above factors result in a self-stressing cement concrete with a high self-stressing value and low gas-permeability. These are the characteristics of the expansion of sulfoaluminate under the condition of under-saturated CaO.

Table 3

Items of comparison				Type-M expansive cement	Aluminate self-stressing cement
(1) Formation of hydration products	$Ca(OH)_2$			Present	Absent
	Formation of ettringite	Mode of formation		$C_3S+3H \rightarrow C_{1.5}SH_{1.5}+1.5CH$ $C_2S+2H \rightarrow C_{1.5}SH_{1.5}+0.5CH$ $CA+3C\bar{S}H_2+2CH+24H \rightarrow C_3A'(CS)_3H_{32}$ $CA_2+6C\bar{S}H_2+5CH+47H \rightarrow 2C_3A(C\bar{S})_3H_{32}$ $C_3A+3C\bar{S}H_2+26H \rightarrow C_3A(CS)_3H_{32}$	$3CA+3C\bar{S}H_2+32H \rightarrow C_3A(C\bar{S})_3H_{32}+2AH_3$ $3CA_2+3C\bar{S}H_2+41H \rightarrow C_3A(CS)_3H_{32}+5AH_3$
		CaO concentration of liquid phase		Saturated	Under-saturated
		morphology		Small size hexagonal	Large size hexagonal prism
		Quantity of ettringite formed in various stages (calculated as SO_3 %*)	Moist curing** (forming skeleton of strength)	ca 6	ca 9
			Water curing** (causing expansion)	ca 1.7	ca 6
			Residual gypsum in concrete products	ca 0.3	ca 1
	Formation of gel phase	Gel phase		C-S-H gel	AH_3 gel
		Mode of formation		from hydration of C_3S and C_2S, not formed in same reaction with ettringite	from hydration of CA and CA_2 with gypsum, formed in same reaction with ettringite
(2) Consistency of ettringite and gel phase and structure of cement paste		Consistency		Not liable to be good	Liable to be good
		Most probable pore radius (1:1 mortar, 28 days)		170 Å	25 Å
		Compressive strength, N/mm^2 (28 days, 1:2 mortar, 3 x 3 x 3 cm cube)		ca 40	ca 50
(3) Properties of hardened cement paste		Ratio of free against restraint expansion (percentage of reinforcing steel = 1.4)		ca 15	ca 5
		Self-stressing value, N/mm^2 (1 : 0.8 : 1.2 concrete, percentage of reinforcing steel = 1.4)		ca 3	ca 6
(4) Properties of self-stressing concrete pipe		Inner-pressure of fracture, N/mm^2 (1 : 0.8 : 1.2 concrete pipe of 300mm diameter)		ca 1.6	ca 2.4
		Resistance to gas permeability, N/mm^2		ca 0.3	ca 1.2

Notes: *Type-M expansive cement contains 8% SO_3, aluminate self-stressing cement contains 16% SO_3.

**Moist curing, room temperature 2 hours +85°C 1.5 hours for Type-M expansive cement and room temperature 6 hours or 40°C 2 hours for aluminate self-stressing cement.
Water curing, room temperature 7-14 days for Type-M expansive cement and 14-28 days for aluminate self-stressing cement.

THE HIGH SELF-STRESSING CEMENTS HAVE BEEN DEVELOPED

Aluminate and sulfoaluminate self-stressing cements have been developed in China. The former is an interground product of high alumina cement clinker with CA and CA_2 as its main constituents and a certain amount of gypsum. The latter is an interground product of calcium sulfoaluminate clinker with $C_4A_3\bar{S}$ and β-C_2S as its main constituents and a certain amount of gypsum. The characteristics of both cements lie in the expansion of sulfoaluminate at the condition of under-saturated CaO. The annual production of each cement amounts to about 20,000 tons and both are being used to manufacture concrete pipes for water,oils and gases.

Recently,improvements have been made in the manufacture of aluminate self-stressing cement concrete. The concrete pipes of 500 mm diameter with self-stressing value up to 8.0-10.0 N/mm^2 and inner pressure of fracture up to 2.4 N/mm^2 have been produced,and put in trial use in penstocks of three water power stations with head up to 160 meters.

PROSPECTS

There had been much controversy about the use of expansive cement for self-stressing concrete during the 3rd Symposium held at london in 1952. Since then it has been used in concrete of low self-stressing value. In view of the fact that the durability of protecting layer of concrete will deteriorate under the extreme expansion of concrete,Polivka(11) emphasized that the practical self-stressing value should not exceed 3.5 N/mm^2. We are of the opinion,however, that with fuller knowledge about the peculiarity of expansion of sulfoaluminate at the condition of under-saturated CaO we can do much to finally solve the problem of the quality of the protecting layer of self-stressing concrete. Now that the high self-stressing cement and its concrete have been developed and concrete with self-stressing value up to 8.0 N/mm^2 have been produced,we can well anticipate that the value of chemical pre-stress will eventually approach that of mechanical pre-stress.

REFERENCES

1. H.Lafuma, Proceedings of the Third International Symposium on the Chemistry of Cement,London, 1952,581-597 (1954)

2. V.V.Mikhailov, Proceedings of the Fourth International Symposium on the Chemistry of Cement, Washington,1960,Vol.2,927-955 (1962)

3. G.L.Kalousek, Klein Symposium on Expansive Cement Concrete,ACI Pub. SP-38,1-20 (1972)

4. P.K.Mehta, M.Polivka, Proceedings of the Sixth International Symposium on the Chemistry of Cement, Moscow, 1974,Vol.3,158-172 (1976)

5. P.P.Budnikov, I.V.Kravchenko, Proceedings of the Fifth International Symposium on the Chemistry of Cement,Tokyo,1968,Part 4,319-330 (1970)

6. V.V.Mikhailov, Klein Symposium on Expansive Cement Concrete,ACI Pub. SP-38,415-468 (1972)

7. H.E.Schwiete, V.Ludwig and Jager, Symposium on Structure of Portland Cement Paste and Concrete, Washington,328-352 (1966)

8. P.K.Mehta, Cement and Concrete Research, Vol.3,No.1,1-6 (1973)
Vol.6,No.6,169-182 (1976)

9. P.K.Mehta,J.Amer.Ceram.Soc.,Vol.56,No.6,315-319 (1973)

10. Xue Jun-gan, Chen Wen-hao and Zhou Shi-fen, Cement and Cement Products,64001 (4) 5-10; 64002 (5) 17-19 (1964)

11. M.Polivka, Klein Symposium on Expansive Cement Concrete,ACI Pub. SP-38,483-487 (1972)

La nature physico-chimique des auto-contraintes des ciments expansifs

Physicochemical nature of own stresses in expanding cements

L.V. NIKITINA, Candidat ès Sciences, Collaborateur scientifique supérieur,
K.G. KRASSILNIKOV, Professeur, Docteur des Sciences Chimiques,
A.I. LAPCHINA, Ingénieur, Institut des Recherches Scientifiques du Béton et du Béton Armé (NIIZhb), Gosstroy, U.R.S.S.

RESUME : Le mécanisme des déformations volumiques des ciments expansifs de compositions différentes est étudié.

Les études complexes des processus physico-chimiques, des auto-contraintes et des déformations ainsi que des variations volumiques, dans les structures soumises aux déformations, a montré que l'augmentation localisée de volume des phases solides dont la formation est le résultat de la réaction du composant-expanseur a pour base l'expansion des ciments. Dans le processus du durcissement des ciments se produit l'augmentation volumique des particules dans la phase expanseuse (ettringite ou $Ca(OH)_2$ qui amène à la naissance dans la structure du ciment durci des contraintes internes (auto-contraintes) σ. A un certain niveau de σ suffisant pour vaincre la résistance de la structure, a lieu la déformation (l'expansion) de la structure. Pour déterminer expérimentalement les auto-contraintes, on a utilisé les méthodes des compensations mécanique et magnétique des déformations d'expansion.

SUMMARY: Mechanism of volumetric strains in expanding cements of different composition has been studied.

It has been shown from complex investigations of physicochemical processes, own stresses and strains as well as from volumetric changes in deformed structures that localized increase in volume of solid phases which are formed as a result of expanding component reaction is the basis of cements expanding. In the process of cements hardening the volume increase of particles in expanding phase (ettringite or $Ca(OH)_2$) leads to development of inner (own) stresses σ in the structure of cement stone. Under a certain critical level σ sufficient for overcoming of structure resistance, the deformation of the structure, or its expanding, takes place. For experimental determination of own stresses there have been used some methods of mechanical and magnetic compensation of expansion strains.

L'un des cas le plus intéressant des propres déformations des structures en ciment est l'augmentation du volume observée lors le durcissement des ciments expansés.

Les études du mécanisme de l'expansion des ciments, présente un intérêt considérable pour la élaboration de la theorie générale des déformations des structures dispersées; aussi ces études sont d'une grande importance pratique pour les developpement de la technologie dans le domaine des ciments et des bétons irrétrécissables, expansifs et autocontraints, étant donné que ciments et bétons mentionnés soient produits sur la base de ces structures.

L'analyse des donnés cités dans les oeuvres littéraires concernant le problème de l'aptitude de ciments a l'expansion montre que, malgré un nombre important des travaux éfectues dans ce domaine et des hypothèses proposées (I-5), le mécanisme de l'expansion du ciment durci n'est pas encore tiré a claire jusqu'à la fin.

La plupart des rechercheurs en envisageant les processus qui se passent dans les systèmes expansives ont principalement accordé leure attention a l'étude des reactions chimiques qui amenent a la formation de la phase d'expansion. Cependant, l'expansion en qualité de l'effet volumique ne peut pas être compris seulement a la base des représentations chimiques. En dehors de l'étude des processus physico-chimiques qui provoquent l'apparition des déformations est tres importante la considerations du côté géométrique des structures poreuses soumises aux déformations, c'est à dire des variations volumiques qui se passent à l'intérieur de la structure simultanement avec la variation volumique des particules isolées dont cette structure est composée.

En étudiant le méchanisme de l'expansion il faut prendre en considération les problemes de la méchanique des déformations, notamment l'interdépendance entre les propriétés de résistance et les proprietés de déformation du ciment durci ainsi que l'interdépendance entre les propres contraintes accompagnant le processus du curcissement des ciments expansifs.

L'objectif de l'ouvrage présent est l'examen de l'ensemble complexe de phénomènes ayant lieu dans les structures expansives.

Les différents types des ciments expansifs d'alumosulfates tels que le ciment d'aluminat gupse (à haute teneur en alumine) (GGC-abreviations russes); le ciment autocontraint (NC), le ciment autocontraint alunitisé (ANC) ainsi que les composantes sur la base de ciment de portland, contenant l'adjuvant CaO (RPC) en qualité de constituant d'expansion (Table I) ont ete les objets de ces études.

Lors la réalisation des les études dans le domaine des processus physico-chimiques ayant lieu pendant le durcissement des ciments mentionnés ont été déterminés:
- la cinétique et le caractère de la cristallisation des phases d'expansion;
- la cinétique de la fixation de l'eau durant le processus de durcissement et d'expansion des ciments;
- la composition de phase des nouvelles formations des hydrates;
- la micro-structure du ciment durci;
- les déformations linéaires des éprouvettes.

TABLEAU I

NN de compositions	Type de ciment	La teneur en % de la masse				
		ciment de portland	ciment d'aluminat	gypse	alunite -700 °C	CaO
I	GGC	-	70	30	-	-
2	GGC-C	-	65	30	-	5
3	NC-N	67	23	I0	-	-
4	NC-T	66	20	I4	-	-
5	ANC	75	-	I0	I5	-
6	RPC	90-99	-	-	-	I-I0

Nous allons nous arreter tout d'abord sur l'examination des compositions expansives les plus repandues c'est à dire des compositions sur la base de sulfo-aluminates - GGC, NC et ANC. Malgré la diversité des hyporthèses proposées expliquant le processus de l'expansion de tels ciments l'opinion est telle que à la base de ce processus est la réaction de la formation de hydro-sulfoaluminate de calcium - d'éttringite - $3CaO \cdot Al_2O_3 \cdot 3CaSO_4 \cdot 3IH_2O$, suivie par l'augmentation en 2,3 fois de volume des phases solides.

Les études que nous avons réalisé montrent que l'ettringite est un produit initial de l'interaction du gypse avec une composante d'aluminate qui se passe pendant le durcissement de tous les types des ciments éprouvés. D'après les données de l'analyse XR et de l'analyse derivatographique (DTA), la formation de l'éttringite est enregistrée dans le ciment durci quelque minutes après le gâchage.

La stabilité d'ettringite durant le durcissement ultérieur est conditionnée surtout par la proportion des minéraux d'aluminate et du gypse dans la composition des ciments éprouvés. Dans la pierre de ciment durci ayant la GGC, et contenant 30% du gypse (composition nº I, table I), l'éttringite formé présente une composition stable et une composition qui ne suleit aucune transformation de phase pendant toute la période du durcissement du ciment. Dans le même temps, un liage un épuisement total du gypse s'étant produit, on peut observer dans certaines compositions de NC-N (composition nº 3, table I) une transition partielle de l'éttringite en mono-sulfo-aluminate de calcium - $3CaO \cdot Al_2O_3 \cdot CaSO_4 \cdot I2H_2O$ (6). Cette transformation de phase est conditionnée par la surabondance de la composante d'aluminate par rapport au gypse dans la composition du ciment et celle-là se passe en parfaite conformité de conditions d'équilibre dans le

systemè de $CaO-Al_2O_3-CaSO_4-H_2O$, étudié minutiensement par D'Ans et par Eick (7).

Les études complexes physico-chimiques étant réalisé il s'est averé, pourtant, que la valeur d'expansion des ciments alumosulfatiques n'est pas liée d'une maniére univalente avec la quantite de l'éttringite formé. Pour affirmer ce fait il suffit de comparer les données sur la déformations des ciments du type GGC et GGC-C que nous avons obtenues. (Les compositions n° I et n° 2, table I) (Fig. I).

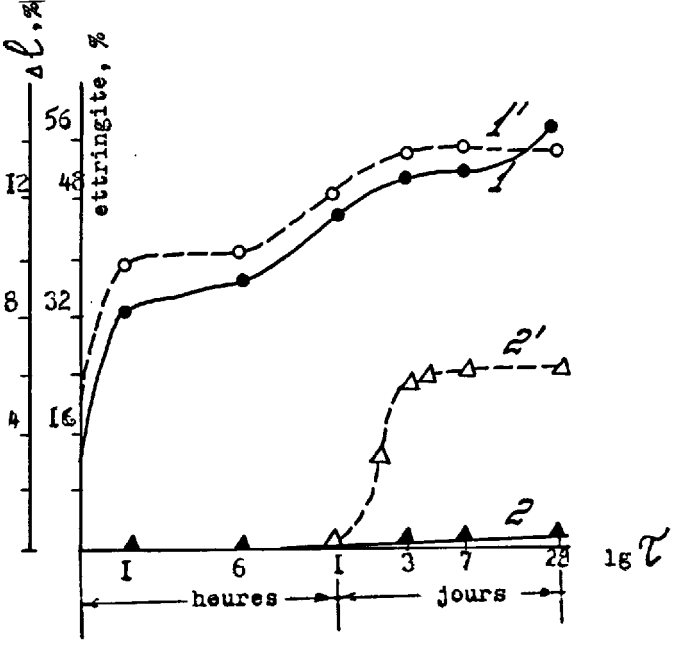

Fig. I - La cinétique de la cristallisation d'ettringite (I,I') et de developpement des déformations d'expansion (2,2') au cours de durcissement de GGC (I,2) et de GGC-C (I', 2').

Comme le montre la figure I, durant le durcissement de deux types de ciments mentionés, se forme à peu près la même quantite d'éttringite (~56%), tandis que les déformations d'expansion dans le cas d'utilisation de GGC ne présentent que 0,I6%, donc dans le cas d'utilisation de GGC-C cette valeur s'approche déjà à 6% vers le 3ème jour de durcissement. Dans les compositions de NC les déformations d'expansion peuvent aussi toucher a des valeurs considérables (4% et plus), alors que la quantité maximale de l'ettringite formé ne dépasse pas 30%, c'est a dire que cette quantité est de 2 fois plus petite que dans les compositions de GGC et de GGC-C considérées plus haut (6,8).

Il est évident qu'il est nécessaire de chercher la cause de cette différence des déformations dans les conditions différentes de la cristallisation de l'éttringite.

Les analyses microscopiques montre (6) que, compte tenu de la phase liquide, la cristallisation de l'éttringite peut se passer soit dans les pores du ciment durci en provoquant les déformations tout à fait médiocres (tout comme dans le cas de GGC), soit bien ce processus se localise sur les grains des aluminates de calcium qui font partie du composant d'expansion. Avec cela une influence déterminante sur le caractère de la cristallisation de l'éttringite est exercée par la teneur en CaO dans la phase liquide du ciment durci. Dans le cas ou la réaction de la formation de l'éttringite se localise sur la surface des particules des aluminates de calcium, ces particules se régenéren peu à peu en peu en un agrégat polycristallin et s'augmentent volume comme un entier unifie. Telles particules deviennent, par conséquent, la source des déformations pour toute la structure dans son ensemble.

Dans les ouvrages (8-9) est montré que le mécanisme analogue d'expansion a lieu aussi dans le cas si nous utilisons CaO et MgO comme les adjuvants d'expansion.

La reaction de hydratation de CaO et de MgO ayant lieu dans la structure durcissante du ciment durci et accompagnée par un plus que double augmentation de volume des phases solides est la cause d'expansion de tels ciments (composition n° 6, Table I). Il est connu que la hydratation de CaO a déjà lieu même si les valeurs de tension de vapeur d'eau sont assez médiocres, c'est a dire en absence de la phase liquide; avec cela est lié, en particulier, son application en qualité de l'agent de dessechement. En se basant sur ce fait certains rechercheurs considérent le processus de hydratation de CaO comme la réaction de phase solide. En tout cas, independamment de mécanisme détaille de cette réaction, il est évident qu'elle est d'un caractère localisé et n'est pas accompagnée par le transport, aux espaces de pores du ciment durci durant son durcissement, de la masse de hydrate au cours de sa formation.

Ainsi, la capacite a la manifestation de déformations d'expansion des structures du ciment ayant des compositions différentes détermine non une simple augmentation de volume des phases solides qui resulte de la réaction du composant d'expansion, mais le caractere local du dégagement des produits de sa hydratation.

Envisageons maintenant le côté géometrique des déformations des structures expansives. Il est possible de supposer, que la déformation observeé pendant le durcissement des ciments expansifs est un certain total de l'ensemble des microdéformations élémentaires dont la naissance est le resultat de l'augmentation du volume des particules du composant expansif faisant partie de leure structure (8). Puisque l'augmentation de volume des particules unitaires du composant d'expansion est à ce qu'il paraît la cause provoquant l'augmentation de volume total de la structure dans l'ouvrage présent nous nous sommes intéressés avant tout au rapport entre l'accroissement de volume total de la structure (V_s) et l'ac-

croissement de volume des phases solides (V_t). La méthodologie de l'étude est décrite en (8). Les modeles des courbes structurales, obtenus pour les différentes compositions expansives sont présentées aux Figures 2 et 3. En faisant l'analyse des courbes on porte avant tout l'attention sur le fait qu'entre les valeurs $_{\Delta}V_s$ et $_{\Delta}V_t$ il n'y a pas de relation linéaire à laquelle on pouvait s'attendre dans le cas où l'expansion de la structure n'était déterminée que par une simple augmentation de volume des phases solides.

Donc, durant la hydratation de GGC, malgré l'augmentation de volume des phases solides resultant de la cristallisation de l'ettringite, le volume de la structure presque ne change pas (Figure 2, courbe I). En tenant compte de ce que $\Delta V_s = \Delta V_t + \Delta V_p$, avec $\Delta V_s \approx 0$ et $\Delta V_t \gg 0$, $\Delta V_t = -{}_{\Delta}V_p$, où V_p - et le volume des pores.

Ainsi, dans le cas de l'absence de la déformation extérieure de la structure, l'augmentation de volume des phases solides résultant de la cristallisation du composant d'expansion est compensée par la diminution de la porosité, c'est à dire, les nouvelles formations en se cristallisant de la solution sursaturée se déposent à l'intérieur des pores remplies par la solution. Cette conclusion, comme il a été déjà montré, est confirmée par un contrôle immédiat au microscope du caractère de la cristallisation de l'ettringite durant la hydratation de GGC.

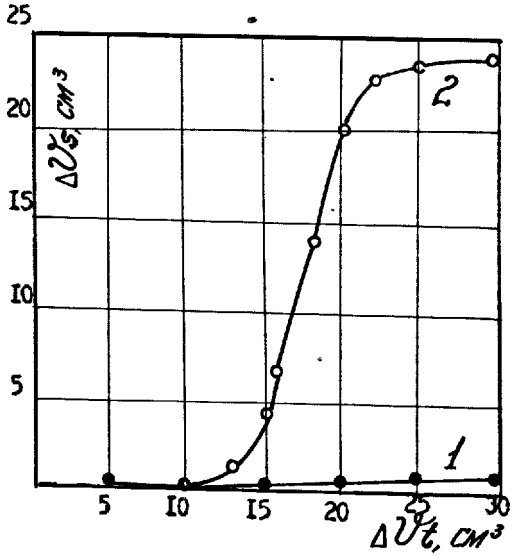

Fig. 2 - La variation de volume des éprouvettes ($_{\Delta}V_s$) en fonction de l'augmentation de volume des phases solides ($_{\Delta}V_t$) au cours de durcissement de GGC (I) et de GGC-C (2).

A l'introduction dans le GGC de l'adjuvant de CaO (composition 2, Table I), à partir d'une certaine valeur critique $_{\Delta}V_t$ le volume de la structure commence à augmenter brusquement (Figure 2, courbe 2). Le changement du caractère de la courbe structurale est dans le cas présent au changement du caractère de la cristallisation de la phase d'expansion de ces ciments - de l'éttringite.

Pour toutes les autres compositions des ciments expansifs (NC, ANC, RPC) qui ont été étudié les courbes structurales représentant le rapport $_{\Delta}V_s = f\,_{\Delta}V_t$ ont le même caractere de "S" pareil a la courbe pour la composition de GGC-C. En qualité d'exemple à la Figure 3 est présentée la courbe du rapport $_{\Delta}V_s$ de $_{\Delta}V_t$ pour RPC contenant 10% de CaO (composition 6, Table I). Avec la courbe principale structurale à la Figure sont aussi présentées les données concernant la cinétique de la hydratation de CaO et le données concernant la fixation de l'eau durant le durcissement de la composition donnee de RPC.

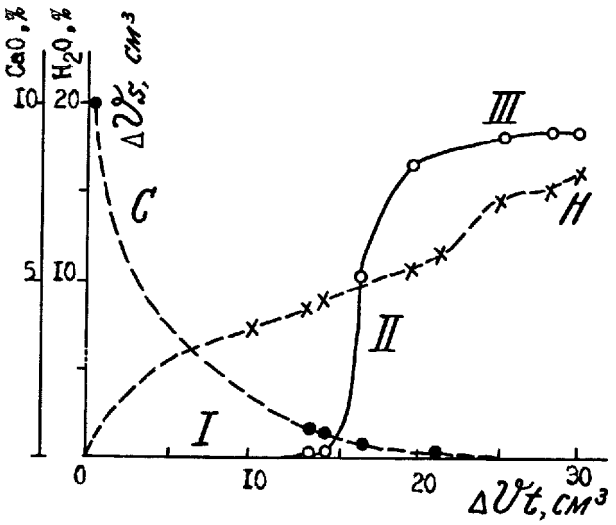

Fig. 3 - La variation de volume de l'éprouvette ($_{\Delta}V_s$) en fonction de l'augmentation de volume des phases solides ($_{\Delta}V_t$) au cours de durcissement de RPC additionne par 10% CaO.

Par la similitude mentionnée dans le caractère des courbes structurales est temoigné le fait que le mécanisme de l'expansion est toujours pareil independamment de la différence dans la nature des composants d'expansion utilisés.

L'analyse des régularités obtenues montre que le processus d'expansion comprend les trois étapes successives et interdépandantes. La section I des courbes structurales (Figure 3), correspondant au stade initial de formation de la structure est caracterisee par l'augmentation de volume des phases solides pour le compte de hydratation des mineraux de clinker de ciment et du des composant d'expansion, le volume de la struc-

ture etant practiquement invariable. Par la suite, l'augmentation localisée de volume des particules du composant d'expansion amène à un accroissement progressif des contraintes internes dans la structure du ciment durci au cours de sa formation. A un moment détermine les contraintes mentionnées touchent à une valeur suffisante pour surmonter la résistance de la structure et puis ces contraintes relaxent et provoquent sa deformation. À la période de l'expansion intensive correspond la section II des courbes structurales. A cette section une accroissement relativement médiocre de ΔV_t provoque une grande augmentation de volume total de la structure et une grande augmentation de volume des pores puisque $\Delta V_s \gg \Delta V_t$ et par consequent, $\Delta V_s \approx \Delta V_p$. L'expansion des éprouvettes prend sa fin, en général simultanément avec l'achévement de la reaction du composant d'expansion.

La section III des courbes structurales est caractérisée par l'augmentation continuée de volume des phases solides qui se realise à présent surtout pour le compte de hydratation des mineraux siliceux du ciment. Ces processus amènent au rétablissement des liaisons déréglées, au compactage de la structure et à l'accroissement de sa résistance mecanique.

Pour confirmer les thèses exposées plus haut ont été effectués les essais directs ayant pour but la détermination expérimentale des propres contraintes qui accompagnent le processus du durcissement des ciments expansifs.

Pour mesurer ces propres contraintes dans les systèmes expansifs sont utilisées les deux méthodes que nous avons mis au point.

La première méthode est basée sur le phenomene de la compensation mécanique des déformations d'expansion du materiau. Cette méthode étant au cours d'élaboration on a adopté en qualité de la caractéristique des contraintes internes la pression la plus petite qui résulte de l'action de la charge extérieure et qui ne provoque pas d'augmentation de volume de la structure. Pour mesurer la valeur mentionnée nous avons créé le special dispositif de mesure qui représente un levier d'équilibrage, muni d'un système automatique de chargement qui effectue son action sur l'éprouvette par l'intermédiaire de poinçon ayant le contact avec sa surface. Au cours de processus d'expansion le ciment durci étudie exerce une pression sur le poinçon ce qui met en marche le système automatique de chargement. D'après la charge indispensable pour le reduction de volume du ciment durci à la valeur initiale on determine l'effort qui se developpe au cours de durcissement des ciments (la pression d'expansion).

La deuxième méthode de mesure des propres contraintes est basée sur l'utilisation des capteurs annulaires magnéto-élastiques crees par TsNIISK Koutcherenko (IO) dont l'anneau rigide en matériau ferromagnetique est l'élement principal.

Pour réaliser les mesures, le capteur est placé au centre de moule cylindrique, après quoi le moule est rempli par la pate de ciment étudiée et les contacts de sortie du capteur sont mis en connexion avec les appareils de mesure. Par suite de l'expansion du ciment durci étant donné qu'il existe un facteur restrictif - la forme, qui empêche sa déformation, les contraintes radiales mécaniques exercent l'action sur la capteur. Avec cela dans le materiau de l'anneau a lieu la modification des propriétés magnétiques par la transformation desquelles en signal électrique on trouve a l'aide des courbes d'etalonnage les valeurs des propres contraintes qui surgissent dans le materiau.

A la Figure 4 sont présentés les résultats de mesure de σ au cours de durcissement de ANC les méthodes citées étant utilisées. Pour faire une comparaison a la Figure sont aussi présentees les courbes de cinétique de la cristallisation de la phase d'expansion du ciment donné - d'ettringite (Courbe I) et de developpement des déformations d'expansion (Courbe 2). Comme on peut voire à la Figure, les courbes de cinétique de developpement des propres contraintes (courbes 3,4) et la courbe de déformations d'expansion, se ressemblent et sont analogues à un S.

Au cours de I5-30 minutes (des le début) on peut observer sur toutes les courbes une courte periode d'induction coincidant avec la période de formation de la structure de la pâte de ciment. A ce stade, l'action du composant d'expansion n'amène pas à l'apparition des contraintes puisque la structure du ciment durci n'a pas encore gagné résistance indispensable.

Par la suite, dans la mesure de durcissement du ciment durci, la cristallisation d'ettringite localisée a la surface des grains de base du ciment amène à un accroissement successif des contraintes à l'intérieur de ce ciment durci. A ce stade, l'essentiel pour le comportement des éprouvettes est l'existence (la présence) ou l'absence de limitation (restriction) de leure déformation. En absence de limitation les propres contraintes ayant touché a un niveau détermine provoquent une expansion considérable du ciment durci (plus de 5%), (Courbe 2), suivie par l'ameublissement de la structure et par l'abaissement de sa résistance. La limitation rigide de la déformation dans la même période étant donnée nous fixons le surgissement et le developpement intensif des propres contraintes (Courbes 3,4). Comme il est montré a la Figure, le developpement des propres contraintes ainsi que l'expansion quia lieu dans le ciment durci en ANC de la composion donnée sont les plus intensifs pendant les 2 heures des le début de hydratation. En comparant les données obtenues avec les résultats des essais physico-chimiques du même ciment on peut voir que la période de developpement intensif des contraintes et des déformations correspond par le temps a une cristallisation la

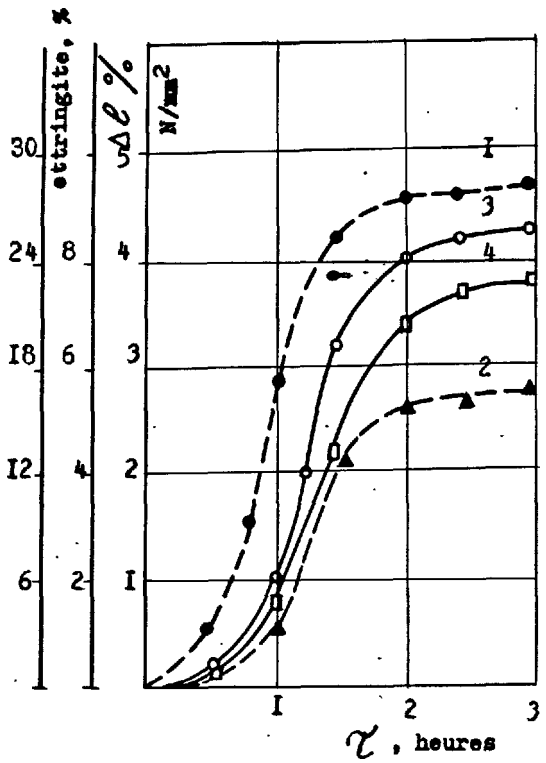

Fig. 4 - La cinétique de cristallisation d'ettringite (I), de developpement des déformations d'expansion (2) et des propres contraintes (3,4) au cours de durcissement de ANC
3 - Les donnés de la méthode des capteurs magnéto-élastiques
4 - Les données de la méthode de la compensation mécanique des déformations d'expansion.

plus active de la phase d'expansion du ciment donné - d'ettringite (Courbe I).

Les études ont montré qu'au cours de durcissement d'autres types des ciment expansifs - de NC et de RPC sont observées les regularites analogues dans la cinétique de developpement des propres contraintes, toutefois, les valeurs maximales de ces contraintes sont parfois plus grandes (8,0-I0,0 N/mm^2)

CONCLUSION

Est étudie la nature physico-chimique des deformation volumiques des compositions expansives des composes differents. Par les méthodes de la composation mécanique des déformations d'expansion d'utilisation des capteurs magnéto-élastiques à été realisé le mesure direct des propres contraintes accompagnant le processus de durcissement des ciments éprouves.

La comparaison des données obtenues avec les résultats des études physico-chimiques montre que c'est les réactions du composant d'expansion amenant à un augmentation localisé de volume des phases solides dans la structure du ciment durci au coure de durcissement qui sont à la base de developpement des propres contraintes et des déformations.

BIBLIOGRAPHIE

I. - H.LAFUMA (I929) "Theorie de l'expansion des liants hydrauliques". Rev. materiaux Constr. N 243-244. (fr.)

2. - V.V.MIKHAILOV (I955) "Le béton armé auto-contraint". Gosstroyizdat. (russe)

3. - I.V.KRAVTCHENKO (I962) "Les ciments expansifs". Gosstroyizdat. (russe)

4. - OUMTCHEDLOV-PETROCJAN, A.G.PHILATOV (I965) "Les composes expansifs à la base de ciment portlans". Stroyizdat. (russe)

5. - P.K.META, M.POLIVKA (I976) "Les ciments expansifs". Dans le Recueil 6eme Congres International sur la Chimie du Ciment", v. 3, Stroyizdat. (russe)

6. - L.V.NIKITINA, Z.M.LARIONOVA, A.I.LAPCHINA et d'autres (I975) "Transformations des phases d'ettringite dans les systèmes expansives". Travaux de NIIZhB, livr. I7, Stroyizdat, 39-55. (russe)

7. - J.D'ANS, H.EIK (I953) "Das System CaO-Al_2O_3-$CaSO_4$-H_2O bei 20°C". Zement-Kalk-Gips, N 9, 302. (allemand)

8. - K.G.KRASSILNIKOV, L.V.NIKITINA, N.N. SKOBLINSKAJA (I976) "La physico-chimie des processus d'expansion des ciments" Dans le Recueil: 6eme Congres International sur la Chimie du Ciment, vol. III, Stroyizdat. (russe)

9. - K.G.KRASSILNIKOV, A.I.LAPCHINA, L.V. NIKITINA (I972) "Les déformations d'expansion au cours de durcissement du ciment portland additionné par CaO" Dans le Rec. "La technologie et l'accroissement de durabilite des structures en béton armé", Stroyizdat. (russe)

I0. - I.N.CHELFER (I97I) Certificat de Paternite N 306338 (URSS). Le capteur magnéto-élastique. Bull. d'Inv. N I9. (russe)

Composition en phases du clinker de ciment alumineux à teneur d'alumine élevée en fonction de la température et du milieu gazeux de cuisson

Phase composition of clinker of high-alumina cement versus calcination temperature and gas medium

T.V. KOUZNETSOVA, Candidat ès Sciences Techniques,
V.P. RIASINE, Candidat ès Sciences Techniques,
V.I. GOUSSEVA, Ingénieur,
V.A. VOROBIEV Ingénieur. NIITzement. Moscou, U.R.S.S.

RESUME : Le système CaO - Al_2O_3 a été étudié par plusieurs chercheurs et à l'heure actuelle la composition de ce système est bien connue. Toutefois, l'analyse de la composition des phases des clinkers industriels montre qu'il est difficile d'obtenir l'équilibre chimique et des phases dans les conditions du four rotatif, et le clinker contient des aluminates de calcium qui diffèrent par leur composition de ceux prévus par le calcul.

C'est pourquoi les auteurs étudièrent le processus de formation des minéraux lors de l'agglomération du clinker dans les conditions de laboratoire, semi-industrielles et industrielles. On a établi la succession de formation des minéraux, la température optimale de cuisson du clinker.

On a montré l'influence qu'exerce le milieu réducteur et l'introduction d'additions dans le mélange cru sur la pureté du produit obtenu et la composition du ciment.

SUMMARY : The CaO-Al_2O_3 system has been studied by many investigators and the composition of the compounds in this system is well known at present. However, analysis of industrial clinker phase compositions reveals that chemical and phase balance is difficult to achieve in rotary furnaces, and the composition of calcium aluminates in clinker differs from the estimated one.

To clairify this point the authors have studied the process of mineral formation during sintering of clinker under laboratory, semi-industrial and industrial conditions. The sequence of formation of minerals and the optimum temperature of clinker sintering have been established.

The influence of the reducing medium and additives to the raw mix on the purity of the target product and cement composition has been shown.

L'ordre de formation des minéraux lors du chauffage du mélange de CaO avec Al_2O_3 fut étudié par beaucoup de chercheurs (1-7) mais jusqu'à présent ils ne sont pas unanimes en ce qui concerne ce problème.

D'après les données du travail (3), lors de la cuisson du mélange cru de 12CaO et $7Al_2O_3$ jusqu'à 1400 °C il se forme le monoaluminate de calcium $CaO \cdot Al_2O_3$ (CA) et seulement à 1450 °C s'achève la fixation complète de la chaux avec la formation de $12CaO \cdot 7Al_2O_3$ ($C_{12}A_7$).

Les calculs thermodynamiques de V. Babouchkine, G. Matvéev, O. Mtchedlov-Pétrossian (2) montrèrent que la composition du minéral primaire varie pour différent rapport entre CaO et Al_2O_3 dans le mélange. Pour la valeur du rapport égale à 1:1, c'est la formation de CA qui est la plus probable, et pour le rapport 1:2, celle de CA_2.

Les auteurs (4, 5) estiment que CA est le produit primaire de la cuisson. T. Robson (6) indique que lors de la cuisson du mélange CaO - Al_2O_3 il y a toujours $C_{12}A_7$, car ce composé se caractérise par une vitesse élevée de croissance des cristaux.

En confirmant cette opinion Scholze et Kumm (7) établirent que 1 % de CaO, Al_2O_3, K_2O, Fe_2O_3 diminue cette vitesse au différent degré, mais dans les conditions relativement identiques la vitesse de croissance des cristaux de $C_{12}A_7$ est supérieure à celle de tout autre aluminate de calcium.

Y. Boutt et V. Timachev (1) estiment que la succession de formation des aluminates de calcium dans la série CA-$C_{12}A_7$-C_3A se conserve lors de la cuisson des mélanges de composition $CaO:Al_2O_3$ = 12:7 ; 1:1 et 3:1. Pour l'excès de l'alumine la synthèse a lieu dans le sens de CA-CA_2-CA_6.

En analysant toutes ces données on peut aboutir à la conclusion qu'il est très difficile d'obtenir l'équilibre chimique dans les conditions du four rotatif et qu'après la cuisson le clinker contiendra des aluminates de calcium qui diffèrent par leur composition des aluminates prévus. La différence entre les compositions en phases théorique et réelle sera plus importante en présence dans la matière crue d'additions : SiO_2, Fe_2O_3, Mn_2O_3, MgO, etc. Leur influence sur les propriétés du ciment est bien connue : SiO_2 fixe Al_2O_3 et CaO en gehlenite, matériau hydrauliquement inerte. Fe_2O_3 forme l'alumoferrite de calcium - le constituant à durcissement lent. MgO dans la composition de la spinelle $MgO \cdot Al_2O_3$ diminue également la résistance du ciment.

Quelques travaux montrent que la silice et les oxydes de fer entrent en petites quantités dans la solution solide d'aluminates de calcium et seulement en présence d'une grande quantité de SiO_2 et Fe_2O_3, ils forment de nouvelles phases dans la composition du clinker de ciment alumineux à teneur d'alumine élevée.

T. Robson se réfère dans son travail (8) à Dayal et Glaser qui affirment que la concentration limite de Fe^{3+} capable de remplacer Al^{3+} dans le réseau de CA est de 4,5 %. Dans ce cas l'hydratation de CA contenant Fe^{3+} est plus rapide que celle du monoaluminate de calcium pur. Les auteurs montrent que CA_2 peut aussi contenir dans la solution solide jusqu'à 5,7 % de Fe et son hydratation s'accélère. Les ions fer peuvent également pénétrer dans le réseau de $C_{12}A_7$.

K. Soudzouki (9) estime que Si et Fe ou Si + Fe pénètrent dans le réseau de CA et modifient ses paramètres, ce qui fait varier l'activité hydraulique de CA.

Le milieu gazeux exerce également une grande influence sur la composition en phases du clinker de ciment alumineux à teneur d'alumine élevée lors de sa cuisson. Dans la référence (10) on suppose que l'oxygène est nécessaire pour la formation du composé $C_{12}O_7$. Dans les conditions réductrices de la cuisson le composé C_5A_3 est stable.

Nos recherches ont pour but d'étudier le processus de formation des minéraux lors de la cuisson des mélanges crus de $CaCO_3$ et $Al(OH)_3$ chimiquement purs, calculés pour la formation de CA et CA_2.

Sur la base des examens aux rayons X, la succession de formation des minéraux, lors du chauffage du mélange de composition $CaO:Al_2O_3$ = 1:2, peut être représentée comme suit :

$$CaCO_3 \xrightarrow{600 \text{ à } 900°C} CaO + CO_2$$

$$CaO + Al_2O_3 \xrightarrow{600 \text{ à } 800°C} CaO \cdot Al_2O_3$$

$$CaO \cdot Al_2O_3 + 11CaO + 6Al_2O_3 \xrightarrow{800°C} 12CaO \cdot 7Al_2O_3$$

$$12CaO + 7Al_2O_3 \xrightarrow{800 \text{ à } 1000°C} 12CaO \cdot 7Al_2O_3$$

$$CaO \cdot Al_2O_3 + Al_2O_3 \xrightarrow{800 \text{ à } 1200°C} CaO \cdot 2Al_2O_3$$

$$12CaO \cdot 7Al_2O_3 + 5Al_2O_3 \xrightarrow{800 \text{ à } 1200°C} 12(CaO \cdot Al_2O_3)$$

$$CaO \cdot Al_2O_3 + Al_2O_3 \xrightarrow{1200 \text{ à } 1400°C} CaO \cdot 2Al_2O_3$$

La décomposition du constituant calcique avec séparation de CaO conditionne son interaction avec Al_2O_3 du mélange cru avec formation de CA et $C_{12}A_7$. L'apparition de l'aluminate $C_{12}A_7$ à côté de CA est une conséquence de la dissociation rapide de $CaCO_3$ dans l'intervalle de 600 à 800 °C avec formation dans le système CaO - Al_2O_3 d'une grande quantité de CaO_{libre}.

Comme la mobilité des ions Ca^{2+} est beaucoup plus grande que celle des ions Al^{3+}, la couche de diffusion des nouvelles formations à la surface limite des phases so-

lides est enrichie en Ca^{2+}. Lorsque la température croît jusqu'à 1200 °C l'activité de Al^{3+} augmente, ce qui contribue à l'accélération de l'interaction de l'alumine avec CaO. Par suite la quantité d'aluminates de calcium dans les agglomérés augmente brusquement, la quantité de $C_{12}A_7$ diminue et CA_2 fait son apparition. $C_{12}A_7$ la température de 1200 °C, lorsque la partie considérable de CaO est fixée en CA, la formation ultérieure du minéral CA_2 a lieu grâce à la réaction d'interaction de CA avec Al_2O_3. $C_{12}A_7$ avec Al_2O_3 forme CA qui forme aussi CA_2 au cours de la réaction avec Al_2O_3.

L'étude microscopique des échantillons cuits montre que sur les grains d'alumine apparaît d'abord une petite couche des produits d'interaction de Al_2O_3 avec CaO et l'épaisseur de cette couche augmente progressivement (fig. 1). Au centre du grain se trouve l'alumine non réagie et aux bords, une frange de nouvelles formations. Avec l'élévation de la température de cuisson, le coefficient moyen de réfraction de la lumière des grains fins des nouvelles formations varie de 1,609 ± 0,002 (à 800°C) jusqu'à 1,650 ± 0,002 (à 1200 °C). Même les échantillons cuits à 1400 °C contiennent, à côté de gros cristaux de CA_2 et CA, des grains d'alumine ayant sur sa surface une frange de nouvelles formations.

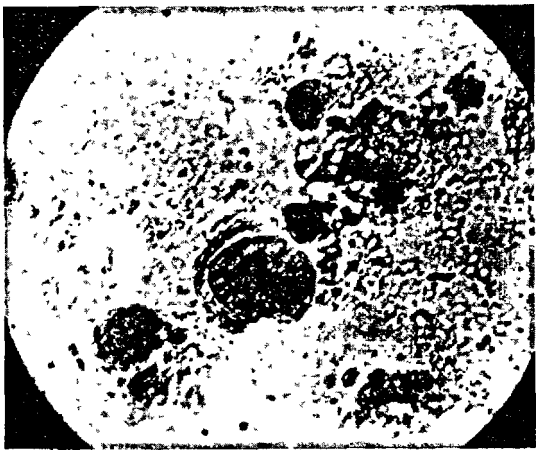

Fig. 1 - Produits d'interaction de l'alumine avec la chaux. Lumière passante, avec l'analyseur, X 600.

Les données obtenues témoignent du processus non équilibré de cristallisation des phases. Après la cuisson à 1400 °C les mélanges calculés pour l'élaboration de CA_2 contiennent réellement, à côté de CA_2 et CA, de l'alumine libre.

Les recherches ultérieures furent menées sur les mélanges avec $CaO:Al_2O_3$ = 1:1. On procédait à la cuisson des échantillons sous forme de granules jusqu'à leur agglomération à 1400 °C. Par examen aux rayons X on a établi qu'il se forme dans le clinker $C_{12}A_7$, CA et il y a Al_2O_3 libre.

On a également établi que le processus de formation des minéraux dépend de la durée et de la température de cuisson. Lorsque le temps de séjour du mélange dans la zone de la température élevée augmente de 10 à 60 minutes, le degré de transformation de CaO croît de 6,5 fois. A en juger d'après l'intensité des raies de diffraction de CA (d = 2,97 Å) et de CA_2 (d = 3,51 Å), à 1300 °C le clinker contient une quantité relativement plus grande de monoaluminate de calcium, à 1350 °C le clinker est représenté par une quantité presque égale de CA et de CA_2, et à 1400 °C la teneur de CA_2 dépasse la quantité de CA dans le clinker.

Notons que les clinkers obtenus par cuisson à la température de 1400 °C ne sont pas monophasés, tandis que les échantillons de CA, CA_2 produits par fusion à 1600 °C ne contenaient pas d'impuretés d'autres phases.

Pour étudier l'influence de Fe_2O_3 sur la composition en phases du clinker et les propriétés du ciment, on a préparé six mélanges à raison d'obtenir CA : le mélange I - sans additions ; les autres mélanges avec addition de Fe_2O_3 en quantité de 0,05; 0,11 ; 1,0 ; 2 et 3 % de la masse du mélange.

Les expériences montrèrent que la température de cuisson des clinkers, avec addition de Fe_2O_3 dans le mélange cru, diminue de 30-70 °C et d'autant plus que la teneur du mélange en Fe_2O_3 est plus élevée.

Les examens aux rayons X permirent d'établir que pour la teneur du mélange en Fe_2O_3 jusqu'à 2 %, la composition en phases du clinker est représentée par le monoaluminate de calcium et une petite quantité de CA_2 et $C_{12}A_7$. Dans ce cas, avec l'augmentation de la quantité de Fe_2O_3 dans le mélange la quantité de CA_2 et de $C_{12}A_7$ diminue, tandis que la quantité de CA augmente (fig. 2). L'augmentation de Fe_2O_3 au-dessus de 2,40 % s'accompagne d'une apparition dans l'échantillon de l'alumoferrite de calcium.

L'étude microscopique des échantillons montre que la préparation de l'échantillon 1 se compose des cristaux sous forme de tables de différentes dimensions. Les indices de réfraction sont N_g = 1,665, N_p = = 1,643. L'addition de Fe_2O_3 dans le mélange cru contribue à la formation de cristaux plus grands. Leurs indice de réfraction augmente jusqu'à N_g = 1,667 à 1,669 et N_p = 1,650 à 1,667.

Les propriétés physico-mécaniques des ciments obtenus (tableau I) témoignent de l'influence favorable exercée par une petite quantité de Fe_2O_3 dans la composition de CA sur ses propriétés. La résistance mécaniques de la pierre de ciment de CA

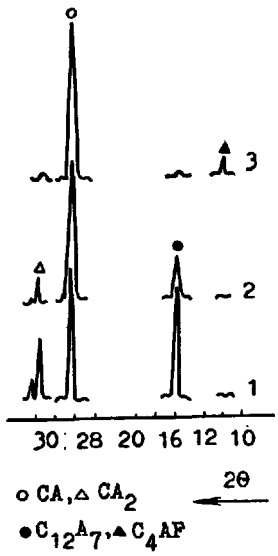

Fig. 2 - Radiogrammes de CA avec différentes additions de Fe_2O_3. 1 - sans addition ; 2, 3 - avec addition de Fe_2O_3 en quantité de 1,2 et 3,7 %.

se trouve en pleine conformité avec la composition en phases du clinker. L'augmentation de la quantité de CA dans le clinker entraîne celle de la résistance de la pierre de ciment. Lorsque la teneur du clinker en Fe_2O_3 se trouve dans les limites de 1,2 à 2,4 %, il se forme pratiquement le produit monophasé contenant seulement CA. La résistance de la pierre de ciment au cours de 24 heures de durcissement augmente respectivement. L'apparition dans la composition du clinker de l'alumoferrite de calcium conduit à une certaine diminution de la résistance du ciment durci.

Tableau I

Quantité de Fe_2O_3 dans le clinker	S, cm^2/g	Prise, heures minutes		Résistance à la compression, kgf/cm^2		
		début	fin	1 jour	3 jours	28 jours
0,006	2770	0-10	1-05	385	407	555
0,14	2880	0-50	1-45	465	582	735
0,60	2780	3-10	5-50	435	627	755
1,20	2780	3-50	6-20	510	640	680
2,40	2800	4-10	7-10	505	680	680
3,70	2800	4-40	7-30	475	623	675

On étudiait l'influence exercée par l'addition de SiO_2 et MgO au mélange cru sur les propriétés du ciment alumineux à teneur d'alumine élevée sur les mélanges calculés pour l'obtention de CA_2. L'échantillon obtenu par cuisson du mélange de matériaux chimiquement purs sans addition de SiO_2 et MgO, se caractérise par une grande quantité de CA à côté de CA_2 et α-Al_2O_3 (fig. 3).

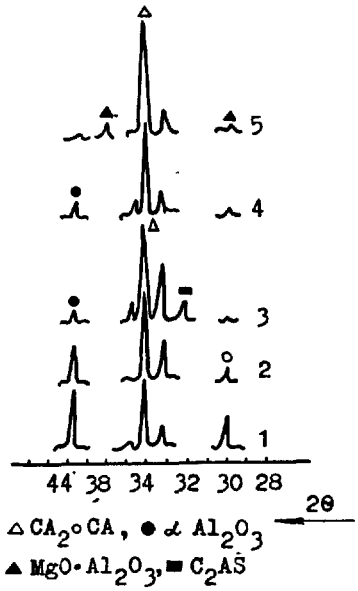

Fig. 3 - Radiogrammes de CA_2 avec additions de SiO_2 et de MgO. 1 - sans additions ; 2, 3 - avec addition de 2 et 4 % de SiO_2 ; 4, 5 - avec addition de 3 et 5 % de MgO.

D'après les calculs, l'échantillon dans lequel étaient introduits 2 % de SiO_2 doit contenir 8 % de gehlenite et l'échantillon contenant 1,5 % de MgO doit avoir dans sa composition 6,5 % de spinelle $MgO{\cdot}Al_2O_3$. Toutefois, sur les radiogrammes de ces échantillons les raies de diffraction avec les distances réticulaires caractéristiques de ces composés, n'étaient pas décelées. On a établi que les échantillons sont représentés principalement par CA_2 à côté duquel il y a α-Al_2O_3, CA mais en quantité plus petite que dans l'échantillon du clinker obtenu par cuisson du mélange cru sans additions. Il est également établi que l'introduction de SiO_2 et de MgO dans le mélange cru modifie la composition en phases du clinker et conditionne l'augmentation de l'activité hydraulique du ciment jusqu'à la limite déterminée. L'accroissement de la résistance du ciment durci s'observe lorsque la teneur du clinker en SiO_2 est jusqu'à 3 % et en MgO jusqu'à 4 %. L'augmentation ultérieure de ces oxydes s'accompagne d'une apparition dans le clinker de la gehlenite et de la spinelle et respectivement d'une diminution de la résistance de la pierre de ciment (fig. 3).

Les recherches ultérieures furent menées avec utilisation du mélange cru préparé à partir du calcaire et de l'alumine technique et contenant (%) : SiO_2 - 0,8 ; Al_2O_3 - 66,4 ; CaO - 18,5 ; Fe_2O_3 - 0,1 ; Mn_2O_3 - 0,05. On étudiait l'influence des additions

pour le mélange cru de minéralisateurs et de modificateurs ainsi que du caractère du milieu gazeux lors de la cuisson du clinker sur sa composition.

Les études de l'influence des additions de $CaSO_4$, CaF_2 et H_3BO_3 en quantité de 1 % de la masse du mélange montrèrent que le processus de clinkérisation s'accélérait en présence de ces additions. Le degré de transformation maximal de Al_2O_3 est observé lors de l'introduction dans le mélange cru de CaF_2.

L'action intensifiante des additions indiquées conduit à une fixation plus complète de Al_2O_3 avec formation de CA, et CA_2 lorsque la quantité de α -Al_2O_3 dans le clinker diminue ; il se forme alors une plus grande quantité de CA_2 par rapport à sa quantité dans le clinker sans additions de minéralisateur.

La variation du rapport $CA:CA_2$ dans le clinker influe respectivement sur la résistance du ciment durci. Dans les premiers délais de durcissement sa résistance (lorsqu'on utilise le clinker obtenu à partir du mélange sans additions) est supérieure à la résistance des autres clinkers et dans les délais avancés cède aux autres clinkers (fig. 4).

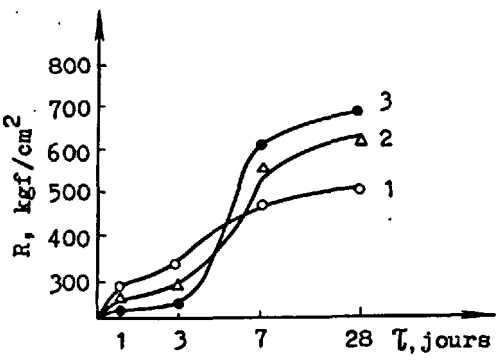

Fig. 4 - Résistance de la pierre de ciment en clinker obtenu par cuisson : 1 - sans additions ; 2 - avec addition de CaF_2 ; 3 - avec addition de H_3BO_3.

La cuisson du mélange cru avec et sans additions indiquées fut effectuée dans le milieu oxydant et réducteur.

Les expériences ont montré que lors de la cuisson dans le milieu réducteur l'introduction des additions dans le mélange cru contribue à la volatilité des oxydes Fe_2O_3 et SiO_2, alors que dans le milieu oxydant leur quantité reste pratiquement invariable.

Les spectres de la résonance paramagnétique électronique (RPE) obtenus à l'aide du radiospectromètre RE-1301 donnèrent les résultats suivants : lors de la cuisson dans l'atmosphère oxydante on observe une grande intensité de 6 raies de la structure hyperfine (SHF), ce qui est dû à la présence d'ions Mn. L'intensité des raies SHF reste pratiquement la même lors du changement du type de l'addition. En même temps, dans le spectre RPE on voit apparaître, avec additions de $CaSO_4$ et CaF_2, une ou deux raies-satellites. L'intensité des raies SHF dans le spectre des échantillons obtenues dans le milieu réducteur tombe brusquement. En comparant l'intensité des raies SHF de l'échantillon sans additions avec l'intensité des raies SHF des échantillons avec additions on peut faire la conclusion suivante : la plus grande influence sur les processus ayant lieu lors de la cuisson est exercée par CaF_2 dont la présence dans le milieu réducteur n'entraîne pas seulement la réduction des ions Fe^{3+} et Mn^{2+} jusqu'à oxyde ou métal mais aussi la sublimation des fluorures de ces éléments (et de SiO_2 dans une certaine mesure), ce qui s'accompagne d'une disparition presque complète des raies SHF. Ceci est confirmé également par l'analyse chimique (tableau II).

Tableau II

Teneur du clinker en oxydes étrangers

n°s des échantillons	Type de l'addition	Milieu oxydant		Milieu réducteur	
I	-	Fe_2O_3, %	SiO_2, %	Fe_2O_3, %	SiO_2, %
1	-	0,1	0,8	0,08	0,80
2	$CaSO_4$	0,1	0,78	0,03	0,72
3	CaF_2	0,11	0,76	0,02	0,70

Ainsi il fut établi que la composition en phases du clinker de ciment alumineux à teneur d'alumine élevée dépend de la température et du caractère du milieu gazeux de cuisson ainsi que de la présence d'impuretés et d'additions de modificateurs dans le mélange cru.

BIBLIOGRAPHIE

1.- Ю.М.БУТТ, В.В.ТИМАШЕВ (1967) Портландцементный клинкер, М., Стройиздат, (en russe).

2.- В.И.БАБУШКИН, Г.М.МАТВЕЕВ, О.П.МЧЕДЛОВ-ПЕТРОСЯН (1972) Термодинамика силикатов, М., Стройиздат, (en russe).

3.- М.Ф.ЧЕБУКОВ (1938) Глиноземистый цемент. Свердловск, ГОНТИ, (en russe).

4.- B. ADOUZE (1961), "Silikates Industr.", 26, n° 4, 179-190 (en français).

5.- W.L. DE KEYSER (1952), "Bull. Sos. Chem. Belge", 60, 516-541 (en français).

6.- T.D. ROBSON (1962), "High - alumina Cement", London (en anglais).

7. -H.SCHOLZE, K.KUMM (1966), "Tonindustrie Ztg", 90, № 12, 559 (en allemand).

8.- Т.Д.РОБСОН (1976) УІ Междун.конгресс по химии цемента, М., (en russe).

9.- К.СУДЗУКИ (1976) Влияние Fe и замещения на процесс образования и гидратацию кальциевого алюмината. УІ Международный конгресс по химии цемента. Т.3, М., Стройиздат, (en russe).

10.- Ю.П.УДАЛОВ, Т.Ю.ЧЕЛИКОВА, З.С.ВИНЕН (1976) К вопросу о характере диаграммы состояния системы $CaO-Al_2O_3$, УІ МКХЦ, М, (en russe).

Chemistry of arresting strength retrogression in structural high alumina cements

Les causes chimiques des baisses ou des limitations de résistance dans les structures en ciment alumineux

P. BHASKARA RAO and V.N. VISWANATHAN, Cement Research Institute of India, M-10, NDSE-II, New Delhi-110049, Inde.

SUMMARY: The conversion of metastable hydrates of high alumina cement has been accepted as a fact to reckon with. One possible method of preventing the formation of cubic C_3AH_6 and arresting strength retrogression would be by providing an alternative but safer path of reaction for hexagonal aluminate hydrates. Such a possibility can be realised through the reaction of these hexagonal hydrates with C-S-H gel leading to the formation of Strätlingite, which contributes to high compressive strength. The success of this method depends on the timing of availability of C-S-H gel for reaction with the metastable aluminate hydrates, before they are converted to C_3AH_6.

A comparative study of the hydration of CA in presence of (i) C-S-H gel and (ii) β-C_2S with varying degrees of fineness of CA has been made. The mineralogical composition and strength development of hydrating specimens were studied as a function of time. While gehlenite hydrate was the major hydration product in all the specimens, no C_3AH_6 could be found at any stage. There was no metastable hexagonal hydrate detectable beyond two weeks of hydration, showing thereby that gehlenite hydrate was readily formed and this precluded any possibility of conversion to C_3AH_6 even in future. Attack of CO_2 on paste specimens produced some $C_4A\bar{C}H_{12}$, while in the mortar specimens, practically free from CO_2 attack, the formation of $C_4A\bar{C}H_{12}$ was negligible. The rate of hydration of β-C_2S is probably enhanced in presence of CA. The mortar specimens showed satisfactory strength development with only gehlenite hydrate as the major hydrated phase.

RESUME: La conversion des hydrates métastables du ciment alumineux a été acceptée comme un fait dont il faut tenir compte. Une méthode éventuelle d' empêcher la formation de C_3AH_6 cubique et d' arrêter la rétrogradation de la résistance serait de prévoir une autre voie, mais plus sûre, de réaction pour les hydrates hexagonaux des aluminates. Une telle possibilité peut être réalisée par la réaction de ces hydrates hexagonaux avec le gel C-S-H menant à la formation de la Strätlingite, ce qui contribue à une haute résistance à la compression. Le succès de cette méthode dépend du moment où le gel C-S-H est disponible pour la réaction avec les hydrates métastables des aluminates avant qu'ils ne soient convertis en C_3AH_6.

Une étude comparée de l'hydratation du CA à divers degrés de finesse et en présence du (i) gel C-S-H et (ii) β-C_2S a été effectuée. La composition minéralogique ainsi que le développement de résistance des échantillons hydratants ont fait l'objet d'une étude en fonction du temps. Alors que l'hydrate de la gehlénite était le produit d'hydratation principal dans tous les échantillons, on n'a pas pu trouver du C_3AH_6 à n'importe quelle étape. Il n'y avait pas d'hydrate hexagonal métastable, qui était décelable au delà de deux semaines d'hydratation, démontrant ainsi que l'hydrate de la gehlénite se formait facilement, et ceci excluait toute possibilité de conversion en C_3AH_6 même à l' avenir. L'attaque du CO_2 sur les échantillons de pâte a produit du $C_4A\bar{C}H_{12}$, alors que dans le cas des échantillons de mortier, qui sont pratiquement exempts de l'attaque du CO_2, la formation du $C_4A\bar{C}H_{12}$ était négligeable. Le taux d'hydratation du β-C_2S est probablement augmenté en présence du CA. Les échantillons de mortier ont révelé un développment satisfaisant de la résistance avec seulment l'hydrate de la gehlénite comme phase importante d'hydrate.

INTRODUCTION

The conversion of high-alumina cement consisting of the transformation of hexagonal aluminate hydrates to the cubic C_3AH_6, has been accepted as a fact to reckon with (1). In spite of several precautions recommended, including the use of low water/cement ratio, service temperature and humidity, it is being increasingly realised that the hexagonal hydrates CAH_{10} and C_2AH_8 can not be permanently stabilised by any of the known physical means (2,3) or through chemical additives (4,5). In this context alumina-belite cements (6) are claimed to be free from the phenomenon of conversion and strength retrogression, but very little is known as to how the formation of C_3AH_6 is prevented on hydration. On the other hand, a recent study on a closely similar system called Porsal cement containing the mineral assemblage, β-C_2S, CA, $C_{12}A_7$ and $C_4A_3\bar{S}$ has revealed the presence of some C_3AH_6 along with gehlenite hydrate and tetracalcium aluminate hydrates in the hydration products (7).

A chemical solution to the problem of formation of C_3AH_6 and moderating, if not arresting, the strength retrogression could be in providing an alternative but safer path for the reaction of the metastable hexagonal hydrates with C-S-H gel leading to the formation of C_2ASH_8 (gehlenite hydrate or Strätlingite), which also contributes to high compressive strength (8). Such a combination of stable hydration products rich in gehlenite hydrate is expected to be resistant to sulphate attack owing to a favourable (C+M)/(A+S) ratio even at the micro level (9). For example, in the case of conventional HAC this ratio is not favourable after conversion where gibbsite and C_3AH_6 phases exist separately at the micro level, although this ratio is unaffected by conversion at the macro level. The success of forming C_2ASH_8 as a major phase depends on the timing of the availability of C-S-H gel for reaction with the metastable aluminate hydrates, before the latter decay by conversion. Towards this end, a comparative study of the hydration of CA in presence of (i) C-S-H gel and (ii) β-C_2S with varying degrees of fineness of the CA component has been made.

EXPERIMENTAL

(i) Materials: Monocalcium aluminate (CA) was prepared by firing at 1400°C a stoichiometric mixture of calcium carbonate and alumina gel. Even after repeated firings the presence of CA_2 and $C_{12}A_7$ in small quantities could not be avoided and the material was used as such. The material was ground to pass through 150 micron sieve and separated into two fractions: (a) -150, +75 micron and (b) -75 micron sizes.

Dicalcium silicate was prepared by standard methods using 0.5% B_2O_3 to stabilise the β-form. The entire material was ground to pass through 75 micron sieve and used as such.

Calcium silicate hydrate (C-S-H) gel was prepared by the hydration of β-C_2S in a slurry form with a water/cement ratio of ten for five months, followed by filtration and vacuum drying at room temperature.

Dehydrated alumina: Chemically pure chromatographic grade alumina (E.Merck, Darmstadt) was used without further treatment.

(ii) Paste hydration studies: Using the coarse and fine fractions of CA respectively two pastes were prepared with a CA/C-S-H gel ratio of 1:2 and a water/solid ratio of four and maintained at 27 ± 2°C. They were denoted as coarse and fine (C and F) pastes.

(iii) Compressive strength: Two series of mortars comprising of the coarse and fine fractions of CA were made with the composition, CA: β-C_2S : Dehydrated alumina = 2:3:10. The water/(CA + β-C_2S) ratio was kept at 1.9. The mortars were cast into cylinders 1.25 cm X 1.25 cm, demoulded after 24 hours of storage in >90% RH atmosphere at room temperature. The cylinders were cured later in water at 27°C. Compressive strengths of cylinders were tested at various ages with the help of a one tonne testing machine provided with necessary arrangement for testing small specimens.

(iv) XRD studies: The pastes as well as mortars were examined for their mineral assemblage at various ages with the help of a Philips 1120 model x-ray diffractometer using Cu-K_α radiation and Ni filter.

(v) Thermal Analysis: TGA and DTA of hydrated pastes aged 11 weeks and cylinders aged 10 weeks were recorded on a Derivatograph (Hungarian Optical Works, Budapest) at 8°C/min.

RESULTS

The mineralogical composition of pastes and cylinder specimens at various ages excluding those minerals present in the starting materials are given in Tables I and II respectively. The typical powder x-ray diffractograms of the pastes at the age of 11 weeks and cylinders at 10 weeks respectively are presented in Fig.1. The mineralogical studies showed that the principal phase formed was always C_2ASH_8 only. No C_3AH_6 was observed in any of the samples.

The paste hydrated specimens showed, besides gehlenite hydrate, a carbonated form of calcium aluminate hydrate, $C_4A\bar{C}H_{12}$ due to the progressive carbonation, to some degree, of the samples inadequately protected against exposure to air. The

TABLE I

Age	Coarse Paste	Fine Paste
5d	C_2ASH_8(s) C_2AH_8(m) CAH_{10}(vw)	C_2ASH_8(s) C_2AH_8(s)
14d	C_2ASH_8(vs) C_2AH_8(w) CAH_{10}(vvw)	C_2ASH_8(vvs) $C_4A\bar{C}H_{12}$(w)
26d	C_2ASH_8(vs) $C_4A\bar{C}H_{12}$(vvw)	C_2ASH_8(vvs) $C_4A\bar{C}H_{12}$(vw)
42d	n.d.	C_2ASH_8(vvs) $C_4A\bar{C}H_{12}$(m)
52d	C_2ASH_8(vs) $C_4A\bar{C}H_{12}$(vw)	C_2ASH_8(vvs) $C_4A\bar{C}H_{12}$(m)
73d	C_2ASH_8(vvs) $C_4A\bar{C}H_{12}$(s)	C_2ASH_8(vvs) $C_4A\bar{C}H_{12}$(s)

vvs: very very strong, vs: very strong,
s: strong, m: medium, w: weak,
vw: very weak, vvw: very very weak

TABLE II

Age	Coarse cylinder	Fine cylinder
7d	C_2ASH_8(s) $C_4A\bar{C}H_{12}$(vw) C_2AH_8(vw)	C_2ASH_8(m) C_2AH_8(vw) $C_4A\bar{C}H_{12}$(vw)
63d	C_2ASH_8(vvs) $C_4A\bar{C}H_{12}$(traces)	C_2ASH_8(vvs) $C_4A\bar{C}H_{12}$(traces)
71d	C_2ASH_8(vvs) $C_4A\bar{C}H_{12}$(traces)	C_2ASH_8(vvs) $C_4A\bar{C}H_{12}$(traces)

minor new phases observed in the pastes were C_2AH_8 and CAH_{10}, which did not persist beyond two weeks. Of the two, C_2AH_8 was more prominent, while CAH_{10} was observed in only one sample in trace quantities.

In the case of cylinders, C_2AH_8 was observed in small amounts only up to seven days and no CAH_{10} was detected at any stage. Carbonation from atmosphere was extremely low, as can be expected in set mortars, and the only carbonated form of aluminate hydrate, $C_4A\bar{C}H_{12}$, was observed only in traces.

The differential thermograms of pastes and cylinder samples, after 11 and 10 weeks of ageing respectively, are presented in Fig.2. The thermograms of both the pastes showed only two major endothermic peaks at

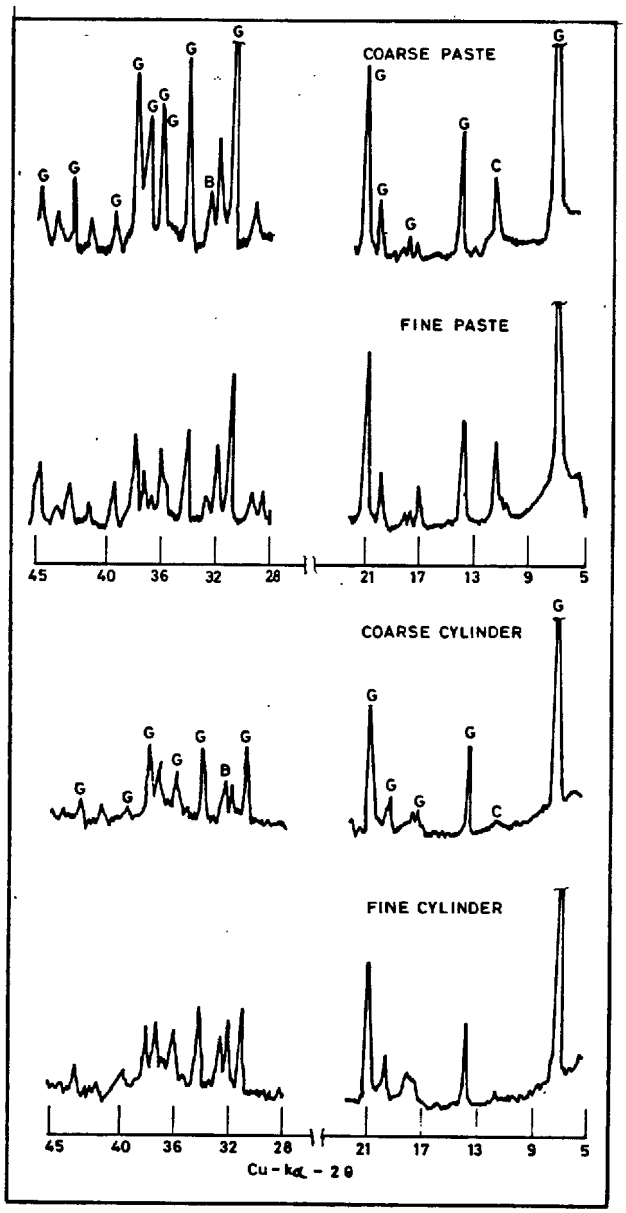

Fig.1 x-ray diffractograms of pastes (11 weeks) and cylinders (10 weeks)
G = C_2ASH_8, B = β-C_2S, C = $C_4A\bar{C}H_{12}$

160°C and 300°C respectively, due to $C_4A\bar{C}H_{12}$. No endothermic peak attributable to C_2ASH_8 (low intensity peak reported at 230°C (10)) was separately visible, perhaps masked by the broad 160°C endothermic peak of the carboaluminate. The thermograms of cylinders showed endothermic peaks at 100°, 150°, 250° and 310°C. The alumina used as aggregate for cylinders also had a small endothermic peak around 140°C due to adsorbed water. In view of this, the first two peaks may be considered as manifestations

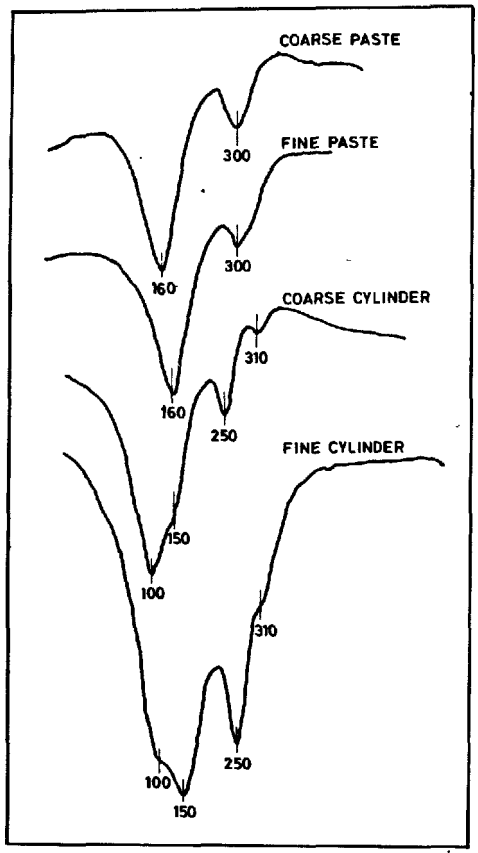

Fig.2 Differential thermograms of Pastes (11 weeks) and cylinders (10 weeks)

of adsorbed water held by alumina and any excess C-S-H gel and part of the combined water of C-S-H gel. The 250°C peak is believed to be due to gehlenite hydrate. However, the sharpness of the peak vis-a-vis broad peaks reported earlier for C_2ASH_8, and the inability to find a similar peak in the pastes where gehlenite hydrate is expected to be in higher concentration not diluted with aggregate, leave some uncertainty in this assignment. The low intensity endothermic peak at 310°C can not be explained at present.

The compressive strengths of cylinders are reported in Table III. The order of strengths of the specimens was markedly lower than those of HAC reported in literature, partly due to high initial water/solid ratio intentionally employed in order to observe whether C_2ASH_8 would be stable, unlike CAH_{10} known to be unstable even under moderately high water/solid ratios. The results of compressive strengths showed that the strength increased progressively with age indicating the continued availability of aluminate hydrate through CA hydration to react with C-S-H gel. The strengths of the fine specimens were always higher than those of the coarse specimens at equal ages.

DISCUSSION

Considering the mineralogical composition of all the specimens and that β-C_2S hydrates through topochemical mechanism in contrast to γ-C_2S which hydrates mostly by a "through solution" mechanism (11), the hydration reactions can be fitted into a generalised scheme, as follows:

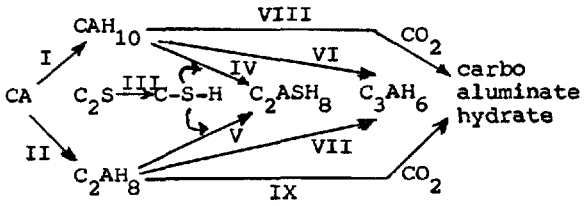

Reactions (I), (II), (III), (VI) and (VII) are well known in literature. Reaction (IV) was also recently reported (8) and the present results support the feasibility of reaction (V) proceeding with a reasonable rate. The effect of atmospheric CO_2 on CAH_{10} and C_2AH_8 is believed to be in the form of (VIII) and (IX), resulting essentially in low carbonate aluminate hydrates, unless CO_2 is deliberately made available in high concentration (3).

TABLE III

Age	Compressive strength, MN/m^2	
	Coarse cylinder	Fine cylinder
1d	0.4	1.0
7d	1.5	2.3
28d	2.6	4.1
56d	n.d.	4.8
85d	4.74	6.0

The absence of CAH_{10} in all the specimens, except in one in trace quantities, shows that the rate of consumption of CAH_{10} is by far greater than its rate of production. The marked absence of C_3AH_6 in all the specimens in spite of the high water/solid ratios, rules out reaction (VI) as the major consumer of CAH_{10}. The lower concentration of carboaluminate as compared to C_2ASH_8 even in the case of pastes leads to the conclusion that reaction (IV) is faster than (VIII). By similar arguments it can be seen that reaction (V) is faster than (IX) and reaction (VII) is very insignificant. The presence of C_2AH_8 in low concentration at least in the initial stages, as against the total absence of CAH_{10} shows that reaction (V) is relatively slower than reaction (IV).

Reaction (III) is of no consequence for pastes and will only determine the progress of reactions (IV) and (V) in cylinders. Even in the case of cylinders the absence of CAH_{10} together with the absence of C_3AH_6 and carboaluminate shows that C-S-H gel is always available in adequate quantity for reaction (IV). The low concentration of C_2AH_8 found is to be attributed to the relative slowness of reaction (V) as compared to (IV) rather than to the non-availability of C-S-H gel. Such a rapid generation of C-S-H gel from β-C_2S is probably because of its consumption by aluminate hydrates, thereby making available a fresh surface of C_2S grains for subsequent hydration. It may, hence, be said that the thickness of C-S-H layer around the C_2S grains is greatly reduced overcoming thereby the hindrance for diffusion of water. Further, the reactions (VI) and (VII) are comparatively slower than (VIII) and (IX) at the concentration of CO_2 available to the system through ordinary air.

The formation of C_3AH_6, being dependent on the availability of CAH_{10} or C_2AH_8, can not take place even in later ages because of the non-accumulation of these phases. Therefore, any strength drop owing to the conversion of hexagonal aluminate hydrates to C_3AH_6 neednot be apprehended because the hexagonal forms are readily fixed up as gehlenite hydrate.

The proportions of β-C_2S and CA in cylinders are adopted from those known in alumina-belite cements and are not necessarily stoichiometric to form gehlenite hydrate. The silicate portion is rather high and, therefore, some C-S-H gel is left unreacted even at long ages. The unreacted C-S-H is indicated by the 150°C peak in thermograms of cylinder samples.

The presence of some C_2AH_8 in the coarse paste and its total absence in fine pastes at 14 days shows the effect of fineness probably because the coarse grains provide the centres for local accumulation of the metastable hydrates. The mineralogy of cylinder specimens is unaffected by the fineness of CA, within the range used in the investigation. However, too coarse a fraction of CA is likely to result in local accumulation of hexagonal hydrates, which may eventually be converted to C_3AH_6 and be unavailable for gehlenite hydrate formation. The compressive strength of fine cylinders is markedly higher than the coarse cylinders at least up to 12 weeks which is self-explanatory.

CONCLUSIONS

The hydration of CA and β-C_2S together gave mainly C_2ASH_8. Higher calcium aluminate hydrates were found as carboaluminates in paste specimens only when there was some access to CO_2. The formation of C_3AH_6 was found to be altogether prevented by the reaction of the metastable hexagonal aluminate hydrates with C-S-H gel and formation of gehlenite hydrate. The progressive formation of C_2ASH_8 resulted in a continuous rise in strength. The ultimate phases formed in set mortars, namely, gehlenite hydrate and some C-S-H gel are stable unless exposed to excess $Ca(OH)_2$ (12), which is an abnormal condition in practice and should be least expected in this system.

Hence, the success of the technology of arresting drop in strength will depend on optimising the properties and fineness of aluminates and β-C_2S such that there is no accumulation of hexagonal aluminate hydrates. The fineness of both components can be increased to improve upon the early strength with the same limitations again that the hydration of CA should not be too fast as to lead to the accumulation of metastable aluminate hydrates. On the other hand a minimum fineness of CA is also required to avoid any local accumulation of hexagonal aluminate hydrates. Further, the presence of small quantities of β-C_2S even after the consumption of hexagonal aluminate hydrates may be beneficial for long-term strength.

REFERENCES

1.- "High alumina cement concrete in buildings", BRE current paper 34/75, Dept. of the Environment, U.K. (1975).

2.- A.M. NEVILLE (1975), "High alumina cement concrete", Halsted press (John Wiley and Sons), New York, pp 16-86.

3.- J. TALABER (1976), "High alumina cements", Proc.VI Intnl. Congr. on Chem. of Cement, Vol. III, Moscow-Stroizdat, pp 124-133.

4.- T.D. ROBSON (1962), "High alumina cement and concretes", I Edition, John Wiley and Sons, New York.

5.- S. UEDA and R. KONDO (1969), Discussion in "Successful prevention of loss of strength in concrete made with HAC", P.K. MEHTA, Proc. V Intnl. Congr. on Chem. of Cement, Part II, Cement Association of Japan, Tokyo, pp 148-152.

6.- L.A. ZAKHAROV (1976), "Alumina-belite cement", Proc. VI Intnl. Congr. on Chem. of Cement, Vol. III, Moscow-Stroizdat, p 153.

7.- S.J. RAINA, V.N. VISWANATHAN and A.K. CHATTERJEE (1978), "Early hydration characteristics of Porsal cement", Zement Kalk Gips, 31, 10, 516-518.

8.- H.G. MIDGLEY and P. BHASKARA RAO (1978), "Formation of Strätlingite $2CaO.SiO_2.Al_2O_3.8H_2O$ in relation to the hydration of HAC", Cem. and Conc. Res., 8, 169-172.

9.- L.J. VICAT (1846), Referred to in F.M. LEA, "The chemistry of cement and concrete", II Edn., Edwin Arnold and Sons, London (1970), p 491.

10.- A. ARIIZUMI (1969), "Formation of hydrated gehlenite through the reaction of clay minerals and lime", Proc. V Intnl. Congr. on Chem. of Cement, Vol.II, Cement Association of Japan, Tokyo, pp 138-147.

11.- M.M. SYCHEV, V.I. KORNEEV, E.N. KAZANSKAYA and I.N. MEDVEDEVA (1973), "Interaction of the β- and γ- forms of calcium orthosilicate with water", J.Appl. Chem. U.S.S.R. (English translation), 46, 530-533.

12.- R. DRON (1976), "Experimental and theoretical study of the $CaO-Al_2O_3-SiO_2-H_2O$ system", Proc.VI Intnl. Congr. on Chem. of Cement, Vol. II, Moscow-Stroizdat, pp 208-213.

The Cement for Use at low Temperatures

Le ciment pour emploi aux températures basses

F. SKVARA RNDr, SCc., Joint Laboratory for Chemistry and Technology of Silicates Czechoslovak Academy of Sciences and Institute of Chemical Technology, Praha,
K. KOLAR, Dipl., Ing.
J. NOVOTNY Docent, Dr. Sc.
Z. ZADAK Dipl. Ing. SCc.,
Z. BAZANTOVA Dipl. Ing. arch., Faculty of Civil Engineering Czech Technical University, Praha, Tchécoslovaquie.

RESUME : Le clinker de ciment, d'une composition chimique usuelle, très fortement broyé, en l'absence de gypse, donne un liant, différent du ciment Portland. Ce liant possède la particularité de faire prise et de durcir, à des températures inférieures à 0°. On a vérifié, sur des éprouvettes de pâte de mortier et de béton, que ce ciment faisait prise et durcissait normalement, à des températures de -35°, en laboratoire, et de -20° sur chantier, lorsque ce clinker était additionné de lignosulfonates, de carbonates ou de bicarbonates alcalins et d'eau. Cette propriété, nouvelle dans la chimie et la technologie du ciment, a donné l'idée d'utiliser ce ciment, sans protection spéciale, pour les constructions à réaliser en hiver.

Le ciment sans gypse est un ensemble comprenant ce clinker, un plastifiant, un retardateur de prise et un accélérateur de durcissement. Les lignosulfonates peuvent être employés comme plastifiants. Les dérivés de la lignine peuvent être partiellement ou entièrement remplacés par le produit de la condensation des phénols sulfonatés et du formaldehyde, ou un sel de l'acide naphtaléno-sulfonique. Le carbonate ou le bicarbonate alcalin peuvent être remplacés par un hydroxyde alcalin. On comprend bien l'influence de chacun de ces composants du ciment sans gypse. L'addition de gypse à ce ciment, dans les mêmes proportions que pour le ciment portland, a un effet défavorable sur ses propriétés rhéologiques.

SUMMARY: Cement clinker of ordinary chemical composition, ground with a grinding aid, but without the presence of gypsum and processed with a low water-to-cement ratio, presents a hydraulic binder which differs from existing portland cements. This binder has the capability of setting and hardening at temperatures below $0^{\circ}C$. The setting and hardening of gypsum-free cement, where a clinker-lignin derivate-alkali carbonate or bicarbonate-H_2O system was predominantly used, was verified in the form of pastes, mortars and concretes under laboratory conditions up to temperatures of $-35^{\circ}C$ and in conditions of an open-air building site up to temperatures of $-20^{\circ}C$. This qualitatively new factor in the chemistry and technology of cement has led to the idea of using this binding agent for construction work without any protection against the weather.

Gypsum-free cement can be described as a clinker-plasticizing agent-set retarder - hardening acceleration agent - H_2O system. Lignosulfonate or sulfonated lignin can be used as plasticizing agents. The lignin derivate can be partially or entirely replaced by the condensation product of sulfonated phenlos with formaldehyde or the salt of naphtalene-sulfonic acid. Alkali carbonate or bicarbonate can be replaced by alkali hydroxide. The influence of individual components in the gypsum-free cement is comprehensive. Gypsum additives to this cement in concentrations normal for portland cement lead to a marked deterioration of rheological characteristics.

The use of ordinary portland cement /which is essentially a clinker-gypsum system/ at temperatures below 0°C is connected with a number of difficulties; at such temperatures it is impossible to achieve a high initial and final strength. The problem of concreting under low temperatures is at present solved on the basis of various methods, one of which is the use of quick-binding cements. These cements must have sufficiently high increments in strength, so that no damage is done by the frost.

A new impetus in the area of quick-binding high-strength cements has been provided by the work connected with the names of P.A.Rebinder and S.Brunauer in which gypsum-free have been studied. Lukyanova, Segalova and Rebinder /1,2/ have studied a clinker-calcium lignosulfonate - H_2O system and designed a calcium lignosulfonate - K_2CO_3 system to control the beginning of the setting of cement pastes. With this combination they were successful in substantially postponing the beginning of the setting process and a marked acceleration of hardening. Brunauer et al./3/ designed a clinker /with a specific surface of 600-900 m^2/kg/- residue of grinding aid - calcium lignosulfonate-K_2CO_3-H_2O system. Excellent results were obtained in pastes, mortars and concretes when this system was used; the achieved strength was higher by several times than those achieved with normal portland cements.

Research /4-6/ carried out in Czechoslovakia since the end of the sixties has led to the development of gypsum-free cements which are call modified quick-binding high-strength cements /MQHC/. By MQHC we have in mind the following system: clinker /with a specific surface of 200 - 3000 m^2/kg/ - a lignin derivate - alkali carbonate or bicarbonate-H_2O. MQHC differs from normal portland cement by a number of characteristics:

a/low porosity of hardened cement stone
b/excellent workability with low water content
c/high short- and long-term strength
d/possibility of substantial acceleration of hardening by small increments of surrounding temperature
e/increased resistance to corrosion.

A highly significant characteristic of MQHC is their capability of setting and hardening at temperatures below 0°C. This new factor in the chemistry and technology of cements is the subject of the present communication.

In the experiments described in this communication, MQHC was made from clinker normally produced at the Czechoslovak Cement Works at Hranice. The grinding of MQHC was done in the absence of gypsum and with grinding aid additives. The MQHC used had a specific surface /Blaine/ of 420, 600 m^2/kg /with a lignin derivate as a grinding aid/ and 900 m^2/kg /with ethylene glykol as a grinding aid/. The chemical composition of the clinker used is given in table I.

Table I.- Chemical Composition of Clinker /in %/

CaO	62,3
SiO_2	19,8
Al_2O_3	6,9
Fe_2O_3	3,8
MgO	3,0
SO_3	0,1
annealing loss	1,6

The produced MQHC were processed into pastes w=0.25, mortars w=0.30 and concretes w=0.33 to 0.35, by using normal technological facilities. For regulating the beginning of the setting process, a sodium lignosulfonate - $NaHCO_3$ system was used, while in the case of the mortars and concretes a further setting regulator was added - sodium potassium tartrate. After the cement pastes were mixed /at temperatures between +10 to +15°C/ they were placed in a nonset state into an environment where temperatures were maintained at constant levels within the range of +20 to -35°C. The strength of the pastes /bodies sized 2.2.2 cm/ was determined after the bodies had been cured for 30 minutes at temperatures of +20°C after taking them out of the air-conditioned area. The results achieved in compression strength are summed up in tables II and III.

Table II.-Compression Strength /MPa/ of Pastes w=0.25, MQHC 420 m^2/kg

days	curing temperature /°C/ +20	+1	-8	-22
1	20	7	3	2
3	50	23	15	5
7	80	42	28	7
28	100	50	40	10

Table III.-Compression Strength /MPa/ of Pastes w=0.25, MQHC 600 m^2/kg

days	curing temperature /°C/ +20	+3	-8	-20	-35
1	60	30	26	7	6
3	100	48	44	12	7
7	110	68	62	16	9
28	118	72	65	23	12
90	120	84	80	32	15
180	122	86	81	33	19

Mortars /with MQHC:sand 1:3/ were made of MQHC and sand at the temperature of +15°C, the water used had a temperature of +3°C.

After the mortar has been mixed, moulds with the samples were placed for 15 minutes into an area with constant temperatures between +20 to -35°C. The moulded bodies /4.4.16 cm/ were left at temperatures of +20°C for 60 minutes before their compression strength was determined. Table IV sums up the achieved compression strengths.

Table IV.-Compression Strength /MPa/ of Mortars w=0.30, MQHC 600 m^2/kg

days	curing temperature /°C/ +20	-8	-20	-35
1	48	5	4	3
3	71	10	7	4
7	82	20	10	7
28	100	36	16	8
90	102	42 *49	26 *38	9
180	110	53 *59	28 *42	10
360	112	- *64	- *60	-

* samples were stored at +20°C after the 28th day.

For the making of concrete /with an MQHC: sand:aggregate 1:3:3, w=0.33/, aggregates at temperatures between +3 and +5°C were used. After preparing the concrete mixture the moulds were immediately transported to an open-air site. The course of temperatures was read from a registration thermometer.The moulded bodies, sized 15.15.15 cm, were tempered at temperatures of +20°C before their compression strength was tested. The results achieved are summed up in table V.

Table V.-Compression Strength /MPa/ of Concrete /1:3:3/ w=0.33,MQHC 600 m^2/kg

days	compression strength	curing temperature /°C/
1	12,1	-8 to -11
3	19,6	-5 to -18
7	43,2	-6 to -19
28	52,1	from the 8th day -6 to +5

Control Experiments at Curing Temperatures of +15°C

days	compression strength
1	35,0
3	69,2
7	78,6
28	79,2

The results achieved indicate, that MQHC processed in the form of pastes, mortars and concretes are capable of setting and hardening at temperatures well below 0°C. This capability is the result of the higher values of hydration heat at the beginning of the hydration process and the higher reactivity of the MQHC components as a consequence of their higher specific surface. The capability of setting and hardening at low temperatures is also caused by the presence of additives which by their cryoscopic effect lower the temperature at which water freezes. The high strength achieved in MQHC in comparison to portland cements are also caused by the possibility of processing the MQHC with a low water content.

Our findings confirm previous data /12/ on the hydration capability of clinker materials at temperatures below 0°C. In the hydration of clinker minerals at low temperatures, anomalous behaviour of water in the porous structure occurs /7/. In such structures water can exist in the form of "modified water", in a liquid state well below 0°C. Such water is then probably capable of a hydration process with clinker minerals even at low temperatures.

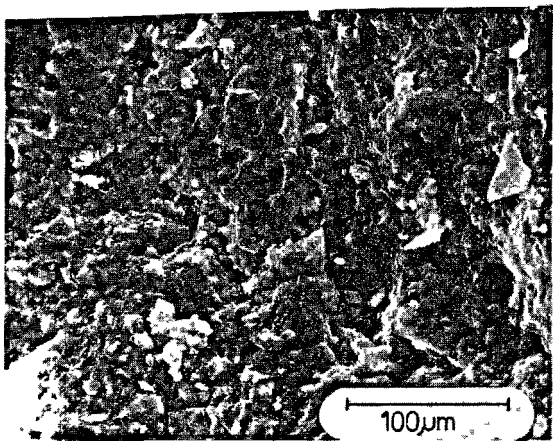

Fig.1 - Fracture surface,paste w=0.25, 360 days, curing at +20°C

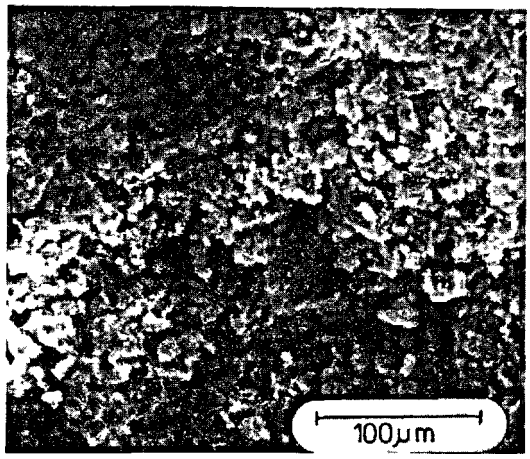

Fig.2 - Fracture surface,paste w=0.25, 360 days, curing at -35°C

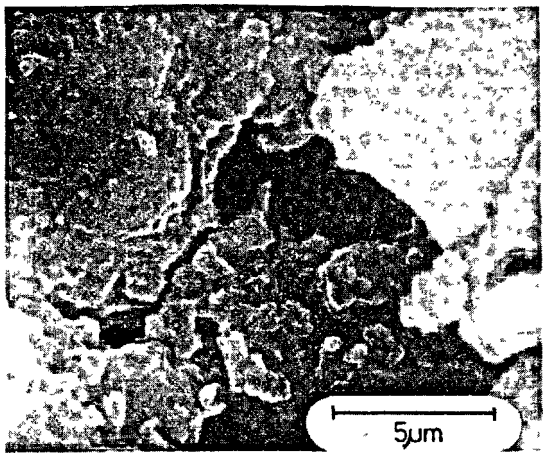

Fig.3 - Detail from fig.2.

Also the structure of hardened cement pastes which have been cured at temperatures in the range of +20 and -35°C were studied. Figure 1. shows the structure of the fracture surface of MQHC pastes /with 600 m^2/kg/, cured at the temperature of +20°C for a period of 1 year, while figures 2. and 3. show the same paste cured without interruption for a 1 year at the temperatures of -35°C /the compression strength achieved was 28 MPa/. On the basis of these microphotographs it is possible to conclude that hydrosilicates and $Ca(OH)_2$ are practically indistinguishable, and also a high degree of compactness. The high number of interfaces indicates the high mechanical strength of hardened MQHC. The influence of lower temperatures during MQHC hardening is apparent by the higher level of development of the crystalline structure /figures 1,2,3/.
The capability of MQHC to set and harden at low temperatures represents a new factor, which makes MQHC qualitatively different from existing portland cements. It should be stressed that the clinkers from which the MQHC were made have the same chemical composition as the clinkers from which normal Czechoslovak portland cements are made. For this reason MQHC represent a higher quality of utilization of clinker, which has a high energy input, than is the case in normal portland cements.

In our experiments we also studied the possibility of a modified use of the clinker - sodium lignosulfonate - alkali carbonate - H_2O system. Our study of pastes /w=0.25/, which set at temperatures between +20 and -30°C, indicates that lignosulfonate can be replaced, for instance by sulfonated lignin. Lignin derivates can partially or completely be replaced by other plasticizing agents, for instance by the condensation product of sulfonated phenols and formaldehyde, the salt of naphtalene sulfonic acid. Alkali carbonates and/or bicarbonate can be replaced by hydroxide. The presence of hydroxide is then manifest by shortening of the beginning of setting.

On the basis of our existing knowledge concerning gypsum-free cements we are able to define them in general terms as a clinker - plasticizing agent - set retarder - hardening acceleration agent - H_2O system. This system includes water because some components must be dissolved in water. The action of individual components within the system is comprehensive. The presence of alkali carbonate in connection with lignin derivate /and probably also in the case of a different plasticizing agent/ causes an improvement of the plasticizing qualities of the lignin derivate, because it prevents the forming of its insoluble calcium salt.

The component which postpones the beginning of the setting process /and makes it possible to process these systems in real time as pastes, mortars and concretes/ are substances based on lignin or carbohydrates which accompany them, or hydroxy-acids, sulfonated phenols and others. Probably also alkali carbonate participates in the process of slowing down setting, as a consequence of carboaluminates. The component which accelerates the hardening process is alkali carbonate and/or bicarbonate or hydroxide. The presence of lignosulfonate in the majority of cases leads to higher increments in strength then when other plasticizing agents are used. The addition of lignosulfonate to a different plasticizing agent is connected with a shortening of the beginning of setting /cf - Table VI./

Table VI.- The Beginning of Setting of Pastes w=0.25 /specific surface of clinker 900 m^2/kg/, +20°C

system	time
clinker+1,8% NaLig+1,2 %Na_2CO_3+0,7% T+ H_2O	2.5 hours
clinker+1,0% NS+ 1,2% Na_2CO_3+ 0,7% T+H_2O	2.5 hours
clinker+1,0% NS+ 0,3% NaLig+ 1,2% Na_2CO_3+ 0,7% T+H_2O	2 hours
clinker+0,8% SF+ 1,2% Na_2CO_3+ H_2O	10 hours
clinker+0,8% SF+ 0,3% NaLig + 1,2% Na_2CO_3+ H_2O	2 hours

Note: NaLig - sodium lignosulfonate
T - sodium potassium tartrate
NS - sodium salt of naphtalene-sulfonic acid
SF - condensation product of sulfonated phenols and formaldehyde

The presence of lignosulfonate seems to influence reactivity of C_3A, when the hydration process is accelerated. The absorption of lignosulfonate on the surface of C_3A, on the other hand, causes a slowing down of the hydration process and the resulting effect is determined by the sum of both precesses /2,8/. Increasing the lignosulfonate to a specific limit means a loss of initial and final strengths. A loss of strength is determined by the irreversible absorption of lignosulfonate in C_3S which blocks further hydration /9,10/.

The presence of sulphates in the studied systems is undesirable after a certain limit. Their presence from the burning process /after a certain limit of SO_3 has been surpassed/, as well as a gypsum additive, causes undesirable changes in volume which can in the long-term even lead to destructions. The negative influence of gypsum in the clinker-lignosulfonate - carbonate - H_2O system during setting with a low water content is apparent made by sulfoaluminates being formed and transformed only after the solid and compact structure of the hydrosilicates has de-

veloped. And this also causes undesirable changes in volume. A gypsum additive to the clinker - lignosulfonate - carbonate - H_2O system in concentrations usual for portland cement also causes an increase in cement paste viscosity, and as a consequence of the forming of an insoluble form of calcium lignosulfonate, a strong decrease in the workability of mortars with a low water coefficient occurs.

Another characteristic of the hydration of gypsum-free cements, so far determined in the clinker-derivate of lignin-alkali carbonate /hydroxide/ - H_2O system, is the limited formation of $Ca(OH)_2$ in initial stage of hydration. This fact follows from the structure of hardened pastes where it is impossible to distinguish between hydrosilicates and $Ca(OH)_2$, and also from the data determined by X-ray diffraction /as also found by Odler, Schönfeld and Dörr/11//.

CONCLUSIONS

Finely ground clinkers of a normal chemical composition processed with a low water-to-cement ratio and in the presence of additives other than gypsum, produce a hydraulic binder which is capable of setting and hardening at temperatures well below 0°C. This qualitatively new factor in the chemistry and technology of mortars has led to the idea of using this binder for construction work in winter conditions.

Our future work will concentrate upon the technology of concreting with these cements under normal and low temperatures and upon a study of the reactions taking place in the hydration of gypsum-free cements.

ACKNOWLEDGEMENTS

The authors of this communication should like to thank the group of employees of building organisation "Pozemní stavby" at Karlovy Vary, who worked under the supervision of Mr.Vojtěch Janda, for their selfless fulfilling of all demanding tests, when during the winter of 1978-79 they were the first in Czechoslovakia to successfully carry out experimental construction work using MQHC without any protection against the weather, during a period when average day-time temperatures reached -8°C.

BIBLIOGRAPHY

1.- O.I.LUKYANOVA, E.E.SEGALOVA, P.A.REBINDER /1957/ "The influence of hydrophilic plasticizer additions on induction period of hydration of portland cement", Doklady Akad.Nauk SSSR 117, 1034-1036.

2.- O.I.LUKYANOVA, E.E.SEGALOVA, P.A.REBINDER /1957/ "The effect of hydrophilic plasticizer additions on the properties of concentrated cement suspensions", Koll.zhurnal XIX, No.1, 82-89.

3.- S.BRUNAUER, M.YUDENFREUND, J.SKALNÝ, I.ODLER /1973/ "Hardened portland cement pastes of low porosity VII.", Summary, Cem. Concr. Res. 3, 279-293.

4.- J.NOVOTNÝ, K.KOLÁŘ, F.ŠKVÁRA, Z.ZADÁK, Z.BAŽANTOVÁ /1979/ "Modified quick binding high-strengths cements", Stavivo /Czechoslovakia/,57, No.2, 44-49.

5.- Research report "High-strength cements, results from years 1967-1974", Faculty of Civil Engineering, Czech Technical University, Praha.

6.- K.KOLÁŘ, F.ŠKVÁRA, J.NOVOTNÝ, Z.ZADÁK, Z.BAŽANTOVÁ, Ger. Offen.No.2,813, 559.

7.- M.SMUTEK /1971/ "Anomalous water/review/ Chemické listy /Czechoslovakia/ 65, 374-396.

8.- E.S.SOLOVYEVA /1971/ "Structure-forming properties of tricalcium aluminate suspensions in the presence of large sulfite waste liquor /SWL/ additions", Koll. zhurnal, XXXIII, 440-444.

9.- P.SELIGMANN, N.R.GREENING /1968/"Studies of early hydration reactions of portland cement by X-ray diffraction", Highway Res.Report, No.62, 80-103.

10.- V.S.RAMACHANDRAN /1972/ "Interaction of calcium lignosulfonate with tricalcium silicate, hydrated tricalcium silicate, and calcium hydroxide", Cem.Concr.Res. 2, 179-194.

11.- I.ODLER, R.SCHÖNFELD, H.DÖRR /1978/"On the combined effect of water soluble lignosulfonates and carbonates on portland cement and clinker pastes II.", Cem.Concr.Res. 8, 525-538.

12.- L.G.SHPINOVA, N.V.BELOV, CH.S.SOBOL, M.A.SANICKIJ /1979/ "Peculiarity of hydration of portland cement at negative temperatures", Doklady Akad. Nauk SSSR 245, No.4, 892-895.

Hydratation du ciment alumineux en présence d'agrégat siliceux et calcaire

Hydration of aluminous cement in the presence of silicic and calcareous aggregate

L. CUSSINO, Recherche et développement, UNICEM S.p.A., Casale Monferrato,
A. NEGRO, Institut de chimie générale et appliquée, Politecnico de Turin, Italie.

RESUME : On sait que les bétons preparés avec du ciment alumineux subissent avec le temps une perte de résistance mécanique à la suite d'une réaction de conversion, pendant laquelle les aluminates de calcium hydrates métastables se transforment en composés plus stables.
Après que les Auteurs aient montrè la possibilité d'une réaction entre les aluminates hydratés et le carbonate de calcium, ils ont voulu étendre leur expérimentation aux ciments alumineux.
Dans ce but, ils ont effectué des essais jusqu'à 5 ans sur des mortiers et bétons en utilisant des agrégats siliceux et calcaires. Les essais mécaniques ont montré que l'agrégat calcaire atténue ou élimine la perte de résistance mécanique des bétons.
L'analyse aux rayons X et à l'ATD, a montré qu'il se produit une réaction entre l'agrégat calcaire et les produits d'hydratation du ciment : la formation de carboaluminate semble limiter la conversion des aluminates de calcium hexagonaux en aluminate cubique.
Les Auteurs attribuent à cette réaction le bon comportement mécanique, dans le temps, des bétons expérimentés.

SUMMARY : It is well known that concretes made with aluminous cement lose their mechanical strength over time following a conversion reaction during which metastable calcium hydrate aluminate are transformed into more stable compounds.
The Authors have shown previously that it is possible that hydrate aluminates react with calcium carbonate and experiments were therefore extended to aluminous cements.
For this purpose, tests were carried out on mortars and concretes using silicic and calcareous aggregates with up to 5-year lives.
Mechanical tests showed that calcareous aggregate attenuates or eliminates the loss of mechanical strenght in mixes.
X-ray and ATD studies showed a reaction between calcareous aggregate and the products of cement hydration : the formation of carboaluminate seems to limit the conversion of hexagonal calcium aluminates into cubic aluminate.
The good mechanical behaviour over time of the mixes experimented is held to be attributable to this reaction.

INTRODUCTION

Le béton préparé avec du ciment alumineux présente des résistances mécaniques remarquables après de courtes périodes de conservation, un caractère réfractaire, une résistance chimique aux sulfates et aux cycles de gel et de dégel. Mais, malheureusement, ce béton présente, dans le temps une diminution de résistances mécaniques et une augmentation de porosité laquelle le rend sensible même à l'aggression chimique. La réaction d'hydratation indiquée ci-après, exprimée sous forme non stoechiométrique, puisque les quantités des produits sont influencées par différents facteurs extérieurs, est la plus importante et se produit pendant les premiers stades de la prise du ciment :

$$CA + H_2O \rightarrow CAH_{10} + C_2AH_8 + AH \qquad [1]$$

Les produits de cette réaction sont métastables : le gel d'alumine se transforme en gypsite AH_3, tandis que le CAH_{10} et le C_2AH_8 se transforment en C_3AH_6 et AH_3 selon les réactions :

$$3CAH_{10} \rightarrow C_3AH_6 + 2AH_3 + 18H_2O \qquad [2]$$

$$3C_2AH_8 \rightarrow 2C_3AH_6 + AH_3 + 9H_2O \qquad [3]$$

Ces réactions sont très importantes car elles influencent les résistances mécaniques des bétons, donc, leur durabilité (1). Cependant, jusqu'à aujourd'hui, il n'y a pas encore eu d'accord sur le mécanisme suivant lequel la conversion des aluminates métastables (CAH_{10} et C_2AH_8) en aluminate stable (C_3AH_6) agirait à l'égard des résistances mécaniques (2).
Certains auteurs, pour limiter les inconvénients dus à la conversion, ont suggéré d'ajouter au béton frais des additifs tels que les tensioactifs, les polysaccharides, les alcools polyoxhydryliques, les sels inorganiques (3).
Selon Mehta (4) le $C_4A_3.SO_3$ empêche pratiquement la conversion des hydrates hexagonaux en hydrate cubique; Ueda et Kondo (5), au contraire, ont trouvé qu'à 50°C, en présence de ce sulfo-aluminate, la conversion se produit quand même et les résistances mécaniques diminuent avec la conservation.
Par contre d'après Collepardi et coll. (6), la conversion trouve un obstacle dans la présence du sulfo-aluminate, avec un effet d'autant plus marqué que la température est plus basse et que l'addition de $C_4A_3.SO_3$ est plus élevée.
Enfin, Ramachandran et Feldmann (2) ont étudié l'hydratation du CA à de faibles rapport eau/liant à 20°C et à 80°C.
Ils ont remarqué que les échantillons hydratés à 80°C présentaient un retrait considérable, contrairement aux échantillons hydratés à 20°C, et que leur résistance mécanique était la plus élevée.
Les méthodes exposées ci-dessus présentent des inconvénients : ou bien elles perdent en efficacité lorsque la température de conservation dépasse la température ambiante, ou bien elles sont difficiles ou chères à réaliser.
Dans un article récent (7) nou avons signalé qu'en hydratant le CA en présence de carbonate de calcium, la conversion des aluminates hydrates CAH_{10} et C_2AH_8 ne se produisait pas, ou bien elle était très limitée par la formation de $C_3A\ CaCO_3\ 11H_2O$.
Les résultats présentés concernent les essais effectués sur des mortiers et des bétons fabriqués avec du ciment alumineux fondu et avec un agrégat calcaire et siliceux.
Une première observation menée sur des échantillons vieillis jusqu'à 5 ans a offert une vue d'ensemble intéressante : les résistances mécaniques du mortier et du béton fabriqués avec un agrégat siliceux avaient subi une détérioration progressive et constante déjà après 28 jours, tandis que le béton avec un agrégat calcaire avait manifesté une amélioration constante de la résistance mécanique que l'on remarque encore à l'échéance de 5 ans.
Sur la base de ces résultats il nous a semblé utile de réaliser une seconde expérimentation dans laquelle, à tous les essais de résistance mécanique étaient associés des analyses chimico-physiques de façon à suivre l'évolution de l'hydratation.
Les résultats de ces observations, menées jusqu'à présent à la fin de deux années, sont indiqués ci-après dans leur expression la plus significative.

PARTIE EXPERIMENTALE

Pour la préparation des échantillons utilisés pour les essais de résistance à compression nous avons employé un ciment alumineux toujours de la même marque dans les deux expérimentations, mais représentés bien sûr par deux échantillons différents. L'analyse chimique des deux échantillons de ciment et celle des agrégats pour mortiers et bétons sont indiquées dans le Tableau I.

TABLEAU I

Oxides	Ciment		Agrégat		
			Siliceux		Calcaire
	N. 1	N. 2	Mortier	Béton	
SiO_2	3,32	2,65	86,60	73,60	0,70
Al_2O_3	39,58	40,50	5,08	6,94	0,18
Fe_2O_3	13,73	12,77	2,13	1,78	0,14
FeO	2,80	3,88	—	—	—
TiO_2	1,90	1,95	—	—	—
CaO	36,80	36,60	1,64	5,23	54,80
MgO	0,59	0,54	0,29	5,27	0,43
K_2O	0,05	0,05	1,27	1,19	0,02
Na_2O	0,04	0,05	1,26	1,55	0,05
SO_3	0,03	0,05	0,00	0,00	0,00
p.a.f.	0,31	0,60	0,85	3,59	42,85

Les alcalins contenus dans les agrégats ne présentent aucune caractéristique de solubilité ni dans l'eau ni dans une solution aqueuse de chaux.
Avec le ciment N. 1 nous avons réalisé les échantillons suivants.

A – Echantillons en mortier plastique type ISO, fabriqués avec du sable siliceux conformément aux Normes Italiennes.
B – Echantillons de béton avec agrégat calcaire : Ø max 25 mm.; courbe granulométrique continue; ciment : 350 Kg./m^3; E/C = 0,50; Slump 9 cm.; tassement par table vibrante; masse volumique au démoulage 2,44.
C – Echantillons de béton avec agrégat siliceux : caractéristiques du béton comme en B, excepté E/C = 0,54; masse volumique 2,44.

Avec le ciment N. 2 nous avons réalisé les échantillons suivants .

D – Echantillons en mortier plastique comme en A.
E – Echantillons en mortier plastique comme en A en utilisant du sable calcaire granulé fractionné dans les même granulométries prévues pour le sable normal.
D' – Echantillons en mortier plastique comme en D et, donc, avec du sable siliceux, mais en utilisant comme liant un mélange à 75/25 respectivement de ciment alumineux et poudre de calcaire broyé à environ 5.000 cm^2/g de surface Blaine.
D" – Echantillons en mortier plastique comme en D', en substituant dans le mélange du liant la poudre siliceuse broyée à environ 4.000 cm^2/g de surface Blaine.
F – Echantillons de béton avec agrégat calcaire concassé : Ø max 20 mm.; courbe granulométrique continue; ciment : 350 Kg/m^3; E/C = 0,60; Slump 8 cm.; tassement par table vibrante; masse volumique 2,41.
G – Echantillons de béton avec agrégat siliceux roulé : caractéristiques du béton comme pour F, excepté E/C = 0,54; Slump 10 cm.; masse volumique = 2,43.
H – Echantillons de béton avec agrégat siliceux comme pour G. Le liant, au lieu d'être seulement du ciment alumineux, se compose d'un mélange à 75/25 respectivement de ciment alumineux et poudre de calcaire à surface Blaine de 5.000 cm^2/g; liant 350 Kg/m^3; E/C = 0,51; Slump 12 cm.; masse volumique = 2,40.

Pour les échantillons A, B et C nous avons retenu les résultats jusqu'à la fin des cinq ans, pour les autres jusqu'à deux ans.
Les échantillons de mortier, après le démoulage, ont été conservés dans l'eau conformément aux Normes Italiennes; les échantillons de béton ont été conservés dans une chambre conditionnée à 20°C ± 1°C et une humidité relative non inférieure à 90%.
Avec les échantillons D' et H nous avons voulu vérifier si une addition au ciment de 25% de pierre calcaire finement broyée provoquait, avec les années, un effet positif sur les résistances mécaniques tant des mortiers que des bétons.
A chaque échéance à laquelle nous avons exécuté les essais mécaniques nous avons effectué l'analyse aux rayons X et l'ADT pour déterminer phases qui se formaient au cours de l'hydratation.

RESULTATS ET DISCUSSION

Le Tableau II presente les résultats des essais mécaniques à compression des mortiers et des bétons fabriqués avec le ciment alumineux.
Les résultats fournis par les échantillons A, B et C sont suffisament éloquents pour démontrer que tant le mortier que le béton avec agrégat siliceux après 28 jours de conservation révèlent une rétrogradation de résistance mécanique, montrant, à 5 ans, une perte de résistance respectivement de 60% et 50% environ.
Par contre, le béton avec l'agrégat calcaire a toujours révélé jusqu'à 5 ans des augmentations de résistance.
Les échantillons D fabriqués avec le ciment N. 2 ont révélé un processus de rétrogradation moins marqué que les échantillons A, en ayant toujours une valeur assez considérable (18,8%).
Le comportment des échantillons E a montré qu'en substituant au sable siliceux le sable calcaire d'une même granulométrie, ou réussit presque à éviter, au moins jusqu'à deux ans, la perte de résistance.

TABLEAU II

Age	Echantillons A	B	C	D	E	D'	D"	F	G	H	
1 j	748	621	519	675	489	581	567	538	526	446	Kg/cm^2
3 j	761	690	536								
7 j	852										
28 j	934	809	579	892	733	744	671	724	730	564	Kg/cm^2
90 j	877	856	508	898	753	848	703	799	681	574	Kg/cm^2
180 j	823	898	413	887	809	888	690	802	628	712	Kg/cm^2
1 an	740	941	302	835	819	882	590	850	552	704	Kg/cm^2
2 ans	609	1065	291	729	803	846	534	873	532	725	Kg/cm^2
5 ans	384	1102	285								

Les valeurs les plus basses de résistance à compression, en termes absolus, par rapport à celles de l'essai précédent découlent de la différence de la nature des sables.
Les résultats des essais sur les échantillons D' et D" mettent en évidence l'effet avantageux de la poudre de calcaire qui, jusqu'à 1 an, réussit à sauvegarder les résistances et à limiter la perte de résistance a 5%, à 2 ans de conservation.

Les échantillons D" révèlent au contraire une aggravation en pour-cent du processus de rétrogradation et donc le renforcement de l'effet négatif de la silice en poudre.
En effet, en comparant ces résultats avec ceux que nous avons obtenus pour les échantillons D, on remarque que la diminution du pourcentage de résistance passe da 18,8 à 24,1.

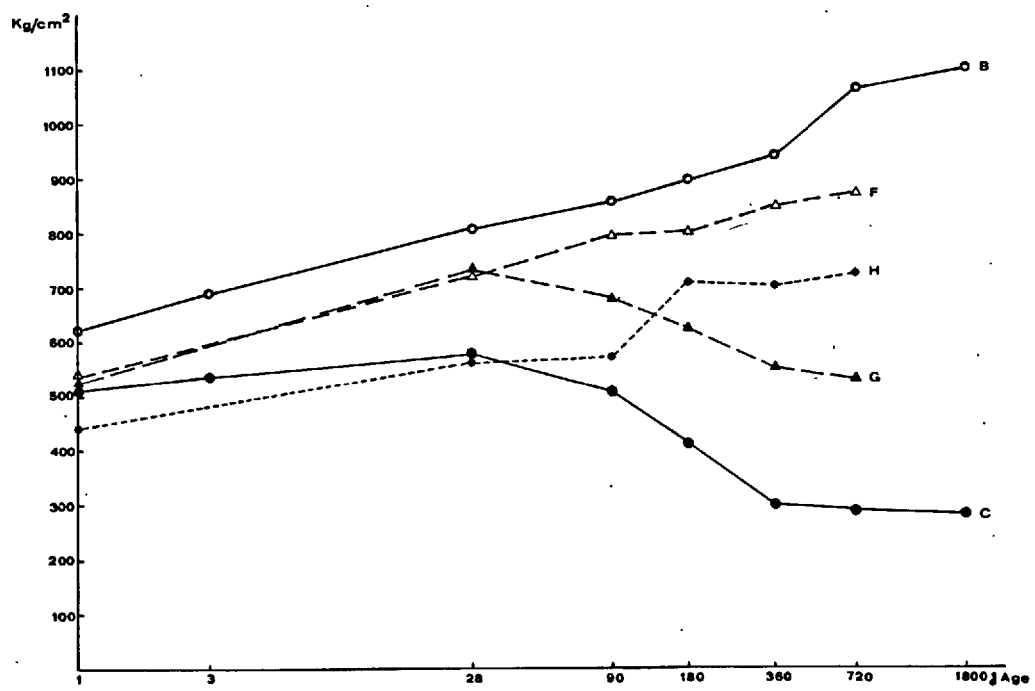

Fig. 1 – Résistances à compression en fonction du temps des bétons B, C, F, G, H

Les résultats offerts par les échantillons F, G, H reproposent des considération analogues à celles qui découlent des résultats des essais sur mortier. En effet, cet échantillon de ciment assure lui aussi des résistances à compression qui augmentent dans le temps s'il est utilisé dans des bétons avec agrégat calcaire, tandis qu'il montre des pertes considérables dans le béton avec agrégat siliceux.
Une confirmation de l'effet positif de la poudre de calcaire est fournie par les échantillons H qui montrent une stabilisation des résistances mécaniques même dans un béton fabriqué avec agrégat siliceux.
Pour mieux montrer leur comportement nous présentons dans la Figure 1 les courbes de résistance mécanique en fonction du temps des bétons B, C et F, G, H.
L'examen aux rayons X a mis en évidence, pour tous les échantillons contenant l'agrégat siliceux, la formation initiale de C_2AH_8 et CAH_{10} et leur transformation ensuite en C_3AH_6 et AH_3.
Pour tous les échantillons contenant l'agrégat calcaire il y a, au contraire formation de CAH_{10} et $C_3A\ CaCO_3\ 11H_2O$ déjà aux premères échéances, tandis que le C_3AH_6 n'apparaît qu'en très petite quantité, dans les bétons après deux ans de conservation (Figure 2).

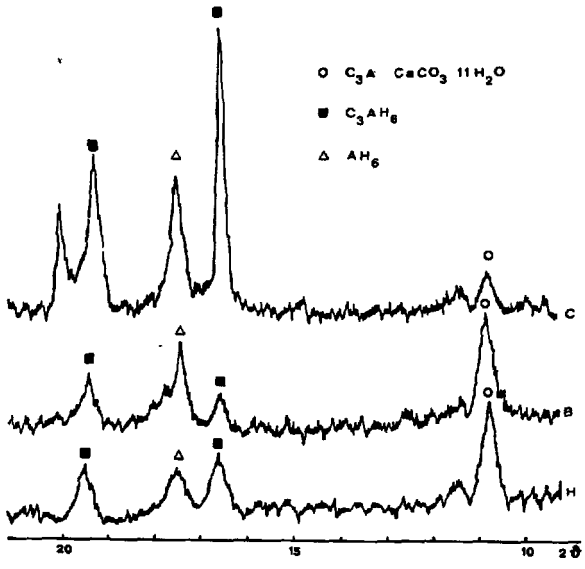

Fig. 2 - Spectres de diffraction X des échantillons B et C après 5 ans, et H après 2 ans

L'ATD confirme les constatations faites par l'examen aux rayons X.
Dans les échantillons fabriqués avec agrégat siliceux, apparaît sur la courbe thermique, après 28 jours, le pic à $\sim$ 330°C attribuable au C_3AH_6 : ce pic augmente en intensité au fur et à mesure que la periode de conservation avance.
Sur les courbes thermiques des échantillons fabriqués avec agrégat calcaire, après 28 jours de conservation, apparaît le pic a $\sim$ 180°C dû au carboaluminate. Le pic du C_3AH_6 ne peut être relevé sur aucune courbe thermique (Figure 3).

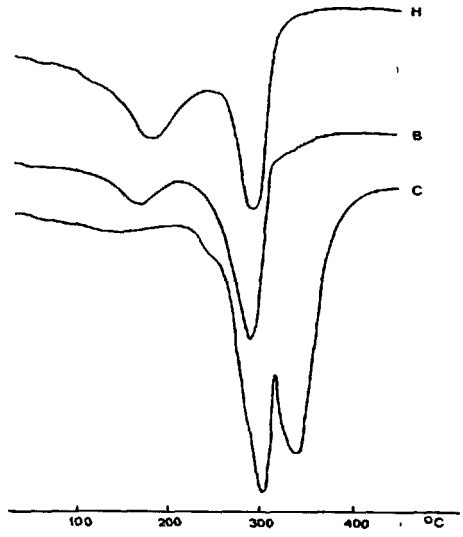

Fig. 3 - Thermogramme des échantillons B et C à 5 ans et de l'échantillon H à 2 ans de conservation

Il est donc confirmé que la présence d'un agrégat calcaire, quelle que soit sa granulométrie, limite la conversion des aluminates hydrates hexagonaux en aluminate cubique : le fait que cette conversion ne se produit pas, ou qu'elle se produit d'une façon très limitée et qu'il se forme du carboaluminate, a comme résultat la progression de résistances mécaniques.
Essayons maintenant d'expliquer le rôle joué par le $C_3A\ CaCO_3\ 11H_2O$, en considérant, avant tout, les variations de volume molaire à la suite des réactions [2] et [3].
Sur la base de l'équation [2], C_3AH_6 et $2AH_3$ occupent ensemble 47,3% de l'espace occupé par $3CAH_{10}$ avant sa transformation : il n'y a aucun doute que l'eau constituant 52,7% du voulume total est responsable de la porosité.
Sur la base de l'équation [3], le solide occupe 66,5% et l'eau 33,9%.

Il est donc évident qu'à la suite de la dessiccation la porosité révèle élevée (8) : d'après certains auteurs (9-11) elle se révèle déterminante pour la chute des résistances mécaniques.
Si, par contre, il se forme de carboaluminate, étant donné son volume molaire élevé, il est à présumer qu'une partie des espaces libres soit occupée par ce composé, avec une réduction de la porosité.
Nous avons vérifié celà en estimant le volume total des pores des échantillons D et E après 28 et 360 jours de conservation au moyen d'un porosimètre à mercure.

TABLEAU III

Echantillons	Conservation 28 jours	360 jours
D	52,69	66,61
E	65,96	38,36

Il est donc confirmé que la conversion provoque une augmentation de porosité, tandis que la formation de $C_3A\ CaCO_3\ 11H_2O$ la réduit de 42% environ. En plus, à l'examen les courbes de répartition du volume des pores indique qu'à l'échéance de 28 jours celles des échantillons D et E sont assez semblables, mais qu'à l'échéance de 360 jours pour l'échantillon D nous avons une accentuation des macro-pores, tandis que l'échantillon E présente une porosité plus fine et uniforme.
En outre la formation de carboaluminate en soustrayant de l'eau et en empêchant la formation de C_3AH_6, réduit probablement la formation des macropores associés à ce composé, ce qui a été mis en évidence par Mehta et Lesnikoff (12) avec des observations au MEB.
Enfin l'habitus lamellaire du $C_3A\ CaCO_3\ 11H_2O$ pourrait jouer un rôle important sur l'empilement des cristaux pour la réalisation d'une structure plus compacte.

CONCLUSIONS

L'emploi d'agrégats calcaires pour préparer des mortiers ou des bétons alumineux, permet d'arriver, même à de longues échéances, à des résistances mécaniques très élevées, grâce au fait que l'agrégat calcaire, réagissant avec les constituants du ciment, donne lieu à du carboaluminate, empêchant ou limitant la conversion et diminuant la porosité du béton.

BIBLIOGRAPHIE

1. - H.G.MIDGLEY et A.MIDGLEY (1975) "The conversion of high alumina cement", Mag. Concrete Res. 91, 59-77
2. - V.S.RAMACHANDRAN et R.F.FELDMANN (1973), "Hydration characteristics of monocalcium aluminate at a low water/solid ratio", Cement Concrete Res. 3, 729-750
3. - T.D.ROBSON (1962), "High alumina cement and concretes", J.Wiley and Sons, New York
4. - P.K.Mehta (1969), "Successful prevention of loss of strength in concrete made with high alumina cement", Proc. V I.S.C.C., Vol. II, pag. 148-151, Tokio
5. - S.UEDA et R.KONDO (1969), Oral discussion, Proc. V I.S.C.C., Vol. II, pag. 151-152, Tokio
6. - M.COLLEPARDI, A.MARCIALIS et R.TURRIZIANI (1972), "The influence of $4CaO\ 3Al_2O_3\ SO_3$ on the hydration of monocalcium aluminate", Il Cemento 3, 179-188
7. - A.NEGRO, L.CUSSINO, A.BACHIORRINI (1978), "The hydration of monocalcium aluminate in the presence of quartz and calcium carbonate", Il Cemento 3, 285-290
8. - J.TALABER (1974), "High - Alumina cement" Principal Paler, Proc. VI I.S.C.C., Moscow
9. - H.G.MIDGLEY (1967), "The mineralogy of set high - alumina cement", Trans. Brit. Ceram. Soc. 66, 161-187
10. - B.COTTIN et P.REIF (1971), "Paraméter physique régissant les properties méchaniques des pâtes pures des liants alumineux", Rev.Mat. Constr. 661, 293-305
11. - A.NEVILLE (1978), "High - alumina cement. A current review", Il Cemento 3, 291-302
12. - P.K.MEHTA et G.LESNIKOFF (1971), "Conversion of $CaO\ Al_2O_3\ 10H_2O$ to $3CaO\ Al_2O_3\ 6H_2O$", J.Amer. Ceram. Soc. 54, 210-212.

The relationship between cement clinker composition and strength recovery of hydrating high alumina cement during conversion

La relation entre la composition du clinker de ciment et la capacité de récupération du ciment alumineux

H.G. MIDGLEY, Concrete Research Laboratory, Civil Engineering Division, The Hatfield Polytechnic, Hatfield, Herts, U.K.

RESUME : Après la baisse de résistance subie par le béton de ciment alumineux (h.a.c.) du fait de la conversion cristalline de ce ciment, une petite récupération de la résistance peut se produite. Cette récupération est attribuée à la présence, dans le ciment, de silicates susceptibles de s'hydrater tardivement (pleochroïte et β-C_2S). Il y a probablement une proportion critique de silice dans ces clinkers, car s'il y avait trop de silice, un silicate inerte (gélénite) se formerait.

SUMMARY: After the loss in strength suffered by HAC concretes during conversion a small recovery in strength may ensue, this recovery is related to the presence of hydratable silicate minerals in the H.A.C. (pleochroite and BC_2S). There is probably a critical amount of silica in the clinker for if too much is present the inert silicate mineral gehlenite will be formed.

INTRODUCTION:

It has been suggested (1,2,3,4,5) that the strength development curves for U.K. manufactured H.A.C. concretes take the form with time the strength rises to a maximum followed by a fall to a minimum and then followed by a small rise in strength. It has been suggested (1) that this recovery in strength may be due to the formation of Stratlingite (C_2ASH_8). On the other hand, some non U.K. H.A.C. concretes may show no such recovery in strength even after 21 years (6.7.)

To see if the composition of the cement clinker has any effect on the strength development curves, three H.A.C. samples have been examined. A, a commercial H.A.C. of U.K. manufacture; B, a commercial H.A.C. of U.S.A. manufacture, and C, a white H.A.C.

EXPERIMENTAL:

The chemical analysis of the cements are given - Table 1 and the mineral composition by QXRD(5) in table 2.

Table 1.
Chemical analysis (wt.%)

	A	B	C
SiO_2	4.0	9.5	0.2
Al_2	37.9	41.6	71.8
CaO	37.5	38.7	27.1
Fe_2O_3	9.8	3.6	C.0
FeO	5.7	-	C.0
SO_3	0.1	0.8	0.3
Na_2O	0.1	0.1	0.1
K_2O	0.1	0.5	trace
Loss on Ign.	0.7	0.1	0.1

Table 2.
Mineral composition of H.A.C. by Q.X.R.D. (wt.%)

	A	B	C
CA	45	30	54
fss*	7	7	1
Wustite	10	6	0
Pleochroite	16	2	0
C_2AS	3	31	0
$C_{12}A_7$	1	20	2
C_2S	4	2	0
CA_6	0	0	42
CT	3	3	1

* ferrite solid solution ($C_2F - C_6AF_2$)

The SiO_2 content ranges from 0.2% in A, to 9.5% in C; the pleochroite content ranges from 16% in A to zero in C, BC_2S from 4 in A to zero in C. The high SiO_2 content (9.5%) of B gives rise to 31% of the inert mineral gehlenite, while the intermediate SiO_2 content (4%) of A produces only 3% gehlenite Pleochroite is considered to be reactive and produce strength (9), BC_2S is highly reactive and strength producing while ghlenite, at normal temperatures is unreactive (10).

The compressive strength of neat cement paste cures (12.5mm side) made with w/c ratios of about 0.27 stored 1 day in moist conditions at 18°C and then in water at 50°C are given in table 3.

Cement A shows the typical strength development cure with a rise to the maximum of 154N/mm^2 at 7 days, the fall to the minimum of 79N/mm^2 at 28 days and the subsequert rise to 105N/mm^2. Cement C shows the rise to the maximum of 138 at 7 days and then the steady fall with no recovery. Cement B shows only a very small strength recovery.

Table 3.

Compressive strength (N/mm^2) of neat cement cubes, W/C 0.27,stored at 18°C 1 day and then in water at 50°C.

Age	1	7	14	28days	3	6	12months
A	150	154	139	79	89	108	105
B	86	72	59	59	31	38	40
C	92	138	124	93	74	66	57

The degree of conversion, Dc,(1), was determined for all specimens table 4. All show a high rate of conversion and eventually a high degree of conversion.

Table 4.

Degree of conversion, Dc,% of pastes cured 18°C 1day and then 50°C.

	1	7	14	28days	3	6	12months
A	15	40	15	65	75	85	90
B	0	40	30	45	65	70	75
C	27	50	55	60	80	80	90

Discussion

Discussion

The amount of strength recovery in N/mm^2 from the minimum to the strength at 1 year are given in table 5; the SiO_2 and silicate mineral contents are also given.

Table 5

Strength recovery of neat cement pastes cured at 50°C; minimum to 1 year strength. SiO_2 content wt%, (table 1), mineral content wt% (table 2)

	Strength recovery	SiO_2	Pleochroite	BC_2S	C_2AS
A	26	4.0	16	4	3
B	9	9.5	2	2	31
C	0	0.2	0	0	0

From the data in table 5 it can be seen that as the amount of pleochroite increases so the amount of strength recovery increases. However, there is no simple relationship between silica content and strength recovery. Cement B with 9.5% SiO_2 but 31% gehlenite and only 2% of pleochroite and BC_2S has a small strength recovery when compared with cement A with 4% SiO_2 but 16% pleochroite and 4% BC_2S and only 3% gehlenite. Cement C shows no strength recovery at 1 year since it contains only 0.2% SiO_2 and no measurable silicate minerals.

Conclusions

It is concluded from an examination of the mineralogy of three high alumina cement that the small recovery in strength observed during the conversion reaction of hydrating HAC following the initial loss in strength may be correlated with the presence of hydratable silica bearing minerals, pleochroite and BC_2S. The strength recovery in absolute terms is not related to the total silica content of the clinker for, if the quantity of SiO_2 is increased too much, the gehlenite, a non-reactive mineral is produced at the expense of the hydratable silicate minerals. It seems likely that there will be a critical amount of silica needed in the cement to produce a maximum strength recovery of H.A.C. concrete during conversion.

REFERENCES:

1. Midgley H.G. and Midgley A. The conversion of high alumina cement. Magazine of Concrete Research Vol. 27, No. 91 June 1975, pp.59 - 77.

2. Robson T.D. High alumina cements and concretes. Contractors Record Limited, London 1962, p.263.

3. Midgley H.G. The mineralogy of set high alumina cement. Trans Brit Ceram Soc. Vol. 66, No. 4. 1967, pp. 161 - 187.

4. Neville A. A study of deterioration of structural concrete made with high alumina cement. Proc. Inst. Civil Engineering, Vol. 25, paper 6653, 1963, pp. 282 - 324.

5. Newman K. Design of concrete mixes with high alumina cement. Reinf. Conc. Rev., Vol. 5, No. 5. March 1960, pp. 269 - 294.

6. Neville A. High Alumina Cement Concrete. The Construction Press, London 1975, p.201.

7. Talaber J. Durabilite des ciments alumineux, RILEM Int. Symp. on the Durability of Concrete, Prague 1961, Final Report 1962, pp.109 - 114.

8. Midgley H.G. The mineralogy of high alumina cement clinker by quantitative X-ray diffraction. To be published

9. Parker T.W. and Ryder J.F. Discussion to paper by T.W. Parker. The constitution of aluminous cement, Proc. 3rd Int. Symp. Chemistry of Cement. London 1952, pp. 524 - 527.

10. Midgley H.G. Melilite from high alumina cement. Discussion to paper by T.W. Parker. The construction of aluminous cement. Proc. 3rd Int. Symp. Chemistry of Cement. London 1952, pp. 515 - 516.

Property and Application of Thermosetting Cement

Propriétés et applications du ciment thermo-durcissant

GUNJI SHIKAMI, HIROFUMI SHIMATANI, RYOICHI SHIKATA, MICHIO MITSUHASHI, Japon.

RESUME : Les ciments thermo-durcissant (ci-après : CTD) sont des ciments composés principalement d'aluminate de calcium, de sulfate de calcium et de silicate de calcium, et dont la prise est ralentie par un agent retardateur.
Ce ciment peut avoir un durcissement rapide, en le chauffant à une température appropriée et en le faisant reposer. Ainsi on peut le malaxer et le mettre en forme, puis après la mise en forme, en faisant une opération de chauffage à 80°C-30 minutes, on peut avoir un ciment ayant un temps de prise long et un durcissement rapide.

On a observé que le durcissement rapide de ces ciments était dû à la formation rapide d'ettringite; cette dernière formation peut être ralentie par un mélange de semi-hydrate de gypse et d'acide citrique.

En faisant chauffer ce ciment à une température de 70 à 80°C on a la formation de l'ettringite en 30 minutes environ, la formation de celle-ci est alors terminée, et après cela il n'y a presque pas d'augmentation ou de diminution de celle-ci.
Le chauffage initial contribue à l'amélioration de la qualité de durcissement rapide ainsi qu'à la stabilisation volumique à long terme. D'autre part, comme on ne chauffe pas pendant longtemps à température élevée, on évite une réduction de la réactivité du C_3S. Le CTD montre une bonne qualité comme liant du béton.

SUMMARY : Thermosetting cement (hereinafter referred to as TSC) mainly consists of calcium aluminate, calcium sulfate and calcium silicate, and its flash setting is prevented by addition of a retarder. With this cement, upon appropriate hot curing before setting time rapid hardening can be obtained. That is, through the heating process at 80°C for 30 minutes after mixing and placing at ordinary temperatures a cement with the longer setting time and rapid hardening is made available.

Flash setting of this kind of cement was known to be on account of rapid formation of ettringite, which thus could be retarded by coexistence of calcium sulfate hemihydrate and citric acid. When this cement is heated prior to setting up to 70 - 80°C, formation of ettringite is accelerated and completed in about 30 minutes, which remains nearly unchanged after that. Therefore, the early heating does much toward improving rapid hardening and stability of volume for a prolonged period. Furthermore restricted hot curring time at high temperatures is also effective to prevent lowering reactivity of C_3S, which contributes to increasing strength of TSC at prolonged period. TSC indicates superior properties as a binder for GRC .

1. Introduction

Trials to receive rapid hardening of cement arrived at a level of hardening in several hours due to development of a regulated cement (it is known as Jet Cement in Japan). It is also possible to make it rapid further, however, the higher in rapid hardening the shorter in setting time, which makes handling of mortar and concrete difficult, thus being limited in rapid hardening.

The authors studied on a cement with rapid hardening in addition to the comparatively longer setting time, and finally succeeded in development of a thermosetting cement with rapid hardening by heating (hereinafter referred to as TSC).

In this report mechanism of retarded setting of TSC, mechanism of early strength appearance as well as optimum heating temperature and time were studied, the results of which are stated below.

2. Hydration of thermosetting cement

As indicated in Table 1, TSC contains as hydraulic compound calcium silicate mainly comprising C_3S, and calcium aluminate mainly comprising CA, to a mixture of which an appropriate amount of insoluble anhydrite and calcium sulfate hemihydrate as well as a little amount of citric acid for adjusting retarded setting are added. The better fineness is favorable, but it is about 7000 cm^2/g in Blaine.

2-1. Setting of thermosetting cement

In Fig. 1 which indicates changes with the passage of time of TSC's heat evolution at ordinary temperatures, the first peak is considered to correspond with formation of ettringite from measurement of XRD. The time of appearance and heat evolution rate of the first peak are known to be markedly retarded by addition of hemihydrate as well as citric acid. The time of appearance of the first peak nearly corresponds with the setting time of those cements made in trial, which indicates that abundant formation of ettringite has resulted in setting of TSC. The comparatively longer setting time is apparently based on the results of chemically controlled formation of ettringite.

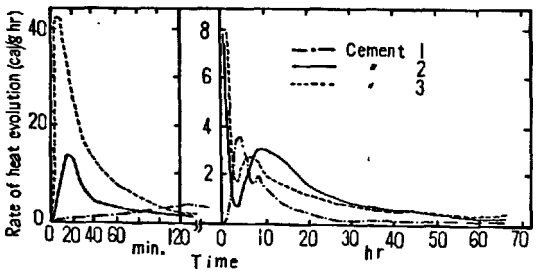

Cement 1: TSC as shown in Table.I.
Cement 2: Cement 1 not containing citric acid
Cement 3: Cement 2 not containing hemihydrate

Fig.1. Effect of hemihydrate and citric acid on the early hydration of TSC at 20°C (W/C=0.65)

2-2. Hydration in heating

Fig. 2 shows the rate of hydration accelerated by heating the TSC paste. When compared with identification with XRD the first peak mainly corresponds with formation of ettringite at every temperature, and in case of 70°C already in the first peak formation of monosulfate is also included. According to Fig. 3, which shows the analytical results of ettringite and monosulfate obtained from stoichiometry[1], the higher the hot curing temperature is, the more formation of monosulfate accelerates, thus it is known that ettringite is formed less and monosulfate is formed more. That is, from the results of Figs. 2 and 3 it is known that prolonged hot curing is not necessary but only 20 - 30 minutes is sufficient to complete formation of ettringite. Fig.4 also supports an accelerated hydration of TSC by heating.

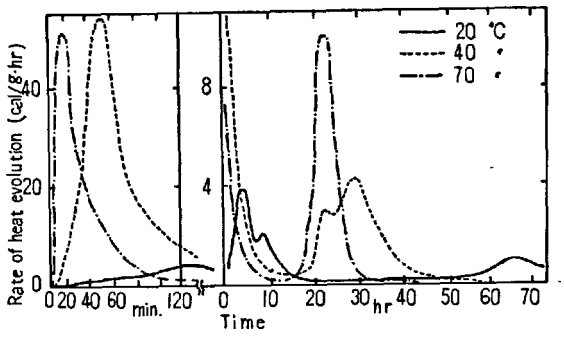

Fig.2. Effect of temperature on heat liberation of TSC. (by conduction calorimeter : (W/C=0.65))

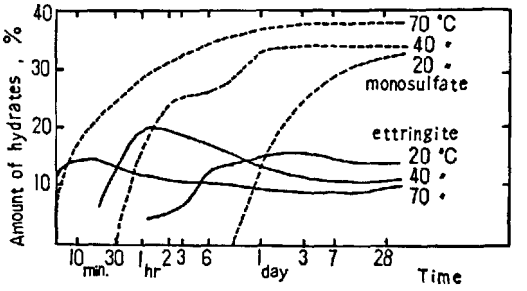

Fig.3. Effect of temperature on the amount of hydrates formed in hardened TSC.

Furthermore, hydration at a high temperature in restricted time followed by 20°C water curing was examined to confirm this point. Fig 5. shows the decreasing rate of hydraulic minerals (hydration rate)

Table.I. Finess, chemical composition and mineralogical composition of TSC

Blaine	chemical composition (%)								mineralogical composition (%)								
(cm^2/g)	Ig.loss	Insol	SiO_2	Al_2O_3	Fe_2O_3	CaO	SO_3	Total	C_3S	C_2S	CA	C_3A	C_4AF	$CaSO_4$	$CaSO_4.1/2H_2O$	$Ca(OH)_2$	Total
6800	2.8	0.1	13.9	9.6	4.4	58.1	9.8	98.7	40	9	7	5	10	11.5	4.5	6	93

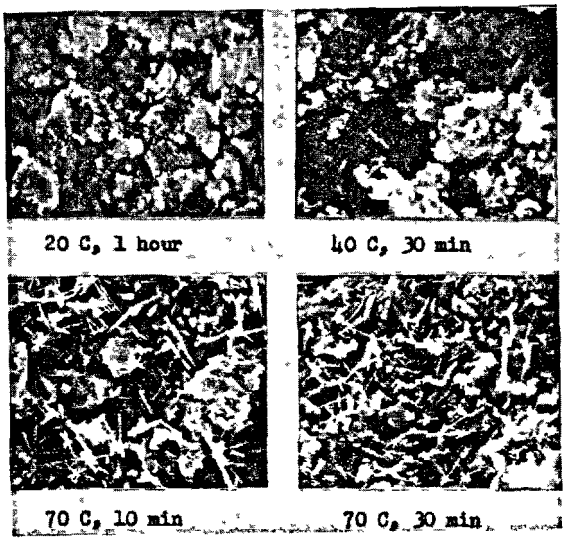

Fig.4. SEM micrograph of hardened TSC.(⊢——⊣:5μm)

obtained for the purpose of knowing a trend of chemical reaction rate with TSC. CA with the lowest reaction rate among calcium aluminates indicated different reaction rate by length of retention time at 80°C. On the other hand Fig. 6 shows formation of ettringite and monosulfate, in which even in 30 minutes of retention time formation of ettringite is completed in an early stage hardly showing an increase in the later period, with only monosulfate being increased. Furthermore when cured at a high temperature for a prolonged period, formation of

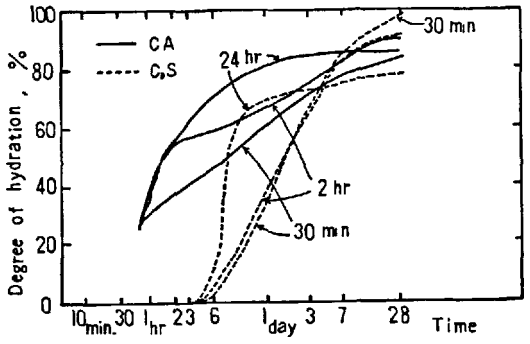

Fig.5. Effect of retention time at 80°C on hydration of C_3S and CA. (by XRD)

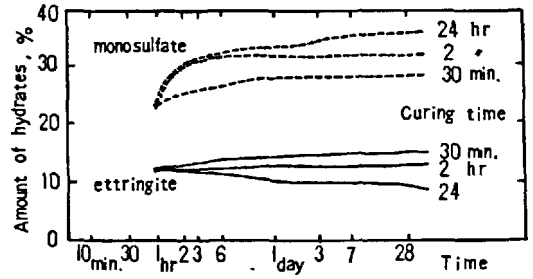

Fig.6. Effect of retention time at 80°C on the amount of hydrates formed in hardened TSC.

ettringite is a little less, which results in a little more of monosulfate.

Thirty minutes after mixing paste was heated for 30 minutes up to 80°C and composition of liquid phase was pursued, the results of which are shown in Fig.7. By heating up to 80°C saturated SO_4^{2-} ion and Ca^{2+} ion decrease and the Al_2O_3 concentration of liquid increases. From this it is known that with hot curing most of ettringite and monosulfate are formed in this period.

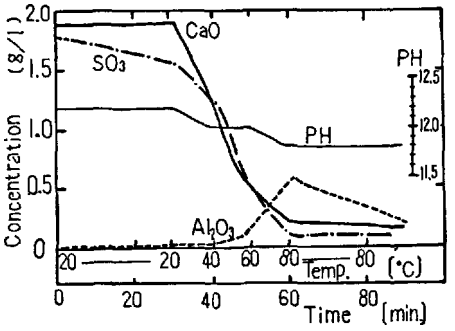

Fig.7. Effect of raising temperature on the composition of liquid phase of TSC. (W/C=10)

On the other hand referring to the reaction rate of C_3S in TSC, as known from Fig.5, the longer the retention time at 80°C is, the more the reaction rate after completion of hot curing increases giving an effect on the strength of about one-day period. However, the reaction rate of the later period decreases on the contrary as the early high temperature curing time is longer, thus making development of strength in the later period lower. (See Fig. 8)

From the above results it was known that the optimum curing of TSC at high temperature is to be 70 - 80°C for from 30 minutes to 2 hours, having formation of ettringite nearly completed, thus high reaction rate of C_3S being maintained.

3. Properties of TSC mortar

The working time of TSC mortar is shorter than that of Portland cement mortar being easily influenced by temperature. With a mortar of S/C = 0.6 - 2, W/C = 0.35 - 0.6 the working time is 1 - 2 hours at ordinary temperatures and 0.5 - 1 hour at 30°C.

Mortar strength differs by heating conditions as shown in Fig. 8. The test results revealed that the early heating at 70 - 80°C for 30 minutes gives the highest strength. When temperature is too low or heating is too short (deficient maturity) damage of texture by expansion is caused in the later period, and too long heating markedly reduces later development of strength, which well corresponds with the results of hydration in heating discussed in 2-2.

Practically, in addition to high strength volume stability must be satisfied. To obtain volume stability for long time it is necessary to complete formation of ettringite in the early stage of heating, and with TSC it can be achieved by means of controlling the amount of ettringite and restricted hot curing at early period.

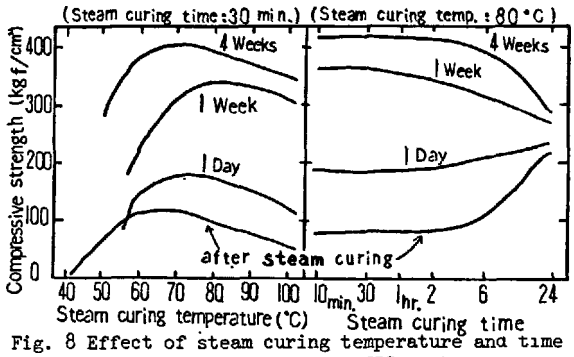

Fig. 8 Effect of steam curing temperature and time on the compressive strength of TSC mortar.

4. Application of thermosetting cement

When used as a binder for GRC, TSC indicates the superior properties as follows:

(1) It enables early release of mold: When GRC was molded by spraying with a glass fiber content of 3 - 5 (wt% / mortar), bending strength of 120 - 180 kgf/cm^2 in one hour was obtained allowing an easy release of mold after steam curing at 80°C for 30 minutes.
(2) It has high strength: GRC using TSC showed an improvement of 20 - 25% in bending strength and 10 - 40% in impact strength compared with that of Portland cement.
(3) It makes deterioration of GRC strength lower: The accelerated deterioration test in hot water at 80°C revealed that TSC showed less deterioration of alkali resistant glass fiber than that of Portland cement, thus decrease of strength with GRC is kept minimum.

In addition to the above, for cement products which require rapid hardening and early release of mold TSC can be used in the same way as Portland cement.

Reference

1. H. Uchikawa, Cement and Concrete Research, Vo. 4, 821 (1974).

Synthèse vers 750°C et propriétés d'un " βC_2S sulfaté"

Synthesis at about 750°C and properties of a sulphated βC_2S

R. STRUILLOU, M. ARNOULD, Centre de Géologie de l'Ingénieur, Ecole des Mines, 60, boulevard Saint-Michel, 75006 Paris, France.

RESUME : On montre qu'on peut obtenir un liant fortement hydraulique par cuisson vers 700-750°C, d'un mélange de nitrate de calcium, de silice et de gypse ($C\bar{S}H_2$). Le $Ca(NO_3)_2$ fond à 561°C, puis se décompose en donnant des vapeurs nitreuses recyclables, et de la chaux qui se combine à la silice. La réaction, en présence d'une phase fondue, est rapide (20 minutes à 750°C). Le produit formé a pour formule chimique approximative

$$Ca_{2-x}\ Si_{1-x}\ S_xO_4 \quad \text{avec } 0 < x < 0,15$$

Cette formule pourrait correspondre à un mélange intime et en toutes proportions de βC_2S et d'un autre minéral de formule hypothétique ($6C_2S$, $C\bar{S}$). Si on a dans le cru la relation molaire $\bar{S} < 0,1(\bar{S}+S)$, l'intégration de $C\bar{S}$ à C_2S est complète. Sinon du $C\bar{S}$ libre en excès subsiste en fin de cuisson. Le produit hydraulique formé présente, en diffractométrie RX, les pics du βC_2S, mais moins hauts, élargis, et légèrement déplacés. Il possède des propriétés hydrauliques bien meilleures que celles du βC_2S pur et donne des résistances à court et moyen terme comparables à celles des ciments portland classiques. Mais si ce produit présente l'avantage de pouvoir être fabriqué à une température relativement basse, sa synthèse, par la voie nitrique, a l'inconvénient majeur de présenter un bilan énergétique nettement plus défavorable que celui des procédés industriels classiques.

SUMMARY : We show that we can get, from a mixture of calcium nitrate, silica and gypsum($C\bar{S}H_2$) a highly hydraulic cement, by burning at about 700-750°C. The $Ca(NO_3)_2$ smelts at 561°C, then decomposes while giving recoverable nitrous vapours and lime which combines with silica. The reaction in the presence of a liquid phase is quick (20 minutes at 750°C). The product so formed has a chemical formula which is approximately

$$Ca_{2-x}\ Si_{1-x}\ S_x\ O_4 \quad \text{with } 0 < x < 0,15$$

This formula could correspond with a mixture homogeneous in all proportions of βC_2S and of another mineral with a hypothetic formula ($6C_2S$, $C\bar{S}$). If the molar relation $\bar{S} < 0,1(\bar{S}+S)$ is realized in the material, $C\bar{S}$ disappears and seems to enter completely into C_2S. In the other case, free $C\bar{S}$ is found after burning. The hydraulic product so formed presents, in X.Rays diffractometry, the rays of βC_2S but less high, wider and a little misplaced. This product has much higher hydraulic properties than pure βC_2S, and gives short and middle-term mechanical resistances comparable with those of classical portland cements. But if this product can be made at a rather low temperature, its synthesis, by the nitric way, has the great disadvantage of presenting a very much defavourable energetic balance than this of classical industrial processes.

Actuellement, toute méthode diminuant la consommation de l'industrie cimentière en produits pétroliers présentarait un intérêt certain, en particulier si elle permettait de remplacer le fuel par une autre source d'énergie. Une voie consisterait à obtenir, à relativement basse température, des liants à propriétés hydrauliques équivalentes à celles des ciments portland à C_3S. Les essais réalisés au Centre de Géologie de l'Ingénieur de l'Ecole des Mines de Paris, avec l'aide financière du Ministère de l'Industrie et du Ministère de l'Equipement, montrent qu'il est possible de fabriquer un tel liant entre 700°C et 750°C.

METHODE D'OBTENTION DU LIANT EN LABORATOIRE

La décarbonatation du calcaire étant très lente au-dessous de 850°C, nous avons remplacé $CaCO_3$ par $Ca(NO_3)_2$ en réalisant, à partir du mélange cru initial (23% SiO_2 + 77% $CaCO_3$), la succession de réactions de base suivantes, avec trempe à l'air des produits en sortie du four :

- en dehors du four :

$$CaCO_3 + 2HNO_3 \longrightarrow Ca(NO_3)_2 + CO_2\uparrow + H_2O \quad (1)$$

- dans le four réglé entre 700°C et 900°C (en général 750°C) :

$$Ca(NO_3)_2 \longrightarrow CaO + (2-x)NO\uparrow + xNO_2\uparrow + \frac{3-x}{2}O_2\uparrow \quad (2)$$

$$SiO_2 + 2CaO \longrightarrow Ca_2SiO_4 \ (\beta C_2S) \quad (3)$$

$Ca(NO_3)_2$ fond à 561°C, dès l'entrée dans le four, et la réaction (3) se réalise donc en présence d'une phase liquide jusqu'à décomposition totale du nitrate par la réaction (2). Dans nos conditions opératoires, les réactions étaient terminées au bout d'environ 20 minutes à 750°C. Les vapeurs nitreuses étaient simplement récupérées à mesure de leur formation, mais elles pourraient être traitées pour reconstitution du stock d'acide nitrique et recyclage. En laboratoire, on peut remplacer l'acide nitrique par le nitrate d'ammonium plus facile d'emploi. Les résultats sont identiques après passage dans le four.

Avec ces réactions de base, on aboutit à un silicate bicalcique de forme β (dit βC_2S) présentant, en diffractométrie RX, des pics élargis et à intensités relatives différentes par rapport aux pics du βC_2S obtenu classiquement par réaction sans nitrate au-dessus de 900°C (fig. 1 A et B). Ceci est l'indice d'une plus mauvaise cristallinité du produit. Ses propriétés hydrauliques restent cependant très médiocres et proches de celles du βC_2S classique en particulier à court terme.

Il n'en est par contre pas de même si on incorpore au mélange cru initial de silice et de calcaire, une faible proportion de gypse ($C\bar{S}H_2$) ou de sulfate de calcium anhydre ($C\bar{S}$) (environ 0,25g de gypse pour un 1g de SiO_2 et 3,3g de $CaCO_3$). Dans ce cas, on obtient, à la sortie du four, un produit très mal cristallisé et doué de propriétés hydrauliques intéressantes. Il présente en diffractométrie RX, les pics du βC_2S mais très faibles, très élargis, mal individualisés et légèrement déplacés par rapport à ceux du βC_2S obtenu en l'absence de $C\bar{S}$. Celui-ci n'apparaît pratiquement pas en diffractométrie RX et semble avoir été incorporé au βC_2S en perdant son individualité. C'est ce βC_2S particulier, très déformé, qui fera l'objet de notre analyse. Nous l'appellerons "βC_2S sulfaté" (fig. 1 C et D).

Il faut remarquer qu'en présence comme en l'absence de sulfate, la transformation de la silice n'est pas totale. On évite la formation d'un excès de chaux libre en diminuant la proportion de calcaire c'est-à-dire en utilisant environ 3g de $CaCO_3$ pour 1g de SiO_2.

PROPRIETES DU "βC_2S sulfaté"

La masse volumique du "βC_2S sulfaté" est d'environ 2,9g/cm^3. En l'absence d'impuretés, il est d'un blanc très franc. A la sortie du four, le produit est très friable et donne facilement, par broyage rapide, de très grandes surfaces spécifiques (5000 à 15000cm^2/g Blaine).

La figure 1 permet de comparer les diffractogrammes RX ($K_\alpha Cu$), réalisés dans les mêmes conditions opératoires, d'une part sur des βC_2S sans sulfate (A et B) cuits, à partir de spongolithe, l'un (A) avec 3% de $CaCl_2$ pendant 2 heures à 1000°C sans nitrate, l'autre (B) pendant 20 minutes à 750°C en milieu nitraté, et d'autre part sur des "C_2S sulfatés" typiques cuits à 750°C pendant 20 minutes en milieu nitraté et obtenus à partir de crus à 6% de gypse ($C\bar{S}H_2$) l'un (C) à poussière de quartz broyé, l'autre (D) à silice organique (spongolithe).

Dans l'ensemble, les pics sont les mêmes, mais leur allure est très différente. La plus mauvaise cristallinité correspond à la silice organique (D), ce qui a été vérifié aussi bien pour la spongolithe que pour des diatomites et pour la gaize, qui donnent des produits équivalents. De plus, le quartz semble favoriser l'appartiion d'une proportion non négligeable de γC_2S non hydraulique (C). Ceci pourrait expliquer que les propriétés hydrauliques des produits à base de silice organique sont sensiblement meilleures que celles des produits provenant de quartz broyé. Cette différence apparaît clairement sur la figure 2 qui montre que sur éprouvettes de pâtes pures (d = 1,2cm ; h = 1,3cm, Méthode DALZIEL-1971) compactées à sec à porosité n = 0,45 et durcies à 40°C, on obtient, au bout de 24 heures, pour les "C_2S sulfatés" cuits à 750°C, des résultats comparables à ceux du CPA400 en partant de silice organique, et à ceux du CPA325 en partant de quartz broyé. Cette figure 2 montre, par ailleurs, que si on remplace 10% du quartz par de la silice organique (spongolithe) on obtient un produit qui se place à peu près à mi-chemin entre le CPA400 et le CPA325. On constate que, parallèlement, la hauteur relative du pic du γC_2S diminue quand la proportion de silice organique augmente.

La figure 3 donne l'évolution dans le temps, à 40°C, des résistances des micro-éprouvettes de type DALZIEL compactées à sec aux porosités n = 0,45 et n = 0,30, d'une part pour un CPA400 et, d'autre part pour "βC_2S sulfaté" obtenu à partir d'un cru à 6% de gypse et à spongolithe.

A partir de 5 heures (0,2 jour), le CPA400 et le "βC_2S sulfaté" sont à peu près équivalents.

La figure 4 permet de comparer les résistances des éprouvettes de pâtes pures gâchées avec un rapport "eau sur ciment" de 0,50 puis vibrées et durcies à 20°C et ceci pour le CPA400, le C_3S pur, le βC_2S classique pur et le "βC_2S sulfaté" obtenu à partir d'un cru à 6% de gypse et à spongolithe.

L'évolution dans le temps du "βC_2S sulfaté" est comparable à celle du C_3S ou du CPA400. Elle est environ 10 à 15 fois plus rapide que celle du βC_2S pur classique non sulfaté.

Quelques essais réalisés sur mortiers normalisés ont donné, pour le "βC_2S sulfaté", des performances comparables à celles du CPA325. Mais on peut se demander si les liants n'ont pas été trop finement broyés (8000cm^2/g Blaine), ce qui les a rendus très avides d'eau et donc inadaptés aux conditions opéra-

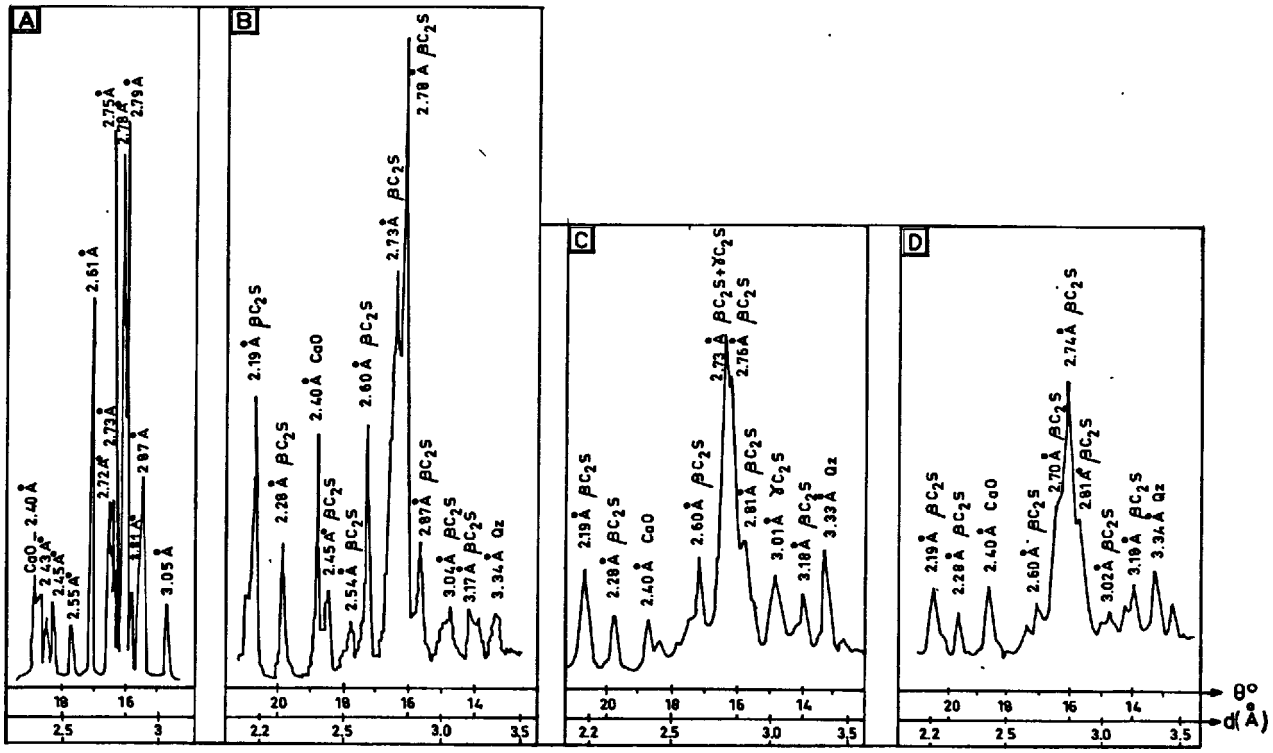

Fig. 1 : Comparaison des diffractogrammes RX ($K_\alpha Cu$) de βC_2S fabriqués dans diverses conditions.

(A) 2h à 1000°C sans nitrate et sans sulfate mais avec 3% de $CaCl_2$ (cru spongolithe)
(B) 20' à 750°C avec nitrate et sans sulfate (cru spongolithe)
(C) 20' à 750°C avec nitrate, 6% de $C\bar{S}H_2$ (cru quartz broyé) - apparition de γC_2S
(D) 20' à 750°C avec nitrate, 6% de $C\bar{S}H_2$ (cru spongolithe).

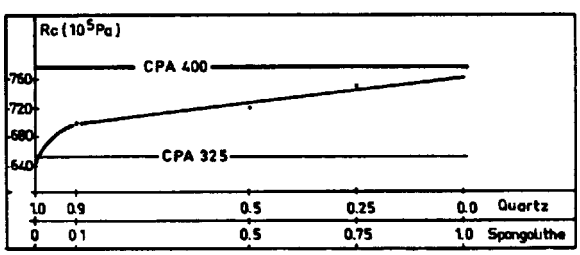

Fig. 2 : Comparaison des résistances en compression R_c, à 1 jour, sur pâtes pures des CPA325 et CPA400 et des "βC_2S sulfatés" obtenus pour diverses proportions "quartz sur silice organique" des crus traités avec 6% de $C\bar{S}H_2$ à 750°C pendant 20 minutes (essais sur micro-éprouvettes compactées à sec à porosité n = 0,45 et durcies à 40°C).

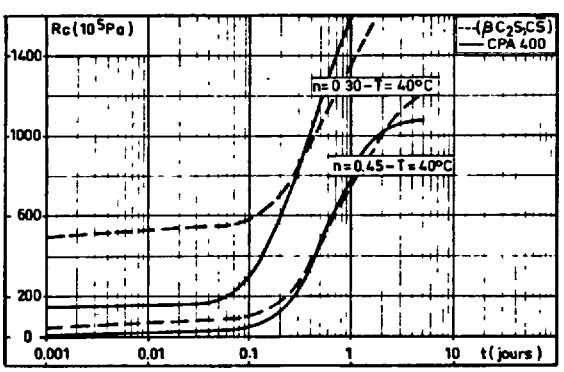

Fig. 3 : Comparaison de l'évolution dans le temps des R_c sur pâtes pures d'un CPA400 et d'un "βC_2S sulfaté" (cru spongolithe à 6% de gypse) - essais sur micro-éprouvettes (d = 1,2cm ; h = 1,3cm) durcies à 40°C après compactage à sec à porosité n = 0,45 ou n = 0,30 .

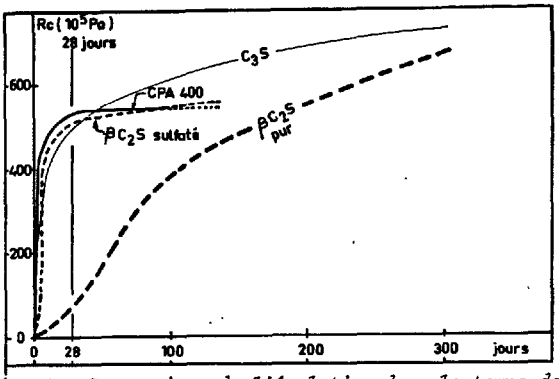

Fig. 4 : Comparaison de l'évolution dans le temps des Rc sur pâtes pures d'un "βC_2S sulfaté" (cru spongolithe à 6% de gypse), d'un CPA400, du C_3S pur et du βC_2S pur classique non sulfaté - essais sur micro-éprouvettes (d = 1,2cm ; h = 1,3cm) gâchées avec E = 0,5C puis vibrées et durcies à 20°C.

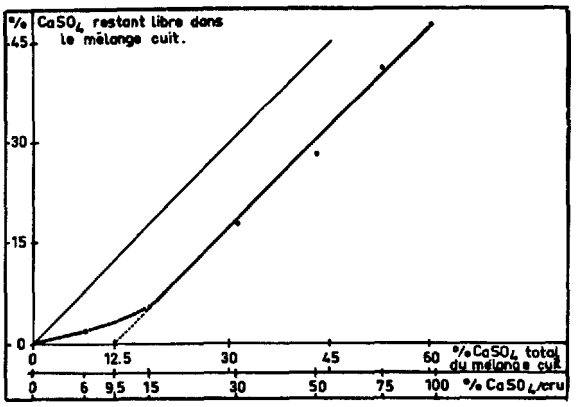

Fig. 5 : Relation entre les quantités totales de $\overline{CS}$ présentes dans les mélanges à "βC_2S sulfaté" cuits et les quantités de $\overline{CS}$ y restant à l'état libre (dosage par diffractométrie RX - étalon interne ZnO).

toires normalisées. Le retrait des mortiers a été légèrement supérieur à celui des mortiers courants, ce qui s'explique par leur richesse en eau due à la finesse du liant.

Tous les résultats cités précédemment correspondent à des liants utilisés sans ajouts d'accélérateurs de durcissement ($CaCl_2$ par exemple). Ceux-ci agissent sur le "βC_2S sulfaté" à peu près de la même façon que sur les ciments portland ordinaires.

MECANISMES DE FORMATION DU "βC_2S sulfaté"

Pour essayer d'interpréter ce qui se passe dans le four lorsqu'on cuit, vers 750°C, un mélange de silice, de nitrate de calcium et de sulfate de calcium, on peut s'appuyer sur deux types d'observations.

D'une part, la figure 5 donne la relation linéaire existant, dans les produits cuits, entre les pourcentages de $\overline{CS}$ libre (dosés par diffractométrie RX - étalon interne ZnO) et les pourcentages totaux de $\overline{CS}$ présents en réalité ($\overline{CS}$ libre + $\overline{CS}$ incorporé). La droite, parallèle à la bissectrice des axes, recoupe l'abcisse pour un pourcentage total de $\overline{CS}$ égal à 12,5% du produit cuit (SiO_2 + CaO + $CaSO_4$), ce qui correspond à 9,5% du produit cru (SiO_2 + $CaCO_3$ + $CaSO_4$). Schématiquement, on peut donc admettre que si le cru contient moins de 9,5% de $\overline{CS}$, celui-ci disparaît à peu près complètement lors de la cuisson et semble donc être incorporé au "βC_2S sulfaté". Au-delà de ce seuil, l'excès de $\overline{CS}$ se retrouve à l'état libre dans le produit cuit. Cependant la première branche curviligne de la figure 4 montre que la réalité est un peu plus compliquée que ce schéma, et que la saturation du βC_2S en $\overline{CS}$ est progressive. En tous cas, si le cru contient moins de 6% de $\overline{CS}$, son incorporation au βC_2S est pratiquement totale.

D'autre part, la figure 6 donne l'évolution, à différents stades de la cuisson à 750°C en milieu nitraté, des composants du système, avec cru de quartz (1g SiO_2 + 3,3g $CaCO_3$). Les phases cristallisées ont été dosées par diffractométrie RX avec la boehmite comme étalon interne. On voit qu'au bout de 4 minutes, il ne reste plus que 25% de quartz cristallisé, alors que le C_2S n'apparaît pas encore. Au bout de 10 minutes, 95% du C_2S est déjà formé alors qu'il reste encore 10% de quartz cristallisé. A la fin de la cuisson, il reste environ 7% du quartz non utilisé.

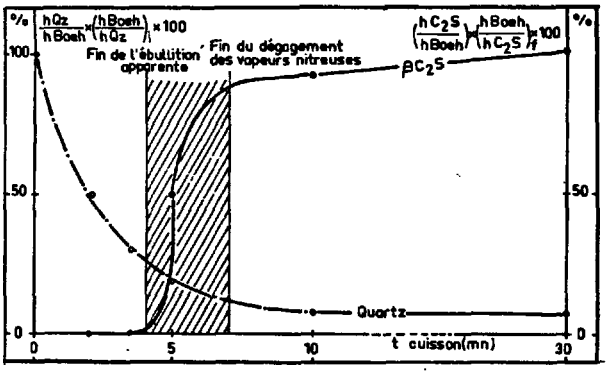

Fig. 6 : Evolution (en %), en fonction du temps de cuisson à 750°C en milieu nitraté de la quantité de quartz cristallisé subsistant dans le mélange, et de la quantité de C_2S formé (dosages par diffractométrie RX - étalon interne boehmite).

Il apparaît donc que le quartz est très rapidement amorphisé, sinon dissous, par le nitrate de calcium fondu. Le C_2S ne se forme qu'à mesure de la décomposition du nitrate de calcium (réaction 2). Il est possible, sinon probable, que $\overline{CS}$ subisse, lui-aussi, une attaque comparable à celle du quartz de la part du nitrate fondu . Dans ces conditions, il est impossible de savoir si le "C_2S sulfaté" se forme par diffusion des ions calcium et soufre à l'intérieur du quartz amorphe mais solide ou à l'état de gel, ou, au contraire, par cristallisation à partir d'un bain fondu nitraté homogène ayant dissous le quartz et le sulfate de calcium.

Quoiqu'il en soit, il semble bien que le C_2S soit susceptible d'incorporer à son réseau cristallin environ 12%, en poids, de $C\bar{S}$, en le déformant légèrement, mais en lui gardant cependant ses caractères cristallographiques de base, en particulier les mêmes pics de diffractométrie RX.

On peut représenter l'ensemble de ces observations en proposant pour le "βC_2S sulfaté", une formule chimique globale :

$$Ca_{2-x}\ S_x\ Si_{1-x}\ O_4 \quad \text{avec} \quad 0 < x < 0{,}15$$

Cette formule ne prétend pas avoir une valeur structurale quelconque. Elle n'est qu'une synthèse commode des observations réalisées.

On pourrait d'ailleurs aussi considérer le "βC_2S sulfaté" comme un mélange intime, et en toutes proportions, de C_2S pur et d'un produit de formule conventionnelle approximative :

$(5\ C_2S,\ C\bar{S})$ ou $(6\ C_2S,\ C\bar{S})$.

Une telle formule est très éloignée de celle du silico sulfate ($2\ C_2S,\ C\bar{S}$) ou sulfo-spurrite non hydraulique (PLIEGO - CUERVO - V.B., GLASSER F.P. 1978-1979). La présence de ce minéral dans notre "βC_2S sulfaté" semble donc devoir être exclue. D'ailleurs il n'y a jamais été identifié sur les diagrammes RX.

CONCLUSION

Il apparaît possible de synthétiser à des températures de l'ordre de 700 à 800°C, des liants à propriétés comparables à celles des ciments portland courants, en partant pratiquement des mêmes matières premières. Le cas du "βC_2S sulfaté" décrit en est un exemple. Il en existe probablement d'autres susceptibles de fabrication industrielle. La méthode utilisée, à 750°C en milieu nitraté, pour la synthèse du "βC_2S sulfaté" n'est pas favorable d'un point de vue énergétique, la consommation globale d'énergie étant de l'ordre du triple de celle des procédés actuels de fabrication de ciment. En effet la réaction (2) de dénitratation est très endothermique. Cette méthode par la voie nitrique ne présenterait donc de l'intérêt que si l'énergie pouvait être fournie à bas prix, par des déchets par exemple, dans un procédé utilisant l'avantage du faible niveau de la température de cuisson (750°C). Mais dans la mesure où on sait que le "βC_2S sulfaté" présente des propriétés hydrauliques intéressantes, on peut espérer trouver une méthode pour le fabriquer d'une façon plus avantageuse du point de vue énergétique.

BIBLIOGRAPHIE

DALZIEL J.A. (1971). "A mini-cylinder test for the rapid determination of cement quality". Cem. Tech. pp. 101-112.

PLIEGO-CUERVO Y.B., GLASSER F.P. (1978). "Role of sulphates in cement clinkering : the calcium silico-sulphate phase". Cement and concrete Res., New-York, vol. 8, pp. 455-460.

PLIEGO-CUERVO Y.B., GLASSER F.P. (1979). "The role of sulphates in cement clinkering : subsolidus phase relations in the system : $CaO - Al_2O_3 - SiO_2 - SO_3$". Cement and concrete Res., New-York, vol. 9, pp. 51-56.

ARNOULD M., PHAN K.D. (1970). "Synthèse de quelques silicates par frittage d'oxydes purs et de minéraux naturels". C.R. 94ème Congrès Nal Stés savantes, Pau 1969, Sciences, t. II, pp. 87-97.

ARNOULD M., ITO K., PHAN K.D. (1973). "Procédé pour l'obtention de wollastonite synthétique". Brevet déposé le 2.08.1973, n°2.239.423.

ARNOULD M., LAVILLE P., STRUILLOU R. (1975). "Procédé pour l'obtention d'anorthite synthétique". Brevet déposé le 22.12.75, n°7539375.

ARNOULD M., STRUILLOU R., ROGER J. (1976). "Procédé pour l'obtention de liants hydrauliques et liants obtenus". Brevet déposé le 5.01.1976, n° 7600115.

BRETON D. (1978). "Contribution à l'étude d'un silicate dicalcique β très réactif synthétisé à 750°C". Thèse 3e cycle Géologie Ingénieur - Ecole des Mines de Paris et Université Paris VI. 121 p.

STRUILLOU R. (1975). "Etude des possibilités de fabrication de liants hydrauliques entre 600°C et 900°C". Rapport rech. au Ministère de l'Industrie

BRETON D., STRUILLOU R. (1977). "Etude des paramètres de fabrication du silicate dicalcique sulfaté par la voie nitrique". Rapport Rech. au Ministère de l'Industrie.

ARNOULD M., STRUILLOU R. (1979). "Possibilités de fabrication de liants hydrauliques entre 700 et 750°C - le βC_2S sulfaté". Rapport Rech. au Ministère de l'Industrie.

BRETON D., STRUILLOU R. (1977). "Essai de synthèse du silicate dicalcique en présence du chlorure ferreux". Rapport Rech. au Ministère de l'Equipement (DBTPC).

Utilisation du ciment sulfaté dans le béton armé de fibres de verre

Application of sulfating cement in glass fibre reinforced concrete

A. PACHTCHENKO, Membre-correspondant de l'Académie des Sciences d'Ukraine, Chef de Chaire des Ciments à l'Institut Polytechnique de Kiev,
H. STARTCHEVSKAIA, Docteur ès Sciences Techniques,
V. SERBINE, Docteur ès Sciences Techniques,
L. KALITA, Ingénieur.

RESUME: On a étudié le ciment contenant le sulfosilicate et le sulfoaluminate de calcium, ainsi que les processus de clinkerisation et du durcissement du ciment sulfaté. On a trouvé que le pH de ce ciment en cours de durcissement est inférieur de 2,0 - 2,5 à celui du ciment portland.

A l'aide de la méthode élaborée on a mis en évidence la stabilité élevée des fibres en verre contenant les oxydes de bore et d'aluminium dans le ciment sulfaté.

On a étudié les propriétés du système verre-ciment sulfaté.

SUMMARY: Cement including calcium sulfo-silicate and calcium sulfo-aluminate has been investigated. Clinker formation and hardening processes of sulfating cement has been studied. It is established that pH of hardening cement is 2,0 - 2,5 units lower than pH of portland-cement.

According to elaborated methods high resistance of alumo-boron-silicate fiber in sulfating cement is determined.

Properties of glass fiber cement in which sulfating cement is used as matrix has been explored.

Il y a assez longtemps que les ciments renforcés de fibres de verre constituent un objet de recherches scientifiques détaillées. On sait que l'armature constituée de fibres inorganiques est très efficace en raison de sa résistance élevée à la rupture par traction et de sa masse volumique faible. On dispose de données sur les méthodes de confection de différents éléments de construction, mais leur mise en oeuvre est freinée par une faible stabilité dans le temps des propriétés mécaniques.

Selon plusieurs auteurs, l'abaissement de résistance mécanique résulte de l'interaction du milieu alcalin du ciment durcissant avec les fibres de verre. Ce point de vue est confirmé par le fait que les fibres de verre perdent leur résistance mécanique après avoir été placées dans des solutions de NaOH, KOH, $Ca(OH)_2$ ayant un pH égal à 12,4 ce qui correspond au pH du ciment durcissant.

La stabilité dans le temps du système verre-ciment peut être améliorée par les méthodes suivantes: utilisation de fibres de verre résistant mieux à l'action des alcalis, enrobage des fibres, introduction des ajouts dans le liant, utilisation de ciments spéciaux ne détruisant pas les fibres de verre.

L'on sait que les fibres de verre se portent bien dans les ciments alumineux, mais ceux-ci ne sont pas largement utilisés en Génie Civil. Ces derniers temps on a élaboré le ciment sulfoalumosilicaté qui peut fournir une solution à ce problème.

Ce ciment est exempt de silicate tricalcique et d'aluminate tricalcique. Ses principaux constituants sont: le sulfoaluminate de calcium $3(CA).CaSO_4$ et le sulfosilicate de calcium $2(C_2S).CaSO_4$. On peut confectionner ce ciment à partir des matières premières suivantes: argile kaolinique, calcaire, gypse. En guise du gypse il est possible d'utiliser le phosphogypse qui est un résidu de la fabrication de l'acide phosphorique et des engrais phosphatés à partir des phosphates.

Etant donné que la composition des phases du clinker sulfaté diffère beaucoup de celle du clinker de ciment portland, on propose la formule suivante pour l'évaluation du coefficient de saturation:

$$CS = \frac{C_o - 0,55A_o - 1,05F_o - 0,7(SO_3)_o}{1,867S_o} \qquad (1)$$

où C_o, A_o, F_o, $(SO_3)_o$, S_o sont les teneurs en CaO, Al_2O_3, Fe_2O_3, SO_3, SiO_2 dans le mélange cru. On suppose que tout le SiO_2 fait partie de $2(C_2S)\cdot CaSO_4$ et de C_2S, ainsi que tout le Al_2O_3 entre dans $3(CA)\cdot CaSO_4$ et C_4AF. L'oxyde de fer entre dans C_4AF.

En outre on introduit le degré de saturation des silicates et aluminates par le gypse (DS_{SO_3}).

$$DS_{SO_3} = \frac{(SO_3)_o - 0,261A_o + 0,166F_o}{0,667S_o} \qquad (2)$$

Lorsque $DS_{SO_3}=1$, on constate la formation des composés: $2(C_2S)\cdot CaSO_4$ et $3(CA)\cdot CaSO_4$ saturés au maximum par le sulfate. Lorsque $DS_{SO_3} > 1$ il y a de l'anhydrite en excès.

Les processus de clinkérisation dans les mélanges des matières premières contenant des sulfates se distinguent de ceux, qui ont lieu lors de la cuisson du clinker portland.

Nous avons étudié les processus de formation des minéraux du clinker dans les mélanges contenant des sulfates. Pour cela on a préparé les mélanges à deux et à trois composants (craie-kaolin et craie-kaolin-phosphogypse). Les mélanges étaient soumis à l'analyse thermique différentielle ainsi qu'à la cuisson entre 600° et 1300°C à des températures par intervalles de 100° avec des paliers de 20 minutes. On a soumis à l'analyse aux rayons X les mélanges obtenus, et on a déterminé la teneur en chaux libre et les pertes au feu.

L'analyse thermique différentielle du mélange craie-kaolin met en évidence deux effets endothermiques aux températures 575° et 930°C et un crochet exothermique à 995°C. Les traces de chaux libre font leur apparition à 700°C, sa teneur maximum est atteinte à 1000°C. A 1300°C il ne reste que

2,8 % de chaux libre. A la température de 1250°C la chaux est combinée à 93,1 %.

La courbe de l'analyse thermique différentielle du mélange contenant du gypse est caractérisée par l'effet endothermique double aux basses températures, dû à la déshydratation du gypse. L'effet endothermique dû à la décarbonatation de la calcite est déplacé de 930° jusqu' à 900°C. On peut juger de l'intensification des processus de formation du clinker d'après les variations de teneur en chaux libre. Elle fait son apparition à 600°C, sa teneur maximum est atteinte à 900°C, à 1300°C il ne reste que 0,8 % de CaO, à la température de 1250°C la chaux libre est combinée à 98,5 %.

L'analyse aux rayons X a démontré que dans les mélanges ternaires les raies du sulfosilicate de calcium ont fait leur apparition à 1000°C et celles du sulfoaluminate à 1100°C.

Les processus d'hydratation des clinkers contenant des sulfates diffèrent de ceux du clinker de ciment portland. Ce sont l'ettringite et l'hydrosilicates du groupe de la tobermorite qui se forment en premier lieu. La chaux libre est absente.

Le durcissement des ciments contenant des sulfates est assez rapide. Leur résistance à trois jours atteint 50-70 % de celle à 28 jours. Il sont plus stables vis-à-vis des sulfates. De tout ceci nous pensons pouvoir conclure, que ces ciments doivent être moins agressifs par rapport aux fibres de verre. Le pH de ces ciments varie aux alentours de 9,8-10,0 ce qui est inférieur de 2,0-2,5 à celui du ciment portland et du même ordre que celui des ciments alumineux.

L'étude de la stabilité des fibres de verre dans les ciments sulfatés, le ciment portland et le ciment alumineux au gypse a été faite par une méthode accélérée.

Nous avons élaboré cette méthode en nous basant sur le fait, que la vitesse de réaction entre le ciment durcissant et les fibres de verre croît avec la température. C'est pourquoi, après avoir déterminé le coefficient thermique d'accroissement de la vitesse de réaction et ayant choisi la température, il est possible de calculer la durée du traitement par étuvage des compositions verre-ciment, ce qui correspondera à la durée et la température d'exploitation de ces compositions dans les conditions naturelles. Comme paramètre caractérisant la résistance des compositions verre-ciment, nous avons choisi la limite de rupture par traction des éprouvettes renforcées de fibres en verre alcalin, non-alcalin et contenant Zr. Les compositions chimiques sont présentées dans le tableau I.

L'armature a permis de réduire la dispersion des résultats d'essais et d'abaisser le coefficient de variation lors des essais paralleles jusqu'à 2-7 %. Ayant fait les essais préalables nous avons évalué le coefficient thermique de croissance de la vitesse de réaction lors d'une montée en température de 10°C, celui-ci étant égal à 2,69 en moyenne. Cela nous a permis d'aboutir à la formule suivante:

TABLEAU I

Compositions chimiques des fibres de verre

Verre	Teneur en oxydes, %						
	SiO_2	Al_2O_3	CaO	MgO	B_2O_3	ZrO_2	K_2O+Na_2O
alcalin	70,12	2,19	6,96	5,49	-	-	15,36
non-alcalin	52,29	16,17	16,48	5,16	9,45	-	0,51
contenant Zr	61,89	2,13	5,39	1,46	-	15,63	13,48

$$t_2 = \frac{t_1}{2{,}69^{\frac{T_2-T_1}{10}}}, \qquad (3)$$

dans laquelle:

t_1 = durée d'exploitation des compositions dans les conditions normales, en heures

t_2 = durée du traitement par étuvage, en heures

T_1 = température d'exploitation des compositions, en °C

T_2 = température de l'étuvage, en °C.

Pour les essais nous nous sommes procurés du ciment obtenu par voie sèche dans un four rotatif 3,5/3,0 x 60 m. La cuisson a été faite à 1280 - 1310°C. La composition minéralogique: $2(C_2S)\cdot CaSO_4$ = 40,14 %, $3(CA)\cdot CaSO_4$ = 15,09 %, C_2S = 27,34 %, C_4AF = 1,52 %. Parallélement on a fait des essais de ciment portland et de ciment alumineux au gypse. Le tableau II montre les caractéristiques des ciments.

Les résultats de ces essais sont présentés dans le tableau III. La résistance des compositions à base du ciment alumineux au gypse s'abaisse dans le temps, comme dans le cas du ciment sulfaté. Mais leur résistance résiduelle après 10 ans est de 2 ou 3 fois supérieure à celle des compositions à base du ciment portland. Il faut noter, que cet abaissement est appréciable jusqu'à l'âge de 5 ans.

TABLEAU II

Caractéristiques des ciments

Ciment	Rapport E/C	Résistance à la rupture par compression, en N/mm², après		
		3j.	7j.	28j.
sulfaté	0,45	19,0	30,0	46,0
portland	0,40	24,3	35,9	47,2
alumineux au gypse	0,30	32,8	38,1	41,0

On a fait l'examen au microscope électronique des surfaces des fibres avant et après les essais accélérés. La surface des fibres dans le ciment portland est recouverte d'une couche continue de produits de réaction du ciment avec le verre et ceci sous forme d'hydrosilicates de différente basicité. La surface des fibres dans le ciment sulfaté ou alumineux au gypse est moins corrodée.

CONCLUSIONS

Les recherches accomplies montrent que le ciment sulfaté est un liant convenant à la

TABLEAU III

Influence du ciment sur la résistance des compositions verre-ciment

Fibres en verre	Résistance à la rupture par traction, en % *						
	1 mois	6 mois	1 an	2 ans	3 ans	5 ans	10 ans
	Ciment portland						
alcalin	67,6	48,1	29,6	16,7	12,0	8,3	7,2
non-alcalin	50,8	30,1	25,4	23,8	19,0	14,3	12,7
contenant Zr	65,0	57,5	53,7	42,5	33,7	20,0	19,4
	Ciment alumineux au gypse						
alcalin	77,2	60,2	55,5	47,2	39,8	17,6	16,3
non-alcalin	77,8	76,2	70,2	53,9	42,8	30,1	28,0
contenant Zr	83,7	80,0	78,5	77,5	76,2	73,7	70,1
	Ciment sulfaté						
alcalin	73,9	51,5	39,1	35,9	33,7	19,6	19,6
non-alcalin	83,7	63,6	44,9	34,5	32,4	28,3	26,0
contenant Zr	90,0	83,3	80,4	75,1	70,5	65,3	63,7

* 100 % correspond à la résistance après 3 - 10 jours.

confection des éléments de construction en béton renforcé de fibres de verre. La production du ciment sulfaté ne comporte aucune difficulté. La température de cuisson plus basse (1250-1280°C) permet de réduire la consommation de combustible. En outre, la possibilité d'utiliser certains déchets de l'industrie chimique présente un interêt pour la protection de l'environnement.

BIBLIOGRAPHIE

1.- W. GUTT, M.A. SMITH (1967)"Studies of SUB SYSTEM CaO-CaO·SiO_2-$CaSO_4$", British Ceramic Society, Vol.66, pp. 557-567.

2. - T.H. TADGIEV, T.A. ATAKOUZIEV et B.H. TADGIEV (1972) "Matériaux inorganiques", Comptes rendus de l'Académie des Sciences de l'URSS, n°9 (en russe).

3. - A.A. PACHTCHENKO (1978) "Nouveaux ciments", p.220 (en russe).

4. - A.A. PACHTCHENKO, V.P. SERBINE, A.P. PASLAVSKAIA, V.R. BONDAR (1978) "Matériaux inorganiques", Comptes rendus de l'Académie des Sciences de l'URSS, n°3, pp. 576-580 (en russe).

4. - A.A. PACHTCHENKO (1979) "Bases physico-chimiques des compositions: liant minéral- fibres de verre" pp. 224 (en russe).

The chemical resistance of high alumina cement concrete

La résistance chimique du béton de ciment alumineux

H.G. MIDGLEY, Concrete Research Laboratory, Civil Engineering Division, The Hatfield Polytechnic, Hatfield, Herts, U.K.

RESUME : Le béton de ciment alumineux (h.a.c.) résiste à l'attaque des sulfates, des chlorures et de l'eau de mer, à condition qu'il ait été préparé correctement et correctement mis en oeuvre. Mais si ce ciment a accompli, en grande partie, sa conversion cristalline et si le béton est fissuré (notamment par la précontrainte), il peut subir une attaque fissurante par les sulfates. L'eau de mer et les chlorures semblent n'entraîner qu'une faible attaque fissurante.

L'hydrolise alcaline et la carbonatation en présence d'hydroxydes alcalins peuvent provoquer la destruction complète du ciment de ces bétons (h.a.c.).

SUMMARY:-

High alumina cement concrete (hacc) is resistant to sulphates, chlorides and sea water if correctly made and used in the correct manner. If, however, the hacc is highly converted and cracked (for example prestressing cracks) then it may be disruptively attacked by sulphates. Sea water and chloride appear to have little disruptive effect.

Alkaline hydrolysis, the carbonation in the presence of alkaline hydroxides can completely disrupt the cement part of hacc.

1. INTRODUCTION:

High alumina cement concrete has the reputation of being a chemically resistant construction material. However, there have been reports that hacc may be vulnerable to sulphate attack (1); chloride attack (2) and may be vulnerable to sea water. Hacc may also be disrupted by atmospheric CO_2 in the presence of sodium potassium hydroxide polutions. This paper reports on the conditions where hacc may be vulnerable.

2. Sulphate attack

Hydrated hac is based on hydrated calcium aluminates which might react with $CaSO_4$ to form ettringite, but it has been shown (2) that only $3CaO\ Al_2O_3\ 6H_2O$, the cubic hydrate formed in conversion of hacc will react.

Hacc with conversion increases in porosity by about 10 %, but if massive hacc is exposed to ground sulphates (e.g. $MgSO_4$), then if fully converted (2) (Dc greater than 90%) ettringite of composition about $6CaO,\ 2Al_2O_3.\ 2.15SO_3,$ $0.02\ SiO_4,\ 0.65\ OH.\ 32H_2O$ will be formed, but even after 18 years the depth of penetration is only about 5mm. These findings are in agreement with laboratory experiments with varying degrees of conversion made with various mixes and w/c ratios (Table 1) and exposed to saturated $CaSO_4$ sclution had penetrations of only a few mm.

Table 1.

Mix composition cement/aggregate	w/c	curing conditions	Dc	Depth of penetrat: :ion
1:3	0.35	1y20°C + 1y sulphate	50	4
1:4½	0.48	do.	30	4
1:6	0.6	do.	30	6
1:3	0.35	9m@ 25 + 1y sulphate	50	3
1:4½	0.48	do.	45	5
1:6	0.60	do.	50	6
1:3	0.35	3m@ 38°C + 1y sulphate	80	3
1:4½	0.48	do.	80	5
1:6	0.60	do.	80	6
1:3	0.35	1month 50°C + 1y sulphate	85	9
1:4½	0.48	do.	90	10
1:6	0.60	do.	90	9

In the case of prestressed hacc beams used for roof support where there has been leakage of rain water through gypsum plasters ($CaSO_42H_2O$), ettringite of composition $6CaO,1.95Al_2O_3.\ 0.21Fe_2O_3.$ $2.51SO_4.\ 0.48OH.\ 32H_2O$ was found, in a few cases to a depth of 20mm. This reaction contributed to the failure of the roof beams (1). The hacc of the beam was highly converted (Dc greater than 90%), but by comparison with massive hacc it was concluded that some other path beside the increase in porosity on conversion is needed for the sulphate ions; and in the case of prestressed beams, microcracks are the most likely.

In another case ettringite was found at least 100mm from the surface of an hacc prestressed beam and the source of the sulphate ions was the Ordinary Portland cement screed of the floor deck; here the beam has cracked by the prestressing. Also the alkaline hydroxide solutions from the O.P.C. concrete had attacked the cement by "alkaline hydrolysis" (see later) which is likely to have made the concrete more vulnerable to sulphate attack.

If hacc concrete is of poor quality, e.g. made with too low a cement content and too high a w/c ratio it will be extremely vulnerable to acid sulphate attack if highly converted. Sewer linings which had been used in a site with acid sulphate ground water from old metallurgical tips showed considerable attack, etrringite of composition $6CaO,\ 1.78,$ $Al_2O_3.\ 0.4\ Fe_2O_3.\ 2.65SO_4.\ 0.07SiO_4.0.29(OH).$ $32H_2O$ was found.

To detect the ettringite in attacked hacc, the following techniques are useful:-

X-Ray diffraction with a characteristic reflection at 9.73Å. Differential Thermal analytical techniques with a strong sharply defined endotherm at about 100°C.

Alkaline hydrolysis

Alkaline hydrolysis of hacc was first described (3) in 1936. This form of attack may completely disrupt the concrete reducing the cement part to a powder. It only takes place in the presence of sodium or potassium hydroxide solutions and CO_2. The alkalies appear to act as carriers for the CO_2 which attacks the cementitious calcium aluminate hydrates to form AH_3 and $CaCO_3$. It must be pointed out that carbonation of hacc in the absence of alkali hydroxides may be beneficial giving an increase in strength (4).

Experimental work has shown that pH alone (triethanolamine) in the presence of CO_2; alkali hydroxides in the absence of CO_2, Sodium and ammonium chloride of high pH in the presence of CO_2 will not cause the decomposition of hacc, but alkali hydroxides in the presence of CO_2 will rapidly decompose the calcium aluminate hydrates.

A number of examples of hacc prestressed beams which have suffered alkaline hydrolysis have shown that the concrete has always produced a fine loose powder which may be brushed away. Mineralogical analysis have shown the products to be AH_3 (either alpha or gamma) and $CaCO_3$.

Chemical analysis of the acid soluble extract of the cement part of the hacc, for Al_2O_3 , K_2O and Na_2O have always shown that the ratio of $Al_2O_3/Na_2O + 0.658K_2O$ (A/TA) to be low.(a high alkali concentration in relation to the Al_2O_3 content of hac - 40%) From a statistical examination of the chemical analysis of U.K. hac the limit of A/TA has been found to be 75.3. From the analysis of 70 samples of hacc which showed powdering the A/TA ratio were 12.3, 25.8, 58.8, 48.4, 52.5, 12.9, while for an equal number of unattacked samples the ratio were 144, 218, 125, 259, 139, 343. By mineralogical techniques of the attacked samples only AH_3 and $CaCO_3$ were found, while in the unattacked samples, CAH_{10}, AH_3, C_3AH_6 etc. were detected. In some samples calcium aluminate hydrates (CAH_{10} and C_3AH_6) were detected but the A/TA ratio was low, 22.9, 26.7, 20.6, 50.3. These samples were considered to be vulnerable. The source of alkali hydroxides is usually external; e.g. from water leaching of porous ordinary Portland cement; but the source may be internal, the extractable K_2O from the micas in the aggregate have been found to provide the alkali hydroxides for alkaline hydrolysis. Alkaline hydrolysis depends on 4 factors; highly permeable concrete, moisture, CO_2 and free alkali hydroxides. Any degree of conversion is vulnerable.

Sea water attack

High alumina cement concrete exposed to sea water will convert very slowly; between 0 - 15% in 34 years; there may be some superficial attack to form ettringite; but the concrete appears to be always sound.

If the hacc is used in a tidal zone then that part which is exposed to the air will convert more rapidly than the submerged part with the concurrent loss in strength due to conversion. However examination of laboratory structure epecimens as well as existing structures whows that even in this region the attack was superficial.

Chloride Attack

No laboratory studies of chloride attack have been carried out and one example of suspected chloride attack of a structure has been seen. A prestressed hacc beam had been exposed to road de-icing salt. One beam had a failure of the end shearing, with exposure of the tendon; the chloroaluminate $C_3A.CaCl_2, 12H_2O$ was detected in the cement part of the hacc but it cannot be established if the formation of this mineral by chloride attack contributed to the failure or if the failure was due to the reduction in passivity to rusting of the tendon by the presence of the chloride ion.

REFERENCES:

(1) S C Bate; Report on failure of Roof beams at Sir John Cass' Foundation and Red Coat School Stepney, B.R.E. Current paper CP58/74, 1974.

(2) H G Midgley and A Midgley. The conversion of high alumina cement, Magazine of Concrete Research, 27, 91 (1975) 59-77.

(3) E Rengade, P. L'Hospitallier, P Durande de Foutmagne Revue des mats. de Constr. et de Trav. Publ. 318, 1936.

(4) E Rask. RILEM Int. Symp Carbonation of Concrete, Wexham 1976.

Ciment expansé composé d'un ciment normal et d'un ajout complexe

Expansive cement conceived on the basis of normal cement and a complex admixture

N.B. DJABAROV, Docteur-Ingénieur et
Y.T. SIMEONOV, Professeur, Docteur-Ingénieur, Laboratoire Central de Mécanique Physique-Chimique, Académie Bulgare des Sciences, Sofia, Bulgarie.

RESUME : Un nouveau type de ciment expansif, composé d'un ciment normal et d'un ajout complexe a été récemment élaboré. Grâce à l'ajout, la structure et les propriétés mécaniques des ciments ordinaires sont modifiées de manière qu'ils se transforment en ciments spéciaux, expansifs.
Suivant les besoins de la construction et de l'industrie des éléments préfabriqués, les ciments normaux peuvent ainsi obtenir les qualités désirées : soit un ciment à retrait compensé, soit un ciment expansif ou bien un ciment autocontraint.

L'expansion des ciments ainsi modifiés peut être contrôlée avec précision et atteindre les valeurs exigées (de 0,1 à 4 % pour un mortier standard de ciment : sable = 1:3 ou béton). L'expansion se produit et se termine définitivement dans les 1 à 3 premiers jours, aussi bien dans la conservation dans l'eau que dans celle à l'air.

Compte tenu de leur grande expansion, ces nouveaux ciments expansifs possèdent des résistances mécaniques relativement élevées. Ils manifestent aussi une résistance contre la pénétration et le passage de l'eau bien augmentée et un fluage et une déformabilité diminués.

SUMMARY : A new typ of expansive cement conceived on the basis of normal cement and a complex admixture was recently elaborated. By means of the admixture the structure and the mechani - cal properties of ordinary cements are modified in such manner that they are transformed in special expansive cements.

According to the needs of construction and prefabricated elements industry the normal cements can obtain the very exactly regulated qualities of a shrinkage compensated cement, or of expansive cement, or of selfstressing cement.

The expansion of the modified cements can be precisely controlled and to receive the needed value - 0,1 to 4 % for standard mortar cement:sand = 1:3 or concrete. The expansion is displaying and is definitively terminated in the initial 1 - 3 days of hardening under water or only on the air.

Comparatively to the great expansion the new expansive cements have high mechanical strengths. They are manifesting also increased resistance against water leakage and diminished creep and general deformation.

Les difficultés d'obtenir un ciment expansif des qualités sûrement reglées et controlées et la complexité de sa technologie de production sont bien connues. Pour surmonter ces defauts au Laboratoire Central de Mécanique Physico-Chimique de l'Académie Bulgare des Sciences ont été entrepris des études visant la modification des ciments normeaux au moyen d'un adjuvant complexe en ciments spéciaux - expansifs. Ainsi le ciment portland devient un liant beaucoup plus universel. Cela découvre la possibilité de le transformer très facilement et conformément aux besoins de la construction et de l'industrie des éléments de construction en ciment de retrait compensé, ou en ciment expansif ou en ciment autocontraint.

Grace à l'adjuvant expansif (AE) au ciment durcis se forme la quantité nécessaire d'ettringite pour rendre sa structure beaucoup plus dense et pour provoquer expansion d'une grandeur désirée. Pour ce but les composents de l'adjuvant contienent les éléments nécessaires pour la formation d'ettringite pendant une période déterminée du durcissement.

La structure du ciment avec et sans l'adjuvant expansif a été étudiée par différentes techniques, mais dans cette brève communication l'effet de l'adjuvant expansif est illustré par l'analyse thermique d'un ciment portland. Sur les figures 1 et 2 sont données schématiquement les courbes de thermogravimétrie différentielle (TGD), d'analyse thermique différentielle (ATD) et de ther - mogravimétrie (TG) après 1 jour de durcissement. Les données expérimentales confirment en générale au point de vue qualitative la présence des produits d'hydratation simi - laires, mais présentent des grandes différences quantitatives. Le ciment durcis avec l'adjuvant expansif contient beaucoup plus d'ettringite. L'analyse prouve aussi que l'hydratation entière est plus avancée. Au contraire - la quantité du portlandit est un peu diminuée.

L'adjuvant "AE" forme l'ettringite supplémentaire indépendement de la composition du ciment employé comme base. Pour cela non seulement le ciment portland normal peut être modifié en ciment expansif, mais aussi d'autre types, comme portland du durcisse - ment rapide, ciment à laitier de haut-fourneau, ciment pouzzolanique etc.

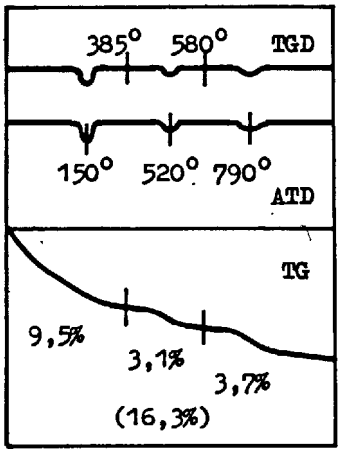

Fig. 1 - Analyse thermique d'un ciment portland normal.

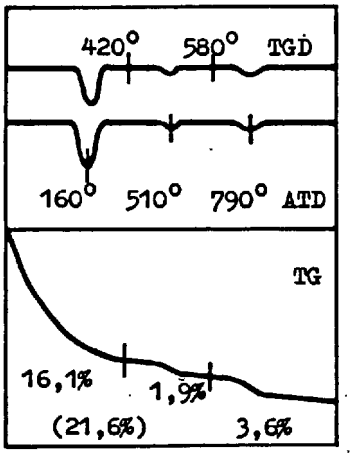

Fig. 2 - Analyse thermique d'un ciment portland normal + l'adjuvant expansif.

Les qualités mécaniques des ciments (déformation, résistance) sont examinées avec un mortier normalisé avec le rapport ciment : sable = 1:3 et rapport E/C = 0,5. La méthode employée est identique à celle qu'on utilise dans plusieur pays comme méthode-standard pour éprouver les qualités des ciments. Cette méthode etait préferée, car elle possède tous les avantage d'une méthode standartisé, usage de même équipement etc. En utilisant

des mortiers plus riches en ciment ou du ciment pur, comme est pratiqué largement pour établir les qualités des ciments expansifs connus, les résultats sont relévés et l'expansion et la résistance obtenues sont beaucoup plus hautes comparées aux résultats obtenus en utilisant le mortier normalisé ou le béton.

Pour prouver l'application d'adjuvant expansif pour différents types des ciments sont donnés des examples d'un ciment du durcissement rapide CPR, de deux ciments portland normal CPN et CPN^{X} et d'un ciment à laitier de haut-fourneau avec differentes quantités de l'adjuvant expansif AE, AE^{X} et AE^{XX}.

Les ciments à laitier de haut-fourneau CLHF sont à peine connus comme base des ciments expansif ou plus tôt d'essai d'obtenir seulement un ciment d'un retrait compensé. Pour cela la production d'un ciment expansif à la base de ces ciments à prix bas presente un intérêt technique et économique particulier.

Les ciments expansifs connus montrent habituelement une expansion seulement en durcissant sous l'eau ou par mouillage abondant - conditions qui sont difficiles à réaliser en pratique. Pour cela les qualités des ciments expansifs conçus à la base d'un adjuvant complexe etaient établies aussi dans des conditions à durcissement seulement à l'air, sans aucun mouillage.

Tableau I montre l'expansion libre du mortier normalisé en conditions du durcissement sous l'eau ou seulement à l'air.

Au tableau II sont donnés quelques examples de l'expansion restreinte du mortier d' un CPN + AE au moyen d'une barre d'acier située longitudinalement dans la prisme. En changeant le diamètre de la barre, sont obtenus differents rapports en % entre la section de l'armature et la section de la prisme du mortier.

Les résultats expérimentaux montrent que tous les types des ciments étudiés peuvent

TABLEAU I

Type du ciment	Expansion libre, %, après jours		
	1	3	28
	Durcissement sous l'eau		
CPR	-	-	-
$CPR+AE^{X}$	0,29	0,38	0,38
$CPR+AE^{XX}$	0,41	1,11*	1,11
CPN	-	-	-
$CPN+AE^{X}$	0,29	0,31	0,31
$CPN+AE^{XX}$	0,89	0,91	0,92
CPN^{X}	-	-	-
$CPN^{X}+AE^{X}$	1,59	1,98	1,98
$CPN^{X}+AE^{XX}$	4,11	4,14	4,14
CLHF	-	-	-
CLHF+AE	0,47	0,49	0,49
$CLHF+AE^{X}$	1,69	1,72	1,72
	Durcissement à l'air		
CPR		retrait	
$CPR+AE^{X}$	0,07	0,09	0,08
$CPR+AE^{XX}$	0,09	0,18*	0,18
CPN		retrait	
$CPN+AE^{X}$	0,05	0,03	0,01
$CPN+AE^{XX}$	0,13	0,12	0,09
CPN^{X}		retrait	
$CPN^{X}+AE^{X}$	0,32	0,30	0,27
$CPN^{X}+AE^{XX}$	0,50	0,46	0,44
CLHF		retrait	
CLHF+AE	0,13	0,13	0,13
$CLHF+AE^{X}$	0,27	0,27	0,25

Remarque*: Pour cettes prismes les mésurements de l'expansion sont faites à l'âge de $7^{ème}$ jour, au lieu de 3^{eme}.

être modifiés en ciments expansifs avec une expansion très justement réglable par la quantité de l'adjuvant expansif. Selon les besoins de la construction on peut obténir dans les conditions du durcissement normalisé une expansion libre de 0,1 à 4 % et de plus. C'est-à-dire on peut obténir selon la valeur de l'expansion tous les types des ciments expansifs: ciment avec un retrait compensé, un ciment d'expansion moyenne et un ciment autocontraint avec une grande expan -

sion. L'expansion se manifeste pendant la période initiale du durcissement et se termine définitivement jusqu'au troisième jour. A l'âge de 28 jours et plus tard le volume est tout-à-fait stable.

En durcissement à l'air les ciments sans l'adjuvant expansif montrent seulement un retrait. En employant l'adjuvant complexe tous les types des ciments changent à fond leur comportement et manifestent une expansion bien exprimée. Cela facilite et enlarge beaucoup l'usage des ciments expansifs conçus à la base des ciments normaux et d'adjuvant.

TABLEAU II

Armature d'acier % de la section de la prisme	Expansion restreinte d'acier de l'armature et du mortier, % après jours		
	1	3	28
0,20	0,22	0,23	0,23
0,44	0,10	0,12	0,12
1,23	0,04	0,04	0,04

L'expansion restreinte est aussi bien exprimée même avec un pourcentage de l'armature assez haut. Cela témoigne les possibilités d'assurer l'obtention d'un ciment autocontraint de haute qualité, qui est objet d'une autre étude spéciale.

Les résistances mécaniques des ciments CPR, CPN, CPN^{X}, CLHF avec ou sans l'adjuvant expansif sont presentées au tableau III. Celles d'un ciment portland normal CPN^{XX}+AE examinées pour une expansion restreinte sont données au tableau IV.

Les résultats expérimentaux montrent qu' il existe une correspondance bien définie entre l'expansion et la résistance mécanique. En réglant le dégré de l'expansion on peut prévoir et obténir une résistance mécanique désirée. Pour le durcissement sous l'eau la résistance initiale pour une expansion de 0,3-0,5 % est à peu près cette du ciment

TABLEAU III

Type du ciment	Résistance en compression, N/mm^2, après jours	
	1	28
	Durcissement sous l'eau	
CPR	19,7	57,2
CPR+AE^{X}	18,0	57,2
CPR+AE^{XX}	14,8	41,9
CPN	11,6	49,0
CPN+AE^{X}	19,4	46,9
CPN+AE^{XX}	9,2	28,4
CPN^{X}	5,4	40,3
CPN^{X}+AE^{X}	3,0	20,9
CPN^{X}+AE^{XX}	1,0	8,6
CLHF	6,9	28,7
CLHF+AE	8,5	33,5
CLHF+AE^{X}	6,6	24,7
	Durcissement à l'air	
CPR	18,0	45,7
CPR+AE^{X}	20,0	52,1
CPR+AE^{XX}	19,0	50,8
CPN	-	41,7
CPN+AE^{X}	-	46,4
CPN+AE^{XX}	-	49,1
CPN^{X}	-	29,8
CPN^{X}+AE^{X}	9,2	33,2
CPN^{X}+AE^{XX}	12,2	31,3
CLHF	3,5	21,4
CLHF+AE	9,8	42,0
CLHF+AE^{X}	5,2	44,2

sans adjuvant expansif (CPR), ou avec 1,2 fois plus haute (CLHF), ou bien 1,7 fois plus haute (CPN). Pour une expansion libre beaucoup plus grande de l'ordre 0,9-1,1 % la résistance est déjà un peu plus basse (CPR et CPN) en comparaison avec les mêmes ciments non modifiés. En augmentant encore l'expansion libre vers 1,7-2 % la résistance est presque égale (CLHF) à celle du même ciment sans adjuvant ou de 40 % plus basse (CPN^{X}). En accroissant l'expansion à une très haute valeur de plus de 4 % (CPN^{X}), quoique les prismes recoivent des fissures,

elles gardent leur intégrité et manifestent certaine résistance mécanique - 20 % par rapport au ciment sans adjuvant. Pour la plupart des ciments avec AE la résistance à l'âge de 28 jours garde en général son rapport envers cette des ciments respectifs, mais sans l'adjuvant. Cela témoigne une bonne accroissement de la résistance méca - nique avec l'avancement du temps, similaire à ce des ciments normaux employés comme base.

Pour le durcissement à l'air, c'est à dire dans les conditions réeles, tous les ciments modifiés en ciments expansifs pour les differentes valeurs de l'expansion (tableau III) possèdent une résistance supérieure à celle des mêmes ciments, mais sans AE. L'accroissement des résistances est particu - lièrement bien éxprimé pour les ciments CLHF.

Les hautes valeurs de la résistance méca - nique comparées aux grandes expansions obtenues s'expliquent par le fait que l'expansion se manifeste à la période initiale du durcissement. A ce temps là le ciment durcissant support beaucoup plus mieux les déformations sans empêcher la formation de la structure et le développement de la résis - tance mécanique.

TABLEAU IV

Armature d' acier, % de la section de la prisme	Résistance en compression du mortier, N/mm^2, après jours	
	1	28
0,20	11,5	37,5
0,44	12,9	40,6
1,23	13,6	38,4

L'étude à conditions restreintes montre qu' en augmentant le pourcentage de l'armature envers la section du mortier la résistance mécanique s'accroît (tableau IV). Cet ac - croissement de la résistance peut être encore plus grand si la restriction de l'ex - pansion est spaciale et non pas seulement dans une direction.

Les qualités des ciments expansifs conçus à la base des ciments normaux et d'un adjuvant expansif etaient étudiées aussi sur éprou - vettes du béton*.

TABLEAU V

Type du ciment	Expansion libre du béton, %, après jours		
	1	3	28
	Durcissement à l'air		
CPN^{XXX}	-0,02	-0,06	-0,09*
CPN^{XXX}+AE	0,06	0,10	0,10
CPN^{XXX}+AE^{X}	0,08	0,12	0,13
$CLHF^{X}$	-0,03	-0,07	-0,11*
$CLHF^{X}$+AE	0,02	0,05	0,04

Remarque*: Le retrait est marqué par "-".

TABLEAU VI

Type du ciment	Résistance en compression du béton, N/mm^2, après jours	
	1	28
	Durcissement à l'air	
CPN^{XXX}	1,3	24,1
CPN^{XXX}+AE	6,1	33,1
CPN^{XXX}+AE^{X}	6,1	28,6
$CLHF^{X}$	0,7	18,0
$CLHF^{X}$+AE	5,3	20,4

Quelques examples du béton d'un ciment portland normal CPN^{XXX} et un ciment à laitier de haut - fourneau $CLHF^{X}$ avec différentes quantités ou sans adjuvant expansif (AE, AE^{X}) sont donnés pour l'expansion libre au tab - leau V et pour la résistance mécanique au tableau VI. Le béton est avec 420 kg ciment pour un m^3 et d'un diamètre des agrégats jusqu'à 20 mm. Le durcissement du béton est à l'air sans d'être mouillé.

Remarque *: Dans les études du ciment expansif à la base du CLHF et des bétons expansifs a pris part aussi Dr.Ing. V. Petkova.

Les résultats expérimentaux montrent que sous l'influence de l'adjuvant expansif le béton, de même que le mortier, change à fond ses propriétés. Au lieu du retrait de 0,09 - 0,11 % jusqu'à 28-ème jour il manifeste une expansion bien exprimée de 0,04-0,13 % pour le même âge.

A cause de sa structure beaucoup plus dense et l'augmentation de la phase cristalline (ettringite) le béton à la base d'un ciment avec l'adjuvant expansif possède une résistance contre la pénétration de l'eau beaucoup plus haute et un fluage réduit par rapport du même béton mais d'un ciment sans l'adjuvant expansif.

Des études durables sur les qualités mécaniques montrent que le fluage du béton à l'âge de presque une et demie année est 0,238 %, tandis que pour la même période celui avec le ciment portland normal modifié par différents quantités de l'adjuvant expansif est seulement 0,183 - 0,216 %. Respectivement les déformations entières des bétons sont pour le normal 0,358 % et pour l'expansif 0,061 - 0,150 %. Ces chiffres prouvent une réduction du fluage sous l'influence de l'adjuvant expansif de 1,1 à 1,3 fois et de la déformation entière de presque 2,4 à 5,9 fois.

Les résultats expérimentaux pour béton d'un ciment à laitier de haut - fourneau montrent la même tendance de réduction du fluage et de la déformation entière par suite de la modification du ciment CIHF à un ciment expansif.

La résistance du béton expansif contre la pénétration de l'eau est 3,5 à 5 fois améliorée en comparaison avec celle du béton des mêmes ciments, mais sans l'adjuvant expansif.

Les résistances mécaniques des bétons (tableau VI) sont augmentées d'une manière expressive par la modification des ciments au moyen de l'adjuvant complexe. L'élévation atteind une très haute valeur de 4,7 à 7,6 fois pour le premier jour et de 1,14 à 1,38 fois pour le 28-ème jour.

La méthode d'obtention des ciments expansifs à la base des differents ciments normaux et d'un adjuvant expansif complexe est brevetée en plusieurs pays et aux Etats Unis, l'Espagne, R. D. Allemagne etc. les brevets sont déjà publiés.

CONCLUSIONS

Une méthode très efficace et facilement réalisable d'obtention des ciments expansifs etait crée. Au moyen d'un adjuvant complexe differents types des ciments ordinaires comme ciment portland normal, ciment du durcissement rapide, ciment à laitier de haut - fourneau etc. sont modifiés à des ciments spéciaux d'une expansion très justement réglable, qui se manifeste et se termine dans les premiers 1 à 3 jours du durcissement. Conformément la valeur de l'expansion on peut obténir tous les types des ciments expansifs: ciment d'un retrait compensé, ciment d'expansion moyenne et ciment autocontraint.

Les nouveaux ciments expansifs montrent une expansion bien exprimée en durcissant sous l'eau ou seulement à l'air sans aucun mouillage.

En réglant le dégré de l'expansion on peut prévoir et obtenir une résistance mécanique désirée. Parce que l'expansion se manifeste seulement à la période initiale du durcissement, quand le ciment durcis support mieux les déformations, les ciments expansifs à la base de l'adjuvant complexe possèdent des hautes résistances mécaniques.

Les ciments expansifs conçus à la base des ciments normaux et d'adjuvant manifestent une résistance contre la pénétration de l'eau bien augmentée et un fluage et déformation entière diminués.

Les qualités des nouveaux ciments expansifs sont prouvées comme par mortier standard, ainsi que par béton.

The structure and characteristics of bleached clinker

Structure et propriétés des clinkers de ciment blanc

K. KARIBAYEV, Doctor-engineer,
K. BEKISHEV, Doctor-engineer,
D. ALDIYAROV, Doctor-engineer,
V. LYSENKO, Kazakh Institute of Chemical Technology, Chimkent, U.R.S.S.

RESUME : Dans cette communication, nous exposons les résultats de recherches sur l'influence des amino-alcools (TEA,MEA)et de liquides silico-organiques sur le processus de blanchiement des clinkers de ciment portland blanc et sur leurs propriétés. On a établi qu'un refroidissement brusque dans une solution aqueuse à 1 à 2 % de mono et de triéthanolamine augmente le coefficient de réflexion diffuse (C.R.D.) du clinker blanc de 5 à 9 %. Le refroidissement brusque dans une solution à 0,5 % des liquides silico-organiques GKG-10 et GKG-11 augmente ce C.R.D. de 8 à 10 % par rapport au blanchiement aqueux. Pour mettre en évidence les conditions optimales de blanchiement du clinker, nous avons déterminé le C.R.D. de quelques constituants du clinker avec leurs éléments colorants, ces clinkers ayant été cuits en milieu légèrement acide et refroidis dans de l'eau additionnée des produits étudiés. L'analyse des données a montré que le refroidissement brusque du clinker, dans des solutions aqueuses, augmente sa blancheur de 2 à 6 %, si l'ajout est de l'oxyde ferrique, et de 5 à 9 %, s'il est de l'oxyde manganeux. A l'aide d'une méthode de résonance paramagnétique électronique, on a constaté un passage partiel des atomes de fer à la position IV-e et de ceux d'oxygène en VI-e. Cela favorise l'affaiblissement de la coloration du clinker et l'apparition d'une ligne d'absorption paramagnétique avec q = 2,040. Les résultats obtenus permettent de constater l'influence importante des additifs étudiés, en solution aqueuse, sur le blanchiement des clinkers contenant du Fe_2O_3 surtout lorsqu'ils sont cuits en atmosphère oxydante. L'influence des conditions de refroidissement des clinkers dans des solutions aqueuses, avec addition de manganèse, se manifeste par une corrélation des atomes de manganèse avec des valences différentes. On a montré que l'adsorption des agents blanchissants à la surface des grains du clinker, lors du blanchiement dans des solutions aqueuses d'amino-alcools ou de liquides silico-organiques, entraîne une amélioration de la broyabilité et de la granulométrie du clinker, et permet de se passer d'agents de mouture.

SUMMARY : Data are reported on the aminoalcohols (TEA, MEA) and silicone liduids influence upon the bleaching process, structure and characteristics of the white Portland cement clinker. The sharp cooling in the I-2% aqueous solutions of monoethanolamine and triethanolamine is established to increase the diffusion reflection coefficient (DRC) of the white clinker by 5-9%. Sharp cooling in the aqueous solutions of the silicone liquids (0,5%) GKG-IO and GKG-II increases DRC of the white clinker by 8-IO%, in comparison with aqueous bleaching. In order to show the optimal conditions of clinker's bleaching we determined DRC of some clinker minerals with dyeing elements, which had been burned in slightly acid conditions and cooled in water and aqueous solutions of chemical additions under study. Data analysis showed that sharp cooling of clinker minerals in aqueous solutions of chemical additives increased the mineral whiteness. If we added ferrous oxide the mineral whiteness increased by 2-6%, if we added the manganese heptoxide the mineral whiteness increased by 5-9%. By the electron paramagnetic resonance method the particle transition of ferrous atoms from tetra coordination to sextant coordination was established it results in relaxation of mineral dyeing and in appearance of paramagnetic absorption lines from q=2,040. Our data allow to establish the cosiderable influence of the aqueous solutions of the additives under study on the mineral bleaching stages with Fe_2O_3 additives, Fe_2O_3 is espacially effective for burning in oxidizing conditions. The influence of cooling conditions of minerals with manganese additives can be seen in different coorelation of manganese atoms in different valente state. The bleaching agents adsorption at the sueface of clinker granules in the process of bleaching in the aqueous solutions of amino alcohols and silicone liquids is shown to intensify the process of clinker grinding to improve the size distribution; it also allows to refuse from using clinker grinding aids.

It is known, that white cement and cement paint manufacture demands the raw materials of a special quality. However, the discovered supplies of limestones and kaolines cannot meet the requirements of still rising demands in cement paint. But the well-known methods of raw materials concentration to remove the dyeing oxides are very expensive and labour-consuming operations. That is why the choice of the technological parameters of clinker burning and cooling processes is more effective, these processes provide the increasing of clinker whiteness.

There are some published data (I), where authors speak about the usage of chemical industry wastes - phosphorus slag, cishtoff white slime as raw components in white Portland cement manufacture. The influence of silicate minerals, calcium aluminate, the degree of saturation and silica modulus on the white clinker DRC value is determined. The abnormal aluminous and silicous modulus, the degree of saturation of silicon by calcium oxide make the directional change difficult in phase composition and white clinker structure while burning. This makes the introduction of mineralizators into the raw meal necessary.

While choosing mineralizators, the electronegativity of anions and cations, being the components of mineralizators, is of great importance. The most effective mineralizator is silicofluoric sodium, its cation has the lowest electronegativity, and anion - the highest, providing He-ion transition from tetrahedral coordination in to the octahedral coordination and formation of fine crystalline structure of the phase composition.(2)

We consider the increasing of clinker's whiteness by sharp cooling in water and in aqueous solutions of different salts and acids to be of great practical and theoretical interest. A.Grachyan and his collegues made detailed investigation of physico-chemical principles of clinker's bleaching in water. (I) According to him, aqueous vapour dissolves in the clinker fusion, and hydrosilicate ions Fe-bonds and O_2 bonds being cleaved by them, provide the formation of Fe-ions octahedral coordination, which has lower dyeing power.

As a result of optimal conditions research of clinker's bleaching, we decided to use different water soluble chemical additives, which are more active, than water, concerning their physico-chemical aspects.

We used such bleaching agents as aqueous solutions of amino alcohols - monoethanolamine (MEA) and triethanolamine (TEA), and also such silicone liquids as sodium ethylsiliconate GKG-IO and sodium methylsiliconate GKG-II . Burning hot clinker was sharply cooled in aqueous solutions of additives with different concentration: DRC was determined with the help of universal photometer (FM-56). The results of the MEA,TEA,GKG-IO, GKG-II solutions influence on clinker bleaching process are shown in table I.

TABLE I

Solution concentration	Cooled clinker DRC, % (as to MC-I4)			
	in TEA	in MEA	in GKG-IO	GKG-II
0	-	-	-	-
0,5	87	9I	93	95
I,0	88	90	9I	93
I,5	90	88	90	93
2,0	94	87	88	9I
3,0	94	86	87	90
4,0	90	86	87	88

Data analysis shows that if optimal concentration of the aqueous solutions for the amino alcohols are TEA - 2,5% and MEA-0,5% respectively, and for silicone liquids - 0,5%, then clinker DRC increases by 7-I0% in comparison with DRC of the water cooled clinker. (3,4). DRC of the water cooled clinker equals to 85%. The increase in reflection capacity of clinker can be explained by the partial reduction of clinker with Fe^{+3} ion solutions along with the formation of ion-grouping Fe^{+3}- O - Fe^{+2}, which is more weaker chromophore, than ion Fe^{+3}.

The investigations of clinker with the help of scanning electron microscope showed, that mineral phases crystals in the clinkers, cooled in the surfactant solutions, were more resorbed, their surface was more effective, in comparison with the surface of water cooling clinker. Fixation of great number of fine crystals in clinker increases the dispersion of light, it provides incresing of clinker's whiteness. Small content of C_4AF in the white clinker made it impossible to fix its structural changes while bleaching with the help of X-ray and infrared spectroscopic analyses, that's why we used the radiospectroscopic method of analysis.

Electron paramagnetic resonance spectra of the white clinker, cooled in water, contain paramagnetic absorption lines in the weak fields region and in the region of free electron factor. The character of absorption is conditioned by Fe^{+3} ions in the four-fold coordination (O_2) and by Mn^{+2} ions in the six-fold coordination.

White clinker, cooled in the TEA solution has the same absorption character, however the intensity of absorption lines in the

region of weak fields considerably decreases at the expense of Fe^{+3} in the four - fold coordination, but Mn lines intensity increases.

It is known (5), that ferriginous compounds fusion dominate in the superficial zones of clinker particles. Fe^{+3} accumulation in the spaces between microcrystals is a favourable factor while clinker bleaching in the aqueous solutions of MEA, TEA, GKGIO GKG-II, which are activated in the process of decomposition by the catalytic action of superheated steam. In the gas-vapour-air atmosphere of the clinker granules molecules and radicals of H_2, CO, CO_2 and other appear, they have the reduction capacity. They diffuse into the clinker granules in the microcracks and micropores, interacting with the surface of cement particles, and partially reducing Fe^{+3}ions to the Fe^{+2} ions.

Considerable increase of the white clinker DRC with the help of aqueous solutions of MEA, TEA, GKG-IO, GKG-II will agree with the data of the chemical analysis of Fe_2O_3 content in the clinkers. (See table II)

TABLE II

Bleaching medium	Solution concentration, %	Fe_2O_3 content, %	Clinker DRC, % (to MS-I4)
Water	-	0,67	85
Triethanolamine	2,0	0,42	94
Monorthanolamine	0,5	0,50	9I
GKG-IO	0,5	0,45	93
GKG-II	0,5	0,40	95

Chemical analysis data about Fe_2O_3 content in the clinkers prove our suggestion, that while clinker bleachind in the aqueous solutions of MEA, TEA, GKG-IO, GKG-II there is some lowering in concentration of dyeing oxide Fe_2O_3 along with the improvement in its whiteness.

We determined the DRC of some clinker minerals with dyeing elements additives, burned in slightly acid conditions and cooled in water and aqueous solutions of TEA, GKG-II. The results show (table III), that the presence of surfactants in the aqueous solutions considerably influence the DRC of minerals dyeing oxides additives, it is connected with the changing of Fe and Mg atoms state in the minerals structure. In comparison with aqueous bleaching C_3S whiteness with Fe_2O_3 additive increases by 2-9%, and with MnO_2 additive it increases by 5-I0% depending on additive. Dicalcium silicate and tricalcium aluminate whiteness also changes depending on bleaching conditions; it exceeds DRC of aqueous bleaching minerals by 2-5% in proportion to amount of introduced dyeing oxides.

Aqueous solutions of TEA, GKG-II most prominently influence the alumoferrous and ferrous phases of cement clinker (table 3). Spectrophotometric analysis showed peaks displacement in the C_4AF reflection curves which was cooled in the additive solutions into the shortlengh part of the visual spactrum, it testifies to the changing of alumoferrits solid solutions structures.

TABLE III

Minerals.	DRC, % (MS-I4), cooled: in water	in TEA solution	in GKG-II solution
C_3S	94	94	96
C_3S + 0,3% Fe_2O_3	83	89	92
C_3S+0,2%MnO	80	87	90
β - C_2S	96	96	98
β-C_2+0,3% Fe_2O_3	86	89	90
β-C_2+ 0,2% MnO	82	88	88
C_3A	96	96	98
C_3A+0,3% Fe_2O_3	84	88	92
C_3A+0,2%MnO	79	82	85
C_4AF	I6	28	32
C_2F	9	I8	22

Considerable effect of C_4AF and C_2F bleaching in the presence of amino alcohols and silicone liquids in the cooling water is explained by the different total surface of contact of the dyeing elements with the reducible gas-vapour phase radicals.

X-ray analysis did not discover any qualitative differences in the mineral bleaching products. Quantitative analysis, determined according to the diffraction reflection changing (d=I,76Å), helped us to state that degree of hydration of tricalcium silicate, tricalcium aluminate of water cooling is IO-I2%, and if we take the degree of hydration of tricalcium silicate,

tricalcium aluminate, cooled in aminoalcohol solutions, it will be lower aminoalcohol presence (MEA, TEA) in the bleaching water causes some redistribution of C_2S diffraction reflection. In this case line intensity increases from d=2,78Å to d=2,79Å. This fact agrees with the formation of some quantity of C_2S form in the mineral, it occurs at the expense of partial reduction of Fe^{+3} to Fe^{+2}, which promotes polymorphic transition to form. If we compare the infra-red spectra of minerals cooled in water and in amino alcohol and silicone liquid solution, we shall see that there is no structural changes in their crystal lattices.

CLINKER GRINDABILITY. Nowadays clinker grinding is the most energy-consuming operation in Portland cement manufacture. For clinker grinding process intensification different surfactants are used, they absorb at the cement particle surface with its polar side, forming protective monomolecular layer, they also decrease intermolecular cohesive forces action, and prevent finely ground material from cohesion.

Partial absorption of amino alcohol and silicone liquid aqueous solutions takes place at the surface of clinker granules during clinker bleaching process of white Portland cement in these solutions, and this intensifies the clinker grinding process. To determine MEA, TEA, GKG-IO, GKG-II aqueous solutions effect as grinding intensifiers, clinker being cooled in water and in additive aqueous solutions was fined in the mill, and in certain periods of time clinker residue was controlled on the sieve N008. The results showed that required specific surface for white Portland cement 3000-3400cm^2/g was established in 50 minutes in the case of water cooling cements, and in 35-40 minutes in the case of cements after cooling in the additive solutions. Therefore, if we use aqueous solutions of MEA, TEA, GKG-IO, GKG-II additives as bleaching agents, there is no sense in using different surfactants at clinker grinding because these additives intensify the grinding process by 20-25% in comparison with water cooling.

Some scientists extablished (6), that rational controlling of cement dispersion degree by improving its granule composition allows to increase its activity and to improve its properties.

Thus, it became obvious that cement obtained from clinkers, bleached in the additive solutions (50 - 57%) has the optimal granulometric composition (0-20 mcm), and fraction quantity 70 - 80 mcm, which hydrates slowly, has 5 - IO%.

CONCLUSIONS

The scientific researches showed that amino alcohols (MEA, TEA) and silicone liquids (GKG-IO, GKG-II) usage as bleaching agents helps to increase the diffusion reflection coefficient of the white clinker by 5-IO% in comparison with aqueous bleaching. The effect is reached at the expense of reducing medium formation in the clinker granule pores at the additive decomposition into molecules and radicals of H_2, CO, CO_2 type.

The rise of clinker mineral whiteness is connected with changing of dyeing element valente state. The less prominent factor is the change of coordination, particularly He-atoms coordination in the bleaching process. Besides, sharp cooling in aqueous solutions of MEA, TEA, GKG-IO, GKG-II allows to obtain mineral crystals of less size.It promotes the whiteness increasing at the expense of increasing the total surface of interaction of reducible molecules and radicals of gas-vapour- phase with clinker microcrystals.

Amino alcohol and silicone liquids aqueous solutions intensify the clinker grinding process at the expense of its adsorption on granule surfaces while bleaching process. That is why we can refuse from using different grinding aids and still grinder's efficiency will be increased.

REFERENCES

I.- A.GRACHYAN, P.GAIDZHUROV and others (I970) "White Portland cement technology Stroyisdat.

2.- I.PONOMAREV, A. GRACHYAN and others (I966) "Mineralized additives influence on cement clinker forming process depending on electronegativity of mineralizator anion and cation", DAN USSR, vol. I66 N2.

3.- K.KARIBAYEV, A.PASCHENKO, K.BEKISHEV and others, USSR Author's Certificate N 447385, "Cement clinker bleaching", 25.IO.74, Bull. 39.

4.- K.KARIBAYEV, A.PASCHENKO, K.BEKISHEV and others, USSR Author's Certificate N 564282, "Method of white Portland cement clinker bleaching", 05.07.77,b.25.

5.- S.CHROMY (I976) "White clinker formation mechanism", VI International Congress on cement chemistry, Stryisdat, vol.3

6.- A.IVANOV - GORODOV (I960) "Granular composition influence on cement solutions strength and freeze resistance", Moscow.

Recherches sur les phases de ferrites de baryum dans la zone fortement basique du système $BaO-Fe_2O_3$

Research studies of the barium ferrites in the upper base part of the system $BaO-Fe_2O_3$

V. VALKOV, Agrégé, Chargé de cours, Candidat ès Sciences Techniques, Institut Supérieur Chimique et Technologique, Sofia, Bulgarie,
A. DENEVA, Maître de Recherches, Candidate ès Sciences Techniques, Institut de Recherches Scientifiques des Matériaux de Construction, Sofia, Bulgarie et,
D. STAVRAKEVA, Agrégée, Chargée de Cours, Candidate ès Sciences Géologiques et Minéralogiques, Institut Supérieur Chimique et Technologique, Sofia, Bulgarie.

RESUME : Des recherches ont été entreprises, au moyen du microscope optique et des rayons X, sur le traitement à haute température et addition de baryte au clinker, de façon à provoquer la formation de diverses ferrites de baryum : BF, B_3F_2, B_2F, B_5F_2, B_3F et B_7F_2. On a observé la formation de BF, B_2F et B_7F_2, mais il a été prouvé que B_3F ne se formait pas, car dans la cuisson en phase solide le B_3F^2 se décompose en un mélange de B_2F et de B_7F_2, et dans la cuisson par fusion il se forme une solution solide de B_7F_2 dans B_2F. Le composé B_7F_2 a pu être analysé aux rayons X.
Les spectres Mössbauer des ferrites BF, B_2F et des constituants B_3F et B_7F_2 ont été obtenus; et il a été constaté la présence, dans ces ferrites, de fer trivalent. On a pu déterminer le nombre et la position des atomes Fe^{+3}, et la probabilité de formation de solutions solides de B_2F dans B_7F_2, au lieu du constituant B_3F.
Ces résultats ont été utilisés pour l'identification des phases ferritiques dans les clinkers baryteux; ils présentent aussi un grand intérêt pour l'étude de la zone fortement basique du système $BaO-Fe_2O_3$.

SUMMARY : Optical-microscopic and X-ray phases researches of constituents, treated at high temperatures, have been carried out for the obtaining of barium ferrites : BF, B_3F_2, B_2F, B_5F_2, B_3F and B_7F_2. The formation of BF, B_2F and B_7F_2 has been confirmed. It has been proved that B_2F does not form itself as an individual compound. At solid phase caking of the constituent for B_3F a mixture is formed from B_2F and B_7F_2, while at its melt crystallization - a solid solution of B_7F_2 in B_2F. X-rays data, for B_7F_2 were obtained.

The Mössbauer ferrites spectra BF, B_2F have been received and the presence of trivalent iron in them, the position numbers of Fe^{+3} and the probability of solid solutions formation of B_2F in B_7F_2, at the constituent for B_3F, have been established.

The results here used for the identification of the ferrites phase of the barium clinkers are of interest in the case of the research studies of the upper basic part of the system $BaO-F_2O_3$.

Le système $BaO-Fe_2O_3$ a été étudié par Goto et Takada, Batti, Kurdowski, Valkov et Boyadjieva (1), (2), (3), (4).

La plus grande part des études est limitée à des constituants d'alcalinité ≤ 2. Les données connues de Kurdowski (3) et Batti (2) pour les constituants plus haute-basiques sont contradictoires. D'après Kurdowski, sauf les ferrites de baryum connus BF, B_2F et BF_6, ils existent encore B_3F, B_5F_3 et B_7F_2, et d'après Batti - une phase de constituant B_7F_2 (On emploie des abréviations acceptées : B - BaO, F - Fe_2O_3).

L'objet de notre étude est d'élucider les phases dans le domaine avec plus haut contenu de BaO, après le composé B_2F, et aussi de caractériser plus pleinement les ferrites de baryum, lesquels, il est possible qu'ils soient dans la composition des clinkers de silicate de baryum.

Des études optico-microscopiques et radiologiques de phases, ont été exécutées, les compositions BF, B_3F_2, B_2F, B_5F_3, B_3F et B_7F_2 et les compositions BF, B_2F, B_3F et B_7F_2 ont été étudiées aussi à l'aide de la spectroscopie de Mössbauer.

Les réactifs de départ $BaCO_3$ et Fe_2O_3 (p.a.) après être précisément dosés et homogénéisés avec de l'eau, puis séchés, sont tamisés, jusqu'à ce que la dernière fronde ait passée au tamis 0,08. Les mixtures obtenues sont briquettées et cuites à une température de 1320°C dans un four à appareils de chauffe en silite, après être restées pendant 10 heures dans le four à la température maximale et deux moutures intermédiaires pour faciliter les interactions des phases solides. Les spécimens ont été soumis à un refroidissement lent (24 heures). En outre, les constituants B_3F et B_7F_2 ont été fondus à la température de 1400°C et brusquement refroidis. Les ferrites obtenus ont été étudiés parallèlement avec ceux provenant de la synthèse de la phase solide.

Les études microscopiques et radiologiques des phases montrent les résultats suivants:

Constituant BaO, Fe_2O_3. Une phase ferrique est établie microscopiquement, laquelle, d'après des données radiographiques - 3,15/10/; 2,73/5/ et 2,68/3/, correspond à BF (4). Le ferrite de monobaryum, en lumière reflétée, se révèle sous l'aspect de formes irrégulières, isométriques, presque carrées et rhombiques ou rectangulaires allongées ou angulaires. La couleur est pris-pâle, faiblement rose,avec une grande capacité de réflexion; anisotropique et présentant un pléochroïsme marqué de réflexion. En lumière traversante il est caractérisé par des couleurs interférentielles gris-blanches ($n_p = 2,14$ et $n_g = 2,23$).

Constituant $3BaO.2Fe_2O_3$. Le produit n'est monophasé. Microscopiquement, en cas de grands agrandissements (900x avec objectifs d'immersion) les deux phases se délimitent clairement. L'une est d'une plus grande capacité de réflexion,, anisotropique et plus claire que l'autre, laquelle est de couleur rose-grise et isotropique. A l'aide des données radiographiques est établie aussi la formation de deux phases ferriques - $BaO.Fe_2O_3$ et $2BaO.Fe_2O_3$.

Constituant $2BaO.Fe_2O_3$. A la synthèse exécutée il se forme un ferrite correspondant à la phase $2BaO.Fe_2O_3$. Dans lumière reflétée, la phase susmentionnée est claire-grise, isotropique, représentée par des sections isométriques, presque carrées. En immersion elle est avec des sections carrées très régulières. Le difractogramme de B_2F montre correspondance avec (4). Quelques différences ont été registrées, principalement auprès les grands angles.

Constituant $5BaO.2Fe_2O_3$. Le modèle est biphasé. L'une des phase est rose-grise et s'inclut dans une autre de couleur jaune. La phase de couleur rose-grise a des sections presque carrées et correspond à B_2F. L'autre - de couleur crème-jaune subit un pléochroïsme de réflexion, elle est anisotropique et par cela elle diffère des décrites BF et B_2F. Selon ses constituants elle doit correspondre à B_3F d'après (3) ou à B_7F_2 d'après (2). Dans le cadre radiologique de ce constituant, outre les distances intersuperficielles de B_2F, se présentent aussi encore deux autres réflexions correspondantes à 3,64-3,69 et 2,10 Å.

Constituant $3BaO.Fe_2O_3$. Dans les épreuves, traitées de manière thermique à une température de 1300°C on observe, microscopiquement, deux phases, analogiquement au constituant B_5F_3. De même. dans le radiogramme de cette épreuve, de pair avec le jeu entier des distances intersuperficielles de B_2F, apparaissent aussi des lignes supplémentaires: 3,66-3,69; 2,09-2,10 Å. Le même constituant, traité thermalement à températures plus hautes - 1400°C jusqu'à obtention de fonte, se caractérise par sa monophasité. Le tableau microscopique du ferrite formé ainsi que son tableau radiographique diffractif correspindent à la phase B_2F. Cela montre que le diagramme de la phase dans le domaine du constituant B_3B répond au diagramme présenté par (2) et que le composé supposé B_3F (3) n'existe pas. Selon (2) la phase B_2F au-dessus de la température eutectique - 1307°C, représente la solution solide de B_7F_2. Donc, le schéma supposé de formation des ferrites pour ce constituant peut être exprimé de la manière suivante: $B_3F \rightarrow B_2F$ (solution solide avec B_7F_2), de la fonte et $3B_3F \rightarrow B_2F + B_7F_2$, au cas de synthèse de la phase solide.

Constituant $7BaO.2Fe_2O_3$. Les phases de cristal des modèles fondus à la température de 1400°C et brusquement refroidis représentent un produit monophasé. Microscopiquement, dans la lumière reflétée, la phase cristalline nouvellement formée est jaune de couleur, avec des sections

idiomorphologiques, rectangulaires ou arrondies, incluses dans des phases vitreuses. En immersion le ferrite synthétisé est vert de couleur, et parfois sa couleur approche le brun. D'après toutes les caractéristiques morphologiques et optiques, la phase B_7F_2 est de système cristallographique rhomboïdal.

La figure 1 montre le diffractogramme ionique de B_7F_2 obtenu de la fonte, lequel peut être accepté comme étalon, faute d'autres données dans la littérature pour ce composé.

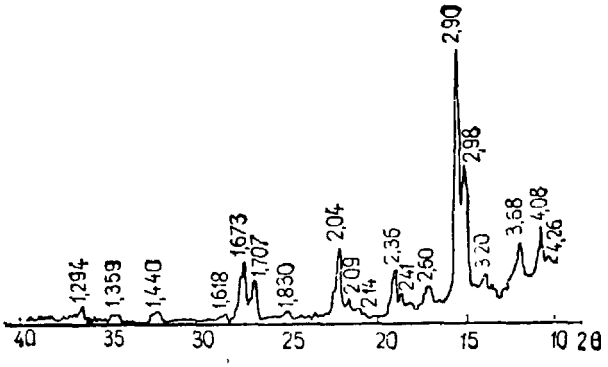

Fig. 1 - Diffractogramme ionique de B_7F_2

Les modèles traités à une température d'environ 1320°C, au cas de cuisson en phase solide, se caractérisent microscopiquement et radiologiquement comme biphasés. Dans des phases pareilles, celle qui prédomine, c'est B_7F_2 et, en moindres quantités - B_2F. Les études des phases, par conséquent, du constituent B_7F_2, confirment pleinement l'aspect de la phase du système, donné par Batti (2), selon lequel, après le constituant eutectique, au-desus de la courbe solide, la phase B_7F_2 représente une solution solide de B_2F dans B_7F_2, de la même manière que représente B_7F_2 dans B_2F, au-dessus de la même courbe de température.

A la Figure 2 est donnée la microstructure de B_7F_2 obtenu de la fonte.

Les ferrites de baryum synthétisés suivant le procédé décrit BF, B_2F, constituants de B_3F et B_7F_2 (les derniers deux de fonte) sont étudiés aussi à l'aide de la spectroscopie de Mössbauer.

Le Co^{57} est utilisé en tant que source, en matrice de palladium.

Les spectres Mössbauer des ferrites de baryum sont donnés à la figure 3, et leurs paramètres - à la Table 1.

Le déplacement isométrique dans les limites au-dessous de 0,4 - 0,5 mm/s indique la présence de fer sous la forme de Fe^{+3}.

Le spectre de $BaO.Fe_2O_3$ montre un champ ma-

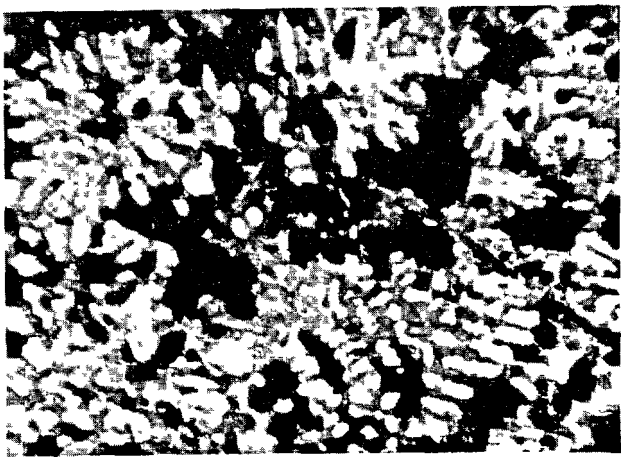

Fig.2 - Formes lumineuses de $7BaO.2Fe_2O_3$ Agrandissement 126x

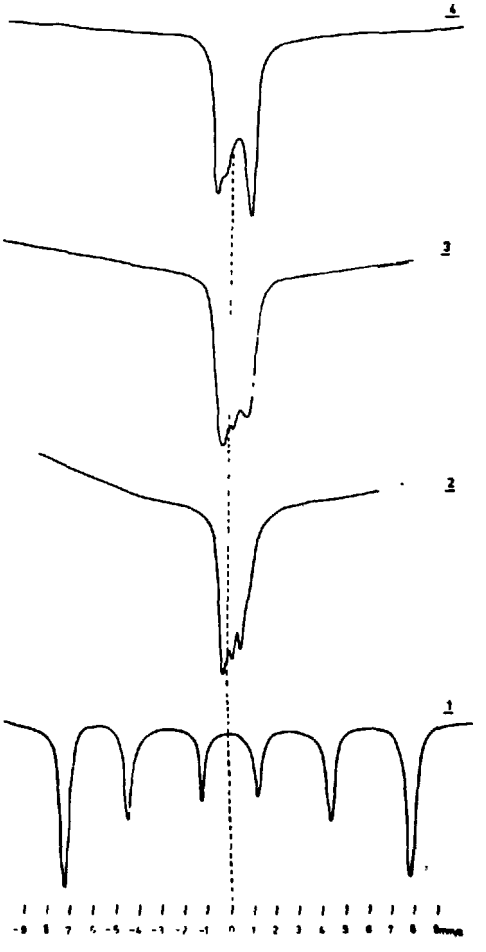

Fig. 3 - Schéma des spectres de Mössbauer des ferrites de baryum: (1) - BF; (2) - B_2F; (3) - constituant B_3F ($B_3F + B_7F_2$-solution solide); (4) - B_7F_2

Table 1

Phase	δ	$\triangle$	H_i
$BaO.Fe_2O_3$	0,19	0,32±0,03	470
$2BaO.Fe_2O_3$	0,16 0,00	0,32 0,64	- -
Constituant $3BaO.Fe_2O_3$ (Solution solide de B_7F_2 dans B_2F)	0,10±0,06 0,30±0,06	0,50±0,06 0,89±0,06	- -
$7BaO.2Fe_2O_3$	0,25±0,10 0,12±0,03	1,26±0,10 1,55±0,03	- -

Remarque:

δ - déplacement isométrique concernant α-Fe, mm/s

$\triangle$ - séparation quadripolaire , mm/s

H_i - champ magnétique local , kOe

gnétique de structure arrangée, laquelle d'après Hi = 470 kOe est proche à la structure du spinelle et du Fe^{+3}, et est probablement dans une coordination sextuple.

L'ion ferrique dans BF se trouve en position une.

L'ion ferrique dans le spectre de B_2F se trouve en deux positions.

Le spectre du constituant B_3F est proche à B_2F, mais il diffère par des changements dans les valeurs numériques des paramètres $\triangle$ et δ des deux positions de l'ion ferrique. C'est le résultat probablement de la formation de solutions solides de B_2F avec B_7F_2.

Le spectre de B_7F_2 diffère catégoriquement de celui de B_2F. La seconde position de l'ion ferrique dans le ferrite, avec $\triangle$= 1,55± 0,03 montre sa présence dans la phase amorphe, à cause de quoi, dans la structure du cristal de B_7F_2 l'ion ferrique est dans un état avec $\triangle$= 1,26±0,06 et avec δ = 0,25±0,06 mm/s.

La grande quantité de phase amorphe ne donne pas la possibilité d'une détermination exacte du spectre de la phase cristal.

Prenant en considération la composition chimique des clinkers de baryum et la formation de ferrites de baryum avec alcalinité ≧ 2, on peut en déduire que B_2F et B_7F_2 ou bien des solutions solides à leur base, représenteront la phase ferrique dans les clinkers de baryum industriels.

CONCLUSIONS

En généralisant les résultats des recherches faites, nous pouvons formuler les conclusions suivantes:

1. Les constituants des ferrites de baryum ont été étudiés microscopiquement et radiologiquements : BF, B_2F, B_3F_2, B_5F_2, B_3F et B_7F_2, et a été confirmée l'existence des phases BF et B_2F. Dans les diffractogrammes d'ionisation obtenus, les distances intersuperficielles correspondent à (4), avec certaines différences dans les grands angles.

2. Le B_3F, décrit par (3), n'a pas été établi ni à la synthèse en phase solide, ni de fonte. Le produit de la synthèse en phase solide sont les deux phases - B_2F et B_7F_2, et de la fonte - solution solide de B_7F_2 dans B_2F.

3. La formation de B_7F_2 est confirmées et, pour la première fois, sont données les distances intersuperficielles caractéristiques.

4. On a établi, à l'aide de la spectroscopie de Mössbauer, la présence de fer trivalent dans les ferrites: BF, B_2F, constituants B_3F et B_7F_2, le nombre des positions de l'ion ferrique dans eux, ainsi que la probabilité pour la formation de solutions solides de B_2F, B_7F_2 dans le constituant B_3F.

5. Les résultats obtenus des études des ferrites de baryum ont été utilisées à la détermination des constituants de clinkers et ciments de baryum à leur base à une échelle semi-industrielle. (5)

BIBLIOGRAPHIE

1.- Y. GOTO et T. TAKADA (1960), "Phase Diagram of the System $BaO-Fe_2O_3$", J. Am. Ceram. Soc., 43, n° 3, 100-101.

2.- P. BATTI (1960), "Diagramma d'equilibrio del sistema $BaO-Fe_2O_3$", Annali di Chimica, 50, n°11, 1461-1478.

3.- W. KURDOWSKI(1973), "Fazy mineralne bogatej w bar cześci ukladu $BaO-Al_2O_3-Fe_2O_3$", Cement-Wapno-Gips, n° 11, 339-350.

4.- V. VALKOV et Hr. BOYADJIEVA (1970), "Ferrites de baryum - production et propriétés", Matériaux de Construction et Industrie des silicates, n°1, 3-6 (en bulgare)

5.- V. VALKOV, A. DENEVA et D. STAVRAKEVA (1978), "Barievi klinkerni minerali i tsimenti na tyakhna osnova", Rapport à la Conférence "Nouvelles Orientations dans le Développement des Matériaux de Construction", Varna, Bulgarie.

Calculation of hypothetically possible potential compositions of high-alumina cements

Calcul des compositions potentielles théoriquement possibles des ciments alumineux

J. CALLEJA, Professor, Consejo Superior de Investigaciones Cientificas, Instituto "Eduardo Torroja" de la Construccion y del Cemento (I.E.T.C.C.) Madrid, Espagne.

RESUME : Malgré la grande complexité des systèmes de phases concernant le ciment alumineux, et le manque de connaissances suffisantes sur sa composition minéralogique, on a tenté dans ce travail d'établir des bases pour calculer quelques-unes de ses compositions potentielles possibles.

Il est évident que ces calculs sont appuyés sur des hypothèses discutables, mais le but principal du travail est celui de chercher une possibilité de corrélation entre les caractéristiques, propriétés et comportement du ciment alumineux "structural" et sa nature minéralogique sur des bases plus solides que celles simplement appuyées sur sa composition chimique.

Il peut être ainsi possible de trouver une aide pour chercher une solution plus complète et satisfaisante aux problèmes de la conversion, de la carbonatation et de l'hydrolyse alcali-carbonique, considérées comme les plus importantes concernant les ciments alumineux, tant du point de vue scientifique que technique.

SUMMARY: Despite the great complexity of the phase systems involved in high-alumina cement and the lack of sufficient knowledge on its mineralogical composition, attempts are made in this paper to establish bases for calculating some of its possible potential compositions.

Of course, such calculations are supported by some controvertible hypothesis, due precisely to the lack of knowledge, but the main aim of this paper is to look for a possibility of correlating some characteristics, properties and behaviours of "structural" high-alumina cement with its mineralogical nature on a more solid base than that barely consisting in its chemical composition.

So, conversion, carbonation and alkali-carbonic hydrolisis considered as principal scientific and technical problems inherent to high-alumina cements could perhaps find an aid to approach to a more complete and satisfactory solution.

1. - INTRODUCTION

A very concise and complet exposition of problems concerning high-alumina cements (HAC in the following), either on the aspects of their fabrication or on particulars related to their utilization has been made by J. TALABER at the VI ICCC, Moscow 1974 (1). Moreover, a survey summarizing the principal items treated at the Symposium on High-Alumina Cements hold in the U.K. (december 1974) has been more recently published (2).

Summarizing in turn the outstanding features of the mentioned exposition by TALABER concerning anhydrous calcium aluminates and HAC, it must be pointed out that the binary and ternary systems C-A and C-A-S are complex, and correspondingly much more so when transformed into the quaternary and quinary systems C-A-S-F and C-A-S-F-F (F=FeO).

Even for a long time the binary system C-A has been controverted, for some authors as NURSE and others have sustained the incongruency of the melting of $C_{12}A_7$ and CA_2 phases in dry atmospheres (3), whilst others either at the same time (as KIESSLING and others -mentioned by UDALOV and others-) or much more recently (as UDALOV and others) have supported the opposite opinion (4), not only regarding the mentioned compounds but also others such as C_5A_3 and CA. Moreover, the nature of the atmosphere (oxidizing for $C_{12}A_7$ and reducing for C_5A_3) seems to be decisive as far as the congruency of the melting of such compounds is concerned. Furthermore, a change of atmosphere during heating may change the phases to one another (4).

According to TALABER (1) the three paragenesis fields of the ternary system C-A-S: $CA-C_{12}A_7-C_2S$, $CA-C_2S-C_2AS$ and $CA-C_2AS-CA_2$ may justify in principle the presence of some of the phases CA_2, CA, $C_{12}A_7$, C_2AS, C_2S. C_2S and C_2AS are always formed in the presence of S: the former if the S content is low, and the latter if it is high. The behaviour of HAC may depend much on the proportions of these phases, in the following way according to SOLACOLU mentioned by TALABER (1): Type I HAC containing mainly $CA + C_{12}A_7$ develops a higher initial strength, whereas those cements of Type II mainly composed by CA and CA_2 develop a lower initial strength, but a more intensive secondary or delayed hardening. In general $C_{12}A_7$ is present in HAC in lower proportions, depending on the C/A ratio and probably on the higher amount of silica present in the cement composition (5).

On the other hand, C_2S behavies as in portland cement. As far as gehlenite C_2AS is concerned, it is considered as a non-desirable component, for it is a non-hydraulic alumina-consuming phase (6).

Much higher complication arises from the presence of a considerable amount of total iron-constituents in HAC (ferric and ferrous oxides, the former of which at least presumably may form calcium ferrites CF and C_2F, as well as solid solutions from C_2F to C_6A_2F (in between C_6AF_2 and C_4AF). A noticeable amount up to 15 % of CF may enter in CA to form another solid solution (1).

Though HAC clinker is formed in most cases through fusion, no crystallization equilibrium is generally reached, so that it is very difficult and risky to apply any calculation of mineral (potential) composition to it, even restricted to the main components of the system C-A-S.

So, it has been not yet quite possible to calculate quantitavely the mineralogical composition of HAC clinker, either from its chemical composition or from that of their raw materials and mixtures. Mineralogical composition of HAC depends on the chemical composition of raw mixture, on heating and cooling (melting temperature and cooling speed), on the oxidizing or reducing atmosphere during the total manufacturing process (4) and on the type of manufacturing technology (melting, sintering or clinkerization). Different phases may result in each case as SUZUKI has pointed out as referred to pure phases and some solid solutions of them (5), so that raw mixtures with the same or very similar chemical composition may result in HAC of different mineralogical composition and/or properties. Nevertheless, the clinker cooling speed and the oxidizing/reducing conditions being almost constant for a given process, and the melting temperature conditioning mainly the ratio Fe^{3+}/Fe^{2+}, in turn taken into account in the chemical composition, this one may be considered as being the only main factor determining the mineralogical composition of HAC.

Anyway, considering that a given stoichiometry is practically mantained in a given manufacturing process, the base for possible calculations of quantitative potentital compositions is the knowledge of the true qualitative mineralogical composition of a given HAC clinker. Nevertheless, characterization of HAC clinker is difficult by several of the most common techniques. As a result, morphology and composition of phases encountered are very different depending on several circumstances. Microscopically CA and C_2AS have been observed in some cases applying suitable techniques (7). But it is well known that quantitative determinations of C_2S by XRD techniques not always is easy, possible or reliable.

So, the lack of sufficient knowledge on mineralogical composition of anhydrous HAC implies a similar lack of knowledge on its hydration processes and hydration products formed, though studies have been made on their mineralogy (8), and mineralogical composition in the system C-A has been determined by means of potential analysis on the basis of phase diagrams, particularly as far as the principal phases CA and CA_2 are concerned (9) (10).

Attempts have also been made to develop potential calculations of anhydrous HAC (11).

These difficulties may be some of the reasons why the main problems affecting "traditionally" to HAC, such as conversion -crystalline transformation of hexagonal hydrates to cubic hydrates-, (12) (13),

carbonation (14) and alcali-carbonic hydrolisis (15) are not yet either fully or satisfactorily explained, as the mechanisms in some cases, and mainly their kinetics, as well as the factors and conditions -for instance, temperature (8)- affecting both, mechanisms and kinetics in most cases, seem not to be sufficiently known. Consequently, neither primary effects derived from such problems (as for instance the loss in strength -and even the strength development (16)-, the liberation of water and the increase of porosity), nor secondary (technical, practical) effects -as for instance refractory behaviour (17) (18) and reinforcement corrosion in reinforced concrete- can be completely or easily avoided or controlled.

2. - FURTHER APPROACHES TO POSSIBLE CALCULATIONS OF HAC POTENTIAL COMPOSITIONS

Independently of the degree of probability, these calculations must be based on conventional and arbitrary hypothesis, more or less justified. Anyway, the corresponding calculations and results may be very diverse. Much more so as each of the hypothesis adopted may present several different alternatives.

The present paper does not consider HAC other than those devised for hydraulic (structural) purposes. So, HAC of the higher contents of A for refractory uses are particularly discarded.

It is admitted that the chemical composition of ordinary structural HAC may usually vary between the following wide limits: A 39 to 42 % (40-42 %); C 37 to 42 % (37-40 %); F+ $\overline{F}$ 9 to 18 % (15-17 %); S 1, 5 to 6 % (1, 5-3 %); T 1 to 2 %. The preceeding wider limits may correspond to broader variations either from country to country (19) (20) or along the time in the same country. This could be the case in Spain. Narrower limits in brackets may correspond to variations observed in more recent time in Spain (21).

It is by no means intended to justify here the important scientific knowledge recently (22) (23) (24) and quite recently (21) gained from theoretical and experimental studies carried out by application of modern XRD, EMP, ROM, etc. techniques to phase equilibria systems of common refractory or structural HAC or to particular HAC. Special mention merits the work in course carried out by R. MARTINEZ and S. DE AZA (21). But it is obvious that the simple ternary system C-A-S is out of consideration for the two latter mentioned cements, owing to their usually high content of total iron compounds and to their relatively low content of S. Otherwise, ternary system C-A-F would be a closer approximation for them, as their three main chemical components amount to more than 90 % of their chemical composition.

From considerations on possible triangles of compatibilities of phases in solid state in both mentioned ternary systems (as in other ternary sub-systems in them), as well as on compositions and primary crystallization fields, it is possible to determine the different possible sequences of crystallization of phases. In fact, it has been recently confirmed that the sequence is CA, ferritic phases and $C_{12}A_7$ in normal fused HAC (21).

Nevertheless, the quaternary system C-A-F-S (22) (23) is a further and closer approach, as the sum of principal chemical components may amount up to about 94 % of the total composition. In a similar manner the authors repeatedly mentioned (21) have established the compatibilities in solid state within the zone of the quaternary system corresponding to fused HAC with a mean chemical composition. According to it, mineralogical compositions might correspond to the quaternary sub-systems

$$CAss\text{-}C_2Fss\text{-}C_{12}A_7ss\text{-}C_2S$$

or

$$CAss\text{-}C_2Fss\text{-}C_2ASss\text{-}C_2S$$

the former being in general more probable, according to the experimental and practical knowledge of hydraulic HAC (21). Practical considerations on hydration show that C_2AS is a non-desirable, non-hydraulically active phase, and that hydration of $C_{12}A_7$ may be very rapid thus impairing setting of HAC. In the same way, according to compositions and primary volumes of crystallization, as well as to the possible eutectic surfaces, the authors (21) have determined the sequence of crystallization. They have concluded that the phases more probably formed for usual compositions of Spanish HAC are

I. $CAss\text{-}C_2Fss\text{-}C_{12}A_7ss\text{-}C_2S$

II. $CAss\text{-}C_2Fss\text{-}C_2ASss\text{-}C_2S$

III. $CAss\text{-}C_2Fss\text{-}C_{12}A_7ss$

their relative probability depending mainly on the chemical composition of the system. It is obvious that systems I and II would be possible for compositions containing noticeable amounts of S; the higher the S content, the more probable the system II as compared with system I.

3. - CALCULATIONS

On the preceeding bases exposed in 2, calculations of potentital compositions have been developped for Spanish fused HAC. Assumptions made for it, according to experimental results of the mentioned recent studies (21) are: i) that ferrous compounds appear as wustite $\overline{F}$, a phase which is compatible with the other aluminous phases in the quaternary system C-A-F-$\overline{F}$, and even with C_2S in the ternary sub-system C_2S-C_2AS-$\overline{F}$; ii) that contrarily to what is generally admitted, the stable phase CT (perowskite), compatible with the other phases, does not appear as such, but in solid solution with the much more abundant ferritic phase; iii) that M (MgO), $\overline{M}$ (MnO), etc., may form solid solutions with other phases.

Consequently, neither $\overline{F}$ not T, M, $\overline{M}$ etc., are taken into account for calculations. They are merely included in what is called "rest" in table I. In this respect it is pointed out that two ways are possible

to simplify calculations: i) to reduce the total chemical analysis of HAC to the four major components (A, C, F, S), whereby values obtained for calculated phases would be higher than actual ones; ii) to include every other minor component in a "rest" (the same for chemical than for potential composition), whereby values obtained for calculated phases would be a little lower than actual ones. The latter way has been preferently choosen in this paper, as it is considered that only the main (hydraulic) phases are important for properties and behaviour of "structural" HAC.

One further assumption is that C_2Fss which may widely vary in composition (at most between the extreme terms C_2F and C_6A_2F) according to the F content, corresponds either to the term C_4AFss -probably more usual (21)-, or to the term C_6A_2Fss in each of the systems I, II and III (sub-cases 1 and 2 of them in the following).

All the calculations are based on percentage contents of oxides expressed in the chemical analysis of HAC (indicated by the small letters corresponding to the symbolic capital letters representing oxidic components), and on the corresponding molar ratios. Final coefficients are given but with only two decimal figures.

3.1. - Calculations in the system I.1:

$$\underline{CAss\text{-}C_{12}A_7ss\text{-}C_4AFss\text{-}C_2S}$$

a) s % of S fix $s.2C/S = 1.866675.s\% = c_1\%$ of C
to form $s.C_2S/S = 2.866675.s\%$ of C_2S
remaining $(c\text{-}c_1) = c_2\%$ of C

b) f % of F fix $f.A/F = 0,638486.f\% = a_1\%$ of A
and $f.4C/F = 1.404687.f\% = c_3\%$ of C
to form $f.C_4AF/F = 3.043174.f\%$ of C_4AF
remaining $(a\text{-}a_1) = a_2\%$ of A
and $(c_2\text{-}c_3) = c_4\%$ of C

c) a_2 % of A fix $a_2.C/A = 0.550007.a_2\% = c_5\%$ of C
to form $a_2.CA/A = 1.550007.a_2\% = (ca)_1\%$ of CA
remaining $(c_4\text{-}c_5) = c_6\%$ of C

d) c_6% of C fix $c_6.7CA/5C = 3.945423.c_6\% = (ca)_2\%$ of CA
to form $c_6.C_{12}A_7/5C = 4.945423.c_6\%$ of $C_{12}A_7$
remaining $((ca)_1\text{-}(ca)_2)$ % of CA

Finally: $C_2S\% = 2.87\ S\%$
$C_4AF\% = 3.04\ F\%$
$C_{12}A_7\% = 4.95\ C\% - 9.23\ S\% - 5.21\ F\% - 2.72\ A\%$
$CA\% = 1.55A\% - 0.99\ F\% - 0.80\ C_{12}A_7\%$
or $CA\% = 3.72\ A\% + 7.36\ S\% + 3.17\ F\% - 3.95\ C\%$

The same equations without terms in F may be applied to the ternary system $CAss\text{-}C_{12}A_7ssC_2S$. On the contrary, if $C_{12}A_7$ cannot be formed, then:

$C_2S\% = 2.87\ S\%$
$C_4AF\% = 3.04\%$
$CA\% = 2.82\ C\% = 5.26\ S\% - 3.96\ F\%$

This is a possible but not probable case.

3.2. - Calculations in the system I.2:

$$\underline{CAss\text{-}C_{12}A_7ss\text{-}C_6A_2Fss\text{-}C_2S}$$

a) As in 3.1

b) f % of F fix $f.2A/F = 1.276973.f\% = a_1\%$ of A
and $f.6C/F = 2.107031.f\% = c_3\%$ of C
to form $f.C_6A_2F/F = 4.384004.f\%$ of C_6A_2F
remaining $(a\text{-}a_1) = a_2\%$ of A
and $(c_2\text{-}c_3) = c_4\%$ of C

c) As in 3.1

d) As in 3.1

Finally: $C_2S\% = 2.87\ S\%$
$C_6A_2F\% = 4.38\ F\%$
$C_{12}A_7\% = 4.95\ C\% - 9.23\ S\% - 6.95\ F\% - 2.72\ A\%$
$CA\% = 1.55\ A\% - 1.98\ F\% - 0.80\ C_{12}A_7\%$
or $CA\% = 3.72\ A\% + 7.36\ S\% + 3.56\ F\% - 3.95\ C\%$

3.3. - Calculations in the system II.1:

$$\underline{CAss\text{-}C_4AFss\text{-}C_2ASss\text{-}C_2S}$$

a) As b) in 3.1

b) s % of S fix $s.2C/S = 1.866675.s\% = c_3\%$ of C
to form $s.C_2S/S = 2.866675.s\% = (c_2s)_1\%$ of C_2S)
remaining $(c_2\text{-}c_3) = c_4\%$ of C

c) c_4 % of C fix $c_4.A/C = 1.818160.c_4\% = a_3\%$ of A
to form $c_4.CA/A = 2.818160.c_4\%$ of CA
remaining $(a_2\text{-}a_3) = a_4\%$ of A

d) a_4 % of A fix $a_4.C_2S/S = 1.689304.a_4\% = (c_2s)_2\%$ of C_2S
to form $a_4.C_2AS/S = 2.689304.a_4\%$ of C_2AS
remaining $((c_2s)_1\text{-}(c_2s)_2)\%$ of C_2S

Finally: $C_4AF\% = 3.04\ F\%$
$CA\% = 2.82\ C\% - 5.26\ S\% - 3.96\ F\%$
$C_2AS\% = 2.69\ A\% - 1.72\ F\% - 1.73_5CA\%$
or $C_2AS\% = 2.69\ A\% + 9.13\ S\% + 5.15\ F\% - 4.89\ C\%$
$C_2S\% = 2.87\ S\% - 0.63\ C_2AS\%$

or $C_2S\% = 2.87\,S\% + 1.08\,F\% + 1.09\,CA\% - 1.69\,A\%$

or $C_2S\% = 3.07\,C\% - 2.87\,S\% - 3.24\,F\% - 1.69\,A\%$

3.4. - Calculations in the system II.2:

$$\underline{CAss\text{-}C_6A_2Fss\text{-}C_2ASss\text{-}C_2S}$$

a) As b) in 3.2
b) As b) in 3.3
c) As c) in 3.3
d) As d) in 3.3

Finally: $C_6A_2F\% = 4.38\,F\%$

$CA\% = 2.82\,C\% - 5.26\,S\% - 5.94\,F\%$

$C_2AS\% = 2.69\,A\% - 3.43\,F\% - 1.73_5\,CA\%$

or $C_2AS\% = 2.69\,A\% + 9.13\,S\% + 6.87\,F\% - 4.89\,C\%$

$C_2S\% = 2.87\,S\% - 0,63\,C_2AS\%$

or $C_2S\% = 2.87\,S\% + 2.16\,F\% + 1.09\,CA\% - 1.69\,A\%$

or $C_2S\% = 3.07\,C\% - 2.87\,S\% - 4.31\,F\% - 1.69\,A\%$

3.5. - Calculations in the system III.1:

$$\underline{CAss\text{-}C_{12}A_7ss\text{-}C_4AFss}$$

a) As b) in 3.1
b) As c) in 3.1
c) As d) in 3.1

Finally: $C_4AF\% = 3.04\,F\%$

$C_{12}A_7\% = 4.95\,C\% - 5.21\,F\% - 2.72\,A\%$

$CA\% = 1.55\,A\% - 0.99\,F\% - 0,80\,C_{12}A_7\%$

or $CA\% = 3.72\,A\% + 3.17\,F\% - 3.95\,C\%$

3.6. - Calculations in the system III.2:

$$\underline{CAss\text{-}C_{12}A_7ss\text{-}C_6A_2Fss}$$

a) As b) in 3.2
b) As c) in 3.1
c) As d) in 3.1

Finally: $C_6A_2F\% = 4.38\,F\%$

$C_{12}A_7\% = 4.95\,C\% - 6.95\,F\% - 2.72\,A\%$

$CA\% = 1.55\,A\% - 1.98\,F\% - 0,80\,C_{12}A_7\%$

or $CA\% = 3.72\,A\% + 3.56\,F\% - 3.95\,C\%$

4. - NUMERICAL EXAMPLES

Application of the preceeding potential calculations to more common ancient and present compositions of some Spanish HAC have been made. Table I shows chemical analysis in terms of the four major components and the "rest" defined in 3. Calculated potential compositions in terms of the phases corresponding to the systems described in 3.1 to 3.6 have been also included in the table. Seven examples have been choosen, the case 3.5a corresponding to the application of calculations in the system III.1 of 3.5, to the chemical composition of case 3.6, also corresponding to the system III.2 of 3.6.

TABLE I

	S	y	s	t	e	m	s
Chem. comp.	3.1	3.2	3.3	3.4	3.5	3.5 a	3.6
A	40.5	40.5	40.5	37.0	39.5	39.0	39.0
C	38.5	39.5	38.5	40.5	36.5	37.0	37.0
S	2.5	2.0	2.5	4.5	-	-	-
F	11.0	9.5	12.5	11.0	12.0	11.0	11.0
R	7.5	8.5	6.0	7.0	12.0	13.0	13.0
Σ	100.0	100.0	100.0	100.0	100.0	100.0	100.0
Pot. comp.	3.1	3.2	3.3	3.4	3.5	3.5 a	3.6
CAss	51.9	43.3	45.9	25.2	40.8	33.8	38.2
$C_{12}A_7$	0.0	0.9	-	-	10.7	19.8	0.6
C_2S	7.2	5.7	2.3	1.5	-	-	-
C_4AF	33.4	-	38.0	-	36.5	33.4	-
C_6A_2F	-	41.6	-	48.2	-	-	48.2
C_2AS	-	-	7.8	18.1	-	-	-
R	7.5	8.5	6.0	7.0	12.0	13.0	13.0
Σ	100.0	100.0	100.0	100.0	100.0	100.0	100.0

Examples show substantial variations in calculated potential compositions, even for very similar chemical analysis. Particular features of this subject may be: i) the different amounts of calculated C_4AFss and C_6A_2Fss in the respective systems, even for the same F content (cases 3.5a and 3.6); ii) the higher values of $C_{12}A_7$ corresponding to the C_4AFss formation, as compared with those corresponding to the C_6A_2Fss formation (cases 3.5 or 3.5a and 3.6); iii) that all these influences and some others related to the A + C sum and/or to the A/C ratio seem to affect the contents of C_2S and/or C_2AS and that of CA, and consequently the properties and behaviour of HAC; iv) that changes introduced in composition of Spanish HAC (ancient case 3.4 as compared with modern cases 3.1 to 3.3) have resulted in an important increase of HAC quality; etc.

5. - CONCLUSION

Stoichiometric consideations and assumptions on formation of possibly existing phases in the extremely complex systems of real and practical -technical, commercial- HAC permit to develop hypothetical potential calculations for such systems; some of the presumably more common of them have been taken into account. Calculations show than even for very similar quantitative chemical compositions or HAC, referred either to percentages of oxides and/or to the ratios between them, may result in different qualitative and/or quantitative potential compositions. It is thought that these differences, when real, may affect to more or less hydraulic anhydrous phases, and to phases with a higher or lower speed of hydration and hardening. It is also thought that this may result in

hydration products of a higher or lower stability -susceptibility to changes provoked by temperature and/or humidity variations or by hydrolitic alkaline processes, carbonation, etc.-. These considerations on the exposed potential calculations might perhaps aid to interpretate the great difference in behaviour of apparently equal or very similar HAC, mainly as far as their bare chemical composition is concerned. As to the calculations applied to the present Spanish HAC with the following rounded mean chemical composition: A = 41.0 %; C = 38.0 %; F = 13 %; R = 5.5 %, its potential composition fits in the system CAss-$C_{12}A_7$ss-C_4AFss, with the following results: CA = 43.6 %; $C_{12}A_7$ = 8.9 %; C_4AF = 39.5 %; R = 8.0 % (R includes S = 2.5 % which is assumed to be in solid solution with some of the other phases). This calculated potential composition agrees well with actual experimental results (21), which confirm the applicability of the mentioned system to the Spanish HAC.

ACKNOWLEDGEMENTS

The author wish to thank Dr. A. de BENITO for his ancient collaboration. And very specially his colleagues Prof. Dr. S. DE AZA and Dr. R. MARTINEZ for their most valuable comments, observations and criticism.

REFERENCES

1.- J. TALABER (1974), "High-alumina cements", VI ICCC (Moscow), Principal Paper.
2.- R. A. BROWN (1975) "Highlights of Symposium on HAC", Cement Technology, nº 2, 59-61.
3.- R. W. NURSE, J. H. WELCH and A. J. MAJUMDAR (1965), "The $CaO-Al_2O_3$ system in moisture-free atmosphere", Trans. Brit. Ceram. Soc., 64, 2, 409-414.
4.- Yu. P. UDALOV, T. Yu. CHEMEKOVA and Z. S. APPEN (1974), "On the character of the $CaO-Al_2O_3$ system diagram", VI ICCC (Moscow) Suppl. Paper III-4.
5.- K. SUZUKI (1974), "Influence of substituted Fe and Si on the formation of calcium aluminate phase and its hydration", VI ICCC (Moscow), Suppl. Paper II-3, 4, 5.
6.- P. KITTL, L. C. POMPEU, A. GOLDSCHMIDT and J. H. C. CASTRO (1978), "Estudio de un clinker industrial aluminoso", V Interamer. Conf. on Materials and Technology, Sao Paulo (Brasil), 245-251.
7.- S. TAKAGI, M. OHTA and G. YAMAGUCHI (1977), "Caractérisation des constituants minéralogiques du clinker de ciment alumineux", J. Ceram. Soc. Japan nº 5, 231-237 (Summary in Bull. Anal. du CERILH, nº 12, ref. 77C 10608, 1977).
8.- H. G. MIDGLEY (1967), "The mineralogy of set high-alumina cement", Trans. Brit. Ceram. Soc., 66, 4, 161-187.
9.- M. JOUNG (1973), "Propriétés hydrauliques des ciments à haute teneur en alumine", Bull. Soc. Fraç. Céram., nº 98, 11-20.
10.- T. W. PARKER (1952), "The constitution of aluminous cement", III, ISCC (London), C&CA, 485-515.
11.- A. DE BENITO (1970), Private comunication. Study carried out at the IETCC (Madrid, Spain), not published.
12.- H. G. MIDGLEY and A. MIDGLEY (1975), "The conversion of high-alumina cement", Build. Res. Establishment, Current Paper CP-72/75.
13.- P. K. MEHTA and G. LESNIKOV (1971), "Conversion of $CaO.Al_2O_3.10H_2O$ to $3CaO.Al_2O_3.6H_2O$", J. Am. Ceram. Soc., nº 4, 210-212.
14.- T. VAZQUEZ, F. TRIVIÑO and A. RUIZ DE GAUNA (1976), "Study on transformations of HAC. Influence of CO_2, temperature, moisture and additions of limestone powder", Monography nº 334 (IETCC, Madrid), pp. 105 (in Spanish).
15.- A. NEVILLE (1978), "High-alumina cement. A current review", II Cemento, 75, 3, 291-302.
16.- H. G. MIDGLEY and J. F. RYDER (1977), "The relationships between mineral composition and strength development of high-alumina cement", Cem. and Concr. Res., 7, 6, 669-672.
17.- J. SAVKOV and J. SULIKOVSKI (1976), "Effect of phase composition of refractory aluminous cements on their utilization", Cem. -Wapno-Gips 30, 10, 281-293.
18.- J. PUIG and F. SANCHEZ-PEREZ (1974), "High-alumina cements and their refractory properties", (in Spanish), Bol. Soc. Esp. Ceram., nº 1, 19-23.
19.- T. D. ROBSON (1962), "High-alumina cements and concretes", Contractors Record Ltd., London, 263 pp.
20.- A. NEVILLE (1975), "High-alumina cement concrete", The Construction Press Ltd., Hornby, Lancaster, Great Britain, 201 pp.
21.- R. MARTINEZ and S. DE AZA (1979), Private Communication. Theoretical and experimental research work on HAC sponsored and financed by CEMENTOS MOLINS, S.A. (Barcelona, Spain), carried out at the Instituto de Cerámica y Vidrio (Madrid, Spain). Ph. D. these of R. MARTINEZ (University of Madrid) directed by S. DE AZA, to be submitted, and papers to be published by both authors.
22.- F. P. SORRENTINO and F.P. GLASSER (1975), "The system $CaO-Fe_2O_3-Al_2O_3-SiO_2$. I. The pseudoternary section $Ca_2Fe_2O_5-Ca_2Al_2O_5-SiO_2$", Trans. Brit. Ceram. Sec., 74, 253-256.
23.- F. P. SORRENTINO and F.P. GLASSER (1976), "Phase relations in the system $CaO-Al_2O_3-SiO_2-Fe-O$. Part. II. The system $CaO-Al_2O_3-Fe_2O_3-SiO_2$", Trans. Brit. Ceram. Soc., 76, 95-103.
24.- T. D. ROBSON (1969), "The chemistry of calcium aluminates and their relating compounds". V ISCC (Tokyo), Vol. 1, 1, 349-365.

Ciments réfractaires alumineux dans le pseudosystème $BaO.Al_2O_3$-$CaO.Al_2O_3$-$MgO.Al_2O_3$-$BaO.6Al_2O_3$-$CaO.6Al_2O_3$

Refractory aluminous cements in the $BaO.Al_2O_3$-$CaO.Al_2O_3$-$MgO.Al_2O_3$-$BaO.6Al_2O_3$-$CaO.6Al_2O_3$ pseudosystem

I. TEOREANU, Professor, Faculty of Chemical Technology, Bucharest, Polytechnical Institute
N. CIOCEA, Scientific - researcher, Bucharest Polytechnical Institute, Roumanie.

RESUME : Une méthode pour obtenir des ciments alumineux de haute réfractairité est de remplacer une partie du CaO contenu dans les ciments alumineux de calcium par MgO, BaO ou SrO. L'oxyde de calcium peut être remplacé en totalité par le SrO ou le BaO.

Le but de ce travail est d'étudier les caractéristiques des masses de ciment réfractaire obtenus par un remplacement total ou partiel du CaO par BaO+MgO. Les auteurs ont déterminé les propriétés physico-mécaniques des masses situées dans le pseudosystème BA-CA-MA-BA_6-CA_6 (B = BaO, C = CaO, M = MgO, A = Al_2O_3) pour des pourcentages de MA de 2o et 5o %, respectivement. Ils ont aussi analysé l'influence exercée par des petites additions de SiO_2 et de Fe_2O_3 (introduites dans le système comme impuretés dans les matières premières) sur les propriétés des ciments alumineux étudiés.

SUMMARY : Aluminous cements possessing high refractoriness may be obtained starting from calcium - containing aluminous cements by means of a partial replacement of CaO by MgO, BaO or SrO. This replacement may be total when barium or strontium oxides are used.

The present work deals with the study of the properties of some masses characterized as aluminous cements, obtained by a partial or total replacement of CaO by BaO+MgO. There were determined the physical - mechanical properties of the masses situated within the BA-CA-MA-BA_6-CA_6 pseudosystem (where B = BaO, C = CaO, M = MgO, A = Al_2O_3), when the MA amount is of 2o and 5o %, respectively.

There was examined, too, the influence of small amounts of SiO_2 and Fe_2O_3 (brought into the system as impurities in the raw materials) on the properties of the aluminous cements studied in this work.

Dans la compositions des ciments alumineux hydrauliques utilisés comme produits réfractaires les constituents majeurs sont les aluminates de calcium. Parmi ces ciments, les plus réfractaires sont ceux à haut contenu d'Al_2O_3 allant, par exemple, jusqu'à 79-81 % Al_2O_3 (1, 2); des travaux et des brévets récents (3, 4) proposent comme méthode de préparation des ciments l'addition de l'oxyde d'aluminium pendant le broyage.

Des données plus récentes (5-13) ont montré qu'on peut aussi obtenir des ciments alumineux de haute réfractairité par le remplacement total ou partiel du CaO contenu dans les ciments alumineux à calcium par MgO, BaO, SrO. Ce remplacement peut être réalisé en totalité dans les cas du BaO et du SrO.

Dans ce travail nous avons étudié les propriétés des quelques masses characterisées comme liants, obtenus par un remplacement total ou partiel du CaO par BaO+MgO. Nous avons déterminé les propriétés physico-mécaniques d'environ 85 masses situées dans la région moins basique du système BaO-CaO-MgO-Al_2O_3, plus exactement dans le pseudosystème BA-CA-MA-BA_6-CA_6, pour des proportions en MA de 2o % et 5o %, respectivement.

Les matières premières utilisées pour la synthèse ont été: carbonate de baryum, carbonate de calcium et carbonate basique de magnesium de pureté chimique et alumine tabulaire (plus de 99,5 % Al_2O_3). Tous les clinkers ont été synthétisés à 154o°C; le temps de cuisson a été 8 heures à cette température.

Pour déterminer le cours des procès de sinterisation et vitrification, nous avons déterminé la porosité des échantillons cuits et nous avons effectué des analyses roentgenographiques (voyez aussi (14)). Les résultats ont montré que pour la quasi-totalité des masses synthétisées l'équilibre thérmique est achevé; les clinkers situés dans la région du BC_2A_4 font exception. Les phases decelées dans les échantillons correspondant au composé BC_2A_4 à 2o % MA et 5o % MA, cuits dans les conditions déjà méntionnées, ont été les suivantes: BC_2A_4 et MA (prédominantes), BA, CA, CA_2. Ces phases ont été observées dans tous les masses à haut contenu potentiel en BC_2A_4.

Pour connaitre les propriétés liantes des masses étudiées dans le pseudosystème BA-CA-MA-BA_6-CA_6, les clinkers ont été broyés jusqu'à un résidu nul sur le tamis de o,o6 mm, et ont été mésurés les valeurs de l'eau de consistance normale, du temps de prise - figure 1 - et de la résistance à compression (sur des échantillons hydratés, gardés en air pour 1, 3 et 7 jours) - figure 2. Les valeurs de l'eau de consistance normale ont été entre 24 et 3o %.

La plupart des ciments obtenus possédent des résistances mécaniques à compression de plus de 1oo daN/cm² après un jour et de 3oo daN/cm² après 7 jours (dans des conditions comparables de synthèse et de mesure, les valeurs pour les échantillons de CA ont été de 3oo daN/cm² après un jour et, respectivement, de 5oo daN/cm² après 7 jours; les meil-

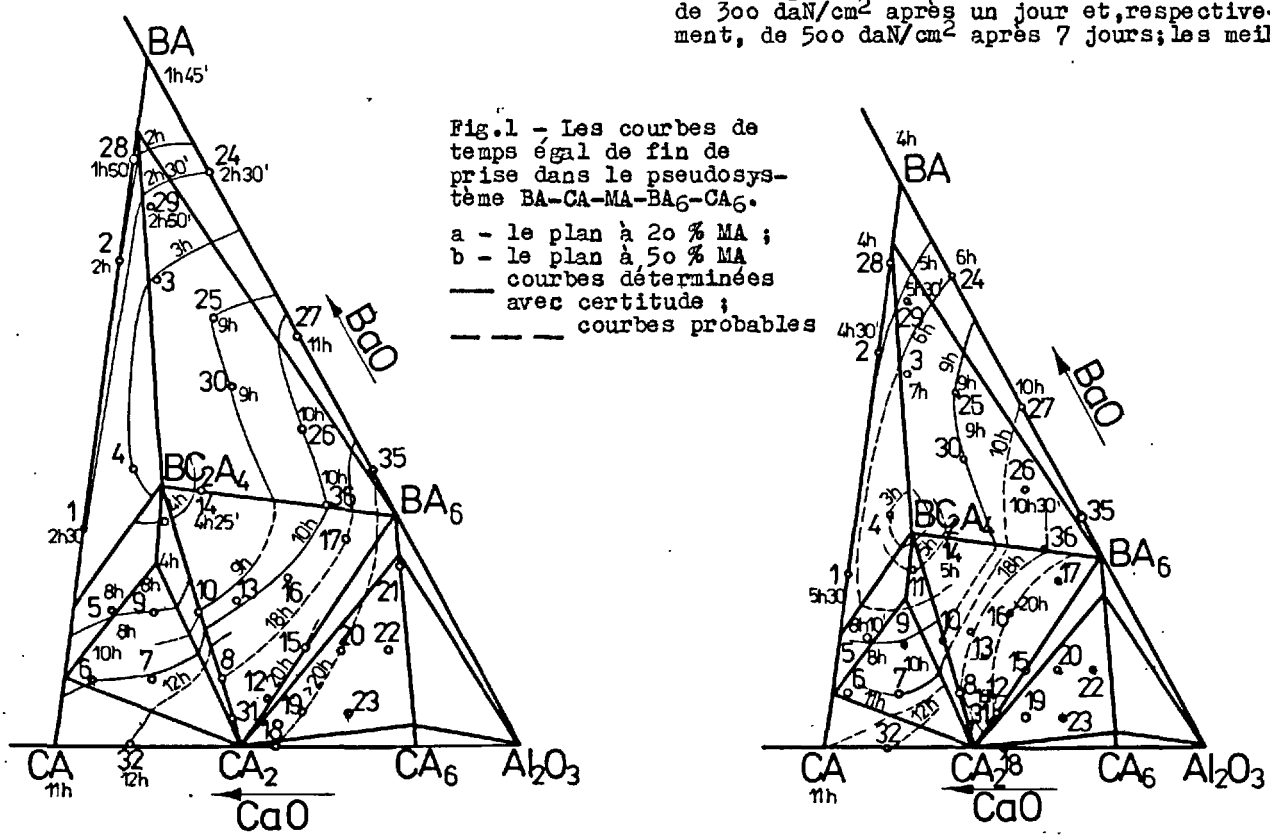

Fig.1 - Les courbes de temps égal de fin de prise dans le pseudosystème BA-CA-MA-BA_6-CA_6.

a - le plan à 2o % MA ;
b - le plan à 5o % MA
—— courbes déterminées avec certitude ;
— — — courbes probables

leurs résultats dans les mêmes conditions ont été 5oo daN/cm² après un jour et 65o daN/cm² après 7 jours).Les courbes dans les figures 1 et 2 sont basées sur ces données.

Nous avons aussi déterminé la réfractairité dont les valeurs sont données dans la figure 3 (pour la plupart des ciments les réfractairités ont été de plus de 175o°C).

L'analyse des courbes de temps égal de fin de prise (figure 1) et de résistance égale à compression après 7 jours (figure 2) montre que les propriétés des ciments synthétisées respectent les régles de paragenèse lorsque l'équilibre thérmique est achevé.

Nous avons mentionné que dans le cas des masses riches en BC_2A_4 l'équilibre est partiellement achevé; de ce motif,le parallélisme entre les propriétés physiques et mécaniques du ciment et sa composition minéralogique potentielle (en conformité avec les régles de paragenèse) n'est pas observé dans tous les cas.

Dans les sous-systèmes BA_{ss}-BA_6-BC_2A_4-MA et BA_{ss}-CA_{ss}-BC_2A_{4ss}-MA les valeurs minimales du temps de fin de prise sont dirigées vers la pointe BA_{ss} ou vers la pointe BC_2A_4. Le temps de prise augmente avec le contenu en spinel magnésien. Les valeurs maximum des résistances mécaniques sont aussi obtenus pour les échantillons riches en BA_{ss}; l'augmentation du contenu en spinel magnésien jusqu'à 5o % ne diminue pas les résistances mécaniques.

Les valeurs de la réfractairité des masses dans les sous-systèms cités plus haut augmentent avec l'augmentation du contenu en BA, BA_6 et MA (figure 3).

Les masses situées dans le sous-système CA_{ss}-BC_2A_{4ss}-CA_2-MA (surtout celles riches en aluminates de calcium), quand sont cuites à 154o°C, possèdent des temps de prise plus longs et les résistances initielles (surtout les valeurs après un jour) sont diminuées. Pour obtenir des valeurs optimales du temps de prise et de la résistance initielle, les masses doivent être cuites à des températures plus basses (environ 15oo°C (15)).

Les compositions situées dans les sous-systèmes CA_2-BC_2A_4-BA_6-MA et CA_2-CA_6-BA_6-MA sont d'une importance pratique réduite en ce que concerne leurs utilisations comme liants.

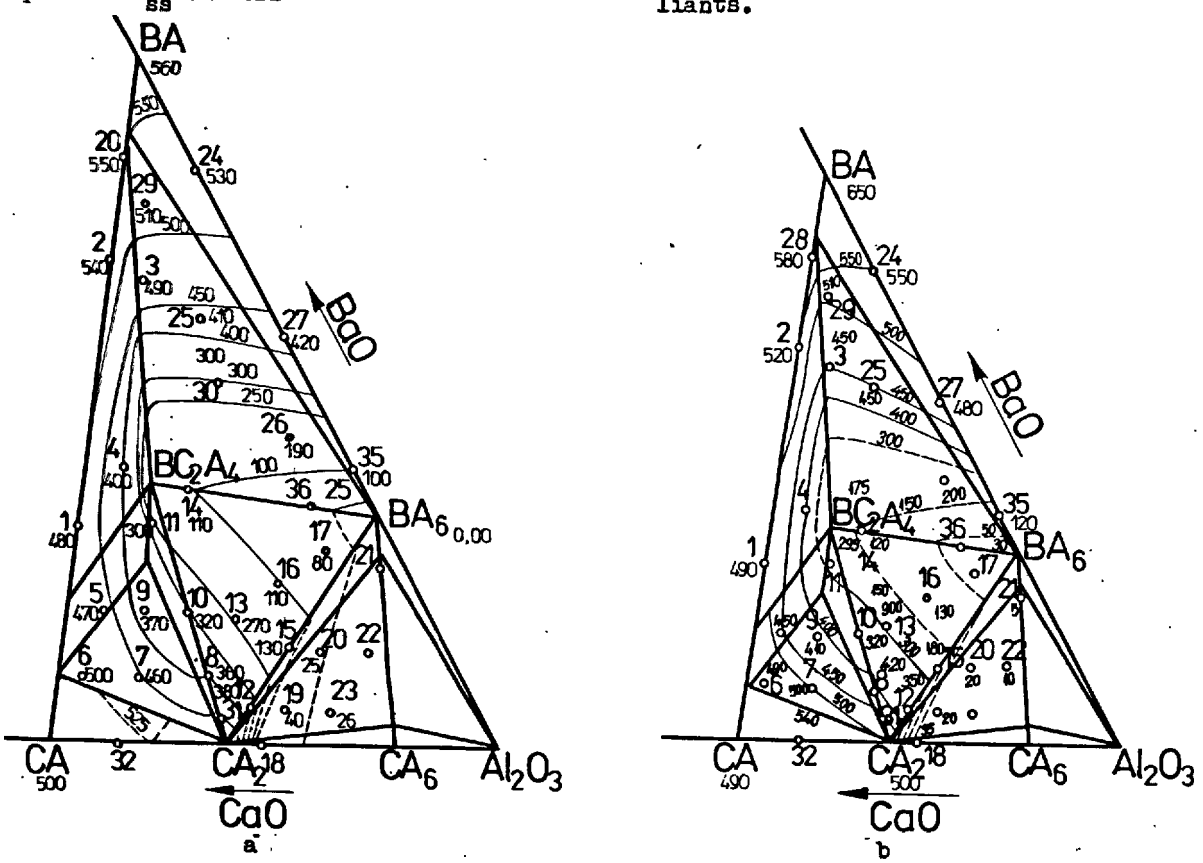

Fig.2 - Les courbes de résistance égale à compression après 7 jours dans le pseudosystème BA-CA-MA-BA_6-CA_6.

a - le plan à 2o % MA; b - le plan à 5o % MA
_____ courbes déterminées avec certitude;
_ _ _ courbes probables

L'étude des propriétés des masses synthétisées nous a montré que les meilleurs valeurs ont été obtenués dans le cas de la masse notée par le symbole BA, qui est composée de 5o % BA et de 5o % MA. L'influence des additions de SiO_2 et de Fe_2O_3, présentes comme impuretés dans les matières premières, a été étudiée sur cette composition, remplaçant une fraction variable d'Al_2O_3 par les additions specifiées plus haut. La composition oxydique du ciment alumineux de baryum et magnésium utilisé comme substance étalon et celle des ciments avec des additions de SiO_2 et Fe_2O_3 sont présentées dans le tableau I.

Les mélanges synthétisés ont été cuits 5 heures à 15oo°C. Quelques propriétés des ciments obtenus sont présentées dans le tableau I.

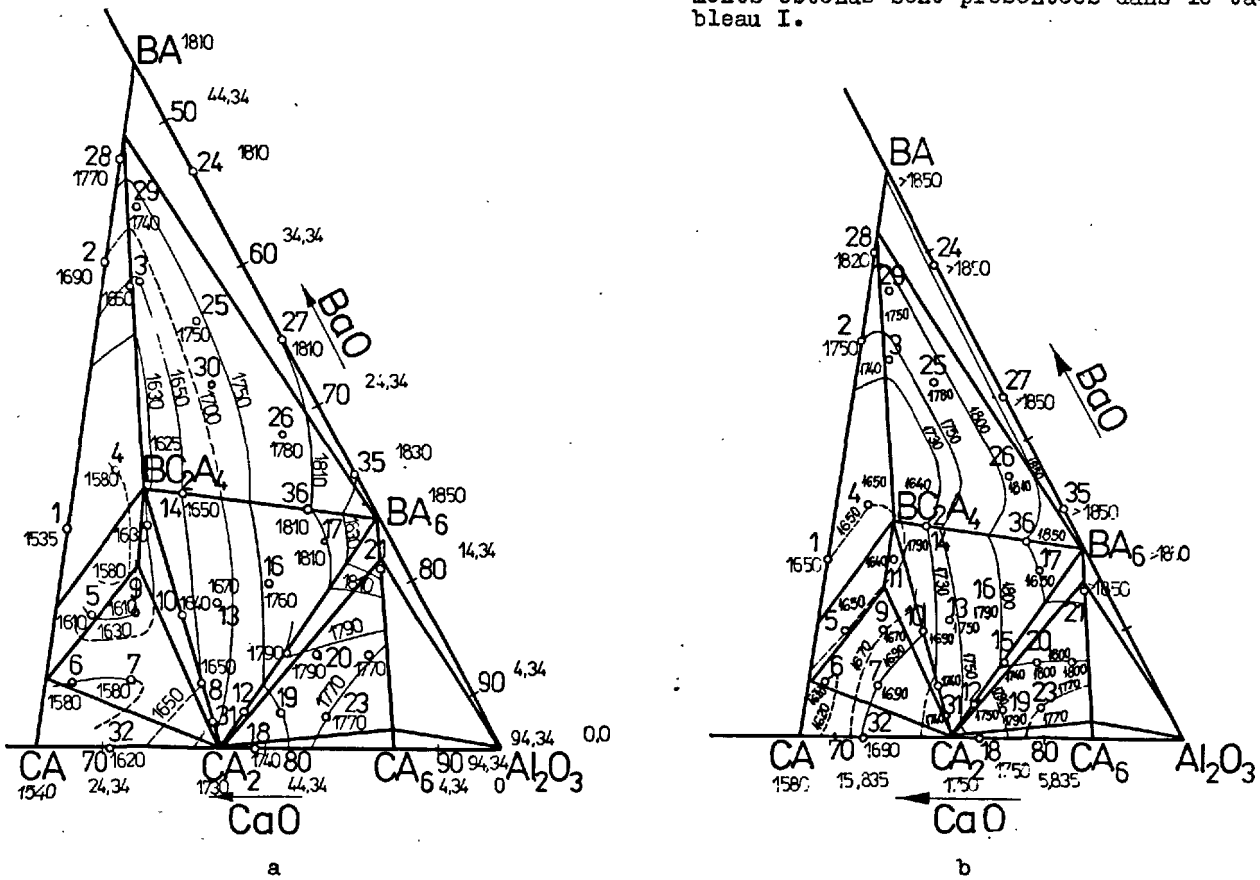

Fig.3 - Les courbes d'isoréfractairité dans le pseudosystème BA-CA-MA-BA_6-CA_6

a - le plan à 2o % MA ; b - le plan à 5o % MA

_____ courbes déterminées avec certitude; _ _ _ _ courbes probables.

TABLEAU I

Symbole de la masse	Composition oxydique, %					Temps de prise, h, min.		Résistance à compression, daN/cm²		Réfractairité, °C
	BaO	MgO	Al_2O_3	SiO_2	Fe_2O_3	Commencement	Fin	après 1 jour	après 7 jours	
BA	3o,1	14,17	55,73	-	-	2h3o min.	4 h	4oo	55o	>187o
1	3o,1	14,17	53,23	2,5	-	3h	6 h	4oo	4oo	181o
2	3o,1	14,17	5o,73	5,o	-	2h3o min.	5 h	3oo	325	175o
3	3o,1	14,17	48,23	7,5	-	4h	7 h	25o	25o	171o
4	3o,1	14,17	53,73	-	2	3h15min.	6 h	325	415	>181o
5	3o,1	14,17	51,73	-	4	3h	6 h	4oo	45o	>181o
6	3o,1	14,17	49,73	-	6	2h3o min.	5 h	375	41o	>181o
7	3o,1	14,17	51,23	2,5	2	4h	6 h	5oo	6oo	181o
8	3o,1	14,17	46,73	5,o	4	3h45 min.	5h3o min.	4oo	475	172o
9	3o,1	14,17	46,23	7,5	2	4h3o min.	6h15 min.	4oo	49o	17oo
1o	3o,1	14,17	47,23	2,5	6	3h3o min.	7h1o min.	21o	33o	179o

Nous avons établi que l'utilisation des matières premières contenant des quantités relativement petites de SiO_2 et de Fe_2O_3 mene à une diminution de la résistance mécanique du ciment et de sa réfractairité. Il nous semble probable que l'action nocive du SiO_2 est plus importante que celle du Fe_2O_3.

CONCLUSIONS

Les données que nous avons présenté, concernant les propriétés des ciments dans le système $BaO-CaO-MgO-Al_2O_3$ montrent que, pour obtenir des ciments de haute réfractairité et d'une haute résistance mécanique, les compositions choisies doivent être situées dans le soussystème $BA_{ss}-BC_2A_4-BA_6-MA$ (dans la région plus riche en BA, le spinel magnésian peut être trouvé en proportions allant jusqu'à 5o %). La cuisson à des températures supérieures à 154o°C n'exerce pas une influence négative sur les propriétés des ciments.

Les masses situées dans le sous-système $BA_{ss}-CA_{ss}-BC_2A_{4ss}-MA$ sont aussi des liants de bonne qualité, dont les propriétés sont en dépendence de la région où se trouvent.

Les masses dans le sous-système $CA_{ss}-BC_2A_{4ss}-CA_2-MA$ possèdent des résistances mécaniques elevées, mais leurs réfractairités sont plus basses. Le danger de la surcuisson paraît plus visible dans le cas des masses riches en CA et CA_2, quand le contenu en BC_2A_4 augmente, les résistances decroissent et le danger de la surcuisson diminue.

Les masses réfractaires situées dans les autres sous-systèmes sont d'une importance technique réduite, compte tenir de leurs propriétés liantes.

L'utilisation des matières premières contenant SiO_2 et Fe_2O_3 (comme impuretés) pour obtenir des ciments étudiés, mene à une diminution de leurs résistances mécaniques et de leur réfractairité. L'influence des ces oxydes (surtout du SiO_2), considerés séparément, semble d'être plus nocive que dans le cas de leur présence simultanée.

BIBLIOGRAPHIE

1. - M.J. SCHMITT (1973) "Les bétons réfractaires - Analyse scientifique et téchnologique", Circulaire d'Informations Téchniques, nr.3, pp.725-742.
2. - x x x "Alcoa Calcium Aluminate Cement CA-25", Alcoa, iunie 1, 1971 - GA2A, Aluminium Company of America, Pittsburgh, P.A. 15219.
3. - G. SADRAN, L. ASSAUD "Ciment alumineux hautement réfractaire et son procédé de fabrication", Brevet nr.1.545.678 - 31 juillet, 1967, Ciments Lafarge, France.
4. - I. TEOREANU, N. CIOCEA (1978) "Cimenturi superaluminoase cu adaosuri inerte", Materiale de Construcţii, vol.8, nr.1, pp.5o-54.
5. - AL. BRANISKI, T. IONESCU, N.DEICA "Cimenturi refractare aluminoase", Brevet nr.51173, ol.11.1967, R.S.România.
6. - N. DEICA, I. DRAGOMAN, N. CIOCEA, C.CAMERMAN (197o) "Contribuţii la fabricarea şi utilizarea cimenturilor şi betoanelor refractare de calitate superioară", Cercetări Metalurgice, nr.11, pp.855-868.
7. - N. CIOCEA (1976) "Cimenturi refractare" (in Roumanian). Thesis, Polytechnic Institute, Bucharest.
8. - I. TEOREANU, N. CIOCEA, M. MUNTEAN, O. SANCU (1974) "Cimenturi aluminoase refractare", Materiale de Construcţii, vol.4, nr.2, pp.62-65.
9. - I. TEOREANU, N. CIOCEA (1975) "Cimenturi aluminoase de stronţiu, bariu şi magneziu", Materiale de Construcţii, vol.5, nr.3, pp.13o-132.
10. - I. TEOREANU, N.CIOCEA (1977) "Einfluss von Magnesiumoxid, Fe_2O_3 und SiO_2, verunreinigungen auf die eigenschaften feuerfester tonerdezemente", Siliconf, Budapest, pp.367-376.
11. - I. TEOREANU, N. CIOCEA "Refractory cements in the pseudosystem $BaO.Al_2O_3-CaO.Al_2O_3-BaO.6Al_2O_3-CaO.6Al_2O_3$" - unpublished work.
12. - D. S. BHUNIA, A.K. MITRA, M.K. CHATTERJEE (1978) "Hydraulic properties of calcium - barium aluminate cements" Indian Ceramics, 2o (2), pp.363-367.
13. - D.S. BHUNIA, A.K. MITRA, M.K. CHATTERJEE (1978) "Hydraulic properties of calcium - strontium aluminate cements" Indian Ceramics, 2o (3), pp.391-395.
14. - I. TEOREANU, N. CIOCEA (1976) "Spezielle Tonerdezemente. Sintermecanismus und technische Eigenschaften der Massen des Teilsystems $BaO.Al_2O_3-CaO.Al_2O_3-MgO.Al_2O_3-BaO.6Al_2O_3-CaO.6Al_2O_3$", Ibausil - Baustoffindustrie, A3 (mai), pp.29-32.
15. - I. TEOREANU, N. CIOCEA (1974) "Consideraţii privind formarea şi proprietăţile unor aluminaţi de calciu", Materiale de Construcţii, vol.IV, nr.1, pp.36-4o.

Hydratation des mélanges silicates-aluminates de calcium

Hydration of calcium silicates and aluminates mixes

B.F. COTTIN, Chef de Service, Laboratoire de Recherche Générale, Lafarge S.A., France.

RESUME : Il est bien connu que les mélanges de ciments Portland et de ciments alumineux peuvent donner, pour certaines proportions, des ciments à prise pratiquement instantanée.

L'étude cinétique des concentrations des solutions de gâchage, et leur comparaison avec le diagramme chaux - alumine - eau, permet de comprendre et d'expliquer, au moins en partie, ces phénomènes.

SUMMARY : It is well known that, for precisely defined proportions, mixes of Portland and high alumina cements give a practically instantaneous setting.

These phenomena are partly understood and explained by comparing kinetic studies of the concentrations of the mixing solutions with the lime - alumina - water diagram.

INTRODUCTION

L'étude de l'hydratation des liants hydrauliques par analyse des filtrats de suspensions de ciments relativement diluées est depuis longtemps utilisée par un certain nombre d'auteurs. Les résultats les plus anciens, et les plus nombreux, se rapportent aux ciments alumineux dont le constituant principal est l'aluminate monocalcique CA. On peut citer en particulier les travaux de ASSARSON (1) - WELLS et CARLSON (2).

Plus récemment, le Professeur Barret et son équipe ont approfondi la connaissance des processus d'hydratation de l'aluminate monocalcique pur et du Ciment Fondu, ciment à haute teneur en alumine fabriqué dans des fours à fusion par Lafarge Fondu International : BESSIERES (3) - BARRET et MENETRIER (4) - BERTRANDIE (5). Leurs essais montrent que l'hydratation de ces ciments suit le schéma : passage en solution - temps de germination - précipitation et correspond très bien au diagramme chaux - alumine - eau étudié en particulier par JONES et ROBERTS (6) - PERCIVAL et TAYLOR (7) - FAURIE-MOUNIER (8).

Le ciment Portland et le C_3S ont aussi été étudiés par l'analyse des filtrats, et nous citerons parmi les derniers auteurs : YOUNG, TONG et BERGER (9) - SLEGERS et ROUXHET (10) - MENETRIER (11). Cette dernière a même pu rattacher les premiers instants de réactions du C_3S avec l'eau au diagramme chaux-silice-eau tel qu'il a été défini par FLINT et WELLS (12) ou GREENBERG et CHANG (13).

L'expérience nous a montré que, aussi bien pour les ciments alumineux que pour les ciments Portland, l'évolution de l'analyse des filtrats de suspensions à rapport pondéral eau/ciment de 10 est bien représentative de la prise des pâtes de rapport E/C 0,5. En particulier, le début de prise coïncide avec le moment où le filtrat des suspensions commence à s'appauvrir en ions en solution, et où des hydrates apparaissent significativement dans le résidu solide. C'est la raison pour laquelle nous avons appliqué la méthode des analyses de filtrats aux mélanges ciment alumineux - ciment Portland, pour lesquels il est bien connu que certaines proportions conduisent à des prises si promptes que le gâchage est impossible.

CONDITIONS EXPERIMENTALES

Nous avons étudié les mélanges 20/80 - 50/50 - 80/20 d'un Ciment Fondu commercial et d'un clinker de ciment Portland broyé sans gypse, dont les caractéristiques sont données ci-après :

Ciment Fondu :

SiO_2	Al_2O_3	Fe_2O_3	FeO	CaO	MgO	TiO_2	p. feu	SS Blaine
4,10	38,90	12,90	3,20	38,45	0,35	2,20	0,25	2890

Clinker de Portland :

SiO_2	Al_2O_3	Fe_2O_3	CaO	MgO	SO_3	p. feu	K_2O	Na_2O	CaO libre
22,95	5,00	2,80	67,60	0,65	0,35	0,45	0,16	0,09	0,70

C_3S	C_2S	C_3A	C_4AF	SS Blaine
59	22	8,5	8,5	3050

Nous avons utilisé la méthode décrite par COTTIN (14)pour les longues échéances dans laquelle l'analyse des oxydes CaO et Al_2O_3 dissous dans le filtrat est complétée par l'examen en diffraction des rayons X du résidu solide, lavé à l'acétone et séché à l'éther sulfurique. Les essais ont été réalisés à la température de 21°C.

RESULTATS DES ESSAIS

Les tableaux I à IV donnent les résultats obtenus aux échéances les plus significatives : concentration du filtrat en CaO et Al_2O_3 (s'il y a lieu) - Rapport C/A molaire des ions en solution - hauteurs des pics de diffraction des rayons X des anhydres résiduels et des hydrates formés dans le résidu sec - pourcentage d'eau liée du résidu sec par perte au feu à 1000°C après lavage à l'acétone et séchage à l'éther.

Echéance	Concentration mg/l		Rapport C/A molaire	Hauteurs de pics en diff. X				Eau liée %
	Al_2O_3	CaO		CA	C_4AF	CAH_{10}	C_2AH_8	
40 mn	1810	1040	1,05	138	69	-	-	0,40
1 h.	1815	1075	1,08	138	69	-	-	0,45
2 h.	1745	1015	1,06	144	66	-	-	1,00
3 h.	1125	715	1,16	117	54	15	21	2,30
4 h.	915	605	1,20	100	51	24	60	18,25
6 h.	770	515	1,22	51	51	66	108	29,90
17 h.	435	370	1,57	c	48	180	165	43,10

TABLEAU I : Ciment Fondu

100 % Fondu

Les résultats obtenus sont classiques et se caractérisent par :

- Une augmentation très rapide des ions en solution dont la concentration atteint en moins d'une heure environ 19,2 millimoles par litre de CaO et 17,8 millimoles par litre de Al_2O_3.
- Une diminution très rapide entre 2 et 3 heures de ces concentrations, avec apparition des hydrates par diffraction X et augmentation significative de l'eau liée.
- La poursuite de l'hydratation avec diminution du C_4AF et surtout du CA résiduels, augmentation des pics de diffraction de CAH_{10} et C_2AH_8, très forte augmentation de l'eau liée et glissement progressif du C/A en solution de 1,05 environ à des valeurs plus importantes.

La cinétique de tous ces phénomènes est caractéristique d'un ciment dont la période dormante se termine un peu avant l'échéance de 3 heures.

Echéance	Concentration mg/l	Hauteurs de pics en D.X.				Eau liée %
	CaO	C_3S	C_3A	CH	C_4AH_{13}	
1 h.	785	180	32	-	-	0,95
3 h.	1035	173	31	-	-	1,55
7 h.	1510	177	32	-	-	1,75
14 h.	1740	175	32	10	-	3,10
23 h.	1655	168	31	195		10,40
26 h.	1620	137	28	237	mal cristallisé	11,40
47 h.	1580	115	26	> 400		14,20
71 h.	1490	104	24	> 400		17,80
103 h.	1470	92	20	> 400		20,40

TABLEAU II : Clinker de Portland

100 % Portland

Dès une heure, la concentration de la chaux en solution est suffisamment élevée pour que l'alumine et la silice ne soient plus significativement décelables. Cette concentration atteint 31 millimoles par litre vers 14 heures, échéance à partir de laquelle apparaissent en diffraction X le premier hydrate bien cristallisé : la chaux hydratée, et une augmentation non négligeable de l'eau liée.

L'hydratation se poursuit relativement lentement pour atteindre vers 100 heures un état où la solution est encore sursaturée par rapport à la chaux hydratée (26 millimoles par litre) et où environ 50 % du C_3S sont hydratés avec 20 %

d'eau liée. La Portlandite diffracte énormément, par contre le C_4AH_{13} paraît plutôt mal cristallisé.

Nous nous trouvons dans le cas de l'hydratation d'un ciment Portland non gypsé, c'est-à-dire où les silicates de calcium anhydres : C_3S sont "empoisonnés" par l'alumine et voient leur hydratation retardée : COTTIN et VIBERT (15).

Echéance	Concentration mg/l		Rapport C/A molaire	Hauteurs de pics en diffraction X					Eau liée
	Al_2O_3	CaO		CA	C_3S	CAH_{10}	C_2AH_8	C_2ASH_8	%
30 mn	1880	1140	1,11	144	62	-	-	-	0,85
1 h.	1940	1170	1,10	135	64	-	-	-	1,10
2 h.	1845	1120	1,10	132	64	-	-	-	1,40
3 h.	1310	820	1,14	105	64	-	ε	-	5,90
4 h.	1110	700	1,15	90	61	28	16	-	13,70
5 h.	1035	655	1,16	77	64	34	24	-	17,80
6 h.	985	640	1,18	59	61	44	29	-	20,50
7 h.	960	630	1,19	39	58	52	29	-	22,7
8 h.	920	605	1,20	38	58	45	32	-	24,3
9 h.	880	585	1,21	24	58	58	32	-	25,2
15 h.	680	525	1,38	12	51	71	18	-	28,0
24 h.	290	465	2,30	ε	48	63	26	37	29,7
32 h.	185	455	4,55	0	30	55	55	89	33,7
48 h.	175	435	4,65	0	26	56	76	133	34,7
96 h.	170	430	4,70	0	20	28	400	123	37,8

TABLEAU III : 80 % Ciment Fondu - 20 % Clinker de Portland

80 % Fondu - 20 % Portland

La mise en solution de la chaux et de l'alumine est au moins aussi rapide qu'avec le Ciment Fondu seul. A l'échéance de 1 heure, les concentrations sont encore plus élevées (21,0 et 19,0 millimoles par litre respectivement pour la chaux et l'alumine). Dès trois heures, les concentrations ont fortement chuté, l'eau liée est relativement importante, et 25% de l'aluminate monocalcique sont hydratés. On peut donc estimer que l'hydratation est commencée, bien que les hydrates n'apparaissent nettement en diffraction X qu'à partir de 4 heures.

Ces hydrates sont d'ailleurs les mêmes qu'avec le Ciment Fondu seul : CAH_{10} et C_2AH_8, mais leur intensité augmente peu avec le temps. Le C/A croît lentement de 1,10 à 1,20, et ne fait un bond au delà de 2 que lorsque C_3S commence à s'hydrater de façon significative après 9 heures. A partir de 24 heures apparaissent les pics de diffraction X d'un nouvel hydrate : la gehlenite hydratée C_2ASH_8. A 96 heures, le CAH_{10} semble diminuer alors que le C_2AH_8 devient très important. Tout CA est hydraté mais seulement les 2/3 de C_3S ont réagi.

Echéance	Concentration mg/l		C/A molaire	Hauteurs des pics en diffraction X								Eau liée
	Al_2O_3	CaO		CA	C_3S	CAH_{10}	C_2AH_8	C_3AH_6	C_2ASH_8	C_4AH_{13}	CH	%
30 mn.	1925	1165	1,10	72	90	-	-	-	-	-	-	0,95
1 h.	1990	1200	1,10	71	85	-	-	-	-	-	-	0,95
2 h.	1985	1195	1,10	66	87	-	-	-	-	-	-	1,40
3 h.	1480	915	1,13	64	88	-	-	-	-	-	-	4,35
4 h.	1125	720	1,17	50	86	10	-	-	-	-	-	9,55
5 h.	1050	685	1,19	45	93	21	-	-	-	-	-	13,75
8 h.	1030	665	1,20	29	98	31	-	-	-	-	-	14,30
10 h.	970	660	1,23	18	94	23	-	-	-	-	-	17,25
14 h.	705	560	1,44	18	86	20	-	-	-	-	-	17,30
24 h.	30	810	50	5	74	0	7	33	138	19	-	24,05
28 h.	25	1135	100	ε	70	-	ε	45	122	25	-	24,40
32 h.	25	1460	115	0	68	-	5	65	135	45	5	24,90
48 h.	15	1530	230	0	65	-	0	60	96	25	12	24,40
80 h.	10	1445	260	0	62	-	-	65	120	35	175	27,60

TABLEAU IV : 50 % Ciment Fondu - 50 % Clinker de Portland

50 % Fondu - 50 % Portland

La mise en solution est encore plus rapide, et les concentrations atteignent à une heure des niveaux encore plus élevés : respectivement 21,5 et 19,5 millimoles par litre pour la Chaux et l'Alumine. Comme précédemment, la chute des concentrations est déjà importante dès trois heures. Cependant ce n'est qu'à 4 heures, et pour une eau liée importante de près de 10 %, qu'apparait le premier hydrate en diffraction des rayons X : le CAH_{10}. Son intensité croît peu, puis disparait après 14 heures, tandis que le CA continue de s'hydrater fortement et l'eau liée de croître. A ce stade, les silicates de calcium ne paraissent pas avoir agi, et le C/A de la solution est d'ailleurs modéré : 1,44.

Echéance	Concentration mg/l		Hauteurs de pics en diffraction X					Eau liée %
	Al_2O_3	CaO	CA	C_3S	C_2ASH_8	C_4AH_{13}	CH	
30 mn	0	925	45	144	7	-	-	5,40
1 h.	-	1040	38	137	7	-	-	6,80
2 h.	-	1170	36	135	8	-	-	6,90
3 h.	-	1300	30	140	11	-	-	8,60
6 h.	-	1360	28	128	12	-	-	10,20
9 h.	-	1455	28	136	18	8	-	10,25
15 h.	-	1650	28	135	16	11	-	11,20
18 h.	25	1650	26	132	12	11	-	11,75
24 h.	20	1655	28	120	15	13	5	12,70
40 h.	5	1645	28	122	22	31	0	12,55
45 h.	0	1665	28	120	21	28	70	17,10
64 h.	0	1650	28	62	15	29	> 300	18,90
88 h.	0	1650	22	52	14	28	> 400	22,00
185 h.	0	1485	21	49	14	55	> 400	24,70

TABLEAU V : 20 % Ciment Fondu - 80 % Clinker de Portland

A partir de 24 heures, alors que presque tout le CA est hydraté, le C_3S commence à réagir. Il en résulte immédiatement la disparition de CAH_{10}, la formation de C_2AH_8 (très peu), de C_3AH_6, de C_2ASH_8 et même de C_4AH_{13}, la disparition presque totale de l'alumine en solution avec une augmentation très importante du rapport C/A.

Entre 24 et 80 heures, la situation évolue relativement peu. Il faut signaler cependant l'apparition de Portlandite et la nouvelle augmentation de la chaux en solution qui atteint les valeurs sursaturées de 26 à 27 millimoles par litre.

20 % Fondu - 80 % Portland

Les résultats se différencient des précédents, et se rapprochent plutôt de ceux trouvés pour le Clinker de Portland seul. En effet l'alumine est pratiquement absente du filtrat, tandis que la chaux en solution croit relativement lentement jusqu'à sursaturation de 29 à 30 millimoles par litre, stable entre 15 et 90 heures.

Le mélange ne se comporte cependant pas comme le clinker de Portland seul car :

- Dès 30 minutes, il y a une quantité d'eau liée non négligeable, avec présence d'un peu de gehlénite hydratée C_2ASH_8.
- Une grande partie du CA s'hydrate pendant les 6 premières heures, avec augmentation de l'eau liée, sans que C_3S ne paraisse beaucoup réagir.
- Le C_4AH_{13} apparait dès 9 heures, alors que la chaux hydratée ne se manifeste nettement qu'à partir de 45 heures, échéance à laquelle C_3S commence à s'hydrater plus rapidement.

Vers 180 heures, la situation se caractérise par la présence persistante de CA anhydre, qui parait en pourcentage moins hydraté que le C_3S. La gehlénite hydratée et le C_4AH_{13} ne fournissent pas des pics de diffraction des rayons X très importants : seule la Portlandite diffracte remarquablement bien.

DISCUSSION DES RESULTATS

Nous avons reporté sur la figure 1 l'évolution, en fonction du temps, des concentrations en CaO des filtrats pour les cinq

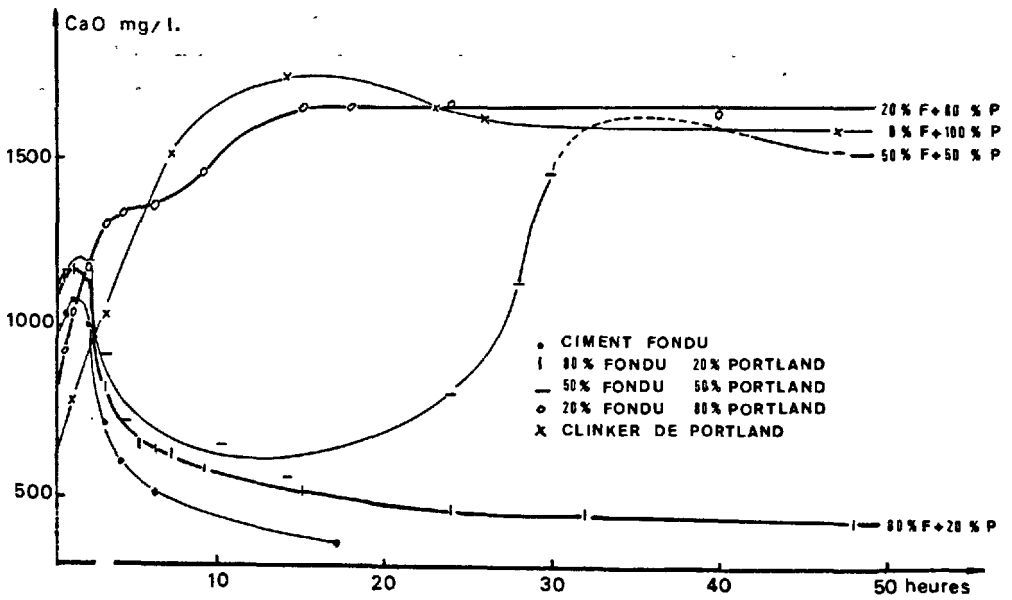

FIG. 1 - Variation de la concentration en CaO des filtrats en fonction du temps

mélanges étudiés. (Les concentrations en alumine ne sont pas représentées pour ne pas alourdir le graphique). Les caractéristiques d'hydratation du Ciment Fondu seul et du mélange 80-20 le plus riche en Fondu obéissent au même principe : passage en solution de la chaux et de l'alumine et précipitation des hydrates au bout d'un temps suffisamment court pour que le palier à sursaturation maximum, et à rapport molaire C/A proche de 1, ait à peine le temps d'être atteint. Lors de l'hydratation, les concentrations en chaux et en alumine chutent rapidement, le rapport molaire C/A ayant tendance à augmenter vers des valeurs de quelques unités.

Le mélange 50-50 se comporte de la même façon en début de réaction avec l'eau, mais à partir d'une vingtaine d'heures, la concentration en alumine se met à tendre vers zéro, la teneur du filtrat en ions calcium atteignant une sursaturation de facteur environ 1,5 par rapport à $Ca(OH)_2$.

Avec le mélange riche en clinker de Portland : 20-80, et avec le clinker pur, le processus d'hydratation est totalement différent dès le début de la réaction : l'alumine n'est jamais significativement présente dans la solution, alors que la concentration en chaux du filtrat atteint rapidement la sursaturation de facteur environ 1,5. L'apparition de la Portlandite en diffraction X ne s'accompagne que d'une très lente diminution de la concentration de la solution, prouvant que les cristaux de $Ca(OH)_2$ formés aux courtes échéances sont beaucoup plus solubles que la chaux hydratée compacte.

Ces caractéristiques d'hydratation, a priori contradictoires, s'expliquent très bien si l'on considère le diagramme $CaO - Al_2O_3 - H_2O$: figure 2. Nous y avons reporté les points représentatifs des concentrations des filtrats des trois mélanges qui s'hydratent en laissant passer de l'alumine en solution. La netteté avec laquelle ces points se

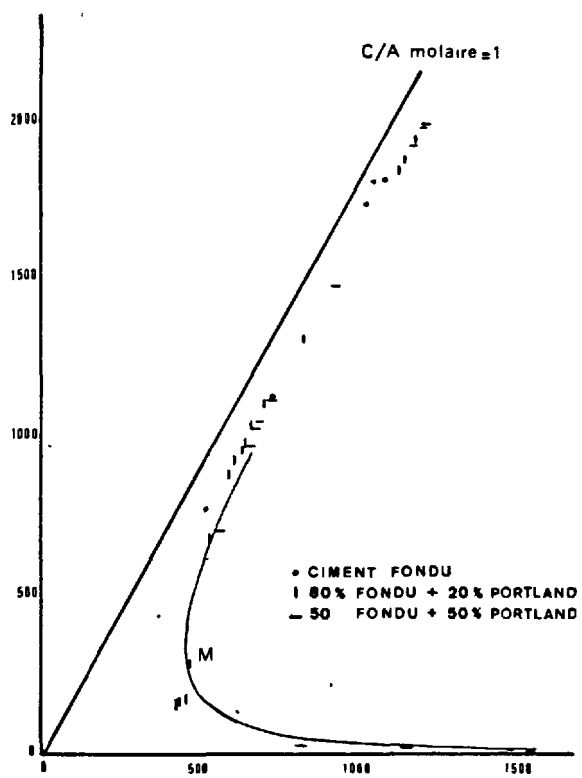

FIG. 2 - Représentation de l'analyse des filtrats dans le diagramme $CaO-Al_2O_3-H_2O$. La courbe représente l'équilibre des hydrates hexagonaux à 21°C (d'après PERCIVAL et TAYLOR).

groupent sur la ligne de précipitation des hydrates hexagonaux, ou son prolongement vers les fortes concentrations, est remarquable. Pour le Ciment Fondu seul et le mélange à 80 % de Fondu, ces points ne franchissent pas le point à tangente verticale M de la courbe de précipitation des hexagonaux (C_2AH_8). Par contre, la plus grande richesse en chaux du mélange 50-50 permet à la solution de décrire la branche C_4AH_{13} de la courbe de précipitation des hexagonaux, où l'alumine en solution est très faible.

Le cas du mélange à 80 % de clinker de Portland, et a fortiori celui du clinker seul, conduit dès les premiers instants d'hydratation à une représentation de la solution de gâchage bloquée sous la courbe C_4AH_{13}, donc sans alumine ou à peu près.

La forme caractéristique du diagramme $CaO - Al_2O_3 - H_2O$ conduit à l'existence de solutions métastables dans deux domaines distincts pour une même concentration en chaux supérieure à 500 milligrammes par litre : cela explique très simplement les comportements en début d'hydratation des ciments alumineux, des ciments Portland et de leurs mélanges.

- Les solutions qui résultent du mélange de l'eau avec le ciment alumineux s'enrichissent en CaO et Al_2O_3 en suivant un chemin proche, mais légèrement sous saturé par rapport à la courbe de précipitation des hydrates. Le temps de prise n'est donc pas instantané et résulte des réactions décrites par l'équipe de BARRET (5).

- Celles qui résultent de l'action de l'eau sur le Portland sont sous saturées par rapport à la courbe des hydrates hexagonaux C_4AH_{13} : le temps de prise est encore de quelques heures et correspond à la longueur de la période d'induction nécessaire pour précipiter les C-S-H et la portlandite.

- Les mélanges de ciments alumineux et Portland suivent l'un ou l'autre chemin, selon qu'il sont riches en l'un ou l'autre des constituants, sauf pour les proportions intermédiaires telles que les passages en solution de l'alumine du ciment alumineux et de la chaux du Portland ont des vitesses équivalentes. Dans ces conditions, le chemin suivi par la solution atteint très rapidement la courbe de précipitation des hydrates hexagonaux, vers le point M. La prise peut être alors rapide, et même instantanée. C'est d'ailleurs pour la même raison que $C_{12}A_7$ et C_3A sont si actifs.

La nature des hydrates formés en fonction du temps est aussi intéressante à observer. Nous avons essayé de la schématiser dans le figure 3 où nous avons tracé les domaines d'existence des divers hydrates formés dans le diagramme : proportions des mélanges en abscisses - temps d'hydratation en ordonnées.

En première approximation, et si l'on considère la séquence des hydrates : CAH_{10} - C_2AH_8, nous pouvons dire que les hydrates deviennent d'autant plus riches en chaux, que pour une échéance donnée le mélange est plus riche en Portland, ou que pour un mélange donné l'échéance est plus grande. La première constatation est évidente ; la seconde provient du fait que les aluminates de calcium s'hydratant plus rapidement que les silicates, la proportion de ciment alumineux hydraté, pour un mélange donné, est d'autant plus élevée que le temps de réaction est plus court.

En réalité les phénomènes sont plus complexes, car il y a formation de grandes quantités du silico aluminate de calcium hydraté C_2ASH_8 qui précipite dans un très large domaine, délimité par la courbe en tirets de la figure 3, lorsque les silicates s'hydratent en même temps que les aluminates.

CONCLUSION

Le diagramme chaux-alumine-eau permet de bien rendre compte des débuts d'hydratation des mélanges ciments alumineux - clinker de Portland : en particulier il montre comment

les mélanges intermédiaires peuvent conduire à des prises promptes, et même des super raidissements, par précipitation immédiate d'aluminates de calcium hexagonaux.

Les phénomènes se compliquent évidemment si la partie silicate du mélange n'est plus un clinker broyé, mais un ciment gypsé : le sulfate de calcium apporte un certain nombre de paramètres supplémentaires liés à sa réactivité (semi hydrate - gypse - anhydrite - proportion et finesse), à celle du C_3A du ciment Portland (cubique - orthorhombique - finesse) et à la vitesse de passage en solution de la chaux (hydrolyse du C_3S - chaux libre).

Cependant le mode de raisonnement proposé reste aisément utilisable dans le cas des mélanges en diverses proportions d'un même ciment alumineux et d'un même ciment Portland.

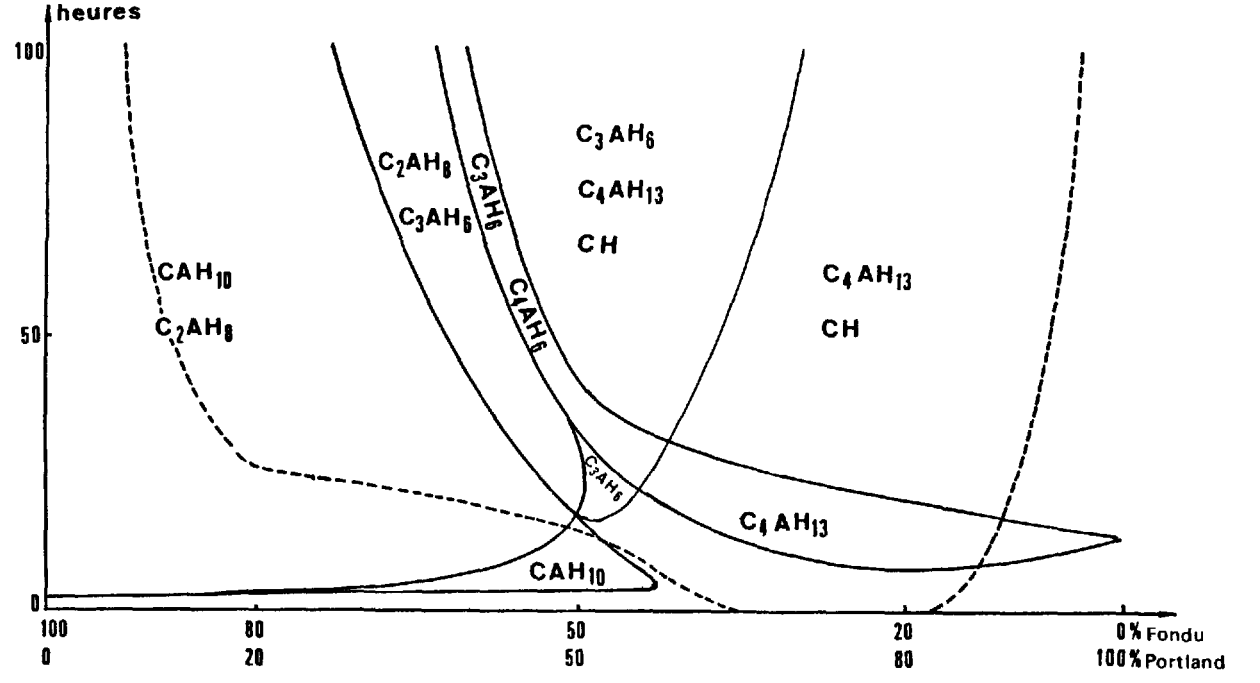

FIG. 3 - Domaines d'existence des hydrates en fonction des proportions relatives Ciment Fondu - Clinker de Portland. C_2ASH_8 est présent au dessus de la courbe en tirets

BIBLIOGRAPHIE

1. ASSARSON G., "The conditions of origin of hydrated compounds in the system CaO - Al_2O_3 - H_2O and the hydration of anhydrous calcium aluminates", Sveriges Geol. Undersökn, Arsbok 30, Ser. C, nº 399 (1936).

2. WELLS L.S., CARLSON E.T., "L'hydratation du ciment alumineux et sa relation avec les équilibres de phase du système chaux-alumine-eau", J. Res. Nat. Bur. Stand., 57, 6, R.P. 2723 (1956).

3. BESSIERES A., "Influence des ensemencements sur la vitesse de précipitation des aluminates de calcium hydratés", Thèse de Docteur de 3ème cycle - Dijon - 10 Juillet 1972.

4. BARRET P., MENETRIER D., "Contribution to the study of the mechanism of aluminous setting", Cem. Conc. Res. Vol. 4, p. 723-733 (1974).

5. BERTRANDIE D., "Contribution à l'étude cinétique de la formation des hydrates dans les solutions aqueuses obtenues à partir du ciment alumineux", Thèse de Docteur de l'université de Dijon, 15 Juin 1877.

6. JONES F.E., ROBERTS M.H., "Le système CaO - Al_2O_3 - H_2O à 25°C", Buid. Res. St., note E, 965, 1960. Indiqué par JONES au 4ème symposium sur la Chimie du Ciment, Washington, 1960.

7. PERCIVAL A., TAYLOR H.F.W., "L'aluminate monocalcique hydraté dans le système CaO - Al_2O_3 - H_2O à 21°C". J. Chem. Soc. 1959, 526, 2629-31.

8. FAURIE-MOUNIER M.T., "Contribution à l'étude du système CaO - Al_2O_3 - H_2O", Revue Mat. Const. Cim. et Bét. nº 635-636 - Août Septembre 1968.

9. YOUNG J.F., TONG H.S., BERGER R.L., "Compositions of Solutions in contact with hydrating Tricalcium Silicate Pastes", J. Amer. Ceram. Soc., 60 (5-6) (1977).

10. SLEGERS P.A., ROUXHET P.G., "The Hydration of Tricalcium Silicate : Calcium Concentration and Portlandite Formation", Cem. Concr. Res., 7 (1) (1977).

11. MENETRIER D., "Contribution à l'étude cinétique de la période initiale d'hydratation de C_3S", Thèse de Docteur es Sciences - Dijon - 15 Juin 1977.

12. FLINT E.P., WELLS L.S., "Study of the System CaO - SiO_2 - H_2O at 30°C and of the Reaction of Water on the Anhydrous Calcium Silicates", J. Res. Nat. Bur. Stand. 12, 751 (1934).

13. GREENBERG S.A., CHANG T.N., J. Phys. Chem. 69 (1), 182 (1965).

14. COTTIN B.F., "Cinétique d'hydratation du ciment Portland en présence de gypse et de sulfate de potassium", Il Cemento Vol. 75 - 177 - Juillet Septembre 1978.

15. COTTIN B.F., VIBERT C., "Poisening of the Hydration of Tricalcium Silicate by soluble Alumina", Papier présenté au 74ème meeting de l'Amer. Ceram. Soc. (1972).

Properties of Super Low Heat Cement concrete

Propriétés des bétons de ciment à très faible dégagement de chaleur

T. GOTO, A. MATSUBARA, K. NAKANO, Japan.

RESUME : Avec l'accroissement des grandes structures en béton armé, la fissuration par contraintes thermiques du béton en masse soulève un problème.

Dans ces conditions, un ciment à très faible chaleur de réaction a été mis au point. Sa chaleur d'hydratation est d'environ 55 cal/g à l'âge de 28 jours, donc beaucoup plus faible que celle du ciment portland normal et même que celle du portland à dégagement de chaleur modéré, soit respectivement de 35 et 20 cal/g de moins.

La résistance et le retrait de ce béton de ciment sont semblables à ceux du béton de ciment portland normal ou à ceux du portland à dégagement de chaleur modéré; son essai de gel et dégel a donné un résultat favorable.
Ses propriétés thermiques aussi sont analogues à celles du béton usuel : coefficient de dilatation thermique de 7 à 9 x 10^{-6}/°C, conductivité thermique de 1.3 à 1.5 kcal/m.h.°C, chaleur spécifique de 0.22 à 0.28 kcal/kg°C, diffusibilité thermique de 0.0022 à 0.0026 m2/h. En outre, son élévation de température au calorimètre adiabatique est beaucoup plus faible que celle des bétons de ciment portland normal et de ciment portland à chaleur modérée pour un même rapport eau-ciment; soit respectivement de 8.8°C et 8.4°C en moins.

En utilisant ces données thermiques expérimentales, on calcule que la température maximale au coeur d'une masse de béton atteint celle mesurée au calorimètre adiabatique dès que l'épaisseur du béton dépasse 4 mètres. Pour une même épaisseur de béton, si l'on emploie ce nouveau ciment à très faible dégagement de chaleur, la température atteinte au coeur de la masse de béton est inférieure respectivement de 8 à 10°C et de 4 à 8°C à celle atteinte avec le ciment portland normal et le ciment portland à dégagement de chaleur modéré. Ce nouveau ciment est donc très efficace pour réduire l'élévation de la température dans une masse de béton.

SUMMARY : Increasing of large reinforced concrete structures, cracking caused by thermal stress has become a serious problem.

For reducing a heat of hydration, Super Low Heat Cement was developed. This cement has extremely low heat of hydration, that is, approximately 55 cal/g at age of 28 days, and it is about 35 and 20 cal/g lower than that of normal portland cement and moderate heat portland cement, respectively.

The strength, shrinkage and resistance to freezing and thawing of the concrete used this cement was about the same as the concrete used normal portland cement.

Thermal properties were also about the same range as the conventional concrete ; coefficient of thermal expansion: 7 - 9x10^{-6}/°C, thermal conductivity: 1.3 - 1.5 kcal/m·h·°C, specific heat: 0.22 - 0.28kcal/ kg.°C, and thermal diffusivity: 0.0022 - 0.0026 m^2/h. At the same water-cement ratio, adiabatic temperature rise of the Super Low Heat Cement concrete was 8.8 °C and 8.4 °C lower than that of normal portland cement and moderate heat portland cement concrete, respectively.

Using the measured thermal characteristic values, the prediction of temperature in mat concrete by numerical computation was carried out. According to the prediction, the maximum temperature rise in the Super Low Heat Cement concrete was 8 -10 °C and 4 - 8 °C lower than those of normal and moderate heat portland cement concrete. It has become evident that use of this cement is very effective for reducing the temperature rise of mass concrete.

INTRODUCTION

In recent year, large reinforced concrete structures have been increasing in Japan.

Such concretes for the structures have comparatively high cement contents, and therefore, thermally induced cracking become a serious problem because of high temperature rise in concrete by heat of hydration of cement.

To prevent such crackings, consideration must be given for mix proportion, practical and curing procedure.But it is a most important thing to use the cement which has satisfactorily low heat of hydration of cement.

For these requirements, Super Low Heat Cement was developed, and mainly consist of high early strength type portland cement clinker and high blaine blast furnace slag. This cement has approximately 55 cal/g of heat of hydration at age of 28 days. Compressive strength of this cement is about the same as that of normal portland cement.

In this report, test results of strength, shrinkage, resistance to freezing and thawing and thermal properties of the concrete using this cement, and the prediction of the temperature in the concrete by numerical computation were described.

RESULTS AND DISCUSSION

1. Properties of Super Low Heat Cement

Chemical and physical properties of Super Low Heat Cement (S.L.H.C.), Normal Portland Cement (N.P.C) and Moderate Heat Portland Cement (M.H.P.C.) are shown in Table-I,II.

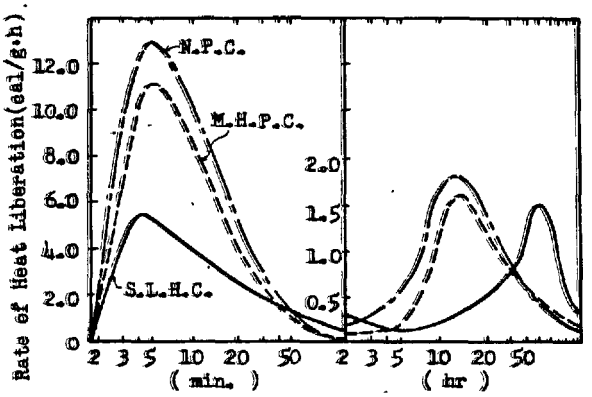

Fig.- 1 Characteristics of the Heat Liberation

As shown in Table-I, heat of hydration of S.L.H.C. is 60 and 70 percent or more of that of N.P.C. and M.H.P.C. at the age of 28 days, respectively. Heat of hydration at age of 7days is 90 percent of that of age of 91 days. Result from heat of hydration test by conduction calorimeter shows that heat of hydration of aluminate at early stage of hydration is especially low (shown in Fig.-1), and the strengthes of this cement is as same as that of N.P.C..

2. Properties of hardend S.L.H.C. concrete

Experiments of hardend concretes were carried out for several mixes shown in Table-III.

Table - I Chemical Properties of Cements used

Type of Cement	Ig.loss	insol	SiO_2	Al_2O_3	Fe_2O_3	CaO	MgO	SO_3	Total	Heat of hydration (cal/g) 7D, 28D,91D
S.L.H.C	0.6	0.3	31.3	11.4	0.8	44.9	4.3	2.7	99.3	52.9 54.9 58.7
N.P.C	0.5	0.3	22.1	5.2	3.2	64.4	3.6	2.0	99.1	81.8 89.3 92.7
M.H.P.C	0.4	0.1	23.7	4.8	4.0	63.7	1.0	1.8	99.5	63.2 76.6 84.7

Table - II Physical Properties of Cement used

Type of Cement	Specific gravity	Specific surface (cm^2/g)	Setting Time initial h - m	Setting Time final h - m	Strength (kgf/cm^2) Compressive 3D	7D	28D	Flexual 3D	7D	28D
S.L.H.C	2.95	5,830	4 - 50	6 - 45	118	261	381	36	61	67
N.P.C	3.17	3,170	2 - 35	3 - 45	134	232	408	32	52	78
M.H.P.C	3.20	3,030	3 - 15	4 - 45	93	150	362	26	37	72

Table - III Mix Proportions of Concretes Tested

Mix	Slump (cm)	W/C (%)	Air (%)	S/A (%)	Unit Weight (kg/m³) W	C	S	G	W.R.A	A.E.A
S - 45	8.0±1.5	45	4.0±0.5	41	160	356	708	1079	0.89	0.042
S - 55	8.0±1.5	55	4.0±0.5	43	159	289	789	1079	0.72	0.017
S - 65	8.0±1.5	65	4.0±0.5	45	161	248	818	1059	0.62	0.011
N - 45	8.0±1.5	45	4.0±0.5	38	164	364	652	1131	0.91	-
N - 55	8.0±1.5	55	4.0±0.5	40	164	300	672	1166	0.75	-
N - 65	8.0±1.5	65	4.0±0.5	42	165	254	757	1111	0.64	-
M - 45	8.0±1.5	45	4.0±0.5	38	155	344	668	1159	0.86	-
M - 55	8.0±1.5	55	4.0±0.5	40	156	284	722	1151	0.71	-
M - 65	8.0±1.5	65	4.0±0.5	42	158	243	769	1129	0.61	-

G_{max}: 20 mm

S: S.L.H.C, N : N.P.C, M : M.H.P.C.

Aggregates used were sea sand (specific gravity: 2.54, finess modulus : 2.79) and crushed stone (specific gravity : 2.69, finess modulus : 6.72).

For concrete of these mixes, compressive, tensile , flexual strength, shrinkage, resistance to freezing and thawing and thermal propertis were tested. Strength test results and relations between compressive strength and cement water ratio are shown in Table-IV and Fig.-2, respectively. These results show that strength of S.L.H.C. concrete is the same or more of those of N.P.C. concrete.

Table - IV Results of Strength Tests

(kgf/cm²)

W/C (%)	Type of Cement	Compressive 7D	28D	91D	Flexual 7D	28D	91D	Tensil 7D	28D	91D
45	S.L.H.C.	-	426	486	-	72.9	74.2	-	35.2	44.9
	N.P.C.	318	420	468	52.7	58.4	62.8	28.9	34.1	36.1
	M.H.P.C.	259	444	512	39.9	54.7	66.8	20.5	30.3	36.2
55	S.L.H.C.	249	348	437	40.4	58.6	58.8	24.4	31.4	42.3
	N.P.C.	239	338	380	47.1	56.0	59,0	24.1	30.9	32.9
	M.H.P.C.	148	282	380	30.6	51.2	58.6	15.3	25.6	31.3
65	S.L.H.C.	-	287	331	-	66.3	74.3	-	27.9	34.4
	N.P.C.	152	215	289	32.1	45.4	49.6	15.1	21.4	25.4
	M.H.P.C.	85	190	285	23.1	44.8	55.2	8.4	20.2	26.6

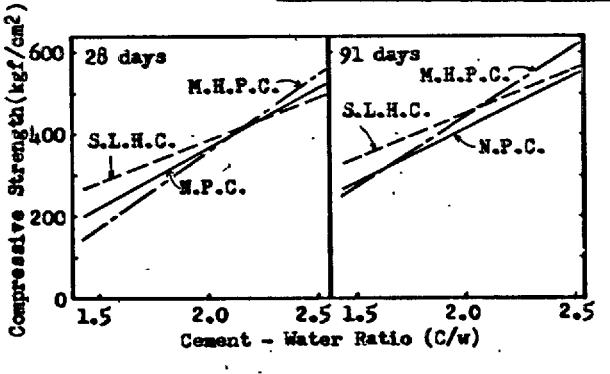

Fig.- 2 Relation between Strength and C/W

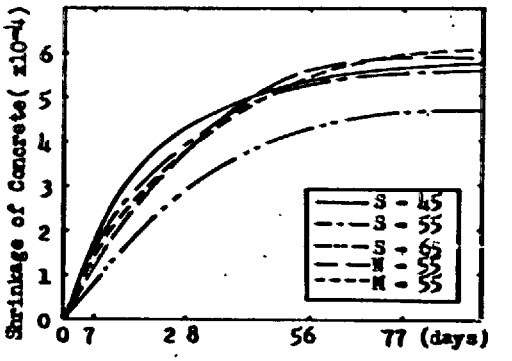

Fig.- 3 Shrinkage of Several Concretes

As shown Fig.-3, shrinkage of S.L.H.C. concrete with 55 percent of water cement ratio is also about the same as that of N.P.C.concrete.

Freezing and thawing test was carried out for S-65 concrete according to ASTM C-666 B method, and there was little reduction of relative dynamic modulus of elasticity.

3. Thermal properties of S.L.H.C. concrete

Thermal properties-adiabatic temperature rise, coefficient of thermal expansion, thermal conductivity, specific heat and thermal diffusivity-were tested for S-45,55,65(S.L.H.C. series), N-55(N.P.C.) and M-55 (M.H.P.C.)concretes.

Test procedures used are;

(1) Coefficient of thermal expansion

Prism specimen (15x15x53 cm) in which mold strain gage(being able to measure temperature) was embedded, was immersed in the water cabinet in which temperature was able to control from 20°C to 70°C. At each temperature, strain and temperature in the concrete were measured.

(2) Thermal conductivity

Plate specimen (30x30x10 cm) heated one side of its surface up to a constant temperature at age of 14 days. When it reached to thermally steady state, thermal current density and surface temperature of opposite side was measured by the thermal current meter(Shotherm HFM, munufactured by SHOWA DENKO CO.,LTD).

(3) Specific heat

Concrete pieces heated up to constant temperature put into the vaccume bottle including constant mass of water, and then temperature rise of water was measured.

(4) Adiabatic temperature rise

Mixed concrete was molded immediately, and temperature was measured continuously and automatically with adiabatic temperature rise testing apparatus from just after molding to age of 7 days.

(5) Thermal diffusivity

Thermal diffusivity was calculated by thermal conductivity, specific heat and density of concrete measured in this test.

The thermal properties are shown in Table-V, and show that coefficient of thermal expansion, thermal conductivity, thermal diffusivity and specific heat of S.L.H.C. concretes are equivalent to those of N.P.C. or M.H.P.C. concretes.

Table - V Thermal Properties of Concretes

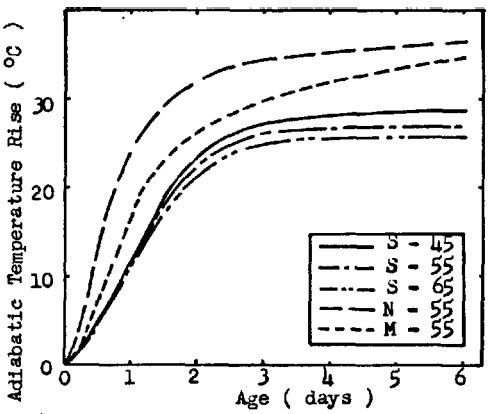

Fig.- 4 Adiabatic Temperature Rise of Concrete

Adiabatic temperature rise (shown in Fig.-4) of S.L.H.C. concretes are very low till 8 hours and after 3 days reaches tonearly maximum temperature, but maximum temperature is very low. Temperature rise curves of S.L.H.C. series are clearly different from those of N.P.C. and M.H.P.C..

On fitting these curves to the formula, curves of N.P.C. and M.H.P.C. concrete fit well to the following formula;

$$T = T_{max.}(1 - e^{-\alpha t})$$

where T : temp. rise (°C), t ; age (days)

$T_{max.}$, α : experimental constant

But curves of S.L.H.C. concretes fit well to the formula, $T = T_{max.}(1 - (1 + \alpha t) e^{-\alpha t})$. From these experimental formulas, $T_{max.}$ of S.L.H.C. concretes are about 8 °C lower than those of N.P.C. and M.H.P.C.

Relation between $T_{max.}$ and cement content of concrete can be expressed as $T_{max.} = 11.1 \log C$, in this test, and when the mix proportion of S.L.H.C. concrete is determined, the maximum temperature rise can be predicted.

4. Prediction of temperature in the concrete mats

The maximum temperature rise in concrete were calculated, using the thermal characteristic values obtained in this test, by Schmidt's method on the unsteady state heat transfer. Relationship between the maximum temperature in concrete and depth of mat concrete is discussed.

Boundary conditions were assumed as follow, (1) at the boundary between concrete and air, thermal thickness of the concrete increased by 0.15 m, (2) at the boundary between concrete and foundation, temperature rise in the concrete was as half as adiabatic temperature rise. Adiabatic temperature rise was obtained from experimental formula and the constants

Kind of Concrete	Coefficient of thermal expansion (x10^{-6}/°C)	Thermal conductivity (kcal/m.h.°C)	Specific heat (kcal/kg.°C)	Adiabatic temperature rise T_{max}	α*	Thermal diffusivity (m^2/h)
S - 45	8.51	1.49	0.28	28.8	1.49	0.0022
S - 55	7.97	1.48	0.24	27.3	1.50	0.0026
S - 65	7.73	1.39	0.22	26.2	1.52	0.0026
N - 55	9.89	1.48	0.28	36.1	1.08	0.0023
M - 55	9.44	1.39	0.28	35.7	0.60	0.0021

*S-45, S-55, S-65; $T=T_{max}(1-(1+\alpha t)e^{-\alpha t})$, N-55, M-55; $T=T_{max}(1-e^{-\alpha t})$

are shown in Table-V.

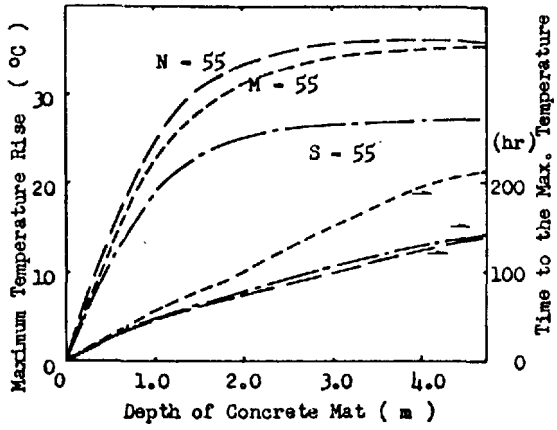

Fig.- 5 Relation between Maximum Temperature and Depth of the Concrete Mat

Results are shown in Fig.-5. When the depth of concretes become over 4 m, maximum temperatures are equivalent to $T_{max.}$ of adiabatic temperature rises. And the time required to reach the maximum temperature increases proportional to the depth, but is defferent some degree to the cement used. In M-55 concrete, the time tend to be longer than others. In either case, when the depth become over 4 m, the time becomes constant. As depth of concrete is over 1 m, maximum temperature in S-55 concrete will be 8 - 10 and 4 - 8 °C lower than in N-55 and M-55 concrete, respectively.

CONCLUSION

Properties of the concrete used Super Low Heat Cement developed newly were investigated, and the temperatures in concrete were calculated, using the thermal characteristic values obtained in this test, by Schmidt's method on unsteady state heat transfer. Relationships between the maximum temperatures in the concretes and depth of the concrete mats were discussed.

From these results the following conclusions can be drawn on Super Low Heat Cement concrete.

1. Strength and shrinkage of the concrete are equivalent to those used Normal Portland Cement.
2. The concrete is durable to freezing and thawing.
3. Thermal properties of concretes are about the same as conventional concretes ; coefficient of thermal expansion: 7 - 9x10^{-6}/°C, thermal conductivity: 1.3 - 1.5 kcal/m·h· °C, specific heat: 0.22 - 0.28 kcal/kg·°C, and thermal diffusivity: 0.0022 - 0.0026 m^2/h.
4. Adiabatic temperature rise of the concrete is 8.8 °C and 8.4 °C lower than that using normal and moderate heat portland cement, respectively.
5. Calculated temperature rises in the concrete mats are 4 - 10 °C lower than conventional concretes.

REFERENCES

1. ACI Committee 207, " Mass Concrete for Dams and Other Massive Structures ", ACI Journal April, 1970
2. McADAMS, W. H., Heat transmission, McGraw-Hill Co., New York, 1954, 43pp.

Solubilité dans l'eau de Ca et CAH_{10} partiellement déshydraté

Solubility of CA and partially dehydrated CAH_{10} in water

P. BARRET, Professeur à l'Université de Dijon, Directeur du L.A. 23 (Réactivité des Solides)
Ph. DUFOUR, Docteur en Chimie Physique, Ingénieur de Recherche (L.A. 23). France

RESUME : La solution obtenue à 21°C à partir de CA monoclinique reste métastable assez longtemps (t > 20h) pour qu'il soit possible d'analyser sa composition : [CaO] ≃ 20.10^{-3} mol.kg^{-1}, C/A ≃ 1,06. On montre que cette solubilité est atteinte et même dépassée par CAH_{10} déshydraté sous vide entre 70°C et 900°C, domaine dans lequel CAH_{10} subit une détérioration progressive de sa cristallinité et devient amorphe, se comportant alors comme une variété allotropique de CA. Le fait que CAH_{10} déshydraté amorphe fasse preuve d'une telle solubilité prouve que son éventuelle réhydratation directe au contact de l'eau est bien moins rapide que son passage en solution.

Cependant, cette solubilité, aussi bien que celle de CA est très inférieure à celle que l'on peut prévoir thermodynamiquement en utilisant les enthalpies libres de référence des partenaires de la réaction de dissolution. L'explication qui est ici proposée est celle de l'intervention d'une étape cinétique d'hydroxylation superficielle de la phase CA anhydre ou déshydratée, par interaction directe avec l'eau liquide. Cette étape précède le transfert en solution des ions de la surface du solide et l'on établit qu'elle participe, par son renouvellement, à une part importante de l'hydratation en même temps qu'elle contribue à plus de la moitié de l'abaissement de l'enthalpie libre dans le passage de CA à CAH_{10}. Il convient donc de ne pas confondre hydratation et précipitation des hydrates.

Les solutions données par CAH_{10} déshydraté amorphe laissent précipiter CAH_{10} comme celles données par CA, mais avec une cinétique différente d'où la possibilité de propriétés hydrauliques. Toutefois, celles-ci ne se manifestent pas par un durcissement de CAH_{10} déshydraté gâché en pâte sans doute en raison de sa grande surface BET. En revanche le durcissement a lieu si la température de déshydratation a dépassé 930°C, température à laquelle la recristallisation de CA est décelée. La mise en évidence par diffraction et microscopie électroniques à haute résolution de domaines distincts recristallisés comme des parties d'un même monocristal de CA suggère que la matrice amorphe, bien que désorganisée, conserve de la structure de CAH_{10} un souvenir suffisant pour induire une telle orientation commune.

SUMMARY : The solution obtained, at 21°C, from monoclinic CA remained metastable for a rather long time (t > 20hr) so that it was possible to study its composition : [CaO] ≃ 20.10^{-3} mol.kg^{-1}, C/A ≃ 1.06. It was shown that this solubility was reached and even exceeded by CAH_{10} dehydrated under vacuum between 70°C and 900°C, range in which CAH_{10} undergoes a gradual deterioration in crystallinity and becomes amorphous, then behaving like an allotropic variety of CA. The fact that amorphous dehydrated CAH_{10} shows such a solubility proves that its possible rehydration on contact with water is less rapid than its passage in solution.

However, this solubility and that of CA as well is much less than may be thermodynamically predicted by using the reference free enthalpies of the components of dissolution. The explanation below is that of the occurrence of a kinetic step of surface hydroxylation of the anhydrous or dehydrated CA anhydrous phase, through direct interaction with liquid water. This step occurs before the transfer into solution of solid surface ions and it is established that it participates, being renewed, largely to hydration while it contributes to half of the decline of the free enthalpy in the conversion from CA to CAH_{10}. Thus, hydration and precipitation of hydrates should not be mistaken.

The solutions resulting from amorphous dehydrated CAH_{10} cause CAH_{10} to precipitate like those resulting from CA but with a different kinetics hence possible hydraulic properties. However, the latter are not shown by hardening of dehydrated CAH_{10} as a paste possibly due its large BET surface. Alternatively hardening occurs if the dehydration temperature is above 930°C, temperature at which recrystallisation of CA is detected. Detection by high-resolution, electron microscope and diffraction of distinct recrystallised domains as parts of the same CA crystal suggests that the amorphous matrix, although it is disorganized, keeps a sufficient picture from the structure of CAH_{10} to induce such a common orientation.

INTRODUCTION

Le durcissement des ciments alumineux est attribué au fait que leur principal constituant, l'aluminate monocalcique CA, donne une solution sursaturée par rapport aux différents hydrates : hydroxyde d'aluminium et aluminates de calcium hydratés ; ces phases apparaissent alors par précipitation conformément au mécanisme proposé dès 1887 par H. Le Chatelier (1).

Il est bien connu que les solutions aqueuses de CA pur atteignent à 21°C des concentrations telles que CaO : $19{,}8.10^{-3}$ mol.kg^{-1}, Al_2O_3 : $18{,}6.10^{-3}$ mol.kg^{-1} (rapport C/A = 1,06). Après une période d'induction d'une vingtaine d'heures, ces solutions laissent précipiter notamment CAH_{10}, qui retiendra particulièrement notre attention, du fait que dans cet hydrate, le rapport C/A est le même que dans l'aluminate anhydre monoclinique CA, bien que la structure soit différente (une récente publication de Taylor et col. (2) considère cette phase comme appartenant au système hexagonal).

Or, nous avons observé expérimentalement que la déshydratation sous vide à relativement basse température (moins de 100°C) de CAH_{10} lui confère une solubilité en chaux et en alumine du même ordre de grandeur que celle de CA et que la solution obtenue laisse à son tour précipiter CAH_{10}. Le produit déshydraté doué de cette propriété apparaît d'ailleurs "amorphe" par diffraction X et électronique.

Ce problème de solubilité nous a donc paru intéressant à étudier ; la première hypothèse venant à l'esprit est que de petits germes de CA monoclinique doivent se former lors de la déshydratation de CAH_{10} à basse température. Les expériences que nous allons décrire n'ont pas confirmé cette hypothèse et c'est ce qui nous a amenés à reconsidérer le problème de la solubilité des phases partiellement déshydratées et anhydres d'un point de vue plus général.

Dès 1961, l'un de nous (3) avait entrepris avec F. Lavanant (4) l'étude de la déshydratation thermique des aluminates de calcium hydratés en mettant pour cela au point la thermogravimétrie (TG) sous pression de vapeur d'eau contrôlée, soit en isotherme, soit en température programmée avec une vitesse de montée linéaire aussi faible que 0,5 deg.heure^{-1}. Mais le problème de la solubilité des phases déshydratées n'avait pas alors été abordé. Des ondulations reproductibles avaient été mises en évidence sur la courbe de TG de CAH_{10}, mais aucun palier caractéristique d'un hydrate intermédiaire stœchiométriquement défini n'avait été décelé. Les autres observations liées à la déshydratation, de l'ambiante à 180°C, sous $P_{H_2O} = 1{,}6.10^{-3}$ N.mm^{-2} étaient : a) la diminution progressive de l'intensité des raies de diffraction X jusqu'à leur disparition quasi totale pour H/A = 4, le produit déshydraté devenant "amorphe", b) la possibilité jusqu'à cette limite d'une réhydratation au contact de la vapeur d'eau, le spectre de diffraction X réapparaissant, mais avec un assez grand retard par rapport à la fixation pondérale de l'eau, c) l'accroissement considérable de la surface spécifique passant de 39 m^2.g^{-1} pour H/A = 6 à 128 m^2.g^{-1} pour H/A = 0,5 , d) le caractère moléculaire de l'eau liée jusqu'à au moins H/A ≈ 3,5 d'après le rapport d'hydrolyse du diborane.

Ces résultats confirmaient et complétaient les conclusions de travaux antérieurs, notamment ceux de Longuet (5), Schneider (6), Carlson (7) et Buttler (8).

Etude expérimentale :

CAH_{10} a été préparé suivant la méthode préconisée par Carlson (9) en agitant soit un ciment alumineux (Fondu Lafarge) soit du CA de synthèse dans de l'eau distillée décarbonatée à 1°C. Dans la gamme d'essais ici décrite et qui a eu un caractère essentiellement exploratoire, les échantillons de 3 g, étalés sur une nacelle de 9 cm^2 d'aire, ont été simplement déshydratés sous vide pendant 4 h, à une série de températures entre l'ambiante et 900°C. Les différentes observations ont été faites à partir de ces échantillons.

Pour affiner les recherches, de nouveaux essais sont actuellement en cours sur des échantillons déshydratés en thermobalance sous pression de vapeur d'eau contrôlée, afin de pouvoir faire la distinction entre le domaine où la déshydratation est réversible et celui où elle ne l'est plus.

Les échantillons de produit déshydraté à différentes températures ont été soumis à un ensemble de tests (10) : dissolution dans l'eau et étude cinétique d'évolution des mélanges solide-liquide et des filtrats prélevés à la concentration maximale ; diffraction X et électronique ; recuits au four à différentes températures ; échauffement sous l'impact du faisceau électronique et observations par diffraction et microscopie électronique à haute résolution ; spectrométrie IR ; analyse thermique différentielle (ATD) et mesure de la surface spécifique (BET).

Résultats :

- Essais de dissolution dans l'eau à 21°C :

Les échantillons préparés comme ci-dessus indiqué peuvent être caractérisés par deux données : la température de déshydratation sous vide θ°C pendant une durée constante et le taux global de déshydratation α, déterminé par perte au feu de l'eau liée résiduelle.

Chacun des échantillons a été soumis à l'essai de dissolution dans l'eau distillée décarbonatée avec un rapport pondéral liquide/solide : $\ell/s = 20$. Pour que les essais soient comparables, la vitesse de rotation de l'agitateur magnétique était soigneusement contrôlée.

La figure (1) rassemble à titre d'exemples quelques-unes des courbes obtenues.

Ces courbes comprennent une branche ascendante de forte pente, correspondant à une grande vitesse de dissolution. Les trois premières passent par un maximum supérieur à 20.10^{-3} mol.kg^{-1} en CaO et Al_2O_3. Après ce maximum, elles présentent une brusque décroissance suivie d'une période de ralentissement puis d'une chute de concentration accélérée. La courbe obtenue après déshydratation à 930°C apparaît comme une limite des précédentes, le pseudo-palier ayant atteint sa longueur maximale (de l'ordre de 6 heures); mais la brusque décroissance initiale ne se manifeste plus après le maximum qui est légèrement inférieur à 20.10^{-3} mol.kg^{-1} en CaO et Al_2O_3. La forme de cette dernière courbe rappelle celle de la courbe d'évolution classique de CA monoclinique pur de synthèse dans un rapport $\ell/s = 20$; mais le temps nécessaire pour que les concentrations maximales soient atteintes est beaucoup plus court (moins de 1 heure au lieu de 4).

Le précipité obtenu dans les essais d'évolution des mélanges eau-produit de déshydratation de CAH_{10} à $\theta < 900$°C, analysé par diffraction X, s'est avéré essentiellement formé de CAH_{10} accompagné, en fin de précipitation, d'une faible proportion de C_4AH_{13} et de

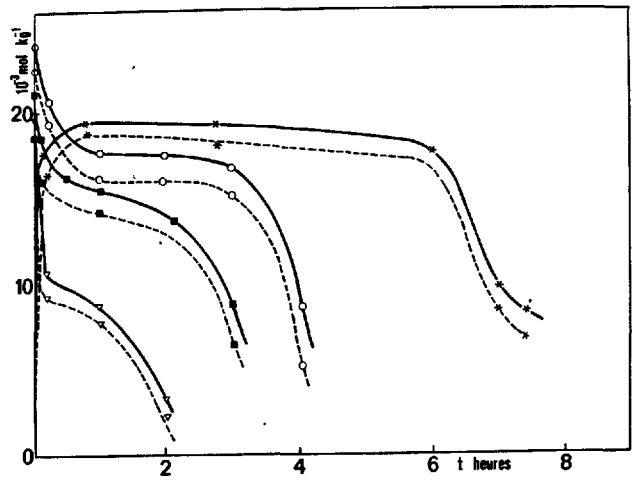

Fig. 1 - Evolution dans l'eau, dans un rapport pondéral ℓ/s = 20 du produit déshydraté à différents taux de déshydratation α de CAH_{10} aux températures suivantes : Δ 90°C (α = 0,74) ; ■ 160°C (α = 0,86) ; o 870°C (α = 0,96) ; ✱ 930°C (α = 1) ; —— CaO ; ---- Al_2O_3.

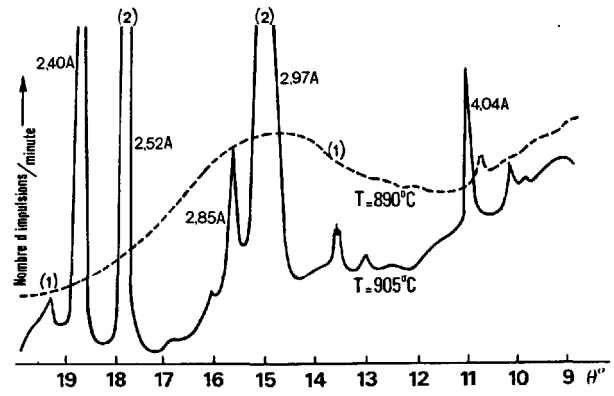

Fig. 2 - (1) Anneau de diffusion à d ≃ 2,9 Å du spectre de diffraction X du produit de déshydratation sous vide de CAH_{10} à θ = 890°C.
(2) Raies de diffraction de CA apparaissant dès la température de déshydratation de θ = 905°C.

carboaluminate en dépit des précautions prises pour protéger de CO_2 le milieu expérimental. Dans le cas des expériences d'évolution de mélanges eau-produit déshydraté à θ > 930°C, le précipité était constitué de CAH_{10}, C_2AH_8 et de gel d'alumine. Il en était de même pour le précipité recueilli en fin d'évolution de filtrats prélevés à la concentration maximale des mélanges eau-produit déshydraté à θ < 900°C.

- Etude par diffraction X et électronique du produit déshydraté :

Lorsque la déshydratation sous vide de CAH_{10} est effectuée pendant d'égales durées (4 h) à des températures successives croissantes, on observe, comme dans les essais effectués en thermobalance sous pression de vapeur d'eau contrôlée, une détérioration progressive de la cristallinité jusqu'à environ 110°C. A 80°C par exemple, les raies de diffraction X à 14 et 7 Å disparaissent. Pour 110 < θ < 300°C le produit de déshydratation apparaît comme "amorphe", présentant par diffraction X et électronique un anneau de diffusion correspondant à une périodicité de d ≃ 2,9 Å pour laquelle la plupart des aluminates de calcium anhydres ou hydratés donnent une raie intense (figure 2). Bien que la solubilité en CaO et Al_2O_3 du produit déshydraté atteigne et même dépasse celle de CA monoclinique de synthèse, aucune raie de diffraction X ou électronique du spectre de cette phase n'apparaît ; cela permet de conclure à l'absence de germes de CA, à moins que leur taille soit inférieure à la longueur de cohérence des rayons X et des électrons.

En revanche, les raies caractéristiques du spectre de diffraction X et électronique de CA commencent à apparaître dans le produit déshydraté lorsque la déshydratation de CAH_{10} a été effectuée dans l'intervalle de température 900°C < θ < 930°C. (figure 2).

Les taches du spectre de diffraction électronique de CA monocristallin apparaissent également à partir du produit amorphe déshydraté à θ < 900°C si l'on augmente suffisamment l'énergie du faisceau incident pour que, sous l'influence du flux d'électrons, la température de l'échantillon s'élève localement à plus de 900°C.

Par interférence du faisceau incident et du faisceau diffracté dans les directions qui correspondent à une ou deux taches du spectre, on met en évidence les familles de plans réticulaires responsables de ces diffractions.

Il est remarquable de constater (figure 3) :
1) que ces plans réticulaires appartiennent à plusieurs domaines monocristallins distincts et éloignés les uns des autres au sein de la matrice de produit déshydraté amorphe ; 2) que néanmoins, les familles de plans réticulaires homologues dans ces domaines sont toujours orientées parallèlement ; 3) que les distances entre leurs plans sont exactement égales à celles qui existent entre les plans de même direction dans la structure de CA monoclinique ; 4) que les franges d'interférences d'orientations différentes, données par des domaines cristallisés distincts et éloignés les uns des autres, peuvent être associées à différents plans h, k, l d'une même zone u, v, w du réseau de CA ; 5) qu'un amas amorphe se transforme toujours, sous le faisceau d'électrons suffisamment accélérés, en un monocristal de CA.

Dans certaines conditions où il est possible de faire apparaître des domaines cristallisés en C_5A_3, les mêmes règles s'appliquent.

- Etude par spectrométrie infrarouge du produit de déshydratation à diverses températures :

Dans l'intervalle : 21 ⩽ θ ⩽ 900°C, la large bande d'absorption comprise entre 500 et 800 cm^{-1} située dans le domaine de vibrations des Al-O diminue progressivement en fonction du taux de déshydratation à mesure que la température augmente, ce qui permet de l'attribuer à l'interaction de l'eau, agissant sur ces vibrations ; il en est de même pour les bandes de déformation de l'eau à 1640 cm^{-1} et de valence OH^- à 3500 cm^{-1} sans que le spectre n'accuse d'importantes

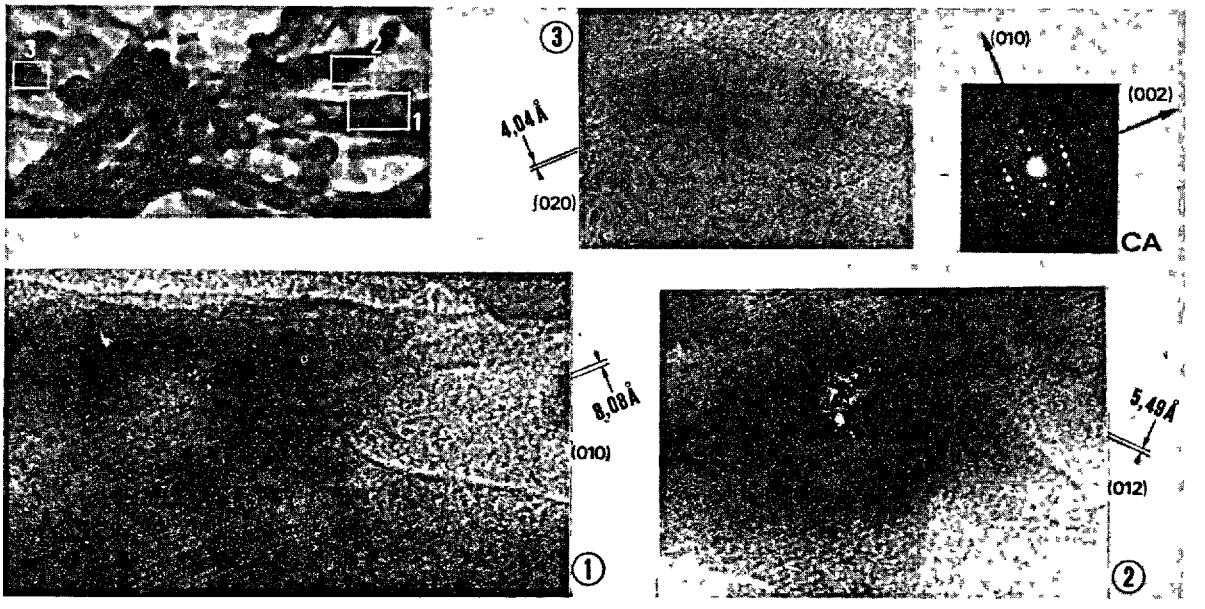

Fig. 3 - Familles de plans réticulaires homologues orientés parallèlement dans trois domaines monocristallins éloignés les uns des autres I, II et III au sein de la matrice amorphe du produit déshydraté. Les interférences correspondent aux directions (010) et (012) de CA.

modifications. Ce n'est qu'au-dessus de 900°C que celui-ci change brusquement d'aspect avec l'apparition des bandes de vibration entre 650 et 850 cm^{-1}, caractéristiques des AlO_4 dans $CaAl_2O_4$ monoclinique (11). L'apparition de ce spectre coïncide donc avec celle des raies de diffraction X et du spectre de diffraction électronique de CA monoclinique, ainsi qu'avec l'apparition de la forme caractéristique de la courbe d'évolution de CA agité dans l'eau. Ces résultats sont en accord avec ceux obtenus en spectrométrie IR par Kondraszenkow et Zigun (12).

- Analyse thermique différentielle :

Les résultats sont également en bon accord avec ceux obtenus par ces auteurs, avec un pic endothermique à 139°C, encadré par deux épaulements, l'un à 107°C, l'autre à 263°C et un pic exothermique à 930°C. De légères variations de ces températures sont observées suivant le mode de préparation de l'échantillon.

- Variation de la surface spécifique en fonction de la température de déshydratation de CAH_{10} :

L'étude de la variation de la surface BET au krypton du produit de déshydratation donne des résultats en bon accord avec ceux obtenus avec F. Lavanant avec l'azote (4) et également avec ceux des techniques précédentes. Au cours de l'amorphisation, la surface spécifique passe de 40 $m^2.g^{-1}$ environ à 140 $m^2.g^{-1}$ lorsque la température de déshydratation sous vide atteint 100°C. Mais une particularité qui demande à être confirmée par l'emploi d'autres gaz est l'apparition de minima dans la courbe de variation de la surface spécifique en fonction de la température de déshydratation, correspondant aux températures des pics et épaulements endo et exothermiques relevés en ATD. Si une telle particularité est aisément explicable pour le point à 930°C, en raison de la cristallisation de CA, une interprétation physique ne peut être aisément donnée pour les points à plus basse température.

- Essais de durcissement des pâtes :

La formation d'une solution à plus de 20.10^{-3} $mol.kg^{-1}$ en CaO et Al_2O_3 à partir des échantillons de CAH_{10} déshydraté entre l'ambiante et 900°C et la précipitation de CAH_{10} de cette solution laissaient supposer que ces échantillons déshydratés gâchés en pâte seraient susceptibles de durcir. Cependant, les essais se sont révélés négatifs : des échantillons déshydratés sous vide à diverses températures entre l'ambiante et 900°C demeurent friables, même plus de 48 heures après gâchage et n'offrent aucune résistance. En revanche, les échantillons déshydratés au-dessus de 930°C, dans lesquels la recristallisation en CA monoclinique s'est produite, donnent lieu à une prise et un durcissement normaux. Le critère de dissolution à 20.10^{-3} $mol.kg^{-1}$ suivi de la précipitation de CAH_{10} apparaît donc comme une condition nécessaire, mais non suffisante de l'existence de propriétés hydrauliques dans le produit de déshydratation.

DISCUSSION

Comment interpréter les observations expérimentales qui paraissent converger vers la description suivante des phénomènes :

Le produit amorphe de déshydratation sous vide de CAH_{10} à $\theta < 900$°C retrouve une solubilité comparable et même supérieure en CaO et Al_2O_3 à celle de CA monoclinique obtenu à $\theta \simeq 1630$°C, bien que, dans ce domaine de températures, aucun germe de CA monoclinique n'ait pu être mis en évidence. D'autre part, quatre faits militent en faveur de l'idée de la conservation par la phase déshydratée amorphe, du souvenir de la

structure de CAH_{10} en dépit de sa désorganisation :
- L'amorçage d'autant plus rapide de la précipitation de CAH_{10} à partir de la solution aqueuse du produit déshydraté que le taux et donc la température de déshydratation ont été plus faibles.
- La cristallisation de domaines amorphes éloignés les uns des autres en des parties d'un même monocristal de CA, ce qui laisse supposer que leur cristallisation a été induite par une matrice ayant elle-même conservé les caractères d'un monocristal de CAH_{10}.
- La diminution progressive en fonction de la température de déshydratation de l'intensité des bandes d'absorption infrarouge sans importantes modifications du spectre jusqu'à 900°C et le brusque changement de celui-ci survenant à cette température avec l'apparition des bandes d'absorption de CA monoclinique.
- L'affaiblissement des raies de diffraction X de CAH_{10} sans aucun déplacement notable, quand le rapport H/A passe de 10 à 4 en même temps que l'augmentation de surface spécifique et la réversibilité de cette transformation par recombinaison de la vapeur d'eau.

Il paraît donc logique d'admettre que le départ de l'eau laisse un solide lacunaire qui, bien que désorganisé et fragmenté, ne subit pas de réarrangement en un nouvel édifice de structure différente tant que la température ne dépasse pas 900°C.

Ce point de vue paraît correspondre à celui exprimé par Buttler et Taylor dans une récente publication (2) : la détérioration croissante de la cristallinité lorsque le rapport H/A tombe au-dessous de 4 peut être attribué au fait que le départ de molécules d'eau supplémentaires peut seulement intervenir par déshydroxylation qui détruit nécessairement les anions hydroxoaluminates, soit :

$$\begin{matrix} Al(OH)_4 \\ Al(OH)_4 \end{matrix} \rightarrow \begin{matrix} AlO_2 \\ Al(OH)_4 \end{matrix} \qquad (1)$$

Le réarrangement structural au-dessus de 900°C peut être représenté en éléments de structure par :

$$\begin{matrix} AlO_2 \\ Al(OH)_4 \end{matrix} \rightarrow \begin{matrix} AlO_2 \\ AlO_2 \end{matrix} \qquad (2)$$

Mais comment peut-on expliquer, en l'absence de germes de CA, l'accroissement de solubilité de la phase amorphe en fonction de son taux de déshydratation, dans le domaine de $\theta < 900°C$?

Il est facile de prévoir par un calcul thermodynamique le sens de la variation de solubilité dans le passage de la phase cristallisée CA à la phase totalement déshydratée amorphe, si l'on admet de considérer celle-ci comme une variété métastable de CA. Lors de ce passage, l'accroissement d'enthalpie libre est :

$\Delta G_t^o = \Delta G_a^o - \Delta G_c^o$ où ΔG_a^o et ΔG_c^o sont les enthalpies libres de formation de la variété amorphe et de la variété cristallisée.

Le passage en solution de l'une ou l'autre de ces variétés est représenté par l'équation :

$$CaAl_2O_{4_s} + H_2O_\ell \rightleftarrows 2[Al(OH)_4]^-_{aq} + Ca^{2+}_{aq} \qquad (3)$$

Soit ΔG_1^o ou ΔG_2^o l'enthalpie libre normale de cette transformation selon que $CaAl_2O_4$ est la variété amorphe ou la variété cristallisée. ΔG_2^o peut être obtenu à partir des données du tableau I.
ΔG_t^o est généralement petit, par exemple $\Delta G_t^o = 4{,}1$ $KJ.mol^{-1}$ dans la transformation SiO_2 vitreuse - tridymite IV ; 1,1 $KJ.mol^{-1}$ dans celle de l'aragonite en calcite.

A l'équilibre avec la solution, si l'on suppose une dissolution congruente de $CaAl_2O_{4_s}$, le produit $x\gamma^{\pm}$ de la concentration molaire massique des ions calcium par le coefficient d'activité est donné par :

$$x\gamma^{\pm} = \left(\frac{K}{4}\right)^{1/3} \qquad (4)$$

TABLEAU I

	$CaAl_2O_4$	$[Al(OH)_4]^-_{aq}$	Ca^{2+}_{aq}	H_2O_ℓ
ΔG^o_{298} KJ.mol^{-1}	- 2206,62	- 1293,25	- 552,51	- 236,96

expression qui provient de la loi d'action de masse avec $y = 2x$; y étant la concentration molaire massique des ions aluminates.

Il y aura deux valeurs K_1 et K_2 de la constante K correspondant à ΔG_1^o et ΔG_2^o.

Le sens de la variation de solubilité $\delta(x\gamma^{\pm})$ pour une petite variation de ΔG_2^o : $\delta(\Delta G_2^o) = \Delta G_t^o$ s'obtient facilement au moyen de l'équation :

$$\delta(x\gamma^{\pm}) = -0{,}210 \frac{\delta(\Delta G_2^o)}{RT} \exp\left[-\frac{\Delta G_2^o}{3RT}\right] \qquad (5)$$

Par exemple pour $\Delta G_t^o = -1$ KJ, $\delta(x\gamma^{\pm}) = 0{,}0106$ mol.kg^{-1}

Il y a donc accroissement de la solubilité en passant de la variété anhydre cristallisée à la variété déshydratée amorphe. Ainsi, on comprend que la déshydratation de CAH_{10} ait pu faire passer sa solubilité dans l'eau de quelques millimoles.kg^{-1} à une valeur supérieure à la solubilité de CA monoclinique, soit plus de 20.10^{-3} mol.kg^{-1}.

Le calcul de $x\gamma^{\pm}$ à partir de l'équation (4) et des données du tableau I dans la même hypothèse $\Delta G_t^o = -1$ KJ donne :

$(x\gamma^{\pm})_1 = 0{,}090$ mol.kg^{-1}

$(x\gamma^{\pm})_2 = 0{,}078$ mol.kg^{-1} ($\delta = 0{,}012$ mol.kg^{-1})

mais pour pousser plus loin le calcul de la solubilité $S = x$, il faudrait exprimer $\gamma^{\pm}$ au moyen de la formule complète de Debye et Hückel. Si $\gamma^{\pm} << 1$, les valeurs de S_1 et S_2 seront très grandes et en tout cas très supérieures à la valeur d'environ 20.10^{-3} mol.kg^{-1} habituellement observée.

Cette constatation ne semble ni fortuite, ni contingente aux incertitudes sur les données thermochimiques. En effet, nous avons vérifié que le calcul à partir des ΔG^o de formation des constituants conduit à des valeurs de la solubilité généralement beaucoup plus élevées que celles qui sont observées ou admises, c'est le cas notamment pour C_3S et C_3A, d'après Stein (13).

Nous proposons une explication à de tels écarts (14) en partant de l'hypothèse d'une hydroxylation superficielle des phases anhydres ou déshydratées par interaction interfaciale directe avec les molécules d'eau. C'est alors la couche superficielle hydroxylée qui se dissout et non la phase solide anhydre. Il faut bien comprendre que l'hydroxylation superficielle est une étape cinétique et qu'elle est constamment renouvelée à mesure que les anions hydroxylés et les cations passent en solution.

A partir de ce postulat, les variations d'enthalpie libre $\Delta G'$ et $\Delta G''$ accompagnant respectivement le passage de l'anhydre CA à l'état superficiellement hydroxylé CA_{sh} et de celui-ci à CAH_{10} peuvent être calculées de deux façons différentes, en prenant comme référence la composition de la solution : a) en équilibre avec CA_{sh}, b) en équilibre avec CAH_{10}. Au point de vue dynamique, le cas a) correspond à la période d'induction de la solution métastable en quasi-équilibre avec CA_{sh} et dont la composition n'est pas changée par la formation des germes de CAH_{10} ; le cas b) correspond à la fin de la précipitation où la vitesse de croissance des germes est très grande de sorte que la solution est en quasi-équilibre avec CAH_{10} ; la dissolution de CA_{sh} ne change pas sa composition.
Les valeurs calculées sont approximativement les mêmes dans les deux cas, c'est pourquoi nous ne développerons ici que le premier mode de calcul a) :
Les réactions qui entrent en jeu sont :
I) Formation de l'état superficiellement hydroxylé :

$$Ca_{Ca} + 2AlO_2 + 4H_2O_{\ell} \rightleftarrows Ca_{Ca} + 2Al(OH)_4$$
$$AlO_2 \qquad\qquad\qquad\qquad AlO_2$$

II) Passage en solution de CA_{sh} :

$$Ca_{Ca} + 2Al(OH)_4 \rightleftarrows Ca^{2+}_{aq} + 2[AlOH_4]^-_{aq} + \left(V''_{Ca} + 2V^{\cdot}_{AlO_2}\right)$$
$$AlO_2$$

III) Précipitation de CAH_{10} :

$$2[Al(OH)_4]^-_{aq} + Ca^{2+}_{aq} + 6H_2O \rightleftarrows Ca[Al(OH)_4]_2,6H_2O \downarrow$$

IV) Formation de gel d'alumine :

$$[Al(OH)_4]^-_{aq} \rightleftarrows OH^-_{aq} + Al(OH)_3 \downarrow$$

Dans le cas a) $\Delta G_{II} = 0$ et $\Delta G' = \Delta G_I$. C'est équivalent d'écrire $\Delta G' = \Delta G_I + \Delta G_{II} = \Delta G_{(I+II)}$. Or la somme des équations I et II est l'équation (3). Par suite : $\Delta G' = \Delta G^o + RT \log_e xy^2(\gamma^{\pm})^3$ avec $\Delta G^o = \Delta G^o_1$ ou ΔG^o_2 suivant que le solide de départ est le produit de déshydratation de CAH_{10} ou CA.
Les valeurs de x et y à introduire dans le calcul sont celles données au début pour la solution métastable à C/A = 1,06, mais y = 2[A]. Donc $x = 19{,}8.10^{-3}$ mol.kg^{-1}, $y = 37{,}2.10^{-3}$ mol.kg^{-1}. L'équation IV n'intervient que pour justifier le fait que C/A > 1, car lorsque C/A → 1, $\Delta G_{IV} \to -\infty$.
Avec $\Delta G^o_2 = 15{,}45$ KJ et en utilisant la formule simplifiée de Debye et Hückel : $\gamma^{\pm} = 10^{-1{,}746\sqrt{x}}$ on obtient $\Delta G' = -14{,}767$ KJ.
Ici $\Delta G'' = \Delta G_{III}$; cette valeur changée de signe est l'affinité chimique de précipitation de CAH_{10} ; notons que dans le cas b), on aurait $\Delta G'' = \Delta G_{II}$ dont la valeur changée de signe serait l'affinité chimique de dissolution de CA_{sh}.
En revenant au cas a)
$\Delta G'' = \Delta G^o_{III} - RT \log_e xy^2.10^{-3(1{,}746\sqrt{x})}$
A partir de la courbe expérimentale de solubilité de CAH_{10} sur le diagramme chaux-alumine-eau, on calcule: $\Delta G^o_{III} = -42{,}572$ KJ. Avec les mêmes valeurs de x et y que pour le calcul de $\Delta G'$, on obtient $\Delta G'' = -12{,}355$ KJ.
La diminution totale d'enthalpie libre $\Delta G = \Delta G' + \Delta G'' = -27{,}122$ KJ correspond au passage de CA à CAH_{10} au contact d'une solution en équilibre avec CA_{sh}. Ainsi, l'hydroxylation superficielle représente une part importante du processus d'hydratation puisqu'elle entraîne la fixation de $4H_2O_{\ell}$ sur 10 et qu'elle abaisse l'enthalpie libre de plus de la moitié de ΔG.

CONCLUSIONS

Hydratation et prise ne doivent donc pas être confondues, une partie de l'hydratation, énergétiquement la plus importante, ne servant qu'à préparer par interaction solide-liquide les espèces aptes à se dissoudre, alors que la prise est due à la précipitation des hydrates à partir de la solution ainsi produite. La déshydratation de CAH_{10} offre un bon exemple de réaction donnant un solide lacunaire non réorganisé qui, bien qu'amorphe, conserve de la structure initiale un souvenir suffisant pour orienter la cristallisation de domaines séparés en un monocristal de CA. Ce solide amorphe se comporte comme une variété plus soluble même que CA, mais qui en pâte ne durcit pas, peut être en raison de sa grande surface spécifique, alors que sa solution laisse précipiter les aluminates hydratés caractéristiques des propriétés hydrauliques.

BIBLIOGRAPHIE

1.- H. Le CHATELIER (1887), "Recherches expérimentales sur la constitution des mortiers hydrauliques", Thèse, Ann. Mines, 11, p. 345.

2.- F.G. BUTTLER, H.F.W. TAYLOR (1978), "Monocalcium aluminate decahydrate : unit cell and dehydration behaviour", II Cemento, 3, p. 147.

3.- F. LAVANANT et P. BARRET (1962), "Contribution à l'étude des différents hydrates de $4CaO,Al_2O_3,nH_2O$" C.R. Acad. Sc. Paris, 255, 1122.

4.- F. LAVANANT (1963), "Contribution à l'étude de quelques aluminates de calcium hydratés", Thèse Ing. Dr. Université de Dijon.

5.- P. LONGUET (1954), "Note sur l'aluminate monocalcique hydraté", Proc. 3rd. Int. Symp. Chem. Cement, London, 1952, 328.

6.- S.J. SCHNEIDER (1959), "Effect of Heat Treatment on the Constitution and Mechanical Properties of some hydrates aluminous cements", J. Amer. Ceram. Soc., 42, 184.

7.- E.T. CARLSON (1957), "Some observations on hydrated monocalcium aluminate and monostrontium aluminate", J. Res. Nat. Bur. Stand., 59, 107.

8.- F.G. BUTTLER (1958), "Study of some hydrated calcium aluminates", PhD Thesis, University of Aberdeen.

9.- E.T. CARLSON (1958), "The lime-alumina-water system at 1°C", J. Res. Nat. Bur. Stand, 61, 1, 2877.

10.- Ph. DUFOUR et P. BARRET (1979), "Solubilité et propriétés hydrauliques du produit de déshydratation de CAH_{10}", C.R. Acad. Sc. Paris,288C, 343.

11.- P. TARTE (1964), "The determination of cation coordination in glasses by I.R. spectroscopy", Proc. int. Conf. Phys. Non-crystal solids", North-Hol. Publish. Comp., Amsterdam, 549.

12.- A.A. KONDRASZENKOW, I.G. ZIGUN (1977),"Transformations dans les aluminates hydratés en fonction de la température", Cement-Wapno-Gips, 6, 142.

13.- H.N. STEINN (1972), "Thermodynamic considerations on the hydration mechanisms of C_3S and C_3A", C.C.R. 2, 167.

14.- P. BARRET et Ph.DUFOUR (1978), "Sur l'existence d'un stade d'hydroxylation superficiel dans l'hydratation de $CaAl_2O_4$", C.R. Acad. Sc. Paris, 286, C, 569.

Méthode de modification des caractéristiques des ciments au moyen des adjuvants

Method for characteristics modification of cements by means of admixtures

Y.T. SIMEONOV, Professeur, Docteur-Ingénieur et
N.B. DJABAROV, Docteur-Ingénieur, Laboratoire Central de Mécanique Physico-Chimique, Académie Bulgare des Sciences, Sofia, Bulgarie.

RESUME : Une nouvelle méthode de modification des caractéristiques des ciments au moyen des adjuvants complexes a été récemment développée. Cette méthode consiste en une action visant un effet physico-chimique bien défini sur la formation de la structure, les propriétés mécaniques des hydrates et leur quantité dans le ciment durcis.

En resultat le durcissement des ciments réels, produits en cimenterie, s'accélère considérablement et leurs résistances mécaniques s'accroissent pendant la période initiale 2 à 7 fois selon le type du ciment. A l'âge de 28 jours et plus tard la résistance des ciments modifiés à l'aide des adjuvants s'accroît constamment et surpasse celle des ciments non modifiés.

Par la méthode en question, qui a une application bien simple, grace aux adjuvants complexes, le ciment portland rapide se transforme en un ciment super-rapide, le ciment portland normal - en ciment portland rapide, les ciments du durcissement lent, comme par exemple le ciment à laitier de haut-fourneau - en ciment à durcissement et résistance normaux comme le ciment portland de haute qualité.

Les bétons à base de ces ciments modifiés accélèrent considérablement leur durcissement et augmentent leurs résistances mécaniques aussi. Le resultat est un effet technique et économique bien établi.

SUMMARY : A new method for characteristics modification of cements by means of complex admixtures was recently developped. This method consist of an action aiming a well defined physico-chemical effect on the structure formation, mechanical properties of hydrates and their quantity in the hardened cement.

In result the hardening of genuine cements i. e. produced in the cement industry is considerably accelerated and their mechanical strengths are augmented in the initial period 2 to 7 times according to the cement typ. On the age of 28 days and later the strength of the modified by means of the admixtures cements is constantly increasing and surpasses this of the not modified cements.

By the method in question, with a quite simple application, due to the complex admixtures the rapid hardening portland cement is transformed in super rapid hardening cement, the ordinary portland cement in rapid hardening portland cement, the slowly hardening cements, as for example the slag cement - in normaly hardening cement with strengths like the high quality portland cement.

The concretes with these modified cements are also considerably accelerating their hardening and are increasing their mechanical strengths. The result is a well expressed technical and economical effect.

Au Laboratoire Central de Mécanique Physico-Chimique de l'Académie Bulgare des Sciences a été recemment développée une nouvelle méthode d'accélération du durcissement des ciments au moyen des adjuvants complexes. Les adjuvants peuvent être introduits préalablement vers les ciments dans les cimenteries ou directement vers le béton a son malaxage.

Cette méthode consiste en une action visante un effet physico-chimique bien défini sur la formation de la structure, les proprié - tés mécaniques des hydrates et leur quantité dans le ciment durcis.

Dans la matrice du ciment en hydratation se forme l'hydrate de sulfoaluminate, qui rend la structure plus dense et joue la rôle de "microarmature". C'est pour cela que la composition des adjuvants complexes est choisie d'assurer tous les élements nécessaires pour la formation d'ettringite supplémentaire indépendamment de la compo - sition du ciment. Les adjuvants complexes contiennent des sels d'aluminium, des sul - fates et de la chaux. A cause de la très haute activité des components alumineux des adjuvants la formation d'ettringite a lieu dans le début du durcissement du ciment à la période ou son effet pour améliorer la résistance mécanique est maximal.

Les études des hydrates en utilisant differentes techniques, comme l'analyse chimique, diffraction des rayons X, microscopie électronique à balayage, l'analyse thermique etc. prouvent que le ciment avec les nouveaux adjuvants contient beaucoup plus d' ettringite et manifeste aussi une hydrata - tion des tous les minéraux du clinker plus avancée, comparé au même ciment, mais sans ces adjuvants. Sur les figures 1 à 4 sont donnés schématiquement des examples d'analyse thermique. Les courbes d'analyse thermique differentielle (ATD), de thermogravimétrie differentielle (TGD) et de thermo - gravimétrie (TG) pour un ciment portland normal et pour un ciment à laitier de haut-fourneau avec ou sans l'adjuvant accélérant respectif, à l'âge d'un jour donnent une idée assez précise sur les changement considérables qui interviennent dans la quantité et la formation de la structure des hydrates sous l'influence des adjuvants.

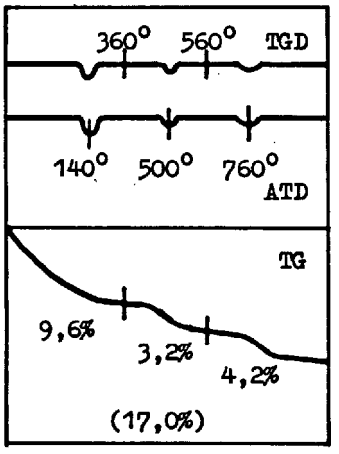

Fig. 1 - Analyse thermique d'un ciment portland normal.

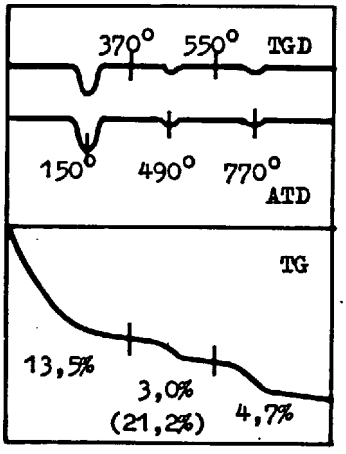

Fig. 2 - Analyse thermique d'un ciment portland normal + adjuvant accélérant.

Les données expérimentales, d'ailleur corroborées aussi par les autres analyses, confirment en général d'une manière quantitative la presence de produits d'hydratation similaires (certain différences dans le dégrée de cristalisation), mais présentent de grandes différences quantitatives. L' effet prédominant, du à l'ettringite, les effets des hydrosilicates et etc., montrent une

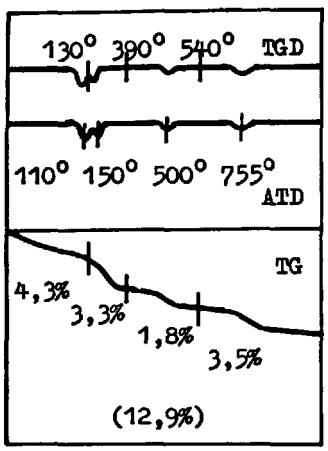

Fig. 3 - Analyse thermique d'un ciment à laitier de haut-fourneau.

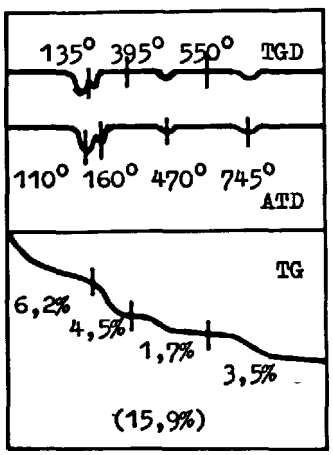

Fig. 4 - Analyse thermique d'un ciment à laitier de haut-fourneau + adjuvant accélérant.

augmentation bien exprimée. Tandis que l'effet pour le portlandite est un peu diminué. Le déplacement des effets pour l'ettringite dans les ciments modifiés vers une température plus haute est une indication pour l'amélioration de la structure cristaline de cet hydrate sous l'influence des adjuvants. Au contraire les effets pour le portlandite dans les ciments avec adjuvants sont déplacés ordinairement vers une température plus basse. Sous l'influence des adjuvants les courbes TG montrent une augmentation bien exprimée de la quantité surtout de l'ettringite, mais aussi des hydrosilicates et d'autre produits hydratés, comme l'hydratation entière des ciments modifiés. Tandis que la quantité du portlandite est un peu diminuée.

En resultat le ciment acquiert l'accélération du durcissement cherchée, sans pratiquement de raccourcir le temps de prise. Sauf la grande amélioration des résistances mécaniques initiales les adjuvants complexes assurent aussi une liaison complète du plâtre ainsi qu'il ne rest libre, ce qui garantie une stabilité de volume du ciment durcis et excitent un accroissement des résistances mécaniques avec l'avancement du temps.

Pour montrer les possibilités d'accélérer le durcissement au moyen de la nouvelle méthode dans cette communication est fait un brèf exposé sur l'augmentation des résistances mécaniques à differentes âges.

Plusieurs types du ciment portland sont choisis pour établir la plus grande universalité de la méthode. Son applicabilité pratique est témoignée par l'usage des clinkers réels , produitent en différentes cimenteries à Bulgarie et à l'étranger.

Les ciments portland de durcissement rapide sont notés en abrégé par CPR, CPR^{X}, CPR^{XX}, les ciments portland normals par CPN, CPN^{X}, CPN^{XX} et les ciments à laitier de haut-fourneau - CLHF, $CLHF^{X}$, $CLHF^{XX}$.

Les propriétés mécaniques de ces trois ciments de chaque type sont examinées à la méthode standard recommandée par RILEM, ISO et Cembureau avec un mortier normalisé de ciment:sable = 1:3, avec un rapport E/C = 0,5 assurant une plasticité assez haute à l'ordre de 150 - 200 mm, établie par la méthode standard. Les resultats sont représentés au tableau I. Ils témoignent que les adjuvants complexes (AA) assurent pour tous les types des ciments une considérable accélération du durcissement.

Pour les ciments de type CPR la résistance mécanique initiale est 1,9 à 2 fois plus

TABLEAU I		
Type du ciment	Résistance à la compression, N/mm^2, après jours	
	1	28
CPR	19,5	49,1
CPR+AA	36,7	60,4
CPR^X	18,2	51,0
CPR^X+AA	34,1	60,8
CPR^{XX}	16,2	52,9
CPR^{XX}+AA	32,2	68,4
CPN	12,7	49,2
CPN+AA	24,0	65,8
CPN^X	12,6	48,7
CPN^X+AA	23,4	56,4
CPN^{XX}	8,9	41,1
CPN^{XX}+AA	18,8	49,7
CLHF	1,7	37,5
CLHF+AA	12,5	49,4
$CLHF^X$	2,4	33,4
$CLHF^X$+AA	9,1	43,7
$CLHF^{XX}$	3,0	39,1
$CLHF^{XX}$+AA	5,9	47,4

haute, ce qui permet d'atteindre la production à la base d'un ciment portland rapide commercial d'un ciment portland super- rapide, ayant une résistance du premier jour très haute de 32 à 37 N/mm^2 (établie par la méthode standard plastique).

Les ciments CPN acquièrent les qualités des ciments CPR d'une haute qualité. La résis - tance initiale augmente de 1,9 à 2,1 fois atteinante 19 à 24 N/mm^2, qui surpasse même celle du CPR, produit en cimenterie.

Les ciments à laitier de haut - fourneau, bien connues avec leurs durcissement lent, sous l'influence de l'adjuvant l'accélèrent de 2 à 7 fois et atteignent le durcissement et la résistance d'un CPN avec 6 à 13 N/mm^2 pour le premier jour.

A l'âge de 28 jours et plus tard la résistance mécanique des tous les types des ciments modifiés au moyen des adjuvants surpasse avec 7,7 à 16,6 N/mm^2 les résistances des ciments non modifiés à la base desquels ils sont concus.

Les résultats expérimentaux témoignent la possibilité de transformer à l'aide des adjuvants complexes différents types des ciments portland à des ciments d'une classe supérieure, ce qui amène à un effet tech- nique et économique bien exprimé.

Les études des ciments modifiés au moyen des adjuvants complexes en béton montrent qu'ils accélèrent considérablement son durcisse - ment et augmentent sa résistance en bon corrélation avec les résultats obtenus en mortier normalisé. Cela assure la possibilité de réaliser plusieurs effets importants. On gagne de productivité en réduisant le temps nécessaire pour le demoulage du béton. Une économie de beaucoup d'énergie peut être réalisée en suprimant le traitement thermique du béton préfabriqué, ou bien en utilisant un traitement fortement raccourci et à une température plus basse. En employant le béton préchauffé sa température est préferable d'être aussi seulement de 30 à 50°C. Une température plus élèvée n'est pas recommandable à cause de pouvoire mieux conserver l' ettringite, ce qui donne aussi un effet économique. La quantité du ciment pour la production d'un m^3 béton peut être fortement réduite. Au lieu du ciment de haute qualité et plus cher on peut utiliser un ciment de qualité et prix beaucoup plus bas.

Les adjuvants accélérants pour les différents types du ciment et leurs méthode d'emploi sont brevetés en plusieurs pays et déjà aux Etats Unis, Suède, R. D. Allemagne, Espagne etc. les brevets sont publiés.

En conclusion on peut dire qu'une méthode très efficace de modification des caractéristiques des ciments au moyen des adjuvants complexes etait inventée et qu'elle donne larges possibilités de transformer diffé - rents types des ciments à une classe supérieure avec des grandes avantages techni - ques et économiques.

Courbe d'instabilité minimale dans une solution métastable de CA

Minimum instability curve in a metastable solution of CA

P. BARRET, Professeur à l'Université de Dijon, Directeur du L.A. 23 (Réactivité des Solides)
D. BERTRANDIE, Docteur de l'Université de Dijon, CNRS (L.A. 23), France.

RESUME : Les conditions d'existence de la longue période de métastabilité (une vingtaine d'heures) que présentent les solutions saturées issues de l'aluminate monocalcique $CaAl_2O_4$ sont étudiées. Or, dans ces solutions, C/A > 1 (1,1) : ceci est justifié par le calcul qui montre que l'affinité chimique de la réaction d'hydrolyse des ions aluminates → ∞ lorsque $[C/A]_\ell \to 1$. Mais pourquoi la formation du gel d'alumine s'arrête-t-elle ? Un phénomène de même nature est observé si la solution est enrichie en chaux : l'enrichissement en chaux critique pour lequel la période d'induction est juste supprimée, est déterminé en fonction du taux de dilution. Le système réagit comme il le fait pour l'alumine, en éliminant spontanément la chaux excédentaire par précipitation d'un aluminate de calcium de rapport $[C/A]_S$ (à l'état solide) > 1, comme C_2AH_8.

Le rapport $[C/A]_\ell$ est ainsi ramené vers 1,1 et une nouvelle période d'induction d'une à plusieurs heures, selon que le précipité primaire est laissé dans la solution ou en est éliminé, coïncide avec le retour de $[C/A]_\ell$ à cette valeur.

Un comportement analogue est observé aux différents taux de dilution de la solution initiale de sorte que trois types de courbes peuvent être mis en place sur le diagramme chaux-alumine-eau : une courbe (m) correspondant aux compositions où la nouvelle période d'induction est observée, encadrée de deux courbes (I) et (II) où la période d'induction primaire est juste supprimée, respectivement par enrichissement en chaux et par enrichissement en alumine.

L'interprétation thermodynamique rend exactement compte de la courbe (m) comme courbe d'instabilité minimale des solutions métastables. Ses points correspondent aux intersections des courbes d'affinité chimique de précipitation du gel d'alumine et de C_2AH_8, qui définissent des valeurs minimales communes des degrés de sursaturation de la solution par rapport à ces hydrates. La courbe (m) apparaît comme une courbe de transition entre ceux-ci. D'autres courbes analogues à (m) ont pu être prévues par le calcul.

SUMMARY : The conditions of occurrence of the long metastability period (about 20 hr.) shown by saturated solutions resulting from monocalcic aluminate $CaAl_2O_4$ were investigated. Now, in these solutions, C/A > 1 (1.1) : this is justified by calculation showing that the chemical affinity of the hydrolysis of aluminate ions → ∞ when $[C/A]_\ell \to 1$. But why does the formation of alumina gel stop ? A similar phenomenon was observed if the solution was enriched in lime : the critical enrichment in lime, for which the induction period is just inhibited, was determined as a function of the dilution ratio. The system reacted, as for alumina, spontaneously eliminating excess lime by precipitation of a calcium aluminate of ratio $[C/A]_S$ (in the solid state) > 1 such as C_2AH_8.

The $[C/A]_\ell$ ratio came back to 1.1 and a new induction period ranging from 1 to several hours coincided with this value, depending on whether the initial precipitate was left within the solution or eliminated.

A similar behaviour was observed for the various dilution ratios of the initial solution so that three types of curve could be reported on the lime-alumina-water diagram : curve (m) corresponding to compositions for which the new induction period was observed, surrounded by two curves (I) and (II) for which the initial induction period was just inhibited by lime enrichment and alumina enrichment, respectively.

The thermodynamic interpretation accounts exactly for curve (m) as a minimum instability curve for metastable solutions. Its points correspond to the intersections of the chemical affinity curves of alumina gel precipitation and of C_2AH_8, which define the common, minimum values of saturation extents of the solution versus these hydrates. Curve (m) appears as a transition curve. Other curves similar to (m) could be calculated.

INTRODUCTION

Lorsque l'aluminate monocalcique anhydre CA passe en solution, celle-ci demeure à l'état métastable pendant une vingtaine d'heures, durée de la période d'induction de nucléation des aluminates hydratés mais il est connu que, aux concentrations maximales atteintes en CaO et Al_2O_3 $[C] = 19{,}8.10^{-3}$ mol.kg^{-1}, $[A] = 18{,}6.10^{-3}$ mol.kg^{-1} à 21°C, le rapport $[C/A]_\ell$ de la solution est supérieur à 1 (1,06), alors que ce rapport dans le solide est $[C/A]_s = 1$. Ce fait peut s'expliquer par la réaction d'hydrolyse :

$$[Al(OH)_4]^-_{aq} \rightleftarrows [OH^-]_{aq} + Al(OH)_3 \downarrow \qquad (I)$$

Mais pourquoi la précipitation de gel d'alumine qui a commencé dans la solution métastable s'arrête-t-elle avant que l'état d'équilibre de la réaction (I) ne soit atteint ? En effet, on calcule facilement, en prenant $K_o = 0{,}63$ comme valeur de la constante d'équilibre de l'équation (I), que la valeur d'équilibre du rapport $[C/A]_\ell$ est 1,630. D'autre part, Le Chatelier (1) avait déjà remarqué que l'adjonction de chaux à la solution métastable de CA provoquait une précipitation prématurée. Ceci est à rapprocher de l'absence de période d'induction dans les solutions aqueuses obtenues au contact d'aluminates anhydres de $[C/A]_s > 1$ comme $C_{12}A_7$ et C_3A et également de l'absence de période d'induction dans la courbe d'évolution d'un ciment alumineux (Fondu Lafarge), dont nous avons établi expérimentalement que l'origine est précisément l'existence comme impureté de $C_{12}A_7$ à quelques pour cent (2). Pour réunir ces faits dans une explication générale, nous avons entrepris un programme expérimental et proposé une interprétation thermodynamique répondant à la question posée (3,4,5).

ETUDE EXPERIMENTALE

Les deux parties du programme expérimental prévu : 1) recherche de la variation initiale de composition à imposer à une solution saturée de CA pour raccourcir ou supprimer la période d'induction, 2) étude cinétique de l'évolution provoquée, ont été effectués à trois températures différentes : 21°C, 8°C et 35°C.

Les trois paramètres dont dépend l'état de la solution métastable étant les fractions anioniques X d'ions OH^-_{aq} et Y d'ions $[Al(OH)_4]^-_{aq}$ et la concentration molaire massique x en ions Ca^{2+}, la façon la plus simple d'imposer à ces paramètres une brusque variation initiale consistait à ajouter à un volume V^o de filtrat saturé de CA, de concentration en CaO : $c^o = n^o_c/V^o$, un volume V d'eau de chaux de concentration $c = n_c/V$. Ces quantités peuvent être calculées approximativement (sans tenir compte des variations des volumes molaires partiels) pour obtenir un mélange de rapport $[C/A]_\ell = r$ et de concentration absolue en chaux c^o/q (facteur de dilution $q > 1$). Les expressions obtenues sont :

$$V = V^o(rq/r^o - 1) \qquad (1)$$

$$c = c^o(r - r^o)/(rq - r^o) \qquad (2)$$

($r^o = [C/A]^o_\ell$ du filtrat saturé)

L'adjonction de chaux fait varier la fraction anionique X en OH^-_{aq} au détriment de la fraction $Y = 1 - X$ en $[Al(OH)_4]^-_{aq}$, tandis que la plus ou moins grande dilution de l'eau de chaux ajoutée agit sur la concentration molaire massique x des ions Ca^{2+} dans le mélange et sur celles y et ψ des anions $[Al(OH)_4]^-_{aq}$ et OH^-_{aq}.

Il convient en effet de noter, qu'en raison de la relation d'électroneutralité :

$$2x = y + \psi \qquad (3)$$

On a : $X = \psi/2x$ et $Y = y/2x$ (4)

Et qu'en outre : $[C/A]_\ell = 1/Y$ (5)

A l'inverse, la fraction anionique Y en $[Al(OH)_4]^-_{aq}$ aurait pu être augmentée au détriment de celle X en OH^-_{aq}, par l'addition d'un aluminate de calcium anhydre de rapport $[C/A]_s < 1$, comme CA_2, mais cette méthode aurait été illusoire, en raison d'une précipitation immédiate de gel d'alumine.

Faute de pouvoir augmenter Y, nous avons eu recours à la simple dilution du filtrat de CA saturé. La dilution ne fait varier ni la fraction Y, car la loi d'action de masse appliquée à (I) donne : $Y = K_o/(1 + K_o)$ (K_o = constante d'équilibre de (I) lue de la droite vers la gauche), ni le degré de sursaturation $\beta = Y/K_o(1 - Y)$ de la solution par rapport au gel d'alumine. Mais, comme l'établiront précisément nos expériences, le degré de sursaturation critique, entraînant une précipitation immédiate, décroît lorsque la dilution augmente d'où la possibilité d'une précipitation de gel d'alumine par simple dilution.

La cinétique d'évolution des solutions en cours de précipitation a été suivie par prélèvements échelonnés dans le temps d'échantillons, à leur filtration en vue d'analyse du filtrat par spectrométrie d'absorption atomique et d'analyse par diffraction X du résidu solide également observé par microscopie électronique à balayage. La solution originelle était un filtrat prélevé au maximum de concentration par agitation soit d'un ciment alumineux, soit de CA pur dans 1000 g d'eau distillée décarbonatée dans un rapport pondéral liquide sur solide : $\ell/s = 10$.

RESULTATS

Essais de dilution à x constant :

Des expériences préliminaires à 21°C ont permis de faire varier la longueur de la période d'induction en ajoutant à 1 l de filtrat saturé d'un ciment alumineux (Fondu Lafarge) de composition : $[C] = 19{,}7.10^{-3}$ mol.kg^{-1}, $[A] = 17{,}60.10^{-3}$ mol.kg^{-1} ($[C/A]_\ell = 1{,}12$), les volumes de solution saturée de chaux donnés dans le tableau I. Cette addition ne fait pratiquement pas varier [C] dans le mélange, mais abaisse [A] et donc augmente $[C/A]_\ell$. En d'autres termes, Y va en diminuant à x constant.

TABLEAU I

Essais	V (ml) ajouté à 1 l	$[C/A]_\ell$	Période d'induction (heures)
B	0	1,12	11
a	36	1,16	6,5
b	54	1,18	3
c	72	1,20	0
d	125,5	1,26	Précipité au cours de l'addition de chaux
e	197	1,34	
f	653	1,85	

Les courbes correspondantes sont rassemblées sur la figure 1 :

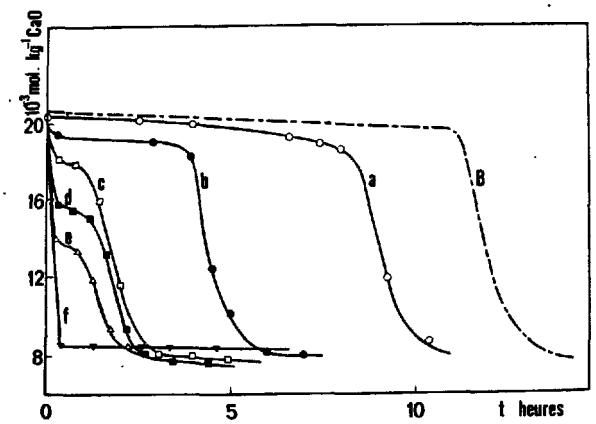

Fig. 1 - Courbes de variation de [C] dans un filtrat saturé B et dans un tel filtrat additionné de chaux en solution saturée : a,b,...pour c, la période d'induction est juste supprimée ; pour d et e le précipité commence au cours de l'addition de chaux.

L'examen de cette figure attire les remarques suivantes :

1) Dans l'essai c, la quantité de chaux ajoutée est juste nécessaire pour supprimer la période d'induction et provoquer une précipitation immédiate.

2) En ce qui concerne la forme des courbes d'évolution : en même temps que le palier ou pseudo-palier est raccourci, une brusque chute de concentration initiale s'installe (courbe b) et s'accentue.

3) Quant à la forme des courbes de vitesse (figure 2), elle est très caractéristique et le minimum correspondant au palier qui subsiste entre les chutes de concentration initiale et finale que nous appelerons respectivement "provoquée" et "spontanée" coïncide avec un minimum du rapport $[C/A]_\ell$. (Y maximum).

4) En ce qui concerne la nature des hydrates apparaissant au début de la précipitation : dans les essais tels que B et a, c'est essentiellement CAH_{10}, tandis que lors de la brusque chute initiale de concentration qui se manifeste dans les essais tels que b c d e, le précipité est formé de C_2AH_8 accompagné seulement dans l'essai b d'un peu de CAH_{10}.

Des résultats semblables peuvent être obtenus en partant de CA pur de synthèse, le rapport $[C/A]_\ell$ à la saturation est généralement un peu plus faible $1,06 < [C/A]_\ell < 1,10$ et le palier plus long (16-21h), mais l'adjonction de volumes croissants de solution de chaux saturée produit des effets analogues à ceux décrits ci-dessus avec un ciment alumineux.

Essais de dilution à Y constant :

Ces essais ont également été menés parallèlement sur le filtrat saturé d'un ciment alumineux et sur celui de CA pur. Le tableau II rassemble les valeurs moyennes d'essais effectués par dilution simple par l'eau distillée décarbonatée de filtrats saturés de CA à 21°C. Les résultats montrent qu'à dilution croissante, une période d'induction de plus en plus courte, jusqu'à l'annulation pour la dilution 2,4, précède la formation de gel d'alumine dont le précipité est presque exclusivement constitué, jusqu'à la valeur $[C/A]_\ell \simeq 1,5$. Notons que le gel d'alumine ne peut plus précipiter si $[C/A]_\ell < 1,63$, valeur qui correspond à la courbe d'équilibre de solubilité de ce constituant sur le diagramme chaux-alumine-eau. Vers $[C/A]_\ell \simeq 1,4$, le gel d'alumine est mêlé à une proportion notable de C_2AH_8, puis pour $[C/A]_\ell < 1,6$, C_2AH_8 précipite seul avec des traces de monocarboaluminate $3CaO,Al_2O_3,CaCO_3,11H_2O$.

TABLEAU II

Dilution	[C] 10^{-3}mol.kg^{-1}	[A] 10^{-3}mol.kg^{-1}	$[C/A]_\ell$	Période d'induction heures
1	20,2	18,7	1,08	20
2	10,1	9,3	1,09	3,3
2,2	9,2	8,5	1,08	2,1
2,3	8,75	8,1	1,08	1,2
2,4	8,4	7,7	1,09	0

Essais de dilution à x et Y variables :

C'est dans ce type d'essais, effectués à 21°C, 8°C, 35°C, qu'a été utilisée la méthode ci-dessus décrite, consistant à ajouter dans un filtrat de CA saturé un volume V de solution de chaux de titre c calculé (relations 1 et 2) pour obtenir un mélange de rapport $[C/A]_\ell = r$ et de concentration en chaux q fois plus petite. Les résultats donnés ici sont ceux des études cinétiques de l'évolution des mélanges dont le rapport $[C/A]_\ell$ a été amené initialement par cette technique à une valeur critique $[C/A]_\ell^* = r^*$, pour laquelle la période d'induction est juste annulée, à une suite de valeurs de x^* décroissantes.

L'allure des courbes d'évolution et de vitesse est analogue à celle des courbes c (figures 1 et 2).

Il n'est pas possible, faute de place, de donner les courbes d'évolution et de vitesse. Celles-ci ont la même allure, respectivement, que les courbes c des figures 1 et 2. La durée du palier intermédiaire est de 0h30 à 1h30 en présence des germes formés au cours de la précipitation initiale. Mais, si ces germes sont éliminés par filtration, cette durée s'étend à plusieurs heures. Dans les essais à 8°C, la précipitation immédiate est encore plus brusque qu'à 21°C et le palier intermédiaire, mieux dessiné, atteint habituellement 1 heure. Au contraire, dans les essais à 35°C, le palier intermédiaire est très atténué et pratiquement remplacé par une discontinuité de la pente des courbes d'évolution, à laquelle correspond un minimum de faible amplitude sur les courbes de vitesse. Mais, dans tous les cas, ce minimum est en bonne coïncidence avec le minimum de la courbe de variation du rapport $[C/A]_\ell$.

Le tableau III rassemble les données les plus caractéristiques relatives à ces évolutions provoquées par addition d'eau de chaux à trois températures différentes, notamment, pour 4 valeurs du facteur de dilution q, les couples de valeurs critiques (x^*, r^*), les valeurs de la fraction d'ions OH^- : X^* et du pH^* qui leurs correspondent, ainsi que les valeurs des mêmes facteurs au minimum de vitesse : (x^m, r^m) et (x^m, pH^m).

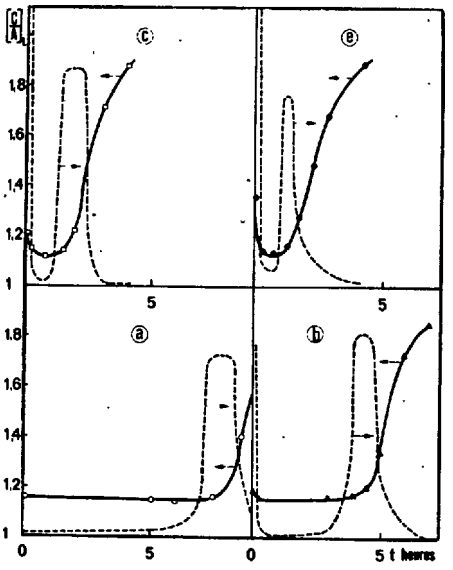

Fig. 2 - --- : vitesse de variation de [C] au cours des essais a, b, c, e du tableau I. —— : variation concomitante de $[C/A]_\ell$: coïncidence des minima.

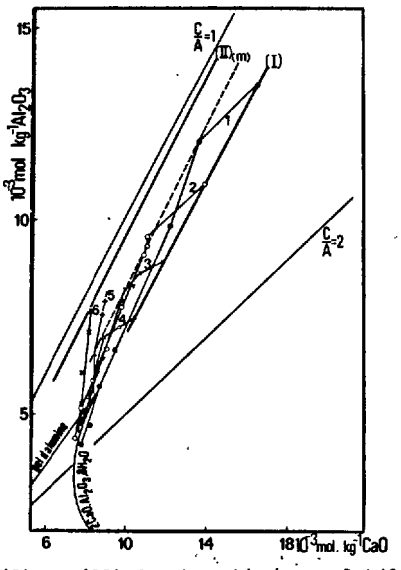

Fig. 3 - (I) et (II) Courbes de supersolubilité de C_2AH_8 et du gel d'alumine. (m) courbe d'instabilité minimale. Les points 1, 2, 3, 4 correspondent aux essais à 21°C du tableau III et les points 5 et 6 aux dilutions 2,2 et 2,4 du tableau II.

TABLEAU III

θ °C	q dilu.	x^* 10^{-3} mol. kg^{-1}	r^*	X^*	pH^*	x^m 10^{-3} mol. kg^{-1}	r^m	X^m	pH^m
21	1,25	16,55	1,23	0,19	11,80	14,00	1,10	0,09	11,40
	1,50	13,95	1,28	0,22	11,79	11,50	1,15	0,13	11,48
	1,75	11,90	1,33	0,25	11,77	10,20	1,20	0,17	11,54
	2,00	10,54	1,41	0,29	11,78	9,50	1,22	0,18	11,53
==	====	=====	====	====	=====	=====	====	====	=====
8	1,25	15,50	1,21	0,17	11,72	13,10	1,09	0,08	11,32
	1,50	13,30	1,25	0,20	11,73	11,20	1,13	0,12	11,43
	1,75	11,20	1,33	0,25	11,75	9,90	1,22	0,18	11,55
	2,00	10,00	1,39	0,28	11,75	8,65	1,28	0,22	11,58
==	====	=====	====	====	=====	=====	====	====	=====
35	1,25	16,00	1,17	0,15	11,68	13,10	1,10	0,09	11,37
	1,50	12,85	1,27	0,21	11,73	11,40	1,18	0,14	11,50
	1,75	11,55	1,32	0,24	11,74	10,60	1,24	0,19	11,61
	2,00	10,55	1,39	0,28	11,77	9,85	1,28	0,22	11,64

Il convient de noter la corrélation qui existe entre les valeurs du rapport $[C/A]_\ell^m$ ou X^* (puisque Y = 1 - X est la pente des droites $[C/A]_\ell$ sur le diagramme chaux-alumine-eau) et celles de x^*, aussi bien d'ailleurs qu'entre $[C/A]_\ell^m$ et x^m : plus la dilution est grande (x petit), plus la fraction d'ions OH^- : X^*, nécessaire au déclenchement immédiat de la précipitation initiale est importante ; il en est de même pour la fraction d'ions OH^- correspondant au palier intermédiaire X^m. Toutefois, le pH, donné par l'expression

$$pH = 14 + Log_{10}(2xX) \qquad (6)$$

varie très peu en fonction de q, qu'il s'agisse de pH^* ou de pH^m et c'est là une propriété remarquable. En outre les valeurs absolues du pH entre pH^* et pH^m ne présentent un écart que de quelques dixièmes d'unités. La température n'a que peu d'influence sur ces valeurs.

La nature des précipités, selon qu'il s'agit de la précipitation provoquée initiale ou de la précipitation spontanée faisant suite au palier (ou période d'induction intermédiaire)et suivant la température, est instructive (tableau IV) :

TABLEAU IV

Précipitation	q	21°C	8°C	35°C
prov.	petit	C_2AH_8+CAH_{10} (traces)	C_2AH_8+CAH_{10} (un peu)	C_2AH_8+AH_3 (traces)
	grand	C_2AH_8 + monocarbo (traces)	C_2AH_8 + monocarbo (un peu)	C_2AH_8 + monocarbo
spont.	petit	C_2AH_8+CAH_{10}	CAH_{10}	C_2AH_8+AH_3
	moyen		CAH_{10}+C_2AH_8 + AH_3	
	grand	C_2AH_8 + monocarbo	CAH_{10} + monocarbo	C_2AH_8 + monocarbo

La différence de nature entre le précipité provoqué immédiat et le précipité spontané différé apparaît clairement : quelle que soit la température, le premier est formé essentiellement de C_2AH_8 avec, à grande dilution, du monocarboaluminate inévitable en raison de l'impureté CO_2. La composition du second est tributaire de la température et peut être comparée à celle du précipité se formant spontanément après une période d'induction plus ou moins longue sans addition de chaux. Ainsi, à 8°C, la précipitation différée donne essentiellement CAH_{10} qui est stable à cette température, tandis qu'à 21°C, c'est C_2AH_8 qui prédomine et à 35°C, CAH_{10} n'est plus stable du tout en raison de la transformation :

$$2CAH_{10} \rightleftharpoons C_2AH_8 + AH_3 + 9H_2O$$

La précipitation forcée initiale se caractérise au contraire par la formation d'un aluminate de calcium hydraté de rapport $[C/A]_s > 1$, ce qui traduit la réaction du système pour éliminer l'excédent de chaux qui lui a été imposé.

Report sur le diagramme chaux-alumine-eau :

Il est d'un grand intérêt de reporter sur le diagramme C-A-H les variations de [C] et [A] accompagnant l'évolution des solutions en fonction du temps. Ainsi, sur le diagramme à 21°C (fig. 3), les points correspondant aux concentrations critiques, tirées des valeurs de x^* et r^* du tableau III, appartiennent à la courbe (I). Les segments de droite tels que 1, 2, 3, 4 représentent la variation de composition consécutive à la précipitation provoquée initiale. Les segments 1 et 2 sont nettement parallèles à la droite $[C/A]_\ell = 2$ parce que le précipité est C_2AH_8. Les segments 3 et 4 ont une pente plus faible car le précipité est un mélange de C_2AH_8 et de monocarboaluminate dont le $[C/A]_\ell$ moyen est > 2. Les extrémités de ces segments, correspondant aux concentrations tirées des valeurs de x^m et r^m du tableau III, pour le minimum de vitesse, appartiennent à une courbe (m) que suivent approximativement les trajectoires du point représentatif de la composition au cours de la précipitation spontanée ultérieure. Par le point correspondant à la dilution 2,4 du tableau II, nous avons fait passer une droite hypothétique (II) qui est censée représenter l'ensemble des compositions critiques conduisant à une précipitation immédiate de gel d'alumine. Faute de pouvoir provoquer expérimentalement un enrichissement relatif en ions $[Al(OH)_4]^-_{aq}$ comme on l'a fait pour les ions OH^-_{aq} à diverses concentrations en Ca^{2+}_{aq}, cette courbe II reste imprécise et ne doit être considérée que comme logiquement probable.

Quel sens attribuer à ces courbes (I), (m) et (II) ?

Au point de vue cinétique, les courbes (I) et (II) peuvent être considérées comme les courbes de supersolubilité respectivement de C_2AH_8 et du gel d'alumine ; c'est-à-dire qu'à l'extérieur de l'étroit couloir qu'elles délimitent, la solution métastable ne peut subsister sans être le siège d'une précipitation immédiate de C_2AH_8 dans le domaine situé à droite de (I) et de gel d'alumine dans celui situé à gauche de (II). La courbe (m) qui représente les compositions auxquelles la solution est remanée spontanément pour corriger, par un précipité approprié, un enrichissement imposé en chaux ou en alumine, a été appelée par nous "courbe d'instabilité minimale". On retrouve les mêmes caractéristiques sur les diagrammes à 8°C et à 35°C.

DISCUSSION

Courbe d'instabilité minimale (m) :

Nous nous proposons de donner une interprétation thermodynamique des courbes d'instabilité minimale, telles que (m) dans une solution métastable. Pour cela, considérons, en plus de la réaction (I), la réaction de précipitation de C_2AH_8 :

$$2[Al(OH)_4^-]_{aq} + 2\ OH^-_{aq} + 2Ca^{2+}_{aq} + 3H_2O_\ell \rightleftharpoons 2CaO,Al_2O_3,8H_2O \qquad (II)$$

Comme la constante d'équilibre de l'équation (I) relative au gel d'alumine, lue de la droite vers la gauche (solubilité) a été désignée à l'aide de l'indice (o), nous conviendrons de réserver les indices 1, 2, 4 aux constantes d'équilibre de solubilité de CAH_{10}, C_2AH_8, C_4AH_{13}. Les valeurs approximatives de ces constantes, calculées à partir des diagrammes chaux-alumine-eau à 21°C (6), 5°C (7) et 50°C (8), sont rassemblées dans le tableau V :

TABLEAU V

°C	K_o	K_1	K_2	K_4
21	1,60	$2,65.10^{-8}$	$1,65.10^{-14}$	$6,50.10^{-26}$
8		$5,23.10^{-9}$	$6,80.10^{-15}$	$4,88.10^{-27}$
35		$1,30.10^{-7}$	$3,0.10^{-13}$	$8,27.10^{-25}$

Avec les notations adoptées [relations (3) et (4)] et en exprimant le coefficient d'activité $\gamma^\pm$ au moyen de la formule simplifiée de Debye et Hückel, soit par exemple à 21°C :

$$\gamma^\pm = 10^{-1,746\sqrt{x}} \qquad (7)$$

les expressions des affinités chimiques relatives aux équations (I) et (II) sont :

$$A_o = RT\ Log_e \frac{1}{K_o}\left(\frac{1}{X} - 1\right) \qquad (8)$$

$$A_2 = RT\ Log_e \frac{16(x\gamma^\pm)^6(1-X)^2X^2}{K_2} \qquad (9)$$

Il est donc possible de construire les courbes représentant, pour différentes valeurs de x, les affinités chimiques en fonction de X. En fait, nous avons porté sur un graphique (figure 4) les valeurs des termes sous Log_e, que nous appelons "degrés de sursaturation" et que nous notons β_o, β_2 en fonction, non de X, mais compte tenu de (6), de ψ ou de pH pour différentes valeurs de x. On constate que les points d'intersection des courbes β_o et β_2, à valeurs de x égales, se placent sur une courbe (m'_4) dont la transformée sur le diagramme C-A-H (figure 5) se confond avec la courbe expérimentale (m).

Toutefois, les coefficients stœchiométriques des équations (I) et (II) sont arbitraires ; les valeurs de β_o et β_2 qui en dépendent le sont donc aussi. Une condition supplémentaire doit être recherchée pour fixer à 1 le rapport moléculaire de $Al(OH)_3$ et C_2AH_8. Cette condition ne peut être qu'une équation chimique reliant ces deux corps dans ce rapport. Comme, en chaque point d'intersection, $\beta = \beta_o = \beta_2$, l'équation suivante, tirée des expressions (8) et (9) doit être satisfaite :

$$\frac{16(x\gamma^\pm)^6(1-X)^2X^3}{1-X} = \frac{K_2}{K_o} \qquad (10)$$

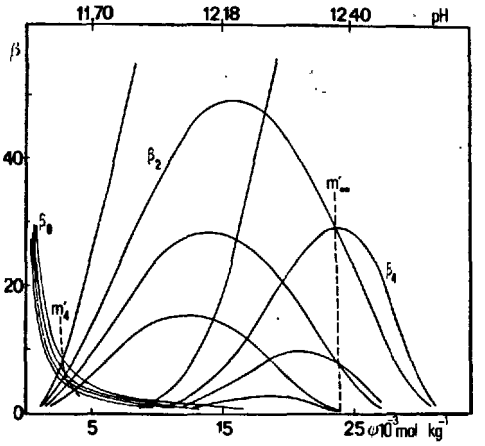

Fig. 4 - Définition des courbes d'instabilité minimale par les interactions m'_4, m'_∞ des courbes des degrés de sursaturation β en fonction du pH.

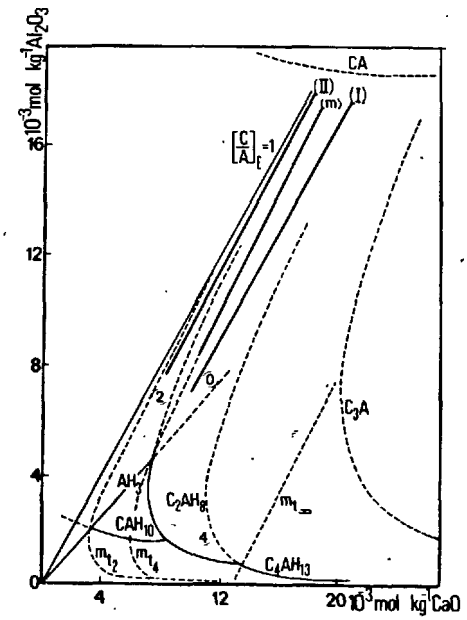

Fig. 5 - Report sur le diagramme C-A-H des courbes d'instabilité minimale théoriques m_{t_4}, m_{t_2}, m_{t_∞}.

Cette équation correspond à l'état d'équilibre de la réaction :

$$2C_2AH_8 \rightleftarrows Al(OH)_3 + [Al(OH)_4]^-_{aq} + 3\,OH^-_{aq} + 2Ca^{2+}_{aq} + \ldots$$
$$\ldots + 3\,H_2O_\ell \qquad (III)$$

On l'obtient en ajoutant à l'équation (I), l'équation (II) inversée. Elle est la condition supplémentaire recherchée. Elle définit la courbe (m_{t_4}) comme courbe d'équilibre de la transformation de C_2AH_8 en gel d'alumine avec libération en solution des ions dans les mêmes proportions stoechiométriques que ceux donnés par la dissolution congruente de C_4AH_{13} :

$$\tfrac{1}{2}\,C_4AH_{13} \rightleftarrows [Al(OH)_4]^-_{aq} + 3\,OH^-_{aq} + 2Ca^{2+}_{aq} + 3H_2O_\ell \quad (IV)$$

La construction de la courbe (m_{t_4}) est donc facile à réaliser : il suffit pour cela de multiplier K_4 par une constante telle que :

$$\sqrt{\alpha K_4} = K_2/K_0 \qquad (11)$$

On obtient $\alpha = 0{,}0016$ et l'on peut aisément vérifier que cette constante est celle de l'équilibre entre phases solides :

$$2C_2AH_8 \rightleftarrows AH_3 + C_4AH_{13} \qquad (V)$$

Nous pouvons prévoir par le calcul d'autres courbes d'instabilité minimale telle que $(m_{t_2}$ ou (m_{t_∞}) marquant respectivement les transformations de CAH_{10} en gel d'alumine et de C_4AH_{13} en C_2AH_8 (figures 4 et 5).

Le prolongement de la courbe d'instabilité minimale dans le domaine des solutions stables constitue la courbe de stabilité maximale de ce domaine.

CONCLUSION

Nous avons défini expérimentalement un étroit couloir sur le diagramme C-A-H délimité par les courbes de supersolubilité du gel d'alumine et de C_2AH_8 et dont la largeur correspond à une petite variation du pH. A l'extérieur de ce couloir, les solutions ne peuvent exister sans précipitation immédiate. A l'intérieur, leur durée de vie est nulle sur les courbes de supersolubilité et maximale sur la courbe (m) dite "d'instabilité minimale" que nous avons définie thermodynamiquement comme correspondant aux intersections deux à deux des courbes de degrés de sursaturation de AH_3 et C_2AH_8 en fonction du pH. Les variations de composition accompagnant l'évolution spontanée des mélanges CA-eau suivent ce chemin. La généralisation de la théorie permet de prévoir d'autres courbes du même type.(*).

BIBLIOGRAPHIE

1.- H. Le CHATELIER (1887), "Recherches expérimentales sur la constitution des mortiers hydrauliques", Thèse, Ann. Mines, 11, p. 345.

2.- P. BARRET et D. MENETRIER (1974), "Contribution to the study of the kinetic mechanism of aluminous cement setting", Cem. and Concr. Res., 4, 723.

3.- D. BERTRANDIE (1977), "Contribution à l'étude cinétique de la formation des hydrates dans les solutions aqueuses obtenues à partir du ciment alumineux", Thèse de Doctorat de l'Université de Dijon.

4.- P. BARRET et D. BERTRANDIE (1979), "Cinétique particulière de précipitation provoquée et spontanée d'une solution métastable d'aluminate monocalcique", C.R. Acad. Sc. Paris, 288 C, 291.

5.- P. BARRET et D. BERTRANDIE (1979), "Courbes d'instabilité minimale d'une solution métastable", C.R. Acad. Sc. Paris, 288 C, 323.

6.- A. PERCIVAL, H.E.W. TAYLOR (1959), "CAH_{10} dans le système C-A-H à 21°C", J. Chem. Soc., 526, 2629.

7.- F.G. BUTTLER, H.F. TAYLOR (1958), "The system C-A-H at 5°C", J. Chem. Soc., 2103.

8.- B. PEPPLER, L.S. WELLS (1954), "The system C-A-H from 50 to 250°C", J. Res. Nat. Bur. Stand, 52, 2, R.P. 2476.

(*)Remerciements : Les auteurs remercient la Société Lafarge pour sa coopération et particulièrement M. Cottin pour les fructueuses discussions sur le diagramme C-A-H.

Influence des conditions de synthèse de l'alumine sur sa réactivité vis-à-vis de la chaux

Influence of the alumina preparation conditions on the reactivity with the calcium oxyde

B. GUILHOT *, J.F. HUGO *, A. MATHIEU **, A. PETIT **, France.

RESUME : De nombreux paramètres peuvent influer sur les propriétés réactionnelles de l'alumine. L'influence du pH de fin de neutralisation du chlorure d'aluminium par l'ammoniaque ainsi que la température de calcination des gels d'alumine ainsi obtenus ont été étudiées.

Le pH de fin de précipitation a un rôle important sur l'état de cristallisation, l'aire spécifique et la teneur en composés chlorés présents dans les gels d'alumine.

Une élévation de la température de calcination atténue progressivement ces différences.

Après broyage et tamisage chaque alumine est mélangée avec du carbonate de calcium. L'évolution du mélange pendant la clinkérisation est suivie au microscope de chauffe.

C'est l'alumine obtenue au pH et à la température de calcination les plus bas qui entraîne le retrait le plus important.

L'analyse par diffraction X des différents clinkers montre qu'une augmentation de la température de clinkérisation provoque une diminution de la teneur en $C_{12}A_7$. Celle-ci est en relation avec le retrait.

On constate que la cinétique d'hydratation est maximale lorsque la température de clinkérisation est voisine de 1350°C.

ABSTRACT : Many parameters can influence the mecanism of the alumina properties. The influences of the pH of the neutralisation reaction of aluminium chloride and ammonium hydroxide and the calcination temperature of alumina gels have been studied.

The pH is an important factor on the cristallisation degree, the specific surface and chloride compound content of the alumina gels. The calcination temperature reduce these differences.

After grinding and screening, each alumina is blend with calcium carbonate. During the clinkerisation the evolution is observed by the heating microscopy technic.

The alumina synthetised with a low pH condition and calcined at low temperature give the largest shrinkage.

X Ray diffraction of the clinkers shows a relation between the clinkerisation temperature, the $C_{12}A_7$ content and the shrinkage. We observe the maximum hydration kinetic when the temperature is about 1350°C.

(x) Ecole des Mines de St Etienne

(xx) LAFARGE Laboratoire Central

INTRODUCTION

Le procédé d'élaboration d'un solide peut avoir une grande influence sur ses propriétés réactionnelles. Dans ce travail nous examinons l'influence :

- du pH de fin de précipitation du gel d'alumine,
- de la température de calcination de l'alumine,

sur sa réactivité vis-à-vis du carbonate de calcium, ainsi que sur l'hydraulicité des aluminates de calcium obtenus.

I) - SYNTHESE des ALUMINES

Les gels d'alumine sont préparés en milieu aqueux selon la réaction :

$$AlCl_3 + 3\ NH_4OH \longrightarrow Al(OH)_3 + 3\ NH_4Cl$$

Les alumines sont ensuite obtenues par calcination des gels.

I-1) - Conditions expérimentales

Une solution de chlorure d'aluminium hexahydraté (300 g/l) est mise dans un réacteur maintenu à 60°C. La solution d'ammoniaque 4 N est ajoutée à vitesse constante (1 ml/mn pour un volume initial de 200 cm^3). Cette vitesse d'introduction a été choisie en fonction de la concentration initiale en ions Al^{3+} et de la température de la solution pour que le système soit le plus proche de l'équilibre (1). L'agitation est maintenue constante quelle que soit la viscosité.

La pHmétrie permet de suivre l'évolution de la réaction.

Afin d'éliminer le sel formé (NH_4Cl), tout en préservant au gel sa structure initiale (2), celui-ci, après filtration, est lavé au soxhlet pendant 24 heures dans le méthanol.

Après séchage à l'étuve à 100°C, le gel est fractionné. Chaque fraction est cuite à une température déterminée (800, 1000 ou 1300°C).

I-2) - Caractérisation

Comme l'ont déjà souligné de nombreux auteurs (3) (4), les gels obtenus à des pH peu élevés sont très désorganisés et contiennent une forte proportion d'anions issus du sel d'aluminium. Par contre, ils contiennent peu de cations provenant de la base utilisée (< 0,35 %). Vers pH 10, les gels obtenus sont pratiquement purs, mais ils ne sont plus amorphes.

L'état de cristallisation joue un rôle important sur l'aire spécifique. C'est ainsi que le gel amorphe a une aire spécifique de 30 m^2/g ; par contre lorsqu'il se présente sous forme de pseudoboehmite, elle est de 300 m^2/g. Cristallisé sous forme de bayerite, elle est alors de 130 m^2/g.

Tableau N° 1

Caractéristiques des gels d'alumine

Sels	pH de fin de neutralisation	analyse thermo-différentielle	analyse thermo-gravimétrique	Pertes au feu	produits chlorés exprimés en $AlCl_3$	Al_2O_3	H_2O	surface spécifique (B.E.T.)	R.X.
A	8,4	75°C (F) 235°C (TF)	300°C (TF)	40,7 %	8,8 %	59,3 %	31,9 %	30 m^2/g	Amorphe
B	9,5	75°C (Tf) 100°C (f) 230°C (F) 275°C (TFf)	150°C (f) 207°C (F)	40,2 %	2,5 %	58,8 %	38,7 %	300 m^2/g	Pseudo-boehmite
C	10,4	70°C (f) 90°C (Tf) 200°C (F) 275°C (TF)	140°C (f) 230°C (TF) 270°C (F)	27,8 %	0,9 %	71,2 %	27,9 %	130 m^2/g	Bayerite + traces de boehmite

Tableau N° 2

Caractéristiques des alumines

alumines	températures de cuisson (5 h sous azote)	R.X.	surfaces spécifiques mesurées par la méthode B.E.T.	surface du pic de T.L. en V.A.	température du pic de T.L.
A	800°C	γ ou η	100 m^2/g	50	315 K
	1000°C	40 % θ + 30 % α	55 m^2/g	140	340 K
	1300°C	α	4,1 m^2/g	10	245 K
B	800°C	γ ou η mieux cristallisé que A 800°	116 m^2/g	50	310 K
	1000°C	98 % θ + 1 % α	60 m^2/g	70	335 K
	1300°C	α	4,2 m^2/g	10	260±20 K
C	800°C	γ ou η mieux cristallisé que B 800°	100 m^2/g	30	315 K
	1000°C	96 % θ + 3 % α	68 m^2/g	75	305 K
	1300°C	α	5,5 m^2/g	25 20	290 K 255±20 K

TL : thermoluminescence.

Des alumines de nature différente sont obtenues selon la température de cuisson de ces gels. A 800°C, les spectres de diffraction X révèlent la présence d'une phase mal cristallisée γ ou η (5). A 1000°C, on note l'apparition de la phase θ en proportion différente suivant la nature du gel initial.

Les surfaces spécifiques des produits, très différentes aux basses températures de cuisson, sont semblables pour des alumines cuites à 1300°C.

L'allure des signaux de thermoluminescence (TL) est différente suivant la température de calcination.

A basse température, les pics sont étalés. A haute température, les pics sont plus étroits (alumine α).

Bien que certains gels (gel A) aient une teneur en composés chlorés relativement importante, les alumines même cuites à basse température ont une teneur en chlore beaucoup plus faible (toujours inférieure à 0,4 %).

II - ELABORATION des ALUMINATES de CALCIUM

II-1) - Préparation du cru

Les crus ont été préparés à partir de gels A, B, C (tableau N° 1) tels quels ou calcinés à 800 et 1300°C. Ces alumines sont désignées par la lettre correspondant à son gel d'origine suivies de sa température de calcination.

Les deux réactants, le carbonate de calcium (PROLABO RP) et l'alumine ont été broyés puis tamisés à 40 microns. Le mélangeage à sec a été effectué successivement au mortier, puis au mélangeur afin de ne pas modifier l'état cristallin des alumines, le rapport C/A molaire choisi étant de 1.

Remarque : le gel B n'a pu être examiné en raison d'une erreur de manipulation.

II-2) - Evolution de la réaction carbonate de calcium-aluminium au microscope de chauffe

Le mélange obtenu est compacté sous forme de cubes de 2 mm de côté qui sont ensuite disposés dans le four d'un microscope chauffant (LEITZ).

Il est possible de suivre en continu, en fonction de la température, la morphologie de l'échantillon (figure 1).

Figure N° 1

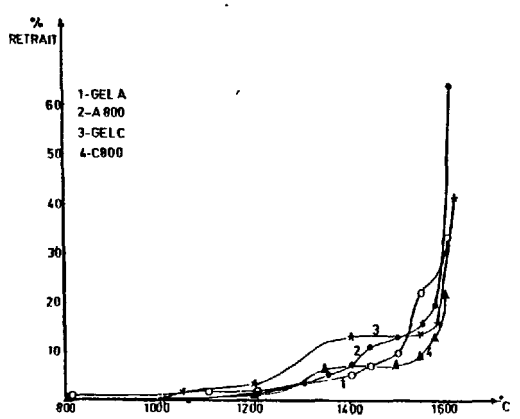

Evolution du retrait géométrique des crus en fonction de la température

Il apparaît que le retrait géométrique des cubes de cru est fonction décroissante de la température de calcination de l'alumine, celui-ci étant maximum pour le gel.

On note d'autre part que le mode d'obtention du gel d'alumine pour une température de calcination donnée (800°C par exemple) a une influence sur le retrait.

A une température de clinkérisation déterminée le retrait est lié à la teneur en $C_{12}A_7$ dans le clinker.

II-3) - Clinkérisation

Des pastilles de cru de 1 g (pressées sous 2 t) sont portées à la température de clinkérisation dans les conditions suivantes :

- montée en température 300°C/h sous air,
- palier de température 1310-1330-1380-1450°C,
- durée de palier 15 mn.

III - CARACTERISATION des ALUMINATES de CALCIUM

Les clinkers ainsi obtenus ont été broyés au mortier puis tamisés à 40 microns. Chaque clinker a été caractérisé :

- par diffraction X,
- par calorimétrie isotherme (25°C).

III-1) - Diffraction X

Les résultats de diffraction X rassemblés dans le tableau N° 3 ne mettent en évidence que la présence de CA - CA_2 - $C_{12}A_7$ (1). Les valeurs indiquées représentent le rapport de l'aire de la raie principale d'un constituant sur la somme des aires des raies principales des constituants présents.

(1) Nomenclature cimentière : C = CaO, A = Al_2O_3.

Tableau N° 3
Diffraction X des clinkers

	GEL A			A 800			A1300			GEL B	B 800			B 1300			GEL C			C 800			C 1300		
θ°C / Phases %	CA_2	CA	$C_{12}A_7$	CA_2	CA	$C_{12}A_7$	CA_2	CA	$C_{12}A_7$		CA_2	CA	$C_{12}A_7$	CA_2	CA	$C_{12}A_7$	CA_2	CA	$C_{12}A_7$	CA_2	CA	$C_{12}A_7$	CA_2	CA	$C_{12}A_7$
1310	21	35	44				19,5	43,5	37,0		17,5	50	32,5	13,8	57,5	28,7	13,8	51,3	34,9	12,8	55,9	31,3	14,6	57,3	28,1
1330	15,2	54,3	30,5	12,5	54,3	33,2	14,7	54,3	31,0		11,4	60,2	28,3	10,2	63,7	26,1	8,7	66,1	25,2	8,6	66,2	25,2	12,1	63,7	24,8
1380	9,8	65,8	24,3	8,1	67,6	24,3	11,6	61,3	27,0		9,7	64,5	25,8	0	73	19	7,5	71,7	20,8	7,9	71,4	20,7	8,5	74,4	17,1
1450	2,5	89,6	7,9	1,7	91,4	10,5	3,5	87,7	8,8		3,5	87,7	8,8	3,5	87,7	8,8	0,9	89,3	9,8	1,5	91,2	7,3	1,9	93,5	4,7

L'examen de ces résultats met en évidence les points suivants :

- le pourcentage de CA croît avec la température de clinkérisation quel que soit le cru initial,
- pour une température donnée de clinkérisation (1330°C par exemple), il apparaît que les alumines issues du gel obtenu au pH le plus élevé (10,4) ont une plus grande réactivité vis-à-vis du carbonate de calcium.
- pour un gel déterminé, une augmentation de la température de calcination de ce gel favorise la cinétique de clinkérisation.

Il ressort de cet examen que l'amélioration de l'état d'organisation du gel constitue un paramètre favorable de la réactivité de l'alumine.

III-2) - Calorimétrie

La cinétique d'hydratation des clinkers a été suivie par calorimétrie, le rapport E/C a été fixé à 1, la masse de l'échantillon étant de de 500 mg.

Les courbes obtenues présentent les caractéristiques classiques des liants hydrauliques.

Figure N° 2

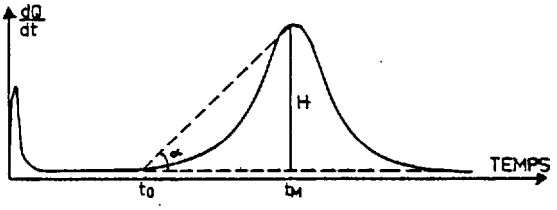

Thermogramme de l'hydratation des aluminates de calcium

L'analyse des courbes calorimétriques montre qu'il est délicat de faire des corrélations significatives entre les conditions d'obtention de l'alumine et la cinétique d'hydratation. On remarque en particulier que l'intensité du pic de mouillage, la période de latence (to), la hauteur du signal calorimétrique (H) sont aléatoires.

Par contre pour comparer les cinétiques d'hydratation nous avons défini un paramètre $\alpha = \frac{H}{tm-to}$ susceptible de rendre compte de la cinétique d'hydratation (accélération moyenne d'hydratation).

Nous avons remarqué que le coefficient α était maximum pour une température de clinkérisation voisine de 1350°C, comme le montre la figure N° 3 relative à la série C et cela quelle que soit l'origine de l'alumine. Par contre le pH de fin de précipitation du gel ne paraît pas constituer un paramètre prépondérant.

Figure N° 3

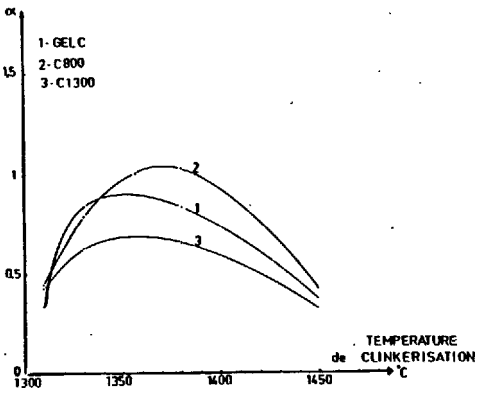

Evolution du coefficient α en fonction de la température de clinkérisation

CONCLUSION

Les alumines hydratées sont préparées en milieu aqueux par neutralisation du chlorure d'aluminium par l'ammoniaque.

Le pH de fin de précipitation (8,4 à 10,4) a un rôle important sur :

- la teneur en composés chlorés (7 à 0,7 %) présents dans les gels d'alumine,
- l'état de cristallisation et l'aire spécifique des gels (30 à 300 m^2/g).

Par contre après cuisson, une élévation de la température de calcination (800 à 1300°C) atténue progressivement ces différences.

Chaque alumine est broyée et tamisée, puis mélangée avec du carbonate de calcium. L'évolution du mélange pendant la clinkérisation est suivie au microscope de chauffe.

L'examen des courbes de retrait en fonction de la température montre qu'une augmentation de la température de calcination de l'alumine provoque une diminution du retrait.

Les analyses par diffraction X des différents clinkers montrent que la teneur en CA est fonction de la température de clinkérisation. On peut aussi noter la relation entre le retrait et la teneur en $C_{12}A_7$.

Il est délicat, compte tenu des résultats obtenus, de faire des corrélations précises entre les conditions d'obtention de l'alumine et la cinétique d'hydratation de l'aluminate de calcium issu de la réaction de cette alumine avec le carbonate de calcium. On constate cependant que l'accélération de la cinétique d'hydratation est maximale lorsque la température de clinkérisation est voisine de 1350°C.

BIBLIOGRAPHIE

1. - C.SERNA, J.L.WHITE, S.L.HEM
J.Pharm. Sci, 1978, 67, 8, 1179.

2. - MATHIEU : Thèse présentée à l'Université de Lyon (1956).

3. - M.C.ASTUCHE, A.HERBILLON
Bull. Soc. Chin. 1962, 1404.

4. - W.V.RAUSCH, H.D.BALE
J.Chem. Chy, 1964, 40, 11, 3391.

5. - HOANG VAN CAN : Thèse présentée à l'Université de Lyon (1968).

High temperature cements with geothermal applications

Ciments pour applications géothermiques

C.A. LANGTON, Graduate Assistant,
E.L. WHITE, Research Associate,
M.W. GRUTZECK, Research Associate and
D.M. ROY, Professor, Materials Research Laboratory, The Pennsylvania State University, University Park, PA 16802, U.S.A.

ABSTRACT: Performance requirements for cements utilized in geothermal and deep oil wells often exceed those of currently available cementing materials, whose upper temperature limits are about 200°C. Experiments undertaken were concerned with finding new cementing compositions and began with a study of the quaternary systems $CaO-Al_2O_3-SiO_2-H_2O$ and $CaO-MgO-SiO_2-H_2O$. Three compositional regions have been delineated as potential high-temperature cements. Region I in the system $CaO-Al_2O_3-SiO_2-H_2O$ intersects the $CaO-SiO_2$ join between 45 and 65 wt % SiO_2. Xonotlite, foshagite, and truscottite crystallized within the temperature range studied and were responsible for favorable cementitious properties of these mixtures. Region II in the system $CaO-Al_2O_3-SiO_2-H_2O$ centers around the anorthite composition, $CaO \cdot Al_2O_3 \cdot 2SiO_2$ and hexagonal anorthite was found to be cementitious. A third region of interest covers a broad band of compositions in the system $CaO-MgO-SiO_2-H_2O$ between about 45 to 65 wt % SiO_2 along the $CaO-SiO_2$ join to about 45 to 55 wt % SiO_2 along the $MgO-SiO_2$ join. Diopside, chrysotile, antigorite, xonotlite, truscottite and foshagite contributed to favorable cementitious properties of these mixtures. Addition of magnesia to the $CaO-SiO_2-H_2O$ join was best accomplished, in view of obtaining desirable physical properties, by the use of calcined chrysotile (asbestos).

Morphology and small size of the crystalline reaction products were, in large part, responsible for the cementitious quality of hydrothermally cured formulations. The following crystal habits resulted in the best cementing materials: needles, fibers, laths, and platelets.

Addition of alkalies to these systems produced several consequences. Addition of up to 10.0 wt % Na_2O and K_2O added as hydroxides on the mixing water, had little effect on bulk compositions between 35 and 55 wt % SiO_2 in the system alkali-$CaO-SiO_2-H_2O$. For mixtures containing over 55 wt % SiO_2, sodium was tied up in pectolite, a silicate phase, above 200°C, 68.9 MPa. At 200°C, 11Å tobermorite plus truscottite crystallized from these compositions. K_2O was tied up in reyerite between 200-350°C for silica-rich mixtures. Bulk compositions approximating $CaO \cdot MgO \cdot 2SiO_2$ were relatively unaffected by the addition of alkalies. However, as little as 0.5 wt % Na_2O added to compositions approximated by $CaO \cdot Al_2O_3 \cdot 2SiO_2$ was found to be deleterious to the hydrothermally cured cements. Analcite, a zeolite with a cubic habit, crystallized between 200-400°C. K_2O (0.5-10 wt %) also resulted in the formation of at least two unknown phases whose presence did not offset the unfavorable effect of analcite.

RESUME :

On demande aux ciments utilisés dans les puits géothermiques ainsi que dans les puits profonds de forage de pétrole une performance qui dépasse souvent celle qu'offrent les matériaux liants que l'on trouve maintenant, et dont les limites d'utilisation se situent aux environs de 200°C. Les expériences que nous avons conduites furent orientées vers la recherche de nouvelles compositions de ciments, en commencant par l'étude des systèmesquaternaires $CaO-SiO_2-H_2O$ et $CaO-MgO-SiO_2-H_2O$. Trois zones de compositions ont été cernées comme ciments potentiels pour usage à température élevée. La Zone I du système $CaO-Al_2O_3-SiO_2-H_2O$ coupe la ligne de conjugaison $CaO-SiO_2$ entre 45 et 65% de SiO_2. La xonotlite, foshagite et truscottite cristallisent dans l'intervallede temperature étudié et sont responsables pour les propriétés liantes de ces mélanges. La Zone II du système $CaO-Al_2O_3-SiO_2-H_2O$ est centrée autour de la composition de l'anorthite, $CaO \cdot Al_2O_3 \cdot 2SiO_2$, et on a trouvé que l'anorthite hexagonale a des propriétés liantes. Une troisième zone d'intérêt couvre une large gamme de compositions dans le système $CaO-MgO-SiO_2-H_2O$ entre environ 45 et 65% de SiO_2, le long de la ligne de conjugaison $CaO-SiO_2$, à environ 45 à 55% de SiO_2 le long de la ligne de conjugaison $MgO-SiO_2$. Le diopside, chrysotile, antigorite, xonotlite, truscottite et foshagite contribuent favorablement aux propriétés liantes de ces mélanges. Le meilleure façon d'incorporer la magnésie dans le système $CaO-SiO_2-H_2O$ pour obtenir les propriétés physiques désirées est d'utiliser du crysotile calciné (amiante).

La morphologie et la petite taille des produits cristallins de réaction sont, dans une large mesure, responsables pour la qualité liante des formulations à prise hydrothermale. Les formes cristallines suivantes produisent les meilleurs liants: aiguilles, fibres, lattes et plaquettes.

L'addition d'alcalis à ces systèmes a des conséquences diverses. Na_2O et K_2O, ajoutés jusqu'à 10% en poids comme hydroxides à l'eau du mélange, n'a que peu d'effet sur les compositions ayant entre 35 et 55% de SiO_2 dans le système $CaO-SiO_2-H_2O$. Dans les mélanges contenant plus de 55% de SiO_2, le sodium est fixé dans le pectolite, phase silicatée, au dessus de 200°C et 68,9 MPa. A 200!c, de la tobermorite (11Å) et de la truscottite cristallisent à partir de ces compositions. Pour des mélanges riches en silice, K_2O est fixé dans la reyerite entre 200 et 350°C. Les compositions autour de $CaO \cdot MgO \cdot 2SiO_2$ sont relativement insensibles aux additions d'alcalis. Toutefois, il fut trouvé que juste 0,5% de Na_2O ajouté aux compositions autour de $CaO \cdot Al_2O_3 \cdot 2SiO_2$ est détrimental aux ciments à prise hydrothermale. L'analcite, une zéolite avec une structure d'halite cubique, cristallise entre 200 et 400°C. K_2O (0,5 to 10% en poids) provoque aussi la formation d'au moins deux phases inconnues dont la présence ne compense pas l'effet défavorable de l'analcite.

INTRODUCTION

Performance requirements for cements utilized in geothermal and deep oil wells often exceed those of currently available cementing materials, whose upper temperature limits are about 200°C (1,2). Experiments undertaken were concerned with finding new cementing compositions, which began with the quaternary systems $CaO-Al_2O_3-SiO_2-H_2O$ and $CaO-MgO-SiO_2-H_2O$. Next the studies were extended to include additions of Na_2O and K_2O to cover broader wall rock and brine composition ranges. Parallel with determination of phase relations, preliminary evaluations of cementing properties were made. The combination of detailed phase- and properties-studies led to delineation of compositional areas having potential geothermal and petroleum well applications. The present paper reports details of the hydrothermal reactions and phase relation determinations, while properties are described elsewhere (1,2).

EXPERIMENTAL PROCEDURES

Starting Materials. Starting materials for phase relation studies included reagent grade oxides, gels, B_2O_3 stabilized βC_2S, commercial portland cements and aluminous cements, silica modifiers (silicic acid, 5 micrometer quartz, Tripoli, perlite, dehydrated silica gel), an alumina modifier (metakaolinite) and a magnesia modifier (calcined chrysotile). X-ray analysis of the Class J oil well cement indicated the presence of βC_2S, quartz, and calcite. Examination of the aluminous cements indicated the presence of CA, $C_{12}A_7$ and C_4AF.

Metakaolinite was prepared by heating high purity kaolinite at 750°C for four hours. The final product was an amorphous reactive aggregate with a bulk composition equivalent to dehydrated kaolinite. Chrysotile serpentine was calcined at 800°C for ten hours to produce a reactive mixture of very fine grained amorphous material, forsterite, and quartz.

Hydrothermal Equipment and Sample Preparation. Two types of autoclaves were used in synthesis studies: (1) Conventional 30 ml cold-seal Tuttle pressure vessels externally heated in Kanthal wound furnace assemblies; (2) 500 ml Inconel cold-seal vessels modified from the Barnes-Rocker Assembly and externally heated in Kanthal pot furnaces.

Preliminary studies were limited to small samples cured in conventional Tuttle pressure vessels. Starting materials, pastes or powders plus water, were placed in noble metal tubes and cured in an open system (tubes were not welded) or in a closed system (tubes were welded and weighed before and after curing to ensure containment). Phase relations were comparable for these preparation techniques which implies negligible ion transport.

Follow-up studies were made on selected formulations showing most potential. Pastes or slurries were cast in 25x50 mm plastic molds and were allowed to set for 30 minutes to 24 hours at room temperature and greater than 95% relative humidity. Then they were removed from the molds and cured in the 500 cc autoclaves. Deionized water was the pressurizing medium in both types of autoclaves.

Curing Conditions. Samples were cured at 200, 250, 300, 350, and 400°C over the pressure range 6.9-68.9 MPa. Pressure had little effect on the run products crystallized. Most experiments were run at 68.9 MPa. Curing times varied from 24 hours to 98 days. Deionized water was used as the pressurizing medium.

Mineralogical Examination. Mineralogical analyses were carried out by x-ray powder diffraction using CuK_α radiation. SEM images were used to describe morphologies of reaction products, and morphologies were then correlated with diffraction patterns. SEM imagery proved to be the most useful technique for identifying minor amounts of phases present.

Physical Property Measurements. Microhardness testing was performed using a Leitz microhardness tester and the Vickers indentation method with a 40X objective. Samples were embedded in epoxy and polished to a one micrometer diamond paste finish. Microhardness measurements were used as an approximation of relative compressive strengths. Compressive strength measurements were made on a Tinius Olsen Testing Machine. Samples were sawed so the tops and bottoms were parallel before testing. Permeability measurements on the larger samples were made with pressurized (up to 5.5 MPa) nitrogen gas flowing through the samples by measuring the displacement of water by the flowing gas. Water permeability was measured using pressurized water (13.8 MPa) flowing through the sample. Viscometers were used to analyze the properties of fresh cement slurries. Both a Brookfield Rheolog model 5XHBT and a Haake Rotovisco RV-3 Viscometer were utilized.

EXPERIMENTAL RESULTS

Compositions were widely scattered throughout the portions of the quaternary systems and selected mixtures are shown in Figures 1 and 2. Since the system $CaO-SiO_2-H_2O$ is a join of both quaternary systems of interest a detailed investigation of compositions between C:S = 2:1 and 1:2 was also undertaken.

$CaO-SiO_2-H_2O$. Initial mixtures were prepared from a variety of starting materials including oxides, gels, and commercially available cements in order to establish approximate phase stabilities and to promote rapid commercial application of new formulations in well cementing. The use of gels was discontinued after initial experimentation resulted in irreproducible phase assemblages. Variations in solubility of the silica modifiers also produced discrepancies in the crystallized phases. Highly soluble forms of silica, such as Tripoli, silicic acid, and perlite, tended to facilitate metastable crystallization of silica-rich hydrates, such as truscottite and wairakite. Coarser grained quartz was slow to dissolve into solution at the temperatures studied and, therefore, produced metastable crystallization of silica-poor phases. These problems were eliminated by the use of 5 micrometer quartz. Differences in silica solubility were attributed to the differences in degree of crystallinity and grain size.

The equilibrium dehydration curve for the reaction xonotlite = wollastonite + water was found to be somewhat lower than previously reported (3-5). In this study, wollastonite was observed to form from xonotlite at 385±5°C and 68.9 MPa within ten days. Reactions were reversed but exact equilibrium conditions are still uncertain because of formation of intermediate or disordered phases, or a very fine scale mechanical mixture. Xonotlite, crystallized over the temperature range of 200-385°C at 68.9 MPa was found to enhance the cementitious properties of hydrothermally cured cements.

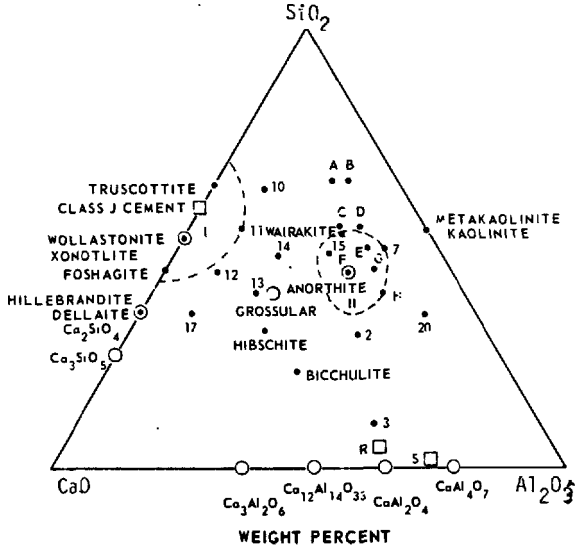

Figure 1. Projection of mixtures and compounds in the system $CaO-Al_2O_3-SiO_2-H_2O$ onto the anhydrous join. Potential hydrothermal cement compositions, Regions I and II, are shown.

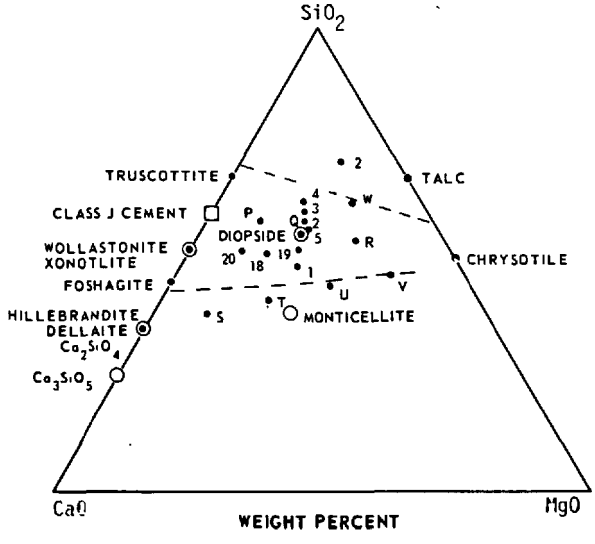

Figure 2. Projection of mixtures and compounds in the system $CaO-MgO-SiO_2-H_2O$ onto the anhydrous join. Potential hydrothermal cement compositions are delineated.

Truscottite crystallized over a wide range of curing conditions. Formation of truscottite in this study was favored by use of the most soluble forms of silica, such as Tripoli, in bulk compositions containing greater than 55 wt % SiO_2. Once crystallized, truscottite persisted throughout the longest runs (90 days) at 250-350°C, 68.9 MPa. The presence of truscottite in run products was not detrimental to the cementing properties of mixtures.

Foshagite crystallized readily between 325 and 400°C from mixtures containing between 40 and 50 wt % SiO_2. The occurrence of the assemblage xonotlite plus foshagite appeared to enhance microhardness and compressive strength measurements.

Carbonation of lime in starting materials resulted in the inadvertent addition of a fifth component, CO_2, to several of the runs. Above 350°C, calcite and a calcium silicate, usually xonotlite, crystallized. Below 350°C, scawtite, a hydrated calcium silicate containing carbonate, formed. The presence of neither phase was found to be detrimental to the physical properties of mixtures investigated.

$CaO-Al_2O_3-SiO_2-H_2O$. Modified commercial cements (Class J oil well cement and alumina cements, R and S), oxide mixtures and βC_2S plus silica and alumina modifiers were cured between 200 and 400°C at 68.9 MPa. Two compositional areas warranting further study are outlined in Figure 1.

Region I extends from approximately 45 to 65 wt % SiO_2 along the $CaO-SiO_2$ join and includes up to 10 wt % Al_2O_3. Phases responsible for the cementing properties within this region are xonotlite, truscottite and foshagite. The addition of up to 10 wt % Al_2O_3 as reactive boehmite [AlO(OH)], or metakaolinite, had no appreciable effect on their formation.

Region II centers around the anorthite composition and extends from about 45 to 65 wt % SiO_2 along the $CaO \cdot Al_2O_3 \cdot SiO_2$ join. Hexagonal anorthite and wairakite, a calcium zeolite, contributed to favorable cementitious properties between 200-400°C. Hexagonal anorthite and wairakite (above 350°C) were only crystallized in run products prepared from types S and R commercial cements plus silica and have been reported to be metastable although they were still present after 98 days (6,7). Crystallization of bicchulite and the hibschite-grossular hydrogarnet series resulted in mixtures with very low compressive strengths. Bicchulite readily formed above 300°C, whereas, variable compositions of the hydrogarnet series crystallized over the entire temperature range studied.

$CaO-MgO-SiO_2-H_2O$. Mixtures in the system $CaO-MgO-SiO_2-H_2O$ were prepared from Class J oil well cement, βC_2S plus silica modifiers (Tripoli or 5 micrometer quartz) and magnesia modifiers (MgO or calcined chrysotile serpentine). A large compositional area of interest is outlined in Figure 2. Crystalline phases responsible for the cementing properties include xonotlite (200-385°C), foshagite (300-400°C), truscottite (200-350°C), diopside (300-400°C), and serpentine polymorphs Chrysotile, the fibrous form of serpentine, crystallized between 250 and 400°C, whereas antigorite, a platy polymorph readily formed below 250°C. Monticellite, an anhydrous magnesium silicate, crystallized between 300 and 400°C. Mixtures containing predominantly monticellite were not cementitious.

Compositions along the joins xonotlite-diopside (325-385°C), diopside-chrysotile (325-400°C) and xonotlite chrysotile (200-385°C) showed the most favorable physical properties and highest microhardness and compressive strength measurements (1,2).

The form in which magnesium was added to the $CaO-SiO_2-H_2O$ join did not effect the phases crystallized. However, the use of calcined chrysotile resulted in much improved physical properties of the slurries as compared to the use of MgO. Addition of up to 10 wt % magnesia to the $CaO-SiO_2-H_2O$ did not significantly effect the stability of hydrated calcium silicate phases.

Table 1. Critical Runs Used for Determination of the Effect of Sodium on Cementitious Compositions

mix code	Composition starting material[1]	Na_2O (wt %)[2]	temperature (°C)	run products[3]
1N	X-O	0.5	400	X
	X-C5Q		200	X
3N		2.0	400	X
			200	X
5N		10.0	400	X
			200	X
6N	A-O	0.5	400	HA+ANA
	A-S5Q		250	HA+ANA
			200	E+d.HA
7N		2.0	400	HA+ANA
			250	HA+ANA
			200	E+d.HA
8N		10.0	400	ANA+HA+TA
			350	ANA+HA
			250	ANA+m.HA
			200	ANA+E+m.HA
9N	D-O	0 5	400	D
	D-C5QCC		200	D
10N		2.0	400	D
			200	D
11N		10.0	400	D+m.P
			200	D+m.P
12N	H-O	0.5	400	H
	H-C		200	H
13N		2 0	400	H
			200	H
14N		10.0	400	H
			200	H+m.P
15N	T-O	0 5	400	T+m.P+m.X
	T-C5Q		350	T+X
			300	T+m.P
			250	T+m.P
			200	d.T+11TOB
16N		2.0	400	P+T
			350	T+X+m.P
			300	T+P
			250	T+d.P
			200	11TOB+d.T
17N		10 0	400	P
			300	P
			250	P+T
			200	11TOB+d.T

[1]Abbreviations used for starting materials have the following meaning: A-O = ANORTHITE COMPOSITION from OXIDES; A-S5Q = ANORTHITE from Brand S CEMENT + 5 μm QUARTZ; D-O = DIOPSIDE COMPOSITION from OXIDES; D-C5QCC = DIOPSIDE from βC_2S + 5 μm QUARTZ + CALCINED CHRYSOTILE; H-O = HILLEBRANDITE COMPOSITION from OXIDES; H-C = HILLEBRANDITE from βC_2S; T-O = TRUSCOTTITE COMPOSITION from OXIDES; T-C5Q = TRUSCOTTITE from βC_2S + 5 μm QUARTZ; X-O = XONOTLITE COMPOSITION from OXIDES; X-C5Q = XONOTLITE from βC_2S + 5 μm QUARTZ.

[2]Na_2O was added as NaOH dissolved in the mixing water.

[3]Abbreviations used have the following meaning: A = ANORTHITE; ANA = ANALCITE; D = DIOPSIDE; E = EPISTILBITE; HA = HEXAGONAL ANORTHITE; H = HILLEBRANDITE; P = PECTOLITE; T = TRUSCOTTITE; TA = TRICLINIC ANORTHITE; TOB = 11Å TOBERMORITE; X = XONOTLITE; d = disordered; m = minor.

EXPERIMENTAL RESULTS II

In view of the range in petroleum and geothermal well wall rock compositions, and also the variations in minor oxide contents of commercial clinker, investigation of a wider range of potential compositions was undertaken. Mixtures with compositions of C:S = 2:1, 1:1, and 1:2, C:A:S = 1:1:2, and C:M:S = 1:1:2, were adjusted with 0.5, 2.0, and 10.0 wt % K_2O and also with Na_2O. Alkalies were added as dissolved hydroxides in the mixing water. Pastes were sealed in noble metal tubes and reacted for 3 to 28 days. Runs were made at 200-400°C at 50° intervals and 68.9 MPa. Both oxide mixtures and modified clinker formulations resulted in crystallization of similar phases after 28 days curing.

Compositions Containing Na_2O. Data for mixtures modified with NaOH are listed in Table 1. Addition of 0.5-10 wt % Na_2O had a negligible effect on run products for compositions approximated by the following compounds: $CaO{\cdot}SiO_2$, $2CaO{\cdot}SiO_2$, and $CaO{\cdot}MgO{\cdot}2SiO_2$. Xonotlite crystallized from mixtures with a C:S = 1:1 plus 0.5-10 wt % Na_2O between 200-400°C at 68.9 MPa.

Similar hydrothermal curing of C:S = 2:1 and C:M:S = 1:1:2 plus up to 10 wt % Na_2O resulted in crystallization of hillebrandite and diopside, respectively. A minor amount of pectolite was detected in these two bulk compositions for samples cured 28 days at 200°C, 68.9 MPa.

On the contrary, a sodium zeolite, analcite, crystallized from a C:A:S = 1:1:2. The amount of analcite present increased at the expense of hexagonal anorthite with increasing sodium content. These two phases coexisted between 400 and 250°C. Below 250°C, epistilbite, another sodium zeolite and hexagonal anorthite crystallized (6). Nucleation and growth of triclinic anorthite from silica-modified aluminous cements was facilitated at 400°C by the addition of 10 wt % Na_2O.

Pectolite, a fibrous Ca,Na silicate, crystallized from silica-rich compositions with a C:S = 1:2 between 250 and 400°C. The amount of pectolite in the run products increased with increasing Na_2O in this bulk composition. It also resulted in formation and persistence of 11Å tobermorite and disordered truscottite at 200°C, 68.9 MPa. This assemblage persisted up to 28 days.

Compositions Containing K_2O. Data for mixtures modified with K_2O added as KOH to the mixing water are listed in Table 2. Addition of 0.5-10.0 wt % K_2O had a negligible effect on run products for mixtures with the following compositions: C:S = 1:1 and C:S = 2:1. Xonotlite readily crystallized from the C:S = 1:1 bulk compositions. Addition of 2-10 wt % K_2O apparently reduced the kinetic barrier for the dehydration reaction xonotlite = wollastonite + H_2O. Dellaite crystallized at 400°C, 68.9 MPa in place of hillebrandite from mixtures with C:S ratio = 2:1 (4).

Diopside crystallized between 300 and 400°C from mixtures adjusted to C:M:S = 1:1:2. Starting materials, including calcined chrysotile formulations, did not affect crystalline products. Below 250°C, an unidentified fibrous phase, U_3, crystallized and persisted through the longest runs of 28 days. X-ray diffraction data for U_3 are presented in Table 3, and its presence in run products was not found to be unfavorable. U_3 may be a potassium-rich 11Å tobermorite.

Table 2. Critical Runs Used for Determination of the Effect of Potassium on Cementitious Compositions

mix code	Composition starting material[4]	K_2O (wt %)[5]	temperature (°C)	run products[6]
1K	X-O	0.5	400	X
	X-C5Q		200	X
3K		2.0	400	X+W
			300	X
			200	X
5K		10.0	400	X+W
			350	X
			200	X
6K	A-O	0.5	400	HA+TA
	A-S5Q		350	HA+TA
			300	HA
			250	HA+U_1
			200	U_1
7K		2.0	400	HA
			350	HA
			300	HA+U_1
			250	U_1
			200	U_1
8K		10.0	400	HA+U_2
			350	HA+U_2+U_1
			300	HA+U_1
			250	U_1
			200	U_1
9K	D-O	0.5	400	D
	D-C5QCC		250	D+U_3
10K		2.0	400	D
			250	D
			200	D+U_3
11K		10.0	400	D
			250	D+U_3
			200	U_3+D
12K	H-O	0.5	400	DEL
	H-C		350	H
			200	H
13K		2.0	400	DEL
			350	H
			200	H
		10.0	400	DEL
			350	H
			200	H
15K	T-O	0.5	400	X+T+d.W
	T-C5Q		350	T+X
			300	T+X
			250	T-R+X
			200	T-R+X
16K		2.0	400	X+d.W
			350	T+X
			300	T-R+X
			200	T-R+X
17K		10.0	400	W+X+T
			350	T+X+U_3
			300	R-T+U_3
			250	R-T+U_3
			200	U_4+R-T

[4]Abbreviations used are given in Table 1, foot-note 1.

[5]K_2O was added as KOH dissolved in the mixing water.

[6]Abbreviations used are given in Table 1, foot-note 3. In addition, the following abbreviations were used: DEL = DELLAITE; R-T = REYERITE-TRUSCOTTITE; T-R = TRUSCOTTITE-REYERITE; U_1-U_3 = UNKNOWNS 1-3 RESPECTIVELY; W = WOLLASTONITE.

Silica-modified aluminous cements adjusted to approximately a composition of C:A:S = 1:1:2 plus 0.5 wt % K_2O produced crystallization of the stable triclinic polymorph of anorthite along with hexagonal anorthite above 350°C, and hexagonal anorthite below 300°C. An unidentified phase, U_1, crystallized below 250°C. U_1 was found in run products cured at 300°C when 2 wt % K_2O was present and at 350°C when 10 wt % K_2O was added. Its stability is questionable. Another unidentified phase, U_2, crystallized between 350 and 400°C from mixtures containing 10 wt % K_2O. X-ray data are presented in Table 3.

The addition of 0.5-10.0 wt % K_2O to bulk composition of C:S = 1:2 produced the assemblage, xonotlite + wollastonite + truscottite at 400°C and truscottite + xonotlite between 300 and 350°C. Reyerite, a hydrated calcium-potassium silicate similar to truscottite, crystallized below about 350°C. U_3, possibly a potassium-rich 11Å tobermorite phase, was also detected in these mixtures containing 10 wt % K_2O and cured between 350 and 200°C.

Table 3. Characteristic d-spacings of Hydrothermally Synthesized Potassium-Silicates

U_1		U_2		U_3	
d	I	*d*	I	*d*	I
4.848	vs	3.633	s	11.334	vs
4.374	s	3.439	m	5.438	m
3.038	m	3.339	m	3.834	w
3.175	m	3.153	w	3.302	w
2.379	m	2.978	w	3.079	s
2.462	w	2.788	s	2.979	s
2.049	w			2.781	s
2.161	w				
1.994	w				

Silica-modified aluminous cements adjusted to approximately a composition of C:A:S = 1:1:2 plus 0.5 wt % K_2O produced crystallization of the stable triclinic polymorph of anorthite along with hexagonal anorthite above 350°C, and hexagonal anorthite below 300°C. An unidentified phase, U_1, crystallized below 250°C. U_1 was found in run products cured at 300°C when 2 wt % K_2O was present and at 350°C when 10 wt % K_2O was added. Its stability is questionable. Another unidentified phase, U_2, crystallized between 350 and 400°C from mixtures containing 10 wt % K_2O. X-ray data are presented in Table 3.

The addition of 0.5-10.0 wt % K_2O to bulk composition of C:S = 1:2 produced the assemblage, xonotlite + wollastonite + truscottite at 400°C and truscottite + xonotlite between 300 and 350°C. Reyerite, a hydrated calcium-potassium silicate similar to truscottite, crystallized below about 350°C. U_3 was also detected in these mixtures containing 10 wt % K_2O and cured between 350 and 200°C.

DISCUSSION

Hydrothermal curing of selected compositions in the systems CaO-SiO_2-H_2O, CaO-Al_2O_3-SiO_2-H_2O, and CaO-MgO-SiO_2-H_2O have been investigated at temperatures from 200-400°C and 6.9-68.9 MPa. Three compositional regions have been delineated as potential well cements. Region I in the CaO-Al_2O_3-SiO_2 system intersects the CaO-SiO_2

join between 45 and 65 wt % SiO_2 and may contain up to 10 wt % Al_2O_3. Xonotlite is the phase responsible for favorable cementing properties of these mixtures, and most silica-modified commercially manufactured well cements lie within Region I. Region II centers around the anorthite composition along the join $CaO \cdot Al_2O_3 - SiO_2$ Formulations prepared from commercial aluminous cements plus silica result in crystallization of the cementitious phase, hexagonal anorthite, between 250-400°C. It did not transform to triclinic anorthite nor did mixtures containing predominantly hexagonal anorthite show a decrease in compressive strength after 98 days. Problems associated with high temperature retardation in setting of these formulations require further research. The third region of interest covers a broad band of compositions in the system $CaO-MgO-SiO_2-H_2O$ between about 45 to 65 wt % SiO_2 along the $CaO-SiO_2$ join and 45 to 55 wt % SiO_2 along the $MgO-SiO_2$ join. Xonotlite, truscottite, foshagite, diopside, and the serpentine polymorphs, chrysotile and antigorite, contributed to the favorable cementitious properties. As previously discussed, these phases form various stable assemblages over specific temperature intervals in the range 200 to 400°C between 6.9 to 68.9 MPa. Addition of magnesia to the $CaO-SiO_2-H_2O$ join was best accomplished, in view of obtaining desirable physical properties, by the use of calcined chrysotile-serpentine (asbestos). Formulations prepared from portland cement adjusted to approximately the diopside composition with silica flour and calcined chrysotile resulted in superior physical properties of both the cements and slurries. As pointed out, it was necessary to add relatively soluble silica to these mixtures in order to prevent the crystallization of monticellite, which once formed, persisted over the range of curing conditions studied, and had an unfavorable effect on the cementitious quality of the cements.

Thermodynamic stability of several cementitious phases within a certain pressure/temperature regime is still questionable since reactions were difficult to reverse. Stability of hexagonal anorthite with respect to the triclinic polymorph has not been definitely demonstrated, although hexagonal anorthite, once crystallized, was not observed to transform to triclinic anorthite (6,7). In addition, the breakdown of truscottite to xonotlite plus silica has been questioned (8). Once crystallized, truscottite persisted in run products for 98 days. Work is presently being conducted to determine the temperature range of crystallization and relative stabilities of the unidentified phases reported here.

Morphology and size of the crystalline or semicrystalline reaction products were both responsible, in large part, for the cementitious quality of hydrothermally cured mixtures. The presence of fine needles, such as xonotlite; fibers, such as truscottite and foshagite; interlocking platelets, hexagonal anorthite; and intergrown needles such as diopside and pectolite, resulted in superior microhardness and compressive strength measurements (2). Cubic crystals such as analcite, grossular-hibschite (hydrogarnet series) and bicchulite, in addition to subhedral to euhedral grains of triclinic anorthite and monticellite, proved deleterious to the cementitious quality of hydrothermally cured mixtures.

Carbonation of free lime in some starting materials resulted in formation of scawtite below about 350°C and calcite above 350°C at 68.9 MPa. Values obtained to date for compressive strength and microhardness measurements indicate acceptable and even superior strengths for carbonate-containing cements.

Addition of up to 10 wt % of either Na_2O or K_2O, as hydroxides dissolved in the mixing water, had minor effect on crystalline run products for bulk compositions between 35 to 55 wt % SiO_2 in the system $Alkali-CaO-SiO_2-H_2O$. This implies that alkalies present in hydrothermally cured normal cements are not "tied up" as stable crystalline phases, and therefore, remain in solution where they are available to react with aggregates or wall rock. The consequences of alkali-aggregate reaction at elevated temperatures and pressures is unknown at the present time. On the contrary, available sodium (up to 10 wt %) was tied up in the silicate phase, pectolite, in mixtures containing greater than about 55 wt % SiO_2 (250-400°C, 68.9 MPa). The presence of 10 wt % Na_2O resulted in the crystallization and persistence of the assemblage 11Å tobermorite plus truscottite at 200°C for up to 28 days. Potassium added to mixtures containing greater than 55 wt % SiO_2 resulted in crystallization of reyerite, and an unidentified reaction product, U_3.

Bulk compositions approximating $CaO \cdot MgO \cdot 2SiO_2$ were also relatively unaffected by the presence of alkalies. Diopside formed as the crystalline product between 200 to 400°C, 68.9 MPa in the presence of 0.5-10 wt % Na_2O and K_2O. The only exception is that addition of 0.5-10 wt % K_2O resulted in formation of an unidentified fibrous phase, U_3, below 250°C. Above 250°C, alkalies are available to react with aggregate, whereas below about 250°C at least some potassium may be tied up in a crystalline reaction product that doesn't appear to be deterious to the cement.

The presence of as little as 0.5 wt % alkalies to bulk compositions approximated by $CaO \cdot Al_2O_3 \cdot 2SiO_2$ was found to produce unfavorable results. Available sodium was "tied up" in analcite, a cubic habit zeolite, over the entire temperature range studied. The availability of potassium facilitated nucleation and growth of triclinic anorthite, an apparently non-cementitious phase, between 350 and 400°C. The availability of potassium also resulted in crystallization of two unidentified phases U_1 and U_2, the presence of which did not offset the adverse effects of analcite and/or triclinic anorthite.

It was concluded that alkali/aggregate (or wall rock) reactions in hydrothermally cured cements could be controlled and possibly eliminated by incorporating alkalies in crystal structures of stable hydrated silicate phases. To accomplish this, bulk composition of cements should be adjusted to greater than 60 wt % SiO_2 with at least 20 wt % relatively soluble silica, such as silica flour or Tripoli. In addition, it was found that sodium added in the form of a NaCl-brine solution used as mixing water had little effect on the run products formed (1,2,9). The affinity of Na^+ for Cl^- was much greater than for silicate complexes under all conditions investigated. Cubic halite crystals were found growing in pores and throughout the bulk paste (1,2).

ACKNOWLEDGEMENTS

This research was supported through DOE sub-contract No. 422272-S, Brookhaven National Laboratory, Upton, Long Island, New York.

REFERENCES

1. ROY, D.M., WHITE, F.L., LANGTON, C.A., and GRUTZECK, M.W., "New High-Temperature Cementing Materials for Geothermal Wells: Stability and Properties," Final Report for Brookhaven National Laboratory, DOE, Sub-422272-S (Nov. 30, 1979).

2. ROY, D.M., WHITE, E.L., LANGTON, C.A., and GRUTZECK, M.W., "Potential New High Temperature Cements for Geothermal Wells," AIME International Symposium on Oilfield and Geothermal Chemistry, Houston, TX, 153-161 (1979).

3. BUCKNER, D.A., ROY, D.M., and ROY, R., "Studies in the System $CaO-Al_2O_3-SiO_2-H_2O$. II: The System $CaSiO_3-H_2O$," American Journal of Science 258, 132-147 (1960).

4. ROY, D.M. and JOHNSON, A.M., "Investigations of Stabilities of Calcium Silicate Hydrates at Elevated Temperatures and Pressures," Proc. Intl. Symposium on Autoclaved Calcium Silicate Building Products, Society of Chemical Industry, London, 114-120 (1967).

5. ROY, D.M. and HARKER, R.I., "Phase Equilibria in the System $CaO-SiO_2-H_2O$," Discussion," Proc. IVth Intl. Symposium on the Chemistry of Cement, Washington, 1960, National Bureau of Standards, Monograph 43, 196-200 (1962).

6. LIOU, G., "P-T Stabilities of Laumontite, Wairakite, Lawsonite, and Related Minerals in the System $CaAl_2Si_2O_8-SiO_2-H_2O$," Journal of Petrology 12, Part 2, 379-411 (1970).

7. ROY, D.M., WHITE, E.L., LANGTON, C.A., and ZIMMERMAN, K.G., "Hydrothermal Calcium Aluminosilicate Cements for Hydrothermal Bonding," Cement and Concrete Research 8, 509-512 (1978).

8. LUKE, K., TAYLOR, H.F.W., and KALOUSEK, G.L., "Geothermal-Well Cements: Formation of Truscottite, Xonotlite and Scawtite," American Ceramic Society 81st Annual Meeting, Cincinnati, OH, April 29-May 2 (1979).

9. NELSON, E.B. and KALOUSEK, G.L., "Effects of Na_2O on Calcium Silicate Hydrates at Elevated Temperatures," Cement and Concrete Research 7, 687-694 (1977).

High strength cement in the $CaO-Al_2O_3-SiO_2-SO_3$ system and its application

Ciments à haute résistance, du système $CaO-Al_2O_3-SiO_2-SO_3$; leurs applications

G. SUDOH, Dr. Eng., Manager of Research Department,
T. OHTA, Senior Research Chemist and
H. HARADA, Research Chemist, Chichibu Cement Co., Ltd., Japan.

SUMMARY : In a $CaO-Al_2O_3-SiO_2-SO_3$ system, clinker containing $C_3A_3 \cdot CaSO_4$, C_2S and free CaO as the principal minerals was obtained when a raw mixture with a suitable chemical composition was burned at a temperature between 1250 to 1300°C using a rotary kiln. It was found that a rapid-hardening and high-strength cement could be produced when this clinker was ground with anhydrite to prepare cement ranging in SO_3/Al_2O_3 molar ratio ($\bar{S}/A$) from 1.3 to 1.9. According to the JIS R 5201 method, the compressive strengths of cement mortars of $\bar{S}/A$ ratio of 1.3 were as follows :

Age	3h	7h	1d	3d	7d	28d
Strength (N/mm^2)	27	38	48	52	54	59

The rapid-hardening and high-strength properties of this cement could be attributed to the formation of needle-like ettringite of 1 to 2 μm with a large specific surface, which filled the inner vacant spaces of the hardened body. Furthermore, the hardened body became stronger due to the hydration of C_2S at later ages.

The cements made from clinkers of this system showed various hydration characteristics which are not normally observed in portland cement. It was also made clear that these cements are applicable to special uses, such as admixtures for soil stabilization and hardening of sludge, as a hydraulic binder in fixation of harmful heavy metals and as a cement for excelsior board.

RESUME : Un clinker, appartenant au système $CaO-Al_2O_3-SiO_2-SO_3$ et contenant principalement : $C_3A_3.CaSO_4$, C_2S et de la chaux libre, a été obtenu en cuisant au four rotatif, entre 1250 et 1300° C un cru de composition chimique appropriée. On a constaté qu'un ciment à durcissement rapide et à haute résistance pouvait être obtenu en broyant ce clinker avec de l'anhydrite, en proportions telles que le rapport molaire ($\bar{S}/A$) soit compris entre 1,3 et 1,9. La résistance à la compression des mortiers de ces ciments, mesurée selon la norme japonaise JIS-R-5201 a été pour un rapport $\bar{S}/A = 1,3$:

Age	3 h	7 h	1 j.	3 j.	7 j.	28 j.
Résistance(N/mm^2)	27	38	48	52	54	59

Le durcissement rapide et les fortes résistances de ces ciments peuvent être attribués à la formation d'aiguilles d'ettringite de 1 à 2 microns, qui remplissent les vides de la structure du ciment durci et augmentent la surface spécifique. De plus, la structure durcie devient de plus en plus résistante, grâce à l'hydratation, à long terme, du C_2S.

Les ciments fabriqués avec ces clinkers présentent des caractéristiques d'hydratation variées, qui n'ont pas été observées avec les ciments portland usuels. Il apparaît que ces ciments peuvent être utilisés pour des applications spéciales : stabilisation des sols - durcissement des boues - fixation des métaux lourds nocifs - ciment à hautes performances.

INTRODUCTION

Some studies (1)(2)(3) have been made or reported about $CaO-Al_2O_3-SiO_2-SO_3$ systems in relation to expansive cement. Most of them, dealing with $C_3A_3 \cdot CaSO_4$, have been undertaken for the main purpose of clarifying the expansive properties of the cement and arriving at a manufacturing method. (Hereafter, $C_3A_3 \cdot CaSO_4$ will be shortened to $C_4A_3\bar{S}$.) The authors found the possibility of applying this system not only to expansive cement but also to a rapid-hardening, high-strength cement and other special admixtures.

Assuming that the ratios or the amounts of $C_4A_3\bar{S}$, free CaO and $C\bar{S}$ in a cement should have much effect on the rate of the formation reaction of ettringite and on its character, the authors investigated the hydration characteristics of cements with various mineral compositions in $CaO-Al_2O_3-SiO_2-SO_3$ systems. Moreover, extending research to the manufacturing of special cements, the authors determined the conditions of mineral composition of cement clinker, burning temperature, grinding and so on.

The present paper is mainly concerned with a high-strength cement using clinker of this system, and deals with the burning reactions and hydration characteristics.

DETERMINATION OF MINERAL COMPOSITION FOR HIGH-STRENGTH CEMENT

The optimum mineral composition for high-strength cement was considered as a result of the following experiments. Three types of clinker were synthesized by use of limestone, two kinds of clay, by-product gypsum and reagent Al_2O_3. The raw materials were mixed at set proportions and ground to 6000 cm^2/g in Blaine specific surface. The raw mixtures were formed into pellets, which were burned in an electric furnace. The clinkers produced were examined by X-ray diffraction analysis to see whether the desired minerals had been formed. The chemical analyses and burning conditions of the clinkers are shown in Table I . The No. 1 clinker contained $C_4A_3\bar{S}$ as its principal mineral, the No. 2 clinker C_2S and the No. 3 clinker free CaO.

Eighteen types of cement were prepared by blending and grinding mixtures of clinkers, anhydrite and quicklime as shown in Table II . Anhydrite was obtained by burning gypsum at 1000°C for 120 min., and quicklime by burning crushed limestone at 1450°C for 80 min. Each cement was ground to 4500 cm^2/g. The compressive strengths of mortars of the cements are also shown in Table II . The testing method was according to JIS R 5201 (W/C = 0.65, 20°C, sand/cement = 2) except that test pieces of $2 \times 2 \times 8^{cm}$ were used.

In the A series shown in Table II , the cements were prepared with $C_4A_3\bar{S}$ and free CaO constant while varying anhydrite and C_2S in amount. The amounts of $C_4A_3\bar{S}$ and free CaO were 41 % and 0 %, respectively. Strengths of mortars increased for all ages with an increase in the amount of anhydrite. The optimum amount of anhydrite for high strength development is estimated to be about 30 %, and in that condition, the SO_3/Al_2O_3 molar ratio ($\bar{S}/A$) is calculated to be about 1.3.

In the B series, the cements were prepared with reference to the mineral composition of A-7 cement which showed good strength proper-

Table I Chemical analyses and burning conditions of synthetic clinkers

Clinker	Chemical composition (%)									Mineral composition (%)					Burning condition	
	ig.loss	insol.	SiO_2	Al_2O_3	Fe_2O_3	CaO	MgO	SO_3	total	$C_4A_3\bar{S}$	C_2S	C_4AF	f-$C\bar{S}$	f-CaO	Temp. (°C)	Time (min)
No. 1	0.1	0.2	2.0	46.7	1.0	38.6	0.1	12.1	100.8	92.0	5.7	3.0	0.1	0	1350	80
No. 2	0.2	0.5	25.1	9.8	1.9	56.4	1.4	3.7	99.0	17.1	72.0	5.8	2.5	0	1380	80
No. 3	0.1	0.1	13.0	7.8	2.5	65.2	0.9	10.3	99.9	12.4	37.3	7.6	14.7	26.8	1320	80

Table II Preparation of cements and respective mortar strengths

Cement	Mixing proportion of synthetic materials (%)					Mineral composition (%)					$\bar{S}/A$ ratio	Compressive strength (N/mm^2)		
	Clinker			Anhydrite	Lime	$C_4A_3\bar{S}$	C_2S	C_4AF	f-$C\bar{S}$	f-CaO		1 d	3 d	28 d
	No.1	No.2	No.3											
A-1	32	68	0	0	0	41	51	5	2	0	0.4	2.5	7.0	13.4
A-2	33	63	0	4	0	41	47	5	6	0	0.5	1.8	9.1	24.4
A-3	34	57	0	9	0	41	43	4	10	0	0.7	6.2	12.3	22.8
A-4	35	52	0	13	0	41	39	4	14	0	0.8	8.5	21.0	28.5
A-5	36	47	0	17	0	41	36	4	18	0	1.0	15.0	25.1	31.2
A-6	37	42	0	21	0	41	32	4	22	0	1.1	17.5	24.4	40.7
A-7	38	36	0	26	0	41	28	3	27	0	1.3	21.2	28.8	51.9
A-8	40	25	0	35	0	41	20	3	36	0	1.6	21.6	27.8	48.2
A-9	42	14	0	44	0	41	12	2	44	0	1.9	21.8	26.9	44.9
A-10	44	4	0	52	0	41	5	2	52	0	2.2	10.2	26.6	33.3
B-1	38	36	0	26	0	41	28	3	27	0	1.3	21.2	28.8	51.9
B-2	38	34	2	26	0	41	27	3	27	0.5	1.3	23.6	28.8	47.4
B-3	38	32	4	26	0	41	27	3	27	1	1.3	20.4	29.4	48.0
B-4	38	28	8	26	0	41	25	3	28	2	1.3	12.1	31.7	52.4
B-5	38	20	16	26	0	40	23	4	29	4	1.4	15.1	32.2	49.6
B-6	38	4	32	26	0	40	17	4	31	9	1.4	40.6	45.4	52.0
B-7	42	0	25	26	7	42	12	3	30	14	1.4	40.8	43.5	44.8
B-8	43	0	13	28	16	41	7	2	30	19	1.4	21.6	18.0	24.5
B-9	44	0	2	30	24	41	3	1	30	25	1.4	25.0	19.5	6.8

ties. The amounts of $C_4A_3\bar{S}$ and anhydrite were fixed at 40～42 % and 27～31 %, respectively, and free CaO and C_2S were varied. When the amount of free CaO came to 9 % as a result of incremental raises, the compressive strength of mortar increased rapidly within 24 hours. However, the strength properties worsened because of undesirable expansion when CaO was added above 19 %.

From the above results, it became clear that a cement of a CaO-Al_2O_3-SiO_2-SO_3 system has the properties of producing rapid hardening and high strength development when the proper mineral composition can be determined.

FUNDAMENTAL STUDIES OF RAPID-HARDENING AND HIGH-STRENGTH CEMENT

Many experiments were conducted on the basis of the above-mentioned results, and as a consequence, a special cement having properties of both rapid hardening and high strength was developed. This cement can also be said to be an energy-saving type as its clinker is burned in a relatively low temperature range of 1250 to 1300°C. The burning reactions and hydration characteristics of the cement are dealt with in the following.

(1) BURNING REACTIONS

The cement clinker has a special mineral composition; it contains $C_4A_3\bar{S}$ and C_2S as the principal minerals, with free CaO amounting to about 9 %, and no free $CaSO_4$ as shown in Table III . This prepared mixture, containing no free $CaSO_4$ in the clinker, prevents volatilization of the SO_3 component, which is very important in preventing environmental pollution.

The raw mixture was prepared by use of limestone, by-product gypsum, aluminous materials and clay to obtain the optimum chemical composition of the clinker as shown in Table

Table III Optimum chemical and mineral compositions of clinker (%)

Chemical composition					Mineral composition			
SiO_2	Al_2O_3	Fe_2O_3	CaO	SO_3	$C_4A_3\bar{S}$	C_2S	C_4AF	f-CaO
11.2	28.1	1.6	52.0	7.1	54	32	5	9

III . The raw mixture, ground to 5500 cm^2/g, was burned in an electric furnace at temperatures varied from 1000 to 1350°C at 50°C increments. The relationships between burning temperatures and clinker minerals were investigated by X-ray. The X-ray diffraction patterns of the clinkers are shown in Fig. 1 .

While C_2AS and $C_{12}A_7$ formed as aluminates in the temperature range of 1000 to 1100°C, $C_4A_3\bar{S}$ became stable above 1150°C with maximum formation in the 1250 to 1300°C range. Silicates coexisting with $C_4A_3\bar{S}$ were $2C_2S{\cdot}C\bar{S}$ and/or C_2S, the former formed mainly in the lower temperature range and the latter in the higher range. $C_4A_3\bar{S}$ began to decompose with the formation of C_3A at 1350°C, and this was accompanied by an extreme decrease in free CaO.

From the above-mentioned results, it was made clear that a temperature range of 1250 to 1300°C is optimum for obtaining clinker containing $C_4A_3\bar{S}$ and C_2S as the principal minerals and a sufficient amount of free CaO.

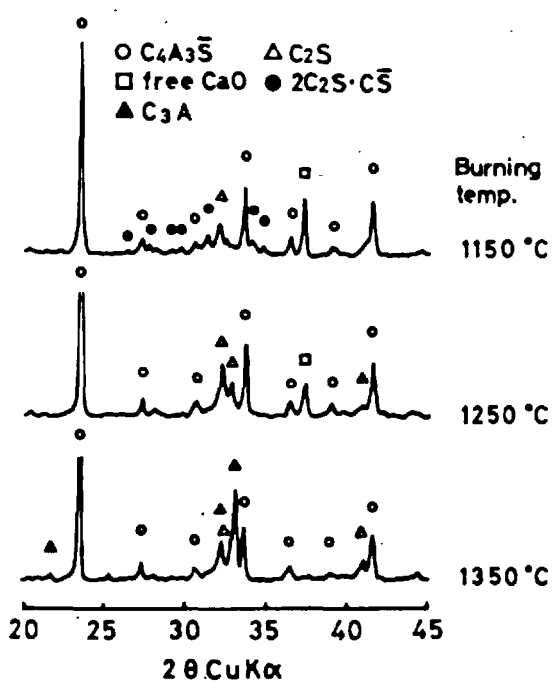

Fig. 1 X-ray diffraction patterns of clinkers

(2) HYDRATION CHARACTERISTICS

Five types of cement of specific surface of 4000 cm^2/g were prepared by blending and grinding mixtures of the clinker and by-product anhydrite. The clinker, prepared to obtain the optimum chemical composition as shown in Table III , was burned at about 1300°C using a test rotary kiln. Table IV shows the preparation conditions of the cements and the compressive strengths of their mortars according to the JIS R 5201 method.

Table IV Preparation of cements and their mortar strengths

Cement	SO_3 (%)	$\bar{S}/A$ ratio	Compressive strength (N/mm²)					
			3 h	7 h	1 d	3 d	7 d	28 d
C - 1	1 0	0.5	7.4	10.0	13.7	13.6	13.9	12.7
C - 2	1 5	0.9	18.5	25.0	32.0	37.4	40.0	40.4
C - 3	2 0	1.3	27.4	38.4	48.5	52.1	53.8	58.8
C - 4	2 5	1.9	17.9	30.3	51.2	60.1	70.8	74.4
C - 5	3 0	2.7	14.5	25.7	38.4	43.3	25.4	18.4
H			—	—	13.8	27.9	28.3	48.6

H: High-early strength portland cement

The strengths of the mortars were increased at all ages when the amount of anhydrite was increased, and the cements showed both rapid-hardening and high-strength properties at SO_3 content of 20 to 25 %, and with $\bar{S}/A$ ratio of 1.3 to 1.9. C-1 cement, having a lesser amount of anhydrite, showed little increase in strength with elapse of time as well as lower strengths at very early ages. C-5 cement, having a larger amount of anhydrite, showed lowering of strength at 7 days due to undesirable expansion cracks. Table V shows compressive strengths in case of standard curing of concretes using various amounts of C-3 cement.

Three types of cement were examined to make clear differences in strength properties through conduction calorimetry, X-ray analysis and scanning electron microscopy. The cements were hydrated in paste form at 20°C and water-cement ratio (W/C) of 0.6. The pastes were sealed in polyethylene sheets, and were allowed to settle down in a room of temperature of 20°C until they could be ex-

Table V Relationships between cement contents and compressive strengths of concretes

Cement	Cement content (kg/m³)	Slump (cm)	Compressive strength (N/mm²)				
			6 h	1 d	3 d	7 d	28 d
C - 3	370	9.0	19.1	44.5	66.0	82.9	87.6
	420	8.5	24.7	55.8	75.0	90.6	96.8
	470	8.0	32.3	61.5	82.2	97.7	103.4
	520	8.0	36.3	65.1	82.5	98.4	103.7
High - early strength p.c.	370	9.5	—	26.8	50.6	58.4	69.2
	520	7.5	—	43.8	62.4	69.2	76.8

Water-reducing admixture : 1.0 % of cement
Retardar : 0.5 % of cement

amined.

All of the heat liberation curves had two peaks as shown in Fig. 2. It is estimated from the results obtained by X-ray analysis (Table VI) that the second peaks correspond to formation of ettringite, which is retarded with additional amounts of anhydrite.

In the case of C-1 cement, heat of hydration decreases at an early stage and monosulfate hydrate forms more stably than ettringite on the first day. As monosulfate hydrate grows in the form of thin plates having vacant spaces which are probably too large to be filled by the hydrate of C_2S, good strength properties cannot be expected in all ages. (Fig. 3(a))

In comparison with the above, the hydrate of C-3 cement having a suitable amount of SO_3 is mainly ettringite. As is shown in Fig. 3 (b), ettringite is formed in needle-like shapes of 1 to 2 μm which fill the inner vacant spaces of the hardened body with a large specific surface, and this provides for high-strength characteristics.

In the case of C-5 cement, as shown in Fig. 3(c), the hydrate is also ettringite, but its form is different from that of C-3 cement; needle-like ettringite aggregates densely surround the cement grains but are formed very little in the vacant spaces. It is estimated that these characteristic forms of hydrate result later in undesirable expansion.

It has been mentioned above that C-3 cement has rapid-hardening and high-strength properties owing to the formation of minute ettringite. Moreover, the hardened structure

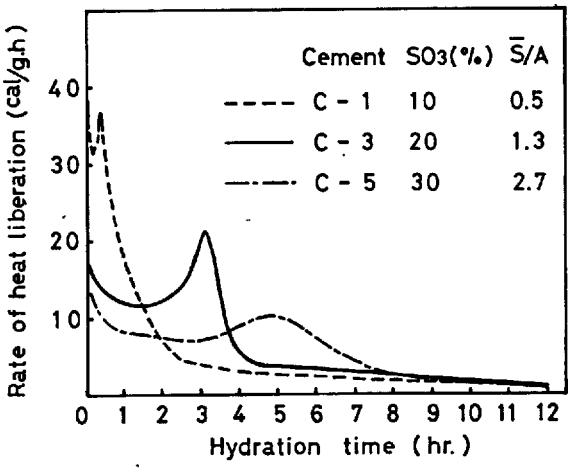

Fig. 2 Heat liberation curves

Table VI Hydration products identified by X-ray analysis

Cement	S̄/A ratio	Hydration time				
		5min.	30min.	90min.	6hr.	24hr.
C - 1	0.5	E	E,M	E,M	E,M	E<M
C - 3	1.3	—	E	E	E	E
C - 5	2.7	—	—	E	E	E

E : $C_3A \cdot 3CaSO_4 \cdot 32H_2O$, M : $C_3A \cdot CaSO_4 \cdot 12H_2O$

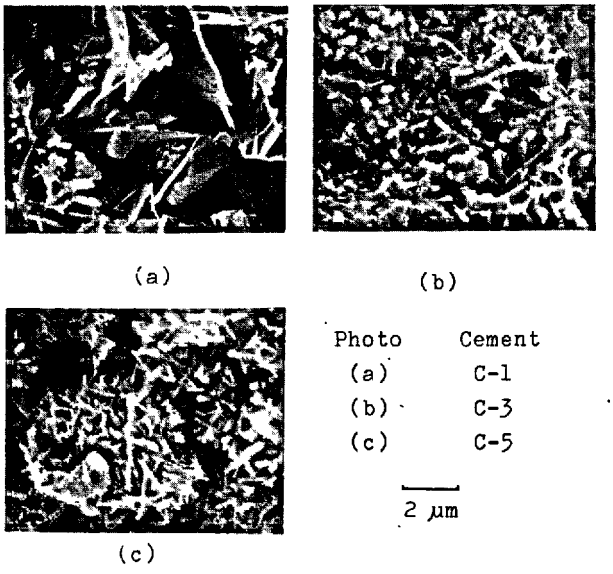

Fig. 3 Scanning electron micrographs of hardened pastes at 1 day

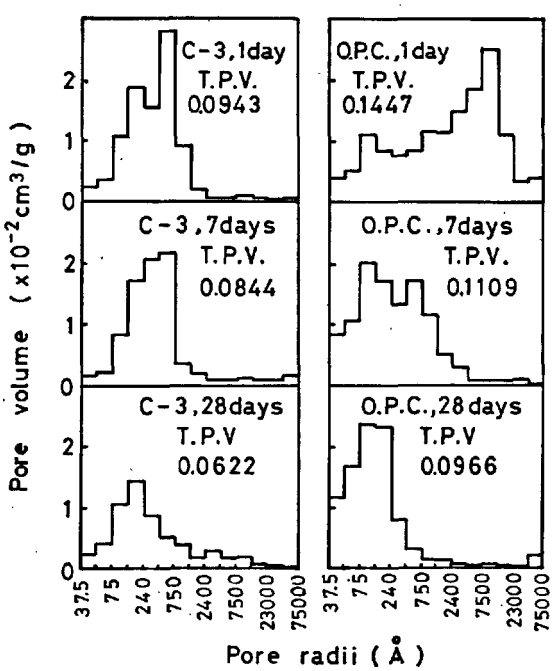

Fig. 4 Pore size distributions of cement mortars

becomes stronger by the hydration of C_2S over long periods of time. Fig. 4 shows pore size distributions of C-3 cement mortars compared with those of ordinary portland cement (O.P.C.) mortars. On comparisons of total pore volumes (T.P.V.) and pore size distributions of C-3 cement mortars with those of O.P.C. mortars, it is easy to understand the reason why C-3 cement exceeds O.P.C. in mortar strength. The T.P.V. of C-3 cement mortar decreases more and more owing to the hydration of C_2S over a long period of time and the hardened body is able to attain a high-strength characteristic.

APPLICATIONS OF CLINKERS OF $CaO-Al_2O_3-SiO_2-SO_3$ SYSTEM

Several kinds of special cement have been developed utilizing clinkers of this system. These types of cement are produced by grinding O.P.C. clinker, blast furnace slag and anhydrite with clinkers of this system which are prepared and burned to give the hydration properties necessary to meet their specific uses.

These cements possess various hydration characteristics due to formation of ettringite which are not seen normally with portland cement, and are applicable to special uses such as admixtures for soil stabilization and hardening of sludge (4), a hydraulic binder in fixation of harmful heavy metals (5) and as a cement for excelsior board.

CONCLUSIONS

Many studies have been carried out regarding clinkers of the $CaO-Al_2O_3-SiO_2-SO_3$ system to clarify expansive properties and to consider utilization as an expansive admixture. As stated in this paper, however, cements of this system have multiple purposes, including that of high-strength cement. This is due to the hydration characteristics of $C_4A_3\bar{S}$ which hydrates in various ways according to the amounts of $Ca(OH)_2$ and $CaSO_4$. It is thought that studies on special types of cement will be advanced further with more specialization in the future, and it may be anticipated that more research works on hydration mechanisms will be carried out employing $C_4A_3\bar{S}$-calcium silicate and/or free CaO-calcium sulfate systems.

REFERENCES

1.- T. NAKAMURA, G. SUDOH and S. AKAIWA (1968), "Mineralogical composition of expansive cement clinker rich in SiO_2 and its expansibility", Proceedings of the Fifth International Symposium on the Chemistry of Cement, Tokyo, IV , 351-365.

2.- S. AKAIWA, G. SUDOH and T. NAKAMURA (1967), "Investigation of volume expansion of $C_4A_3(SO_3)$", Cemento Gijutsu Nenpo, XXI , 156-162.

3.- M. COLLEPARDI, R. TURRIZIANI and A. MARCIALIS (1972), "The paste hydration of $4CaO{\cdot}3Al_2O_3{\cdot}SO_3$ in presence of calcium sulphate, tricalcium silicate and dicalcium silicate", Cement and Concrete Research, Vol. 2, No. 2, 213-223.

4.- Chichibu Cement Co., Ltd. (1979), Gekkan Haikibutsu, Vol. 5, No. 51, 78-82, and Vol. 5, No. 54, 64-68.

5.- T. MARUTA, I. UCHIDA, K.KATO (1978), "Fixation of harmful heavy metals with cement of calcium sulfoaluminate type", Cemento Gijutsu Nenpo, XXXII , 116-119.

Système aluminate de calcium - gypse - chaux - eau

On the calcium aluminate - gypsum - lime system

A. BONIN, Ingénieur de Recherche, Laboratoire de Recherche Générale, Lafarge S.A.,
B. CARIOU, Ingénieur, Laboratoire de Recherche Appliquée, Lafarge S.A., France.

RESUME : La mise au point des ciments expansifs de type M a montré le rôle important de la chaux vis-à-vis de la cinétique de gonflement de ces liants. L'expansion étant obtenue grâce à l'hydratation, en ettringite, du C_3A du clinker de Portland, en présence de gypse, une étude de cinétique de formation d'ettringite a été menée à partir des constituants purs.

Avec l'aluminate tricalcique C_3A, stoechiométrique pour la formation de l'ettringite, la présence de chaux en quantité inférieure à 1 % suffit pour bloquer pratiquement les réactions.

Dans le cas d'autres aluminates de calcium, où la chaux intervient en tant que réactant, elle provoque d'abord une accélération de la cinétique, puis un ralentissement pour les plus fortes proportions, plus ou moins marqué selon l'aluminate étudié.

SUMMARY : The studies about the shrinkage compensating cements of type M had shown that the kinetics of their expansion are very affected by the lime. The increase in volume is due to the C_3A hydration into ettringite, in the presence of gypsum. Therefore, we investigated the kinetics of ettringite formation from the pure components.

With the tricalcium aluminate C_3A, which is stoechiometric for ettringite formation, a content of lime as low as one percent is able to stop the reactions nearly completely.

In the case of other calcium aluminates, the lime is involved in the reactions as a reagent : at first it induces an increase in the kinetics ; then, for larger contents, a retardation more or less significant according to the calcium aluminate in question.

INTRODUCTION

Au cours de nos études de liants hydrauliques divers (ciment portland, spéciaux, prompts, expansifs ...), nous avons été constamment confrontés au problème de l'hydratation des aluminates de calcium (C_3A - $C_{12}A_7$ - CA - $C_4A_3\bar{S}$) en présence de quantités plus ou moins grandes de sulfate de calcium et de chaux ou corps libérant de la chaux. C'est ainsi que nous avons été amenés à étudier des systèmes séparés - aluminate de calcium - gypse - chaux - eau. Nous nous proposons de faire la synthèse des résultats que nous avons obtenus.

Les aluminates de calcium des essais ont été préparés par cuisson au four électrique, de mélanges stoechiométriques des oxydes de base. Nous avons considéré qu'ils étaient purs, quand par diffraction des rayons X, on ne décelait plus la présence des produits de départ (CaO libre en particulier), ni celle d'aluminates autres pouvant se former de manière transitoire.

Les techniques d'investigation utilisées ont été essentiellement :

- La microcalorimétrie isotherme qui nous permet d'enregistrer les dégagements de chaleur de réaction dès le contact de l'anhydre et de l'eau.

- La diffraction des rayons X pour identifier les hydrates formés et suivre la consommation des anhydres.

- Dans certains cas, la mesure de l'eau liée par perte au feu à 1000° sur échantillons dont l'hydratation est stoppée par lavage à l'acétone et séchage à l'éther.

SYSTEME C_3A - GYPSE - CHAUX - EAU

De nombreux auteurs (1 - 5) ont étudié ce système en raison de son importance dans les ciments Portland. Ils ont dans leur ensemble adopté un rapport molaire gypse/C_3A toujours inférieur à 0,4. Pour notre part, ayant été amenés à cette étude pour des questions de raidissement inhabituel, nous avons préféré opter pour un rapport plus élevé car aux premiers instants de l'hydratation, le C_3A en périphérie des grains (donc au contact de la solution) est tel que le rapport gypse/C_3A est certainement très grand. D'autre part, le seul hydrate se formant durant les premières minutes de l'hydratation étant l'ettringite, nous avons choisi la proportion de trois moles de gypse pour une de C_3A.

Ce mélange de base a été hydraté seul ou en présence d'une solution saturée de chaux, ou d'ajouts de chaux hydratée solide allant de très faibles teneurs jusqu'à 10 % (E/C = 1,0).

Le graphique N° 1 et le tableau N° I illustrent les réactions.

De l'ensemble de ces résultats, nous remarquons que :

- Dans tous les cas, le seul hydrate formé est l'ettringite.

- L'hydratation du témoin (C_3A + 3 gypses) est rapide et sans période dormante. On peut estimer que la réaction est effectuée à 60 % à 1 heure et à 85 % à 24 heures. Il n'apparaît aucun bloquage.

- Un ajout de 0,1 % de chaux hydratée semblerait accélérer la réaction d'hydratation. Par contre, 0,3 % la ralentit fortement, 0,5 % la bloque presque et 1 % la rend inexistante.

- Le gâchage avec une solution saturée de chaux (correspondant à 0,15 % de chaux hydratée) la ralentit fortement.

En résumé, il faut admettre que l'hydratation du mélange C_3A + 3 gypses ne se bloque pas mais qu'il suffit de très peu de chaux hydratée pour la ralentir et même la stopper.

Pour les ciments, STEINOUR (6), STEIN (7), COTTIN (8), COLLEPARDI (9) admettent qu'en présence de gypse l'hydratation du C_3A est ralentie par la formation d'une coquille d'ettringite imperméable et protectrice. Nos observations ne sont pas en contradiction avec cette hypothèse et nous

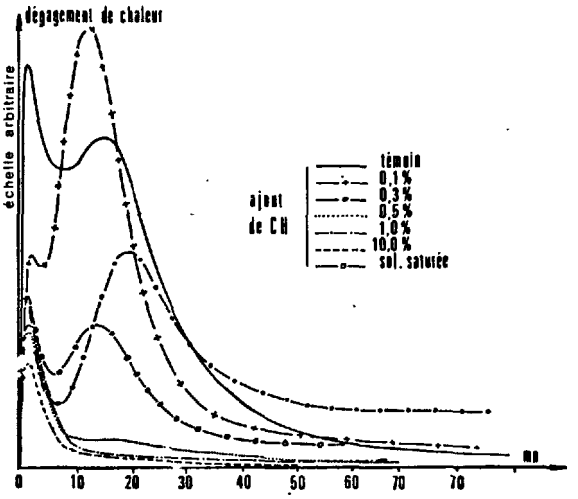

GRAPHIQUE N° 1 - Microcalorimétrie des mélanges C_3A + 3 Gypse avec teneurs croissantes en $Ca(OH)_2$

Echéances	C_3A + 3 SO_4Ca			+ Sol. sat. de chaux		+ 0,3 % $Ca(OH)_2$	
	Int. RX		p. f. 1000°	Int. RX	p. f. 1000°	Int. RX	p. f. 1000°
	Ettr.	Gypse		Ettr.		Ettr.	
0	0	150	16,7 %	0	16,7	0	16,7 %
5 mn	28	122	24,4 %	10	19,7	ε	19,4 %
20 mn	161	78	45,2 %			13	20,3 %
25 mn				102	27,6		
60 mn	167	58	48,2 %	140	41,9	45	27,2 %
24 h.	>230	20	61,8 %				

TABLEAU N° I - Cinétique de formation de l'ettringite du mélange C_3A + 3 Gypses seul ou en présence de chaux

ajoutons que c'est grâce à la chaux (libre ou d'hydrolyse du C_3S) saturant rapidement la solution en ions Ca^{++} que la coquille peut être bloquante, car moins bien cristallisée. S'il venait à manquer de la chaux en solution, l'ettringite formée assurerait moins bien son rôle protecteur, ou hydraterait plus de C_3A et on risquerait le raidissement.

SYSTEME $C_{12}A_7$ - GYPSE - CHAUX - EAU

Lors de l'étude de produits spéciaux, nous avons considéré l'hydratation du système à base de $C_{12}A_7$, dilué dans un inerte (mélanges du tableau N° II).

en poids				en mole		
inerte	$C_{12}A_7$	$C\bar{S}H_2$	CH	$C_{12}A_7$	$C\bar{S}H_2$	CH
80	20	15	0	1	6	0
			1			0,95
80	20	30	2	1	12	1,87
			3			2,81
80	20	45	4	1	18	3,75
			5			4,68
80	20	52	6	1	21	5,62
			8			7,50

dans tous les cas

TABLEAU N° II - Proportion pondérale et molaire des constituants des divers mélanges

Si on écrit les réactions théoriques d'hydratation de ces mélanges, avec les proportions extrêmes de chaux et en combinant le maximum de sulfate sous forme de sulfoaluminate (tri ou mono), on est conduit aux équations suivantes.

15 % $C_{12}A_7 + 6\,C\bar{S}H_2 \xrightarrow{aq} C_3A\,3\,C\bar{S}H_{32} + 3\,C_3A\,C\bar{S}H_{12} + 3\,AH_3$ (1)

Gypse $C_{12}A_7 + 6\,C\bar{S}H_2 + 9\,CH \xrightarrow{aq} 6\,C_3A\,C\bar{S}H_{12} + AH_3 + 3\,CH$ (1 A)

30 % $C_{12}A_7 + 12\,C\bar{S}H_2 \xrightarrow{aq} 4\,C_3A\,3\,C\bar{S}H_{32} + 3\,AH_3$ (2)

Gypse $C_{12}A_7 + 12\,C\bar{S}H_2 + 9\,CH \xrightarrow{aq} 5/2\,C_3A\,3\,C\bar{S}H_{32} + 9/2\,C_3A\,C\bar{S}H_{12}$ (2 A)

45 % $C_{12}A_7 + 18\,C\bar{S}H_2 \xrightarrow{aq} 4\,C_3A\,3\,C\bar{S}H_{32} + 3\,AH_3 + 6\,C\bar{S}H_2$ (3)

Gypse $C_{12}A_7 + 18\,C\bar{S}H_2 + 9\,CH \xrightarrow{aq} 11/2\,C_3A\,3\,C\bar{S}H_{32} + 3/2\,C_3A\,3\,C\bar{S}H_{12}$ (3 A)

52 % $C_{12}A_7 + 21\,C\bar{S}H_2 \xrightarrow{aq} 4\,C_3A\,3\,C\bar{S}H_{32} + 3\,AH_3 + 9\,C\bar{S}H_2$ (4)

Gypse $C_{12}A_7 + 21\,C\bar{S}H_2 + 9\,CH \xrightarrow{aq} 7\,C_3A\,3\,C\bar{S}H_{32}$ (4 A)

Selon ces équations, en l'absence d'ajout de chaux hydratée, il se forme toujours une quantité constante d'alumine libre. Le gypse est excédentaire pour les teneurs de 45 et 52 %. On obtient un mélange de mono et trisulfo pour le produit à 15 % de gypse et de l'ettringite pour les autres.

Un ajout de chaux hydratée au mélange à 15 % de gypse ne permet de combiner qu'une partie de l'alumine et tout le sulfate est sous forme de monosulfoaluminate.

Par contre, un ajout de 9 moles de chaux aux autres produits permet de combiner toute l'alumine et tout le gypse en un mélange de mono et trisulfo pour 30 et 40 % de gypse et en ettringite pure pour 52 %.

Nous avons déterminé les temps de prise Vicat et identifié semi quantitativement par diffraction des RX les phases présentes après 24 heures d'hydratation. Le tableau N° III donne les résultats obtenus.

Nous ne donnons que les courbes calorimétriques du mélange à 30 % de gypse, les autres étant semblables : graphique N° 2. On constate que :

- En diffraction X, on n'observe jamais l'alumine qui, quand elle existe, doit être sous forme amorphe.

- Les produits sans ajout de chaux hydratée se comportent comme le prévoient les équations 1 - 2 - 3 - 4.

- L'ajout de chaux hydratée au produit à 15 % de gypse ne provoque pas de phénomènes en contradiction avec l'équation 1A. Par contre, pour les produits à 30 - 45 et 52 % de gypse, on ne trouve aucun des comportements décrits par les équations 2A - 3A et 4A : il existe une teneur critique en chaux, croissante avec la teneur en gypse, pour laquelle on observe une discontinuité de comportement :

- En dessous de cette valeur, les réactions sont fortement accélérées (temps de prise très raccourcis, augmentation importante du premier pic de calorimétrie). La presque totalité du gypse ainsi que toute la chaux sont consommés et le seul hydrate observé est l'ettringite.

- Au dessus de cette valeur, la situation est complètement inversée. Les réactions sont bloquées (absence de fin de prise, diminution importante du premier pic de calorimétrie, disparition totale du second). La quantité d'ettringite faite est réduite de moitié et il reste toujours de fortes quantités de gypse et de chaux hydratée.

L'explication de ces phénomènes n'est pas évidente. A priori, on pouvait penser que l'alumine amorphe libérée par l'hydratation des produits sans chaux, gênerait le contact du $C_{12}A_7$ avec la solution et ralentirait les réactions ; mais que par contre des ajouts de chaux consommant cette alumine permettraient d'accélérer l'hydratation. Cette hypothèse va dans le sens de nos observations d'une part en ce qui concerne les mélanges à 15 % de gypse et d'autre part pour ceux à 30 - 45 et 52 % à condition de ne pas dépasser la valeur critique d'ajout de chaux.

En ce qui concerne les blocages des produits plus riches en chaux, il faut faire intervenir comme dans le cas du C_3A une protection du $C_{12}A_7$ par une pellicule d'ettringite dont la cristallisation (donc la plus ou moins grande imperméabilité) est influencée par la concentration en chaux de la solution. En supposant qu'il y ait compétition entre la cinétique de consommation de la chaux par l'alumine et sa vitesse de mise en solution, pour de faibles teneurs en chaux où la consommation l'emporterait, la solution ne serait jamais saturée en Ca^{++} alors que pour les plus fortes elle le serait rapidement. Dans ces conditions, la coquille d'ettringite mieux cristallisée aux faibles ajouts de chaux serait moins bloquante tandis qu'aux forts ajouts, moins bien cristallisée, elle isolerait plus efficacement le $C_{12}A_7$ de la solution.

Une telle explication est en accord avec les résultats trouvés pour le C_3A où des quantités infimes d'ajout de chaux suffi-

CH ajoutée	15 % de Gypse						30 % de Gypse					45 % de Gypse					52 % de Gypse				
	Prise mn		I. RX				Prise mn		I. RX			Prise mn		I. RX			Prise mn		I. RX		
	D.	F	ettr.	gyps.	M sulf.	CH	D.	F	ettr.	gyps.	CH	D.	F	ettr.	gyps.	CH	D.	F	ettr.	gyps.	CH
0	165	205	49	5	0	0	180	225	85	30	0	135	215	90	193	0	150	210	85	145	0
1	40	140	44	7	5	3	15	40	80	25	0	20	50	72	121	0	30	60	80	156	0
2	20	40	41	10	12	4	25	pas de fin de prise	45	159	11	40	55	85	43	0	10	20	82	119	0
3	30	40	38	6	11	2	45		50	193	16	50	pas de fin de prise	35	318	10	15	30	88	107	0
4	25	50	31	7	15	4	50		43	216	17	55		47	326	14	120	pas de fin de prise	38	479	14
5	25	50	27	0	15	5	45		47	226	20	60		34	297	21	pas de début de prise		32	440	19
6	45	65	25	0	20	5	40		42	230	29	60		38	319	23			57	233	22
8	45	75	20	0	20	9	30		43	308	31	60		29	348	27			49	313	28

TABLEAU N° III - Temps de prise et phases présentes après 24 heures d'hydratation

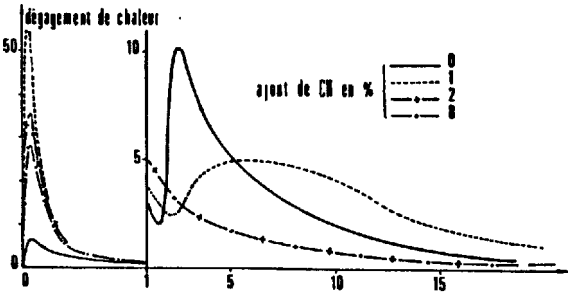

GRAPHIQUE N° 2 - Courbes de dégagement de chaleur lors de l'hydratation du mélange à 30 % de gypse pour divers ajouts de CH

sent pour bloquer l'hydratation, car dans ce système il n'y a pas d'excès d'alumine et la chaux d'ajout, aussi faible soit-elle, n'est jamais consommée et donne rapidement des solutions saturées en Ca^{++}.

SYSTEME CA - GYPSE - CHAUX - EAU

Un tel système est susceptible de se rencontrer dans les ciments prompts, constitués d'un mélange d'alumineux et de portland gypsé. Pour l'étudier, nous avons réalisé l'hydratation des mélanges du tableau N° IV.

en mole				en mole		
CA	$C\bar{S}H_2$	CH		CA	$C\bar{S}H_2$	CH
1	1	0		1	3	0
1	1	0,5		1	3	1
1	1	2/3		1	3	2
1	1	4/3		1	3	3

TABLEAU N° IV - Composition des mélanges de CA-Gypse et chaux étudiés

Les équations d'hydratation des mélanges à une mole de gypse peuvent s'écrire :

$$CA + C\bar{S}H_2 \xrightarrow{aq} 1/3\ C_3A\ 3\ C\bar{S}H_{32} + 2/3\ AH_3 \qquad 5$$

$$CA + C\bar{S}H_2 + 0,5\ CH \xrightarrow{aq} 1/3\ C_3A\ 3\ C\bar{S}H_{32} + 1/6\ AH_3 + \tfrac{1}{2}\ CA \qquad 5\ A$$

$$CA + C\bar{S}H_2 + 2/3\ CH \xrightarrow{aq} 1/3\ C_3A\ 3\ C\bar{S}H_{32} + 2/3\ CA \qquad 5\ B$$

$$CA + C\bar{S}H_2 + 4/3\ CH \xrightarrow{aq} 1/3\ C_3A\ 3\ C\bar{S}H_{32} + 2/3\ CA + 2/3\ CH \qquad 5\ C$$

On remarque que le mélange équimolaire de CA et de gypse s'hydrate en libérant 2/3 de moles d'alumine. Un ajout de n moles de chaux permet de consommer n moles d'alumine mais entraine aussi une augmentation de n moles de CA non hydraté. En ce qui concerne les équations 5 A - 5 B - 5 C, il y a risque de formation de monosulfoaluminate mais qui ne devrait pas se manifester à l'échéance de 24 heures.

Les équations théoriques d'hydratation des mélanges à 3 moles de gypse peuvent s'écrire :

$$CA + 3\ C\bar{S}H_2 \xrightarrow{aq} 1/3\ C_3A\ 3\ C\bar{S}H_{32} + 2\ C\bar{S}H_2 + 2/3\ AH_3 \qquad 6$$

$$CA + 3\ C\bar{S}H_2 + CH \xrightarrow{aq} 1/3\ C_3A\ 3\ C\bar{S}H_{32} + C\bar{S}H_2 + 1/3\ AH_3 \qquad 6\ A$$

$$CA + 3\ C\bar{S}H_2 + 2\ CH \xrightarrow{aq} C_3A\ 3\ C\bar{S}H_{32} \qquad 6\ B$$

$$CA + 3\ C\bar{S}H_2 + 3\ CH \xrightarrow{aq} C_3A\ 3\ C\bar{S}H_{32} + CH \qquad 6\ C$$

Dans le cas des mélanges sans chaux, on a un gros excès de gypse et on libère 2/3 de moles d'alumine. L'ajout de n moles de chaux permet de consommer n moles de gypse et n/3 moles d'alumine : pour n = 2, l'hydratation du mélange conduit à 100 % d'ettringite.

Nous avons réalisé l'hydratation de ces mélanges au calorimètre à conduction. Les résidus de calorimétrie à 24 heures après stoppage d'hydratation ont été examinés en diffraction des RX pour juger de l'avancement des réactions. Le tableau N° V donne les estimations de la consommation des phases de départ. Les graphiques N° 3 et 4 donnent les courbes de dégagement de chaleur d'hydratation.

mélanges à 1 mole de gypse					mélanges à 3 moles de gypse			
mole de CH ajoutée	% CA consommé	% $C\bar{S}H_2$ consommé	% CH consommé		mole de CH ajoutée	% CA consommé	% $C\bar{S}H_2$ consommé	% CH consommé
0	70	69	-		0	100	27	-
0,5	73	quasi totale	100		1	60	62	100
2/3	64		100		2	55	66	100
4/3	55		95*		3	72	80	26

TABLEAU N° V - Estimation de la consommation des phases de départ des mélanges à 1 et 3 moles de gypse (* présence de C_4AH_{13})

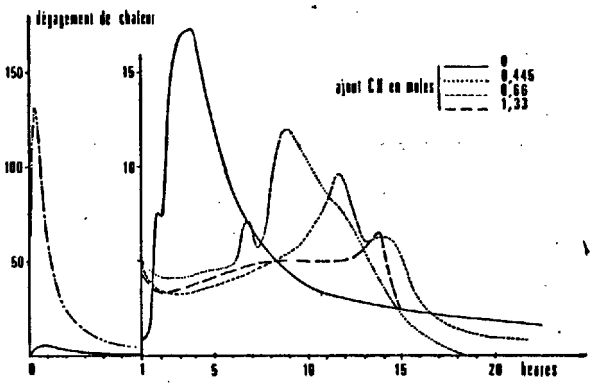

GRAPHIQUE N° 3 - Courbes de dégagement de chaleur des mélanges CA + $C\bar{S}H_2$ pour divers ajouts de CH

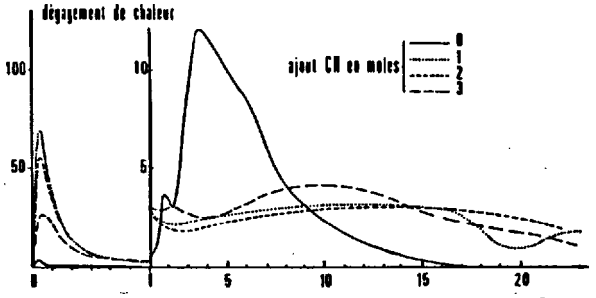

GRAPHIQUE N° 4 - Courbes de dégagement de chaleur des mélanges CA+3$C\bar{S}H_2$ pour divers ajouts de CH

On constate que :

- Le seul hydrate formé est l'ettringite. On ne voit pas l'alumine par diffraction des rayons X (elle est donc sous forme amorphe comme dans le cas du $C_{12}A_7$). Dans tous les cas où les équations d'hydratation prévoient que la chaux hydratée se combine à l'alumine, on observe effectivement une consommation totale de l'ajout pratiqué.

- Pour les mélanges à une mole de gypse, la réaction est effectuée conformément à l'équation 5 et le degré d'avancement à 24 heures est de 70 %. La majeure partie de la réaction se produisant après 1 heure. En ajoutant de la chaux, on accroit considérablement le premier pic (sensiblement de 15 fois) et on retarde en les diminuant légèrement les pics situés après 1 heure. L'augmentation du 1er pic est indépendante de la teneur en chaux, par contre, le retard des autres est croissant avec l'ajout pratiqué. De toute manière, les réactions sont à peu près totales à 24 heures.

- Pour les mélanges à trois moles de gypse en absence de chaux, on consomme tout le CA et le tiers du gypse comme le prévoit l'équation 6 . La réaction est totale à 24 heures (la plus grande partie s'effectuant après 1 heure). En ajoutant 1 mole de chaux, on augmente fortement le premier pic (sensiblement de 7 fois) mais on retarde fortement les autres pics en les écrasant. A 24 heures, les réactions ont un degré d'avancement réduit à 60 %. En continuant à augmenter l'ajout de chaux, on obtient une nette décroissance du 1er pic sans changer notablement les autres. Le degré d'avancement à 24 h de la réaction s'en trouve un peu diminué.

En résumé, on peut retenir qu'en présence d'une faible quantité de gypse, l'ajout de chaux hydratée accélère l'hydratation surtout dans les premières minutes et qu'on observe aucun blocage. En présence de quantités plus grandes de gypse les ajouts successifs de chaux, après avoir fortement accéléré l'hydratation, la ralentissent notablement sans tou-

tefois provoquer de blocage absolu.

SYSTEME $C_4A_3\bar{S}$ + GYPSE + CHAUX + EAU

Un tel système se rencontre dans les ciments expansifs de type M. Pour l'étudier en laboratoire, nous avons réalisé l'hydratation des mélanges du tableau N° VI.

$C_4A_3\bar{S}$	$C\bar{S}H_2$	CH	$C_4A_3\bar{S}$	2 $C\bar{S}H_2$	CH	$C_4A_3\bar{S}$	8 $C\bar{S}H_2$	CH
1	0	0	1	2	0	1	8	0
1	0	0,43	1	2	0,26	1	8	0,27
1	0	0,92	1	2	0,68	1	8	0,55
1	0	2,00	1	2	1,43	1	8	1,41
1	0	4,00	1	2	2,28	1	8	3,00
1	0	6,00	1	2	4,00	1	8	6,00
1	0	10,00	1	2	6,00	1	8	10,00

TABLEAU N° VI - Composition molaire des mélanges de gypse et de chaux étudiés

Les équations d'hydratation de ces mélanges sont :

$$C_4A_3\bar{S} \xrightarrow[aq]{} C_3A\,C\bar{S}H_{12} + 2\,AH_3 \qquad 7$$

$$C_4A_3\bar{S} + 8\,CH \xrightarrow[aq]{} C_3A\,C\bar{S}H_{12} + 2\,C_4AH_{13} \qquad 7\,A$$

$$C_4A_3\bar{S} + 2\,C\bar{S}H_2 \xrightarrow[aq]{} C_3A\,3\,C\bar{S}H_{32} + 2\,AH_3 \qquad 8$$

$$C_4A_3\bar{S} + 2\,C\bar{S}H_2 + 6\,CH \xrightarrow[aq]{} 3\,C_3A\,C\bar{S}H_{12} \qquad 8\,A$$

$$C_4A_3\bar{S} + 8\,C\bar{S}H_2 \xrightarrow[aq]{} C_3A\,3\,C\bar{S}H_{32} + 2\,AH_3 + 6\,C\bar{S}H_2 \qquad 9$$

$$C_4A_3\bar{S} + 8\,C\bar{S}H_2 + 6\,CH \xrightarrow[aq]{} 3\,C_3A\,3\,C\bar{S}H_{32} \qquad 9\,A$$

On voit que $C_4A_3\bar{S}$ s'hydrate en monosulfo avec libération d'alumine. Un ajout de 8 moles de chaux permet de fixer cette alumine en C_4AH_{13}. En présence de 2 moles de gypse et 6 moles de chaux, on obtient du monosulfo pur et pour 2 moles de gypse et 6 moles de chaux, de l'ettringite pure.

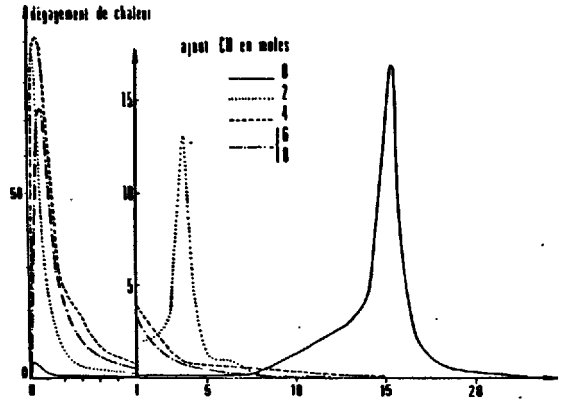

GRAPHIQUE N° 5 - Courbes de dégagement de chaleur des mélanges $C_4A_3\bar{S}$ + n CH

Le tableau N° VII donne les phases obtenues par hydratation durant 24 heures. Les graphiques N° 5 - 6 - 7 montrent les courbes de dégagement de chaleur pendant les réactions.

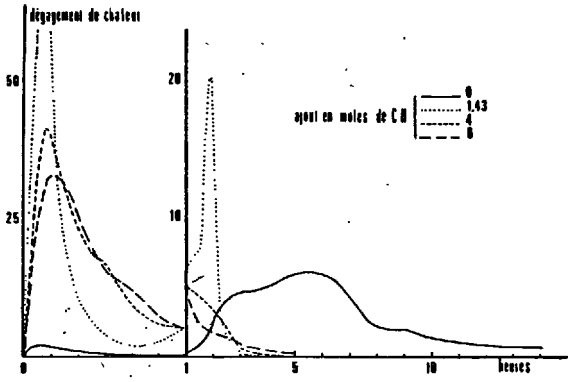

GRAPHIQUE N° 6 - Courbes de dégagement de chaleur des mélanges $C_4A_3\bar{S}$ + 2 $C\bar{S}H_2$ + n CH

On remarque que :

- Le $C_4A_3\bar{S}$ seul s'hydrate de manière prépondérante en monosulfoaluminate selon l'équation 7 et l'alumine visible en diffraction des rayons X est mieux cristallisée. En accord avec l'équation 7 A l'ajout de CH permet de fixer l'alumine sous forme de C_4AH_{13}. Dans tous les cas, les réactions ont un degré d'avancement de 95 % en moyenne à 24 heures. Les microcalorimétries montrent en présence de CH une très forte accélération des phénomènes se traduisant par un premier pic considérablement augmenté et un déplacement des seconds pics vers les temps les plus courts. Nous n'observons jamais de blocage.

- Le mélange à deux moles de gypse s'hydrate en ettringite en accord avec l'équation 8 . L'alumine formée est amorphe. Un ajout progressif de chaux permet d'obtenir, en accord avec l'équation 8 A un mélange de plus en plus riche en monosulfoaluminate. Nous ferons, en ce qui concerne les cinétiques de réaction, les mêmes remarques que pour le $C_4A_3\bar{S}$ seul (en particulier l'absence de blocage).

- Le mélange à 8 moles de gypse, en absence de chaux, est complètement hydraté, à 24 heures, en ettringite. Il reste beaucoup de gypse et l'alumine libérée (équation 9) est amorphe. Des ajouts progressifs de chaux augmentent le premier pic de calorimétrie et font disparaître les seconds. Il semblerait que les réactions soient accélérées, cependant,

$C_4A_3\bar{S}$							$C_4A_3\bar{S}$ + $C\bar{S}H_2$							$C_4A_3\bar{S}$ + 8 $C\bar{S}H_2$				
moles CH ajoutées	% de consommation de		I. R X				moles CH ajoutées	% de consommation de			I. R X			moles CH ajoutées	% de consommation de			I. R X
	$C_4A_3\bar{S}$	CH	Mono	Ettrin.	C_4AH_3	AH_3		$C_4A_3\bar{S}$	$C\bar{S}H_2$	CH	Ettrin.	Mono	C_4AH_{13}		$C_4A_3\bar{S}$	$C\bar{S}H_2$	CH	Ettrin.
0	96	-	132	20	40	oui	0	93	≃ 100	-	220	0	0	0	100	37	100	190
0,4	97	100	105	ε	70	oui	0,26	91	"	100	187	0	0	0,27	"	27	"	167
1,0	95	"	122	ε	68	ε	0,68	97	100	"	155	ε	0	0,55	"	26	"	130
2	94	"	130	0	Très mal cristallisé	ε	1,43	90	"	"	185	ε	0	1,41	"	19	"	145
4	92	"	125	0		0	2,28	96	"	"	151	45	ε	3,0	≃100	62	"	181
6	93	"	136	0		0	4,00	90	"	"	92	82	35	6,0	78	11	≃ 100	196
8	96	"	145	0		0	6,00	93	"	"	39	86	66	10,0	56	42	16	102

TABLEAU N° VII - Consommation des anhydres et apparition des phases hydratées à 24 h des mélanges $C_4A_3\bar{S}$ + gypse en fonction des ajouts de chaux hydratée

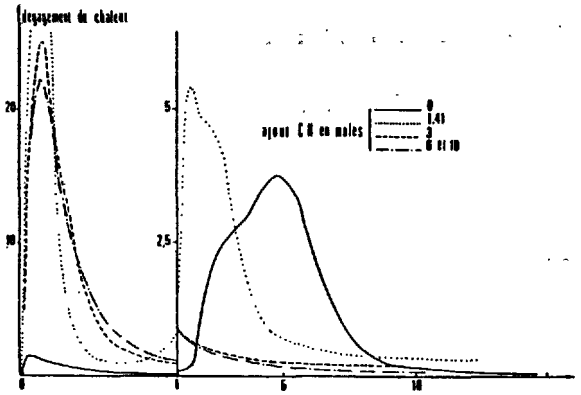

GRAPHIQUE N° 7 – Courbes de dégagement de chaleur des mélanges $C_4A_3\bar{S} + 8\ C\bar{S}H_2 + n\ CH$

on voit par diffraction des rayons X que globalement la quantité de $C_4A_3\bar{S}$ réagissant décroit notablement à partir d'un ajout de 6 moles de chaux (stoechiométrie de l'ettringite) qui n'est pas entièrement consommé. En forçant l'ajout de chaux hydratée, on ralentit encore l'hydratation. Il y a là un début de blocage des réactions moins caractérisé que pour le C_3A et le $C_{12}A_7$ mais qui ne fait aucun doute.

En résumé, tous les mélanges $C_4A_3\bar{S}$ – gypse en absence de chaux hydratée s'hydratent rapidement. L'ajout de chaux hydratée accélère les réactions chaque fois que l'on favorise la formation de monosulfo et les ralentit quand on cherche à former l'ettringite pure.

CONCLUSION

Les mélanges d'aluminate de calcium, de gypse et de chaux peuvent avoir des comportements, lors des réactions d'hydratation, très différents selon la nature de l'aluminate de base et des hydrates susceptibles de se former.

On peut schématiquement considérer trois cas.

– Les mélanges ont la stoechiométrie pour la formation de monosulfoaluminate : Les réactions sont alors rapides et complètes sans phénomène de blocage (cas de $C_{12}A_7$ – CA – $C_4A_3\bar{S}$). La formation passagère d'un peu d'ettringite aux faibles échéances n'altère pas les cinétiques.

– Les mélanges ont la stoechiométrie pour la formation d'ettringite : On assiste alors en présence de CH à des blocages plus ou moins caractérisés. Ces blocages sont d'autant plus marqués que le C/A de l'aluminate de départ est plus grand (dans l'ordre C_3A – $C_{12}A_7$ – $C_4A_3\bar{S}$ – CA).

– Les mélanges intermédiaires où les hydrates formés sont des mélanges de monosulfo, d'ettringite, de C_4AH_{13} et d'alumine (le plus souvent amorphe). Chaque fois que ces teneurs en gypse et en chaux augmentent et favorisent une proportion relative d'ettringite un peu prépondérante, on assiste à des blocages ou ralentissements.

En ce qui concerne l'alumine amorphe, elle aurait tendance à ralentir les réactions (sans doute en gênant la mobilité des ions en solution) et de faibles ajouts de chaux permettant de la consommer, surtout aux faibles échéances, accélèrent considérablement l'hydratation dans les premières minutes.

Le point qui nous parait le plus important à souligner est le rôle bloquant de l'ettringite quand celle-ci se forme en présence de chaux excédentaire (Au tout début des réactions quand très peu d'ettringite s'est formée, on peut considérer qu'il y a de la chaux excédentaire même pour de faibles teneurs).

En fait, il faut raisonner en possibilité de sursaturation en ions Ca^{++} dans la solution où précipite l'ettringite. Plus cette sursaturation a de risques d'être élevée (même momentanément), plus l'ettringite sera mal cristallisée et en conséquence plus bloquante.

A chaque fois que, dans des ciments, interviendra un système aluminate de calcium – gypse – chaux, il conviendra de s'intéresser aux conditions de précipitation des hydrates et les quelques conclusions de ce papier sont de nature à aider les raisonnements.

En particulier, ne faudrait-il pas voir là l'explication de la fausse prise carbonate ? En effet, il est plus séduisant de penser que c'est le manque momentané de Ca^{++} en solution (due à la précipitation de calcite) qui modifierait la cristallisation de l'ettringite permettant une hydratation accrue du C_3A, génératrice de raidissement, plutôt que d'admettre que c'est la très faible quantité de calcite (bien cristallisée et n'entrainant pas d'eau) qui provoque l'épaississement de la pâte.

BIBLIOGRAPHIE

1. COLLEPARDI M., BALDINI G., PAURI M., CORRADI M., Tricalcium aluminate hydration in the presence of lime, gypsum or sodium sulfate. CCR. Vol. 8, pp. 571–580 – 1978.
2. MEHTA P.K., Effect of lime on hydration of pastes containing gypsum and calcium aluminates or calcium sulfo aluminates, Journal of the American Ceramic Society., Vol. 56, N° 6, pp. 315–319.
3. SCHWIETE H.E., LUDWIG U., JAGEA F., Recherches sur le système 3 CaO. Al_2O_3 – $CaSO_4$ – CaO – H_2O, Zement Kalk Gips, Juin 1964, N° 6, 229–36.
4. STEIN H.N., Reacties van tricalciumaluminaat tijdens de cementharding : feiten en problemen, Klei en Keram, Nederl. 1974, N° 1 – 2, 10.
5. JAWED I., GOTO S. and KONDO R., Hydration of tetracalcium aluminoferrite in presence of lime and sulfates, CCR, Vol. 6, pp. 441–454, 1976.
6. STEINOUR H.H., "Setting of Portland Cement : A review of Theory, Performance and Control". Res. Lab., Portland Cement Assoc. Dept Bull. N. 98, 124 (1958).
7. STEIN H.N., Silicates Ind. 28 (3), 141–45 (1963).
8. COTTIN B., Hydratation et expansion des ciments. Ann. Chim. Fr., 1979, 4 pp. 139–144.
9. COLLEPARDI M., CORRADI M., BALDINI G., PAURI M., Meccanismo d'azione del gesso sull'idratazione dell'alluminato tricalcico. Il Cemento – 75ème Anniversario 169, 176.

High strength slag-alkaline cements

Ciments de laitier alcalin, à haute résistance

V.D. GLUKHOVSKY, Professor, Dr. Technical Sciences,
G.S. ROSTOVSKAJA, Cand. Technical Sciences,
G.V. RUMYNA, Cand. Technical Sciences, Institute of Civil Engineering, Kiev, U.R.S.S.

RESUME : Vers les années 50 de notre siècle, furent découvertes les propriétés liantes hydrauliques de composés chimiques contenant Li, Na, K, Rb, Cs ...; en 1960, leur mélange avec des produits hydrauliques entra dans la pratique courante de l'industrie de la construction; il s'agissait alors à la fois de métaux alcalins et alcalinoterreux.
C'est le cas des ciments de laitier alcalin, qui ont été étudiés et fabriqués, non seulement en U.R.S.S., mais aussi en Pologne et brevetés en R.D.A., en R.F.A., en Grande Bretagne, en France et au Japon.

Les ciments de laitier alcalin sont obtenus par broyage des laitiers granulés produits par la métallurgie et l'électrothermie des minerais phosphoreux, avec addition d'une solution d'un composé de métaux alcalins, de façon à produire la réaction alcaline.

Les produits de l'hydratation de ces ciments sont : la silice acide et des hydrosilicates de calcium à faible basicité du type hydronephelite, natrolite, paragonite et muscovite; ils ne contiennent pas de chaux libre, ni hydroaluminates, ni hydrosulfoaluminates, ni hydrosilicates de calcium à forte basicité.

La résistance de ces ciments varie de 400 à 1200 kg/cm2. En ce qui concerne leur résistance à la corrosion, ils surpassent les ciments résistant aux sulfates; en ce qui concerne la vitesse de durcissement, ils sont comparables aux ciments alumineux.

SUMMARY : In the fifties of our century hydraulic binding properties of the compounds of Li, Na, K, Rb, Cs, were discovered and in 1960 mixed hydraulic binding systems were put into practice in the construction industry; these consistinf of both alkali and alkaline-earth metals. Belonging to them are the slag-alkaline cements which are investigated and manufactured not only in the USSR but in Poland and are patented in the GDR, FRG, Great Britain, France and Japan.

The slag-alkaline cements are ground products of granulated metallurgical and electrothermophosphorous slags with solutions of alkaline metals compounds added to them and producing alkaline reaction.

The hydration products of the slag-alkaline cements comprise silicic acid, low-basicity calcium hydrosilicates, as well as alkaline hydroalumosilicates of the hydronephelite, natrolite, paragonite and muscovite group; they contain no free lime, hydroaluminates, hydrosulphoaluminates and high-basicity calcium hydrosilicates.

The strength of the slag-alkaline cements ranges from 400 to 1200 kgf/cm2. In corrosion stability they excel the sulfate-resisting cement and in speed of the strength reaching - high alumina cement.

According to the forecasts, special-purpose concretes Grades up to 4000 will be developed by 2000, while the concretes of Grades 1400 will become a common everyday occurence (1). Along this line of development it is proposed to increase concrete crack resistance and tensile strength; speed up strength growth; enhance abrasion- and frost resistance; reduce heat release during hydration; reduce permeability, etc.

The target set in this country is to considerably increase the production volume of high-strength cements by the 1980-ies and to get concretes Grades 600-1000 in volumes sufficient to meet the construction industry demands (2).

To solve these problems, the activity of the known cements has to be enhanced and new high-strength binding substances developed.

However, the research of many years in the field of enhancing the grades of the Portland cements, generalized in the publications of L.D.Yershov (3) and I.V.Kravchenko (4), shows that the possibilities of raising the activity of the system Portland cement - water are so far limited: neither the variations of mineralogical composition of the clinker, nor the increase of the specific cement surface right up to 900 m^2/kg do not allow to enhance its grade to a considerable degree. In all cases, when determined by GOST 310.4-76, it remains within the range 500-700. On account of that the highest grade of industrially produced cement to GOST 10178-76 is limited by 600.

Notwithstanding the fact that the Portland cement will, probably, remain the determining binding substance in the nearest discernable future, we set a task to develop new highly-active mineral binding substances which would substantially enhance the strength of concretes, their frost- and corrosion resistance, and other qualities, as well as to consideranly extent the raw materials basis of the fillers.

The essence of the idea of creating such binders consists in the exclusion from the cement composition of highly-basic minerals (C_3A, C_3S and C_4AF) whose hydration products either have no essential effect on the synthesis of cement stone strength (C_3AH_6, $CdOH_2$) or enhance its reaction capacity (C_3AH_6, C_4AH_{13}, C_2SH_2, $Ca(OH_2)$ and in the introduction instead of them of caustic alkalis ensuring hydration of alumosilicate substance of the cement.

To solve this problem helped the discovery in 1957 of hydraulic binding properties in the compounds of alkaline metals - the elements of the basic subgroup of the first group of D.I.Mendeleev's periodic system - Na, K and Li. As a result of this alkaline cements of the system R_2O-R_2O_3-SiO_2 (6,7) were obtained which served as a pre-requisite for the development of alkaline - alkaline-earth alumosilicate cements represented by the system of oxides R_2O-RO-R_2O_3-SiO_2, where: R_2O - oxides of alkaline metals Li_2O, Na_2O, K_2O; RO - oxides of alkaline-earth metals MgO, CaO, SrO; R_2O_3- amphoteric oxides Al_2O_3, Fe_2O_3, Cr_2O_3, etc.

A variety of these cements are the slag-alkaline nonhydraulic binding substances which are the products of ground granulated metallurgical or electrothermophosphorous slags mixed with solutions of the compounds of sodium and potassium alkali metals producing alkaline reaction (8, 9).

Caustic alkali ROH, nonsilicate salts of weak acids R_2CO_3, R_2SO_3, R_2S, RF, etc; silicate salts type R_2O (0.5-2.5) SiO_2, alumosilicate salts type $R_2OAl_2O_3$(7) can be used as alkali components of the slag-alkaline cements.

A distinguishing feature of these compounds as compared to similar calcic ones in their matchlessly great solubility. Therefore, the composition of substances participating in the process of condensing the slag-alkaline binding dispersions into a water-resisting stone differs from the composition of substances ensuring the synthesis of the water-resisting stone of calcium binders despite the fact that calcium oxide is present in the system.

By the composition of hydration products these cements can be described as a mixture of two hydraulic binding substances - alkaline alumosilicates and alkali-earth silicates.

Their hydration products are represented, mainly, by silicic acid, low-basic calcium hydrosilicates of the CSH(B) group with d=3.07; 2.71; 2.11; 1.82Å, as well as by alkaline hydroalumosilicates of hydronephelite type ($R_2OAl_2O_3 \cdot 2SiO_2 \cdot nH_2O$) with d=6.28; 3.66; 3.28; 2.80; 2.08Å; natrolite ($R_2OAl_2O_3 \cdot 3SiO_2 \cdot nH_2O$) with d=6.7; 4.10; 3.77; 2.82Å); analcite ($R_2OAl_2O_3 \cdot 4SiO_2 \cdot nH_2O$) with d=5.60; 3.45; 2.94; 2.09Å); muscovite and paragonite ($R_2O \cdot 3Al_2O_3 \cdot 6SiO_2 \cdot nH2O$) with d=4.39; 3.18; 2.52Å). Apart from these, encountered are gismondite ($CaOAl_2O_3 \cdot 2SiO_2 \cdot nH_2O$), hydrogarnets, and mixed sodium-calcic and potassium-calcic hydroalumosilicates. They contain none of the new formations, such as free lime, hydroalumosilicates, hydrosulphoaluminates and highly-basic calcium hydrosilicates characteristic of the Portland cement.

The solubility of low-basic calcium hydrosilicates is within the range of 0.035 to 0.05 g/l, whereas the solubility of alkaline hydroalumosilicates is still lower. All of them are less soluble and more chemically stable than the determining highly-basic, and, consequently, more reactive new formations characteristic of the Portland cement stone (highly-basic calcium hydroaluminates and hydrosilicates and free lime the solubility of which is 0.5 to 1.3 g/l).

The specific features of chemical and mineralogical composition, the structure and nature of the new formations render singu-

lar properties to the slag-alkaline binders owing to which the latter can be used as special cements.

So, the slag-alkaline cements are distinguished by high strength which, depending on the chemical nature of the alkaline component is within the range of from 400 to 1200 kgf/cm^2 when testing bar samples made of cement mortar of 1:3 ratio, the samples being fabricated and tested to GOST 310.4-76. As to their corrosion resistance in waters with low hydrocarbonate hardness, in sulphate, magnesian and in sea water these cements surpass not only the common one but the sulphate-resisting cement as well. They are distinguished by low heat release, this being explained by low hydration energy of alkali metal ions (K - 82, Na - 99 kcal (g-ion) as compared to alkaline-earth metals (Ca - 361 kcal(g-ion). This permits their use in the construction of heavy monolithic structures, such as dams. Their construction is 4 to 5 times lower than that in the Portland cement.

Slag-alkaline cements on the basis of low-modulus silicate salts (Mc = 0.5 - 1.5) are high-speed cements: by the rate of strength gathering, after three days of hardening, they surpass not only the high-speed Portland and slag-Portland cements but the alumina cement as well. Thus, at the age of 24 hours the strength of these cements is 350, at the age of two days - 550, at the age of 3 days it is 750 kgf/cm^2. Further on, unlike the alumina cement, the slag-alkaline cement continues to gather speed rapidly, so that by the 28th day it comprises 1000-1200 kgf/cm^2.

Since the freezing temperature of concentrated water solutions of alkali metal compounds is considerably far below zero, the slag-alkaline cements can be used in winter concreting.

According to data of S.P.Mukhamedhalejeva, the slag-alkaline concretes are used to their best advantage in structures used under cold-temperature conditions. This is due to the fact that, unlike the water-satu rated Portland cement stone, in freezing of water-saturated slag-alkaline stone to minus 15 - minus 20°C there is no spasmodic expansion of the substance filling the pores as a result of sudden freezing of the undercooled water. The cooling of a slag-alkaline stone right down to minus 30°C causes none whatsoever freezing destruction, this being explained by its porous structure (with the gellous pores prevailing), by the porous space containing alkali in the form of true solution whose freezing temperature is considerably below the freezing temperature of water and by gradual freezing-out of ice from the solution. Frost destruction of the slag-alkaline stone occurs, mainly, at the cooling down to minus 40°C and below. That, in particular, explains also the high frost-resistance of concretes on the slag-alkaline cement basis, the resistance exceeding 1000 cycles. The slag-alkaline cements are also resistant to high temperatures, this permitting their use in the production of heat-resistant concretes.

Even the inferior-grade slag-alkaline cements, such as grade 400, enable to obtain concretes of grade 500-700, whereas for the traditional concretes of the same grades Portland cement of grades 500-600 is required. The cements of grades 1000-1200 can be employed for production of concrete grades 1000-1200, i.e. of concretes whose production, by the American predictions, is planned only by the year 2000.

The slag-alkaline cements extend the raw material basis of high-strength concretes, because they do not require the concentration of aggregates, permit the exclusion of coarse aggregates and the use of fine sands and sandy loams as fine aggregates. This is explained by the interaction of caustic alkalis springing up in the process of cement hydration with the aggregate agrillaceous minerals enveloping the particles of sandy and dust-like fractions, this resulting in the formation of unsoluble alkaline hydroalumosilicates. The latter, along with the products of slag-alkaline cement hydration, are partially cementing the sandy particles of the aggregate and completely the dust-like particles.

The pilot-plant production of the slag-alkaline cements and concretes on their basis was started in 1960, and their industrial production, in 1964.

By joint collaboration with the Scientific Research Institute of Cement, The Scientific Research Institute of Reinforced Concrete and other leading research and educational institutions of the country the standardization of the activity and other properties of the industrially-produced slag-alkaline cements was carried out (9) in 1977-1979.

Thus, high-strength cements grade 1000-1250 were obtained at plants producing and utilizing slag-alkaline cements in the cities of Perm, Tula, Krivoj Rog, Alma-Ata and Tashkent. The results of determining the activity of industrially-produced slag-alkaline cements based on various types of slags and alkali components are generalized and presented in a Table below.

Table

Activity of slag-alkaline cements, depending on slag basicity and chemical nature of alkaline component

Slag type	Ultimate strength, kgf/cm^2, when used as alkaline components			
	soda ash	soda-alkaline melt	sodium disilicate	sodium metasilicate
Basic	450/65	500/70	1000/90	950/60
Neutral	400/60	600/90	900/90	1250/128
Acid	380/60	600/90	800/90	1050/120
Thermophosphorous (basic)	500/65	550/85	1000/85	1150/130

Note: over-the-line figure - compression strength
under-the-line figure - bending strength.

These cements are used for the production of concrete grades 1000-1600 distinguished by high watertightness, high density, corrosion-, heat-, and frost resistance.

There can be no doubt that the new possibilities opened by the slag-alkaline cement in the field of the synthesis of artificial building conglomerates will, in due time, exclude the use of blast-furnace, electrothermophosphorous and the like slags for the production of low-grade slag Portland cements, Portland cement clinker, various aggregates, etc. But even now these cements command sufficiently broad raw material resources. It can be supplied by that amount of blast-furnace, electrothermophosphorous and other types of slag produced by the industry at the present time.

Thus, the analysis of the condition of the slag raw material resources in the USSR indicates that, even with the slag Portland cement production volume left unchanged, the amount of slag which could be used for the production of slag-alkaline cements would comprise over 45 mill. t (10). Organized production of slag-alkaline cements from the mentioned amount of slags will essentially increase the resources of constructional binding substances.

A considerable production volume of various slags is also noted in other countries. So, according to the figures of 1970-1973, the annual output only of blast-furnace slags comprised: in the USA - 22.8; Japan - 28.0; France - 14.1; FRG - 13.8; Great Britain - 11 mill. t (10).

Undoubtedly, the most efficient field of slag utilization is their use in cement production.

The raw material resources of the alkaline components can be presented by the following substances:

a) commercial products: soda, potash, sodium fluoride produced by the chemical industry, and soluble alkaline silicates (sodium silicate solutions with silicate modulus 0.5 to 2.5);

b) side products: alkali melts, soda-alkaline melt, sodium metasilicate, etc.;

c) natural soda.

Sodium sulphate and sodium chloride serve as raw materials for the production of alkaline components, the resources of the former being practically unlimited.

Considering that the slag-alkaline cements are distinguished by a number of specific properties, they find their most expedient application in jobs on the level with the high-strength, high-speed and sulphate-resisting Portland cements, as in many cases instead of the alumina cement.

In the USSR a fifteen to twenty year experience has been accumulated in the production and service of concrete structures based on such cements which confirmed their high technological properties and service reliability.

Beginning with 1972 the slag-alkaline cements are studied and at present are produced in Poland. The results obtained in the studies and adoption of these materials in the building industry by the scientists of the Krakow Mining and Metallurgical Academy under the guidance of the Member of the Academy E.Grzymek are indicative of their efficiency (11).

In addition to that, building materials on the basis of slags and alkaline components are being developed from 1972 in other countries as well, this being confirmed by patents published in the GDR, FRG, Great Britain, France and Japan.

The above facts signify that the application of new cements containing the compounds of alkali and alkali-earth metals in the building industry is successfully expanding.

Their use in the Soviet Union made it possible to double the grade of construction cements and concretes, as well as to extend the range of aggregates, in particular the use of barkhan sands.

The economic efficiency of slag-alkaline cements is obtained through the utilization of industrial by-products, as well as due to high strength and long service life of structures made on their basis.

In addition, their efficiency rises when the grey iron and slag are produced in a combined process: as usual, molten iron and slag are poured out of the blast furnace. The slag is first granulated, then ground with simultaneous drying in air-pressure mills. Steam released from the blast furnaces can serve as heat source for slag drying and for operation of the air-pressure mills. In this case the grey iron and ground slag are produced simultaneously. The capital investment per 1 t of ground slag should not exceed 5-10 roubles. For the binder an alkaline component, such as sodium silicate, is also necessary. Its consumption comprises 5 to 8%, i.e. about 65 kg per one ton of slag. Thus, the capital investment for the alkaline component will comprise 50x0.005=3.25 roubles per one ton of binder, the total being 10·0.935+ +3.25=12 to 13 roubles. The capital investment per one ton of Portland cement is 40 roubles.

CONCLUSIONS

1. Hydraulic binding substances, - slag-alkaline cements grade 400-1200, have been developed and adopted in the industry. They are distinguished by high corrosion resistance, surpass the alumina cement by the rate of strength gathering, exhibit high density and low heat release. These properties predetermine their expedient use in special types of construction.

2. Slag-alkaline cements were introduced into construction practice in the USSR (1960) and in Poland (1974). An experience of many years (15 to 20 years) has been accumulated in the USSR in the production and operation of concrete structures based on such cements, confirming their high technological properties and operational reliability.

3. The raw material resources for these cements are provided by blast-furnace, electrothermophosphorous and other types of metallurgical slags combined with alkali-containing products both basic (soda, potash, sodium silicate solutions, etc.) and industrial by-products (soda-alkaline melt, soda melt, sodium metasilicate, etc.)

4. The net cost of slag-alkaline cements is lower than that of the Portland cements. Their economic efficiency is obtained by the utilization of inexpensive industrial by-products as well as due to the high strength and long service life of the structures.

REFERENCES

1. Journal of the American Concrete Institute (1971), August, No.8, vol.68, pp. 581-589.

2. УШ Всесоюзная конференция по бетону и железобетону.Тезисы докладов.М., 1977, "Стройиздат", стр.3-27.

3. Ершов Л.Д. /1975/. Высокопрочные быстротвердеющие портландцементы, К., "Будівельник".

4. Кравченко И.В. /1976/. Быстротвердеющие и высокопрочные портландцементы".Материалы УІ международного конгресса по химии цемента, М., т.3,стр.6-20.

5. Глуховский В.Д. /1959/. Грунтосиликаты, К.,Госстройиздат,стр.58-110.

6. Глуховский В.Д. /1967/. ГрунтосилІкатнІ вироби І конструкцІІ. К.,"БудІвельник", стр.36-58, стр.82-93.

7. Глуховский В.Д.,Пахомов В.А. /1978/. Шлакощелочные цементы и бетоны. К., "БудІвельник",стр.23-77.

8. Глуховский В.Д. /1976/. Материалы УІ Международного конгресса по химии цемента, М., т.3, стр.345-346.

9. Глуховский В.Д. /1979/. Щелочные и щелочно-щелочноземельные гидравлические вяжущие и бетоны. К., "Вища школа", стр. 50-118, 180-220.

10. Романенко А.Г. /1977/. Металлургические шлаки.М.,"Металлургия", стр.5-18.

Structure et propriétés de l'alynite et du ciment d'alynite

Structure and properties of alinite and alinite cements

B. NOUDELMAN, Professeur, Docteur ès Sciences,
M. BIKBAOU, Candidat ès Sciences,
A. SVENTSITSKI, Candidat ès Sciences, Institut des Recherches Scientifiques et des Projets des Matériaux de Construction de Tachkent et
V. ILUKHINE, Docteur ès Sciences, Institut de Cristallographie de l'Académie des Sciences de l'U.R.S.S.

RESUME : L'alynite, silicate tricalcique nouveau, est la phase minérale principale des ciments obtenus à partir des matières premières traditionnelles, avec addition de chlorure de calcium, d'après la technologie du sel élaborée en U.R.S.S.

L'analyse de la structure cristalline du minéral a démontré que la particularité distinctive principale de la constitution de l'alynite est la position des atomes de chlore dans une structure ferme, composée de huit cations de calcium, ce qui conditionne les propriétés spécifiques du silicate tricalcique avec des anions de O - Cl mélangés.

L'étude des particularités de la structure et des propriétés de l'alynite a permis d'établir qu'il existe au moins quatre modifications allotropiques du minéral - γ, β, α' et α ; avec cela, les formes de haute température sont caractérisées par le système cubique.

Le minéral est caractérisé par un nombre considérable de défauts de cristallisation sous forme de vacances d'oxygène et de ses associations. La haute symétrie du réseau cristallin du minéral se trouve en corrélation avec la capacité du minéral à contenir un grand nombre d'éléments; par rapport à l'alite, l'alynite dissout de 1,5-2,0 fois d'éléments modifiants de Al, de Fe, de Mg, etc.

La présence des atomes de Cl dans la structure de l'alynite assure des avantages importants à ces ciments par rapport au ciment portland connu : températures de formation plus basses (1000-1100°C), facilité de cristallisation dirigée, haut degré de solubilité des éléments additifs et modifiants, faible résistance au broyage, haute capacité d'hydratation.

Des ciments d'alynite sont caractérisés par la solidité et l'activité assez hautes, la pierre de ciment à sa base est caractérisée par une morphologie spécifique des formations hydratées.

Les particularités de la constitution et des propriétés de l'alynite déterminent les perspectives de la création des ciments nouveaux qui permettront de réduire les frais d'énergie pour la cuisson du clinker; leurs qualités techniques seront améliorées.

SUMMARY : Alinite - the new highly-based calcium silicate - is the main mineral phase of cement clinker which are produced from the traditional raw materials with addition of calcium chloride by the new salt technology, being developed in the USSR. The analysis of crystallographic structure of the mineral has shown, that the main feature of alinite is the peculiar position of chlorine atoms surrounded by eight calcium atoms which is stipulated by the specific properties of the new silicate with mixed "O-Cl" anions.

The existance of at least four modifications of alinite - $\gamma, \beta, \alpha', \alpha$ has been established, and high-temperature forms have cubic syngonia. As for alinite, the mineral is characterized by a considerable number of defective centers, namely, oxygen vacancies and their associations with other atom vacancies. High crystallographic symmetry of alinite correlates with its ability to dissolved considerable number modifying elements - Al, Fe, Mg etc. in 1,5-2 times more than the known alite.

The presence of chlorine atoms in the structure of alinite calls forth a number of advantages of alinite cements in comparison with the portland cement - lower formation temperatures (1000-1100°C) and easier realization of directed crystallisation, the higher grade of grindability and dissolution of mixed and modifying elements, and high ability of interaction with water.

Alinite cements are notable for great activity and strength. Alinite cements stones are characterized by specific morphology of hydrated new formations.

The peculiarities of structure and properties of alinite determine the possibilities of creating new cements on the basis of alinite with less power consumption (energy) and with better construction properties.

L'un des constituants les plus importants du clinker de ciment, obtenu d'après la technologie de basse température (technologie de sel) est l'alynite, silicate de calcium nouveau(2). Ce compose cristallise en système quadratique, le groupe de Feudoroff est = I $\bar{4}$2m. Une cellule elementaire avec des paramètres a = IO.47I; c=8.6I4Å contient neuf atomes indépendants - trois Ca, un Si, quatre O et un Cl. Le comptage des multiplicités des positions cristallographiques aboutit à la formule chimique de l'alynite: $Ca_{11}(Si,Al)_4O_{18}Cl$ avec z = 2.

D'ici la densité calculée = 3.10 g/cm^3, tandis que sa valeur expérimentale-3.075g/cm^3. Selon les données de l'analyse structurale aux rayons X, de grands cations de Ca sont disposés dans trois positions cristallographiques différentes et leur entourage est différent. Ca_2 (dans un point particulier sur l'axe 4) se trouve au centre d'un cube suffisamment correct avec des distances Ca-O = 2.5II-2.52I Å et des arêtes O-O=2.646-3.025 (l'excentricité du cube = 1.14).

Ca_3 se trouve aussi dans une position particulière sur l'axe $\bar{4}$ dans une face latérale, octaèdre aplati avec des distances equatorielle Ca-O=2.432Å et méridionale (le long de l'axe $\bar{4}$) = 2.154Å. Enfin, Ca_1 se trouve en position générale et a six anions voisins: cinq atomes de O (Ca-O=2.270-2.529) et un atome de Cl éloigné à 3.271 Å. Le polyèdre de coordination pour Ca_1 est un octaedre, mais le Ca fortement modifié est déplacé du plan equatoriel vers la moitié "d'oxygène" de l'octaèdre. Le cation de Si(Al) plus petit est localise dans un tétraèdre standard avec Si - O = I.629 - I.666 Å.

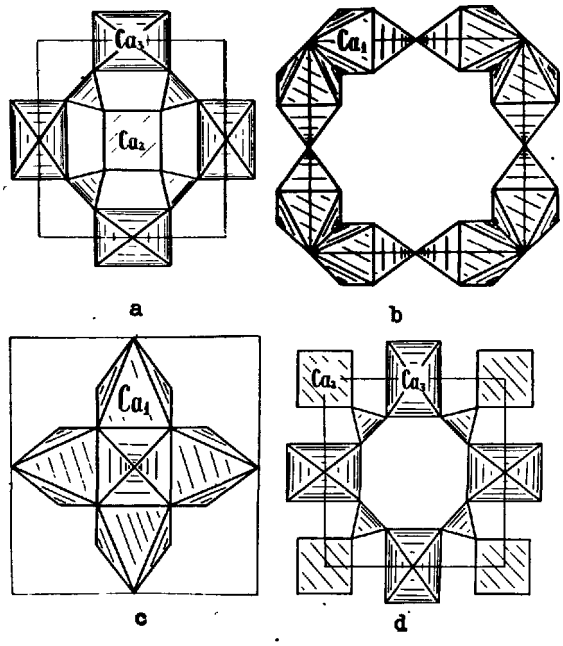

Fig.I. Couches caractéristiques de la structure cristalline de l'alynite. Les polyèdres de calcium avec les atomes de calcium dans les positions cristallographiques différentes sont représentés shématiquement.

Il est commode de représenter la structure cristalline de l'alynite composée des couches plates parallèles au plan x O$_y$ et alternant le long de [00I] Ces couches sont au nombre de six par cellule dont quatre sont représentees sur la fig. I-a-d dans l'ordre de leur alternance. Le caractère de la jonction des chouches en carcasse tridimensionnelle est illustré par la fig.2 représentant l'axonométrie de la moitié de la cellule élémentaire en polyèdres; les couches sont écartées l'une de l'autre le long de l'axe c, pour que la figure soit plus claire.

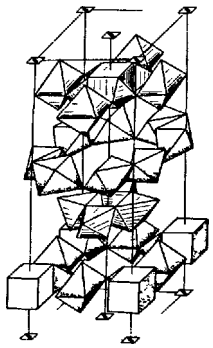

Fig.2. L'axonométrie I/2 d'une cellule élémentaire de l'alynite. La suite des couches (de haut en bas) correspond a a-d sur la fig.I.

Si à l'intérieur de la couche les polyèdres sont liés par les sommets et les arêtes, les couches elles-mêmes se trouvent liées par les arêtes et les faces des Ca-octaèdres. On peut le voir d'une façon claire sur la fig.3 qui représente la section de la structure de l'alynite à la hauteur de y = 0.

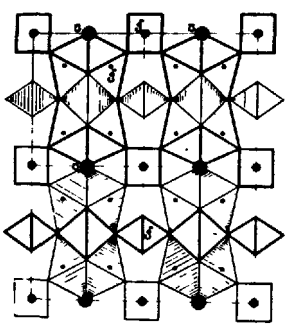

Fig.3. Section d'une cellule d'alynite, y=0. La couche des polyèdres de Ca est représentée.

Chaque atome de chlore attire vers lui huit Ca-octaèdres qui se lient en couples par les faces et forment un claster tétragonal symétrique autour de l'axe de quatrième ordre. Les groupes de claster sont liés le long le l'axe C par les Ca_2-cubes en formant une colonne dont la section longitudinale est representee sur la fig.4.

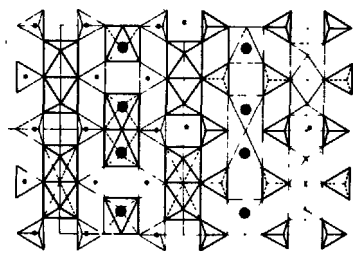

Fig.4. Section d'une cellule d'alynite, y = I/4. Représentation des canaux avec les tetraèdres de SiO_4.

De l'autre côté, chaque couple de Ca_I-octaèdres se repose sur les arêtes d'un Ca_3-octaedre (fig.3) qui, de cette façon, formé un élément de liaison entre les groupements de Ca_I, identiques en translation le long de l'axe a (b). Il faut noter que la distance Ca Ca_I-Ca_3 est de l'ordre de 3 Å. De cette façon les groupements de Ca_I liés par les Ca_3-octaèdres, forment un clàster infini à des noyaux multiples ayant la forme d'un réseau carre avec une épaisseur = c/2.

Ces réseaux identiques en translation le l long de c sont liés par les Ca_3-cubes et par les sommets des Ca_I- et des Ca_3-octaèdres. Une famille des réseaux est liée avec une translation initiale I. Ces deux familles se croisent mutuellement et forment une carcasse tridimensionnelle très dense avec des canaux etroits le long de [001], ou les tétraèdres sont disposés par c/2.

De cette façon, la particularité caractéristique de la structure cristalline de l'alynite est la position des atomes de Cl dans l la fermeture constituée par huit atomes de calcium ce qui conditionne le caractere specifique de cette formation ainsi que l'originalité des propriétés du silicate nouveau avec des anions de O-Cl melanges; des materiaux contenant ce silicate ont, eux aussi, des propriétés originales.

Cette particularité de la constitution du minéral a été brevetée en URSS en tant que la découverte n° 2I0(3); elle conditionne la présence dans ce minéral des complexes avec des liaisons hétérodesmiques des cations dans les fragments O-Ca-Cl ainsi que le caractère specifique du minéral et des ciments qui le contiennent. Le spectre de l'absorption infrarouge de l'alynite (Bekman, KBr) est représenté par les oscillations valentes et asymétriques des groupes de SiO_4 et de AlO_4 (tabl.I).

Les bandes de l'absorption avec des fréquences de 560-400 cm^{-1} et se rapportent aux oscillations de déformation des complexes de SiO_4 au-dessous de 350 cm^{-1} elles sont mélangées avec des bandes des oscillations de deformation des tetraèdres de AlO_4. Les bandes de l'absorption à 730 et 760 cm^{-1} se rapportent aux oscillations valentes des groupes de AlO_4 dont la présence temoigne que les atomes de silicium dans l'alynite sont remplacés par les atomes de l'aluminium; ceci se trouve en accord avec les donnees de l'analyse structurale.

La valeur de la séparation des oscillations valentes asymétriques ($\Delta\nu_{as}$ = 40 cm^{-1}) et l'intensité relative ν_s des oscillations (~ 0.6I) témoignent la présence d'une deformation insignifiante des groupes de SiO_4 dans l'alynite. Un nombre considérable de bandes est observé dans le domaine des spectres des ondes longues ; il est difficile de les identifier. Ce domaine est caracterisé par les oscillations des anions SiO_4 et par celles de déformation des tetraèdres de AlO_4.

Les spectres ESR de l'alynite ont été obtenus sur les poudres des cristaux à l'aide du radiospectromètre RE-I30I fonctionnant dans l'étendue de 3 cm; à 298 et 77°K l'irradiation des cristaux du minéral a été effectuée à l'aide de l'appareil PXM - γ - 20, avec une dose de $I0^{19}$ roentgens.

Le spectre ESR de l'alynite irradié différe de celui de l'alite (4) par des lignes de l'absorption intense dans le domaine g=2.0I-2.04; de telles lignes caractérisent généralement des centres perfores formés sur les propres défauts de reseau cristallin du minéral. Aux températures habituelles, la concentration totale des centres paramagnetiques formes sur les defaunts du réseau des cristaux de l'alynite est ~ $I0^{19}$ spin/g ce qui dépasse sensiblement celle de l'alite pour la même dose de l'irradiation.

Un recuit consécutif du minéral irradié à 20 - 300°C avec l'enregistrement des spectres ESR nous a permis de déterminer les centres perfores caractéristiques pour Al occupant les positions dans les tetraèdres de AlO_4. Des centres analogiques ont été décrits pour l'alite. Le spectre ESR de l'alynite irradié et cuit à I80°C contient des

Tableau I. Identification des bandes d'absorption infrarouge de l'alynite

Classification des bandes d'absorption															
Bandes valentes							Bandes de deformation								
SiO_4				AlO_4			SiO_4		SiO_4 (δ_s) et AlO_4(δ_{as}, δ_s)						
ν_{as}			ν_s	ν_{as}			δ_{as}								
936	928	918	837	760	730		560	500	385	370	353	333	324	309	
902	896						430	398	295	28I	270	250	23I	22I	208

lignes avec $g_\perp = 2.0161$ et $g_\parallel = 2.0024$ ($A = 7,4$G). La cuisson à 195°C permet de découvrir dans l'alynite des centres perforés dans la sphère même de coordination des atomes du chlore; le spectre ESR de ces centres découvre des lignes à quatre composantes avec $g = 2.0081$ et $A = 4,0$ G (fig.5).

Fig.5. Spectre ESR de l'alynite irradié. Le recuit a 195°C, 10 min.

La structure extrafine des lignes d'absorption s'explique par l'interaction des trous avec le noyau de Cl^{35} (I=3/2, contenu naturel est 75,4%). Il est probable que la nature des centres perforés s'explique par la présence d'une quantité considérable d'aluminium (4% de la masse du minéral calculée à partir de Al_2O_3), ainsi que par une certaine friabilité du réseau cristallin du minéral dûe à la présence d'une grande quantité des places vacantes dans le réseau.

L'alynite constitue 60-80% de la masse du clinker; la composition chimique de l'alynite dans le clinker varie dans les limites proches, en fonction de la quantité des éléments alliants de Al, de Fe, de Mg, de Cl et d'autres contenus dans les matières premières. L'alynite dans le clinker cristallise sous forme des prismes, des plaques hexagonales, des aiguilles qui sont le plus souvent les débris et les cristaux défigures avec le faciès d'octaèdre quadratique.

Les dimensions des cristaux de l'alynite dans les clinkers différents peuvent varier dans les limites assez larges - à partier des portions d'une micron jusqu'aux centaines de microns. La microscopie optique permet d'observer la structure fine, moyenne et à gros grains des clinkers d'alynite. Et avec cela, dans tous les cas la cristallisation de l'alynite est assez distincte, à la surface des cristaux il y a des hachures, quelquefois on observe des macles polysynthetiques. Les études au microscope électronique permettent de déterminer d'une façon nette le caractère de la cristallisation de l'alynite dans le clinker (fig.6).

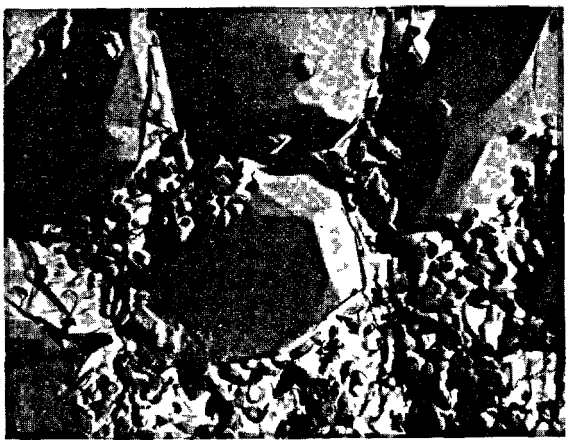

Fig.6. Cristaux de l'alynite dans le clinker. Répliques de charbon atténuees de platine, x 4000.

Le coefficient de réfraction des cristaux de l'alynite N = 1.709±0.001. En fonction de la nature et de la quantité des éléments alliants le coefficient de réfraction des cristaux de l'alynite peut s'élever à 1.714-1.715. Nous avons effectué une étude de la solubilite des éléments alliants sur l'alynite polycristallin dans lequel nous avons introduit de différentes concentrations des oxydes de Al, Fe, Mg, Ba, K, Na, P, et B. La cuisson de l'alynite avec les admixtions indiquées et l'analyse des phases des produits de la cuisson effectuée à l'aide de la diffractometrie aux rayons X nous ont permis de déterminer les valeurs suivantes des limites de la solubilité des éléments alliants dans l'alynite (% de la masse du minéral): Al_2O_3 - 4.5; Fe_2O_3 - 3.0, MgO - 3.0, BaO - 2.5, K_2O, Na_2O - moins de 0.5, P_2O_5, B_2O_3 - 1.0

Les valeurs indiquées peuvent varier dans les limites ± 10%; en cas de la présence complexe des éléments dans les produits de la cuisson on y observe jusqu'à ± 20% de la valeur absolue.

La contenance considerable des éléments dans le réseau cristallin de l'alynite liee à la haute symétrie de la structure et de sa "friabilité", explique les oscillations de la température de la fusion. En fonction de la composition chimique et de la quantité des admixtions alliantes la température de la fusion de l'alynite varie dans les limites de 1420 - 1490°C. La limite supérieure correspond à l'alynite avec un minimum d'impuretes. Le poids spécifique de l'alynite = 3.075 g/cm³; il peut aussi varier d'une facon insignifiante en fonction de la nature et de la quantité des éléments alliants.

Nous avons également effectué des études de l'alynite à basses temperatures qui representent un grand intérêt pour l'étude de la chimie physique de l'alynite. Ces études ont été effectuées la méthode de l'analyse structurale aux rayons X a l'aide du diffractomètre DRON-I muni d'un dispositif d'étu-

de à haute température aux rayons X GPVT - I500. L'échantillon étudié contenait des monocristaux de l'alynite de dimension de 3 mm émiettés jusqu'aux dimensions de 50 microns. L'analyse des changements du tableau de diffraction à l'élevation de la température a permis de faire ressortir 4 séries principales de diffractions à intensite variable synchronisée.

Nous avons découvert la convertibilité des processus en cas du réchauffement ou refroidissement de l'alynite ce qui permet de considérer toutes les quatre séries en tant que les modifications polymorphes: 3 séries de refractions des formes de haute température, à savoir: β, α' et α ont été determinées dans le cadre de la symetrie cubique (voir le tableau 2).

Tableau 2

Donnees de la diffractométrie aux rayons X des modifications de l'alynite

L'alynite a la température du milieu extérieur (γ)			I050°C (β)			II90°C (α')			II90°C (α)		
Cellule tétragonale à capacités centrées a = I0.47I4 ± 0.00I9 Å.			Cellule cubique à faces centrées a=7.865±0.009 Å.			Cellule cubique à capacités centrées a = II.82±0.02 Å.			Cellule cubique à faces centrées a = 8.060 ± 0.005 Å.		
hkl	d	I	hkl	d	I	hkl	d	I	hkl	d	I
03I	3.235	22	III	4.54	22	2II	4.82	44	III	4.65	22
222	2.808	I00	200	3.93	27	222	3.4I	2	200	4.03	32
040	2.6I8	26	220	2.784	I00	32I	3.I54	I00	220	2.850	I00
I4I	2.436	9	3II	2.370	I2	330	2.782	40	3II	2.430	9
240	2.342	5	222	2.272	5	420	2.647	I8	222	2.326	2
042	2.237	4	400	I.966	38	422	2.4I4	6	400	2.0I5	34
033	2.2I8	I0	33I	I.802	4	43I	2.322	9	33I	I.850	7
004	2.I54	20	420	I.758	7	440	2.086	9	420	I.802	I4
5I0	2.054	5	422	I.607	23	530	2.026	4	422	I.646	42
34I	2.035	5	5II	I.5I2	4	600	I.97I	25	5II	I.552	6
I43	I.903	8	440	I.39I	7	6II	I.9I8	2	440	I.425	7
440	I.85I	I9				620	I.87I	9			
350	I.796	2				63I	I.743	3			
600	I.745	5				550	I.670	4			
053	I.692	I2				552	I.6I0	4			
352	I.658	I2				642	I.580	9			
253	I.6I0	I0									
035	I.545	I5									
07I	I.474	6									

Le clinker d'alynite utilisé pour la production du ciment contient, d'habitude, de 60 a 75% d'alynite. Pour la production du ciment a durcissement rapide et du superciment on utilise le clinker contenant jusqu'à 80 % d'alynite. Le reste de la masse du clinker contient l'orthosilicate, L'aluminate et le ferrite de la chlorure de calcium. La proportion de ces phases n'est pas strictement limitée; elle est déterminee par le choix des matières et la destination du clinker produit.

La haute activité d'hydratation des ciments d'alynite s'explique par les particularités de la structure de l'alynite (Présence des atomes "actifs" de Cl dans un motif structural original du réseau cristallin du silicate nouveau, un grand nombre des défauts du réseau cristallin), par la composition de la phase liquide de la solution de ciment (faible contenu d'alcalis, présence de Cl, concentration élevee de Ca), par la composition et la structure des nouvelles formations hydratées (formation sur la surface de l'alynite d'une enveloppe hydratée metastable, permeable et relativement bien cristallisée). Les particularites indiquées assurent une hydratation intense et le durcissement des ciments d'alynite aux températures normale et au-dessous de zero (jusqu'à -5°C), ainsi qu'au traitement thermique et humide.

Puisque le clinker d'alynite a une haute porosité et une haute capacité de broyage, il est possible d'utiliser ces qualités pour intensifier l'hydratation et le durcissement des ciments en augmentant la finesse de broyage. Ainsi, par exemple, quand la surface spécifique du ciment portland est 3000cm^2/g et celle du ciment d'alynite 4500cm^2/g, les consommations spécifiques d'énergie électrique sont identiques et font environ 30kwh/t.

Il faut souligner qu'à la différence du ciment portland, une telle augmentation de la surface specifique du ciment d'alynite n'exige pas une quantité d'eau plus grande, mais, par contre, moins grande. Les valeurs minimales de la quantité d'eau nécessaire eau/cim = 0.225-0.235 caractérisent les ciments d'alynite a surface specifique 4500 ± 200 cm^2/g.

Le sulfate de calcium introduit sous forme de calcium de gypse, de phosphogypse ou de borogypse est une composante obligatoire du

ciment d'alynite. Mais il ne joue pas le role de ralentisseur de la prise comme dans le cas du ciment portland;par contre c'est un intensificateur du durcissement.

Le contenu optimal de gypse dans le clinker d'alynite variant dans les limites 2-3,5% (calculées pour SO_3) assure une augmentation de l'activité du ciment sans additions de I.5-2.5 fois ce qui depasse la vitesse moyenne de l'hydratation de l'alite de I.5-2.5 fois. L'hydratation rapide de l'alynite et l'apport constructif de la phase d'aluminate assurent un durcissement rapide du c ciment d'alynite dans le bas âge. En fonction du degré de dispersion du ciment la resistance des échantillons à l'âge de 24 heures est égale à 5-8% de l'activite de marque du ciment.

Le processus de la formation de la structure de la pierre de ciment ne cesse pas après la fin de l'hydratation de l'alynite (voir la fig.7 a).

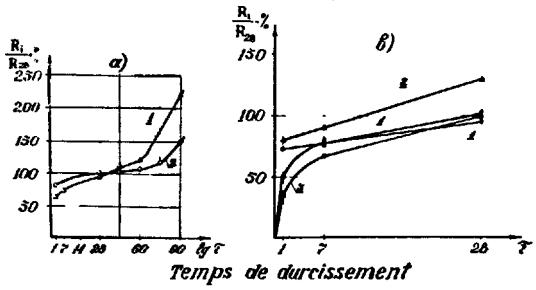

Fig.7. Cynetique du durcissement des ciments d'alynite (a) et des bétons (b):

a) - I - ciment à S_{sp}= 3600cm^2/g et le contenu de l'alynite à 60%; 2 - ciment à S_{sp}= 4080cm^2/g et le contenu de l'alynite à 75%.

b) - I - de ciment d'alynite à durcissement normal;
- 2 - de même après le traitement à la vapeur;
- 3 - de ciment portland à durcissement normal;
- 4 - de même après le traitement à la vapeur.

Nous croyons que ce phenomène s'explique par la recristallisation des hydrosilicates primaires du type C_2SH_2 en hydrosilicates secondaires du type CSH. Ce processus est suivi de la cristallisation de $Ca(OH)_2$, de l'augmentation du degré de polymérisation des hydrosilicates des déformations de retrait, de la reduction du contenu d'eau de cristallisation et de l'augmentation du contenu de l'hydrosilicate.

Nous supposons la possibilité de la formation des hydrosilicates de la chlorure de calcium au cours de l'hydratation et du durcissement de l'alynite, dont témoigne la morphologie originale des formations nouvelles cristallisant sous forme de pétales et de plaques très fines. Le contenu des ions libres de Cl dans la pierre de ciment de l'âge different ne dépasse pas 0.6% de la masse. A l'âge plus mûr ce contenu varie généralement dans les limites de 0.3-0.4%.

La perméabilité de la pierre de ciment d'alynite est de 5-I0 fois inferieure à celle du ciment portland ce qui est lié aux différences dans leurs monostructures. Cette propriété assure une haute stabilite d'exploitation du béton d'alynite armé.Les bétons à la base du ciment d'alynite découvrent une résistance de 20-30% supérieure a celle des bétons à la base du ciment portland pour les dépenses identiques du ciment.

Un grand avantage des bétons à la base du ciment d'alynite traités à la vapeur est l'accroissement intense de leur résistance dans le processus du durcissement ulterieur dans les conditions normales (voir la fig. 7,b). A l'âge de 28 jours, cela assure un accroissement de la résistance des échantillons traités à la vapeur de I5-25% par rapport aux echantillons à durcissement normal.

Ces recherches ont contribué à obtenir des ciments de haute resistance et des bétons des marques 600-700.

CONCLUSIONS: La distinction principale de la constitution de l'alynite, nouveau silicate tricalcique de calcium contenant le chlore, est la présence des atomes du chlore dans les noeuds du réseau cristallin du minéral dans un complexe structural original sous forme d'un atome de Cl entoure de huit atomes de calcium.

Le caractère decrit de la présence du chlore dans la structure conditionne les propriétés spécifiques de l'alynite - formation aux températures I000-II00°C, haute symétrie des réseaux cristallins de ses modifications, haut degré de solubilités des elements modificants,faible résistance au broyage, haute capacité d'hydratation, morphologie originale des formations hydratées nouvelles.

Les qualités découvertes de l'alynite et des ciments à sa base permettent de considerer ce liant nouveau en tant qu'un concurrent sérieux du ciment portland traditionnel.

BIBLIOGRAPHIE

I. B.NOUDELMAN (I976) VI Congres international sur la chimie du ciment "Clinkerisation dans la fusion de sel de la chlorure de calcium", tome I, pp.2I7-22I (russe).

2. V.ILUKHINE, N.NEVSKY, M.BIKBAOU et R.HOWIE (I977).Nature,"Crystal structure of alinite", v.269, n 5627, pp.397-398, english.

3. Bulletin des découvertes et des inventions (I979),diplôme n°2I0,n°22, p.3 (russe).

4. M.BIKBAOU, Y.BOUTTE, V.TIMACHEV (I976) Nouvelles des écoles supérieures secondaires.La chimie et la technologie chimique. "L'étude du silicate tricalcique par la méthode de la spectroscopie". XVIII, v.6, pp. 936-966 (russe).

Comportement de divers phosphates avec des constituants des ciments

Behaviour of various phosphates with contituents of cements

P. BARRET, Professeur à l'Université de Dijon, Directeur du Laboratoire de Recherches sur la Réactivité des Solides (L.A. 23),
C. BENES, Maître-ès-Sciences, (L.A. 23),
D. BERTRANDIE, Docteur de l'Université de Dijon, CNRS (L.A. 23),
J. MOISSET, Directeur Recherche et Développement Technique de la Société Lafarge, France.

RESUME : Le problème de l'adjonction de phosphates alcalins dans certains ciments alumineux (SECAR 71) se pose pour diverses applications. Dans ce travail, les interactions possibles sont étudiées d'un point de vue fondamental, d'une part dans le domaine basse température (à l'ambiante et entre 0 et 100°C), d'autre part entre 100 et 1000°C. Dans le domaine basse température, l'influence de 5 % en poids d'hexacyclophosphate de sodium commercial sur l'évolution du SECAR agité dans l'eau est déterminée, ainsi que sur l'évolution d'un tel mélange gâché en pâte. Par la mise en œuvre de divers moyens analytiques et calorimétriques, il a été établi que la prise phosphatique a lieu dans la période initiale et qu'elle fait avancer la prise hydraulique de plusieurs heures bien que les ions sodium libérés maintiennent un taux élevé d'alumine en solution.

Dans le domaine (100 - 1000°C), les transformations subies par différents types de phosphates de sodium : dihydrogénomonophosphate, hexacyclophosphate, sont systématiquement suivies à partir d'échantillons soit secs, soit gâchés avec de l'eau. Dans ces deux cas (à sec ou en présence d'eau), des essais analogues sont effectués comparativement sur des mélanges des mêmes phosphates avec différents oxydes : CaO, Al_2O_3 et avec du SECAR 71. Les produits de réaction sont analysés en fonction de la température.

SUMMARY : The problem of adding alkaline phosphates in some aluminous cements (SECAR 71) is raised for various applications. The present work, the possible interactions are studied from a fundamental newpoint, on the one hand, in the low temperature range (room temperature and between 0 - 100°C), on the other, between 100 and 1000°C. In the former range the influence of 5 % weight of marketed sodium hexacyclophosphate on the evolution of SECAR stured in water is determined, as well as the influence upon the evolution of such a mixture as paste. Using various analytical and calorimetric means it was established that phosphate setting occurs during the initial period and accelerates hydraulic setting by several hours although the sodium ions released keep a large extent of alumina in solution.

In the 100 - 1000°C range, the transformations undergone by various types of sodium phosphates : dihydrogenemonophosphate, hexacyclophosphate were systematically followed either with dry samples or mixed with water. In both cases (dry or with water) similar tests were made comparatively with mixtures of the same phosphates with different oxides : CaO, Al_2O_3 and SECAR 71. The reactions products were studied versus temperature.

INTRODUCTION

L'étude des réactions des phosphates avec différents oxydes présente de nombreuses applications. Certains phosphates sont utilisés dans les ciments dentaires (1), (2) ; d'autre part lorsque des phosphates sont ajoutés au Portland (3), (4), (5), (6), les phénomènes observés lors de la prise sont complexes.

Le maintien de la cohésion d'un béton réfractaire jusqu'à la prise céramique, entre dans le cadre de cette étude. Les études antérieures à caractère fondamental sont peu nombreuses : Kingery (7) signale les possibilités de liaison par réaction de l'acide orthophosphorique avec des oxydes métalliques. La thèse présentée par Bouvier d'Yvoire (8) concerne l'étude de phosphates d'aluminium et de fer trivalent. Dans son mémoire, Forest (9) apporte une contribution à la recherche de nouveaux liants gâchés avec une liqueur phosphorique.

Nous nous proposons de préciser les conditions dans lesquelles s'effectue la "prise phosphatique" *, et d'analyser les réactions et les mécanismes qui entrent en jeu. Pour cela nous avons effectué deux types d'expériences portant :

1) sur l'évolution d'un mélange de SECAR 71 et de 5 % d'hexacyclophosphate de sodium par agitation dans l'eau, dans un rapport pondéral liquide/solide : $\ell/s = 10$, afin de situer dans le temps les réactions conduisant à la prise phosphatique et à la prise hydraulique, et d'étudier leurs interactions ; des essais sont effectués parallèlement sur des pâtes en utilisant l'effet thermique comme moyen de détection.

2) sur l'évolution thermique entre l'ambiante et 1000°C d'échantillons de dihydrogénomonophosphate de sodium (NaH_2PO_4) et d' "hexacyclophosphate de sodium" d'origine industrielle (principal constituant : $(NaPO_3)_6$).

L'évolution d'échantillons soit secs, soit humidifiés est étudiée dans deux séries d'essais menés parallèlement sur des échantillons purs et sur des mélanges de ces phosphates avec différents oxydes. Les essais ici rapportés n'ont qu'un caractère exploratoire, une étude en thermobalance étant actuellement effectuée dans des conditions de température et de pression de vapeur d'eau plus précises.

ETUDE EXPERIMENTALE

I - Etude à température ambiante :

a) Etude cinétique : L'influence d'une adjonction de 5 % d'hexacyclophosphate de sodium industriel sur l'évolution du SECAR 71 *** est analysée en suivant la cinétique des réactions en solution aqueuse. Pour cela, le SECAR 71 pur (puis le mélange SECAR 71 + 5 % d'hexacyclophosphate de sodium) est agité dans de l'eau (rapport pondéral $\ell/s = 10$), à 21°C. L'évolution du système en fonction du temps est suivie point par point par prélèvements et dosages, par spectrométrie d'absorption atomique, des concentrations en solution, exprimées en CaO et Al_2O_3. (Notées [C] et [A]).

b) Essais en pâte : La prise du ciment mettant en jeu des phénomènes exothermiques, nous avons étudié la prise du SECAR 71 pur, puis du mélange SECAR 71 avec 5 % d'hexacyclophosphate de sodium en tenant compte de cet effet thermique. Le gâchage est effectué dans un rapport $\ell/s = 0,33$.

Pour cette étude, deux montages ont été réalisés. (1 et 2) :
1) Le dispositif est constitué d'une nacelle cylindrique de 40 mm de diamètre et 20 mm de hauteur contenant le ciment, enfermé dans une enceinte en polystyrène expansé, et dans laquelle plonge un thermocouple ATE-BTE. Il s'agit donc d'une analyse thermique effectuée dans un système adiabatique.

2) Le second montage peut être considéré comme un système "adiabatique amorti", l'échantillon est étalé en couche mince sur une grande face d'une plaque de cuivre parallélépipédique (78x37x7 mm) de façon à évacuer rapidement la chaleur dégagée et maintenir l'échantillon dans des conditions quasi-isothermes. Cette plaque de cuivre constitue, avec une autre plaque identique à laquelle elle est reliée par un fil de constantan, un ensemble de deux couples cuivre-constantan montés en différentielle. Les deux plaques sont isolées thermiquement l'une de l'autre et placées dans un boitier isolant en polystyrène expansé. Ce montage permet de situer dans le temps les divers dégagements de chaleur pouvant intervenir au cours de l'évolution de l'échantillon gâché avec de l'eau sans que les réactions ne soient perturbées par une élévation notable de température.

II - Etude dans le domaine de température 100-1000°C :

a) Essais exploratoires : Afin d'élucider le problème, des essais de décomposition thermique ont été effectués de 100°C à 1000°C, dans un four tubulaire thermorégulé. L'échantillon (4g) placé dans une capsule en platine, est porté à la température désirée et y est maintenu pendant une heure à l'atmosphère libre. Lorsque les essais ont eu lieu sur les échantillons gâchés préalablement, le rapport pondéral ℓ/s était de 0,3. Les essais effectués sur les phosphates seuls seront notés essais (A).

Par la suite, des mélanges de ces phosphates avec, soit de l'alumine, soit de la chaux ont été calcinés dans les mêmes conditions. Ces essais seront appelés B. Enfin des expériences comparatives (essais (c)), ont été effectuées encore dans les mêmes conditions, sur des mélanges phosphate + SECAR 71, et phosphate + SECAR 71 + alumine.
Tous ces échantillons sont analysés par diffraction des rayons X et chromatographie sur couche mince.

Remarque : Alors que dans les mélanges industriels la proportion en masse des phosphates ne dépasse pas 5 %, un rapport de 50 % a été utilisé ici, afin de pouvoir obtenir des informations analytiques précises par diffraction X et chromatographie. Mais, en dépit de cette forte teneur en phosphates, l'oxyde reste en excès dans la réaction de combinaison, comme le prouvent les spectres de diffraction X pris après le traitement thermique.

b) Etude en thermogravimétrie (TG) dans un domaine de température plus restreint : Ce travail, juste commencé, a permis de reprendre les essais de décomposition thermique, sous pression de vapeur d'eau contrôlée, mais seulement dans le domaine de température 80 - 400°C au moyen d'une thermobalance à hélice de silice, type Mac Bain. La pression de vapeur d'eau y est maintenue non saturante grâce à la thermorégulation à 80°C de ses parois et du tube réacteur ainsi que des canalisations et des vannes. Elle peut être régulée à une valeur constante grâce à un point froid constitué par un réservoir d'eau thermorégulée. Les variations de masse de l'échantillon sont enregistrées par un procédé optique (10, 11). Une thermobalance du même type mais qui permettra de couvrir le domaine de température 80 - 1000°C est en cours de réalisation.

A titre exploratoire, il est procédé à une analyse en montée linéaire de température ; mais pour plus de précision, l'échantillon est soumis, sous pression de vapeur d'eau constante à des paliers successifs, de température progressivement croissante, les écarts étant de faible amplitude : 5°C, dans les domaines où des transformations ont lieu. En outre, les échantillons sont analysés par diffraction des rayons X et par chromatographie sur couche mince (C.C.M).

RESULTATS ET DISCUSSION

I - Etude à température ambiante.

a) Etude cinétique : Les courbes d'évolution du SECAR 71 pur et du mélange avec l'hexacyclophosphate de sodium ont été tracées, en suivant la variation de la concentration en alumine et en chaux dans la solution, en fonction du temps d'agitation. Les résultats obtenus sont reportés sur les courbes de la figure 1 :

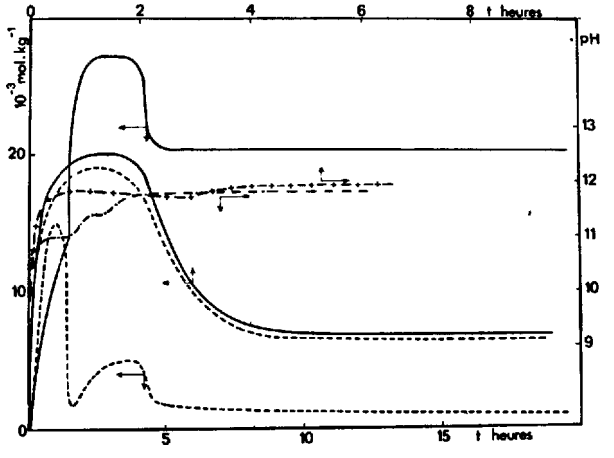

Fig. 1 - Courbes de l'étude cinétique donnant l'évolution des concentrations [C] et [A], ainsi que du pH en fonction du temps.
Echelle du bas : mélange SECAR 71 + 5 % hexacyclophosphate de sodium en présence d'eau (ℓ/s = 10).
Echelle du haut : SECAR 71 pur + eau (ℓ/s = 10).
——: [A] ; - - - : [C] ; -•-•-: pH du mélange avec phosphate ; -+-+- : pH du SECAR 71 seul.

En ce qui concerne le SECAR 71 pur, la courbe présente un maximum à [C] = 19.10^{-3} mol.kg^{-1} et [A] = 20.10^{-3} mol.kg^{-1}. Les valeurs de [C] et [A] restent constamment très proches l'une de l'autre pendant toute l'évolution. La précipitation massive des aluminates de calcium hydratés débute 2h30 après le début de l'expérience. Puis [C] et [A] restent pratiquement constantes : ([C] = $6,8.10^{-3}$ mol.kg^{-1}, [A]= $7,2.10^{-3}$ mol.kg^{-1}) avec $[C/A]_{\ell}$ = 0,94.

La figure 1 montre aussi les courbes obtenues lorsque 5 % d'hexacyclophosphate de sodium industriel sont ajoutés au SECAR 71. Pendant une période initiale de 1h30, la chaux et l'alumine en solution ne sont pas dosables par spectrométrie d'absorption atomique, car une précipitation spontanée se produit dans le filtrat en présence d'HCl. Néanmoins ces dosages ont été effectués par volumétrie (complexométrie avec l'E.D.T.A).

Le précipité blanc et colloïdal, apparaissant dans le filtrat en présence d'HCl, analysé en C.C.M. donne des taches de triphosphate et de phosphates plus lourds. L'analyse X de ce précipité après calcination à 1000°C, montre qu'il est constitué d'un mélange $Al(PO_4)$ et $Al(PO_3)_3$.

Les courbes d'évolution du SECAR 71 en présence d'hexacyclophosphate de sodium sont très différentes de celles obtenues avec le SECAR 71 seul. La concentration de la chaux en solution passe par un maximum ([C] = 15.10^{-3} mol.kg^{-1}) après 1 heure d'agitation à 21°C. Entre 1 h et 1h30, cette concentration diminue brusquement, jusqu'à [C] = $1,8.10^{-3}$ mol.kg^{-1}. Aux environs de 3h, la chaux atteint 5.10^{-3} mol.kg^{-1}, pour se stabiliser ensuite à $1,5.10^{-3}$ mol.kg^{-1}. La concentration en alumine augmente rapidement mais régulièrement, et atteint le maximum pour 27.10^{-3} mol.kg^{-1} après 2h d'agitation. Au bout de 4h, [A] diminue mais reste voisine de 20.10^{-3} mol.kg^{-1}. Ainsi, après la précipitation, le rapport $[C/A]_{\ell}$ tend vers 0,075. Parallèlement, une courbe représentant le pH de la solution en fonction du temps a été tracée. Elle révèle deux "sauts" de pH, l'un à 1h30 (moment où [C] chute), l'autre vers 3h (lorsque les concentrations [C] et [A] arrivent à leur maximum). Puis le pH reste constant à 11,8.

Lors de ces essais, des échantillons de filtrat, prélevés respectivement après 10 mn, 1h, 2h, 3h, 4h, 8h et 11h, ont été analysés par C.C.M. Les taches observées sont nettement séparées sur le chromatogramme, ce qui permet d'identifier :
- à 10 mn, un monophosphate et des polyphosphates à longues chaînes (chaîne phosphorée > 4P),
- à 1h, un diphosphate, ainsi que du tricyclophosphate et des phosphates à longues chaînes,
- à partir de 2h (jusqu'à 11h), le chromatogramme ne présente plus aucune tache, ce qui permet de conclure à la précipitation à peu près complète de tous les anions phosphates.

Ces résultats laissent penser que l'hexacyclophosphate de sodium subit très rapidement une hydrolyse interne, avec ouverture des cycles et formation d'ions phosphates (ou polyphosphates), réagissant avec les ions Ca^{++} pour donner un précipité de phosphate de calcium insoluble ; d'où la nette diminution observée de [C] dans la solution. En revanche, la précipitation des phosphates de calcium laisse les ions Na^{+} en solution, de sorte que la teneur élevée de celle-ci en alumine s'explique par le fait qu'elle s'y trouve sous forme d'aluminate de sodium.

b) Essais en pâte : Deux types d'essais ont été effectués comparativement sur du SECAR 71 frais, puis sur le mélange de ce ciment alumineux avec 5 % d'hexacyclophosphate de sodium. Les courbes obtenues à partir des dispositifs 1 et 2 sont reportées ci-dessous (figure 2).

L'essai 1 montre qu'un processus exothermique intervient dès le gâchage et arrive à son terme au bout de 45 mn. D'après nos expériences d'évolution à ℓ/s = 10, cet effet thermique doit correspondre à la précipitation de phosphate de calcium. En fait, avec le dispositif (1), adiabatique, les résultats diffèrent suivant le taux de remplissage de la cellule de mesure. Ainsi pour un taux de remplissage de 100 % (cavité entièrement emplie), l'écart de température au sommet du premier pic peut être évalué à 34,6°C pour le SECAR pur, (figure 2, trait plein), à 28°C pour le mélange avec le phosphate (figure 2, pointillés). L'influence de cette élévation de température sur la prise hydraulique est importante

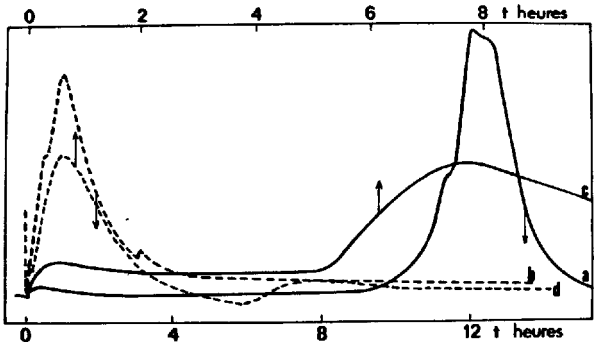

Fig. 2 - Courbes d'analyse thermique.
Dispositif (1) ; ℓ/s = 0,33 :
a : SECAR 71 seul.
b : SECAR 71 + 5 % hexacyclophosphate de sodium.
Dispositif (2) ; ℓ/s = 0,30 :
c : SECAR 71 seul.
d : SECAR 71 + 5 % hexacyclophosphate de sodium.

puisque celle-ci se traduit par un second pic de faible amplitude (écart de 4°C) débutant à 3h10. Il convient de noter les épaulements traduisant une succession de processus chimiques.

Avec le dispositif (2), les essais sont effectués sur 1 g de ciment et un rapport ℓ/s = 0,3, dans des conditions adiabatiques, quasi isothermes. La figure 2 montre les résultats obtenus, d'une part avec du SECAR 71 pur (trait plein), d'autre part avec le mélange ciment + 5 % hexacyclophosphate de sodium.

Dans le premier cas, la prise s'effectue après 5h, et la différence de température observée est $\Delta\theta$ = 0,2°C, ce qui correspond à une quantité de chaleur $\Delta Q \simeq 13,7$ J pour 1 g de ciment, valeur certainement inférieure à la réalité en raison de la fuite thermique.

Dans le second cas, une élévation de température de 0,27°C a lieu 5 mn après le gâchage ($\Delta Q \simeq 18,5$ J par g de matière), le pic de la prise hydraulique n'apparaissant qu'après 4h, avec $\Delta\theta$ = 0,05°C ($\Delta Q \simeq 3,4$ J).

Ces essais qui possèdent un caractère préliminaire seront complétés par des mesures microcalorimétriques ; ils ont permis de déterminer la succession temporelle des phénomènes.

II - Etude dans le domaine de température 100-1000°C.

a) Essais exploratoires : Dans le tableau I, sont rassemblés les résultats des essais (A), portant sur le dihydrogénomonophosphate de sodium et sur l'hexacyclophosphate de sodium, soit secs, soit gâchés avec de l'eau dans le rapport pondéral ℓ/s = 0,3.

Il convient de noter qu'après la formation intermédiaire de diphosphate, se forme à partir de 300°C, du tricyclophosphate qui subsiste jusqu'à 600°C, quel que soit le produit de départ.

A 700°C, la C.C.M. permet de révéler la présence de polyphosphate à longue chaîne (> 3 P), amorphe aux rayons X.

Dans le tableau II sont présentés les résultats des essais (B) d'évolution thermique des mélanges de

TABLEAU I

Essais Température (°C)	DHP anhydre	HCP anhydre	DHP + H_2O	HCP + H_2O
100°C	CCM : MP RX : NaH_2PO_4	CCM : HCP RX : amorphe	CCM : MP RX : NaH_2PO_4	DP + TP + TCP + HCP RX : $Na_2H_2P_2O_7$
200°C	CCM : DP RX : $Na_2H_2P_2O_7$	HCP amorphe	MP + DP $Na_2H_2P_2O_7$	DP $Na_2H_2P_2O_7$
300°C	TCP RX : $Na_3P_3O_9$ + $(NaPO_3)_x$	TC $Na_3P_3O_9$	MP + DP + TCP $Na_3P_3O_9$	
400°C à 600°C	TCP $Na_3P_3O_9$	TCP $Na_3P_3O_9$	TCP $Na_3P_3O_9$ + traces $(NaPO_3)_x$	DP + TCP $Na_3P_3O_9$ + $Na_2H_2P_2O_7$
700°C à 1000°C	PP RX amorphe	PP amorphe	PP amorphe	PP amorphe

* Remarque sur notations :
DHP : dihydrogénophosphate de sodium ; NaH_2PO_4
HCP : hexacyclophosphate $(NaPO_3)_6$. MP : monophosphate.
DP : diphosphate. TP : triphosphate. TCP : tricyclophosphate. PP : polyphosphate (P > 4).

TABLEAU II

Essais :	NaH_2PO_4 (2g) + H_2O			$(NaPO_3)_6$ (2g) + H_2O		
T°C	CaO (2g)	Al_2O_3 (2g)	SECAR (2g)	CaO (2g)	Al_2O_3 (2g)	SECAR (2g)
100	MP	MP RX : Al_2O_3	MP RX : SECAR	MP + DP + TP	MP RX : Al_2O_3	MP RX : SECAR
200 à 500	MP + DP + TP + TCP	MP + DP + TCP	MP + DP RX :SECAR $Ca_2P_2O_7$ $Ca_3(PO_4)_2$	MP + DP + TP + TCP	MP + DP RX : Al_2O_3	MP + DP RX :SECAR $\alpha NaCaPO_4$ $\beta Ca_2P_2O_7$
600 à 1000	MP	MP RX : Al_2O_3	MP RX :SECAR Al_2O_3 $NaCaPO_4$	MP	MP	MP RX :Al_2O_3 + $\alpha NaCaPO_4$

SECAR 71 exempt d'alumine, avec CaO, Al_2O_3, dans les proportions indiquées, gâchés à l'eau (ℓ/s = 0,3). Dans chaque cas, les transformations et combinaisons des phosphates avec les oxydes se produisent à température relativement basse (θ < 400°C).

A θ > 600°C, seule la tache du monophosphate apparaît sur le chromatogramme.

Dans tous les cas, la preuve d'un excès d'alumine ou

de SECAR 71 est apportée par diffraction X, de sorte que, bien que les phosphates soient en forte proportion (50 % massique), leur combinaison avec les oxydes peut se faire complètement.

Enfin, le tableau III contient les résultats des deux essais effectués sur les mélanges des monophosphates et polyphosphates avec Al_2O_3 et SECAR 71, gâchés à l'eau dans un rapport $\ell/s = 0,3$.

TABLEAU III

Mélanges / T°C	DHP (1g) + Al_2O_3 (1g) + SECAR 71 (1g) + H_2O	HCP (1g) + Al_2O_3 (1g) + SECAR 71 (1g) + H_2O
100°C	CCM : MP	MP + DP
200°C à 400°C	MP + DP	MP + DP RX : Al_2O_3 excès + Secar
400°C à 1000°C	MP	MP RX : Secar + Al_2O_3 + $CaNaPO_4$

Pour 200°C < θ < 400°C, le chromatogramme permet de déceler un mélange de mono- et diphosphates. Au-delà de 400°C, ne subsiste que le monophosphate.

La transformation diphosphate → tricyclophosphate n'a donc lieu que lorsque les phosphates ne sont pas mélangés avec des oxydes. Dans le cas contraire, que ce soit avec Al_2O_3 ou CaO ou le SECAR 71, il se forme directement du monophosphate.

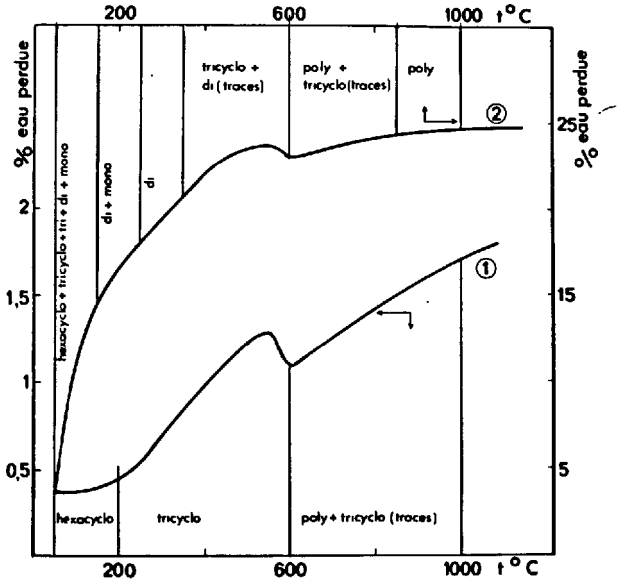

Fig. 3 - Courbe d'évolution thermique de l'hexacyclophosphate de sodium industriel.
(1) : hexacyclophosphate de sodium seul.
(2) : hexacyclophosphate de sodium + H_2O ($\ell/s = 0,3$).

La décomposition thermique de "l'hexacyclophosphate de sodium" industriel présente une courbe d'évolution en fonction de la température qui se caractérise par un minimum de masse à 600°C. Une telle courbe, donnant le pourcentage d'eau perdue en fonction de la température est tracée figure 3.

TABLEAU IV

T°C chauffage	NaH_2PO_4 t°C point froid : 25°C	$(NaPO_3)_6$ t°C point froid : 25°C
150°C	Δm = 0 C.C.M. → MP	Δm = 0 C.C.M. → PP + traces TCP et TP
210°C	Δm : perte de $1H_2O$/mole. C.C.M. : DP + traces PP	Δm = 0
445°C	Δm : perte de $2H_2O$/mole. C.C.M. : TCP + traces PP	Δm ≃ 1,4 % H_2O C.C.M. : TCP + traces PP

Le minimum coïncide avec la transformation du tricyclophosphate cristallisé, produit de décomposition de l'hexacyclophosphate à 200°C, en polyphosphate vitreux à longue chaîne.

b) Premiers résultats en thermogravimétrie (TG) : Les courbes de déshydratation du dihydrogénophosphate de sodium et de l'hexamétaphosphate industriel sont représentées figure 4. Les produits de décomposition sont analysés comme précédemment par C.C.M. (tableau IV).

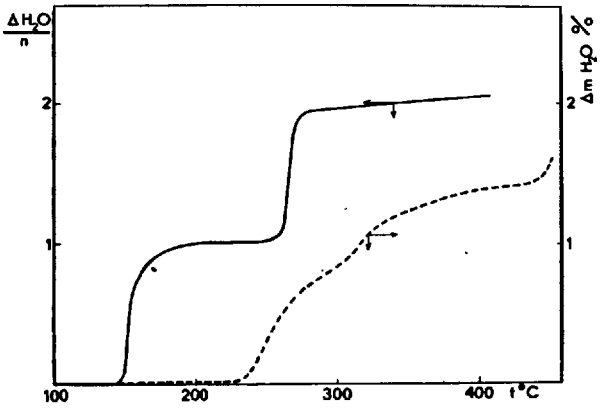

Fig. 4 - Courbes de déshydratation, sous $3,2.10^3$ Pa de pression de vapeur d'eau en fonction de la température.
——— : dihydrogénophosphate de sodium.
$\frac{\Delta H_2O}{n}$: nombre de moles d'eau perdues par mole de produit.
---- : hexacyclophosphate de sodium industriel.
$\Delta m H_2O$: pourcentage en masse d'eau perdue.

Il doit être noté que la pression de vapeur d'eau maintenue constante par la thermorégulation du "point froid" a eu peu d'influence sur le taux de déshydratation atteint à une température donnée.

Ces résultats, obtenus dans des conditions mieux définies, confirment, dans le domaine de température qu'ils ont pour le moment permis d'explorer (80°C < θ < 400°C), les conclusions tirées des essais de décomposition thermique point par point.

CONCLUSION .

A température ambiante, l'étude cinétique en solution à ℓ/s = 10 permet de constater que l'hexacyclophosphate de sodium met un certain temps à s'hydrolyser. Pendant cette période, la concentration en CaO dans le filtrat augmente jusqu'à un maximum de 15.10^{-3} mol.kg^{-1}. Puis une compétition entre l'hydrolyse interne de l'hexacyclophosphate de sodium et la précipitation du phosphate de calcium peut expliquer l'allure de la courbe obtenue.

Une analyse par C.C.M. du filtrat indique que les ions "phosphate" ont disparu de la solution après 4h de réaction. Pour ce même temps de réaction, la forte teneur en Al_2O_3 observée peut s'expliquer par la formation d'un aluminate de sodium soluble, due aux ions Na^+ apportés par le cyclophosphate. La succession des phénomènes est également traduite par la variation du pH.

Cette étude montre, qu'à la température ambiante la prise "phosphate" s'effectue avant la prise hydraulique, commence dès le gâchage avec l'eau et l'hydrolyse interne du phosphate cyclique ; ceci est confirmé également sur pâte (ℓ/s = 0,3) au moyen des courbes de dégagement de chaleur en fonction du temps. L'intensité de la prise hydraulique est alors affaiblie par rapport à celle du SECAR 71 pur.

En montée progressive de température, entre l'ambiante et 1000°C, les états successifs de décomposition de l'hexacyclophosphate de sodium ont été mis en évidence, notamment, la formation du tricyclophosphate entre 300 et 600°C et celle de polyphosphates au-delà de 600°C. Par contre en présence de divers oxydes, le tricyclophosphate n'est pas formé mais la réaction évolue vers l'apparition de monophosphate dès 600°C.

Dans les expériences d'évolution à ℓ/s = 10, et en pâte avec 5 % d'hexacyclophosphate de sodium, il n'avait pas été possible de mettre en évidence directement par analyse (rayons X, C.C.M) le phosphate de calcium présent dans le précipité. Sa formation avait été déduite d'une part de la courbe thermique, d'autre part de la disparition des ions "phosphate" en C.C.M.

En dernière minute, nous donnons les résultats d'une expérience complémentaire qui a consisté en une simulation, par mélange de 5 g d'hexacyclophosphate de sodium dans 1 l d'eau de chaux de concentration initiale $[C]_0$ = $22,2.10^{-3}$ mol.kg^{-1}. Ceci correspondrait sensiblement à la concentration maximale atteinte par la chaux dans l'expérience à ℓ/s = 10 avec l'hexacyclophosphate.

Dans une durée analogue (1h 45) il s'est formé un précipité blanc, amorphe en diffraction X, (anneau de diffusion aux alentours de d_{hkl} = 7,3 Å, pouvant correspondre à α-$Ca_3(PO_4)_2$).

L'analyse par C.C.M. du précipité a montré la présence d'ions monophosphate et triphosphate.

On notera également, que l'hydrolyse interne de l'hexacyclophosphate de sodium (5g) dans 1 l d'eau sans addition de chaux, est beaucoup plus lente, puisqu'après un temps d'agitation de 15h, la C.C.M. révèle des traces de monophosphate, de tricyclophosphate, mais une proportion encore importante d'hexacyclophosphate.

BIBLIOGRAPHIE

1.- M. ANZAI, K. TAKEDA, M. SATO, K. KOMIYAMA, Y. NOMOTO, N. SAITO (1974), "Studies on silicate cement ", Jour. of Nihon University ; school of dentistry, 3, 16.

2.- C.E. SEMLER (1976), "A quick-setting wollastonite phosphate cement", Ceram. Bull., 55, (11), 983.

3.- W. GUTT, M.A. SMITH (1974), "Studies of phosphatic portland cements", VIe congrès internat. des ciments, Moscou.

4.- W. LIEBER (1974), "The influence of phosphates on the hydration of portland cement", VIe congrès internat. des ciments, Moscou.

5.- I.G. LUGININA (1974), "Effect of phosphorus on cement stone properties", VIe congrès internat. des ciments, Moscou.

6.- J.E. CASSIDY (1976), "Phosphate bonding then and now", Bull. Amer. Ceram. Soc., 55, (4), 443.

7.- W.D. KINGERY (1950), "Fondamental study of phosphate bonding in refractories", Jour. Amer. Ceram, Soc., 33, (8), 239-250.

8.- F. BOUVIER D'YVOIRE (1961), "Contribution à l'étude des phosphates d'aluminium et de fer trivalent", Thèse, Paris.

9.- J. FOREST (1963), "Contribution à la connaissance de ciments liés par l'acide orthophosphorique et à l'étude de certains phosphates d'aluminium", Thèse, Paris.

10.- P. BARRET (1957), "Dispositif de projection et d'enregistrement optique des élongations d'une balance à hélice de quartz", Bull. Soc. Chim. Fr. 165, 912.

11.- F. LAVANANT (1963), "Contribution à l'étude de quelques aluminates de calcium hydratés", Thèse Docteur-Ingénieur, Dijon.

---

* La signification du terme "prise phosphatique" peut être contestée : certains auteurs l'appellent plutôt "liaison phosphatique".

** Nous rappelons que le SECAR 71 est un ciment alumineux à 70 % d'alumine.

*** SECAR 71 exempt d'alumine signifie pour nous SECAR 71 sans addition supplémentaire d'alumine.

Problème de l'utilisation des sous-produits minéraux dans la production des liants

Use of mineral sub-products in binder manufacturing

P. BOJENOV, Docteur ès Sciences, Professeur, Ecole du Bâtiment, Léningrad, U.R.S.S.,
B. GRIGORIEV, Candidat ès Sciences, Chargé de Cours, Ecole du Bâtiment, Léningrad, U.R.S.S.

RESUME : La fusion des métaux ferreux et non-ferreux, la combustion des combustibles et d'autres opérations sont suivies, à grande échelle, par des processus analogues à la formation des clinkers. La composition chimique de la partie minérale des minerais et des combustibles, les conditions thermiques déterminent la formation de l'orthosilicate du calcium. Les sous-produits contenant β-C_2S sont à utiliser non seulement comme un composant des matières premières des crus de ciments, mais aussi pour la fabrication des ciments composés.

Sont proposées des méthodes d'activation des propriétés liantes des sous-produits, en utilisant le mécanisme de l'adsorption intérieure entre les cristaux et un procédé d'évaluation des propriétés liantes des sous-produits d'après les coefficients de base. Il a été constaté que le progrès dans la création de nouveaux ciments à la base de sous-produits de l'industrie est intimement lié à l'étude de leur composition chimique et de phase, et de la technologie de la fabrication du produit essentiel.

SUMMARY: The processes similar clinker formation occur under ferrous and non-ferrous métal fusion, combustion of combustible and in other branches of industry in large scale. Chemical composition of the mineral part of ores and combustibles and temperature conditions determine the calcium orthosilicate formation.

It is shown that subproducts containing β - C_2S are useful not only as a raw material component of cement charges but also for the separate cement fabrication.

The methods of subproduct's astringent properties activation using the mechanism of inner adsorbtion between crystal as well as the way of subproduct's astringent properties estimation by the bases coefficient are offered.

It is infered that the success in the creation of new cements on the basis of industry subproducts is closely connected with their phase and chemical structure exploring, with comprehensive in interference in technology of the product fabrication.

L'analyse de l'état des ressources en matières premières utilisées pour la production des liants, d'une part, la pratique du bâtiment, d'autre part, prouvent que les ciment bélites, notamment le ciment de Portland, conserveront leur rôle essentiel dans l'avenir proche et même dans l'avenir plus éloigné.

La base cristallochimique pour la fabrication du ciment de Portland est la suivante: élimination de l'eau des minéraux stratifiés et stratifiés en bande; reconstruction et destruction des méthastructures; décarbonisation du carbonate de calcium et réfection de la grille de la calcite trigonale (rhomboèdre) en structure cubique de l'oxyde de calcium; combinaison postérieure de la chaux et de la silice et formation du silicate bicalcique et tricalcique. Dans ces conditions la nature de liaison entre les éléments de structures des matériaux de base change ce qui conditionne l'activité hydraulique des silicates de calcium formés. L'adaptation réciproque des éléments de tétraèdres silice-oxygène et colonettes (bandes) des octaèdres de calcium est fonction de plusieurs facteurs dont la température. Elle rend plus facile la réalisation des structures orthosilicates de calcium. Dans les conditions réeles de la production du clinker, en général, l'état d'équilibre n'est pas atteint dans le système, et les nouvelles formations surgies sont à l'état méthastable.

Des processus analogues ont lieu à une grande échelle pendant la production des métaux ferreux et non ferreux, la combustion des combustibles solides ainsi que dans certaines branches de l'industrie chimique.

Le volume sommaire de la production à la base des matières premières minérales mis sur le marché mondial augmente progressivement. Ainsi, suivant des données incomplètes, au début du XX^{e} siècle, la production annuelle en était 140 millions de tonnes, elle a atteint près de 3 milliards en 1975, on attend pour 1980 plus de 10 milliards.

Actuellement, les entreprises faisant usage des éléments dispersés dans l'écorce terrestre se developpent d'une manière intense. Pour en fabriquer 1 tonne il faut traiter des dizaines et même des centaines de tonnes de minérais.

Or, on peut supposer que le volume annuel des matières premières minérales extraites de l'écorce terrestre atteindra 150- 200 milliards de tonnes vers l'année 2000.

Nombreuses sont les entreprises où les matières premières mises en oeuvre pour la fabrication du produit essentiel sont soumises à un traitement thermique à une température qui souvent ne dépasse pas 1200- 1300°C. Mais, comme le rendement du produit essentiel ne fait qu'une partie insignifiante des matériaux traités, les frais principaux d'énergie, de combustible, de main-d'oeuvre sont dépensés, fait paradoxal, à la modification, l'enrichissement, le chauffage et la séparation des sous-produits.

Comme le produit essentiel ne peut être fabriqué sans ces dépenses et, d'autre part, puisque la composition chimique et les conditions thermiques de la partie minérale favorisent la formation de l'orthosilicate du calcium, on peut bien comprendre l'aspiration des spécialistes du ciment de coopérer avec les branches d'industrie produisant des sous-produits pareils.

Une intervention raisonable dans les procédés technologique en vue d'obtenir des sous-produits d'une composition de phase et de qualité requises est devenue une nécessité vitale de notre époque. L'industrie présente des exemples concluants de la résolution de cette tâche.

Le traitement complexe de la roche

apatitonéphéline pour la production du ciment, de l'alumine, du sodium et de la potasse réalisé en URSS est rendu possible grâce à l'étude approfondie de la composition chimique et de phase des sous-produits, grâce à la modification appropriée de la technologie de production de l'alumine en vue d'augmenter le rendement de ß - C_2S.

En théorie, il est possible de corriger la charge et mener le processus de manière à assurer la formation du silicate tricalcique en quantité égale à celle renfermée dans le ciment de Portland, c'est-à-dire, fabriquer le clinker du ciment portland sans déchets.

Mais cela aurait pour conséquence la réduction du rendement des appareils pour le produit essentiel; et la modification des paramètres techniques du fonctionnement des appareils entraîne une augmentation des pertes du produit essentiel et une consommation de combustible due à l'accroissement de la masse de la roche traitée pour le compte du calcaire complémentaire.

C'est pourquoi dans les techniques du ciment est devenue courante la méthode de la mise en oeuvre des sous-produits contenant le silicate bicalcique, des laitiers, des boues etc. comme un des composants de la charge des matières premières. Ils ont déjà passé le stade de formation de C_2S ce qui rend la formation du silicate tricalcique plus facile, réduit la consommation de combustible et d'énergie électrique à 20-50%, tout en assurant la bonne qualité du ciment de Portland (1,2).

Pourtant la formation, à la base de ces produits, des liants indépendants, ne cédant en qualité au ciment de Portland semble être plus perspectif.

L'expérience de la production, en URSS, des ciments de néphéline à la base des boues de néphéline, sous-produit de production de l'alumine, qui contient 85% ß - C_2S, a prouvé que ces ciments peuvent avoir un usage courant pour la fabrication des pièces en béton armé et en béton céllulaires (3,4).

L'expérience prouve que les boues de néphéline de diverses entreprises, contenant à peu près la même quantité d'orthosilicate du calcium, possèdent une activité hydraulique variée. Cela résulte, évidemment, de la différente action stabilisante des additions comprises dans les matières premières traitées qui, étant adsorbées aux limites des grains, sont aptes à régler la formation de C_2 dans des modifications et exercent une influence sur la dimension et la forme des cristaux. A l'aide du mécanisme de l'adsorbtion intérieure entre les cristaux, on peut augmenter l'activité de ß - C_2S et du liant lui-même par une seconde cuisson à une température basse.

La faculté forte exprimée de l'orthosilicate du calcium de dissoudre des additions diverses, d'une part, l'étude approfondie de la conduite des additions dans différentes conditions, d'autre part, laissent à rechercher de nouvelles voies d'activation du silicate bicalcique. C'est ainsi que le problème de l'usage des sous-produits contenant C_2S peut avoir un autre sens. C'est pourquoi au VI Congrès à Moscou, le professeur P.Bojenov a proposé de l'examiner comme une question spéciale au Congrès futur.

Un autre problème spécial: influence de l'excédent de chaux sur la stabilisation d'une forme de l'orthosilicate de calcium, nouvelle répartition de l'oxyde de calcium en phases dans les systèmes contenant C_2S sous l'influence des ions halogènes et certains oxydes des éléments de transition.

Les essais nous ont montré qu'il est possible d'obtenir un ciment du clinker avec KH =0,67 en présence de l'oxyde de chrome et de manganèse dont l'activité est

50-55 MPa en 7 jours et 65-70 MPa en 28 jours.

On a fait usage de ce procédé pour l'accroissement de l'activité des liants à la base des sous-produits, contenant l'orthosilicate du calcium.

Une autre possibilité d'activation des propriétés liantes de tels systèmes est leur transformation en un état hydraté et un traitement thermique postérieur du produit d'hydratation à une basse pression. Le ciment ainsi fabriqué dont la composition, à côté d'autres phases, contenait ß- C_2S à l'état des cristaux fins a formé, aux conditions de durcissement normales, une pierre d'une résistance assez élevée - 40 MPa. Ce procédé de fabrication des liants n'exige pas de hautes températures, nécessaire pour le synthèse des minéraux de clinkers suivant les techniques du ciment de Portland.

L'état de l'orthosilicate de calcium en cristaux fins des sous-produits a été défini par une charge supplémentaire en chaux de certaines espèces de laitiers et par le réglage du régime de traitement thermique. Il en résultent des liants ayant l'activité de 40 à 100 MPa.

L'étude des déchets agglomérés dans les terris présente un problème spécial.

Sous l'influence des agents atmosphériques, la composition chimique et la composition de phase des déchets dans les terris se modifient. L'hydratation des compositions silicates et d'autres, leur carbonisation par l'acide carbonique de l'air ont des conséquences défavorables sur les propriétés hydrauliques des déchets. Pourtant, même alors la situation n'est pas irrémédiable.

C'est ainsi que l'étude de la composition de phase des fractions fines des laitiers de haut-fourneau pulvérisés, produits ensemble avec les alliages ferreux et enrichis par l'alumine, à permis à A.Boldyrev et à ses collaborateurs de fabriquer un ciment de silicate alumineux dont les propriétés se rapproche à celles des ciments alumineux (1).

P.Bojenov, B.Grigoriev ont montré que par l'addition de NaOH, Na_2CO_3, CaCl et d'autre combinaisons est atteinte une considérable activation des laitiers qui contiennent jusqu'à 25% du carbonate de calcium sous l'aspect de vaterite et jusqu'a 15% de vollastonite.

V.Glouckovski et ses collaborateurs (5) après avoir étudié l'influence des additions sur l'activité des laitiers ont formé un ciment nouveau, substance liante en laitier alcalin dont les propriétés peuvent rivaliser et même dépasser celles des ciments portlands.

Pour apprécier les propriétés liantes (hydrauliques) des sous-produits, laitiers et cendres y compris, on fait usage courant comme caractéristique chimique des modules divers. Pourtant, l'étude de différents laitiers a prouvé que parfois leur activité effective ne correspond pas aux valeurs données des modules. La raison en est l'absence de logique mathématique et chimique dans la formule des modules, ce qui empêche leur emploi en qualité de caractéristique chimique de n'importe quel sous-produit silicate. A une valeur constante de module, l'activité des liants, produits à la base de diverses matières peut différer de manière sensible.

P. Bojenov a proposé le "Coefficient de base" qui, contrairement aux modules, ne prévoit plus la simple somme des oxydes, mais tient compte de la succession des opérations dans les nouvelles formations du produit.

$$\text{Coef.de base} = \frac{(CaO+0,93\ MgO+0,6\ R_2O)-(0,55Al_2O_3+0,35\ Fe_2O_3+0,7\ SO_3)}{0,93\ SiO_2}$$

où CaO, MgO, SiO_2 est la teneur globale des oxydes.

L'analyse de cette formule donne la possibilité au technologue d'estimer les matières premières dont il se sert et les corriger.

Dans notre rapport nous avons analysé quelques espèces de sous-produits contenant, en règle générale, l'orthosilicate du calcium. Cependant, l'industrie produit d'autres matériaux, notamment ceux qui comprennent le silicate Mg et dont on peut faire usage pour la production des liants.

Le developpement postérieur de la production des ciments traditionaux et la création de nouveaux ciments à la base des sous-produits de l'industrie peut être assuré par l'étude de la composition de phase des sous-produits, par l'intervention raisonnable dans la technologie de la fabrication du produit essentiel, enfin, par la mise au point d'une méthode de la correction de leurs propriétés, dont l'augmentation de l'activité hydraulique.

Bibliographie

1. Boldyrev A., Lourié U., Oguianova E., Kouznetsov P. (1940). Production du ciment de Portland, URSS, 10-11 et 235-236.
2. Bojenov P., (1946), Le ciment de néphéline Lenisdat, URSS.
3. Bojenov P.,(1963), Utilisation complexe des matières premières minérales pour la production des matériaux de construction, Stroïsdat, URSS.
4. Bojenov P. et Kavalérova V. (1966) Les boues de néphéline, Stroïsdat, URSS.
5. Glouckovski V.,(1979), Les bases théoriques des ciments alcalins, alcalino-terreux et des bétons, Dans le livre "Liants hydrauliques alcalins et alcalino-terreux et les bétons " "Vischaia Chkola", Kiev, URSS.

Activation mécano-chimique du silicate dicalcique technogène

Mechanochemical activation of technogenic bicalcium silicate

V.I. AKOUNOV, Candidat ès Sciences Techniques,
A.M. DMITRIEV, Candidat ès Sciences Techniques,
S.D. MAKACHEV, Ingénieur,
G.P. LITVINOV, Ingénieur,
V.I. JARKO, Candidat ès Sciences Techniques,
G.V. ZAVADSKI, Ingénieur,
B.E. YOUDOVITCH, Candidat ès Sciences Techniques, NIITzement, Moscou, U.R.S.S.

RESUME : Le niveau insuffisant des résistances initiales empêche, partiellement dans le cas de β- C_2S, (complètement pour ce qui est de γ - C_2S) la mise en oeuvre, en tant que composants hydrauliquement actifs, des sous-produits technogènes de l'industrie de l'alumine, notamment du β -C_2S ou du γ C_2S

Le passage dans un broyeur à jet de mélanges composés de 70 % de clinker ordinaire et de 30 % de β-C_2S technogène, additionnés de gypse, donne un ciment dont l'activité initiale est sensiblement supérieure à celle des ciments provenant des broyeurs à boulets.

La baisse de l'énergie d'activation de l'hydratation, que l'on observe lors de la pulvérisation par jet, a pour effet un relèvement sensible du taux d'utilisation de l'énergie potentielle contenue dans β- C_2S et le clinker de ciment Portland industriel, et permet d'organiser sur cette base une production rentable des ciments d'activités différentes.

SUMMARY : Reduced growth of strength at the early stage of hardening limits the use of technogenic by-products of alumina industry containing β - C_2S and excludes the use of by-products containing γ - C_2S as hydraulically active components of cement.

Jet grinding of mixture comprising 70% of ordinary clinker and 30% of technogenic β - C_2S with gypsum renders cement with considerably increased initial activity as compared with cement crushed in a ball drum mill.

Reduction of hydration activation energy by jet grinding ensures considerable increase in the degree of utilization of the potential energy stored in the technogenic β - C_2S and industrial portland cement clinker and provides for economic production of cements of various activity.

L'exposé (1) traite des raisons pour lesquelles il serait utile d'activer le silicate bicalcique qui se crée lors du traitement thermique des minéraux dans le système $CaO - SiO_2$, ou bien dans les systèmes minéraux comprenant le système sus-mentionné, notamment lors de l'extraction de l'alumine par agglomération des alumosilicates. Les sous-produits, comprenant le silicate bicalcique en quantités toujours croissantes, ce qui est lié à l'extension de la production d'alumine, doivent être utilisés dans d'autres industries dans le cadre d'une technologie sans rejets. L'activité hydraulique du silicate bicalcique permet l'utilisation des sous-produits qui comprennent ce minéral, avant-tout, pour la production des ciments. L'introduction du silicate bicalcique technogène dans la composition du ciment, par broyage, avec un clinker portland, constituerait un procédé simple dont la réalisation est la plus facile. Cependant, l'accroissement ralenti de la résistance pendant la période initiale de durcissement (jusqu'a 72 heures) empêche l'utilisation, en tant que constituants hydrauliquement actifs, des sous-produits a $\beta - C_2S$ - partiellement, et a $\gamma - C_2S$ - patiquement dans leur totalité. Dans ce contexte, les procédés d'activation mecanique et chimique du silicate dicalcique technogène, passes en revue dans la presente communication, acquièrent une importance considerable.

PRINCIPES D'ACTIVATION MECANIQUE ET CHIMIQUE

Sous le nom d'activation mécano-chimique des matériaux, on comprend généralement l'élévation de leur réactivité (dans les réactions chimiques) à la suite des modifications de structure par le traitement mécanique, notamment par broyage. Le traitement mécanique peut être effectué au préalable. Dans ce cas, son effet d'activation doit se conserver, au moins, jusqu'au début de la réaction chimique intensifiée. Mais ce genre de traitement peut être également opéré pendant la réaction; cette activation est la plus efficace, quoique sensiblement plus compliquée du point de vue matériel, c'est plutot une technologie du demain bien qu'il existe des licences, d'application pratique peu sure, ainsi que deux ou trois solutions techniques valables.

Les modifications de la structure apparaissant lors de l'activation mécano-chimique se prêtent à la classification suivante : 1° modification statiques, c'est-à-dire qui se conservent en permanence dans la structure activée, 2° modifications dynamiques gardées pendant un certain temps et qui disparaissent spontanément, 3° modifications mixtes qui incluent à la fois les deux types de modifications précédentes.

Du point de vue de la physique du corps solide, les modifications statiques sont conditionnées par les défauts du réseau cristallin, dus au changement de place des atomes dans les noeuds et les interstices des noeuds, ainsi qu'aux variations dans le nombre et l'emplacement des lacunes. L'augmentation quantitative de ces changements peut être considérée formellement, ou liée de fait à l'accroissement de la densité de dislocations dans le réseau cristallin de la matière jusqu'à son amorphisation complète (2,3).

Naturellement, de tels changements de la structure lors du traitement mécanique de la matière peuvent être enregistrés avec succès, par la méthode de la radiographie. Les changements dynamiques de la structure survenant au cours de l'activation mécano-chimique des matériaux sont conditionnés par les défauts, apparaissant et disparaissant, dans les enveloppes électroniques des atomes qui constituent le réseau cristallin. Il est généralement admis aujourd'hui que lors de la dispersion de la matière, une partie des électrons se trouvent séparés de leurs atomes par les interfaces apparaissantes, ce qui provoque un excès du potentiel électrostatique à la surface et entraine des variations correspondantes du niveau Fermi, c'est-à-dire de l'énergie moyenne des électrons dans les zones extérieures du réseau cristallin (4). La valeur de cet excès du potentiel peut être stable et alors les variations de la structure engendrées par ce potentiel, peuvent etre envisagées comme défauts statiques. Cependant, dans bien des cas, l'excès du potentiel Fermi, après la dispersion, a une tendence à se diminuer, par exemple à la suite de l'émission à partir de la surface des électrons excédentaires durant un certain temps qui suit la pulvérisation. Une telle émission exo-électronique a été observée pour la première fois sur le gypse par Kramer (5). C'est ce qu'on appelle aujourd'hui "effet Kramer". Parmi les autres modifications, conditionnant la baisse du niveau excédentaire du potentiel Fermi des matériaux activés, on peut citer l'adsorption des molécules de gaz, et notamment, du gaz carbonique et/ou de l'oxygène contenu dans l'air, des molécules d'eau qui constituent l'humidité naturelle, etc. Les défauts du réseau cristallin disparaissant pendant cette réaction peuvent aussi etre considérés comme modifications dynamiques provoquées par l'activation. Elles sont enregistrées grace aux procédés indirects, compte tenu des techniques modernes. En particulier, l'émission exoélectronique (effet Kramer) est observée au moyen des capteurs à pointe à rayons X, puisque l'énergie des électrons émis est assez importante (6). Jusqu'à présent, on ne trouve pas de critères théoriques de structure, qui conditionnent la présence ou l'absence de l'effet Kramer à la suite de l'activation mécano-chimique des matériaux. Aussi, le type des modifications dynamiques du réseau cristallin des matériaux activés n'est-il défini que par voie expérimentale.

PULVERISATION PAR JET EN TANT QUE METHODE D'ACTIVATION. On connait toute une série de méthodes d'activation mécano-chimique de matériaux par dispersion. Le broyage en broyeurs à cylindres en est un procédé d'activation préliminaire très ancien, utilisé par l'homme pour des processus physiques et chimiques divers tels que pyrométallurgie, panification, fabrication d'objets en céramique, etc. Au XIX-e siècle, ce procédé a

été en partie remplacé par broyage à tambour, notamment, dans des moulins à tubes remplis de corps broyants nécessaires à la mouture (boulets, cylpebs, etc). Dans les années cinquante de notre siècle, afin d'accroître l'efficacité de l'activation préliminaire, on recourt largement aux broyage par percussion et par vibration, deux inventions datant d'une vingtaine d'années, ainsi qu'à un traitement par désintégration. De tous ces procédés relativement nouveaux, seule la mouture par vibration est utilisable dans le cas de l'activation du silicate bicalcique, les autres ne permettant que l'obtention d'un produit assez grossier par comparaison à la finesse des ciments ordinaires. Les expérimentations sur broyage par vibration du silicate bicalcique technogène, effectuées à le NIITzement dans les années soixante, ont donné des résultats positifs. Cependant, elles n'ont pas trouvé d'application industrielle en raison de certaines particularités de construction du broyeur vibrant, de son faible rendement et du taux d'usure élevé de la garniture, par rapport aux moulins à tambours ordinaires. La pulvérisation par jet a été proposée, en tant que méthode d'activation mécano-chimique préliminaire des liants, par un des auteurs du présent exposé, dans les années soixante (7). Par rapport aux autres engins de broyage, le procédé en question se caractérise par un niveau plus élevé (d'un ordre de grandeur) de la consommation d'énergie par unité de volume utile, un équipement peu encombrant donc une quantité moindre de matériaux mis en oeuvre pour sa construction, l'absence de pièces mobiles, de corps broyants, de séparateurs, d'où un taux moins élevé (de deux ordres de grandeur) d'usure des organes de travail, un fonctionnement silencieux, sans parler des avantages intrinsèques résidant dans la nature physique meme de cette méthode d'activation mécano-chimique. Son atout principal consiste dans une propagation à vitesse supersonique des ondes de choc et, comme corollaire, une éventualité très minime de relaxation des contraintes apparaissant dans le réseau cristallin.

Outre l'augmentation du rendement de l'énergie dépensée pour le broyage, cela garantit le taux maximum de formation des défauts statiques et le taux maximum de maintenance de défauts dynamiques provoqués pendant la pulvérisation par jet de la matière à activer. Cela assure une utilisation efficace de la pulvérisation par jet du clinker portland et de ses mélanges avec le laitier granulé de haut fourneau, en tant que méthode de la fabrication des ciments à haute résistance dont la surface spécifique est pour une resistance egale, d'environ 1000 cm^2/g inférieure à celle des ciments analogues obtenus dans les broyeurs à tube (8).

MATIERES UTILISEES PENDANT LES EXPERIENCES. Clinker portland industriel, β - C_2S technogène (boue de bélite, résidu d'extraction d'alumine à partir de néphéline) et γ - C_2S - produit de synthèse par cuisson dans le four pilote rotatif de la cimenterie expérimentale de le NIITzement - avaient un composé chimique illustré par le tableau I. Les analyses pétrographique et aux rayons X ont prouvé la présence dans le clinker d'alite de la série monoclinique des modifications, de β - C_2S et de C_3A tétragone; dans β - C_2S technogène, on remarquait la présence d'impuretes ordinaires de gehlenite, de wollastonite et de minéraux alcalins, le tout avec 80% de la matière de base. Le γ - C_2S contenait près de 20% de β - C_2S, ce qui correspond parfaitement à la composition des rejets issus de la transformation industrielle des produits de kaolinite de la valorisation du charbon en alumine.

TABLEAU I

Composition chimique des matériaux, en %

Oxydes	Clinker	β - C_2S semi-produit	γ - C_2S
Pertes à la calcination	0,21	2,76	0,35
SiO_2	21,56	30,52	35,00
Al_2O_3	4,69	2,79	0,22
Fe_2O_3	4,52	2,52	0,10
CaO	64,97	56,67	63,70
CaO (libre)	0,05	néant	0,40
MgO	1,46	-	traces
SO_3	0,53	-	traces

RESULTATS DES EXPERIENCES. Chacune des matières précitées, ycompris les mélanges préparés d'avance et constitués à 70% de clinker à 30 % de β et γ -C_2S avec 5% de gypse ont subi une pulvérisation par jet dans un engin de la série USV-300. Les matériaux obtenus ont été analysés au sujet de la radioactivité, au moyen d'un compteur de rayons X directif d'après la méthode (9) et utilisés pour la fabrication d'échantillons (conformément aux Normes GOST 310 - 76) avec du sable (rapport 3 à 1), afin d'évaluer leur activité hydraulique. L'usage, pendant la pulvérisation, de divers agents porteurs d'énergie - tels que l'air ou la vapeur d'eau - prouve que ces agents exercent un effet considérable sur l'activité hydraulique et la radioactivité des matériaux obtenus. Dans le cas, présent, on a fait usage de vapeurs d'eau.

La granulométrie des matériaux obtenus par pulvérisation par jet se distingue des matériaux de la mouture à boulets, qui ont la surface spécifique identique (déterminée d'après la méthode de la perméabilité à l'air) par la valeur légèrement supérieure de l'ascension n (tangente de l'angle d'inclinaison) de la droite - anamorphose de la répartition des particules selon leurs dimensions, dans le système Rosine-Rammler - Sperling-Bennett : n = 1,1-1,3 , pour la pulvérisation par jet, et 0,7-0,9 pour le broyage à boulets.
On a établi l'existence, pendant environ 24 heures après la pulvérisation par jet, de β - C_2S, ainsi que du clinker portland, d'une émission exo-électronique à partir de

la surface de leurs particules. Le γ-C_2S est, paraît-il, exempt de ce phenomene. L'intensite d'emission des particules clinker est inferieure par rapport a β - C_2S, proportionnellement au contenu de ce mineral dans le clinker; ceci permet de considérer β - C_2S comme cause de l'emission, puisqu'il fait partie du clinker. L'activité hydraulique de β - C_2S, et plus particulièrement, de γ - C_2S n'est pas forte par rapport aux données assez favorables sur l'activite du melange technogene clinker portland - β - C_2S (tableau II).

TABLEAU II

Caractéristiques de résistance des matériaux obtenus par broyage a boulets (I) et par jet (II)

Caracteristiques	Matériaux, parties en masse								
	Clinker 100 Gypse 3		Clinker 70 β-C_2S 30 Gypse 5		Clinker 70 γ-C_2S 30 Gypse 5		β-C_2S 100		γ-C_2S 100
	I	II	I	II	I	II	I	II	II
S, 1000 cm^2/gr	3,4	3,3	3,4	3,5	3,7	3,7	3,4	3,8	8,2
E/C	0,4	0,4	0,4	0,4	0,4	0,4	0,42	0,4	0,43
DE, mm*	113	111	113	113	113	113	107	109	113
R_P, 1j	39	32	26	24	3	10	0	0	4
Kgf/cm^2 3j	51	54	44	48			0	0	6
Kgf/cm^2 7j	59	62	49	54			0	9	9
Kgf/cm^2 28j	68	78	59	66			26	33	23
R_C, 1j	94	153	62	67	10	49	0	0	15
Kgf/cm^2 3j	246	281	194	233			0	0	17
Kgf/cm^2 7j	342	345	254	340			0	12	18
Kgf/cm^2 28j	409	481	343	419			76	78	43

* degré d'étalement

EXAMEN DES RESULTATS. Les données de l'émission exo-électronique coincident, dans leur ensemble, avec les resultats du travail (9) a la suite duquel on a constate la presence exclusive de cette emission dans C_2S (β-forme, a ce qu'il paraît), hormis le reste des mineraux clinker. Le diagramme X des poudres de tous les materiaux pulverisées prouve qu'il n'y a pas lieu d'appréhender l'existence d'une multiplication des dislocations, et moins encore d'une amorphisation des particules dans les couches superficielles, en comparaison avec le broyage a boulets dans des broyeurs de laboratoire.

Au contraire, il peut y s'agir de l'intensification des pics d'analyse d'alite (51,7°), de β - C_2S (15,5°) et de γ - C_2S (29°) apres la pulvérisation par jet, par rapport au broyage a boulets. Ceci atteste la densité moinsforte des dislocations dans les materiaux pulverises par jet et, par consequent, l'existence des interfaces plus planes. Les microphotos des preparations d'immersion de certaines fractions du clinker prouvent, qu'apres le broyage par jet, les grains sont moins rugueux: une partie de la surface des grains est constituee, a la difference du broyage a boulets, par le plan de clivage. Mais les projections visibles sur les epreuves temoignent que, souvent apres la pulverisation par jet, se forment les grains aux angles aigus de moins de 1 rad, alors que chez les particules issues du broyage a boulets, les angles aigus ne dépassent jamais 1,4 rad et, si besoin est de former un angle aigu solide, celui-ci est cree par deux angles obtus, comme on le voit sur le schema (Fig.1).

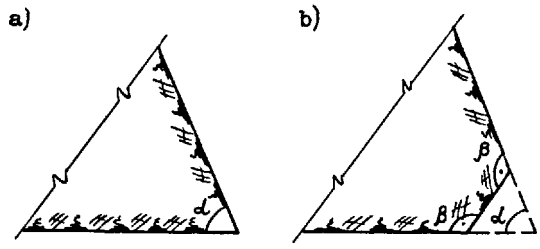

Fig.1; Une particule obtenue par jet (a) et par boulets (b) ayant un angle solide egal entre les faces (schema).

La soumission de la répartition des particules selon les dimensions, pendant la pulverisation par jet, a l'equation Rosine-Rammler-Sperling avec le coefficient d'uniformite $n \approx 1$ est conditionnee (10), d'apres l'analyse theorique, par l'absence de relaxation au cours de la pulverisation, et par la domination exclusive de l'action percutante. Lors du broyage a boulets, qui constitue une combinaison des actions percutante et abrasive (11), les angles aigus, formés dans les particules apres l'action percutante, deviennent obtus sous l'effet de frottement. Le phenomène des angles aigus, des particules de materiaux obtenus par jet, rend plus accessible leur volume interieur pour les reactions chimiques heterogenes, et accelère, on le sait (12), leur continuation dans le temps. C'est la que nous sommes enclins de voir l'effet essentiel d'activation offert par la pulverisation par jet. L'activation du reseau cristallin n'aura d'effet sur la surface des particules qu'avec un taux de dispersion tres eleve, allant jusqu'a 8000 cm^2/g de γ - C_2S.

L'importance des exo-électrons pour l'acti-

vité hydraulique est aussi prouvée. En effet, le taux de consistance de la pate de ciment normale produite à partir du clinker fraichement moulu avec du gypse en poudre, se réduit d'une façon exponentielle dans le temps (13); il en est de meme pour la valeur d'émission exo-électronique. Cet effet n'est pas utilisé exprès pendant nos expérimentations puisque, d'une manière générale, il n'est guère réalisable que pendant la production complexe des ciments et bétons ce qui est réservé pour l'avenir. C'est pourquoi, pendant ces expériences, le gâchage hydraulique des matériaux pulvérisés par jet s'effectuait au bout des 24 heures après la pulvérisation et l'arret total de l'émission exo-électronique. Cependant, même dans ces conditions, la pulvérisation par jet du mélange constitué à 70% par clinker industriel et à 30% par β - C_2S avec 5% de gypse, a permis d'obtenir un ciment à activité initiale considérablement elevée par rapport au ciment de la meme composition mais pulvérisé dans un tambour broyeur à boulets. Son taux de résistance correspond au portland ordinaire, (classe 400, Normes GOST 10178-76), ou bien au ciment type 1 ASTM C-150.

Pour trouver la cause de l'accroissement accéléré de la résistance de ce ciment, en comparaison avec un ciment analogue broyé par boulets, il a fallu toute une série d'analyses (ingénieur N.V.TSOUKANOVA) qui avaient pour objectif d'étudier la vitesse d'hydratation dans un milieu dont la température variait.

Les résultats de ces expériences attestent que la pulvérisation par jet peut etre considérée comme un procédé qui réduit la valeur énergétique d'activation de l'hydratation des ciments et augmente le degré d'utilisation de l'énergie potentielle accumulée dans un clinker et β - C_2S technogène.

CONCLUSIONS.

La technologie rationnelle de la production des ciments qui comprennent β - C_2S technogène, peut se baser sur la pulvérisation par jet du mélange de cette matière avec du clinker industriel et du gypse. Ce procédé permet d'obtenir des ciments à activité variable, y compris des homologues du portland ordinaire (type 1, Normes ASTM), lorsqu'ils contiennent 30% de β -C_2S technogène environ; cela revient à la réduction de 30% des dépenses en énergie lors de sa production. Pour utiliser γ- C_2S, il faut des efforts d'activation supplémentaires. Sont particulièrement prometteuses les possibilités qui sont tracées dans un de nos ouvrages et qui concernent l'activation des C_2S par les agents énergétiques sous haute température permettant de combiner dans un meme engin (broyeur à projection) les processus de pulvérisation, de séchage et du traitement thermique de haute température (14). Cela amène dans la couche superficielle deshydratée de β - C_2S, l'apparition de zones activées du réseau cristallin qui accélèrent le processus d'hydratation. Actuellement, on procède à la mise au point de cet engin en Union Soviétique.

BIBLIOGRAPHIE :

1. - A.S.BOLDYREV (1980) "Ciments à haute teneur en silicate bicalcique et monocalcique et leur application". Rapport présenté au VIIème Congrès (en français)

2. - Г.С.ХОДАКОВ (1972) "Физика измельчения". М., "Наука", 307 с, (en russe).

3. - Р.ШРАДЕР (1969) "Новые примеры из области механохимии". II Всевоюзный симпозиум по механохимии и механоэмиссии твердых тел, тезисы докладов, Фрунзе (en russe).

4. - Ф.Ф.ВОЛЬКЕНШТЕЙН (1973) "Физико-химия поверхности полупроводников". М., "Наука", 399 с, (en russe).

5. - J.KRAMER (1949) Zeitschrift für Physik, 125, N° 11/12, 739-756, (en allemand).

6. - Н.И.КОБОЗЕВ (ред) (1962) "Экзоэлектронная эмиссия". М., ИЛ с, (en russe).

7. - В.И.АКУНОВ (1967) "Струйные мельницы" М., "Машиностроение", (en russe).

8. - Ю.И.ДЕШКО, В.И.АКУНОВ, В.Л.ПАНКРАТОВ, Н.И.ФЕРЕНС, В.П.ШЕЛУДЬКО, Г.В.ЗАВАДСКИЙ (1976) "Получение высокопрочного и быстротвердеющего цемента". VI Междунар. конгр.по химии цемента, т.III 23-24, (en russe).

9. - Д.М.МАМБЕТОВ, В.Ф.РЕСНЯНСКИЙ, К.Ш.ШАТЕМИРОВ (1969) "Электронная эмиссия с некоторых минералов цемента". II Всесоюзный симпозиум по механохимии и механоэмиссии твердых тел, Фрунзе, с 6, (en russe).

10. - В.И.АКУНОВ, Б.Э.ЮДОВИЧ, Т.А.АРБЕКОВА, Г.П.ЛИТВИНОВ (1979) "Генерация поверхности и зерновой состав продуктов измельчения в струйных мельницах". "Цемент", в печати, (en russe).

11. - Р.ГИЙО (1964) "Проблема измельчения материалов и ее развитие". М., Стройиздат, 112 с, (en russe).

12. - Б.ДЕЛЬМОН (1972) "Кинетика гетерогенных реакций". М., "Мир", 554 с, (en russe).

13. - М.Т.ВЛАСОВА, В.Н.КАЛЬЯНОВА, Б.Э.ЮДОВИЧ (1979) "О водопотребности цементов различного зерного состава". "Цемент", в печати (en russe).

14. - В.И.АКУНОВ, Ю.И.ДЕШКО, С.Д.МАКАШЕВ, Г.П.ЛИТВИНОВ (1978) "Струйное измельчание - эффективный метод повышения гидратационной активности белитового шлама". У Всесоюзное совещание по химии и технологии цемента. Краткие тезисы докладов. М., ВНИИЭСМ, 218-219, (en russe)

The development of the structure of CA and CA_2 type high alumina cement clinkers and the properties of cements

Formation des clinkers des ciments alumineux des types CA et CA_2 ; propriétés de ces ciments

J. TALABER, Professor, Director, Ph. D. Central Research and Design Institute for Silicate Industry, Budapest, Hungary, et
K. DOLEZSAI, Ph. D., Head of Sci.Dept. Central Research and Design Institute for Silicate Industry, Budapest, Hungary.

RESUME : La disparition des composants initiaux et la formation des phases intermédiaires et finales des crus de ciment alumineux à base de CA ou de CA_2 ont été étudiées aux rayons X dans des fours de laboratoire.

On a observé que pour les ciments à base de CA, en augmentant l'intensité de la cuisson, on accroissait la proportion de CA, mais que du CA_2 était toujours détectable. Un composé intermédiaire $C_{12}A_7$ est aussi formé.

Pour les ciments à base de CA_2, on observe un accroissement continu du CA_2 et la formation de deux composés intermédiaires : CA et $C_{12}A_7$.

Des expérimentations, en laboratoire et en usine pilote, ont montré que, pour les ciments à base de CA, la proportion maximale de CA est obtenue par une cuisson modérée. Ce maximum coïncide avec la plus grande résistance initiale du ciment. Si l'on augmente l'intensité de la cuisson, on diminue à la fois la proportion de CA dans le ciment, et sa résistance initiale.

SUMMARY: The disappearing of the starting components as well as the formation of the intermediate and final phases of monocalcium-aluminate- and calcium-dialuminate-type raw meals were followed by X-ray investigation using heating chamber.

It was stated that at CA-composition the amount of CA increases upon increasing the burning intensity, and beside it CA_2 can be detected too. Intermediate $C_{12}A_7$ is also formed.

At CA_2 composition the amount of CA_2 is continuously increasing and intermediate CA and $C_{12}A_7$ are also formed.

Laboratory and pilot plant burning experiments also proved that in case of CA composition the maximal CA is achieved by the less intensive burning. This maximum coincides with that of the initial strength of cement. Upon increasing the burning intensity both CA and the initial strength of cement are decreasing.

The physical-mechanical properties of white high alumina cements depend on their Al_2O_3 content and the way of burning.

It is known from literature that the high initial strength is mainly due to CA. Rapid hardening is caused by CA that is why the conditions of forming the maximal amount of CA in the CA and CA_2 type clinkers is investigated in the following.

THE FORMATION OF CA AND CA_2

When burning raw mixtures corresponding in their composition to the above mentioned two calcium aluminates besides the basic mineral other calcium aluminates partly of intermediate, partly of constant character are formed as a function of sintering temperature and time /1,2,3/.

According to recent publications on the CaO-Al_2O_3 systems /1,4/ CA and CA_2 melt incongruently. Among the calcium aluminates of intermediate character the $C_{12}A_7$ is formed only in the presence of moisture /the moisture being present in air is sufficient/ and in the burnt CA one can almost always find CA too, if during burning a partial melting appears for when an incongruently melting compound is crystallizing out from the melt, a perfect state of equilibrium can rarely be achieved.

For the investigation of the CA and CA_2 formation a Jeol type X-ray diffractometer equipped with heating chamber was used. The maximum heating temperature of the chamber is 1773 K.

Since our aim was the definition of the conditions at which the maximal amount of CA is formed and not the determination of the absolute amount of minerals, the changes were followed by measuring the most characteristic peaks of the individual minerals.

Raw meal compositions corresponding to CA and CA_2 were prepared using alumina, limestone and in some cases lime hydrate. The CaO + Al_2O_3 content - referred to the loss on ignition free state - amounted to 99 %.

The raw meals were heated at a rate of 10°/min. Between 1173 and 1773 K the heating was interrupted at every 100° increase stage for 30 minutes and the material was maintaned at those temperatures to have the equilibrium state being achieved and following this the X-ray patterns were made.

The experiments with CA were repeated four times: twice using limestone and twice lime hydrate as basic material while that with CA_2 only once using lime hydrate.

Fig.1. shows the average data of the four CA syntheses. On the abscisse the temperature, on the ordinate the heights of the 0,240 nm CaO, 0,208 nm Al_2O_3, 0,268 nm $C_{12}A_7$, 0,298 nm CA and 0,349 nm CA_2 peaks are plotted.

Besides the continuous decrease of the peak characterising the initial CaO and Al_2O_3, the reflection of $C_{12}A_7$ appears at 1173 K then, after reaching a maximum, it disappears

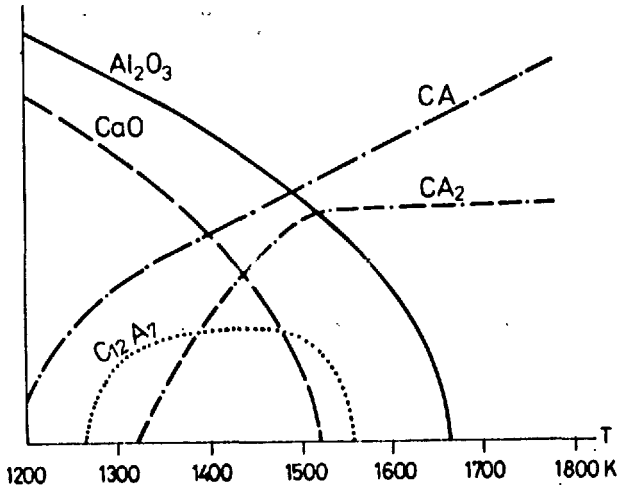

Fig. 1.- Formation of calcium aluminates from raw meals of CA composition as investigated by X-ray diffractometer equipped with heating chamber

at 1550 K.

The CA_2 appears at 1320 K, its reflection intensity increases up to 1520 K then remains constant up to the possible maximal heating temperature - 1770 K. It may be supposed that upon a further temperature rise and subsequent cooling of the material besides CA the amount of CA_2 would also decrease due to the tendency to approach the state of equilibrium.

This is confirmed by the X-ray patterns of the materials of CA composition melted in laboratory arch furnace and sintered in laboratory furnace where besides the CA peaks CA_2 reflections of minor intensity can also be observed.

On the basis of these investigations it can unambiguously be stated that in the case of a composition corresponding to CA the maximal amount of CA can be obtained by elevating the temperature or by melting.

Fig. 2. shows the phase composition relations in the process of heating the mixtures with a composition corresponding to CA_2. These relations are more simple than those of CA type mixtures.

The intensity of the initial CaO and Al_2O_3 reflections are continuously decreasing here, too. The peak showing CA formation appears at 1200 K. Its intensity increases up to 1400 K and thereafter begins to diminish.

The CA_2 and $C_{12}A_7$ reflections appear at 1470 K. The intensity of the CA_2 peaks increases continuously with the temperature while that of the $C_{12}A_7$ reflections decreases. Using extrapolation it seems to be probable that in the final equilibrium state only CA_2 is

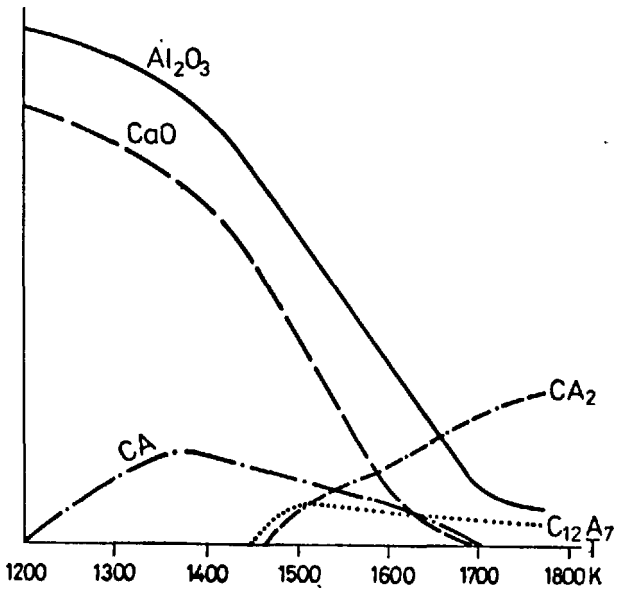

Fig. 2. - Formation of calcium aluminates from raw meals of CA_2 composition as investigated by X-ray diffractometer equipped with heating chamber

present which is supported by other investigations, too.

In case of CA_2 composition the maximal intensity of CA reflections - in contrast with the CA composition - can be observed at a relatively low temperature i.e. far away from the state of equlibrium.

PHYSICAL-MECHANICAL PROPERTIES OF THE CEMENT AS A FUNCTION OF THE WAY OF SINTERING

In order to investigate the relationships between the intensity of burning, the formation of crystalline CA and the strength, CA and CA_2 type raw meals were burnt at 1473, 1623 and 1723 K with sintering times of 2 and 4 hours in a silite rod heated electrical laboratory furnace.

The clinkers cooled in the furnace were ground to a specific surface of 400 m²/kg and the strenth tested according to the Hungarian Standard Specs. MSZ 4702/9/74 requiring the compressive strength at 3 days age to reach the minimal values as listed below:

Al_2O_3 content < 70 %	34,3 MPa
Al_2O_3 content > 70 %	24,5 MPa

The compressive strength of the products of CA composition is shown in Fig.3. while in Fig.4. the 0,298 nm peak height of the X-ray pattern, in Fig.5. the compressive strength of CA_2 and in Fig.6. the 0,349 nm peak height can be seen.

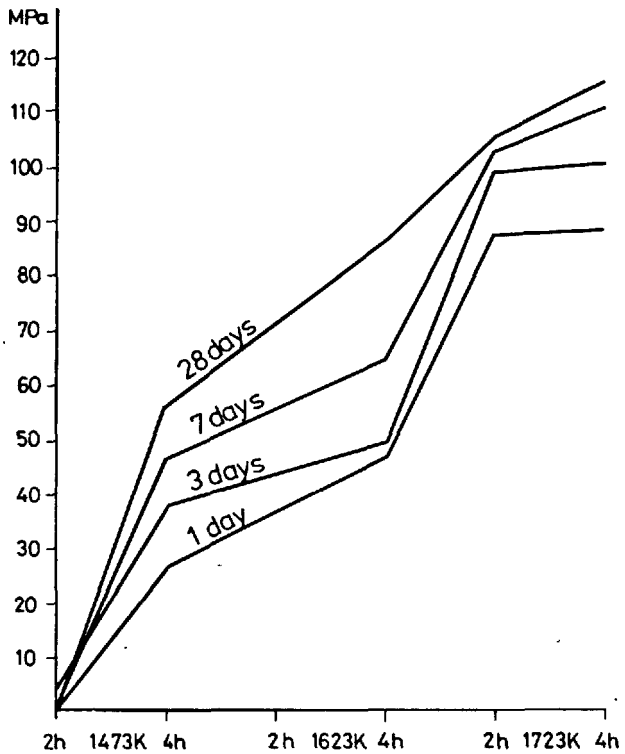

Fig.3. - Change of the compressive strength as a function of burning temperature and time of CA composition cement burnt and ground in laboratory

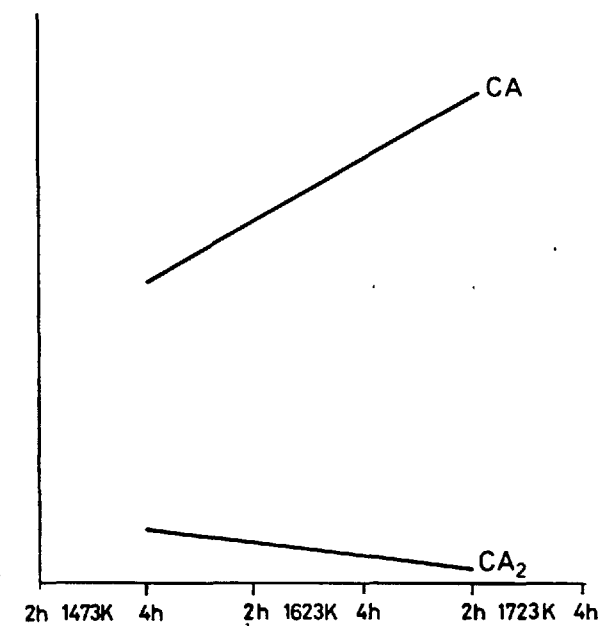

Fig.4. - Change of the 0,298 nm CA and 0,349 nm CA_2 peak heights as a function of burning temperature and time of CA type clinker burnt in laboratory

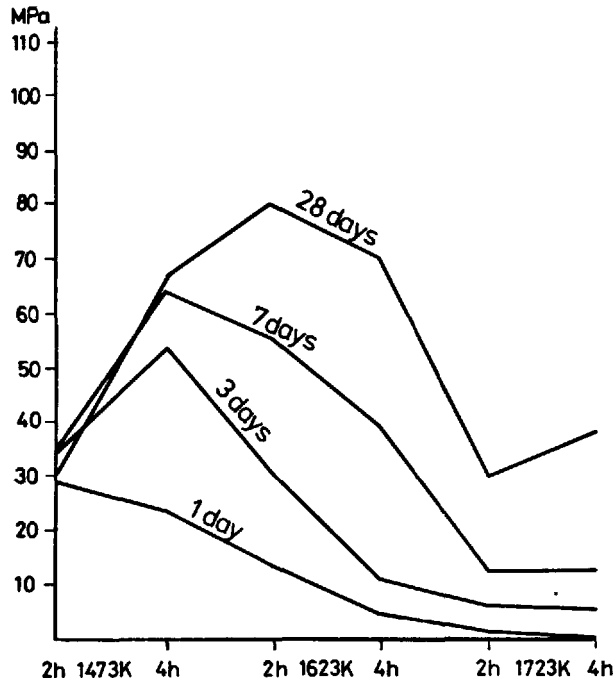

Fig.5. - Change of the compressive strength as a function of burning temperature and time of a CA_2 composition cement burnt and ground in laboratory

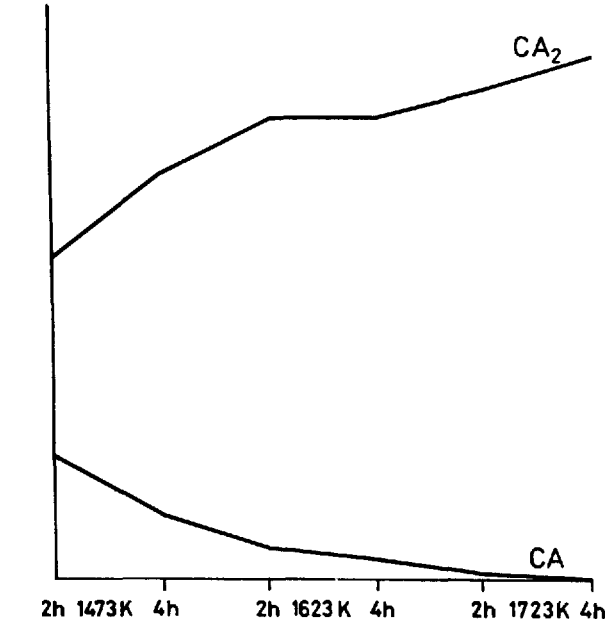

Fig.6. - Change of the 0,298 nm CA and 0,349 nm CA_2 peak heights as a function of burning temperature and time of a CA_2 type clinker burnt in laboratory

TABLE I

Clinker burning temperat. K	duration hours	free CaO %	Insoluble in hydrochlor. acid resid. %
CA type			
1473	2	7,71	21,6
1473	4	1,80	12,7
1623	2	0,53	11,5
1623	4	0	4,1
1723	2	0	6,3
1723	4	0	5,1
CA_2 type			
1473	2	0,53	37,9
1473	4	0,21	41,1
1623	2	0,05	53,6
1623	4	0	52,3
1723	2	0	62,7
1723	4	0	58,0

Table I. - The free CaO content and the insoluble residue of CA and CA_2 type clinkers synthetized in laboratory

Table I. shows the free CaO-content and the insoluble in hydrochloric acid residue of the cements.

The strength of the CA-type cement burnt at 1473 K for 2 hours is lowered by the large amount of free CaO. Upon increasing the temperature and sintering time the strength and - as it has been stated by the investigation of the CA forming process - the height of the 0,298 nm CA peak is also continuously increasing.

In the X-ray pattern of the product burnt at 1473 K for 4 hours the line of $C_{12}A_7$ - even if only in traces - can be found. Moreover, in the pattern of the sample burnt at 1723 K for 2 hours the presence of CA_2 can be observed.

In case of the CA_2 composition the Al_2O_3 being present in larger amount binds the CaO of smaller amount more rapidly thus the CA is formed quickly and at a lower temperature.

According to our investigations the maximum of the CA-peak can be observed after the burning at 1473 K for 2 hours but it may be supposed that also in case of a less intensive burning it would further increase since in Fig,4. only the descending part of the curve can already be seen.

The strength of the with the lowest intensity burnt material is in this case, too, diminished by the free CaO but the amount of it is considerably less than in the case of

the similarily burnt CA-composition thus its strength is ten times higher than that of the former one.

The highest strength value is achieved by burning at 1473 K for 4 hours. The maximums of CA peak-intensity and strength do not coincide which is due to the larger amount of free CaO remaining after a less intensive burning.

Further on, the strength and the intensity of the CA-peak decrease continuously while the CA_2 reflection increases.

The change of the strength and CA-reflections according to a maximum curve as well as the continuous increase of CA_2 correspond to the tendency that was found by investigating the products of CA_2 composition.

The amount of the insoluble in hydrochloric acid residue is big and as contrasted to the CA-composition mixture, it is increasing with intensified burning.

In order to prove as well as to prepare the utilization of our laboratory results a raw meal corresponding in its composition to CA_2 was also burnt in the 10 meter long rotary kiln of our pilot plant.

The data of burning temperature, free CaO and the insoluble in hydrochloric acid residue are given in Table II. while in Fig.7 the strenths, in Fig.8. the 0,298 nm peak heights of CA and 0,349 nm ones of CA_2 are shown.

TABLE II

Clinker mark	Burning temperature K	Free CaO % original	Free CaO % after storage	Insoluble in hydrochloric acid %
I.	1373-1423	2,83	0,15	35,3
II.	1423-1473	1,63	0,25	39,1
III.	1473-1573	0,17	-	42,0
IV.	1573-1673	traces	-	39,0
V.	1773	0	-	41,7

The cements marked with I. and II. were stored under atmospheric conditions in order to neutralize the effect of free CaO since their strengths could not be determined due to rapid setting. In this way the strength-reducing effect of free CaO was eliminated even for the less intensively burnt material, too.

The tendencies are the same as in the laboratory experiments but the actual values show some deviation due to changes in the way of burning and the sensitivity of testing.

In case of the CA_2-composition both in laboratory experiments and in those ones made in pilot plant it can be observed that with

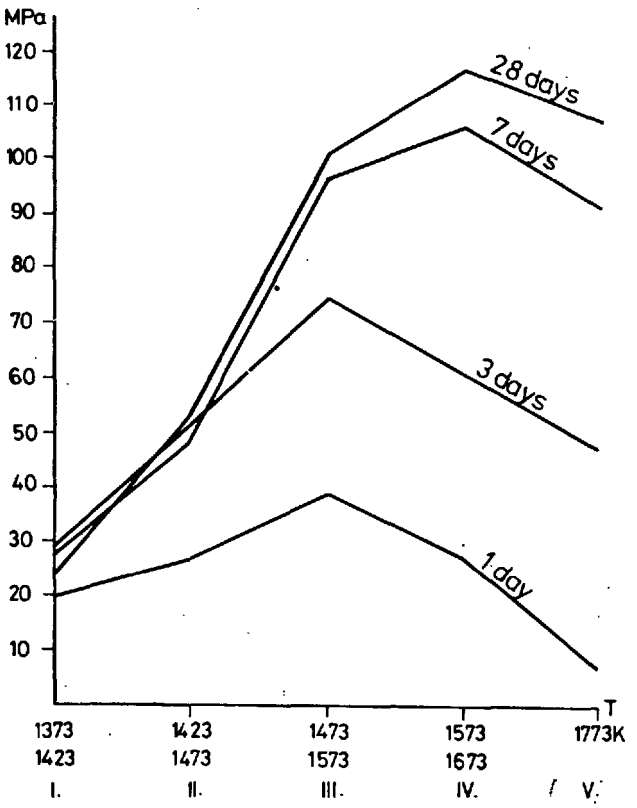

Fig.7. - Change of the compressive strength as a function of burning temperature of a CA_2 composition cement burnt in pilot plant and ground in laboratory

the increase of hardening time the maximum of strength is shifted towards the more intensive burning. The probable cause of this phenomenon is that here hydration of the less soluble and more slowly hardening CA_2 is already beginning.

CONCLUSIONS

The early strength of high alumina cements is proportional with their CA-content. The conditions of maximal CA-formation were stated by comparing the characteristic peak heights measured by X-ray investigation using heating chamber.

The amount of crystalline CA in the clinker composition corresponding to CA is continuously increasing with intensified burning. Meanwhile intermediate $C_{12}A_7$ and CA_2 are also formed. The amount of $C_{12}A_7$ changes according to a maximum curve then disappears. CA_2 does not fully disappear even in melted CA supporting its nature of incongruent melting.

In the clinker composition corresponding to CA_2 CA disappears after a relatively low temperature maximum. Intermediately $C_{12}A_7$ is also formed. The amount of crystalline CA_2 is continuously increasing with the intensification of burning.

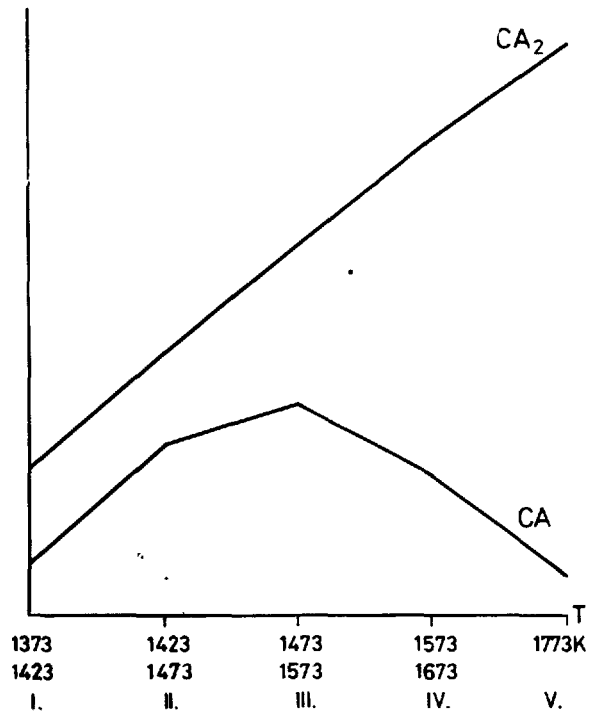

Fig.8. - Change of the 0,298 nm CA and 0,349 nm CA_2 peak heights as a function of burning temperature of a CA_2 composition clinker burnt in pilot plant rotary kiln

Laboratory and pilot plant clinker burning experiments prove the CA-formation tendencies determined by the X-ray investigation using heating chamber as well as the relationships between CA formation and 3 days age strengths.

Consequently, clinkers of CA composition giving high strength can be produced by intensive burning or by melting. In case of CA_2 composition the burning should be carried out very softly at the temperature of the maximal CA formation. Care should be taken, however, that no free CaO remains in the clinker because this would diminish the strength. According to our investigations the optimal amount of free CaO is 0,2 %.

With prolonged storing time the maximal strengths of test specimens are shifted towards the more intensive way of burning.

LITERATURE

1. - A.J. MAJUMDAR /1967/ "Studies on individual constituents of high alumina cements", Silicates Induus triels, No.9., p.297-3o7

2. - K. DOLEZSAI - I. VARGA /1978/ "Principal and technical problems of high alumina cement production", SZIKKTI Research Report /in Hungarian/

3. - L.N. ZABOTINA - G.D.URÜVAEVA /1979/ "Interaction of CaO and Al_2O_3 at the synthesis of calcium aluminate made under different conditions of heat treatment, Izv.Him.Nauk.,2., 4., pp. 73-76 /in Russian/

4. - A. PETZOLD - W. HINZ /1978/ "Silicate Chemistry" VEB Deutscher Verlag für Grundstoffindustrie, Leipzig /in German/

Possibilités de l'intensification des propriétés liantes des matériaux à la base du C_2S

Possibilities of increasing the binding properties of materials rich in C_2S

P.I. BOJENOV, Docteur ès Sciences, Professeur, Institut du Bâtiment, Léningrad, U.R.S.S.,
B.A. GRIGORIEV, Candidat ès Sciences, Chargé de Cours, Institut du Bâtiment, Léningrad, U.R.S.S.,
G. OVTCHARENCO, Ingénieur, Institut du Bâtiment, Léningrad, U.R.S.S.

RESUME : A la base des lois de correspondance structurale, on trouve des cations, susceptibles de stabiliser les modifications des orthosilicates de calcium à haute température. Du point de vue des idées sur l'adsorbtion interne entre les cristallites, il est proposé un mécanisme de stabilisation β-C_2S par la chaux en excès. Par la voie expérimentale, il est démontré que l'activité des ciments bélites peut être considérablement augmentée par un réglage judicieux de la distribution des additions.

Il est proposé une explication du mécanisme d'activation de l'orthosilicate du calcium obtenu dans les réactions topotaxiques de déshydratation des hydrosilicates dans le vide. Il est constaté que le silicate bicalcique est apte à former, dans les conditions normales de durcissement, une pâte durcie ayant une résistance considérable.

Il est proposé une explication de l'activation hydrothermale en présence de SiO_2 et CO_2.

SUMMARY: On the basis of the structural accordance low the cations which can stabilizate high-temperature modifications of the calcium orthosilicate were ascertained.

The stabilization mechanism of β - C_2S with abundunt lime was proposed from the position of intercrystal interior adsorbtion ideas. It was shown experimentally that under regulation of additions distribution one can essentially increase an activity of belit cements.

The activation mechanism of the calcium orthosilicate as a product of topotaxic reactions of dehydratation of high based hydrosilicate in vacuume was explained. There was found that double - calcium silicate obtained as a result of dehydratation side by side with CaO, under normal conditions of hardening was capable to form a stone of rather high strength.

The hydrothermal activation of C_2S in the presence of SiO_2 and CO_2 was explained.

L'activité hydraulique des orthosilicates du calcium est fonction d'une part, de la façon complète ou incomplète de la succession des fragments structuraux des chaux et, d'autre part, de la mode de formation d'une modification de C_2S.

La succession de la structure des chaux semble être plus grande dans les modifications α, α' et β, elle n'est que partielle dans celles de $\gamma - C_2S$ (1).

L'analyse de la loi de correspondance structurale et l'usage des notions du dynamisme de SiO_2 nous a permis de proposer un modèle théorique sur lequel ont été révélés des cations essentiels susceptibles de stabiliser des modifications C_2S aux températures élevées.

La particularité des structures avec des cations tels que Cr^{2+}, Mn^{2+}, Ca^{2+}, Sr^{2+}, Ba^{2+}, Na^{+}, K^{+} etc. réside dans le fait que pour assurer les conditions de la loi de correspondance structurale les tétraèdres Si doivent s'unir dans des diorthogroupes. La stachyometrie des orthosilicates anhydres ne permet pas de réaliser de telles associations, et pour assurer la commensurabilité de l'arête du tétraèdre Si avec celle du cation polyèdre, les gros cations doivent avoir une coordination supérieure à 6.

Le passage d'une partie de Ca^{2+} au polyèdre à 7 sommets permet de stabiliser $\beta - C_2S$.

Or, le mécanisme de cette stabilisation n'est pas encore révélé définitivement. Il y a une particularité: pour la stabilisation $\beta - C_2S$ il est nécessaire, pour une courte durée, de chauffer une seconde fois à une température modérée ($\sim 1000^{o}C$) les produits de la cuisson primaire du mélange

$$CaO : SiO_2 \simeq 2{,}2 : 1.$$

L'analyse du mécanisme de distribution des ions additifs dans les corps polycristallins nous a donné la possibilité de proposer une explication du procédé de stabilisation du point de vue de l'adsorbtion intérieure entre les cristallites (AI) étudiée pour les systèmes métalliques par B.Archarov. (2)

La particularité de la distribution des ions additifs, compte tenu la AI, réside dans le fait que dans la réaction primaire, à la phase solide, les ions additifs, essentiellement, sont localisés dans l'espace entre les cristallites et y égalisent ainsi les maximums énergétiques. Ceux-ci sont dûs aux déformations considérables de la grille cristalline à l'endroit des joints des cristallites.

Ces ions sont appelés horophiles. Une seconde cuisson à basse température permet d'éliminer la hétérogénéité locale des phases pour le compte de la diffusion des ions additifs au fond des cristallites (là, ils peuvent stabiliser une certaine modification).

C'est en réglant la distribution des additions dans les polycristallites qu'il est possible de modifier essentiellement les propriétés des métaux (2), des céramiques, des liants clinkers, ce qui est prouvé par les résultats des essais sur les ciments bélites (tableau 1) fabriqués des clinkers KH = 0,67 additionné de 1% d'oxyde de chrome. Le réfroidissement se faisait soit par une trempe sous l'eau, soit par un lent refroidissement dans le four. Dans le premier cas reste une hétérogénéité locale des phases, dans le deuxième cas elle est partiellement évitée.

Pour créer des centres actifs d'hydratation, des cuissons de deux types ont été effectuées à une température basse: un recuit à courte durée et celui à une durée plus prolongée. Coformement à l'hypothèse de travail, les ions horophiles devaient diffuser dans la masse des cristaux

en faisant"ameublir" les zones entre les cristallites. Pendant le recuit à courte durée le processus n'est pas terminé, et la microhétérogénéité locale est conservée, elle doit disparaître au recuit plus prolongée.

De même a été effectué le recuit dans le vide. Dans ce cas la défectivité des zones entre les cristallites devait accroitre, due à l'apparition des places vacantes de l'oxygène dans l'oxyde du chrome.

cates, ou bien des structures semblables à tilléites, adhèrent encore de l'autre côté du mur portlandite.

Dans les réactions topotaxiques de déshydratation, des hydrosilicates à fort cuisson doivent se dégrager en CaO et $\gamma - C_2S$ (à la structure la plus stable). Mais comme la désydratation est réalisée aux températures modérées de 500-900°, en présence des chaux à dispersion fine, le mécanisme de AI est mis en action qui

Tableau I

Activité des ciments bélites en fonction des conditions de refroidissement et du recuit des clinkers

Conditions de fabrication des clinkers		Temps de recuit min	Activité MPa	
refroidissement	cuisson		7 jours	28 jours
A l'air	A l'air	5 30	4,6 3,2	5,9 3,5
Dans le four	Dans le vide	5 30	5,0 4,4	5,9 4,9
La trempe	A l'air	5 30	6,9 5,6	12,6 10,9
	Dans le vide	5 30	8,0 6,0	16,0 12,0
Une cuisson		-	5,0	8,5

Cette conception relative au comportement de CaO horophile au cours de la stabilisation $\beta - C_2S$ explique bien le fait, noté pour la première fois par Keevil, et Thorvaldson[3], que dans certains cas c'est justement cette modification qu'on obtient pendant la désydratation des hydrosilicates du calcium à haute base; cette conception explique aussi des données contradictoires concernant la modification obtenue de C_2S après la déshydratation TSH (C_3SH_2). (4)

Il est connu que dans les hydrosilicates de calcium à haute base, parmi des fragments structuraux, on peut relever des murs portlandites auquels adhèrent d'un côté ou de deux côtés des blocs orthosili-

transforme $\gamma - C_2S$ en β modification. La vitesse de cette réaction est limitée par le degré de récristallisation de CaO, c'est-à-dire par l'impossibilité de former la solution solide $\gamma - C_2S + CaO$. Pour obtenir des produits de la réaction topotaxique de déshydratation des hydrosilicates à haute base à l'état de dispersion fine on peut faire usage de la déshydratation dans le vide (analogue à la décarbonisation) (5).

Afin d'obtenir de telles compositions liantes une synthèse des hydrosilicates de calcium a été réalisée dans le rapport $C/S \geqslant 2$ (TSH, C_5S_2H et d'autres) avec leur déshydratation ultérieure à la tempé-

rature de 500-900° à l'air et dans le vide.

Les données du tableau 2 montre que le silicate bicalcique, résultat de la déshydratation, dans les conditions normales de durcissement est susceptible de former une pierre d'une résistance assez élevée. La présence de ß - C_2S dans le produit de la déshydratation accroît l'activité des système liants.

cations difficiles à commesurer, dans les produits hydratés, des tétraèdres isolés peuvent s'unir en diorthogroupes (Si_2O_7), puisque une partie de CaO de C_2S passe en portlandites, et la présence (OH^-) permet de construire des combinaisons hydratés en conservant partiellement - C_2S et en formant, d'autre part, des bandes tilléites (la réalisation des diorthogroupes).

Tableau II

Activité des produits de la déshydratation des hydrosilicates de calcium à hautes bases

Produits hydratés	Conditions de déshydratation °C, Pression	Contenu des phases des produits cristallins	Activité MPa	
			7 jours	28 jours
TSH	670°C atmosphère	C_5S_2H, CaO	8,5	13,6
	vide	C_2S CaO, C_5S_2H	15,0	29,6
	900°C atmosphère	γ + ßC_2S, CaO	7,5	15,0
	vide	ß + γ C_2S, CaO	38,0	46,0
C_5S_2H	635°C atmosphère	C_2S, CaO, C_5S_2H	6,9	10,0
	vide	ß C_2S, CaO, C_5S_2H	18,7	24,1
	700°C atmosphère	C_2S, CaO	8,7	13,3
	vide	ß + γ C_2S, CaO	31,6	42,3
	900°C atmosphère	γ - C_2S, CaO	6,4	8,9
	vide	ß + γ C_2S, CaO	26,1	35,0
Les boues hydratés de néphéline	700°C vide	ß + γ C_2S, CaO	18,5	20,0
	800°C vide	ß + γ C_2S, CaO	25,6	28,3
	900°C vide	ß + γ C_2S, CaO	8,8	9,6

La succession des fragments structuraux dans les réactions de déshydratation des silicates de chaux des ciments était indiquée en (6) pourtant la manifestation de la loi de coordenance structurale dans des combinaisons anhydres et hydratés, selon notre avis, se réalise avec un changement du degré de dynamisme SiO_2 et détermine l'accroissement des réactions d'hydratations des orthosilicates de calcium dans certaines conditions.

Cette affirmation s'explique par le fait que, si dans C_2S anhydre l'unité essentielle dynamique SiO_2(7) doit se faire correspondre aux arêtes des polyèdres de. Exemple caractéristique: la structure du dellaite stable dans des larges limites. Ainsi, dans les conditions favorisant la formation partielle de diorthogroupes la réaction d'hydratation doit s'accroître. Ces conditions sont notamment: présence des groupes OH^- (F^-) (traitement hydrothérmal) présence de SiO_2 ou CO_2 (ou bien des deux) pour la formation des structures. L'accroissement de la vitesse d'hydratation C_2S en présence de SiO_2 ou de CO_2 était enregistré expérimentalement à plusieures reprises (8). En utilisant ces réactions à la base des boues de néphéline, nous avons obtenu des matériaux de construc-

tion qui jouissent de bonnes propriétés d'exploitation.

Bibliographie.

1. Ilukhin V.V. et Kasak V.F. (1976), Discussion, VI^{e} Congrès International de chimie des ciments. Stroïsdat, p.74,
2. Arkharov V.I., (1976) " Une des nouvelles directions du développement de la science des matétiaux ", Mecanique physico-chimique des matériaux, vol.12, N 5.
3. Keevil N.B. and Thorvaldson T., (1936) Canadian Journal of Research, 14, p.20.
4. Kheiker D.M. et Zalkind A.I. (1961). Ouvrages de l'Institut des Recherches Scientifiques Asbestociment (11).
5. Mikhail R. (1963), Sh.I.Phys.Chem.37 (10).
6. Kasak V.F., Kouznetsov V.A., TlukhinV.V. Lobatchev N.V., (1977), " Croissance des cristaux dans les solutions hydratés à haute température ", Ed. " Nauka ", p.66
7. Belov N.B. (1976). Essai de la minéralogie structurale, Ed. " Nedra ".
8. Teilor X.F.Y. (1969) Chimie des ciments, Ed. des livres sur le bâtiment.

Analyse de la composition granulométrique des ciments de forages pétroliers

Study of the grain composition of oil-well cements

V.S. BAKCHOUTOV, Candidat ès Sciences Techniques,
KH. AL-VARDI, Candidat ès Sciences Techniques,
Tchjao PIN-KHOUAN, Candidat ès Sciences Techniques, Institut I.M. Goubkine de l'Industrie Pétrochimique et du Gaz de Moscou,
M.K. NIKOLAEVA, Candidat ès Sciences Techniques, Institut de Recherches Scientifiques de l'Information et de l'Economie, Industrie des Matériaux de l'U.R.S.S.

RESUME : L'analyse de la composition granulométrique de plus de 70 ciments pour forages pétroliers connus précédemment et élaborés par les auteurs, de composition et de destination différentes, a permis d'établir, pour chaque ciment, des valeurs optimales de la dimension et de la quantité des diverses fractions et de déterminer le paramètre D (dimension conventionnelle moyenne des particules) qui peut caractériser la composition granulométrique. On a obtenu des équations de régression linéaire décrivant la relation entre le paramètre D et les propriétés technologiques principales des mortiers de ciment et de la pierre de ciment à base de ces derniers, ce qui permet de les "prédire" encore au stade de broyage des ciments sans ou avant les essais techniques, et d'obtenir les matériaux ayant les propriétés requises. L'influence considérable qu'exerce la composition granulométrique sur les propriétés des ciments pour forages pétroliers et sur la structure physique du ciment durci a permis de conclure à la nécessité de son contrôle au cours du broyage du ciment. A cet effet, on a mis au point un procédé rapide de détermination de la composition granulométrique de ces ciments dans les conditions industrielles. Il a été établi que les dépendances entre le paramètre D, la perméabilité et la porosité du ciment durci ont un caractère linéaire.

SUMMARY : Study of over 70 different oil-well cements made it possible to establish the optimal grain size and amount of fractions and to determine parameter D, an arbitrary average size of particles which may be used to characterize grain composition. Equations of linear regression describing the relationship between parameter D and important technological properties of cement mortars and stones were obtained which enable to predict these properties at the grinding stage before or without technological tests and to obtain oil-well cements with required properties. Strong effect of grain composition on oil-well cement properties and cement stone physical structure was established. It necessitates control of grain composition during grinding. An express method for determining grain composition of oil-well cements under production conditions was developed. Linear dependence between parameter D and permeability and porosity of the cement stone was established.

On a étudié tant les ciments de colmatage ordinaires que les ciments de colmatage allégés (CCA), allégés expansifs (CCAE), expansifs (CCE) et alourdis (CCL), élaborés par les auteurs et produits par mélangeage ou broyage simultané des constituants dans un désintégrateur du modèle D-7210 ou dans un broyeur à boulets (1).

Il a été établi que un CC (ciment de colmatage) ordinaire de broyage industriel se caractérise par une basse teneur en petites fractions hydrauliquement les plus actives (de 0 à 5 μm - 12 % ; de 5 à 40μm - 50 % ; jusqu'à 40μm - 60 %). Les auteurs ont prouvé qu'il est possible de régler la composition granulométrique des CC ordinaires en modifiant le régime du traitement par désintégration, ce qui augmente la teneur en fractions de 0 à 5μm de 12 à 64 % et plus, la teneur totale en fractions de 0 à 40μm pouvant atteindre 99 %. Ceci conduit à l'accroissement de l'activité hydraulique du liant en entier, car grâce à la présence d'une quantité considérable de petites particules de gypse, de C_3A, de C_3S et C_4AF très actifs, le processus de durcissement se trouve considérablement intensifié. Pour éclaircir la relation entre la granulométrie et les propriétés des ciments de colmatage on a introduit le paramètre D :

$$D = \frac{R_1 \Pi_1 + R_2 \Pi_2 + \ldots + R_n \Pi_n}{\Pi_1 + \Pi_2 + \ldots + \Pi_n} \quad \text{ou}$$

$$D = \frac{\Sigma R_i \Pi_i}{\Sigma \Pi_i} \quad (\mu m),$$

où R_i est la dimension moyenne des particules dans la gamme de mesure, μm ;
Π_i, la teneur en fraction de la gamme de mesure donnée, %.

Le paramètre D caractérise la dispersité du ciment de colmatage du point de vue de sa granulométrie en général. Comme sa valeur est proche de celle de la dimension moyenne de toutes les particules du ciment, il est appelé dimension moyenne conventionnelle des particules. Lors du traitement des données obtenues par la méthode de corrélation, on a révélé une dépendance linéaire ($y = ax + b$) entre les propriétés des ciments étudiés (y) (degré d'étalement, temps de prise, temps d'épaississement, résistance à la compression et perméabilité à l'eau) et la grandeur D(x). Le coefficient de corrélation, caractérisant le degré d'interdépendance linéaire de x et de y, s'est avéré assez élevé (0,85 à 0,99) et était calculé d'après la formule

$$r = \frac{\left[\frac{1}{n} \Sigma (x_i y_i) - \overline{xy}\right]}{\sigma_x \sigma_y},$$

où $x = D_i$ est le paramètre caractérisant la dimension moyenne conventionnelle des particules ; y_i, le paramètre caractérisant les propriétés du ciment (E est le degré d'étalement, I, la prise initiale et F, la prise finale, σ_{comp}, la résistance à la compression, K_{perm}, la perméabilité à l'eau) ; n, le nombre d'expériences (tabl.I).

Compte tenu des paramètres indiqués, l'équation de régression linéaire était ramenée à la forme

$$y = \bar{y} + r \frac{\sigma_y}{\sigma_x} (x - \bar{x}),$$

où σx, σy sont les écarts quadratiques moyens ;
$r \frac{\sigma_y}{\sigma_x}$ est le coefficient angulaire (coefficient de régression de y par rapport à x).

En connaissant la composition granulométrique (D), on peut prédire, par le calcul, avec une précision assez élevée, toutes les propriétés technologiques principales des ciments de colmatage encore au stade de leur broyage, sans procéder aux essais techniques. De la même façon, mais partant cette fois des exigences concrètes sur la qualité du ciment de colmatage (par exemple la résistance), on peut déterminer pour ce dernier la valeur optimale de D, i.e. la composition granulométrique.

Il est établi que pour les CC ordinaires la valeur optimale de D se trouve dans l'intervalle de 12 à 15 μm et pour les CC ordinaires dont le degré de dispersion est élevé, dans l'intervalle de 8 à 9μm. Les équations de régression pour les ciments principaux sont données dans le tableau I.

Le trait caractéristique des CCA de broyage industriel est une basse teneur en fraction de 0 à 5μm, qui est de 20 % ; la teneur en fraction de 40 à 210μm est près de 31 %. Lors du traitement par désintégration du CCA-1, on peut régler sa composition granulométrique de sorte que la teneur en fraction de 0 à 5μm augmente de 2 fois et plus et la teneur en fraction de 40 à 210μm diminue de 15 à 20 fois. Ceci augmente fortement la résistance de la pierre de ciment CC pour tous les délais de durcissement, ce qui est très important, car la résistance de la pierre de ciments allégés est habituelle faible. L'étude de la variation de résistance et de temps de prise de CCA-1 en fonction de la valeur de D a montré que pour le degré d'étalement égal à 18 cm, la composition granulométrique optimale est la suivante: D = 14μm pour E/C = 1,1 et D = 6,3μm pour E/C = 1,6.

On a étudié dans ce travail la composition granulométrique et les propriétés des ciments de colmatage allégés expansifs, élaborés par les auteurs, avec additions de l'oxyde de calcium (CCAE-1) et de la boue de chromates (CCAE-2). Pour CCAE-1 utilisé dans l'intervalle de température de 20 à 90 °C, la valeur optimale de D se trouve dans les limites de 7 à 8μm pour E/C = 0,9 ; de 4 = 5μm pour E/C = = 1,1. L'augmentation de la teneur en fractions de 0 = 5μm de 2,5 fois conduit

TABLEAU I

Equations de régression

I. CC de composition ordinaire

Propriétés du ciment*	CC ordinaire de broyage industriel	Propriétés du ciment*	CC à degré de dispersion élevé ($F \leqslant 40\mu m$)
1	$E=5,48+0,71D$	2	$I=264+15,38D$
2	$I=214,4+14,47D$	3	$F=288,9+31,6D$
3	$F=352,5+14,74D$	4	$I=48,94+8,16D$
4	$I=91,4+2,4D$	5	$F=117,33+5,82D$
5	$F=154,14+2,07D$	7	$\sigma_{comp}=348,2-31,3D$
6	$T=77+3,74D$	8	$\sigma_{comp}=624,1-41,8D$
7	$\sigma_{comp}=202-2,65D$		
8	$\sigma_{comp}=385,4-6,6D$		

II. CC allégés**

Propriétés du ciment*	CCA-1	Propriétés du ciment*	CCA-2
2	$I=469,4+108D$	1	$E=16+0,367D$
3	$F=588,3+20,2D$	4	$I=57,8+4,46D$
4	$I=68,86+3,8D$	5	$F=101,2+6,54D$
5	$F=185,2+6,3D$	8	$\sigma_{comp}=171,6-4,08D$
6	$T=19,18D-70,55$	10	$K_{perm}=(7,4+2,6D)10^{-4}$
7	$\sigma_{comp}=15,4-0,42D$	Gel-ciment	
8	$\sigma_{comp}=162-4,43D$	1	$E=3,88+1,34D$
9	$K_{perm}=(2,12D-10,8)10^{-1}$		
10	$K_{perm}=0,0023D-0,0123$	4	$I=8,827+9,166D$
		5	$F=68,77+11,47D$
		8	$\sigma_{comp}=73,13-2,5D$
		10	$K_{perm}=(11,3D-71,62)10^{-3}$

III. CC allégés expansifs

Propriétés du ciment*	CCAE-1	Propriétés du ciment*	CCAE-2
1	$E=11,86+0,67D$	4	$I=68,33+18,3D$
4	$I=113,4+4,72D$	5	$F=139,6+4,13D$
5	$F=255,8+7,9D$	8	$\sigma_{comp}=179-4,43D$
8	$\sigma_{comp}=128,4-1,52D$		

IV. CC expansifs

Propriétés du ciment*	CCE-1	Propriétés du ciment*	CCE-2
1	$E=11,99+0,326D$	1	$E=4,54+0,57D$
2	$I=97,89+11,36D$	4	$I=32,95+3,75D$
3	$F=153,04+14,22D$	5	$F=54,15+4,34D$
4	$I=51,825+3,59D$	7	$\sigma_{comp}=210,23-4D$
5	$F=127,34+4,415D$		
7	$\sigma_{comp}=195,73-5,32D$		
8	$\sigma_{comp}=256,345-4,276D$		

V. CC alourdis

CCL-1		CCL-2	
4	$I=51,+1,7D$	4	$I=52,1+1,47D$
5	$F=192,25+13,6D$	5	$F=296,7+0,84D$
7	$\sigma_{comp}=287,6-4,1D$	7	$\sigma_{comp}=98,1-0,37D$
10	$K_{perm}=(1,80-22,2)10^{-3}$	10	$K_{perm}=(2,50-3,03)10^{-3}$

CCL-3		CCL-4	
4	$I=244+5,5D$	4	$I=119+0,99D$
7	$\sigma_{comp}=162,84-2,75D$	7	$\sigma_{comp}=113,5-0,84D$
10	$K_{perm}=(4D-47)10^{-3}$	10	$K_{perm}=(2,92D-6)10^{-3}$

CCE-3		CCE-4	
4	$I=36,87+1,96D$	4	$I=42,8+3,37D$
5	$F=49,31+22,84D$	5	$F=111+2,57D$
7	$\sigma_{comp}=244,7-8,03D$	7	$\sigma_{comp}=159,2-3,8D$
10	$K_{perm}=(2,683D-11,1)10^{-3}$	10	$K_{perm}=(14+3,36D)10^{-3}$

Notes pour le Tableau I :
* Propriétés des ciments de colmatage
1) Degré d'étalement (F), cm
2) Prise initiale à 22 °C (I), mn
3) Prise finale à 22 °C (F), mn
4) Prise initiale à 75°C (I) mn
5) Prise finale à 75°C (F), mn
6) Temps d'épaississement à 75 °C (T), mn
7) Résistance à la compression à 22 °C (σ_{comp})
8) Résistance à la compression à 75 °C (σ_{comp})
9) Perméabilité à l'eau du ciment durci après deux jours, 22 °C (K_{perm}), millidarcy
10) Perméabilité à l'eau du ciment durci après deux jours, 75 °C (K_{perm}), millidarcy
** Compositions des ciments de colmatage
CC - ciment portland pour colmatage
ciments allégés :
CCA-1-50 p.pond. de CC + 50 p.pond. de la gaize ; CCT-2-70 p.pond. de CC + 30 p.pond. de la gaize
Gel-ciment-75 p.pond. de CC + 25 p.pond. de la bentonite
ciments allégés expansifs :
CCAE-1-55 p.pond. de CC + 15 p.pond. de CaO + 35 p.pond. de la gaize
CCAE-2-50 p.pond. de CC + 20 p.pond. de la boue de chromates + 35 p.pond. de la gaize
ciments expansifs :
CCE-1-100 p.pond. de CC + 15 p.pond. de CaO + 5 p.pond. de la gaize
CCE-2-100 p.pond. de CC + 15 p.pond. de CaO + 20 p.pond. du sable
CCE-3-60 p.pond. de CC + 15 p.pond. de CaO + 40 p.pond. du sable
CCE-4-60 p.pond. de CC + 20 p.pond. de la boue de chromates + 40 p.pond du sable
ciments alourdis :
CCL-1-60 p.pond. de CC + 40 p.pond. de la magnétite
CCL-2-40 p.pond. de CC + 60 p.pond.de la magnétite
CCL-3-50 p.pond. de CC + 50 p.pond. des résidus de pyrites
CCL-4-50 p.pohd. de CC + 50 p.pond. de l'hématite

à l'accroissement de 3 fois de la résistance de la pierre de ciment CCAE-2 durant les premiers deux jours, l'augmentation graduelle de la teneur en petites fractions s'accompagnant toujours d'accroissement de résistance. Pour CCAE-2 qu'on recommande d'utiliser aux températures de 90 à 120 °C, la valeur optimale de D se trouve dans les limites de 14 à 15 μm. L'accroissement de la valeur optimale de D qui suit la hausse de la température correspond en gros aux conclusions faites auparavant pour CC ordinaire.

On a également étudié l'influence de la composition granulométrique sur les propriétés des ciments de colmatage expansifs (CCE) ayant une grande expansion (jusqu'à 6 %) à base d'oxydes (en particulier, avec addition d'oxyde de calcium). L'analyse des résultats des études du CCE-1, utilisé essentiellement pour la cémentation des puits à la température jusqu'à 75 °C, montre que tant à 22 °C qu'à 75 °C on observe l'accroissement de résistance à la compression du ciment durci à mesure que la teneur en petites fractions augmente ; la tendance à l'accroissement continu de la résistance avec le temps se conserve, bien que la vitesse de cet accroissement diminue graduellement.

La valeur optimale de D pour le ciment en question avec E/C = 0,5 se trouve dans l'intervalle de 14 à 16 μm. Une conclusion analogue a été faite pour CCE-2 avec addition de 20 % de sable, utilisé à des températures jusqu'à 90 °C, bien que ce ciment se caractérise également par une certaine diminution de résistance avec le temps lorsque la teneur en petites fractions augmente. On a procédé à des études analogues pour CCE destinés aux températures plus élevées.

On a également étudié l'influence qu'exerce la composition granulométrique sur les propriétés des ciments de colmatage alourdis (CCL) de composition différente (2). Les CCL-1 et 2 avec magnétite se caractérisent par ce que même une variation relativement petite de teneur en petites fractions de 0 à 5 et de 5 à 10 μm, conditionnée par la technique de broyage, conduit à une augmentation notable de leur résistance. Ainsi, l'accroissement de la teneur en fractions 0-5 μm de 12,2 à 19,6% et en fractions 5-10 μm de 25,5 à 31,6 % conduit à l'augmentation de résistance de 14,6 à 20,6 MPa à l'âge de deux jours, la perméabilité de la pierre de ciment diminuant de trois fois. Avec l'accroissement de la teneur en magnétite, ces dépendances restent en vigueur, bien que la résistance diminue en valeur absolue.

Le domaine de D optimal pour CCL avec magnétite se trouve, pour les rapports E/C = = 0,35 et 0,38 dans l'intervalle de 20 à 22 μm.

On a également étudié la relation entre la composition granulométrique des ciments de colmatage, la composition chimico-minéralogique des différentes fractions constitutives et la structure physique du ciment durci. Il a été admis que telles ou telles fractions du ciment se trouvent parfois surenrichies, par rapport à la teneur moyenne, en constituants de clinker déterminés. Pour vérifier cette supposition, on a divisé une série de ciments en 15 fractions (y compris en 8 fractions dans l'intervalle de 0 à 40 μm) et en procédant à l'analyse quantitative aux rayons X, on a déterminé la teneur de chaque fraction en minéraux essentiels. Ensuite on a construit les diagrammes de variation du pourcentage de ces minéraux en fonction de la dimension moyenne des particules de ciment. L'hypothèse a été confirmée et on a établi que la teneur du ciment en chaque minéral a ses maxima et minima dans des intervalles

déterminés de dimension des particules de ciment, constants pour chaque mineral, et ceci quels que soient le type du ciment, la cimenterie et le mode de broyage. Ainsi, la quantité maximale de C_3S est contenue dans les petites particules de ciment de dimension variant de 3 à 12 μm et la quantité minimale, dans des particules plus grandes de dimension de 50 à 100 μm ; la teneur en C_3S des fractions de 0 à 12 μm dépasse sa teneur dans le ciment de départ de 25 à 30 %, et dans les fractions de 50 à 100 μm elle est 1,5 à 2 fois plus petite que dans le ciment de départ. Ceci permet d'intensifier considérablement le processus de durcissement lorsque la teneur du ciment en petites fractions augmente jusqu'à une valeur optimale déterminée pour chaque ciment (3, 4).

On a émis une hypothèse d'après laquelle la structure physique de la pierre de ciment (en particulier la micromorphologie de sa surface, la porosité et la perméabilité) est conditionnée, de façon déterminée, par sa granulométrie, surtout au cours du durcissement précoce, et peut donc être "programmée" à l'avance au stade de broyage du ciment et aisément réglée au besoin.

Les analyses de la micromorphologie du clivage de la pierre de ciment par la méthode de microscopie électronique à balayage ont confirmé cette hypothèse et montré qu'aux délais précoces (2 jours après le gâchage) la pierre (fig. 1, c et d) se compose en général des particules d'à peu près la même dimension prédominante (D) que le ciment de départ (fig. 1, a et b), ces particules étant fixées l'une à l'autre par le "gel" des nouvelles formations hydratées. Ceci est caractéristique pour CC composé des fractions fines (fig. 1,a) et pour CC de broyage plus grossier (fig. 1,b).

Il est naturel que s'il existe une telle dépendance pour les particules de ciment formant la carcasse de la pierre de ciment, il devrait exister une dépendance analogue pour les pores formés par ces particules (5). Pour évaluer quantitativement ces phénomènes, on a pris pour base le nomogramme connu du professeur V.S. Danuchevski et du candidat ès sciences techniques K.A. Djabarov, d'après lequel on peut déterminer la relation entre E (porosité totale de la pierre de ciment), R (rayon moyen des pores) et K_{perm} (perméabilité à l'eau) (fig. 2,a). Sur la base des données expérimentales disponibles sur la granulométrie et la perméabilité à l'eau du ciment durci à l'âge de deux jours, on a construit un diagramme montrant la dépendance de K_{perm} par rapport à la dimension moyenne conventionnelle D des particules de ciment. Comme il est apparu, cette dépendance a un caractère linéaire. En disposant de la valeur expérimentale de E pour une valeur déterminée de D et de la perméabilité à l'eau K_{perm}, on déterminait d'après le nomogramme la valeur de R en construisant de cette façon le diagramme de dépendance de R par

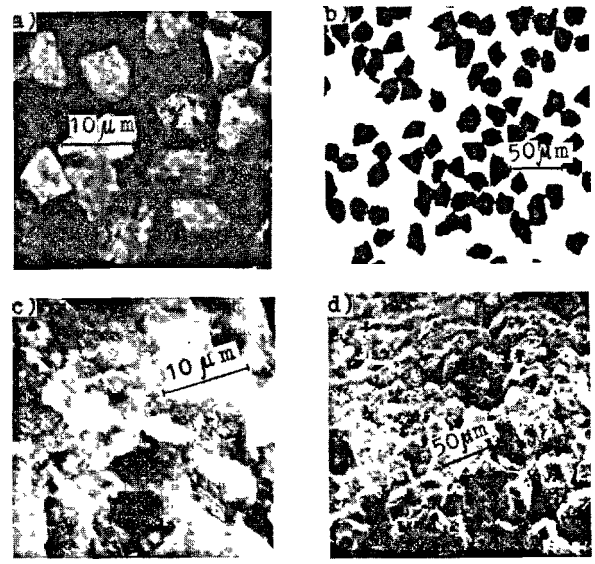

Fig. 1 - Influence de la composition granulométrique du ciment de colmatage sur la microstructure de la pierre de ciment.
a, c) CC de broyage fin (fractions de<40μm) S_{sp} = 3900 cm^2/g ; D = 8,83 μm ; rayon moyen des pores R = 0,05 μm
b, d) CC de broyage industriel S_{sp} = 2890 cm^2/g ; D = 24,76 μm ; rayon moyen des pores R = 0,16 μm

rapport à D, qui a, lui aussi, un caractère linéaire (fig. 2,b). Les dépendances linéaires établies de K_{perm} et de R de la pierre de ciment par rapport à sa composition granulométrique, qui se manifestent surtout pour les délais de durcissement précoces, témoignent d'une possibilité réelle de réglage de la microstructure de la pierre de ciments pour colmatage encore au stade de son broyage, ce qui a une grande importance pratique.

Nous avons élaboré un procédé rapide simplifié de détermination du paramètre D par l'analyse pétrographique *) des particules de ciment en immersion, qui consiste dans la détermination de la valeur moyenne (diamètre) soit des particules de ciment elles-mêmes dans l'échantillon moyen, soit des cristaux d'alite bien visibles dans ces dernières.

Les équations de régression obtenues montrent qu'entre ces grandeurs et le paramètre D existe une dépendance linéaire (fig. 3).

---

*) Ce travail était fait avec la participation du pétrographe V.I. Goussev.

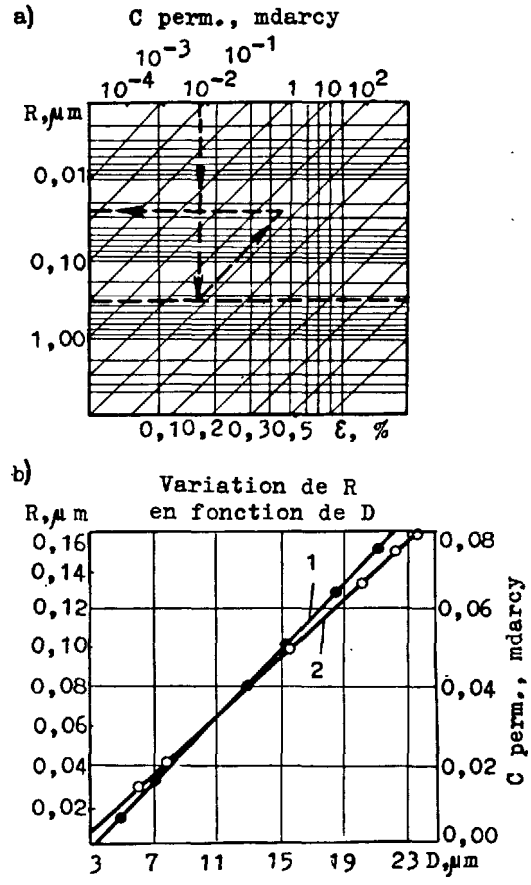

Fig. 2 - Relation entre la dimension moyenne conventionnelle des particules du ciment (D) et la structure physique de la pierre de ce ciment (porosite-1 et permeabilite-2). Temperature de 75 °C, temps de durcissement de deux jours. (a - les donnees de V.S. Danuchevski et K.A. Djabarov) ; Cp - coefficient de permeabilite a l'eau, mdarcy ; R - rayon moyen des pores, μm ; porosite totale - ε ; variation de R en fonction de D ; D - dimension moyenne conventionnelle des particules de ciment, μm.

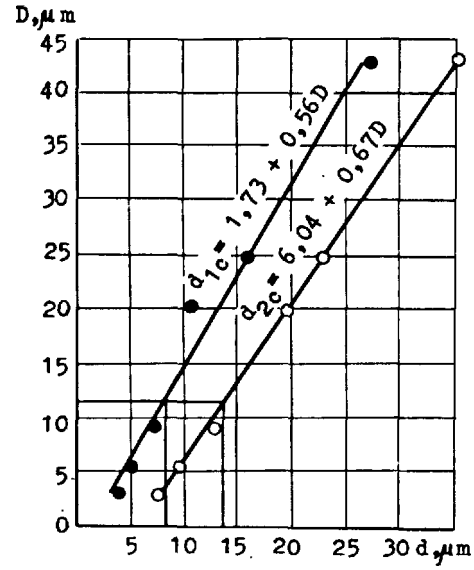

Fig. 3 - Variation de dimension moyenne des cristaux d'alite d_1(I) et des particules de ciment d_2(2) en fonction de la dimension moyenne conventionnelle des particules D (d_1 et d_2 sont determines petrographiquement, D est determine par le calcul d'apres les donnees de l'analyse de la composition granulometrique du ciment ; d_c - d calcule).

CONCLUSION

L'analyse des résultats de ce travail montre que la composition granulometrique des ciments de colmatage determine pour beaucoup leurs principales proprietes technologiques : etalement, temps de prise et duree d'epaississement, resistance, porosite et permeabilite. En reglant la composition granulometrique au cours du broyage du ciment, on peut regler par la meme les proprietes indiquees, en les choisissant pour la resolution de tel ou tel probleme concret. Ceci permet de conclure sur la necessite, lors du broyage des ciments de colmatage, du controle de leur composition granulometrique afin d'en optimiser le degre de finesse et les proprietes technologiques.

BIBLIOGRAPHIE

I.- Г.С.ХОДАКОВ (I972) "Физика измельчения" Изд. "Наука", Гл.ред.физ.-мат.литературы, М., 9-4I, (en russe).

2.- Х.АЛЬ-ВАРДИ, В.С.БАКШУТОВ, ЧХАО ШИН-ХУАН (I976), "Влияние гранулометрического состава утяжеленных тампонажных цементов на прочность цементного камня", Сборник "Экспресс-информация", серия "Геология, бурение и разработка газовых месторождений", М., Изд. ВНИИЭГазпром, № 24, I4-I8, (en russe).

3.- Х.АЛЬ-ВАРДИ, И.Ф.ТОЛСТЫХ, В.С.БАКШУТОВ, ЧХАО ШИН-ХУАН (I977) "Об оптимальном гранулометрическом составе тампонажных цементов", Сборник "Экспресс-информация", серия "Геология, бурение и разработка газовых месторождений", М., Изд. ВНИИЭГазпром, № 3, 7-I2, (en russe).

4.- Б.ВЕРИНСКИ (I976) "Влияние гранулометрического состава цемента на его свойства", УI Международный Конгресс по химии цемента, М., Стройиздат, т. 2, книга I, I76-I79, (en russe).

5.- Ю.В.ЧЕХОВСКИЙ, Л.Е.БЕРЛИН, "О кинетике формирования поровой структуры цементного камня", УI Международный Конгресс по химии цемента, М., Стройиздат, т. 2, книга I, 294-297, (en russe).

Aspect cristallochimique du durcissement des ciments pour forages pétroliers

Crystallochemical aspect of hardening of oil - well cements

V.V. ILIOUKHINE, Docteur ès Sciences Physico-Mathématiques, Institut de Cristallographie de l'Académie des Sciences de l'U.R.S.S.,
V.S. BAKCHOUTOV, Candidat ès Sciences Techniques, Collaborateur Scientifique au Laboratoire de Cémentation des Puits de l'Institut I.M. Goubkine de l'Industrie Pétrochimique et du Gaz,
A.N. LIOUSSOV, Docteur ès Sciences Economiques, Professeur, Directeur de l'Institut de l'Information et de l'Economie de l'Industrie des Matériaux de Construction,
M.K. NIKOLAEVA, Candidat ès Sciences Techniques, Secrétaire Scientifique, Moscou, U.R.S.S.

RESUME : On a étudié dans ce travail le mécanisme et la cinétique de la cristallisation ainsi que la structure cristalline des monocristaux d'hydrosilicates et d'hydroaluminates de calcium de composition différente, qui se forment lors du durcissement des ciments pour forages pétroliers, dans les conditions spécifiques des forages (de -10°C jusqu'à + 300°C et des pressions allant jusqu'à 150 MPa) en contact avec les milieux salins concentrés (jusqu'à 80 % par rapport à la stauration), etc.

On a établi que les réactions d'hydratation, au cours desquelles le type et la structure des phases hydratées se constituent, peuvent se produire en solution ou de façon topotactique. Les cristaux hydratés stables qui se forment dans les pâtes de ces ciments sont principalement constitués de formations régulières des types suivants : enchevêtrement, interpénétration, concrétion. Le développement de ces dernières formations cristallines, dans la pâte durcissante, dès le début de l'hydratation, grâce au choix de la composition stoechiométrique du clinker et au choix de la composition du liquide, est le principe essentiel qui permet de contrôler la cristallochimie de ces sortes de ciment, et d'accroître leur efficacité.

SUMMARY : The work investigates the mechanism, kinetics of crystallization and cristalline structure of monocrystals of calcium hydrosilicates and hydroaluminates of different composition which are formed at hardening of oil-well cements under the specific conditions of the wells (-10 °C +300 °C, pressures up to 150 MPa) and on contact with concentrated salt media (up to 80 % saturation), etc.

It has been found out that the hydration reactions wherein the type and structure of the hydrate phases are formed can take place both through the solution and topotactically. The main form of stable existance of hydrate crystals in the oil-well cement stone are regular concretions of the following main types : intergrowth, interpenetration and combinations thereof. Increase of their number for a given crystalline phase within the volume of the hardening system at the beginning of hydration, either by introduction from the outside or by formation in the bulk of the hardening system owing to selection of the composition and stoichiometry of the solid (binder) and liquid (mixing medium) phases, is the main principle of crystallochemical control of the oil-well cement hardening processes with a view to instensifying the latter.

Les processus d'interaction cristallochimique des phases hydratées apparues entre elles et avec les minéraux du liant de départ, i.e. les processus de concrétion des cristaux, jouent un rôle essentiel dans la formation de la structure résistante de la pierre.

Les particularités cristallochimiques de la structure des phases hydratées principales (parmi celles présentes dans les systèmes durcissants de ciments de colmatage), à savoir les hydrosilicates de calcium (HSC), de composition différente et de formule générale :

$$\left\{Ca_x \left[Si_y(O,OH)_z\right] \cdot (H_2O)_m \cdot \left[Ca(OH)_2\right]_n\right\},$$

où x, y, z > 0, m, n ⩾ 0,
et les hydroaluminates de calcium et les complexes formés à leur base de composition différente et de formule générale :

$$\left\{Ca_x \left[(Al_y, Fe_m)\cdot R_z\right] \cdot (H_2O)_n \cdot \left[Ca(OH)_2\right]_p \cdot \left[Al(OH)_3\right]_q\right\},$$

où x, y, z > 0 ; m, n, p, q ⩾ 0, $R\text{-}O^{2-}$, $(OH)^-$, Cl^-, $(SO_4)^{2-}$, etc., se forment encore au stade de leur état préembryonnaire. Une vraie solution moléculaire qui apparaît au cours de la dissolution des constituants de départ du liant, se compose d'abord de complexes séparés, ayant une organisation structurale déterminée, de trois types: les complexes de solvates ordinaires du type $[CaO\text{-}H_2O]$, $[SiO_2\text{-}H_2O]$ et $[Al_2O_3\text{-}H_2O]$ ayant la structure de la phase initiale, les complexes des nouvelles formations du type $[xCaO\cdot ySiO_2\cdot zH_2O]$ et $[xCaO\cdot yAl_2O_3\cdot zH_2O]$ apparaissant de façon épitaxiale-topotactique et ayant la structure du constituant de départ, et les complexes dits "de transport" - par exemple pour les hydrosilicates de calcium, ce sont les complexes du type $[(Ca\text{-}Si)R_z] \cdot (H_2O)_m \cdot (OH)_{\overline{n}}$, où R est un ion alcalin dit "de transport" (Na^+, K^+, Li^+).

Dans ce cas, la formation des phases hydratées (par exemple, des hydrosilicates de calcium) a lieu lorsque les ions de transport substituent, encore en solution, de façon isomorphe l'ion Ca^{2+} dans ses complexes, ce qui entraîne la diminution de leurs dimensions (vu que le nombre de coordination, par exemple Na^+, est de deux fois inférieur à Ca^{2+}), la diminution de la masse et l'accroissement de leur mobilité. De plus, on assiste en même temps à la substitution aux atomes de O dans les chaînes (Si-O) des groupes $(OH)^-$ qui, pour un volume identique à celui des atomes de O, ont une charge ionique deux fois moindre. Ceci conduit à la rupture de longues chaînes (Si-O), ce qui augmente la disposition des éléments de la solution pour l'association régulière.

Avec l'accroissement de sursaturation, la quantité de ces complexes de transport et de leurs associés par unité de volume augmente et lorsqu'ils sont proches l'un de l'autre, les forces d'attraction mutuelle les réunissent en groupements construits en présence des éléments de régularité spatiale. Ce sont justement la structure et la quantité de ces groupements qui prédéterminent la structure du germe et son type.

Dans ce travail on a posé le problème d'élaboration et d'étude des monocristaux de certaines phases de HSC et de leurs agrégats, des conditions de leur apparition et de détermination des frontières des champs de stabilité dans une large gamme des conditions initiales (1-3).

La cristallisation hydrothermale dans le système $CaO\text{-}SiO_2\text{-}ROH$ (R-Na, K, Li) était réalisée dans l'intervalle de températures de 200° à 700° et de pressions de 100 à 300 MPa, imitant les conditions des puits profonds, d'après la méthode connue, avec variations du rapport CaO/SiO_2 (pond.) = = 0,25 à 5,0 et celles de la concentration de l'alcali de 0 à 60 %.

Au cours de la cristallisation hydrothermale se manifesta le rôle "catalytique" de Na^+ qui est proche, du point de vue cristallochimique, du cation "matriciel" des hydrosilicates, à savoir Ca^{2+} : les produits principaux de la synthèse étaient des monocristaux de différents HSC de 10 mm environ de longueur et de près de 3 mm de diamètre (fig. 1) ; dans certains cas (synthèse dirigée), on a obtenu des monocristaux de composition mixte (Na, Ca).

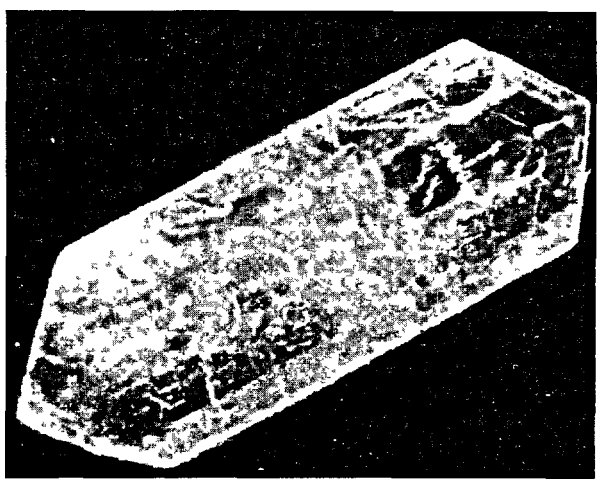

Fig. 1 - Monocristal de Ca-chondrodite de composition C_5S_2H (lumière passante, x100)

L'analyse cristallochimique des processus de synthèse des HSC de telle ou telle structure a montré que la formation et la croissance des HSC sont dues à l'aptitude de Ca à construire des incréments de structure caractéristiques de telles ou telles conditions concrètes, lorsque le matériau

de construction "non calcique" est disposé dans les chambres et les couloirs de la cage principale en Ca (4). La silice est une "charge" principale ; selon N.V. Bélov (4), la molécule neutre de SiO_2 à deux liaisons potentielles Si-O et de configuration "angulaire" (exigée par la chimie quantique) (O-Si-O ~ 109°) est une unité dynamique sous forme de laquelle la silice passe d'une construction à l'autre ; c'est justement cette molécule "angulaire" SiO_2 qui forme dans les structures de HSC l'unité statique, le tétraèdre de Si. Les exigences énergétiques de réalisation des liaisons potentielles de la molécule "angulaire" de SiO_2 lors de la formation de l'ossature structurale de tel ou tel HSC s'expriment par le postulat cristallochimique sur la conformité dimensionnelle des arêtes des polyèdres de Ca et des tétraèdres de Si. Les motifs silico-oxygénés qui se fixent dans les structures des HSC : tétraèdres isolés, diorthogroupes, triorthogroupes, rubans, gaufres, etc., suivent entièrement les aires de croissance primaires en polyèdres de Ca. Ainsi, pour les HSC faiblement basiques et hautement polymérisés de type xonotlite-hillébrandite-tobermorite de faciès fibreux, les éléments structuraux principaux silico-oxygénés - les rubans à anneaux octagonaux $[Si_6O_{17}]_\infty^{10-}$ ou les gaufres $[Si_{12}O_{31}]_\infty^{14-}$ à base de ces rubans - correspondent aux colonnes triples ou (dans la hyllebrandite et les tobermorites) aux couches d'octaèdres de Ca en cas d'une correspondance complète des périodes de répétition des éléments structuraux indiqués le long de l'axe "b" ; pour les éléments [Si-O] cette période est égale à n·7,3 Å, pour les éléments [Ca-O] à 2n·3,65 Å. Dans ce cas, dans xonotlite $Ca_6[Si_6O_{17}] \cdot (OH)_2$ les parois (couches d'octaèdres de Ca alternants) sont "fixées" entre elles par les rubans $[Si_6O_{17}]_\infty^{10-}$, dans la hyllebrandite $Ca_{12}[Si_6O_{17}] \cdot (OH)_4 \cdot 12Ca(OH)_2$ les unités structurales "de xonotlite" sous-mentionnées "s'alternent" en quelque sorte avec les couches de portlandite $(Ca(OH)_2$, et, dans la tobermorite $Ca_{10}[Si_{12}O_{31}] \cdot (OH)_6 \cdot nH_2O$ (n = 3, 8, 18), le motif cristallin est un réseau gaufré formé lors de la condensation et du "chevauchement" mutuel des mêmes rubans $[Si_6O_{17}]_\infty^{10-}$; ce fait témoigne avant tout de la similitude cristallochimique des éléments principaux de la structure résistante du ciment durci.

Du point de vue cristallochimique, l'hydratation du liant peut suivre deux voies - celle de solution et topotactique. Dans les deux cas, au début, a lieu l'interaction des ions H^+, $(OH)^-$, des dipôles d'eau avec le cristal du minéral de départ, ce qui fait que sa couche superficielle (de la couche monomoléculaire jusqu'aux milliers de couches atomiques) se trouve déformée et détruite par la suite.

Au début de l'hydratation, lorsque le système contient beaucoup de phase liquide et le degré de polymérisation des radicaux $[Si_xO_y]^{z-}$ et $[Al_xO_y]^{n-}$ est peu élevé, la cristallisation se fait essentiellement moyennant la solution, car, dans ces conditions, il est plus facile d'ordonner des éléments structuraux relativement petits des hydrates en réseau cristallin. A ce stade il apparaît habituellement beaucoup d'hydrates différents faiblement polymérisés. Mais par la suite commence à prédominer la voie topotactique de formation des phases hydratées. Si l'on considère, par exemple, l'hydratation des minéraux principaux (siliceux) des ciments de colmatage, on voit se former deux groupes d'hydrates : à base de la structure de β - ou γ -C_2S se forment la chondrodite calcique $Ca_5[SiO_4]_2 \cdot (OH)_2$ ou $2C_2S \cdot CH$, la dellaïte (phase Y) $Ca_6[Si_2O_7] \cdot [SiO_4] (OH)_2$, l'afwillite $3CaO \cdot 2SiO_2 \cdot 3H_2O$ faiblement polymérisés fortement basiques ; sur la base de la structure de la wollastonite β -$CaO \cdot SiO_2$ se forment la xonotlite $Ca_6[Si_6O_{17}] \cdot (OH)_2$, la hillebrandite $Ca_6[Si_6O_{17}]_2 \cdot (OH)_4 \cdot 12Ca(OH)_2$ ou $C_2SH(B)$, les phases de tobermorite du type $Ca_{10}[Si_{12}O_{31}] \cdot (OH)_6 \cdot nH_2O$ et d'autres HSC faiblement basiques hautement polymérisés.

La structure résistante de la pierre de ciments de colmatage est formée par des agrégats réguliers (prédominants) et des agrégats irréguliers des cristaux (5) (fig. 2). Les germes des agrégats réguliers se forment principalement avec des sursaturations élevées par déposition, sur la face conventionnelle du cristal primaire, de l'associés des atomes ou des ions en position maclée (le plus souvent antiparallèle).

Fig. 2 - Agrégats de cristaux de HSC du groupe de la chondrodite (lumière passante, avec analyseur, x10)

A partir des associés "maclés" ainsi apparus il se forme des agrégats réguliers : la plupart des HSC fortement basiques sont maclés d'après les lois périclinique et de Manebach (fig. 3) ; les HSC faiblement basiques se caractérisent par le maclage et la formation des agrégats parallèles dans la direction parallèle à l'axe d'allongement du cristal, ce qui est dû à leur fa-

ciès fibreux-filiforme. Il convient de noter que seuls les cristaux analogues sur le plan structural et chimique présentent en règle générale des agrégats réguliers.

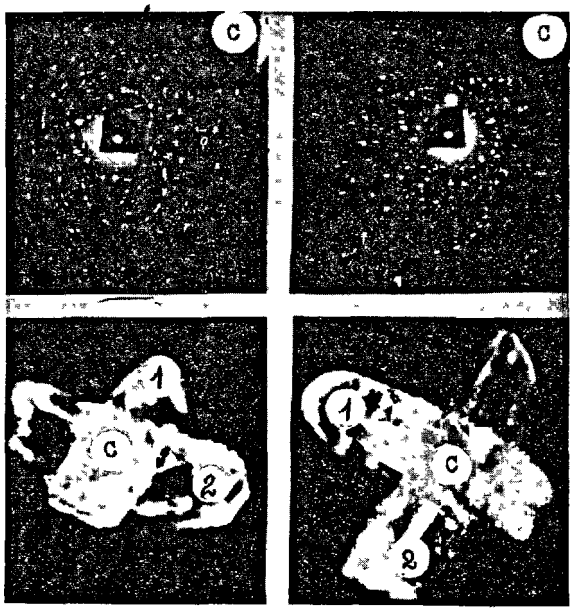

Fig. 3 - Diagrammes de Laue de la zone de contact (C) des agrégats de cristaux de HSC du groupe de la chondrodite (structures d'enchevêtrement)

La concrétion de ces cristaux se réalise par l'accolement des éléments identiques de leur structure : pour HSC par exemple ce sont les couches octaédriques de portlandite et les radicaux de degré de polymérisation voisin. Dans le premier cas a lieu une concrétion "classique" d'après des lois déterminées : de maclage polysynthétique, périclinique, de Manebach, etc., et dans le deuxième cas, une "couture" de polymérisation avec la formation des structures résistantes spatiales de durcissement (5). La concrétion régulière des cristaux de composition différente peut avoir lieu d'après le schéma de Royer-Friedel avec une correspondance relative de leurs paramètres réticulaires dans la zone des contacts. Les agrégats de ce type sont caractéristiques d'une grande classe de cristaux hexagonaux lamellaires des aluminates hydratés de calcium et de composés complexes à base de ces derniers.

Les agrégats réguliers se forment au stade de germination lorsque la probabilité d'apparition de la zone de contact à peu de défauts est maximale. D'après nos données, la dimension des microcristaux qui forment intensément des macles au stade de germination ne dépasse pas 10^{-5} cm et leur particularité caractéristique est une aptitude manifeste à la croissance ultérieure.

Les cristaux mal orientés d'un même type structural et les cristaux de types structuraux différents donnent des agrégats irréguliers.

Ainsi donc, la structure cristalline résistante de la pierre de ciment de colmatage est une carcasse formée par des agrégats réguliers relativement grands (jusqu'à 10^{-2} cm), des cristaux individuels des phases hydratées et leurs agrégats (textures) basés dans l'espace intergranulaire et sur les grains en cours d'hydratation du liant de départ, "fixée", aux points de contacts, par le "gel" des nouvelles formations hydratées (6) qui est également représenté par les microgermes des agrégats réguliers, des cristaux individuels et de leurs agrégats dont la dimension est inférieure à 10^{-5} cm.

En mettant en évidence les régularités de l'interaction cristallochimique des cristaux des minéraux composant la pierre de ciments de colmatage, on a réussi à formuler un procédé de réglage cristallochimique des processus de leur durcissement (dans le but d'intensification) grâce à l'augmentation de la quantité de phase cristalline stable (agrégats et cristaux individuels) dans le volume du système durcissant aux stades d'hydratation précoces (7, 8). On peut l'atteindre par deux voies : soit par "renforcement mécanique" du système en y introduisant des HSC "prêts" et/ou leurs constituants, soit par "autorenforcement" du système en créant les conditions pour l'apparition spontanée de ces phases hydratées (dites intensificateurs cristallochimiques de durcissement - ICD) grâce au choix de la composition et de la stoechiométrie des phases solide et liquide.

Les exigences principales envers ICD sont les suivantes : ils doivent être analogues du point de vue chimique et structural à la masse principale des cristaux d'hydrates qui sont stables dans des conditions concrètes données ; les cristaux de ICD doivent avoir une dimension de 10^{-6} à 10^{-5} cm, le faciès de préférence filiforme et l'aptitude à une croissance ultérieure intense, i.e. à l'accolement avec leurs semblables et la matrice de ciment. Les ICD contribuent à l'apparition spontanée d'un grand nombre d'agrégats stables des hydrates au stade précoce de durcissement, remplissent les fonctions de supports d'orientation pour les hydrates apparaissant dans le système principale, augmentent la concentration totale de la phase cristalline aux stades d'hydratation précoces, accélèrent chimiquement les réactions d'hydratation grâce à l'évacuation des nouvelles formations (ions, complexes) des zones de réaction et "renforcent" de façon purement mécanique le système en cours de durcissement, ce qui entraîne une amélioration notable de sa structure physique et des propriétés de résistance (fig. 4).

Fig. 4 - Zone de contact des ICD de renforcement avec la matrice de ciment (réplique de platine-carbone, x10000)

L'introduction dans le système durcissant des ICD du type de HSC de composition, structure, dimension, degré de perfection, etc., différents qui représentent les phases métastables synthétisées lors de l'interaction des solutions aqueuses saturées de la chaux et de l'acide silicique, en quantité de 1 à 3 % par rapport à la masse du ciment conduit à l'accroissement de résistance de la pierre de ciment d'une valeur allant jusqu'à 60 % (7, 8).

Des résultats positifs furent également obtenus par introduction simultanée dans le système du ciment durcissant de colmatage des constituants individuels de HSC-CaO ou de $Ca(OH)_2$ avec des formes différentes de SiO_2.

L'utilisation en tant que ICD, dans les solutions allégées, de la chaux anhydre qui, en combinaison avec le constituant siliceux très fin hydrauliquement actif, (gaize), permet d'augmenter considérablement la quantité de HSC aux délais de durcissement précoces, a permis d'obtenir, pour la densité de la solution de l'ordre de 1,5 g/cm^3, un ciment durci avec σ_{flex} après deux jours de durcissement à 75 °C, de l'ordre de 2,0 à 2,5 MPa et σ_{comp} de l'ordre de 7,0 MPa, i.e. dépassant de plus de deux fois les ciments ordinaires de ce type.

On a élaboré par un procédé analogue une série de ciments de colmatage expansifs (CCE) de grande expansion, utilisant en tant que constituants des ICD les oxydes de calcium et de magnésium cuits à des températures différentes en combinaison avec le sable quartzeux (9,10).

Comme un exemple de réalisation pratique de l'"autorenforcement", on peut citer la solution alcaline de potassium (SAP) pour colmatage qui sert à la cémentation des puits à des températures positives peu élevées et négatives(11,12).Le problème principal, à savoir l'accroissement de résistance de la pierre à +5 à -10 °C, fut résolu par application en qualité de liquide de gâchage d'une phase liquide spéciale qui ne gèle pas à t < 0 °C et sert d'intensificateur des processus de durcissement ; lors du durcissement il se forme des ICD, phases hydratées supplémentaires donnant un agrégat cristallin normal et stable dans ces conditions.

CONCLUSION

L'application des méthodes de modification cristallochimique des processus de durcissement des solutions pour colmatage à base de liants minéraux permet d'élever rapidement et avec les dépenses minimales la vitesse de durcissement et la résistance du ciment durci ainsi que d'améliorer sa microstructure. La reproductibilité des résultats est alors très élevée, ce qui permet de considérer comme très avantageuse la méthode cristallochimique de réglage des processus de durcissement des ciments de colmatage ayant pour but leur intentsification.

BIBLIOGRAPHIE

1. Ю.М. БУТТ, В.В. ТИМАШЕВ , В.С. БАКШУТОВ (1969) "Способ получения кристаллов гидросиликатов кальция". Авторское свидетельство СССР № 234373, "Бюллетень изобретений", 1969, № 4, (en russe).
2. Ю.М. БУТТ, В.В. ТИМАШЕВ, В.С. БАКШУТОВ, В.В. ИЛЮХИН, В.А.ИЛЮХИН, В.А. КУЗНЕЦОВ, М.К. ГРИНЕВА "Способ получения монокристаллов гидросиликатов кальция". Авторское свидетельство СССР № 298532, "Бюллетень изобретений", № II, (en russe).
3. Ю.М. БУТТ, В.В. ТИМАШЕВ, В.С. БАКШУТОВ, В.В. ИЛЮХИН, В.А. КУЗНЕЦОВ, М.К.ГРИНЕВА. (1971) "Способ получения изометрических и нитевидных монокристаллов гидросиликатов кальция". Авторское свидетельство СССР № 298531, "Бюллетень изобретений", № II,(en russe).
4. Е.Н. БЕЛОВА, Л.Н. ДЕМЬЯНЕЦ, В.В. ИЛЮХИН, В.С. БАКШУТОВ (1972) "Гидротермальный

синтез силикатов (германатов) в свете их кристаллохимии". Труды IУ Всесоюзного совещания по росту кристаллов. Цахкадзор. 228–234, (en russe).

5. Ю.М. БУТТ, В.В. ТИМАШЕВ, В.С. БАКШУТОВ, В.В. ИЛЮХИН, С.П. ГОЛОВАЧЕВ (I970) "Закономерности образования кристаллов и кристаллических сростков гидросиликатов кальция (ГСК) в твердеющем цементном камне". "Цемент", № 9, I4–I6, (en russe).

6. Х.Ф.В. ТЕЙЛОР (I974) "Кристаллохимия продуктов гидратации портландцемента". Труды УI Международного Конгресса по химии цемента, Москва, Стройиздат, т.2, книга I, I92–207, (en russe).

7. Ю.М. БУТТ, В.В. ТИМАШЕВ, В.С. БАКШУТОВ, В.В. ИЛЮХИН (I97I) "Способ интенсификации процессов твердения минеральных вяжущих". Авторское свидетельство СССР № 900444, "Бюллетень изобретений", № I3, (en russe).

8. Ю.М. БУТТ, В.В. ТИМАШЕВ, В.С. БАКШУТОВ, В.В. ИЛЮХИН, Г.Д. ЛУКАЦКИЙ, М.М. ПАНОВА (I97I) "Бетонная смесь". Авторское свидетельство СССР № 296726, "Бюллетень изобретений", № 9, (en russe).

9. В.С. ДАНЮШЕВСКИЙ, В.С. БАКШУТОВ, ЧЖАО ПИН-ХУАН (I972) "Расширяющийся тампонажный цемент с большой величиной расширения на основе окиси кальция". "Цемент", № I, I4, (en russe).

I0. V.V. SIMONOV, V.S. BAKSHUTOV, D.A.P. SAGUA, J. PIN-KHUAN (1976) "New expanding cement for ultra deep wells" Third Adriatic Symposium an oil well drilling, Zagreb, 102–104, (en anglais).

II. В.В. СИМОНОВ, В.С. ДАНЮШЕВСКИЙ, В.С. БАКШУТОВ, В.Н. НИКИТИН, В.В. ИЛЮХИН (I977) "Тампонажный раствор". Авторское свидетельство СССР № 578435, "Бюллетень изобретений", № 40, (en russe).

I2. В.В. СИМОНОВ, В.С. БАКШУТОВ, В.В. БОНДАРЕНКО, В.Н. НИКИТИН, В.П. ДЕТКОВ, А.И. ЧАЙНИКОВ. "Тампонажный раствор". Авторское свидетельство СССР по заявке № 250I377/03 с приоритетом от 2I.06.77, (en russe).

Application of activated calcium aluminate clinker to quick hardening cement

Utilisation d'une pouzzolane artificielle alumino-calcique dans la fabrication d'un ciment à durcissement rapide

K. ISOZAKI, Research Chemist,
S. SAKAMAKI, Assistant to Research Manager,
K. NAKAGAWA, Senior Research Manager, Denki Kagaku Kogyo Co., Ltd., R and D Department of Omi-Plant, Japan.

RESUME : On a étudié la relation entre la résistance et le processus d'hydratation d'un ciment spécial préparé en mélangeant du clinker de ciment portland avec 20 % de sulfate de calcium et d'un aluminate de calcium activé; ce dernier était obtenu par fusion au four électrique, puis refroidissement brusque, d'un cru approprié. Des mélanges de cette sorte sont utilisés industriellement dans la fabrication des ciments expansifs du type M et dans celle des ciments à haute résistance initiale.

En faisant varier le rapport C/A de cette pouzzolane artificielle et sa proportion dans le ciment, on peut obtenir diverses sortes de ciments à prise rapide. L'augmentation de ce rapport C/A peut accroître les résistances à 1 heure, 7 jours et 28 jours, mais la prise peut devenir trop rapide pour pouvoir être contrôlée. En augmentant l'addition du gypse, les résistances à 3 et 24 heures augmentent, et le ciment devient plus maniable.

Il a été établi que les propriétés de ces ciments dépendent de la vitesse de la formation de l'ettringite et de l'hydratation du C_3S, et que l'on peut maîtriser ces facteurs par réglage du mélange. Une optimisation de ces ciments à prise rapide est possible.

SUMMARY: The relation between the strength and hydration process of the special cement which was prepared by admixing ordinary portland cement with 20%(wt.) of the admixture consisting of calcium sulfate and calcium aluminate clinkers made by quenching after electric melting thereof was examined. The admixtures of this kind are industrially applied to the M-type expansive cement, quick hardening cement and high strength cement.

Various kinds of quick hardening cements can be obtained by varying the C/A ratio of clinker. When the C/A ratio is raised, the strength can be improved per 1 hour, 7 days, and 28 days. but the setting is so rapid that in most cases the control of setting time is difficult. When anhydrite content is increased, there is a tendency that the 3 hour and 24 hour strengths can be increased, and the workability can be also improved.

We have made it clear that the characteristics of quick hardening cement can be determined by the yield and formation timing of ettringite and hydration of C_3S, and these factors can be controlled by said admixtures. Whereby it has been made possible to plan ideal quick hardening cement.

1. INTRODUCTION

We have already reported a part of the method for producing electrically melted calcium aluminate clinker (1) and the application thereof to expansive cement (1,2), quick hardening cement (2), and high strength cement (3,4). The present report discusses more in detail on the basic properties of said calcium aluminate clinker when applied to the quick hardening cement. And, there are reported the hydration process of the cements added with the admixtures prepared by changing C/A ratio of clinker and anhydrite (Type II-calcium sulphate) content, the structures of cement stone, morphology of hydrates and the effects given to the mechanical strength, and such like basic data which become the guidlines for planning ideal quick hardening cement.

2. PREPARATION of SAMPLES

The samples which were prepared by mixing calcium oxide and bauxite at predetermined blending ratios were melted at a temperature in the range of from 1500°C to 1700°C for about one hour and blown by air to quickly cool off. Regarding the calcium aluminate clinkers which were used in this test, the following three kinds of compositions are given below. (Table I)

TABLE I

Chemical composition of clinkers (wt%)

Name of clinker	C/A	CaO	Al_2O_3	SiO_2	f-CaO	blaine (cm^2/g)
A	1.10	48.7	44.1	2.5	0.3	5720
B	0.92	43.9	47.7	3.4	0.1	5530
C	0.65	36.1	55.5	3.8	0.1	5540

TABLE II

Chemical composition of admixtures

Name of admixture	C/A	clinker/ II-$CaSO_4$	$\bar{S}/A$ (SO_3/Al_2O_3)
A_1	1.10	1/1	1.33
A_2	1.10	1/1.5	2.00
A_3	1.10	1/2	2.66
B_1	0.92	1/1	1.23
B_2	0.92	1/1.5	1.84
B_3	0.92	1/2	2.46
C_1	0.65	1/1	1.06
C_2	0.65	1/1.5	1.59
C_3	0.65	1/2	2.11

Table II shows the compositions of 9 kinds of admixtures prepared by adding anhydrite to calcium aluminate clinker. Table III shows the chemical composition of ordinary portland cement.

TABLE III

Chemical Composition of ordinary portland cement (wt%)

ig.loss	insol.	SiO_2	Al_2O_3	Fe_2O_3	CaO
0.7	0.3	22.0	4.8	3.2	64.9

MgO	SO_3	Na_2O	K_2O	f-CaO	blaine(cm^2/g)
1.9	1.9	0.40	0.44	0.7	3110

3. EXPERIMENTAL

The quick hardening cement was prepared by mixing 20% by weight of admixture with 80% by weight of ordinary portland cement. The ratio of water and the cement was 0.41. As the retarder, 0.8% by weight of the mixture of citric acid and potassium carbonate in the ratio of 1:3 to the cement was added. The mixing was carried out in such a manner that water was poured into a vessel to dissolve the retarder, and the quick hardening cement was added thereto and stirred. The curing was carried out at 20°C. 80%rh.

The paste specimen having arrived at the predetermined age was crushed into particles whose particle sizes were respectively from 5.0mm to 2.5mm, and below 1.7mm and the sample whose particle size was from 5.0mm to 2.5mm was subjected to D-drying treatment for two days, and was used as the sample for measuring evaporable water, non-evaporable water (1000°C, 1 hr), pore volume (mercury pressure porosimeter) and observation by scanning electron microscope (SEM). The sample whose particle size was below 1.7mm was washed with ethanol for terminating hydration, and was subjected to the measurement of X-ray diffraction. The heat liberation curve of hydration was obtained by conduction calorimeter, and the compressive strength test was carried out by using 1:2 mortar (4x4x16 cm beam).

4. RESULTS AND DISCUSSION

4-1 HYDRATION PROCESS

The hydration of C_3S is remarkably affected by the C/A ratio of clinker. There is a tendency that the hydration of C_3S is more retarded as the C/A ratio is lower. This tendency holds true not only in the case of early stage of age but also in the case of 28 day age. The effect of anhydrite content is differed more or less by the composition of clinker. (Fig. 2)

Regarding the formation of ettringite, the effect of the C/A ratio is great. In Series A (C/A=1.10), the abrupt formation of ettringite started right after the pouring of water, and the yield arrived slowly at the maximum in 14 days. The formation of ettringite was milder in Series B (C/A=0.92) than in Series A, but the yield of ettringite became constant around one day age, and after the 14th day, the yield thereof became lowered. In Series C (C/A=0.65), the ettringite formation reaction in early age was milder and the vigorous reaction was brought about from 2 to 12 hours, and the yield arrived at the maximum in about one day, and thereafter the yield is abruptly reduced. When the C/A ratio is low and anhydrite content is high, the reaction in the early age is retarded. When the C/A ratio is low and anhydrite content is low, the formation timing of calcium aluminate monosulfate hydrate is accelerated and the yield becomes increased.

The retarding mechanism of hydration of C_3S is considered as follows. While the ettringite producing reaction is vigorously carried out, the crystalline nucleation for C_3S hydration to enter into acceleration period cannot be sufficiently carried out (5). Therefore, it is considered that as the C/A ratio is lower, the delayed period is prolonged.

The reaction between calcium aluminate clinker and anhydrite has the tendency to be more delayed as the C/A ratio is lower, and this can be explained by the protective coating film forming mechanism which controls ion dissolution. It can be confirmed that by the SEM photograph that the clinker enriched more with Al_2O_3, the crystal growing reaction of fine ettringite is more delayed, and this phenomenon is also considered to be related to the concentration of Ca ion.

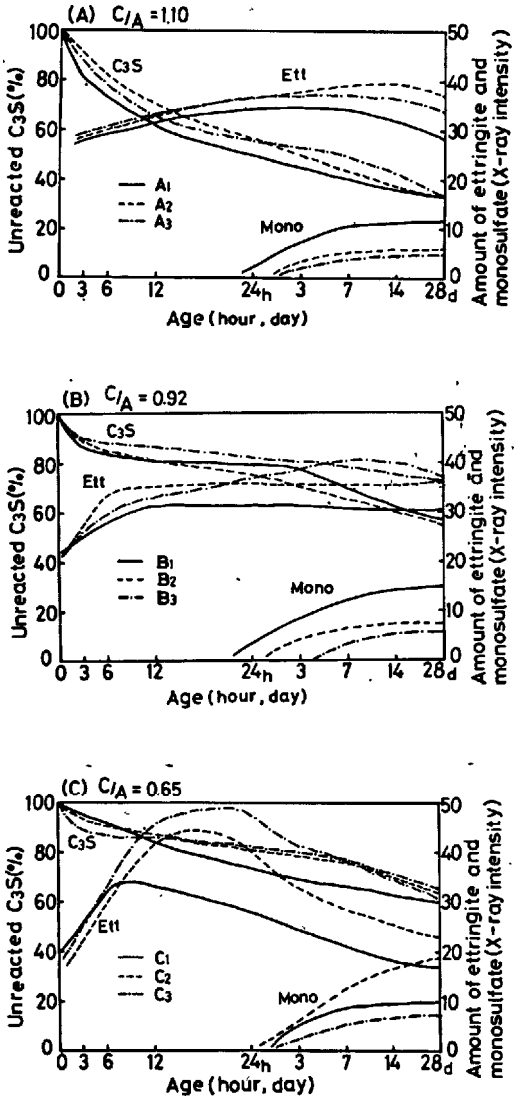

Fig. 1 - Hydration of C_3S and fromations of ettringite (Ett) and calcium aluminate monosulfate (Mono).

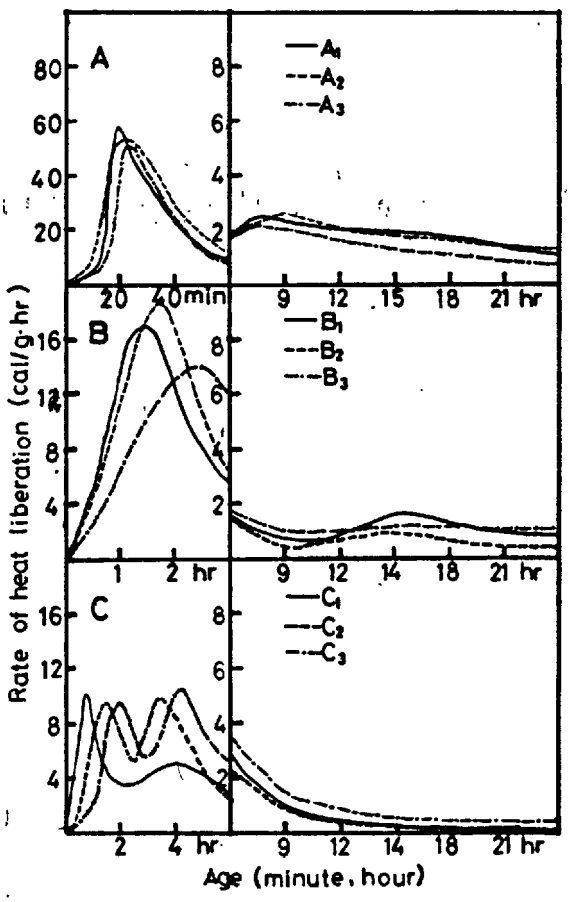

Fig. 2 - Rate of heat liberation.

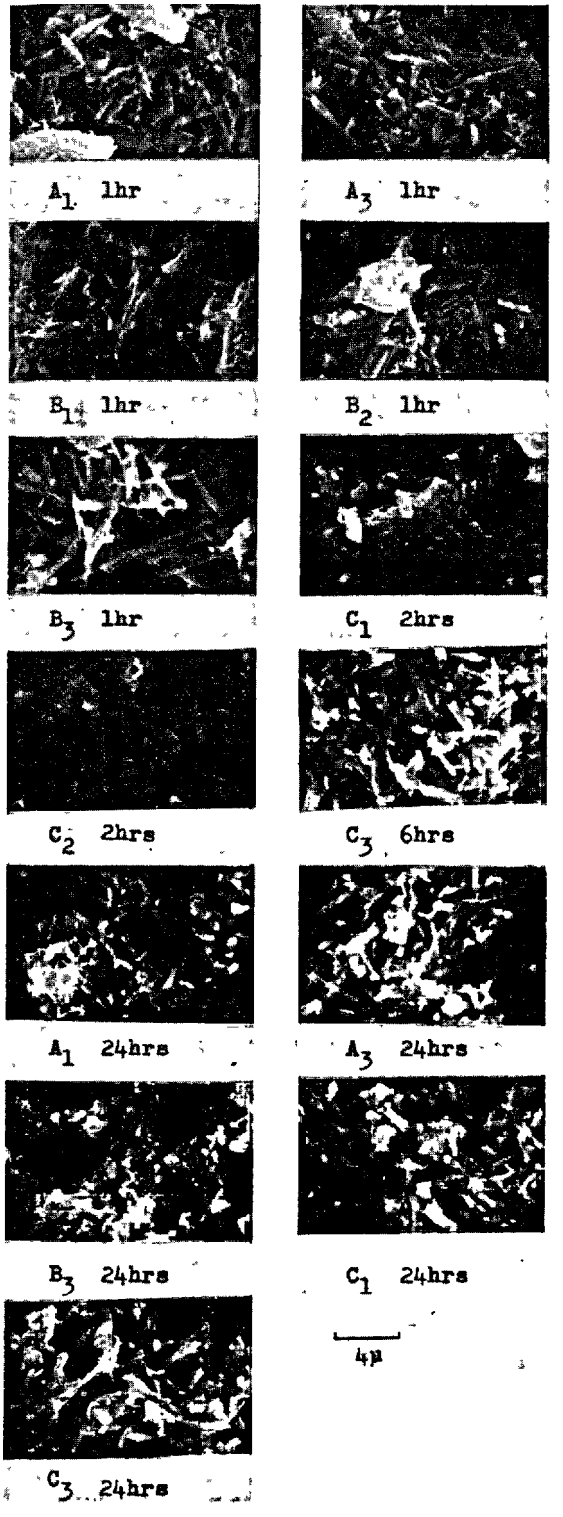

Fig. 3 - Morphology of hydrates (by SEM).

The above described hydration process can be vouched by the heat liberation curve of hydration. The height of the first peak of Series A is about 6 times that of Series C, and is deeply related to the yield of ettringite.
On the other hand, as the anhydrite content becomes larger, the position of the first peaks of Series A, B, and C are delayed and the heights thereof are lower, and the lower the C/A ratio is, the greater the above mentioned tendency is. The appearance of the second peak in Series C is caused by the delay of ettringite producing reaction. The second peaks of Series A and B are overlapped with the first peaks, and therefore the second peaks are not present. (Fig. 2) The size of heat liberation peak caused by C_3S hydration is almost identical with the results of X-ray diffraction.

Fig. 3 shows the morphology of the hydrates by means of SEM. The diameter of ettringite crystal grows in the range of from 0.2 to 0.4 μ and the length thereof in the range of from 3 to 4 μ within 2 hour age in Series A and B and there is not so much difference from those of the sample of 28 day age. In Series C, the sample of 3 hour age, ettringite takes on such a morphology as fine and wide rectangular form and covers the surface of the calcium aluminate particles, said ettringite is also turned into the same morphology and size as in the case of Series A and B in several hours. Calcium aluminate monosulfate hydrates take on remarkably hexagonal morphology before 24 hour age.

4-2 HYDRATE STRUCTURE AND HYDRATION DEGREE

Fig. 4 shows the relation between the non-evaporable water of cement stone and SO_3/Al_2O_3 ($\bar{S}/A$) of the admixture. Throughout all the ages Series B shows high values regardless of anhydrite content, and above all, B_3 shows the highest value and little pore volume. (Fig.5) In Series B, it is remarkable that pore volume ranging from 1000 to 10000 Å which belongs to capillary pore is less than Series A and C. In Series A and B, pore volume from 2000 to 4000 Å is abruptly reduced in 3 hour to one day age, and the pore volume in Series C ranging from 3000 to 9000 Å is reduced over the 3 hour age to one day age, but the pore volume ranging from 1000 to 2500 Å remains unchanged. This is considered to have been caused partially by the morphological change of ettringite in the early stage of the reaction. The C/A ratio rather than anhydrite content overwhelmingly affects non-evaporable water, pore volume and pore size distribution.

Fig. 6 shows the relation thereof to the heat of hydration and Series A takes extremely high value in one hour age, and Series A and B take almost the same values in 3 hour age.

In 24 hour age, there is a tendency that when the C/A ratio is higher, heat of hydration become higher, but the increase in the heat of hydration of B_3 is great.

Regarding the relation between the degree of hydration and the structure of hydrates, not only the kind, morphology and quantity of hydrate are important factors, but also the hydration process is a very important factor.

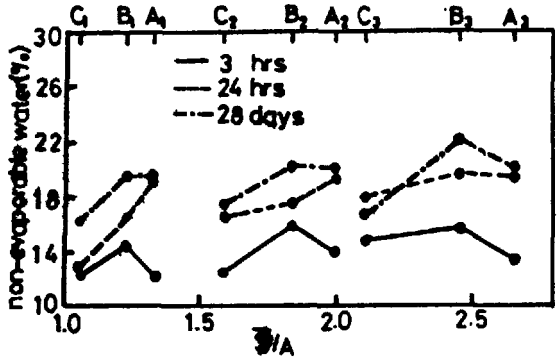

Fig. 4 - Relation between non-evaporable water and $\bar{S}/A$ of admixture.

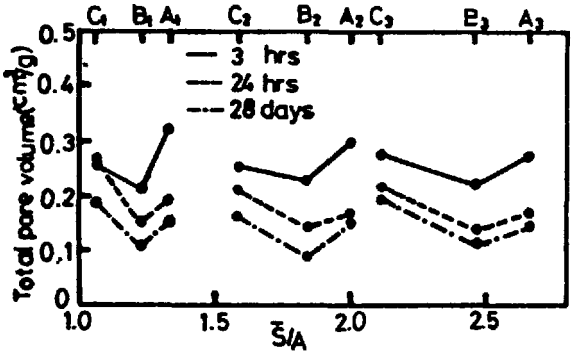

Fig. 5 - Relation between total pore volume (75-75000 Å) and $\bar{S}/A$ of admixture.

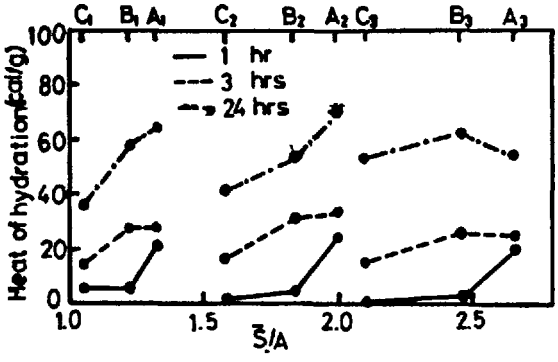

Fig. 6 - Relation between heat of hydration and $\bar{S}/A$ of admixture.

4-3 STRENGTH DEVELOPMENT AND SETTING TIME

The production of ettringite contributes much to the development of primary strength as is apparent in jet cement (5) and it is considered that the hydration of C_3S affects the development of long period strength. In regard to the strength development against unit heat of hydration, up to 24 hour age, Series C is the highest when compared with Series A and B, but the hydration of C_3S is considered to have contributed not so much to the strength development, and in a long period age, no strength development can be observed when the hydration of C_3S has been carried out. This phenomenon is considered to have been caused by the structual change of the conversion of ettringte to calcium aluminate monosulfate hydrate and the carbonation. On the contrary, when the C/A ratio is high, the dependability on C_3S hydration is increased. (Fig. 7, 8) Therefore, not only the yield of ettringite, but also hydration process become an important factor.

As the important characters of quick hardening cement, workability, strength development in the early stage of the reaction, and the stability in long period age can be given, but the degree of importance of said factors can be, of course, varied in accordance with the applications thereof. As is shown in Fig. 9, when much handling time is desired to be taken, there are three ways to solve the problem; i.e., (i) the C/A ratio be controlled lower (ii) the amount of anhydrite be increased; and (iii) the amount of retarder be increased.

When quick setting is desired, the opposite ways are recommended to be taken. Generally speaking, it is not clever to use a large amount of retarder, and when the C/A ratio is controlled to be too low, the strength development becomes poor.

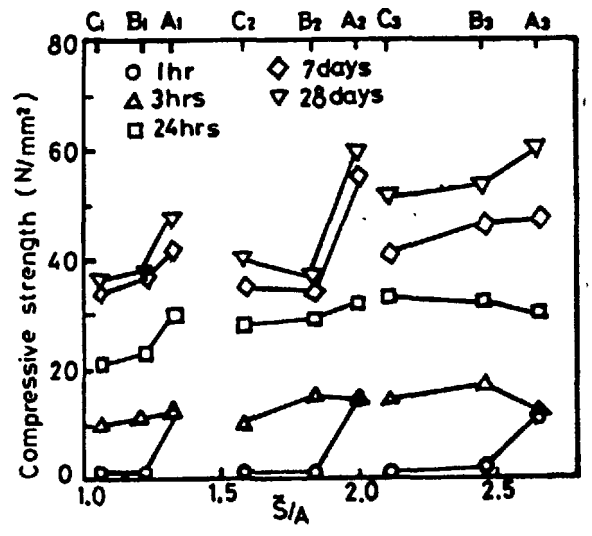

Fig. 7 - Relation between compressive strength and $\bar{S}/A$ of admixture.

For example, when quick setting is more desired, A (C/A=1.10, $\bar{S}$/A=1.33) is appropriate, and this is applied to the chemical grout. On the other hand, when the development of 2-3 hour strength and 7-28 day strength are desired by taking a proper handling time, B_3 (C/A=0.92, $\bar{S}$/A=2.46) composition is appropriate, and this composition is now being applied to urgent repair.

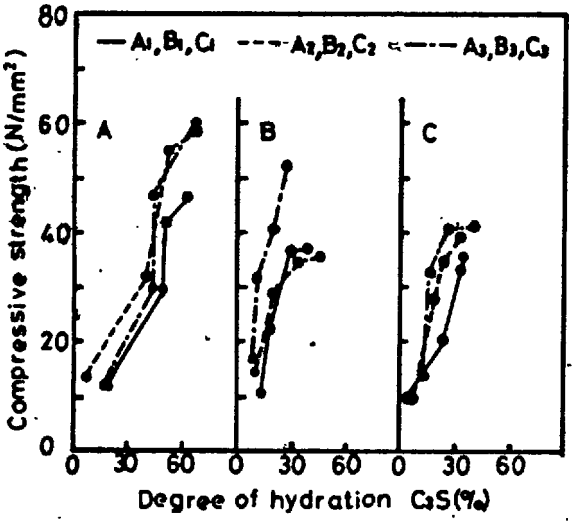

Fig. 8 - Relation between compressive trength and degree of C_3S hydration.

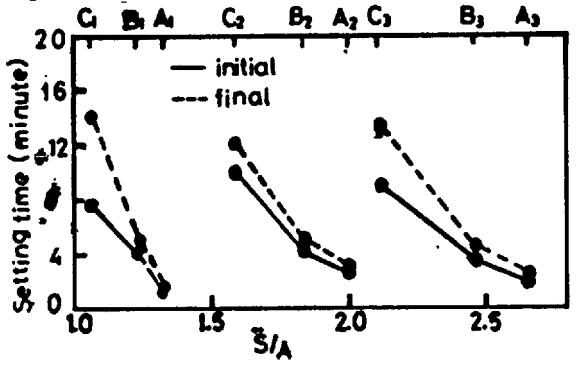

Fig. 9 - Relation between setting time and $\bar{S}$/A of admixture (the retarder 0.8% by weight to cement).

5. CONCLUSION

The hydration process, strength and workability of the special cement which was prepared by adding ordinary portland cement to 20% of the various kinds of admixtures prepared by changing the composition of the electrically melted calcium aluminate clinker and anhydrite content were examined, and the following facts have been made clear;

The C/A ratio affects more to the hydration of silicate phase and ettringite producing reaction than anhydrite content, and brings about strength development and determines the structure of cement stone.

There is a tendency that when the C/A ratio is raised, quicker hardening property can be attained, and when the amount of anhydrite to be added is increased, hardening become slowed down, but the effect of the C/A ratio is overwhelming.

When the C/A ratio is lowered too much, handling time can be taken sufficiently, but it is impossible to expect the high strength development. In the neighbourhood of C/A=0.9, excellent workability can be attained when the anhydrite content is high, and strength development can be expected, and cement stone of high quality can be obtained, and therefore, the cement whose C/A ratio is in the neighbourhood of 0.9, having high anhydrite content is considered to be appropriate as quick hardening cement for general constructions.

REFERANCE

1.- T. SATO, K. NAKAGAWA and K.HIRANO (1974), " Production of expansive cement clinker by electric furnace", The VI Inter. Symp. Chem. Cement, Moscow, sp III-5.

2.- N. MIYAKE, K. NAKAGAWA and J. ISOGAI (1975), "Basic properties of calcium sulfoalminate admixtures for cement", CAJ Review of the 29th General Meeting, 82-85.

3.- K. NAKAGAWA, Y. WATANABE, I. MINO and T. KITSUTA (1974), "Adoption of electrofused calcium sulfoaluminate clinker for ultra high strength concrete", The VI Inter. Symp. Chem. Cement, Moscow, sp III-1.

4.- K. ISOZAKI, K. NAKAGAWA and Y. WATANABE (1978), "Studies on the strength of high ettringitic cement stones steam cured at normal pressure", CAJ Review of the 32th General Meeting, 42-43.

5.- H. UCHIKAWA and K. TSUKIYAMA (1973), "The hydration of jet cement at 20°C", Cement and Concrete Research, 3, 263-277.

Role of Expansive additive CaO in expansive cement

Rôle d'une addition de CaO expansive dans les ciments expansifs

U. YAMAZAKI, H. KAMIAKA and S. KOBAYASHI, Japan.

RESUME : Les auteurs ont effectué des recherches sur le comportement des pâtes et mortiers de ciments expansifs, lorsqu'on leur ajoute séparément ou ensemble les composés expansifs suivants : CaO - $CaSO_4$ - $C_4A_3\bar{S}$ et CA. Ils ont étudié tout d'abord l'addition de CaO.

L'expansion des éprouvettes de mortier de ciment expansif additionné de CaO expansive commence dès que la résistance à la compression de ces éprouvettes atteint quelques kgf/cm^2. Elle est due à la formation massive de $Ca(OH)_2$ à partir de CaO non hydraté.

Si, en plus de CaO, on ajoute $CaSO_4$, l'expansion est augmentée. Ceci semble dû à l'effet retardateur de $CaSO_4$ sur l'hydratation de CaO.

SUMMARY : This paper describes the results of investigations on the behaviors of the expanding additive CaO in cement paste and mortar specimens, as one of the studies on the roles of the expanding additives. CaO, $C_4A_3\bar{S}$ and $CaSO_4$ in expansive cement.

The expansion of expansive cement mortar specimen with expansive additive CaO starts at the time when the compressive strength of the mortar reached to several kgf/cm2. This expansion is caused and increased by the successive formation of massive $Ca(OH)_2$ formed from the unhydrated CaO.

The expansion of expansive cement mortar specimen with CaO is promoted by the additional $CaSO_4$ because the amounts of the unhydrated CaO is increased by the retarding effect of $CaSO_4$ on the hydration of CaO.

Introduction

Many studies of the mechanism of the expansion of expansive cement have been reported. There are some hypotheses of the expansion mechanism, for example, the crystalization 1) 2) the dusting 3) and the swelling 4).

In order to make clear the role of expansive additive CaO in expansive cement, the behaviors of hydration of CaO in expansive cement were investigated in this study.
The expansion of mortar specimen was continuously observed from the early stage of hydration by the Automatically Restraining Apparatus (ARA).5). The processes of hydration studied by employing Scanning Electron Microscopy (SEM), conduction calorimeter, X-ray diffraction techniques.

Experimental procedure

Cements used are listed in Table I. CaO was calcinated in electric furnace at 1500°C. CaO calcinated was ground to 10 % residue on 170 mesh sieve.
$CaSO_4$ was ground to 8000 cm2/gr. Blaine.

Table I. Mix proportion of ordinary portland cement and expansive components

	Proportion			
	CaO	$CaSO_4$	C_4A_3S	ordinary portland cement
A	0	0	0	100
B	3	0	0	97
C	3	3	0	94
D	3	6	0	91
E	0	6	0	94
F	2	5	2	91

1) The length changes of the mortar specimens (cement:sand:water=1:2:0.6) under the restrained condition were measured by the ARA. The loading equipment of the ARA is shown in Fig. 1. The mortar specimen cured at 20°C was demoulded at 7 hours after casting. The demoulded specimen was wrapped with polyethylene sheet and was set on the loading stage. The expansion of the specimen was continuously measured from 7 hours after casting.
The expansion of mortar specimen which was "remoulded" by the following methods at 7 hours after casting was also measured with the ARA.

a) a mortar specimen of ordinary portland cement premixed with 0.5-3.0% CaO was demoulded at 7 hours and was crushed into pieces and was moulded again to keep the initial size (5Ø x 10 cm) by a press.
b) Ordinary portland cement mortar demoulded at 7 hours was crushed into pieces by the same way as (a) mixed with 0.5-3.0% CaO and then moulded again by the same way as (a).

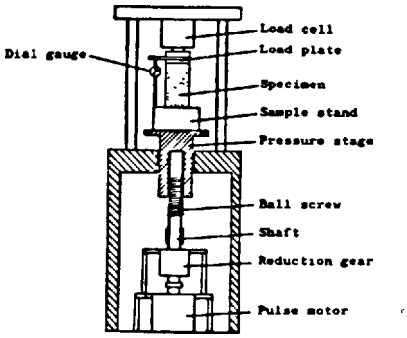

Fig.1. Schematic diagram of the load stage equipment for uniaxial restraining of specimen

2)The amounts of CaO and $CaSO_4$ in expansive cement pastes were determined with the XRD by the internal standard method. The paste sample was mixed with the standard MgO in cyclohexanol.6)
3)The rate of heat liberation was measured with the conduction calorimeter.
4)The structure of hardened expansive cement paste was observed by SEM and EPMA.

Results

1) The linear expansion curves of the specimens (A-F) are shown in Fig. 2. The expansion of each specimen started at about 7 hours after casting, and reached to the maximum by 3 days. The expansions of the specimens (B,C,D and F) were more than 5×10^{-4}, while the expansion of the specimen E with $CaSO_4$ only was very small.

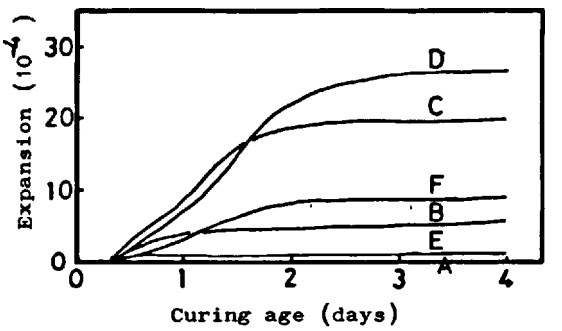

Fig.2. Expansion curves of cement (A-F)

2)Expansion curves of the remoulded mortars by the method, (a) and (b) are shown in Fig. 3. Fig. 4 shows the relations between the added contents of CaO and the expansion of the remoulded mortar specimens at 3 days. In each case, the more CaO was added, the larger the expansion of the specimen became.

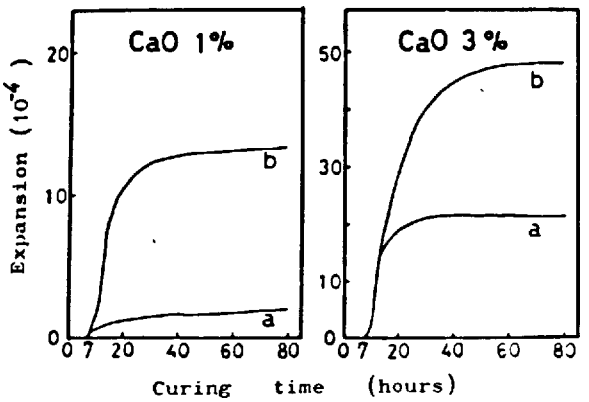

Fig.3. Expansion curves of mortars added CaO 1% and 3%
(a) premixed
(b) mixed at 7hours after casting

3)As a result of XRD analysis, it was recognized that one-third of added CaO remained at the age of 7 hours in the specimen B with 3 % CaO, while a half of both CaO and $CaSO_4$ remained in the specimen D with CaO 3 % and $CaSO_4$ 6 % at the same age.

4)The amounts of unhydrated CaO in $CaO-H_2O$ system and in $CaO-CaSO_4-H_2O$ system were calculated from the measurement of the heat of hydration of the systems. The results obtained show that the hydration of CaO in $CaO-CaSO_4-H_2O$ system was retarded by $CaSO_4$ (Fig. 5).

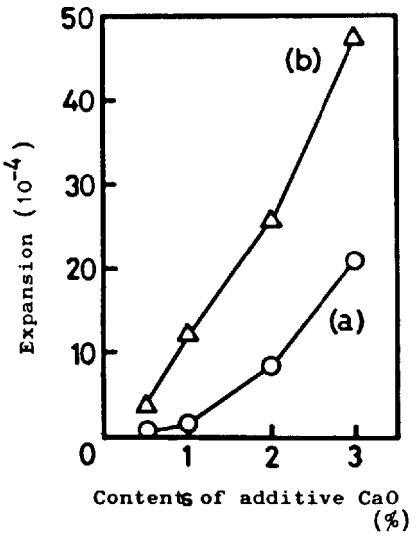

Fig.4. Relation between expansion at 3 days and contents of additive CaO(%)
(a) premixed
(b) mixed at 7hours

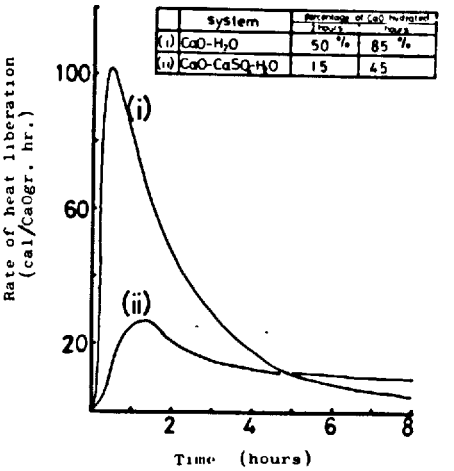

Fig.5. Influence of $CaSO_4$ on the hydration of CaO (water/solid=0.6)
(i) $CaO-H_2O$ system
(ii) $CaO-CaSO_4-H_2O$ system
($CaO:CaSO_4$=1:1)

5) In Fig. 6 are shown the typical figures of the massive reaction products observed only in the expanded paste specimens B,C, D and F. These reaction products were recognized to be $Ca(OH)_2$ by EPMA.

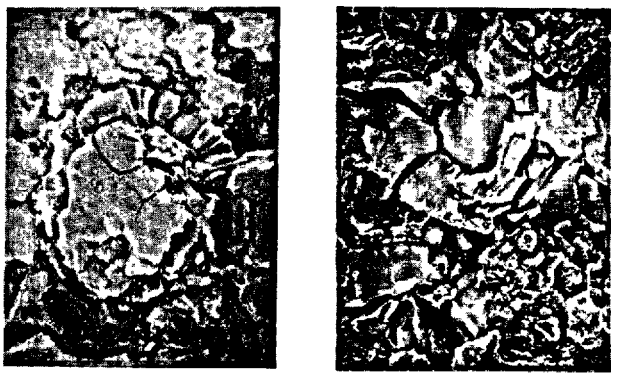

Discussion

The typical relations between the expansion curve of the mortar specimen D and the reaction processes of the corresponding expansive cement are shown in Fig.7
Though it was suggested from the rate of

heat liberation, the amounts of $Ca(OH)_2$ and the decrease of expanding additives CaO and $CaSO_4$ of the specimen D that the hydration reaction of expansive cement D proceeded in 7 hours, and that the expansive components reacted in 7 hours. The expansion of this specimen was detected just after the age of 7 hours, when the compressive strength of this specimen attained to about 3 kgf/cm2.

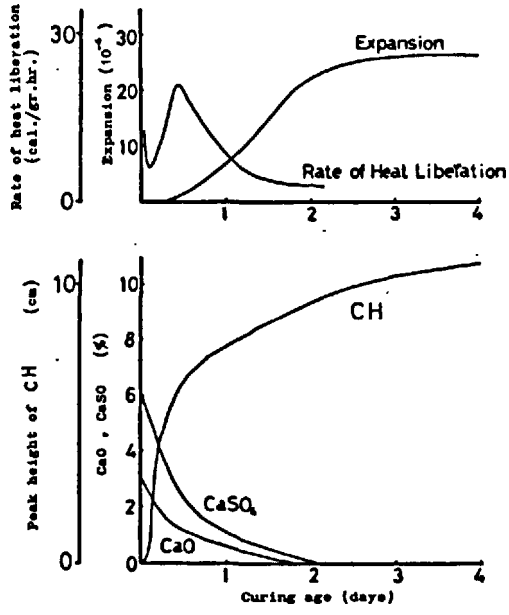

Fig.7. Typical patterns of the rate of heat liberation curve in cement paste, expansion curve in mortar and contents of CaO, $CaSO_4$ and produced CH in paste, in case of expansive cement D
($CH=Ca(OH)_2$)

When more than 1 % CaO remains in the expansive cement mortar at 7 hours, as plotted in (b), Fig.4, the mortar shows considerable expansion.
Though a half of CaO hydrated before the age of 7 hours, however, the expansion of mortar specimen was not observed as shown in Fig.7. This is for the reason that as cement gel is movable to fill up the space of water consumed in hydration of CaO at the earlier age, the structure of mortar specimen absorbes the expanding force originated from the hydration of CaO. In other words, while CaO grains increse their volume 1.8 times by hydration, the total volume ratio of $Ca(OH)_2$/ CaO and H_2O decreases to 90 % as a whole structure. Therefore the mortar specimen shows no expansion, when the cement gel is movable.

After 7 hours, it is not easy for cement gel to fill up the space of H_2O because the matrix possesses some rigidity. And $Ca(OH)_2$ as shown in Fig. 6 produced from unhydrated CaO. In this case, the hydration of unhydrated CaO to $Ca(OH)_2$ brings out the change of volume by about 1.8 times as a whole. Therefore, the mortar specimen shows expansion.
When $CaSO_4$ coexists in the expansive cement including CaO, the hydration of CaO is restrained as observed in $CaO-CaSO_4-H_2O$ system with conduction calorimeter. This retarding effect of $CaSO_4$ in hydration of CaO is caused because the solubility of $Ca(OH)_2$ is decreased by dissolution of $CaSO_4$ and because the surface of CaO is covered with the tighter film layer of $Ca(OH)_2$ which was recognized by means of optical microscopic observation by the authors.
This phenomenon is also recognized in the expansion reaction of expansive cement specimen with additional CaO and $CaSO_4$.
The expansion of expansive cement mortar specimen with CaO is promoted by the additional $CaSO_4$ because the amounts of the unhydrated CaO is increased by the retarding effect of $CaSO_4$ on the hydration of CaO.

Conclusion

1) The expansion of expansive cement mortar specimen with expansive additive CaO starts at the time when the compressive strength of the mortar reached to several kgf/cm2. This expansion is caused and increased by the successive formation of massive $Ca(OH)_2$ formed from the unhydrated CaO.
2) The expansion of expansive cement mortar specimen with CaO is promoted by the additional $CaSO_4$ because the amounts of the unhydrated CaO is increased by the retarding effect of $CaSO_4$ on the hydration of CaO.
3) In many cases, the massive $Ca(OH)_2$ formed the hydration of the unhydrated CaO is observed in the expanded specimen with expansive additive CaO.

Reference

1. Chatterji S. and Jeffery J.M., Mag. Concrete Research Vol.18, N°55, 1966, pp 65-68
2. M. Okushima, R. Kondo, H.Mugusuma and Y. Ono, Proc. 5th Int.Symp. Chemistry of Cement, Tokyo, 3, 419 (1968)
3. Ramachandran V.S., Sereda P.J. and Feldman R.F., Nature Vol. 201, No.4916, 18 January 1964, pp 288-289
4. Mehta P.K., Cement and Concrete Research Vol. 3, No.1, 1973, pp 96-97
5. U. Yamazaki, S.Kobayashi, H. Kamiaka and K. Sugiura, CAL., Review of the 34th General Meeting, 1979,
6. W. Ohnemüller and I. Zimmerman, Zement Kalk Gips, No.5, 1970, pp 203-205.

THÈME VI

Les pâtes de ciment : rhéologie, évolution des propriétés et des structures

Cement pastes : rheology, evolution of the properties and structures

Président : M. DIAMOND (U.S.A.)

SOUS-THÈME VI-0

Structure et rhéologie des pâtes fraîches de ciment*

R. A. HELMUTH
Portland Cement Association
U. S. A.

* Cet exposé constitue le rapport principal du sous-thème VI - 0 qui, parvenu trop tardivement, n'a pu être publié dans le volume 1 réservé aux rapports principaux.

INTRODUCTION

Les propriétés des pâtes fraîches de ciment portland, présentent un grand intérêt, car les propriétés des bétons en découlent. Cet intérêt est très général en ce qui concerne les caractéristiques du ciment qui influent sur la consistance, la maniabilité et la prise du béton. La maîtrise des propriétés rhéologiques du béton frais doit avoir des conséquences importantes, sur le choix de la composition du béton et sur les moyens de malaxage et de mise en oeuvre.

Les examens au microscope des coupes de béton normalement durci, montrent que chaque grain de l'agrégat est enrobé dans une matrice de pâte de ciment durcie, des films de cette pâte séparant complètement ces grains les uns des autres. Le béton frais doit acquérir cette sorte de structure, dans la période de repos qui précède la prise. Cependant, durant le malaxage et la mise en oeuvre du béton, les grains de sable ou ceux du gros agrégat, auront fréquemment entre eux des contacts directs. Ces contacts directs, créeront des forces de frottement; les effets sur les divers grains interféreront et s'ajouteront pour réduire la fluidité de la pâte de ciment elle-même.

Bien que des progrès aient été faits dans la connaissance des phénomènes et l'établissement de relations entre la rhéologie du béton et celle de la pâte de ciment (1-5), la plupart des essais standardisés sur les ciments, les mortiers et les bétons sont purement empiriques; et les résultats de ces divers essais semblent difficilement comparables. Par exemple, un ciment très finement broyé, peut exiger dans une pâte pure plus d'eau de malaxage et avoir une consistance plus raide, qu'un ciment plus grossièrement broyée; mais il faut aussi exiger moins d'eau de malaxage (ou avoir une plus grande fluidité) s'il est essayé dans un mortier plastique, par suite de la diminution du nombre des contacts des plus gros grains de ciment avec les grains du sable, dans le mortier.

Les essais de détermination de la consistance du béton ou du mortier, consistent à mesurer leur déformation sous l'action de la gravité, ou la progression de leur déformation(ou le temps nécessaire pour obtenir une déformation donnée) sous l'action d'impacts répétés, ou de vibrations et de la granité. De tels essais donnent des résultats numériques, relevant d'échelles arbitraires, qui n'ont aucun rapport simple avec les propriétés physiques, bien définies, telles que la viscosité ou le seuil de rigidité (contrainte minimum de cisaillement provoquant l'écoulement). Le "slumptest" est considéré comme mesurant la consistance du béton frais, et le facteur de compactage; alors que le "V.B. test", mesure la viscosité apparente (6). Cependant, il a été constaté qu'aucun essai ponctuel, comme ceux-ci ne pouvait fournir une mesure valable de la fluidité et de la maniabilité des bétons dans toute la gamme des conditions possibles (3, 7). La raison en est, qu'il y a une grande différence entre l'état de la pâte, avant et après le début de l'écoulement. Il est de pratique courante d'utiliser la vibration pour fluidifier les bétons frais trop raides, et permettre leur mise en oeuvre dans les moules. Les structures faibles dans la pâte sont alors détruites par des cisaillements énergiques ou par la vibration. La pâte est dite avoir alors la consistance fluide. La consistance du béton, lors de sa mise en place par vibration est due, au moins en partie, aux caractéristiques rhéologiques de sa pâte de ciment, dans son état fluidisé (1). La résistance du bétin frais à la déformation et à l'écoulement, dans l'état statique, doit aussi être liée, au moins en partie, au seuil de cisaillement de la pâte de ciment.

La résistance de la pâte de ciment portland au cisaillement, dépend, à la fois, du temps et de la vitesse de la déformation. Elle dépend aussi de la durée du malaxage et de son intensité. Les pâtes de ciment sont normalement thixotropiques, c'est-à-dire que leur résistance au cisaillement s'amoindrit lors de l'écoulement de la pâte, par suite de la rupture progressive, des liaisons de floculation entre particules. L'hydratation du ciment a des effets à court terme (prise rapide, fausse prise), aussi bien qu'un raidissement normal progressif. Le comportement à l'écoulement peut cependant être très complexe, même pour un seul ciment, et les comparaisons entre divers ciments peuvent être fortement affectées par des variations des méthodes d'essais ou de l'appareillage utilisé.

Les propriétés des pâtes fraîches de ciment portland, sont aussi intéressantes, dans les recherches sur les autres caractéristiques du ciment. Par exemple, l'étude des propriétés des pâtes fraîches est utilisée, pour déterminer l'influence de la distribution granulométrique du ciment, ou pour mesurer l'action, sur les réactions d'hydratation initiales, des teneurs plus ou moins fortes en gypse ou en autres additifs. Dès le début du mélange eau ciment, le processus de la dissolution et de la formation des hydrates, provoque des changements progressifs dans la structure et les propriétés rhéologiques de la pâte.

STRUCTURE DE LA PATE FRAICHE

Les ciments portland modernes sont moulus en poudre fine, qui n'a qu'un très faible pourcentage de grains supérieurs à 74 microns ou inférieurs à 1 micron. La taille des grains, est le résultat de nombreuses factures aléatoires, qui se produisent à la fin du broyage, et tendent à transformer certains grains arrondis en grains anguleux. La distribution granulométrique rapportée à des grains sphériques de diamètre équivalent, en se basant soit sur la vitesse de sédimentation, soit sur la surface spécifique, donne une bonne approximation.

Les ciments modernes ont généralement des surfaces spécifiques de l'ordre de 300 à 500 m^2/kg (soit 3000 à 5000 cm^2/gr), mesurées par la perméabilité à l'air à l'aide de méthodes telles que celle de Lea et Nurse, ou celle de Blaine (ASTM C. 204). Certaines méthodes, telles que l'A.S.T.M. C 115 utilisant le turbidimètre de Wagner, conduisent à des valeurs beaucoup plus faibles, parce que la teneur en particules les plus fines est sous estimée. Certaines autres méthodes sédimentométriques mesurent la teneur des ciments en fines particules, en bon accord avec les méthodes de perméabilité à l'air. Par contre, les valeurs des surfaces spécifiques mesurées par adsorption d'azote (méthode BET), sont bien plus grandes, que celles mesurées par perméabilité à l'air, parce que l'adsorption mesure aussi la surface des hydrates, et celle d'autres petites particules collées à la surface des grains de ciment, aussi bien que celles des fissures et peut être même celle de certains pores du ciment. Il semble que la surface spécifique mesurée par la méthode Blaine, soit mieux appropriée à l'étude de l'écoulement ou de la sédimentation,

que celle mesurée par la méthode B.E.T., parce que l'eau enrobe les grains de ciment d'une couche lisse, qui supprime l'influence des petites irrégularités de la surface des grains.

Les pâtes fraîches de ciment sont initialement une suspension épaisse de grains de ciment dans l'eau de malaxage. La structure de cette suspension dépend du rapport eau ciment, et de la distribution granulométrique du ciment. Elle dépend aussi des forces qui s'exercent entre particules, et des forces d'attraction de l'eau à la surface des grains solides, qui a leur tour, dépendent de l'ionisation et de la concentration des solutions. Dans les solutions diluées, les grains de ciment doivent normalement floculer, c'est-à-dire s'agglomérer en amas distincts appelés flocons, qui sédimentent rapidement. Les flocons ainsi formés, à partir de ciment ordinaire, dans les solutions diluées, ont un rapport eau ciment d'environ : 0,4. Dans les suspensions épaisses, que sont les pâtes de ciment, les flocons isolés sont amalgamés, à l'état statique dans un grand floculant continue unique. Les grains ne sont pas uniformément répartis dans une telle structure; Certains flocons réunissent plus de grains que la concentration moyenne, mais laissent entre eux des intervalles remplus d'eau. A l'intérieur de ces flocons les grains tendent à réduire les intervalles entre particules, de façon à réduire l'énergie potentielle. Powers a appelé ceci l'état floculé (1).

Pendant le malaxage, les grains de ciment tendent à se disperser plus uniformément dans l'eau, et il y a une rupture généralisée des liaisons entre flocons; ceci est la cause de la thixotropie (chute de la résistance au cisaillement) des pâtes de ciment. Si l'on opère à vitesse de cisaillement constante, un équilibre structurel (peut être résultant de la distribution granulométrique des flocons) est atteint au bout de quelques minutes, produisant une viscosité apparente constante. Il y a aussi un processus de neutralisation empêchant la structure de se reconstituer. Lorsque le malaxage est arrêté, la structure floculée statique se reforme graduellement. Bien que la pâte soit fluide durant le malaxage, elle prend, dans son état statique, une structure floculée, correspondant à un état faiblement solide, mais ayant un seuil de cisaillement défini.

Certains additifs organiques (réducteurs d'eau) sont utilisés pour accroître la fluidité des bétons, ou pour réduire leur teneur en eau, pour une même fluidité. L'examen au microscope, montre que pour des teneurs en additifs suffisantes les grains de ciment sont tous séparés, au lieu d'être floculés. Il y a lieu de penser, que ceci résulte de l'adsorption de l'additif à la surface des grains de ciment, qui provoque ainsi une neutralisation des charges, et la création, entre grains de ciment, de forces répulsives.

Un tel concept peut être utilisé pour visualiser la structure d'une pâte fraîche de ciment, comme indiqué, à titre de modèle simple sur la figure (1). Les frais y sont représentés sous forme de sphères, de diamètres équivalents correspondant à la distribution granulométrique d'un ciment de 430 m^2/kg de surface spécifique. La grande demi-sphère du fond, représente un grain de 30 microns de diamètre. Les intervalles entre grains sont remplis par de l'eau et par des grains plus petits. La figure correspond à un rapport

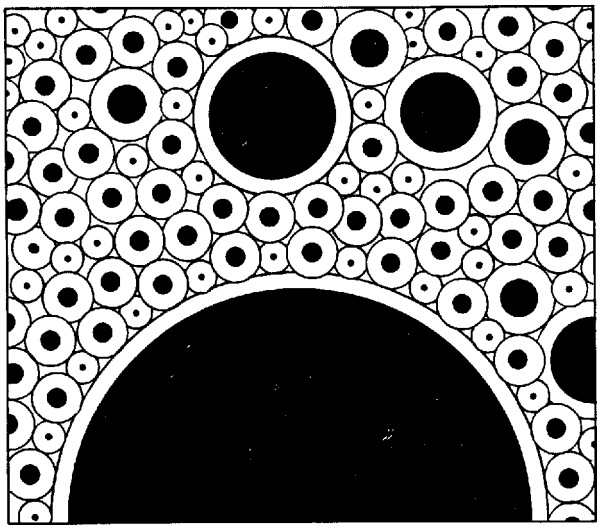

Fig. 1 - Modèle simple de grains sphériques dispersés, dans la structure d'une pâte fraîche de ciment, pour un rapport eau ciment de 0,5 et un ciment de 430 m^2/kg (8)

eau ciment de : 0,5. Lorsque l'eau est fortement attirée à la surface des grains, chacun de ces grains est enrobé d'un film d'eau continu; si le ciment est dispersé par un vigoureux malaxage, ou si l'on utilise un additif réducteur d'eau, l'épaisseur de ces films tend à s'uniformiser. Une première approximation de cette épaisseur est donnée par le rayon hydraulique : le volume de l'eau de malaxage divisé par la surface spécifique. Pour le ciment et la teneur en eau de la fig. 1, cette épaisseur est d'environ : 1,2 microns, soit à peu près le dixième du diamètre moyen des grains de ciment. Bien que ce modèle soit plus proche d'une solution dispersée que d'une pâte de ciment, l'épaisseur du film d'eau reste la même. Une seconde approximation peut être obtenue en tenant compte de l'eau contenue dans les grands interstices entre grains(2,9). Les réactions d'hydratation initiales peuvent aussi être considérées, selon un modèle plus réaliste de la structure de la pâte fraîche. La dissolution rapide du gypse et des alcalis, dans l'eau de malaxage, produit des hydroxydes et des sulfates de sodium, de potassium et de calcium. Grâce au gypse destiné à régulariser l'hydratation de l'aluminate tricalcique, un enrobage de sulfo-aluminate se forme sur les grains d'aluminate tricalcique, ce qui arrête leur réaction d'hydratation initialement très rapide. Environ 10 % du C_3A peut être hydraté dans les dix premières minutes(10); après quoi la réaction d'hydratation du C_3A est beaucoup plus lente, jusqu'à épuisement du gypse, ce qui ne se produit généralement qu'à la fin de la prise. La profondeur de l'attaque dans le C_3A, au début (10 %) de la réaction peut être estimée à : 0,1 micron. Si le produit de la réaction est de

l'éttringite très compacte, la surface du C_3A est enrobée d'une couche épaisse d'environ : 0,8 micron. Rapidement, la moitié du gypse est consommée dans cette réaction initiale; si le gypse a une surface spécifique initiale d'environ 800 m^2/kg, et si chaque grain de gypse se dissous sur une même épaisseur, cette épaisseur est de 0,5 micron environ. Après cette réaction initiale la surface spécifique de particules de gypse résiduelles est inférieure à la moitié de cette valeur, et la surface spécifique du ciment est diminuée de 30 m^2/kg environ. Cependant, la surface spécifique mesurée au B.E.T. augmente par suite de la formation des produits de l'hydratation; si ces hydrates se forment à la surface des grains de ciment, ils peuvent avoir un effet négatif sur la fluidité à ce moment. La formation de l'ettringite peut, elle-même, réduire la teneur en eau libre de la pâte de ciment d'environ : 0,02 g/g de ciment, pendant cette même période (10 %) de l'hydratation.

Tous ces processus initiaux influent sur la surface spécifique, et sur la teneur en eau libre, donc sur l'épaisseur du film d'eau d'enrobage, pendant la période de latence. La réaction initiale d'hydratation des silicates peut avoir un petit effet, sur la structure des pâtes fraîches de ciment, à moins qu'un vigoureux malaxage soit poursuivi, décapant continuellement les hydrates à la surface des grains. Après cette période de latence, des cristaux de chaux hydratée commencent à se former dans la solution; ceci accélère l'hydratation des silicates, et des cristaux de silicate de calcium hydraté se forment sur la surface correspondante des grains solides, et croissent sous forme d'aiguilles. La prise normale se produit alors, résultant de l'entrecroisement de ces hydrates; la recristallisation de l'ettringite peut aussi contribuer à la prise (10).

DEFORMATION ET COMPORTEMENT FLUIDE

La consistance des pâtes fraîches de ciment, après cette période de prise, varie si fortement, avec la composition du ciment et avec le temps, qu'un seul appareil de mesure ne peut suffire à en couvrir toute l'étendue. Les viscosimètres, spécialement les viscosimètres à cylindres coaxiaux, sont généralement utilisés avec les pâtes les plus fluides, dont le seuil de cisaillement va jusqu'à 200 Pa (2000 dynes/cm^2) et dont la viscosité apparente, va jusqu'à plusieurs milliers mPa/s (= centipoises). Récemment un mini slup test, a été jugé très pratique, pour comparer les fluidités de pâtes de diverses compositions (11). Dans cet essai, un petit cône est rempli avec la pâte à essayer, puis soulevé de façon que la pâte s'écoule et forme un pâté; l'aire de ce pâté, donne la mesure de la consistance. Pour des pâtes plus rigides, des essais de pénétration, tels que l'aiguille de Vicat , sont mieux adaptés à la mesure de la teneur en eau qui donne la consistance normale, ainsi qu'à la mesure du début et de la fin de la prise. Un appareil automatique, le rhéographe décrit par Bombled (12 - 13), mesure les seuils de cisaillement par des essais de pénétration, sur un large éventail de pâtes à résistances très variées, depuis environ 30 jusqu'à plus de $1,5 \times 10^5$ Pa. Il recouvre donc tout le domaine, depuis l'extrémité des mesures faites au viscosimètre à cylindres coaxiaux, jusqu'aux valeurs de début et de fin de prise mesurées à l'aiguille de Vicat, qui correspondent approximativement respectivement a : 2×10^4 et 1×10^5 Pa.

La figure 2 donne des exemples de courbes mesurées au rhéographe, sur des pâtes de ciment de rapport eau ciment égal à 0,25, avec des ciments de différentes finesses (13). Les seuils de rigidité (résistance au cisaillement) sont calculés, pour des forces nécessaires pour produire une pénétration de 20 mm, à l'aide d'une ou de plusieurs sondes, dont les diamètres varient de 1 à 12 mm. Les valeurs initiales du seuil de rigidité sont, parfois, plus grandes par suite de la faiblesse du rapport eau ciment. La consistance normale des pâtes correspond approximativement à un seuil de rigidité de 2000 Pa. Deux de ces pâtes étaient plus raides que la consistance normale. Ces courbes peuvent être utilisées pour définir et calculer les divers paramètres qui interviennent dans la prise du ciment; début et fin de prise, vitesse de prise, durée de la période de latence, pendant laquelle le seuil de rigidité est pratiquement constant. A des teneurs en eau plus fortes, le début de ces courbes est presqu'horizontal.

Malgré le fait que de tels essais statiques montrent clairement l'existence de seuils de rigidité dans les pâtes de ciment ordinaires, les résultats obtenus avec les viscosimètres dynamiques ne donnent souvent pas de valeurs bien définies de ces seuils. La vitesse de déformation par cisaillement en fonction de la contrainte de cisaillement, peut être représentée par des courbes; lorsque ces mesures sont faites à l'aide de viscosimètre rotatifs (voir fig. 3), on constate que les résultats dépendent considérablement de l'histoire de la déformation des pâtes et du type d'appareil utilisé.

Le comportement des pâtes de ciment, lors de cette déformation, peut, suivant la nature des pâtes et le type d'appareil utilisé, être classé en quatre catégories. 1) newtonien, 2) Binghamien, 3) pseudo-plastique et 4) dilatant. En outre les courbes peuvent présenter un comportement réversible, entre thixotrotique (chute de seuil de cisaillement) et anti-thixotropique (augmentation du seuil de cisaillement). Le comportement antithixotropique semble être du à un processus de retour de thixotropie, qui doit, cependant, être distingué de la dilatance, qui elle aussi, provient d'une augmentation du seuil de cisaillement mais pour d'autres raisons.

ECOULEMENT NEWTONIEN ET BINGHAMIEN

Quand la vitesse de cisaillement γ, est proportionelle à la contrainte de cisaillement τ, l'écoulement est dit newtonien, ou à viscosité constante.

Les pâtes de ciment ne sont normalement pas newtoniennes, mais peuvent le devenir très rapidement, en y ajoutant des quantités suffisantes de certains additifs réducteurs d'eau (14 - 17). Les pâtes de ciment ont approximativement le comportement d'un solide plastique de Bingham, avec un seuil de rigidité E, et une viscosité U, de telle façon que :

$$\gamma = \frac{1}{U} (\tau - E) . \qquad (1)$$

Les résultats des mesures rhéologiques faites sur les pâtes de ciment, sont souvent représentés graphiquement (comme sur la fig. 3), en portant en abscisse la résistance au cisaillement (ou le couple de torsion du viscosimètre rotatif), et en ordonnée la vitesse de cisaillement (ou la vitesse de rotation) (2).

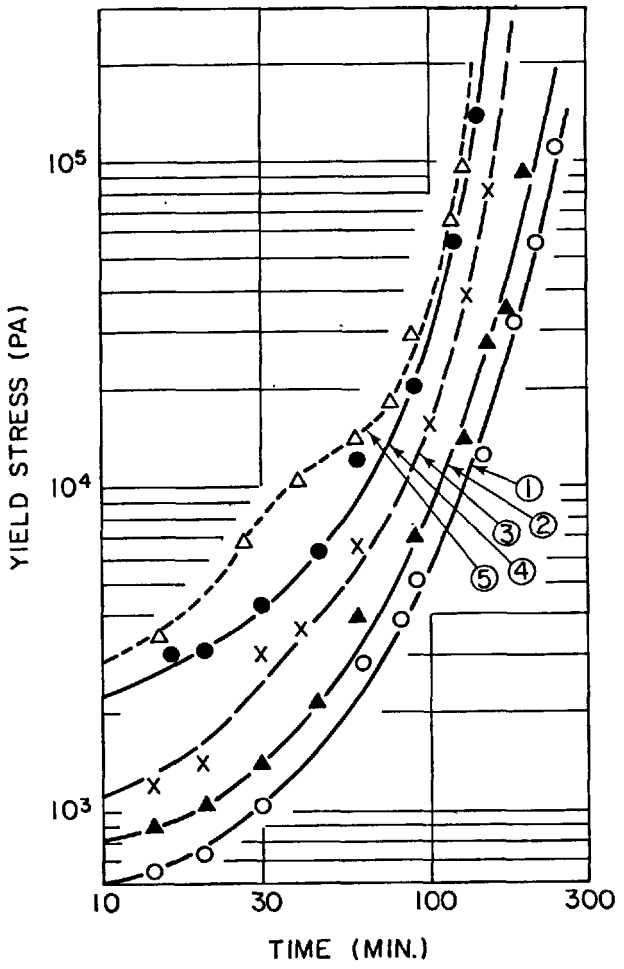

Fig. 2 - Courbes relevées au rhéographe, sur des pâtes (clinker broyé plus 5 % de gypse, à un rapport E/C de 0,25) pour des ciments de finesses variées : 1) 201 m^2/kg; 2) 248,5 m^2/kg; 3) 307 m^2/kg; 4) 403 m^2/kg; 5) 511 m^2/kg (13).

Dans de tels diagrammes, les fluides newtoniens sont représentés par une ligne droite passant par l'origine (E= 0 dans l'équation : 1). Les solides plastiques de Bingham sont aussi représentés par une droite, mais ne passant plus par l'origine, dans ces cas, la pente de la droite est égale à l'inverse de la viscosité plastique; la viscosité apparente est $\frac{\tau}{\gamma}$, c'est-à-dire l'inverse de la pente de la droite qui relie l'origine à un point de la courbe. Donc, même si la viscosité plastique est constante, la viscosité apparente dépend de la vitesse de cisaillement, et peut être beaucoup plus grande que la viscosité plaqtique, aux faibles valeurs de la vitesse de cisaillement, par suite de l'existence d'un seuil de rigidité non nul.

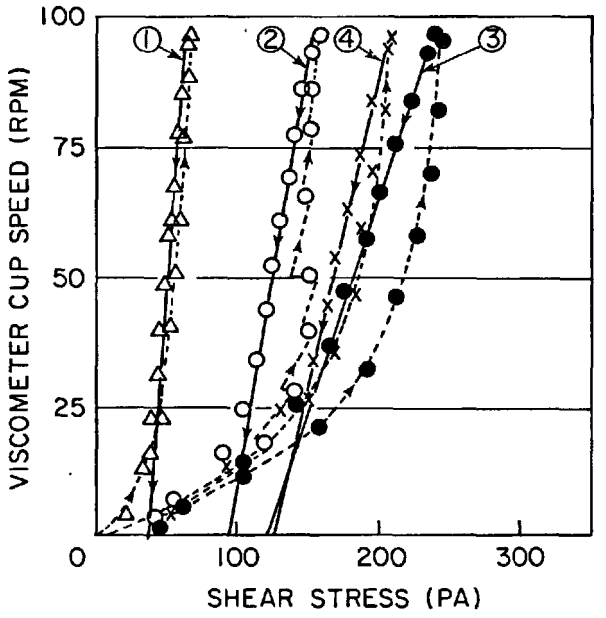

Fig. 3 - Courbes relevées au viscosimètre rotatif pour diverses pâtes de ciment : 1) E/C = 0,4; 2) E/C = 0,25, à vitesse constante et à l'équilibre; 3 et 4) E/C = 0,32; 3 immédiatement après malaxage; 4 immédiatement après la première mesure (2)

PSEUDOPLASTICITE

Les seuils de rupture mesurés au viscosimètre sur les pâtes de ciment, réelles, ne sont pas définis aussi nettement que dans le modèle plastique de Bingham. Au lieu d'une droite, les couples de valeurs mesurées: vitesse de cisaillement vs, contrainte de cisaillement, peuvent figurer une courbe graduellement croissante depuis l'axe des contraintes pour tendre vers une droite (fig. 3), ce comportement est appelé : pseudoplastique ou plastique thixotropique. La portion droite de cette courbe, peut être utilisée, en la prolongeant vers les vitesses de cisaillement décroissantes, pour obtenir par extrapolation la valeur du seuil de rigidité. La partie courbe peut résulter de la combinaison d'un écoulement non uniforme de l'échantillon, et de la nature thixotropique du matériau, notamment si le viscosimètre comporte un espace trop large entre les deux cylindres coaxiaux (1).

Dans l'essai des pâtes de ciment dans les viscosimètres à cylindres coaxiaux, l'écoulement peut ne pas devenir immédiatement uniforme. Ainsi, quelques glissements peuvent se produire, à la surface des cylindres, des parties de la pâte étant décollées des parois, et s'écoulant, alors que d'autres y restent adhérentes. La vitesse de cisaillement des parties décollées, donc en mouvement, est alors bien plus grande que celle indiquée par la vitesse de rotation relative des cylindres. Paroifs la totalité de la pâte glisse d'une façon apparemment uniforme. Ces phénomènes ont

été étudiés en détail, en utilisant des cylindres lisses et des cylindres cannelés, et en faisant varier la vitesse de cisaillement et la nature des pâtes (18).

Dans une approche différente, Legrand (19), utilise un viscosimètre comportant une série de pales radiales, plongeant dans un grand volume d'échantillon. La variation du couple de torsion en fonction du temps, pendant la période d'écoulement non uniforme, a été analysée, pour déterminer le seuil de rigidité, la contrainte de cisaillement, et la vitesse de cisaillement, pour diverses valeurs constantes de la vitesse de rotation.

DILATANCE

Il y a un passage progressif entre les propriétés de l'écoulement plastique thixotropique et le comportement dilatant (réduisant la résistance au cisaillement), lorsque le volume des solides augmente dans les mortiers et les ciments (19). Quand la proportion de ces volumes solides dépasse environ 0,6, la résistance au cisaillement augmente avec la vitesse de cisaillement, et une augmentation du volume se produit alors. La courbe est alors concave vers l'axe des déformations, au lieu d'être convexe comme dans le cas de la fig. 3. Ces effets résultent de modifications dans l'arrangement mutuel des grains de ciment, de façon à permettre le mouvement relatif de ces grains, le long des surfaces de rupture. Il en résulte une augmentation moyenne des interstices entre grains dans la direction perpendiculaire à la direction du cisaillement. L'eau est alors amenée à pénétrer dans ces interstices élargis, et la résistance au cisaillement dépend, par conséquent, de la vitesse du cisaillement et de la perméabilité du matériau. D'autre part, du fait que l'eau et les solides sont peu compressibles, un peu d'air tend à pénétrer dans le matériau. Cet air ainsi piégé, fournit l'espace d'expansion, sans exiger d'écoulement d'eau supplémentaire.

Ces interactions entre grains produisent un accroissement rapide du seuil de rigidité et de la viscosité apparente, lorsque la proportion en volume des solides dépasse environ 0,6 et lorsque le matériau n'est pas vibré. Lorsque le matériau est vibré, le comportement à l'écoulement est transformé, et cette transition vers la dilatance se produit alors seulement lorsque la proportion en volume des solides est un peu supérieure (0,62).

Les mêmes considérations s'appliquent aussi aux pâtes de ciment à très faible rapport eau ciment. Une concentration en volume de ciment de 0,6 (40 % en eau du volume total), correspond à un rapport eau ciment en poids de 0,21. Des courbes typiques de dilatance ont été obtenues, pour des rapports eau ciment de cet ordre, avec des pâtes de clinker broyé, fluidisées avec des additions de lignosulfonate et de carbonate soluble (17, 20).

THIXOTROPIE

Il a été démontré (3, 18, 21, 22), que dans des conditions expérimentales appropriées (vitesse de cisaillement constante, écoulement uniforme),le couple de torsion T_o, mesuré dans un viscosimètre à cylindres coaxiaux, variait exponentiellement avec le temps depuis la valeur T_o, jusqu'à une valeur d'équilibre T_E, selon la formule :

$$T = T_E + (T_o - T_E)e^{-Bt} \qquad (2)$$

où B est une constante qui dépend de la vitesse de cisaillement (ou de la vitesse angulaire) et des propriétés de la pâte. Les valeurs de B sont de l'ordre de 0,04 s^{-1}. L'équilibre est atteint en 1 ou 2 minutes. Depuis T_o jusqu'aux diverses valeurs de T_E, la forme des courbes peut varier considérablement, en ce qui concerne les vitesses de cisaillement (déformations et contraintes), selon la durée des augmentations (courbes croissantes) ou des diminutions (courbes descendantes) de ces vitesses de cisaillement (méthode de Green). La fig. 3 montre des exemples de comportements thixotropiques des pâtes de ciment, au cours de tels essais (2). On y distingue quatre manifestations de la thixotropie apparente :

1. La courbure des courbes ascendantes, indique une diminution de la viscosité lorsque la vitesse de cisaillement augmente.

2. Les courbes ascendantes correspondent à des contraintes de cisaillement plus fortes (pour des vitesses de cisaillement identiques) que celles des courbes descendantes.

3. La courbe 2 montre la diminution de la contrainte de cisaillement pour une vitesse de rotation du viscosimètre constante.

4. La courbe 4 montre des contraintes de cisaillement plus faibles, lorsque l'on recommence immédiatement l'essai de la courbe 3.

Non seulement, la boucle d'hystérésis de la courbe 4 est déplacée vers les contraintes de cisaillement les plus faibles (et les viscosités plastiques les plus faibles) mais encore la boucle 3 est plus grande que la boucle 4; ce qui implique qu'il y ait davantage de ruptures de liaisons dans le premier cycle que dans le second. Dans des conditions d'essai standardisées, les aires de ces boucles d'hystérésis, ont été utilisées pour mesurer la proportion des ruptures des liaisons thixotropiques. Des tentatives ont aussi été faites pour déterminer quantitativement l'énergie nécessaire, par unité de volume pour produire ces ruptures des liaisons thixotropiques lorsqu'on opère à vitesse de cisaillement constante (3, 22).

Une autre manifestation de la thixotropie a été observée, dans des essais, où la vitesse de cisaillement maximum augmentait avec le nombre de cycles. Dans ce cas les boucles aussi évoluent vers des contraintes et des viscosités plastiques plus faibles, ce qui implique qu'il y ait davantage de ruptures de liaison aux vitesses de cisaillement élevées (3).

ANTITHIXOTROPIE ET EFFETS DU MALAXAGE

Des résultats obtenus dans des viscosimètres à cylindres coaxiaux, ont montré, des seuils de rigidité bien définis, et des viscosités plus faibles, pour des faibles vitesses de cisaillement; ceci dépendait du degré de dispersion des grains de ciment par un malaxage approprié et du type de viscosimètre employé, et notamment de l'étroitesse de l'espace entre cylindres. Bien que Greenberg et Meyer (24) ait publié en 1963 que pour obtenir un écoulement uniforme, il leur avait été nécessaire de réduire cet espace à 1,0 mm environ,

la plupart des résultats publiés depuis, ont été obtenus avec des espaces trop larges pour éviter cet effet instrumental. Un autre facteur peut être la douceur de marche de la machine, et l'absence de vibrations de l'appareil, les vibrations et les chocs peuvent provoquer des écoulements non uniformes aux faibles valeurs des seuils de résistance. Roy et Asaga (15) ont récemment publié des résultats obtenus avec un viscosimètre de 0,7 mm d'espace entre cylindres, dans lesquelles les courbes croissantes sont remarquablement linéaires, avec des seuils de rigidité bien définis, c'est-à-dire un comportement presque Binghamien (voir fig. 4). Par contre, des viscosimètres comportant des espaces plus larges entre cylindres (4 mm et plus) ont montré un comportement pseudoplastique sans seuils de rigidité bien définis (2, 22, 25). Il y a lieu de noter que les courbes d'hystérésis de la fig. 4 sont très différentes de celles des autres publications. Non seulement, elles montrent des seuils de rigidité bien définis, pour des contraintes de cisaillement croissantes, mais aussi des boucles d'hystérésis comportant une importante antithixotropie ou réduction de la résistance au cisaillement; notamment, des contraintes plus élevées se produisent sur les courbes descendantes que sur les courbes ascendantes, pour une même vitesse de cisaillement. Le viscosimètre et les méthodes utilisés par Roy et Asaga ont donné des résultats entièrement dépourvus de comportement plastique-thixotropique. D'autre part, l'une des raisons de la grande surface des boucles d'hystéresis antithixotropique, semble être la très faible vitesse des essais (15 minutes par cycle) alors qu'habituellement ces cycles ne durent que quelques minutes. Désormais, une durée plus longue doit être attribuée à la fois aux ruptures de liaisons thixotropiques et à la recouvrance.

Plusieurs expérimentateurs ont observé à la fois des comportements thixotropiques et antithixotropiques sur les mêmes pâtes (23, 24, 25) essayées, à différents âges après malaxage. Des courbes pseudoplastiques ont été obtenues à des vitesses plus rapides (cycles de 2 à 3 minutes) que celles utilisées par Roy et Asaga. Les vitesses d'essai plus rapides laissent moins de temps pour la recouvrance thixotropique des pâtes fraîches. Même, les résultats obtenus ont montré que peu de temps après le malaxage, les pâtes étaient habituellement légèrement antithixotropiques, mais qu'après quelque temps de repos (30 à 45 minutes) elles devenaient thixotropiques. Cependant, quand après un certain temps de repos, la pâte était agitée, par des essais répétés, la courbe évoluait de la forme thixotropique, à la forme antithixotropique. Après un temps de repos plus long (2 à 3 heures) la pâte devenait très fortement thixotropique à l'approche de la prise, sauf si elle était continuellement agitée. Cette action de l'agitation conduit à penser que l'intensité du malaxage initial doit aussi influer sur la fluidité de la pâte, ce qui est bien connu, depuis déjà quelque temps.

Les malaxeurs mécaniques capables de produire un malaxage énergique et uniforme sont habituellement utilisés, peut être par intermittence, pour produire des pâtes de meilleure fluidité, après un malaxage assez long (5 à 10 minutes). Si la pâte est malaxée pendant 30 secondes, au moins, elle subira une prise rapide, qui est due, pense-t-on, à un collage des grains entre eux, par suite des produits de la réaction initiale avec l'eau, formés à leur surface. Bien qu'un temps de malaxage de 1 minute puisse être assez long

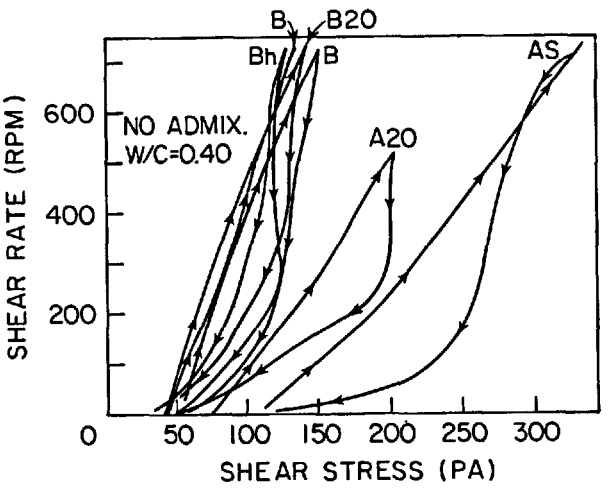

Fig. 4 - Courbes relevées au viscosimètre rotatif, pour des pâtes malaxées suivant six méthodes différentes, mais avec un même E/C = 0,40 (15)

pour supprimer cette prise rapide, il peut ne pas être suffisant, pour produire une dispersion correcte, ou pour éliminer la fausse prise due à la formation de gypse, à partir de semi-hydrate qui pouvait être présent dans le ciment. Ces cristaux de gypse forment une structure faible, qui peut être brisée par un malaxage ou un remalaxage.

Un malaxage énergique continu, peut aussi briser les structures de floculation des grains de ciment, qui sont responsables du comportement thixotropique. Des mesures, telles que celles indiquées sur la figure 3, pour diverses séries de malaxage d'une durée de 5 minutes chacune, dans un malaxeur planétaire, ont montré, qu'en augmentant la vitesse de malaxage de 150 tours/minute à 450 tours/minute, on abaissait les boucles d'hystérésis à des contraintes de cisaillement plus faibles, et qu'on rétrécissait ces boucles vers un comportement plastique presque réversible, du type Bingham (non thixotropique). Des résultats analogues ont été obtenus lorsque les temps de malaxage, à la vitesse de 250 tours/minute étaient portés de 3 à 20 minutes. Dans toutes ces mesures, faites avec des pâtes ayant un rapport eau ciment de 0,35, on a constaté que la viscoplasticité, indiquée par la courbe décroissante, diminuait progressivement avec l'intensité et la durée du malaxage. Cependant, pour un rapport E/C de 0,25, on atteignait le seuil de rigidité après environ 5 minutes de malaxage (2).

Une étude des effets du malaxage à haute intensité, sur des pâtes ayant un rapport eau ciment de 0,45, ont montré que la viscoplasticité passait par un minimum, mais que les seuils de rigidité augmentaient progressivement avec la durée du malaxage depuis 10 jusqu'à 50 Pa (2). Un malaxage énergique semble briser très rapidement la thixotropie et améliorer la fluidité, mais si ce malaxage est prolongé l'abrasion des grains augmentera le seuil de rigidité et la viscoplasticité.

En utilisant des mélangeurs à grande vitesse, pour malaxer des pâtes de E/C égal à 0,5, on a trouvé que le seuil de rigidité initial (à 15 minutes) augmentait progressivement de 22 à 52 Pa, et que les viscoplasticités diminuaient de 21 à 47 mPa/s, lorsque la durée du malaxage passait de 1 à 10 minutes (23). La température finale du mélange était de 25°C. Après une hydratation de 3 heures, la température augmentait quand la durée du malaxage croissait, ce qui dénote la persistance des effets de la durée du malaxage. En outre, les pâtes malaxées pendant une minute étaient thixotropiques, et le devenaient encore plus, avec la durée de l'hydratation, tandis que les pâtes malaxées pendant 10 minutes étaient initialement antithixotropiques, mais devenaient, après deux heures d'hydratation, encore plus thixotropiques que les pâtes malaxées pendant 1 minute. Un malaxage à très grande vitesse (10 000 tours/minute), comportant un refroidissement externe, a été utilisé pour produire des pâtes à faible ressuage (26). On pense que son principal effet, a été de remanier les minces couches d'hydrates formés à la surface des grains de ciment, et de les disperser dans la pâte, qui a ainsi atteint une consistance épaisse.

Les résultats inscrits sur la figure 4, ont été obtenus principalement pour déterminer l'influence de l'intensité du malaxage sur les courbes d'écoulement. Il n'a pas été procédé à des variations de la durée de ce malaxage énergique, mais on constate cependant de grandes variations dans les propriétés rhéologiques. Six sortes de malaxage, d'intensité croissante, ont été essayées. Le processus AS est celui de la méthode ASTM C 305, utilisant un malaxeur planétaire Hobart à faible (140 tours/minute) ou à moyenne (280 tours/minute) vitesse. Le processus A 20 comporte le malaxage pendant 20 minutes à faible vitesse. Le processus B 20 est celui du standard API utilisant un mélangeur à grande vitesse pendant 1 minute à titre de malaxage préliminaire, suivi d'un malaxage de 20 minutes à faible vitesse dans un gobelet B, Bl et Bh sont d'autres variantes du processus de malaxage dans un mélangeur à grande vitesse, comportant des malaxages à faible (3 500 tours/minute) et grande (17 000 tours/minute) vitesse, mais sans dépasser un temps de malaxage de 1 minute. De telles variations dans l'intensité du malaxage n'ont qu'une incidence mineure sur la fluidité. La fig. 4 montre que les seuils de rigidité et les viscoplasticités, de toutes ces pâtes mélangées et malaxées sont sensiblement plus faibles que celles des pâtes malaxées moins énergiquement. Cependant, après addition de 1 % du poids du ciment, d'un additif superplastifiant formé d'un condensat de sulfonate de formaldéhyde de β naphtalène (additionné d'un retardateur de prise), ces variations ont été pratiquement supprimées, notamment les seuils de rigidité sont alors voisins de zéro. Les boucles d'hystérésis sont beaucoup plus minces que celles de la figure 4; les pentes de ces courbes sont à peu près les mêmes que celles obtenues avec des pâtes sans additif malaxées très énergiquement.

Plusieurs des divers types de comportement fluide, obtenus par divers expérimenteurs peuvent être expliqués qualitativement par des ruptures de liaisons thixotropiques et une certaine recouvrance, se produisant pendant et après les divers malaxages et les processus d'essais. Dans cet esprit, il est utile de considérer que la force et le nombre des liaisons intergranulaires, dans les structures floculées, sont des fonctions du temps. Le développement des ruptures thixotropiques et de la recouvrance peut être exprimé dans de tels termes (3), qui permettent aussi de définir un degré de floculation. Bombled et d'autres ont attribué la thixotropie à des variations du degré de floculation, qu'ils ont défini de façon mesurable, par le rapport entre la dimension moyenne des agglomérats floculés et la dimension moyenne des grains (2). Cette définition ne peut pas donner une mesure exacte de la résistance au cisaillement de la structure floculée, mais elle permet d'expliquer les comportements complexes qui ont été observés. Pour ce faire, on admet que le degré de floculation peut être représenté qualitativement en fonction du temps, pendant et après le malaxage comme indiqué sur la fig. 5.

Deux courbes sont présentées : 1) La courbe L-LR correspond à un malaxage à faible intensité pendant un temps M, puis à une recouvrance le long de la courbe LR si la pâte est laissée au repos, 2) La courbe H-HR qui correspond à une pâte malaxée énergiquement (mais pas assez longtemps pour produire d'autres effets) et sa recouvrance. Une décroissance exponentielle des courbes est observée, à la fois pour la période des ruptures et celle de la recouvrance; mais la durée constante de la recouvrance semble être au moins dix fois plus grande que la période des ruptures. Ceci est cohérent avec des durées des périodes de rupture de l'ordre de 1 minute (3, 21), et des durées de la recouvrance, indiquées par le changement de l'écoulement antithixotropique en écoulement thixotropique, de 30 à 45 minutes (23, 25). Un point important est que ces pâtes à cause de leur haut degré de floculation, ou à cause d'un malaxage et d'une recouvrance insuffisants, donneront lieu à davantage de ruptures thixotropiques, que les pâtes plus complètement dispersées par un malaxage énergique.

Les pâtes plus complètement dispersées subiront une recouvrance plus rapide après malaxage, et tendront vers un comportement antithixotropique si le processus de la recouvrance se superpose aux modifications imposées par l'essai de mesure. Cependant si la pâte malaxée énergiquement est laissée au repos après le malaxage, le degré de floculation retrouvera le même niveau que celui de la pâte malaxée à faible intensité pendant quelque temps P, comme montré sur la fig. 5.

Les variations du degré de floculation provoquées par l'essai lui-même apparaissent, pour un seul cycle, sur la fig. 6, les courbes du haut et du bas ayant été obtenues à l'aide d'un viscosimètre, en maintenant constantes les vitesses des variations de vitesse du cisaillement, comme indiqué sur la partie basse de la figure. La courbe en forme de S, montre les variations du degré de floculation de la pâte, lorsque la vitesse croît lentement au début de l'essai. Pendant l'essai, le degré de floculation diminue lentement, seulement aux faibles vitesses de cisaillement initiales; mais décroit plus rapidement pour les plus grandes vitesses de cisaillement, puis de nouveau, plus lentement, pour les faibles vitesses de cisaillement de la fin de l'essai. D'autre part, si la pâte au repos a récupéré sa recouvrance, à une vitesse appréciable, comme indiqué sur la courbe de recouvrance R, la courbe obtenue résulte de la superposition de deux effets qui ressemblent à ceux de la courbe T. La courbe T peut varier entre les positions

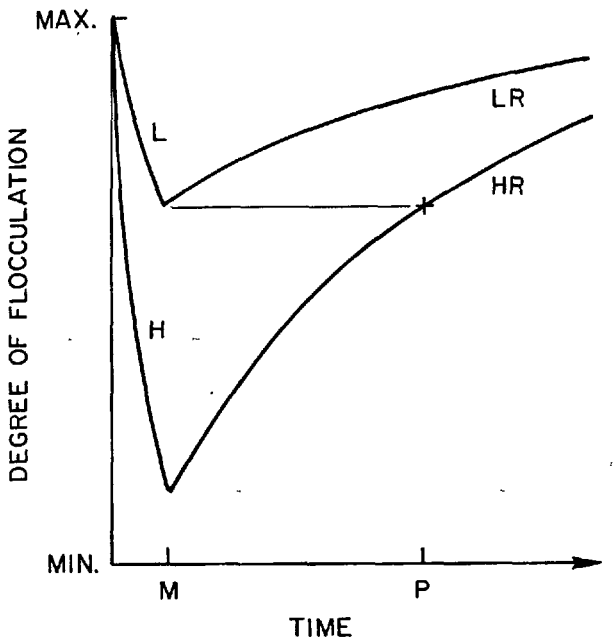

Fig. 5 - Variations du degré de floculation des grains de ciment dans des pâtes, pendant un malaxage à haute intensité H, ou à faible intensité L, et pendant la recouvrance, la pâte étant mise au repos après le malaxage

extrêmes S et R, selon les conditions de l'essai, et peut être considérée comme thixotropique ou antithixotropique selon l'effet qui prédominera au cours de l'essai.

FACTEURS INFLUANT SUR LA FLUIDITE

La finesse du ciment et le rapport eau ciment de la pâte fraîche sont les deux principaux facteurs qui influent sur la fluidité. Ces deux facteurs commandent ensemble l'épaisseur moyenne des films d'eau d'enrobage des grains et l'espacement intergranulaire. Malgré le fait que les pâtes normales de ciment sont dans l'état floculé dès qu'elles sont au repos, le concept de l'épaisseur moyenne des films d'eau, semble être assez valable pour caractériser les propriétés rhéologiques. Pour déterminer les effets de la teneur en eau, de la finesse et d'autres facteurs plus ou moins simples, Legrand a étudié systématiquement le comportement fluide des pâtes et mortiers confectionnés avec des poudres fines de calcite ou d'autres matériaux (19). Des essais analogues mais moins complets ont été effectués avec des ciments. La valeur maximum du seuil de rigidité de telles pâtes au repos, E_o, avant les ruptures thixotropiques provoquées par l'essai, est étroitement liée à la concentration en volumes solides C, suivant la formule :

$$E_o = Ae^{a'C - 0,5)} \qquad (3)$$

dans laquelle A et a sont des paramètres déterminés par l'expérience. Quand les pâtes sont vibrées, les seuils de rigidité sont nuls. Les valeurs de C s'étalent de 0,475 à 0,677 pour les ciments portland; ce qui correspond à des valeurs du rapport eau ciment variant de 0,15 à 0,35. Bien que le comportement de ces pâtes, passe, pour ces valeurs de C, par une transition entre l'état plastique thixotropique et l'état dilatant, l'équation (3) représente bien les résultats obtenus pour toutes ces valeurs de C.

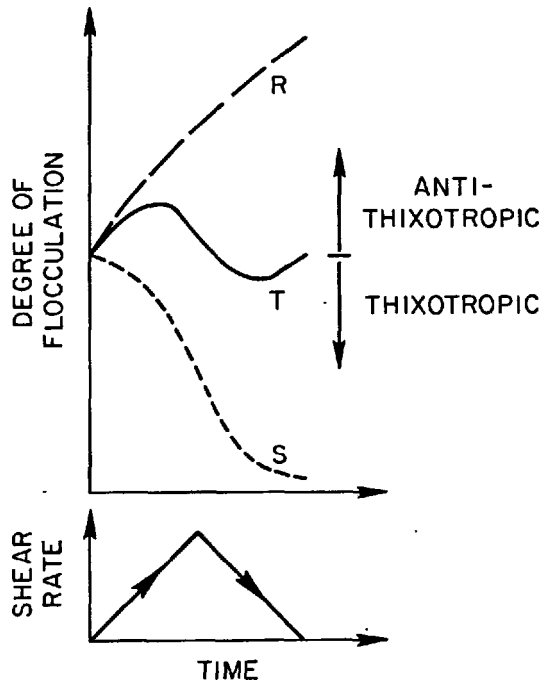

Fig. 6 - Variations du degré de floculation des grains de ciment, dans des pâtes pendant leur essai au viscosimètre rotatif, au cours d'un seul cycle. La courbe S correspond à une pâte à recouvrance lente après malaxage. La courbe R correspond à une pâte à recouvrance rapide. La courbe T montre la superposition de ces deux effets S et R.

Les valeurs de a dans l'équation (3) dépendent de la nature et de la forme des grains, mais sont indépendantes de la surface spécifique et de la distribution granulométrique du matériau; les valeurs de a s'étalent entre 23 et 48 selon que les grains sont sphériques ou anguleux. La valeur de A augmente rapidement avec la surface spécifique du ciment, jusqu'à dépasser environ 100 Pa.

Une relation analogue, a été trouvée, entre la concentration en volumes solides C et la contrainte de cisaillement τ, mesurée à des vitesses constantes de la déformation par cisaillement, pendant que la pâte est vibrée :

$$\tau = Be^{b(C - 0,5)} \qquad (4)$$

dans laquelle B et b sont des paramètres déterminés par l'expérience. Cette relation est applicable aux valeurs de C inférieures à la transition entre comportement dilatant et comportement pseudoplastique. Dans ce cas, b dépend de la vitesse du cisaillement, de la nature du matériau et de la forme des grains,

mais est indépendant de la surface spécifique et de la distribution granulométrique. b atteint un maximum d'environ 26 pour une vitesse de déformation de 40 s^{-1}. La valeur de B croît aussi avec la vitesse de cisaillement et la surface spécifique, atteignant plusieurs centaines de Pa pour les ciments finement broyés.

Les formules (3) et (4) représentant les résultats expérimentaux sont utiles, parce qu'elles permettent d'identifier certains facteurs qui peuvent influer sur la fluidité dans les systèmes les plus simples; la formule (4) est aussi vérifiée pour les pâtes de ciment portland pendant leur vibration. Les résultats obtenus avec des pâtes de ciment portland non vibrées, ont aussi été étudiés, dans le but de déterminer les véritables relations fonctionnelles et de mieux comprendre le rôle des facteurs qui influencent la fluidité. Les résultats obtenus au viscosimètre et indiqués sur la fig. 3, montrent la diminution des seuils de rigidité et des viscosités quand la teneur en eau augmente. Une série d'essais, effectués sur des pâtes de ciment portland ordinaire d'une finesse Blaine de 447 m^2/kg, avec des rapports eau ciment très variés, ont donné les résultats exposés au tableau I.

TABLEAU I

Rapport E/C en poids g/g	Seuil de rigidité (Pa)	Viscoplasticité en mPa.s
0,4	81	39
0,45	39	22
0,5	25	16
0,6	9	12
0,7	6,4	8,5
0,8	1,6	5,8

Des résultats correspondant à des rapports E/C plus faibles sont donnés sur le tableau II, qui comportent à la fois des mesures faites au viscosimètre et au rhéographe (2)

Bien que l'on ait employé différents ciments et diverses méthodes de malaxage, ces deux ensembles de résultats donnent des valeurs analogues pour le seuil de rigidité en fonction de la teneur en eau.

TABLEAU II

Rapport E/C en poids g/g	Seuil de rigidité Pa
0,24	1900
0,32	130
0,36	65
0,40	30
0,50	8,5

Les résultats de la fig. 2, montrent l'influence des variations de la surface spécifique du ciment, sur les valeurs initiales du seuil de rigidité, pour des pâtes ayant un rapport E/C de 0,25; ils montrent aussi comment ces valeurs évoluent pendant la prise. L'effet de la finesse du ciment est aussi montré sur le tableau III, pour des pâtes à rapport E/C 0,4, et aussi pour d'autres pâtes dont le rapport E/C a été fixé par la condition d'avoir pour ces pâtes un même seuil de rigidité (2)

TABLEAU III

Surface spécifique m^2/kg	Seuil de rigidité pour E/C = 0,4 (Pa)	E/C en poids pour E = 30 Pa	Distance entre grains en microns *
235	14,0	0,35	2,0
278	26,5	0,44	2,3
329	75,0	0,475	2,2
442	165,5	0,55	1,9
560	>250,0	0,58	1,6

* distance calculée à l'aide de la formule (5) en fonction de la surface spécifique.

Comme on peut s'y attendre, en considérant l'épaisseur des films d'eau et les distances intergranulaires, l'augmentation de la surface spécifique, augmente progressivement le seuil de rigidité pour une même teneur en eau. De même, la teneur en eau nécessaire pour obtenir un seuil de rigidité de 30 Pa augmente systématiquement avec la surface spécifique. Bombled pense que les distances intergranulaires restent approximativement constantes, si la teneur en eau augmente avec la surface spécifique, de façon à maintenir constant le seuil de rigidité (2). La distance intergranulaire (2 fois l'épaisseur du film en microns) est donnée par la formule :

$$d = 2 \times 10^3 \frac{E/C - 0,12}{S} \qquad (5)$$

où E/C est le rapport eau ciment, S la surface spécifique du ciment, et 0,12 la proportion de l'eau intersticielle, qui ne contribue ni à l'épaisseur des films ni aux espaces intergranulaires, comme indiqué sur la fig. 1. On voit sur le tableau III que les valeurs de d sont approximativement constantes.

En plus des formes fonctionnelles (3) et (4), des équations ont été élaborées pour représenter la relation entre la fluidité du ciment et sa finesse. Les résultats du tableau II, ont été utilisés pour établir la formule suivante, valable pour S constante.

$$E_o = \frac{0,124}{(E/C - 0,15)^{3,97}} \qquad (6)$$

Cette formule a été obtenue par la méthode des moindres carrés. Pour obtenir le meilleur ajustement, la teneur en eau qui ne contribue pas à l'écoulement, doit être prise égale à 0,15. Les résultats du tableau III, ont été tracés sur un diagramme logarithmique, dont la pente a permis d'obtenir la formule

$$E_o = 4{,}47 \times 10^{-9} S^{4{,}01} \qquad (7)$$

Le fait que les exposants dans les deux formules (6) et (7) soient pratiquement égaux, montre à nouveau, que le seuil de rigidité est étroitement lié à la surface spécifique et à la teneur en eau. Toutefois, ces données semblent donner aussi de bons ajustements pour d'autres exposants, et d'autres relations, par suite du faible nombre et de la faible précision de ces données.

La relation fonctionnelle entre la viscoplasticité apparente, la teneur en eau et la surface spécifique devient plus compliquée. Dans une étude (9), la viscosité apparente a été trouvée égale à :

$$\eta = 13(d')^{-0,6} - 1 \qquad (8)$$

où d' est un paramètre utilisé pour mesurer l'espacement intergranulaire; il s'exprime en microns par la formule :

$$d' = \frac{(E - E_a)^2}{S} 10^3 \qquad (9)$$

dans laquelle les teneurs en eau E et E_a, ainsi que la surface spécifique S, sont calculées par unité de pieds du ciment. La valeur de E_a, la teneur en eau imposée par l'essai standard, est d'environ 0,3. Ceci conduit à penser que les relations fonctionnelles entre la viscosité et la teneur en eau, peuvent différer considérablement de celles correspondants aux seuils de rigidité pour le ciment portland.

ADDITIFS REDUCTEURS D'EAU

Les observations au microscope ont, maintes fois, confirmé que les grains de ciment étaient dispersés par les additifs réducteurs d'eau (2). On a longtemps pensé que cette dispersion était le résultat de la neutralisation des charges superficielles et de la réduction des forces attractives intergranulaires. Les additifs assez récents appelés "super réducteurs d'eau", tels que le formaldehyde melamine sulfoné (type M) ou le formaldéhyde naphtalène sulfoné (type N), sous forme de condensats ne créent pas de retards importants à l'hydratation. Ils peuvent toutefois, être employés à des concentrations beaucoup plus fortes (plus de 1 % en poids de ciment) que celles que l'on utilisait habituellement avec les additifs aux lignosulfonates. Ce dernier type d'additif provoque habituellement des retards importants à des concentrations quelque peu supérieures à 0,1 %, que cet additif contienne ou non du sucre (27).

Daimon et Roy (28) ont mesuré la loi d'adsorption du condensat de formaldéhyde naphtalène sulfoné par les grains de ciment dans l'eau, ils ont trouvé que celle-ci correspondait à une isotherme de Langmuir. Ils ont aussi montré qu'avec le ciment utilisé (393 m^2/kg) et avec des proportions d'additifs d'environ 1,5 %, presque tout le composant actif était adsorbé (environ 20 % n'était pas adsorbable); mais quand on augmentait fortement cette proportion d'additif, une part rapidement croissante, restait en solution. Les mesures du potentiel zéta des grains les plus fins du ciment, ont montré que ses variations en fonction de la proportion d'additif suivait une isotherme d'adsorption de Langmuir, atteignant des valeurs d'environ 50 mV, au maximum de l'adsorption (29). Des essais d'écoulement des mortiers ont aussi montré un accroissement similaire en fonction de la proportion d'additif. Des mesures faites au viscosimètre rotatif ont montré que les seuils de rigidité initiaux, qui variaient de 40 à 100 Pa (selon l'énergie du malaxage) pour la pâte pure à 0,4 d'eau, diminuaient jusqu'à zéro pour une proportion d'additif de 1 %. La viscosité apparente, diminuait aussi de 500 environ à 200 mPa/s environ, si la pâte était malaxée peu énergiquement (ASTM); mais cette diminution était très faible si la pâte était malaxée très énergiquement (API), comme indiqué dans la discussion de la figure 4.

L'adsorption de deux additifs du type N et de deux polymères du système à haut poids moléculaire, par les ciments, a pu être portée (30) jusqu'à 0,5 % du poids du ciment. Pour les additifs du type N, la loi d'adsorption était du type isotherme de Langmuir; pour le polymère du styrène elle a été du type H (forte affinité). Les mesures de vitesse de sédimentation, avec des additifs du type N, de suspensions diluées de ciment dans l'eau (3 g dans 28,5 ml) ont montré la bonne séparation des grains; car la vitesse de sédimentation diminuait quand on ajoutait l'additif jusqu'à une proportion de 0,4 % en poids du ciment.

Petri (14) a mesuré la viscosité apparente des pâtes de ciment, à l'aide du viscosimètre rotatif de Brookfield, avec ou sans ajout d'additifs divers. Ces ajouts ont atteint 1,6 % du poids du ciment. On a constaté, en accroissant l'ajout d'additifs du type N, une diminution progressive du seuil de rigidité, de la viscosité et de l'aire des boucles d'hystérésis, par augmentation et diminution de la vitesse de cisaillement, jusqu'à ce qu'un comportement newtonien soit obtenu, pour une proportion de 1,2 % d'additif. Un autre additif essayé par Petri l'hexamétaphosphate de sodium, a produit son effet maximum pour une proportion d'environ 0,5 %.

Petri a aussi tenté de déterminer la relation fonctionnelle, autre la viscosité apparente η de la pâte de ciment, et la concentration en volumes solides C. Les résultats concernant les pâtes de ciment sans additif n'ont satisfait aucune des nombreuses équations théoriques de l'électroviscosité. Ceci n'est pas surprenant, car ces équations ont été établies dans l'hypothèse d'un comportement newtonien. Cependant, Petri, a trouvé que pour les pâtes contenant 1 % d'additif du type N, les mesures faites sur les suspensions correspondaient remarquablement au modèle théorique de sphères, de dimensions égales, et sans attractions mutuelles, dans une suspension très concentrée; dans ce cas on a :

$$\eta = \eta_o (1 - 1{,}35\ C)^{-2,5} \qquad (10)$$

Les recherches continuent sur l'emploi de lignosulfonate comme additif réducteur d'eau, particulièrement

dans les pâtes à faible rapport eau ciment. On y ajoute du carbonate soluble pour éviter un retard de prise excessif. Odler et coll. (17) ont étudié les propriétés rhéologiques des pâtes de ciment portland (à 6 % de gypse), avec ou sans lignosulfonate de sodium additionné de carbonate de soude, et des pâtes de clinker pulvérisé, avec les mêmes additions. Il fut ajouté jusqu'à 1,25 % de chacun de ces deux additifs, et quand ils étaient tous les deux ajoutés on a observé un effet fluidifiant et régulateur de prise. La finesse variait de 340 à 850 m^2/kg. Lorsque le ciment était gypsé, le temps de prise était réduit, mais sur les produits non gypsés ces additifs produisaient un comportement normal à la prise et un durcissement accéléré. Les mélanges à rapport eau ciment aussi bas que 0,225 étaient suffisamment fluides pour pouvoir être essayés au viscosimètre rotatif. Comme indiqué précédemment, on observa un comportement avec épaississement de ces pâtes. Dans une autre étude (31), utilisant du lignosulfonate de calcium, et du carbonate de potassium, des difficultés apparurent au-dessous d'un rapport eau ciment de 0,25, pour l'essai de ces pâtes dans un viscosimètre rotatif. Ces pâtes sont décrites comme ayant une consistance caoutchouteuse. D'autres expérimentateurs ont utilisé des lignosulfonates avec $NaHCO_3$, pour produire des pâtes, ayant des rapports eau ciment variant de 0,22 à 0,24, qui se sont montrées "automontantes", mais qui avaient des propriétés rhéologiques très complexes; elles semblaient avoir des propriétés élastoplastiques, difficilement caractérisables en termes normaux (20).

COMPOSITION DES CIMENTS ET HYDRATATION

Pour les ciments dont les premières réactions d'hydratation ont été correctement contrôlées, les propriétés rhéologiques, pendant la période de latence, ne dépendaient pas beaucoup de la composition de ces ciments. Une étude portant sur douze ciments de divers types, a conclu, que, sauf pour un ciment à prise régularisée, la composition chimique et minéralogique du ciment, avait peu d'influence, sur le comportement rhéologique, comparativement à l'influence de la teneur en eau et de la finesse du ciment (25). Cependant, l'eau nécessaire à rendre fluide une pâte, augmente d'une façon significative avec la proportion de C_3A et d'alcalis; elle en dépend autant que de la distribution granulométrique (32). En outre, le sulfate de calcium doit être sous une forme convenable, pour contrôler les réactions initiales des aluminates et empêcher la fausse prise (24 - 33). Cependant, si les mesures au viscosimètre sont poursuivies assez longtemps au cours de l'hydratation, l'effet de la teneur en C_3A devient progressivement plus important. Des mesures faites sur des ciments contenant des teneurs en C_3A variant de 0 à 14 %, ont montré une faible variation du seuil de rigidité, de la viscoplasticité ou de l'aire des boucles d'hystérésis, pendantles 45 minutes suivant le malaxage (23). Cependant, deux heures après malaxage, la thixotropie, représentée par l'aire des boucles d'hystérésis, augmentait fortement quand la teneur en C_3A dépassait 2 %. Le seuil de rigidité, lui aussi commençait à croître avec la teneur en C_3A après 2 heures. La viscoplasticité n'a, cependant, pas sensiblement présenté le même effet même après 3 heures.

Wittmann (34) a étudié l'effet d'un additif du type M, sur la viscosité des pâtes de ciment, ayant un rapport eau ciment de 0,6, à des âges supérieurs à 7 heures. Pour les pâtes sans additif, les courbes de la viscosité en fonction du temps, ont montré, pour différentes vitesses de rotation du viscosimètre, une augmentation du temps d'hydratation plus grande que celle obtenue au rhéographe (fig. 2). Pour une vitesse de rotation de 80 tours/minute, la viscosité apparente augmentait d'environ 2000 à l'origine jusqu'à plus de 20000 mPa/s, après environ 4 heures. Ces valeurs paraissent extraordinairement élevées. Avec 1,5 % d'additif, la viscosité initiale tombe à une valeur d'environ 50 mPa/s, et montre au bout d'une heure ou deux, un comportement très proche du comportement newtonien idéal. Après environ 3 heures, la viscosité n'est plus newtonienne, et la vitesse de cisaillement augmente jusqu'à près de 20000 mPa/s, à 80 tours minute, après environ 7 heures. Des études entreprises sur plusieurs ciments différents ont donné des résultats analogues, sauf pour un ciment du type PZ 550, qui exige un plus fort porcentage d'additif pour retarder l'augmentation de la viscosité. Ceux-ci, et bien d'autres résultats, comme ceux indiqués sur la fig. 2, montrent que le raidissement de la pâte au cours de la prise, suit, normalement, un processus progressif. Ce processus résulte des réactions d'hydratation initiales, et il est affecté par certains facteurs qui accélèrent ou retardent l'hydratation.

CONCLUSION ET DISCUSSION

Il apparaît à la lecture de la littérature disponible, qu'il y a encore d'importantes lacunes dans notre connaissance de la rhéologie des pâtes fraîches de ciment. On a tenté, avec difficulté, d'exprimer quantitativement les résultats en fonction des propriétés des matériaux, et d'établir des relations entre la concentration et les propriétés du ciment. Un résultat, au moins partiel, est le suivant : le processus de malaxage des pâtes de ciment, et les méthodes de mesure de leurs propriétés rhéologiques, influent sur les propriétés à mesurer. Il semble souhaitable d'étudier la rhéologie des pâtes de ciment, dans un état de dispersion des grains dans l'eau, comparable à celui qui existe dans les pâtes du béton. Pour cette raison T.C. Powers préconise l'emploi de mélangeurs à grande vitesse, parce qu'il pense que les vitesses de cisaillement des pâtes de ciment dans les malaxeurs à béton, sont au moins aussi énergiques, que dans les malaxeurs de pâte à ciment des laboratoires. Nous avons vu récemment des résultats qui montrent des différences sensibles entre les malaxeurs de chantier et les malaxeurs des essais normalisés. Il serait alors prudent, si cela n'a pas encore été fait, de commencer par définir l'intensité du malaxage désirée; ensuite on pourrait concentrer nos efforts sur les pâtes ainsi malaxées. Des considérations analogues peuvent intervenir, en ce qui concerne les types très variés de viscosimètres rotatifs. Des expérimentations très soignées ont, d'autre part, été entreprises, sur les appareils de mesure, dont la conception et les dispositions constructives, peuvent empêcher des mesures quantitatives, car ne créant pas un malaxage uniforme et régulier, ou provoquant des ruptures de l'écoulement. Il apparaît que ce problème a été bien perçu par certains expérimentateurs, et que plusieurs méthodes valables vont apparaître permettant de réaliser des essais reproductifs. Peut être, on pourrait mettre au point des méthodes valables de comparaison des divers essais rhéologiques, soit en choisissant un ciment standardisé bien défini servant d'étalon, soit en utilisant un matériau inerte ayant des propriétés rhéologiques proches de celles du ciment.

En ce qui concerne les interprétations théoriques, la situation pouvait aussi, être sensiblement améliorée. Petri (14) considère la théorie des suspensions fluides, de grains chargés électriquement par un électrolyte, c'est-à-dire l'électroviscosité. Les équations complexes qui représentent la viscosité de telles suspensions, font appel aux paramètres électriques des potentiels de double couche, aussi bien qu'à la concentration en volumes solides C, et à la viscosité du liquide. Sous leur forme réduite, la plus simple, ces équations donnent :

$$\eta = \eta_o (1 + kC) \qquad (11)$$

qui, pour k = 2,5 donne l'équation bien connue d'Einstein. Ceci met en évidence une imperfection flagrante de la théorie, lorsqu'on l'applique aux systèmes, tels que les pâtes de ciment, dans lesquels les forces intergranulaires provoquent une floculation et la formation d'une structure, ayant un seuil de rigidité non nulle, dépendant de la vitesse de déformation, et une thixotropie, c'est-à-dire un comportement non newtonien.

Néanmoins, les recherches sont parvenues à nous fournir une compréhension qualitative et parfois même semi-qualitative du comportement complexe des pâtes fraîches de ciment. Plusieurs formules empiriques, donnant semble-t-il satisfaction, ont été établies pour relier les propriétés rhéologiques des pâtes fraîches, à la surface spécifique du ciment, et à sa concentration dans l'eau. Cette matière semble méritée des recherches complémentaires, l'objectif étant de pouvoir prévoir à l'avance, de façon sûre, les propriétés rhéologiques des pâtes fraîches de ciment, en fonction de la composition du ciment et de ses propriétés physiques.

Le développement rapide de l'emploi de réducteurs d'eau organiques et d'autres additifs dans le béton, et l'apparition de nouveaux additifs, a provoqué maintes recherches sur leur action sur les propriétés rhéologiques des pâtes de ciment. De telles recherches ont généralement pour but de connaître l'efficacité d'additifs particuliers. Cependant, puisque le comportement rhéologique des pâtes de ciment contenant des additifs est plus simple que celui des pâtes sans additif, il doit être possible d'établir les véritables relations fonctionnelles qui commandent l'état dispersé, puis, ensuite, s'attaquer aux problèmes des pâtes floculées à divers degrés.

BIBLIOGRAPHIE

1. T. C. Powers (1968), "Rheology of Freshly Mixed Concrete," The Properties of Fresh Concrete, John Wiley, New York. (In English)

2. J. P. Bombled (1974), "Rheology of Mortars and Fresh Concrete: Studies of the Interstitial Cement Paste," Ciments, Betons, Platres, Chaux (Rev. Mater. Constr.), No. 688, 137-155. (In French)

3. G. H. Tattersall (1976), "The Workability of Concrete," Publ. 11.008, Cement and Concrete Assoc., England. (In English)

4. D. W. Hobbs (1976), "Influence of Aggregate Concentration Upon the Workability of Concrete and Some Predictions from the Viscosity-Elasticity Analogy," Mag. Concr. Res., 28, No. 97, 191-202. (In English)

5. M. Barrioulet and C. Legrand (1977), "Influence of the Interstitial Paste on the Flow Ability of Fresh Concrete. The Importance of the Water Retained by the Aggregates," Materials and Structures, 10, No. 60, 365-373. (In French)

6. G. H. Tattersall (1976), "Relationships Between the British Standard Tests for Workability and the Two-Point Test," Mag. Concr. Res., 28, No. 96, 143-147. (In English)

7. M. Barrioulet and C. Legrand (1978), "Study of Intergranular Friction in Fresh Concrete. New Ideas on the Flow of Vibrated Fresh Concrete," Materials and Structures, 11, No. 63, 191-197. (In French)

8. C. W. Richards and R. A. Helmuth (1975), "Expansive Cement Concrete - Micromechanical Models for Free and Restrained Expansion," Stanford Univ. CE-TR-191. (In English)

9. K. Rendchen (1976), "Influence of Various Cements on Flow Behavior and Stability of Cement Suspensions," Beton: Herstellung Verwendung, 26, No. 9, 321-325. (In German)

10. F. W. Locher, W. Richartz and S. Sprung (1976), "Setting of Cement. Part 1: Reaction and Development of Structure," Zement-Kalk-Gips, 29, No. 10, 435-442. (In German)

11. W. F. Perenchio, D. A. Whiting and D. L. Kantro (1978), "Water Reduction, Slump Loss, and Entrained Air-Void Systems as Influenced by Superplasticizers," in Superplasticizers in Concrete, CANMET, Ottawa, 295-324. (In English)

12. J. P. Bombled (1971), "Rheograph for the Rheologic Study of the Stiffening of Pastes. Application to the Setting of Cement," Rev. Mater. Constr., No. 673, 256-277. (In French)

13. J. P. Bombled (1976-7), "Setting Time Measurements for Cement Pastes - Rheograph and Automatic Prisometer CERILH," Ciments, Betons, Platres, Chaux (Rev. Mater. Constr.), No. 699, 113-124; No. 709, 355-362. (In French)

14. E. M. Petri (1976), "Effect of Surfactant on the Viscosity of Portland Cement-Water Dispersions," Ind. Eng. Chem., Prod. Res. Dev., 15, No. 4, 242-249. (In English)

15. D. M. Roy and K. Asaga (1979), "Rheological Properties of Cement Mixes: III. The Effects of Mixing Procedures on Viscometric Properties of Mixes Containing Superplasticizers," Cement and Concr. Res., 9, No. 6, 731-739. (In English)

16. H. Reul (1978), "Rheological Investigation of Cement Suspensions with Fluidizing Agents," Beton: Herstellung Verwendung, 28, No. 10, 360-361. (In German)

17. I. Odler, U. Duckstein and Th. Becker (1978), "On the Combined Effect of Water Soluble Lignosulfonates and Carbonates on Portland Cement and Clinker Pastes, I. Physical Properties," Cement and Concr. Res., 8, No. 4, 469-480. (In English)

18. C. R. Dimond and G. H. Tattersall (1976), "The Use of the Coaxial Cylinders Viscometer to Measure the Rheological Properties of Cement Pastes," in Hydraulic Cement Pastes: Their Structure and Properties, Publ. 15.121, Cement and Concrete Assoc., England, 118-133. (In English)

19. C. Legrand (1972), "A Contribution to the Study of Fresh Concrete Rheology," Materials and Structures, 5, No. 29, 275-295; No. 30, 379-393. (In French)

20. S. Diamond and C. Gomez-Toledo (1978), "Consistency, Setting, and Strength Gain Characteristics of a 'Low-Porosity' Portland Cement Paste," Cement and Concr. Res., 8, No. 5, 613-621. (In English)

21. R. Lapasin, V. Longo and S. Rajgelj (1976), "Rheological Behavior of Cement Pastes," Il Cemento, 73, No. 2, 91-101. (In Italian and English)

22. R. Lapasin, V. Longe and S. Rajgelj (1979), "Thixotropic Behavior of Cement Pastes," Cement and Concr. Res., 9, No. 3, 309-318. (In English)

23. M. Ish-Shalom and S. A. Greenberg (1960), "The Rheology of Fresh Portland Cement Pastes," in Proc. 4th Int'l. Symp. on Chemistry of Cement, NBS Monograph 43, Vol. II, 731-744. (In English)

24. S. A. Greenberg and L. M. Meyer (1963), "Rheology of Fresh Portland Cement Pastes: Influence of Calcium Sulfates," Highway Res. Record, No. 3, 9-29. (In English)

25. I. Odler, Th. Becker and B. Weiss (1978), "Rheological Properties of Cement Pastes," Il Cemento, 75, No. 3, 303-307. (In Italian and English)

26. S. A. Markestad (1976), "The Gukild-Carlsen Method for Making Stabilized Pastes of Cements," Materials and Structures, 9, No. 50, 115-117. (In English)

27. V. S. Ramachandran (1978), "Effect of Sugar-Free Lignosulfonates on Cement Hydration," Zement-Kalk-Gips, 31, No. 4, 206-210. (In German)

28. M. Daimon and D. M. Roy (1978), "Rheological Properties of Cement Mixes: I. Methods, Preliminary Experiments, and Adsorption Studies," Cement and Concr. Res., 8, No. 6, 753-764. (In English)

29. M. Daimon and D. M. Roy (1979), "Rheological Properties of Cement Mixes: II. Zeta Potential and Preliminary Viscosity Studies," Cement and Concr. Res., 9, No. 1, 103-110. (In English)

30. R. Kondo, M. Daimon, and E. Sakai (1978), "Interaction Between Cement and Organic Polyelectrolytes," Il Cemento, 75, No. 3, 225-230. (In English)

31. K. M. Hanna and A. Taka (1977), "Rheological Properties of Low-Porosity Cement Pastes," Zement-Kalk-Gips, 30, No. 6, 293-297. (In German)

32. J. Gebauer and W. Schramli (1974), "Variations in Water Requirement of Industrially Produced Portland Cements," Bull. Am. Ceramic Soc., 53, No. 2, 161-168. (In English)

33. G. Frigione (1978), "The False Set of Portland Cement Pastes," Il Cemento, 75, No. 3, 207-224. (In Italian and English)

34. F. H. Wittmann (1979), "Influence of Water Reducing Admixtures on the Rheological Behavior, Capillary Shrinkage and Structure of Cement Paste," Silicates Industriels, 44, No. 1, 5-13. (In English)

SUB-THEME VI-0

Structure and rheology of fresh cement paste*

R. A. HELMUTH
Portland Cement Association
U. S. A.

* This communication constitutes the principal report of sub-theme VI-0 which was received too late to be published in the volume 1 "Principal Reports".

INTRODUCTION

The properties of fresh portland cement pastes are of interest primarily because of their relationship to the properties of concrete. Of universal interest are the characteristics of cements that influence the consistency, workability, and setting characteristics of the concrete. Understanding how to control the rheological properties of fresh concrete is important for the economical proportioning of concrete mixtures and the proper mixing and placement of concrete.

Microscopic examinations of sections of normal hardened concrete show each aggregate particle to be suspended in a matrix of hardened cement paste with films of paste completely separating the particles. Hence, the fresh concrete must have had this kind of structure in the quiescent state at the time of setting. However, during the mixing and placement of the concrete, the coarse aggregate and sand particles must come into frequent direct contact. Such direct contact between aggregate particles results in frictional forces and particle interference effects in addition to the resistance to flow of the cement paste itself.

Although progress in the development of an understanding of the relationship between the rheology of concrete and cement paste has been made (1-5), most standard testing procedures for cements, mortars, and concretes are purely empirical and results obtained by different tests may appear to be inconsistent. For example, a more finely ground cement may have a higher water requirement or a stiffer consistency than a coarser cement in a cement-water paste, but may have a lower water requirement (or greater flow) when tested in a plastic mortar because of a smaller amount of interference by the largest cement particles to the motion of sand particles in the mortar.

Tests to measure concrete or mortar consistencies include those that measure deformation due to the force of gravity, and the cumulative deformation (or time to a given deformation) under repeated impact or vibrational and gravitational forces. Such tests yield numerical results on arbitrary scales which have no simple relationship to any well defined physical properties such as yield value (minimum shear stress for flow) or viscosity. The slump test has been shown to be a measure of the yield value of fresh concrete, and the compacting factor and Vebe tests are measures of the apparent viscosity (6). However, it has been shown that no single-point test provides an adequate measure of the flow properties and workability of concretes under various conditions (3,7). One reason for this is that there is an important difference between the state of the paste before and after it has begun to flow. It is common practice to use vibration to cause stiff fresh concrete mixtures to flow readily into place in the forms. Weak structures in the paste are broken down by steady shear or by vibration. The paste is then said to be in the fluidized state. The consistency of concrete while it is being placed by vibration is due, at least in part, to the rheological characteristics of its paste component in the fluidized state (1). The resistance of fresh concrete to deformation and flow when in the static state must also be due, at least in part, to the yield value of the cement paste.

The resistance of portland cement paste to shear is both time and shear strain rate dependent. It also depends upon mixing time and intensity. Cement pastes are normally thixotropic, or shear thinning, as a result of progressive breakdown of the flocculent structure of the particles as the paste is forced to flow. Hydration of the cement has some short term effects (brief mix set, false set) as well as the normal progressive stiffening. The flow behavior can therefore be very complex for even a single cement and comparisons between cements can be strongly affected by variations in methods of test and equipment employed.

The properties of fresh portland cement paste are also of interest relative to research on other characteristics of cements. For example, study of the properties of fresh pastes is useful in determining how cement particle size distributions might be improved, or how the gypsum content and other additions can be varied to obtain proper control of the early hydration reactions. From the time of initial mixing of the cement with water, the processes of solution and formation of hydrates cause progressive changes of the structure and rheological properties of the paste.

FRESH PASTE STRUCTURE

Modern portland cements are ground to a fine powder in which only a few percent of the cement is coarser than 74 μm, or finer than 1 μm. The particle shapes are the result of random multiple fracturing of the polymineralic clinker during finish grinding and tend to vary in shape from somewhat rounded to more angular grains. Hence, particle size distributions using equivalent spherical diameters for equal sedimentation velocities or surface areas should be good approximations.

Modern cements commonly have specific surface areas of 300-500 m^2/kg (3000-5000 cm^2/g), as measured by air permeability methods such as those due to Lea and Nurse or Blaine (ASTM C204). Some methods, such as the ASTM C115 Wagner Turbidimeter method, yield much lower values because the amounts of the finest particles are

underestimated. Certain other sedimentation methods determine amounts of fine cement particles that yield specific surface areas in close agreement with air permeability methods. By contrast, the values of the specific surface areas of cement as determined by nitrogen adsorption (BET method) are much larger than the air permeability values because adsorption methods determine the surface areas of the hydrates and other very small particles adhering to the surfaces of the cement particles, as well as the cracks, fissures and perhaps some of the pores in the clinker particles. It appears that the Blaine surface areas are more appropriate for use in the consideration of flow or sedimentation than the BET values because the water flow around the particles defines a smooth cement particle - water interface and does not detect minor irregularities of the particle surfaces.

Fresh cement pastes are initially a thick suspension of the cement particles in the mixing water. The structure of this suspension depends upon the water-cement ratio and the particle size distribution of the cement. It also depends upon the interparticle forces and attraction of the water to the solid surfaces, which in turn depends upon surface charges, ionic species and concentrations in solution, and sorption from solution. In dilute suspensions cement particles normally will flocculate, forming separate clusters of particles called floccules; these settle rapidly. Floccules formed from ordinary cement in dilute suspensions have a water-cement ratio of about 0.4. In the thick suspensions we call cement pastes, the separate floccules in the static state merge into a single continuous large floc. The particles are not uniformly distributed in such a structure; there are aggregations of higher than average particle concentrations between which are water-filled interstices. Within these aggregations the particles tend to have smaller interparticle separations corresponding to minimum potential energy configurations. Powers has called this the flocculent state (1).

During mixing, the cement particles tend instead to become more uniformly dispersed in the water. There is a continuous breaking down of the structure during mixing; this is the origin of the thixotropic, or shear-thinning, behavior of cement pastes. At any constant rate of shear an equilibrium structure (perhaps floccule size distribution) is reached within several minutes, resulting in a constant apparent viscosity. There is also a counteracting process of structure reformation. When the mixing is stopped, the static floc structure gradually forms again. Although the paste is a fluid during mixing, the floc structure is a weak solid, with a finite yield value, in the static state.

Certain organic (water-reducing) admixtures are used in concrete to improve its flow properties or reduce the water requirement for flow. Microscopic examinations show that when suitable amounts of such admixtures are used, the cement particles are completely dispersed in the water instead of being in the flocculent state. This is believed to be a result of adsorption of the admixture molecules on the cement particle surfaces, neutralization of charges, and the development of static repulsive forces between cement particles.

Some of these concepts can be used to visualize the structure of fresh cement pastes in terms of a simple model (8) as depicted in Fig. 1. The particles are represented

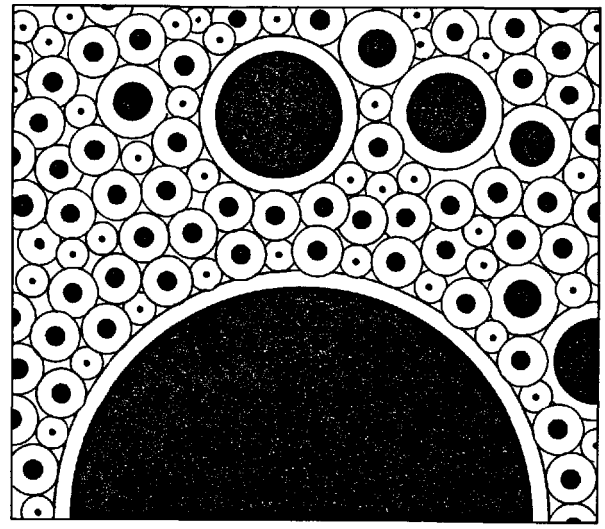

Fig. 1 - Simple dispersed spherical particle model of the structure of fresh cement paste of 0.5 water-cement ratio; 430 kg/cm^2 cement (8).

as spheres of sizes given by the equivalent spherical diameters of the particle size distribution curve typical of a cement of 430 m^2/kg specific surface area. The large half-sphere at the bottom represents a 30 μm particle. The spaces between large particles are filled with smaller particles and water. The figure is drawn for a paste with a water-cement ratio of 0.5. Because the water is strongly attracted to the particle surfaces, each particle is shown with a continuous film of water; if the cement is dispersed by vigorous mixing or with the use of a water-reducing admixture, the thicknesses of these films will tend to equalize as much as possible. A first approximation to the average thickness of these films is given by the hydraulic radius: the volume of water divided by the specific surface area of the cement. For this cement and water-cement ratio, the average film thickness is about 1.2 μm, only about one-tenth of the mass median particle diameter. Although the model is better suited to dispersed cements than

for pastes in the flocculent state, the average value of the film thicknesses will be the same. Second approximations have been proposed which consider the interstitial water outside of the films (2,9).

The early hydration reactions of the cement must also be considered in more realistic models of fresh paste structure. The initial rapid solution of the gypsum and alkali phases in the cement results in an aqueous solution of the hydroxides and sulfates of sodium, potassium, and calcium. With proper gypsum control of the hydration of the tricalcium aluminate, a sulfoaluminate coating is formed which almost stops the C_3A hydration after the rapid initial reaction. About 10% of the C_3A may hydrate in the first few minutes (10), after which the C_3A hydration is very slow until the gypsum is depleted, which usually occurs after final set. The depth of the reaction into the C_3A during the initial (10%) reaction can be estimated to be about 0.1 μm. If the reaction product is densely packed ettringite, these C_3A surfaces would be coated with a layer of about 0.8 μm. Nearly half of the gypsum would be consumed in this initial reaction; if the gypsum had an initial specific surface area of about 800 m^2/kg and if each gypsum particle dissolved to equal depths, the depth would be about 0.5 μm. After this reaction the specific surface area of the remaining gypsum particles would be less than half this value, so that the specific surface area of the cement would be reduced by about 30 m^2/kg. However, the BET surface area would be increased by formation of hydration products; if these hydrates form on the cement particle surfaces, they should not have any adverse effect on flow at this stage. Ettringite formation would by itself reduce the free water content of the paste by about 0.02 g/g cement for the same (10%) reaction.

All of these initial processes affect the specific surface area, free water content and, therefore, the water film thicknesses during the dormant period. The initial hydration reaction of the silicate surfaces should have little effect on the fresh paste structure unless vigorous mixing is continued so that the hydrates are continuously abraded from the surface. After the induction period, crystals of calcium hydroxide begin to form out of solution; this accelerates the hydration of the silicates and the formation of calcium silicate hydrate in acicular growths over all of the available solid surfaces. Normal setting occurs as a result of the intergrowth of these hydrates; ettringite recrystallization may also contribute to the setting (10).

DEFORMATION AND FLOW BEHAVIOR

The consistencies of fresh cement pastes up to the time of set vary so widely with composition and time that no single method of measurement suffices for the entire range. Viscometers, especially coaxial cylinders viscometers, are commonly used for the more fluid pastes with yield stress values up to about 200 Pa (2000 $dynes/cm^2$) and apparent viscosities of up to several thousand mPa·s (= centipoise). Recently, a mini-slump cone test has also been found useful for comparing flow properties of cement pastes of different compositions (11). In this test a small cone filled with paste is lifted so that the paste flows out to form a pat; the area of the pat is used as a measure of the consistency. For stiffer pastes, penetration tests such as Vicat needles are more suitable for the determination of the water content for normal consistency and the initial and final set times. A versatile automatic instrument, the rheograph described by Bombled (12,13), measures the yield value by penetration tests over a very wide range of paste shear strengths, from about 30 to more than 1.5×10^5 Pa. It therefore somewhat overlaps the upper part of the range of coaxial cylinders viscometers and extends the range beyond the Vicat initial and final set yield values, which were found to correspond to shear strengths of 2×10^4 and 1×10^5 Pa, respectively.

Figure 2 gives five examples of rheograph curves for cement pastes made at water-cement ratios of 0.25 with cements of different finenesses (13). The yield values (shear strengths) are calculated from the force required to produce a penetration of 20 mm by one of several probes ranging in diameter from 1 to 12 mm. The initial yield values are, in these cases, rather high because of the low water-cement ratio. Normal consistency pastes have initial yield values of about 2000 Pa. Two of these pastes were stiffer than normal consistency. These curves can be used to define and calculate various parameters useful in characterizing the setting of cements, such as the initial and final set times, the rate of setting, and a time period analogous to the dormant period, during which the yield value is approximately constant. At higher water contents, the early part of the curve is nearly horizontal.

Despite the fact that such static tests clearly show the existence of a yield value for ordinary cement pastes, the results obtained dynamically with viscometers often do not indicate well defined yield values. The shear strain rate versus shear stress curves obtained with rotational viscometers (see Fig. 3) depend strongly on the flow history of the pastes and also on the apparatus used. Depending on the paste composition and testing conditions, cement pastes exhibit flow behavior approximating any of four main types: 1) Newtonian, 2) Binghamian, 3) pseudoplastic, and 4) dilatant. In addition, the

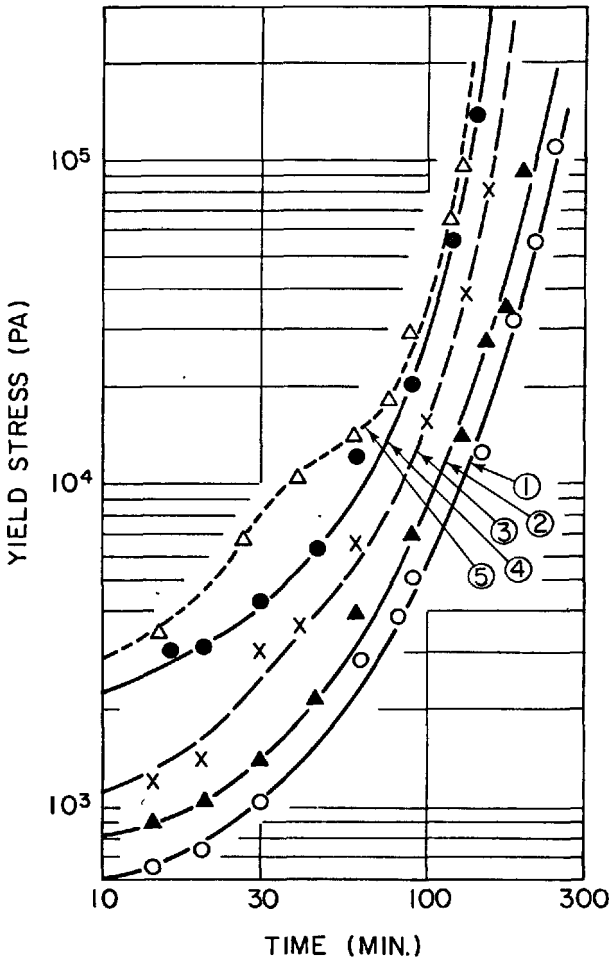

Fig. 2 - Rheograph curves for cement pastes (ground clinker plus 5% gypsum at 0.25 water-cement ratio) for cements of various finenesses. 1) 201 m^2/kg; 2) 248.5 m^2/kg; 3) 307 m^2/kg; 4) 403 m^2/kg; 5) 511 m^2/kg (13).

curves may indicate reversible, or thixotropic (shear thinning), or antithixotropic (shear thickening) behavior. Antithixotropy seems to be a manifestation of the thixotropic recovery process, which should, therefore, be distinguished from dilatancy, which is also shear thickening but for other reasons.

NEWTONIAN AND BINGHAMIAN FLOW. When the rate of shear strain, $\dot{\gamma}$, is directly proportional to the shear stress, τ, a fluid is said to be Newtonian with a constant coefficient of viscosity.

Cement pastes are not normally Newtonian but can become very nearly so with additions of sufficient amounts of certain water-reducing admixtures (14-17). Cement

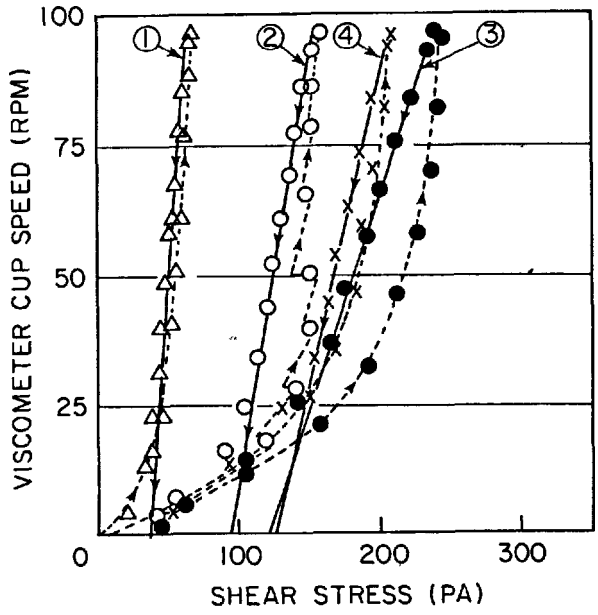

Fig. 3 - Rotational viscometer curves for several cement pastes. 1) w/c = 0.4; 2) w/c = 0.35, held at constant speed for equilibration; 3,4) w/c = 0.32; 3 immediately after mixing; 4 immediately after the first measurement (2).

pastes often approximate a Bingham plastic solid with a finite yield value, f, and plastic viscosity, U, so that:

$$\dot{\gamma} = \frac{1}{U}(\tau - f) \qquad (1)$$

Results of rheological measurements on cement pastes are often presented graphically (as in Fig. 3) with the shear stress (or torque in a rotational viscometer) as the abscissa and the shear strain rate (or rotational speed) as the ordinate (2). In such plots, Newtonian fluids yield straight lines through the orgin (f = 0 in Eq. 1). Bingham plastic solids yield straight lines with an intercept at f; in this case the slope of the straight line is the reciprocal of the plastic viscosity; the apparent viscosity is $\tau/\dot{\gamma}$, i.e., the reciprocal of the slope of a line through the origin to any point along the line of Eq. 1. Hence, even if the plastic viscosity is constant, the apparent viscosity is shear rate dependent and may be very much higher than the plastic viscosity at low shear rates because of the finite yield value.

PSEUDOPLASTICITY. The yield values indicated in viscometer tests of cement pastes are not as sharply defined as in the Bingham plastic model. Instead, plots of shear rate vs shear stress may curve gradually upward from the stress axis to an approximately linear portion (Fig. 3) and are

termed pseudoplastic or plastic-thixotropic. This linear portion, or the reverse at decreasing shear rates, may then be used to estimate the yield value by extrapolation. The curved portion may be a result of the combination of non-uniform flow of the sample and the thixotropic nature of the material in instruments in which the gap between the cup and bob in the viscometer is too wide (1).

During testing of cement pastes in coaxial cylinders viscometers, uniform flow may not be immediately achieved. Instead, some slippage occurs, with a portion of the paste flowing and a portion remaining as a plug. The shear rate in the flowing portion is then much higher than indicated by the speed of rotation and the gap width. Eventually the entire volume of paste flows apparently uniformly. These phenomena have been investigated in some detail using both smooth and serrated cylinders in connection with time and shear rate dependence studies of cement pastes (18).

In a different approach, Legrand (19) used a viscometer with a set of radial blades immersed in a much larger cup of sample. The variation of the torque with time through the non-uniform flow period was analyzed to determine the yield value, the shear stress and shear strain rate at constant rotor speeds.

DILATANCY. There is a progressive transition of flow properties from plastic-thixotropic to dilatant (shear thickening) behavior as the volume concentration of solids is increased in mortars of cement fineness (19). When the volume fraction of solids exceeds about 0.6, the resistance to shear increases with shear rate and volume expansion occurs during shear. The curve is then concave to the shear stress axis instead of convex as for the curves in Fig. 3. These effects are a result of changes in the packing of the particles that are required to permit the particles to move past one another along shear surfaces. The result is increased average separations of particles in the direction perpendicular to the direction of shear. The water is then required to flow into the enlarged separations and the resistance to shear, therefore, depends upon the shear rate and the permeability of the material to such flow. Also, since water and the solids have small compressiblities, some air will tend to be drawn into the mixture to provide the necessary dilatancy during shearing during mixing. This entrapped air provides the capacity for dilation without requiring as much water flow.

These particle interference effects produce rapid increases in the yield value and apparent viscosity as the volume concentration of solids exceeds about 0.60 when the material is not vibrated. When the material is vibrated the flow behavior is altered, but this transition to dilatancy occurs at only slightly higher (0.62) volume concentration of solids.

These same considerations also apply to the cement paste itself at very low water-cement ratios. A volume concentration of cement in water of 0.6 (40% water by volume) corresponds to a water-cement ratio of 0.21. Dilatant type curves have been obtained at water-cement ratios in this range in ground clinker pastes fluidized with lignosulfonate and soluble carbonate additions (17,20).

THIXOTROPY. It has been shown (3, 18, 21-22) that under proper experimental conditions (constant rate of shear, uniform flow) in a coaxial cylinders viscometer the initial torque, T_o, decays exponentially with time, t, to an equilibrium value T_E according to:

$$T = T_E + (T_o - T_E)e^{-Bt} \qquad (2)$$

where B is a breakdown constant which depends upon the shear strain rate (or angular speed) and properties of the paste. Values of B are of the order of 0.04 s^{-1}. The breakdown process reaches essential equilibrium in 1 or 2 minutes. Since T_o may be several times T_E, this process may have a considerable effect on the shapes of shear rate vs shear stress curves obtained, depending on the time allowed for each point at increasing (up curve) and then decreasing (down curve) rates of shear (Green's method). Figure 3 shows examples of the thixotropic behavior of cement pastes in such tests (2). There are four manifestations of the apparent thixotropy shown.

1. The curvature of the up curve indicates decreasing viscosities with increasing shear strain rates.

2. The up curves have higher shear stresses (at equal shear rates) than the down curves.

3. Curve 2 shows the decrease in shear stress while the paste is mixed in the viscometer at constant speeds.

4. Curve 4 shows lower shear stresses upon immediately repeating the curve 3 test.

The hysteresis loop 4 is not only shifted to lower shear stresses, (and lower plastic viscosities) but loop 3 was also larger than loop 4, indicating more breakdown during the first cycle than during the second cycle. For standard test conditions the areas of the hysteresis loops so formed have been used as a measure of the amount of breakdown of the thixotropic structure (23). Attempts have also been made to determine quantitatively the energy per unit volume required for the

thixotropic breakdown process from constant rate of shear tests as with Eq. 2 (3,22).

Another manifestation of thixotropy is shown in tests in which the maximum shear rate is increased in successive cycles. When that is done the loops also shift to lower stresses and lower plastic viscosities, indicating more breakdown at higher shear rates (3).

ANTITHIXOTROPY AND THE EFFECTS OF MIXING. Obtaining results with coaxial cylinders viscometers that show well defined yield values and lower viscosities at low shear rates seem to depend upon the degree of dispersion of the cement particles by adequate mixing and use of viscometers with very narrow gap widths. Although Greenberg and Meyer (24) reported in 1963 that to obtain uniform flow it was necessary for them to use a gap width of about 1.0 mm, much of the published data has been obtained with gaps too wide to avoid instrumental effects. Another factor may be the smoothness of operation and freedom from vibration of the equipment; vibration or shocks may initiate non-uniform flow at low yield stresses. Recently published data obtained by Roy and Asaga (15) using an improved viscometer with a 0.7 mm gap showed remarkably linear up curves with distinctly indicated yield values, i.e., nearly Binghamian behavior (see Fig. 4). By contrast, viscometers with larger (4 mm or more) gaps give results indicating pseudoplastic behavior with no distinct yield value (2,22,25). It should be noted that the hysteresis curves in Fig. 4 are considerably different from most other published data. Not only do they show distinct yield values at increasing shear stress, but the hysteresis loops show considerable antithixotropy or shear thickening, that is, higher stresses occurred on the down curves than on the up curves at equal shear rates. The viscometer and procedures used by Roy and Asaga yielded results largely free of the plastic-thixotropic behavior often observed. Also, one reason for the large area of the antithixotropic hysteresis loop appears to be that the test was conducted more slowly (15 minutes/cycle) than in the usual few minutes. Hence, more time was allowed for both the thixotropic breakdown and recovery processes.

Several workers have observed both thixotropic and antithixotropic behavior of the same pastes (23,24,25) at different times after mixing. Pseudoplastic curves were obtained at faster rates (2-3 minutes/cycle) than used by Roy and Asaga. The faster testing rate allows less time for thixotropic recovery of freshly mixed pastes. Even so, their results showed that shortly after mixing the pastes were usually slightly antithixotropic, but after some time at rest (30-45 minutes) became thixotropic. However, when the paste after

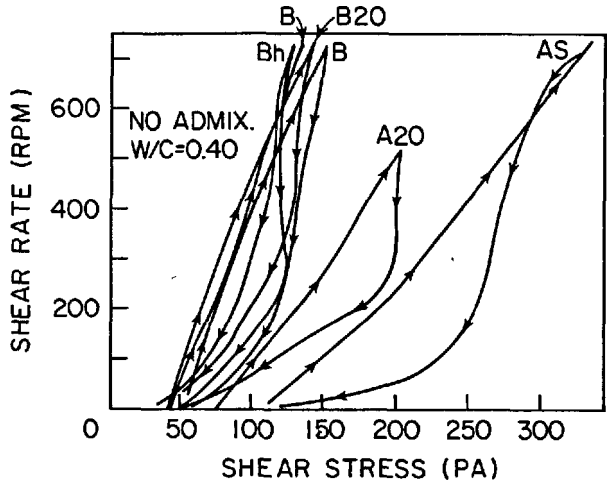

Fig. 4 - Rotational viscometer curves for pastes mixed by six different methods, w/c = 0.40 (15).

being at rest was agitated by repeated testing, the type of flow curve changed from thixotropic to antithixotropic. At rest for longer times (2-3 hours), the pastes became very strongly thixotropic as setting approached unless continuously agitated. These effects of agitation suggest that the initial mixing intensity should also affect the paste flow properties, and this has been known for some time.

Mechanical mixers capable of producing a uniformly and vigorously mixed paste are normally used, perhaps intermittently, for long enough time periods (5 - 10 minutes) to produce pastes of the best flow properties. Inadequate or excessive mixing increases the paste stiffness. If the paste is mixed for only 30 seconds or less, it will suffer brief-mix-set, thought to be caused by cementing together of the grains by the reaction products formed on their surfaces by the rapid initial reactions with water. Although a mixing time of 1 minute may be long enough to eliminate brief-mix-set, it may not be long enough to effect adequate dispersion or to eliminate false-set due to the formation of gypsum from hemihydrate that may be present in the cement. These gypsum crystals form a weak structure which can be broken down by continued mixing or remixing.

Continuous vigorous mixing also breaks down the flocculent structure of the cement particles responsible for the thixotropic behavior. Measurements like those shown in Fig. 3 for different batches mixed 5 minutes each in a planetary mixer showed that increasing the mixing speed from 150 rpm to 450 rpm shifted the hysteresis

loops to lower shear stresses, and narrowed the loops to a nearly reversible (nonthixotropic) Bingham plastic type behavior. Similar results were obtained when the mixing time at 250 rpm was increased from 3 to 20 minutes. In both of these sets of measurements, made with pastes at a water-cement ratio of 0.35, the plastic viscosity indicated by the down curves decreased progressively with mixing time and intensity. However, at a w/c of 0.25, the yield values reached a minimum after about 5 minutes of mixing (2).

A study of the effects of high intensity mixing of 0.45 water-cement ratio pastes showed that a minimum was reached for the plastic viscosity, but that the yield values increased progressively with mixing time from 10 to 50 Pa (2). Intense mixing appears to produce very rapid thixotropic breakdown and improved flow, but if it is prolonged, abrasion of the particles will increase the yield value and plastic viscosity.

When high speed blenders were used to mix pastes at a w/c of 0.5, it was found that the initial (15 minute) yield values increased progressively from 22 to 52 Pa and the plastic viscosities increased from 21 to 47 mPa·s as the mixing time increased from 1 to 10 minutes (23). The final temperature of the mixes was 25°C. At hydration times up to 3 hours, these increases with mixing time became even greater, indicating a persistent effect of these differences in mixing times. In addition, the pastes mixed for 1 minute were thixotropic and became more so with hydration time, whereas the pastes mixed 10 minutes were antithixotropic initially, but became even more thixotropic after 2 hours than the 1 minute pastes. High speed (10,000 rpm) mixing with external cooling has been employed to produce pastes with reduced bleeding (26). It is believed that the main effect was that the mixing removed thin layers of hydrates formed on the cement grains and dispersed these in the paste to produce a thick consistency.

The results in Fig. 4 were obtained primarily to determine the effect of mixing intensity on the flow curves. They do not include prolonged high intensity mixing, but still show wide variations in the rheological properties. Six different mixing procedures of increasing intensities were used. Procedure AS was the ASTM C305 procedure using a Hobart planetary mixer at low (140 rpm) and medium (280 rpm) speed. Procedure A20 was mixing for 20 minutes at low speed. Procedure B20 was the API standard procedure using a high-speed blender for 1 minute after preliminary mixing, followed by 20 minutes of low speed mixing in a beaker. B, Bl and Bh are other variations of procedures with the high-speed blender including blending at low (3,500 rpm) and high (17,000 rpm) speed, but for not more than 1 minute. Such variations in mixing intensity with the high-speed blender had only minor effects on the flow behavior. Fig. 4 shows that the yield values and plastic viscosities of all the blender-mixed pastes were substantially less than the less intensively mixed pastes. However, with the addition of 1 percent by weight of the cement of a superplasticizing admixture of the β-naphthalene sulfonate formaldehyde condensate (with added retarding component), such variations in mixing procedures had no appreciable effect; with the admixture the yield values were all nearly zero. The hysteresis loops were much thinner than those of Fig. 4, with slopes for the up curves about the same as the most intensely mixed pastes without the admixture.

Many of the different types of flow behavior obtained by different research workers can be qualitatively understood in terms of the thixotropic breakdown and recovery processes that occur during and after different mixing and testing procedures. For conceptual purposes it is useful to consider the strength and number of bonds between particles in the floc structure as a function of time. The extent of the thixotropic breakdown or recovery can then be expressed in such terms (3), which could also be used to define a degree of flocculation. Bombled and others have attributed the thixotropy to changes in the degree of flocculation, which he defined in terms of measurable quantities, the ratio of the median size of the agglomerates of particles to the mass median particle size (2). This definition may not be an exact measure of the structurally related resistance to shear, but it provides a conceptual basis for explaining the complex behavior observed. To do this it is assumed that the degree of flocculation can be qualitatively represented as a function of time during and after mixing as shown in Fig. 5. Two curves are shown: 1) curve L-LR which corresponds to low intensity mixing for a time M, and recovery if left undisturbed along the curve LR, and 2) curve H-HR which corresponds to a paste mixed at high intensity (but not for so long as to produce other effects) and its recovery. Exponential decay curves are assumed for both the breakdown and recovery curves, but the time constant for recovery is assumed to be at least ten times that of the breakdown curve. This is consistent with a comparison of breakdown time constants of the order of one minute (3,21) with recovery times indicated by changes from antithixotropic to thixotropic flow curves in 30 to 45 minutes (23,25). The important point is that pastes with a high degree of flocculation, either because of inadequate mixing or subsequent recovery, will be subject to more thixotropic breakdown during the test than pastes more completely dispersed by intense mixing.

The more completely dispersed pastes will undergo more rapid recovery after mixing and will tend to show antithixotropic behavior if this recovery process is superimposed upon the changes caused by the test itself. However, if the paste mixed at high intensity is allowed to stand before testing, the degree of flocculation will have recovered to the same level as that of the paste mixed at low intensity at some time P shown in Fig. 5.

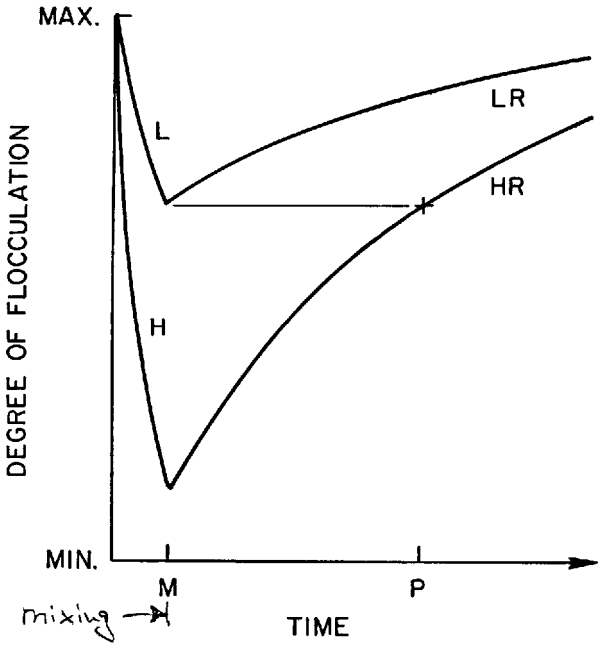

Fig. 5 - Changes of the degree of flocculation of particles in cement pastes during mixing at high intensity H, and low intensity L, and recovery while at rest after mixing HR and LR.

The changes in degree of flocculation caused by the test itself are sketched in Fig. 6 for a single cycle, up curve and down curve in a viscometer, at constant rates of change of rate of shear as shown in the lower part of the figure. The S shaped dashed curve, S, indicates the changes in the degree of flocculation of a paste that was increasing relatively slowly when the flow test began. During the test the degree of flocculation decreases only slowly at the initial low rates of shear, but decreases more rapidly at the highest shear rate, and then more slowly again at the low rates of shear at the end of the test. If, on the other hand, the undisturbed paste would have been recovering at an appreciable rate as shown by the recovery curve R, the curve obtained as a result of superposition of the two effects should resemble curve T. The position of curve T will vary between the extremes S and R, depending upon the testing conditions, and would be referred to as thixotropic or antithixotropic depending on which effect predominates during the test.

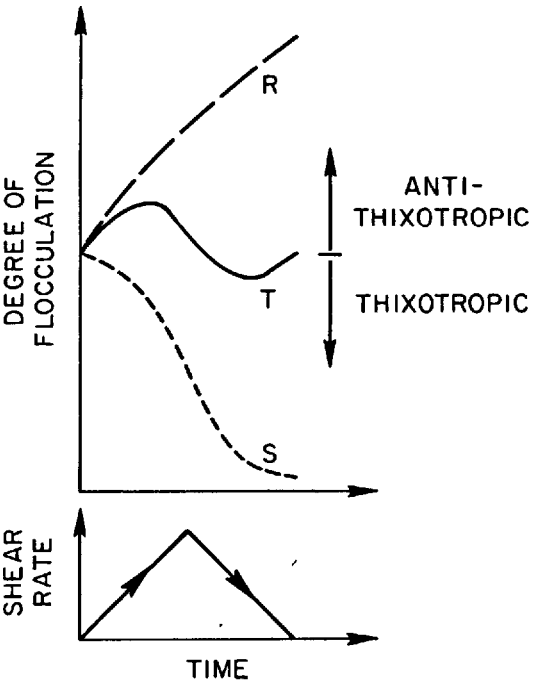

Fig. 6 - Changes of the degree of flocculation of particles in cement pastes during testing in a rotational viscometer during a single up-curve, down-curve cycle. S: curve for changes during test of paste that was recovering slowly after mixing, R: recovery curve of paste recovering rapidly after mixing, T: superposition of the two effects.

FACTORS AFFECTING FLOW

The fineness of the cement and the water-cement ratio of the fresh paste are two of the most important factors affecting flow. These two factors together determine the average water-film thicknesses and interparticle spacings. Despite the fact that normal cement pastes are in a flocculent state when at rest, the average water-film thickness concept appears to have some validity in determining their rheological properties. To determine the effects of water content, fineness, and other factors uncomplicated by the effects of cement hydration, Legrand systematically studied the flow behavior of pastes and mortars made with fine powders of calcite and other materials (19). Similar but less complete results were obtained with cements (5). The maximum yield value of such pastes at rest, f_o, before any thixotropic breakdown during the test, was found to depend on the volume concentration of solids, C, according to:

$$f_o = Ae^{a(C - 0.5)} \quad (3)$$

in which A and a are parameters determined from the data. When the pastes were vibrated, the yield values were essentially zero. C values ranged from 0.475 to 0.677; for portland cements these volume concentrations would correspond to a range of water-cement ratios from 0.15 to 0.35. Although the flow behavior of these pastes went through a transition from plastic-thixotropic to dilatant behavior in this range, Eq. 3 applied over this entire range of solids concentrations.

The value of a in Eq. 3 depends on the material and shape of the particles, but is independent of the specific surface area or particle size distribution; values ranged from 23 to 48 for spherical to angular particles. The value of A increases rapidly with the specific surface area for powders of cement finenesses up to values of about 100 Pa.

A similar dependence on the volume concentration of solids was found for the shear stress, τ, measured at constant rates of shear strain while the paste was vibrated:

$$\tau = Be^{b(C - 0.5)} \quad (4)$$

in which B and b are parameters determined from the data. This relation applies for values of C less than the transition from dilatant to pseudoplastic behavior. In this case b depends upon the rate of shear strain, nature of the material and shape of the particles, as well as being independent of the specific surface area and particle size distribution. The value of b approached a maximum of about 26 at a strain rate of 40 s^{-1}. The value of B also increased with the rate of shear strain and the specific surface area, reaching values of several hundred Pa for powders of cement fineness.

The formulation of experimental results represented by Eqs. 3 and 4 is useful because it permits the identification of certain factors affecting the flow behavior in simpler systems; Eq. 4 was also verified for portland cement pastes while vibrated. Data for portland cement pastes without vibration have also been examined in attempts to determine the true functional dependencies and to better understand the factors controlling the flow. Viscometer data was given in Fig. 3 which showed the decreasing yield values and viscosities with increasing water content. A set of data covering a wider range of water-cement ratios for pastes made with an ordinary portland cement of Blaine fineness 447 m^2/kg is given in Table I.

TABLE I

Water-Cement Ratio g/g	Yield Value Pa	Plastic Viscosity mPa·s
0.4	81	39
0.45	39	22
0.5	25	16
0.6	9	12
0.7	6.4	8.5
0.8	1.6	5.8

Values at lower water-cement ratios are given in Table II, which must include both viscometer and rheograph data (2). Although different cements and mixing procedures were used, these two sets of data show similar variations of the yield values with water contents.

TABLE II

Water-Cement Ratio g/g	Yield Value Pa
0.24	1900
0.32	130
0.36	65
0.40	30
0.50	8.5

The data in Fig. 2 show the effect of variation of the specific surface area of a cement on the initial yield values in pastes of 0.25 water-cement ratio and how these values vary with time through setting. The effect of cement fineness is also shown in Table III for pastes at water-cement ratios of 0.4, and also for another set of pastes made at the water-cement ratio required to give equal yield values (2). As might be expected from

TABLE III

Specific Surface m^2/kg	Yield Value at w/c = 0.4 Pa	w/c for f = 30 Pa g/g	Interparticle Distance* µm
235	14.0	0.35	2.0
278	26.5	0.44	2.3
329	75.0	0.475	2.2
442	165.5	0.55	1.9
560	>250.0	0.58	1.6

*Calculated from Eq. 5 using indicated Specific Surface.

consideration of the water film thicknesses and interparticle distances, increasing the specific surface area progressively increases the yield value at constant water

content. Also, the water content required to obtain a yield value of 30 Pa increases systematically with the specific surface area. Bombled suggested that the interparticle distances remain approximately constant as the water content increases with the surface area to maintain the constant yield value (2). The interparticle distance (2 X the water-film thickness in μm) was calculated from:

$$d = 2 \times 10^3 \frac{w/c - 0.12}{S} \quad (5)$$

in which w/c is the water-cement ratio, S is the specific surface area of the cement, and 0.12 is an estimate of the amount of interstitial water which does not contribute to the water-film thicknesses or interparticle spacings as indicated in Fig. 1. The values of d in Table III are seen to be approximately constant.

In addition to the functional forms of Eqs. 3 and 4, numerous other exponential and power law equations have been used to describe the dependence of flow properties on water content and cement fineness. The data of Table II at constant S was used to obtain:

$$f_o = \frac{0.124}{(w/c - 0.15)^{3.97}} \quad . \quad (6)$$

by the method of least squares. To do this the value of the water content not contributing to flow was varied to obtain the value 0.15 for the best fit. The data in Table III was fitted simply by determination of the slope and intercept of the logarithmic plot to obtain:

$$f_o = 4.47 \times 10^{-9} S^{4.01} \quad (7)$$

The fact that the exponents in both Eq. 7 and 8 are nearly equal again indicates that the yield value is closely related to the ratio of the surface area to part of the water content. However, the data seem to yield equally good fits for various exponential and power law relationships because of the limited range and accuracy of the data.

The functional dependence of the apparent or plastic viscosity on water content and specific surface becomes even more complex. In one study (9) the apparent viscosity, η, was found to be given by:

$$\eta = 13(d')^{-0.6} - 1 \quad (8)$$

where the quantity d' used as a measure of the interparticle spacing in μm was calculated from:

$$d' = \frac{(w - w_a)^2}{S} 10^3 \quad (9)$$

in which the water contents, w and w_a, and the surface area, S, are expressed per unit weight of cement. The value of w_a, the water requirement by a standard test, was about 0.3. This suggests that the functional dependence of the viscosity on the water content may differ considerably from that for the yield values for portland cements.

WATER REDUCING ADMIXTURES. Microscopic observations have repeatedly confirmed that the cement particles are dispersed by water-reducing admixtures (2). It has long been believed that this dispersion is the result of neutralization of surface charges and the reduction of attractive forces between particles. The relatively new "super" water-reducing admixtures, such as the sulfonated melamine formaldehyde (M-type) and sulfonated naphthalene formaldehyde (N-type) condensates do not strongly retard cement hydration. They can, therefore, be used at concentrations considerably higher (over 1% by weight of cement) than normally practical with lignosulfonate type admixtures. The latter type usually causes significant retardation at concentrations somewhat higher than 0.1%, whether they are sugar-free or not (27).

Daimon and Roy (28) measured the adsorption of a sulfonated naphthalene formaldehyde condensate by cement particles in water and found that the data yielded a Langmuir isotherm. It was also shown that with the cement used (393 m^2/kg) and with additions of the admixture up to about 1.5%, nearly all of the active component was adsorbed (about 20% was not adsorbable), but when larger amounts were added the amount in solution increased rapidly. Measurements of the zeta potential of the finer cement particles showed variation with the amount added similar to the Langmuir adsorption isotherm, reaching values of about -50 mV at maximum adsorption (29). Mortar flow values also showed a similar increase with admixture content. Rotational viscometer measurements on cement pastes gave initial yield stress values which decreased from 40 - 100 Pa (depending on mixing intensity) for the plain paste at 0.4 water-cement ratio to zero at 1% addition. The apparent viscosity was also reduced from about 500 to about 200 mPa·s if the paste was mixed at low intensity (ASTM), but only very slightly if mixed at high intensity (API), as indicated in the discussion of Fig. 4.

The adsorption of two N-type admixtures and two high molecular weight styrene polymers in cements was determined (30) at additions up to 0.5% of the weight of cement. For the N-type admixture the adsorption isotherms were of the Langmuir type; for the styrene polymer they were of H (high affinity) type. Sedimentation rate measurements with the N-type admixture in dilute cement-water suspensions (3 g in

28.5 ml) indicated dispersion of the particles by a progressive decrease from the sedimentation rate with no admixture to very low values at additions of 0.4% by weight of cement.

Petri (14) measured the apparent viscosities of cement pastes with a Brookfield rotational viscometer with and without several admixtures. Additions up to 1.6% by weight of cement were used. With increasing amounts of an N-type admixture he showed the progressive decrease of yield value, viscosity, and the area of the hysteresis loops at increasing and decreasing shear strain rates until Newtonian behavior was obtained with 1.2% of the admixture. Another admixture tested by Petri, sodium hexametaphosphate, produced its maximum effect at about 0.5% addition.

Petri also attempted to determine the functional dependence of the apparent viscosity, η, of cement pastes on the solid volume concentration, C. Data for cement pastes without admixtures did not fit any of several theoretical equations from electroviscosity. This is not surprising since the theory used has given only equations of Newtonian form. However, Petri did find that his data for pastes containing 1% of the N-type admixture indicated that the suspensions behaved remarkably like a theoretical model for nonattracting spheres of equal size at high concentrations, for which:

$$\eta = \eta_o \ (1 - 1.35 \ C)^{-2.5} \qquad (10)$$

There is continuing research on the use of lignosulfonate water-reducing admixtures, especially in low water-cement ratio systems. Soluble carbonate additions are used to overcome excessive retardation. Odler et al (17) studied the rheological properties of portland cement (6% gypsum) pastes with and without sodium lignosulfonate and sodium carbonate additions, and ground clinker pastes with the same additions. Additions of up to 1.25% of each were used, but only when both additives were present was a fluidizing and set-regulating effect obtained. Finenesses ranged from 340 to 850 m^2/kg. When gypsum was present the setting time became much shorter, but without gypsum these additives produced normal setting behavior and rapid strength development. Water-cement ratios as low as 0.225 were fluid enough to be tested in a rotational viscometer. As noted earlier, these pastes showed shear thickening behavior. In another study (31) using calcium lignosulfonate and potassium carbonate, difficulties in testing 0.25 water-cement ratio pastes in a rotational viscometer were reported. The pastes were described as having a rubbery consistency. Other workers have used sulfonated lignins with $NaHCO_3$ to produce pastes of 0.22 to 0.24 water-cement ratios which are self-leveling but of complex rheological character; they seem to have elastic-plastic properties not readily characterized in normal terms (20).

CEMENT COMPOSITION AND HYDRATION. For cements in which the early hydration reactions are properly controlled, the flow properties during the early dormant period do not depend very strongly on the compositions of the cements. One study of 12 cements of different types concluded that, except for a regulated set cement, the chemical and mineralogical composition seemed to be of little importance for flow compared to water content and cement fineness (25). However, the water requirement for flow has been shown to increase significantly with the C_3A and alkali contents, as well as depending on the particle size distribution (32). In addition, the calcium sulfate must be in a form suitable for control of the early aluminate reactions and the prevention of false set (24,33). However, if viscometer measurements are continued for longer hydration times, the effect of the C_3A content becomes increasingly important. Measurements using cement of C_3A contents ranging from 0 to 14% showed little variation of the yield stress, plastic viscosity or the area of the hysteresis loop during the first 45 minutes after mixing (23). However, after 2 hours the thixotropy indicated by the area of the hysteresis loop increased strongly with C_3A content above 2%. The yield stress also began to increase with C_3A content at 2 hours. The plastic viscosity, however, did not show this same strong effect until 3 hours.

Wittmann (34) examined the effect of additions of an M-type admixture on the apparent viscosities of cement pastes at a water-cement ratio of 0.6 at ages up to 7 hours. For pastes without the admixture the viscosity versus time curves for different viscometer rotor speeds showed increases with hydration time rather like the rheograph curves in Fig. 2. At a rotor speed of 80 rpm, the apparent viscosity increased from about 2,000 initially to over 20,000 mPa·s after about 4 hours. These reported values seem extraordinarily high. With 1.5% of the admixture added, the initial viscosity dropped to a value about 50 mPa·s, and exhibited nearly ideal Newtonian behavior for 1 to 2 hours. After about 3 hours the viscosity became non-Newtonian and shear rate dependent as it increased to nearly 20,000 mPa·s at 80 rpm at about 7 hours. Studies with several different cements yielded similar results except for a PZ 550 type, which required higher percentages of admixture to retard the increase in viscosity. These and many other results, such as those in Fig. 2, show that the stiffening of the paste through setting is normally a progressive process. This process is a result of the early hydration reactions and is affected

by any factors which accelerate or retard the hydration reactions.

CONCLUDING DISCUSSION

It is apparent from the available literature that there are still substantial gaps in our knowledge of the rheology of fresh cement pastes. It has proven difficult to quantify the results in terms of material properties and their functional dependencies on the cement properties and concentrations. This is at least partially a result of the fact that the procedures used to mix cement pastes and to test the flow properties affect the properties to be measured. It appears that it would be desirable to study the rheology of cement pastes in a state of dispersion of the particles in water that is comparable to the state of the paste as it is normally used in concrete. For this reason T. C. Powers advocated the use of high speed blenders because the shear rates in the paste in concrete during mixing were believed to be at least as high as in the most vigorous laboratory mixer. We have seen recent results that show substantial differences between such mixing techniques and other common test methods. It would appear prudent to definitely establish what mixing intensity is required, if that has not already been done, and then to concentrate research efforts on adequately mixed pastes. Similar considerations apply to the use of rotational viscometers of various designs. Much otherwise careful work has been done with equipment that may by its design preclude quantitative determination of the material properties because of non-uniform flow, or by the failure to take non-uniform flow properly into account. It appears that the problem is well appreciated in some quarters and that several equally valid test methods will emerge that can be used to obtain reproducible results. Perhaps some kind of standard test sample of cement, or an inert material of similar rheological properties, should be made available to permit comparison of rheological test methods.

The situation with respect to theoretical interpretation could also be substantially improved. Petri (14) reviewed the theory of flow of suspensions of charged particles in an electrolyte, i.e., electroviscosity. The complex equations for the viscosities of such suspensions contain the electric double layer parameters as well as the volume concentration, C, of the solids, and the viscosity of the liquid, η_o. When reduced to its simplest terms the general equation becomes:

$$\eta = \eta_o (1 + kC) \qquad (11)$$

which is the well known Einstein equation when k is 2.5. This reveals an obvious shortcoming of the theory as presently developed for systems like cement pastes in which interparticle forces cause flocculent structure formation, finite yield values, shear rate dependence, and thixotropy, i.e., non-Newtonian behavior.

Nevertheless, research has given us a good qualitative or even semi-quantitative understanding of the complex behavior of fresh cement pastes. Several apparently satisfactory empirical equations have been established which relate certain rheological properties of the fresh pastes to the specific surface area of the cement and concentration of the cement in water. This matter appears to deserve further study with the objective of being able to predict with confidence the rheological properties of fresh cement pastes from the cement composition and physical properties.

The increasing use of organic water-reducing and other admixtures in concrete and the development of new admixtures have stimulated many studies of their effects on the rheological properties of cement pastes. Such studies are usually aimed at assessing the effectiveness of individual admixtures in concrete. However, since the rheological behavior of cement pastes containing certain admixtures is simpler than that of plain pastes, it may be possible to determine the true functional dependencies for the dispersed state, and then attack the problem of pastes in various degrees of flocculation.

BIBLIOGRAPHY

1. T. C. Powers (1968), "Rheology of Freshly Mixed Concrete," The Properties of Fresh Concrete, John Wiley, New York. (In English)

2. J. P. Bombled (1974), "Rheology of Mortars and Fresh Concrete: Studies of the Interstitial Cement Paste," Ciments, Betons, Platres, Chaux (Rev. Mater. Constr.), No. 688, 137-155. (In French)

3. G. H. Tattersall (1976), "The Workability of Concrete," Publ. 11.008, Cement and Concrete Assoc., England. (In English)

4. D. W. Hobbs (1976), "Influence of Aggregate Concentration Upon the Workability of Concrete and Some Predictions from the Viscosity-Elasticity Analogy," Mag. Concr. Res., 28, No. 97, 191-202. (In English)

5. M. Barrioulet and C. Legrand (1977), "Influence of the Interstitial Paste on the Flow Ability of Fresh Concrete. The Importance of the Water Retained by the Aggregates," Materials and Structures, 10, No. 60, 365-373. (In French)

6. G. H. Tattersall (1976), "Relationships Between the British Standard Tests for Workability and the Two-Point Test," Mag. Concr. Res., 28, No. 96, 143-147. (In English)

7. M. Barrioulet and C. Legrand (1978), "Study of Intergranular Friction in Fresh Concrete. New Ideas on the Flow of Vibrated Fresh Concrete," Materials and Structures, 11, No. 63, 191-197. (In French)

8. C. W. Richards and R. A. Helmuth (1975), "Expansive Cement Concrete - Micromechanical Models for Free and Restrained Expansion," Stanford Univ. CE-TR-191. (In English)

9. K. Rendchen (1976), "Influence of Various Cements on Flow Behavior and Stability of Cement Suspensions," Beton: Herstellung Verwendung, 26, No. 9, 321-325. (In German)

10. F. W. Locher, W. Richartz and S. Sprung (1976), "Setting of Cement. Part 1: Reaction and Development of Structure," Zement-Kalk-Gips, 29, No. 10, 435-442. (In German)

11. W. F. Perenchio, D. A. Whiting and D. L. Kantro (1978), "Water Reduction, Slump Loss, and Entrained Air-Void Systems as Influenced by Superplasticizers," in Superplasticizers in Concrete, CANMET, Ottawa, 295-324. (In English)

12. J. P. Bombled (1971), "Rheograph for the Rheologic Study of the Stiffening of Pastes. Application to the Setting of Cement," Rev. Mater. Constr., No. 673, 256-277. (In French)

13. J. P. Bombled (1976-7), "Setting Time Measurements for Cement Pastes - Rheograph and Automatic Prisometer CERILH," Ciments, Betons, Platres, Chaux (Rev. Mater. Constr.), No. 699, 113-124; No. 709, 355-362. (In French)

14. E. M. Petri (1976), "Effect of Surfactant on the Viscosity of Portland Cement-Water Dispersions," Ind. Eng. Chem., Prod. Res. Dev., 15, No. 4, 242-249. (In English)

15. D. M. Roy and K. Asaga (1979), "Rheological Properties of Cement Mixes: III. The Effects of Mixing Procedures on Viscometric Properties of Mixes Containing Superplasticizers," Cement and Concr. Res., 9, No. 6, 731-739. (In English)

16. H. Reul (1978), "Rheological Investigation of Cement Suspensions with Fluidizing Agents," Beton: Herstellung Verwendung, 28, No. 10, 360-361. (In German)

17. I. Odler, U. Duckstein and Th. Becker (1978), "On the Combined Effect of Water Soluble Lignosulfonates and Carbonates on Portland Cement and Clinker Pastes, I. Physical Properties," Cement and Concr. Res., 8, No. 4, 469-480. (In English)

18. C. R. Dimond and G. H. Tattersall (1976), "The Use of the Coaxial Cylinders Viscometer to Measure the Rheological Properties of Cement Pastes," in Hydraulic Cement Pastes: Their Structure and Properties, Publ. 15.121, Cement and Concrete Assoc., England, 118-133. (In English)

19. C. Legrand (1972), "A Contribution to the Study of Fresh Concrete Rheology," Materials and Structures, 5, No. 29, 275-295; No. 30, 379-393. (In French)

20. S. Diamond and C. Gomez-Toledo (1978), "Consistency, Setting, and Strength Gain Characteristics of a 'Low-Porosity' Portland Cement Paste," Cement and Concr. Res., 8, No. 5, 613-621. (In English)

21. R. Lapasin, V. Longo and S. Rajgelj (1976), "Rheological Behavior of Cement Pastes," Il Cemento, 73, No. 2, 91-101. (In Italian and English)

22. R. Lapasin, V. Longe and S. Rajgelj (1979), "Thixotropic Behavior of Cement Pastes," Cement and Concr. Res., 9, No. 3, 309-318. (In English)

23. M. Ish-Shalom and S. A. Greenberg (1960), "The Rheology of Fresh Portland Cement Pastes," in Proc. 4th Int'l. Symp. on Chemistry of Cement, NBS Monograph 43, Vol. II, 731-744. (In English)

24. S. A. Greenberg and L. M. Meyer (1963), "Rheology of Fresh Portland Cement Pastes: Influence of Calcium Sulfates," Highway Res. Record, No. 3, 9-29. (In English)

25. I. Odler, Th. Becker and B. Weiss (1978), "Rheological Properties of Cement Pastes," Il Cemento, 75, No. 3, 303-307. (In Italian and English)

26. S. A. Markestad (1976), "The Gukild-Carlsen Method for Making Stabilized Pastes of Cements," Materials and Structures, 9, No. 50, 115-117. (In English)

27. V. S. Ramachandran (1978), "Effect of Sugar-Free Lignosulfonates on Cement Hydration," Zement-Kalk-Gips, 31, No. 4, 206-210. (In German)

28. M. Daimon and D. M. Roy (1978), "Rheological Properties of Cement Mixes: I. Methods, Preliminary Experiments, and Adsorption Studies," Cement and Concr. Res., 8, No. 6, 753-764. (In English)

29. M. Daimon and D. M. Roy (1979), "Rheological Properties of Cement Mixes: II. Zeta Potential and Preliminary Viscosity Studies," Cement and Concr. Res., 9, No. 1, 103-110. (In English)

30. R. Kondo, M. Daimon, and E. Sakai (1978), "Interaction Between Cement and Organic Polyelectrolytes," Il Cemento, 75, No. 3, 225-230. (In English)

31. K. M. Hanna and A. Taka (1977), "Rheological Properties of Low-Porosity Cement Pastes," Zement-Kalk-Gips, 30, No. 6, 293-297. (In German)

32. J. Gebauer and W. Schramli (1974), "Variations in Water Requirement of Industrially Produced Portland Cements," Bull. Am. Ceramic Soc., 53, No. 2, 161-168. (In English)

33. G. Frigione (1978), "The False Set of Portland Cement Pastes," Il Cemento, 75, No. 3, 207-224. (In Italian and English)

34. F. H. Wittmann (1979), "Influence of Water Reducing Admixtures on the Rheological Behavior, Capillary Shrinkage and Structure of Cement Paste," Silicates Industriels, 44, No. 1, 5-13. (In English)

On Hardening Mechanism of Portland Cement Paste

Mécanisme du durcissement de la pâte de ciment portland

J. MITUZAS, Cand.Sc. (chemistry), Head of the Laboratory,
A. KAMINSKAS, Cand. Sc. (Technics), Director of the Institute,
A. MITUZAS, Cand. Sc. (Technics), Head of the Laboratory, "VNII teploizoliscija" Vilnius, USSR.

RESUME : Cette communication étudie le processus de formation de gel de tobermorite et de composés de silico-hydrato-aluminate et de silico-sulfo-aluminate, lors de l'hydratation des ciments portland, en présence de gypse et pour diverses valeurs du rapport eau sur ciment. De nouveaux résultats expérimentaux sur l'évolution de ces composés sont exposés, ainsi que sur les phases de transition qui apparaissent lors de l'attaque des constituants du ciment par les sulfates.

Un modèle schématisant le mécanisme de l'hydratation et du durcissement du ciment est présenté, dans lequel les constituants hydratés ne sont plus considérés isolément, mais dans l'ensemble complexe de tous les composés. Les résultats expérimentaux exposés permettent de mieux comprendre les processus dans les systèmes hétérogènes de ciments portland durcis. Ceci pourrait servir de base à une nouvelle conception du durcissement du ciment.

SUMMARY : Formation processes of tobermorite gel, silicohydroaluminate and silicosulphoaluminate compounds are discusses and new data on development of these compounds in hydrated cement are given in this paper. Phase transitions occuring during the destruction of Portland cement compounds by sulphate attack in the cement-water system of different composition in the presence of gypsum are studied.

A hardening mechanism (hydration) scheme of Portland cement in water is given, in which the reaction products are shown not as separate hydrated compounds, but as complexes of these compounds. The obtained data provide a better understanding of processes occuring in heterogeneous systems of hardening Portland cements, what in its turn may serve as a base for new conception about processes occurring during cement hydration.

INTRODUCTION

Up to now different opinions exist on hydrated compound formation mechanism and phase composition of hardening Portland cement.

According to recent theoretical views and experimental data on hydration and hydrolysis of the main minerals of Portland cement in aqueous medium saturated with lime (at initial hardening periods also with SO_4^{2-} ions) at room temperature may be expressed by the following chemical equations:

1. $C_3S + aq \longrightarrow CaO \cdot SiO_2 \cdot aq + (3-m)\ CH$
2. $C_2S + aq \longrightarrow CaO \cdot SiO_2 \cdot aq + (2-m)\ CH$

T - gel
m = 0,8-2,0

3. $C_3A + aq \longrightarrow C_3AH_6$ — cubic
4. $C_3A + CH + aq \longrightarrow C_4AH_{13}$ — hexagonal
5. $C_2(A,F) + CH + aq \longrightarrow C_3(A,F)H_6$ — cubic
6. $C_2(A,F) + 2CH + aq \longrightarrow C_4(A,F)H_{13}$ — hexagonal
7. $C_3A + gypsum + aq \longrightarrow C_3A \cdot 3CaSO_4 \cdot H_{31}$ — hexagonal
8. $C_3A \cdot 3CaSO_4 \cdot H_{31} + 3C_3A \cdot H_6 + CH + aq \longrightarrow 3\ C_3A \cdot CaSO_4 \cdot H_{12} + C_4AH_{13}$ — solid solution.
9. $C_3(A,F)H_6 + gypsum + aq \longrightarrow C_3(A,F) \cdot 3CaSO_4 \cdot H_{31}$ — hexagonal
10. $C_3(A,F) \cdot 3CaSO_4 \cdot H_{31} + 3/C_3(A,F)H_6/ + CH + aq \longrightarrow 3/C_3(A,F) \cdot CaSO_4 \cdot H_{12}/ + C_4(A,F)H_{13}$ — solid solution

However, the results obtained by us in the investigation of phase composition of different Portland cements curing many years in water at room temperature /1,2/, enable us to give the another interpretation of cement hardening mechanism and changes in its phase composition, which was partly published in the materials for the Sixth Congress on Chemistry of Cement /1/.

DISCUSSION OF THE RESULTS

Earlier results obtained by us /1/ about the existence of complex compound $C_3A \cdot CaSiO_3 \cdot aq$ in hardening cements and its formation through liquid phase and decomposition under the action of gypsum present in the system etc. were supported by other authors, who carried out experiments with the help of modern apparatus /3/. However, literature dealing with these questions is quite scarce.

It is known, that at the end of setting period, the duration of which depends on mineralogical composition of Portland cement, its dispersion, crystalline structure of particles, temperature of surrounding atmosphere and etc. all elements composing Portland cement are always observed in different amounts in liquid phase. In this case the liquid phase is a non equilibrium system of dissolved components of $C-A-F-S-SO_4-H$ order. Immediately upon contact with water, Portland cement minerals interact with it and ettringite is precipitated topochemically in the form of small crystals of irregular shape. In alkali solutions, with/without traces of SO_4^{2-} ions, compounds possessing the structure of ettringite are unstable. More stable crystals are formed as a result of recrystalization of ettringite through the liquid phase. After a few days of interaction between Portland cement and water separation of ettringite begins and is ussually accompanied by the separation of monosulphate at the same time. This phenomenon results from the presence of $/Al(OH)6/^{3-}$ ions in solution and depends on Portland cement mineralogical composition and hardening conditions. Interaction of ortho- and pyro- ions of silicic acid and Ca^{2+} and OH^- ions results in formation of microcrystalline precipitates of $2CaO \cdot SiO_2 \cdot aq$ and $3CaO \cdot 2SiO_2 \cdot aq$ types of almost colloidal sizes combined to precipitates formed topochemically earlier and of an analogical composition. T-gel formed only from calcium salts of ortho- and pyro silicic acid is of such a nature.

Simultaneously with the appearance of T-gel (after a period of 6-12 h, when water is added to Portland cement) formation of silicates of higher degree of polycondensation begins through liquid phase and calcium silicate hydrates of more complex composition than T-gel are formed.

Investigations carried out by us show, that silicic acid in liquid phase of hardening Portland cement is present as $(SiO_4)^{4-}$, $(Si_2O_7)^{6-}$ and $(Si_3O_9)^{6-}$ ions (higher degrees of polycondensation are possible) or in the form of a coagulated sol.

It is known, that in hardening Portland cement paste of normal composition uncombined gypsum disappears during the period of 10-20 h, when water is added and in Portland cements without iron compounds (white cement) after 2-3h, while the concentration of $/Al(OH)_6/^{3-}$ ions in the liquid phase increases with time.

The presence of silicic acid ions of different polycondensation degrees and also $/Al(OH)_6/^{3-}$ ions in solution determine composition and structure of compounds formed through the liquid phase. Ettringite and monosulfate in liquid phase interact with silicic acid ions of higher polycondensation degree forming large complexes $C_3A \cdot Ca/SiO_3, SO_4, (OH)_2/aq$ and $C_3A \cdot 3Ca/SiO_3, SO_4, (OH)_2/aq$ the composition of which corresponds to solid solutions $C_3A \cdot CaSiO_3 \cdot H_{12} - C_3A \cdot CaSO_4 \cdot H_{12} - C_3A \cdot Ca(OH)_2 \cdot H_{12}$ and $C_3A \cdot 3CaSiO_3 \cdot H_{31} - C_3A \cdot 3CaSO_4 \cdot H_{31} - C_3A \cdot 3Ca(OH)_2 \cdot H_{31}$ /1, 3, 5/. Compound $C_3A \cdot nCaSiO_3 \cdot aq$ /1/ serves as nucleus for such complexes.

X-ray diffraction pattern of these complex compounds corresponds to that of ettringite or monosulfate aluminate /3, 5/. The above mentioned complexes are formed either through the liquid phase in hydration process of initial aluminate phases or as a result of further conversion in liquid

phase of new formations originally formed by the hydration of C_3A.

In hardened Portland cement paste of normal composition (with limited amount of gypsum) above mentioned complexes are in equilibrium and retain stability until a disturbance of this equilibrium occurs as a result of the appearance or an increase in gypsum content in the system, e.g. as in the case of sulphate-gypsum attack. The presence of significant number of SO_4 ions in the system leads to the decomposition of silicate complexes with separation of inert $CaO \cdot SiO_2 \cdot aq$ and ettringite crystals stable under the given conditions - $C_3A \cdot 3CaSO_4 \cdot H_{31}$ and also to transformation of C_4AH_{13} compound to ettringite through liquid phase. Ettringite decomposes cement stone due to an increase in its volume.

A new equilibrium among the components of the system is achieved after gypsum attack. As it is known, hydration process of C_4AF mineral and mechanism of formation of hydrated compounds during Portland cement hardening is similar to that occuring during C_3A mineral hydration, however, it has its specific pecularities. At the relationship of A/F = 1 in initial phase C_4AF reaction products are equimolar quantities of C_3A and C_3F in solid solution, composition of which may be expressed by general formula C_6AFH_x /6/. Crystalline structure of this compound is similar to that of cubic minerals C_3AH_6 and C_3FH_6.

Compound C_3FH_6 was not identified by X-ray diffraction in hydrated Portland cement of normal composition. Not in all the investigated specimens was the presence of mixed crystals (solid solutions) of $C_{3(4)}(A,F)$ composition identified. In our research chemical phase analysis has shown the formation of complex X_2 of $C_{3(4)}(A \cdot nCaSiO_3, F)$ aq composition/1/. This shows the appearance of mixed crystals of $C_{3(4)}(A,F)H_x$ composition through liquid phase, aluminate component of which forms the above mentioned complex with calcium salt of metasilicic acid in solution. Formula of complex X_2 may be written as follows:

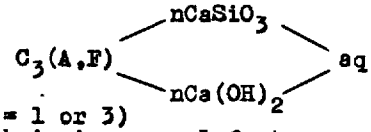

(n = 1 or 3)

Such is in general features, the hypothesis suggested by us about structure the formation mechanism and the formation of new compounds in hardening Portland cements. The hydration of minerals in hardening Portland cement is not isolated, but surrounded with compounds interacting with one another, then the hydration process in Portland cement of a normal composition may be expressed by the following equations:

a) hardening of Portland cement clinker (free of gypsum):

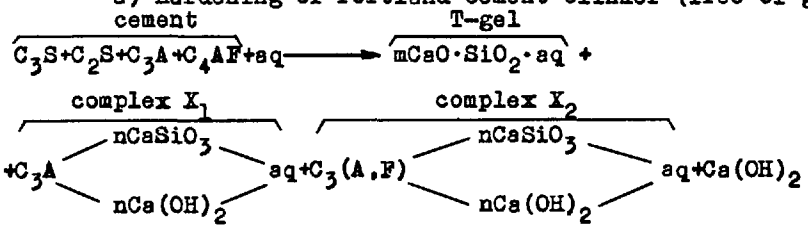

b) hardening of Portland cement of normal composition (3-6% gypsum):

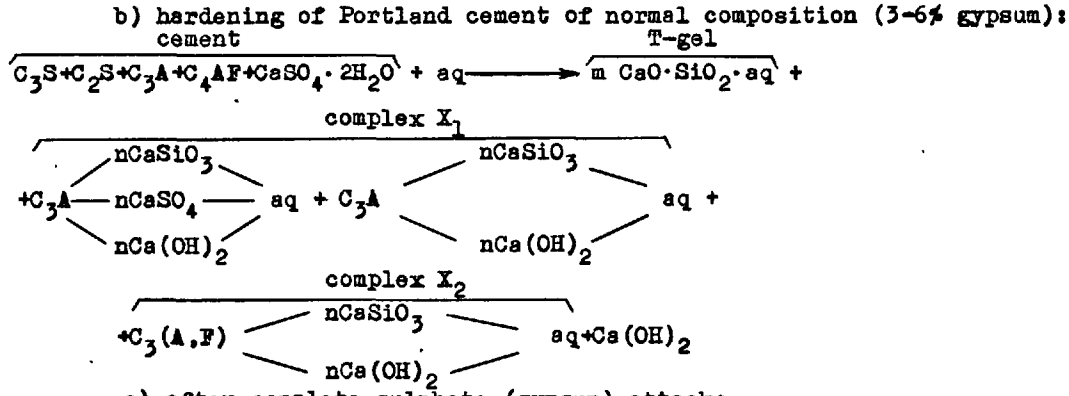

c) after complete sulphate (gypsum) attack:

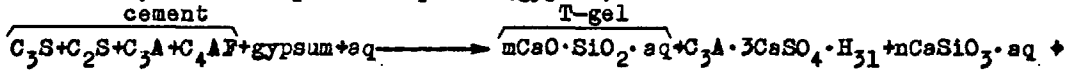

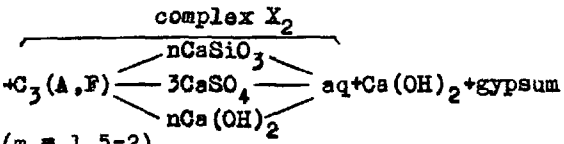

(m = 1.5-2)
(n = 1 or 3)

The data obtained in the investigations carried out by the authors of this paper show that in normal hydrated Portland cements (with 3-6% of gypsum) ettringite $C_3A \cdot 3CaSO_4 \cdot H_{31}$ in pure form is absent but it is included in the composition of complex $C_3A \cdot 3Ca/SiO_3, SO_4, (OH)_2/ \cdot aq$.

Sulphate (gypsum) attack develops gradually only with the increasing of gypsum concentration in the system followed by the decomposition of complex X_1 /1,2/ and cement stone. At the end of attack nearly all the X_1 decomposes into separate $CaSiO_3 \cdot aq$ compounds and ettringite. This process may be observed by the gradual increasing of $CaSiO_3 \cdot aq$ in boiling H_3BO_3 solution with a rise in gypsum concentration in the system. Apparently the complex X_1 contains ettringite in amount which does not decompose the complex itself. The increase of ettringite amount for some reason (e.g. in the case of sulphate-gypsum attack) results in decomposition not only that part of complex X_1 where ettringite entered earlier and also that part, which had not contained it, e.g. compounds $C_3A \cdot nCaSiO_3 \cdot aq$ and C_4AH_{13}. As a result of this separate inert components possessing no binding properties are formed which convert Portland cement stone into a formless mass.

Portland cement hydration process analysis data show, that the end of these processes - strength of Portland cement stone - is the result of total mineralogical composition of cement stone, space distribution of hydration products, crystalline structure of hydrated compounds, their crystal forms and degree of dispersion. Portland cement stone taken as a whole should be looked upon as a texture containing all necessary elements of strength. The main framework of the texture consists of interlocked rigid crystals of $Ca(OH)_2$ and calcium hydroaulfoaluminates entering complex X_1. Interspaces in this bearing framework are filled densely with T-gel and remaining part by complex X_1 of fine crystalline structure. The remaining interframework is filled with mostly colloidal substance of T-gel and with complex X_2 - $C_3(A \cdot nCaSiO_3, F) \cdot aq$ formed on the base of ferrite phase.

CONCLUSIONS

1. It was found, that solid phase of completely hydrated Portland cement of common composition consists of: 25-40% T-gel, 35-50% complex X and 15-20% $Ca(OH)_2$.

2. T-gel contains only 50-60% SiO_2 of the amount present in hardened Portland cement paste in the form of salts of calcium ortho- and pyro- silicic acid. The remaining SiO_2 amount in the form of calcium salts of metasilicic acid (may be of the highest degree of polycondensation) enters the more larger silicohydroaluminate complexes (complex X), the nucleus of which is made up of compound $C_3A \cdot nCaSiO_3 \cdot aq$ (n=1 or 3).

Thus, not all the SiO_2 present in the system enters T-gel in hardened Portland cement as is claimed by the generally accepted conception. The latter conception is based on the data obtained in the investigations, in which specimens of the material (hardened Portland cement paste) during their preparation for phase analysis by the molybdenum method are extracted by HCl solution.

However immersion of hardened Portland cement specimens in HCl solution even of low concentration completely decomposes the above mentioned complex X. Thus silicic ions of higher degree of polycondensation belonging to the complex X pass into solution and then they are estimated as a part of T-gel. Further research work must be carried out in this field.

BIBLIOGRAPHIE

1. Mituzas J.I., Kaminskas A.J., Mituzas A. J.(1976) Novye dannye o fazovom sostave tverdejushchego cementnovo kamnya. Shestoi mezhd. kongress po khimii tsementa. Tom II, kniga I. M., Stroiizdat, s.275-277.

2. Mituzas J.I., Mituzas A.J.(1973) Sb.trudov VNII teploizolyatsii, v.7, Vilnius, p.205-246.

3. Regourd M., Hornain H. and Mortureux B. (1976) Evidence of Calcium Silicoaluminates in Hydrated Mixtures of Tricalcium Silicate and Tricalcium Aluminate. "Cement and Concrete Research", vol.6, p.p. 733-740.

4. Schwiete H.E., Ludwig U., Jäger P.(1964) Untersuchungen im System $3CaO \cdot Al_2O_3$ - $CaSO_4$ - CaO - H_2O. "Zement-Kalk-Gips". No 6, 229-236.

5. Flint E.P., Wells L.S. (1944) "J.Research NBS", 33, 471.

6. IV mezhd. kongress po khimii tsementa (1964) M., Stroiizdat, s.213-317.

Estimation of Chemical Bonding in Hardened Cement Paste and Its Implications

Les liaisons chimiques dans les pâtes de ciment durcies et leurs conséquences

S. CHATTERJI, M.Sc., D.Phil., Research Scientist, H + H-INDUSTRI A/S, Lundtoftevej IA, DK 2800 Lyngby, Denmark.

SUMMARY: The existence of chemical bonding between the cement hydration products has been postulated by different workers to explain some properties of cement pastes. To form a stable three dimensional body the chemically bonded particles must form a fairly dense three dimensional net work. No attempts seem to have been made to quantify the preponderance of chemical bonding in a cement paste from its fundamental requirements. Most fundamental of these requirements is the juxtaposition of appropriate atoms or ions. Basing on this requirement only, the maximum probability of formation of a single chemical bond between two particles can be calculated. Other requirements reduce this maximum. From the above maximum probability it is possible to estimate the extent of three dimensional net work of particles bonded by single chemical bonds. For a water cured paste it is extremely low i.e. chemical bonding plays a negligible role in the structure of a cement paste. Implications of this result as regards the properties of pastes and the aggregate-paste bonding are discussed.

RÉSUMÉ: Plusieurs chercheurs ont formulé l'hypothèse que l'existence de liaisons chimiques entre les produits d'hydratation des ciments pouvaient apporter une explication à certaines propriétés des pâtes de ciment. Pour former un corps à trois dimensions stable, les particules liées chimiquement doivent former un réseau à trois dimensions suffisamment dense. Il n'a été fait aucune étude quantitative sur la prépondérance des liaisons chimiques dans une pâte de ciment à partir de ses exigences fondamentales. L'exigence fondamentale prédominante est la juxtaposition des atomes ou des ions appropriés. A partir de cette seule exigence, on peut calculer la probabilité maximale de formation d'une liaison chimique unique entre deux particules. D'autres exigences réduisent ce maximum. A partir de cette probabilité maximale ci-dessus, il est possible d'évaluer l'étendue du réseau à trois dimensions des particules liées par des liaisons chimiques uniques. Pour les pâtes conservées dans l'eau, le résultat est extrèmement faible, c.à.d. que les liaisons chimiques jouent un rôle négligeable dans la structure des pâtes de ciment. Un débat est ouvert actuellement sur les implications de ces résultats en ce qui concerne les propriétés des pâtes et les liaisons chimiques des pates-agrégats.

Formation of chemical bonds among cement hydration products has been postulated by different workers to explain some of the properties of cement paste e.g. limited swelling capacity, wet strength etc. (1,2,3). No attempt has been made to estimate the probability of its formation from the pre-requisites of bond formation. These requisites are (i) right types of bond forming atoms or ions have to be juxtaposed within the bond forming distance of about 3Å; (ii) the nearest neighbours of either of the bond forming atoms should not interfere with the bond formation; (iii) after the bond formation the spatial disposition of the bonded atoms should satisfy the required bond angle e.g. Si-O-Si, Ca-O-Si etc. In this paper an attempt will be made to estimate the probability of bond formation from the pre-requisites. Of these requisites the first is the least restrictive and yields the maximum probability. The other two requisites reduce the probability of bond formation sharply and as such their application will be deffered. It is to be noted that the application of the first requisite only is equivalent to an assumption that the material is composed of a random collection of atoms or ions.

After mixing cement with water it takes some time before the paste is capable of carrying any load; though the anhydrous cement grains start to hydrate from the time water is added. The initial hydration products form at isolated places round the anhydrous grains and the water-filled intergranular spaces get filled up by hydration products formed subsequently (4,5,6). When the hydration products from different sources approach each other due to growth or nucleation they do so in random orientation. To perform the functions for which it has been postulated the chemical bonding among these randomly oriented hydration products have to be fairly extensive.

Of the total hydration products of cement only a small part is crystalline and well characterized e.g. $Ca(OH)_2$, ettringite, but the characteristics of the major constituent namely calcium silicate hydrate (CSH) are disputed except that it is composed mainly of positive and negative ions. Various morphologies have been reported for CSH (7); however, analyses of the reports indicated that all these are derived from needle-shaped CSH (8,9) except for the product which form very early (10). The diameter of CSH needles have been reported from 500 to 2000Å (11,7); the latter value refers to needles coated with metal films of unknown thickness. The needles are generally reported to be about a micrometer long. The chemical bond formation among these CSH needles is what has been postulated in 1,2,3.

If a cement paste is kept saturated from the beginning, as is the normal practice in cement testing or some application, the space between the hydration products will be filled by water. Experiments with contacting silica glass surfaces in atmospheres of different relative humidities (rh) showed that upto about 50% rh the surfaces remain in contact. Above this rh the surfaces are disjoined by a water film whose thickness increases with rh and can be as high as 500Å at 100% rh i.e. each surface can have an absorbed water film of about 250Å thickness (2). In a saturated cement paste the CSH needles will also have absorbed water films and will be subjected to a similar disjoining force (1,2). To form chemical bonds between two CSH needles their respective water films have to be thinned down, against the disjoining force, to that in equilibrium with 50% rh; thereafter van der Waals forces will bring the needles still closer (2). This thinning down can only occur when the movements of the needles are restricted whilst the needles are approaching each other due to growth.

Consider two CSH needles which, by chance, have come within the bond forming distance. If they can form a bond at the point of their nearest approach, which can withstand the disjoining force, then further bond formation may occur by accreation of solids round the bond. The first bond formation can occur if oppositely charged ions face each other. The probability of that occuring is given by

$$P_1 = (0.x)(0.y) \text{ ----------[1]}$$

where 0.x and 0.y are the fractional volumes occupied by the positive and negative ions in the needles. When the needles are of similar composition then P_1 will approach its maximum value of 0.25. The probability of forming two bonds at the first instance is p_1^2 and so on.

It now remains to find the strength of a chemical bond and that of the disjoining force. In a silicate structure the Si-O bond is generally considered to be the strongest bond at room temperature. In quartz a single Si-O bond has a strength of 5.98×10^{-4} dyne-Å (12). From the properties of quartz it can be calculated that the average cross-sectional area of a Si-O bond is $5.23 Å^2$. These values will be taken as the average values for bonds in CSH needles.

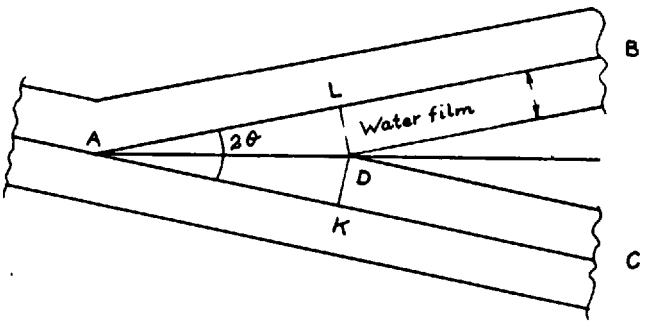

Fig. 1 Shows the geometry used to estimate the disjoining force between two needles.

Fig. 1 schematically shows a principal section through two bonded needles AB and AC together with their absorbed water layers. Upto K and L the water absorption is hindered and the region AKL will be subjected to the disjoining force. The disjoining pressure, ΔP at any small region along AK or AL is given by $\Delta P = (RT/V_M)\cdot(\ln h_1/h_2)$, where h_1 is the rh corresponding to the film thickness at the region, h_2 is the ambient rh (100%), V_M is the mol. volume of the absorbed water and the other symbols have their usual meanings (1). At 25°C the disjoining pressure adjacent to A will be $\Delta P = (RT/V_M)\cdot(\ln 50/100) = -9.55\times10^{-8}$ dynes/A^2, and K or L will be zero. The disjoining pressure will decrease away from the line AD along the circumference of the needles. This is schematically shown in Fig. 2.

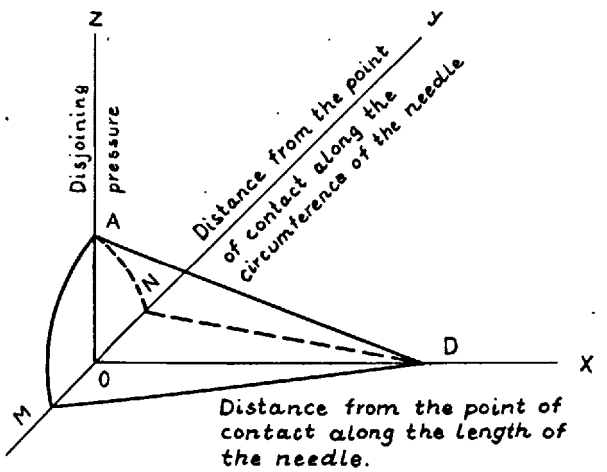

Fig. 2 Shows the area on which the disjoining force acts.

The total disjoining force will be that acting on the surface MAND of Fig. 2. The area of the surface MAND depends on the angle 2Θ, at which the needles approach each other. Further calculation will be simplified if instead of using the whole MAND surface only 25A wide strip surfaces, tangential to and centered on AK and AL, are considered. At any point along the length there will be a negligible drop in the disjoining pressure across the width of the strips, though the disjoining pressure will drop from A to K or L. The average disjoining pressure ΔP_{av} is given by

$$\Delta P_{av} = (RT/V_M)\cdot(2\int_{50}^{100} \ln h_1/h_2 dh) = -4.23\times10^{-8}$$

dynes/A^2

The total disjoining force, F, will be 25. AK.ΔP_{av} dynes. In other words water will be forced against the bond with the above force. To break the bond, the water front has to move by 2.6A and the work done will be 2.6.F dyne-A. Equating 2.6.F with the bond energy 5.98×10^{-4} dyne-A gives AK as 217 A.

The absorbed water film on a silica glass surface is about 250A thick (2). The corresponding film thickness for CSH is not known, but for further calculations, it will be assumed to be 100A. This gives Θ as 24.7° i.e. two needles approaching at an angle more than 49.4° will be able to form a stable bond. Thus of the total number of needles that can approach a needle only those approaching at 49.4° or above are capable of forming stable bonds and of these only about one-fourth (0.25) can actually form bonds. This gives the overall probability

$$P_t = (1-\text{Cos}\ (90-49.4))\cdot P_1 = 0.06 \text{ ------[2]}$$

That is out of 16 approaching needles only 1 will be able to form a stable bond. To get a three dimensional load bearing structure some of the needles need to form at least 3 bonds, which requires on the average some 48 needles to approach each of them to bond forming distances -- a highly unlikely figure in a not so dense random packing of needles.

Note that in the above order of magnitude estimation the effects of the other two pre-requisites have been ignored, which could not be done in the case of real solids. In this context it is of interest to note that in the case of hardened plaster of Paris cement, where all the three requisites could be explicitely taken into account, P_t is 1 in 22000 even when the effect of the disjoining force is ignored i.e. chemical bonding plays no part in this cement (13). This conclusion is supported by the electron microscopic study of set plaster of Paris blocks (14). However, set plaster of Paris is of a limited swelling type and is capable of carrying load when saturated i.e. these

properties are not dependent on chemical bond formation.

From the above it can be inferred that
(a) chemical bonding among the cement hydration products plays very little, if any, part in determining the properties of cements.
(b) in a moist paste the hydration products are separated by films of water. This physical picture of a paste is identical to that proposed by Chatterji and Jeffery (11). From the above picture it follows that
(i) the tensile strength of a paste will be determined by the intervening liquid films and for a given paste will have a maximum (15). Moreover, the tensile strength of the liquid phase will set an ultimate upper limit to the tensile strength.
(ii) compressive strength will have no such limit and be determined by the shear strength of the needles (16).
(iii) during the first drying of a paste, the particles which are separated from each other by thinner water films will be brought nearer to each other from those separated by thicker water films i.e. fine cracks will form (17). These cracks are responsible for the irreversible shrinkage on first drying.
(iv) the potential points of crack formation during drying will also be points at which hydration products will be able to slide over each other or rearrange easily i.e. they will act as sites of creep (18).

Chemical bond formation between CSH and concrete aggregates has been postulated by different workers to explain differences in properties of concrete made with different aggregates. Most natural aggregates are polycrystalline and are often polymineralic. Due to the crystalline nature of aggregates all the three pre-requisites have to be taken into account even for a single bond formation and as a result its probability will be very low. In other words in a concrete the nature of bond between CSH and aggregates is the same as that between CSH particles (19).

REFERENCES

1. - T.C. POWERS (1968) "Mechanism of shrinkage and reversible creep of hardened cement paste". The structure of concrete. Cement & Concrete Assoc. London, 319-344.

2. - F.H. WITTMANN (1973) "Interaction of hardened cement paste and water". J. Am. Ceram. Soc. 56, No. 8, 409-415.

3. - A. BENTUR et al (1979) "Creep and drying shrinkage of calcium silicate pastes. III". Cement and Concrete Research. 9, 83-96.

4. - W. CZERNIN (1960) "A few unsolved problems of cement hydration". IVth Inter. Symp. Chem. Cement, Washington, 725-729.

5. - S. CHATTERJI and J.W. JEFFERY (1966) "Three dimensional arrangement of hydration products in set cement pastes". Nature. 209, 1233-1234.

6. - D.D. DOUBLE, A. HELLAWELL and S.J. PERRY (1978) "The hydration of Portland cement". Proc. Royal. Soc. London. 359, 435-451.

7. - S. DIAMOND (1976) "Cement paste microstructure - an overview at several levels". Hydraulic cement pastes: Their structure and properties. Cement & Concrete Assoc., London, 13-14.

8. - S. CHATTERJI (1974) "Microstructure of magnesium oxychloride cements". Nature. 250, 443.

9. - S. CHATTERJI (1979) "A discussion of the paper "A multi-method study of C_3S-hydration"". Cement and Concrete Research. 9, 391-392.

10. - S. CHATTERJI and J.W. JEFFERY (1963) "Studies of early stages of paste hydration of different types of Portland cements". J. Am. Ceram. Soc. 46, 268-273.

11. - S. CHATTERJI and J.W. JEFFERY (1967) "Strength development in calcarious cements". Nature. 214, 556-561.

12. - L. PAULING (1966) "The nature of the chemical bond". Cornell Univ. Press., New York. 85.

13. - S. CHATTERJI (1974) "Load bearing structures and crystal intergrowth". Nature. 252, 383-384.

14. - N. WHITNEY, S. CHATTERJI and J.W. JEFFERY (1979) "Mechanics of failure of plaster of Paris blocks in different types of stresses". Cement Tech. 1, 171-173.

15. - A. Grudemo (1974) "Strength vs structure in cement pastes". Preprint, VIth Inter. Symp. Chem. Cement, Moscow.

16. - S. POPOVICS (1974) "Strength development of Portland cement paste". Preprint, VIth Inter. Symp. Chem. Cement, Moscow.

17. - S. CHATTERJI (1979) "Analyses of techniques of measuring physical properties of cement paste to obtain microstructural information". Bull. Am. Ceram. Soc. 58, 233-234.

18. - B.R. GAMBLE and J.M. ILLSTON (1976) "Rate of deformation of cement paste and concrete during regimes of variable stress, moisture-content and temperature". Hydraulic cement pastes. Their structure and properties. Cement & Concrete Assoc., London. 297-311.

19. - S. CHATTERJI and J.W. JEFFERY (1971) "The nature of the bond between different types of aggregates and Portland cement". Indian Concr. J. 45, 346-349.

On main formulae of cement stone and concrete strength

Formules fondamentales de la résistance des mortiers et bétons

I.P. VYRODOV, G.P. PADALKINA, U.R.S.S.

RESUME : La présente communication étudie le durcissement en fonction du rapport eau sur ciment $\frac{E}{C}$.

Une formule générale en a été déduite, permettant de calculer la résistance des mortiers et bétons; elle dérive (sous certaines restrictions) des formules déjà connues, mais elle est plus simple et plus pratique.

Deux termes antagonistes de cette formule révèlent une analogie avec l'action réciproque des forces moléculaires. L'analyse des données théoriques et expérimentales permet de comprendre le sens physique des paramètres utilisés, et d'aboutir à des calculs numériques.

De nombreuses expériences, et notamment des expériences sur du béton lourd, ont montré la bonne concordance entre les valeurs calculées selon la formule proposée et les résultats expérimentaux. Cette formule permet donc, en fonction du paramètre $\frac{E}{C}$ de calculer à l'avance les résistances.

SUMMARY : Relationship between strength and watercement ratio ($\frac{W}{C}$) has been under investigation in this study. Generalized formula of cement stone and concrete strength has been deduced. It contains (under certain restrictions) formerly known and more simple formulae used in practice. There have been specified two antogonistic addenda what allowed to establish the identity with intermolecular forces developed in the system. Analysis of theoretical and experimental data resulted in revealing the physical significance of strength parameters and estimating their numerical values. Using the extensive experimental material, in particular taking as an example heavy concrete, the proper correspondence of the experimental and theoretical strength estimated according to the generalized formular has been shown. The formular reflects variations of the main factor ($\frac{C}{W}$) and strength parameters while approaching the value of the predicted strength.

The watercemnt ratio is one of the most significant factors that determines not only conditions of hydration and new formation recrystallization, but also processes including formation of physicomechanical properties of the binding systems to be solidified. This strength factor was first formalized by Bolomeo to estimate the concrete strength: $\frac{W}{C}=\chi^{-1}$

$$R=AR_{\mu}(Z-b), \qquad (1)$$

where

A and b - certain coefficients,

R_{μ} - cement activity.

However this formular can be the proper approximation only in the restricted interval$_Z$ Fig.1 (Typical experimental relationships R(Z) taken from a series of trials are given in this figure).This fact is taken as a principle of the approximation curve using either a series of straight segments (a broken curve) or a single averaging straight line in some not exact technological calculations. Such an approximation as a consequence of experience conceals the true behaviour of strength relative to the watercement ratio as well as the fundamental properties R(Z) which can be used by specialists. To clear up a general nature of Z effect on formation of strength, there has been used a Stochastic approach in the works / 1-3 / what resulted in better approximation

$$R=Az\ (\alpha+z) \qquad (2)$$

as compared with (1). Further generalization / 4-7 / allowed to establish the strength formula

$$R=\eta_1 z(\alpha+z)\ (\eta_2+z)^{-2} \qquad (3)$$

wherein

α - autohesive-cohesive factor

η_1, η_2 - factors which meaning will be revealed later on.

For theoretical interpretation ratios (3) are given as

$$R=\eta_1\eta_2(\eta_2-\alpha)y^{-2}+\eta_1\left[1+(\alpha-2\eta_2)y^{-1}\right]= \\ =R_1+R_{II}=R_{III}\ , \qquad (4)$$

where

$$y=z+\eta_2$$

Let $R(z)=R_I+R_{II}=R_{III}$ (Fig.2)

Singling out addenda R_I and R_{II} from the summary strength $R=R_{III}$ reflects the fact that cement stone and concrete are both resistant to the mechanical compression and tension as well. It means that there exist mutual interaction forces R_I (autohesive-cohesive interaction: adhesion) and repulsion forces R_{η} between there particles. It is evident that the system is also exposed to overmolecular forces of mechanical tensions of strengthening and weakening together with the interaction F_I and repulsion forces F_2 of intermolecular interaction.

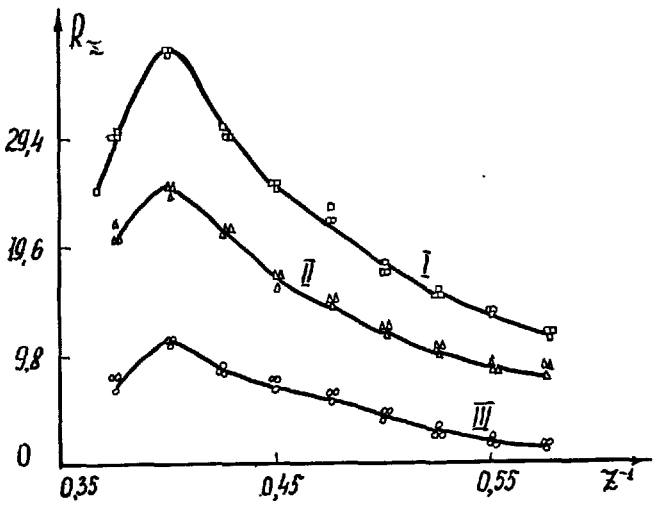

Fig.1

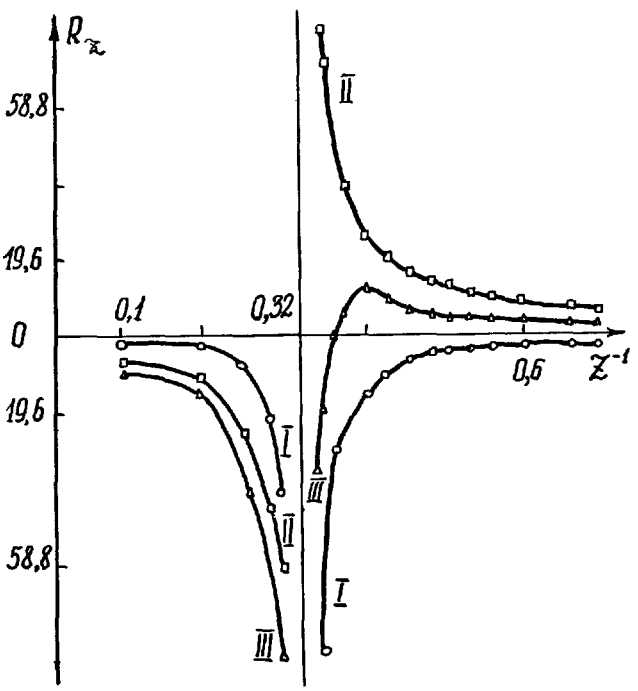

Fig.2

In this connection data of Fig.1,2 are compared with the known curves of intermolecular forces of interaction F_1 which are dependent upon a spacing between molecules r, and the result is that there is similarity in behaviour of the summary forces of interaction $F(r)=F_1(r)+F_2(r)$, and the summary compression strength $R_{compr.}(z^{-1})=R_1(z^{-1})+R_2(z^{-1})$. The antibate character of these curves determines the choice of the strength factor:while comparing tension strength $R_{tension}(z^{-1})$ with F(r) the symbate character of the curves mentioned above as well as curves R_1, R_2, and F_1,F_2 has been established. It is the second peculiarity that proves availability of interparticle interaction forces. As to the third peculiarity of values $R_1(z^{-1})$ and $R_2(z^{-1})$ it exhibits itself in diminishing these values up to zero while r increases. Decreasing of strength $R(z^{-1})$ with growth can be explained by analogy with the behaviour F(r): distance increase between the interacting particles. The more complex system is however characterized by other effects, which can be traced in

the formula (4).

The more comprehensive analysis reveals an influence of different strength factors taking into account links that exist between the phenomenological factors and $_2$ and cement activity $P_{cem.}$, cement consumption $Ц^{x}$: $\eta_1 = \alpha R_Ц$, $\eta_2 = V_Ц^{*}$, where

α - transition factor between cement strength and concrete strength

γ - factor that reflects the water excess value relative to stechiometry

Evaluation of data on building cement and concrete as well as experimental studies carried out by us made it possible to establish numerical values of factors α, η_1, η_2.

Analyses showed that value α in all cases studied above for concretes having the same base (portlandcement) can be taken for constant $\alpha = -1.054$: α means from 0.9 to 1.7 depending upon a type of inert (concrete) aggregate, setting conditions, way of testing; γ - a value of water excess and equals to $- 2{,}8.10^{-4}$, it is the same for cements with identical solidifications (setting) base. Formula (3) with these factors can be used to evaluate ordinary and high-strength concrete having standard setting rate and age of 28 days on portlandcements and inert (concrete) aggregates that meet the requirements of standards. The following concrete aggregates have been used: gravel with grain size $_{max}$=80 mm, granite broken (crushed) stone, pumice, lightweight aggregate, anyiskaya pumice.

Results of actual and estimated factors on heavy concrete compression strength having a 28-day age have been compared in Table. Gravel with grain size up to 80 mm and building quartz sand with module of coarseness 2.56.2.59 mm are taken as inert aggregates. In accordance with the evaluations carried out $W/_C$-ratio has been varied in the range of 0.38-0.74, and cement consumption - in the range of 200-350 kg/m^3. Cement activity has been changed in the range of 39.2-55.8.

Comparison of heavy concrete strength with the estimated one

Table

Z	Ц Cement consumpt kg/m^3	R Cement activity MIIa	$R_{compr.}$ Actual	$R_{compr.}$ Estimated according to (3) MIIa	Deviation %	Estimated according to Bolomea MIIa	Deviation %
1.50	290	55.52	24.71	28.23	-12.4	31.16	+32.6
1.89	258	39.24	28.16	29.77	-5.3	30.93	-22.5
1.90	260	45.13	26.78	29.23	-8.3	35.82	-25.2
2.22	236	39.24	27.57	29.52	-6.6	38.54	-28.4
2.50	190	45.15	37.38	36.78	-1.6	51.82	-27.8
2.50	200	49.05	40.12	40.12	0.0	56.55	-29.1
2.50	280	39.24	32.64	32.57	+0.1	45.01	-27.6
2.73	210	49.05	46.27	43.67	+7.2	51.93	-11.0

Continuation of table

1	2	3	4	5	6	7	8
3.50	300	55.52	51.60	54.83	-5.8	96.37	-46.4
4.00	320	55.52	57.78	57.78	0.0	112.64	-48.7
4.50	350	55.52	63.86	60.15	+6.1	129.03	-50.5

It is clear from the table that with change of cement activity formula ( ) shows the higher precision rate as compared with the widely used Bolomea formula.

In conclusion we can assume that the generalized formula (3) offerred by us for estimation of concrete and cement stone strength, and which carries in its base the quadratic dependence R (z), allows to predict strength R by way of selecting parameters α, η_1, η_2 and the main strength factor z as well.

LITERATURE CITED

1.- Выродов И.П. Элементы теории прочности цементного камня. Труды Кубанского СХИ, II/39/, Краснодар, I963, стр.40-49; I3/4I/, Краснодар, I968, стр.252.

2.- Выродов И.П. О некоторых вопросах физико-химии гетерогенных систем применительно к минеральным вяжущим веществам. Докт.дис. Харьков, I964.

3.-Выродов И.П. О некоторых основных аспектах теории гидратации минеральных вяжущих веществ и формирования прочности цементного камня. Докт.Дис. Ленинград, I970.

4.- Выродов И.П., Падалкина Г.П. Обобщенная формула зависимости прочности бетона от водоцементного отношения. Известия СКНЦ ВШ, серия "Технические науки", №3, I977, стр.I05.

5.- Выродов И.П. Физико-химические основы процессов гидратации и формирования прочности в вяжущих системах и перспективы развития теории. В книге "Гидратация и твердение вяжущих". Уфа, I978, стр.204-2I3.

6.- Выродов И.П. Об основных аспектах развития теории по физико-химическим основам процессов гидратации и формирования физико-механических свойств в вяжущих системах. Краткие тезисы докладов на V Всесоюзном научно-техническом совещании по химии и технологии цемента М. I978, стр.88.

7.- Выродов И.П., Падалкина Г.П. Об уточнении зависимости прочности бетона и цементного камня от различных факторов-показателей прочности. Межвед. сборник "Физико-химические основы процессов гидратации и гидратационного твердения вяжущих систем". Краснодар, I979.

Accroissement de la résistance du ciment portland par introduction des constituants de cristallisation (germes)

Increase of portland cement strength at introduction of crystallizing components (crents)

A.M. DMITRIEV, Candidat ès Sciences Techniques,
M.T. VLASSOVA, Candidat ès Sciences Techniques,
B.E. YUDOVITCH, Candidat ès Sciences Techniques,
A.K. ZAPOLSKI, Docteur ès Sciences Techniques,
I.V. KRAVTCHENKO, Docteur ès Sciences Techniques,
L.M. SAZONOVA, Ingénieur, NIITzement, Moscou et Institut de la chimie colloïdale et de la chimie de l'eau, Kiev, U.R.S.S.

RESUME : On a étudié le problème d'accroissement de la résistance du ciment portland et de ses constituants par l'introduction d'un constituant complémentaire, dit constituant de cristallisation, car il cumule les fonctions de réactif de démarrage et d'amorce de la formation de deux porteurs de résistance principaux : hydrosilicates de calcium et ettringite. Ce constituant est étudié sur l'exemple du mélange $Al_2(SO_4)_3$, $Al_2(SO_4)_2.(OH)_2$, $Al(OH)_3$ et SiO_2(coll.) introduit dans la composition du ciment. L'accroissement de la résistance initiale de ce dernier est dû à la formation d'une quantité complémentaire d'ettringite et de sa meilleure répartition autour des granulats. L'augmentation de la résistance à long terme est due à l'accélération de l'hydratation de l'alite et à l'élévation du degré d'homogénéité de la structure submicroscopique des hydrosilicates de calcium, produisant une diminution des microtensions internes au niveau du granulat. On a commencé la production de ces ciments aux constituants de cristallisation (germes).

SUMMARY : Increase of strength of portland cements and its components by introduction of an additional component has been studied. The additional component has been called "crystallizing" since it combines the functions of the initial reagent and of seed for formation of two main carriers of strength, calcium hydrosilicates and ettringite. An $Al_2(SO_4)_3$, $Al_2(SO_4)_2\cdot(OH)_2$, $Al(OH_3)$ and SiO_2 (col.) mixture introduced into the cement composition was studied. The cement early strength increase of the latter stems from formation of additional amounts of ettringite with increasing the fraction of its regular concretions, whereas the late hardening strength increase stems from accelerated hydration of alite and increase of homogeneity of calcium hydrosilicate submicrostructure which indicates decrease of the natural microstresses level in their aggregates. Industrial production of cements with crystallizing components (crents) has been started.

INTRODUCTION. La voie principale d'accroissement de la résistance du ciment passe actuellement par une optimisation successive des paramètres technologiques de sa production à chaque opération entrant dans le cycle technologique, à commencer par le choix de la composition et de la dispersité des matériaux bruts jusqu'au choix de la granulométrie optimale des ciments (1 à 3), les améliorations dues aux modifications technologiques isolées de la production et apportées au résultat final - activité hydraulique du ciment - n'étant pas de simples termes additifs, l'accroissement total de la résistance est toujours inférieur à la somme des contributions isolées. C'est pourquoi les technologues ont conclu qu'il existe une limite de résistance du ciment, impossible à dépasser par les procédés technologiques traditionnels. Il est donc nécessaire d'étudier ses causes microstructurales et sur cette base tracer les voies à suivre pour augmenter la résistance.

PARTICULARITES DE LA STRUCTURE SUBMICROSCOPIQUE DES CIMENTS DURCIS A HAUTE RESISTANCE ET DU MICROMECANISME DE DESTRUCTION. Les études de la structure submicroscopique d'hydratation des ciments à haute résistance, obtenus à l'aide de la technologie classique (3, 4), montrèrent que la résistance de la structure d'hydratation du ciment portland à l'âge de 1 à 3 jours (20 à 40 MPa) est conditionnée par le réseau cristallin biphasé tridimensionnel en fibres rigides inflexibles d'ettringite et d'hydrosilicates de calcium C - S - H (II). Ce réseau recouvre les pores entre les particules de départ du ciment entourées d'hydrates. Après 4 à 6 h de durcissement, les mailles du réseau sont remplies successivement par la "matrice" (autres produits d'hydratation) - en premier lieu par C - - S - H (II) - en commençant par les particules de départ, tandis que les mailles "inachevées" continuent à se construire et se fixent au réseau et à l'agrégat à l'aide des zones de portlandite et C - S - H (II). La particularité principale de la structure d'hydratation des ciments à haute résistance consiste en moindres dimensions des mailles de son réseau, des zones d'ettringite, de portlandite et C - S - H (II). La deuxième particularité due à l'hydratation rapide est le volume plus petit des pores capillaires, leurs dimensions plus faibles et la densité plus grande (3). Une résistance élevée liée à ces particularités microstructurales rapproche le ciment hydraté des autres matériaux de construction dont la résistance croît également avec la diminution des dimensions des éléments structuraux (5).

Le micromécanisme de destruction de la structure d'hydratation est envisagé en détail dans le rapport de stand de Y.I. Papiachvili et de certains d'entre nous au Congrès actuel. La conclusion tirée des observations se ramène au fait que la fissure principale de destruction dans la matrice armée par le réseau se propage par sauts. L'extension des zones de fissuration spontanée est liée de façon antibatique, tout comme dans les autres matériaux (5, 6), à la dimension moyenne des éléments structuraux. Ceci conditionne justement l'existence de la limite de la résistance pratique des ciments, qu'on augmente par des méthodes technologiques classiques. Lors de l'essai des échantillons à haute résistance l'accroissement des zones de fissuration sous charge s'accompagne d'effets acoustiques fort caractéristiques, comparables à une détonation.

JUSTIFICATION DE L'INTRODUCTION DES CONSTITUANTS DE CRISTALLISATION (CRENTS) DANS LE CIMENTS. Nous partons de la nécessité, pour l'accroissement ultérieur de la résistance, d'arrêter ou de prévenir la fissuration de la matrice - "gel" des hydrosilicates. Une des idées maîtresses, à savoir la diminution de la concentration des contraintes près des sommets de microfissures dans les plans normaux à leurs trajectoires (7), n'est discutée en détail que pour les bétons (8). Vu que, pour le mécanisme existant de destruction, les contraintes normales dans la matrice sont celles de traction, les travaux pour la réalisation de cette idée doivent en premier lieu être orientés sur la création des zones de compression perpendiculaires au plan de la fissure, i.e. disposées le long des axes du réseau de fibres de renforcement. Ceci est technologiquement réalisable seulement par l'introduction dans la structure d'hydratation du ciment de la phase fibreuse expansive immergée dans le gel préalablement comprimé par cette dernière. Par conséquent, ce gel doit être présent, si c'est possible, dès le début de la cristallisation de la phase expansive. A cette fin le gel et la phase expansive immergée dans ce dernier doivent être spécialement "amorcés" par introduction dans la composition du ciment du constituant complémentaire dit constituant de cristallisation (crents) (3). Dans ce cas nous nous sommes attendus à l'accroissement équivalent de la résistance et de la résistance à la fissuration. Les lignes qui suivent traitent de l'argumentation chimico-technologique du procédé en question. Il existe également d'autres orientations et lignes directrices dans ce domaine, mais leur examen sort du cadre de cette communication.

MODE OPERATOIRE. MATERIAUX DE DEPART. Par cuisson répétée d'après la technique habituelle on a synthétisé les principaux minéraux de clinker $C_3S(M)$, $C_2S(\beta)$, $C_3A(T)$, C_4AF, tous de pureté de 95 à 98% ; le clinker comprenant (%) $C_3S(R)$-63, $C_2S(\beta)$-18, $C_3A(T)$-7, C_4AF-11, R_2O-0,25 % était cuit dans un four industriel de 127 mètres. Comme additions on a utilisé : silicagel récemment précipité cuit à 750 °C (2 h) et broyé jusqu'à son passage complet à travers le tamis n° 008 (coll. SiO_2) ; $Al_2(SO_4)_3$ recristallisé incluant les impuretés d'$Al(OH)_3$, $Al_2(SO_4)_2 \cdot (OH)_2$ (jusqu'à 30 %) ; métakaolinite obtenue par cuisson (620 °C, 1,5 h) du concentré de kaolinite de 90 % et broyée jusqu'à son passage par le tamis

n° 008 ainsi que $CaSO_4$ dihydraté recristallisé et séché à 60 °C (1 jour). En outre, on a utilisé le constituant de cristallisation industriel synthétisé pour nous à l'un des combinats chimiques par traitement thermoacide de l'argile.

METHODOLOGIE DES ESSAIS. Les constituants de clinker étaient broyés jusqu'à obtenir 0,1-0,3 % du résidu sur le tamis n° 008, et le clinker - jusqu'à obtenir la surface spécifique de 3440 cm^2/g avec des résidus sur les tamis n° 02 - 0,3 % et n° 008 - 4,3 % ; à partir d'eux et de leurs mélanges avec additions on a préparé des échantillons de 1,4x1,4x1,4 cm, 2x2x2 cm ainsi que de 4x4x16 cm avec du sable (1:3) d'après les normes en vigueur en U.R.S.S. (GOST 310-76). Les échantillons fabriqués étaient laissés à l'air pendant 24 h à 22 ∓ 1 °C et à l'humidité de 100 % et ensuite mis dans l'eau à la même température. Après l'essai de résistance les échantillons étaient soumis à l'analyse thermique différentielle et à l'analyse aux rayons X. Des portions de la phase liquide étaient prises pendant 3 h par méthode d'extrusion à la presse.

RESULTATS DES EXPERIENCES. Les indices de résistance des échantillons et les résultats de détermination du degré d'hydratation aux rayons X sont donnés dans les tableaux I, II, III. Les résultats des expériences permettent de faire les conclusions suivantes :

1. L'introduction du constituant de cristallisation (crent) augmente considérablement la résistance de C_3S pur à l'âge de 28 jours. Un gain de résistance notable était observé en présence de C_3A et du gypse. La présence de la bélite dans le mélange de minéraux abaisse ces effets utiles. Lors de l'introduction complémentaire dans le mélange de C_4AF, la résistance de la structure d'hydratation baisse brusquement pendant 7 jours de durcissement.

2. Indépendamment de la composition du mélange de minéraux, l'introduction du constituant de cristallisation (crent) aboutit à l'augmentation de sa résistance. Le gain de résistance minimal est observé dans le mélange C_2S + C_3A (90 + 10), le gain maximal - pour C_3S pur hydraté.

3. Parmi les additions utilisées en qualité de réactifs de départ et de germes pour la synthèse du gel et de la phase expansive plongée dans le gel, c'est SiO_2 (coll.) et son mélange avec $Al_2(SO_4)_3$ qui se sont avérés les plus efficaces pour la résistance des échantillons de 28 jours. La métakaolinite et ses mélanges avec d'autres additions sont moins efficaces, mais ils assurent tous le gain de résistance en comparaison du ciment témoin (tableau II). Toutes les additions réduisent quelque peu les durées de prise.

4. L'étude de la composition de la phase liquide, les données de l'analyse thermique différentielle et de l'analyse aux rayons X montrent qu'en présence de SiO_2 (coll.), de $Al_2(SO_4)_3$, de métakaolinite et de constituant de cristallisation industriel, en raison de l'abaissement initial de la concentration de SiO_2 et Al_2O_3 dans la phase liquide et de la diminution de la concentration de CaO, après 1 jour de durcissement il se forme des quantités complémentaires d'ettringite et d'hydrosilicates de calcium dont la basicité n'est pas encore déterminée. Ceci confirme le rôle des additions en tant que réactifs pour leur formation. Le degré d'hydratation du ciment diminue d'abord (après 1 jour) pour augmenter ensuite (après 3 jours et plus), bien que la résistance augmente déjà après 6 h de durcissement.

5. Selon les données présentées partiellement dans le rapport de stand cité, la microstructure des nouvelles formations varie vers une ettringite facettée plus nettement et vers un arrangement plus fin et plus régulier des hydrosilicates dans la masse totale des nouvelles formations.

TABLEAU I

Caractéristique des mélanges de constituants de clinker avec le constituant de cristallisation (crent) industriel (C)

Composition des mélanges, parties en masse						Rapport eau/ciment	Résistance à la compression, kgf/cm^2		
C_3S	C_2S	C_3A	C_4AF	C	Gypse		1j.	3j.	28j.
100	-	-	-	-	-	0,4	209	214	619
100	-	-	-	5	-	0,4	301	385	765
100	-	-	-	10	-	0,4	362	500	836
100	-	-	-	15	-	0,4	494	543	763
90	-	10	-	-	-	0,4	300	431	731
90	-	10	-	5	-	0,4	188	181	357
90	-	10	-	-	5	0,4	288	490	742
90	-	10	-	5	5	0,4	298	443	888
90	-	10	-	10	5	0,4	329	541	872
80	20	-	-	-	-	0,4	0	31	331
80	20	-	-	10	-	0,4	0	227	617
80	10	10	-	-	-	0,5	38	178	278
80	10	10	-	10	-	0,47	43	212	426
80	10	10	-	-	5	0,4	164	301	591
80	10	10	-	10	5	0,4	306	414	752
64	15	4	14	-	-	0,42	0	89	398
64	15	4	14	10	-	0,4	0	66	462
64	15	4	14	-	5	0,4	84	219	631
64	15	4	14	10	5	0,4	119	275	745

Les résultats des essais des propriétés du ciment additionné de constituant de cristallisation (crent) industriel (tableau III), dont la majeure partie n'est pas donnée ici vu la place insuffisante, témoignent de l'absence d'écarts notables par rapport aux indices de référence, à

l'exclusion de la résistance élevée et du fluage légèrement augmenté.

TABLEAU II

Caractéristique des mélanges du ciment (95 % de clinker +5 % de gypse) avec additions

Composition des mélanges, parties en masse				Degré d'hydratation de C_3S, %		Résistance à la compression, kgf/cm^2 (E/C=0,35)		
Ciment	SiO_2 coll.	Métakaolline	Sulfate Al*)	1j.	3j.	1j.	3j.	28j.
100	-	-	-	49	56	75	300	610
100	3	-	-	45	65	137	363	1 050
100	-	3	-	46	61	150	438	825
100	-	-	1	42	54	150	450	900
100	3	3	-	39	56	150	463	950
100	3	-	1	44	59	131	463	1176
100	-	3	1	47	57	137	488	900
100	3	3	1	41	63	143	463	750

*) Dans l'eau de gâchage.

TABLEAU III

Caractéristique des ciments avec additions (d'après GOST 310-76)

Composition du ciment, parties en masse			$S, cm^2/g$	Eau/ciment	Résistance à la flexion/compression, kgf/cm^2			
Clinker	gypce	addition			1j.	3j.	7j.	28j.
94	6	-	3900	0,4	25/122	47/270	59/446	69/539
94	6	aérocyle 10	4300	0,45	23/110	42/247	54/430	63/587
94	6	crent 10	3890	0,4	42/232	61/387	66/526	80/732

DISCUSSION DES RESULTATS. Une amélioration relative de la cristallisation de l'ettringite, y compris l'accroissement de la part de ses agrégats réguliers, surtout de la part des cristaux croissant radialement à partir des grains du ciment, ainsi que l'augmentation du degré d'homogénéité de la structure submicroscopique des hydrosilicates de Ca, plus notable dans les échantillons d'âge avancé, prouvent que les quantités complémentaires de ces phases, qui se forment au stade précoce, servent en réalité de germes cristallins, au moins en ce qui concerne le caractère de leur influence. Puisque les ciments et les minéraux aux additions considérées ne démontrent pas de proportionnalité directe (qui a lieu dans la situation habituelle jusqu'à 24 heures) entre la surface spécifique, le degré d'hydratation et la résistance et, de plus, la durée de la période inductive d'hydratation devient plus courte, on peut tirer la conclusion que la vitesse d'hydratation est limitée, au stade de la période d'induction, par la germination. Par la suite, les germes apparus à ce stade créent des difficultés pour le stade suivant (cinétique) d'hydratation, qui n'influent pas sur la résistance. Par contre, le troisième stade d'hydratation contrôlé par diffusion (après 24 heures de durcissement) est de nouveau accéléré par ces germes.

Pour expliquer ce phénomène, notons que les produits d'hydratation du ciment préparés à l'avance ne sont pas efficaces pour la réduction de la période d'induction à la température normale du milieu. Ceci n'est pas lié à leur surface spécifique insuffisante ou, au contraire, à une mauvaise taille des cristaux, mais à la perte, lors du vieillissement, de la capacité initiatrice, ce qui est dû semble-t-il à la compensation des charges des centres actifs sur leur surface à cause du réarrangement, par vacances et par trous, de la structure qui a lieu sous cette surface et/ou à l'addition des adatomes de l'atmosphère. Dans les germes actifs la compensation des charges a lieu au stade cinétique du processus et une partie des radicaux libres est utilisée pour cela.

C'est pourquoi ces germes ralentissent quelque peu le déroulement du processus justement à ce stade. Mais ce ralentissement influe de façon favorable sur la taille et la distribution dans le volume du système des produits du stade cinétique, abaisse leur hétérogénéité de concentration et les niveaux de contraintes internes, car l'interaction des germes actifs formés et des radicaux libres a lieu d'abord là où ces derniers dominent quantitativement, ce qui a pour résultat leur distribution plus régulière. De plus, autour des sources de radicaux libres (grains du ciment) leur absorption limite les possibilités d'agrégation prématurée des nouvelles formations. Ceci conditionne un déroulement plus libre du stade suivant de diffusion du processus et explique également le fluage élevé de ces structures d'hydratation.

Le gain de résistance des ciments à l'âge de 1 à 3 jours n'est conditionné que par l'optimisation de la microstructure et de plus par l'accroissement du degré d'hydratation et, par conséquent, une quantité moindre de pores.

Les germes actifs introduits par les constituants de cristallisation se distinguent

de ceux formés dans les systèmes ordinaires par la quantité, la distribution et le temps de formation - durant la période d'induction - tandis que normalement les germes apparaissent vers sa fin. On sait que les germes actifs jouent en général un rôle principal dans la cohésion et l'adhésion des systèmes de ciment (9), mais ce qui compte surtout c'est la courte durée du stade de leur activité élevée, passée jusqu'à présent presque inaperçue, sans parler des processus conditionnant la suppression de leur activité. Mais c'est justement ces processus qui sont responsables d'une brusque diminution de l'adhésion des systèmes de ciment aux agrégats et substrats dès l'achèvement de la prise, et de l'absence de cohésion après la dispersion de la matière durcie. Nous pensons également que les résultats positifs obtenus avec le traitement aux ultra-sons ou avec une vibration répétée des systèmes de ciment, proposée par S.V. Chestoperov, peuvent être expliqués par le blocage des processus de suppression de l'activité des germes. La même explication est également possible en ce qui concerne l'influence positive de l'atmosphère sans CO_2, découverte par Y.S. Malinine et son équipe et décrite dans leur communication à ce Congrès.

CONCLUSION. Les résultats exposés partiellement plus haut et les travaux similaires effectués par I.F. Ponomarev, I.A. Kryjanovskaïa, Y.M. Syrkine avec collaborateurs et figurant aussi au Congrès ont servi de fondement scientifique pour commencer la production industrielle à l'une des cimenteries de l'U.R.S.S. du ciment à haute résistance additionné de constituants de cristallisation (crents).

BIBLIOGRAPHIE

1.- И.В.КРАВЧЕНКО (1976) "Быстротвердеющие и высокопрочные цементы", VI Междунар. конгр. по химии цемента, т.Ш, 6 - 20, (en russe).

2.- И.В.КРАВЧЕНКО, М.Т.ВЛАСОВА, Б.Э.ЮДОВИЧ (1971) "Высокопрочные и особо быстротвердеющие портландцементы", М., Стройиздат, 232 с, (en russe).

3.- И.В.КРАВЧЕНКО, Т.В.КУЗНЕЦОВА, М.Т.ВЛАСОВА, Б.Э.ЮДОВИЧ (1979) "Химия и технология специальных цементов", М., Стройиздат, 208 с, (en russe).

4.- Ю.С.МАЛИНИН, У.И.ПАПИАШВИЛИ, Б.Э.ЮДОВИЧ (1977) "О морфологических основах структуры цементного камня", Доклады АН СССР, 233, 4, 653-656, (en russe).

5.- В.М.ЕНТОВ (1976) "О роли структуры материала в механике разрушения", Известия АН СССР, МТТ, n° 3, 110-118, (en russe).

6.- J.F.KNOTT (1973) "Fundamentals of Fracture Mechanics", L., Butterworths, 273p, (en anglais).

7.- J. COOK, J.E.GORDON (1964) "A mechanism for control of crack", Proc. Roy. Soc., A282, 508, (en anglais).

8.- А.Е.ШЕЙКИН, Ю.В.ЧЕХОВСКИЙ, М.И.БРУССЕР (1979) "Структура и свойства цементных бетонов", М., Стройиздат, 344 с, (en russe).

9.- А.Ф.ПОЛАК (1966) Гидратация мономинеральных вяжущих веществ", М., Стройиздат, 208 с, (en russe).

Influence of sulfonated naphtalene on the fluidity of cement pastes

Influence de la naphatline sulfonée sur la fluidité des pâtes de ciment

M. COLLEPARDI, Professor of Materials Technology and Applied Chemistry,
M. CORRADI, Doctor in Industrial Chemistry,
G. BALDINI, Doctor in Industrial Chemistry and
M. PAURI, Doctor in Industrial Chemistry,
Department of Materials Science, University of Ancona, Italy
Research and Development Laboratory, MAC Mediterranea Additivi Cementi, Treviso, Italy.

RESUME : On a examiné, grâce à un test de mini-slump, l'influence de la naphtaline sulfonée (monomère) et de la naphtaline-sulfonée-condensée (polymère) sur les propriétés rhéologiques des pâtes de ciment. L'influence du moment de l'addition de ces produits sur la fluidité des pâtes de ciment a également été étudiée.
Les mesures d'adsorption, de potentiel Zéta, de calorimétrie, de diffraction de rayons X et d'analyse thermique ont été effectuées sur les pâtes de ciment/
En ajoutant une dose inférieure à 0.5 % en poids du ciment de polymère en poudre, on augmente notablement la fluidité de la pâte, alors que l'hydratation du ciment reste pratiquement la même. Des dosages supérieurs en polymère (1 - 1,5 %) augmentent la fluidité de façon négligeable et provoquent un retard de l'hydratation du ciment durant la période d'induction. Par contre, l'addition du monomère ne provoque aucune modification significative de la fluidité ou de l'hydratation.

Le moment de l'addition du polymère influence également la fluidité des pâtes de ciment et la vitesse d'hydratation durant la période d'induction. On a observé d'intéressantes relations entre l'adsorption du polymère, le potentiel Zéta et la fluidité de la pâte de ciment.

SUMMARY :

The influence of sulfonated naphtalene (monomer) and sulfonated naphtalene condensate (polymer) on the rheological properties of cement pastes determined by mini-slump test was examined. The influence of time of addition of these products on the fluidity of the pastes was also studied.

Adsorption, zeta potential, calorimetry, XRD and thermal analysis (DTG) were also carried out on the cement pastes.

With dry polymer additions lower than 0.5 % by weight of cement, fluidity of the paste is remarkably increased, whereas the cement early hydration is substantially the same. Higher dosages of dry polymer (1 - 1.5 %) increase fluidity to a lower extent and cause stronger retardation in the cement hydration during the induction period. Conversely, no substantial change neither in the fluidity nor in the early hydration rate was caused by the addition of the monomer.

The time of addition of the polymer also affects the fluidity of cement pastes, and the cement hydration rate during the induction period, increasing fluidity and retarding the cement hydration. Some interesting relationships between polymer adsorption, zeta potential, and paste fluidity were found.

INTRODUCTION

All the properties of the hardened concrete proportionally improve by reducing the water/cement (w/c) ratio of the fresh mix. However, the w/c ratio cannot be decreased under certain limits because of the reduction in the workability of the fresh concrete. The so-called super-water-reducers or superplasticizers can be used as additives that permit a concrete to have about 25 % of the mixing water removed without reduction in workability or a strong increase in workability (for example : from 20 mm to 220 mm in slump) without a significant change in all the properties of the hardened concrete. Combination of the two effects can also be obtained.

A large number of works has been devoted to study the properties of fresh and hardened concrete containing commercial superplasticizers (1). However, relatively few papers have been published to explain the effect of the superplasticizers on the water-cement system. In particular, few data (2-6) have appeared about the effect of pure chemical products used as superplasticizers on the physical-chemical changes of the cement pastes.

Superplasticizers are substantially based on sulfonated naphtalene-formaldehyde polymers or sulfonated melamine-formaldehyde polymers (7). The purpose of the present paper is to examine the influence of sulfonated naphtalene as a monomer and sulfonated naphtalene formaldehyde condensed polymer on the physical-chemical properties of a cement paste. Moreover the effect of the time of addition of the additives on the same properties were also studied.

EXPERIMENTAL

Materials

Ordinary portland cement was used and Table 1. shows its chemical analysis. Pure sodium salt of naphtalene sulfonic acid (monomer) and sodium sulfonated naphtalene formaldehyde condensate (polymer) both produced as dry powders by MAC Spa were utilized. An aqueous solution of the sulfate-free polymer (wt % solid = 40) shows a viscosity of 40 cp and a specific gravity of 1.224 g/cm^3 at 20°C. Tap water with a specific conductance of 480 mho . cm^{-1} was used.

Table I - Chemical analysis of cement

SiO_2	=	20.80 %
Al_2O_3	=	5.51 %
Fe_2O_3	=	2.99 %
CaO	=	63.60 %
MgO	=	0.85 %
K_2O	=	0.38 %
Na_2O	=	0.19 %
SO_3	=	1.75 %
L. O. I. (950°C, 1h)	=	2.00 %
Blaine surface area	=	3.850 cm^2/g

Cement pastes were prepared at 20°C by mixing for 5 min 50 g of cement and enough water to obtain w/c ratio of 0.3 or 2. In a first series of experiments the monomer or the polymer were added to cement with mixing water. In a second series of experiments the solid additives were added 2.5 min after mixing and then the pastes were mixed again for other 2.5 min. Both polymer and monomer additions are expressed as percent by weight of cement. It must be taken into account that commercial superplasticizers are aqueous solutions generally containing from 20 to 40 % of the dry polymer used in the present work.

Techniques

The following experiments were performed : Minislump tests, polymer adsorption on cement, zeta-potential, isothermal calorimetry, X-ray diffraction analysis (XRD), differential thermal gravimetry (DTG). All the measurements were carried out at 20°C with polymer or monomer addition with mixing water or after 2.5 min the mixing had begun.

In the minislump tests (8) the pastes were prepared only with w/c ratio of 0.3, adding each time a different dosage rate of polymer or monomer, and the pat areas (in cm^2) were measured after five minutes of mixing.

The magnitude of surface adsorption of the monomer or the polymer upon the cement particles was determined by U.V. absorption spectroscopy in the 220-230 mm absorption band due to a sulfonated naphtalene group present in both the polymer and the monomer. Fifty grams of cement and 15 ml (w/c = 0.3) or 100 ml (w/c = 2) of polymer or monomer solution of known concentration were mixed continuously for 5 minutes. In the delayed addition tests the dry polymer or the monomer was added after 2.5 min of mixing with tap water and then the paste was mixed again for other 2.5 min.

The liquid phase was then separated by filtration under vacuum. Each solution was diluted to the optimum concentration and brought to pH 6.5 before spectroscopic measurement. The quantities adsorbed were calculated by differences in concentration of polymer or monomer of the liquid phase before and after adsorption.

The zeta potential measurements were performed using a Laser Zee Meter by Pen Kem Inc. which is based on electrophoretic technique (9) and gives the results directly in millivolt. Zeta potential of colloidal particles is measured by determining the rate at which these particles move in a known electric field.

Zeta potential measurements were performed only with w/c ratio of 2. The samples for the measurements were prepared by mixing continuously 50 g of cement, 100 ml of water and a certain amount of additive for 5 minutes, then separating the liquid phase by vacuum filtration. Small portion of original paste was added to the filtered liquid phase and a suspension (0.5 g of solid/liter) was obtained with the same ionic

strength of the original paste and diluted enough to be observed to the microscope of the Laser Zee Meter.

Heat evolution as a function of time was determined according a method previously described (10) by using an isothermal conduction calorimeter. In the delayed addition tests, the polymer or the monomer was added after 2.5 min by injecting a saturated water solution so that the resulting final w/c ratio was 0.3, and then mechanically vibrating for 2.5 min.

XRD and DTG analysis were also performed on the hydrated cement pastes with a w/c ratio of 0.3.

DISCUSSION OF RESULTS

In fig. 1 the influence of monomer and polymer additions on the flowability of cement pastes measured by the minislump test is shown. No substantial change in the flowability is recorded by adding the monomer both in mixing water and after 2.5 min of mixing, whereas very drastic increase in the minislump is caused by the polymer. However, the influence of the polymer is quite affected by the time of addition.

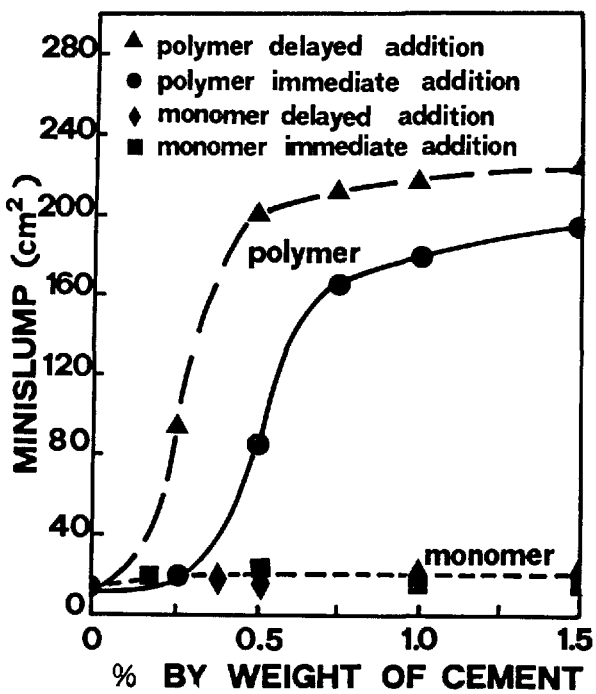

Fig. 1 - Influence of polymer or monomer addition on flowability (minislump) of cement pastes (w/c = 0.3).

A delayed addition of the polymer seems to be more effective particularly in the lower dosage range. For example, 0.25 % of polymer raises the minislump from 15 cm^2 to 95 cm^2, when the admixture is added to the cement paste after 2.5 min after mixing had begun, while a negligible increase (from 15 cm^2 to 20 cm^2) is observed if the same amount of polymer is added with the mixing water. With a delayed addition of 0.5 % of polymer, the minislump rises to 200 cm^2, while no significant further increase is recorded with higher amounts of additive. On the other hand, the minislump arrives at 160 cm^2 if about 0.75% of polymer is added with the mixing water, with only minor changes in flowability for higher percentages of addition.

In Fig. 2 the amount of polymer or monomer adsorption by cement as a function of the percentage of admixture added to cement paste is shown. The polymer is much more adsorbed than the monomer. Moreover, the adsorption of the polymer depends on the w/c ratio of the paste and on the time of addition, whereas these parameters do not substantially affect the adsorption of the monomer.

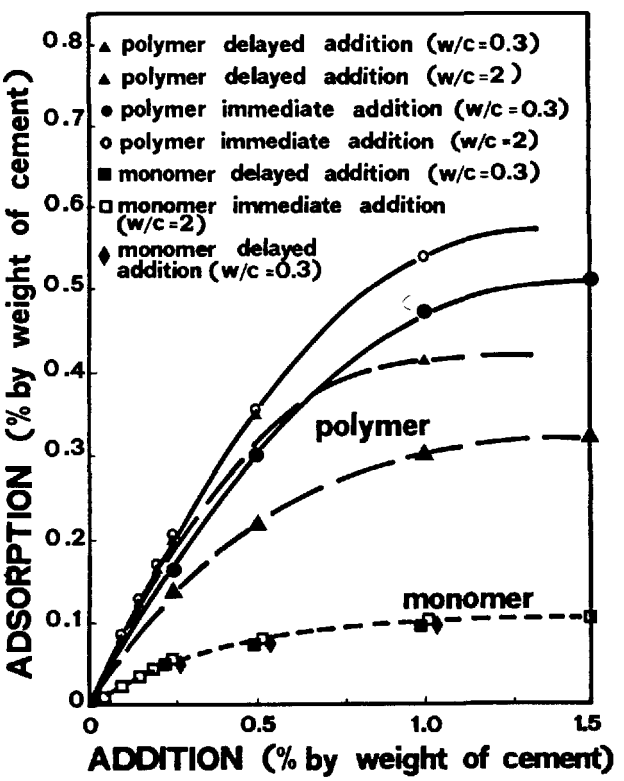

Fig. 2 - Polymer or monomer adsorption on cement as a function of addition.

Polymer adsorption appears to be higher with a higher w/c ratio whereas one would expect the contrary due to the greater polymer concentration in the aqueous phase of the paste with a lower w/c ratio (0.3). Three mechanisms, all related to the larger amount of mixing water, could possibly explain the higher adsorption in the paste with a higher w/c ratio : a) a larger amount of hydrated cement; b) a better dispersion of cement

particles; c) a lower concentration of ions coming from cement phases that could interfere with the polymer adsorption.

Adsorption seems to be greater when the polymer is immediately added with the mixing water. It is possible to think that the polymer adsorbed by cement particles in the early stage of hydration is coated by initial hydration products such as ettringite, and in this way it becomes unaffective in terms of electrical surfaces properties. By this way the nominal adsorption, calculated by difference between the polymer concentration in water before and after mixing with cement, really includes a certain part of polymer incorporated in the hydrated products of cement. Moreover, when the polymer addition is delayed, there is a much higher concentration of ions coming from cement and these could interfere with the polymer adsorption to a greater extent.

Fig. 3 shows the ratio between the concentration of admixture in the liquid phase after and before the

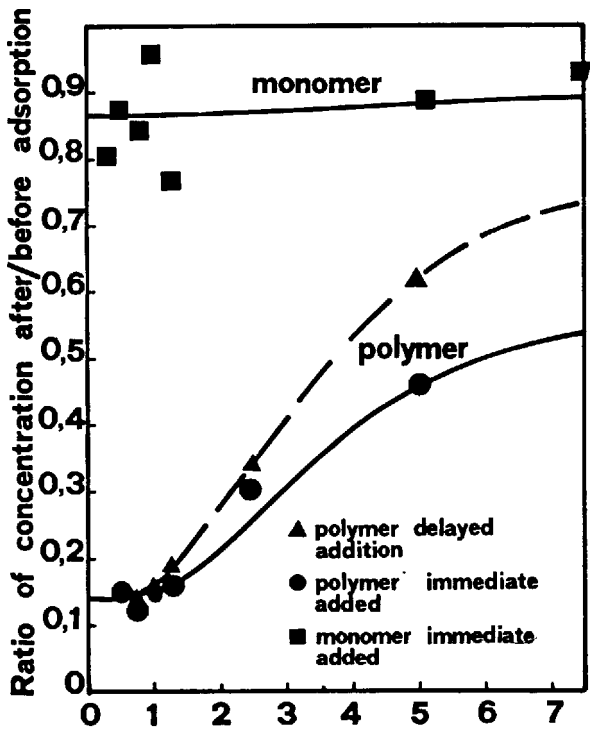

Fig. 3 - Relationship between the admixture concentration in the liquid before and after adsorption (w/c = 2).

adsorption experiments (after/before) as a function of the initial concentration (before) for both polymer and monomer. The after/before concentration ratio is substantially constant for the monomer indicating that about 85 % of the product always remains in the liquid phase. On the other hand, the after/before concentration for the polymer decreases by decreasing the polymer initial concentration in the liquid phase. However this ratio tends to about 0.15 by extrapolating the initial concentration to zero. Daimon and Roy (5) found 0.20 for the extrapoled value of the after/before concentration ratio and concluded that 20 % of their original admixture (sulfonated naphtalene formaldehyde condensate) was to be considered unadsorbable. By assuming that the monomer is the only unadsorbable impurity present in the "polymer", one could conclude that the percentage of monomer is about 23.5 % (= 20/0.85) in the sulfonated naphtalene formaldehyde condensate used by Daimon and Roy and about 17.6 % (=15/0.85) in the polymer of the present work.

In Fig 4. the zeta potential as a function of the polymer or monomer addition is shown. No substantial change in the zeta potential is caused by the monomer independently of the time of addition, whereas a remarkable increase in the zeta potential is recorded in the presence of polymer. So a certain relationship exists between flowability, adsorption on the cement surface and zeta potential. In fact the monomer does not modify flowability of the cement paste (Fig. 1) and at the same time it is adsorbed to a negligible extent on the cement surface (Fig. 2) and causes only insignificant changes in zeta potential (Fig. 4). On the other hand, polymer addition increases flowability

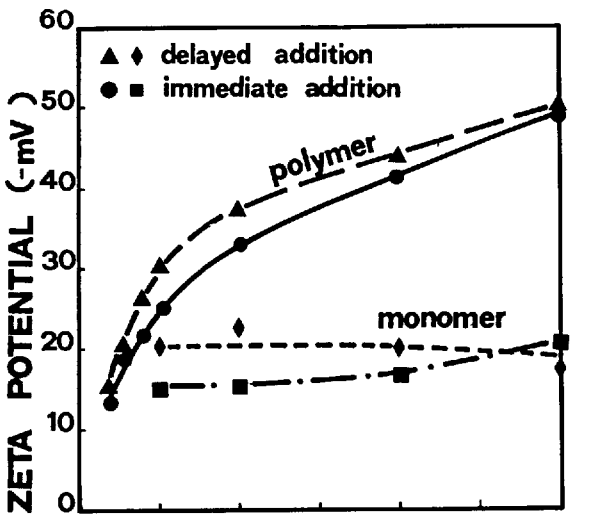

Fig. 4 - Zeta potential as a function of polymer or monomer addition.

(Fig. 1) and zeta potential (Fig. 4) and it is remarkably adsorbed on the cement surface (Fig. 2). This would confirm (6) that the dispersing effect of the superplasticizer is caused mainly by the change in

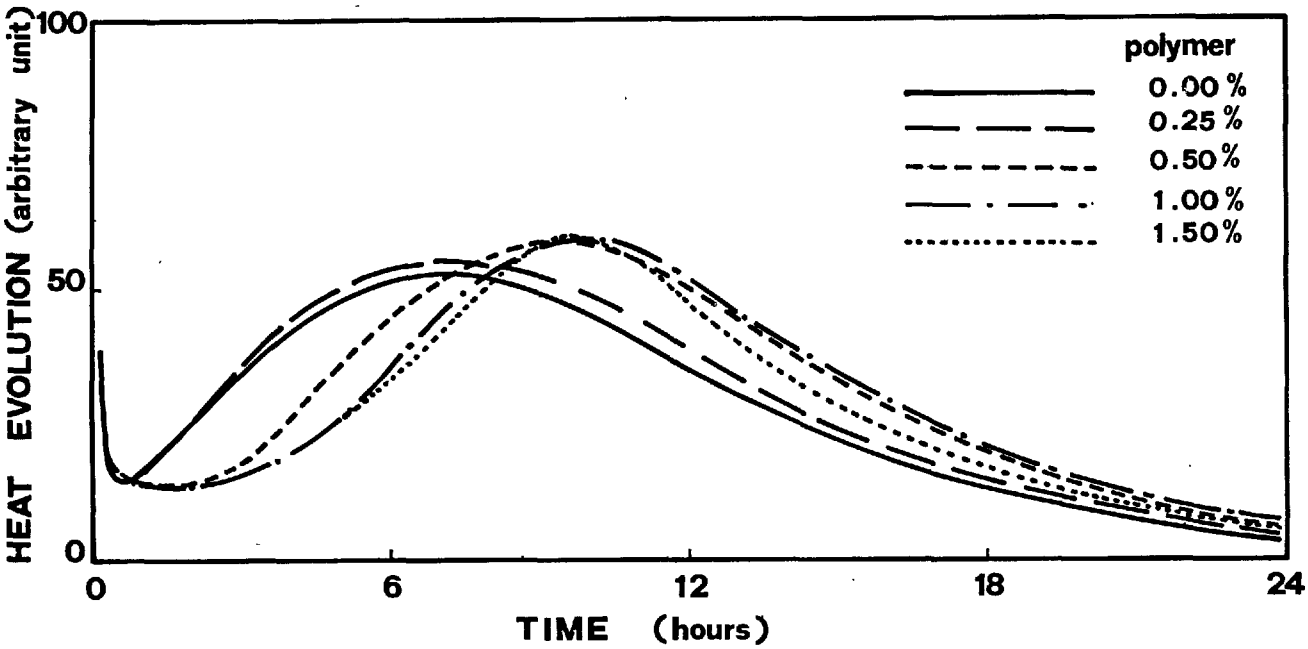

Fig. 5 - Heat evolution rate of cement pastes with different dosage rates of polymer as a function of time.

zeta potential as a function of polymer adsorption on the cement particles. However, some other effect must be taken into account to explain that a delayed polymer addition causes larger increases in flowability and zeta potential, whereas the amount of adsorbed polymer is lower than the one for immediate addition of admixture with mixing water. This would confirm the above mentioned hypothesis that a certain part of the polymer is incorporated within the hydrated product formed during the initial mixing time (2.5 min), so that the effective amount of polymer adsorbed on the hydrated cement surface would be larger in the delayed polymer addition. This seems to be confirmed by the results concerning the polymer addition on the hydration rate, as it is seen further on.

Fig. 5 shows heat evolution rate of the cement in the presence of different amount of polymer added with the mixing water. No substantial change in the heat evolution curve is recorded with a polymer addition of 0.25 %. In the presence of higher amounts of polymer the induction period is proportionally delayed, whereas the hydration rate in the acceleratory period is not substantially changed, so that the time of the heat evolution peak is increased by some hour. With a delayed polymer addition the retarding effect is slightly increased particularly when larger amounts of polymer (0.5 - 1.5 %) are used.

In Fig. 6 the X-ray line at 2.18 Å ($C_3S + C_2S$) is reported as a function of the time for immediate polymer addition. Free calcium hydroxide analysis by DTG confirms that higher dosages of additive (0.5 - 1.5 %) and particularly delayed addition cause a more remarkable retardation in the C_3S and C_2S hydration.

Isothermal calorimetry, XRD and DTG show that the monomer (0.25 - 1.5 % by weight of cement) does not change the hydration rate independently of the time of addition.

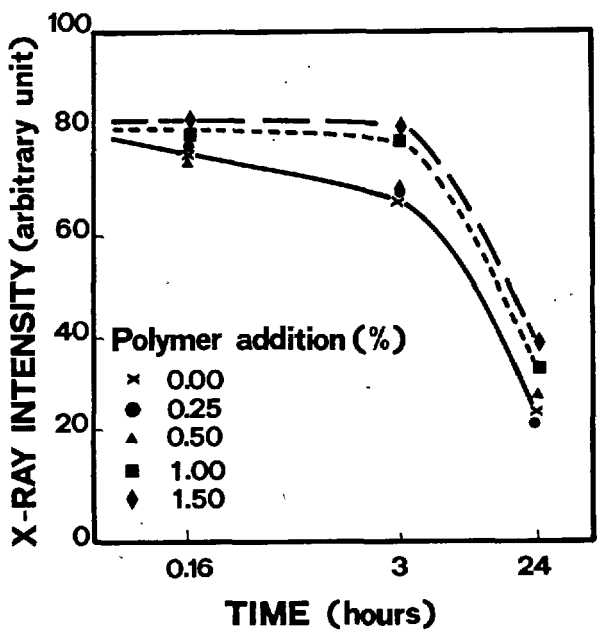

Fig. 6 - X-Ray intensity of cement pastes with immediate addition of different dosage rates of polymer as a function of time.

According Kondo (2) type I anionic surfactants having an hydrophilic group (-SO_3Na) at the end of the molecule, when present more than a critical amount, are closely adsorbed on cement particle (Fig. 7a). On the other hand, for type II anionic surfactants, having hydrophilic groups in the molecule, a "flat" adsorption occurs instead of "close" adsorption (Fig. 7b). Kondo found that the hydration of cement was strongly retarded when more type I surfactants were added than a critical amount, while in the case of type II the retarding effect became gradually larger with increasing amount of surfactants. Kondo found that the sulfonated naphtalene monomer is a type I anionic surfactant and its critical amount is about 0.3 - 0.4 % by weight of cement, whereas the sulfonated naphtalene-formaldehyde condensed polymer is a type II anionic

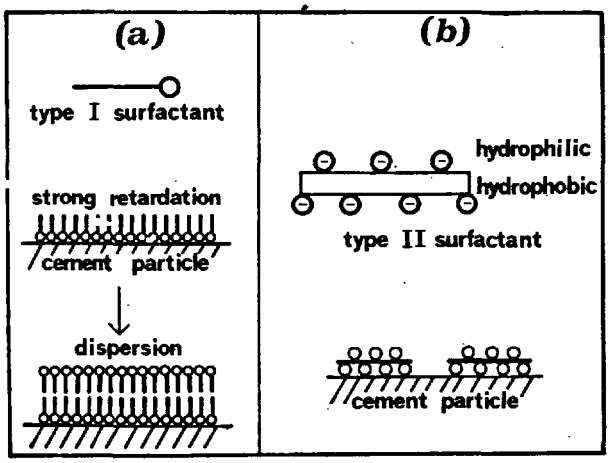

Fig. 7 - Schematic illustration of "close" (a) and "flat" adsorption (b) of anionic surfactants on cement (2).

surfactant. The results of the present paper do not confirm the data of Kondo concerning the behaviour of the monomer, since the cement hydration rate was not changed by monomer addition of 0.25 - 1.50 %. On the other hand no significant adsorption (Fig. 2) or change in the zeta potential (Fig. 4) were recorded. However the authors of the present paper found that the flat polymer adsorption suggested by Kondo is at moment the most convincing mechanism to explain the influence of the polymer on the flowability of fresh mixes.

CONCLUSIONS

It seems that there is a certain relationship between the dispersing effect of the admixture and the retarding effect on the cement hydration. Monomer addition neither affects the cement hydration rate nor influences the flowability of the cement paste, while the product is adsorbed on the cement surface to a negligible extent and the zeta potential does not significantly change. On the other hand, polymer addition increases the flowability of the cement paste and retards the cement hydration rate. It is significantly adsorbed on the cement surface and does change the zeta potential. The effect of the polymer increases by increasing the dosage rate and delaying the addition time. With a dry polymer addition of 0.25 - 0.50% by weight of cement corresponding to that of liquid commercial superplasticizer the dispersing effect is good enough without any significant retarding effect in the hydration rate. With higher dosage rate (1 - 1.5 % of dry polymer by weight of cement), corresponding to three-four times the normal dosage of a liquid commercial superplasticizer, the retarding effect is significantly increased whereas the flowability is not substantially improved.

The results of the present paper would suggest that a certain number of sulfonic groups all linked to a naphtalenic-methylenic polymer chain is essential to a flat adsorption (2) and then to an increased dispersing effect.

REFERENCES

(1) Proceedings of an International Symposium "Superplasticizers in Concrete" held in Ottawa, Canada, 29-31 May 1978.

(2) R. KONDO (1976) "Cement and Cement Hydrate with Organic Reactions", Report to the Ministry of Education, n°3, 35-48.

(3) M. COLLEPARDI and M. CORRADI (1979), "High Strength and Reliable Concretes", Silicates Industriels, Vol. 44, n°1, 13-22.

(4) K. HATTORI (1978), "Experiences with Mighty Superplasticizer in Japan" in ref.1, Vol.I, 49-86.

(5) M. DAIMON and D.M. ROY (1978) "Rheological Properties of Cement Mixes : I Methods, Preliminary Experiments, and Adsorption Studies", Cem. Concr. Res. 8, 753-764.

(6) M. DAIMON and D.M. ROY (1979) "Rheological Properties of Cement Mixes : II Zeta Potential and Preliminary Viscosity Studies", Cem. Concr. Res. 8, 103-110.

(7) Joint Working Party, Cement Admixtures Assn. & Concr. Assn., Superplasticizers in Concrete, Cem. Concr. Assn., Wexham Springs, UK 1976.

(8) W.F. PERENCHO, D.A. WHITING and D.L. KANTRO (1978) "Water Reduction Slump Loss and Entrained Air Void Systems as Influenced by Superplasticizers", in ref. 1, Vol.1, 295-324.

(9) T.M. RIDDICK (1968), "Control of Colloid Stability through Zeta Potential", pp.372, Zeta Meter Inc., New York.

(10) M. COLLEPARDI, M. CORRADI, G. BALDINI and M.PAURI (1978) "Tricalcium Aluminate Hydration in the Presence of Lime, Gypsum or Sodium Sulfate", Cem. Concr. Res. 8, 571-580.

Influence of Microstructure on the Creep and Drying Shrinkage of Calcium Silicate Pastes

Influence de la microstructure sur le fluage et le retrait au séchage des pâtes de silicate de calcium

Arnon BENTUR, Senior Lecturer, Department of Civil Engineering, Technion, Haifa, Israel,
Joseph H. KUNG, Fellow, Division of Building Research, National Research Council, Ottawa, Canada,
Richard L. BERGER, Professor of Civil Engineering and Ceramics Engineering, University of Illinois, Urbana, Illinois,
J. Francis YOUNG, Professor of Civil Engineering and Ceramics Engineering, University of Illinois, Urbana, Illinois,
N.B. MILESTONE, Principal Scientist, Chemistry Division, D.S.I.R. Petone, New Zealand,
Sidney MINDESS, Associate Professor of Civil Engineering, University of British Columbia, Vancouver, Canada,
F.V. LAWRENCE, Professor of Civil Engineering and Metallurgy, University of Illinois, Urbana, Illinois, U.S.A.

RESUME : Des mesures du retrait des pâtes de C_3S, de β-C_2S et de ciments portland ont été faites et analysées en fonction de deux composantes de la porosité:

l'eau contenue dans les capillaires (CD) et celle retenue par les gels de C.S.H. (GD)

Ces deux composants ont été déduits des pertes de poids au séchage.

Le premier composant (CD) est en corrélation avec la macro-porosité (diamètre des pores compris entre 25 et 300 A); le second (GD) avec la microporosité (diamètre des pores < 25 A). Le retrait total est en corrélation avec la somme de ces deux porosités, bien mieux qu'avec le volume total des pores. Une meilleure corrélation a été observée entre le retrait total et un certain facteur structural Z , calculé à partir de la distribution des pores, caractérisée par la surface spécifique mesurée par l'adsorption d'azote, et celle mesurée par adsorption de vapeur d'eau et par le degré de polymérisation des silicates. Le fluage dépend aussi de la microstructure, mais plus spécialement du degré de polymérisation des silicates.

ABSTRACT: Shrinkage data for C_3S, β-C_2S and ordinary portland cement pastes are analyzed in terms of contribution from the "pore components" (capillary drying.["CD"] shrinkage) and the "C-S-H component" (gel drying. ["GD"] shrinkage). These two contributions are determined from shrinkage-weight loss curves obtained during drying. CD shrinkage correlated reasonably well with total mesoporosity (pores $\geq$ 25-300 Å diameter) and GD shrinkage with mesoporosity (pores < 25 Å diameter) as determined by mercury porosimetry. Thus, total shrinkage shows a correlation with the sum of the volumes of mesopores and micropores, rather than with the total pore volume. A better correlation with total shrinkage is obtained using a structure factor (Z), which is calculated from the pore size distribution using nitrogen adsorption, surface area from water vapor adsorption, and the degree of silicate polymerization. It is thought that problems in determining the degree of silicate polymerization in substituted C-S-H may affect the value of Z for portland cement pastes. Creep also depends on microstructural factors, particularly the degree of silicate polymerization.

INTRODUCTION

The drying shrinkage and creep of cement paste and concretes have been the subject of numerous investigations which have resulted in many conflicting models. Creep and shrinkage are often regarded either as the result of a single mechanism, or the result of several mechanisms which each control deformations in a limited relative humidity range. However, it has recently been pointed out (1,2) that time dependent deformations may be the result of the superposition of several mechanisms, effective over the same relative humidity range. This may in part be the reason for the conflicting results and theories which can be found in the literature.

In previous work (2-6) the microstructural and chemical changes occurring during creep and shrinkage of calcium silicate pastes were studied. It was concluded that shrinkage is the result of two types of mechanisms:

Mechanism CD (Capillary drying) - Capillary effects which take place in the "pore component," which represents the pores larger than 25 Å diameter. Signifcant capillary stresses can only develop in the mesopores (25-300 Å) and therefore this pore fraction is mainly responsible for the CD mechanism.

Mechanism GD (Gel drying) - Loss of water from the "C-S-H component," which includes the pores smaller than 25 Å diameter (micropores). In these pores, no capillary effects can take place.

A detailed discussion of these mechanisms is given elsewhere (2) and is only briefly reviewed here. Mechanism CD is considered more influential, but not dominant, in low degree of hydration (α) pastes. Capillary stresses cause an irreversible collapse of pores in the diameter range of 40 to 100 Å which is accompanied by a reduction in the nitrogen surface area [$S(N_2)$]. The GD mechanism has a contribution at all degrees of hydration, but becomes more important at high degrees of hydration. The reduction in spaces between the C-S-H surfaces is accompanied by an increase in the formation of Si-O bonds which can be detected by silicate structure analysis. Condensation of the C-S-H structure also leads to irreversible shrinkage.

This interpretation suggests that shrinkage strains and shrinkage-weight loss curves should be sensitive to the microstructure and chemical composition of the hydrated pastes. The driving force for CD shrinkage is expected to be related to the volume and size distribution of the mesopores while the driving force for GD shrinkage is related to the volume and size distribution of the micropores. The internal stresses induced by movement of water out of these pores will result in shrinkage. The magnitude of this shrinkage will depend not only on these stresses, but also on the rigidity of the paste structure which resists them. For example, the presence of stable crystalline phases like CH and a more stable silicate skeleton of the C-S-H (as exhibited by higher degree of silicate polymerization) are expected to result in reduced shrinkage.

Such aspects of shrinkage can be clarified if changes in time dependent deformations are studied in parallel with changes in microstructure and chemical composition of hydrated pastes. This paper describes the results of such an investigation, in which pastes of C_3S, β-C_2S, and ordinary portland cement (OPC) cured at 4°, 25°, and 65°C were studied. Correlations between total shrinkage, CD and GD shrinkage and various structural parameters such as pore size distribution, surface area and degree of

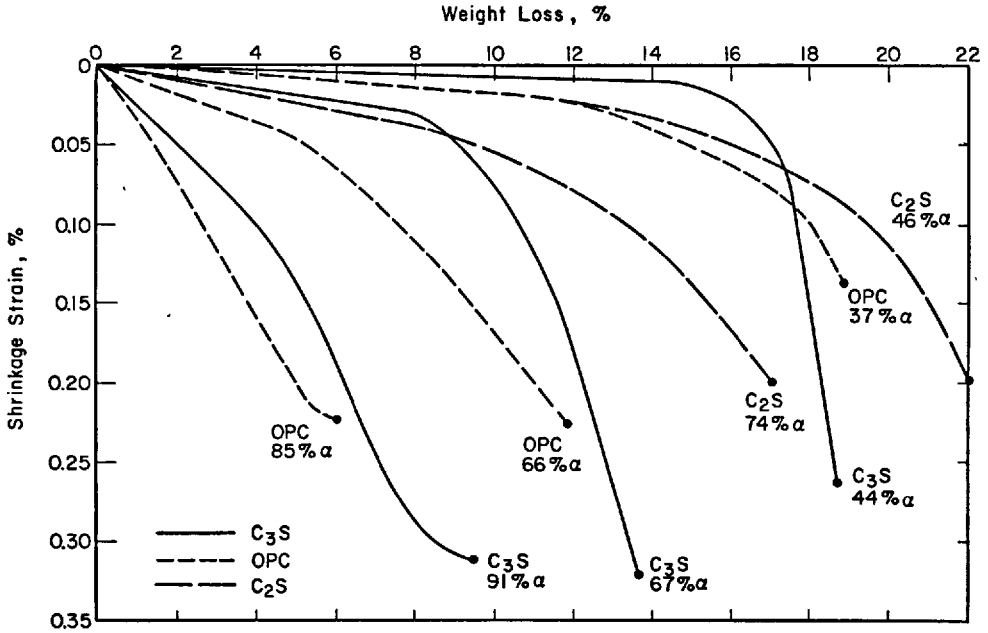

Fig. 1. Shrinkage-weight loss curves determined during drying of pastes of C_3S, β-C_2S and ordinary portland cement (% α indicates degree of hydration).

silicate polymerization were established. A brief discussion of microstructural influence on creep is also given.

EXPERIMENTAL

The C_3S and β-C_2S used in this study are described elsewhere (3); a commercial Type I cement was also used. Details of specimen preparation and testing are to be found in previous papers (2,4,6).

RESULTS AND DISCUSSION

Porosity-Shrinkage Relationships

Some typical shrinkage-weight loss curves are shown in Figs. 1 and 2.

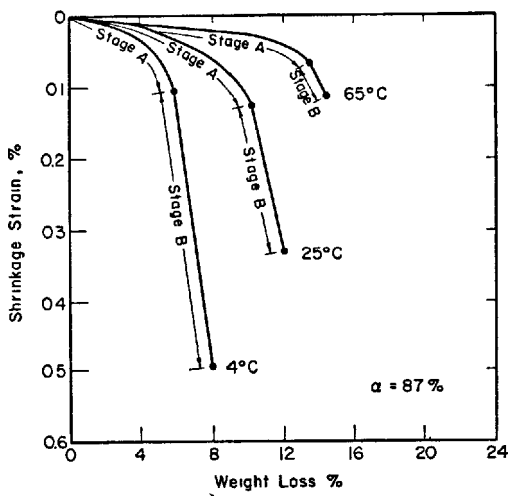

Fig. 2. Effect of curing temperature on the shrinkage-weight loss curves of C3S pastes.

It can be seen that the shape of the curves is very sensitive to the chemical composition of the hydrating compound (Fig. 1) and to the curing temperature (Fig. 2). An increase in curing temperature is associated with a reduction in the shrinkage values and slopes of the shrinkage-weight loss curves (Fig. 2).

In Fig. 3 typical mercury intrusion porosimetry (MIP) curves for well hydrated C_3S pastes cured at 25°C and 65°C, and OPC and β-C_2S pastes cured at 25°C are presented. It can be seen that these pastes have different pore structures and these differences may be correlated with the changes in the shrinkage characteristics of these pastes. For example, the coarser pore structure in β-C_2S pastes is associated with the higher weight loss for these pastes (Fig. 1) and is consistent with SEM observations (7). On the other hand OPC pastes have less pore volume below 250 Å than C_3S pastes and this may account for its lower shrinkage values. A similar qualitative explanation can be given in the case of C_3S cured at 25°C and 65°C; the high temperature pastes have much less porosity in the range of diameters lower than 250 Å which can explain their smaller shrinkage values.

It was suggested in the introduction that CD shrinkage is related to the volume and structure of the mesopores and that GD shrinkage is related to the volume of the micropores. The information contained in shrinkage-weight loss curves and pore size distribution curves may be used to test the validity of the statement by determining whether such correlations can be found. The mesopore volume was determined from the MIP curves and the micropore volume from the difference between total porosity and the MIP cumulative pore volume, down to pores of 25 Å diameter. In order to analyze the shrinkage curves in terms of the two mechanisms, the observed shrinkage strains must be separated into the contributions of mechanism CD and mechanism GD. This was previously done (2) by dividing shrinkage-weight loss curve into two stages, A and B, as shown in Fig. 2. Stage A is believed to represent the CD shrinkage, while stage B is attributed to the GD shrinkage; the significance and limitation of this simplified approach have been discussed in detail (2).

In Fig. 4, the CD and GD shrinkage values as determined from the shrinkage weight-loss curves are plotted against mesoporosity and microporosity. In both cases, shrinkage increases with porosity, as would be expected. It should be pointed out that the data include systems which are different in many aspects - chemical composition, curing conditions and α - and yet, they all seem to fit a reasonable linear relationship. Combining the two curves will yield a relation between total shrinkage and the volume of pores smaller than 300 Å (Fig. 5b). It is interesting to compare this plot with that of shrinkage versus total porosity where no distinct correlation can be observed (Fig. 5a).

Shrinkage-Microstructure Relationships

The data presented in Figs. 4 and 5 indicate that differences in shrinkage behavior can be accounted for by differences in pore structure. However, it should be noted that there is still considerable scatter in the data which suggests that, although pore structure parameters have considerable influence on shrinkage, other parameters must be taken into account. For example, the size distribution of the micropores and mesopores and the degree of silicate polymerization of the C-S-H component are thought to be important. In view of the complexity of the cement paste structure and the uncertainty with regards to its detailed chemical composition and microstructure, it is extremely difficult to develop a quantitative model taking all these factors into account. However, in a separate set of experiments (6) an attempt was made to define some of these parameters and derive an empirical relation which would correlate with shrinkage better than the simple relations discussed above. Three parameters are considered in this analysis.

(1) The pore volume and pore size distribution of the mesopores are considered. The cumulative pore volume was best expressed using a weighted function which considers the relative importance of the pores in the size distribution with regard to their induced stress that will be generated during drying:

$$V^* = \Sigma V_i(D_i) \cdot F(D_i) \qquad (1)$$

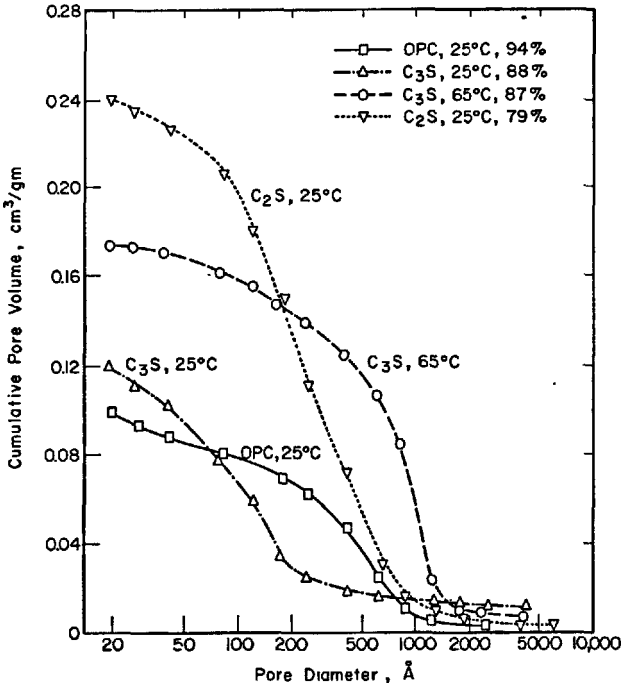

Fig. 3. Mercury porosimetry curves of pastes of C_3S, β-C_2S and ordinary portland cement

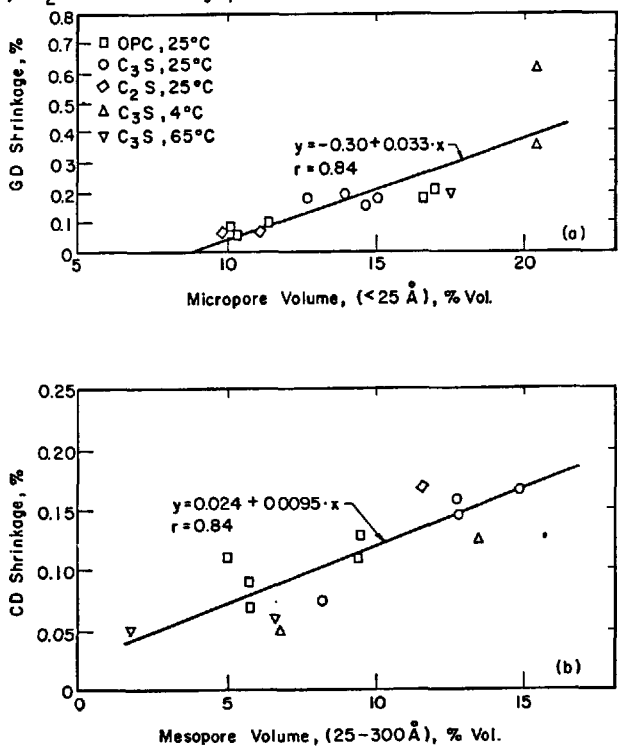

Fig. 4. (a) GD shrinkage vs. microporosity of hardened pastes. (b) CD shrinkage vs. mesoporosity of hardened pastes. (Best-fit straight line shown in each case.)

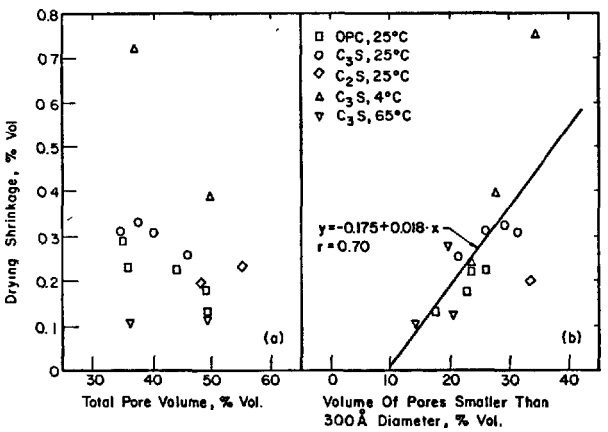

Fig. 5. (a) Total drying shrinkage vs. total pore volume. and microporosity. (Best-fit straight line shown.) (b) Total drying shrinkage vs. total mesoporosity.

where: V* is the effective cumulative pore volume; V_i is the pore volume at the corresponding pore diameter D; $F(D_i)$ is the weighted function, which was taken as $300/D_i$; 300 Å being taken as the upper size limit of the mesopores. A better fit of the experimental data was obtained if V* is calculated using N_2 adsorption data rather than MIP data.

(2) Water measured surface area, $S(H_2O)$ was chosen as a parameter representing the effect of microporosity.

(3) The nonvolatile content (N) was used as an estimate for the degree of silicate polymerization of the C-S-H (4) and it represents its stableness and ability to resist the shrinkage stresses.

On the basis of an empirical approach it was found that a good linear relationship (correlation factor of 0.97) could be obtained (Fig. 6) between shrinkage and an effective structure factor (Z) as defined in Eq. 2.

$$Z = \frac{V^* \cdot S(H_2O)}{N} \qquad (2)$$

This empirical relationship indicates that if various physical and chemical parameters are considered at the same time it is possible to account for differences in shrinkage in a wide variety of microstructures. For example a high degree of silicate polymerization [C_3S cured at 65°C (5)] is associated with a reduction in shrinkage, while an increase in mesoporosity [C_3S + $CaCl_2$ (5,8)] or $S(H_2O)$ tends to enhance shrinkage. Z depends only on the properties of the C-S-H component and the pore component. Thus, as a first estimate it can be assumed that the "CH component", or the residual unhydrated material has little ability to resist shrinkage stresses.

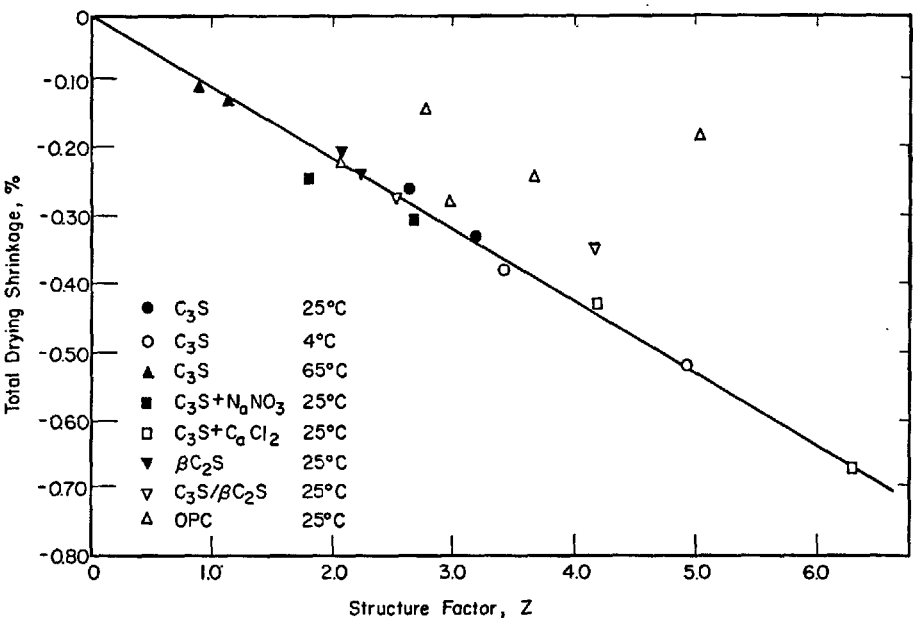

Fig. 6. Total drying shrinkage of C_3S and β-C_2S pastes vs. the effective structure factor, Ż (Best fit straight line shown.)

It should be noted that the quantities used to calculate Z are determined on reference pastes. Since it has been observed (4) that changes in pore distribution and silicate polymerization occur during shrinkage experiments, Z will change with the history of the paste. A reduction in V* and an increase in N are observed on drying, resulting in a lower Z and hence lower shrinkage on second drying. Such behavior is well documented in the literature (9,10).

It should also be noted that three of the points calculated for OPC show considerable deviation from the best-fit line (which was determined from data for pastes of the calcium silicate pastes only). As can be seen in Table 1, OPC pastes have much lower values of N than C_3S pastes of comparable degrees of hydration. It is likely that in the case of OPC the N values may not provide a good assessment of silicate polymerization, because it is well known that C-S-H can undergo isomorphous replacement of Si^{4+} by Al^{3+} or S^{6+}, and that a substituted C-S-H will be formed in OPC pastes. Lentz (11) has shown that Al-O-Si bonds are readily cleaved by TMS derivatization and that the silicate network in aluminosilicates is disrupted where aluminum is substituted. For example, sodalite derivatizes as an orthosilicate and natrolite as a linear trisilicate, which correspond to the arrangements of silica tetrahedra as determined by x-ray diffraction. Also, Rio (12) observed that C-S-H formed from C_3S in the presence of gypsum had a lower degree of silicate polymerization than C-S-H formed in the absence of sulfate ions. It is noteworthy that whereas monomeric silicate (SiO_4^{4-}) in hydrated C_3S pastes can be wholly attributable to unhydrated C_3S (13,14) considerable SiO_4^{4-} is observed in OPC pastes that are completely hydrated (15-17).

TABLE I

Comparison of Polysilicate Contents (N) of C_3S and OPC Pastes Hydrated at 25°C (values of α given in parentheses).

Nominal α	C_3S	OPC
40%	14*(42)	4 (37)
50%	24 (55)	4 (48)
60%	-	6 (60)
70%	20 (68)	-
80%	22 (78)	9 (80)
85%	23 (88)	12 (85)

*Wt percent of total silicate in hydrated fraction.

Creep-Microstructure Relationships

The influence of microstructure on creep strains has not been studied in the same detail as shrinkage. Initial results indicate (1) that creep and shrinkage arise from different structural changes and that the two processes are fundamentally different. For example, the pore component does not influence basic creep, which is to be expected since moisture loss does not occur. However, as in the case of shrinkage, the degree of silicate polymerization is an important parameter in determining creep behavior. Both creep and shrinkage are reduced when the C-S-H component has a higher polysilicate (N) content; (determined at 96% rh) as has been observed also by Parrott (18-20).

An interesting observation in the present studies was the increase in $S(N_2)$ (Table 2) that was observed in several different systems, e.g., C_3S, C_2S and OPC, but occurs only in well-hydrated systems.

TABLE II

N_2 Surface Area of Well-Hydrated C_3S and OPC Pastes Treated for Basic Creep and Shrinkage.

	C_3S*	OPC#
Control	18.1	13.6
Shrinkage	16.3	13.3
Basic Creep	32.5	39.1

*Hydrated for 90 days. #Hydrated for 150 days

What is the cause of this increase cannot be determined with certainty but it has been suggested (1) that it is the result of an internal dilation in the C-S-H component. This dilation will oppose the bulk creep strain and hence reduce its value. It appears that internal dilation can only occur in a stable C-S-H component with a high polysilicate content; in the less stable C-S-H component of young pastes, internal dilation is reduced or may even become negative due to the large differential movement that can take place between C-S-H particles and which contribute to the measured creep of the bulk specimen. The precise response of the C-S-H component to stress influences the extent to which further polymerization can occur on subsequent, or concomitant, drying.

ACKNOWLEDGMENTS

This work was supported by National Science Foundation Grant ENG-75-00422. We thank Prof. S. Diamond for helpful discussion and for the use of the mercury porosimeter.

REFERENCES

1. A. Bentur, R. L. Berger, F. V. Lawrence, N. B. Milestone, S. Mindess, and J. F. Young, 1979. "Creep and Drying Shrinkage of Calcium Silicate Pastes III. Hypothesis of Irreversible Creep and Drying Shrinkage," Cement and Concrete Research, 9(1) 83-95.

2. J. F. Young, R. L. Berger and A. Bentur, 1978. "Shrinkage of Tricalcium Silicate Pastes: Superposition of Several Mechanisms," Il Cemento, 3, 391-397.

3. S. Mindess, F. V. Lawrence and J. F. Young, 1978. "Creep and Drying Shrinkage of Calcium Silicate Pastes I. Pretreatment and Mechanical Properties," Cement and Concrete Research, 8(6), 591-600.

4. A. Bentur, N. B. Milestone and J. F. Young, 1978. "Creep and Drying Shrinkage of Calcium Silicate Pastes II. Induced Microstructural and Chemical Changes," Cement and Concrete Research, 8(6) 721-732.

5. A. Bentur, N. B. Milestone, J. F. Young and S. Mindess, 1979. "Creep and Drying Shrinkage of Calcium Silicates Pastes IV. Effect of Accelerated Curing," Cement and Concrete Research, 9(2), 161-170.

6. J. H. Kung, 1978. "Shrinkage of Calcium Silicate Pastes," Ph.D. Thesis, University of Illinois.

7. J. F. Young and H. S. Tong, 1977. "Microstructure and Strength Dev elopment of Beta-Dicalcium Silicate Pastes With and Without Admixtures," Cement and Concrete Research, 7(6), 627-636.

8. R. L. Berger, J. H. Kung and J. F. Young, 1976. "Influence of Calcium Chloride on the Drying Shrinkage of Alite Pastes," J. Test. Evaln., 4(1), 85-93.

9. R. A. Helmuth and D. H. Turk, 1967. "The Reversible and Irreversible Drying Shrinkage of Hardened Portland Cement and Tricalcium Silicate Pastes," J. PCA Res. Dev. Labs., 9(2), 8-21.

10. R. F. Feldman and E. G. Swenson, 1975. "Volume Change on First Drying of Hydrated Portland Cement With and Without Admixtures," Cement and Concrete Research, 5(1) 25-36.

11. C. W. Lentz, 1964. "Silicate Minerals as Sources of Trimethylsilyl Silicates and Silicate Structure Analysis of Calcium Silicate Solutions," Inorganic Chemistry, 3, 574-579.

12. A. Rio, 1974. "Approaching a Macromolecular Characterization of the C_3S Hydration Process," Supplementary Paper #67, Proceedings, Sixth International Symposium on the Chemistry of Cement, Moscow.

13. L. S. Dent Glasser, E. E. Lachowski, K. Mohen, and H. F. W. Taylor, 1978. "A Multi-Method Study of C_3S Hydration," Cement and Concrete Research 8(6) 733-740.

14. A. Bentur, N. B. Milestone and J. F. Young, unpublished observations.

15. C. W. Lentz, 1966. "The Silicate Structure Analysis of Hydrated Portland Cement Paste," in Symposium on the Structure of Hardened Cement Paste and Concrete, Highway Research Board Special Report 90, 269-283.

16. E. E. Lachowski, 1979. "Trimethylisilylation as a Tool for the Study of Cement Pastes (2) Quantitative Analysis of the Silicate Fraction of Portland Cement Pastes," Cement and Concrete Research, 9(3), 337-342.

17. A. K. Sarkar and D. M. Roy, 1979. "A New Characterization Technique for Trimethylsilylated Products of Old Cement Pastes," Cement and Concrete Research, 9(3), 343-352.

18. L. J. Parrott, 1976. "Effect of a Heat Cycle During Moist Curing When the Deformation of Hardened Cement Paste," in Hydraulic Cement Pastes: Structure and Properties, 189-204 (Cement Concr. Assoc., Wexham Springs, Slough, UK)

19. L. J. Parrott, 1977. "Recoverable and Irrecoverable Deformation of Heat-Cured Cement Paste," Mag. Concr. Res., 29(98) 26-30.

20. L. J. Parrott, 1977. "Basic Creep, Drying Creep and Shrinkage of a Mature Cement Paste After a Heat Cycle," Cement and Concrete Research 7(5) 597-604.

Rhéologie et hydratation du ciment sous l'influence des facteurs extérieurs

Rheology and hydration of cement at outer influence

I.B. ZACEDATELEV, Docteur ès Sciences, chef de laboratoire, Teploproekte,
B.D. TRINKER, candidat ès sciences, chef de laboratoire, Teploproekte, et
Yu.S. TCHERKINSKY, docteur ès sciences, chef de laboratoire NIL PCMMTP, Moscou, U.R.S.S.

RESUME : Les processus réels d'hydratation du ciment et de formation de la structure de la pierre de ciment se caractérisent par leur dépendance des facteurs extérieurs, ces processus pouvant suivre leur cours dans des conditions non-stationnaires de température, déshydratation partielle et humidification répétées du système durcissant.

On a étudié, pour la première fois, la viscosité des suspensions de ciment à l'aide de la rhéocinétique. La construction des courbes rhéocinétiques pour les températures 293-353°K et la détermination des constantes de vitesse ont permis d'obtenir des équations d'Arrhénius. Ces équations permettent de caractériser la nature du processus de changement de viscosité selon l'énergie d'activation, ainsi que l'intensité de l'effet thermique sur ce processus.

Les propriétés rhéologiques de la pâte de ciment durcissante du début de la prise jusqu'à la fin de la prise ont été déterminées à l'aide d'un plastomètre selon la valeur de contrainte limite de cisaillement. Il est montré que l'emploi du plastomètre conique permet d'évaluer les temps de prise bien fondés physiquement, contrairement à ce qu'on obtient à l'aide de l'aiguille de Vicat. A l'aide des courbes plastométriques on peut juger du processus de formation de structure, y compris des phénomènes anormaux, tels que la fausse prise.

L'utilisation d'une famille de plastogrammes obtenues expérimentalement dans des conditions isothermes permet de construire des courbes plastométriques pour des régimes thermiques non-stationnaires.

On a proposé, en vue de prédire les caractéristiques cinétiques du processus d'hydratation du ciment sous l'influence des facteurs extérieurs, une méthode de recherche et une construction de dispositif pour déterminer la cinétique de dégagement calorifique dans des conditions d'échange extérieur de chaleur et de masse.

SUMMARY: Distinctive feature of real processes of cement hydration and cement stone structure formation is dependence of these factors on outer influence. At this time cement hydration and structure formation process may proceed at conditions of nostationary temperature regime, partial dewatering and repeated moistening of setting system. Rheokinetic method was used for the first time at investigation of viscosity of cement suspensions. Plotting of rheokinetic curves at temperature 293-353°K and determination of velocity constants permitted to obtain equations for description of rheokinetic processes including Arrhenius' equations. Such equations give possibility to characterize nature of process of change of viscosity depending on value, of activation power and also intensity of thermal influence on this process.

Rheological properties of hardening paste up to complete setting are determined by plastometric method depending on value of limit shear stress. It is showed that usage of conical plastometer for determination of setting time permits to obtain physically well-founded values as distinct from applied test method by Vicat device. Plastometric curves permit to evaluate course of structure formation process including anomalous phenomens such as false setting.

Usage of system of plastograms obtained experimentally for isothermal conditions permits to plot by graphic method the plastometrical curves for nonstationary temperature regimes.

Method and construction of device for determination of kinetics of heat liberation at conditions of outer heat and mass change is suggested for prediction of kinetic characteristics of cement hydration process at conditions of outer influence.

Selon le principe de la méthode rhéocinétique (1), si le système est soumis aux processus chimiques ou physico-chimiques, on peut, pour la description de la cinétique de ces processus, employer les équations cinétiques de dépendance de la viscosité spécifique ($\eta_{уд}$) du temps (τ). Dans le plus simple cas on peut comparer l'équation de viscosité d'Einstein avec l'équation formelle de la cinétique chimique et obtenir l'équation rhéocinétique, par exemple, de premier ordre, sous forme différentielle:

$$\frac{d\eta_{уд}}{d\tau} = k\eta_{уд} \qquad (1)$$

où K est la constante de vitesse d'accroissement de viscosité.

Par construction, d'après les données expérimentelles, des équations cinétiques $\eta_{уд} = f(\tau)$ en coordonnées normales ($\eta_{уд}$-τ), semi-logarithmiques ($\lg\eta_{уд}$-τ) où fractionnaires ($\frac{1}{\eta_{уд}}$ - τ), il est possible de déterminer l'ordre du processus (nul, premier ou second, respectivement) et de calculer la rhéocinétique de vitesse d'accroissement de viscosité. La détermination des valeurs des constantes rhéocinétiques (K_T) pour températures différentes permet d'employer l'équation d'Arrhénius pour le processus rhéocinétique sous forme

$$K_T = A_0 \exp(E_R/RT) \qquad (2)$$

où A_0 est le facteur pré-exponentiel, E_R est l'énergie d'activation du processus rhéocinétique, R ist la constante des gaz, T est la température.

Bien entendu, on ne peut étudier à l'aide de rhéométrie que le processus de formation de structure à l'étape initiale, quand l'accroissement de viscosité n'est dû pratiquement qu'à la formation de structure par coagulation. Mais cette étape, très importante du point de vue technologique, peut être décrite avec des équations physiques assez correctes.

Il est à noter que l'équation (1) contient la viscosité spécifique. Pour déterminer l'énergie d'activation du processus rhéocinétique des suspensions des ciments on peut employer la viscosité.

Et, enfin, quand à la concentration de la suspension de ciment, les essais ont démontré que des dépendances satisfaisantes peuvent être obtenues quand le rapport eau-ciment est de 0,4 à 0,6.

Des courbes rhéocinétiques ont été obtenues pour les températures 303, 313, 323, 333, 353°K, et l'on a calculé les valeurs de K_T correspondantes. L'équation expérimentale d'Arrhénius pour les suspensions de ciment a la forme suivante:

$$K_T = 5{,}16 \cdot 10^3 \exp\left(-\frac{1000}{RT}\right) \qquad (3)$$

L'équation (3) permet de calculer le processus de formation de structure du système simulé ciment-eau, y compris avec des constituants secondaires, pour des différentes températures. Elle est d'interêt, puisque l'énergie d'activation relativement basse indique que l'interaction des particules de la suspension de ciment conduisante à l'accroissement de viscosité est bien faible, ce qui caractérise notamment la formation de structure par coagulation.

L'évaluation des propriétés du ciment à base des caractéristiques rhéologiques, c'est à dire méchanico-structurales, permet de déterminer les valeurs des periodes de formation et de durcissement de la structure, donc, des temps de prise de la pâte de ciment (2,3).

On a étudié les caractéristiques rhéologiques de la pâte de ciment en comparaison avec les caractéristiques standardes.

Pour mesurer la contrainte limite de cisaillement on a adopté la méthode de plastomètre conique. Parallèlement on a déterminé les temps de prise avec l'aiguille de Vicat à l'aide de l'instrument APSS (GOST 310-60). La cinétique d'accroissement de la résistance plastique (P_m) de la pâte de ciment est représentée sur fig. 1.

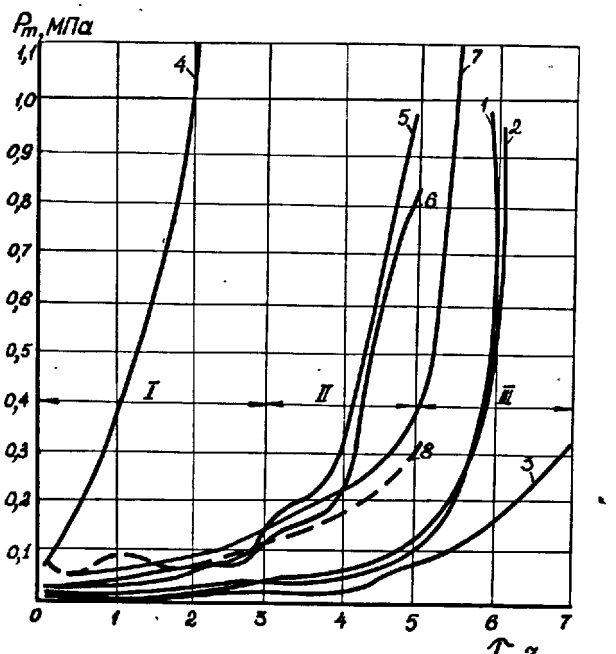

Fig. 1. Variations de résistance plastique de la pâte de ciment à consistance ordinaire: 1 - sans adjuvants; 2 - 0,2% CD ; 3 - 0,2% CD + 1% $NaNO_2$; 4 - 0,1% CD + 2% $CaCl_2$; 5 - sans adjuvants; 6 - 0,2% CD ; 7 - 0,2% CD + 1% $NaNO_2$; 8 - effet de prise "fausse"; 1,2,3,4,8 - 298°K; 5,6,7 - 333°K

La première période (3-4h) continue du début de gâchage jusqu'à la première inflexion de la courbe et se caractérise par formation d'une structure coagulante réversible. La résistance plastique de la pâte accroit très lentement et atteint à la fin de cette période 0,025-0,2 MP_a.

La deuxième période se trouve dans l'intervalle entre la première et la deuxième inflexions des courbes (élévation des courbes sur la plastogramme). La transition de structure coagulante à structure coagulante-cristalline au cours de la deuxième période se produit dans 3-5h après gâchage. La résistance plastique de pâte atteint à la fin de cette période 0,1-0,5 MPa.

Le début de la troisième période se caractérise par formation de structure cristalline-coagulante. Dans cette période la résistance du système "ciment-eau" accroit en avalanche, les courbes étant presque parallèles à l'axe d'ordonnées. La vitesse d'accroissement de résistance est de 0,6-0,8 MP_a/h.

Comme il a été démontré par les expériments, en général les courbes plastométriques sont d'un caractère hyperbolique et peuvent être décrites par l'équation générale suivante:

$$P_m = e^{\tau - A} - \frac{\tau^2(\tau - B)}{C} \qquad (4)$$

où P_m est la résistance plastique; τ est le temps; A, B, C sont des coefficients dépendants du type de ciment et des constituants secondaires.

L'élévation de température de durcissement de la pâte de ciment ou l'introduction des constituants secondaires conduisent à la diminution de durée de la première et de la deuxième périodes, et, dans des cas particuliers, à la disparition de toutes les deux périodes ou seulement de la deuxième période. La cinétique de formation de structure du ciment portland à prise "fausse" est caractérisée par la courbe 8 (fig. 1).

Les temps de début et de fin de durcissement de la pâte de ciment obtenus avec l'aiguille de Vicat coincident, dans l'essentiel, avec les caractéristiques obtenues à l'aide du plastomètre conique. La première inflexion des courbes correspond au moment initial de la prise de la pâte de ciment, la deuxième correspond à la fin de la prise (ou elles different d'eux à 10-20 min). Le remplacement de l'aiguille de Vicat par le plastomètre conique et la construction des courbes plastométriques permettent d'effectuer le contrôle permanent du processus de formation de structure de la pâte de ciment, ce qui est de grande importance, surtout dans des conditions d'actions extérieurs thermiques, chimiques et mécaniques sur le système "ciment-eau" durcissant.

La prédiction du processus de formation de structure dans des conditions non-stationnaires de température peut être effectuée sur la base des résultats d'étude de la résistance plastique effectuée pour de différents régimes isothermes. Une famille de plastogrammes isothermes pour un certain type de système durcissant (pâte de ciment, mortier de ciment) peut être défini comme champ plastométrique isotherme. Il a été possible d'employer la méthode de construction graphique, sur ce champ, de variation successive de P_m en fonction de température.

Les valeurs de P_m obtenues par expériments, ainsi que celles calculées, dans des conditions d'élévation uniforme de température sont représentées sur fig. 2.

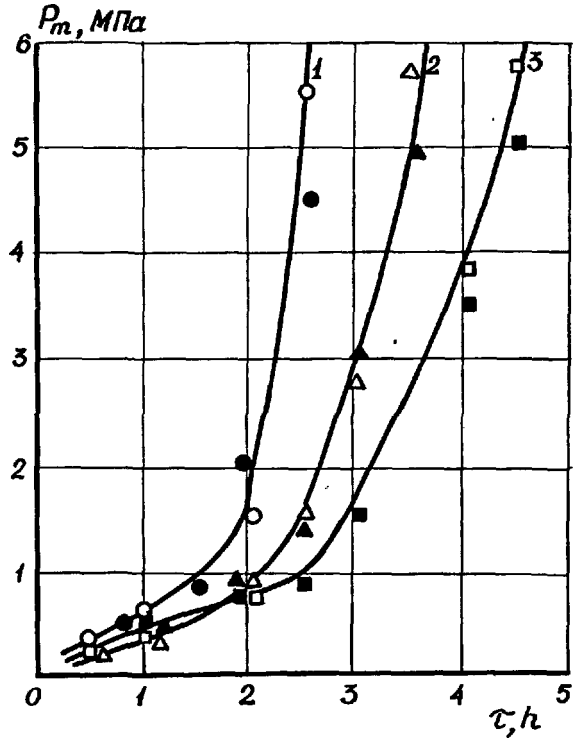

Fig. 2. Variations de résistance plastique du mortier au stade d'élévation de température à vitesse suivante: 1 - 30°/h; 2 - 15°/h; 3 - 10°/h; ●,▲,■ - données expérimentales; ○,△,□ - données calculées

En vue de déterminer le caractère de cinétique d'hydratation et de formation de structure du ciment dans des systèmes réels sous l'influence de divers facteurs extérieurs, on a adopté la méthode expérimentale de mesurage de chaleur d'hydratation dans le calorimètre différentiel. Contrairement aux méthodes bien connues, le matériau à étudier a été soumis au chauffage et refroidissement supplémentaires programmés, ce qui a permis d'effectuer des recherches aussi dans les régimes thermiques non-stationnaires (4). Pour étudier la cinétique d'hydratation dans les conditions d'échange

de masse avec le milieu ambiant, on a mis au point de spéciales méthodes et constructions de vases calorimétriques (5).

Il est démontré par les résultats d'expériments que l'influence sur le taux d'hydratation du ciment et sur la résistance de la pierre de ciment de l'eau evaporée est assez faible quand sa quantité ne dépasse pas 10% de l'eau de gâchage. Quand l'évaporation atteint 20 et 30% de l'eau de gâchage le dégagement calorifique abaisse les premiers trois jours à 18 et 25% et la résistance relative abaisse en même temps à 59 et 61% respectivement.

Les résultats d'étude de l'influence de conservation préalable ont montré que, si l'évaporation atteint, par exemple, 20% d'eau de gâchage immédiatement après gâchage, ainsi qu'après conservation pendant 8 et 16h avant l'évaporation, les courbes de cinétique de dégagement calorifique coincident.

Les résultats de recherche de structure de pierre de ciment durcissante dans les conditions d'évaporation de 10 à 30% d'eau de gâchage ont montré une teneur élévée en pores intermédiaires à rayon $10^3...10^4$Å en comparaison aux conditions standardes de durcissement.

Pour prédire la chaleur d'hydratation du ciment à la déshydratation partielle (ΔB) on peut poser le dégagement calorifique ($Q_{\Delta B}$) au moment τ égal au dégagement calorifique spécifique sans pertes d'humidité (Q_o) au moment

$$\tau_o = \frac{\tau_o}{\tau_{\Delta B}} \cdot \tau \qquad (5)$$

où, selon S.A. Chifrine,

$$\frac{\tau_o}{\tau_{\Delta B}} = 1 - 0{,}01\,\Delta B, \qquad (6)$$

$$\text{alors } Q_{\Delta B} = Q_o \left(\frac{\tau_o}{\tau_{\Delta B}} \cdot \tau\right) \qquad (7)$$

Les processus d'hydratation dans les conditions réelles peuvent contenir pas seulement la déshydratation partielle du système durcissant, mais aussi l'humidification répétée. La singularité du processus d'hydratation dans ces régimes est illustrée par l'intensité de dégagement calorifique (fig. 3). Le régime d'humidification du ciment durcissant après la déshydratation partielle emmène à l'intencification du dégagement calorifique au moment initial, mais ensuite l'intensité du processus d'hydratation s'abaisse par comparaison avec des échantillons ayant durci dans les conditions standardes.

L'humidification répétée emmène à l'accroissement de résistance de la pierre de ciment, pourtant cet effet est en rapport inverse avec la durée des processus d d'échange de masse. Ainsi, quand la durée de conservation préalable est 6h, l'humidification répétée après l'évaporation emmène à l'accroissement de résistance à 50% en comparaison au régime sans humidification, tandis qu'après 16h de conservation cet effet n'a atteint que 8%.

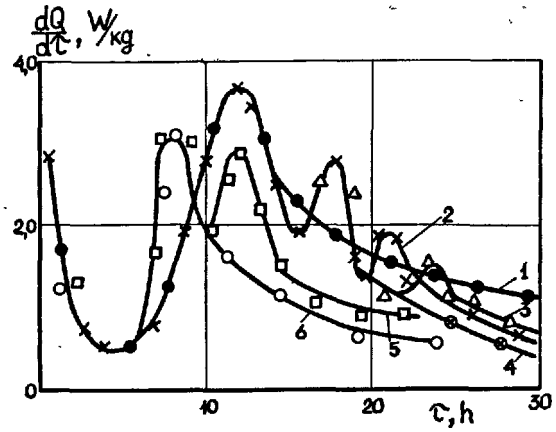

Fig. 3. Intensité de dégagement calorifique dans des conditions non-stationnaires d'humidité: 1 - conservation normale; 2 - $\tau_{пред.}$ = 16h, ΔB = 20%, début d'humidification = 2h après l'évaporation; 3 - comme 2, mais début = 6h après l'évaporation; 4 - comme 2, mais sans humidification; 5 - $\tau_{пред.}$ = 6h; ΔB = 30%; début d'humidification = 2h après l'évaporation; 6 - comme 5, mais sans humidification.

L'efficacité d'humidification répétée pour l'évaluation des caractéristiques cinétiques d'échange de chaleur abaisse aussi au fur et à mesure qu'augmente la période entre la fin d'évaporation et le début d'humidification répétée.

Conclusions

L'étude de viscosité des suspensions de ciment à l'aide de la méthode rhéocinétique permet d'obtenir des caractéristiques rhéologiques fondamentales et de comprendre la nature des interactions délicates qui sont au fond de la formation de structure à différentes températures.

Pour contrôler la qualité du ciment, il est avantageux de remplacer l'évaluation des temps de prise avec l'instrument de Vicat par la détermination de résistance plastique avec le plastomètre conique.

Les résultats d'études des processus d'hydratation du ciment quand il y a l'échange de masse avec le milieu ambiant permettent d'approcher le phénomène de la résistance "critique" du ciment durcissant (la résistance critique est la valeur de la résistance initiale après l'obtention de

laquelle l'évaporation de l'eau libre ne produit aucun effet sur la résistance du ciment).

BIBLIOGRAPHIE

1. - TCHERKINSKY Yu.S. (1977) "O vozmojnosti reokinetitcheskogo izoutchenia reaczi polimerisatsii i depolimerisatsii", Vissocomolecoularnie soedinenia (A), XIX, N 3, 459, russe.

2. - REBINDER P.A., YAMPOLSKY B.A. (1948) "Issledovanie strouctourno-mekhanitcheskikh svoistv dispersnikh sistem metodom conitcheskogo plastometra", Colloidny journal, t. 10, vip. 8, russe.

3. - TRINKER B.D., YITZ G.N. (1974) "Reologuitcheskie kharacteristiki tcementnogo testa i rastvornoi smeci", Sbornik troudof VNIPI Teploproect "Spetsialnie betoni i soorougenia", vip. 30, russe.

4. - ZACEDATELEV I.B. (1976) "O temperatournoi funktzii teploti guidratatcii tcementa", Troudi VI Mejdounarodnogo congressa po khimii tcementof, 11, 34, russe.

5. - ZACEDATELEV I.B., CHIFRINE S.A. (1978) Certificat d'auteur d'invention N 612167, Otkritia, isobretenia, promichlenie obrastci, tovarnie znaki, N 23.

Le retrait autogène de la pâte de ciment durcissante

Autogenous shrinkage of the hardening cement paste

M. BUIL, Docteur-Ingénieur, L.C.P.C. *,
J. BARON, Docteur ès Sciences Physiques, L.C.P.C. **, France

* depuis juillet 1979 à LAFARGE S.A.
** depuis novembre 1979 à LAFARGE S.A.

RESUME : Cet article traite du retrait autogène de la pâte de ciment Portland durcissante, en liaison avec les phénomènes de fissuration précoce du béton. Il existe deux méthodes de mesure de la déformation spontanée d'une pâte de ciment. La méthode unidimensionnelle (= mesure de la distance entre deux plots ancrés dans l'éprouvette) semble en pratique mieux adaptée que la méthode volumétrique (= mesure d'un volume de liquide déplacé par l'éprouvette).

La déformation spontanée d'une pâte de ciment Portland, mesurée dans l'essai unidimensionnel, fait apparaître trois phases successives : un premier retrait, un gonflement et un second retrait ou retrait de durcissement.

Il existe une corrélation expérimentale entre la fissuration précoce des bétons et la vitesse maximale de second retrait ; ceci justifie une étude approfondie du mécanisme du retrait de durcissement.

Le retrait de durcissement est proportionnel à la chaleur d'hydratation, à partir d'un certain temps d'hydratation. On considère que cette relation est perturbée au début du durcissement par la superposition du phénomène de gonflement. On a également constaté la proportionnalité entre la contraction Le Chatelier (= variation du volume absolu de l'eau et du ciment) et le dégagement de chaleur, à partir de quelques heures d'hydratation. Le phénomène de contraction Le Chatelier intervient dans le mécanisme du retrait de durcissement. En effet, il provoque une autodessiccation de la pâte de ciment, et donc un retrait semblable au retrait de dessiccation, l'eau partant non plus vers l'extérieur, mais "vers l'intérieur" de l'éprouvette. On a constaté, sur un ciment donné, que l'ordre de grandeur du retrait d'autodessiccation est semblable à celui du retrait de durcissement. Dans l'état actuel de nos connaissances, l'hypothèse de l'autodessiccation est jugée suffisante pour expliquer le phénomène du retrait de durcissement.

SUMMARY : This paper deals with the autogenous shrinkage of the hydrating Portland cement paste, in connection with the phenomenon of the early cracking of concrete. There are two measurement methods of the cement paste autogenous straining. The unidimensional method (= measurement of the distance between two studs sunk into the test-bar)proves better, in practice, than the volumetric method (= measurement of the volume of liquid displaced by the cement paste sample).

The autogenous strain of a Portland cement paste, recorded in the unidimensional test, is splitted into three stages = a first shrinkage, a swelling and a second shrinkage or hardening shrinkage.

The hardening shrinkage maximum rate is experimentally correlated to the early cracking of concrete ; for this reason, an extensive research on the hardening shrinkage is needed.

The hardening shrinkage is proportional to the hydration heat, from a certain hydration time onwards. It is thought that this proportionality is disturbed in the beginning of hardening by the superposition of the swelling phenomenon. The chemical shrinkage (Le Chatelier shrinkage) (= absolute volume change of water plus cement) is also proportional to the heat evolution , from a few hydration hours onwards. The chemical shrinkage operates in the hardening shrinkage mechanism. As a matter of fact, it induces an autodessication of the cement paste, and consequently a shrinkage similar to the dessication shrinkage , the water evolving "inwards" the sample instead of outwards. It was noticed, with a given cement, that the autodessication shrinkage reaches the same magnitude as the hardening shrinkage . In the present state of knowledge, it is found that the autodessication hypothesis is adequate to explain the hardening shrinkage phenomenon.

L'étude du retrait autogène de la pâte de ciment durcissante a une importance certaine pour la compréhension des phénomènes de fissuration précoce des bétons. Des recherches sur le retrait autogène sont menées au Laboratoire Central des Ponts & Chaussées depuis 1964. Nous présentons ici une synthèse rapide de ces recherches, avec les résultats les plus récents.

I - Le retrait de durcissement et sa mesure simplifiée

1- La mesure de la déformation autogène

Il existe deux méthodes de mesure. La première, souvent utilisée, consiste à mesurer un volume de liquide déplacé (1, 2, 3, 4, 5, 6). L'éprouvette est isolée du liquide par une membrane souple. La deuxième méthode consiste à faire des mesures unidimensionnelles = on suit le déplacement d'un capteur ancré dans l'échantillon (7, 8, 9). Ces deux méthodes sont peu sûres dans les premières heures d'hydratation. Dans la méthode volumétrique, des phénomènes de ressuage et de compression de l'éprouvette par la membrane peuvent changer la nature de la mesure (10). Dans la méthode unidimensionnelle, les frottements perturbent l'essai jusqu'au moment de la prise.

D'après la forme typique des courbes de déformation de pâtes de ciment Portland dans l'essai unidimensionnel (fig. 1), on distingue trois phases successives de déformation que l'on peut appeler a) premier retrait, b) gonflement, c) second retrait ou retrait de durcissement.

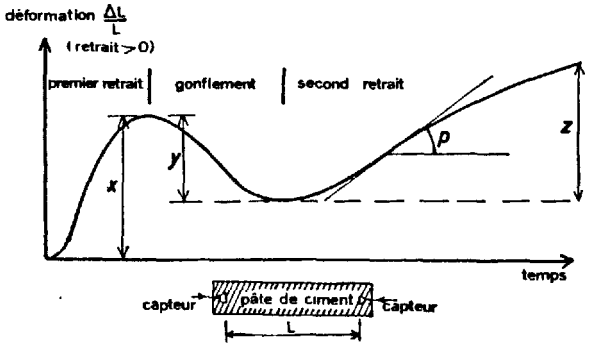

x: valeur maximale du premier retrait
y: valeur maximale du gonflement
z: valeur maximale du second retrait
p: vitesse maximale de second retrait

fig.1 Déformation d'une pâte de ciment dans l'essai unidimensionnel

a) le premier retrait commence 1 à 3 heures après le malaxage et dure 2 à 4 heures, il coïncide donc approximativement avec la prise et constitue une part intégrante du retrait plastique. Le premier retrait reste assez faible par rapport au retrait plastique d'une éprouvette exposée à une atmosphère non saturée, c'est pourquoi l'étude du premier retrait autogène ne paraît pas revêtir une grande importance pratique.

b) le gonflement n'apparaît généralement pas dans l'essai volumétrique. Mais il est probable que dans un tel essai, il est masqué par des phénomènes de réabsorption d'eau de ressuage et de compression par la membrane de la pâte encore faiblement cohérente (10). C'est pourquoi nous pensons que l'essai unidimensionnel est seul représentatif des déformations dans les heures qui suivent la prise.

La durée et l'amplitude du gonflement varient beaucoup suivant les ciments, même à l'intérieur d'une même classe de résistance. Pour certain ciment riche en C_3A et sous-dosé en gypse, il peut n'y avoir aucun gonflement, à peine un ralentissement momentané du retrait. Pour un dosage en gypse un peu plus élevé, le gonflement ne dure qu'une heure ou deux et peut échapper à l'observation tant que les déformations ne sont pas enregistrées. Cependant, pour de nombreux ciments, la période de gonflement dure entre 10 et 20 heures et le gonflement maximal est de l'ordre de 4 10^{-4} (pour E/C = 0,27). Le gonflement dépend de la quantité de chaux libre restant non hydratée à la fin de prise : il augmente fortement avec la température (11). L'influence du dosage en eau reste à préciser.

c) second retrait : Il se manifeste après la fin de prise : à déformations égales, les contraintes en jeu sont donc beaucoup plus fortes pour le second retrait que pour le premier. La valeur maximale de second retrait peut atteindre 1,5 10^{-3} (en $\frac{\Delta L}{L}$), ceci dans des conditions isothermes et, évidemment, en l'absence d'évaporation. Il faut plusieurs jours, parfois 7 et plus, pour atteindre cette valeur maximale. Le second retrait dépend du rapport E/C . Il diminue lorsque E/C augmente, pour s'annuler pratiquement à E/C > 0,35. Lorsque les essais sont faits sans précautions particulières, une déformation d'origine thermique (résultant de l'échauffement de l'éprouvette en cours d'hydratation) se superpose aux déformations précédentes. Cette déformation dépend beaucoup, évidemment, des conditions d'essais et, notamment, de la taille des éprouvettes. Souvent, sur des éprouvettes prismatiques de 7.7.28 cm, un retrait thermique se superpose pendant quelques heures au second retrait ; la vitesse de refroidissement de l'éprouvette est alors de 0,5 à 1°C par heure en sorte que les vitesses de retrait thermique et de second retrait peuvent être du même ordre. Comme il a été dit plus haut, il est préférable de séparer les deux effets ; pour maintenir constante au degré près la température interne de l'éprouvette, on peut :

. réduire la taille de l'éprouvette (exemple : cylindre de 2 cm de diamètre, 16 cm de hauteur, moule en laiton),

. noyer un circuit de refroidissement par air dans l'éprouvette au moment du coulage (9).

2 - Fissuration et retrait de durcissement

La vitesse maximale de second retrait varie considérablement suivant les ciments, même à l'intérieur d'une même classe de résistance (fig. 2). Pour E/C = 0,27, les valeurs s'étalent de 0,2 à 7 10^{-5} par heure ; il semble que, en gros, plus le gonflement dure longtemps, plus la vitesse maximale de second retrait est faible ; cette vitesse augmente quand le rapport eau/ciment diminue (12). Il a été avancé que (9) le risque de fissuration précoce après prise était d'autant plus grand que la vitesse maximale de second retrait était plus élevée. Cette hypothèse a été émise après constatation d'une corrélation expérimentale entre les deux phénomènes. Cette fissuration de second retrait se superposerait à la fissuration par retrait thermique, dont le mécanisme, proposé par Springenschmidt (13), est le suivant : au cours de la montée en température, sous l'effet de la chaleur d'hydratation, le béton est mis en compression et subit une déformation plastique. Lors de la descente en température, les contraintes de compression s'annulent pour une température t_1 supérieure à la température ambiante t_0, car du fait du vieillissement du matériau, il y a eu diminution de la longeur d'équilibre de l'éprouvette (longueur pour laquelle les contraintes appliquées sont nulles). La température diminuant encore, le béton est mis en traction. La fissu-

ration est d'autant plus importante que la différence $t_1 - t_0$ est plus élevée.

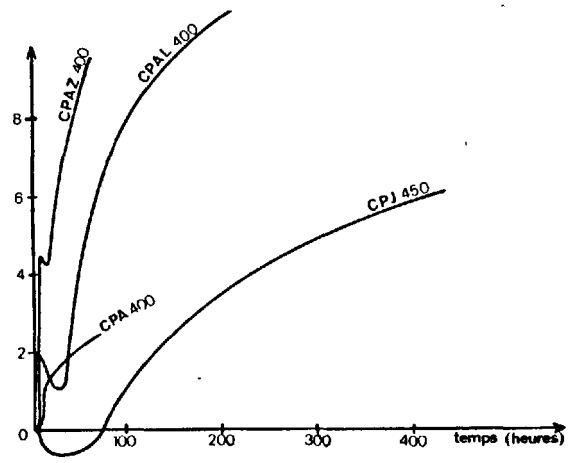

fig.2 Déformation de la pâte de ciment au premier âge pour différents ciments.

3 - Mesure simplifiée du retrait de durcissement

Etant donné l'intérêt de la mesure de la vitesse maximale de second retrait pour la détermination du risque de fissuration, un essai simplifié de second retrait a été mis au point au L.C.P.C. afin de disposer d'une mesure de routine (12). Dans cet essai, la mesure de déformation est faite verticalement sur des éprouvettes cylindriques (L = 160 mm, Ø = 20 mm) contenues dans des moules en laiton (figure 3)

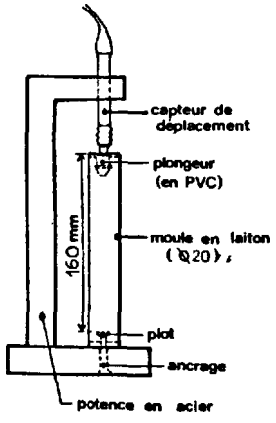

fig.3 Mesure simplifiée du second retrait

Les essais de répétabilité dans un même laboratoire et de reproductibilité inter-laboratoires font apparaître des coefficients de variation respectivement de 8 % (sur 15 essais) et 13 % (sur 6 laboratoires). On obtient le même résultat dans l'essai simplifié (fig.3) et l'essai de recherche (fig. 1)à partir du maximum de gonflement (l'enfoncement du plot sous l'effet de la pression du capteur perturbe l'essai simplifié jusqu'à cet instant).

II - Le retrait de durcissement et la cinétique de l'hydratation

1 - Déformation isotherme après prise et dégagement de chaleur

On a étudié la déformation en fonction du dégagement de chaleur pour divers ciments et des rapports E/C de l'ordre de 0,25. Les ciments utilisés étaient des mélanges de clinker et de gypse à différents dosages (3 clinkers et 4 dosages par clinker). On constate que les courbes deviennent linéaires et parallèles entre elles à partir d'un certain temps (48 heures par exemple) pour deux des clinkers utilisés et quel que soit le dosage en gypse (9).

Lorsque le gonflement est inexistant, la courbe est linéaire sur toute son étendue. A partir de cette observation, on a proposé une méthode graphique pour séparer les phénomènes de gonflement et de retrait (9).

Le gonflement et le retrait sont supposés être deux phénomènes indépendants qui se superposent, le gonflement prédominant en début d'hydratation, le retrait l'emportant ensuite. On propose de considérer le retrait comme caractérisé par une relation linéaire entre chaleur et déformation, le gonflement s'obtient alors par différence (figure4).

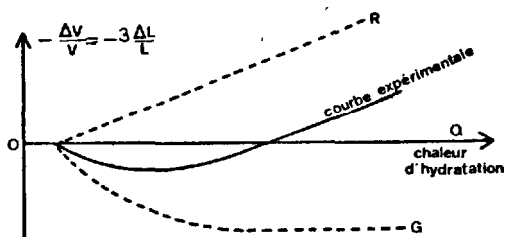

fig.4 Séparation graphique du retrait R et du gonflement G

2 - Contraction Le Chatelier et dégagement de chaleur

La contraction Le Chatelier, qui est la diminution du volume total (volume de l'eau + volume du ciment) au cours de l'hydratation, est un phénomène différent du retrait de durcissement. Le retrait de durcissement est une variation de volume apparent, inférieure de plus d'un ordre de grandeur à la contraction Le Chatelier, qui est une variation de volume absolu. Nous verrons (au § III) que la contraction Le Chatelier joue un rôle important dans le mécanisme du retrait de durcissement.

Powers a montré (14) l'existence d'une relation linéaire entre la contraction Le Chatelier et le dégagement de chaleur. Cette relation était établie à partir de 7 jours d'hydratation. Nous avons pu vérifier que cette relation reste valable à partir de quelques heures à l'aide d'un appareil permettant l'enregistrement automatique de la contraction Le Chatelier (15).

Nous avons trouvé le coefficient de proportionnalité suivant (voir aussi figure 5), valable pour différents CPA :

$$\frac{dQ}{dt} \simeq 2{,}0\,\frac{dE_i}{dt}$$

Q : dégagement de chaleur en cal/g ciment anhydre initial
Ei : contraction L.C. en mm3/g " " "

les expériences de Powers donnent en accord avec nos résultats :

$$1{,}7\,\frac{dE_i}{dt} < \frac{dQ}{dt} < 2{,}0\,\frac{dE_i}{dt}$$

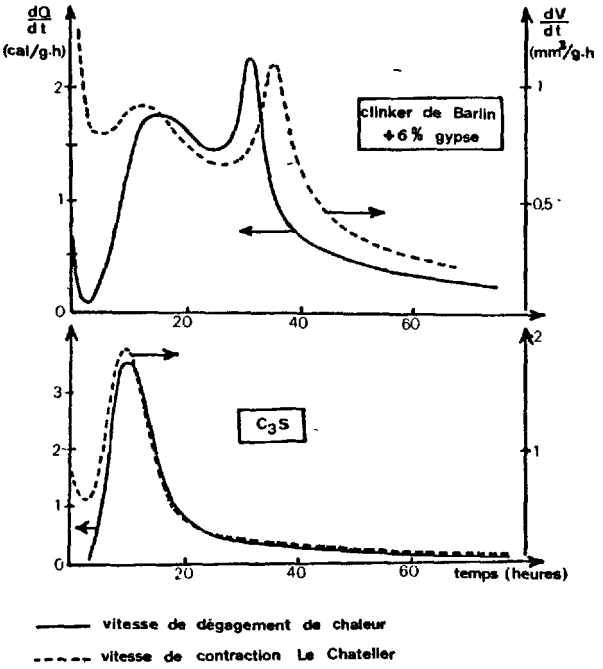

fig.5 Exemples de comparaison des courbes de dégagement de chaleur et de contraction Le Chatelier.

Nous avons constaté une divergence dans les premières heures d'hydratation, où la contraction Le Chatelier est proportionnellement beaucoup plus importante que le dégagement de chaleur. Cette différence pourrait provenir de la contraction du volume du liquide interstitiel de la pâte lors du passage en solution d'ions électropositifs comme Ca^{++} (il y a électrostriction de l'eau au voisinage de l'ion, l'ordre de grandeur de la contraction qui en résulte peut être assez important = la dissolution de 0,5 cm3 de $Ca(OH)_2$ dans 1000 cm3 d'eau donne environ 999,5 cm3 de solution, soit une contraction d'environ 1 °/₀₀(15)).

3 - Contraction Le Chatelier et autodessiccation

La contraction Le Chatelier, lorsqu'elle se produit dans une éprouvette de pâte de ciment conservée en empêchant tout échange d'eau avec le milieu, se traduit par l'apparition de vides gazeux à l'intérieur de l'éprouvette. Il en résulte une diminution de la pression partielle de vapeur d'eau en équilibre avec la pâte de ciment, c'est-à-dire une autodessiccation. Si l'isotherme de l'éprouvette était une courbe unique, la diminution de la pression partielle P/Po serait donnée par cette courbe en y reportant la perte de poids équivalente en volume à la contraction Le Chatelier. En réalité, on a un phénomène d'hystérésis dans les courbes de désorption-adsorption (16) et tous les points compris entre les deux courbes extrêmes sont des points "d'équilibre".

Dans le cas de l'autodessiccation, on se situe à une pression de vapeur comprise entre les limites établies par ces 2 courbes. L'autodessiccation peut être observée directement par mesure de l'hygrométrie dans une enceinte fermée contenant une pâte de ciment durcissante (17, 18). On constate que l'hygrométrie d'équilibre peut descendre jusqu'à environ 75 % lorsque le rapport E/C est suffisamment bas (de l'ordre de 0,25).

III - Retrait autogène par autodessiccation

Une explication du mécanisme de retrait de durcissement a été proposée depuis longtemps (19, 20). Elle consiste en ceci : l'hydratation engendre une autodessiccation et donc un retrait analogue au retrait de dessiccation, l'eau partant non plus vers l'extérieur mais "vers l'intérieur" de l'éprouvette. Nous allons étudier ici le problème de la vérification quantitative de cette hypothèse.

1 - Les méthodes de mesure du retrait d'autodessiccation

L'Hermite et coll. (21) ont procédé à une estimation quantitative du retrait d'autodessiccation et l'ont comparé au retrait de durcissement. Leur méthode était la suivante : des pâtes de ciment (E/C = 0,25) étaient conservées sous eau puis exposées à 50 % d'humidité relative à diverses échéances (2 j, 8 j, 30 j, 90 j, 180 j) avec mesures de la déformation, du poids et de la quantité d'eau non évaporable. Des éprouvettes étaient aussi conservées dans le mercure, ce qui constitue un mode de conservation du type protégé. La courbe de retrait dans le mercure a été portée en fonction de la quantité d'eau absorbée intérieurement (= quantité d'eau correspondant en volume à la contraction Le Chatelier). Les auteurs ont trouvé que cette courbe appartenait à la famille des courbes de retrait de dessiccation (retrait - quantité d'eau évaporée) à différents âges (elles sont toutes à peu près semblables). Ils en ont déduit que le retrait de durcissement résultait bien de l'autodessiccation.

La méthode de L'Hermite présente des inconvénients : la structure d'une pâte de ciment n'évolue pas de la même façon selon le mode de conservation, il n'est pas certain que le retrait d'évaporation soit le même pour une éprouvette conservée sous eau ou protégée. Il est aussi difficile de raisonner sur une courbe globale de retrait sous mercure, puisque le phénomène de gonflement se superpose au retrait de durcissement en début d'hydratation.

Nous avons utilisé une méthode différente pour l'estimation du retrait d'autodessiccation : nous avons mesuré des pentes, ou plutôt des petites variations à partir d'un instant t considéré. On peut ainsi travailler sur des éprouvettes de retrait de dessiccation et de durcissement qui ont la même structure à l'instant t et qui n'évoluent pratiquement pas en cours d'essai. Nous avons évalué sur des éprouvettes de pâte de ciment de mêmes rapports E/C et à un instant donné :

- la vitesse de contraction Le Chatelier $p_1 = \frac{d\left(\frac{\Delta P}{P}\right)}{dt}$,

  la contraction $\frac{\Delta P}{P}$ étant exprimée en perte en poids équivalente au volume de la contraction Le Chatelier. (On a utilisé un appareil enregistrant en continu la contraction sur des éprouvettes d'environ 1 cm3 avec une précision d'environ 1°/₀₀).

- le taux de retrait de dessiccation $p_2 = \frac{d\left(\frac{\Delta L}{L}\right)}{d\left(\frac{\Delta P}{P}\right)}$.

  Il s'agit de la pente à l'origine de la courbe retrait-perte en poids mesurée sur une éprouvette

conservée en empêchant tout échange d'eau avec le milieu jusqu'au moment de l'essai et de forme cylindrique Ø = 3,5 cm - L = 10 cm. La précision de cet essai est mauvaise, elle est estimée à 30 %.

- la vitesse du retrait de durcissement $p_3 = \frac{d(\frac{\Delta L}{L})}{dt}$ mesurée à l'aide de l'essai simplifié de second retrait.

En faisant l'hypothèse très simplificatrice (voir discussion sur l'isotherme, § II -3) que la contraction Le Chatelier provoque une diminution de la pression partielle d'équilibre égale à la diminution provoquée par l'évaporation d'une masse d'eau équivalente sur une éprouvette de même structure, nous obtenons la vitesse du retrait d'autodessiccation p_4 à l'instant considéré

$$p_4 = \frac{d(\frac{\Delta L}{L})_{auto.}}{dt} = p_1 \times p_2$$

Si p_3 et p_4 sont du même ordre de grandeur, nous pourrons en déduire que l'autodessiccation explique une part importante du retrait de durcissement.

2 - Résultats

Nous avons procédé aux essais décrits plus haut sur un ciment du type CPA (analyse chimique, tableau 1) et pour un rapport E/C = 0,25

tableau 1

SiO_2	Al_2O_3	Fe_2O_3	CaO	MgO	SO_2	TiO_2	Na_2O	K_2O
21,02	5,40	2,20	63,24	0,89	3,15	0,32	0,10	0,38 %

insoluble

2,27 %

pour t = 48 h, moyenne 6 essais: $p_1 = 0,16.10^{-3}\ h^{-1}$

moyenne 4 essais: $p_2 = 1,7.10^{-2}$

moyenne 4 essais: $p_3 = 0,24.10^{-5}\ h^{-1}$

$p_4 = p_1 \times p_2 = 0,27.10^{-5}\ h^{-1}$

Nous constatons que p_3 et p_4 sont du même ordre de grandeur: Nous avons vérifié ce résultat pour des temps supérieurs à 48 h, mais avec une précision de plus en plus mauvaise, les vitesses p_1 et p_3 devenant de plus en plus faibles.

Ce résultat confirme, pour le ciment choisi, que l'hypothèse du retrait par autodessiccation semble suffisante pour expliquer le retrait de durcissement. Mais cette conclusion devra être vérifiée pour d'autres types de ciment. On ne peut également exclure l'hypothèse que d'autres mécanismes, d'un ordre de grandeur inférieur ou égal, puissent se superposer au retrait d'autodessiccation, étant donnée la mauvaise précision des essais. Le retrait de carbonatation nous fournit un exemple d'un tel mécanisme (le retrait provient d'une dissolution de l'hydroxyde de calcium sous l'effet des contraintes de retrait de dessiccation, avec reprécipitation du carbonate de calcium dans les zones de faibles contraintes (22).

CONCLUSION :

Les principaux éléments auxquels nous sommes parvenus sont les suivants :

1) la fissuration précoce des bétons est en relation avec le retrait de durcissement (ou retrait autogène après prise). Il existe un appareil simple permettant de mesurer la vitesse maximale de ce retrait de durcissement et donc d'évaluer le risque de fissuration précoce.

2) le retrait autogène après prise, comme la contraction Le Chatelier, est proportionnel au dégagement de chaleur.

3) la contraction Le Chatelier avant prise paraît liée à des phénomènes de dissolution.

4) l'autodessiccation résultant de la contraction Le Chatelier semble expliquer une part importante du retrait de durcissement.

BIBLIOGRAPHIE

1 - R. L'HERMITE et J.J. GRIEU (1952), "Etudes expérimentales récentes sur le retrait des ciments et bétons", Ann. Inst. Tech. Bâtiment Trav. Publ., Paris, n° 52-53, 491.

2 - W. CZERNIN (1956) "Uber die Schrumpfung des erhärtenden Zementes", Zement-Kalk-Gips, n° 12, 525-530.

3 - M. DEL CAMPO (1959) "A new method to study the early volume changes on the neat cement paste", Bull. RILEM, 4, 18-23.

4 - F.O. SLATE et R.E. MATHEUS (1967) "Volume changes on setting and curing of cement paste and concrete from zero to seven days", Journal of the American Concrete Institute, n° 1, 34-39.

5 - Y. YAMAZAKI, T. MONJI, K. SUGIURA (1974) "Early age expanding behaviour of mortars and concretes using expansive additives of $CaO-CaSO_4-4CaO.3Al_2O_3.SO_3$ system" VIth Int. Symp. on the Chemistry of Cement, Moscou.

6 - G.D. DE HAAS, P.C. KREIJGER, E.M.M.G. NIEL, J.C. SLAGTER, H.N. STEIN (1975) "The shrinkage of hardening cement paste and mortar", Cement and Concrete Research, 5, 295-320.

7 - F.S. FULTON (1963) "The early dilatation of Portland cement pastes", Portland cement institute, Laboratory report SF-7, Johannesburg.

8 - J.BARON (1968) "Mesure du premier retrait des bétons hydrauliques", Bull. Liaison Lab. P. & Ch., n° 31, 81-92.

9 - J. BARON (1971) "Fissuration du béton par hydratation localement différée du ciment", Rapp. Rech. Lab. P. et Ch., n° 15, Paris.

10 - J. BARON et M. BUIL (1979) "Remarques à propos de l'article "Mechanical features of chemical shrinkage of cement pastes", Cement and Concrete Research, 9, 545-547.

11 - S.J. LAGINHA, M. GUERREIRO (1969) "Autogenous and hygrometric expansion of mass concrete", Journal of the American Concrete Institute, n° 9, 716-719.

12 - J. BARON, N. EL KASSEM, B. GUIEYSSE (1977) "Mise au point d'un essai simplifié de second retrait" Bull. Liaison Lab. P. et Ch., n° 89, 39-44.

13 - R. SPRINGENSCHMID, P. NISCHER (1973) "Untersuchungen über die Ursache von Querrissen im jungen Beton" Beton und Stahlbetonbau, 9, 221-226.

14 - T.C. POWERS, T.L. BOWNYARD (1946-1947) "Studies of the physical properties of hardened Portland cement paste" Proc. American Concrete Institute, 41, pp. 101-132,249-336,469-504,549-602,669-712, 815-880,933-992.

15 - M. BUIL (1980) "Contribution à l'étude du retrait de la pâte de ciment durcissante" Rapp. Rech. Lab. P. et Ch., n° 92., Paris.

16 - R.F. FELDMAN (1968) "Sorption and length-change scanning isotherms of methanol and water on hydrated Portland cement", Vth Int. Symp. on the Chemistry of Cement, Tokyo.

17 - L.E. COPELAND, R.H. BRAGG (1955) "Self-dessication in Portland cement pastes", Research and Development Laboratories of the P.C.A., Res. Dept. Bull., n° 52,

18 - F. WITTMANN (1968) "Surface tension shrinkage and strength of hardened cement paste", Matériaux et Constructions, N° 6, 547-552.

19 - H.E. DAVIS (1940) "Autogenous volume changes of concrete", American Society for Testing Materials, Proc., 40, 1103-1140.

20 - M.A. SWAYZE (1942) "Early concrete volume changes and their control", Journal of the American Concrete Institute, 13, 425-440.

21 - R. L'HERMITE, J. CHEFDEVILLE, J.J. GRIEU (1949) "Nouvelle contribution à l'étude du retrait des ciments", Annales I.T.B.T.P., n° 106, 1-27.

22 - T.C. POWERS (1962) "A hypothesis on carbonation shrinkage" Research and Development Laboratories of the P.C.A., Res. Dept. Bull. n°146.

Influence of Phase Composition of Portland Cements on the Resultant Properties of their Pastes Processed by Steam Curing

Influence de la composition du ciment sur les caractéristiques des pâtes durcies et chauffées

Z. SAUMAN, Professor, Research Institute of Building Materials, Brno
F. VAVRIN, Professor, Technical University, Brno, and
J. CERNA, RNDr, Research Institute of Building Materials, Brno, Tchécoslovaquie.

RESUME : Des pâtes ont été préparées avec dix sortes de ciment portland et chauffées à la vapeur à 80°. Ces ciments avaient des surfaces spécifiques très voisines, et des courbes granulométriques semblables.

On a constaté que les caractéristiques physiques et mécaniques des pâtes durcies dépendaient principalement de la teneur en alite, tandis que la bélite et le C_3A n'avaient qu'une influence secondaire.

Les différences de résistance de ces pâtes, de composition de phases et de granulométrie analogues peuvent être imputées à des solutions solides différentes dans l'alite et à des structures internes différentes de celle-ci, bien qu'aucune différence significative n'ait pu être décelée dans les dimensions des cristaux du clinker.

La microstructure de ces pâtes diffère peu de celles traitées à la température normale (25°); la différence provient essentiellement de la formation, dans les premières, de cristaux de tobermorite en forme d'aiguilles, mais dont la cristallisation est imparfaite.

SUMMARY : The pastes prepared from 10 types of portland cements were subjected to steam curing at 80°C. The cements were characterized by very close specific surface values and not too different granulometries.

It was found that the main influence onto the physical and mechanical properties of the hardened pastes is exerted by the alite contents, whereas belite and C_3A, respectively are characterized by practically secondary effect.

Differences in the strengths of cement pastes showing similar phase and granulometric composition can be attributed to the character of solid solutions in the alite and to the internal structure of the latter, since no significant differences have been found in the dimensions of the crystals of this main clinker component.

The microstructure of the pastes is somewhat different from the samples that have been treated at normal temperatures (25°C), mainly due to the formation of rod-shaped particles of "crystalically imperfectly developed tobermorite".

INTRODUCTION

In the course of previous experimental work (1,2) carried out at the Research Institute of Building Materials in Brno there were found certain differences in the microstructure of cement pastes treated at normal room temperature and by steam curing. It appeared expedient to study this phenomenon in greater detail and above all to determine the relationship between the phase composition of the cements and the physical and chemical properties of the pastes prepared from them. For actual work there were employed 10 types of commercial clinkers ground in a programmable manner with 5% gypsum rock in such a way that their specific surface approached the value of 3500 $cm^2.g^{-1}$ (Blaine). The pastes prepared from these cements (W/C = 0,32) were processed after 1 hour rest by steam curing at 80°C with an isothermal holding period of 2, 4, 8 and 24 hours, 3 and 7 days.

After density and strength determination the phase composition of the pastes, including porosity was ascertained, and their microstructure was studied. As can readily be seen from the results of this work as well as from recent papers (3-8), the hydration mechanism as well as the mutual relations between the degree of hydration and the properties of the cement pastes have not yet been clarified in a satisfactory manner and are therefore the subject of studies in quite a number of research establishments.

ANALYSIS OF RESULTS OBTAINED

The enclosed table I shows the phase composition of the clinkers studied with the aid of the light microscopic analysis.

TABLE I

Clinker designation	Contents of determined component (%)					
	C_3S	C_2S	C_3A	$C_6A_xF_y$	free CaO	Σ
AR	59,2	23,1	11,9	5,8	traces	100,0
BB	69,1	13,2	6,2	6,9	3,6	99,0
CI	57,5	26,5	14,3	1,1	0,4	99,8
HR	73,5	9,8	8,8	6,2	1,7	100,0
HS	59,9	22,2	10,3	6,1	1,5	100,0
KD	60,6	16,8	10,0	6,7	5,1	99,2
MA	65,0	15,2	4,4	15,3	traces	99,9
ME	74,0	9,1	8,6	8,1	0,2	100,0
ML+/	72,2	12,4	4,5	7,8	2,1	99,0
MO+/	69,6	8,6	14,8	4,5	1,2	98,7

+/ In the clinker there was also identified a certain quantity of α-C_2S which could not, however, be expressed in per cents as the differentiation from the belite mass was rather difficult.

On the prepared cements there was carried out a granulometric analysis with the aid of a Coulter Counter instrument; the results are summarized in Table II.

TABLE II

Design. of cement	Measured interval in μm (%)					
	<4,5	4,6-11,5	11,6-23,0	23,1-36,5	36,6-58,0	>58,0
AR	8,1	22,5	24,1	19,7	21,1	95,5
BB	3,3	22,8	29,8	19,1	16,5	91,5
CI	9,7	21,2	23,5	16,9	22,0	93,3
HR	2,5	23,8	30,0	22,3	18,1	96,7
HS	9,2	25,2	24,8	20,0	18,9	98,1
KD	6,1	24,4	26,9	19,3	17,4	94,1
MA	7,9	24,0	22,1	18,0	20,7	92,7
ME	4,3	17,0	20,5	15,8	22,6	80,2
ML	8,1	20,1	19,1	17,3	23,3	87,9
MO	8,3	21,1	22,6	20,2	22,7	94,9

The highest quantity of the finest fraction (<11,5 μm) is exhibited by the HS cement, whereas the sample ME is characterized by the lowest contents of this fraction.

The contents of alite, belite and C_3A in the treated pastes were determined by X-ray diffraction methods. It was found that after a 7 day hydration more than one third of the alite remains in its original unhydrated state. An exception are the cements ML and MO, where the residual contents represent less than one third of the original quantity. In all the samples after a 7 day treatment there was identified more than one half of still unreacted belite contents. With the exception of MO sample, 1-3% C_3A could be identified even after the longest treatment.

The resultant compression strength values are given in Table III.

TABLE III

Compres. strenght values ($N.mm^{-2}$)	2 h	4 h	8 h	24 h	3 d	7 d
AR	32,0	49,8	52,8	60,0	81,5	82,6
BB	34,5	60,2	76,6	86,4	95,7	107,6
CI	26,4	50,8	65,6	85,8	90,7	92,6
HR	43,1	67,3	78,7	91,0	102,5	110,5
HS	27,8	44,1	51,1	58,6	68,8	80,9
KD	37,5	51,8	74,4	93,2	95,4	103,1
MA	24,1	41,0	66,4	72,9	100,4	101,1
ME	27,9	60,1	71,7	83,5	95,5	101,0
ML	24,8	52,4	80,5	99,1	111,7	113,6
MO	20,2	57,2	75,8	95,1	102,3	105,3

In order to give more instructive information the early (2 h) and final strength (7 d) values are plotted in Figs. 1 and 2,

together with the indication of cements phase composition.

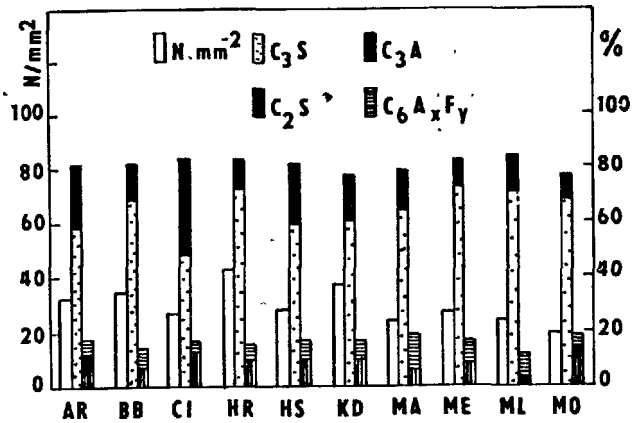

Fig. 1 - Compression strength of cement pastes after 2 hour treatment.

It follows explicitly from the above data that the major influence onto the attained strengths is exerted by alite. The relatively low early strength value (2 h) for the ME paste (27,9 $N.mm^{-2}$) is caused by almost 20% the >58,0 µm fraction amounting almost to 20%. In the case of ML and MO samples, which are also characterized by a marked alite content, the relatively low early strengths are caused by a higher total porosity in comparison with the remaining pastes during the first hydration stages. Only the sample KD is characterized by a relatively pronounced early strength (43,1 $N.mm^{-2}$) which is out of proportion with regard to the present alite quantity (60,6 %).

Cement pastes samples CI, AR and HS which contain the highest quantities of belite (26,5 - 22,2 %) exhibit the lowest compression strength values after 7 days of treatment.

Also the increased C_3A content did not positively influence the attained early strengths, as could perhaps have been assumed.

As has been shown experimentally, the differences in the size of the alite particles have not been substantial enough to influence the strength differences of the tested pastes in apparently principal manner.

Thus the main cause seems to be in the character of the contained solid solutions and in the internal structure of the alite itself.

The microstructure of the steam cured pastes (80°C) differs from those treated at room temperature (25°C) mainly by the fact that there is also formed the C-S-H-gel in the form of isometric particles which are mutually linked with the formation of the rod-shaped "crystalically imperfectly developed tobermoritic phase", in which in some cases there can seen the indication of

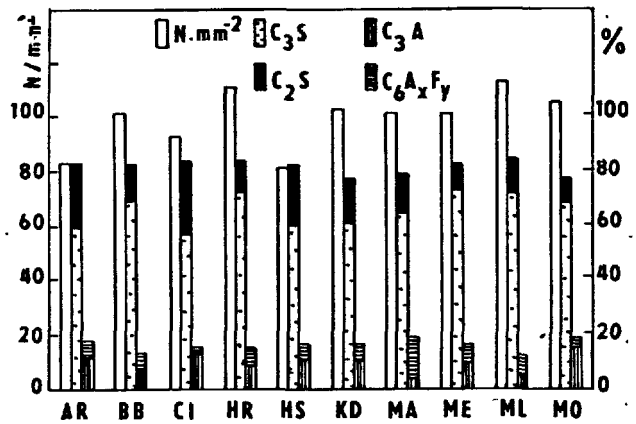

Fig. 2 - Compression strength of cement pastes after 7 day treatment.

zoning original formations (Fig.3).

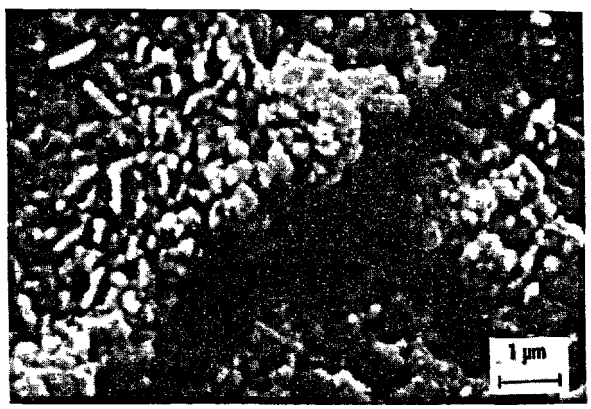

Fig. 3 - Paste of MA cement (7 days, 80°C).

Typical portlandite crystals are often mutually intergrown, as a consequence of their formation in different periods of time or growth at different rate which can positively influence the strength of the cement paste (Fig. 4).

The "Type I" C-S-H-gel according to Diamond (4) which forms a fibrous structure, could be identified only sporadically, and the same applies to crystals which should, in accordance with their morphology, correspond to $C_4A\bar{S}H_{12}$, but belong to portlandite.

A very frequent case of microstructure is the phenomenon when needle-shaped C-S-H-gel particles of very small dimensions intergrow the tabular portlandite crystals (Fig. 5).

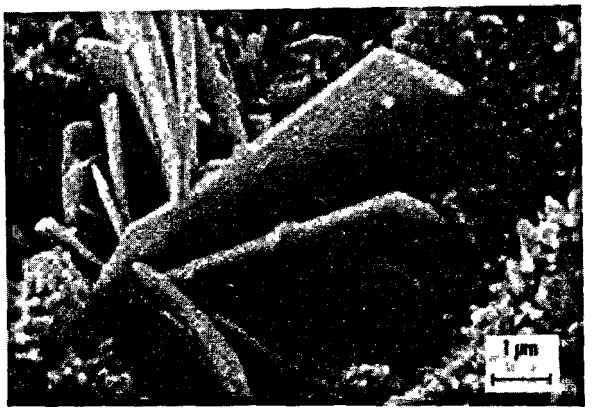

Fig. 4 - Paste of MO cement (24 h, 80°C).

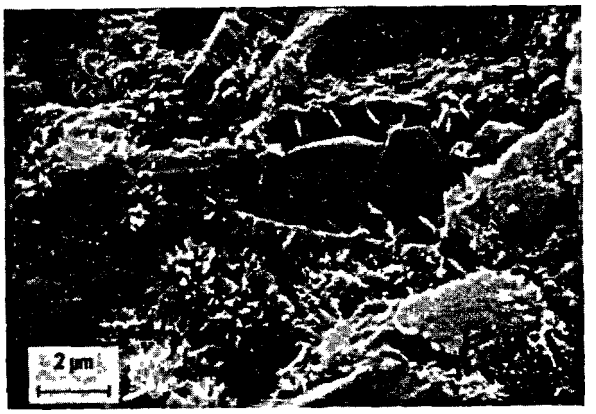

Fig. 5 - Paste of HS cement (24 h, 80°C).

CONCLUSION

Pastes from 10 cement types of approximately same specific surface were treated for the various periods of time at 80°C and it was found that the major influence onto the physical and mechanical properties is exerted by alite contents whereas belite and C_3A, respectively exhibit only an unpronounced effect. The resultant differences in the strengths of samples having a close phase composition and a not too different granulometry are not caused by the difference in the dimensions of alite crystals, but are apparently related to the character of the contained solid solutions as well as the actual structural arrangement of this major clinker component.

REFERENCES

1.- Z. ŠAUMAN (1964), "Clarification of the Reactions of Portland and Slag Cements under Hydrothermal Conditions", Research Report Building Materials Research Institute Brno (in Czech).

2.- Z. ŠAUMAN and J. ČERNÁ (1969), "Structure and Properties of Cement Pastes", Research Report Building Materials Research Institute Brno (in Czech).

3.- S. DIAMOND (1972),"Identification of Hydrated Cement Constituents Using a Scanning Electron Microscope - Energy Dispersive X-ray Spectrometer Combination", Cem.Concr.Res. 2, 617-632.

4.- S. DIAMOND (1976),"Cement Paste Microstructure - an Overview at Several Levels", Proc.Conf.Hydraul.Cem.Pastes-their Struct.Anal.Properties (Sheffield).

5.- A. GRUDEMO (1979),"Microcracks, Fracture Mechanism and Strength of the Cement Paste Matrix", Cem.Concr.Res.9, 19-34.

6.- J. SKALNÝ, I.JAWED and H.F.W. TAYLOR (1978), "Studies on Hydration of Cement-Recent Developments", World Cem.Technol. 9, 183-195.

7.- D.D. DOUBLE, A. HELLAWELL and S.J.PERRY (1978), "The Hydration of Portland Cement", Proc.R.Soc.London,A 359, 435-451.

8.- J.P. BERNARD (1978), "Le durcissment des pâtes de ciment Portland", Cement bétons platres chaux, 359-366.

Calculations of Strength Development from the Coumpound Composition of Portland Cement

Calcul du développement de la résistance des ciments portland à partir de leur composition

Sandor POPOVICS, Department of Civil Engineering, Drexel University, Philadelphia, Pennsylvania 19104, U.S.A.

RESUME : On a comparé quatre méthodes de calcul de la résistance des ciments portland, en fonction de leur âge, de leur finesse de broyage et de leur composition chimique :
le modèle linéaire
le modèle exponentiel
le modèle du second degré complet
le modèle du second degré partiel

Un exemple numérique illustre l'application de ces méthodes. Les équations 4, 10 et 11, ainsi que les formules dérivées de l'équation 12, dans le modèle exponentiel, constituent des nouveautés.
Le modèle exponentiel fournit une preuve indirecte de l'action du C_3A comme catalyseur de l'hydratation des silicates de chaux.

SUMMARY : The paper compares methods of calculation for the strength development of portland cement in terms of age, fineness and compound composition. The following four methods are investigated :
the linear methods
the exponential formulas
the complete formula of second degree
the trunkated formula of second degree.

A numerical example illustrates the application of the methods. Eqs. 4, 10 and 11 and the derivation of Eq. 12 from the exponential cement model are new.

The exponential cement model also provides indirect evidence that the C_3A acts as a catalyst in the hydration of the calcium silicates.

The paper compares several old and new methods of calculation for the strength development of portland cements in standard mortars of ASTM C 109 type. The independent variables are: compound composition, age at testing, and fineness. Equations 4), 10) and 11) and the derivation of Eq. 12) from the exponential cement model have not been published before.

This paper is the continuation of the papers the writer presented at the IV. and V. International Symposia on the Chemistry of Cement.

The Linear Cement Models

The mathematical form of the first such model is, as follows:

$$f = \text{Strength} = a(C_3S) + b(C_2S) + c(C_3A) + d(C_4AF) \qquad 1)$$

where the symbols in parentheses represent the calculated (Bogue) percentages by weight of the compounds, and a, b, c, and d are empirical coefficients (parameters). A set of the coefficients for Eq. 1) are presented in Table 1. These are valid for standard Ottawa-sand mortars of ASTM C 109 and C 190 types.

Strengths calculated by Eq. 1) and the pertinent parameters of Table 1 for Cement No. 24 of Gonnerman's (1) are shown in Figure 1 along with the experimental values. The composition of this cement is:

$C_3S = 41\%$; $C_2S = 37\%$; $C_3A = 7\%$; $C_4AF = 12\%$.

Several attempts have been made to improve the linear model. Blaine and his co-workers introduced a large number of additional variables. (2) Their formulas for portland cements in Ottawa-sand mortars of ASTM C 109 type are as follows:

$$f_1 = -2029 + 18.19C_3S + 224.7SO_3 + 349.1\,K_2O - 168.8\,\text{Loss} - 228.2\,\text{Insol} + 0.5509S_s - 16.82\,\text{Air} \qquad 2a)$$

$$f_3 = -2950 + 41.51C_3S + 22.05C_3A + 432.5\,SO_3 + 327.3\,K_2O - 249.9\,\text{Loss} + 0.7573S_s - 49.55\,\text{Air} \qquad 2b)$$

$$f_7 = -4131 + 56.16C_3S + 90.45C_3A + 378.1SO_3 + 592.8\,K_2O - 39.24\,MgO - 68.66\,\text{Loss} + 1.07\,S_s - 59.99\,\text{Air} \qquad 2c)$$

$$f_{28} = 1075 + 42.08C_3S + 53.03C_3A + 23.60C_4AF + 0.5729S_s - 95.61\,\text{Air} \qquad 2d)$$

$$f_{365} = 6518 - 103.4C_3A - 687.7\,Na_2O + 0.4345S_s - 100.2\,\text{Air} \qquad 2e)$$

$$f_{1825} = 5331 + 16.25C_2S - 85.22C_3A - 1091Na_2O - 107.9MgO + 0.5375S_s - 507.8\,\text{Insol} - 106.5\,\text{Air} \qquad 2f)$$

$$f_{3650} = 7833 + 18.77\,C_2S - 161.5\,C_3A - 71.0C_4AF - 1578Na_2O - 723\,\text{Insol} + 0.2496\,S_s - 122.2\,\text{Air} \qquad 2g)$$

where

TABLE I - Coefficients for Eq. 1) (1)

Curing of specimens: in moist room at normal temperature up to 28 days, then in water.

	Coefficients, psi						
Age / Compound	1 d	3 d	7 d	28 d	3 m	1 y	2 y
	2-in. Plastic Mortar Cubes, 1:2.75 Mix by Weight for Compressive Strength						
C_3S	8.5	27.4	40.0	48.8	55.7	61.8	70.7
C_2S	0.3	-1.1	-5.1	19.1	62.9	80.6	82.2
C_3A	11.3	24.1	58.4	100.1	56.4	5.6	-12.5
C_4AF	-6.5	-9.8	-0.2	30.8	39.7	39.6	27.2
	1:3 Standard Ottawa Sand Briquets for Tensile Strength						
C_3S	2.1	3.6	4.6	5.0	4.7	4.6	4.9
C_2S	0.3	0.8	1.3	3.8	6.1	6.4	6.1
C_3A	4.6	6.3	7.1	7.1	4.4	2.1	0.9
C_4AF	0.4	3.7	3.5	4.0	4.0	2.6	2.2

The conversion factor from psi to MPa is 0.0069.

f_t = standard compressive strength of mortar at the age of t days, psi,

C_3S, C_2S, C_3A and C_4AF = calculated (Bogue) amounts of the four cement compounds, percent by weight,

SO_3, K_2O, Na_2O, and MgO = sulfate, potassium, sodium and magnesium contents, respectively, percent by weight,

Loss = loss on ignition, percent by weight,

S_s = fineness of cement by the air-permeability (Blaine) method, cm^2/g,

Air = air content of the fresh mortar, percent.

The conversion factor from psi to MPa is 0.0069.

Using again Cement No. 24 from Gonnerman's investigation with the estimated values of Air = 1%, SO_3 = 1.8%, K_2O = 0.4%, Na_2O = 0.6%, MgO = 2.8%, Loss = 0%, Insol = 0.2%, and S_s = 2700 cm^2/g, the strength values calculated by Eqs. 2a) through 2f) are presented in Figure 1.

In another effort, Alexander presented a simplified two-component linear model (3) for the cube strengths of 2.75 standard Ottawa-sand mortars under wet curing:

$$f_3 = -1477 + 24.64\,C_3S + 40.43\,C_3A + 0.484S_s \quad 3a)$$

$$f_7 = -1245 + 41.16\,C_3S + 78.84\,C_3A + 0.355S_s \quad 3b)$$

$$f_{28} = 286 + 27.25\,C_3S + 146.96\,C_3A + 0.384S_s \quad 3c)$$

where the symbolds are identical with the symbols of Eqs. 2a) through 2g).

The conversion factor from psi to MPa is again 0.0069. Strength values calculated by Eqs. 3a) through 3c) for Cement No. 24 are presented in Figure 1.

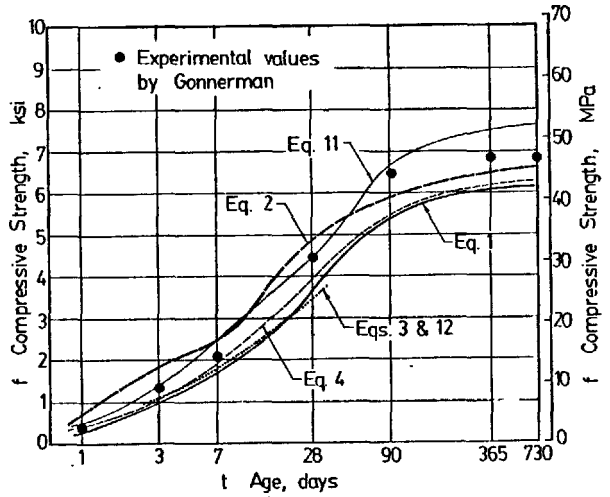

Figure 1. Comparison of compressive strengths estimated for the same cement. The specimens were 2-in. (5-cm) cubes of 1 : 2.75 Ottawa-sand mortar made with Cement No. 24 from the series of Gonnerman's. (1) Lines represent values calculated by formulas as marked; points represent experimental values by Gonnerman. The cement composition is: C_3S = 41%; C_2S = 37%; C_3A = 7%; and C_4AF = 12%

The Direct Exponential Model

Another approach is the following formula for the calculation of compressive and tensile strengths of standard, non-air-entrained mortars of ASTM C 109 and C 190 types:

$$f_t = f_{90}\,\frac{1 - pe^{-b_1 t} - (1-p)e^{-b_2 t}}{1 - pe^{90b_1} - (1-p)e^{-90b_2}} \quad 4)$$

where

f_t = estimated mortar strength at the age of t days, psi

f_{90} = strength parameter representing the mortar at the age of 90 days.

For the standard compressive strength of non-air entraining cements in Ottawa-sand mortars:

$$f_{90} = 5500S_s/S_o \text{ (psi)} \quad 5)$$

For the compressive strength of the same cements and mortars as above but when the curing takes place in moist air instead of water:

$$f_{90} = 5900S_s/S_o \text{ (psi)} \quad 6)$$

For the tensile strength of standard briquette but with moist-air curing:

$$f_{90} = 580 \text{ (psi)} \quad 7)$$

t = age of the specimen at testing, days,

p = computed C_3S content of the portland cement, percent/100,

b_1 and b_2 = rate parameters which are independent of the strength, age, and C_3S and C_2S contents, but may be a function of the temperature, C_3A content, fineness and any other factor that influences the course of hydration (minor constitutents, gypsum content, admixtures, water-cement ratio, curing and testing methods, etc.), 1/day.

For the compressive strengths of Ottawa-sand mortar cubes made, cured and tested according to ASTM C 109, the following b parameters are valid:

$$b_1 = 0.2S_s/S_o \quad (1 \text{ day}) \quad 8)$$

$$b_2 = 0.005C_3A\,S_s/S_o \quad (1 \text{ day}) \quad 9)$$

For the tensile strength of Ottawa-sand briquettes according to ASTM

C 190, the following b parameters are valid:

$b_1 = 0.80 S_s/S_o$ (1 day)

$b_2 = 0.02 C_3A\ S_s/S_o$ (1 day)

S_s and S_o = Specific surface of the cement in question, and that of a typical Type I cement, respectively. In the case of Kliegar's LTS cements (4) S_s was usually taken for Type III cements as 2600 cm^2/g (Wagner), and for the other cement types as 1800 cm^2/g (Wagner). S_o was usually taken as 1800 cm^2/g (Wagner).

The conversion factor from psi to MPa is 0.0069. Strength values calculated by Eq. 4) with Eqs. 6), 8) and 9) for cement No. 24 are shown again in Figure 1.

Eq. 4) is an advanced form of the earlier exponential cement model for relative strengths. (5)

Eq. 4) can also be used to estimate the strength at any age from the experimentally obtained strength of the mortar in question at a given age. For instance, the strength at any age can be estimated from the measured 3-day strength if t = 3 is substituted for 90 in the formula:

$$f_t = f_3 \frac{1 - pe^{-b_1 t} - (1 - p)e^{-b_2 t}}{1 - pe^{-3b_1} - (1 - p)e^{-3b_2}} \qquad 10)$$

where the symbol are the same as the symbols for Eq. 4).

Values calculated by Eq. 10) with Eqs. 8) and 9) from the 3-day compressive strength of the Ottawa-sand mortar cubes made with Gonnerman's Cement No. 24 are also shown in Figure 1.

A considerable amount of evidence has been published to show that the exponential cement model is well supported by experimental data. (6) - (9) It is highly unlikely that such a good fit could have been obtained without a fundamental similarity between the hardening process represented by this model, and the actual process. Therefore, it seems safe to say that the C_3A acts as a catalyst on the hydration of the calcium silicates, as indicated by the structure of the model. (10)

Note that both Eq. 4) and Eq. 10) are also suitable for the estimation of concrete strengths. This, however, is the topic of another paper.

Quadratic Models

If one expands the exponential terms in Eq. 4) into the well-known series, and omits the terms of higher degrees, the following formula of second degree is obtained:

$$f_t = g + hC_3S + iC_3S \times C_3A + jC_3A + kS_s \qquad 11)$$

where g, h, i, j and k are experimental parameters that are independent of the compound composition of the cement but may be affected by any factor that influences the strength development. Reliable best-fit values for these parameters are not available at this time.

If one assumes that the term of jC_3A is negligible, then Eq. 11) provides the formulas recommended by Alexander (3):

$$f_3 = -1248 + 22.32\ C_3S(1 + 0.030\ C_3A) + 0.468S_s \qquad 12a)$$

$$f_7 = -772 + 34.20\ C_3S(1 + 0.043\ C_3A) + 0.329S_s \qquad 12b)$$

$$f_{28} = 1129 + 15.36\ C_3S(1 + 0.181\ C_3A) + 0.325S_s \qquad 12c)$$

where the symbols and the limits of validity are the same as those for Eqs. 2a) through 2g). The conversion factor from psi to MPa is 0.0069.

Using again Cement No. 24 from Gonnerman's investigation, the strength values calculated by Eqs. 12a) through 12c) are practically the same for this cement as those by Eqs. 3a) through 3c) shown in Figure 1.

Conclusion

All the presented formulas are suitable for the estimation of the strength developing capacity of portland cements, although none of them is completely satisfactory. The reason for this is that none of the formulas includes all the factors that affect the strength development of a cement. Nevertheless, it appears that the exponential model, that is Eq. 4), is perhaps the most promising partly because it is more in accordance with accepted concepts of cement chemistry than the other models, and partly because it contains only two parameters.

References

1. Gonnerman, H. F., "Study of Cement Composition in Relation to Strength, Length Changes, Resistance to Sulfate Waters and to Freezing and Thawing, of Mortars and Concrete", Proceedings ASTM, Vol. 34, Part II, 1934, pp. 244-295.

2. Blaine, R. L., Arni, H. T., and Defore, M. R., "Compressive Strength of Test Mortars" Section 7. Interrelations between Cement and Concrete Properties, Part 3, Building Science Series 8, U. S. Department of Commerce, National Bureau of Standards, Washington, D. C., 1968, pp. 1-65.

3. Alexander, K. M., "The Relationship Between Strength and the Composition and Fineness of Cement", Cement and Concrete Research, Vol. 2, No. 6, November, 1972, pp. 663-680.

4. Klieger, P., "Long-Time Study of Cement Performance in Concrete - Chapter 10. Progress Report on Strength and Elastic Properties of Concrete", ACI Journal, Proc. Vol. 54, December, 1957, pp. 481-504.

5. Popovics, S., "A Model for the Kinetics of the Hardening of Portland Cement", Highway Research Record No. 192, Highway Research Board, Wachington, D. C., 1967, pp. 14-35.

6. Popovics, S., "Berechnung der Festigkeitsentwicklung von Morteln und Betonen unter Berucksichtigung der Klinkerphasen des verwendeten Portlandzementes" Referate. (Calculation of the Strength Development of Mortars and Concrete from the Compound Composition of the Portland Cement Used), Betonstein-Zeitung, Vol. 34, No. 11, November, 1968, pp. 587-590.

7. Popovics, S., Effect of Kinetics on the Ultimate Strength of Portland Cement Pastes, (Published In Russian), Beton i Zhelezobeton, Moscow, March, 1972, pp. 23-24.

8. Popovics, S., "Phenomenological Approach to the Role of C_3A in the Hardening of Portland Cement Pastes", Cement and Concrete Research, Vol. 6, No. 3, May, 1976, pp. 343-350.

9. Popovics, S., Concrete Making Materials, McGraw-Hill Book Company, New York, etc. and Hemisphere Publishing Corporation, Washington, D. C. etc. 1979.

10. Popovics, S., "Strength Development of Portland Cement Paste", The VI. International Congress on the Chemistry of Cement, Supplementary Paper, Section II, Moscow, September, 1974.

The Distribution of Evaporable water in hardened cement paste (h.c.p)

La distribution de l'eau évaporable dans les pâtes durcies de ciment

S. SABRI and
J. M. ILLSTON, Division of Civil Engineering. The Hatfield Polytechnic, Hatfield, Herts, U.K.

RESUME : Nous avons étudié la répartition de l'eau évaporable dans les pâtes de ciment durcies, en utilisant une méthode thermogravimétrique semi-isotherme et une méthode dérivée de la thermogravimétrie.

Ces mesures permettent de distinguer deux sortes d'eau évaporable. Les variations des quantités d'eau de chaque sorte ont été déterminées expérimentalement, en fonction des durées d'hydratation, de l'humidité relative ambiante, de la température et du rapport eau/ciment. Nous en avons conclu que l'eau évaporable dans les pâtes de ciment durcies n'est pas due uniquement à l'eau physiquement adsorbée, mais aussi à l'eau de combinaison de certains hydrates, instables quand la teneur en eau interne de la pâte varie.

SUMMARY: The distribution of evaporable water in h.c.p. was studied using a simultaneous semi-isothermal method of thermogravimetry and derivative thermogravimetry.

The measurements allow quantitative differentiation between two different types of evaporable water in h.c.p. The variations in the amount of each type in response to changes in curing period, relative humidity, temperature and water-cement ratio were determined experimentally.

It is concluded that the evaporable water in h.c.p. is not present solely as physically adsorbed water but also as a structural component of some hydrates that are not stable with regard to changes in moisture content.

INTRODUCTION

Knowledge of the distribution of evaporable water in h.c.p. is essential for a realistic interpretation of sorption and length change measurements. A series of measuring methods are reported in the literature by means of which attempts are made to establish criteria to distinguish between the different types of water in h.c.p. None of these methods, however, succeeds in separating quantitatively the different classes of evaporable water present in h.c.p.

In the following, such a method of determining the distribution of water in h.c.p. is demonstrated, using a semi-isothermal thermogravimetric method.

EXPERIMENTAL

Specimen Preparation:

A type I cement was mixed at a water cement ratio (W/C) of 0.47, cast as hollow cylindrical tubes of wall thickness 1 mm, external diameter 32 mm, and length 100 mm, in specially designed perspex moulds (1), stored at 20°C for one day in 100% R.H chamber, demoulded and then cured at 20°C in deionized water until tested.

The samples used for the determination of the distribution of evaporable water by the semi-isothermal TG/DTG method were broken pieces taken from the 1 mm tubes. The initial weight of the sample was always between 10 and 12 mg. Essentially similar results were obtained using samples in a powder form. Powdered samples were not used, however, to avoid additional carbonation occurring during conditioning, grinding and placing in the furnace.

Apparatus and Experimental Conditions:

A TG 750-thermobalance (Stanton Redcroft, London, UK) was used with N30 μV-preamplifier and N42 Derivative unit (Linseis Messegerate GmbH, Self, W. Germany). The TG, DTG and temperature curves were recorded simultaneously on a Linseis multi-pen recorder.

All semi-isothermal TG/DTG experiments were carried out at a heating rate of 5°C/min, chart speed 100 mm/h and in a dynamic atmosphere of CO_2 free air of constant water vapour pressure equal to the saturation vapour pressure of water at 20°C, at a rate of 25 ml/min. This relatively high water vapour pressure was chosen because it is thought to delay the start of the desorption of that part of evaporable water that is more tightly bound to the solid and consequently facilitates the separation of the peaks.

The Semi-isothermal Thermogravimetric Procedure:

The features of the semi-isothermal technique used in this study are essentially the same as those used by El-Jazairi and Illston in reference (2). As the rate of weight change reaches a maximum (at a peak) and starts to decrease, the temperature programmer is switched from dynamic heating to the isothermal condition for 30 minutes. At the end of the 30 minutes isotherm the temperature programmer is again switched to dynamic heating until the next peak is reached.

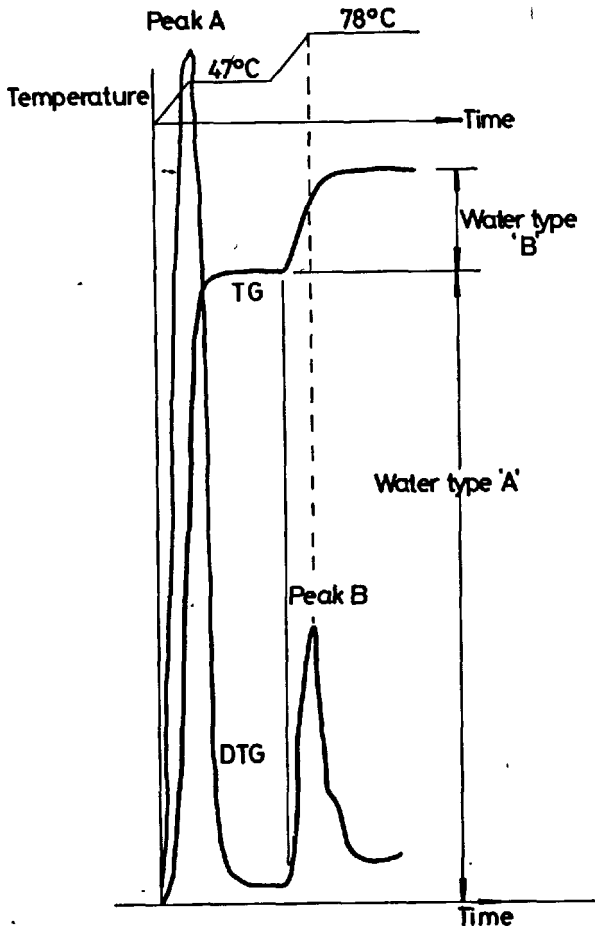

Fig. 1: Typical semi-isothermal TG/DTG curves for a saturated sample of h.c.p.

Fig.(1) shows typical semi-isothermal TG/DTG curves for a saturated h.c.p. sample hydrated for only one day. The semi-isothermal TG/DTG method allows the separation of TWO main peaks on the DTG curve in the temperature range 20° to 100°C. The two types of water corresponding to the lower and the higher temperature peaks are designated water type "A" and water type "B" respectively. W_A and W_B are defined as the weight of water type "A" and the weight of water type "B" per unit weight of dry paste respectively.

For samples cured for one day only, the first peak occurs at about 47°C and the second peak occurs at 78°C. The temperature of each peak increases with the curing period up to 28 days, after which they remain constant at about 54° and 90°C for peak "A" and peak "B" respectively.

RESULTS

Effect of Curing Period:

The amount of water type "A" was found to be practically constant all through the curing period from 1 day up to 2 years. The amount of water type "B" on the other hand increases steadily with the curing period. A plot of the experimental values of W_B against W_n is shown in Fig.(2), it gives a straight line of the form

$$W_B = .023 + .276\ W_n \quad \ldots\ldots\ldots (1)$$

where W_n is the non evaporable water per unit weight of ignited paste. Equation (1) can be used to determine the amount of water type "B" in saturated samples by measuring W_n alone. This helps to determine any changes that might occur during drying or heating in the amount of water type "B" relative to its originally saturated state without the complicating factors arising from continued hydration during relative humidity or temperature changes.

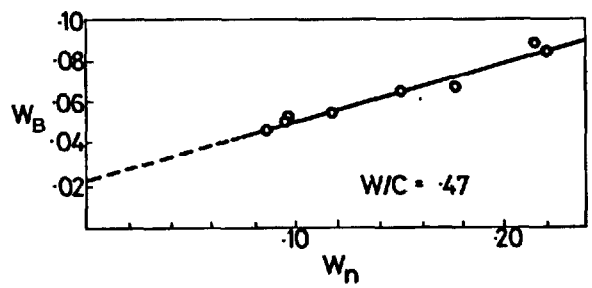

Fig. 2: W_B vs W_n plot for saturated h.c.p.

Effect of Drying and Wetting:

In order to determine how each type of evaporable water in h.c.p. changes with relative humidity, semi-isothermal TG/DTG experiments were performed on samples conditioned to different levels of R.H. The samples were initially cured for 28 days in water before conditioning. To correct for any additional hydration that occurs during conditioning at high levels of R.H, the quantity W_B/W_{Bo} is used instead of W_B to plot the correct isotherm of water type "B". W_{Bo} is the amount of water type "B" that should have been present in the sample if it was continuously kept in water as calculated from the value of W_n of partially dried sample, using equation (1).

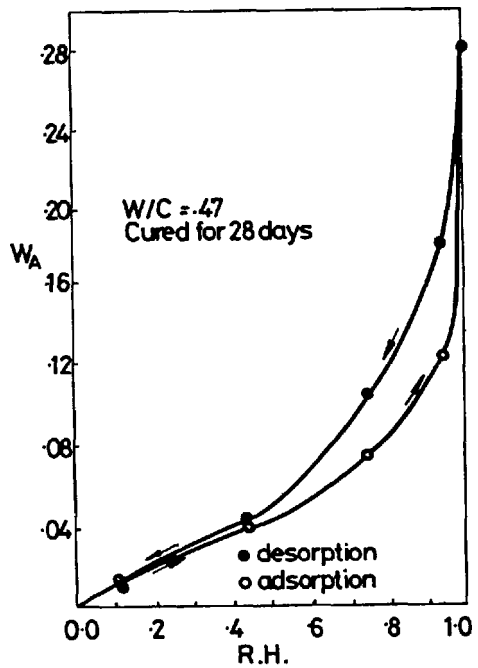

Fig. 3: Adsorption - desorption isotherm of water type "A".

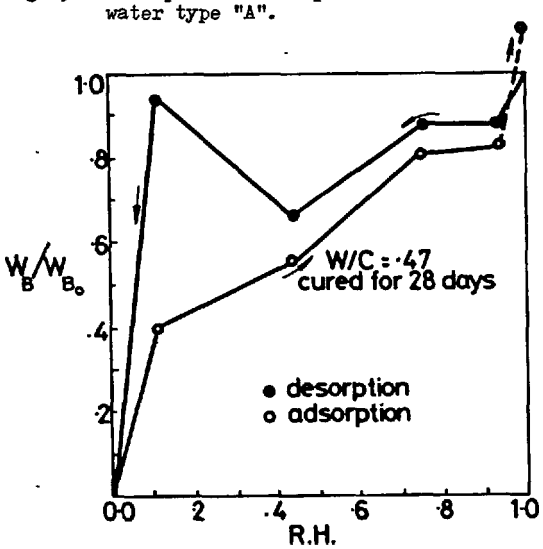

Fig. 4: Adsorption - desorption isotherm of water type "B".

The isotherms of water type "A" and water type "B" are shown in Fig. (3) and Fig. (4) respectively, where it can be seen that:

1. Water type "A" is present at all relative humidities and its amount decreases as relative humidity decreases.

2. The isotherm of water type "A" is reversible in the lower humidity range, a hysteresis loop is present at high humidities and closes at about 35% R.H.

3. Most of water type "B" is lost below 11% R.H.

4. Even at the highest relative humidity used (namely 94% R.H) some of water type "B" is lost from the sample.

5. Between 100 and 11% R.H a minimum is observed in the amount of water type "B" retained by the sample.

6. On adsorption, W_B increases throughout the full humidity range.

A large hysteresis loop is observed at all levels of R.H, and the difference is particularly large at 11% R.H.

Perhaps the most important result with regard to the effect of drying on the distribution of evaporable water in h.c.p. is that a definite increase in W_B occurs due to drying on rewetting. The increase in W_B (of the order of about 20%) due to a drying cycle to 11% R.H and back to saturation is about twice the increase due to drying to 44 or to 0% R.H.

Effect of Temperature:

Heating in the dry condition has very little effect on the distribution of evaporable water in h.c.p. as measured by the semi-isothermal TG/DTG method. Heating in water, however, produces a substantial decrease in W_B; especially at temperatures higher than about $45^{\circ}C$.

Effect of W/C Ratio:

Semi-isothermal TG/DTG runs were performed on saturated fully hydrated samples of h.c.p. made with different W/C ratios. The amount of water type "A" per unit non-evaporable water increases with W/C ratio, while the amount of water type "B" per unit non-evaporable water appears to be constant for samples made with low W/C ratio. For samples made with W/C ratios higher than about 0.4, W_B/W_n decreases with W/C ratio.

DISCUSSION:

The adsorption-desorption isotherm of water type "A" shows the characteristics of physically adsorbed water. Water type "A" must include both capillary and gel water according to the classification of Powers and Brownyard (3) since about 49% of the evaporable water present in samples made with W/C ratio of 0.23 (which according to Powers contains no capillary pores) is present as water of type"A".

The sorption isotherm of water type "B" shows a hysteresis loop extending over the low relative humidity range, which is a feature of crystals in which water is withdrawn from the structure.

Water type "B" is probably due to the dehydration of one or more of the hydrates in h.c.p. that are not stable with relative humidity such as C-S-H gel and ettringite.

Water in ettringite can contribute only to water type "B" that forms during the first day of hydration. The rest of water type "B", which as Fig. (3) indicates, increases linearly with W_n, would therefore be due to the dehydration of the C-S-H component of the paste.

A practical implication of the identification of water type "A" as physically adsorbed water, is that the surface area covered by water type "A" can be determined by applying the BET equation to its isotherm, without the complications arising from the loss and gain of the hydrate water type "B".

It is interesting to note that if we assume that water type "B" in C-S-H gel is present as a monolayer of water adsorbed between two surfaces and calculate the surface area covered by water type "B", the value of the total surface area covered by both types of water in saturated samples is about 680 m^2/gm of dry paste. This value is in close agreement with the value of 660 m^2/gm of dry paste reported by Winslow and Diamond (4) for saturated samples using low-angle X-ray scattering method. Moreover, heating at $105^{\circ}C$ in water reduces the surface area of saturated samples irreversibly by about 50% and also reduces irreversibly the amount of water type "B" by about 50%. This suggests that water type "B" is probably present in C-S-H gel as a monolayer of water separating the basic structural units composing the gel particles.

The increase in W_B on rewetting after drying suggests that drying causes neighbouring structural units that are partially or totally separated by water type "A" in the initially saturated state to approach each other creating, irreversibly, more spaces of type "B".

CONCLUSIONS:

The semi-isothermal TG/DTG method described above is a useful method for studying the properties and the distribution of evaporable water in h.c.p.

Evaporable water in h.c.p. can be divided into two types. The first type includes the water present in the pores of the paste as well as the physically adsorbed water on the free surfaces of the solid, and the second type is regarded as a structural component of some hydrates that are not stable with regard to changes in moisture content such as C-S-H gel and ettringite.

REFERENCES:

1. S. SABRI, "The response of hardened cement paste to changes in ambient relative humidity and temperature".
A PhD thesis to be submitted to the University of London (1979).

2. B. EL-JAZAIRI and J.M. ILLSTON, "A simultaneous semi-isothermal method of thermogravimetry and derivative thermogravimetry, and its application to cement pastes".
Cement and Concrete Research, Vol. 7 (1977).

3. T.C. POWERS and T.L. BROWNYARD, "Studies of the physical properties of hardened portland cement paste".
J.A.C.I. (1947).

4. D.N. WINSLOW and S. DIAMOND, "Specific surface of hardened portland cement pastes as determined by small angle X-ray scattering".
Journal of American Ceramic Society, Vol. 57, No. 5, May (1974).

Effect of cement kind on chemical and drying shrinkage

Influence du type de ciment sur le retrait chimique et hydraulique

V. DORKIN, Docent, All Union Polytechnical Institute (WZPI) Moscow, and
Yu. ZAITSEV, Professor, All-Union Polytechnical Institute (ZWPI) Moscow, U.R.S.S.

RESUME : On a étudié séparément le retrait chimique et hydraulique sur des éprouvettes en pâte de ciments portlands ayant des teneurs différentes en C_3S, C_2S, C_3A.

Les déformations chimiques et hydrauliques ont été mesurées en fonction du temps. On a constaté que les retraits chimique et hydraulique dépendaient essentiellement de la minéralogie du ciment et du rapport E/C.

SUMMARY: Separately chemical and drying shrinkage of hardened cement paste on various portland cements (with different content of C_3S, C_2S and C_3A) has been studied.

Chemical and drying shrinkage strain values as function of time are given. It is shown that both chemical and drying shrinkage strain depends significantly on the mineralogical composition of cement. Effect of w/c ratio on chemical and drying shrinkage strain is analysed.

INTRODUCTION

Shrinkage of hardened cement paste and concrete can be considered as consisting of 3 components: drying shrinkage, chemical shrinkage and carbonisation shrinkage (1,2). Chemical shrinkage seems to be one of the most fundamental properties of hardened cement paste, because it is connected only with hydration process and does not depend on the environment effects as the drying and carbonisation shrinkage do. Nevertheless chemical shrinkage is significantly less investigated as compared to drying shrinkage. In this study chemical shrinkage of hardened cement paste made on different cements was investigated. At the same time drying shrinkage of companion specimens was studied too.

MATERIALS

Table 1 shows the composition of cements used in this study.

Cement paste with three fixed water/cement ratio (0.26; 0.28; 0.30) was compacted in hermetic cylindrical moulds with the following size: diameter d = 40 mm, height h = 160 mm. Specimens were cured at 20 ± 0.5°C for a period of 18 hours (cements No. 1-4) or 2 hours (cement type No. 5). Shrinkage of the cement paste at an earlier age (i.e. plastic shrinkage) was not investigated because the chemical shrinkage does not contribute significantly to the plastic shrinkage (3,4).

APPARATUS

Chemical shrinkage was investigated on completely cealed specimens, which were immersed into toluol. Toluol is liquid having nearly the same density as water and is practically dissoluble in it. Use of liquid insulation allowed to combine the container for specimen and the support for measurement of specimen strain. Container was made from quartz to eliminate probable deformation induced by temperature changes.

Drying shrinkage was investigated on unsealed specimens in quartz supports, by 70 ± 2% r.h. and 20 ± 0.5°C in special climatic chambers.

RESULTS

Typical results of tests - chemical shrinkage strain ε_{ch} and drying shrinkage strain ε_{dr} are shown in Fig. 1.

As can be seen from Fig. 1, chemical shrinkage strain are equal to 20-30% of drying shrinkage strain. Character of chemical shrinkage curves differs significantly from that of drying shrinkage curves - the former always have an ascending part (dilatation of cement paste), the latter as a rule (with the exception of the cement No. 3) have it not. The effect of mineralogical composition of cement on shrinkage strain of both kinds is shown in Fig. 2, where related strain values $\varepsilon_{ch}/\varepsilon_{ch}^{*}$ $\varepsilon_{dr}/\varepsilon_{dr}^{*}$ are given; ε_{ch}^{*} and ε_{dr}^{*} are values of ε_{ch} and ε_{dr} respectively at the end of the test, i.e. by t = 672 h.

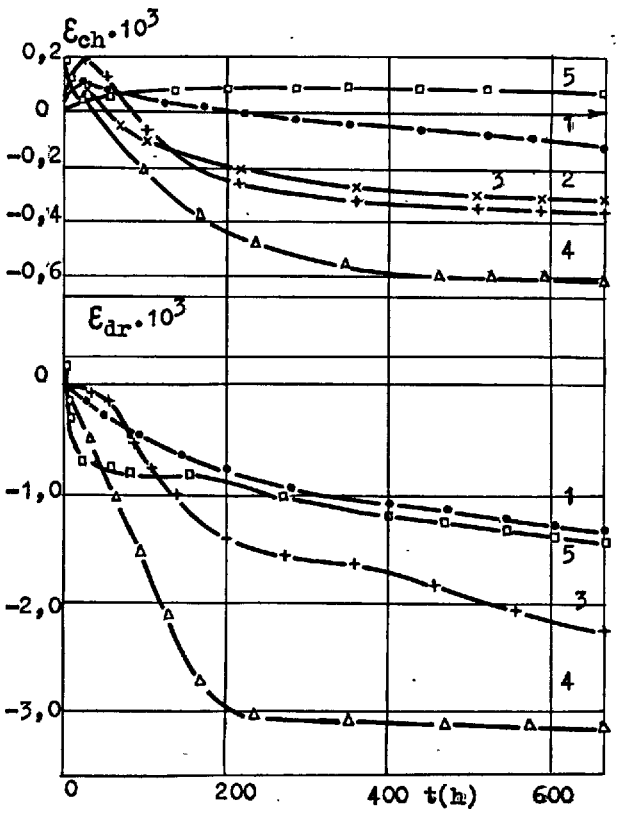

Fig. 1. Chemical and drying shrinkage as a function of time

It can be seen from Fig. 2, that for drying shrinkage the mineralogical composition effects rather the absolute values of strain than the character of shrinkage curves; for chemical shrinkage, on the contrary, both the absolute strain values and the character of shrinkage curves (especially at the beginning of the test) are significantly affected by mineralogical composition of cement.

In an effort to find out quantitative connections between mineralogical composition of cement and shrinkage strain we have considered ε_{ch}^{*} - and ε_{dr}^{*} - values as functions of the content of C_3A - see Fig. 3. Reasons to choose the C_3A - content as a parameter were the following. On the one hand the presence of the C_3A accelerates hydration of C_3S (5), which can accelerate shrinkage process too. On the other hand

TABLE I

No. Material	Composition, %			
	C_3S	C_2S	C_3A	C_4AF
1. Low alumina portland cement	66	15	4	13
2. Low alumina portland cement	56	21	4	13
3. Middle alumina portland cement	57	14	6	15
4. High alumina portland cement	60	12	8	14
5. Alumina gipseous cement*)	-	-	-	-

*) Al_2O_3 = 45.25%, CaO = 42.45%, SiO_2 = 9.77%, S = 1.25%; gipsum is used to regulate the hardening of cement paste.

the content of C_3A varied in our cements in a relatively wide range as compared to other components of cement. It was assumed that $\varepsilon_{ch} = 0$ at the moment of maximal dilatation of cement paste . As can be seen from Fig. 3 both chemical and drying shrinkage strain increases nearly linearly with the increasing of the C_3A content. Similar results for only drying shrinkage of two kinds of cement were obtained in (6,7) by C_3A content equal to 0.1% and 12%. Water cement ratio effects the shrinkage strain slightly. Nevertheless it is obvious that this effect is different for drying and chemical shrinkage: the more is W/c the more is drying shrinkage and the less is chemical shrinkage strain.

CONCLUSIONS

Chemical shrinkage strain are equal to 20-30% of drying shrinkage strain. Both chemical and drying shrinkage strain depends significantly on the mineralogical composition of cement. Both chemical and drying shrinkage strain increases nearly linearly with the increasing of the C_3A content. Effect of W/c ratio is different for drying and chemical shrinkage: drying shrinkage strain increases and chemical shrinkage strain decreases with the increasing of W/c ratio.

REFERENCES

1. A.M. NEVILLE (1963), Properties of Concrete. London, 344 pp.
2. S.V. ALEKSANDROVSKIJ (1973), Calculation of concrete and reinforced concrete structures on fluctuations of temperature and humidity with respect on creep. Moscow, Strojizdat (in Russian), 432 pp.
3. R. L'HERMITE (1960), Volume change of Concrete, Proc. 4th Int. Symp. on Chemistry of Cement, Washington, pp. 659-694.
4. F.H. WITTMANN (1976), On the Action of Capillary Pressure in Fresh Concrete. Cem. Concr. Res., vol. 6, No. 1, pp. 49-56.
5. A. CELANI, A. MOGGI, A. RIO (1968), The Effect of C_3A on the Hydration of C_3S and Portland Cement. Proc. 5th Int. Symp. on Chemistry of Cement, Tokio, parts I-IV, pp. 248-249.
6. M. VENAUT (1968), Influence du ciment sur le retrait hydraulique apres prise. Int. Coll. on the Shrinkage of Hydraulic Concretes. Madrid, II.
7. G.P. TOGNON* (1968), Le retrait d'hydratation du ciment en relation a certaines caracteristiques physiques et a la composition chimico-mineralogique des clinkers y relatifs. Int. Coll. on the shrinkage of Hydraulic Concretes. Madrid, II-I.

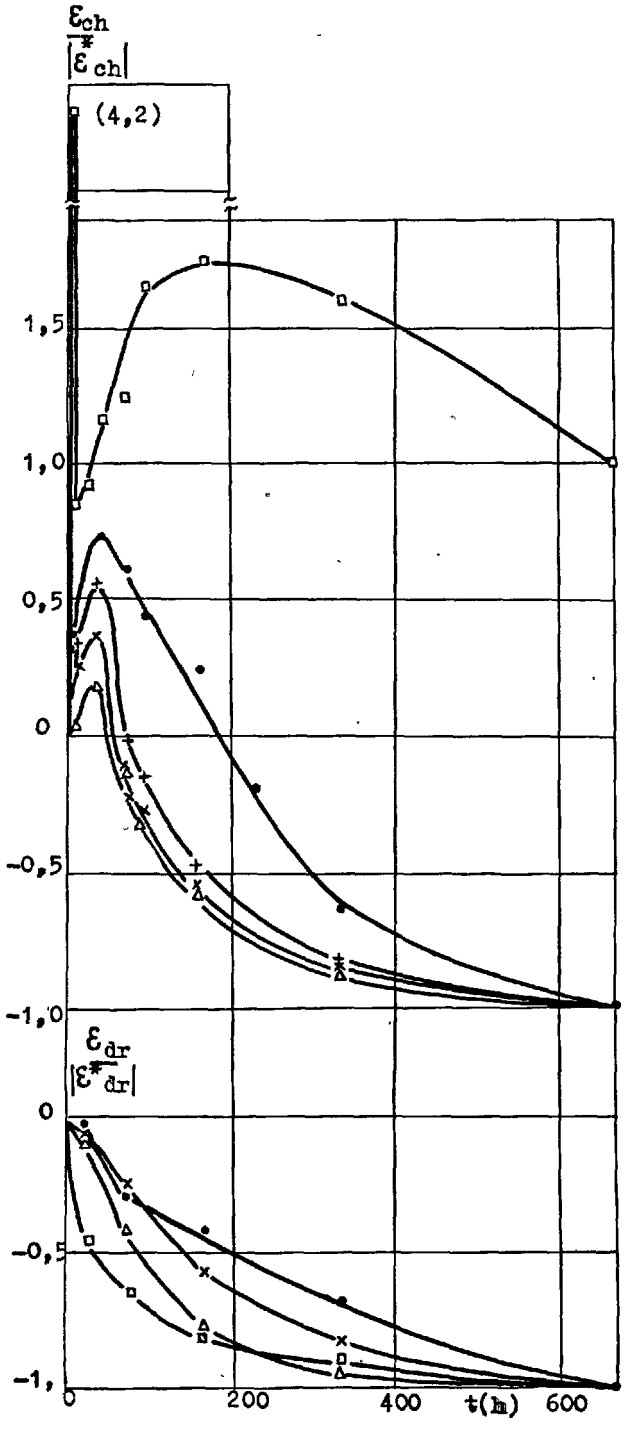

Fig. 2. Related chemical and drying shrinkage strain as a function of time

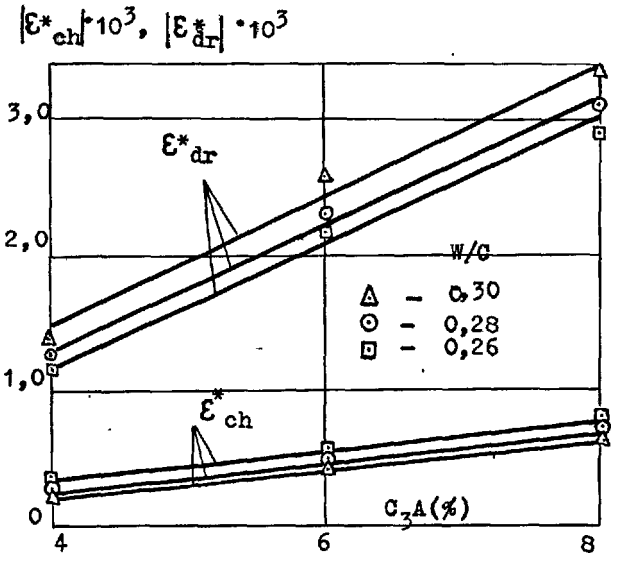

Fig. 3. Chemical and drying shrinkage strain at the end of the test as a function of C_3A content

Ageing and Drying of Tricalcium Silicate Pastes

Vieillissement et séchage des pâtes de silicate tricalcique

N.B. MILESTONE, Scientist, Chemistry Division, Department Scientific and Industrial Research, Petone, New Zealand.

SUMMARY

Trimethylsilylation has been used to study changes in the silicate phase composition upon ageing and drying of tricalcium silicate pastes dried at varying relative humidities from 75% rh to 11% rh. Drying is shown to have a pronounced effect on the distribution of the silicate phases in the C-S-H gel.

Drying pastes to 33% rh or less causes irreversible changes in the distribution of silicate phases in the gel. Monosilicate is not present and the amount of polysilicate increases as drying is increased. No increase in polysilicate with time is noted.

For pastes dried to 53% or 75% rh, monosilicate is present in the gel but the amount decreases with time (half-life of approximately one and a half weeks). The amount of polysilicate in the gel increases with time without any increase in the degree of hydration indicating an ageing effect.

The ageing effect is considered to be a silicate condensation reaction and could explain the age dependent changes in creep and shrinkage of pastes and surface area changes noted by other workers.

RESUME : On a utilisé du triméthylsilyl pour étudier les variations de la composition des phases silicatées, au cours du vieillissement du séchage de pâtes de silicate tricalcique soumises à des atmosphères desséchantes, ayant des humidités relatives variant de 75 % à 11 %. On a observé que le séchage a un effet prononcé sur la distribution des phases de silicate dans le gel de C-S-H.

Les pâtes desséchées à 33 % d'humidité relative, ou moins, subissent des variations irréversibles de cette distribution du silicate dans le gel. Le monosilicate disparaît et la proportion de polysilicate augmente avec le séchage. Cette proportion de polysilicate n'augmente pas avec le temps.
Dans les pâtes desséchées entre 53 % et 75 % d'humidité relative, le monosilicate est présent dans le gel, mais sa proportion diminue avec le temps (diminution approximative de moitié en une semaine et demi). La proportion de polysilicate dans le gel augmente avec le temps, sans que l'on observe d'accroissement de l'hydratation ou du vieillissement.

Le vieillissement semble dû à une polymérisation, ce qui peut expliquer les variations avec l'âge du retrait et du fluage des pâtes et de leur surface spécifique, signalées par d'autres chercheurs.

INTRODUCTION

Changes in some of the properties of cement and calcium silicate pastes that cannot be accounted for by changes in degree of hydration (α) or porosity have been noted by several workers. These changes may be accounted for by an ageing or maturing process, occurring in the microstructure of the CSH gel.

Parrott[1] noted that creep was reduced in samples stored at high humidity and loaded at later ages as compared to samples with the same degree of hydration loaded at early ages. In later work[2] he showed that heat treatment produced a similar effect. Parrott attributed this effect to continued polymerization of the silicate in the CSH gel after hydration had ceased and using the method devised by Funk and Frydrych[3], was able to show that increased polymerization occurred.[2]

Hunt et al[4] reported that drying affected the measured values of surface areas. For pastes stored between 40 and 60% rh they found a time-dependent decrease in the surface area determined using N_2 and suggested this effect was due to some form of an ageing mechanism.

Changes upon heating dried tobermorite gels were attributed to changes in silicate polymerization by Collepardi et al[5]. Funk[6], in his studies on the ageing of tobermorite gels, was able to measure an increase in the amount of polysilicate.

Changes in silicate pastes are normally considered to occur in the C-S-H gel. The gel is amorphous and generally indirect methods must be used for study. These usually involve severe drying. Drying has been shown to affect the physical properties of amorphous C-S-H gel in cement paste. Irreversible changes in basal spacings of C-S-H(I) upon drying were noted by Gutteridge and Parrott[8].

A new method, pioneered by Lentz[9] and perfected by Tamas et al[10] for cement pastes gives a direct method of examining the chemical structure of silicates in a paste without the need for harsh drying. Trimethylsilyl derivatives are formed which prevent further polymerization and permit analysis by gas-liquid chromatography (glc) and gel-permeation chromatography.

Workers at the University of Illinois[11-15] applied several techniques, including those of silylation, to a series of pastes subjected to creep and shrinkage. They noted that differences in drying caused differences in the nonvolatile polysilicate component of the pastes[12,13]. Further work on the structural properties of the pastes[14] showed that the amount of polysilicate correlated with time suggesting a time dependent ageing process. The percentage polysilicate in the paste was also shown to increase with temperature[15] and it was found that pastes hydrated at 4°C contained monomer in the gel.

This paper describes a study of the changes in silicate structure of tricalcium silicate pastes dried to various relative humidities and the effects of storing these pastes at the different humidities.

EXPERIMENTAL

C_3S pastes (w/s = 0.5) were mixed in vials under N_2 and hydrated at 21°C. After hydration the vials were opened and quickly hand-ground under a large inverted funnel through which dry nitrogen was flushed before being immediately equilibrated at relative humidities of 75%, 53%, 33% and 11% rh. Samples for derivatization were taken at 24 hours, one week, four weeks and eight weeks. The degree of hydration was determined using non-evaporable water loss and checked by X-ray diffraction (XRD) for several samples.

Derivatization was carried out using the method of Tamas et al with the quantities of the reagents doubled to counter the effects of the extra water added in the samples conditioned at high rh's. Quantitative glc was carried out using the standard described by Milestone[16]. Polymeric silicate (more than 6 Si-O linkages) was determined gravimetrically by heating the mixture of derivatives at 180° for 24 hours. The percentage of oligosilicates (units of 3-6 Si-O linkages) was determined by difference and is subject to an error of ± 3% in actual value. Results are expressed as a percentage of total silica in the paste.

RESULTS

The amounts of the various silicate phases in C_3S pastes derivatized after 24 hour equilibration are shown in Table I and monomer and polysilicate percentages plotted in Figure 1.

TABLE I

α	Silicate Phase	Relative Humidity 75%	53%	33%	11%
0.55	Monomer (I)	64(19)*	51 (6)	51 (6)	45 (0)
	Dimer (II)	27	25	26	27
	Polysilicate	3.0	3.6	5.0	6.0
	Oligosilicate	6	20	18	22
0.65	Monomer (I)	40 (5)	36 (1)	35 (0)	35 (0)
	Dimer (II)	46	48	45	46
	Polysilicate	6.4	8.0	8.1	9.1
	Oligosilicate	8	8	12	10
0.78	Monomer (I)	29 (7)	26 (4)	27 (5)	23 (1)
	Dimer (II)	60	58	48	54
	Polysilicate	9.5	11	11.3	12.4
	Oligosilicate	1	5	14	11
0.86	Monomer (I)	25(11)	23 (9)	20 (6)	19 (5)
	Dimer (II)	55	58	54	55
	Polysilicate	13.2	15.8	16.8	18.9
	Oligosilicate	7	3	9	7

Figures expressed as % total silica.
* Percentage of gel monomer

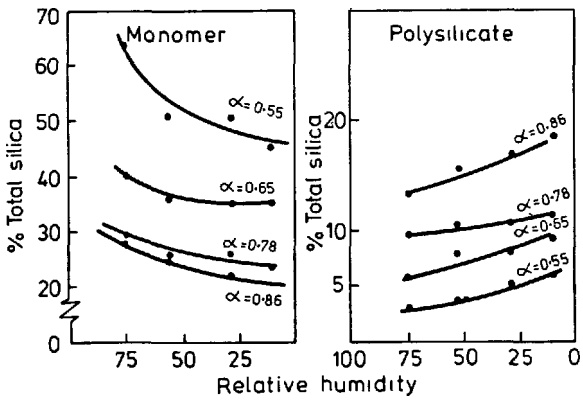

Fig 1. Silicate Phase Changes with Drying.

At the lower degrees of hydration, the amount of monomer present can largely be accounted for by unhydrated C_3S present in pastes dried below 53% rh. At α = 0.78 and 0.86 only for the pastes dried at 33% rh or less can the percentage of monomer be related by to the content of unhydrated C_3S. For pastes equilibrated at higher relative humidities the percentage of monomer is greater than can be accounted for by unhydrated C_3S but as the pastes are dried the amount of monomer decreases until a constant value is obtained at 11% rh.

(See Fig 1)

Little systematic variation in percentage of dimer appears to occur as samples are systematically dried. However, there does appear to be an increase in oligosilicate on increased drying especially with α = 0.55 but the error in oligosilicates is so large that no significant change is noted at $\alpha > 0.78$.

The effects of storage at the various relative humidities on phase composition are shown in tables II-IV, selected results are plotted in figure 2.

There is little change with time for any phase in pastes equilibrated at 11% rh. However, for all pastes equilibrated at 33% rh or higher, there is an increase in polysilicate with time. This is accompanied by a decrease in monomer content and a slight increase in dimer content with time.

Results obtained from cement pastes cured in the same manner were difficult to interpret and the results are not shown. Berger et al[14] suggested that foreign ions such as Al and S could cause an apparent reduction in polysilicate by substituting in the silicate structure and the presence of these ions may complicate the changes observed for the cement pastes.

TABLE II

Relative Humidity	Phase	α = 0.65 Time (Weeks) 0	1	4	8
11%	Monomer (I)	35 (0)*	36 (1)	34 (0)	35 (0)
	Dimer (II)	46	46	46	48
	Polysilicate	9.1	9.1	10	10
	Oligosilicate	10	9	10	7
33%	Monomer (I)	35 (0)	33 (0)	33 (0)	-
	Dimer (II)	45	43	48	-
	Polysilicate	8.1	8.6	8.5	9.1
	Oligosilicate	12	15	10	-
53%	Monomer (I)	36 (1)	37 (2)	35 (0)	34
	Dimer (II)	48	44	47	48
	Polysilicate	8.0	7.0	13.0	10.1
	Oligosilicate	8	12	5	8
75%	Monomer (I)	40 (5)	38 (3)	36 (1)	35
	Dimer (II)	46	44	44	45
	Polysilicate	6.4	9.1	10.8	12.1
	Oligosilicate	8	9	9	8

Figures expressed as % total silica
* Percentage of gel monomer

TABLE III

Relative Humidity	Phase	α = 0.78 Time (Weeks) 0	1	4	8
11%	Monomer (I)	23 (1)*	20 (0)	21 (0)	24 (2)
	Dimer (II)	54	57	52	55
	Polysilicate	12.4	12.5	11.8	12.7
	Oligosilicate	11	10	15	8
33%	Monomer (I)	27 (5)	25 (3)	19 (3)	23 (1)
	Dimer (II)	48	45	45	50
	Polysilicate	11.3	11.4	14.9	15.2
	Oligosilicate	17	19	21	12
53%	Monomer (I)	26 (4)	24 (2)	21 (0)	22 (0)
	Dimer (II)	58	45	55	57
	Polysilicate	10.8	10.8	13.8	17.8
	Oligosilicate	5	20	10	13
75%	Monomer (I)	29 (7)	27 (5)	21 (0)	21 (0)
	Dimer (II)	60	59	64	59
	Polysilicate	9.5	10.9	12.9	14.9
	Oligosilicate	1	3	1	5

Figures expressed as % total silica
* Percentage of gel monomer

TABLE IV

Relative Humidity	Phase	α = 0.86 Time (weeks) 0	2	8	12
11%	Monomer (I)	19 (5)	17 (3)	18 (4)	17 (3)
	Dimer (II)	55	56	53	53
	Polysilicate	18.9	15.4	17.6	17.9
	Oligosilicate	7	12	11	12
33%	Monomer (I)	20 (6)	19	17	19 (5)
	Dimer (II)	54	56	60	54
	Polysilicate	16.8	17.8	17.3	18.1
	Oligosilicate	9	7	6	9
53%	Monomer (I)	23 (9)	19	17	17 (3)
	Dimer (II)	58	57	60	58
	Polysilicate	15.8	16.3	17.3	17.4
	Oligosilicate	4	8	6	8
75%	Monomer (I)	25 (11)	20	15	15 (1)
	Dimer (II)	55	55	59	56
	Polysilicate	13.2	15.2	17.1	17.8
	Oligosilicate	6	10	9	9

Figures expressed as % total silica
* Percentage of gel monomer

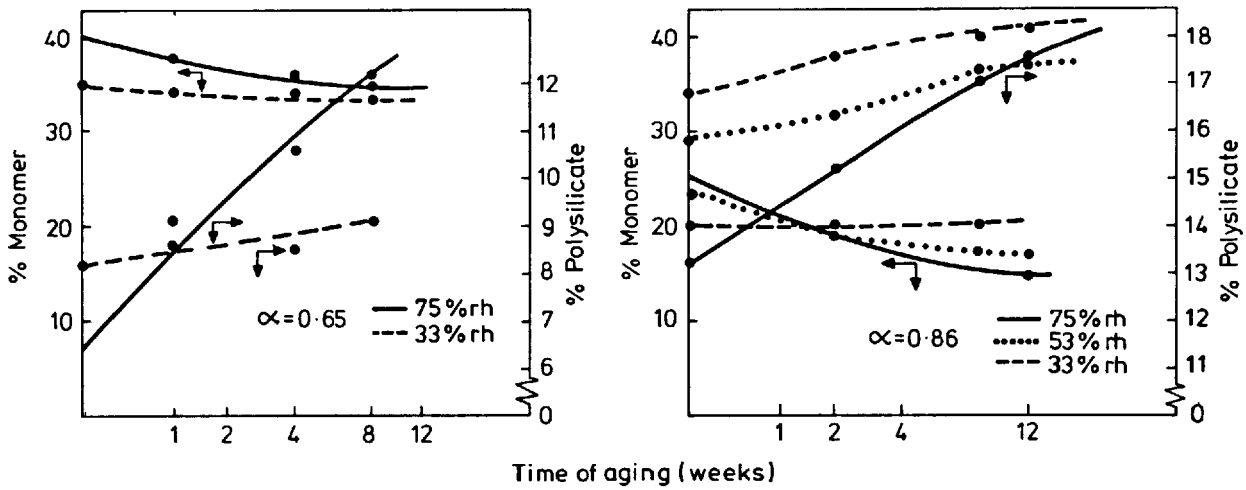

Fig 2. Effect of Silicate Composition on Ageing.

DISCUSSION

The phase composition changes as hydration proceeded were similar to those reported by other workers[9,10,12]. There is a decrease in monomer content with a subsequent increase in dimer followed more slowly by an increase in polysilicate content. Small amounts of oligosilicates are present, especially those due to linear trimer and cyclic tetramer. After an initial increase in the amount of these species, there is a decrease to a low constant value as hydration proceeds.

The most marked changes occurring in the paste on drying are the decrease in monomer content, together with the general increase in polysilicate content. (Fig 1) There is little systematic change in the amount of dimer present on drying pastes at all values of α. A slight increase in the amount of oligosilicates occurs upon drying but this is pronounced for α = 0.55. An initial increase in the amount of trimer was noted by Sarkar and Roy[17] in cement pastes that had been vacuum dried. Dent Glasser et al[18] showed that all the monomer present in their samples could be accounted for by unhydrated C_3S in the pastes. However, their pastes were vacuum dried. Monomer contents for the pastes dried to 11% rh in this study also closely relate to the amount of unreacted C_3S. For the less severely dried pastes more monomer is present than can be accounted for by unreacted C_3S and it is thus clear that some monomer must be present in the C-S-H gel.

Rothbaum and Rohde[19] postulated that in silica polymerization in dilute solutions, the monomer preferentially reacted with polymeric silica units rather than another monomer unit, since the amount of dimers and higher species in solution was low. A similar reaction could explain the lack of large dimer increase upon drying, together with the slight increase in oligosilicates and the large increase in polysilicate. In the sample with α = 0.55, there is very little polymer present before drying and so condensation of monomer with dimer and oligosilicates occurs giving the large oligosilicate increase rather than a high polysilicate increase.

There is little change with time of the proportions of the silicate phases for pastes dried at 11% rh. (Tables II-IV). After the increase caused by drying no further ageing takes place. It has been noted that processes such as creep do not occur in well dried pastes[20] and irreversible changes occur upon drying CSH(I)[8].

For α ⩾ 0.65 the changes upon ageing are significant. Polysilicate increases with time, especially in pastes equilibrated at 75% and 53% rh, with a consequent reduction in monomer (See Fig 2). The gel monomer (obtained by subtracting the silica due to unhydrated C_3S and shown by the figures in brackets in tables I-IV) decreases with an approximate half-life of 1½ weeks.

For the pastes with α = 0.65 and 0.86 the results plotted in Fig 2 show that the greatest changes occur when the pastes are equilibrated at 75% rh. The time-dependent monomer decrease has almost reached zero after 8 weeks for α = 0.65 and 10 weeks for α ≐ 0.86 but the amount of polysilicate continues to increase with time. Thus ageing is not associated solely with the loss of gel monomer but there must be continued contribution from the dimer and oligosilicates. The values of α in pastes equilibrated at 75% rh were analysed by XRD. Non-evaporable water analyses repeated at

the end of the experiment showed a slight decrease but XRD showed no significant change in α. The decrease in non-evaporable water could be expected if a continued polymerization reaction occurred since some will escape as evaporable water.

When Bentur et al[15] found evidence for monomer in the gel at 4°C, the amount was pronounced only at low values of α and in young pastes, and decreased with time as the polysilicate was formed. They postulated that in the process monomer $\xrightarrow{1}$ dimer $\xrightarrow{2}$ polysilicate, the rate determining step was that of dimer to polysilicate. However this was based on results obtained from pastes derivatized after 11% rh drying. It is clear that drying can give a false picture of the relative proportions of the various phases. Thus the rate constant for step 2 may not be very much less than that for st p 1 which would mean that in the young saturated paste a considerable proportion of gel still exists as monomer. When a young paste is dried the capillary forces would force the silicate units closer together, especially those of the monomer which are likely to exist in solution, creating a condition where polymerization is likely to occur.

In an aged, but not dried, paste all the gel monomer will have reacted, although the polysilicate formed may be of a different nature. In the results discussed by Bentur et al[13], drying caused large increases in polysilicate content of pastes with α = 0.42 but the changes were not marked in pastes with α = 0.68. However, in this case the pastes had been stored for some time and so could not be considered young.

It is possible that some monomer is formed during the derivatizing process but this amount is likely to be small. Derivatization trials with 14Å tobermorite and xonotolite show that crystalline hydrous polysilicates derivatize as 97-98% of polymer[21]. Further after four weeks of 'ageing' at 75% rh the pastes show little more monomer than expected from unhydrated material.

The above results show that monomeric silicate exists in the C-S-H gel of fresh silicate pastes. It has not been detected previously because pastes have been severely dried.

CONCLUSIONS

When an immature silicate paste is dried, there is an increase in the amount of polysilicate present in the paste together with a decrease in the amount of monomer. For pastes dried at rh's higher than 33% monomer is present in the gel.

An ageing process occurs in pastes equilbrated at rh's greater than 33% rh with the greatest change occurring at 75% rh. Polysilicate content increases with time and the gel monomer content decreases with a half-life of approximately 1½ weeks.

These processes can be explained by a process of silicate polymerization where further Si-O-Si bonds are formed on drying or ageing.

REFERENCES

1.- L.J. PARROTT (1973),"An Examination of the Effects of the Age of Loading upon the Creep of Hardened Cement Paste", Mag. Concr. Res. 25(85(197-200.

2.- L.J. PARROT (1977), "Basic Creep, Drying Creep and Shrinkage of a Mature Cement Paste after a Heat Cycle", Cem. Concr. Res. 7(5) 597-604.

3.- H. FUNK and R. FRYDRYCH (1966), "The Degrees of Anion Condensation in Silicic Acids and Silicates," Highway Research Bd. Special Report 90 284-290.

4.- C.M. HUNT, L.A. TOMES and R.L. BLAINE (1960). "Some Effects of Aging on the Surface Area of Portland Cement Paste", J. Res. Natl. Bur. Stds A 64(2) 163-169 (1960).

5.- M. COLLEPARDI, L. MASCIDDA and G. USAI (1971), "The Kinetics and the Mechanism of Ageing of Tobermorite Gel", Il Cemento 68, 3,9,13,19 (English Translation).

6.- H. FUNK (1965), "Chemical Alterations of Poorly Crystallized Calcium Silicate Hydrates by Hydrothermal Treatment", Symp. Autoclaved Calcium Silicate Building Products, London. Pub Soc. Chem. Ind. 1965.

7.- K.S. BIRRELL and M. FIELDS (1968), "Amorphous Constituents: in Soils of New Zealand Pt II. N.Z. DSIR Soil Bureau Bull 26(2) 39-49.

8.- W.A. GUTTERIDGE and L.J. PARROTT (1977) "A Study of the Changes in Weight, Length and Interplanar Spacing induced by Drying and Wetting Synthetic CSH(I). Cem. Concr. Res 6 357-360

9.- C.W. LENTZ (1966), "The Silicate Structure Analysis of Hardened Portland Cement Paste",ref 3 269-283.

10.- F.D. TAMAS, A.K. SARKAR and D.M. ROY (1976), "Effect of Variables upon the Silylation Products of Hydrated Cements,: Conf. Hydraulic Cement Pastes, Sheffield. Pub. C. and CA.

11.- S. MINDESS, J.F. YOUNG and F.V. LAWRENCE Jr.(1978), "Creep and Drying Shrinkage of Calcium Silicate Pastes, I, Specimen Preparation and Mechanical Properties", Cem. Concr. Res. 8 591-600.

12.- A. BENTUR, N.B. MILESTONE and J.G. YOUNG (1978), "Creep and Drying Shrinkage of Calcium Silicate Pastes, II, Induced Microstructural and Chemical Changes", Cem. Concr. Res. 8 721-732.

13.- A. BENTUR, R.L. BERGER, F.V. LAWRENCE Jr, N.B. MILESTONE, S. MINDESS and J.F. YOUNG (1979), "Creep and Drying Shrinkage of Calcium Silicate Pastes, III, A Hypothesis of Irreversible Stains", Cem. Concr. Res. 9 83-96.

14.- R.L. BERGER, A. BENTUR, N.B. MILESTONE and J.H. KUNG (1979), "Structural Properties of Calcium Silicate Pastes, I, Effect of the Hydrating Compound". J. Amer. Ceram. Soc. July/Aug.

15.- A. BENTUR, R.L. BERGER, J.H. KUNG, N.B. MILESTONE and J.F. YOUNG (1979), "Structural Properties of Calcium Silicate Pastes, II, Effect of Curing Temperature". J. Amer. Ceram. Soc. July/Aug.

16.- N.B. MILESTONE (1977), "A New Method of Quantitative Silylation of Silicates", Cem. Concr. Res. 7 345-346.

17.- A.K. SARKAR and D.M. ROY (1979), "A New Characterization Technique for Trimethylsilylated Products of Old Cement Pastes", Cem. Concr. Res. 9 343-352.

18.- L.S. DENT GLASSER, E.E. LACHOWSKI, K. MOHAN and H.F.W. TAYLOR (1978), "A Multimethod Study of C_3S Hydration" Cem. Concr. Res. 8 733-740.

19.- H.P. ROTHBAUM and A.G. ROHDE (1979) "Kinetics of Silica Polymerization and Deposition from Dilute Solutions between 5°C and 180°C." Accepted Jnl Coll. Interface Sci.

20.- A.M. NEVILLE (1970), "Creep of Concrete: Plain Reinforced and Prestressed." Chapt. 6. Pub. North Holland.

21.- N.B. MILESTONE (1979). Unpublished results.

On the effect of preventing drying shrinkage cracks of expansive cement concrete

Action préventive contre les fissures et retrait du ciment expansif dans les bétons

J. ISOGAI, Senior Research Chemist
S. NAKAYA, Civil Engineer,
H. NISHIMURA, Research Chemist, Denki Kagaku Kogyo Co., Ltd., R and D Department of Omi-Plant, Japon.

SUMMARY : In the field of civil and architectural engineering in Japan, the usefulness of the calcium sulfoaluminate expansive admixture has come to gain a wide public acceptance.

In the case of concrete using the calcium sulfoaluminate expansive admixture, the amount of the free shrinkage due to drying in the nonrestraint state is less than ordinary concrete, and also the extensibility of concrete is greatly increased by expansion.

In the studies, preventive effects on the drying shrinkage cracks by the reduction of drying shrinkage and the increase of extensibility were elucidated chemically.

And, it was made clear that the extensibility of expansive cement concrete increases in proportion to the amount of capillary pores formed by expansion, and also the amount of drying shrinkage decreases in proportion to the amount of Ettringite formed in capillary pores.

RESUME : Au Japon, l'emploi, en génie civil et dans le bâtiment, d'additions produisant du sulfoaluminate de calcium expansif, connait un certain développement.

Dans les bétons utilisant de telles additions, le retrait non contrarié, dû au séchage, est plus faible que celui des bétons ordinaires, et leur expansion en est bien augmentée.

Des études ont permis d'élucider les phénomènes chimiques qui, dans ces bétons, diminuent les risques de fissuration de retrait, par réduction de ce retrait et augmentation de l'expansion.

Il a été clairement établi que l'expansion de ces bétons croissait proportionnellement au volume des pores capillaires créés par l'expansion, et que le retrait hygrométrique diminuait proportionnellement à la quantité d'ettringite formée dans ces pores.

1. INTRODUCTION

In the field of civil and architectural engineering in Japan, expansive admixture of calcium sulfoaluminate type, which are being used in quantities with a purpose of reducing drying shrinkage cracks or of introducing chemical prestress, have gained a wide public acceptance because of its usefulness[1].
The concrete using the calcium sulfoaluminate expansive admixture is characterized by less free shrinkage amount on drying in a nonrestrained state than ordinary concrete and also a remarkable increase in the extensibility of concrete by expansion.
In the studies, with an intention of elucidating chemically the aforesaid characteristic properties of the concrete using the calcium sulfoaluminate expansive admixture, experiments with the following three subjects were carried out:
1) the elucidation of hydration process for cement paste, 2) the elucidation of expansion phenomenon for cement mortar, and 3) the elucidation of preventive effect on drying shrinkage cracks for concrete and the quantitative grasping of its preventive effect.

2. EXPERIMENTS

The results of chemical analyses for the calcium sulfoaluminate expansive admixture and the normal portland cement used in the experiments are given in Table 1.

TABLE I

	ig. loss	in-sol	SiO_2	Al_2O_3	Fe_2O_3	CaO	MgO	SO_3
P.C.	0.8	0.1	21.9	5.1	3.0	64.2	1.2	2.1
C.S.A.	1.2	0.6	2.9	11.0	0.5	52.8	1.0	29.5

The main mineral composition of the expansive admixture includes 15.7% $C_4A_3\bar{S}$, 13.0% $C_{12}A_7$, 16.9% free-CaO, 52.6% $CaSO_4$ and the rest.

2-1 PASTE EXPERIMENTS FOR ELUCIDATING HYDRATION PROCESS

With an object of making clear the hydration process of normal portland cement paste which is added the calcium sulfoaluminate expansive admixture (hereinafter referred to as CSA expansive admixture). a cement paste of a water-cement ratio of 0.40 was prepared by using a 11% CSA expansive admixture-mixed normal portland cement. And, expansion due to hydration in the early period were measured by a Le Chatelier simplified expansion tester and then hydration process was investigated in detail by using X-ray diffraction, a differential thermal balance, and a scanning electron microscope.

2-2 MORTAR EXPERIMENT FOR ELUCIDATING EXPANSION PHENOMENON

In the experiments, with a purpose of investigating the change in the fine pore structure of hardened mortar with the hydration and expansion of expansive cement, a cement mortar of a cement-sand ratio of 1 : 2 and a water-cement ratio of 0.45 was prepared by using 0,7, 11, and 15% CSA expansive admixture-mixed normal portland cement. Using a scanning electron microscope, the shapes of Ettringite and calcium hydroxide, which are causative of expansion, were observed and also by a mercury porosimeter, the variation in the fine structure of hardened mortar was investigated.

2-3 CONCRETE EXPERIMENTS FOR MAKING CLEAR PREVENTIVE EFFECT ON CRACKS DUE TO DRYING SHRINKAGE

Table 2 shows the mix proportion of concrete and also Fig. 1 illustrates concrete specimens for crack development.
In the experiments, with a purpose of quantitatively making clear the effect of reducing drying shrinkage and the effect of preventing cracking for the case where a CSA expansive admixture-mixed ordinary portland cement concrete (hereinafter referred to as expansive concrete) was cured under water at 20°C for a definite period and then dried at 20°C, 60%RH, an examination was made of a relation between the fine structure of hydrate in paste portion of concrete and its mechanical characteristics.

TABLE II

	W/C (%)	S/A (%)	CSA (%)	Unit weight(kg/m^3) C	CSA	W	S	G
Plain concrete	537	39	0	300	0	161	753	1187
CSA concrete	537	39	10	270	30	161	753	1187

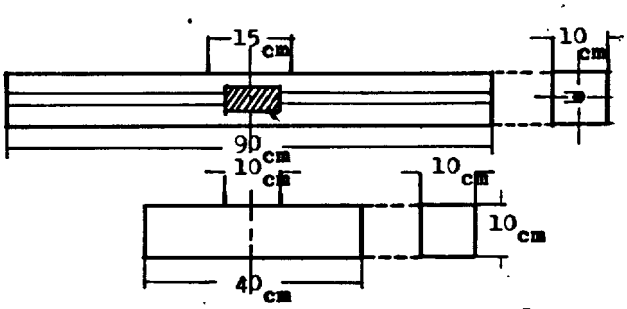

Fig.1-Dimension of the test pieces for evaluating shrinkage cracks and free expansion-shrinkage of concretes.

3. EXPERIMENTAL RESULTS AND CONSIDERATIONS

3-1 ELUCIDATION OF HYDRATION PROCESS OF PASTE[2]

The early expansion developing curve of paste, obtained by a Le Chatelier simplified expansion tester, is shown in Fig. 2, and also the result on the powder X-ray diffraction for hardened cement paste is given in Fig. 3 and 4.

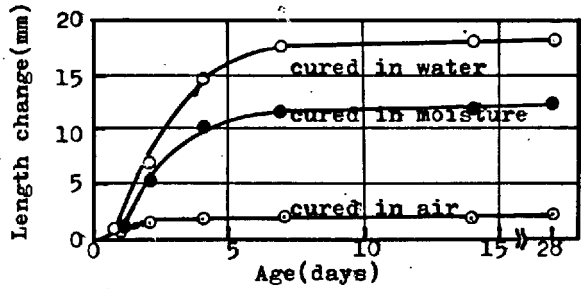

Fig.2-Early expansion developing curves of paste by a Le Chatelier Simplified expansion tester.

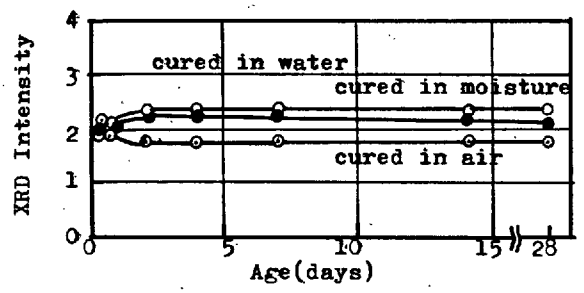

Fig.3-X-ray diffraction intensity of Ettringite produced at each age.

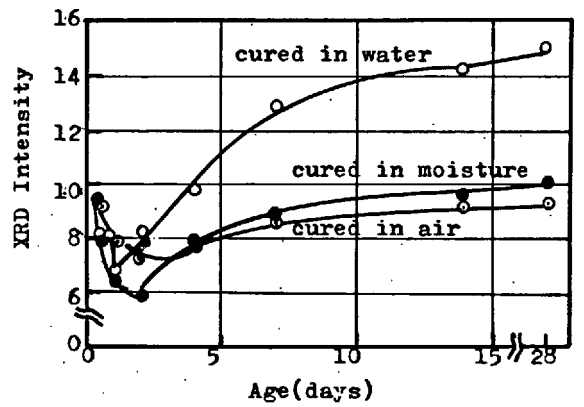

Fig.4-X-ray diffraction intensity of $Ca(OH)_2$ produced at each age.

The crystalline Ettringite, which is considered to be one of the causes of expansion of the CSA expansive admixture, reaches a saturation at the age of approx.
16 hours regardless of curing conditions, after which no change was observed in the Ettringite. The fact gives a ground that expansion amount is not necessarily related to the amount of formation of Ettringite, similarly to the case with long ages. The early expansion developing curve as shown in Fig. 2 indicates that the crystalline Ettringite does not take part in the expansion development of hardened cement paste.
The result on the dehydration curve of Ettringite obtained by a differential thermal balance is given in Fig. 5.

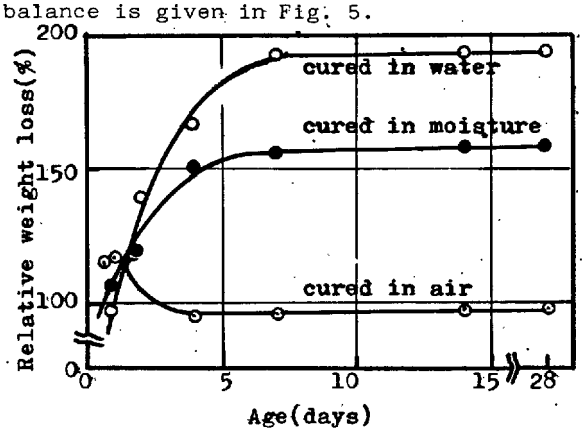

Fig.5-Relative weight loss curves of Ettringite measured by differential thermal balance.

The result shows that it is related to the early expansion developing curve shown in Fig. 2, showing the presence of noncrystalline Ettringite such that powder X-ray diffraction fail to detect.
And, crystalline $Ca(OH)_2$, as shown in Fig. 4, which is formed by the hydration of free-CaO, seems to somewhat relate to the expansion of cement paste.
In consequence, it was made clear from an investigation into the hydration process of hardened CSA expansive cement paste under varying curing conditions that the hardened cement paste expanded in proportion to the amount of formation of noncrystalline Ettringite and the amount of formation of crystalline $Ca(OH)_2$.

3-2 ELUCIDATION OF EXPANSION PHENOMENON OF MORTAR[3]

Since the hydration process of the CSA expansive cement was made clear from basic experiments with cement paste, an investigation was made on how the constitutional structure of hardened cement mortar is changed by expansion due to hydration.
The result on the observation of the fine structure of hardened cement mortar by a scanning electron microscope is given in Fig. 6, and also the result on the measurements of expansion is given in Fig. 7.
In the case of normal portland cement mortar the hexagonal calcium hydroxide crystals and calcium silicate hydrate crystals were merely observed. And, in the case of a 7% CSA-added mortar of less expansibility, comparatively large needle-like crystal suspected to be formed in voids by a through solution reaction was observed, but fine Ettringite considered to be formed by a topochemical reaction was not almost observed. For a 11% CSA-added mortar which shows optimum expansion amount, two forms of Ettringites were recognized and also $Ca(OH)_2$ crystals were observed. And, for a 15% CSA-added mortar which shows great expansion amount, great amounts of fine Ettringite were observed, indicating that the fine Ettringite crystals have a close relevance to expansion.
Fig. 8 shows the pore size distribution of

capillary pores obtained by a mercury porosimeter in terms of the fine structure of hardened mortar.

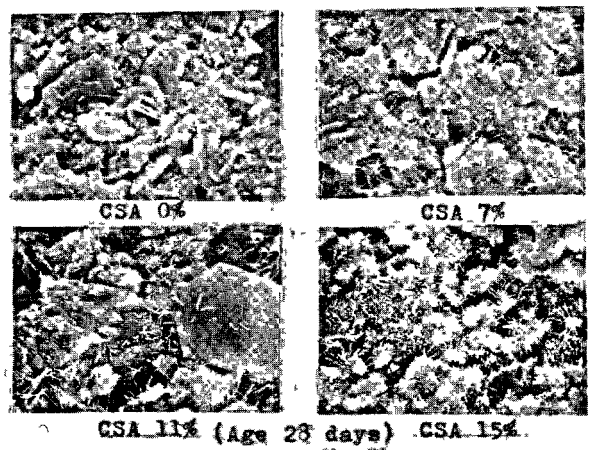

Fig.6-Scanning electron micrographs.

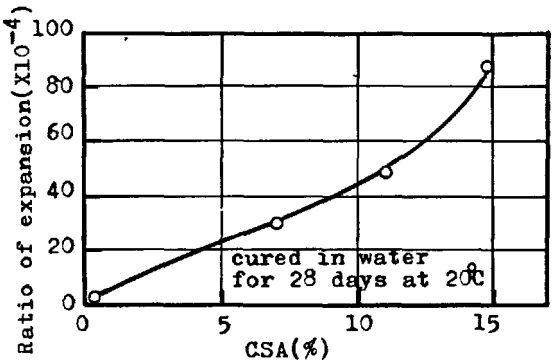

Fig.7-Ratio of free expansion of expansive cement mortars.

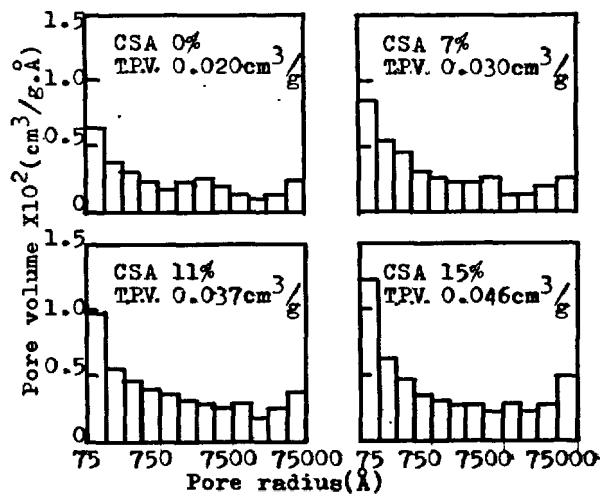

Fig.8-Pore size distributions of expansive cement mortars cured in water for 28 days at 20°C.

From Fig. 8, it was proved that the fine structure of hardened expansive cement mortar is greatly increased its capillary pores of a fine pore radius of 75 to 1400 Å by expansion. In other words, the expansion phenomenon due to hydration of hardened cement mortar is proved to accompany an increase in capillary pores within a specific range.

3-3 ELUCIDATION OF PREVENTIVE EFFECTS ON CRACKS DUE TO DRYING SHRINKAGE FOR CONCRETE[4]

As a result of basic experiments with cement mortar, the fine pores of the hardened CSA-mixed cement mortar are made clear to be increased within a specific range as a result of expansion due to hydration.

Thus, experiments on the development of cracks for concrete were made with an intention of making clear preventive effects on the drying shrinkage cracks of the CSA expansive admixture having such an expansion characteristic.

In Fig. 9, the amount of free shrinkage accompanying the drying of nonrestrained test specimens is given. The amount of drying shrinkage of the CSA concrete is 10 to 30% less than the ordinary concrete, and particularly lowest in case where water curing was made for approx. 7 days in the early period.

Fig. 10 gives the change in the amount of shrinkage accompanying the drying of restrained specimens for crack development. Cracks developed at the shrinkage of 100 x 10^{-6} to 200 x 10^{-6} for the ordinary concrete, whereas for the CSA concrete, no cracks developed even at the shrinkage of 400 x 10^{-6} to 500 x 10^{-6}. In short, the CSA concrete has a greater extensibility than the ordinary concrete, indicating that cracks are hard to develop in the CSA concrete.

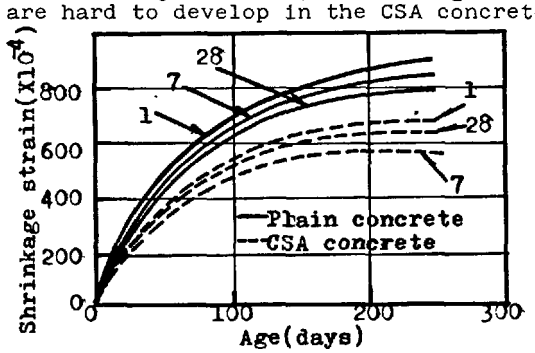

Fig.9-The change of the strain due to drying shrinkage of nonrestrained test pieces.

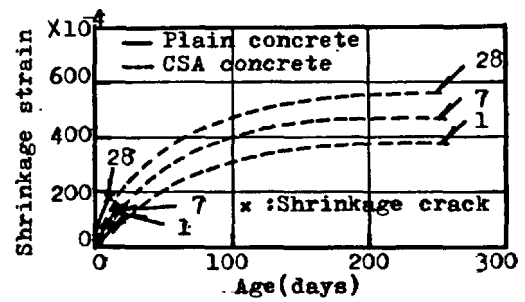

Fig.10-The change of the strain due to drying shrinkage of restrained test pieces.

Although little difference in mechanical properties between the CSA concrete and the ordinary concrete was recognized, the time when cracks develop in the restrained test specimens was entirely different, as shown in Fig. 10.
In the case of the CSA concrete, it is made known that the extensibility is increased by expansion arising from the formation of fine Ettringite caused by a topochemical reaction and the growth of crystals from $Ca(OH)_2$ gel formed by the hydration of free-CaO. The fine voids formed by expansion, consisting of independent fine voids of a pore radius of 75 to 1400 Å, disperse and absorb the drying shrinkage stress. From a point of view of mechanics, creep increases and an effect of relaxing internal stress (drying shrinkage stress) resulting from drying is produced, whereby suppressing the development of cracks When being placed in a dried state, comparatively large Ettringite crystals are formed by a through solution reaction, where no expansion takes place and the constitution of hardened concrete is made denser, resulting in an effect of reducing the drying shrinkage amount of concrete.
In the case of the CSA concrete, the age at which cracks develop is greatly delayed as compared with the case with ordinary concrete. However, the fact can be noticed only from the observation of cracking, but not by prediction.
Thus, the prediction of the drying shrinkage cracking resistance of the CSA concrete was tried by using the values of early expansion characteristics and strength characteristics[5] and the following equation was proposed.

$$K_{cr} = \varepsilon_b \times \sigma_c / \varepsilon_f \qquad (1)$$

Where Kcr is index of drying shrinkage crack durability, ε_b is max. restrained expansion rate, ε_f is max. free expansion rate, and σ_c is compressive strength at the time of max. expansion.
As understood from the equation(1), the greater the value of Kcr, the greater is cracking resistance.
In this report, the equation(1) is a mere proposal. Further investigations on relations between data obtained at experimental room and the data obtained from actual structures will be made and then more accurate experimental equation will be given.

4. CONCLUSION

In order to elucidate effects on the drying shrinkage cracks of concrete using a calcium sulfoaluminate expansive admixture, experiments with (1) the elucidation of the hydration process of cement paste, (2) the elucidation of the expansion phenomenon of cement mortar, and (3) the development of cracks of concrete were carried out and obtained the following results:
1) The causative factors of expansion of the CSA expansive admixture are the formation reaction of fine noncrustalline Ettringite and the growth of crystals from $Ca(OH)_2$ gel.
2) Expansion due to hydration greatly increases capillary voids of a pore radius of 75 to 1400 Å in expansive cement mortar.
3) The extensibility of expansive concrete becomes greater in proportion to the increment of capillary voids by expansion arising from the formation of needle-like fine Ettringite by a topochemical reaction during the early period of hardening and also the growth of crystals from $Ca(OH)_2$ gel formed by the hydration of free-CaO.
4) The free shrinkage amount of expansive concrete becomes smaller in proportion to the amount of formation of comparatively large Ettringite by a through solution reaction in the capillary voids, whereby the constitution of hardened concrete is made denser.

LITERATURE

1.- M. Kokubu (1973), "Use of Expansive Components for Concrete in Japan"., ACI, sp 38.

2.- Jun Isogai, Akira Saito, and Mitsuo Takahashi (1977), Annual Report of the Cement Association of Japan(Cemento Gijutsu Nenpo), 31, 66 to 70.

3.- Jun Isogai (1975), "Properties of Hardened $3CaO.3Al_2O_3.CaSO_4$-$CaSO_4$-CaO expansive cement at later age", Annual Report of the Cement Association of Japan(Cemento Gijutsu Nenpo), 29, 126 to 130.

4.- Nobuo Miyake, Jun Isogai, Akira Kinoshita and Katsuhisa Endo (1976), "Preventive Effects on Drying Shrinkage Cracks of Concrete by adding CSA Expansive admixture, Annual Report of the Cement Association of Japan(Cemento Gijutsu Nenpo), 32, 70 to 73

5.- Publication is on hand.

The evolution of the structure of cement paste investigated by radiometric emanation method

L'évolution de la structure de la pâte du ciment étudiée par la méthode radiométrique d'émanation

V. BALEK, M.Sc. Ph.D., Nuclear Research Institute, Rez, Czechoslovakia,
V. SATAVA, Prof., D.Sc., Institute of Chemical Technology, Prague, Czechoslovaquia,
J. DOHNALEK, M.Sc., Ph.D., Building Research Institute, Technical University, Prague, CSSR.

RESUME : La méthode radiométrique d'émanation (MRE), fondée sur la mesure des gaz inertes radioactifs échappés des échantillons, donne la possibilité d'obtenir des informations sur la grandeur de la surface interne et sur les changements du coefficient de diffusion de ces gaz dans les systèmes étudiés. On décrit un mode d'application original de la MRE à l'étude de l'hydratation de la pâte du ciment. On a pu observer, d'une façon continue, les changements de structure au cours de tout le processus étudié, dans des conditions choisies d'humidité et de température.

Une comparaison des résultats de la MRE avec les méthodes en usage habituel démontre que la MRE livre de nouveaux aspects sur le mécanisme de la formation de la pierre du ciment; on pourrait l'appliquer par exemple à la détermination de la quantité optimum de gypse comme additif pour le réglage de la prise du clinker du ciment portland. On a aussi démontré les avantages de la mesure en continu de la vitesse d'émanation et des changements de structure de la pierre du ciment au cours du séchage et de la déshydratation. Les résultats ont confirmé l'hypothèse du caractère réversible de la structure de la pierre du ciment.

L'avantage de l'appareil MRE, produit commercial de Netzsch, consiste dans la possibilité de la mesure automatique dans un régime programmé. Du point de vue de la sécurité du travail avec les radioisotopes en question, en utilisant des concentrations en traces, un laboratoire chimique bien équipé peut effectuer ces mesures. La méthode radiométrique d'émanation peut devenir un instrument nouveau pour l'étude de l'hydratation de la pâte du ciment et de l'influence des différents facteurs.

SUMMARY : The radiometric emanation method (REM) based on the measurement of radioactive inert gases released from the samples studied gives the possibility of obtaining information on the size of the inner surface area and on the changes of the diffusion coefficient of these gases in the investigated systems. In this paper an original kind of application of REM in the investigation of the hydration of cement paste is described. By means of REM it was possible to study the changes of structure during the whole hydration process investigated continuously and under the conditions of the required humidity and temperature.

From the comparison of the results found by REM with those obtained by commonly used methods it follows that REM affords new insights into the evolution of the structure of a cement stone; it might be applied e.g. to the determination of the optimum amount of gypsum added to the regulation of the setting of Portland cement clinker. The advantages of the continuous measurement of emanation rate were further shown on the investigation of the changes of structure of the Portland cement stone during drying and rehydration. The results corroborated the view of reversible character of the structure changes of a cement gel.

The advantage of the REM apparatus, produced commercially by Messrs.NETZSCH, consists in the possibility of automatic measurement in a programmed regime. Even a well equipped chemical laboratory complies with the requirements of safe work with radioisotopes in question in the given trace concentration. The radiometric emanation method possesses all preconditions for becoming a new tool for the investigation of the hydration of cement paste and of the influence of various factors on this process.

INTRODUCTION

The study of processes occuring after the mixing of cement with water usually consists in stopping the process after chosen time intervals and investigating the morpbology and nature of phases present in the system. On the basis of the data obtained the hypothesis explaining the mechanism of the whole process is searched for. This discontinuous technique brings a number of experimental and interpretation difficulties.

The aim of this contribution is to show certain possibilities of studying the hydration and the setting of cement paste given by the radiometric emanation method (REM) which makes it possible to follow continuously the changes of structure in the system investigated.

PRINCIPLE OF THE RADIOMETRIC EMANATION METHOD

The radiometric emanation method (REM) is based on the measurement of radioactive inert gases, e.g. of radon, released from the material investigated. Before the measurement, it is usually necessary to incorporate the radioactive gas into the material under study, in other words to label the material with a radioactive isotope. This labelling can be achieved by a number of methods (1), e.g. by the incorporation of trace amounts of thorium or radium isotopes into the sample. These isotopes represent a constant source of the radioactive emanation-radon. The atoms of radon ^{220}Rn can be produced for example by the decay of thorium ^{228}Th emitting alpha radiation

$$^{228}Th \xrightarrow{\alpha} {}^{224}Ra \xrightarrow{\alpha} {}^{220}Rn \xrightarrow{\alpha} \qquad /1/$$

The inert gas does not react with the material under study and it is released from this material as a result of both the recoil energy - which every atom gains when formed by the decay of radium - and the diffusion to the surface of the sample. The radioactivity of gas makes possible its detection in trace amounts, causing thus the high sensitivity of the method. In practice, the rate of the release of the radioactive inert gas from the sample is measured which is denoted as the emanation rate. The relation valid (1) for the emanation rate E of a grain or of a set of isolated grains of a solid is

$$E = S\left[k + (D/\lambda)^{1/2}\right]\rho \qquad /2/$$

where S - is the specific surface area of the solid, k - is a constant independent of temperature, D - is the diffusion coefficient of radon in the material investigated, λ - is the decay constant of radon, ρ - is the density of the solid.

Hence, by measuring the rate of the radon release we can obtain an information on the changes of diffusion coefficient of radon in the material investigated and the changes of the boundary area between solid and liquid phases which occur during microstructural transformations in the system investigated.

EXPERIMENTAL

Materials used

Portland cement PC 400 (specific surface area 0.86 m^2g^{-1})
ground Portland cement clinker (specific surface area 1.90 m^2g^{-1})
precipitated gypsum, R.G. (specific surface area 3.0 m^2g^{-1}
The phase composition of ground Portland cement clinker was as follows:
C_3S - 69.7 %, C_2S - 11.0 %, C_3A - 8.2 %, C_4AF - 6.4 %, free CaO 1.29 %.

Preparation of labelled samples

The procedure applied to the radioactive labelling of investigated materials consisted in the impregnation of the original feed materials with a solution containing trace amounts of parent radionuclides of the inert gas. Carrier-free parent radionuclides present in the impregnation solution are practically immediately adsorbed on the surface of the sample and as a result of the recoil of radium or radon during the radioactive decay of the parent nuclides in question they penetrate into the bulk of the material into the depth of approximately 1 /um. In the samples of cement pastes produced from PC 400 the labelling occured at the beginning of hydration by the adsorption of ^{228}Th and ^{224}Ra nuclides from the mixing water. Ground Portland cement clinker or gypsum were labelled at least one week before the mixing with water. The labelling of cement clinker was performed by its impregnation in acetone solution with trace amounts of ^{228}Th and ^{224}Ra. The labelled gypsum was prepared by the hydration of plaster with an aqueous solution containing trace amounts of ^{228}Th and ^{224}Ra radionuclides.

The activity of the samples of aqueous suspensions of binding materials was equal to $5x10^3$ - $5x10^5$ Bq at the mass of 2 g.

Equipment for REM measurements

The REM measuring equipment is shown schematically in Fig. 1. It consists of following parts: the carrier gas circuit, the measuring cell into which the sample is placed, the system of detection and registration of radioactive gas released from the sample, the chamber with the detector of alpha activity, connected with the counts-rate meter, and the equipment keeping the sample at the required experimental conditions (temperature, humidity, chemical composition of the gas medium). The data of the counts-rate meter are presented digitally and registered by a recorder or a printer with a perforated tape output.

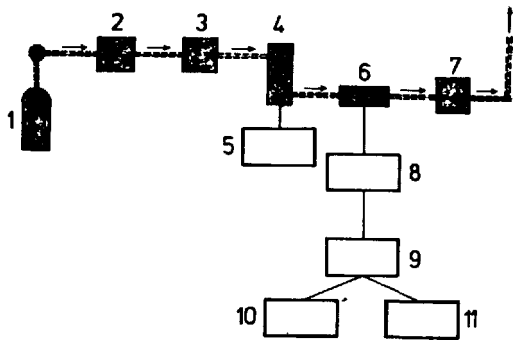

Fig. 1 - The scheme of the apparatus for radiometric emanation method: 1 - the carrier gas supply, 2 - flow-stabilizer and flow-meter of the carrier gas, 3 - equipment for the regulation of humidity and chemical composition of the carrier gas, 4 - measuring cell with the sample, 5 - temperature controller of the measuring cell, 6 - chamber for radioactivity detection, 7 - flow-meter for the carrier gas, 8 - counts-rate meter, 9 - digital voltmeter, 10 - printer, 11 - recorder

This equipment, which is a part of a series of equipments for simultaneous thermal analysis DTA-TG-ETA produced by Messrs. NETZSCH (3) allows to perform the measurements under various conditions maintained automatically according to the given program (temperature, humidity, flow-rate of carrier gas, gas pressure).

The measurement was carried out as follows. The vessel containing the sample of paste was placed instantly after the mixing of the binder with water into the measuring cell. Air, used as a carrier gas, passed in the immediate proximity of the sample and carried the released atoms of radon into the measuring chamber. The constant flow rate (0.7 ml s^{-1}), temperature (20 ±2 °C) and relative humidity (95 ±3 %) of the carrier gas were secured after passing through the measuring chamber the radioactive emanation was carried into the ventilation of the chemical laboratory. When the sensitivity of the structure of cement stone to the humidity changes of medium was investigated, the measurement was carried out in a gas (air) medium with the relative humidity of 65 ±3 % with the aim to achieve the drying of the sample.

Further parameters measured

Besides REM the time dependence of other physical quantities which can characterize the course of processes taking place in the cement paste on hydration was investigated. Specific surface area (S) was determined by the method of Nelsen and Eggertsen (2). Porosity (PS) and distribution of the size of pores in the range from 7.5 nm to 7500 nm were measured by the method of mercury porosimetry (apparatus produced by Carlo Erba, type AG 65). Penetration resistance (R) was determined as the ratio of the strength needed for the penetration of a cylindrical indentor into the setting cement paste to the cross-sectional surface of this indentor (4). Ultrasonic longitudinal wave propagation rate (v_L) was determined by means of the apparatus RECO (GDR) with the transducer with natural frequency. The beginning und the period of setting, and/or the end of setting of cement paste were established by the standard Vicat test. The time course of hydration reaction was followed continuously by conductivity calorimetry (5).

RESULTS AND DISCUSSION

I. THE EVOLUTION OF STRUCTURE OF CEMENT PASTE DURING SETTING

Fig. 2 shows the time dependence of the rate of radon release from two samples of cement pastes prepared from the labelled PC 400 with the cement-water ratio w/c = = 0.28 (sample I) and w/c = 0.55 (sample II). From the comparison of the curve I in Fig.2 with the time dependence of the change of penetration resistance (R) (Fig. 3, curve 1) and with the rate of ultrasonic wave propagation (v_L) (Fig. 3, curve 2) it is evident that the increase of the emanation rate of the sample of cement paste corresponds to the time dependence of (R) and (v_L) and the beginning of the increase of the emanation rate E corresponds quite exactly to the beginning of setting determined by the Vicat test (see the hatched region in Fig. 3).

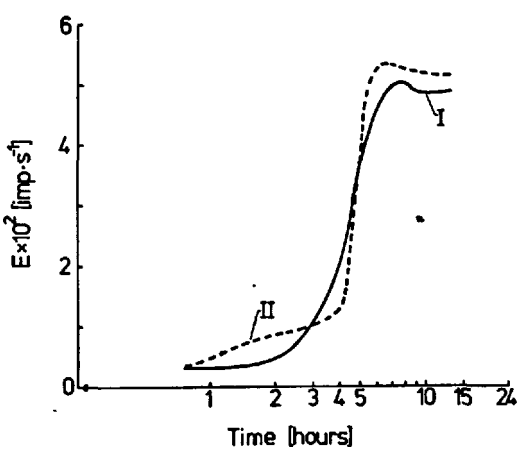

Fig. 2 - Time dependence of the emanation rate E of the samples of cement paste with the w/c = 0.28 (curve I) and w/c = 0.55 (curve II)

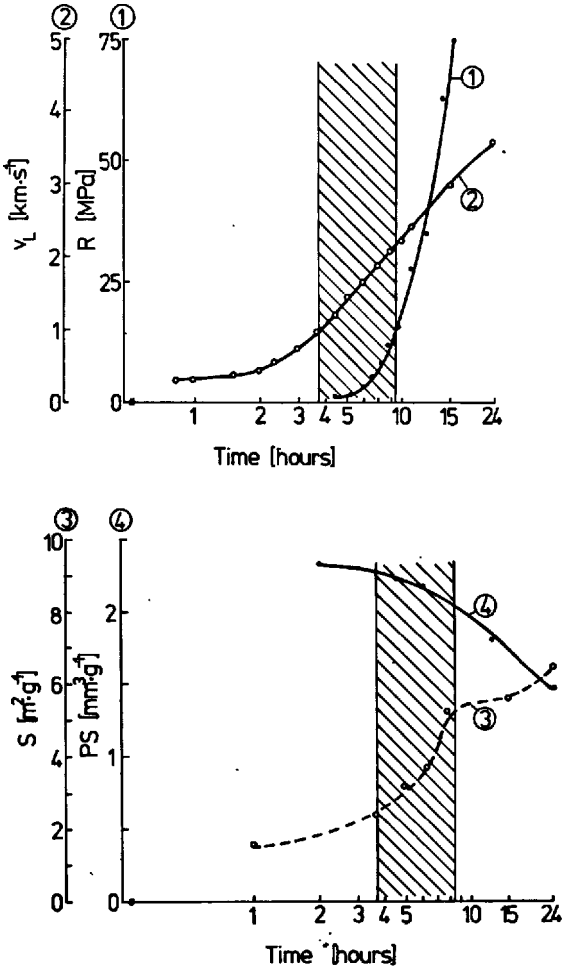

Fig. 3 - Time dependence of the measured physical parameters characterizing the hydration of the sample I (see curve I in Fig. 2):
penetration resistance (R) - curve 1;
ultrasonic wave propagation rate (v_L) - curve 2; specific surface area (S) - curve 3, and capillary porosity (PS) - curve 4.

The increase of the emanation rate in Fig. 2 is caused evidently by the increase of the specific surface area of the solid phase brought about by the rising amounts of hydration products, the specific surface area of which is by several orders of magnitude higher than the specific surface area of the original cement grains (6). The correctness of this explanation is proved also by the time course of the specific surface area shown in Fig. 3, curve 3. The decrease of the capillary porosity in the course of the process (curve 4 in Fig. 3) does not limit the curve of the emanation rate. Therefore, it can be supposed that the capillary porosity in the measured range of the pores (size from 7.5 nm to 7500 nm) does not influence the diffusion coefficient of radon in the material investigated.

Also the investigation of the structure of pores of the samples I and II led to the same conclusion. After 12 hours setting the volume ratio of capillary pores in the sample II was approximately 2x higher than in the sample I, while the emanation rate of both samples is about the same (see Fig. 2).

Thus it seems that the structure of gel hydration products is independent of the values of w/c ratios of the studied samples I and II. The plateau which appears on the curve of the emanation rate in the region of the end of setting (independent of the w/c ratio of the samples) corresponds also to the course of the specific surface area of the solid phase and it is probably caused by the decrease of the surface area of the sample. This effect can be ascribed most probably to the transition of ettringite to C_4ASH_{13} which takes place after the consumption of gypsum in the reacting system.

The following monotonous increase of the emanation rate is caused by the increase of the surface area of the hydration products of C_3S and C_3A building the cement gel.

As a further evidence of applicability of radiometric emanation method are shown the results of the investigation of the influence of gypsum admixture on the initial period of hydration of ground Portland cement clinker. The time dependence of the emanation rate of the suspension of ground clinker with the admixture of 0, 2, 4, and 6 % of gypsum together with the corresponding dependence of changes of penetration resistance are shown in Fig. 4. The specific surface area of clinker was chosen higher, in order to show the processes taking place in the suspension in the initial period of hydration more distinctly.

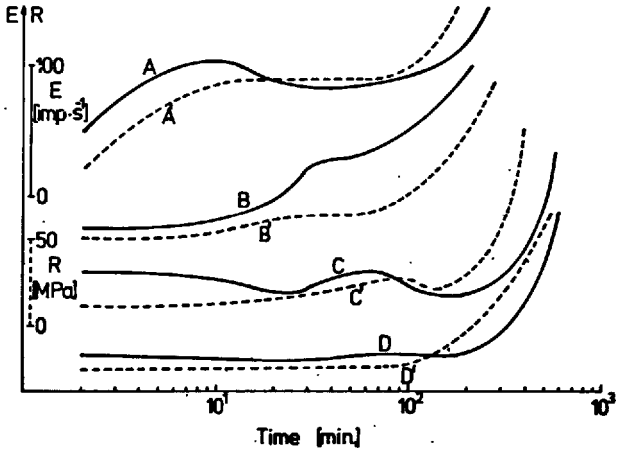

Fig. 4 - Time dependences of emanation rate (E), (curves A,B,C,D) and of penetration resistance (R), (curves A´,B´,C´,D´) of the samples of ground Portland cement clinker with the admixture of 0 - 6 % of gypsum: curves A,A´ - sample withouth gypsum, B,B´ - 2 %, C,C´ - 4 %, D,D´ - 6 % admixture of gypsum. In all samples the clinker was labelled with radioisotopes.

The increase of the emanation rate of the suspension of the ground clinker without gypsum (Fig. 4, curve A) is caused by hydration of C_3A which results in instantaneous hardening (Fig. 4, curve A´). Even if the amount of the reacted C_3A in this initial period is relatively low (7), it can be judged from the pronounced effects on the emanation curves A,A´ that the product causing the hardening has a large surface area. Further increase of emanation rate accompanied with the increase of penetration resistance occuring after a certain incubation period, can be ascribed to the increase of specific surface caused by the hydration products of C_3S, C_2S and of remaining C_3A.

The moderate decrease of emanation rate during the incubation period is probably the result of recrystallization of hydrated calcium aluminates giving most probably C_4AH_{13}. The changes of penetration resistance are less pronounced in this period.

The hydration of ground cement clinker in the presence of gypsum is also demonstrated by the increase of emanation rate (Fig. 4, curve B) which takes place, however, with a certain delay. It can be supposed that it corresponds to the formation of ettringite with a high specific surface area. From the curve B´ in Fig. 4 it can be seen that this process is also accompanied with the increase of penetration resistance. However, if the system contains a higher amount of gypsum (curve C´ in Fig. 4) the increase of penetration resistance of the sample is lower, goes through a maximum and decreases again.

From the course of the emanation rate (curve C in Fig. 4) it can be concluded that ettringite formed recrystallizes, its surface area decreases and also its binding abilities go down (see curve C´, Fig. 4).

At an even higher content of gypsum the effect on the curve of emanation rate is less pronounced (see Fig. 4, curve D) and the effect on the curve of penetration resistance disappears completely (Fig.4, curve D´). As the amount of the ettringite formed in all the samples studied is the same (the degree of C_3A hydration is independent of the presence of gypsum (7)) and because the emanation rate of the sample represented by the curve D, Fig. 4,increases only insignificantly, we have to suppose that relatively large particles of ettringite with a low surface area are formed in this case. The low number of the large particles of ettringite is incapable of forming a continuous structure which would result in hardening of the system investigated (curve D´,Fig.4).

The evidence that the measured emanation rate provides an information on the character of structure of newly formed phases mainly, characterized by large surface area, is demonstrated by the REM curves in Fig. 5. From this figure it follows that the character of REM curves is practically identical regardless of the fact which of the both solid phases (gypsum or ground cement clinker) is labelled with a radionuclide.

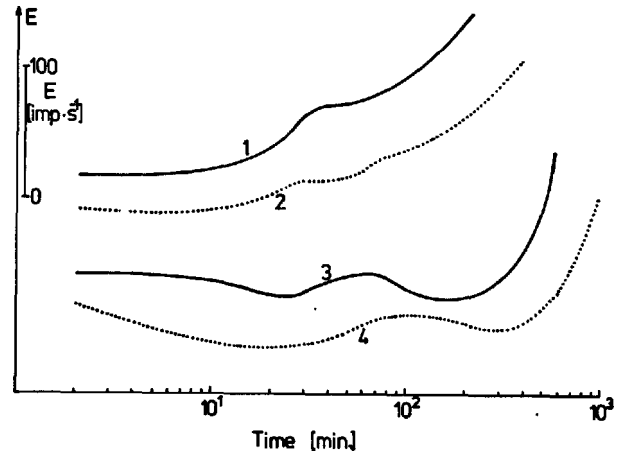

Fig. 5 - Time dependences of emanation rate (E) of samples of water suspension of Portland cement clinker with the admixture of 2 % of gypsum (curve 1 and 2) and 4 % of gypsum (curve 3 and 4). In the samples both cement clinker (curve 1 and 3) and gypsum (curve 2 and 4) were labelled with radioisotopes.

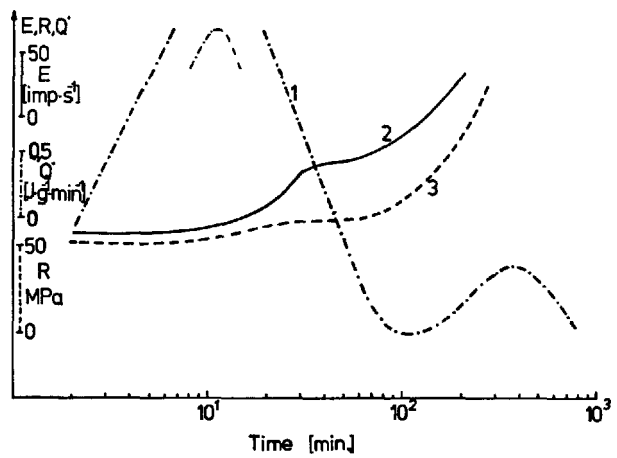

Fig. 6 - Time dependences of the release of hydration heat (curve 1), emanation rate (curve 2) and penetration resistance (curve 3) of the sample of a water suspension of Portland cement clinker with 2 % of gypsum. For REM measurements in the preparation of the sample gypsum labelled with radioisotopes was used.

Fig. 6 shows the curves obtained by three different methods during the investigation of the setting binder suspension. Each of these curves reflects the course of hydration processes from a different point of view. While the calorimetry (curve 1) provides an information only on the achieved degree of transformation of all hydration reactions, the other two methods (curve 2 and 3) give the picture of the structure

of the investigated system which occur as a result of the hydration reactions; these structure changes determine the plasticity of binder suspensions and therefore are most important from the practical point of view.

The radiometric emanation method could be applied to the determination of the optimum amount of gypsum added to the Portland cement clinker, similarly as the calorimetric method (8). Such an amount of admixtured gypsum could be considered as optimum that just brings about the disappearence of the effect caused by the formation and recrystallization of ettringite (see Fig. 4). The advantage consists again in the completely continuous and fully automated measurement of emanation release rate.

II. CONTINUOUS INVESTIGATION OF THE SENSITIVITY OF CEMENT GEL STRUCTURE TO THE CHANGES OF HUMIDITY

In the region of cement paste setting the emanation rate is controlled first of all by the increase of the surface area of hydration products. In the following stages of the process, when the hydration reaction is controlled by the diffusion of water to the non-hydrated cement grains, the change of surface area with time is low and a less pronounced rise of emanation rate gradually takes place.

However, it became evident that the pronounced changes of emanation rate occur when the cement stone is kept in the gas medium with the various water vapour pressure. Fig. 7 shows the dependence of emanation rate E of the sample of cement stone after 14 days of hydration, on the time of keeping in the air medium with a various water vapour pressure.

The samples were gradually put into air atmosphere with 95 ±3 % humidity and then measured in a stream of air with 65 ±3 % humidity. The saturation of the samples with water during their storage in air with 95 ±3 % humidity results in the increase of emanation rate, while the drying in the course of measurement causes its rapid decrease. From the data obtained it also follows that with the increasing time of saturation the relative rise of emanation rate gradually decreases though its absolute values keep increasing.

Simultaneously, it was verified that on keeping the sample in the air with high relative numidity the mass of the samples rose as a result of saturation of the samples with water; during the measurement, which was carried out in the air with a lower relative humidity the mass of samples usually decreased.

The changes of the emanation rate observed cannot be caused by the changes of specific surface area which in the time period of the emanation rate measurement changes only insignificantly; thus beeing the result of the changes of radon diffusion rate in the system investigated. The changes of the diffusion coefficient are raised by structure transformations in the cement gel. The sensitivity of REM to the effects described is

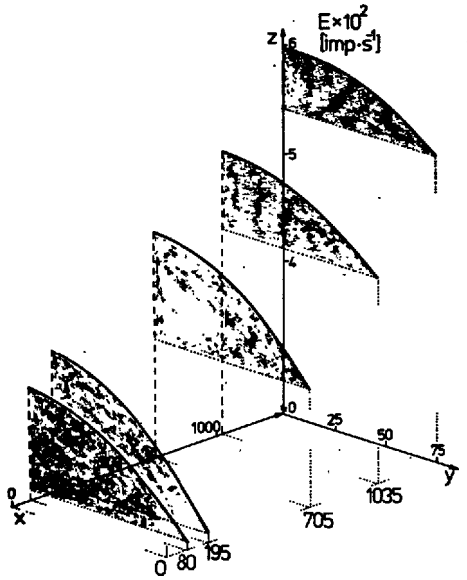

Fig. 7 - Time dependence of the emanation rate E of the sample of Portland cement stone (w/c = 0.28, time of sample aging 14 days) on the time of storage in the air medium with various water vapour pressure. x-axis = time of storage /min/ of the sample in the air medium of 95 ±3 % humidity, y-axis = time of storage /min/ of the sample in the air medium with 65 ±3 % humidity, z-axis = emanation rate E of the sample /imp s^{-1}/.

probably given by the fact that the size of gel pores is comparable with the diameter of the diffusing radon atoms /d = 0.42 nm/; the changes of size of gel pores are therefore clearly expressed on the emanation rate curve.

A possible direct influence of water molecules on the values of the emanation rate of the cement stone samples was eliminated by following experiments. A sample of hydrated plaster was measured using the same procedure as for the cement stone. The structure of plaster has (contrary to that of cement stone) the character or a rigid skeleton which does not undergo structure changes caused by drying the sample or its saturating with water. With this sample the effects on the REM curve shown in Fig. 7 did not appear. The emanation rate values of the hardened plaster paste saturated with water and of the same sample after its drying were practically identical.

The presented results of emanation release rate measurements of the hardened cement stone suggest that during the water saturation of the sample as well as during its drying the continuous changes of its diffusion coefficient take place. If we accept the hypothesis about the layer arrangement of the C-S-H gel, the results can corroborate the views supposing that the layers of the dried C-S-H gel are not permanently

drawn together and that the action of water can cause their drawing away as a result of penetrating of water into the gel pores (9).

CONCLUSIONS

The potentialities of the application of the radiometric emanation method to the investigation of hydration and setting of the cement paste were shown. REM not only complements the commonly used experimental methods but also provides new views on the processes taking place during the evolution of cement stone structure.

The advantage of REM consists in the possibility of the continuous investigation of the changes of structure during the whole duration of the process of setting of the cement paste namely under the conditions of required humidity, temperature and chemical composition of the gas medium around the sample. This gives the possibility to investigate the ways of influencing the process of setting e.g. by temperature or admixtures, under the conditions interesting from the point of view of both science and technology.

We have shown the possibility of continuous investigation of the changes of cement stone structure on drying and rehydration of the sample, not necessitating any additional interference with the measured samples which would cause undesirable changes in the structure of the sample studied.

Radiometric emanation method possesses all preconditions for becoming a new source of information on the evolution of structure of binding systems.

By parallel measurement of two released radioactive gases, REM makes possible to discern also the role of surface area and diffusion in the emanation release rate of the sample measured. This can give more complete information on the structure evolution of the systems investigated.

The commercially produced apparatus for radiometric emanation measurements by NETZSCH (F.R.G.) is fully automated and a well equipped chemical laboratory is suited, complying with the requirements of the safety of work with radioactive isotopes in the trace concentration, when the REM apparatus have to be employed.

REFERENCES

1.- V. BALEK (1977), "Emanation thermal analysis", Thermochim. Acta, 22, 1-157

2.- F.M. NELSEN, F.T. EGGERTSEN (1958), "Determination of Surface Area - Adsorption Measurements by a Continuous Flow Method", Anal. Chem., 30, N° 8, 1387-1390.

3.- W.D. EMMERICH, V. BALEK (1973), "Simultaneous Application of DTA, TG, DTG and Emanation Thermal Analysis", High Temp. - High Pressures, 5, 67.

4.- V. ŠATAVA (1955), "Ein Gerät zur rheologischen Untersuchung des Erstarrungsverlauf der Bindemittel", Silikattechnik, 6, 338.

5.- H.N. STEIN (1961), "Influence of Some Additives on the Hydration Reactions of Portland Cement - I", J. appl. Chem., 11, 474-482.

6.- H.F.W. TAYLOR (1964), "The Chemistry of Cement", Academic Press, London.

7.- F.W. LOCHER, W. RICHARTZ, S. SPRUNG (1976), "Erstarren von Zement", Zement-Kalk-Gips, 29, 435-442.

8.- W. LERCH (1948), J. Amer. Concr. Inst., 44, 743.

9.- D.N. WINSLOW, S. DIAMOND (1974), "Specific Surface of Hardened Portland Cement Paste as Determined by Small-Angle X-Ray Scattering", J. Amer. Ceram. Soc., 57, N° 5, 193-197.

Interaction of cement minerals with water

Interaction des composants du ciment avec l'eau

P.F. RUMYANTSEV, Doctor, Institute of Silicate Chemistry of the Academy of Sciences of the USSR, Leningrad, U.R.S.S.

RESUME : Le durcissement des ciments est lié aux processus d'interaction chimique entre les composants solides du ciment et un liquide. De tels processus peuvent aussi se produire au cours de la cuisson du clinker.

Jusqu'ici on avait établi que l'interaction chimique entre les minéraux solides du ciment et les liquides, dans les systèmes de ciments, se produisait non pas régulièrement sur toute la surface des grains, mais sur des zones séparées, donc localement.

Pour représenter le processus chimique qui se produit, on a établi les équations suivantes :

$$V = \frac{A}{D} e^{-\frac{E}{RT}} \qquad W = W_0 [1 - e^{-kt^n}] \qquad V = \frac{\bar{u}\, n.\varepsilon.S}{4\nu}$$

L'utilisation de ces formules permet d'obtenir de nouvelles informations scientifiques sur la vitesse et le mécanisme du durcissement du ciment, et sur le processus de cuisson du clinker. Elle permet aussi d'établir un modèle mathématique pour l'automatisation des techniques de fabrication du ciment.

SUMMARY : Hardening of cements is related with the processes of chemical interaction between solid cement minerals and a liquid. Such processes can also take place during the burning of cement clinker.

It has been established hitherto that the chemical interaction between solid minerals and liquids in cement systems proceed not uniformly throughout the surface of the minerals but on its separate parts , i.e. locally.

To describe the chemical processes which proceed by the indicated mechanism, the following equations can be used:

$$V = \frac{A}{D} \cdot e^{-E/RT} ; \qquad W = W_0 \left[1 - \exp(-kt^n)\right] . \qquad V = \frac{\bar{u}\, n\, \varepsilon\, S}{4\, \nu}$$

The use of these formulas permits to obtain new scientific information about the rate and the mechanism of hardening of cements, of the burning of clinker as well as to create the mathematical model for the automatization of technological processes in cement inductry.

The processes of chemical interaction between solids and liquids are widely spread in nature and technique. They are realized during the hardening of cements and burning of clinker, and being heterogeneous in their nature they proceed according to the scheme:

solid A + liquid B = solid C.

If one assumes that A, B, C can be represented by several components, then it becomes apparent that the study of these processes is a complicated and difficult task. The latter may explain a considerable lag in the development of theoretical conceptions and in the establishment of kinetic regularities of such processes as compared to homogeneous.

For the last two decades several comprehensive monographs of basic importance have been published on kinetics of homophase processes /1-4/, whereas the publications on kinetics of heterogeneous process are of less important, private character /5/. No universal methods of the determination of the rates of such processes exist.

In recent years we carried out investigations on the kinetics of interaction between cement minerals and liquids at high and room temperatures. Some common results of these studies are reported in the present communication.

The chemical interaction of solid cement minerals with a liquid proceeds in three stages:
1. Chemical interaction between the particles of solid substance and the liquid at the phase interface.
2. Diffusion of the decomposition products of solid substance or of the interaction products between solid and liquid into the bulk of the liquid.
3. The formation of new liquid and solid phases in solution up to the crystallization of the solid phase.

All these stages first proceed consecutively and then simultaneously. The rate of the process will be determined on the whole by the stage with a lower rate. Taking account of this fact and introducing the parameter characterizing the surface area of the solid body permitted to use the kinetic equations which were earlier derived for simple processes.

To describe the temperature dependence of the rate, the well-known experimental Arrhenius equation was used, the parameter taking into consideration the surface area having been introduced as a constituent member of the pre-exponential multiplier:

$$V = \frac{A}{D} \cdot e^{-E/RT} \qquad (1)$$

The use of the given formula permitted to determine the effective activation energies of the processes studied and to conclude which of the stages plays the determining role in each process.

In several cases the change in value of the effective activation energy with increasing temperature was established what permitted to reveal the new character of interaction and to fix temperatures at which these processes proceed. The reasons of non-constancy of the effective activation energies were changes in the chemical composition of the liquid phase or the appearance of the film of new formations on the surface of the primary solid sample.

The experimental data on the isothermal processes were successfully analyzed with the aid of the well-known Kholmogorov-Erofeev equation

$$W = W_0 \left[1 - \exp(-kt^n)\right] \qquad (2)$$

The analysis of the above given formulas permitted to find that for the burning of cement clinker the dissolution is the limiting factor, whereas for the hydration process of calcium aluminates and for the interaction of alumina and silica with phosphoric acid it is the diffusion.

The first stage, namely the interaction on the phase interface is a less studied stage being of the greatest interest from the view-point of the kinetics of heterophase processes.

The chemical interaction on the solid-liquid interface is a topochemical process whose mechanism can be represented as follows /6-8/.

On the active surface of the mineral particles the polar molecules or ions are adsorbed what results in the formation of a polymolecular layer in which the orientation of dipoles leads to the appearance of the interphase jump of potential, therefore the dissolution of the particles is accompanied by intense diffusion flows of new formations.

The orientation of polar molecules is most expressed in the adsorption layer near the interface and it decreases with increasing distance from the surface forming chains which intergrow deep into the liquid layer.

Thus the diffusion flows during dissolution are polarizing factors.

The oriented polarization of polar groups orders and determines, under conditions of crowdness, the controlled character of gel formation and crystallization. However, this concept requires precision as it is based on the more or less uniform activity of the total surface and suggests the presence of the uniform front of interaction. Under real conditions the deviation from the mechanism spoken of is observed in most cases. Thus, for example, during the dissolution of cement minerals the dispersion of the initial particles takes place in the liquid phase of clinker; during the hydration of calcium aluminates figures of etching are clearly observed; during the hydration process of calcium aluminates and interaction of single crystals of alumina and silica with phosphoric acid the new formations ap-

pear only at the separate parts of the surface and only later when these parts increase and merge the solid layer is formed.

Thus, the dissolution proceeds more preferably in the reactive parts or in the active centers which play an essential role during the dissolution of solid materials (like the case of their decomposition).

By "active centers" we mean atoms located in the crystal lattice defects emerging on the surface. Such atoms possesss the lowest coordination in the lattice as compared to the other atoms on the surface, and therefore they are most reactive. The form and the area of such parts are determined by the surface defects.

The migration of atoms located in the lattice defects from the crystal to the liquid causes in turn the formation of new reactive parts the role of which is played by atoms which were formerly connected with the ones that passed into solution.

To explain the formation of new reactive parts by analogy with Garner /9/, we suggest the model of local branched chains. Recently it became clear that the group of topochemical reactions can be divided into two subgroups. In one of them the chain branched reaction proceeds only on the surface, large parts (centers) being formed in the point of branching. In the second sub-group the chains are not limited by the points on the outer crystal surface but penetrate also into the depth thus causing the cracking of crystals. In the first case when the supersaturated solution (with respect to the other interaction products) has been formed, the layer of solid new formations may appear.

The results of many works confirm the applicability of the mechanism under discussion.

Thus, studies on the dissolution of clinker minerals in the liquid phase showed the presence of topochemical dissolution referred to the second sub-group. The branching of the chains into the depth of the crystal can proceed along the lines and planes of dislocation or along the mosaic planes. A visual example of such a mechanism is the dissolution of sugar in water or in tea.

Crystal defects are widely spread in cement minerals and, as shown in the works of Butt and Timashev /10, 11/, they influence considerably the physico-chemical properties, the activity during the interaction with water included.

Studies on the hydration of calcium aluminates performed on single-crystal samples led to establish the first type of local chain branched reactions with the formation of the film of calcium hydroaluminates which slows down considerably the interaction process between the initial solid sample and water.

Consequently, the earlier suggested scheme which describes the uniform front of interaction between the particles of liquid and solid bodies on the surface of the latter and the diffusion of the interaction products into the deeper layers of the liquid should be corrected with taking into consideration the occurrence of local active parts on the surface. It is obvious that the front of interaction will not be uniform. It will have the form of semispheres what should cause a strong deviation from the diffusion mechanism adopted in the first scheme into the direction of its complexity. The latter can also be due to the fact that in some cases the appearance of the film formed of the liquid-solid interaction products takes place on the surface of the solid sample.

For such a mechanism, from Eq.(1), the number of acts of chemical interaction on the unit surface per unit time is equal to one fourth of the product of the average rate of the molecule motion, $\bar{u}$, by the number of particles (molecules) of the liquid per 1 cm^3, n, and by the probability of reaction in collision, ε , :

$$V_s = \frac{\bar{u}\, n\, \varepsilon}{4} \qquad (3)$$

The rate of the solid-liquid reaction can be described as the product of V_s (from formula (3)) by the full value of the solid body surface, S, divided by the volume of reactive system, v :

$$V = \frac{\bar{u}\, n\, \varepsilon}{4} \cdot \frac{S}{v}$$

The value of the average rate of the particles (molecules) motion in these two formulas is determined following the formula

$$\bar{u} = \left(\frac{8kT}{\pi m}\right)^{1/2} \qquad (4)$$

and the reaction probability in collision according to the formula

$$\varepsilon = n_s \sigma_s\, p\, e^{-E/RT} \qquad (5)$$

Here n_s is the number of active parts per unit surface; σ_s is the area of one active part; p is the probability of orientation or the steric factor; $n_s \sigma_s$ is the total area of the active parts per 1 cm^2 of the surface.

Thus, the rate appears to be proportional to the number of reactive particles, and the value

$$k = \frac{\bar{u}\, \varepsilon}{4} \cdot \frac{S}{v}$$

can be regarded as the effective constant of the first order value for reaction of the particles with the surface.

It should be noted in this case that the value of n is the concentration of particles (the number of particles per 1 cm^3) near the surface. If the reaction proceeds very rapidly, then as a result of consumption of the particles near the surface the concent-

ration of them will be lowered and the non-uniform distribution of particles will take place in the system. The rate of reaction will also depend on the rate of diffusion of particles towards the surface. But in those cases when the film of new formations appears on the surface of the solid body (which was already mentioned), the reaction rate will depend on the rate of diffusion of particles through the film.

Now turn again our attention to formula (4). By substituting the values of $\bar{u}$ and $\bar{\varepsilon}$, one obtains the unfolded equation of the form

$$V = \left(\frac{8kT}{\pi m}\right)^{1/2} \frac{n_s \sigma_s p e^{-E/RT}}{4} \frac{S}{\vartheta} n \qquad (6)$$

By uniting the constant values into one value, we obtain the Arrhenius equation in the form which was used by us earlier for a study of the dissolution of clinker minerals:

$$V = S A e^{-E/RT} \qquad (7)$$

The given mathematical method shows, firstly, the correct use of Arrhenius equation for the analysis of our experimental results, and secondly, it discovers the meaning of the pre-exponential multiplier for the case of heterogeneous processes.

CONSLUSION

The use of the fundamental kinetic equations for a study of the mechanism and of the rate of interaction between cement minerals and a liquid permits to gain new information of great scientific importance which can be applied in mathematical modelling of the automatization processes of cement technology.

Further development of investigations in this field should be made using new methods and directed toward the more profound study of the elementary acts of chemical interaction, especially on the surface of cement minerals.

REFERENCES

1.- N.M. Emanuel', D.T. Knorre (1974) "A course of Chemical Kinetics", Nauka, Moscow.

2.- N.N. Semenov (1958) "On Some Problems of Chemical Kinetics and Reactivity", Nauka, Moscow, 1967.

3.- "Development of Conceptions in the Field of Kinetics of Catalysis and Reactivity", Ed. Ya.T. Eidus (1967), Nauka, Moscow

4.- "Progress in Chemical Physics in the USSR", Ed. N.M. Zhavoronkov (1967), Nauka, Moscow.

5.- P. Barre (1976) "Kinetics of Heterogeneous Processes", Mir, Moscow.

6.- B.V. Deryagin (1964) "Dimeric and Three dimentional Aspects of the Surface Phenomena", In: Collection of Papers of the 2nd Confer. on the Surface Strengths, Nauka, Moscow, p.3-9.

7.- I.F. Efremov, M.M. Sychev, O.M. Rozental' (1973) "Some Problems of the Mechanism of Hardening of Cement Pastes", Zhurn. Prikl. Khim. 46, n° 1, 261-268.

8.- M.M. Sychev (1971) "Some Problems of Hardening of Binding Materials", Izv. Akad. Nauk SSSR, Ser. Neorgan. Materialy 7, n°3, 391-401.

9.- W.E. Garner and H.R. Hailes (1933) "Thermal Decomposition and Detonation of Mercury Fulminate", Proc. Royal Soc. Ser. A, 139, 576-595.

10.- Yu.M. Butt and V.V. Timashev (1962) "Different Forms of Alite and their Hydration activity", In: Proceed. 6th Confer. on the Experim. and Technical Mineralogy and Petrography, Publ. House Acad. Sci. USSR, Moscow, p.243-250.

11.-Yu.M. Butt, V.V. Timashev (1965) "Portland Cement Clinker with a Given Structure and its Preparation on the Base of High-Quality Cements", Zhurn. Vsesoyuz. Khim. Obshchestva, 10, n°5, 551-557.

Estimating strength from cement composition

Prévision des résistances à partir de la composition du ciment

L.P. ALDRIDGE, Scientist, Chemistry Division, DSIR, Private Bag, Petone, New Zealand.

SUMMARY : Simple equations have been found which predict the compressive strength at 3, 7, 28, 91 and 365 days from the Bogue compositions of C_3S, C_3S+C_2S, C_3A and specific surface. The equations were determined using multiple regression analysis of data from 114 cements. The standard deviations of the calculated compressive strengths range from 2.8 to 3.6 and the square of the multiple regression coefficients ranges from 0.73 to 0.86.

The equations are empirical equations as the coefficients could not be used to predict the individual component effect. While the equations are shown to fit the strengths of concretes produced from New Zealand cements they should be used with caution by workers wishing to apply them to other cements.

The major factors influencing compressive strength were shown to be the Bogue composition and the specific surface of the cements. Minor oxides had a small effect on the compressive strength.

RESUME : Des formules mathématiques simples ont été établies, permettant de prévoir la résistance à la compression des ciments à 3, 7, 28, 91 et 365 jours, en fonction de leur surface spécifique et de leur composition, selon Bogue, en C_3S, $C_3S + C_2S$ et C_3A. Ces formules ont été établies au moyen de nombreux calculs statistiques de régression portant sur les résultats expérimentaux de 114 ciments. L'écart type des valeurs ainsi calculées varie entre 2,8 et 3,6, et les coefficients de corrélation entre 0,73 et 0,86.

Ces formules sont empiriques; aussi ne doivent elles pas être utilisées pour apprécier l'action de l'un des composants du ciment. Bien que ces formules aient montré une bonne corrélation avec la résistance des bétons confectionnés avec des ciments de Nouvelle Zélande, elles doivent être utilisées avec précaution pour être appliquées à d'autres ciments.

Les facteurs les plus importants, qui déterminent la résistance à la compression, sont la composition selon Bogue et la surface spécifique des ciments. Les oxydes mineurs ont un effet réduit sur cette résistance à la compression.

INTRODUCTION

Despite the efforts of a number of workers the relationship between cement composition and the compressive strength is still not fully understood. Alexander (1) reviewed the attempts of some authors to relate strength to the composition and specific surface of cements. He used empirical equations, derived by multiple regression analysis, to relate the 3, 7, and 28 day compressive strength of cement pastes to the specific surface and the Bogue C_3S and C_3A composition.

There were indications from earlier work carried out by the author (2) that the compressive strength of concretes made from New Zealand cements gave better fits than Alexander's samples (1). In this study simple equations were generated to predict the compressive strengths at ages up to one year. The effects of additional variables on the regression equations were studied.

EXPERIMENTAL

Materials

The 114 cements studied were from a series of samples which had been taken at monthly intervals over a five year period from five cement works (A-E) and for which chemical analyses were available. The compressive strengths at 3, 7, 28, 91 and 365 days were determined using the New Zealand Standard (NZS 3122:1974) method which uses 100 x 200 mm concrete cylinders and a water cement ratio of 0.50. Coefficients of variation of the strengths have been found by repeated within-laboratory testing to be less than 2.5%. The specific surface was measured using the air permeability method. Bogue compositions were calculated after subtacting the free lime from the CaO content and assuming that all the manganese was present in the ferrite phase. Ranges of the Bogue compositions, the amount of the minor oxides, the specific surface, free lime, insoluble residue and compressive strength are shown in Table I.

Multiple Regression Analysis

The methods and limitations of multiple regression analysis are well known (3,4). In this study R denotes the multiple correlation coefficient and gives the fraction of the total variation about the mean compressive strength explained by the regression equation, s denotes the standard error estimate, an estimate of the standard deviation of the calculated compressive strength derived from the regression equation, and r denotes a correlation coefficient between two variables. The computer program (SHARE Library Number 360D-13.6.008) used in this study has been described (3).

A number of problems in regressions involving cement composition were identified by Alexander (1). Some variables were highly correlated with each other; these were C_3S with C_2S (r=0.9) and C_3A with C_4AF(r=0.8). Furthermore the sum of the variables C_3S,C_2S, C_3A and C_4AF is a constant and so these four variables are not independant.

A number of preliminary fits were carried out to determine which variables to include in the regression equations. It was then decided to use the variables in the initial equations which would be expected from cement chemistry to be the most influential. The variable C_4AF was not included in the regression equations and instead of C_2S the variable (C_3S + C_2S) or the sum of the silicate phases was used. C_3S was not highly correlated to (C_3S + C_2S) as r=0.35. Equations 1, 2, 3, 4 and 5 were fitted by multiple regression to all samples and also those from individual works : and the values of R^2 obtained are shown in Table II. If the additional variables gave a significant increase to the degree of fit (determined by an F test at the 5% level) then this is indicated by an asterisk in Table II.

$$CS = b_0 + b_1 C_3S + b_2 C_3A + b_3 Sp\text{-}S \quad (1)$$

$$CS = b_0 + b_1 C_3S + b_2 C_3A + b_3 SO_3 + b_4 Sp\text{-}S \quad (2)$$

$$CS = b_0 + b_1 C_3S + b_2 (C_3S+C_2S) + b_3 C_3A + b_4 Sp\text{-}S \quad (3)$$

$$CS = b_0 + b_1 C_3S + b_2 (C_3S+C_2S) + b_3 C_3A + b_4 SO_3 + b_5 Sp\text{-}S \quad (4)$$

$$CS = b_0 + b_1 C_3S + b_2 (C_3S+C_2S) + b_3 C_3A + b_4 SO_3 + b_5 TiO_2 + b_6 MgO + b_7 Na_2O + b_8 K_2O + b_9 Mn_2O_3 + b_{10} fr\text{-}l + b_{11} IR + b_{12} Sp\text{-}S + b_{13} P_2O_5 \quad (5)$$

where CS is the compressive strength, b_0 to b_{13} are empirical coefficients, Sp-S is the specific surface, IR is the insoluble residue and fr-l is the free lime.

RESULTS AND DISCUSSION

The results from Table II show that regression equation 3 gave significantly better fits than equation 1 when fitting strengths from all of the cements. Equation 5 which included the extra variables, free lime, the minor oxides and insoluble residue gave a more significant fit (at the 5% level) than equation 3 for all the compressive strengths except that at 7 days. It was not possible to determine which of the additional variables gave by itself a significant improvement to the fit. Mallow's Cp statistic (3), gave many alternative choices between combinations of variables and none of these combinations were duplicated at different ages of the compressive strength.

It is recommended that equation 3 be used for predicting the compressive strength of New Zealand cements. (See Table III). Although equation 5 gave a statistically better fit the maximum increase of R^2 (0.04) does not warrant the trouble of including the additional terms. It is possible that the co-

TABLE I

Range of composition of samples from cement works A - E (%) with specific surface (M^2/kg) and compressive strength of concrete (MPa)

	Overall	A	B	C	D	E
C_3S	32 - 73	46 - 72	55 - 68	54 - 73	39 - 55	32 - 61
$C_3S + C_2S$	68 - 82	78 - 82	74 - 78	74 - 79	68 - 74	72 - 79
C_3A	4 - 11	5 - 11	6 - 9	4 - 9	5 - 7	4 - 11
TiO_2	.08 - .46	.15 - .22	.15 - .46	.12 - .39	.08 - .32	.17 - .27
MgO	.45 - 5.3	.66 - 1.20	1.2 - 2.1	.45 - 1.6	4.2 - 5.3	.47 - 4.0
SO_3	1.0 - 3.1	1.4 - 2.8	1.9 - 2.9	1.9 - 2.6	1.0 - 2.4	1.6 - 3.1
Na_2O	.11 - 1.0	.11 - .25	.20 - .31	.20 - .31	.7 - 1.0	.16 - .28
K_2O	.04 - .67	.15 - .38	.31 - .47	.21 - .67	.04 - .22	.23 - .51
Mn_2O_3	0 - 1.4	.06 - .15	.03 - .11	.10 - 1.4	0 - 0.08	.01 - .04
P_2O_5	.02 - .28	.10 - .22	.06 - .16	.09 - .28	.10 - .14	.02 - .24
IR	.01 - .88	.02 - .33	.01 - .30	.02 - .35	.05 - .88	.01 - .07
fr-l	.18 - 3.1	.44 - 2.4	.50 - 2.4	.18 - 1.6	1.3 - 3.1	.53 - 1.3
Sp-S	280 - 550	310 - 490	300 - 487	290 - 390	300 - 385	280 - 550
Compressive Strengths						
3 day	10 - 40	16 - 39	21 - 33	15 - 29	10 - 19	10 - 40
7 day	15 - 55	28 - 55	33 - 46	26 - 44	19 - 33	15 - 54
28 day	33 - 68	49 - 68	48 - 59	43 - 60	33 - 45	33 - 66
91 day	44 - 72	59 - 72	55 - 68	52 - 66	43 - 55	53 - 70
365 day	50 - 78	63 - 78	58 - 70	56 - 70	50 - 61	60 - 73
No of cements	114	20	14	34	14	32

IR = insoluble residue, fr-l = free lime

TABLE II

R^2 after fitting equations 1 - 5

Compressive strength (days)	3	7	28	91	365
Equation	All Cements				
1	.84	.84	.62	.33	.20
2	.85	.84	.62	.34	.22
3	.86*	.86*	.78*	.76*	.74*
4	.87	.86	.78	.76	.74
5	.88*	.88	.82*	.81*	.78*
	Cement from Works A				
1	.92	.87	.68	.52	.22+
2	.94	.88	.69	.54	.24+
3	.95	.88	.70	.53	.22+
4	.96	.88	.71	.54	.25+
	Cement from Works B				
1	.77	.66	.49+	.53	.43+
2	.76	.71	.60	.53	.44+
4	.89	.92	.73	.70	.72
	Cement from Works C				
4	.32+	.29+	.15+	.29+	.40+
5	.56+	.54+	.47+	.64+	.70
	Cement from Works D				
1	.28+	.77	.60	.50+	.38+
2	.68	.79	.75	.75	.68
4	.69	.79	.76	.77	.69
	Cements from Works E				
1	.94	.94	.79	.67	.65
2	.94	.94	.80	.68	.67
3	.95	.95	.80	.67	.66
4	.95	.95	.80	.68	.68

* Denotes that the R^2 is significantly improved

\+ Denotes that the regression is not significant

TABLE III

Regression equation 3

	b_0	b_1	b_2	b_3	b_4	R^2	s
3 day	-55	.34	.36	.64	.073	.857	2.8
7 day	-68	.53	.48	1.11	.079	.857	3.6
28 day	-83	.32	1.2	1.14	.049	.776	3.7
91 day	-82	.57	1.6	.52	.038	.757	3.2
365 day	-69	-.08	1.6	.42	.034	.733	2.9

efficients of equation 3 in Table III could apply to the compressive strengths of concretes made from any Portland cements. The equations have been derived from New Zealand cements and workers using other cements should not use these equations before testing them on cements whose composition, specific surface and compressive strength is known.

Cements from different works did not give the same coefficients in the regression equations. Table IV gives the coefficients when equation 1 was fitted to the 3, 7 and 28 day compressive strengths of cements from, all the works, works A, works E, and works A and E. Coefficients are seen to vary considerably. The coefficients of the regression equations cannot be used therefore with any confidence to predict the effect on compressive strength of individual components.

TABLE IV

Coefficients of regression equation 1

Cement Works	b_0	b_1	b_2	b_3	R^2	s
3 day						
All	-30	.??	.64	.073	.84	2.9
A	-47	.86	1.74	.032	.92	2.4
E	-26	.32	.58	.072	.93	2.5
A & E	-29	.46	1.72	.072	.92	2.6
7 day						
All	-34	.58	1.12	.078	.84	3.8
A	-32	1.09	.98	.087	.87	3.4
E	-33	.57	1.10	.079	.94	3.2
A & E	-34	.71	.75	.071	.91	3.5
28 day						
All	2.5	.45	1.14	.045	.61	4.9
A	35	.64	-.87	-.018	.68	3.1
E	9.1	.45	.22	.050	.78	4.0
A & E	12.1	.50	.22	.038	.73	4.1

The values of the standard deviations of the calculated compressive strength, s, are higher than the standard deviations of the observed compressive strength s_o. For 3 day compressive strength s = 2.8 MPa and s_o lies between 0.4 and 1.0 MPa while for the 365 day strength s = 2.9 MPa and s_o lies between 1.6 and 1.9 MPa. Furthermore the standard deviations of the compressive strength calculated by the method of error estimation from near neighbours (3) by the computer program was approximately the same as s suggesting that the fitting procedure could not be taken any further with the present variables.

The high values of R^2 obtained when equation 3 was fitted implies that the compressive strength of concrete for New Zealand cements is largely dependent on the composition and specific surface of the cement. The fit attained is surprising considering the errors of accuracy in the Bogue compositions (6). The percentage of variance not explained when equation 5 was fitted to all of the cements varied between 12 and 22% (calculated from R^2 values in Table II). This unexplained variance could be due either to the unreliability of the Bogue compositions, or to factors other than the Bogue compositions, the minor oxides and the specific surface. In an earlier paper (2) it was shown that better composition estimates gave no improvement to the degree of fit of equation 1 and therefore it can be concluded that it is the additional factors which are significant in modifying compressive strength. The nature and role of these other factors has been reviewed by Chatterjee (5) and examples of these factors are the crystal size of the alite, defects present in the alite crystals and impurities present in alite.

CONCLUSIONS

A simple equation has been generated which predicts the compressive strength of concrete at 3, 7, 28, 91 and 365 days.

Eighty percent of the variance is explained by the regression equations and the standard deviation of the calculated compressive strength is about 3 MPa.

ACKNOWLEDGEMENT

I would like to thank Mr J. Clelland of Central Laboratory, Ministry of Works and Development, who supplied all the compressive strength data, and for his help and advice. I also thank Mr R.A. Kennerley and Mr L.M. Smith for many useful discussions and Drs W.C. Tennant and G.J. Gainsford for their help and advice.

REFERENCES

1.- K.M. ALEXANDER (1972), "The relationship between strength and the composition and fineness of cement", Cement and Concrete Research, 2, 663-680.

2.- L.P. ALDRIDGE, "Accuracy and precision of an x-ray diffraction method for analysing Portland cements." To be submitted Cement and Concrete Research.

3.- C. DANIEL, F.S. WOOD, J.W. GORMAN (1972), "Fitting equations to data - Computer Analysis of multifactor data for scients and engineers", Wiley-Interscience.

4.- N.R. DRAPER, AND H. SMITH (1966), "Applied Regression Analysis", Wiley, Chapters 6-8.

5.- A.K. CHATTERJEE (1979), "Phase composition, microstructure, quality and burning of Portland cement clinkers - a review of phenomenological interrelations - Part 1 and 2", World Cement Technology, 10, 124-135, 165-173.

6.- L.P. ALDRIDGE (1978), "International Cement Analysis Study. Part 4: Comparison of Results", Chemistry Division, DSIR, New Zealand Report CD 2267.

The Effect of Cement Composition on the Cracking Resistance

L'influence de la composition du ciment sur la résistance à la fissuration

Z. TSILOSANI, D.Eng. Professor, Head of Department,
G. DALAKISHVILI, M.Eng. Engineer, Institute of Structural Mechanics and Seismic Stability, As.Sc.GSSR.
and
S. KAKICHASHVILI, M.Sc. Head of Department, Institute of Cybernetics, Ac.Sc.GSSR.

RESUME : Sont exposés les résultats d'étude sur la résistance à la fissuration au cours du durcissement de mortier de ciment-sable fabriqué à partir de six différents types de ciments. La naissance des fissures a été étudiée à l'aide de l'interférométrie holographique permettant de fixer l'apparition des fissures avant que cela soit possible par d'autres méthodes. Sont également décrits les dispositifs permettant d'évaluer la résistance à la fissuration au cas où le retrait du béton et la charge mécanique agissent en même temps. En plus, il a été noté que cette méthode rapprochait les résultats d'essais du béton en laboratoire de ceux obtenus au cours d'exploitation de la structure en béton.

La période entre le début de l'observation et le moment de détection des fissures sur les échantillons est prise pour la mesure de résistance à la fissuration, et l'on a effectué la comparaison des propriétés des ciments ayant différentes compositions minéralogiques et différentes teneurs en constituants non-calcines.

Les auteurs proposent d'utiliser cette méthode d'interférométrie holographique pour déterminer la grandeur d'extensibilité limite du ciment durci et du béton.

SUMMARY: The results of studies of the cracking resistance of a hardened cement-sand solution prepared of 6 different kinds of cement are presented. Cracking is studied using the method of holography interferometry which enables to detect cracks at earlier stages than it van be done with other methods. Devices used to evaluate the cracking resistance in case of a combined action of shrinkage and mechanical load are described. The laboratory conditions for testing concrete are shown to be close to those in a real structure.

Assuming the time elapsing from the beginning of observation of specimen to the moment of detection of a crack, as a measure of the cracking resistance, cements of different mineral compositions and different contents of unbaked components are compared.

The authors suggest to apply the method of holography interferometry to evaluate the ultimate extensibility of cement stone and concrete.

The problem of crack formation in concrete and reinforced concrete units has long long become a matter of concern of engineers and researchers. Cracks result in the decrease of the supporting power and duarbility of units deterioration of their service characteristics, not to mention the appearance of the structure.

Cracks are caused by various reasons-external mechanical loads or strains induced by the irregularity of settlement of supports, shrinkage and thermal strains of concrete, etc. On the other hand, resistance of concrete and reinforced concrete to cracking also depends on a number of factors, the most important among them being a tendency of concrete to an intensive development of the shrinkage strain and creep of cocnrete and its ultimate tensile strength.

The great variety of factors causing cracking as well as those contributing to the cracking resistance of concrete makes it difficult to predict the degree of danger. This has evidently given rise to the great number of methods created for evaluation of the cracking resistance of concrete. Hence seem to emerge different interpretations of the idea of the "cracking resistance of con-crete".

An attempt has been made (I) to classify the so far suggested methods of evaluation of the cracking resistance of cocnrete. These are indirect and direct methods and those based on mdelling a conérete structure. The indirect methods of evaluation of the cracking resistance consist in the accounting for the degree of tightness of the cement stone shrinkage strain by the counter-action of a coarse filling(with non-reinforced concrete) and reinforcement (with reinforced concrete). The cracking resistance is calculated using coeffi-cients, the latter being derived from the concrete specifications: the ultimate tensile strength and the ultimate compressive strengrh, the ultimate extensibily, the elastic modulus, the shrinkage strain value, the coefficient of internal fric-tion,the intensity of external mass-exchange and internal moisture transfer and others Some investigators suggest to deduce the cracking resistance from the mineral composition of cement and other factors,

It should be pointed out that the a.m. indirect methods require the knowledge of some characteristics which are not defined during standard conventional tests of concrete; for instance, the ultimate extensibility of concrete is not always evaluated and even the method of its evaluation is not unique, every investigator using different experimental means and experience, and the literature providing rather different values of the ultimate extensibility of concrete. Also the value of loose and, especially, tight settlement of concrete is not always available.

The methods of evaluation of cracking resistance based on modelling a concrete structure are doubtlessly interesting,altough most of them are within the sphere of laboratory research or are too simplified and can provide results not reasonable enough practically.

The suggested direct methods of evaluation of the cracking resistance and, in particular, the method of the ring(2), which is widely used in laboratory, is quite simple, but it enables to evaluate the resistance to cracking resulting from shrinkage only; while our point of interest is the resis-tance to cracking resulting from shrinkage and external mechanical loads.This will bring the laboratory conditions closer to the field where the elements of constructions are subjected to the forces of shrinkage as well as forces developing from the proper weight and external mechanical load. The effect of the simultaneous forces of shrinkage and external mechanical load is not a more sum of the effects of these two forces(3). While studying the mineral composition of cement regarding the cracking resistance, we used a special device which enabled to evaluate the cracking resis-

tance under the effects of shrinkage and external load. The method of Holography interferometry was used to observe the process of emergence and development of Cracks (4).Holography has become a widely used means of checking important parts of machines,aircraft,etc. In building it has been used but seldom, in particular, in testing concrete and reinforced concrete.However, a number of advantages of the holography methods over the conventional ones, and a common tendency to lower the prices of testing devices on the whole, rose interest to them in researchers and engineers. Thus, when the method of holography interferometry is used to test strain, it does not require any special surface characteristics(roughness,moisture), or the size of tensometers, not to mention the complicated procedure of sticking and wiring the letter, the whole picture of the strain over the surface under observation being obtained easily, which is not the case when the method of electrotensometry is used. Holography interferometry has also advantages over other optical methods,such as the method of photoelasticity,as it does not require any optically sensitive material which often fails to imitate closely the actual characteristics of concrete and reinforced concrete(5)

TABLE I

Cement No	Kind of cement	Kind and amount of unburnt component
I.	Portland cement low heat output and low alkaline content	Diatomite, I5%
2.	Portland cement	" "
3.	Portland cement	Addition, I5%
4.	Portland cement	Blast furnace granulated slag,I5%
5.	Slag Portland cement	Blast furnace granulated slag,50%
6.	Puzzolanic Portland cement	Pumice, 35%

Below the test results of 6 kinds of cement with different mineral compositions are given (Tables I and 2). Specimen of cement-sand mixtute (maximum grain size of the filling -5mm), 4 x 4 x I6 cm, were made, reinforced with two steel rods of 3 mm diameter. The cement -to-filling and water-to-cement rations in the samples were the same. The samples were kept in water to avoid craking due to heat and water treatment. The samples were loaded by means of a special device (Fig. I). The applied force was 0.7 of the load causing observable cracks. It was defined through short - run tests of twin samples.

TABLE II

Cement No	Mineral composition				Grout of normal tickness %	Strength N/mm^2
	C_3S	C_2S	C_3A	C_4AF		
I.	45.0	32.0	4.5	I5.0	26.0	42.0
2.	60.0	I7.0	4.2	I5.0	23.0	50.8
3.	58.0	I9.0	4.0	I6.0	27.5	5I.5
4.	56.I	I5.9	9.4	I5.7	25.0	50.2
5.	56.5	I5.0	9.7	I5.95	26.5	4I.0
6.	37.2	35.3.	I4.8	9.55	32.7	39.7

To take the interferogram the loaded samples were laid on a special rack.(Fig.2) . The holograms were taken by a single-mode He-Ne laser (6328Å wave length) of 50 mW power, using the method of double exposition and a two-beam scheme. The intervals between expositions had been defined previously, the time of each exposure was 1 minute.

Figs. 3-6 present a part of the interferograms. The specimen numbers correspond to the cement numbers given in Table 2. The first interferogram (Fig.3) has rare broad transversal interference bands which indicate a weak development of strain along the longitudinal axis of the samples. The first specimen has a surface crack which as the subsequent interferograms

prove, does not develop any more.

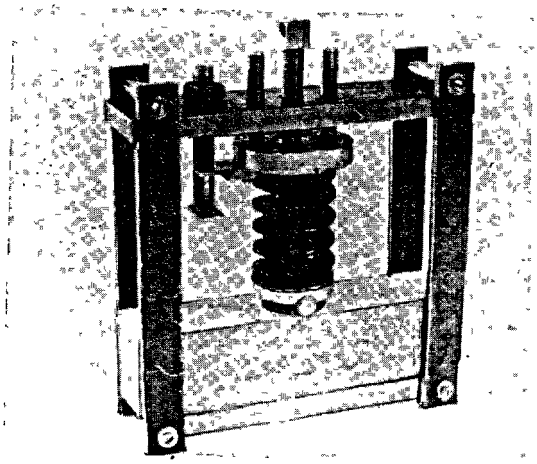

Fig.I. The loading device

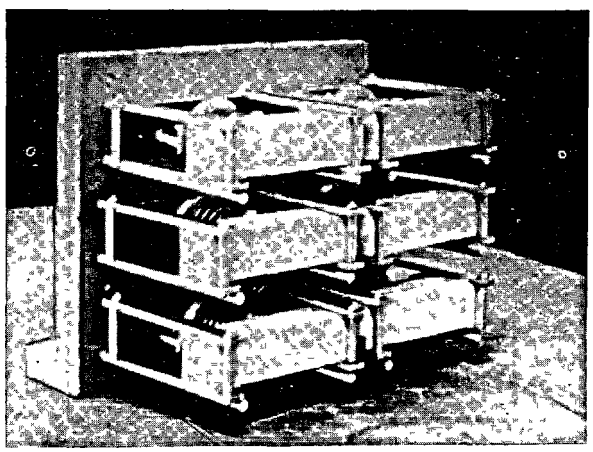

Fig.2. The rack with the specimen

For I4 hours following the loading of the specimen, the interference bands grew denser(Fig. 4), indicating an intensified process of strain of the stretched side of the specimen, which resulted from a combined effect of shrinkage and erternal load. After I6 post-loading hours cracks appeared in 4 specimen in the following order: 6,3,I and 4. After I8 hours (Fig.5) was seen in specimen 5, while after 20 hours (Fig. 6) in sample 5.

Cracking could be observed in the shape of the interference bands. While the material under study was intact, the interference bands were free of breaks and never crossed. As soon as cracks formed, orientation of the bands either changed, or they crossed or broke up.

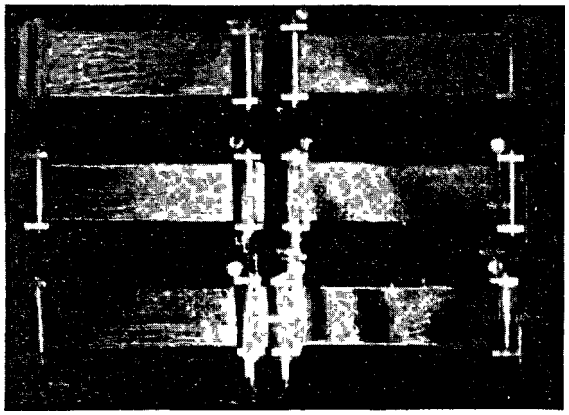

Fig. 3. An interferogram of the specimen 2 hours after the loading. The numbers of the same as correspond to the numbers of the cement types in the Tables.

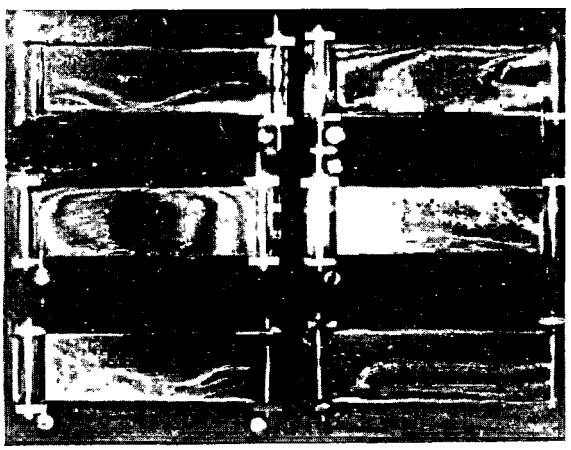

Fig. 4. An interferogram of the specimen I4 hours after the loading

Proceeding from the existing direct methods of evaluation of the cracking resistance, let us assume the time elapsing from loading a specimen to crack formation (i.e., the time when the typical breaks of the interference bands appear on the interferogram) as its measure. Then the kinds of cement under

study can be classified in the following way. The best crack-resistant kind is Portland-cement without any active mineral addition (cement No.1). Even a negligible amount of addition (as low as 15% of the cement weight) reduces the cracking resistance quite significantly (cement No 3).

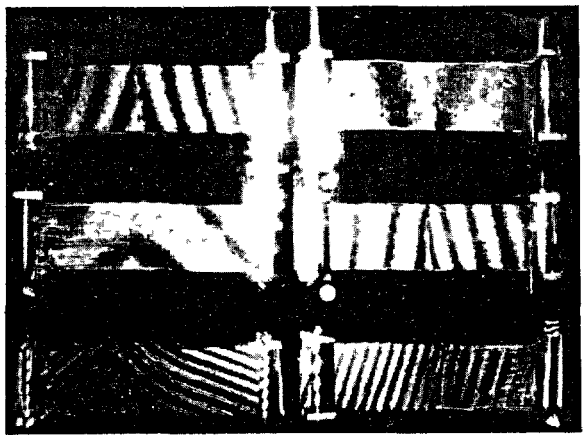

Fig. 5. An interferogram of the specimen 18 hours after the loading.

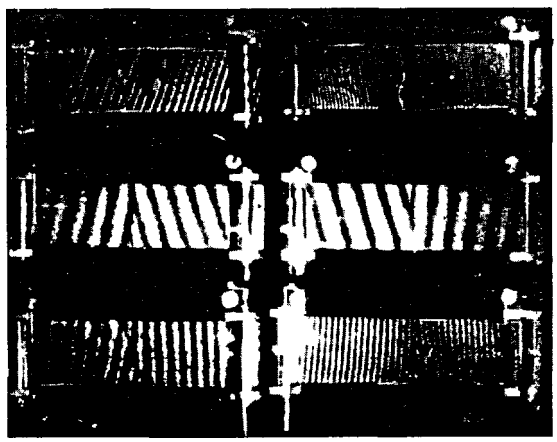

Fig. 6. An interferogram of the specimen 20 hours after the loading

The lowest crack resistance was displayed by puzzolan Portland cement (cement No 6). It should be also noted that the mineral composition of clinker did not seem to affect the cracking resistance value of cement as active mineral additions did.

It could be thus concluded that changes in the character of the interference bands provide information on cracking much earlier than it can be observed visually of even though a 24 x magnifying glass. As the interferogram enables to evaluate also the strain value of an object, the method of holography interference can be recommended to find the values of ultimate extensibility of concrete, although it will require finding the length of the extended section as the basic value in evaluating the strain

CONCLUSIONS

The described method of comparative evaluation of the cracking resistance of cement stone and concrete employs the method of holography interferometry. It has been suggested to evaluate the cracking resistance under a combined action of shrinkage and external mechanical load. A special device has been designed to prove the idea;

The method of holography interferometry ensures detection of a crack at an earlier stage of its development than other existing methods (visual observation of the specimen, application of tensometers, the ultrasound). Thus a better accuracy of evaluation of the ultimate extensibility of concrete is made possible.

Comparison of the cracking resistance test results for 6 kinds of cement has demonstrated that the cracking resistance depends predominantly on the active mineral additions in cement. The role of the mineral composition of cement seemed insignificant as compared with the role of additions.

REFERENCES:

1.- Composition, structure and characteristics of cement concretes. Edited by G.I.Gorchakov, Moscow, Stroiizdat 1976 (in Russian).

2.- ROBERT LHERMITE. Idees Actueles sur la Technologie du Beton, Paris, 1955.

3.- Z.N.TSILOSANI, A.V.SAKVARELIDZE. Structural changes in the drying cement stone. 6-th International Congress on

the chemistry of cement. Proc., V.II, book 1, 1976 (in Russian).

4.- R.J.COLLIER, C.B. BURCHARDT, H.L.LIN. Optical Holography, Bell Telephone Laboratories, Murray Hill, New Jersey, 1971.

5. - G.K.DALAKISHVILI, SH.D.KAKICHASHVILI, Z.N.TSILOSANI. Concrete shrinkage deformation research by holographic interferometry method. International conference on optical computing in research and development, Visegrad, 1977.

La structure de pierre de ciment de nouveaux types de béton

A structure of the cement stone of the new types of concrete

K. GORIAINOV, Professeur, Chef de Chaire de Matériaux Thermo-isolants et Ceramique,
A. STCHASTNII, Docteur ès Sciences, U.R.S.S.

RESUME : Cette communication expose les résultats d'observations faites au microscope électronique sur la structure fine des ciments hydratés, notamment dans des bétons à granulats de laitier. Le grossissement du microscope électronique variait de 211 à 46.800.

Les éprouvettes de ciment étaient moulées; certaines étaient comprimées sous une pression de 200 MPA. Leur résistance à la compression atteignait 70 MPA.

Des éprouvettes de béton ont été comprimées à la pression de 5 MPA (R_c = 90 MPA).

On a étudié des éprouvettes de pâtesde ciment, imprégnées après durcissement jusqu'à saturation, par des *suspensions de ciment*.

On a constaté une disposition bien homogène des cristaux d'hydrates; dans les bétons à granulats de laitier on a observé des fils cristallins d'un diamètre compris entre 300 et 600 Å, et d'une longueur de 0,3 à 0,4 microns.

On a constaté que l'imprégnation, par une suspension de ciment, diminuait la porosité et la perméabilité des éprouvettes.

SUMMARY: The report gives the results of the study or the microstructure of the cement stone and concretes on the slag fillers.

There have been used an electron microscope with a resolving power from 211 till 46800.

The samples of the cement stone made under the pressure of 200 MPA and without it have been investigated. Compression strength of the samples Rc reached 70 MPA.

There have been also studied the samples from the concrete saturated with the cement suspension.

The homogeneity of disposition of the new particles have been concrete consists of crystal filaments of diameter 300-600 Å and length 0,3-0,4 MKM.

There was also proved that saturation with the cement suspension increases waterproofness of the concrete.

On a effectué des études de la structure du mortier de ciment moulée (pressée) et du béton de laitier dans les buts de fabrication des bétons à haute résistance avec une structure homogène.

On a fait aussi des études d'imprégnation de béton par solution colloidale (suspension de ciment et d'eau) pour augmentation de résistance à la compression et d'imperméabilité à l'eau.

On a étudié l'influence de temps de durcissement sur la structure de différents types de béton au moyen de micrographie. La micrographie est faite avec orientation sur un et deux points de surface.

La caractéristique de pierre de ciment est fixé dans le tabl.I.

Tableau I

Ns	Rapport E/C	Agrandissement	Mode de traitement	
			Durcissement pendant 12 h dans les conditions normales	Traitement thermique avec t°80
1	0,28	6330	12	-
2	0,28	6330	12	4
3	0,28	6330	12	4
4	0,28	12660	12	-
5	0,1 x)	6330	12	6

La micrographie a fixé le premier stade d'hydratation après 12 heures de durcissement dans les conditions normales (des.1-2). On a pu voir les particules de dimension de 1 MKM à 25 MKM. On a pu aussi fixer la structure de stratification de $Ca(OH)_2$ et C-S-H. On a pu observer les pores de dimension de 20 MKM en forme d'étoile et parallélépipède rectangle.

x) On a fait le pressage de 200 MPA/cm^2 pendant la fabrication de pâte de ciment avec E/C = 0,15 - 0,1

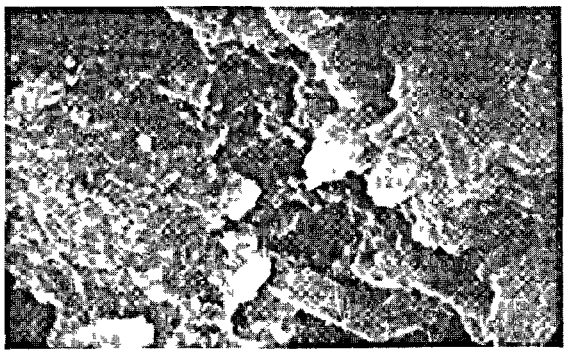

Des.1

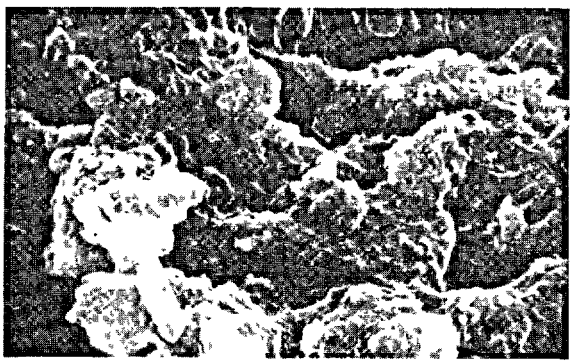

Des.2

Après le traitement thermique pendant 4 heures on peut voir les particules lamellaires de dimension et de configuration différentes. Sur ces particules sont vus les agrégats ronds de ø 0,6-0,8 MKM. (des.3d) ainsi que les fibres (des.4). Sur les surfaces lisses de particules sont observées les pores de dimension de 500 à 4000 A°.

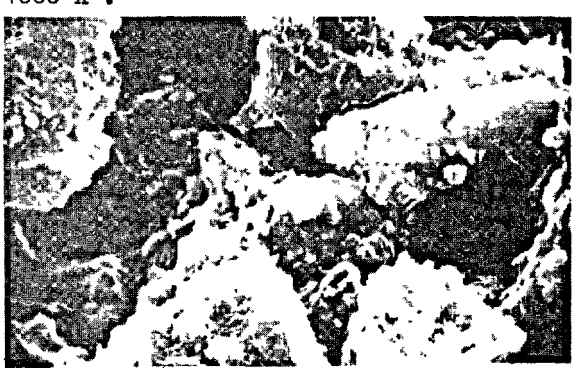

Des.3

Des.4

La quantité des agrégats ronds est augmentée sur les éprouvettes pressées (des.5a).

La micrographie a indiqué que la microstructure de bétons de laitier se presente les fils cristalliques de ∅ 300-600 A° et de longueur 0,3-0,5 MKM (des.6).

L'espace entre les fils est remplie par les masses gélifiantes.

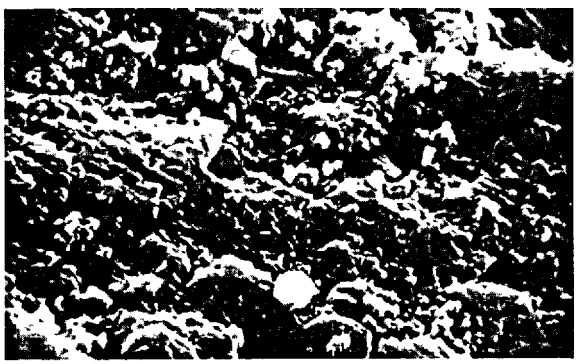

Des.5

Des.6

La composition de bétons de laitier était suivante: 350 kgs de ciment et 1700 kgs de laitier granulé pour 1 m^3 de béton. Le rapport E/C est égale de 0,6.

Les éprouvettes sont compactées par vibration et pressage. Rc de béton est égale de 92-93 MPA.

On a effectué les études de macroporosité de pierre de ciment imprégnée par suspension de ciment et d'eau sous pression.

K.Goriainov et R.Lorétova ont élaboré la méthodologie de mesure de macroporosité de pierre de ciment.

On a fait des essais de deux sortes d'éprouvettes: les éprouvettes étuvées sous l'action de t°80 et celles-ci imprégnées de la suspension de ciment et d'eau. On a préparé la suspension par le mélange de 2 parties d'eau et 1 partie de ciment.

Les caractéristiques essentielles de matériaux en question sont indiquées dans le tabl.II.

Tableau II

Masse volumique de mat.kg/m^3		MPA	Résistance à la compression MPA/kgs	Caractéristique d'éprouvettes
Après l'étuvage	Dans 28 jrs de durcissement	Dans 28jrs de durcissement	Dans 28jrs de durcissement	
2078	2058	14,6	0,075	non-imprégnées
2150	2180	20,8	0,965	imprégnées

On a mesuré les pores de dimension de 10 MKM à quelques millimètres. On a fait le calcul de pores sur la surface de 2 x 2 cm.

Les résultats des essais sont fixés dans le tabl.III.

Tableau III

Ns de rectangle	Eprouvette non-imprégnée	Eprouvette imprégnée
1	25,1	13,4
2	23,6	16,1
3	10,7	12,5
4	20,4	15,9
moyenne	20%	15%

Les dimensions de pores de 75 MKM à 5 mm prédominent dans le plan de quantité les petites macropores de dimension 123-250 MKM. La superficie intérieure de pores d'éprouvettes imprégnées á été couverte de couche de suspension de ciment durcis d'épaisseur de 50-75 MKM. Ce phénomène change les propriétés d'éprouvettes imprégnées.

La structure d'éprouvettes imprégnées est plus homogène que celle-ci d'éprouvettes non-imprégnées.

Les éprouvettes imprégnées ont la plus haute imperméabilité que celles-ci non-imprégnées (0,05 MPA pour les éprouvettes non-imprégnées, 0,2-0,3 MPA pour les éprouvettes imprégnées).

CONCLUSIONS

1. L'essais de structure de pierre de ciment montre que non-homogénéité observée de produits d'hydratation de ciment dépend de degrés d'agrandissement.

2. On a découvert aussi que la saturation de pierre de ciment augmente la imperméabilité à l'eau et diminu sa porosité.

TITRES DE DESSINS

1. Micrographie à microscope de balayage de l'éprouvette de pierre de ciment à E/C de 0,23 sans pression dans 12 h de durcissement dans les conditions normales.

2. Micrographie à microscope de balayge de l'éprouvette de pierre de ciment à E/C de 0,28 sans pression dans 12 h de durcissement et 4 h de traitement thermique sous l'action de $t^{o}80$.

3-4. Micrographie à microscope de balayage de l'éprouvette de pierre de ciment à E/C de 0,28 sans pression dans 12 h de durcissement et 4 h de traitement thermique sous l'action de $t^{o}80$.

5. Micrographie à microscope de balayage de l'éprouvette de pierre de ciment à E/C de 0,1 sous pression spécifique de 200 MPA dans 12 h de durcissement dans les conditions normales et 4 h de traitement thermique sous l'action de $t^{o}70$.

6. Béton de laitier pressé (augmentation en 12660).

Structure and composition of compounds in some fully hydrated cement pastes

Structure et composition de certaines pâtes de ciment totalement hydratées

A.E. MOORE, Materials Research Department, Cement and Concrete Association, Slough U.K.

RESUME : S'il est broyé jusqu'à moins de 10µm, le clinker de ciment peut être totalement hydraté dans un délai de 60 à 90 jours. A cette finesse, les micro-cylindres (50 mm2 de section transversale) peuvent être pressés à sec pour une porosité de 60 % et un rapport d'hydratation eau/ciment de 0.5. Ils atteignent une résistance à la compression d'environ 70 MPa après 28 jours à 20°C et peuvent donc être considérés comme une pâte de béton.

Une étude aux rayons X révèle la formation des phases suivantes : portlandite, C-S-H, AFt et AFm. La phase C-S-H présente environ quatre réflexions hk0 mais aucune 001. La phase AFt présente un mode ettringite, y compris la diffraction 101, qui la distingue de la thaumasite. La phase AFm présente une ou deux réflexions hk0, y compris celle à 2.86 - 2.87 et une 001 ou plus.

L'étude au microscope électronique ne peut déterminer que les éléments de poids atomique de 11 et plus; l'analyse des hydrates doit donc être basée sur des proportions.

Les quatre phases contiennent les cinq éléments Ca, Si, Al, Fe et S, bien que Al et S ne soient pas toujours présents dans la phase portlandite. Les plus petites concentrations d'atomes étrangers se trouvent dans cette dernière -$Ca(OH)_2$- soit environ 0.3 d'atomes Si et 0.05 d'atomes Fe par 10 Ca. Les autres phases démontrent une différence de composition considérable, aussi bien entre les différents échantillons que dans chaque échantillon. Les quantités totales d'atomes étrangers sont plus grandes qu'on ne pensait possible précédemment. Le rapport C/S varie en C-S-H entre 1.25 et 4.0, et le total AL+Fe+S varie de 0.1 à 0.9 du Si. La phase AFt contient du Si et du Fe, bien qu'il y ait moins de Fe que de Si et le rapport Al:(Si+Fe) est environ 2:1. La phase AFm contient plutôt plus de Fe et moins de Si que la phase AFt. S est toujours insuffisant (en partie en raison de la perte dans le microscope électronique) dans la phase AFt aussi bien que dans la phase AFm.

Le rapport Fe/(Al+Fe) est toujours inférieur dans les phases AFt et AFm et plus élevé dans la phase C-S-H que dans le clinker anhydre.

SUMMARY: Cement clinker, if ground to less than 10 µm, can be fully hydrated in 60-90 days. At this fineness micro-cylinders (50 mm^2 cross-sectional area) can be dry-pressed to 60% porosity, giving 0.5 water/cement ratio on hydration. These reach a compressive strength of about 70 MPa after 28 days at 20°C, and may therefore be regarded as being representative of paste in concrete.

Analysis by X-ray diffraction shows the compounds formed to be portlandite, C-S-H, AFt and AFm phases. The C-S-H shows about four hk0 reflections but no 001. The AFt shows an ettringite pattern including the 101 diffraction that distinguishes it from thaumasite. The AFm phase shows one or two hk0 reflections including that at 2.86 - 2.87 and one or more 001.

Analytical electron microscopy can only determine elements with atomic number equal to or greater than 11, and analyses of hydrate phases must therefore be based on ratios.

All four phases contain the five elements Ca, Si, Al, Fe and S although Al and S are sometimes absent from portlandite. The latter - $Ca(OH)_2$ - shows the smallest concentrations of foreign atoms about 0.3 Si and 0.05 Fe atoms per 10Ca. The other phases show considerable variation in composition both between different samples and within each sample. The total levels of foreign atoms are larger than has previously been considered likely. The C/S ratio varies in C-S-H between 1.25 and 4.0, and the total AL+Fe+S varies from 0.1 to 0.9 of the Si. The AFt phase contains both Si and Fe, though less Fe than Si, with Al:(Si+Fe) about 2:1. The AFm phase contains rather more Fe and less Si than does the AFt. S is always deficient (only in part due to loss in the electron microscope) in both AFt and AFm.

The ratio Fe/(Al+Fe) is always lower in the AFt and AFm phases and higher in the C-S-H than in the anhydrous clinker.

INTRODUCTION

Lawrence (1) has shown that there is a sharp change in aqueous phase composition during cement hydration when the (SO_4^{--}) ion is no longer available; (Ca^{++}) decreases while (OH^-) and the alkali metals increase; SiO_2 also increases though it remains very low. It is well known that alumino-ferrite trisulphate (AFt) phase forms before SO_4 depletion and monosulphate types (AFm) thereafter, but it seemed possible that different C-S-H compositions might form during these regimes. In order to approximate the early and late hydration situations, samples were made with cement clinker or with excess gypsum added.

In addition, the XRD pattern of C-S-H* is notoriously disordered, and it was hoped that, at full hydration it might be easier to resolve in the absence of lines from the anhydrous phases. Cement of normal fineness does not hydrate completely at normal water-cement (w/c) ratios in times up to 100 years, and even at w/c = 5 or more may require ten years to react completely. However, if the cement is ground so that no particles are larger than 10 μm, an OPC will hydrate completely in about two months. If the ground cement is dry-pressed into small right cylinders (2) the porosity attainable is about 60%; this gives a w/c of about 0.5 when hydrated by evacuating the cylinders and allowing water to replace the vacuum. Thus a fully hydrated paste may be obtained at w/c similar to those used in practice. Another advantage of this technique is that flash set problems do not occur, and the samples may be made from ground clinker without added gypsum.

Experimental

Three clinkers, chosen to cover a wide range of chemical and compound composition, (A,B and C in Table I) were ground in an agate swing-mill to a specific surface of about 1400 m^2/kg, (this gives an average particle size of 5-6 μm). Clinkers B and C were also combined with gypsum (laboratory grade) in weight ratio 9:1. Specimens were prepared by compressing the dry powder into right cylinders of 50 mm^2 cross section with about 60% porosity; these were put in a vacuum desiccator kept at 20°C, evacuated for at least ½ hr and then water at 20°C was allowed to replace the vacuum. The cylinders were kept in water at 20°C until testing; two being tested for compressive strength at each age:- 1,2,4, 8,16,32 and 64 days.

The crushed cylinders from A,B and C were stored in methanol, but when it was found that AFt phase is rendered X-ray amorphous by 8 days of this treatment, samples from BG and CG were stored in iso-propyl alcohol, or taken straight from water.

X-ray diffraction photographs were taken (on a Nonius Guinier camera) as soon as possible after crushing, and XRD traces (on a Philips vertical-circle diffractometer) of the samples at maximum hydration.

Samples were prepared for analytical electron microscopy by grinding and dispersing ultrasonically in iso-propyl alcohol, and then taking up a drop of the liquid on a carbon-coated grid. The Kratos CORA Analytical Electron Microscope allows particles in the sample to be examined in transmission and by electron diffraction, and to be analysed for elements of atomic number ⩾11 by energy-dispersive analysis of X-rays emitted from the back of the sample. Thus compositions which contain H,O,N or C cannot be analysed completely and analysis must be based upon ratios of elements.

TABLE I

	A	B	C
SiO_2	21.7	24.22	20.76
Fe_2O_3	1.89	6.65	1.99
Al_2O_3	4.45	3.61	5.26
CaO	66.40	61.31	66.30
MgO	2.36	0.82	1.90
SO_3	0.50	0.61	1.02
Na_2O	1.20	0.13	0.15
K_2O	0.22	0.30	1.35
P_2O_5	0.12	0.18	0.03
TiO_2	0.43	0.22	0.30
Mn_2O_3	0.06	0.09	0.06
Loss on Ign.	0.59	1.96	0.96
	99.92	100.10	100.08
Insoluble residue	0.41	-	0.26
Free CaO	1.24	0.06	0.19
Potential compound composition			
C_3S	69	29	74
C_2S	10	48	3.6
C_3A	8.5	0	10.6
C_4AF	6	17	6
C_2F		1	
Composition by QXDA			
Alite	82	24	78
Belite	$3(C_2S)$	56	6
Ferrite	4	16.5	6
C_3A	8	0	8

Chemical and XRD analysis of clinkers

Identification of phases in the electron microscope

Calcium hydroxide was easily identified by its thin hexagonal plates and strong hexagonal diffraction pattern. AFt phases were prismatic and showed no diffraction pattern; they bubbled vigorously in the electron beam and probably decomposed even before counting could begin. Lachowski et al (3) showed that the AEM analysis even of natural ettringite was deficient in sulphur, and to some extent in calcium, by comparison with the classical chemical analysis, but that synthetic calcium aluminate monosulphate was much more stable: they found S/Ca = 0.23, (Theoretical 0.25).

AFm phases could sometimes be recognised as uniform thin plates, and sometimes gave one or two diffraction spots, but were generally not distinguishable from C-S-H, by morphology or electron diffraction.

C-S-H never gave diffraction patterns, and both AFm and C-S-H often showed damage after analysis.

* Cement chemical nomenclature
C = CaO, S = SiO_2, A = Al_2O_3, F + Fe_2O_3, M = MgO, H = H_2O, $\bar{S}$ = SO_3

Results

Strength Development (Table II)

Clinkers A and C developed strength very rapidly and were virtually completely hydrated at 16 days; addition of gypsum to C accelerated hydration slightly and increased strength by about 30%. Clinker B did not reach full hydration (even at 128 days) but showed about 30% more strength than clinkers A and C at 64 days; gypsum addition accelerated the reaction considerably and increased strength by about 25%, but hydration was still not complete at 64 days.

Both microscopy (in reflected light) and XRD confirmed the presence of small amounts of belite and F_{ss} in the B and BG samples at 64 days, and the absence of anhydrous phases in A, C and CG at 64 days was confirmed by XRD.

TABLE II

Age	Crushing Strength (MPa)				
	A	B	C	BG	CG
1	-	-	38.0	9.4	45.6
2	52.4	0.9	-	28.4	63.3
4	65.5	4.6	52.7	39.4	70.1
8	-	15.7	62.5	44.6	81.6
16	69.2	27.6	63.9	63.5	83.6
32	69.6	73.4	64.7	93.4	82.1
64	71.1	85.8	64.0	109.7	88.3

Strength development of micro-cylinders

X-ray Diffraction

As expected AFt phases were absent from A,B and C; AFm phases showed 001 reflections at 8.1 and 7.6 Å, which for pure materials would indicate carbonation; (normal care was taken to avoid CO_2 contamination during preparation, using CO_2-free water for hydration etc., but the cylinders were exposed, damp, during compression testing). These lines are both present, though weaker, in the XRD traces from CG and that at 8.1Å, also weak, in BG. A fairly sharp line at 2.87Å is probably also due to an AFm (hk0) reflection, but there was no similarly shape line at 1.66Å.

Table III lists broad reflections which were either probably or possibly due to C-S-H. Those which appear only in samples B and C are likely to be due to AFm phases, while those which appear at similar intensity in B and BG, C and CG are more likely to be due to C-S-H. The first two lines listed are overlapped by strong ettringite lines, so it is impossible to tell whether they are present in BG and CG. The reflections at 4.03 and 2.015Å could thus be 002 and 004 for the 8.1Å AFm phase, though the 2.015 are rather more alike in intensity than the 8.1Å.

The reflections at 1.82 and 1.66Å have a half peak width of 2 degrees 2θ (i.e. 1.84 - 1.80Å and 1.674 - 1.654Å) and could be said to indicate C-S-H I but none of the other lines make a convincing case for this, and the presence of a wide halo from 3.2 - 2.7Å does not help the identification. In the light of the results to be reported from the analytical electron microscopy this is perhaps not surprising. The line at 2.275Å is wholly unaccounted for; it has not been previously recorded for a C-S-H, but it is present in all four diffraction patterns, at $\frac{1}{4}$ to $\frac{1}{5}$ the intensity of the line at 1.88Å.

TABLE II

B	BG	C	CG	Assigned to
4.4	Ett.	4.4	Ett.	?
4.03	Ett.	4.03	Ett.	AFm ?
3.035	3.035	3.035	3.035	C-S-H or calcite
2.54	-	2.54	-	AFm ?
2.45	-	2.45	-	AFm ?
2.275	2.275	2.275	2.275	C-S-H ?
2.015	2.015	2.015	2.015	AFm ?
1.82	1.82	1.82	1.82	C-S-H
1.66	1.66	1.66	1.66	C-S-H + AFm ?

Broad X-ray reflections, possibly or probably due to C-S-H

Analytical Electron Microscopy

All particles were analysed for any elements present between atomic number 11 (sodium) and 30 (zinc). Ca, Si, Fe, Al and S appeared in the great majority of analyses with Mg, Na or K in many, and Cl, Ti or Mn and occasionally Zn in a few.

It was found convenient to convert all counts to atom ratios (not molar) with a base of 10 Ca. This showed that most particles could be grouped into Si 2-10, (Al+Fe)$\lesssim$2, or (Al+Fe) 2-10, Si$\lesssim$2, or nearly pure Ca (i.e. calcium hydroxide). But a few particles with high Mg (1 - 2.5) fell outside this scheme. By assuming that Mg replaces Ca and re-calculating to a base of 10 (Ca+Mg) these particles fell within the high Si, low (Al+Fe) field i.e. C-S-H, and all further calculations were made to this ratio.

Of the high (Al+Fe) particles, none showed sulphar content as high as the 5.0 required for ettringite and few even the 2.5 required for monosulphate. Lachowski et al (3) finally assigned the fields shown in Fig.1 on the basis of morphology and

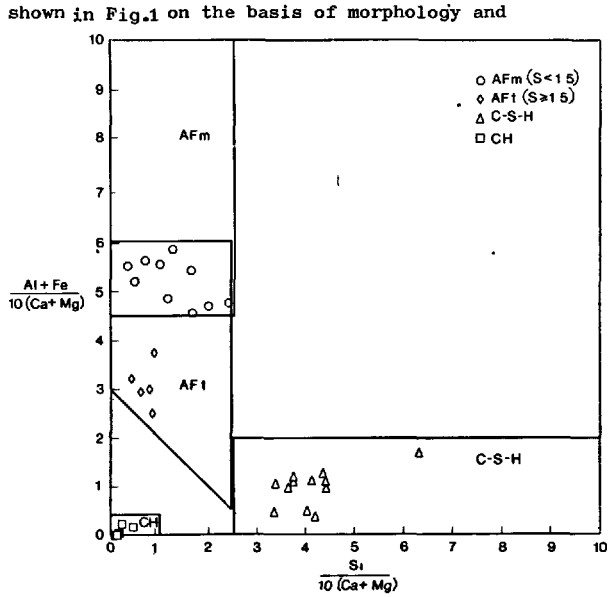

Fig.1 - Composition zones for hydrate phases as atom ratios to 10(Ca+Mg) with particles from B and BG plotted.

diffraction pattern, with AFm and AFt distinguished by $S < 1.5$ and $S > 1.5$ respectively.

The fields are defined as:-

C-S-H	$2.5 < Si < 10$, $(Al+Fe) < 2$	
CH	$Si < 1.0$, $(Al+Fe) < 0.4$,	$S \leq 0.4$
AFt	$Si < 2.5$, $(Al+Fe+Si) > 3$, $(Al+Fe) < 6.0$	$S \geq 1.5$
AFm	$Si < 2.5$, $4.5 < (Al+Fe) < 10$,	$S < 1.5$

Particles from samples B and BG only are shown plotted in Fig.1 to avoid confusion.

C-S-H

Table IV shows mean and S.D. or range for the six major elements in C-S-H particles from all five samples, calculated as atom ratios to 10(Ca+Mg), together with $\Sigma Al + Fe$, $\Sigma Al + Fe + Si$ and $\Sigma Al + Fe + Si + S$, and the ratio Fe/(Al+Fe). The variability is very large; this was also shown by Gard et al (4) for C_3S pastes and is much greater than experimental error. However, the mean composition appears to be $Si \sim 5$, $(Al+Fe) \sim 1$ and S, if available, up to 1, this corresponds to a Ca/Si ratio of 2, but a Ca/Si equivalent more like 1.5. The only significant difference between the without and with-gypsum samples is that in sulphur content between B and BG.

TABLE IV

Sample	A	B	BG	C	CG
No. of analyses	16	4	8	12	20
Ca	9.5	9.8	9.9	9.8	9.6
S.D.	0.69	0.13	0.09	0.26	0.64
Si	5.5	5.8	4.8	5.5	4.3
S.D.	1.75	1.04	1.41	1.16	1.23
Al	0.7	0.5	0.4	0.7	0.7
S.D.	0.31	0.02	0.13	0.26	0.42
Fe	0.3	0.6	0.6	0.2	0.2
S.D.	0.18	0.16	0.25	0.14	0.10
S	0.3	0.2	0.9	0.3	0.6
Range 0.1→	1.0	0.3	1.8	1.3	1.7
Mg	0.5	0.2	0.1	0.3	0.4
Range 0.0→	1.7	0.3	0.2	0.7	2.9
Al+Fe	1.0	1.1	1.0	1.0	0.9
Al+Fe+Si	6.4	6.9	5.8	6.5	5.2
Al+Fe+Si+S	6.6	7.1	6.7	6.8	5.8
Fe/(Al+Fe)	0.31	0.60	0.57	0.24	0.24
S.D.	0.08	0.12	0.08	0.08	0.07

C-S-H Compositions Atom ratios to 10(Ca + Mg)

Several other parameters change consistently with gypsum addition, but with this variability and sample size these changes are not significant, although they may indicate trends.

There is some indication that mean Si content decreases as S increases, but this is not born out in individual results. However, the individual results for BG and CG do show significant positive correlations between S and (Al+Fe). (Both significant at 0.001 level; Fe/S in BG and Al/S in CG also both significant at .001 with a slightly lower r). The author suggests that this might be due to maintenance of charge balance ($R_2O_3 + SO_3 \equiv 3\ SiO_2$) but Taylor (5) considers this unlikely in such a disordered structure.

The parameter with the lowest coefficient of variation is Fe/(Al+Fe) and this is clearly correlated with the same ratio for the anhydrous starting materials, which is 0.21, 0.54 and 0.19 for A, B and C respectively.

Calcium hydroxide

This phase is the easiest to recognise in the electron microscope and, as the electron diffraction pattern survives the analysis, there is every reason to expect the analysis to be accurate. Of 18 particles analysed, all contained Si (mean 0.34 atoms /10 Ca), none contained Mg, 14 contained Fe (mean 0.05), while only 4 contained Al, and 9, mainly from BG and CG contained S (mean 0.06).

It seems possible that this small amount of Fe, taken up in preference to Al even in the low Fe/(Al+Fe) samples, may be Fe^{++} which has survived the clinkering process in the reduced state.

AFt and AFm phases

Mean compositions for the same six elements are given in Table V for the samples in which these phases occurred. Samples BG and CG were expected

TABLE V

	AFm					AFt	
	A	B	BG	C	CG	BG	CG
N	5	8	1	2	2	5	9
Ca	10.00*	9.7	10.0	9.9	10.0	10.0	9.8
S.D.	0.04	0.32				0.04	0.35
Al	5.1	2.7	2.9	4.0	5.6	2.6	2.4
S.D.	0.09	0.72				0.74	0.78
Fe	1.0	2.4	1.9	0.7	0.2	0.5	0.3
S.D.	0.68	0.74				0.37	0.2
Si	1.1	1.3	1.2	1.3	0.2	0.7	0.9
S.D.	0.91	0.77				0.19	0.7
S	0.5	0.4	0.9	0.5	0.6	2.5	2.6
S.D.	0.15	0.09				0.87	0.75
Mg	0.0	0.3	0.0	0.2	0.0	0.0	0.1
Range 0.0→	0.09*	0.88		0.31		0.05	0.44
Al+Fe	6.1	5.0	4.8	4.7	5.8	3.1	2.7
Al+Fe+Si	7.2	6.4	6.0	6.0	6.0	3.8	3.7
Al+Fe+Si+S	7.7	6.7	6.9	6.5	6.6	6.3	6.2
Fe/(Al+Fe)	.0.16	0.47	0.39	0.14	0.04	0.18	0.13
S.D.	0.08	0.14				0.15	0.10

Compositions of AFm and AFt phases
Atom ratios to 10(Ca+Mg)

to contain AFt rather than AFm and only a very few AFm were found; but there is no explanation for the difficulty experienced in finding AFm in C.

The AFm phase is only distantly related to monosulphate; it contains substantial amounts of Si. and much less S then theoretical; furthermore the (Al+Fe)/10 Ca is in many cases greater than the 5

*Single value for MgO = 0.09, others 0.0

required to fill the octahedral site, and the excess must be accommodated in interlayer sites together presumably with OH^- and CO_3^{2-} anions, and a silicate ion of unknown constitution.

The AFt phase is neither ettringite nor iron-ettringite; it contains considerable Si and certainly less S (even allowing for loss in the electron microscope) than theoretical. Lachowski et al (3) showed that the most satisfactory way to describe the data was to assume that (Ca+Mg+K) occupy Ca sites, and (Al+Fe+Si) the octahedral sites, even though it has been shown that Si can occupy the channel sites. Because of the possible loss of Ca during the analysis they considered that attempts at further refinement are unjustified.

A most interesting point is the low Fe content in AFt from both BG and CG; the maximum Fe/(Al+Fe) in BG was only 0.39 compared with 0.54 in the anhydrous clinker. It has always been assumed that, if available, Fe would enter the ettringite structure almost as easily as Al, and in this clinker there is no question of it being unavailable as there is virtually a single interstitial phase of composition $C_4A_{.34}F_{.66}$.

Unidentified phases

Two types of particles were not assignable to any of the compositions discussed above. Some were probably composite, with an analysis lying between AFm and C-S-H zones.

Another phase was clearly losing Ca during analysis. This was detected in samples A, B, BG and CG. When calculated as ratios to 10 Si, the analyses were fairly consistent:-

Al 0.25 - 1.0, S 0.1 - 0.55, Fe 0.2 - 0.5, (Al+Fe+S) $\leq$1.6.

and by extrapolating back to the start of the analysis for one case, where three sequential counts were taken, Ca/Si about 2. Lachowski et al (3) found that gyrolite, a hydrothermally-produced calcium silicate hydrate ($C_2S_3H_2$) also loses Ca during analysis, but there is no other resemblance to these particles.

DISCUSSION

Table VI shows Fe/(Al+Fe) for the anhydrous starting materials and for the hydrate phases formed from them, together with S.D. where available. Tested as follows, the ratios differ significantly, in BG between C-S-H and AFt at .001, in CG between C-S-H and AFt at .01, in A between C-S-H and AFm at .01. This disproportionality is more likely to be due to rejection of Fe by the AFt and AFm phases rather than to preferential take-up of Fe by the C-S-H. The C-S-H structure is so disordered that it probably acts simply as a sink for Fe, the very small amount taken up by the CH being insufficient to affect the balance.

The levels of cross-contamination found in this work are somewhat greater than those found by Lachowski et al (3) for normally ground cements at ages to 28 days, as might be expected, but probably give a not unrealistic picture of the levels to be expected after long hydration times in real concrete with thermal and humidity variations to assist ionic migration.

TABLE VI

	A	B	BG	C	CG
Anhydrous clinker	0.21	0.54	0.54	0.19	0.19
C-S-H	0.31	0.60	0.57	0.24	0.24
S.D.	0.08	0.12	0.08	0.08	0.07
AFt			0.18		0.13
S.D.			0.15		0.10
AFm	0.16	0.47	0.39	0.14	0.04
S.D.	0.08	0.14	-	-	-

Fe/(Al + Fe) for anhydrous clinkers and hydrated phases.

The XRD and analytical results tend to support Taylor's most recent (6) views on the structure of C-S-H. The few broad C-S-H spacings are consistent with "small fragments of Ca - O layers, perhaps some tens of Å large and only rarely parallel to each other".

If Al, Fe and S were substituting for Si in a long chain polymer, then at the (Al+Fe+S) levels which have been found, Si chains would rarely exceed 3 units long, and marked differences in polymerisation would be found between C_3S pastes and cement pastes. This is not the case and hence supports Taylor's view that silica "polymersation does not give rise to long chains but to small, roughly equidimensional clusters".

The author further suggests that the (Al+Fe+S), if they are not substituting for Si or affecting silica polymerisation, may be acting as nuclei for the growth of AFt or AFm phases and hence promoting intergrowth and bonding of hydrate phases.

CONCLUSIONS

The C-S-H in fully hydrated cement pastes is extremely variable in composition, Ca/Si varying from 1.25 to 4.0; with Al, Fe and S each up to $\frac{1}{5}$ of the calcium, and (Al+Fe+S) from 0.1 to 0.9 of the Si. The structure probably does not contain either layers or chains of silicate ions, but "roughly equidimensional clusters".

The AFm phase is equally variable in composition, and probably only slightly more ordered structurally, having some evidence of plate morphology and layer structure. It contains considerable Si, more than it does S, which is well below theoretical, and takes up a lower Fe/(Al+Fe) than is available from the clinker.

The AFt phase gives a complete ettringite XRD pattern, but is defective in both Al and S; there is considerable Si present and rather less Fe; some Si is certainly in octahedral sites but some may also be in channel sites.

The calcium hydroxide contains about 3 Si atoms and 0.5 Fe atoms per 100 Ca, and is well crystallised with thin hexagonal plate morphology.

Acknowledgements

The author is indebted to Prof. H.F.W. Taylor and Dr E Lachowski not only for the use of COA, but for continual help and discussion and to Mr J A Dalziel for making and testing of micro-cylinders.

REFERENCES

1. - C.D. LAWRENCE (1966), "Changes in composition of the aqueous phase during hydration of cement pastes and suspensions" Special Report 90, Structure of Portland Cement Paste and Concrete, Highway Research Board, Washington, D.C. 379-391.

2. - J.A. DALZIEL (1971), "A mini-cylinder test for the rapid determination of cement quality", Cement Technology, Vol.2, No.4, 105-112.

3. - E.E. LACHOWSKI, K. MOHAN, H.F.W. TAYLOR and A.E. MOORE (1980), "Analytical Electron Microscopy of Cement Pastes", Part II Pastes of Portland Cements and Clinkers. To be offered to J. Amer. Ceram. Soc.

4. - J.A. GARD, K. MOHAN, H.F.W. TAYLOR and G. CLIFF (1977), "Analytical Electron Microscopy of Hydrated Cements." Part I Tricalcium Silicate Pastes. To be offered to J. Amer. Ceram. Soc.

5. - H.F.W. TAYLOR. Personal communication.

6. - H.F.W. TAYLOR (1979), Engineering Foundation Conference on "Cement Production and Use" at Rindge, New Hampshire, U.S.A., June 1979. To be published by Engineering Foundation.

Influence of fly-ash on the rheology of cement pastes

L'influence de la cendre volante sur la rhéologie des pâtes de ciment

Ya. IVANOV, Ph.D. Head of Department of Rheology, and
S. ZACHARIEVA, Eng. Central Laboratory of Physico-Chemical Mechanics, Bulgarian Academy of Sciences, Sofia, Bulgary.

RESUME : Les pâtes de ciment, comme matériaux inorganiques, ont des comportements rhéologiques extrêmement complexes et différents. Ce comportement est le résultat de la composition polyminéralogique du ciment et de son processus d'hydratation. La cendre volante prend une part de plus en plus grande dans la production du ciment. Elle influence aussi bien les processus d'hydratation, le durcissement du ciment et ses propriétés mécaniques, que le comportement rhéologique des pâtes de ciment.

Cette communication analyse des résultats expérimentaux concernant l'influence de la proportion de cendre volante dans le ciment, de sa composition chimique et de sa surface spécifique sur les propriétés rhéologiques de la pâte. On montre que la cendre volante provoque un comportement non-Newtonien remarquable de la pâte. Les caractéristiques rhéologiques des pâtes augmentent avec l'augmentation de la cendre volante dans le ciment. L'incorporation de cendre volante au ciment entraîne des modifications importantes de la cohésion et du frottement interne de la pâte.

SUMMARY: Cement pastes as inorganic materials demonstrate an extremely complex and diverse rheological behaviour. This is due to the polymineral composition of cement and the process of hydration, progressing in time. Fly-ash finds more and more application in cement production. It influences the process of hydration and cement hardening, physico-mechanical properties as well as the rheological properties and behaviour of cement pastes.

In this contribution the influence of quantity, dispersity and chemical composition of fly-ash on the rheological properties of cement pastes is analysed. It is shown that the fly-ash induces a noticeable non-Newtonian behaviour in the pastes. The rheological characteristics increase with increasing fly-ash content. A marked change in cohesion and internal friction is observed in the case of fly-ash/cement pastes-mixtures.

1. INTRODUCTION

The properties of fresh concrete are of great importance to building technology. Knowledge of these extremely complex and diverse properties is conductive to the correct determination of mix proportion, the manner of transportation and placing of concrete mixtures. Cement paste is a constituent of concrete. In order to obtain a deeper understanding of the properties of fress concrete it is necessary to understand those of cement pastes. It was shown in previously published rheological measurements [1,2,3] that the hydraulic admixtures like trass and slag changed to a marked degree the rheological characteristics of paste. This paper contains an experimental study of cement pastes with fly-ash.

The interest in the rheological properties of fly-ash cement pastes is due to the increasing use of them in the cement industry. Its influence on the process of hydration, of cement hardening, as well as on the physico-mechanical properties of the cement and concrete, were widely studies and discussed. The flow behaviour of cement pastes with fly-ash has not been studied in the past. The reasons for this lack of attention are probably the difficulty in preparing the samples, and the poor reproducibility of the fly-ash composition and properties.

2. RHEOLOGICAL CHARACTER OF CEMENT PASTES

Numerious investigations have shown that cement pastes are structured, disperse systems. They are on the boundary between solids and liquids on the "rheological tree" of M-Reiner. The Rheological vehaviour of very highly concentrated (with low water/cement ratio) pastes can be approximated by coulomb/s equation [4,5]:

$$\tau = \sigma \operatorname{tg} \alpha + C \qquad (1)$$

In this case the yield stress is proportional to the applied shear stress and the tangent of the angle of internal friction. The deformation is manifested by the shifting of layers in the contact zone. The system is a discontinuous medium whose shear resistance resumbles the character of dry friction. The rheological properties of such pastes were shown in [4].

The flow behaviour of fluid and plastic cement pastes obeys Bingham's equation:

$$\tau = \tau_o + \eta \frac{dv}{dt} \qquad (2)$$

It is a case when a volumetric deformation takes place without interruption of continuity. The resistance to the deformation has a pure viscous character and depends on the deformation rate.

Most of the pastes, however, are between these boundary cases. In several conditions they possess both properties inherent to the materials with viscoplastic flow, and those with dry friction.

It has previously been shown that the rheological properties of these systems can be characterized by the following characteristics: viscosity, cohesion, interal friction and yeild value [4,5].

3. EXPERIMENTAL RESULTS AND DISCUSSION

The rheological characteristics were obtained:
(a) for the liquid pastes from a specially constructed measuring device with kungled surfaces on a coaxial cylinder rotational viscometer. Thus, slip phenomena was eliminated, and a steady shear takes place in the substance medium. The flow curves of cement pastes with different water/cement ratios and fly-ash concentrations are seen in Figs. 1-3;
(b) for the very concentrated cement pastes by means of the method discribed in [4,5,6].

Table 1 shows the chemical composition of used fly-ash as well as its dispersity (specific surface). Their chemical activity was 36 and 63 $cm^2\ gr^{-1}$. In both cases normal portland cement with S = 3400 $cm^2\ gr^{-1}$ was used.

3.1 INFLUENCE OF FLY-ASH ON THE RHEOLOGICAL BEHAVIOUR AND PROPERTIES OF CEMENT PASTES

Fig. 1 illustrates how the flow curves change with an increase of fly-ash in cement pastes. These curves, as well as the curves in Fig. 2 and Fig. 3 (for constant fly-ash content but different concentration of pastes), show that the pastes have non-Newtonian flow. So, they correspond to the Bingham model in the general outline. However, these exist some peculiarities in the rheological behaviour of the pastes which must be noted. In the case of lower fly-ash disperisty (No. 1) with incsreasing fly-ash content, the plastic flow becomes more significant (curves 1-4 in Fig. 1). Pastes with higher dispersity of fly-ash (No. 2) demonstrate the flow behaviour which seems like pseudo plastic rather than real plastic (curves 1-4). Both pastes have a Bingham yeild value and, at higher shear rates, the stress increases nearly linearly with the rate of shear. Therefore, a structural (apparent or Binghamian) viscosity may be calculated from the slop of the curve. The same peculiarities can be observed in the case of a constant cement/fly-ash ratio with a change of paste cencentration - water/cement ratios (Fig. 2 and Fig. 3). From these data it is seen that the pastes with high fly-ash content as well as with high concentrations (low water/cement ratios) are both characterized by a marked increase of τ at low and high values of D. Calculations indicate an approximate dependence on the square of the concentration. Hence there is a good agreement to the theory [8]. It must be pointed out that the rise of τ depends also on the dispersity of fly-ash. It indicates that the flow of pastes in the flocculated and flocculent state (as classified by Powers in [7]) has to be considered separately for each case.

Table 2 illustrates how τ_o (yield value) varies with the fly-ash content for a range of water/cement ratios of cement pastes. The results show that for the same concentration of the pastes τ_o rises exponentially with increasing fly-ash. This rise also depends on the water/cement ratios and the

dispersity of the fly-ash.

Table 3, Table 4 and Table 5 show respectively how η_0 (maximal Newtonian), η (structural), and η_m (minimal Newtonian) viscosities vary with the content of fly-ash for different water/cement ratios of pastes. The comparison of these experimental results with those of τ_0 indicates the same relation of each of them with studied factors (fly-ash content, water/cement ratios, and dispersity of admixture). From the structural (η) and minimal Newtonian (η_m) viscosities data (Table 4 and Table 5), as well as the previous figures, it is seen that these pastes have lower resistance to the flow after the apparent yield (or yield value) than those of cement with trass [12]. At the same time they demonstrate a higher resistance to the flow than those of cement with slag [1,2]. The viscosity of all the systems can be represented by the modified money equation [10].

Experimental results obtained with very highly concentrated cement indicate that its pastes obey Coulomb's equation. Some of the results are shown in Fig. 4 and Fig. 5. The date from Fig. 4 illustrates how C and K = tg α varies with change of fly-ash content. It is seen that for several concentrations of pastes (water/cement ratio), as well as dispersity of fly-ash, C passes through the max value (curve C' for water/cement = 0.3). When the quantity of water is different, notwithstanding that it corresponds to the "normal thickness" of pastes (measured in accordance with the standards in force for the cement), with an increase of fly-ash the rise of C was observed. Internal friction (K = tg α) indicates a decrease in both these cases.

Fig. 5 illustrates how C and K vary with the change of fly-ash content for a range of concentrations (water/cement ratios), besides those corresponding to the "normal thickness" of pastes. The change of these characteristics corresponds to the relations noted in [4]. The difference is only in the speed of the change, and in the values of C and K. Tested pastes with fly-ash have a lower speed of change and bigger values for C = f(w) and K = f(w) than those shown in [4].

4. CONCLUSION

The experimental investigations indicate that fly-ash has a marked influence on the rheological behaviour and on the flow properties of cement pastes. The systems are plastic- or pseudo plastic-like flow which becomes significant for high fly-ash content. They show Bingham yield stresses. The study of very highly concentrated cement pastes with fly-ash shows the behaviour which can be characterized by the existence of C and K. The latter change with an increase of fly-ash in pastes, as well as an increase of concentration of the pastes. The reason for their change is not clearly understood yet. It may be related to the dense particle packing and to their surface characteristics, which became very important in the highly concentrated pastes.

TABLE 1. Chemical composition and dispersity of used fly-ash.

Values	fly-ash No. 1	fly-ash No. 2
S_1O_2 %	61.0	60.2
Al_2O_3 %	21.4	23.0
Fe_2O_3 %	6.8	6.0
CaO %	2.0	2.1
MgO %	1.0	1.5
SO_3 %	3.0	2.3
S cm^2 gr^{-1}	4650	5150

TABLE 2. Effect of concentration and dispersity of fly-ash on τ_0 (N/m^2) of cement pastes

fly-ash No.	cement fly-ash ratio (%)	water/cement ratio 0.45	0.55	0.65	0.70
1	100 : 0	46	13	6.2	4.5
	80 : 20	58	18	8	6.5
	65 : 35	77	35	11	9.5
	50 : 50	185	66	20	16.0
	35 : 65	238	89	48	32.0
	0 : 100	160	70	34	26.0
2	80 : 20	77	35	10	8
	65 : 35	150	63.5	37	19
	50 : 50	254	80	48	30
	35 : 65	-	124	64	47
	0 : 100	-	248	110	89

TABLE 3. Change of η_o (Ns/m^2) of cement pastes depending on the concentration and dispersity of fly-ash

fly-ash no.	cement fly-ash ratio (%)	water/cement ratio 0.45	0.55	0.65	0.70
1	100 : 0	8.28	3.05	2.07	1.14
	80 : 20	17.52	5.17	2.22	1.81
	65 : 35	28.59	11.99	3.41	3.00
	50 : 50	45.20	19.36	5.74	4.91
	35 : 65	117.58	36.88	16.14	11.28
	0 : 100	65.94	23.05	9.68	5.43
2	80 : 20	23.05	8.54	2.48	2.07
	65 : 35	50.30	19.36	9.31	4.05
	50 : 50	87.61	27.66	10.40	6.62
	35 : 65	-	-	20.75	13.06
	0 : 100	-	81.99	32.28	22.35

TABLE 4. Influence of concentration and dispersity of fly-ash on η (10^{-1} Ns/m^2) of cement pastes

fly-ash No.	cement fly-ash ratio (%)	water/cement ratio 0.45	0.55	0.65	0.70
1	100 : 0	3.1	1.10	0.4	0.29
	80 : 20	5.5	1.61	0.63	0.44
	65 : 35	7.1	2.56	0.96	0.73
	50 : 50	14.0	4.90	1.72	1.27
	35 : 65	18.4	7.51	3.52	2.62
	0 : 100	32.1	9.05	3.07	2.19
2	80 : 20	7.10	3.18	0.83	0.59
	65 : 35	11.39	5.36	2.68	1.52
	50 : 50	16.06	7.93	3.72	2.30
	35 : 65	18.11	9.91	5.64	3.70
	0 : 100	32.60	19.07	9.15	7.34

TABLE 5. Effect of concentration and dispersity of fly-ash on η_m (10^{-2} Ns/m^2) of cement pastes

fly-ash no.	cement fly-ash ratio (%)	water/cement ratio 0.45	0.55	0.65	0.70
1	100 : 0	10	4	2	1
	80 : 20	34	12	3.8	2
	65 : 35	46	16	6	4.2
	50 : 50	75	31	10.4	7
	35 : 65	96	41	20	13.2
	0 : 100	203	68	18.8	12.5
2	80 : 20	47	23	6	4.2
	65 : 35	75	34.5	18	9
	50 : 50	86	45	25.5	16.8
	35 : 65	95	57	33	21.5
	0 : 100	-	84	60	44

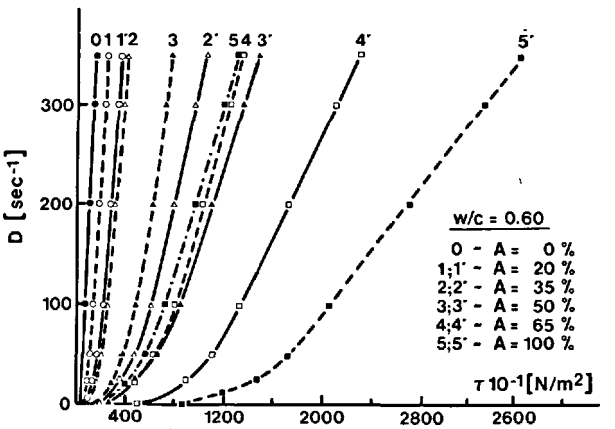

Fig. 1 - Influence of the fly-ash contents (A%) in the cement on the flow of the paste (pastes with fly-ash No. 1 are indicated as 1, ...5, and those with No. 2 as 1' .....5').

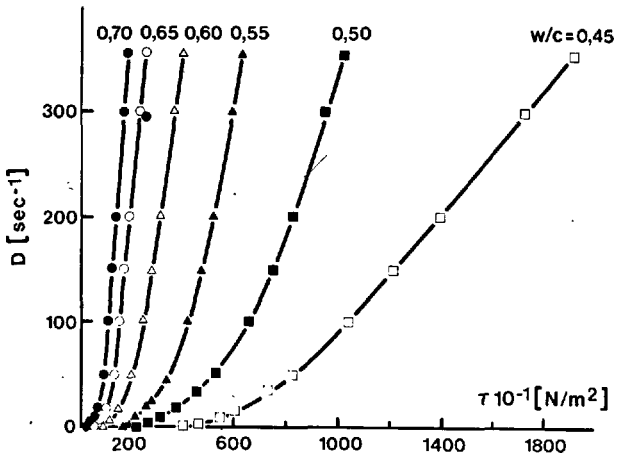

Fig. 2 - Flow curves for the cement pastes with fly-ash No. 1 (cement: fly-ash ratio = 65 : 35%).

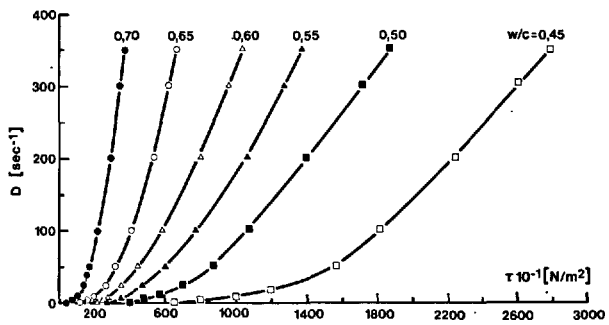

Fig. 3 - Flow curves for the cement paste with fly-ash No. 2 (cement: fly-ash = 65 : 35%).

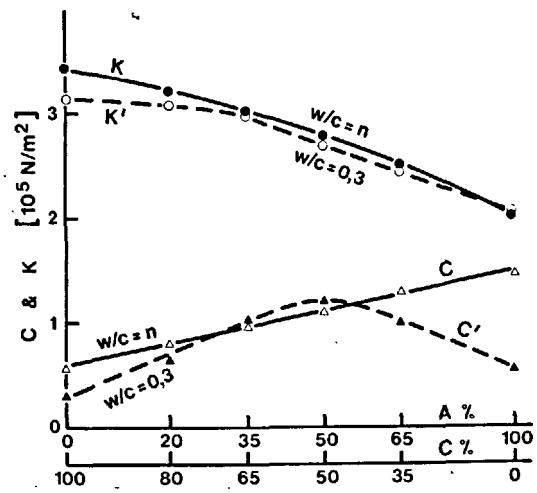

Fig. 4 - Influence of fly-ash contents in the cement on C and K (for n see text).

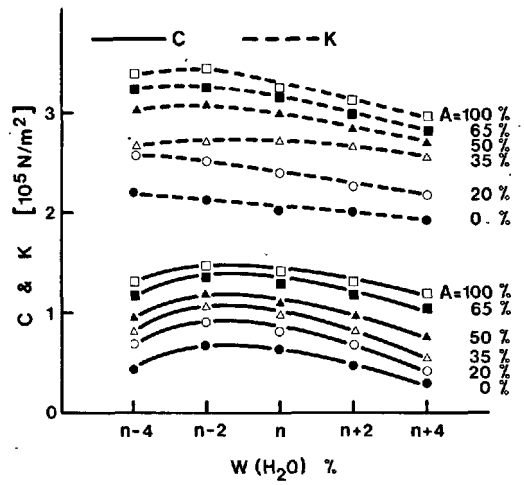

Fig. 5 - Change of C and K with fly-ash content in cement and water/cement.

REFERENCES

1. Y. IVANOV, E. STANOEVA (1976), "On the effect of some factors on the rheological behaviour of cement pastes", Proceeding of the VIIth Intern. Congr. on Rheology, Sweden, 360-361.

2. Y. IVANOV, E. STANOEVA (1979), "On the influence of cement composition and other factors on the rheological behaviour of cement pastes", Silicates Industriels, Belg., (in press).

3. Y. SIMEONOV, Y. IVANOV, E. STANOEVA (1979), "A study of cement pastes' tixotropy", Physico-Chimitcheska Mechanica", No. 6, Bulgar., 32-41.

4. Y. IVANOV, Y. SIMEONOV, (1974) "Rôle des éléments fins dans le comportement rhéologique des bétons frais", Rheol. Acta., 717-720.

5. J.P. BOMBLED, Révue des materiaux de construction, No. 571, 582, 590, 594.

6. T.C. POWERS (1968), The Properties of fresh concrete, Acad. Press, N.Y.-L.

7. R. BUCHARDAL, J.E. THIMM (1945), J. Appl. Phys., 16, 344-352.

8. Y. IVANOV, E. STANOEVA, A. TSENOVA (1977), "On the rheology of cement pastes", Proc. of Ist National Conf. on Mechanics and Technology of Composite Materials, Bulg., 521-525.

L'effet des propriétés physico-chimiques du ciment sur la structure et la résistance du ciment hydraté

The Effect of Physico-Chemical Properties of Cement on Structure and Strength of Cement Stone

A.Ph. POLAK, Dr. ès Sc. Professeur, Directeur de l'Institut des Recherches Scientifiques des Constructions Industrielles "NIIPROMSTROI", Ufa. U.R.S.S.
V.V. BABKOV, Cand. ès Sc., Chargé de cours, Directeur-Adjoint de l'Institut des Recherches Scientifiques des Constructions Industrielles "NIIPROMSTROI", Ufa. U.R.S.S.

RESUME : L'article présente une description quantitative des phases principales de formation de la structure et du développement de la résistance du ciment hydraté : la dissolution du liant, la nucléation, la formation de structures coagulantes et cristallines. L'article montre aussi le mécanisme de la soudure des cristaux.

Les principaux facteurs structurels et mécaniques qui influencent la résistance du ciment hydraté sont aussi examinés dans cet article.

Les auteurs proposent une description du mécanisme de rupture, une méthode de prévision des résistances et les moyens d'optimiser la structure.

Les auteurs montrent aussi qu'une corrélation considérable existe entre la structure du ciment hydraté et sa résistance ultérieure et que ces facteurs sont prédéterminés par la composition minéralogique et la structure géométrique du liant original.

SUMMARY: The paper quantitatively describes the main stages of structure formation and strength development of cement stone: dissolution of binder, nucleation, formation of coagulational and crystalline structures. The mechanism of crystal intergrowth is also shown.

The basic structural and mechanical factors influencing the strength of resulting cement stone are examined.

The description of failure mechanism is proposed, the strength of cement stone is estimated and means of its structure optimisation are shown.

The authors demonstrate that cement stone structure and its strength are to a considerable extent interrelated and predetermined by mineralogy and geometric structure of the initial binder.

Une description quantitative de formation des systèmes disperses peut être realisee à base mathématique qui fourni une description de la structure geometrique de ces systèmes.

En absence des forces de liaison entre les particules et une distribution aléatoire des particules en volume, le système peut être caracterisé par six parametres primaires: Π_m - porosite, V_m - volume, S_m - superficie, N_m - nombre des particules dans l'unité de volume; $\bar{a}$, $\bar{h}$ - valeurs moyennes des dimensions des particules et la distance qui les separe. Ces parametres sont liés entre eux par quatre equations:

$$\left.\begin{aligned} \bar{a}\, S_m = m_1 V_m, \quad S_m^3 = m_2 V_m N_m, \\ V_m + \Pi_m = 1, \quad \bar{h} V_m = m_3 \Pi_m \bar{a}, \end{aligned}\right\} \quad (1)$$

où m_1, m_2, m_3 - sont les modules de dispersion du système, qui réflechit l'influence de la forme des particules et la distribution d'accord aux dimensions /1/. Pour des confirgurations et distributions concretes on peut les obtenir par des calcules; pour les systemes polidisperses ce sera:

$$m_1 = \frac{2(1+\nu)(1+2\nu)}{3\nu} \frac{\psi_1 \psi_2}{\psi_3}; \quad m_2 = \frac{8(1+2\nu)^3}{\nu^2} \frac{\psi_2^3}{\psi_3^3}, \quad (2)$$

où ν - est le paramètre de forme des particules qui est égal à la relation entre la dimension longitudinale et transversale; ψ_i - moments de distribution de i-tième puissance (pour un système monodisperse ces seront $\psi_1 = \psi_2 = \psi_3 = 1$).

A la base des paramètres primaires (1) on peut calculer les paramètres secondaires; il en resultent pour les nombres $\mathcal{Z}_\kappa^{(2)}$, et l'aire $F_\kappa^{(2)}$ des contacts dans l'unité d'aire et les aires des contacts dans l'unité de volume $F_\kappa^{(3)}$ les relations suivantes:

$$\mathcal{Z}_\kappa^{(2)} = S_m^2 \frac{13\nu}{2(1+2\nu)}, \quad (3)$$

$$F_\kappa^{(2)} = V_m^2, \quad F_\kappa^{(3)} = \tfrac{1}{2} S_m V_m. \quad (4)$$

Aprés le gâchage le système du liant se dissoud au cours de hydratation et par consequence la dimension caracteristique et la quantité des particulres diminuent. En consideration de cette circonstance on introduit le fonction du temps t, qui represente la degrée de hydratation du liant θ ($\theta \in [0,1], t \in [0,\infty]$). On peut demontrer /1/ que les parametres du système dissolvant du liant (indiex x) se modifient en forme suivante:

$$\left.\begin{aligned} V_x = V_{x0}(1-\theta), \quad S_x = S_{x0}(1-\theta)^{\frac{1+\kappa}{3}}, \\ \bar{a}_x = \bar{a}_{x0}(1-\theta)^{\frac{1+2\kappa}{3}} \quad N_x = N_{x0}(1-\theta)^{\kappa}, \end{aligned}\right\} \quad (5)$$

où $V_{x0}, S_{x0}, \bar{a}_{x0}, N_{x0}$ - sont les valeurs des paramètres au commençement du processus; κ - degrée, dependant de la fonction de distribution des particules selon les dimensions (pour un système monodisperse $\kappa = 0$, pour une distribution équilibrée $\kappa = 0{,}25$). Si x_0 - represente la consommation du liant pour unité de volume de pâte (gr./cm^3), S_{ox} - superficie spécifique du liant (gr./cm^2), γ_x - densité (gr./cm^3), alores si $t = 0$, $\theta = 0$ on aura:

$$\left.\begin{aligned} V_{x0} = x_0/\gamma_x, \quad S_{x0} = x_0 S_{ox}, \\ \bar{a}_x = m_{1x}/S_{ox}\gamma_x, N_{x0} = x_0 \gamma_x^2 S_{ox}^3. \end{aligned}\right\} \quad (6)$$

Dans les systèmes sans recristallisation la quantite des cristaux du hydrate de formation nouvelle (index y), qui est égal à la quantité des germes cristallins au debut du processus, ne se change pas /2/ et le processus de croissance dans un système monomineral est caracterisé pour des relations suivantes:

$$\left.\begin{aligned} V_y = V_{y1}\theta, \quad S_y = S_{y1}\theta^{2/3} \\ \bar{a}_y = \bar{a}_{y1}\theta^{1/3} \quad N_y = N_{y1} = \text{const}, \end{aligned}\right\} \quad (7)$$

dont $V_{y1}, S_{y1}, \bar{a}_{y1}, N_{y1}$ - representent les valeurs des parametres au moment quand le processus de termine.

Si ϑ est le coefficient d'agrandissement du volume au moment de transformation du liant en hydrate, $\mathcal{Z}_0$ - la quantité des germes du hydrate dans l'unité de superficie du liant (cm^{-2}), alors au moment quand le processus de hydratation est fini ($\theta = 1$) nous aurons

$$\left.\begin{aligned} V_{y1} = V_{x0}\vartheta, \quad S_{y1} = m_{2y}^{1/3} V_{y1}^{2/3} N_{y1}^{1/3}, \\ \bar{a}_{y1} = m_{1y}/m_{2y}^{1/3}\left(V_{y1}/N_{y1}\right)^{1/3}, N_{y1} = x_0 S_{ox} \mathcal{Z}_0 \end{aligned}\right\} \quad (8)$$

Comme l'indiquent les équations (7) et (8) la structure geometrique du hydrate est determinée par la structure geometrique originelle du liant (x_0, S_{ox}) et sa composition mineralogique (ϑ, m_i, $\mathcal{Z}_0$).

Les systèmes des équations ci-dessus sont valides non seulement pour des liants monominéraux, mais pour des ciments aussi, bien que les parametres dans ce cas ont un caractère integral.

Si on connait la quantité spécifique des germes, il est possible de calculer les paramètres de structure du hydrate (7) en voie de devéloppement. L'évaluation théorique de la valeur $\mathcal{Z}_0$ est realisée en forme suivante. Supposons que v_x est la vitesse de venue du matériau dissoud dans la solution (selon la théorie de Nernst-Chukarev) comme consequence de la dissolution de la phase originale, v_0 et v_y - sont les vitesses de formation des germes du hydrate et leur croissance suivante (d'après Volmer) et les corrections de Polak /2/. Dans ce cas

$$v_x = K_x(\alpha_\infty - \alpha), \quad (9)$$

$$v_0 = K_0 \exp\frac{-u_0}{\ln^2\alpha}, \quad v_y = K_y \exp\frac{-u_y}{\ln^2\alpha}, \quad (10)$$

$$u_0 = 2\left(\frac{\psi}{\kappa T}\right)^3 \chi_0, \quad u_y = 2\left(\frac{\psi}{\kappa T}\right)^3 \chi_y, \quad (11)$$

dont K_x, K_0, K_y - sont les constants de vitesse des processus correspondants (cm./s.); α, α_∞ - degré actuel de sursaturation de la solution et sursaturation

sur la superficie des particules du liant, $\varphi = 2\delta_0 \sigma$ – énergie conventionelle d'arrachement d'une molecule, δ_0 – paramètre du réseau cristallin (cm), σ – énergie spécifique superficielle de la phase solide du liant dans la solution, $0 < \chi_i < 2$ – coefficient de la inhomogénéité physico-chimique /2/.

Considerons la dimension caractéristique des germes d'après Thompson

$$a_0 = 2\delta_0 \frac{\varphi}{\kappa T} \cdot \frac{1}{\ln \alpha} . \qquad (12)$$

En applicant la condition d'équilibre dynamique de venue de la substance dissolvante et sa déviation pour formation des germes du hydrate après le moment de termination de la germination, on peut obtenir le rapport de $\mathcal{Z}_0$ des paramètres du système

$$\mathcal{Z}_0 = \gamma_1 (\alpha_\infty - \alpha_n) \frac{\kappa_x}{\kappa_y} \cdot \frac{\varphi}{\kappa T} \cdot \frac{\chi_y}{\delta_0^2} \cdot \frac{\ln^2 \alpha_n}{u_y} \exp \frac{u_y}{\ln^2 \alpha_n} , \qquad (13)$$

où γ_1 – est le coefficient, compte tenu de la configuration du germe.

Admettant que $\gamma_1 = 0{,}15 \ldots 5$, $\alpha_\infty - \alpha_n \approx 1{,}1$, $\kappa_x/\kappa_y = 10^{-5} \ldots 10^{-4}$, $\varphi/\kappa T = 2 \ldots 3$, $\chi_y = 0{,}2 \ldots 1$, $\delta_0 = (7 \ldots 10) 10^{-8}$ cm, $u_y = 3 \ldots 8$, $\alpha_n = 3{,}2$ on reçoit

$$\mathcal{Z}_0 = 5 \cdot 10^7 \ldots 2 \cdot 10^{13} \ \mathrm{cm}^{-2} . \qquad (14)$$

Au course des recherches directes nous avons obtenue pour le gypse le valeur $\mathcal{Z}_0 \approx 10^7 \mathrm{cm}^{-2}$, mais pour le gel du ciment durci, calculé d'accord à la superficie spécifique $\mathcal{Z}_0 \approx 10^{13} \mathrm{cm}^{-2}$, qui corresponde assez bien à cette gamme.

Les cristaux du hydrate sont les particules colloïdales, qui dans la solution propre sont entourées d'un champ de force $\mathcal{P}(h)$, l'intensité duquel est déterminée par des forces d'attraction de van-der-Vaals et par des forces de répulsion d'origine diverses /3/. Deriaguine, Landau, Overbeck et Fervey ont indiqués que à une distance déterminée entre les particules h_i ($i = 1,2,3$) les valeurs $\mathcal{P}_i$ ($i = 1,2,3$) = 0; par conséquence les énergies potentielles du système $\mathcal{E}_i$ ($i = 1,2,3$) touchent à ses valeurs extremales. A la distance h_1 et h_3 on a $\mathcal{E}_{1,min}$ et $\mathcal{E}_{3,min}$; le système est en équilibre et se forment des structures de coagulation proches et lointaines. En outre, à une distance h_2 on trouve une barrière énergetique $\mathcal{E}_{2,max}$; en traversant cette barrière les particules peuvent passer de la distance h_3 à la distance h_1 (dans ce cas $h_1 < h_2 < h_3$).

Cette traversée joue un rôle trés important dans le durcissement du système, parce qu'une structure cristalline peut être formée seulement à une distance de h_1 et moins.

Les principes de coagulation des systémes colloïdaux découverts par Deriaguine et al. ont été developpés par les auteurs. Comme consequence d'une fluctuation de distance h_2 où h_3 des zones d'ameubilissement et de consolidation se forment dans le volume du système et, sous certains conditions, ces zones se transforment dans des pores et des agrégats stables (fig.1). Il y a une certain relation entre le potentiel chimique du liquid au dedans d'agrégat $\mu(h)$, en dehors d'agrégat $\mu(\infty)$ et la pression du fractionnement $\mathcal{P}(h)$:

$$\mu(\infty) - \mu(h) = g_0 \mathcal{P}(h) , \qquad (15)$$

où g_0 – est le volume d'un mole. Si a_κ – est le diamètre d'agrégat, Π – la porosité interne d'agrégat, σ – l'énergie d'interface "agrégat-milieu extérieur", on peut déterminer l'énergie de formation adimensionelle d'un agrégat u_κ

$$u_\kappa = -\frac{\pi a_\kappa^3}{6} \Pi \frac{\mathcal{P}}{\kappa T} + \pi a_\kappa^2 \Pi \frac{\sigma}{\kappa T} . \qquad (16)$$

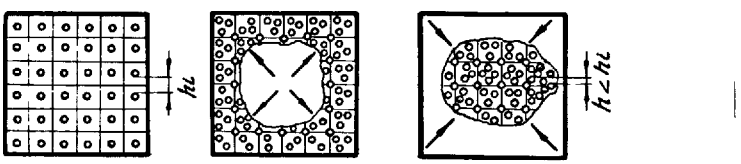

Fig.1 – Schema de formation des pores et des agrégats.

La stabilité de ces agrégats, d'après Gibbs et Volmer, demande que $du/da = 0$, $d^2u/da^2 < 0$, ce que donne, après des calculs simples, (eq. 16) l'énergie de formation et les dimensions des agrégats stables:

$$u_\kappa = \frac{16\pi}{3} \cdot \frac{\Pi \sigma^3}{\kappa T \mathcal{P}^2} ; \quad a_\kappa = \frac{4\sigma}{\mathcal{P}} . \qquad (17)$$

Realisons une consolidation imaginaire du système colloïdal jusqu'une distance entre les particules, puis separons le système en deux et coulissons les parties jusque la distance h_i; nous pourrons observer alors la formation d'interface, qui peut être expressée pour la formule suivante:

$$2\Pi\sigma = \int_{h_i}^{\infty} \mathcal{P}\, dh . \qquad (18)$$

Ainsi en conditions égales $\sigma = \sigma(h)$ et alors $a_\kappa = a_\kappa(h)$. Pour definir la valeur moyenne de dimension du agrégat, nous considerons que la distribution des agrégats selón leur dimensions, par analogies avec les oeuvres de Volmer /7/, suivit une loi exponentielle:

$$d N_\kappa = N_{\kappa m} e^{-u_\kappa} du_\kappa , \qquad (19)$$

où $N_{\kappa m}$ – corresponde au total des agrégats. Puis nous considerons que autour de h_i ($i = 1,3$) la pression change d'accord à la loi lineaire:

$$\mathcal{P} = \mathcal{P}_m (\xi - 1) , \quad \xi = h/h_i . \qquad (20)$$

Alors pour le diamètre moyen d'agrégat et la quantité des particules dans un agrégat nous aurons:

$$\bar{a}_\kappa = \int_0^\infty a_\kappa e^{-u_\kappa} du_\kappa = \left(\frac{h_i \kappa T}{\mathcal{P}_m}\right)^{1/2} \frac{1}{\Pi^{1/2}} \left(\frac{3}{2\pi}\right)^{1/4} \Gamma(5/4) (2\pi) \qquad (21)$$

$$\bar{n}_\kappa = V \frac{a_\kappa^3}{a^3} = \left(\frac{h_i \kappa T}{\mathcal{P}_m}\right)^{3/4} \frac{V}{\Pi^{3/2}} \left(\frac{3}{2\pi}\right)^{3/4} \Gamma(3/4) . \qquad (22)$$

Si le volume minimal d'un agrégat correspond à $\bar{n}_\kappa = 6$, alors $\bar{n}_\kappa > 6$ represente les

conditions de formation des agrégats. En vertu de (22) ces conditions auront la forme suivante:

$$\Omega_\kappa = \frac{h_i \kappa T}{g_m a_i^4} \cdot \frac{V^{2/3}}{\Pi^2} > 0{,}4 , \qquad (23)$$

où V - la densité (concentration de volume), a - dimension des particules dans un agrégat. La porosité interne est égal à

$$\Pi = \frac{h}{h + ma} . \qquad (24)$$

Si nous aurons $ma \gg h$,alors $\Pi = h/ma$. Dans ce cas nous reçevrons de la formule (23) la formule suivante:

$$\Omega = \frac{\kappa T}{g_m h_i a_i^2} . \qquad (25)$$

A mesure que progresse le processus de hydratation, le diametre des cristaux du hydrate a augmente, tandis que la concentration C de la solution diminue; mais la pression du fractionnement augmente aussi. Ce pourquoi nous avons une perte totale de la capacité de formation d'une structure de coagulation dans le système. Ce fait a été prouvé en forme experimentale par Segalova et Rebinder /4/ et la formule (25) confirme ce fait en forme théorique.

Chukine et al./5/ dans ces études on mesures la resistance des contacts et ont établis, qu'il y a deux types des contacts, dont la valeur de resistance diffère pour deux ordres de grandeur et même plus. Les contacts plus faibles etaient formés par coagulation, tandis que les plus resistants etaient du type de cristallisation. La preuve thermodynamique de la possibilité de formation des contacts a été donné dans nos études /6/. Le mécanisme de formation des contacts dans ce cas est connecté avec une migration bidimensionnelle des molecules dans la couche mobile d'adsorption. Les molecules individuelles ou en paires de la couche mobile d'adsorption diffusent dans l'espace libre entre les particules. Alors ces molecules d'un cristal peuvent se réunir avec les molecules du cristal opposé. Ainsi se forment des ponts estables, qui se transforment posteriorement en contacts cristallins.

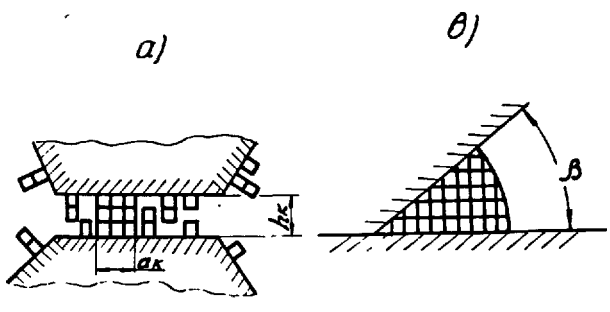

Fig.2 - Schema de formation d'un contact cristallin.

Les calculs thérmodynamiques /6/ confirment que la formation des ponts des contacts d'accord à la fig.2a est possible sous la condition, que la dimension de l'espace ne soit pas en excès de la valeur

$$h_\kappa \approx \frac{\delta_2}{2}\left\{\frac{\ln\alpha}{\ln\alpha^*} + \left[\left(\frac{\ln\alpha}{\ln\alpha^*}\right)^2 + \frac{4\varphi}{\kappa T}\cdot\frac{1-\chi}{\ln\alpha^*}\right]^{1/2}\right\} \approx (1\ldots 1{,}1)\delta_2 \qquad (26)$$

La longueur du bord d'un germe stable sera égal à (a_2 - le bord du germe bidimensionel)

$$a_\kappa = \frac{a_2}{1 + (1-\chi)a_2/h_\kappa} \qquad (27)$$

Quand $\chi \geqslant 1$ les conditions d'assemblage deviennent défavorables: ce fait indique, que l'assemblage peut être accomplie d'un façon satisfaisant seulement entre des cristaux pures et de même composition chimique.

La condensation de la phase solide dans un espace cunéiforme entre les particules (fig.2b) procede en forme automatique, toutefois que l'angle β soit moins d'une valeur critique $\beta < \pi(1-\chi)$.

En somme,la rigidité du ciment durci dépende du gel du ciment, qui est un conglomérat des cristaux, joint dans les points du contact. La caracteristique principale qualitative du gel est le haut degre de hétérogénéité mécanique et structurelle. Il est exprésse par la hétérogénéité des caractéristiques de resistance des éléments structurels et,d'autre part, par l'inhomogénéité en état de tension. La dispersion des valeurs de resistance est la consequence de la différence de dimension des cristaux /7-9/. Les dimensions typiques des cristaux des hydrates basiques (diamètre des cristaux filiformes et aciculaires , épaisseur des cristaux en forme des plaques) varient dans des bornes assez etendue: de $5.10^{-7}\ldots 2.10^{-6}$cm. pour des cristaux des hydrosilicates de calcium et jusque 10^{-4}cm. et plus pour des cristaux de hydrosulfoaluminate et hydroxyde de calcium.

L'influence de dimension d sur la resistance R_c pour des cristaux hydratés du ciment a été établie par Boutte et Timachev et al./8/. Dans cette étude nous proposons la relation suivante /9/ pour description de la fonction $R_c = f(d)$,qui est en rapport avec les resultats des essais:

$$R_c = R_m \left(d_*/d\right)^n , \qquad (28)$$

où R_m - est la resistance théorique dans la phase de cristallisation, d_* - la dimension d'un cristal "parfait", - le taux de reduction de la resistance avec la croissance du dimension de d .L'hétérogénéité dans la distribution des tensions dans les contacts et dans les cristaux a comme base la différence dans la direction des cristaux d'un agrégat, l'inconstance des rapports entre les aires des contacts et les cristaux des éléments structurels et d'autres imperfections.

Considerons la rupture des cristaux d'un agrégat aux contacts resistants. Sans prendre en consideration la déformation

des contacts et considerant la constance du module de Young, on peut dire, qu'avec des tensions uniformes nous aurons des sollicitations égals dans des cristaux ayant la même direction. En ce cas une charge exterieure détruit les cristaux faibles, avec une redistribution de la charge entre les éléments plus resistants. Dans cet état intermédiaire la charge sur l'unité d'aire peut être expressée par l'équation:

$$R = \tfrac{1}{3} R_m V_m \left(d_*/d\right)^n \int_{d_o}^{d} \varphi(d)\, dd, \quad (29)$$

où $\varphi(d)$ est la fonction de distribution des cristaux d'accord aux dimensions, - dimension du cristal le plus grand, resté intact $(d_m \leq d \leq d_o)$.

Une croissance de la charge extérieure et stabilisation d'état sont possibles seulement jusqu'un certain stade. A une certaine charge la stabilisation devient impossible et ce processus se transforme dans une avalanche destructive, qui a pour consequence une destruction totale de tous les elements de la structure. Ce niveau de charge critique corresponde à la resistance du système cristallin R_{cs}, la valeur de cette resistance peut être reçue à l'aide d'analyse (29) à extremum de d. Pour une distribution regulière $\varphi(d) = \frac{1}{d_m - d_o}$ et avec $d_o \geq d_*$ nous aurons

$$R_{cs} = \tfrac{1}{3} R_m V_m \left(d_*/d_o\right)^n \frac{d_o}{d_m - d_o} \cdot \frac{(n-1)^{n-1}}{n^n} \quad (30)$$

La formule (30) est juste si $d_o \leq d_{cr} \leq d_m$, $n > 1$. En absence des ces conditions la resistance peut être exprimée par la relation

$$R_{cs} = \tfrac{1}{3} R_m V_m \left(d_*/d_m\right)^n. \quad (31)$$

Pour une distribution regulière et $d_o \leq d_*$ et sous la condition que $d_* \leq d_{cr} \leq d_m$ la resistance corresponde à la formule (30). Si la dernière condition n'est pas remplie, on aura:

$$R_{cs} = \tfrac{1}{3} R_m V_m \int_{d_o}^{d_*} \frac{1}{d_m - d_o} dd = \tfrac{1}{3} R_m V_m \frac{d_* - d_o}{d_m - d_o}. \quad (32)$$

Des calculs pareils peuvent être realisés pour d'autres fonctions de distribution normale aussi.

Une evaluation quantitative de la resistance d'un gel du ciment durci par le corps cristallin, pour plusieurs fonctions de distribution, a donnée des valeurs de resistance à la rupture de 80 à 200 MPa (dans ce cas les valeurs de repère des parametres de la structure $V_m \approx 0{,}72$; $R_m \approx 4 \cdot 10^3$ MPa; $d_* \approx 5 \cdot 10^{-6} \ldots 10^{-5}$ cm, $d_o \ldots d_m \approx 5 \cdot 10^{-7} \ldots 10^{-4}$ cm, $n \approx 1{,}2 \ldots 1{,}6$).

Une analyse des formules obtenues indique, que la voie principale d'accroissement de resistance des structures cristallines, ayant des contacts bien développés, est un acroissement de la dispersité des cristaux.

Si les contacts sont faibles et ont une aire limitée, la destruction de la soudure aura lieu à travers des contacts. Le mécanisme de destruction et la resistance de la structure dans ce cas seront defini par la surcharge des contacts, en relation aux cristaux correspondants et l'inhomogenéité de l'état de tension dans les contacts. Si la resistance du contact de phase est égaé à R_m, la condition intermédiaire de la structure sous une charge sera defini par l'équation:

$$R = \tfrac{1}{3} R_m V_m \eta \int_{\eta}^{\eta_m} \varphi(\eta)\, d\eta, \quad (33)$$

dont $\varphi(\eta)$ est la fonction de distribution de la phase cristalline sur des aires relatives η.

Une analyse d'équation (33) à extremum de η pour une distribution uniforme simple $\varphi(\eta) = \frac{1}{\eta_m - \eta_o}$ donne des formules suivantes de resistance d'une soudure à travers des contacts:

$$R_{cs} = R_m V_m \frac{\eta_m^2}{12(\eta_m - \eta_o)} \quad \text{pour } \eta_o \leq \eta_m/2, \quad (34)$$

$$R_{cs} = \tfrac{1}{3} R_m V_m \eta_o \quad \text{pour } \eta_o \geq \eta_m/2, \quad 0{,}5 \leq \eta_o/\eta_m \leq 1. \quad (35)$$

Calcul de la resistance d'une soudure à travers des contacts pour plusieurs fonctions caracteristiques $\varphi(\eta)$ dans le gamme de changement des parametres $0{,}2 \leq \eta_m \leq 1$, $0{,}1 \leq \eta_o/\eta_m \leq 0{,}5$ donne une valeur de resistance à la rupture de 25 à 150 MPa.

Le durcissement de la structure dans la zone des contacts peut être obtenu en augmentant la quantite des contacts par developpement d'aire des contacts et consolidation de la phase de contacts et aussi par égalisation des aires relatives des contacts. L'état de tension dans les contacts en dernier cas sera uniforme et la force portante des tous les contacts sera épuisée simultanément, avec une effectivité maximale.

Le second facteur d'influence sur la resistance du ciment durci est la porosité. Mais dans ce cas la resistance du ciment durci ne doit pas être relationée avec la porosité capillaire, mais avec la concentration des produits de hydratation, c'est-à-dire le facteur "gel-espace" Φ. Cette relation se doit au fait, que la superficie de destruction du ciment durci se forme à travers de la structure du gel du ciment et par des pores capillaires, laissant les inclusions dures des particules du clinker nonhydraté intacts.

La formation de la structure du ciment durci dans ce niveau se realise par une "couture" des flocules de la masse cristalline hydratée. L'aire des contacts entres les flocules du gel $F_g^{(2)}$ dans la superficie de destruction peut être expressée par la formule (4)

$$F_g^{(2)} = \Phi^2. \quad (36)$$

Si la structure est uniforme et les mailles des pores individuelles ont le même type géométrique, ayant la même charge, alors la resistance de la structure sera égal à

$$R_{cim} = R_{cs}\,\Phi^{2}. \qquad (37)$$

Une structure réel est inhomogéne et ce fait est confirmé par une distribution des compacités locales ρ (facteur Φ), qui conduit à une tension inhomogène et une surcharge des certains microvolumes ayant des valeurs petits ρ. Le mécanisme de destruction d'une structure pareille est échelonné et lié à une destruction anticipés des cellules surchargées /10/; l'état intermediaire du système sera expressé par l'équation

$$R = R_{cs}\,\rho^{2}\int_{\rho}^{\rho_m}\varphi(\rho)\,d\rho, \qquad (38)$$

dont $\varphi(\rho)$ - est la fonction de distribution des compacités locales $\rho_0 \le \rho \le \rho_m$ aceptant que la gamme de changement du paramètre ρ est $\Phi = \int_{\rho_0}^{\rho_m}\rho\,\varphi(\rho)\,d\rho$.

Pour une distribution locale uniforme la formule de resistance du matériau poreux aura la forme suivante:

$$R_{cim} = R_{cs}\,\frac{4\,\rho_m^{3}}{27\,(\rho_m-\rho_0)}. \qquad (39)$$

Cette formule est justifiée si $\rho_0 \le 2/3\,\rho_m$ Faut de remplir cette dernière condition alors $R_{cim} = R_{cs}\,\rho_0^{2}$. Une évaluation quantitative de la formule (39) et des formules correspondantes aux autre fonctions caractéristiques aussi, y compris la loi de distribution normale, indique que ces formules peuvent être approximées pour la relation, qui s'approche à la formule de Powers

$$R_{cim} = R_{cs}\,\Phi^{s}, \qquad (40)$$

dont $s = 2{,}5\ldots3{,}5$, dependant de $\varphi(\rho)$ Les calculs ont montrés, que les pertes de resistance du ciment durci, comme consequence de la inhomogénéité mécanique et structurelle sont égales à 50...100, mais comme consequence de la porosité capillaire - à 3...10.

CONCLUSIONS: La structure et la resistance des liants hydratés de la pierre à ciment sont predéterminées par la minéralogie et la structure du ciment. Les états principaux de la formation de la structure sont la germination et la formation des structures coagulantes et cristallines. La resistance du ciment durci est déterminée par la resistance des cristaux individuels des hydrates, liés aux points des contacts et par la porosité aussi. Cette resistance est relativement faible à cause de l'inhomogénéité des structures géométriques et minéralogiques. A base des formules théorétiques proposées par les auteurs, on peut faire des prévisions des proprietés du ciment durci.

LITERATURE:

1. - А.Ф.ПОЛАК, В.В.БАБКОВ, Ю.Ф.ДРАГАН, В.Н.МОХОВ (1978), "МАТЕМАТИЧЕСКАЯ МОДЕЛЬ СТРУКТУРЫ ПОЛИДИСПЕРСНОЙ СИСТЕМЫ". - В кн.:"ГИДРАТАЦИЯ И ТВЕРДЕНИЕ ВЯЖУЩИХ". Уфа, с.3-11.

2. - А.Ф.ПОЛАК (1966), "ТВЕРДЕНИЕ МОНОМИНЕРАЛЬНЫХ ВЯЖУЩИХ ВЕЩЕСТВ". М., СТРОЙИЗДАТ, 208с.

3. - Б.В.ДЕРЯГИН, Л.Д.ЛАНДАУ (1945), "ТЕОРИЯ УСТОЙЧИВОСТИ СИЛЬНО ЗАРЯЖЕННЫХ ЛИОФОБНЫХ ЗОЛЕЙ И СЛИПАНИЯ СИЛЬНО ЗАРЯЖЕННЫХ ЧАСТИЦ В РАСТВОРАХ ЭЛЕКТРОЛИТОВ". - ЖУРНАЛ ЭКСПЕРИМЕНТАЛЬНОЙ И ТЕОРЕТИЧЕСКОЙ ФИЗИКИ, т.15, вып.11, с.663-682.

4. - П.А.РЕБИНДЕР, Е.Е.СЕГАЛОВА (1952), "НОВЫЕ ПРОБЛЕМЫ КОЛЛОИДНОЙ ХИМИИ МИНЕРАЛЬНЫХ ВЯЖУЩИХ МАТЕРИАЛОВ". - "ПРИРОДА", № 12, с.45-52.

5. - Е.Д.ЩУКИН, Е.А.АМЕЛИНА, С.И.КОНТОРОВИЧ (1978), "ФИЗИКО-ХИМИЧЕСКИЕ ИССЛЕДОВАНИЯ ЗАКОНОМЕРНОСТЕЙ ФОРМИРОВАНИЯ ДИСПЕРСНЫХ ПОРИСТЫХ СТРУКТУР". - КОЛЛОИДНЫЙ ЖУРНАЛ, № 5, с.938-945.

6. - А.Ф.ПОЛАК (1966), "КИНЕТИКА ГИДРАТАЦИИ И РАЗВИТИЯ КРИСТАЛЛИЗАЦИОННОЙ СТРУКТУРЫ СРАСТАНИЯ МОНОМИНЕРАЛЬНЫХ ВЯЖУЩИХ ВЕЩЕСТВ ТИПА ПОЛУВОДНОГО ГИПСА". - КОЛЛОИДНЫЙ ЖУРНАЛ, т.22, вып.6, с.689-701.

7. - А.Ф.ПОЛАК (1976), "КИНЕТИКА СТРУКТУРООБРАЗОВАНИЯ ЦЕМЕНТНОГО КАМНЯ". У1 МЕЖДУНАРОДНЫЙ КОНГРЕСС ПО ХИМИИ ЦЕМЕНТА, том П, книга 1. М., СТРОЙИЗДАТ, с.64-68.

8. - М.К.ГРИНЕВА, Ю.М.БУТТ, В.В.ТИМАШЕВ, В.С.БАКШУТОВ (1971), "ПРОЧНОСТЬ НА РАСТЯЖЕНИЕ МОНОКРИСТАЛЛОВ РЯДА ПРИРОДНЫХ И СИНТЕТИЧЕСКИХ ГИДРАТИРОВАННЫХ КАЛЬЦИЕВЫХ СИЛИКАТОВ". - ТРУДЫ МХТИ им.МЕНДЕЛЕЕВА, № 68, М., с.234-237.

9. - А.Ф.ПОЛАК, В.В.БАБКОВ, В.Н.МОХОВ (1978), "ПРОЧНОСТЬ ЦЕМЕНТНОГО КАМНЯ". В кн.: "ГИДРАТАЦИЯ И ТВЕРДЕНИЕ ВЯЖУЩИХ". Уфа, с.56-69.

10. - В.В.БАБКОВ, В.Н.МОХОВ, Ю.Г.НУРИЕВ, А.Ф.ПОЛАК (1977), "МЕХАНИЗМ РАЗРУШЕНИЯ И ПРОЧНОСТЬ ХРУПКИХ ПОРИСТЫХ МАТЕРИАЛОВ". - ТРУДЫ НИИПРОМСТРОЯ, вып.22, Уфа, с.122-132.

Scanning Electron Microscopic Observations of Cracking in Portland Cement Paste

Observations des fissures de pâtes de ciment au microscope électronique

Sidney DAIMOND, Purdue University, and
Sidney MINDESS, University of British Columbia, U.S.A.

SUMMARY:
A device has been designed and constructed to permit observation of cracking of specimens loaded within the stage of a scanning electron microscope. The specimen configuration is that of the "compact tension" specimens used in plane strain measurements of fracture toughness. Preliminary observations on portland cement pastes indicate that the cracks are long, narrow, approximately parallel-sided, mostly unbranched except near the tip, and only approximately straight. Close observation indicates that the cracks occur as assemblages of relatively short straight segments set at small angles to each other. The effects of successive displacements of the loading device viewed at the same place along the crack are complex.

RESUME:
Un appareillage a été conçu et construit pour permettre l'observation de la fissuration sous charge d'échantillons, à l'intérieur d'un microscope électronique. La configuration des échantillons est du type "à contrainte concentrée", utilisé dans la mesure des déformations planes avec ruptures fragiles. Les premières observations des pâtes de ciment ont montré que les fissures sont longues, étroites, approximativement parallèles aux bords, le plus souvent non ramifiées, sauf près des extrémités, et à peu près droites. Des observations plus poussées ont montré que ces fissures se présentent sous la forme d'une suite de segments droits, relativement courts, et faisant entre eux de petits angles. L'effet de déplacements successifs de l'appareil de chargement, observé du même point le long d'une fissure, est complexe.

INTRODUCTION

The nature of the origin and development of cracks in hardened portland cement pastes, as well as in mortars and concretes, is of continuing concern. Cracking obviously results in damage and failure of specimens in strength testing, and the propagation of cracks under mechanical loading has been the subject of much investigation and theoretical development. With cement and concrete materials, crack development and propagation at stresses far below those required to induce structural failure are common occurrences. Such cracks, arising as a result of freezing, excessive shrinkage, or attack through environmental agencies, contribute significantly to concrete durability problems by rendering access to the interior of exposed concrete structural members relatively easy.

Despite the importance of the cracking problem in concrete, understanding of how real cementitious materials behave in terms of crack initiation and propagation is meagre. Efforts to apply the concepts of linear elastic fracture mechanics, notably successful in dealing with relatively homogenous, non-particulate materials like steel, have not been particularly successful. In part this may be due to the paucity of observational information on the way in which small cracks first originate and then propagate through cement paste and mortar matrices. Observations at a level fine enough to be meaningful in this context have not heretofore been pursued with any degree of consistency in the cement field.

In the present work, we describe and illustrate preliminary results obtained with a device specially constructed to permit close observation and photomicrographic recording of cracks generated within the scanning electron microscope (SEM). The work reported here is confined to cement paste; results obtained by similar means on mortar specimens will be submitted for publication elsewhere.

INSTRUMENTATION

The device used here is specially designed to be accommodated within the specimen stage area of the ISI Super III-A scanning electron microscope in use in the laboratory of the first-named author at Purdue University. Details of the device and its functioning will be published elsewhere (1).

The specimen configuration is essentially that of the compact tension specimen described in ASTM E 399-78, Plane Strain Fracture Toughness of Metallic Materials (2), except that the present specimens are slightly narrower. A dimensioned drawing is provided as Fig. 1. The specimen may be described as a rectangular solid with a 13-mm long narrow (0.7 mm) notch cast in one end. Steel posts 3 mm in diameter are cast on either side of the notch. In operation circular steel bearings are placed over the posts and a wedging device is advanced by electric motor so as to spread the posts apart and induce tensile stresses concentrated at the root of the notch. A drawing of the loading assemblage is given as Fig. 2. The geometry is defined in such a fashion as to permit calculation of the stress intensity factor at the root of the notch. The entire assemblage is mounted in the specimen stage of the SEM. In operation the area at the root of the notch is located and held under observation while the motor is activated to advance the wedge until cracking just

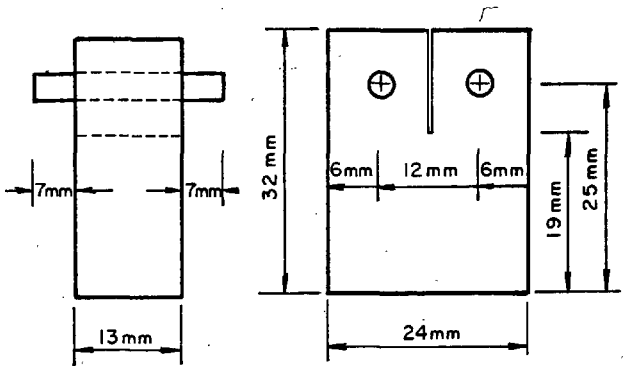

Fig. 1. Configuration and Dimensions of Cement Paste Compact Tension Specimens.

occurs. The motor is immediately shut off, and the extent and details of the crack produced are observed and microphotographs made. When this process is completed the motor is again actuated for an arbitrary period and the crack extended; then the drive is turned off and the enhanced crack configuration again documented. This process is repeated several times until the crack propagates completely across the specimen and failure occurs.

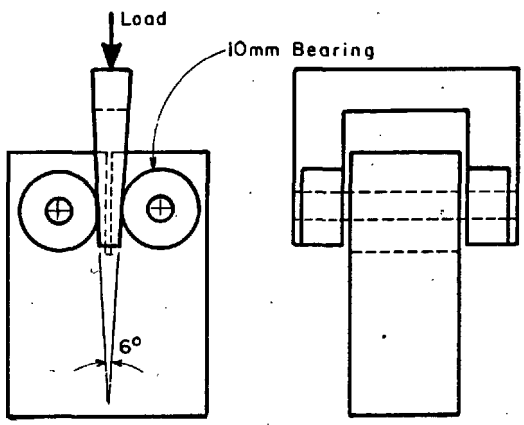

Fig. 2. Configuration of Wedge-Loading Device

Wedges of various wedge angles have been used, including 3^{0}, $4\frac{1}{2}^{0}$, and the 6^{0} angle shown in Fig. 2.

SPECIMEN PREPARATION

The portland cement pastes used in this study were prepared from ordinary (ASTM Type I) portland cements and were cast into specially-designed molds machined so as to provide the configuration shown in Fig. 1. The casting process was assisted by vibration. After casting the specimens were sealed within the molds for 24 hours, then demolded, and cured under saturated limewater for various periods.

In preparing the specimens for the SEM it was found undesirable to attempt to evacuate the relatively thick specimens to permit application of a conductive coating. It was found that specimens that had been

air cured for some time could be examined in the SEM without benefit of such coatings, at least at the relatively modest magnifications required to document the crack geometry. While some loss of water undoubtedly occurs for such specimens within the SEM, this seems neither to interfere with SEM observation nor to contribute visibly to cracking or extension of cracks formed by the mechanical loading device. It was found that application of a layer of silver dag ("silver paint") on the vertical end of the specimen away from the notch, which contacts a metal plate in the specimen holding device, is sufficient to provide proper electrical grounding for the specimen, and charging effects were not a problem. The SEM was operated at 5 KeV and at 15 KeV at various times, without much difference in results being observed.

RESULTS

The appearance of the area at the root of the cast-in-place notch of a typical cement paste specimen mounted in the SEM before application of the wedge loading is shown in Fig. 3. This specimen was cast at w:c 0.5, cured for approximately 24 hours in the mold, for an additional period of two weeks in saturated limewater, and then exposed to laboratory ambient air for several weeks before examination.

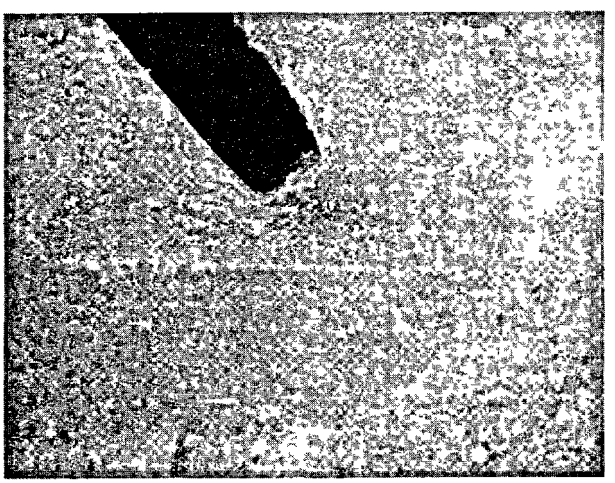

Fig. 3. Area At the Root of the Cast Notch Before Loading. Original Magnification 30x.

The appearance of the same area after application of the initial loading just sufficient to produce cracking is shown as Fig. 4.

As a result of the wedge-loading action a long, relatively narrow crack is generated. In this specimen the crack width near the root of the notch was approximately 30 μm, and it extended to a detectable distance of approximately 10 mm away from the notch; that is, the aspect ratio of the initially formed crack was well over 300. The width of this crack gradually diminishes in the direction of propagation, approaching a minimum clear detected width of about 3 μm near the end. This is commensurate with the sizes of the smaller hydrated cement and cement grains, and the definition of the crack is lost in the general discontinuity of the cement paste.

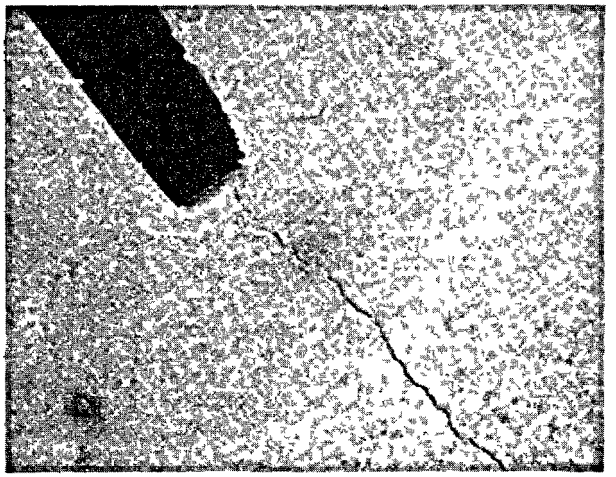

Fig. 4. Crack Produced in Specimen as a Result of Initial Application of Wedge Loading. Original Magnification 30 x.

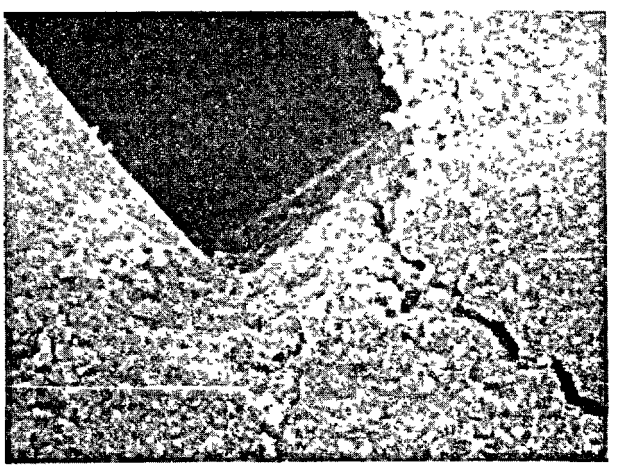

Fig. 5. Detailed View of Portion of Crack Shown in Fig. 4. Original Magnification 100x.

As indicated in Fig. 5, the crack is not quite straight and parallel sided, as is assumed in many fracture mechanics treatments, but rather is shown to be an assemblage in a zig-zag pattern of short segments, each of the order of 60 μm or so in length. There are a few individual hydrated cement grains visible at the surface in Fig. 5 that have not completely separated from either side, apparently bridging over short segments of the crack; however with these few exceptions, the crack depicted in Fig. 4 seems continuous.

This is not quite true for the regions beyond that shown in Fig. 4. At two or three places near the tip of the crack where the crack has narrowed significantly, the trace of the crack at the surface appears to terminate, and a seemingly parallel crack displaced from it occurs and continues onward. In two cases a short intermediate segment extending back toward the notch and the segment extending forward toward the tip can be observed. An illustration of such an area is shown as Fig. 6. The trend of the crack direction in this area has

wandered to the left from the general upper left to lower right orientation. It should be specifically understood that only the surface of the specimen can be observed, and it is possible that the underlying crack within the specimen may be continuous despite the interruptions shown by the trace on the surface.

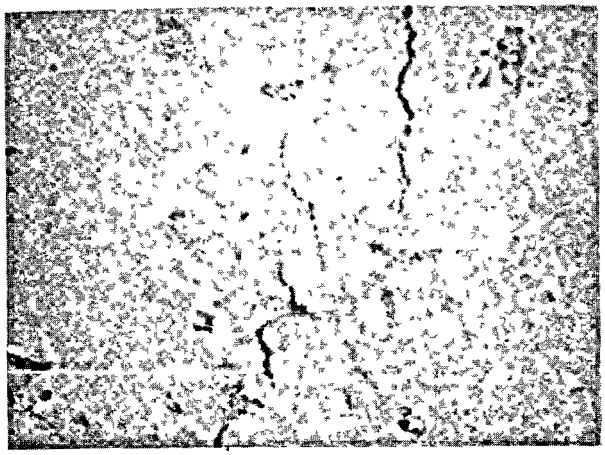

Fig. 6. Illustration of Apparent Discontinuity in Trace of Crack at Surface. Notch is Upward And to the Left. Original Magnification 300x.

The observations so far illustrated may be summarized as indicating that mechanically-induced cracks in cement paste specimens of this type are basically long, narrow, parallel-sided, and unbranched in character. However, when examined closely and at enlarged magnifications it appears that these descriptors are only approximately true.

The question arises as to how such cracks compare with the crack pattern produced by drying shrinkage rather than mechanical loading, for specimens of the same configuration. An answer is provided in Fig. 7, which shows the general crack pattern produced in a specimen of the same type, age, and w:c ratio as previously examined, which has been exposed to a 105° C. temperature drying oven for half an hour and then evacuated in a sputter coating device prior to examination in the SEM. No mechanical loading has been applied.

It is seen that the drying shrinkage crack originates at the root of the precast notch in the same general area as a mechanical loading crack and is in some respects similar to it. The outstanding obvious difference is that the drying shrinkage crack pattern in Fig. 7 is repeatedly branched, branching occurring at intervals of about 2.5 mm. It is apparent that the stress distribution arising from shrinkage is very much different from that designed to be induced in the specimen by the mechanical loading system.

The gold-palladium conductive coating applied to this specimen permits examination of the crack in greater detail than is possible otherwise. Fig. 8 shows the area immediately surrounding the point of intersection of the second branch crack from the root of the notch in the lower center part of Fig. 7, at an enlarged scale. The crack width here is approximately 30 μm. The distinctly particulate character of the hardened cement paste is quite apparent, individual grains being clearly detected. Examination down the

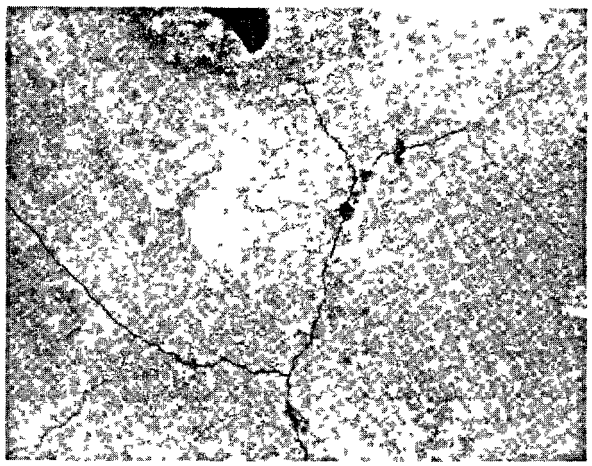

Fig. 7. Cement Paste Specimen Showing Shrinkage Crack Pattern Arising From Partial Oven Magnification 9x.

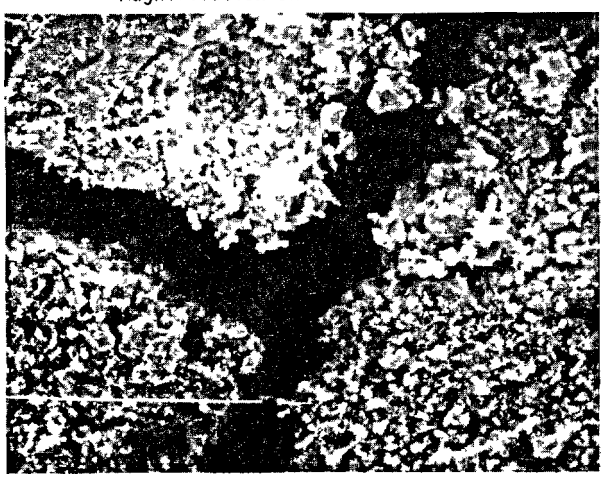

Fig. 8. Higher-Magnification View of the Area Surrounding the Second Shrinkage Crack Branch in Fig. 7 Above. Original Magnification 500x.

crack disclosed that, as expected, the crack is approximately, but not perfectly parallel sided.

As has been mentioned previously, with the present apparatus it is possible to extend the initially-formed crack several times before failure occurs. Distinctive areas of the crack may thus be re-examined after successive displacements to form a better picture of the crack extension process.

An example of the type of comparison that is possible is provided in Fig. 9. Fig. 9A on the left is the appearance of the initial crack as it emanated from the notch in the first comparatively heavy loading of a w:c 0.5 cement paste specimen cured in lime-water for approximately two weeks and subsequently in air for a like period. Fig. 9B on the right is the same area taken at the same magnification after the crack has been extended and widened by additional displacement of the wedge.

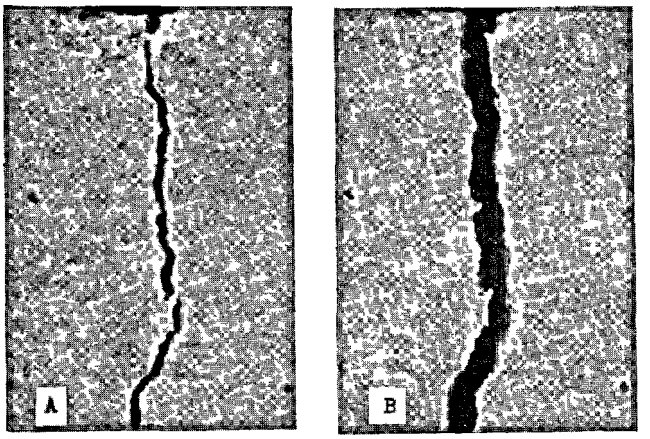

Fig. 9. Comparison Between Appearance of Initial Crack (A, left) and Widened Crack (B, right) at Point of Initiation At Precast Notch. Original Magnification 27x.

The crack in this region is widened from approximately 60 μm to approximately 180 μm. The additional displacement produces an apparent straightening effect on the appearance of the crack.

A further effect is illustrated in Fig. 10. While it is usually the case that the crack starts off in a direction normal to the end of the notch, there is usually a certain amount of wander from this direction, as can be seen in the lower part of Figs. 9A and 9B. This tendency is accentuated with increasing distance from the notch. In segments not trending in the predominant crack direction the displacements produced by the extension of the crack are complex. As is particularly apparent in Fig. 10B, the crack sides are no longer parallel in such segments, and the three-dimensional geometry of the crack may be other than that inferred from its trace at the surface of the specimen. This is despite the fact that the specimen geometry is designed to insure cracking under plane strain conditions.

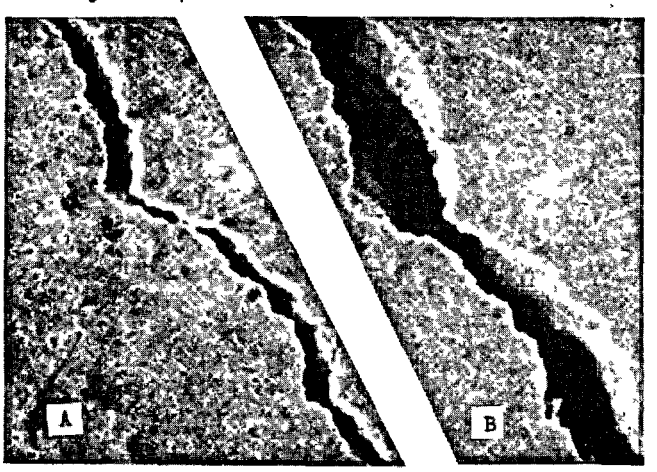

Fig. 10. Comparison Between Appearance of Initial Crack (A, left) and Widened Crack (B, right) In Area Where Crack Direction Has Wandered From The Designed Direction. Original Magnification 135x.

The region depicted in Fig. 10 is more than half way from the notch to the end of the specimen; the cracks here are narrower than those depicted in Fig. 9. At the widest part in Fig. 10A the crack is only about 30 μm wide; at the narrow zone just below the sharp jog near the center of the figure it is only about 7 μm wide. In contrast, after the crack extension, the widest part of the crack is almost 150 μm across.

The particular crack depicted in Fig. 10 has not branched between the root and the area depicted. The first visible branch was found several mm beyond this point, and its appearance at the first stage is shown in Fig. 11A, on the left. The notch is in the upward direction. It appears that continuation of the smooth flow of crack extension would have been along the right hand branch, but that for some reason a left-hand branch intersecting the smooth path at a sharp angle was also produced. As can be seen in Fig. 11B on the right, on further crack extension, the left hand branch is clearly active and dominant, and the right hand branch is entirely unaffected by the crack extension process. This observation seems to hold good generally where branching is found; one branch is "active" and widens under the crack extension process, while the other is inactive and unaffected.

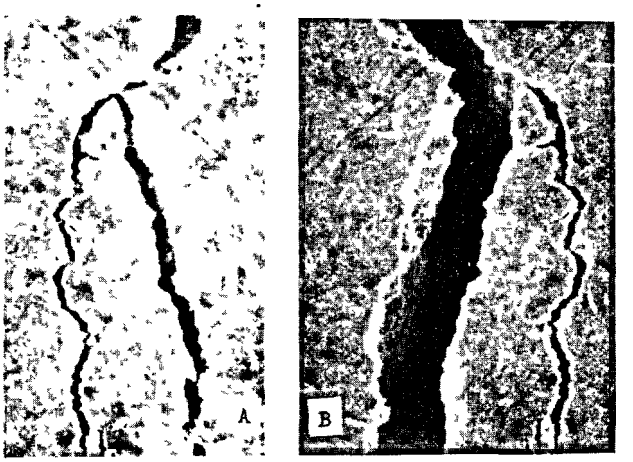

Fig. 11. Detail of Crack Extension Effects at Point of Branching Showing That Only One Branch Is "Active" in Crack Extension: A, (left) is Initial Crack, B (right) is Crack After Extension by Additional Wedge Displacement. Original Magnification 135x.

It has been mentioned previously that the initially formed cracks are difficult to trace to their tips, since they narrow and become indefinite as their width approaches that of the general run of cement paste grains. Generally some branching is found before the crack peters out completely. Fig. 12A provides an illustration of such a zone, near but definitely not at the tip of the initially formed crack. The effect of additional crack extension on such a zone is seen in Fig. 12B, on the right. While only a single crack is primarily active, and the side branches are unaffected, there seems to be a splitting action leaving the hinge configuration evident in the center of Fig. 12B.

A number of mortar specimens have also been examined by the method reported here. These examinations suggest that cracking in mortars is considerably more

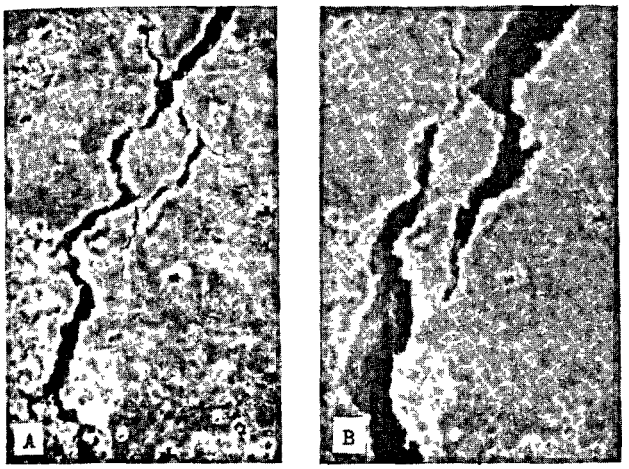

Fig. 12. Detail of Branched Area Near Original Crack Tip: A (left) is Initial Crack, B (right) is Same Area After Crack Extension. Original Magnification 135x.

complex than cracking in cement pastes, due to the larger scale disturbances associated with the sand grains. The cracks bend at larger angles, branching is much more frequent, and a far less straightforward pattern results.

CONCLUSIONS

The present work indicates that cracks in cement paste induced by a carefully defined mechanical loading system designed to produce plane strain conditions tend to be approximately straight and to run in the defined direction. However, they actually consist of a linked series of short segments that zig-zag back and forth around the direction of propagation. The cracks are unbranched except for a very few side branches produced far from the initiating point. Where such branching occurs only one branch is mechanically active, as indicated by repeat observations after further crack extension. The cracks are approximately, but not completely parallel sided, and narrow somewhat toward the tip. The tip area itself cannot be observed with confidence with the present experimental setup.

The influence of variations in such cement paste parameters as w:c ratio, degree of hydration, presence of admixtures, etc. on the nature of the cracks developed remain to be established, but are expected to be minor.

ACKNOWLEDGEMENTS

This paper represents a contribution from the Joint Highway Research Project, Purdue University, in cooperation with the Department of Civil Engineering, University of British Columbia. The SEM fracture device was constructed in the latter department, and the contributions of Messrs. B. Merkli, R. Postgate and W. Schmitt to the successful development of the device are gratefully acknowledged.

REFERENCES

(1)- S. Mindess and S. Diamond, "A Preliminary Study of Crack Propagation in Mortar," prepared for submission to Cement and Concrete Research.

(2)- American Society for Testing and Materials, (1978), Annual Book of ASTM Standards, Part 10 Designation E 399-78, pp. 512-533.

Analysis on fluidity of cement paste and mortar

Recherches sur la fluidité de la pâte et du mortier de ciment

S. NAGATAKI, Dr. Associate Professor, Dept. of Civil Eng. Faculty of Eng., Tokyo Institute of Technology, and
S. KAWANO, Researcher, Tunnel Section, Public Works Research Institute, Ministry of Construction, Japan.

RESUME : Récemment, on a fait beaucoup d'études sur la fluidité de la pâte et du mortier de ciment, dues à l'augmentation de l'emploi de ces derniers dans les matériaux d'injection tels que le béton prépakt et le mortier liquide.

Dans les anciennes recherches, on avait l'habitude de considérer, au point de vue rhéologique, la pâte de ciment et le mortier frais, comme des corps de Bingham. Ce texte suggère que de tels fluides soient plutôt considérés comme des corps visqueux ayant des réactions chimiques et une hystérésis des contraintes. Le comportement thixotropique semble affecter la fluidité considérablement. La rationalité de la suggestion ci-dessus est confirmée par les résultats des expériences faites avec et sans emploi de plastifiants ordinaire ou super, au moyen de divers appareils tels que les viscosimètres à rotation ou à tubes, et des appareils d'essai destinés spécialement aux bétons prépakts.

SUMMARY : In recent years, with the increase in use of cement paste and cement mortar in grouting materials such as prepacked concrete and grouted mortar, there have been many studies on the fluidity of cement paste and mortar.

Whereas it was customary to regard fresh cement paste and mortar as Bingham bodies in the analysis on their fluidities in past researches, this report suggests that such fluids should rather be considered as structural viscous bodies possessing chemical reactions where the hysteresis of strain and thixotropic behavior are seemed to greatly affect fluidity. The rationality of the above proposition is substantiated with results obtained from experiments with and without the use of ordinary or super-plasticizers, by means of various apparatus such as the rotation viscometer, the tubular viscometer and testing apparatus specially designed for prepacked concretes.

FOREWORD

Attempts have been made from a fairly long time ago to analyze the fluidity of still unhardened (hereafter called fresh) mortar by rheological techniques, but the greater part of these research works assumed fresh mortar and concrete to be Bingham bodies trying to judge their fluidities using the two rheological quantities of shearing yield value and coefficient of plasticviscosity. However, there are various problems about clarifying the fluidity of actual fresh mortar and concrete by this method, and even before that, it is difficult to measure shearing yield values and coefficients of plasticviscosity themselves. The reasons for this are cited as being the existence of slippage at the sample boundary plane and the thixotropy of cement paste in measurement with the rotation viscometer, and it may be said that practically no research has been done to analyze these phenomena. In addition, it appears difficult to clarify the special fluidities of fresh mortar and concrete using superplasticizers with the above method.

In view of the above, experiments and observations were made in the present study considering it necessary to start out with examinations of the real natures of the fluidity characteristics of cement paste and mortar in their fresh states returning to the very basis, and to grasp by all means the true picture of fluidity. In the analysis of flow characteristics in this study, it was considered that the factor making fluidity complex is the viscosity structure of cement paste, and a comparison study was made with the thinking on structurally viscous fluidities of suspension systems (1). As a result, it was concluded that cement paste possesses a reactive property, and it is more rational to handle it as a structurally viscous fluid highly influenced by hysteresis of strain.

OUTLINE OF EXPERIMENTS

Materials Used

The materials used in the experiments were ordinary portland cement manufactured by Nihon Cement Co. (Saitama Plant), Fuji River sand of F.M. of 1.96 cut by a 1.2 mm sieve, Pozzolith No. 5L (25% solution) as a normal type of water-reducing admixture, and Mighty 150 as a superplasticizer.

Mix Proportions

From the necessity of measuring fluidity, consistency of the degree of grout mortar for so-called prepacked concrete was made the standard. The particulars are sand-cement ratios of 0, 0.5 and 1.0, water-cement ratios varied between 0.30 and 0.55, with Pozzolith added 0.25% by weight of cement, and Mighty between 0 to 0.75% by weight of cement, all of the mixes being such that fluidities could be measured with the apparatus described below within the limits that they would not segregate.

Mixing

After preparing the temperatures of the various materials so that temperature as mixed would be in the range of 20±2°C, sand and cement were dry-mixed for 2 minutes, and after introduction of the other materials, full mixing was done for 3 minutes. Following this, the mix was left standing for 5 minutes to eliminate the influence of false setting, and measurements were made after further mixing for 1 minute.

Measurements by Rotation Viscometer

The rotation viscometer was a coaxial-cylinder, outer cylinder-rotation type, with the outer cylinder of diameter 160mm by 180mm and inner cylinder of diameter 100mm by 120mm for sample thickness of 30mm, and the speed of the outer cylinder was 0 to 100rpm.

In order to measure the angular velocity distribution in the radial direction of samples, reference points were provided at the circular frame at radii of 55, 65 and 75 mm. Then, the movements of reference points and the outer cylinder during fluidity measurements were filmed by 16 mm camera, and this film was examined by a motion analyzer (2). The shear rate at the various points inside the rotation viscometer were obtained by the equation below according to the deviation angle Ω between reference points.

$$\dot{\gamma}_A = 2\dot{\Omega}/\{1 - (\frac{R_i}{R_o})^2\}$$

where

R_i : inner reference point radius
R_o : outer reference point radius

Measurements were made causing the outer cylinder revolutions to go from 0 to 30rpm and back, with measurements on two round trips. The apparent shear rate in these cases was about 20 sec^{-1} at maximum.

Measurements by Tublar Viscometer

With a tubular viscometer, it is possible for measurements to be made of a shear rate range of about 5 sec^{-1} to about 100-400 sec^{-1}. The fluidity curve was obtained in the form of apparent fluidity curve by the equations below from the flows inside the tube and differences in head.

$$\tau_A = \frac{\rho H R_o}{2L}$$

$$\dot{\gamma}_A = \frac{4V}{R_o}$$

where

τ_A : apparent shear stress (g/cm^2)
$\dot{\gamma}_A$: apparent shear rate (1/sec)
R_o : tube diameter (cm)
L : tube length (cm)
H : head difference (cm)
ρ : mortar density (g/cm^3)
V : average flow velocity (cm/sec)

RESULTS OF EXPERIMENTS

Fig. 1 is an example of a fluidity curve obtained from the range of diameter from

55mm to 65mm thought to be uninfluenced by wall surfaces inside a rotation viscometer. As indicated in the figure, both fresh cement paste and mortar clearly show shear rate thinning flows. However, on looking at the decreasing speed or down curves, in contrast to the increasing speed or up curves, the apparent viscosity after flow either increases or decreases. According to the classifications by Ish-Shalome (3), plain fresh cement paste presents anti-thixotropy in the initial stage after mixing where apparent viscosity is increased by flow, goes through a stage of non-thixotropy with elapse of time, and then moves on to thixotropy where apparent viscosity is increased by flow. On applying these classifications to all of the tasted fresh pastes and mortars at the initial stage after mixing, all mixes plain and using the ordinary water-reducing admixture showed anti-thixotropy, but mixes containing the superplasticizer 0.5% or more by weight of cement showed thixotropy in spite of it being the initial stage after mixing. Generally, when a superplasticizer is added 0.5% or more by weight of cement, it is said cement particles are almost completely dispersed into primary particles with flocks not formed, and consequently, it is surmised that the thixotropic character seen at the initial stage after mixing is greatly influenced by whether or not there are flocks.

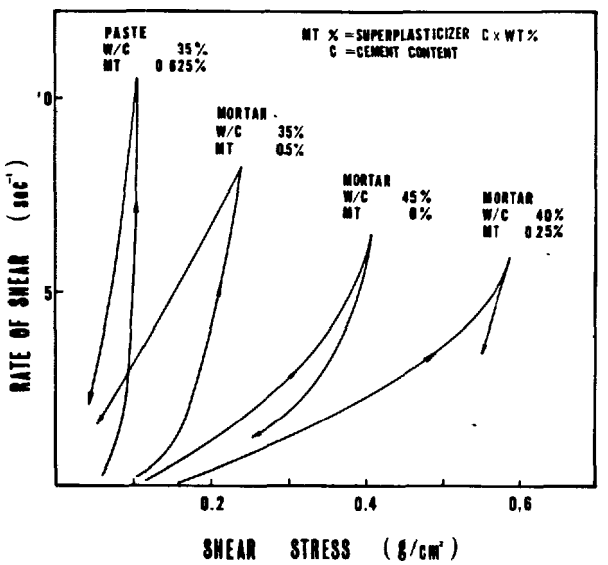

Fig. 1 - Consistency curves by couette type rotation viscometer

Next, examples of fluidity curves obtained by tubular viscometer at a higher range of slip velocity are shown in Fig. 2. The fluidity curves of fresh pastes and mortars indicating thixotropy show approximately linear behaviors in this range. As for those which indicated anti-thixotropy, they show shear rate thinning flow in this range also, and it is surmised that the structure of the interior of the paste is continuing to change even in the high shear rate range. (It may be considered that viscosity actually is changing in the direction of tube length due to thixotropic behavior, but here, in order to qualitatively grasp the fluidity of mortars, the average fluidity curves for the tube lengths were determined.)

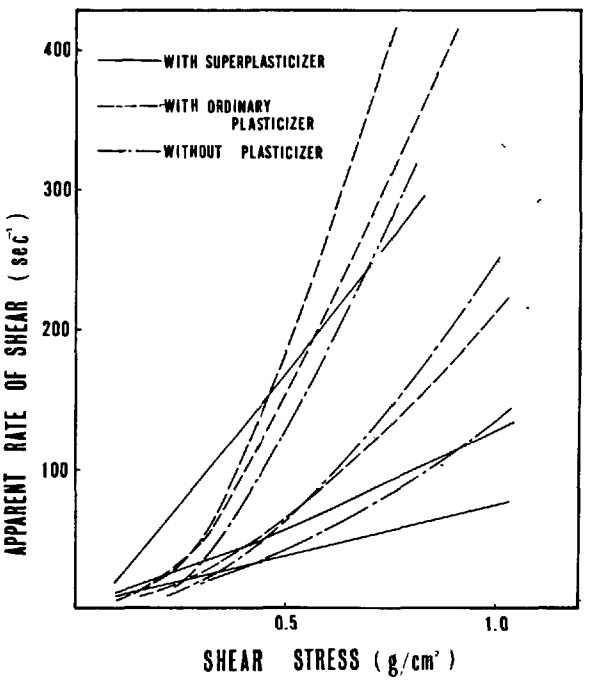

Fig. 2 - Consistency curves by tubular viscometer

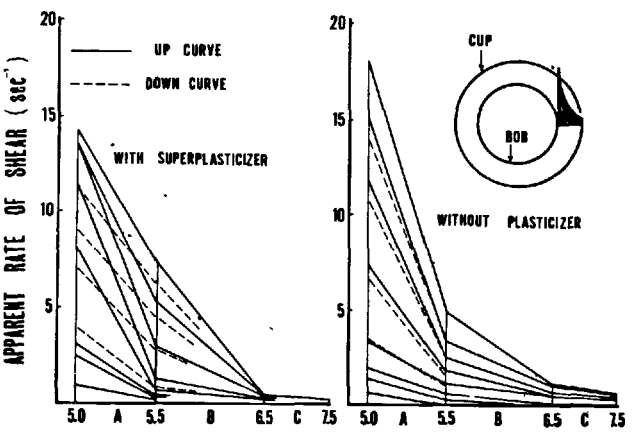

Fig. 3 - Distribution of rate of shear in a container of rotation viscometer

Fig. 3 shows the results of shear rate distributions in the radial directions of samples in the rotation viscometer followed by time intervals in accordance with rotation speed variations. This graph is of a nature that if a sample of uniform viscosity, the various measuring points when connected will

indicate a straight line. However, as shown in the figure, the tendency seen with actual fresh paste is that for the fresh paste at the left which demonstrated anti-thixotropy, it is indicated that the sample became extremely fluidized in the vicinity of the inner cylinder with increase in the angular velocity of rotation viscometer, and moreover, the shapes of the curves up and down are more or less the same. Past research works handle this phenomenon as slippage of the sample at the wall surface, but the sample is clearly extremely fluidized in observations during measurements, and it is felt necessary to analyze this phenomenon considering it as an element of the fluidity characteristics of cement mortar rather than as being due to slippage. When such a property is defined as "concentration of shear rate," this phenomenon of concentration of shear rate is thought to be a property contradictory at first glance to the property of anti-thixotropy of apparent viscosity due to flow.

On the other hand, with the fresh paste shown at the right which demonstrated thixotropy, although there is a tendency in this case also for shear rate to be concentrated at the vicinity of the inner cylinder at the start of revolution of the rotation viscometer, with increase in speed, the increase in shear rate near the inner cylinder hits a ceiling, and the portion at which shear rate increases gradually moves toward the outside (defined as "dispersion of shear rate"). And at the down curve the variation in the shear

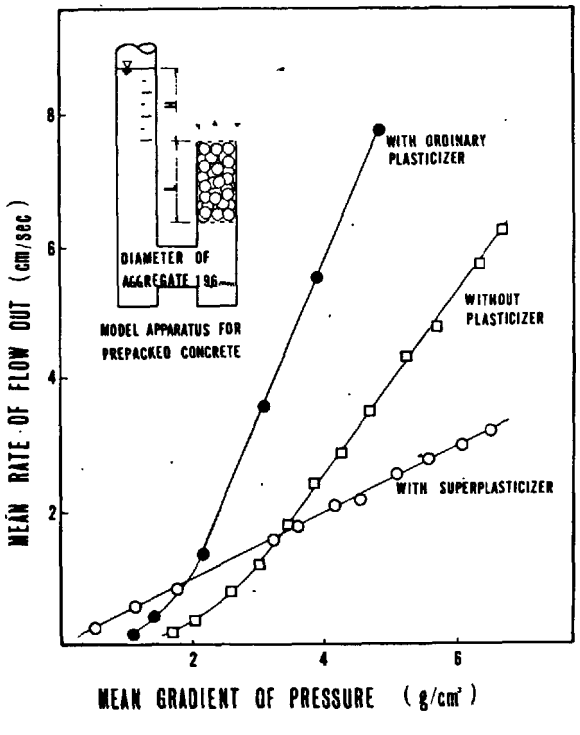

Fig. 4 - Consistency curves by model apparatus

rate becomes roughly uniform so that the curves up and down are completely different, but especially with the down curve it is indicated that the tendency is similar to that of a sample having a so-called uniform viscosity.

CONSIDERATIONS

In systematizing the various flows of these fresh cement pastes demonstrating anti-thixotropy and thixotropy and arranging and considering them, it appears to be rational for explanations to be made thinking of a viscosity structure introducing the reactivity of cement also in the concept of fluidity of a suspension system the viscosity of which is determined by the structural variations of flocks, in other words, agglomerated bodies. Thereupon, the viscosity structure in cement paste is considered divided into the two parts below.

Firstly, one is caused by flocks and is defined here as "primary structure." Flocks during flow show a stable agglomerated state in accordance with shear rate, and because of this, a primary structure generally shows an equilibrium flow curve. Consequently, in these experiments, it may be considered that this curve configuration indicates shear rate thinning flow.

The other viscosity structure is one that is considered to be due to causes such as gelation of leached components of cement, defined here as "secondary structure." The secondary structure is considered not to have an equilibrium flow curve, is destroyed with flow, and is indicated only by a hysteresis flow curve. In general, since relatively great energy is required for destruction or formation of a primary structure, and formation and growth of a flock require collision between primary particles or flocks, it is considered that in case an equilibrium structure is possessed at a high shear rate, formation the structure is accelerated more when flowing at low shear rate rather than when standing still.

In contrast, it appears the secondary structure is readily destroyed, and is swiftly reformed after stoppage of flow, and within the scope of these experiments, formation seemed to occur in several seconds to several tens of seconds. The strength of the secondary structure appears to be influenced by concentration of cement paste, sand-cement ratio, and water reducing admixture. However, in any event, it is thought the behavior of a secondary structure is that of a elastic one against impact stress or low stress, above which the behavior is viscous with there being a character of destruction with increase in strain.

Considering that the differences of thixotropy and anti-thixotropy appearing during measurement of flow of fresh mortar, or the phenomena of concentration and dispersion of shear rate of samples in rotation viscometers were

produced as a result of the primary and secondary viscosity structures being tangled with each other, the following explanations may be made.

Firstly, when a superplasticizer is added in large amount, and when considering that cement is dispersed into primary particles and flocks do not exist in the cement paste, a primary structure will not exist, and the viscosity structure will be a secondary structure only. Therefore, fresh paste and mortar of such mix proportions indicate thixotropy with secondary structure, the phenomenon of dispersion of shear rate is produced.

On the other hand, in case of existence of flocks as with plain paste and mortar, the two viscosity structures of primary and secondary will exist together. In such case, the primary structure in the paste during mixing or agitation approaches equilibrium at a high shear rate, and with stopping of the mixer, the secondary structure is rapidly formed ahead of the primary structure, and the primary structure is maintained at equilibrium in a high shear rate range. (This phenomenon will be called "memory of preceding shear rate.")

In measurements by ratation viscometer, since the shear rate itself is lower than the shear rate the mortar was subjected to during agitation, after the secondary structure has been destroyed formation of the primary structure is accelerated and anti-thixotropy is produced. In this case, however, inside the sample in the rotation viscometer, the secondary structure is first destroyed in the vicinity of the inner cylinder at the start of rotation and this part is fluidized with low viscosity memorized in the high shear rate, there will be concentration of shear rate produced due to the influence of the secondary structure in farther outside. In the down part, formation of a primary structure is seen in the vicinity of the inner cylinder, and perhaps due to this in two continuous round-trip measurements there was a tendency for concentration of shear rate to be alleviated the second time compared with the first.

The secondary structure in the cement paste gradually becomes stronger with time through hydration, and as according to Ish-Shalome, paste that had shown anti-thixotropy will come to show thixotropy, and it is thought later the difference of primary and secondary disappears to proceed toward setting.

As described above, whereas analyses of fluidities of fresh mortar and concrete had been made in the past assuming Bingham bodies, the present study has carried out examinations providing fairly bold hypotheses in order to be able make explanations including the peculiar phenomena recognized when superplasticizers are used in analyzing fluidities of fresh mortar and concrete. Admittedly, there has been a fair amount of heavy-handedness in explaining the phenomena grasping the fluidities of fresh mortar and concrete as is. However, within the scope of the experiments conducted in this study, it is felt that by separating the viscosity structure of cement paste into primary and secondary structures it has been possible to adequately explain at least qualitatively the flow properties of fresh paste and mortar.

However, it was not possible to distinctly grasp the influence of sand particles in the present experiments, where especially, in case of high sand-cement ratio, there will be the influence of interlocking of sand particles. As others, there will be the influence of air bubbles, and so long as a viscosity structure itself is physico-chemical, the variation in the condition due to the influence of temperature will be a very important factor. In regard to these, while endeavoring further to make it possible to quantitatively grasp the viscosity structure, it is thought necessary to carry out further analyses on the influences of the above factors.

SUMMARIZATION

The results obtained in this study may be summarized as follows:

1) The flows of cement paste and mortar in fresh states are not simply Bingham flows, but basically are shear rate thinning flows.

2) When a superplasticizer is added approximately 0.5% or more by weight of cement, fresh paste and mortar show thixotropy. Following this, they show flows close to Newtonian flows. Ordinary fresh pastes and mortars other than the above show anti-thixotropy, and have a tendency of becoming extremely fluidized at the boundary plane of the rotation viscometer during flow.

3) Two forms are conceivable regarding the viscosity structure in cement paste. One is flocculation of cement particles, and the other is gelation of the paste as a whole. The former is viscosity structure similar to the flow of a suspended system, while the latter is one which is simply thixotropic, but in a cement paste the two influence each other, and make the flow of cement paste extremely complex through the structural form, hysteresis of strain, and time-dependent change, etc. due to reaction.

REFERENCES

1. K. Umeya : Proceedings of the Cement Association of Japan, XXX, p.19, (1976). Others

2. S. Nagataki et al.: Proceedings of the Cement Association of Japan, XXIX, p.207 (1975).

3. Ish-Shalome et al.: National Bureau of Standards Monograph, 43, 2, 731, 1962

Préhydratation superficielle des ciments et son influence sur le processus de durcissement

Surface pre-hydration of cements and its influence on hardening process

Y.S. MALININE, Docteur ès Sciences Techniques,
V.P. RIAZINE, Candidat ès Sciences Techniques,
L.S. BATOUTINA, Ingénieur,
N.D. KLICHANIS, Ingénieur,
B.E. YOUDOVITCH, Candidat ès Sciences Techniques, NIITzement, Moscou, U.R.S.S.

RESUME : Il est proposé un nouveau procédé d'intensification du processus de durcissement du ciment, par un pré-traitement à l'air humide épuré de CO_2. Ceci provoque la formation sur tous les grains non encore hydratés de ciment, d'enveloppes hydratées semi-perméables; en donnant à ces enveloppes une épaisseur optimale, on accélère l'hydratation ultérieure du ciment.

On a établi que pour tous les ciments fraîchement broyés, ce traitement, poursuivi pendant un temps optimal, variable suivant le type du ciment, améliorait les résistances, les propriétés rhéologiques et la durabilité. Cette préhydratation superficielle des ciments modifie la composition et la structure des hydrates formés au cours de l'hydratation ultérieure.

On a montré qu'il existait des différences sensibles dans la composition de ces derniers hydrates, selon que le prétraitement à l'air humide s'effectuait en présence ou en absence de CO_2.
Ce procédé : traitement du ciment par préhydratation en atmosphère humide débarrassée de CO_2, peut être recommandé pour accroître l'activité du ciment.

SUMMARY : A novel technique for intensifying the cement hardening process by pre-treating it with CO_2-free high-humidity air is proposed. The technique provides for creating semi-permeable shells of new formations having optimum thickness around the particles of the unhydrated cement. These shells accelerate the process of hydration of the cement.

It has been established that treatment of all freshly-ground cements by the above method at an optimum time which differs with each cement grade, improves the cement strength, plasticity and life characteristics.

Surface pre-hydration of cements and their component clinker minerals changes phase composition and structure of the hydration products at further hardening. The considerable differences in the phase composition of new formations are shown in the case of surface hydration with high-humidity air in the presence and absence of atmospheric CO_2.

The method of surface pre-hydration in a high-humidity air free from CO_2 may be recommended for increasing activity of cement.

Les processus se déroulant lors du stockage du ciment dans l'atmosphère humide continuent à attirer notre attention malgré l'expérience presque séculaire de leur étude. On sait que l'hydratation superficielle dans l'atmosphère humide entraîne habituellement le ralentissement de la prise et la diminution de l'hydraulicité du ciment. Toutefois, les exceptions, qui ne sont pas rares, à cette règle générale conduisent à la nécessité de nouvelles études. Ainsi, au IV-ième Congrès sur la chimie du ciment W.C. Hansen (1) fit la communication sur l'apparition d'une fausse prise due à l'action sur le ciment de l'air humide ; il expliqua ce phénomène par l'"ulcération" de la surface des particules, augmentant la surface spécifique de réaction lors de l'interaction ultérieure avec de l'eau. J. Gebauer (2) aboutit à la conclusion que dans ce cas c'est C_3S qui est activé avant tout, mais d'autres chercheurs sont d'avis que l'activation des aluminates exerce une plus grande influence (3). Fut également notée la désactivation de C_3A lors du stockage du ciment à l'air humide ou lors du broyage du ciment en présence d'humidité dans le broyeur (4, 5). Cette contradiction est liée au niveau de la teneur du ciment en composés alcalins et à la composition des aluminates. Selon (3), une fausse prise est due en particulier à la présence dans les aluminates de $C_{12}A_7$. Dans un de nos travaux nous avons montré la disposition des ciments comprenant NC_8A_3 pour le mottage et la fausse prise (6, 7). L'hydratation superficielle peut avoir lieu à l'air complètement sec, car une quantité d'eau introduite dans le broyeur pour le refroidissement ou avec le laitier granulé est suffisante pour provoquer cette hydratation ; lors du stockage du ciment dans le silo la température élevée conduit à l'hydratation de C_3A par l'eau de cristallisation provenant du gypse (8). Ce phénomène s'observe également en cas de broyage fin du ciment, C_3S et C_3A étant soumis eux aussi à l'hydratation superficielle (3, 6). Ceci est dû évidemment à la formation de liaisons de valence libres saturées en eau adsorbée.

Le rôle du gaz carbonique atmosphérique présente un intérêt tout particulier. Les difficultés d'ordre linguistique sont évidemment la cause de ce que l'observation importante de B. Beke (9) sur l'adsorption de CO_2 par le ciment broyé est peu connue. Ceci témoigne d'une grande activité du gaz carbonique en tant qu'agent capable de prendre part à la saturation des centres actifs de la surface du ciment. En même temps, dans les ciments finement broyés on peut observer souvent, surtout lorsqu'il y a beaucoup de vapeur dans les broyeurs, des grains de carbonates (10), ce qui témoigne d'une importance considérable de cette interaction rapide. Toutefois, on se représente le plus souvent la carbonisation comme un processus lent, ce qui est vrai pour les bétons mais ne l'est guère pour l'hydratation superficielle du ciment dans le milieu air-vapeur.

En partant de ces considérations, deux d'entre nous ont abouti à l'hypothèse que l'élimination de CO_2 de l'atmosphère, lors de l'hydratation superficielle du ciment, pourrait prévenir la saturation des centres actifs avec formation de $CaCO_3$ inerte et accélérer l'hydratation du ciment grâce à la découverte d'une nouvelle surface pour l'interaction ultérieure. Dès les premières expériences cette hypothèse fut confirmée (11). Dans cette communication on donne les résultats d'études plus détaillées de ce problème.

MATERIAUX DE DEPART. Dans nos expériences nous avons utilisé des constituants de clinker synthétisés par cuisson et des clinkers industriels de composition différente (Tableau I) broyés avec et sans gypse dans le broyeur d'essais jusqu'à obtenir une surface spécifique de 3000 à 3500 cm^2/g (d'après la méthode de perméabilité à l'air).

TABLEAU I

Composition des clinkers industriels, % en masse

n°s	Pertes à la calcination	SO_3	Na_2O	K_2O	C_3S	C_2S	C_3A	C_4AF
1	0,15	0,78	0,08	0,73	49	30	3	14
2	0,68	0,30	0,14	0,35	52	25	1	16
3	0,88	0,26	0,29	0,30	58	19	5*)	15
4	0,17	0,35	0,15	0,22	58	21	7	13
5	0,05	0,44	0,20	0,30	60	17	7	14
6	0,51	0,20	0,12	0,22	67	11	3	17

*) 50 % de NC_8A_3.

METHODOLOGIE DES ETUDES. Les constituants de clinker et les ciments étaient soumis à la conservation dans l'atmosphère d'air humide avec et sans CO_2 dans des conditions statiques (exsiccateurs) et dynamiques (succion à travers la couche) pour simuler respectivement la conservation dans les sacs et les silos à la température normale du milieu. Après la fin de la préhydratation de durée déterminée, ces matériaux étaient étudiés par les méthodes de l'analyse thermique différentielle, de l'analyse aux rayons X et par la méthode électronique microscopique et utilisés pour la préparation des éprouvettes afin de déceler l'influence des conditions de la préhydratation superficielle sur la structure d'hydratation ; ensuite la structure de leurs fragments était étudiée par les méthodes susmentionnées. Ces échantillons étaient conservés, dans les régimes habituels, à l'air humide à CO_2 et dans l'eau. Pour tenir compte de la température du milieu on a procédé aux expériences dans deux cimenteries. Des silos industriels (un silo à chaque cimenterie) étaient pré-

alablement équipés d'un système d'épuration de l'air utilisé pour l'aérage contre CO_2 atmosphérique. L'efficacité de l'épuration était contrôlée par titrage d'une solution alcaline barbotée par le gaz. On a étudié les échantillons moyens du ciment stocké pendant des durées différentes dans les silos aménagés et les silos ordinaires aérés par l'air avec CO_2, par les méthodes de l'analyse physico-chimique et contrôlé leur hydraulicité. Quelques résultats obtenus sont donnés plus bas.

RESULTATS DES EXPERIENCES. ADSORPTION DE L'EAU EN PRESENCE ET EN L'ABSENCE DE CO_2. Sur la figure 1 sont représentées les données sur la sorption pondérale de l'humidité par les minéraux et ciments en présence et en l'absence de CO_2, de l'air dont l'humidité relative est de 100 %. Les données obtenues témoignent que la série d'activité des minéraux quant à l'absorption de l'humidité sans CO_2 : $NC_8A_3 > C_3A > C_3S > C_4AF > \beta - C_2S$, est en bon accord avec les résultats des nouvelles études sur l'absorption des agents tensio-actifs à partir des solutions benzéniques (12) et de la phase de vapeur (20) et traduit donc l'activité relative et la concentration des microzones de réaction sur la surface des minéraux. La série d'activité pour l'absorption d'humidité en présence de CO_2 se présente sous une autre forme : $NC_8A_3 > C_4AF > C_4AF > C_3A > C_3S > \beta - C_2S$.

Une analyse plus détaillée d'un échantillon d'alumoferrite utilisé dans ces expériences a montré que dans ce dernier il y a des marques de décomposition réductrice avec la formation éventuelle des microzones de $C_{12}A_7$ conformément au mécanisme proposé dans (13) : $C_4AF = C_{12}A_7 + C_2F + CF + C$. Cependant ceci n'influait pas sur l'activité du minéral en l'absence de CO_2. La présence de CO_2 augmente en général la quantité d'humidité absorbée par les minéraux, de sorte qu'on ne peut pas parler de l'"intoxication" des zones de réaction actives en présence de CO_2, c'est pourquoi on préfère le terme de "saturation". La vitesse et le degré d'absorption de l'humidité par les ciments est en somme en bon accord avec les données pour les minéraux, compte tenu d'une composition en phases différente des ciments. Ceci n'est pas étonnant : dans les conditions de l'expérience on a exclu l'effet d'écran exercé sur un minéral dans le ciment par un autre et si l'humidité du milieu était de 100 %, les différences connues dans le submicrorelief de la surface des minéraux séparés n'avaient pas d'importance (10) ; pour une pression relative plus basse de la vapeur d'eau, ces différences conduisaient à une adsorption prédominante de l'humidité sur C_3S (du milieu dont l'humidité relative est inférieure à 70 %) en comparaison de C_3A dans le travail (3). Ce fait explique également les données de Gebauer (2) sur l'activation de l'alite.

Il faut tout spécialement souligner une activité superficielle élevée du ciment contenant NC_8A_3 qui dépassait tous les autres en ce qui concerne la vitesse et la

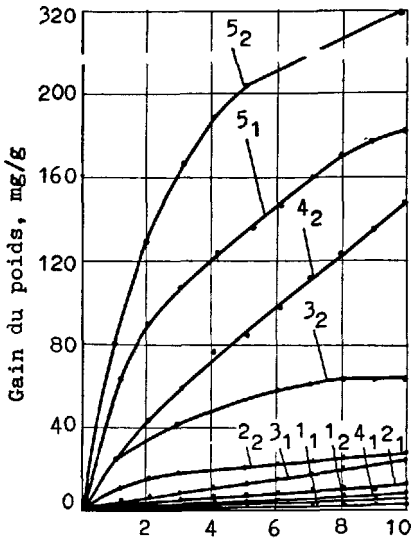

Fig. 1a

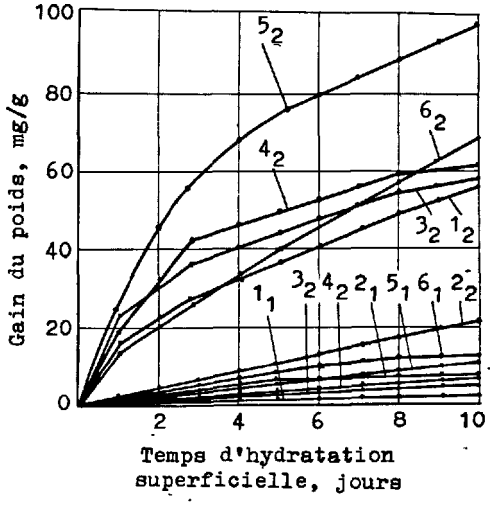

Fig. 1b

Fig. 1 - Cinétique de la sorption de la vapeur d'eau par a) les constituants de clinker et b) les ciments. a) 1_1; 2_1; 3_1; 4_1; 5_1 - C_2S ; C_2S ; C_3A ; C_4AF ; NC_8A_3 - courbes d'absorption d'humidité sans CO_2 ; 1_2; 2_2; 3_2; 4_2; 5_2 - idem, en présence de CO_2 atmosphérique. b) 1_1; 2_1; 3_1; 4_1; 5_1; 6_1 - courbes d'absorption d'humidité par les ciments de 1 à 6 sans CO_2 ; 1_2; 2_2; 3_2; 4_2; 5_2; 6_2 - idem, en présence de CO_2 atmosphérique.

quantité d'humidité absorbée, surtout en présence de CO_2. D'autre part, il est bien connu que NC_8A_3 présente une activité moindre que C_3A lors de l'hydratation dans le milieu aqueux (14). Pour expliquer cette contradiction, on peut évidemment s'adresser aux idées développées dans le travail (15) où NC_8A_3 est considéré comme un système complexe comprenant les microzones des oxydes de Na et de Ca libres ainsi que de $C_{12}A_7$. Il va de soi que la diminution de solubilité de la chaux grâce aux ions Na dans la phase liquide, qui limite l'activité hydraulique de NC_8A_3, est remplacée par l'intensification de l'adsorption de H_2O et de CO_2 atmosphériques sur la surface contenant Na^+. L'activité de $C_{12}A_7$ s'explique partiellement par la présence sur sa surface d'électrons libres (14).

Comme il fallait s'y attendre, les études de la composition en phases des hydrates superficiels formés montrèrent la formation de $CaCO_3$ et des carbo-aluminates ou de leurs solutions solides avec ferro-aluminates lors de l'hydratation de C_3S, C_2S et de C_3A, C_4AF respectivement, sous l'action de CO_2 de l'air. Les autres produits d'hydratation superficielle étaient identiques dans les deux milieux, mais il y avait les distinctions principales quantitatives et structurales suivantes. Lors de la préhydratation dans le milieu avec CO_2, il se forme sur la surface des particules de ciments et de C_3S des quantités importantes de $Ca(OH)_2$ cristallin fixé nettement par toutes les méthodes physico-chimiques, alors que les hydrosilicates de calcium formés ne sont repérables, même dix jours durant, ni par méthode pétrographique ni aux rayons X. Lors de la préhydratation dans le milieu sans CO_2, il se forme principalement $Ca(OH)_2$ amorphe et on peut fixer les hydrosilicates de Ca bien qu'en petite quantité. Par conséquent, en présence d'humidité CO_2 sature les microzones actives de la surface des constituants de clinker et en accélère, lors de l'hydratation superficielle, la destruction du réseau cristallin en contribuant à la séparation des complexes calcio-oxygénés au profit de la couche externe des particules. Il faut prendre en considération que les centres actifs dans les microzones de réaction de la surface de tous les constituants de clinker ne sont représentés que par les ions Ca et O (18). En détachant les ions Ca et O, le CO_2 contribue à la formation dans la couche externe des particules de centres de cristallisation tout faits - germes en $Ca(OH)_2$ cristallin moins soluble dans l'eau lors de l'hydratation ultérieure que $Ca(OH)_2$ amorphe. On peut supposer que les hydrosilicates qui apparaissent après la préhydratation dans le milieu privé de CO_2 peuvent également servir de centres de cristallisation pour C-S-H (II) lors de l'hydratation "aqueuse" ultérieure. On en vient ainsi à la conclusion que la présence de CO_2 dans l'air peut conduire à l'augmentation de la teneur en portlandite lors de l'hydratation ultérieure du ciment, et l'effet utile de la préhydratation du ciment par l'air humide libre de CO_2 (11) est dû à la diminution de la teneur relative en portlandite et à l'augmentation de la part des hydrosilicates de calcium.

ACTIVITE D'HYDRATATION DE C_3S ET DES CIMENTS APRES LA PREHYDRATATION SUPERFICIELLE DANS DEUX MILIEUX. En résumant brièvement les résultats des expériences, notons que le traitement de C_3S et des ciments par l'air humide au cours de 1 à 10 jours en présence de CO_2 atmosphérique entraîne une perte considérable de l'hydraulicité de 20 à 70 % à mesure que le temps de traitement croît. Par contre, en l'absence de CO_2, l'activité de C_3S et des ciments augmente (tableau II). Dans ce cas l'optimum de temps de traitement est de 3 à 7 jours. Le gain de résistance est de 20 à 50 % de la résistance des échantillons témoins (et même beaucoup plus si l'on tient compte de la diminution d'activité en présence de CO_2). Le traitement ultérieur dans ce milieu diminue la résistance tant dans les conditions statiques que dynamiques. Les expériences industrielles ont confirmé le fait que l'absorption de CO_2 à partir de l'air d'aération peut être appliquée en pratique pour augmenter l'activité du ciment (voir tableau II). Dans ce cas le temps de conservation ultérieure dans le silo du ciment traité n'est pas limité.

TABLEAU II

Rapport entre la résistance de C_3S et des ciments et la durée de durcissement, kgf/cm^2

Matériau	Traitement	3 jours	7 jours	28 jours
C_3S	T	205	271	403
	I	281	364	532
	II	180	266	311
Ciment n°2 (voir tabl. I)	T	150	240	300
	I	235	310	378
	II	140	200	265
Ciment n°2*	T	97	196	347(302**)
	I	136	222	412(410**)
	II	-	-	-
Ciment n°4	T	197	316	486
	I	226	359	567
	II	138	265	326
Ciment n°4*	T	197	320	503(397**)
	I	226	367	515(515**)
	II	-	-	-

Note : T - échantillon témoin. I - préhydratation superficielle par l'air humide sans CO_2. II - idem, en présence de CO_2 atmosphérique. *) Ciments industriels aérés dans les conditions industrielles et essayés

d'après GOST 310-60. **) Après la conservation de 6 mois.

Il est établi également que cet effet ne concerne pas seulement l'accroissement de résistance, car après le traitement le besoin en eau diminue et la maniabilité des materiaux a base de ce ciment se trouve améliorée. Lors de son stockage ultérieur a l'air, l'activité ne diminue pas au cours de 6 mois. Nous expliquons ce fait par un effet d'écran exercé sur les particules par une couche comprenant C-S-H (II) dont la carbonisation, comme il est connu de (19), est de trois ordres de grandeur plus lente que celle de la portlandite.

ETUDE DE LA COMPOSITION EN PHASES DES PRODUITS D'HYDRATATION ET DE LA STRUCTURE D'HYDRATATION DE C_3S ET DES CIMENTS PREHYDRATES DANS DEUX MILIEUX. On a mis à l'étude les échantillons de C_3S et de ciments durcis sans prehydratation et après la prehydratation dans deux milieux : avec CO_2 et sans CO_2. Comme on supposait, les résultats de l'analyse thermique différentielle et de l'analyse aux rayons X avaient permis de fixer après 3, 7, 28 jours de durcissement l'accroissement de teneur en portlandite dans une série d'échantillons II > T > I tant dans C_3S que dans les ciments hydratés étudiés. Il est difficile de faire une évaluation quantitative sûre de la teneur en hydrosilicates, c'est pourquoi on a préféré l'étude de la submicrostructure par la méthode électronique microscopique, ce qui a permis d'obtenir certaines preuves d'une cristallisation complète et nette d'hydrosilicates de Ca dans les échantillons prehydratés en l'absence de CO_2.

Dans l'immédiat nous nous proposons de publier les données obtenues pour les autres minéraux et ciments. On y observe des différences notables dans la teneur des échantillons en carboaluminates et en C_3AH_6 ainsi qu'une formation anomale du gel d'hydroxyde de Al. Ces différences exercent une influence considérable sur la résistance du matériau. Font semble-t-il exception les matériaux a agrégats carbonatés, car on sait que la formation des carboaluminates dans les zones de transition a un effet positif (19).

BIBLIOGRAPHIE

1.- W.C. HANSEN (1962), "False set in Portland cement" - IV International Symposium of the Chemistry Cement, Washington, 1960. Procedings, NBS Monograph, v. 2, 387-403 (en anglais).

2.- I. GEBAUER (1978), "Technologische Möglichkeiten zur Vermeidung des Frühansteifens von Zement". Verfahrenstechnik der Zementherstellung VDZ Kongress, 1977, Bauverlag, Wiesbaden-Berlin, 682-685 (en allemand).

3.- Б.Э. ЮДОВИЧ, М.Т. ВЛАСОВА, В.Н. КАЛЬЯНОВА, В.И. ГУСЕВА (1977) "Поверхностные явления в высокомарочных портландцементах и ложное схватывание". Труды НИИЦемента, № 46, с 40-56, (en russe).

4.- T. KODAMA, T. NIEDA (1975), "The deterioration of quality and the aeration phenomenon of sacked cement left in the air for a longtime". Rev.29th.Gen. meeting Cem.Assoc.Jap., Tokyo, 62-64.

5.- S. SPRUNG (1974), "Einfluß der Mühlenatmosphäre auf das Erstarren und die Festigkeit von Zement", Zement-Kalk-Gips, B.27, 259-268 (en allemand).

6.- Ю.С. МАЛИНИН, В.П. РЯЗИН, Л.С. БАТУТИНА, А.С. ШЕВЦОВ (1977) "Устранение причин комкования цементов" Цемент, № 7, с 17-18, (en russe).

7.- W. RICHARTZ (1973), "Einfluß der Lagerung auf die Eigenschaften des Zements". Zement-Kalk-Gips, 26, N° 2, 64-67 (en allemand).

8.-S. SPRUNG (1978), "Einfluß der Lagerungsbedingungen auf die Zementeigenschaften" кн. в ссылке (2), 686-695 (en allemand).

9.-B. BEKE (1963), "Apritaselmelet.Akad. Kiado, Budapest, 132-139 (en hongrois).

10- О.М. АСТРЕЕВА, Л.Я. ЛОПАТНИКОВА (1959) "Петрография вяжущих материалов", Москва, с. 164, (en russe).

11- Ю.С. МАЛИНИН, Н.Д. КЛИШАНИС (1970) "Способ получения портландцемента" Авт. св-во СССР, № 261232, БИ № 4, (en russe).

12- Г.М. ТАРНАРУЦКИЙ, Б.Э. ЮДОВИЧ, И.В.КРАВЧЕНКО (1977) "Исследование адсорбции ПАВ на цементе и составляющих его минералах". Труды НИИЦемента, № 32, с.74-91, (en russe).

13- З.Б. ЭНТИН, Б.Э. ЮДОВИЧ, М.Т. ВЛАСОВА и др. (1978) "Модель жидкофазного механизма образования алита в спекаемом портландцементном клинкере. Тезисы докладов на У Всесоюзн. совещании по химии цемента, Москва, с.67-68, (en russe).

14- Ю.С. МАЛИНИН, В.П. РЯЗИН, К.Г. КОЛЕНОВА (1972) "Свойства соединения NC_8A_3 и его влияние на гидравлическую активность клинкера", Цемент, № 1, с.20-21, (en russe).

15- А.И. БОЙКОВА, В.А. ПОНОМАРЕВА, А.И. ДОМАНСКИЙ, М.М. ПИРЮТКО (1976) "Состав и гидратационная активность алюминатной фазы клинкера", Цемент, № 6, с.20-22 , (en russe).

16- Б.Э. ЮДОВИЧ, М.Т. ВЛАСОВА и др. (1978) "Особобыстротвердеющие цементы для сборного железобетона", Москва, с.60, (en russe).

17- S. BRUNAUER (1957) "Surface energies of solids" II International Congress of Surface activitg. Proceedings, v. 2 , London, с 17-21, (en anglais).

18- М.А. СОРОЧКИН, А.Ф. ЩУРОВ, Н.Б. УРЬЕВ (1970) "Воздействие углекислого газа

как метод интенсификации процессов гидратации цемента". Доклады АН СССР, т.194, № 1, с 149-151, (en russe).

19.- I. FARRAN (1956) "Revue des Matériaux de Construction", N° 492, c.191-209, (en français).

20.- Ф.Л. ГЛЕКЕЛЬ (1979) "Коллоидный журнал", № 4, (en russe).

Structure and thermal creep of cement paste

Structure et fluage thermique de la pâte de ciment

L.J. PARROTT, Dr, Cement and Concrete Association, Slough, U.K.

SUMMARY : The effects of temperature history upon the creep of concrete must be considered if analyses of the stresses in engineering structures are to be realistic. Recent studies indicate that the creep behaviour of concrete subjected to variable temperatures is largely controlled by the cement paste matrix. An important feature of the creep of cement paste is that heating prior to loading reduces creep while virgin heating after loading greatly increases creep. The objectives of the present work are to identify changes in cement paste that cause or correlate with this particular creep behaviour, so that reliable advice concerning the prediction and control of thermal creep can be provided. Heating a mature, saturated cement paste from 20°C to 60°C was found to have little effect upon the bound water content as determined by thermogravimetry. Quantitative X-ray diffraction results also indicated that continued hydration of the cement minerals was not significant. Changes in silicate structure due to heating were observed and in particular an increase in polysilicate formation was noted. Some changes in sorption behaviour were also observed. The measured creep rates correlated closely with changes in polysilicate formation for a variety of conditions which included heating prior to loading and heating after loading. The results are considered in terms of a simple hypothesis in which the creep rate increased when a load-bearing part of the cement paste structure suffered a phase change. Thus heating prior to loading limited the potential for further phase change and consequently reduced creep whilst virgin heating after loading produced a large phase change and a substantial increase in creep.

RÉSUMÉ : Les effets de la température sur le fluage du béton doivent être pris en considération si l'on veut que les analyses de contraintes dans les ouvrages de génie civil soient valables. De récentes études indiquent que le fluage du béton soumis à des températures variables est largement contrôlé par le comportement de la pâte de ciment. Une caractéristique importante du fluage de la pâte de ciment réside dans le fait que son chauffage avant mise en charge réduit considérablement le fluage alors que son chauffage uniquement après mise en charge l'augmente considérablement. Le but des travaux actuels est de déterminer quels changements se produisant dans la pâte de ciment provoquent ce comportement directement ou indirectement afin que des conseils plus judicieux puissent être offerts à l'égard de la prédiction et du contrôle du fluage thermique. Le chauffage d'une pâte de ciment saturée ayant atteint la maturation, de 20°C à 60°C, s'avéra avoir peu d'effet sur la teneur en eau latente déterminée par thermogravimétrie. Les résultats d'une radiodiffraction quantitative indiquèrent également que l'hydratation permanente des minéraux du ciment n'était pas significative. Des changements furent observés dans la structure des silicates; une augmentation des polysilicates fut en particulier notée. Des changements d'absorption furent également observés. Les taux de fluage mesurés étaient étroitement liés aux changements observés dans la formation de polysilicates dans diverses conditions y compris le chauffage avant mise en charge et après mise en charge. Les résultats permettent d'émettre le simple hypothèse selon laquelle le taux de fluage augmente lorsqu'une partie portante de l'ouvrage en pâte de ciment subit un changement de phase. Ainsi, le chauffage de la pâte avant la mise en charge limite les possibilités d'autres changements de phase et réduit donc le fluage alors qu'un chauffage uniquement après la mise en charge entraîne un changement de phase important et par conséquent une augmentation considérable du fluage.

INTRODUCTION

An earlier report showed that the creep of cement paste was very sensitive to temperature history and that heating of even a mature cement paste after loading increased creep considerably (1). This increase was not associated with continued hydration of the cement as assessed by quantitative X-ray diffraction measurements or thermogravimetry (2). There were indications that the pore structure of the paste was modified during heating (2) and this may have influenced the creep behaviour. Changes in the silicate structure of the paste were also observed and these changes and their relationship with the measured creep are the main subject of the present paper.

EXPERIMENTAL

The creep experiments have already been reported in detail (1) so only the main features of the experiments will be described here. 12 x 12 x 110 mm prisms of saturated, hardened cement paste (water/cement ratio = 0.47 by weight) were loaded at ages of 28 or 189 days and creep strains were measured at 20°C. The temperature of certain prisms was raised from 20°C to 60°C (8°C/hour) at ages of 42 or 203 days and the resultant increase in creep was observed. Control samples of the cement paste were crushed and ground to a fine powder (particle size <0.3 mm) at preselected intervals throughout the creep test. Immediately after grinding, the powder was used for analysis of the silicate structure of the cement paste. The method (3) involved dissolving the powdered cement paste in methanolic hydrochloric acid to yield a silicic acid and then complexing the silicic acid with ammonium molybdate. The formation of the resulting, yellow coloured molybdosilicic acid complex was monitored continuously with the aid of a spectrophotometer. The rate of formation of the molybdosilicic acid complex was slower the higher the degree of condensation of the original silicic acid. With suitable analysis of the reaction curve (3) the silicate structure of a cement paste could be determined in terms of:

a) Proportion of silicate present as monomer
b) " " " " " dimer
c) " " " " " polymer
d) Complexing reaction rate constant for polysilicate, which is related to its degree of condensation
e) S_{300}, the amount of silica unreacted after 300 seconds of complexing.
This is a parameter that is approximately proportional to the product of the proportion of polysilicate and its average degree of condensation (3).

RESULTS AND DISCUSSION

The creep results shown in Figure 1 clearly illustrate the large increases in creep that are associated with heating after loading. Figure 1 also shows the development of S_{300} with age at 20°C and after heating to 60°C: it can be observed that there is a striking similarity to the creep curves. One aim of this study was to check the hypothesis that a phase change in a load-bearing part of the cement paste structure would increase creep because of the local increase in compliance associated with the molecular rearrangement. The changes in creep after heating

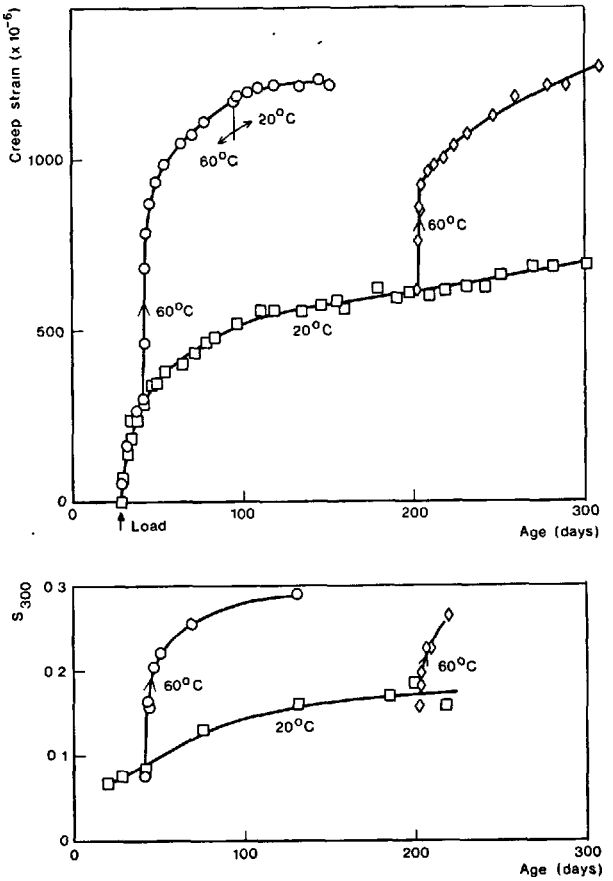

Fig. 1 Development of creep strain and S_{300}, a measure of polysilicate formation, with age and temperature.

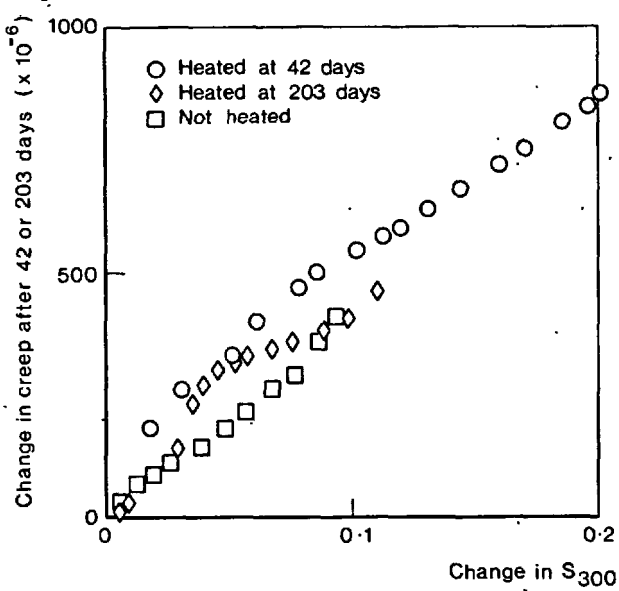

Fig. 2 Change in creep versus corresponding change in polysilicate as indicated by S_{300}.

are plotted in Figure 2 against the corresponding estimates of the changes in $S_{3\,00}$. Figure 2 also contains data pertaining to creep and polysilicate development at 20°C. It can be seen that although there is some dispersion of the results, for different temperature histories the measured creep is fairly closely related to concurrent changes of the polysilicate and may thus be regarded as consistent with the hypothesis above. It should be noted, however, that the initial creep measured at 20°C during the two weeks after loading develops very rapidly and does not correlate with $S_{3\,00}$. It seems from creep recovery tests that the initial creep is associated with the development of a small recoverable component of creep while the creep that correlates with polysilicate development is mainly irrecoverable. The mainly irrecoverable nature of the creep associated with heating would be expected from the hypothesis above and is consistent with earlier work (4) which demonstrated that heating prior to loading reduced the irrecoverable component of creep but not, to any great extent, the recoverable component.

The nature of polysilicate formation was studied using the analytical technique outlined in reference 3. At 20°C hydration of the Portland cement involved very little change in the proportion of polysilicate between ages of 28 and 220 days and the increase in $S_{3\,00}$ could be attributed mainly to an increase in the degree of condensation of the polysilicate. However, heating at 60°C increased both the proportion of polysilicate and its degree of condensation. The increase in proportion of polysilicate after the start of heating was accompanied by a decrease of similar magnitude in the proportion of dimer. Heating to 60°C at an age of 203 days did not cause any significant change in the proportion of monomer. This was consistent with the observed constancy of the alite and belite concentrations and of the bound water content (2) under the same conditions, if it was assumed that monosilicate derived from the anhydrous cement. Such an assumption seems reasonable on the basis of the C_3S hydration studies of Dent Glasser et al (5). Thus it appears that at 60°C polysilicate is formed at the expense of disilicate hydrates while at 20°C polysilicate development involved conversion of existing polysilicate to a more highly condensed form. This difference in behaviour at the two temperatures may be partly responsible for the dispersion of the results in Figure 2.

The present study has some bearing upon the prediction and control of creep in concrete structures, particularly where the concrete is likely to be heated. It appears from Figure 2 that the components of creep strain that were termed flow and transitional thermal creep by Illston and Sanders (6) may be similar in nature. It may therefore be profitable to relate the sum of these components (i.e. the total irrecoverable creep) to a function that embodies the relationship between temperature history and polysilicate development. A further corollary of the present study is that a major part of creep seems to be related to changes in the main hydration products of Portland cement, the calcium silicate hydrates. Thus control of creep is unlikely to be affected by controlled selection of the aggregate or the cement. The most effective means of minimising creep at the present time is to heat the concrete before loading; however this may not completely eliminate transitional thermal creep (1).

Relationships between the creep and microstructure of calcium silicate hydrates (CSH) have recently been examined by workers at the University of Illinois (7). Their results showed that basic creep (i.e. creep without drying) was associated with an increase in surface area measured by nitrogen although the surface area measured by water and the silicate structure were unaffected by sustained loading. The data were interpreted in terms of new surface being exposed to nitrogen as a result of micro-shearing or relative sliding of CSH crystallites. Distortion and buckling of the thin crystallites under sustained load could presumably cause an increase in surface available to nitrogen also. This second possibility can explain the high creep strains that were observed in the present study after the creep prisms had been heated:- Redistribution of water in the micropores of cement paste occurs after heating but published data (8) and the present results on unloaded prisms indicate that equilibrium is achieved very rapidly (i.e. a few hours) compared with the development of transitional thermal creep. Indeed close examination of initial transitional thermal creep strains indicates that during the first 10 hours after heating only 10% of the additional creep developed. Thus enhanced micro-shearing of water between crystallites was not thought to be a dominant process for creep at 60°C. However internal rearrangement of silica at 60°C could enhance distortion of the crystallites under sustained load and the rate of creep would then be related to the rate of polysilicate development, as indicated in Figure 2.

On a more general level it should be noted that the concept of creep being related to a phase change is not confined to the effects of silicate structure changes. Greenwood and Johnson (4) accounted for the increase in creep of metals during heating by a thermally induced structural transition. Also reanalysis of some earlier work by the author (10) indicates that carbonation can induce internal changes in cement paste that enhance creep. The effect is illustrated in Figure 3 and can be

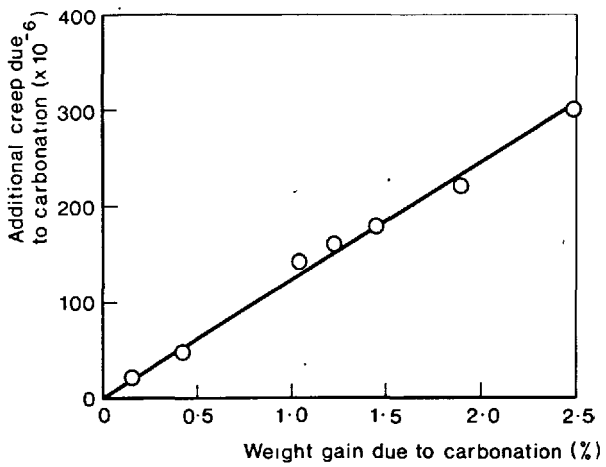

Fig.3 Increase in creep versus weight gain for carbonating cement paste

explained by a mechanism similar to the one proposed by Powers (11) for carbonation shrinkage: creep is increased due to chemical erosion of the load-bearing cement hydrates. There is also evidence to suggest that with very early ages of loading (i.e. less than 7 days) creep is enhanced by simultaneous hydration of the cement (12).

The present work is in its infancy and before any mathematical models of creep can be reliably developed further experimental data on creep and changes in structure are required. In the author's laboratory a study of the relationship between creep and the physical and chemical structure of hydrated C_3S is in progress. The study will include a close examination of pore structure changes for a range of load and temperature histories.

CONCLUSION

The experimental results relating to creep, physical structure and chemical structure of a saturated cement paste suggested that long-term creep at 20°C and the increase in creep after the temperature of the loaded prism was raised to 60°C were closely related to the development of polysilicate in the cement hydrates.

ACKNOWLEDGEMENTS

The author gratefully acknowledges the assistance of the following members of the Materials Research Department of the Cement and Concrete Association with the experimental work and the reporting of this project: Mr W A Gutteridge, Mr J A Martin, Dr C D Pomeroy and Mr M G Taylor.

REFERENCES

1. - L.J. PARROTT (1979), "A study of the transitional thermal creep in hardened cement paste", Magazine of Concrete Research, Vol.31, No.107, June, 99-103.

2. - L.J. PARROTT (1979), "Changes in saturated cement paste due to heating", Cement and Concrete Association Technical Report 42.528, August.

3. - L.J. PARROTT AND M.G. TAYLOR (1979), "A development of the molybdate complexing method for analysis of silicate mixtures", Cement and Concrete Research, Vol.9, No.4.

4. - L.J. PARROTT (1977), "Recoverable and irrecoverable deformation of heat-cured cement paste", Magazine of Concrete Research, Vol.29, No.98, March, 26-30.

5. - L.S. DENT GLASSER, E.E. LACHOWSKI, K.MOHAN and H.W.F. TAYLOR (1978), "A multi-method study of C_3S hydration", Cement and Concrete Research, Vol.8, No.6, 733-740.

6. - J.M. ILLSTON AND P.D. SANDERS (1974), "Characteristics and prediction of creep of a saturated mortar under variable temperature", Magazine of Concrete Research, Vol.26, No.88, September, 169-179.

7. - A.BENTUR, R.L. BERGER, N.B. MILESTONE, S. MINDESS, F.V. LAWRENCE, JR and J.F.YOUNG (1979), "Creep and drying shrinkage of calcium silicate pastes. Part III A hypothesis of irreverisble strains", Cement and Concrete Research, Vol.9, No.1, 83-96.

8. - R.A. HELMUTH (1961), "Dimensional changes of hardened Portland cement pastes caused by temperature changes", Proc. Highway Research Board, Vol.40, 315-336.

9. - G.W. GREENWOOD and R.H. JOHNSON (1965), "The deformation of metals under small stresses during phase transformations", Proc. Royal Society, Series A, Vol. 283, No. 1394, January, 403-422.

10. - L.J. PARROTT (1975), "Increase in creep of hardened cement paste due to carbonation under load", Magazine of Concrete Research, Vol. 27, No.92, September, 179-181.

11. - T.C. POWERS (1962), "A hypothesis on carbonation shrinkage", Journal of P.C.A. Research and Development Laboratories, Vol.4, No.2, May, 40-50.

12. - R.S. GHOSH (1972), "Creep of Portland cement at early ages", Materials and Construction, Vol. 5, No. 26, 93-97.

The effect of the water reducer addition on the rheological properties of cement pastes

L'influence de l'addition de fluidifiants sur le comportement rhéologique de pâtes de ciment

R.LAPASIN, Istituto di Chimica Applicata e Industriale, Universita di Trieste,
V. LONGO, Istituto di Chimica Applicata e Industriale, Universita di Trieste,
S. RAJGELJ, Istituto di Scienza delle Costruzioni, Universita di Trieste, Italie.

RESUME : On a étudié l'influence de l'addition de trois fluidifiants à base de lignosulfonates et d'un superplastifiant à base de résines de mélamine sur le comportement rhéologique de pâtes de ciment.
Les essais expérimentaux effectués ont permis de déterminer, pour différentes vitesses de déformation, la contrainte de cisaillement maximale, la cinétique de destruction et la contrainte de cisaillement d'équilibre.
On a observé la présence, pour chaque fluidifiant examiné, d'une concentration critique relativement aux divers aspects considérés : la dépendance du temps, la contrainte de cisaillement d'équilibre et maximale, le comportement thixotropique. En ce qui concerne le comportement en fonction du temps (du type partiellement thixotropique), on a trouvé que la fonction de transfert τ-t peut être décrite par deux modèles, pour des valeurs de $\dot{\gamma}$ différentes, et que le type de fonction de transfert ne dépend pas de la nature et de la concentration du fluidifiant, tandis que son amplitude est affectée par la concentration en fluidifiant. La concentration atteint une valeur critique au minimum de l'amplitude. L'étude des valeurs d'équilibre et maximales montre que, lorsque la concentration du fluidifiant augmente, la viscosité d'équilibre diminue, tandis que la viscosité maximale atteint un minimum et ensuite augmente dans le cas des lignosulfonates et reste presque invariable dans le cas du superplastifiant. Le comportement thixotropique a été caractérisé par des grandeurs significatives, en particulier par un paramètre structurel; le paramètre de distance d , évalué sur la base d'essais effectués précédemment sur des pâtes sans additifs pour différents rapports eau/ciment et SSB. La destruction thixotropique maximale a lieu à la concentration critique. L'étude de l'influence des additifs sur le paramètre d a montré que l'adsorption superficielle ne suffit pas à expliquer entièrement l'action des fluidifiants à base de lignosulfonates.

SUMMARY : In the present work the influence of the addition of three lignosulphonate-based water reducers and of a melamine resin-based superplasticizer on the rheological behavior of cement pastes is evaluated.

The experimental tests permitted the determination, at different shear rates, of maximum shear stress, breakdown kinetics and equilibrium shear stress.

It was observed that, for each water reducer tested, there is a critical concentration relative to the various aspects considered: time-dependence, equilibrium and maximum shear stresses, thixotropic behavior. As regards the time-dependent behavior (partially thixotropic type), it was found that the transient τ-t can be described by two models, for different $\dot{\gamma}$ and that the type of transient is unaffected by the type and concentration of the water reducer, while its amplitude is dependent on the water reducer concentration. The concentration reaches its critical value, when the amplitude is at a minimum. An examination of equilibrium and maximum values shows that, as the water reducer concentration increases, equilibrium viscosity decreases, while maximum viscosity reaches a minimum beyond which it increases for the lignosulphonates and remains nearly constant for the superplasticizer. The thixotropic behavior was characterized through significant quantities, among which a structural parameter, the distance parameter d as derived from previous tests on pastes without additives at different water/cement ratio and SSB. The maximum thixotropic breakdown is reached near the critical concentration. The study of the influence of additives on the parameter d showed that the action of lignosulphonates-based water reducers cannot by fully accounted for by surface adsorption.

INTRODUCTION

The characteristics of a hardened cement paste such as compressive strenght, compactedness, impermeability, dimensional stability etc. improve with decreasing water content, upon which the workability of the fresh paste, necessary for a correct placeability, is inversely dependent. The water content of the mix must be properly selected to realize a compromise between the characteristics of the paste in the hardened and in the fresh state.

When it is necessary to obtain mixes with both high fluidity and excellent mechanical properties, water reducing admixtures, are added to the cement pastes.

In fact, when treated with water reducers, cement pastes undergo significant changes in rheological behaviour. Their viscosity decreases in the fresh state, while the characteristics of the pastes do not change appreciably in the hardened state.

So, it is possible to improve the workability of a mix at a given water content and to reduce the water content of a mix without modifying its workability.

The viscosity reduction can derive from the adsorption of water reducers onto cement particles and/or hydration products. The adsorption determines the breakage of inter particles links and the resulting dispersion of the particles (1-6). The dispersing effect can be connected with variations of zeta potential, and solid-liquid affinity, and/or steric hindrance action(7). Besides, admixtures can exert a physical action by lowering the surface tension of dispersing medium (1, 8-9). The addition of water reducers can result in a strong reduction of the rate of hydration process so that part of the hydration water remains free and can contribute to the fluidity of paste (10-11). The mode of action and effectiveness in improving the rheological properties of a paste depend on the chemical composition of the additive. Some admixtures which provide a particularly good dispersion of the cement agglomerates and are known as "superplasticizers" are based essentially on sulphonated naphtalene formaldehyde polymers or sulphonated melamine-formaldehyde polymers.

Studies carried out on different products have made it possible to locate optimum concentrations of water reducers in correspondence of which maximum viscosity reduction is attained (3-4). For superplasticizers, the viscosity reduction does not change appreciably beyond the optimum concentration. Therefore the effectiveness and the optimum concentration of a water reducing admixture has to be evaluated chiefly from the results of rheological measurements.

Many studies have been carried out on the rheological behavior of cement pastes, but many problems are still open, concerning the preparation of specimens, the characteristics of the measuring instruments and the experimental procedures.

In the present work, the variations of shear- and time-dependent properties of cement pastes with the addition of different types of water reducing admixtures and different concentrations of a same water reducing admixture were investigated with the aim to evaluate their effectiveness and to determine their optimum concentrations with respect to the properties considered.

For a global estimation of optimality from the technological point of view, a number of additional tests will be needed, to check that there are no adverse side effects, that the mechanical behavior in the hardened state is good, and, in the rheological field, the workability loss with time is negligible.

MATERIALS AND EXPERIMENTAL PROCEDURE

All the pastes were prepared from Portland Cement 425(density d = 3060 Kg/m^3, specific surface S_s = 1.105 m^2/cm^3 (equivalent to Blaine surface area SSB = 361 m^2/Kg), oversize screening residue: 1.2 on 90μ and 2.9 on 63μ) and tap water (hardness 20°F, pH 7.5).
The added water reducers were:
F1, .25 ÷ 2% refered to cement weight
F2, .10 ÷ 2% refered to cement weight
F3, .10 ÷ 2% refered to cement weight
F4, .25 ÷ 4% refered to cement weight
F1, F2, F3 belong to the class of lignosulphonates, while F4 is a superplasticizer based on melamine resins.

The cement volume fraction Φ is .449 (equivalent to water/cement ratio w/c = .4), in some checking tests .483 (equivalent to w/c = .35).

Each mix was prepared first by hand with a spatula and then mixed in a vanomixer, at two speeds, according to the following stirring time sequence (as specified for the mixing of standard mortar specimens) : 30s at v_1, 30s at v_2, 90s at rest, 60s at v_2 (v_1 = 36.65 rad/s, v_2 = 45.03 rad/s).

The rheological measurements were carried out at 25°C, with the rotating coaxial cylinder viscometer Rotovisko Haake 1, using the measuring heads Mk 50 and 500 and the device MV III with smooth cylinders (cup diameter 42 mm, bob diameter 30.4 mm, bob height 60 mm).
The measurable shear stress range is 15 ÷ 510 Pa.

Several experimental approaches have been proposed for the rheological characterization of cement pastes. They differ in the instruments and methods employed, so that the results obtained often differ too. The majority of the approaches are based on the use of coaxial cylinders viscometers, with smooth or serrated surfaces, with large or small clearance. The most frequently used method is the hysteresis cycle and either the up-curve or the down-curve is

taken as the representative flow curve. Both curves depend upon the shear acceleration and the maximum shear rate reached in the cycle, and therefore they cannot characterize uniquely the rheological behavior of a material.

In this work the rheological tests were performed at constant shear rates by using a new fresh sample for each shear rate. In this manner it was possible to determine, at different shear rates, the maximum shear stress, the breakdown kinetics and the equilibrium shear stress and from these values to draw the equilibrium flow curve.

RESULTS AND DISCUSSION

Transient behavior

When subjected to shear, cement pastes undergo a breakdown of their structure, which is not rebuilt in rest conditions. Fig. 1 gives an example of the partially thixotropic breakdown of the pastes, as it appears from the transient shear stress τ-time t obtained at constant shear rate $\dot{\gamma}$.

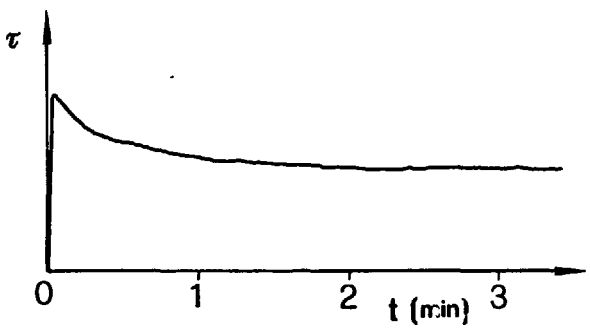

Fig. 1 - Typical transient behavior at constant shear rate

At low shear rates, the transients τ-t can be described satisfactorily by the model I:

$$\tau = \tau_e + C \exp(-Bt) \quad [1]$$

$$C = \tau_{max} - \tau_e \quad [2]$$

and, at higher shear rates, by the model II:

$$\tau = \tau_e + C_1 \exp(-B_1 t) + C_2 \exp(-B_2 t) \quad [3]$$

$$C_1 + C_2 = \tau_{max} - \tau_e \quad [4]$$

Similar transients have been determined by Tattersall (12) in a study of the influence of various technological parameters on the time dependent behavior of pastes. Tattersall states that different transient types can be noticed only by using coaxial cylinders with smooth surfaces.

The concentration and the type of water reducer do not substantially affect the type of transient. The transient amplitude (measured by C or $C_1 + C_2$) is larger at higher shear rates. The water reducer concentration influences the transient amplitude more than the breakdown kinetics, and a concentration can be found at which the transient amplitude reaches its minimum value.

Equilibrium and maximum shear stresses

As regards the equilibrium flow curves, it is impossible to find, among the models proposed (13-16), a single one suitable for all the pastes examined. In fact the progressive addition of water reducer influences the shape of the curves, as Fig. 2 shows.

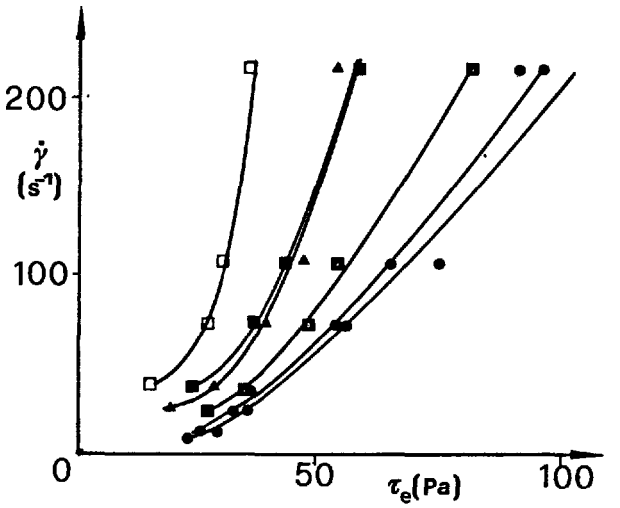

Fig. 2 - Equilibrium shear stress vs. shear rate for cement pastes containing F2 (Φ = .449; c = 0 (●), .1 (●), .3 (◘), .5 (■), 1 (□), 1.5 (▲))

Thus, the effect of the water reducer addition on the equilibrium behavior can be examined by comparing the viscosity values η_e at the various shear rates. Fig. 3 shows how viscosity decreases with increasing concentration of the water reducer. The maximum viscosity reduction amounts to 60% for F1, F2, F3 and to 85% for F4.

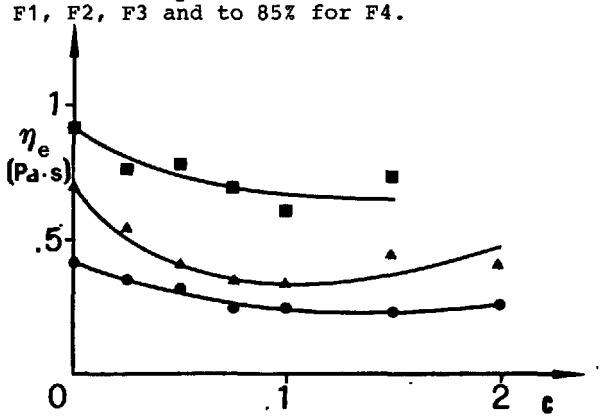

Fig. 3 - Equilibrium viscosity vs. F1 concentration (Φ = .449; $\dot{\gamma}$ = 216 s^{-1} (●), 108 s^{-1} (▲), 36 s^{-1} (■))

The initial stress overshoots τ_{max} determined at the various shear rates and the corresponding viscosity η_{max} define the rheological behavior of the structure initially present in the material at rest. Fig. 4 shows how the progressive addition of water reducer determines the pronounced shifting of τ_{max} curves towards the $\dot{\gamma}$ axis.

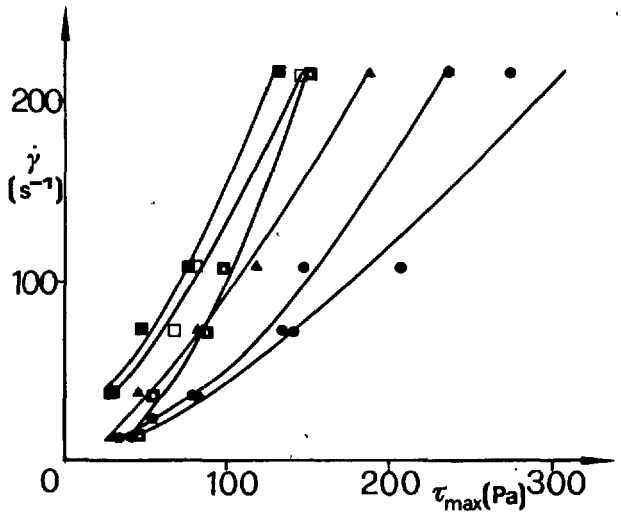

Fig. 4 - Maximum shear stress vs. shear rate for cement pastes containing F2 (Φ = .449; c = 0 (●), .1 (⊙), .3 (⧈), .5 (■), 1 (□), 1.5 (▲))

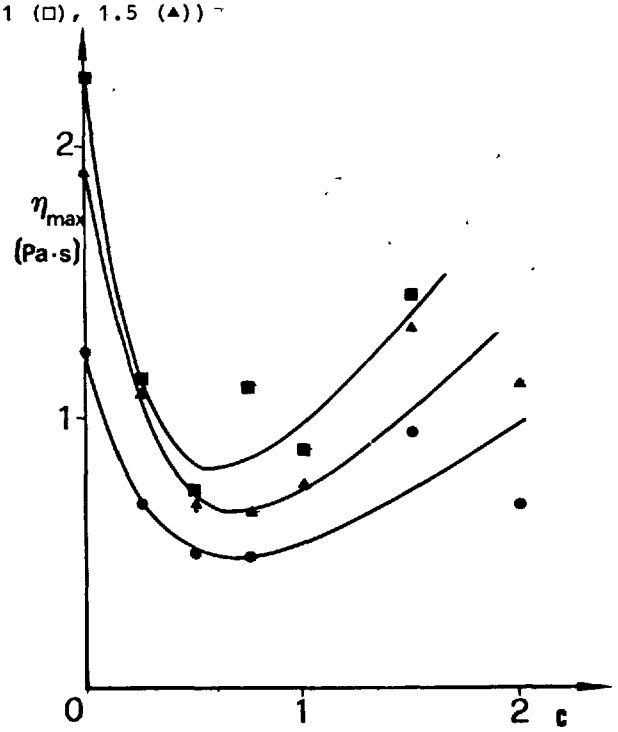

Fig. 5 - Maximum viscosity vs. F1 concentration (Φ = .449; $\dot{\gamma}$ = 216 s^{-1} (●), 108 s^{-1} (▲), 36 s^{-1} (■))

By plotting η_{max} versus the concentration of water reducer c, as in Fig. 5, it can be noted that there exists a critical concentration c_c at which η_{max} reaches its minimum value. The critical c_c is about .5 for F1, F2 and F3, and the corresponding reduction of η_{max} is about 65÷70 per cent. For F4, the critical concentration c_c is about 2.5 with a η_{max} reduction of about 85 per cent.

For concentrations higher than c_c, η_{max} increases with addition of water reducer for F1, F2 and F3, while η_{max} remains nearly constant for F4. It is shown in Fig. 6 which reports the η_{max} values relative to the highest shear rate tested. A similar comparison is impossible at lower shear rates owing to the too low viscosity values for F4.

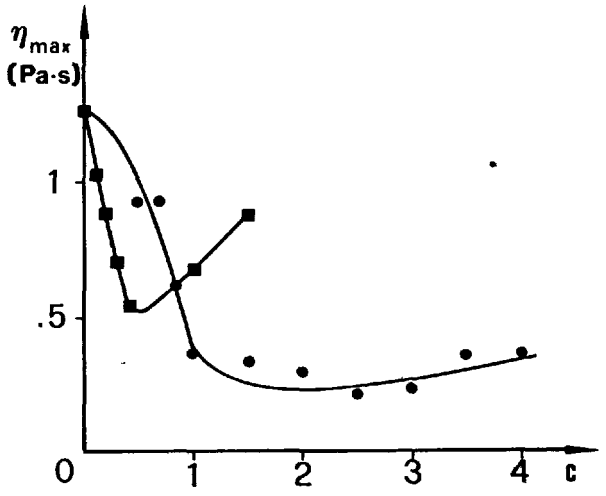

Fig. 6 - Maximum viscosity vs. water reducer concentration at $\dot{\gamma}$ = 216 s^{-1} (Φ = .449; F2 (■); F4 (●))

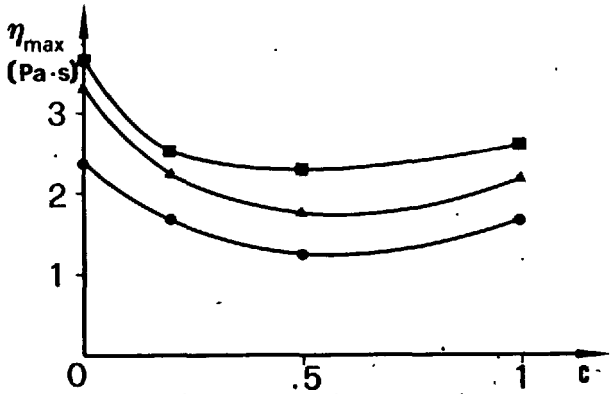

Fig. 7 - Maximum viscosity vs. F1 concentration (Φ = .483; $\dot{\gamma}$ = 216 s^{-1} (●), 108 s^{-1} (▲), 36 s^{-1} (■))

Similar results are obtained at a cement volume fraction of .483 for both equilibrium and maximum data. The viscosity reduction is less marked, as it can be seen in Fig. 7.

Thixotropic behavior

A comparison between the equilibrium and maximum values of shear stress shows the marked effect of the water reducer addition on the apmplitude of the thixotropic behavior. The variation of amplitude with shear rate can be described, according to Lin (17), by the parameter λ:

$$\lambda = \frac{\tau_{max} - \tau_e}{\tau_{max}} \qquad [5]$$

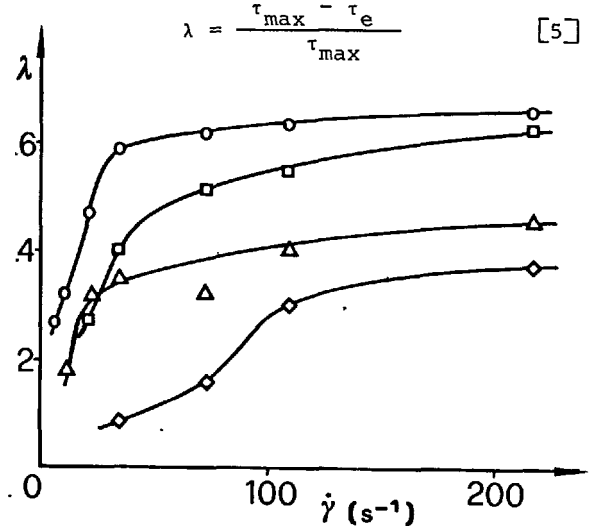

Fig. 8 - Parameter λ vs. shear rate at different F3 concentrations
(Φ = .449; c = 0 (○), .3 (△), .5 (◇), .75 (□))

As shown in Fig. 8, λ increases as $\dot{\gamma}$ increases. At any shear rate, the minimum value of λ is reached near the critical concentration c_c.

For a comparison between different systems, it is more convenient to consider the area A comprised between the curves $\tau_e - \dot{\gamma}$ and $\tau_{max} - \dot{\gamma}$ in the $\dot{\gamma}$ range considered (18). The breakdown area A can be interpreted as a measure of the density of power expended to break part of the interparticle links initially present in the structure at rest and to pass to an equilibrium structure.

The plots of A vs. water reducer concentration clearly indicate that the amount of thixotropic behavior is reduced to its minimum value near the critical concentration c_c. Fig. 9 reports the plot A vs. c relative to F3.
For F4 it was impossible to determine the values of the breakdown area A at the highest water reducer concentration, because the viscosity values corresponding to the lowest shear rates were too low to be experimentally determined.

In a previous paper (18), the breakdown area A has been correlated with a distance parameter d, defined by:

$$d = \frac{1 - \Phi}{\Phi} \frac{1}{S_s} = \frac{w/c}{SSB} \qquad [6]$$

through the relationship:

$$A = D \exp(-fd) \qquad [7]$$

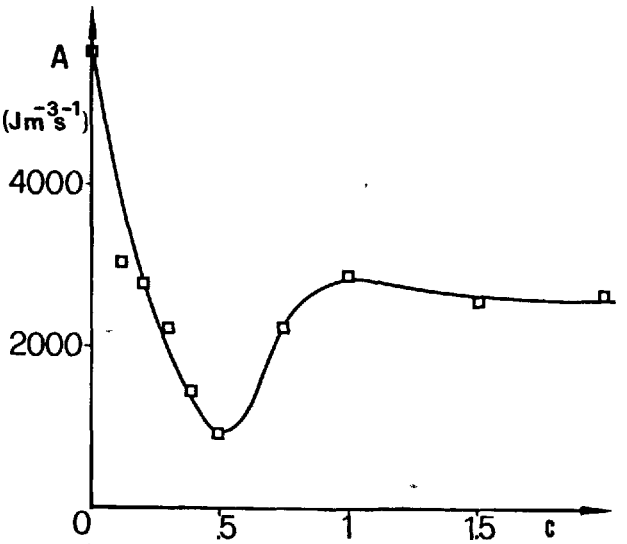

Fig. 9 - Breakdown area A vs. F3 concentration (Φ = .449)

where $D = 1.24 \cdot 10^6$ J·m^{-3}·s^{-1} and $f = 51$ kg·m^{-2}
From the value of the breakdown area it is possible to determine, through eq. [7], an equivalent distance parameter, and hence to individuate the water/cement ratio of the pastes without water reducer having an equivalent time dependent behavior.

Table I

water reducer type	c_c	w/c	$(w/c)_{eq.}$	c_c	w/c	$(w/c)_{eq.}$
F1	.5	.40	.50	.5	.35	.38
F2	.5	.40	.47	.5	.35	.40
F3	.5	.40	.51	.5	.35	.40
F4				2.5	.35	.48

Table I reports examples of such an equivalence for the optimum water reducer concentrations. The comparison of the equivalent w/c ratios clearly shows the effectiveness of the superplasticizer F4.

It is interesting to compare the results obtained for different systems having different Φ and water reducer concentration on the basis of the d/d$_o$ ratio (where d and d$_o$ are the distance parameters of the systems with and without water reducer, respectively) and of a concentration parameter k, defined by:

$$k = \frac{c_s}{\Phi} \qquad [8]$$

where c_s is the surface concentration of water reducer

$$c_s = \frac{c\,\rho_c}{S_s} \qquad [9]$$

Thus, it is possible to give a generalized representation of all the results relative to a given water reducer, for all the reducers belonging to the class of lignosulphonates.

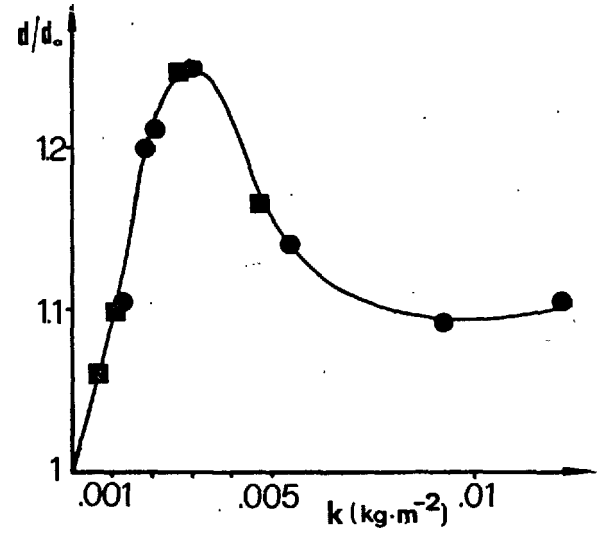

Fig. 10 - Ratio d/d_0 vs. concentration parameter k for F2 (Φ = .449 (●), .483 (■))

Fig. 10 shows that the maximum increase of the distance parameter (and, correspondingly, the maximum reduction in the thixotropic behavior of the pastes) is reached in the vicinity of a well defined k value, namely k_c. If c_{sc} and C_c are the c_s value and the concentration of water reducer (expressed in g/m^3), corresponding to the maximum increase of d/d_0, respectively, it follows that:

$$c_{sc} = k_c \Phi \qquad [10]$$

$$C_c = k_c S_s \Phi^2 = k_c \cdot (S_s \Phi) \Phi \qquad [11]$$

The condition of maximum reduction is obtained for a surface concentration c_{sc}, proportional to the cement volume fraction Φ. If the mode of action of the water reducer (lignosulphonate) should derive only from the adsorption of water reducer on the surface of the cement particles, the above mentioned condition wolud be reached for a well defined value c_{sc}, independent of the cement volume fraction Φ. The optimum concentration of the water reducer C_c is proportional to the product of the total surface of the cement particles and the total cement volume (see eq. [11]). Therefore, the mechanism through which a water reducer acts cannot be explained merely through its adsorption on the cement particles. The results of the rheological tests appear to agree with those of the chemical and microscopical analyses reported in the literature (19).

CONCLUSIONS

The transients τ-t can be described satisfactorily by two models, for different $\dot{\gamma}$. The concentration and the type of water reducer do not substantially affect the type of transient, while its amplitude is dependent on the water reducer concentration. A concentration can be found at which the transient amplitude reaches its minimum value.

As the water reducer concentration increases, η_e decreases, while η_{max} reaches a minimum value beyond which it increases for the lignosulphonates and remains nearly constant for the superplasticizer.

The thixotropic behavior is characterized through significant quantities, as the Lin parameter, the breakdown area and the distance parameter. The maximum thixotropic breackdown is reached near a critical concentration. The study of the influence of a concentration parameter on the distance parameter shows that the action of lignosulphonates-based water reducers cannot be fully explained by surface adsorption.

REFERENCES

1.- P.HEWLETT, R.RINOX, (1977), ACI Journal, n. 5, N.6-N.11.

2.- F.M.ERNSBERGER, W.G.FRANCE, (1945), Ind. Eng. Chem., 37, n. 6, 598-600.

3.- E.M.PETRIE, (1976), Ind. Eng. Chem., Prod. Res. Dev., 15, n. 4, 242-249.

4.- A.A.PASHCHENKO, N.N.KRUGLITSKII, V.I. KOVALEVSKII, I.F.RIDENKO, (1974), Ukr. Khim. Zh. (Russ.Ed.), 40, n. 5,492-495.

5.- M.PAPADAKIS, (1955), Rev. Mater. Construct., n. 476, 1-48.

6.- I.I.KLIMASHCHIN, U.D.MAMADZHANOV, B.Z. ASILOV, (1975), Izv. Akad. Nauk. Uzb. SSR Ser. Tekh. Nauk, n. 6, 64-66.

7.- M.DAIMON, D.M.ROY, (1978), Cem. Concr. Res., 8, 753-764.

8.- J.BONZEL, E.SIEBEL, (1974), Beton, n.1, 20-24, n. 2, 59-63.

9.- P.SCHMINCKE, (1977), Zement u. Beton, n. 2, 44-47.

10.- F.MASSAZZA, U.COSTA, E.CORBELLA, (1977), Proc. Conf. "Reaction of Aluminates during the Setting of Cements", Univ. Technol. Eindhoven, April 13-14.

11.- P.DIERKES, E.HAYEK, (1975), Chem. Kunstst. Altuell, 29, n. 2, 71-74.

12.- G.H.TATTERSALL, (1978), Univ. of Sheffield, Rep. BS 45.

13.- E.BINGHAM, (1922), "Fluidity and Plasticity", McGraw-Hill, New York.

14.- H.PIERZCHALA, (1970), Tonind.-Z., n. 8, 331-336.

15.- W. von BERG, (1979), private communication.

16.- K.WESCHE, W. von BERG, (1973), Beton, n. 1, 21-27.

17.- O.C.C.LIN, (1975), Chem. Tech., 5, n. 1, 51-60.

18.- R.LAPASIN, V.LONGO, S.RAJGELJ, (1979), Cem. Concr. Res., 9, 309-318.

19.- F.MASSAZZA, M. TESTOLIN, (1979), private communication.

Sorption of N_2 and n-C_4H_{10} on hydrated cements

Etude porométrique de ciments hydratés par adsorption de N_2 et de n-C_4H_{10}

C.D. LAWRENCE, Materials Research Department, Cement and Concrete Association, Slough, and
F.G.R. GIMBLETT, and
K.S.W. SING, School of Chemistry, Brunel University, Uxbridge, U.K.

RESUME : L'observation porométrique révèle un affaissement de la microstructure des ciments hydratés, au cours d'un séchage normal. En comparant des pâtes soumises à différents séchages isothermes, on a constaté que des micropores présents dans les pâtes rapidement séchées et conservées à température ambiante étaient absents dans les pâtes lentement desséchées.

Des analyses αs, utilisant la silice TK 800 comme étalon, ont donné des résultats semblables avec l'azote à -196°C et avec du butane à 1°C. Pour les pâtes rapidement séchées et conservées à température ambiante, les diagrammes αs s'infléchissent au-dessus d'une pression relative de 0,4, ce qui indique, à la fois, la présence de mésopores en forme de fissures, et l'absence de condensat capillaire pendant l'adsorption. Le condensat capillaire est présent, au cours de l'adsorption de N_2 ou de n-C_4H_{10} par des pâtes lentement desséchées, ou par des pâtes traitées à l'autoclave.

SUMMARY : Sorption data give evidence for a partial microstructural collapse in hydrated cements during normal drying. From a comparison of a large number of isotherms, it is deduced that micropores are present in rapidly dried pastes that have been cured at room temperature, but are possibly absent from slowly dried systems. α_s analyses, using silica TK 800 as a reference, are similar for nitrogen at -196°C and butane at 1°C: on rapidly dried pastes cured at room temperature, the α_s plots are curved above a relative pressure of 0.4, indicating both the presence of slit-shaped mesopores and the absence of capillary condensate during adsorption. Capillary condensate is present during N_2 or n-C_4H_{10} adsorption on slowly dried pastes, or on autoclaved systems.

INTRODUCTION

Variations in the method and rate of drying result in microstructural changes which complicate the interpretation of sorption isotherms on hydrated cements. Reported investigations have usually employed a single standardised preparation procedure, thus avoiding this difficulty, but in so doing have failed to detect a basic characteristic of these systems (1,2). Uncertainty in the qualitative interpretation of data arises because reference isotherms are not available on materials closely related to hydrated cements. To circumvent these difficulties, approximately 350 N_2 isotherms have been determined on 60 specimens, making it possible to eliminate random discrepancies and arrive at well-founded data for the different preparation procedures; an initial analysis is carried out by comparing the shapes of N_2 isotherms within this set of data.

Experimental

Hardened cement pastes and hydrated suspensions were prepared at room temperature from commercial cements and from laboratory cements made in the $CaO-SiO_2-Al_2O_3-Fe_2O_3$ system (Table I identifies the systems discussed in this report). Some cement/water mixes were hydrated for limited periods at 190°C in an autoclave or laboratory bomb, but most systems were stored under water at room temperature for most of their cure. At the beginning of the study, samples were generally dried by evacuation at room temperature for extended periods through a trap cooled at -79°C (d-dried) then stored dry until a final outgassing at room temperature through a trap cooled with liquid nitrogen, immediately before determining the sorption isotherm. Most of the isotherms subsequently obtained were on freshly crushed hydrated systems placed in the sorption apparatus while still saturated with water, and dried by direct outgassing through a trap cooled with liquid nitrogen. Solvent replacement procedures (3,4) were adopted towards the end of the study as a means of removing some of the free water, before outgassing.

The quantity of nitrogen sorbed at -196°C was determined in a conventional volumetric apparatus (5), and a gravimetric procedure was employed to obtain butane isotherms at 1°C. Two microbalances (C.I. Electronics Ltd, Mk2C) were incorporated in the butane system, so allowing two samples to be examined at the same time; butane gas was admitted from a cylinder of Instrument Grade n-butane (99.5% purity) and withdrawn by a rotary pump via two solenoid valves which were operated by a Data General Nova 2 computer,

TABLE I

Specimen	Cement	w/c	age	Compressive strength MNm^{-2}
OPC1/.5/1081	OPC-1	.5	1081	58
SRPC1/.18/505	SRPC-1	.18	505	273
OPC2/10/4750	OPC-2	10	4750	-
C2S1/.5/2267	belite-1	.5	2267	39
OPC1/.5/2500	OPC-1	.5	2500	48
C3S2/.08/2297	alite-2	.08	2297	438
C3S1/.47/42	C3S-1	.47	42	-
C3S3/.4/415	alite-4	.40	415	113

controlling the pressure of butane to preset points throughout the isotherm. Weight changes were recorded at 100 mg full scale sensitivity to 0.01 mg, and pressures were recorded to 0.0001 atmospheres by means of a pressure transducer (Druck Ltd, PDCR60, 1 bar).

N_2 Sorption Data

The shapes of nitrogen adsorption isotherms on hydrated cements conform to Type 2 in Brunauer's classification, and show Type B or D hysteresis loops between adsorption and desorption branches in de Boer's classification which close or almost close at relative pressure 0.45. Wide ranges of isotherm shape have been obtained in the present study. To analyse the cause of this variability, the data have been divided into groups of similarly shaped isotherms, after normalising at relative pressure 0.4, treating the lower and upper pressure regions independently. The number of separate sorption runs in each group varies between 10 and 60; representative isotherms have been drawn through each group. Data on hydrated cements in the lower relative pressure region are illustrated in Figure 1A by isotherms B to I which show a trend to a flatter shape; the corresponding isotherm for silica TK 800,

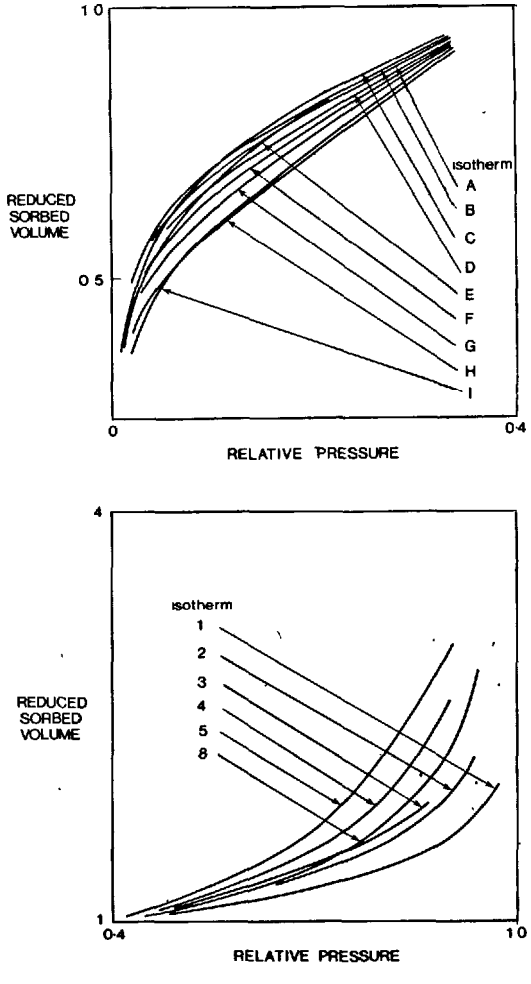

Fig. 1 - Representative N_2 isotherms on hydrated cements normalised at a relative pressure 0.4: 1A, low pressure; 1B, high pressure

a well-documented hydrous oxide (6), is isotherm A. Sorption data at higher relative pressures are treated similarly and are illustrated in Figure 1B by representative isotherms 1 to 5; they show a trend to steeper rates of N_2 uptake; the corresponding data for silica TK 800 is isotherm 8. A positive correlation is indicated between these two groups, suggesting that it may not be permissible to interpret the lower and upper regions of isotherms independently.

When samples are directly outgassed from the saturated state, the nitrogen sorption data at low relative pressures can be represented by isotherms B,F,G, or H; these same isotherms are found with d-dried samples and with samples dried at 100°C; they have relatively sharp knees. When organic solvents are employed to displace free water, nitrogen sorption data can be represented by isotherms C, E or I at low relative pressures; these isotherms have relatively rounded knees. At higher pressures, drying by direct outgassing usually results in isotherms 2 or 3, while drying at 100°C or d-drying leads to isotherm 4 for porous pastes and to isotherm 5 for dense pastes. After displacement of free water with methanol, specimens usually yield N_2 sorption data approximating to isotherms 1 or 2. At low relative pressures nitrogen sorption data on autoclaved specimens may usually be represented by isotherm H, and these data are unaffected by pre-treatment with methanol. Soaking a d-dried specimen in methanol causes sorption data to change from isotherm G to isotherm I. The additional effect on isotherm shape of prolonging pretreatment with methanol is negligible for paste specimens, but N_2 isotherms on suspension hydrated cement become steeper with increasing period in methanol.

For the specimens examined, BET surface areas lie between 0.4 and 183.3 $m^2 g^{-1}$, on the basis of outgassed sample weights; BET 'C' constants for hydrated cements lie about a mean of 82 with a standard deviation for the population of 42.

TABLE II

Specimen	Drying procedure	N_2 BET surface m^2/g	Butane uptake at P/P° = .4 g/g
SRPC1/.5/347	direct outgas	89.6	.0134
OPC1/.5/1081	d-dried + badly stored	-	.0040
OPC1/.5/1081	d-dried	82.5	.0194
OPC1/.5/2500	methanol	119.9	.0258
C3S3/.4/415	100 dried	-	.0245
C3S1/.47/1	direct outgas	8.3	.0019
C3S1/.47/7	methanol	106.2	.0190
C3S1/.47/28	methanol	138.3	.0277
C3S1/.47/42	methanol	139.8	.0210
C3S1/.47/42/2H	methanol	113.4	.0259
C3S1/.47/42/4H	methanol	128.6	.0336
OPC2/10/4750	methanol	183.1	.0355
silica TK 800	direct outgas	155.1	.0325

Outgassing of saturated samples directly produces larger surface areas than either d-drying or drying at 100°C; also dry storage causes a significant reduction in surface. Drying by displacing free water with methanol usually results in a substantial increase in surface; BET 'C' constants are significantly reduced by pretreatment with methanol, e.g. they are reduced on average from 106 to 59 in the case of dense pastes.

The surface areas of paste specimens OPC1/.5/1081 and SRPC1/.18/505 are increased after 15 day's soaking in methanol but are not further changed by prolonging the period in methanol; BET 'C' constants are also unchanged by prolonging the soaking in methanol. In contrast the suspension hydrate OPC2/10/4750 at first continues to increase in surface area with increasing time in methanol, but at 330 days the surface area falls unexpectedly after an accidental halt to agitation of the methanol suspension, then increases again at 380 days when agitation has recommenced; during this halt the suspension settles and forms a dense sediment which gives a reduced surface area of about 1/3 the previous value.

$n\text{-}C_4H_{10}$ Results

A limited number of butane sorption isotherms are available at the present time, however it seems possible to state that isotherm shapes on hydrated cements are modified by the method of sample preparation adopted. As the isotherms exhibit very shallow knees, an analysis of this region of the isotherms is not feasible; differences in the shapes of hysteresis loops at moderate and high relative pressures are clearly visible and examples of three these isotherms are illustrated in Figures 2 to 4. The desorption isotherms for samples pretreated with methanol have a relatively acute approach to the ordinate at P/P°=1, in contrast to the asymptotic approach of nitrogen isotherms, suggesting that a definite mesopore volume is defined by butane but not by nitrogen. The weights of butane sorbing onto samples at relative pressure 0.4 are compared to nitrogen BET surface areas in Table II: a general correspondence between these values is apparent though some exceptions may be genuine; a detailed analysis may be possible when more data are available.

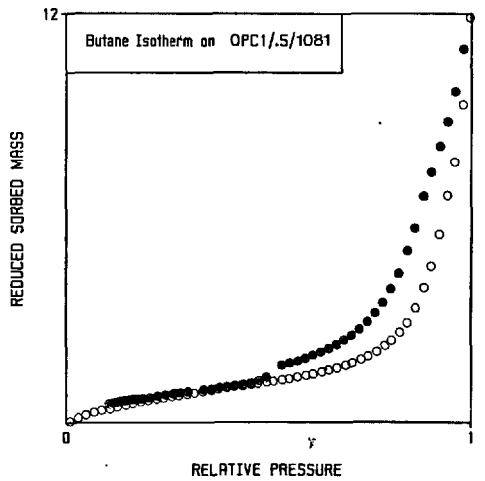

Fig. 2 - Butane isotherm on hydrated cement paste OPC1/.5/1081 d-dried and badly stored.

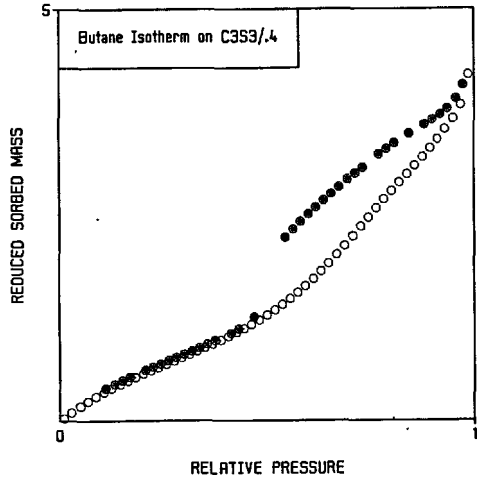

Fig.3 - Butane isotherm on hydrated alite cement paste C3S3/.4/415 dried at 100°C.

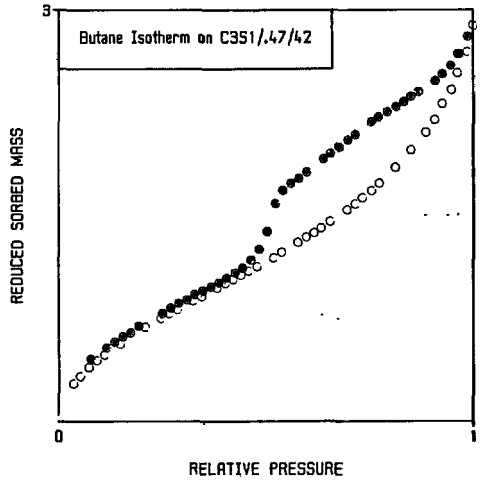

Fig. 4 - Butane isotherm on hydrated C_3S paste C3S1/.47/42/4H dried by presoaking in methanol.

DISCUSSION

The nitrogen sorption results seem to provide evidence for a collapse of pore structure, leading to loss of free surface during drying under normal conditions that may be prevented, at least partially, by pretreatment with methanol. The evidence from pretreatment of d-dried specimens with methanol suggests that methanol does not readily open up pores that have already collapsed, though the behaviour of the suspension hydrate specimen shows that slow expansion of some microstructures can take place in methanol. The erratic changes in surface area of the suspension hydrated cement suggests that its morphology is one that allows close packing of particles when agitation ceases, so forming loose aggregations which can exclude nitrogen from a substantial fraction of their surface after removal of methanol. The obvious model for these hydrate particles is a platelet. When saturated cement specimens, cured at room temperature, are treated with methanol, usually both the quantities of nitrogen sorbed (or the BET surface areas) and the shapes of isotherms at low relative pressures are changed. The results for different specimens after pretreatment with methanol are:-

(a) OPC2/10/4750; a large change in isotherm shape plus an erratic change in surface area, depending on the degree of agitation.

(b) OPC1/.5/1081; some change in isotherm shape plus a large increase in surface area.

(c) C2S1/.5/2267; some change in isotherm shape plus an initial increase in surface area followed by a reduction to the surface area of the untreated sample.

(d) OPC1/.5/2500; a change in isotherm shape but no change in surface area.

(e) SRPC1/.18/505; a change in isotherm shape plus a large increase in surface area.

(f) OPC1/.5/1081 (d-dried); a large change in isotherm shape but no change in surface area.

A change in isotherm shape is thus universally obtained when samples are pretreated with methanol but the quantity of nitrogen sorbed is not always increased. A possible explanation is that the chemical nature of the solid surfaces is modified to different extents for the different specimens by chemisorption of methanol: sorption isotherms of certain alcohols on hardened cement pastes provide evidence for this chemisorption (8); the reduction in N_2 BET 'C' constants after pretreatment with methanol may also be considered evidence for this effect.

Nitrogen is physically sorbed onto solid surfaces at -196°C, but changes in the chemical nature of surfaces can somewhat influence the data since the nitrogen molecule contains an electrical quadrupole which interacts with any charged species in the surfaces (7). For butane and other aliphatic hydrocarbons, electrical quadrupoles and dipoles are absent so their sorption data are less sensitive to the chemical nature of the surface. If it is provisionally assumed that pretreatment with methanol results in an energetically more uniform surface chemistry for the outgassed specimens, then patterns of nitrogen sorption that reflect physical structure may be revealed among these treated specimens. Experimentally all methanol soaked room temperature cured paste specimens produce low relative pressure sorption data represented by isotherms C or E, with the exception of the very dense specimens C3S2/.08/2297 which gives isotherm I; suspension hydrate OPC2/10/4750 yields isotherm G and d-dried OPC1/.5/1081, isotherm I; autoclaved pastes yield isotherm H. From these results normal density pastes may be provisionally assigned the largest volume of micropores since these pastes give isotherms with most pronounced knees, the presence of micropores resulting in enhanced sorption in this region of the isotherm. From considerations of N_2 isotherm shapes and the degree of crystallinity shown in Stereoscan pictures, autoclaved pastes may contain a negligible volume of micropores.

The shapes of isotherms in the higher relative pressure region, where multilayer adsorption and

capillary condensation can occur, are probably less influenced by specific interactions between nitrogen molecules and solid surfaces: experimentally isotherms on silica TK 800 are similar in shape to isotherms 2 or 3 on hydrated cements, in the relative pressure interval 0.4 to 0.75. Those hydrated cements yielding isotherms 4 or 5 show enhanced rates of uptake of nitrogen compared to non-porous silica, thus capillary condensation is probably taking place during adsorption. Hydrated cement specimens giving nitrogen sorption data represented by isotherms 1, 2 and 3 have similar or reduced rates of uptake compared to non-porous silica; several possible explanations may be given for this behaviour:-

(i) Specimens may be non-porous or only contain very large diameter mesopores (isotherms may then be expected to be identical to the TK 800 standard).

(ii) Specimens may contain slit-shaped pores that fill with liquid nitrogen at high relative pressures only when multilayers of nitrogen molecules adsorbing on the flat opposing faces of the slits eventually touch, as the relative pressure rises.

(iii) Micropore filling takes place in specimens at lower relative pressures, resulting in higher sorbed volumes at relative pressures below 0.4 than are required by simple multilayer sorption on the open surface remaining at $P/P^{\circ}=0.4$.

Examination of the data shows that all rapidly dried pastes produce sorption data that may be represented by isotherms 1, 2 or 3. Since the discussion of low relative pressure isotherms given above has suggested that micropores are present in these specimens, explanation (iii) is the most likely.

A standard method of elucidating microstructures from sorption isotherms is the construction of α_s plots (7). The normalised isotherms are plotted against those of a non-porous reference material of similar chemical constitution: a straight line plot along the diagonal is obtained when the shape of the hydrated cement isotherm is identical to that of the reference. Deviations above this diagonal at higher relative pressures are generally interpreted as capillary condensation while deviations below this diagonal may be interpreted to indicate the presence of slit-shaped mesopores or the presence of micropores. Examples of α_s plots are shown in Figures 5 to 7 using silica TK 800 as the reference. Capillary condensation occurs during adsorption in:-

(a) Autoclaved specimens

(b) Specimens dried at 100°C

(c) Dense d-dried paste specimens

(d) Some d-dried porous paste specimens

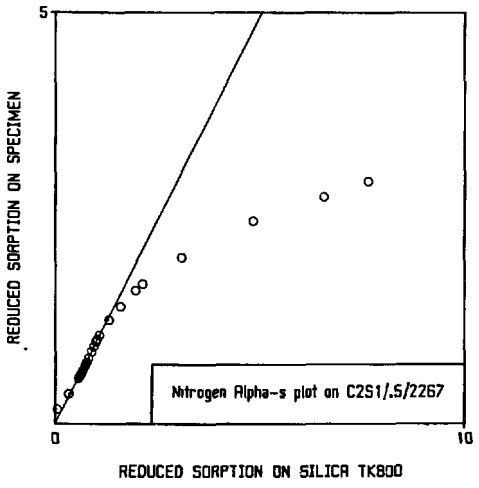

Fig. 5 - Nitrogen α_s plot on hydrated belite cement paste C2S1/.5/2267 directly outgassed while saturated.

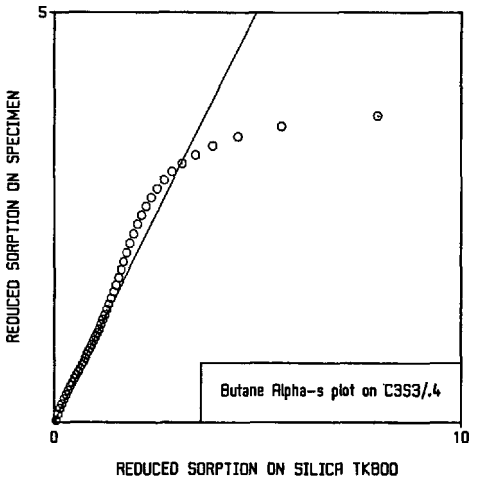

Fig.6 - Butane α_s on hydrated alite cement paste C3S3/.4/415 dried at 100°C.

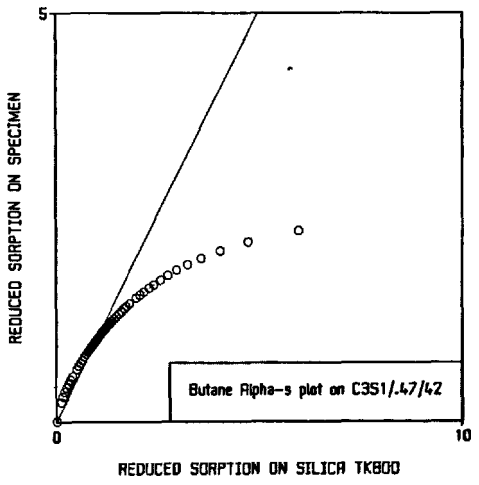

Fig. 7 Butane α_s plot on hydrated C_3S paste C3S1/.47/42 dried by presoaking in methanol.

A downward deviation of the α_s plots occurs in the case of isotherms on:-

(e) Room temperature cured specimens that are outgassed directly from the saturated state in the sorption apparatus (with the exception of the suspension hydrate)

(f) Room temperature cured specimens that are pretreated with methanol (with the exception of the suspension hydrate)

(g) Most porous d-dried specimens.

In agreement with the contention that methanol pretreatment prevents collapse of micropores, paste samples pretreated with methanol show increased downward deviations in their α_s plots compared to those on the corresponding untreated pastes. The α_s plots for butane isotherms show a general similarity to those for nitrogen isotherms: because of the less specific nature of the interaction between the butane molecule and solid surfaces, the interpretation of butane α_s plots, especially at low relative pressures, can be more certain - deviations above the diagonal at relative pressures below 0.4 provide additional evidence for the presence of micropores. The fact that α_s plots continue to deviate from the diagonal line at relative pressures above 0.4 suggests that a slit-shaped mesopore model is appropriate. A rigid slit-shaped pore model has been adopted for clay mineral compacts that yield nitrogen isotherms with the characteristics of isotherms 1, 2 and 3 (9), but if the hydration products are flexible lamillae, slit-shaped pores may be expected to form between them that are able to swell to limited extents as gas is condensed; unlike a rigid structure, the filling of pore space could be complete below the limiting pressure for capillary condensation (at $P/P^o=0.45$) (10) and still account for the sorption data.

CONCLUSIONS

The structure of hydrated cement pastes cured at room temperature and rapidly dried, appears to be dominated by platy particles or lamellae that form slit-shaped mesopores and micropores. Small pores develop if these lamellae are allowed to collapse together, for example during slow drying, that behave as hollow cylinders or spheres in which N_2 or $n\text{-}C_4H_{10}$ condenses during adsorption.

REFERENCES

1. - C.D. LAWRENCE (1978), "An examination of possible errors in the determination of nitrogen isotherms on hydrated cments" Technical Report 42.520 Cement and Concrete Association.

2. - E.E. BODOR, J. SKALNY, S.BRUNAUER, K.HAGYMASSY and M. YUDENFREUND (1970), "Pore structure of hydrated calcium silicates and Portland cements by nitrogen adsorption". J. Colloid and Interface Science, 34, pp 560-570.

3. - G.G. LITVAN (1976), "The variability of nitrogen surface area of hydrated cement paste", Cement and Concrete Research, 6, pp 139-144.

4. - J.J. SWANSON (1979), "The porous nature of pulpwood fibres", Swiss-British Symposium 'Characterisation of Porous Solids', Neuchatel. Edited by S.J. Gregg, K.S.W.Sing and H.F. Stoeckli. Society of Chemical Industry, pp 339-342.

5. - S.J. GREGG and K.S.W. SING (1967), "Adsorption surface area and porosity", London, Academic Press.

6. - D.H. EVERETT, G.D. PARFITT, K.S.W. SING and R. WILSON (1974), The SCI/IUPAC/NPL project on surface area standards. J. Applied Chemistry and Biotechnology, 24, pp 199-219.

7. - S.J. GREGG and K.S.W. SING (1976), "The adsorption of gases on porous solids", Surface and Colloid Science, 9, Edited by E. Matyevic, John Wiley.

8. - R.SH. MIKHAIL and S.A. SELIM (1966), "Adsorption of organic vapours in relation to the pore structure of hardened Portland cement pastes", Highway Research Board, Special Report 90, pp 123-134.

9. - L.A.G. AYLMORE (1974), "Gas sorption in clay mineral systems", Clays and Clay Minerals, 22, pp 175-182.

10. - C.G.V. BURGESS and D.H. EVERETT (1970), "The lower closure point in adsorption hysteresis of the capillary condensation type", J. Colloid and Interface Science, 33, pp 611-614.

Réglage de la formation de la structure et des propriétés du ciment

Control of structure formation and properties of cement

I.F. PONOMAREV, Directeur de l'Institut,
I.A. KRYJANOVSKAIA, Candidat ès Sciences Techniques,
A.G. KHOLODNYI, Candidat ès Sciences Techniques, Institut "Youjguiprotzement", U.R.S.S.

RESUME : On a étudié le mode de réglage, dans de larges limites, des propriétés du ciment par introduction dans sa composition de diverses quantités d'un composé cristallisé sulfoalumino-siliceux. On a montré que lors du broyage du mélange des trois constituants (clinker-portland, gypse et cristallisé), on peut obtenir, par la seule variation du rapport entre constituants, un ciment portland très résistant et des ciments expansifs, dont le temps de prise peut varier des valeurs ordinaires jusqu'aux valeurs très petites, de 5 à 8 minutes.

A l'aide d'un ensemble de méthodes d'étude physico-chimiques (radiographie, spectroscopie infrarouge, dérivatographie, microscopie électronique), on a mesuré les variations en quantité des hydrosilicates, des hydrosulfoaluminates et de l'hydroxyde de calcium qui se forment lors du durcissement des ciments à teneur différente en composé sulfoaluminosiliceux et on a montré que ces variations conditionnent les différentes propriétés techniques des ciments.

SUMMARY: A method of controlling cement properties within a wide range has been investigated. The method resides in introduction of different amounts of a crystallizing component of sulfoalumosilicate composition into the cement. It is proved that when crushing a three-component charge of conventional portland cement clinker, gypsum and crystallizing component, il will suffice to vary relationship of the components for obtaining high-strength portland cement and expanding cements the setting periods of which may be varied from regular to very short ones (5 to 8 min).

A complex of physical and chemical methods of investigations has been used (radiography, IRS, derivatography, electronic microscopy) to determine variations of the amounts of hydrosilicates, hydrosulfoaluminates and calcium hydroxide formed at hardening of cements with different content of the sulfoalumosilicate component and it has been shown that these variations dictate different technical properties of cements.

Introduction of the sulfoalumosilicate component into cement considerably increases homogeneity of the cement structure thus increasing cement strength.

Pour produire des ciments de types spéciaux on met habituellement en jeu les divers procédés technologiques qui introduisent des restrictions indésirables à tous les stades de production, à partir du choix des matières brutes pour la cuisson du clinker jusqu'aux paramètres de broyage du ciment. Afin de simplifier le processus technologique on a mis au point le mode de réglage des propriétés du ciment au stade de son broyage par introduction des constituants de cristallisation spéciaux dont la composition peut être assez variée. Dans ce travail on donne les résultats des recherches sur l'utilisation du constituant de cristallisation sulfoalumosiliceux.

La composition en phases du produit sulfoalumosiliceux (ou PSAS) est très complexe. D'après les données des analyses pétrographiques, aux rayons X, électrono-microscopiques, spectroscopiques aux rayons infrarouges *), les composés siliceux PSAS se caractérisent par la présence de couches $(Si_2O_5)_n$ à structure perturbée et du complexe absorbé, qui font preuve de l'activité élevée lors de l'interaction avec la solution aqueuse du ciment durcissant. La présence dans la composition de PSAS de composés solubles dans l'eau qui alimentent la phase liquide de la pierre de ciment durcissante en ions Al^{3+}, Ca^{2+} et SO_4^{2-} est aussi une particularité de ce produit.

L'étude des propriétés des ciments, contenant une quantité différente de PSAS et du gypse, a permis d'établir qu'avec accroissement de la teneur en ces additions le temps de prise devient plus court et l'expansion du ciment augmente, tandis que les indices de résistance commencent par croître pour diminuer ensuite. Ceci rend possible, en faisant varier le rapport entre le clinker-portland, PSAS et le gypse, l'élaboration du ciment portland très résistant et des ciments expansifs à prise différente, en utilisant le même clinker pour la production de ces ciments spéciaux à destination différente.

L'étude des processus d'hydratation et de durcissement des ciments contenant les différentes quantités du produit sulfoalumosiliceux et du gypse était effectuée avec utilisation de la microscopie électronique, de la spectroscopie infrarouge, de la radiographie quantitative, de la dérivatographie, de l'analyse chimique des solutions aqueuses de la pierre de ciment durcissant. A titre de comparaison on a étudié également le ciment portland ordinaire. L'analyse de la composition de la solution aqueuse des échantillons de ciment durci montre que le durcissement des ciments avec PSAS a lieu en conformité avec les lois caractéristiques du ciment portland ordinaire. On peut voir nettement l'interliaison entre la concentration de CaO et de R_2O dans la solution. Il est établi que la chimisorption des ions de métaux alcalins par les constituants PSAS amorphisés en forme de gel entraîne la diminution de la concentration de R_2O et l'accroissement de la teneur en CaO dans la solution, ce qui provoque l'augmentation dans la composition des ciments avec addition PSAS de la quantité de l'ettringite (grâce à la diminution de sa solubilité) et du gel hydrosiliceux (vu l'adsorption plus intense de CaO à partir de la phase liquide par les constituants PSAS). Une concentration accrue de Al_2O_3 et SiO_2 dans la solution aqueuse des ciments contenant PSAS confirme également le fait que l'addition prend une part active dans les processus d'hydratation.

Selon les données de l'analyse aux rayons X, de la spectroscopie infrarouge et de la dérivatographie, les ciments durcissants ayant une teneur différente en PSAS se caractérisent par une composition des phases similaire des hydrates et une succession analogue de leur formation au cours du durcissement. Le premier des hydrates (4 mn d'hydratation) qui apparaît toujours dans la pierre de ciment est l'ettringite (réflexions à 9,8; 5,6 Å sur les radiogrammes, bandes d'absorption de 1130 cm^{-1}, 3450 cm^{-1} sur les spectres infrarouges, endoeffet avec le minimum à 140°C sur les dérivatogrammes); ensuite on fixe la formation de $Ca(OH)_2$ (réflexions à 4,9 ; 2,6 Å; 500 à 540°C) et d'hydrosilicates de calcium (bande d'absorption de 970 à 980 cm^{-1} sur le spectre infrarouge, endoeffet dans l'intervalle de 160 à 180°C sur les dérivatogrammes). Un trait distinctif des spectres infrarouges des ciments avec PSAS est l'élargissement des bandes d'absorption dans le domaine de 970 à 980 cm^{-1} avec accroissement de la quantité de PSAS dans le ciment, ce qui témoigne de l'augmentation de la quantité des hydrosilicates de calcium amorphisés dans la composition des hydrates.

La caractéristique qualitative des ciments analysés témoigne donc du fait que les hydrates de ciment durci sont principalement représentés par l'ettringite, les hydrosilicates et l'hydroxyde de calcium. La quantité de ces phases dans les ciments analysés, déterminée à l'aide de la radiographie et de la dérivatographie, est donnée dans le tableau ci-dessous. Dans ce tableau les ciments sont disposés dans l'ordre d'accroissement de leur teneur en PSAS.

Le degré d'hydratation de l'alite était déterminé de façon radiographique d'après l'intensité de réflexion à 1,76 Å selon la méthode proposée par M.E.Jmodikova, V.I.Korneev (1) et la quantité de l'ettringite, d'après l'intensité de réflexion à 9,8 Å selon Kh.G.Smoltchik (2). La quantité de $Ca(OH)_2$ était déterminée d'après les dérivatogrammes. Les données obtenues témoignent de l'accroissement de la teneur des échantillons en ettringite avec augmentation de la quantité de PSAS dans le ciment. La plus grande différence dans la teneur en ettrin-

---

*) Les recherches étaient effectuées avec participation de V.F.Gribko, L.N.Skrynnik, O.M.Vodovosova, T.Y.Chtchetkina, A.A.Lazareva.

Tableau

Résultats des déterminations quantitatives des hydrates de ciment durci

type du ciment	temps d'hydratation	Quantité, %			Degré d'hydratation de l'alite,%
		de l'ettringite	de l'eau du gel	de $Ca(OH)_2$	
Ciment portland	4 mn	-	-	-	6
	3 h	-	-	-	6
	12 h	5,0	3,7	1,1	30
	1 j	6,2	5,6	2,2	32
	3 j	5,0	7,3	2,4	66
	7 j	5,0	9,1	3,3	70
	28 j	4,8	10,8	3,4	70
Ciment a haute résistance	4 mn	-	-	-	6
	3 h	6,2	1,17	-	19
	12 h	7,0	3,8	0,8	38
	1 j	6,2	6,3	1,1	44
	3 j	6,8	7,1	2,4	58
	7 j	7,0	7,8	2,6	63
	28 j	5,5	10,7	3,3	71
Ciment expansif	4 mn	5,5	1,8	-	16
	3 h	10,0	3,8	-	25
	12 h	9,8	6,2	0,7	40
	1 j	9,0	7,3	0,7	45
	3 j	7,5	8,0	1,1	56
	7 j	10,0	12,2	1,9	69
	28 j	10,7	16,2	-	78
Ciment expansif à prise rapide	4 mn	5,9	1,7	-	-
	3 h	15,5	3,1	-	4
	12 h	12,5	5,2	-	27
	1 j	11,0	7,0	-	30
	3 j	10,2	13,2	-	32
	7 j	7,5	14,0	0,6	57
	28 j	9,4	15,4	-	65

gite est observée aux stades précoces de durcissement (jusqu'à 3 jours). L'hydroxyde de calcium cristallin entre en quantité maximale dans la composition des échantillons du ciment portland. Avec augmentation de la part de PSAS dans le ciment, la concentration de $Ca(OH)_2$ dans la pierre de ciment diminue. Ce phénomène est dû évidemment à la variation du degré d'hydratation de l'alite, à l'interaction de la chaux avec l'addition PSAS, à la formation de $Ca(OH)_2$ sous forme de gel. Le degré d'hydratation maximal de l'alite est observé dans le ciment expansif; un accroissement ultérieur de la teneur en addition PSAS conduit au ralentissement de l'hydratation de l'alite, ce qui est dû évidemment au blocage de ses grains par une quantité complémentaire de l'hydrogel qui se forme à partir de PSAS.

Il est établi que la structure de la pierre de ciment avec addition PSAS se distingue de la structure des échantillons en ciment portland par une plus grande homogénéité. Les facteurs contribuant à l'accroissement du degré d'homogénéité sont: 1) disposition uniforme des particules finement dispersées de PSAS dans le volume des échantillons du ciment; 2) formation simultanée à partir des particules de PSAS de l'ettringite et des hydrosilicates de calcium qui se trouvent en contact étroit; 3) réduction de la quantité et de la dimension des cristaux de $Ca(OH)_2$. Le deuxième facteur est le plus important parmi les facteurs énumérés d'accroissement du degré d'homogénéité de la structure du ciment durci. La figure 1 donne différentes variantes de disposition mutuelle des hydrosilicates de calcium et de l'ettringite.

La structure du ciment-portland durci sans addition PSAS se caractérise par ce qu'après 7 jours de durcissement les cristaux d'ettringite sont enchevêtrés avec les hydrosilicates de calcium fibreux (fig.1a). Aux stades suivants de durcissement (28 jours) les régions de la structure, formée par l'ettringite et les hydrosilicates de calcium fibreux, se trouvent en contact avec des agglomérations serrées des particules le plus finement dispersées du gel hydrosiliceux (fig.1b).

Comme on le voit sur le dessin, les agglomérations serrées d'hydrosilicates de calcium ne sont pas en contact avec tous les cristaux d'ettringite mais seulement avec ceux qui se trouvent disposés à la périphérie de la région formée par l'ettringite et des hydrosilicates de calcium fibreux. Dans le ciment avec addition PSAS (fig.1c,d), lors de l'interaction avec la solution aqueuse de la pierre durcissante, les particules de PSAS donnent, comme on le voit sur la photo, l'ettringite et les hydrosilicates de calcium le plus finement dispersés, qui sont étroitement enchevêtrés l'un avec l'autre. Il est indéniable que ces régions de la structure se caractérisent par une plus grande homogénéité que les contacts entre la structure compacte d'hydrosilicates et la structure plus meuble d'hydrosilicates et d'hydrosulfoaluminates du ciment portland durci.

En évaluant les différences entre la structure de la pierre de ciment portland ordinaire et celle de ciment avec addition PSAS il convient donc de souligner qu'en l'absence d'addition la structure de la pierre de ciment se caractérise par la présence des régions séparées de la pierre formées par les agglomérations serrées des particules d'hydrosilicates et les cristaux prismatiques d'ettringite. Dans les ciments avec addition PSAS, grâce à la formation des cristaux d'ettringite et d'hydrosilicates de calcium finement dispersés à partir de la même phase initiale - particules de PSAS - la disposition spatiale des hydrates étant conservée, à la place des particules de départ il se forme une structure plus homogène de la pierre de ciment. La différence entre les structures de types décrits de la pierre de ciment est schématisée sur la figure 2.

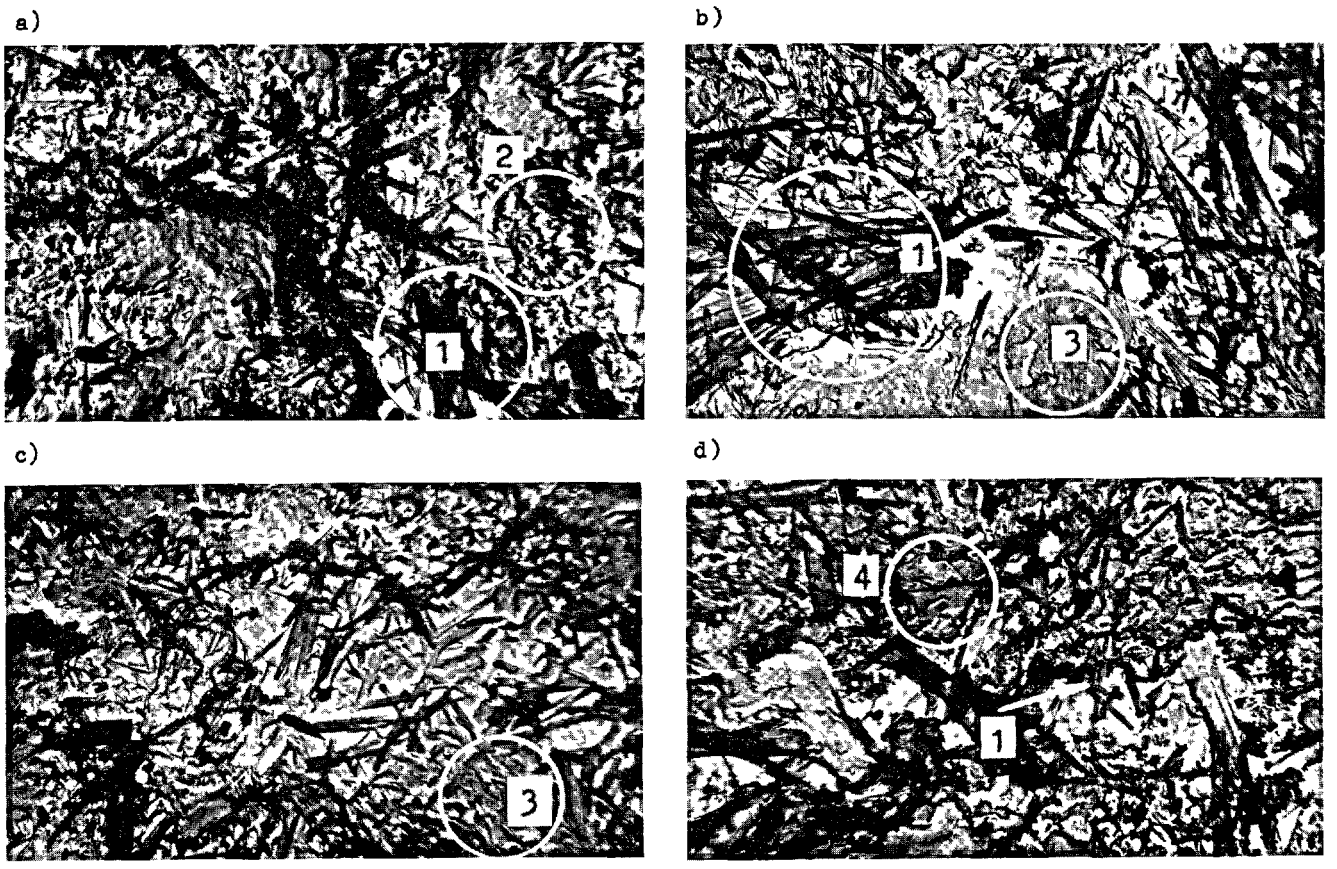

Fig.1.Disposition mutuelle des cristaux d'ettringite et des hydrosilicates de calcium dans la structure de la pierre de ciment. a - ciment portland ordinaire après 7 jours de durcissement; b - idem après 28 jours; c - ciment avec addition PSAS après 7 jours de durcissement; d - idem après 28 jours.
1 - ettringite; 2 - hydrosilicates de calcium fibreux; 3 - agglomérations serrées des hydrosilicates de calcium finement dispersés; 4 - particules de PSAS; 8000^{x}.

En comparant les résultats obtenus lors de l'analyse de la formation de gel du ciment durci avec les données de la détermination quantitative des hydrates on aboutit à la conclusion suivante: l'accroissement de la résistance du ciment avec addition PSAS aux différents stades de durcissement (jusqu'à 7 jours) s'explique par l'augmentation de la quantité de l'ettringite et une structure plus homogène de la pierre. L'accroissement de la résistance des échantillons de ce ciment après 28 jours de durcissement, lorsque la quantité des hydrates y est à peu près au niveau du ciment portland ordinaire, s'explique par une structure plus homogène de la pierre de ciment.

Comme le montrent les études, l'expansion du ciment durcissant avec addition PSAS a lieu pour la teneur en ettringite de 8 à 9%. On sait (3,4) qu'une teneur considérable de la pierre durcissante en ettringite est une condition nécessaire mais non pas suffisante pour l'expansion. L'expansion peut apparaître seulement dans le cas où la croissance des cristaux d'ettringite a lieu au stade de formation des contacts de cristallisation dans la structure qui rendent le système cohérentet déterminent un certain niveau de résistance mécanique.

Dans les ciments analysés avec addition PSAS, l'enveloppement des cristaux d'ettringite par les particules d'hydrogel, qui crée le niveau requis de résistance de la structure formée, est un des facteurs contribuant à l'expansion..

La non-coïncidence dans le temps de la fin de l'expansion du ciment durci (3 jours) et l'obtention d'une quantité maximale de l'ettringite (dans les limites de 12 h) s'expliquent par ce que l'expansion continue grâce à la recristallisation et à la croissance des cristaux d'ettringite sans variation ou même avec diminution de leur quantité totale (Fig.3).

En même temps cette croissance des cristaux grâce à laquelle l'expansion ne cesse pas ne détermine pas par elle-même la cinétique de l'expansion. Ainsi, lors du durcissement du ciment expansif et du ciment expansif à prise rapide la croissance des cristaux d'ettringite a lieu avec une vitesse différente, et la cinétique de l'expansion de ces ciments est pratiquement identique.

La cinétique de l'expansion dépend essentiellement de la quantité du gel d'hydrosilicate, de la valeur de l'adhésion du gel d'hydrosilicate aux cristaux d'ettringite

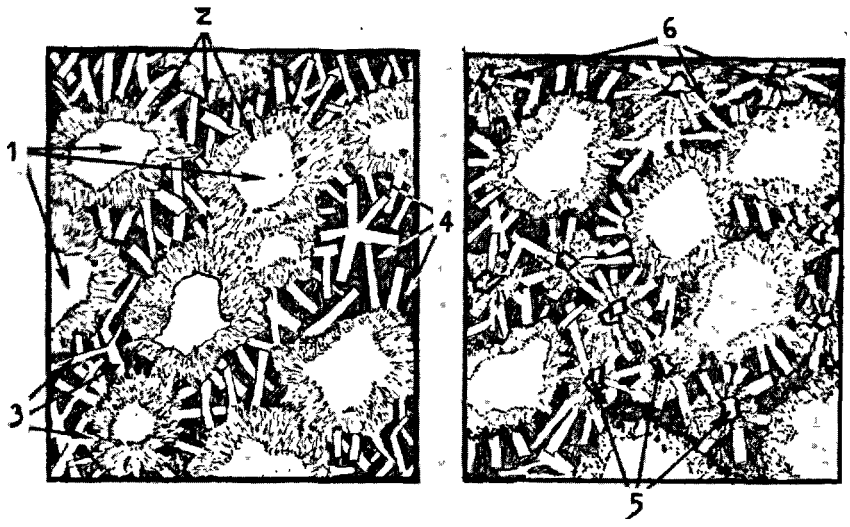

Fig.2. Représentation schématique des structures de la pierre de ciment a) sans PSAS, b) avec PSAS. 1 - restes des grains initiaux du ciment; 2 - régions de la structure compacte secondaire d'hyrosilicates; 3 - ettringite; 4 - hydrosilicates de calcium fibreux; 5 - particules de PSAS restantes; 6 - régions de la structure compacte et secondaire d'hyrosilicates entre cristaux d'ettringite.

et du degré d'homogénéité de la structure du ciment durci. Ces facteurs ont des valeurs proches pour les deux ciments expansifs étudiés.

Sur la base des recherches effectuées, on peut donc conclure que l'addition PSAS agit sur des aspects différents du processus de durcissement du ciment portland. Le plus important est que l'addition est une source des nouvelles formations d'hydrosilicates et d'hydrosulfoaluminates. Ceci conduit à une variation notable de la formation de structure. Les cristaux d'ettringite apparaissent près des particules de départ de PSAS se trouvent en contact étroit avec les agglomérations serrées des particules finement dispersées d'hydrosilicates de calcium. Quant au ciment portland ordinaire, le nombre de ces contacts y est petit grâce à la formation des régions de cristaux d'ettringite isolées du reste de la structure.

Cette différence de principe dans la formation de gel avec les variations de quantité des hydrates de ciment durci fait que la même addition peut communiquer au ciment des propriétés différentes.

Il est expérimentalement établi que la durabilité de la pierre de ciment avec PSAS ne cède pas à celle du ciment portland. Ceci est lié à la composition des hydrates caractéristique du ciment portland et à leur disposition qui est dans la structure du ciment durci plus uniforme que dans le ciment portland et qui exclue le danger de contraintes internes.

CONCLUSIONS

On a étudié le mode de réglage dans de larges limites des propriétés du ciment en introduisant lors du broyage du clinker-portland les diverses quantités du constituant

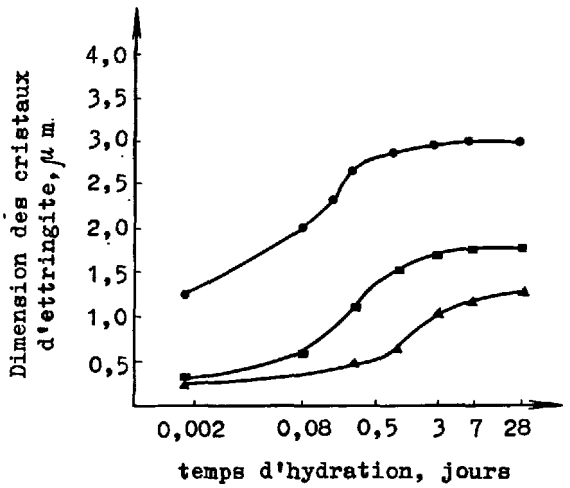

Fig.3. Variation de dimension des cristaux d'ettringite dans la pierre de ciment avec le durcissement —▲—▲— - ciment portland très résistant, —■—■— - ciment expansif, —●—●— - ciment expansif a prise rapide.

de cristallisation sulfoalumosiliceux. Ceci permet d'élaborer sur la base d'un seul clinker des ciments spéciaux à destination différente: ciment portland très résistant et ciments expansifs dont le temps de prise peut être réglé dans de larges limites.

A l'aide d'un ensemble de méthodes d'études physico-chimiques on a établi qu'à la base de ce mode de réglage des propriétés du ciment se trouvent les variations de quantités des hydrosulfoaluminates, de l'hydroxyde et des hydrosilicates de calcium, qui

se forment au cours du durcissement, et l'accroissement de l'homogeneite de la structure du ciment durci en presence d'addition sulfoalumosiliceuse.

BIBLIOGRAPHIE

I.- М.Е.ЖМОДИКОВА, В.И.КОРНЕЕВ (I970) , "Степень гидролиза твердых растворов трехкальциевого силиката". Труды Гипроцемента, вып. 37, с. 49-57, (en russe).

2.- H.G.SMOLCZYK (1962) "Ein zweckmaßiges röntgenographischen Verfahren zur quantitativen Untersuchung hydratisierenden zemente", Tonindustrie-Zeitung, N 10, s. 261-267, (en allemand).

3.- К.Г.КРАСИЛЬНИКОВ, Л.В.НИКИТИНА, Н.Н. СКОБЛИНСКАЯ (I976) "Физико-химия процессов расширения цементов". Труды шестого международного конгресса по химии цемента, т.Ш, с.I73-I79, (en russe).

4.- П.П.БУДНИКОВ, И.В.КРАВЧЕНКО (I973) "Расширяющиеся цементы", У международный конгресс по химии цемента, с.45I-455, (en russe).

Influence de la composition chimique des lignosulfonates sur l'hydratation et la plastification des ciments

Influence of chemical structure of lignosulfonates on hydration and plastification of cements

G.M. TARNAROUTSKI, Candidat ès Sciences Techniques, NIITzement, Moscou,
N.V. GRIBANOVA, Ingénieur, Filiale de VNIIB, Perm.,
G.M. TELYCHEVA, Candidat ès Sciences Chimiques,
V.N. SERGUEEVA, Docteur ès Sciences Chimiques, de l'Académie des Sciences de Lettonie, Institut de la Chimie du Bois de l'Académie des Sciences de Lettonie, Riga, U.R.S.S.

RESUME : On a établi l'augmentation et la diminution respectivement des effets plastifiant et entraîneur d'air des lignosulfonates dans les systèmes ciment-eau lorsque la masse moléculaire croît jusqu'à 14 000 - 16 000, l'optimum d'après le critère de plastification. L'accroissement de l'entraînement d'air est obtenu par diminution de la masse moléculaire et du rapport molaire des groupes sulfo- et méthoxyles. On peut accélérer l'hydratation des ciments avec lignosulfonates et augmenter l'effet plastifiant de ces derniers en introduisant dans la partie liophobe de leurs molécules les groupes polaires aminés et en augmentant le pourcentage de la fraction molaire des groupes hydroxyles. En choisissant un lignosulfonate de masse moléculaire et de composition fonctionnelle données et le procédé de modification de sa structure, on peut obtenir un plastificateur pour ciment, aux effets plastifiant et entraîneur d'air requis, qui ne ralentit pratiquement pas l'hydratation et le durcissement du ciment.

SUMMARY : Increase and decrease of plastifying and air-entraining effects respectively of lignosulfonates in cement-water systems at increase of molecular weight to 14 000 - 16 000 (optimum as regards the plastification criterion) have been established. Increase of air-entraining is achieved by decreasing molecular weight and the molar ratio or sulfo and methoxy groups. Acceleration of hydration of cements with lignosulfonates and intensification of the plastifying effect of the latter are due to introduction of amino-containing polar groups into lyophobic part of their molecules and by increasing content of molar fraction of hydroxy groups.

By selecting lignosulfonates with preset molecular weight and functional composition, as well as the method of modifying of its structure it is possible to obtain a plastifier for cement with the required plastifying and air-entraining action which practically does not decelerate hydration or hardening of cement.

INTRODUCTION. Vu l'effet technique et économique obtenu grâce à l'introduction dans les ciments et bétons des plastifiants, le volume de leur application dans l'industrie des matériaux de construction pour le réglage des propriétés techniques et de construction et la diminution de la consommation de ciment ainsi que pour l'accroissement de la longévité des pièces en béton et en béton armé, croît constamment. En tant que ressources de matières premières pour la production industrielle en grande série de ces additions, on utilise largement les lignosulfonates techniques (LST).

Un grand nombre de travaux est consacré à l'étude du problème de l'influence des caractéristiques du ciment, de la composition du mortier et du béton, des régimes de mélangeage, de compactage et de durcissement sur l'efficacité de l'action des LST. On a prêté beaucoup moins d'attention à la dépendance entre les propriétés chimiques et physico-chimiques des lignosulfonates et leur qualité en tant que plastifiant (1).

L'hétérogénéité de la lignine naturelle, les particularités des processus de délignification du bois ainsi que de la transformation biochimique et de la concentration par évaporation des lessives déterminent une composition chimique différente des lignosulfonates, en particulier leur polydispersité. Des données disponibles (2) témoignent de la dépendance qui existe entre les propriétés consistantes et rhéologiques des systèmes de ciment et l'action dispersante des lignosulfonates qui est déterminée principalement par leur masse moléculaire (MM) et la composition fonctionnelle.

Dans la présente communication on envisage l'influence qu'exercent les lignosulfonates de MM et de composition fonctionnelle différentes sur l'hydratation et la plastification du ciment.

MATERIAUX ET TECHNIQUE D'ETUDES. Des lignosulfonates de sodium purs furent obtenus à partir des LST, le produit marchand obtenu par transformation biochimique de la lessive sulfitique provenant de la cuisson du bois à base de Na ou à base mixte de Ca-Na. L'élimination des hydrocarbures et le fractionnement étaient réalisés par des méthodes fondées sur la capacité des lignosulfonates de former des complexes (3, 4). La destruction d'un complexe formé était réalisée par la solution alcaline. En éliminant les cations des lignosulfonates contenant un excès d'alcali, on a obtenu des acides lignosulfoniques à partir desquels, par substitution au cation d'hydrogène d'autres cations de valence différente, on a obtenu des lignosulfonates (LS) de sodium, d'ammonium, de calcium et de fer. La distribution des masses moléculaires (DMM) des LS est établie sur des colonnes chromatographiques remplies de gel Sefadex G-75(5). Le calcul des MM était effectué d'après les gel-chromatogrammes des LS dans le diméthylsulfoxyde d'après la méthode (6).

On a obtenu un grand nombre de fractions dont les fractions extrêmes étaient utilisées dans les expériences en tant que fractions macromoléculaire (FMM) et bas-moléculaire (FBM).

Pour expliquer l'influence du rapport des groupes hydrophiles et hydrophobes dans les LS, on a déterminé la teneur en groupes méthoxyles (OCH_3) et sulfoxyles (SO_3H) d'après la méthode (7). Pour déterminer la teneur en groupes acides, y compris les groupes sulfoxyles et carboxyles, ainsi qu'en hydroxydes phénoliques, on a utilisé la méthode de conductimétrie à haute fréquence.

On réduisait la quantité de groupes hydroxyles dans la molécule de LS par leur "fermeture", c.-à-d. par la formation des éthers avec le sulfate de diméthyle. La teneur totale en groupes hydroxyles était déterminée par la méthode d'acétylation dans des micro-ampules scellées.

En plus de LST et de fractions certaine de LS, on a utilisé, dans les expériences, des échantillons de lignosulfonates techniques modifiés (LSTM) et de fractions macromoléculaire (FMMM) et bas-moléculaire modifiées (FBMM) de LS obtenues par le traitement des LST et des fractions correspondantes de LS par les amines et leurs dérivés.

Dans les expériences on a utilisé le clinker de composition chimico-minéralogique suivante (% en masse) : pertes à la calcination = 1,47, SiO_2 = 21,66, Al_2O_3 = 4,61, Fe_2O_3 = 4,89, CaO = 65,22, MgO = 1,46, SO_3 = 0,15, R_2O = 0,44, CaO_{libre} = 0,32, C_3S = 61, C_2S = 15, C_3A = 5, C_4AF = 15.

Les plastifiants étudiés étaient introduits dans la composition du ciment lors de son broyage ou avec l'eau de gâchage lors de la préparation du mortier. Les ciments étaient élaborés par broyage, dans un moulin d'essais à deux chambres, jusqu'à S = 3000 ± 100 cm^2/g. L'action plastifiante des agents tensio-actifs était évaluée d'après l'étalement du cône standard sur la table vibrante (d'après GOST 310.4-76, annexe 1), ainsi que d'après la valeur de viscosité de la pâte à structure non détruite avec le rapport E/C = 0,50, en qualité de capteur de viscosité on a utilisé un viscosimètre rotatif "Réotest 2".

Pour évaluer l'influence des plastifiants sur la cinétique et le degré d'hydratation du ciment, on a étudié la composition de la phase liquide de la pâte, et les échantillons durcis étaient soumis à l'analyse thermique différentielle et à l'analyse aux rayons X.

La teneur en air du mortier était évaluée par la méthode de compression et les indices de résistance, d'après GOST 310.4-76 lors du durcissement normal et de l'étuvage.

RESULTATS DES EXPERIENCES. L'efficacité d'action des LS, qui se distinguent par leur MM et la composition fonctionnelle, était comparée pour un effet plastifiant égal s'exprimant par un accroissement de 15 à 25 % de la plasticité du mortier et par une diminution de 1,5 à 3 fois de la viscosité de la structure pratiquement non détruite de la pâte de ciment (η_0). La quantité de LS nécessaire pour obtenir cet effet était de 0,10 à 0,17 % *) (fig. 1). L'augmentation de la quantité de plastifiant jusqu'à 0,30–0,50 % s'accompagnait d'un accroissement de plasticité du mortier de 1,5 à 2 fois et d'une diminution de la grandeur η_0 de 8 à 10 fois. Parallèlement, la limite conventionnelle de la fluidité et la contrainte de cisaillement limite de la pâte de ciment se trouvaient diminuées. Les données obtenues témoignent que les FMM des LS se caractérisent par une action plastifiante plus élevée en comparaison des FBM dans l'intervalle de dosage de 0,10 à 0,20 %. Les MM des fractions de LS avec action plastifiante maximale se trouvaient dans les limites de 10 000 à 15 000. L'extension des limites supérieure et inférieure conduisait en règle générale à la diminution de l'effet de plastification. Toutefois, lorsque la quantité d'agent tensio-actif s'élève jusqu'à 0,50 %, l'action plastifiante de FBM augmente beaucoup plus que pour FMM. L'effet plastifiant le plus élevé était observé lorsqu'on utilisait LS d'ammonium.

La capacité d'entraînement d'air de LS, indépendamment du cation, augmentait avec la diminution de MM. On observait l'effet maximal d'entraînement d'air lors de l'introduction de FBM de LS d'ammonium et surtout de sodium. L'augmentation dans la molécule de LS des groupes hydrophiles, tout d'abord grâce à l'augmentation de la quantité d'hydroxyles phénoliques et des groupes sulfoniques, de même que leur modification par les amines et leurs dérivés, contribue au renforcement de l'action plastifiante et à la diminution de l'effet d'entraînement d'air complémentaire des LS.

D'après les données de l'analyse thermique différentielle, de l'analyse aux rayons X et la cinétique de la variation de composition de la phase liquide, l'introduction de 0,10 à 0,17 % de plastifiants étudiés ne conduit pas à un ralentissement notable de l'hydratation du ciment (Tableau I). En font exception seulement FBM de sodium et FBM de fer. Il faut noter qu'un ralentissement plus considérable des processus d'hydratation était observé lors de l'introduction de FBM.

*) Ici et dans le texte suivant la quantité de LS est calculée pour le corps sec en % de la masse du ciment.

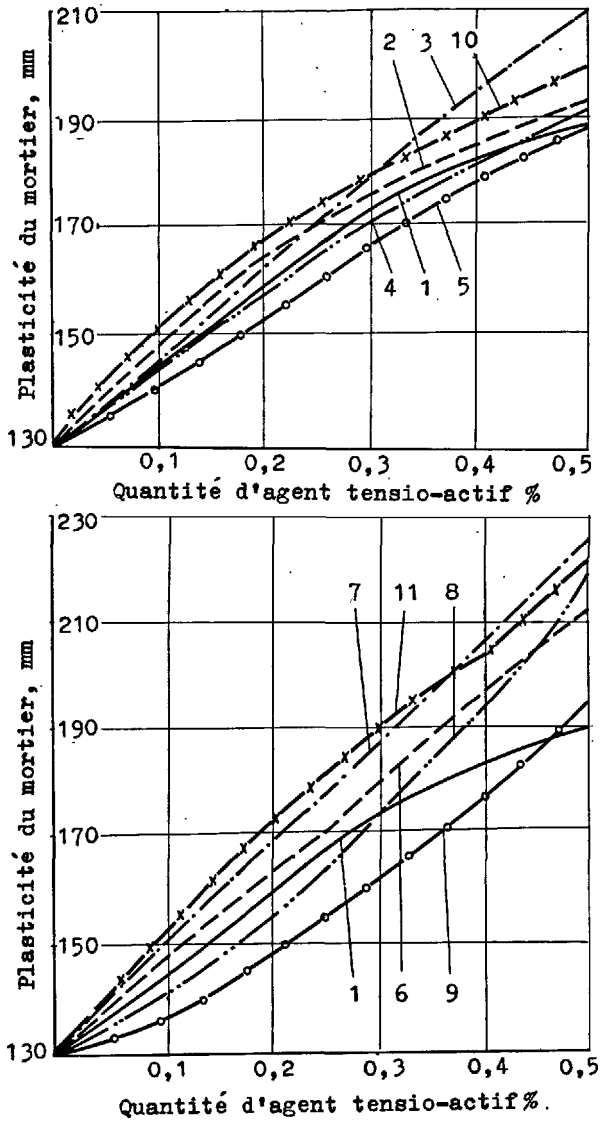

Fig. 1 – Action plastifiante des LS.
1 – LST, 2 – FMM de Na, 3 – FMM de NH_4, 4 – FMM de Ca, 5 – FMM de Fe, 6 – FBM de Na, 7 – FBM de NH_4, 8 – FBM de Ca, 9 – FBM de Fe, 10 – FMMM de Na, 11 – FBMM de Na

Avec l'augmentation de la quantité d'agents tensio-actifs jusqu'à 0,30–0,50 %, on observait le ralentissement des processus d'hydratation du système indépendamment de MM : l'aire de l'effet de déshydratation des hydrosulfoaluminates sur les thermogrammes diminuait, ce qui témoignait de la diminution de la quantité d'éttringite et

du degré d'hydratation ; à côté de la forme cristalline de $Ca(OH)_2$ (480 °C) était fixé l'effet étendu de l'hydroxyde de calcium amorphe (420 à 450 °C). Le degré d'hydratation du ciment avec agent tensio-actif diminuait de 20 à 40 %. FBM de LS de sodium manifesta la plus forte action ralentissante. On observait une influence positive des LS sur les processus d'hydratation après le traitement par les amines et leurs dérivés.

TABLEAU I

Influence des LS sur le degré d'hydratation du ciment

Dénomination de l'addition	Degré d'hydratation d'après C_3S, %			
	1 jour		28 jours	
	Quantité d'addition, %			
	0,15	0,50	0,15	0,50
Sans agents tensio-actifs	38	38	82	82
LST	37	24	81	74
FMM de Na	34	22	83	77
FMM de NH_4	39	27	80	76
FMM de Ca	38	30	81	74
FMM de Fe	38	31	78	74
FBM de Na	30	19	82	71
FBM de NH_4	40	24	82	77
FBM de Ca	34	22	80	76
FBM de Fe	28	21	77	72
FMMM de Na	39	32	85	80
FBMM de Na	34	28	82	78

L'action ralentissante sur l'hydratation du ciment des hydrates de carbone et des acides organiques, entrant dans la composition de l'échantillon étudié des LST en quantité de 8,5 %, ne devenait assez perceptible que lors de l'introduction des LST en quantité de 0,50 %. Toutefois il faut noter que les LST épurés d'hydrates de carbone, surtout leurs FMM, diminuaient sensiblement, dans nombre de cas, le temps de prise du ciment.

Les données obtenues sur la résistance des échantillons (Tableau II) montrèrent qu'indépendamment de la quantité de surfactifs, les FMM étaient plus efficaces que les FBM en cas de traitement à la chaleur humide. Lors du durcissement normal des échantillons, surtout lorsqu'on introduit des quantités élevées de plastifiant, l'effet des LS dépend faiblement de MM. L'accroissement de la quantité de groupes hydroxyles et la modification des LS indépendamment de leur MM entraînèrent l'augmentation des indices de résistance du ciment.

DISCUSSION DES RESULTATS. Les différences notées plus haut en ce qui concerne l'efficacité de l'action des LS de MM différente s'expliquent par leur pouvoir d'adsorption

TABLEAU II

Dénomination des additions et leur quantité, %	Entraînement d'air complémentaire, %	Résistance limite à la compression, MPa, des échantillons d'après		
		GOST 310.4-76		GOST 310-60
		de durcissement normal		étuvés
		3 jours	28 jours	1 jour
Sans surfactifs	-	21,3	40,4	20,8
LST 0,18	3,0	21,1	41,2	16,3
FMM de Na 0,10	2,4	23,4	43,4	19,0
FMM de NH_4 0,10	2,2	23,7	42,1	20,5
FMM de Ca 0,17	1,6	23,2	44,0	18,4
FMM de Fe 0,17	0,8	21,0	43,6	18,3
FBM de Na 0,15	3,8	19,2	39,5	15,7
FBM de NH_4 0,12	3,2	24,2	43,1	18,3
FBM de Ca 0,15	2,2	21,9	39,7	18,0
FBM de Fe 0,15	1,6	18,7	41,0	16,5
FMMM de Na 0,10	1,2	24,6	46,5	22,2
FBMM de Na 0,08	2,6	22,9	44,3	17,4

différent sur la surface des particules du ciment et de ses nouvelles formations hydratées. On sait que, les autres conditions étant égales, le pouvoir d'adsorption des LS croît avec leur MM (1). L'effet dispersif des LS dans les systèmes de ciment augmente avec l'augmentation de leurs MM jusqu'à une limite déterminée, après quoi il commence à diminuer (2). Ceci est en accord avec nos données sur une action plastifiante plus élevée des FMM en comparaison des FBM.

Selon l'hypothèse faite dans (8), l'action plastifiante des agents tensio-actifs dans les systèmes ciment-eau peut être expliquée par la formation des systèmes de faibles H-liaisons, due à l'interaction de l'eau avec les centres électronégatifs de la partie lyophobe des molécules du surfactif. Les autres effets sont secondaires. Comme le montrent les spectres infrarouges, de "fortes" H-liaisons se forment dans la couche potentielle remplie d'eau près de la surface des particules du ciment (9). Pour prévenir leur formation, il faut recouvrir cette couche par la partie lyophobe d'une molécule du surfactif. C'est pourquoi l'action plastifiante des agents tensio-actifs doit croître avec la longueur de la partie lyophobe jusqu'à ce qu'elle atteigne l'épaisseur critique de la couche potentielle, i.e. avec l'augmentation de leurs MM. En effet, les FMM des LS en quantité (0,10 à 0,15 %), assurant le recouvrement des centres actifs de la surface, sont plus efficaces que les FBM dont la quantité doit être sensiblement plus gran-

de pour atteindre le même but. Toutefois, lors de l'introduction d'une quantité élevée de surfactif ce qui fait qu'un grand nombre de molécules restent non adsorbées, la capacité du surfactif de diminuer la tension superficielle, à la limite phase liquide-air, devient un facteur important. Grâce à la solubilité plus élevée, cette capacité croît plus fortement pour les FBM, ce qui est peut-être la cause d'un renforcement sensible de leur action plastifiante lors de l'introduction du surfactif en quantité à peu près égale ou supérieure à 0,50 %.

Outre une longueur correspondante de la partie lyophobe de la molécule du surfactif, la plastification nécessite le blocage des fortes H-liaisons des molécules d'eau par les systèmes ("icebergs") de "faibles" H-liaisons. C'est pourquoi l'effet de plastification doit croître lorsqu'on introduit dans la partie lyophobe des molécules, des groupes polaires renforçant l'électronégativité de leurs centres actifs. Ceci explique l'augmentation de l'effet plastifiant lors de la substitution au cation d'ammonium du cation de sodium et de la modification des lignosulfonates par les amines et leurs dérivés. La valeur de l'effet dépend alors de la structure du groupe aminé joint et se détermine principalement par la densité électronique sur l'atome d'azote.

Lors de l'introduction des agents tensioactifs hydrosolubles, l'effet d'entraînement d'air complémentaire s'explique par la réduction de la tension superficielle sur l'interface solution du surfactif-air, qui dépend de la concentration des molécules du surfactif restant dans la solution après son adsorption. C'est pour cette raison que les FBM de LS, qui possèdent un pouvoir adsorbant réduit en comparaison des FMM, se caractérisent par une action d'entraînement d'air et moussante plus élevée. Ces effets augmentent avec l'accroissement de la concentration des LST dans la solution, la diminution de MM et du degré de sulfonation des LS (2). Les LST à base d'ammonium possèdent le plus grand pouvoir moussant tandis que les LST à base de sodium se caractérisent, même aux faibles concentrations, par une grande stabilité de la mousse (10). Ces derniers possèdent également une action d'entraînement d'air plus élevée par rapport aux LS de calcium et de fer. La modification des LS conduit à l'accroissement de leur MM et respectivement à la diminution de leur pouvoir d'entraînement d'air et de leur pouvoir moussant.

L'influence des lignosulfonates sur les indices de résistance du ciment dépend de leur action ralentissante sur les processus d'hydratation du ciment et du pouvoir d'entraînement d'air des LS, le premier facteur exerçant une influence plus sensible sur la résistance du ciment au cours du durcissement normal et le second, lors du traitement à la chaleur humide. Il convient aussi de noter l'importance de l'élévation du pouvoir plastifiant des LS, ce qui permet d'obtenir le même effet plastifiant avec une quantité moindre d'addition et, donc, d'affaiblir les facteurs négatifs influant sur la résistance du ciment.

CONCLUSION

L'analyse des données obtenues témoigne de la nécessité d'aborder de manière différencielle le problème d'élaboration des additions sur la base des LST en fonction de leur destination. On a établi qu'il est possible d'obtenir un plastifiant pour le ciment à base des LS, qui aurait une action plastifiante et d'entraînement d'air requise et qui ne ralentirait pratiquement pas l'hydratation et le durcissement du ciment.

BIBLIOGRAPHIE

1. В.Н. СЕРГЕЕВА, Г.М. ТАРНАРУЦКИЙ, Н.В.ГРИБАНОВА, Г.М. ТЕЛЬШЕВА (1979) "Лигносульфонаты как пластификаторы цемента",Химия древесины, вып. 3, с. 3-12, (en russe).

2. А. КОБАЯСИ, Т. ХАГА, К. САТО (1967), "Диспергирующий и воздухововлекающий эффект лигносульфонатов", Мокудзай гаккайси, т. 13, 3, с. 113-122.

3. F.E. BRAUNS Recovery of lignosulfonates. US Patent № 3.297.676 от 10.01.67, (en anglais).

4. М.Н. ЦЫПКИНА, И.М. БАЛАШОВА (1959) "Осаждение лигносульфонатов комплексной солью", Журнал прикладной химии, т. 32, I, с. 166-170, (en russe).

5. Г. ДЕТЕРМАН (1970), "Гель-хроматография", "Мир", М., с. 105, (en russe).

6. А.Д. АЛЕКСЕЕВ, В.М. РЕЗНИКОВ, Б.Д. БОГОМОЛОВ, О.М. СОКОЛОВ (1969), "Исследование полидисперсности лигнина Бьеркмана", Химия древесины, вып. 4, Рига, с.49-50, (en russe).

7. Г.Ф. ЗАКИС, Л.Н. МОЖЕЙКО, Г.М. ТЕЛЬШЕВА (1975), "Методы определения функциональных групп лигнина", "Зинатне", Рига , с. 16-80, (en russe).

8. Г.М. ТАРНАРУЦКИЙ, Б.Э. ЮДОВИЧ (1978) , "Физико-химические основы гидрофобизации и пластификации цемента поверхностно-активными веществами", Тезисы докладов, VI Всесоюзное совещание по химии и технологии цемента, М., с. 33, (en russe).

9. Г.М. ТАРНАРУЦКИЙ, Б.Э. ЮДОВИЧ, И.В.КРАВЧЕНКО (1977), "Инфракрасная спектроскопия ПАВ, адсорбированных на клинкерных минералах", "Технология специальных цементов", Труды НИИЦемента, вып. 32, М., с. 92, (en russe).

10. Г.М. ТАРНАРУЦКИЙ, Г.Ю. ВАСИЛИК, Ю.С.МАЛИНИН (1978), "Применение технических лигносульфонатов в производстве цементов", Гидролизное производство, Реф. сборник,вып.11(100),с.11,(en russe).

Testing methods for the set of pastes and mortars

Méthodes de détermination de la prise des pâtes et mortiers

Dr. M. MAULTZSCH and
U. MEINHOLD, Federal Institute for Testing Materials (Bundesanstalt für Materialprüfung (BAM) Berlin, R.F.A.

RESUME : Des mesures de la prise des pâtes et mortiers de ciment ont été faites par différentes méthodes et comparées entre elles. La prise des pâtes est déterminée par un essai de pénétration, notamment par l'aiguille de Vicat. Sous certaines conditions et en choisissant convenablement le corps de pénétration, on peut caractériser de façon qualitative l'influence de certains facteurs sur l'évolution de l'hydratation. Les facteurs pris en compte ont été : le rapport E/C, la température et le dosage en adjuvant.

Les essais de prise sur mortiers normalisés sont plus proches des exigences de la pratique. Ainsi des changements, en fonction du temps, du comportement plastique, peuvent être décelés par le "flow test". La fausse prise, le raidissement prématuré et d'autres irrégularités du processus de prise peuvent être ainsi déterminés quantitativement, ainsi que l'action des adjuvants. Des exemples montrent que les résultats obtenus sur les pâtes se transposent difficilement aux mortiers, alors que les résultats obtenus sur mortiers et sur bétons sont comparables.

SUMMARY: Measurement data of cement pastes and mortars are compared. The set of pastes is tested with the penetration method e.g. according to Vicat. Under special conditions and selecting a suitable penetration body it is possible to record qualitatively certain influences on the process of hydration, namely the water/cement ratio, the temperature and adding quantity of chemical admixtures for concrete. More suitable for the requirements in practical use are set tests on standardized mortars. Thereby the temporal change of the plastic behaviour is to be determined by the flow test. False set, premature stiffening and other irregularities in the process of setting as well as the action of admixtures, can be recorded quantitavely. By examples it is shown, that test results of set for pastes are only comparable to a certain extend to those of mortars, whereas mortar and concrete react comparable with each other.

INTRODUCTION

The setting of cement pastes and mortars is being tested according to the penetration test of Vicat (1) since the beginning of the 19th century. Originally this was done to distinguish qualitatively between the fast setting within a few hours and the slow setting within any length of time. The development of cement and concrete technology during the last decades has made it necessary to get more exact knowledge of the setting process. As far as the Vicat test was used quantitatively it has been overestimated in many cases with regard to the certainty and the importance of the measurements. On the other hand there is no other method for cement pastes that gives us any reliable data comparatively as little expended energy as this test.

Besides insufficient attention is paid to the differences of changes in consistency of mortars and concretes referred to the setting of cement and those of pastes.

SETTING OF CEMENT PASTES

The needle penetration method of Vicat may provide reasonable set test values for normally setting cements. Prerequisite is always keeping precisely the same conditions and a careful test procedure (2). The fixings of this point by international standards are not sufficient.

The penetration depth of the needle, plotted versus time, shows a more or less steep s-like shape as a rule (figure 1 top). This shape of the curve does not even change if a cement tends to "false set" or "premature stiffening". However, if irregularities of setting become stronger the penetration depth values may vary erratically so that only a fitting curve leads to a result. In figure 1 bottom the setting of a paste containing a retarder admixture is plotted. Apparently this admixture has promoted the formation of spacially limited portions, stiffening starts from these. In former studies this effect sometimes is mentioned as "insular formation". It causes an irregular penetration of the slim Vicat needle. It shall be remembered here that the volume displaced by the Vicat needle is a very small one indeed, but the needle regarded as a pressure foot causes the considerable compressive stress of 3 N/mm^2.

The above mentioned irregularities of the test values do not occur if a conical penetrator instead of the needle is used because its penetration volume is larger. McCormick and Cowgill (3) had already pointed to the greater precision of the test working with a cone, two inches in base diameter, to determine the water content of mortars. The slender cone proposed by us makes it possible for example to find out the "false set" and the "premature stiffening" or the stiffening secondary effect due to some concrete admixtures. The curves for instance drawn in figure 2 are based on numerous measurements with a conical penetrator the diameter of which is 1 mm at the bottom and 9 mm at the height of 40 mm respectively. Using this cone one cannot measure the setting time as defined in the standards, but it makes perceptible such properties of cements that influence directly the consistency changes dependent on time.

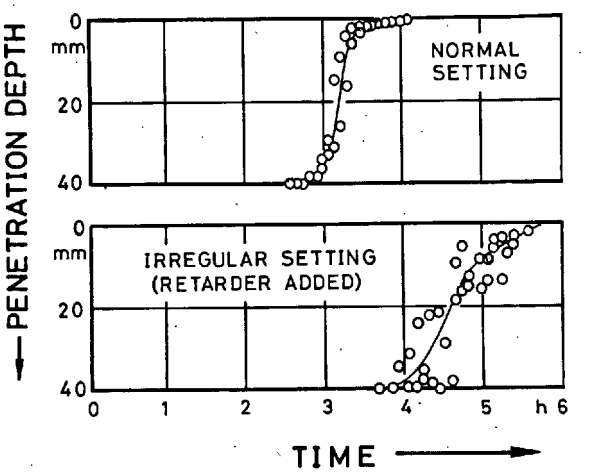

Fig. 1 - Vicat test on cement pastes. Penetration depth versus time.

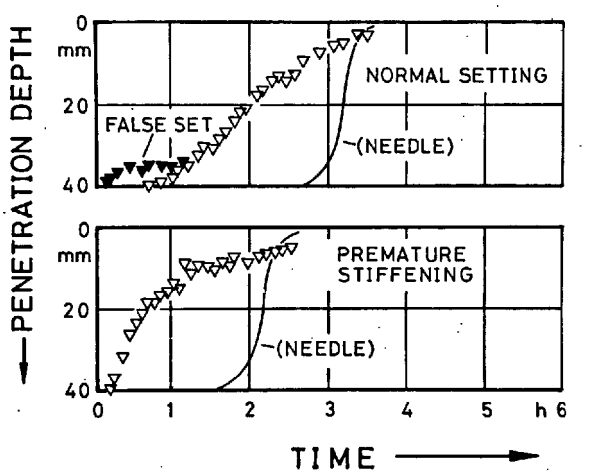

Fig. 2 - Modified Vicat test on cement pastes. Penetration depth of a conical penetrator versus time.

The regulations for setting time determination laid down in cement standards do not make much sense. This is because they are based on penetration depth values lying within the respective flat sections of the s-like curve. That means of course that the spread of the values is very large. For the determination of setting times it is more suitable to elect a point out of the steep curve path, e.g. at the penetration depth of 20 mm. In most cases the spread will be re-

duced to ± 5 minutes. In this way the influence of the water/cement-ratio can be determined on a large scale (fig. 3). In these experiments two ordinary portland cements Z 45 F of nearly equal fineness were used. It is significant that small variations of the w/c-ratio produce large changes of setting time only for one of the cements.

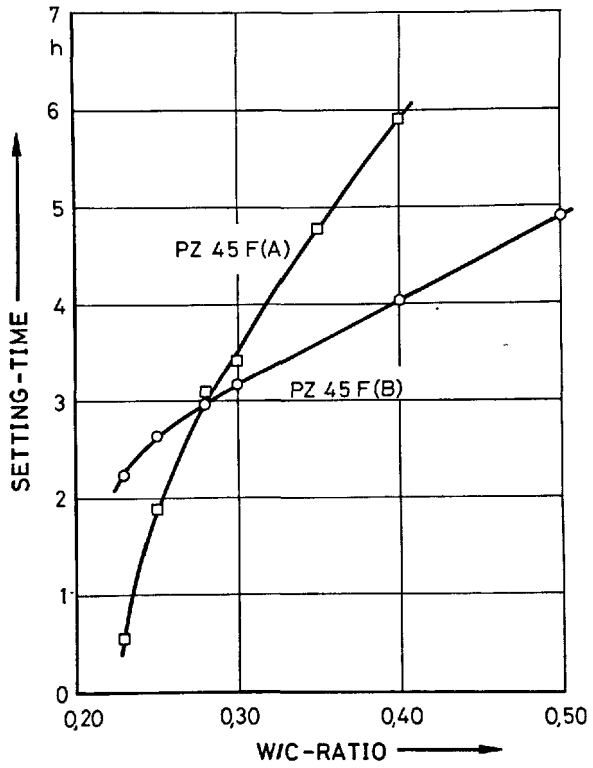

Fig. 3 - Influence of the w/c-ratio on the setting time of cement pastes for two different cements "A" and "B".

Figure 4 shows the influence of the dosage rate of a retarding admixture on the setting time of a portland cement. The amount of time in which the needle reached only 20 mm penetration depth was defined as the setting time in this case too. Initial or final setting time values as defined by standards could not be determined at all or with sufficient precision for most of the mixtures. With a certain quantity of admixture depending on the w/c-ratio slow-setting is reverted to quick-setting rather abruptly. The importance of these measurements with regard to practical use will be referred to later.

SETTING OF MORATRS AND CONCRETES

The purpose of determining the setting times of cements is, with regard to practical application, to point out the length of time during which mortars and concretes are workable. It has been proven, however, that the stiffening behaviour of cements in pastes is

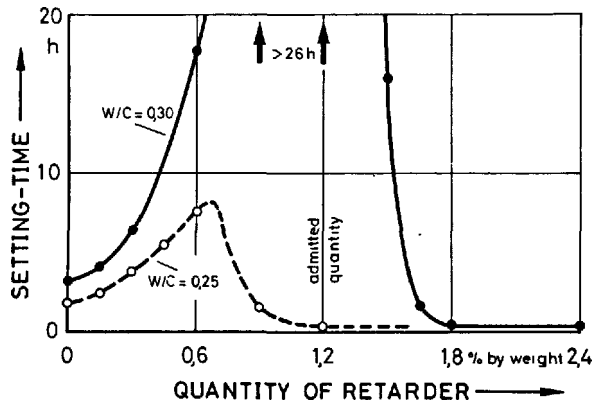

Fig. 4 - Setting time of cement pastes versus quantity of retarder admixture.

different from that in mortars or concretes. But it is a disadvantage that stiffening tests on concretes are very laborious. Furthermore most of the methods for testing the consistency of concretes fail in accuracy, or their applicability is limited (4). Particularly the penetration tests on concretes hardly indicate any useful results.

During the last years we made numerous measurings of the time-dependent consistency changes of concretes using the German standard flow table. The flow development in time has been mentioned on other studies referring to the influences of some admixtures, particularly of plasticizers (5, 6). But the extent of these investigations is not adequate to evaluate the workability in principle. Working with this background, investigations with the aid of flow tests on standardized mortars adduced satisfactory results (7). Provided with a suitable test procedure, it is possible to even quantitatively recognize factors of influence on the stiffening behaviour.

The flow of mortars is determined by the flow table apparatus standardized in DIN 18 555 (similar to that in ASTM C 230-68). The conical mold for the mortar has a basic diameter of 10 cm. The table is to be dropped through a height of 10 mm once per second and the flow is the resulting diameter of the mortar mass after a certain number of drops.

In order to precisely determine the stiffening the flow value should originally be on a high level, and test mortars initially should have a good flow capability. This may be affected by the cement content, the water/cement-ratio, and the number of drops. Originating with the standard mortar specified for testing cements, a small increase of cement content proved to be favorable. The investigations described subsequently were carried out with mortars of mix proportion 1 : 2,7 by weight. If the water/cement-ratio is varied within a reason-

able range, flow values correspond directly and linearly, even after some hours after mixing and additionally affected by admixtures (figure 5).

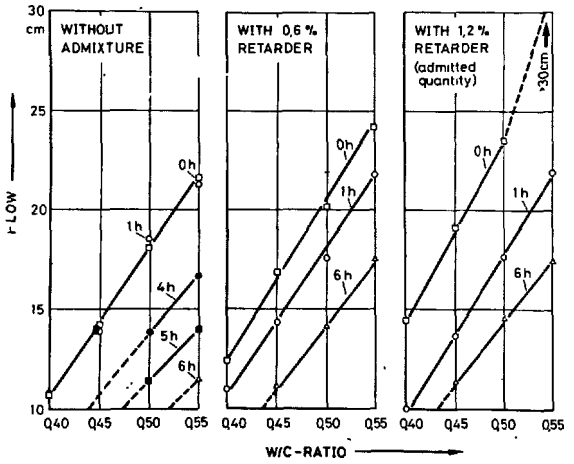

Fig. 5 - Flow of mortars with and without admixture at different hydration times versus water/cement-ratio.

Figure 6 shows the flow correlating to the number of drops while different w/c-ratios are given. With growing numbers of drops flow values increase a little underproportionally. For further investigations the w/c-ratio was fixed at 0,50 and the number of drops at 20. Under these conditions most of the cements produce initial flows of about 20 cm.

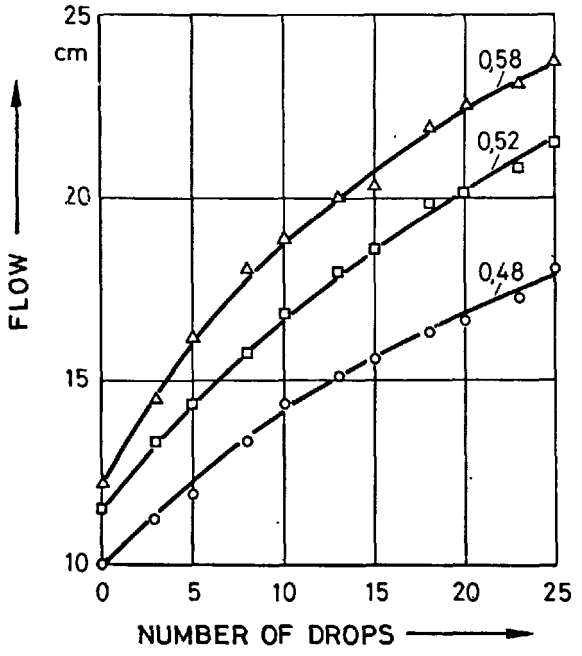

Fig. 6 - Flow of mortars with different w/c-ratios versus number of drops.

The hydration process leads to the stiffening of the mortar and to a continuous decrease of the flow depending on time. The values of normal setting cements generally fall into the hatched area of figure 7. But otherwise this test method makes it possible to definitely recognize setting irregularities such as false set or premature stiffening. False set always leads to a slight increase of flow values during the initial time period. On the other hand premature stiffening can be recognized by a remarkable steep fall of the curve within the first hour after mixing.

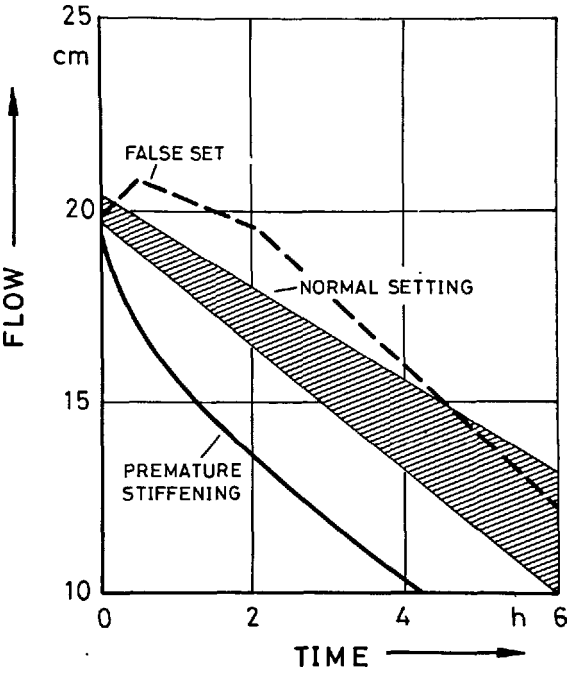

Fig. 7 - Flow of modified standard mortar versus time.

In many cases of practical use concrete admixtures are added to affect consistency or stiffening. The mode of action of these reagents, such as plasticizing, retarding, accelerating, may be determined with sufficient accuracy by the proposed test method. Here also the modified standard mortar with increased cement content and the w/c-ratio 0,50 stood the test. During the first hours measurements of flow should be performed in 30 min intervals at the most. When testing admixtures of accelerating or stiffening effect, time intervals should be shortened (8).

This way for example many setting retarders were tested. With respect to numerous different cements it could be proven that retarding effects, i.e. to preserve a certain consistency, did not occur before 2,5 - 4 hours after mixing, while within the initial period a conspicuous stiffening of the mortar was observed. Figure 8 shows flow curves of mortars with various quantities of retarder

admixtures in comparison to non-retarded mortars, using three different w/c-ratios.

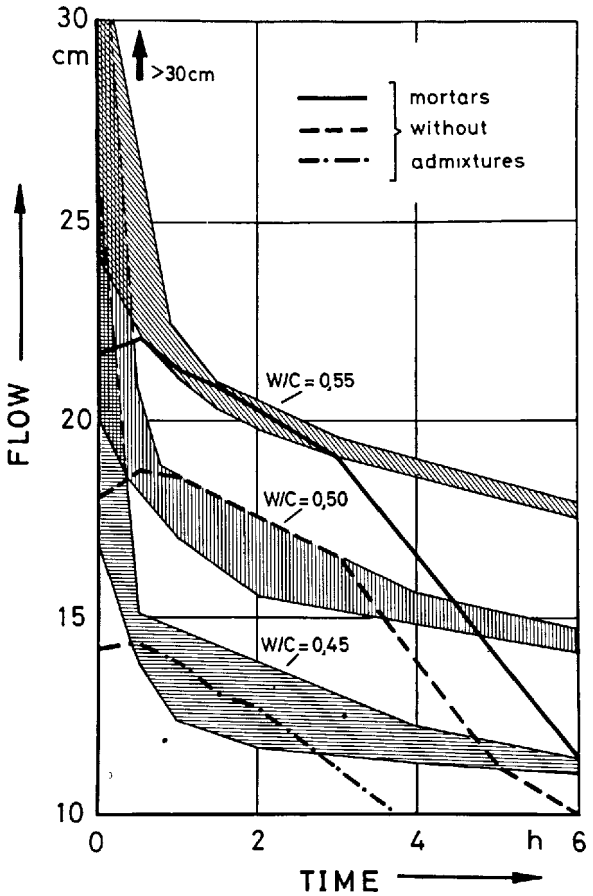

Fig. 8 - Effect of a retarder on the flow of mortars. The hatched area covers the values for different admixture quantities.

The admixture's influence on the consistency within the first half hour is evident. It should be mentioned that the non-retarded mortar tended to false set due to the chosen cement. During the next 2 hours all retarded mortars show nearly the same stiffening behaviour as those without admixtures. Only later the retarded mortars stiffen slowly as compared to the normal set of the non-retarded mortars. This behaviour seems to be independent of the water/cement-ratio. Merely the premature stiffening effect becomes stronger with the decrease of w/c-ratio and the increase of dosage. Other retarders, those without plasticizing effect, also led to flow development in time that differed from that of admixture-free mortars not before 2,5 - 4 hours.

Figure 9 answers the question regarding the influence of the dosage that was already mentioned. Immediately after mixing, the retarder used here plasticizes the mortar more and more with increasing addition, as is well known of lignosulphonates. But the early stiffening effect grows at the same rate. Therefore after one hour all the mortars have the same flow independent of the dosage of retarder. Further stiffening is affected differently only by very small additions, but exceeding a certain quantity the dosage does not induce any differences in stiffening behaviour. All measured values are covered by the hatched area in the graph, i.e. in spite of increasing admixture quantities the setting of the mortars is retarded equally. This result appears to be in contradiction to the values determined by needle penetration tests on pastes of the same cement and retarder (see fig. 4). There is no reversion to quick-setting of the mortars. It must be concluded that with respect to the workability of mortars and concretes the needle test is unsuitable and may even cause an erroneous rating of consistency behaviour. Results of tests on the setting of cement pastes cannot be transferred to the consistency development in time of mortars and concretes. On the other hand it was previously deduced that flow values of modified standard mortars determined by the proposed method correlate very well at any time to those of comparable standardized concretes (7).

However, the Vicat needle test may point to discontinuities of the hydration process with certain addition quantities. For example the mortars with high retarder content being of good workability even after six hours failed in strength development. Finally they crumbled if stored under water. In this case the striking reversion in set observed in the tests on pastes indicates problems with the hardening process rather than trouble with the workability.

CONCLUSIONS

With regard to tests on the set of pastes three conclusions result from the investigations and interpretations of many references as well: 1st, the traditional Vicat test should be improved by recording continuously the determined values of penetration depth versus time and by redefinition of the setting time on the basis of a medium penetration depth; 2nd, results of penetration tests on pastes should not be the only criterion for the setting of mortars and concretes; better results will be obtained using a conical penetrator; 3rd, the needle test is suitable to detect qualitatively certain effects on the hydration process.

Setting tests on mortars require an acceptable expenditure of work. Under certain conditions the results correspond to those obtained by tests on concretes. Based on satisfactory experiences on a large scale, a method of setting test is proposed using a standardized mortar with increased cement content. Normal setting, false set, and premature stiffening respectively may be determined by this method.

Furthermore effects of admixtures on the

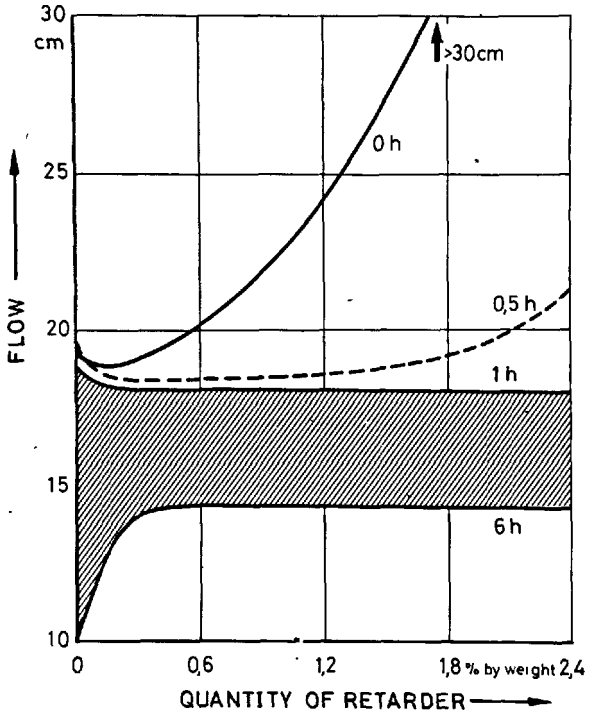

Fig. 9 - Flow of modified standard mortar versus quantity of retarder admixture at different hydration times.

consistency or the stiffening may be characterized even quantitatively. However, it must be pointed out that a favorable workability of mortars or concretes, particularly of those containing admixtures, does not necessarily guarantee favorable hardening and strength development.

REFERENCES

1.- L.J. VICAT (1818), "Recherches expérimentales sur les chaux de construction, les bêtons, et les mortiers ordinaires", Paris.

2.- M. MAULTZSCH (1977), "Zur Messung des Erstarrens von Zementpasten", BAM-Amts- u. Mitteilungsblatt, 7, 146-148.

3.- F. McCORMICK and J.T. COWGILL (1965), "Sensitivity of a conical penetrator to variations in mortar mix parameters", J. Franklin Inst., 279, 464-471.

4.- TH. DRATVA (1978), "Messung der Betonkonsistenz. Vergleich der Prüfstreuung und Empfindlichkeit von sieben Methoden", Schweizer. Bauz., 96, 11-14

5.- O. HALLAUER (1978), "Einfluß langer Rührzeiten auf die Betoneigenschaften", beton, 28, 131-135.

6.- H. REUL (1979), "Untersuchungen an Fließmitteln", beton, 29, 247-249.

7.- U. MEINHOLD, M. MAULTZSCH, and P. SCHIMMELWITZ (1978), "Untersuchungen zur Wirkung von Erstarrungsverzögerern auf die Verarbeitbarkeit von Beton", Betonwerk + Fertigteil-Technik, 44, 485-491.

8.- J. HOROWITZ, Z. KALMAR, and F. TAMAS (1978), "Effect of plasticizing admixtures upon the rheological properties and the hardening of concrete", Silic. Ind., 43, 101-108.

Influence des sulfates sur les comportements rhéologiques des pâtes de ciment et sur leur évolution

Influence of sulfates on the rheological behavior of cement pastes and on their evolution

J.P. BOMBLED, C.E.R.I.L.H., France

RESUME

Les sulfates jouent un rôle important non seulement en fabrication des liants mais encore et surtout lors de leur utilisation dans les mécanismes rhéologiques et d'hydratation ainsi que pour la durabilité.

Pour chercher à comprendre leur action sur le plan rhéologique à l'état frais et sur les évolutions précoces (prise, raidissements) ou ultérieurs (résistances, variations dimensionnelles) on a étudié d'une part différents sulfates calciques (gypse, plâtre, anhydrite naturel, phosphogypse) et d'autre part un certain nombre de sulfates non calciques (Li, Na, Mg, Al, K, Mn, Fe, Cu, Zn, Ba, Pb, NH_4) ; les essais ont porté sur deux clinkers de teneur différente en C_3A (3 et 14 %).

Comme les cinétiques et les équilibres de dissolution régissent en grande part tous les phénomènes initiaux, l'étude a débuté par l'examen de la solubilité et de la vitesse de dissolution ainsi que les facteurs qui l'influencent (température, finesse, ions communs); y compris la répercussion du moment d'incorporation du sulfate (au broyeur, dans le clinker broyé, dans l'eau, dans le malaxeur).

Il ressort des essais que la rhéologie des pâtes de ciment fraîches résulte de la conjonction de l'effet de floculation et de l'action retardatrice sur l'hydratation précoce des aluminates : selon la composition minéralogique du clinker et la cinétique de dissolution, l'incorporation d'un sulfate peut se traduire, soit par une fluidification (apparente), soit par une rigidification.

L'évolution dans les premières heures (période de mise en œuvre) montre aussi que, suivant la quantité de sulfate disponible ou non consommée, on peut voir l'action fluidifiante ou rigidifiante suivie soit par un effet retardateur soit par un effet accélérateur sur la phase silicate.

D'une façon générale, les activités observées dans presque tous les cas se classent à peu près dans l'ordre des vitesses de dissolution.

Les conséquences sur les propriétés des pâtes durcies confirment ce qui est déjà bien connu dans ce domaine.

SUMMARY

The sulfates play an important role, not only in the fabrication of binding materials, but also and chiefly in their use in rheological and hydration mechanisms, and for the durability.

Different calcium sulfates (gypsum, plaster of Paris, natural anhydrite, phosphogypsum) and on the other hand sulfates of other metals (Li, Na, Mg, Al, K, Mn, Fe, Cu, Zn, Ba, Pb, NH_4) were studied in order to attempt an understanding of their action on the rheological field at fresh state and upon early (set, stiffening) or further (strength, dimensional variations) evolutions ; the tests were made on two clinkers with different C_3A-contents (3 and 14 %).

As dissolution kinetics and equilibriums govern in a large extent all initial phenomena, the research began with the examination of the solubility and speed of dissolution as well as factors which influence on it (temperature, fineness, common ions), including the effect of the point of time of the incorporation of the sulfate (into the mill, into the ground clinker, into the water, into the mixer).

The tests show that the rheology of fresh cement pastes results from the conjunction of the effect of flocculation and of the retarding action upon the early hydration of the aluminates : according to the mineralogical composition of the clinker and to the dissolution kinetics, the incorporation of a sulfate determines either a seeming fluidization or a stiffening.

The evolution during the first hours (pouring period) shows also that according to the disposable or unconsumed quantity of sulfates, the fluidizing or stiffening action can be followed either by an extended retarding effect or an accelerating effect on the silicate phase.

Generally, the activities observed in almost all the cases are classed approximately in the same order as the dissolution speeds.

The consequences on the properties of hardened pastes confirm what is already well known in that field.

1. INTRODUCTION

Les sulfates et notamment les sulfates calciques peuvent jouer un rôle soit en fabrication (minéralisateurs, fabrication combinée clinker-SO_4H_2), soit comme composants de liants (sursulfatés, expansifs,...), soit comme adjuvant modifiant la rhéologie et les vitesses d'hydratation (accélération des silicates et du laitier, retardement des aluminates,...) ; les ions sulfates interviennent aussi dans les problèmes de durabilité (attaques d'eaux agressives par exemple).

Ajoutons que le souci de protection de l'environnement et de valorisation de déchets industriels rend disponibles des quantités considérables de sulfates de calcium "chimiques" (phosphogypse par exemple) dont l'incorporation dans les ciments est envisagée.

Il en résulte qu'une meilleure connaissance des mécanismes d'action des divers sulfates sur le comportement rhéologique à l'état frais et sur l'évolution ultérieure (prise, raidissements, durcissement, variations dimensionnelles) revêt un intérêt capital.

2. GENERALITES

2.1 Floculation

A partir du contact eau-ciment, dans la séquence des phénomènes (mouillage, floculation, pénétration, hydrolyse, dissolution, solvatation, hydratation, diffusion, sursaturation et précipitation) c'est en particulier la floculation qui conditionne le comportement rhéologique de la pâte fraîche ; néanmoins, il ne faut pas oublier que les premières liaisons dues à l'hydratation précoce peuvent aussi empiéter sur la période de mise en œuvre (état frais).

Nous avons montré depuis longtemps [1] que l'état de floculation des pâtes de ciment dépend de la nature des minéraux (potentiel de surface et homogénéité de répartition des charges) et de la nature (valence, dimension) des ions compensateurs provenant des éléments dissous ou des adjuvants (épaisseur de la double couche de Gouy, quantité d'eau "bloquée").

Il ressort de nos études antérieures que la floculation est en grande partie responsable du comportement visco-plastique Binghamien des pâtes de ciment fraîches (cohésion, thixotropie,...) et ipso facto de la cohésion de la pâte interstitielle des bétons, grandeur qui est une des composantes de la plasticité des bétons frais [2].

2.2 Dissolution

Comme pour les minéraux du clinker, les conditions du passage en solution des sulfates (et surtout leur vitesse) est l'élément capital pour comprendre les mécanismes rhéologiques précoces qui nous intéressent. Mais il faut aussi tenir compte du phénomène très important de solvatation (dû à l'interaction des ions avec les molécules du solvant), c'est-à-dire la fixation autour des ions d'un essaim considérable de molécules d'eau, ce qui modifie la mobilité, la diffusion, la quantité d'eau libre, etc...

Rappelons que l'équilibre ionique des solutions est régi par la loi de dilution d'OSTWALD:

$$\text{Produit de solubilité : } K_{ps} = \frac{[A^+][r^-]}{A\Gamma} = \frac{\alpha^2}{1-\alpha} C^n \qquad (1)$$

(pour fixer les idées, à 18/25 °C :
$K_{ps} = 2{,}5\ 10^{-5}$ pour $SO_3Ca.2H_2O$
$= 1{,}3\ 10^{-5}$ " $Ca(OH)_2$).

L'évolution, dans les premiers instants, sera la conjonction des cinétiques de dissolution des éléments très rapidement solubles (C_3A, sulfates, éléments alcalins, grains "colloïdaux") en résumé :

La solubilité des sulfates calciques dépendra :

- de leur taux d'hydratation (et éventuellement des conditions de déshydratation ; cf paragraphe 3),
- de la température, la solubilité décroît pour les dissolutions exothermiques et pour les corps formant des hydrates (ce qui est le cas), figure 1 (a) ,
- de la conséquence de la loi de dilution par la présence d'autres ions, communs (Ca^{++}, SO_4 des clinkers) ou non (hydroxyle OH^- par exemple), figure 1 (b).

La vitesse de dissolution dépendra de la surface en contact (figure 2), de la constitution du sulfate (figure 3) et dans une certaine mesure de l'agitation et de l'ordre d'incorporation, on peut noter sur la figure 2 qu'au-delà de ∿ 3000 cm^2/g, la surface spécifique du gypse joue peu, la dissolution est quasi instantanée.

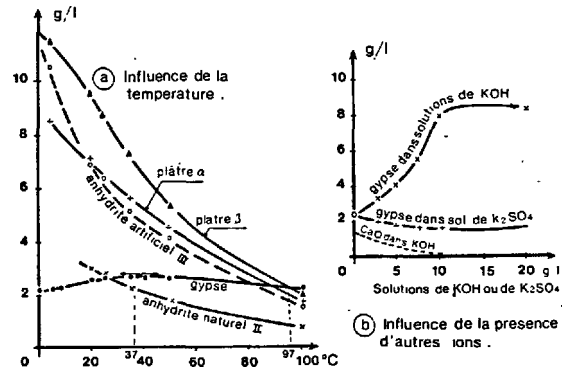

Fig 1 . Solubilite des sulfates calciques .

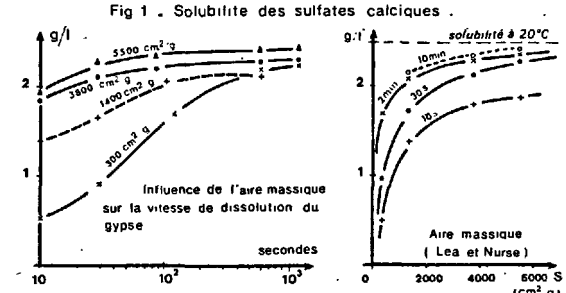

Fig 2 . Vitesse de dissolution et aire massique .

2.3 Corollaire

Le comportement rhéologique à l'état frais sera le résultat de la conjugaison de plusieurs processus plus ou moins échelonnés dans le temps :

- les gros anions (SO_4^{--}, OH^-) viennent préférentiellement se fixer sur les grains électropositifs des aluminates et modifier l'équilibre électrocinétique des interactions intergranulaires (liaisons de floculation).
- par ses ions Ca^{++}, le sulfate de calcium joue le rôle de réducteur de solubilité à l'égard du C_3A et par conséquent retarde l'apparition de liaisons d'hydratation précoces [3] et [4].
- l'affinité des sulfates et des aluminates conduit aussi à la formation de sulfo-aluminates qui consomment les ions SO_4^{--} dont l'épuisement permet à nouveau, à terme, la reprise de la dissolution et de l'hydratation du C_3A avec le raidissement concomitant.

- enfin comme anions forts (donnant des sels calciques plus solubles que les silicates de Ca), s'ils ne sont pas épuisés les ions SO_4^{--} contribuent à accélérer l'hydratation de C_3S d'où de nouvelles liaisons prenant le relai dans les premières heures pendant l'évolution rhéologique.

3. MATERIAUX UTILISES

3.1 Clinkers (Tableau I)

Deux clinkers, de teneurs en C_3A différentes, et broyés à deux finesses ont été sélectionnés.

Tableau I

Clinker	Analyses minéralogiques par diffraction X (%) C_3S	C_2S	C_3A	C_4AF	Teneur en éléments mineurs (%) SO_3	K_2O	Na_2O	MgO	chaux libre	Aire massique Blaine (cm^2/g)
"A"	77	15	3,2 *	4,3	0,43	0,25	0,13	0,86	0,40	I 3600
						Σ 0,38 %				II 4600
"B"	62	18	14 **	5	0,44	1,10	0,28	1,04	1,25	I 3600
						Σ 1,38 %				II 4600

* forme cubique ** orthorhombique

3.2 Sulfates (Tableau II)

Quatre sulfates de Ca, parmi lesquels deux ont été broyés à deux finesses, ont été choisis.

Tableau II

Sulfates (provenances)	Minéraux	Déterminations chimiques p f	SO_3	Na_2O K_2O	MgO	Aire massique Blaine (cm^2/g)
gypse (Vaux / Seine)	$SO_4Ca,2H_2O$ + quartz et calcite	22,0	43,3	0,10	abs	(1) 3800 (2) 5500
Anhydrite naturel (Thionville)	SO_4Ca contient aussi du gypse	5,1	54,1	0,20	0,60	(1) 3500 (2) 7200
Plâtre (Prolabo)	$SO_4Ca,0,5H_2O$ + anhydrite	7,9	50,2	0,03	0,50	2700
Phosphogypse* neutralisé épuré (Douvrin)	presque entièrement forme de semi hydrate	5,6	53,5	abs	0,40	6900

* Impureté majeure soluble . P_2O_5 8 mg l

Pour les sulfates non calciques on a choisi : Li, Na, Mg, Al, K, NH_4, Mn, Fe, Cu, Zn, Ba et Pb.
La Figure 3 illustre les vitesses de dissolution.

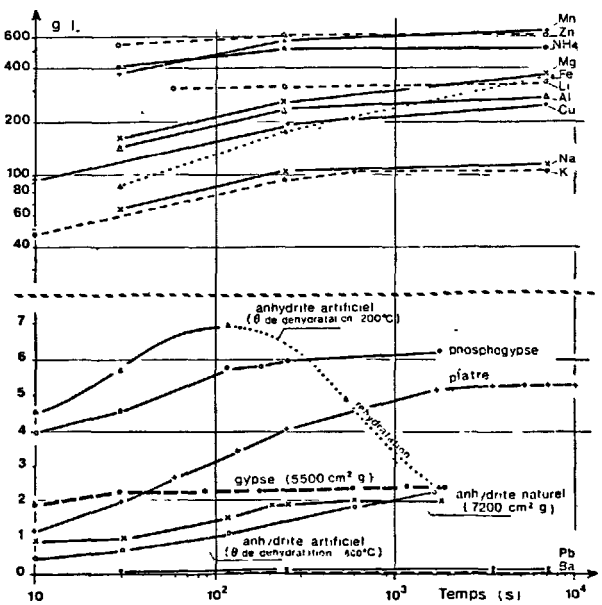

Fig 3 . Vitesse de dissolution des différents sulfates . (eau distillée 20°C)

Ce qu'il faut retenir de la Figure 3, c'est que les sulfates calciques ont une solubilité intermédiaire entre des substances quasiment insolubles (SO_4Ba, SO_4Pb) et la plupart des autres sulfates choisis et, par ailleurs, l'extrême rapidité de la plupart des dissolutions (∿ 80 à 90 % de la saturation après 10 secondes) ; notons que l'anhydrite naturel est presque aussi soluble que le gypse mais sa vitesse de dissolution est plus lente.

4. MOMENT D'INCORPORATION DU GYPSE

Dans la suite des essais, pour des raisons pratiques, les sulfates seront homogénéisés à sec dans le clinker broyé ; comme les équilibres de solubilité sont liés au passage en solution d'autres éléments très solubles provenant du clinker, il était utile de connaître l'influence du moment d'incorporation du sulfate. Dans ces conditions, 5 mélanges ont été étudiés avec 5 % en poids du gypse G1.

- (a) gypse et clinker broyés ensemble,
- (b) gypse et clinker mélangés à l'état de poudre,
- (c) gypse mêlé à l'eau de gâchage,
- (d) gypse introduit au début du malaxage (1 min après le mouillage du clinker),
- (e) gypse incorporé en fin de malaxage (1 min avant la fin d'un malaxage de 5 min).

Le Tableau III résume quelques uns des principaux résultats.

Tableau III

Grandeurs mesurées	Moment d'incorporation a	b	c	d	e	Clinker sans sulfate N
Seuil de cisaillement f de la pâte fraîche* (Pa)	54	72	55	92	155	210
Début de prise Vicat** (min)	100 (0244)	80 (0260)	55 (0260)	75 (0267)	130 0294	115 0296
Résistance en compression à 28 jours (MPa)	111	110	95	985	81	79
Retrait à l'air à 28 jours 50 % HR (µm m)	1630	1910	2000	2000	2090	5060

- Clinker BI 14 % C_3A 3600 cm^2/g
* mesures au viscosimètre à cylindres coaxiaux E C 0 40
** essais en pâte pure à consistance égale (2000 Pa) (entre parenthèses le E C)

R_c à 2 et 28 j ⟶ : N < e < c et d < a < b
retrait à 28 j ⟶ : a < b < c et d < e < N
f (exigence en eau inverse) et prise cf. fig 4 et 5.

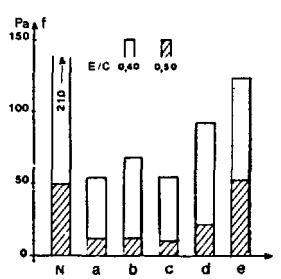

Fig 4 . Mesure du seuil de cisaillement f au viscosimètre .

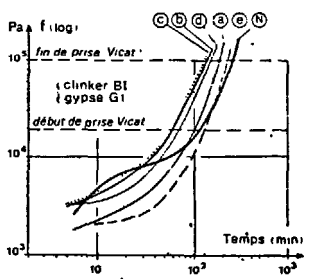

Fig 5 . Evolution de la prise au rhéographe BOMBLED .

Notons que dans le cas du broyage simultané, les finesses respectives sont certainement en raison inverse des broyabilités et sont par conséquent différentes de celles des Tableaux I et II.

Le renflement caractéristique de la courbe de la pâte sans gypse (fig. 5) et les effets fluidifiant initial et accélérateur ultérieur seront explicités au chapitre 6 (figure 14).

5. RHEOLOGIE DE LA PATE INTERSTITIELLE DE CIMENT FRAICHE

Toutes les mesures ont été faites au viscosimètre à cylindres coaxiaux CERILH [5] ; la figure 6 montre les différents aspects possibles des rhéogrammes enregistrés et les divers comportements rhéologiques observables.

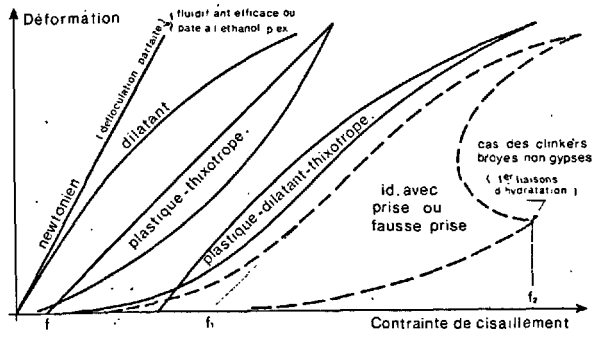

Fig 6 - Differents types de rheogrammes .

La grandeur la plus significative de ces fluides Binghamiens (ou pseudo) étant leur seuil de cisaillement, c'est celui-ci qui sera étudié (les mesures ont toutes été effectuées 5 min après la fin du malaxage).

5.1 Influence de la teneur en C_3A

Nous avons montré, dans une étude précédente [1], que, dans l'eau pure, les aluminates sont initialement défloculés et dispersés ; en revanche, ils forment très rapidement des liaisons en fonction des conditions spatiales (serrage et teneur en eau) : le comportement des pâtes de ciment sera donc la combinaison de ces deux effets contradictoires (figure 7).

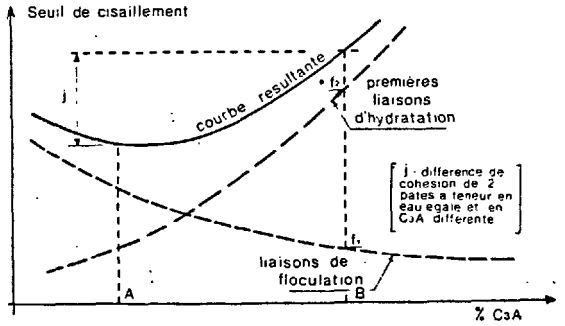

Fig 7 . Rheologie et teneur en C_3A .

Par conséquent, les corps qui présentent en même temps une action floculante et un effet retardateur du C_3A, comme c'est le cas généralement pour les sulfates, conduiront à un comportement différent selon la teneur en C_3A du clinker.

Sur la figure 8 qui illustre la conclusion précédente dans le cas des clinkers "A" et "B", on peut faire les observations suivantes :

- E représente la différence d'exigence en eau à caractéristique rhéologique égale (pour 2 teneurs en C_3A),
- J même signification que figure 7,
- F effet floculant (rigidifiant),
- R action retardatrice initiale sur le C_3A dans les premiers moments (fluidification apparente).

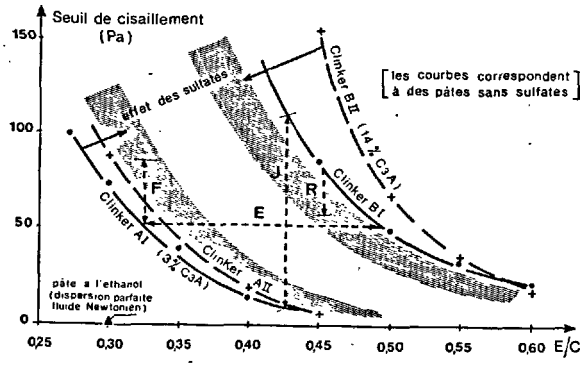

Fig 8 . Seuil de cisaillement en fonction du rapport E/C .

On peut noter que l'influence de la finesse de mouture se répercute moins sensiblement sur le clinker à faible teneur en C_3A.

5.2 Action des sulfates calciques

L'incorporation de sulfates conjugue les deux effets indiqués ci-dessus et conduit à une courbe de principe analogue présentée figure 9 et confirmée par les nombreux résultats qui ont permis de construire la figure 10.

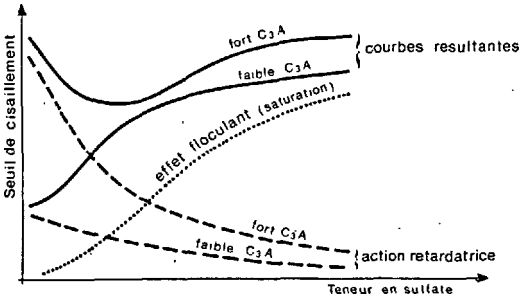

Fig 9 . Schéma de l'action des sulfates calciques .

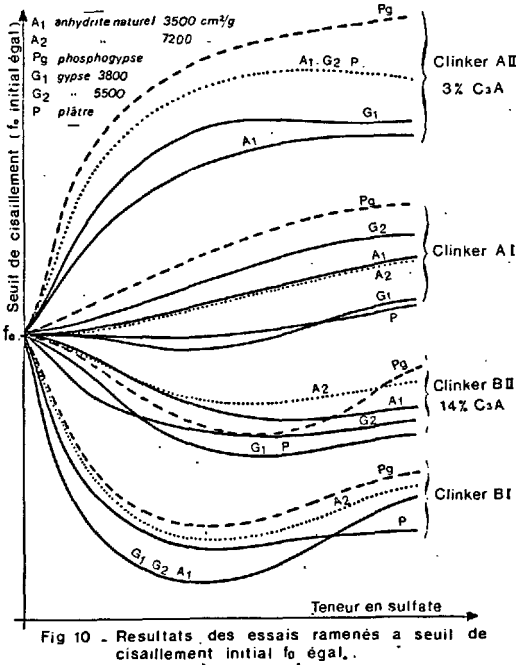

Fig 10 . Resultats des essais ramenés a seuil de cisaillement initial f_0 égal .

Ces courbes font toutefois ressortir très nettement l'effet limité de la floculation dans le cas du clinker pauvre en C_3A.

D'une façon générale, il apparaît que l'action des sulfates calciques, aussi bien floculante que retardatrice, s'échelonne à peu près dans le rapport de leur vitesse de dissolution (sauf pour l'action retardatrice du phosphogypse à cause de ses impuretés solubles).

La figure 11 illustre l'effet d'agglomération des grains et l'influence d'un sulfate.

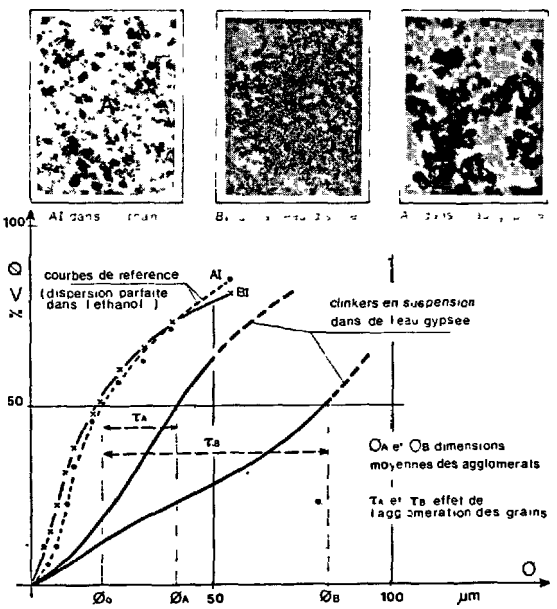

Fig 11 - Sedimentometrie . Floculation

5.3 Action des sulfates non calciques

L'action fluidifiante (apparente ou retardatrice) ou les raidissements observés sont résumés sur la figure 12.

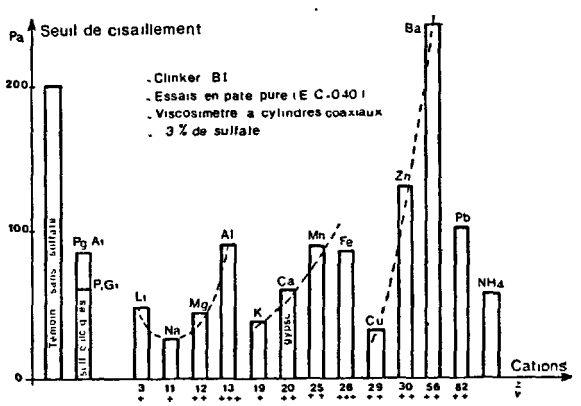

Fig 12 . Influence des sulfates non calciques .

6. EVOLUTION RHEOLOGIQUE DE LA PATE DE CIMENT PENDANT LES PREMIERES HEURES

6.1 Moyen d'étude

L'évolution du seuil de cisaillement a été suivie à l'aide du rhéographe, mis au point au CERILH [6] et [7], lequel permet des mesures depuis la fin du malaxage jusqu'au-delà de la fin de prise VICAT et fournit un certain nombre de grandeurs (figure 13).

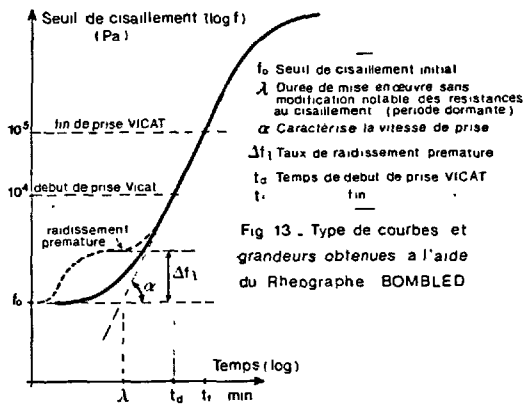

f_0 Seuil de cisaillement initial
λ Durée de mise en œuvre sans modification notable des résistances au cisaillement (période dormante)
α Caractérise la vitesse de prise
Δf_1 Taux de raidissement prematuré
t_d Temps de debut de prise VICAT
t_f fin

Fig 13 - Type de courbes et grandeurs obtenues a l'aide du Rheographe BOMBLED

La figure montre que des raidissements précoces peuvent ne pas être décelables avec les moyens habituels trop peu sensibles et que seule une méthode comme celle-ci peut y parvenir.

Néanmoins, même s'ils ne sont pas mesurables facilement, ces raidissements pendant la période de mise en œuvre sont toujours rédhibitoires pour la maniabilité et ce doit être, par conséquent, le domaine de choix des études rhéologiques.

6.2 Action des sulfates calciques

Le renflement caractéristique des raidissements est systématique pour les pâtes de clinker broyé non gypsées. La figure 14 montre plusieurs cas possibles de l'action d'une addition.

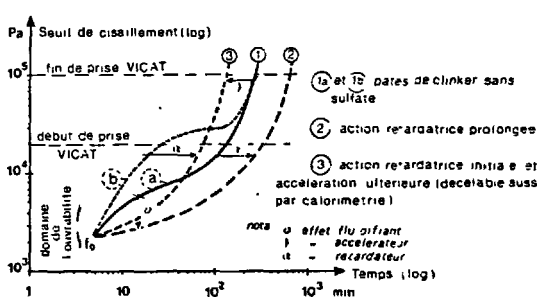

1a et 1b pates de clinker sans sulfate
2 action retardatrice prolongee
3 action retardatrice initiale et acceleration ulterieure (decelable aussi par calorimetrie)
nota a effet fluidifiant
b - accelerateur
c - retardateur

Fig 14 - Action du gypse par exemple .

L'effet (3) devrait plutôt se produire s'il reste suffisamment de sulfate "libre", c'est-à-dire : soit pour une forte teneur en sulfate, soit pour une faible teneur en aluminate, ou encore une vitesse de dissolution lente (anhydrite naturel, broyage grossier, chaleur).

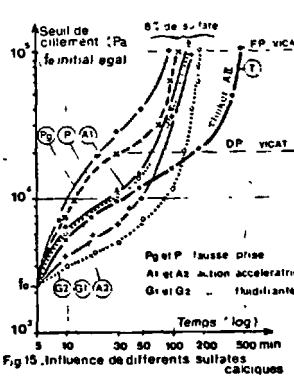

Fig 15 . Influence de differents sulfates calciques

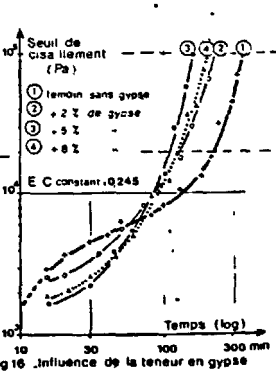

Fig 16 . Influence de la teneur en gypse

Les essais ont porté, comme pour la viscosimétrie, sur les 2 clinkers, les 2 finesses de mouture et les 4 sulfates à trois teneurs ; les figures 15 et 16, sélectionnées parmi les résultats, confirment bien le schéma précédent.

6.3 Action de sulfates non calciques

Les résultats obtenus sont résumés pour le clinker BI sur la figure 17 ci-après ; on peut diviser les modes d'action en trois catégories :

- les cations accélérateurs (Li, Na, K),
- les ions colmateurs très retardateurs et généralement fluidifiants (Pb, Ba),
- les substances gélifiant l'eau interstitielle, provoquant un raidissement notable (Al, Zn, Fe).

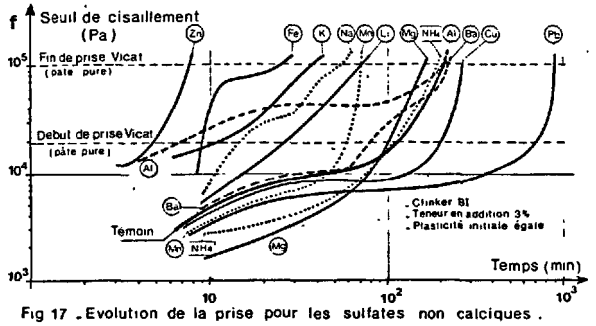

Fig 17 - Evolution de la prise pour les sulfates non calciques.

7. ACTION DES DIFFERENTS SULFATES ETUDIES SUR LES PROPRIETES DES PATES DURCIES

La figure 18 illustre les résultats obtenus pour les résistances en compression en pâte pure à 1 et 28 jours avec les deux clinkers, pour les sulfates de Ca et avec le clinker BI seulement pour les non calciques.

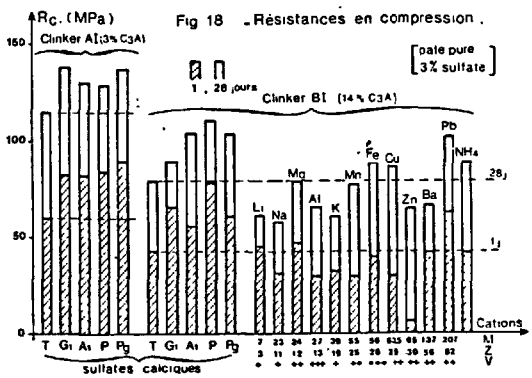

Fig 18 - Résistances en compression.

La figure 19 donne un aperçu des variations dimensionnelles pour les mêmes matériaux.

On sait que la teneur en sulfate doit être modulée à la composition minéralogique du clinker, à sa teneur en éléments rapidement solubles (C_3A, alcalins) et à la finesse de mouture ainsi qu'à la vitesse de dissolution du sulfate ; il existe généralement à chaque âge un optimum donnant les résistances maximales et le retrait minimal.

Parmi les non calciques, les sulfates de Cu et de Pb semblent donner des résistances comparables à celles des sulfates de Ca (en particulier, le sel de Pb qui allonge notablement les temps de prise mais accroît sensiblement les résistances à 1 et 28 jours), en revanche les retraits sont toujours plus élevés.

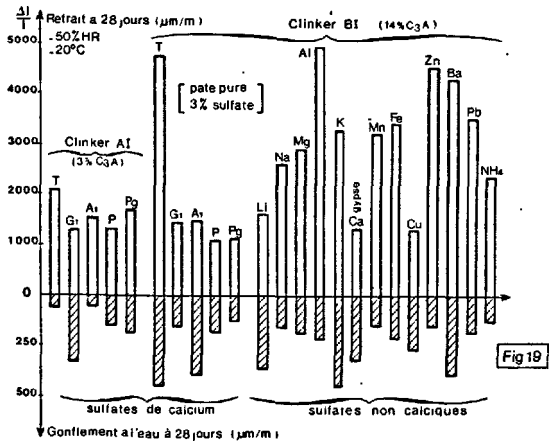

Fig 19

8. CONCLUSION

L'action des sulfates sur les clinkers est multiple : floculants, réducteurs de solubilité des aluminates, colmateurs, accélérateurs des silicates.

Le seuil de cisaillement des pâtes fraîches de ciment Portland est le résultat des liaisons de floculation et d'hydratation précoce : les sulfates augmentent les premières et diminuent les secondes en fonction de la teneur en C_3A (et de la solubilité et de la teneur en sulfate) ; il peut y avoir prédominance de l'un ou de l'autre effet (de même pour l'exigence en eau à cohésion égale). L'évolution de la prise étaye ces observations et y ajoute l'accélération éventuelle des silicates par le sulfate non consommé par les aluminates. L'action sur les pâtes durcies confirme la nécessité des sulfates calciques pour de bonnes performances des ciments.

9. BIBLIOGRAPHIE SOMMAIRE

[1] J.P. BOMBLED : Rhéologie des mortiers et des bétons frais : Etude de la pâte interstitielle du ciment. (R.M.C. n° 688, mai-juin 1974).
[2] J.P. BOMBLED : Rhéologie des bétons frais. (R.M.C. 1/1974).
[3] A. JOISEL : Le sulfate de calcium constituant et adjuvant des ciments. (R.M.C. n° 667).
[4] A. JOISEL : Les adjuvants du ciment. (Ed. de l'auteur, 1973).
[5] J.P. BOMBLED : Viscosimètre à cylindres coaxiaux pour l'étude des pâtes de ciment. (R.M.C. n° 683, oct. 1973).
[6] J.P. BOMBLED : Rhéographe pour suivre l'évolution des pâtes. (R.M.C. n° 673, oct. 1971).
[7] J.P. BOMBLED : Prisométrie des pâtes de ciment. (R.M.C. n° 699 et n° 709).
[8] SEMINAIRE RILEM sur les sulfates.

Effect of mix rheology, admixtures and salts upon physical and mechanical properties of hardened cement pastes

Action combinée des adjuvants et des additions de sel sur les propriétés physiques et mécaniques des pâtes de ciment durcies

B.E. SCHEETZ, Research Associate,
E.L. WHITE, Research Associate,
D. WOLFE-CONFER, Senior Research Technician, and
D.M. ROY, Professor, Materials Research Laboratory, The Pennsylvania State University, University Park, Pennsylvania 16802, U.S.A.

SUMMARY: The interrelationships between the rheological properties of ordinary cement slurries and viscous pastes and the mechanical and physical properties of their hardened composites have been investigated. The cement slurries, made from an ASTM Type I and an API Class C cement, were modified by addition of two superplasticizing admixtures, a sulfonated melamine formaldehyde condensate (A14) and a sulfonated naphthalene formaldehyde condensate (A3). The interactions between the admixtures and brines are important since these composites may be exposed to brines at elevated temperatures (geothermal applications) and to bedded evaporite deposits (in a possible nuclear waste disposal site).

Rheological properties of cement slurries were measured at different shear rates to explore properties related to pumpability in the mixes. The shear stress for both the Type I and the Class C cement slurries was found to decrease with increasing superplasticizer concentration and with increasing salt content at a 1% admixture concentration. However, the rheological properties of both cement pastes were very erratic below 15 wt/o NaCl. In the presence of 25 wt/o NaCl the fluidities of the pastes were 2 to 3 times greater at ≤1% superplasticizer concentrations but changed rapidly in contact with additional amounts of either superplasticizer.

The setting times for the Type I cement slurries systematically increased with increased admixture concentrations; however, the Class C cement had the opposite trend. The possible reason for these behaviors are discussed. The bulk densities for all specimens were measured and variations with curing time, admixture content, and nature of mixing waters were discussed.

The microhardness measurement was utilized as a criterion to determine the strength of a specimen. Generally, the hardness increased with increasing curing time. Variation in hardness values for samples prepared from various cements and mixing water (with or without additives) were also discussed. A very distinct difference in hardness between the samples prepared with deionized water and admixture and saturated sodium chloride and admixture exists. The deionized water prepared samples were fully 40% stronger than the salt-admixture prepared samples.

RESUME :
Les relations entre les propriétés rhéologiques de barbotines de ciments ordinaires ainsi que de pâtes visqueuses et les propriétés mécaniques et physiques de leurs composés durcis ont été étudiées. Les barbotines de ciment, préparées a partir de ciments ASTM type I et API Classe C, furent modifiées par l'ajout de deux adjuvants superplastifiants, un condensé sulphoné de formaldéhyde de mélamine (A14) et un condensé sulphoné de formaldéhyde de naphtalène (A3). Les interactions entre les adjuvants et les saumures sont importantes vu que ces composites peuvent être exposés à des saumures à des températures élevées (applications géothermales) ainsi qu'à des depôts d'evaporite (dans un site éventuel de stockage de déchets radioactifs).

Les propriétés rhéologiques des barbotines de ciment furent mesurées à différentes vitesses de cisaillement afin d'explorer les propriétés en rapport avec l'aptitude au pompage des mélanges. La force de cissaillement pour les pâtes du Type I et de la Classe C diminue lorsque la concentration de superplastifiant augumente ainsi qu' avec une augmentation du taux de sel lorsque l'on utilise 1% d'adjuvants. Toutefois, les propriétés rhéologiques des deux pâtes de ciment deviennent erratiques lorsque l'on utilise moins de 15% (en poids) de NaCl. En présence de 25% (en poids) de NaCl, les fluidités des pâtes sont 2 à 3 fois supérieures pour des concentrations de superplastifiants ≤ 1%, mais changent rapidement au contact d'ajouts supplémentaires d'un des duex superplastifiants.

Le temps de prise des pâtes de ciment du Type I est systématiquement alongé lorsque l'on augmente la concentration des adjuvants contrairement au ciment de la Classe C. Les raisons possibles pour ces phénomènes sont exposées. Les densités de tous échantillons furent mesurées et leurs variations avec le temps de prise, le taux d'adjuvants et la nature des eaux de mixage sont rapportees.

La microdureté fut utilisée comme critère pour déterminer la résistance d'un échantillon. En général, la microdureté augmente avec le temps de prise. La variation de la dureté d'échantillons préparés à partir de différents ciments et eaux de mixage (avec on sans additifs) est aussi rapportée. Il existe une différence très nette entre la dureté d'échantillons préparés avec de l'eau dé-ionisée et des adjuvants et celle d'échantillons préparés avec de l'eau saturée en chlorure de sodium et des adjuvants. Les échantillons préparés avec de l'eau dé-ionisée sont 40% plus resistants que ceux préparés avec l'eau saturée en NaCl.

INTRODUCTION

Effective sealing of penetrations into a nuclear waste repository (1), or through rock strata made for the purpose of extracting geothermal energy (2,3) will demand the development of cementitious composite materials for closure of the holes, or for cementing of the casings. The composites will need to possess long-term stability (4) coupled with ease of emplacement. Fundamental to the geothermal applications is the exposure of these cementitious composites to mineral-laden brines at elevated temperatures (2,3); while, for the nuclear waste disposal application, the most conceptually-advanced repository in the U.S. (5) is designed for siting in bedded evaporite deposits. The research results presented here were carried out to address certain intrinsic materials performance and property questions, dictated by the requirements of potentially important applications of cementitious materials where they will perform in the presence of halide phases:

(1) Effects upon the chemical and physical properties of such composites prepared with superplasticizing admixture and salt combinations: Are there potential interactions that would affect the integrity of the composites?

(2) Effects of alkali halides and superplasticizers upon the rheological properties of "pumpable" cementitious slurries: Because cement formulations for downhole emplacement are usually designed to be pumped under turbulent flow conditions (large Reynold's numbers) it is necessary to determine any such effects.

(3) Interactions of halides with the superplasticizers, that will affect the "pumpability" of the slurries: Do any significant changes occur with time?

The purpose of the following experiments was therefore to address the questions of potential interaction between halide phases present in the expected geological environment and the cementitious mixes that might be emplaced in the geomedia.

EXPERIMENTAL

Ordinary commercial cements were used in these studies as much as possible, modified by chemical additions to achieve additional desirable chemical and physical properties. The cements used included an ASTM Type I and an API Class C. Table 1 gives chemical analyses of these cements. Three commercial superplasticizers, one sulfonated melamine formaldehyde condensate (A14), and one sulfonated naphthalene formaldehyde condensate (A3), were employed in the studies.

All cement preparations were conducted following ASTM C305 procedures; samples were mixed with either deionized water, or sodium chloride saturated solutions and maintained at a w/c of 0.3, compacted into polyethylene molds on a vibrating table for 60 seconds, and cured for 24 hours at greater than 90% relative humidity (1). The molds were then removed, and the samples were cured under selected fluids, saturated $Ca(OH)_2$ or saturated NaCl, contained in sealed glass jars at room temperature and 60°C. The nomenclature used is as follows:

cement type	w/c	mixing water	% admixture	curing water	curing temp.
I	0.3	NaCl*	1	$Ca(OH)_2$	RT
I	0.3	DW	0	NaCl	60.

*The concentration of NaCl in the solution is not included as solid in the designated water:solid ratio; DW = deionized water.

Table 1. Chemical composition (major constituents) of Type I and Class C cements

	Type I (I-5)	Class C (C-2)
SiO_2	20.82	21.2
Al_2O_3	5.24	2.7
Fe_2O_3	2.90	5.1
CaO	62.88	65.4
MgO	3.20	0.8
SO_3	2.88	2.5
CO_2	ND	ND

Compressive strength (ASTM C109), microhardness (Vickers), density (1), water and gas permeability (6), bond strength, phase composition by x-ray diffraction, setting times (ASTM C191), and rheological properties (7) were determined to aid in the interpretation of potential interactions.

RESULTS AND DISCUSSION

These experiments were designed to investigate various properties of cementitious materials relevant to their placement and performance in contact with salt-saturated environments. Initial experiments were designed to compare the effects of deionized mixing water vs. saturated NaCl mixing water; the effect of the interaction of a fixed concentration (1%) of a superplasticizer with NaCl added to the mixing water; the effect of the type of curing water [sat. $Ca(OH)_2$ or sat. NaCl], and in a limited number of tests the effects of curing at elevated temperatures.

X-ray Diffraction Phase Determination. Very little difference in the resultant hydration products could be recognized between the samples that were prepared with and without an admixture. The phases identified by x-ray diffraction (XRD) were portlandite [$Ca(OH)_2$], β-C_2S, C_3S* and the calcium chloroaluminate hydrate "Friedel's salt" (8). Also recognized in these diffractograms were a large amorphous contribution to the x-ray diffraction pattern centered at ~25°2θ, and the contribution of a phase that possesses intense low angle diffuse background which usually left the chart, beginning in the range of from 6 to 10Å. Table 2 is a summary of the recognized phases. The present XRD data were obtained for qualitative phase identification; the references therefore necessarily reflect only trends of the reactions.

Table 2. Phases identified by x-ray diffraction

	curing time (days)	admixture (A3)*									
		0%					1%				
0.3 NaCl-$Ca(OH)_2$-RT†	7	P	B	C	lb		P	B	C	lb	
	28	P	B	C			P	B	C		
	56	P	B			k	P	B	C		k
0.3 NaCl-NaCl-RT	7	P	B	C	lb		P	B	C	lb	
	28	P	B	C		k	P	B	C		ka
	56	P	B	C		a	P	B	C		ka
0.3 DW-$Ca(OH)_2$-RT	7	P	B	C	lb		P	B	C		
	28	P	B	C		a	P	B	C		a
	56	P	B	C			P	B	C		
0.3 DW-NaCl-RT	7	P	B	C	lb		P	B	C	lb	
	28	P	B	C		k	P	B	C		k
	56	P	B				P	B	C		

†Nomenclature in order: w/c ratio, mixing water, curing water, curing temperature.

P = portlandite, B = β-C_2S; C = C_3S; lb = low angle background; k = Friedel's salt ($3CaO{\cdot}Al_2O_3{\cdot}CaCl_2{\cdot}10H_2O$); _ = 60°C cured sample; a = amorphous background; A3* = sulfonated naphthalene formaldehyde condensate.

*Cement abbreviations: C = CaO, S = SiO_2, A = Al_2O_3, F = Fe_2O_3.

Bulk Density. Bulk density is a routinely measured control property which, when all other factors are equal, confirms reproducibility of sample preparation (i.e., replicates should agree within a high degree of precision). It is also a useful measurement for indicating trends. Therefore, such densities were measured for each sample in this series of experiments, as mass per unit volume, after removal from the curing solution, saturated, surface dry (see Table 3).

The relative comparisons are as follows: (1) With the exception of two compositions which showed significant departures, a specimen of a particular composition was found to maintain its density (within ±1.5 percent), not changing with curing time (8 of 12 were within ±1 percent). (2) The admixture-containing samples as a group showed the lowest overall variation as a function of time. (3) The de-ionized water preparations showed less variation than the salt-saturated mixing water specimens. (4) Within the deionized mixing water group, samples prepared with admixtures at a single age were essentially identical.

It should be noted that the specimens made with saturated NaCl mixing water actually contain considerably higher total solids content. Thus it had been expected that this group of samples would possess considerably higher densities. In fact, only a single sample set (that with both NaCl mixing and curing water, no admixture, and cured at room temperature) showed considerably higher densities than other comparable samples. Thus, the salt-saturated samples departed significantly from expected ideal behavior.

Microhardness. Following earlier work (9) which showed that a relationship exists between microhardness and porosity for certain families of cement-like materials, a relation between microhardness and bulk density was also established (10,11), which is indirectly related to strength. The microhardness of every sample was determined using the Vicker's technique (10); data are given in Table 4. The general trend found for all samples was an increase in hardness with increasing curing time. The hardness increase ranged from 10% to 70% in some instances with the average increase approximating 30%. The reference neat paste (without admixture or NaCl) cured at 60°C showed the most rapid increase in hardness and also possessed the greatest hardness. Generally the samples prepared with deionized water and Type I cement were harder than those prepared with salt. All of the samples using deionized mixing water produced harder products than those samples prepared with salt mixing water. The former samples generally maintained their strength with respect to the latter samples as a function of time. A very distinct difference in hardness exists between the admixture-containing samples prepared with deionized water and those prepared with saturated sodium chloride. The samples prepared with deionized water are fully 40% stronger than the salt-admixture prepared samples.

Permeability. One of the most effective predictive measures of the potential for mass transport through a particular medium is its permeability (6). If a cementitious material is going to be an effective barrier to the transfer of fluids and their contents, it must possess a permeability less than or equal to that of the surrounding rock. The permeability measurements recorded in this experimental sequence were all made with nitrogen, using the Klinkenberg extrapolation to infinite pressure, giving an approximate liquid permeability. The values obtained for the entire specimen set, range from about 0.1 microdarcy to tens of microdarcies. No obvious trend is apparent in these data as a function of the admixture's presence. All those samples prepared with deionized water appear to have permeabilities that are less than or equal to the values obtained for the saturated sodium chloride mixing water samples. The data are reported elsewhere (12).

See Table 3, page VI-175

Table 4. Microhardness vs. curing time for sodium chloride treated Type I pastes

		time (weeks)		
		1	4	8
I-0.3 NaCl-0-$Ca(OH)_2$-RT	3A	41.5	53.0	63.8
I-0.3 NaCl-1-$Ca(OH)_2$-RT	1A	36.3*	50.7*	50.3*
I-0.3 NaCl-0-$Ca(OH)_2$-60	3A'	49.0	63.0	55.2
I-0.3 NaCl-0-NaCl-RT	3B	44.8	50.5	77.0
I-0.3 NaCl-1-NaCl-RT	1B	36.8*	45.3*	52.9*
I-0.3 NaCl-0-NaCl-60	3B'	53.0	60.0	51.4
I-0.3 DW-0-$Ca(OH)_2$-RT	4A	59.8	59.1	66.7
I-0.3 DW-1-$Ca(OH)_2$-RT	2A	57.1*	69.4*	63.9*
I-0.3 DW-0-$Ca(OH)_2$-60	4A'	59.1	81.0	81.8
I-0.3 DW-0-NaCl-RT	4B	55.5	62.6	66.7
I-0.3 DW-1-NaCl-RT	2B	54.1*	63.9*	67.3*
I-0.3 DW-0-NaCl-60	4B'	52.4	66.4	58.7

*with admixture

OVERVIEW OF PHYSICAL PROPERTIES

Microhardness measurements showed a general increase with curing time, which would be indicative of generally increased strength. The samples prepared with deionized water were generally superior to those prepared with saturated salt solutions. This gives rise to a suggestion that optimized cementing compositions possibly may not involve preparation with saturated salt solutions. On the other hand, samples prepared with deionized water and cured in a 20% salt solution were generally equal to or superior to any of the former samples.

Further, it is realized also that microhardness of the present samples cannot be expected to follow a strictly linear relationship with bulk density for two reasons: (1) The salt-saturated samples cannot be compared strictly with ordinary silicate cement samples because of major compositional difference. NaCl intrinsically has a lower hardness than silicates; although its addition serves to increase density of the composites, it does little to increase the hardness. (2) The density of samples containing only bound (non-evaporable) water would be the more appropriate property for correlation with microhardness, rather than the saturated bulk density, which includes a component of non-structural water. The latter adds little to the strength. Therefore, the above correlation, while showing trends, does not

constitute a quantitative relationship. It will be important to find whether there are correlations with dry (110°C) density, and to further characterize the cement composites' mechanical properties.

Although general trends can be ascertained that suggest that the sodium chloride based formulations do not form as good a composite as similar formulations without the salt, there was no specific evidence of superplasticizer-salt interactions.

Rheological Properties. The questions addressing the potential influence upon the setting times and rheological properties, which affect pumpability do indirectly suggest that interactions occur.

Literature references (13,14) state that in the presence of brines no adverse effects occurred between the saline mixing waters and commercial oil well cementing admixtures. Both of the above references, however, failed to identify the general class of admixtures or to provide any specific details of the nature of any experimentation that was conducted.

All viscosity measurements were made on a Brookfield Model 5X HBT. Other measurements in the laboratory have been carried out with a Haake Rotovisco instrument (7), and calibrations using standard Newtonian liquids have shown agreements in calculated viscosities from the two instruments to within 3-6% (15). The Brookfield instrument was chosen for the current studies for convenience, as well as for the instrument's ability to permit measurement of mortars as well as pastes. The torques at 8 different shear rates were determined in successive order from the largest to the smallest (measurement duration 1 min.), followed by a 1 minute rest, then determined with successively larger shear rates. The total time required for the measurement after mixing was approximately 17 minutes.

Figures 1 and 2 contain data sets for the instrument reading given in millivolts, which is proportional to rheological shear stress, versus added sodium chloride solids in weight percent. The data are graphically presented for one rotor speed (10 rpm), which is proportional to shear rate; this represents an intermediate value of the 8 rates determined. The data in Figure 1 suggest a nearly monotonically decreasing shear stress with increasing salt content (at 1% concentration: wt admixture solids/weight cements, of both the sulfonated naphthalene and melamine formaldehyde condensate superplasticizers). The Type I cement alone undergoes somewhat more erratic behavior but with roughly the same trend. The Class C cement in Figure 2 behaves in a similar fashion with a monotonically decreasing shear stress with increased salt concentrations. The exception to this is the mixture of Class C cement with the sulfonated naphthalene superplasticizer (A3) which is approximately a factor of 3 more fluid than the remaining 2 samples. In both sets of experimental data, erratic behavior occurs in the rheological properties of the pastes below 15 wt/o NaCl.

Typical of the rheological properties with varying superplasticizer concentrations are the data presented in Figure 3, where the shear stresses with increasing superplasticizer concentration generally appear to decrease monotonically. However, in the presence of 25 wt/o sodium chloride, the pastes typically are a factor of 2 to 3 more fluid at low superplasticizer concentrations (less than or equal to 1%) but rapidly

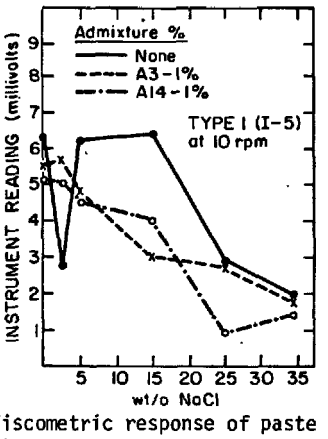

Figure 1. Viscometric response of paste vs. % NaCl in mixing water.

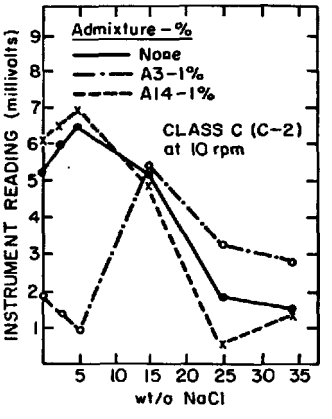

Figure 2. Viscometric response of paste vs. % NaCl in mixing water.

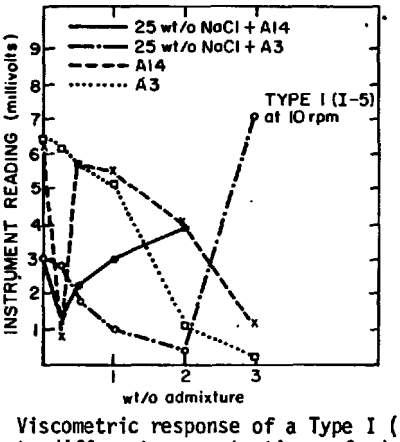

Figure 3. Viscometric response of a Type I (I-5) cement paste to different concentrations of admixtures and NaCl.

change in their fluidity in contact with larger concentrations of either superplasticizer.

Setting Times. Extensive measurements were made of setting times of the variety of pastes (1,16). Initial measurements performed on the neat cement Type I (I-5) pastes with increasing admixture concentrations

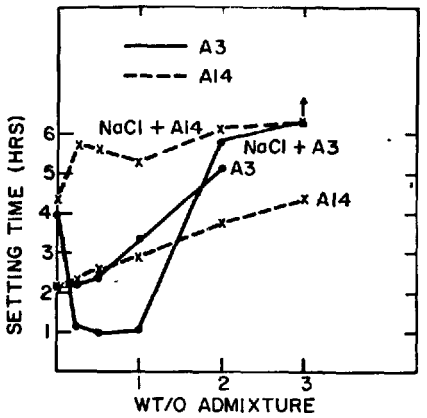

Figure 4. Effects on initial setting time of Type I cement of varying amounts of water-reducing agents in the presence of 25 wt/o NaCl.

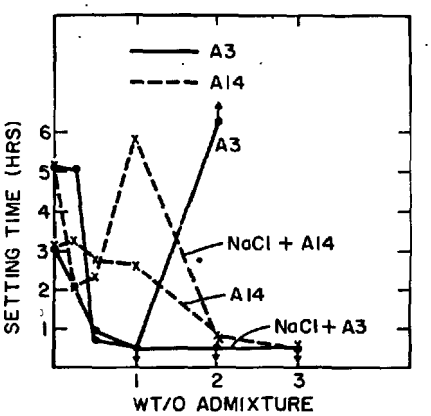

Figure 5. Effects on initial setting time of Class C cement of varying amounts of water-reducing agents in the presence of 25 wt/o NaCl.

indicated a systematic increase in setting times with increasing admixture content. Variations due to the chemical type of admixture were observed especially at the large concentration levels (Figure 4). The Class C (C-2) cement, however, exhibited the opposite trend of setting faster with increased admixture concentrations with very erratic results occurring for the chemically different admixtures at concentrations above 1 wt/o (Figure 5).

The explanation for these observations may lie in a combination of the physical properties of the individual grinds for each cement, and its chemistry. The chemical compositions given in Table 1 show both a lower alumina (and resultant lower C_3A) and slightly lower SO_3 content in cement C-2; and C-2 has a slightly higher specific surface area.

The setting times of the Type I (I-5) cement (Figure 4) in the presence of 25 wt/o NaCl generally indicate a trend toward the retardation of setting with increased admixture concentrations. The sulfonated naphthalene formaldehyde condensate A3 behaves erratically, acting as an accelerator at low concentration and as a retarder at higher concentrations. The Class C (C-2) cement exhibited a trend of acceleration of the setting with increased admixture concentrations.

In the four data sets presented, the sulfonated melamine formaldehyde condensate for the most part behaves in a more nearly predictable manner than the sulfonated naphthalene but the Class C (C-2) cement responds in a more predictable manner than the Type I.

Additional experiments with 1% admixture and varying salt concentrations up to saturation further substantiate these observations (16).

CONCLUSIONS

Phase characterization of cement pastes prepared with various combinations of ingredients (including presence or absence): mixing water, admixture, curing water; and curing temperature was made. The calcium chloroaluminate hydrate, Friedel's salt, was characteristic of many specimens which either included NaCl in their mix or curing solution. Physical properties studies of the products of cement pastes prepared with superplasticizers in the presence of sodium chloride suggest that the cured products typically are less predictable and often inferior to those of the analogue formulations prepared without the presence of sodium chloride. E.g., these are typified by similar permeability values but with a larger, more erratic scatter in the measured values for the salt-containing samples.

Investigations of the rheological properties of these pastes in the presence of sodium chloride are more revealing experiments. The data presented herein suggest that potential interactions do exist between the superplasticizers (irrespective of the formulation or type of admixture) and salt to produce erratic behaviors. Fortunately, the erratic behavior appears to be limited to low salt concentrations (at low superplasticizer levels) or at relatively high superplasticizer concentrations at more nearly typical working salt-concentrations. This trend, fortunately, will minimize their erratic behavior for certain applications: during emplacement of a slurry the mix most likely will become enriched in salt as it is pumped into an evaporite formation. Data in Figures 2 and 3 would suggest that this circumstance will have little effect upon the rheological properties as compared to the impossible circumstance in which the concentration of admixture increased.

When designing cementitious mixes for geothermal cementing, there would appear to be little advantage, and possible disadvantage, to including salts in the initial mixes (2,3). For plugging applications in evaporites, factors involved with the individual situation would have to be considered. From the present data, either salt-containing mixes or non-salt-containing ones apparently could be emplaced; but other factors relating to longevity would also have to be considered for their final evaluation (4).

ACKNOWLEDGEMENT

The research reported herein was sponsored through subcontracts from the U.S. Department of Energy and administered by the Office of Nuclear Waste Isolation, Battelle Memorial Institute, Columbus, OH.

REFERENCES

1. D.M. ROY, B.E. SCHEETZ, E.L. WHITE, and M. DAIMON, "Borehole Cement and Rock Properties Study: Part A, Borehole Plugging Cement Studies," ONWI-5 Annual Progress Report, ONWI/SUB/78/E512-00500, Oct. 30 (1978), 130 pp.

2. D.M. ROY, E.L. WHITE, C.A. LANGTON, and M.W. GRUTZECK, "Potential New High Temperature Cements for Geothermal Wells," Proc. 1979 SPE Intl. Symp. Oilfield & Geothermal Chemistry, Jan. 22-24, 1979, Houston; pp. 153-161.

3. D.M. ROY, E.L. WHITE, C.A. LANGTON, and M.W. GRUTZECK, "New High Temperature Cementing Materials for Geothermal Wells: Stability and Properties," Final Report to DOE, Contract EY-76-C-02-1016, Nov. 30 (1979).

4. D.M. ROY, M.W. GRUTZECK, and P.H. LICASTRO, "Evaluation of Cement Borehole Plug Longevity," Report No. ONWI-30, Topical Report for ONWI (Feb. 1979), 35 pp.

5. U.S. Dept. of Energy, Proc. Natl. Waste Terminal Storage Program Information Meeting, ONWI-62 (Oct. 30, 1979), 232 pp.

6. E.L. WHITE, B.E. SCHEETZ, D.M. ROY, K.G. ZIMMERMAN, and M.W. GRUTZECK, "Permeability Measurements on Cementitious Materials for Nuclear Waste Isolation," pp. 471-478 in Scientific Basis for Nuclear Waste Management, Vol. 1; Proc. Symp. on 'Science Underlying Radioactive Waste Management,' Materials Research Society Annual Meeting, Boston, MA, Nov. 28-Dec. 1, 1978; Ed. G.J. McCarthy.

7. D.M. ROY and K. ASAGA, "Rheological Properties of Cement Mixes. III. The Effects of Mixing Procedures on Viscometric Properties of Mixes Containing Superplasticizers," Cem. Concr. Res. 9 (6), 731-740 (1979).

8. H.G. SMOLCZYK, "Chemical Reactions of Strong Chloride-Solutions with Concrete," Proc. Fifth Intl. Symp. Chem. Cement, Tokyo, Vol. III, pp. 274-280 (1968).

9. I. SOROKA and P.J. SEREDA, "The Structure of Cement-Stone and the Use of Compacts as Structural Models," Proc. Fifth Intl. Symp. Chem. Cement, Tokyo, Vol. III, pp. 67-73 (1968).

10. G.R. GOUDA, "Preparation and Characterization of Very High Strength Hot Pressed Cement Pastes," PhD Thesis, The Pennsylvania State University (August 1975); also G.R. GOUDA and D.M. ROY, Cem. Concr. Res. 5, 551-564 (1975).

11. S.O. OYEFESOBI, "Novel Processing of Cement Phase: A Comparison," PhD Thesis, The Pennsylvania State University (1976); also S.O. OYEFESOBI and D.M. ROY, Cem. Concr. Res. 7, 165-172 (1977).

12. B.E. SCHEETZ, D.M. ROY, E.L. WHITE, and D. WOLFE-CONFER, "Comparison of Tailored Cement Formulations for Borehole Plugging in Crystalline Silicate Rocks and Evaporite Mineral Sequences," Proc. Symposium on 'Science Underlying Radioactive Waste Management,' Materials Research Society Annual Meeting, Boston, MA, Nov. 1979 (in press).

13. K.A. SLAGLE and D.K. SMITH, "Salt Cement for Shale and Bentonnitic Sands," J. Petrol. Tech. 187-194 (1963).

14. W.C. CUNNINGHAM and D.K. SMITH, "Effect of Salt Cement Filtrate on Subsurface Formation," J. Petrol. Tech. 239-263 (1968).

15. K. ASAGA, unpublished work.

16. D.M. ROY, P.H. LICASTRO, B.E. SCHEETZ, E.L. WHITE, M.W. GRUTZECK, and K. ASAGA, "Borehole Cement and Rock Properties Study, Task I: Borehole Plugging Cement Studies," ONWI/SUB/78/E512-00500-2 (Task I), Quarterly Progress Report (March 30, 1979).

Table 3. Bulk density of sodium chloride treated samples versus curing time

		admixture					
		1 week		4 weeks		8 weeks	
		without	with	without	with	without	with
I-0.3NaCl-0-$Ca(OH)_2$-RT	3A	1.94		1.91		1.94	
I-0.3NaCl-1-$Ca(OH)_2$-RT	1A		1.88		1.85		1.88
I-0.3NaCl-0-$Ca(OH)_2$-60	3A'	1.87		1.88		1.87	
I-0.3NaCl-0-NaCl-RT	3B	2.07		1.95		2.02	
I-0.3NaCl-1-NaCl-RT	1B		1.93		1.87		1.88
I-0.3NaCl-0-NaCl-60	3B'	1.94		1.96		1.90	
I-0.3DW-0-$Ca(OH)_2$-RT	4A	1.89		1.88		1.90	
I-0.3DW-1-$Ca(OH)_2$-RT	2A		1.90		1.90		1.91
I-0.3DW-0-$Ca(OH)_2$-60	4A'	1.86		1.90		1.89	
I-0.3DW-0-NaCl-RT	4B	1.94		1.91		1.91	
I-0.3DW-1-NaCl-RT	2B		1.91		1.90		1.91
I-0.3DW-0-NaCl-60	4B'	1.92		2.00		1.93	
Average (kg/dm^3)		1.93±07		1.91±0.04		1.92±0.05	
			1.91±0.02		1.88±0.02		1.90±0.02

Influence of structure on fracture mechanism of hardened cement paste

L'influence de la structure sur le mécanisme de rupture des pâtes de ciment durcies

Yu. ZAITSEV, Professor, All-Union Polytechnical Institute (WZPI) Moscow, U.S.S.R.

RESUME : On a étudié l'influence de la structure poreuse des pâtes de ciment durcies sur le mécanisme de leur rupture et sur leur résistance mécanique. On en a déduit un modèle mathématique du processus. Ce modèle tient compte de la distribution différente des pores dans la pâte de ciment. On a analysé le développement de la rupture par la méthode de Monte-Carlo.

SUMMARY: Influence of porous structure of hardened cement paste on its fracture mechanism and mechanical strength is investigated. A mathematical model of fracture process is developed. The model takes into account different distribution of size of pores in a sample of hardened cement paste. Using Monte-Carlo method crack propagation is analyzed.

INTRODUCTION

Many contributions devoted to deformation and fracture of hardened cement paste, mortar and concrete are to be found in the literature (1-3). Most attemps, however, are mainly based on phenomenological approach and do not analyze theoretically the basic laws of fracture process.

In an effort to fill this gap we have made attempt to give a theoretical description of crack propagation and fracture process in a porous and viscoelastic material such as hardened cement paste.

DEVELOPMENT OF INITIAL CRACKS

Let us examine the process of crack propagation in the porous material under uniaxial compession. The simplest element to be investigated in an idealized structure of a porous material is a cylindrical hole in a homogeneous and isotropic plate. For a short time loading it is possible to neglect the phenomenon of creep and to assume that the large mass of the material outside the zone adjacent to the crack acts elasticly. The stress distribution around a cylindrical hole is well known (Fig. 1). Methods of fracture mechanisc make it possible to define the relation between a value of the external load $q(q_0)$ and length of a crack at the lines of maximum tensile stress. This relation is given by the following expression (4):

$$q = \sqrt{\frac{\pi E \gamma}{2r}} \sqrt{\frac{(1+\lambda)^2}{(1+\lambda)^2 - 1}}, \quad (\lambda = l/r)$$

where E is elastic moduli and γ is the effective surface energy density of hardened cement paste. Experimentally estimated values of γ are given in (5).

SIMULATION OF CRACK PROPAGATION IN HARDENED CEMENT PASTE

Expression given above can be applied as long as the crack length l is small as compared to the distance of individual pores, i.e. as long as the interaction between two mutual approaching cracks is negligible. Therefore the propagation of two interfering cracks (Fig. 2) and finally the crack propagation in a material with pores distributed at random (Fig. 3,a) has been studied. In this model which is fairly close to a realistic porous structure of hardened cement paste. The random pore distribution was generated by a digital computer. The results obtained by one computer realization of Monte Carlo method are shown in fig. 3,b,c. Mathematical basic for such calculation uses the methods of fracture mechanisc and was described in (4). The sum of the length of all individual cracks as a function of the applied load has been calculated. Each time two pores become connected by merging of two growing cracks there is a sudden increase in the total crack length until a critical value is reached when the cracks propagate without any increase of external stress.

Simulation of crack propagation described above makes it possible to estimate the effect of pore size distribution on the fracture mechanism, mechanical strength and strain behavior of hardened cement paste. It was found that with the increasing mean size of pores by the constant quantity of pores, the ultimate load will decrease.

With the increasing maximum size of pores by the constant mean size and the constant quantity of pores, the ultimate load will decrease too. The main results are shown in fig. 4. It was also found that with the increasing mean and (or) maximum size of pores by the constant quantity of pores, or with the increasing number of pores of constant size, the probability of a splitting mode of fracture (as shown in fig. 3,c) will decrease and the probability of shear mode of fracture will increase. At the latter case an inclined crack crossing the areas mostly weakend with pores will propagate (fig. 3,d).

CONCLUSION

A new and basic approach to simulate crack propagation in hardened cement paste has been described. Simulated crack patterns agree reasonably well with experimental findings. Therefore it seems that a solid basic for further investigation has been provided.

REFERENCES

1. R. L'HERMITE (1961), Les deformations du beton. Cahiers de la recherche theorique et experimentale sur les materiaux et les structures. Paris.
2. S.P. SHAH, S. CHANDRA (1968), Critical stress, volume change and microcracking of concrete. ACI Journal, 65, p. 770.
3. A.M. NEVILL (1970), Creep of concrete: Plain, Reinforced and Prestressed, North-Holland Publishing Company, Amsterdam.
4. F. WITTMANN, Yu. ZAITSEV (1974), Verformung und Bruchvorgarg poroser Baustoffe bei kurzzeitiger Belastung und Dauerlast. Deutscher Ausschuss fur Stahlbeton, Heft 232, pp. 65-145.
5. F. RADJY, T.C. HANSEN (1973), Fracture of Hardened Cement Paste and Concrete. Cement and Concrete Research, 3, No. 4, pp. 343-361.

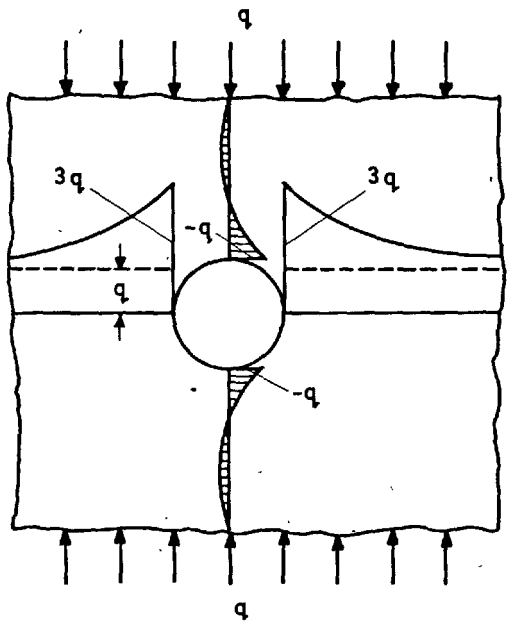

Fig. 1. Stress distribution in a homogeneous material around a circular pore

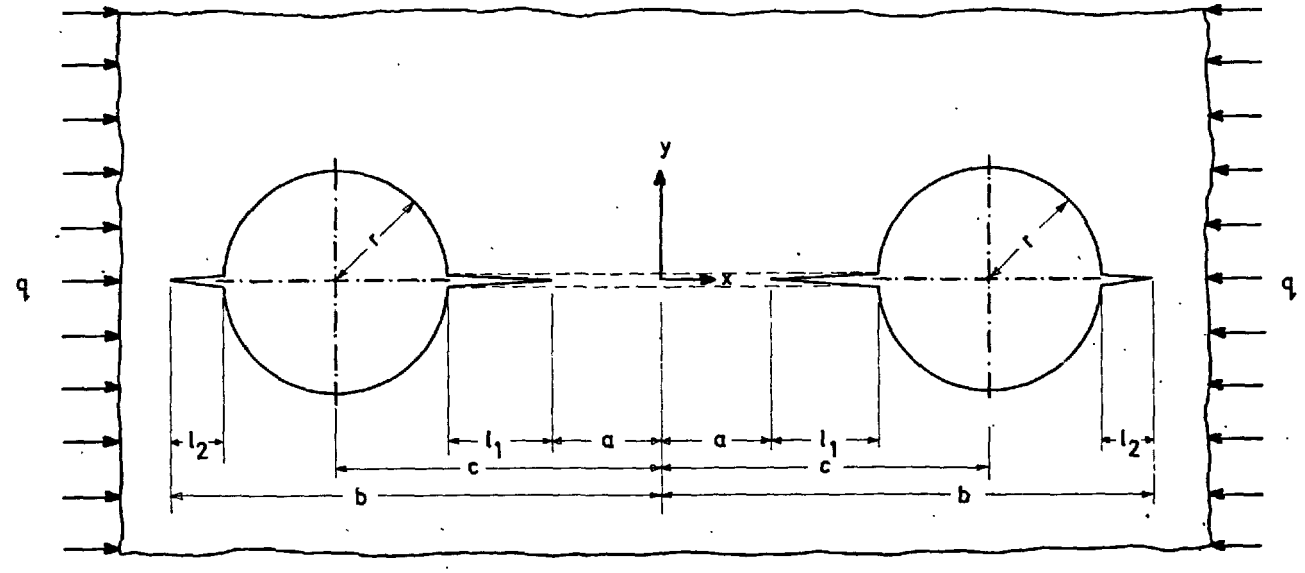

Fig. 2. Development of cracks near two neighboring pores is completed by the coalescing of the cracks and the formation of one crack (dottet line) passing through the two pores

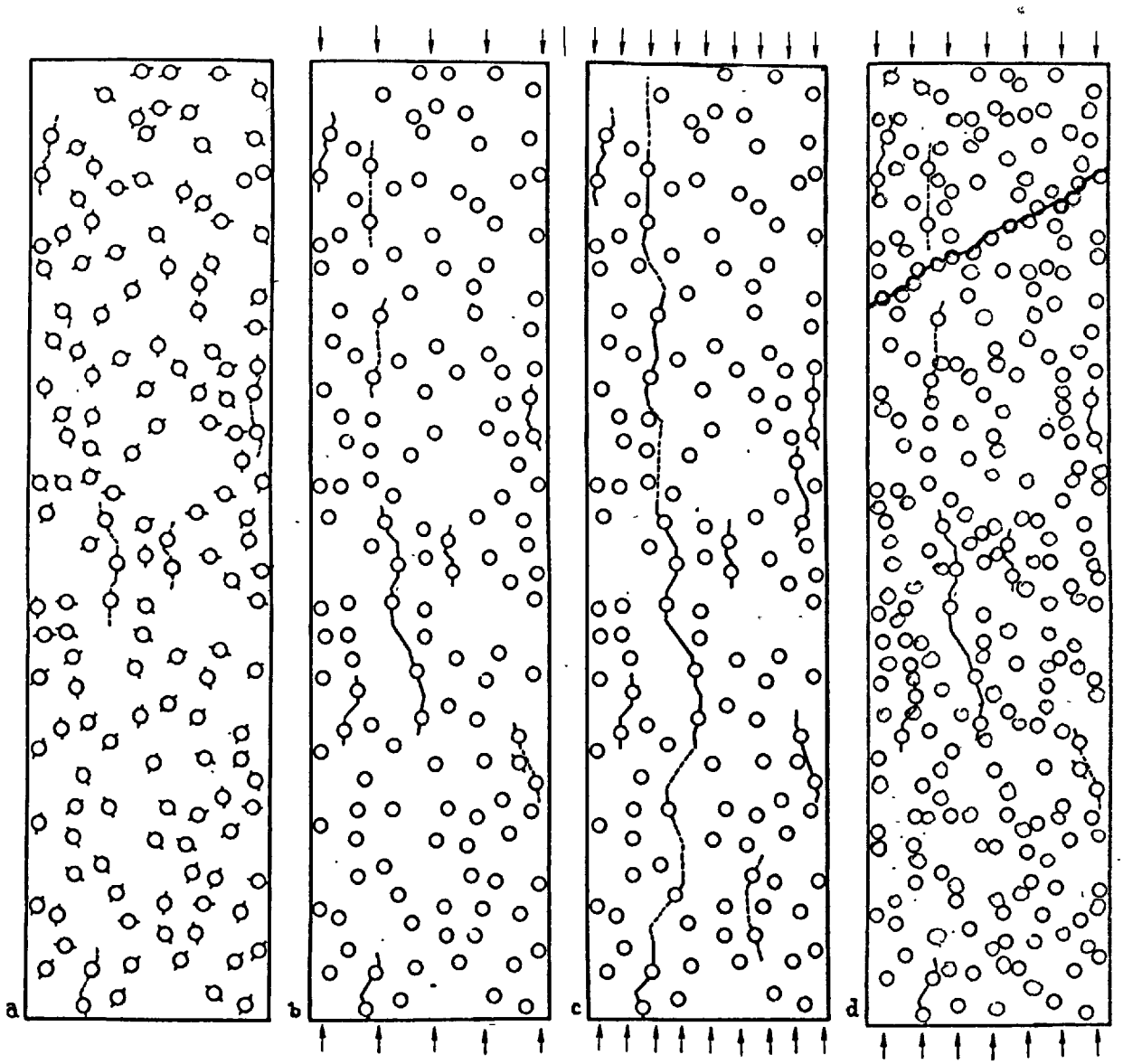

Fig. 3. Simulated crack propagation in a two-dimensional model of hardened cement paste; a - unloaded model; b,c - two different stages (middle and final) of crack propagation; c - the final stage of crack propagation in a model of another structure (great number of pores)

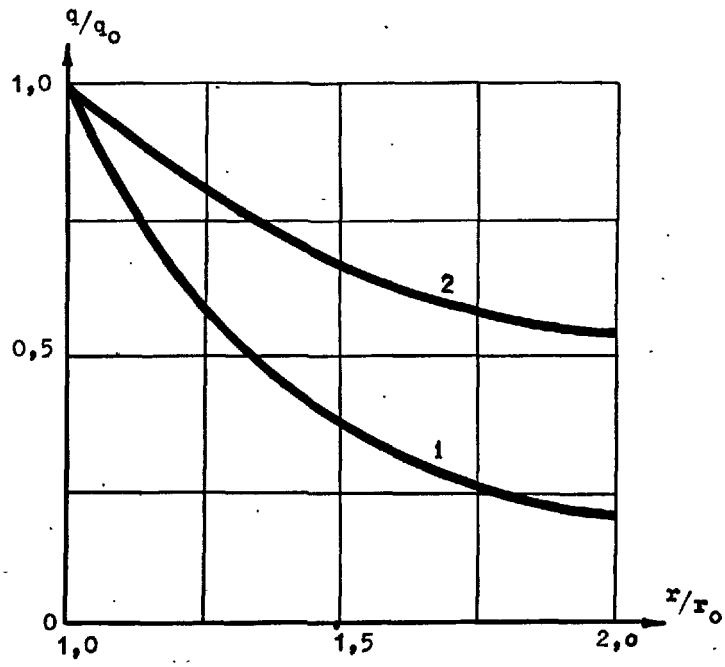

Fig. 4. Related ultimate load q/q_o as a function of the related radius of pores r/r_o; 1 - effect of change of the mean radius of pores by the constant quantity of pores; 2 - effect of change of the maximum radius of pores by the constant mean radius and the constant quantity of pores

Capillary pore structure and permeability of hardened cement paste

Structure des pores capillaires et perméabilité des pâtes durcies de ciment

B.K. NYAME and Dr. J.M. ILLSTON, Division of Civil Engineering,
The Hatfield Polytechnic, Hatfield, Herts, U.K.

RESUME : La relation entre la perméabilité à l'état saturé, la porosité et la distribution des pores dans les pâtes de ciment durcies, a été étudiée par la méthode de porométrie au mercure et séchage à 105°C, pour des valeurs variées, du rapport eau/ciment, et des durées d'hydratation.

On a trouvé que la relation entre la perméabilité et la porosité, en fonction du rapport eau/ciment variait avec la durée de l'hydratation. Un maximum a été observé dans la courbe de distribution des pores; ce maximum est relié étroitement et uniquement à la perméabilité, indépendamment de la durée de l'hydratation et du rapport eau/ciment.

SUMMARY:- The relationships between saturated permeability, porosities and the pore size distributions of hardened cement paste as influenced by water/cement ratios and times of hydration were studied by the techniques of mercury porosimetry and drying at 105°C.

It was found that the permeability - porosity relationship for hardened cement paste of different water/cement ratios is not the same for different times of hydration. A maximum continuous pore size was identified from the pore size distributions which closely and uniquely relates to permeability irrespective of time of hydration or water/cement ratio of the pastes.

INTRODUCTION:

It is known that the permeability of hardened cement paste is mainly dependent on the capillary pore volume (1) Studies of the pore size distributions of hardened cement paste (2,3,4) generally indicate the existence of a threshold diameter, which is interpreted to correspond to the 'minimum geometrically continuous' pore size in hardened cement paste. The present work was performed to enable a closer study to be made of the relationship between the permeability of hardened cement paste and its porosity and pore size distributions with the particular purpose of finding the significance of the threshold diameter in relation to permeability.

EXPERIMENTATION:

Ordinary Portland cement (D25) with composition C_3S; 64%, C_2S; 13%, C_3A; 6.8%, C_4AF; 7.3%, $CaSO_4$; 3.6% was mixed with distilled water at w/c ratios in the range 0.23 to 1.00, and hydrated continuously in water for periods up to 20 months. Truncated conical shaped samples of between 10 - 20mm thick were used for the steady state permeability tests. The steady state permeability method used is described elsewhere (5); it basically involves the use of silicone rubber sealing jacket cut to fit tightly to the sides of the specimens prior to mounting in high pressure permeameters. The conical shape of the specimens aids the formation of a seal between the silicone rubber jacket and the specimen. Steady state flows were measured with cathetometers by monitoring the changes in level of the water meniscus in outflow capillary tubes.
The total porosity, from the saturated and surface dry condition, was estimated from the water contents determined by drying at 105°C. The pore size distributions were determined by mercury intrusion porosimetry (Carlo Erba Series 200 model) for the samples at the conclusion of the steady state permeability measurements. The pore radius was calculated using equation 1 for cylindrical pores, a contact angle of 140° and a surface tension of mercury of 0.48N/m^2 being assumed.

$$r = \frac{75{,}000}{P} \qquad (1)$$

where r = pore radius (A)

P = applied pressure (kg/cm^2)

The differential pore size distributions were evaluated from equal volume divisions of the penetrated pore volume and equation 2. (6)

$$\frac{dv}{d\log r} = \frac{P}{2.303}\,\frac{dv}{dp} \qquad (2)$$

where v = intruded pore volume (cm^3/g)

The maximum continuous pore radius, r_{oo}, was defined to correspond to the pore radius at which dv/dp has a maximum value.

RESULTS:

Fig. 1. shows the effects of hydration on permeability for pastes of water/cement ratios 0.23, 0.47, 0.71 and 1.00. The permeability values represent the mean values obtained from between 3 to 8 samples, and typically the coefficients of variation for permeability at each w/c ratio were in excess of 50%.

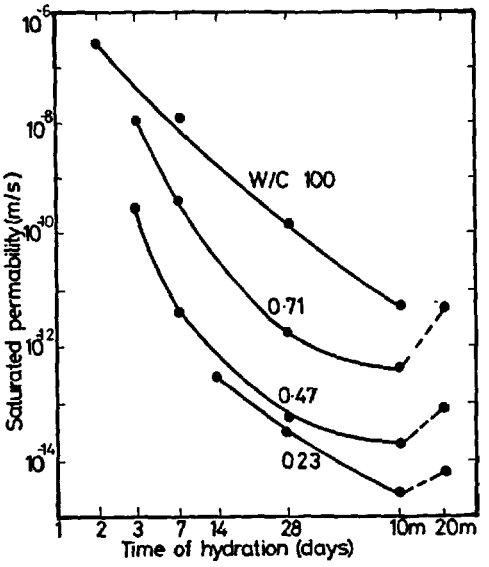

Fig.1.- Effects of hydration on permeability of hardened cement pastes of different water/cement ratios.

The pore size distributions for the age at 28 days are given in Figs. 2a and 2b, again showing the differences between the four water/cement ratios. The values of the maximum continuous pore radius, as previously defined are identified on Fig. 2b and located on the cumulative pore size distributions of Fig. 2a.

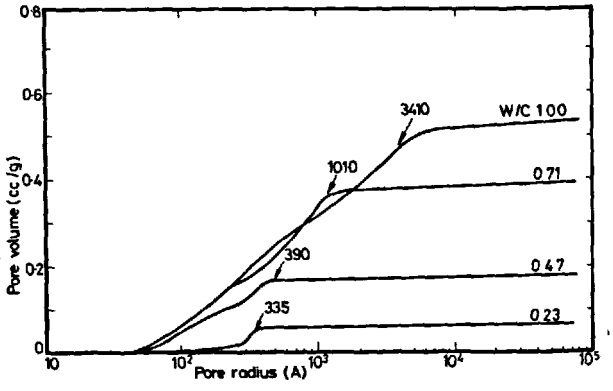

Fig.2a: Effect of water/cement ratio on the cumulative pore size distributions of hardened cement pastes hydrated in water for 28 days.

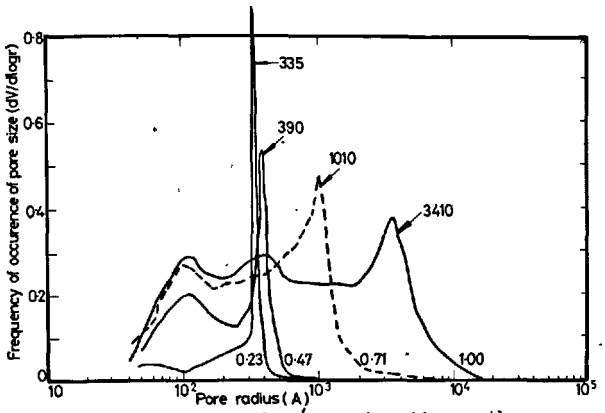

Fig. 2b: Effect on water/cement ratio on the differential pore size distributions of hardened cement pastes hydrated in water for 28 days.

Fig.3. shows the variation in the maximum continuous pore size with w/c ratios and time of hydration, and it can be seen that, except at the highest w/c ratio, r_{∞} reduces to a steady-state value after 28 days of hydration.

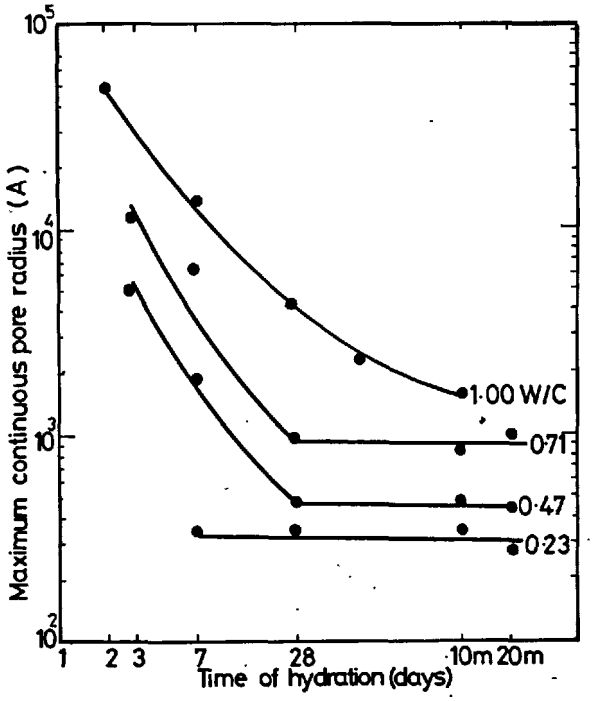

Fig.3: Effect of water/cement ratio and time of hydration on the maximum continuous pore radius of hardened cement paste.

The results are summarised in Figs. 4 and 5 which show the multivalued nature of the relationship between permeability and total porosity, which contrasts with the unified relationship of permeability to the maximum continuous pore radius.

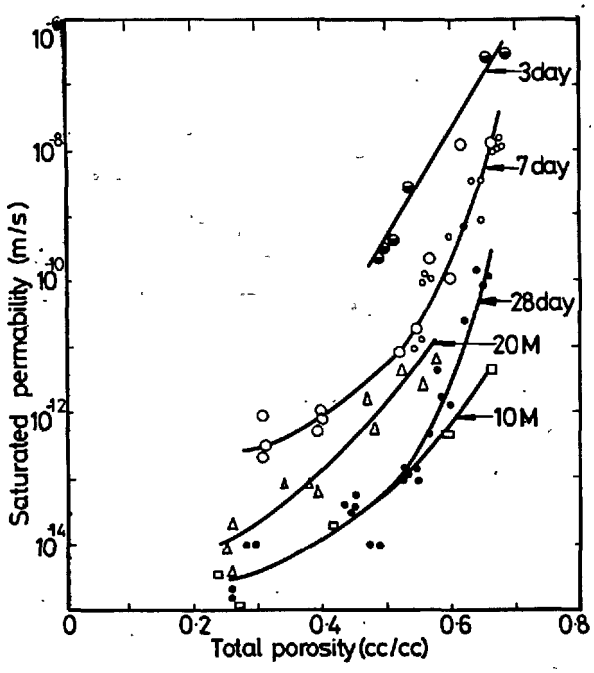

Fig.4: The relationships between total porosity and saturated permeability of hardened cement paste.

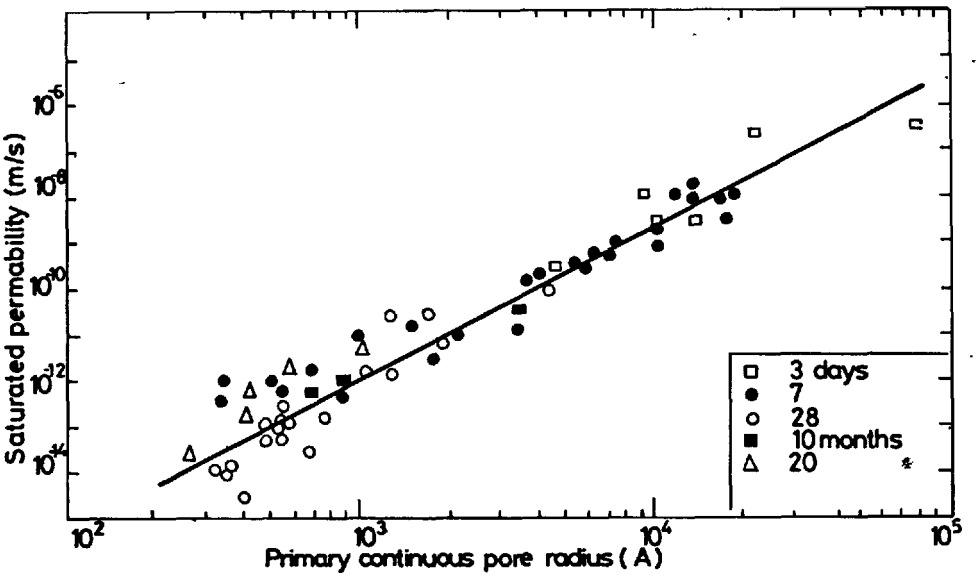

Fig. 5: The relationship between the maximum continuous pore radius and saturated permeability of hardened cement paste.

The relationship between the maximum continuous pore radius and permeability of hardened cement paste was found by linear regression to be

$$K = 1.684\ r_{\infty}^{3.284} \times 10^{-22} \qquad (3)$$

with a correlation coefficient of 0.9576 where

K = permeability (m/s)

r_{∞} = maximum continuous pore radius (A)

The constants for the relationship between total porosity, ϵ, and permeability, K, fitted to the equation of the form

$$K(t) = K_o(t) \cdot \epsilon^{b(t)} \qquad (4)$$

are given in Table 1.

Table 1: Constants of regression for the relationship between total porosity and permeability of hardened cement paste.

Time of hydration (days)	$K_o(t)$ m/s	b(t)	Correlation Coefficient
3	$4.19\ 10^{-5}$	16.18	0.8811
7	$3.00\ 10^{-7}$	12.98	0.8323
28	$1.57\ 10^{-10}$	9.02	0.7031
10month	$2.25\ 10^{-11}$	6.44	0.9378
20month	$3.88\ 10^{-10}$	7.95	0.9661

DISCUSSION:

It is often considered that, as a first approximation, permeability and porosity of hcp are uniquely related. Fig.4. clearly demonstrates that this is reasonably true only for different water/cement ratios at a given time of wet curing; it does not hold when the changes in porosity are caused by continuing hydration. In other words, the changes in pore structure resulting from hydration are very different from those resulting from different water/cement ratios. The reduction in permeability accompanying hydration is shown in Fig. 1, which also indicates that there may be a reversal of this trend if wet curing is prolonged. It is noticeable that Figs. 1 and 3 exhibit similar patterns, so that permeability and the maximum continuous pore radius are apparently related. That this is indeed so, is evident from Fig. 5.

The general shapes of the differential pore size distributions (Fig. 2b) include a maximum peak towards the upper end of the range of pore sizes, and it follows that the radius corresponding to this peak is representative of a considerable proportion of the pore volume. Winslow and Diamond[2] visualised the penetration of mercury at the upper end of the pore size spectrum to be analogous to flow through the main continuous channels of a river system whilst the penetration below the peaks correspond to flow through local side channels. Since the larger pores are likely to offer the least resistance to water flow, it is not unreasonable to deduce that the majority of the flow will occur in the volume represented by the peak radius i.e. by the maximum continuous pore radius. The reasonable correlation of Fig. 5. certainly supports this view, and it may

be further concluded also that the considerable proportion of small pores carry very little of the permeating water.

The changes in the maximum continuous pore radius with water/cement ratio and hydration (Fig. 3.) suggest that it is representative of the spaces between cement grains, which become partially filled with the advance of hydration products. While no geometrical description is possible, it is of interest that, with the exception of the 1.00 water/cement ratio, the partial filling appears to cease at 28 days, thus implying that hydration after this time consists of a densification of existing structures rather than the deposition of new material within the maximum continuous pore channels between adjacent grains.

CONCLUSIONS:

(1) Total porosity of hardened cement paste is not uniquely related to permeability but depends on whether the change in porosity derives from differences in water/cement ratio or times of hydration.

(2) The maximum continuous pore radius, as defined here, is related to permeability and is representative of the size of pore in which the water flows.

ACKNOWLEDGEMENTS:

The authors are indebted to Science Research Council of the U.K. for financial support.

REFERENCES:

1. Powers T C, Brownyard T L
'Studies of the physical properties of hardened Portland cement paste'.
(Nine parts) Proc. ACI, Vol.43, Oct. 1946 - April 1947.

2. Winslow D N, Diamond S
'A mercury porosimetry study of the evolution of porosity in Portland Cement'
Journal of Materials, JMLSA, Vol.5, No.3.
Sept. 1970, pp. 564 - 585.

3. Diamond S, Dolch W L
'Generalised log-normal distribution of pore sizes in hydrated cement paste'
Journal of Colloid and Interface Science, Vol.38
No.1. p. 234 - 244, (1972)

4. Sellevold E J
'Mercury porosimetry of hardened cement paste cured or stored at 97°C'
Cement and Concrete Research, Vol. 1, No.3.
p. 399 - 404 (1974)

5. Nyame B K
'Permeability and Pore structure of hardened cement paste and mortar'
A PhD thesis submitted to the University of London, September 1979, p. 48 - 64.

6. Orr C.
'Review of the mercury porosimeter technique'
Powder Technology. Vol.3, p. 117, (1969)

Influence des résines de synthèse fluidifiantes sur la rhéologie et la déformation des pâtes de ciment avant et en cours de prise

Influence of fluidifying synthetic resins on the rheology and deformation of cement pastes before and during the setting

A.M. PAILLERE, Docteur ès Sciences, Chef de Section "Produits Nouveaux" au Département des Bétons et Métaux, Laboratoire Central des Ponts et Chaussées, Paris, et
Ph. BRIQUET, Ingénieur E.C.S., Chef de groupe "Adjuvants et additifs" à la Section des Produits Nouveaux, L.C.P.C. Paris, France.

RESUME : La différence de comportement entre les résines de synthèse tensioactives et les lignosulfonates est surtout mise en évidence en étudiant l'action de ces produits lorsqu'ils sont introduits au cours de la prise du ciment.

Leur effet défloculant devient très marqué par rapport aux plastifiants réducteurs d'eau à base de lignosulfonate dans le cas des éléments de diamètre inférieur à 20 µ. Cette défloculation agit sur le comportement rhéologique du béton et sur l'hydratation du ciment.

Les déformations en cours d'hydratation de la pâte semblent être sensiblement modifiées par le naphtalène sulfonate lorsque ce produit est introduit dans l'eau de gâchage, c'est-à-dire dans des conditions ne correspondant pas à son effet optimum.

Ceci se traduit sur béton par un temps de fissuration plus avancé.

SUMMARY : The difference about the behaviour between synthetic tensioactive resins and lignosulfonates is particularly shown up by studying the action of these products when put during the setting of cement.

Their defloculating effect becomes very pronounced with regard to water-reducing plasticizers countaining lignosulfonates in caseof particules below 20 micrometers. This defloculation influences the rheological behaviour of concrete and the hydratation of cement.

The deformations in process of hydratation of the paste seem to be appreciably modified by naphtalene sulfonate when this product is introduced in batch water i.e. in its not optimum use.

So, the cracking time of concrete takes place sooner.

INTRODUCTION

Les exigences croissantes des techniques et des chantiers, les ouvrages d'art à ferraillage souvent très dense, ont eu pour conséquence, au cours des dernières années, d'estimer que, pour certaines réalisations, les adjuvants "classiques" n'étaient plus adaptés. Pour répondre aux besoins des utilisateurs, on a vu apparaître des produits à formule chimique très élaborée qui, en apportant des améliorations notables à certaines caractéristiques du béton, permettent d'élargir les domaines d'emploi de celui-ci. C'est le cas tout particulièrement des résines de synthèse qui sont à la base de la composition d'une nouvelle famille de produits ayant une action particulière sur la maniabilité ou fluidité des mortiers et bétons hydrauliques. Dès la commercialisation de ces produits qui ont reçu des appellations diverses, telles que "superplastifiants", "superfluidifiants" ou "fluidifiants", il s'est posé la question de savoir s'ils constituaient une nouvelle famille par rapport aux plastifiants"classiques" et si leur mode d'action était différent.
Du point de vue chimique, ce sont des solutions aqueuses à pH neutre de mélamine formaldéhyde ou de dinaphtyl-méthane sulfonate de sodium ou de calcium. Leur action fluidifiante, qualifiée par certains de spectaculaire, est très variable et assujettie à de nombreux paramètres. Les recherches et expérimentations sur chantier ont montré qu'elle ne se produit de façon incontestable que lorsque les produits sont introduits après confection des mortiers ou bétons hydrauliques, de préférence juste avant leur mise en oeuvre (1). Mélangés à l'eau de gâchage, c'est-à-dire utilisés au moment de la fabrication du béton, les résines de synthèse agissent de façon analogue aux lignosulfonates ou autres produits tensioactifs qui constituent les plastifiants.

Influence des résines de synthèse sur la rhéologie des pâtes de ciment

La différenciation entre les deux familles d'adjuvants (plastifiants et fluidifiants), basée sur le comportement rhéologique du béton final, a été mise en évidence sur pâte de ciment en mesurant sa viscosité à l'aide du viscosimètre à cylindres coaxiaux type CERILH (2)(3).

En effet, tel qu'il apparaît dans les figures 1a et 1b, l'introduction de lignosulfonate (produit n° 3) ou de résines de synthèse (produits n° 1 et n° 2) au moment de la confection de la pâte, n'entraîne, du point de vue de la viscosité, aucune différence caractérisant chacune des familles chimiques. En revanche, introduits en différé, c'est-à-dire 30-60-120 minutes après fabrication de la pâte de ciment, les fluidifiants conduisent à des viscosités comprises entre 0,4 et 1,6 Poises et ceci 2h après fabrication. Quant au plastifiant, il n'améliore plus de façon notable, à partir d'une heure la viscosité de la pâte qui devient même supérieure à celle du témoin quand le plastifiant est introduit 2h après confection.

Afin d'approfondir ces résultats marquant la différence d'action entre les diverses familles chimiques d'adjuvants, nous avons effectué des mesures de viscosité des pâtes, dans lesquelles les produits, dont la composition chimique variable est donnée dans le tableau n° I, étaient introduits en différé jusqu'à 3h après confection.

Fig. 1 : Viscosité des pâtes de ciment adjuvantées en fonction du temps d'attente et de leur nature chimique.

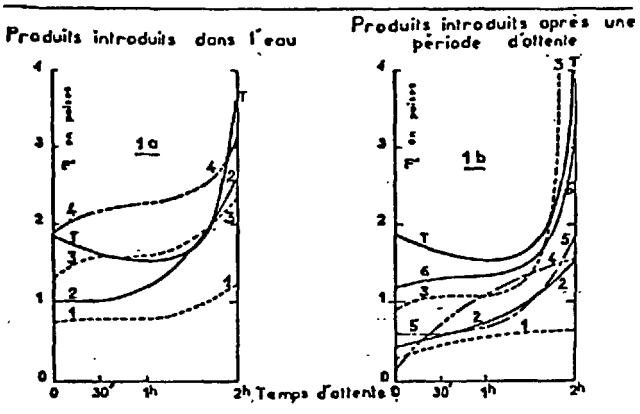

TABLEAU N° I

Nature chimique des adjuvants utilisés

Code	Extrait Sec (%)	Nature Chimique
N° 1	20	Résine mélamine formaldehyde sulfonate de sodium
N° 2	40	Dinaphtylméthane sulfonate de calcium (poids moléculaire 500)
N° 3	39	Lignosulfonate de sodium + ester phosphorique
N° 4	16	Lignosulfonate de sodium + traces de naphtalène sulfonate
N° 5	27	Dinaphtylméthane sulfonate de sodium (65 %) lignosulfonate de sodium (35 %)
N° 6	35	Lignosulfonate de calcium
N° 7	30	Lignosulfonate de sodium + alkylphenol oxyethylené
N° 8	40	Naphtalène formaldehyde sulfonate de sodium (poids moléculaire 2000)
N° 9	30	Gluconate de calcium + alkylaryl sulfonate

Les essais effectués confirment les résultats précédents et la mesure de la viscosité à 3h montre que le classement, du point de vue rhéologique, s'effectue de façon très nette en fonction de la nature chimique des produits (Figure 2).

Viscosité des adjuvants introduits en différé en fonction du temps d'attente et de leur nature chimique Figure 2

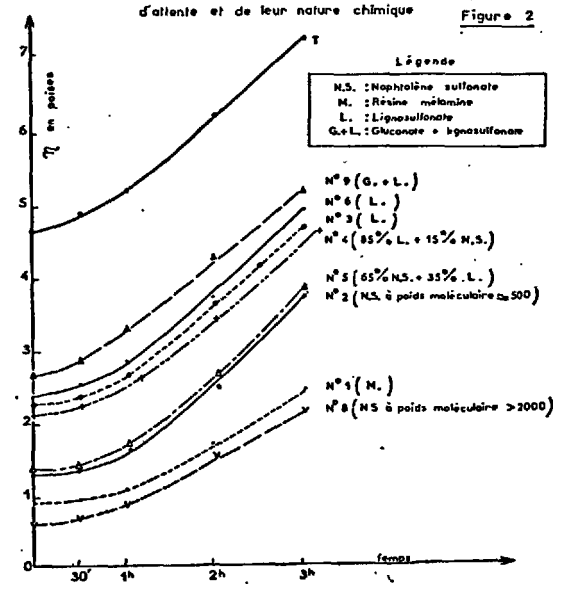

Viennent en tête, du point de vue pouvoir fluidifiant, avec des viscosités à 3h de la pâte, comprises entre 2 et 2,6 poises :

- la résine naphtalène sulfonique de poids moléculaire $>$ 2000 (n° 8),
- la résine mélamine (N° 1).

Ensuite on trouve avec des viscosités plus élevées (3,8 à 4 P) :

- le naphtalène sulfonate à poids moléculaire $\simeq$ 500 (n° 2),
- le mélange 65 % naphtalène sulfonate à poids moléculaire $\simeq$ 500 et 35 % de lignosulfonate (N° 5).

Avec une viscosité de la pâte de 4,5P, le produit n° 4 (riche en lignosulfonates avec de très faibles proportions de naphtalène sulfonate) se place très près des produits n° 3 et 6 (plastifiants classiques à base de lignosulfonate).

Le produit n° 9, constitué de gluconate de calcium conduit à la pâte la plus visqueuse (6 Poises).

Il apparaît ainsi que l'introduction en différé des fluidifiants est bien le mode d'utilisation optimum de ces produits. Leur action devient dans ce cas très marquée et ils se distinguent très nettement des plastifiants. La mesure de la viscosité des pâtes adjuvantées semble permettre de classer les produits suivant leur efficacité et leur nature chimique.

Pouvoir défloculant des résines de synthèses

L'abaissement du seuil de cisaillement des pâtes de ciment constaté avec les fluidifiants est relié au pouvoir défloculant des produits. De nombreuses recherches ont été effectuées sur les propriétés défloculantes des composés tensioactifs (4) (5).

L'effet plastifiant et retardateur des lignosulfonates a été expliqué en partie par l'état défloculé des grains de ciment en présence de ces produits. Nous avons donc recherché s'il existait une différence significative entre le pouvoir défloculant des résines de synthèse et les lignosulfonates et si cette caractéristique n'était pas sélective vis-à-vis de la granularité des grains de ciment.

L'étude de l'aptitude à la défloculation ou dispersion des grains de ciment dans l'eau a donc été menée sur les produits caractérisant chacune des familles d'adjuvants (fluidifiants et plastifiants) sur un ciment brut et sur les trois coupes granulométriques suivantes :

- ultrafines (0/10 µ) comprenant 98 % d'éléments $>$ 5 µ,
- fines moyennes (0/20 µ) comprenant 78 % d'éléments compris entre 5 et 20 µ,
- gros éléments (0/100 µ) comprenant 80 % d'éléments compris entre 20 et 80 µ.

La distinction entre les fluidifiants et les plastifiants étant très nette du point de vue de la viscosité, dans le cas de l'introduction du produit différé après confection de la pâte, nous avons recherché si ce phénomène se reflètait de même dans la défloculation des grains de ciment.

Les essais ont donc été réalisés sur chaque produit du tableau n° I, introduits, d'une part dans l'eau de dispersion du ciment, et d'autre part avec un temps d'attente après le mélange eau-ciment variant entre 5 minutes et 2h 30.

Le tracé des courbes granulométriques des ciments a été reconstitué à partir des mesures de défloculation effectuées à l'aide du sédimentomètre Prot et de la pipette d'Andreasen.

Les mesures de défloculation des grains avec les adjuvants, mélangés à l'eau avant dispersion du ciment, ne laissent pas apparaître de différence significative de comportement entre les diverses compositions chimiques des produits (Fig. 3).

Figure N° 3 **COURBES GRANULOMÉTRIQUES**

Reconstituées à partir des grains de ciment défloculés (Sédimentomètre Prot).

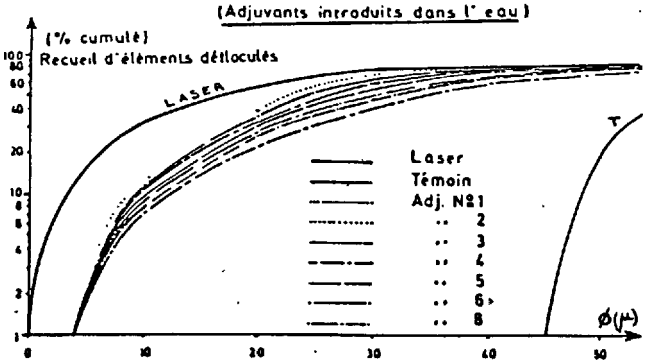

L'état de floculation des grains de diamètre compris entre 0 et 45 µ est total dans le cas du ciment seul: aucun grain inférieur à 45 µ n'a été mesuré, les éléments fins se sont groupés en donnant de gros grains. La granularité se trouve de ce fait complétement modifiée, tout semble se passer comme si le ciment était constitué de grains de dimensions comprises entre 45 et 100 µ.

En revanche l'addition de lignosulfonate ou de résines de synthèse conduit à une dispersion meilleure des éléments fins qui se trouvent partiellement individualisés. Cette dispersion est sensiblement la même quelque soit le produit utilisé.

Lorsque l'emploi de l'adjuvant a lieu en différé, (Fig. 4) on constate que la défloculation des grains 0/20 µ, obtenue avec les résines de synthèse (N° 2 - 1 5 - 8), est plus élevée que dans l'expérience précédente. Ceci est fortement marqué dans le cas du naphtalène sulfonate commercialisé en tant que fluidifiant (produit n° 2). Par contre, les produits à base de lignosulfonate en fortes proportions (3 - 4 - 6) défloculent moins bien que lorsqu'ils sont introduits dans l'eau de gâchage.

Une étude plus approfondie par coupe granulométrique confirme que la dispersion des grains de ciment obtenue avec les résines mélamine et naphtalène sulfonate est supérieure à celle des lignosulfonates dans le cas des ultrafines et fines moyennes, c'est-à-dire pour les grains compris entre 0 et 25 µ (Fig. 5a, 5b, 5c).

Figure N° 4. **COURBES GRANULOMÉTRIQUES**

Reconstituées à partir des grains de ciment défloculés (Sédimentomètre Prot).

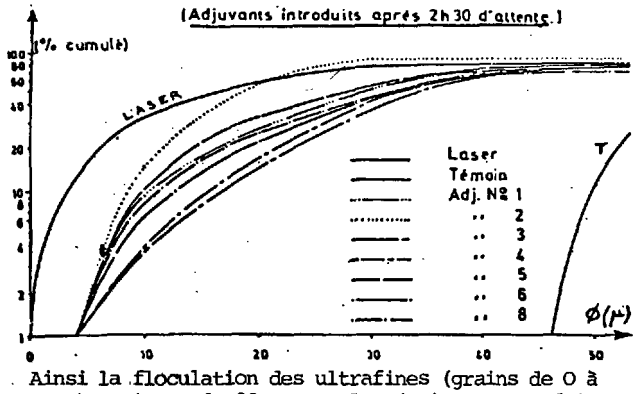

Ainsi la floculation des ultrafines (grains de 0 à 10 μ), qui est de 82 % pour le témoin sans produit et de 73 % pour le lignosulfonate, passe à 36 % et 30 % pour la résine mélamine et le naphtalène sulfonate respectivement.

COURBES GRANULOMÉTRIQUES Reconstituées à partir des grains défloculés (adjuvants introduits après 2h30)

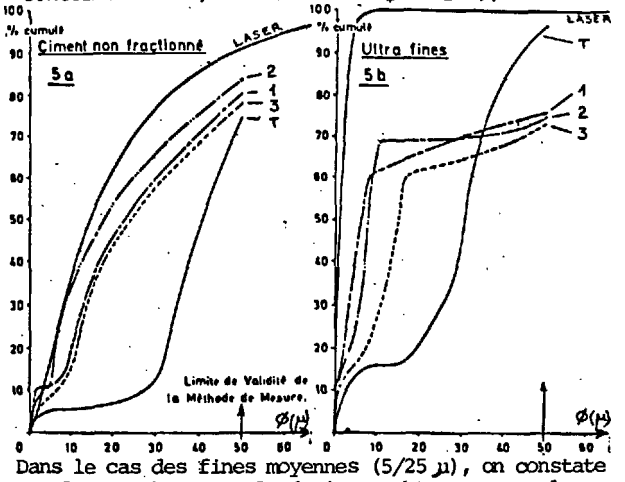

Dans le cas des fines moyennes (5/25 μ), on constate que les courbes granulométriques obtenues avec les suspensions de ciment contenant du naphtalène sulfonate et de la résine mélamine sont très proches (ou confondues) jusqu'à la granulométrie de 8 μ, de celle déterminée au laser. Pour 10 μ, la floculation est d'environ 20 à 15 % pour les résines de synthèse et de 25 % pour le lignosulfonate.

Pour les grains supérieurs à 40 μ, la différenciation n'est pas significative (Fig. 5d), les granularités obtenues avec les différents produits étant sensiblement les mêmes.

D'une façon générale on peut dire que les fluidifiants dispersent plus efficacement que les plastifiants les éléments fins du ciment, c'est-à-dire les grains entre 0 et 20 μ. On remarque de même que la floculation des grains, due à l'absence de produit tensioactifs, conduit à des courbes granulométriques témoin totalement différentes des courbes réelles obtenues par laser. Par contre, les tensioactifs en général permettent d'obtenir des dispersions granulaires dans l'eau conduisant à des courbes granulométriques ayant même allure générale que celle déterminée au laser. Toutefois, quel que soit le produit, la défloculation des éléments fins n'est pas totale et il subsiste toujours un pourcentage variable de grains agglomérés. Ceci entraîne un plus fort pourcentage de grains de dimensions supérieures que celui existant réellement dans le ciment.

Si l'efficacité, du point de vue de la défloculation des grains, est systématiquement plus importante dans le cas des fluidifiants, elle est variable suivant le produit et le moment auquel il a été introduit dans le milieu eau-ciment. La figure 6 montre l'évolution de l'aptitude à la défloculation des grains de ciment de 20 μ que possèdent les principaux fluidifiants et plastifiants en fonction du temps auquel ils sont introduits.

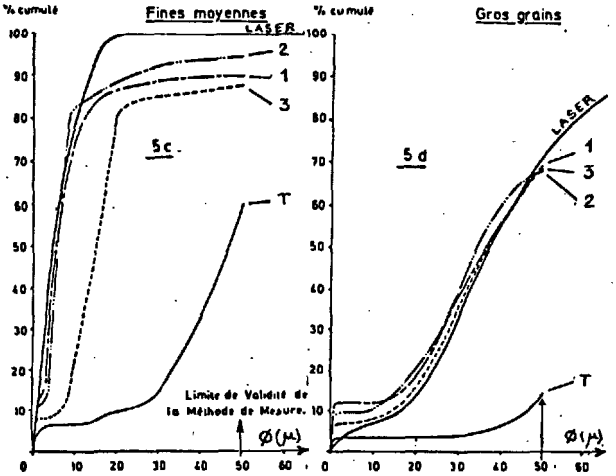

Ainsi l'utilisation optimale, du point de vue de la défloculation, de la résine mélamine (N° 1) se place après un temps d'attente compris entre 60 et 120 minutes après dispersion du ciment dans l'eau. Le comportement du naphtalène sulfonate à poids moléculaire ≃ 500 (n° 2) ainsi que du mélange 65 % de naphtalène sulfonate et 35 % de lignosulfonate (n° 5) semble moins pointu que la résine mélamine. Toutefois, l'efficacité de ces deux produits, est plus accentuée vers 120 minutes pour le n° 5 et 150 minutes pour le n° 2.

Le naphtalène sulfonate à plus haut poids moléculaire (n° 8) présente un pouvoir de défloculation assez constant entre 15 et 20 minutes pour diminuer rapidement après.

Les lignosulfonates (n° 4 et 6) possèdent un maximum d'aptitude à la défloculation entre 5 et 60 minutes.

Pour chaque fluidifiant, l'efficacité du point de vue de l'amélioration des propriétés rhéologiques des mortiers et des bétons sera fonction, en plus de sa composition chimique, d'une part du moment auquel il sera introduit dans le mélange eau-granulats-ciments, et d'autre part de la granularité du ciment lui-même.

Dans le cas d'un ciment riche en éléments fins, les fluidifiants, et tout particulièrement le naphtalène sulfonate du même type que celui du produit n° 2, présentent une efficacité très marquée. Cette efficacité diminuera ou s'atténuera d'autant plus que la mouture du ciment sera plus grossière. Pour certaines granularités et temps d'introduction, il n'y aura pas de

différence sensible entre un lignosulfonate et une résine de synthèse fluidifiante.

Figure 6

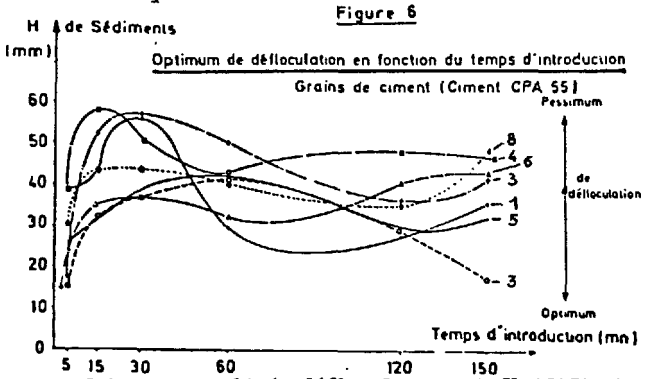

Toutefois, ces qualités défloculantes et fluidifiantes des produits, liées à la granularité des grains de ciment, ne sauraient être dissociées de la nature chimique des constituants prépondérants dans les fractions granulaires étudiées (Tableau II).

TABLEAU II

Analyse chimique des différentes fractions granulaires (CPA 55)

	Ultra fines	Fines Moyennes	Gros grains	Ciment CPA 55 non fractionné
Chaux libre	1,25	1,04	0,25	0,59
Ca SO_4	31,48	9,69	2,78	5,10
Ca SO_4 $2H_2O$	39,82	12,26	3,53	6,45
C_4 AF	4,92	5,83	6,32	6,08
C_3 A	9,06	12,79	12,58	12,71
C_3 S	64,82	66,62	45,21	63,43

La fixation préférentielle du fluidiant par le C_3A a été montrée au cours de recherches antérieures (6). Cependant, compte-tenu que ces fractions granulaires d'ultrafines et fines moyennes ont relativement la même teneur en C_3A que le ciment, mais sont par contre surdosées en SO_4 (ou en gypse : Ca SO_4 $2H_2O$), il semble bien qu'il y ait ainsi une adsorption préférentielle des résines de synthèse sur le gypse. Cette adsorption préférentielle, liée à des familles de produits (structures globulaires pour le naphtalène sulfonate et filandreuse pour le lignosulfonate par exemple), conduit à une configuration du film de produit fixé sur les grains de ciment plus épaisse dans le cas de la résine mélamine et du naphtalène sulfonate (Fig. 6a) que dans le cas des lignosulfonates (fig.6b)

La séparation entre les grains est donc favorisée et la défloculation est, de ce fait, plus marquée.

Déformations de la pâte de ciment en cours d'hydratation

Compte-tenu de ces résultats, il était permis de penser que la présence de fluidifiant dans une pâte de ciment en cours d'hydratation devait se traduire par un comportement différent de celle-ci. En effet, l'étude des courbes de déformation aux jeunes âges des pâtes de ciment en fonction du temps, avec et sans adjuvants, à l'aide de l'appareil de mesure du second retrait (7) fait apparaître, lorsque les adjuvants sont introduits dans l'eau de gâchage, qu'il existe une différence très nette dans l'allure de la partie "gonflement" des courbes de déformation des pâtes de ciment contenant du naphtalène sulfonate, par rapport aux pâtes contenant des produits à fort pourcentage en lignosulfonates (Fig. 7).

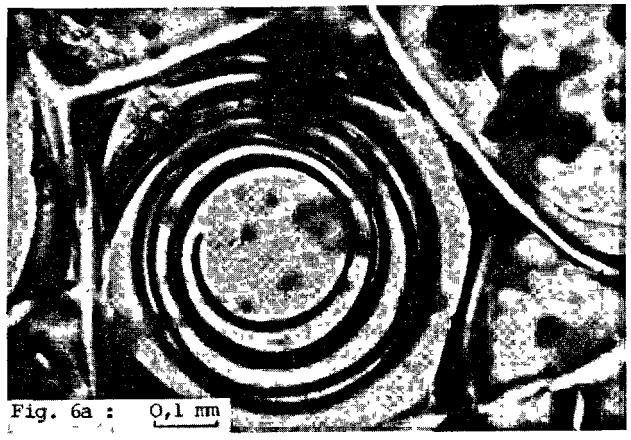

Fig. 6a : 0,1 mm

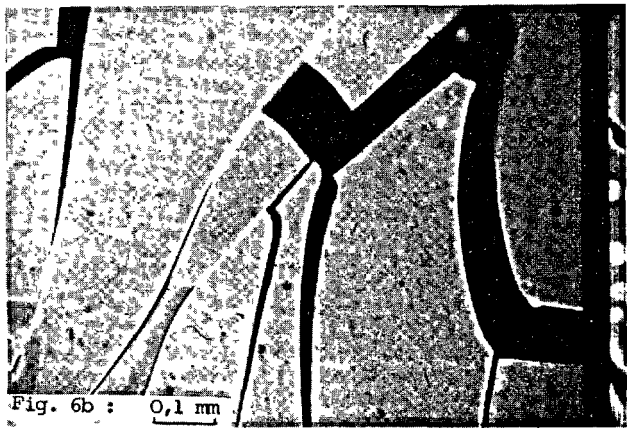

Fig. 6b : 0,1 mm

La présence de naphtalène sulfonate entraîne systématiquement un gonflement de la pâte en cours d'hydratation, très supérieur à celui de la pâte témoin ou adjuvantée avec d'autres produits. Toutefois, les vitesses maximales de second retrait ne se diffécient pas significativement d'une famille chimique à une autre.

FIG:7 INFLUENCE DE LA NATURE CHIMIQUE DE L'ADJUVANT SUR LES COURBES RETRAIT-GONFLEMENT DES PATES DE CIMENT

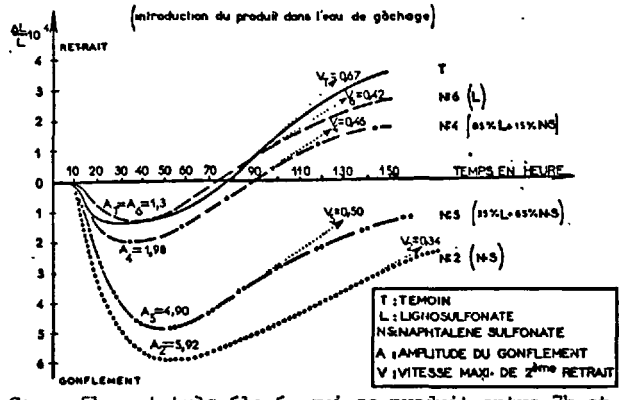

Ce gonflement très élevé, qui se produit entre 7h et 65h après gâchage de la pâte de ciment dans l'eau adjuvantée de naphtalène sulfonate, ne se produit plus

lorsque ce produit est introduit en différé (1h après confection dans l'exemple présent). Au contraire, il semblerait que, dans ce cas, le gonflement mesuré, bien qu'inférieur à celui du témoin, soit plus important dans le cas des lignosulfonates.

Ce phénomène de gonflement élevé de la pâte de ciment en cours d'hydratation se répercute sur la fissuration du béton. Ainsi l'étude comparative faite au banc de fissuration L.C.P.C. (8) entre des bétons avec et sans lignosulfonate et naphtalène sulfonate montre que ce dernier, mélangé à l'eau de gâchage, entraîne une fissuration du béton légèrement retardée par rapport au témoin mais nettement plus rapide par rapport au lignosulfonate (Tableau III).

TABLEAU III

	Age du béton au moment de la fissuration	
	Produit introduit dans l'eau de gâchage	Produit introduit 1h après confection du béton
Béton témoin	20h	-
Béton+lignosulfonates	73h	44h
Béton+naphtalène sulfonate	32h	72h

A l'instar des constatations faites sur les courbes de gonflement des pâtes de ciment, ce comportement est inversé lorsque le naphtalène sulfonate est introduit 1h après confection du béton. Dans ce cas, la fissuration est retardée alors qu'elle devient plus précoce (comparativement) avec le béton adjuvanté au lignosulfonate.

Par ailleurs, les courbes des contraintes engendrées par les déformations en fonction du temps, enregistrées dès la mise en place du béton dans le banc de fissuration, ont des allures totalement différentes dans l'un ou l'autre cas.

Les contraintes engendrées par le retrait du béton dans lequel le naphtalène a été introduit dans l'eau de gâchage sont enregistrées à partir de 21h et entraînent rapidement la fissuration (32h). Alors que dans l'autre cas, elles ne se développent qu'à 33h, c'est-à-dire après la fissuration intervenue dans le béton précédent. Le rapport des vitesses de retrait respectives est de 2,13.

CONCLUSION

Cette étude a permis de cerner le mode d'action des résines de synthèse fluidifiantes (mélamine et naphtalène sulfonate) et de les différencier des tensioactifs (lignosulfonates, etc...) employés habituellement en tant que plastifiants.

Il est apparu ainsi que l'efficacité de ces produits est étroitement liée au moment de leur introduction dans le mélange eau-ciment-granulats. D'une façon générale, et quelle que soit la nature chimique, les résines de synthèse utilisées en différé (30 minutes et plus après fabrication des mélanges hydrauliques) présentent un effet fluidiant très élevé, les démarquant nettement des lignosulfonates.

En revanche, il n'existe pas de différenciation significative entre les divers adjuvants lorsqu'ils sont introduits dans l'eau de gâchage.

Cette fluidification est reliée à une défloculation notable des grains de ciment de diamètre $< 20\ \mu$.

Le pouvoir défloculant des résines de synthèse dépend aussi du moment d'introduction du produit et semble lié à une adsorption préférentielle sur les grains de gypse et de C_3A du ciment Portland.

Une particularité des fluidifiants à base du naphtalène sulfonate est qu'ils entraînent une augmentation importante du gonflement des pâtes de ciment en cours d'hydratation lorsqu'ils sont utilisés dans l'eau de gâchage, c'est-à-dire au minimum de leur performance. Ceci n'est pas sans influence sur la fissuration du béton qui se trouve être accélérée dans ce cas et pour cette famille chimique de produits.

Le comportement à la fissuration d'un béton additionné de naphtalène sulfonate peut être donc complétement différent suivant le mode d'introduction du produit. Ceci peut revêtir une grande importance dans le cas des constructions en béton.

BIBLIOGRAPHIE

(1) Commission Permanente des Liants Hydrauliques et des Adjuvants du Béton "Règlement technique de l'agrément " ed. Synad - Paris.
(2) AM.PAILLERE-Ph.B "Etude comparative du comportement rhéologique et mécanique des bétons avec plastifiants et fluidifiants" Colloque International sur la rhéologie des matériaux industriels - Mons 1977 - Revue Silicates Industriels.
(3) J.P. BOMBLED "Rhéologie des mortiers et des bétons frais, influence du facteur ciment" Proceedings of RILEM Leeds - mars 1973 - Vol. I.
(4) IVANOV F.M.T. et al. "Les bétons de ciment avec plastifiants" Dorizdat - Moscou 1952.
(5) C. LEGRAND "Détermination des caractéristiques rhéologiques des corps viscoplastiques à thixotropie partielle" Cahiers Groupe Français de Rhéologie Tome III - Avril 1973.
(6) R. SIERRA "Action des fluidifiants sur les processus d'hydratation du ciment et de ses constituants Colloque International sur les adjuvants du béton Mons 77 - Revue Silicates Industriels.
(7) J. BARON "Fissuration du béton par hydratation localement différée du ciment" Rapport de Recherches n° 15 - mars 71 - L.C.P.C. Paris.
(8) A.M. PAILLERE - J.J. SERRANO "Appareil d'étude de la fissuration du béton - Bulletin de Liaison des Laboratoires des Ponts et Chaussées n° 83.

Effect on micro-additives on properties of concretes

Influence des micro-additifs sur les propriétés des bétons

L.N. POPOV, Dr. Sc. All-Union Polytechnical Institute (WZPI), Moscow, U.R.S.S.

RESUME : Le processus de durcissement du béton de ciment et de formation de sa structure et de ses propriétés dépend non seulement du ciment portland utilisé pour sa fabrication, mais aussi des micro-additifs dispersés dans le ciment. Les micro-additifs sont introduits dans le ciment portland au broyage du clinker de ciment avec des roches ou des déchets industriels. Ils peuvent aussi être introduits dans le béton, lors de son malaxage, sous forme d'agent dispersif, ou bien sous forme de fraction des agrégats. Il ne faut pas considérer le micro-additif comme un adjuvant inerte. L'examen de la structure et des propriétés des bétons de ciment à agrégats fins a mis en évidence que les micro-additifs améliorent la granulométrie générale du béton, ce qui garantit une certaine diminution de la consommation du ciment. Les bétons à agrégats fins avec addition de micro-additif ont une structure dense et ont les mêmes grandeurs de résistance et de déformabilité que celles des bétons ordinaires.

SUMMARY: Process of hardening of concrete and formation of its structure and properties depends not only on the portland cement but also on the disperse additivs - microaggregate. Microaggregate can be inserted into Portland cement composition together with rock products or waste products of the industry during grinding of cement clinker.

Microaggregate is a disperse fraction of aggregate and can be inserted also into concrete mixture together with its other component.

Microaggregate cannot be considered as an inert additiv. Investigation of the structure and properties of fine-corned cement conretes has been showed that the addition of microaggregate improves the general granulometric composition of aggregate and allows to decrease cement content in concrete. At the same time fine-corned concretes with added microaggregate have the same strength- and strain-properties as common plain concretes.

INTRODUCTION

Hardened cement paste is a three-phase system (solid phase - water - air) and has a capillar-porous structure. It consists of clincer particles not fully hydrated; gel, including gel pores; cristalls of calcumoxydhydrat etc.; and also capillar pores and air voids (1). Hardened cement paste can be considered as "microconcrete". Clincer particles have not only higher strength as compared to cement gel, but also high bond strength with gel. Thus "microconcrete" can be considered as a composition material, reinforced with clincer particles (2).

Structure and strength of hardened cement paste depends significantly on the fineness of pulverizing and granulometrical composition of Portland cement (3,4).

In some investigations it was found that mostly active part of cement consists of the fraction 5-20 mcm; the fraction 20-40 mcm can also be considered as an active. On the other hand the fraction 40-60 mcm and more coarse particles play a role of micro-aggregate. It is found that these particles have a positive effect on the structure and properties of hardened cement paste. It can be assumed that use of special microaggregate can also lead to a positive effect.

As such microaggregate can be used rock materials and disperse waste product of the industry (ash, slays, etc.) (5).

Microaggregate can be inserted into Portland cement composition together with rock products or waste products during grinding of cement clinker. Microaggregate can be also inserted into concrete mixture together with other components (6).

Microaggregate cannot be considered as an inert additiv. Using different experimental methods (chemical, physico-chemical etc.) it is possible to appraise the activity of microaggregate of a given kind and to analyse its effect on structure and strength of hardened cement paste (7).

It can be supposed (analogously to common plain concrete) that the weakest link in the structure of hardened cement parte is the interface between microaggregate particles and matrix.

Thus the density and strength of the interface effects significantly the strength and strain behaviour of cement concretes.

MICROSCOPICAL INVESTIGATION OF THE INTERFACE MICROAGGREGATE-MATRIX

Fine-corned concrete with aggregate consisting of waste product from the mining industry - oreless particles of quartzit, both sand-like and with 5 - 20 mm dimensions is a relatively new kind of concrete.

These materials can be used as aggregates for fine-corned concrete. This kind of concrete will be widely used for manufacturing of thin-walled and other reinforced concrete structures.

Fine-corned concrete has higher homogeneity, higher tensile strength, higher water resistance and higher dynamic strength as compared to common plain concrete (8). Waiste products contains disperse particles (< 100 mcm) which can be considered as microaggregate.

We have investigated interface between these particles and matrix (hardened cement parte) with the help of electron microscope UEMV-100 K. This investigation was based on the replic method and used specimens of hardened cement parte at the different age (from some days to 3 months).

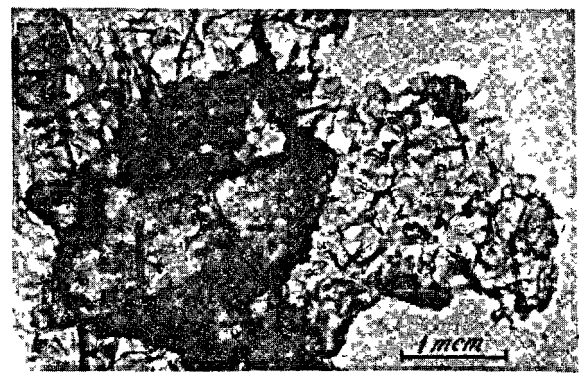

Fig. 1. Electron micrograph of hardened cement paste with microaggregate particles at the age of 90 d.

From Fig. 1 it can be seen than microaggregate formed particles have dense contacts with hardened cement paste. Bounderies are "smeared", which indicate on the chemical reaction between quarzit particles and hydration products of Portland cement (9). On the investigated areas of specimen practically no pores, cracks or woids was observed. It confirms a positive influence of microaggregate on the structure of hardened cement paste.

INVESTIGATION OF MICROHARDNESS OF THE INTERFACE MICROAGGREGATE-MATRIX

Microhardness was investigated with the help of microhardness measuring apparatus PMT-3. It was found that microhardness of the interface between microaggregate and matrix was higher than the microhardness of matrix, but a little lower than for interface between quartz particles and matrix - see Fig. 2.

It was also found that at the age of 30 d the maximal depth of the interface layer between microaggregate particles and matrix is equal to 20-30 mcm.

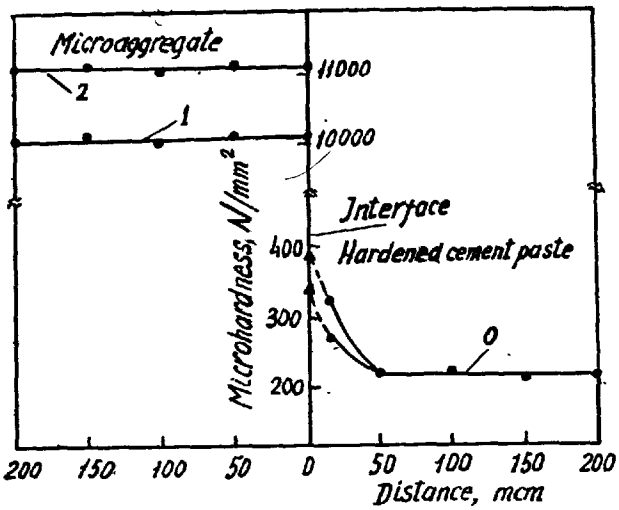

Fig. 2. Microhardness of microaggregate particles hardened cement paste (0); of the interface between matrix and quartzit (1); of the interface between matrix and quartz (2): • - experimental data; ▲ - interpolated values of microhardness.

COMPRESSION STRENGTH OF HARDENED CEMENT PASTE CONCRETE WITH MICROAGGREGATE

It was found, that by the replacement of 10%; 20% and 30% from clinker to the respective quantity of microaggregate the strength of hardened cement paste at the age of 28 d decreases (by 7, 14 and 20% respectively). On the other hand, the coefficient of use of clincer was found to be higher as compared to the hardened cement paste on the pure Portland cement. The coefficient of use of clincer was found to be much higher for concrete made with addition of microaggregate (6).

We have also investigated strength and strain behavior of fine-corned concrete, made with aggregate consisting of waist product of mining industry (fine sand and oreless particles 5-20 mm). Disperce waist product of mining industry (ferro-quartzit) was also used as microaggregate instead of 25% of common sand.

The investigation has showed that microaggregate improved the general granulometric composition of aggregate. It was possible to get fine-corned concrete with the cubic strength of 44, 55 and 67 N/mm^2 at the age of 28d by cement expense 300, 400 and 500 kg/m^3 respectively. This values are approximately by 10% higher as compared to the strength of common concrete with aggregate of crushed granite.

It was also found that the fine-corned concrede described above has lower (or equal) shrinkage and creep strains as compared to the common concrete with aggregate of crushed granite.

The results described above have been used for design and manufacture of reinforced concrete slabs for industrial buildings in the USSR.

CONCLUSIONS

Microaggregate inserted into concrete mixture improved its general granulometric composition. Microaggregate cannot be considered as an inert additiv. Particles of microaggregate have dense contacts with the hardened cement paste. Fine-corned concrete with aggregate of waste products of mining industry with addition of microaggregate have approximately the same strength and strain properties as the common concrete with aggregate of crushed granite.

REFERENCES

1.- А.В. ВОЛЖЕНСКИЙ, Ю.С. БУРОВ, В.С. КОЛОКОЛЬНИКОВ (1979), "Минеральные вяжущие вещества", Стройиздат, 280-283.

2.- Г.И.ГОРЧАКОВ (1976), "Состав и структура и свойства цементных бетонов", Стройиздат, 27-34.

3.- А.Е. ШЕЙКИН (1974), "Структура, прочность и трещиностойкость цементного камня". Стройиздат, 85-91.

4.- B. BEKK (1965), Einige Fragen der Zementvermahlung. "Zement-Kalk-Gips", No. 5, 259-270.

5. - А.В. ВОЛЖЕНСКИЙ, Л.Н. ПОПОВ (1961), "Смешанные цементы повторного помола и бетоны на их основе", Госстройиздат, 73-75.

6.- Л.Н. ПОПОВ (1978), "Строительные материалы из отходов промышленности","Знание", 25-26.

7.- Л.Н. ПОПОВ, Е.В. ЗВЕЗДИНА (1978), "К выбору методики оценки гидравлической активности микронаполнителей" Сб. трудов ВЗПИ. Выпуск 110, 10-15.

8.- Ю.М. БАЖЕНОВ (1978), "Технология бетона" "Высшая школа", 177-182.

9.- О.П. МЧЕДЛОВ-ПЕТРОСЯН (1971), "Химия строительных материалов". Стройиздат, 153.

Conceptual and mathematical models for tricalcium silicate hydration

Modèles qualitatifs et quantitatifs pour l'hydratation du silicate tricalcique

James M. POMMERSHEIM, James R. CLIFTON, Geoffrey FROHNSDORFF, U.S.A.

SUMMARY : Based on conceptual models for the stages in the hydration of tricalcium silicate, a mathematical model was formulated and solved using analytical techniques and the computer. The separate resistances in the mathematical model correspond to the phenomenological stages of the conceptual models. The mathematical model accounts for both diffusion through growing, interpenetrating spherical product layers and chemical reaction at the hydrate-cement interface, as expressed by a dimensionless modulus proportional to the ratio of the diffusion rate to the reaction rate.
Low values of the modulus indicate that chemical reaction rate controls the hydration process while high values indicate that hydrate diffusion is the controlling mechanism. The model assumes quasi-steady-state growth but allows for the depletion of water from solution as hydration proceeds. Model input allows for different particle sizes, water to cement ratios; and initial temperatures, while model output predicts the degree of hydration, the porosity and the overall structure of the hydration products, all as functions of time. Comparison of model output with available degree of hydration data gave a reasonable fit between the model and the data, with physically realistic values found for model constants.

RESUME : En se basant sur des modèles qualitatifs de l'hydratation du silicate tricalcique, un modèle mathématique a été imaginé, puis calculé grâce à des analyses techniques et en utilisant un ordinateur. Les résistances indiquées par le modèle mathématique correspondent aux phases phénoménologique des modèles qualitatifs. Le modèle mathématique tient compte à la fois, de la diffusion à travers la structure, et de la réaction chimique à l'interface eau-ciment; il dépend d'un facteur sans dimension, proportionnel au rapport de la vitesse de diffusion à la vitesse de réaction.
Les basses valeurs de ce facteur correspondent au cas où le processus d'hydratation est commandé par la vitesse de la réaction, alors que ses hautes valeurs correspondant au cas où ce processus est commandé par la vitesse de diffusion. Ce modèle permet de représenter la croissance dans un état quasi stable; mais il permet aussi de représenter ce qui se passe quand on vide l'eau qui servait à l'hydratation. Le modèle est valable pour diverses granulométries et divers rapports E/C; il indique en fonction du temps et de la température initiale, le degré d'hydratation, la porosité et la structure interne des produits de l'hydratation. En comparant les résultats du modèle et ceux de l'expérimentation, on constate un accord raisonnable, pourvu que les constantes physiques du modèle soient bien choisies.

Introduction

To develop an improved method for predicting the performance and durability of cement and concrete, the mathematical modeling of the hydration of portland cement and dependent phenomena has been undertaken [1]. Because tricalcium silicate (C_3S)* is the major constituent of portland cement, and since it, along with dicalcium silicate, is principally responsible for the strength development of cement, the hydration of C_3S was mathematically modeled. The model allows prediction of the degree of hydration and the amounts of reactants consumed and hydration products formed. The major details of this model are outlined in this paper.

In a recent review article [2] the mathematical modeling of cement systems, including C_3S, has been summarized. The mathematical model developed by Kondo and Ueda [3], although similar in some respects to that developed here, is less comprehensive. Their model is based upon an analogous three layer system which takes into account the disappearance of the middle layer. However, it does not allow for resistance due to the hydration reaction itself and, in addition, the model was found to be improperly derived. Further, Kondo and Ueda did not test their model against the hydration data presented in the same paper [3].

Development of the Model

The mathematical model was developed based upon generally accepted conceptual models [3, 4, 5] which describe the principal stages in C_3S hydration (refer to table 1).

In developing the model it was presumed that the system of hydrating particles remains isothermal and that their hydration rate is not dependent on their position within the system. In addition, C_3S particles were presumed to be uniform in size and spherical as were the hydrate layers forming around the particles.

Basically the problem is conceived as involving diffusion of chemical reactant species (water and ions) through ever-thickening spherical layers of precipitated porous products to the interface between the C_3S core and the innermost hydrate layer [3], dissolution of ions from the C_3S and their hydration near this interface, diffusion of soluble product ions back out through deposited hydrate layers, and precipitation of insoluble products. Insoluble species precipitate as separate C-S-H hydrate layers (so-called inner and outer hydrate) both within and on the outside of the growing hydrated particles. A middle product (or barrier) layer is postulated as forming between the inner and outer hydrate layers at very early times and then disappearing [3]. It acts as a barrier to the diffusion of water into the particle and/or the diffusion of ions away from the particle. The middle product layer may be an impermeable solid which dissolves (or becomes more permeable) with time [3], or it may consist of a diffuse layer of adsorbed calcium ions contributing to an electrical double layer around the particle [4]. Its disappearance may mark the end of the induction period and the beginning of the acceleratory period [3-7].

Most growth of calcium hydroxide crystals occurs in the bulk solution between particles. It is postulated that the growth of calcium hydroxide and the outer hydrate layers decreases the (intergranular) porosity and results in restricted or hindered diffusion of chemical species to the particle surface.

Figure 1 is a schematic representation of a single spherical hydrating C_3S grain shown sometime before the acceleratory period has been completed [7]. Both inner and outer hydrate layers are shown along with the middle product layer. Inner hydrate is presumed to form only within the original boundary (radius R) of the C_3S grain. The hydrate layers consist of two different (C-S-H) gels that are formed in different stoichiometric amounts, b_i, but in constant proportion to one another. The hydrates can have different C/S ratios. Dimensions shown in Figure 1 include R, the original radius of the particle; r_i, the radius of the unhydrated solid C_3S core; r_o, the outside (particle) radius; and x, the thickness of the barrier layer. Concentrations of species in solution (between grains) are denoted as C_o.

Considering the system to be the pores of the particle depicted in Figure 1, and assuming spherical particle symmetry with no internal production or consumption of chemical species and constant diffusivity D, a mass balance for the pore liquid for each species yields:

---

* Conventional cement chemistry nomenclature is used here:

$$C = CaO, \quad S = SiO_2, \quad H = H_2O.$$

$$\frac{D}{r^2} \cdot \left[\frac{\partial}{\partial r} r^2 \frac{\partial C}{\partial r} \right] = \frac{\partial C}{\partial t} \qquad (1)$$

$$0_i < r < r_o < r$$

The concentrations C will vary with both radial position r and time t. Equation (1) will be valid for each chemical species in the hydrate layers surrounding the particles. It will apply to the pores of the inner and outer hydrates as well as those of the middle layer. In each region equation (1) is subjected to two boundary conditions and one initial condition. The initial condition for the model presumes uniform concentrations at time zero. Boundary conditions are prescribed at the interfaces between regions. There is equality of component fluxes at r = R and r = R + x. At the outside of the particle, where diffusivities are much greater than within the hydrating mass, concentrations are taken equal to the concentrations present in the bulk liquid.

At the unhydrated core ($r=r_i$) the boundary condition equates the flux of the diffusing reactant species N to the surface rate of chemical reaction R, so that:

$$-N = -D \frac{\partial C}{\partial r} = R = k C \qquad (2)$$

Equation (2) describes a first order irreversible reaction with reaction velocity constant k. If the temperature is constant, k will also be constant.

To obtain an expression for the degree of hydration α, a mass balance is made at the hydrating interface:

$$-\rho a \frac{dr_i}{dt} = D \left(\frac{\partial C}{\partial r}\right)_{r = r_i} \qquad (3)$$

where a is the moles of water reacted per mole of C_3S consumed and ρ is the solid molar density of C_3S. In this development a single chemical reaction is presumed whose overall stoichiometry is presented in Figure 1. a, b and c are stoichiometric coefficients. Equation (3) equates, on a surface area basis, the moles of solid C_3S which dissolve to the moles of water which react with the C_3S at the particle core.

Application of the given boundary and interface conditions to equation (1) yields the following differential equation:

$$-\frac{d\tau}{\tau} = \left(\frac{1}{my^2} + \frac{1}{y} - 1 \right) + \frac{D_i}{D_x} \frac{x}{R}$$

Resistances: Reaction/Diffusion in Inner Hydrate; Middle Layer Diffusion

$$+ \left(\frac{D_i}{D_o} 1 - \frac{R}{r_o}\right) y^2 \, dy \qquad (4)$$

Diffusion in Outer Hydrate

where:

τ is the characteristic time, $\frac{aR\rho^2}{C_o D_i}$

y is the reduced radius, r_i/R

D_x is the diffusivity through the middle layer

D_i is the diffusivity through the inner hydrate layer

D_o is the diffusivity through the outer hydrate layer

m is kR/D_i (reaction-diffusion modulus)

The development of equation (4) presumes that the thickness of the barrier layer x remains much less than the particle size R and also presumes that the growth of the precipitate layers is quite slow so that quasi-steady state can be assumed. This assumption has been tested mathematically using available hydration data [3] and found to be reasonable. The solution of the equation with its one initial condition (y = 1 at t = 0) will predict the radius of the unhydrated core r_i as a function of time. It will also predict the degree of hydration α since:

$$\alpha = 1 - y^3 \qquad (5)$$

Hydration Sub-models

To solve equation (4) separate geometric and mass transfer sub-models have been developed for the geometric ratio r_o/R, the diffusivity ratios D_x/D_i and D_o/D_i, and the middle layer thickness x.

The sub-model for the geometric ratio r_o/R was developed by accounting for the volume of the outer hydrate formed at a given degree of hydration. The sub-model for the barrier layer thickness was derived allowing the barrier layer to disappear at a rate proportional to the product of its surface area and the liquid concentration gradient between the surface of the barrier layer and the bulk solution.

D/D_i, the ratio of diffusivities of the barrier layer to the inner hydrate, was set constant, while D_o/D_i, the ratio of diffusivities of the outer to the inner hydrate was expressed as a power function of solution-porosity [8]. As the porosity of the solution decreased, this ratio became much less corresponding to increased diffusional resistance in the outer hydrate. Solution porosity was determined as a function of the degree of hydration by accounting for the total volume of solid products which are formed.

Equation (4) is written in dimensionless form. Each term on the right side represents a separate resistance to diffusion. This includes resistances to reaction and diffusion in the inner hydrate, diffusion in the middle layer, and diffusion in the outer hydrate. The dimensionless time $d\tau/\tau$ can be viewed as a measure of the sum of the times needed for the diffusing molecules to pass through each of the separate resistances. The resistance to diffusion in the outer hydrate is initially zero since $r_o = R$. As time proceeds and the particle radius r_o increases, the resistance to diffusion through the outer hydrate eventually becomes the dominant resistance.

The first term in the right side of equation (4) represents the resistance to diffusion through the inner hydrate along with reaction at the interface between the inner hydrate and the unhydrated core. The modulus m (equal to $k R/D_i$) is a dimensionless parameter which measures the relative importance of reaction to diffusion. If the rate of hydration is high (large k), or the C_3S particles are large

(large R), or the diffusion coefficients are low (small D_i), m will be large and diffusion through the the inner hydrate will be the controlling resistance. Any one of high k, large R or small D_i can make the modulus m significantly greater than unity. In this case, the controlling factor is the diffusion process since it will determine the overall rate of hydration. Diffusion will be more likely to control the process when the permeability or porosity of the inner hydrate is low, resulting in low values of D_i, and when the temperature is high, resulting in higher values of k. Increases in temperature raise the reaction rate much more rapidly thanthe diffusion rate.

The analysis of the model as well as numerical solutions to the model to the model indicates that each resistance listed below equation (4) becomes dominant in turn. Thus, at early times (before formation of any middle layer), the combined effects due to reaction and diffusion in the initially thin inner hydrate predominate. At later times (induction period and beginning of the acceleratory period) the resistance of the middle layer becomes dominant. At still later times, in the final period of hydration, the dominant resistance shifts to diffusion through the outer hydrate layers. The transition between periods is more or less abrupt depending on the specific values of model parameter sets. An advantageous feature of the model is its ability to give estimates of the relative values of the three resistances.

Model Output

The general mathematical model and the geometric and mass transfer submodels can be solved using numerical techniques and the computer. The following output variables can be obtained as a function of time:

> (1) degree of hydration and hydration rate, α and $d\alpha/dt$, (2) core and particle radii, r_i and r_o, (3) amount of free and combined water, (4) amount of calcium hydroxide formed (5) amount of C-S-H gel formed (6) intergranular porosity, and (7) rate controlling process.

To illustrate the application of the model consider Figure 2 which shows a plot of log (1-y) vs. log t/τ. (1-y) is the radius fraction of hydration while t/τ is a dimensionless hydration time. Experimental hydration data, indicated by circles, is shown from one hour to six months after mixing of C_3S with water. This data, taken from Kondo and Ueda [3], was collected under controlled conditions and represents what is considered to be the best current available set of C_3S hydration data. Particle sizes had a range from 2 to 5μm, the ratio of water to C_3S was 1.0, and the temperature was 25°C.

The solid curve was taken from a computer output of the mathematical model. Known parameters were substituted into the model and sub-models while unknown parameters were selected which gave a reasonable fit between the model and the data. In all cases parameeters were chosen which had physically realistic values. For parameter sets which give reasonable fits to experimental data, sensitivity analyses were performed on each parameter to determine effects on the deviations between the measured and predicted variables. In addition, as parameters of particular interest, particle size, hydration temperature, and water to C_3S ratio, were varied over suitable ranges and their effects determined using the computer model. In addition, overall hydration curves have been determined using the model for the hydration of particles exhibiting a range of particle sizes.

Recent conceptual models [8,9] consider the possibility that a barrier layer may form just outside the core of the unhydrated particle with two additional hydrate layers located outside the barrier layer. The barrier layer is postulated to be a semi-solid having a low C/S ratio. The present model can be modified to treat this case. In this way the sensitivity of the model to the location of the barrier layer could be tested. The general mathematical model will be applied to the hydration of C_2S and other simple cement systems. It is also planned to determine if the model can be used to predict the performance characteristics of portland cement.

References

1. Pommersheim, J. M., and Clifton, J. R., "Mathematical Modeling of Tricalcium Silicate Hydration," Cement and Concrete Research, (to be published).

2. Pommersheim, J. M. and Clifton, J. R., "Mathematical Modeling of Cement Systems," _____.

3. Kondo, R. and Ueda, S. "Kinetics and Mechanisms of the Hydration of Cements", Proceedings of the International Conference on the Chemistry of Cement, Tokyo, pp. 203-255 (1968).

4. Tadros, M. E., Skalny, J. and Kalyoncu, R. S., "Early Hydration of Tricalcium Silicate," Journal of the American Ceramic Society, pp. 344-347 (1976-Jul/Aug).

5. de Jong, J. G. M., Stein, H. N., and Stevels, J. M., "Hydration of Tricalcium Silicate," Journal of Applied Chemistry, 17, pp. 246-250 (1967).

6. Odler, I. and Dörr, H., "Early Hydration of Tricalcium Silicate II. The Induction Period, Cement and Concrete Research, 9, pp. 277-284 (1979).

7. Williamson, R. B., "Solidification of Portland Cement," Progress in Materials Science, 15 (No. 3), pp. 189-285 (1972).

8. Petersen, E. E., Chemical Reaction Analysis, Chpt. 5., Prentice-Hall Inc., (1965).

9. Dent Glasser, L. S., Lachowski, E. E., Mohan, K., and Taylor, H. F. W., "A Multi-method Study of C_3S Hydration," Cement and Concrete Research, 8, pp. 733-739 (1978).

10. Skalny, J., Jawed, I., and Taylor, H. F. W., "Studies on Hydration of Cement-Recent Developments," World Cement Technology, 9, pp. 183-195 (1978).

TABLE 1. STAGES IN TRICALCIUM SILICATE HYDRATION

Stage Designation	Duration Seconds	Hydration Rate	Heat Evolution Rate	Solution Ion Concentrations		Possible Controlling Mechanism(s)
				Ca^{2+}	Si^{4+}	
1. Early Period	$0-10^3$	moderate	high to moderate	rises rapidly past saturation	rises rapidly past saturation then falls rapidly to saturation	reaction/diffusion in solution and precipitation
2. Induction	10^3-10^4	low	low	rises slowly to 1.5 times saturation	remains at[1/] saturation	diffusion through barrier layer/inner product
3. Acceleratory	10^4-4x10^4	high	high to moderate	starts to fall to saturation	remains at saturation	disappearance of barrier layer/hydration reaction and diffusion/ (Precipitation of $Ca(OH)_2$ in solution)[3/]
4. Post-Acceleratory Period	$>4x10^4$	low to very low	low to very low	falls to saturation[2/]	remains at saturation	diffusion through inner and outer product layer

1/ Saturation defined with respect to calcium silicate hydrate (C-S-H) gel.
2/ Saturation defined with respect to calcium hydroxide.
3/ Different phenomena control different parts of acceleratory period.

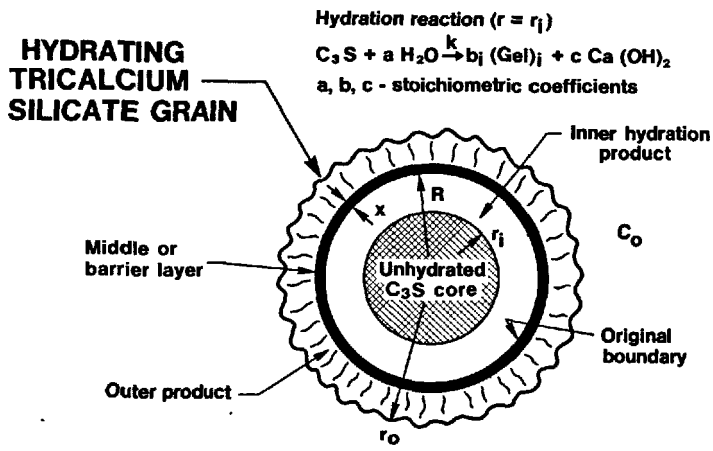

FIGURE 1
Schematic Representation of Hydrating C_3S Grain

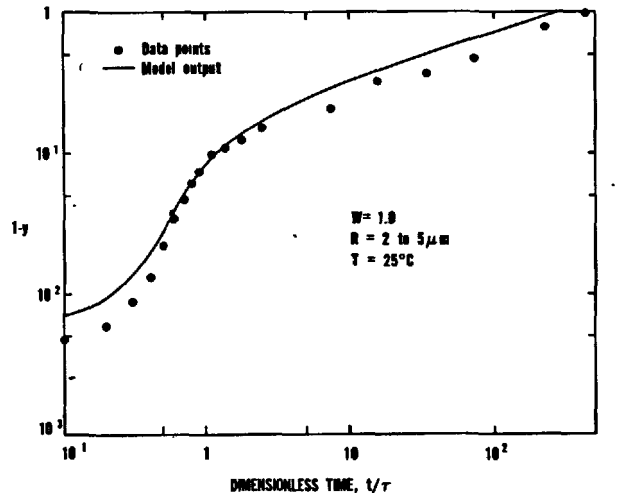

FIGURE 2
Comparison between experimental data and model predictions

Répartition des différentes formes d'eau dans la structure des pâtes pures des C_3S et de ciment Portland

Distribution of different forms of water in the structure of pure slurries of C_3S and Portland Cement

R. SIERRA, Docteur ès Sciences Physiques, Laboratoire Central des Ponts et Chaussées, Paris, France.

RESUME : En associant les méthodes de la spectroscopie moléculaire (spectrométrie infrarouge, résonance magnétique nucléaire et méthode diélectrique de spectroscopie d'absorption hertzienne) avec les méthodes d'analyse thermique, il a été possible d'établir la répartition des diverses formes d'eau, moléculaire et hydroxylique, dans la structure des pâtes de C_3S ou de ciment Portland.

Cette répartition de l'eau est faite tant sur le plan de la localisation que du mode de liaison des molécules d'eau et des hydroxyles. Elle permet ainsi de compléter le schéma de l'unité structurale du C-S-H. En outre, elle montre que l'eau des micropores n'est pas une eau simplement adsorbée mais une eau structurée, donc rigidifiée, par liaison hydrogène.

SUMMARY : By associating the methods of molecular spectroscopy (infrared spectrometry, nuclear magnetic resonance and the dielectric method of hertzian absorption spectroscopy) with thermal analysis methods, it was possible to establish the distribution of the different forms of water (molecular and hydroxylic) in the structure of slurries of C_3S or portland cement.

This distribution of water is done both from the viewpoint of location as well as from that of the bonding of the molecules of water and hydroxyls. It thus makes it possible to complete the diagram of the structural unity of C-S-H. In addition, it shows that the water in the micropores is not simply adsorbed water but one which is structured and, hence, rigidified by hydrogen bonding.

I. INTRODUCTION

La pâte de ciment durcie est un corps cohérent poreux. Sa matrice solide est constituée par les produits d'hydratation du ciment initial dont l'agencement détermine la porosité. L'extrême division des produits d'hydratation fait que la taille des vides est essentiellement du domaine des micropores.

L'eau, toujours présente dans une pâte durcie est répartie à la fois dans les micropores et dans la structure des hydrates. Dans les micropores, ses propriétés varient suivant les paramètres géométriques, physico-chimiques et structuraux de la matrice solide. On distingue en général : l'eau libre, l'eau de sorption (chimisorbée ou physisorbée) l'eau combinée qui peut être soit moléculaire (cas de l'eau de cristallisation ou d'enclathration), soit hydroxylique. Dans la texture de la pâte, l'eau est essentiellement une eau de sorption, l'eau libre n'existant que dans les macropores et les cavités.

Les méthodes de spectroscopie moléculaire sont les plus adaptées à l'étude de l'eau adsorbée. Nous les avons appliquées aux pâtes de ciment durcies en les associant avec l'analyse thermogravimétrique type Mac Bain qui permet de faire le bilan du contenu en eau. Par l'interprétation des résultats obtenus, nous avons essayé d'établir un schéma textural. Pour des raisons évidentes de simplification, nous avons axé l'investigation sur les pâtes de C_3S.

II. TECHNIQUES EXPERIMENTALES

1) Thermogravimétrie en atmosphère contrôlée (à la thermobalance type Mac Bain).

Le tableau I et la figure 1 résument les résultats obtenus pour un hydrosilicate calcique du type C-S-H(I) et pour un gel de C-S-H extrait d'une pâte durcie.

Etat d'hydratation	Conditions de dessiccation	C-S-H (I)	Gel C-S-H
2	Apres ± à température ambiante en atmosphère saturante	$C_{1,52}\,S\,H_{2,42}$	$C_{1,75}\,S\,H_{2,58}$
1	Sous 14 torrs de vapeur d'eau : palier entre 40 et 70°C		$C_{1,75}\,S\,H_{1,59}$
	Sous $\geq 10^{-2}$ torr de vapeur d'eau palier entre 20 et 40°C	$C_{1,52}\,S\,H_{1,56}$	
0	Apres dessiccation equivalente à séchage D, ($\sim 5.10^{-3}$ torr).	$C_{1,52}\,S\,H_{1,02}$	$C_{1,75}\,S_{1,11}$

Tableau 1 - Détermination des états d'hydratation d'un gel de C-S-H et de C-S-H(I) par thermogravimétrie sous vapeur d'eau.

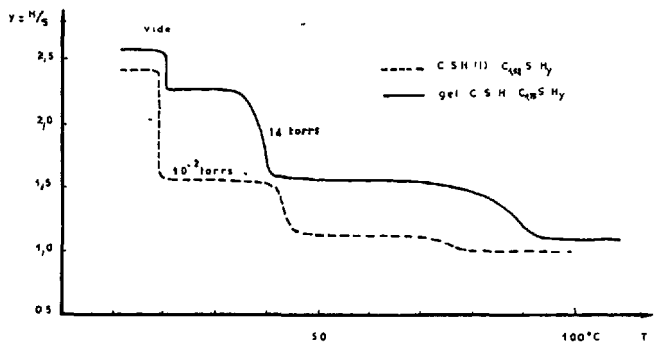

Fig 1 - Courbes d'analyse thermogravimétrique isobare de deux échantillons de gel C-S-H.

Bien qu'il existe une certaine imprécision sur le rapport molaire eau sur silice donc sur H, on voit qu'il existe trois états d'hydratation. Le premier état correspond au séchage D ; il n'y a pas d'eau de sorption. Le second, "état I", est tel qu'approximativement une demi-mole d'eau reste fixée par "mole" de silicate. Le troisième, "état 2", est tel qu'une mole d'eau environ s'est ajoutée à la mole silicatée, par rapport à l'état précédent.

2) Spectrométrie infrarouge

La spectrométrie infrarouge permet de distinguer aisément l'eau hydroxylique de l'eau moléculaire. Dans certains cas, elle peut renseigner sur la localisation, l'orientation et même l'environnement des molécules d'eau, lorsque celles-ci sont adsorbées.

Nous avons plus particulièrement examiné la réponse donnée dans la gamme spectrale 2500-4000 cm^{-1} , en opérant avec la résolution maximale du spectromètre Leitz III G, soit 300 traits par millimètre.

Le spectre présenté figure 2 correspond à un gel de C-S-H extrait d'une pâte durcie et séché sous vide primaire. Il consiste en un énorme massif dissymétrique dont l'importance, tant en absorbance qu'en largeur spectrale (3700 à 2500 cm^{-1}) indique le grand nombre d'hydroxyles mis en jeu et surtout l'importante dispersion des fréquences de vibration de

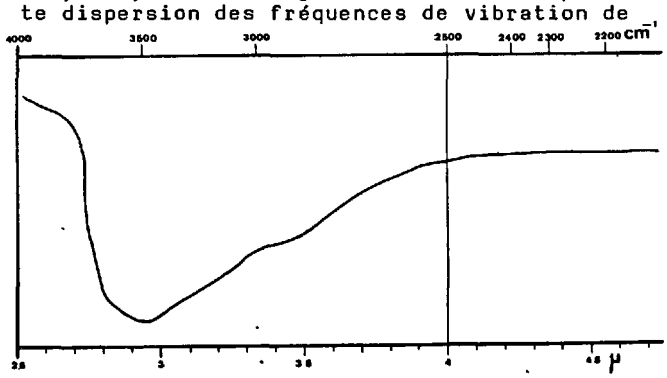

Fig.2 - Spectre d'absorption infrarouge d'un gel C-S-H extrait d'une pâte durcie ; domaine des vibrations de valence des hydroxyles.

valence des liaisons O-H. La partie comprise entre 3400 et 2500 cm^{-1}, restant stable après chauffage prolongé ou après deutériation, correspond à des vibrations d'hydroxyles internes(association de tétraèdres SiO_4^{4-} par liaison H. Entre 3600 et 3400 cm^{-1} on a les vibrations correspondant aux liaisons H des hydroxyles superficiels.

3) Résonance magnétique nucléaire

La résonance magnétique des spins protoniques appliquée à l'étude de l'eau dans les argiles, gels de silice, zéolites, etc... a donné des résultats intéressants, notamment en ce qui concerne la mobilité et parfois la localisation des molécules d'eau dans la couche adsorbée.

Nous avons utilisé la technique à large bande. Celle-ci s'avère nécessaire chaque fois que l'on a affaire à des structures gelées, ce qui est le cas des couches d'eau au contact du solide.

Les mesures faites à la température de 21 °C, sont récapitulées dans le tableau II. Les résultats, donnés en largeur de raies et en temps de relaxation transversale T_2 sont déduits de l'enregistrement de la dérivée première de la courbe d'absorption.

Réf.	Echantillon Désignation	Etat d'hydratation	Caractéristiques de résonance (largeurs de raies ΔH en oersted et T_2 calculé en microsecondes). 1 ΔH	1 T_2	2 ΔH	2 T_2	3 ΔH	3 T_2
A	Gel C-S-H $C_{1,75}\ S\ H_{1,11}$ après séchage D	0	Néant					
B	id. $C_{1,75}\ S\ H_{2,28}$ après ↕ p/p_0 0,71	1 à 2	0,15	440	≈0,67	≈103	1,03	67
C	id. après ↕ avec vapeur D_2O à p/p_0 = 0,84	1 à 2	0,13	530	≈0,56	≈124	0,99	67
D	id. tel quel $C_{1,75}\ S\ H_{2,58}$	2	0,12 à 0,13	551 à 530	-	-	-	-
E	Pâte $C_3S + D_2O$ E/L = 3	1 à 2	0,12	451	?	?	≈0,95	68

Tableau II - Résultats de résonance magnétique nucléaire.

Dans une étude combinant A.T.D., R.M.N. large bande et R.M.N. à écho de spin, Englert et Wittman(1) ont proposé les attributions suivantes : 0,2 oe pour l'eau des macropores ($r_h > 10^{-5}$ cm), 0,3 oe pour l'eau des micropores et 0,6 oe pour celle des espaces interfoliaires. Compte tenu de l'acquis des méthodes d'investigations précédemment examinées, nous proposons : que le premier signal, ΔH=0,1 à 0,2 oe corresponde à l'eau multicouche des micropores ; que le second corresponde à l'eau adsorbée en première couche monomoléculaire et le troisième à une eau interfeuillet (dont les protons ne sont pas échangeables par les deutérons).

4) Spectroscopie hertzienne d'absorption diélectrique

Cette étude, décrite par ailleurs (2) nous a permis d'appréhender le comportement diélectrique de l'eau adsorbée sur les pâtes de C-S-H et de ciment durcies en procédant par analogie avec le comportement sur les gels de silice.

L'absorption qui se produit à la fréquence de 1 kHz dans le domaine de température 140-175° K ressort d'une polarisation dipolaire du type Debye de l'eau adsorbée. Nous avons mis en évidence que ce domaine était en réalité constitué de deux bandes. La première B_α se situant vers 140-150° K se caractérise par une énergie libre d'activation de l'ordre de 0,37 eV. Elle ne se manifeste que pour de très faibles valeurs du taux de recouvrement moléculaire ($\theta < 1$ ou 2). Elle résulterait d'un mécanisme d'orientation des molécules d'eau, après rupture pour chacune d'elles de la liaison hydrogène qu'elle possède avec le site d'adsorption hydroxylique du produit. La seconde bande B_β se produit à plus haute température (160-175° K) et nécessite une énergie libre d'activation de 0,58 eV. Elle serait due à un mécanisme de polarisation par orientation de molécules d'eau avec rupture pour chacune d'elles, des deux liaisons hydrogène qui la relient à deux sites hydroxyliques voisins.

III. PROPOSITION DE REPARTITION DES DIVERSES FORMES D'EAU

1) Eau dans la structure du gel C-S-H

Il est maintenant bien établi que la particule élémentaire de gel de C-S-H est une lamelle constituée selon Kantro et al (3) de deux ou trois feuillets (fig.3).

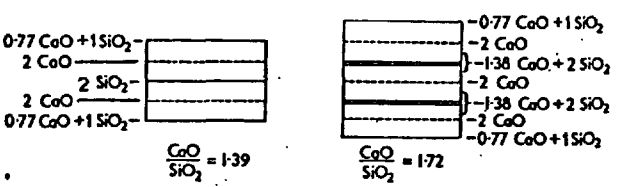

Fig. 3 - Modèles de la structure du C-S-H (a- à deux feuillets ; b - à trois feuillets).

Nos résultats de mesure de surface spécifique (227 $m^2.g^{-1}$) et de composition chimique ($C_{1,77}\ S\ H_{1,25}$) sont compatibles avec le modèle à trois feuillets pour lequel les valeurs théoriques correspondantes sont 252 $m^2.g^{-1}$ et $C_{1,72}\ S\ H_y$.

Nous définissons une unité structurale comme étant le motif atomique de la lamelle. Elle comprend trois pseudo-mailles (ou motif atomique du feuillet) dont les paramètres ont été établis par Megaw et Kelsey (4). Par pseudo-maille, il y a deux "molécules $C_x\ SH_y$ et sa section basale est de 20,35 $Å^2$.

a) eau hydroxylique

Nous avons montré qu'après séchage D, seule l'eau hydroxylique subsiste (I.R., R.M.N.). La thermogravimétrie à la balance Mac Bain permet de préciser qu'il y a deux molécules d'eau hydroxylique par pseudo-maille (cas de l'échantillon dont la maille contient deux "molécules" $C_{1,75}\ S\ H_{1,11}$).

Ces hydroxyles, d'après la spectrométrie infrarouge sont en partie internes (vibration de valence vers 3650 cm^{-1} et en partie externes (silanols libres vibrant vers 3700 cm^{-1}). Ils peuvent être portés, soit par des atomes Si, soit par des atomes Ca (notamment par les ions Ca^{2+} fixés sur la surface pour compenser l'électronégativité de la surface). Or, par section basale, ils ne peuvent être plus de deux. Il n'y a qu'un tétraèdre et demi de SiO_4^{4-} par couche dans la maille. De toute manière, ils ne peuvent se lier au maximum qu'à deux molécules d'eau (au premier niveau) puisque l'aire d'encombrement moléculaire de celle-ci est de 11,4 $Å^2$.

b) eau interfeuillet

La thermogravimétrie à la balance Mac Bain nous a indiqué que, pour une hygrométrie comprise entre le vide donné par le silica-gel (soit environ 10^{-2} torrs) et 80 %, la pseudo-maille contient une molécule d'eau supplémentaire. Cette eau ne peut être qu'interfeuillet. La R.M.N. révèle en effet une eau moléculaire de faible degré de liberté donnant un signal vers 1 oe et un temps de corrélation de 5.10^{-7} s rad^{-1} . La méthode diélectrique montre que jusqu'à $\theta = 1$, il n'y a pas d'absorption dipolaire Debye.

2) Eau dans les pores

Il s'agit plus précisément de l'eau adsorbée à la surface des lamelles.

Lorsque la pression relative est de l'ordre de 0,8, on a d'après les résultats de la thermogravimétrie isobare, l'état 2 d'hydratation ; la "molécule de C-S-H" ou demi-pseudo-maille contient 2,5 molécules d'eau globale. L'unité structurale qui comprend trois de ces pseudo-mailles renferme donc une quinzaine de molécules d'eau dont six sous forme hydroxylique et quatre dans les espaces interfoliaires. Il reste donc en moyenne cinq molécules fixées sur les deux faces basales de la lamelle. L'eau des faces latérales est négligeable, l'épaisseur étant de la trentaine d'angströms par rapport à des longueur et largeur de l'ordre de plusieurs microns.

La spectro-infrarouge et la R.M.N. mettent en évidence la présence d'une eau moléculaire relativement liée ; la première par la manifestation des vibrations d'hydroxyles liés par pont d'hydrogène (entre 3400 et 3600 cm^{-1}) ; la seconde par un signal de largeur de raie d'environ 0,6 oe.

La méthode diélectrique donne une bande d'absorption B_α lorsque θ est compris entre 1 et 2 à 3. Les molécules d'eau concernées, qu'elles soient fixées sur un hydroxyle isolé attenant au support ou qu'elles soient liées à d'autres molécules d'eau, ne peuvent se réorienter sous l'effet du champ que si leur liaison se fait par un seul pont H.

Nous sommes maintenant en mesure de donner une représentation de l'eau fixée à la surface des lamelles. Compte tenu de ce qu'il ne peut y avoir plus de deux molécules d'eau par section basale, les raisons étant les mêmes que pour l'eau interfeuillet, nous pouvons envisager deux schémas (fig.4). Ceux-ci diffèrent avec le plus ou moins grand rapprochement des silanols superficiels : A correspond à des silanols adjacents, B à des silanols isolés. Le bilan du contenu en eau joint à la figure permet de se rendre compte que les valeurs du taux de recouvrement θ et de teneur en eau y (rapportée à la demi-pseudo-maille) concordent avec les déterminations expérimentales.

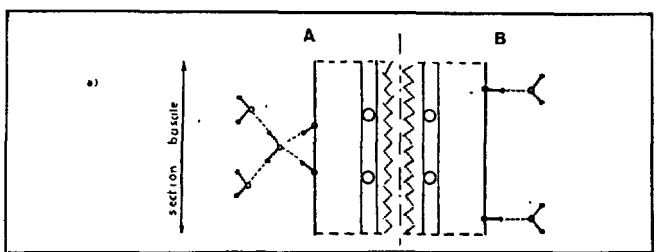

b)

		Contenu en molécules d'eau selon		
		Schéma A	Schéma B	Résultats expérimentaux
= Eau dans l'unité structurale				
- Eau sous forme hydroxylique	N_{OH}	6	6	
- Eau interfeuillet	N_I	4	4	
- Eau globale externe	N_E	6	4	
Total	N_T	16	14	environ 15.
= Eau monocouche sur faces externes	Σ	4	4	
= Taux de recouvrement - θ apparent	$\frac{N_I+N_E}{\Sigma}$	$\frac{10}{4}$ = 2,5	$\frac{8}{4}$ = 2	
- $\theta \to$ relaxation B_α		2	2	2
= Rapport eau sur silice $y = N/S$	$\frac{N_T}{S}$	$\frac{16}{6}$ = 2,65	$\frac{14}{6}$ = 2,34	2,5

Fig. 4 - Schéma (a) et bilan (b) de répartition de l'eau pour une lamelle de C-S-H de composition $C_{1,75}\ S\ H_{2,5}$ (estimation du contenu correspondant à une maille de section basale de l'ordre de 20,35 $Å^2$).

Il ressort de cette discussion que pour $p/p_0 = 0,8$, l'eau extérieure aux lamelles est une eau adsorbée en première couche dont les molécules sont disposées suivant les schémas A et B en fonction de la densité hydroxylique superficielle.

L'eau adsorbée au-delà de la première couche n'a pas été spécialement étudiée. Elle est également liée mais d'une façon nettement plus lâche que la précédente, et ce, d'autant plus que l'on s'éloigne de la surface du solide. C'est elle qui est à l'origine du premier signal R.M.N. ($\Delta H \approx 0,13$ oe) et de la bande B_β d'absorption diélectrique.

IV. SCHEMA TEXTURAL PROPOSE

Pour des raisons exposées par ailleurs (2), nous avons retenu comme modèle de texture celui proposé par Feldman et Sereda (5) et que nous représentons figure 5.

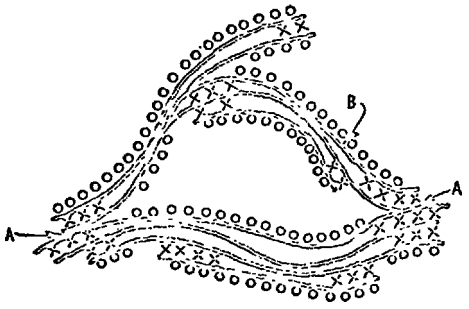

Fig. 5 : Modèle de texturation du gel C-S-H
A - soudures ou liaisons interparticulaires
B - feuillets de C-S-H
X - eau interfeuillet
O - eau adsorbée.

Nous allons examiné plus particulièrement les formes de liaison de l'eau dans les espaces vides de la texture.

1) Micropores interlamellaires

Les micropores qui représentent une part très importante du volume total et par suite de la surface totale des vides de la pâte, ont un rayon hydraulique moyen de l'ordre de 5 Å, alors que les pores dits "plus gros" ont un rayon moyen de l'ordre de 10 A (6).

A un rayon hydraulique de 5 Å correspond un espacement interlamellaire de 10 Å. Dans de tels espaces, l'eau soumise aux effets des champs de forces des surfaces qui se font vis-à-vis est en quelque sorte polarisée dans toute son épaisseur et par suite présente *une structuration*. Le schéma de la figure 6A donne un exemple de la façon dont les molécules d'eau sont liées et de ce fait agencées dans un micropore d'une dizaine d'angströms. Rappelons que l'épaisseur moyenne d'une monocouche d'eau définie statistiquement lors d'une physisorption est de l'ordre de 2,5 Å, soit le diamètre de la molécule. Ce schéma nous a été inspiré par celui que Hair et Hertl (7) ont proposé pour l'eau adsorbée sur un gel de silice et soumise aux effets d'une seule surface du solide (un gel de silice a de relativement gros pores (fig. 6B). La validité du schéma se trouve justifiée par les résultats de l'étude diélectrique. Le recouvrement de chaque surface se fait de telle sorte que pour la quantité d'eau correspondant à une monocouche physique, les molécules d'eau sont nécessairement disposées en deux niveaux. Tant que les deux seconds niveaux ne sont pas remplis, les molécules donnent, sous l'effet du champ alternatif, une bande d'absorption Debye dipolaire du B_α correspondant à une énergie libre d'activation U de 0,37 eV, ce qui traduit l'existence de liaison H simple. Lorsque les deux niveaux médians sont remplis, on a une structuration telle que toutes les molécules d'eau sont doublement liées par pont H, d'où une absorption du type B_β (U = 0,58 eV).

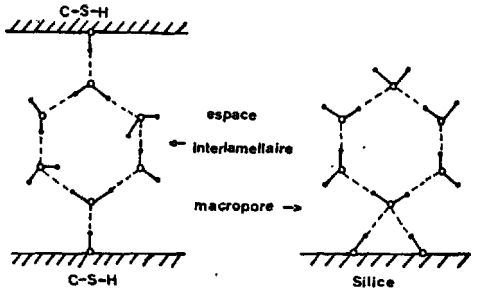

Fig. 6 - Représentation de la disposition des molécules d'eau adsorbées
A - modèle proposé pour l'eau des espaces interlamellaires dans le gel C-S-H.
B - modèle d'Hair et Hertl pour l'eau adsorbée dans les pores du gel de silice.

2) espaces interfoliaires

L'eau de ces espaces est considérée comme partie intégrante du schéma structural de C-S-H. Par conséquent, elle apporte une contribution à la cohésion intrinsèque de la lamelle, en liant les trois feuillets qui la composent.

La nature de cette liaison peut être précisée par l'étude diélectrique. En effet, lorsque le taux de recouvrement est égal ou inférieur à 1 il n'y a pas d'absorption de relaxation. D'après la figure 4, il n'y a au plus pour $\theta = 1$ que deux molécules d'eau par section basale logées dans les espaces interfoliaires. Cette eau qui ne se manifeste dans la mesure diélectrique ni à U = 0,37 eV, ni à 0,58 eV doit être encore plus fortement liée. Nous suggérons, en nous inspirant du modèle retenu par Mamy pour la montmorillonite (8) que chaque molécule d'eau soit triplement liée, donc comme dans la glace (fig. 7).

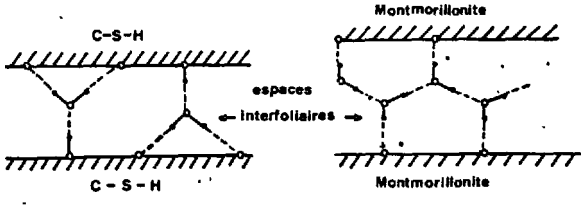

Fig.7 - Représentation de la disposition des molécules d'eau adsorbées :
A - modèle proposé pour l'eau des espaces interfoliaires dans le gel C-S-H.
B - modèle de Mamy pour l'eau des espaces interfoliaires dans la montmorillonite.

V. CONCLUSION

L'association des méthodes de spectrométrie moléculaire nous a permis d'une part, de répartir les différentes formes d'eau dans la structure et la texture d'une pâte durcie de C_3S et/ou de ciment, d'autre part d'apprécier les énergies de liaison des molécules d'eau, soit entre elles, soit avec la matrice solide. Nous avons ainsi montré que l'eau des micropores interlamellaires présente une structuration résultant de liaisons H et que celle des espaces interfoliaires est rigidifiée comme la glace. Il paraît donc certain que ces deux formes d'eau contribuent pour une certaine part à la cohésion des pâtes de ciment et ce, sur la base de liaisons hydrogène.

BIBLIOGRAPHIE

(1) ENGLERT,G., WITMANN,F., NUSSBAUM M., 1971, Zement Kalk Gips, 7, 312-6, 4, 165-74, (All).

(2) SIERRA,R., a) 1974, Contribution à l'étude de l'hydratation des silicates calciques hydrauliques, Thèse, Rennes, (Fr).

b) 1974, idem, Rapport de recherche LCPC, Paris, n° 39, (Fr).

(3) KANTRO, D.L., BRUNAUER, S., WEISE, C.H., a) 1962, Advances in chemistry, 33, 199-219, b) 1962, Journal of Physical-chemistry, 66,1804-9, (Ang).

(4) MEGAW, H.D., KELSEY, C.H., 1956, Nature, 177, 390, (Ang).

(5) FELDMAN, R.F., 1972, Cement Concrete Research, 2 (4), 493-8, (Ang).

(6) MIKHAIL, R.SH., KAMEL, A.M.; ABO EL ENEIN, S.A., 1969, Journal of Applied chemistry, 19, 324-8, (Ang).

(7) HERTL, W., HAIR, M.L., 1969, Nature, 223 (5211), 1150-1, (Ang).

(8) MAMY, J., 1968, Thèse, Paris, (Fr).

THÈME VII

Réaction aux interfaces entre ciment et granulat dans les bétons et mortiers

Interface reactions between cement and aggregate in concrete and mortar

Président : M. IDORN (Danemark)

Pore size distribution and permeability of hardened cement pastes

Distribution de la Taille des pores et perméabilité des pâtes de ciments durcies

P.K. MEHTA and D. MANMOHAN, Université de Californie, Berkeley, U.S.A.

SUMMARY: Portland cement pastes hydrated with different water-cement ratios from 0.3 to 0.9 were investigated at 28 days, 90 days, and 1 year for pore size distribution and permeability. The pore size analyses were carried out by mercury intrusion technique, and the permeability was determined from flow of water under pressure in thin specimens of hardened cement pastes.

A correlation was found between the permeability of cement paste and the volume of pores greater than 1320 Å diameter. Irrespective of the age of hydration and water-cement ratio, as long as a specimen of hardened paste did not contain pores greater than 1320 Å, its permeability remained insignificantly low.

RÉSUMÉ: Des pâtes de ciment hydratées à différents rapports eau/ciment (de 0,3 à 0,9) ont été étudiées à 28 jours, 90 jours et 1 an quant à leur distribution de la taille des pores et leur perméabilité. Les mesures de la taille des pores ont été effectuées par la technique de pénétration du mercure et la perméabilité a été déterminée à partir d'un écoulement d'eau sous pression dans des échantillons minces de pâtes de ciment durcies.

Une corrélation a été trouvée entre la perméabilité de la pâte de ciment et le volume des pores de diamètre supérieur à 1320 Å. Indépendamment du temps d'hydratation et du rapport eau/ciment et aussi longtemps que l'échantillon de la pâte de ciment ne contenait pas de pores supérieurs à 1320 Å, sa perméabilité est restée insignifiante.

INTRODUCTION

It is generally known that durability of concrete exposed to aggressive aqueous environments is greatly affected by the permeability of the hardened cement paste which is the binder in concrete. Powers (1) reported the influence of water-cement ratio on porosity and permeability of portland-cement pastes, however, there is little information in published literature on the relationship between pore-size distribution and permeability. In this paper, the results of an investigation on determination of this relationship are described.

PROCEDURE

A commercial ordinary portland cement with the following potential composition was used for this investigation: 63% C_3S, 17% C_2S, 6% C_3A, and 7% C_4AF. Using 0.3, 0.4, 0.5, 0.6, 0.7, 0.8, or 0.9 water-cement ratio by weight, cement pastes were molded in plastic vials into 25 by 38 mm cylindrical specimens. Special techniques reported in detail elsewhere (2) were adopted to prevent bleeding and air entrainment. At 24 hours, the specimens were demolded and stored in lime water until ready for testing at 28 days, 90 days and 1 year.

For measurement of pore size distribution, 3-4 g pieces were cut from the cylindrical specimens. Hydration was stopped with an acetone wash, and the remaining pore water was removed by drying the specimens to constant weight at 70°C under vacuum for 24 hours. Data on bulk density and total porosity was also obtained from these specimens. In addition, degree of hydration was determined on 100°C-dried specimens by igniting them at 900°C. The pore size analysis was carried out by a commercial mercury intrusion apparatus capable of recording pore diameters down to 45 Å. Permeability was determined by applying D'Arcy's equation to the flow rate of water through cylindrical specimens of 25 mm diameter and 7.5 + 0.5 mm thickness. The water pressures applied ranged from 1.4 MPa for the high water-cement ratio specimens, to 10.3 MPa for water-cement ratios 0.6 and less. Reproducibility of the data was ensured by duplicate or when necessary by triplicate tests.

RESULTS AND DISCUSSION

The results from the tests on permeability, bulk density, total pore volume and degree of hydration are shown in Table 1. The results show that for water-cement ratios of 0.3 and 0.4, with increasing hydration, the bulk density increased significantly with corresponding reduction in total pore volume. However, in the 0.5-0.9 water-cement ratio range, the bulk density as well as the total porosity remained essentially unchanged between 90 days and 1 year. The pastes made with 0.6, 0.7, 0.8 and 0.9 water-cement ratios were about two-third hydrated at 28 days, three-fourth at 90 days, and about 80 percent at 1 year. Correspondingly, there were significant changes in the physical characteristics of the pastes between 28 and 90 days curing period, but only insignificant changes were observed between 90 days and 1 year. Since similar degrees of hydration at given periods were recorded for the pastes made with water-cement ratios 0.6 and above, the pore size distribution data for these pastes only is used below for discussion purposes.

Table 1 Characteristics of cement pastes made with varying water-cement ratios

water-cement ratio	age	bulk density, g/cc	total pore volume cc/g	degree of hydration, percent	permeability, $X10^{-11}$ cm/sec
0.3	28 days	1.89	n.a.	54.59	1
	90 days	1.88	0.117	57.34	0.6
	1 year	1.94	0.130	64.68	0.4
0.4	28 days	1.65	n.a.	61.93	2.0
	90 days	1.70	0.196	64.68	1.0
	1 year	1.75	0.184	71.56	1.0
0.5	28 days	1 50	0.295	64.22	3
	90 days	1.57	0.253	71.10	3
	1 year	1.57	0.247	75.23	1
0.6	28 days	1.26	0 417	64.22	23
	90 days	1.33	0.368	73.85	3
	1 year	1.33	0.362	77.06	2
0.7	28 days	1.18	0.470	64.22	220
	90 days	1.24	0.414	75.23	18
	1 year	1.24	0.409	79.82	14
0.8	28 days	1.09	0.531	65.14	963
	90 days	1.12	0.501	75.23	77
	1 year	1.12	0.503	79.82	45
0.9	28 days	0.91	0.713	66.06	4100
	90 days	0.99	0.622	75.23	175
	1 year	0.99	0.619	79.82	76

*n.a. = not available

EFFECT OF WATER-CEMENT RATIO ON PORE SIZE DISTRIBUTION

The pore size distributions for all the 28-day pastes are compared in Fig. 1. From the plots it can be concluded that with increasing water-cement ratios, the cumulative volume of pores at any given diameter and the threshold diameter increased significantly. The threshold diameter is the diameter of the largest pore present at which mercury begins to penetrate into the pores of the specimens.

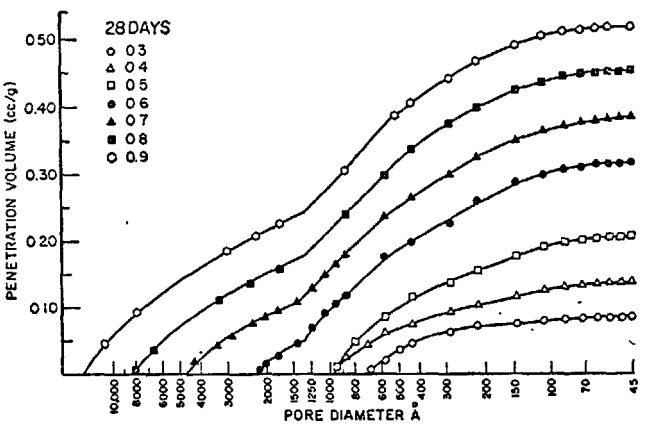

Fig. 1 The effect of varying water-to-cement ratio on pore size distributions, 28 days.

From Fig. 1, two distinct slopes are apparent in the 0.6, 0.7, 0.8 and 0.9 water-cement ratio plots, the breakpoint being 1320 Å; and in the range 45 to 1320 Å the plots appear to be parallel to each other. The data for the above specimens was then replotted in Fig. 2 after subtracting the volume of pores > 1320 Å from the total mercury-intrusion pore volume.

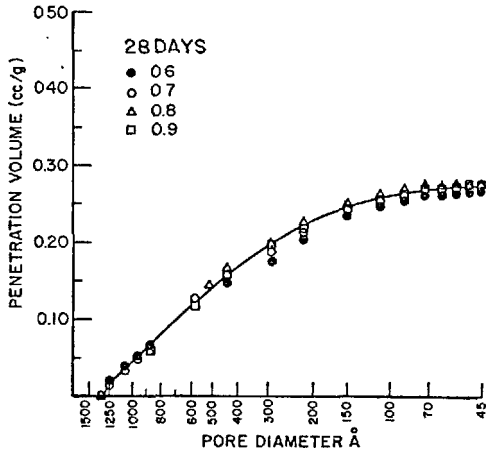

Fig. 2 The pore size distribution of < 1320 Å pores in 0.6-0.9 water-to-cement ratio specimens, 28 days.

Surprisingly, it was found that a single curve could fit the 1320-45 Å pore size distribution data of the 28-day old cement pastes made with 4 different water-cement ratios (Fig. 2). This shows that in hardened cement pastes, the increase in total porosity resulting from increasing water-cement ratios manifests itself in the form of large pores only. In this study, the large pores are defined as those which were intruded by mercury at or below 9.0 MPa applied pressure, i.e., the pores greater than 1320 Å diameter. It is possible that this breakpoint at which the small pores end and the large pores begin (the pores representing the unfilled void spaces between clusters of the hydration products) is influenced by the materials and the methods used in this investigation. However, the present investigators are convinced that for the purposes of understanding and control of the engineering properties of hardened cement pastes, an arbitrary breakpoint value, for instance at about 1000 Å or 0.1 μm, between the large or macro pores and small pores would be useful. It may be noted that the small pores envisaged here include the gel pores (6-16 Å) of Powers (1) and the meso pores of Brunauer et al (3).

EFFECT OF AGE OF HYDRATION ON PORE SIZE DISTRIBUTION

The pore size distribution plots for the 0.9 and 0.7 water-cement ratio pastes at the three ages of hydration, namely, 28 days, 90 days, and 1 year, are shown in Figs. 3 and 4. The plots in Figs. 3 and 4 are typical of the plots obtained for the other water-cement ratio pastes. In general, with increasing age of hydration there was reduction in the threshold diameter, and the cumulative volume of pores at any given diameter. It was observed that the pore size distributions were not uniformly affected by increasing age of hydration. This is probably because as long as there are sufficient void spaces in a hydrating cement system, viz pores > 1320 Å, then following the path of least resistance the hydration products tend to fill these voids first, thus causing little or no change in the 1320-45 Å range. This phenomenon is associated with a significant decrease in the threshold diameter but only insignificant decrease in the volume of pores > 45 Å. Once the larger spaces, in this instance > 1320 Å are filled, further hydration appears to effect the entire pore size distribution.

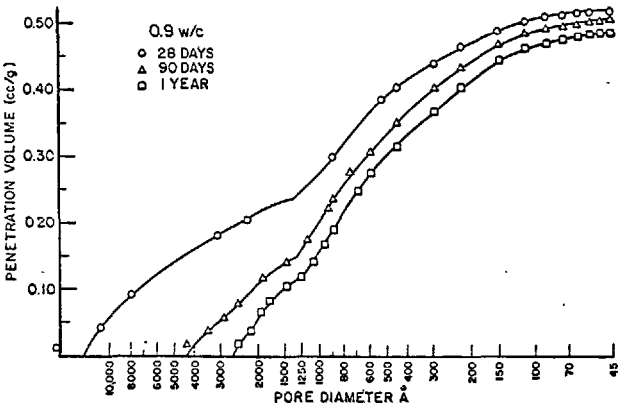

Fig. 3 The pore size distributions, 0.9 water-to-cement ratio.

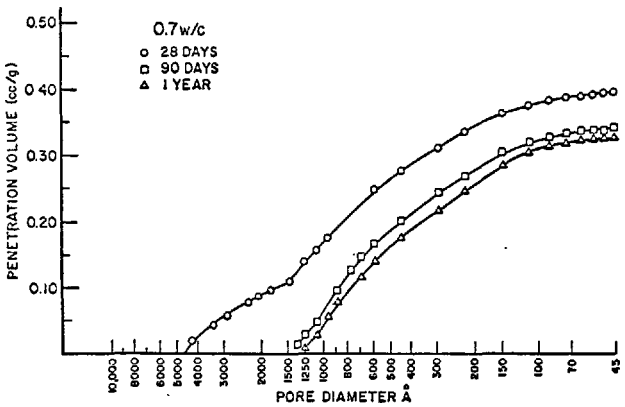

Fig. 4 The pore size distributions, 0.7 water-to-cement ratio.

For example, with increased hydration, the 0.9 water-cement ratio paste (Fig. 3), which had a large volume of pores > 1320 Å present at all test ages, showed major changes in threshold diameter but little change in the total volume of pores > 45 Å. However, in the 0.7 water-cement ratio paste (Fig. 4) for which most pores > 1320 Å were filled between 28 and 90 days, there was correspondingly a large decrease both in the threshold diameter and the volume of pores > 45 Å. Once the > 1320 Å pores were filled, the pore size distributions changed uniformly with further hydration between 90 days and 1 year.

RELATIONSHIP BETWEEN PERMEABILITY AND POROSITY

From the data in Table 1 it is concluded that the experimentally determined values of the permeability coefficient (K_1) are in general agreement with Powers (1). For instance, at any age, the permeability coefficient increased exponentially with increase in water-cement ratio or total pore volume of the cement pastes. Also generally, the permeability coefficient decreased exponentially with increasing age or degree of hydration.

However, it is also concluded from the data that a knowledge of the total volume of pores is not sufficient to accurately predict the permeability of a cement paste. For example, the permeability coefficient for the 1-year old 0.8 water-cement ratio paste was found to be much lower than the 28-day old 0.7

water-cement ratio paste in spite of the fact that the former had a greater total pore volume. On examining the pore size distribution and permeability data it is apparent that large pores, viz > 1320 Å, played a more important role in determining the permeability than the smaller pores. In the case under discussion, the large pores in the 0.8 water-cement ratio paste were filled at 1 year, whereas in the 0.7 water-cement ratio paste at 28 days, a substantial volume of these pores was still present. This shows that in order to develop a more reliable relationship between pore structure and permeability of a hardened cement paste, it would be better to take into consideration several parameters from the pore size distribution, rather than depend on the total porosity alone.

PREDICTING PERMEABILITY FROM PORE SIZE DISTRIBUTION

Using certain parameters from the pore size distribution data as independent variables and the permeability coefficient as the dependent variable, a multiple regression analysis was carried out for setting up a mathematical model from which permeability could be predicted. The pore size distribution was arbitrarily divided into volume of pores >1320 Å, and volume of pores in the 290-1320 Å range. Dividing these volumes by the total mercury intrusion porosity, the effect of pore volume in the 45-290 Å range was taken into consideration. These normalized values of pore volumes in the > 1320 Å and 290-1320 Å range were designated as V_1 and V_2, respectively. Threshold diameter (TD), the largest pore diameter at which the flow of mercury is established in the specimen, was visualized as another important parameter influencing the permeability of a cement paste. Finally, the modified total porosity (MTP), which is equal to total pore volume divided by the degree of hydration, was another parameter used in this study. The modified total pore volume was found more useful to the model than the unmodified pore volume, because reduction of large pores which affected permeability greatly is a function of the degree of hydration. It should be noted that three of the four independent variables proposed here are available from the pore size distribution analysis, and the modified total porosity is obtained from the experimental data on total porosity and degree of hydration.

Table II Input data for the computer program

Water-Cement Ratio	Age	ln K_1	V_1	V_2	TD	MTP
0.3	90 days	-0.51	0.000	0.735	600	0.267
	1 year	-0.92	0.000	0.719	560	0.200
0.4	90 days	0.00	0.000	0.609	760	0.302
	1 year	0.00	0.000	0.559	760	0.256
0.5	28 days	1.099	0.000	0.628	1000	0.466
	90 days	1.099	0.000	0.632	860	0.356
	1 year	0 00	0.000	0.548	720	0.329
0.6	28 days	3.135	0.189	0.552	2200	0.652
	90 days	1.099	0.000	0.653	1150	0.497
	1 year	0.693	0.000	0.618	1100	0.470
0.7	28 days	5.394	0.278	0.481	4600	0.734
	90 days	2.890	0.029	0 676	1400	0.552
	1 year	2.639	0.000	0.662	1250	0.536
0.8	28 days	6.870	0.385	0.440	7800	0.817
	90 days	4.344	0.250	0.523	3500	0.668
	1 year	3.807	0.051	0.633	1550	0.629
0.9	28 days	8.319	0.442	0.404	14000	1.080
	90 days	5.165	0.300	0.500	4000	0.829
	1 year	4.331	0.234	0.503	2600	0.774

Plots of permeability coefficient against each one of the independent variables suggested the exponential relationship of the type:

$$K_1 = \exp(aV_1 + bV_2 + cMTP + dTD + e)$$

where a,b,c,d, and e are constants. Therefore, the permeability values were converted to their natural logarithm (ln K_1) before input into the computer for the multiple regression analysis. The analysis was carried out using the canned program SPSS (Statistical Package for Social Sciences). The input data for this program is shown in Table II. The results gave the following values of the constants for determining the coefficient of permeability of a specimen, with a known mercury intrusion pore size distribution and a known degree of hydration:

$$K_1 = \exp(3.84V_1+0.20V_2+0.56\times10^{-6}TD+8.09MTP-2.53) \quad (i)$$

The accuracy of prediction of permeability by this equation, as reflected by the statistical r^2 value, was found to be 95 percent. In other words, in the present study 95 percent of the variation in the permeability results could be taken care of by the independent variables V_1, V_2, TD, and MTP. Thus, the model for predicting permeability of hardened cement pastes can be used with a good degree of accuracy. Calculations show that on average, the predicted value of the permeability coefficient will deviate from the actual value by 0.61 cm/sec only.

The relationship between permeability and V_1, permeability and MTP, and permeability and TD were also investigated separately. The significant effect of > 1320Å pores on permeability is evident from the plot in Fig. 5 which shows an exponential increase in ln K_1 with increasing V_1. Straight line relationships, also shown in Fig. 5, were found when ln K_1 was plotted against either MTP or ln TD. The corresponding mathematical expressions for these relationships are

$$\ln K_1 = 2.85 \ln TD - 18.51 \quad (ii)$$

$$\ln K_1 = 10.91 MTP - 3.38 \quad (iii)$$

The coefficients of determination calculated for equations (ii) and (iii) are 0.96 and 0.94, respectively. These coefficients are a measure of the accuracy of the fit for the experimental data; and for a perfect linear fit the value is 1.

CONCLUSIONS

Investigations on the pore size distribution and permeability of portland cement pastes hydrated with 0.3 to 0.9 water-cement ratios showed that the pastes made with 0.6 to 0.9 water-cement ratios contained substantial volume of large pores, i.e., pores > 1320 Å diameter. In these high water-cement ratio pastes, the pore size distribution at 28 days was found to remain essentially the same in the 45-1320 Å range, because with the increasing water-cement ratio the increased porosity manifested itself in > 1320 Å pores.

Since the large pores were found to have a greater influence on permeability than small pores, it is concluded that the pore size distribution data, rather than total porosity, provides better opportunity for developing accurate correlations with permeability. It is also concluded that permeability can be computed from a mathematical model which uses input from the pore size distribution data.

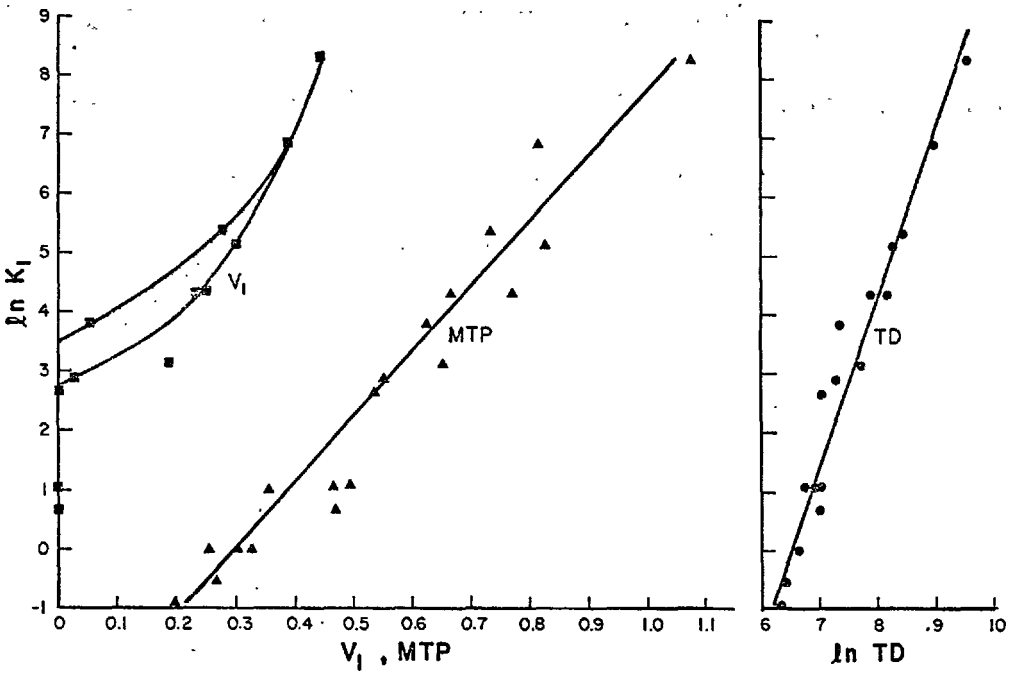

Fig. 5 Relationship Between V_I, MTP, TD and Permeability

ACKNOWLEDGEMENT

The work reported in this investigation was supported by a grant from the U.S. National Science Foundation.

REFERENCES

1. T.C. Powers, "Structure and Physical Properties of Hardened Portland Cement Paste", Journal of the American Ceramic Society, Vol. 41, pp. 1-6, (1958).

2. D. Manmohan, "Studies on the Microporosity and Permeability of Hardened Cement Paste", Doctor of Engineering Dissertation, University of California, Berkeley, pp. 21-46, June 1979.

3. S. Brunauer, J. Skalny, I. Odler, "Complete Pore Structure Analysis", Pore Structure and Properties of Materials RHEM-IUPAC. Part I C3-26 (1973). Academia, Prague.

Liaison pâte de ciment Portland - Granulats naturels

Bond between Portland cement paste and native aggregates

M. CONJEAUD, Ingénieur de Recherche, Laboratoire de Recherche Générale Lafarge S.A.,
B. LELONG, Chef de Service, Laboratoire de Recherche appliquée Lafarge S.A.,
B. CARIOU, Ingénieur, Laboratoire de Recherche appliquée Lafarge S.A., France.

RESUME : La liaison pâte granulat entre des ciments riche et pauvre en C_3A et des granulats naturels, quartz et calcaire, a été étudiée en mesurant son interaction sur les résistances en flexion et en compression de mortiers d'un type spécial, et en déterminant le nombre de granulats cassés à la rupture.

Des essais complémentaires avec le calcaire ont mis en évidence L'influence de la forme des granulats et de leur rugosité de surface sur les propriétés mécaniques de ces mortiers.

Des observations en microscopie électronique à balayage ont permis de suivre, en fonction de l'échéance, le déplacement des surfaces de moindre résistance par rapport à l'interface pâte-granulat.

SUMMARY : The c ement paste -aggregate bond was studied by measuring tensile and compressive strengths of special type mortars which allowed to determine the number of aggregates fractured during the flexion shear. Two industrial Portland cements, respectively C_3A - poor and C_3A - rich, and two native aggregates, quartz and limestone, were used for the study.

In the case of limestone, supplementary tests showed the influence of the shape and surface texture of the aggregates on the mechanical properties of mortars.

Scanning electron microscopy investigations allowed to follow the shift versus time, of the lower strength surfaces from the cement paste - aggregate boundary.

L'étude des liaisons entre granulats et pâte de ciment a fait l'objet de nombreux travaux et tous les auteurs s'accordent à considérer que ces liaisons jouent un rôle prépondérant dans l'acquisition des propriétés mécaniques des bétons. Le développement des caractéristiques de ce matériau hétérogène est lié à de très nombreux paramètres et si les problèmes attachés au choix des granulats ou des liants et à leurs conditions de mise en oeuvre ont été depuis longtemps étudiés, l'examen des mécanismes de liaison entre la pâte de ciment et les granulats n'a été abordé que beaucoup plus récemment.

C'est ainsi que FARRAN (1), l'un des premiers à envisager de manière systématique l'étude des mécanismes de liaison et à en souligner les divers types, a montré que l'adhérence n'est pas simplement due à la forme et à l'état de surface des grains, mais que la nature minéralogique des granulats et celle des hydrates qui se forment à leur contact jouent un rôle prépondérant. Ces résultats soulignent le caractère hétérogène du matériau étudié. Cette idée, reprise par MASO (2), conduit à envisager l'existence autour des granulats, d'une auréole de cohésion variable, plus faible que celle de la masse du liant. Des mesures de microdureté (3) et la mise en évidence, au niveau de la zone de transition de variations de composition de la pâte (4), confirment cette hypothèse.

Beaucoup d'autres travaux ont été poursuivis selon diverses voies, s'attachant à préciser les types de liaison (5) et leurs mécanismes de formation, mettant notamment en évidence l'influence des réactions entre le calcaire et les phases alumineuses des liants sur la formation de liaisons de type épitaxique dues à la présence des hydrates formés et à la nature minéralogique des granulats (6 à 10).

D'autres études ont permis de préciser la morphologie de la zone de contact (11, 12, 13), soulignant soit l'enrichissement en portlandite de la couche de contact (14, 15, 16), soit les caractéristiques physiques de l'auréole de transition, notamment les variations d'épaisseur et de porosité qui expliquent l'existence d'une zone de moindre cohésion (17, 18).

Enfin, certains travaux ne considèrent que les caractéristiques mécaniques des liaisons pâte/granulats et précisent les conditions de développement des microfissures dans le béton (19, 20). Malgré l'abondance des résultats déjà acquis, il a semblé utile de préciser les relations entre les types de liaisons pâte/granulats et les propriétés mécaniques des bétons. On entend par types de liaison ceux qui peuvent être définis par des paramètres faciles à appréhender et aisément mesurables à une échelle relativement grossière, tels que la présence de composés chimiques définis à l'interface granulats/liants ou la nature, la forme, l'état de rugosité de la surface des granulats. Cette approche ne préjuge donc nullement de la nature exacte, mécanique, physique ou chimique de la liaison.

Nous présentons les principaux résultats de nos essais destinés à préciser l'importance des différents types de liaisons précédemment définies. Les examens ont été faits d'une part à l'échelle macroscopique, au niveau des performances et de l'aspect des ruptures ; d'autre part, à l'échelle microscopique, par l'observation au microscope électronique à balayage.

METHODES EXPERIMENTALES

Pour faciliter les observations, nous avons utilisé des mortiers 1/1 à 1/1,5 de granulats monodimensionnels (entre 4 et 5 mm de diamètre). Nous avons adopté un E/C pondéral voisin de 0,30 qui conduit à une bonne aptitude à la mise en place, sans ségrégation des granulats.

Les éprouvettes 4 x 4 x 16 cm ont été conservées à 20°C, pendant 24 heures en salle humide puis sous eau jusqu'aux échéances de 2 - 7 - 28 et 90 jours. Nous avons alors mesuré les résistances à la flexion et à la compression, et déterminé par comptage la proportion de granulats cassés sur la surface de rupture par flexion.

Tous les échantillons, aux échéances de 7 et 90 jours, ont été examinés au microscope électronique à balayage. Pour cette étude, les restes d'éprouvettes, après mesure des résistances, ont été fracturés au marteau, et les surfaces de fracture fraiches ainsi dégagées ont été immédiatement mises sous vide et métallisées pour éviter toute hydratation et carbonatation ultérieures. Le fait de préparer les échantillons par fracture au marteau crée des contraintes, et entraine la formation de fissures qui n'existaient pas initialement dans l'éprouvette de mortier. Mais ceci n'est pas en fait un inconvénient car ces fissures provoquées passent par les surfaces de moindre résistance et nous renseignent sur leur cheminement au voisinage des granulats.

Outre ces examens sur fractures, des sections polies ont été exécutées à l'échéance de 2 jours pour observer au microscope optique la répartition, entre les granulats, des grains de ciment en fonction de leur taille.

RESULTATS MACROSCOPIQUES

Deux séries d'essais ont été réalisées : l'une, avec deux granulats roulés et deux ciments différents pour étudier l'éventualité des liaisons physicochimiques et leur rôle sur les résistances ; l'autre avec un seul ciment et un seul type de granulat diversement traité, pour tester l'influence de sa forme et de son état de surface sur les propriétés mécaniques.

Première série d'essais

Des mortiers 1/1 au E/C = 0,30 ont été réalisés avec deux ciments Portland du type CPA 400, l'un riche en C_3A : 13 %, l'autre pauvre en C_3A : 3 %.

Nous avons utilisé du calcaire dur roulé très pur (type urgonien provenant d'alluvions fluvio-glaciaires würmiennes de la région d'Auberive en Royan - Isère, de résistance à la pénétration 2100 MPa) et du quartz roulé très pur (gisement de sable kaolinique de la région de Barbières - Drôme).

Nous recherchions, en employant des granulats roulés, à minimiser les accrochages mécaniques liés à leur forme et à leur état de surface. En réalité, nous avons pu constater par observation au microscope électronique à balayage, que l'un et l'autre de ces granulats présentent une même rugosité de surface, importante au niveau du micron. De ce fait, des accrochages mécaniques sont possibles avec la pâte, liés à cet état de surface, mais du même ordre de grandeur avec les deux séries de granulats.

Les résultats (tableau I) font apparaitre globalement un pourcentage de granulats cassés très faible, même à 90 j.

TABLEAU I

ciment à	granulats	2 jours		90 jours	
		Flexion MPa	% granulats cassés	Flexion MPa	% granulats cassés
3 % C_3A	calcaire	5,4	3	9,1	22
	quartz	5,8	5	9,1	18
13 % C_3A	calcaire	8,0	13	9,3	14
	quartz	7,9	9	8,7	15

Pour une même échéance, les résistances à la flexion sont indépendantes du granulat : elles ne font que refléter la meilleure résistance initiale du ciment riche en C_3A.

Cependant, à l'échéance de 90 jours, et avec le ciment riche en C_3A, la diffraction X nous a révélé, au contact du seul granulat calcaire, la présence de monocarboaluminate de calcium hydraté : C_3A, $C\bar{C}$, 12 H. Il existe donc bien une réaction chimique dans ce cas, mais qui ne parait pas entrainer une amélioration significative de la résistance du mortier correspondant.

Elle ne parait pas non plus favoriser l'adhérence pâte-granulat puisque, pour une échéance donnée, les pourcentages de granulats cassés par la rupture ne sont pas significativement différents.

Ces résultats permettent de conclure, puisque les granulats ont des possibilités d'accrochage mécanique voisines (même rugosité - même forme roulée) les réactions physico-chimiques qui se produisent avec la pâte n'influencent pas l'accrochage, tout au moins aux échéances examinées.

Deuxième série d'essais

Le fait de n'observer qu'un pourcentage de granulats cassés relativement faible doit pouvoir s'expliquer par l'utilisation de produits roulés. C'est pourquoi nous avons réalisé une autre série d'essais, avec un seul ciment CPA 400 de teneur moyenne en C_3A : 7 % et un seul granulat calcaire, de même origine que précédemment, mais de formes et d'états de surface variés. Ces granulats ont été :

- polis par usure dans un broyeur sans boulet avec de l'alumine comme abrasif pour obtenir des formes arrondies et de faibles rugosités de surface ce qui entraine peu d'accrochages mécaniques

- concassés ce qui donne des formes anguleuses et des rugosités de surface plus grandes d'où de bons accrochages mécaniques (voir fig. 1 - 2)

- attaqués par une solution d'acide chlorhydrique diluée ce qui permet d'obtenir des formes et des rugosités de surface intermédiaires entre les granulats polis et les granulats concassés.

Les mortiers 1/1,5 ont été gâchés au E/C de 0,28.

Comme précédemment, les conditions de préparation des mortiers étant identiques, toute différence entre les résultats obtenus ne pourra provenir que de différence au niveau de l'adhérence pâte-granulat. Globalement, on observe (Tableau II) qu'en fonction de l'échéance le % granulats cassés et les résistances en compression et flexion augmentent régulièrement avec les granulats concassés. Alors qu'avec les granulats polis le % granulats cassés est faible et n'évolue pas, la résistance à la compression n'augmente que faiblement et la résistance à la flexion presque pas du tout. Avec les granulats attaqués à l'acide, les résultats sont in-

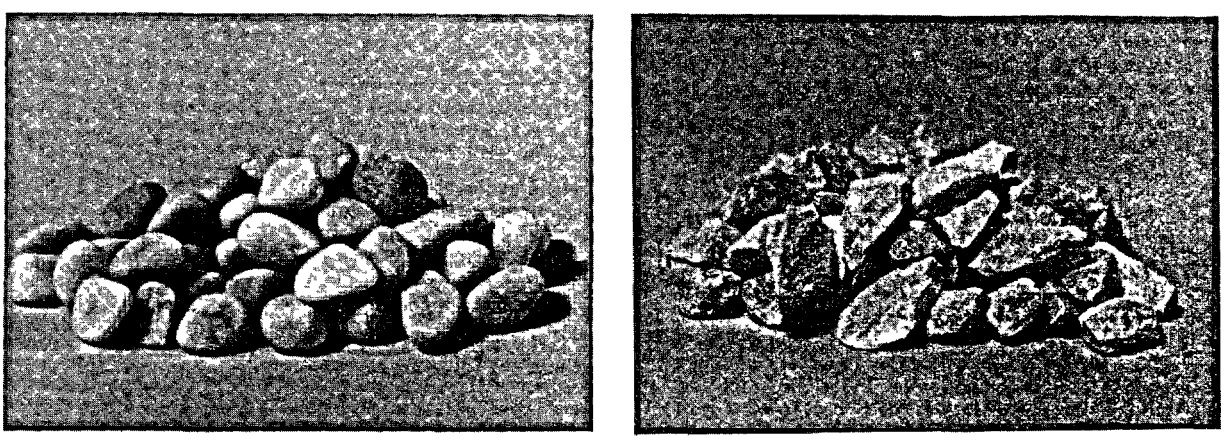

FIGURE 1 - Formes - (a) Granulats polis, (b) Granulats concassés

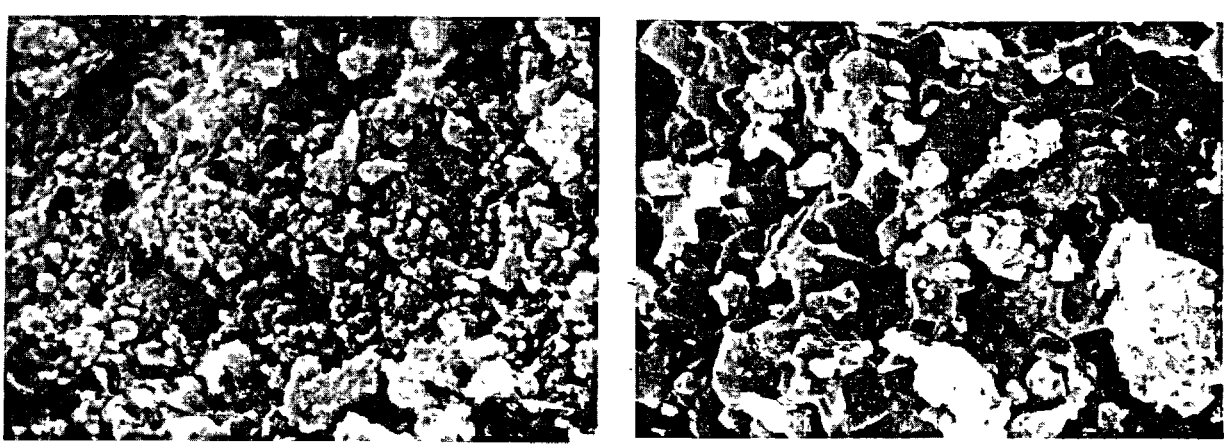

FIGURE 2 - Aspect de la surface - (a) Granulats polis, (b) Granulats concassés 5 µm

TABLEAU II					
avec granulats	Échéances en jours	2	7	28	90
polis	% Granulats cassés	7	17	11	11
	Flexion MPa	7,5	8,0	7,9	8,3
	Compression MPa	46,6	61,4	73,4	76,8
	Compression/Flexion	6,2	7,7	9,3	9,3
attaqués à l'acide	% Granulats cassés	28	32	33	27
	Flexion MPa	7,9	8,5	8,1	8,6
	Compression MPa	51,9	61,5	75,7	77,9
	Compression/Flexion	6,6	7,2	9,3	9,1
concassés	% Granulats cassés	39	52	57	62
	Flexion MPa	8,2	9,8	10,7	11,3
	Compression MPa	55,4	68,9	81,4	94,1
	Compression/Flexion	6,8	7,0	7,6	8,3

termédiaires, plus proches de ceux obtenus avec les granulats polis.

Nous avons porté les résultats de compression et flexion en fonction du % granulats cassés (Figure 3). On remarque que la résistance à la compression dépend de l'échéance, donc de la résistance de la pâte, et aussi du % granulats cassés lorsque celui-ci augmente, la résistance propre des granulats participant alors à la résistance du mortier. Ce nombre de granulats cassés dépend lui-même de la qualité de l'adhérence pâte-granulat. On voit que la résistance à la compression dépend de la résistance de la pâte et de l'adhérence pâte-granulat. La résistance à la flexion, par contre, paraît dépendre principalement du % de granulats cassés, et moins de l'évolution de la résistance de la pâte. Les résultats se regroupent sur une courbe d'allure exponentielle qui met en évidence l'intérêt d'obtenir, par une bonne adhérence pâte-granulat, un % granulats cassés élevé. La résistance à la flexion apparaît donc, proportionnellement, plus liée à la qualité de l'adhérence pâte-granulat que la résistance à la compression d'où une diminution du rapport compression/flexion lorsque l'adhérence pâte-granulat s'améliore.

A partie de la même variété de granulats calcaires durs et en ne faisant varier que leurs formes et leurs états de surface, nous avons pu obtenir, à 90 jours : une adhérence médiocre (polis) ne conduisant qu'à 11 % de granulats cassés à la fracture et une très bonne adhérence (concassés) entrainant 62 % de granulats cassés à la fracture avec une amélioration de 17,3 MPa en compression et 3,0 MPa en flexion. Ceci montre bien l'importance de la contribution des accrochages mécaniques à l'adhérence pâte-granulat.

RESULTATS MICROSCOPIQUES

L'examen à 2 jours des sections polies en microscopie optique fait apparaître dans tous les cas un enrichissement en fines particules de ciment autour des granulats. On a là un effet semblable à celui de la peau du béton : les gros grains de ciment ne peuvent pas être au contact du granulat, car, même s'il y a contact en quelques points, il y aura toujours de la place entre eux et le granulat pour des grains plus fins. Mais il peut aussi se produire, en plus, un effet d'attraction électrostatique sur les particules fines.

Cet enrichissement en fines particules explique l'hydratation, un peu plus rapide au contact des granulats qu'au coeur de la pâte, observée en diffraction X.

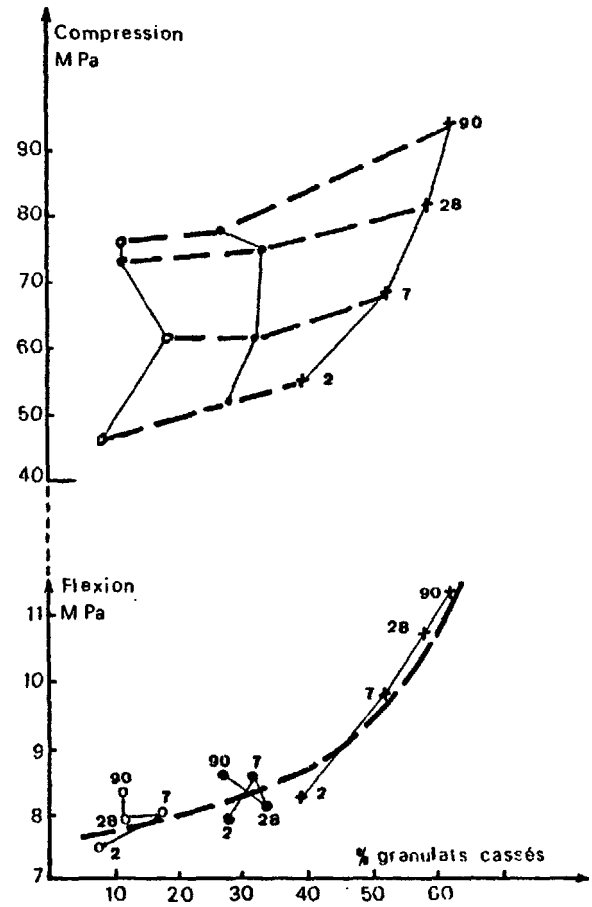

FIGURE 3 : Granulats polis o , attaqués acide • , concassés + .

L'examen au microscope à balayage à 7 jours et 90 jours des fractures des mortiers dans lesquels on a fait varier respectivement le ciment (un riche en C_3A, un pauvre en C_3A), la nature des granulats (un calcaire, un quartz) et l'état de surface des granulats (calcaire poli, concassé, et attaqué par HCl dilué) permet de dégager les conclusions suivantes :

1) il y a enrichissement en $Ca(OH)_2$ au contact des granulats dans tous les cas et aux 2 échéances considérées. Cet enrichissement en $Ca(OH)_2$ peut s'expliquer par l'augmentation locale du E/C due au mouillage des granulats, favorisant la précipitation de gros cristaux de $Ca(OH)_2$. Mais on n'observe pas d'orientation préférentielle de ces cristaux de chaux que la fracture fait apparaître stratifiés par clivage (fig. 4),

2) il n'y a pas de différence décelable de comportement à l'interface pâte-granulat entre les 2 ciments pour un même granulat, ni entre les 2 granulats pour un même ciment.

3) statistiquement, l'accrochage de la pâte de ciment sur le granulat, se fait aussi bien avec $Ca(OH)_2$ qu'avec le CSH (fig. 5).

4) dans tous les cas, les surfaces de moindre résistance s'éloignent de l'interface pâte-granulat quand l'échéance

FIG. 4 : Précipitation de $Ca(OH)_2$ auprès des granulats 5 µm

FIG. 5 : Accrochage de CH et CSH sur les granulats 1 µm

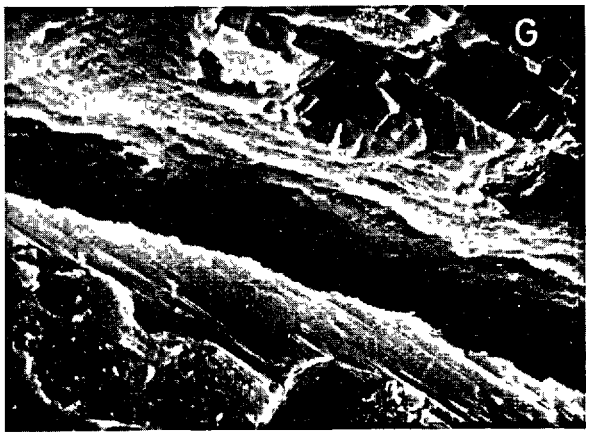

FIGURE 6 : Echéance 7 jours - (a) Granulats polis, (b) Granulats concassés, G = Granulat 5 µm

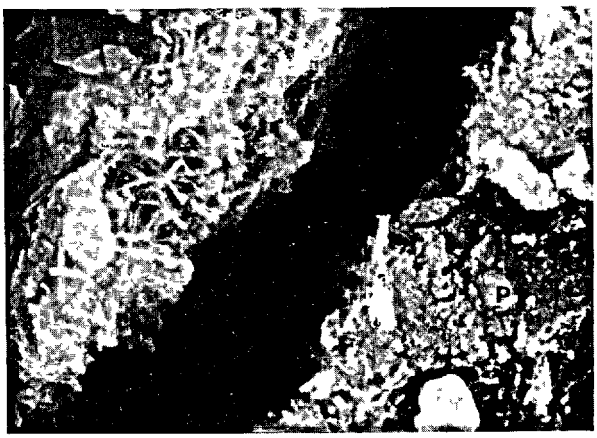

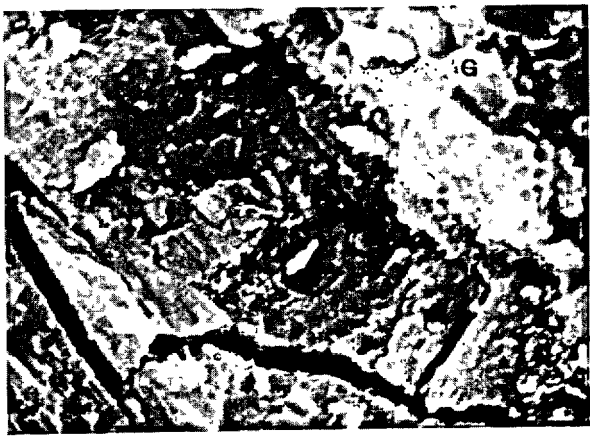

FIGURE 7 : Echéance 90 jours - (a) Granulats polis, (b) Granulats concassés, G = Granulat, P = Pâte 5 µm

augmente ; mais, à une échéance donnée, il y a une influence significative de la rugosité et de la forme des granulats sur la distance entre la surface de moindre résistance et l'interface pâte-granulat : celle-ci augmente progressivement quand on passe des granulats polis (de forme arrondie et lisse) → granulats attaqués à HCl dilué (de forme arrondie mais un peu rugueux) → granulats concassés (anguleux et très rugueux) (fig. 6, 7).

Ce dernier point peut s'expliquer ainsi : quand un mortier subit un choc, s'il n'y a pas du tout d'adhérence entre le granulat et la pâte, la fissure suivra l'interface pâte-granulat. Par contre, dès qu'il commence à y avoir adhérence pâte-granulat, il y a compétition (au niveau de la résistance globale) entre une ligne de rupture longue suivant le contour du granulat, et une ligne droite, plus courte, dans la pâte, et ceci entraine, aussi bien l'éloignement statistique dans le temps de la surface de rupture par rapport à l'interface pâte-granulat que son éloignement en fonction de la rugosité.

CONCLUSION

L'utilisation de mortiers de granulats monodimensionnels et la détermination des résistances de ces mortiers avec évaluation du pourcentage de granulats cassés à la rupture en flexion, se sont avérées une méthode très riche pour évaluer l'adhérence pâte-granulat et son interaction sur les propriétés mécaniques. La microscopie électronique à balayage a permis de compléter ces résultats par observation directe de l'interface pâte-granulat.

Bien que l'on ait confirmé l'existence de réactions chimiques entre le calcaire et le C_3A du ciment, nos essais ont montré qu'au moins jusqu'à 90 jours et pour les granulats étudiés, les accrochages mécaniques liés à la rugosité et surtout à la forme des granulats sont prépondérants pour l'adhérence.

Une amélioration dans l'adhérence influe directement sur les résistances en flexion et dans une moindre part sur les résistances en compression.

On a confirmé la précipitation préférentielle de CH auprès des granulats. Mais surtout on a mis en évidence l'existence d'une surface de moindre résistance qui est à l'interface pâte-granulat aux courtes échéances, et qui s'éloigne ensuite dans la pâte et ce d'autant plus que les granulats sont rugueux et anguleux. Cette surface de moindre résistance paraît être l'équivalent des zones de transition souvent signalées, et nous pensons que les recherches futures devraient porter sur les moyens les plus judicieux à utiliser (granulats spéciaux ou synthétiques, traitement de surface de granulats traditionnels) pour diminuer la faiblesse de cette zone.

BIBLIOGRAPHIE

1. J. FARRAN (1956), Contribution minéralogique à l'étude de l'adhérence entre les constituants hydratés des ciments et les matériaux enrobés. Thèse – Toulouse.
2. J.C. MASO (1967), La nature minéralogique des agrégats facteur essentiel de la résistance des bétons à la rupture et à l'action du gel. Thèse – Toulouse.
3. LYUBINOVA et PINUS (1962), Crystallisation structure in the contact zone between aggregate and cement in concrete. Colloid Journal. Vol. 24 – n° 5.
4. J. GRANDET (1971), Contribution à l'étude de la liaison entre la pâte de ciment et les terres cuites. Thèse-Toulouse.
5. F.H. WITTMANN (1972), Etude de la force d'adhésion en fonction du mouillage. Colloque RILEM – Toulouse.
6. J. FARRAN et J.C. MASO (1964), De l'emploi des substitutions calcaires pour l'amélioration des agrégats à béton. Rev. Mat. Constr. n° 586-587, 195-203.
7. P. TERRIER (1972), Contribution de recherches sur l'hydratation des ciments au problème de la liaison dans le béton. Colloque RILEM – Toulouse.
8. L. CUSSINO et G. PINTOR (1972), Recherche sur le comportement différent de granulats calcareux et siliceux dans les agglomérés, en fonction de la composition minéralogique du ciment. Il Cemento – n° 4 – 255-268.
9. L. CUSSINO, M. MURAT, A. NEGRO (1976). Studio chimico-fisico dell'aderenza tra il cemento ed aggregati calcarei e silici nelle malte. Il Cemento – n° 2, 77-89.
10. C. PERRY et J.E. GILLOTT (1977), The influence of mortar-aggregate bond strength on the behaviour of concrete in uniaxial compression.Cement and Concrete Research. Vol. 7, 553-564.
11. T.J. LYUBIMOVA, P.A. REBINDER (1971), Etude au microscope électronique à balayage et au microscope optique de la structure de cristallisation de liants hydrauliques, au cours de leur durcissement dans la zone de contact avec les granulats.Dokl. Acad. Nauk SSSR – T. 201 n° 5 – 1167-1169.
12. J.P. OLLIVIER (1975), Etude de la liaison entre la pâte de Ciment Portland et les granulats par observation directe au microscope électronique par transmission. Thèse – Toulouse.
13. B.D. BARNES, S. DIAMOND, W.L. DOLCH (1979), Micromorphology of the interfacial zone around aggregates in Portland Cement mortar. J. Amer. Ceram. Soc. Vol. 62, n° 1-2, 21-24.
14. N. THAULOW, T. KNUDSEN (1975), Quantitatives microanalyses of the Reaction Zone between Cement Paste and Opal. Symposium on Alkali Aggregate Reactions – Reykjavik.
15. R. ZIMBELMANN (1978), Zur Frage der Festegkeitssteigerung bei Beton. Betonwerk Fertigteil Technik – n° 2 – p. 89-96.
16. D.J. PINCHIN, D. TABOR (1978), Interfacial phenomena in steel fibre reinforced cement, I. Structure and strength of interfacial region. Cement and Concrete Research. Vol. 8, p. 15-24.
17. J. FARRAN, R. JAVELAS, J.C. MASO, B. PERRIN (1972), Etude de l'auréole de transition existant entre les granulats d'un mortier et la masse de la pâte de ciment hydraté. Colloque RILEM – Toulouse.
18. B. PERRIN (1974), Observation en microscopie électronique des caractères morphologiques de la liaison pâte de ciment durci matériaux associés. Thèse – Toulouse.
19. T.T. HSU, F.O. SLATE (1963), Tensile bond strength between aggregate and Cement Paste or Mortar. J. Amer. Concrete Institute. Vol. 60, n° 4, 465-486.
20. M.A. TAYLOR, B.B. BROMS (1964), Shear bond strength between Coarse Aggregate and Cement Paste or Mortar. J. Amer. Concrete Institute, Vol. 61, n° 8,. 937-956.

Approche analytique de la dédolomitisation des granulats dans le béton durci

Analytic approach of dedolomitization of agregates in concrete

F.X. DELOYE, Docteur Ingénieur,
A. BERNARD, Chef du Groupe "Méthodes Thermiques",
A. POINDEFERT, Assistante,
Laboratoire Central des Ponts et chaussées - Service de Chimie, France.

RESUME : La dédolomitisation est susceptible d'affecter les bétons confectionnés à partir de calcaires dolomitiques. Ce phénomène est régi par le couple de réactions de double décomposition : $CaMg(CO_3)_2+2NaOH \rightarrow Ca\downarrow CO_3+Mg\downarrow(OH)_2+Na_2CO_3$, puis : $Na_2CO_3+Ca(OH)_2 \rightarrow Ca\downarrow CO_3+2NaOH$, où l'hydroxyde alcalin est régénéré tant que le béton contient de la portlandite. Il s'agit donc en fait d'une catalyse homogène.

En raison de la nature des oxydes mis en cause, la détection de la dédolomitisation n'est pas possible par analyse chimique. Seule l'investigation minéralogique fine est en mesure de le faire.

D'une part, la thermogravimétrie en atmosphère inerte permet le dosage de la portlandite ($Ca(OH)_2$) et de la brucite ($Mg(OH)_2$). D'autre part, l'association du dosage précis de CO_2 avec l'analyse thermique différentielle sous anhydride carbonique permet la détermination simultanée de la dolomite ($CaMg(CO_3)_2$) et de la calcite ($CaCO_3$).

L'introduction de ces données dans l'analyse minéralogique d'un béton durci contenant des granulats dolomitiques permet de mettre en évidence une éventuelle dédolomitisation et d'en connaître le degré d'avancement.

SUMMARY : Dedolomitization might affect concretes made up from dolomitic limestones. This phenomenon is governed by following reaction pair of double decomposition : $CaMg(CO_3)_2+2NaOH \rightarrow Ca\downarrow CO_3+Mg\downarrow(OH)_2+Na_2CO_3$, then : $Na_2CO_3+Ca(OH)_2 \rightarrow Ca\downarrow CO_3+ 2NaHO$, where alkali is regenerated as long as concrete contains portlandite. Thus, it is in fact an homogeneous catalysis.

Because of the nature of the oxides involved, it is not possible to detect the dedolomitization by means of a chemical analysis but this can be attained by a detailed mineralogical investigation.

On one hand, thermogravimetry in inert atmosphere allows to determine the proportions of portlandite and brucite, on the other hand, the combination between the precice determination of the proportions of CO_2 and the differential thermal analysis in a carbon dioxide medium makes it possible to simultaneously determine the dolomite ($CaMg(CO_3)_2$) and the calcite ($CaCO_3$) .

With help of these data, the mineralogical analysis of hardened concrete containing dolomitic aggregates allows for an eventual dedolomitization to be detected and thus for its progress to be known.

La dolomite est le nom du minéral constitutif des dolomies ; sur le plan chimique il s'agit du carbonate double de calcium et de magnésium de formule $CaMg(CO_3)_2$.

On rencontre communément la dolomite en association avec la calcite dans les marnes et certains calcaires appelés pour cette raison "calcaires dolomitiques" lesquels sont souvent assez durs. Ceci explique qu'en France dans le Midi Méditerranéen où ils sont abondants, ces derniers aient été fréquemment utilisés dans la construction et employés sans précaution particulière pour la confection des mortiers et bétons.

La dolomite est difficilement attaquée par l'acide chlorhydrique à froid (1) et sa solubilité dans l'eau pure est légèrement inférieure à celle de la calcite, par contre au sein du béton fortement basique la présence d'alcalis libres peut déclencher un cycle dit de dédolomitisation (2) caractérisé par la chaine de réactions :

$$CaMg(CO_3)_2 + \overset{(K)}{2NaOH} \rightarrow Ca\underset{\downarrow}{CO_3} + Mg\underset{\downarrow}{(OH)_2} + \overset{(K_2)}{Na_2CO_3}$$

$$\text{dolomite} + \text{alcali libre} \rightarrow \text{calcite} + \text{brucite} + \text{carbonate alcalin}$$

$$\overset{(K_2)}{Na_2CO_3} + Ca(OH)_2 \rightarrow Ca\underset{\downarrow}{CO_3} + \overset{(K)}{2NaOH}$$

$$\text{carbonate alcalin} + \text{portlandite} \rightarrow \text{calcite} + \text{alcali libre}$$

Il s'agit d'une catalyse homogène que l'on peut écrire :

$$CaMg(CO_3)_2 + Ca(OH)_2 \rightarrow 2Ca\underset{\downarrow}{CO_3} + Mg\underset{\downarrow}{(OH)_2}$$

$$\text{dolomite} + \text{portlandite} \rightarrow \text{calcite} + \text{brucite}$$

où l'alcali libre, catalyseur est perpétuellement régénéré, donc une faible proportion de celui-ci dans le béton est parfaitement capable de provoquer la dédolomitisation jusqu'à carbonatation complète de la portlandite, pouvant entraîner la décohésion du liant.

La nature des oxydes mis en cause dans cette réaction CaO,MgO, Na_2O ou K_2O, CO_2, qui appartiennent tous à la fois au ciment et aux granulats du béton ne permet pas de mettre en évidence par voie chimique une éventuelle dédolomitisation. Seule une investigation minéralogique fine est en mesure de déterminer si celle-ci a effectivement eu lieu.

Sur le plan minéralogique la chaine de réactions fait intervenir quatre minéraux : dolomite, portlandite, calcite et brucite, dont les trois premiers sont initialement présents dans le béton.

En raison de la solubilité très faible de la brucite, le phénomène est nécessairement lié à la présence de ce minéral détectable par diffractométrie des rayons X ; mais cette présence n'est pas suffisante, en effet la brucite observée peut dans certains cas provenir de l'action prolongée d'eaux contenant de la magnésie même en faible quantité. Ceci est particulièrement vrai pour les bétons de fondation.

En pétrographie, on peut distinguer la dolomite de la calcite par coloration spécifique (3) et observer une éventuelle épigenie. Mais si cette technique s'applique fort bien aux roches compactes, sa transposition au béton se heurte à la présence de la pâte de ciment.

En fin de compte, la dédolomitisation ne peut être mise en évidence et surtout quantifiée avec certitude qu'à l'aide d'un bilan minéralogique complet du matériau.

Tout d'abord, grâce à "l'analyse allégée" (4), il faut établir la composition que devait avoir le béton lors de sa mise en place, y compris la composition approchée du ciment. Ensuite, à l'aide des méthodes spécifiques à l'analyse minéralogique (5), il est nécessaire de déterminer les teneurs respectives, actuellement présentes des quatre minéraux mis en cause par la réaction. Enfin le calcul du bilan minéralogique réel et sa comparaison avec la composition initiale doit permettre de rendre compte du phénomène par le transfert d'une partie de la dolomite et de la portlandite vers la calcite et la brucite. La comparaison en question repose essentiellement sur le dosage précis de ces quatre minéraux dans le béton.

En raison de sa sensibilité trop faible, la diffractométrie des rayons X ne peut pas être mise à contribution pour doser directement ces minéraux alors qu'elle est d'un grand secours pour les identifier. Par ailleurs, ceux-ci ont leurs anions en commun deux à deux, OH^- et CO_3^{--}.

Les méthodes thermiques choisies pour effectuer les dosages font intervenir la dissociation en utilisant les départs d'eau ou d'anhydride carbonique. Mais dans les conditions opératoires, certaines recombinaisons ont lieu et il est important d'en tenir compte. Il en résulte que les dosages des quatre minéraux sont liés.

DOSAGE DE LA BRUCITE ET DE LA PORTLANDITE

En thermogravimétrie, sous atmosphère inerte, avec une vitesse de montée en température relativement lente (60 °C par heure), les paliers de déshydratation de la brucite et de la portlandite sont séparés et bien définis, 300 °C à 330 °C pour la brucite et 360 °C à 450 °C pour la portlandite.

En conséquence, le dosage de ces deux espèces minérales à partir de leur eau de constitution ne présente pas de difficulté, des vérifications ayant été faites pour avoir la certitude que dans le cas d'un béton de ciment portland aucune décomposition d'aluminate ne vient se superposer aux effets thermiques précédents.

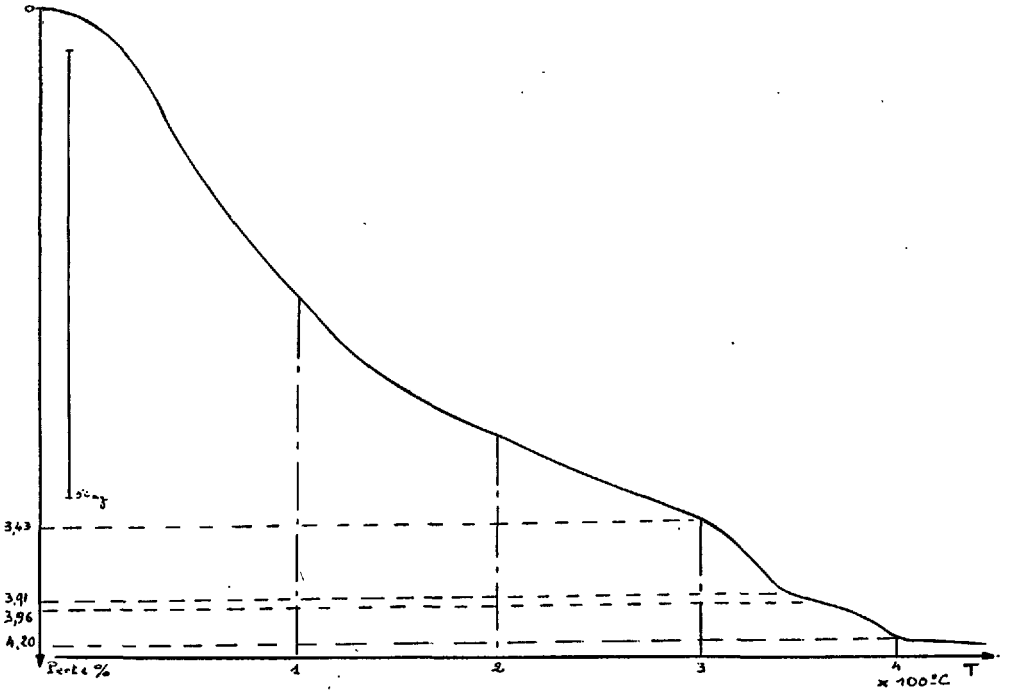

Fig. 1 - Thermogravimétrie d'un béton dolomitique.

La courbe (figure 1) montre le thermogramme d'un béton dolomitique auquel 2 % environ de brucite a été ajoutée pour bien montrer la séparation des deux paliers de déshydratation.

DOSAGE DE LA DOLOMITE ET DE LA CALCITE

La détermination simultanée des teneurs en calcite et en dolomite est plus délicate car, d'une part la dolomite est un carbonate double et d'autre part la calcite provient de différentes origines. C'est pourquoi le dosage de ces deux minéraux est effectué par une combinaison de l'analyse thermique différentielle sous atmosphère CO_2 et du dosage chimique de l'anhydride carbonique.

Plusieurs méthodes ont été publiées pour déterminer d'une façon précise la teneur en CO_2 d'origine minérale d'un béton (5), (6). Elles sont toutes pondérales mais fondamentalement différentes. Aussi semble-t-il opportun de rappeler le principe de celle qui parait donner le meilleur résultat et dont la normalisation a été proposée (7).

Le matériau est attaqué à chaud par une solution d'acide ortophosphorique, en présence d'acétate de cuivre destiné à fixer l'hydrogène sulfuré éventuellement formé. L'anhydride carbonique libéré par cette attaque est entraîné par un gaz vecteur inerte, séché puis recueilli sur un absorbant spécifique et pesé.

En analyse thermique différentielle, le thermogramme d'un béton dolomitique réalisé sous atmosphère CO_2 avec enregistrement Δt-temps, présente les différences suivantes par rapport à celui obtenu dans l'air (figure 2).

- Disparition du pic endothermique à 480 °C du à la déshydratation de la portlandite : ce minéral se carbonate.

- Dans la zone de température 700 °C-1000 °C remplacement du pic multiple par deux pics endothermiques bien distincts : le premier vers 770 °C correspond à la décarbonatation de la partie magnésienne de la dolomite. Le second vers 925 °C est dû à la dissociation de la partie calcique de la dolomite et de différents carbonates de calcium (calcite des granulats et de carbonatation du ciment ainsi que le carbonate formé en cours d'essai à partir de la portlandite).

Les aires de ces deux pics de décarbonatation sont proportionnelles aux teneurs en CO_2 lié à MgO et à CaO, leur utilisation permet donc en tenant compte des recombinaisons et de la teneur en CO_2 "total" de doser simultanément la calcite et la dolomite présentes dans l'échantillon. La justification complète de ces dosages sortirait du cadre de la présente communication (8).

La méthodologie suivante a été retenue pour la réalisation du dosage des quatre minéraux impliqués dans la dédolomitisation :

1) Déterminer par thermogravimétrie en atmosphère inerte les teneurs en brucite et en portlandite à partir de leur eau de constitution.

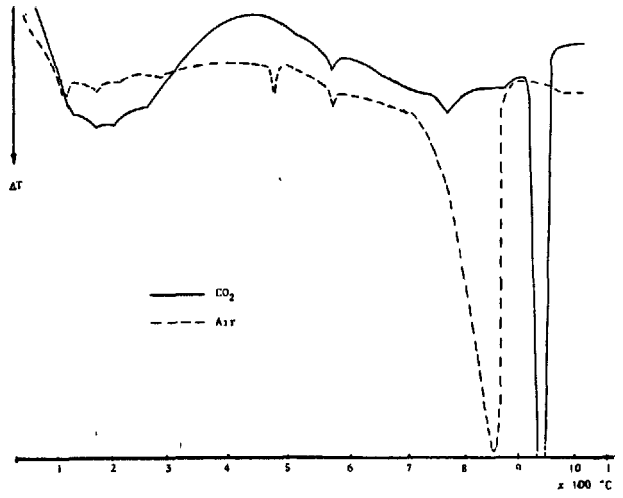

Fig. 2 - Analyse thermique différentielle d'un béton dolomitique.

2) Déterminer la teneur en anhydride carbonique d'origine minérale selon le processus décrit précédemment (7).

3) Soumettre la béton à l'analyse thermique différentielle en atmosphère CO_2 et mesurer les aires des deux pics de décarbonatation.

4) Calculer les teneurs en calcite et en dolomite à partir de ces éléments (8). Dans les calculs la teneur en CO_2 "total" à prendre en compte est la somme : CO_2 d'origine minérale plus CO_2 correspondant à la carbonatation de la portlandite pendant l'essai.

5) Déduire de la teneur en calcite ainsi calculée, la teneur en carbonate de calcium correspondant à la carbonatation de la portlandite. Il est alors possible d'effectuer les calculs de transferts minéraux qui permettent de conclure à l'existence d'une dédolomitisation.

CONCLUSION

Les développements qui précédent ont montré que l'on pouvait quantifier une dédolomitisation éventuelle à partir des bilans minéralogiques. Ceci grâce à la détermination précise des teneurs en calcite, dolomite, portlandite et brucite d'un béton dolomitique.

A l'heure actuelle aucune dédolomitisation n'a pu être mise en évidence avec certitude dans les échantillons que nous avons examinés, ce qui ne signifie pas que le phénomène en question n'ait pas lieu dans les bétons. Par ailleurs, la cinétique de cette réaction est très lente.

Il faut enfin remarquer que la nature même du cycle de réactions mis en jeu limite, en l'absence d'apport alcalin par le milieu extérieur, la transformation, à la quantité de dolomite correspondant à la carbonatation de la totalité de la portlandite présente.

BIBLIOGRAPHIE

1.- G. BLOT "Essai de mise au point d'une technique de calcidolomimétrie par la méthode de Dietrich-Frühling", Bull. Liaison Labo. P. et Ch., 80, Nov-Déc. 1975, 25-28.

2.- F.M. PELLERIN "Les altérations des maçonneries carbonatées de tunnels ferroviaires anciens" thèse, Paris VI, Juin 1978.

3.- J. JUNG "Précis de Pétrographie", Masson ed., Paris, 1960.

4.- F.X. DELOYE "L'analyse minéralogique, Application aux bétons durcis en liaison avec la pérennité des ouvrages", rapport de recherche L.C.P.C. n° 83, Paris, 1978.

5.- I.A. VOINOVITCH et al. "L'analyse minéralogique des sols argileux", Eyrolles ed., Paris, 1971.

6.- C. DUVAL "Traité de microanalyse minérales" Tome IV, Presses Scientitiques Internationale, Paris, 1957.

7.- Projet de norme française, P.15.512, Mars 1979.

8.- A. BERNARD, A. POINDEFERT et F.X. DELOYE "Dosage de la brucite, de la calcite et de la dolomite dans les bétons. Importance pour l'étude des dégradations par la magnésie", Bull. Liaison Labo. P. et Ch. (à paraitre).

Cement paste-quartz bond in autoclaved concretes

Adhérence ciment-quartz dans les bétons autoclavés

F. MASSAZZA, Professor of Applied Chemistry, Italcementi, Laboratorio Chimico Centrale, Bergamo, Italy,
M. PEZZUOLI, B.Ch. Italcementi, Laboratorio Chimico Centrale, Bergamo, Italy.

RESUME : En employant des granulats de quartz, les bétons autoclavés peuvent atteindre des résistances supérieures à 150 N/mm2. Cette résistance élevée doit être partiellement attribuée à des réactions qui se produisent à l'interface pâte de ciment-quartz. Les observations au MEB ont indiqué que dans ces bétons l'adhérence du quartz à la pâte de ciment est plus forte que la cohésion de la pâte de ciment même. L'analyse à la microsonde électronique a montré que la zone intermédiaire entre le quartz et la pâte de ciment devient plus riche en calcium et plus pauvre en silicium en s'éloignant du granulat.

Les mesures de microdureté ont montré que la couche intermédiaire est plus dure (et a donc une résistance mécanique plus élevée) que la masse de la pâte.

Les surfaces de quartz polies autoclavées dans de l'eau additionnée de ciment ont été profondément corrodées et couvertes de cristaux fibreux de tobermorite 11 Å.

Sur la base des résultats expérimentaux, on peut supposer que la forte liaison à l'interface granulat-pâte dépend de
- l'interconnexion mécanique de la pâte de ciment avec la surface corrodée du quartz,
- l'accolement épitaxique des cristaux de tobermorite sur ceux de quartz.

SUMMARY: By using quartz aggregates, autoclaved concretes can attain compressive strengths over 150 N/mm^2. This high strength must be partially attributed to reactions occurring at the cement paste-quartz interface. SEM observations indicated that in these concretes the adhesion of the quartz to the cement paste is stronger than the cohesion of the cement paste itself. Electron microprobe analysis showed that the intermediate zone between quartz and cement paste becomes richer in calcium and poorer in silicon by moving away from the aggregate.

Microhardness indentations showed that the intermediate layer is harder (and therefore it has higher mechanical strength) than the bulk paste.

Polished quartz surfaces autoclaved in mother cement liquor appeared to be deeply corroded and covered with fibrous crystals of 11 Å tobermorite.

Based on the experimental evidence, it can be assumed that the strong bond at the aggregate-paste interface depends on
- the mechanical interlock of the cement paste with the corroded quartz surface
- the epitaxis intergrowth of the tobermorite crystals on the quartz ones.

1. INTRODUCTION

It has recently been proved that autoclaved concretes whose mechanical compressive strengths attain 180 N/mm^2 or anyhow exceed 150 N/mm^2 can be obtained. An important aspect of these results lies in the fact that they can be made by usual materials and procedures. The only concern consists in selecting the materials and the working modes (1).

Compared with identical concretes cured under ordinary conditions, these concretes have quadruple compressive strength, triple modulus of rupture and splitting tensile strength and nearly double modulus of elasticity (2).

Other peculiar characteristics are the almost linear trend of the curve $\varepsilon = \varepsilon(\sigma)$ and the conchoidal fracture which passes through both the mortar and the aggregate grains and does not follow the boundaries of the grains, as it occurs in ordinary concretes.

It must be noticed that these results without precedent were obtained by using quartz aggregates whereas the outcome was less brilliant with other materials: for instance strength was less than the half by utilizing calcareous aggregates (3).

If the apparent ductility of ordinary concrete under short-term loading, shown by the curving shape of the stress-strain curve, represents the cumulative effects of progressive microcracking (4), the almost rectilinear trend of the curve $\varepsilon = \varepsilon(\sigma)$ found for very high strength concretes (1) proves that in this case microcracks only form immediately before failure.

All these facts lead to think that the exceptional mechanical characteristics of these autoclaved concretes must be attributed not only to the known improvement in strength of the cement paste (cement + silica powder) (5) but also and chiefly to the paste-aggregate bond.

In the present paper the particular conditions occurring at the aggregate-cement paste interface are examined and the experimental results explaining the exceptional mechanical characteristics of this new concrete are shown.

2. EXPERIMENTAL

To determine the causes of the strong bond between cement paste and aggregate owing to the hydrothermal treatment, the alterations suffered by the quartz surface when it comes into contact with cement paste or cement mother liquor were examined.

2.1 The initial tests were carried out on mortar cubes made as shown in table I.

Table I - Composition of the steam cured mortars

Binder	Rapid hardening portland cement	50 g
	ground silica	20 g
Crushed quartzite	(fract. 0-2 mm)	120 g
	(fract. 2-3 mm)	20 g
Water		30 g
Superplasticizer (25 wt.% solution)		1.5 g

The binder consisted of a homogeneous mix of 50 weight parts of a rapid hardening portland cement and 20 parts of silica powder ground to a Blaine specific surface of 4500 cm^2/g. The aggregate was a quartz sand (SiO_2 = 98%) having a continuous particle size distribution already used in previous works (1). It was deprived of the coarser fractions to facilitate the microscopic study of the autoclaved material.

A superplasticizer was used to reduce the water/binder ratio and thus to improve the compactness of the mortars.

After mixing, the samples were introduced into 17.3x17.3x17.3 mm metal cubic moulds, compacted on a jolting table and prestored at 20°C and 100% R.H. for 5-8 hours.

Afterwards the cubes were removed from the moulds, introduced into a small laboratory autoclave and subjected to a double steam curing: 5 hours at atmospheric pressure at 70°C and 15 hours under pressure at 190°C.

A heating rate of 0.7°C/min. and a cooling rate of about 1.0°C/min. were maintained in all the preparations.

The X-ray diffraction analysis of the autoclaved material showed the presence of quartz and 11 Å tobermorite, typical product of the hydrothermal reactions between cement and quartz (6)(7)(8) as well as lime and quartz (9)(10)(11).

After curing, the cubes were crushed and the obtained fragments, after metalization with Au, were examined under the scanning electron microscope.

Figures 1 and 2 show that the fracture surface con-

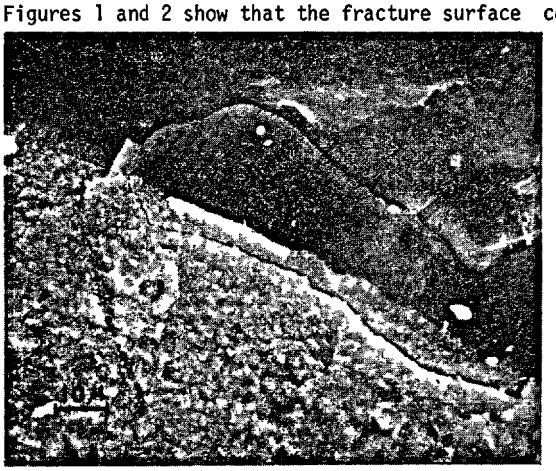

FIG. 1 - Broken surface of autoclaved concrete - S.E.I. 1000 X

cerns both the quartz aggregate (upside) and the cement paste. By examining the two figures it is also possible to notice that the contact between cement paste and aggregate is continuous and intact as well as that the fracture lines do not coincide with the cement paste-quartz interface.

This means that the steam curing yields a stronger quartz-cement paste bond than the cohesion of the cement paste itself. This results is opposite to what found for concretes cured at ordinary temperature, where the fracture almost always occurs along the boundaries of the aggregate (4)(12)(13).

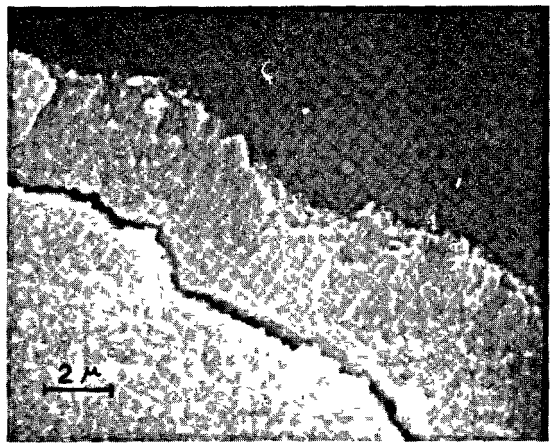

FIG. 2 - Detail of the preceding micrography - S.E.I. 6000 X

The alterations suffered by the quartz surface because of the combined action of cement and steam curing were observed on a quartz fragment ground, polished and covered with the paste of the binder.

After the aforesaid curing cycle, the fragment was sectioned perpendicularly to the polished surface in order to examine the quartz-cement paste interface. One of the obtained sections was polished and metallized with Be.

Figures 3, 4 and 5, taken by the scanning electron microscope, show that the boundary between quartz and cement paste is no longer sharp and rectilinear but appears to be more or less modified.

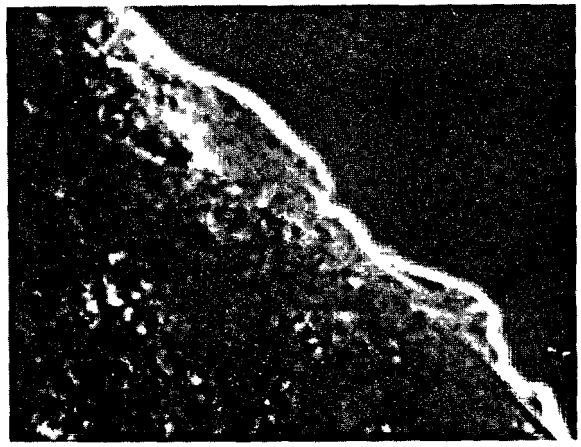

FIG. 3 - Polished surface of autoclaved concrete - S.E.I. 1000 X

This is the evidence that a chemical reaction has altered the interface.

A confirmation of this change is given by the electron microprobe analysis of the contact zone quartz-cement paste: by passing from the first to the second, a decrease in the Si content and an increase in the Ca one is observed, as figures 6 and 7 show.

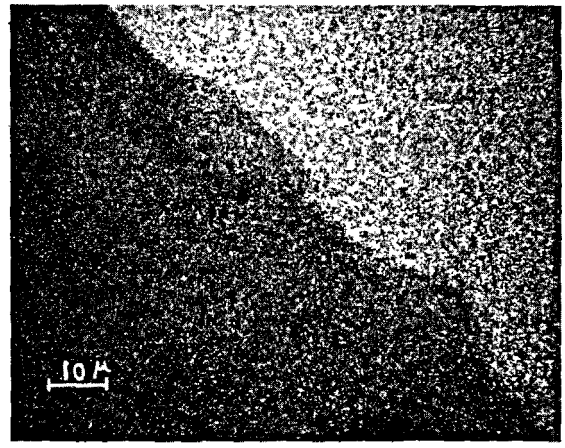

FIG. 4 - Preceding surface. Distribution image of silicon - SiK_α 1000 X

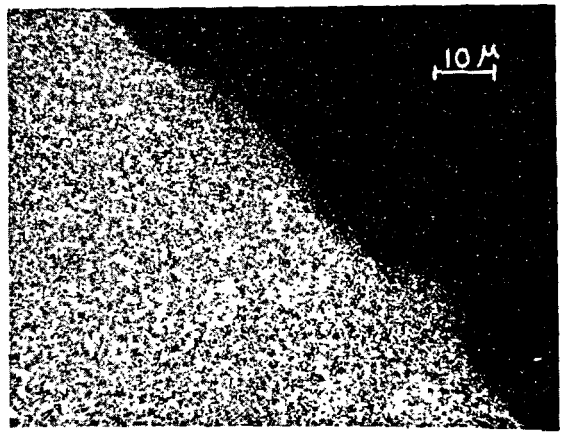

FIG. 5 - Preceding surface. Distribution image of calcium - CaK_α 1000 X

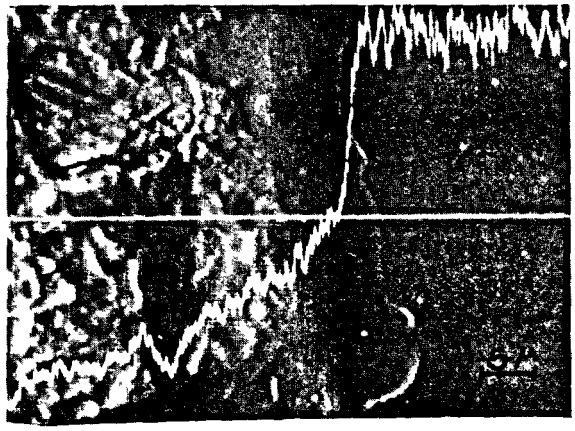

FIG. 6 - Polished surface of autoclaved concrete - Line profile of silicon (SiK_α) S.E.I. 2000 X

The trend of the two concentration curves shows that a layer about 5 μm thick, having progressively varying composition, is in contact with quartz. These data seem to prove that AITKEN and TAYLOR'S (8) hypothesis

is right. These Authors assume that, around the quartz grains, there is probably a zoning of calcium silicate hydrate characterized by a low C/S ratio near the quartz grains and by a higher ratio a little farther.

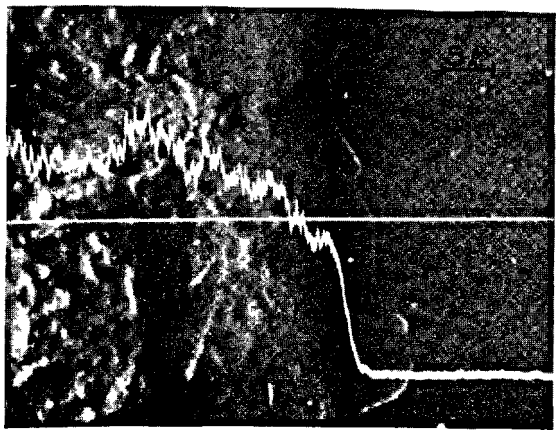

FIG. 7 - Preceding surface. Line profile of calcium (CaK_α). S.E.I. 2000 X

The different composition of the intermediate layer with respect to the cement paste affects its mechanical properties. In fact its mean microhardness has appeared to be twice that of the paste and 1/6 of that of quartz. It is reminded that the intermediate layer of ordinarily cured concretes is, on the contrary, weaker and has a microhardness half that of the paste (14).

Because of the extremely small sizes of the crystals forming the intermediate layer and the cement paste, the microhardness indentation has simultaneously concerned many crystals and therefore the obtained values are the result of an integration. This consideration is not valid for the quartz aggregate grains which are composed of $\sim 4 \times 10\ \mu m$ crystals and for which the indentation (diagonal $\sim 6.5\ \mu m$) can have only concerned one or some contiguous crystals.

The mechanical strength of cement pastes can be calculated by determining the corresponding microhardness (15)(16) but, for the purposes of this work, it is sufficient to state that the higher microhardness of the intermediate layer also means higher mechanical strength than that of the bulk paste.

To show the changes caused by the hydrothermal treatment to the surface of the aggregate, a fragment of quartz was ground, polished, maintained in diluted HCl (1:10) for 30 minutes and finally washed with distilled water. The paste of the binder was applied on the polished surface and the whole was steam cured by following the above mentioned working modes.

After the thermal treatment the paste was removed, partly mechanically and partly by diluted HCl (1:10) and, after metalization with Au, the quartz surface was re-examined under the scanning microscope. As figure 8 shows, the quartz surface appears to be irregularly but clearly corroded.

2.2 Since quartz is very likely to be attacked by the mixing water rather than the cement, a fragment of quartz having a ground and polished surface was steam cured in cement mother liquor. The mother liquor was prepared by shaking one part of rapid hardening portland cement with 10 parts of CO_2 free distilled water for 30 minutes and then by filtering it.

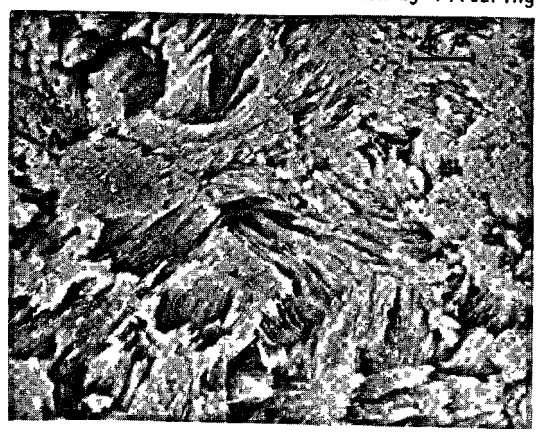

FIG. 8 - Surface of quartz polished, covered with cement paste, autoclaved and washed with HCl 1:10. S.E.I. 3000 X

After autoclaving, the fragment was washed with water, vacuum dried, metalized with Au and observed under the scanning electron microscope. As figure 9 shows, the polished surface appears to be covered with a layer of fibrous entangled crystals, obviously produced by the reaction between quartz and mother liquor.

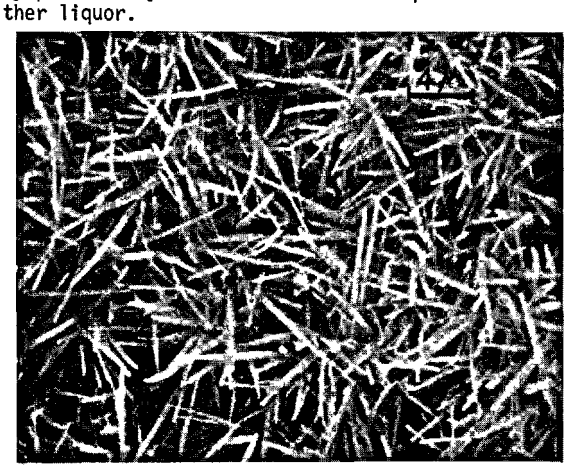

FIG. 9 - 11 Å tobermorite developed on a quartz surface polished and autoclaved in cement mother liquor. S.E.I. 3000 X

The solubilization of these newly formed crystals by diluted HCl (1:10) has evidenced the quartz surface which has appeared corroded (see figure 10). The appearance of the surface also indicates that the quartz crystals have underwent a different attack depending on their orientation.

The product formed on the quartz surface was not enough to be easily examined and studied. For this reason, that is to increase the yield of the reaction, steam curing was repeated by replacing the quartz fragment with an equal amount of quartz sand having the same origin but a surface higher by about 100 times.

FIG. 10 - Preceding surface after washing with HCl 1:10 - S.E.I. 1000 X

The quartz grains autoclaved in the cement liquor were washed before with distilled water and then with ethanol. Afterwards they were vacuum dried at room temperature.

The autoclaved material was subjected to X-ray diffraction analysis and it showed to be only formed of quartz and 11 Å tobermorite.

The tobermorite fibres covering the aggregate were solubilized by cold diluted HCl (1:10) and analyzed by atomic absorption. Different preparations gave a C/S ratio equal to 0.90 on the average.

The hydrothermal reaction is accompanied by a decrease in the pH and the CaO content of the contact solution.

3. DISCUSSION

In the steam cured very high strength concretes (compressive strength >150 N/mm^2) the cracked surfaces show that the cement paste-quartz bond is stronger than the tensile strength of the cement paste.

The examination under the electron microscope showed that an intermediate layer having different composition from that of the cement paste forms in contact with the quartz aggregate. In fact the C/S ratio the more increases the farther the interface.

This layer has a microhardness (~10 N/mm^2) which is twice that of the cement paste.

Microhardness is usually measured on individual crystals and therefore its high values do not necessarily involve a high mechanical strength of the bulk material.

Nevertheless when the fineness of the structure is such that each indentation involves many crystals, the microhardness is indicative of the mechanical characteristics of the bulk material. This condition occurs in the cement paste and it was proved that microhardness is representative of its compressive strength and its modulus of elasticity (15)(16).

Therefore the higher microhardness of the intermediate layer with respect to the paste, found in the present work, corresponds to a higher mechanical strength. This fact can be related to the different C/S ratio.

As for the strong bond existing at the aggregate-paste interface, it can be observed that the intermediate layer is deeply embedded in the grains of the aggregate because of the corrosion suffered by quartz. This fact positively affects the bond but such a factor is probably secondary and the strong adhesion between cement paste and quartz must mainly be attributed to the overlap and the epitaxis intergrowth of the tobermorite crystals on the quartz ones. The process of epitaxis intergrowth is not a mere absorption caused by London-van der Waals' forces but a real crystallochemical reaction involving the lattices of the two phases as though a two-dimensional chemical compound were formed by the action of chemical valences (17).

This explanation is strengthened by the fact that the mechanical strengths of these steam cured concretes do not decrease as the ambient moisture increases (18), as on the contrary it is noticed in ordinary concretes (19) and in cement pastes (20)(21).

This decrease is due to the disjoining action of water when it penetrates among the particles forming the cement paste or between cement and aggregate and which is able to considerably reduce van der Waals's force (22).

Since in the epitaxis intergrowth the distance between the two crystalline phases is of the order of magnitude of the lattice distances, no phase, liquid or gaseous, can penetrate into the interface between the two phases (23).

Therefore the material subjected to the compressive test must not show a different strength depending on whether the environment is wet or dry.

Other factors can have favoured an epitaxis overgrowth of tobermorite on quartz. For example, epitaxis is favoured by the temperature rise (17) and this can explain the fact that the strong quartz - cement paste bond does not occur at ordinary temperature.

Also the differences of composition noticed for the cement paste, richer in silica at the interface with the aggregate, can have facilitated the epitaxis overgrowth of tobermorite on quartz by an increased analogy of their crystal lattices.

4. CONCLUSIONS

By autoclaving concretes containing quartz aggregates, compressive strengths over 150 N/mm^2 are obtained. This result is partly related to the fact that the aggregate-cement paste bond is, in this case, stronger than the cohesion of the paste itself. This can be attributed to both a deeper embedding of the hydration products in the quartz grains corroded by the contact solution and the epitaxis intergrowth of 11 Å tobermorite crystals on the quartz ones.

REFERENCES

1.-TOGNON G.P., COPPETTI G., URSELLA P. (1978), "Very high strength concretes for precasting: production technology and characteristic properties", 9th Int. Congr. Precast Concr. Industry (Wien), 1-39, 1-46, (Eng.)

2.-TOGNON G.P., URSELLA P., COPPETTI G. (1979), "Design and properties of concretes with strength over 1500 kg/cm^2", presented at the American Concrete Institute An-

nual Convention (Milwaukee), (Eng.)

3. - TOGNON G.P., URSELLA P., COPPETTI G. (1977), "Calcestruzzi ad altissima resistenza per la prefabbricazione",
L'Industria Italiana del Cemento, 47, 699-706, (It.)

4. - SHAH S.P., SLATE F.O. (1968), "Internal Microcracking, mortar-aggregate bond and the stress-strain curve of concrete",
The Structure of Concrete and its Behaviour under Load (London 1965), 82-92, (Eng.)

5. - MENZEL C.A. (1934), "Strength and volume change of steam-cured portland cement mortar and concrete",
Journal of the American Concrete Institute, 31, 125-148, (Eng.)

6. - KALOUSEK G.L., ADAMS M. (1951), "Hydration Products formed in cement pastes at 25 to 175°C",
Journal of the American Concrete Institute, 23, 77-90, (Eng.)

7. - SANDERS L.DEAN, SMOTHERS W.J. (1957), "Effect of tobermorite on the mechanical strength of autoclaved portland cement-silica mixtures",
Journal of the American Concrete Institute, 54, 127-139, (Eng.)

8. - AITKEN A., TAYLOR H.F.W. (1962), "Steam curing of cement-quartz pastes",
Proc. 4th Int. Symp. on the Chemistry of Cement, (Washington, 1960), I, 285-290, (Eng.)

9. - AITKEN A., TAYLOR H.F.W. (1960), "Hydrothermal reactions in lime-quartz pastes",
J. Appl. Chem., 10, 7-15, (Eng.)

10.-KONDO R. (1967), "Kinetics study on hydrothermal reaction between lime and silica",
Autoclaved Calcium Silicate Bldg.,Proc.Pap.Symp., (London, 1965), 92-100, (Eng.)

11.-CHAN C.F., SAKIYAMA M., MITSUDA T. (1978), "Kinetics of the CaO-quartz-H_2O reaction at 120°C to 180°C in suspensions",
Cement and Concrete Research, 8, 1-5, (Eng.)

12.-ALEXANDER K.M., WARDLAW J., GILBERT D.J. (1968), "Aggregate-cement bond, cement paste strength and the strength of concrete",
The Structure of Concrete and its Behaviour under Load (London, 1965), 59-81, (Eng.)

13.-BACHE H.H., NEPPER-CHRISTENSEN P. (1968), "Observations on strength and fracture in lightweight and ordinary concrete",
The Structure of Concrete and its Behaviour under Load, (London, 1965), 93-108, (Eng.)

14.-LYUBIMOVA T.Yu., PINUS E.R. (1962), "Crystallization processes of structure formation in the contact zone between the filler and the binder in cement concrete",
Kolloid. Zh., 24, 578-587, (Russ.)

15.-SEREDA P.J. (1972), "Significance of microhardness of porous inorganic materials",
Cement and Concrete Research, 2, 717-729, (Eng.)

16.-BEAUDOIN J.J., FELDMAN R.F. (1975), "A study of mechanical properties of autoclaved calcium silicate systems",
Cement and Concrete Research, 5, 103-118, (Eng.)

17.-EITEL W. (1964), "Epitaxis phenomena",
Silicate Science, 1, 204-212, (Academic Press), (Eng.)

18.-Unpublished data

19.-TROXELL G.E., DAVIS H.E., KELLY J.W. (1968), "Composition and properties of concrete", 254-255, (McGraw-Hill), (Eng.)

20.-SEREDA P.J., FELDMAN R.F. (1966), "Effect of sorbed water on some mechanical properties of hydrated portland cement pastes and compacts",
High.Res. Board, Special Report, n° 90, 58-72, (Eng.)

21.-WITTMANN F. (1968), "Surface tension shrinkage and strength of hardened cement paste",
Matériaux et Constructions, 1, 547-552, (Eng.)

22.-WITTMANN F.H. (1972), "Etude de la force d'adhésion en fonction du mouillage",
Liaison de Contact dans les Matériaux Composites utilisés en Génie Civil (Toulouse), 1, 174-184, (French)

23.-FARRAN J. (1956), "Contribution minéralogique à l'étude de l'adhérence entre les constituants hydratés des ciments et les matériaux enrobés",
Revue des Matériaux, 490, n° 1-2, 155-172,191-209, (French).

Etude du contact zinc - Pâte de ciment Portland

Study of the contact zone between zinc and Portland cement paste

G. ARLIGUIE, Assistante,
J. GRANDET, Professeur : I.N.S.A. Département du Génie Civil, U.P.S. Toulouse,
R. DUVAL, Professeur, France.

RESUME : On étudie d'abord le comportement électrochimique du zinc dans des solutions simulant le milieu pâte de ciment Portland, puis les constituants formés à l'interface zinc-pâte de ciment Portland.

En immergeant des éprouvettes de zinc dans des solutions saturées de chaux, on décèle la formation sur la surface du métal d'un composé complexe et insoluble d'hydroxyzincate de calcium. Les mesures électrochimiques ont montré que ce composé passivait le zinc.

Après ces expériences effectuées en solution de simulation on a étudié, par diffractométrie X, la nature des constituants hydratés de la pâte de ciment durcissant au contact d'une éprouvette de zinc. On a pu mettre en évidence l'existence d'ettringite et d'hydroxyzincate de calcium dans la zone de pâte proche du métal ; par contre, on ne décèle pas de portlandite dans les premiers jours suivant la prise. L'observation des surfaces de rupture entre le zinc et la pâte de CPA a été faite au microscope optique puis au microscope électronique à balayage. Nous avons ainsi pu déterminer la limite de la zone d'influence du zinc dans la pâte et son évolution en fonction du temps.

SUMMARY : We studied firstly the electrochemical behaviour of zinc immersed in the solution representing the fresh Portland cement paste. Then, we observed the constituents formed at the interface between zinc and Portland cement paste.

By immersing the zinc specimens in the saturated lime solution, we found the formation of an insoluble composite of calcium hydroxyzincate. The electrochemical measurements showed that this composite formed the passive zinc.

We also studied the hydrated constituents setting up at the contact between cement paste and zinc by the X-ray diffraction analysis. The results showed that the existance of ettringite and calcium hydroxyzincate occurred in the zone of cement paste nearly to the metal. On the other hand, we have not found portlandite in this zone during the first days after setting.

The breaking surface between zinc and Portland cement paste was also observed by the optical microscope and the scanning electron microscope. Consequently, we can determine the boundary of the influence zone of zinc in the cement paste and its evolution in the function of time.

Pour obtenir une protection des armatures d'acier noyées dans un béton soumis à des milieux agressifs, on a parfois recours à la galvanisation. Cependant, le comportement du zinc au contact d'un béton n'est pas encore totalement éclairci (1 à 7).

Nous avons procédé d'une part à l'étude du comportement électrochimique du zinc dans des solutions simulant le milieu pâte de ciment Portland, et d'autre part à l'analyse par diffractométrie X des constituants formés dans la zone de contact zinc-pâte de ciment Portland.

ETUDE ELECTROCHIMIQUE

Le comportement électrochimique de matériaux métalliques au contact de béton a déjà été abordé en utilisant des solutions de simulation approchées, le plus souvent des solutions saturées de chaux. Ces études ont apporté des renseignements intéressants sur les produits de corrosion formés en milieu basique, mais ce dernier est différent du milieu complexe créé par la pâte de ciment Portland. Par la suite, des travaux effectués par P. LONGUET et COLL (6) ont permis d'extraire et d'analyser le liquide interstitiel existant à l'intérieur d'un béton.

Nous avons tout d'abord entrepris l'étude électrochimique du comportement du zinc dans des solutions de simulation tenant compte du milieu réel afin de voir quelle était l'influence des divers composants de cette solution sur le métal. Nous avons utilisé des solutions saturées de chaux, des solutions alcalines, et enfin des solutions mixtes chaux-alcalins.

Dans des solutions saturées de chaux, nous avons mis en évidence la formation, sur la surface du zinc, d'une couche passive constituée par un composé complexe insoluble d'hydroxyzincate de calcium $Ca\ Zn_2\ (OH)_6,\ 2\ H_2O$. Nous avons pu constater que ce composé jouait un rôle protecteur vis-à-vis de certains agents agressifs, plus particulièrement des ions chlorures (7).

Dans des solutions alcalines, le zinc est fortement attaqué avec formation de zincates solubles.

Enfin, nous avons réalisé des essais dans des solutions mixtes chaux-alcalins, de façon à approcher la composition du milieu interstitiel réel de la pâte de ciment. Cette étude a montré le rôle particulier de la chaux qui contribue à former l'hydroxyzincate de calcium. Pour des concentrations faibles en potasse la couche d'hydroxyzincate recouvre totalement la surface du zinc. Pour des concentrations plus fortes, on observe une attaque parfois importante due à un mécanisme de corrosion par micropiles galvaniques ; de l'oxyde de zinc se forme au détriment de l'hydroxyzincate de calcium passif. La présence d'oxyde de zinc n'est décelable que pour de fortes teneurs en alcalins

Après ces expériences effectuées en solution de simulation nous avons étudié, par diffractométrie X, la nature des constituants hydratés formés par une pâte de ciment Portland durcissant au contact du zinc.

PREPARATION DES ECHANTILLONS

Les éprouvettes de zinc se présentent sous forme de cylindres dont une section plane (1 cm^2) a été polie sur papier abrasif jusqu'au grain 1200.

La teneur en zinc des échantillons utilisés est de 99 %.

Après polissage, les cylindres de zinc sont soumis aux ultra-sons, rincés à l'alcool, puis séchés. Une pâte de ciment CPA 55 R dont le rapport E/C est égal à 0,29 est coulée sur la section polie. Tous les échantillons sont conservés dans une ambiance à 20° C et 100 % d'humidité relative.

METHODE D'ETUDE

Après démoulage, on rompt mécaniquement l'éprouvette mixte. On analyse, par diffractométrie X, les sections de rupture côté pâte.

L'épaisseur de la pellicule adhérente au métal est déterminée par microscopie optique. Ensuite, on observe les surfaces de rupture au microscope à balayage. Puis on étudie des sections de pâte de ciment parallèles à la surface de rupture. Pour celà, on enlève des couches de pâte de ciment par abrasion et on détermine la quantité recueillie par double pesée afin d'en déduire l'épaisseur de la couche détachée (8).

Chaque nouvelle section obtenue est examinée par diffractométrie X. On peut ainsi dresser la carte des constituants présents depuis la surface du métal jusqu'au coeur de la pâte de ciment.

CONSTITUANTS DANS LA ZONE DE CONTACT

Nous avons étudié des éprouvettes mixtes à différents âges. Les résultats sont présentés d'une manière schématique dans la figure 1.

A un jour, le diagramme X effectué sur la face de rupture côté zinc montre la présence d'hydroxyzincate de calcium et, en quantité beaucoup plus faible, d'oxyde de zinc et d'ettringite. La portlandite n'apparait pas. De nombreux grains de ciment anhydre restent accrochés sur le métal (raies de diffraction de C_3S). L'observation au microscope à balayage nous permet de voir que l'hydroxyzincate de calcium recouvre déjà en grande partie la surface du zinc.

Sur la face de rupture côté ciment, on ne décèle pas de portlandite par diffraction X, et le diagramme obtenu traduit une faible hydratation de la pâte. Par abrasions successives parallèlement à la surface de rupture, les raies de diffraction X de la portlandite n'apparaissent qu'à une distance de 100μ du contact et augmentent au fur et à mesure que l'on s'en éloigne. L'ettringite est présente dès le contact, mais en faible quantité. On note l'absence d'hydroxyzincate de calcium sur cette face. La rupture s'est donc produite à la limite de la zone constituée essentiellement par l'hydroxyzincate de calcium. Ce composé se forme par action de la chaux sur l'oxyde de zinc, ce qui explique l'absence de portlandite dans les 100 premiers microns de la pâte.

A deux jours, la rupture de l'éprouvette mixte se produit en laissant, comme précédemment, une fine pellicule adhérente sur la surface du métal et quelques amas de grains de ciment.
Côté zinc, le diagramme de diffraction X indique la présence des mêmes composés qu'à un jour ; on note que l'hydroxyzincate de calcium et l'ettringite apparaissent en quantité un peu plus importante.

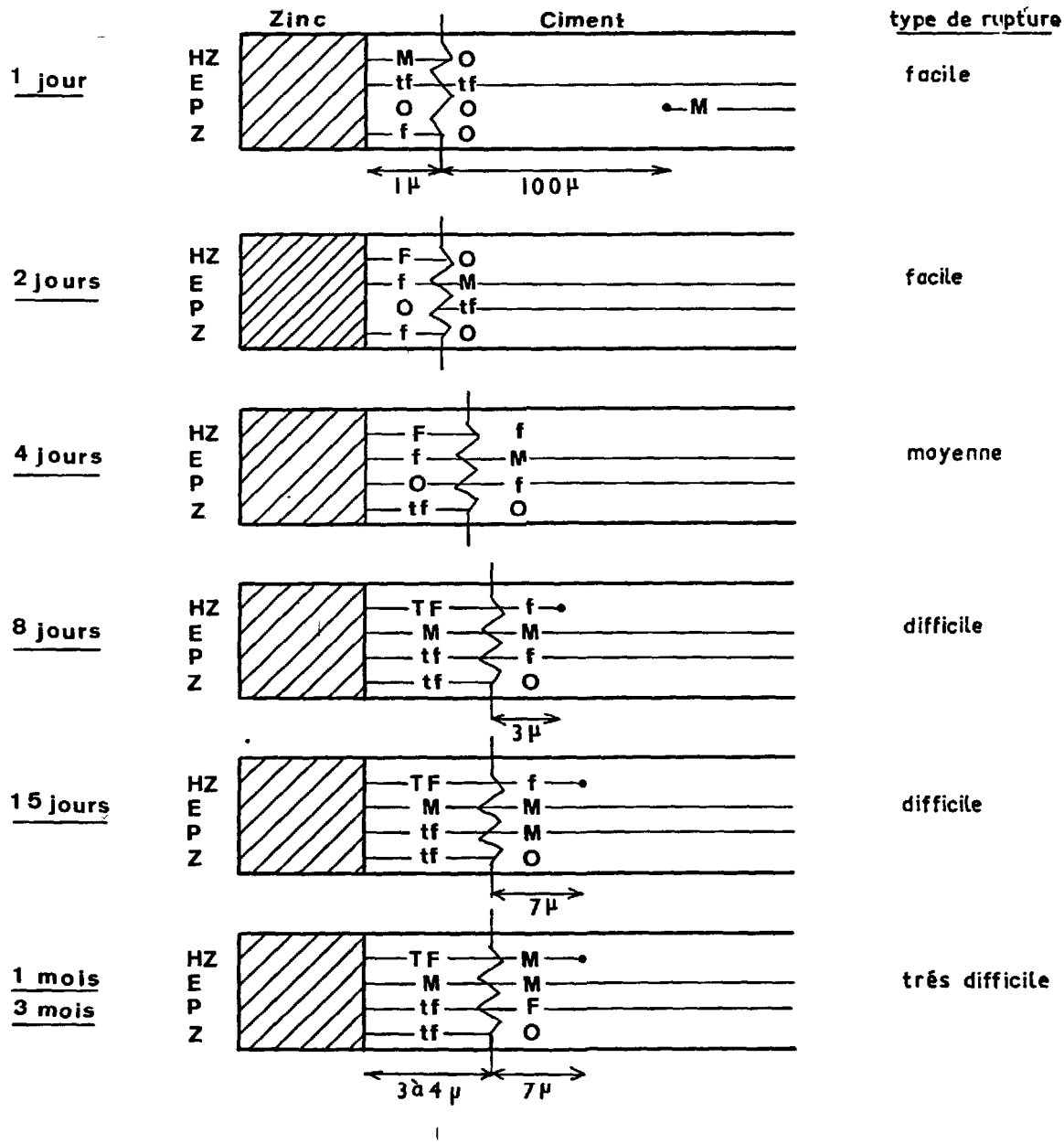

FIGURE 1 - "Evolution de la zone de contact en fonction du temps"

Notations utilisées : HZ = hydroxyzincate de calcium
E = ettringite
P = portlandite
Z = oxyde de zinc

Intensité du pic principal de diffraction du composé : TF = très importante
F = importante
M = moyenne
f = faible
tf = très faible

Absence du composé : 0

Limite du domaine d'existence du composé : —•

Au microscope à balayage, on observe que l'hydroxyzincate est le premier dépôt sur le zinc, la pâte de ciment la recouvrant par endroits (figure 2)

FIGURE 2 : "Surface de rupture côté zinc après un contact de 2 jours" -(x 2000)-

Côté pâte, il apparaît un peu de portlandite. Le diagramme obtenu sur cette face de rupture montre que l'hydratation de la pâte est retardée par la présence du zinc : les raies de C_3S sont plus importantes qu'au coeur de la pâte.

A quatre jours, les résultats sont très différents. Au voisinage du contact, l'hydratation du ciment s'est accélérée : l'intensité des raies du C_3S est analogue à celle obtenue au coeur d'une pâte de ciment de même âge.

L'hydroxyzincate de calcium se trouve en quantité notable de part et d'autre de la rupture. Sur la face de rupture côté zinc, nous n'avons que les raies principales de l'hydroxyzincate, alors que toutes les raies apparaissent sur la face ciment (figures 3 et 4). Sur cette dernière, on remarque que la portlandite se trouve encore en quantité plus faible que dans le coeur de la pâte. Par contre, la formation de l'ettringite n'est pas influencée par la présence du zinc ; elle présente une cristallisation analogue à celle observée au contact de supports inertes.

A quinze jours, la séparation mécanique entre le cylindre de métal et la pâte est très difficile.
La mesure de l'épaisseur de la pellicule adhérente au microscope optique donne des résultats variables selon la zone observée, en moyenne 4 μ.

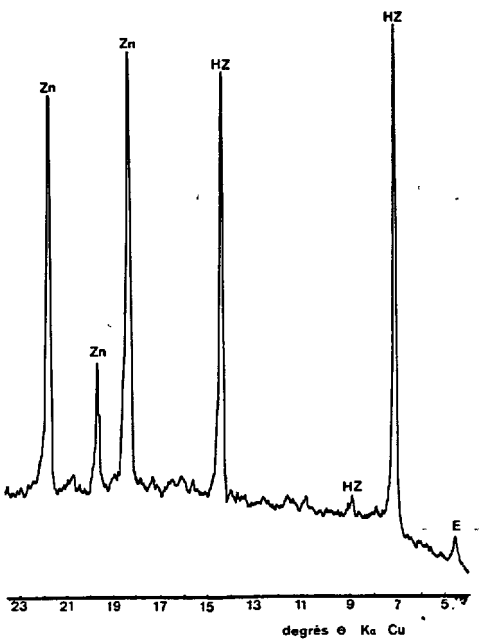

FIGURE 3 : "Enregistrement diffractométrique de la surface de rupture côté zinc après un contact de 4 jours"

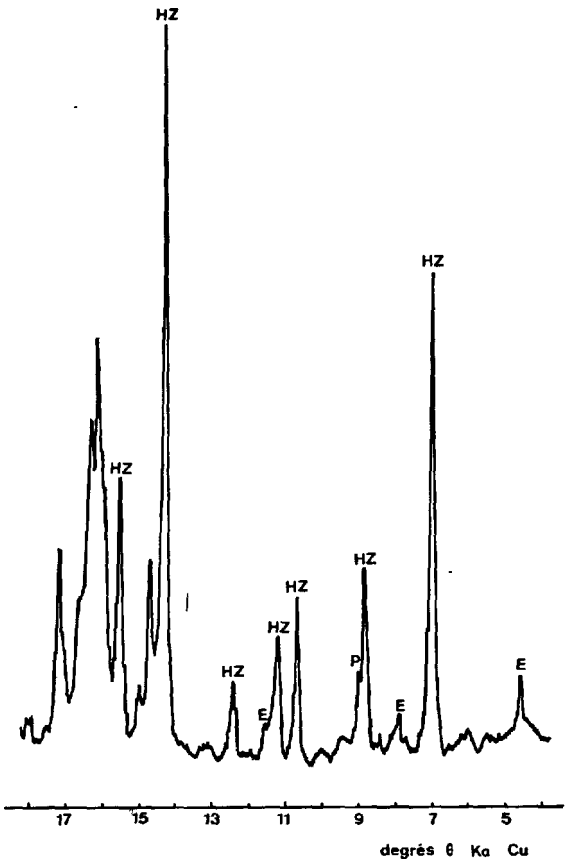

FIGURE 4 : "Enregistrement diffractométrique de la surface de rupture côté ciment après un contact de 4 jours.

La rupture se fait dans la couche d'hydroxyzincate de calcium puisqu'il apparaît sur les diagrammes de rayons X de chaque surface de rupture. Ceci est confirmé par l'observation au microscope à balayage qui montre des fractures sur les cristaux d'hydroxyzincate, la couche d'hydroxyzincate recouvre la quasi-totalité de la surface du zinc (figure 5). Par abrasions successives et analyses par diffractométrie X, on décèle la présence d'hydroxyzincate jusqu'à une distance de 10μ du zinc.

A un mois de durcissement, on ne note plus d'évolution quant aux constituants présents sur les surfaces de rupture.
Au contact de la pâte de ciment Portland, l'oxyde de zinc se trouve en quantité très faible, parfois, il n'est même pas décelé. Ceci confirme les résultats obtenus par les essais électrochimiques effectués en solution de simulation.

FIGURE 5 : "Surface de rupture côté zinc - Cristaux obtenus à 15 Jours" -(x 1500)-

CONCLUSION

L'étude du contact entre le zinc et les pâtes de ciment Portland confirme les résultats obtenus en solution de simulation : l'hydroxyzincate de calcium forme, à partir de la chaux, une couche continue et protectrice sur le zinc.
De plus, la méthode employée nous a permis de suivre l'évolution des constituants dans la zone de rupture. Nous avons tout d'abord noté qu'au contact du zinc, l'hydratation de la pâte de ciment Portland est retardée pendant les quatre premiers jours suivant la confection des éprouvettes mixtes. Nous avons d'ailleurs obtenu des résistances mécaniques faibles. Par la suite, l'accrochage entre la pâte de ciment et la surface polie du zinc est efficace ; il est ainsi fréquent d'obtenir des amas de pâte de ciment restant accrochés sur la surface métallique.
L'hydroxyzincate de calcium se forme dès le premier jour suivant le gâchage. Le rôle essentiel de la chaux dans la formation de ce composé est mis en évidence par le fait qu'on ne décèle pas de portlandite dans la zone de pâte proche du métal. La composition de cette zone évolue jusqu'à l'obtention d'une couche d'hydroxyzincate recouvrant la quasi-totalité de la surface du zinc. Une fois la formation de l'hydroxyzincate de calcium achevée, l'hydratation de la pâte se poursuit normalement.

BIBLIOGRAPHIE

(1) - G. REHM, A. MAMMKE (1970) "Untersuchungen über recktionen des zinks unter Einwirkung von Alkalien im Hinblick auf das Verhalten verzinkter Stähle im Beton" - Betonstein - Zeitung, n° 6, pp 360-365, Allemand.

(2) - M. BRACHET, A. RAHARINAIVO (1975) "Des aciers à haute résistance, galvanisés, utilisables comme armatures de béton précontraint" - Matériaux et Constructions, 8, n° 46, p. 323, Français.

(3) - I. CORNET, T. ISHIKAWA, B. BRESLER (1968) Materials Protection, 7, n° 44, Anglais.

(4) - P. LONGUET, P. PEGUIN, M. RUBAUD, A. ZELWER (1973) "Bases expérimentales de l'étude électrochimique du comportement des métaux en présence du béton" - Corrosion TPF, vol. 21, n° 3, p. 155, Français.

(5) - P. PEGUIN, M. RUBAUD, A. ZELWER (1976) Bulletin RILEM 9, 55, 187, Français.

(6) - P. LONGUET, L. BURGLEN, A. ZELWER (1973) "La phase liquide du ciment hydraté" - Revue Matériaux de Construction et T.P., 676, 35, (Français).

(7) - R. DUVAL, G. ARLIGUIE (1974) "Passivation du zinc dans l'hydroxyde de calcium, en égard au comportement de l'acier galvanisé dans le béton" - Mémoires Scientifiques Revue Métallurgie, 71, 5, Français.

(8) - J. GRANDET, J.P. OLLIVIER (à paraître) "Nouvelle méthode d'étude des interfaces ciment-granulat" - 7ème Congrès International de la Chimie des ciments, (Paris, 1980), Français.

Electrochimie des pâtes de ciment

Electrochemistry of cement pastes

V.I. BABOUCHKINE, Professeur, Docteur ès Sciences Techniques, VODGEO,
A.S. KOCHMAI, Ingénieur,
O.P. MTCHEDLOV-PETROSSIAN, Professeur, Docteur ès Sciences, Techniques, KhICI, U.R.S.S.

RESUME : L'hydratation et le durcissement des pâtes de ciment engendrent des processus électrochimiques dont la spécificité est conditionnée par les propriétés semi-conductrices des minéraux du clinker, la présence de défauts structuraux et de lacunes chargées. L'interface des phases solide et liquide d'un liant en voie d'hydratation peut être assimilé à un système de couches bipolaires en interaction. Le phénomène d'hydratation du ciment s'accompagne d'une séparation volumétrique de charges et de l'apparition de forces pondéromotrices, ce qui est une des raisons possibles de la manifestation de propriétés liantes.

Il est établi de façon expérimentale l'existence d'une sensible différence de potentiels entre les phases dans le système "liant-eau" engendrée par une distribution déséquilibrée de charges, du type Donnan, et des courants de diffusion.

On montre que toutes les pâtes de ciment en voie de durcissement possèdent une haute activité électrochimique. Par suite la phase liquide contenue dans les micropores du gel-ciment se trouve dans un état particulier et ne s'identifie pas à la phase liquide dégagée.

La détermination des potentiels de diffusion et électrocinétiques des pâtes de ciment permet de décrire de façon judicieuse le phénomène de durcissement surtout à ses débuts.

SUMMARY : Hydration and hardening of cement pastes are accompanied by electrochemical processes the peculiarities of which are dictated by semiconductor properties of clinker minerals, presence of structural defects and charged vacancies. The boundary between the solid and liquid phases of the binder being hydrated may be considered as a system of interacting double electric layers. The cement hydration process involves spatial separation of charges and appearance of pondermotive forces which is one of the possible reasons for manifestations of the binding properties.

It has been found out experimentally that the binder-water system comprises considerable inter-phase difference of potentials stemming from unbalanced distribution of Donnan type charges and diffusion flows.

It has been shown that hardening cement pastes feature high electrochemical activity. Therefore, the liquid phase contained in micropores of cement gel is in a particular state and does not correspond to the liquid pase liberated.

Determination of diffusion and electrokinetic potentials of cement pastes provides for rational description of the hardening processes, especially at the initial stages thereof.

La pâte de ciment qui durcit constitue un système colloïdo-cristallin déséquilibré hétérogène. Après gachage sur l'interface des phases solide et liquide se forme une charge électrostatique et une couche bipolaire (CB) que cette charge conditionne. Dans les pâtes de ciment sont ainsi amorcés des phénomènes électrochimiques qui jouent un rôle important dans le mécanisme commun de durcissement. C'est la raison de l'intérêt croissant pour l'électrochimie des liants. Toutefois nos idées en ce domaine ont un caractère fragmentaire et se rapportent pour l'essentiel aux propriétés électrocinétiques des pates de ciment (1, 2, 3).

Dans les pâtes de ciment s'amorcent des phénomènes électrochimiques déjà observés dans les colloïdes, les suspensoïdes et les corps capillaire-poreux, mais la spécificité du système "ciment-eau" engendre des phénomènes particuliers. Cette spécificité est due à la structure des substances liantes de départ, à leur métastabilité par rapport à l'eau et la nature exothermique de l'hydratation.

Il est établi que les minéraux du clinker - portland possèdent des propriétés de semiconducteurs (5). Cela signifie que la distribution de la charge de la CB du coté de la phase solide n'est pas localisée à la surface mais pénètre dans le volume. L'existence de défauts structuraux et de lacunes chargées conditionne la réactivité des minéraux du clinker. Quant aux impuretés on peut leur imputer la variation du mode de conductibilité d'un quelconque des minéraux du clinker et l'accroissement de concentration de défauts structuraux. Une grande concentration de défauts à la surface de l'alite accroit brusquement son pouvoir absorbant. Des études ont montré qu'à la surface de C_3S se rencontre des centres actifs où s'effectue le transfert d'électrons aux molécules absorbées avec formations d'ions chargés négativement (6).

Le déplacement de CB sur l'interface "minéral de clinker-eau" dans le volume des phases liquide et solide assure un caractère volumétrique aux phénomènes superficiels pendant l'hydratation des liants. Des forces pondéromotrices sont ainsi engendrées auxquelles on peut attribuer l'action à grande distance observée des formations hydratées.

Les grandeurs mesurables pouvant caractériser la CB est sa capacité et son potentiel électrocinétique ζ . Dans les pates de ciment le potentiel ζ est de nature complexe, car les différentes composantes des systèmes étudiés varient en grandeur et par le signe de leur charge superficielle. Les études réalisées ont montré que les minéraux du clinker C_2S, C_3S et les produits de leur hydratation rappelant le tobermorite, ont une charge superficielle négative. C_3A, C_4AF et les produits de leur hydratation, de même que le gypse, l'ettringite, $Ca(OH)_2$ ont au contraire une charge superficielle positive dans le milieu aqueux. Le potentiel ζ total des pates de ciment est négatif et conserve cette polarité durant tout le processus de durcissement ne variant qu'en grandeur absolue.

Les particularités de structure de la CB dans le système "liant-eau" se manifestent le plus nettement dans le cas de C_3S. Selon les concéptions modernes il se produit au début une absorption de molécules d'eau à la surface de l'alite et une dissolution congruente avec formation d'un hydrosilicate primaire du type $C_3S \cdot nH_2O$. Sous l'effet de pénétration du champ de molécules de H_2O adsorbées à travers la surface C_3S, les groupements siloxanes $\equiv Si - O - Si \equiv$ se polarisent, et, en se rompant partiellement, forment les groupements $\geqslant \overset{-}{S}i - O\,H^+$. L'hydrosilicate $C_3S \cdot nH_2O$ joue le rôle de pellicule de gel semiperméable et déséquilibré qui empeche le contact direct de l'alite avec l'eau. La vitesse d'hydratation chutant, on passe à la période dite "d'induction". Durant cette période l'hydrosilicate $C_3S \cdot nH_2O$ est métastable par rapport à l'eau, s'hydrolyse rapidement en formant des pellicules en hydrosilicates secondaires avec $\frac{CaO}{SiO_2} < 3$. Ces processus provoquent la saturation et la sursaturation de la phase liquide par rapport à $Ca(OH)_2$.

Il se produit sur les groupements $\geqslant Si - O^-H^+$ une adsorption orientée des molécules polaires de l'eau. En remplissant le rôle de lents états de surface, les groupements $\geqslant Si - O\,H^+$ constituent un écran pour le volume du semiconducteur C_3S, le champ de molécules de H_2O adsorbées n'agissant que sur la partie diffuse de la CB en phase liquide. À la surface des hydrosilicates secondaires il peut alors s'amorcer une absorption partielle de co-ions OH^- de sorte que la concentration maximale de contre-ions Ca^{2+} se produit avant celle d'ions OH^-.

Cette hypothèse permet d'expliquer pourquoi avec l'hydratation de C_3S il se forme à la fin de la période d'induction un excès d'ions Ca^{2+} perturbant l'électroneutralité de la phase liquide (7). La figure 1 montre la formation de la CB lors de l'hydratation du C_3S en conformité avec le modèle du processus décrit.

Evidemment il se forme dans ce cas un système de CB en interaction. La première CB (interne) se forme sur l'interface de C_3S et du gel d'hydrosilicate qui passe par trois stades de développement et contient des quantités variables de H_2O et de concentrations d'ions Ca^{2+} et OH^- en état de saturation et de sursaturation. La seconde CB (externe) se forme sur l'interface du gel d'hydrosilicate et de la phase liquide libre.

Au cours du processus d'hydratation on voit de nouvelles interfaces entre les phases solide et liquide, tandis que les porteurs de charge de la substance de départ se trouvant au début dans la phase solide près de l'interface s'en éloignent en profondeur de l'épaisseur de la couche de nouvelles formations hydratées. Les ions OH^- étant absorbés de façon sélective par le gel d'hydro-

silicate et les contre-ions Ca^{2+} de signe opposé repoussés par l'interface qui se déplace, il se forme dans les phases solide et liquide des charges volumétriques de signe opposé. Il se produit une différenciation de charges qui dure tant que la différence de potentiels amorcée entre les phases solide et liquide ne soit compensée par la différence des potentiels électrochimiques entre les ions correspondants des deux phases.

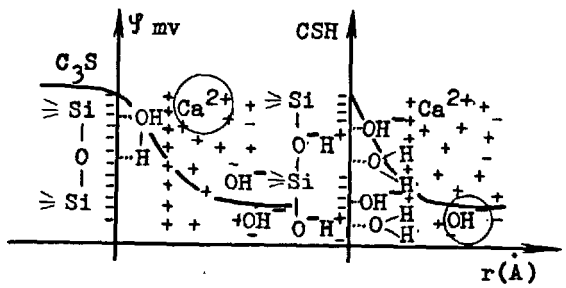

Fig.1. Structure de la couche bipolaire dans le système "C_3S - H_2O"

Avec l'acquisition d'une certaine grandeur $\Delta\psi$ un flux de diffusion électrique d'ions peut se mettre à traverser la pellicule de gel et, partant, la phase liquide se trouve sursaturée en ions Ca^{2+}, qui sont partiellement retenus par les hydrosilicates. Il se forme ainsi un gel stable (tertiaire) d'hydrosilicate de calcium à teneur élevée en chaux mais en maintenant le rapport $\frac{CaO}{SiO_2} < 3$.

Le flux de diffusion électrique élève fortement la perméabilité de la péllicule de gel. La période d'induction s'achève et une hydratation intense du liant s'amorce.

On a étudié la différence de potentiels entre les phases solide et liquide dans les suspensions et les pates en voie d'hydratation. Le rapport eau-ciment des suspensions du liant était de 5,0. La différence de potentiels était mesurée entre deux électrodes en chlorargent placées respectivement dans le précipité et au-dessus de la solution de la suspension. Le potentiel d'asymétrie des électrodes ne dépassant pas 0,5 mV. Le rapport eau-ciment des pates était de 0,5. Dans ce cas la différence des potentiels était mesurée au cours du filtrage sous pression de la phase liquide, l'une des électrodes en chlorargent contactant avec la pâte de ciment et l'autre avec la solution séparée. La grandeur de la pression de régime était 146 MPa.

La figure 2 montre la variation de la différence de potentiels ($\Delta\psi$) entre les phases solide et liquide de la suspension de ciment (courbe I) et de la pâte de ciment (courbe II) en fonction du temps d'hydratation (τ). Dans les deux cas il est possible d'établir les mêmes régularités.

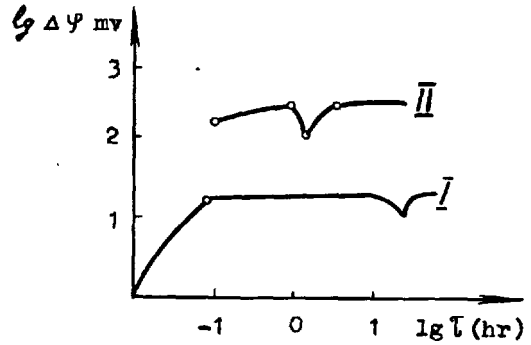

Fig.2. Variation de la différence de potentiels entre les phases
I) dans les suspensions de ciment,
II) dans les pâtes de ciment

Au début de l'hydratation de la suspension durant 4 à 5 minutes, la grandeur $\Delta\psi$ atteint rapidement 15 mV. Ensuite, $\Delta\psi$ s'accroît lentement durant 14 heures, phénomène s'expliquant par la différenciation des charges. La diminution subséquente de la grandeur $\Delta\psi$ est, vraisemblablement, due au flux de diffusion électrique à travers le gel de ciment. La seconde hausse de $\Delta\psi$ est également en rapport avec la différenciation des charges engendrée par la formation du gel au cours de l'intense hydratation. Simultanément il se produit un développement de la structure de la suspension du liant. Au début de l'hydratation de la pâte de ciment (6 à 8 min) la grandeur $\Delta\psi$ monte à 160 mV. Ensuite en une heure $\Delta\psi$ s'accroît jusqu'à 250 mV. Vraisemblablement, c'est dû à la séparation des charges durant la période d'induction. A la fin de la période d'induction le flux de diffusion électrique provoque la diminution de $\Delta\psi$. La seconde élévation de $\Delta\psi$, comme précédemment, est en rapport avec la différenciation des charges engendrée par la formation ultérieure du gel. En même temps s'amorce le processus de prise de la pâte de ciment en voie de durcissement. A la fin de prise, après 3,5 heures de durcissement, l'élévation de $\Delta\psi$ se ralentit fortement.

La différenciation des charges n'est pas la seule cause de l'apparition de la différence de potentiels entre les phases solide et liquide de la pâte ou de la suspension de ciment. L'autre raison de l'engendrement de $\Delta\psi$ est la distribution irrégulière d'ions entre la phase liquide composant les micelles colloïdales du gel de ciment et la

phase liquide libre. Cette distribution est propre à tous les systèmes colloïdaux et aboutit en conditions d'équilibre, à l'apparition du potentiel de Donnan

$$\varphi_D = \frac{RT}{Z_i F} \ln \frac{a_i}{\tilde{a}_i} \qquad (1)$$

où a_i est l'activité du i-ème ion dans la solution libre; $\tilde{a}_i$ - l'activité du i-ème ion dans la solution liée; R - la constante de gaz parfaits; F - le nombre de Faraday; Z_i - la charge du i-ième ion (compte tenu de son signe).

Cependant le gel de ciment de la pâte qui durcit se trouve dans un état qui est loin de l'équilibre thermodynamique. Aussi dans le cas étudié ne peut-on parler que du potentiel du type Donnan (ε_D) mais dans des conditions de déséquilibre et transitoires. La différence entre φ_D et ε_D a un caractère de principe et la grandeur ε_D ne peut être calculée sur la base de l'équation (1).

Outre la grandeur ε_D il faut tenir compte des potentiels liés aux flux de diffusion dans les microcapillaires. On sait que le gel de ciment est traversé par de nombreux microcapillaires dont le rayon est de l'ordre de l'épaisseur de la CB. Dans ces capillaires la phase liquide est soumise à une forte action des surfaces chargées. Ceci a des effets sur de nombreuses propriétés physico-chimiques de la solution, en particulier sur la viscosité, la permittivité, la force ionique. Sous l'effet de la charge superficielle l'activité des ions de la phase liquide et leur mobilité se modifient. Le nombre de transfert de co-ions diminue donc, tandis que celui de contre-ions augmente. Il en résulte des courants de diffusion ainsi qu'un phénomène de conductibilité superficielle dont il faut tenir compte au cours de la détermination de la grandeur du potentiel ζ d'après les mesures électrocinétiques.

Ainsi donc la différence entre les potentiels des phases solide et liquide se détermine dans le gel de ciment par le potentiel du type Donnan (ε_D) et le potentiel de diffusion φ_d. La somme de ces potentiels doit être considérée comme le potentiel de la membrane du gel de ciment : $\varphi_m = \varepsilon_D + \varphi_d$.

L'apparition du potentiel de diffusion au cours du durcissement de la pâte de ciment a été étudié dans la chaîne électrochimique

$$\underset{= 0,02}{Ag,AgCl,KCl_{m_1}} = \left| \begin{matrix} \text{pâte de} \\ \text{ciment} \\ E/C=0,5 \end{matrix} \right| KCl_{m_2} = 0,01\ \underset{Ag}{AgCl},$$

où m_1 et m_2 sont les molalités des solutions de KCl; E/C étant le rapport eau-ciment dans la pâte.

La figure 3 montre la variation de la grandeur φ_d en fonction du temps de durcissement de la pâte de ciment (courbe I). La nature de la courbe $\varphi_d = f(\tau)$ témoigne que la pâte de ciment, déjà dès le début de gâchage modifie sensiblement le nombre de transfert de co-ions et de contre-ions, c'est-à-dire possède une activité électrochimique marquée. Le nombre de transferts peut être calculé d'après la formule connue

$$t_+ = \frac{\varphi_d}{2\frac{RT}{ZF}\ln\frac{f_1 m_1}{f_2 m_2}} \qquad (2)$$

où t_+ est le nombre de transferts du cation; f_1 et f_2 - les coefficients d'activité des solutions KCl.

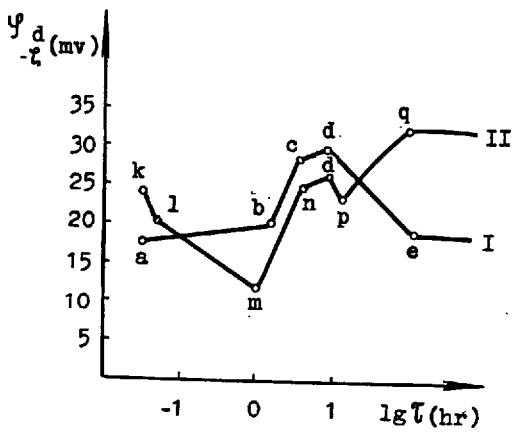

Fig.3. Caractéristiques électrochimiques des processus de durcissement de la pâte de ciment
I) par rapport au potentiel de diffusion
II) par rapport au potentiel électrocinétique

Après le choix des molalités le nombre de transferts d'ions K^+(t_{k^+}) dans la solution libre équivaut à 0,49. Deux minutes après gâchage t_{k^+} atteint 0,53 (point "a"), Δt étant égal à 8%. Une heure et demi après le début du durcissement (point "b") t_{k^+}=0,58, tandis que Δt = 19%. Ensuite les nombres de transferts varient brusquement et au point "c" correspondant à 3,5 heures de durcissement t_{k^+}=0,85, tandis que Δt = 73%.

La période de durcissement entre les points "b" et "c" correspond évidemment à celle de l'épaississement de la pâte de ciment par coagulation et formation de nombreux micropores ainsi que du fait de l'amorçage du développement de la structure. Après 8 heures de durcissement t_{k^+} atteint dans la pâte 0,88 et Δt 79% (point "d"). Par la suite la grandeur t_{k^+} commence à diminuer et après un durcissement de 18 jours la pâte acquiert une valeur stable égale à 0,56 (Δt=14%). La chute de Δt est une indication de l'affaiblissement de l'activité électrochimique après la transformation de la pâte en pierre de ciment. La raison en peut être la variation de la structure de la CB comme celle du rayon des pores. Aussi

pour une description complète des phénomènes électrochimiques dans les pâtes de ciment faut-il étudier la variation du potentiel ζ au cours du durcissement. Si l'on introduit une correction à la conductibilité superficielle, la grandeur ζ sera indépendante du rayon des capillaires et des pores.

La figure 3 représente la variation de la grandeur du potentiel ζ en fonction du temps de durcissement de la pâte de ciment (courbe II). Au début de durcissement le potentiel ζ atteint -24 mV (point "k"), ensuite, durant environ une heure, il diminue en valeur absolue jusqu'à -12 mV (point "ℓ"). La diminution du potentiel ζ est due à la saturation électrolytique de la phase liquide du fait d'intenses processus d'hydratation. Ensuite, durant la période d'induction on assiste à la formation de la pellicule de gel qui absorbe de façon spécifique les coions de la solution. De ce fait la concentration de la charge électrostatique superficielle augmente. Ces deux processus aboutissent à la compression de la partie diffusive de la CB et, partant, à la diminution du potentiel ζ.

D'un autre côté la différenciation volumétrique des charges et la diminution de la concentration d'ions dans la phase liquide par cristallisation conduit à une forte augmentation de la grandeur ζ (intervalle m - n). L'apparition de courants de diffusion et la poursuite de l'hydratation de particules originaires du liant relentissent la croissance du potentiel ζ puis l'obligent à diminuer (intervalles n - o et o - p). Le développement de structures cristallines du liant en voie de durcissement et le rearrangement des ions dans la CB par absorption sélective provoquent de nouveau l'élévation de la grandeur ζ (intervalle p - q).

La confrontation des courbes $\varphi_d = \varphi(\tau)$ et $\zeta = \zeta(\tau)$ montre que malgré une différence apparente elles caractérisent de façon univoque le processus de durcissement. C'est ainsi qu'à la période d'accroissement de l'activité électrochimique de la pâte de ciment correspond une rapide augmentation du potentiel ζ. Le ralentissement de l'activité électrochimique s'accompagne de celui de la grandeur ζ. La diminution du potentiel ζ s'amorce durant la période de la baisse d'activité électrochimique de la pâte.

Habituellement la coagulation de particules hydratées du liant est reliée à la diminution de la grandeur du potentiel ζ. Mais pour les systèmes lyophiles auxquels appartiennent les pâtes, cette interdépendance n'est pas obligatoire. De surcroît les expériences montrent que le développement de la structure primaire irréversible dans les pâtes de ciment débute au cours de l'élévation du potentiel ζ. Selon nous la coagulation et la prise des pâtes de ciment est due à l'action des forces pondéromotrices apparaissant avec la différenciation volumétrique des charges. L'effet de différenciation des charges au cours de l'hydratation des ciments peut être considéré comme une des causes de l'apparition de propriétés liantes. Si l'on admet que l'énergie de différenciation des charges est fournie par la chaleur d'hydratation il devient alors clair pourquoi tous les liants interagissent avec l'eau de façon exothermique.

CONCLUSIONS

L'analyse théorique ainsi que des études expérimentales ont montré que la pâte de ciment doit être considéré comme un système électrochimique particulier. L'interface des phases solide et liquide d'un liant qui s'hydrate est constitué par un ensemble de couches bipolaires en interaction. Les forces pondéromotrices développées au cours de la séparation volumétrique des charges peuvent être l'une des raisons de la manifestation des propriétés liantes.

Cette hypothèse est confirmée par l'existence d'une différence importante de potentiels entre les phases au cours de la décantation des suspensions de liant et le filtrage sous pression de la phase liquide à partir des pâtes de ciment. La différence de potentiels entre les phases dans le système "liant - eau" est loin d'être un artifice, elle est due à une distribution déséquilibre des charges du type Donnan et d'une importante activité électrochimique des suspensions et des pâtes de ciment.

Dans des systèmes colloïdaux équilibrés la différence entre les potentiels chimiques des phases liée et libre se compense par la pression osmotique. La différence de potentiels chimique entre les ions de même signe liés et diffusant librement se compense par la pression osmotique et la différence entre les phases des potentiels électriques. Dans le système déséquilibre "liant - eau" par contre la compensation ne s'établit pas et la pression osmotique atteint même 19 à 54 MPa (4). La scission provoquée par cette pression aboutit à la déformation et à la rupture de nouvelles formations de gel ainsi qu'à la dilatation sensible du liant en cas de cohésion du système.

La différence de potentiels entre les phases solide et liquide doit être prise en compte au cours des études des processus d'hydratation et de durcissement. Il faut souligner tout particulièrement que la mesure des paramètres tels le pH, la concentration active d'ions, la conductivité électrique, etc. doit être faite directement sur la pâte de ciment et non pas sur la phase liquide extraite de cette dernière (8).

Le développement de connaissances sur les processus électrochimiques dans les pâtes de ciment, sur leur nature et leurs particularités peuvent être utilisées de façon efficace dans le but de modification orientée des propriétés des liants. Cela concerne en premier lieu le choix d'adjuvants chimiques et d'actions électromagnétiques externes à des fins de réglage des délais de prise et des conditions de durcissement des pâtes de ciment.

BIBLIOGRAPHIE

I.- ЕИ.Ведь, Е.Ф.Жаров, Г.М.Бакланов, Ж.А.Бреценко, Ю.В. Гордеев и А.Н.Голодовникова (I972), "Твердение портландцемента в ранние сроки, Будівельні матеріали і конструкції, №3, с.30-3I, (en ukrainien).

2. - Г.Дж.Вербек и Р.А.Хельмут (I972), "Структура и физические свойства цементного теста", Пятый Международный конгресс по химии цемента, с.269, (en russe).

3. - А.А.Старосельский, А.Г.Ольгинский и Ю.А.Спирин (I976),"Электрокинетические свойства цементного камня", Шестой Международный конгресс по химии цемента, т.II, кн.2, с.I92-I95, (en russe).

4. - О.П.Мчедлов-Петросян и В.И.Бабушкин (I976) "Термодинамика и термохимия цемента", Шестой Международный конгресс по химии цемента, т.II, кн.I, с.I4-I6, (en russe).

5. - J.Phatak and A.Chattergi (1963), "Semiconductivity and cementing action in hydraulic-bond type cement", Nature, v.197, n°4868, 40-43, (en anglais).

6. - P.Fierenz et J.P.Verhaegen (1976), "Propriétés nucleophiles des surfaces de silicate tricalcique", Cement and Concrete Research, v.6, n°1, 103-111, (en anglais).

7. - J.F.Young, H.S.Tong and Berger (1977), "Compositions of solutions in contract with hydrating tricalcium silicate pastes", Journal American Ceramic Society, v.60, n°5-6, 193-198, (en anglais).

8; - A.S.Koszmaj, O.P.Mczedlow-Petrosjan, A.W.Uszerow-Marszak (1973),"Wybrane zagadnienia z dziedziny pH-metrii zaczynow cementowych", Cement Wapno Gips, n°4, 109-110, (en polognais).

Some aspects and a new method of evaluating the sulphate resistance of cements

Quelques considérations sur la résistance des ciments à l'action des sulfates ; nouvelle méthode de mesure de cette résistance

M. REVAY, Ph.D. Senior Sci. Officer, Central Research and Design Institute for Silicate Industry, Budapest, Hungary; and
R. KOVACS, Ph. D., Deputy Head of Sci. Department, Central Research and Design Institute for silicate Industry, Budapest, Hungary.

RESUME : Les causes des variations de la résistance à l'action des sulfates de divers ciments ont été étudiées, en examinant leurs compositions de phase et leurs textures; on a tenté d'en déduire une explication précise du mécanisme de la corrosion par les sulfates.
Au cours de ces recherches (en utilisant et en améliorant les méthodes actuelles, bien connues, d'appréciation de la résistance aux sulfates) une méthode plus sensible, relativement rapide, fiable, en bonne concordance avec l'expression pratique et susceptible d'une normalisation internationale a été élaborée, pour apprécier la résistance des ciments à l'action des sulfates.

SUMMARY: The causes of the different sulphate resistance of various types of cements were interpreted using phase composition and texture investigations and an attempt was made to find a more accurate explanation of the sulphate corrosion mechanism.

In the course of the research - using and further developing the elements of some well known methods of investigating the sulphate resistan ce - a more sensitive, relatively rapid, reliable method well conforming the practical experience and being suitable for international standardization was elaborated for the investigation and evaluation of the sulphate resitance of cements.

INTRODUCTION

The predominant part of subsoil waters in Hungary have high sulphate concentration. That is why the study of the causes bringing about sulphate corrosion, the factors influencing the sulphate resistance of cements and the methods of its testing are of great importance for us. In the following besides the discussion of some theoretical problems a short summary of our recent work made in this field is given.

VOLUMETRIC CHANGES AND SULPHATE CORROSION

As it is known the volume of the compounds formed during the hardening of a cement-water mix is smaller than the total volume of the cement and water /1,2/. Thus after the solid structure has been developed a cement stone of considerable porosity is formed which usually shows some shrinkage later on.

The frequently observed swelling phenomenon cannot thus be understood in the first moment since in the porous cement stone there are always eneough free room for the new formations. There is no doubt that the expansion is caused by processes accompanying the volumetric increase of the solid phase but although hydratation is also of similar nature it does not cause expansion. According to some authors /3,4,5/ expansion takes place when the crystalline pressure of the new compounds formed during topochemical processes affects the solid structure, while others/6,7/ deny the possibility of such processes.

As it is known, sulphate corrosion is caused by the expanding effect of the sulphate-containing secondary hydrate compounds formed due to the sulphate ion penetration from subsoil waters into the cement stone /3,4,5,6/.

As a fact, the higher quantity of the Al_2O_3 content of the cement is bound in the form of C_3A the stronger tendency to sulphate corrosion can be observed /9,10/. Calcium-aluminate-sulphate-hydrates, however, may develop also from other Al_2O_3-containing phases so it is not quite clear why C_3A-less ferro-Portland cements are more sulphate resistant than ordinary cement containing practically the same amount of Al_2O_3. The "protecting effect" of the iron hydroxide gel suggested by some authors does not explain the smaller sulphate sensibility of the Al_2O_3 being present in the vitreous phase in the calcium aluminates of lower lime saturation /e.g. $C_{12}A_7$/ and in hydraulic admixtures /2,3,8/, as well as the better sulphate resistance of high alumina-te cements containing little Fe_2O_3 /11/.

Our experiments were devoted to find answers to the above questions.

INVESTIGATIONS ON THE MECHANISM OF SULPHATE CORROSION

In our experiments 20x20x80 mm cement paste specimens were prepared from cements of quite different sulphate resistance with a water/cement ratio of 0,26. One part of them was stored in water while the other part transferred for storage into a 4,4% Na_2SO_4 solution after two weeks. Strength tests of these specimens were carried out at ages from 1 to 365 days whereafter their pieces were subjected to various physical-chemical investigations.

The results of strength-tests proved the exponential relationship between porosity and strength stated by many authors /12,13,14/ to be valid for the cements stored in water but not for those stored in sulphate solution. This shows that for the latter ones the strength is determined not by their porosity but by micro- and macrocrackings. An explanation is attempted on the base of structural investigations.

Fig.1 shows some typical X-ray diffractograms.

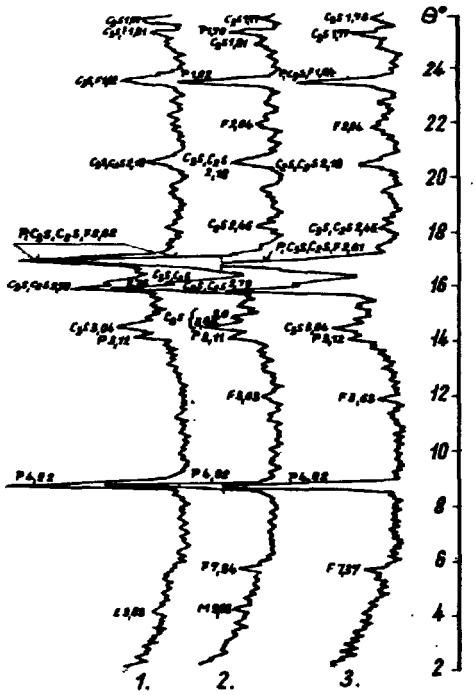

Fig.1 - X-ray patterns of various type cements after curing 14 days in water and further on in sulphate solution
a/ Portland cement; b/ moderate sulphate resistant and c/ sulphate resistant cement
E=ettringite; M = monosulphate; G = gypsum
F = ferrite phase; P = portlandite

It can be observed that in Ferrari-type cements the intensity of the calcium-aluminate-ferrite peaks is quite remarkable even after storing in sulphate solution for a relatively long time. This indicates that the dissolution rate of the Al_2O_3 content of the cement is considerably less than that of the cements containing alumina mostly in C_3A phase. Concentration relations in this

case enable the Al_2O_3 content of the cement to practically crystallize in the form of primary calcium-aluminate-sulphate-hydrates. This process keeps going on even with sulphate ions penetrating from outside. If a large amount of C_3A is, however, present, the initial aluminium-ion concentration will be higher and the amount of the dissolving sulphate is not sufficient to form from the dissolved ions exclusively sulphate containing hydrate compounds so a certain amount of primary calcium aluminate hydrates also precipitates beside them. The latter, upon the effect of the sulphate solution penetrating from outside convert into secondary calcium-aluminate-sulphate-hydrates. Textural investigations give information on the mechanism of their formation.
These results are illustrated by pore size distribution diagrams of some typical probes obtained by the mercury penetration method /Fig.2./.

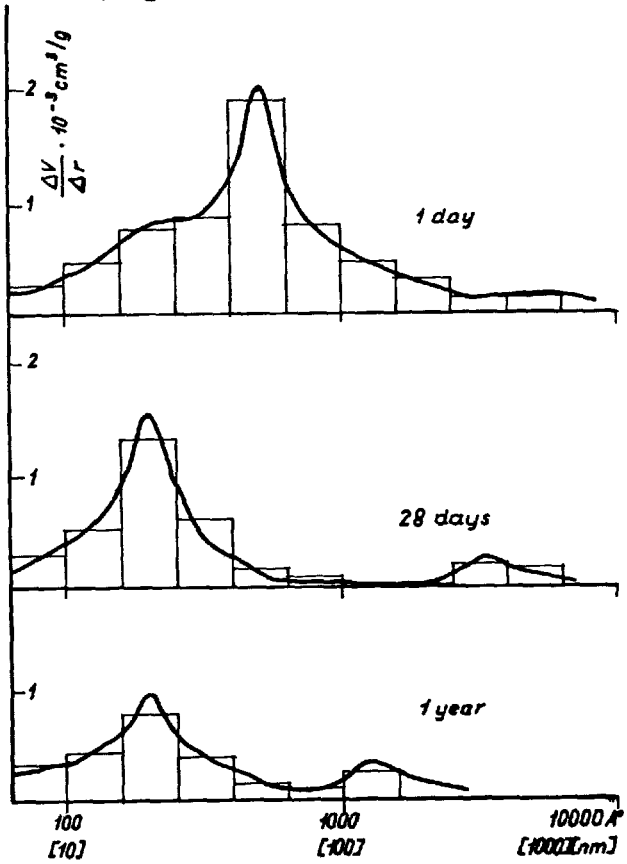

Fig.2 - Pore size distribution curves of a Portland cement after curing in water for a/ 1 day; b/ 28 days; c/ 1 year

On the differential pore size distribution curves of the cements stored in water two peaks of pore size frequency can be identified the position of which is shifted towards smaller pore diameters with the progress of the hydration. The phenomenon can be so interpreted that the location of the peak corresponding to the larger pore radii represents the average distance between the individual cement particles which decreases with the new formations precipitating up on them as upon nucleation bases. The peak corresponding to the smaller pore radius represents the distance between the particles of the new formations and also decreases with the progress of the hydration accompanied with their growth.

Upon the effect of sulphate solution the change in the pore structure of various cements shows significant differences depending on their sulphate resistence/Fig.3/.

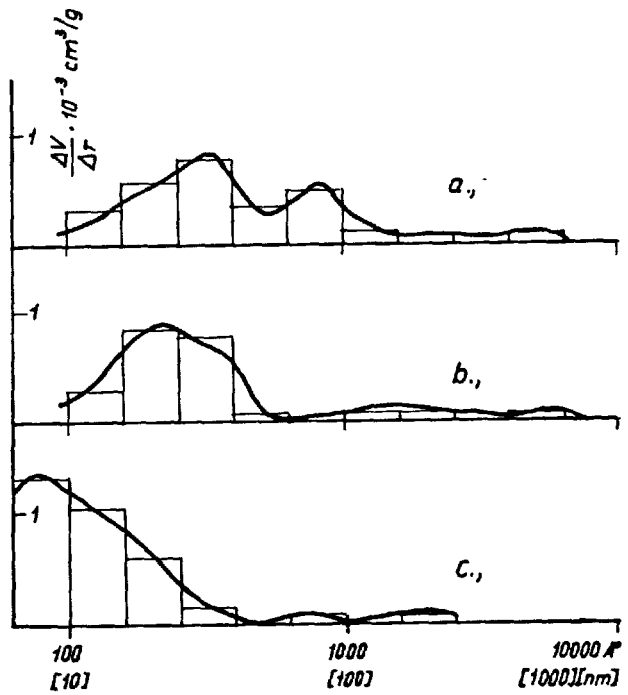

Fig.3 - Pore size distribution curves of various type cements after curing 14 days in water and further on in sulphate solution
a/ Portland cement; b/ Portland blastfurnace slag cement; c/ sulphate resistant cement

On the pore size distribution curves of the most sulphate resistant /Ferrari-type/ cements the peak corresponding to the larger pore radius decreases considerably while that one belonging to the pores of smaller diameters broadens remarkably. This phenomenon - although less definitely - can be observed for heterogeneous cements, too. At the same time it cannot at all be seen in the case of cements containing C_3A.

This shows that in cements of higher sulphate resistance the primary sulphate hydrates due to the change in the concentration relations and to the more free migration of ions, are formed in larger pores thus increasing the density. In less sulphate resistant cements, however, the dominant part of the secondary sulphate hydrates are formed in the smaller pores among the previously developed hydrate compounds. As far as these

smaller pores contain oversaturated solutions the process due to the hindered diffusion takes place much more localizedly /a "quasi topochemical process"/. This causes expansion and cracking while the pores of large size are preserved, so in case of Ferrari type cements the formation of secondary sulphate hydrates is hindered by the slower dissolution of Al_2O_3 while for heterogeneous cements - by the lower concentration of calcium ions.

These regularities, however, bear only of tendencious character and due to differences in production technologics there are significant variations even in the sulphate resistance of identical type cements. Therefore the solution prescribing the application of certain type cements at places of sulphate corrosion danger cannot be regarded as safe. It would be necessary to determine the effective sulphate resistance of the cements by testing. That is why we have dealt in detail with the problems of testing the sulphate resistance of cements too.

ELABORATION OF A NEW METHOD FOR TESTING THE SULPHATE RESISTANCE OF CEMENTS

The numerous known testing methods may, on the base of qualifying parameters, be classified into three groups. These are methods based on:

- chemical analysis
- the measurement of changes in the length of specimens /with supplementary gypsum addition or without it/
- the measurement of the changes in the strength of specimens

The most important methods were controlled by laboratory experiments. The results are summarized in the following:

The methods based on chemical analysis may at most be only informatory.

The methods testing the decrease in strength are on the one hand very time-consuming /although the modification - elevation of the temperature of the sulphate solution - suggested by Mehta and Gjorv/8/ may help in this/, on the other hand the opposite /porosity-decreasing and expanding/ effects of the volume growth of the solid phases make, in the initial one-two months, the results uncertain.

Among the methods based on measuring the expansion the main shortcoming of the methods using gypsum-overdosage is that they under estimate the sulphate-resistance of the cements containing hydraulic admixtures. Moreover, these methods characterize rather the tendency of the cement to gypsum expansion than its sulphate resistance.
By methods without gypsum-overdosage even after a relatively long time cannot be achieved such big variations in the expansion of the different type cements that would enable a reliable evaluation. For these reasons we attempted to elaborate a more rapid and more sensible method.

In this work we started from the following considerations:

- the new method should fit well to the standard prescriptions of the physico-mechanical testing of cements;
- the size of the specimens should not be too small in order to diminish the standard deviation of results but it should have the largest possible surface-volume ratio and a porous structure in order to secure the better sulphate effect;
- the sulphate resistance of the cement should be evaluated through the expansion value.

In developing the new method we set out from the Locher-method /15/ since it contained some elements of the above requirements. /The essence of it is that test specimens of 10x40x160 mm size made of standard cement mortar are at first stored in water for 14 days and then transferred into a 4,4% sulphate solution, the sulphate resistance being estimated on the base of the expansion measured at the age of 56 days./
With the intention to accelerate the method and to improve its sensitivity we applied

- steam-curing for the pre-hardening of the specimens and
- standard sand of incomplete granulometry for preparing the specimens in order to increase their porosity.

Concerning steam-curing a worry may rise that compared with hardening at normal temperature in this case a cement stone of different phase composition and texture may form, that may influence the sulphate corrosion, too. On the other hand, however, it should be taken into account that a large amount of steam-cured concrete is also being exposed to sulphate effect and to determine their corrosion resistance just such a method is expected to give adequate results.

The phase composition investigations proved, in agreement with other authors /17,18/ that regarding the composition of the hydrate phases formed there is no significant difference between the two ways of hardening.

Further, the textural investigations /Fig.4/ proved that among the steam-curing parameters /75; 85; 95° and 2; 4 and 24 hours/ the curing at 85°C for 2 hours ensures a pore structure most similar to that developed at normal temperature /see curves a/ and b/ in Fig.2/.

Fig.5 shows the influence of the hardening parameters upon the sulphate expansion of a cement. It can be seen that by a properly choosen steam curing /85°C, 2 hours/ the absolute value of expansion can be considerably increased as compared to that after a two-week pre-hardening at normal temperature. This makes the evaluation easier and improves the reliability of the testing method.
The density of the specimens was decreased in such a way that - preserving the 1:3 cement/sand ratio - the fine fraction of the three ones of sand was omitted.

Results here not cited show that incomplete granulometry itself does not cause a significant change if the pre-hardening takes

place

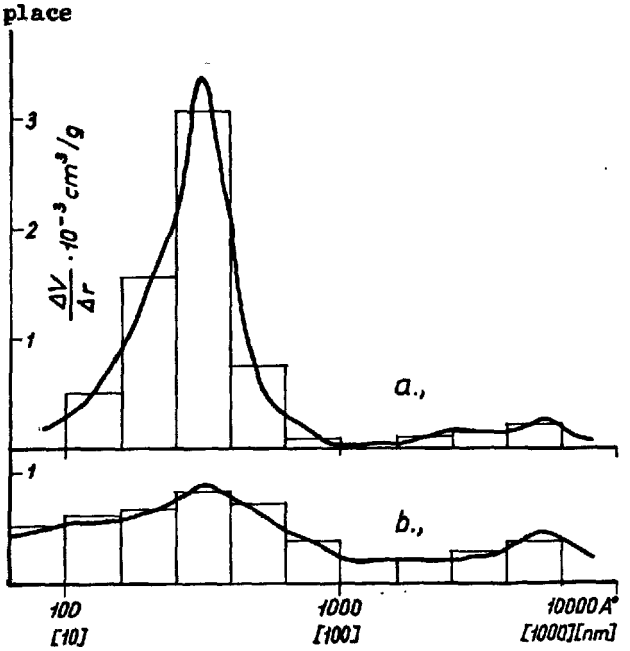

Fig.4 - Pore size distribution curves of a Portland cement after steam-curing for a/ 2 hours at 85°C b/ 24 hours at 85°C

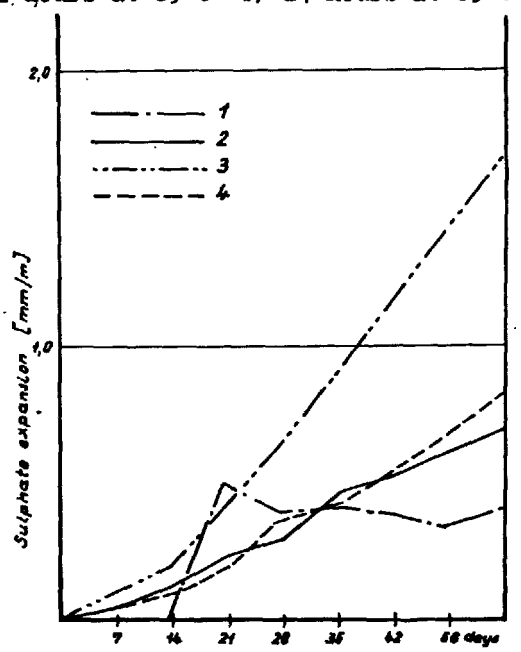

Fig.5 - Sulphate expansion of Portland cement specimens cured in water for 14 days/1/ and steam-cured for 24 hours at 75°C /2/, 2 hours /3/ and 4 hours /4/ at 85°C

place at normal temperature. At the same time its simultaneous application together with pre-hardening by steam-curing results in a manifold increase of the expansion value.
Fig.6 proves that the sequence of sulphate

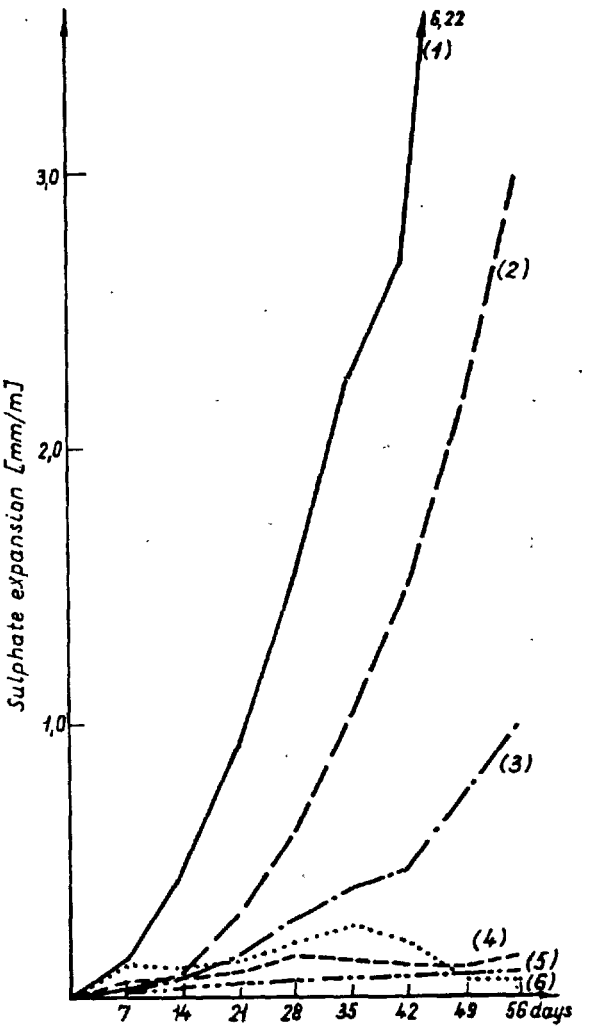

Fig.6 - Sulphate expansion of various type cements by the new method
1 - Portland cement; 2 - Portland blasfurnace slag cement; 3 - Portland fly ash cement; 4 - moderate sulphate resistant cement 5 and 6 - sulphate resistant cements

resistance of various cements as tested by the new method is in good agreement with the practical experience and the results got by the Locher method, the difference being in the much higher expansion values of the individual cements considerably exceeding the error limit of the measurement.

Reproducibility tests were conducted in our institute as well as by some home and foreign institutions. The reassuring results made it possible to publish the method in the "Technical Prescriptions" /19/ organically fitted into the Hungarian Standard series for cement testing.

Concerning the sulphate resistance of the main Hungarian cement types on the base of

Fig.6 it can be stated that as it was expected, the most sulphate resistant one is the Ferrari type cement not containing C_3A and the less resistant the pure Portland cement of high C_3A content.

It is noteworthy from the point of effective covering the demands on sulphate resistant cements that the expansion practically does not increase remarkably up to an AM value of about 1,2 on the one hand and that the sulphate resistance of heterogeneous cements, including fly ash cements, is also considerable on the other.

However, as it has been pointed out, reliable meeting the requirements in sulphate resistant cements is only possible on the base of factual testing. This became practicable due to the relative rapidity /28 days/ of the suggested new method.

On the base of the experiences and results got thus far a prescription was elaborated in which the selection of cements applicable in subsoil waters of different sulphate concentration is based up on the chemical and physical composition /aluminate module, C_3A-content/ of the cement but upon the sulphate expansion determined by our method.

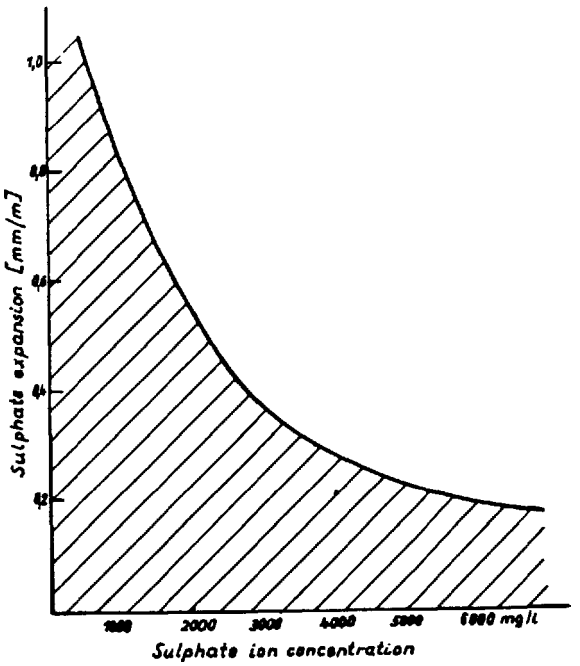

Fig.7 - Diagram for the determination of the applicability of cements in sulphate containing waters of various concentration based on their expansion as tested by the new method

Fig.7 shows the permissible sulphate ion concentrations as a function of the 28 days swelling value.
This solution gives the possibility to exclude the cements of although appropriate chemical composition but of poor sulphate resistance /due to some production technological causes/ and to utilize the cements having a less advantageous chemical composition but showing better sulphate resistance as determined by our method. Such a practice enables the more secure and more economic covering the demands on sulphate resistant cements.

LITERATURE

1.- LE CHATELIER /1898/ Bull.Soc. d'Encouragement

2.- H.KÜHL /1952/ Zement Chemie, Berlin

3.- T.THORWALDSON /1952/ Symp.Chem.Eng. London

4.- H.LAFUMA /1932/ Recherches sur les... Paris

5.- F.E.JONES /1938/ Symp.Chem.Cem., Stockholm

6.- A.F.POLAK /1966/ The hardening of binding materials composed of one mineral, Stroizdat, Moscow /in Russian/

7.- T.Ju.LJUBIMOVA,P.A.REBINDER /1971/ Dokl. Acad.Nauk.SSSR,Vol.200,No.3.,p.657 /in Russian/

8.- P.K.MEHTA, O.E.GJORV /1974/ J.of Testing and Evaluation,2, 6

9.- F.FERRARI /1940/ Tonindustrie Zeitung 58, p.636

10- F.FERRARI /1941/ Tonindustrie Zeitung 59, p.533

11- J.TALABÉR /1956/ Építőanyag, 8, p.5 /in Hungarian/

12- C.D.LAWRENCE /1977/ Yearbook of the Cement and Concrete Association

13- T.C.POWERS, T.L.BROWNYARD /1947/ J.Am. Conc.Inst.Proceedings, 43.,

14- W.J.DUCKWORTH /1953/ J.Am.Ceram.Society, 36

15- I. MEDGYESI /1977/ Cand. Dissertation /Theses/ Hung.Acad.Sci.,Budapest

16- I. MEDGYESI, L. AMRICH /1977-1978/ Építőanyag, Vol.29-30, No.12-1, pp.504-510 and pp.19-25 /in Hungarian/

17- S. MIRONOV, L. MALININA /1964/ Accelerating the setting of concretes, Stroizdat, Moscow, /in Russian/

18- G. KALOUSEK, F. ADAMS /1953/, J.Am.Concr Inst., p.23.

19- Technical Prescriptions No. MI-523/8 /1979/, Budapest /in Hungarian/

Effects of Raw Materials and Addition of Alkali on the Hydrothermal Reaction in Quartz and Lime System

Influence des matières premières et d'une addition d'alcali sur la réaction hydrothermique entre quartz et chaux

K. ASAGA, Dr. Research Associate,
M. DAIMON, Dr. Associate Professor,
S. GOTO, Dr. Research Associate,
R. KONDO, Dr. Professor,
Dept. of Inorganic Materials, Tokyo Institute of Technology, Japan.

RESUME : Cette étude concerne la synthèse de cristaux aciculaires ou fibreux d'hydrates et de silicates de calcium par le traitement hydrothermique d'un ensemble quartz-chaux. Dans cette synthèse, il est nécessaire de diriger la solubilité et la vitesse de dissolution des matières premières.
L'étude a été exécutée à 150°C-210°C, employant $CaCO_3$, $Ca(OH)_2$, et SiO_2 comme matières premières et des alcalis comme additifs.

La solubilité et la vitesse de dissolution de la chaux ont diminué quand on a employé $CaCO_3$ et $Ca(OH)_2$ avec des additifs alcalins.

Par contre, la solubilité et la vitesse de dissolution de SiO_2 ont augmenté avec l'addition d'alcalis. Ces additifs alcalins ont aussi affecté la stabilité des hydrates.

Dans le système $Ca(OH)_2$ - SiO_2 - NaOH, un cristal aciculaire de pectlite a été formé. Dans le système $Ca(OH)_2$ - SiO_2 - KOH, la tobermorite est devenue stable en augmentant la concentration en KOH, même à température élevée, et la proportion molaire Ca/Si des matières premières s'est étendue. On a obtenu des cristaux de tobermorite longs et fibreux de 200 µm de longueur dans le système $CaCO_3$ - SiO_2 - KOH; et on a observé un cristal aciculaire non identifié, mais semblable à un zéolite dans le système $CaCO_3$ - SiO_2 - K_2CO_3.

SUMMARY : This study concerned with the synthesis of needle or fibrous crystals of calcium silicate hydrates by hydrothermal reaction. In the synthesis of these fibrous crystals, it is very necessary to control the solubility and the rate of solution of raw materials. The study was carried out at 150°-210°C using $CaCO_3$, $Ca(OH)_2$ and SiO_2 as raw materials and alkalis as additives.

The solubility and rate of solution of lime when using $CaCO_3$ and $Ca(OH)_2$ with alkaline additives decreased.

On the other hand the solubility and rate of solution of SiO_2 increased by the addition of alkalis. Alkaline additives also affected the stability of hydrates.

In the system $Ca(OH)_2$ - SiO_2 - NaOH, needle crystal of pectlite was formed. In the system $Ca(OH)_2$ - SiO_2 - KOH, tobermorite became stable with the increase of KOH concentration at higher temperatures and wider Ca/Si molar ratio of raw materials. Very long fibrous tobermorite of about 200 µm in length was obtained in the system $CaCO_3$ - SiO_2 - KOH and also unidentified but zeolite-like needle crystal was observed in the system $CaCO_3$ - SiO_2 - K_2CO_3.

INTRODUCTION

Asbestos have long been used as the alkali resistive fiber in many building materials, but it is going to be difficult to use a large quantity because of the shortage of resources and injuary to human body. It will be nessesary to develop the new alkali resistive fiber instead of asbestos. Tobermorite and xonotolite are the tipical fibrous or needle hydrates obtained from hydrothermal reaction in the system of silica and lime, and have been studied from the view points of phase equiribium, crystal chemistry and kinetics of reaction (1, 2, 3, 4, 5). It is necessary to control the solubility and the rate of dissolution of raw materials, in order to synthesyse these fibrous crystals.

It is effective to use the additives to control the solubility of raw materials. The effects of aluminum ion have recently been clearifed (2, 4, 5, 7, 8, 9). There were also lots of studies on the effects of alkalis (6, 10, 11, 12, 13). But the role of those additives has not been discussed precisely. In addition to these studies, products and reaction rate were investigated by using the various kind of silica and lime materials (2, 14, 15). But there were very few studies using $CaCO_3$ as raw materials because of the very low solubility.

In the present study, the effect of various alkalis on the hydrothermal reactions in the $Ca(OH)_2$ or $CaCO_3$-SiO_2-H_2O system, and the reactivity of $CaCO_3$ were systematically studied. And the synthesis of needle or fibrous crystals was attempt in the above hydrothermal system.

EXPERIMENTAL PROCEDURES

Quartz, with the particle diameters of 6-10μm and 10-20μm, $Ca(OH)_2$ and $CaCO_3$ were used as the raw materials. LiOH, NaOH, KOH, K_2CO_3 and Na_2CO_3 solutions were used as the alkali resorces. 1-4g of raw mixes, with the Ca/Si ratio of 0.6-1.2, and water or alkali solutions were thoroughly mixed to having the w/c ratio between 10 and 40. Then they were processed at 150-210°C, for 1-10 days in the 60ml autoclave rotated at 25rpm. The products were dried at 110°C and examined by X-RD, SEM, TG-DTA and so on.

The solubility of SiO_2, $Ca(OH)_2$ and $CaCO_3$ was measured by colorimetric and atomic absorption.

RESULTS AND DISCUSSION

$Ca(OH)_2$ - SiO_2 - alkali system

Unreacted $Ca(OH)_2$ and SiO_2 were not detected by X-RD, in the alkali free system when processed at 180°C and 210°C for 3-10 days. Tobermorite was produced at c/s = 0.8, and xonotolite at c/s = 1.0, 1.2. These results agreed with the Kondo(2) and Taylor(1).

(1) $Ca(OH)_2$ - SiO_2 - NaOH, Na_2CO_3 system

Pectolite was produced in 1 N NaOH at 180°C or 0.15 N NaOH at 210°C. The range of pectolite formation was agreed with the results of Blakman(12) and Nelson(13). Pectolite was formed as needle crystals simillar to xonotolite with maximum length 150μm. The pectolite crystal seemed to grow larger than that of xonotlite. The same results were obtained when Na_2CO_3 was used instead of NaOH.

(2) $Ca(OH)_2$ - SiO_2 - KOH, K_2CO_3 system

The results in this system were very different from the Na containing system, and tobermorite or xonotlite were obtained. Fig.1 shows the products after 3-10 days reaction in the presence of KOH. The unreacted $Ca(OH)_2$ and SiO_2 were also not detected by X-RD. The conditions of the formation of tobermorite and xonotlite did not differ from alkali free system when KOH concentration was lower than 0.3 N. But at heigh KOH concentration, the formation of tobermorite was extended to the range of higher c/s and higher temperature. These tobermorite had the lath shape and grew larger than those in alkali free system, as shown in Fig.2

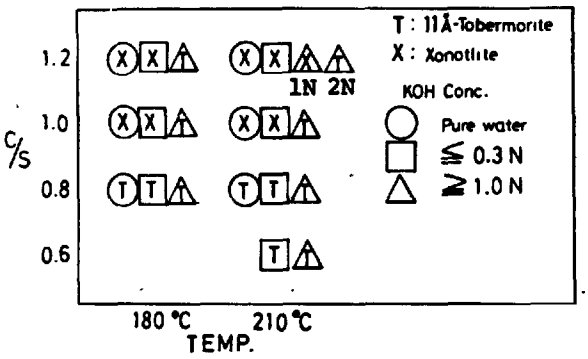

Fig. 1 - Reaction products of the $Ca(OH)_2$-SiO_2 - KOH system after treated for 3-10 days

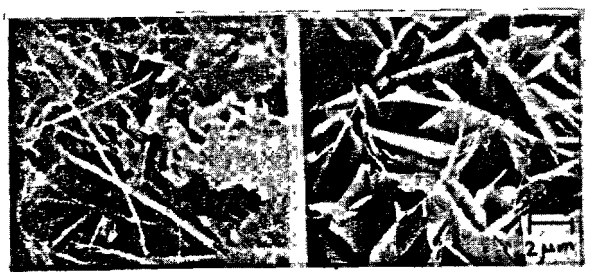

alkali free 1N KOH

Fig. 2 - The SEM photographs of the tobermorite c/s = 0.8, 180°C, 5 days

X-RD pattern had more sharp peak, and the peak of (400, 008) separated to (400) and (008). These results suggested that KOH increased the crystalinity of tobermorite and retarded the transformation to xonotlite.

Fig.3 shows the change in the values of d(hlℓ), (220), (400), (008) of tobermorite with the concentration of KOH.

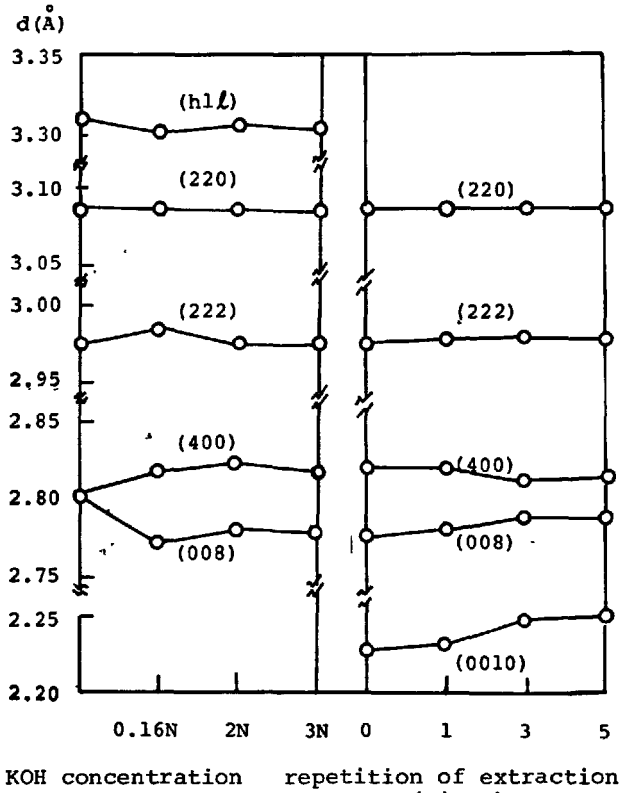

Fig. 3 - Changes in the d(h.k.l) of the tobermorite with concentration of KOH; 180°C, 3 days. and Changes in the d(h.k.l) of the tobermorite obtained at 1 N KOH, with the washed with water.

The peak near the 2.80Å separated into 2 peakes, and the values of d(400) became larger, the values of d(008) became smaller. The values d(002) and (0010) became smaller too. However the other values did not change largely. Accordingly, K^+ ions seemed to exist in the interlayer spaces of the tobermorite. The values of d(008) did not change with concentration of KOH, suggesting the limited amount of K^+ ions, which could enter between tobermorite layers.

The values of d(008) became larger, when the tobermorite was washed with distild water, and (400) peak and (008) peak became nearly one peak as shown in Fig.3. K^+ ions were liberated into the washed water. It was suggested that the K^+ ions exsisted in the interlayer spaces of the tobermorite were loosely bounded and easily dissolved.

(3) $Ca(OH)_2$ - SiO_2 - mixed alkali system

Fig.4 (a) shows the products obtained by reaction at 180°C for 3 days, in the mixed alkali solutions. The total alkali concentration was 1 N, and c/s and w/s were 0.8 and 20. Tobermorite and pectolite coexisted at the condition of KOH : NaOH = 0.2 : 0.8, K_2CO_3 : Na_2CO_3 = 0.2 : 0.8. At the heigher concentration of KOH or K_2CO_3, tobermorite was the only product. Pectolite was produced as increasing the Na^+ ion concentration without effected from the KOH.

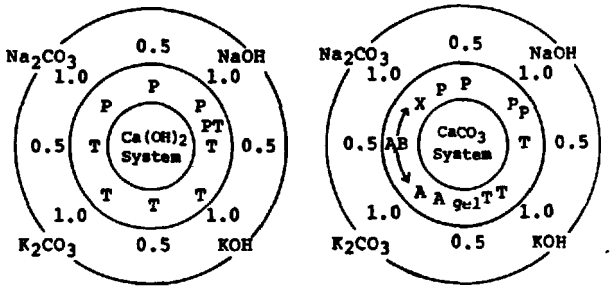

T; tobermorite
A; AB; needle crystal
X; not reacted

Fig. 4 - Reaction products of the $Ca(OH)_2$, $CaCO_3$ - mixed alkali solution system, c/s = 0.8. concentration of alkali 1 N, 180°C, 3 days.

(4) $Ca(OH)_2$ - SiO_2 - LiOH system

The reaction with LiOH was very different. Considarable amounts of unreacted $Ca(OH)_2$ and SiO_2 were observed, and Li_2SiO_3 was obtained as the products and no hydrate was detected by X-RD. Fig.5 shows the S.E.M. microphotograph of the sample treated at 180 °C for 3 days.

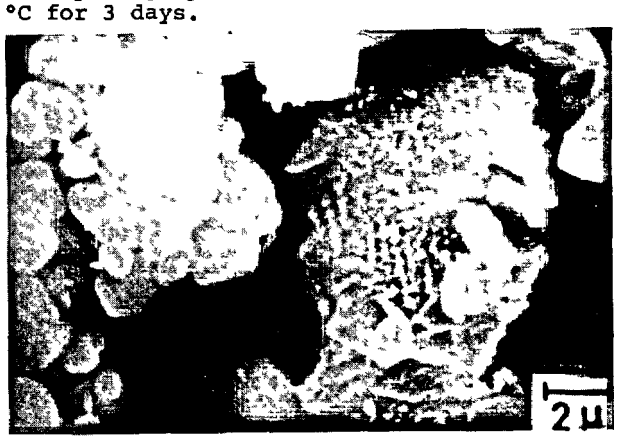

Fig. 5 - Reaction products of the $Ca(OH)_2$ - SiO_2 - LiO_2 system; c/s = 0.8, 1 N LiOH, 180 °C, 3 days.

The prasmatic or polyhedronic crystals of Li_2SiO_3 were observed, but lath or fibrous crystals did not exist in the samples. Lots of quartz particles were covered with small dense products which seemed to retard the reaction.

3 - 2 $CaCO_3$ - SiO_2 - Alkali system

No products was obtained, in the systems of $CaCO_3$ - SiO_2 and $CaCO_3$ - KOH, at 180°C for 5 days.

(1) $CaCO_3$ - SiO_2 -KOH system

The experiments were carried out in 0.5 N - 2 N KOH solution at 150-210°C for 3-10 days. The unreacted or unsoluble SiO_2 was not detected, but unreacted $CaCO_3$ was observed in the all experiments. The only products was the tobermorite except the case of 0.5 N KOH, where the gel products were obtained. These tobermorite crystals had the same character as the products in $Ca(OH)_2$ - SiO_2 - KOH system. Fig.6 shows the change in the morphology of the products. The morphology of the tobermorote changed from lath to fibrous crystal with the processing time.

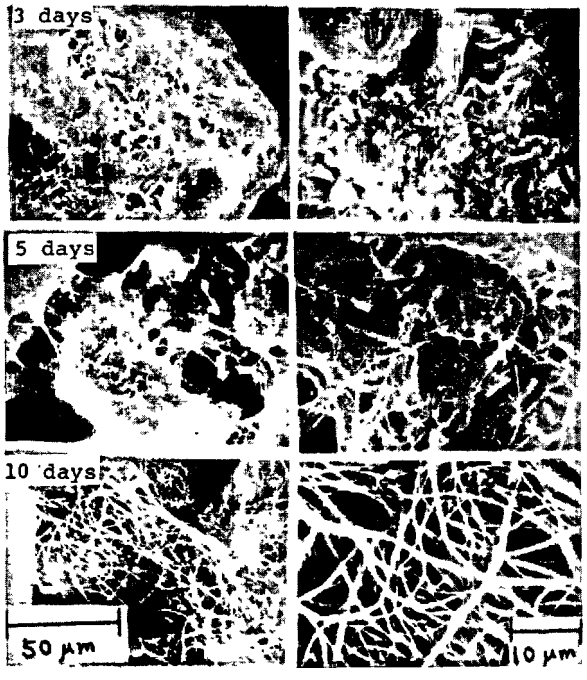

Fig. 6 - Change in the morphology of the products in the $CaCO_3$ - SiO_2 - KOH system; c/s = 0.8, 1 N KOH, 180°C.

Fig.7 shows the long fibrous tobermorite with the length of 200μm. The mix with c/s = 0.8 was treated in 2 N KOH solution at 180°C for 10 days.

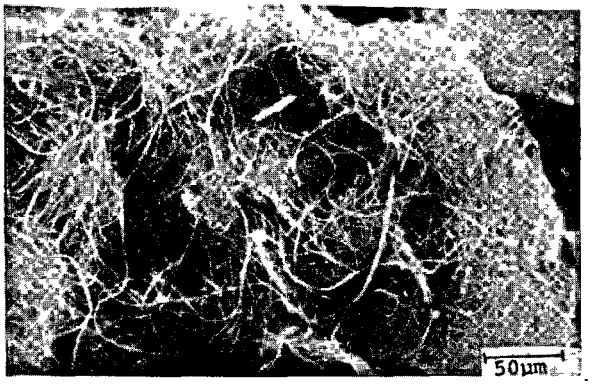

Fig. 7 - SEM photograph of the long fibrous tobermorite; c/s = 0.8, 2 N KOH, 180°C, 10 days.

Fig.8 shows the changes in the amounts of reacted $CaCO_3$ with the concentration of KOH. The amounts of reacted $CaCO_3$ were measured from weight loss by T.G. The reaction rate of $CaCO_3$ increased with the increasing KOH concentration. About 80% of the $CaCO_3$ was reacted at the 2 N KOH within 3 days, but reaction did not proceed over 85% even after 10 days. It seemed to be difficult to react untill the $CaCO_3$ was completly consumed.

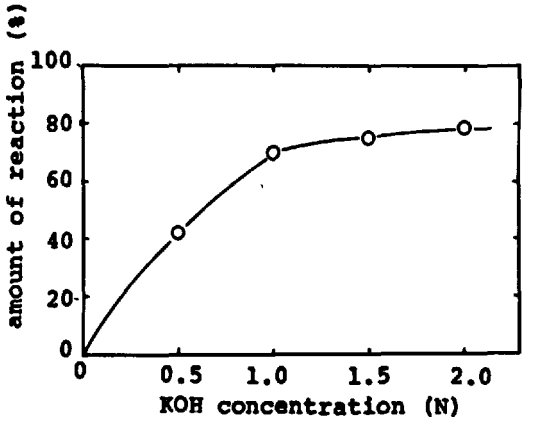

Fig. 8 - Changes in the amounts of reacted $CaCO_3$ with the concentration of KOH; c/s = 0.8, 180°C, 3 days.

Fig.9 shows the change in SiO_2 and CaO concentration of solution with the processing time, in the system $CaCO_3$ - SiO_2 - KOH. The methods of measurement was mentioned in the previous paper (16). The concentration of SiO_2 was about 2g/l at 6hr of proceeding time and did not change largely as the time proceeded. This concentration was much larger

than that case without alkali. On the other hand, the concentration of CaO increased slowly as the time proceeded, and kept almost constant at about 0.3mg/l after 3 days, which was extremely smaller than the SiO_2 concentration.

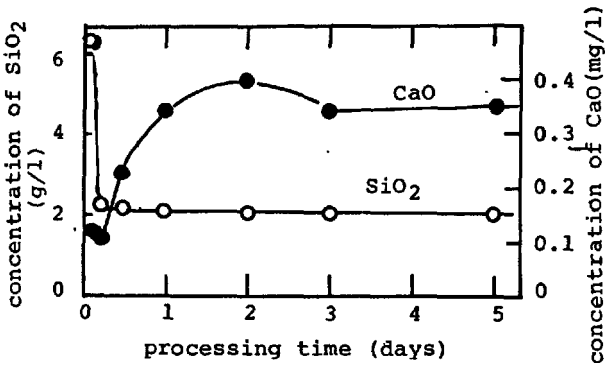

Fig. 9 - Changes in SiO_2 and CaO concentration of the solution in the $CaCO_3$ - SiO_2 - KOH system with the processing time, c/s = 0.8, 180°C, 3 days.

Tobermorite grew surrounding the $CaCO_3$ particles and detected by X-RD after 1hr. The crystalization of tobermorite was more rapid than the case of $Ca(OH)_2$ - SiO_2 - KOH system. α- C_2SH or C-S-H grew the SiO_2 particles in the $Ca(OH)_2$ - SiO_2 - KOH, in which concentration of CaO was larger than that of SiO_2 at early stages. The reaction products should grow surrounding the particles having relatively smaller solubility. These results suggest the reaction mechanisms of this system should be as follows. At first, SiO_2 was dissolved by KOH, and the concentration of SiO_2 increased. Then SiO_2 reacted with $CaCO_3$ producting the tobermorite around the $CaCO_3$ particles. The reaction began retarded when product layer became thick.

(2) $CaCO_3$ - SiO_2 - K_2CO_3 system

The reaction was carried out at 150-210°C for 3-5 days, with c/s = 0.5-1.0, w/s = 20 and 1-4 N K_2CO_3. Needle shaped crystals are shown in Fig.9. $CaCO_3$ but no SiO_2 was observed in all samples. The crystal sizes were about 50-200 μm in length. From the results of the D.T.A, T.G, IR, X-RD and chemical snalysis, the chemical composition of this crystal was found to be $K_2O{\cdot}2CaO{\cdot}10SiO_2{\cdot}6H_2O$. And it was dehydrated with 2 steps at 195-380°C. This was supposed to be a new compound which sould be similar to some kind of zeolites such as rhodesite [$KNaCa_2(H_2Si_8)5H_2O$] or mountenite [$KNaCa_2(HSi_8O_2)5H_2O$].

No reaction product was observed in the system of $CaCO_3$ - SiO_2 - Na_2CO_3 at 150°C-210°C

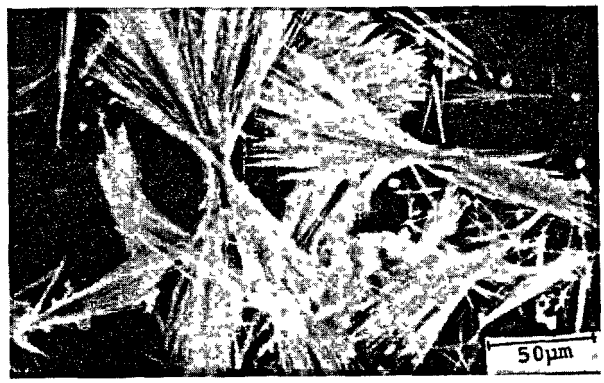

Fig. 10 - SEM photograph of the needle crystal produced in the $CaCO_3$ - SiO_2 - K_2CO_3 system; c/s = 0.8. 2 N K_2CO_3 180°C, 3 days.

(3) $CaCO_3$ - SiO_2 - mix alkali system

Fig.3 (b) shows the products obtained by the reaction of the mixture of 1 N alkali at 180°C for 3 days. Where, A is the needle crystal above mentioned, AB is the needle cristal had the slitly different X ray pattern, which could not be identified whether it was consisted only one crystal or mixture of two crystals. Tobermorite and these needle crystals were not produced together at the same time, and no crystal but gel material was observed at the condition of KOH : K_2CO_3 = 0.5 : 0.5. Comparing the results of $Ca(OH)_2$ and $CaCO_3$ system, tobermorite and pectlite were produced when either alkali or calucium resorces was the carbonate, however needle crystals were only produced when both alkali and calcium resorces were carbonate and the solution had to include K^+ ions.

The precise reaction mechanism could not be discussed by these results but the role of CO_3 was very significant and interesting, in spite of CO_3 was not included in both the products as tobermorite and the needle crystals.

CONCLUSION

The hydrothermal reactions in $Ca(OH)_2$ - SiO_2 and $CaCO_3$ - SiO_2 system were studied at 150-210°C using various kind of alkali solutions. Pectolite was produced, in the $Ca(OH)_2$ - SiO_2 system at 180°C with 1 N NaOH or Na_2CO_3, or at 210°C. When the concentration of NaOH or Na_2CO_3 was higher than 0.1 N. The pectolite was needle or fibrous crystal with maximum length of 150μm. Tobermorite and xonotolite were produced in the $Ca(OH)_2$ - SiO_2 system treated with KOH or K_2CO_3. Tobermorite became stable with increase of KOH or K_2CO_3 concentration at high temperature and wide c/s ratio of raw materials. No hydroration product but

Li_2SiO_3 was obtained in the presence of LiOH.

The tobermorite obtained in the presence of KOH or K_2CO_3 contained K^+ ions in the interlayer space. X-RD pattern of (400) and (008) peakes separated. The interlayer distance was 11.15Å which was slightly smaller than that of usual tobermorite, and easily shifted to usual distance by dissolving the K^+ ions from the interlayer site when samples were washed with water. The thermal analysis suggested that it was anomalous type.

No reaction was observed without alkali, in the $CaCO_3$ - SiO_2 - system, but about 80% of $CaCO_3$ reacted within 3 days in the presence of 1 N KOH. The same products in the case of the $Ca(OH)_2$ system were obtained with NaOH, KOH and LiOH, which were pectolite, tobermorite and xonotorite, and Li_2SiO_3 respectively. These hydrates seemed to be grown longer compaired with $Ca(OH)_2$ system. The long fibrous tobermorite with the length of 200μm was obtained in the presence of 1 N KOH. In this system the solubility of $CaCO_3$ and SiO_2 were about 0.3 mg/l and 2g/l respectively. A new compound of needle shaped crystal the chemical composition of $K_2O \cdot 2CaO \cdot 10SiO_2 \cdot 6H_2O$ was obtained in the presence of K_2CO_3. The long needle crystal with 150μm with length was obtained. This needle crystals were obtained only when both of alkali and Calcium resorces were carbonate, and the solution had to include the K^+ ions.

REFERENCES

1.- H.W.F. Tayler (1968), "The Calcium Silicate Hydrate", Proc. 5th. Int'l. Symp. Chem. Cement, Tokyo., 2, 1-26.

2.- R. Kondo (1965), "Kinetics Study on Hydrothermal Reaction between Lime and Silica", Proc. Symp. Autoclaved Calcium Silicate Building Products, 92-97.

3.- R. Kondo, K. Lee and M. Daimon (1976), "Kinetics and Mechanism of Hydrothermal Reaction in Lime - Quartz - Water System" (In Japanese), Yogyo Kyokai-shi, 84, 573-578.

4.- K. Lee, M. Daimon, K. Asaga, T. Nishikawa, and S. Goto (1977), "Role of the Microstructure of Reaction Products on Hydrothermal Reaction Rate in Lime - Quartz - Water System" (In Japanese), Yogyo Kyokai -shi, 85, 14-19.

5.- C.F. Chan, M. Sakiyama and T. Mitsuda (1978), "Formation of 11Å Tobermorite from Mixture of Lime and Colloidal Silica with Quartz", Cement and Concrete Research, 8, 135-138.

6.- R. Kondo, S. Ohsawa, H. Matsumaru, M. Kitamura and T. Kato (1967), "The Hydrothermal Reactions between Lime and Siliceous Materials" (In Japanese), Cement Gijutsu Nenpo, 21, 92-100.

7.- R. Kondo, S.A.Abo-El-Enein and M. Daimon (1975), "Kinetics nad Mechanism of Hydrothermal Reaction of Granulated Blast Furnace Slag", Bul. Chem. Soc. Japan, 48, 222-226.

8.- S.A.Abo-El-Enein, R.Sh. Mikahail, M. Daimon and R. Kondo (1978), "Surface Area and Pore Structure of Hydrothermal Reaction Products of Granulated Blast Furnace Slag", Cement and Concrete Res., 8, 151-160.

9.- S.A.S. El-Hemaly, T. Mitsuda, and H.F.W. Tayler (1977), "Synthesis of Normal and Anomalous Tobermorite", Ibid., 7, 429-438.

10.- T. Yoshii and G. Sudo (1959), "Effects of Na_2O on the Reaction of Calcium Silicate Hydrates" (In Japanese), Cement Gijutsu Nenpo, 13, 80-86.

11.- G. Unemi and K. Higaki (1968), "Effect of Alkali on the Character of Calcium Silicate Hydrate" (In Japanese), Cement Gijutsu Nenpo, 22, 83-88.

12.- E.A. Blakeman, J.A. Grad, C.G. Ramsay and H.F.W. Taylor (1974), " Studies on the System Sodium Oxide-Calcium Oxide-Silica-Water", J. Appl. Chem. & Biotech. 24, 239-245.

13.- E.B. Nelson and G.L. Kalousek (1977), "Effects of Na_2O on Calcium Silicate Hydrate at Elevated Temperature", Cement and Concrete Research, 7, 687-694.

14.- K. Suzuki, K. Asakawa, Y. Tuchida, S. Ito and K. Hukuo (1977), "Hydrothermal Reactivity of Powdered Quartz of Different Origins with Lime" (In Japanese), Yogyo Kyokai-shi, 85, 440-447.

15.- S.O. Oyefesobi and D.M. Roy (1976), "Hydrothermal Studies of Type V Cement-Quartz Mixes", Cement Concrete Research, 6, 803-810.

16. K. Lee, M. Shimura, M. Daimon and R. Kondo (1977), "Chemical Composition of Solution in Hydrothermal Reaction of Lime-Quartz-Water System" (In Japanese), Yogyo Kyokai-shi, 85, 282-286.

Volume Instability of Porous Solids : Part I

Instabilité en volume de solides poreux

G.G. LITVAN (Senior Research Officer),
Division of Building Research, National Research Council of Canada, Ottawa, Ontario, Canada.

RESUME : L'adsorption de NO_3Na en solution aqueuse fait subir à un verre poreux de silice saturé d'eau une variation de longueur de 27×10^{-5}. L'échantillon a subi une variation irréversible de longueur de 50×10^{-5} $\Delta\ell/\ell$. L'isotherme ressemble beaucoup à celle obtenue pour l'adsorption de la vapeur d'eau par le verre sec et présente une hystérésis sur l'ensemble des concentrations. L'expansion de 325×10^{-5} $\Delta\ell/\ell$ a été trouvé, lors de l'attaque du verre poreux par NaOH 0.2 N; et un changement de longueur de 125×10^{-5} $\Delta\ell/\ell$ a eu lieu durant la dissolution en $C\ell H$ 1.0 N d'un échantillon de ciment hydraté (e/c = 0.6).

Lorsqu'on a lessivé la chaux d'une pâte de ciment (e/c = 0.6) avec du glycol d'éthylène, on a observé une variation de 120×10^{-5} $\Delta\ell/\ell$. Ces résultats introduisent une donnée additionnelle qui pourrait expliquer le processus de détérioration des solides poreux exposés à certains produits chimiques, par exemple l'attaque par le sulfate et par l'eau de mer, et la réaction alcali-agrégat.

SUMMARY: A 27×10^{-5} fractional length change occurred in a water-saturated porous silica glass on adsorption of $NaNO_3$ from aqueous solution. The specimen suffered a 50×10^{-5} $\Delta\ell|\ell$ irreversible length change after determination of the extension adsorption isotherm. The isotherm greatly resembles that obtained on water vapour adsorption by dry glass, and exhibits marked hysteresis in all concentration regions. An expansion of 325×10^{-5} $\Delta\ell|\ell$ was found while porous glass was under attack from 0.2 N NaOH; and 125×10^{-5} $\Delta\ell|\ell$ length change occurred during the dissolution in 1.0 N $HC\ell$ of a 0.5 W/C hydrated cement specimen. On leaching lime from 0.6 W/C cement paste with ethylene glycol, 120×10^{-5} $\Delta\ell|\ell$ was observed. These results introduce an additional factor that may explain the deterioration process of porous solids exposed to some chemicals, for example, in alkali aggregate reaction, sulfate attack and seawater attack.

INTRODUCTION

Mechanical breakdown is the most common and most important form of concrete deterioration usually associated with volume change. Several causes of volume change are known. Thermal expansion does not normally result in damage, but under certain conditions, as when large temperature gradients are created, it can be disruptive. Stresses, usually non-uniform in nature, are created by secondary effects of the temperature change, including change in moisture content and phase change.

By far the largest group of causes of excessive volume instability in concrete comprises phenomena involving chemical reactions. These may involve interaction of one or more constituents of the concrete, or some component or components of the concrete and a substance originating from the environment. Hydration during setting and alkali aggregate reaction are examples of the former; sulfate attack, carbonation, seawater attack, and corrosion of the reinforcing steel belong to the latter category. In characterizing these expansions Calleja (1) employs the terms intrinsic and extrinsic, depending on the type of reaction.

Examination of the pertinent literature makes it clear that the mechanism of expansion is far from understood, although the causal relation between volume instability and the chemical processes is well established. A review of alkali aggregate reaction by Diamond (2) clearly indicates that no consensus concerning the mechanism of expansion exists. Similarly, as discussed by Hansen (3), several explanations have been put forward with regard to sulfate attack. Mather too has stated (4) that in spite of extensive studies fundamental aspects of the sulfate attack on cement are poorly understood, including the relation between the physical properties of the material surrounding the newly formed hydrated sulfate and the amount of expansion, and the effect of restraint on expansion. Further work to elucidate the mechanism of expansion of hydrated cement paste due to chemical attack is warranted and desirable.

The present contribution deals with the dimensional changes of water-saturated porous solid in response to change in concentration of non-aggressive aqueous $NaNO_3$ solution with which it is in contact. In addition, length changes have been observed during leaching and dissolution.

EXPERIMENTAL

Dimensional changes were measured in a stainless steel cell (Fig.1). The 28 by 6 mm specimen (c) was clamped to the base (b) and connected to the transformer core (g) through a floating jaw (d) and extension rod (f). The Trans-tek #240 .000 linear variable differential transformer (h) was housed in a double-walled section of the cell so that temperature could be maintained to ±0.05°C with the aid of a Colora thermostated circulating pump.

The transformer, which has a ±1.27 mm working range with ±0.5% linearity, was supplied with 6 V dc from a Hewlett Packard Model 6102 power source (stability better than 0.01%).

Corning glass code 7930, porous 96% silica glass specimens were purified by continuous heating in air to 400°C. To restore the hydroxyl groups on the surface, specimens were stored for five days in simmering distilled water. Cement specimens were cut from a 31 mm diameter cylinder that had been cured in lime water for two years. The specimens, when placed in the cell, were fully saturated with water and care was taken to maintain this condition during the transfer procedure. After attainment of constant length (fluctuation less than $\pm 0.5 \times 10^{-5}$ $\Delta\ell/\ell$ in 24 h) water was replaced by the appropriate solution through the filling tube (e) with the aid of a syringe.

RESULTS

I. Length changes of the porous 96% silica glass (immersed in aqueous $NaNO_3$ solution) in response to a change in solute concentration are shown in Fig.2. The reference length, i.e., the origin of the plot, is the equilibrium state of the glass fully saturated with water. Its length is approximately 200×10^{-5} $\Delta\ell/\ell$ longer than in the dry state. Each point indicates constancy of dimensions attained in 14 days, on the average. The run, not yet complete, has lasted 254 days.

The shape of the adsorption branch of the isotherm resembles the well-known extension isotherm of the porous glass-water system (5,6), shown in Fig.3.

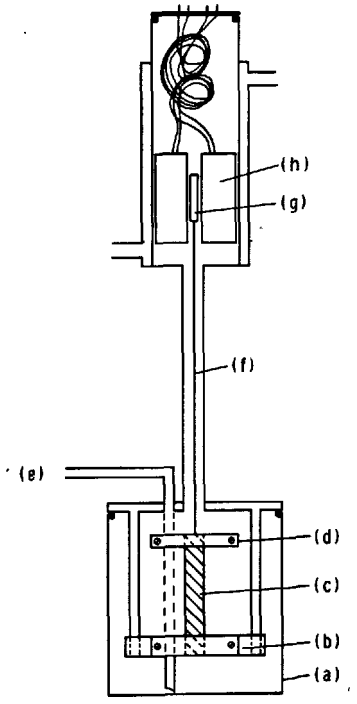

Fig.1 - Schematic diagram of extensometer. For explanation see text.

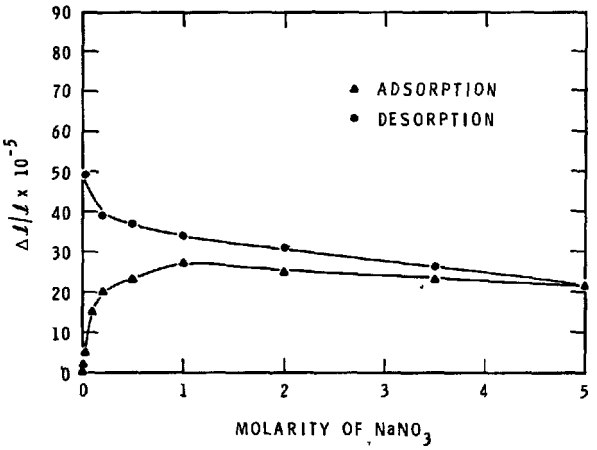

Fig.2 - Extension isotherm of the porous 96% silica glass - aqueous $NaNO_3$ solution system.

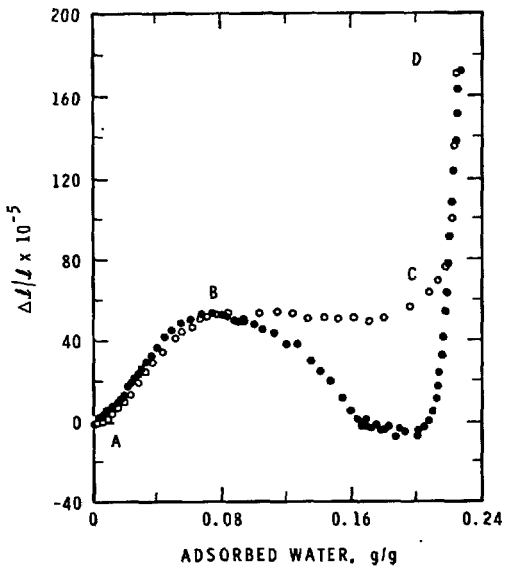

Fig.3 - Extension isotherm of the porous 96% silica glass-water system.

At low concentrations the curve for the $NaNO_3$-glass system rises rapidly to 27 x 10^{-5} $\Delta\ell/\ell$; at concentrations higher than 1 mole/ℓ it decreases slightly, but monotonously, reaching 21 x 10^{-5} $\Delta\ell/\ell$ at 5 molar concentration. This is the only major difference from the water extension isotherm (Fig.3), which undergoes a large expansion of approximately 100 x 10^{-5} $\Delta\ell/\ell$ in the final stages of saturation (i.e. between points C and D).

Amberg and McIntosh (5) attribute the expansion between C and D (Fig.3) to flattening of the menisci, increasing spreading force of the adsorbed film in filled pores, and further adsorption in wide channels. Because no menisci are present in adsorption from solution, no expansion at high concentrations is to be expected in the present experiments. Its absence supports the meniscus flattening hypothesis postulated for the vapour adsorption method.

The desorption branch of the $NaNO_3$-H_2O-glass system differs from that of the water-glass system in at least two major aspects: there is no contraction on diminishing saturation, and the volume changes are not reversible in any concentration region. Most significantly, hysteresis and continous expansion were observed on decreasing concentrations.

II. The dimensional changes observed during dissolution of porous glass in 0.2 N NaOH are shown in Fig.4. The 5 mm thick glass disintegrated in 82 h. Except for the last 3 min, the sample expanded continuously. The total fractional expansion was 326 x 10^{-5} $\Delta\ell/\ell$. Feldman and Sereda (7) reported expansion at a rapid but decreasing rate on treating porous silica glass with alkali, but their experiment was not carried to complete dissolution. The present findings appear to be consistent with the results obtained on leaching of sodium borosilicate glasses with sulfuric acid. Krasikov et al (8) found 0.16 to 0.2% expansion on complete leaching of 2 mm thick glass specimens. The observed 0.326% ultimate increase in length on dissolution of glass, though very substantial, is merely a fraction of that obtained in other similar experiments (to be reported elsewhere). The magnitude of expansion depends on several factors, but the weight of the extension rod and transformer core assembly in the present experimental arrangement is considered to have decreased it.

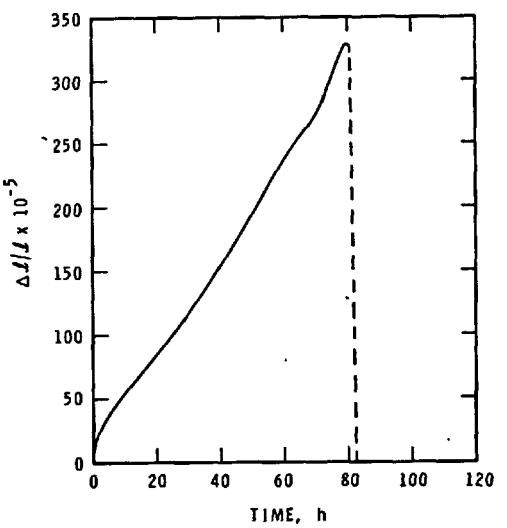

Fig.4 - Length changes of a porous 96% silica glass immersed in 0.2 N aqueous NaOH, as a function of time.

III. On immersion of a water-saturated hydrated cement paste specimen in aqueous 1.0 N HCℓ solution, monotonous expansion was observed until nearly complete disintegration. The dimensional change versus time of contact plot (Fig.5) is very similar to that of Fig.4, although there are some differences. The magnitude of the expansion is about one third that of the glass-NaOH system. The curve is slightly convex rather than somewhat concave, as in the previous case, and the dissolution occurred after 10.6 instead of 82 h of contact time.

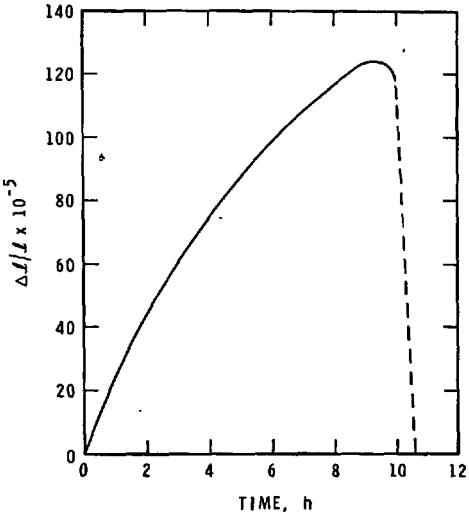

Fig.5 - Length changes of a hydrated cement paste specimen (W:C = 0.5), immersed in 1.0 N aqueous HCℓ, as a function of time.

IV. Calcium hydroxide can be leached from portland cement paste with ethylene-glycol (9). The concomitant length changes associated with leaching a water-saturated hydrated neat cement specimen (W:C = 0.6) are shown as a function of time in Fig.6.

An over-all expansion of 110 x 10^{-5} $\Delta\ell/\ell$, with respect to the fully water-saturated state, took place after approximately 800 h of leaching at room temperature.

An unusual feature of the curve is the fairly substantial contraction, -26 x 10^{-5} $\Delta\ell/\ell$, recorded in the first 5 h following replacement of water with ethylene glycol.

Very recently, Midgley (10) reported that ethylene glycol leached out the free lime in cement paste and also attacked the calcium bearing phases. These findings have to be kept in mind when considering the implications of the present results.

DISCUSSION

Although expansion of active carbon on adsorption from solution was observed by Pawlow (11) over 50 years ago, it appears that a detailed extension isotherm has not been reported until now and its existence was not really expected. It is surprising that on immersion in $NaNO_3$ solution the glass specimen expanded 25 x 10^{-5} $\Delta\ell/\ell$ units beyond the length it reached on complete saturation with water (Fig.2). This expansion is about half as much as that which takes place when dry glass becomes 80% saturated with water (see Fig.3, sections A to C).

The relatively large effect of an inorganic salt on dimensions is even more significant in view of the well-documented phenomenon of salt rejection (12,13). In fact, the adsorption isotherm for water on porous silica glass containing various amounts of NaCℓ strongly suggests that salt is excluded from the first monolayer (13,14). The length changes observed in the present work seem to be due to concentration changes of the liquid held in the centre of the capillaries, separated by at least one water layer from the glass surface. Further marked decrease in length as the $NaNO_3$ concentration increased beyond 1 mole/ℓ may be caused by decrease in adsorption in the vicinity of the surface, as has been reported by Mukerjee and Anavil for the ionic surfactants-porous glass system (14).

The pronounced hysteresis of the $NaNO_3$-glass isotherm (Fig.2) indicates that on traversing the concentration region that extends from pure water to saturated solution, length changes were probably caused by more than a mere change in the concentration, or by the structure of the ionic double layer on the surface. The length in pure water is greater by approximately 50 x 10^{-5} $\Delta\ell/\ell$ after the run. This is a preliminary value only, subject to change when equilibrium will have been reached. The possibility that irreversible change was caused by corrosion of the substrate must also be considered.

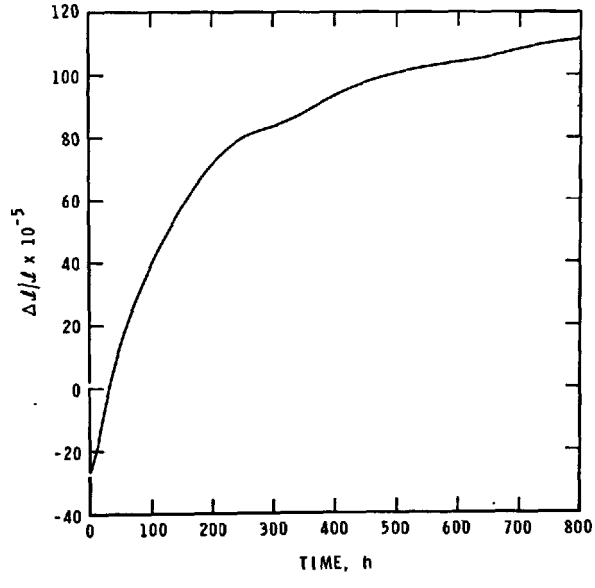

Fig.6 - Length changes of a hydrated cement paste specimen (W:C = 0.6), immersed in ethylene glycol, as a function of time.

The similarity of curves obtained on the dissolution of porous glass in NaOH and hydrated cement paste in HCℓ in the first instance, and on leaching of porous glass in acid and cement paste in ethylene glycol in the second, suggests that the reported results are of general validity. For the purpose of this discussion, this hypothesis will be accepted and some very brief comments concerning the implications for hydrated cement will be made.

The very large expansion during complete dissolution is an important factor with regard to an explanation of the mechanism of volume expansion due to chemical attack. Osmotic pressure, crystallization pressure, and mechanical pressure exerted by the volume requirement of the reaction product, which is greater than the space available, plus gel formation followed by water adsorption have all been suggested as causes of volume expansion of cement on chemical attack. It is fair to say, however, that none of these theories is entirely satisfactory.

In searching for understanding of the causes of volume instability of porous solids under chemical attack the solid matrix itself has not been considered responsible for volume change, but was assumed to expand passively in response to an internal pressure generated in the void space (e.g. crystallization or osmotic pressure). The present results, although preliminary, clearly indicate that changes occurring on the surface - whether sorption of inert ions or dissolution of either a constituent of a non-homogeneous matrix or a portion of the entire solid - result in expansion of a magnitude that induces cracking. It appears that such alteration of the surface energy is sufficient for the disjoining pressure to become dominant. If correct, this assumption offers a simple, credible and unified explanation of a number of deterioration processes leading to excessive volume instability and cracking.

ACKNOWLEDGEMENT

The author is indebted to H. Schultz for carrying out the experimental work.

REFERENCES

1.- J. CALLEJA (1978), "L'expansion des ciments," Il Cemento, Vol.75, No. 3, 154-164.

2.- S. DIAMOND (1975), "A Review of Alkali-Silica Reaction and Expansion Mechanisms," Cem. Concr. Res., Vol.5, No. 4, 329-346.

3.- W.C. HANSEN (1968), "The Chemistry of Sulphate-Resisting Portland Cements in Performance of Concrete," In Performance of Concrete, by E.G. Swenson (Ed.), Symposium in honour of Thorbergur Thorvaldson.

4.- B. MATHER (1969), "Sulfate Soundness, Sulfate Attack, and Expansive Cement in Concrete," Vol.II, RILEM Symposium on the Durability of Concrete, Academia Prague.

5.- C.H. AMBERG and R. MCINTOSH (1952), "A Study of Adsorption Hysteresis by Means of Length Changes of a Rod of Porous Glass." Can. J. Chem., Vol. 30, No. 12, 1012-1032.

6.- E.W. SIDEBOTTOM and G.G. LITVAN (1971), "Phase Transitions of Adsorbates; Part 2 - Vapour Pressure and Extension Isotherms of the Porous-Glass and Water System below 0°C." Trans. Faraday Soc., Vol. 67, Part 9, 2726-2736.

7.- R.F. FELDMAN and P.J. SEREDA (1961), "Characteristics of Sorption and Expansion Isotherms of Reactive Limestone Aggregate," J. Amer. Conc. Inst., Vol. 58, No. 2, 203-241.

8.- S.E. KRASIKOV, O.S.MOLCHANOVA and L.A. ORLOVA (1963), "Volume Changes in the Leaching of Sodium Borosilicate Glasses," Zh. Prikl. Khimii, Vol. 36, No. 7, 1398-1403.

9.- F.M. LEA (1970), "The Chemistry of Cement and Concrete," London, Arnold, p. 108.

10.- H.G. MIDGLEY (1979), "The Determination of Calcium Hydroxide in Set Portland Cements," Cem. Concr. Res., Vol. 9, No. 1, 77-82.

11.- P.N. PAWLOW (1927), "Uber die Quellung aktiver Kohle," Kolloid Zeitschr, Vol. 42, No. 2, 112-119.

12.- K.A. KRAUS, A.E. MARCINKOWSKY, J.S. JOHNSON; and A.J. SHOR (1966), "Salt Rejection of a Porous Glass," Science, Vol. 151, 14 Jan. 194-195.

13.- G.G. LITVAN (1973), "Phase Transitions of Adsorbates; V. Aqueous Sodium Chloride Solutions Adsorbed on Porous Silica Glass," J. Coll.Interface Sci., Vol. 45, No. 1, 154-169.

14.- P. MUKERJEE and A. ANAVIL (1975), "Adsorption of Ionic Surfactants to Porous Glass: The Exclusion of Micelles and other Solutes from Adsorbed Layers and the Problem of Adsorption Maxima in Adsorption at Interfaces." (K.L. Mittal, Ed.), Am. Chem. Soc. Symp. Series No. 8, p. 107.

Studies on unsoundness of clinker with below 3.5 percent MgO content

Etudes sur le manque de solidité d'un clinker d'une teneur en MgO inférieure à 3,5 pour cent

S.K. CHOPRA, K.C. NARANG, S.P. GHOSH and
K.M. SHARMA, Cement Research Institute of India, New Delhi, India.

RESUME : Bien qu'il y ait différents points de vue sur les limites admissibles de teneur en M_gO des ciments, la limite maximale permise par les spécifications internationales sur le ciment portland ordinaire est de 6 pour cent. Par ailleurs, les chercheurs sont généralement d'accord sur le fait que les clinkers ayant une teneur en M_gO de 3,5 pour cent ou moins ne manqueront pas de solidité. Cependant, dans certains cas exceptionnels, les clinkers ayant une teneur en M_gO inférieure à 3,5 pour cent ont manifesté un manque de solidité, et la présente communication rend compte des recherches sur les causes du manque de solidité de ces clinkers. Des études sur des clinkers de laboratoire, spécialement préparés et ayant une teneur en M_gO de moins de 3,5 pour cent ont montré qu'en plus de la finesse du mélange cru, du ciment définitif et des conditions de refroidissement, plusieurs autres paramètres tels que la teneur en C_3A, la morphologie et la microstructure des phases du clinker jouent un rôle important dans l'expansion autoclave des ciments. La corrélation entre le manque de solidité des clinkers, c'est à dire l'expansion autoclave, et leurs propriétés minéralogiques microstructurelles et autres propriétés physico-chimiques a fait l'objet d'une étude. Certaines directives pour prévoir le caractère peu solide du clinker sur la base des propriétés physico-chimiques et minéralogiques des clinkers sont aussi proposées.

SUMMARY : Although there are different opinions about the permissible limits of MgO content in cements, the maximum which is permitted in some of the world standard specifications on ordinary portland cement is 6 percent. Also, there is general agreement amongst the researchers that clinkers having MgO content of 3.5 percent or less will not be unsound. However, in certain exceptional cases clinkers having MgO content below 3.5 percent have shown unsoundness and this paper reports the investigations on the causes of unsoundness in such clinkers. Studies on specially prepared laboratory clinkers with less than 3.5 percent MgO content have indicated that in addition to the fineness of the raw mix, final cement and the conditions of cooling, several other parameters, such as C_3A content, morphology and microstructure of clinker phases also play a significant role in causing autoclave expansion in cements. The interrelations between unsoundness of clinkers i.e, autoclave expansion, and their mineralogical, microstructural and other physico-chemical characteristics have been studied. Certain guidelines for predicting unsound character of clinker on the basis of physico-chemical and minoralogical properties of clinkers have also been suggested.

INTRODUCTION

While it is generally understood(1,2,3) that the autoclave expansion in clinkers with MgO content higher than 5% suddenly jumps to higher values, a paradoxical situation prevails as some clinkers with higher MgO content ($\geq$5%)are observed to be sound and on the other hand clinkers with MgO content much below this level show unsoundness ($>$0.8% autoclave expansion). Number of reports (2,3,4) have appeared dealing with unsoundness of high magnesia ($>$5.0%) clinkers but a few deal (5,6,7) with problems facing some of the plants where at times clinkers with lower MgO content show autoclave unsoundness. This cannot be straightaway explained either on the basis of level of MgO content, SO_3 or alkali content which generally are of the same magnitude or even C_3A content which on the average ranges between 5 and 12 percent in the Indian clinkers.

Studies on some commercial clinkers and specially prepared laboratory clinkers were therefore taken up to examine the unsound behaviour in low MgO clinkers and to determine the relative importance of different factors responsible for autoclave unsoundness. Based on these studies , a hypothesis which could explain the causes of unsoundness in low MgO clinkers ,is proposed.

Experiments: The occurance of expansive constituents and their physical state is directly governed by the properties of raw materials, raw mix fineness, burning and cooling schedule etc(8). While the influence of these parameters is known for the manufacture of high MgO clinkers, experiments were designed to study their influence in the manufacture of lower MgO content clinkers. Raw mixes with following potential phase composition were planned and studied in 2 series of experiments : C_3S $\approx$45 and$\approx$55 percent; C_3A $\approx$ 7-8%, 10-11% and 14-15 percent; MgO $\approx$0.2, 1, 3 and 4 percent.

Series 1 Raw mixes with three different levels of fineness i.e. 1,3% on 72 mesh sieve and 10% on 170 mesh sieve were prepared and their potential phase composition varied in terms of MgO content(1and 3%) and C_3A level (7-15%). The mixes were fired in a laboratory kiln at 1450°C and cooled under normal ambient conditions.

Series 2:Raw mixes with different potential phase composition were fired at 1450°C for same retention time and subjected to two different cooling rates:

a) Clinker removed from furnace at 1450°C and cooled to ambient temperature (rapid cooling);

b) Clinker cooled in the furnace at the rate of 8-10°C/min. upto 1100°C and cooled in air to ambient temperature (slow cooling)

Clinkers obtained for series 1 and 2 were examined using standard analytical,XRD and microscopic techniques. Cements prepared from these clinkers (with optimum SO_3 content and fineness 3000 cm^2/g) were studied for their expansion and strength characteristics. The autoclaved cement pastes were examined by XRD, IR spectroscopy,electron and optical microscopy for determining the nature of autoclaved products.

Series 3: Mineralogical ,physical & microstructure properties of two unsoundcommercial clinkers with MgO content below 5 percent were also examined. Cements were prepared at various fineness levels (2250-5000 cm^2/g) to investigate the influence of fineness of cement on autoclave expansion in these two clinkers.

Results and Discussions

Series 1: Effect of fineness of raw mix: In addition to the mineralogical composition ,the reactivity of the raw mix components is known (8) to be significantly influenced by homogeneity and fineness.It is reported that not more than 0.5 percent of silica particles above 0.2mm size and 5 percent calcite particles above 0.15mm size should generally be present in high LSF (0.95) mixes. For raw mixes of lower LSF value,relatively higher proportions of coarse particles can, however, be tolerated. The rate of reaction is greatly affected by grain size which inturn affects the formation and distribution of alite, belite and minor phases in them. For our studies raw mixes with LSF 0.89-0.95 have been used as shown in Table 1:

Table 1: Properties of Raw Mixes

Raw Mix No.	HM	AM	LSF	SM	Clinker No
1	1.96	1.85	0.90	1.84	1,2 and 3
2	1.89	1.10	0.91	1.58	4,5 and 6
3	2.06	1.58	0.89	2.81	7 and 8
4	2.02	2.44	0.93	1.81	24
5	1.99	1.46	0.90	2.08	28
6	1.90	1.74	0.91	1.50	30
7	2.08	3.0	0.91	2.33	32
8	2.16	1.48	0.95	2.44	33
9	2.17	2.23	0.95	2.50	34

Results in Table 2A show that mineral composition ofclinkers in series 1 appears to be close to the potential, phase composition except for clinker 3 and 6 which have been prepared from raw mixes with 10% residue on 170 mesh sieve. Clinker 3 and 6 have alsoshown a tendency to dust on cooling and storage due to conversion to C_2S phase. Free lime content of all the clinkers was found to be low and as a result all the clinkers passed the Lechatelier expansion test (expansion $<$10m).

Optical microscopic studies also show that except clinker 3 and 6, all other clinkers in the series have well developed alite and belite grains, alite being predominantly in hexagonal shape and almost free from belite inclusions. Intergranular alite and belite assembelage, is also rare. The interstitial phase occurs as ground mass preferably around C_3S grains. Presence of periclase crystals in clinkers with MgO content $\sim$1% is rarely observed & wherever observed occassionally varies in 2-6μ size range. In clinkers with MgO content $\sim$ 3% the size of periclase is of the order of 4-12μ. XRD lines for major phases do not show any significant shift thus indicating that formation of normal phases has occured in clinkers of series 1.

Results in Table 2B show good development of strength of cements made from clinkers of series 1 which are also affected by change in raw mix fineness. Cement 3 and 6 which show overall poor strength are also the cements observed to be poor

Table 2A : Effect of fineness of raw mix on clinker composition and autoclave expansion - Series 1

Raw mix No	Residue on 72/170 mesh %	Free lime content of clinker	Phase composition of the clinkers					Autoclave expansion %
			C_3S	C_2S	C_3A	C_4AF	MgO	
1	1	0.10	55.23	13.22	10.18	18.57	1.16	0.02
1	3	2.39	45.63	20.48	10.30	18.42	1.25	0.03
1	10(170 mesh)	1.35	5.25	59.31	14.88	17.99	1.16	0.11
2	1	0.30	42.25	22.81	8.06	23.41	1.10	0.10
2	3	1.86	47.92	17.50	7.82	22.16	1.24	0.15
2	10(170 mesh)	2.50	10.21	55.63	10.80	21.28	0.90	0.12
3	1	0.06	30.24	46.63	7.67	11.86	2.76	0.18
3	3	0.24	28.63	47.96	7.56	11.86	2.99	0.22
4	1	Nil	41.58	28.76	9.55	15.41	2.97	0.04
4	3	0.66	41.15	29.32	9.91	15.43	2.93	0.19

Table 2 B: Physical characteristics of cements made from clinkers of Series 1

Clinker No	% residue on 72 mesh/170 mesh sieve	Setting time (min)		Lechatelier Expansion mm	Autoclave Expansion %	Compressive strength Kg/cm^2		
		IST	FST			3 day	7 day	28 day
1	1	143	182	1.5	0.02	400	611	697
1	3	165	193	1.5	0.03	443	505	675
1	10(170 mesh)	163	198	1.0	0.11	149	152	286
2	1	140	190	1.0	0.10	353	429	502
2	3	173	225	0.5	0.15	328	498	581
2	10(170 mesh)	135	180	0.5	0.12	168	238	389
3	1	168	218	1.5	0.18	223	298	512
3	3	160	205	1.0	0.42	268	358	518
4	1	-	-	1.0	0.04	317	368	-
4	3	-	-	1.0	0.19	213	341	546

in C_3S content. Lechatelier expansion, autoclave expansion and setting time characteristics have not been affected directly and all the cements are observed to be sound in autoclave test.

Series 2 : Role of C_3A, MgO content in clinkers and effect of cooling rates:

From the results in Table 3A it can be observed that neither the level of C_3A nor the cooling rate of clinkers with 1% and below MgO content is decisive for soundness of clinkers as both the rapid and the slowly cooled clinkers are observed to be sound. Lechatelier expansion of all the clinkers was found to be below 2mm eliminating thereby the effect of free lime and SO_3 contributions to autoclave expansion. The effect of C_3A content becomes however, apparent for clinkers with MgO level about 3% in which case the autoclave expansion increases suddenly for slowly cooled clinkers with high C_3A content. While clinkers with about 7% C_3A and 3% MgO levels are observed to be sound, clinkers with 15% C_3A and 3% MgO become unsound in autoclave test. These results lead to conclusions that rapidly cooled clinkers allow high MgO content compared to slowly cooled clinkers and this tolerance of MgO in slowly cooled clinkers decreases with increasing C_3A content. This is further supported by the data in Table 3A, as the slowly cooled clinkers with MgO content $\approx$ 4% are observed to be unsound at all levels of C_3A (> 7%) even when C_3S content is maintained as high as 56%. A direct application of these results in India could be that in plants where cooling rates are likely to be rather slow and MgO content in raw materials relatively higher, a lower alumina modulus of raw mix may be designed in order to obtain sound clinkers.

The data in Table 3B show that among the three parameters i.e. C_3A, MgO and rate of cooling the last has more significant effect on strength characteristics. Slowly cooled clinkers show invariably poor strength development. Comparatively lower strengths of slowly cooled clinkers is more significant at 28 days age. The drop in strength is also affected by C_3A level as when it is high in clinkers, the drop in strength is maximum.

Microstructure of sound and unsound clinkers:

Rapidly cooled clinkers with upto 4 percent MgO and 15 percent C_3A content show good granulometery and are characterised by idioblastic C_3S and C_2S grains in separate clusters. Sizes of C_3S grains range from 4-18μ for smaller grains and 40-80μ for larger grains. Prismatic elongated grains of C_3S are predominant (Fig 1 and 2). C_2S grains range between 4-16μ for smaller and 40-75μ for larger grain. Ferrite and aluminates phase is evenly distributed between both C_3S and C_2S. MgO inclusions are fairly uniform and vary in size range between 12-16μ in C_3S and 4-12μ in C_2S, on average being >10μ in size.

Slowly cooled clinkers are distinctly poorer in granulometery, have relatively more and larger inclusions specially of MgO grains. Cluster formation, large crystal growth and instability of phases appear to be the main features of these clinkers. C_3S grains are larger 40-120μ and

Table 3A: Effect of C_3A/MgO content and cooling rate on clinker characteristics Series 2

Clinker No	Free CaO	Compound composition					Lechatelier expansion		% autoclave expansion	
		C_3S	C_2S	C_3A	C_4AF	MgO	Rapid cooling	Slow cooling	Rapid cooling	Slow cooling
4	0.30	42.25	22.81	8.06	23.41	1.10	1.50		0.03	
7	1.50	30.24	46.63	7.67	11.86	2.76	1.50 /	1.0	0.18 /	0.23
33	1. 06	56.56	20.00	7.11	10.00	4.05	2.00 /	2.0	0.13 /	6.33
28	0.50	42.98	32.85	9.55	12.86	0.19	1.00 /	1.0	0.05 /	0.05
2	2.39	45.63	20.48	10.30	18.42	1.25	1.50		0.03	
34	0.42	56.83	19.36	11.20	7.69	4.06	1.00 /	1.5	0.10 /	8.60
30	0.68	39.26	30.27	13.33	15.02	0.17	0.50 /	1.0	0.06 /	0.18
32	0.06	38.42	37.42	14.87	7.11	0.92	1.00 /	1.5	0.03 /	0.20
24	0.66	41.15	39.32	15.43	9.91	2.93	1.00 /	1.0	0.19 /	6.50

Table 3 B : Effect of C_3A/MgO and Cooling conditions on Clinker characteristics Series 2

Clinker No	Cooling rate	Compressive strength (Kg/cm^2)			Le chatelier Expansion mm	Autoclave Expansion %
		3 days	7 days	28 days		
28	Rapid	304	393	550	1.00	0.05
	Slow	315	363	470	1.00	0.12
30	Rapid	200	318	496	0.50	0.06
	Slow	217	296	440	1.00	0.10
32	Rapid	255	335	472	1.00	0.03
	Slow	205	279	358	1.50	0.20
24	Rapid	213	341	546	1.00	0.19
	Slow	221	279	314	1.00	6.50
34	Rapid	315	410	486	1.00	0.10
	Slow	325	368	432	1.50	8.60
33	Rapid	-	-	-	2.00	0.13
	Slow	354	467	503	2.00	6.33

have less defined boundaries. Periclase grains vary in 5-25μ size range. C_2S grains are also relatively larger (35-90μ) and mostly irregular in shape. MgO inclusions are present frequently in liquid phase as periclase crystals ranging in size from 20-25μ (Figs 3 and 4).

From all the above results it appears that sudden increase in autoclave expansion of slowly cooled clinkers may be due to differential rate of hydration of alite/belite and periclase crystals. In rapidly cooled clinkers which are characterised by small grains of alite as also of periclase, the strength development appear to be faster due to hydration of alite & the structure of cement paste can accomodate the expansion of periclase which itself is finely and uniformly divided. On the other hand in slowly cooled clinkers, the larger grains of alite/belite appear to hydrate rather slowly and hence show poor strength development. The structure of cement paste in this case appears to be unable to contain the expansion due to periclase hydration which is also not uniformly distributed. This hypothesis also seems to be supported by the results in Table 4 which shows that periclase quantity alone can not explain the unsound behaviour of slowly cooled clinkers. Results of IR spectroscopy, electron microscopy (Fig 5) and XRD studies on autoclaved products of various clinkers also support the observations. Fig 6 shows a clear brucite peak at 3700 cm^{-1}, the intensity of which increases with larger MgO and C_3A content in clinkers. XRD studies of autoclaved products also show similar pattern.

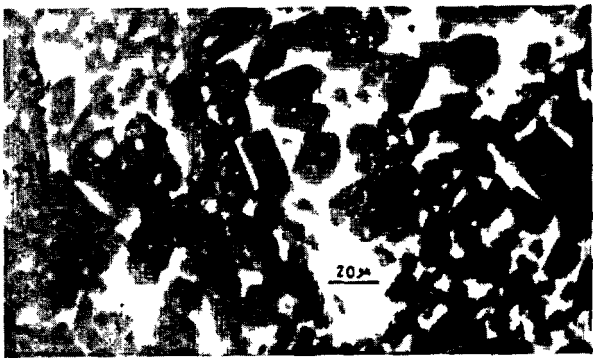

Fig.1 Optical microphotograph of rapidly cooled clinker (Clinker 24).

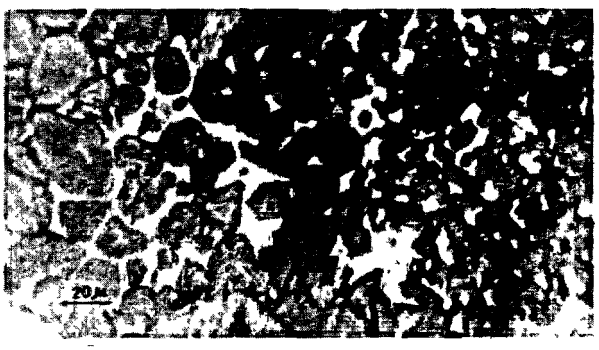

Fig.2 Optical microphotograph of rapidly cooled clinker (Clinker 34).

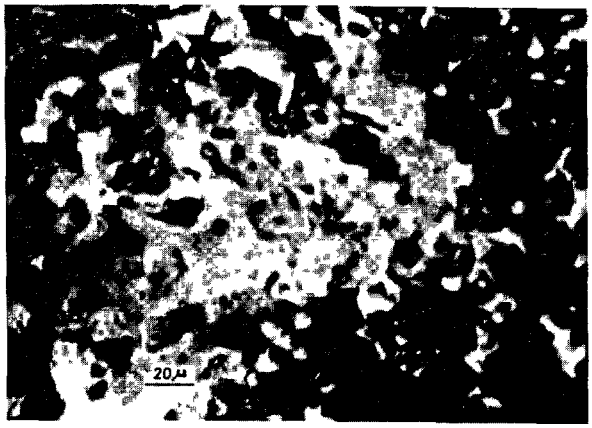

Fig.3 Optical microphotograph of slowly cooled clinker (Clinker 24).

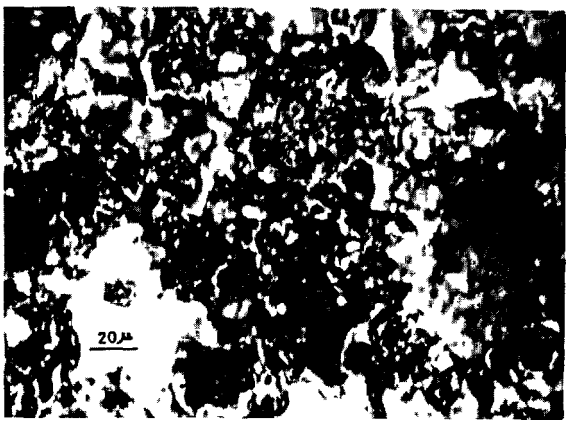

Fig.4 Optical microphotograph of slowly cooled clinker (Clinker 34).

Table 4: Free MgO content of clinkers Series 2

Clinker No	Cooling rate	Free MgO	
		Chemical	XRD
32	Rapid	Nil	0.50
	Slow	Nil	0.50
24	Rapid	1.03	0.80
	Slow	1.88	1.64
33	Rapid	2.53	2.94
	Slow	3.03	3.53
34	Rapid	2.49	2.60
	Slow	2.90	3.40

Series 3: Effect of fineness of cement on unsoundness

Table 5 shows the physicochemical and mineral characteristics of two commercial clinkers with MgO content lower than the permissible limit of 6%. Various studies including XRD and optical microscopy investigations show that these clinkers are characterised by low free lime, high large size alite, high periclase content and very poor granulometery (Fig. 7) Autoclave expansion of cements of normal fineness (3000 cm^2/g) is observed to be very high. The data also shows that the autoclave expansion of these clinkers can be reduced significantly by increasing fineness, so much so that one of the clinker becomes sound (<0.8% expansion) (Fig.8). Refiring of these clinkers followed by rapid cooling also renders the clinkers sound. In general the two clinkers show characteristics of slowly cooled clinkers.

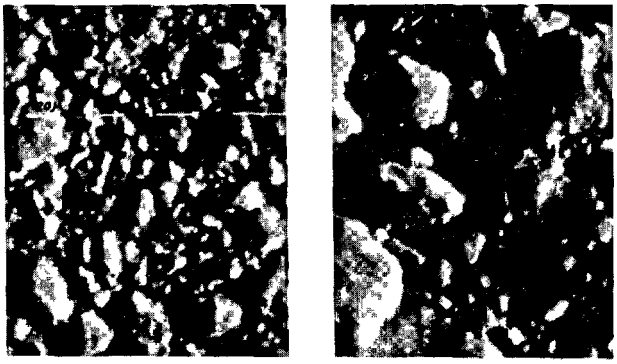

(a) (b)

Fig 5: Scanning Electron microphotographs of autoclaved cement paste of (a) sound and (b) unsound clinkers.

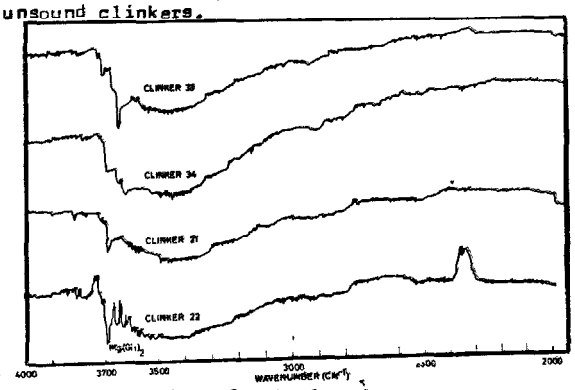

Fig 6: IR spectra of autoclaved cement pastes of unsound clinkers.

Table 5 Characteristics of Commercial unsound clinkers

Clinker No	Phase composition						Le chatelier/Autoclave Expansion at fineness level (cm^2/g)						
	C_3S	C_2S	C_3A	C_4AF	MgO	Free lime	2250	2500	2750	3000	3500	4000	5000
21	68.30	10.10	7.68	8.54	4.52	0.35	-	0.90/ 9.85	-	1.00/ 9.50	-	1.00/ 9.05	1.00/ 5.92
22	59.89	14.49	9.29	9.03	4.92	0.02	1.00/ 7.06	1.00/ 7.66	1.00/ 7.42	1.00/ 4.24	1.00/ 1.39	1.00/ 0.24	-

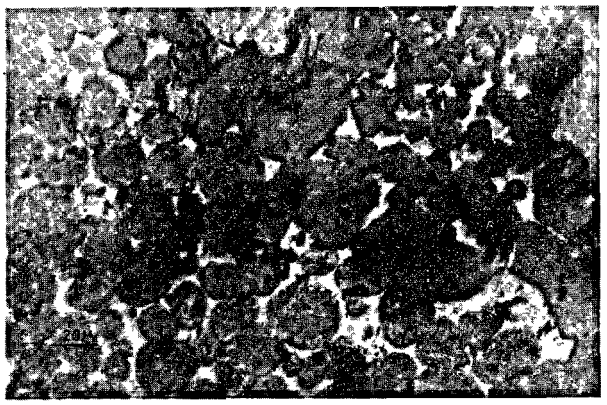

Fig 7. Optical microphotograph of unsound commercial clinker (Clinker 22)

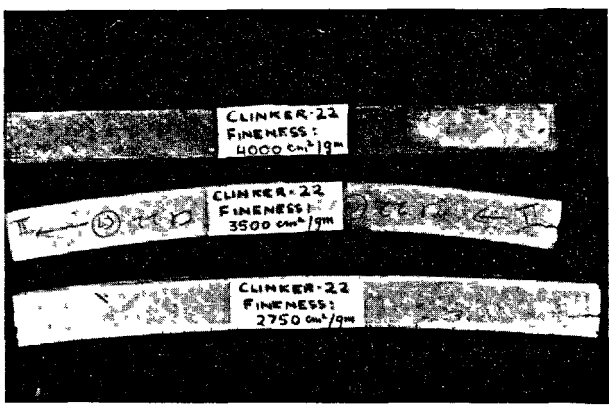

Fig 8. Effect of fineness of cement on autoclave expansion (Clinker 22).

CONCLUSIONS

Amongst the different factors responsible for the manifestation of autoclave unsoundness in low MgO clinkers, C_3A content, rate of cooling and granulometry of clinkers have been found to be the more important parameters. Unsound clinkers prepared in the laboratory were found to be characterised by unevenly distributed larger than usual alite and periclase crystals inspite of total MgO content being less than 4%. These clinkers are also characterised by relatively poorer strength development when compared with sound clinkers. The sudden jump in autoclave expansion may be explained on the basis of hydration characteristics of various phases in particular the alite and periclase grains. Alite particles being larger and more ordered in slowly clinkers, appear to hydrate slowly and result in poor strength development under autoclave conditions which is not sufficient to contain the expansion due to hydration of periclase and thus resulting in failure in the soundness test (autoclave expansion 0.8%). On the other hand small size and disordered alite in rapidly cooled clinkers hydrates rapidly to develop good strength to contain the periclase expansion and may accomodate expansion, even when MgO content in clinkers is upto the maximum permissible limit (6%).

The occasional unsoundness in commercial clinkers with MgO content below permissible limit can also be ascribed due to these reasons in additon to the presence of large size periclase crystals in such clinkers. However, in such cases fineness of the ground cement also becomes an overriding parameter because it reduces the size of both the alite and periclase grains as is evident from the fact that one of the clinkers becomes sound when ground to a particular fineness. For situations in plants where such occurrence is likely, either the rate of cooling or the raw mix properties should be adjusted so as to achieve a microstructure in clinkers which allows the formation of small sized alite grains only, alternatively in clinkers where microstructure of the desired granulometry is not obtained, grinding the clinkers to higher fineness could be adopted as an effective measure to obtain sound cement.

ACKNOWLEDGEMENT

The work reported here is part of the R&D programme of the Institute and the report is being communicated with the permission of the Director General, Cement Research Institute of India, New Delhi.

BIBLIOGRAPHY

1. - H.F. Gonnerman etal. (1953), Investigations of the Hydration Expansion characteristics of Portland Cements, PCA Bulletin, 45,(Eng)

2. - S.K. Chopra et al (1973), Utilization of High Magnesia Limestones in the Manufacture of Cement, CRI publication SP-6-73.

3. - J. Calleja and C. Delolmo (1974), Expansion of Cements and Methods to Determine it. VIth International Symposium on Chemistry of Cement, Moscow.

4. - O. Henning and V.D. Luong (1973), Clinker Formation and Hydration of High Magnesia Portland Cements BRE Translation No 1754

5. - F. Gille (1952), Investigations of the Magnesia Expansion of Portland Cement, Schriftenreihe Der Zement Industrie., HEFT 10.

6. - G. Goggi (1971), Contribution to th study of the Soundness of Cements, BRE Library Communication 1609.

7. - C. Schmitt-Henco (1974), Magnesium oxide content of clinker, Autoclave Test nd Soundness. VI International Symposium on Chemistry of Cement, Moscow, 110-113.

8. - F.M. Lea (1970), The Chemistry of Cement and Concrete, 132-144.

9. - A. Stahel and W. Schramli (1969), The Behaviour of Magnesia in Clinker under different Cooling Conditions. Zement-Kalk-Gips, 22 (9), 407-13

Mechanisms and Kinetics on Neutralization of Concrete in Sea Water

Mécanisme et cinétique de la neutralisation des bétons dans l'eau de mer

T. AKIBA, Senior Research Chemist,
K. MINEGISHI, Dr. Eng., Chief Research Chemist, and
G. SUDOH, Dr. Eng., Manager of Research Department, Chichibu Cement Co., Ltd, Japan.

SUMMARY : Concrete structure in sea water suffer attack owing to the chemical reaction between cement components, either unhydrated or hydrated, and dissolved salts. Studies were made on mechanisms of sea water attack, mainly in relation to kinetics on neutralization of hardened concrete.

The rate of neutralization can be expressed as $L^2=k_e(t-t_i)$ in the first approximation, where L is the neutralized depth, k_e the neutralization rate constant experimentally obtained, t the time of immersion, and t_i the induction period. The above equation suggests that the rate determing process of neutralization in sea water is diffusion process.

Chemical reaction by sea water attack is assumed to occur at a boundary which corresponds to the neutralized depth. Thus, we can apply the following equation:

$$k_t = \frac{2D\varepsilon\Delta C}{C_o\xi} = fk_e$$

The rate constant of neutralization is calculated in consideration of the material transfer of Cl ion. In consideration of the magnitude of the f value, the above rate equations seem to be reasonable and applicable to the practice.

RESUME : En eau de mer, les ouvrages en béton sont soumis à des attaques dues à des réactions chimiques entre les constituants, hydratés ou non, de leur ciment et des sels dissous dans l'eau de mer. Des études ont été entreprises sur le mécanisme de cette attaque de l'eau de mer, principalement sur la cinétique de la neutralisation du béton durci.

En première approximation, la vitesse de la neutralisation peut être représentée par la formule : $L^2 = k_e (t-t_i)$ où L est la profondeur neutralisée, k_e une constante qui est déterminée expérimentalement, t le temps d'immersion, et t_i le "temps de latence".

Cette équation suggère que le processus de neutralisation du béton dans l'eau de mer est un phénomène de diffraction.

La limite de la zone atteinte par la réaction chimique de l'attaque par l'eau de mer correspond à la profondeur neutralisée. Nous pouvons alors appliquer l'équation suivante :

$$k_t = \frac{2\,D.\varepsilon.\Delta C}{C_o\,\xi} = f.k_e$$

La constante de la vitesse de neutralisation est calculée en fonction de la diffusion des ions Cℓ . Compte tenu de l'importance de la valeur f, les équations ci-dessus sont applicables, raisonnablement, dans la pratique.

INTRODUCTION

Studies on the durability of cement mortar and concrete in sea water have been made mainly in connection with the resistivity of cement hydrates and corrosion of reinforcing steel. Sea water attack which seems to be unavoidable on hardened cement is regarded as an example of the reaction of porous solid with gas or liquid which diffuses into the former.

One of the authors (1)(2) has studied the rate of neutralization of cement mortar in relation to the carbonation mechanisms, and found a relationship between the rate and the pore structure.

In a similar way, studies were made on sea water attack to make clear the mechanisms and kinetics. In this experiment, the degree of sea water attack, penetration rate of Cl ion, neutralized depth and pore size distribution of concrete were measured and the rate of neutralization due to sea water attack were discussed.

SEA WATER ATTACK AND NEUTRALIZATION

There are many causes affecting the durability of concrete in sea water, such as the chemical action of dissolved salts, the crystallization of salts within the concrete under condition of alternate wetting and drying, the frost action, the mechanical attrition and impact by waves, the bacterial oxidation and the corrosion of reinforcement embeded in it.

It is considered that the stability of concrete depend on three facters: denseness, cement content and chemical resistance of the cement hydrates to sea water.

Many investigations on sea water attack of hardened cement studied by tricalcium aluminate and lime content in relation to the expansive crystallization of ettringite due to the presence of sulfate, however recently some studies (3)(4) have been made on the influence of Cl ion on cement products. R. Kondo et al. (5) have studied the rate of diffusion of various ions in cement paste and showed the importance of the rate of neutralization on hardened cement in relation to the corrosion of reinforcing steel.

Neutralization of concrete is important phenomenon not only on resistivity of cement hydrates but on the corrosion of reinforcing steel. The corrosion rate indicated is proportional to the diffusion of oxygen on steel surface in the presence of the corrosive medium. The final result of the corrosion process is the formation of a thick rust layer which exerts sufficient tensile forces within the concrete to crack and cause spalling of the concrete cover.

In an alkaline solution, such as the calcium hydroxide solution in set cement, a protective oxide film forms over the steel. The stability of the film depends on the maintenance of certain minimum pH value, 10.5(6).

Thus the rate of neutralization should be taken into account. In the later part of this paper, it will be discussed in relation to pore structure.

EXPERIMENTAL

To examine the durability of concrete in sea water, long time soaking test was started at 1973, and five years test was carried out. In this report, studies were made on the mechanisms of sea water action mainly in connection with the neutralization.

In this experiment, ordinary portland cement (O), moderate heat portland cement(M) and sulfate resisting cement(S) as shown in Table I were used in comparison, and the mix properties of concrete are given in Table II.

The size of the specimens molded is ϕ15x30 cm. After being cured in water for 7 days, the specimens were soaked in sea water at tidal zone or the place in which tidal action was excluded for selected times of exposure. Chemical composition and some properties of the sea water are shown in Table III.

After the compressive strength measurement, each exposed specimen was cut perpendicular to the length with a diamond cutter and the penetration depth of Cl ions was determined with colorimrtric method (7), then the neutralization depth was determined with 1% phenolphtalein solution.

Some of the sea water attacked specimens were sliced perpendicular to the direction of penetration. And samples of surface part and inner part were crushed for such tests as the quantification test by X-ray diffraction, chemical analysis containning water soluble Cl ion and IR.

The pore size distribution of mortar parts separated from several specimens were also measured with a mercury pressure porosimeter.

RESULTS

Table I Chemical analysis of cement used

		Composition (%)							
		ig-loss	insol	SiO_2	Al_2O_3	Fe_2O_3	CaO	MgO	SO_3
Ordinary	portland cement (O)	0.7	tr.	22.2	5.2	3.1	64.7	0.9	1.8
Moderate	heat portland cement (M)	0.7	0.3	23.3	4.3	3.7	64.0	0.9	2.2
Sulfate	resisting cement (S)	0.6	tr.	22.3	2.8	5.1	64.8	0.9	1.7

Table II Mix properties of concrete

		Slump (cm)	Air Content (%)	W/C (%)	S/a (%)	Unit weight (kg/m^3) Water	Cement	Sand	Gravel
O1	Ordinary portland cement	8	4.5	50	38.5	150	300	715	1162
O2				65	40.8	151	232	781	1152
S1	Sulfate resisting cement			50	39.7	148	296	744	1146
S2				65	42.0	149	229	810	1133

Mix properties of moderate heat portland cement(M1) are similar to S1.

Table III Chemical composition and some properties of the sea water

pH	Specific gravity	Composition (mg/l) Na^+	Kt^+	Ca^{++}	Mg^{++}	Cl^-	SO_4^{--}
7.9	1.021	9496	365	370	1400	17047	2481

Degree of Sea Water Attack

The writers (8) reported on the chemical resistivity of cements in sulfate solutions and artificial sea water, and found a relationship between the amount of C_3A and detrioration. In this experiment, the difference in cements on compressive strength measurement seem to have no signifficant effect.

Fig. 1 shows the x-ray diffraction intensity of ordinary portland cement concrete soaked at tidal zone in relation to the depth in specimens and the soaking time.

The amount of calcium hydroxide decreases in the surface layer after 3 years immersion. and gradually decreases in inner parts.

Hydrated chloroaluminate (Fridel's salt) is found at the 7 cm depth on the 3years soaking specimen, and decreases in later stage.

In the case of the investigation about the low C_3A content cements, similar results to the O3 cement as illustrated in Fig. 1 are obtained.

The exact consideration in relation to sea water action will be discussed separately.

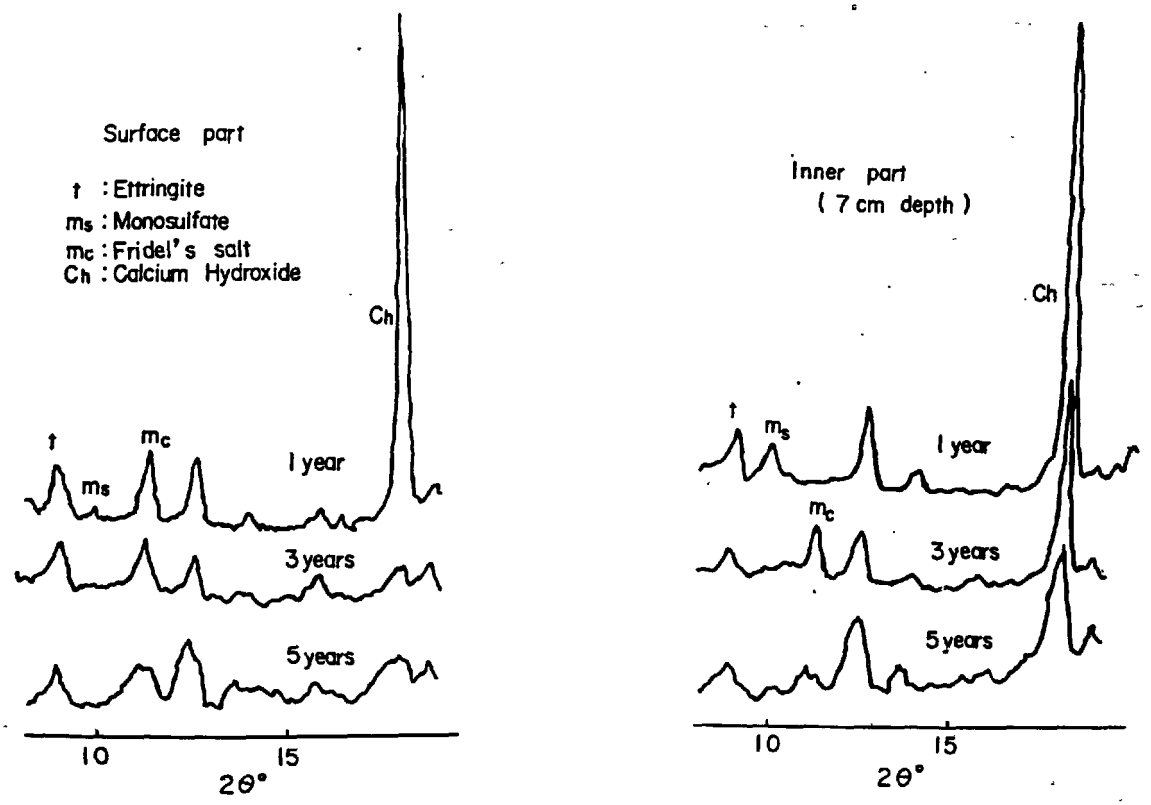

Fig. 1 X-ray diffraction intensity of the ordinary portland cement concrete (O1)

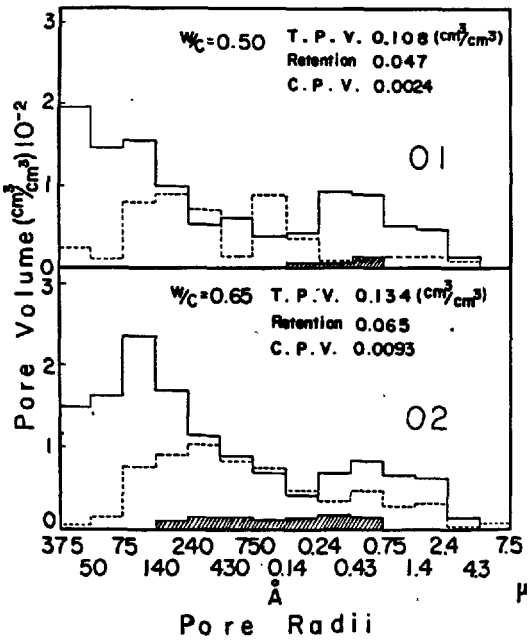

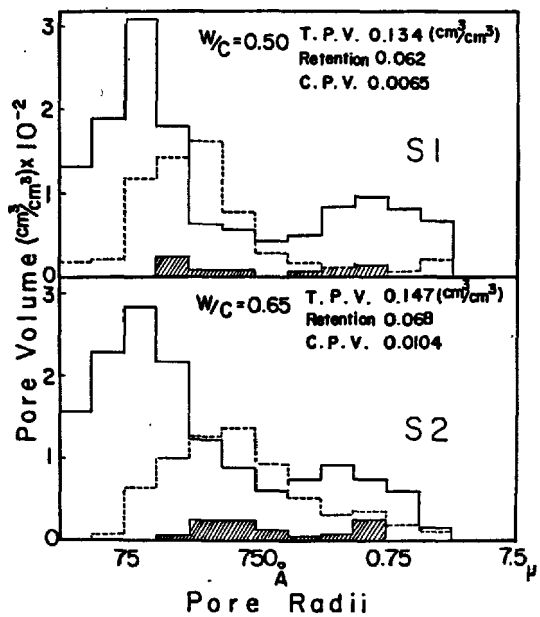

Fig. 2 Pore size distribution of specimens exposed for 1 year

——— : showing the ascending
----- : showing the descending
≈≈≈ : showing the C.P.V.

Pore Size Distribution

The determination of pore size distribution is useful in consideration of the mechanism of sea water attack on set cement.

The pore size distribution of O and S cement concrete immersed for 1 year at tidal zone are shown in Fig. 2.

The measurement of pore size distribution by mercury pressure porosimeter based on the model of cylindrical pores, but hysteresis in mercury porosimetry is due to the existence of the ink-bottle pores. Such a pore consists of a big cavity connected with the remaining pore system by a narrow neck.

In this experiment, the Reverberi method (9) which utilizing the difference between the ascending and descending branches of the curve for evaluating the broad and narrow part of the pores independently, was applied on hardened cement.

One of the authors (2) has studied the through pore size distribution determined by back diffusion and applied to the rate of neutralization by carbonation reaction.

In Fig. 2, T.P.V. shows the total accessible pore volume calculated by ascending branch and Retention means the volume of mercury by descending way. C.P.V. shows the cylindrical pore volume which seems to be comparable with the through pore.

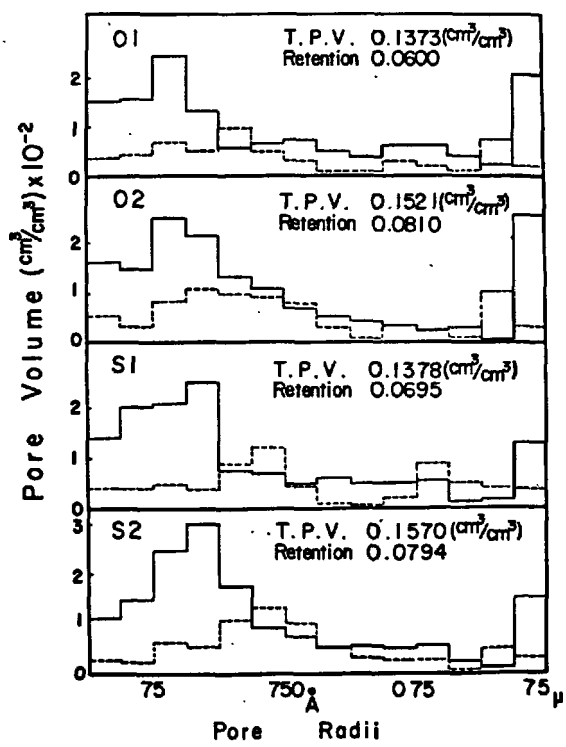

Fig. 3 Pore size distribution of specimens exposed for 5 years

In the case of the determination of micro through pore under 0.1 μm diameter, the measurement by mercury porosimeter is superior to gas diffusion determination on account of the reason that the latter can not determine the pore size distribution of micro through pore under 0.1 μm diameter.

The pore size distribution of specimens cured for 5 years are illustrated in Fig. 3 . By the reaction of sea water attack, the pore structure of hardened cement is affected and the great difference is the increase of large accessible pores which seems to be due to the leaching of calcium hydroxide. The increase in O cement is slightly greater than in S cement.

Penetration Rate of Cl Ions

The penetration of calcium chloride were studied in connection with de-icing agents in cement, and it was found that the phenomenon was governed by diffusion process (7) . We studied the rate in relation to the rate of neutralization and the corrosion of steel.

The penetrated depth of Cl ions in concrete are shown in Fig. 4 . The linear plot of depth as a function of $\sqrt{t}$ supports the rate determing process is diffusion. The value of diffusion coefficient of O1, O2, S1 and S2 are 2.2, 3.5, 2.5 and 9.2×10^{-8} cm^2/sec respectively. These values are about thousand times smaller than the diffusion coefficient of chloride ion in water as mentioned in other papers (5)(7)..

The chemical reaction of chloride with hydrates and the interaction between the surface and diffusing ions could be responsible for the decrease in the diffusion coefficient of chloride. The reason that the value of S cement is greater than other cements also could be considered in view of above mentioned and the difference of C.P.V..

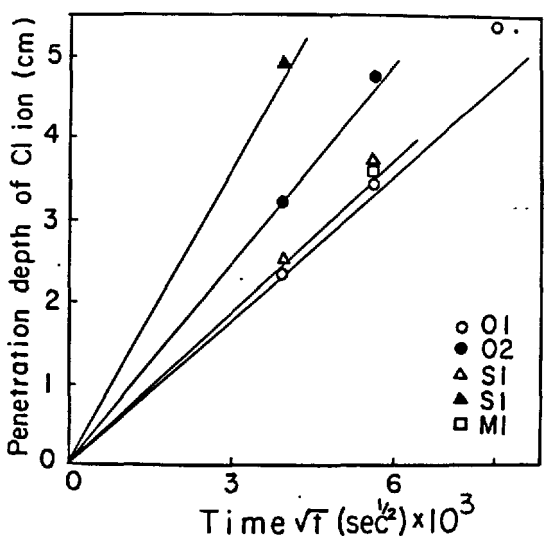

Fig. 4 Relationship between penetrated depth of chloride and time

In this experiment, the corrosion of steel embeded in 5 cm depth was not observed even at 5 years test.

Neutralization Rate of Concrete

The neutralization rate of the specimens are illustrated in Fig. 5 .

The rate of neutralization can be expressed as $L^2 = k(t-t_1)$, in the first approximation where L is the neutralized depth, t is time, t_1 is induction period and k is a constant. Therefore the value k shows the ease of neutralization.

The difference in cements seems to have no signifficant effect. The water-cement ratio shows the greatest effect. The values of the rate constant of each specimens are compared in Table IV.
In this experiment, the difference in exposed places was not observed.

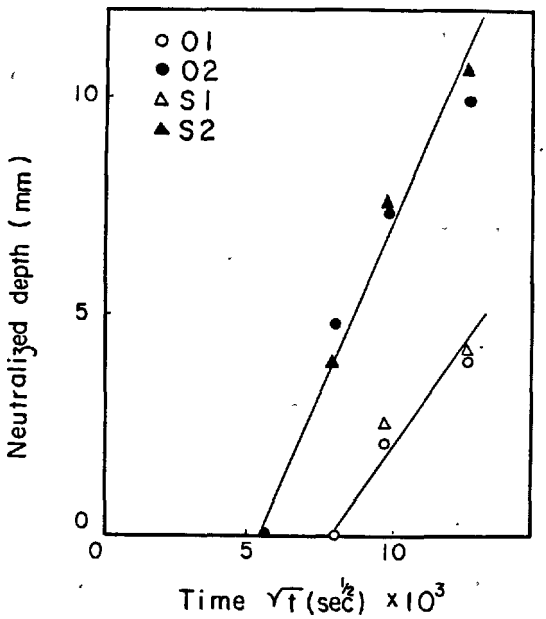

Fig. 5 Relationship between neutralized depth and time

DISCUSSION ON THE RATE OF NEUTRALIZATION

Induction Period in Neutralization

Neutralization does not occur immeadiately even on the surface which is in direct contact with sea water. The length of the induction period varies with the water-cement ratio of specimen, and in the case of W/C= 0.65 and 0.5 , the length of the induction period are 1 year and 2 years respectively. These differences occur depending chiefly on their pore structure and the rate of chemical reaction of pore surface between cement hydrates and sea water components.

Rate Equation on Neutralization

The rate of neutralization of various

specimens are shown in Fig. 5 . In the first approximation, the rate can be expressed by the equation,

$$L^2 = k_e(t-t_i) \quad (1)$$

where
L is the neutralized depth
t is the soaking time
t_i is the induction period
k_e is the neutralization rate constant experimentally obtained

The equation suggests that the rate determing process is diffusion, because this type of equation can be derived when the rate of reaction controlled by diffusion as shown in the former study (1).

Nevertheless the boundary between the two parts, neutralized and unneutralized, can not be clearly distinguished, the chemical reaction by sea water attack is assumed to occur at the boundary, and the concentration of chloride in solution is zero at the boundary. Thus, we can apply the following equation,

$$k_t = \frac{2D\varepsilon\Delta C}{C_0\rho} = f \cdot k_e \quad (2)$$

where
D is the diffusion constant of Cl (1.763×10^{-5} cm^2/s)
ΔC is the difference of concentration of Cl (4.8×10^{-4} mol/cm^3)
ε is the porosity of the specimen(cm^3/cm^3)
C_0 is the amount of free calcium hydroxide (mol/g mortar)
ρ is the density of the mortar(g/cm^3)
k_t is the theoretical neutralization rate constant
f is the tortuosity

Rate Constant of Neutralization

The rate constant of neutralization is calculated in consideration of the material tranfer of Cl ions, and the calculated values for specimen O1, O2, S1 and S2 are shown in Table IV.

As for the value of ε, C.P.V.(ε_c) were adopted. The amount of calcium hydroxide assumed the reactant is calculated based on the result that the cement paste contains 0.22g calcium hydroxide on ignited sample. The value is multiplied by 2 because of the molar ratio correction.

Table IV Rate constant and tortuosity

	O1	O2	S1	S2
$C_0\rho$	3.16×10^{-4}	2.42×10^{-4}	3.08×10^{-4}	2.38×10^{-4}
ε_c	0.0024	0.0093	0.0065	0.0104
k_e	2.1×10^{-9}	4.8×10^{-9}	2.1×10^{-9}	4.8×10^{-9}
k_t	1.3×10^{-8}	6.5×10^{-8}	3.6×10^{-8}	7.4×10^{-8}
f	6.1	14	16	15

In consideration of the magnitude of the f value which is empirically expected to be in the order of 10, the equation seems to be applicable to the neutralization of hardened cement in sea water.

CONCLUSION

In this report, the rate of neutralization of concrete in sea water was studied in relation to the pore structure, and it is found that the equation(1) and (2) seem to be applicable in practice.

The rate constant of neutralization in sea water is $2\sim5\times10^{-9}$ cm^2/s and it is interesting that the value is simillar to the rate constant of neutralization by carbonation measured by Hamada; 4.3×10^{-9} cm^2/s (10).

REFERENCES

1.-R. KONDO,M. DAIMON and T. AKIBA (1968) "Mechanisms and Kinetics on Carbonation of Hardened Cement", Proc. of 5th Symposium on Chemistry of Cement, Tokyo, 402-409.
2.-M. DAIMON, T. AKIBA and R. KONDO (1971) "Through Pore Size Distribution and Kinetics of the Carbonation Reaction of Portland Cement Mortars",J. Am. Cer. Soc., 54, 423-428.
3.-H.G. SMOLCZYK (1969), "Concrete in Strong Chloride Solutions", Rilem Intern. Symp. Durability of Concrete, Preliminary Report, C-113-126.
4.-W. RIEDEL (1973) "Corrosion Resistance in Solutions of Magnesium Salts", Zement Kalk Gips, 26, 286-296.
5.-R. KONDO, M. SATAKE and H. USHIYAMA (1974),"Diffusion of Various Ions in Hardened Portland Cement", CAJ Review of 28th General Meeting, 41-43.
6.-R.W. Nurse (1964),"Slag Cement" The Chemistry of Cements , Academic Press, London and New York.
7.-M. COLLEPARDI,A. MARCIALIS and R. TURRIZIANI (1972),"The Penetration of De-icing Agents in Cement Pastes", il cemento, 143-149.
8.-G. SUDOH, T. AKIBA and K. ARAI (1975), "Chemical Resistivity of Cements in Sulfate Solutions and Artificial Sea Water" 3rd Intern. Ocean Development Conference, Tokyo, 231-242.
9.-M. SVATA (1971/72),"Determination of Pore Size and Shape Distribution from Porosimetric Hysteresis Curves" Powder Technol., 5, 345-349.
10.-M. HAMADA(1968),"Neutralization(Carbonation) of Concrete and Corrosion of Reinforcing Steel", Proc. of 5th Symposium on Chemistry of Cement, Tokyo,343-369.

Orientation des hydrates au contact des granulats

Orientation of hydration products near aggregate surfaces

J. GRANDET, Professeur,
J.P. OLLIVIER, Maître-Assistant
I.N.S.A., Département de Génie Civil - Université Paul Sabatier, Toulouse, France.

RESUME : La croissance orientée des cristaux de Portlandite dans l'auréole de transition qui entoure les granulats du béton y favorise la propagation des fissures et influe sur les résistances mécaniques. Nous avons étudié l'orientation des cristaux de Ca $(OH)_2$ dans la pâte de ciment Portland durcissant contre différents supports (quartz, calcaires, polyéthylène). Nous avons réalisé des enregistrements diffractométriques X sur des sections de pâte parallèles à l'interface pâte-support, et tracé sur les courbes I = f(log d). I est un indice d'orientation qui prend une valeur supérieure à 1 lorsque le cristal est orienté et d la distance entre le plan d'analyse et l'interface pâte-support. Jusqu'à une distance d_0 du support appelée limite d'orientation, I est supérieur à 1 et I = f(log d) est représenté par une droite. Au-delà de d_0, on n'observe plus d'orientation préférentielle.

Parmi les paramètres étudiés, nous montrons que la limite d'orientation des cristaux de Portlandite dépend de la quantité d'eau de gâchage : d_0 augmente avec E/C.

La pente de la droite I = f(log d) $\{d < d_0\}$ dépend, parmi les paramètres étudiés :

- de la nature du support ;
- de l'âge des éprouvettes ;
- de l'hygrométrie de conservation.

Cette pente caractérise l'aptitude des granulats à orienter les cristaux de Portlandite et la croissance de cet hydrate sur les germes déjà existant.

SUMMARY : The oriented growth of Portlandite crystals in the interfacial zone around aggregates, allowing the evolution of hair-cracks, influences the mechanical resistance. In this paper, we study the orientation of Ca $(OH)_2$ crystals in Portland cement paste hardening with different aggregates (quartz, polyethylene, limestone). Successive sections of cement paste parallel to the contact interface are studied by X-ray diffraction. The curves I = f(log d) are then plotted ; where I is an orientation index which is greater than 1 when the crystal is oriented, d is the distance between the contact interface and the analysed section. It is obvious that I is greater than 1 at the distance up to d_0, so-called the limit of orientation, and I = f(log d) is represented by the straight lines. Beyond the distance d_0, the Portlandite crystals have no particular orientation.

Among parameters studied, it is shown that the orientation limit of Portlandite crystals depends on the amount of mixing water : d_0 increased with E/C ; the slope of curves I = f(log d), for$(d < d_0)$, depend on :

- the nature of aggregate ;
- the curing time ;
- the humidity of conservation.

This slope characterizes the aptitude of aggregates for the orientation of Portlandite crystals and the growth of this hydrate from the nucleus.

Dans un béton la croissance des cristaux de Portlandite à l'intérieur de l'auréole de transition qui entoure les granulats joue un rôle important dans la mesure notamment où la formation de couches cristallines orientées favorise la propagation des fissures et contribue à diminuer les résistances mécaniques. Nous avons montré, dans une autre communication à ce Congrès International de la Chimie des Ciments (1), qu'il était possible de caractériser cette orientation en déterminant par diffractométrie X, la variation de l'ordre cristallin et la limite d_0 de la zone orientée dans la pâte, cette valeur d_0 pouvant être considérée du point de vue de l'orientation comme la limite d'influence du granulat dans la pâte.

Nous rappelons brièvement le processus expérimental mis au point à cette fin. Des éprouvettes cylindriques sont confectionnées dans des moules en matière plastique de la manière suivante : le granulat cylindrique de diamètre 2 cm est poli sur une face, l'état de surface final étant obtenu avec du diamant de finesse 5 µm. Dès la fin du polissage, la pâte de ciment est coulée sur cette face. Le ciment utilisé est du ciment Portland CPA 55 R (Norme N F P 15 - 301) dont les caractéristiques sont données dans le tableau I.

Composition chimique (%)		Composition de Bogue (%)	
Insolubles	1,08	C_3S	55
SiO_2	21,4	C_2S	24
Al_2O_3	5,3	C_3A	10
Fe_2O_3	2,3	C_4AF	7
CaO	64		
MgO	1,4		
K_2O	0,49		
Na_2O	0,04		
SO_3	2,98		
Perte au feu (CO_2+H_2O)	1,02		
Cl^-	0,01		
S	0,01		
Finesse Blaine : 320 $m^2\ kg^{-1}$			

Tableau I : Caractéristiques du ciment utilisé (CPA 55 R)

Les éprouvettes sont conservées dans l'air à 20°C ± 0,2°C et à humidité relative contrôlée. Après durcissement, les collages sont rompus et l'orientation de la Portlandite dans la zone de contact côté pâte est analysée en fonction de la distance d, plan d'analyse-face du granulat, par diffractométrie X.

Dans ce travail, nous appliquons cette méthode à l'analyse d'un certain nombre de paramètres susceptibles de modifier la croissance des cristaux de Portlandite : la nature du granulat, la quantité d'eau de gâchage, la durée et l'humidité relative de conservation. Au cours de ces essais, nous n'avons modifié ni la nature du ciment, ni la température de cure.

I - RESULTATS EXPERIMENTAUX

Dans cette dernière partie, nous exposons l'influence des différents paramètres étudiés sur les courbes I = f(log d), en particulier sur la limite d'orientation d_0 et sur la pente de la droite obtenue pour $d < d_0$. Nous analyserons la signification de ces grandeurs et leur variation dans une seconde partie.

I.1 - Influence de la nature du granulat

Les paramètres constants ont les valeurs suivantes :

- E/C de gâchage = 0,29 liant : CPA 55 R ;
- conservation à 20°C et 100 % d'humidité relative ;
- durée de conservation = 1 jour ;

Les granulats utilisés sont :

- marbre de Mosset, grosseur moyenne ≃ 2 mm ;
- marbre de Calacata, grosseur moyenne des grains ≃ 40µm ;
- quartz de Montredon Labessonie ;
- polyéthylène.

Avec ces granulats, la rupture se produit dans la pâte, l'épaisseur de la pellicule adhérant sur le support, généralement quelques micromètres, est mesurée par microscopie optique. L'orientation de la Portlandite, caractérisée par son indice I - rapport du quotient de l'intensité des raies (001) et (101) à la valeur 0,74 caractéristique de la désorientation statistique - varie dans la pâte en fonction de la distance d à l'interface selon les courbes de la figure 1.

Les différentes courbes I = f(log d) correspondant aux divers granulats convergent toutes vers le point {log 40 µm, 1}. Les cristaux de Portlandite restent donc orientés sur une distance de 40 µm, comptée à partir de l'interface, ceci, quelquesoit le granulat utilisé. Par contre, les pentes des courbes varient selon la nature des supports, ces derniers ayant donc une propension différente à orienter les cristaux de Portlandite.

Côté support, il est encore possible de déterminer l'indice d'orientation des cristaux de Portlandite par diffractométrie X, les valeurs trouvées sont très élevées (souvent supérieures à 50). Comme nous le

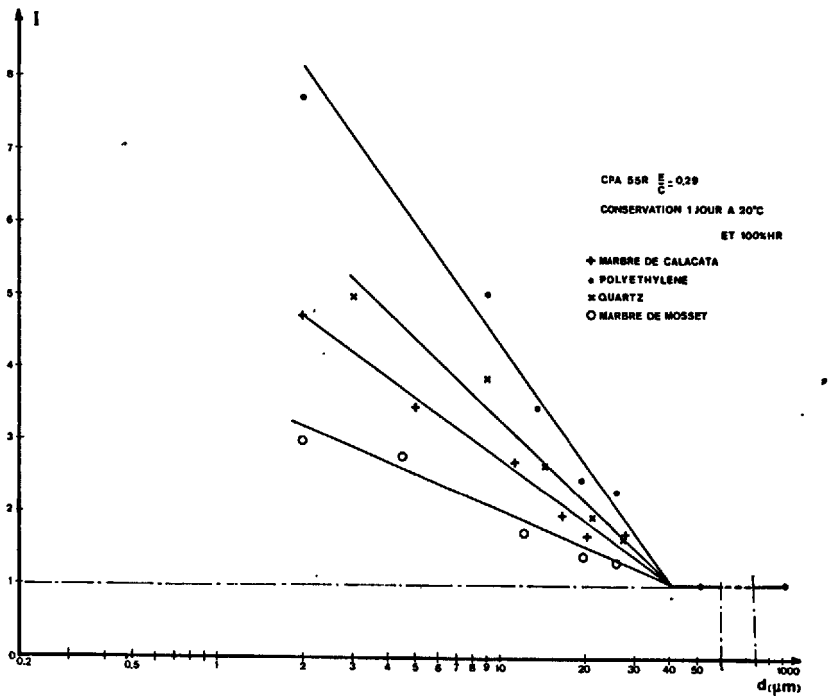

FIGURE 1 : Influence de la nature des granulats

montrons par ailleurs (1), celles-ci ne peuvent pas être portées sur la courbe I = f(log d), néanmoins, ce résultat permet de confirmer que dans le voisinage immédiat des granulats, les cristaux de CH croissent avec leur axe [001] perpendiculaire à l'interface.

I.2 - Influence du rapport E/C de gâchage

Les éprouvettes sont préparées avec du marbre de Calacata et conservées 3 jours à 20°C et 100 % d'humidité relative.

Les courbes I = f(log d) obtenues avec différentes valeurs de E/C de gâchage sont représentées à la figure 2. Les limites d_0 d'orientation de la Portlandite augmentent avec la quantité d'eau de gâchage. Les pentes des droites I = f(log d) $\{d<d_0\}$ restent identiques pour un granulat et un ciment donnés.

I.3 - Influence de la durée de conservation

Des éprouvettes analogues aux précédentes sont confectionnées avec une pâte E/C = 0,29 et des éprouvettes de marbre de Calacata. Conservées à 100 % d'humidité relative, elles sont rompues à différents âges.

Les courbes de la figure 3 représentent la variation de l'indice I en fonction de log d : au cours du vieillissement des éprouvettes, la limite d'orientation d_0 des cristaux de Portlandite n'est pas modifiée : par contre, la pente des droites I = f(log d) $\{d < d_0\}$ augmente avec l'âge. En outre, pour des durées de conservation supérieures à deux mois, la méthode d'analyse ne permet pas de déceler de modification de cette pente.

L'ordre des pentes des droites I = f(log d) $\{d < d_0\}$ observé à 1 jour avec différents granulats (marbre de Mosset, marbre de Calacata, quartz, polyéthylène) est conservé au cours du vieillissement des éprouvettes.

I.4 - Influence de l'humidité relative du milieu de conservation

Des pâtes de ciment gâchées avec E/C = 0,29 sont coulées sur des granulats de quartz et conservées 8 jours dans des atmosphères à 50, 75 et 100 % d'humidité relative.

Les courbes I = f(log d) sont tracées après rupture

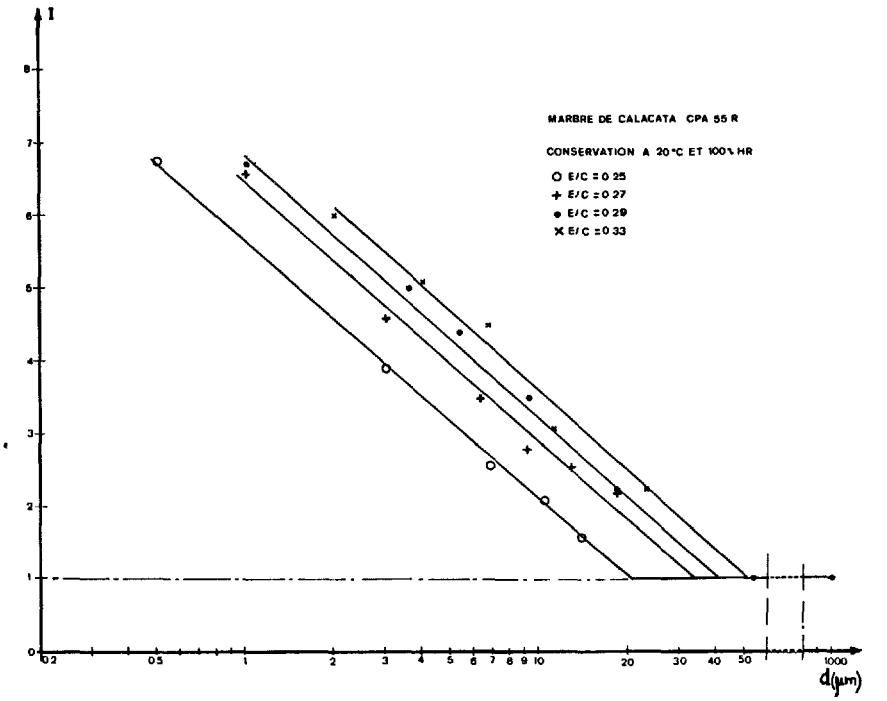

FIGURE 2 : Influence du E/C de gâchage

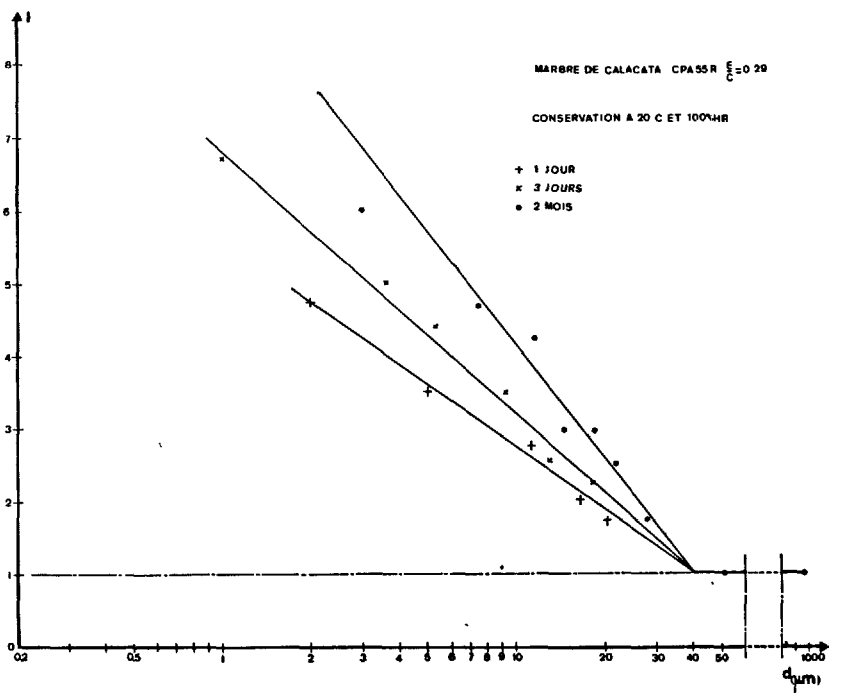

FIGURE 3 : Influence de la durée de conservation

des éprouvettes. Les droites obtenues (figure 4) convergent toutes vers le point $\{\log 40\,\mu m,\ 1\}$, la limite d'orientation d_0 n'est donc pas influencée par l'hygrométrie de l'ambiance de conservation ; par contre, la pente des droites $I = f(\log d)\{d < d_0\}$ augmente avec l'humidité relative.

II - ANALYSE DES RESULTATS

Avant de proposer une analyse de ces courbes, il est utile de remarquer que l'indice d'orientation ne représente pas la quantité de Portlandite et de noter que des résultats analogues à ceux présentés sont obtenus lorsque les paramètres fixés varient : les valeurs absolues de d_0 et de la pente des courbes peuvent alors être modifiées mais les sens de variation observés restent analogues à ceux indiqués précédemment.

Les courbes $I = f(\log d)$ permettent de caractériser l'orientation des cristaux de Portlandite dans la pâte de ciment à la distance d du granulat. En-deçà de la limite d'orientation d_0, l'indice I varie et les modes de germination et de croissance des cristaux sont tels que $I = f(\log d)$ est une droite. La pente de cette droite peut traduire deux phénomènes :

- l'aptitude des granulats à orienter les germes de Portlandite à leur contact ;

- la croissance en cours d'hydratation des cristaux de Portlandite sur ceux déjà existant.

Les résultats de la figure 1 montrent que la taille des grains et la nature minéralogique des granulats influencent l'orientation des cristaux de Portlandite formés à leur voisinage dans la pâte de ciment ; elle augmente lorsque les grains du support sont plus petits et quand sa surface est plus réactive. Il est peut-être possible d'expliquer ces résultats par le fait que la germination des cristaux d'hydrates se produit en priorité sur les défauts de la structure du support, en particulier sur les joints de grains. Par contre, lorsque le granulat réagit avec la pâte de ciment, la formation des couches orientées de Portlandite est perturbée par la libéraiton d'ions et la constitution de composés intermédiaires qui en résultent. La nature des granulats n'affecte pas la limite d'orientation d_0, celle-ci n'étant fonction, parmi les paramètres étudiés, que de la quantité d'eau de gâchage.

La durée de conservation ne modifie pas l'ordre des pentes observé sur la figure 1 (marbre de Mosset, marbre de Calacata, quartz, polyéthylène). Ainsi, si si l'on admet que, pour un âge et une pâte donnés, la quantité de Portlandite à une distance d quelconque du granulat est la même, quelquesoit la nature de celui-ci, les résultats que nous avons obtenus expliquent, en partie, les bonnes propriétés mécaniques des bétons de granulats calcaires (2) : la propagation des fissures à travers les cristaux de Portlandite y serait rendue plus difficile du fait de leur orientation plus faible.

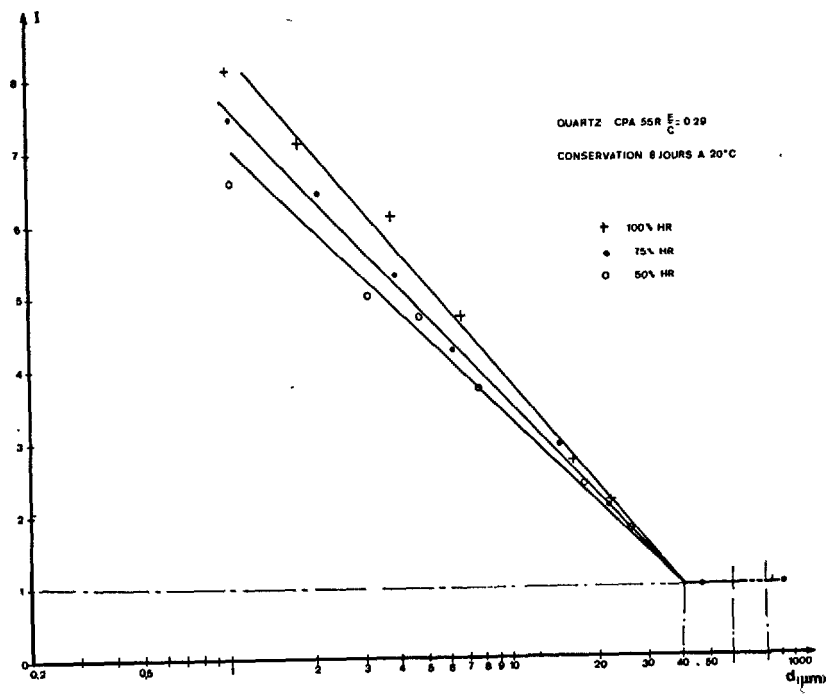

FIGURE 4 : Influence de l'humidité relative de conservation

Les autres courbes correspondent à des modifications de l'état d'hydratation de la pâte. Lorsque cette hydratation est plus avancée du fait de l'augmentation de l'hygrométrie ou de la durée de conservation, la pente de la droite $I = f(\log d) \{ d < d_0 \}$ augmente. Ainsi, à une distance de l'interface inférieure à d_0, l'orientation des cristaux de Portlandite augmente avec le degré d'hydratation. Ce résultat pourrait s'expliquer par le mode de croissance des cristaux sur des germes déjà existant. A cet égard, des essais complémentaires en microscopie électronique à balayage ont montré qu'au voisinage du marbre, la croissance de la Portlandite était de type dendritique selon des directions [u, v, o] (figure 5), ce qui entraîne un renforcement de l'orientation existant aux premiers âges.

III - CONCLUSION

Nous avons montré que la pente de la droite $I = f(\log d) \{ d < d_0 \}$ et la limite d'orientation d_0, traduisent de manière notable des différences de cristallisation de la Portlandite dans l'auréole de transition. Cette technique peut donc être utile à l'étude de l'influence des différents paramètres de composition et de cure sur le comportement mécanique des bétons et, par voie de conséquence, aider à indiquer dans quel sens il conviendrait d'agir sur les constituants et les conditions d'hydratation pour améliorer la liaison pâte de ciment-granulat.

BIBLIOGRAPHIE

(1) GRANDET J., OLLIVIER J. P. (1980) "Nouvelle méthode d'étude des interfaces ciment-granulats". Septième Congrès International de la Chimie des Ciments , PARIS (Français)

(2) MASO J. C. (1967) "La nature minéralogique des agrégats, facteur essentiel de la résistance des bétons à la rupture et à l'action du gel". Thèse TOULOUSE (Français).

FIGURE 5 : Croissance dendritique de la Portlandite

Effect of pozzolanic reactions on the mechanical properties of glass fiber reinforced cement

Les effets des réactions pouzzolaniques sur les propriétés mécaniques de ciment armé de fibres de verres

S. OHSAWA, Officier de Technique, et
R. KONDO, Dr. Professeur,
Dept. Inorg. Matières, Faculté de Technologie Institut de Technologie de Tokyo, Japon.

RESUME : Pour diminuer l'alcalinité de la matrice ciment, dans le ciment armé aux fibres de verre et réduire ses dégradations, on ajoute au ciment portland diverses sortes de pouzzolanes et de laitier. Des éprouvettes ont été confectionnées avec des ciments comportant de tels ajouts, et des fibres de verre résistant aux alcalis, ou fibres de verre du type E. Après conservation humide, on a examiné la corrosion des fibres de verre de ces éprouvettes, et mesuré la réduction de leurs propriétés mécaniques.

Les résultats ont montré que, même avec les verres résistant aux alcalis, les résistances mécaniques des éprouvettes diminuaient avec le temps. Mais la corrosion des verres résistant aux alcalis est seulement superficielle, et elle provoque une augmentation de l'adhérence des fibres à la matrice. Ce phénomène peut être attribué au fait que les hydrates du ciment pénètrent à l'intérieur des bottes de fibres. Le résultat est cependant une augmentation de la fragilité.

En remplaçant une partie du ciment par un zéolite, du métakaolin ou du verre de silice, on diminue la corrosion des fibres. En somme, les pouzzolanes, qui ont une grande affinité pour la chaux, sont efficaces pour réduire cette corrosion.

SUMMARY : For the purposes of decreasing the alkalinity of cement matrix in glass fiber reinforced cement and to minimize the degradation of mechanical properties of the composite, various kinds of pozzolanic materials or slag are added to portland cement. The composites consisted of the above materials, cement and alkali-resistant glass fibers or E-glass fibers are prepared and cured. The corrosion of glass fibers is compared and the changes of mechanical properties of composites are determined.

The results show that even alkali-resistant glass fiber is used, the strength of the composites decreases with passage of curing time. As alkali-resistant glass fiber is corroded only slightly and sticks with matrix so tightly, the reverse effect of cement to the reinforcing fiber is considered. This phenomenon must be attributed to the packing of cement hydrates into the bundle of fibers resulting in increasing the brittleness.

Replacing a part of portland cement by either zeolite, metakaolin or silica glass, the corrosion of glass fibers effectively decreases. On the whole, the pozzolanic material which has high reactivity with $Ca(OH)_2$, is effective for decreasing the corrosion of glass fibers.

INTRODUCTION

As a representative of ordinary glass fibers, E-glass fiber is easily deteriorated with time in high alkali environment as in hardened portland cement. In order to prevent this phenomenon, plastic coating etc. have been attempted on the glass fibers. Still, there is insufficient success reported. At present, the following methods are considered to be the solution:

1. To produce the excellent alkali-resistant glass fibers.
2. To make the cement matrix lower in alkali content.

Concerning the first method, it is well known that ZrO_2 is effective in increasing alkali resistance. Majumdar and Ryder (1), on the basis of data obtained by Bacon and Raggon (2), confirmed that the glass in Na_2O-SiO_2-ZrO_2 system was excellent in alkali resistance. These glass fibers are called "Cem-FIL" and commercially available nowadays. The effectiveness of ZrO_2 on the alkali resistance has been confirmed by several scientists (3, 4, 5).

Concerning the second method, it is believed that the alkalinity of cement matrix can be lowered by substituting a part of portland cement with pozzolan. Addition of pozzolans is also favorable for energy saving in cement production, and reducing of heat liberation in the hydration of cement.

In connection with pozzolan, Massazza (6) published a general report. Costa and Massazza (7) showed that the hydration of Italian pozzolan slowed down at a certain stage, and about 70% of pozzolan still remained at 90 days. Majumdar (8) reported that the decrease in strength of glass fiber reinforced cement could be improved by adding fly ash. However, the reactivity of fly ash was found to be unexpectedly small by Kondo and Ohsawa (9).

As mentioned above, Italian pozzolan is not always highly reactive like fly ash. Further, as suggested by the authors (9), Italian pozzolans contain considerable alkali, which is released gradually during hydration.

The first purpose of this study is to find the pozzolanic materials which are effective for preventing the corrosion of glass fibers. The second purpose is to clarify the possibility of preventing the decrease of strength of glass fiber reinforced cement by protecting the glass fibers from corrosion.

Excellent quality pozzolanic materials such as hakudo (porous opal), opal, zeolite etc. are produced in Japan. Therefore, by substituting a part of portland cement with such materials, the corrosion of glass fibers is expected to be prevented.

MATERIALS AND EXPERIMENTAL METHOD

Glass Fibers, Cement and Pozzolanic Materials

The physical properties, chemical composition and density of the glass fibers used are tabulated in Table 1 and 2. The glass fibers are chopped E-glass fibers and chopped alkali-resistant glass fiber "Cem-FIL".

Ordinary portland cement is used, and Italian pozzolans (Segni, Bacoli, Baia and Sacrofano), opal, hakudo (porous opal), zeolite (clinoptilolite), metakaolin, fly ash, silica gel and silica glass are used as substituting materials. In addition, granulated blast-furnace slag (called "slag" for simplification) having latent hydraulic property is also used. The chemical composition of these materials is tabulated in Table 3. The nature and sources of these materials, except the opal used in this experiment (from Satsuma-Iojima), were previously noted elsewhere by the authors (9).

Italian pozzolans, opal, zeolite and silica gel are ground, sieved and only those finer than 88μm are used. Hakudo, metakaolin, silica glass and slag are originally finer than this size. The particle size distribution, Blaine fineness and density of these materials are shown in Fig. 1.

Preparation and Curing of Specimens

Before using, pozzolanic materials and slag are kept at 35°C, 100% RH until saturated. However, the moisture absorption of the materials used is less than 5 wt% except that of silica gel which is about 30 wt%. Therefore, the moisture content of each material is not taken into consideration.

According to the composition, the specimens used in this experiment are divided into three groups.

1. 100 wt% portland cement, and 70 wt% portland cement + 30 wt% pozzolanic material (or slag) dried at 105°C
2. Specimen 1 + 5 wt% E-glass fibers
3. Specimen 1 + 5 wt% Cem-FIL

The size of the specimen is 2×2×8cm and water to solid ratio is 0.4.

Since the fluidity of the cement paste con-

Table 1 - Physical properties of glass fibers

	E-glass fiber	Cem-FIL
Fiber length(mm)	12	12
Diameter of fiber filament(μm)	10	13
Number of filaments in a strand	408	204
Tensile strength(kg/mm^2)	352	255
Young's modulus (kg/mm^2)	7380	7140

Table 2 - Chemical composition and density of glass fibers (wt%)

	SiO_2	ZrO_2	Al_2O_3	Fe_2O_3	B_2O_3	CaO	MgO	Na_2O	K_2O	Density
E-glass fiber	54.0	-	13.9	0.1	11.0	17.3	3.4	0.13	0.03	2.54
Cem-FIL	61.4	16.8	0.77	0.06	0.002	5.28	0.02	14.4	0.62	2.64

Table 3 - Chemical composition of portland cement, pozzolanic materials and slag (wt%)

	SiO_2	Al_2O_3	Fe_2O_3	CaO	MgO	Na_2O	K_2O	SO_3	Others
Portland cement	22.5	5.0	3.1	64.6	1.2	0.42	0.58	2.0	IL 0.7
Segni	45.10	19.23	10.02	9.78	4.48	0.76	6.17	0.19	IL 4.23
Bacoli	53.59	18.03	4.41	8.19	1.13	3.12	7.92	0.47	IL 3.41
Baia	55.36	22.07	3.03	3.16	1.31	3.82	6.23	tr.	IL 4.62
Sacrofano	87.61	3.60	0.40	0.39	0.07	tr.	tr.	0.99	IL 7.08
Opal	96								
Hakudo	94.1	2.8	0.4	0.2			0.2		TiO_2 1.2
Zeolite	68.0	10.1	1.4	2.1	0.5		3.4		$+H_2O$ 9.7, $-H_2O$ 4.0
Georgia kaolin	45.42	38.79	0.31	0.35		0.13	0.02		TiO_2 1.53, IL 13.79
Fly ash	50.30	24.73	6.26	7.07	2.31		1.24	0.64	B_2O_3 0.25
Silica gel	99								
Silica glass	99.5	0.3	0.05		0.01		0.01		
Slag	34.13	16.25	tr.	41.52	4.82				MnO 0.50, P_2O_5 tr., Fe 0.68, FeO 0.87, S 1.02

taining slag and fly ash is remarkable, 50 wt% of sand (standard quartz sand for cement testing) has to be added. In this series of experiment, 5 wt% of glass fibers is added to the mixture of cement, fly ash (or slag) and sand.

After mixing by automatic cement mixer, the slurry of the mixture is molded into a rectangular specimen and cured at 35°C, 100% RH for 24 h. Then it is removed from the mold, and subjected to different curings as follows:

1. Directly cured at 80°C, 100% RH for 24 h.
2. Specimen, after having been treated as in 1, is subjected to further curing at 35°C, 100% RH for 3 months.
3. Same as 2 but curing time is 6 months.
4. Directly cured at 35°C,100% RH for 4 weeks.
5. Directly cured at 35°C,100% RH for 3 months.
6. Directly cured at 35°C,100% RH for 6 months.

For the specimens without glass fibers and for those with E-glass fibers, all the above curings are performed, and for those with Cem-FIL, the curings of 1, 3, 4 and 6 are performed. Further, for the specimens containing Sacrofano, only those curings of 1, 3, 4 and 6 are performed on the specimens without glass fibers and with Cem-FIL, and the specimens with E-glass fibers are not made due to lack of the quantity of Sacrofano.

Measurement of Strength

After a certain period of curing, bending and compressive strengths of the specimens are measured. Then, the hydration of specimens is stopped by D-dry method (10).

Determination of Free CaO and Free Alkali

The amount of free CaO of the specimens without glass fibers is determined by using glycerol and ethyl alcohol as the solvent (11).

The determination of free alkali is as follows : the specimen without fibers is ground, sieved and the particles between 44 and 88 μm in diameter are collected. 0.5 g of these particles is put in a beaker and 50 ml of deionized water is added. The suspension is stirred for 30 min. at room temperature to let the alkali dissolve, and then filtered. The filtrate is analyzed by flame emission spectrophotometer.

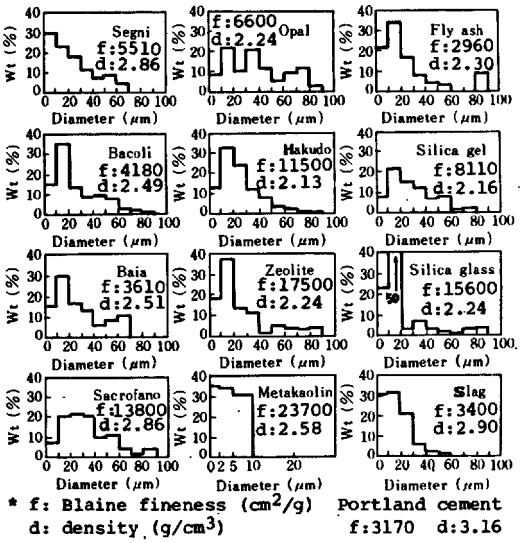

* f: Blaine fineness (cm^2/g) Portland cement
d: density (g/cm^3) f:3170 d:3.16

Fig. 1 - Particle size distribution, fineness and density of the materials used.

Observation by SEM

The degree of corrosion of glass fibers is observed by scanning electron microscope (SEM). The hydrates stuck around the fibers are removed by washing the specimen in 2N HCl for a few minutes.

RESULTS

Free CaO and Free Alkali

The relation between free CaO and curing time is shown in Fig. 2. For convenience, the amount of free CaO is calculated on ignited basis and per unit weight of cement. In both curings, the specimens with either metakaolin, silica gel, zeolite, silica glass or Sacrofano contain small amount of free CaO. The authors studied pozzolanic reactivity thermodynamically, and metakaolin was proved to have an excellent reactivity (9).

The amount of free alkali is tabulated in Table 4. The amount of free Na and K shows the similar tendency depending on the added

pozzolan. However, there is no relation between the amount of free alkali and the tendency in corrosion of glass fibers.

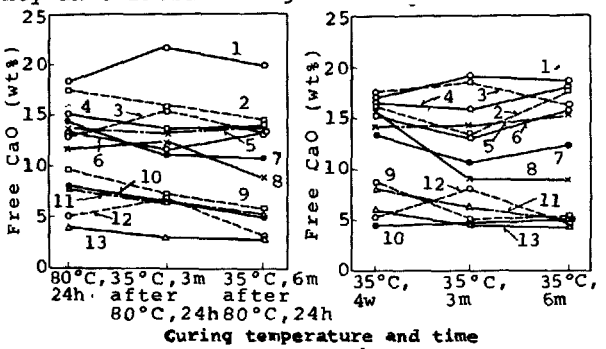

1. Portland cement
2. Slag
3. Segni
4. Baia
5. Fly ash
6. Bacoli
7. Opal
8. Hakudo
9. Silica glass
10. Sacrofano
11. Zeolite
12. Silica gel
13. Metakaolin

Fig. 2 - Relation between the amount of free CaO and curing time.

Table 4 - Free alkali in the specimen cured at 35°C for 6 months (wt%)

	Na	K
Portland cement	0.17	0.27
Segni	0.16	0.65
Bacoli	0.31	0.69
Baia	0.34	0.66
Sacrofano	0.03	0.04
Opal	0.03	0.02
Hakudo	0.04	0.04
Zeolite	0.52	0.39
Metakaolin	0.10	0.14
Fly ash	0.20	0.26
Silica gel	0.02	0.01
Silica glass	0.12	0.18
Slag	0.15	0.23

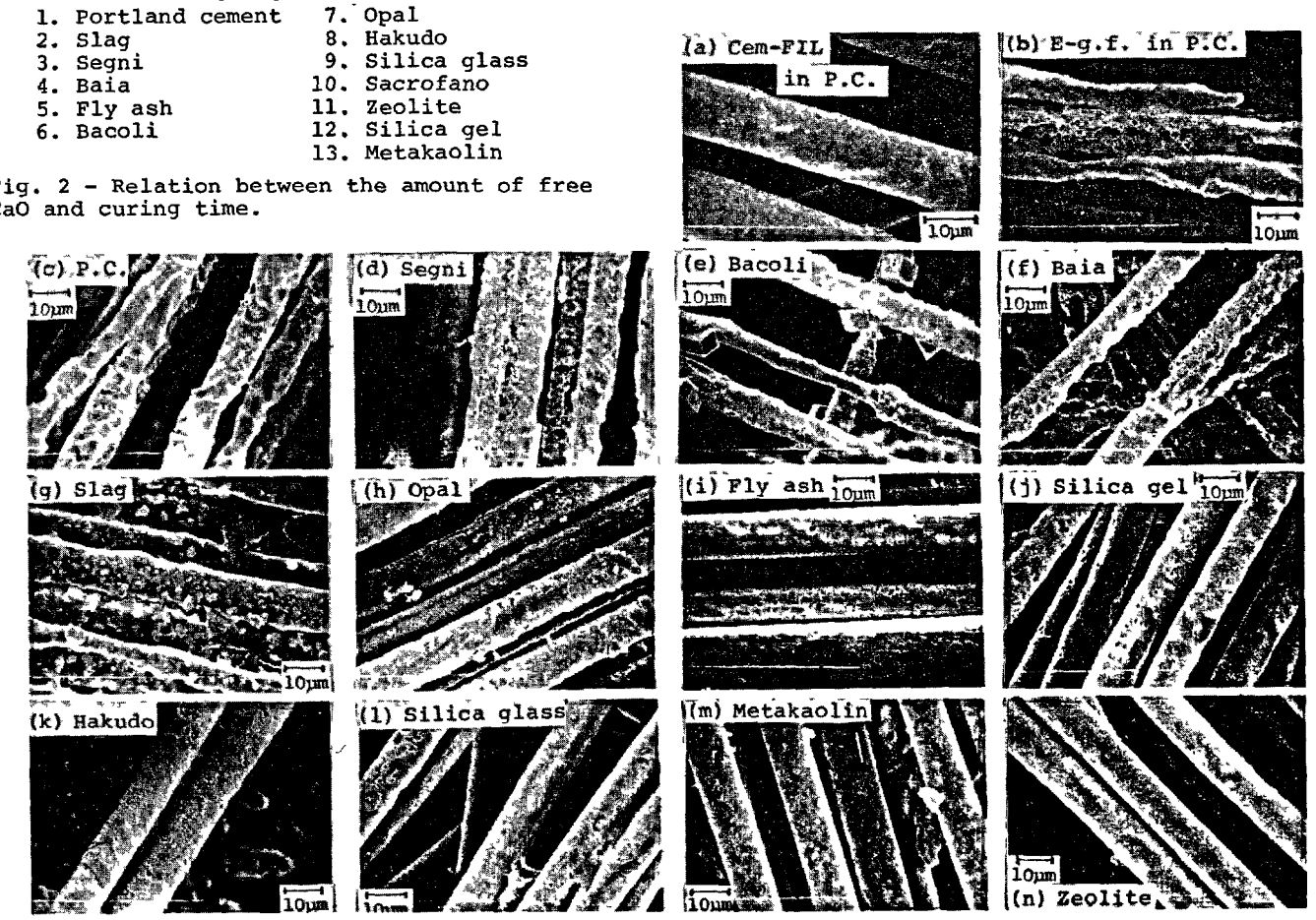

Fig. 3 - Scanning electron micrographs of the surfaces of extracted glass fibers.*
*E-glass fibers except (a) which is Cem-FIL; cured at 35°C for 6 m after curing at 80°C for 24 h except (b) which is cured at 35°C for 3 m after curing at 80°C for 24 h.

Observation by SEM

Fig. 3 (a) shows Cem-FIL in the specimen of portland cement only, cured under the condition 3 mentioned above. Although this is the most severe curing condition against glass fibers, remarkable corrosion can not be seen. The effectiveness of preventing the corrosion is shown in comparison with each other in Fig. 3. By the micrographs, the degree of corrosion of glass fibers can be arranged in the following order: portland cement=Segni=Bacoli =Baia→slag→opal=fly ash→silica gel→hakudo→ silica glass→metakaolin→zeolite. In the specimens containing a little amount of free CaO, i.e., those with highly reactive pozzolanic materials, the corrosion of glass fibers is decreased.

DISCUSSION

Bending Strength

The reinforcement of hardened cement with fibers is effective especially for tensile strength. It is difficult to discuss directly on the results of bending strength of the specimens containing fibers since the strength varies with time. Majumdar (8) used the following equation, and Clifton and Frohnsdorff (12) introduced the original reference of the equation:

$$\sigma_c = \eta_o \eta_1 \sigma_f V_f + \sigma_m V_m \quad \text{----- 1}$$

where, σ_c, σ_f and σ_m are the strength for the composite, fiber and matrix respectively; V_f is the volume fraction of the fiber and V_m is the volume fraction of the matrix; and η_o and η_1 are efficiency factors for the orientation and effective length of the fibers, respectively.

The authors incorporate the strength decreasing parameter K of the matrix due to pores into equation 1, then, it is as follows:

$$\sigma_c = \eta_o \eta_1 \sigma_f V_f + K \sigma_m V_m \quad \text{----- 2}$$

By using equation 2, the strength charged by glass fibers can be shown as follows:

$$\eta_o \eta_1 \sigma_f = \frac{\sigma_c - K \sigma_m V_m}{V_f} \quad \text{----- 3}$$

η_o and η_1 can not be estimated, but these values are constant independent of curing time. Therefore, the effectiveness of reinforcement of fibers in composite can be clarified by estimating $\eta_o \eta_1 \sigma_f$. In general, mixture rule deals with tensile strength, but it is postulated in this study that bending strength is nearly proportional to tensile strength.

K is estimated by postulating that the first term of equation 2 is 0 in the specimen of portland cement only, cured under above condition 3, which is the most severe condition and E-glass fibers are supposed to be completely corroded. Substituting the values, σ_c=115, σ_m=178, V_m=0.968 into equation 2, K equals 0.667. This value is used for all the calculations. The relation between $\eta_o \eta_1 \sigma_f$ and curing time is shown in Fig. 4. The results of the specimens with Italian pozzolans are omitted since they are remarkably corroded.

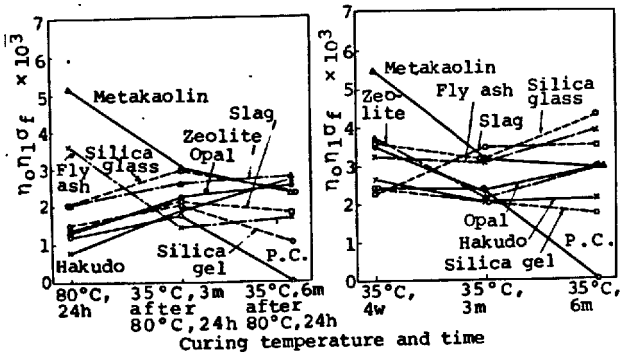

Fig. 4 - Relation between $\eta_o \eta_1 \sigma_f$ and curing time.

The following aspects can be clarified from Fig. 4.

1. Comparing the specimens cured at 80°C for 24 h and those cured at 35°C for 4 w, the strength of fibers in former one is lower.
2. In the specimens directly cured at 80°C for 24 h at first, the strength at 3 m increases except those with metakaolin or fly ash, while, those cured at 35°C, the strength at 6 m increases except that of portland cement.
3. The fibers in the specimen with metakaolin shows considerably high strength initially, but deteriorate with time and at 6 m, the strength is almost the same as the others.

Considering the results by SEM and the value, $\eta_o \eta_1 \sigma_f$, the above result 1 may be attributed to the higher corrosion of E-glass fibers in the specimen cured at 80°C for 24 h. The result 2 may be attributed to the increase in effectiveness of reinforcement, caused by the sticking of glass fibers with matrix. And the increase in effectiveness of reinforcement must be greater than the decrease of strength caused by the corrosion of E-glass fibers. Further the hydration proceeds, the tight sticking results in increasing the brittleness of the structure, and thus, the effectiveness of reinforcement is decreased.

Grimer and Ali (13) indicated that the strength of the composites made from E-glass fibers and low alkaline matrices such as super sulphated or alumina cements decreased at long curing ages. Cohen and Diamond (14) found that the strength of AR-glass fibers removed from cast composite retained the same level of strength as they had at initial stages. According to Nair (15), the effectiveness of the fibers decreased by the packing of cement hydrates into the bundles of fiber strands.

The result 3 seems to be attributed to the decrease of reinforcement of E-glass fibers since the packing may be remarkable in the specimen with metakaolin which is very fine and excellent in reactivity. As seen in Fig. 3, the corrosion of E-glass fibers is comparatively slight in the specimen with metakaolin.

Table 5 shows $\eta_o \eta_1 \sigma_f$ of the specimens reinforced with Cem-FIL. The values at 6 m are smaller than those at 4 w.

Table 5 - $\eta_o \eta_1 \sigma_f$ of the specimens reinforced with Cem-FIL

	$\eta_o\eta_1\sigma_f$ (×10³) 35°C, 4w	35°C, 6m
Portland cement	5.72	2.45
Segni	6.97	3.09
Opal	10.25	5.07
Zeolite	8.91	5.70
Metakaolin	12.94	10.83
Fly ash	6.52	6.02

As shown in Fig. 3, Cem-FIL is corroded only slightly and sticks with matrix so tightly, the reverse effect of cement to the reinforcing fiber is considered. This phenomenon must be attributed to the packing of cement hydrates into the bundle of fibers resulting in increasing the brittleness.

Relation between Compressive Strength and the Amount of Free CaO

The effect of reinforcement of fibers is small against compressive strength, and strength is rather decreased due to pores included with fibers at preparation of specimens. The following correlation can be given between the ratio of compressive strengths of the specimens with fibers to that without fibers and the amount of free CaO.

$$\frac{S_c}{S_m} = a - b \ln L$$

S_c and S_m are compressive strengths of the specimen with and without fibers respectively; L is the amount of free CaO per unit weight of matrix; and a and b are constants. The relation between S_c/S_m and the amount of free CaO is shown in Fig. 5.

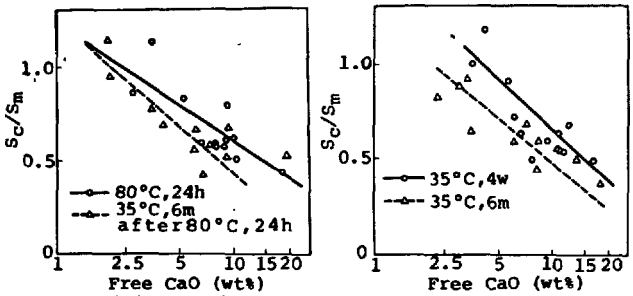

(a) Specimens with E-glass fiber

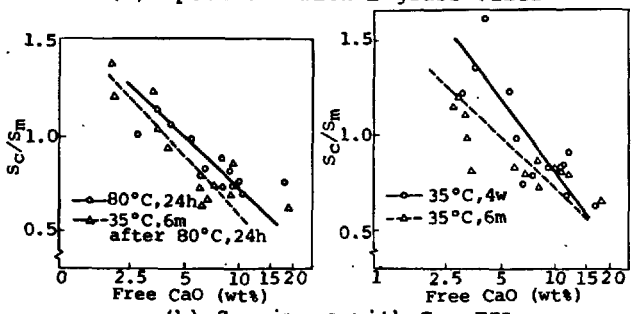

(b) Specimens with Cem-FIL

Fig. 5 - Relation between S_c/S_m and the amount of free CaO.

The following results are obtained from Fig. 5:

1. The lower the amount of free CaO, the higher the value S_c/S_m.
2. S_c/S_m is higher in the specimens with Cem-FIL than that with E-glass fibers.
3. S_c/S_m is higher at short curing time than that at long curing time.

Compressive strength can be considered to be a kind of shear strength. Therefore, compressive strength is decreased if the effectiveness of reinforcement of fibers is decreased. The phenomena 1, 2 and 3 can be considered to be attributed to the corrosion of glass fibers, "packing" and "tight sticking" mentioned above.

ACKNOWLEDGMENT

The authors wish to thank Prof. F. Massazza for supplying the Italian pozzolans.

REFERENCES

1.- A.J. Majumdar and J.F. Ryder (1968), "Glass fibre reinforcement of cement products", Glass Technol., 9, No.3, 78-84.

2.- F.R. Bacon and F.C. Raggon (1959), "Promotion of attack on glass and silica by citrate and other anions in neutral solution", J. Am. Ceram. Soc., 42, No.4, 199-205.

3.- S. Motoi and K. Urushibara (1976), "Alkali-resistant glassy fibers and their composites" (in Japanese), Gypsum and Lime, No. 140, 25-34.

4.- T. Baak, C.F. Rapp, H.T. Hartley and B.E. Wiens (1968), "Chemical durability of a soda-lime glass with TiO_2, GeO_2, ZrO_2 and $AlPO_4$ partially substituted for SiO_2", Am. Ceram. Soc. Bull., 47, No.8, 727-730.

5.- H. Ohta and Y. Suzuki (1978), "Chemical durability of glasses in the systems SiO_2-CaO-Na_2O-R_mO_n", ibid., 57, No.6, 602-604.

6.- F. Massazza (1976), "Chemistry of pozzolanic additions and mixed cements", il cemento, 73, No. 1, 3-38.

7.- U. Costa and F. Massazza (1977), "Factors determining the development of mechanical strength in lime-pozzolana pastes", Proc. 12th Conference on Silicate Industry and Silicate Science, 537-552.

8.- A.J. Majumdar (1974), "The role of the interface in glass fibre reinforced cement", Cem. Concr. Res., 4, No.2, 247-266.

9.- R. Kondo and S. Ohsawa (1979), "Reactivities of various silicates with calcium hydroxide and water", J. Am. Ceram. Soc., 62, No.9-10.

10.- L.E. Copeland and J.C. Hayes (1953), "Determination of non-evaporable water in hardened portland cement paste", ASTM Bull. 194, No.12, 70-74.

11.- R. Kondo (1966) "Kinetic study on hydrothermal reaction between lime and silica", Proc. Symp. Autoclaved Calcium Silicate Building Products, 1965, 92-97.

12.- J. Clifton and G. Frohnsdorff (1975), "Fiber-reinforced cementitious materials", Cements Research Progress 1974, Am. Ceram. Soc., 201-204.

13.- F.J. Grimer and M.A. Ali (1969), "The strengths of cements reinforced with glass fibres", Mag. Concr. Res., 21, No.66, 23-30.

14.- E.B. Cohen and S. Diamond, "Validity of flexural strength reduction as an indication of alkali attack on glass in fiber reinforced cement composites", Proc. RILEM Symp. 1975 Fiber Reinforced Cement and Concrete, 315-325.

15.- N.G. Nair, "Mechanics of glass fiber reinforced cement", ibid., 81-93.

Bond strength in very high strength concrete

L'adhérence dans le béton à très haute résistance

G.P. TOGNON, Chem. Eng., Italcementi S.p.A. - Laboratorio Chimico Centrale - Bergamo (Italy),
P. URSELLA, Chem. Eng., Italcementi S.p.A. - Laboratorio Chimico Centrale - Bergamo (Italy),
G. COPPETTI, Chem. Eng., Italcementi S.p.A. - Laboratorio Chimico Centrale - Bergamo (Italy).

SUMMARY: The exceptional mechanical properties of autoclaved concretes (VHSC, compr. strength $\geqslant$150 N/mm^2)are attributed to a strong chemical bond between cement matrix and aggregate. This bond and consequently the mechani - cal and elastic properties of these concretes decrease if the quartzy aggregates are substituted for others partially or not reactive with the hydrolysis lime of cement.
By using quartz, jasper, granite, basalt and limestone, autoclaved concretes and, as a comparison, normally cured concretes were made. The carried out tests show that the ratios of the mechanical strengths of the autoclaved concretes to those of the corresponding normally cured ones are a function of the aggregate reactivity and, in particular, of its quartz content. These ratios range between 1.18 for limestone and 2.29 for quartz.
The type of aggregate and the thermal treatment do not cause considerable variations in the moduli of elasticity of concrete, but they strongly modify the stress-strain curves.
The inelastic phenomena, such as the local plasticization and microcracking, appear the more intense the stronger the bond at the interface. Subsequent loading and unloading cycles applied to normally cured concretes give similar $\sigma - \varepsilon$ curves, independent of the aggregate and characterized by large hysteresis areas. On the contrary the same cycles applied to autoclaved concretes produce a drastic reduction in these areas. This decrease appears to be particularly marked in the concrete containing quartz aggregates, which indicates the formation of a strong aggregate-cement matrix bond.
The comparison of the elastic yields (ratios of the areas under the loading and unloading curves) of the auto - claved concretes further confirms the importance of this bond. In fact a rapid decrease in the elastic yield occurs in concretes containing not reactive aggregates for stresses over 60%, whereas this yield is nearly constant and very high (90%) up to failure in concretes containing quartz aggregates.

RESUME: Les caractéristiques mécaniques exceptionnelles des bétons autoclavés (VHSC, resistance à la compres. $\geqslant$ 150 N/mm^2) sont attribuées à la présence d'une forte liaison chimique entre matrice en ciment et agrégat. Cette liaison, et donc les caractéristiques mécaniques et élastiques des bétons, diminuent en remplaçant les agrégats quartzeux par d'autres partiellement ou pas du tout reactifs avec la chaux d'hydrolyse du ciment.
En employant quartz, jaspe, granite, basalte et calcaire, on a préparé des bétons autoclavés et, par comparaison, des bétons durcis dans des conditions normales. Les essais effectués ont mis en évidence que les rapports entre les résistances mécaniques des bétons autoclavés et celles des correspondants bétons non autoclavés sont fonc - tion de la réactivité de l'agrégat et, en particulier, de sa teneur en quartz. Ces rapports sont compris entre 1.18 pour le calcaire et 2.29 pour le quartz.
Le type d'agrégat et le traitement thermique n'entraînent pas de variations considérables des modules d'élasticité du béton, mais ils modifient nettement les courbes contrainte-déformation.
Les phénomènes non élastiques, tels que la plasticisation locale et la microfissuration, se manifestent d'une intensité d'autant plus basse que l'adhérence à l' interface est plus forte. Des cycles successifs de chargement et de déchargement appliés aux bétons durcis dans des conditions normales ont donné des courbes $\sigma - \varepsilon$ pareilles, indépendantes du type d'agrégat et caractérisées par des aires d'hystérésis larges. Au contraire les mêmes cycles appliés aux bétons autoclavés ont causé une réduction drastique de ces aires. Cette réduction a été particulièrement marquée pour le béton contenant des agrégats quartzeux, ce qui indique la formation d'une forte liaison entre agrégat et matrice en ciment.
La comparaison des rendements élastiques (rapport entre les aires au-dessous des courbes de chargement et de déchargement) des bétons autoclavés a ultérieurement confirmé l'importance de cette liaison. En effet, pour des contraintes supérieures à 60% de la charge maximale dans les bétons contenant des agrégats non reactifs, il y a une diminution rapide du rendement alors que dans les bétons contenant des agrégats quartzeux, ce rendement est presque constant et très élevé (90%) jusqu'à la rupture.

1. INTRODUCTION

The mechanical strength and the inelastic deformation of concretes under load are affected by the composite nature of the material and particularly by the matrix -aggregate interface, the latter being the weakest point of the concrete (1)(2)(3)(4)(5).
The mechanical properties of very high strength concretes (VHSC, compr. strength $\geqslant 150$ N/mm^2)(6) and their elastic behaviour are not justifiable if a substantial improvement in the interface bond is not recognized. The strengthening of such a bond, which appears as a "weld bead" between cement matrix and siliceous aggregate, was already pointed out in a previous paper (7) and justified by electron microscope observations and microhardness measurements (8).
In order to verify the relationship between interface bond and elastic and mechanical properties of VHSC made with quartzy aggregates, the effects caused by the substitution of quartz for aggregates having different nature were evaluated in the present work.

2. EXPERIMENTAL

2.1 The materials used for the tests were:

a) Aggregates
The concretes were made with five different aggregates, all excellent for the preparation of ordinary concretes which, owing to the different chemical composition, showed different capabilities of fixing the hydrolysis lime of cement in autoclave.
Table I shows the five aggregates together with the respective total and quartzy SiO_2 content and their mechanical properties measured on 50 mm diam., 100 mm high cylindrical specimens.
The same table gives their "reactivity" with respect to cement, expressed as mechanical strength of autoclaved specimens consisting of 55 parts of 525 Ptl cement and 45 parts of aggregate ground to a Blaine specific surface of 4500 cm^2/g.

Table I: Properties of the aggregates

Aggregate	Compressive strength N/mm^2	Modulus of elasticity N/mm^2	Poisson's ratio	Total SiO_2 %	Quartzy SiO_2 %	Reactivity N/mm^2
Barzana quartz	n.d.	72150	0.05	95.9	86.2	152.5
Jasper	n.d.	76500	0.11	85.1	54.4	109.5
Granite	226	33600	0.09	72.9	30.8	82
Limestone	174	58500	0.17	0.4	0.3	55
Basalt	334	103500	0.24	43.6	1.1	53
Cement paste	-	-	-	-	-	80

Mixing water: 26%
Curing cycle: presteaming 16 h at 20°C
autoclaving 10 h at 190°C

The aggregates, divided into four fractions, had a maximum diameter of about 8 mm.

b) Binder
A mixture of high strength and rapid hardening portland cement (525 class) and quartz ground to the same fineness as the cement was used.

c) Water
The w/b ratio was maintained rather low owing to the use of a superplasticizer assuring a good workability of the mix.

d) Superplasticizer
A naphthalene sulphonate formaldehyde condensate (25 wt % solution) was used.
The concretes were made according to the proportions and the working modes already used (6) and summarized in Tables II and III.
Concretes cured under normal conditions (T = 20°C, R.H. = 100%) were made as a comparison; in this case the binder was only cement.

TABLE II: Composition of concretes

Concretes cured at 20°C, R.H.100%	Components of the mixture	Autoclaved concretes
	Binder	
500 - 500 kg/m^3	525 Ptl cement Ground silica	410 / 200 610 kg/m^3
	Aggregate	
1650 kg/m^3	fract. 0-1.5 mm 20% 1.5-3 mm 35% 3-6 mm 20% 6-8 mm 25%	1550 kg/m^3
	Superplasticizer	
2.5 wt. % of the binder	naphthalene sulphonate formaldehyde condensate (25 wt.% solution)	2.5 wt. % of the binder
0.42	Water/binder ratio	0.35

TABLE III: Thermal treatment

Presteaming	about 17 h at 20°C
Low pressure steam curing	8 h at 60°C
Rate of temperature rise	0.7°C/min
High pressure steam curing	24 h at 190°C
Rate of temperature rise	0.7°C/min

2.2 Testing modes

The concretes were cast into prismatic moulds and, after autoclaving or a 21 day curing, they were cored to obtain 70 mm diam., 200 mm high cylinders. These leveled and ground up to a flatness allowance lower than 25 μm, were used to determine the compressive strength, the elastic properties and the strain energy ratios.
The strains were measured by eight resistance strain gauges having a 30 mm gauge length: four of them were directed to the load and four were orthogonal to it. The detection system was a data logger arranged so as to give the deformation values with a sensitivity of $1 \cdot 10^{-6}$ or $0.1 \cdot 10^{-6}$ and the stress values with a sensitivity of 0.01 N/mm^2.
The data were taken every 60 min up to 90÷95% of the maximum load and afterwards every 10 sec. The testing machine operated at constant increase of load equal to $2 \cdot 10^{-6}$/sec.
The strain energies were measured by using the same working modes, except that the transducers were inductive instead of resistive. The samples were submitted to a series of 5 or 6 loading and unloading cycles; after each cycle, the load was increased by about 1/5 of the maximum strength of the specimen. By repeating the sequence of the cycles on several specimens, one per each cycle, significant differences in the hysteresis loop did not appear.

3. RESULTS

The values of mechanical strength are shown in Table IV. The secant moduli of elasticity and Poisson's ratios, given in Table V, were determined for stresses ranging between 2 and 22 N/mm^2.

TABLE IV: Compressive strength (N/mm^2) of normally cured and autoclaved concretes

(70 mm diam., 200 mm high cylindrical specimens)

Concretes with aggregates of	Normally cured 28 days	Normally cured 60 days	Autoclaved
Limestone	68	75	88.5
Basalt	82.5	91.5	117
Granite	72.5	86.5	141.5
Jasper	69.5	71.5	148
Quartz	72.5	78	179

TABLE V: Secant modulus of elasticity and Poisson's ratio

Stresses between 2 and 22 N/mm^2

Concretes with aggregates of	E(N/mm^2)		Poisson's ratios (μ)	
	normally cured	autoclaved	normally cured	autoclaved
Limestone	38650	34540	0.270	0.235
Basalt	42050	47270	0.220	0.230
Granite	24680	28210	0.170	0.160
Jasper	35510	39620	0.170	0.168
Quartz	37790	45050	0.171	0.137

In a second series of tests, the samples were deformed up to and beyond the maximum load, by determining the values of σ_z, ε_z towards the load axis and the circumferential strain ε_θ. It was possible to plot the $\varepsilon_z = \varepsilon_z(\sigma_z)$, $\varepsilon_\theta = \varepsilon_\theta(\sigma_z)$ curves and those of the derivative variables $\mu(\sigma_z) = \frac{\varepsilon_\theta}{\varepsilon_z}$ e $\frac{\Delta V}{V}(\sigma_z) = |\varepsilon_z| - 2|\varepsilon_\theta|$.

The $\sigma_z = \sigma(\varepsilon_z)$ curves were interpolated by a parabola passing through the origin (for 10 or more degrees of freedom, the determination index ≥ 0.999) (9)(10).

The values of the coefficients "b" and "c" of the interpolating parabolas are shown in Table VI (for σ in N/mm^2).

Table VII gives the values of the critical loads, expressed as percentage of the maximum load: σ' relevant to the load at which the curve $\mu(\sigma_z)$ deviates from the rectilinear trend and σ'' corresponding to the load at which $\Delta V/V$ (σ_z) reaches the maximum value.

Based on the loading and unloading σ-ε curves, the strain energy was determined by integrating the area under the curves themselves; the ratio of the strain energy during unloading to the one during loading was defined as "elastic yield".

Table VIII shows the values of the elastic yields for loads as percentage of the maximum load.

4. DISCUSSION

- The ratio of the mechanical strength of autoclaved concretes to the one of the corresponding concretes

TABLE VI: Coefficients b and c of the interpolating parabolas $\sigma = b\varepsilon + c\varepsilon^2$

Concretes with aggregates of	b	c
Normally cured		
Limestone	0.040142×10^6	-6.58974×10^6
Basalt	0.048158	-7.76454
Granite	0.031212	-3.50825
Jasper	0.041999	-6.56471
Quartz	0.040494	-6.29148
Autoclaved		
Limestone	0.043246×10^6	-5.54026×10^6
Basalt	0.060456	-7.93733
Granite	0.034894	-1.57885
Jasper	0.041718	-1.42230
Quartz	0.051007	-2.37339

TABLE VII: Critical loads expressed as percentage of the maximum load

Concretes with aggregates of	σ' %	σ'' %
Normally cured		
Limestone	76.83	96.17
Basalt	74.02	92.19
Granite	76.51	88.77
Jasper	77.13	95.97
Quartz	72.86	94.57
Autoclaved		
Limestone	80.68	94.90
Basalt	82.87	94.78
Granite	85.00	91.94
Jasper	78.69	93.97
Quartz	89.23	97.69

normally cured for 60 days varies versus the aggregate. The values of 1.18 and 1.28, obtained by using limestone and basalt respectively, indicate that autoclaving does not improve strengths considerably. On the contrary, different results are obtained with granite, jasper and quartz whose ratios increase to 1.64, 2.07 and 2.29.

As previously pointed out (6), it is the quartz content of the aggregate that has a determining effect on the strength increase.

- The thermal treatment in autoclave does not involve appreciable variations in the secant moduli of elasticity (Young's modulus): the latter increase by about 10-20%, except for concretes containing limestone. This result is in agreement with the fact that the modulus of elasticity of the matrix, made up of the finest part of the concrete, rises by about 30% after autoclaving.

TABLE VIII: Elastic yield versus load (in % with respect to the maximum strength of the sample)

Concretes with aggregates of	20	40	60	80	90	100
Normally cured						
Limestone	96	90	79	65	58	45
Basalt	93	85	77	66	58	45
Granite	82	77	70	61	54	45
Jasper	96	92	85	75	69	55
Quartz	93	86	77	67	61	50
Autoclaved						
Limestone	97	94	92	88	86	n.d.
Basalt	97	96	93	87	83	n.d.
Granite	87	87	87	84	83	n.d.
Jasper	98	97	96	94	92	n.d.
Quartz	97	97	96	94	93	n.d.

- On the contrary the stress-strain curves, determined up to cracking and represented by the interpolating parabola, depend on both the autoclaving and the aggregate.
This deviation from the ideal elastic trend (rectilinear) was related, by different Authors (11)(12), to the formation of microcracks and local phenomena of plasticization.
The results of Table VI show that the values of the coefficient "c" for the concretes with quartz, granite and jasper reduce, after autoclaving, by about one third of the corresponding values of normally cured concretes. For the concrete with calcareous and basaltic aggregates, the thermal treatment does not involve considerable variations of "c".
By assuming that the matrix, notwithstanding the different nature of the fine part of the aggregates, can be considered substantially the same for all the types of concrete, the variations of "c" must be attributed to the reaction between silica of the aggregates and lime of the matrix. Therefore it must be thought that the inelastic phenomena, such as the local plasticization and microcracking, proceed with much lower intensity versus the applied load when the reaction at the interface occurs.

- By examining the values of σ' and σ'' shown in Table VII, it can be noted an obvious difference between autoclaved and normally cured concretes as regards the first critical load corresponding to the beginning of the microcracking indicated by the increase in Poisson's ratio (2)(13). On the contrary, no significant difference is observed for the second critical load. This should lead to suppose that once cracking has begun, even if for higher loads, the percent load of the initial increase of the concrete volume (maximum value of $\Delta V/V$), is about equal for autoclaved and normally cured concretes.

- To catch the difference in the elastic behaviour of the different concretes, it is useful to represent their σ-ε curves in subsequent loading and unloading cycles (14). Figures (1a) and (1b) relevant to two concretes cured under normal conditions, containing basalt and quartz aggregates respectively, show substantially analogous curves. After autoclaving, the behaviour of the concretes themselves is modified: the hysteresis areas undergo a considerable reduction, as shown in figures (2a) and (2b); this decrease appears to be particularly marked in the quartz concrete owing to the formation of an aggregate-cement matrix bond.

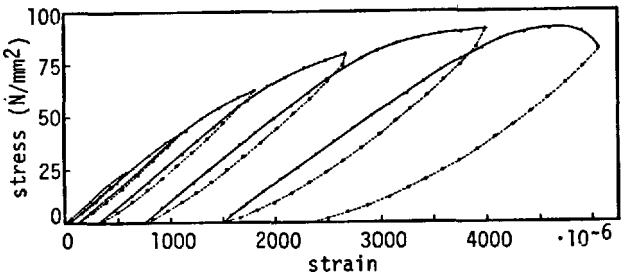

FIGURE 1a: σ-ε curves in subsequent loading and unloading cycles for normally cured concrete containing basalt aggregate

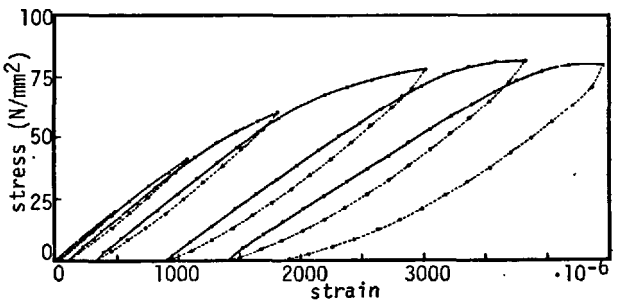

FIGURE 1b: σ-ε curves in subsequent loading and unloading cycles for normally cured concrete containing quartz aggregate

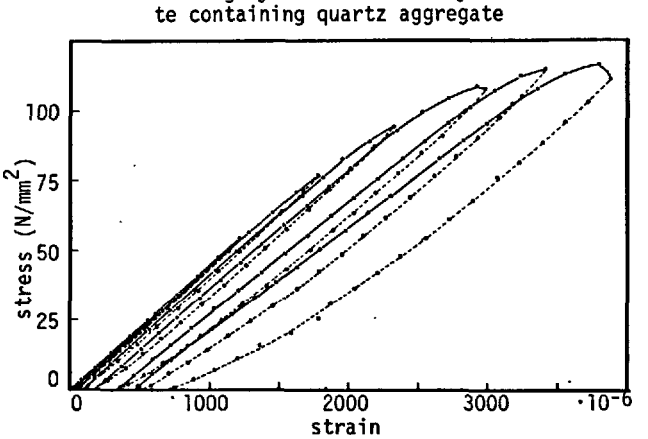

FIGURE 2a: σ-ε curves in subsequent loading and unloading cycles for autoclaved concrete containing basalt aggregate

The comparison among the behaviours is more significant if the values of the elastic yield, given in Table VIII, are examined. All the autoclaved concretes, for stresses up to 50% of the applied load, have about the same elastic yield; for higher stresses, the elastic yield is nearly constant and very high up to about failure in concretes containing quartzy aggregates (quartz and jasper), whereas a rapid decrease occurs in concretes with not reactive aggregates. In

fact 90% is exceeded for stresses of 90% of the maximum load. As regards the same concretes cured under normal conditions, 90% of the elastic yield is obtained by not exceeding 20÷40% of the maximum load.

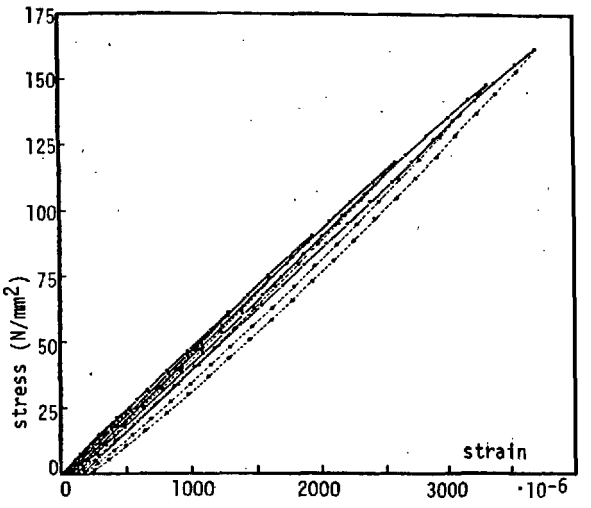

FIGURE 2b: σ-ε curves in subsequent loading and unloading cycles for autoclaved concrete containing quartz aggregate

The foregoing is pointed out by the curves shown in Fig. 3 concerning the elastic yield of the concrete containing not reactive aggregates (basalt) and of the one with highly reactive aggregates (quartz). The difference in the two behaviours for loads over 60% is an index of the increase in the load at which cracking begins, owing to the formation of an interface bond having higher strength.

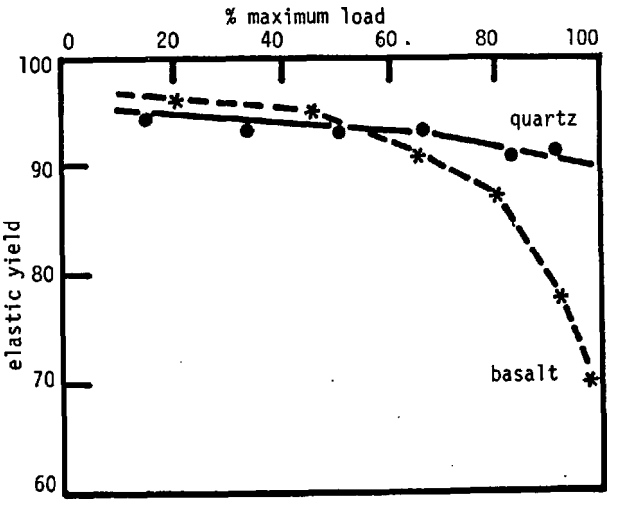

FIGURE 3: Elastic yield versus percentage of maximum load for autoclaved concretes containing basalt and quartz aggregate

5. CONCLUSIONS

Since it was possible to obtain a significant gain in strength in a VHSC by transforming it from binary system, typical of an ordinary concrete, to an almost homogeneous product, the main phenomena of this conversion due to the silica-lime reaction at the interface were investigated.
Actually the VHSC containing reactive aggregates show, when the "weld bead" has formed, only a slight deviation under load from the theoretical linear trend (elastic trend). Moreover the elastic yields, related to the formation of cracks at the interface (the weakest point of concrete), strongly increase, that is they shift towards higher percent values of the maximum load.

REFERENCES

(1) SHAH S.P., WINTER G. (1968) "Inelastic behaviour and fracture of concrete"
ACI Publication SP-20, 5-28 (Eng.)

(2) SHAH S.P., CHANDRA S. (1968) "Critical stress, volume change, and microcracking of concrete"
J. Amer. Concr. Inst. 65 (9), 770-81 (Eng.)

(3) MASO J.C. (1969) "La nature minéralogique des agrégats, facteur essentiel de la résistance des bétons à la rupture et à l'action du gel"
Revue des Matériaux No. 647/48, 247-76; No. 649, 321-30 (French)

(4) SWAMY R.N. (1971) "Aggregate-matrix interaction in concrete system"
Int. Conf. on Structure, Solid Mechanics and Engineering Design in Civil Engineering Materials, Southampton, U.K., 1969, 301-15 (Eng.)

(5) TANIGAWA Y. (1976) "Model analysis of fracture and failure of concrete as a composite material"
Cement and Concrete Research 6 (5), 679-90 (Eng.)

(6) TOGNON G.P., COPPETTI G., URSELLA P. (1978) "Very high strength concretes for precasting: production technology and characteristic properties"
9th Int. Congr. Precast Concrete Industry, Wien 1978, I/39-46 (Eng.)

(7) TOGNON G.P. (1977) "Calcestruzzi ad altissima resistenza per la prefabbricazione"
L'Ingegnere Libero Professionista (11), 889-901 (Ital.)

(8) MASSAZZA F., PEZZUOLI M. "Cement paste-quarz bond in autoclaved concretes"
Presented at 7th Int. Congr. on the Chem. of Cement, Paris 1980 (Eng.)

(9) MURZEWSKI J. (1971) "Random structure of a quasi-homogeneous material"
Int. Conf. on Structure, Solid Mechanics and Engineering Design in Civil Engineering Materials, Southampton, U.K., 1969, 105-16 (Eng.)

(10) WANG P.T., SHAH S.P., NAAMAN A.E. (1978) "Stress-strain curves of normal and lightweight concrete in compression"
J. Amer. Concr. Inst. 75 (11), 603-11 (Eng.)

(11) JENKINS G.M. (1971) "The influence of fine microfissures on mechanical properties"
Int. Conf. on Structure, Solid Mechanics and Engineering Design in Civil Engineering Materials, Southampton, U.K., 1969, 67-73 (Eng.)

(12) SWAMY R.N., KAMESWARA RAO C.V.S. (1973) "Fracture mechanism in concrete systems under uniaxial loading"
Cement and Concrete Research 3 (4), 413-27 (Eng.)

(13) BERNTSSON L., HEDBERG B., MALINOWSKI R. (1971)
"Triaxial deformations by uniaxial compressive load on heat-cured and high-strength concrete"
Int. Conf. on Structure, Solid Mechanics and Engineering Design in Civil Engineering Materials, Southampton, U.K., 1969, 799-813 (Eng.)

(14) SPOONER D.C., DOUGILL Y.M. (1975) "A quantitative assessment of damage sustained in concrete during compressive loading"
Magazine of Concrete Research 27 (92), 151-60 (Eng.)

Some problems of the chemistry of adhesion, Cement hardening and the strength of cement stone

Adhérence aux granulats, durcissement et résistance de la pâte de ciment durcie

M.M. SYCHEV, Leningrad Lensoviet Technological Institute, Leningrad, U.S.S.R.,
L.B. SVATOVSKAYA, Leningrad Institute of Railway Engineers, Leningrad, U.S.S.R.

RESUME : En prenant pour base les transferts, entre atomes, de leurs électrons périphériques, on a élaboré un modèle chimique, qui permet l'étude de l'adhérence du ciment aux granulats; il permet aussi d'examiner les aspects chimiques de la cohésion des pâtes de ciment durcies, et de la résistance des mortiers.

SUMMARY: The role of phenomena connected with electron transfer, the chemical model, of cohesion and adhesion contacts, are presented and the chemical aspects of cement adhesion are considered and the nature of cement stone strength is discussed.

Some problems connected with the chemistry of cement pastes and mortars condensation including the problems of hydration mechanism are dealt with.

Initial Hydration Stages Connected with the Transfer of Charges- electrons, protons. One of the stages of cementing phase formation is the breaking of the bonds -O-Ca-O- in cement minerals which are partly polarised, nevertheless they cannot be broken by the water polar molecules and are most probably broken by protonation (1,2). The bonds of -O-type are broken only in the alkali medium as a result of complex-formation with OH^- groups increasing silicon coordination number to five or six (3). The protons concentration is not great in water, it is determined by the degree of water dissociation. The authors think, however, that the supplier of protons in water may also be dissociative adsorption, i.e. the dissociation of water molecules on the active centres of solid phase surface. The adsorption on the active centres is accompanied by partial transfer of electron density according to the link: active centre - adsorbed molecule. The process of charge transfer, therefore, may be influenced from outside by introducing corresponding substances - activators. Activators may be substances with electron-donor or acceptor properties, these are oxidizing or reducing agents. Their influence will be felt at the stage of donor-acceptor element of hydration mechanism of cement minerals and of hardening kinetics. Experiments made by the authors showed (4,5) that the activators introduced into cement paste in the amounts of 0.5 - 3% produce great effect upon the kinetics of hydration and hardening. Substances containing free and easily excited electrons such as d-10 metals (Cu, Zn), p-metals with high quantum number n (Pb), simple and complex slightly soluble semiconductors (B, Si_2O, Sb_2S_3) i.e. electron donors inhibit the hydration and hardening processes often reducing early strength (24 hours) to zero. While electron acceptors d 2-8 metals, substances containing elements with high and mean oxidation degrees (inorganic oxidizing agents), lead to the acceleration of hydration and to a considerable growth of early strength.

Physico-chemical investigations showed that the inhibition of hydration and hardening due to substances which are electron-donors takes place as a result of stopping or inhibiting the hydration of silicate cement component while the aluminate component is often hydrated in a usual manner. In the contact of cement minerals with an electrolyte into which an oxidizing or reducing agent is introduced the change of oxidation-reduction potential of the solution leads to the change of electrostatic potential in the interface as a result of which the interchange of charges may take place through the interface boundary - the injection of electrons or holes (i.e. the mineral surface will lose some of its electrons) that will affect the concentration of active centers.

The process of deactivation in introducing powdered copper which loses its electron according to the schedule:

$$2\,Cu - 2\,e = 2\,Cu^{+1} \qquad (1)$$

is reduced to the transfer of an electron onto the surface of silicate minerals probably according to the system of H-bonds:

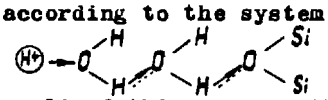

(2)

As a result of this process the proton loses its activity and for some time it does not decompose the silicate. But the electron may happen to reach an active centre of the silicate and to attenuate it.

Atoms of oxygen concentrating positive charges (holes) around themselves are likely to be taken for active centres. The result of this electron effect is the retardation of hydration and hardening decreasing the amount of combined water, the absence in the X-ray patterns and derivatopatterns of $Ca(OH)_2$ effects. Activation process should in this case be concerned with the increase of active centres concentration due to the transfer of electrons from the surface of the clinker minerals to an acceptor and due to the increase of holes concentration. Besides, the acceleration of the proton transfer according to Scheme 2 by H-bonds may also lead to activation. And, indeed, in the presence of d 2-8 metals (acceptors) and also of certain oxidizing agents the increase of combined water amounts takes place along with the growth of early strength as well as the increase of the intensity of $Ca(OH)_2$ effects.

Cement Paste Condensation. The reaction of powder and mixing liquid leads to the increase of S/l relation developing with time (selfdrying of the system), to the increase of solid phase surface at the expence hydrate generation up to 100-500 m^2/gr and to warming up due to hydration heat. The intergrain condensation beside these processes is connected with the interaction of the liquid with the surface of cementing phases and the filler, the initial action of which is the process of metting and the formation of hydrogen and donor-acceptor bonds. At the early stages of hardening up to 50% of water is bound by the surface forces according to the NMR data which results in the structurized state of the greater part of the liquid for which quasisolid properties are characteristic. So, the initial strength of the stone during setting is partly determined by the cohesion properties of water interlayers enveloping solid particles .

Continuous combination of water into hydrates and the inner suction (drawing off) lead to the reduction of water interlayers among solid particles. In the outcome the water molecules from aquaous interlayers are transformed into surface hydrate phases - the components of hardening structure:

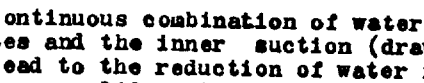

The fact that the grains may be linked by surface hydrates is due to bridge water molecules being a liquid phase component and a cementing phase structural component simultaneously, the saturated solutions of crystalline hydrates being relative in composition to their crystal structure.

Warming up of the system due to the hydration heat, metastability of the amorphous hydro-silicate phases, local pH change contribute to the proceeding of polycondensation processes:

$$\equiv Si\text{-}OH + OH\text{-}Si \equiv \xrightarrow[\Delta pH]{\Delta t} \equiv Si\text{-}O\text{-}Si \equiv + H_2O$$

and to the formation of strong contacts owing to the bonds $\equiv Si\text{-}O\text{-}Si \equiv$ playing considerable part in forming the strength of cement stone, 50% of the strength being connected with the contacts of polycondensation nature.

Chemistry of Cement Stone Strength. The authors showed (6,7) the existance of correlation between crystallochemical, energy and thermodynamical characteristics of the phases of new formations and the strength of cement stone. Lafuma considered cement stone strength to be determined by hydrogen bonds. Calculations showed (8), however, that the activation energy of bonds breaking up in the destruction of cement stone is 26 k. cal/mole, it supports the conception of one of the authors (9) that the donor-acceptor bonds of the type: $= Ca - O \begin{matrix} < H \\ < H \end{matrix} > O =$ contribute to the strength properties as well as the bonds formed on the basis of polycondensation processes (10). According to (11), the activation energy of bonds breaking up in the destruction of cement stone dehydrated at 400°C (when up to 50-60% strength is lost) is equal to 95 k.cal/mole This values is equal to the bond energy. which corresponds to the contacts of polycondensationn nature.

The experiments made by the authors (12) showed that the early strength of cement stone is connected with the amount of combined water by power relation $\sigma = kc^n$, where n is the exponent that is greater than 1 and it may reach the values equal to 2 or even 3. It supports the necessity to form at the early stages of hardening the phases with large quantities of crystal water of complex compound type or double salts (13) which are the carriers of cement stone early strength in quick-hardene cements such as hydro-halogen-sulpho-aluminate and sulpho-ferrite cements.

Chemical Aspects of Cement Stone Adhesion. It should bee taken into consideration in the analysis of chemical aspects of cement adhesion that the surface of the filler, binding agent (a binder) and cementing phases are presented by oxygen, calcium, silicon and aluminium, aluminium and silicon atoms appearing on the surface being hydroxylable (≡Al - OH ≡ Si - OH). In the hardening cement dispersion one may distinguish the following types of contacts: a) a section of a binder particle surface - a part of the surface of cementing phase particle (adhesion contact), b) the contact of the sections of cementing phase particle surfaces between themselves. Such a contact may be both of cohesion character (two particles of hydrosilicates(and an adhesion one (hydro silicate particle - $Ca(OH)_2$ crystal), c) a section of cementing phase surface - a section of the filler surface (an adhesion contact), d) the section of a cementing phase particle - the surface of cementing part (a brick or a concrete one) - an adhesion contact.

The foundation of the initial adhesion contacts is wetting connected with the formation of hydrogen bonds with surface hydrogen atoms which occupy a great part of the surface, being of larger size. Hydrogen bonds play a great role in forming the initial strength of torkret-compositions connected with the quasisolid properties of boundary water films linking solid phase particles. The cohesion properties of such films are also connected with hydrogen bonds. Adhesion contacts, however, are stronger because they are formed due too hydrogen bonds polarized by surface atoms. Besides, they introduce stronger donor-acceptor bonds into the strength of adhesion contacts

$$= Ca - O \begin{matrix} < H\ldots \\ < H\ldots \end{matrix}$$

Ion exchange processes play a certain part in forming adhesion contacts with the filler surface.

Literature Sited.

1. M.M.Sychev. "Inorganic Glues". Izd.Hhimiya. Leningrad. 1974.
2. V.V.Danilov. "Proceedings of the Sixth International Congress on the Chemistry of Cement". Vol.2. Book 1. Stroiizdat. Moscow. 1976.
3. V.S.Balitskii. "Experimental Investigation of Crystallization". Nauka. Moscow. 1978.
4. M.M.Sychev, L.B.Svatovskaya. "Cement". No.4.1979.
5. L.B.Svatovskaya. Zh.Prikl.Khim. Vol.53. No.4. 1980.
6. L.B.Svatovskaya, M.M.Sychev. Zh.Prikl. Khim. 52. No.11. 1979.
7. L.B.Svatovskaya, M.M.Sychev. "Inorganic Materials", Vol.16. No.4.
8. G.M.Sergeeva, V.D.Kharlob. "Proceedings of Leningrad Engineering Construction Institute". No.105. Leningrad. 1974. pp. 145-158.
9. M.M.Sychev. Zh. Prikl.Khim. Vol.51. No. 4. 1978.
10. M.M.Sychev. "Cement". No.11. 1978.

11. A.N.Bahtibaev, A.Kadirbskov, V.R.Regel. "All-Union Seminar on the Physics of Composite Materials". P.T.I. Leningrad. 1978, pp.146-151.

12. L.B.Svatovskaya, M.M.Sychev, I.M.Yahnitch in "Hydration and Hardening of Cement". No.3. 1979.

13. L.B.Svatovskaya, M.M.Sychev in "Hydration and Hardening of Binders." Ufa. 1978.

Nouvelle méthode d'étude des interfaces ciment-granulats

New method for the study of cement-aggregate interfaces

J. GRANDET, Professeur,
J.P. OLLIVIER, Maître-Assistant,
I.N.S.A., Département de Génie Civil - Université Paul Sabatier - Toulouse, France.

RESUME : Un granulat modifie dans son voisinage la cristallisation des hydrates d'une pâte de ciment. On décrit une technique d'étude permettant de mettre en évidence l'orientation de cristaux d'hydrates dans la zone proche du granulat.

Des enregistrements diffractométriques X sont réalisés sur des sections de pâtes de ciment parallèles à l'interface pâte-granulat et de plus en plus éloignées de celle-ci. L'étude est effectuée sur une zone d'environ 100 µm autour des granulats. L'orientation des cristaux, notamment de Portlandite, est mesurée à partir des intensités des raies caractéristiques de différentes familles de plans cristallographiques. On définit un indice d'orientation indépendant de la puissance délivrée par le tube de rayons X, ainsi que de la quantité de cristaux d'hydrates présents dans le volume de pâte analysé.

Les différentes sections de pâtes étudiées sont obtenues par abrasion. Il est possible de réaliser des analyses sur des sections distantes entre elles d'environ 1 µm. On montre que cette technique ne modifie pas, à l'échelle des mesures effectuées, l'organisation géométrique des hydrates dans la zone analysée. Cette méthode permet de déterminer la variation de l'indice d'orientation des cristaux à partir de l'interface pâte-granulat et de délimiter la zone d'influence du granulat dans la pâte de ciment.

SUMMARY : The crystallisation of hydration products around aggregates is not of the same manner as occured in the bulk portland cement paste. The orientation of hydrated crystals in the contact zone is studied with a new method.

Different sections parallel to the cement paste-aggregate interface are observed by XED technic. These investigations were done around aggregates up to 100 µm thick. The orientation of crystals, Portlandite for example, is measured from the intensity ratio of diffraction peak caracteristics. We defined an orientation index which is independant of the power delivered by X ray tube and the quantity of hydrate crystals contained in the volume of analysed paste.

The different sections of studied pastes are obtained by the abrasion. The distance between two successive sections is about 1 µm. We found that the geometrical arrangement of crystals in the analysed zone is not destroyed during the preparation of specimens. It is then possible to study the variation of the orientation index in the interfacial zone and to define the influence zone of aggregate in the cement paste.

Dans un béton de ciment Portland, la pâte forme autour des granulats une auréole de transition (1) dans laquelle la cristallisation des hydrates est différente de celle existant dans une pâte pure. Cette auréole est le point faible des bétons car il s'agit d'une zone de moindre cohésion dans laquelle se propagent les fissures. Plusieurs auteurs ont signalé que dans cette zone, la Portlandite (CH) se formait en grande quantité relativement au reste de la pâte et cristallisait en couches orientées, l'axe [001] étant perpendiculaire au support (2,3). Ce type de croissance étant évidemment favorable à la propagation des fissures par clivage des cristaux, nous avons mis au point une méthode permettant d'étudier, suivant des plans parallèles au support, l'orientation des cristaux de Portlandite dans la zone constituant l'auréole.

La diffractométrie X sur échantillons en masse est une technique bien adaptée à ce problème car la variation de l'orientation des plans réticulaires d'une espèce cristalline se traduit par une modification des intensités relatives des raies observées sur le diagramme de diffraction.

REALISATION DES EPROUVETTES D'ESSAIS

Il n'est pas facile d'étudier dans un béton, la croissance cristalline des hydrates au voisinage d'un granulat de forme quelconque ; aussi, nous avons choisi un modèle simple, constitué d'une éprouvette mixte granulat-pâte de ciment.

Le granulat se présente sous forme d'un cylindre de 2 cm de diamètre (la hauteur du faisceau X étant de 1 cm, on évite ainsi l'influence des parois latérales).

La pâte de ciment Portland est coulée contre une section plane du granulat dont le polissage a été effectué avec différents abrasifs jusqu'à une granulométrie de 5 µm, de manière à obtenir un état de surface permettant d'une part la localisation de l'interface après confection des éprouvettes et, d'autre part, la réalisation dans la pâte, de tranches successives de quelques micromètres d'épaisseur parallèles au support.

Les éprouvettes, placées dans leur moule en matière plastique (Ø 2 cm), sont conservées dans des atmosphères contrôlées à 20°C ± 0,2°C et sous différentes humidités relatives. Au moment choisi pour son observation, l'éprouvette est démoulée, puis rompue. Avec les granulats utilisés (quartz, marbre, polyéthylène) et le mode de conservation choisi, la rupture se produit dans la pâte selon un plan parallèle au support et à une distance très faible de ce dernier.

Pour chaque essai, la section polie du granulat est observée au microscope optique (x 625), afin de mesurer l'épaisseur de la pellicule de pâte adhérente. On constate qu'elle est formée d'un tapis continu de cristaux présentant quelques aspérités. Du fait de celles-ci et compte tenu de la profondeur de champ du microscope optique, l'incertitude sur la mesure de l'épaisseur de la pellicule peut être estimée à 1 µm.

REALISATION DES SECTIONS DROITES SUCCESSIVES PARALLELES AU PLAN DE L'INTERFACE

L'étude de la variation de l'orientation des cristaux de Portlandite dans la pâte de ciment à partir de la face de contact nécessite la réalisation de sections droites successives et parallèles au plan du granulat. Nous avons procédé par abrasion. On peut penser a priori que cette technique risque de modifier l'arrangement des cristaux ; nous étudierons ce problème dans la suite de ce travail. La face plane de pâte de ciment révélée par la rupture de l'éprouvette mixte est polie à sec sur un disque d'abrasif de grain 22 µm. Le disque est placé dans un récipient en matière plastique de manière à recueillir tous les produits d'abrasion dont la masse est ensuite mesurée par double pesée au 1/10ème de mg.

Pour connaître l'épaisseur de pâte enlevée , nous avons supposé, en première approximation, que la masse volumique des constituants de l'auréole était identique à celle du reste de la pâte. Nous avons donc déterminé, par pesée hydrostatique, les masses volumiques d'échantillons témoins coulés et conservés dans les mêmes conditions que les pâtes des éprouvettes mixtes.

ENREGISTREMENTS DIFFRACTOMETRIQUES

L'orientation d'un constituant cristallin peut être caractérisée au moyen d'un couple de raies de diffraction : celles-ci doivent appartenir à deux familles de plans différentes, le plan d'orientation du cristal étudié faisant partie de l'une d'elles. En outre, il faut éviter le choix de raies perturbées par un autre constituant.

Ainsi, pour caractériser l'orientation des cristaux de Portlandite dont le plan (001) - d = 4,90 Å - a tendance à croître parallèlement au support (ce qui se vérifie en faisant diffracter la pellicule adhérant sur le support), nous avons choisi la raie de diffraction correspondant à ce plan, ainsi que celle indexée (101) - d = 2,628 Å - qui n'est que peu perturbée par la raie du silicate tricalcique située à 2,59 Å.

Les diagrammes ont été réalisés au moyen d'un goniomètre équipé d'un tube avec anticathode de cuivre. Une fois le couple de plans réticulaires choisi, nous avons mesuré, sur l'enregistrement diffractométrique de la face étudiée, les intensités des pics correspondant par rapport au fond continu et calculé leur rapport

$$R = \frac{I(001)}{I(101)}$$

Nous avons opéré de même, figure 1, sur le diagramme de poudre d'une pâte de ciment Portland - E/C = 0,29 - âgée de 1 jour. Le rapport $R_0 = \frac{I(001)}{I(101)}$ trouvé, est égal ici à 0,74, valeur donnée par les fiches ASTM pour ces raies de la Portlandite*.

---

* De même que certains auteurs (4,5), nous avons parfois constaté de légères variations de ce rapport. Toutefois, l'imprécision commise en mesurant les hauteurs de pics au lieu de leur surface nous autorise à utiliser la valeur habituelle 0,74.

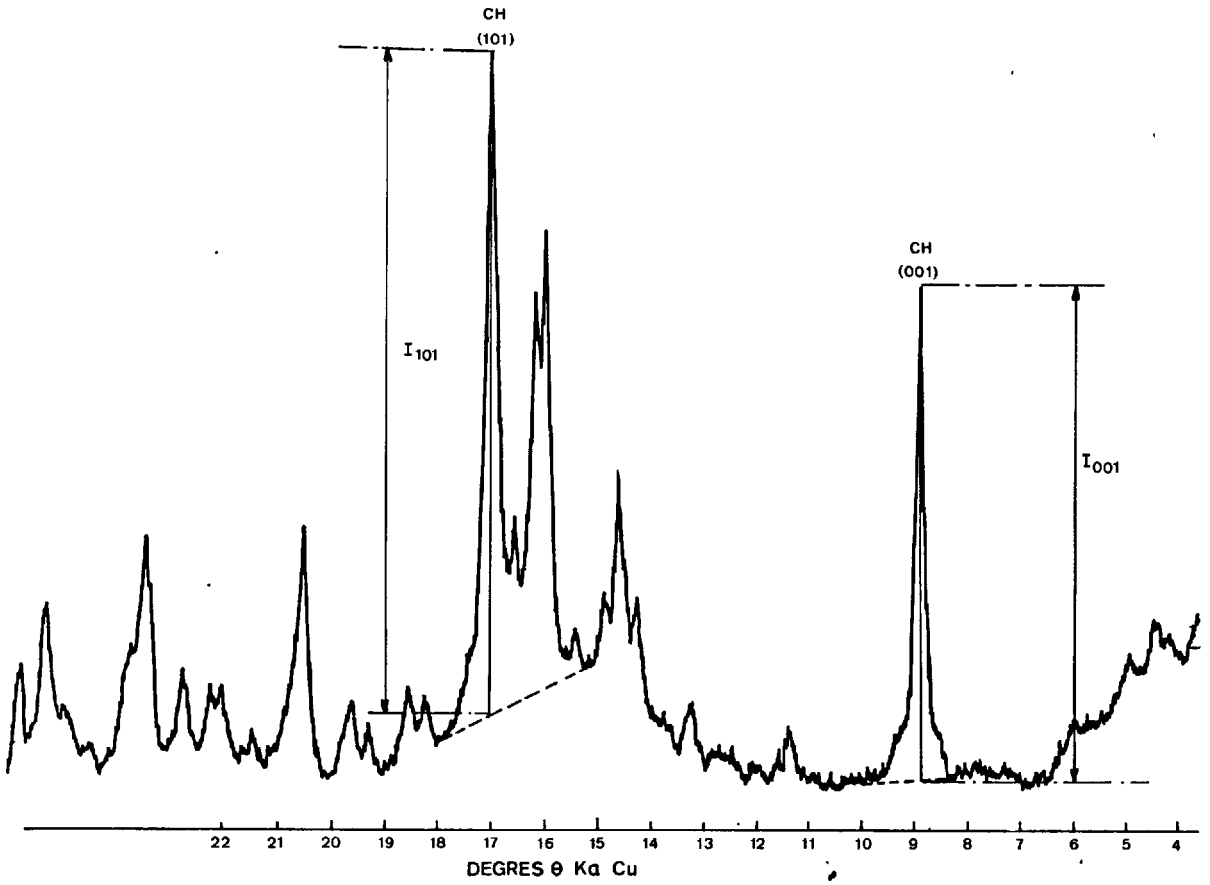

FIGURE 1 : Mesure de l'intensité des raies du diagramme de diffraction

DEFINITION D'UN INDICE D'ORIENTATION

Pour quantifier l'orientation observée sur le diagramme, nous définissons l'indice d'orientation :

$$I = \frac{R}{Ro}$$

Dans le cas des cristaux de Portlandite, l'indice vaut :

$$I = \frac{I(001)/I(101)}{0,74}$$

Cet indice est indépendant de la puissance délivrée par le tube de rayons X, ainsi que de la quantité d'hydrates formés dans le volume analysé. Il ne caractérise pas uniquement l'orientation des cristaux de la face apparente de l'éprouvette car le faisceau diifracté intègre l'orientation des cristaux situés en arrière de cette face, dans la masse de l'échantillon où le rayonnement incident pénètre. La pénétration du faisceau suit la loi $i = i_0 \exp(-\mu\rho x)$ dans laquelle i est l'intensité transmise à travers l'épaisseur x d'un matériau de masse volumique ρ et de coefficient d'absorption massique μ ; i_0 étant l'intensité incidente. La pénétration du faisceau est indépendante, pour une longueur d'onde du faisceau X donnée, des conditions d'analyse.

Ainsi, nous voyons que l'indice I ne représente pas l'orientation des cristaux de la seule face apparente mais intègre les orientations de tous les cristaux du volume analysé. Compte tenu de la loi de variation exponentielle, un plan intervient d'autant plus dans l'intensité recueillie qu'il se trouve plus proche de la surface apparente.

L'analyse diffractométrique, côté support, de la pellicule de ciment adhérant sur le granulat après rupture permet également de définir un indice d'orientation. Sa valeur numérique est supérieure à celle obtenue par l'analyse de la surface côté pâte de ciment alors que l'orientation statistique des cristaux situés sur les deux faces révélées par la rupture est vraisemblablement la même. En fait, les valeurs de ces deux indices ne peuvent pas être égales car la mesure du premier intègre, vers le support, une fine pellicule de cristaux très orientés, alors que dans la détermination du second, ce sont des cristaux moins orientés, situés vers le coeur de la pâte de ciment, qui participent à l'intensité diffractée.

REPRESENTATION GRAPHIQUE

Après mesures de l'épaisseur de la pellicule adhérant sur le support,de la masse prélevée par abrasion et de la masse volumique de la pâte, il est possible de

situer la face apparente de l'échantillon par rapport au support ; soit d cette distance.

Les intensités des raies de diffraction d'un constituant, ainsi que la valeur I de l'indice d'orientation, varient avec d. A titre d'exemple, la figure 2 représente cette évolution pour un contact quartz-pâte de ciment (E/C = 0,29) conservé 7 mois à 20°C en atmosphère saturée.

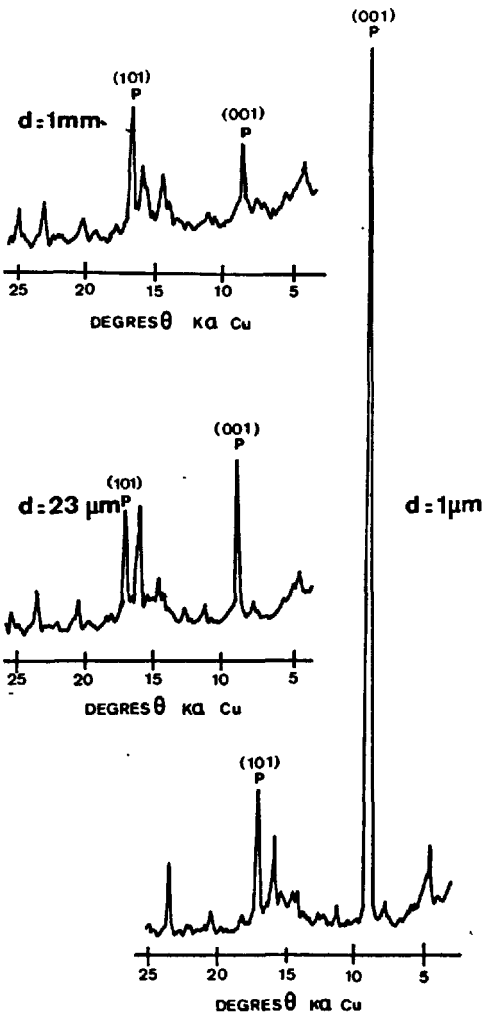

FIGURE 2 : Evolution du diagramme de diffraction d'une section de la pâte avec d, distance au granulat

Si l'on construit, en coordonnées semi-logarithmiques la courbe I = f(log d), on constate qu'elle est formée de deux demi-droites (cf. la figure 3, relative au contact étudié figure 2). La forme de cette courbe permet de définir d_0, limite d'orientation des cristaux de Portlandite dans la pâte de ciment. En-deçà de cette limite, l'orientation des cristaux de Portlandite croît lorsque l'on s'approche du granulat ; au-delà, elle est totalement désorientée. La pente de la droite I = f(log d) $\{ d < d_0 \}$ est une autre caractéristique de ces courbes dont nous montrons par ailleurs (6) qu'elle représente l'aptitude du granulat à orienter les cristaux de Portlandite ainsi que le mode de croissance de cet hydrate dans l'auréole de transition.

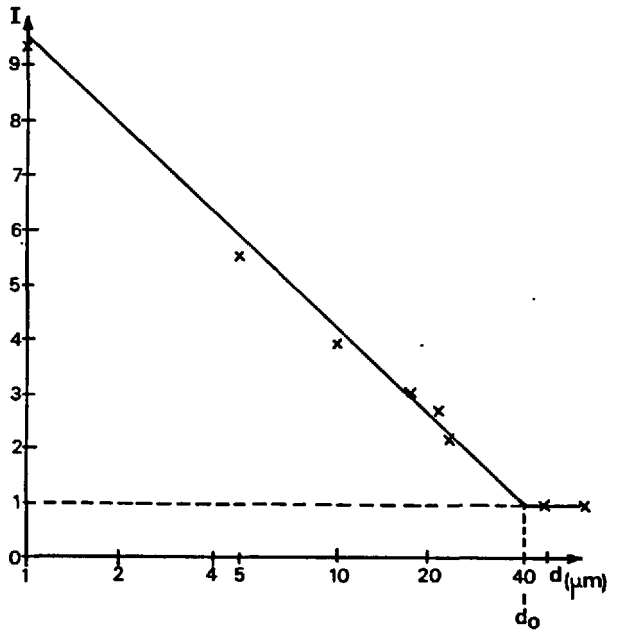

FIGURE 3 : Variation de l'indice d'orientation I de la Portlandite en fonction de la distance d au granulat

ANALYSE DE LA METHODE D'ETUDE

Nous avons montré que cette méthode permet de caractériser les variations de l'orientation des cristaux de Portlandite au voisinage d'un granulat. Afin de s'assurer que ce résultat n'était pas dû à l'abrasion mécanique, nous avons effectué des mesures analogues sur un échantillon dont les faces successives étaient obtenues par amincissement ionique. Dans l'appareillage utilisé (EDWARDS IBMA2) l'éprouvette de pâte est bombardée sur toute sa section par 13 faisceaux d'ions argon, ce qui réalise un décapage uniforme. Avec ce procédé d'amincissement très lent (environ 0,5 µ m par heure), l'arrangement des cristaux n'est pas modifié et les courbes d'orientation I = f(log d) sont analogues à celles obtenues par abrasion. D'autres essais effectués suivant notre méthode (7) ont, en outre,

montré que le polissage mécanique d'une pâte pure ne créait pas d'orientation préférentielle des cristaux de Portlandite.

Cette méthode d'étude, dont nous avons pu constater la fidélité, permet donc de caractériser la variation de l'orientation des cristaux de Portlandite dans une pâte de ciment Portland située au voisinage d'un granulat et de délimiter la zone d'influence de celui-ci. Cette méthode peut également être utilisée pour étudier l'orientation d'autres hydrates des liants hydrauliques dans le cas où ils cristallisent en quantité suffisante, les aluminates de calcium hydratés des ciments alumineux, par exemple.

BIBLIOGRAPHIE

(1) PERRIN B. (1974) "Observation en microscopie électronique des caractères morphologiques de la liaison pâte de ciment durci-matériaux associés" Thèse (Français)

(2) BARNES B. D., DIAMOND S., DOLCH W. L. (1978) "The contact zone between Portland cement paste and glass "aggregate" surfaces". Cement and Concrete Research, vol. 9, 233 (Anglais)

(3) AL KHALAF M. N., PAGE C. L. (1979) "Steel-mortar Interfaces : microstructural features and mode of failure". Cement and Concrete Research, vol. 9, 197 (Anglais)

(4) SIERRA R. (1974) "Contribution à l'étude de l'hydratation des silicates calciques hydrauliques". Rapport de recherche n° 39, L. C. P. C. (Français)

(5) GRUDEMO A. (1977) "Strength-structure relationships of cement paste materials". C. B. I. Report 6 - 77 (Anglais)

(6) GRANDET J., OLLIVIER J. P. (1980) "Orientation des hydrates au contact des granulats". Septième Congrès International de la Chimie des Ciments Paris (Français)

(7) GALLIAS J. L. (1979) "Analyse et réglage du fonctionnement du diffractomètre de rayons X. Application à l'influence du polissage des échantillons en masse sur les diagrammes de diffraction". D. E. A. de Génie Civil - I. N. S. A. Toulouse (Français).

Effects of interface reaction between blast furnace slag and cement paste on the physical properties of concrete

Effets de la réaction d'interface entre le laitier de haut-fourneau et la pâte de ciment sur les propriétés physiques du béton

S. NAGATAKI, Dr. Associate Professor, Dept. of Civil Eng. Faculty of Eng. Tokyo, Institute of Technology
and
M. TAKADA, Researcher, Central Research Lab., Nisso Master Builders Co., Japon.

RESUME : Dans les dernières années, à cause du manque d'agrégats fins de bonne qualité et de l'économie des ressources, on a tenté d'utiliser le laitier granulé de haut fourneau comme agrégat fin du béton. Pourtant, selon les résultats des expériences de laboratoire, on a trouvé que si le béton contenant le laitier de haut fourneau est gardé en atmosphère sèche, il aura tendance à perdre peu à peu sa résistance, après une période d'à peu près 6 mois. De plus, on a trouvé que, dans les mêmes conditions, le retrait par desséchement est plus petit que dans le cas où on a employé des agrégats ordinaires, tandis que la valeur du fluage est à peu près la même. On pense que cela est dû à la réaction d'interface entre le laitier de haut fourneau et la pâte de ciment; par conséquent, des recherches ont été faites sur les substances formées en surface au moyen de SEM et EPMA. Les résultats montrent que, par desséchement, des fissures se forment sur cette surface et les fissures déterminent largement les propriétés physiques du béton gardé en atmosphère sèche.

SUMMARY : In recent years, in view of a shortage of good quality fine aggregates and saving of resources, attempts have been made in the application of granular blast furnace slag as fine aggregate in concrete. However, according to results from experiments in the laboratory, it is found that if the concrete having blast furnace slag as fine aggregate were to be kept under dry atmosphere, then there will be a tendency for the strength to fall after the age of approximately 6 months. Also, it is found that under similar dry atmospheric condition, drying shrinkage is smaller than when ordinary fine aggregate is used but the amount of creep is approximately the same. The reason is assumed to be due to the interface reaction between the blast furnace slag and the cement paste and investigations were therefore made on the substances formed on the boundary surface by means of SEM and EPMA. Results indicated that upon drying, cracks develop on this surface and the existence of such cracks determines greatly the physical properties of concretes kept under dry atmosphere.

FOREWORD

In recent years, because of the shortage of good-quality fine aggregates brought about as river aggregates have become depleted, and with the objective of effective utilization of blast furnace slag being produced in excessive quantity as a by-product, research and development for application of blast furnace slag sand (hereafter abbreviated as slag sand) as fine aggregate for concrete have been actively going on in the steel industry to begin with and in the Japan Society of Civil Engineers, the Architectural Institute of Japan and the construction industry, and progress has been made to a point that a proposal for standards for using slag sand has been prepared based on the results of these research works.

However, it was only 5 or 6 years ago that work was started on the applicability of slag sand at the various research institutions, and therefore, it cannot be said that confirmation of macroscopic characters such as mechanical properties and durability at long-term age of concrete using slag sand, and evaluation of the potential hydraulicity of slag sand are adequate.

In view of the above, the study reported here was made on the influence on the physical properties of concrete, particularly, long-term soundness, of the existence of a hydration reaction layer produced through the potential hydraulicity of slag sand. Parenthetically, the bond mechanism and micro structure at the interface between slag sand and cement paste were observed by scanning electron microscope, and the correlations with macroscopic properties such as strength, modulus of elasticity and volume change properties of mortar at long-term age are discussed.

OUTLINE OF EXPERIMENTS

Materials Used and Mix proportions

The cement used was ordinary portland cement, the results of physical tests thereof being as shown in Table 1. The fine aggregates were the 2 varieties of slag sand (A, B) as shown in Table 2 and a river sand used for comparison purposes.

In the mix proportions of mortar used for the experiments, water-cement ratios were of the three levels of 0.40, 0.50 and 0.65, flow values were maintained constant at 190±5mm in all cases, and the fine aggregate quantities satisfying these conditions were obtained by preliminary tests. The unit contents for the various mix proportions are given in Table 3.

Strength Tests and Length Change Tests

The respective tests were performed on specimens kept under the curing conditions indicated in Table 4. The specimen dimensions were 10 dia.×20cm ht. for strength tests, 10×10×50cm for drying shrinkage tests, while creep test specimens were uniaxially restrained specimens of the kind shown in Fig. 1, the cross section being 10×10cm and length 40cm. Measurements of drying shrinkage of creep specimens were made following the dial gauge method according to JIS A 1124.

Scanning Electron Microscope (SEM) Examinations

SEM examination specimens were taken breaking specimens which had been used for length change tests. The sizes of specimens were about 0.5cm in length, 0.5cm in width and 0.3 cm in thickness, and those specimens happening to contain numerous particles of sand not more than 1 mm in size were selected and used for examinations.

Table 1. Test results of cement

SPECIFIC GRAVITY	BLAINE (cm^2/g)	SETTING (h-m) INI.	SETTING (h-m) FIN.	FLOW (mm)	COMP.STRENGTH (kg/cm^2) 3(day)	7	28
3.15	3,220	2-18	3-35	254	121	214	404

Table 2. Physical properties of fine aggregates

FINE AGGREGATE		SPECIFIC GRAVITY	ABSORPTION (% BY WT.)	FINESS MODULUS
RIVER SAND		2.62	1.81	2.84
GRANULATED SLAG SAND	A	2.67	3.82	2.65
	B	2.68	1.05	2.55

Table 3. Mix proportions of mortar

(UNIT:kg/m^3)

FINE AGGREGATES	W/C=65% W	C	S	50% W	C	S	40% W	C	S
RIVER SAND	276	425	1550	266	531	1488	264	660	1386
SLAG SAND A	295	459	1498	287	573	1420	282	706	1320
SLAG SAND B	329	506	1366	312	623	1309	304	760	1216

Table 4. Curing conditions

	Curing condition
N- 7	dry-curing for 2 years, after water-curing for 7 days.
N-28	dry-curing for 2 years, after water-curing for 28 days.
N-91	dry-curing for 2 years, after water-curing for 91 days.
N	water-curing for 2 years

(Note) water-curing : 20°C
dry-curing : 20°C, 50%RH

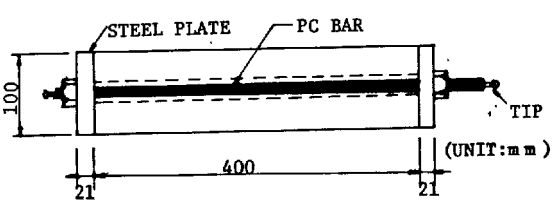

Fig. 1. Creep test specimen

INTERFACE REACTION BETWEEN SLAG SAND AND CEMENT PASTE

Hydration Reaction of Slag Sand

Photo. 1 is from SEM examination of slag sand (A) mortar continuously cured in water for 2 years. This photomicrograph clearly shows that a hydration reaction layer is produced between slag sand and cement paste during long-time curing in water, and moreover, that the hydration reaction layer has grown to a thickness of about 3μ.

Photos. 2-4 are of slag sand (B) mortar cured in water for 7, 28 and 91 days, respectively, and then dried in air for 2 years under the conditions of 20°C, 50% RH. Since these were dried for a long period after curing in water the conditions are different from the result shown in Photo. 1, and these photomicrographs show that with mortar cured in water for short periods (N-7, N-28), the hydration layer is thin (about 0.3-1.0μ) and of porous constitution, but as the period of curing in water becomes long (N-91), the hydration reaction layer is of denser and thicker constitution (about 2μ).

The thickness of the hydration reaction layer of granulated slag, according to the method of Kondo and Osawa[1] (quantification of unhydrated granulated slag in cement using the methanol salicylate method), is about 0.5μ at the age of 7 days, but retardation of reaction is said to begin occurring when the thickness of the reaction layer becomes 0.35-0.50μ. However, the results of examination by SEM as shown in Photos. 2-4 appear to indicate that the hydration reaction layer surrounds the unhydrated part of slag sand along the interface between slag sand and cement paste and fills the gap with the cement paste in the form of gradual growth with increased age of curing in water.

An example of river sand mortar is shown in Photo. 5 for comparison, and quite naturally, in spite of the outer sides of particles being covered by crystals of $Ca(OH)_2$, there is no reaction layer to be seen at all inside river sand.

Influence of Drying on Hydration Reaction Layer

Photos. 2-4 indicate the forms of hydration layers in case of drying under fairly severe conditions for a long period of time, but as can be seen in Photos. 2 and 3, the hydrated layers of slag sand are fairly coarse compared with the case of continuous curing in water, and along with something gap-like recognized, there are microcracks (about 0.1μ) existing along the interface between hydrated layer and cement paste.

Regarding the widths of these microcracks, when taking into account problems in examination techniques such as that examination specimens were prepared breaking beam specimens, or that specimens were dehydrated because of the high-vacuum conditions when making SEM examinations, it cannot be simply concluded that such crack widths are produced only due to air-drying. However, as a result of SEM examinations of replica films prepared by the single-stage replica method in order to differentiate from cracks produced due to being maintained in a condition of high vacuum, when curing in water was continued formation of cracks was not seen, but in case of dry-curing, microcracks were formed along the interface, while with river sand mortar observed in a state of high-vacuum as shown in Photo. 5 such microcracks were not recognized, and so it is thought the abovementioned cracks were unmistakenly formed at the interfaces during the long-term drying process.

It should be noted though, that at the present stage it is not clear whether the cause is brittleness of the hydration reaction layer produced on slag sand due to drying, or slight tensile stresses produced from drying where bond between the hydration reaction layer and cement paste was weak.

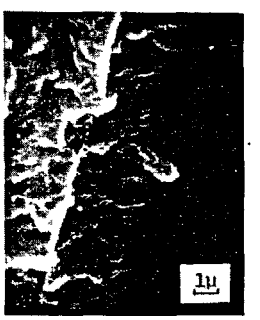

Photo. 1. Slag sand(A) N (W/C=50%)

Photo. 2. Slag sand(B) N-7 (W/C=40%)

Photo. 3. Slag sand(B) N-28 (W/C=40%)

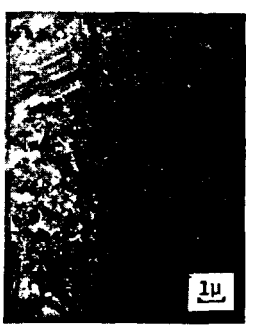

Photo. 4. Slag sand(B) N-91 (W/C=40%)

Photo. 5. River sand N-91 (W/C=50%)

PHYSICAL PROPERTIES OF CONCRETE

Mechanical Properties

Regarding the mechanical properties of concrete using slag sand, as already described in detail in many research reports, when continuously moist-cured over a long period of time, the characteristic is for strength to gradually increase, and it has been confirmed that this strength is equal to that when good-quality river sand has been used. However, these experimental results were obtained under conditions favorable to slag sand, in effect, in a moist state where the potential hydraulicity can be readily brought out, whereas it has been reported that when dried for a long period of time there is a tendency for compressive strength and static modulus of elasticity to be greatly inferior compared with concrete using river sand[2]. It is thought such a characteristic of the macroscopic properties suggests that there are close relationships with the microscopic and the physical properties of concrete. Therefore, in this study, the properties of strength variations accompanying drying were compared by coefficient of brittleness considered to be the index of existence of microcracks first produced in concrete.

Fig. 2 and 3 show the results of strength tests of mortar using the slag sands A and B and the river sand indicated in Table 2 by the relations between compressive strength (σ_c) and coefficient of brittleness (σ_c/σ_t). Fig. 2 gives the results after curing in water and Fig. 3 those after dry-curing under the conditions shown in Table 4. After water-curing (before drying), the strength properties of slag sand mortar show a trend more or less similar to those of river sand mortar. However, after dry-curing for 2 years (after drying), the coefficient of brittleness becomes fairly high compared with river sand mortar as shown in Fig. 3, and it is clearly indicated that reduction in tensile strength due to drying is especially prominent.

Fig. 4 gives the result of measurements of dynamic modulus of elasticity, also an index sensitively indicating the existence of microcracks in concrete, and as it clear in this graph it is recognizable that deterioration in quality due to drying is greater than for river sand mortar.

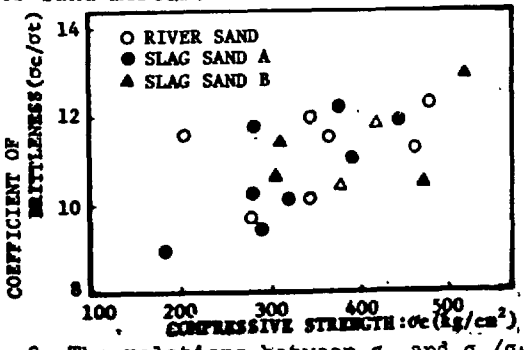

Fig. 2. The relations between σ_c and σ_c/σ_t (before drying)

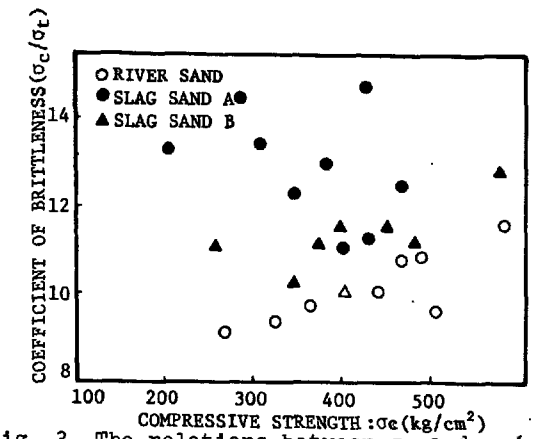

Fig. 3. The relations between σ_c and σ_c/σ_t (after drying)

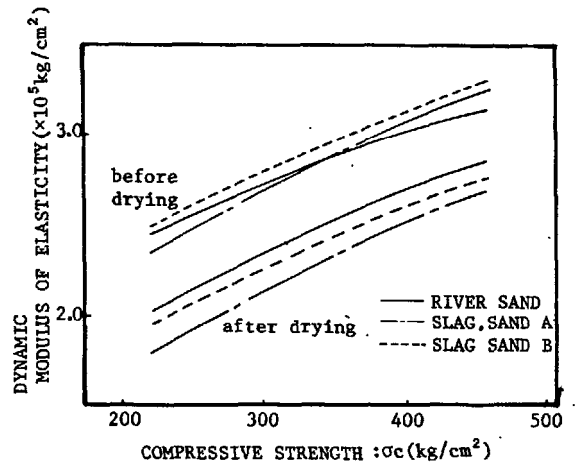

Fig. 4. The relations between compressive strength and dynamic modulus of elasticity

Volume Change Properties Under Water-Curing Conditions

The formation of hydration reaction products of slag sand, as confirmed by SEM examination is that of growth toward the interior of the particle with the original shape of the particle intact. Accordingly, if the reaction were to progress continuously over a long term taking this form, it is thought there is no possibility for expansion and cracking of concrete due to reaction products of slag sand or for breakage of particles accompanying progress in reaction.

Fig. 5 indicates an example of expansive strain of slag sand mortar in moist condition (20°C, in water) in relation to age cured in water. According to this graph, regarding the expansive strain of slag sand mortar, although there is a slight difference in trend compared with river sand mortar such that expansion appears at an early stage, it is not a significant difference, and it may be said that soundness is roughly equal to that of

river sand.

Fig. 6 indicates the creep properties similarly under water-curing conditions, the relation between specific creep and age after loading, when loading was done after standard curing for 28 days followed by continued curing in water. The specific creep of slag sand mortar is larger than that of river sand mortar and the difference gradually increases with increased age after loading. The reason for this is thought to be that slag sand mortar requires a higher unit paste content to obtain the same flow as river sand mortar, and compared by specific creep/unit cement content also, since the value for slag sand mortar is still larger, it is thought the plasticity of the hydrated layer produced at the slag sand influences the creep properties of slag sand mortar.

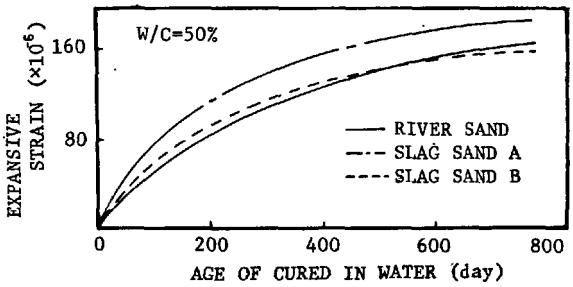

Fig. 5. Expansive strain of slag sand mortar (in water)

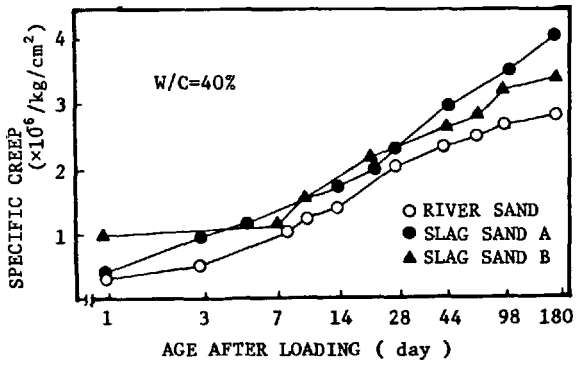

Fig. 6. The creep properties under water-curing conditions

Volume Change Properties Under Dry-Curing Conditions

Fig. 7 shows the volume change properties at drying age of 6 months in terms of the relation between drying shrinkage and specific creep. There is a tendency recognized where in spite of slag sand mortar having drying shrinkage smaller than for river sand mortar, its specific creep is equal or larger.

In general, the drying shrinkage of concrete using slag sand is said to be smaller than in the case of using river sand, and the causes of this are thought to be the latent hydraulicity of slag sand, the finely-divided powder effect, and water retention. However, in order to comprehensively explain such phenomena as the results in Fig. 3 and Fig. 7, in effect, that strength reduction due to drying is prominent, and that drying shrinkage is small but specific creep is of about the same degree as river sand mortar, it was thought reasonable to consider them assuming that microcracks are formed in the interior of slag sand mortar.

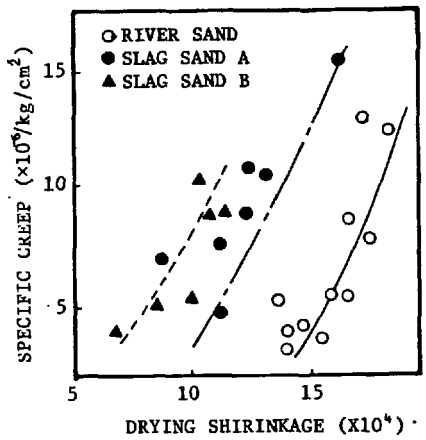

Fig. 7. The relations between drying shrinkage and specific creep

AFTERWORD

As a result of examination of the relationship between the microscopic form of hydration reaction layers produced in slag sand and the macroscopic properties of slag sand mortar, it was confirmed that the various properties of slag sand mortar may be aptly explained by the interface reaction between slag sand and cement paste.

However, there are still many points remaining unclarified about hydration of blast furnace slag, and regarding also the hydration reaction layer produced at the surface of slag sand observed in the present study, the reaction mechanism, the process of reaction layer formation, and crystallization of hydrates are completely unexplained. Therefore, it is necessary for further close investigations to be made of the hydrate structure of the hydration reaction layer and the characteristics of the hydrates, and their relationships with the macroscopic characters indicated by mortar and concrete to be examined.

REFERENCES (in Japanese)

1. R. Kondo and H. Osawa: "Study on Quantification of Granulated Blast Furnace Slag and Hydration Reaction Rate of Slag in Cement", Journal of the Ceramic Association of Japan, Vol. 77 (2), 1969.

2. S. Nagataki, A. Yoneyama and M. Takada: "Properties of Concrete Using Granulated Blast Furnace Slag Sand", Proc. 1st Annual Presentation Meeting on Research in Concrete Technology, May 1979.

L'influence des procédés de fabrication des clinkers sur la résistance des ciments à l'action des eaux sulfatées

Influence of the manufacturing processes of clinkers on the cement resistance to sulphate waters action

M. NADU, Ingénieur docteur, Chercheur scientifique principal, Institut de Recherches Hydrotechniques (I.C.H.), Bucarest, Roumanie.

RESUME: On présente une étude comparative de laboratoire concernant le degré de corrosion par les eaux sulfatées, d'eprouvettes de mortier confectionnées avec plusieurs ciments.
Les clinkers des différents ciments :

- sont caractérisés par diverses teneurs potentielles des principaux constituants, notamment C_3S , C_3A et C_4AF;
- proviennent de cimenteries équipées d'installations differant entr'elles par la voie de fabrication (humide ou demi-sèche) et par le régime thérmique de cuisson et de refroidissement.

L'analyse des résultats prouve que :

- la structure réelle et la résistance des ciments à l'action des eaux sulfatiques s'avèrent parfois plus sensiblement influencées par certains paramètres de fabrication que par la composition potentielle des clinkers ;
- parmi ces paramètres, ceux qui concernent le régime de cuisson et le régime de refroidissement du clinker (dans la zone finale du four et dans le refroidisseur), sont particulièrement importants.

SUMMARY : A comparative laboratory investigation on the sulphate waters corrosion degree of mortar test is presented. The cement clinkers :

- are characterized by various potential contents of the main constituents : C_3S, C_3A and C_4AF ;
- come from cement plants equipped with installations differing by the manufacturing process (wet or semi-dry) and by the thermal burning and cooling conditions .

The results analysis prouves that :

- the real structure and the resistence of the cements to the action of sulphate waters are sometimes more sensitive to the influence of certain manufacturing parameters than to the potential phase composition of the clinkers ;
- between those parameters, the clinker burning and cooling conditions in the final zone of the kiln and in the cooler are particularly important.

Notations et abréviations utilisées :

C_3A; C_3S ou V : teneur réelle des constituants respectifs ou du verre

$\underline{C_3A}$, $\underline{C_3S}$ ou $\underline{V}$: teneur calculée pour le clinker trempé à partir de 1450°(Dahl/1/)

$\overline{C_3A}$, $\overline{C_4AF}$, $\overline{C_3S}$, $\overline{C_2S}$: teneur potentielle en C_3A etc

CPA: ciment portland artificiel

A : $C_4AF + C_3A$ ou $\overline{C_4AF} + \overline{C_3A}$

A': $C_4AF + 2C_3A$ ou $\overline{C_4AF} + 2\overline{C_3A}$

E, F et T : symboles pour les cimenteriers

E, F', X, Y, Z: symboles pour les fours et pour les ensembles d'échantillons des clinkers(ou des ciments obtenus d'eux)

K_n: coefficient de stabilité, après n mois de conservation des eprouvettes dans la solution agressive, calculé par la rélation :

$$K_n = \frac{R_{ns}}{R_{ne}}$$ où R_{ns} (et R_{ne}) sont les résistances moyennes des eprouvettes conservées en solution agressive (et en eau)

K_{nE} ou K_{nX} etc.: K_n moyen pour les ciments de l'ensemble E (ou X) etc.

m.s.: "migration sélective" ou deshomogénéisation de la phase liquide du clinker

M : intensité présomptive de la m.s.

M_E ou M_X etc.: M moyenne pour les ciments de l'ensemble E (ou X) etc.

Q_{sp} : consommation spécifique de combustible du four (Kcal/Kg clinker)

R : vitesse présomptive de refroidissement du clinker

R_f: R à la zone aval du four

R_{fE} ou R_{fX} etc.: R_f moyenne pour les clinkers de l'ensemble E ou X etc.

R_r : R ou refroidisseur

R_{rE} ou R_{fX} : R_r moyenne pour les clinkers de l'ensemble E (ou X) etc.

Introduction

Dans les laboratoires de l'ICH de Bucarest on utilise depuis 20 ans une méthode directe proposée par Kind/2/, pour déterminer la résistance des ciments à l'action des eaux sulfatées. Normalisée en Roumanie, sur la base des avantages qu'elle presente /3a/, cette méthode consiste à suivre le comportement en solution agressive de petites éprouvettes prismatiques de mortier. Le critère quantitatif pour l'appréciation de l'agressivité d'une solution sur le ciment donné, est exprimé par la valeur K_n. Des différences de 0,1 sur les K_n de deux ciments comparés s'avèrent significativement différentes de zero, si le mode opératoire normalisé (standard roumain STAS 2633-74) est soigneusement suivi. L'eau agressive utilisée pour les recherches presentées, c'est une solution saturée de $CaSO_4 \cdot 2H_2O$, donc pas trop riche en ions SO_4^{2-} (1500 mg/dm^3), proche des eaux séléniteuses naturelles. Les exigences des normes pour les CPA résistants aux eaux sulfatées contiennent des restrictions pour les teneurs potentielles des phases du clinker. Il s'agit des restrictions pour les phases aluminoferritiques qui peuvent être conçues biunivoquement s'il s'agit d'A, de C_3A, de C_4AF, de A ou de A' sur un graphique F=f(A) et des restrictions pour les silicates. On peut remarquer que les exigences valables en divers pays différent, souvent, moins au fond qu'au modalités formmelles de symboliser les restrictions (Fig.1). Le support scientifique principal de ces normes, c'est le comportement spécifique aux sulfates des ciments à constituants purs, bien que maintes travaux expliquent que ces ciments sont exempts de la présence des constituants mineurs, des solutions solides et des particularités structurelles des clinkers industriels: l'hydratation des ciments industriels riches en C_4AF, conduisent à des solutions solides résistants aux eaux sulfatiques(Cirilli et Malquori); cf.à Carlson, la formation des hydrogranates stables à ces eaux est possible à des températures usuelles etc. (cf.réf./3b/.

On va exemplifier pour des situations particulières, l'influence des procedés de fabrication des clinkers sur la résistance sulfatique des ciments.

Procédés de fabrication et valeurs K_n

La plupart des ciments étudiés sont preparés par mouture de laboratoire, en conditions comparables de clinkers industriels dont le tableau 1 précise brièvement les procédés de fabrication. Il faut excepter une série de

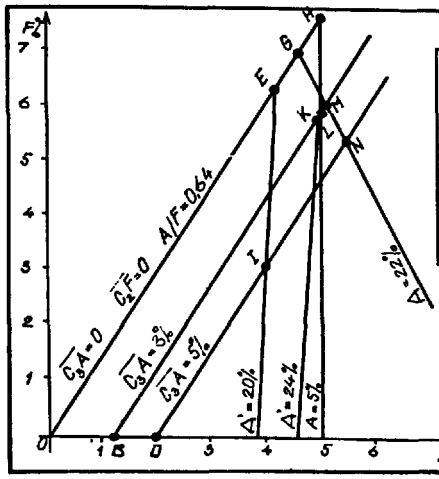

Pays	Standard	Conditions techniques	
		Pour les phases qui contiennent A et F (domaine admissible sur le diagramme)	Pour les silicates
Roumanie	STAS 3011-78	OBMG	$C_3S < 55\%$
RDA	TGL 16691-82	OBKH	—
RFA	DIN 1164-78	OBLH	—
URSS	GOST 22266-76	ODNB	$C_3S < 50\%$
USA	ASTM c 150-74	ODIE	—

Abreviations utilisées:
$\overline{C_4AF} + \overline{C_3A} = A$
$\overline{C_4AF} + 2\overline{C_3A} = A'$

Points mal lisibles:
$M = \{A = 22\} \cap \{\overline{C_3A} = 3\}$
$L = \{A = 5\} \cap \{\overline{C_3A} = 3\}$
$K = \{A' = 24\} \cap \{\overline{C_3A} = 3\}$
$H \approx \{A' = 24\} \cap \{A = 5\} \cap \{\overline{C_3A} = 0\}$

Figure 1: Exigences des normes pour les CPA résistants aux eaux sulfatées à $\overline{C_3A} \geq 0$

TABLEAU I

Cimenterie	Four et refroidisseur	Nombre d'échantillons	Type de clinker	Procédé de fabrication des clinkers analysées	Q_{sp} Kcal/Kg
E	E	18	Ferro-portland A/F < 1,38	Voie demi-sèche, four "Lepol", ø3.2 x 32m, refroidisseur rotatif	~ 1ooo
F'	F'	2o		Voie humide, four ø3 x 88m, refroidisseur planétaire	~ 16oo
T	X	2	Portland A/F=2,16	Voie humide, four ø2.7 x 2.9 x 5om, refroidisseur rotatif	~ 2ooo
T	Y	2		Voie humide, four ø3 x 88m, refroidisseur planétaire	~ 16oo
T	Z	2		Voie humide, four ø4 x 3.6 x 15om, refroidisseur à grille	~ 135o

15 ciments alumineferritiques (ferroportland) qui proviennent de compesants purs syntetisés et moulus en laboratoire par Velica /4/ et dont le tableau II présente la composition et les valeurs K_n. D'autres données résultent:

- du tableau III, on l'on compare la variation de composition et l'incidence de cette variation sur les K_n, pour trois ensembles de ciment ferroportland: ceux a constituants purs et ceux provenus des 18 clinkers E et des 2o clinkers F';
- du tableau IV pour exemplifier l'incidence de la différenciation des compositions potentielles et réeles sur K_{nE} et sur K_{nF}
- du tableau V pour la composition potentielles et les K_n des 6 CPA normals X, Y et Z. La simultanéité de chaque échantillonage a été assurée.

A noter que: (i) les données experimentales des tableaux II, III et IV sont complémentaires a celles d'une communication antérieure /3b/; (i,i) hormis les echantillons du four X qui contiennent de la chaux libre (~o,8 %), la présence du C libre n'a pas été signalée.

TABLEAU II

Echantillon n°	Teneur, %						K_6
	C_3S	C_2S	C_3A	C_4AF	A	A'	
148	5o	35	1	14	15	16	o,86
149	5o	3o	1	19	2o	21	o,72
15o	5o	25	1	24	25	26	o,59
153	5o	2o	1	29	3o	31	o
154	5o	34	4	12	16	2o	o,39
155	5o	28	4	18	22	26	o,35
156	5o	22	4	24	28	32	o
157	5o	17	4	29	33	37	o
158	5o	3o	8	12	2o	28	o
159	35	5o	1	14	15	16	o,96
16o	35	45	1	19	2o	21	o,81
161	35	4o	1	24	25	26	o,76
162	35	35	1	29	3o	31	o,54
163	35	49	4	12	16	2o	o,94
164	35	32	4	29	23	27	o

TABLEAU III

Caractéristiques analysées (notations usuelles)	Echantillons de ciment		
	(15), fabriqués en laboratoire à partir de constituants purs	(18), des clinkers produits par la cimenterie E	(2o), des clinkers produits par la cimenterie F'
Variations des teneurs des principaux constituants :			
	teneurs réelles	teneurs potentielles	
% C_3S	35 et 5o	29 ... 56	49...65
% C_3A	1,4 et 8	1 ... 6	o... 9
% C_4AF	12...29	16...24	12...21
% (C_4AF + 2C_3A)	16...37	23...28	22...33
Incidences sur les valeurs K_n			
Hausse % C_4AF pour mêmes % C_3S et % C_3A	Baisse jusqu'à $K_6 = 0$	Pas d'influence significative	
Hausse % C_3S pour mêmes % C_3A et % C_4AF	Baisse jusqu'à $K_6 \leq 0,54$	Pas d'influence significative	
Hausse % C_3A pour mêmes % C_3S et % C_4AF	Baisse jusqu'à $K_6 = 0$	Baisse jusqu'à $K_{12} = 0$	Baisse jusqu'à K_{12} = = 0,9 (et exceptionnellement pour $C_3A > 7$ jusqu'à K_{12} = 0,75)

TABLEAU IV

Echantillon n°	Cimenterie	A/F	Constitution, % — Potentielle $\overline{C_3S}$	$\overline{C_2S}$	$\overline{C_3A}$	$\overline{C_4AF}$	Calculée x) C_3S	C_2S	V	Réele xx) C_3S	V	C_3A	K_{12}	Interprétation des résultats (On a noté les implications par →)
75	E	o,87	48	29	3,6	17,3	4o	29	29	47	∿4	3	o,76	$C_3A \approx \overline{C_3A}$; $V \ll \underline{V}$ ou et
76	E	o,88	55	21	3,9	18,7	47	2o	31	56	∿5	3,5	o,7o	$C_3S \approx \overline{C_3S} > \underline{C_3S}$ → R_{rE}
89	F'	o,9o	61	16	3,7	16,o	54	15	27	55	∿22	0	1,o7	$C_3S \approx \underline{C_3S} < \overline{C_3S}$
74	F'	1,26	56	26	7,o	13,o	46	23	27	47	∿2o	<1	1,o8	$V \approx \overline{C_3A + C_4AF} \leq \underline{V}$ → $R_{rF'}$ > $K_{nF'}$; $C_3A \ll \overline{C_3A}$

x) D'après Dahl xx) Résultée d'observations microscopiques

TABLEAU V

Cimenterie	Four	Composition potentielle		K_n
Premier echantillonage				
T	X	C_3S=6o	C_3A=13	K_{12}=o,47
T	Y	C_2S=19	C_4AF=6	K_{12}=o,67
T	Z			K_{12}=o,69
Deuxième echantillonage				
T	X	C_3S=62	C_3A=13	K_4 = 0
T	Y	C_2S=17	C_4AF=6	K_4 = o,3
T	Z			K_{12}=o,78

Analyse des résultats

Les présomptions basées sur les paramètres technologiques du tableau 1 et les données experimentales sont comparées au tableau VI. Pour le mieux comprendre s'avère utile un court rappel de quelques publications tenant de la technologie chimique de la fabrication des clinkers.

Theorie de la m.s. D'après Titeiu qui a étudié le phenomène, il s'agit d'une migration de la phase liquide, du noyau vers la périphérie du granule; elle est sélective par ce que M est plus intense pour F et C que pour A et S. Implications; il

y a plus de C_3A à l'intérieur qu'à la périphérie, d'ou l'on voit l'effet negatif de la m.s. sur la résistance sulfatique des ciments. Tiţeiu a remarqué aussi que M est en hausse: (i) pour les crus qui développent une phase liquide abondante et fluide; (i,i) au cas d'une flamme ferme (d'une zone courte de clinkerisation)/5/.

A partir du tableau I on peut présumer selon le critère (i,i) les inegalités 1 et 4 (tableau VI).

Sur le refroidissement du clinker. Il y a deux etapes ou R influence la structure et les propriétés des clinkers, notamment les K_n: (i) pendant la solidification de la phase liquide, (i,i)après solidification par transformations polymorphes des silicates.
L'étape (i) a lieu dans la zone aval du four et (s'il y a encore de phase liquide dans les granules sortis du four),dans le refroidisseur. A propos de l'influence de R(soit R_r ou/et R_f) sur les K_n,on admet: (j) qu'au fur et à mesure d'une hausse de R, la teneur en C_3A devient plus petite que celle de $\overline{C_3A}$, au compte des aluminates de basicité réduite, des solutions solides ou du verre; (jj) que le C_3A est plus sensible aux sulfates que les autres formes des aluminates de calcium;(jjj) que, finalement une hausse de R implique une hausse des K_n. Comme on verra, cette théorie reste valable, même pour les ciments pauvres en C_3A (à rapport $A/F < 1{,}38$) bien qu'il est vrai que pour des tels clinkers, la trempe rapide conduit à moins de C_3S que le $\overline{C_3S}$, à une mauvaise cristalisation de l'alite et donc a des ciments à propriétés techniques générales moins favorables /6-10/.

TABLEAU VI

No.	Présomptions basée sur les paramètres technologiques	Conclusion des essais
1	$M_E > M_F \rightarrow K_{nE} < K_{nF}$	Cf. tableau IV et /3b/: $K_{nE} < K_{nF}$
2	$R_{fE} < R_{fF} \rightarrow K_{nE} < K_{nF}$	
3	$R_{rE} < R_{rF} \rightarrow K_{nE} < K_{nF}$	
4	$M_X > M_Y > M_Z \rightarrow K_{nX} < K_{nY} < K_{nZ}$	Cf. tableau V: $K_{nX} < K_{nY} < K_{nZ}$
5	$R_{fX} > R_{fY} > R_{fZ} \rightarrow K_{nX} > K_{nY} > K_{nZ}$	
6	$R_{rX} < R_{rY} < R_{rZ} \rightarrow K_{nX} < K_{nY} < K_{nZ}$	

Interpretation: Excepté les inegalités 5, les présomptions basées sur les paramètres technologiques concordent aux conclusions des essais.

Au point de vue des paramètres thermiques des installations du tableau I,on peut admetre théoriquement :
- que R_f depend essentiellement du débit d'air secondaire, donc pour un même excès d'air on aura une fonction croissante $R_f = f(Q_{sp})$. Si cette implication s'avére pratiquement importante on peut présumer les inegalités 2 et 5 (tableau VI). S'il y a encore de phase liquide dans le clinker sorti du four, des inégalités analogues sur les R_r sont également possibles ;
- que pour des raisons thermiques (transfert de chaleur, étancheité de joints four-refroidisseur), les R_r baissent en ordre suivant des types de refroidisseur : à grille, planetaire, rotatif /11/. On peut donc présumer valables les inégalités 3 et 6 (tableau VI).

L'étape (i,i) a lieu géneralement au refroidisseur. Les phases solidifiées subissent au cas des petites R_r les transformations: $C_3S \rightarrow \beta C_2S + C$ à 1250^oC et $\beta C_2S \rightarrow \gamma C_2S$ à 650^oC. La dernière(accompaghée par pulvérisation) ne s'est pas produit pour aucun des clinkers étudiés. Quant à la première (si elle n'est pas évitée par une hausse de R_r quand le C_3S reste en état de surfusion), on peut l'identifier par la présence de la chaux libre, dont l'influence négative sur les K_n est connue /6,7/
C'est une nouvelle raison de considérer valable l'inégalité 6 (tableau VI).
L'examen de résultats conduit aux remarques suivantes :
a) Les exigences des normes pour les CPA sulfatoresistants sont justifiées par les recherches presentées:
- totalement au cas des essais sur constituants purs; les valeurs K_n baissent sensiblement (jusqu'à zéro) si la composition des clinkers à $C_3A \geq 0$ est en dehors des limites de la figure 1. Les résultats du tableau II concordent tant aux normes qu'aux conclusions des travaux classiques;
- en moindre mesure et seulement par rapport au C_3A au cas des essais sur clinkers industriels.Les autres caractéristiques n'influencent pas significativement les K_n, même s'ils sont en dehors des exigences normalisées (tableaux III,IV et /3b/).

b) Il y a des différences essentielles de sensibilité aux sulfates des clinkers *ferro*-portland produits par les cimenteries E et F'. Du à un cumul de causes, les valeurs K_n s'avérent plus grandes et moins influencées par les variations de composition (notamment pour le C_3A) pour les ciments de la série F', par rapport à ceux de la série E. Les incidences du spécifique du cru (structure, teneur en alcalis etc), de la façon dont chaque cimenterie et chaque cuisseur conduit le processus, ainsi que d'autres facteurs, sont évidemment possibles. Mais toute une série d'explications, liées aux caractéristiques des procédés de fabrication des clinkers, capables d'impliquer des différenciations du traitement thérmique de cüisson et de refroidissement, restent irréfutables.

c) L'incidence des paramètres technologiques sur les K_n des CPA provénus des clinkers (produits par les fours X, Y et Z) de la cimenterie T est évidente. Les K_{nX} diffèrent sensiblement des K_{nY} et essentiellement des K_{nZ}, malgré que les compositions potentielles des clinkers X, Y et Z sont les mêmes. Des clinkers également riches en $\overline{C_3A}$ peuvent conduire à des CPA très sensibles aux sulfates (pour les échantillons X), mais aussi à des CPA de résistance sulfatique rélativement élevée (pour les échantillons Z).

d) Pour les cimenteries E et F', toutes les prévisions basées sur les paramètres technologiques envisagés (valeurs M, R_f et $R_{f'}$) paraissent expliquer, en même sens, les valeurs différentes pour les K_n (les inégalités 1, 2 et 3 du tableau VI). Mais, pour la cimenterie T, seuls les paramètres M et $R_{f'}$ conduisent à des prévisions similaires aux conclusions des essais (les inégalités 4 et 6). Quant aux valeurs présumées pour R_{fX}, R_{fY} et R_{fZ}, l'inégalité 5 conduit à une fausse prévision. Pour le cas des fours de la cimenterie T, les implications sur la résistance sulfatique de la relation $R_f = f(Q_{sp})$, (implications assez désobligeantes pour les actuels efforts d'économie de combustible) se prouvent exemptes d'importance pratique.

Conclusions

Le traîtement thérmique dans la fabrication du clinker (c'est-à-dire le caractére du chauffage et la vitesse de refroidissement), peüt affecter, plus qu'on puisse croire, favorablement ou défavorablement, la résistance aux sulfates du ciment obtenu.

Les chemins d'obtenir des CPA résistants aux eaux sulfatées, doivent être cherchés, non seulement à partir de la composition et de la réactivité des crus, de la qualité de diriger le processus de cuisson, etc.

Il y a des cimenterie qui, en fonction de la conception des installations thérmiques disponibles, peuvent réaliser du ciment à résistance sulfatique satisfaisante, à partir de crus de composition normale. Les exemples donnés prouvent l'oportunité d'une étude systématique de l'influence des divers types de fours, de refroidisseurs et de procédés de fabrication sur la résistance sulfatique des ciments.

Bibliographie

1.-DAHL L.A.(1939), réf./6-9/

2.-KIND V.V.(1955), "Corrosion des ciments et des bétons", russe, Moscou

3.- NĂDU M.a)(1969), "De l'appréciation de la résistance des ciments aux eaux sulfatées sur la base des différentes méthodes usuelles", Colloque RILEM, Prague, aussi Rév. Matér. Constr., Fr., 654, p.61-67; b)(1979), "On the sulfate resistance of the hardened cement paste" 6 ISCC Moscou

4.-VELICA P.(1970), Thèse, Institut de Construction, roum., Bucarest

5.-TITEIU O.(1973), "La migration séléctive de la phase liquide du clinker" roum, Materiale de construcţii 3,1, p.1, Bucarest

6.-BOGUE R.H.(1955), "The chemistry of Portland cement", New York

7.- LEA F.M., (1970), "The chemistry of cement and concrete", London

8.-SOLACOLU S.(1968), "La chimie physique des silicates techniques", (roum), Bucarest

9.-TEOREANU I (1967), "La technologie des ciments et des bétons", roum., Bucarest

10.-VOLJENSKY A.V., BUROV I.S., KOLOKOLNIKOV V.S., (1979), "Liants minérals, russe, Moscou

11.-LURIE I.S.(1963), "Le ciment portland", russe, Leningrad.

12.-STEOPOE A.(1970), "La durabilité du béton" Paris

Effect of chloride penetration on the properties of hardened cement pastes

Effet de la pénétration des chlorures sur les propriétés des pâtes de ciment durcies

H.G. MIDGLEY and J.M. ILLSTON, Division of Civil Engineering, The Hatfield Polytechnic, Hatfield, Herts, U.K.

RESUME : Les effets des ions de chlorures ayant pénétré dans la pâte durcie du ciment ont été étudiés par DTG, QXRD, analyse chimique et la porosimétrie. On en a déduit que plus la proportion de E/C est élevée, plus la pénétration des ions de chlorure est profonde; la concentration en ions Cl suit une loi déterminée, en fonction de la profondeur de la pénétration. Les chlorures réagissent avec les aluminates de chaux du ciment pour former un chloro-aluminate complexe : $C_3A\ CaCl_2\ 12\ H_2O$. Tout le chlorure présent n'est pas fixé dans ce complexe; une partie reste libre. La quantité de chlorure fixé ne dépend pas de la teneur en C_3A du clinker, puis des hydrates des aluminates de chaux coexistent avec le chloro-aluminate. La pénétration du chlore altère les pores; plus la concentration en chlorures est élevée et plus petits sont les pores attaqués.

SUMMARY: The effects of chloride ions penetrating hardened cement pastes (hcp) have been investigated by DTG, QXRD, chemical analysis and mercury intrusion porosimetry. It has been found that the higher the w/c ratio the greater the penetration of chloride ions; the concentration with depth of penetration follows a power relationship. Chloride reacts with the calcium aluminates in the cement to form the complex chloroaluminate $C_3A\ CaCl_2\ 12H_2O$. Not all the chloride present is bound up in the mineral some is left as free chloride. The quantity of bound chloride found does not depend on the amount of C_3A in the unhydrated cement since calcium aluminate hydrates occur in the hcp with the chloroaluminate. Chloride penetration alters the pores in the hcp, the greater the chloride concentration the smaller the pores formed at the expense of the slightly larger ones.

INTRODUCTION:

Chloride ions present for example in sea water can penetrate hardened cement pastes (hcp) with either deleterious effects due to reaction with the calcium aluminates in the cement, or beneficial effects due to changes in the form of hydration of calcium silicates.

To investigate these effects hcp's of 0.23, 0.47 and 0.71 w/c ratio using an ordinary Portland cement were prepared as cylinders 70mm high x 23mm diam. They were moist cured for 24 hours; demoulded and placed in water at 20°C for 1 month. The cylinders were then protected on the long side and at one end by tightly fitting rubber sheaths. The protected cylinders were placed in 3 conditions, maintained at 20°C;

(a) Water(w)($Ca(OH)_2$ solution produced by keeping hcp in the water).
(b) Sodium chloride solution 30g/litre (s) (equivalent to sea water concentration) and sodium chloride solution 150g/litre (5s) (equivalent to 5 x sea water concentration).

After 6 months the cylinders were removed from the solutions, demoulded from the sheaths and split into 5 equal mini cylinders. Each mini cylinder was examined by the following techniques:
Derivative Thermogravimetry (DTG);
Semi isothermal Derivative Thermogravimetry (SiDTG);
Quantitative X-ray diffraction (QXRD);
chemical analysis for chlorides and pore size distribution and porosity by mercury intrusion porosimetry.

RESULTS

The total chloride penetration was found to obey a power relationship, Table 1, where it can be seen that there was only a slight penetration in the specimens made with a w/c ratio of 0.23; the values of chloride as wt% were for the top 14mm 0.26 for s and 0.46 for 5s. For the 0.47 w/c ratio specimen there was more penetration to a greater degree; the wt% chloride for s was 0.55 and for 5s 0.90. The 0.71 w/c ratio specimens had about the same depth of penetration but there was a greater concentration at the top 1.12% for s and 2.43 % for 5s conditions; roughly twice for the higher w/c ratio.

The chloride ions which penetrate the hcp may react with the calcium aluminates to form the complex calcium chloroaluminate $3CaO.Al_2O_3.CaCl_2.12H_2O$; or react with the calcium silicates to form complex chloride bearing calcium silicate hydrates (C-S-H); or they may remain as free chloride ions in the fine capillaries.

Table 1

Penetration of chloride ions into hcp at 6 months.

$c = kd^{-m}$
c = concentration of chloride ion wt%
d = distance into hcp in mm
k = constant reflecting depths of penetration
m = slope of relationship $mc = k' + m.\ln d$
r = correlation coefficient of linear regression.

Mark	k	m	r	Chloride wt% in bottom 14mm	Chloride wt% in top 14mm
0.23/s	17.3	-0.08	0.82	0.00	0.26
0.23/5s	22.4	-0.10	0.73	0.00	0.46
0.47/s	27.6	-0.68	0.99	0.03	0.55
0.47/5s	27.6	-0.42	0.85	0.02	0.90
0.71/s	27.6	-0.75	0.85	0.10	1.13
0.71/5s	27.6	-0.65	0.83	0.14	2.43

QXRD determination of the calcium chloroaluminate hydrate shows that there is a considerable proportion of the chloride ions not locked up the crystalline salt but must be present in the C-S-H. or as free ions.

The general mineralogy of the hcp as determined by DTG, SiDTG and QXRD shows that chloride penetration into the hcp has little effect on the quantities of calcium aluminate hydrates; the calcium sulphoaluminate hydrates or calcium hydroxide present. The chloroaluminate hydrate does not appear to be formed at the expense of the other calcium aluminate hydrates and so must be formed by reaction with the anhydrous aluminates in the unhydrated cement present.

No detectable increase in the quantity of C-S-H with chloride penetration was found for specimens made with w/c ratios of 0.23 and 0.47; but with the hcp of w/c ratio 0.71 a detectable increase in C-S-H was found for the specimen stored in sodium chloride solutions.

The results of the porosity and pore size distribution as measured by mercury intrusion porosimetry are given in Table 2. From this data it can be seen that specimens made with a w/c ratio of 0.23 have a large maxima of pores at 560Å pore radius with smaller maxima.

Table 2

Porosity cm^3/g; Pore volume cm^3/g; at selected pore radii for hcp.

Mark	Porosity	Pore value at - Å 560	400	335	270	230
0.23/w	0.058	0.0029	0.0168	0.0087	0.0049	0.0027
0.23/s	0.058	0.0025	0.0167	0.0101	0.0056	0.0035
0.23/5s	0.058	0.0005	0.0035	0.0119	0.0124	0.0030
0.47/w	0.122	0.0671	0.0147	0.0098	0.0136	0.0109
0.47/s	0.146	0.0006	0.0043	0.0195	0.0176	0.0122
0.47/5s	0.132	0.0000	0.0032	0.0156	0.0136	0.0130
0.71/w	0.265	0.0098	0.0261	0.0185	0.0243	0.0191
0.71/s	0.278	0.0201	0.0329	0.0193	0.0249	0.0215
0.71/5s	0.221	0.0037	0.0221	0.0281	0.0233	0.0162

at 400 and 355Å pore radii. With exposure to NaCl solutions (150g/l) the largest maxima shifts to 400Å pore radius, and there is an increase in the pore volumes at 335 and 270Å pore radii.

For the hcp made with a w/c ratio of 0.47 the pore volumes at 560 and 400Å pore radii are roughly equal in water storage; with exposure to sodium chloride solutions the absolute pore volume at 560Å decreases, as does that at 400Å but to a small degree while the pore volume of pores of radii 335 and 270Å increase.

With hcp made with a w/c ratio of 0.71 the pore volume of pores of 400Å pore radius reduce in the presence of chloride ions, pore volume of pores of 335Å radius increases slightly, but no change in the pore volume of pores of 220Å radius could be detected.

GENERAL CONCLUSIONS

(1) Chloride ions penetrate hcp, the greater the w/c ratio the greater the amount of penetration

(2) At the highest w/c ratio used, (0.71), more C-S-H is produced in the presence of sodium chloride.

(3) Chloride ions react with the calcium aluminate ($3CaO.Al_2O_3$) of the unhydrated cement to form

$3CaO.Al_2O_3.CaCl_2.12H_2O$,

but not all chloride ions present so react.

(4) Chloride ion penetration into hcp alters the pore size distribution, the greater the chloride present the smaller the pores formed.

Résistance du béton aux attaques physico-chimiques

Resistance of concrete to physico-chemical attack

M. REGOURD, H. HORNAIN, P. LEVY, B. MORTUREUX, C.E.R.I.L.H., France

RESUME

La résistance du béton aux attaques physico-chimiques dépend d'un grand nombre de paramètres dont certains ont été considérés séparément : composition chimique et minéralogique du ciment (teneur en C_3A, nature de la phase ferritique, teneur en laitier et en pouzzolanes), composition du béton (nature minéralogique des granulats), milieu de conservation (eau de mer artificielle, mer Méditerranée, Océan Atlantique, solutions de $MgSO_4$), traitement préalable (carbonatation).

Les mécanismes de dégradations ont été reliés à l'évolution de la microstructure du matériau , à l'aide du microscope électronique à balayage (MEB), de la microsonde électronique de Castaing, de la diffraction des rayons X (DRX). Les examens ont été complétés par des mesures de gonflement et de résistances mécaniques.

SUMMARY

The resistance of concrete to physico-chemical attack depends on a large number of parameters of which certain were considered separately : the chemical and mineralogical composition of the cement (C_3A content, nature of the ferrite phase, slag and pozzolana content), composition of the concrete (mineralogic nature of the aggregates), area of conservation (artificial sea water, Mediterranean Sea, Atlantic Ocean, $MgSO_4$ solutions), pre-treatment (carbonation).

The degradation mechanism has been related to the evolution of the microstructure of the material by means of Scanning Electron Microscope, Electron Probe Microanalysis and X-ray Diffraction. The examinations were completed by measurements of swelling and mechanical resistances.

Bien composé et correctement mis en œuvre, le béton est généralement stable vis-à-vis des agents agressifs courants. Toutefois, tous les facteurs conditionnant la pérennité d'un ouvrage en béton n'étant pas toujours maîtrisés, il importe de prendre un certain nombre de précautions destinées à prévenir les dégradations ultérieures. Le mécanisme de ces dégradations fait intervenir de nombreux paramètres en relation avec les caractéristiques du ciment et du béton, la nature de l'agent agressif, les conditions d'exposition. Nous considérerons ici quelques uns des facteurs qui conditionnent la résistance chimique du ciment vis-à-vis des sulfates et de l'eau de mer, et dans le cas de la réaction alcalis-granulats.

1. RESISTANCE CHIMIQUE DES CIMENTS VIS-A-VIS DES SULFATES ET DE L'EAU DE MER

1.1 Mécanisme d'attaque

Deux phénomènes physico-chimiques principaux entrent en jeu :

- (1) Expansion et fissuration par formation très localisée d'ettringite. Les contraintes sont dues à une ettringite "naissante" mal cristallisée (fig. 1). Les cristaux bien formés n'apparaissent qu'après fissuration quand ils disposent de l'espace nécessaire à leur croissance.
- (2) Dissolution de $Ca(OH)_2$ et des C-S-H qui deviennent plus poreux (fig. 2).

Selon P.K. MEHTA, le gonflement de l'ettringite serait dû à une adsorption d'eau [1,2].

En eau de mer, la cristallisation de chloro-aluminates $C_3A.CaCl_2.10H_2O$ ralentit l'attaque du ciment. Dans les solutions contenant des ions Mg^{2+} (eau de mer, $MgSO_4$), l'échange $Mg^{2+} \rightarrow Ca^{2+}$ conduit à la formation de $Mg(OH)_2$ et de C-S-H où la chaux peut être remplacée progressivement par le magnésium pour donner des (C,M)-S-H ainsi que le montre l'analyse des silicates hydratés de la zone superficielle d'une éprouvette de pâte pure de CPA ayant séjourné 3 mois en eau de mer (tableau I).

	Zone superficielle	Zone interne
CaO	18,2	37,5
SiO_2	29,2	27,1
MgO	22,4	0,7
Al_2O_3	2,3	2,8
Cl	∿ 3,6	∿ 4,6
SO_3	∿ 1,5	∿ 0,6
C/S	0,7	1,5
C+M/S	1,8	1,5

Tableau I - Analyse à la microsonde de Castaing des C-S-H dans un CPA conservé 3 mois en eau de mer.

Les chloro-aluminates et les sulfo-aluminates ne sont pas stables à long terme dans l'eau de mer et les solutions chargées en sulfates. Dans une solution à 5% de $MgSO_4$, ils donnent naissance au gypse (fig. 3). En eau de mer, le chloro-aluminate se transforme en ettringite (fig. 4) qui peut disparaître à son tour de sorte que dans les zones fortement altérées de bétons anciens on ne retrouve parfois que $CaCO_3$ et des M S H [3].

L'hydrotalcite $Mg_2Al_2CO_3(OH)_{16}4H_2O$ en plaquettes hexagonales (fig. 5) a pu être mise en évidence dans certains produits, notamment dans un mortier de ciment alumineux conservé en eau de mer depuis 1920.

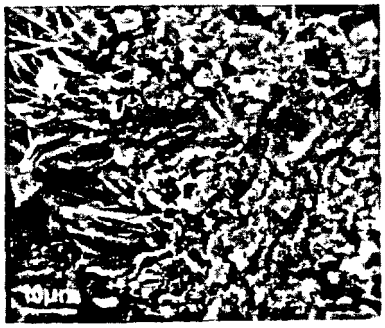

Fig. 1 - Ettringite expansive.

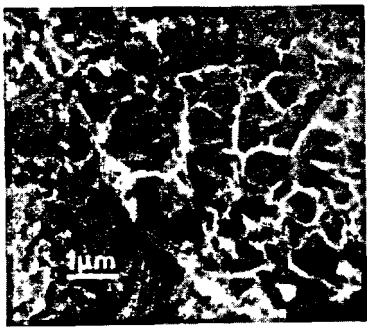

Fig. 2 - C-S-H alvéolaire.

Fig. 3 - Transformation chloro-aluminate-gypse dans $MgSO_4$.

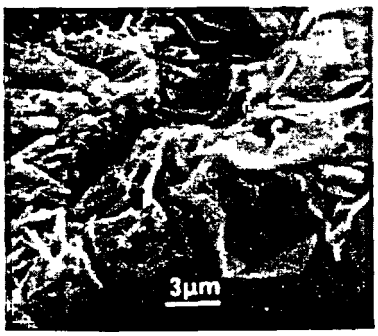

Fig. 4 - Transformation chloro-aluminate-ettringite en eau de mer.

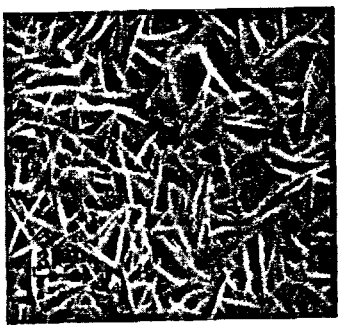

Fig. 5 - Hydrotalcite

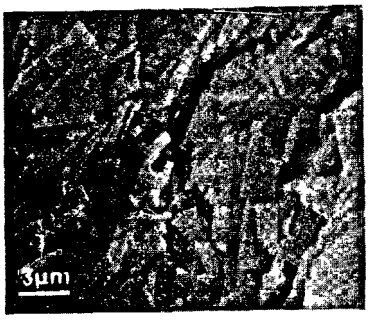

Fig. 6 - Thaumasite.

L'altération des mortiers riches en chaux peut être en relation avec la formation de thaumasite $CaCO_3$ $CaSiO_3CaSO_4 15H_2O$ qui résulte souvent de la transformation d'ettringite avec laquelle elle coexiste, par fixation de CO_2 et SiO_2 [4]. Ce minéral a été observé dans différents ouvrages maritimes où il correspondait à un stade avancé de dégradation (fig. 6).

1.2 Influence de la composition minéralogique du ciment.

La composition potentielle de Bogue ne donne souvent que des valeurs indicatives différentes de celles plus exactes mesurées par diffraction des rayons X (Tableau II).

1.2.1 Teneur en C_3A : C_3A est le minéral déterminant dans le processus d'expansion, mais d'autres facteurs peuvent interférer tels que le taux de gypse, la composition de la phase ferritique, etc ... Le tableau II regroupe les résultats obtenus sur 12 ciments dont 7 CPA. Après deux ans de conservation, en immersion totale, en eau de mer naturelle, en laboratoire les éprouvettes 2 x 2 x 16 cm de mortier ISO confectionnées à partir des CPA à faible teneur en C_3A ont des gonflements faibles. Toutefois, les ciments 6 et 8 contenant respectivement 9,5 et 6 % de C_3A ont un comportement médiocre : le CPA n° 6 est surgypsé ; le CPA n° 8 contient une phase ferritique réactive plus alumineuse que C_4AF (Tableau IV).

Une deuxième série d'essais a été effectuée sur 12 clinkers synthétisés en laboratoire où l'on a fait varier les teneurs en C_3S, C_2S, C_3A et $C_2(A,F)$. A partir de ces clinkers broyés à 3500 $cm^2.g^{-1}$ et gypsés ont été confectionnés des prismes 2 x 2 x 16 cm de mortier ISO conservés en eau de mer artificielle pendant 4 ans. Les résultats sont rassemblés dans le tableau III et illustrés par la figure 7. Les ciments à teneur en C_3A supérieure à 10 % ont été détruits.

N°	C_3A	C_4AF	C_3S	C_2S	Gonglements en $\mu m.m^{-1}$
13	< 1	21	65	11	1685
14	< 1	23	52	23	1740
15	< 1	22	35	34	1980
16	6,5	16,5	60	10	1740
17	4	18	53	18	1940
18	5	16	38	36	1750
19	10	13,5	60	12	2130
20	8	14	54	16	2060
21	8	15	40	25	1880
22	13	8	57	16	détruite
23	14	8	47	22	-id-
24	13	9	39	32	-id-

Tableau III - Composition minéralogique et gonflements après 4 ans en eau de mer des 12 clinkers synthétiques.

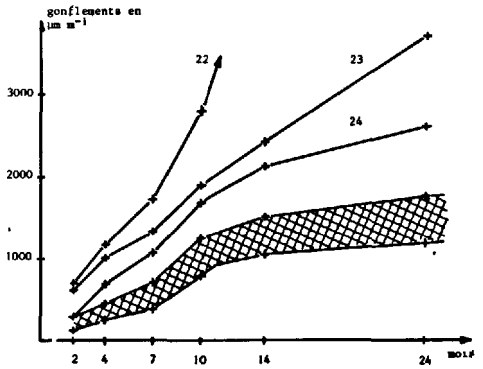

Fig. 7 - Gonflements en fonction de la teneur en C3S et C_3A

N° et type de ciment			CPA 1	CPA 2	CPA 3	CPA 4	CPA 5	CPA 6	CPA 7	CPA 8	CPAL 9	CPF 10	CPF 11	CLK 12
Composition minéralogique	BOGUE	C_3S	69,2	50,5	55,5	35,8	60,1	49,4	45,6	56,3	CPA 7 + Laitier 20 %	CPA 7 + Laitier 30 %	CPA 8 + Laitier 30 %	CPA 4 + Laitier 80 %
		C_2S	17,7	26,2	15,7	31,8	12,2	21,6	21,3	15,0				
		C_3A	4,1	1,6	9,3	11,8	7,4	7,6	14,0	10,0				
		$C_2(A,F)$	3,9	13,6	9,9	7,6	7,1	7,3	8,4	10,0				
	DRX	C_3S	68	57	58	54	60	55	49	54	40	38	40	n.d.
		C_2S	17	22	19	18	15	18	20	18	15	11	12	
		C_3A	5	2,5	3	11	8,5	9,5	18	6	13,5	11,5	4	
		$C_2(A,F)$	2,5	11	12,5	6	5	5,5	5,5	12	5	3	7	
SO_3 (dosage chimique)			1,87	2,33	2,51	3,25	3,41	4,46	2,93	2,16	2,50	3,80	3,17	3,30
Finesse Blaine ($cm^2.g^{-1}$)			3300	3100	2140	2670	3920	3300	3300	2890	2900	3350	2880	3320
Gonflements $\mu m.m^{-1}$	ATLANTIQUE		400	550	600	950	3400	6000	1600	2250	2400	2150	1700	400
	MEDITERRANEE		600	500	900	1550	1025	4100	1100	800	1350	1250	1200	600

Tableau II - Composition minéralogique, finesse et gonflements en eau de mer après 2 ans.

1.2.2 Teneur en phase ferritique : Tous les essais indiquent que les ciments à forte teneur en C_4AF sont stables dans l'eau de mer. La cristallisation "ménagée" d'ettringite à partir de la solution n'est pas expansive. Toutefois les compositions se rapprochant de C_6A_2F se comportent moins bien [5]. C'est le cas du ciment n° 8 qui, malgré sa faible teneur en C_3A (6 %), se dégrade. Ce CPA contient 12 % d'une phase ferritique plus riche en chaux et en alumine que C_4AF (tableau IV).

MgO	Al_2O_3	SiO_2	CaO	Fe_2O_3	A/F	C/A+F
3,5	20,8	4,1	51,7	19,8	1,64	2,81

Tableau IV - Analyse à la microsonde de la phase ferritique du ciment n° 8.

1.2.3 Teneur en silicate tricalcique : La résistance chimique des ciments à teneur élevée en C_3A est d'autant moins bonne que leur teneur en C_3S est plus élevée. C'est le cas des ciments 22, 23 et 24 contenant 13 % de C_3A et respectivement 57, 47 et 39 % de C_3S (tableau III et fig. 7). L'influence de C_3S est moins nette dans les ciments où C_3A est inférieur à 10 %.

1.2.4 Teneur en SO_3 : Des essais de laboratoire ont montré qu'il existe un gypsage optimal qui dépend de la composition minéralogique et de la finesse du ciment. Les ciments fins à granulométrie resserrée, gypsés à l'optimum, ont un comportement amélioré dans l'eau de mer. L'amélioration est en relation d'une part avec leur plus grande compacité et leur taux d'hydratation plus élevée et d'autre part avec la présence d'une plus grande quantité de C_3A disponible rapidement pour former de l'ettringite primaire non expansive. Les proportions d'alumine restant pour une cristallisation ultérieure d'ettringite expansive sont réduites.

1.3 Influence des ajouts sur la résistance des ciments vis-à-vis de l'eau de mer et des sulfates.

1.3.1 Teneur en laitier : Tous les ciments contenant au moins 60 % de laitier sont stables. En deça de cette valeur, la tenue du ciment dépend de la composition du clinker et de celle du laitier [6]. La bonne résistance chimique des ciments de laitier est due à leur teneur en chaux plus faible que celle des CPA et à la nature des hydrates formés dont la composition, la concentration, la distribution et la texture sont différentes. $Ca(OH)_2$ est moins abondant ; les C S H sont plus riches en Al_2O_3 et MgO mais moins riches en CaO (tableau V).

	CPA - (3 mois)		CLK - (3 mois)	
	eau douce	eau de mer	eau douce	eau de mer
C/S	1,8	1,8	1,5	1,5
Al_2O_3	3,1	2,4	8,0	6,0
MgO	∿ 1,0	∿ 1,0	n.d.	∿ 5,0

Tableau V - Composition des C-S-H au contact des grains de clinker dans un CPA et dans un CLK (microsonde de Castaing).

Les examens et analyses au microscope électronique à balayage montrent que les C-S-H formés sont compacts et que leur composition demeure relativement proche de celle du laitier anhydre (fig. 8). Les quantités d'ettringite et de chloro-aluminates formés dans les ciments au laitier conservés en eau de mer sont généralement plus importantes que dans les CPA.

Mais la cinétique et le mode de cristallisation sont différents : l'ettringite apparaît par un processus relativement lent de passage en solution et de cristallisation. La distribution des cristaux est plus diffuse. Ils sont plus courts, plus fins, souvent intimement mélangés aux C-S-H et peu visibles en fractographie au MEB dans les échantillons compacts.

Les ciments n° 1 à 12 décrits dans le Tableau II font l'objet d'une étude à long terme dans le cadre de la COPLA (Commission Permanente des Liants Hydrauliques et Adjuvants) en collaboration avec les Laboratoires maritimes et le Laboratoire Central des Ponts et Chaussées.

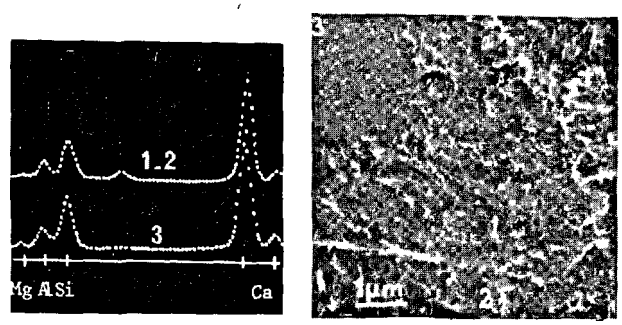

Fig. 8 - Texture et composition des C-S-H au contact d'un grain de laitier dans un CLK.

1.3.2 - Teneur en pouzzolanes : Cinq pouzzolanes dont les caractéristiques générales sont rassemblées dans le tableau VI ont été testées en eau de mer artificielle, [7].

Pouzzolane	Type	Finesse $cm^2.g^{-1}$	Fixation de CaO Unités arbitraires
Tuff	Zéolithe	5600	100 à 21 jours
Trass	Zéolithe	7000	93 "
Phlégréenne	Verre 50 %	2900	47 "
Volvic	Verre 20 %	4300	39 "
Cendre vol.	Verre 90 %	5000	30 "

Tableau VI - Caractéristiques des pouzzolanes.

Cinq CPAZ (20 % pouzzolane) ont été confectionnés avec un même ciment de composition : 60 % C_3S ; 15 % C_2S; 8,5 % C_3A ; 5 % C_4AF ; 3,4 % SO_3 ; 2 % MgO ; 1,5 % CaO libre. Deux séries de prismes 2 x 2 x 16 cm de mortiers ISO conservés préalablement 28 jours en atmosphère humide ont été immergées l'une dans l'eau douce, l'autre dans l'eau de mer artificielle. Les résistances en compression et les gonflements, après 2 ans en eau de mer, sont donnés respectivement sur la fig. 9 et dans le tableau VII.

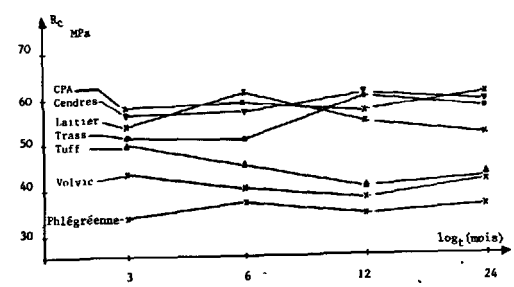

Fig. 9 - Résistances en compression des CPAZ conservés 2 ans en eau de mer artificielle.

D'après ces résultats on observe que : le CPA demeure assez stable après 2 ans ; le trass, très réactif, donne de bons résultats ; les cendres volantes, qui ne commencent à réagir que tardivement, ont un bon comportement ; la pouzzolane phlégréenne de granulométrie grossière a des résistances faibles mais sensiblement constantes ; le tuff, très réactif, donne des résultats satisfaisants en eau douce mais moins

bons en eau de mer où, dès 3 mois, le gonflement est supérieur à celui des autres ciments ; la pouzzolane Volvic réagit lentement et dans les conditions de l'essai son influence n'est pas très favorable.

	3 mois	6 mois	1 an	2 ans
CPA	470	750	1130	1340
Tuff	630	1030	1220	1560
Trass	470	840	1160	1440
Phlégréenne	380	470	750	1090
Volvic	440	690	1130	1410
Cendre vol.	340	720	810	1130

Tableau VII - Gonflements des CPAZ en $\mu m.m^{-1}$.

Les analyses par DRX des mortiers conservés en eau de mer révèlent la présence d'ettringite et de chloro-aluminates. Mais les différences essentielles portent sur l'intensité des raies de $Ca(OH)_2$ dont la diminution n'est pas due uniquement à l'effet pouzzolanique comme le montre la comparaison avec les enregistrements effectués sur les mêmes échantillons en eau douce. Ainsi dans le CPAZ au tuff, la dissolution de la chaux est maximale [fig. 10 (a) et 10 (b)].

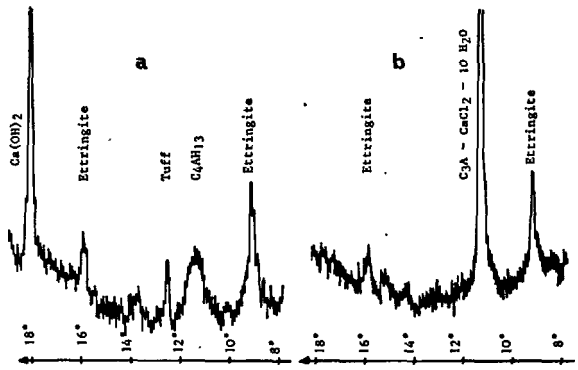

Fig. 10 - Enregistrements diffractométriques du CPAZ au tuff conservé 2 ans en eau douce (a) et en eau de mer (b).

Le CPAZ à la pouzzolane phlégréenne est peu altéré. De même le ciment au trass renferme encore des quantités appréciables de $Ca(OH)_2$. Le ciment aux cendres contient, à deux ans, beaucoup d'ettringite et de chloro-aluminates ; la dissolution de la chaux y paraît importante. L'altération de ce ciment se traduit par une chute importante des résistances en flexion.
Le CPAZ à la pouzzolane de Volvic, peu réactive, contient beaucoup d'ettringite dont les raies sont 4 à 5 fois plus intenses que dans le CPA témoin ou le CPAZ au trass.

Les résultats obtenus montrent que la tenue des CPAZ en eau de mer dépend de leur composition chimique et minéralogique, de leur réactivité, de leur finesse et vraisemblablement de la composition du clinker de base (teneur en C_3A). Leur stabilité n'est pas toujours en relation avec l'effet pouzzolanique, comme le montre l'exemple du tuff très réactif, mais donnant un comportement médiocre en eau de mer.

1.4 Influence du mode conservation

Le tableau II indique que l'eau de la Méditerranée est moins agressive que l'eau de l'Atlantique.

L'immersion alternée, jointe aux variations climatiques (gel, ensoleillement), est parfois plus préjudiciable au béton que l'immersion totale. L'abaissement de la température accroît le gonflement des CPA ; mais l'addition de laitier améliore le comportement du ciment ainsi que le montre la fig. 11 relative à des essais de laboratoire sur prismes 4 x 4 x 16 cm conservés 1 an en eau de mer artificielle.

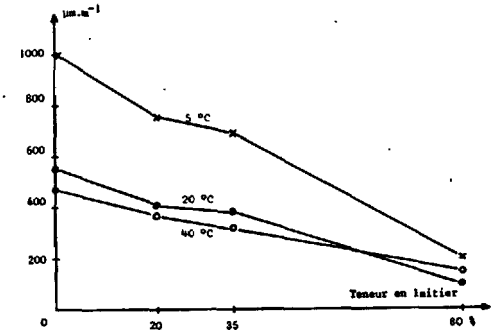

Fig. 11 - Gonflement en fonction de la teneur en laitier et de la température en immersion totale.

La carbonatation naturelle ou artificielle des bétons renforce leur résistance aux sulfates [8, 9]. Des essais effectués sur mortier ISO confectionnés à partir de 3 ciments A, B, C renfermant respectivement 15, 9, 5 % de C_3A, conservés dans une solution de 5 % de $MgSO_4$, ont montré qu'un traitement préalable sous CO_2 annulait le gonflement des 3 ciments (fig. 12) et diminuait fortement la pénétration des ions Cl^- (tableau VIII).

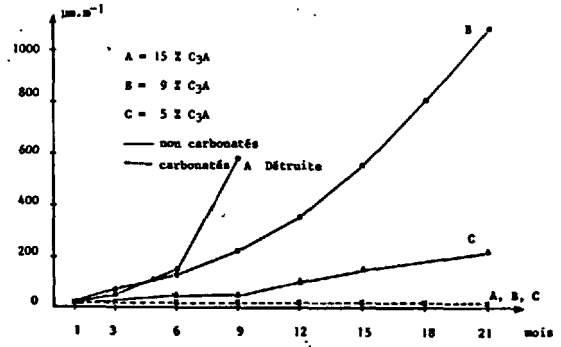

Fig. 12 - Gonflements dans $MgSO_4$ des mortiers carbonatés (immersion totale), et non carbonatés.

		Conservation préalable	
		60j CO_2	60j H_2O
Ciment à 11 % de C_3A	0 - 2 mm	0,110	0,380
	2 - 4 mm	0,089	0,361
	4 - 6 mm	0,005	0,291

Tableau VIII - Dosage potentiométrique de Cl^- (10 jours dans l'eau de mer).

2. INFLUENCE DE LA NATURE MINERALOGIQUE DES GRANULATS

La présence dans le béton de granulats feldspathiques et micacés (schistes, gneiss, granites) peut être à l'origine de dégradations à la suite de réactions du type alcalis-silicates, qui conduisent à la formation de gels expansifs contenant SiO_2, CaO, Na_2O, K_2O, H_2O. Les gels se forment au contact du granulat et parfois sur le granulat entre les lits micacés. La composition moyenne suivante a été observée : CaO = 16 % ; SiO_2 = 53 % ; K_2O = 3 % ; Na_2O = 6 %. Les gels sont associés à des cristaux en plaquettes, plus ou moins efflorescents, déposés sur les granulats [fig. 13 (a) et 13 (b)]. Il s'agit de silicates de calcium et de potassium du type tobermorite dont la teneur en K est d'autant plus élevée qu'on avance vers l'intérieur du granulat. On observe que l'ettringite et la thaumasite sont fréquemment associées aux dégradations dues aux réactions alcalis-silicates.

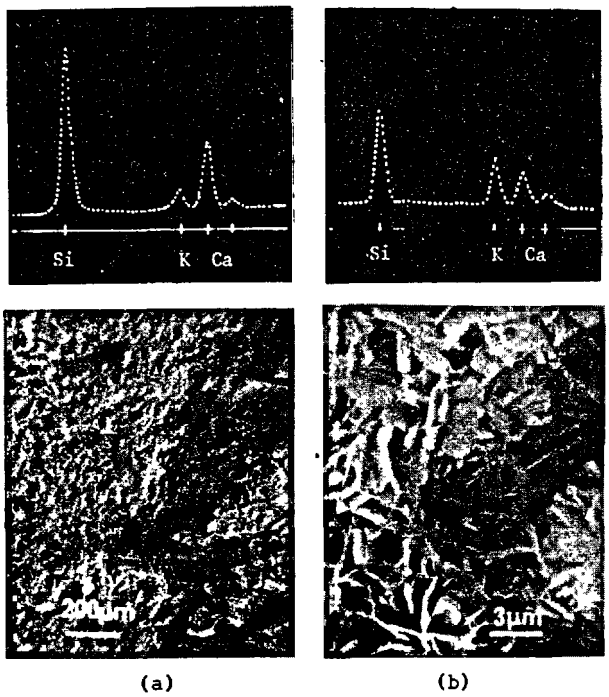

(a) (b)

Fig. 13 - Texture et composition du gel (a) et des cristaux (b) en contact avec le granulat

3. CONCLUSIONS

- L'expansion des bétons dans les eaux sulfatées est due à la formation "d'ettringite naissante" mal cristallisée.

- Pourvu qu'ils soient correctement gypsés et qu'ils ne contiennent pas d'autres phases réactives, les ciments où C_3A ne dépasse pas 10 % sont stables en eau de mer.

- Les ciments à forte teneur en C_4AF sont stables. Mais le comportement est moins bon dans le cas des solutions solides proches de C_6A_2F.

- Une grande finesse combinée à un gypsage optimal améliore la tenue aux sulfates.

- L'addition de laitier est favorable. Les C-S-H sont plus compacts et de composition moins riche en chaux et plus riche en Al_2O_3 et MgO que celle des CPA.

- L'effet des pouzzolanes, généralement favorable, ne dépend pas seulement de leur activité pouzzolanique.

- La carbonatation renforce la résistance chimique des ciments.

- La présence de granulats feldspathiques ou micacés peut entraîner des dégradations du type alcalis-réaction indépendamment de la teneur propre en alcalins du ciment.

4. BIBLIOGRAPHIE

[1] MEHTA (P.K.) : Mechanism of expansion associated with ettringite formation.
Cem. Concr. Res., Vol. 3, (1973), p. 1-6.

[2] MEHTA (P.K.), FAICHUNG HU : Further evidence on expansion of ettringite bu water adsorption.
Communication Commission RILEM 32 RCA, Athènes, 14-15 mars 1978.

[3] REGOURD (M) : L'action de l'eau de mer sur les ciments.
Annales I.T.B.T.P., Supplément au N° 329, juin 1975, Série Liants Hydrauliques n° 25, p. 87-102.

[4] REGOURD (M), HORNAIN (H), MORTUREUX (B), BISSERY (P), EVERS (G) : Ettringite et thaumasite dans le mortier de la digue du large du port de Cherbourg.
Annales de l'I.T.B.T.P., N° 358, févr. 1978, Série Liants Hydrauliques n° 28, p. 3-13.

[5] FRIGIONE (G), MARRA (S) : Influence of the isomorphous replacement Fe→Al on the technological characteristics of tricalcium aluminate.
Il Cemento, oct.-déc. 1975, n° 4, p. 173-180.

[6] LOCHER : Zur Frage des Sulfatwiderstandes von Huttenzementen.
Z.K.G., 19 (1966), 395-401.

[7] MORTUREUX (B), HORNAIN (H), GAUTIER (E), REGOURD(M) Comparaison de la réactivité de différentes pouzzolanes.
Communication à ce Congrès.

[8] CALLEJA (J) : Topics on beneficial aspects of concrete carbonation.
RILEM International Symposium on Carbonation of Concrete. Wexham Springs, 5-6 avril 1976.

[9] REGOURD (M) : Carbonatation accélérée et résistance des ciments aux eaux agressives.
International Symposium on Carbonation of Concrete Wexham Springs, 5-6 avril 1976.

Fly Ash and Alkali Aggregate reaction

Les cendres volantes et l'alcali-réaction des agrégats

W. GUTT, P.J. NIXON, M.E. GAZE, Grande-Bretagne.

RESUME : On étudie les réactions qui se produisent dans le système eau, C_3A, $Ca(OH)_2$, K_2SO_4 avec et sans addition de cendres volantes. On confirme le rôle des sulfates alcalins neutres, qui augmentent la teneur en hydroxyde des solutions des pores de ciment; on montre que la présence de cendres volantes accroît le taux de réaction aux premiers âges de durcissement. On discute les résultats expérimentaux par rapport au mécanisme par lequel les cendres volantes peuvent réduire la dilatation due à l'alcali-réaction des agrégats (ARA). La question de savoir si les cendres volantes peuvent avoir en pratique une influence sur la neutralisation de l'ARA reste un sujet discutable.

SUMMARY : The reactions occurring in the system water, C_3A, $Ca(OH)_2$, K_2SO_4 with and without the addition of fly ash have been studied. The role of neutral alkali sulphates in increasing the hydroxyl content of cement pore solutions has been confirmed and the presence of flyash has been shown to increase the rate of reaction at early ages. The experimental results are discussed in relation to the mechanism by which flyash can reduce expansion due to alkali aggregate reaction. Whether flyashes can be relied upon to counteract AAR in practice, remains an issue which is controversial.

INTRODUCTION

Soon after Stanton discovered that alkali aggregate reactivity (AAR) was the cause of damage to concrete in the USA(1) he found that such damage could be alleviated by adding finely ground reactive material to the concrete mix. Since then it has been claimed that a wide variety of natural and artificial pozzolanas and materials such as granulated blastfurnace slags with latent hydraulic properties can mitigate damage due to AAR. A series of eleven flyashes from different British power stations have been investigated at BRE for their effectiveness in preventing deleterious expansion due to AAR using the ASTM test (C441) which employs pyrex glass as the standard reactive aggregate. All the ashes tested reduced expansion and there were only small differences between the effectiveness of the different ashes. The differences that were found between ashes did not correlate with the alkali content of the ash and the best correlation was found with some measure of the pozzolanic activity of the ash, in particular with the results of the Lea test(2). The results of this investigation will be published in more detail.

In order to gain a more basic understanding of the mechanism by which flyashes can reduce expansion due to AAR a series of experiments have been started to examine the composition of solutions in contact with flyash/Portland cement mixtures. As a preliminary step the reaction by which the alkalinity of the pore solution in Portland cement concrete is enhanced in the presence of alkali metal salts and the effect of flyash on this reaction has been investigated.

In Portland cement clinker the alkali metals occur preferentially in a potassium-sodium sulphate solid solution and in this form they are most readily soluble. Diamond(3) has proposed that enhanced hydroxyl ion concentrations in the pore solution of hydrated cement come about when the sulphate ions react with the calcium aluminates in the cement, precipitating ettringite. This enables the dissolution of more calcium hydroxide (produced by the hydration of the calcium silicates) thus preserving the solution equilibria of a saturated solution of calcium hydroxide. In fact for this to happen calcium ions in the solution must also be involved in the reaction. A possible reaction sequence would therefore be:

$$Ca(OH)_2 \rightleftharpoons Ca^{2+} + 2(OH)^-$$

$$4CaO.Al_2O_3.19H_2O + 3Ca^{2+} + 3SO_4^{2-} + 13H_2O \rightarrow$$

$$3CaO.Al_2O_3.3CaSO_4.31H_2O\downarrow + Ca(OH)_2$$

The final result would be precipitation of ettringite and a pore solution richer in alkali hydroxides.

As a first step in the investigation we have therefore examined the reactions taking place between tricalcium aluminate, potassium sulphate and a saturated lime solution and the effect that the presence of flyash has on these reactions.

EXPERIMENTAL

In the first series of reactions approximately 0.5 g of laboratory prepared tricalcium aluminate was reacted in a sealed plastic flask with 75 ml of water, 25 ml of 0.4N K_2SO_4 and about 1 g of freshly ignited CaO. The quantity of CaO was judged sufficient to provide an excess over that required for reaction. The contents of the flask were stirred with a magnetic stirrer and the reaction was carried out at room temperature. After the designated reaction period the solid material was separated from the solution by centrifuging and the solution was transferred to a 200 ml volumetric flask. The solids were washed once with distilled water, re-centrifuged and the washings transferred to the volumetric flask which was then made up to 200 ml with distilled water. 25 ml aliquots of this solution were used for the determination of:

(a) total alkalinity by titration against N/20 HCl
(b) calcium by titration against EDTA
(c) sulphate gravimetrically by precipitation as $BaSO_4$

The separated solids and portions of the diluted solutions were evaporated to dryness and examined by X-ray powder diffraction using a Guinier Focussing camera.

The second series of reactions was carried out similarly but with the inclusion of 5 g of flyash. The ash used had the following characteristics:

total alkali metals - 3.35 wt% as equivalent Na_2O

available alkali metal - 1.58 wt% as equivalent Na_2O (determined according to ASTM C311)

pozzolanic activity according to Lea test(2) - a strength difference of 17.6 MN/m^2 for a mix containing 30% ash. This classifies it among the more pozzolanic flyashes.

RESULTS

The results of the chemical analyses of the solutions from the two series of reactions are given in Table 1 and the phases identified by X-ray powder diffraction in the residues after evaporation of the reaction solutions and in the solids separated by centrifuging are listed in Table 2.

The chemical analytical results for both series show the removal of calcium and sulphate ions from solution. The precipitate is shown by the X-ray diffraction results to be calcium sulpho-aluminate hydrate, both 'high' and 'low' sulphate forms being detected. The solution becomes effectively one of potassium and hydroxyl ions with increased alkalinity compared with the initial calcium hydroxide solution.

In the presence of flyash however the reaction proceeds very much more quickly, going to completion by 7 days whereas without the flyash the reaction is not complete at 28 days. In the solution containing flyash there is a slight reduction in alkalinity at 28 days and also a slight rise in the sulphate content of the solution although the calcium level in solution has continued to fall.

DISCUSSION

The results obtained for the solution containing C_3A, $Ca(OH)_2$ and K_2SO_4 support Diamonds proposal(3)

TABLE 1

Mix	Reaction period	Composition of 25 ml aliquots of reaction solution				% of K_2SO_4 reacted(b)
		Total alkalinity (ml of N/20 HCL required to neutralise)	Alkalinity from Reaction(a)	CaO (mg/25 ml)	SO_4^{2-} (mg/25 ml)	
$C_3A/K_2SO_4/Ca(OH)_2$	7 days	25.5	12.5	18.3	28.0	53
	14 days	23.35	16.0	10.3	18.55	69
	28 days	26.3	20.1	8.6	7.3	88
$C_3A/K_2SO_4/Ca(OH)_2$ + flyash	1½ hours	19.6	2.3	24.3	-	9(c)
	1 day	20.05	7.0	18.3	43.7	27
	7 days	26.9	24.95	3.05	nd	100
	14 days	26.55	24.7	2.5	nd	100
	28 days	23.85	23.7	0.2	3.0	95

nd - not detected

(a) - total alkalinity less the calculated OH^- from residual CaO

(b) - calculated from the residual SO_4^{2-} in solution except (c) which was calculated from the alkalinity

TABLE 2

Mix	Reaction period	Phases detected by X-ray powder diffraction	
		Residue after evaporation of solution to dryness	Solids separated by centrifuging
$C_3A/K_2SO_4/Ca(OH)_2$	7 days 14 days 28 days	K_2SO_4 $K_2Ca(CO_3)_2$	$Ca(OH)_2$, $CaCO_3$, strong ettringite some 'low sulphate'(a)
$C_3A/K_2SO_4/Ca(OH)_2$ + flyash	1½ hour	K_2SO_4, $Ca(OH)_2$	$Ca(OH)_2$, some 'low sulphate'(a)
	1 day	K_2SO_4, $Ca(OH)_2$	weaker $Ca(OH)_2$, 'low sulphate'(a) trace ettringite
	7 day	$K_2CO_3 1\frac{1}{2}H_2O$, $K_2Ca(CO_3)_2$	mainly ettringite trace $Ca(OH)_2$
	14 day	$K_2Ca(CO_3)_2$	
	28 day	$K_2Ca(CO_3)_2$	

(a) the low sulphate form of calcium sulpho-aluminate hydrate

regarding the mechanism whereby neutral alkali sulphates can increase the hydroxyl content of a cement pore solution. It has been shown that removal of sulphate ions from solution is coupled with the appearance in the solid precipitate of ettringite and/or the 'low sulphate' form of calcium sulpho-aluminate and at the same time the alkalinity of the solution is raised above that of a saturated $Ca(OH)_2$ solution and is finally almost completely converted to a KOH solution. Similar observations have been made by Lawrence(4).

When flyash is added to the reactants the same removal of calcium and sulphate ions from solution accompanied by an increase in the alkalinity of the solution is observed but the rate of reaction is greatly accelerated and the reaction is complete within 7 days. A similar acceleration in the rate of removal of calcium hydroxide from a paste of C_3A, $Ca(OH)_2$ and gypsum when natural pozzolanas were present has been noted by Collepardi et al(5). They commented that the rate of reaction was too rapid to be accounted for by the usual lime-pozzolana reaction. In the reaction observed here there is evidence of the effect of the lime-pozzolana reaction continuing to reduce the lime in solution after all the sulphate has been precipitated as calcium sulpho-aluminate but in this initial period the main reaction seems to be the same as in the system without flyash.

The reactions occurring at early ages are of particular importance in seeking an explanation for the action of pozzolanas in reducing the expansion due to alkali aggregate reaction as in the experiments carried out at BRE in which pyrex has been used as the reactive aggregate in mortar bars with a high alkali content, the effectiveness or otherwise of the pozzolana is clearly apparent by the time of the 14 day measurement. It is therefore reasonable to look for explanations in the results described above.

The most obvious explanation for the action of pozzolanas in reducing expansion due to AAR is that they reduce the alkalinity of the pore solution by removing the free lime which is the primary source of hydroxyl ions. However the results reported here show that on the contrary, at these early ages the alkalinity of the pore solution is enhanced in the presence of flyash. Alternatively then it could be that the rapid increase in alkalinity in the flyash system induces reaction at such an early age that the cement matrix is soft enough to accommodate it and that all available alkalis or reactive aggregate is consumed in this early reaction.

The other relevant feature of the results is the very rapid removal of the calcium from solution by precipitation as calcium sulpho-aluminate. This depletion of calcium (and possibly the release of alkali metal ions from the flyash) means that the gel produced by attack of the alkaline solution on the siliceous aggregate has a relatively much higher alkali metal to calcium ratio. Vivian has shown(6) that if the ratio of alkali to reactive material is very high the expansion is reduced and has suggested that this is because a gel with a high alkali to silica ratio is fluid and does not produce expansive pressure whereas Krogh(7) has investigated synthetic gels and found that gels with a high percentage of calcium are rigid and non-expansive. It can therefore be postulated that gels with a high alkali/low calcium content may be too fluid to cause expansion. Although there is as yet no direct experimental evidence for this, Chatterji(8) has demonstrated that the complete removal of free $Ca(OH)_2$ suppresses alkali-silica reaction even when excess alkali metal salt, including hydroxide, is present in the structure.

There must always be some doubt about the extent to which the rates of reaction found in these very dilute solutions relate to those in a cement paste. Lawrence(4), however, has studied the rates of combination of sulphate and release of alkali in cement-water systems with water/cement ratios varying from 0.5 to 50 and has found that they were independent of the water/cement ratio provided a saturated lime solution could be formed very quickly by the cement.

CONCLUSIONS

Studies of the reactions occurring in the system water, C_3A, $Ca(OH)_2$, K_2SO_4 confirm the role of neutral alkali sulphates in increasing the hydroxyl content of a cement pore solution. Similar reactions have been found in the presence of flyash but the rate of reaction is very much greater. No reduction in alkalinity at early ages due to the presence of flyash has been found but there is much more complete removal of calcium from solution.

These observations suggest that the action of pozzolanas in reducing expansion due to AAR may either be due to an acceleration of the rate of reaction so that it takes place while the cement matrix is still soft or to the rapid and complete removal of calcium ions from solution and the consequent effect on the properties of the gel.

Whether flyashes can be relied upon to counteract AAR in practice remains an issue of some controversy requiring further research.

ACKNOWLEDGEMENT

The work described has been carried out as part of the research programme of the Building Research Establishment of the Department of the Environment and this paper is published by permission of the Director.

REFERENCES

1 Expansion of concrete through reaction between cement and aggregate, T E Stanton, Am Soc Civil Eng, Proc 66, pp 1781-1811, 1940

2 The testing of pozzolanic cements, F M Lea, Cement Technology, Vol 4, No 1, pp 3-7, 1973

3 A review of alkali-silica reaction and expansion mechanisms: Part I, Alkalis in cement and in concrete pore solutions, S Diamond. Cement and Concrete Research, Vol 5, No 4, pp 329-346, 1975

4 Structure of Portland cement paste and concrete, C D Lawrence, Highway Res Board, Special Report 90, 1966

5 The effect of pozzolanas on the tricalcium aluminate hydration, M Collepardi, G Baldini, M Pauri and M Gorradi, Cement and Concrete Research, Vol 8, No 6 pp 741-752, 1978

6 Studies in Cement-aggregate reaction, R H Jones and H E Vivian, Bulletin 256, CSIRO, Melbourne, Australia, 1950

7 Examination of synthetic alkali-silica gels, H Krogh, Proc of Symposium on Alkali-Aggregate Reaction Preventive Measures, Reykjavik, Aug 1975

8 The role of $Ca(OH)_2$ in the breakdown of Portland cement concrete due to alkali-silica reaction. S Chatterji. Cement and Concrete Research, Vol 9, No 2, pp 185-188, 1979

Importance et conditions d'une étude et d'une évaluation rationnelle de la durabilité et de la sécurité à long terme du béton dans les eaux agressives

Importance and conditions of rational study and design of the durability and long-term safety of concrete in aggressive waters

O. VALENTA, Ingénieur-Docteur, Prague, Tchécoslovaquie.

RESUME : L'étude de la sécurité et de l'économie des constructions en béton, soumises à des eaux agressives, doit être basée sur une méthode rationnelle nouvelle, et sur des notions scientifiques de caractère quantitatif.

Dans le monde entier, les méthodes actuellement utilisées sont empiriques et imprécises; de plus elles ne se prêtent pas à une approche rationnelle de l'effet à long terme des diverses ambiances. La prévision quantifiée à long terme, de l'action du milieu ambiant doit être faite, en tenant compte de la durabilité recherchée et de l'évolution de l'ambiance.

Une solution rationnelle doit être fondée sur le choix des matériaux du béton, sur la technologie de fabrication et le contrôle du béton, sur la cinétique du mouillage et sur les réactions chimiques d'attaque du ciment. Elle doit tenir compte notamment des recherches de base sur la cinétique de ces réactions chimiques, en fonction de la nature du ciment.

SUMMARY: Safe and economic design of concrete structures in aggressive waters must be based on the new rational method and scientific notions of quantitative character.

Empiric and inaccurate methods used by the standards of the whole World do not provide the possibility of such a rational acces to the complex question of the long-term effect of any liquid environment.

Quantification of the long-term effect of environment in the period of required durability on the base of objective prognosis for the environment development.

Conditions of rational solution based on complex access and regulation of effect: choice of materials (cement), technology and control of concrete, kinetics of its wetting, of the proper chemical reactions and of concrete structure deterioration.

Need of systematic scientific and basic research and of quantitative kinetics of the main chemical reactions with cement of different character. Importance and application of functional models.

New requirements on hydrogeological investigation and acquaintance of basic properties of concrete mainly of the pore-system in relation to the water and to its chemical effect on concrete and its components including the reinforcement. Claims on the research and testing of concrete and its components.

Requirements of the world practice, research and the conception of the theme VII of the Congress 1980.

1. INTRODUCTION

Les questions de la durabilité des ouvrages d'art en général et du béton et des constructions en béton en particulier sont devenues dans tout le monde téchniquement développé par principe une question de la qualité et de l'économie de longue terme. Il s'agit des questions de caractère scientifique, technique et économique qui ont une rélation étroite à l'optimalisation de la solution complexe basée sur la minimalisation des dépenses totales: d'investement, d'exploitation, d'entretien, de protection et de la liquidation.

On se trouve aussi dans le stade de la responsabilité morale des ouvrages qui doivent servir aussi aux générations futures et on se trouve inévitablement devant la nécessité de revaloriser les critères incorectes de l'économie de court terme, des épargnes momentanées surtout dans les dépenses d'investement au préjudice des possibilités de développement future et de la durabilité des ouvrages de génie civil et des dépenses de maintenance élevés liées aux éxigences élevées sur la maintenance par le travail manuel et qualifié.

Malgré que les questions de la durabilité du béton et d'autres matériaux poreaux, non-métalliques ne sont pas encore complétement résolues surtout pour l'action combinée des conditions réelles et par rapport à la cinétique quantitative de la détérioration - il est nécessaire de résoudre dans cet état des notions incomplètes dans tout le monde - avec sûreté et rationnellement le choix des matériaux, la technologie propre du béton et d'autres matériaux ainsi que les travaux de conctruction, du point de vue de la durabilité définie et exigée par le maître de l'oeuvre dans les conditions spécifiques de long terme du milieu hydrogéologique, climatique et d'exploitation.

2. LES METHODES UTILISEES JUSQU'A PRESENT POUR LA SOLUTION DE LA SECURITE A LONG TERME ET DE LA DURABILITE DES OUVRAGES DE GENIE CIVIL SUR LA BASE DES RECOMMANDATIONS ET DES DIRECTIVES

L'analyse des normes valables dans différents pays techniquement développés montre leur insuffisances quant à l'application à la solution rationnelle, objective et quantitative des questions de la durabilité spécifiée du béton dans un milieu agresif en général et sous l'action des eaux agressives en particulier.

Le besoin d'assurer la sécurité des parois des tunnels du Metro de Prague pour la période de 100 ans a introduit dans la solution scientifique et technique le facteur décisif de l'action à long terme du milieu sur les matériaux et les constructions: le temps défini. Aucune norme dans tout le monde ne donne pas la solution objective et d'un dimensionement des ouvrages souterrains comme mûrs des tunnels. Il était alors nécessaire de chercher, de formuler et d'appliquer une solution, une méthode nouvelle et convenable sur la base de l'effet quantifié de l'action de long terme du milieu des eaux agressives souterraines.

De l'autre côté, même les propriétés du béton et de son système poreux décisives pour la réaction des eaux agressives avec le béton: la perméabilité, l'élévation capillaire et la surface interne ouverte n'étaient pas jusqu'à présent l'objet d'une quantification compétente et de l'expression en unités mesurables et contrôlables. La perméabilité du béton et d'autres matériaux poreux en est le facteur le plus important une fois exprimé par le coefficient de perméabilité k en cm/sec. Malheureusement, les essais normalisés dans différents pays ne offrent pas du tout, malgré son importance pour l'évaluation quantitative de l'effet des eaux agressives sur la structure et les propriétés du béton dans une période définie et par suite sur la durabilité des bétons. Le coefficient de perméabilité seul, proprement déterminé par une méthode convenable est l'indicateur quantitatif de la perméabilité des matériaux poreux comme béton. Ceci conduit à la revendication catégorique de la détermination et du contrôle du coefficient de la perméabilité k cm/sec par un essais convenable, non seulement pour le béton mais aussi pour le terrain ambiant.

Les normes existantes ne fournissaient aucun guide dans ce sens ni pour les essais propres ni du point de vue de la nécessité d'une expression quantitative de la perméabilité du béton. La connaissance de ce coefficient est nécessaire non seulement pour le béton seul mais aussi pour les matériaux ambiants (le terrain), qui décident de l'accès des eaux agressives vers le surface de la construction en béton et joue le rôle décisif dans la cinétique de la détérioration du béton, qui après tout est la résultante de la cinétique résultante de l'écoulement des eaux agressives dans le milieu ambiant et dans le béton ainsi que de la cinétique des réactions agressives des eaux souterraines avec les composants du béton surtout avec le ciment.

Pour la détermination rapide et sure du coefficient de la perméabilité k cm/sec du béton et d'autres matériaux poreux - nouvelle méthode introduite et vérifiée par l'auteur et basé sur la cinétique de l'écoulement non-stacionnaire à travers le système poreux est recommandé comme la base de l'étude théorique et expérimental de la cinétique de la détérioration des matériaux par les eaux agressives.

Les normes existants de tout le monde ne connaissent pas en général cette méthode objective de la solution quantitative de l'effet de longue durée du milieu agrésif, liquide sur le béton et n'offrent pas même les bases nécessaires pour une solution logique, quantitative et objective de la

durabilité et de la sécurité à long terme des ouvrages de génie soutarrain . Même par leur conception générale elles sont insuffisantes et non-convenables pour une solution économiquement important.

3. LES CONDITIONS ET LE CADRE D'UNE SOLUTION RATIONELLE, OBJECTIVE ET QUANTITATIVE DE LA SECURITE A LONG TERME ET DE LA DURABILITE DES CONSTRUCTIONS EN BETON DANS DES EAUX AGRESSIVES

Une solution objective et sûre de la sécurité à long terme et de la durabilité des constructions en béton dans le milieu agressif de n'importe quel caractère et intensité est possible seulement sur la base de l'effet quantitatif de longue durée des agents du milieu sur le matériel de construction et sur la construction dans la période planifiée ou exigée de l'exploitation de la construction. L'effet du milieu naturel est donné par l'ensemble des effets des agents différents séparément et en combinaisons, que l'on peut définir par l'analyse du milieu et par la cinétique de la teneur (concentration) des agents différents. La condition d'une solution avec succès consiste dans l'accès complexe à la question compliquée à résoudre et dans les solutions convenables de tous les étapes partielles de l'action des eaux souterraines sur le béton.

La condition principale y est dans la connaissance des conditions réelles du milieu des eaux souterraines qui vont exercer une action sur le béton et sur la construction en béton pendant une longue période surtout du point de vue hydrogéologique et de l'écoulement des eaux souterraines une fois l'ouvrage terminé.

L'étude hydrologique du chantier futur doit alors s'occuper de ces stades importants:
a) nature et état de long terme des eaux souterraines avant l'ouverture des travaux, les travaux de terrassement,
b) importants stades transitoires pendant l'exécution des travaux,
c) long terme conditions de l'écoulement des eaux souterraines dans les conditions nouvelles modifiées et de leur variations quant à leur caractère - ce qui représente le stade le plus important pour la durabilité d'un ouvrage concret. Ceci souligne l'importance d'un pronostic scientifique et objectif des conditions hydrogéologiques de l'ouvrage terminé pendant son exploitation de long terme.

Le facteur principal des exigences sur la solution technique et économique de la sécurité à long terme d'une ouvrage est représenté par l'action propre à long terme de l'eau agressive souterraine sur le béton et l'ouvrage en béton, ses parties importantes et sur son ensemble - la cinétique de la détérioration progressive proprement dite et son effet intégré dans la période de la durabilité exigée de l'ouvrage T_r. Et de cet effet intégré résultent tous les mesures logiques et objectives qui doivent assurer la durabilité exigée de l'ouvrage et que l'on peut diviser en ces groupes:

a) aménagement convenable de l'ambiance aqueuse de l'ouvrage et de la construction conduisant à la réduction de l'effet nocif sur le béton et l'ouvrage y compris le traitement des eaux;

b) la technologie du béton proprement dite basée sur le choix des matériaux convenables et sur la perméabilité réduite du béton;

c) protection superficielle du béton contre le contact excessif avec l'eau.

Ce travail prétentieux doit faire l'objet principal de l'étude approfondie et des travaux propres du projet d'exécution dans le stade de la préparation des travaux.

La solution réussite de cette question doit être assurée aussi par une collaboration étroite avec la recherche qualifiée et ses travailleurs d'une part et avec les organisations de l'investigation du sol et du milieu agressif de la construction d'autre part.

Quant à la recherche propre de la technologie du béton durable on doit affronter toute une série des questions nouvelles jusqu'à présent non-résolus, surtout de la cinétique des procès physiques et chimiques accompagnant la détérioration progressive du béton avec perte de ses propriétés fondamentales et importantes: perméabilité, résistance mécanique et l'homogénéité.

Trois méthodes existent pour la solution de la cinétique propre de la détérioration du béton:

a) étude théorique de la cinétique quantitative des procès et réactions chimiques se trouvant à la base l'action de la détérioration progressive du béton et de ses composantes par les eaux souterraines. De cet étude peuvent sortir les guides pour la mise en oeuvre du béton et son traitement par les moyens convenables du caractère physique et chimiques.

b) étude expérimentale sur les modèles fonctionnels en béton (Fig. 1)

c) long terme observation scientifique de l'effet quantitatif du milieu sur le béton et ses propriétés.

Dans l'intérêt de la solution accélerée et objective de ces questions insistantes et importantes de la sécurité à long terme, de l'économie et de la durabilité des ouvrages en béton soutarrains, il est nécessaire de profiter des avantages et des succès de chacune d'eaux. En même temps il faut se rendre compte que l'observation à long terme des ouvrages choisis a un caractère plutôt verificatif que théorique malgré le fait qu'elle éxige un contrôle complex des matériaux, de la technologie et des propriétés du béton pendant la mise en oeuvre des ouvrages choisis pour une telle

observation scientifique. C'est une tâche très prétentieuse même pour la coopération internationale effectuée dans le cadre des commissions spéciales techniques comme celle de la RILEM - CDC.

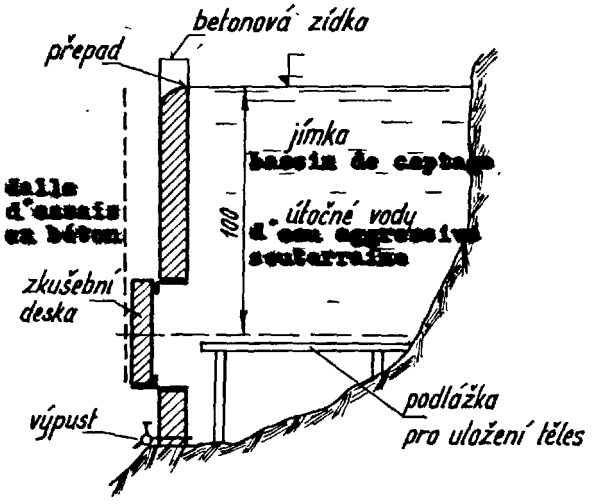

Fig. 1 - Modèle fonctionnel de l'étude et de contrôle de l'effet des eaux souterraines - agressives sur le béton.

L'étude de cette commission a effectué la classification internationale quant à l'importance des différents agents agressifs du milieu pour les constructions en béton avec ce résultat:

1. corrosion de l'armature
2. les sulfates,
3. gel et mouillage alterné et les acides.

Il est dommage que ce résultat d'une enquête internationale ne fut pas respecté dans le choix et la formulation des thèmes concernant la sécurité de long terme et la durabilité des constructions en béton.

Alkali Aggregate Reaction with Opaline Sandstone

La réaction alcaline des agrégats avec du grès opalin

Dennis LENZNER and Udo LUDWIG, Institut für Gesteinshüttenkunde, RWTH Aachen, R.F.A.

RESUME : Les résultats de quelques recherches en laboratoire sur l'alcali réaction des agrégats (RAA) dans le béton sont exposés.

Il est démontré que la réactivité dangereuse de l'agrégat est inversement proportionnelle à sa porosité.

Le développement de la dégradation est mieux déterminé par la mesure du gonflement en combinaison avec la mesure de la fréquence de résonance que par la mesure du seul gonflement.

L'humidité atmosphérique minimale nécessaire pour le développement de la RAA est déterminée à 85 % hr. Au-dessus de cette limite, la vitesse de la réaction est proportionnelle à l'humidité.

Une accélération de la RAA, par exemple par une élévation de la température, par une augmentation de l'humidité ou par un fin broyage des agrégats réactifs, réduit la dégradation finale.

Un conditionnement à sec initial du béton augmente la dégradation par la RAA. Avec des grains gros (plus de 0,5 mm de diamètre), seules des expériences de longue durée donnent des résultats certains.

SUMMARY: The results of some laboratory investigations on the concrete damaging alkali-aggregate reaction (AAR) with opaline sandstone are reported.

It is shown that the damaging reactivity of the aggregate is inversely proportional to its porosity. The development of the damage is better detected by measurement of the expansion together with resonance frequency measurement than by the observation of the expansion alone.

The minimum atmospheric humidity needed for a progressing AAR is discovered to be 85 % rh. Above this limit, the reaction rate is proportional to the humidity.

An acceleration of the damaging AAR, i.e. through raised temperature, high humidity, or fine crushing of the reactive aggregate reduces the final damage.

Initial dry storage of the concrete increases the damage due to the AAR.
With coarse reactive aggregate (more than 0.5 mm in diameter) only long-therm tests give reliable results.

INTRODUCTION

The alkali-aggregate reaction (AAR) may cause considerable damage to concrete which contains soluble silica within its aggregate. By the reaction between the alkalies solved in the pore solution and the reactive aggregate components, locally osmotic pressures are built up if sufficient humidity is available, which may exceed the strength of the concrete. Part of the then generated cracks are microscopically small. They cause an extension and a loosening of the structure which can be measured through macroscopic extension and decrease of strength.

In the following some results of research on the influence of different parameters on the AAR are presented. Some of these tests have been running for more than four years.

EXPERIMENTAL

To determine the dangerous alkali reactivity of an aggregate, mortar bar tests show the most reliable results.

The mortar used in the following experiments is made with a Portland cement (PZ 45 F) with an alkali content of 0.9 wt-% Na_2O equivalent.

In contrast to other published investigations, no special cement-rich mix is used, but the mortar is composed and prepared according to the German standard DIN 1164, which means the composition of cement : aggregate : water beeing 1 : 3 : 0.5. The aggregate is standard sand. The opaline sandstone is crushed to a grain size of 0.09 to 0.5 mm and is added in amounts of 4 wt-% of the aggregate as replacement of the corresponding sand fraction. With this mortar in any case six prismatic specimens of the dimensions 1 x 4 x 16 cm are made. For the extension measurement the bars are equipped with gauge points to fit into a comparator. After 24 h of humid storage, the specimens are demolded. They are stored in slightly evacuated desiccators above water.

To determine the progressing damage due to the AAR at different intervals mass, length change and resonance frequency are measured. The comparator is equipped with a dial gauge with a resolution of 0.01 mm. The zero measurement is performed after the demolding of the specimens.

The resonance frequency is measured with the EG-meter according to Kottas (1). Together with the density and the length of the specimen, the resonance frequency yields Young's modulus, which is proportional to the square of the resonance frequency. In all the reported tests, the length change and the change of the bulk density are small compared to the change of the resonance frequency. Therefore an increase of the resonance frequency indicates an increase of Young's modulus which means a consolidation of the structure whereas a decrease of the resonance frequency suggests a weakening of the specimen.

REACTIVE AGGREGATE

Throughout all tests opaline sandstone from Schleswig-Holstein was used as reactive aggregate. The modifications of the reactive aggregate in Schleswig-Holstein are described by Niemeyer (2).

Sixty percent of the opaline sandstone which was at the authors' disposal looked grey-white, the rest grey-green. First investigations revealed considerable differences in its mineralogical composition and its porosity.

See figure 1

page VII - 123

Fig. 1 X-ray deflection pattern of opaline sandstone with different bulk densities

The x-ray deflection pattern shows that the material with bulk densities of more than 2.1 g/cm^3 only contains quartz and calcite. The less dense material contains cristobalite and only small amounts of quartz and calcite. Therefore the aggregate was assorted according to its colour and its bulk density. Table 1 shows the porosity, the specific surface area, and the calcite content of the different fractions which was measured thermogravimetrically.

	bulk density g/cm^3	density g/cm^3	porosity vol-%	sp. surface area m^2/g	calcite content wt-%
	1.13	2.53	55.3	15.1	8.5
grey-	1.47	2.62	45.8	20.5	30
white	1.87	2.57	27.2	10.1	35
	2.34	2.74	15.0	1.9	96.6
	1.20	2.84	57.8	35.3	2
	1.37	2.75	50.2	34.8	6
grey-	1.70	2.61	34.9	26.1	2
green	1.91	2.44	21.7	30.7	2.8
	2.05	2.38	13.9	18.0	7.7
	2.60	2.72	4.4	4.2	55.7

Tab. 1 Properties of opaline sandstone

Ludwig and Bauer (3) have already reported, that the porous opaline sandstone causes no damage. The tests were extended to lower porosities. Fig. 2 shows the expansion and the resonance frequencies of the specimens containing different fractions of the opaline sandstone. The least porous reactive aggregate causes the most severe damage.

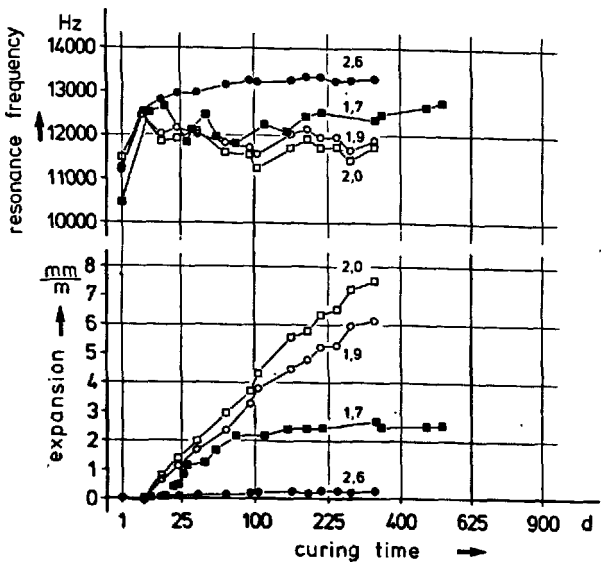

Fig. 2 Expansion and resonance frequency of mortar bars containing opaline sandstone with different bulk densities

The material with a bulk density of 2.6 g/cm^3 does not contain opal, which shows cristobalite structure in the x-ray analysis (see Fig. 1), and is not reactive. The tests show that opaline sandstone with a porosity of 50 vol-% or more does not cause damage within the test period of nearly 500 days when reacting with the cement alkalies. The osmotic pressures are then degenerated within the pore space of the aggregate and not transmitted to the concrete structure. At lower porosities the damage is inversly proportional to the porosity the lower limit being determined by the mineralogical composition.

MINIMUM HUMIDITY

For the AAR to proceed, the concrete must contain free water. The diffusion processes which lead to the AAR presuppose a pore liquid in the concrete. On the other hand, the osmotic pressures result from the imbibition of water by the reaction products. In order to determine the minimum atmospheric humidity required for the AAR, one series of specimens at a time was cured at different humidities. The opaline sandstone in these tests has a bulk density of 1.9 g/cm^3.

To adjust the atmospheric humidity, sulphuric acid of different concentrations is used. In the first instance, the humidities are adjusted to about 40 % rh, 60 % rh, 80 % rh, 90 % rh and more than 95 % rh.

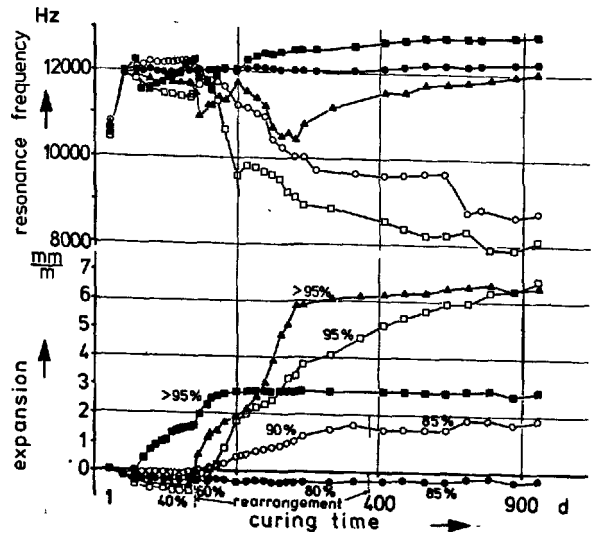

Fig. 3 Expansion and resonance frequency of mortar bars stored at different relative humidities

The specimens stored above water already expand clearly within 15 days and after about 100 days, they reach their final expansion of 2.8 mm/m. At the lower humidity of 90 % rh the AAR cannot be observed before about 50 days. The expansion increases more slowly due to the lower water supply. The reduction of the resonance frequency, however, is more pronounced than that of the specimens stored above water. The specimens stored at humidities of 80 % rh and less only show drying shrinkage. Therefore, after 42 days, the specimens are rearranged from 60 % rh and 40 % rh to more than 95 % rh and 95 % rh. Then these specimens expand rapidly and their resonance frequency decreases accordingly. Again, the specimens stored above water expand faster and reach their final expansion earlier than those stored at the lower humidity of 95 % rh. The former reach their final expansion of 6 mm/m after about 200 days. This value is about twice as much as the expansion reached by the specimens which were stored above water from the beginning of the test.

The specimens rearranged from 40 % rh to 95 % rh expand more slowly but the reduction of their resonance frequency and therewith their structural damage is more severe. They do not reach their final expansion until after 900 days.

The results show that a reduced moisture availability does not diminish the damage due to the AAR but only delays it. Because of the longer reaction period, the concrete damages are more severe at the lower humidity. Furthermore, a high humidity is necessary for the rehealing process. This is an additional reason for the greater damage at the lower humidity. The same holds true for the specimens stored at 90 % rh. They expand very slowly. After 360 days their expansion amounts to only 1.6 mm/m. This expansion, however, is accompanied by a marked decrease in the resonance frequency.

The storage at 80 % rh does not cause an expansion or a decrease in the resonance frequency within the period of 360 days. Therefore, in order to determine the minimum humidity needed for the AAR, the specimens stored initially at 80 % rh and 90 % rh are rearranged to about 85 % rh after 360 days.

Thereafter, the specimens formerly stored at 80 % rh do not show effects of the AAR up to 1000 days. The rearrangement from 90 % rh to 85 % rh results in a delay in the expansion reaction. After a dormant period of about 200 days, the specimens expand a little. This inferior expansion is accompanied by a distinct decrease in the resonance frequency, a clear indication of the recommencing AAR.
The results show that for a damaging AAR a minimum humidity of about 85 % rh is needed.

RESIDUAL HAZARD

After a test period of 1000 days all specimens were rearranged to the high humidity of more than 95 % rh in order to determine the residual reaction potential of the reactive aggregate. To accelerate the reaction, two specimens from each series were stored at 40°C. The specimens which had been stored above water before show no reaction. Their content of opaline sandstone has reacted completely.

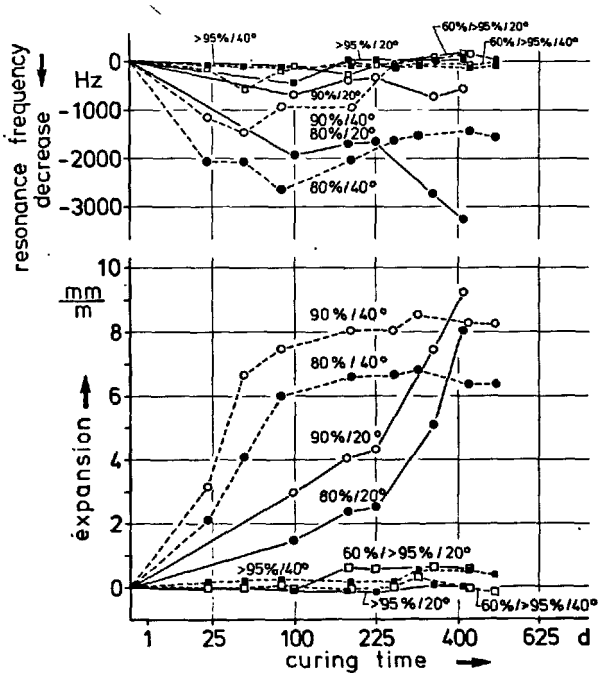

Fig. 4 Residual hazard after 1000 days storage at different humidities

The specimens which have been stored near the minimum humidity expand after the rearrangement by up to 9 mm/m. This expansion is more than the expansion of the specimens which were rearranged to the high humidity at earlier ages. The higher temperature causes an acceleration of the reaction. This acceleration, however, reduces the final damage as detected in other test series (4).

The decrease in the resonance frequency of the specimens formerly stored at 80 % rh is stronger than that of the specimens rearranged from 90 % rh. The structure of the latter, at the time of the rearrangement, is damaged to such an extent that the reaction intensified by the high humidity hardly causes new microcracks. The expansion is achieved by the widening of the existing cracks. This has no effect on the natural frequency. On the other hand, the structure of 80 % rh-specimens is at the time of the rearrangement practically undamaged. The osmotic pressure due to the AAR causes the generation of microcracks and this is indicated by the decrease in the resonance frequency.

The results show that an aging of concrete in a dry atmosphere markedly increases the risk of damage through the AAR. The explanation is that fresh concrete can yield to swelling pressures through plastic deformation. Thereby part of the pressure is cancelled. But the rigid structure of older concrete does not allow plastic deformations. Therefore more cracks are formed and the damage is more severe.

GRAIN SIZE OF THE REACTIVE AGGREGATE

Another example of a delayed reaction's causing more damage than a fast reaction is provided by the investigation of the influence of the grain size of the reactive aggregate on the AAR.
Four test series with the granulometric fractions 0,09 - 0.5 mm; 0.5 - 1 mm; 1 - 3.15 mm; 3.15 - 5 mm of the opaline sandstone were prepared.

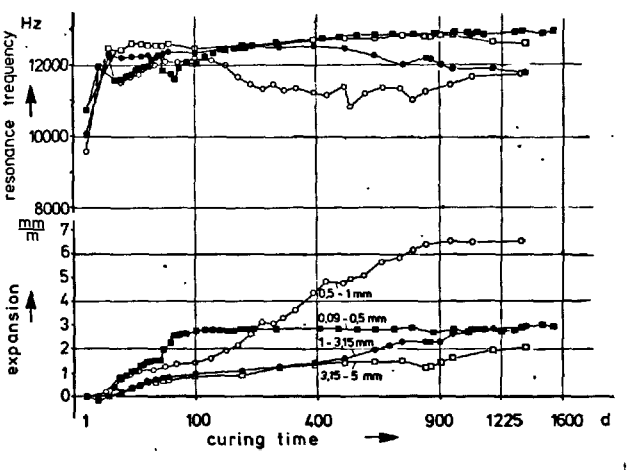

Fig. 5 Expansion and resonance frequency of mortar bars containing opaline sandstone of different grain sizes

The specimens containing the finest reactive aggregate (0.09 - 0.5 mm) attain their ultimate expansion after a period of about 100 days humid storage. Then their resonance frequency increases continuously.

The structure reheals as the first reaction products solidify through the reaction with lime and thus cement the cracks.

The specimens containing the fraction 0.5 - 1 mm exceed the expansion of the former after 225 days and reach their final expansion only after more than 900 days. This slow expansion is accompanied by a continuous decrease in the resonance frequency. The frequency does not indicate the beginning of the rehealing process until after more than 800 days.

The mortar bars containing the coarser reactive aggregate fractions expand more slowly but after 1200 days the expansion of the specimens containing the fraction 1 - 3.15 mm exceed the expansion of the bars with the finest fraction. The decrease in the resonance frequency of the specimens with the coarse fractions after 1000 days clearly indicates the progress of the damage due to the AAR.

Another result of these tests is that investigations over limited periods of one or two years may in some cases only give limited information about the parameters influencing the AAR.

REFERENCES

1. - H. KOTTAS (1964), "Das Resonanzverfahren zur Messung mechanischer Schwingungen und Materialeigenschaften", Zeitschr. f. Instrumentenkunde 72, 7, 199-204.

2. - E.A. NIEMEYER (1973), "Betonzuschlag in Schleswig-Holstein", Vorbeugende Maßnahmen gegen Alkalireaktion im Beton, Schriftenreihe der Zementindustrie 40, 37-56.

3. - U. LUDWIG, W. BAUER (1976), "Untersuchungen zur Alkali-Zuschlag-Reaktion", Zement-Kalk-Gips 29, 9, 401-411.

4. - D. LENZNER, U. LUDWIG (1978), "Alkali-aggregate reaction with opaline sandstone from Schleswig-Holstein", Proc. Fourth Intern. Conf. Effects of Alkalies in Cement and Concrete, West Lafayette USA, 11-34.

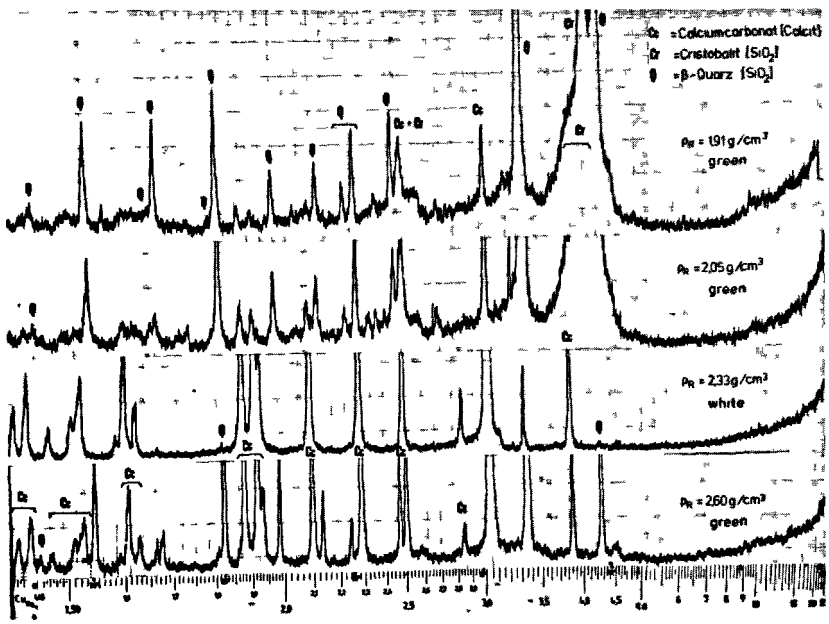

Fig. 1 X-ray deflection pattern of opaline sandstone with different bulk densities

Resistance of hardened cement mortar to magnesium chloride solution

Résistance d'un mortier au ciment durci à une solution de chlorure de magnésium

Y. SUZUKAWA, Dr. Central Research Laboratory, Ube Industries, Ltd. Japan.

RESUME : Des échantillons de mortier faits avec divers types de ciment commercial ont été immergés dans des solutions contenant 1, 4, et 25 g. de $MgCl_2$/l pendant un an.

Les résultats de l'essai ont montré que le ciment Portland de laitier de haut fourneau, avec une teneur élevée en laitier a une bonne résistivité, comme nous l'avons décrit précédemment dans notre rapport. Aucune relation n'a été observée entre la diminution de la résistance du mortier et la teneur en C_3A du ciment Portland.

La détérioration du mortier de ciment durci est principalement due à une augmentation de la porosité du mortier produite par la dissolution de $Ca(OH)_2$.

SUMMARY : Mortar specimens made with various types of commercial cement were immersed in solutions containing 1, 4, and 25 g. $MgCl_2$/l. up to 1 year.

Test results showed that portland blast-furnace slag cement with a higher content of slag has a good resistivity as reported previously. No relationships were observed between the decrease in mortar strength and the C_3A content of portland cement.

The deterioration of hardened cement mortar is due mainly to an increase in the porocity of mortar caused by the dissolution of $Ca(OH)_2$.

Four types of portland cement, i.e., ordinary (1), moderate heat of hydration (2), high early strength (3), and sulfate resistant (4), portland blast-furnace slag cement (5), and portland fly-ash cement (6) were used. Chemical compositions and Blaine specific surface are shown in (Table I).

TABLE I

Sample No.	Loss on ignition	Insoluble residue	SiO_2	Al_2O_3	Fe_2O_3	CaO	MgO	SO_3	Free CaO	Sp. surface sq.cm. per g.
1	0.7	0.4	21.4	5.7	3.4	63.9	1.4	2.1	0.5	3250
2	0.7	0.4	23.1	4.3	4.0	63.5	1.5	2.0	0.1	3250
3	0.9	0.8	20.4	5.0	2.7	65.3	1.3	2.6	1.1	4270
4	0.5	0.4	22.4	3.1	4.7	64.8	1.3	2.1	0.1	3700
5	0.1	0.3	28.2	12.5	1.6	50.0	3.2	2.2	0.2	3630
6	1.1	22.8	17.2	4.9	2.7	48.4	1.1	1.5	0.4	3090

EXPERIMENT AND RESULTS

Mix proportion of cement : sand : water of the mortar used is 1 : 2 : 0.65. Size of specimen for compressive strength test is 4 x 4 x 16 cm. and that for expansion test is 1 x 1 x 11.25 inch.

After molding, these specimens were cured in moist closet for 1 day and then cured in water for 6 days. After this period, they were cured in water or in $MgCl_2$ solution at 20°C until the time of test. The concentration of $MgCl_2$ solution used is 1, 4, and 25 g. $MgCl_2$ per litre, respectively.

At the ages of 1, 4, 13, 26, and 52 weeks, mortar strength and expansion were measured. After strength test, mortar specimens were cut from the surface at an interval of 5 mm. into four parts with equal thickness. These cutting specimens were subjected to chemical and X-ray analyses and electron microscopic observation. Total pore volume and pore size distribution were also measured.

Compressive strength ratio of mortars cured in solution containing 25 g. $MgCl_2$/l. and those cured in water up to the age of 52 weeks is shown in (Table II).

Within the scope of this experiment, no relations were observed between the decrease in compressive strength ratio and the content of C_3A in portland cement.

TABLE II

Sample No.	Compressive strength ratio		
	Curing period in weeks		
	4	26	52
1	84	64	47
2	87	63	58
3	91	67	62
4	88	65	53
5	104	100	94
6	95	65	63

In the expansion of mortar cured in $MgCl_2$ solution, portland fly-ash cement mortar showed a little higher value, but the other cement mortars showed approximately the same value as compared with the expansion of corresponding specimens cured in water.

The surface of mortar specimens immersed in $MgCl_2$ solution was covered with a white colour film, consisting mainly of $Mg(OH)_2$ as reported by Kalousek and Benton (1), and the formation of $C_3A \cdot CaCl_2 \cdot 10H_2O$ was also found.

Riedel (2) has already reported that in solution containing a large amount of $MgCl_2$, magnesium oxychloride $Mg_2(OH)_3Cl \cdot 4H_2O$ is formed. In the present experiment up to the concentration of 25 g. $MgCl_2$ per litre, however, no formation of this compound was found.

The amount of water-soluble Cl ion of each cutting specimens of hardened cement mortar cured in 25 g. $MgCl_2$ per litre solution is shown in (Figure 1).

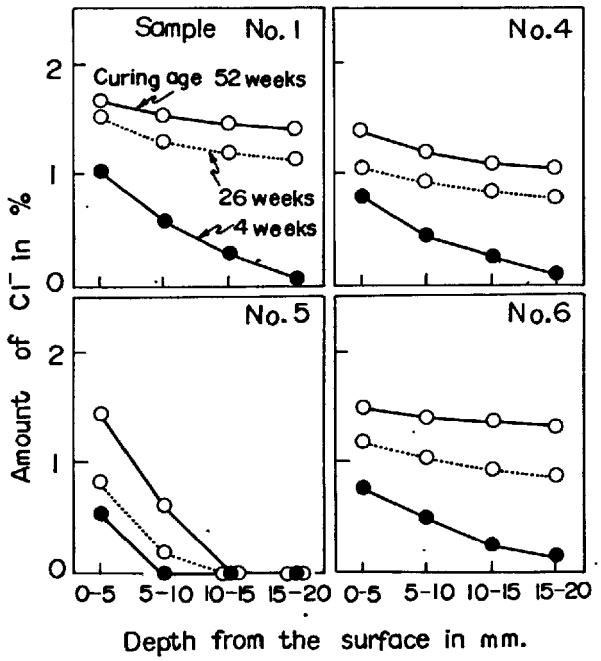

Fig. 1 - Amount of water-soluble Cl ion

The results showed that in portland and portland fly-ash cement mortar the penetration of Cl ion reaches already up to the centre portion at the age of 26 weeks and in portland blast-furnace slag cement mortar the penetration occurs up to 10-15 mm. from the surface at the age of 52 weeks.

Total pore volume was measured with sample crushed into a size of 5-1.2 mm. by using the mercury porocimeter. These values of specimens cured in water and of those cured in 25 g. $MgCl_2$/l. solution are shown in (Figure 2).

Figure 2 showed that only a slight difference is observed at the age of 4 weeks. However, at the age of 52 weeks, the value showed a large difference with the exception of portland blast-furnace slag cement mortar.

Based on the results obtained in Table II and Figure 2, the decrease in compressive strength ratio is related intimately to the increase in total pore volume.

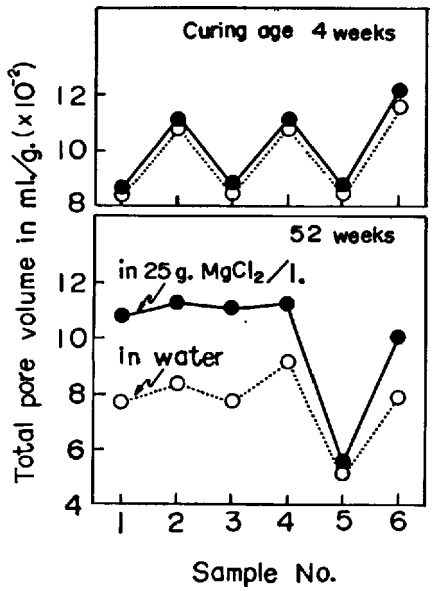

Fig. 2 - Total pore volume

CONCLUSION

The deteriration of hardened cement mortar in $MgCl_2$ solution is due mainly to an increase in the porocity of mortar caused by the dissolution of $Ca(OH)_2$. This dissolution is expressed by the following chemical equation:

$$Ca(OH)_2 + MgCl_2 = Mg(OH)_2 + CaCl_2.$$

No relations were observed between the decrease in mortar strength in $MgCl_2$ solution and the C_3A content of portland cement.

BIBLIOGRAPHY

1. - G. L. Kalousek and E. J. Benton (1970), "Mechanism of seawater attack on cement pastes", J. Am. Concrete Inst., 67, 187-192.

2. - W. Riedel (1973), "Die Korrosionsbeständigkeit von Zementmörteln in Magnesiumsalzlösungen", Zement-Kalk-Gips, 26, 286-296.

Morphology and microstructure of cement paste/rock interfacial regions

Morphologie et microstructure de la pâte de ciment à la surface des granulats

C.A. LANGTON, Graduate Assistant, and
D.M. ROY, Professor of Materials Science, Materials Research Laboratory, The Pennsylvania State University, University Park, U.S.A.

RESUME : Cette étude est basée sur le fait qu'une relation importante peut exister entre, d'une part la structure et la morphologie de la zone interfaciale entre la pâte de ciment et les agrégats et, d'autre part, la formation et la propagation de microfissures. Les éprouvettes ont été préparées à 27, 60 et 90°C sous des pressions de 0,1, 6,9 et 68,9 MPa. La morphologie et le mode de fracture le long de la zone interfaciale du ciment Portland et des cailloux dépendent de la réactivité des agrégats ainsi que du taux d'hydratation de la pâte de ciment.

Une région formée de deux couches apparaît dans la zone interfaciale entre les agrégats non réactifs et la pâte du ciment. La morphologie interfaciale est caractérisée par un film mince de C-H (C-S-H) à partir duquel des particules de C-H-S semblent croître. En plus des particules de C-H-S, des cristaux de plus grande taille de $Ca(OH)_2$ semblent rattacher la zone interfaciale à la pâte et, par conséquent, les agrégats à la pâte. Lorsque le taux d'hydratation augmente, une plus grande quantité de pâte est fixée à la zone interfaciale. Des examens tous les 6 mois montrent que la zone interfaciale conserve une structure formée de 2 couches.

Contrairement à la région à 2 couches formée sur un agrégat non réactif et contrairement aussi à ce qui a été publié sur les surfaces réactives, nous avons trouvé 4 couches interfaciales sur des surfaces réactives. La surface réactive des agrégats est d'une manière typique recouverte d'une couche de S-C-K-H à partir de laquelle des particules de S-C-K-H semblent croître. Ces deux couches forment la Zone I. Les particules S-C-K-H de la Zone I sont recouvertes d'un second film de C-S-H (C-H) contenant relativement plus de calcium que de silicium et pas d'alcalis. Ici encore les particules de C-H-S semblent croître à partir de cette couche, rattachant ainsi la zone interfaciale à la pâte de ciment.

Des groupes indépendants de fissures dues au retrait sont observés dans les Zones I et II. Toutefois, ces fissures sont beaucoup plus nombreuses dans la Zone I (S-C-K-H). La fracture se propage typiquement en marches à travers chaque couche de la zone interfaciale.

Des pressions élevées furent utilisées pour augmenter les contacts entre la pâte et la surface des cailloux et furent aussi combinées avec une température élevée pour accroître la vitesse d'hydratation. La rugosité du gravier n'a pas d'effet majeur sur la structure de base de l'interface.

ABSTRACT: The present investigation was based on the likelihood that an important relationship might exist between the structure and morphology of the cement paste/aggregate (wall rock), interfacial region and the initiation and propagation of microcracks. Curing conditions included temperatures of 27, 60, and 90°C and pressures of 0.1, 6.9, and 68.9 MPa. The morphology and mode of fracture at the interfacial region formed between portland cement and rock were both dependent on reactivity of the aggregate and degree of hydration of the cement paste. A two layered zone developed in the interfacial region between non-reactive aggregates and portland cement paste. The interfacial morphology is characterized by a thin film of C-H (C-S-H) from which C-S-H particles appear to be growing. In addition to C-S-H particles, larger crystals of $Ca(OH)_2$ appear to attach the interfacial region to the bulk paste and thereby the aggregate to the bulk paste. As the degree of hydration increased, more bulk paste became attached to the interfacial region. Where the interfacial region was exposed in six month runs it still appeared as a two layer zone.

In contrast to the two-layered region formed on an unreactive aggregate and previously reported on reactive surfaces, four interfacial layers were characteristically present on reactive surfaces. The reactive aggregate surface was typically overlain by a S-C-K-H film from which S-C-K-H particles appeared to be growing. These two layers make up Zone I. S-C-K-H particles on Zone I were attached to an overlying second film containing relatively more calcium than silicon and no alkali, C-S-H (C-H) film. Again, C-S-H particles appeared to be growing from this film and attaching the interfacial region to the bulk paste. Independent sets of shrinkage cracks were observed in both Zones I and II. However, they were much more abundant in Zone I (S-C-K-H Zone). Fracture typically took place in a step-like manner across each layer of the interfacial region.

The effect of elevated pressures was to increase the contact between paste and rock surface and, when combined with elevated temperature, to increase also the hydration rate. Surface roughness of the rock resulted in no major effect upon the basic structure of the interface.

INTRODUCTION

The present investigation is based on the likelihood that an important relationship exists between the structure and morphology of the interfacial region formed at a cement paste/aggregate (wall rock) contact, and the initiation and propagation of microcracks. The characteristics of this region may be responsible for eventual failure through decreased strength and/or permeability. Previously, little attempt has been made to relate microstructure to microcracking or to evaluate them in terms of measurable physical properties (1-3). Characterization of the morphology of the interfacial region formed between portland cement and various substrates is particularly important if cement or concrete is to be used as a containment material for potentially harmful substances, such as radioactive waste stored in mined underground repositories. The type of interfacial morphology developed on specific rocks is a means of classifying them as reactive or nonreactive. Accurate characterization of the interfacial region also may be a method of early detection of reactive materials. Data concerning the morphology of the interfacial region are presented here; the relation between cement/rock interfacial regions and permeability and bond strength are discussed elsewhere (4,5).

EXPERIMENTAL PROCEDURE

Curing conditions chosen for this study included temperatures of 27, 60 and 90°C and pressures of 0.1, 6.9, and 68.9 MPa. Experiments conducted at ambient temperature, 0.1 MPa, were carried out in temperature-controlled, constant-humidity chambers; higher pressure runs were made in stainless steel autoclaves. Temperatures below 100°C were regulated in a water bath. Mineral oil was used as the heat-transfer medium in longer term runs. Curing times of relatively short duration (most of which were less than three days) were intended to study the interfacial morphology as a function of temperture and pressure with little or no cement/aggregate interaction. Longer term experiments, up to six months, were also conducted to determine the nature and extent of the aggregate/cement reaction.

Pastes were prepared according to ASTM procedure C305 using a low alkali portland type I cement. Low-alkali cement was chosen to prevent extensive rapid reaction from masking the interfacial morphologies and time-dependent characteristics. A w/c ratio of 0.40 was used. Chemical analysis of the cement is as follows:

Portland Type I Cement

CaO	= 64.99	MgO	= 2.09
SiO_2	= 21.00	SO_3	= 2.61
Al_2O_3	= 5.22	Na_2O	= 0.08
Fe_2O_3	= 2.90	K_2O	= 0.74

"Aggregates" (rock slices) used included: Tuscarora quartzite, 95% quartz with a silica cement; a siltstone member of the Juniata formation containing approximately 25-30% matrix of illite and about 65% quartz; the Valentine limestone, 99.9% calcium carbonate; Beltane opal from Sonoma county, California, containing cristobalite and minor amounts of tridymite and alunite.

These rocks were slabbed, cored, and cut into discs 19.1 mm in diameter and 6.4 mm thick. One face was ground to 600 grit, the other left as sawn. Rock samples were stored at room temperature and 100% relative humidity according to ASTM procedure C227.

The cement paste/rock disc samples were cast in polyethylene molds and set for 12 hours at 25°C and greater than 95% relative humidity. The specimens were then cured for 1, 3, 7, and 28 days. Three- and six-month runs also were made. Some high-temperature, high-pressure experiments were also conducted in which setting and curing conditions were identical. Sample geometry is illustrated in Figure 1.

After samples were removed from the autoclaves, the cement cylinders were cut longitudinally and placed in liquid nitrogen for 15 minutes. The samples were then freeze-dried on a cold-plate vacuum desiccator for 48 hours to stop further hydration and to remove free water. One longitudinal half of the sample was fractured along the interface and the complementary halves (paste and aggregate) were gold coated. In some cases, the other longitudinal half of the sample was used to make polished sections perpendicular to the interface. All samples were stored over magnesium perchlorate until viewed under a Scanning Electron Microscope with energy dispersive x-ray analysis.

RESULTS

In preliminary experiments, samples were set at 25, 60, and 90°C and 100% relative humidity for 12 and 24 hours. The result of increasing setting time and temperature was to increase the degree of hydration. However, the basic structure of the interfacial region remained relatively unchanged after the setting period (even for the opaline aggregate).

Figure 2 shows the morphology of the interfacial region formed on a Valentine limestone surface. The sample was cured for 24 hours at 60°C and 0.1 MPa pressure. This morphology is representative of the interfacial

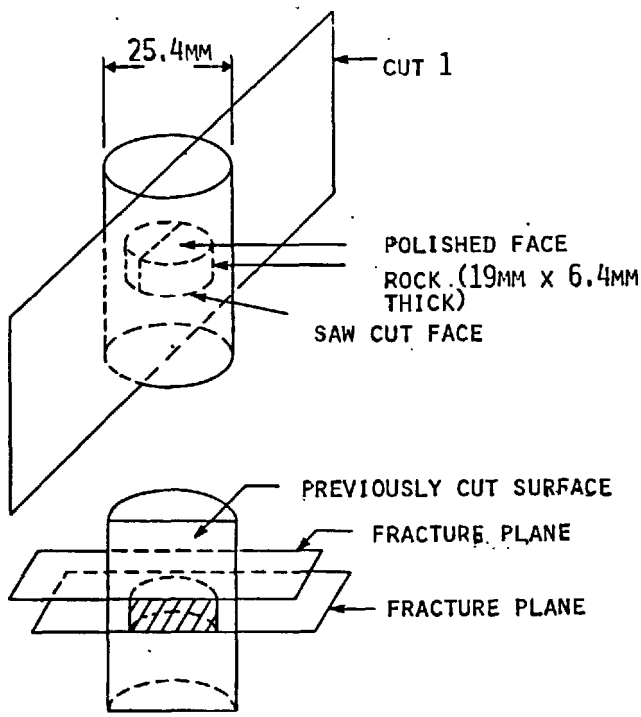

Figure 1. Geometry of sample preparation.

regions formed with other types of rock when samples were subjected to similar curing conditions. In all cases, fracture occurred through void spaces between hydrating cement grains and through voids formed between the hydration of shells of partially hydrated cement grains and their unhydrated cores. The rock portion of the fractured surface appears coated with fine acicular C-S-H gel and hexagonal $Ca(OH)_2$ crystals ranging in size up to about 20 μm. In addition, numerous partially hydrated cement grains are attached to the rock surface.

The paste half of the sample appears as partially hydrated cement grains covered with fine C-S-H gel growing perpendicular to the grain surfaces and hexagonal $Ca(OH)_2$ crystals growing in some of the pore spaces.

Figure 3 shows the morphology of the interfacial region formed on a similar limestone surface in a sample cured for three days at 60°C and 0.1 MPa pressure. The structure formed after three days is similar to that formed after 24 hours. However, fewer partially hydrated cement grains are attached to the rock surface and, therefore, the layer of C-S-H gel is more clearly exposed. $Ca(OH)_2$ crystals are still attached to the rock surface and in some places are coated with patches of acicular C-S-H gel.

The paste half of the sample is more hydrated after three days. Patches of well-crystallized equant hydrogarnets were also observed and are more common at the higher temperatures. Hexagonal $Ca(OH)_2$ crystals were found in pores and between hydrating cement grains.

Energy dispersive x-ray (EDX) analyses of the C-S-H gel formed during the first day of hydration indicated that the average Si:Ca ratio increased slightly with increasing temperature. Qualitative compositional analysis of the calcium hydroxide within a given sample indicated a compositional range from almost pure $Ca(OH)_2$ to appreciable amounts of Si, Al, and S. In places, large $Ca(OH)_2$ crystals were observed engulfing smaller $Ca(OH)_2$ grains and partially hydrated cement grains. The solubility of lime in water at 90°C is approximately 1/2 the solubility at 25°C. As temperature was increased from 25°C to the curing temperature, calcium apparently precipitated out of solution and grew to form these large $Ca(OH)_2$ crystals.

Secondary deposits of $Ca(OH)_2$ resembling small closely spaced platelets have been reported filling open spaces near the interface after about three days for samples cured at 25°C (1-3). This structure was not typical of the interfacial regions formed at higher temperatures and pressures. However, it was observed lining voids presumably formed by air bubbles trapped in the cement.

One effect of pressure on the morphology of the interfacial region is to increase the contact between the cement and rock. Figure 4 shows the interfacial region developed after curing for three days at 90°C and 68.9 MPa. This figure shows the paste half of the sample taken from the unpolished side of the Tuscarora quartzite. After three days, most of the C-S-H gel and $Ca(OH)_2$ formed at the interface are attached to the paste. The C-S-H paste forms a blanket-like texture made up of interlocking rosette structures.

Figure 5 again shows the paste half of the sample; the other half is polished quartzite. The sample was cured for seven days at 90°C and 68.9 MPa. The medium-gray, smooth-textured area in the center of the figure is a portion of the $Ca(OH)_2$ film which was deposited on the rock surface shortly after it came in contact with the paste. When the sample was fractured, part of the thin lime film remained attached to the rock, and part to the bulk cement.

Figure 6 shows the aggregate half of a sample cured for seven days at 90°C and 68.9 MPa. The aggregate in this case was unpolished Juniata siltstone. Hexagonal $Ca(OH)_2$ crystals, dense C-S-H gel, and partially hydrated clinker grains are attached to the siltstone surface and masks the interfacial morphology after only seven days curing. This was also the case for limestone and quartzite aggregates.

Samples containing Valentine limestone, Tuscarora quartzite and Juniata siltstone, when cured for periods of up to 28 days, showed continued hydration. When samples were broken, fracture occurred through the bulk paste above the interface. Most of the hydration products formed during these studies thus remained attached to the bulk paste. It was therefore difficult to detect changes in and/or characterize the interfacial morphologies of these three relatively non-reactive rock types.

An entirely different type of interfacial morphology was detected in samples containing opaline aggregates cured seven days to six months at 27°, 60° and 90°C over the entire pressure range studied. (Three-day samples showed morphologies similar to those previously discussed.) Fracture was observed to take place typically in layered steps from the aggregate surface upwards through the interfacial region and then the bulk cement paste. The interfacial region between the reactive opaline rock and the low alkali Type I cement was characterized by two zones each of which was made up of a thin film on which semicrystalline or gel particles appeared to be growing. Figure 7 is an SEM stereo image of the two-zoned interfacial region developed on a reactive opaline rock. The opaline substrate is exposed in the upper left of the image. It is overlain by a thin film, from which particles appear to be growing, Interfacial Zone 1. Shrinkage cracks were most likely induced in the desiccation necessary for SEM/EDX analysis. An enlargement of the gel particles in Zone I is shown in Figure 8.

Zone II is seen in Figure 7 overlying the particles on Zone I. Interfacial Zone II is also characterized by a film on which particles appear to be growing. Figure 9 is an enlarged view of Zone II which typically consists of a porous film covered with C-S-H gel particles.

An EDX-qualitative chemical analysis from area A, Figure 7, is plotted in Figure 10a. Zone I has a silica-rich potassium-calcium composition. Comparative analyses of the film versus the particles in this interfacial zone indicated a slightly higher Si:Ca ratio for the film. A chemical analysis of Zone II is shown in Figure 10b and can be seen to contain a relatively higher Ca:Si ratio and no potassium, in contrast to the analyses of Zone I.

Bulk cement paste is shown in Figure 7 in the lower right corner and also in the left corner of Figure 9. It appears to be attached to the interfacial region of the C-S-H gel particles growing on the film in Zone II.

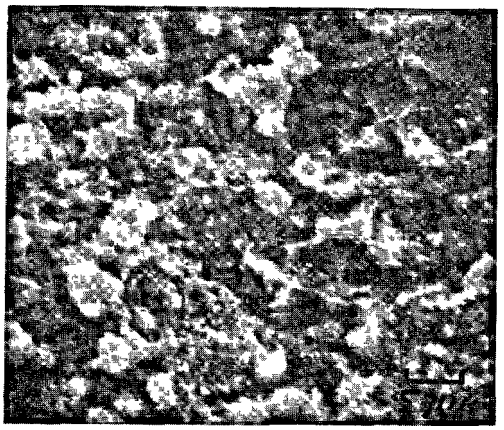

Figure 2. Morphology of interfacial region formed between paste and Valentine limestone cured 24h at 60°C and 0.1 MPa is characterized by C-S-H gel particles, partially hydrated clinker, and hexagonal $(Ca)OH_2$ crystal attached to the rock surfaces.

Figure 3. Interfacial region formed between paste and Valentine limestone cured for 3d at 60°C and 0.1 MPa is characterized by an increase in the amount of C-S-H gel particles and a decrease in partially hydrated clinker attached to the rock surface.

Figure 4. Intergrowth of C-S-H gel particles attached to the complementary paste half of the fractured sample is characteristic of the interfacial region formed between type I cement and unpolished Tuscarora quartzite surface, cured 3d at 90°C and 68.9 MPa.

Figure 5. A thin patchy film of $Ca(OH)_2$ is also characteristic of the interfacial region formed between type I cement and a polished Tuscarora quartzite surface cured 3d at 90°C, 68.9 MPa. The thin $Ca(OH)_2$ film is shown attached to the bulk paste by interlocking C-S-H particles.

Figure 6. Hexagonal Ca(OH) crystals, dense C-S-H gel and partially hydrated clinker grains are attached to the Juniata siltstone surface after 7d curing at 90°C and 68.9 MPa.

DISCUSSION AND CONCLUSIONS

The morphology and mode of fracture through the interfacial region formed between portland cement paste and rock are both dependent on the reactivity of the aggregate (solubility in a high-pH solution caused by hydrolysis of uncombined free water in cement pastes to produce hydroxyl ions) and the degree of hydration of the cement paste (sodium and potassium are released into solution by the formation of ettringite which ties up sulfate ions previously combined with alkalies). The net effect of reactive rocks used as aggregates in portland cement has been termed alkali-aggregate reaction. In this study the degree of cement hydration was found to increase with increasing time and temperatures up to 90°C. Aggregates were classified as reactive and unreactive based on morphologies developed in the interfacial region after curing for six months. Valentine limestone (99.0% calcium carbonate), Tuscarora quartzite (95% quartz plus silica cement), and Juniata siltstone (25-30% illite matrix plus 65% quartz) were found to be non-reactive; Beltane opal was reactive.

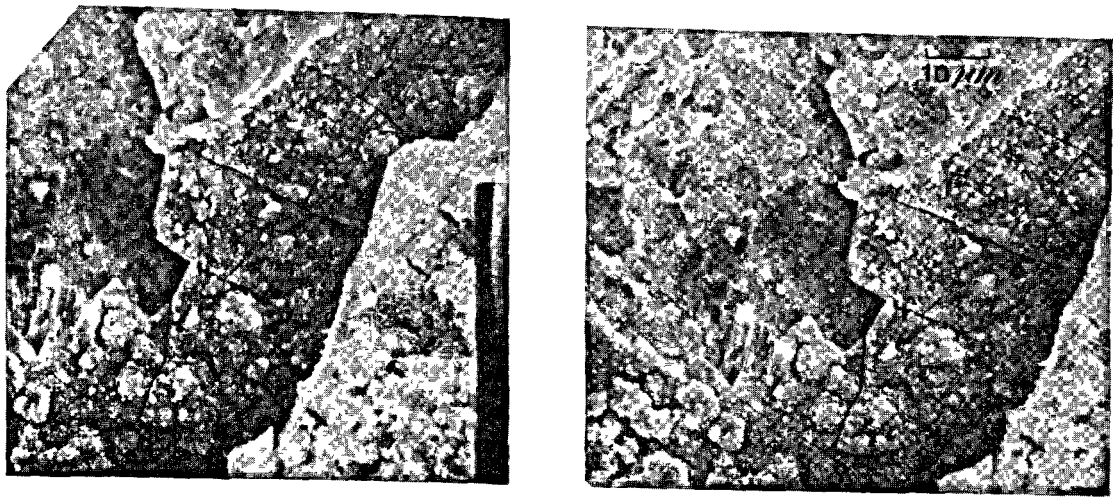

Figure 7. Stereo image of the interfacial region developed between reactive Beltane opal and type I cement cured 21d at 60°C, 0.1 MPa. The opaline substrate (upper left) is overlain by an S-C-K-H film on which S-C-K-H gel particles appear to be growing (Zone I). These particles are overlain by a C-S-H (C-H) film from which C-S-H gel particles appear to be growing (Zone II). These C-S-H particles attach the interfacial region to the bulk paste shown at the lower right.

Figure 8. Magnification of S-C-K-H gel particles from Interfacial Zone I.

Figure 9. Magnification of C-S-H porous film and C-S-H gel particles making up Interfacial Zone II.

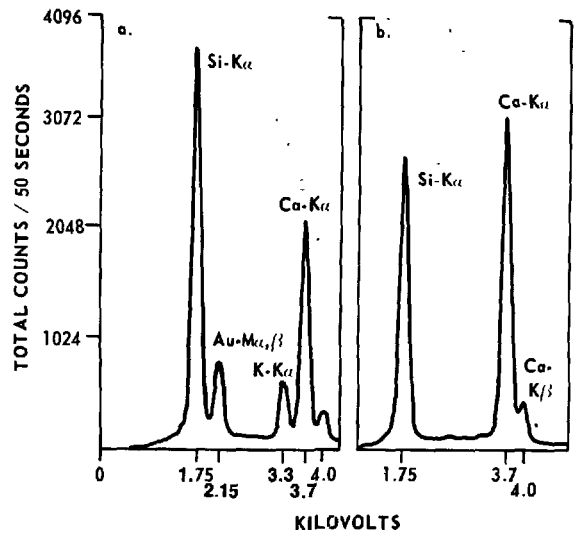

Figure 10. (a) Energy dispersive x-ray analysis of S-C-K-H gel particles within area A, Figure 7. (b) Energy dispersive x-ray analysis of C-S-H gel particles within area B, Figure 7.

Figure 11 is a schematic diagram of the characteristic two-layer zone developed in the interfacial region between a non-reactive aggregate and portland cement paste. The interfacial morphology is characterized by a thin film of C-H (C-S-H) from which C-S-H particles appear to be growing. In addition to C-S-H particles, larger crystals of $Ca(OH)_2$ appear to attach the interfacial region to the bulk paste and thereby the aggregate to the bulk paste. As the degree of hydration increased, more bulk paste became attached to the interfacial region, making further characterization of the aggregate-film contact difficult. Where the interfacial region was exposed in six-month runs it still appeared as a two-layer zone.

A schematic diagram of the morphology of the inter-

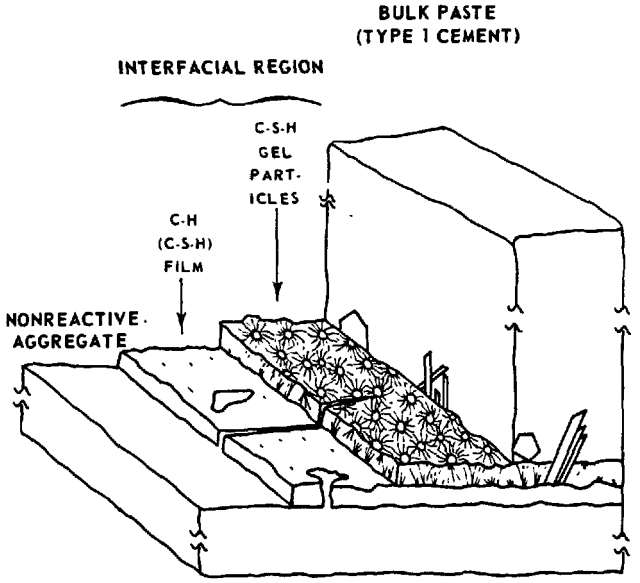

Figure 11. Schematic diagram of the interfacial region formed between a non-reactive silica substrate and Type I cement paste.

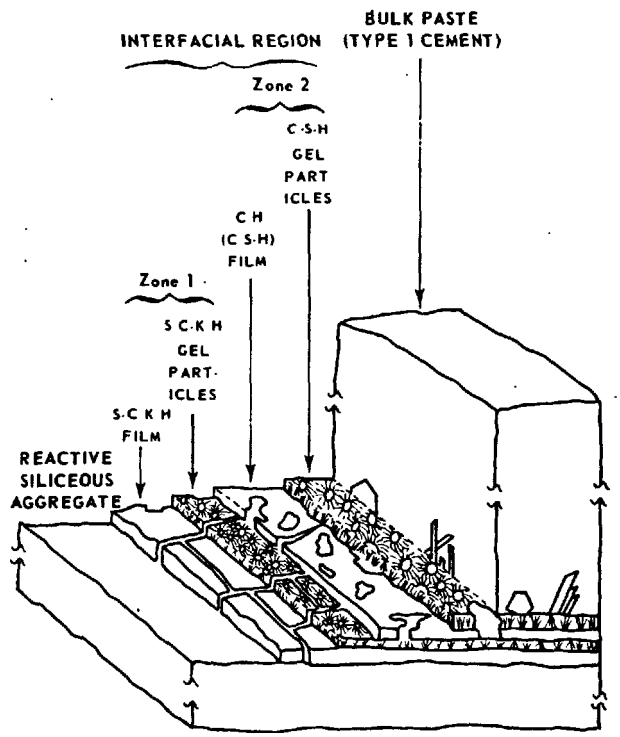

Figure 12. Schematic diagram of the interfacial region formed between a reactive silica substrate and Type I cement paste.

facial region which developed on a reactive aggregate surface is shown in Figure 12. In contrast to the two-layered region formed on an unreactive aggregate and previously reported on reactive surfaces (1-3,6), four interfacial layers characteristically were present on reactive surfaces. The reactive aggregate surface was typically overlain by a S-C-K-H film from which S-C-K-H particles appeared to be growing. These two layers make up Zone I. S-C-K-H particles on Zone I were attached to an overlying second film containing relatively more calcium than silicon and no alkali, C-S-H (C-H) film. Again, C-S-H particles appeared to be growing from this film and attaching the interfacial region to the bulk paste. Independent sets of shrinkage cracks were observed in both Zones I and II. However, they were much more abundant in Zone I (S-C-K-H Zone). Fracture typically took place in a step-like manner across each layer of the interfacial region.

The effect of elevated pressures was to increase the contact between paste and rock surface, and, when combined with elevated temperature, to increase also the hydration rate. Surface roughness of the rock resulted in no major effect upon the basic structure of the interface.

ACKNOWLEDGEMENT

This research was supported through DOE subcontract No. E512-00500, Office of Nuclear Waste Isolation, Battelle Memorial Institute, Columbus, OH.

REFERENCES

1. BARNES, B.D., S. DIAMOND, and W.L. DOLCH, American Ceramic Society Journal 62, 21-24 (1979).

2. BARNES, B.D., S. DIAMOND, and W.L. DOLCH, Cem. Concr. Res. 8, 233-244 (1978).

3. BARNES, B.D., PhD Thesis, School of Civil Engineering, Purdue University (1976).

4. ROY, D.M., et al., "Borehole Cement and Rock Properties Study-Part A: Borehole Plugging Cement Studies," Annual Report for ONWI, Sub/78/E512-00500, Report No. ONWI-5, Appendix IV (Oct. 1978).

5. ROY, D.M., "Borehole Cement and Rock Properties Study-Task I: Borehole Plugging Cement Studies," Quarterly Progress Report for ONWI/SUB/78/E512-00500-1, 26-32 (Dec. 1978).

6. HADLEY, D., PhD Thesis, School of Civil Engineering, Purdue University (1972).

Interface phenomena and durability of concrete

Phénomènes à l'interface et durabilité du béton

G.P. TOGNON, Chem. Eng. Italcementi S.p.A. - Laboratorio Chimico Centrale - Bergamo - Italy,
S. CANGIANO, Chem. Eng. Italcementi S.p.A. - Laboratorio Chimico Centrale - Bergamo - Italy.

RESUME : En opérant sur des éprouvettes de mortier de ciment cylindriques, coulées autour d'un cylindre coaxial en calcaire ou en quartz, on a confirmé l'existence d'une porosité particulière (rayons compris entre 150 et 300 Å) à l'interface du mortier et de la pierre; elle semble due à des discontinuités dans les liaisons.

Après autoclavage, cette porosité, déjà réduite dans les éprouvettes à noyau calcaire après une cure normale, semble disparaître complètement, notamment dans les éprouvettes à noyau de quartz. Des mesures conductimétriques ont, en outre, montré que cette zone interfaciale était particulièrement perméable à NaCl. La profondeur de la pénétration du NaCl dans cette zone dépend étroitement de la dimension des pores.

L'addition d'un entraîneur d'air augmente cette perméabilité à 20°; l'augmentation est plus importante avec le noyau calcaire qu'avec le noyau quartzeux, par suite probablement de l'accroissement des discontinuités de liaison du fait des bulles d'air. Toutefois, des éprouvettes comportant un entraîneur d'air, et soumises à des cycles de gel/dégel ont montré que l'augmentation de la perméabilité de la zone interfaciale était plus faible que celle produite, dans les mêmes conditions, sur des éprouvettes sans entraîneur d'air.

SUMMARY: By testing cement mortar specimens with a cylindrical limestone or quartz inclusion in the centre, the existence of a peculiar porosity (radii between 150 and 300 Å) was confirmed at the mortar-aggregate interface, attributable to bond discontinuities. After autoclaving, such a porosity, already reduced in normally cured specimens with calcareous inclusion, appears to be almost suppressed especially in specimens with quartz inclusion. Moreover conductimetric measurements showed that the interface, compared with the mortar, is the site of a preferential penetration of a NaCl solution. The magnitude of this penetration must be related to the volume of pores there existing.
The addition of an air-entraining admixture is liable for an increase in the interface penetration at 20°C. This increase is more marked in the specimens with calcareous aggregate because of the greater extent of the bond discontinuities due to the formation of bubbles at the interface. Nevertheless the lower interface penetration observed after freeze/thaw cycles in air-entrained specimens compared with the plain ones proved that the air-entraining admixture restrains the frost action also at the interface.

1. INTRODUCTION

As known, the contact zone between cement matrix and aggregate plays an important role in the development of the mechanical strength of concrete, especially of the very high strength one (1, 2).
For some types of aggregates, having suitable chemical and mineralogical composition, a crystallochemical interaction is added to the interface interaction of physical type (3, 4). The former can be due to an epitaxis intergrowth between carbonated portlandite crystals and calcareous aggregates in concretes cured at ordinary temperature (3) and between quartz aggregate and tobermorite 11 Å in autoclaved mortars (5).
The discontinuities always present at the aggregate-matrix interface, which would appear already reduced in the case of epitaxis with calcareous aggregate (3), ought to be almost absent owing to the hydrothermal lime-silica reaction. In fact, in this case, the formation of a "weld bead" was observed around the aggregate (1).
It is reasonable to think that the durability of concrete is affected by the type of interaction (physical and crystallochemical), as was found for the mechanical strength. In fact the interface layer can be more permeable to water or saline solutions than the matrix or the aggregate itself.
The purpose of this work is to prove the existence of a higher permeability in the interface zone due to a peculiar porosity and to verify whether the substantial strengthening of the interface bond, observed in very high strength concretes (2, 5), yields a decrease in permeability, so improving the durability of concrete to freeze/thaw cycles.

2. EXPERIMENTAL

The materials used in the different tests are:

- very high strength portland cement (class 525)
- quartz containing 86.2% quartz silica
- limestone containing 99.4% $CaCO_3$
- binder obtained by mixing the cement and the quartz ground to a Blaine specific surface of 4500 cm^2/g at the 1 : 1.66 ratio respectively.

Two types of mortar were prepared by using these materials; an ordinary one, with cement, for specimens to be water-cured at 20°C, and another with binder for specimens to be autoclaved. The composition of the two mortars is shown in Table I.

TABLE I: Composition of mortars

Materials and mix ratios		Cement mortar %	Binder mortar %
525 Ptl cement	(C)	45.8	28.6
Ground silica (4500 cm^2/g)	(S)	-	17.2
Quartz (fract. 0 ÷ 0.83 mm)		54.2	54.2
W/C ratio		0.4	-
W/C + S ratio		-	0.4
C/Sand ratio		1 : 1.8	-
C + S/Sand ratio		-	1 : 1.18

Besides these, mortars containing an air-entraining admixture (saponified VINSOL resin) in the rate of 2‰ of the binder were made. The air content in the fresh mixes was about 8%.
The adopted curing conditions are given in Table II.

TABLE II: Curing conditions

Normal	Autoclaved	
Immersion in water at 20°C for 28 days	Presteaming	about 17 h at 20°C
	Low pressure steam curing	8 h at 60°C
	Rate of temperature rise	0.7°C/min.
	High pressure steam curing	24 h at 190°C
	Rate of temperature rise	0.7°C/min.

2.1 Determination of the porosity in the interface zone

To determine the porosity and the pore distribution in the interface zone, porosimetric measurements were carried out by a mercury porosimeter in the range of the pore radii between 75 and 75 000 Å (6).
The measurements were performed on the specimens indicated in the first column of Table III. The specimens 5 to 8 consisted of a cylindrical calcareous or quartz core surrounded by a ring of binder paste.

TABLE III: Porosimetric values concerning the individual materials, the specimens and the interface zone

Materials	Measured volume of pores (cm3/g) (a)	Calculated volume of pores (cm3/g) (b)	Volume of the interface pores (cm3/g) (a-b)
1) Limestone (cylinders: h = 15 ø = 8 mm)	0.0070	-	-
2) Quartz (cylinders: h = 15 ø = 8 mm)	0.0022	-	-
3) Normally cured binder paste	0.0737	-	-
4) Autoclaved binder paste	0.0072	-	-
5) Normally cured binder paste + limestone	0.0346	0.0252	0.0094
6) Autoclaved binder paste + limestone	0.0098	0.0071	0.0027
7) Normally cured binder paste + quartz	0.0463	0.0360	0.0103
8) Autoclaved binder paste + quartz	0.0061	0.0047	0.0014

The section of the specimens is shown in the detail of figure 2.
The second column of Table III shows the pore volume determined experimentally in the different specimens. The third column lists the porosity values calculated from the porosity values of the individual components (aggregate and binder paste), their weighted ratio considered.
The difference between the measured and the calculated porosimetric values is reasonably attributable to the porosity of the interface zone.
Table III allows the following observations: in the normal curing, the interface porosity of the specimen with calcareous inclusion is lower, even if slightly, than the one of the specimen with quartz aggregate; the difference reverses when the specimens are autoclaved.
Autoclaving reduces the porosity drastically, namely: by about seven times in the specimens with quartz inclusion and by about three times in the ones with calcareous inclusion.

The pore size distribution in the interface zone of the normally cured specimens is shown in figure 1.

As can be seen, there is a peak in the pore range between 150 Å and 300 Å; the peak is more marked and shift

ed to wider radii for the specimen containing quartz. Since these peaks are not present in the binder paste and in the aggregate, it is reasonable to attribute them to discontinuities in the interface zone.

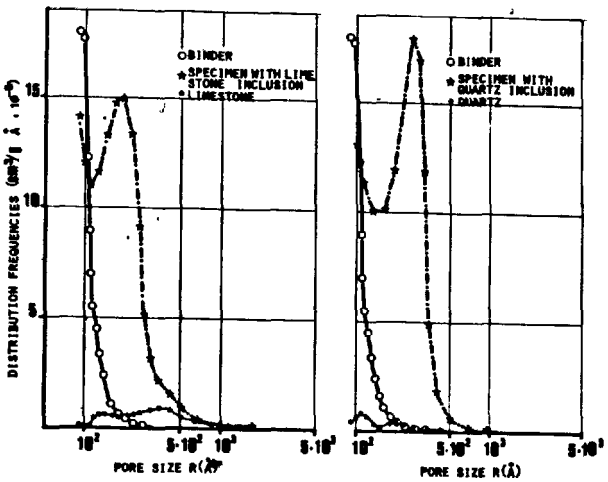

FIG. 1: Pore size distribution of normally cured specimens (20°C - fog room)

On the contrary, this peak lacks in the autoclaved specimens. Here the two curves take a continuous trend which decreases as the radius increases. Moreover, especially in the above-mentioned range, they show a more marked porosity in the sample containing the calcareous inclusion than the one of the sample with quartz inclusion.

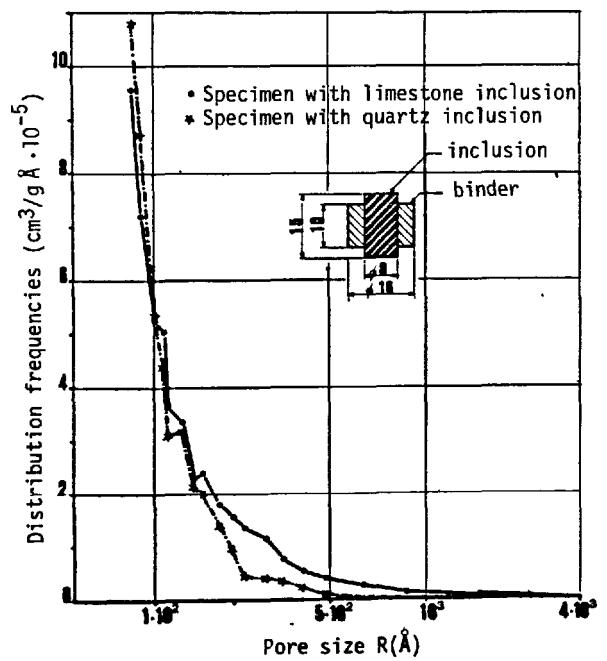

FIG. 2: Pore size distribution of autoclaved specimens

The presence of a certain porosity at the paste-quartz inclusion interface was confirmed experimentally as follows. Some specimens having the shape shown in the detail of figure 2 were subjected to mercury penetration at increasing pressures. After each treatment, the paste was detached from the quartz cylinder by according to the tensile splitting test.
This procedure led to determine the pressure values at which the mercury begins and ends the penetration at the interface.

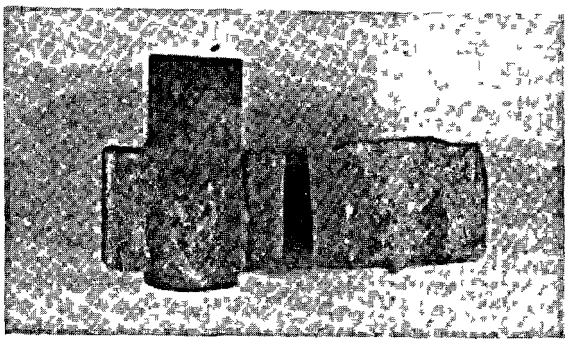

FIG. 3: Autoclaved specimen with quartz inclusion split after mercury penetration at 250 atm

Figure 3 shows that, at 250 atm pressure necessary for filling the pores having $r \geq 300$ Å, the contact surfaces of the two components (binder paste and aggregate) are not yet blackened by the metal. This means that the penetration of mercury has not yet occurred. The figure also shows pieces of mortar still strongly bonded to the aggregate core.
On the contrary, at 400 atm pressure (pore $r \geq 150$ Å), the mercury penetrated the specimen.

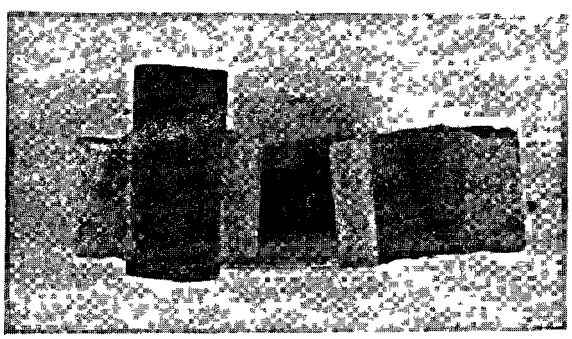

FIG. 4: Autoclaved specimen with quartz inclusion split after mercury penetration at 400 atm

As figure 4 shows, the penetration occurred mainly at the interface. In fact the mercury blackens the surfaces in contact with the quartz core and the binder paste, but it does not concern the real mass of the binder paste. This fact confirms that the interface porosity, also by autoclaving, is located in a wider range of radii (150-300 Å) than the one of the binder.

2.2 Permeability of the interface and the cementitious matrix

To evaluate the permeability of the interface layer and the mortar, measurements of electrical conductivity were carried out on special specimens subjected to penetration of a NaCl solution.
The electrical conductivity of the hardened and wet

cement pastes was recently (7) described by a model consisting of an equivalent circuit composed of four parallel resistances. In this model, the total conductance of the system is given by the sum of the following conductances:

γo = inherent conductance of the paste
γad = conductance of the adsorbed water films
γelk = conductance depending on the electrokinetic processes
γely = electrolytic conductance.

By considering this model, the Authors tried to maintain the effect of the three first terms constant by always operating in alternating current, at the same frequency and with equal "cells" for all the specimens. Under these conditions, the differences of conductivity among the different specimens were only attributable to the term γely which depends on the amount and the number of ionic species participating in the electrolytic conduction.
The conductimetric tests were carried out on mortar prisms (10 x 10 x 4 cm) whose upper part was provided with a cylindrical cavity (Ø = 5 cm, h = 2 cm) suitable for accomodating a 3% NaCl solution (figure 5).

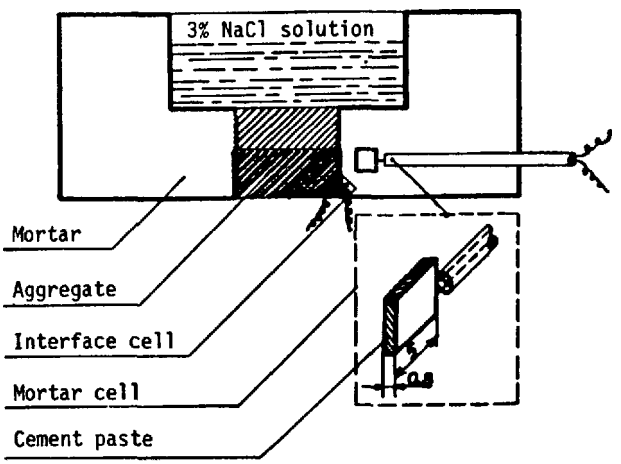

FIG. 5: Specimen and arrangement of conductimetric cells for penetration tests

Before casting the mortar, an aggregate cylinder (Ø = 2.2 cm, h = 2 cm) was placed in the centre of a suitably shaped mould. Moreover, a measurement "cell", represented in the detail of the same figure 5, consisting of two platinum electrodes (5 x 5 mm) 0.8 mm distant from each other and between which a cement paste (w/c = 0.5) was previously cast, was carefully introduced into the mould at the distance of 3.5 mm from the aggregate inclusion and at the depth of 1 cm. Another cell (interface cell) adherent to the aggregate cylinder was placed at the same depth as the previous one. Its construction was carried out as follows. The first electrode was drawn on the cylinder by a silver colloidal suspension and immediately covered by a thin layer of cement paste (w/c = 0.5) whose thickness was determined by weighing. The second electrode was drawn on this paste again by the silver suspension. The conductimetric tests were performed continuously at 20°C and during freeze/thaw cycles by working with a conductimeter having a 1 kHz operating frequency, judged as optimum for conductimetric tests on cement pastes (8) under a 200 mV tension.

2.2.1 Permeability at 20°C

As for the normally cured specimens, the increase in conductivity was always indicated at first by the cell at the interface and then by the one embedded in the mortar. Indeed, the latter did show no significant conductimetric signal since the specimen cracked at varying times but anyhow subsequent to those of appearance of the signal at the interface.

TABLE IV: Times of appearance of the conductimetric signal at the interface

Type of specimen	Hours from the beginning of the permeation
Ordinary mortar + calcareous inclusion	4
Ordinary air-entrained mortar+calcareous inclusion	2.5
Ordinary mortar+quartz inclusion	1
Ordinary air-entrained mortar+quartz inclusion	0.5

Table IV shows the times of appearance of the conductimetric signal at the interface. They were measured from when the NaCl solution was poured into the cavities of the specimens.

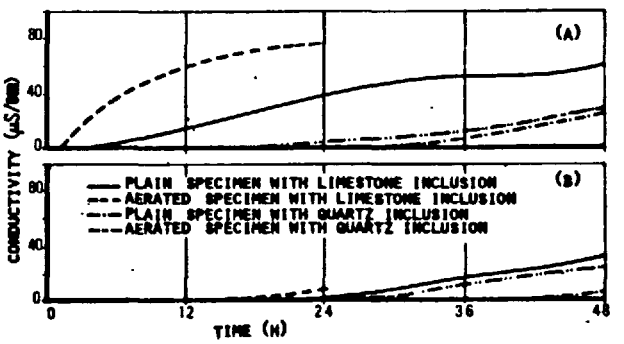

FIG. 6: Conductivity curves at the interface (A) and in the mortar (B) of autoclaved specimens stored at 20°C and 50% R.H.

Figure 6 gives the conductivity trend measured on autoclaved specimens. These did never show cracking because of their high strength.
The recorded data show that, for all the specimens, the conductimetric signal appears before at the interface than in the mortar and, at least in the first 48 hours, it takes ever-increasing values at the interface compared with those of the mortar. Obviously this means that the interface zone constitutes a preferential way to permeation.
The permeation in the mortar is affected, owing to the side diffusion, by the rapidity of its occurrence at the interface. In fact more rapid increases in conductivity were noticed in the mortar of the specimens whose interface revealed a quicker permeation.
The normally cured specimens (Table IV) with quartz inclusion showed more rapid permeations at the interface than those of specimens with calcareous inclu

sion.
The autoclaving of the specimens containing quartz aggregate strongly reduces the permeability and causes a considerable delay in the appearance of the conductimetric signal compared with what observed in the normally cured specimens (see figure 6).
On the contrary the same behaviour is not recorded for the specimens with calcareous aggregate. In this case the autoclaving, compared with the normal curing, does not involve a substantial decrease in permeability.
In all cases, the addition of air-entraining admixture causes the appearance of the conductimetric signal in advance and therefore it increases the permeability.

2.2.2 Permeability during freeze/thaw cycles

Figure 7 shows the conductivity values measured during freeze/thaw cycles in the air (cooling or heating rate: 5°C/h - storage at extreme temperatures (+20°, -20°): 4 h) in the interface zone and in the mortar of autoclaved specimens.

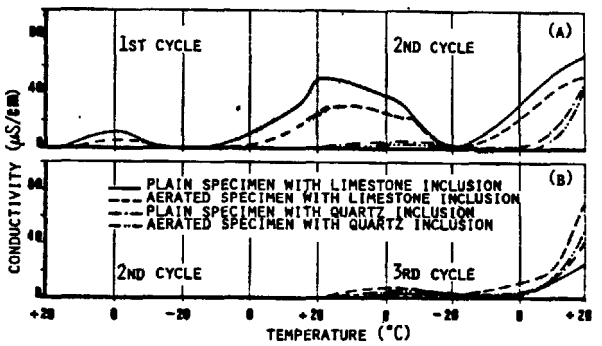

FIG. 7: Conductivity curves at the interface (A) and in the mortar (B) of autoclaved specimens subjected to freeze/thaw cycles

It was not possible to work on the normally cured specimens because of the aforesaid phenomenon of cracking. The curves are affected by the effect of the thermal alternances on the conductivity and the permeation. Both phenomena are progressively reduced by a decrease in temperature until they are partially blocked.
At about -8°C, a rapid drop in conductivity is observed when the water begins freezing in the pores of the paste placed between the electrodes of the two cells.
Figure 7 shows that, similarly to what occurs in the case of the permeation at 20°C, the specimens with calcareous inclusion have a higher interface conductivity than the one of the specimens with quartz inclusion.
The addition of air-entraining admixture causes a decrease in permeation at the interface for both types of specimens, that is an opposite behaviour to the one occurring at 20°C.
The comparison of the curves of figures 6 and 7 evidences that, at the end of the cycles, the interface shows higher conductivity values than those attained in the same period of time by the analogous specimens stored at 20°C, except for the air-entrained one with calcareous inclusion.
On the contrary an appreciable increase in conductivity is measured in the mortar only after the 3rd cycle.

3. DISCUSSION

The normal curing gives the specimens with calcareous inclusion a lower interface porosity by 10% than the one of specimens with quartz inclusion. This fact must be related to the formation of an epitaxial-type additional bond at the mortar-limestone interface (3).
The considerable reduction in the interface porosity occurring in the autoclaved specimens with quartz aggregate must be attributed to the existence of wide surfaces of lime-silica reaction. On the other hand the presence of a residual interface porosity confirms that not all the surface of the aggregate is involved by the reaction.
The reduction in the interface porosity also observed in the autoclaved specimens with calcareous aggregate, even if less marked than in other specimens, is likely due to the fact that the reaction products between ground silica and hydrolysis lime covering the aggregate (9) partially fill the discontinuities at the interface. Actually these discontinuities are still visible under the electron microscope (1).
The autoclaved plain specimens with calcareous aggregate show a considerably higher permeability at the interface than the one of specimens with quartz inclusion, even if the respective interface porosities are of the same order of magnitude (0.0027 and 0.0014 cm^3/g). This is related to the fact that the NaCl solution by exerting its disjoining action (3, 10), can penetrate only the zones where there is no epitaxis intergrowth. In the case of calcareous inclusion, the interface bond mainly occurs by physical cohesion whereas wider and broader interaction zones of crystallochemical type form on the quartz one.
Microscopic observations showed that the autoclaved and normally cured air-entrained specimens with calcareous inclusion have a higher concentration of bubbles at the interface than the one found at the quartz-mortar interface (figures 8 and 9).

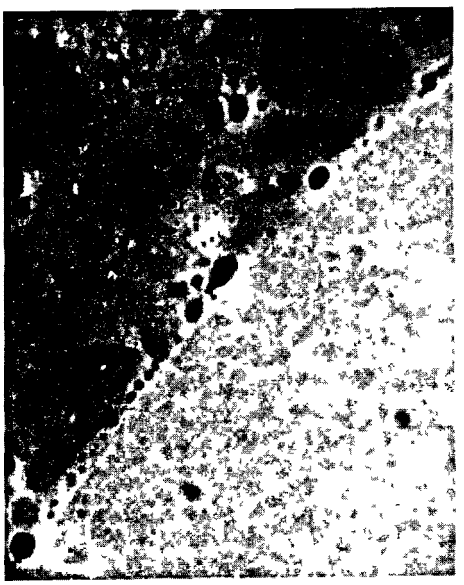

FIG. 8: Air bubbles present in the mortar (upper left side) and at the calcareous inclusion - mortar interface - 10 X

This explains the insignificant difference of permeability between air-entrained and plain specimens when

the inclusion is quartzy and the considerable difference when the inclusion is calcareous.

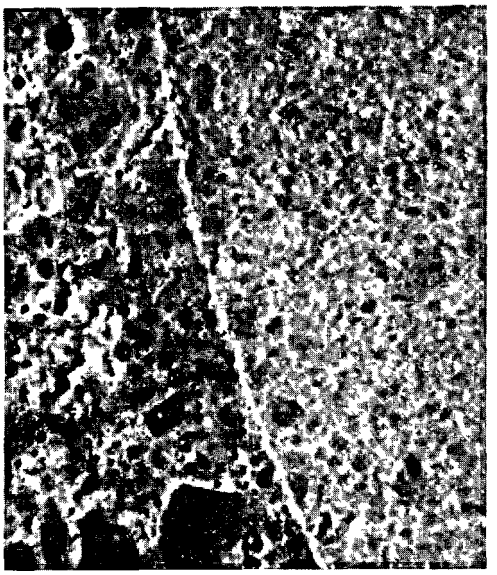

FIG. 9: Air bubbles present in the mortar (left side) and lacking at the quartz inclusion-mortar interface - 10 X

The bubbles at the interface form discontinuities and determine a higher permeation at 20°C but, in case of freezing, they act as pressure compensation chambers. In this way they prevent or anyhow retard the disaggregating action of frost (figure 7).

4. CONCLUSIONS

The layer at the interface constitutes a zone of higher porosity liable for the experimentally observed preferential permeation.
The obtained results, besides confirming the hypothesis about the higher sensibility to frost of the interface zone, indicate that the bond strengthening owing to the lime-silica reaction involves an appreciable reduction in the permeability of this zone when the specimens are subjected to freeze/thaw cycles. Nevertheless this permeability is always higher than the one observed in the mortar.

REFERENCES

1. TOGNON G.P. (1977), "Calcestruzzi ad altissima resistenza per la prefabbricazione", L'Ingegnere Libero Professionista, (11), 889-901 (It.)
2. TOGNON G.P., URSELLA P., COPPETTI G. (1980),"Bond strength in very high strength concrete", 7th Int. Congr. Chem. Cem., Paris (Eng.)
3. FARRAN J. (1956), "Contribution minéralogique à l'étude de l'adhérence entre les constituants hydratés des ciments et les matériaux enrobés", Revue des Matériaux, (490-491), 153-172; (492), 191-209 (French)
4. WITTMANN F.H. (1972), "Etude de la force d'adhésion en fonction du mouillage", Coll.Int.RILEM/INSA: Liaison de contact dans les matériaux composites utilisés en génie civil - I, (Toulouse, 22-24 nov. 1972), 174-184 (French)
5. MASSAZZA F., PEZZUOLI M. (1980), "Cement paste-quartz bond in autoclaved concretes", 7th Int. Congr. Chem. Cem., Paris (Eng.)
6. ALONGI V. (1964), "Metodi per la determinazione della microstruttura in materiali porosi", Cronache di Chimica, (6), 16-25 (It.)
7. SCHULTE Ch., MADER H., WITTMANN F.H. (1978),"Elektrische Leitfähigkeit des Zementsteins bei unterschiedlichem Feuchtigkeitsgehalt", Cement and Concrete Research, 8, 359-368 (Ger.)
8. CALLEJA J. (1952), "Effect of current frequency on measurement of electrical resistance of cement paste", Journal of the American Concrete Institute, 24, (Proc. 49), 329-332 (Eng.)
9. BARNES B.D., DIAMOND S., DOLCH W.L. (1979), "Micromorphology of the interfacial zone around aggregates in portland cement mortar", Journal of the American Ceramic Society, 62, 21-24 (Eng.)
10. WITTMAN F.H. (1973), "Interaction of hardened cement paste and water", Journal of the American Ceramic Society, 56, 409-415 (Eng.)

INDEX DES AUTEURS
AUTHORS INDEX

D

E

F

G

H

I

J

K

L

M

N

O

P

R

S

T

U

7e Congrès International de la Chimie des Ciments

7th International Congress on the Chemistry of Cement

VOLUME IV

RAPPORTS GENERAUX - POSTERS - SEMINAIRES

GENERAL REPORTS - POSTERS - SEMINARS

PARIS 1980

7e Congrès International de la Chimie des Ciments

7th International Congress on the Chemistry of Cement

VOLUME IV

RAPPORTS GENERAUX - POSTERS - SEMINAIRES

GENERAL REPORTS - POSTERS - SEMINARS

PARIS 1980

EDITIONS SEPTIMA - 14, rue Falguière,
75015 PARIS (France)

Imprimé en France - 1981.

TABLE DES MATIERES
CONTENTS

ALLOCUTIONS

RAPPORTS GENERAUX

POSTERS

THEME I

THEME II

THEME III

THEME IV

COMMUNICATIONS

SEMINAIRES

SEMINAIRE A – Rôle du C_3A sous toutes ses formes dans l'hydratation des ciments et leur attaque par les sulfates

THEME 3 - Hydration of C_3A in cements.
Hydratation de C_3A dans les ciments.

THEME 4 - Hydration of C_3A in the presence of admixtures.
Hydratation de C_3A en présence d'adjuvants.

SEMINAIRE B - Insolubilisation à l'aide de liants hydrauliques des ions métalliques contenus dans les boues industrielles

SEMINAIRE C - Economies d'énergie vues prospectives (Président, M.-A. Guy)

SEMINAIRE D – Influence des caractéristiques du ciment sur les propriétés du béton

ALLOCUTIONS

Séance inaugurale - 30 Juin 1980

ALLOCUTION DE M. R. POITRAT

Président du Syndicat National des Fabricants de Ciments et de Chaux
Président du 7e Congrès International de la Chimie et Ciments

Nous sommes particulièrement heureux d'accueillir en France le 7ème Congrès International de la Chimie des Ciments.

Au nom de l'Industrie Cimentière Française et en mon nom personnel, il m'est agréable d'exprimer à l'ensemble des congressistes mes souhaits cordiaux de bienvenue à Paris, et tout particulièrement à ceux d'entre vous qui sont dans notre capitale pour la première fois.

Les plus hautes autorités françaises ont marqué l'intérêt qu'elles portaient à cette manifestation. Le Chef de l'Etat, M. Valéry Giscard d'Estaing,lui a accordé son Haut Patronage, et le Comité d'Honneur qui a été constitué a reçu l'adhésion de :

- M. Raymond Barre, Premier Ministre,
- M. Jean-François Poncet, Ministre des Affaires Etrangères,
- M. Michel d'Ornano, Ministre de l'Environnement et du Cadre de Vie,
- Mme Alice Saunier-Seité, Ministre des Universités,
- M. Joël Le Theule, Ministre des Transports
- M. Jean-François Deniau, Ministre du Commerce Extérieur,

et de M. Pierre Aigrain, Secrétaire d'Etat auprès du Premier Ministre - Chargé de la Recherche.

M. André Giraud, Ministre de l'Industrie, nous a fait, pour sa part, le grand honneur d'accepter de prendre la parole au cours de la présente séance inaugurale. Nous aurons le plaisir de l'accueillir dans un instant.

Et nous avons aussi la joie d'avoir parmi nous deux des plus éminentes personnalités du monde scientifique :

- le Professeur André Guinier, Membre de l'Académie des Sciences, qui, dans les laboratoires de la Faculté des Sciences d'Orsay,a su communiquer sa foi à de nombreux chercheurs;
- le Professeur Henri **Lafuma**, élève et collaborateur d'Henry Le Chatelier, dont il a maintenu la présence permanente et vivante parmi nous en poursuivant au CERILH, Centre de Recherches de l'Industrie Cimentière française, les travaux de l'éminent savant qui avait été son maître.

Je suis sûr d'être l'interprète de l'ensemble des congressistes en exprimant aux Professeurs Guinier et Lafuma la profonde reconnaissance de l'industrie cimentière mondiale.

o
o o

Six années se sont écoulées depuis le précédent Congrès qui s'était tenu à Moscou; six années qui n'ont pas effacé l'excellent souvenir qu'en ont gardé les participants.

Six années qui ont été marquées par de profondes évolutions dans la quasi totalité des secteurs industriels du monde, et notamment dans ceux dont les activités exigent d'importantes quantités d'énergie. C'est pourquoi nous avons souhaité que l'organisation de cette nouvelle rencontre puisse bénéficier des travaux réalisés dans le monde entier.

Un Comité Scientifique International a été constitué dans cet esprit, auquel ont été appelés à participer les plus éminents spécialistes internationaux.

Présidé par M. François Le Bel, ce Comité s'est attaché, depuis quatre années, à choisir et définir de façon précise les questions à étudier.

Deux de ses membres nous ont malheureusement quittés au cours de ces travaux : le Professeur Kondo et le Docteur Peter.
Je m'incline ici devant leur mémoire.

o
o o

L'activité de l'industrie cimentière a connu, entre les années qui ont suivi la seconde guerre mondiale et 1973, un rythme de progression continu, de l'ordre de 6 à 7 % par an en moyenne.

De 102 millions de tonnes en 1948, la production du monde passait à 314 millions de tonnes en 1960, 589 millions de tonnes en 1970 et 717 millions de tonnes en 1973.

Après 1973, cette évolution a subi les à-coups économiques nés de la crise de l'énergie; ainsi, le taux de croissance moyen des cinq dernières années s'est établi à 3 % et la production de 1979, avec 860 millions

de tonnes, n'est que de 20 % supérieure à celle de 1973.

Mais cette moyenne recouvre des situations fort diverses allant de la stagnation, voire de la récession dans certains grands pays producteurs, à un développement considérable dans d'autres pays.

o
o o

Ainsi donc, cette crise de l'énergie a profondément marqué la période qui s'est écoulée entre le Congrès de Moscou et notre présente Assemblée. Le renchérissement du fuel-oil lourd et celui, bien qu'à un degré moindre, des autres sources d'énergie, ont bien évidemment incité les cimentiers à porter leurs efforts sur l'adoption de dispositions permettant de réduire leur consommation en combustible. Dans tous les pays, la recherche s'est orientée sur les moyens d'économiser l'énergie en général et les produits pétroliers en particulier.

En premier lieu, s'est engagé un mouvement général de reconversion vers le procédé de fabrication par voie sèche, qui permet une économie de thermie à la tonne de ciment appréciable.

Dans la même optique, est apparu l'intérêt d'une utilisation plus large de constituants secondaires dans la composition du ciment. En effet, pendant une longue période, le problème du coût de l'énergie ne se présentait pas avec l'acuité actuelle; les usines étaient conçues essentiellement pour la production de ciments Portland purs et l'on se préoccupait peu de les adapter à l'utilisation d'ajouts réactifs. Il faut cependant souligner que quelques pays, dont la France, produisent depuis des décennies des ciments contenant du laitier de haut-fourneau, des pouzzolanes, ou des cendres volantes de centrales thermiques et l'emploi de ces ajouts, dans des proportions définies par les normes, permet à la fois d'obtenir des produits dont les qualités spécifiques les rendent souvent préférables aux ciments purs tout en réalisant des économies appréciables d'énergie. L'expérience ainsi acquise a conduit d'autres pays à étudier la possibilité d'avoir recours aux types d'ajouts dont ils peuvent disposer, dans des conditions économiques acceptables. Une extension de cette utilisation se manifeste et il est permis de penser que cette tendance se développera dans un très proche avenir.

Enfin, un grand effort a été amorcé pour diminuer la consommation de produits pétroliers en substituant le charbon au fuel-oil lourd. Cette recouversion au charbon est particulièrement indiquée en cimenterie, notre industrie ayant la rare faculté de pouvoir utiliser des charbons de qualité secondaire à forte teneur en cendres, sans que cette utilisation pose, dans le domaine de la chimie des ciments, de problèmes autres que ceux de la composition du cru, qui peuvent être résolus sans grandes difficultés.

o
o o

Cette obligation devant laquelle l'industrie cimentière s'est trouvée de consacrer une attention particulière aux problèmes de l'énergie ne l'a pas empêchée de se préoccuper parallèlement, au cours des six dernières années, de l'amélioration de la qualité de ses produits : les résistances mécaniques exigées par les ouvrages modernes, en béton précontraint notamment, les résistances chimiques aux ambiances agressives dues à l'eau de mer ou à certaines pollutions, ont fait l'objet d'études approfondies.

Ce 7ème Congrès va montrer que d'importants progrès ont été réalisés dans le domaine de l'utilisation des constituants secondaires, ainsi que dans celui de la qualité depuis le Congrès de Moscou. Il montrera également que les chercheurs, face à la rapidité de l'évolution des conditions économiques, se sont attachés à dégager les conclusions les plus utiles aux applications technologiques et à réduire ainsi le temps de réponse de la recherche que nous connaissions jusqu'alors.

Dix-neuf rapports principaux, près de trois cents communications individuelles, les exposés et les conclusions de quatre séminaires spécialisés ont fait ou feront l'objet de publications qui constituent incontestablement les meilleures références des connaissances actuelles en matière de recherche sur nos produits.

Nous présenterons dans un instant, sous la forme d'un diaporama et d'un divertissement un bref rappel de l'histoire du ciment et de la construction. Les Congrès de la Chimie des Ciments s'inscrivent dans cette histoire. Et le Septième du nom qui s'ouvre aujourd'hui montrera que notre industrie, bien que traditionnelle par ses origines, est capable d'une adaptation rapide et efficace aux situations nouvelles.

Je vais passer maintenant la parole à M. Raymond Peltier, Ingénieur Général des Ponts et Chaussées, Secrétaire Général du Congrès, qui vous donnera des informations précises sur le déroulement de cette manifestation qu'il a eu la lourde charge d'organiser avec le concours du CERILH.

Mais auparavant, et en terminant, laissez-moi vous exprimer tous les voeux que je forme pour le plein succès de vos travaux, me réjouir des échanges de vues bénéfiques qu'ils vont permettre de réaliser et vous faire part de ma conviction que ce septième Congrès International de la Chimie des Ciments constituera une date importante pour une meilleure connaissance scientifique des produits que nous fabriquons, cette connaissance étant la condition nécessaire du progrès économique ainsi que du développement de l'industrie cimentière mondiale.

Séance inaugurale - 30 Juin 1980

DISCOURS DE M. A. GIRAUD

Ministre de l'Industrie

Monsieur le Président, Mesdames, Messieurs,

Permettez-moi tout d'abord de dire combien je suis heureux de me trouver parmi vous et de souhaiter la bienvenue aux nombreux congressistes étrangers, issus d'une cinquantaine de pays, que nous accueillons aujourd'hui pour le 7ème Congrès International de la Chimie des Ciments.

Par une sorte de coïncidence, vos congrès se tiennent dans des années portant des millésimes qui retiennent l'attention : 1968, 1974, 1980. La conjonction de ces réunions avec des évènements où sont posées, de façon plus aiguë, des questions économiques et des questions de société qui engagent l'avenir des nations, semble faite pour illustrer que les scientifiques sont pris désormais, eux aussi, dans les urgences, que de leurs trouvailles dépend la solution de problèmes majeurs, et que leurs recherches répondent à des attentes intenses, même si elles sont quelquefois confuses.

Cela est vrai, permettez-moi de le souligner, tout autant dans des industries de base que dans des industries de pointe. Les progrès éblouissants de l'électronique ou de la biologie, qui profitent d'ailleurs aussi aux industries de matériaux de construction, pourraient par instants faire perdre de vue qu'il reste un grand nombre de besoins fondamentaux et simples, exigeants en énergie et incompressibles. Ces consommations fondamentales ne méritent pas moins d'attention que les autres; elles aussi déterminent les formes de notre civilisation et participent à nos réussites comme à nos échecs. Elles sont en outre, pour les pays moins pourvus, parmi celles dont la satisfaction est la plus pressante.

Les Thèmes du Congrès :

Les thèmes que vous avez retenus pour le Congrès sont d'une grande diversité; ils se regroupent cependant autour de deux préoccupations centrales qui montrent bien la continuité de la volonté d'adaptation de ces industries :

- Comment obtenir une meilleure qualité des ciments, c'est à dire obtenir des ciments plus résistants, plus réguliers, donc plus sûrs, mais aussi mieux adaptés à leur emploi,
- Comment économiser au maximum l'énergie nécessaire à leur fabrication.

A - La qualité :

Sur le premier point, nous constatons l'importance du progrès technologique et l'interdépendance des différentes branches d'un système technique; ainsi, par exemple, grâce à la puissance des moyens d'investigation modernes, dont le pouvoir séparateur en particulier s'améliore toujours et avoisine maintenant quelquefois la dizaine d'angströms, la connaissance et la maîtrise de la structure des matériaux complexes que sont les ciments peut progresser comme progresse aussi celle des mécanismes de formation de leurs produits d'hydratation dans des ambiances agressives.

Le fabricant pourra ainsi mener sa fabrication de façon à obtenir les meilleures caractéristiques de son produit pour un usage déterminé.

De même, au stade de la fabrication du béton, la liaison granulats-pâte de ciment a fait l'objet de recherches particulières, qui ont conduit à la constatation que les cristaux qui se forment au contact des granulats sont différents de ceux qui se forment dans la pâte de ciment. Une meilleure connaissance de cette zone intermédiaire devrait permettre d'en renforcer la liaison granulat-ciment.

Prolongeant la recherche afin de mieux maîtriser les éléments qui déterminent les qualités du ciment, on trouve l'effort d'optimisation de la gestion de la qualité. C'est naturellement le reôle des normes. Les nouvelles normes françaises de ciment, entrées

en vigueur en 1979, garantissent à l'utilisateur des produits mieux définis, plus réguliers et mieux contrôlés. Elles se définissent essentiellement par référence aux performances, c'est à dire à ce qui est le plus directement utile à la mise en oeuvre du produit, plutôt que par référence à la composition, laquelle est laissée plutôt à la disposition du fabricant pour obtenir les performances prescrites.

Cet effort de modernisation des normes ne se limite pas à la France, mais s'insère dans un mouvement plus vaste, à l'échelon européen.

B - Les économies d'énergie.

Le deuxième thème que vous abordez de façon préférentielle est d'une importance manifestement cruciale. La crise énergétique a frappé de plein fouet l'industrie cimentière, grosse consommatrice.
J'ai déjà abordé ce thème par le biais des normes; en effet, la transformation des normes a permis des économies d'énergie considérables, grâce à l'adjonction de produits secondaires. C'est un champ où la recherche française est bien avancée; où chaque point d'ajout de ces constituants secondaires permet une économie de combustible de l'ordre de 1 %. En général il est possible d'aller jusqu'à 30 % de produits secondaires, et pour certains usages même davantage. L'adjonction de produits secondaires au clinker peut permettre de régler des problèmes d'utilisation de sous-produits industriels; plusieurs pays ont pris, de longue date, l'habitude d'utiliser le laitier de haut-fourneau; l'usage des cendres volantes de centrales thermiques,moins ancien, tend à se répandre.

A côté de cette évolution récente et fortement liée à la recherche, citons parmi les choix qui, sur le plan industriel, contribuent à réduire la consommation énergétique, le fait que le procédé de fabrication par voie sèche tend, partout où cela est possible, à remplacer les anciens procédés par voie humide.

En France, dans l'ensemble, les efforts réalisés permettent d'économiser déjà presque 400.000 tonnes de fuel annuelles. Et le Gouvernement français, pour sa part, a tenu à encourager l'industrie dans ce sens par des aides financières.

Enfin, l'industrie du ciment s'oriente vers des sources d'énergie bon marché : bitumes lourds et produits pétroliers difficilement valorisables, et plus encore: charbon.

Si vous me permettez de citer encore le cas de la France, l'industrie cimentière y est une des premières, sinon la seule à être déjà bien engagée dans cette voie, et elle peut espérer que ce combustible représentera 75 % de sa consommation d'énergie en 1985.
Si le recours au charbon ne pose pas aux fabricants de ciment de problème majeur, il impose un effort d'organisation des approvisionnements, qui n'est d'ailleurs que la première étape d'un retour général au charbon dans l'industrie. Il me plait de souligner que l'industrie cimentière y fait oeuvre de progrès.

D'autres voies encore pourront conduire sans doute à des économies d'énergie : ainsi par exemple l'amélioration des échanges de chaleur dans les fours, la réduction et la récupération des pertes thermiques, la fabrication de clinker à plus faible température, et la réduction de la consommation d'énergie au niveau du broyage.

Je parlais, en commençant, des dates significatives de vos congrès ... On pourrait presque tracer un parallèle entre ces dates et les thèmes choisis :
1968 est une année où est devenue visible à tous l'émergence de la revendication de la qualité de la vie, qui commence par la qualité des produits et la limitation des nuisances. Ces préoccupations ne nous ont plus quittés, et les progrès accomplis ont été considérables.

1974 est pour chacun l'année où le monde a commencé à prendre conscience de la nécessité de réaliser une croissance plus sobre en énergie, et de trouver des alternatives au pétrole. Ici encore, ces préoccupations nous sont demeurées, et à vous aussi dans la profession cimentière elles sont restées un grand souci.
Mais quel sera le thème qui poindra en 1980 ? Je ne me hasarderai pas à en formuler un sur le plan général, mais je prends le risque d'en proposer un pour les cimenteries. Si nous réfléchissons bien, et si nous nous demandons où se trouve l'avenir du ciment, il apparaît que ce n'est pas principalement dans les pays industrialisés avancés. Même si, aujourd'hui en France, quelques mesures sont prises pour soutenir la conjoncture dans le bâtiment, il est clair que ni en France, ni dans l'ensemble du monde industrialisé, ne se trouvera rien de comparable aux immenses besoins

des pays en voie de développement et à démographie à croissance rapide.
Que peut-on envisager afin de faciliter la satisfaction de ces besoins ? Je suis persuadé qu'une orientation d'une partie des recherches vers le développement de technologies spécifiques, qui tiennent compte des gisements, des conditions industrielles, de la nécessité de disposer d'unités de production plus petites et plus dispersées dans certains cas, bref de l'ensemble des différentes caractéristiques rencontrées dans les pays en voie de développement pourrait être un facteur important pour permettre à ces pays de se donner rapidement les infrastructures et le parc immobilier qui leur sont nécessaires.

L'importance de ces différents thèmes n'échappera à personne; aussi conclurai-je, si vous me le permettez, Mesdames et Messieurs, en souhaitant aux congressistes - j'espère que ce n'est pas contradictoire - à la fois un agréable séjour dans notre capitale et des discussions et des réflexions qui seront fertiles, j'en suis sûr, pour l'ensemble de l'humanité.

Séance de clôture - 4 Juillet 1980

CONCLUSIONS DU CONGRES PAR M. F. LE BEL

Président du Comité Scientifique du Congrès

Après ces journées passionnantes (le qualificatif n'est pas trop fort), des devoirs m'attendent : l'un est facile et agréable : vous remercier toutes et tous; l'autre, plus difficile et probablement très incomplet ; établir un bilan; bilan qui, heureusement, ne peut être encore que très provisoire.

Si la raison majeure du succès de ces journées a été votre présence vivante, leurs fruits sont l'apport extraordinaire que vous avez fait à l'industrie cimentière mondiale par les textes mis à sa disposition. Ils sont très nombreux : l'ensemble des rapports principaux, l'ensemble des communications, et enfin celui des rapports généraux et les conclusions des tables rondes, ainsi que vos interventions dans les discussions concernant les thèmes de ce Congrès.

Sa préparation matérielle a été élaborée avec beaucoup de minutie, par un Secrétariat Général intelligent et actif, animé par mon ami Raymond PELTIER, Ingénieur Général des Ponts et Chaussées, que je tiens à remercier tout spécialement, sans oublier Mme J. CARDEY, sa fidèle collaboratrice, pour son rôle obscur, mais déterminant. L'aide efficace et bienveillante de notre Syndicat National des Fabricants de Ciments et de Chaux doit être mise en vedette, car sans elle rien n'était possible. Je tiens donc à remercier tout particulièrement son Président, M. Raymond POITRAT, et son Délégué Général, M. Gilbert DENOIX, auprès desquels nous avons toujours trouvé un patronage efficace, une grande compréhension, et enfin des fonds qui, hélas, sont toujours délicats à trouver.

La préparation intellectuelle de ce Congrès doit être également évoquée, car elle fut originale quant à sa conception et efficace quant à ses résultats.

Originale, car elle a été conçue et organisée par un groupe de travail international qui, bénévolement, avec passion et sérieux, a choisi les thèmes, les a précisés, faisant appel, pour en parler, aux sommités internationales les plus compétentes que vous avez pu entendre pendant ce Congrès.
Je tiens donc à remercier devant vous tous les membres de ce Comité Scientifique International pour leur collaboration amicale et efficace durant plus de deux ans à la préparation intellectuelle du Congrès.

Je me plais à souligner également l'assistance scientifique de haut niveau que nous ont apportée les Universités françaises, les chercheurs du C.E.R.I.L.H. et ceux des Sociétés cimentières et des Services Officiels français.

Un bilan intellectuel.

L'amélioration de nos connaissances sur les clinkers industriels ou de laboratoires et sur leurs composants est indispensable, car l'évolution des technologies de fabrication est permanente avec ses retombées sur les spécificités des produits fabriqués même si les matières premières, c'est à dire les entrées du système, ne changent pas. Par exemple, au cours des dix dernières années, chauffe avec un mazout riche en soufre, four avec échangeurs verticaux à cyclônes, dé-

poussiérage rigoureux des fours, recyclage des poussières, sont des raisons suffisantes pour concentrer des éléments mineurs tant et si bien que la composition potentielle des clinkers correspondants s'en est trouvée modifiée; ceci pour le plus grand bien de certains utilisateurs (des sulfates alcalins, donc des ciments rapides), pour le plus grand dommage de certains autres (concentration par recyclage du thallium.

Ce qui prouve d'ailleurs que le contrôle minutieux de ce que l'on produit ne doit échapper ni aux producteurs, ni aux consommateurs; ce mot "contrôle", pris au sens anglo-saxon du terme, implique donc recherches et laboratoires, car il vaut mieux prévoir que subir. C'est là une partie des missions pratiques de nos congrès, qui doivent chercher les messages issus de la recherche, susceptibles d'être appliquées dans l'industrie à délai aussi bref que possible.

Aussi comment établir un bilan de ce Congrès? C'est l'affaire de tous les congressistes, car je pense que chacun y a trouvé de quoi rassasier provisoirement sa faim de savoir et exciter son désir d'en savoir plus.

Je rappellerai ici que les recommandations faites à l'intention des rédacteurs de communications précisaient que les travaux présentés à notre Congrès devaient :

1. autant que possible concerner des produits industriels, sans exclure toutefois les préparations en laboratoire;

2. être orientés dans des directions favorables aux économies d'énergie.

Nous pensons que ces recommandations ont été bien perçues, car les retombées pratiques de ce Congrès sont nombreuses et nous montrent que la recherche de base, orientée, peut déboucher sur le marché plus rapidement qu'on pouvait le penser. Cela est un encouragement solide pour les chercheurs, car, dans bien des cas, leur efficacité est liée aux dialogues fructueux qu'ils peuvent nouer avec les exploitants et les utilisateurs.

Le nombre des communications écrites a été élevé : 290 pour le congrès, 130 pour les séminaires, plus 155 posters.

Le nombre des participants aussi, si on le compare aux congrès précédents :
Tokyo : 572 - Moscou : 708 - et Paris : 880

Les rapports principaux : 19
Les rapports généraux : 7

Toute cette nourriture intellectuelle est dense et diversifiée; l'assimiler complètement demandera une longue réflexion, donc du temps, c'est à dire une période dormante, à l'issue de laquelle les fruits essentiels de ce Congrès cristalliseront; bilan et vues sur l'avenir suivront.

Quelques faits saillants m'ont particulièrement frappé : c'est un peu de la pêche à la ligne que je fais ici; ce ne sera donc pas un examen complet. Vous m'en excuserez sans doute, et les poissons seront présentés trop en vrac peut-être, d'autant que je suis avant tout industriel et ingénieur, tenté par la science certes, car son pouvoir d'attraction est devenu irrésistible du jour où les chercheurs sont devenus des pédagogues.

Le sujet du Thème 1 est une innovation dans un tel Congrès, qui s'intéressait jadis plus aux structures et propriétés des clinkers qu'à la philosophie de leur genèse.

Or l'évolution des moyens de production, pour obtenir des produits réguliers, nous a conduits à étudier les corrélations multiples qui existent entre matières premières et produits finis, et, de ce fait, à prédéterminer avec une grande précision les conditions requises pour fabriquer, de façon très régulière, des produits spécifiques déterminés : choix des matières premières et leur traitement, c'est à dire choix optimal des procédés.

Les recherches sur ces corrélations ont alors une portée scientifique et industrielle qui dépasse le stade de la curiosité scientifique.

Les notions de réactivité des minéraux naturels ou artificiels se sont précisées dans les esprits du fait de l'invention et de la mise au point de nouveaux équipements de laboratoire; ils permettent de juger des structures moléculaires, des structures cristallines, et, ainsi, de définir des critères de choix, dont les retombées dans l'art de l'ingenierie cimentière sont très importantes.
Si le séminaire sur les économies d'énergie nous a permis de mieux connaître ce qui se passe dans le domaine des technologies actuelles de fabrication, des idées intéressantes sur leurs prolongements ont été proposées.

D'un point de vue plus fondamental, en se basant sur des théories de la migration ionique en milieu fondu, deux résultats importants ont retenu notre attention :

- la fabrication du silicate tricalcique chloré avec inclusion d'aluminium et de magnésium (bain fondu de $CaCl_2$ à 1000/1100°) minéral plus réactif que le silicate tricalcique bien connu;
- la fabrication du β C_2S sulfaté dans un bain fondu me semble très importante et ouvre peut-être de nouvelles voies pour l'utilisation rationnelle des énergies dégradées.

Dans les séances concernant les thèmes 2, 3, 4, un accord presque général est apparu sur les phénomènes de prise; en particulier, celui de la mise en solution de la silice et de sa migration dans le milieu aqueux, expliquant que la formation du silicate monocalcique hydraté CSH ne se forme pas seulement de façon topochimique, mais aussi dans le bain grâce à cette diffusion ionique.

C'est un fait très important, et les hypothèses présentées pour analyser ce phénomène de prise et l'expliquer sont beaucoup plus homogènes que dans le passé.

Une foule de résultats ont été exposés sur la qualité des ciments, en fonction de leurs dosages en clinker, en laitier et en pouzzolanes. Les structures propres de ces éléments se précisent chaque jour davantage, ainsi que leurs réactivités. Aussi les mélanges de ces éléments broyés ensemble ou séparément, à des dosages différents, donnent ils toute une palette de produits hydrauliques dont les thèmes 5 et 6 ont mis en valeur les propriétés, grâce à un arsenal de méthodes d'essais très diverses; ces méthodes d'essais intéressent plus particulièrement les phénomènes de rhéologie des pâtes de ciment, leur mode de durcissement, l'évolution de la porosité au cours de la formation du squelette, les raisons des résistances et le rôle fondamental joué par l'eau liée.

L'étude de la porosité en particulier nous a montré que granulométrie des pores structuraux et granulométrie des pores capillaires ont une incidence fondamentale sur les résistances à la traction des pâtes durcies et sur leur résistance aux eaux agressives.

Je me permettrai de citer à cet égard l'intérêt des études sur les ciments de laitier, qui nous ont montré que, dans les pâtes durcies, la répartition granulométrique des pores capillaires est plus régulière que dans celle des ciments Portland purs, et que c'est probablement une des explications de leurs meilleures résistances à la traction et résistances aux eaux agressives.

Le thème 7 est venu clôturer ce Congrès; et là aussi, ce thème 7 est un peu une nouveauté comme le thème 1, car nous avons pensé que si les pâtes de ciment sont intéressantes à étudier, leur rôle dans les bétons l'est aussi; le ciment est principalement fait pour le béton, et de son bon emploi dépend grandement la qualité de la construction.

Nous mentionnerons en particulier les très intéressantes études présentées sur les liaisons pâtes-agrégats, sur les migrations ioniques dans la pâte pendant la prise, sur la qualité de la structure de contact et la découverte des échanges d'ions entre pâte et agrégat; tout cela est prometteur et demande réflexion néanmoins, car grande résistance et fragilité sont souvent corrélatives; or si le béton, matériau composite par excellence, doit résister à de nombreuses sollicitations sans faillir, il doit aussi avoir une certaine aptitude à la déformation.
J'ai eu le plaisir de constater que l'ensemble des rapports rédigés à l'occasion de ce Congrès forme vraiment une chaîne continue, du thème I au thème 7, dont les retombées pratiques sont, comme nous venons de le voir, très importantes; des lacunes restent à combler, bien entendu; heureusement elles seront en partie les raisons d'être du prochain Congrès auquel nous souhaitons déjà bonne chance.

Conclusion :
Je vous l'ai dit; tout cela n'est qu'un survol très rapide et peut-être peu significatif. La matière est en effet très dense; il nous faut donc digérer ce qui a été écrit ou dit. Pour essayer de faire une bonne synthèse des apports de ce Congrès, si ce n'est pas abuser de la gentillesse de nos Présidents de thèmes, je leur demanderai de résumer en quelques pages, pour la fin de l'année, le bilan de leur intervention et de celles de leurs collaborateurs, que je remercie tous bien vivement pour la qualité très exceptionnelle de leurs prestations. Elles rejoignaient, bien que quelquefois apparemment lointaines, nos préoccupations communes au service des pâtes de ciment, des mortiers et des bétons, qui peuvent être résumées en une phrase d'un de nos amis bien connu :
"Il est important de prendre en considération le fait que la morphologie, la porosité, la densité et la composition chimique sont des facteurs interdépendants, qui déterminent les caractéristiques des résistances."

o
o o

Avant de terminer, j'aimerais aborder rapidement avec vous quelques données sur l'avenir de l'Industrie Cimentière, dont les retombées sur les programmes de recherche ne sont pas négligeables, loin de là.
Par quelques exemples, on peut imaginer l'échelle des économies d'énergie et des investissements que représente une politique raisonnable des ajouts.
Les prévisions des Nations Unies nous disent que de 1980 à l'An 2000, c'est à dire en 20 ans, la production cimentière dans le monde va croître de 850 MT (195 kg par habitant) à 1 500 MT (238 kg par habitant), c'est à dire s'accroître de 650 MT.
Taux de croissance : 2,88 % par an; c'est à dire que le nombre des usines nécessaires à assurer ce surcroît de production exigé par le marché en 2000 pourrait être de 650 usines de 1 MT/an, ce qui correspond donc à la création annuelle de 33 usines de 1 MT/an.

Chaque année, de 1980 à 2000, ces cimenteries s'implanteront dans des pays les plus divers dans tous les domaines, dont les stades de développement sont différents; il s'agira donc d'usines adaptées à chaque marché et à chaque conteste (dont le contexte géologique), à la cadence figurative de mise en route suivante :

1 usine de 1 MT/an tous les 10 jours
et cela pendant 20 ans.

Estimation du montant annuel de l'investissement pour 1 T de production annuelle de CPA :
1 000 F :
1 000 x 33 M = 33 milliards de francs

Consommation supplémentaire annuelle de fuel correspondante :
33 x 100.000 T. = 3,3 MT de fuel.

Réaliser ce programme pose des cas de conscience graves; il ne s'agit pas de construire des usines en série, car celles-ci sont dans la généralité des cas mal adaptées aux

contextes locaux; hélas, nous constatons qu'il en est souvent ainsi. Pourquoi ?

L'expérience prouve qu'en général le problème est mal posé, ou insuffisamment précisé; en particulier, les études préalables ne sont pas poussées aussi loin que l'ont recommandé nos amis du thème I. Par ailleurs, les leçons apportées par les thèmes II, III et IV devraient ouvrir les yeux des responsables sur les économies d'investissement et d'énergie, réalisables par une bonne connaissance des ressources géologiques de leurs pays.
L'expérience prouve que la nature a été généreuse et qu'aucun pays n'est dépourvu de cette manne. Un énorme effort de formation universitaire appliquée doit être donc entrepris. Voilà un programme passionnant pour les chercheurs qui doivent devenir bons pédagogues, et le sont en fait, comme nous l'avons vu ces jours-ci.

Nous venons de parler du programme de construction de 33 usines de 1 MT/an de ciment Portland
L'expérience prouve que, dans bien des cas, même avec des ajouts peu réactifs, un bon clinker peut supporter 30 % d'ajouts réguliers, et ce d'autant qu'ils sont broyés séparément à une granulométrie appropriée.
Il en résulterait une économie annuelle d'investissement de 10 usines de fabrication de clinker, donc de 10 millions de tonnes de clinker. Soit, en se basant sur un coût de construction de 600 frs par tonne de clinker fabriquée annuellement, pour un coût de 1000 frs par tonne de ciment CPA produite, une économie annuelle de :

600 x 10 M. = 6 milliards de francs

L'économie annuelle supplémentaire de fuel serait de 0,1 x 10 M = 1 million de tonnes de fuel ou d'équivalent fuel.
Il est intéressant de constater qu'au prix de 1000 frs la tonne de blé, cela correspondrait au prix de 6 millions de tonnes de blé, ce qui permettrait de nourrir, en pain, l'excédent annuel de la population du monde.

Une autre constatation : en l'An 2000, la production mondiale de ciment sera très probablement de 1.500 MT; ajoutons à ce tonnage (en supposant que les clinkers seront de bonne qualité et le broyage bien contrôlé) 5 % d'ajouts, réactifs ou non, broyés très finement; les ciments correspondants ne se porteront pas plus mal, et souvent mieux; cela est certain pour les CPA.

Ce tonnage d'ajouts sera de 75 MT. Il permettrait donc d'arrêter pendant deux ans les investissements-lignes de production de clinker :

Economies 600 x 75 MT = 45 milliards de frs

Economies de fuel :

75 x 100.000 = 7,5 MT d'équivalent fuel.

Ne trouvez-vous pas que cela en vaut la peine ?

Une autre constatation :
En l'An 2000, la quantité de carbone envoyée dans l'atmosphère sous forme de CO_2 sera (en désignant le clinker par K)

300 kg CO_2 par tonne de clinker

100 kg de C par T de K(part de CO_3Ca)
70 kg de C par T de K(part de fuel)
---
170 kg de C par T de K, c'est à dire 0,17 T

1.500 MT ciment ~ 1.000 MT de K → 0,17Tx1000 M = 170 MT de C par an

Cette estimation peut donner des idées, nous le verrons plus tard.

Je serais heureux que nations, investisseurs et bureaux d'engineering soient conscients de ces gains possibles. L'adaptation des technologies aux conditions locales devient une nécessité certes, mais encore faut-il bien connaître les buts poursuivis dans l'u-

tilisation des produits hydrauliques. Une connaissance de plus en plus approfondie de leurs comportements est donc une autre nécessité et, dans ce sens, nos Congrès et ceux qui suivront ont rempli et rempliront leurs missions.

Pour conclure, je m'aventurerai dans un domaine un peu plus prospectif et qui tient peut-être du rêve sait on jamais ?
Les combustibles fossiles sont la propriété d'un certain nombre de nations, mais d'autres nations en sont complètement dépourvues, ou le seront avant la fin du siècle. Cela pose, pour ces dernières, un déséquilibre dans leur balance des paiements, soluble quelquefois au prix de lourds sacrifices; s'ils deviennent insupportables, il leur faudra trouver d'autres solutions.

Si nous examinons dès maintenant, en France par exemple, les prix de l'énergie électrique, nous arrivons aux résultats suivants, rapportés au kwh produit en usine :

Origine	Nucléaire	Fuel	Charbon
Investissement	6,70	4,44	5,16
Exploitation	2,55	2,52	2,85
Combustible	4,27	26,56	14,28
Total partiel	13,52	33,52	22,29
Majoration pour désulfuration		2,80	2,50
Total	13,52	36,32	24,79

c'est à dire qu'à court terme :
le kwh-fuel coûtera 3 fois plus cher que le kwh nucléaire,

le kwh-charbon coûtera 2 fois plus cher que le kwh nucléaire.

Nous savons déjà que les réserves de la France en énergies fossiles seront rapidement négligeables, et que d'autre part nos réserves en uranium naturel sont évaluées à 100.000 T , c'est à dire l'équivalent en énergie électrique des réserves de pétrole de la mer du Nord; mais utilisées dans les surgénérateurs, elles représentent trois fois les réserves de l'Arabie Saoudite; elles représentent donc un atout énergétique puissant, qu'il serait peut-être temps de tester dans le cadre de notre industrie (en l'An 2000, 50 % de l'énergie électrique sera d'origine hydraulique et nucléaire).

Pour le broyage des ajouts, pas de problème, bien entendu, mais dans celui des clinkers c'est une autre histoire. Quelles voies choisir ?

1. La fusion dans le four électrique ?
   Des essais ont permis de réaliser des clinkers fondus très réactifs, après trempe très énergique (les cristaux de C_3S sont très petits).
   Mais le bilan est mauvais du fait de la mauvaise récupération de la chaleur sensible des clinkers.
   Le frittage serait-il possible par cette voie ? Pourquoi pas.

2. Chauffe avec l'hydrogène (fournie par l'électrolyse ou décomposition catalytique de l'eau dans les piles atomiques)
   Combustion de cet hydrogène dans l'air ou dans l'oxygène ?
   Evidemment, la mise au point d'une telle combustion de l'hydrogène pose des problèmes, mais ils ne sont pas insolubles.
   Nous y reviendrons in fine.

3. Fabrication du $C_2S\beta$ à 700°, en utilisant de l'énergie dégradée disponible; par exemple, la combustion hydrogène oxygène, qui permettrait de fabriquer le C_3S et l'énergie dégradée pourrait être utilisée pour ce $C_2S\beta$ dont on nous a montré que la réactivité est assez voisine du C_3S à condition d'en fabriquer dans certaines conditions.

4. Activation des produits d'addition par broyage séparé.
   On pourrait multiplier les exemples; ils sont faciles à trouver. Mais les études correspondant à ces souhaits demanderont des efforts financiers importants et de la réflexion. Cela en vaut la peine,

d'autant que du rêve à la réalité le chemin est court quelquefois.

Enfin, l'utilisation de l'hydrogène comme carburant pose des problèmes; on en parle suffisamment dans la presse pour que je ne revienne pas sur le sujet.

Mais il est un produit qui pourrait être intéressant : c'est le gaz carbonique pur, CO_2pur, porteur éventuel d'hydrogène, pour lequel MOBIL a pris récemment un brevet.
En présence d'un catalyseur adéquat, on peut passer du CO_2 au méthanol ou plus directement aux carbures d'hydrogène, qui, par polymérisation, peuvent redonner des produits voisins de l'essence du commerce.

Le problème est donc d'obtenir du CO_2 pur.

L'industrie cimentière en serait elle capable ? Pourquoi pas ? Si les matières premières sont, d'une part du calcaire pur, d'autre part de la silice pure; tout cela broyé finement bien entendu.

La fabrication de C_3S ou de C_2S β dégage, si la combustion hydrogène-oxygène est bien réglée, uniquement du CO_2.

Les cimentiers seraient donc capables, dans des conditions à préciser, de fabriquer un CO_2pur, donnant ainsi une nouvelle voie de fabrication d'un combustible utilisable dans les futures automobiles.

Tout cela n'est qu'un schéma, mais pourquoi pas ? Le carbone est encore abondant sur notre glpbe, mais pas pour tous les pays, et, à terme, à quel prix. Et quelles autres conditions pour ceux qui n'en ont pas ?
Alors pourquoi ne pas réfléchir à cette voie?

Je m'arrête donc là; peut-être parmi vous existe-t-il le chercheur qui nous dira si cette voie est fiable, mais surtout économique. Merci.

Séance de clôture - 4 Juillet 1980

ALLOCUTION DE M. R. POITRAT

Président du Syndicat National des Fabricants de Ciments et de Chaux
Président du 7e Congrès International de la Chimie des Ciments

M. LE BEL vient de nous donner des chiffres qui situent bien la place occupée par l'industrie cimentière à l'échelon mondial.

Personnellement je ne vous en donnerai qu'un. J'ai essayé de prévoir à quelle époque la production cimentière mondiale atteindrait le milliard de tonnes. Eh bien, très vraisemblablement, ce chiffre sera atteint en 1986, date de notre prochain Congrès. Une image vous permettra de vous représenter ce qu'est un milliard de tonnes de ciment. Si nous les chargions sur des bateaux de 100.000 tonnes et que nous mettions ces bateaux les uns derrière les autres, le convoi ainsi formé s'étendrait sur deux mille kilomètres.

De toutes les industries lourdes, l'industrie cimentière est sans conteste la plus développée sur notre planète. Le calcaire et l'argile se rencontrent pratiquement partout et il est peu de pays qui ne possèdent de cimenteries ou n'aient des projets pour en implanter. C'est dire la nécessité impérieuse de la recherche en ce domaine et, par là, toute l'importance de nos rencontres.

Aussi, en ouvrant Lundi dernier, ce 7ème Congrès International de la Chimie des Ciments, c'est avec beaucoup de conviction que je souhaitais un plein succès à vos travaux, conscient que j'étais de la somme de réflexion et d'expérience dont ils allaient être l'aboutissement.

Après ce que vient de dire M. Le Bel, j'ai la profonde satisfaction de constater que ce souhait a été vraiment exaucé. Non seulement les inscriptions au Congrès ont dépassé nos prévisions, puisque 54 nations ont été ici représentées par près d'un millier de congressistes, mais la fréquentation aux séances a été exceptionnelle aussi bien pour les réunions de travail plénières tenues dans cette salle, que pour les séminaires du premier jour ou les posters qui ont connu toute la semaine une grande affluence.

Par ailleurs, l'exposition a été aussi très fréquentée. Je me suis entretenu avec bon nombre d'exposants et j'ai recueilli chaque fois le même écho, chacun s'estimant satisfait de l'attention que vous avez portée aux matériels exposés.

Sans doute, le soin apporté à la préparation de ce Congrès n'est pas étranger à sa réussite. Le Comité Scientifique International qu'a présidé M. LE BEL a effectué un excellent travail et je suis heureux de le féliciter en votre nom aujourd'hui.

Nous avons tenu à ce que vous receviez avant le Congrès les rapports principaux et vous avons distribué le premier jour deux tomes de communications. Ceci représente, vous vous en doutez, une documentation considérable dont il faudra beaucoup de temps avant d'épuiser la richesse. Vos bagages vont s'en trouver quelque peu alourdis, je le crains, mais vous n'attacherez sûrement qu'une importance mineure à cet inconvénient.

Il a fallu collationner et traduire près de trois cents communications, relancer les retardataires de façon à ce que toutes ces communications soient prêtes en même temps, au moment voulu. Tout cela n'a pas été facile, mais seul le résultat comptait et il est là.

Je suis sûr d'être votre interprète en remerciant M. Raymond Peltier, Secrétaire Général du Congrès, qui n'a ménagé ni son temps, ni sa peine pour mener à bien cette tâche considérable. Il a été secondé avec ardeur dans cet accomplissement par l'équipe du CERILH, tout particulièrement par son Président, M. Charreton, et son Directeur Général, M. Méric, ce dernier cumulant sa participation à la réalisation du Congrès et sa mission de Président de thème. Et personne n'a non plus garde d'oublier, dans tout ceci, le rôle de Mme Cardey qui, depuis deux ans, est la véritable cheville ouvrière de l'organisation de cette semaine de rencontre.

Le rôle des organisateurs n'est d'ailleurs pas terminé. Vous savez que nous avons encore un document à vous faire parvenir; il s'agit des actes les plus importants de cette semaine de travail, et en particulier des rapports généraux et des comptes rendus des séminaires.

Vous allez donc recevoir, dans un délai raisonnable, un quatrième volume, qui viendra ainsi compléter votre documentation. Je ne doute pas que vous ayez ainsi à disposition dans votre bibliothèque une véritable mine de références, dont vous saurez tirer le plus grand profit.

o
o o

Lundi dernier, je vous avais également souhaité, dans mon allocution inaugurale, la bienvenue à Paris, et j'avais exprimé le désir que ce Congrès soit une occasion fructueuse de rencontres et d'échanges de vues.

C'est à vous qu'il appartient de dire si cet objectif a été atteint.

Nous avons fait de notre mieux pour vous donner un aperçu de notre capitale. Il était bien évidemment impossible, en si peu de soirées, de faire davantage; nous avons opté pour le maximum de diversité dans notre choix, en espérant vous donner le désir de revenir à Paris.

Le précédent Congrès a eu lieu à Moscou en 1974, présidé par M. Boldyrev. Il a rencontré le succès que l'on sait et je tiens encore à dire à M. Boldyrev combien tous les participants ont goûté leur séjour dans sa capitale.

Le prochain Congrès aura lieu en 1986 dans un lieu qui vous sera indiqué tout à l'heure par celui-là même qui nous y invitera.

Devant le progrès de vos recherches et le nombre toujours croissant des résultats dans des domaines diversifiés, la question a été posée de savoir si l'intervalle de six années entre nos rencontres n'était pas un peu trop important. En fait, je pense difficile de changer nos traditions à cet égard, compte tenu des délais nécessaires à la préparation d'une telle réunion.

Il faut, en effet, laisser aux chercheurs, aux professeurs et aux savants le temps nécessaire pour mener à bien leurs travaux, et nous avons vu, tout au long de ces journées que dans le domaine du ciment plusieurs mois, et parfois plusieurs années, étaient nécessaires pour tirer des conclusions de certaines expériences. Une suggestion a été faite qui méritera sans doute d'être étudiée et approfondie. Il s'agirait de la création d'un noyau permanent qui se réunirait entre les Congrès, à la fois pour faire le point des dernières découvertes et préparer les prochaines rencontres. Il y a là une idée à creuser.

o
o o

J'arrêterai ici mon propos, mais avant de donner la parole à M. de Assis Basilio qui a une communication importante à vous faire, je voudrais vous remercier tout d'abord en mon nom personnel pour le très grand plaisir que j'ai pris à vous rencontrer au cours de cette semaine, et au nom de l'industrie cimentière française pour être venus si nombreux et vous être montrés si attentifs à ce Congrès.
Si vous emportez le sentiment d'en avoir retiré un enrichissement à la fois sur le plan scientifique, sur le plan culturel, et sur celui de l'amitié, ce sera pour nous la meilleure récompense.

Séance de clôture - 4 Juillet 1980

ALLOCUTION DE M. DE ASSIS BASILIO

Président de l'Association Brésilienne du Ciment Portland

Monsieur le Président,
Mesdames, Messieurs,

M. POITRAT a créé un "suspense" en parlant de notre prochain Congrès - le huitième - sans en indiquer le lieu, mais en passant la parole au délégué du Brésil.
Je dois vous dire que depuis deux ou trois ans, au cours des réunions du Comité Scientifique International du Congrès, nous avons, à plusieurs reprises, évoqué cette question. Et sans que l'on sache très bien comment cela s'est produit, un beau jour le Brésil a été pressenti pour organiser ce huitième Congrès.

L'Industrie cimentière brésilienne et M. le Ministre d'Etat de l'Industrie et du Commerce du Gouvernement brésilien ont donné leur accord. Nous sommes conscients de la grande responsabilité que nous prenons, mais nous nous sentons en mesure de l'assumer. Aussi, je propose à votre Assemblée de choisir le Brésil comme lieu du 8ème Congrès International de la Chimie des Ciments (vifs applaudissements dans toute la salle)

Je vous remercie de votre approbation.
Je vous signale que s'il fait parfois très chaud dans le nord et le centre du Brésil, à cette époque de l'année, qui pour nous correspond à l'hiver, il ne fait pas plus chaud à Rio et à São Paulo qu'à Paris actuellement.
São Paulo est le centre industriel du Brésil; c'est une très grande ville, environ douze millions d'habitants, extrêmement active, mais où se posent malheureusement parfois des problèmes de pollution atmosphérique.
Par contre, Rio dispose de kilomètres de plage et bénéficie d'un air marin très pur et d'un ensoleillement agréable; en outre, il y a à Rio une vie nocturne qui incite à la détente.

L'apport technique des Congrès Internationaux de la Chimie des Ciments est toujours très marquant. Les sessions au cours desquelles sont examinés et discutés les problèmes les plus aigus qui se posent aux cimentiers, aboutissent généralement à des conclusions d'une grande importance pratique, par leurs conséquences sur la technologie des ciments et des bétons. Je citerai par exemple le problème de l'hydratation de l'aluminate tricalcique, sur lequel s'étaient déjà penchés les Congrès précédents, et sur lequel notre présent Congrès a apporté une grande clarté.

Nous espérons que le 8ème Congrès sera dans la ligne de ce 7ème Congrès, et nous apportera de nouveaux progrès. Nous avons demandé à tous ceux qui ont participé à l'organisation, si réussie, de ce 7ème Congrès, en particulier à MM. PELTIER, LE BEL et POITRAT, de nous aider de leurs conseils, dans la préparation du 8ème Congrès.

Nous espérons pouvoir compter sur votre participation à tous, en 1986, au Brésil. Nous espérons aussi voir arriver les jeunes générations de techniciens, qui auront la charge de poursuivre les recherches sur le ciment, ce matériau si largement utilisé, mais qui, malgré tous nos efforts, ne nous a pas encore dévoilé tous ses secrets.

Merci encore à tous; et je vous donne rendez-vous en 1986, au Brésil, pour notre 8ème Congrès.

Séance de clôture - 4 Juillet 1980

ALLOCUTION DE M. A.S. BOLDYREV

Vice-Ministre de l'Industrie des Matériaux de Construction de l'U.R.S.S.

Mesdames, Messieurs,

Je pense que nous avons tous bien fait de tenir ce congrès en France, et à Paris. Le ciment en profitera sûrement.

Le congrès de Paris laissera une trace profonde dans l'esprit des spécialistes et aura une grande importance pour les praticiens. Ce congrès a été plus représentatif que les précédents puisqu'il a attiré les plus grands spécialistes de 55 pays du monde, s'occupant de tous les aspects des problèmes complexes d'obtention de clinkers de ciments Portlands et d'utilisation rationnelle des ciments dans les bétons.

Nous avons entendu des exposés très intéressants, donnant un éclairage nouveau aux questions de la chimie et de la technologie des ciments.

Il est aussi très important que ce congrès se soit fait l'écho de questions vitales, dont dépend le développement à venir de l'industrie cimentière : on y a discuté des possibilités d'économiser l'énergie et d'utiliser des sous-produits et des déchets industriels.

On a examiné avec soin les questions d'utilisation des laitiers, des cendres, des ajouts hydrauliques naturels pour fabriquer des ciments composés, qui jouent un rôle important dans la diminution des dépenses énergétiques. Une grande attention a été portée aux ciments spéciaux. On a abordé sous un jour nouveau les problèmes théoriques, l'hydratation des ciments et les nouvelles méthodes d'intensification du durcissement et d'amélioration des caractéristiques de résistance mécanique par emploi d'adjuvants.

Le système des rapports principaux, des séminaires, des affiches commentées et des communications écrites, ainsi qu'un large échange de vues, ont permis aux participants du congrès de prendre connaissance d'une quantité énorme d'informations.

Je pense que les participants seront d'accord avec moi pour dire que l'organisation de ce congrès a été admirable, que l'hospitalité française s'y est manifestée de façon authentique par le soin dont tous les participants ont été entourés, par l'organisation d'une bonne détente, qui leur a permis de découvrir les curiosités de Paris.

Ce congrès aura eu une grande importance scientifique.

Permettez-moi d'exprimer au nom de tous, les remerciements des participants à MM. POITRAT, LE BEL, MERIC, PELTIER et à tous ceux qui les ont aidés dans l'organisation irréprochable du congrès.

o
o o

Permettez moi de transmettre également au Président du congrès la lettre que l'un des plus vieux spécialistes du monde des ciments, élève et traducteur russe de Henry LE CHATELIER, père de la chimie des ciments, a écrite: je veux parler du Professeur I.F. PONOMAREV, aujourd'hui âgé de 98 ans.

o
o o

Permettez-moi enfin de souhaiter à tous les participants de ce congrès une bonne santé, beaucoup de bonheur, et un travail fructueux pour le développement de la science des ciments et la préparation du prochain congrès.

Je vous remercie.

Lettre de M. I.F. PONOMAREV, Professeur à l'Institut Polytechnique de Novocherkask (URSS) aux participants du 7ème Congrès International de la Chimie des Ciments, à Paris.

"Chers participants au Congrès,

"Recevez mes cordiales salutations et mes "voeux de succès pour les travaux de ce Con-"grès de portée mondiale.

"Ce Congrès a lieu à Paris, où Henry Le Cha-"telier a fait ses travaux de recherche "scientifique et a écrit son remarquable ou-"vrage "La silice et les silicates"*
"Je lui ai toujours été très reconnaissant "de m'avoir autorisé à imprimer la traduc-"tion russe de cet ouvrage et de m'avoir "fait parvenir en plus sa photographie, ain-"si que des corrections et des compléments, "qui n'ont été publiés que dans l'édition "russe.

"Recevez les amicales salutations d'un vieux "spécialiste des silicates".

I.F. PONOMAREV
Professeur

faite à Novocherkask (URSS)
le 25 Juin 1980

* Paru en 1914, chez Hermann, 574 pages.

RAPPORTS GENERAUX

par les

PRESIDENTS DE THEME

THEME I

Influence des matières premières des combustibles et des procédés de fabrication sur la structure et les propriétés des clinkers

par R. BUCCHI et J.-P. MERIC

Quatre rapports principaux (de MM. BUCCHI, SPRUNG, TIMASHEV et MERIC) et près de soixante communications originales de différents Auteurs constituent une mise à jour très complète des connaissances sur les différents sujets de ce thème.

Les principaux sujets traités sont les suivants :

1.- La réactivité des crus.
2.- La physico-chimie de la phase liquide.
3.- L'influence des additions et des composés mineurs sur les réactions de clinkérisation.
4.- La structure du clinker en fonction des paramètres de fabrication.
5.- La mécanique de la fragmentation et son application aux broyeurs industriels.
6.- La broyabilité du clinker et des constituants secondaires.

1.- LA REACTIVITE DES CRUS

Deux grandeurs distinctes rendent compte de la manière dont le cru se transforme en clinker : l'aptitude à la cuisson et la réactivité. Cette transformation est caractérisée par plusieurs paramètres :

- α qui est le degré de combinaison de la chaux dans les composés formés,
- CaO_f qui est le pourcentage de CaO libre,
- t la température,
- θ le temps.

L'aptitude à la cuisson est en général représentée dans un espace à trois dimensions par la fonction reliant α à t et θ ou par la fonction reliant CaO_f à t et θ. De cette représentation on peut déduire les relations entre deux variables, la troisième restant constante. Ces différentes relations permettent de quantifier l'aptitude à la cuisson d'un cru.

La réactivité, par ailleurs, est définie comme la vitesse d'une réaction ou d'un ensemble de réactions à une température donnée. Dans le cas d'un cru de cimenterie, on mesure souvent la réactivité moyenne apparente de la cuisson.

Il se révèle que ni la mesure de l'aptitude à la cuisson ainsi qu'elle vient d'être définie, ni celle de la réactivité moyenne, ne sont adaptées à la caractérisation complète d'un cru. Cette caractérisation complète pourrait sans doute être approchée par l'étude de trois valeurs de réactivité moyenne dans trois intervalles de température :

Δt_1 : 500°C - 1000°C
Δt_2 : 1000°C - 1300°C
Δt_3 : 1300°C - 1450°C

Ces trois intervalles sont suggérés par l'identification des différentes réactions qui précèdent ou accompagnent la clinkérisation.

L'aptitude à la cuisson dépend de la saturation en chaux et de la réactivité des matières. La réactivité des matières, c'est-à-dire la vitesse à laquelle elles se combinent, est fonction de SM, TM, de la dimension des grains, de leur nature minéralogique et de leur état d'activité au moment où elles entrent en combinaison. Ce dernier point est capital pour expliquer la différence de réactivité d'une même matière lorsqu'elle se trouve dans des crus différents. L'explication de ces effets est fondée sur les lois de la diffusion solide, notamment sur les relations entre les coefficients de diffusion solide et l'énergie d'activation de la matière. Cette énergie d'activation dépend elle-même des défauts de structure des solides en présence. D'autres paramètres, notamment ceux de la phase liquide comme la viscosité, la mobilité ionique et la tension superficielle jouent également un rôle essentiel.

U. LUDWIG et S.E. IBRAHIM ont établi une relation entre l'aptitude à la cuisson mesurée en termes de durées nécessaires à différentes températures pour atteindre $CaO_f \leq 2\%$ et certains de ces paramètres (figure 1).

$$B_{c,t} = \left[0{,}04 \sum_{20}^{300} HE + 0{,}043\,(K_{st}\,III^2 - 90^2) - 0{,}114\,SA^2\right] - e^{0{,}0126\,(1360-t)}$$

$r = 0{,}94$

$B_{c,t}$ = Aptitude à la cuisson calculée à t°C.
ΣHE = Somme des influences de "hétérogénéité"
$K_{st}III$ = Kalkstandard sel. SPHON.
SA = Phase liquide sel. DAHL à 1360° C.
t = Température.

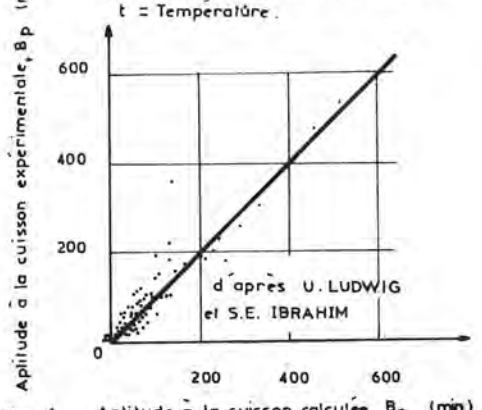

Fig. 1

P. GOMA a établi une fonction qui prend en considération même la présence et la teneur de quelques composés mineurs.

S. CHROMY a mis en évidence l'importance de la granulométrie du calcaire et du quartz pour l'aptitude à la cuisson.

2.- LA PHYSICO-CHIMIE DE LA PHASE LIQUIDE

Le rapport de V.V. TIMASHEV présente une théorie unitaire des propriétés de la phase liquide et de la cinétique de formation de C_3S en s'appuyant sur des connaissances obtenues par les chercheurs russes. Une communication supplémentaire particulièrement remarquable sur la cristallogenèse dans les microzones des grains de clinker est apportée par V.V. TIMASHEV en collaboration avec A.P. OSSOKINE et E.N. POTAPOVA.

Le milieu fondu est l'intermédiaire grâce auquel l'alite peut se former. La température à laquelle la phase liquide se forme, ses propriétés physico-chimiques et la quantité formée déterminent la cinétique de dissolution des grains de CaO et de bélite en fonction de leur dimension et de leur état d'activation, ainsi que la cinétique de diffusion de Ca^{2+}, O^{2-} et $Si_xO_y^{z-}$ vers les zones de naissance et de croissance des cristaux d'alite. Les trois paramètres cités contrôlent donc la micro et la macrostructure du clinker.

Le milieu fondu présente un caractère fortement ionique. Il est composé essentiellement d'ions Ca^{2+} O^{2-} SiO_4^{4-} et de deux groupes MeO_x d'ions amphotères Al et Fe^{3+} : il s'agit d'abord d'ions tétraédriques MeO_4^{5-} où le métal est fortement lié à l'oxygène et présentant un caractère acide et ensuite d'ions octaédriques MeO_6^{9-} présentant un caractère basique, facilement dissociables en Me^{3-} et $6O^{2-}$ et par conséquent plus mobiles que les ions tétraédriques. Les propriétés du bain sont donc différentes selon le déplacement de l'équilibre acide-base

$$MeO_4^{5-} \rightleftharpoons Me^{3+} + 4O^{2-}$$

Ce déplacement est fonction de la nature et de la concentration des ions de composés mineurs. Ces propriétés peuvent être traduites par trois paramètres principaux : la viscosité, les coefficients de diffusion et la tension superficielle.

En principe, la viscosité η diminue lorsque le potentiel ionique Z/a (et l'énergie de liaison Me-O) des éléments dans le bain augmente. Ainsi s'expliquent l'action défavorable de K^{1+} et Na^{1+} et celle favorable de F^{1-}, Cl^{1-}, Ti^{4+}, S^{6+}, P^{5+}, Mg^{2+}.

La présence simultanée d'éléments différents ne permet pas de cumuler les effets lorsque ceux-ci s'exercent dans le même sens, mais elle peut compenser partiellement des effets opposés ; ainsi les sulfates alcalins réduisent la viscosité qui, par ailleurs, augmente brusquement lorsque $[K_2O] + [Na_2O] > [SO_3]$. Il est à noter que Mg^{2+} compense K^{1+} et Na^{1+}. Les effets simultanés des quatre éléments les plus fréquents dans les crus (K^{1+}, Na^{1+}, S^{6+}, Mg^{2+}) sont représentés par les courbes d'isoviscosité de la figure 2.

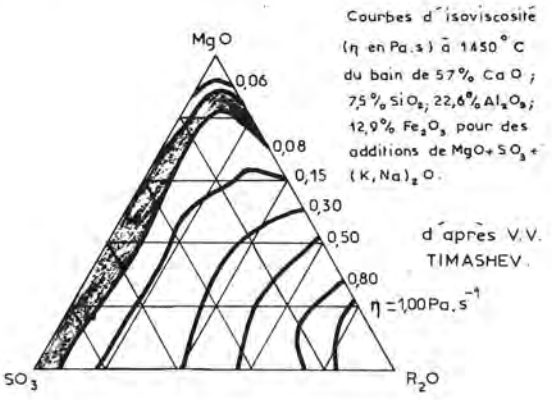

Fig. 2

Les ordres de grandeur des coefficients de diffusion D sont :

Ca : 10^{-9} m²/s

Al, Fe : 10^{-10} m²/s

Si : 10^{-11} m²/s

Les dimensions des lacunes dans le bain de l'ordre de 1.1Å justifient l'hypothèse suivant laquelle Ca^{2+}, Al^{3+}, Fe^{3+} (rayon ionique 1 Å) diffusent par trous, tandis que les ions plus grands SiO_4^{4-}, AlO_4^{5-}, FeO_4^{5-} diffusent plus lentement par déplacement.

Les grandeurs η et D agissent sur la vitesse I de dissolution par diffusion de CaO et de C_2S (figure 3), ainsi que sur la vitesse de formation de C_3S.

On suppose qu'il existe deux mécanismes pour cette formation en raison de l'apparition de phénomènes de liquidation. Dans les zones bélitiques (acides) du bain, ce sont I_{C_2S} et $D_{Ca^{2+}}$ qui contrôlent le processus. En conséquence, les cristaux d'alite croissent sur les cristaux de bélite pour se substituer à eux. Dans les zones les plus basiques (surtout en présence de K^{1+} et Na^{1+}) I_{C_2S} est plus élevé et le processus est contrôlé par I_{CaO} : dans ce cas, la bélite se corrode en se dissolvant dans le bain. L'alite précipite de manière homogène et des vides se forment à la place des grains de chaux.

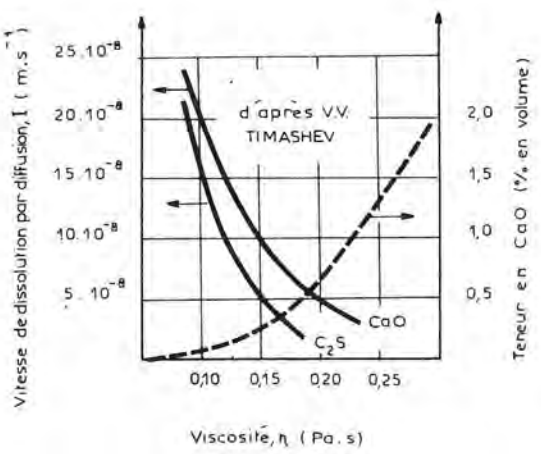

Fig. 3

La cristallisation et l'agglomération des particules, c'est-à-dire la granulation du clinker, sont essentiellement influencées par la quantité de masse fondue, par sa viscosité et par sa tension superficielle σ (B.S. ALBATS et Coll.). V.V. TIMASHEV démontre que la fonction reliant la dimension moyenne des grains de clinker à la tension superficielle est linéaire (figure 4). Cette relation est vérifiée sur les installations industrielles et elle donne un moyen d'action sur la granularité du clinker en faisant varier la quantité et les propriétés de la phase liquide.

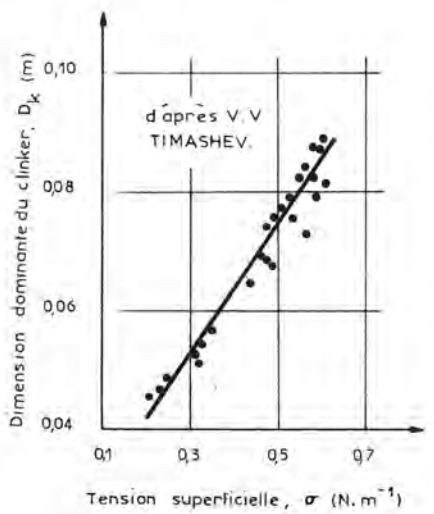

Fig. 4

3.- L'INFLUENCE DES ADDITIONS ET DES COMPOSES MINEURS SUR LES REACTIONS DE CLINKERISATION

R.BUCCHI a examiné onze éléments mineurs dans 141 crus industriels. Les plus fréquents sont, par ordre de concentration : MgO, K_2O, SO_3, Na_2O, TiO_2.

En ce qui concerne les alcalis, on vient de voir que lorsqu'ils sont en excès stoechiométrique par rapport à SO_3, ils dégradent les propriétés de la phase liquide. En outre, ils créent, comme l'a montré SPRUNG, des circulations nuisibles dans le four et des anomalies dans la prise du ciment. Souvent les alcalis semblent donc indésirables.

MgO présente de nombreux aspects positifs qui sont souvent méconnus. En effet, il s'agit d'un minéralisateur et d'un fondant efficace qui peut être admis à des concentrations supérieures à celles qui sont annoncées, à condition cependant qu'il soit finement cristallisé et bien dispersé dans la masse fondue. Ces conditions sont d'autant mieux remplies que le cru est finement broyé et qu'il contient du SO_3 et des fluorures (Y.V. NIKIFOROV et R.A. ZOSOULIA). On retrouve ainsi le rôle bénéfique des sulfates, rôle qui est cependant contesté par les travaux de N.H. CHRISTENSEN et V. JOHANSEN ; W.A. KLEMM et I. JAWED.

Les résultats concernant TiO_2 (D. KNÖFEL, 1977-1979) concluent à un rôle positif.

Le rôle des fluorures déjà connu a été réexaminé. F^{1-} favorise la dissociation de $CaCO_3$ d'une manière plus ou moins marquée selon le cation associé à l'ion F^-(figure 5 S.N. GHOSH). Dans le système C-A-F-S, F^{1-} étend le domaine d'existence du C_3S à des intervalles de composition plus grands. Il élargit le domaine de phase primaire des solutions solides de $C_{12}A_7$, mais il restreint celui du C_3A (A.K. SARKAR et R.M. SMART). Il augmente de 2 à 2,5 fois la vitesse de formation de l'alite par l'intermédiaire d'un accroissement de la phase liquide et des vitesses de diffusion (N.H. CHRISTENSEN et V. JOHANSEN). Plusieurs travaux ont comparé l'efficacité de l'ion SiF_6^{2-} et de l'ion F^-, mais sans conclure de manière indiscutable. L'action de F^{1-} est renforcée par la présence de MgO et de SO_3, surtout du point de vue de la cinétique de clinkérisation, de la structure du clinker et des résistances mécaniques qui sont plus élevées même à des échéances brèves, notamment lorsque TM = 1,5 ainsi que W.A. KLEMM et I. JAWED le montrent.

L'ion Cl^{1-} améliore les propriétés de la phase liquide et comme l'ion F^{1-}, il est un fondant et un minéralisateur efficace. Le chlore présente un certain nombre d'inconvénients qui proviennent du caractère

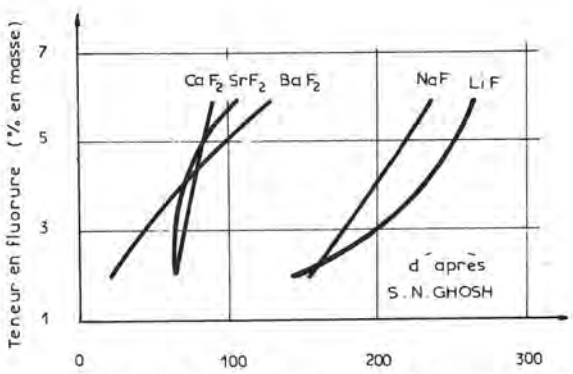

Fig. 5

volatil des chlorures alcalins et du fait que sa concentration dans le clinker atteint des niveaux très faibles (0,01%). Cl^{1-} catalyse la formation de $2C_2S.CaCO_3$ (spurrite) et provoque des croûtages, des collages, des anneaux, soit dans le four, soit dans le préchauffeur. S. SPRUNG fixe à 150 ppm la concentration en chlore dans un cru au-delà de laquelle, si K_2O est supérieur à 2%, il est nécessaire de by-passer les fumées des fours avec préchauffeur à suspension. R. BUCCHI constate, qu'en dessous d'une concentration de 50 ppm, le fonctionnement du four est dans tous les cas régulier pour ce type de four. Le remède à ces inconvénients du chlore, préconisé par H.M. SYLLA (1974), est de bloquer Cl^- en chloro-apatite à l'aide de phosphate, ce qui a été confirmé par M. KOVACS et K. BENYEI. 0,8% de P_2O_5 dans le cru réduit la formation de spurrite, mais son élimination complète ne se fait que vers 1,5%. Cette teneur en P_2O_5 peut être dangereuse pour la qualité du produit, même si V. V'IKOV et Coll. (1967) considèrent qu'elle est tout à fait tolérable dans les clinkers ayant une saturation en chaux basse.

4.- LA STRUCTURE DU CLINKER EN FONCTION DES PARAMETRES DE FABRICATION

Les minéraux du clinker sont des solutions solides hors d'équilibre contenant des impuretés dans les différentes phases. L'activité hydraulique plus ou moins élevée provient essentiellement des défauts et distorsions du réseau provoqués par les substitutions isomorphes, soit homo, soit hétérovalentes, ainsi que par le refroidissement. La structure fine des phases est responsable de la concentration et de la répartition des impuretés qu'elles contiennent : grossièrement, l'alite peut en contenir 4%, la bélite 6%, l'aluminoferrite jusqu'à 10% et l'aluminate jusqu'à 13% (A.I. BOIKOVA).

Dans un rapport très important, P. GOURDIN, E. DEMOULIAN, F. HAWTHORN et C. VERNET ont étudié, par une approche statistique, les relations entre l'alite, le C_3A, les résistances mécaniques, les espèces minéralogiques du cru, les composés mineurs et le procédé de fabrication de 60 clinkers industriels. Ils ont trouvé des formes d'alite très diverses :

M_{Ib} : 47% des cas
M_{IIb} : 35% des cas
R : 18% des cas

Le C_3A est cubique dans 48% des cas et rarement tétragonal (8%) ; dans 43% des cas les deux formes coexistent simultanément.

L'association d'alite R avec du C_3A cubique est fréquente dans les crus quartzeux pauvres en MgO et en alcalis mais présentant un excès de SO_3 sur K_2O. Les résistances de ces clinkers à 7 et à 28 jours sont supérieures à la moyenne.

Les clinkers provenant de crus "illitiques" riches en magnésie et en alcalis non saturés par les sulfates, alcalis qui sont par conséquent disponibles pour entrer dans les réseaux de C_3S et de C_3A, contiennent le plus fréquemment une alite M_{Ib} et un C_3A tétragonal. En outre, si les teneurs en Na_2O sont élevées, on constate également la présence de C_3A cubique. On constate que l'alite R n'est jamais associée avec le C_3A tétragonal.

Les clinkers contenant de l'alite M_{IIb} et de l'aluminate cubique (ou cubique ou tétragonal) donnent les résistances les plus élevées, tandis que les clinkers contenant de l'alite M_{Ib} ont des résistances inférieures à la moyenne.

Les relations entre composition, conditions de cuisson, structure microscopique et résistances mécaniques sont discutées dans trois communications : celles de Y. ONO, de S. TAKAGI et A. KAWASHIMA et de B.V. VOLCONSKI et Coll.. La figure 6 donne l'équation de Y. ONO pour l'évaluation de la résistance en fonction des paramètres géométriques et optiques du clinker.

5.- LA MECANIQUE DE LA FRAGMENTATION ET SON APPLICATION AUX BROYEURS INDUSTRIELS

Le rendement énergétique de la fragmentation par rapport à l'énergie de surface libérée est très faible, de l'ordre de 1%.

Si on rapporte le rendement du broyage à l'énergie de fissuration, c'est-à-dire à l'énergie nécessaire au déplacement d'une fissure, on trouve encore des chiffres très modestes inférieurs à 10%.

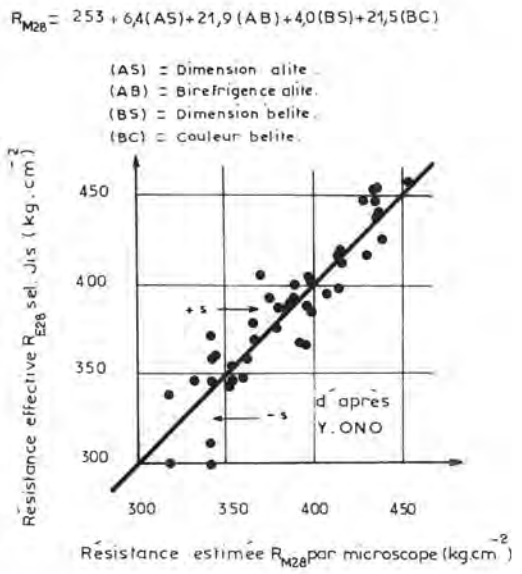

Fig. 6

Un peut comparer les rendements des différents modes de broyage entre eux. On constate alors que ces rendements se situent dans un intervalle dont les extrêmes sont dans un rapport dix.

Les pertes énergétiques analysées par J.P. MERIC dans son rapport sont de quatre types :

- celles dues aux déformations plastiques qui entraînent une dissipation énergétique dans la matière même ;
- l'énergie élastique excédentaire communiquée au matériau pour la propagation de la fissure ;
- les pertes dues au manque de sélectivité des corps broyants qui communiquent à la matière plus d'énergie qu'il n'est nécessaire pour créer le champ de contraintes (ce qui se traduit par des réagglomérations) ;
- les pertes mécaniques.

H. HORNAIN et M. REGOURD communiquent des mesures de l'énergie spécifique de fissuration du clinker γ_F comprises entre 12 et 22 J.m^{-2}, ce qui signifie que l'énergie théoriquement nécessaire pour libérer une surface de 3500 cm^2/g est de 1.65 kWh/t, alors que celle des broyeurs industriels est de l'ordre de 40 kWh/t. Le rendement par rapport à l'énergie de fissuration qui est ainsi mis en évidence est de 4%.

En comparant les différents modes de fragmentation, on constate que l'écrasement lent est très sélectif et présente les rendements les plus élevés. Il est réalisé dans les broyeurs à meules, mais d'une manière imparfaite seulement.

La percussion par masse tombante est le mode de broyage le moins sélectif, étant donné que les corps broyants attaquent tous les grains, les plus fins comme les plus gros, avec une énergie égale. Le rendement diminue très rapidement lorsque la finesse augmente. Cette diminution peut être freinée par deux remèdes : l'utilisation de corps broyants de petite dimension (mini pebs) ou des séparateurs à air qui éliminent les grains les plus fins.

La projection de matière sur une enclume pourra donner naissance à une troisième génération de broyeurs très sélectifs avec un rendement amélioré, à condition que l'on sache maîtriser les problèmes technologiques posés par l'utilisation de ciments à spectre granulométrique étroit. Une revue très claire de ce problème est présentée par Y. LE JEAN. La figure 7 illustre la sélectivité du broyeur à projection.

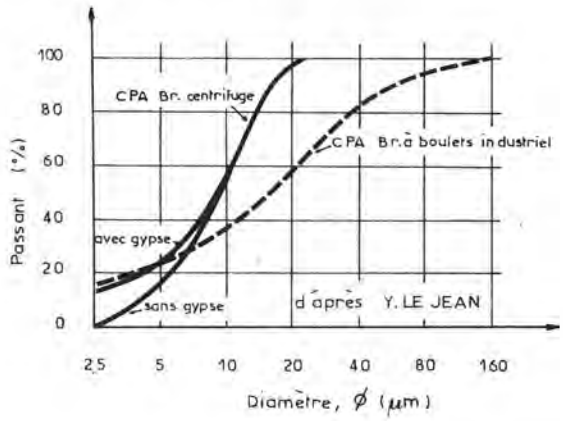

Fig. 7

A première vue, il semble que des progrès considérables peuvent être faits dans le domaine du broyage du cru et du ciment car les outils actuels ont des rendements médiocres et réagglomèrent les grains.

Dans le cas du cru, cette conclusion est indiscutable puisque, comme l'a montré R. BUCCHI, la réactivité du cru est plus élevée lorsque le spectre granulométrique est resserré.

Dans le cas du clinker, on arrive à la même conclusion en ce qui concerne la réactivité vis-à-vis de l'eau. Un spectre granulométrique étroit conduit à d'excellentes performances hydrauliques mesurées sur éprouvettes normalisées. Cependant, l'influence d'un tel spectre sur la rhéologie est négative. Si l'on considère la qualité du béton, qui résulte à la fois des propriétés rhéologiques et hydrauliques, le bilan est loin d'être indiscutablement positif, mais il pourra s'améliorer lorsque l'on saura encadrer le spectre granulométrique du clinker par des compléments fins et grossiers inertes qui amélioreront le comportement rhéologique tout en conservant les bonnes propriétés hydrauliques.

La possibilité de préparer des ciments consistant en fractions presque monogranulaires de matière active (clinker ou laitier) et de particules inertes ayant une granulométrie complémentaire pour un remplissage optimal reste un des thèmes fondamentaux de la science du broyage avec un double objectif : l'économie d'énergie de broyage, l'économie de clinker pour une même qualité du béton.

6.- LA BROYABILITE DU CLINKER ET DES CONSTITUANTS SECONDAIRES

Les clinkers les plus faciles à broyer sont ceux dont la concentration en microfissures est la plus élevée. L'état de fissuration dépend à son tour de la structure, de la composition minérale et de la vitesse de refroidissement du clinker. Le module d'élasticité et le coefficient de dilatation thermique permettent d'expliquer la bonne broyabilité de C_3S et la mauvaise broyabilité de C_2S (H. HORNAIN et M. REGOURD). D'autre part, I.F. PETERSEN montre que les clinkers industriels sont d'autant plus broyables que l'aire des pores par unité de volume est plus élevée (figure 8). Celle-ci dépend à son tour de la finesse des cristaux et de la quantité de phase liquide (figure 9).

Pour la préparation de ciments composés, il apparaît que la règle de broyer séparément les composants, que l'on applique si le composant le moins actif du point de vue hydraulique est aussi le plus difficile à broyer, soit à réviser à la lumière de résultats présentés par OPOCZKY et T.K. MRAKOVICS. Le bon choix entre broyage simultané et broyage séparé doit, en effet, tenir compte, non seulement de la broyabilité des composants, mais aussi de leur tendance à la réagglomération (indice d'uniformité de la distribution de ROSIN RAMMLER) de leurs proportions respectives et du type de circuit de broyage, ouvert ou fermé, utilisé.

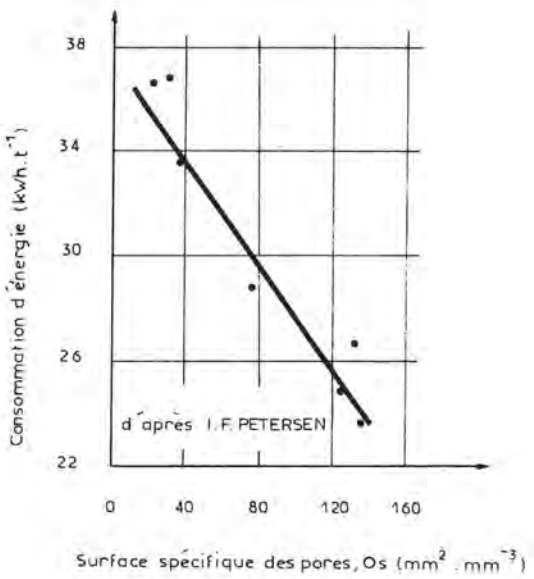

Fig. 8

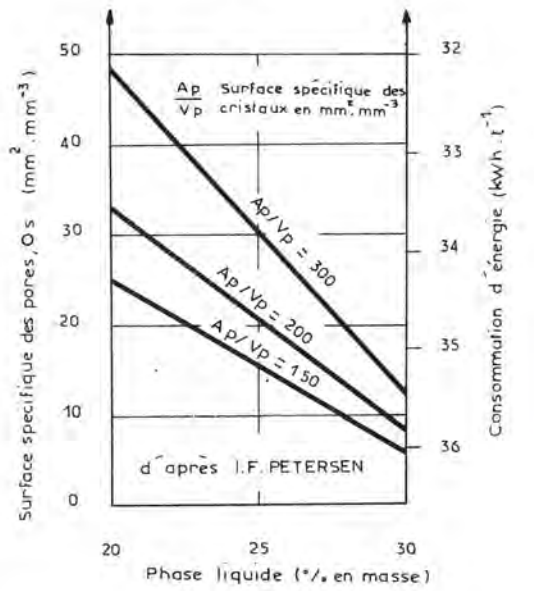

Fig. 9

W. KURDOWSKI et Z. WELISZEK rappellent que le broyeur à ciment, dont la fonction première est de libérer des surfaces nouvelles, est également un réacteur chimique alimenté

par l'énergie de broyage presque entièrement dégradée en chaleur qui vient s'ajouter à la chaleur propre du clinker.

Les réactions qui se déroulent dans le broyeur conduisent à la formation de semi-hydrate, de syngénite, d'ettringite. Elles dépendent du type de broyeur et de son régime de fonctionnement. Les auteurs établissent ainsi que la syngénite peut se former à partir de K_2SO_4 et de sulfate de calcium hydraté ou semi-hydraté à condition que la température s'élève au-dessus de 75°C et que la tension de vapeur d'eau passe un certain seuil (figure 10).

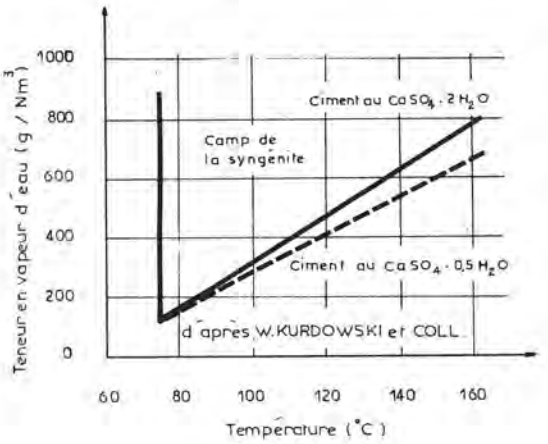

Fig. 10

CONCLUSION

Sur ce dernier sujet, nous terminons cette présentation, malheureusement trop rapide, des progrès les plus récents dans la connaissance des transformations physico-chimiques intervenant dans la fabrication du clinker et du ciment.

L'objectif qui est poursuivi par tous les laboratoires qui travaillent sur ces sujets est double :

d'abord maîtriser les transformations chimiques pour faire face à la très grande variabilité des matières premières ; il s'agit en effet pour le cimentier de passer d'une matière crue, particulière et souvent hétérogène, à un produit régulier parfaitement défini et adapté au marché ;

ensuite choisir parmi les transformations qui sont possibles celles qui exigent la dépense d'énergie la plus faible.

En raison de ces deux contraintes, souvent contradictoires, l'on aboutit à des procédés de plus en plus complexes, difficiles à régler et à stabiliser, qui vont exiger, de la part des constructeurs et des exploitants, une analyse approfondie des phénomènes physico-chimiques.

Les communications présentées à ce Congrès démontrent que cette analyse progresse rapidement, grâce à la collaboration très étroite des scientifiques et des industriels.

° ° °

RESUMES DES DEBATS DE LA TABLE RONDE

U. LUDWIG
Institut für Gesteinshüttenkunde, RWTH Aachen

Remarks on the burnability of cement raw materials.

I would like to give only a short summary here specially of the latest results of our working groups on the burnability of industrial raw mix for the production of Portland cement clinker.

Together with G. Ruckensteiner and S.E. Ibrahim we found that increasing values for the standard lime and for the heterogeneous coarse material, > 90 and > 20 µm, respectively, lead to an increase and increasing values for the molten fraction at sintering temperature to a decrease in the time needed for well burned clinker under otherwise constant conditions.

With respect to the kiln feed we have not been able to decide up to now whether granules or nodules on the one hand or powdered material on the other give the best values for burnability, or whether they have any influence at all. The cause is the formation of active states during dehydration and decarbonization at meal-like feed, and from these results the formation of meal granules and adhesives on the rotating laboratory burning equipment. So, we did not succed in direct burning of meal feed. But we are of the opinion that these active states of the meal during heating up are the primary cause of the formation of adhesives and meal rings in the kiln and the pre-heater system. Their stabilization by alkalies and others is a secondary effect but of no less importance.

According to the burning temperature it is of little practical interest that A. Wolter

refined the lowest temperature of C_3S formation to 1264°C instead of 1250°C. Of greater importance for the cement production is the stable formation of alites already at 1200°C and their unstable formation above 1160°C. From our work with additional additives in amounts of 0.5 wt.-% to alite only fluorine leads to a further lowering of the alite formation temperature to 1100°C. Finally, fluorine-alite is already formed at 925°C. From these results one can conclude that the formation of Portland cement clinker should be possible for below 1360°C. Besides we know from the work with D. Bürger that the low temperature alites and alinites have sufficient hydraulic properties. - Our revision on O. Philipp's work with several raw meals together with H. Bomas showed only in some cases a more rapid lime combination by using a high heating rate. - F. Bayer found in his experimental work that rapid heating, slow cooling up to 1250°C and rapid cooling again afterwards result in best mortar strength (DIN 1164).

From the above-mentioned great influence of the coarse and heterogeneous particles of the raw mix one can conclude that cement manufacturers should try to improve the grindability of the raw mix and the effectiveness of the separator by the use of surface active substances. H. Glock found a marked lowering of coarse particles > 90 and > 25 µm diameter, with the help of such substances.

A more extensive summary of our work on the influences on burnability of Portland cement raw mixes will be published shortly. I am indebted to C.A. Mulhern for his revision of the English text.

H. BRAUN
Holderbank Gestion et Conseils S.A.-Suisse

Comportement des mélanges crus à la cuisson

Le comportement à la cuisson d'une matière première ne se réfère pas seulement à l'aptitude à la cuisson, mais comprend tous les facteurs d'une importance technique lors de la cuisson, soit l'aptitude à la cuisson, la formation du croûtage, la volatilité (des alcalis, du soufre et du chlore), la formation de la poussière et la granulométrie du clinker.

Les facteurs les plus importants influençant l'aptitude à la cuisson sont la saturation en chaux, le module silicique et la quantité des grains de quartz et de calcite au-dessus d'un certain diamètre critique des grains. Basé sur un très grand nombre d'essais, nous avons établi un modèle mathématique des effets exercés par ces facteurs sur l'aptitude à la cuisson de tout mélange cru à ciment, modèle qui permet d'optimaliser la préparation et la cuisson du cru.

Le comportement du cru à la cuisson aux températures inférieures est aussi important. D'un échauffement trop lent de quelques crus résulte une diminution de la réactivité de la matière cuite.

Pour caractériser la formation du croûtage et la volatilité, nous avons développé des tests spéciaux.

La performance d'un ciment Portland peut être attribuée jusqu'à environ 90% à la chimie du clinker correspondant. Parmi les facteurs chimiques ce sont notamment les sulfates d'alcalis qui influencent surtout le développement de l'hydratation. La performance d'un ciment n'est souvent pas celle qui pourrait être attendue sur la base des propriétés du clinker, parce que non seulement le clinker, mais également le broyage et le stockage influencent sensiblement les propriétés du ciment.

A. BOIKOVA
Institute of Silicate Chemistry of the USSR Academy of Sciences, Leningrad

Remarks on Alinite

Alinite, a high-basic Al-Cl-calcium silicate differs strongly from alite in composition, structure and properties.

The peculiarity of alinite is that aluminium and chlorine, together with the main elements Ca, Si and O, participate in the formation of a specific structure arrangement in the form of mixed anionic network consisting of oxygen and chlorine atoms (1, 2).

Based on the structural analysis the authors propose the idealized formula of alinite as $Ca_{11}(Si_{0.75}Al_{0.25})_4O_{18}Cl$; the tetragonal cell contains two formula units.

However, under real synthesis conditions the alinite single crystals obtained by the authors always contained Mg and Fe.

The X-ray diffraction pattern of alinite is different from either of well-known patterns of triclinic (T_I, T_{II}, T_{III}), monoclinic (M_I, M_{II}, M_{III}) and rhombohedral alites.

The presence of chlorine in the structure provides the lower formation temperature of this mineral compared to alite (1000-1100°C instead of 1400-1500°C).

Alinite is highly reactive with water and shows high long term strength.

Although alinite is the main constituent of alinite clinker (a clinker of the low-temperature synthesis), the problem of alinite cannot solve the clinker problem as a whole due to a number of reasons.

The mineralogical phase composition of alinite clinker is rather complex, and the influence of other phases on the properties of clinker (and cement) should be noticeable.

However, the character of interrelation between these phases and chlorine is unknown.

Some other facts are also unknown such as the real composition of phases in the alinite clinker, isomorphic impurities in them, the distribution of impurities of the raw mixture (mainly of chlorine) among these phases.

Due to imperfect homogenization of the initial raw mixture and to the non-equilibrium conditions of the annealing of clinker the satisfactory combining of chlorine by the clinker constituents may hardly be attained.

Apparently in this case one should not exclude the possibility of obtaining the alinite analogs with more "quiet" elements in structure than chlorine.

It is also important to know the thermal stability of alinite and of the other phases of alinite clinker.

The study of the interaction process of alinite, the other phases and the alinite cement with water is of greatest practical and scientific significance. The main problem of this trend is the behaviour of chlorine during the hydration, in particular the probability of its entering into the structure of hydrates.

The composition, structure and properties of hydrates containing chlorine are also of great interest.

The problems mentioned are only part of the scientific tasks to be solved in the course of production and investigation of the alinite clinker.

References :

1.- V.V. ILYUKHIN, N.N. NEVSKY, M.J. BICKBAU and R.A. HOWIE (1977) "Crystal structure of alinite" - Nature 269, n° 5627, 397-398.

2.- V.V. ILYUKHIN, N.N. NEVSKY, R.A. HOWIE, M.J. BICKBAU, N.V. BELOV (1977) "Crystal structure of alinite" - Doklad. Akad. Nauk. URSS, 237, n° 4, 834-836.

P. GOURDIN
Société des Ciments Français, Centre d'Etudes et de Recherches de GUERVILLE

Polymorphisme de l'alite et du C_3A. Statistiques. Remarques complémentaires.

La question du polymorphisme des composés du clinker est complexe puisque l'alite est soit triclinique, soit monoclinique ou trigonale et que le C_3A peut être cubique, orthorhombique ou monoclinique. Le Séminaire A a montré que la forme tétragonale du C_3A n'existe pas, ce qui simplifiera un peu ces remarques.

Notre contribution à ce Congrès a été de montrer que l'alite des clinkers industriels est, le plus souvent, monoclinique et que l'alite trigonale fait plutôt figure d'exception puisque nous ne l'avons rencontrée que 11 fois sur 60 clinkers examinés. Le C_3A est cubique (29 clinkers) ou orthorhombique (5 clinkers) ou sous les deux formes simultanément (26 clinkers).

Nous voyons donc que :

- l'alite trigonale est plutôt une exception;
- l'alite monoclinique (M_I et M_{II}) est très fréquente ;
- l'alite triclinique est absente, sauf dans un échantillon exceptionnel, ayant séjourné longtemps dans le four rotatif et décrit dans une autre communication.

Nous ajouterons que l'alite trigonale est toujours associée au C_3A cubique dans nos clinkers industriels.

On peut alors se poser deux questions : pourquoi voit-on telle ou telle forme dans les clinkers industriels ? et quelle est la forme la plus favorable aux meilleures résistances à la compression des ciments portland correspondants ?

Pour répondre à ces questions nous avons dressé des Tables de Fréquence des formes allotropiques observées dans les clinkers en face des principales caractéristiques des mélanges crus, des clinkers et des ciments portland correspondants. Nous sommes arrivés aux trois conclusions suivantes :

1.- Parmi les ciments portland qui développent les plus hautes résistances à la compression se trouvent ceux dont l'alite est de forme trigonale et le C_3A de forme cubique.

2.- L'alite trigonale et le C_3A cubique se voient plus fréquemment dans les clinkers où SO_3 est en excès par rapport à K_2O, après formation de K_2SO_4.

3.- Les clinkers dans lesquels SO_3 est en excès par rapport à K_2O proviennent des mélanges crus dont la silice est sous forme de quartz et de kaolinite, c'est-à-dire sans composés alcalins et clinkérisés avec du fuel-oil ordinaire, à 4% de soufre.

De ces conclusions, on peut supposer que l'alite trigonale renferme plus de SO_3 dans sa structure et moins de MgO, K_2O et P_2O_5 que l'alite monoclinique. Cette supposition, à partir de 60 clinkers industriels, confirmerait les analyses que Mme REGOURD a présentées à Copenhague en 1972 et à Moscou en 1974, selon lesquelles "l'alite trigonale contient moins de MgO et plus de SO_3 que l'alite monoclinique". Ainsi comprenons-nous l'importance pratique du polymorphisme de l'alite et du C_3A.

H.W. POLLITT
Blue Circle Technical, England

1.- Reactivity of raw mix predicted by its physico-chemical properties.

There can be no question that the reactivity of the individual species present in raw material depends on the size, shape and perfection or imperfection of the crystal forms in which they appear, with special reference to their purity and the regularity of the lattice structure and the fine structure of the boundary surfaces. In other words the lattice energy, occurrence of defects, minor constituents and surface energy are all as important as Prof. BUCCHI has indicated in his Summary Paper on this theme. Also important are the presence of reducing compounds and the homogeneity of the ground and blended raw materials both of which can materially influence the temperature/time/atmosphere regime required in the kiln, i.e. what we call the combinability.

The question is directed at our ability to predict. Immediately, the difference in viewpoints of the academic and the industrial scientist becomes apparent. Of course both can agree that any means of accurate prediction of necessary process parameters must be valuable in principle. But in practice it is also necessary that the procedures leading to a prediction should represent an economy in time and cost over the already existing methods of measuring combinability. In my view, the procedures for determining on a representative scale, as distinct from on a few individually prepared crystals, the lattice energy, defect occurrence and surface energy for the range of materials present in one raw mix would be far more time-consuming and expensive than is the relatively simple combinability test. It could be argued that after the acquisition of sufficient data in an early phase the balance would eventually swing in favour of the predictive method. This would be more likely if the range of raw materials of interest were restricted. Unfortunately, as Prof. BUCCHI has pointed out, cement has to be made where there is a market for it and we have to use the materials that lie within economic reach. Those of us whose interests are worldwide are constantly encountering new forms of the necessary minerals. For a predictive method to be universal in application, the investigative early phase would in fact prove to be extensive and expensive.

Apart from the case of works with a limited range of mineral and crystal forms, where there should be little difficulty anyway in understanding combinability, I believe that the most useful approach is to continue with intelligent performance, and interpretation, of combinability tests resorting to more refined methods of study only when unusual aspects of the materials are revealed by those tests ; in other words what we are already doing.

2.- Influence of grinding on cement properties.

It is well known and has been stated by Dr. MERIC and others that alite and C_3A are more brittle than belite and the ferrite phase. In principle therefore it would not be surprising to find more alite and C_3A in the finer fractions and more belite and ferrite in the coarser fractions of clinker in cement. This simple principle can however be modified, for example, according to the method of preparation of the raw meal and the burning and cooling regimes. These factors influence the sizes of the unground crystals and indeed their brittleness. Rapidly cooled celite, e.g., may contain little or no crystalline ferrite owing to its glassy form. Another important factor is the overall clinker composition with especial reference to silica ratio and liquid content. The whole field of possibilities is obviously enormous. But taking the simple principle already stated as a centre line of thought, it is broadly true that the lower the silica ratio and therefore the higher the liquid content the less obvious are the signs of segregation of the four phases : conversely the higher the silica ratio the more obvious will be those signs of segregation. But of course in real clinkers the impurity of all the phases can again modify the picture.

Heterogeneity at random is bound to occur in clinker nodules unless the distances between unlike particles in the decarbonated nodules are small and closely grouped about their mean. This is why fine grinding and efficient blending of the raw meal are vital for fuel economy and clinker quality. Radial heterogeneity in a nodule can arise in two principal ways. First, as Dr. SPRUNG has said in answering M. VON EUW, if the coal

in a coal-fired kiln is not ground finely enough then quite apart from the important effects on flame characteristics, the molten ash will fall in the burning and decarbonating zones primarily. In cases where the raw material has already nodulised this means that the centre of the nodule is overlimed and the surface of the nodule is underlimed because the Works Chemist has provided in the raw meal an excess of lime intended to react with the acidic coal ash. There are many beautiful photomicrographs of such clinker showing belite concentrations round the surface and free lime in the interior of the nodule. Similar effects can occur as a result of coatings, clinker rings and other anomalous deposits breaking away.

The second form of radial heterogeneity arises in the very hard burning of high silica ratio materials. The clinker nodules tend to be friable and to be surrounded by a sugary deposit of alite crystals alone. The extent to which this is due to kiln and/or cooler conditions varies.

° ° °

CONCLUSIONS RESUMEES SUR LE THEME I PAR LES PRESIDENTS

1.- Dans les six années qui se sont écoulées depuis le Congrès de Moscou on a vu apparaître d'importantes et remarquables contributions à la connaissance des propriétés et des mécanismes physicochimiques qui interviennent dans la fabrication du ciment. Les principaux domaines couverts par ces contributions sont les suivants :

- la réactivité des crus et de leurs composants,
- la cinétique de la diffusion solide-solide et solide-liquide,
- la micro et macrostructure du clinker,
- et enfin, la mécanique et mécanochimie du broyage.

Une attention toute particulière a été apportée au rôle d'échange de la phase fondue et plus particulièrement à l'influence de sa composition, notamment en éléments mineurs, sur les principaux paramètres qui la caractérisent.

Bien que tous les aspects de ces problèmes ne soient pas encore éclaircis, l'état actuel des progrès réalisés est tel qu'il est possible d'espérer des retombées rapides sur la technologie et donc sur l'industrie où des changements décisifs sont à attendre.

2.- Les discussions de la table ronde ont démontré que la cuisson en four rotatif, outre qu'elle présente un bilan thermique imparfait, ne permet pas de conserver aux solides originels ou aux néoformations qui proviennent du cru un niveau élevé d'activité susceptible de favoriser la vitesse de combinaison. Le séjour prolongé des matières à des températures inférieures à celles d'apparition de la masse fondue alors que la décarbonatation est déjà accomplie, contribue au "vieillissement" des matières et favorise l'évolution des structures vers des états stables peu réactifs. Il en résulte une diminution des vitesses de toutes les réactions de diffusion qui se produisent avant ou après l'apparition de la phase liquide.

Il est à prévoir que dans un proche avenir, on assistera à des tentatives sans doute nombreuses pour modifier le processus qui se déroule dans "l'intervalle mort" entre 1000° et 1300°C environ ; il s'agira d'utiliser éventuellement des types d'installations différents de ceux actuellement connus.

3.- Un autre domaine dans lequel il faut s'attendre à des progrès techniques d'une importance non négligeable est celui du broyage.

Les procédés de comminution fine par projection constituent un espoir concret d'une grande portée ; ses possibilités sont loin d'avoir été entièrement explorées. Ce type de broyeur porte les matériaux à un niveau de réactivité très élevé, mais ce niveau est tel que les propriétés rhéologiques des ciments s'en trouvent perturbées par des réactions de surface trop précoces. Ce problème devra être maîtrisé avant d'envisager son utilisation pour le broyage du ciment et il s'agit là d'un objectif pour les recherches des années à venir.

Le broyage du cru pourra également être amélioré par l'utilisation du broyeur à projection car il est possible que la très grande réactivité des matériaux préparés dans ce type de broyeur puisse permettre d'élaborer des crus de cimenterie ayant des cinétiques de cuisson nettement plus élevées que celles qui sont couramment obtenues par des broyages dans les broyeurs à boulets ou à meules. Dans ce cas les effets secondaires sur la rhéologie des produits ne présenteront pas la même gêne que pour le ciment.

La sélectivité du broyage par projection permettra de concevoir des ciments composés particulièrement performants. Dans ce cas, le but ne se limite pas seulement à l'économie dérivant du remplacement d'une partie du clinker par des constituants ayant un contenu énergétique plus bas, mais s'étend au con-

traire à un objectif plus ambitieux qui est la réalisation de ciments reconstitués à partir de fractions granulométriques définies, ces ciments permettant de confectionner des bétons présentant des propriétés rhéologiques adequates pour des rapports E/C faibles.

4.- Il est impossible de ne pas évoquer pour terminer les composés mineurs du clinker. L'influence qu'ils exercent sur les équilibres de phase, sur la cinétique des réactions, sur les propriétés du clinker, ainsi que sur la régularité du fonctionnement du four, est, depuis longtemps, l'objet de recherches actives et approfondies. Ce chapître de la recherche cimentière est cependant loin d'être terminé. Il reste l'un des domaines d'investigation les plus prometteurs, surtout lorsqu'il s'agit de la possibilité d'obtenir des types d'alite stables à plus basse température ou des types de bélite plus actifs hydrauliquement que ceux qui sont actuellement fabriqués.

THEME II

Hydration of Pure Portland Cements

by F.W. LOCHER

1. Synopsis

There are 2 principal reports and 51 basic reports on Theme II "Hydration of Pure Portland cements". The first principal report by J. Skalny and J.F. Young deals with the course of cement hydration, the second principal report by H.F.W. Taylor and D.M. Roy provides a general view of the composition and structure of the compounds which form in cement hydration and can occur as constituents of hardened cement paste. The 51 basic reports can be divided into 7 fields as shown in table 1.

Table 1: Classification of the basic reports of Theme II

Theme II: Hydration of pure Portland Cements
Basic Reports

A	*Theory of Hydration*	2
B	*Methods of Investigation*	4
C	*Initial Reactions*	18
D	*Ettringite*	2
E	*Hydration of Silicates*	12
F	*Effect of Admixtures*	9
G	*Compounds in Hardened Cement Paste*	4
		51

This classification shows that more than 3/4 of the basic reports are concerned with the fields of "initial reactions", "hydration of calcium silicates" and "effect of admixtures".

It is the task of the general report to present a summary of the principal and basic reports. On the basis of the congress contributions this report will attempt to describe in particular the processes in hydration which, in our opinion, are of special importance regarding the practical aspects of setting and hardening of cement. If the opinion of our institute is particularly stressed it should be understood as a stimulus for the discussion which will follow.

2. Summary of the course of reaction

A large number of investigations have shown that the course of cement hydration can be divided into 3 stages. The most important connexions are illustrated in figure 1. In both diagrams the division of the abscissa shows the duration of hydration; on the left of the ordinate the content of nonhydrated tricalcium aluminate (top) and tricalcium silicate (bottom) and on the right the content of non-evaporable water (top) and newly-formed calcium hydroxide (bottom) are shown.

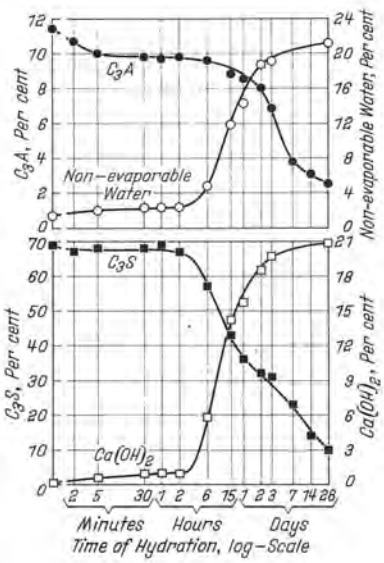

Figure 1: Hydration of tricalcium aluminate and tricalcium silicate in Portland cement

The course of the 4 curves illustrates that the initial reaction which starts immediately after the mixing of the cement stops after 15 minutes at the latest. The dormant period, which lasts for a few hours, follows and practically no or only a very weak chemical reaction occurs. Then the actual cement hydration starts in which the hydration prod-

ucts are formed which are essential for the hardening.

Tricalcium aluminate and calcium sulfate added for control of setting are primarily involved in the initial reaction. In the first minutes after mixing the tricalcium silicate mainly only releases calcium hydroxide to the solution. Certain initial reactions can also be expected from calcium aluminate ferrite and dicalcium silicate but the extent of the reaction is very low.

3. Reaction of tricalcium aluminate with calcium sulfate

The amount of tricalcium aluminate involved in the initial reaction does not depend on the addition of calcium sulfate. This is shown by studies of the course of hydration of ground cement clinker with and without the addition of gypsum. The results are shown in figure 2.

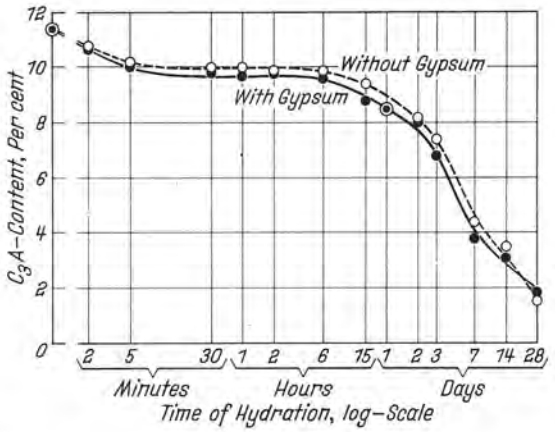

Figure 2: Hydration of tricalcium aluminate in ground Portland cement clinker with and without addition of gypsum

It shows that the reduction in the content of tricalcium aluminate as a result of hydration ist practically the same with and without the addition of gypsum. The addition of gypsum thus influences neither the quantity of tricalcium aluminate, which reacts in the first minutes after the mixing of the cement, nor the start and end of the dormant period. The retarding effect of the calcium sulfate on the setting is thus not due to the inhibition of a chemical reaction.

The calcium sulfate does, however, have a very important influence on the type of reaction products occuring in the first minutes and the structure formed by them. These processes can be followed by studies with the scanning electron microscope. Without the addition of calcium sulfate relatively large crystals of tabular calcium aluminate hydrate form which are responsible for the rapid setting as they produce a rigid structure shortly after mixing (figure 3).

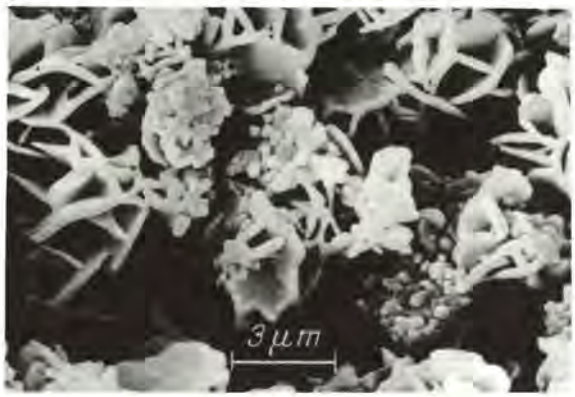

Figure 3: Structure of paste from ground Portland cement clinker without addition of gypsum 30 minutes after mixing

With the addition of calcium sulfate ettringite forms in the shape of very small particles on the surface of the cement grains (figure 4) which are so fine-grained that they cannot produce a rigid structure.

Figure 4: Structure of paste from ground Portland cement clinker with addition of gypsum 30 minutes after mixing

The orderly retarded setting of the cement paste starts during the dormant period as a consequence of a recrystallization of the ettringite in which the small crystals are dissolved and the larger crystals grow so that they can bridge over the space between the grains of cement and produce a rigid structure (figure 5).

Only that proportion of tricalcium aluminate which goes into solution in the first minutes of hydration until the start of the dormant period is involved in these reactions. The amount varies from cement to cement and is

between 0.3 and 2.0 percent by weight in relation to the total clinker.

Figure 5: Structure of paste from ground Portland cement clinker with addition of gypsum 4 hours after mixing

It does not only depend on the total amount of tricalcium aluminate but to a greater degree on other influences too. It increases, for example, if the cement clinker is burned and slowly cooled in a reducing atmosphere. It grows with decreasing grain size and decreasing width of grain size distribution. Also it is greater the higher the temperature during hydration of the cement. On the other hand, this amount of tricalcium aluminate involved in the initial reaction with calcium sulfate can change during the grinding and storage of the cement. A more or less large share of the tricalcium aluminate available for the initial reaction can react with water vapour without the participation of calcium sulfate and can form very fine-grained calcium aluminate hydrate on the surface of the tricalcium aluminate which only reacts very slowly with sulfate. Consequently the amount of tricalcium aluminate, which can react immediately after the mixing of the cement with the added calcium sulfate, decreases. Such prehydration must be expected if water is improperly injected into the cement mill, if the cement is stored outside, or if cement is stored in a silo and the gypsum still contained in the cement after grinding dehydrates slowly at an increased temperature.

The greatest possible retardation of setting occurs when the share of tricalcium aluminate which goes into solution in the first minutes after the mixing of the cement, i.e. before the start of the dormant period, is combined on the surface of the cement grains completely as fine-grained ettringite.

If the sulfate supply in the solution is not sufficient to bind the amount of tricalcium aluminate going into solution during the initial reaction as ettringite, monosulfate and/or calcium aluminate hydrate also occur, besides ettringite, in the shape of large tabular crystals (figure 6) which cause quick setting.

Figure 6: Structure of Portland cement paste with a sulfate supply which is too low

If the sulfate supply in the solution during the initial reaction is too great e.g. as a result of too high a content of hemyhydrate, so-called secondary gypsum (figure 7) is formed, apart from ettringite, and also generates solidification. If the secondary gypsum forms very quickly and if the amount is so small that it can be consumed before the start of the dormant period by reaction with the tricalcium aluminate still going into solution at this time, so-called false setting occurs.

Figure 7: Structure of Portland cement paste with a sulfate supply which is too high

If the amount of secondary gypsum is so great that it cannot be consumed before the start of the dormant period the early solidification remains, so the formation of secondary gypsum causes quick setting.

For the greatest possible retardation of setting it is thus necessary to adjust the sulfate supply in the solution to the amount of tricalcium aluminate going into solution during the initial reaction. If the amount of tricalcium aluminate is low the addition of gypsum is sufficient for this, but if it is relatively high the cement should contain hemihydrate which goes into solution much faster and in greater quantities than the gypsum. To retard setting it has thus proved useful to add a mixture of gypsum and natural anhydrite whose proportion of gypsum must be adjusted to the reactivity of the tricalcium aluminate and to grind the cement at a temperature that the gypsum is completely dehydrated to hemihydrate. The proportion of natural anhydrite which goes into solution more slowly serves to maintain a certain sulfate supply for a time after the end of the dormant period as it promotes further hydration reactions.

Dehydration of the gypsum in grinding also has the advantage that during the subsequent storage in the silo the formation of coating is avoided and the cement properties remain constant. Coating on the wall of the silo is usually due to the fact that the water contained in the gypsum escapes at a high temperature, diffuses to the colder silo wall, concentrates there and causes chemical reactions which lead to solidification.

As a result of the prehydration described above part of the water expelled from the gypsum reduces the amount of tricalcium aluminate available for the initial reaction with sulfate. On the other hand, the sulfate content of the solution increases, as the hemihydrate forming during the dehydration of the gypsum goes into solution more quickly and in greater amounts. The result can be false or quick setting, usually acceleration of the setting. For this reason it is advisable, as far as possible, not to take any water into the cement silo, especially not with the gypsum, if high temperatures cannot be avoided in the silo. The storage temperature which can cause these reactions to occur is the lower the longer the cement remains in the silo. For 7-day storage it is approximately 60 to 70 °C.

4. Hydration of calcium silicates

The amount of tricalcium silicate reacting in the first minutes after mixing is in the order of 1 % (figure 8). Little is known of the influences on the extent of this reaction. Various results suggest that just as in the case of tricalcium aluminate, the chemical composition, the crystal structure and its degree of disorder are of importance.

The start and end of the dormant period are different with tricalcium silicate and tricalcium aluminate. The addition of calcium sulfate has no effect on the dormant period of the tricalcium aluminate; in the case of tricalcium silicate the dormant period is shortened by the calcium sulfate. This means that the calcium sulfate still contained in the solution after the dormant period accelerates the hydration of tricalcium silicate and as a result increases the initial strength.

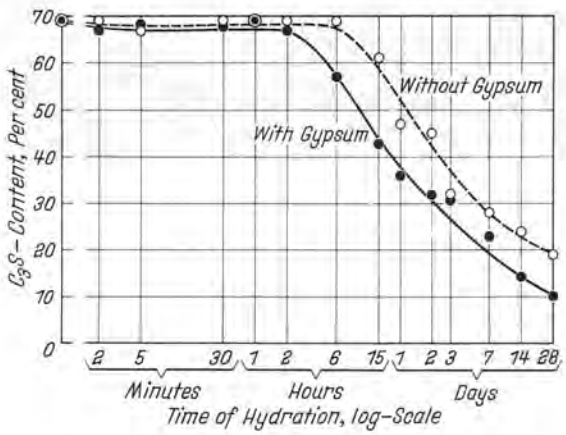

Figure 8: Hydration of tricalcium silicate in ground Portland cement clinker with and without addition of gypsum

The dormant period of the tricalcium silicate in the cement is approximately 4 hours with hydration under normal temperature conditions. It can practically not be reduced by finer grinding of the cement. This means that the hardening of the cement only starts after this time and that a certain initial strength can be expected at the earliest only after approximately 6 hours. If greater strengths are desired earlier the hydration products of other compounds must be used, e.g. calcium aluminate hydrates and/or monosulfate or similar compounds as with regulated set cement or jet cement.

A certain initial reaction can also be expected for dicalcium silicate. The dormant period occuring afterwards is much longer than with tricalcium silicate. Thus for the development of the initial strength only the hydration of the tricalcium silicate is important. It practically does not start until after the dormant period when the reaction between tricalcium aluminate and calcium sulfate responsible for setting has been concluded, i.e. when the first structure of ettringite and maybe monosulfate or secondary gypsum has formed which is rigid but has relatively large pores and whose strength is thus very low. The hydration products of the tricalcium silicate gradually fill these

pores. Als the degree of filling increases, the strength also grows. In order to achieve a high degree of filling with a low degree of hydration of the tricalcium silicate, the first structure should have as few pores as possible. This happens if before the dormant period only very fine-grained ettringite and no large crystals of monosulfate or secondary gypsum have formed, i.e. if during the initial reaction the sulfate supply in the solution was adjusted to the reactivity of the tricalcium aluminate. But even in the caseof ideal adjustment differences in the packing density of the initial structure may occur and it can be assumed that the pore space increases with increasing ettringite content, i.e. with increasing reactivity of the tricalcium aluminate. Also the shape of the ettringite is important which depends on the composition of the solution, especially on its alkali content.

The hydration products which produce the first structure form relatively quickly during the initial reaction before the dormant period. The tendency to form a more or less rigid very porous first structure is thus particularly great during the inital reaction. For this reason it is advisable during this time to mix the cement paste, mortar or concrete very intensely. The first structure then forms during the dormant period because of recrystallization processes which are much slower so that a first structure with fewer pores can form.

Various research results and observations show that the hydration products of tricalcium silicate and dicalcium silicate can only fill the pores which were previously filled with water. This would mean that the hydration of calcium silicates is also a process which at least partly runs via the solution. The conclusion for the practice of cement application results from the fact that during the initial hardening even a short drying out of the concrete should be avoided as with rewetting under normal pressure the water connot penetrate all pores afterwards. As a result these pores can no longer be filled with hydration products.

5. Effect of admixtures

Even small additions of inorganic or organic compounds can greatly change the course of the hydration reaction. Studies by W. Richartz with a large number of different substances have shown that 3 groups can be distinguished according to the effect on the initial reaction and the length of the dormant period. This is illustrated in figure 9.

In the first group are substances which shorten the dormant period of the tricalcium silicate. They promote the reaction of the tricalcium aluminate during the initial reaction, but do not influence the initial reaction of the tricalcium silicate and the dormant period of the tricalcium aluminate. According to studies made so far, only chlorides, formates and thiocyanides have this effect.

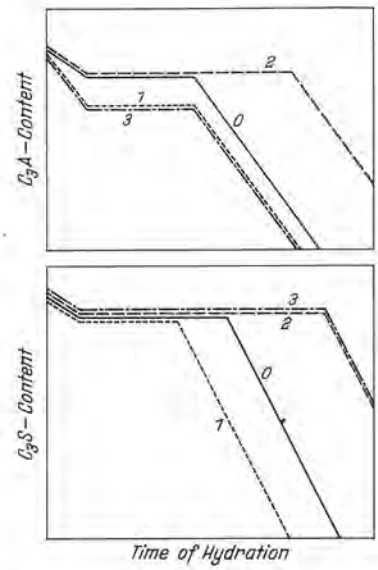

Figure 9: Effect of admixtures on hydration of tricalcium aluminate and tricalcium silicate in Portland cement

As a result of the increased reaction of tricalcium aluminate at the start of hydration more ettringite is formed as long as the sulfate supply in the solution is sufficient; otherwise more monosulfate or other aluminate compounds are formed. As a result of the shortened dormant period of the tricalcium silicate hardening also starts more quickly.

The substances in the second group do not affect the reaction of tricalcium aluminate and tricalcium silicate during the initial reaction but increase the dormant period of both compounds. In this group are, for example, phosphates, tartrates and citrates soluble in water. The result of the longer dormant period of the tricalcium silicate is that hardening starts much later. As the reaction of tricalcium aluminate does not change before the start of the dormant period the amount of ettringite formed during the initial reaction remains the same. Setting is retarded all the same, however. Studies carried out with the scanning electron microscope have shown that the admixtures of this group greatly change the crystallization behaviour of the ettringite. Instead of needle-shaped, very thin crystals, the ettringite forms in the shape of short columns with larger diameters which grow very little also during the dormant period. It can be assumed that the change in the ettringite crystallization causes the retarding effect in the setting.

The substances in the third group increase

the amount of tricalcium aluminate which reacts at the beginning of hydration but do not change the dormant period of the tricalcium aluminate, do, however, increase the dormant period of the tricalcium silicate. In this group are, for example, sugar, triethanolamine and zinc oxide.

With normal composition of the cement clinker, the increased amount of tricalcium aluminate reaction during the initial reaction results in quick setting, which is generally caused by the formation of monosulfate besides ettringite. Due to the increased dormant period of the tricalcium silicate, strength also develops much later.

The effect of all additions depends to a great extent on the amount added. The typical effect of each addition can only be seen when certain minimum concentrations are exceeded. This is particularly important, for example, for triethanolamine which only inhibits hardening if its concentration, related to cement, is more than 0.1 %. With concentrations of 0.02 to 0.05 %, when used as a grinding aid, changes in the setting and hardening are not yet to be expected.

The type of effect is also to a great degree dependent on temperature. The initial reaction of tricalcium aluminate is not changed, for example, by citric acid at a temperature of 20 °C but is greatly increased at 35 °C.

The effect of additions is also greatly influenced by the solution behaviour of the calcium sulfate. Citric acid and citrates retard, for example, to a large degree the dissolution and rehydration of the hemihydrate. As a result the supply of sulfate during the initial reaction decreases. This can either be an advantage or disadvantage depending on the reactivity of the tricalcium aluminate in the cement.

The effects of the additions described so far were chemical processes. The additions change the amount of the substances involved in the chemical reactions and as a result influence the type and amount of the reaction products and their crystallization behaviour. It is, however, possible that surface effects are also involved which promote the dispersion of the cement particles in the mixing water solution. In the case of plasticizers, particularly of super-plasticizers, we assume these effects to prevail or to be the sole effect.

Discussion on the Principal Paper of SKALNY and YOUNG

by Prof. H.N.STEIN
Laboratory for Colloid Science
Vakgroep Elektrochemie
University of Technology
EINDHOVEN, THE NETHERLANDS

C_3A HYDRATION : FACTS UNEXPLAINED BY THE SKALNY MECHANISM :

C_3A hydration is a complicated process, as well appears from the mechanism proposed by Dr SKALNY and Dr YOUNG, and I feel somewhat guilty in having to drawn the attention of the audience to some facts which cannot easily be understood on the basis of this mechanism, indicating that the truth must be more complicated still.

1. - Addition of $Ca(OH)_2$ crystals to a C_3A + water paste does not accelerate the hydration of C_3S, as should be expected on the basis of SKALNY's mechanism, but rather retards it (1). This is explained by SKALNY and YOUNG through poisoning of the $Ca(OH)_2$ crystals in their function as nuclei, silicate ions being regarded as a poison in this respect (2). It remains unexplained, however, why this poisoning is more pronounced in the presence of added $Ca(OH)_2$ than in its absence ; $Ca(OH)_2$ cannot be expected to increase the silicate ion concentration.

2. - Congruent dissolution of C_3S is found, when precautions are taken against precipitation of calcium silicate hydrates from the solution. The most thorough investigation in this respect is by KOHLSCHUTTER (3), who achieved freedom from precipitation of C-S-H by working either in very dilute suspensions, or by leading a stream of water through a thin C_3S bed.

It might be argued that these data are not indicative on C_3A hydration in pastes, because of the different water/C_3A ratio. However, it should be noted that congruent dissolution of C_3S is also found in dilute suspensions in which an important parameter, viz. the pH, has been adjusted such as to resemble paste conditions in early hydration stages (e.g., pH = 11.75 or 12) (4). This is not accounted for by the SKALNY mechanism, where, without any interaction with other C_3S particles, preferential leaching of Ca^{2+} and OH^- ions into the solution is postulated from the start of the hydration onwards.

Both phenomena are consistent, however, with the formation of a first, strongly retarding hydrate, and its conversion into a second, less retarding one ; the conversion being stimulated by low initial $[Ca^{2+}]$ and $[OH^-]$. It should be noted that this hypothesis also provides for a natural explanation of the accelerating effect of amorphous silica on C_3S hydration (5).

It is not necessary that the first hydrate has a composition C_3SH_n, although it would be natural to expect that it has a higher C/S ratio than the second, less retarding hydrate. Neither it is surprising that the first hydrate cannot be seen by electron microscopy (5), since it may originate through penetration of water into the C_3S.

References

1. - J.G.M. de JONG, Ph.D. Thesis, Eindhoven 1968, p. 30.

2. - M.E. TADROS, J. SKALNY and R.S. KALYONCU, J. Amer. Ceram. Soc. 59, 344 (1976).

3. - H.W. KOHLSCHUTTER, Proc. Intern. Symp. Reactivity of Solids, Gothenbrug 1952, part 2, p. 671 : Chem. Abstr. 48, 12387 b.

4. - K.G. Mc CURDY and H.N. STEIN, Cement and Concrete Research 3, 247 (1973).

5. - H.N. STEIN and J.M. STEVELS, J. Appl. Chem. (London) 14, 338 (1964).

INTERVENTION

DU Professeur O.P. MTCHEDLOV-PETROSSIAN

Je voudrais exprimer ma satisfaction à propos de ce qu'un des fondateurs de la cristallochimie moderne du ciment, le Professeur Taylor, qui enfin, après une discussion de 20 années, a suggéré l'idée que les processus de base relatifs au durcissement de la pierre de ciment sont déterminés, dans les conditions normales par les phénomènes évoluant au stade colloïdale et formant la porosité. La cristallochimie joue ici un rôle secondaire.

En ce qui concerne la discussion des participants de la table ronde au sujet de la nature des forces conditionnant la prise, il convient de dire qu'il n'y a qu'à considérer la caractéristique énergétique (thermodynamique et thermochimique) du processus de prise de ciment portland pour comprendre clairement que tous les processus déterminant la prise se déroulent pendant la période de l'hydratation active des aluminates.

Les études effectuées par le Professeur Roy et le Professeur Séréda ont montré que les phases de silicate sont également soumises à la prise sous l'influence de température et de pression. Cependant, ce fait n'a aucun rapport avec la prise des ciments portland habituels.

I would like to express satisfaction that Prof. Taylor, one of the founders of modern cement crystal chemistry, at last after our 20-year discussion has said that the main processes of cement stone hardening under normal conditions are determined by the fenomena taking place during colloid phase and forming porosity. Crystal chemistry acts here a secondary part. As to the argument between the participants of the discussion on the nature of the forces motivating hardening, it might be well to point out that one should anly look upon energetic (thermodynamic and thermochemical) characteristic of portland cement hardening process to clear yp that all the processes determining hardening proceed in the period of aluminates active hydration.

Prof. Roy and Prof. Serada have showed that silicate phases also harden on exposure to temperature and pressure, but this has no relation to the hardening of ordinary portland cements.

CONCLUSIONS DE LA TABLE RONDE

par le Professeur I. BARRET

Ce thème était divisé en deux sous-thèmes et 8 questions essentielles appartenant à ces sous-thèmes ont été abordées :

Sous-thème 2.1 : Mécanismes d'hydratation

Sujet n° 1 :
Un résumé des résultats du Séminaire sur l'aluminate tricalcique est fait par Mme REGOURD d'où il ressort en premier lieu, en ce qui concerne les phénomènes aux interfaces C_3A/eau et C_3A/solution de chaux, qu'à la suite de la communication de P. BARRET et D. BERTRANDIE, la dissolution congruente de C_3A peut être admise, ce qui, d'après H.N. STEIN n'est pas incompatible avec les valeurs positives du potentiel ζ qu'il a observées sur les hydrates hexagonaux et cubiques se formant durant l'hydratation de C_3A et qui correspondent à une extraction préférentielle des ions aluminates favorisée par l'adjonction de NaOH. La plupart des contributions soulignent l'idée que dans la phase liquide, les concentrations locales tout près de C_3A diffèrent des concentrations loin de C_3A et que ces concentrations locales jouent un grand rôle dans la formation des hydrates et sur la vitesse d'hydratation de C_3A.

L'influence de Na_2O sur la vitesse d'hydratation de C_3A reste controversée. En fait, deux questions se posent :

1°) Na_2O retarde-t-il ou accélère-t-il l'hydratation de C_3A ?

2°) Na_2O en solution solide avec C_3A agit-il de la même façon qu'une quantité équivalente de NaOH ajoutée séparément ? La plupart des publications concluaient à un retard par Na_2O certaines, comme celles de BUTT, à une accélération.

Les communications au Congrès ne mettent pas fin à ce désaccord puisqu'elles se partagent en nombre à peu près égal entre les deux thèses. Les opinions sont divisées également en ce qui concerne la réponse à donner à la seconde question et de nouvelles expériences devront être imaginées.

Les avis sont également partagés pour attribuer le rôle retardateur à l'hydratation de C_3A en présence de gypse, soit à la couche d'ettringite elle-même (communications de GHORALE, HEINZ, LUDWIG, MESKENDAHL et WOLTER), soit à une couche de C_4AH_{13} (CHATTERJI) s'interposant entre la couche d'ettringite et C_3A.

Dans les discussions ont été évoquées les différentes possibilités de formation de l'ettringite, plus ou moins amorphe autour des grains de C_3A et cristallisée à plus grande distance, les interactions entre C_3A et C_3S pour donner des silicoaluminates.

D'après ODLER, l'adsorption de sulfate sur C-S-H empêcherait l'ettringite de se former. B. COTTIN souligne le rôle retardateur de C_3A au cours de l'hydratation de C_3S dans le développement des résistances.

Sujet n° 2 :
Après le rapport général exposé par F.W. LOCHER, la discussion porte sur le processus d'hydratation du ciment Portland dans la période initiale et particulièrement sur le point de savoir si la prise est la conséquence, comme le pense F.W. LOCHER, de la présence dans le ciment Portland, d'aluminate tricalcique et de gypse, et s'explique par la constitution d'une structure rigide à base de gros cristaux. Un défaut de gypse entraînerait la prise rapide par formation de gros cristaux tabulaires d'aluminates de calcium hydratés peu de temps après le mélange avec l'eau. Une proportion convenable de gypse, se combinant exactement sous forme de fines particules d'ettringite avec l'aluminate tricalcique dissous durant les premières minutes donnerait la prise retardée, s'expliquant par la recristallisation en gros cristaux, pendant la période dormante des particules d'ettringite initiales incapables, en raison de leur finesse, de donner une structure rigide.

L'attribution de la prise uniquement à la présence d'aluminate tricalcique et de gypse est controversée notamment par F. YOUNG, qui pense que C_3S contrôle la prise plus que C_3A, mais que celui-ci est impliqué dans la fausse prise. B. COTTIN demande comment alors expliquer, si la prise est due à la recristallisation de l'ettringite, le mécanisme de la prise de C_3S pur et parfois des clinkers non gypsés, ainsi que celle des ciments fortement surgypsés dans laquelle l'hydratation de C_3A peut être bloquée pendant des semaines ?

D'autres questions vont dans le même sens. La formation des hydro-silicates dès la période initiale et pendant la période dormante doit donc être impliquée dans la prise, mais il est certain qu'il doit être tenu

compte non seulement de la chimie des hydrates, mais aussi de la structure.

Sujet n° 3 :
La discussion engagée sur la "période dormante" révèle l'existence de deux conceptions différentes. La première, qui est celle de F.W. LOCHER et qui est partagée par TAYLOR et par de nombreux auteurs tels que DE JONC, STEIN, STEVELS, ODLER et DÖRR, TADROS et col., DOUBLE, BIRCHHALL, JENNINGS et PRATT, DENT-GLASSER et beaucoup d'autres, admet un véritable arrêt de la réaction. Cet arrêt est attribué à la constitution, dans la période initiale, de barrières de diverses natures laissant seulement diffuser les ions Ca^{2+}_{aq} et OH^{-}_{aq} mais non les ions silicates :

couche protectrice d'hydrate primaire, membrane semi-perméable développant une pression osmotique, couche semi-fluides d'ions silicates riches en protons et de molécules d'eau. Dans cette conception, la nucléation de C-H et de C-S-H n'intervient pas pendant la "période dormante"; c'est pourquoi cette période est aussi appelée "période d'induction"; la nucléation de C-H et de C-S-H n'a lieu qu'au début de la période suivante dite de post-induction ou d'accélération.

La seconde conception soutenue par P. BARRET à partir des expériences faites par ses collaborateurs en coopération avec la Société LAFARGE, et partagée notamment par C. VERNET et col. suppose un processus continu depuis l'instant initial du mélange, les diverses périodes ci-dessus décrites n'étant que le résultat d'une autorégulation du système fermé, sous l'influence des facteurs cinétiques dont les valeurs locales dépendant de sa propre évolution.

Ce processus se décompose en une étape interfaciale liquide-solide d'hydroxylation par protonation des ions O^{2-} et SiO_4^{4-} qui deviennent des sites superficiels à mesure qu'ils sont découverts par ceux qui, déjà hydroxylés, passent en solution. Cette étape mobilise pratiquement toute l'eau qui entrera dans la composition des hydrates C-H et C-S-H. Les concentrations ioniques locales résultent de l'apport congruent des ions Ca^{2+}, OH^{-} et silicates en régime établi, de leur diffusion et de leur consommation par précipitation au-delà d'une certaine sursaturation. La sursaturation la plus élevée est atteinte au voisinage immédiat de l'interface C_3S-solution qui est un lieu privilégié de nucléation, toujours accessible aux molécules d'eau auxquelles le dépôt de C-S-H n'oppose pas une barrière étanche. La composition et l'état de condensation de la silice dans ces C-S-H dépend à une température donnée de la concentration de la chaux et de la silice dans la phase liquide, indépendamment du rôle éventuel d'impuretés.

Dans cette conception, la "période dormante" n'est une période d'induction que pour l'hydroxyde de calcium puisque le C-S-H se forme depuis la période initiale. La quantité de C-S-H ayant précipité à l'instant t est étroitement corrélée à la quantité de chaux accumulée dans la phase liquide car $(3 - \alpha)$ moles de chaux passent en solution lorsque α moles de C-S-H de rapport molaire $C/S = \alpha$ ($\alpha < 3$) précipitent.

Sujet n° 4 :
F.W. LOCHER amène précisément la discussion sur les causes de la période d'induction : recouvrement protecteur, membrane semi-perméable, zone frontière semi-fluide et sur les facteurs qui contrôlent la nucléation à la fin de la période d'induction.

L'effet ralentisseur d'une concentration élevée dans la phase liquide indépendamment de toute barrière est illustré par P. BARRET en présentant des courbes de taux d'hydratation en fonction du temps établies comparativement à l'aide d'une suspension de C_3S agité soit dans l'eau, soit dans une solution de chaux sursaturée (35.10^{-3} mole.kg^{-1}) dans le même rapport $\ell/s = 10$.

Alors que le taux d'hydratation croît régulièrement dans le premier cas depuis l'instant initial, il demeure presque nul dans le second cas pendant la même durée (4 heures). Le décalage dans les deux taux d'hydratation se conserve par la suite. Mme DELLA ROY et J. SKALNY objectent que la situation est différente dans une pâte où le rapport $\ell/s \leqslant 1$ et dans une suspension de rapport $\ell/s = 10$.

Ainsi pour différents rapports ℓ/s, on obtiendrait différents types de C-S-H. Dans un milieu dilué, il ne se formerait pas de C-S-H de type I comme avec C_3S en pâte, mais du C-S-H du type II (en nid d'abeilles).

Bien qu'en outre, dans une pâte, le milieu soit stagnant, il est remarquable que la durée de la "période d'induction" ne varie que de 4 à 6 heures et que la concentration maximale atteinte par la chaux ($\simeq 36.10^{-3}$ mole.kg^{-1}) reste la même lorsque le rapport ℓ/s passe de 0,5 à 10.

Cela paraît indiquer que les facteurs cinétiques jouant un rôle essentiel dépendent peu des masses des phases en présence et l'on pense tout naturellement que de tels facteurs sont les concentrations ioniques en solution, étant entendu que la réalisation des concentrations locales des diverses espèces dépend du rapport ℓ/s et du fait que le milieu est agité ou stagnant.

Sujet n° 5 :
La dissolution de C_3S est elle toujours incongruente ?
C'est la question posée à F. YOUNG par Mme REGOURD. Les partisans de l'incongruence de la dissolution de C_3S prennent comme argu-

ments les mesures de potentiel ζ qui dans les suspensions est trouvé > 0, ce qui est interprété comme un indice du passage préférentiel des ions Ca^{2+} en solution et de leur adsorption à la périphérie des grains. Le passage sélectif des ions Ca^{2+} et OH^- dans la phase liquide est souvent considéré comme l'effet de la présence à la périphérie des grains d'une couche protectrice à propriétés semi-perméables, comme on l'a vu plus haut dans le cas des pâtes. Mais F. YOUNG estime que dans les conditions utilisées par P. BARRET et col., de flux rapide de solvant à travers une couche de C_3S, la dissolution est probablement congruente.

Sujet n° 6 :
La discussion vient sur l'effet des sulfates alcalins sur C_3S.
J. SKALNY souligne leur effet accélérateur sur l'hydratation de C_3S, dû probablement à leur influence sur la solubilité de $Ca(OH)_2$. D'après Mme REGOURD, les sulfates alcalins augmentent la réactivité des aluminates plutôt en agissant sur la réaction entre sulfate de calcium et C_3A qu'en augmentant la réactivité propre de C_3A. Pour F.W. LOCHER, la présence de sulfates alcalins dans le clinker entraîne la formation d'une solution d'hydroxydes alcalins à pH élevé susceptible de provoquer une modification des premiers hydrates et donc de la résistance finale. J. SKALNY exprime son accord sur le fait que la résistance finale dépend des premiers hydrates produits.

Les questions posées par les intervenants ont été généralement des invitations à préciser certains points restés obscurs ou sans réponses dans les problèmes discutés. Par exemple, il est demandé par M. BAILEY si le panel est d'accord sur le fait que la microscopie électronique montre la formation de C-S-H durant la "période dormante" lorsque la concentration en ions silicates dans la solution est faible; M. BENSTED demande si ce n'est pas une simplification de discuter de la sursaturation des ions Ca^{2+} et OH^- pendant la période dormante et de ne pas parler des autres cations et anions sûrement impliqués. Pour M. STEIN, le mécanisme d'hydratation de C_3S présenté par J. SKALNY et F. YOUNG se heurte à deux objections : la dissolution congruente initiale de C_3S quand la précipitation à partir de la solution n'intervient pas et le rôle retardateur, plutôt qu'accélérateur de $Ca(OH)_2$.

D'autres questions tendent à faire préciser certains détails des mécanismes proposés par F.W. LOCHER sur l'influence de proportions relatives plus ou moins importantes de C_3A et de gypse. Par exemple, M. WALL demande si une plus grande différence dans le temps de prise entre le ciment Portland ordinaire et les "sulphate resisting cements" ne devrait pas être attendue, tandis que M. HELMUTH s'interroge sur la cause du retard à l'hydratation de C_3A puisqu'il s'observe avec ou sans la présence de gypse ?

Le Professeur FIERENS fait remarquer que l'influence des défauts dans les solides n'a pas été assez rappelée dans les discussions et cite à ce propos les observations par S.E.M. rapportées dans la publication de D. MENETRIER, D.K. Mc NAMARA, I. JAWED et J. SKALNY sur les premières secondes de contact entre β C_3S et l'eau, valables également pour C_3S et mettant en évidence une dissolution préférentielle aux joints de grains ainsi qu'une distribution non uniforme des produits d'hydratation à la périphérie des grains.

Sous-thème 2.2. : Structure et composition des hydrates.

Sujet n° 1 :
La discussion s'engage sur le problème des structures et des degrés de cristallinité. D'après F.H.W. TAYLOR, le degré de cristallinité du C-S-H est très faible. Alors que l'idée majeure de F.D. TAMAS est que la résistance des ciments est liée au degré de condensation des ions silicates dans le C-S-H, TAYLOR, qui est d'accord sur le fait que les ions silicates subissent une polymérisation au cours du temps, ne voit aucun lien entre la résistance des ciments et le degré de polymérisation. Pour lui, l'organisation des C-S-H repose sur celle de la chaux plus que sur celle de la silice. Ce serait les feuillets Ca-O qui commanderaient la morphologie. La question actuellement sans réponse certaine est celle de savoir si la polymérisation donne des chaines de silicates. D'après BERNAL, c'est l'enchevêtrement des matériaux qui confère la résistance.

F.H.W. TAYLOR est d'accord avec F.W. LOCHER sur le point que la structure des C-S-H initiaux influe sur la forme finale des hydrates produits et pense que les hydrates qui se forment tard dans l'évolution sont de type morphologique III dans la nomenclature de DIAMOND (grains formés de particules à peu près équidimensionnelles dans toutes les directions).

Sujet n° 2 :
Mme M. REGOURD revient sur les conclusions du Séminaire sur C_3A pour souligner l'influence des adjuvants sur l'hydratation de C_3A et notamment le retard provoqué sur celle-ci par le lignosulfonate de calcium. Il apparaît clairement, à la suite de la communication de V.S. RAMACHANDRAN que ce retard est dû à l'adsorption sur C_3A du lignosulfonate qui s'adsorbe également sur les aluminates hydratés hexagonaux. Cependant, pour F. MASSAZZA qui a étudié l'hydratation de mélanges de C_3A et de gypse en présence de lignosulfonate de sodium et de condensat de naphtalène sulfoné et de formaldéhyde dans le but d'éclaircir les causes de l'action fluidisante exercée par ces substances sur les pâtes de ciment, C_3A non encore hydraté n'adsorbe pas ces adjuvants. Ce sont les sulfoaluminates hydratés qui absorbent des quantités considé-

rables de ces adjuvants et cela cause des modifications morphologiques dans les cristaux d'ettringite qui apparaissent sous forme de petites aiguilles au lieu de gros cristaux fibreux. Cette morphologie différente pourrait expliquer, au moins partiellement, l'action exercée par ces superfluidifiants sur la rhéologie des pâtes de ciment. En outre, ce feutre microcristallin sur les grains de $C_3\bar{A}$ empêcherait son hydratation.

D'autre part, le changement de signe du potentiel ζ qui passe de + à - en présence de lignosulfonate et de carbonate de sodium ou d'un adjuvant à base de polymère de naphtalène sulfoné, pourrait, d'après les expériences de M. COLLEPARDI contribuer à la fluidisation.

D'autres modes d'action sont évoqués, notamment la formation de complexes en solution, par certains des intervenants.

En conclusion générale, il apparaît que de nombreux progrès ont été accomplis grâce à la mise en oeuvre de méthodes expérimentales nouvelles : ESCA, AUGER, S.E.M. et T.E.M.S.C.A.N., triméthylsilylation, chromatographie en couche mince, spectrométrie de masse et grâce à une meilleure utilisation des moyens analytiques plus traditionnels. Cependant, il faudra encore du temps pour que les nouvelles données soient prises en compte dans les interprétations et leur permettent de triompher des nombreuses idées préconçues, qui retardent le progrès dans les connaissances et leurs possibilités d'application à la technologie du ciment.

CONCLUDING REMARKS

by F. W. LOCHER

The panel descussion and general discussion dealt with the subjects of
1. Initial reactions,
2. Hydration of calcium silicates and
3. Influence of admixtures.

The summary below contains the main conclusions which can be drawn from the contributions to the congress and the discussion.

1. INITIAL REACTIONS

In the first minutes after mixing, the share of tricalcium silicate, dicalcium silicate, tricalcium aluminate and calcium aluminate ferrite decreases slightly by 1 % due to reaction with water. This is followed by the induction period which lasts for several hours during which the share of the 4 clinker compounds is not further reduced or is only reduced very slightly. After the induction period, which can vary in length for the 4 clinker compounds, the hydration reactions occur in which compounds essential for hardening form, in particular calcium silicate hydrates.

Basically two reaction mechanisms are considered the cause of the induction period:
1) Blocking of the surface mechanisms of the cement constituents and
2) Hindrance of the crystallization of the hydration products.

A blocking of the surface may be caused by various ions or molecules accumulating from the pore solution, by the development of a less permeable cover of metastable hydration products or by the dissolving of certain elements, e.g. Ca^{2+}, resulting in a less reactive surface layer richer in SiO_2.

A hindrance of crystallization may occur if at first a certain oversaturation in calcium hydroxide has to be attained so that the nucleus of crystallization with a critical size, necessary for the rapid formation of the hydration products, can form.

The cause of setting appears to be the formation of a more or less rigid network of hydration products which develop during the first reaction before the induction period. The agglomeration of the cement particles and of the first hydration products as a result of surface forces probably also play a major role here.

Hydration products which are involved in the formation of the first network are primarily calcium aluminate hydrates and/or calcium aluminate sulphate hydrates. Calcium silicate hydrates may also be involved in Portland cement; in pastes of pure tricalcium silicate they are the only cause of setting.

A large number of studies have shown that the setting of Portland cement depends to a large degree on the reaction between tricalcium aluminate and sulphate. The share of tricalcium aluminate which dissolves directly after the cement is mixed until the beginning of the induction period, reacts with the sulphate from the alkali sulphate of the clinker and from the calcium sulphate which is contained in the cement in the form of admixed gypsum, hemihydrate, soluble anhydrite and/or natural anhydrite. Depending on the share of quantities in the solution, ettringite, monosulphate, calcium aluminate hydrate and/or gypsum then forms. The greatest possible retardation always occurs when the share of tricalcium aluminate dissolved before the beginning of the induction period is bound solely as ettringite.

It is generally assumed that the retardation of the setting by the admixture of calcium sulphate is due to a corresponding retardation of the chemical reaction. This is in contrast, however, to the finding that the calcium sulphate admixture does not retard the hydration of the tricalcium aluminate and tricalcium silicate in the period important for setting. This would mean that it is not pimarily the quantity of newly-formed hydration products which are important for setting but their tendency to form a rigid structure as a result of recrystallization. Here the agglomeration of the cement particles as a result of surface forces could play a decisive role. The calcium sulphate admixed as a set retarder, would thus prevent the share of tricalcium aluminate dissolved at the beginning of hydration and maybe also the share of calcium aluminate ferrite, crystallizing as coarse-grained, structure-forming calcium aluminate hydrate but it would settle as a thin cover of fine-grained ettringite on the surface of the cement particles. The cause of setting would then be the slow formation of a structure of recrystallized ettringite. On the other hand, it is also possible that the calcium silicate hydrate is involved in the formation of the first structure which is very important for setting. At the time, however, at which setting normally begins, the quantity is much lower than that of the other hydration products. It is thus improbable that in the case of Portland cement the formation of calcium silicate hydrate controls the setting.

2. HYDRATION OF THE CALCIUM SILICATES

In the hydration of the calcium silicates, calcium silicate hydrate occurs as a reaction product to which the hardened cement paste owes its strength in particular. Despite extensive research it is not yet possible to give a generally accepted description of the formation of the calcium silicate hydrate, its chemical composition and its structure.

During the initial reaction before the induction period a small share of the calcium silicates are dissolved either congruently if calcium and silicate ions go into solution in the same quantities in which they are originally contained in the silicates or incongruently if more calcium ions are dissolved.

The calcium silicate hydrate which occurs as a reaction product does not have a uniform composition; the ratio of CaO/SiO_2 varies in the range of between approx. 1.5 and 3.0. It may contain larger quantities of foreign substances, in particular aluminium, iron, alkalies and sulphate.

During hydration the silicic acid polymerizes. The degree of polymerization appears to be greater the slower the calcium silicates hydrate.

The arrangement of the calcium and silicate ions in the calcium silicate hydrate is closer to the amorphous state than to the regular arrangement in a crystal lattice. There does not appear to be any connexion between the degree of crystallinity and the mechanical properties of hardened cement paste.

3. INFLUENCE OF ADMIXTURES

Admixtures of foreign substances soluble in water can retard or accelerate the hydration of the cement compounds, can influence the change of hydration products already formed or can alter the zeta-potential, i.e. the surface charge of the solid particles and their agglomeration behaviour. Chlorides, nitrates and nitrites accelerate hardening because they increase the initial reaction of the tricalcium silicate and tricalcium aluminate and reduce the induction period of both constituents. Compounds of heavy metals soluble in water, e.g. zinc, lead and copper, increase the induction period of the tricalcium silicate and thus retard hardening. As, on the other hand, they increase the initial reaction of the tricalcium aluminate, they increase the amount of ettringite formed at the beginning. The result may be a rapid start of setting and a higher heat of hydration. Glucose and lignosulphonate can have a similar effect.

The effect of all admixtures depends largely on the amount added. It also depends on whether and to what degree the admixtures influence the solution behaviour of the calcium sulphate and Ca^{2+} ion concentration of the solution.

Surface-active admixtures reduce, in particular, the viscosity of the cement paste but do not greatly change the setting and hardening. Without admixtures, agglomerates form in the cement paste shortly after mixing as the solid particles attract each other under the effect of surface forces. As a result the viscosity of the cement paste increases. This process is increased by sulphate ions in the mixing water solution. Surface-active substances, e.g. melamine compounds, reduce the viscosity greatly as they change the surface charge of the particles and thus reduce the tendency to agglomerate.

THEME III

Structure des laitiers et hydratation des ciments de laitier

par M. VON EUW

Messieurs les Présidents,
Mesdames,
Messieurs,

1. PREAMBULE.

Mes éminents collègues du Comité Scientifique ont eu l'extrême indulgence de me confier la Présidence du Thème consacré aux laitiers et ciments de laitier. Je les en remercie et je souhaite ne pas les décevoir par ce trop bref exposé.

Les travaux présentés à ce 7ème Congrès International de la Chimie des Ciments sont soumis à 3 directives émises par le Comité Scientifique :

- présenter essentiellement un caractère scientifique et non pas technologique.
- concerner des produits élaborés industriellement, sans toutefois exclure des préparations en laboratoire.
- orienter les recherches dans des directions favorables aux économies d'énergie.

30 communications, 3 rapports principaux et 8 posters présentés par 13 pays rendent compte des résultats obtenus depuis le Congrès de Moscou dans les études visant à relier les phénomènes d'hydraulicité à la structure des laitiers. Le fait que les travaux exposés concernent des laitiers ou scories industriels aboutit à une diversité d'informations que j'ai essayé de mettre à profit pour établir le lien indispensable entre composition-structure et réactivité. En permettant de mieux comprendre les phénomènes en jeu, tant dans l'élaboration que dans l'utilisation de ces sous-produits industriels, une contribution importante est apportée à l'objectif général des économies d'énergie.

Cette préoccupation de valoriser des sous-produits d'origines diverses en les faisant entrer dans la production des liants, soit dans la Cimenterie, soit en dehors de cette Industrie, conduit à distinguer, d'une part, l'origine des produits, d'autre part, leurs modes d'activation.

Afin d'établir une certaine cohérence entre les communications, je traiterai d'abord des laitiers de haut-fourneau et des ciments correspondants. Les problèmes posés par les laitiers d'aciérie et les scories de métaux non ferreux seront discutés ensuite.

2. LAITIERS DE HAUT FOURNEAU.

2.1. CARACTERISATION.

Les méthodes utilisées se rapportent à l'analyse chimique, à la structure et à l'hydratation.

2.1.1. Méthodes chimiques.

Parmi les diverses méthodes retenues pour caractériser les laitiers, l'analyse chimique est certainement la plus courante. Il existe deux possibilités d'utiliser les résultats de l'analyse élémentaire, soit le calcul d'indices ou modules, soit le calcul de la composition minéralogique potentielle.

Les auteurs qui utilisent les indices chimiques relient la réactivité des laitiers à leur basicité. Les nombreuses formules adoptées expriment le rapport pondéral ou molaire des éléments basiques aux éléments acides; certaines tiennent compte du rôle amphotère de l'alumine.

SMOLCZYK dans son rapport principal, après avoir fait une étude critique de ces indices établit une régression multiple entre les teneurs des constituants et les résistances. Il précise cependant que les coefficients dépendent beaucoup du clinker utilisé.

La critique que nous pouvons faire à l'emploi des indices est que ceux-ci définissent des limites, mais ne permettent pas d'établir une relation réelle. Ceci d'autant plus qu'elles ne prennent en compte qu'une partie de la composition. C'est pourquoi les calculs de corrélation multiple appliqués aux laitiers par SMOLCZYK donnent de meilleurs résultats.

.../...

DEMOULIAN ajoute aux propositions de SMOLCZYK la prise en compte d'autres éléments de l'analyse tels que Cl, Ti, F, S, ainsi que la somme des minéraux dosée par microscopie optique.

Les corrélations multiples de SMOLCZYK et celles de DEMOULIAN montrent que l'appréciation de l'hydraulicité par les nombreux modules chimiques habituels ne concernant que les éléments majeurs sont insuffisants. Ceux qui placent l'alumine au dénominateur comme formateur de réseau donnent de moins bons résultats que ceux qui l'introduisent au numérateur comme modificateur de réseau; c'est probablement la raison qui a fait choisir le rapport $\frac{Al_2O_3}{SiO_2}$ pour sélectionner les laitiers hydrauliques en URSS, ainsi que l'avait relaté SATARINE au Congrès de Moscou.

Le rôle de MnO a été traité en tant qu'élément mineur respectivement par SMOLCZYK et DEMOULIAN, mais certains laitiers en renferment des proportions importantes, ainsi que le signale TANEJA. Cet auteur a étudié des laitiers indiens renfermant 3 à 7 % de MnO, et il a vérifié que les ciments métallurgiques correspondants font preuve d'une bonne hydraulicité. Un tel résultat pourrait paraître infirmer la règle classique selon laquelle MnO a une influence négative sur la valeur hydraulique des laitiers. En fait SOLACOLU avait montré dans une étude publiée en 1964 que le rôle de MnO pouvait être soit négatif, soit neutre, soit positif selon la basicité du laitier. A l'examen il apparaît que le laitier de ROURKELA, qui a été étudié par TANEJA, se place dans la catégorie peu basique définie par SOLACOLU. Ceci explique que malgré son taux élevé de MnO, les résistances du ciment soient conformes aux normes indiennes.

Une autre façon d'utiliser l'analyse élémentaire est le calcul de la composition minéralogique potentielle proposée par GOURDIN et introduite par DEMOULIAN dans ses corrélations multiples.

Les minéraux qui cristallisent lors de la dévitrification complète des laitiers dans le système SiO_2, Al_2O_3, CaO, MgO ont une structure à base de chaînes SiO_3^{2-}, ou de doubles tétraèdres $Si_2O_7^{6-}$, ou encore de tétraèdres simples SiO_4^{4-}. Les auteurs ont observé une relation entre les bonnes résistances développées par certains laitiers et les structures à base de tétraèdres simples dans les minéraux de la composition potentielle.

2.1.2. Méthodes basées sur la structure.

Si la composition chimique joue un rôle essentiel dans la valeur hydraulique des laitiers, leur structure est non moins prépondérante. On sait depuis longtemps que l'état vitreux est indispensable, mais des précisions viennent d'être apportées quant aux méthodes basées sur la structure.

FIERENS par la mesure de l'exoémission électronique a pu apprécier les défauts de surface agissant comme centres de formation des germes de sels hydratés. L'auteur a mis les taux d'exoémission en corrélation avec les résistances en compression de microéprouvettes de laitier gâchées à la soude.

HAWTHORN a relié les résistances ISO de ciments à haute teneur en laitier aux dimensions des hétérogénéités du verre mesurées par diffusion centrale des rayons X.

SMOLCZYK examine la répartition des minéraux par microscopie optique; il en déduit que les germes cristallins bien dispersés dans la masse vitreuse, ont une influence favorable à l'hydraulicité.

Mme REGOURD a recristallisé par chauffage à 850° 7 laitiers de compositions différentes. Elle a constaté que la réactivité est fonction du taux de gehlénite dans la mélilite. Il s'agit là d'une méthode rapide d'appréciation de l'hydraulicité qu'il est d'ailleurs possible de recouper par le calcul en utilisant l'analyse chimique.

DRON montre que les taux de dissolution en milieu sodique de la silice, de l'alumine et de la chaux, sont en relation directe avec la basicité et la teneur en alumine du laitier; ceci est en accord avec les résultats d'HAWTHORN opérant sur les mêmes laitiers, et se trouve d'ailleurs illustré par ceux des essais mécaniques ISO.

2.1.3. Méthodes basées sur l'hydratation du laitier.

A priori, il semble logique de vouloir relier le taux d'hydratation aux résistances mécaniques mesurées sur éprouvettes.

Mme REGOURD travaillant sur des pâtes pures de ciment CHF, préparées à partir des laitiers retenus par DRON et HAWTHORN, trouve une bonne relation entre le taux de laitier hydraté et les résistances mécaniques.

De même, elle trouve une bonne relation avec la chaleur d'hydratation, et elle conclut avec E. GAUTIER et leurs collaborateurs, que dans la comparaison de la réactivité des laitiers, la calorimétrie se révèle être une méthode très sensible.

.../...

DAIMON préconise de son côté la détermination du degré d'hydratation par l'extraction sélective des phases.

En définitive, quels que soient les procédés d'appréciation de l'hydraulicité, tous doivent se référer aux résultats donnés par les mesures de résistances mécaniques, et ces essais sont effectués sur des mélanges laitier/clinker.

Malheureusement, les résultats obtenus ne sont pas seulement fonction de la qualité du laitier, mais de celle du clinker, du taux de gypsage et de la finesse des constituants ainsi que de l'échéance retenue.

2.2. STRUCTURE ET REACTIVITE DES LAITIERS.

2.2.1. SMOLCZYK reprend dans son rapport principal la théorie de ZACHARIASEN selon laquelle le verre de laitier est un réseau à trois dimensions, plus ou moins déformé. Le silicium y forme des tétraèdres SiO_4^{4-} plus ou moins polymérisés. Les charges négatives de ces groupes anioniques (Tétraèdres, doubles tétraèdres, chaines) sont compensées par les charges positives des cations. Ces cations, dont le rayon ionique est plus grand que celui du silicium, sont situés dans les cavités où ils jouent le rôle de modificateur du réseau. Le degré de polymérisation des tétraèdres SiO_4^{4-} est alors d'autant plus petit que la part des cations modificateurs est plus grande à l'intérieur du réseau. Il en résulte pour le verre correspondant une plus grande instabilité, donc une plus grande réactivité chimique.

L'ion Ca^{2+} avec la coordinance 6 est le modificateur de réseau responsable en majeure partie de l'activité du laitier, ce qui explique l'usage de l'indice CaO/SiO_2. L'aluminium et le magnésium, apparaissent dans le réseau des laitiers avec les coordinances 4 et 6 soit comme formateurs, soit comme modificateurs. Ceci explique la place qui leur est donnée dans certains indices d'hydraulicité.

2.2.2. ROIAK considère que les différences existant entre les cations dans le réseau, constituent un facteur essentiel de l'activité du laitier. Selon cet auteur les dépenses en énergie de rupture de la liaison Me - O doivent en effet varier avec la position du cation. Il y a création de conditions favorables au passage du cation en solution aqueuse si l'énergie cinétique des molécules d'eau et l'énergie de liaison Me - O, affaiblie dans le milieu aqueux, sont du même ordre.

De telles conditions sont réalisées avec un optimum de cations modificateurs dont le passage en solution perturbe l'électro- neutralité locale.

Approfondissant sa théorie reliant l'hydraulicité à la structure, ROIAK fait apparaître par résonnance paramagnétique électronique la présence de centres paramagnétiques sur les tétraèdres SiO_4 de la structure vitreuse, alors qu'ils sont absents des structures cristallines.

Cet auteur explique que le début du processus d'hydratation est la dissolution du liant, mais que ce processus se poursuit par la polymérisation des radicaux hydratés. Ce phénomène de polymérisation contribue à la formation de particules gélifiantes qui adsorbent à leur surface les cations déjà passés en solution, d'où la formation des hydrosilicates des métaux correspondants.

ROIAK démontre de cette manière qu'il existe entre la partie non hydratée du laitier vitreux et les hydrosilicates de calcium, une couche intermédiaire gélifiante de faible basicité.

2.2.3. DRON dans sa communication, propose une théorie statistique de la structure. Il assimile la structure du verre de laitier à celle d'un liquide constitué de silicates fondus et il fait ressortir que la longueur des éléments de la structure des silicates fondus n'est pas uniforme comme dans un cristal : elle est distribuée suivant une progression géométrique. La longueur et la ramification de ces éléments, qui dépendent de la quantité d'ions modificateurs de réseau, conditionnent la réactivité.

2.2.4. Il faut ajouter à celà que certains éléments mineurs, tels que Na et K, par leur rôle modificateur de réseau améliorent la réactivité du laitier tel que l'ont montré DEMOULIAN et ses collaborateurs, ainsi que SMOLCZYK.

2.2.5. On peut par ailleurs mettre en évidence dans les laitiers industriels, l'existence de microhétérogénéités correspondant à un degré supérieur d'organisation locale. A la suite d'autres chercheurs, c'est ce qu'ont vu également HAWTHORN et ses collaborateurs par des études de diffusion centrale aux rayons X. Ces auteurs ont montré expérimentalement que les diamètres des microhétérogénéités, compris entre 300 et 900 Å, sont une résultante de la composition chimique et de l'histoire thermique du laitier.

L'hydraulicité des laitiers varie pour les cas étudiés par HAWTHORN en sens inverse du diamètre des microhétérogénéités.

Ces expériences pourraient être interprétées en se rapprochant des théories de SOLACOLU et BUSCH relatées par SATARINE au Congrès de Moscou.

Par ailleurs, on observe dans la plupart des laitiers des cristallisations visibles au microscope optique.

.../...

DEMOULIAN et ses collaborateurs ont identifié les différentes espèces cristallines présentes en utilisant la diffraction des rayons X, l'examen au microscope électronique à balayage, puis, la microsonde de Castaing.

Ces cristaux sont de la merwinite et de la mélilite. La présence de ces minéraux influence favorablement la réactivité hydraulique des laitiers. Les auteurs ont dosé, selon les cas examinés, de 0 à 30 % de cristaux. Il semble qu'il existe un optimum de cristallisation qui est fonction de la composition pour chaque type de laitier. Cet optimum est lié en particulier à la composition et au traitement thermique du laitier.

On peut être tenté d'expliquer le rôle positif d'une cristallisation partielle, par la modification de la composition chimique du verre dans un sens favorable à sa réactivité. Ainsi la cristallisation de la merwinite enrichit le verre en alumine et éléments mineurs.

2.2.6. Dans une autre optiqueROPER a étudié la morphologie de 8 laitiers d'origines diverses obtenus avec des procédés de trempe différents, tels que la trempe à l'eau, la trempe à l'air et le bouletage. ROPER observe que selon le mode de refroidissement les grains de laitiers sont constitués de verres hétérogènes et de particules aciculaires. Il explique que partant d'un laitier fondu d'une composition globalement basique, les hétérogénéités dues au mode de refroidissement peuvent entraîner la séparation de particules aciculaires plus ou moins développées et de composition acide.

2.2.7. Enfin, une particularité intéressante de la texture des laitiers a été étudiée par COURTAULT. COURTAULT s'intéresse aux gaz dissous et aux gaz occlus. Il a analysé les gaz occlus après extraction par broyage sous vide et il a constaté que l'aptitude au broyage et la réactivité des laitiers sont améliorées par l'existence de ces gaz occlus.

2.3. HYDRATATION DU LAITIER.

2.3.1. Les travaux récents communiqués au Congrès relancent la discussion de deux théories en complément des explications développées par ROIAK dans son analyse de la structure et de la réactivité des laitiers vitreux : la réaction dissolution-diffusion-cristallisation appelée par certains "trans-solution", et la réaction topochimique.

2.3.2. Réaction "trans-solution".

DRON interprète la solubilisation initiale du laitier comme le passage sélectif en solution d'entités structurales analogues à celles de la rankinite et de l'aluminate monocalcique.

Les ions Ca et les ions aluminates et silicates en solution s'accumulent jusqu'à sursaturation et précipitation sous forme de C S H et d'aluminates hydratés.

VERNET considère à la fois les comportements simultanés du clinker et du laitier mis ensemble en présence d'eau. Il a étudié pour cela 16 ciments à fortes teneurs en laitier et les a comparés au Portland fait avec le même clinker.

L'auteur analyse en continu l'évolution des concentrations ioniques dans des suspensions de rapport $\frac{\text{eau}}{\text{ciment}} = 4$. Il résulte de cette étude que le laitier et le clinker se dissolvent simultanément, mais à des vitesses différentes. Le clinker agit sur la vitesse de dissolution du laitier, et réciproquement la consommation de chaux par le laitier augmente la vitesse de dissolution de l'alite.

L'auteur désigne ces interactions sous l'appellation de "couplages chimiques". Il trouve une similitude dans les actions réciproques des chaleurs dégagées par les réactions d'hydratation, et par analogie il les nomme "couplages thermiques".

VERNET par ses expériences montre la simultanéité des pics de flux thermiques et des variations de concentration des ions en solution.

L'examen des courbes de concentration ionique fait apparaître pour tous les ciments de laitier l'existence de quatre périodes au cours de l'hydratation.

Il faut en retenir que dès la première période le laitier participe à la saturation de la solution en même temps que le clinker; et ceci est une notion nouvelle que l'auteur prouve en se basant sur les différences de concentration ionique en relation avec les différents laitiers et le clinker correspondant.

Mme REGOURD confirme la participation précoce du laitier aux réactions d'hydratation en s'appuyant sur les résultats de mesure de la chaleur d'hydratation et sur l'identification au microscope à balayage et par diffraction des rayons X des minéraux hydratés formés : en effet, l'abondance de l'ettringite n'est justifiée que par la consommation de l'alumine du laitier. Les travaux de Mme REGOURD et ceux de VERNET, par des voies différentes, viennent à l'appui des conceptions de ROIAK sur la structure des laitiers grâce auxquelles l'auteur explique l'hydraulicité par la réaction de dissolution-diffusion-cristallisation.

.../...

2.3.3. Réaction topochimique.

Bien que Mme REGOURD et VERNET démontrent assez clairement par leurs expériences que l'hydratation s'effectue par dissolution et cristallisation, cette conception n'est pas partagée par tous les chercheurs. Ainsi, ABO EL ENEIN écrit que les grains de laitier réagissent topochimiquement avec la solution d'hydroxyde de calcium, et DRON, de son côté, n'exclut pas la possibilité de réactions pouzzolanique et topochimique à partir du squelette laissé par l'attaque hydrolytique préalable.

DAIMON exposant ses propres travaux et ceux de KONDO dans son rapport principal suppose que le laitier s'hydrate topochimiquement et il met d'ailleurs l'accent sur l'inhibition de la réaction d'hydratation par la formation de couches d'hydrates faiblement perméables enrobant les grains. Cette inhibition lui apparaît très rapide avec les activants alcalins.

De toute façon, la discussion reste ouverte sur le principe même du processus d'hydratation, lequel d'ailleurs n'est pas propre aux laitiers. Heureusement, la plupart des chercheurs s'accordent sur la nature des hydrates formés.

2.3.4. Hydrates formés.

Les travaux de Mme REGOURD, de TEOREANU, de SERSALE, de ABO EL ENEIN, de VERNET, et leurs collaborateurs, montrent tous la formation de C S H, de portlandite, d'ettringite et de monosulfoaluminate.

Cependant, TEOREANU étudiant le système laitier - chaux - gypse - eau, trouve qu'il se forme transitoirement de la géhlénite hydratée C_2 S A H_8 qui se transforme à long terme en hydrogrenat. A ce sujet, DRON précise que la géhlénite hydratée ne peut se former qu'après la disparition de la chaux.

VERNET, lui, pense avoir trouvé un sulfuroaluminate de calcium hydraté, ou une solution solide de CaS dans l'aluminate et qui seraient analogues au monosulfoaluminate. Il a révélé la formation probable de ce nouvel hydrate dans son étude de la cinétique d'hydratation des ciments à fortes teneurs en laitier.

Enfin, MASCOLO a préparé par synthèse des hydroxydes doubles de Mg et Al et les produits carbonatés correspondants. Il pense que la résistance aux sulfates s'explique par la formation préférentielle de ces produits carbonatés.

2.3.5. Chaleur d'hydratation.

La chaleur d'hydratation ou plutôt la chaleur dégagée à une échéance donnée est liée à la fois à l'enthalpie de chacune des réactions et à la cinétique de l'hydratation.

A ce sujet, les conceptions de "couplages chimiques" et de "couplages thermiques" énoncées par VERNET et ses collaborateurs, selon lesquelles le clinker et le laitier ont des interactions aboutissant à l'augmentation des taux de réaction de chacun de ces constituants, trouve une confirmation dans les travaux de TOTANI. Nous comprenons en effet du travail de TOTANI que la chaleur d'hydratation de l'alite ou du clinker est augmentée dans les ciments au laitier du fait de l'interaction des constituants.

2.4. MODES D'ACTIVATION CHIMIQUE.

Nous avons vu que pour être effectives, les réactions d'hydratation exigent que le laitier soit maintenu dans un milieu à pH suffisant quel que soit le processus, dissolution - précipitation ou topochimique.

2.4.1. Activations non calciques.

Selon les utilisations plusieurs modes d'activation sont proposés, autres que l'activation calcique : VOINOVITCH a étudié et préconisé l'emploi des métasilicates de sodium; il a défini le dosage en fonction de la température; il a mis au point un liant qu'il nomme silicociment, lequel est constitué de laitier broyé additionné éventuellement de gypse naturel ou chimique et de filler calcaire.

VOINOVITCH précise que des travaux similaires effectués par des chercheurs Soviétiques et Polonais ont abouti à des résultats analogues.

SATARINE parvient à préparer des bétons armés à plus hautes performances mécaniques que les bétons de Portland en ajoutant un activant polyminéral sulfoalumino-siliceux. Cette action qui se manifeste sur les résistances à tous les âges est conservée dans le cas d'un traitement thermique humide. Selon l'auteur, ces hautes performances sont dues à la formation précoce d'une carcasse d'ettringite remplie d'hydrosilicates de calcium. SATARINE insiste sur la densité de la structure favorisée par la naissance ultérieure de gels de boehmite et de gypsite.

2.4.2. Activation sulfo-calcique par le clinker et le gypse.

Bien sûr, l'activant le plus étudié et le plus employé à ce jour reste le clinker de portland. La plupart des auteurs étudiant l'hydratation des laitiers utilisent des mélanges laitier/clinker.

SMOLCZYK dans son étude déjà citée sur les corrélations entre composition et résistances, constatait une forte influence de la nature du clinker dans le cas de ciments à 60 et 75 % de laitier.

.../...

HAWTHORN lui, a eu pour objectif de préciser le rôle du type de clinker avec les trois laitiers déjà cités utilisés au dosage de 80 %.

Une expérimentation portant sur 7 clinkers couvrant un large éventail de composition minéralogique a montré que :

1. L'influence de la qualité du clinker n'est pas importante avant 2 jours.

2. De meilleures performances sont obtenues à 28 jours avec les clinkers riches en alite et en C_3A tétragonal.

3. L'accroissement de résistances jusqu'à un an est essentiellement fonction de la finesse du laitier.

L'étude a aussi montré que le gypsage optimal est fonction de la finesse du laitier, du temps de réaction et de la teneur en C_3A du clinker.

Par ailleurs, le surgypsage d'un ciment de laitier du type CLK à finesse peu poussée est très préjudiciable aux résistances.

Enfin, je rappellerai que DRON avait précisé que la chaux et le gypse sont de véritables réactifs, alors que la soude ne joue qu'un rôle de catalyseur.

2.5. TRAITEMENTS THERMIQUES.

Mme REGOURD, GAUTIER et leurs collaborateurs ont étudié l'influence de la température sur les courbes de durcissement de ciments CHF.

Après traitement thermique à 50°, les différences entre 7 laitiers de diverses qualités sont pratiquement effacées, mais le niveau des résistances atteint dans tous les cas, reste inférieur à celui que l'on obtient à 20°.

En revanche, un traitement à 80° montre un comportement différent très favorable aux ciments les moins réactifs à 20°, et très défavorable aux ciments les plus réactifs.

Mme REGOURD a montré avec l'aide du microscope électronique à balayage que dans le cas du CHF peu réactif à 20°, un traitement à 80° aboutit à un aspect normal des hydrates, alors que dans le cas du CHF réactif, ce même traitement engendre des amas de monosulfoaluminates provoquant une texture hétérogène, laquelle est peu favorable à la cohésion du mortier.

GOVOROV a voulu étudier le comportement dans un traitement hydrothermal jusqu'à 285° de laitiers synthétiques pour une gamme de composition très large sortant du domaine habituel des laitiers sidérurgiques.

GOVOROV rappelle que dans le traitement hydrothermal à 250° les laitiers dont la structure est faite de tétraèdres isolés ou de groupements limités, c'est-à-dire, les laitiers mélilitiques, donnent des hydrogrenats, alors que ceux dont la structure est faite de chaines de tétraèdres, donnent de la tobermorite. Ces deux types d'hydrates sont eux-mêmes constitués comme les produits anhydres d'origine, soit de tétraèdres ou de groupements isolés, soit de chaînes.

L'auteur trouve que le passage en solution de la silice est d'autant plus retardé que la structure est compliquée.

La chaux accèlère aussi bien le passage de la silice en solution que sa recombinaison en hydrosilicate de calcium; cela a pour effet d'avancer le début du durcissement, mais GOVOROV précise que l'addition optimale de CaO est limitée à une valeur de 0,3 à 0,8 %.

Cette étude trouve une application dans l'utilisation des coulis de laitiers pour puits de forage profonds.

HOOTON a étudié l'autoclavage de laitiers bouletés en mélanges ternaires avec du ciment portland et de la farine de silice, soit en pâte pure, soit en mortier. Il a trouvé que les résistances à la compression sont considérablement augmentées par l'addition de farine de silice.

2.6. CONTROLE DE LA COMPOSITION DES CIMENTS DE LAITIER.

Nous venons de voir que les laitiers de haut-fourneau activés de différentes manières peuvent donner des ciments hydrauliques. Ces ciments se caractérisent par des performances mécaniques et chimiques égales ou même supérieures à celles des portlands selon l'échéance considérée. Il est cependant indispensable comme pour tous les types de ciments de garantir la régularité de leur qualité. Cette régularité dépend à la fois de la réactivité des constituants et de leurs proportions.

La surveillance de ces proportions nécessite de disposer de méthodes de contrôle rapides et précises.

DEMOULIAN a apporté une contribution intéressante à la résolution de ce problème en proposant la dissolution sélective du clinker et du gypse dans une solution sodique de EDTA et de triethanolamine à pH = 11,5 $\pm$ 0,1. Dans ces conditions, le laitier est insoluble et son dosage est obtenu directement par filtration.

.../...

2.7. UTILISATIONS DIVERSES DES LAITIERS ET SCORIES.

Je voudrais rappeler l'utilisation des laitiers et scories comme matières premières dans la préparation des mélanges crus pour ciment portland, ce qui conduit à une sensible économie d'énergie.

Parmi les utilisations nouvelles des laitiers il faut enfin citer les études de BELETSKAIA et LOUGUININA ainsi que de KLUKHOVSKY pour la production de clinker d'un type nouveau à base de laitier et d'additions alcalines.

Par ailleurs, une proposition originale est faite par SOULEIMENOV pour corriger les laitiers par addition de poussières alcalines de cimenterie dans le laitier fondu au moment de la granulation.

3. AUTRES LAITIERS ET SCORIES.

3.0. La période actuelle d'économie amène les industriels du monde entier à valoriser les sous-produits de toutes origines, c'est le cas pour les laitiers de métallurgies diverses, allant des laitiers d'aciéries aux laitiers de la métallurgie du zinc, du nickel, du cuivre, etc...

Alors que les laitiers de hauts fourneaux se caractérisent par une hydraulicité latente, les scories d'aciéries ayant une composition chimique riche en chaux combinée, sont directement hydrauliques, les autres au contraire doivent être activées.

Les laitiers de métaux non ferreux ont par contre une structure tout à fait différente et se comportent le plus souvent comme des pouzzolanes.

3.1. SCORIES D'ACIERIES.

La plupart des scories d'aciéries n'avaient pas jusqu'à maintenant été employées comme liants hydrauliques étant donné leur composition chimique non adaptée. Cette non-adaptation réside principalement dans l'insuffisance de silice et surtout d'alumine, ainsi que dans un large excès d'oxyde de fer, de chaux libre, et souvent de magnésie.

GEORGES et SORENTINO ont étudié en remplacement du spath fluor un nouveau fondant synthétique désigné CAMFLUX apportant les éléments manquant à la scorie et qu'ils mettent en oeuvre dans le convertisseur B.O.P au début de l'affinage.

Cette opération améliore à la fois la composition et l'homogénéité de la scorie. Elle rend cette dernière hydraulique et supprime le gonflement.

Les auteurs ont étudié l'hydraulicité de la scorie améliorée en suivant la fixation de l'eau et le dégagement de chaleur en fonction du temps. Ils en ont conclu que la valeur hydraulique de tels produits est malgré tout insuffisante, et qu'il est nécessaire de les additionner de ciment portland, comme pour les laitiers de haut-fourneau afin d'obtenir des résistances convenables.

Cependant, il existe des laitiers d'aciéries dont la composition chimique est telle que la teneur en C_3S en fait des produits directement hydrauliques.

Ce sont des produits de ce type qui ont été étudiés par WANG Yu Ji.

L'étude pétrographique de cet auteur indique comme constituants: du C_3S en quantités variables, du C_2S, du C_2F et des solutions solides de FeO et de MgO ainsi que de la chaux libre.

L'auteur relie à la teneur en C_3S les résistances à 28 jours données par de tels laitiers normalement gypsés, mais il élimine ceux qui renferment plus de 3 % de chaux libre, étant donné leur forte tendance à l'expansion.

LUO SHOUSEN étudie également les scories d'aciéries et s'attache particulièrement à définir l'état de la magnésie en vue de remédier au gonflement qu'elle provoque.

LUO a travaillé avec 6 scories d'origines différentes dont la teneur en magnésie varie de 6 à 18.

Cet auteur a montré que la magnésie est inoffensive si elle est combinée à l'état de composés silicatés, ou si elle se trouve en solution solide avec FeO et MnO.

L'auteur précise que dans les scories réductrices MgO est à l'état de périclase et que les ciments qui seraient fabriqués avec de telles scories seraient détruits à l'autoclavage. En revanche, il existe pour les scories oxydantes une teneur optimale en magnésie définie par le rapport $\frac{MgO}{FeO + MnO}$ lequel doit rester inférieur à 1.

Pour éviter le gonflement LUO propose d'utiliser par mélange avec du clinker de portland les scories où MgO est combiné à l'état de silicates et il remédie à l'expansion des laitiers réducteurs riches en périclase en les additionnant, soit de sulfate de magnésium, soit de laitier de haut fourneau granulé, soit de matières siliceuses telles que les cendres volantes. Il propose également un traitement de carbonatation en l'absence de gypse.

Par ailleurs, le problème de l'hydratation de la magnésie a été étudié par MASCOLO et MARINO qui ont synthétisé les hydroxydes doubles de Mg et Al identifiés dans les produits d'hydratation des laitiers de haut fourneau en présence de chaux.

Ces auteurs ont montré que des laitiers à forte teneur en MgO sont capables de résister à l'attaque des sulfates parce que les tétraèdres SO_4^{2-} pénètrent difficilement dans la structure des hydroxydes doubles.

.../...

Ils constatent accessoirement une carbonatation facile de ces hydroxydes pour former un carboaluminate de magnésium hydraté. Peut-être peut-on trouver là une explication aux bons résultats obtenus par LUO SHOU SUN dans son traitement de carbonatation pour annihiler l'expansion du périclase.

3.2. SCORIES DE METAUX NON FERREUX.

CARLES GIBERGUES étudie les scories hydrauliques résultant de la fabrication du magnésium. Ces scories se composent de deux parties distinctes, l'une pulvérulente, composée de C_2S gamma et d'aluminate $C_{12}A_7$, l'autre granulée, renfermant du $C_2S\beta$ dans une matrice vitreuse hétérogène; la granulation par trempe à l'eau de cette seconde partie de la scorie hydrate partiellement l'aluminate en C_3AH_6.

La cinétique d'hydratation est évidemment différente pour la scorie fusante et pour la scorie granulée, ce qui s'explique partiellement par l'état anhydre de l'aluminate dans le premier cas et par sa préhydratation partielle dans le second cas.

Le mélange de ces scories donne d'excellents résultats en technique routière, mais prises séparément elles peuvent trouver leur utilisation dans la préfabrication de matériaux manufacturés.

L'auteur propose de produire des matériaux cellulaires en ajoutant aux scories fusantes de la poudre d'aluminium, et de fabriquer des éléments très résistants par autoclavage du laitier granulé broyé.

Les auteurs qui ont étudié les scories de la métallurgie du cuivre et du nickel, s'accordent à leur trouver une structure et des propriétés pouzzolaniques.

BARAGANO s'attache à montrer les qualités pouzzolaniques des scories de la métallurgie du cuivre.

Ces laitiers vitrifiés et finement granulés à l'eau ont une composition chimique pratiquement exempte de chaux, mais en revanche très riche en silicate ferreux détectable sous forme de cristaux de fayalite en aiguilles.

Il est permis de penser que la présence de silice soluble résultant de la décomposition de la fayalite par la chaux, explique les résultats positifs obtenus par l'auteur dans tous les tests de pouzzolanicité qu'il a appliqués.

Il faut cependant remarquer que ces scories utilisées sous forme de ciments à la pouzzolane par mélange avec du portland réagissent plus lentement que les pouzzolanes naturelles, mais que les résistances obtenues après 60 jours sont du même ordre.

Par ailleurs, de tels produits résistent excellemment aux attaques chimiques et aux épreuves climatiques.

Les scories de la métallurgie du nickel ont une composition et des propriétés pouzzolaniques analogues à celles de la métallurgie du cuivre; c'est ainsi que LANEUVILLE, étudiant ces scories, aboutit dans ses recherches aux mêmes résultats que BARAGANO. Il précise que d'autres auteurs, tel que THOMAS, ont également démontré les propriétés pouzzolaniques des scories de la métallurgie du plomb.

Nous voyons donc qu'il y a là des sources importantes de sous-produits utilisables en cimenterie pour la préparation de ces ciments particulièrement appréciés pour leurs propriétés spécifiques que sont les ciments pouzzolaniques.

BOLDYREV met en valeur les tonnages très importants de résidus industriels disponibles en U.R.S.S. et parmi ceux-ci des scories de métaux non ferreux. Les compositions chimiques de ces scories sont voisines de celles annoncées par BARAGANO d'une part, et LANEUVILLE d'autre part, avec en particulier la présence de fayalite.

BOLDYREV développe des explications très approfondies du processus d'hydratation de ces scories. Il ajoute que le verre alumino ferro siliceux de ces scories est responsable de leur comportement pouzzolanique de la même façon que la silice active et le verre alumino-siliceux.

* * *

THEME III - DISCUSSION DU PANEL

Membres du Panel :

M. M. VON EUW, Président de Thème .
Prof. M. DAIMON, Professeur à l'Institut de Technologie de Tokyo, JAPON.
Dr R. DRON, Ingénieur au Laboratoire Central des Ponts et Chaussées, FRANCE.
M. B. ENTINE, NII Cement Department Chief, Cand. Sci. (Techn.) de Moscou, U.R.S.S.
M. le Prof. FIERENS, Doyen de l'Université de l'Etat de Mons, BELGIQUE.
M. LUO SHOUSUN, Ingénieur Cement Research Institute, Beijing, CHINE.
Dr M. REGOURD, Chef du Département Microstructures, C.E.R.I.L.H., FRANCE.
Dr H.G. SMOLCZYK, Forschungsgemeinschaft Eisenhüttenschlacken, Diusburg, R.F.A.

1. STRUCTURE ET REACTIVITE

M. VON EUW :

- "Je souhaiterai que nous discutions d'abord des recherches liant la structure et la réactivité hydraulique.

J'ai retenu des différents travaux sur la structure des laitiers "dits vitreux" que le verre de laitier est constitué de tétraèdres SiO_4 plus ou moins polymérisés. Le réseau est déformé par l'insertion d'une certain nombre de cations dont le rayon est plus grand que celui du silicium.

Dès 1932, ZACHARIASEN expliqua que les cations modificateurs de réseau conditionnent le degré de polumérisation. Il résulte de cette conception de la structure, que le nombre de tétraèdres simples est d'autant plus grand que les cations modificateurs de réseau occupent plus de place ; en conséquence, la réactivité chimique est elle-même d'autant plus grande. Cette explication n'apparaît pas suffisante. Elle est maintenant précisée par des travaux récents."

- "M. le Professeur ROIAK a particulièrement étudié la dépolymérisation des ions complexes silicium-oxygène par les cations Aluminium et Magnésium. Prof. ENTINE voulez-vous nous apporter quelques informations sur les travaux de ROIAK ? "

Prof. Z.B. ENTINE :

- "Les travaux scientifiques russes et plus particulièrement ceux du Prof. ROIAK ont montré que l'oxygène joue un rôle déterminant dans l'activité des laitiers fondus. Les ions modificateurs du réseau exercent leur action sur l'état énergétique de l'oxygène, sur la polymérisation ou la dépolymérisation des complexes ions-oxygène, c'est-à-dire sur l'état vitreux. L'état énergétique des ions Al et Mg a aussi une grande influence. Il faut accroître la teneur en aluminium pour obtenir une bonne activité du laitier, liée au fait que Al prend une valence 6+ et contribue à la dépolymérisation des ions dans le laitier. Cette valence 6+ a été confirmée par spectroscopie d'absorption infrarouge et résonance paramagnétique électronique. Le magnésium joue un rôle moins marqué que celui du calcium. Il peut y avoir démixtion de la masse fondue en deux phases et cristallisation partielle. Ces deux phénomènes, démixtion et cristallisation partielle ont, à mon sens, une très grande influence sur la réactivité et n'ont pas été suffisamment étudiés car des laitiers ayant des compositions identiques peuvent avoir une réactivité différente. Ceci permet d'expliquer l'effet des éléments mineurs Ti et Mn et l'hétérogénéité qu'ils entraînent.

- "M. DRON, en étudiant la réactivité du laitier granulé, vous avez été conduit à proposer une théorie statistique de la structure. Votre approche s'écarte-t-elle en cela des conclusions de ROIAK ?"

M. R. DRON

- "La conception du verre à laquelle je me réfère part de la structure du verre de silice. Elle s'apparente à celle du cristal de quartz qui est formé de tétraèdres SiO_4 dont chaque sommet est commun à deux tétraèdres. La liaison Si-O a un caractère covalent extrêmement marqué, avec une hybrication sp^3 qui détermine les directions de valence à 109°28', l'angle Si-O-Si étant à 180°.

Dans le verre, les angles O-Si-O restent proches de 109°, mais les angles Si-O-Si s'écartent notablement et de façon aléatoire de 180° de sorte qu'on cesse d'avoir un réseau au sens cristallographique du terme, avec répétition du motif par une opération de translation, mais on conserve un pseudo réseau.

Un verre de silicate peut être considéré comme un verre de silice modifié. Il dérive de celui-ci par une opération de coupure des ponts silicium-oxygène-silicium par suite de la réaction :

$$Si\text{-}O\text{-}Si + O^{2-} \longrightarrow Si\text{-}O^{-} + {}^{-}O\text{-}Si$$

Le réseau obtenu diffère du réseau primitif à la façon d'un filet dont on aurait sectionné au hasard une partie des mailles (Fig. 1, Fig. 2).

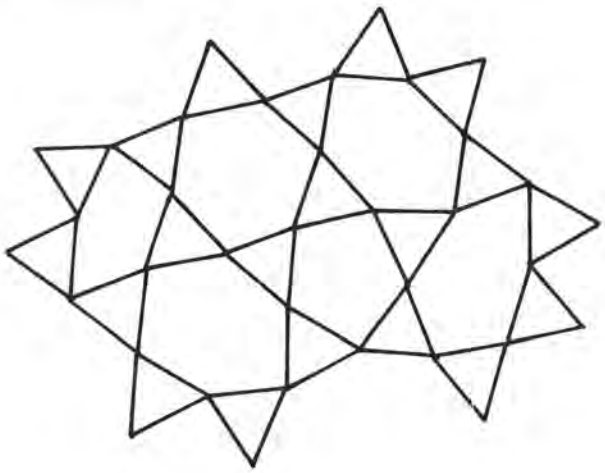

Fig. 1 - Pseudo réseau du verre de silice.

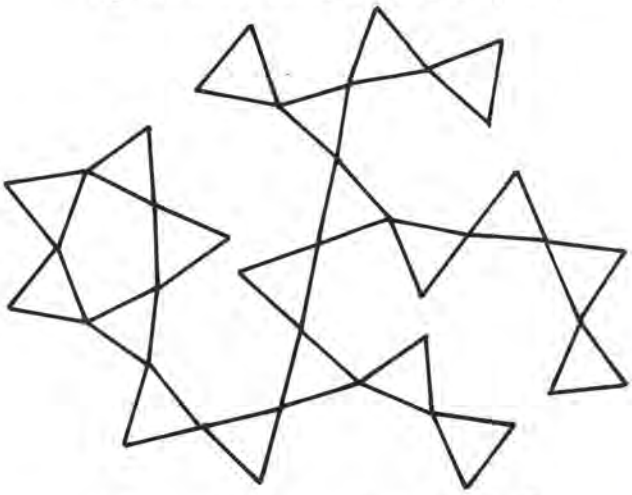

Fig. 2 - Sectionnement du réseau par O^{2-} dans un verre de silicate

Ma conception diffère donc un peu de celle de **M. ROIAK**, en ce sens que je considère que l'agent modificateur n'est pas le cation (Ca^{2+} par exemple) mais l'anion O^{2-} apporté par la chaux. Cet anion disparaît en tant que tel dans la réaction de coupure des ponts.

Les tétraèdres, qui initialement étaient tous de même nature puisqu'ils comportaient tous, quatre oxygènes pontants, vont constituer maintenant cinq espèces différentes selon le nombre d'oxygènes pontants qu'ils auront conservé :

Les espèces X avec quatre oxygènes pontants occupent des positions de croisement de chaînes et les espèces Y (trois) des positions de bifurcation de chaînes. Les espèces E (deux) sont des éléments de chaînes et les espèces Z (un seul) des extrémités de chaîne. Il convient d'ajouter à ces quatre espèces l'espèce S qui n'est autre que le tétraèdre SiO_4^{4-} isolé.

La statistique permet de dénombrer ces espèces moyennant certaines hypothèses simplificatrices. J'ai pu étendre par ce moyen le dénombrement dans les systèmes à moyenne teneur en silice que constituent les laitiers.

Les agents formateurs du réseau sont bien entendu le silicium mais également l'aluminium qui, dans les milieux basiques, est toujours tétracoordonné. Il semble occuper dans le laitier préférentiellement les sites X (croisement de chaînes).

L'ion calcium se place à proximité des oxygènes porteurs de charges et forme entre eux des ponts de nature électrovalente, facilement détruits par l'eau.

Le magnésium, auquel la plupart des auteurs font jouer un rôle semblable à celui du calcium, a un caractère ionique moins marqué et peut même former, dans des composés cristallisés comme l'akermanite, des structures covalentes. Quoi qu'il en soit, le pont oxygène-magnésium-oxygène est moins facilement hydrolysé que le pont oxygène-calcium-oxygène, de sorte que tout se passe comme si, partiellement du moins, le magnésium jouait un rôle de formateur de réseau."

M. VON EUW :

- "J'ai retenu également que la structure du verre n'est pas seulement hétérogène à l'échelle atomique, mais que plusieurs chercheurs ont observé dans la masse vitreuse des hétérogénéités assimilables à des globules de verre non miscibles.

D'autres auteurs se sont consacrés à l'identification et au dosage des cristaux qui apparaissent en plus ou moins grandes proportions pendant la trempe du laitier.

Enfin, les défauts qui existent à la surface du verre semblent constituer des centres de formation de germes lors de l'hydratation."

- "**M. le Professeur FIERENS** que pensez-vous de ces aspects différents de la structure des laitiers ?"

Prof. P. FIERENS :

- "Les cristaux "parfaits" qui correspondent à un ordre structural très rigoureux sont très rares. A l'autre bout de l'échelle, les verres "parfaits", caractérisés par un désordre maximum, sont tout aussi peu fréquents.

L'état cristallin et l'état vitreux réels présentent un certain nombre de défauts de structure de divers types qui constituent souvent des centres actifs jouant un rôle prépondérant dans la réactivité des solides.

C'est la raison pour laquelle il est illusoire de bâtir une théorie de l'hydratation des ciments, des laitiers et des liants pouzzolaniques sans faire intervenir les défauts de structure. Ces défauts sont des lacunes, des interstitiels, des dislocations, des joints de grains, des impuretés, etc ...

Par exemple, dans le verre de laitier, des défauts peuvent se situer à l'interface des microhétérogénéités qui ont été identifiées sous forme de globules vitreux non miscibles par **HAWTHORN** ou de microcristaux par **DEMOULIAN, MORTUREUX, ROIAK** et d'autres. Il me paraît évident que l'accroissement de réactivité du laitier n'est pas dû aux cristaux eux-mêmes mais bien, je le répète, aux défauts apparaissant à l'interface avec le substrat vitreux.

La thermoluminescence et l'exoémission électronique sont deux techniques qui permettent de caractériser les défauts de structure à la surface des échantillons et notamment sur le plan énergétique. Ces défauts causent, dans le matériau, des élévations locales de l'énergie libre qui entraînent la diminution de l'énergie d'activation du processus d'hydratation. Les travaux effectués dans mon laboratoire sur l'hydratation de la géhlénite, de laitiers synthétiques et de laitiers industriels montrent que le mode de trempe a une grande répercussion sur les caractéristiques énergétiques et entropiques des défauts de l'état vitreux.

Néanmoins, si l'on veut tirer un enseignement pratique à propos de l'influence de la trempe sur le pouvoir hydraulique des laitiers, il ne faut pas séparer ce paramètre et le facteur relatif à la composition chimique élémentaire quantitative. Pour un laitier de composition chimique donnée, deux modes de trempe différents peuvent conduire à des réactivités variant de 1 à 270, alors que pour un laitier d'une autre composition, les deux modes de trempe n'ont pratiquement aucune influence sur la vitesse d'hydratation. Dans le second cas, il ne sert à rien de tenter d'améliorer le pouvoir hydraulique du laitier en agissant sur le mode de trempe. Au contraire, dans le premier, une telle étude est très bénéfique.

Cette conclusion me paraît avoir un grand intérêt au niveau de la pratique industrielle."

M. VON EUW :

- "J'ajouterai en ce qui concerne les microcristaux dosés par **DEMOULIAN** et également par **MORTUREUX**, que la merwinite apparaît comme l'espèce principale.

Je serais tenté d'avancer que la cristallisation de la merwinite aurait pour conséquence l'enrichissement du verre en alumine et éléments mineurs, ce qui est favorable à l'hydraulicité."

- "**M. DRON** partagez-vous cette hypothèse ?"

M. R. DRON :

- "Je partage cette hypothèse. Si le milieu est enrichi en alumine, il a plus de chance de réagir car Al est l'élément le plus fragile en milieu basique. Le magnésium est par contre renforcé."

2. CARACTERISATION

M. VON EUW :

- "Les explications de l'hydraulicité par la structure ne nous suffisent cependant pas. En effet, dans la pratique industrielle, nous avons besoin de caractériser les laitiers et pour cela diverses méthodes sont en concurrence."

- "Dr SMOLCZYK, pouvez-vous nous dire comment vous utilisez les résultats de l'analyse élémentaire, et surtout quelle importance vous donnez aux éléments mineurs ?"

Dr H.G. SMOLCZYK :

- "A lot of most complicated hydraulic formulas for granulated blast-furnace slag are not more precise than very simple formulas of the type CaO/SiO_2. If a precision of more then 90 % (r^2) is demanded, then it is necessary to include some minor elements. We introduced only MnO, alkali and P_2O_5 in our formulas with best results.

In the very interesting formulas of DEMOULIAN, GOURDIN, HAWTHORN and VERNET, all the minor elements are explicitly dealt with. This does not necessarily mean a contradiction to our opinion. The amounts of TiO_2, fluor, chloride and crystalline particles in our 24 slags and their range of variation have been far too small for statistical evaluations. We fully agree with the opinion of M. DEMOULIAN that the glass-content has some influence on the hydraulic properties and that the chloride naturally has a very strong positive influence."

M. VON EUW :

- "Mme REGOURD, votre méthode calorimétrique permet-elle de faciliter la sélection des laitiers ?"

Mme REGOURD :

- "La calorimétrie à conduction est une méthode sensible et rapide dans la comparaison de la réactivité des ciments au laitier. Si les mesures sont effectuées à 40 °C, température à laquelle les hydrates formés sont les mêmes que ceux qui apparaissent à 20 °C, un classement de différents laitiers peut être connu avant la quinzième heure d'hydratation. Les courbes de la Figure 1, relatives à des ciments de haut fourneau CHF (70 % de laitier), montrent que le maximum du flux de chaleur est nettement moins intense et décalé dans le temps avec les CHF 2 et 3 qu'avec le CHF 1, plus encore avec les CHF 4 et 5. Par contre, la courbe du CHF 1 prouve la participation simultanée du laitier et du clinker portland aux premières réactions d'hydratation : le pic le plus intense se place au même moment pour les deux ciments et le rapport entre l'énergie libérée par le CHF 1 et l'énergie libérée par le CPA est très supérieur à la proportion de clinker (28,5 %) dans le ciment au laitier.

Le même classement des laitiers se retrouve dans la comparaison de l'évolution, en fonction du temps, des résistances mécaniques en compression sur mortier ISO. La distinction est particulièrement marquée à 7 jours (Fig. 2) et plus nette, à la même échéance, que lors de l'estimation du degré d'hydratation en pâte pure par la méthode de dissolution. Elle reste toutefois moins rapide que la calorimétrie."

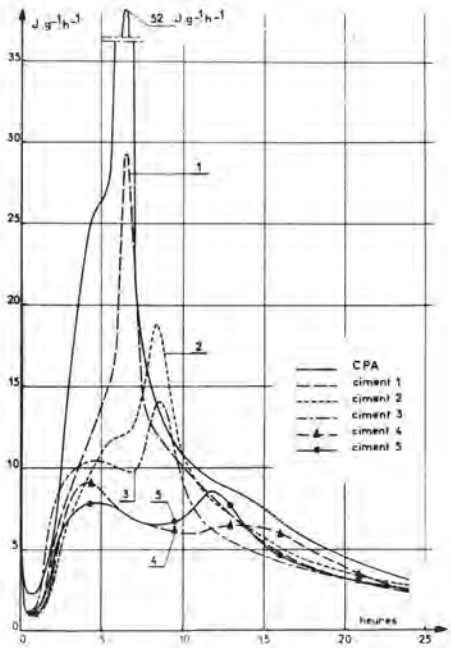

Fig. 1 - Chaleur d'hydratation à 40 °C d'un CPA et de cinq ciments de haut fourneau CHF.

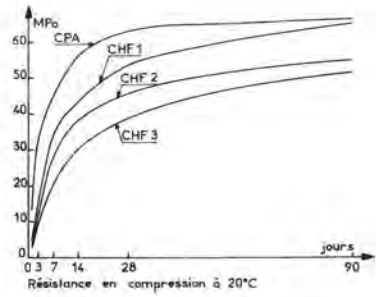

Fig. 2 - Evolution des résistances mécaniques en compression des mortiers ISO du CPA et des CHF 1, 2 et 3.

M. VON EUW :

- "Le regretté Prof. KONDO mesurait le degré d'hydratation par extraction sélective des phases, M. le Professeur DAIMON souhaitez-vous nous parler de cette méthode ?"

Prof. M. DAIMON :

- "When I was asked to prepare a paper on the mechanism and the kinetics of hydration of slag, one question was how to measure the change and degree of slag hydration with hydration time. Obviously, we should find a suitable method for the quantitative analysis of slag in order to determine the degree of slag hydration and the selective method of dissolution

by **Prof. KONDO** seems to me the only method which have enough accuracy for this purpose. in this method, hydration products are almost completely dissolved by organic acid solution while unhydrated slag remains undissolved (principal Paper III.2.2). It is necessary to have several independent methods for such fondamental and important measurement. We know that the conduction calorimeter is very useful as mentionned before but we cannot obtain the reaction rate itself. The determination of evaporable water, free lime, free gypsum and so on should also be performed to know the full picture of the slag hydration."

Prof. P. FIERENS :

- "La caractérisation des laitiers, sur le plan de leur pouvoir hydraulique, paraît pouvoir se faire en mesurent la vitesse de progression du degré d'hydratation. En effet, la détermination de l'augmentation du degré d'hydratation en fonction du temps conduit à un classement de différents ciments au laitier conforme à la séquence correspondant aux résistances mécaniques respectives à des échéances données.

C'est ce qui ressort des travaux de Mme **REGOURD** et de ceux du **Prof. DAIMON.** C'est également ce que j'ai pu observer moi-même sur des échantillons d'un même laitier trempés selon des modes différents, mettant de plus en évidence le rôle joué par des défauts de structure caractérisés par exoémission électronique.

Ces considérations méritent cependant un commentaire supplémentaire montrant qu'il est nécessaire de distinguer l'usage qui peut être fait d'une part, de la mesure du degré d'hydratation et d'autre part, la détermination de la vitesse de l'augmentation de ce dernier dont il est question plus haut.

S'il est évident que le degré d'hydratation d'un ciment de laitier est un facteur important contribuant aux résistances mécaniques, il est essentiel de souligner que ce n'est pas le seul. Mes travaux ont montré que, pour quatre échantillons d'un même laitier trempés selon des modes différents , pour un même degré d'hydratation, la résistance à la compression prenait les valeurs respectives de 50, 41, 35 et 29 MPa.

Ceci montre sans ambiguïté qu'il n'y a pas de relation quantitative simple entre le degré d'hydratation et les résistances mécaniques et qu'à côté du degré d'hydratation interviennent d'autres paramètres, tels que la texture des hydrates qui dépend notamment des conditions de formation et de croissance des cristaux de ces produits et, en particulier, de la vitesse de cette dernière.

Je crois que beaucoup de progrès restent à accomplir à ce niveau, notamment par l'étude dynamique des microstructures des pâtes en cours de durcissement en relation, d'une part, avec les conditions présidant à la croissance des cristaux d'hydrates formés et, d'autre part, avec le développement des propriétés mécaniques et des caractéristiques rhéologiques.

Enfin, il y a tout lieu de croire que les observations faites dans mon laboratoire à propos de l'hydratation de laitiers industriels, pourraient être étendues aux ciments de laitier et aux ciments portland."

3. MECANISME DE L'HYDRATATION

M. VON EUW :

- "Nous avons vu que la structure et la composition chimique conditionnent la réactivité des laitiers. J'aimerai que l'on discute maintenant du mécanisme de l'hydratation.

- " Est-on arrivé à concilier la théorie de **LE CHATELIER** et celle présentée au Congrès de Londres en 1952 par **HANSEN** sur la réaction topochimique ? Je ne connais pas l'opinion des chercheurs chinois ; **M. LUO SHOUSUN**, comment comprend-on en Chine le mécanisme de l'hydratation des ciments de laitier ?"

M. LUO SHOUSUN :

- "We have studied the effect of magnesia in steel slags, so we have not done much work on slag hydration and we do not have anytaing to comment."

Prof. Z.B. ENTINE - (à la demande de M. VON EUW, point de vue des chercheurs russes) :

- "Le point de vue du **Prof. ROIAK** est relatif à l'influence des valences 6 par rapport à l'oxygène sur la réaction d'hydratation des laitiers. Il y a dans le verre un accroissement des liaisons de type ionique et une diminution des liaisons de type covalent. Les ions modificateurs passent en solution et sont remplacés par des ions qui, de valence 4, prennent la coordination 6. Les liaisons Si-O sont affaiblies et ces radicaux passent en solution. Les ions hydratés calcium s'éloignent de la zone d'influence des grains de laitier alors que les ions hydratés siliciques restent dans cette zone d'influence. Les ions Al et Mg ont une position intermédiaire.

Dans la seconde étape du processus d'hydratation, il y a interaction entre les éléments basiques au voisinage des grains de laitier et les éléments siliciques, avec formation de gel d'hydrosilicate et d'aluminates hydratés. Dans la mesure où la brucite n'a pas été mise en évidence, on peut considérer que Mg entre également dans la composition des hydrosilicates et aluminates hydratés. Les néoformations constituent une couche qui enveloppe les grains anhydres mais est séparée des grains eux-mêmes par des éléments dont la basicité est inférieure à celle des éléments entrant dans les néoformations.

Cette interprétation du **Prof. ROIAK** est vraisemblablement correcte dans son ensemble mais certains éléments de détail ne sont pas admis par tous les spécialistes."

Intervention du Prof. M. SCHULTZ :

- "Je voudrais vous faire part des idées des spécialistes des verres en ce qui concerne les laitiers. La structure du verre peut être envisagée du point de vue de la structure de phase et du point de vue du problème du voisinage. L'expérimentation permet de se faire une idée de la structure de phase, en particulier la démixtion et la cristallisation, mais les verriers sont actuellement très concernés par le problème essentiel du voisinage immédiat. Je suis d'accord avec le **Prof. ENTINE**, mais dans les problèmes oxydo-basiques, il faut surtout mettre l'accent sur les questions d'échanges électroniques entre atomes. Mes travaux ont montré que la formation des composés de coordination est essentielle dans les

problèmes de structure des verres. Il faut donc absolument aborder les échanges électroniques au niveau de Al^{4+} et Mg^{4+}."

M. VON EUW :

- " Quelle est l'opinion de M. le Prof. DAIMON pour le Japon ?"

Prof. M. DAIMON :

- " Before beginning our discussion, I think we have better to get agreement in the definition of the word topochemical. When I say topochemical reaction, I mean that the reaction product exists at the place where original unhydrate was, when it is observed by electron microscopy. Therefore, the pseudomorphic hydrate which is stated in the Principal Paper by Mme REGOURD, should be identical to the topochemical hydrate in this definition. The topochemical reaction can be dissolution and precipitation process if the precipitation takes place very close to the surface of the unhydrated grains and forms a product layer. Such a product layer surrounding the remaining unhydrate tends to play a very important role in the kinetics of hydration especially when the transportation of a certain species through this layer is the rate determining step in the whole hydration reaction. I am feeling that the discussion of hydrolytic reaction is going to show us the potential hydration reactivity of slag and we will be able to have a better understanding of practical reaction rate in the course of topochemical discussion but we know very well that we have so many things left to be solved yet."

M. VON EUW :

- "Mme REGOURD, votre Rapport principal traite des phénomènes d'hydratation et des hydrates formés. Nous serions très intéressés de connaître votre avis : dissolution-cristallisation ou topochimie ? "

Mme M. REGOURD :

- "La réponse du Prof. ENTINE et celle du Prof. DAIMON effacent, me semble-t-il, les désaccords entre les partisans de la théorie topochimique et ceux de la théorie de la dissolution-cristallisation. Favorable à la théorie de LE CHATELIER, dissolution-diffusion-précipitation, je voudrais illustrer mon propos à l'aide de deux microfractographies prises au microscope à balayage et qui figurent dans le Rapport principal III.2 11.

La première photo représente une lamelle porte-objet sur laquelle a été déposée une goutte de suspension de laitier dans une solution normale de soude. Le grain de laitier est couvert de C-S-H et des cristaux de géhlénite hydratée C_2ASH_8 ont précipité loin du grain anhydre. Mais sur la lamelle elle-même, nous observons clairement des silicates hydratés C-S-H. La présence de silice dans l'hydrosilicate, loin du grain de laitier anhydre, peut être considérée comme une preuve du processus dissolution-diffusion-précipitation.

La seconde photo montre un grain de laitier dans une pâte de 90% laitier + 10% gypse. Le grain de laitier est effectivement entouré d'une couche d'hydrate dont la formation pourrait être interprétée comme le résultat d'une réaction topochimique. Mais, dans ce cas, les forces de liaison entre grain anhydre et hydrate progressant vers le centre du grain devraient être des liaisons fortes et le C-S-H ne devrait pas se détacher aussi facilement du grain anhydre. Par contre, ce C-S-H pseudomorphique me semble être l'image du caractère limité de la diffusion des ions au travers de la solution dans la pâte de ciment. L'hydrate insoluble précipite en grande partie là où la sursaturation de la phase aqueuse interstitielle est la plus forte c'est-à-dire à proximité de la surface réactive du grain de laitier. Une autre fraction d'hydrate peut précipiter, loin du grain, dans des régions moins saturées et sa composition ne sera pas exactement la même que celle du C-S-H formé à l'interface grain anhydre-solution. Ces notions de distance de diffusion et précipitation ont été clairement mises en évidence par M. VERNET dans une communication à ce Congrès grâce aux observations simultanées de la phase solide et des analyses ioniques des solutions.

Fig. 1 - Activation sodique : C-S-H sur le grain de laitier et sur la lamelle porte-objet, cristaux de C_2ASH_8

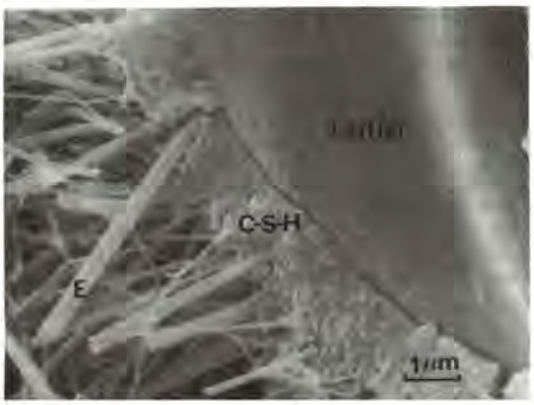

Fig. 2 - Activation sulfatique : ettringite et C-S-H compact autour du grain de laitier.

La texture du C-S-H provenant de l'hydratation du laitier est différente de celle formée à partir des silicates du ciment portland. Elle est plus dense et moins bien structurée : elle apparaît amorphe à l'observation microscopique (Fig. 2). Au voisinage immédiat des grains anhydres, le C-S-H du laitier a une composition plus riche en alumine et en magnésie que le C-S-H du clinker. Les analyses à la microsonde

électronique révèlent un enrichissement très net en Mg de la couche d'hydrate entourant les grains de laitier (Fig. 21 (a), Communication principale III. 2/21). La diffusion de Mg apparaît donc très limitée. C'est un point particulier que le Prof. ENTINE a mentionné et qui demande de nouvelles études approfondies bien que la présence de $Mg(OH)_2$ n'ait pas été décelée.

La faible porosité du C-S-H du laitier joue un rôle important dans la résistance chimique des ciments au laitier, en s'opposant à la diffusion des ions agressifs tels que Cl^- et SO_4^{2-} contenus dans l'eau de mer (Fig. 21 (c), Communication principale III. 2/21)."

M. VON EUW :

- "Les travaux communiqués par M. VERNET semblent en effet bien faire une démonstration intéressante de la théorie de la dissolution-cristallisation applicable aux ciments de laitier.

Ce chercheur présente d'ailleurs un poster expliquant sa méthode. Nous pourrions lui demander de nous résumer ses résultats."

M. C. VERNET :

- "Nous avons appliqué les méthodes développées dans le poster à l'étude de nombreux ciments pour lesquels nous avons fait des observations simultanées des phases solides et de la solution correspondante. Ces observations nous conduisent à penser que le mécanisme de dissolution-cristallisation de LE CHATELIER s'applique à l'hydratation des ciments de laitier, comme à celle des ciments portland. En effet, il existe une correspondance permanente entre la composition ionique et les vitesses de réaction des phases solides. Les concentrations résultent de la différence entre les flux ioniques de dissolution et de précipitation : tant que cette différence n'est pas nulle, l'énergie libérable (après hydroxylation superficielle des anhydres) est utilisée à maintenir un certain taux de sursaturation, moteur de la cristallisation et de l'évolution du système vers l'équilibre thermodynamique, qui ne peut être atteint que lorsque les anhydres ont disparu, et que la vitesse de précipitation tend vers zéro.

Cette sursaturation est illustrée par la première figure, où l'on voit le trajet du point figuratif (F) des concentrations en chaux et silice, qui se déplace dans le diagramme chaux-silice eau pendant la lixiviation du ciment portland. Dès les premières minutes, F parvient en R_1 dans le domaine sursaturé qui se trouve au-dessus de la courbe (G - correspondant à l'équilibre du C-S-H). Le trajet R_1-R_2 est de nature cinétique : c'est le résultat d'une compétition entre la vitesse de dissolution et la vitesse de précipitation, qui est ici très grande : en effet, ce trajet est voisin de la courbe (M - correspondant à la nucléation rapide de C-S-H), établie par D. MENETRIER. Malgré la dilution par l'eau de lixiviation, ce qui devrait produire une sous-saturation, le point F continue ensuite un trajet voisin de la courbe G, mais toujours dans le domaine sursaturé.

Voilà bien une preuve expérimentale de l'existence d'un mécanisme de dissolution-précipitation. Mais ceci n'exclut aucunement l'intervention des phénomènes à l'interface réactionnelle, par exemple :

1°) Au premier contact avec l'eau, la formation d'une couche hydroxylée, par chimisorption d'eau, ce qui est prévu par les calculs du Prof. BARRET, et observé par le Prof. FIERENS, qui a montré l'existence de "défauts" électroniques de la surface où cette réaction est plus intense.

2°) Des phénomènes de chimisorption d'ions calcium libérés par la dissolution et créateurs de barrières de potentiel. Ceci a été observé par la mesure du potentiel ζ et plus récemment, par spectroscopie de photo-électrons (mesures de D. MENETRIER et de M. REGOURD).

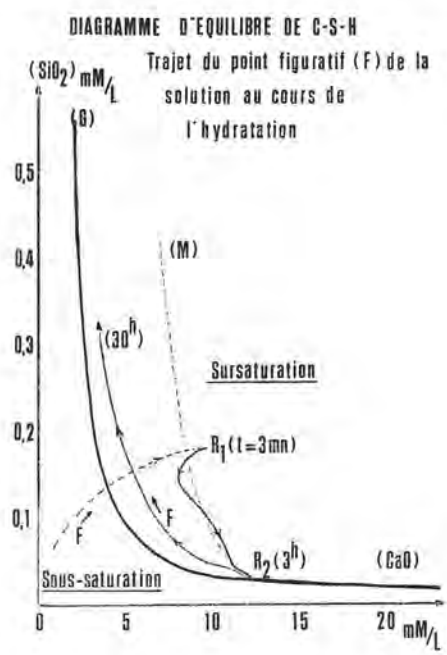

Fig. 1 - Diagramme d'équilibre de C-S-H.

Le mécanisme de LE CHATELIER, qui implique une composition ionique commandée par des paramètres cinétiques, nous a amené à introduire deux concepts nouveaux qui en sont la conséquence :

- d'une part, le concept de couplage entre phases,
- d'autre part, le concept de distance de précipitation.

Le couplage entre phases permet d'analyser la "personnalité" de chaque ciment, y compris celle des ciments de laitier, ce que nous allons illustrer par la Figure 2. Ce diagramme simplifié montre l'évolution de 5 paramètres durant 3 des 4 périodes de l'hydratation d'un ciment à 75 % de laitier. Pendant la période II ou "période dormante", la solution se sursature en chaux. Comme l'a très bien expliqué F. YOUNG, il y a de bonnes raisons expérimentales de penser que la croissance de la portlandite est alors empêchée par un empoisonnement (par la silice dissoute), jusqu'au temps t_2, où la sursaturation est telle que cette croissance peut s'effectuer. Il y a alors précipitation de la portlandite, annoncée ici par la chute de conductance, au début de la période III (courbe[1]). Toutes les vitesses de réaction augmentent alors : celle du laitier, dont la teneur diminue de manière significative (courbe [2]), celle de C_3S, qui augmente le flux thermique et celle de C_3A (qui est ici une solu-

tion-solide orthorhombique, riche en sodium et potassium et dont la vitesse est repérée par l'ion Na^+ qui sert de traceur) (courbe [3] , en bas).

La précipitation de la portlandite a donc produit un couplage des réactions :

- par effet chimique (sur C_3S) en abaissant la teneur en chaux dissoute,
- par un effet thermique (couplage C_3S-C_3A),
- et par les deux ensemble (effet thermique et chimique sur le laitier).

En conséquence, il se forme du C-S-H et de l'ettringite, plus rapidement que pendant la période précédente. Ceci, d'une part consomme de l'eau libre et, d'autre part, crée dans les mortiers des structures liantes nouvelles, ce qui aboutit à une modification rhéologique qui n'est autre que la prise. Il y a donc coïncidence temporelle entre la vitesse maximale de formation de l'ettringite et la période de la prise, mais ce n'est pas une raison pour affirmer que l'ettringite est la cause du phénomène : les vitesses de formation du C-S-H et de la portlandite passent également par un maximum durant cette période.

Au temps t_3, la relative accélération des réactions du C_3A et du laitier conduit à la disparition du gypse, qui ne se produit, dans les mélanges riches en laitier, que par une participation du laitier. Cette disparition est suivie d'une chute brutale de la teneur en SO_4^{--} de la solution : ceci produit la transformation de l'ettringite en monosulfoaluminate, au temps t_4, signalé par le minimum de conductance et par un deuxième pic de flux thermique. Il y a, à nouveau, accélération de toutes les réactions, dont celle du C_3A et celle du laitier, qui atteint ici sa vitesse maximale.

Figure 2

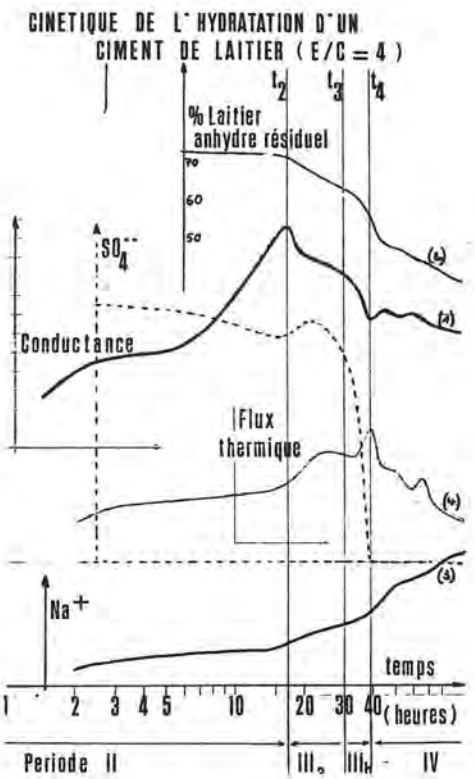

Dans le cas des ciments finement broyés, ceci peut même produire la dissolution de la portlandite: la disparition du gypse a donc entraîné un couplage de toutes les réactions, y compris celles des hydrates.

Un autre exemple de couplage est donné dans le Tableau I qui montre la réaction du laitier dès les premières minutes : la consommation de la chaux libérée par le Clinker C7 varie en sens inverse de la basicité des laitiers (donnée par le rapport C/S).

Tableau I - Exemples de couplages chimiques laitier-clinker.
(Période I : t = 10 min)

Ciments :	Clinker C 7 et Laitier A	Laitier B	Laitier C	C 7 CPA
(Ca^{++})mM/L	14	1	6	17
C/S des laitiers :	1,33	1,24	1,18	

Le deuxième concept, concept de "distance de précipitation", permet d'interpréter, dans le mécanisme de LE CHATELIER, les variations dans le temps et dans l'espace de la microstructure des hydrates, variations particulièrement importantes dans le cas des ciments de laitier. Notre étude expérimentale de la cinétique de précipitation des C-S-H permet, en effet, de calculer la distance d parcourue par les ions silicate depuis l'interface de dissolution jusqu'au site de précipitation. Comme le montre la Figure 3, cette distance des écarts $(X_0 - X)$ entre concentrations

Figure 3

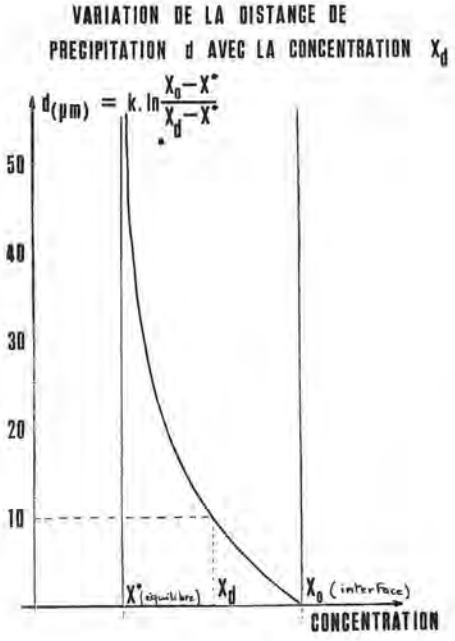

à l'interface et concentration à l'équilibre et (X_d - X), entre concentration à la distance d et concentration à l'équilibre. Plus le taux de sursaturation est élevé et plus le gradient de diffusion à partir de l'interface est élevé, plus la distance d devient faible. La Figure 4 montre que la majeure partie des C-S-H va se former à une distance très faible des grains, de l'ordre de l'épaisseur de la couche de diffusion, mais que cependant une certaine proportion d'hydrates peut se former à une distance plus grande, là où la solution est moins sursaturée : on peut donc s'attendre à des différences de structure et de composition entre ces hydrates, formés à des vitesses différentes et dans des zones où les concentrations sont différentes. Et effectivement, la microstructure des ciments de laitiers hydratés correspond bien à ce schéma : on y observe divers types de C-S-H, dont certains cristallisent à grande distance et viennent combler les pores : ceci donne aux ciments riches en laitier une faible porosité et améliore leur résistance en milieux agressifs. De la même façon, le concept de distance de précipitation permet d'expliquer le mode de croissance particulier du C-S-H dans les ciments portland ou le C_3S.

Figure 4

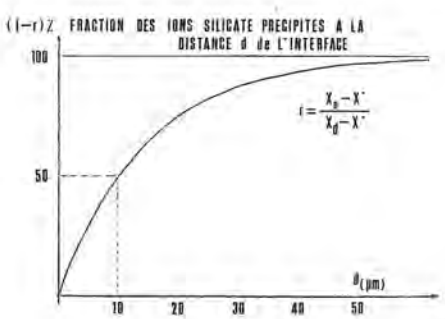

Ces deux concepts, couplage entre phases et distance de précipitation, qui sont l'aboutissement d'un travail expérimental, sur des ciments industriels, et non pas de considérations théoriques basées sur des interprétation de phénomènes pris isolément, permettent donc de replacer le mécanisme de LE CHATELIER dans le contexte de toutes les observations connues, sans négliger les phénomènes de surface ou de diffusion qui l'accompagnent."

4. PROPRIETES PARTICULIERES DES CIMENTS DE LAITIER

M. VON EUW :

- "Il est connu que les ciments de laitier présentent l'avantage d'une faible chaleur d'hydratation et également la qualité d'une grande résistance aux attaques chimiques.

Une autre propriété spécifique de ces ciments est leur très grande résistance à la diffusion des chlorures. Cette propriété est probablement liée à la faible porosité des pâtes de ciments de laitier signalée par plusieurs auteurs dont SERSALE.

Dr SMOLCZYK nous aimerions vous entendre sur ce sujet."

Dr H.G. SMOLCZYK :

- "The high resistance of BFC against the diffusion of chlorides into the concrete is "State of Knowledge" meanwhile. Another wellknown fact is the very low permeability of BFC_s. The reason for this advantageous effect of the blast-furnace slag is not a distinctly lower total porosity of the cement paste. The reason is the distinctly lower amount of bigger pores with ratio of > 300 A or > 1000 A which decreases with increasing slag content. The result of this favourable pore-size distribution is an elevated resistance against the penetration of salt-solution and ions, for sure.

However , this explanation is not sufficient. We meanwhile know that even the diffusion of sodium-chloride is a much more complicated reaction than the mere moving of the dissolved salt through capillary pores. In our studies on concretes in 3 mol NaCl-solution, we compared the quantitative amounts of penetrated Na- and Cl-ions. It became evident that the molar ratio of chloride to sodium was 2 to 1 instead of 1 to 1. That means that a chemical reaction evidently did occur and hydroxil-ions had to move out of the concrete."

5. LAITIERS D'ACIERIE

M. VON EUW :

- "Nous avons discuté uniquement jusqu'ici des laitiers de haut fourneau. Il me paraît juste et intéressant d'aborder maintenant les recherches sur les laitiers d'aciérie et ensuite sur les scories de métaux non ferreux.

Plusieurs auteurs proposent de valoriser les propriétés hydrauliques des laitiers d'aciérie.

. WANG YU JI classe ces laitiers en fonction de leur teneur en C_3S et CaO libre.

. GEORGES et SORRENTINO modifient la composition en cours d'affinage de la fonte pour donner aux scories BOP des propriétés hydrauliques."

- " M. LUO SHOUSUN vous avez présenté une brillante communication consacrée aux laitiers d'aciérie. Voulez-vous, en particulier, nous faire part de vos conclusions sur l'influence de MgO ? Vous préconisez aussi un ajout de $MgSO_4$ pour éviter l'expansion du périclase. Comment expliquez-vous cette action ?"

- "The initial idea of using steel slag to make cement in China dates back to the early seventies. Today, the annual production of steel slag cement amounts to more than 100,000 tons not including the steel slag used directly as binder in the making of concrete products. The gypsum steel slag cement, made at the plant in Pekin, has a 28 day compressive strength of 44N/mm^2. The mortar brick which is made from this has a cement/sand ratio of 1 to 3 and W/C about 0.3. The slag cement concrete made with cement/aggregate ratio of about 1 to 4 after carbonation treatment has a 28 day compressive strength of 20 to 30 N/mm^2. Both the cement mortar and concrete specimens have proved to be sound after autoclaved tests. The present contribution deals mainly with the relationship between the form and the content of magnesia (the used steel slag from the open hearth and the electric furnace) and the long term durability or soundness of the cement made thereby. According to the author's investigation with optical microscope and actually diffraction pattern studies, the steel slags were found to exist in three forms : firstly, in the form of combined states mainly as merwinite or monticellite, secondly, in the form of free state as periclase and thirdly, in the form of RO phase.

The long term soundness of the steel slag cements as accesses from results of autoclave tests is related with a form or state of magnesia and the radical contained in the diverted oxide present as RO phase.

The chemically combined magnesia has not, but the free apparently has harmful effect. The effect of magnesia in form of RO phase on soundness of cement is determined by the magnesia to ferrous oxide plus manganese oxide ratio. The cement is sound when the ratio is said to be less than 1, but it is often unsound when the ratio exceeds 1. The long term soundness of the resulting steel slag from the electric furnace can be favorably improved by the addition of magnesium sulfate or a preparation of siliceous materials or granulated blast-furnace slag and further by carbonization treatment."

6. SCORIES DE METAUX NON FERREUX

M. VON EUW :

- " Ces produits s'apparentent plus à des pouzzolanes artificielles et je craindrais d'empiéter sur le domaine du Thème IV. En effet, les travaux de LANEUVILLE sur les scories de nickel et ceux de BARAGANO sur les scories de cuivre sont basés sur les méthodes d'essais des pouzzolanes. Ils mériteraient à mes yeux d'être discutés par le Prof. MASSAZZA."

- "Cependant, les scories de la métallurgie du magnésium, étudiées par CARLES-GIBERGUES sont douées de propriétés hydrauliques. Nous serions donc heureux d'entendre M. CARLES-GIBERGUES".

M. A. CARLES-GIBERGUES :

- "Le laitier de magnésium provient de l'Usine de Marignac qui produit du magnésium selon le procédé Magnetherm. On réduit la dolomite, préalablement décarbonatée, par du ferrosilicium additionné de bauxite. Le magnésium se dégage à l'état de vapeur ; le four est alors ouvert puis retourné au-dessus d'une fosse pleine d'eau. On recueille ainsi un laitier granulé, poreux, friable, de granulométrie comprise entre 0,2 et 10 mm. Par ailleurs, une fraction moins importante du bain (le tiers environ) reste collée aux parois du four : elle se refroidit lentement à l'air et se délite en une poudre qui constitue le laitier fusant (surface spécifique voisine de 1800 cm^2. g^{-1}). Ce laitier est très différent des laitiers de fonte.

a) - Par sa composition chimique tout d'abord :

L'examen du Tableau I montre qu'il est beaucoup plus basique que les laitiers de fonte Thomas français.

Tableau I : Compositions chimiques moyennes des laitiers de :

	Magnésium	Fonte Thomas
SiO_2	25	31 - 36
Al_2O_3	14	11 - 18
CaO	54,2	42,2 - 45,4
MgO	3,9	3,8 - 5
$i = CaO/SiO_2$	2,17	1,25 - 1,45

b) - Par sa composition minéralogique ensuite :

Le laitier fusant est presque entièrement cristallisé : à l'état essentiellement de γ-C_2S et, en faibles quantités, sous forme de périclase et d'aluminate de calcium $C_{12}A_7$. Le laitier granulé, pour sa part, est largement cristallisé. La **Figure 1**, qui est une interprétation d'examens à la microsonde électronique montre que les cristaux, pour leur grande majorité, sont de gros individus (30 à 80µm) de silicates bicalciques, α' et β, au sein d'une matière interstitielle, vitreuse, hétérogène. Cette dernière est globalement caractérisée par un rapport molaire $\frac{C + M}{S + A}$ proche de 2. La prépondérance de l'aluminium sur le silicium (11 Al pour 2 Si) a amené, localement, des différenciations en petits cristaux d'aluminates de calcium directement hydratés, au cours de la trempe, en C_3AH_6. En outre, au contact des cristaux de C_2S, on note des concentrations en magnésium, qui correspondent soit à du périclase, soit à de la forstérite (M_2S).

COMPORTEMENT AU CONTACT DE L'EAU

A la différence des laitiers de fonte, les 2 formes de ce laitier de magnésium, prises séparément ou conjointement, manifestent des propriétés hydrauliques sans qu'il y ait besoin de les activer.

La fraction fusante réagit rapidement au contact de l'eau : les premiers composés hydratés sont décelables moins de 2 heures après le gâchage. L'aluminate C_2AH_8 est le produit initial de l'hydratation. Par la suite, il disparaît progressivement. A terme, la phase hydratée responsable du durcissement du laitier fusant gâché avec de l'eau est un système ternaire dont le constituant principal C_2ASH_8 est associé à 2 aluminates de calcium hydratés : C_4AH_{13} et C_3AH_6.

Le laitier granulé, même broyé à une finesse comparable à celle de la fraction fusante, est moins réactif : les premiers hydrates ne s'observent qu'à 1 jour. Il s'agit d'aluminate de calcium hydratés et de géhléni-

te hydratée. A long terme C_4AH_{13} devient prépondérant et C_2ASH_8 est, ici, minoritaire. La formation de C-S-H est probable, mais difficile à mettre en évidence.

Figure 1 - Grain de laitier granulé.

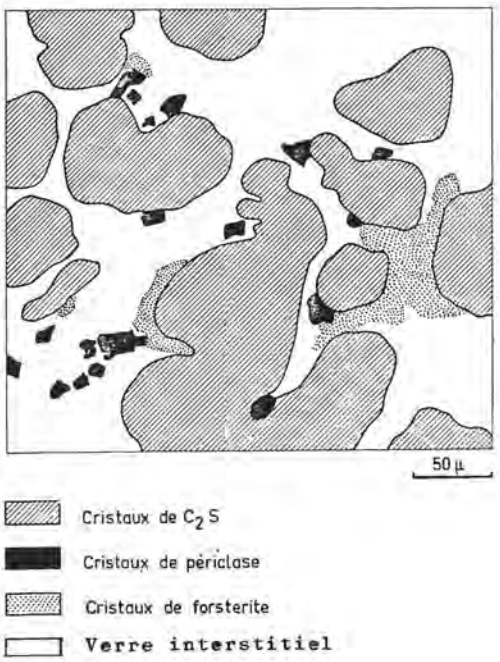

Les deux fractions étant associées, on note l'apparition initiale de C_2AH_8. Mais son existence est brève ; C_4AH_{13} et C_2ASH_8 se développent alors à même vitesse. Là encore, la foramtion de C-S-H est probable.

EMPLOI COMME LIANT, EN PATE PURE, DES 2 FORMES ASSOCIEES

L'élaboration d'un liant optimal conduit donc à associer les deux fractions, après un broyage préalable du laitier granulé. Cette opération est économiquement possible dans un broyeur à barres comme le montre la Figure 2 où la broyabilité du laitier de magnésium de Marignac se révèle bien supérieure à celles de laitiers de fonte.

Nous avons étudié le durcissement de pâtes pures réalisées à partir de mélanges, en proportions variables. Ces essais confirment bien la réaction mutuelle des 2 formes puisque, comme on peut le constater sur le Figure 3, le fuseau correspondant aux mélanges est toujours largement au-dessus des courbes relatives aux deux constituants séparés.

CONCLUSIONS : PERSPECTIVES D'EMPLOIS

En conclusion, un liant intéressant peut être obtenu en associant le laitier fusant et le laitier granulé broyé dans des proportions identiques à celles de leur production à savoir, respectivement, 1/3 et 2/3. Ceci n'est pas limitatif et l'on peut, par exemple, envisager 3 autres formes d'emplois.

1) - **Mélange utilisé, sans broyage de la phase granulée, en technique routière.** L'addition de 10 à 15 % du mélange optimum à une grave siliceuse a permis d'atteindre des résistances à la compression simple de 7,2 MPa.

2) - **Fabrication de matériaux cellulaires.** En incorporant 1 ‰ de poudre d'aluminium à un mélange, on a obtenu des masses volumiques de 1 T/m^3 pour une résistance à la compression de 6 MPa et un coefficient de conductivité thermique $\lambda = 0,15\ W.m^{-1}.°C^{-1}$.

3) - **Fabrication de matériaux autoclavés.** L'autoclavage du laitier granulé broyé a déjà conduit à des matériaux dont les résistances atteignent 78 MPa."

Figure 2 - Broyabilité du laitier granulé.

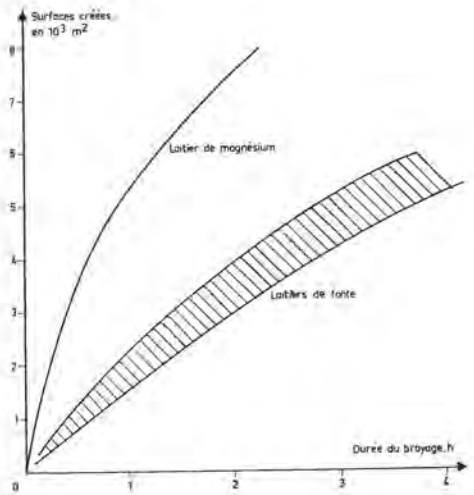

Figure 3 - Résistance mécanique en fonction du temps.

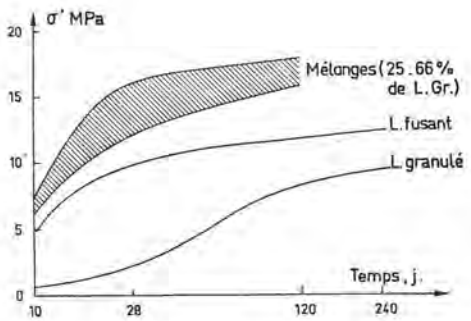

* * *

DISCUSSION

by LOU ZONGHAN

It was a great pleasure for us to read Mr. Daimon's paper on the mechanism and kinetics of slag cement hydration; we would like to say something.

Our and other researchers'works in China proved, when only gypsum is added to the acid slag (don't be added any lime or clinker), it has no strength. With the same way, the synthesized C_2AS or CAS_1 of slag glass will reach the same result too. That is to say, only gypsum can not activate the latent hydraulic property of slag. On the other hand, when a suitable amount of $Ca(OH)_2$ is added to slag, the slag cement produces strength to some extent, but it is still lower. Granulated blastfurnace slag is an unstable glassphase in the system $CaO-Al_2O_3-SiO_2$. The alkaline circumstance in aqueous solution created by lime or clinker, stimulates the activity of slag, brings about the partial disintegration of slag and formation of hydraulic calcium silicate. When the gypsum exists, ettringite will be formed too. The formation of ettringite decreases the concentration of ions Ca^{++} SO_4^{--} and AlO_2^- in solution, thus upsets the certain solid-liquid equilibrium established before, and promotes the alkaline stimulation. The fact that the essential function of gypsum to promote the reactivation of alkaline stimulation is generally called "sulphate stimulation". Therefore, we think the alkaline stimulation as a prerequisite for the sulphate stimulation, and the sulphate stimulation further promotes the alkaline stimulation. The continuous activation of the latent hydraulic property of slag is based on multiply repeated action of the above mentioned two stimulations.

An important problem we should pay attention to is the alkality of supersulphate cement. If there were no suitable alkality in liquid phase, slag could not be activated and disintegrated. Meanwhile, it is obvious from the phase diagrams of system $CaO-Al_2O_3-H_2O$ and $CaO-CaSO_4-H_2O$ that the solution of $CaSO_4$, especially of Al_2O_3 is seriously inhibitted in saturated solution or nearly saturated with CaO, this fact shows that the high alkality should restrict the formation of ettringite and exertion of latent hydraulic property of slag. Furthermore, the above mentioned conclusions were proved from measuring the reacted slag, the reacted $CaSO_4$, the combined water, the heat of hydration, and the strength in the mixture of slag, gypsum and various amount of lime.

In fact, the sulphate stimulation develops fully in supersulphate slag cement with 3-5 % clinker and excessive gypsum, whereas the alkaline stimulation plays an important role in slag Portland cement which consists of 40-60 % clinker and less gypsum. It is clear from above expositions that the two different kinds of slag cement bring out different conditions of hydration, in which hydrated products form in different circumstances and offer different characteristics of properties, for example, ettringite would be different in quantity, growing rate, morphology, transformation, stability and expansion.

Therefore, there are different requirements for the chemical composition of slag for two kinds of slag cement. The requirements for slag portland cement were mentioned in principal reports, as to supersulphate cement, because ettringite is formed much more during hydration and hardening, the suitable amount of Al_2O_3-content and CaO/Al_2O_3 ratio of slag is necessary. For the most kinds of slag in China, the relation between the strength of supersulphate cement and the

($2Al_2O_3$ + CaO) values is showed as following diagram :

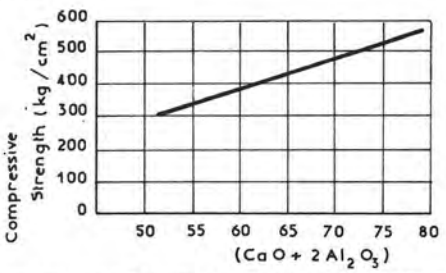

Fig. Relation between chemical composition and compressive strength

We believe, while the researches on mechanism of slag cement hydration and activation of latent hydraulic properties are being carried out deeply, a prospect to make fully effective use of slag in cement industry will appear before us.

CONCLUSIONS

M. VON EUW :

- " Mesdames et Messieurs,

Au terme de cette matinée, je voudrais tenter de tirer les conclusions de nos travaux.

1. - Les laitiers de haut fourneau et les clinkers de ciment portland sont généralement associés en proportions variables pour constituer différents types de ciments.

On attache couramment aux laitiers ainsi utilisés le terme "d'ajout", c'est-à-dire qu'ils sont considérés comme des auxiliaires du clinker. Cette notion mérite d'être révisée si l'on en juge par les communications consacrées au mécanisme de l'hydratation. Nous avons vu en effet que le laitier et le clinker agissent réciproquement sur leur propre cinétique d'hydratation.

En clair, ceci veut dire qu'il faut optimiser les mélanges en choisissant, si l'on en a les moyens, les "couples de constituants" avec chacun leur finesse propre. La Cimenterie n'est-elle pas la plus apte à réaliser cette opération ?

2. - Nous pouvons grâce aux récentes recherches, faire une analyse de la structure :

- le réseau plus ou moins dépolymérisé de tétraèdres SiO_4,
- les hétérogénéités décelée dans la masse du verre.
- les cristaux ayant germé pendant le refroidissement,
- et les défauts observables en surface, sont autant d'éléments de la structure qui conditionnent la réactivité.

3. - Si nous ajoutons à nos connaissances de la structure, les résultats des recherches sur la cinétique de l'hydratation et sur l'identification des hydrates, nous croyons pouvoir comprendre le mécanisme de l'hydratation.

4. - Ces connaissances étant acquises, il reste à tirer le meilleur parti des propriétés spécifiques de ces sous-produits mis à notre disposition par les diverses métallurgies.

Les chercheurs ont consacré leurs efforts à apprécier la réactivité des laitiers et à optimiser l'utilisation de leur potentiel hydraulique.

Nous avons les moyens de mieux maîtriser l'activation par le clinker et le gypse ; d'autres modes d'activation, étrangers à l'Industrie Cimentière, ont été imaginés.

Enfin, de très récents travaux ont montré que le traitement thermique des bétons de ciment de laitier doit être adapté à chaque ciment, c'est-à-dire à chaque couple laitier-clinker, compte tenu d'un optimum de gypsage.

5. - Les chercheurs qui se sont penchés sur les problèmes posés par l'utilisation des laitiers et scories ont pleinement répondu aux objectifs fixés pour notre Congrès. Leurs travaux, poursuivis tant dans le domaine de la structure que dans celui des phénomènes d'hydratation, constituent des recherches de base. Ces recherches ouvrent la voie à l'amélioration des produits existants et à la création de produits nouveaux.

Bien sûr, les sidérurgistes et les métallurgistes se soucient d'abord de la production du métal; il n'en reste pas moins que nous pouvons souhaiter et soutenir un effort de recherche et d'adaptation des procédés, afin de réduire cet aspect de "fatalité" appliqué aux laitiers et aux scories.

Ces sous-produits méritent dans les circonstances actuelles une attention particulière si l'on veut bénéficier de leur potentiel énergétique.

Remerciements :

Je me fais un devoir et un plaisir de féliciter les auteurs de toutes les Communications, des Rapports principaux et des Posters, ainsi que les Membres du Panel pour leur participation hautement compétente à la discussion des sujets traités.

Je renouvelle mes remerciements aux Personnalités qui m'ont confié la Présidence de ce Thème, ainsi qu'à toute l'assistance pour l'attention qu'elle a témoignée à nos exposés et à nos discussions."

* * *

THEME IV

Structure of pozzalana and fly-ash and the hydration of pozzolanic and fly-ash cements

by F. MASSAZZA

1. NATURE AND CONSTITUTION OF POZZOLANAS

The classification of pozzolanas is a problem still open as they are formed of materials very different from one another in chemical and mineralogical composition, structure and origin.
Actually most of these materials resemble typical Italian pozzolanas, which gave the name to the whole group only in the properties of reacting with lime and of hardening in the presence of water.
The writer made a tentative classification, presented to the Congress of Moscow, which can constitute the base for an useful discussion even if it cannot be considered as perfect (1). Other criteria of classification are contained in Sersale's (2) principal paper and this points out the difficulty of grouping very different materials from one another in a general scheme.
In this report the materials having pozzolanic behaviour will be often called "pozzolana" in the above-mentioned meaning, that is without making any specific reference to the real pozzolanas of the Neapolitan and Latial regions.

1.1 Natural pozzolanas

The great difference in chemical and mineralogical composition and morphology of natural pozzolanas is pointed out in paper (3). It confirms that Rhine trass and Neapolitan tuff contain a small amount of vitreous phase but they are rich in zeolitic phases. In the former chabazite prevails and analcime, feldspar and quartz (10-12%) are present. In the latter herschelite is the major component besides minor amounts of analcime and potassium feldspars. Flegrean (Naples) and Volvic (Puy-de-Dôme) pozzolanas are very rich in glass (50 and 25% respectively). Of course these pozzolanas also contain many crystalline minerals such as, for the flegrean ones, sanidine, analcime, potassic zeolite, quartz, augite and dolomite and, for the Volvic one, abundant andesite, quartz, diopside and magnetite. A high silica microcrystalline pozzolana (70.45% SiO_2) essentially consists of opal, traces of quartz and crystobalite, dolomite and phosphates.
A diatomite rich in (~ 50%) and a gaize sample poor in (~ 15%) amorphous silica, used for a study on the hydration of pozzolana-containing cements (4), contain appreciable quantities of quartz and glauconite. The former contains also clayey minerals whereas the latter is particularly rich in calcite (~ 45%).

1.2 Artificial Pozzolanas

1.2.1 Fly ashes from coal

The chemical and mineralogical composition of coal ashes is less varying than the one of natural pozzolanas: generally silica ranges between 48 and 53%, alumina between 23 and 28%, iron oxide between 7 and 10% whereas lime does not exceed 3% (3)(5)(6)(7)(8). Quartz and sillimanite (5) as well as mullite and magnetite (3) are present besides the predominant vitreous phase.
The chemical composition can appreciably vary from the fraction < 40 μm to the one included between 40-80 μm since, if the mineralogical composition is qualitatively the same, the crystallized phases prevail in the fines (5).
Fly ahses can contain considerable amounts of cenospheres which, because of their low apparent density, can be separated in disposal lagoons and used to produce insulating materials (9).
An often neglected constituent of fly ashes is coal. If present in amounts higher than certain levels, it makes fly ashes unusable since it stains the concrete and adsorbs the admixtures (7). In theory coal can be eliminated by sieving since it is generally concentrated in the coarse fractions (> 100 μm), or rather by flotation and combustion. However all these procedures have a cost which limits their possibilities of application. In the practice the only valid solution seems to build and to power plants giving fly ashes containing not more than 2-3% of residual coal (7).

1.2.2 Fly ashes from lignite or sub-bituminous coal

The composition of fly ashes from lignite and sub-bituminous coal is different from the one of coal in that they contain considerable amounts of free calcium oxide which can reach 28% (10).
During combustion free lime forms instantaneously, as proved by the very small sizes of its crystals which adhere to the surface of the vitreous particles (5) (17).
The chemical composition of these materials is much more varying than the one of coal fly ashes (11), even within the same deposit, with variations in the silica content also of 13% (12). Obviously this variability has repercussions in the mineralogical composition, as can be noticed in table I.
All these ashes contain considerable amounts of vitreous material and different crystalline minerals. Among these, quartz, mullite, hematite, magnetite, CaO, C_2S (α, β) anhydrite, $C_{12}A_7$, C_2F and C_3A besides traces of calcite, periclase and C_4A_3S were recognized.
The composition of the vitreous mass can be very different from the average one of the sample and the glass can be even richer in alumina than silica (10).
The composition of the vitreous particles and therefore their refractive index can considerably vary and this allowed five types of glass to be distinghished (11). The three first types have refractive indexes ranging between 1.620 and 1.640 (vitreous melilite), between 1.670 and 1.720 (glasses perhaps of the system C-F-S since their colour varies from yellow to yellowish brown), between 1.720 and 1.735 (brown or brownish black glasses rich in calcium); the two others are opaque and porous. Glasses of type 2 and 3 have a good hydraulicity because of their high calcium content.
Lignite ashes are richer in glasses of type 2 and 3 than the common coal fly ashes.

1.2.3 Melted ashes

In U.S.S.R. the new thermoelectric power plants produce coal slags, at the liquid state, which are granulated with water (5). Their chemical composition widely varies (SiO_2 35-65%, Al_2O_3 10-25%, CaO 1-50%, FeO up to 20%) and consequently not only the percentage of the vitreous phases but also their composition considerably change.
The recognized crystalline phases, sometimes present in appreciable amounts, are mullite, gehlenite, pseudowollastonite and β-C_2S. Of course the presence of glass involves the absence of free lime.
The hydraulic activity of these products increases as the CaO content rises but if the $\frac{CaO+MgO}{SiO_2+Al_2O_3}$ ratio exceeds 1, slags tend to be mainly crystalline and the hydraulic activity drops sharply. If however slag has a composition similar to the one of portland cement clinker, its crystallization gives rise to a material containing considerable amounts of alite and belite and having higher hydraulic properties (5).

2. EVALUATION OF POZZOLANIC ACTIVITY

The problem relevant to the determination of the pozzolanic activity of a material was the object of thorough studies, clearly summarized in chapter 5 of Sersale's (2) principal paper.
Two reports were presented about the subject which has important technological implications. In the former it is shown that, if the standardization of the method is stricter, Chapelle's test can become more precise. By operating with different cements containing pozzolanas of different origin (natural, melted and fly ashes), a good correlation between amount of lime fixed by pozzolana and amount of vitreous phase determined by X-rays was found (13).

TABLE I

Reference	12	11	10	16	5
Free CaO	X	5-15%	28%	X	7-20%
Glass	X	X	34%	X	X
Quartz	X		5%	X	
Mullite	X				
Hematite	X		4%		
Magnetite	X		4%		
βC_2S	X	X	14%		
C_3A				X	
$C_{12}A_7$	-	X			
C_2F	-	X			
$CaSO_4$	-	X	15%	X	X

The decrease with time in the lime present in pastes consisting of one part of lime and four parts of pozzolana can be taken as a measure of the pozzolanic activity of the material. The lime dosage was carried out by X-ray diffraction analysis and it allowed the pozzolanic activity of six studied natural and artificial materials to be clearly differentiated (3). The same study evidenced that the classification of pozzolanas based on the combined lime corresponds to the classification according to the B.E.T. specific surface, so confirming the importance of this parameter on the activity of pozzolanas (3).
Starting from the ascertainment that both chemical and mechanical methods are not able to give an exhaustive evaluation of the pozzolanicity of a material, a new method was proposed. By measuring the mortar strength and the combined lime, four quantities are defined: pozzolanic activity, reactivity, efficiency and relative pozzolanic efficiency.
The overall synthetic characterization is expressed by the index of pozzolanic quality equal to the product of the "pozzolanic reactivity" by the "pozzolanic reactive efficiency" (20).
Anyhow the review of the methods to evaluate pozzolanas has once more pointed out the absence of a simple general method valid for all the materials having pozzolanic behaviour (2) (18).
This conclusion depends on that no general correlation seems to exist between the mechanical strength of pozzolana containing-pastes and the different parameters which, each time, are taken as a measure of the pozzolanic activity (15).

3. POZZOLANA-LIME MIXES

3.1 Reaction between lime and pozzolana

Sersale's (2) and Takemoto's (18) principal papers examine in detail the mechanism of the lime-pozzolana reaction and the factors affecting the pozzolanic activity. These factors are chemical composition, quantity of active phases, structure, morphology, fineness, specific surface a.s.o.
As regards the compounds forming owing to the lime-pozzolana reaction, the previous results were confirmed, that is most compounds are the same forming during the hydration of portland cement.
The contribution dealing with this subject concern both natural and artificial pozzolanas. Pozzolanas consisting of lignite or sub-bituminous coal practically behave as an artificial mix of pozzolana and lime since they are formed of vitreous particles accompanied by smaller particles of free lime (4) (11). Therefore these ashes have a good hydraulicity in themselves. In the lime-pozzolana mixes the fixed lime increases as the duration of the reaction prolongs and, at least till 21 days, as the B.E.T. specific surface increases (3). Generally grinding improves the fineness of fly ashes which, being formed of compact microspheres, have a very low B.E.T. surface but it does not appreciably modify the one of natural pozzolanas. Zeolitic pozzolanas react with lime more rapidly than the ones having vitreous structure (3).
The w/s ratio does not affect the mechanism of reaction between the vitreous part of fly ashes and lime but it only acts on the rate of the different reactions (10).
As for lignite fly ashes the pozzolanic reaction occurs naturally after the hydration of free calcium oxide. By mixing a calcareous lignite ash at w/s = 0.2, free lime decreases linearly as far as to disappear after about 180 days (10), whereas portlandite begins appearing after four hours and ettringite after seven hours. The latter reaches its maximum after about 90 days together with the disappearance of $CaSO_4$. By operating with higher water amounts (w/s=10), free lime disappears after 15 days, portlandite appears after about one hour and ettringite after about one hour and a half (10).
In a lignite ash containing C_3A the X-rays showed that ettringite starts forming before half an hour after the beginning of mixing. Plates of monosulphate hydrate ($C_4A\bar{S}H_{12}$) begin appearing after 4 hours (16). C-S-H gel, probably of type I, is visible under SEM after about 28 days. These gel particles are likely the product of the pozzolanic reaction between glass and lime. The delay in their formation also indicates the slowness of glass to begin the reaction (16). Also in other cases the formation of C-S-H and of other hydrates, such as $C_2A\bar{S}H_8$, occurs at longer ages, even by operating with diluted suspensions at w/s = 10 (10).
Besides participating in the pozzolanic reaction, free lime contained in lignite ashes activates, together with the often present $CaSO_4$, the hydration of glasses, C_2S and other constituents (11). The activating action of free CaO seems to be proved by the fact that lignite ash, melted at 1,350 - 1,450°C and then quenched, looses its hydraulicity since free lime is combined. Indeed it could be maintained that the pozzolanic reaction cannot occur in the absence of free lime.

Nevertheless, it can be assumed that high calcium ashes, similar in composition to metallurgical slags, are activated by $Ca(OH)_2$ and $CaSO_2$.
Type I calcium silicate hydrate was also found in fly ashes from sub-bituminous coals. These products form by peeling off the outer surface of the ash particles which would be covered by a coating of calcium compounds (12). The final hydration products would be essentially ettringite wrapped up by tobermorite gel (11).
The addition of sodium chloride accelerates the hydration of free lime contained in lignite ashes, the formation of calcium aluminate hydrates and, through the pH decrease, the hydration of silicates. This fact is pointed out by the higher heat of hydration evolved by ashes in the presence of salt (11).
The lime pozzolana reaction can be accelerated by steam curing (3) (5) (10). Interesting results giving a contribution to the interpretation of the variability in the Ca/Si ratio of C-S-H gel were obtained by comparing the reactions of a volcanic glass and a silica glass (SiO_2 99.97%) mixed with lime at different ratios (17). The tests were performed at temperatures ranging between 70 and 100°C, for reaction times between 2 and 120 days but at a constant water/solid ratio=20.
As for the volcanic glass it was found that the initially formed C-S-H and C-S-H(I) transform into 10 Å tobermorite after 20 days and subsequently into 11 Å tobermorite. The microanalysis showed that the former tobermorite has a higher Ca/Si ratio than the latter (about 1.15 compared with 0.93). The same occurs for the Ca/(Si+Al) ratio. On the contrary for the silica glass it was possible to observe the transformation of the initially formed CSH into 14 Å tobermorite having a Ca/Si ratio included between 0.64 (microanalysis)and 0.82 (chemical analysis). The addition of alumina to silica glass tends to decrease the basal spacing and, if the duration of the reaction prolongs, it tends to give Al-substituted 11 Å tobermorite. 12 Å tobermorite or tacharanite and 10 Å tobermorite form as intermediate phases in the presence of alumina. What obtained suggests that each tobermorite having different basal spacing may be a well-crystallized form of C-S-H(I) of different Ca/Si ratio.
As regards the morphology of the hydration products it was observed that, if the hydration products of lignite fly ashes are mostly fibrous after 28 days, hexagonal particles are not lacking (12). These products rich in calcium form on the surface of the spherical ash particles and cause their mutual cementation (12). At first the appearance of the vitreous spheres is unaltered but after seven days the corrosion of their surface and their disaggregation are noticed (16).

3.2 Physical and mechanical properties

The presented contributions only considered the physical and mechanical properties of sub-bituminous and lignite ashes. These ashes are used because of self-hydraulic properties suitable to make mortars and concretes (11) and gravel and ash mixes (10).
Lignite fly ashes have a rather rapid set. In fact, depending on the w/s ratio, set begins between 30 and 75 minutes (10) (11) and, in the presence of C_3A, between 15 and 45 minutes (16). Gypsum retards set as it does in cement (11). Below 25°C, a temperature decrease considerably slows down the initial set. The effect is more marked at high w/s ratios (10).
The set of calcareous lignite ashes mixed with water was attributed at first to the formation of portlandite and then to ettringite (10), or directly to the latter (16).
Excellent micrographs show that set is really due to ettringite needles protuding from the individual ash spheres, often perpendicularly, and acting as connection bridges (16).
Generally the presence of free calcium oxide makes the lignite and sub-bituminous coal ashes unsound. The pastes, even if made with different w/s ratios (0.166--0.30), show the same typical behaviour: after an initial volumetric shrinkage the samples swell rapidly and considerably in times ranging between 10 and 40 hours, depending on the water content. Initial shrinkage is attributed to the volume decrease accompanying the water-lime reaction whereas swelling, and therefore cracking and disaggregation of the pastes, are ascribed to the formation and crystallization of ettringite (10).
However it is also reported that the use of lignite ashes containing up to 15% free lime causes no negative effect on the soundness of mortars and concretes (11). Expansive ashes added in small amounts (3-5%)to coarse aggregates (e.g. road gravel) cause no unsoundness and give strengths over 15 N/mm^2 to the mix.
By mixing sub-bituminous coal ashes with water in order to attain the highest density (12-20%), it is possible to obtain materials that, after 28 days' wet curing, have strengths ranging between 0.7 and 6.3 N/mm^2.
Nevertheless these samples, immersed in water, disintegrate before two weeks (12). The great differences in strength and hardening rate of these samples must be attributed, more than to pozzolanic reactions having different rates, to the different content in promptly reactive calcium silicates and aluminates (12).
Opposite results were obtained with lignite ashes which, in spite of their free lime content, gave strength of 29.0 and 33.4 N/mm^2 at 7 and 28 days. These values increase to 33.4 and 44.8 N/mm^2 respectively if gypsum is added or to 44 and 56.4 N/mm^2 respectively by addition of NaCl (11).
To conclude, the available information about fly ashes containing free lime is contradictory and insufficient to preconize their use in the field of hydraulic binders. Therefore their knowledge needs to be deepened by studying their chemical and physical properties and their applicative characteristics.

4. POZZOLANA-PORTLAND CEMENT MIXES

4.1 Reactions in mixes containing cement and pozzolana

In pozzolana-containing cements the hydration reactions of clinker and pozzolana can be considered separately, even if to a certain extent they occur simultaneously. In fact the pozzolanic reaction, which is anyhow slower than the hydration reaction of clinker, can take place only after the hydrolysis of alite and belite has formed $Ca(OH)_2$.
As regards the pozzolanic reaction, since the components mainly involved are SiO_2, Al_2O_3, Fe_2O_3 and CaO, it is not surprising if the obtained products are the same forming during the hydration of clinker. The subject is exhaustively treated in the wide and documented chap. 3 of Takemoto's principal paper (18), where the process and the mechanism of hydration of the systems formed by pozzolana with the clinker constituents and portland cement are examined. Here, of course, the main points of the contributions dealing with this subject are recalled.
X-rays showed that cements made with different pozzo-

lanas give the same hydrated phases even if the quantitative ratios can be different (4). The value of B.E.T. specific surface of the hydrated pastes depends on the nature of pozzolanas. In any case it is higher than the one of the control cement and it presents a maximum value at 28 days' curing (4). Also the pore distribution depends on the type of pozzolana and the duration of curing (19).
At 7 days' hydration the pozzolanic reaction has already begun (20) even if the contribution given by the pozzolanic material to the hydraulic properties of clinker would occur only at relatively long ages: 6 months, 1 year and longer (13). Nevertheless it was indicated that the reactions involving pozzolana begin already after 3 days (8), or even after 1 day (19), that is before the time reported by other Authors.
A layer of C-S-H forms on the surface of the ash grains owing to the attack of the solution supersaturated with $Ca(OH)_2$. This layer, which appears in the form of plates and discs, has a lower Ca/Si ratio than the fibrous C-S-H (outer and inner) forming on the clinker grains (20).
Aluminate hydrates and ettringite, forming initially, transform afterwards into monosulphate and the solid solution C_3A ($CaSO_4$, $Ca(OH)_2$).H_{12} (4) (19). After one year, cements containing 20% of different types of pozzolana show the presence of ettringite, C_4AH_{13}, C-S-H and $Ca(OH)_2$ (4) (3). C-S-H forming on the ash and pozzolana grains has a lower Ca/Si ratio than the cement paste (3). At long terms the ash-cement hydration products have morphology similar to the one of type I and III calcium silicates (8). In any case the peculiar morphology depends on the clinker composition, the hydraulic activity of ash, its fineness, its quantity and the degree of hydration reached at a given time (20).
The lower early strength of cements containing pozzolanic additions is attributed to the fact that the interaction products between the grains of pozzolana (burnt shale) and the solution supersaturated with $Ca(OH)_2$ appear in the form of needle-shaped crystals which are not able to grow continuously in length and have few and weak points of contact. Another cause contributing to decrease early strengths lies in that the additions accelerate the hydrolysis of clinker silicates. This results in the formation of many and short filaments having few points of contact with one another. Subsequently these elements entangle forming a thick skeleton and the cement paste increases in strength (20).
Another factor contributing to retard the hardening of fly ash-containing cements is the slowing down of the C_3A+C_4AF hydration. In fact by adding fly ashes to C_3A+C_4AF separated from the clinker silicates by maleic acid methanolic solution, it was seen that the hydration of the two compounds is much slower than the one observed when an equal amount of ground quartz is added. It was even noticed that fly ashes have a higher retarding effect than gypsum (8). Pozzolanas also decrease the hydration rate of synthetic C_3A but in the presence of $CaSO_4.2H_2O$ they cause an acceleration. In this case, the pozzolana accelerates the hydration of tricalcium aluminate since its grains offer the precipitation sites of the formed ettringite. The reaction rate of C_3A also depends on the nature of pozzolanas (composition, specific surface, capacity of ion exchange) (19).

4.2 Physical and mechanical properties

4.2.1 Influence of the nature and the proportion of constituents

Owing to the relative slowness with which the reaction between clinker hydrolysis lime and pozzolana proceeds, the pozzolana-containing cements generally have lower early strengths and higher ultimate strengths than control cements.
In any case the strength of the pozzolana-containing cements depends on the nature of pozzolana (3)(8)(10)(13) and its content, at both short and long ages. Similarly, the highest strength obtainable from an ash depends on the composition of clinker (21).
The replacement of 10-35% portland cement with pozzolanas of different nature (9000 Blaine) yield, before 28 days, a lower mechanical strength (in ISO mortar) than the portland cement ground to 3200 Blaine. Till 11 days and at 20°C the strength of mortars decreases proportionally to the increase in the ash content (22). This fact indicates that, till this age, ashes give no contribution to strengths. However after 28 days the strengths at 20°C decrease less than proportionally to the ash content and this shows that the pozzolanic reaction has begun (22).
Also the free calcium hydroxide content of the pastes justifies the mechanical behaviour of mortars. In fact $Ca(OH)_2$ is proportional to the clinker content till 11 days' curing at 20°C but it is lower than the proportional value for longer times (or higher temperatures) (22).
In a study extended to six different natural and artificial pozzolanas it was noticed that a correlation between lime fixed in pure pastes and compressive strength in ISO mortars only exists between six months and one year (3).
Tests carried out on mortars made with many cements containing pozzolanas of different origin showed that, as from 180 days, it is possible to correlate the increase in the long term-strength with the amount of fixed lime measured by the modified Chapelle's test (13).
Of course, if the pozzolana is added in excess, a part of it cannot find the lime which to react with. Therefore the addition of 45% pozzolana justifies that the strengths of the blended cements were always lower than those of the control portland cement, till 300 days (4).
By replacing 20% of a portland cement with a fly ash, it was observed that in ISO mortars the strengths of the blended cement exceed those of the control cement after about 150 days' curing (6). However the overtaking moment also depends on the composition of clinker since it was seen that mixes of clinker, containing more than 8% C_3A, and fly or melted ashes exceed the strengths of control cements already between 28 and 90 days, depending on their preparation (13).
The long term-strength increase as the ash content increases (within certain limits) is explained not only by the well-known pozzolanic effect but also by the fact that ashes retard the C_3A and C_4AF hydration. This has, as a counter-effect, the possibility of increasing the volume of calcium silicates (8).
At the same w/c ratio, the ash content increase is accompanied by a slump increase of concretes (8) but it must be reminded that ground ashes demand more water than the original ones (5).
Tests on concretes showed that the replacement of 15% portland cement with fly ashes increases strengths at both 3 days and 91 days' curing, whereas the substitution of 30% improves strengths only after about two months. Higher contents always give lower strengths than the control sample (8).
Chapter 4 of Takemoto's (18) principal paper summarizes the works that, after the Moscow Congress, were carried out to relate the mechanical strength of pozzolana-containing cements to many variables. The

strengths of pozzolanic cements depend , as the one of portland cements, on the texture of the hardened pastes, the composition of the hydrated phases, the capillary and gel porosity, the shape of the gel pores, the pore size distribution and, of course, the nature of pozzolana.

4.2.2 Influence of temperature

The temperature rise accelerates the hardening of pozzolana-containing cements as it does for portland cements. At 80°C it was observed that only 1/25 of the time demanded operating at 20°C is necessary to reach a certain strength (3). At higher temperatures portland cements show a strength decrease whereas those containing 35% ashes indicate a sharp increase which reaches the maximum value at 28 days (22).
Curing temperatures above 20°C (35-80°C) improve the strength of a cement containing 20% fly ashes more than it does for the control portland cement (6). Also by using steam curing, the cements containing fine fractions (< 40 μm) of a fly ash show lower strengths than those containing coarser fractions (40-80 μm) (5).

4.2.3 Influence of fineness

The addition of fly ashes to portland cement having the same fineness involves a 28 day strength decrease. A longer grinding time improves the compressive strength but increases the energy consumption (7). From this standpoint it would be suitable to mix portland cement with already very fine ashes.
Anyhow it must be considered that the grindability of ashes and pozzolanas is generally higher than clinker and therefore in the intergrinding the fine fractions are richer in ash and the coarse ones in clinker. Since the latter is the constituent that more contributes to the short and medium-term strengths, it is understood why the early strengths of blended cements are often lower than portland cement (6) (21). Therefore it is clear that the fineness of clinker needs to be increased in order to obviate this inconvenience (6).
In fact the pregrinding of clinker, followed by an intergrinding, produces 10-20% ash cements having mechanical strengths practically equal to those of the control cement in the 1-90 day range and higher after 180 days' curing (21). The optimum parameters of this process, such as time and specific surface, depend on the quality of clinker and ash (21).
To find the best conditions of grinding, as regards both mechanical strength and energy consumption, the grinding of fly ash-containing cements can be carried out according to different ways. With 15% fly ash, the best performances were obtained by intergrinding, whereas with a content of 30% the best results were achieved by separated grinding (7). It is obvious that different results can be obtained by using other materials but, as a general rule, this procedure allows the best grinding conditions to be chosen. In any case it was seen that at constant specific consumption (kwh/t), the short term-strengths improve if clinker is ground more finely whereas the 90 day strengths increase if ashes are ground longer.
Till 1-3 months cements containing the finest fractions of two fly ashes (< 40 μm) show lower strengths than cements containing the coarser fractions (40 - 80 μm), whereas subsequently this behaviour reverses.
This fact is explained by observing that the fine fractions have a much higher surface than the coarse ones. Therefore the annular volume filled with the liquid phase forming around the ash grains at the beginning of the hydration is on the whole higher. Subsequently when the pores are filled enough with the newly formed compounds the strength of cements containing the finest fractions become higher (5).

4.3 Heat of hydration

The addition of pozzolana (or limestone) decreases the heat of hydration but accelerates the appearance of the maximum thermal effect. The latter action is attributed to the fact that pozzolanas, since they absorb lime from the solution, accelerate the hydration of clinker whereas limestone reacts, with considerable thermal effect, with C_3A forming $C_3A.CaCO_3.12H_2O$. Moreover, all the additions have a dispersing action, which facilitates the contact of water clinker. Simultaneously their grains act as crystallization nuclei during the early hydration (8). This acceleration of the hydration process is confirmed by the fact that a lite disappears more rapidly in the cements containing additions (4).

4.4 Dosage of pozzolana in cements

The dosage of the pozzolana contained in a blended cement constitutes a problem of increasing importance. An interesting attempt was made on this subject by using the quantitative X-ray diffraction analysis (Q X DA) to determine the index of crystallinity of the pozzolanic addition, defined by the ratio:

$$M = \frac{I_{tidi} - I_A}{I_{tidi}} \times 100$$

where:

I_{tidi} = total integrated diffracted intensity
I_A = integrated diffracted intensity of "amorphous halo"

The tests were limited to fly ashes, but also in this case acceptable results are obtained only when the ash used in calibration has an index of crystallinity similar to the one of the unknown mix (23).

4.5 Durability

While it is generally accepted that the resistance to the chemical attack of pozzolana-containing cements is higher than portland cements, doubts arise on the ability of these cements to efficaciously protect the reinforcement. The pozzolanic reaction, as it fixes lime, reduces the alkalinity and therefore it accelerates the neutralization caused by carbon dioxide in the air. However, it is reported that in fly ash-containing mortars not all lime is fixed and the remainder is anyhow sufficient to maintain a pH = 12.5 in the solution and therefore to assure a good protection to the reinforcement (22).
The results of a 10 years' study on the influence of fly ashes on the neutralization of concrete, where the classical method of the colouring by phenolphthalein was used, are given in contribution (24). The test showed that, at the same workability, the depth of neutralization decreases as the cement dosage becomes higher and increases as the ash content rises. The depth of

neutralization results to be proportional to the square root of the time, with a coefficient of proportionality increasing with the w/c ratio. The depth of neutralization results to be inversely proportional to the 28 day strength, regardless of the addition of fly ashes. Anyhow the depth of neutralization of concretes having strengths over 40 N/mm^2 practically tends to zero. It is lower for long cured concretes and, very interesting fact, for the ones in the open. The mechanical strength of cement mortars containing pozzolana (45%) is higher than the one of the control portland cement if they were immersed for three years in solutions containing 2% Na_2SO_4 and $MgSO_4$. It is lower if they have been water-cured for the same period of time. Indeed the strength of pozzolanic mortars cured in water or in the two solutions is the same (4).

To conclude this necessarily short review on pozzolanas and pozzolanic cements it can be noticed that their use is growing and that about this matter studies and research are spreading all over the world. This means on one hand that pozzolana containing-cements have excellent performances and on the other they offer economical advantages above all in connection with the energy saving that they allow.

REFERENCES

1. MASSAZZA F.
Chemistry of pozzolanic additions and mixed cements
6th International Congress on the Chemistry of Cement (Moscow, 1974) 65 pp.

2. SERSALE R.
Structure and characterization of pozzolana and fly ash
This Congress vol. I - IV-1/3-1/18

3. MORTUREUX B., HORNAIN H., GAUTIER E., REGOURD M.
Comparison of the reactivity of different pozzolanas
This Congress vol. III - 110-115

4. GRZYMEK J., ROSZCZYNIALSKI W., GUSTAW K.
Hydration of cements with pozzolanic additions
This Congress vol. III - 66-71

5. DMITRIEV A.M., ENTINE Z.B., GOLDSTEIN L.J., CHATOKHINA L.P.
Hydration, morphology and properties of ash cements
This Congress vol. III - 98-103

6. DALZIEL J.A.
The effect of curing temperature on the development of strength of mortar containing fly ash
This Congress vol. III - 93-97

7. ALSTED NIELSEN H.C.
Preparation of fly ash cements
This Congress vol. III - 72-77

8. CABRERA J.G., PLOWMAN C.
The influence of pulverized fuel ash on the early and long term strength of concrete
This Congress vol. III - 84-92

9. RAASK E.
Utilization of pozzolanic and cenospheric ashes
This Congress vol. III - 1-6

10. CHARLES-GIBERGUES A., THENOZ B., VAQUIER A.
Hydration mechanism of a fly ash produced from calcareous lignite
This Congress vol. III - 53-59

11. LIU HUAKUN, LU ZHONGYA, LIN SHENGJIE
Composition and hydration of high calcium fly ash
This Congress vol. III - 7-12

12. JOSHI R.C., WARD M.A.
Cementitious fly ashes - structural and hydration mechanism
This Congress vol. III - 78-83

13. RAVERDY M., BRIVOT F., PAILLERE A.M., DRON R.
Appreciation of pozzolanic reactivity of minor components
This Congress vol. III - 36-41

14. VERHASSELT A.
Characterization of the pozzolanicity of fly ash
This Congress vol. III - 116-121

15. MASSAZZA F., COSTA U.
Factors determining the development of mechanical strength in lime-pozzolana pastes
XII. Conference on Silicate Industry and Silicate Science - SILICONF I (Budapest, June 1977) - 537 - 552

16. DIAMOND S.
Hydration reactions of C_3A contained in an unusual flyash
This Congress vol. III - 19-23

17. HARA N., INOUE N.
Formation of 10 Å and 14 Å tobermorite from pozzolanic glassy silica
This Congress vol. III - 13-18

18. TAKEMOTO K., UCHIKAWA H.
Hydration of pozzolanic cement
This Congress vol. I - IV-2/1-2/29

19. UCHIKAWA H., UCHIDA S.
Influence of pozzolana on the hydration of C_3A
This Congress vol. III - 24-29

20. YANEB I., RADENKOVA-YANEVA M., LAZAROV I., TCHULEVA E.
Structure of the products of hydration of cement with shale ash
This Congress vol. III - 42-47

21. KOVACS R.
The influence of the production technology of fly ash cements upon their hydration and hardening
This Congress vol. III - 104-109

22. OWENS P.L., BUTTLER F.G.
The reactions of fly ash and portland cement with relation to the strength of concrete as a function of time and temperature
This Congress vol. III - 60-65

23. GUTTERIDGE W.A.
An examination of ordinary portland cement blended with pulverised-fuel ash
This Congress vol. III - 48-52

24. TSUKAYAMA R., ABE H., NAGATAKI S.
Long-term experiments on the neutralization of concrete mixed with fly ash and the corrosion of reinforcement
This Congress vol. III - 30-35

ROUND TABLE

F. Massazza (Italy) Chairman, K. Takemoto (Japan) and R. Sersale (Italy), principal reporters, Messrs. A.M. Dmitriev (USSR), R. Magnan (France), P. Longuet (France), J. Skalny (USA) participated in the round table on Theme IV.
The round table examined and discussed numerous subjects whose scientific and practical importances was pointed out in the principal papers and the contributions presented to the Congress.
The conclusions reached can be shortly summarized as follows:

a) Evaluation of the pozzolanic activity

The pozzolanic activity, even if it is the object of many studies, was not yet a simple definition and its evaluation cannot be obtained through an only test. In fact none of the different experimented methods showed to have a general validity since each method generally tends to take, as an index of the pozzolanic activity, a particular property which instead constitutes only one of the numerous parameters characterizing a pozzolanic material. As a consequence, the different methods give good results if a certain family of materials, characterized by the constance of certain parameters, is considered whereas they fail when they are extended to other materials.

b) Structure and composition of pozzolanas and their reactivity

The reactivity of natural and artificial pozzolanas depends on many chemical, structural and morphological factors. All pozzolanas are characterized by the presence of (vitreous, amorphous or zeolitic) phases rich in silica unstable in the presence of calcium hydroxide. The reactivity of these phases mainly depends on the chemical and mineralogical composition and the BET specific surface. In fact vitreous phases of different composition and pozzolanic activity can be found in certain pozzolanas whereas in others the reactivity can be lowered by reducing their specific surface through thermal treatment and causing the vitreous phases to crystallize.
In some countries, besides the traditional coal fly ashes, also basic fly ashes begin to be used. They result from the combustion on lignites and sub-bituminous coal which can contain up to 28% free lime and therefore be self-hardening.
The negative consequences of the presence of not combined CaO in mortars and concrete were pointed out by different research. Nevertheless it was also reported that lignite ashes containing up to 15% CaO do not cause volume instability probably because the CaO grains are very small and hydrate before the hardening process starts. The problem of the basic fly ashes, which is already important today and will be still more in the future, demands other thorough studies to verify the fields and limits of use of these materials.

c) Relationship between chemical reactivity and mechanical strength

No doubt that there is a relationship nature-reactivity-performances of pozzolanas.
Nevertheless it is not yet possible to foresee their performances even if their nature or reactivity is known. In fact the former are conditioned by several factors, sometimes badly known. For example by using a given pozzolana considerably different performances can be obtained by mixing it with different clinkers.

d) Difference between natural and artificial pozzolanas

The differences between natural and artificial pozzolanas are not deeper than those existing in each group. In this connection it is sufficient to remember the considerable differences findable among natural, vitreous and zeolitic pozzolanas. The most homogeneous group is perhaps represented by coal fly ashes whose genesis and composition are very similar.

e) Importance of pozzolanas in the energy saving

The importance of pozzolanas in the energy saving is emphasized by the following data relevant to 1979.
About 6 millions of tons of natural and artificial pozzolanas were used to make cements in USSR. Italy used about 5 millions of tons of pozzolanas for the manufacture of about 15 millions of pozzolanic cements. In France, besides natural pozzolanas, one million of tons of fly ashes was used to make different types of cement. These data are obviously partial but give an idea of the importance that pozzolanic materials have in the cement industry, taking into account that natural and artificial pozzolanas are largely used also in many other countries. Considering that substituting ten tons of portland cement for as many of pozzolana involves a saving of about one ton of fuel, it is possible to have a clear idea of the amount of energy saving allowed by the use of pozzolanas.

f) Performances of cements containing pozzolanic additions

As for the performances of pozzolana-containing cements, the fact that they are used all over the world is the best proof of their excellent characteristics.
Some deficiencies in the performances observed in pozzolanic cements compared with portland cements can sometimes be attributed to unsuitable technological cycles of production rather than to intrinsic quality deficiencies of the former.
As for durability and chemical attack resistance, it is possible once more to refer to the ancient works, especially the ones built by the Romans with mortar and pozzolanic concretes, but also recent studies indubitably prove the favourable action exerted by pozzolanas.

Mechanism of the pozzolanic reaction

The study of the mechanism of reaction of pozzolanas has recently been faced in a new light which could give an important contribution to the knowledge of these materials.
For this reason R. DRON was asked to present the results obtained in the laboratory of Ponts et Chaussées of which we give a short summary.

"Les feldspaths, qui sont les constituants essentiels des pouzzolanes, appartiennent à la classe des tectosilicates. Leur structure cristalline résulte d'un arrangement de tétraèdres $Si^{4+}(O^{2-})_4$ et $Al^{3+}(O^{2-})_4$ dans lequel chaque oxygène est commun à deux tétraèdres et peut donc être considéré comme n'appartenant que pour moitié à un tétraèdre donné. Les tétraèdres s'organisent en un édifice complexe qui laisse des cavités dans lesquelles se logent les cations alcalins et alcalino-terreux. Les verres pouzzolaniques sont constitués des mêmes tétraèdres, mais l'arrangement de ceux-ci est désordonné.

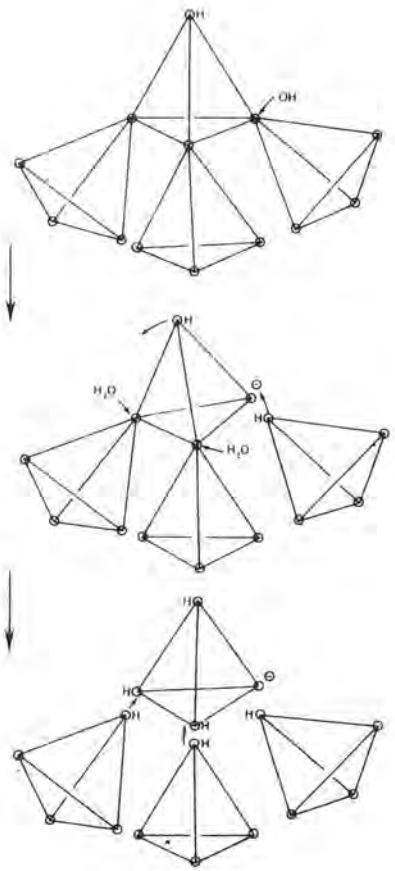

Mécanisme d'attaque alcaline des pouzzolanes

Les silicates et les aluminates de calcium hydratés sont également formés d'un arrangement de tétraèdres, mais ceux-ci sont indépendants, étant constitués d'ions tels que $AlO_4H_4^-$ et $SiO_4H_3^-$. Le passage de la phase anhydre, où les tétraèdres sont à oxigènes communs aux phases hydratées où ils sont indépendants se fait donc nécessairement par l'intermédiaire d'une individualisation de ces entités sous une forme qui ne peut être que ionique.
Dans l'hypothèse d'un mécanisme suivant le modèle de Le Chatelier, on distinguera trois étapes

a) L'étape d'attaque
Considérons un assemblage tétraédrique à oxigènes communs et intéressons-nous à un tétraèdre superficiel. Celui-ci peut comporter, à la différence des tétraèdres "profonds", un sommet libre, occupé par un ion OH^-. Ce tétraèdre peut être décroché par une solution basique de la façon suivante:
- un ion OH^- est attiré par l'ion central (Si^{4+} ou Al^{3+}) de l'un des tétraèdres supports. Il expulse l'oxygène de liaison, provoquant le basculement du tétraèdre superficiel qui n'est plus lié que par une arête autour de laquelle il peut pivoter, et qui présente maintenant un excès de charge égal à −1, ce qui lui confère une forte affinité pour l'eau (fig.);
- le même processus pourrait provoquer la rupture des liaisons résiduelles, mais la présence d'une charge négative excédentaire tend à éloigner les ions OH^-.
L'hydrophilie du site ionique crée favorise une coupure par des molécules H_2O libérant ainsi un ion tétraèdrique qui sera soit l'ion $SiO_4H_3^-$ soit l'ion $AlO_4H_4^-$.

b) L'étape de diffusion
L'ion libéré par l'attaque diffuse dans la solution, c'est-à-dire que sous l'effet de l'agitation thermique il s'éloigne progressivement de la surface originelle.

c) L'étape de cristallisation des hydrates
La présence dans la solution d'ion Ca^{2+} provoque, à partir d'une certaine concentration d'ions silicate et aluminate déterminée par les produits de solubilité des hydrates, une instabilité thermodynamique qui entraîne la cristallisation.
Elle conduit à la formation de composés hydrates dont la nature est définie par les règles générales qui gouvernent le système $CaO-Al_2O_3-SiO_2-H_2O$.
Dans la pratique courante où des quantités importantes de chaux sont utilisées, les produits d'hydratation sont l'aluminate tétracalcique hydraté et le silicate de calcium hydraté".

Formation of tobermorites from pozzolanic materials

The characterization of calcium silicate hydrates represents a still open problem and was the object of many contributions presented to this Congress. One of these studies, involving the lime-pozzolana reaction, was summarized by N. Hara who, together with N. Inoue obtained different types of tobermorite characterized by different composition and basal planes (10 Å, 11 Å and 14 Å) by starting from mixes containing lime with a natural pozzolana or a silica glass.
The reactions were performed between 70 and 100°C with varying ratios of composition to processing duration. Depending on the starting material and the working conditions, tobermorites of different basal plane form. In any case the formation of tobermorite passes through the formation of CSH.
Starting from volcanic glass, the initially formed CSH transforms into 10 Å tobermorite after 20 days and afterwards into 11 Å tobermorite. Microanalysis show-

ed that the former has a Ca/Si ratio ≃ 1.5 and the latter ≃ 0.93. On the contrary starting from silica glass, CSH transforms into 14 Å tobermorite with a Ca/Si ratio ranging between 0.64 (microanalysis) and 0,82 (chemical analysis).
The presence of aluminium tends to decrease the basal plane.
The obtained results suggest that each tobermorite different basal distance is a well crystallized form of CSH having different Ca/Si ratio.

How to grind fly ash cements to obtain the best performance and the highest energy saving

A communication particularly interesting for practical purposes was summarized by H.C. Alsted Nielsen who considered the manufacture of fly ash-containing cements as regards both performances and energy consumption.
In particular the different grinding and mixing modes which can be industrially performed were analyzed. The choice of the process depends on the clinker/fly ash ratio but also on the main objects that manufacturers want to obtain, that is low energy consumption or high mechanical strengths.
For instance, for cements containing up to 15% fly ashes, intergrinding gives excellent results, but with higher contents the best results are attained by separate grinding.
This has the advantage of modifying the development of the cement strength according to the requirements of the market. In particular, by distributing the grinding energy suitably between clinker (+ gypsum) and fly ashes, mechanical strengths at short ages can considerably be improved.
The Author only considered one type of fly ashes and one type of clinker, but the arguments and experiences carried out have a general character and therefore they are susceptible of being used as a guide in the preparation of cements containing fly ashes and natural pozzolanas.

Influence of pozzolana on the early C_3A hydration

Some Authors mentioned in the synthesis of communications that fly ashes and pozzolanas retard the hydration of C_3A+C_4AF separated from clinker silicates and synthetic C_3A. Since Collepardi found rheological changes besides retardation effects, he was asked to summarize his experiences.
When C_3A hydrates in the presence of pozzolanas, the heat evolution curves are quite lower (see fig.). The influence of pozzolanas is slight when C_3A hydrates in the presence of lime and gypsum. Moreover, when a volcanic natural pozzolana (Segni) is substituted by a silica rich diatomaceous pozzolana (Sacrofano) the retarding effect becomes more evident. This retarding effect would indicate that some adsorption of pozzolana on C_3A surface can occur. The adsorption would be lower when both lime and gypsum are present, probably for the presence of "colloidal" ettringite coating the C_3A grains as stated by Metha (J. Am. Ceram. Soc.1973) and Collepardi et al. (Cem. Concr. Res. 1978).
In the C_3A sample containing both calcium hydroxide and the volcanic pozzolana a rheological change from a stiff paste to a flowing one is observed during 10-30 min. of hydration, while the laminar crystals of hexagonal hydroaluminate (C_2AH_8 and C_4AH_{13}) are transformed into the cubic crystals of C_3AH_6.

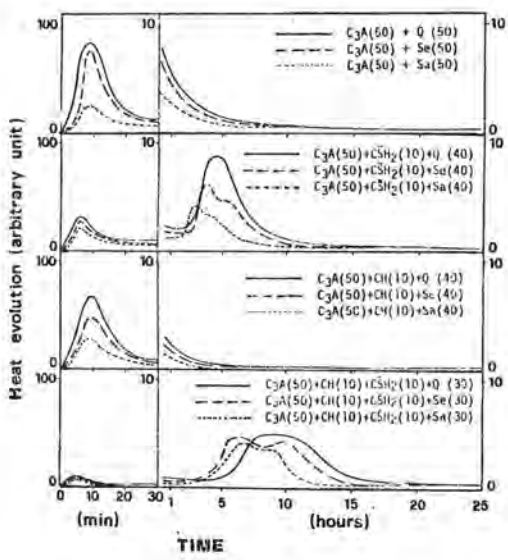

- Heat evolution curves for C_3A hydration in the presence of lime (CH), gypsum ($C\bar{S}H_2$), quartz (Q), Segni pozzolana (Se) or Sacrofano pozzolana (Sa).

Generally the transformation from the hexagonal crystals into the cubic phase occurs after the setting of C_3A paste. However, when this transformation, for some reasons, is anticipated and the system is still in a plastic state the stiff paste is changed into a flowing one. The change in the morphological character of the hydrated products is caused by the presence of both lime and the volcanic pozzolana but the mechanism is not yet known. A similar phenomenon was pointed out by Traetteberg and Grattan-Bellew (J. Am. Cer. Soc. 1975) on pure C_3A pastes. However, in this case, the change in the morphology of hydroaluminates and then in the rheological properties was ascribed to high water/solid ratios and high temperatures - caused by large samples liberating remarkable heat of hydration - as both these parameters favour the transformation from hexagonal hydroaluminates into the cubic phase.

DISCUSSION

Different participants asked questions most of which received an immediate answer whereas others, for lack of time, were not examined during the session. However all of them are presented here together with the relative short answers.

J. BENSTEND's question

There is some evidence in portland cement containing fly ash that alkali hydroxide rather than calcium hydroxide is making the major contribution to pozzolanicity. It thus follows that chemical tests for pozzolanicity need to take full account of this possibility. What are the panel's views on the role of alkali hy-

droxide as opposed to calcium hydroxide in determining pozzolanicity in such situation?

Réponse de P. LONGUET

Sur le plan des principes nous sommes d'accord avec Monsieur Bensted sur le rôle des alcalis dans le développement de l'effet pouzzolanique, et sur l'intérêt qu'il y aurait à en tenir compte pour définir un test chimique d'appréciation de l'activité pouzzolanique.
La difficulté serait sans doute de définir le milieu réactionnel convenable assurant une solubilité telle à l'hydroxyde de calcium que la concentration en ions Ca^{2+} reste supérieure à celle provenant de l'équilibre de solubilité des composés calciques hydratés susceptibles de se former. Il y a là certainment une série d'études qui seraient très profitables à une connaissance plus complète de l'effet pouzzolanique.

Question de E. DEMOULIAN

A quoi peut-on attribuer le retard de prise des ciments qui contiennent des cendres volantes?

Réponse de P. LONGUET

Si ce retard n'est pas attribuable à la composition particulière de la cendre: par exemple des impuretés existant naturellement dans le charbon initial (l'exemple du Zn a été signalé) soit provenant de combustibles ajoutés au charbon au niveau du brûleur de la chaudière (huiles usées renfermant des additifs tel le sulfure de molybdène...), la réponse n'est pas évidente. Peut-être faudrait-il vérifier si les propriétés adsorbantes particulières des cendres volantes ne déplacent pas les équilibres ioniques initiaux de la phase aqueuse de la pâte de ciment dans un sens comparable à l'addition d'un retardateur?

Question de E. DEMOULIAN

Influence de la réactivité chimique de la pouzzolane sur la structure et la composition des hydrates formés. (Question au Panel).

R. SERSALE's reply

The chemical reactivity of pozzolanas does not seem to appreciably affect the structure and composition of the newly formed hydrates.
In fact, starting from natural pozzolanas of different eruptive areas, the principal products originating after the reaction with lime and liable for the binding action are constantly: calcium silicate and tetracalcium aluminate hydrates.
In the light of the experimental research carried out so far, the determining role of the chemical reactivity of pozzolana is likely to be limited to a substantial influence on the formation kinetics of the newly formed phases.

S. DIAMOND's question

It has often been thought that reactivity of flyash or pozzolanic glasses may be related in part to the state of strain in the glass, is there any convenient method available to measure this?

R. SERSALE's reply

Direct methods for evaluating the state of strain in incoherent glasses, like fly ashes or pozzolanas, probably cannot provide reliable results, even if, no doubt, strain favours reactivity.
By means of physico-chemical techniques, such as evaluation of the heat of solution, dilatometric analysis, high sensitivity thermal differential analysis, a relative and indirect determination of the strain can often be obtained provided glassy samples have the same chemical composition but different thermal history.

U. LUDWIG's question

What is your opinion about the maximum replacement of portland cement with pozzolana free of lime with respect to carbonation and:
a) influence on ultimate strength
b) influence on the carbonation rate

F. MASSAZZA's reply

a) Italian pozzolanic cements usually contain around 33% of pozzolana. Practically as much pozzolana is added as much is necessary to combine the hydrolysis lime of clinker (pozzolanicity test ISO R 863). Higher amounts of pozzolana would not react and therefore would reduce mechanical strengths. In pozzolana-containing cements, all the other conditions being equal, the change in mechanical strengths as a function of pozzolana content shows a nearly linear decrease at short ages but presents a maximum after about 28 days. The early and ultimate strengths of a pozzolanic cement depend, of course, on the quality of pozzolanas (active phase content, their nature, BET specific surface, a.s.o.).
b) Latest research by Longuet et al. (Rev.Mat.Constr. 1973, Silicates Ind. 1976) and Diamond (Il Cemento 1977) proved that the solution filling the pores of the cement paste is practically free of calcium hydroxide ($Ca^{++} < 10^{-3}M$) and essentially consists of alkali hydroxides.
Therefore the resistance to the carbonation of concrete does not appear to be attributed to the presence or absence of calcium hydroxide in the pore solution, but it must be sought in other factors such as, for instance, the permeability of CO_2 of the cement paste. Anyhow it must be reminded that appreciable amounts of free calcium hydroxide are always present in the pastes of pozzolanic cements, even when very active pozzolanas rich in silica ($SiO_2 > 80\%$) and poor in lime ($CaO < 0.5\%$) are used.

G.K. MOIR's question

I would like your reactions to the observation that not only need the pozzolana be assessed by strength test but that clinker rather than $Ca(OH)_2$ should be used as factors such as the available alkali and sulphate may influence reactivity. Further, perhaps the most important property of the pozzolana with regard to strength up to 28 days is the influence upon concrete workability (rheology) and consequently w/c ratio.

Réponse de R. MAGNAN

Il a été noté par différents auteurs que les connaissances actuelles ne permettaient pas de relier les ca-

ractéristiques chimiques d'une pouzzolane et d'un clinker et la réactivité du mélange.
Il est donc nécessaire pour connaître la qualité d'une pouzzolane de faire des tests mécaniques en utilisant les matériaux réels. C'est-à-dire la pouzzolane et le clinker contenant ses éléments secondaires, sulfate, alcalis, etc....
Il est bon de distinguer deux types de réactivité. La réactivité chimique qui est la vitesse de réaction chimique avec l'eau et la réactivité physicochimique qui est la vitesse d'acquisition des résistances mécaniques. Il est en effet possible d'avoir une réactivité chimique élevée par exemple en augmentant la surface spécifique des produits sans avoir de résistances élevées, car la surface spécifique élevée exigera pour une théologie acceptable un E/C élevé dont on connaît les effets néfastes.
Une bonne pouzzolane correspond au meilleur compromis entre une réactivité chimique la plus élevée possible et une surface ou activité de surface vis à vis de l'eau, la plus faible possible.

T. PATZIAS's question

What happens to Al_2O_3 of fly ash with low (or high) CaO content during the hydration of pozzolanic cements to explain their improved sulphate resistance?

F. MASSAZZA's reply

A good portion of Al_2O_3 of pozzolanas and presumably also of fly ashes, enters the lattice of C-S-H. Once the best sulphate resistance of the pozzolanic cement paste was simply attributed to the low $Ca(OH)_2$ content that made ettringite unstable. Today this fact is ascribed to a lower permeability of the cement pastes toward the SO_4^{--} ion. In its turn this higher impermeability is attributed to the presence of a higher amount of gel and to differences in its composition and structure.

K. POPOVIC's question

Since most pozzolana-containing cements demand more water for a same consistency and therefore a higher cement dosage to obtain the same strength, is it possible to talk about energy saving?

F. MASSAZZA's reply

Considering that not all pozzolanic cements, and particularly those containing fly ashes, demand more water than portland cements, it was found that by using Italian pozzolanic cements containing about 1/3 of natural pozzolanas it is necessary to increase the w/c ratio on the average by 0.01-0.02 to have the same slump given by plain portland cements. This difference is slight and therefore also the increase in the cement dosage required to have the same 28 day-strength is small. Needless to say that later on the strength of a pozzolanic cement will increase more than a portland one.

E. RAASK's question

I should like to ask for opinion of the Panel if it is further while to investigate further chemical methods of pozzolanic activity tests to supplement the accepted mechanical tests.

Réponse de R. MAGNAN

Il a été reconnu par les différents auteurs que seuls les tests mécaniques permettent de mettre en évidence la qualité d'une pouzzolane et son activité.
Les tests mécaniques ont l'inconvénient d'être lents et sont donc peu pratiques pour le contrôle continu d'une fabrication industrielle.
Mais dans ce cas, s'agissant généralement d'un clinker défini et d'un materiau d'addition préalablement testé, il peut être intéressant de faire des tests chimiques qui donnent rapidement une mesure de variations éventuelles de la pouzzolane et qui permettent ainsi de s'assurer de la régularité du produit.
La méthode chimique permet alors de diminuer le nombre de tests mécaniques mais ne peut être considérée que comme une méthode indicatrice.

V. RAMACHANDRAN's question

One of the important research problems should concern itself to activate the reaction between lime and a pozzolana for obtaining higher early strength development. Are there any new catalysts being investigated recently?

Réponse de P. LONGUET

Il est bien établi que le développement des caractéristiques mécaniques lié à la présence de pouzzolanes dans un ciment est par nature un phénomène lent. Des résistances mécaniques élevées aux premiers âges avec un ciment pouzzolanique ne pourront donc être obtenues qu'indirectement:
- Soit en accélérant les réactions propres au clinker présent en espérant compenser la baisse de résistance à long terme qui en résulte par l'effet pouzzolanique lui-même.
- Soit en ajoutant un système donnant rapidement une résistance initiale (intérêt plus particulier pour le démoulage rapide).
Des résultats intéressants ont été obtenus par addition de ciment alumineux (ciment fondu) ou d'aluminate de sodium, mais à vrai dire il s'agit là d' effets différents de ceux attribués habituellement aux produits accélérateurs dont l'action est plutôt de nature catalytique.

A. SAMARIN's question

Is it possible to utilize brown coal fly-ash in concrete? Our experience is that these ashes are high in magnesia and alkalis, have little or no pozzolanic values and cause corrosion of reinforcing steel.
Is it possible, in the opinion of the panel, to overcome these problems?

Réponse de P. LONGUET

La réponse est difficile puisque vous décrivez vous-même vos cendres de lignite avec des teneurs élevées en magnésie et en alcalis, avec peu ou prou de propriétés pouzzolaniques et de plus apportant des risques de corrosion des armatures (à cause de la présence de teneurs élevées en sulfates vraisemblablement). Tout au plus, si elles sont assez fines, pourrait-on envisager leur addition comme charge plus ou moins inerte pour compléter la courbe granulométrique du ciment et améliorer les propriétés rhéologiques lors du gâchage. Il conviendrait alors de vérifier les points suivants:

- Extinction complète de la chaux libre et de la magnésie libre présentes dans les cendres.
-Absence de quantités importantes (1 ou 2% au maximum).
-Teneur en sels solubles compatibles avec l'absence d'apparition d'efflorescences à la surface des bétons réalisés.
- Définition des raisons du risque de corrosion des armatures: concentration élevée en solfates (à compenser par une addition modérée des cendres au ciment), présence éventuelle de chlorures (à proscrire pour les ciments destinés à la précontrainte).

Question de W. SCHRAMLI

Specifier le ciment aux cendres volantes selon sa performance plutôt que selon sa composition a l'inconvénient que l'aspect durabilité est negligé car il est difficile de la mesurer.
Est-ce-qu'il est fait en France pour attribuer, dans le cadre des normes, à l'aspect durabilité l'importance qu'il mérite?

Réponse de P. LONGUET

Nous ne pensons pas que le fait de connaitre la composition d'un ciment aux cendres volantes puisse permettre d'établir la durabilité du béton correspondant.
En France les normes définissent certes des performances mais indiquent aussi les limites supérieures des teneurs en produits d'addition des différents liants hydrauliques.
Votre question pose plutôt le problème de la définition d'un béton de référence, à partir duquel des critères de durabilité pourraient être effectivement mieux définis.

Question de J. PUIG

Comment pouvez vous utiliser les cendres à basse teneur en CaO libre (10%) en les séparant des autres, plus grosses, à forte teneur en CaO libre (20%)? Avec 25% de cendres à 10% de chaux libre, avez vous une bonne stabilité de volume? A quel essai? L'aiguille ou l'autoclave?

Réponse de M. DMITRIEV

Les cendres sont directement séparées en fractions aux centrales thermo-électriques où les cendres à dispersion grossière ayant une forte teneur en CaO libre se précipitent aux premiers champs du filtre électrique horizontal, tandis que les cendres à basse teneur en CaO libre et à dispersion fine sont amenées dans le dernier champ de ce filtre. En cas d'utilisation des cendres à fine dispersion, le ciment subit n'importe quels essais concernant la stabilité de volume.

B.S. RAUQUEKAR's question

Regarding "Basic Flyashes", is it necessary to add "active or ground silica", when manufacturing portland-pozzolana cement using basic flyashes?
With such additions is it possible to have a better strength development?

Réponse de M. DMITRIEV

La fabrication du ciment pouzzolanique avec l'utilisation des fractions fines de la cendre basique n'exige pas d'additions de la silice active.
Si l'on utilise les fractions grossières de la cendre ayant une haute teneur en CaO libre, il est possible d'effectuer une certaine quantité d'additions contenant de la silice active. Les meilleurs résultats sont obtenus en cas de 15-25% de cendre, en fonction de sa dispersion.

CONCLUSIONS

The conclusions that can be drawn from the principal reports, the written and oral contributions as well as the discussions can be summarized as follows.
The use of pozzolanic materials shows the following advantages:

- The production of cements that must not only be considered as substitutes of portland cements, but also as cements having some improved characteristics, such as heat of hydration, shrinkage, creep, durability, etc.

- The reduction in the energy consumption and the building costs of the cement factories. In fact the possibility offered by the pozzolanic additions to increase the cement production without a corresponding heat consumption or plant enlargement is doubtless stimulating.

- Finally pozzolanic cements allow the utilization of residues from other processings that, as fly ashes, constitute a serious ecologic problem still today.

The number and the quality of the presented works, both those having an eminently scientific character and those with more practical purposes, are the most convincing proof of the interest that subject "pozzolana" arises all over the world.

To conclude this general report the Chairman of Theme IV would like to thank the principal reporters, the Authors of the written and oral communications and the participants in the round table and the discussion for the valid contribution they gave to the success of this section.

THEME V

Ciments spéciaux

par F. de ASSIS BASILIO

I - INTRODUCTION -

1. Le Comité Scientifique International a chargé un représentant de l'Amérique Latine de présider le 5ème Thème du Congrès, probablement en hommage aux spécialistes de ce continent lointain, dont la production annuelle de ciment a atteint près de 60 millions de tonnes en 1978.

Le Brésil, mon pays, a produit dans les cinq dernières années les tonnages suivants de ciments de toutes sortes :

1975 - 16.737.458

1976 - 19.146.794

1977 - 21.122.927

1978 - 23.202.867

1979 - 24.873.654

Tableau

Production de ciment Portland en Amérique Latine, en 1978 :
Chiffres en tonnes par année :

Amérique Centrale	3.126.259
Argentine	6.316.129
Bolivie	257.008
Brésil	23.202.867
Colombie	4.140.000
Chili	1.176.698
Equateur	976.060
Mexique	14.055.720
Paraguay	166.777
Pérou	2.047.348
Uruguay	683.300
Vénézuéla	3.349.794
Total:	59.497.960

Source : Asociacion de Fabricantes de Cemento Portland - La industria argentina del cemento Portland : anuario 1978. Buenos Aires, 1979, p.39.

L'item relatif au Brésil fut obtenu par le Syndicat National de l'Industrie du Ciment, Rio de Janeiro.

o

o o

L'Industrie cimentière au Brésil, comme d'ailleurs dans un grand nombre de pays d'Amérique Latine, a créé, en 1936, l'Association Brésilienne du Ciment Portland, à laquelle appartiennent toutes les cimenteries du pays (actuellement 57 usines).

L'Association du Brésil possède un Centre Technique du ciment, situé à Sao Paulo, et des laboratoires d'essais et de recherches comprenant quatre départements :
physico-chimie,
chimie,
béton et ciment (essais physiques)
et sol-ciment.

Le laboratoire a des techniciens, des ingénieurs chimistes, des géologues et des ingénieurs civils; il travaille avec les équipements normaux d'essais et de recherche (XRD, ATD, microscopie optique, etc...)

2. Le Thème 5 : Ciments spéciaux, a été divisé en trois sous-thèmes :

- Sous-thème 5.1., dont le Rapporteur Principal, M. C.M. GEORGE (U.K.) a présenté un travail intitulé "Ciments alumineux". Une synthèse des récentes publications (1974-1979).

- Sous-Thème 5.2., dont le Rapporteur Principal, M. W. KURDOWSKI (Pologne) a présenté un travail intitulé "Ciments expansifs".

- Sous-Thème 5.3., dont le Rapporteur Principal, M. A.S. BOLDYREV (URSS) a présenté un rapport intitulé "Autres ciments (ciments à haute teneur en C_2S actif) et leurs utilisations".

3. Le Président du Thème 5 a reçu 41 communications et 3 rapports principaux, qui traitent respectivement :

- du sous-thème 5.1. Ciments alumineux :
  16 travaux qui proviennent des pays suivants : France (6), Royaume-Uni (3), Italie, URSS, Roumanie, Inde, Hongrie, Chili et Espagne (1 chacun)

- du sous-thème 5.2. Ciments expansifs :
  10 travaux qui proviennent des pays suivants : Chine (2), France, URSS, Roumanie, Pologne, Japon, Bulgarie, Etats-Unis, et Egypte (1 chacun)

- du sous-thème 5.3. Autres ciments :
  19 travaux qui proviennent de :URSS (10), Japon (3), Bulgarie (2), France, Etats-Unis, R.F.A. et Tchécoslovaquie (1 chacun)

4. On peut y voir la préoccupation générale d'orienter les recherches sur des bases scientifiques sans oublier :

a) l'économie du combustible dans la fabrication de ciment, notamment en cherchant des nouveaux types de ciments à température de clinkérisation inférieure à 1200° voire même à des températures inférieures à 1000°C.

b) l'utilisation des déchets ou sous-produits industriels. L'utilisation des laitiers et des cendres volantes est déjà bien connue, mais il y a d'autres sous-produits qui méritent attention.

Ces deux directives furent traitées en détail dans presque tous les travaux provenant de l'URSS, comme par exemple dans le Rapport Principal du sous-thème 5.3 de M. BOLDYREV, concernant l'utilisation des boues rouges (déchets de la fabrication de l'alumine à partir de la néphéline) dans la fabrication du ciment, car cette boue peut contenir jusqu'à 80 % de β-C_2S.

5. On constate aussi qu'il existe un nombre croissant de nouveaux types de ciments alumineux, avec une teneur variable en aluminates, et des ciments alumineux associés aux ciments Portland avec ou sans ajouts.

L'étude de l'influence sur l'hydratation et les propriétés des ciments alumineux des composés mineurs comme SO_3, Cl, Ba, Ti, Mn, et d'autres a été présentée dans plusieurs travaux.

Quelques travaux insistent sur l'intérêt d'utiliser l'alunite $Ca_{11}(Si,Al)_4O_{18}Cl$ dans la fabrication des ciments expansifs.

6. Ce rapport général est divisé en trois parties, correspondant chacune à un sous-thème.

o
o o

Sous-thème 5.1. - Ciments alumineux.

1.0 - Rapport principal
"Ciments alumineux : une synthèse des récentes publications (1974-1979)
C.M. GEORGE - U.K.

1.1 - "Hydratation du ciment alumineux en présence d'agrégat siliceux et calcaire".
L. CURSINO et A. NEGRO - Italie.

1.2 - "Solubilité dans l'eau de CA et CAH_{10} partiellement déshydraté"
P. BARRET et Ph. DUFOUR - France

1.3 - "Composition en phases du clinker alumineux à teneur d'alumine élevée, en fonction de la température et du milieu gazeux de cuisson".
T.V. KOUZNETSOVA, V.P. RIASINE, V.I. GOUSSEVA et V.A. VOROBIEV - URSS

1.4 - "Ciments réfractaires alumineux dans les pseudosystèmes $BaO.Al_2O_3$ - $CaO.Al_2O_3$ - $MgO.Al_2O_3$ - $BaO.6Al_2O_3$ - $CaO.6Al_2O_3$".
I. TEOREANU et N. CIOCEA - Roumanie

1.5 - "Courbes d'instabilité minimale dans une solution métastable de CA".
P. BARRET et D. BERTRANDIE - France

1.6 - "Hydratation des mélanges silicates-aluminates de calcium".
B.F. COTIN - France

1.7 - "Les causes chimiques des baisses ou des limitations de résistance dans les structures en ciment alumineux"
P. BHASKARA RAO et V.N. VISWANATHAN - Inde -

1.8 - "Formation des clinkers des ciments alumineux des types CA et CA_2; propriétés de ces ciments".
J. TALABER and K. DOLEZSAI - Hongrie -

1.9 - "Influence des conditions de synthèse de l'alumine sur sa réactivité vis à vis de la chaux".
B. GUILHOT, J.F. HUGO, A. MATHIEU et A. PETIT - France

1.10- "Comportement de divers phosphates avec des constituants des ciments"
P. BARRET, C. BENES, D. BERTRANDIE et J. MOISSET - France -

1.11- "La résistance chimique du béton de ciment alumineux"
H.G. MIDGLEY - U.K.

1.12- "La relation entre la composition du clinker de ciment et la capacité de récupération du ciment alumineux"
H.G. MIDGLEY - U.K.

1.13- "Microstructure et hydratation des ciments à haute teneur en alumine".
P. KITTL, J.H.C. CASTRO, L.C. POMPEU - Chili.

1.14- "Calcul des compositions potentielles théoriquement possibles des ciments alumineux".
J. CALLEJA - Espagne.

1 - Le rapport principal du sous-thème 5.1 a été présenté par M. G.M. GEORGE, Directeur Technique de Lafarge Fondu International.

Son rapport de 24 pages contient une synthèse des récentes publications (1974-1979) présentées depuis le Congrès de Moscou. Il a examiné ainsi 103 publications récentes.

Examinons les principales questions traitées par les auteurs des travaux présentés dans ce sous-thème 5.1. :

2. Conversion (Transformation cristalline des ciments alumineux hydratés).

2.1 - Le rapporteur principal aborde cette question et même prend position de la façon suivante (p.2)
"Les publications les plus importantes concernant les résistances à long terme et la conversion montrent clairement que les ciments alumineux se transforment relativement vite (quelques mois ou années) dans pratiquement toutes les conditions d'utilisation; donc la propriété de durcissement rapide doit être exploitée seulement en considérant les résistances après conversion, et en utilisant un faible rapport eau/ciment".
Et il continue : "CAH_{10} est l'hydrate principal formé à 20°C ou moins, à partir de CA; C_2AH_8 prédomine autour de 30°C et ces deux hydrates se transforment en C_3AH_6, d'autant plus rapidement que la température est plus élevée (phénomène de conversion)".

Si la situation se présente comme un fait inévitable, il y a cependant un certain nombre d'études pour trouver une solution de nature physique ou chimique qui puisse empêcher la conversion.

2.2 - Les auteurs de la communication 1.7 affirment que "la conversion du ciment alumineux ... est un fait que l'on doit accepter". Mais ils se préoccupent cependant de trouver une solution pour éviter ou réduire cette conversion par l'addition de β-C_2S. "En hydratant ensemble du CA et du β-C_2S on obtient surtout du C_2ASH_8 (gehlenite hydratée ou strätlingite)".
Et ils arrivent à la conclusion :
"Le succès de la technologie d'arrêt de la chute de résistance dépend de l'optimisation des propriétés et de la finesse des aluminates et du β-C_2S de façon à ne pas accumuler les aluminates de calcium hydratés" (p.7). Malheureusement, ils n'ont présenté de résultats d'essais de résistance à la compression que jusqu'à 85 jours, mais sans réduction de résistance.

MIDGLEY dans sa communication 1.12 présente des résultats de conversion et de récupération; on y voit que le ciment ayant le plus grand pourcentage de β-C_2S a la plus grande récupération.

Presque toutes les 14 communications ont traité, plus ou moins, de ce problème de la conversion.

2.3 - Dans la communication 1.1. présentée par CURSINO et NEGRO, les auteurs se montrent plus optimistes quant à la possibilité d'éviter la conversion; ils préconisent à ce sujet l'addition de poudre calcaire broyée à environ 5000 cm2/g au ciment alumineux, dans la proportion 20/80. Ils ont réalisé plusieurs essais; les résultats des essais de résistance à la compression de béton, dosé à 350 kg/m3 avec e/c=0,75 avec agrégats calcaires (courbe F) avec e/c = 0,50 (courbe B), montrent que les résistances à la compression ont toujours augmenté jusqu'à 1800 jours.

L'essai fait avec des agrégats siliceux, mais avec un mélange 25/75 de poudre calcaire et de ciment alumineux, et avec un e/c de 0,51 a présenté aussi des résultats de résistance à la compression toujours croissante jusqu'à 1800 jours (courbe II). Par contre, les effets de la conversion sont visibles dans des essais faits sans poudre calcaire.

Ces conclusions semblent compléter ce qui se trouve dans le rapport principal (p.10) :
"En présence de $CaCO_3$, le CAH_{10} est moins produit à toutes les températures; mais l'apparition de C_3AH_6 est aussi réduite en faveur de l'apparition de mono-carbo-aluminate hydraté $C_3A.CaCO_3.11H_2O$. On en conclut que la vitesse de conversion est plus basse en présence de $CaCO_3$ et que la formation de carbo-aluminates à la place de C_3AH_6 doit réduire la porosité et donc améliorer la résistance des bétons de ciment alumineux".

En effet, les auteurs du travail 1.1. ont fait des considérations théoriques en se basant sur les réactions connues :

$$3\ CAH_{10} \rightarrow C_3AH_6 + 2AH_3 + 18H_2O \qquad (2)$$

$$3C_2AH_8 \rightarrow 2C_3AH_6 + AH_3 + 9H_2O \qquad (3)$$

"L'équation (2) montre que C_3AH_6 et 2 AH_3 occupent ensemble 47,3 % de l'espace occupé par 3 CAH_{10} avant sa transformation; il n'y a aucun doute que l'eau constituant 52,7 % du volume total est responsable de la porosité. Sur la base de l'équation (3), le solide occupe 66,5 % et l'eau 33,9 %.

Pour compléter cette étude, les auteurs ont déterminé, à l'aide d'un porosimètre à mercure, la porosité de deux échantillons de mortier après 28 jours et 360 jours, l'un avec du sable siliceux, et l'autre du sable calcaire. Les résultats obtenus sont :

siliceux 28 jours 52,69 % 360 jours 66,61%

calcaire 28 jours 65,96 % 360 jours 38,36%

"Ce qui montre une réduction de la porosité du mortier de 42 %".

2.4 - Avec le même objectif, P.K.MEHTA avait présenté au Congrès de Tokyo un travail sous le titre "Prévention de la perte de résistance des bétons de ciments alumineux". Il a employé comme additif 5 % en poids du ciment, du $C_4A_3\bar{S}$ et a obtenu des résultats favorables sur un ciment alumineux d'origine américaine.

KONDO cependant a aussi fait des essais avec le même additif et n'a pas obtenu de résultats satisfaisants.

3. Composition minéralogique.

Plusieurs travaux traitent de cette question: quels sont effectivement les composés qui se forment dans la production industrielle du ciment alumineux et dans quelles conditions ?

Le rapporteur principal du sous-thème 5.1 fait un tour d'horizon sur les principales recherches faites depuis 1974, en commençant par les aluminates de calcium les plus importants, $C_{12}A_7$, CA et CA_2 avec la relation C/A décroissante et les alumino-ferrites de calcium.

Dans le travail 1.14 CALLEJA a considéré comme possible la formation de CA, $C_{12}A_7$, C_2S, C_4AF, C_6A_2F et C_2AS, d'après des ciments alumineux produits en Espagne.

Dans le travail 1.3 de KUZNETSOVA, les auteurs montrent que "la composition à teneur en alumine élevée dépend de la température et du caractère du milieu gazeux (oxydant ou réducteur) de la cuisson, ainsi que de la présence d'impûretés ou d'additions de modificateurs dans le mélange cru".

On voit bien l'énorme difficulté de prévoir, en partant de la composition chimique du clinker, sa composition potentielle, comme l'avait fait, il y a une cinquantaine d'années, M. BOGUE, pour le calcul de la composition potentielle du clinker Portland.

C'est pourtant ce que M. CALLEJA a tenté de faire en présentant dans son travail 1.14 les équations, basées sur la stoechiométrie des réactions, pour des ciments alumineux correspondant à la composition suivante :

A entre 39 et 42 %; C de 37 à 42 %, F de 9 à 18 %; S de 1,5 à 6 % et T de 1 à 2 %, qui correspond aux ciments alumineux d'Espagne.

Il a admis trois systèmes en vue de faire les calculs; en partant de la composition chimique du clinker alumineux, il a pu calculer une composition potentielle qui, d'après ses observations, serait en accord avec la composition potentielle mesurée.

4. Hydratation.

4.1. Les auteurs du travail 1.2 ont cherché à éclaircir une question relative à la solubilité de la chaux et de l'alumine, du CAH_{10} déshydraté sous vide à des températures supérieures à 100°C "la solution obtenue laisse à son tour précipiter CAH_{10}". C'est une étude assez complexe et qui doit aider à la compréhension de certaines questions relatives à l'hydratation des ciments alumineux.

4.2. Les auteurs du travail 1.5 ont fait une étude théorique minutieuse et sont arrivés à des courbes sur le diagramme C-A-H de supersolubilité du gel d'alumine et du C_2AH_8, limitée par la courbe "d'instabilité minimale". (p.6)

4.3. L'auteur du travail 1.6 a fait des études sur des mélanges de ciment alumineux (fondu) et ciment Portland, broyés sans gypse (voir le travail 3.11), en proportions variables. Il arrive à établir la composition probable des hydrates pour les mélanges étudiés, dans le domaine du système C-A-H.

4.4. Les auteurs du travail 3.13 ont étudié au microscope électronique à balayage l'évolution de l'hydratation, pendant les premières minutes après l'addition de l'eau, des aluminates synthétisés en laboratoire.
Ils signalent, dans l'hydratation du $C_{12}A_7$ vitrifié, un mécanisme de "défoliation" (?) et présentent l'explication probable de ce mécanisme (p.3).

5. Clinkérisation.

Les travaux 1.8 et 1.9 donnent des renseignements précieux sur les composés du clinker alumineux.

5.1. Les auteurs du travail 1.8 ont présenté une étude remarquable sur les conditions de formation du $C_{12}A_7$, CA et CA_2 en fonction de la température d'après des minutieuses déterminations faites par XRD. Une conclusion par exemple, le maximum de CA fut obtenu à la température de 1473° après 2 heures de cuisson au four de laboratoire (p.4).

5.2. Les auteurs du travail 1.9 ont fait une recherche sur la clinkérisation, en laboratoire, de l'alumine et de $CaCO_3$ calcinées à 1310°C, 1330°C, 1380°C et 1450°C. Par XRD ils présentent au tableau 3 les variations des compositions du clinker obtenu en CA_2, CA et $C_{12}A_7$.

6. Autres études.

6.1 - Les auteurs du travail 1.10 ont étudié le ciment alumineux : SECAR 71 (contenant 70 % d'Al_2O_3 additionné de sodium sous la forme de $(NaPO_3)_6$ et de dihydrogénophosphate de sodium NaH_2PO_4.

Comme conclusion "l'étude montre qu'à la température ambiante la prise "phosphate" s'effectue avant la prise hydraulique.... L'intensité de la prise hydraulique est alors affaiblie par rapport à celle du SECAR 71 pur".

6.2 - Le travail 1.4 étudie un ciment réfractaire alumineux avec substitution totale ou partielle du CaO par BaO et MgO. Les auteurs ont fait de nombreuses recherches dans le pseudosystème BA-CA-MA-BA_6-CA_6 et arrivent à une composition sans CaO ayant une résistance à la compression de 400 da N/cm2 à 1 jour et 550 da N/cm2 à 7 jours, et une réfractairité de 1870°C.

6.3 - Le travail 1.11 traite de la résistance chimique du ciment alumineux à l'eau de mer et aux eaux sulfatées. L'auteur attire l'attention sur l'hydrolise alcaline, c'est à dire celle due à l'action du sodium et du potassium en présence de CO_2, et d'humidité, dans un béton assez perméable.

o
o o

Sous-thème 5.2 - Ciments expansifs.

2.0 - Rapport Principal "Ciments expansifs"
Rapporteur Principal : W. KURDOWSKI - Pologne.

2.1 - "Rôle d'une addition de CaO expansive dans les ciments expansifs".
V. YAMASAKI, H. KAMTAKA and S.KOBAYASHI - Japon -

2.2 - "Ciment expansé d'alun et béton précontraint"
WU CHUNG-WEI and WAUG YAN-SHENG - People's Republic of China.

2.3 - "Expansion du sulfo-aluminate en solution sous saturée en CaO"
XUE JUN-GAN, CHEN WEN-HAO and XU JI-ZHI - People's Republic of China -

2.4 - "Système aluminate de calcium-gypse-chaux-eau"
A. BONIN et B. CARIOU - France -

2.5 - "La nature physico-chimique des autocontraintes des ciments expansifs"
L.V. NIKITINA, K.G. KRASSILNIKOV et A. LAPCHINA - URSS -

2.6 - "Sur le mécanisme de l'expansion des ciments expansifs" -
V. MALDOVAN et N. BUTUCESCU - Roumanie -

2.7 - "Ciment expansé composé d'un ciment normal et d'un ajout complexe".
N.B. DJABAROV et Y.T. SIMEONOV - Bulgarie -

2.8 - "Oxyde de magnésium, additif producteur d'autocontrainte dans la masse du béton".
P.K. MEHTA, D. PIRTZ and G.J. KOMANDANT - USA -

2.9 - "Pâtes de clinker dilaté, compressé après hydratation".
R.S. MICHAIL, S.A. ABO-EL-ENEIN et S. HANAFI - Egypte -

1. Le Rapporteur Principal du sous-thème 5.2 est le Professeur KURDOWSKI, du Centre de Recherches de l'Industrie des Matériaux de Construction, en Pologne. Son rapport présente une appréciation générale sur plusieurs ciments expansifs actuellement utilisés dans la construction et sur ceux qui sont encore en phase d'étude et de recherche. Son travail de 11 pages s'est appuyé sur une bibliographie sélectionnée de 59 publications.

Les ciments expansifs ont normalement deux emplois distincts : produire une expansion qui annule les effets du retrait, ou produire une expansion du béton capable de conduire à la précontrainte des armatures.

Dans le rapport principal ces deux emplois sont étudiés, en indiquant, par exemple, qu'en URSS on fabrique des ciments expansifs capables de produire "un potentiel expansif (pression d'expansion) de 20 kg/cm2, 40 kg/cm2 et 60 kg/cm2 respectivement". Ces deux derniers sont destinés à la précontrainte.

Les ciments expansifs les plus utilisés au monde sont examinés dans le rapport principal. Les types K et M sont bien connus (1, p.1) ainsi que le M-S; mais on voit croître l'intérêt pour d'autres types de ciments, dont quelques uns sont signalés dans le rapport principal dans les travaux présentés:

- les ciments SCT et SCN ont été étudiés par MICHAILOV ainsi que le ciment WEC. Le ciment SCT doit avoir une cure hydrothermique suivie de cure à l'eau à la température normale : il se produit pendant la cure normale du monosulfoaluminate $3C_3A.C\bar{S}.H_{12}$ qui subit une évolution vers l'ettringite (2, p.432).

- des ciments expansifs, utilisant des additifs, largement utilisés au Japon.

2. Nous allons attirer l'attention sur certains aspects, en vue de faire une synthèse des travaux présentés .

3. Mécanisme de l'expansion.

L'ettringite est actuellement le composé expansif le plus important, mais comment se forme-t-elle ?

MEHTA, cité dans le rapport principal, a démontré, en se basant sur des observations SEM, que"l'ettringite se forme, en règle générale, par cristallisation dans une solution". Mais dans le rapport principal on trouve aussi que "indépendamment de l'hypothèse de MEHTA, plusieurs auteurs continuent à considérer que l'expansion peut être causée par des transformations locales des phases anhydres en hydrates".

En effet, dans le travail 2.5. de NIKITINA (p.3), on voit que "dans le cas où la réaction de formation de l'ettringite se localise sur la surface des particules d'aluminates de calcium, ces particules se régénèrent peu à peu en un agrégat polycristallin et augmentent de volume comme un cristal unique. De telles particules deviennent alors la source de déformations pour toute la structure dans son ensemble"

On voit aussi, dans le travail 2.6. de MOLDOVAN (p.4) que "l'hydratation du ciment E (expansif) en pâte, est caractérisée par l'apparition de produits d'hydratation du type ettringite à la surface des grains anhydres", comme on peut le voir sur la microphoto (fig.2) de 30.000x.

Mais il signale aussi que "dans le cas du ciment A (Portland), ce qui caractérise l'hydratation c'est l'apparition des produits d'hydratation via la solution dans l'espace intergranulaire" et il conclut "la vraie cause de l'expansion c'est la formation d'ettringite à la surface des grains anhydres en présence d'une solution saturée en $Ca(OH)_2$ et en l'absence d'Al_2O_3 en solution".

4. Pression d'expansion et pression de cristallisation.

Dans le rapport principal, on attire l'attention sur les trois niveaux de la pression d'expansion adoptés en URSS (norme ?) soit 20 kg/cm2, 40 kg/cm2 et 60 kg/cm2.

On voit que dans le travail 2.5 de NIKITINA (p.5)on s'est préoccupé de mesurer la pression d'expansion et on a envisagé deux méthodes. La deuxième méthode consiste à vérifier "la charge indispensable pour réduire le volume du ciment durci à sa valeur initiale. On détermine ainsi l'effort qui se développe au cours du durcissement de ces ciments (pression d'expansion)".

Les auteurs du travail 2.6 MOLDOVAN et BUTUCESCU considèrent que "des pressions de cristallisation locales déterminent l'augmentation du volume du système déformable". Une explication semblable a été donnée dans la recherche de KROSILNIKOV présentée au Congrès de Moscou.

On voit cependant très peu de données quantitatives au sujet de la pression de cristallisation et de son influence sur la pression d'expansion, depuis que la question a été posée, par exemple, par KALOUSEK et BENTON et a provoqué une contestation de LEVI BROWN (4, p.187 et 5 p.646) en 1970.

5. Influence du CaO dans l'hydratation des ciments expansifs.

5.1 - Les auteurs du travail 2.3 présentent des références de plusieurs chercheurs; certains considèrent que la saturation en CaO de la phase liquide est indispensable pour avoir des ciments expansifs; d'autres affirment le contraire, c'est à dire qu'il faut avoir dans la phase liquide une solution sous-saturée en CaO.

Les auteurs ont alors procédé à une expérimentation rigoureuse, en comparant l'hydratation d'une pâte d'aluminates de calcium pour auto-contrainte avec une sous-saturation en CaO dans la phase liquide, et un ciment alumineux du type M. en condition de saturation en CaO dans la phase liquide. Au tableau 3, ils présentent des résultats très favorables à la condition de sous-saturation. Les auteurs ont une large expérience de l'emploi de ce type de ciment auto-contraint dans la fabrication de tuyaux en béton précontraint depuis 20 ans.

5.2 - Les auteurs du travail 2.4. traitent de l'influence de la chaux dans l'hydratation d'un ciment expansif type M. Ils ont étudié le système $C_4A_3\bar{S}$ - Gypse-chaux-eau, et les condition pour la formation du $C_3A.C\bar{S}.H_{12}$ et du $C_3A.C\bar{S}.H_{32}$ et la formation intermédiaire de ces deux composés avec en plus du C_4AH_{13} et de l'alumine (p.6).

5.3 - Dans le travail 2.1. les auteurs ont étudié l'effet de l'addition au ciment Portland de la chaux (3 % et 6 % de CaO), du sulfate de chaux (3 % et 6 % de $CaSO_4$) et de $C_4A_3\bar{S}$ (2 % à 5 %). L'addition de 3 % de CaO et 6 % de $CaSO_4$ a conduit à une expansion convenable (courbe D de la fig. 2)

6. Ciment expansif avec additifs.

6.1 - Le rapport principal traite de la fabrication d'un ciment obtenu par mélange de clinker Portland, d'alumine activée entre 600°C et 800°C, et de gypse; le produit actif de ce ciment est l'ettringite.

6.2 - Le travail 2.2 traite aussi d'un ciment expansif obtenu par mélange d'alumine naturelle (contenant 20 % à 50 % de $K_2SO_4.Al_2(SO_4)_3.4Al(OH)_3$) de clinker Portland, d'anhydrite et de cendres volantes ou de laitiers.

Les auteurs ont utilisé le porosimètre à mercure et ont confirmé par des essais la cristallisation de l'ettringite dans les pores, après sa formation dans la phase liquide.

Ce ciment est employé pour la fabrication de tuyaux précontraints en béton, en Chine (environ 2000 km par an).

6.3 - Le travail 2.8 présente un ciment ayant comme additif MgO, en envisageant l'emploi de ce ciment à la fabrication du béton expansif pour barrage. Les auteurs montrent que la calcination de MgO à haute température conduit à un produit d'hydratation très lent ou inerte. Par contre la calcination de MgO entre 900 et 950°C, avec broyage pour obtenir des grains de 300 à 1180 µm, additionnés de 5% de ciment Portland, peut donner un ciment expansif capable de neutraliser le retrait des bétons des barrages.

7. Etudes diverses.

7.1 - Le travail 2.9 présente une recherche sur des pâtes de ciments expansifs soumis, après hydratation, à une forte compression de 50 kg/cm2 jusqu'à 500 kg/cm2.

Comme conséquence, on observe une réduction appréciable de la porosité. L'étude comporte des observations morphologiques sur la microstructure des hydrates.

7.2 - Le travail 2.7 traite d'un additif complexe au ciment Portland ou aux laitiers, capable de produire des expansions de 0,1 % à 0,4 %. Le produit est breveté dans plusieurs pays.

o
o o

Sous-thème 5.2 - Bibliographie.

1 - KALOUSEK, G.L. - Development of expansive cements. - American Concrete Institute - Klein symposium on expansive cement concretes, ACI Committee 223. Detroit, 1973, p.1-19 (Special Publication SP-38).

2 - MIKHAILOV, V.V. - Stressing cement and self-stressed structures in the USSR. - American Concrete Institute - Klein symposium on expansive cement concretes, ACI Committee 223. Detroit, 1973. p.415-482 (Special Publication SP-38).

3 - MEHTA, P.K. - Scanning electron micrographic studies of ettringite formation. Cement and Concrete Research, 6(2): 169-182, Mar./Apr. 1976.

4 - KALOUSEK, G.L., BENTON, E.J. - Mechanism of seawater attack on cement pastes. American Concrete Institute, Proc.,67 (2) - 187-192, Feb. 1970.

5 - BROWN L.S. Discussion of the paper Mechanism of seawater attack on cement pastes. American Concrete Institute, Proc. 67(8) - 646-648, Aug. 1970.

o
o o

Sous-thème 5.3 - Autres ciments.

3.0 - Rapport Principal "Autres ciments (ciments à haute teneur en C_2S actif) et leurs utilisations".
A.S. BOLDYREV - URSS -

3.1 - "Structure et propriétés des clinkers de ciment blanc"
K. KARIBAYEV, K. BEKISHEV, D. ALDIYAROV et V. LYSENKO - URSS -

3.2 - "Propriétés des bétons à très faible dégagement de chaleur"
A. GOTO, A. MATSUBARA et K. NAKANO - Japon -

3.3 - "Activation mécano-chimique du silicate bicalcique technogène"
V.I. AKOUNOV, A.M. DMITRIEV, S.D. MAKACHEV, G.P. LITVINOV, V.I. JARKO, G.V. ZAVADSKI, B.E. YONDOVITCH - URSS.

3.4 - "Possibilités de l'intensification des propriétés liantes des matériaux à la base du C_2S"
P.I. BOJENOV, B.A. GRIGORIEV et G. OVTCHARENCO - URSS -

3.5 - "Synthesis at about 750°C and properties of a sulphated β-C_2S".
H. STRUILLOU et M. ARNOULD - France -

3.6 - "Utilisation du ciment sulfaté dans le béton armé de fibres de verre"
A. PACHTCHENKO, H. STARTCHEVSKAIA, V. SERBINE et L. KALITA - URSS -

3.7 - "Aspect cristallochimique du durcissement des ciments pour forages pétroliers".
V.V. ILIOUSKHINE, V.S. BAKCHOUTOV, A.N. LIOUSSOV, M.K. NIKOLAEVA - URSS.

3.8 - "Analyse de la composition granulométrique des ciments de forages pétroliers".
V.S. BAKCHOUTOV, K.H. Al. VARDI, M.K. NIKOLAEVA - URSS -

3.9 - "High temperature cements with geothermal applications"
C.A. LAUGTON, E.L. WHITE, M.W. GRUTZECK et D.M. ROY - USA -

3.10- High strength cement in the $CaO-Al_2O_3$ SiO_2-SO_3 system and its applications"
G. SUDOH, F. OHTA et H. HARADA - Japon

3.11- "Investigations on two special cements"
Y. EFES - R.F. ALEMAGNE

3.12- "Structure et propriétés de l'alunite et du ciment d'alunite".
B. NOUDELMAN, M. BIKBAOU, A. SVENTSITSKI et V. ILUKHINE - URSS -

3.13- "High strength slag-alkaline cements"
V.D. GLUKHOVSKI, G.S. ROSTOVSKY et G.V. RUMYNA - URSS -

3.14- "Recherches sur les phases des ferrites de baryum dans la zone fortement basique du système $BaO-Fe_2O_3$.
V. VALKOV, A. DENEVA et D. STAVRAKEVA Bulgarie -

3.15- "Le ciment pour emploi aux températures basses".
F. SKVARA et J. NOVOTNY - Tchécoslovaquie.

3.16- " Property and application of thermosetting cement".
GUNJI SHIKAMI - Japon -

3.17- "Méthode de modification des caractéristiques des ciments au moyen des adjuvants".
Y.T. SIMEONOV et N.B. DJABAROV - Bulgarie -

3.18- "Problème de l'utilisation des sous-produits minéraux dans la production des liants"
P. BOJENOV et B. GRIGORIEV - URSS -

I. M. A.S. BOLDYREV, du Ministère de l'Industrie des Matériaux de Construction de l'URSS, a présenté son rapport principal, de 17 pages sous le titre "Autres ciments, ciments à haute teneur en C_2S actif, et leurs utilisations" en s'appuyant sur une bibliographie sélectionnée de 50 textes.

2. Le sous-thème 5.3 peut être commenté d'une façon plus commode en le subdivisant en quatre parties :

a) ciments à C_2S actif

ces ciments ont été étudiés dans le rapport principal et dans les travaux 3.3., 3.4, 3.5 et 3.6.

b) ciments pour colmatage des puits pétroliers.

les travaux 3.7, 3.8 et 3.9 se rattachent à ce type de ciment.

c) ciments à haute résistance initiale

3 travaux : 3.10, 3.11 et 3.13, traitent des ciments à haute résistance initiale.

d) autres ciments.

3. Ciments à C_2S actif.

3.1 - Le rapport principal montre l'intérêt attaché en URSS à l'utilisation, dans la fabrication du ciment, de produits technogènes secondaires comme par exemple la boue rouge : déchet de la fabrication de l'alumine, en partant de la néphéline comme matière première, et qui existe en abondance. "Le procédé fournit, à titre de sous-produit, un schlamm de néphéline à teneur en eau allant jusqu'à 50 %, la matière solide contenant 80 à 90 % de $\beta-C_2S$" (p.2).

Dans son rapport principal, l'auteur signale aussi l'utilisation du "Schlamm de cendres", des lignites bruns extraits dans la région de Moscou, dont la matière solide est constituée de 70 à 75 % de $\beta-C_2S$.

Dans les deux cas, le schlamm est considéré comme "un produit de départ très efficace pour la fabrication du clinker et un constituant du ciment portland". En utilisant ce schlamm comme matière première associée au calcaire, trois usines produisent actuellement du ciment. "Dans toutes ces usines le rendement des fours rotatifs est de 30 % plus élevé, et la consommation unitaire de combustible de 20 à 25 % plus basse que dans les fours du même type lors de la cuisson des matières premières traditionnelles" (p.9)

Le rapport principal traite aussi du "Ciment Portland Bélitique (CPB) renfermant plus de 20 % de bélite technogène". La somme de la bélite, additif au clinker Portland, et de la bélite du clinker donne la teneur totale en bélite.

L'expérience a montré qu'avec 45 % de bélite on obtient un ciment Portland bélitique qui atteint des résistances à la compression de l'ordre de 25 à 30 MPa à 28 jours et près de 55 MPa à six mois (fig. 4).

3.2 - Dans le même but, les auteurs du travail3.3 ont présenté une étude sur l'activation mécano-chimique du C_2S technogène, en utilisant le broyage par percussion, par vibration et finalement par jet déjà utilisé en Russie.

Un mélange de 70 % de clinker portland avec 30 % de β et de γ - C_2S et 5 % de gypse a été soumis à un broyage par jet (équipement russe série USU - 300) et "les résultats obtenus sont considérablement plus élevés que ceux obtenus, pour une même composition, dans un broyeur à boulets". Le taux de résistance obtenu "correspond au Portland ordinaire (classe 400, Normes GOST 10178-76) ou bien au ciment type 1 ASTMC - 150.

3.3 - Dans le travail présenté par STRUILLOU et ARNOULD (3.5) on produit du"β-C_2S sulfaté" à partir d'un cru à 6 % de gypse et à spongolithe, en utilisant une phase nitreuse intermédiaire. "L'évolution de la résistance dans le temps du β-C_2S sulfaté est comparable à celle du C_3S où du CPA 400. Elle est environ 10 à 15 fois plus rapide que celle du β-C_2S pur, classique, non sulfaté.

L'examen par diffraction RX du β-C_2S avec ou non la phase nitreuse intermédiaire, montre des pics dans le diffractogramme, bien distincts. Les auteurs attirent l'attention sur le fait que les réactions de clinkérisation s'effectuent en 20 minutes à la température de 750°C (beaucoup plus basse que celle de clinkérisation du β-C_2S pur).

3.4 - Des considérations théoriques sont présentées par les auteurs du travail 3.4 sur l'activation chimique du β-C_2S.

4 - Ciments pour des puits pétroliers.

4.1 - Dans son rapport principal, l'auteur signale (p.13) les expériences faites avec "un ciment de colmatage bélitique technogène et siliceux", qui a été préparé à partir d'un mélange d'un produit bélitique technogène et d'un sable quartzeux dans un rapport de 70:30 à 30:70, et broyé jusqu'à l'obtention d'une surface spécifique de 2 à 4 milliers de cm2/g. "Ce ciment a bien durci sans qu'on ait recours à des activants tels que le ciment Portland ou le gypse, dans les essais réalisés" à des températures comprises entre 150 et 300°C et avec des pressions allant de 500 à 700 atm."

4.2 - Les auteurs de l'excellent travail 3.7 ont traité des "intensificateurs cristallochimiques de durcissement ICD". Dans certaines conditions, les liants additionnés de ces "intensificateurs" en solutions aqueuses saturées de chaux et d'acide silicique, en proportion de 1 à 3 % par rapport à la masse du ciment, accroissent leur résistance d'une valeur allant jusqu'à 60 % (p.5).

Ils ont aussi fait des recherches sur des ciments de colmatage expansif de grande expansion utilisant en tant que constituants des ICD et des oxydes de calcium et de magnésium cuits à des températures différentes avec du sable quartzeux.

4.3 - L'importance de la granulométrie des ciments de colmatage est l'objectif principal des auteurs du travail 3.8. Ils montrent par exemple que "l'augmentation,dans la proportion de 2,5 fois, de la teneur en fractions de 0-5 mm, conduit à un accroissement de 3 fois de la résistance du ciment CCAE-2 (ciment expansif allégé) durant les premiers jours".

4.4 - Enfin, les auteurs du travail 3.9 ont présenté une recherche, encore en cours, sur des ciments pour forages profonds.

Ils ont examiné plusieurs compositions possibles dans les deux systèmes $CaO-Al_2O_3-SiO_2-H_2O$ et $CaO-MgO-SiO_2-H_2O$.

5 - Ciments à haute résistance initiale.

5.1 - Les auteurs du travail 3.10 ont fait des nombreuses recherches dans le système $CaO-Al_2O_3-SiO_2-SO_3$ et finalement sont arrivés à un ciment ayant la composition potentielle suivante : $C_4A_3\overline{S}$-54%; C_2S-32%; C_4AF-5 % et CaO-(libre) 9 %. Ce clinker fut obtenu à température de 1300°C et fut broyé à 5500 cm2/g. Il est important d'observer que si la température de clinkérisation atteint 1350°C, le $C_4A_3\overline{S}$ se décompose et donne C_3A. Ce ciment a présenté les résistances suivantes dans un béton de 420 kg/m3 de ciment (en N/mm2) : à 6h: 24,7 - à 1 jour:55,8; à 3 jours: 90,6 et à 28 jours : 96,8.

5.2 - L'auteur du travail 3.11 présente un ciment super-rapide, obtenu par un mélange de 82 % en poids de clinker Portland, et 18 % de ciment alumineux, avec des additifs et du gypse pour le contrôle de la prise. Le mélange est broyé à 5580 cm2/g. Ce ciment atteint

5 N/mm2 à 2 heures, selon l'essai normal (DIN 1164).

Les essais sur cubes de 20 cm de côté de ce béton, selon la norme DIN 1048 ont donné, après 2 heures, des résistances de 3 à 6,5 N/mm2 (rapport e/c de 0,70 et 0,45) à 28 jours, respectivement 30,2 et 46,6 N/mm2, et à 360 jours une résistance 20 % plus élevée.

Ce travail contient aussi l'étude d'un ciment pouzzolanique.

5.3 - Les auteurs du travail 3.13 donnent des informations sur un ciment fabriqué avec des laitiers de hauts-fourneaux, des laitiers électrothermo-phosphoreux et d'autres types de laitiers métallurgiques, additionnés de produits basiques contenant des alcalis (sodium, potassium, solutions de silicate de sodium) et de sous-produits industriels (fusion de soude-alcaline, de soude, métasilicate de sodium, etc.).

Ce ciment, en usage en Russie depuis 1960, donne des résistances à la compression (mesurées selon la norme GOST 310.4.76) de :

à 1 jour : 350 kg/cm2

à 2 jours : 550 kg/cm2

à 3 jours : 750 kg/cm2

et à 28 jours : 1000 à 1200 kg/cm2

6. Autres ciments.

6.1 - Ciment blanc - travail 3.1.
Dans cette communication, les auteurs exposent les résultats de recherches sur l'influence des amino-alcools (mono et triétanolamine) et de liquides silico-organiques (éthil ou méthilsiliconate de sodium) sur le processus de blanchiement des clinkers de ciment Portland blanc.

Ils ont obtenu une amélioration sensible du coefficient de réflexion diffuse.

6.2 - Ciment à très faible chaleur d'hydratation - travail 3.2.
Les auteurs ont fait des recherches en mélangeant un ciment de haute résistance initiale et du laitier de haut-fourneau, et ont obtenu un ciment à dégagement de 55 cal/g de chaleur à 28 jours.

6.3 - Béton armé de fibres de verre - travail 3.6.
Les auteurs ont fait des recherches sur un "ciment exempt de C_3S et de C_3A. Ses principaux constituants sont : le sulfo-aluminate de calcium $3(CA).CaSO_4$ et le sulfosilicate de calcium $2(C_2S)CaSO_4$". Ce ciment, d'après les auteurs, donne des résistances semblables à celles du ciment Portland et assure une meilleure durabilité quand il est employé dans le béton armé de fibres de verre.

6.4 - Ciment d'alynite - travail 3.12.
Les auteurs traitent d'un ciment breveté en URSS. L'alynite a la formule chimique : $Ca_{11}(Si,Al)_4O_{18}Cl$. Le ciment d'alynite est obtenu à partir des matières premières traditionnelles, avec addition de chlorure de calcium. "L'alynite constitue 60-80 % de la masse du clinker". Les auteurs ont présenté une étude très poussée de la structure atomique de l'alynite.

6.5 - Ferrites de baryum - travail 3.14.
Les auteurs ont présenté les résultats d'une recherche du système $BaO-Fe_2O_3$ et ont cherché à caractériser les composés suivants : BF, B_3F_2, B_5F_2, B_3F et B_7F_2 (B = BaO et $F = Fe_2O_3$).

L'étude est minutieuse et les auteurs concluent que le B_3F ne doit pas se former et que le B_7F_2 a été confirmé pour la première fois dans cette étude.

6.6 - Ciment pour emploi aux basses températures - travail 3.15 -
Les auteurs ont étudié un ciment Portland sans gypse, mais avec addition d'un dérivé de lignite et d'un carbonate alcalin (K_2CO_3) ou de bicarbonate. Le clinker est broyé très fin (de l'ordre de 10.000 cm2/g). Les résistances obtenues à des températures de - 20°C et - 35°C sont de l'ordre de 23 et 12 MPa à 28 jours.

6.7 - Ciments thermo-durcissants (CTD) - Le travail 3.16 traite du CTD qui est composé principalement de C_3S, de CA et C_4AF et $CaSO_4$ (anhydryte avec addition d'acide citrique pour contrôler le temps de prise). Ce ciment est utilisé avec une cure à la température de 80°C pendant 30 minutes à 2 heures. Il présente la propriété de ne pas attaquer les fibres alcalines de verre du béton armé avec ces fibres.

6.8 - Adjuvants pour ciment - travail 3.17 -
Les auteurs ont breveté dans plusieurs pays un type d'adjuvant qui peut être additionné au ciment, au malaxeur ou en fabrique. D'après ces auteurs, on peut obtenir une résistance à la compression plus élevée du ciment à l'essai normal ou dans le béton à 28 jours.

6.9 -Utilisation de sous-produits minéraux dans la production des liants - travail 3.18
Les auteurs, comme le Rapporteur Principal, attachent une grande importance à l'utilisation de sous-produits et de déchets industriels pour la fabrication des liants.

DISCUSSION

par T.V. KUZNETSOVA

concernant la communication de J. Calleja "Calcul des compositions potentielles théoriquement possibles des ciments alumineux".

Contrairement au ciment portland, il n'existe pas jusqu'à présent de méthodes fiables pour calculer la composition minéralogique des ciments alumineux à partir des résultats de l'analyse chimique. C'est pourquoi l'approche du professeur J.Calleja mérite une très grande attention et une haute appréciation. Cependant nous voulons souligner les circonstances pouvant conduire aux erreurs dans les calculs:

1. En cas des ciments alumineux fondus, il est nécessaire de maintenir un certain régime de refroidissement, car le refroidissement rapide provoque la formation d'une phase vitreuse qui modifie la composition réelle du clinker par rapport aux calculs.
2. En cas de production du clinker des ciments alumineux par frittage, l' équilibre de phase dans le four industriel est obtenu à grand-peine et dépend considérablement de la température et du milieu gazeux de cuisson, ainsi que de la présence d'impuretés dans les crus. Nos recherches montrent que SiO_2, MgO, Fe_2O_3 peuvent former les solutions solides avec $C_{12}A_7$, CA et CA_2 en quantité de 2-3%.

Il est nécessaire d'en tenir compte lors des calculs de la composition de phase du clinker.

DISCUSSION

par T.V. KUZNETSOVA

concernant la communication de U. Yamazaci, H. Kamiaka et S. Kobayschi "Role of expansive additive CaO in expansive cement".

La présence de la chaux dans les ciments expansifs influe, en effet, sur la formation de leurs propriétés (expansion, autocontrainte, résistance). Cependant, de notre point de vue, le rôle de CaO consiste en concentrations de la chaux dans le système qui modifie la cinétique et les conditions de formation d'ettringite déterminant l'expansion du ciment. Nos recherches montrent que la cristallisation de l'ettringite primaire à partir de la solution sursaturée conduit à l'étanchéité et à l'amélioration de la pierre de ciment. La formation de l'ettringite secondaire par suite de l'interaction de la solution diffusée contenant Ca^{2+} et SO_4^{2-} par rapport aux aluminates hydratés de calcium, hydroxyde d'aluminium ou par rapport aux cristaux d'ettringite mène à l'expansion de la pierre de ciment.

DISCUSSION

par A.S. BOLDYREV

I.Activation chimique de $2CaO \cdot SiO_2$

Je pense qu'avant de parler de l'activation chimique du β-silicate bicalcique il faut dire quelques mots à propos de sa stabilisation.

La tendance du C_2S au polymorphisme dans la série $\alpha \rightarrow \alpha' \rightarrow \beta \rightarrow \gamma$ et le changement d'activité d'hydratation du silicate bicalcique, lié à ce fait, ont déterminé la poussée à de nombreuses recherches concernant la stabilisation des formes de haute température du C S. Du point de vue de l'utilisation industrielle de certains déchets, la conversion $\beta - \gamma$ a une très grande importance, car il n'existe pas jusqu'à présent d'une opinion commune relative à l'activité d'hydratation du $\gamma - C_2S$.

Les principes essentiels de stabilisation cristallochimique consistent en substitution isomorphe cationique et anionique dans la structure du C_2S. On peut utiliser en qualité des stabilisateurs de nombreux oxydes (K_2O, Na_2O, MgO, BaO, Al_2O_3, Cr_2O_3, P_2O_5, etc).

Dans ce cas, on peut également utiliser des additions complexes comprenant les différents cations et anions. En principe, l'activation du $\beta - C_2S$ est obtenue à l'aide de constituants additifs, plus basiques que Ca^{2+} et plus acides que Si^{4+}.

Dans mon rapport concernant le thème Y j'ai cité les résultats des expériments relatifs à la production d'un grand lot industriel de ciment alumosilicate aux laitiers obtenus lors de la fonte bauxite. Le laitier se composait de $\gamma - C_2S$ et d'aluminates de calcium à faible basicité ce qui a permis d'obtenir le ciment dont l'activité a été de 250-400 kgf/cm^2.

Il y a des données témoignant que le laitier friable obtenu lors de la production des ferro-alliages et se composant pour 70-80% de $\gamma 2CaO \cdot SiO_2$, en cas d'utilisation de ses suspensions aqueuses à la température élevée, montre la prise avec du sable (30-50 %) et forme la pierre de ciment possédant une haute thermostabilité. Le $\gamma 2CaOSiO_2$ actif a été obtenu à NIIciment 1 lors du broyage du ciment contenant 30% de $\gamma 2CaOSiO_2$ dans le broyeur à projection.

Cependant au niveau de nos connaissance d'aujourd'hui il est plus préférable d'avoir affaire à β $2CaO \cdot SiO_2$.

II. Ciments de bélite pour colmatage à base des pâtes néphélines

Grâce au développement en U.R.S.S. de l'industrie du pétrole et du gaz le besoin en ciments pour colmatage a augmenté d'une manière brusque.

L'enfoncement des forages jusqu'à 7-10 M. mètres a mené à l'élévation des températures atteignant 200°C et à l'augmentation de la pression jusqu'à 120 atmosphères techniques absolues.

Les eixgences pour la pierre de ciment concernant sa densité, étanchéité à l'eau et, enfin, sa résistance à la corrosion par l'eau minéralisée ont considérablement augmenté.

A présent, l'U.R.S.S. produit environ de 3 millions de tonnes de ciments pour colmatage ayant 8-12 types différents satisfaisant aux conditions spécifiques du colmatage thermostables, on a élaboré et on utilise avec succès le ciment silicueux de bélite "BKC". Il comprend la pâte néphéline (β $2CaO \cdot SiO_2$) et le sable quartzeux broyé avec rapport de 3:1 ou 1:1.

Les ciments ci-dessus sont caractérisés par le retardement de la prise aux températures élevées, retardement du durcissement initial, ainsi que par une haute thermostabilité et la stabilité de la composition. Ces ciments sont les meilleurs pour les forages à haute température.

Pour les forages ultraprofonds, où il est nécessaire de monter le mortier de ciment presque jusqu'à la tête du forage, en vue de séparer la rangée de niveaux, on nous a obligé d'élaborer un ciment spécialement allégé ayant un rapport élevé eau/ciment et des additions minérales actives, ainsi qu'une grande surface spécifique. Pour les forages où règnent les températures de 120-180°C on utilise le ciment comprenant 50-60 parties de pâte néphéline, 25-30 parties de sable quartzeux et 10-15 parties d'additions hydrauliques.

III.Au sujet de la fabrication et de l'utilisation des ciments mixtes à base du ciment portland et du ciment alumineux

On n'utilise pas les mélanges de ciment portland et de ciment alumineux, car ils diminuent brusquement la résistance et montrent le temps de prise minimum.

On a élaboré en U.R.S.S. un ciment expansif (RPC) se composant de clinker portland (60-65%), de ciment alumineux (5-7%), de gypse naturel (7-10%) et d'additions hydrauliques (20-25%).

Les études du ciment ont montré que même pendant les premières heures d'hydratation on observait la formation de l'hydrosulfoaluminate de calcium ayant la forme de trisulfate qui détermine l'activité et le degré d'expansion du ciment.

DISCUSSION

by LU CHUN-XUAN

In China, red slime, a by-product consisting mainly of dicalcium silicate and formed in the manufacture of alumina, has been utilized in the cement industry for more than ten years. To date the red slime (dry basis) utilized amounts to 1.5 million tons. More than 5 million tons of various kinds of cement made from red slime, such as ordinary portland cement, oil well cement and red slime-sulfate cement have been manufactured.

The chief constituents of the red slime are as follows:

β-C_2S	$C_3AS_xH_y$	NAS_2H_2	FH_n	$CaCO_3$	CT
50-60	5-10	5-10	4-7	2-10	2-5

The specific surface of the red slime is about 4200-5000 cm^2/g. The melting point is about 1250-1270°C. The viscosity of the molten mass is low and its fluidity fair. When the red slime is proportioned with a suitable amount of limestone residue, also an industrial by-product of the alumina works, the resultant raw slurry has good burnability in clinkering.

Table I shows the chemical composition of the clinker made from the red slime and the physical properties of the cement.

Table I

SiO_2	Al_2O_3	Fe_2O_3	CaO	MgO	K_2O+Na_2O	C_3S	C_2S	C_3A	C_4AF	sp surf (cm^2/g)	setting		comp str (N/mm^2)		
											ini	fin	3d	7d	28d
20.78	5.59	5.58	63.24	1.24	1.13	50.54	21.44	5.45	16.98	3115	2:50	4:41	37.3	47.9	61.7

Since the red slime is low in silica and high in iron oxide content, repeated experiments have been carried out on an industrial scale to produce clinkers of low silica and high iron oxide content. The silica moduli of the clinkers made are as low as 1.12-1.56 and the iron moduli are from 0.6 to 1.0. The physical properties of the cements made from the clinkers are normal, as shown in Table II.

Table II

No.	L.S.	S.M.	I.M.	C_3A+C_4AF	f-CaO	sp surf (cm^2/g)	setting		comp str (N/mm^2)		
							ini	fin	3d	7d	28d
1	0.924	1.56	0.98	25.35	1.09	3075	1:52	3:23	46.6	58.1	67.8
2	0.942	1.36	0.80	26.67	1.10	3085	2:16	3:43	46.1	60.0	68.5
3	0.929	1.12	0.95	34.15	0.79	3060	2:08	3:29	41.6	55.2	61.1
4	0.888	1.43	0.84	26.47	0.75	3125	2:19	3:23	40.9	54.3	64.5

If a suitable mineralizer is added to the raw slurry to produce the clinkers shown in Table II, the free lime content in the clinkers may drop down to about 0.5% even if the alkali content of the clinkers is as high as 2%.

The cement made from such clinkers has the following good features, that is, lower heat of hydration, better resistance to sulfate attack and frost action, and lower permeability as compared with ordinary portland cement. This cement has been used with non-reactive aggregate in hydraulic structures and good results have been obtained.

Conclusion des échanges de la table ronde

par M. SOUSTELLE et B.F. COTTIN

Ce thème était divisé en trois sous-thèmes et cinq questions essentielles appartenant à ces sous-thèmes ont été abordées.

Sous-thème V.I: Ciments alumineux

Sujet n° 1 : A la suite de la communication de L. CUSSINO et A.NEGRO sur l'hydratation du ciment alumineux en présence d'agrégats siliceux et calcaires, il est maintenant bien établi qu'une réaction se déroule entre les aluminates hydratés et le carbonate de calcium pour former des carbo-aluminates. Cette réaction se déroule aux dépens de la conversion de CAH_{10} en C_3AH_6. Ce carbo-aluminate formé a une influence favorable sur la liaison pâte-granulat, ce qui provoque une forte augmentation des résistances.

Il est particulièrement intéressant que les auteurs prolongent leur expérience qui a déjà cinq ans, pour prouver que les résistances se maintiennent pour des échéances plus longues. Il est cependant étonnant que les résistances se dégradent aussi vite que l'annoncent les auteurs en présence des agrégats siliceux, et il conviendrait d'examiner avec plus d'attention l'influence du rapport E/C dans les deux cas, et particulièrement en présence de calcite.

Tous les intervenants ont noté l'importance d'une bonne définition de la température aussi bien au moment de l'hydratation que pendant la conservation, car il y a une très grosse influence de ce paramètre sur les résultats obtenus.

Deux problèmes majeurs, auxquels aucune réponse n'est encore apportée, restent posés :

- Quelle est l'influence de la présence d'alcalins ?
- Quelle est la stabilité des carbo-aluminates en présence d'agents agressifs ?

Sujet n° 2 : A la suite de la communication de J. CALLEJA sur le calcul de la composition potentielle des ciments alumineux, la question est posée pour savoir si ce calcul extrêmement intéressant de l'auteur est applicable dans tous les cas.

Il est évident que prévoir les phases par l'utilisation de formules analogues à celles de BOGUE est du plus haut intérêt pour le fabricant de ciments alumineux fondus. Malheureusement, alors que pour le ciment Portland les formules de BOGUE donnent une bonne approximation des phases en présence, le problème est plus difficile dans le cas des ciments alumineux préparés par fusion.

Parmi les causes de ces difficultés, on peut citer :

- le nombre de phases décelées (par diffraction X, microscopie ...) est toujours supérieur à celui autorisé par la règle de GIBBS (écarts importants à l'équilibre).
- l'existence d'une partie vitreuse dans la masse du ciment,
- l'importance des solutions solides.

Un gros progrès apporté par le calcul du Professeur CALLEJA vient du fait qu'il tient compte d'une manière rigoureuse de certaines solutions solides et notamment des phases alumino-ferrites; mais il est certain que la généralisation de ces formules est limitée par les écarts à l'équilibre, plus ou moins importants selon les cas, et inévitables.

Sous-thème V.2 : Ciments expansifs.

Sujet n° 1 : Au sujet de la communication de P.K.MEHTA, D. PIRTZ et G.J.KOMANDANT sur l'addition d'oxyde de magnésium pour la production de ciment expansif, il est très clairement montré que le maximum de l'expansion est obtenu par une température de calcination de 900°C avec des particules de dimensions comprises entre 380 et 1180 m. Mais il est évident que les résultats sont encore à l'échelle du laboratoire et bien que très prometteurs, ils n'en sont pas encore au stade industriel, et en particulier, le comportement des grandes masses n'a pas été encore étudié.

Sujet n° 2 : Les causes de la pression d'expansion des ciments expansifs : différentes causes de cette pression sont analysées par la table ronde. Sans qu'il soit possible de connaître leurs poids respectifs, on relève :

- les causes liées à la pression de cristallisation qui peut être due, soit à la transformation en travail de la variation d'enthalpie libre de la

transformation, soit à la présence d'une solution sursaturée dans des capillaires, ce qui l'empêche de précipiter,

- les causes liées à la pression osmotique,
- les causes liées au fait que l'ettringite formée est mal cristallisée et se présente sous forme de gel qui provoque le gonflement.

Sujet n° 3 : La formation de l'ettringite est elle favorisée par la sous ou la sursaturation en chaux ? Se forme-t-elle au contact des cristaux d'aluminate ou au contraire loin de ceux-ci dans la solution ?

Le modèle de B. COTTIN répond à l'ensemble de ces questions :
Dès le mélange du ciment avec l'eau, les différents types d'ions suivants passent en solution :

- les ions calcium issus du C_3A, des sulfates, de la chaux;
- les ions sulfates, issus des sulfates de calcium,
- Les ions aluminiques, issus du C_3A.

Les ions diffusent, à partir de la surface des constituants, de sorte que, en un point donné de la solution, les concentrations augmentent à des vitesses et jusqu'à des niveaux, fonctions du lieu géographique du point considéré, de la réactivité des phases et de leurs proportions relatives. Le schéma suivant représente les "fronts de dissolution" en fonction des temps croissants 1-2-3, dans un cas où, pour simplifier le dessin, nous avons mis ensemble la chaux et le sulfate de calcium.

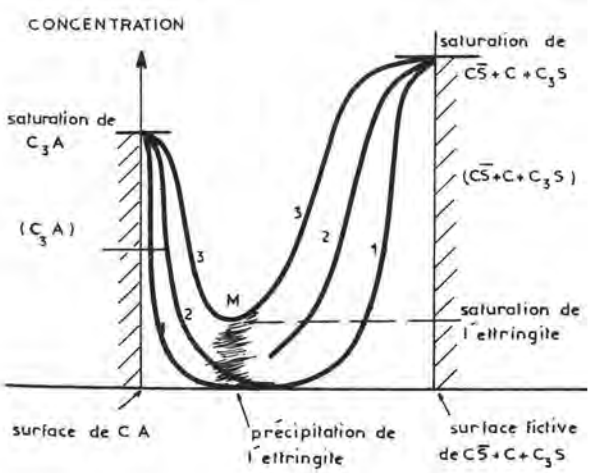

La saturation par rapport à l'ettringite (l'hydrate le moins soluble du système C-A-$\bar{S}$-H) sera donc atteinte en un point (M sur notre schéma) où cet hydrate précipite. Ce point M se situe à une distance d'autant plus petite de la surface de C_3A que la vitesse de passage en solution de C_3A sera plus faible par rapport à celle des autres constituants. Lorsque le C_3A est peu actif, et la chaux libre + semi hydrate très actifs et en grande quantité, la précipitation d'ettringite peut se produire très près de la surface de C_3A :

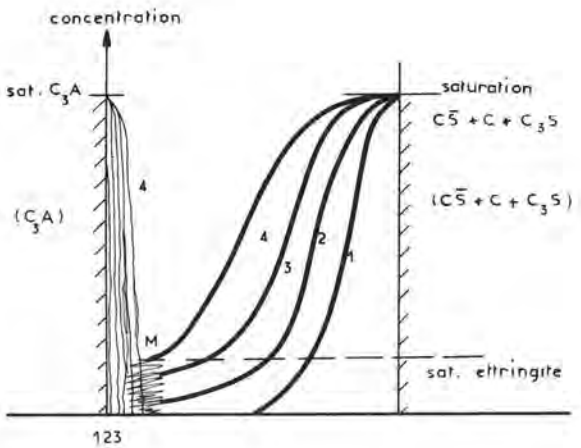

Ceci répond à la deuxième partie de la question.
Pour la première partie, il faut considérer que l'apport de chaux en solution par C_3S et la chaux libre écarte la stoechiométrie de tous les ions en solution de celle de l'ettringite, et diminue la solubilité de l'ettringite. Il en résulte un déplacement du point M vers la gauche, c'est à dire une précipitation plus proche de la surface de C_3A. La sous-saturation relative en chaux a l'effet inverse (addition de complexants du calcium par exemple). Comme le volume, donc la quantité d'ettringite formée est d'autant plus petit que le point M est plus proche de la surface de C_3A, il est possible de conclure (et l'expérience le vérifie) que la sursaturation en chaux induit une précipitation d'ettringite en moins grande quantité, et probablement moins bien cristallisée. La sous-saturation a évidemment l'effet inverse.

Sous-thème V.3 : Autres ciments

Sujet n° 1 : Stabilisation et activation du βC_2S :

Les différentes interventions mettent en évidence qu'il est possible de préparer une phase βC_2S qui a des propriétés analogues à C_3S, mais que cette phase doit être stabilisée. Elle peut l'être de trois manières :

- par la présence d'ions de métaux lourds dans le réseau du silicate : ions trivalents (Cr, Fe, Al, B), ion tétravalent (Ti),
- par la présence d'anions divalents (SO_4^{2-}) ou trivalents (phophates) en solution solide dans le réseau du silicate,
- par la présence de cations alcalins dans le réseau du silicate.

Dans les trois cas, on forme de véritables solutions solides.

Examinons ces différents cas et les conséquences qu'entraînent ces adjonctions d'ions au réseau du βC_2S par l'intermédiaire de la neutralité électrique :

a) la présence de cations trivalents ou tétravalents en substitution d'ions calcium divalents dans un réseau a pour conséquence, comme le montre le schéma, la présence de lacunes de calcium. Par exemple, pour deux ions trivalents on obtient une lacune de calcium.

Ca^{2+}	□	Ca^{2+}	Ca^{2+}
SiO_4^{4-}	SiO_4^{4-}	SiO_4^{4-}	SiO_4^{4-}
Cr^{3+}	Ca^{2+}	Cr^{3+}	Ca^{2+}

Schéma 1

Introduction de chrome dans un réseau βC_2S

b) la présence d'anions divalents ou trivalents en substitution d'ions silicates (tétravalents) a, comme le montre le schéma 2, pour conséquence la présence des mêmes lacunes de calcium (pour un ion sulfate, on obtient une lacune de calcium).

Ca^{2+}	□	Ca^{2+}	Ca^{2+}
SiO_4^{4-}	SO_4^{2-}	SiO_4^{4-}	SiO_4^{4-}
Ca^{2+}	Ca^{2+}	Ca^{2+}	Ca^{2+}

Schéma 2

Introduction de SO_4^{2-} dans le βC_2S

c) la présence de cations alcalins monovalents de petites dimensions, en insertion dans le réseau a pour conséquence, comme le montre le schéma 3, la présence des mêmes lacunes de calcium.

Ca^{2+}	□	Ca^{2+}		Ca^{2+}
SiO_4^{4-}	SiO_4^{4-}	SiO_4^{4-}	Na^+	SiO_4^{4-}
Ca^{2+}	Ca^{2+}	Ca^{2+}	Na^+	Ca^{2+}

Schéma 3

Introduction d'un alcalin en insertion dans βC_2S

Il semble donc, en définitive, que l'élément de base qui stabilise cette phase βC_2S et qui sans doute l'active, soit la présence de lacunes de calcium dans le réseau.

Pour introduire dans ce réseau ces différentes impuretés qui induisent ces lacunes, il est clair qu'une méthode qui passe par une phase liquide et une coprécipitation, est plus efficace qu'une méthode de diffusion à l'état solide.

THEME VI

Cement pastes : rheology and evolution of properties and structures

by Professor S. DIAMOND

I. INTRODUCTION

This general report represents an effort to assess the large body of information submitted to the Congress related in various ways to the characteristics of cement pastes. A total of four principal papers and forty communications are included in this portion of the Congress activity. The topics covered are broken down into four general areas, loosely relating to (a) rheological and other characteristics of fresh cement pastes, (b) the formation and evolution of structure in hardened cement paste, (c) the properties of mature cement paste, and (d) mathematical models attempting to describe structure or strength development. The topics are far from mutually exclusive and are not exactly coincident with the areas covered by the authors of the principal papers, but they serve as a convenient framework for review and analysis.

It should be pointed out at the outset that the opinions expressed in this general report are entirely the personal views of the writer and should be so regarded. The writer apologizes in advance for any statements which misconstrue the results or the interpretations of any of the contributors whose work is mentioned.

II. RHEOLOGICAL CHARACTERISTICS OF FRESH CEMENT PASTES

Rheology of Plain Pastes and Concrete

It is especially fitting to discuss the rheology of cement paste and concrete at an International Congress to be held in Paris. The accomplishments of what might be loosely termed the French school of cement and concrete rheology certainly deserve special acknowledgement, and the contributions of such workers as LeGrand, Bombled and other French colleagues are evident in the view provided in the principal paper of Helmuth (1) and in papers contributed to this portion of the Congress.

Strictly speaking, this Congress is concerned with cement and cement paste rather than with concrete *per se*, but it is apparent that the rheological characteristics of fresh paste are of concern primarily because of their influence on the flow behavior and workability of concrete. It has become recognized in recent years that most fresh mortars and concretes behave approximately as Bingham fluids, whose yield stress and plastic viscosity parameters are at least conditioned by the flow characteristics of the cement paste portion. Naturally, concrete flow behaviour also reflects particle interactions between aggregate grains, and the pattern of behavior may be modified by the effects of vibration used in placing the concrete.

Despite efforts by various workers to put testing of flow behavior and "workability" of concrete on a rational basis, nearly all fresh concrete testing continues to be done by arbitrary empirical methods such as the slump, flow, Vebe, compaction factor and Vicat tests. In their contribution to this Congress Maultzsch and Meinhold (2) describe and report on certain proposed improvements in several of these tests, especially the mortar flow test. Such improvements may certainly prove to be helpful, but they do not really address the question of properly characterizing concrete and mortar in rheological terms.

Most of the concern with rheological matters at this Congress is of course not with concrete but with cement paste. Two central questions appear to emerge:

(1) How does one properly characterize and understand the rheological behavior of a given cement paste, and

(2) What are the changes in behavior that follow from changes in cement characteristics, or from incorporation of mineral or chemical admixtures, especially superplasticizers?

Evaluation of the rheological characteristics of cement pastes may be easier than evaluation of concretes because of the reduced level of particle interaction, but even so it is an extremely difficult and demanding field.

Rheological characteristics of suspensions are normally determined in terms of flow curves. For most substances the method of mixing does not seriously affect the flow behavior of the resulting suspension, nor does the suspension change character in response to ongoing chemical reactions while its flow behavior is being determined. Unfortunately, cement paste is uniquely sensitive to details of the mixing procedure for a variety of reasons, and hydration continuously modifies the flow characteristics of the paste, even through the apparent "dormant" period. Both of these features have been discussed in detail by Helmuth (1).

To a reasonable first approximation, the flow characteristics of fresh cement paste are those of Bingham fluids. The behavior is quite obviously the result of the state of flocculation existing in the suspensions, which for pastes not incorporating water-reducing or superplasticizing admixtures is practically complete. As an illustration, sedimentation data for "control" pastes reported in the communication by Palliere and Briquet (3) show no particles sedimenting at effective diameters below about 45 µm, all individual particles below this size being bound in flocs. In ordinary pastes of the usual range of water contents sufficient bonding develops between flocs that some minimal level of shear stress (the Bingham yield stress) must be applied for continuous flow to be initiated. The flow units actively moving at low shear rates are quite obviously flocs and not individual particles. However, if flow is maintained at higher rates by application of shear stresses substantially higher than the yield stress the flocs tend to break down to smaller flow units and the suspension "thins" over some finite period to an equilibrium state characteristic of the particular shear rate. The flowing paste then continues in this state while flow is maintained. If shearing slows or stops the suspension tends to recover its original state of flocculation.

Two complementary descriptive parameters emerge from this picture. The primary parameter is the flow curve, in principle a plot of shear stress-shear rate points, each corresponding to an equilibrium state of the flowing suspension. Of secondary interest but of importance in special situations is a mathematical description of the rate of thinning

and of the rate of recovery of the original structure at each shear rate. The two types of information together constitute an appropriate description of the flow characteristics of a given paste at a given time after mixing (or as close to a given time as the data can reasonably be acquired). Note that the implication is that each measurement at a given shear rate is properly carried out on a separate batch of paste, with the times of mixing of the batches appropriately staggered.

A considerable amount of perhaps avoidable complication has entered the literature on cement paste rheology as a result of flow testing carried out on certain modern coaxial cylinder viscometers. These are highly sophisticated, but in the writer's opinion highly inappropriate instruments for characterizing the flow behavior of cement pastes. Part of the problem is associated with the transient (or sometimes permanent) inhomogeneity in the flow accross the gap, referred to by various workers in their communications to this Congress and elsewhere. The other feature is the interaction of the first with the way such instruments are operated. Rather than maintaining a constant shear rate and measuring torque (shear stress) over time until equilibration is established, in these instruments the shear rate is increased continuously according to a program selected by the investigator, and then decreased continuously to zero in a like time period. The torque or shear stress is measured continuously and "up" and "down" flow curves are produced automatically. The paste is never in an equilibrated condition at any shear rate. In such flow curves hysteresis loops, *i.e.* displacements of the downcurve with respect to the upcurve, are commonly observed, and a rounding off toward the origin at low shear rates is a common feature. As indicated by Helmuth (1) these responses are conventionally described as "thixotropic" or "antithixotropic" loops and pseudoplastic behavior, respectively. Much effort and attention has been expended in efforts to provide structural interpretations explaining these observations, even though "thixotropic" and "antithixotropic" behaviour can succeed each other in successive runs with the same paste.

In their communication to this Congress, Nagataki and Kawano (4) suggest that these effects may be manifestations related to the development and breakdown of a somewhat nebulous "secondary structure" relating to gel formation and distinct from the floc structure of the pre-existing paste. This is in contrast to the interpretation in terms of varying rate of breakdown and recovery of the floc structure as outlined by Helmuth (1). The present writer feels that these effects may have more to do with the properties of the different viscometers and shearing schedules selected by the investigators than with the flow behaviour of the cement pastes *per se*. In his view attempts to analyze such transient behavior have not been particularly fruitful and are not likely to be so in the future.

The flow curve determined as a succession of equilibrium states is for most cement pastes approximately that of a Bingham fluid, and as such is adequately characterizable in terms of the simple parameters of yield stress and plastic viscosity. This approach has been taken in most of the relevant contributions to this Congress, and the results stated are at least approximately comparable with each other. One should mention that, as indicated by Helmuth (1), pastes too stiff to be tested in conventional viscometers may still be characterized in terms of yield stress in specially devised instruments generally called rheographs or plastometers.

Values of yield stress usually recorded for cement pastes may range from a few Pa to several thousand Pa shortly after mixing, and of course these increase drastically with the progressive stiffening that accompanies the approach to set. A number of equations relating yield stress to such factors as water:cement ratio and cement fineness have been cited by Helmuth (1).

Values of plastic viscosity are most appropriately quoted in units of Pa-s, with some workers preferring to use mPa-s (Pa-s x 10^{-3}) since 1 mPa-s equals 1 centipoise, the traditional unit of viscosity. Cement paste plastic viscosities are normally in the range of tens of Pa-s unless water reducers or superplasticizers have been incorporated, in which case they are much reduced. For comparison, water at room temperature has a (Newtonian) viscosity of 0.001 Pa-s, glycerol 1.7 Pa-s.

As indicated by Helmuth (1) variations in the relative amounts of the different clinker components seem to produce only minor rheological effects, except possibly for augmented C_3A contents. On the other hand, the amount and form of the calcium sulfate interground with the clinker may have profound influence on the rheological characteristics of the paste. A significant contribution to this Congress is the paper by Bombled (5) in which the rheological influence of various forms of calcium and other sulfates are sorted out. The effect of the sulfate depends on its solubility, and equally important, on its rate of dissolution. In C_3A-poor cement pastes, sulfate in solution remains in high concentration and acts as a strong flocculant, as a reducer of the solubility of calcium aluminates, and eventually as an accelerator of silicate hydration. With high C_3A content cements these effects are modified by rapid precipitation of the calcium aluminate sulfate hydrates and concomitant removal of sulfate from solution.

Admixture Effects in Rheology

The influence of mineral and especially of chemical admixtures on the rheology of fresh portland cement pastes may be profound, and a large proportion of the contributed Congress papers on rheology are concerned with this general subject.

One mineral admixture extensively employed in many countries is flyash (pulverised fuel ash). The contribution by Ivanov and Zacharieva (6) is concerned with measurements of the influence of two specific flyashes on cement paste rheology; in fact, the rheology of a complete spectrum of mixes of the two components was examined. The flyash-bearing pastes were found to yield markedly higher yield stress values and somewhat higher plastic viscosities than did the reference cement pastes.

The influence of water-reducing and superplasticizing chemical admixtures is naturally in the opposite direction. These substances function as dispersants, modifying the development of the usual floc structure, or resulting in the partial or even complete dispersion of pre-existing flocs when added after the main mixing step. The result is a marked lowering of both the yield stress and the plastic viscosity, *i.e.* a fluidification of the paste. This translates in concrete practice to a reduced water requirement for the maintenance of normal workability characteristics of the concrete.

Lignosulfonates have been used as water-reducing agents for many years. In the contribution of Tarnaroutski *et al.* (7) the influence of the molecular weight of the lignosulfonate and of the content of various functional groups on the dispersing effectiveness of lignosulfonates are explored. The technically important influences of these variations in molecular structure on air entrainment and on set retardation are also described.

The influence of the dosage rate of several different lignosulfonate water reducers on the flow characteristics of fresh cement paste are described and analyzed in detail in the contribution of Lapasin *et al.* (8). It was found that the general type of transient or "breakdown" behavior between the initial state and the equilibrium state at a given shear rate is not affected by the dosage rate but the amplitude or relative extent of the breakdown effect is concentration dependent, and it goes through a minimum at some critical concentration. Initial viscosity values also show this effect, but equilibrium viscosity values decreased monatonically with concentration. The flow curves exhibit a rounding at low shear rates, and the authors have chosen not to discuss estimates of Bingham yield stresses.

The rheological and the floc-dispersing effects of a number of lignosulfonate-related admixtures (classified as "surfactants" by the authors) and of melamine- and napthalene- based superplasticizers were studied as functions of time of addition in an interesting contribution by Palliere and Briquet (3). The state of dispersion attained in each instance was followed by measurement of the size distribution of settling particles or flocs using a laser-based particle size measuring device, and comparison of this to the size distribution of the original cement. The superplasticizers were found to be more effective dispersants than the surfactants and were found to be even more effective when added after delays of as much as 2½ hours after mixing. In some of the trials complete dispersion to primary particles was indicated.

Further studies of the mechanism of dispersion were reported in a contribution by Collepardi *et al.* (9), who compared the effects produced by varing concentrations of a sulfonated naphthalene-formaldehyde condensate based superplasticizer with those produced by its monomer. Small addition (*ca.* 0.5 percent by weight of cement) of the superplasticizer increased fluidity markedly, but additional dosage increments to three times this level had comparatively little incremental effect, despite increases in measured zeta potential accompanying these additional dosage increments. It appears from this report that cement paste should be largely dispersed if a zeta potential of the order of -35 mV can be attained. Interestingly, it was found that the sulfonated naphthalene monomer was without effect. In agreement with the results of Palliere and Briquet (3) it was found that delayed addition of the superplasticizer increased its effectiveness, especially in the lower dosage range.

A study of the combined effects of superplasticizer and salt addition on the rheological and other characteristics of cement paste was reported in the contribution of Sheetz *et al.* (10). Such a combination might be found in salt-affected wells cemented with superplasticized portland or oil well cements. Increasing a salt content (up to as much as 35 weight percent NaCℓ) was found to reduce the viscosity, but the effect was erratic at lower salt concentrations and varied with the type of cement used.

In his principal paper Helmuth (1) briefly describes the results of experiments with cements in which gypsum is replaced by a mixture of a lignosulfonate and an alkali carbonate, the two together acting as a highly efficient dispersant and fluidifier. At high water contents pastes prepared in this manner are thin Newtonian or almost Newtonian fluids. At low water contents (water:cement ratios as low as 0.20) such pastes are peculiar in that they flow without measureable yield stress but only at relatively slow rates: attempts at application of high shear rates produce sudden quasi-dilatant stiffening in a manner not yet adequately described. Concretes formulated with such cements may be of considerable future interest (11).

III. THE FORMATION AND EVOLUTION OF STRUCTURE IN HARDENED CEMENT PASTES

Processes of Structure Formation

Fresh cement paste inevitably becomes stiffer and stiffer, and at some point passes from a system of flocs in concentrated suspension, to a porous viscoelastic skeletal solid capable of supporting applied stresses at least for the short times without significant deformations. This conversion constitutes set. The set paste continues to evolve toward a progressively more rigid porous solid which becomes, roughly speaking, elastic and brittle in character. In this section some of the details of this complex process of structure and strength development will be discussed, with consideration of the properties of the 'mature" paste left for the next portion of this report.

What might be called the chemical aspects of this process, that is, the hydration reactions *per se* and the chemical and "nanostructural" characteristics of the hydration products formed, are discussed in the General Report of Theme II by Locher (12), and in the principal papers of Skalny and Young (13) and Taylor and Roy (14), respectively. There is naturally a considerable overlap to be expected between the "hydration" aspects and the "structure formation" aspects of the same basic process.

The structure forming processes in hardening cement paste seem exceedingly difficult to characterize properly, in part perhaps because it is always harder to understand a rapidly changing physical system than a static one. There have been relatively few contributions to this Congress dealing with the structure forming processes *per se*. However, considerable progress seems to have been reported on methods of altering these processes so as to produce superior products.

The rheological behavior of progressively hardening cement pastes almost to the time of set has been followed by a plastographic method by Zacedatelev *et al.* (15), who investigated the effects of varying temperatures and of changing water content. Equations were proposed to describe the stiffening process as influenced by these parameters.

An extremely ingenious new method for indirectly following the change taking place as cement paste hardens is described in the contribution of Balek *et al.* (16). In this so-called "radiometric emission method" the cement is radiolabeled in such a way that radon gas is constantly produced within the cement grains. The gas is emitted from the specimen at a rate which depends on the diffusion coefficient for the gas within the particles, and their surface area.

The evolution of structure as cement paste sets and hardens causes changes in both these characteristics, which result in concommitant changes in the rate of emission of radon from the sample. Changes in the structure by Vicat needle determinations or by hydration measurements are clearly mirrored by corresponding changes in the rate of emission of the gas during and after set. The interpretation is somewhat complicated by the fact that the two governing parameters, diffusion rate and surface area, are changing in opposite directions as the setting and hydration responses proceed.

The processes of structure formation in hardening cement paste may be followed by many different methods, as the foregoing suggest. However, it seems to the writer that perhaps the most informative and satisfying, if non-quantitative, method available today is that of direct examination and description of progressive changes in microstructure as observed in scanning electron microscopy of specimens of progressively increasing age.

As indicated by Sereda, Feldman, and Ramachandran in their principal paper (17), proper interpretation of such investigations depends on an appropriate selection of fields to be examined, since the structure changes at different rates in different parts of even the same specimen, and is never homogeneous. Nevertheless, these problems are not insuperable and the writer is somewhat disappointed at the relative lack of consideration of such results as are already in the literature in the principal papers of both Sereda *et al*. (17) and of Wittmann (18). The relative scarcity of new information of this type in the contributed papers on structure formation is a further disappointment.

To partly remedy this lack, the writer offers the following generalized description of structure development in portland cement paste based on his own scanning microscope observations and those of others. The pastes concerned are ordinary portland cement pastes hydrated under the usual ambient conditions, and not influenced by admixtures.

For such pastes, visible evidence of the earliest hydration can be seen as thin filmy bodies developing on the surfaces of cement grains, at first being rather difficult to distinguish from small chips of ground clinker also often found adhering to such surfaces. Relatively few visible AFt (rod-shaped) particles are seen in the first few hours. As hydration speeds up at the end of the dormant period it can be seen that a thin shell is developed around most of the clinker grains, and clusters of Type I (elongated) C-S-H gel particles and some AFt rods, project outward radially from these "kernals". Thin films of calcium hydroxide become visible in the pore spaces and around other particles, and in some areas Type II (reticulated network) C-S-H gel is observed. As time passes much additional C-S-H gel is produced, and it begins to be clear that a continuous skeleton is being formed by contacts between C-S-H grains and AFt rods projecting from adjacent cement grain kernals. These contacts become reinforced by additional deposits of hydration product, often not of any particular shape. Hexagonal calcium hydroxide crystals appear, and these grow laterally and finally begin to get thicker, in the process invading and engulfing previously deposited C-S-H gel. In occasional and usually isolated areas small clusters of thin hexagonal plates of AFm products are developed, recognizable by a characteristic edge-to-face contact habit. "Hadley grains" start to appear for higher water:cement pastes; that is, apparent dissolution and removal of cement grain material takes place from within the shells formed earlier around the cement grains, leaving a zone of vacant space between the shall and the reduced cement grain within it. As hydration procedes further, general deposition of C-S-H gel hydration product seems to take the form of masses of small and indefinite Type III C-S-H grains, and in some areas of infilling material without visible particle structure (at the magnifications available in the SEM). It become progressively more difficult to pick out individual particles in many, but not all areas. In some originally highly porous areas, separate and distinct hydration product particles of various types may continue to be distinguished indefinitely. The final "mature" cement paste is an amalgam of these features. Increases in strength may continue long after no further microstructural changes are visible, presumably due to continued infilling and tightening of the existing structure.

Significant changes in the above pattern may be produced by admixtures of various kinds, by heat treatment with or without the use of steam, or by various other physical or chemical treatments that may be imposed.

Bond Formation

Among the topics discussed in the principal paper of Sereda *et al*. (17), there is extensive discussion of the nature of the bonds thought to be formed between individual cement hydration particles in the process of hardening, leading to the solid skeletal "xerogel" visualized by Wittmann (18). In following this discussion and others like it, it is not clear to the writer what the "particles" involved are presumed to be. For example, it is uncertain from many of the arguments presented whether discussion postulates bonding between clearly defined individual particles coming into contact across gaps, such as the radial C-S-H Type I particles meeting across the gap between two separate kernels, *i.e.* cement grains, or whether the postulated bonding is within smaller structural units, perhaps thin sheets, within such particles. Also one wonders whether the term "bond" is really being used in a mechanical sense to merely connote adhesion or cohesion between two adjacent particles, or in the more precise chemical sense where electron transfer (or sharing) between closely spaced and precisely-oriented atoms is implied. Certainly one sees little indication of what atom is being bonded to what other atoms across what bond length and what bond energies are involved. Collepardi (19) is quoted by Sereda *et al*. (17) as suggesting that Si-O-Si bonds are formed across contacts of pre-existing C-S-H particles. This may be true, but the indirect evidence adduced for this conclusion is far from convincing. On the other hand, the picture of Ubelhack and Wittmann (20) also cited by Sereda *et al*. suggests that thin water films continue to separate adjacent "bonded" particles, and thus that the attractive forces involved are primarily long range polar forces ("van der Waals' forces") subject to modification with changes in local environmental conditions, especially RH. This would appear to be a completely opposite concept.

In his contribution to the present Congress Chatterji (21) attempts to calculate the probability

of formation of permanent chemical bonds across two intersecting C-S-H needles and concludes that such bonding is exceedingly unlikely. However, it seems to the writer that the arbitrary assumptions made in the calculations render the conclusion open to question.

In their principal paper, Sereda *et al.* (17) also refer to the ideas of Rehbinder *et al.* (22) concerning the formation of so-called "crystallization contacts" across particles, as controlled by the level of supersaturation with respect to the substances involved. Certainly dissolution and recrystallization at contacts of such well-defined substances as calcium carbonate is well known to occur and to develop strong bonding in, for example, carbonate rocks. If the writer's understanding of the concept of Rehbinder *et al.* is correct, the inference is that particles become bonded by the same kinds of specific, permanent chemical bonds that hold the atoms together within a single particle, and the recrystallization at contacts, once made, should be permanent.

After considerable thought, the writer must admit that it appears to him that in the present state of knowledge, not very much reliable or even useful information concerning the bonds between particles has been adduced.

Effects of Admixtures and Altered Conditions of Hydration

It has previously been mentioned that the development of structure in cement pastes can be modified considerably by application of admixtures or by altering the conditions under which the structure formation is taking place. Specific influences of various admixtures, primarily dissolved chemical admixtures, are extensively discussed in the principal paper of Sereda *et al.* (17).

A number of contributions to this Congress record the results of research in which various solid admixtures are used to influence the course of development of the cement paste structure. Changes induced by inclusion of special crystallizing components, so-called "crents", are described in the contribution of Dmitriev *et al.* (23). These substances are blends of aluminum sulfates or hydroxysulfates with silica gel, gypsum, and in some cases dehydroxylated kaolinite. Used in substantial proportions, *ca.* 10 percent of the cement, they are reported to enhance the early formation of ettringite (resulting in early strength gain), and subsequently to accelerate C_3S hydration. Ponomarev *et al.* (24) illustrate the effects of such additions on the developing microstructure, and show how variations in content of such admixtures can result in development of a high-strength cement, an expansive cement, or a rapid-hardening expansive cement.

The mode of action of a somewhat different solid admixture has been clearly documented in the interesting contribution of Isogai *et al.* (25). The admixture used in this case was a blend of anhydrite, free lime, $C_4A_3\bar{S}$, and $C_{12}A_7$. The expansive effect produced is indicated as being the result of topochemical formation of very fine "non-crystalline ettringite" and of some extra $Ca(OH)_2$, both produced over a period of several days after setting. The expansion was definitely not associated with the large, well-formed ettringite particles developed early in the hydration process.

The solid admixtures discussed above are highly reactive chemically. The influence of less reactive solid admixtures on the evolution of structure and strength may also be considerable. In their report Popov *et al.* (26) illustrate the influence of the inclusion of "microaggregate", mostly quartzitic ground rock particles, on the structure produced. A general homogenization and densification is reported. The writer would infer that such effects may be associated with modifications of the gross floc structure that normally develops in the fresh cement paste.

Methods of modifying the evolution of structure by altering the conditions under which hydration is taking place or by post-hydration manipulations have been reported by various contributors. The contribution of Gorianov and Stchastnii (27) illustrates the effects of pressing, hot-pressing, and of exposure to saturated cement pore solution. A somewhat more commercially viable method of altering the development of structure is steam curing, and the contribution of Sauman *et al.* (28) reports on studies in which pastes of 10 different cements, each well characterized chemically and granulometrically, are steam cured for various periods. It appears that differences in the rate of strength development for the different cements is conditioned primarily by differences in alite content, and secondarily by variations in the character of the alite solid solutions. Variations in content of C_2S or of C_3A, and differences in alite grain size seem to be unimportant.

A somewhat novel method of influencing the development of structure and strength in cement paste by pretreating the cement with CO_2-free high humidity air is described in the contribution of Malinine *et al.* (29). Freshly ground cements so exposed are said to develop semipermeable shells of "prehydration product" which accelerate the cement hydration process once water is added. Premature carbonation that would attend the use of moist air not specially purified was said to be counterproductive.

IV. THE STRUCTURE OF HARDENED CEMENT PASTE

Structure of the Solid

Having examined (albeit imperfectly) the processes of structure formation we now turn to a consideration of the structure and properties of the "mature" material. There is no sharp dividing line separating paste still in process of formation from "mature" paste, but certainly 28-day old paste is mature for all practical purposes and for some purposes pastes at much earlier ages might well be so designated.

The usual pattern in most modern material science developments is that one studies the structure of a material on the basis that one should be able to understand, predict, and modify its properties most efficiently after its structure is understood. This approach has been quite successful in metallurgy and in ceramics. To date it has not been followed very successfully with respect to cementitious materials, perhaps because the structure is too complicated to be very well understood.

In his principal paper on this subject, Wittman (18) describes the structure of hardened cement paste as comprising a solid "xerogel", water, and pore space. In contrast with most other materials, the solid

part of cement paste is unusually and sensitively linked with the water component, in part because the solid is composed of hydrates, in part because physical characteristics of the solid are unusually sensitive to water content and even to changes in ambient RH. Details of the pore structures seem also intimately bound up to this sensitivity, and it is very difficult indeed to trace through the interrelationships involved.

The chemical and crystallographic characteristics of the several solid phase components normally present have been cogently summarized in the principal paper of Taylor and Roy (14). Hardened portland cement paste prepared under the usual ambient conditions is an assemblage of almost amorphous C-S-H gel of variable chemical composition and morphological type, of calcium hydroxide, of some AFt (red-shaped) and AFm (hexagonal platy) calcium aluminate sulfate hydrates of variable compostion, and of whatever unhydrated cement remains. The C-S-H gel is usually considered to be the dominant component, so much so that some workers tend to lose sight of the existence of the other components when interpreting cement paste behavior.

The nature of this C-S-H component has been the subject of much investigation and considerable dispute for many years. The current status of ideas on its internal structure is expertly summarized by Taylor and Roy (14). The structure has only a small degree of order. The well-known Feldman and Sereda model rests primarily on interpretations of measured changes in various characteristics (length change, stiffness, rate of helium penetration, and adsorption-desorption responses) as functions of RH, rather than with structural investigations by the classic tools of structure determination (x-ray diffraction, electron diffraction, infrared spectroscopy, mass spectroscopy, chemical analysis, etc.) This model is discussed at length in the principal paper of Sereda *et al.* (17). The so-called "Munich model" is not really a description of the structure of the C-S-H gel but a mathematical explanation of paste characteristics, based on thermodynamic calculations, water sorption isotherms, and experimental measurements of creep, shrinkage, strength, and other parameters, again primarily as functions or RH. This model is discussed briefly in the principal paper of Wittmann (18).

Recently, the term "xerogel" has been introduced into the cement literature by Wittmann to describe the solid "skeletal" portion of hardened cement paste. In the classical colloid literature a xerogel is a dried gel retaining its original structure after the fluid phase has been removed. Its use to represent the skeletal structure of hardened cement paste is strictly speaking a departure from the older usage. One should also guard against the inference that the solid component is only a small volume fraction of the total colloidal system, as might be implied from the adjective "skeletal" since the solids normally constitute 60 or 70 percent or more of the volume of mature pastes.

Details of the chemical composition of individual particles of this solid as dispersed ultrasonically from specially-prepared hardened cement paste are reported in the contribution of Moore (30). The cement used was ground ot unusual fineness (all particles less than 10 μm), pressed into pellets, and hydrated by water drawn into the pellets by capillary action. Hydration carried out in this manner was found to be completed in about 3 months. Individual particles were analyzed in an analytical electron microscope, using thin film calculations which avoid various corrections otherwise necessary. The many C-S-H gel particles examined showed a wide range in chemical composition, with Ca:Si ratio varying from 1.25 to 4.0, and with Aℓ, Fe, and S collectively present within wide limits of 0.1 to 0.9 atoms per atom of silicon. AFm and AFt particles contained large contents of Si, and S and Aℓ were seriously deficient in them, specially in the AFm particles. These compositional ranges, and variations from one particle to another particle are similar to those also reported by Lachowski *et al.* (31) for ordinary cement pastes of lesser maturity.

The contribution of Mituzas *et al.* (32) is specifically concerned with the distribution of the silica among the components present in hardened pastes. These workers conclude, apparently from complexiometric measurements, that a very considerable proportion of the silica in cement pastes is bound into unstable "complexes" with the ettringite and monosulfate phases, and that much less C-S-H gel is present than is normally assumed.

Pore Structure

Attempts at characterization of the pore structure constitute a surprisingly large portion of the experimental work that has been done on the structure of hardened cement paste. Of interest here are the volume, size distribution, and shape of the pores involved. These range in size over many orders of magnitude, the largest being of the order of millimeters, the smallest of nanometers, or even, by some definitions, of the sizes of spaces left vacant by the removal of individual water molecules on drying. Much of the size range is amenable to investigation by mercury intrusion porosimetry: the finer pores are usually investigated by methods involving gas or vapor adsorption or desorption studies. An extensive review of the subject has been provided in the principal paper by Sereda *et al.* (17), and a brief treatment is given by Wittmann (18). As pointed out by these authors, no method is free from difficulties and uncertainties of interpretation.

A number of papers communicated to this Congress are concerned with pore size measurement and interpretation. The relationship between pore size distributions as measured for a spectrum of cement pastes of varying age and water:cement ratio and the corresponding saturated permeabilities measured for the same pastes is explored in an outstanding contribution by Nyame and Illston (33). A power function relationship of surprising precision was developed between a characteristic radius of the paste determinable from the mercury intrusion curve and the permeability. The radius involved is that of the maximum in the dv/d log r plot set up using divisions of equal volume intrusion, and is considered to be representative of the effective size of the continuous pore system through which most of the water flows. The radius involved is near the upper end of the measured size distribution, and is analogous to the "breakthrough diameter" of Winslow and Diamond (34).

An investigation of cement paste pore structure by mercury porosimetry was reported in the communication by Bozhinov and Borovski (35) and it was again confirmed that the water:cement ratio exercises the major influence in setting the distribution of pore sizes in the resulting paste. A modest supervening

influence ascribable to cement fineness was also detected.

At the other end of the pore size range, inferences about the status of micropores in hardened cement paste were drawn by Lawrence *et al.* (36) from an extensive series of nitrogen and butane adsorption isotherms on pastes that had been dried in several different ways. In this contribution it is suggested that micropores available to nitrogen are present in rapidly dried pastes but not in slowly dried pastes. On the other hand, for the latter the isotherms are interpreted as suggesting the presence of slit-shaped mesopores that appear not to be present if the pastes are dried rapidly.

The alteration of pore structure with drying condition inferred by Lawrence *et al.* is an illustration of the general pattern of reports of the instability of hardened cement paste structure, especially with respect to changes brought about by drying. These changes seem only partly reversible on rewetting. Much of this literature is discussed in the principal papers of Sereda *et al.* (17) and of Wittmann (18). Wittmann suggests that such changes necessarily involve a rearrangement in such a way that the surface area is reduced and the structure coarsened. Measurements of surface area by low-angle x-ray scattering reported some years ago by Winslow and Diamond (37) suggest that dried pastes indeed exhibit only about half the surface area of the same pastes before drying, but that immersion in water restored the original area. Permanent reduction in surface area was found to take place only if the pastes were heated in water.

Structure, Creep, and Status of Water

Regardless of the permanence of surface area changes, it is well known that significant shrinkage occurs in cement pastes on drying, and that some of the shrinkage so produced is not recoverable. Shrinkage also occurs in the normal sequence of hydration even in the absence of any drying effects, and one must be careful to distinguish this so-called "autogenous" shrinkage from drying shrinkage.

The separate magnitudes of the two phenomena have been studied by Dorkin and Zaitsev (38) in their contribution of this Congress, as functions of water:cement ratio for several cements of widely varying composition. Typically, autogeneous shrinkage was found to amount to about 30 percent of the magnitude of the drying shrinkage. Both were found to be larger in magnitude for pastes made from cements with higher C_3A contents, and autogenous shrinkage was found to decrease, rather than increase, with water:cement ratio.

Explanations for some of these observations are forthcoming from the detailed study of autogenous shrinkage by Buil and Baron (39). In this contribution the processes were clearly shown to involve a sequence of initial (plastic) shrinkage starting a few hours after mixing, followed by an intermediate stage of expansion, and then a final stage of "hardening shrinkage" after set. The latter was confined to low water:cement ratio pastes (w:c 0.35 and below), and it was considered to be caused by self-desiccation, the water being evolved inward to the interior of the specimen rather than outward to the surrounding atmosphere as in drying shrinkage.

Drying shrinkage is often coupled with creep, a related manifestation of the instability of cement paste. Both are generally thought to be conditioned partly by the pore structure of the paste, partly by the characteristics of its solid component. It appears that both shrinkage and creep may in turn affect the structure, leading to an extremely complex situation. Several of the contributions to this Congress provide some insight into this situation.

The drying shrinkage behavior of a number of thin-walled cylinder specimens of C_2S, C_3S, and cement paste was very carefully determined as the starting point for an interesting set of interpretations provided in thecontribution of Bentur *et al.* (40). These workers divide the observed drying shrinkage into "capillary" - and "gel" - related portions on the basis of shrinkage-weight loss curves. The magnitude of the former is related primarily to the content and size distribution of mesopores, *i.e.* pores in the range of 2.5 to 30 nm radius, which the authors consider to be active in developing capillary shrinkage stresses. The gel-related portion, attributed to drying-induced structural changes in the C-S-H gel component, is related to the volume of micropores (of radius below 2.5 nm), to the surface area, and to the silica polymerization status of the C-S-H gel. An overall effective shrinkage factor is developed which encompassed an empirical combination of the parameters mentioned, and this is shown to be a good linear predictor of total drying shrinkage.

As an illustration of the instability effect, the contribution of Milestone (41) reports the measured effects of drying and of aging at intermediate RH values on the state of polymerization of silica within the C-S-H gel of young C_3S pastes. Drying (to 11% RH) produces a decrease in monomer content and an increase in polysilicate content, the changes being completed rapidly. Equilibration at higher RH values was found to slowly produce changes in the same directions; Milestone especially noting gradual and progressive increases in polysilicate content at RH values of 75% and to a lesser extent, at 50%. Monomeric silica was shown to exist in the gel portion of fresh C-S-H pastes never exposed to lowered humidities.

The changes found by Milestone to result from drying or from aging seem to be similar in character to those occurring in young cement pastes loaded in creep at 20°C and then subjected to rapid temperature increase to 60°C while under load, as reported in the interesting contribution of Parrott (42). The increase in degree of polymerization was parallelled by a rapid increase in creep rate observed. The enhanced creep component stemming from the change is non-recoverable. Parrott indicates that previous work had indicated that heating of similar pastes not under load had reduced, rather than increased the non-recoverable creep component. Parrott concludes that the enhanced creep rate is due to a structural reorganization involving the enhanced silica polymerization. On the basis of the reasoning of Bentur *et al.* (40), one might expect paste with more highly polymerized C-S-H gel to exhibit reduced, rather than enhanced creep capacity, in view of the stiffening effect thought to be associated with a higher degree of polymerization.

The behavior of hardened portland cement paste is generally considered to be influenced not only by the structure of the solid and by the size distribution and character of the pores present, but also by the varying status of the water present in the pores and within the solid components. Investigations into the status of cement paste water have been reported for many years. Unfortunately, it has proven to be exceedingly difficult to reach any sort of consensus, since the results seem to vary markedly with the method of study.

In his principal paper (18) Wittmann cites a four-fold subdivision of water in cement paste into (a) bulk water in large pores, (b) water of reduced chemical potential in medium-sized pores, (c) "structured" water condensed into pores between 3 and 10 nm in radius, and (d) adsorbed water on surfaces in layers not exceeding 2½ monolayer thicknesses. The distinctions were made on the basis of freezing behavior.

In their interesting contribution to the present Congress, Sabri and Illston (43) report that a physical separation of two distinct types of water in cement pastes can be effected by a semi-isothermal mode of operation of TGA and differential TGA apparatus, in which heat increase is stopped once a peak start to come off. They were able to consistently separate the water removal process into peaks coming off isothermally at between 47° and 54°C (depending on age of the pastes), and peaks coming off between 78° and 90°C, again as a function of age. Measurements were made of specimens of various ages and water:cement ratios, and of specimens that had been conditioned to various RH values before the investigation. These workers conclude that water removed in the first peak ("type A water") includes all of the pore water and the physically adsorbed water as well, and that water removed in the second peak ("type B water") is structural or hydration product water removed from C-S-H gel or other hydration products. The amount of this "structural" water is reduced on pre-exposure of saturated pastes to even slightly reduced RH conditions, e.g. 94% RH, but most of it is retained against drying at 11% RH.

A somewhat different type of study on the status of water in hardened cement paste is provided in the contribution of Sierra (44), who reports on measurements of IR, broad-band proton spin NMR, and dielectric behavior of C_3S and portland cement pastes. The results are interpreted as indicating that water in the finest pores and on the surfaces is extensively hydrogen bonded, and a definite picture of the structural location of water molecules and the status of their hydrogen bonding to specific Si-O sites in a postulated C-S-H gel structure was provided. In the opinion of the writer, and of Taylor and Roy (14), the gel structure postulated as the framework, which is the 2- or 3-layer tobermorite sheet structure of Kantro, Brunauer, and Weise (45) is not likely to be an appropriate representation of the actual C-S-H gel structure.

The writer would also suggest that several points be considered by those workers concerning themselves with the status of water in hardened cement paste: (a) results from a number of laboratories in several countries indicate conclusively that at least the "water" in larger pores of cement paste that can be expressed by application of high pressures is not water at all, but is rather a concentrated solution of sodium and potassium hydroxides, and (b) ordinary "bulk" water is highly structured and at ordinary temperatures is extensively hydrogen bonded. What one must investigate is the change in structure brought about the local environment, both chemical and physical, of the various regions within the hardened cement paste.

Crack Formation and Propagation

The various properties and characteristics of hardened cement paste so far discussed are of considerable scientific interest. However, their practical importance rests on whatever bearing they may have on the engineering properties of cementitious materials. Strength is clearly the engineering property of greatest interest in this connection.

In the principal paper of Wittmann (18) strength in hardened cement paste is seen to be limited by crack formation; in the principal paper of Sereda *et al.* (17) it is specifically linked to the pore structure. In the contribution by Zaitsev (46), the influence of pore structure on crack formation and hence on strength in cement paste is explored in a Monte Carlo model of failure in compression. The model assumes a random distribution of pores of the appropriate sizes is present, and that as the system is loaded, cracks extend from the pores along the line normal to the direction of maximum tensile stress. As loading is increased, favorably located cracks from adjacent pores join together, each junction constituting a sudden increase in crack length. This process is followed by computer simulation until a critical crack length is achieved and failure occurs without additional loading.

New methods allowing the study of actual development of cracks in real specimens are described in two contributions to this Congress. Tsilosani *et al.* (47) describe a holographic interferometer method of depicting and studying the state of strain in concrete being subjected to simultaneous mechanical and shrinkage stresses. The onset of cracking is clearly depicted by modifications in the interference bands observed. Thus comparative cracking resistance and measured values to time-to-first-significant-cracking can be compiled for concrete specimens made from various cements or exposed to various preliminary treatments. The results obtained suggest that even modest contents of mineral additions may lower the cracking resistance of concrete but that it is not greatly affected by variations in cement composition.

The prospects for furthering an understanding of the microstructural basis for the cracking and fracture behavior of cement paste would seem to be enhanced by applications of a device described in the contribution of Diamond and Mindess (48). A compact tension fracture mechanics specimen arrangement has been constructed in such a way that it may be included and loaded within the specimen stage of a scanning electron microscope. Thus direct observation of the formation and propagation of cracks produced under controlled conditions can be attained within the scanning electron microscope. Preliminary microscopic observations relating to the geometry, branching characteristics, and displacements of cracks produced in cement pastes are reported.

V. MATHEMATICAL MODELING OF CEMENT PASTE STRUCTURE AND STRENGTH DEVELOPMENT

The development of mathematical models to describe the evolution of the hydration processes and the development of strength in hardened cement paste and concrete seems not very well advanced. The discrepancy between the possibilities and the practical results so far attained is pointed out in the principal paper of Cheine (49), who considers that a lack of fundamental rigor exists in defining the important characteristics of the starting materials and of the hydration products. This is explainable in view of the inherent complexity of cementitious systems as is obvious from the preceding sections of this report.

Contributions in this area generally attempt to model either the hydration processes in more or less chemical terms or else model strength development, usually empirically or by application of statistical or regression formalisms.

"Chemical"-type treatments are provided in contributions by Rumyantsev (50), and by Pommersheim *et al.* (51).

The former provides a general mathematical treatment of solid-liquid reactions, with application both to high temperature clinker-melt reactions and to cement hydration. A rate process equation in which the surface area is subsumed in the pre-exponential term was suggested to express the temperature dependence of the processes, the Kholmogorov-Erofeev double exponential equation was suggested for fitting to isothermal processes, and an equation developed on the basis of local branched chain reactions was suggested instead of the usual treatment of solid liquid reactions proceding by slow diffusion through a uniformly-increasing thickness of coating.

A specific mathematical model for the hydration of uniformly-sized C_3S particles was elegantly developed in the contribution of Pommersheim *et al.* (51). This model assumes progressive development of both "inner" and "outer" hydration product layers, and the temporary development and subsequent disappearance of a barrier layer between them. The essence of the model is contained in a dimensionless parameter expressing the ratio of the rate of diffusion through the expanding layer of hydrate to the rate of chemical reaction at the core-hydrate interface. Based on realistic inputs of particle size, water: cement ratio, and temperature, the model is shown to predict reasonable values of the degree of hydration as a function of time, and to fit the experimental data of Kondo and Ueda (52) for the hydration of closely-sized C_3S particles.

An extensive mathematical treatment describing both hydration and strength development in hardened cement paste is provided in the contribution of Polak and Babkov (53). In contrast to the paper discussed previously, these authors apparently do not attempt to compare the mathematical formalism developed to actual data for either hydration or strength development processes.

The remaining papers in this area are concerned exclusively with providing mathematical descriptions of strength development, and with its variation under different conditions.

The principal paper of Cheine (49) reports a highly sophisticated time-series analysis of the "activity", *i.e.* the strength developing capacity of the product being produced by a particular slag-cement factory. Seasonal fluctuations are shown to occur, loosely correlated with variations in the C_3S plus C_2S content of the clinker, but the major factors influencing the strength developing capacity are said to be the specific proportions of slag, gypsum, and clinker, and the fineness of grinding. Equations relating strength at any age to the activity measured in tests at early ages are suggested.

In other contributions, a generalized formula for the estimation of the strengths of concretes and of cement pastes is suggested by Vyrodov and Padalkina (54), a comparison of several equations for the calculation of expected strength from cement compound composition and fineness is provided by Popovics (55), and a set of regression equations relating strengths of concrete to calculated Bogue cement compositions for a range of New Zealand cements is provided by Aldridge (56).

VI. ACKNOWLEDGEMENTS

This report was written during periods in which the writer was an academic visitor at the University of Aberdeen and at Imperial College. The writer expresses his appreciation for the hospitality provided by Professor H.F.W. Taylor and by Professor P.L. Pratt at their respective institutions, and for travel support by the Science Research Council of the U.K.

REFERENCES

1. - R.E. HELMUTH (1980) "Structure and Rheology of Fresh Cement Paste" Principal Paper VI-0, this Congress.
2. - M. MAULTZSCH and U. MEINHOLD (1980) "Testing Methods for the Set of Pastes and Mortars" this Congress.
3. - A.M. PAILLERE and Ph. BRIQUET (1980) "Influence of Fluidifying Synthetic Resins on the Rheology and Deformation of Cement Pastes Before and During the Setting" this Congress.
4. - S. NAGATAKI and S. KAWANO (1980) "Analysis of Fluidity of Cement Paste and Mortar" this Congress.
5. - J.P. BOMBLED (1980) "Influence of Sulfates on the Rheological Behavior of Cement Pastes and on their Evolution" this Congress.
6. - Ya. IVANOV and S. ZACHARIEVA (1980) "Influence of Flyash on the Rheology of Cement Pastes" this Congress.
7. - G.M. TARNAROUTSKI, N.V. GRIBANOVA, G.M. TELYCHEVA, and V.N. SERGUEEVA "Influence of Chemical Structure of Lignosulfonates on Hydration and Plastification of Cement" this Congress.
8. - R. LAPASIN, V. LONGO, and S. RAJGELJ (1980) "The Effect of the Water Reducer Addition on the Rheological Properties of Cement Pastes" this Congress.
9. - M. COLLEPARDI, M. CORRADI, G. BALDINI, and M. PAURI (1980) "Influence of Sulfonated Napthalene on the Fluidity of Cement Pastes" this Congress.

10. - B.E. SHEETZ, E.L. WHITE, H. WOLFE-CONFER, and D.M. ROY (1980) "Effect of Mix Rheology, Admixtures, and Salts upon Phsyical and Mechanical Properties of Hardened Cement Pastes" this Congress.

11. - S. DIAMOND (1980) "An Alternative to Gypsum Set Regulation for Portland Cements" World Cement Technology, 11 (3) 116-121.

12. - F.R. LOCHER (1980) "Hydration of Pure Portland Cements" General Report II, this Congress.

13. - J.P SKALNY and J.F. YOUNG (1980) "Mechanisms of Portland Cement Hydration" Principal Paper II-1, this Congress.

14. - H.F.W. TAYLOR and D.M. ROY (1980) "Structure and Composition of Hydrates" Principal Paper II-2, this Congress.

15. - I.B. ZACEDATELEV, B.D. TRINKER, and YU. S. TCHERKINSKY (1980) "Rheology and Hydration of Cement at Outer Influence" this Congress.

16. - V. BALEK, V. SATAVA, and J. DOHNALEK (1980) "The Evolution of the Structure of Cement Paste Investigated by Radiometric Emanation Method" this Congress.

17. - P.J. SEREDA, R.F. FELDMAN, and V.S. RAMACHANDRAN (1980) "Structure Formation and Development in Hardened Cement Pastes" Principal Paper VI-1, this Congress.

18. - F.H. WITTMANN (1980) "Properties of Hardened Cement Paste" Principal Paper VI-2 this Congress.

19. - M. COLLEPARDI (1973) "Pore Structure of Hydrated Tricalcium Silicate" Proc. Int. Congr. Colloid and Surface Chem. (IUPAC), Prague, Vol. 1, B25 - B49.

20. - H.H. UBELHACK and F.H. WITTMANN (1976) "Dynamics of the Development of Structure in Colloids and Brownian Motion" J. de Phys. pp. C6-269 to C6-271.

21. - S. CHATTERJI (1980) "Estimation of Chemical Bonding in Hardened Cement Paste and its Implications" this Congress.

22. - P.A. REHBINDER, E.E. SEGALOVA, E.A. AMELINA, E.P. ANDREEVA, S.I. KONTOROWICH, O.I. LUKYANOVA, E.S. SOLOVYEVA, and E.D. SHCHUKIN (1974) "Physico-Chemical Aspects of Hydration Hardening of Binders" Proc. Sixth Int. Congr. Chem. of Cement, Moscow, Vol. II, Book I, 58 - 64.

23. - A.M. DMITRIEV, H.T. VLASSOVA, B.E. YUDOVICH, A.K. ZAPOLSKI, I.V. KRAVTCHENKO, and L.M. SAZANOVA (1980) "Increase of Portland Cement Strength at Introduction of Crystallizing Components (Crents)" this Congress.

24. - I.F. PONOMAREV, I.A. KRYJANOVSKAIA, and A.G. KHOLODNI (1980) "Control of Structure Formation and Properties of Cement" this Congress.

25. J. ISOGAI, S. NAKAYA, and H. NISHIMURA (1980) "On the Effect of Preventing Drying Shrinkage Cracks of Expansive Cement Concrete" this Congress.

26. - L.N. POPOV (1980) "Effect of Micro-additive on the Properties of Concrete" this Congress.

27. - K. GORIANOV and A. STCHASTNII (1980) "A Structure of Cement Stone of the New Types of Concrete" this Congress.

28. - Z. SAUMAN, F. VAVRIN, and J. CERNA (1980) "Influence of Phase Composition of Portland Cements onto the Resulting Properties of their Pastes Produced by Steam Curing" this Congress.

29. - Y.S. MALININE, V.P. RIAZINE, L.S. BATOUTINA N.D. KLICHANIS, and B.E. YOUDOVITCH "Surface Prehydration of Cements and its Influence on Hardening Process" this Congress.

30. - A.E. MOORE (1980) "Structure and Composition of Compounds in some Fully Hydrated Cement Pastes" this Congress.

31. - E.E. LACHOWSKI, K. MOHAN, H.F.W. TAYLOR and A.E. MOORE (1980) "Analytical Electron Microscopy of Cement Pastes. Part II. Pastes of Portland Cements and Clinkers" J. Amer. Ceram. Soc. (in press).

32. - J. MITUZAS, A. KAMINSKAS, and A. MITUZAS (1980) "On Hardening Mechanism of Portland Cement Paste" this Congress.

33. - B.K. NYAME and J.M. ILLSTON (1980) "Cappillary Pore Structure and Permeability of Hardened Cement Pastes" this Congress.

34. - D.N. WINSLOW and S. DIAMOND (1970) "A Mercury Porosimetry Study of the Evolution of Porosity in Portland Cement Pastes" J. Materials (ASTM) 5, 564-585.

35. - G. BOZHINOV and N. BOROVSKY (1980) "Pore Structure of Cement Stone and its Influence on the Mechanical Properties of Concrete" this Congress.

36. - C.D. LAWRENCE, F.G.R. GRIMBLETT, and K.S.W. SING (1980), "Sorption of N_2 and n-C_4H_{10} on Hydrated Cements" this Congress.

37. - D.N. WINSLOW and S. DIAMOND (1974) "Specific Surface of Hardened Portland Cement Paste as Determined by Small-Angle X-ray Scattering" J. Amer. Ceram. Soc. 57 193 - 197.

38. - V. DORKIN and Yu ZAITSEV (1980) "Influence of Type of Cement on Chemical and Drying Shrinkage" this Congress.

39. - M. BUIL and J. BARON (1980) "Autogeneous Shrinkage of the Hardening Cement Paste" this Congress.

40. - A. BENTUR, J.H. KUNG, R.L. BERGER, J.F. YOUNG, N.B. MILESTONE, S. MINDESS, and F.V. LAWRENCE (1980) "Influence of Microstructure on the Creep and Drying Shrinkage of Calcium Silicate Pastes" this Congress.

41. - N.B. MILESTONE (1980) "Ageing and Drying of Tricalcium Silicate Pastes" this Congress.

42. - L.J. PARROTT (1980) "Structure and Thermal Creep of Cement Paste" this Congress.

43. - S. SABRI and J.M. ILLSTON (1980) "The Distribution of Evaporable Water in Hardened Cement Paste (h.c.p.)" this Congress.

44. - R. SIERRA (1980) "Distribution of Different Forms of Water in the Structure of Pure Pastes of C_3S and of Portland Cement" this Congress.

45. - D.L. KANTRO, S. BRUNAUER, and C.H. WEISE (1962) J. Phys. Chem. 66 1804 - 1809.

46. - YU. ZITSEV (1980) "Influences of Structure on Fracture Mechanism of Hardened Cement Paste" this Congress.

47. - Z. TSILOSANI, G. DALAKISHVILI, and S. KAKICHISHVILI (1980) "The Effect of Cement Composition on the Cracking Resistance" this Congress.

48. - S. DIAMOND and S. MINDESS (1980) "Scanning Electron Microscopic Observations of Cracking in Portland Cement Paste" this Congress.

49. - V.I. CHEINE (1980) "Mathematical Models of Alterations of the Properties of Cement Paste with Time" Principal Paper VI-3 this Congress.

50. - P.F. RUMYANTSEV (1980) "Interactions of Cement Minerals With Water" this Congress.

51. - J.M. POMMERSHEIM, J.R. CLIFTON and G. FROHNSDORFF (1980) "Conceptual and Mathematic Models for Tricalcium Silicate Hydration" this Congress.

52. - R. KONDO and S. UEDA (1968) "Kinetics and Mechanisms of the Hydration of Cements" Proc. Vth Int. Symp. Chem. Cements, Tokyo, 203 - 255.

53. A. Ph. POLAK and V.V. BABKOV (1980) "The Effect of Physico-Chemical Properties of Cement on Structure and Strength of Cement Stone" this Congress.

54. I.P. VYRADOV and G.P. PADALKINA (1980) "On Main Formula of Cement Stone and Concrete Strength" this Congress.

55. - S. POPOVICS (1980) "Calculations of Strength Development from the Compound Composition of Portland Cement" this Congress.

56. - L.P. ALDRIDGE (1980) "Estimating Strength from Cement Composition" this Congress.

Intervention à la table ronde

par C. LEGRAND

Comme l'a souligné le Professeur DIAMOND dans son rapport général, de nombreuses communications de ce thème donnent des résultats de mesures rhéologiques, effectuées essentiellement à l'aide de viscosimètres coaxiaux. Les auteurs se servent bien entendu de ces résultats pour interpréter les phénomènes observés tout en reconnaissant, pour la plupart d'entre eux, que ces résultats sont différents suivant l'appareil de mesure utilisé. Il y a donc là un problème important et on est en droit de se demander quelle est la confiance que l'on peut accorder à des mesures effectuées sur les pâtes de ciment dans de telles conditions.

Une première source d'erreur réside dans le non respect des hypothèses qui ont servi à établir les formules donnant la contrainte et la vitesse de déformation. On peut rapidement citer quelques exemples :
- le fluide doit être homogène. Or, les mesures sur les pâtes de ciment se poursuivent parfois au-delà de dix minutes et des phénomènes de sédimentation peuvent alors intervenir de façon non négligeable et conduire à des augmentations apparentes de viscosité qu'il ne faudrait pas alors attribuer à autre chose;

- l'écoulement doit être laminaire. On voit trop souvent donner des interprétations abusives à des rhéogrammes qui changent d'allure pour des vitesses angulaires élevées, alors que, tout simplement l'installation d'un régime turbulent rend inapplicables les équations classiques de la viscométrie;

- il ne doit pas y avoir de mouvement relatif entre le milieu et les cylindres de l'appareil. Ceci est bien connu et je n'insisterai pas plus sur les dangers qu'il y a à utiliser des cylindres lisses;

- enfin, et ceci est capital, l'écoulement doit être stable; cela signifie notamment que la vitesse de rotation du cylindre mobile doit être constante et égale à celle de l'axe d'entraînement du système. La vitesse de déformation du dynamomètre mesurant le couple résistant doit donc être nulle. Nous savons tous que ceci n'est pas le cas avec les pâtes de ciment qui présentent une structure floculée qui se détruit au fur et à mesure qu'elle est cisaillée, provoquant une thixotropie partielle.

Une deuxième source d'erreur réside, en supposant que les hypothèses dont je viens de parler sont respectées, dans l'évaluation du gradient de vitesse à partir des caractéristiques de l'appareillage, de la vitesse de rotation et du couple résistant mesuré sur l'axe.

Ceci ne pose pas de problème particulier lorsque le corps étudié a un comportement linéaire (newtonien ou binghamien). Par contre, de nombreuses difficultés surgissent dans les autres cas, notamment parce que la détermination du gradient de vitesse dans l'espace annulaire dépend de la loi de comportement que l'on cherche justement à obtenir. Il existe heureusement des solutions plus ou moins précises et plus ou moins lourdes à mettre en oeuvre; je voudrais citer, parmi les communications de ce thème, celle de NAGATAKI et KAWANO, qui ont étudié, par cinémographie directe, la répartition des gradients de vitesse dans l'espace annulaire.

En tout état de cause, déterminer ce gradient à l'aide des formules classiques, qui supposent a priori le comportement linéaire pour trouver, en définitive, un comportement qui ne l'est pas, n'est pas une approximation, mais une erreur.

Je voudrais maintenant revenir sur la destruction de la structure par le cisaillement (structural breakdown) qui conduit à des effets de thixotropie partielle. A mon avis, avec un viscosimètre classique, deux choses seulement sont mesurables. D'une part, le seuil de cisaillement initial, c'est à dire celui de la pâte vierge de tout cisaillement, qui dépend essentiellement des forces de liaison intergranulaires, et, d'autre part, la viscosité finale de la pâte, une fois que la stabilité de l'écoulement est atteinte, c'est à dire après la destruction de toutes les liaisons qui devaient être détruites. Le rapport de ces deux valeurs me paraît être une bonne caractéristique de la thixotropie du milieu. Celle-ci est, toutefois, incomplète puisqu'on ne prend en compte que l'état initial et l'état final. Mais, comme je l'ai signalé tout à l'heure, les mesures intermédiaires ont peu de signification. J'ai déjà montré, il y a quelques années (*) qu'il existait un couplage important entre le milieu d'essai et l'appareil de mesure et que, suivant la vitesse de rotation et la rigidité du dynamomètre, on pouvait trouver à une même pâte plusieurs comportements rhéologiques.

Mais alors, comment faire pour obtenir des résultats significatifs ?

Peut-être faut il utiliser des viscosimètres travaillant non plus à vitesse d'entraînement constante, mais à contrainte imposée et tracer ainsi des courbes de fluage en vitesse de déformation.

Peut-être faut-il au contraire tracer des courbes de relaxation en contrainte à vitesse de déformation constante, en utilisant alors des dynamomètres à la fois précis et très rigides ?

Le problème n'est, à ma connaissance, même pas abordé à l'heure actuelle et je souhaitais le poser. Ce n'est, en définitive, qu'en trouvant de vraies caractéristiques mécaniques qu'on arrive à mieux connaître le comportement rhéologique des pâtes, et pas seulement d'ailleurs de ciment.

(*) C. LEGRAND - Détermination des caractéristiques rhéologiques des corps viscoplastiques à thixotropie partielle - Cahiers du Groupe Français de Rhéologie - III - n° 2 (Avril 1973)

Intervention

par Yu M. BAZHENOV

L'application de modèles et de méthodes mathématiques à la technologie des ciments et des bétons implique de faire appel à des méthodes d'essais et des caractéristiques nouvelles des matériaux, car les méthodes normalisées, traditionnelles, ne permettent pas de faire les calculs avec la précision nécessaire, compte tenu des possibilités des ordinateurs.

En Union Soviétique, à l'Institut "Ecole des Travaux Publics de Moscou (MISI im Kujbysheva), on a élaboré une méthode d'appréciation des propriétés des pâtes de ciment dans la masse même des bétons, en tenant compte de ce que le comportement d'une pâte est alors différent de celui d'une pâte pure. Les propriétés des matériaux dépendent notablement des granulats, de la composition du béton, et d'autres facteurs.

Par suite de l'influence des forces de surface, les grains du granulat diminuent notablement la maniabilité des bétons frais ainsi que les délais de prise.
Pour avoir la même maniabilité que celle de la pâte de ciment, on est conduit à augmenter le rapport eau/ciment des mortiers et des bétons. On peut apprécier l'influence globale d'un granulat en utilisant un coefficient d'influence particulier, qui indique la quantité d'eau supplémentaire à ajouter pour le granulat, afin de ne pas modifier les propriétés du béton frais (sa maniabilité, les délais de prise, etc.)

Par exemple, pour avoir un affaissement du cône sur table vibrante de 17 cm (170 mm), il faut, pour un ciment donné, que $(e/c)_c = 0,3$, tandis que pour un mortier 1:2, il faut que $(e/c)_m = 0,44$. Le coefficient d'influence du sable sera alors égal en % à :

$$K_s = \frac{(e/c)_m - (e/c)_c}{2} \; 100 = 7 \; \%$$

Les sables courants utilisés dans la construction ont un coefficient K_s compris entre 4 et 11 % suivant leur grosseur et les propriétés de leur surface.

Pour déterminer les coefficients d'influence d'un sable K_s ou d'un gravillon K_g on fait des essais comparatifs sur une pâte de ciment, un mortier et un béton.

Nous utilisons des mortiers 1:2 et des bétons 1:2:3. La consistance d'une gâchée correspond à la consistance normale de la pâte de ciment.

Si l'on connait les coefficients d'influence du granulat et si l'on sait comment les propriétés de la pâte de ciment varient en fonction de divers facteurs, on peut prévoir les propriétés des mortiers et des bétons avec une grande précision de calcul. Pour cela on fait appel à une nouvelle notion, celle du rapport (eau/ciment) efficace ou effective, qui indique le comportement réel d'une pâte de ciment dans un béton.

Dans ce but, de la quantité totale d'eau on déduit la quantité nécessaire pour compenser l'influence du granulat sur les propriétés du béton frais :

$$(e/c)_{ef} = \frac{e - K_s S - K_g G}{c}$$

où S et G sont les teneurs en sable et gravillons concassés respectivement.

Ainsi, par exemple, pour une gachée de béton 1:2:4, ayant un rapport total de (eau/ciment) $e/c = 0,6$ $K_s = 0,07$ (7 %) et $K_g = 0,02$ (2 %), le rapport efficace déterminant le comportement de la pâte de ciment dans le béton sera

$$(e/c)_{ef} = 0,6 - 0,07.2 - 0,02,4 = 0,38$$

Pour construire des modèles mathématiques définissant la rhéologie des bétons frais, compte tenu de la rhéologie des pâtes de ciment, en plus des valeurs de $(e/c)_{ef}$, il faut connaître la teneur en pâte de ciment dans les bétons.

Les meilleurs résultats sont obtenus en introduisant la notion de teneur effective, qui ne tient pas compte de toute l'eau, mais seulement de celle qui détermine le rapport eau/ciment efficace.

$$p_{ef} = \frac{c}{1000} \left[\frac{1}{\rho} - (e/c)_{ef} \right]$$

ou c désigne le dosage du ciment en kg.
ρ la densité du ciment.

On peut faire des essais comparatifs, déterminer $(e/c)_{ef}$ et p_{ef} en utilisant des adjuvants ou en travaillant à des régimes technologiques de fabrication différents, afin d'en déterminer l'efficacité. Ces caractéristiques permettent de prévoir avec suffisamment de précision le temps et les conditions de durcissement d'une pâte de

ciment et d'un béton. Ces facteurs exercent une influence déterminante sur la structuration ultérieure d'un béton et sur ses propriétés finales.

La méthode examinée ci-dessus a permis d'augmenter la précision des calculs faits avec l'aide d'ordinateurs. A l'avenir il nous faut chercher de nouvelles méthodes ou des méthodes semblables permettant d'augmenter la précision des calculs technologiques et économiques.

REFERENCES BIBLIOGRAPHIQUES

1) BAZHENOV Yu. M., Teknologiya betona, (La technologie des bétons), Strojizdat, Moscou, 1978.

2) BAZHENOV Yu. M., GORCHAKOV G.I.,ALIMOV L. A. VORONIN V.V., Poluchenie betona zadannykh svojstv, (Obtention de bétons de propriétés voulues), Strojizdat, Moscou, 1978.

3) BAZHENOV et all. Strukturnye kharekteristiki betona (Caractéristiques structurales des bétons), Beton i zhelezobeton, n° 9, 1972.

REVIEW and CONCLUSIONS

by SIDNEY DIAMOND

The activities/encompassed in Theme VI consisted of the following parts:

(a) Four principal papers prepared respectively by Helmuth, by Sereda, Feldman, and Ramachandran, by Wittmann, and by Cheine.

(b) A total of 39 contributed papers by authors from thirteen countries.

(c) A general report prepared and delivered by the undersigned.

(d) A total of 29 posters prepared by authors from seven countries.

(e) A Round Table discussion.

(f) A final session of questions for the Round Table members.

In conformance with the general regulations of the Congress, the individual principal papers were not delivered by their authors but were summarized by the general reporter.

The principal paper by Helmuth (VI-0) covered structure and rheology of fresh cement paste. Helmuth discussed certain characteristics of cement paste as a disperse particle-fluid system whose particles are flocculated unless an effective dispersant has been incorporated into the mix, and introduced a simplified model in which all the individual particles, of whatever size, have water films of equal thickness surrounding them. The flow characteristcs of pastes in terms of Bingham parameters were elucidated, and complications of dilatant, pseudoplastic, thixotropic behavior were discussed. The changing behavior of pastes under repeated shear cycles were attributed to a balance between thixotropic breakdown and recovery, and various cement and solution characteristics that modify flow behavior were reviewed.

The principal paper by Sereda, Feldman, and Ramachandran (VI-1) provided a review of a number of aspects of structure formation and development in hardened cement pastes, particularly those aspects in which major contributions had been made by the NRC Canada group. The paper was subdivided into several independent subsections, the first of which involved the formation and nature of bonds, bond strength, and bonding as related to material structure and behavior. This was followed by a section on porosity and pore size distributions in hardened cement paste. A third section on physical factors controlling structure and strength development was followed by a final section on the influence of admixtures.

The principal paper by Wittmann (VI-2) reviewed aspects of the characteristics and behavior of hardened cement paste seen as a system comprising a solid skeletal structure with an intrinsic pore system, the latter usually containing water; the presence or absence of the water exerts a profound influence on the mechanical characteristics of the system. A survey of the commonly experienced mechanical behavior features of cement paste and their origins in the nature and microstructure of the system completed this review.

The principal paper by Cheine (VI-3) comprised primarily a treatment of time variation in the strength-producing quality of the output of a particular blended cement plant and an exposition of sophisticated mathematical procedures for the analysis of such variation.

The 39 contributed papers encompassed a wide variety of topics, but may be loosely grouped into (a) nine papers on the rheological and other characteristics of fresh cement paste, with many of them dealing with modifications produced by superplasticizers and other admixtures, (b) ten papers dealing generally with the formation and evolution of structure in hardened cement pastes and the bonding developed therein, (c) fourteen papers relating to the structure and properties of hardened cement pastes: and finally, six papers on mathematical modeling of hydration and strength development. One of the most interesting contributions in this last area, a paper by Knudsen, was perhaps inappropriately assigned to Theme I and is found in that portion of the Contributions volume of the Proceedings.

The general report, prepared and delivered by the undersigned, was an attempt to synthesize as much as possible of the important features of the principal reports and the principal papers. Because of the magnitude of the task and the restrictions on length of report and on time of delivery at the Congress, the general report was necessarily somewhat superficial in character. The writer hopes that the effort was useful to Congress participants and will be of help to later readers of the final Congress volume.

The large set of posters exhibited at the Theme VI session of the Congress was something of a surprise to the writer, who did not have an opportunity to examine their contents prior to the Session. Abstracts of these posters are available in the final volume of the Congress proceedings.

In conformity with the established format of the Congress a Round Table panel was assembled to discuss and answer questions pertaining to this portion of the Congress activity. The panel was chaired by the undersigned and consisted of Messrs LeGrand (France), Helmuth (USA), Sereda (Canada), Ramachandran (Canada), Wittmann (Switzerland), Mchedlov-Petrossyan (USSR), Bombled (France), and Mindess (Canada). A portion of

the round table period was devoted to brief expositions by those of its members who were authors of principal papers of their most significant points and any changed viewpoints since the principal papers were prepared. Several questions were then posed to the panel by the Chair, relating to specific topics of concern that had arisen from prior discussions. The questions posed were in brief form: (1) Is there any experience, or consensus, on what sorts of shear rates might be expected to obtain in the usual run of concrete mixing practices, so that rheological tests might be carried out at such shear rates? (2) What, if anything, happens to the preexisting floc structure of fresh paste on setting and hardening? (3) Whether the usual colloidal concepts in general use are really appropriate to describe the behavior of the set synthetic cement paste or stone, and (4) Whether the brittle failure characteristics associated with high-strength concretes were a necessary and intrinsic feature of high strength portland cement systems, or whether one could expect modification of this sometimes undesirable behavior as a result of future development? Time did not permit discussion of all these questions but the consensus suggested that it is not possible to define a definite range of shear rates for the concrete mixing operation, which varies enormously with equipment and circumstances, and that the floc structure of fresh cement paste is probably carried over intact to the hardened paste, and this may have important consequences for the behavior of the latter.

In a final session a relatively large number of questions from the floor were handed in for discussion by the panel, but time permitted response to only a few of these. A number of Congress participants requested time to make brief ad hoc presentations, but it was the painful duty of the undersigned to have to refuse all these requests as inconsistent with the format and time available for the session. He regrets this very much and hopes that on future occasions sufficient time might be set aside for such vital and important communications.

As a general conclusion, the undersigned is of the opinion that Theme VI of the Congress was adequately carried out and that the purposes of summarizing progress in the relevant areas since the Moscow Congress in 1974 were in general achieved, despite frustrations due to format and shortage of time. He would like to acknowledge with great thanks, the tremendous efforts of the Congress organizers, the exceedingly fine facilities placed at the disposal of the Congress participants, and the excellent work of the simultaneous translators who were crucial to the successful functioning of this multilingual assembly.

THEME VII

Interface reactions between cement and aggregate in concrete and mortar - bond strength and durability

by G.M. IDORN

SUMMARY: As introduction is discussed a contrast in the present cement and concrete situation: The cement manufacturing process has reached high industrial efficiency, and civil engineering has proven capable to match the social demands on ever increasing building and construction development, while application of chemical knowledge is too confined to stimulate the creation of contemporary concrete processing technology methods and procedures.

In this context the various aspects of adherence (bond) and durability are discussed on the basis of the contributions to the theme, and selected information from elsewhere.

The advantage is stipulated for application of thermodynamics and reaction-kinetic concepts in studies of the processing of concrete seen as an entirety from the stage of mixing, through placing, curing and performance until ultimate degradation.

Consequently, cement-aggregate reactions and the creation and characteristics of adherence are discussed as primarily dependent upon conversion of "intrinsic" energy, while attack of saline waters is considered as promoted by "intrusive" energy. The adherence between cement paste and reinforcement bars, fibre reinforcement and the effects of pozzolans are dealt with as special issues within this framework.

Contributions on hydrothermally created bond-strength and morphology in cement mortars are treated as elements of future innovative technology development.

Ways and means are suggested for making concrete technology research effective as support to the civil-engineering development of concrete usages.

RESUME:Comme introduction, est discuté une contradiction dans la situation actuelle concernant le ciment et le béton:
"Le procédé de fabrication de ciment a atteint une efficacité industrielle élevée et l'art du génie civil s'est montré capable de répondre aux demandes sociales du développement accéléré dans le bâtiment et la construction, tandis que l'application de la connaissance chimique est trop limitée pour stimuler la création contemporaire des méthodes et procédures technclogiques".

Dans ce contexte, est discuté les aspects divers concernant l'adhérence et la durabilité, ceci sur la base des contributions au thème et des informations d'ailleurs.

L'avantage est invoqué de l'utilisation des conceptes thermo-dynamiques et réaction-kinétiques dans les études de la fabrication du béton dans leur ensemble à partir de la phase de préparation et le coulage, la maturation et performance jusqu'à la dégradation ultime.

Par consequence, les réactions ciment-agrégats et la créàtion d'adhérence sont considérées comme principalement dépendante de la conversion d l'énergie "intrinsique", tandis que l'attaque des eaux salines est considérée comme créé.par la conversion de l'énergie "intrusive". Dans ce cadre est traité spécialement les problèmes d'adhérence entre la pâte de ciment et les fers de renforcement, les fibres de renforcement et l'influence des pouzzolanes.

Sont traitée à titre d'éléments d'innovation technologique l'influence des conditions hydrothermiques aux l'adhésion et la morphologie des mortiers de ciment.

Des méthodes et procédures sont suggérées afin d'améliorer l'efficacité de la recherche dans la technologie de béton, comme appui à l'industrie des oeuvres de génie civil.

INTRODUCTION

The preceding sessions of the 7th International Congress on the Chemistry of Cement have demonstrated that cement manufacture now possesses remarkable abilities for applying cement chemistry knowledge to match the increasing pressures from the depletion of the resources. Also the elaborate evolution of ordinary and special cement characteristics based upon deliberate utilization of chemical knowledge has been convincingly illuminated, and has shown an impressive integration of independent and industrial research, or, if so preferred: of non-**mission**, basic, and mission-orientated, applied research.

Thus, cement manufacture with its storage tank of cement chemistry knowledge is prepared to serve the needs for vastly increasing uses of cement during the forthcoming decades.

Meanwhile, concrete construction design has pioneered energy conservation throughout the post-war period by enabling considerable increases of imposed loads relative to dead loads of structures and buildings, and also by invention of system and modular building's design etc. Concrete construction execution has concurrently created management of large-scale, mechanized erection operations to earlier unthinkable extents and rates of execution. This synergetic civil engineering development of concrete uses has now made cement a fundamental primary material for the functions and further progress of all human societies.

Therefore, there are obvious reasons why the present congress could have had a concluding session to concentrate on the opportunities for industrial research and development of cement using processes and products, by utilizing the available cement chemistry knowledge. And there are in fact incipient moves in this direction among the contributions to this session.

However, the prevailing feature in actual cement using practice is not industrial innovation, but rather that major constructions, for instance, in the energy producing and the infrastructure sectors, are requested to be designed for higher levels of performance reliability than before, while concurrently repairs and replacements of deteriorated concrete are showing unacceptably increasing consumption of the available resources.

With these trends outfolding: higher performance requirements confrontated with increasing deterioration, the established civil engineering concepts for the structural utilization of concrete, relying on simple, empiric specimen-testing and on equally simplified measures of the capabilities of cements, do not suffice. They cannot provide the specified initial and lasting performance qualities of structures and products, let alone stimulate to significant technology progress.

The civil engineering establishments are unable to change this situation, because this requires physico/chemical manipulations in concrete processing beyond the general acceptance systems. This is why it is cement chemistry knowledge which is facing great opportunities and obligations in updating of the technologies for cement uses.

It is the aim of the present general report to assess the potential impact of cement chemistry in counteracting the actually growing concern about insufficient concrete durability. This is to be accomplished by analysing the delivered contributions and other recent acquisitions of relevant knowledge. In this connection the adherence (bond) between matrix and aggregates will be considered as having an important role.

Whilst the attainable assessments from the analyses may prove to be incompatible with several rules and regulations in current engineering practice, the backfire on efforts to develop concrete technology and its research is hoped to be considerable, and in particular with regard to the use of cement-chemistry knowledge in obedience of the conditions under which concrete is made and required to perform.

SURVEY OF CONTRIBUTIONS

During the Fourth International Symposium on the Chemistry of Cements in 1960 F.M. Lea (1) suggested the adherence between cement paste and aggregate as a subject worth of exploratory research. Since then many studies in this field have appeared, among which the comprehensive survey by Alexander and Gilbert (2) is emphasized. The present principal paper (3) and the adhering contributions (4), (5), (6), (8), (9) bring forward new concepts and methods of investigations regarding the nature of adherence under various circumstances, while (10), (11), (12), (13) in particular deal with hydrothermal reaction conditions.

The principal paper, (14), on the durability of concrete, is a comprehensive, critical review of the complex problems and accumulated knowledge in this field.

The reaction kinetics of cement paste hydration as influencing the characteristics of concrete is discussed in (15) and (16).

An expansive mechanism for porous solids, e.g. hardened cement paste, as a feature in concrete deterioration processes is suggested in (17), while the importance of the pore-size distribution and its measurement is emphasized in (18).

The "intrinsic" reactivity between cement paste and aggregates is treated in (19) and (20), which deal with alkali-silica reactions. These are also mentioned in (5), in relation to adherence, and in (25 - see below) in connection with studies of seawater attack. Dedolomitization is discussed in (21), and the particular effects of pozzolans upon the chemical resistance of

glass fibre in cement paste are demonstrated in (22).

The "intrusive" reactivity of aggressive solutions on concrete is discussed in (23), the practical basis of which is aggressive, sulphate bearing ground waters, which also is the background for the contribution (24).

In more general, the aggressivity of sulphates, though with emphasis on sea waters is discussed in (25), (26) and (27), in the latter emphasizing the influence of cement manufacture parameters on the C_3A-content and sulphate resistance of cements.

The special effects of chlorides are treated in (28) and (29).

The discussion in (30) on the influence of the MgO-content on the quality of cements is an interesting example of the "chemical alertness" in research in a developing country, where exploitation of hitherto unknown raw materials must be important. Implicitly the paper also shows, however, that concrete technology research in the "old world" has not contributed sufficient information on the autoclave-test for MgO as a reliable model for the behaviour of concrete, which hardens under atmospheric pressure at temperatures below 100°C.

The above introduced designations: "intrinsic" and "intrusive" reactivity gives a distinction between chemical reactions between the constituents - cement paste and aggregates - of concrete, and reactions by chemically aggressive solutions, primarily attacking cement paste while penetrating into concrete from the environment.

Admittedly, this is a crude distinction which neglects two important things:

(1): Any of the chemical processes concerned involves heat transfer and humidity exchange, i.e. energy conversion in the entire system: concrete and environment.

(2): The reaction kinetics encompass the entire energy conversion in concrete from the commencement, i.e. setting and hardening of the cement paste, until the ultimate stage of thermodynamic equilibrium of the reacting phases of the system is reached.

When these two basic conditions are observed it becomes clear that adherence must be conceived:

(1) as created during the early hydration of the cement paste

(2) as subject to continuous transition during concrete performance

(3) as the seat of migration of substances during any "intrinsic" or "intrusive", deleterious process.

Herewith adherence is "brought in place" as an integral part of the research on concrete durability. At the same time it is implicitly stated that interpretation of experimental or theoretical model studies of durability need clarification of the "model" thermodynamics and reaction kinetics in relation to those of the intended applications.

THE ENERGY CONCEPT

A certain fraction of the chemical energy in cement is converted into bond-forces between the cement-paste components and the surfaces of aggregate particles, fibre and reinforcement bars etc. during the setting-hardening process, see TABLE 1. The creation of these bond-forces is decisive for that the conglomerates of cement, water and aggregates, can become useable building materials.

ENERGY INPUT
Available energy in cement: 1450-1900 kJ/kg cement
ENERGY CONVERSION
1. The creation of stable, intrinsic bond-forces and morphological structures of solids, solutions and air in cement paste during the setting and hardening phases of processing.
2. The concurrent creation of bond-forces between cement paste components and aggregate particles, fibre and reinforcement bars.
ENERGY CONSUMPTION
3. The development and consumption of heat during hydration as the driving force of the chemical reactions between cement and water.
4. The development and consumption of energy in additional chemical reactions, as e.g. with pozzolans, admixtures.
5. The consumption of energy in rheological deformations, microcracking etc.
ENERGY PRESERVATION
6. The preservation of energy in cement particles, at less than complete hydration (available for subsequent hydration during performance).

TABLE 1.
The energy input/output feature in the manufacture of concrete and cement products. The energy-efficiency is represented by the energy conversion into thermodynamic stable hydrates and bond-forces within the cement paste, and gluing the cement paste to the aggregate particles. The energy conversion is decisive for the performance, while the energy consumption as heat is important in modern manufacture economy and efficiency.

POWER AND INCINERATION PLANTS
Cooling channels Coal storage basins Chimneys Foundations
OFF-SHORE PLATFORMS
Submerged sub-structures Super-structures in wetting/ drying zones
HIGHWAYS AND BRIDGES
Pavements Sidewalks Bridge decks Draining mains and wells etc.
WATERWAYS AND DAMS
Natural, acidified waters Polluted waters due to urbanisation, strip-mining etc.
SEWER MAINS AND CLEANING PLANTS
Domestic waste water Industrial and agricultural waste waters
TUNNEL AND MINE SHAFT LININGS
DEEP BOREHOLE CASINGS AND PLUGS
SWIMMING POOLS

TABLE 2.
Types of structures of importance in modern societies, and exposed to environmental energy, the aggressive effects of which are enhanced by heat, alternate heating/cooling, concentrated aggressive solutions and low pH in waters etc.

During use in practice the materials are exposed to transformations induced by additional available energy, intrinsic and intruding from the environments. The durability depends upon, how the entire system of materials and environments converge towards ultimate thermodynamic equilibrium.

The research associated with cement industry has until recently concentrated upon energy conversion in cement manufacture, which per unit of product is by far the most energy-intensive category of cement/ concrete production.

The engineering and construction sector has traditionally been concerned with energy, primarily as (1): potential energy in structural masses, and (2): kinetic energy in mass transport during construction operations, but not with monitoring of the conversion of the available energy in cement in the making of products or concrete.

RAPID HARDENING CEMENTS
HIGH CEMENT-CONTENT
WATER REDUCING AND DISPERSING ADMIXTURES
INTENSE, HIGH-FREQUENCY VIBRATION
HIGH-TEMPERATURE CURING
EARLY FORM REMOVAL
RAPID DRYING
HOT ENVIRONMENT
ABRUPT COOLING
EARLY IMPOSING OF LOAD

TABLE 3.
Characteristics of concrete manufacture conditions, encompassing as well neglectance of "good practice" as sophisticated construction operations and precast and product manufacture.

Conceptual research on energy conversion in cement uses - during manufacture and while being used - is therefore rather homeless, yet acquiring increasing impact on both cement industry and engineering practice.

The problems herein are aggravating with the modern development of concrete usages.

Much concrete is now exposed to more severe environmental aggressivity than incorporated in the philosophy of conventional research. TABLE 2 exemplifies some such performance exposures.

Particular references are given in (23) and (24) to aggressive sulphatic ground-waters in East Europe (foundations, tunnel linings etc.). More severe problems with aggressive ground-waters are met in the Middle East, as described for instance by Fooke and Collis (31), and in hot regions elsewhere.

Warm, aggressive waters are also met increasingly in construction work for industrial production, in the infrastructure sector, and in areas with condensed habitation. Acidification of natural waters, due to air-borne pollution, or to strip-mining or agricultural and foresting development etc. is in progress, and in developing countries the increasing accumulation of masses of people in townships with primitive urbanisation facilities may create severe chemical pollution of surface- and ground-waters, often in connection with considerable changes of levels and availability of water for consumption.

In the temperate and cold regions the intensive de-icing practice to facilitate road- and highway utilization in winter seasons is adding chemical energy to the deleterious effects of freezing-thawing. The processes concerned are still not quite satis-

FIGURE 1
Configuration of the "constructive" energy conversion during the making of concrete. The hydration of cement paste results in the creation of inherent strength and cement paste-aggregate bond.
Concrete is a material of excellent durability, if adequately cured, whereas "destructive" energy may result in acceleration of deterioration, if the processing does not facilitate efficient energy conversion, as for instance by too rapid release of the heat of hydration during early curing.

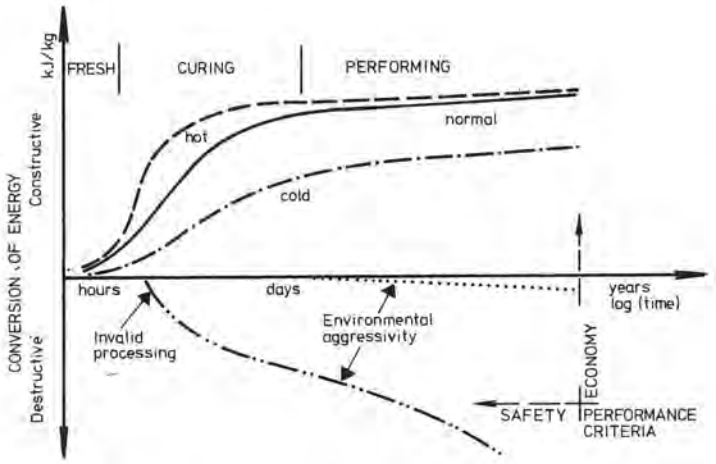

factorily explained, yet demanding increasing resources for repair to pavements, sidewalks and bridge-decks. It is unexplored, but likely, that saline run-off melting water may enhance the aggressivity of ground-water towards concrete exposed to capillary suction from beneath.

Severe stress conditions are also to be anticipated for much concrete during the manufacture phase, due to the intensity of the development and transfer of heat of hydration under conditions which are incompatible with the prevailing research methodology. TABLE 3 exemplifies such manufacture conditions, which are in contrast to that most laboratory experiments concerning adherence and durability research are made at "room temperature" conditions $\sim 20^{o}C$. However, some researchers do apply supplementary experimental series at higher constant temperatures in order to investigate accelerating effects of heat, see e.g. (5), (19), (22), (25). (Even the use of steam-cured cement mortar specimens are recommended (24) for comparison of the sulphate resistance of different cements).

The traditionally accepted custom to work "isothermic" surely facilitates communication and broad interpretation of findings among researchers. The logical basis is that development and transfer of heat during the setting/hardening process are of no significance in small mortar or paste specimens if dealt with in the temperature/humidity constancy of modern laboratory conditions. Such experiments, therefore, represent adequately homogeneous models of cement paste and mortar behaviour. Correspondingly, adherence and durability studies usually interpretate the behaviour of concrete, as if it is isothermic hardened (mostly at $20^{o}C$, 100% RH), and also rely upon comparable, simplified models of aggressive exposures.

The reaction kinetics of cement hydration as decisive for the adhesion within the cement paste and for the cement-aggregate adherence is discussed on the basis of electro-chemistry in (15) and (16). And in a general way the incompatibility of current experimental and standard-specification practice on the one side, and the actual conditions for the making and uses of cement products and concrete is emphasized in (23), thus sustaining several statements on this issue in the principal paper on durability, (14).

It is characteristic that deleterious energy conversion during concrete performance appears visible as cracking, expansion, distortion, spalling, dissolution etc., and these phenomena are recognizable and empirically comparable when used as measures for durability criteria by laboratory experiments, as e.g. reflected in (19) regarding alkali-silica reactions, (25) regarding sulphate attack, and other contributions.

In contrast, the early damages due to excessive rates of energy conversion and consumption during cement paste hydration - barred further hydration, plastic shrinkage thermal conditioned microcracking - do not appear in the conventional laboratory practice and are therefore in general not experienced by researchers to develop in field scale concrete.

To the studies of adherence and durability are therefore coming to belong, not only initially deleterious effects of modern concrete manufacture, but also synergetic effects in field concrete of invalid processing plus subsequent added "destructive" energy from the environments (or inherently available energy) in contrast to protected experimental models.

FIGURE 1 configurates that in principle these problems express the need to introduce energy conversion during cement hydration processing, and during subsequent additional conversion of inherent and environmental available energy, i.e. an overall reaction-kinetic concept, in the research.

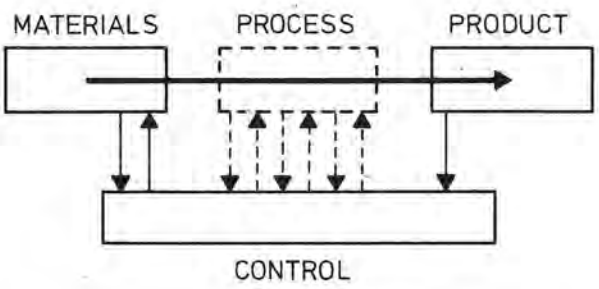

FIGURE 2
Process control in industry consists of check on the primary materials and their entrance in the processing, monitoring of the manufacturing operations with on-line recording of influential process parameters, and final check on the products' compliance with the desired characteristics.
Concrete manufacture is virtually without on-line process control and possibility to monitore that the process results in the required concrete characteristics. And these are largely tested on specially protected test specimens, which do not reflect the impact of the process-parameters on the ultimate characteristics of the concrete as it is placed for permanent performance.
(From Idorn (32)).

The mentioned dialectic "contraposto": the aggravated impact of "destructive" energy on modern concrete behaviour on the one side, and the still prevailing use of simple experimental models, which deliberately eliminate reaction-kinetics from the research on the other side, is also reflected in the principles of concrete control in practice, versus monitoring process-control in high-technology industries, as shown in FIGURE 2, from Idorn (32). It appears: standard concrete control relies exclusively on the testing of the materials and of control specimens, which are not representative of the ultimately attained product, in contrast to the monitoring principle, which continuously records how the processing technology will result in that the specified ultimate characteristics be reached. Also in this context it is apparent that the heat development and consumption during cement hydration is to be considered a valid means of monitoring, and therefore must be taken into consideration in the further progress of research.

The emphasis on cement clinker mineral composition in several contributions notably (24), (25), (27), are demonstrating, how far cement industries have utilized cement chemistry research to conduct their predominant intents for making concrete durable against attack of sulphates in aggressive solutions.

The discussed new aspects in modern cement using technology indicate, that energy additional to that from the cement has commenced to gain relatively more influence than the chemical energy in the cement itself, both on the course of the concrete manufacture processing and on the behaviour during performance. This trend in the background for research, does not degrade the importance of cement chemistry knowledge, but invites to more comprehensive utilization of basic chemistry in the planning and interpretation of technology oriented research.

The contributions (10), (11), (12), (13), (22), are demonstrating the impact of adherence and durability as technology development issues of innovative process and product development with cements, showing that industry exploitation of market potentials have commenced to play a part - glass fibre reinforcement, autoclaved lime/silica technology etc. To complete this picture of a "renaissance dawn" to come for new development of cementitious materials, contributions on superplasticizers and on polymer-impregnation are missed and must be sought elsewhere.

Practically any of the mentioned new developments are closely associated with the energy situation, either as means of savings - as e.g. pozzolans, superplasticizers -, or as means for the attainment of exceptional adherence and durability - e.g. polymer-impregnation - or as enabling less voluminous and lighter products - e.g. glass fibre reinforcement.

A more complete analysis on adherence and durability with respect to the perspectives of the energy situation and to the issues seen in a context of thermodynamics and reaction kinetics is not warranted by the presented contributions, but none the less needed to point towards. This is particularly so, because the frequently met attitude that concrete is an energy extensive building material, does not hold true, when the total quantity of concrete produced - by now about 7000 million tons a year - and the 1980-2000 period's need for increases are considered. The contributions therefore are to be considered forerunners for a decisive orientation of more research to meet these demands, including elimination of unforeseen failure risks and of unreasonable repair needs, as the "defensive" strategy goals, and higher energy efficiency of cement uses as the "offensive" strategy.

THE PARTICULAR IMPORTANCE OF HEAT

In a general way it is widely known that heat is a driving force in the chemical process of cement paste hydration, and accelerates the strength development, if not lost to the environments. During many years' evolution of concrete technology the heat

development was, however, so insignificant in practice that it seemed justified to neglect this category of energy consumption as a parameter in research. The post-war need for winter-concreting broke the barrier of this inheritance, and monitoring of concrete making in cold weather which utilized the heat of hydration was developed and implemented in practice, based on combined utilization of works by Powers and introduction of maturity functions, Nerenst (33). The development of steam curing initiated long-term research at the former Concrete Research Laboratory, Karlstrup on the problems of monitoring the concrete processing by high-levels of heat development early during hydration, and Idorn in (34) suggested heat of hydration introduced as a general parameter in research.

Through continued work by Freiesleben-Hansen (35), (36) and others, computerised design/monitoring systems, by which the heat/strength development can be precalculated and continuously controlled, have now been established.

The gist of the concurrent technology development is that cement chemistry and cement production technology jointly with the civil engineering demands on rapid construction and early high strength concrete now often compress the development of heat during the phase of curing in much modern concrete. Consequently, thermal stresses develop, which exceed the mechanical resistance capability of the cement paste at early maturity stages. Invalidity - microfractures - caused this way, are irreparable, and become seats of deterioration, promoted e.g. by too abrupt cooling, and by later "intrinsic" and "intrusive" aggressivity.

This issue is implicitly treated in the contributions underlying the present general report, but deserves, in the opinion of the writer, to be profoundly taken into consideration in research on adherence and durability. This is not only to create means for effective utilisation of the energy converted into heat during hydration, but also because the complex of processes during hydration of cement and performance of concrete are all very sensitive to the time/temperature history of the material. Moreover, calculated development of energy saving requires theoretical and technological elucidation of the role of heat in processing.

CEMENT PASTE-AGGREGATE REACTIONS

Alkali-silica reactions are by nature hydration reactions and must be assumed to obey a time/temperature relationship akin to that which is established for the formation of calcium-silica-hydrates and alumina-compounds in cement paste. They depend upon mass-transport of $(Na, K)^+$ and $(OH)^-$ions through the interface-precipitates into the structure of siliceous aggregate particles. While this structure is being disrupted by

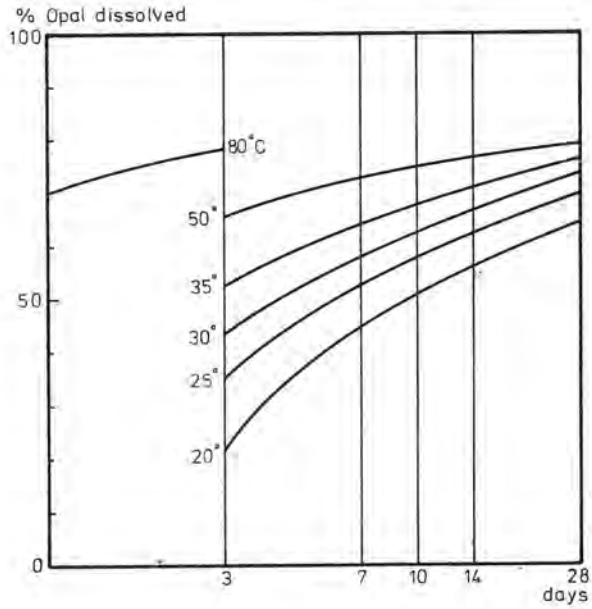

FIGURE 3
Graphic configuration of table 2 in Gutteridge and Hobbs (40) showing the percentage of Beltane Opal dissolved in 3 M NaOH at different temperatures and lengths of time of exposure. From Idorn (41)

the OH^-ions, SiO_2 is,in a gel-phase, migrating back through the interface, or through cracks opened by accumulated pressure in the particles, to precipitation as alkali-silica gel or lime-alkali-silica gel outside the particles. These are diluted as a consequence of the reactions and are left, either fractured due to the created interior pressure, or exceedingly weakened, if not completely converted into a gel or sol.

The rate and extent of alkali-silica reactions depend upon the concentration of $(Na, K)^+$ in solution relative to the Ca^{++}-concentration. It is significant that $(Na, K)^+$ suppress the concentration of Ca^{++} in the liquid of cement paste, see e.g. Malquori (37) and Lea (38), and increase the pH, thus facilitating the attack on siliceous aggregates.

The course of alkali-silica reactions are also significantly influenced by temperature, inter al because the solubility of $Ca(OH)_2$ is suppressed at rise of temperature, see e.g. Greenberg and Brunauer (39) who gave the thermodynamic functions for the solution of calcium hydroxide in water.

Also the solubility in alkali-hydroxide of reactive silica increases with temperature, as for instance shown by Gutteridge and

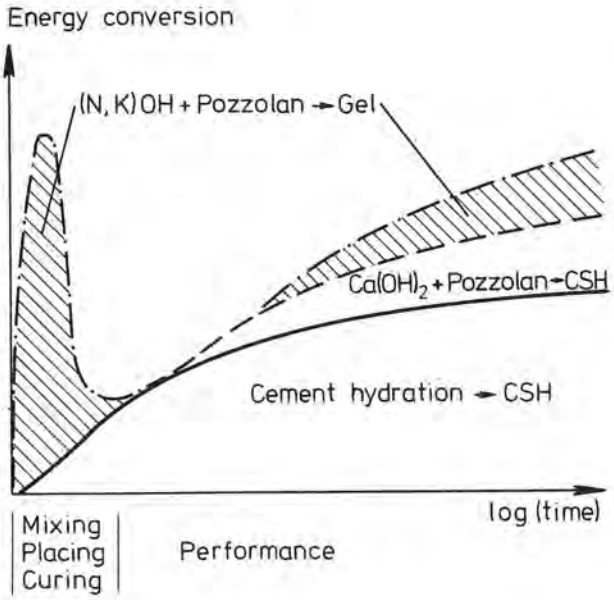

FIGURE 4
Qualitative comparison of the reaction kinetics of the hydration of cement in the presence of alkalies and pozzolans. At high heat of hydration, alkali-pozzolan reactions may forerun the intended lime-pozzolan reactions, but the developed alkali-silica gel may be metastable and alkali-reactions be renewed at later stages, e.g. at high exposure temperatures.

Hobbs (40) in experiments with finely ground Beltane Opal. Data for North-German opal, referred to in (19) corroborate these findings. Gutteridge and Hobbs' findings were discussed by Idorn (41), see FIGURE 3, emphasizing that the rapid dissolution at temperatures up towards 80°C (>50% dissolved in 1 day at 80°C) corresponds much more to the circumstances in modern concrete manufacture, than does the common use of 20°C isothermic storage of mortar bar specimens in the research. It must be kept in mind that an exposure of finely ground opal in concrete to 80°C would at the same time suppress the $Ca(OH)_2$ concentration considerably, and increase the pH towards 13.5-14.0 dependant upon the available quantities of soluble alkalies.

For several reasons these observations are important to consider in the planning and interpretation of the research.

First, alkali-silica reactions may in our time, due to increased concrete temperatures during early curing (high cement-content, high-strength cements etc.), outfold much faster than corresponding to the conventional concepts. Thus, the reactions may induce early cracking or be completely released while the "green" concrete is still deformable.

Second, in concrete, which is permanently exposed to elevated temperatures, continuous alkali-silica reactions will also continue to suppress the solution of $Ca(OH)_2$. It must also be considered that alkalies may be available from silicate minerals in certain aggregates, see e.g. Lemish(42), Malinowski et al (43),and (25).

Third, the viscosity of the C(N,K)S-H system surely depends upon its composition, as discussed e.g. by Krogh (44) and Struble (45), but must also be expected to depend upon the actual temperature level. This means that penetrability of gel of low viscosity into the surrounding, porous matrix must be considered in reaction kinetic studies as alternative to any pressure building up mechanism. Brown (46), Kennedy and Mather (47), and Idorn (48) have observed evidence of such "gel-impregnation" into ambient cement paste, though in concrete, which probably never experienced temperatures higher than about 30-35°C, and was exposed to cold climate conditions during its performance.

Fourth, the influence of pozzolans on alkali-silica reactions must be evaluated under consideration of

(1) the contents of soluble alkalies in pozzolans plus cement,

(2) the solubility of the silicious pozzolanic constituents in the given concentration of the alkaline solvent,

(3) the time/temperature dependency of the entire reacting system,

(4) the possible influence upon the reactions of constituents other than soluble silica, in particular alumina-compounds.

A quantitative analysis of these matters would lead the general report into a far too comprehensive investigation of contributions to the preceding sessions, and also to thorough reexamination of many older observations on alkali-silica reactions.

Qualitatively, FIGURE 4 is a summary of the presented, exemplified observations, and stipulates that:

(a) In modern concrete alkali-silica reactions may be pronounced during the concrete manufacture phase, and their effects may differ from those usually studied by research. Any laboratory study of the reactions should identify its time/temperature characteristics, and implementation for engineering practice must be on such basis.

(b) In modern concrete with pozzolans, it be natural, fly ash, silica dust etc. alkali-pozzolanic reactions may forerun lime-pozzolanic reactions, dependant upon temperatures, nature of pozzolans, alkalies in cement etc.

(c) The thermodynamic stability of alkali-silica gel compounds with more or less lime may not be reached in concrete within the phase of manufacture and curing. Observations by Nepper-Christensen and Nielsen (49) on the rise and decline of bond in experiments with glass marbles as aggregates sustain this observation. Also, ion-migration e.g. with external heat or additional chemical energy (e.g. de-icing, aggressive waters) may re-activate alkalies to renewed reactions with available silica. The protective effect of pozzolans is therefore not an a-priori matter of fact, in accordance with an observation referred to in (20).

(d) The development of adherence between any siliceous aggregate and cement paste is a matter of alkali-silica reactions under the conditions outlined above, and the dissolution of the silica-structure by OH^- is an essential feature, remarkable even in ancient concrete with high $Ca^{++}/(Na,K)^+$ ratio, see e.g. Idorn (50), referring to part-dissolution of the surface-layer in siliceous sand particles in a 600-year old lime-mortar and in Roman concrete from Cæsarea.

The results by Gutteridge and Hobbs, (40), and those referred to in (19) showed that even in "highly reactive" silica some 20-40% substance was undissolved in 3M NaOH after 28 days at 20-80°C, and related this to the presence in the opal of sub-microscopic/microscopic crystalline silica. This sustains earlier "reactivity ratings" from opal and pyrex-glass as the "most" reactive, through volcanic glass towards chalcedony, quartzite to crystalline quartz as practically non-reactive in concrete. As appears from the above discussion, such ratings should be re-examined with the entire "reacting concrete system" as the basis.

Turriziani and Rio (51) demonstrate another feature of interest in comparison with the Gutteridge and Hobbs results. They compared the so-called Florentin base-acid attack on two different pozzolans. The highest silica content (88%) gave the highest dissolution (53% SiO_2 in 28 days), indicating that for low-silica pozzolans, which also encompass some fly-ashes, the preventive effects towards alkali-silica reactions may be much less than for other ones, even if different alkali-contents are not considered.

The presence of calcium-alumina-sulphates in "aureoles", (4), (5), and their precipitation in dependence of the concentration of alkalies, see the solubility study (20), indicate that investigations with time/temperature sequences simulating concrete curing conditions would be rewarding for studies of the behaviour of the alumina compounds of the cements in cement-aggregate reactions.

Extended research on cement-aggregate reactions with slag cements could also be of interest, and it seems natural in this connection to include more work to examine the hypothesis presented in (17), because expansions within the cement paste itself might also be connected with the migration tendencies for ions in the metastable compounds. Also further studies of the pore-systems, as dealt with in (18), would belong to elucidation of the effects of hydration at higher temperatures than 20°C, since alternate precipitation/dissolution phenomena might profoundly change the pore-systems.

The newer development of cement paste with exceptionally low water-content and high degrees of compaction deserves much research for identification of their behaviour with regard to cement-aggregate reactions. Some of this category of cement paste possess strong alkaline liquids, but only in minute quantities, and this must be assumed in the long run to influence the character of interface reactions and also the stability of created bond forces.

THE CREATION OF INTERFACE

Fundamentally, the interface commences to be created when thin films of water are formed on aggregate surfaces during the mixing of concrete. Alkalies from the cement dissolve immediately in the liquid, and lime commences to be released by the hydration reactions. From this outset, with its concurrent creation of strong OH^- concentrations, any of the following cement-aggregate reactions may proceed in the interface-zone, dependent upon the available constituents and the conditions for mass-transport and energy-conversion in the system: pore-liquid - interface - interior of aggregate particles.

1. Basic Feature:

$Ca(OH)_2$ precipitates in the liquid "surface-film" on the aggregate particles during the hydration, and creates a solid "aureole", which in the course of time develops or enhances crystalline orientation and bonding or intergrowth with the matrix and with the aggregate surfaces.

2. Siliceous Aggregate:

Free OH^-ions break up the surface layer of the aggregate particles, and therewith the reactions may practically cease. In this case an alkali-(lime)-silica complex inside and outside the original surface becomes a significant element of the "aureole", which may completely intergrow with the outermost surface regions.

If the OH^-ions penetrate deeper into the particles the reactions may (1): either entirely transform the siliceous structure into alkali-(lime)-silica gel, which may build up sufficient hydraulic pressure on the surrounding cement paste through the interface-precipitates to impregnate the surrounding cement paste with gel, or to cause it to fracture. Or partial dissolution (low-permeability aggregate) may create local pressure regions within the

particles, and cause fracturing of the particles to proceed out into the cement paste. After fracturing due to swelling of gel in particles, dilute gel will flow out in the cracks and may become a significant constituent of the concrete.

3. Silicate Aggregate:

The free OH^--ions in the liquid of the paste may break up the structure in low-silica, glassy or crystalline, silicate rocks and release alkalies. These will add to the $(Na,K)^+$- and OH^--concentration. If such dissolution also releases free SiO_2-structures, these may become seats of formation of alkali-(lime)-silica gels.

4. Dolomithic Aggregate:

The free OH^--ions may break up the Ca-Mg-carbonate bondings, giving $CaCO_3$ plus $Mg(OH)_2$ plus Na_2CO_3, which in turn may react with $Ca(OH)_2$ to form more $CaCO_3$, and regenerate Na^+ and OH^-. The dissolution and migration of ions may encompass silica in aggregates, e.g. as in opaline-magnesium-limestone, or even in quartz, thus establishing a link to alkali-silica reactions. Thorough transformation of the interface precipitates and weakening of the interior of aggregates seem to be characteristic of dedolomitization rather than creation of expansive pressure in the reacting particles.

5. Calcium-Carbonate Aggregates:

There is evidence that intergrowth-reactions occur in the initially precipitated $Ca(OH)_2$-"aureole" on the surfaces of calcium-carbonate aggregate, and in the course of time both calcium-carbonate/calcium-hydroxide may exhibit diagenetic interlayer-growth and the CSH of the paste may develop similar phenomena. However, representative observations are still scarce.

A marked zonality in the composition of interface-layers is demonstrated in (5), and also dealt with in other contributions. Such phenomena were observed early in the history of petrographic examinations of concrete and referred to in numerous publications. The zonality has also frequently been found along internal cracks in concrete, and even on concrete surfaces (D-cracking "deposit cracking" (?)). Poole, in (52) demonstrated remarkable zonality in the interface-layers as a consequence of dedolomitisation. Apparently, one must anticipate that when the cement-aggregate system exhibits intensive migration of ions and substances, then will also variations in the physico/chemical circumstances tend to favour selective dissolution/precipitation phenomena.

It is not a priori possible to evaluate such diagenetic transitions as converging towards increased performance quality and equilibrium, or as contributions to deterioration, and also the position of cracks, for instance in a zonal interface system, ought to be cautiously interpretated at the present stage of knowledge.

There are no contributions which deal with the creation of interface with slag cements, at "natural" concrete curing conditions. The matter of particular interest in this respect is the limited availability of $Ca(OH)_2$ without appreciably high $(Na,K)^+$-concentration.

Thus, the creation of adherence and the stability of early formed interface compounds with slag cements need further research. It seems likely that in particular with slag cements the inherent reactivity of the cement paste itself should be examined in accordance with Litvan's hypothesis (17).

Some authors (3), (13), refer to the occurence of air-bubbles in interface zones. One ought to have in mind that compaction of fresh cement paste under some circumstances may cause tiny air-bubbles to adhere to the surface of aggregate particles, a purely physico/mechanical conditioned phenomenon.

ADHERENCE BETWEEN CONCRETE AND REINFORCEMENT

The adherence between the cement paste in concrete and reinforcement bars is discussed in (8) with zinc and cement paste as special experimental materials, implicitly referring to the possible passivating role of zinc-coating on steel-reinforcement bars. The development of calcium -hydroxyzincate is found as the interface reaction product in lime-solutions, whereas the presence of alkalies promote the formation of zinc-oxides, and soluble zincates are formed in pure alkaline solutions.

The electro-chemistry concepts on hydration, presented in (15) and (16) are also important for further exploration of the reaction-kinetics of the cement paste-metallic adherence and of the reaction products.

It seems likely that in a few years' time more research on the nature of cement paste-reinforcement adherence phenomena will become an important facet of further refinement of concrete construction design. Hitherto, transfer of stresses from concrete to reinforcement bars has been approached empirically with laboratory cast beams, columns, panels etc. as the basis for stress/strain and rupture-measurements and calculations. But effective transfer of stresses through identified interface phases have not been studied as an integral part of civil engineering design. It is therefore indicative of a trend for future research to designate (22) a pioneering study in this field, although with glass-fibre as the reinforcing agent, not ordinary steel bars, and therefore of interest for application in cement-product industries, rather than in civil engineering construction development.

Considering steel reinforcement, even the initial dissolution of alkalies and CaO in the liquid of fresh concrete will cause Fe to be dissociated and Fe^{++} to precipitate in a sequence with Ca^{++} as hydroxides

FIGURE 5
Concrete structure in a Middle East country. The concrete is thoroughly cracked due to severe corrosion of the reinforcement bars with expansive forces developed during the formation of corrosion-products. The corrosion is probably enhanced by capillary suction of salts from the groundwater, and definitely by the temperature-conditioned acceleration of all the involved physico/chemical processes.

creating a passivating layer at pH∿12-13.5 as a stable barrier against further corrosion. However, if the pore-liquid of the cement paste is neutralized by access of O_2 or CO_2 or by saline solutions with SO_4^{--} and Cl^-, further electrolytic dissociation will be promoted, and more Fe-hydroxides and complex salts will precipitate. This course of reaction (requiring available free energy) is destructive for the adherence and also for the concrete as such.

In hot countries the activation energy level enhances the course and rate of corrosion. FIGURE 5, from Idorn (32) is a typical example of structural failure attained in a course of 5-6 years in an exotic climate. FIGURE 6 is a configuration of the corrosion features which are characteristic of such environments. Fe^{+++} compounds are precipitated instead of the ferrous-compounds, and this causes pH to decrease to 2-3, see e.g. Bastiansen et al (53), and strong acids to accumulate in pockets created by the expansive pressure which develop because the trivalent, complex hydroxides are 2-3 times more voluminous than are the divalent ferro-hydroxides. Possibly also osmotic pressures and crystallisation pressure exerted by gypsum, see e.g. Dreyer-Jørgensen (54), are involved. As can be seen in FIGURE 5 the release of energy is powerful enough to create deep, longitudinal cracks over reinforcement bars of which there after a few years' time may be only complex Fe^{+++} hydroxides etc. and no load-bearing capability left.

FIGURE 6
The sketch outlines the mechanisms of corrosion of reinforcement bars in concrete in warm, saline environments, and also the primary reactants and resulting corrosion products. The configuration is deducted from experienced cases of complete disappearance of metallic iron in a few years' time concurrent with the devastating exertion of expansive pressure from the corrosive "cells".

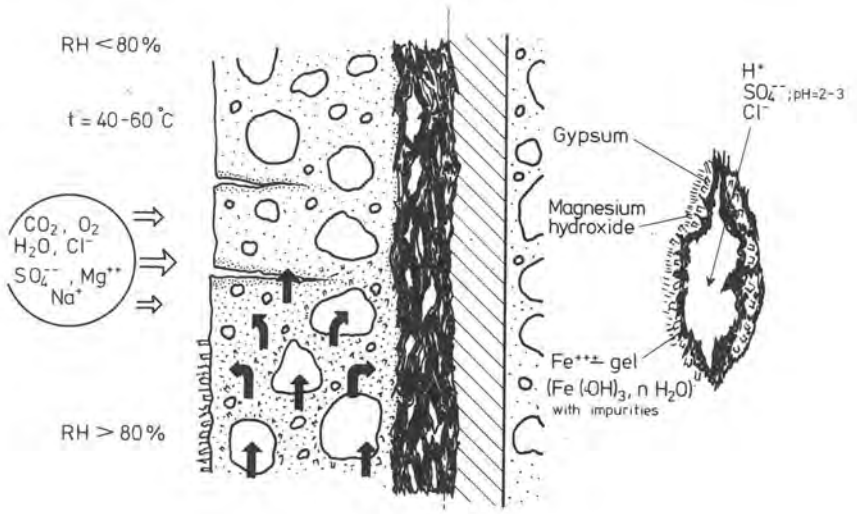

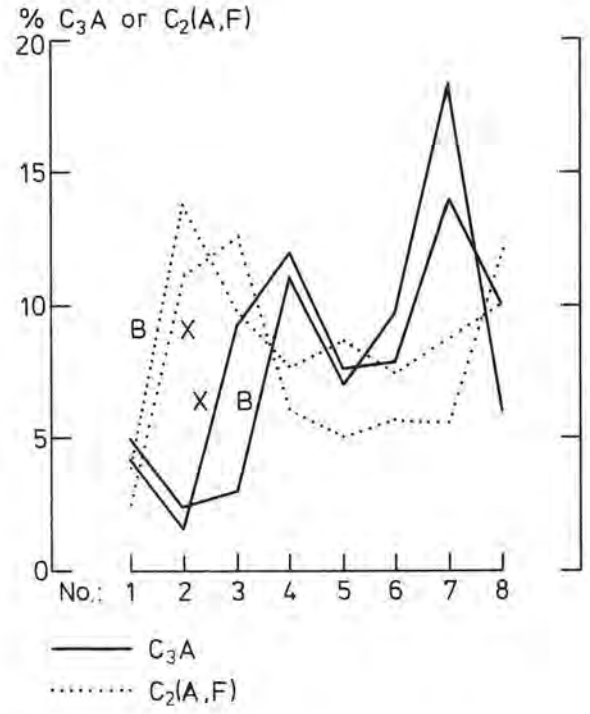

FIGURE 7
C_3A and $C_2(A,F)$ contents, Bogue-calculated (B) and XRD-measured (X), of eight ordinary portland cements, referred to in (25).

Both in hot and temperate regions the progression of corrosion after the initial formation of passivating Fe- and Ca-hydroxides as the adherence "aureole" around reinforcement bars may be caused either by high cement-content with initial heat-induced microfracturing during the hydration, or by the use of too low cement-content which cannot provide sufficient impermeability and strength to the concrete to prevent access of O_2, CO_2 or saline waters for reaction with the reinforcement. Also many other factors under the heading "good or bad concrete practice" are involved.

Consequently, the nature and stability of the adherence between cement paste and reinforcement are important, both for the composite, statical function of reinforced concrete, and for the performance reliability of concrete structures. The conditions for the design of optimum concrete composition and of concrete making procedures therefore also depend upon further progress of the research on the nature and characteristics of the adherence phenomena.

THE EFFECTS OF SALINE WATERS

Besides the question of different reaction-kinetics in laboratory mortar specimens and in structural concrete, there is one problem emanating from the contributions (23), (24), (25), (26) and (27) on sulphate resistance of cements and concrete, which in particular deserves a general discussion. This is the registration and the stipulated influence of the C_3A-content in cements on the resistance of concrete to the aggressivity of saline sulphate waters.

Criteria	Sample No:							
	1	2	3	4	5	6	7	8
$C_3A < 10\%$ B&X	+	+	+	-	+	+	-	-
$C_2(A,F) < 10\%$ B&X	+	-	-	+	+	+	+	-
$B-X \leq 2.5\%$	+	-	-	+	-	+	-	-

TABLE 4
Suitability (+ or -) of the eight ordinary portland cements referred to in FIGURE 4, evaluated according to the criteria: $C_3A < 10\%$ (B&X), for sulphate resistance, $C_2(A,F) < 10\%$ for strength capability, and $B-X < \pm 2.5\%$ for reducing ambiguity. Cements Nos 1 and 6 meet the criteria.

Schrämli (55) revealed considerable ambiguity among researchers about the net benefit by specifying the use of low C_3A cements for concrete. He also found a remarkable discrepancy between Bogue-calculated and XRD-measured contents of C_3A in cement clinkers.

The principal paper (14) discusses these uncertainties, and further information is extractable from (25). FIGURE 7 shows the C_3A and the $C_2(A,F)$ contents of eight portland cement samples, Bogue-calculated (B) and XRD-measured (X), respectively (originating from (25), table II). For C_3A the difference between B and X varies from 0.3% (sample 5) to 6.3% (sample 3). For $C_2(A,F)$ the difference varies between 1.4% (sample 1) and 3.5% (sample 5). It also appears that a low C_3A-content may or may not be obtained by a high $C_2(A,F)$-content, compare for instance sample 1 and 2. The quality of the eight cements as regards sea water attack is compared in TABLE 4 by introduction of the following three criteria:

(a): $C_3A < 10\%$, both by B and X - as a reasonable sulphate resistant limitation.

(b): $C_2(A,F) < 10\%$, both by B and X - because the ferrite-compounds are not strength-contributors and thus represent energy waste in concrete.

(c): $B-X < \pm 2.5\%$ both for C_3A and $C_2(A,F)$ so as to reduce the ambiguity of the classification of the cement composition for the consumer.

It appears that cement sample No.1 and No.6 comply with these three criteria. However,

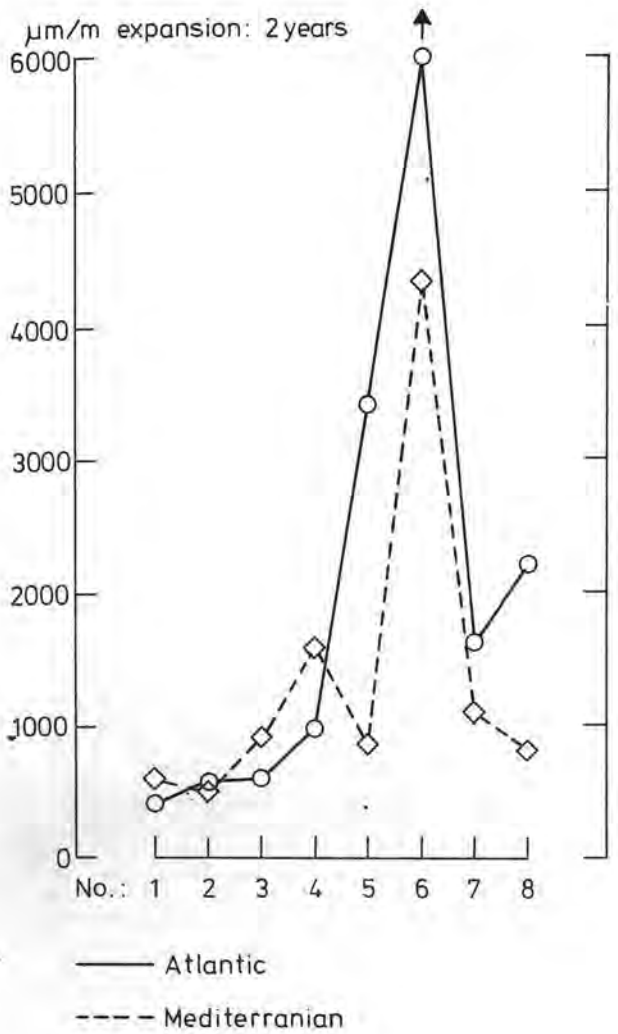

FIGURE 8
Expansion, after 2 years in sea water (Atlantic and Mediterranian), of mortar bars made with the eight ordinary portland cements, referred to in FIGURE 5 and TABLE 4. Cement No.6 which meets the three quality criteria in TABLE 4 shows the highest expansions. Cement No.7 with 14 or 18% C_3A (B or X) shows much less expansions. Cement No.1 is good according to all four criteria.

when the expansions of mortar bars in sea water, as displayed in FIGURE 8, are added as a fourth criterion, then only cement No.1 can be said to comply, since No.6 has the highest expansions of all samples, while cement No.7 with 14% (B) or 18% (X) C_3A shows much less expansions.

The results reported in (27) about correlations between the C_3A-content (Bogue-calculated) and particular burning/cooling circumstances during the cement manufacture, sustain recent results by Locher (56). It appears that considerable variations in C_3A-content for one brand of cement may occur in dependence of the cooling conditions, which may well be at variance in cement manufacture under forced changes of fuel, use of mineral admixtures, cost-savings efforts etc. The principal paper (14) does discuss these matters in more detail, and also their influence on the resistance of cements to sulphatic solutions of other clinker components etc.

Thus, altogether a very complex picture exists. This is what the general report must emphasize, because engineering practice in general is served by advisory or compulsory regulations based upon simplifications, which have a weakening basis in the now attained cement chemistry knowledge.

The aggressivity of chlorides under rather specific circumstances are discussed in (28) and (29). There is a broad background for supplementary investigations in serious problems for construction and building:

(1): Continuous progress of deterioration of highways, sidewalks, bridges etc. where de-icing is common practice in winter seasons.

(2): Permanent exposure to temperate saline waters in swimming pools.

(3): Penetration into concrete of saline ground-waters and wind-borne seawater spray in hot countries.

It is characteristic for chloride attack that both concrete and reinforcement are practically defenseless, if the energy activation level is high, and the concrete permeabel. This is why quantitative assessments of exposure conditions as germinating the release of the destructive energy conversions have good chances to exhibit big returns on research investments.

FIBRE REINFORCEMENT

For many years asbestos fibre have been used as reinforcement in cement based products to provide excellent adherence and durability characteristics attained by empiric, technical development. In recent years glass-fibre have been developed as alternative reinforcing agent. The particular aspects of adherence, and of the stability of the interface structure and constituents, are presented in (22).

It is shown that if the bond is enhanced between fibre and cement matrix there may appear a concurrent decrease of strength of the glass substance, and thus a reduction of durability of the product. It is also shown that the presence of pozzolans in the cement matrix greatly reduces the corrosion of the fibre surfaces. There does not seem to be a correlation between the amount of free alkali in the specimens and the degree of glass corrosion, while curing at high

temperatures (80°C) does aggravate the corrosion, a finding which is in accordance with the results by Gutteridge and Hobbs, referred to above. These observations confirm that a more complete study of the beneficial effects of the various pozzolans might provide additional knowledge of considerable practical interest.

Supplementary investigations of these matters must be anticipated to be important for the further innovation of fibre-reinforced products. The interface phenomena might be found in particular to be sensitive to the processing conditions, to the type and dimensions of fibre materials, to the use of superplasticizers and special pozzolans, to the alkalinity of the matrix etc. A wide range of opportunities are thus awaiting determined industrial exploitation.

POZZOLANIC MATERIALS

The effects of pozzolans in glass-fibre reinforced products are discussed in (22) as a deliberate aid against deleterious alkali-silica reactions. Historically, pozzolans have been widely used as a means of cement (energy) saving, to moderate heat development during curing, and to improve sulphate resistance of concrete. The present intensification of the use of pozzolans for the utilization of fly ashes and other types of siliceous materials from dust-collectors raises issues for the research, which have not been much pursued for a number of years. Malquori (37) compiled convincing evidence that pozzolan-granula in cement paste are corroded and surrounded by layers of gel-like, hydrated calcium silicates. Thus, the high specific surface of the pozzolans was found greatly to enhance the kind of reactions which are designated creation of adherence or bond, if the pozzolanic material has the size of aggregate particles, instead of cement fineness. Malquori also refers to reactivity of the alumina in pozzolans, which in the presence of sulphates react to give calcium-sulpho-aluminates.

The different quality of pozzolans as means for increasing the sulphate resistance of concrete is mentioned in (25), but the role of alkalies and of the initial reaction kinetics remains to be described.

The various available fineness of pozzolans, from about that of ordinary cement or less (some fly ashes) to more than 15000 cm^2/g (ferro-silicon dust, or refined fly ash), or even 24000 cm^2/g (metakaolin) and the influence of particle shape of the pozzolanic particles - rounded spheres, partly hollow in case of fly ashes, glass splints in case of volcanic tuff etc., or fragments with high internal surface as the Greek Santorin Earth or the Danish diatomaceous earth, also remain to be examined in depth, and the differentiated effects identified.

Alkalies were found by Malquori (ibid) to combine into the calcium-silicate-gel complex. However, it was noted that the presence of alkalies has influence on the reaction-kinetics, among other things due to its suppression of the solubility of calcium hydroxide. The observations do not allow conclusions as to whether the fixation of alkalies early during pozzolanic reactions is permanent and stable, or merely loose and liable to transition.

Turriziani and Rio (51) found that the reaction between lime and silica is the initial reactivity, also in cases where alumina takes part in the further reactions, and becomes absorbed in the precipitated gel-complex. (The alkali-content of the pozzolans was not given).

These scattered evidence serves the purpose to stipulate the importance of thorough investigations of the systems N,K - C - S - Al,Fe - H_2O under real reaction conditions in concrete and in cementitious products, also when siliceous aggregates are used in cement fineness as pozzolanic, mineral admixtures to improve adherence or durability or both at the same time.

HYDROTHERMAL PROCESSING

Hydrothermal reactions have for many years been utilized on account of the intensive creation of adherence-forces and the high degree of ultimate stability it is possible to attain with mixtures of $CaCo_3$, SiO_2 and H_2O during a brief processing time.

In (10) the synthetis of fibrous CSH crystals by hydrothermal reactions is reported. The solubility of lime was found to decrease in the presence of alkalies, while the solubility of silica increased when the system contained alkalies. Different compositions of the reacting system therefore gave different reaction products: tobermorite, xonotlite, pectolite etc. The influence of the alkalies was conspicuous, the most spectacular result being the manufacture of "rock-wool" fibre of lengths $\sim$200 µm. These were obtained with C/S = 0.8 and treatment in a 2N KOH solution at 180°C for 10 days. In general $CaCO_3$ dissolved much slower than did SiO_2 and fibre was only obtained when both alkali and calcium sources were carbonates, and K^+ions were present. There were no reactions observed without alkalies.

Compressive strengths over 150 N/mm^2 have been reached with autoclaved concrete, using quartz aggregates, (11). The high strength is attributed to intense interface reactions resulting in 11 Å crystalline tobermorite intergrowing with silica in the corroded surface of the quartz aggregate. In (12) it is shown that decreasing contents of quartz in the aggregate resulted in less strength. Rapid decrease of elastic yield (ratio of strain energy during unloading to the one during loading) occurred in concrete with non-reactive aggregates for stresses $\sim$60% of failure, whereas the elastic yield was constant and high (90%) up to failure in concrete with quartz aggregates.

Special experiments, referred to in (13)

disclosed that under certain circumstances an air-bubble porosity structure may appear associated with the cement paste aggregate interface. Autoclaving nearly eliminated the pores in the case of quartz aggregates, and this also increased the frost resistance.

Altogether, the mentioned contributions invite to further studies of the interface creation and composition at hydrothermal conditions, and in particular to additional exploratory research on the influence of alkalies on the reaction kinetics and the thermodynamic equilibria of the CSH systems at hydrothermal conditions.

THE FUTURE RESEARCH

In 1941 G. Kalousek (57) said:

" ---- the mechanism of the expansion of concrete is as complicated as the setting and hardening phenomena. For this reason the need of fundamental research as to the ultimate products of reaction for conditions simulating the normal exposure of concrete is definitely indicated. Phase-equilibria studies will show the end products of reaction".

This statement may be read as an early anticipation that expansion, as a phenomenon of deterioration, is one among the mechanisms of energy conversion and their consequences in concrete, which need to be understood.

Maybe it is today too much of a generalisation to say that cement paste hardening, cement paste-aggregate (and pozzolanic) reactions, corrosion of reinforcement, and saline water attack are merely each their species of hydration reaction. However, this seems closer to the truth, than to consider causes of early deterioration exploitable by means of 20°C isothermic laboratory models. And for some years it has been possible to make on-line recording of the temperature development in concrete during the curing phase, and to connect the thermocouples to a maturity-computer, whereby the early stress/strength development in the concrete can be calculated continuously, and the processing-monitoring can be used to change the course of hardening if need be, according to predesigned criteria and methods.

Practising of this technology can improve the durability of concrete considerably, and, in fact, the attainable benefits do not require more knowledge from chemical research than what Kalousek outlined in 1941: "to understand concrete under the conditions which govern its making".

The problem for research in this respect therefore is primarily in the second category of the R&D entirety: Development. In other words, it is a problem of cohesive technology system approach and instrumentation.

Progress along this line requires that market opportunities can be envisaged. The total concrete production in the world is of the order of magnitude of 60-70.000 million m^3 up till now, and at present are added about 3000 million m^3 a year. The production will converge towards at least 9000 million m^3 of concrete a year at the end of the century (corresponding to a world consumption of 300 kg cement per capita annually at year 2000) if things go unchanged.

With the present development of microprocessors such market potentials are attractive for the monitoring system and equipment industries, also because the market is a mix of innumerable big and small concrete-making customers. The attractiveness also stems from the increasing concern about performance reliability of concrete structures, or in other words: about adherence and durability.

Nuclear Power Agencies are presenting requirements for borehole-plugging materials of 1000 years' trustworthy behaviour, while power plants, and many other kinds of construction must be reliable without repair need for 30-40 years' use.

In contrast USA in 1978 estimated a 6.3 billion $ budget for repairs alone to Highway Bridge decks, and about 105,000 bridges needing repairs. Comparable data from elsewhere are not easily accessible, but a great part of early concrete construction works - dams, harbours, bridges, tunnels etc. - in many countries are approaching total depreciation or are in fact long overdue, but now very expensive to replace. And concurrently, the real depreciation periods are going short where aggressive environments play a part, while the need for the use of concrete to new construction and building development is increasing and the cost of repair-concrete may exceed that of construction-concrete by a factor of 10. At the same time repairs are unduly contributing to depletion of the materials-, energy- and capital-resources.

These inherent contradictions in the situation:

"Data and methodologies are available to improve the durability of concrete structures. The need to do this is broadly acknowledged as urgent, while the perspectives for growing demands on the materials are equally obvious",

ought to stimulate the research community to launch effective R&D-efforts based upon cement chemistry application in accordance with the conditions for the making and performance of concrete.

An immediate look at the theme-contributions does not indicate, however, that the cement and concrete manufacturers and users are preparing for remarkable upgradings of concrete technology research and development. To advance the utilization of knowledge accumulated by the congress in the prevailing systems will therefore become long-term shoehorning efforts on the part of the researchers.

But farther away from the research benchwork, certain changes in the environments are appearing, which must be considered - also for the planning of the present scientific priorities in the research.

Steel-, fuel- and power-industries are in the commencement of an era which will make them users and producers of limestone, slag, fly ashes and gypsum etc. in quantities which in several countries will exceed the present cement production - though by far the future needs for inorganic binders.

Chemical industries have only a few years ago commenced to develop powerful, liquid admixtures, not yet more than empirically combined with the above primary materials, and synthetic fibres. And the border-land between inorganic and organic polymers is also in an early phase of exploration.

Electronic industries are awaiting acceptance of processing technology in concrete production, but prepared to implement soft- and hardware.

These categories of industries possess comprehensive R&D-organisations with established knowledge of effective planning and management, and experience with "transfer into technology". Besides, they have elaborate, professional R&D-education, as appears e.g. in the work of EIRMA (European Industrial Research Management Association) and IRI (Industrial Research Institute) etc.

Thus, there is, strategically considered, more capability available for forceful efforts to make concrete durable than as yet called upon for investments.

Although one must realize that the present congress was not requested to outline new research strategies and the present report accordingly only can point towards the new incitaments for adjustments of the research, it is timely to say as a terminating statement, that the germination of new advances in concrete durability must have cement chemistry research as the driving force. But also, that fruitful harvesting depends upon more than that.

CONCLUSIONS

It is in accordance with the principal paper (14) to say that the complexity of the theme: interface reactions, is too comprehensive to make an adequate synthetis possible in one paper. This has, also for the general report, necessitated severe restrictions on the discussions of the individual contributions, and is the reason why the following concluding statements refer both to matters discussed above, and to items, which it has not been possible to deal sufficiently with, despite their importance for research and practice.

There are seven concluding statements, referring both to scientific problems and to those connected with the utilisation of the research in practice.

Herewith an attempt is made to stimulate the researcher in seeing under which circumstances, i.e. chemical and physical conditions, the material concrete is made and used so that dialogues within the research communities may enhance alertness about desirable adjustments to forthcoming work. At the same time, the general report aims at explaining to the civil-engineer that the rentability of building and construction with concrete can be considerably improved by application of modern chemical knowledge rather than by reliance on mechanistic models of concrete behaviour as the basis for specifications and working procedures.

To promote these views results in the risk that researchers may find the scientific discussion too superficial, while the civil-engineer may still consider the concepts too far from current practice to be of immediate economic advantage.

This risk is accepted, and the seven concluding statements are as follows:

1. Adherence and durability are inseparable fields of studies within the framework of diagenetic alterations of concrete in the course of time.

Consequently: research experiments with "static" mechanical disruption must be appreciated as momentary flashlights on the nature of concrete, while development or degradation of characteristics under isothermic laboratory storage must be interpretated as "linearly projected" reflections of the reaction kinetics in real concrete.

2. The refinements during recent years, of measurements of cement clinker compositions is a valuable asset for reevaluation of the importance of cement properties for the behaviour of concrete.

The various ways of counting the C_3A-content of cements is an example of how civil-engineering now needs the service of cement chemistry for more nuanced information on cement characteristics, corresponding to the demands on concrete in widely different environmental and manufacture situations.

3. Evaporation during concrete manufacture and performance is a major physical factor influencing the consequences of the energy conversions in concrete.

The omittance of physically conditioned aggressivity in the principal papers and the general report was a decided restriction in order to overcome the work and to maintain the cement chemistry as over-all issue of the congress. Admittedly, the physical factors belong to the energy conversion concept, and cannot be neglected. A recent observation is the contribution by Nixon et al (58) on changes of alkali-concentrations through a body of concrete, and the possible influence on partial localization of deleterious alkali-reactivity. Many observations on the validity of mortar-bar "pessimum proportions" as a means of preventive safeguards for practice may need revisions, when alkali-ion migration is acknowledged to be important also in this way. Also in general, the significance of evaporation for salt-concentrations in concrete is known, in particular in hot countries.

4. The swelling mechanisms of cement paste compounds and of substances migrating in the pores of concrete and through the interface regions between cement paste and aggregate, need to be better understood and explained. Their good and bad effects in manufacture and performance of concrete need to be assessed.

Four different issues are in particular calling for the attention of research to the benefit of practice:

(1). Which swelling mechanisms are relevant in the cement paste itself, see (17), with different types of cement and under the processing and performance conditions relevant for concrete in cold, temperate and hot regions, and with/without additional swelling mechanisms in the system?

(2). Which consensus is attainable among chemical researchers regarding the swelling/non-swelling characteristics of alkali-silica gel with/without lime etc.? Reference is made to recent work by L. Dent Glasser (59) and others. In continuation: is swelling gel in cracks in concrete able to exert accumulated hydraulic or hydrostatic pressure on surrounding masses of concrete? And in contrast: May gel-phases in pores of cement-matrix and interfaces have advantageous effects, e.g. as buffers, or by decreasing the permeability?

(3) Can the development of pressure-exerting gel be deliberately prevented by predesign of procedures to give "stable"-gel-compositions which eventually will converge towards crystalline compounds?

(4) Which basic conditions determine the permanent stabilisation-effects of pozzolanic SiO_2 and/or Al_2O_3?

5. The availability of a vast storage of chemical knowledge for launching powerful industrial development of cement-based processing technology and creation of new products could be a way to solve durability problems associated with present technique and technology.

Recent years have seen many attempts to promote new products on cement basis, with a higher "end-value" factor than concrete. The research on durability could have untraditional off-springs in this direction. As one example, cement-based, adequately fibre-reinforced boards for permanent shuttering would offer effective protection for less expensive mass-concrete behind.

6. The R&D-systems need to advance the utilization of chemistry in the development of concrete technology for more energy-effective use of concrete.

The powerful development of effective R&D management and planning in industrial environments are examplifying that the capability exists to restructure cement/concrete research so as to absorb as well market opportunities as social needs. The ever increasing use of concrete and the concurrent concern about performance reliability strongly point in the direction of more attention to these matters, both from industries, engineering firms, governments, and international organisations.

7. The presented knowledge at the congress contains much information, which could be extracted as guidelines for improvements in practice, and for educational purposes, not least for the benefit of the developing countries.

The formation of a group of researchers and practising professionals is suggested for attaining consensus on urgent issues discussed at the theme session, and to establish cohesive contacts and gain impact on future congresses and on institutions etc. so as to advance fruitful, basic and applied chemical research for concrete technology.

REFERENCES *

1.- LEA, F.M., "Cement Research: Retrospect and prospect". Paper I-2, Chemistry of Cement. Proceedings of the Fourth International Symposium. Washington 1960. pp 5-8. Nat.Bur. of Standards Monograph 43 - Vol.I.1962.

2.- ALEXANDER, K.M., WARDLAW, I. and GILBERT, D.J., "Aggregate-cement bond, cement-paste strength and the strength of concrete". International Conference on the Structure of Concrete. Cement and Concrete Association 1968.

3.* MASO, J.C., "The bond between aggregates and hydrated cement paste". Principal paper, theme 7, sub-theme 1.

4.- CONJEAUD, M., LELONG, B. and CARIOU, B. "Bond between Portland cement paste and native aggregates".

5.- LANGTON, C.A. and ROY, D.M., "Morphology and Microstructure of Cement Paste/Rock Interfacial Regions".

6.- GRANDET, J. and OLLIVIER, J.P., "Orientation of hydration products near aggregate surfaces".

7.- GRANDET, J. and OLLIVIER, J.P., "New method for the study of cement-aggregate interfaces".

8.- ARLIGUIE, G., GRANDET, J. and DURAL, R., "Study of the contact zone between zinc and Portland cement paste".

9.- NAGATAKI, S. and TAKADA, M., "Effects of interface reaction between blast furnace slag and cement paste on the physical properties of concrete".

*References 3 through 30 are contributions to the 7eme Congres Internationale de la Chimie des Ciments. Paris 1980. They are referred to in the text without author's name, i.e. only by number.

10.- ASAGA, K., DAIMON, M., GOTO, S. and KONDO, R., "Effects of Raw Materials and Addition of Alkali on the Hydrothermal Reaction in Quartz and Lime System".

11.- MASSAZZA, F. and PEZZUOLI, M., "Cement paste-quartz bond in autoclaved concretes".

12.- TOGNON, G.P., URSELLA, P. and COPPETTI, G., "Bond strength in very high strength concrete".

13.- TOGNON, G.P. and CANGIANO, S.,"Interface phenomena and durability of concrete".

14.- CALLEJA, J., "Durability". Principal paper. Theme 7, sub-theme 2.

15.- SYCHEV, M.M. and SVATOVSKAYA, L.B., "Some problems of the chemistry of adhesion, Cement hardening and the strength of cement stone".

16.- BABOUCHKINE, V.I., KICHMAI, A.S. and MTCHEDLOV-PETROSSIAN, O.P., "Electrochemistry of cement pastes".

17.- LITVAN, G.G., "Volume Instability of Porous Solids: Part I".

18.- METHA, P.K. and MAMMOMAN, D., "Pore size distribution and permeability of hardened cement pastes".

19.- LENZNER, D. and LUDWIG, U., "Alkali Aggregate Reaction with Opaline Sandstone".

20.- GUTT, W., NIXON, P.J. and GAZE, M.E., "Fly Ash and Alkali Aggregate Reaction"

21.- DELOYE, F.X., BERNARD, A. and POINDEFERT, A., "Analytic approach of dedolomitization of aggregates in concrete".

22.- OHSAWA, S. and KONDO, R., "Effect of pozzolanic reactions on the mechanical properties of glass fiber reinforced cement".

23.- VALENTA, O., "Importance and conditions of rational study and design of the durability and long-term safety of concrete in aggressive waters".

24.- REVAY, M. and KOVACS, R., "Some aspects and a new method of evaluating the sulphate resistance of cements".

25.- REGOURD, M., HORNAIN, H., LEVY, P. and MORTUREUX, B., "Resistance of concrete to physico-chemical attack".

26.- AKIBA, T., MINEGISHI, K. and SUDOH, G., "Mechanisms and Kinetics on Neutralization of Concrete in Sea Water".

27.- NADU, M., "Influence of the manufacturing processes of clinkers on the cement resistance to sulphate waters action".

28.- MIDGLEY, H.G. and ILLSTON; J.M., "Effect of chloride penetration on the properties of hardened cement pastes".

29.- SUZUKAWA, Y., "Resistance of hardened cement mortar to magnesium chloride solutions".

30.- CHOPRA, S.K. NARANG, K.C., GHOSH, S.P. and SHARMA, K.M., "Studies on unsoundness of clinker with below 3.5 percent MgO content".

31.- FOOKES, P.G. and COLLINS, L., "Problems in the Middle East". Reprint of five articles from CONCRETE. A Viewpoint Publication, Cement and Concrete Association 1977. 6 pp.

32.- IDORN, G.M., "The Concrete Future". Danish Concrete Institute. 1980. 37 pp.

33.- NERENST, P., "Computation of freezing resistance of concrete at early ages". RILEM symposium: Winter Concreting, Copenhagen 1956. Proceedings, Session C, pp. 1-33.

34.- IDORN, G.M., "Hydration of portland cement paste at high temperature under atmospheric pressure". Proceedings, Fifth International Symposium on the Chemistry of cements. Session III-4a. Tokyo 1970. pp. 411-28.

35.- FREIESLEBEN HANSEN, P., "Hærdningsteknologi 1. Portlandcement". Aalborg Portland og BKF-centralen. 1978. 143 pp.

36.- FREIESLEBEN HANSEN, P., "Hærdningsteknologi 2. Dekrementmetoden". Aalborg Portland og BKF-centralen. 1978. 148 pp.

37.- MALQUORI, G., "Portland-Pozzolan Cement". Paper VIII-3. Chemistry of Cement. Proceedings of the Fourth International Symposium. Washington 1960. National Bureau of Standards. Monograph 43-Vol.II, pp. 983-1001.

38.- LEA, F.M., "The Chemistry of Cement and Concrete". 2nd Edition 1956. E. Arnold (Publishers Ltd.) 637 pp.

39.- GREENBERG, S.A. and COPELAND, L.E., "The Thermodynamic Functions for the Solution of Calcium Hydroxide in Water". Bulletin 116. Portland Cement Association 1960. 7 pp.

40.- GUTTERIDGE, W.A. and HOBBS, D.W., "Some Chemical and Physical Properties of Beltane Opal Rock and its Gelatinous Alkali Silica Reaction Product". Cement and Concrete Research. Vol.10 No.2, March 1980. pp 183-93.

41.- IDORN, G.M. - Discussion to ref.40 Cement and Concrete Research. In press.

42.- LEMISH, J. Discussion to "Chemical Reactions Involving Aggregates" by Bredsdorff et al. Chemistry of Cement. Proceedings of the Fourth International Symposium. Washington 1960. Nat. Bureau of Standards. Monograph 43 - Vol.IV. pp. 796-99.

43.- MALINOWSKI, R., SLATKINE, A. and BEN-YAIR, M., "Durability of Roman Mortars and Concretes for Hydraulic Structures at Caesarea and Tiberias". RILEM International Symposium - Durability of Concrete - Final Report - Praha 1961. Czechoslovak Academy of Sciences, Praha 1962. pp. 531-44.

44.- KROGH, H., "Examination of synthetic alkali-silica gels". Symposium on Alkali-Aggregate Reaction. Preventive measures. Reykjavik 1975. pp. 131-65.

45.- STRUBLE, L.J., "Swell and other Properties of Synthetic Alkali Silica Gels". Thesis submitted to the Faculty of Purdue University. 1979. 150 pp.

46.- BROWN, L.S., "Some Observations on the Mechanics of Alkali-Aggregate Reaction". Bulletin 54. Portland Cement Association 1955. 12 pp.

47.- KENNEDY, Th. B. and MATHER, K., "Correlation Between Laboratory Accelerated Freezing and Thawing and Weathering at Treat Island, Maine". Journal of the American Concrete Institute 50 (1953): 2, pp. 119-41.

48.- IDORN, G.M., "Studies of disintegrated Concrete". Part I-V. Progress Report N_2-N_6. The Danish National Institute of Building Research and the Academy of Technical Sciences. Copenhagen 1961-64. pp. 77, 47, 66, 45, 81.

49.- NEPPER CHRISTENSEN, P. and NIELSEN, T. P.H., "Model Determination of the Effect of Bond between coarse Aggregate and Mortar on the Compressive Strength of Concrete". Journal of the American Concrete Institute. 66(1969):1. pp. 69-72.

50.- IDORN, G.M., "Durability of Concrete Structures in Denmark". Teknisk Forlag. Copenhagen 1967. 208 pp.

51.- TURRIZIANI, R. and RIO, A., "High chemical Resistance Pozzolanic Cements". Paper VIII-54. Chemistry of Cement. Proceedings of the Fourth International Symposium. Washington 1960. National Bureau of Standards. Monograph 43 - Vol.II. pp. 1067-73.

52.- POOLE, A.B. and SOTIROPOULOS, P., "The Interaction of Alkalies with Dolomite and Quartz in Experimental Concrete Systems". Proceedings of the Fourth International Conference on the EFFECTS OF ALKALIES IN CEMENT AND CONCRETE. Purdue University 1978. Publication No. CE Mat-1-78 Purdue University 1978. pp. 163-79.

53.- BASTIANSEN, R., ROSENQUIST, I.Th. and MOUM, J., "Bidrag til belysning af visse bygningstekniske problemer ved Oslo-områdets alun-skifere". Norges Geotekniske Institut. Publication No. 22 Oslo 1957. 69 pp.

54.- DREYER-JØRGENSEN, K., "Setting Expansion of Gypsum". Proceedings of the Fourth International Symposium on the Reactivity of Solids. Amsterdam 1960. pp. 638-42.

55.- SCHRÄMLI, W., "An attempt to assess beneficial and detrimental effects of aluminate in the cement on concrete performance". World Cement Technology, March and April 1978. Vol.9, Nos 2 and 3. pp. 2-11.

56.- LOCHER, F., "Influence of burning conditions on clinker characteristics". World Cement Technology. March 1980. pp. 67-73.

57.- KALOUSEK, G., Discussion of a paper by Charles P. Berkey: The Nature of the Processes leading to the Disintegration of Concrete, with special Reference to Excess Alkalies". Journal of the American Concrete Institute. Vol.37. Supplement Nov. 1941. pp. 692-1 - 692-3.

58.- NIXON, P.J., COLLINS, R.J. and RAYMENT, P.L., "The concentration of Alkalies by Moisture Migration in Concrete - A Factor Influencing Alkali Aggregate Reaction". Cement and Concrete Research. Vol.9 No.4 1979. pp. 417-24.

59.- GLASSER, L.S.D., "Osmotic Pressure and the Swelling of Gels". Cement and Concrete Research Vol.9 No.4 1979. pp. 515-18.

DISCUSSION

by V.I. BABUSHKIN

. In my address I considered it essential to emphasize an important contribution of electrochemical phenomena to the process of hydration and structure formation of the cement, as well as to the cement stone and concrete corrosion processes.

We have experimentally proved that the hydration process, just as any other process producing solution and causing formation of new phases, is accompanied by volumetric separation of electric charges and creation of membrane potentials with values equal to the sum of the Donnan and the diffusion potentials of the inequilibrium type. The inequilibrium state of binder - water systems distorts compensation of the difference of chemical potentials, of tied and free diffusing ions due to interphase electric potentials and the osmotic pressure, which may amount to 19-54 MPa and can cause deformation and destruction of gel films around hydrating particles, as well as volumetric changes in binder - water systems.

Investigations have revealed that the e electrochemical phenomena also play a certain role in contact zone formation along the cement stone - aggregate boundary. But here it is necessary to take into account not only the charge sign and the electrokinetic potential value but also a possibility of the surface hydrofilization.

We applied the above-mentioned notions to explain the mechanism of sulphate and salt corrosion as well as the destructive action of the reinforcing steel rust products upon the protective coating of concrete.

A "pass of potential" experimental procedure for the electrokinetic potential determination in the specified dispersion systems can give the greatest degree of reliability, with allowance for surface conductance.

The investigation of electrochemical characteristics should be conducted simultaneously with determination of construction, of new formation crystallization rate in hardening and corrosing, and of pore size distribution. At that a special attention should be paid to the osmotically dangerous pores in which the rate of filling up with new formations particles is higher than in large-size pores and gel pores.

DISCUSSIONS

by TANG MING-SHU

Concerning the mechanism of alkali-silica reaction, some aspects seem worthy of consideration.

1. According to repeated observations on the polished surface of mortar containing opal, the expansion is almost always found to have taken place before the reaction product becomes fluid. Besides, the expansion may still increase after cracks have appeared in the mortar. So the water imbibition and swelling theory proposed by Vivian[1] and Brown[2] seems reasonable.

If we assume that the expansion is caused mainly by water imbibition and swelling, it will be insignificant whether there is a semi-permeable membrane or not, and therefore the expansion will have nothing to do with the composition of a semi-permeable membrane.

2. How to explain the effect of various factors, such as the amount and size of reactive aggregate and alkali content, on the alkali-silica reaction? It should be noted that the expansion is caused by chemical reaction, but at the same time, it is also a physical phenomenon. Therefore, both physical and chemical factors should be taken into consideration. According to Vivian's[1] and ourself's investigation, we have mentioned[3] that the expansion is related to the following factors: (a) number of active centers, i. e., the number of particles of reactive aggregate per unit volume of mortar; (b) the amount of alkali for unit area of reactive aggregate; (c) the expansive force generated by each particle as a result of alkali-silica reaction. The magnitude of the force depends on the degree of reaction and the total surface area of the particle; (d) the tensile strength of the cement paste. As the overall linear expansion measured includes both the micro and macro cracks formed in the mortar, so factors (c) and (d) should be considered.

According to the above views, the results of the experiments of many authors designed to study the influence of various factors can be explained.

3. It is just what Diamond[4] has stated that the competitive reaction theory suggested by Powers[5] is only a hypothesis which has not been confirmed by experiments. The theory is not satisfactory in explaining the influence of various factors. For example, Powers calculated by using Woolf's data the $CaO_{adsorbed}/Na_2O_{adsorbed}$ ratios in the reaction process and suggested that no expansion would take place if the ratio attains a certain value. Upon using all the data offered by Woolf and following the same method of calculation, it shows that in case the difference of the ratio of adsorbed CaO to adsorbed Na_2O between "safe" and "unsafe" reaction is so small, then it is difficult to explain the reason of expansion

As to the reason why low alkali cement does not cause expansion, it is probably ascribed to the much less extensive reaction of the reactive aggregate and not to the "safe" reaction. This has been proved by repeated microscopic observations on the degree of reaction of reactive aggregate (opal) in low alkali Portland cement.

Alkali-silica reaction is a complex problem. Mr. J. Calleja had a good proposal. He suggested that further researches in this field should be based on a wide interdisciplinary cooperation.

References
1. H. E. Vivian, Australian Council for Scientific and Industrial Research, Bulletin, (256), 1950; Australian Journal of Applied Science, 2 488-494, 1951.
2. L. S. Brown, Bulletin ASTM, (205), 40, 1955.
3. Tang Ming-shu and Xue Wan-rong, Journal of the Chinese Silicate Society, 2 (2), 110-117, 1963.
4. S. Diamond, Cement and Concrete Research, 5, (4), 329-347, 1975.
5. T. C. Powers and H. H. Steinour, ACI, Journal, Proc. 51, 497, 1955; Proc. 51, 585, 1955.

The authors stated:"There is no essential difference between the hydration in the system pozzolana-cement and that in the system pozzolana-$Ca(OH)_2$ and pozzolana-cement compound". In a general sense, the above statement is true. However, as portland cement inevitably contains a certain amount of alkali, some sort of alkali-silica reaction might occur at certain stage of cement-pozzolana reaction.

Alkali-silica reaction may be represented by the equation

$$2NaOH+xSiO_2+yH_2O = Na_2O\cdot xSiO_2\cdot(y+1)H_2O$$

The $Ca(OH)_2$ released in the hydration of portland cement may react with $Na_2O\cdot xSiO_2$ to liberate alkali. The regenerated alkali can once again penetrate into the particles of the reactive aggregate. As the particles of pozzolanic additives are very small, they will all be eventually transformed into C-S-H and other hydrates while most of the alkali ions will migrate into the solution. It should be noted that at certain stage of the reaction, K^+ and Na^+ ions do not necessarily go into pore solutions; on the contrary, they may penetrate into the inner part of the pozzolana particles.

Even though the pozzolana may itself contain alkali, at certain stage of the reaction, it still tends to absorb alkali from the pore solution of cement paste instead of releasing it into the solution. We have made mortar cubes using a high alkali cement and a tuff rock as aggregate which contains 0.88% Na_2O and 2.59%

K_2O, with a particle size of about 1mm. After one month curing, the tuff particles were observed to have been surrounded by reaction rims which contained much more alkali than the particles themselves as detected with EDAX (Fig.1)

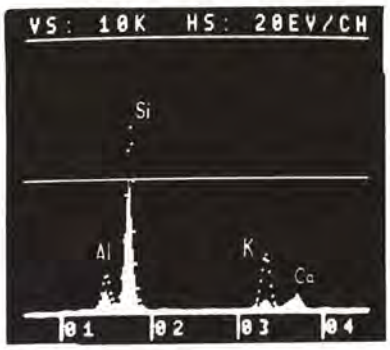

EDAX detection of reaction-rim and unreacted tuff particle.
△ — reaction-rim
▲ — unreacted particle

Recently, ion-concentrations of pore solution of cement paste were determined with pressing technique [1]. The results showed that when portland cement clinker contains alkalis, the pH value of the pore solution may be greater than 13.0, sometimes as high as 13.7. It is assumed that high concentrations of R^+ and OH^- ions might affect the reaction process of pozzolana-cement. Diamond [2] in his experiment has shown that the mortar bar expansion may typical alkali-silica reactions. As the particle size of pozzolanic additives is small as compared with aggregates, the amount of alkali for unit surface area will be less. In the mean time, the expansive stress caused by such small particles may be distributed evenly and hence expansion will be inhibited. But in certain stage, the reaction of pozzolana-cement may be likened to alkali-silica reaction. Naturally, further study is needed to determine to what extent the influence of alkali could be.

In the investigation into the reaction mechanism of the system of pozzolana-cement, it might be appropriate to take into consideration the chemical and physical processes of the alkali-silica reaction, especially when the pozzolanas used contain opal or volcanic glass as described in this article.

References

1. P.Longuet, Revue des Materiaux, 676, 35, (1973)
2. S.Diamond and N.Thaulow, Cement and Concrete Research, 4, (4), 591-607, (1974)

CONCLUDING REMARKS

by G.M. IDORN.

Final conclusions regarding achievements and issues requiring further attention and research within the fields of interface reactions in concrete and mortars - based upon the written contributions, including posters, to the theme, the panel contributions and the terminating question and answer part of the session.

The discussions during the session on theme VII underlined that there is now a considerable coherence and progress of ongoing research on sub-theme one : adherence (bond-strength) between aggregates and cement paste, not least based upon comprehensive work in France. Also the adherence between cement paste and metallic reinforcement and glass-fibre, and grout to host rocks in subterranian works, is treated , as well as the enhanced interface reactions created by the high activation energy at hydrothermal treatments.

Contributions are missed about such a "down to earth", but economical important issue as bonding by repairs of new to older concrete, and neither the excessive bond-qualities obtainable with the use of organic polymers as admixtures nor by impregnation have found interested supporters.

Also the more fundamental problems with inherent bonding within cement paste constituents and the binding capability created by pozzolanic reactions remain to be considered in conjunction with the research reported in theme II, III and IV (though principally much governed by the same forces as paste/aggregates adherence).

The difference of the interface-character in dependence of calcareous or siliceous aggregates is now more clear than before (although not applicable in terms of "performance" - value of high or low bond-strength in concrete in practice). It is also obvious that in the case of siliceous aggregates the interface reactions must in any case be considered metastable editions of gel-producing alkali-silica reactions, i.e. bond-creating without expansive pressure formation, but appreciably penetrating into the structural build-up of the aggregates, and not necessarily long-term dependable. With calcareous aggregates the bond-creation seems more restricted to the aggregate surface and the innermost part of the "aureole" zone and the bond-forces to be nearer to, what metallurgists and some authors designate "epitaxial" growth. With dolomithic aggregates a sort of "hybrid" reactivity seems established, since these reactions do release alkalies and do break up the interior $Ca/MgCO_3$ structure of the aggregates, but do not produce swelling gel, except probably with siliceous-magnesium lime stone, which ought to be considered very susceptible to combined dedolomitization and alkali-silica reactions, i.e. to weakening bonding-creation (and gave rise to the pioneer studies of alkali-silica reactions in USA in the forties).

The stage of knowledge now attained seems ripe for systematic application of reaction kinetics and thermodynamics in the further research. This is enhanced by the aim of the American presentation - to gain knowledge on 1000 years or more performance stability of cementitious plug materials for deep boreholes. In this study the long-term geophysico/chemical exposure approaches hydrothermal conditions, which according to the Italian and Japanese contributions on industrial autoclaving processing brings about much more intensive interface reactions than found at ordinary temperature levels.

It is an interesting paradox, that the long-term stability aiming American studies find alkali-silica reactions an identifiable factor in the interface with a siliceous aggregate. This a reminder that even at ordinary temperatures the convertible energy in the high-alkaline environment with soluble silica is sufficient to cause considerable transitions in the entire system beyond those intentionally monitored during the hydration process.

The special bond-creating reactions with glass fibre, metallic reinforcement, and the influence of pozzolans, different cement types and different environments etc. altogether emphasize that the creation, preservation or possible deterioration of adherence as an integral feature of the entire system must be considered dynamically.

The thoroughness of the principal paper on sub-theme 2 : durability, makes is easy for students of the individual contributions to find supplementary information within the area of cement-aggregate reactions, the effects of aggressive solutions on concrete and the available counter-measures etc.

There are, however, still many loose ends, for instance, concerning alkali-silica reactions. Even if consensus is approaching that:

1. expansive pressure can develop both within a (compact) partially reacting siliceous aggregate particle, or

2. during complete dissolution of a porous, readily reacting particle, or

3. cause gel to dissipate out into ambient paste while concurrently releasing expansive pressures

it still remains a mystery for the construction engineer, and is untouched by research, how pressure in discrete aggregate particles, usually in the sand fractions, can accumulate so as to crack and displace large parts of concrete masses. No contributions have as yet dealt with the expansive power of dilute

gel in cracks and pores in the concrete - the only medium seemingly available for exertion of a continuum of hydraulic pressure in excess of the strength and weight of concrete masses.

It is another inconclusive situation emerging from the contributions, that beyond excessive limitation of the alkali-content and of the amount of free pore-liquid in concrete there are no safe precautions against deleterious alkali-silica reactions established for application in construction practice, where reactive aggregates are used.

Surely, pozzolanic reactivity is principally an innocuous edition of alkali-silica reactions. But the laboratory examinations have not yet presented reliable models for conversion of the results to match the conditions in engineering practice, among other things with regard to the long-term stability of the pozzolanic reaction products. This seems a prolific field for further research, in particular if thereby the means for the use of high alkali cements without risks could be elucidated.
A possible further step in this direction is indicated by the deliberate utilization of the alkalies in cement as prerequisite for making fibrous CSH by hydrothermal processing as demonstrated in a Japanese contribution, while the advantageous use of alkali-hydroxides as hydration activators jointly with dispersing agents is discussed elsewhere in the congress program. Thus altogether, the historic, monotonous designation of alkalies as primarily deleterious ought to be reviewed, also now in view of the energy expenditure for their removal in much cement manufacture and the presence of soluble alkalies in many natural and synthetic pozzolanic materials.

Concerning the deleterious attack of saline solutions on concrete it is convincingly established that the conventional measurements of the C_3A-content of cements are qualitatively and quantitatively insufficient. Partly due to this observation but also to the common use of simplified laboratory models in studies of saline aggressivity, it seems reasonable to assume that C_3A in cements is of relatively minor importance for concrete performance than are many factors which have been less counted with as influential in conventional concrete technology and regulations.

Among the constituents of aggressive saline constituents sulphates are the primary subject of the presented studies. However, modern de-icing practice in the cold regions, and urbanisation in hot countries underline in each their way the implications of more complex salinity and ought to stimulate further studies of their possible synergetic effects, for instance in sea water attack and combined with alkali-silica reactions.

The two mentioned extremes of exposures also underline the urgency of introducing reaction-kinetics in the research. Energy conversion is rapid and violent in both cases, despite the fact that the available added energy in the one case is chemical, in the second primarily physical.

Preceding the effects of either exposure is, however, the hydration phase during the concrete making. The presentation of the general report exemplified, that by ordinary construction practice about 30 years ago the heat development in concrete during curing slowly caused interior temperatures to rise to about 30-40°C and to descend slowly again towards environmental levels in a temperate region, while modern concrete in an exotic environment jumped beyond 80°C in 12-14 hours, and down to the environment in about 50-80 hours thereafter. This latter time/temperature history is quite common in modern construction and precast works, and may through the overfeed with convertible energy during early curing often cause severe initial microfracturing in the cement paste. Thus, further research must study the physico/chemical aggressivity during performance as possibly superimposed upon initially invalidated structures of the concrete. This requires clarification of the reaction kinetics and thermodynamics in the entire system of concrete making and performance including the environmental energy impact. As pointed out in the principal paper, several contributions inter al from USSR and East-Europe and the general report, such research, operating with concrete as it is made and used in our time, must gain priority over continued work with laboratory experimental specimens, which are kept entirely protected against the effects on an increasing fraction of the energy conversion in concrete in practice.

The contribution from India on the significance of MgO in cements in conjunction with a discussion during session V brought the issue into focus that developing countries must revise numerous conventional concepts and methods for which the feasibility is questionable, both in view of general advance of knowledge and to their particular conditions. This attitude may in turn become a gift to further advance regarding durability in the old world.

Alertness is also required towards the outfolding impact of new materials in concrete making from industries other than cement, because the technology is to be profoundly influenced hereby, and improvement of durability and adherence under these circumstances require high priority to cement chemistry knowledge in the research and development.

At present it is impossible to analyse in depth the issues dealt with in Theme VII in relation to the achievements in the preceding themes. It is clear, however, that the performance of concrete is a matter of how it was prepared and made as much as of how it is exposed during performance. And all the way through, the cement chemistry knowledge must be applied as an entity and any specialist of the preceding themes must be aware of the performance of concrete in practice as the terminal criterion of reliability.

TERMINATING REMARKS

by G.M. IDORN, Chairman

During the congress in Moscow in 1974 I said in the concluding remarks to the presentation of the paper on polymer cement materials, that in advocating more determined industrial R & D to make concrete innovations like in high technology industries - I felt much like the figure in a well-known Danish children's book : "Paul alone in the world".

I was speaking entirely concerning the general pressure of retrogradation of research to come with the economy crises, while at the same time inventors from USA and USSR at thatmeeting threw light on exciting, qulte new opportunities within the field I had reported on.

Today I don't feel nearly as much like such a Paul.

This is because we have been confronted with an enormous capability of cement chemistry knowledge, which is notyet applied to realise the manifold opportunities for making concrete durable, hereunder for the creation of effective and stable bond-forces between the various phases of the composite normally called concrete.

Let me terminate the business of this session - relying not only upon what we have discussed since 9 O'clock this morning, but also upon much more, which we have not yet assimilated effectively from the preceding sessions - in summarizing some among the challenging opportunities we are facing, and thereby also your obligations, because civil engineering cannot anymore develop concrete technology to provide satisfactory durability without profound assistance from cement chemistry.

I - Ensure initial quality of concrete to be gained during manufacture in obedience of the governing inherent and environmental conditions. In other words :

Harmonize environmental aggressivity and characteristics of concrete by design of the material composition, the making, and the performance characteristics. Crudely speaking, observe :

Chemical reactions x heat represent energy.

Design and monitor for energy efficiency.

II. Identify and make use of the advantages of alkalies with :

Pozzolans and fly ashes
Slags
Superplasticizers
etc.

III. Harmonize the chemical identification of cements for the users with adequate measurement techniques into unambiguous formulae and recommendations.

IV. Intensify R & D innovations like :

"Sandwich" solutions, i.e. permanent cement-product formwork
Fibre reinforcement
High-strength and high-density concrete, etc.

V. Educate research and practice :

1. Abandon the use of 20°C isothermic storage of cement paste, mortar and concrete as representative for construction conditions.

2. Beware of exaggerated spectacularity of SEM and STEM features.

3. Remember and use research also from the pre-electronic instrument era and continue to utilize the petrographic microscope.

4. Let research gatherings not merely be stimulating sanctuarity occasions for research, but request evaluations of their outcome in terms of development opportunities.

If these guidelines are broadly implemented, then I am confident that the presently increasing lamentations about problems with concrete durability will soon become inferior to significant progress.

This is why I don't hesitate to predict that your aim will be to present remarkable realisation of existing opportunities for development, when your preparation for the 1986-congress on cement chemistry begins on Monday morning, July 7th.

With this challenge, I thank you all for the contributions and attendance realized in such ways that our theme and session hardly at all have needed to have a chairman.

I also want to vote a thank from all of us in attendance to acknowledge the foresight in choice of the subjects, of the panel, and of the principal authors. I do hope that we have injected valid stimuli into the further work on the issues to the satisfaction of the organizers.

And last but not least : many thanks to all those anonymous helpers behind the screen : typist, secretaries, technical staff and interpreters. Your assistance to our performance today has been second to none.
Session 7 is terminated.

POSTERS

THEME I

Influence des matières premières des combustibles et des procédés de fabrication sur la structure et les propriétés des clinkers

Influence of raw materials, fuels and manufacturing processes on clinker structure and properties

---

Etudes thermochimiques de la formation du clinker

Thermochemical investigations in clinker formation

M. KOUGUIA, Guiprotsement, Leningrad, URSS.

Les méthodes thermiques telles que la méthode des chaleurs de dissolution et la méthode thermique sous forme traditionnelle et modifiée, ont été utilisées pour l'étude des différences dans le comportement lors du traitement thermique des mélanges crus de ciment sur la base des matières premières provenant des différents gisements de l'Union Soviétique; Ces différences s'expriment par: a) la succession de la formation des minéraux; b) les limites de température de formation des constituants de clinker et de la phase liquide; c) la distribution des dépenses thermiques selon les températures. Les caractéristiques contribuant à un déroulement rapide et complet des réactions à l'état solide ne sont pas toujours favorables pour la formation de l'alite en présence dela phase liquide. Les particularités dégagées du comportement des mélanges crus peuvent servir de base pour l'estimation du comportement des mélanges crus dans les fours rotatifs industriels.

The thermochemical methods of investigations such as thermal and and solution heat methods, both conventional and modified, were used to study distinctions in behaviour of cement raw mixtures, when heated, composed of raw materials from different deposits of the USSR.

These distinctions are expressed in: a) sequence of mineral formation; b) temperature ranges of clinker minerals and liquid phase formation; c) heat distribution with temperature;

Raw mix features contributing to fast and complete proceeding of reactions in the solid state do not always prove to be favourable for alite formation in the liquid phase presence. The revealed particularities of raw mixtures behaviour may serve as a basis when estimating the behaviour of raw mixtures in industrial rotary kilns.

En ce qui concerne les particularités caractéristiques et la présence d'effets thermiques sur les courbes ATD des mélanges bruts, les avis sont partagés [1,2,3,4,5].

Auteur et al.ont effectué un examen des mélanges bruts industriels de plusieurs cimenteries de l'Union Soviétique (plus de 40)

Les charges ont été examinées par la méthode de l'analyse thermique différentielle sous forme traditionnelle et sous forme modifiée, par la méthode thermogravimétrique et par celle des chaleurs de dissolution. Leurs caractéristiques chimiques et granulométriques correspondaient à celles qui sont généralement admises dans la production. Les résultats ont montré que les différences les plus caractéristiques se situent sur les courbes ATD dans le domaine de 1100 à 1450°C. Les données ainsi obtenues, auxquelles s'ajoutent les analyses des matières premières utilisées par les usines, ont permis d'établir une classification des mélanges bruts industriels. Pour le premier groupe de ces mélanges, on a enregistré sur les courbes ATD deux effets exothermiques de formation des minéraux dans le domaine de 1200 à 1350°C et un effet endothermique d'apparition d'une phase liquide dans l'intervalle de 1340 à 1390°C. Pour ce groupe, on utilise le plus souvent des calcaires à gros cristaux, des constituants argileux avec prédominance d'hydromicas et de caolinites, d'argillites et d'aleurolites.

Le second groupe, plus nombreux, est constitué par les mélanges présentant un exo-effet et un endo-effet de fusion. Ici, on utilise essentiellement comme matières premières des calcaires organogènes, la craie, des constituants argileux sous forme de compositions naturelles de divers minéraux argileux, des cendres. Sur les courbes ATD des schlamms du troisième groupe, assez nombreux eux aussi, les effets exothermiques de formation de minéraux étaient absents et on n'a enregistré qu'un maximum endothermique de fusion.

Les usines de cette catégorie utilisent essentiellement des calcaires tendres, des craies, des constituants argileux avec prédominance des variétés mixtes et montmorillonitiques,des schlamms contenant de l'orthosilicate de calcium. La présente communication expose les résultats des recherches effectuées sur les représentants types des trois groupes précités en vue d'établir les causes des différents comportements des mélanges bruts vis-à-vis du chauffage, traduits par les courbes ATD,et aussi pour élucider l'influence exercée par certains facteurs.

A cet effet, on a exécuté, outre l'ATD, des expériences relatives à la cinétique de l'assimilation de l'oxyde de calcium, on a déterminé les pertes survenant dans les produits de cuisson lors de la calcination, on a opéré des analyses cristallooptiques et radioscopiques des phases, déterminé les chaleurs de dissolution.

Les Tableau 1 et 2 résument les données fournies par les analyses chimiques, des caractéristiques minéralogiques et certaines autres, qui mettent en évidence que les transformations les plus importantes sont intervenues dans le mélange du 3e groupe vers 1200°C.

Toutefois, les produits de la cuisson à 1400°C des mélanges du premier et du deuxième groupes ont les pertes par calcination et la teneur en CaO_{libre} inférieures à celles du troisième essai, ce qui prouve que vers 1400°C les processus de formation de minéraux ont été plus marqués dans le mélange du premier groupe par rapport au mélange 2 et surtout au mélange 3.

La chaleur de dissolution du clinker se compose des $Q_{diss.}$ des minéraux individuels qui le constituent et de la phase liquide vitriforme, aussi varie-t-elle d'une façon complexe et non univoque, suivant la température à laquelle est exposée la matière considérée, ce qui ressort à l'évidence du Tableau 2. Dans le but de vérifier, pour avoir plus de certitude, les résultats obtenus, on a aussi effectuées des recherches sur des mélanges bruts synthétiques, présentant les caractéristiques suivantes: CS = = $0,90 \pm 0,02$; n = $2,0 \pm 0,2$; p=$1,2 \pm 0,2$. Le mélange A contenait, outre le calcaire et les résidus de calcination, de l'argile hydromicacée et caolinitique, le mélange B,de l'argile hydromicacée, le mélange C, de l'argile montmorillonitique, et le mélange D, del'argile caolinitique. La figure 1 représente les portions à haute température de leurs courbes ATD, obtenues sur l'appareil "Mettler". Les effets thermiques globaux de formation des matières du clinker

Tableau 1

Compositions chimique et minéralogique et caractéristiques physiques des mélanges bruts des trois groupes et des produits de leur cuisson

Caractéristiques			Mélanges bruts		
			1	2	3
Composition chimique	Teneur en Oxydes, %, en calculant en matière solide	P.P.C.	34,19	33,37	34,90
		SiO_2	14,45	14,98	14,23
		Al_2O_3	3,97	2,96	3,80
		Fe_2O_3	1,57	329	2,48
		CaO	42,72	42,26	42,67
		MgO	1,05	1,06	0,75
		SO_3	0,01	0,25	0,35
		K_2O	0,95	0,89	0,90
		Na_2O	0,23	0,33	0,25
		TiO_2	0,17	0,15	0,19
			99,31	99,54	100,52
		C.S.	0,88	0,86	0,89
		n	2,61	2,40	2,27
		p	2,53	0,90	1,53
Composition minéralogique	Constituants aluminosilicatés	Schiste argileux, minéraux argileux, hydromica, caolinite	Argile, minéraux argileux: hydromica, montmorillinite		Argile, beaucoup de matières organiques, montmorillonite
	Constituants carbonatés	Calcaire	Craie		Craie
Finesse de mouture	Refus de tamisage sur la claie n°02	1,6	1,8		2,2
	Refus de tamisage sur la claie n°008	12,4	7,7		7,0
P.P.C. produits de cuisson	1200 °C	33,55	33,20		25,56
	1400 °C	0,5	4,01		6,29

et de la phase liquide, calculés à partir des données relatives à l'allure de l'assimilation de la chaux au cours des cuissons des mélanges bruts synthétiques effectuées au laboratoire [6] figurent dans le dessin 2 et sont en assez bon accord avec les effets thermiques observés sur les courbes ATD (fig.1).

L'analyse des phases par diffraction des rayons X à haute température et l'analyse des phases par diffraction des rayons X dans les produits de cuisson des mélanges synthétiques ont montré que dans le domaine de 1000 à 1200°C il y avait, dans la charge C, disparition du quartz, accroissement de la teneur en C_3A, formation de bélite nette.

Dans le mélange D, la bélite ne s'est formée qu'aux températures supérieures à 110°C (c'est-à-dire que sa formation est décalée de 100 à 150°C par rapport au mélange C);en plus, au-delà de 1200° il y a eu une cristallisation intense de l'alite. Il s'ensuit que dans cette charge la synthèse des principales matières formant clinker s'est produite à des températures plus élevées et dans un intervalle plus étroit de températures.

Les charges à base des argiles hydromicacée et mixte occupent une position intermédiaire entre les mélanges C et D quant aux caractéristiques qu'elles manifestent lors du traitement thermique.

L'analyse thermogravimétrique des mélanges bruts industriels et synthétiques a montré (Tableau 2) que la décarbonisation s'y produit selon un mécanisme complexe et s'effectue en deux étapes, les valeurs des énergies d'activation pour la dissociation des carbonates à la seconde étape étant, en règle générale, supérieures à E_a de la première étape.Les résultats obtenus avec les échantillons synthétiques ont confirmé et complété les données obtenues avec les mélanges bruts industriels, en montrant bien, d'une part, le rôle que joue la nature minéralogique des constituants lors de

Tableau 2

Caractéristiques thermochimiques des mélanges bruts des trois groupes

			Mélanges bruts		
			1	2	3
Caractéristiques thermiques	Pertes de poids	Combustion des matières organiques et déshydratation	3,1	3,0	4,1
		Décarbonisation	31,1	30,4	27,7
	Energie d'activation de la décarbonisation	Stade I	-	14,5	21,0
		Stade II	-	40,9	41,9
	Températures caractéristiques	Température du début de décarbonisation	780	740	760
		Température de la décarbonisation maximale	980	955	970
		T_{max} exotherm. I	1260	-	-
		II	1305	1300	-
		T_{max} endotherm.	1355	1370	1360
Chaleur de dissolution, cal/g		1200°C	-	558	563
		1400°C	-	575	584

la formation du clinker, surtout au stade des réactions intervenant dans la phase solide, et del'autre, elles donnent lieu à penser que la cause essentielle de l'absence des effets thermiques de formation de minéraux sur les courbes ATD des quelques uns des mélanges bruts au-dessus de 1000°C réside vraisemblablement dans une formation précoce de C_2S, simultanément avec le processus de décarbonisation, dissimulée sur les courbes thermiques par un endo-effet et la dissociation du carbonate et la coincidence, selon [7], de l'état actif de l'oxyde de calcium et des minéraux appartenant aux alumino-silicates, modifiés sous l'effet de la chaleur, et la formation d'alite étalée le long de l'échelle de températures,à cause de la combinaison entravée de CaO avec le silicate dicalcique recristallisé. Il est possible que le ralentissement du dernier stade de formation du clinker est dû lui aussi à la recristallisation de l'oxyde de calcium non entré en réaction. A la lumière des recherches dont il est question, on comprend aiséement pourquoi un schlamm (E) se prete difficilement à l'agglomération, malgré les bonnes apparences de la matière première (craie et compositions argileuses à partir des minéraux d'hydromicas, de caolinite et de montmorillonite).Dans les expériences que l'auteur a exécutées avec ses collègues [8] dans les conditions industrielles, aux fours mesurant 5x185 m , en utilisant des schlamms d'une composition plus grossière (le constituant argileux étant représenté

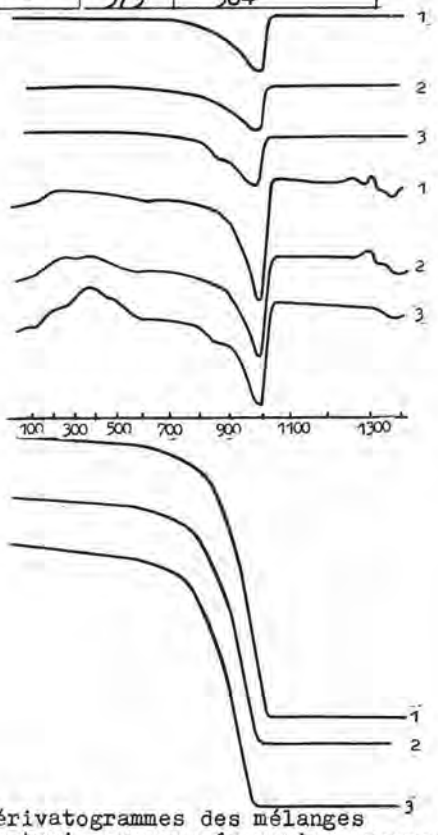

Fig.1. Dérivatogrammes des mélanges bruts des trois groupes: 1-premier groupe; 2 - deuxième groupe; 3 - troisième groupe

par un limon), en comparaison des schlamms couramment utilisés le constituant carbonaté étant le meme (la craie), on a constaté que la consommation spécifique de chaleur a diminué de 3% et les pertes avec les poussières, rapportées aux matières premières sèches, ont diminué de 2%. Ce dernier résultat est du au décroissement de la teneur de la matière à cuire en granules de petite taille.

C'est ce qui a permis de supposer qu'en cas de schlamms à base de limons un traitement thermique moins intensif est nécessaire dans la zone d'agglomération pour faire entrer la chaux en réaction et pour achever la formation du clinker, par rapport aux matières premières plus tendres.

Compte tenu des résultats obtenus, une circonspection s'impose quant aux recommandations de la communication 9 sur l'utilisation souhaitable des argiles montmorillonitiques dans la fabrication du ciment.

Les données que nous avons obtenues s'accordent avec celles de la communication 10, qui mettent en évidence que l'aptitude de certains mélanges à la formation de la bélite est différente de celle à la formation de l'alite.

Il ressort de ce qui vient d'être dit que la nature minéralogique des matières premières joue un role important dans la formation du clinker, en déterminant le stade du processus qui se déroule en phase solide et ayant par là des incidences sur l'agglomération définitive en phase liquide, et que l'analyse thermique conjuguée à d'autres méthodes de la thermochimie permet de pronostiquer les aptitudes réactionnelles des mélanges bruts.

REFERENCES

1. Рамачандран В.С. Применение дифференциального термического анализа в химии цементов. М., Стройиздат, 1977

2. Lach V., Rosova M. Stavivo 55, N°44, 1977.
3. Courtault B. Revue des matériaux de construction. N°569-573, 1969 (en français).
4. Kramer H. Zement-Kalk-Gips N°8, 1958 (en allemand).
5. Forest J. Silicates industriels N°6-9, 1973 (en français).
6. Коугия М.В., Гнедина И.А. Труды НИИцемента, вып. 42, 1977
7. Макашев С.Д. Цемент № I, 1970
8. Шлионский Ю.С., Иванова Л.К., Коугия М.В. Труды НИИцемента (в печати)
9. Pernica M. Silikaty N°4, 1974.
10. Имлах Л.А., Хофменнер Ф. Труды VI Международного конгресса по химии цемента. М., 1974.

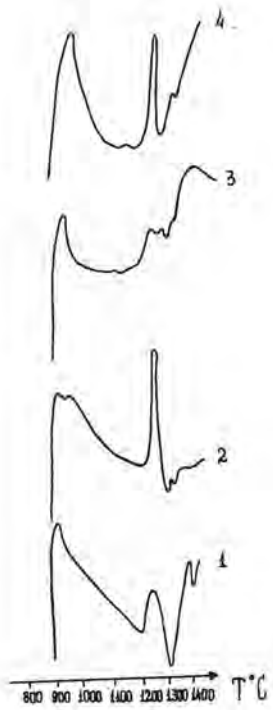

Fig.2. Zones de hautes températures des courbes ATD pour les mélanges bruts synthétiques: 1-mélange A; 2-mélange B; 3-mélange C; 4-mélange D

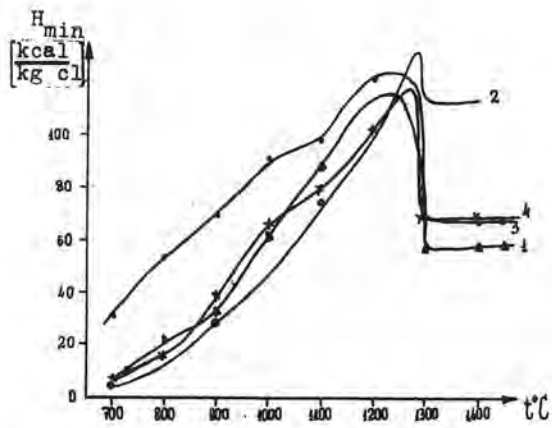

Fig.3. Effets thermiques globaux de formation de minéraux: 1-mélange A; 2-mélange B; 3-mélange C; 4-mélange D

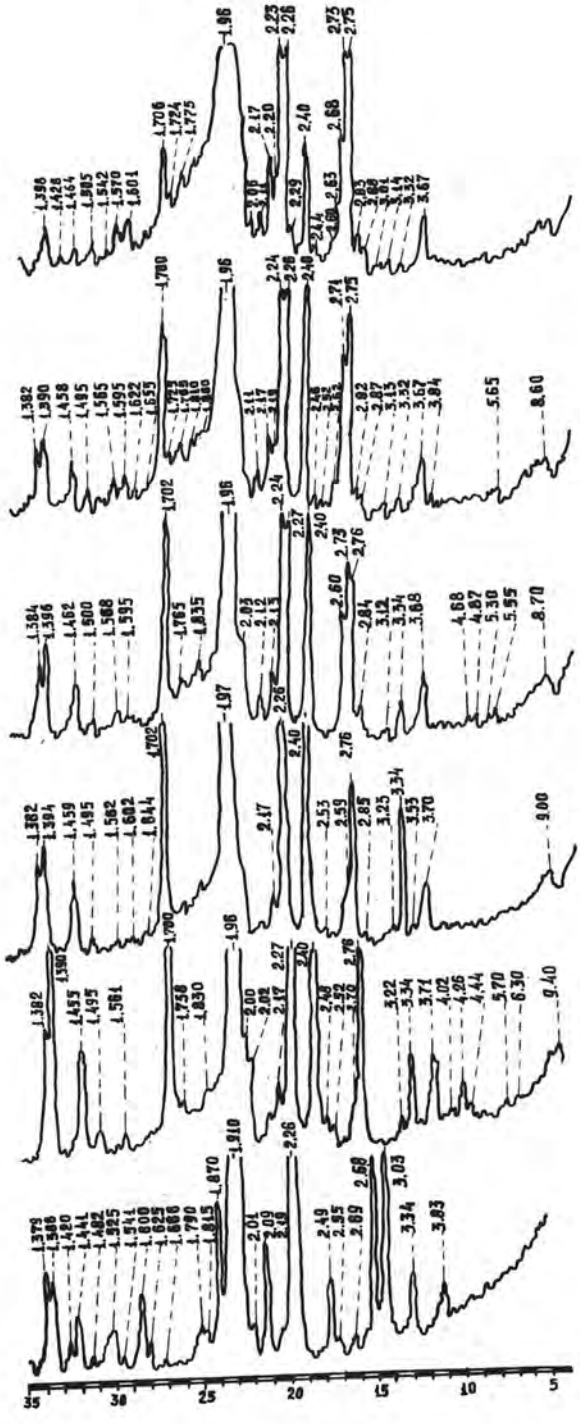

Fig.4. Diffractogrammes du mélange brut C: 1-initial; 2-700; 3-800; 4-900; 5-1000; 6-1200 °C

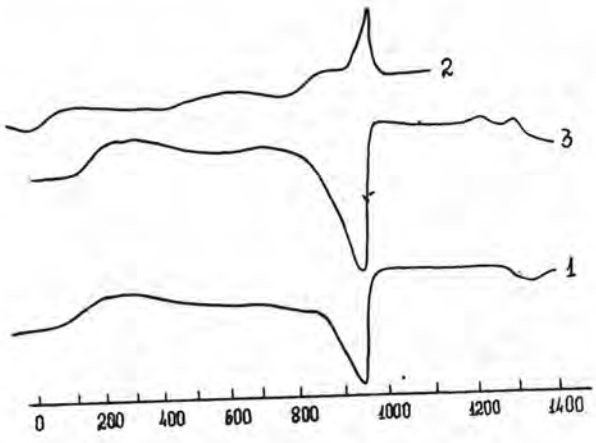

Fig.5.Dérivatogrammes du mélange brut E: 1-prise d'essai industrielle; 2-effet exothermique de formation de C_2S; 3-mélange contenant du marshallite

Influence of temperature, grain size and the amount of added water on the development of the porosity and surface size during the hydration of C_3S

Influence de la température, de la granulométrie et du dosage en eau sur le développement de la porosité et de la surface spécifique du C_3S hydraté

R. TRETTIN and W. WIĘKER, Zentralinstitut für Anorganische Chemie der Akademie der Wissenschaften der DDR - Berlin - RDA

Summary:

The change of the specific surface areas of hydrated C_3S was measured by nitrogen adsorption in dependence on the temperatur (5-75 °C), the water/solid ratio and the grain size.
After the end of the induction period the specific surface area of the hydrated pastes increases strongly, goes through a maximum after 10 up to 168 hours depending on the reaction conditions. The occurence of this maximum can be interpreted as a result of the formation of highly dispersed x-ray amorphous calcium hydroxide.
At the end of the induction period the specific surface area of hydration products increases exponentially and gives a maximum at the same time at which the hydration heat evolution has its maximum too. The hight of this maximum becomes lower as the temperature of hydration decreases, the grain size and the water/solid ratio increases. The following reduction of surface of hydration products is in high degree dependent on the temperatur.
The pore-size distribution was calculated from the nitrogen sorption isotherm data in C_3S hydrated for 28 days. It was obtained, that with increasing temperatur, W/C ratio and particle size the quantity of pores having a radius smaller than 20 Å is larger.

RESUME : Les variations de la surface spécifique du C_3S hydraté ont été mesurées par adsorption d'azote, en faisant varier la température (5 à 75°C), la granulométrie et le dosage en eau. Après une période de latence, cette surface spécifique augmente fortement, et atteint un maximum au bout de 10 à 168 heures, suivant les conditions opératoires. Le maximum semble résulter de la formation de chaux amorphe.

Après la période de latence, la surface spécifique croît exponentiellement avec le temps et atteint son maximum en même temps que la chaleur d'hydratation. Ce maximum diminue si la température s'abaisse, ou si la dimension des grains et la teneur en eau augmentent. Cette diminution dépend principalement de la température.

La distribution granulométrique des pores a été mesurée, par adsorption d'azote, après 28 jours d'hydratation. La dimension moyenne des pores est de 20 Å ; elle augmente avec la température, la dimension des grains anhydres et le dosage en eau.

1. Introduction

From the literature /1,2/ it is known, that the hydration of C_3S is accompanied with a strong increase of the BET surface, which is attributed to the formation of the CSH-phases. The purpose of our investigations therefore was to look for relationships between the surfacesize developed and the reaction products formed in the different stages of the hydration process.

2. Experimental

Pure C_3S (free CaO = 0,2 % by weight, triclinic modification) ground to a Blain fineness of 3500 cm^2/g was used. At appropirate times the hydration was stopped and the water was removed by treating with alcohol and ether and then the samples were dried by evacuation. All operations were performed in a CO_2-free atmosphere. The quantity of nitrogen adsorbed at - 196 °C was determined in a volumetric apparatur. The specific surface areas were abtained from the BET region adsorption isotherms. Pore structure analyses of samples were performed using the method of Brunauer and coworkers /3/. X-ray diffraction was used for quantitative determination of unreacted C_3S in the hydrated samples. The result obtained were used for the determination of degree of hydration.
The $Ca(OH)_2$ formed during the hydration was determined by a modified extraction method of Franke /4/ and by x-ray diffraction.

3. Results and Discussion

The measured changes in the surface area for C_3S samples (W/C = 0,5) hydrated at 25°C is shown in Fig. 1.A. Immediately after the contact of the C_3S with water occurs a first increasing of the surface area. After this it remains nearly constant up to 2 hours.As can be seen from curve 1 in Fig. 1.A, in the further progress of the hydration the surface area is then converted to a increase again up to 56 days. The formation of the maximum of the surface area of the hydrated pastes is remarkable and agrees to the results reported by Harade et al /5/ and Kondo et al/6/.

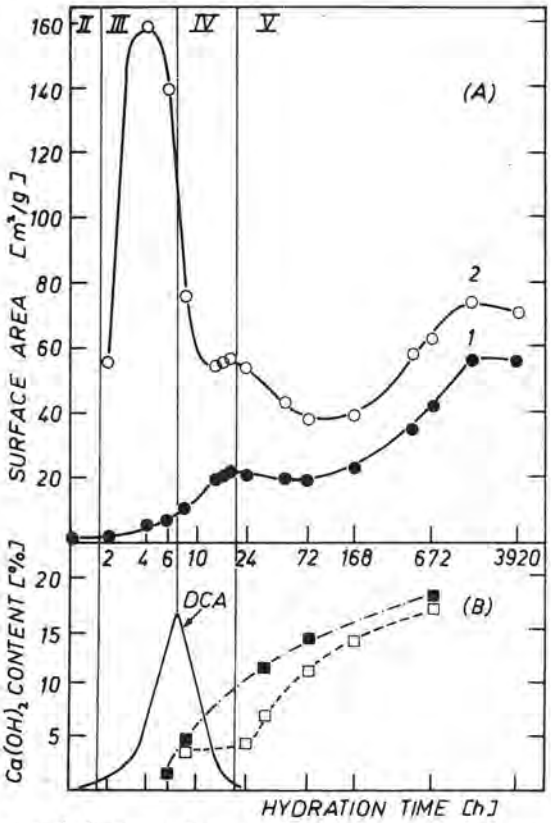

Fig.1.(A) Specific surface area of the dried paste (curve 1) and the products of hydration (curve 2) of C_3S (W/C = 0,5) hydrated at 25 °C in function of the time of hydration.
(B) Heat evolution measured by differential calorimetry and the calcium hydroxide content determined by the extraction (■) and XRD (□) methods as function of the time of hydration.

If the specific surface area is related to the amount of hydrated C_3S (Fig.1.A, curve 2) it is seen that at the end of the induction period the surface area increases exponentially which coincides with the period of maximum hydration heat evolution measured by differential calorimetry (DCA). With decreasing heat evolution the surface area of hydration products decreases to (Fig.1.A;

stage III). This decrease is caused by the growth of calcium hydroxide and calcium silicate hydrate. The following maximum of surface areas in the stage IV coincides with the prevously mentioned maximum of specific surface area of hydrated pastes (curve 1). To understand why this is formed we investigated the liberation of calcium hydroxide from the C_3S because there are no indications that in this reaction period a transformation of the C-S-H phases occur. The calcium hydroxide content was determined by the chemical extraction as well as by XRD method. The results of both methods show partially remarkable differences, especially in the reaction time between 8 and 48 hours (Fig. 1.B). This difference can be explained by the assumption that a past of the calcium hydroxide is present in an amorphous form, so that it cannot be determined by XRD-methods, which was prevously suggested by Brunauer and Kantro /7/. As can be seen from Fig. 1.A and B, the maximum of surface area (in stage IV) coincides with the maximum amount of amorphous calcium hydroxide. This means that the amorphous part of the $Ca(OH)_2$ exists in a highly dispersed form.

Additional informations we got by proton spinlattic relaxation time (T_1) measurments, the results of which are shown in Fig. 2.

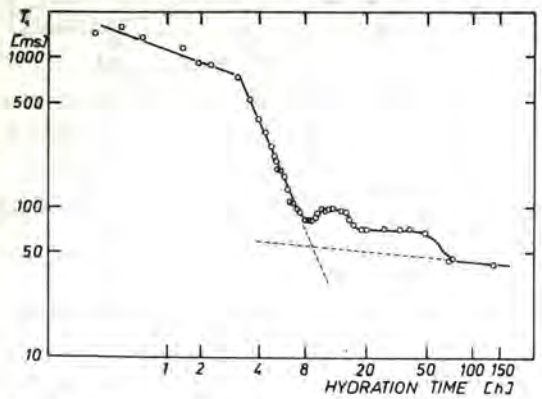

Fig. 2. Course of proton spin-lattic relaxation times (T_1)as a function of time of hydration for C_3S (W/C = 0,5; 25 °C).

After 2 hours T_1 begins to decrease lineary. Beginning from nearly 8 hours T_1 increases a littel bit and after a small maximum at 10-18 hours is formed the T_1-values decrease again. Similar results of T_1 measurements, made on C_3S pastes were reported by Kocuvan and coworker /8/. This maximum of T_1 coincides with the already mentioned maximum of highly dispersed calcium hydroxide content of samples and the maximum of the surface formed in the hydration of C_3S. Therfore it is assumed that the observed change in the spin-lattic interraction of the protons is connected with the formation and later cristallisation of the highly dispersed practically amorphous calcium hydroxide. The origin of the amorphous $Ca(OH)_2$ is not quite clear now, but we assume like Tadros et al /9/ that the cristallisation of the calcium hydroxide is poisoned by silicateanions. Additional measurements of specific surface area of the hydrated pastes of C_3S at 5 °C and 75 °C show as can oe seen in Fig. 3.,

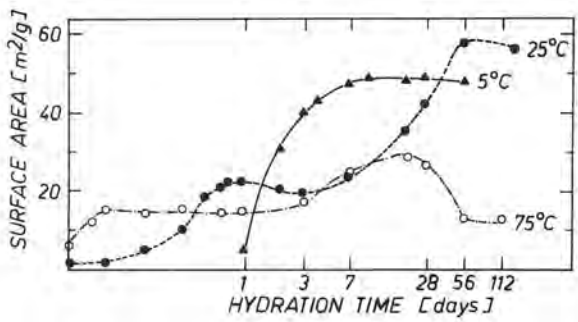

Fig. 3. Specific surface area of a dried C_3S paste (W/C = 0,5) hydrated at different temperatures in function of the time of hydration

that the maximum are shifted to shorter reaction times with increasing reaction temperature. This effect is in accordance with the heat evolution, the maximum of which is also shiffed to shorter reaction times with an increase in temperature.

For the hydration products can be observed besides the shortening of the period up to the rapid surface area development by raising the temperatur an increase of the

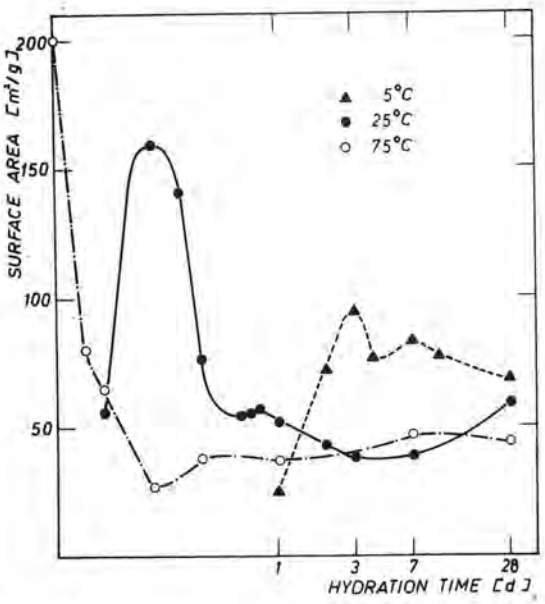

Fig. 4. Specific surface area of the hydration products of C_3S (W/C = 0,5) hydrated at different temperatures in function of the time of hydration

hights of the surface maximum (Fig. 4.). This increase of the hights of the maximum coincides with an increasing of the hydration rate in the early hydration stages. From the pore-size distribution was obtained, that with increasing temperatur the quantity of pores having a radius smaller than 20 Å is larger.

Another factor influencing the surface development in the C_3S hydration is the grain size of the starting material. Fig.5. gives the results of surface measurments of C_3S hydration products in dependence of the grain size.

It shows that the surface developed increases with decreasing grain size. Furthermore the decrease in grain size results in a shortening of the time needed for the beginning of the surface development. The specific surface of the hydration products formed during the acceleration period increases considerable with a decrease in grain size. From the porevolume distribution curves Fig. 6. it is seen that with decreasing

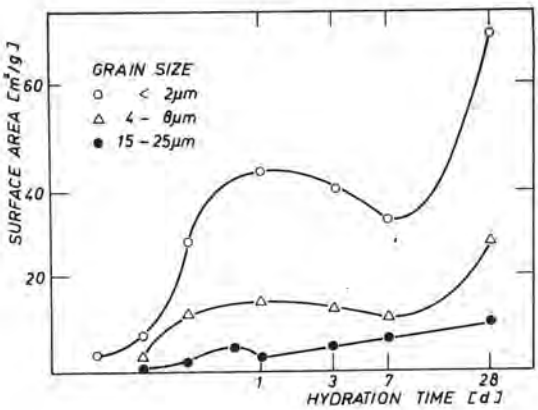

Fig. 5. Specific surface area of a dried C_3S paste (25 °C; W/C = 0,4) different grain sizes as function of the time of hydration.

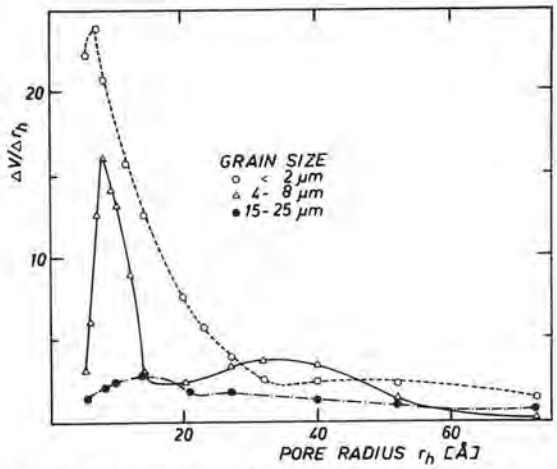

Fig. 6. Pore-size distribution of 28-day-old hydrated C_3S samples (25 °C; W/C = 0,4) for different grain sizes.

grain sizes a strong increase of pores with radii smaller than 20 Å is connected.

The variation of the water/C_3S ratio gives only small differences in the surface development during the C_3S hydration. But it is pointed out, that the pore-size distribution is shifted to smaller pore radii with decreasing water/C_3S ratio.

References

/1/ KANTRO, D.L., BRUNAUER, S. and WEISE,C.
J. Amer. Chem. Soc. 66 (1962) 1804

/2/ SKALNY, J., ODLER, I.
J. Colloid Interface Sci. 40 (1972) 199

/3/ BRUNAUER,S., MIKHAIL,R. and BODOR, E.E.
J. Colloid Sci. 24 (1967) 451

/4/ FRANKE, B.
Z. anorg.allg.Chemie 247 (1941) 180

/5/ HARADA, T., OHTA, M. and TAKAGI, S.
J. Ceram. Soc. Japan 86 (1978) 195

/6/ KONDO, R. and DIAMON, M.
J. amer. Ceram. Soc. 52 (1969) 503

/7/ BRUNAUER, S. and KANTRO, D.L.
in: The Chemistry of Cement Vol. 1,
pp. 287-309 Academic Press, London and
New York, (1964)

/8/ KOCUVAN, I., URŠIČ, J. and BARBIČ, L.T.
Silikattechnik 30 (1979) 22

/9/ TADROS, M.E., SKALNY, J. and KALYONCU,R.
J. Amer. Ceram. Soc. 59 (1976) 344.

Determination of specific surfaces of co-grinded materials with different grindabilities

Détermination des surfaces spécifiques des matériaux de différentes broyabilités après leur broyage simultané

Dr. S. TSIMAS, Dr. V. KASSELOURIS, Dr. CH. FTIKOS, Dr. G. PARISSAKIS,
HERACLES General Cement Co. - National Technical University of Athens,
Lab. of Inorg. and Anal. Chemistry, Greece.

SUMMARY : It is well known that by co-grinding materials of different grindabilities the desired granulometric curve is not always achieved. The prediction of the granulometry as well as the final specific surfaces becomes more difficult when these materials are co-grinded in different proportions.

The aim of this study is, in the case of co-grinding clinker and Santorin earth, to determine the resulting specific surfaces of each of these materials.

Thus, it has been found that by increasing in the mixture the proportion of Santorin earth (which is easier to grind than clinker) the final values of the specific surfaces of both the materials are decreased. More specifically by grinding clinker and Santorin earth in proportion 70:30 and 60:40 the fraction of 3-30 µm is significantly decreased.

RESUME : On sait qu 'en broyant ensemble des matériaux de broyabilité différente, la courbe granulométrique obtenue est déficiente.

La prévision de la granulométrie et des surfaces spécifiques finales s'avère plus difficile quand ces matériaux sont broyés ensemble dans des proportions différentes.

L'objet de cette étude, dans le cas du broyage du clinker et de la terre de Santorin, consiste à déterminer les surfaces spécifiques de chacun de ces matériaux dans le mélange.

Aussi on a trouvé qu'en augmentant dans ce mélange la proportion de la terre de Santorin (plus facile à broyer que le clinker) les valeursfinales des surfaces spécifiques de deux matériaux diminuent. Plus particulièrement en broyant du clinker et de la terre de Santorin dans les proportions 70:30 et 60:40 la fraction 3-30µm diminue d'une façon significative.

1. Introduction

From previous works (1,2,3) it has been proved that co-grinding of clinker with a pozzolan leads to the production of cements which show various advantages, especially with respect to their physical properties compared to Portland cements.

Pozzolans are, by nature, easier to grind than clinker, which means that with the same consumption of energy, the finenesses attained from pozzolan are far greater than those from clinker. In addition the co-grinding of these materials which have different grindabilities, results in a great differentiation concerning the final resulting specific surfaces of each one (4,5). The specific surface of each constituent must be known taking into consideration that both the pozzolanic material and clinker demonstrate their beneficial properties over limit values of specific surface. The prediction of the granulometry, as well as the final specific surfaces, becomes more difficult when these materials are co-grinded in different proportions. The aim of this study is in the case of co-grinding clinker and Santorin earth (S.e) to determine the resulting specific surfaces of each of these materials providing a systematic analysis of the weight percentages of the materials to be ground.

2. Experimental

2.1. Procedure

a) Co-grinding with 10,20,30,40% of Santorin earth. The mixture has been tested at Blaine finenesses of 3350, 3700 and 4150 cm^2/g. Thus 12 mixtures have been tested in total. These co-grindings have been worked out in a 510 mm x 340 mm laboratory mill. Both clinker and Santorin earth had previously been ground in the same mill separately, yielding the curves in fig. 1

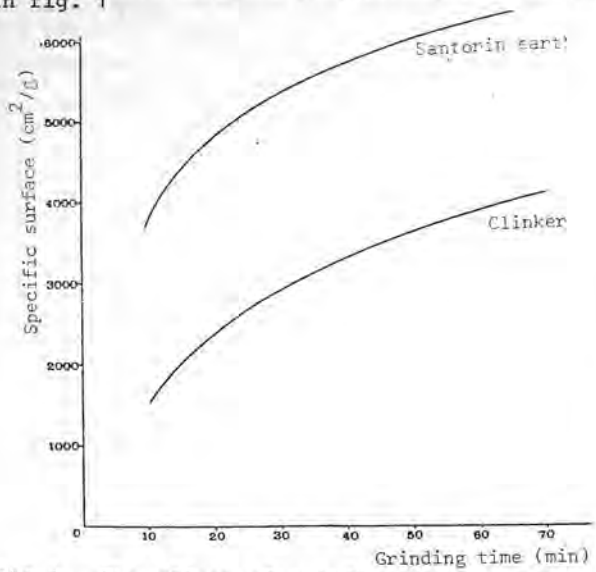

Fig 1. The effect of grinding time on the specific surfaces of clinker and Santorin earth.

These curves in combination with the Bond Indeces (clinker 14Kwh/S.t, S.e 12,1 Kwh/S.t) indicate the difference in grindability between the above materials.

b) Granulometric analysis of each sample, by sieving for the range 90-56 μm and by the use of the Alpine method for the range 56 -11 μm. Apparatuses used in both methods allow for further treatment of separated fractions (5.6).

c) Determination of pozzolanic material in each fraction. This determination is based on the amount of insoluble residue after a suitable chemical treatment.

d) Calculation of the specific surface for both the pozzolanic material and the clinker on the basis of the formula (7,8)

$$S_B = \frac{3}{p} \cdot \frac{x}{r}$$

where p = density of a constituent
x = the percentage of a constituent in each fraction
r = the average radius of a fraction

This calculation followed an extension of the granular gradation curves for the range below 11 m.

2.2 Verification of the method

A total of 14 experiments has been conducted in order to secure accuracy of the method. In these experiments clinker and Santorin earth of known specific surfaces were mixed together. The results of the above experiments are presented in the following table I, where the specific surfaces are measured with Blaine apparatus.

TABLE I. Measurements of the accuracy of the method

CEMENTS			CLINKER		
Spec. surf.		Deviation	Spec. surf.		Deviation
Meas.	Calc.	%	Meas.	Calc.	%
3360	3356	0,1	3200	3198	0,0
3360	3302	1,7	2890	2931	1,4
3300	3310	0,5	3000	3149	5,0
3350	3419	2,0			
3620	3609	0,4	SANTORIN EARTH		
3350	3399	1,5	4340	4396	1,3
3360	3344	0,4	5800	5783	0,3
3350	3289	1,8	6000	5790	4,7

2.3 Results and discussion

The results attained are summarized in Table II.

TABLE II. Specific surface of each constituent

S.e %	Spec. surf. of the mixture cm^2/g (Blaine)					
	3350		3700		4150	
	Cl.	S.e	Cl.	S.e	Cl.	S.e
10	2980	7100	3500	7680	3830	8200
20	2840	5820	3280	6800	3630	6950
30	2680	5650	3170	5600	3380	5900
40	2600	5070	3030	5450	3120	5700

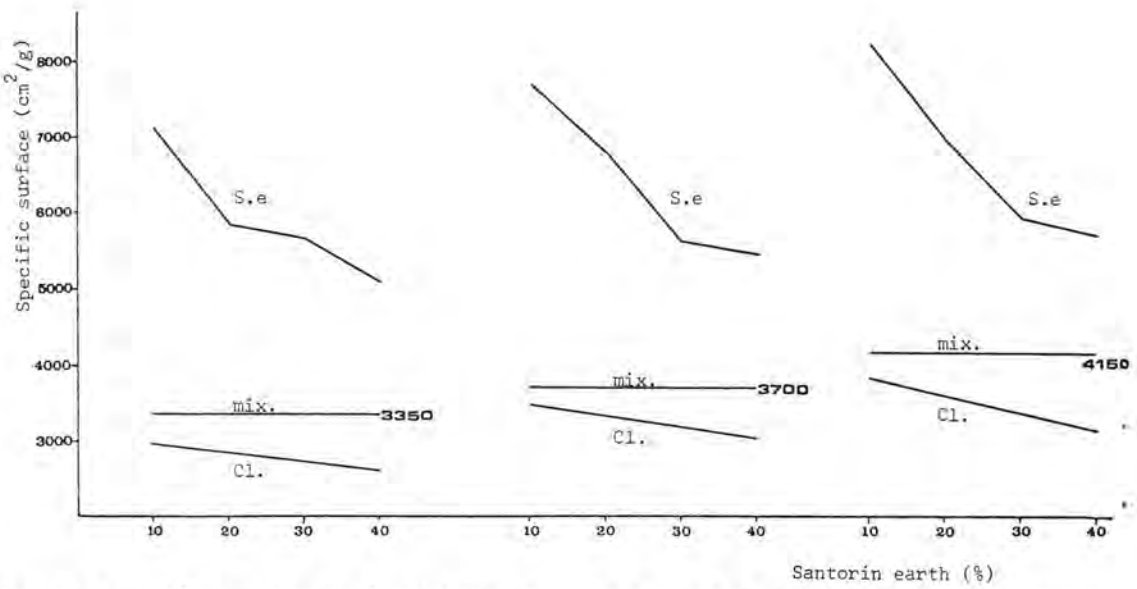

Fig. 2. The specific surfaces of clinker, Santorin earth and their mixture for several percentages of Santorin earth and several finenesses of the mixture.

a. From Table II and the relative Figure 2, it appears that:
- The specific surfaces of each material are considerably differentiated during their co-grinding with decreased specific surface in case of clinker and increased specific in case of Santorin earth.

- An increase in the percentage of Santorin earth results in decreased values of specific surface for both clinker and Santorin earth compared to their respective values when the Santorin earth percentage in the mixture is less.

b. Similar conclusions are derived from the observation of Fig. 3 which depicts the changes in the specific surface of clinker in relation to the mixture's specific surface, for various percentages of Santorin earth. It is noticed that when the Santorin earth percentage is increased, the clinker's specific surface is increased at a more pronounced rate for the range 3350-3700 cm^2/g than for that between 3700-4150cm^2/g.

c. On the basis of Fig. 3, the specific surface of the mixture may be calculated by taking into consideration the percentage of Santorin earth in it, so that the specific surface of clinker reaches a certain value. Specifically, if clinker should have a fineness of 3050± 50cm^2/g (Blaine), the suggested specific surfaces (Blaine) of the mixture are as follows:

3400± 50cm^2/g	for a mixture	with	10%	Santorin	earth	
3500± 50cm^2/g	" "	"	"	20%	"	"
3650± 50cm^2/g	" "	"	"	30%	"	"and
3800± 50cm^2/g	" "	"	"	40%	"	"

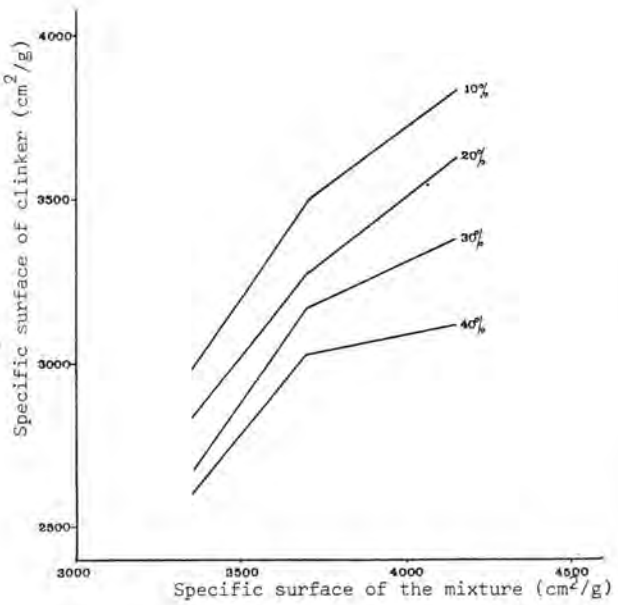

Fig. 3. Relationship between the specific surfaces of clinker and mixture for several percentages of Santorin earth.

d. Table III shows the percentages of mixtute and its constituents in the 3-30μm fraction. As it is clearly seen from this table an increase in S.e. causes a decrease of the % of clinker in the above mentioned fraction.

TABLE III. Percentage of materials for the 3-30μm fraction.

S.e	3350			3700			4150		
	Cem.	Cl.	S.e	Cem.	Cl.	S.e	Cem.	Cl.	S.e
10	53.0	53.5	46.0	52.5	53.0	40.0	59.0	59.0	49.0
20	50.5	50.0	51.0	47.0	48.0	40.0	50.0	51.0	42.5
30	45.5	44.5	48.5	43.0	44.0	40.0	41.5	44.5	38.0
40	41.0	41.5	40.5	44.5	42.0	45.0	45.0	44.0	48.0

3. Problems arising form grinding materials of different grindability and suggested solutions

From the above it is concluded that an increase in the Santorin earth percentage complicates the co-grinding process and leads to smaller specific surfaces both for clinker and Santorin earth. Moreover, the above mentioned increase results in a decrease of the 3-30 μm fraction.

This reduced grindability of the constituents may be attributed to the following:

a) The overgrinding of Santorin earth during its co-grinding with clinker is partly due to the latter's behaviour as a grinding medium. Thus, an increase in Santorin earth proportion and a corresponding decrease in clinker make the clinker's role as a grinding medium less significant and therefore, grinding is made more difficult.

b) Due to its smaller bulk density a higher proportion of Santorin earth causes an in crease in the loading of the mill. As a consequence, the passing of clinker through the mill is made difficult.

Solutions to these problems which are more pronounced for percentages higher than 20% are suggested below.

As laboratory testings have shown, Santorin earth forms a 75% residue on the 90 μm sieve. Thearfore, for the separation of the 25% fine fraction the use of an air-separator is recommended on an industrial scale. In this way the overgrinding of this fraction is eliminated, while operations in the mill's second compartment are facilitated.

A change in the gradation of grinding media inside the mill is necessary, especially in the second compartment, so that the quantity of the grinding media of small diameter is considerably increased.

Bibliography

1.- TERRIER, P., MOREAU, M. (1966): Rev. Mater. Constr., 613 379-96, 441-51.

2.- FTIKOS, C. (1977): Study of the pozzolanic action in cement pastes during their hydration process. Diss Thesis, Nat. Tech. Univ. Athens.

3.- FTIKOS, C., PARISSAKIS, G. (1975): Pozzolans and their action during hydration of cement pastes. 2nd Hellenic Concrete Conference, Thessaloniki, Greece.

4.- BOMBLED,J.P. (1965): Rev. Mater. Constr., 593 61-75.

5.- MUSIKAS, N. (1970): Rev, Mater. Constr., 652-3, 21-35.

6.- A.F.NOR. (1968), E.P. 3576.

7.- A.S.T.M. (1968), STP 473.

8.- ALLEN, T. (1975): Particle size measurement, Chapman and Hall, London 122, 395.

Influence of MgO on phase composition of PC-clinker and on cement properties

L'influence de la magnésie sur la composition de phases du clinker Portland et sur les propriétés du ciment

K. POPOVIC, Civil and Construction Engineering Institute, Faculty of Construction Sciences, University of Zagreb,
A. BEZJAK, Faculty of Pharmacy and Biochemistry, University of Zagreb Yougoslavie.

SUMMARY: According to X-ray diffraction results, the increase from 0 to approx. 2.5% MgO content in clinker (potential composition: C_3S 57, C_2S 23, C_3A 10 and C_4AF 10%) causes considerable lowering of C_3A and belite, with simultaneous increase in alite and ferrite phase content. Opposite effects are, however, the consequence of MgO additions exceeding 2.5%. The intensities of these phase changes are closely associated with the cooling rate of sintered mixes.

Despite the said differences in phase composition, cements without and those with MgO addition were found to be quite similar in respect to the rate of hardening. The heat of hydration has exhibited the expected changes brought about by various C_3A contents in clinkers.

X-ray diffraction has also established that the degree of hydration (α) of alite does not significantly differ for MgO and MgO-free samples.

RÉSUMÉ: Les résultats de la diffraction des rayons X indiquent que l'augmentation de 0 a environ 2.5 % de la teneur en magnésie dans le clinker (composition potentielle: C_3S 57%, C_2S 23%, C_3A 10% et C_4AF 10%) cause une diminution considérable de C_3A et de la bélite, avec une augmentation simultanée de la teneur en alite et en phase ferritique. Si toutefois l'addition de MgO dépasse 2.5%, on obtient des effets opposés. Les intensités de ces changements des phases sont étroitement liées à la vitesse de refroidissement des mélanges cuits.

Malgré les différences mentionnées dans la composition des phases on a constaté que les ciments avec et ceux sans addition de MgO sont similaires quant a la vitesse de durcissement. La chaleur d'hydratation a montré les changements prévus résultant des teneurs différentes en C_3A dans les clinkers.

La diffraction des rayons X a aussi confirmé que le degré d'hydratation (α) de l'alite ne diffère pas significativement pour les échantillons renfermant la magnésie et les échantillons qui ne la contiennent pas.

1. INTRODUCTION

Magnesium oxide is of particular interest in cement manufacture mainly due to the unsoundness of the product that it can bring about if present in greater amounts. When exploring various mineralizers in order to improve the sintering process of white cement, however, the addition of MgO to the raw mix was observed to significantly affect the phase composition of the clinker. Several researchers [1-5] have noticed certain changes in the phase composition of clinker under the influence of MgO, and the present work describes the results of systematic investigations concerning the effect of magnesia on the phase composition and on some cement properties.

2. EXPERIMENTAL PROCEDURES

2.1. The influence of MgO on the phase composition of clinker was studied on the C_3S-C_2S-C_3A system corresponding to white cement, and also on the system of normal portland cement clinker C_3S-C_2S-C_3A-C_4AF. Table 1 shows the potential mineral composition of the observed clinkers.

TABLE I
Potential mineralogical composition of clinker samples

Clinker	Phase content (wt %)			
	C_3S	C_2S	C_3A	C_4AF
W-1	55	30	15	-
W-2	5	75	20	-
W-3	15	65	20	-
W-4	32	48	20	-
W-5	48	32	20	-
W-6	75	5	20	-
W-7	25	25	50	-
N-1	57.1	24.5	7.6	9.9
N-2	65	15	10	10
N-3	50.6	39.4	10	-
N-4	48.8	38	10	3.3
N-5	47	36.5	10	6.6
N-6	45	35	10	10

Several tests were carried out on the C_3S-C_2S system too with varying variations in the potential proportion of particular minerals.

The clinkers were synthetized from pure chemicals (W-2 to W-7 and N-3 to N-6) and also from industrial raw materials (W-1, N-1 and N-2) containing practically no magnesia. MgO was added to the raw mix in the amount up to 5% by weight of clinker. The samples were sintered in a laboratory electric furnace of the "Kanthal" type at 1450°C and remained at the sintering temperature for one hour. Cooling was effected in two ways: the majority of samples were subjected to rapid colling being exposed to room temperature; with the other samples slow cooling was applied from the sintering temperature to the temperature of 1300°C in order to allow the melt to crystallize in equilibrium with the solid phase, and then the samples were cooled rapidly being exposed to room temperature. X-ray diffraction served to establish the phase composition of the clinkers.

2.2. The influence of MgO on cement properties was studied on the system of normal portland cement by comparing MgO-free samples with those containing the amount of MgO that brought about the greatest phase changes. MgO-free industrial raw mixes were used and the sintering was carried out at 1450°C, with rapid cooling.

The potential composition computed according to Bogue's formulas and the actual phase composition of the observed clinkers determined by X-ray diffraction are given in Table II.

TABLE II
Composition of clinkers for cement properties examinations (Wt %)

	MgO free		2.3% MgO	
	Bogue	X-ray	Bogue	X-ray
C_3S	57	50	55.6	60
C_2S	23	30	22.5	20
C_3A	10	10	9.8	3
C_4AF	10	5	9.8	9
MgO	-	-	2.3	0

The clinkers were subsequently ground to Blaine fineness of 3200 cm^2/g, with the addition of gypsum (2.9% SO_3). In the cements obtained, determinations were performed of the strengths and of the heats of hydration.

X-ray diffraction was applied to determine the degree of hydration of alite over the period of three days.

3. RESULTS AND DISCUSSION

3.1. The investigation of the C_3S-C_2S-C_3A system has established that MgO, if added up to the "characteristic " amount of approximately 2%, brings about lowering of the aluminate and C_2S-phase with a parallel increase in the alite content. The addition of MgO in amounts greater than 2% had the opposite effects e.g., an increase in the C_3A and C_2S contents and a decrease in the alite content. Figure 1 (left) shows such changes in the intensity of diffraction peaks for individual minerals obtained on clinker W-1. In case of raw mixes with very high proportion of alite, there is no increase in alite content; instead free CaO appears in the clinker (Fig. 1 - right).

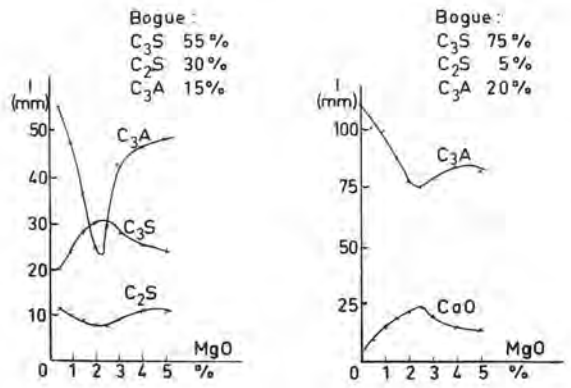

Fig. 1 - Phase changes in system C_3S-C_2S-C_3A caused by MgO (intensities of X-ray peaks)

The "characteristic" magnesia content causing the greatest changes in phase composition is proportional to the potential C_3A content in clinker: it amounts to 2% for the clinker with 15% C_3A, 2.3% for the clinker with 20% C_3A and about 4% if the mix contains 50% C_3A (Fig. 2). It is also in mix W-7 that the addition of MgO causes the appearance of free CaO, instead of an increase in alite.

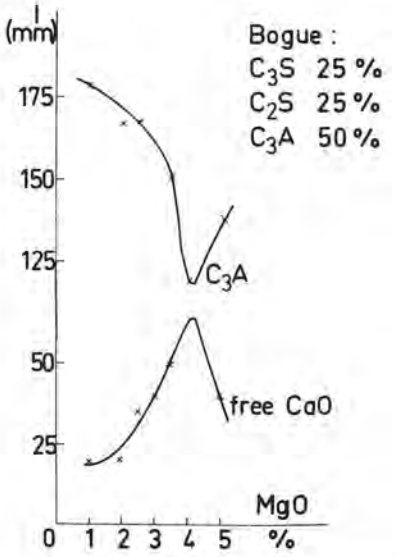

Fig. 2 - Phase changes in system C_3S-C_2S-C_3A (sample with 50% C_3A) caused by MgO (intensities of X-ray peaks)

Free MgO as periclase appears only if the MgO amount in the mix is greater than the "characteristic" one. This is particularly interesting in mix W-7 potentially incorporating 50% C_3A.

In the C_3S-C_2S-C_3A-C_4AF system the addition of MgO, up to its "characteristic" value also reduces the C_3A and C_2S amounts in clinker with a parallel increase in the contents of C_3S and the ferrite phase. MgO content exceeding the "characteristic" one will produce opposite effects in that case too. Typical changes in the proportion of clinker minerals determined in clinker N-2 are presented in Figures 3 and 4.

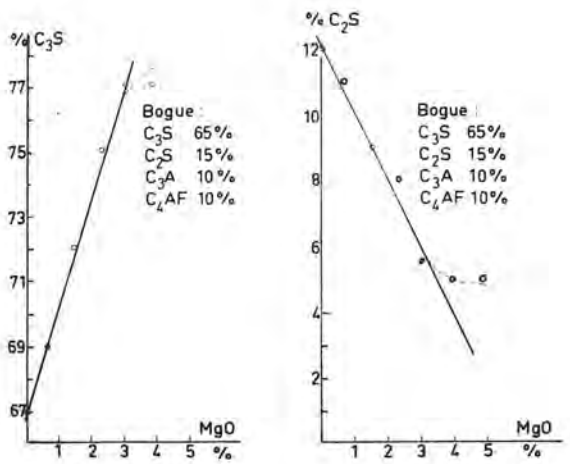

Fig. 3 - Changes in C_3S- and C_2S-phase content (system C_3S-C_2S-C_3A-C_4AF) caused by MgO (quantitative X-ray analysis)

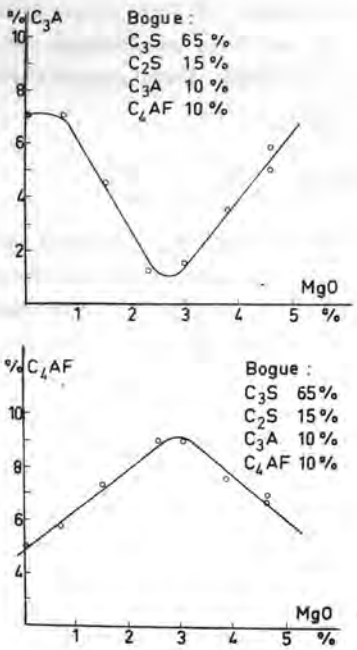

Fig. 4 - Changes in C_3A- and C_4AF-phase content (system C_3S-C_2S-C_3A-C_4AF) caused by MgO (quantitative X-ray analysis).

A further effect of magnesia addition is the change in the composition of the ferrite phase. Based on the position of diffraction peaks it has been established that, depending on the MgO present, the ferrite phase has the composition, shown in Table III.

TABLE III

Ferrite phase composition depending on MgO content

% MgO	mol % C_2F	mol % C_2A
0	45	55
0.7	55	45
1.5	62.5	37.5
2.3	65	35

Free MgO as periclase appears also in this system only if the amount of MgO added is greater than the "characteristic" value.

All the described effects were noticed only in case of rapid cooling.

The phase changes are the due to differences in the amount and composition of the liquid phase during sintering which result from the different MgO proportions in the raw mix. In the slowly cooled clinkers, where the melt has crystallized in equilibrium, no changes in phase composition have been noticed caused by magnesia. Neither in the C_3S-C_2S system where the reaction at 1450°C occurs almost exclusively in the solid phase, the addition of MgO did not affect the phase composition regardless of whether rapid cooling or slow cooling was applied.

3.2. The determination of strengths of cements obtained from MgO-free clinkers and those with MgO added (Table II) has yielded the results shown in Table IV, whereas Table V presents the heats of hydration of the same cements determined by the vacuum flask method.

TABLE IV

Compresive strengths of cements with and without MgO (N/mm^2)

	1 day	3 days	7 days	28 days
Cement paste (w/c=0.4) 1x1x4 cm				
MgO free	11.8	25.7	48.7	77.2
2.3% MgO	9.6	27.8	43.0	87.2
Cement mortar (1:3) (w/c=0.5) 2x2x20 cm				
MgO free	13.4	30.0	43.4	63.0
2.3% MgO	12.9	27.1	42.0	60.7

TABLE V

Heat of hydration of cements with and without MgO (cal/g)

	3 days	7 days
MgO-free	85.5	92.7
2.3% MgO	74.9	82.3

The results clearly indicate that the determinations of the heat of hydration for cements without and those with MgO exhibit differences that have been expected owing to the different proportion of C_3A in the clinkers from which the cements were made.

The strengths developed in cements not containing magnesia, however, do not significantly differ, from those in cements with MgO despite the considerably higher alite content in cements with MgO additon. It appears that the proportion of C_3A in cement has a very important role in strength development, particularly at early ages; as already mentioned C_3A proportion is much lower if cement contains MgO; thus the higher alite content in the cement with MgO is compensated.

The study of alite hydration over a 3-day period has proved that its degree of hydration is similar in samples with and those without MgO, the hydration rate being, however, slightly higher in cements with MgO (Fig.5).

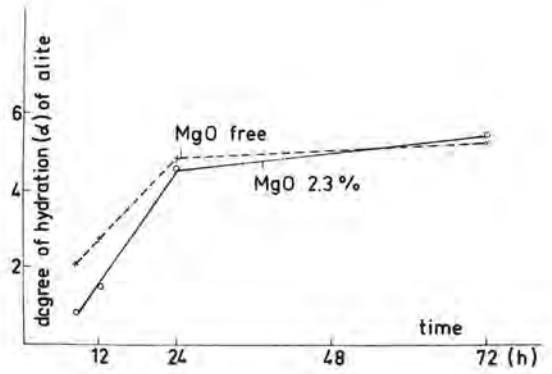

Fig. 5 - Rate of hydration of alite for cements with and without MgO

Because of the great lowering of C_3A content under the influence of MgO, considerable changes in the sulfate resistance of cement can also be expected. Such investigations are in progress.

ACKNOWLEDGEMENT

The assistance of JUCEMA, Association of the Yugoslav Cement Producers, in allowing the authors to use its laboratory equipment during the investigations described is gratefully acknowledged.

REFERENCES:

1.- F.M. LEA (1970), The Chemistry of Cement and Concrete, Edward Arnold, London.

2.- H.Krämer and H.Strassen (1960), Proceedings of the Fourth International Symposium on the Chemistry of Cement, Washington, Vol I, 32-33.

3.- K.MIYAZAWA, and K.TOMITO (1966), "Der Einfluss von MgO auf die Eigenschaften des Portlandzementes", Zement-Kalk-Gips 19, No.2, 82-85.

4.- E.SPOHN, E.WOERMANN, and D.KNOEFEL,(1969) "Eine verfeinerte Kalkstandardformel", Zement-Kalk-Gips 22, No. 2, 55-60.

5.- Yu. NIKIFOROV, R.A.ZOZOLYA, and N.M. IVANOVA (1974), "Role played by Magnesia in Clinker and Cement Technology", The VI International Congres on the Chemistry of Cement, Moscow, Supplementary paper, Section I, I-3.

A method for determination of free CaO ($Ca(OH)_2$) in binding materials

La détermination de la chaux libre dans des matériaux cimentés

A. MITUZAS, Cand. Sc. (technics), Head of the Laboratory,
J. MITUZAS, Cand. Sc. (chemistry), Head of the Laboratory,
L. RAMANAUSKIENE, engineer, « Akmencementas », N. Akmené, USSR.

RESUME : Nous avons élaboré et vérifié une méthode de détermination à la température ambiante du CaO ou $Ca(OH)_2$ libres dans les briques hollandaises et autres matériaux cimentés durcis.

Comme solvant, on peut se servir d'éthylène-glycol déshydraté ou son mélange avec un de ses composés de la classe des alcools en ajoutant $Ca(NO_3)_2$, $Sr(NO_3)_2$ $BaCl_2$ etc. Avant l'analyse, on fait bouillir le solvant avec un des produits ajoutés, puis on le fait refroidir jusqu'à la température ambiante. Le solvant amené au pH nécessaire est prêt à l'utilisation.

L'analyse est faite à un pH constant contrôlé d'une façon potentiométrique. Cela permet de faire la mesure d'une façon automatique suivant le schéma pH-mètre-bloc de titrage automatique -enregistrement des résultats.

SUMMARY: A method for determination of free CaO or $Ca(OH)_2$ in clinkers, Portland cements, other binding materials and their hardened products at room temperature has been developed and checked by authors.

Anhydrous ethylene glycol or its mixture with one of compounds from group of alcohols with $Ca(NO_3)_2$, $Sr(NO_3)_2$, $BaCl_2$ or other dehydration agents can be used as solvent. Before the analysis solvent is subjected to boiling and subsequent cooling to room temperature.

The analysis is carried out at constant pH, which is controlled with the help of potentiometer. This allows to carry out the automatic analysis according to the following scheme: pH - meter-block for automatic titration -recording of the results.

INTRODUCTION

At present determination of free CaO or $Ca(OH)_2$ amounts is one of the important problems in chemistry and technology of binding materials. Many scients are carrying out research work in this field in different contries (1,2).

Among well-known methods for free CaO ($Ca(OH)_2$) determination the following ones find an extensive use: 1)Emmly modified by Bogue and Lerch (3); 2) Branderburg,s one (4); 3) Franke modified more than once and at present time to be used in the form proposed by Pressler,Brunauer,Kantro and Weise (6) in which either variation of extraction time (TVM) or solution (SVM) amount are assumed.

Methods (3,4,5) are based on selective dissolution of free CaO ($Ca(OH)_2$) in specimen under investigation in corresponding solvents at their boiling temperature and so according to the method (6) the material to be analyzed can be treated in a certain solvent at boiling temperature and as well at room temperature with the following determination of free CaO transited into solution by voluminous methods.

However the specificity of methods (analyzing at boiling temperature /3,4,5/ or the separation of the material to be analyzed by filtering (5,6) rusult in some difficulties in the case of automatization and evaluation of experimental results for instrumental methods employment for analysis (potentiometric, coulometric,titration,etc.).

The method developed by the authors of this paper allows to carry out the analysis of free CaO ($Ca(OH)_2$) content in binding materials and products of their hardening at room temperature and simultaneously solves the problem of automatic system development for a given component analysis.

I. EXPERIMENTAL PROCEDURE

In the series of experiments it was found that the temperature increase during the treatment of ethylene glycol [x] with addition of different dehydrating salts of type $Ca(NO_3)2$, $Sr(NO_3)_2$,$BaCl_2$,LiCl etc.with the following cooling of solution to room temperature results in always increasing intensity of CaO ($Ca(OH)_2$) dissolution. The highest reactivity relative to CaO ($Ca(OH)_2$) has been attained after boiling with following cooling of pure ethylene glycol (boiling temperature (b.p.) 197°C) with $Ca(NO_3)_2$ addition.Further in the present work pure ethylene glycol with $Ca(NO_3)_2$ addition (60 mg to 1 ml ethylene glycol) boiled in the period of 5 min.and cooled under the stream of water to room temperature was used as solvent.Boiling is carried out in Erlenmeyer flask with reflux condeser supplied with tube filled with soda lime and Bunsen valve not allowing air access to the content in the flask.

After solvent boiling and cooling acetonitrile (1 ml CH_3CN to 5 ml of ethylene glycol) has been added for viscosity decreasing. This aprotic solvent not showing acidity properties possesses of a relatively high dielectric constant (ε = 37,5) and plays an important role at the employment of potentiometric analysis methods,which were used by us in the present work.

In reality the analysis was carried out in mixed solvent consisting of polar (ethylene glycol) and aprotic (CH_3CN) components at the ratio of 5:1.

Thus pH of prepared solvent has attained 9,25[xx] by addition of 1% KOH solution in ethylene glycol.

Glass electrode with H^+ function was used as indicator electrode and silver chloride electrode filled with saturated water solution of potassium chloride served as reference one.

After attaining required pH of solvent the material to be analyzed [xxx] was placed in certain amounts into the cell for titration and after switching on magnetic stirrer automatic titration system was switched on. During the analysis proceeding solvent pH with substance to be analyzed was in the range of 9,20-9,25.pH reducing to 9,20 was caused by cell inertness after addition of next portion of titrant,particulary in the final stage of determination. 0,2N solution of dehydrated benzoic acid in isopropanol has been used as titrant.

The principal scheme of potentiometric titrometer is given in Fig.1.

The final moment of titration is considered achieved when pH variation of solvent does not exceed 0,05 in the period of 20 min.

2.EXPERIMENTAL RESULTS

For the evaluation of the suggested method reliability the determinations of CaO ($Ca(OH)_2$) were carried out on the same specimens by other well-known chemical methods. The following methods developed by different authors were employed:Emmly,s modified by Bogue and Lerch (3);Branderburg (4); Franke modified by Pressler and etc. (6).

Short characteristics of employed materials are given in Table 1 and experimental results - in Table II.

---

[x] Treatment temperature was controlled by addition of corresponding alcohols. In this work the following alcohols were used:isopropanol (b.p.-82,5°C); propyl alcohol (b.p.-97°C); isobutyl alcohol (b.p. - 108°C);butyl alcohol (b.p.-118°C); amyl alcohol (b.p.-138°C);cyclohexanol (b.p.-161°C).

[xx] In some cases pH of the medium was different.

[xxx] In a given series of experiments all specimens to be analyzed have been ground to fineness of 40 μm in jasper mortar.No cautions were taken against action of surrounding atmosphere to specimens during their grinding.

Table I. Composition of Employed Materials

Index	SiO_2	Al_2O_3	Fe_2O_3	CaO	MgO	R_2O	SO_3	Oth.	Loss of ignition	
K	21,12	6,80	3,65	62,37	3,52	1,00	0,48	0,81	0,25	Clinker from rotary kiln.
C_o	20,35	6,53	3,84	60,95	3,05	0,84	1,76	1,55	1,13	Portland cement hydrated over different periods of time x/
B_o	20,96	6,20	4,13	64,70	2,66	0,60	0,48	0,09	0,18	Portland cement hydrated during 13 years.
B_1	20,12	5,95	3,97	63,47	2,50	0,58	2,28	0,33	0,80	Portland cement hydrated during 9 years.
$Š_1$	22,80	6,22	1,00	65,16	1,50	0,14	1,82	0,22	1,14	Portland cement hydrated during 13 years.
D	2,75	R_2O_3=	1,17	45,12	6,40	-	-	1,09	43,47	Dolomite limestone
R	20,10	5,96	4,04	56,97	3,50	1,77	1,80	2,54	3,32	Probe from calcination zone of rotary kiln.

Table II. CaO Amount (%) in Investigated Specimens xx/

Index	Methods			Suggested method	
	Emmly(mod.by Bogue and Lerch)	Branderburg,s	Franke (mod.by Pressler etc) xxx	CaO	Analysis time (min.)
K	0,20	0,28	-	0,33	55
C_o^o	11,80	12,66	-	11,30	120
C_o^1	9,09	8,78 8,85	-	9,10	120
C_o^3	10,03	11,07	-	10,12	90
C_o^7	10,43 10,23	11,35	-	10,79	110
C_o^{28}	11,39	13,06	-	11,90	180
C_o^{90}	11,76	13,32	-	11,88	130
B_o	18,54	22,04	18,54	19,67 19,57	270 xxxx/ 210
B_1	17,99	19,37	17,88	18,44 18,31 18,58	270 xxxx/ 210 240
$Š_1$	12,61	15,12	12,47 12,45	14,22 14,29 14,26	270 xxxx/ 210 240
D	74,53	76,73	74,29	74,12	12
R	11,35	11,43	11,47	11,49	40

x/ 1 day - C_o^1; 3 days - C_o^3 ;7 days - C_o^7;28 days -C_o^{28};90 days - C_o^{90} ; curing (80°C) -C_o^o

xx/CaO content calculated on Calcined material.

xxx/ Variant TVM been used.CaO amount calculated after dissolution in 60,90 and 120 min. The final point of titration has been determined potentiometrically in the point of titration curve inflection (pH =3,05)

xxxx/ pH = 9,35

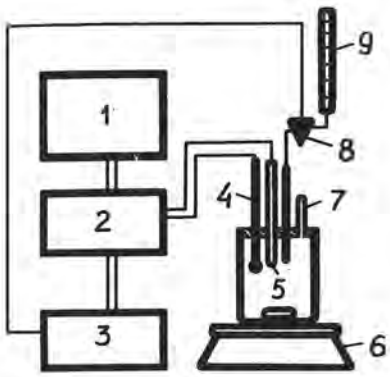

Fig.1. The priciple scheme of automatic potentiometric titrometer.

1 - recorder; 2 - pH-meter;3 - automatic block for titration;4 -indicator electrode; 5 - reference electrode;6 -magnetic stirrer; 7 - tube with ascarite; 8 - magnetic valve; 9 - microburette.

3.DISCUSSION OF RESULTS

Data given in Table II show,that CaO content determined by the suggested method in investigated materials are in good correlation with results obtained by Emmly and Franke methods,excluding quantities found in Portland cements hydrated over a long period of time. Amounts of CaO determined by Branderburg,s method mainly exceed that obtained in the work carried out by other methods. Most likely this is caused by partly dissolution of other components of binding materials (2).

Considering data on CaO ($Ca(OH)_2$) in Portland cements hydrated over a long period of time (B_0,B_1,$\check{S}_1$),results obtained by us are as if in "the middle" amoung the data obtained by Branderburg,s method and Emmly and Franke one. X-ray patterns[x] obtained on separate specimens after their treatment at room temperature and also at boiling temperature (Fig.2) show the absence of $Ca(OH)_2$ peaks indicating that really complete dissolution of $Ca(OH)_2$ crystals has occured.Treatment of ethylene glycol with dehydrating salts at elevated temperatures leads to compound[xx]formation,composition of which was not determined in this work.Although namely this new compound of solvent favours dissolution of calcium silicate hydrates or calcium aluminate hydrates at pH<9,0,and that of $Ca(OH)_2$ only at higher pH.

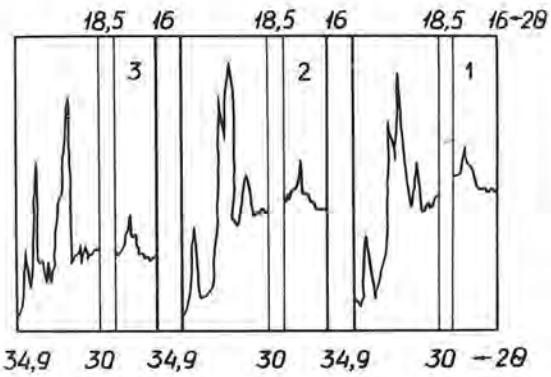

Fig.2.X-ray patterns of some investigated specimens.

1 - $\check{S}_1$ after treatment by suggested method; 2 - $\check{S}_1$ after treatment by Franke method (TVM); 3 - B_1 after treatment by suggested method.

Separate experiments showed,that the dissolution even of large single crystals (hexagonal plates 3-4 x 0,5-0,6 mm) $Ca(OH)_2$[xxx] proceeds with significant rate.The scheme of dissolution rate of $Ca(OH)_2$ single crystals in the above mentioned solvent is shown in Fig.3.

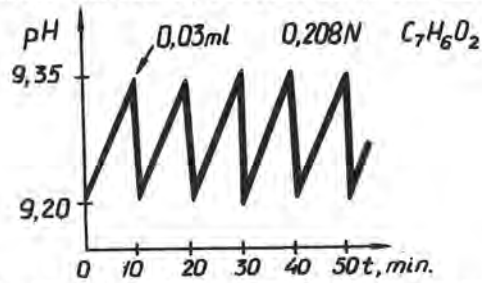

Fig.3. $Ca(OH)_2$ single crystals dissolution rate at room temperature.

The attention is drawn by the fact,that dissolution proceed at constant rate,i.e. reaction rate is proportional to specific area of the material to be dissolved.

Filtrate analysis on the presence of SiO_2, Al_2O_3 etc. after complete $Ca(OH)_2$ dissolution was employed for the proposed method verification.After the separation of insoluble part by filtration the obtained filtrate was subjected to vacuum distillation (10 mm Hg column) in which ethylene glycol and acetonitrile were eliminated[xxxx].The remaining solid substance must consist of the initial $Ca(NO_3)_2$ and SiO_2,Al_2O_3 etc. in the case of their transition into filtrate during the dissolution of the investigated material.Heat treat-

---

x/ Wide range diffractometer of the type DPOH - 1,5.CuK_{oc} radiation; tube current capacity 20 mA ; voltage - 32 kV.

xx/ pH of ethylene glycol with dissolved $Ca(NO_3)_2$ (60 mg $Ca(HO_3)_2$ in 1 ml if ethylene glycol) before boiling attains ~ 7,1 and after it increases to 8,5-8,6.

xxx/ Single crystals were grown by diffusive method at the temperature of 52°C in 3 weeks. NaOH and $CaCl_2$ served as components of reaction.

xxxx/ In a given case the analysis proceeding is described after treatment of $\check{S}_1$ (Table II).

ment of the similar system must proceed according to

$$k\ Ca(NO_3)_2 + \begin{cases} SiO_2 \\ Al_2O_3 \end{cases} \xrightarrow{t^oC} \longrightarrow \begin{matrix} C_2S \\ + \\ C_3A \end{matrix} + (k-5)\ CaO \qquad (I)$$

Free CaO decrease must point to the presence of other components besides to $Ca(NO_3)_2$x/. However after solid substance firing at the temperature of 1100°C in the period of 30 min. it was obtained free CaO = 98,93% i.e. really at the purity grade of $Ca(NO_3)_2$ used agent. This point to the absence of the components of SiO_2, Al_2O_3 type in filtrate after durable treatment of cement stone in the above mentioned solvent.

REFERENCES

1. - H.G.Midgley (1979), Cement and Concrete Research, 9, 77-82.
2. -"Химия цементов", под ред.Х.Ф.У.Тейлора, Стройиздат, М., стр.216-217, 1969.
3. - R.H.Bogue."The chemistry of portland cement",2 nd.Ed.,Reinhold,New York,p.p. 98-99,1955.
4. - R.H.Bogue "The chemistry of portland cement",2 nd. Ed., Reinhold,New York, p.p.100,1955.
5. Ф.М.Ли."Химия цемента и бетона",Стройиздат, М., стр.109, 1961.
6. - E.E.Pressler,S.Brunauer,D.L.Kantro, C.H. Weise (1961).Analytical Chemistry, 33, 877-882.

---

x/ In separate experiments it was established that used solvent does not affect separate minerals C_3S, C_2S, C_3A, C_4AF.

On the composition of cement minerals

Sur la composition minérale du ciment

A. BOIKOVA, Doctor, Institute of Silicate Chem. of the USSR Academy of Sci. Leningrad,
A. ESAYAN, Engineer, Institute of Silicate Chem. of the USSR Academy of Sci. Leningrad,
V. LAZUKIN, Engineer, Institute of Silicate Chem. of the USSR Academy of Sci. Leningrad.

RESUME : Les compositions des phases de cinq clinkers industriels du ciment Portland ont été étudiées à l'aide d'un appareil Camebax du type MB-1.

Pour faire un calcul quantitatif des éléments, les produits types suivants ont été synthétisés : des solutions solides de C_3S avec Na_2O, K_2O, MgO, Al_2O_3, Fe_2O_3; C_3S avec MnO; C_3S avec TiO_2; C_2S avec P_2O_5; C_3A avec Na_2O; C_4AF avec MgO; C_6A_2F avec Na_2O, MgO, MnO, SiO_2, TiO_2; un verre contenant SO_3.

Les données de l'analyse par microsonde électronique sur les compositions des minéraux du ciment (les phases du clinker) permettent de faire quelques conclusions générales.

Chacune des impuretés de la matière première peut être présente dans tout minéral du ciment.

La composition des cristaux d'une même phase du clinker est différente, par suite des conditions de non-équilibre de leur formation.

La phase aluminate est l'objet d'une attention spéciale. La quantité la plus grande des impuretés est distribuée dans sa structure.

SUMMARY : The compositions of phases of five commercial Portland cement clinkers were studied using a Camebax apparatus of the type MB-1.

To make a quantitative calculation of the elements, the following standards were synthesized: solid solutions of C_3S with Na_2O, K_2O, MgO, Al_2O_3, Fe_2O_3; C_3S with MnO; C_3S with TiO_2; C_2S with P_2O_5; C_3A with Na_2O; C_4AF with MgO; C_6A_2F with Na_2O, MgO, MnO, SiO_2, TiO_2; a glass containing SO_3.

Electron microprobe data on the composition of cement minerals (clinker phases) permit some general conclusions.

Each of the impurities of raw material can be present in any cement mineral.

The composition of crystals of one and the same clinker phase is different due to non-equilibrium conditions of their formation.

The aluminate phase deserves special attention. The greatest amount of impurities is distributed in its structure.

Electron-probe microanalysis of the composition of Portland cement minerals (clinker phases) permits some general conclusions:

1. Inhomogeneous mixing of initial raw materials as well as the non-equilibrium conditions of the clinker burning and of the formation of crystal phases may result in different compositions of crystals of the same clinker phase.

Such phases can exist in clinker in at least two crystal forms (for example belite, alite, aluminate).

At the same time the different composition of the crystals of one and the same phase may lie within the composition range of one modification.

It was also observed that the impurity distribution in one crystal is non-uniform. As a rule, the compositions of the center and of the edges of such a crystal are different.

2. Each of the impurities of raw material can be present in any cement mineral.

However, the preferable distribution of impurities among minerals depends on the peculiarities of crystal structure. So the octahedral positions in the aluminoferrites are most convenient for Mg occupansy. Such elements as Ti, Mn, Cr are also distributed

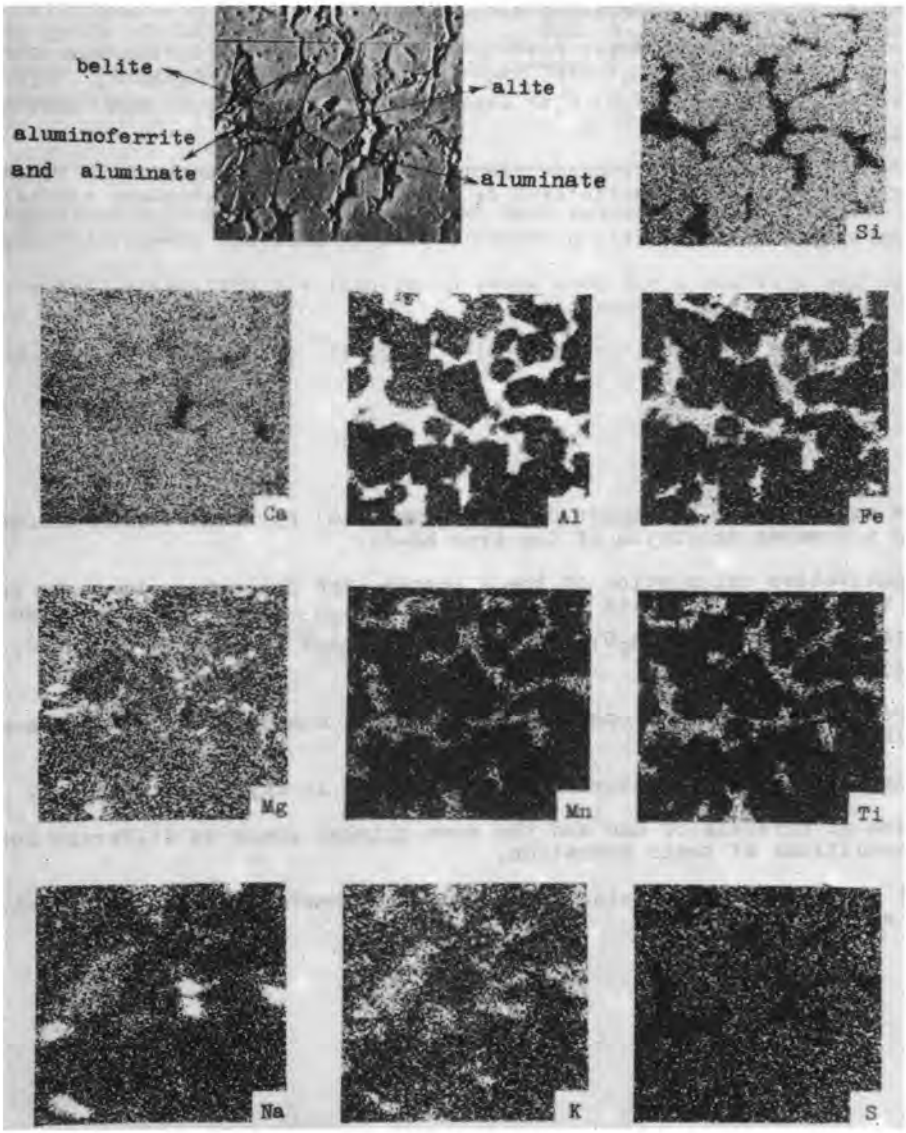

EPMA photograph of clinker

preferentially in the aluminoferrites. The large cations of Na prefer the crystal lattice of C_3A with large holes.

Owing to the possible substitution $CaAl \rightleftharpoons NaSi$ both the aluminate and aluminoferrite contain a considerable amount of Si. P,S,K are preferentially distributed in belite.

For each of the phases there is a most characteristic set of impurities: for alite - Mg,Al,Fe,Na,K (Cr,Ti,P a.o.); for belite - Mg,Al,Fe,K,P,S (Cr a.o.); for aluminate - Na,Si,Fe,Mg,K a.o.; for aluminoferrite - Mg,Si,Ti,Mn,Na (Cr,K a.o.).

Each phase can also form without some impurities (see Table). So the clinker may contain magnesium-free crystals of the aluminate and belite phases.

TABLE
COMPOSITIONS OF CLINKER PHASES IN OXIDES
The least and the greatest amount of oxides are given (wt %)

Phases / Oxides	Alite	Belite	Aluminate	Aluminoferrite
CaO	69,0 72,7	60,3 64,4	52,3 58,7	45,5 50,7
SiO_2	23,8 26,4	28,0 33,8	3,5 5,6	2,0 5,5
Al_2O_3	1,1 2,7	1,4 3,1	26,4 35,0	17,3 22,9
Fe_2O_3	0,4 1,5	0,3 1,8	2,9 7,1	19,4 26,2
MgO	0,5 1,4	0,4 0,8	0,0 2,1	2,3 5,4
Na_2O	0,1 0,3	0,0 1,1	0,2 4,0	0,0 0,9
K_2O	0,1 0,3	0,6 1,3	0,3 0,8	0,0 0,3
P_2O_5	0,0 0,5	0,2 0,8	0,0 0,1	0,0 0,3
SO_3	0,0 0,4	0,0 0,8	0,0 0,4	0,0 0,3
Mn_2O_3	0,0 0,1	0,0 0,1	0,0 0,1	0,1 0,8
TiO_2	0,0 0,3	0,0 0,4	0,0 0,4	0,5 1,8

3. The analysis of our results and those of other authors shows that the smallest amount of impurity oxides is present in alite (~4 wt%); belite contains a greater amount of impurities (~6 wt%). The amount of impurities increases sharply in aluminoferrites (~10-11 wt%).

Of special attention is the composition of the aluminate phase. This phase contains the greatest amount of impurities (~13 wt%).

Besides, its composition is most variable because it is greatly influenced by accidental factors, first of all by the presence of the neighbouring phases.

So, as a rule, its Fe_2O_3 content is overstated due to the influence of aluminoferrite intergrowths. According to the results of the synthesis of the aluminate phases under laboratory conditions the Fe_2O_3 content does not exceed 4-5 wt %.

4. The $CaO:Al_2O_3:Fe_2O_3$ ratio in the aluminoferrite phase of the clinkers investigated is close to 6:2:1 but not to 4:1:1.

In alite and belite the $CaO:SiO_2$ ratio is, as a rule, higher than 3:1 and 2:1 respectively.

5. Inaccuracies in the determination of the compositions of clinker phases can be due to several reasons: to the superimposition of one phase on another, especially if the parts close to the crystal edge are chosen for the analysis; to the intergrowth of one phase with another; to the presence of microinclusions of one phase in another.

Thus the possiblity of using EPMA is limited by the size of the crystal analyzed.

Investigation of alumoferrite calcium crystallization processes

Etude de processus de cristallisation des alumoferrites de calcium

A.M. DMITRIEV,
M.T. VLASSOVA,
B.E. YOUDOVITCH,
S.I. IVACHTCHENKO, Niitsement, Moscou, U.R.S.S.

On a étudié l'influence des différentes additions catalytiques sur les processus de cristallisation de la phase alumoferritique du clinker. On a proposé le modèle du mécanisme de la formation des alumoferrites de calcium de composition différente en fonction de la concentration de l'addition introduite et des conditions thermiques de la cuisson du clinker. Ce modèle est fondé sur la relation établie pour la première fois entre la position d'un élément catalytique dans le tableau périodique des éléments de D.I.Mendéléev et la composition de la phase alumoferritique en cours de cristallisation. On a révélé la dépendance entre la composition et la structure de la phase alumoferritique et la broyabilité et l'activité d'hydratation du clinker de ciment portland.

The influence on the alumoferrite clinker phase crystallization processes of different catalytic additions have been studied. Model mechanism of different composition alumoferrite calcium formation depending on the concentration of an addition introduced and thermal conditions of clinker burning has been proposed. This model mechanism is based on a first determined interrelationship between catalytic element position in the Periodic Mendeleyev's system of elements and crystallizing alumoferrite phase composition. Dependence between composition and structure of alumoferrite phase and grindability and hydration activity of portland cement clinker is exposed.

Calcium aluminoferrites represent a series of solid solutions of general formula $2CaO \cdot (Al_2O_3)_x \cdot (Fe_2O_3)_{1-x}$ where x varies from 0 to 0.7 and constitue a considerable part of Portland cement clinker (up to 15%). Their composition and structure have a significant effect on hydraulic activity of cements.

At present many researchers consider that the hydraulic activity of "pure" minerals of calcium aluminoferrites in creases with the ratio Al_2O_3/Fe_2O_3 although some data indicate that the highest hydraulic activity is displayed by Fe_2O_3-enriched aluminoferrite phase.

Possessing considerable isomorphic capacity calcium aluminoferrites may accomodate in their crystal lattice various micro-impurities (Mg,Si,Ti,Mn,Cr,Na,K,Ca,Al,Fe,Sr, Ba, SO_3) /1-3/ which makes the problem of most hydraulically active aluminoferrite phase more difficult to solve. Analysis of results obtained in NIITSEMENT and in work /1/ shows that,despite the complex dependence between hydraulic activity and composition and nature of microimpurities, a general tendency of increase of hydraulic activity of bot "pure" and modified calcium aluminoferrites with increase of Al_2O_3 content exists. Accordingly in this work we studied means of enhancing hydraulic activity by changing the composition of aluminoferrite phase, introducing various microadditives (CuO, ZnO, P_2O_5,BaO, Ni_2O_3,Mn_2O_3) into raw cement charges.

The synthesis of calcium aluminoferrites modified by the microadditives mentioned above is described in /4/.The amount of the modifying ion in the aluminoferrite phase was monitored by methods of rational chemical analysis and atomabsorption spectroscopy and its composition by petrographic, chemical and X-ray phase methods of analysis. The composition of calcium aluminoferrites was determined from calibrated plots by reflection at d=1.92 A, which is the most sensitive characteristic of aluminoferrite phase variation /2/.

Roentgenograms of the aluminoferrite phase show that on addition of BaO the peak at d=1.92 A is shifted to lower values, and in the presence of CuO, ZnO,Mn_2O_3,Ni_2O_3, P_2O_5 to higher values of the diffraction angle (Table 1). As follows from Table 1, calcium aluminoferrites of composition $C_6A_{1.5}F$ crystallize from clinker melt without additives. Introduction of a basic oxide (BaO) decreases the amount of aluminoferrite phase and enriches it with iron oxides. The presence of acidic components (CuO,ZnO,Ni_2O_3, Mn_2O_3, P_2O_5) increases the amount of aluminoferrite phase and enriches it with Al_2O_3 which was also confirmed by petrographic data. The following general tendency is observed (Table 1,Fig.1): with increase of the acidic properties of additives, characterized by electronegativity (E.N.), ionic potential (Z/r) and bonding energy between cation and oxygen (E_{Me-O}), calcium aluminoferrite compositions are shifted to a higher degree towards increasing Al_2O_3/Fe_2O_3 ration. According to the increasing effect on the composition of crystallizing calcium aluminoferrites (facilitating crystallization of calcium aluminoferrites enriched with Al_2O_3, except for BaO), the elements studied may be arranged in the following sequence (Fig.1):

Ba Mn Ni Zn Cu P

A similar sequence with only slight deviations is formed when arranging these elements according to increasing acidic properties.

Most researchers explain variation of aluminoferrite phase composition by different solubility of Al_2O_3 or calciuma aluminates in liquid phase of ferrite composition due to reduction of viscosity occurring at higher temperatures of clinker burning or on introduction of mineralizers into the raw mixes. However, this does not explain many experimental facts, e.g. why increase of viscosity of liquid phase caused by addition of P_2O_5 is accompanied by shift of aluminoferrite phase composition towards formation of C_8A_3F.

Since viscosity of the clinker melt is determined by its structure it would be more correct to associate variations in calcium aluminoferrite composition not with viscosity variation, but with restructuring of the clinker liquid phase "structure"

Table 1

B No.	Additive	Characteristics of the cations formed on dissociation of the additives			Position of peak with d=1.92 A	Al_2O_3/Fe_2O_3 ratio (mol.) in aluminoferrite phase
		Electronegativity (Pauling)	Bonding energy with oxygen kcal; Avogadro number	Ion potential, Z/r		
1	BaO	0.9	29	1.49	47°20[1]	$A_{1.4}/F$
2	-	-	-	-	47°21[1]	$A_{1.5}/F$
3	Mn_2O_3	1.4-1.5	36	2.5-6.7	47°28[1]	$A_{1.76}/F$
4	Ni_2O_3	1.8	36	2.9	47°31[1]	A_2/F
5	ZnO	1.6	43	2.41	47°33[1]	$A_{2.16}/F$
6	CuO	2.0	29	2.78	47°38[1]	$A_{2.5}/F$
7	P_2O_5	2.1	104	14.3	47°42[1]	A_3/F

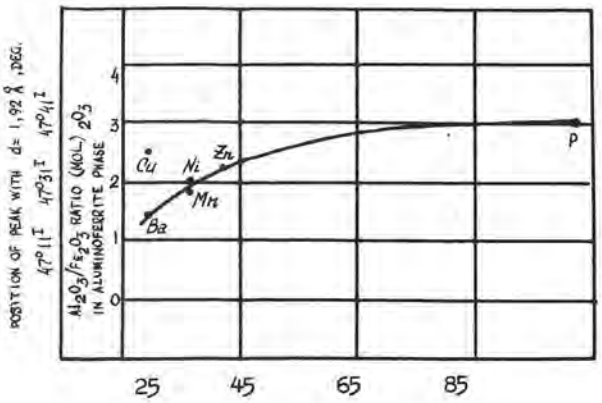

Fig. 1a. Composition of aluminoferrite phase depending on the bonding energy between the introduced cation and oxygen

under the effect of temperature of additives. One should also take into account that only change of structural features of amphoteric elements Al and Fe should effect the composition of the crystallizing aluminoferrite phase, whereas viscosity of the melt is determined by the presence of not only aluminoferrooxygen complexes, but also of other large radicals (e.g. PO_4^{3-}) which frequently have a decisive a effect on viscosity of the clinker melt /5/, but do not noticeably affect the mechanism aluminoferrite phase formation.

Clinker melts are a highly basic (60% of CaO) aluminoferrosilicate phase in which under certain temperature conditions in the presence of certain amounts and types of microadmixtures a dynamic equilibrium exists between various coordination forms of amphoteric elements Al and Fe, and the direction in which this equilibrium is shifted is determined by acid-base properties of the system. The intensity of the shift, which determines the absolute value of viscosity change, depends on the acid-base characteristics of the dissolved ions /5/. $2CaO \cdot Fe_2O_3$, $5CaO \cdot 3Al_2O_4$ or $12CaO \cdot 7Al_2O_3$ and CaO are usually considered real components of solid solutions and formation of the aluminoferrite phase crystallizing from the melt occurs, in the final analysis, when "populating" octahedral and tetrahedral positions by aluminum and iron ions.

It may be concluded from analysis of the published data /6-9/ on the ratio of tetrahedrally and octahedrally coordinated iron and aluminum ions in the structure of aluminoferrite phase (Table 2) that with increase of A/F ratio in the calcium aluminoferrite composition that amount of octahedrally coordinated iron atoms increases, whereas the number of tetrahedrally coordinated FeO_4^{5-} complexes decreases. The few studies which point to a similar dependence for Al coordinated ions require additional verification with modern methods of physico-chemical analysis. From the available data on structural arrangement of Al and Fe ions in calcium aluminoferrites the following model of the mechanisme of aluminoferrite phase formation depending on the concentration of the additive and the temperature conditions of clinker burning may be proposed. Increase of clinker burning temperature or the presence of additives in the raw mix which exhibit acidic properties in the melt (in our case CuO, ZnO, Mn_2O_3, Ni_2O_3, P_2O_5) shifts the dynamic equilibrium towards increase of the number of Al and Fe atoms in octahedral coordination and decrease of the number of tetrahedral complexes. This was confirmed previously in the study of IR absorption spectra of sharply cooled melts /5/. This will cause fluctuations in the melt with structural similarity to Al_2O_3 -enriched calcium aluminoferrites (Table 2).

Table 2

Ratio of tetrahedral and octahedral iron and aluminum ions in the structure of calcium aluminoferries

No.	Value of x in the formula of calcium alumino-ferrites	Composition of aluminoferrite phase	Amount of complexes in aluminoferrite phase, %			
			FeO_4	FeO_6	AlO_4	AlO_6
1	0.824	$C_8A_{3.30}F_{0.70}$	14.0	84.0	-	-
2	0.789	$C_8A_{3.16}F_{0.84}$	18.0	82.0	-	-
3	0.750	C_8A_3F	100.0	0	33.0	66.0
4	0.747	$C_6A_{2.24}F_{0.76}$	23.0	77.0	-	-
5	0.724	$C_6A_{2.17}F_{0.83}$	23.0	77.0	-	-
6	0;681	$C_6A_{2.04}F_{0.96}$	26.0	74.0	-	-
7	0.667	C_6A_2F	26.7	73.3	-	-
8	0.628	$C_4A_{1.256}F_{0.744}$	28.0	72.0	-	-
9	0.500	C_4AF	24.0	76.0	76.0	24.0
10	0.500	C_4AF	25.0	75.0	75.0	25.0
11	0.498	$C_4A_{0.996}F_{1.004}$	32.5	76.5	-	-
12	0.344	$C_6A_{1.032}F_{1.968}$	38.0	62.0	-	-
13	0.321	$C_6A_{0.963}F_{2.037}$	38.8	61.2	-	-
14	0.0	C_2F	50.0	50.0	-	-

This facilitates crystallization of the latter from the clinker liquid phase modified by Cu, Zn, Mn, Ni, P ions. The same occurs on increase of clinker burning temperature. The intensity of variation of Al and Fe ion coordination (i.e. composition of the aluminoferrite phase) is determined by the magnitude of the acid-base properties of the additives: the more acidic the element the greater the Al_2O_3-enrichement of the aluminoferrite phase (Fig.1). Addition of BaO into the raw increases bysicity of the system resulting in formation of additional AlO_4^{5-} and FeO_4^{5-} and in reduction of the number of octahedra, thus shifting the aluminoferrite phase composition towards C_6AF_2 (Fig.1).

It should be noted that variation of aluminoferrite phase composition with temperature conditions or addition of microadmixtures should presumably by determined by a combination of many factors; solubility of Al_2O_3 and calcium aluminates in clinker melt, redox properties of the additives, appearance in the system of liquation regions, etc. The determining factor affecting the mechanism of this process is however variation of acid-base properties of the clinker melt.

In order to verity the proposed route of increase of hydraulic activity of cements, clinkers with KH=0.93; n=1.8; p=1.1 with addition of Zn and Cu oxides were synthesized.

X-ray phase and petrographic analyses showed that the phase composition of the test and dummy clinkers practically coincide (59-62 % of C_3S; 17-19% of C_2S; 4-5 % C_3A and 16-19% of aluminoferrite phase). Modifications of clinker minerals were the same: monoclinnic for alite and -form for dicalcium silicate. The composition of the aluminoferrite phase, isolated by chemical methods, in the clinker modified by Zn and Cu ions was shifted towards Al_2O_3-enriched calcium aluminoferrites as compared with dummy clinker.

The clinker was well sintered, showed a more uniform granulometric distribution, better grindability and its hydraulic activity was in average by 50-80 kg/cm^2 higher than of the dummy clinker.

Hence, the proposed model of formation of aluminoferrite phase of various composition based on the established relationship between the position of the added element in the Periodic table and the composition of the crystallizing calcium aluminoferrites makes it possible to carry out a directed search for effective additives which significantly affect the composition of the aluminoferrite phase. This is becoming especially important lately since the traditional means of increasing the grade of cements have been exhausted and directed change of aluminoferrites phase composition of clinkers is an additional method of enhancing hydraulic activity of cements.

REFERENCES

1. Smirnova L.V., Boikova A.I. Composition and Properties of Aluminoferrite Phase

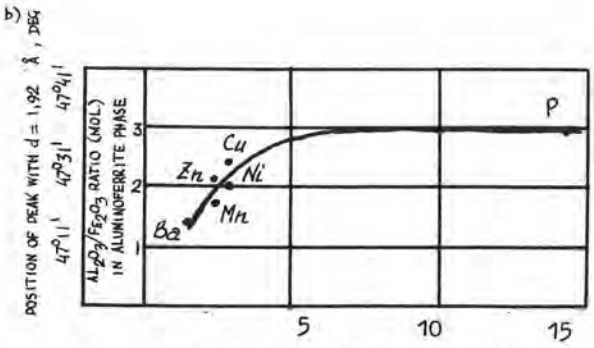

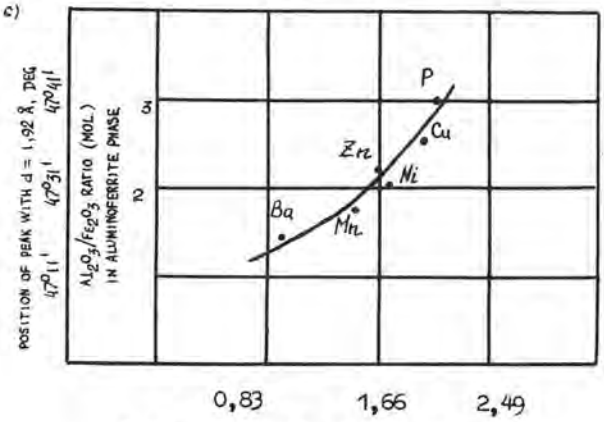

Figs. 1b, 1c. Composition of aluminoferrite phase depending on electronegativity (c) and ion potential of the introduced cation (b)

of Clinker, Tsement, 1977, No.9 (in Russian).
2. Jamaguchi G., Takagi S; The Analysis of Portland Cement Clinker; - Proc. Of the Fifth Int.Symp.on the Chem.of Cement; Tokio, 1969, p.1, vol.1.
3. Fletcher I.E. The Composition of the Tricalcium aluminoate and Ferrite phases in Portland Cement Determined by the Use of Electronprobe macroanalyser. - Mag. of Concrete Res., 1969, vol.21, No.66.
4. Ivashchenko SI.I, Vlasova M.T. et al. The Possibilities of Increasing Hydraulic Activity of Portland Cement. Tsement, 1979, No.7 (in Russian).
5. Ivashchenko S.I.I Study of the Effect of Melt Properties on Processes of Clinker Formatioa. Thesis of Candidate's Dissertation. Moscow, 1976 (in Russian).
6. Boikova A.I., Ekimov S.P., Grishchenko Distribution of Trivalent iron the Structure of Calcium Aluminoferrites. Tsement, 1978, No.6 (in Russian).
7. Smitch K.D. Crystallographic Changes with the Substitution of Aluminum for Iron in Dicalcium Ferrite. - Acta Cryst., 1962, vol. 15, No.11.
8. Pobell F., Witmann F. Replacement of Fe^{3} by Al^{3} in Calcium Aluminate Ferrite. - Physics Letters, 1965, vol.19, No.3.
9. Grenier J.C., Pouchani M., Hagenmuller P. Evaluation des interactions magnétiques dans les phases dérivés du ferrite bicalicique $Ca_2Fe_2O_3$. Mat.Res.Bull.,1976, vol.22, No.6.

Shales and their working-over solid by-products in portland cement production

Schistes et déchets solides de leur transformation dans la production du ciment portland

Y.I. SIDOROVITCH, Institut de Géologie et de Géochimie des Combustibles Fossiles de l'Académie des Sciences de l'Ukraine, U.R.S.S.

La masse inorganique des schistes combustibles est représentée sous forme générale par les carbonates de calcium dans le mélange avec les argiles, rarement par les argileg. La masse organique (kérogène) se compose d'hydrocarbures. Ainsi les schistes sont en meme temps les matières premières de ciment et le combustible.

Lors de la combustion dans les foyers des générateurs de vapeur et de la pyrolyse des schistes on obtient les déchets solides ayant dans sa composition le silicate dicalcique en quantité de 20 à 60%. Il est mieux d'utiliser ces déchets lors du broyage du ciment portland ou, s'ils contiennent le kérogène résiduel, en qualité du combustible secondaire. Les schistes mélilitiques possèdent un effet fluidifiant des boues de ciment crues et peuvent être utilisés en général au lieu des argiles.

Ionorganic substance of oil shales is represented in general by calcium carbonates mixed with clay, rarely by clay alone. Organic substance (kerogen) consists of hydrocarbons. Thus shales are simultaneously raw material and fuel.

In the process of burning in boiler furnaces and after pyrolysis, solid byproducts are received, that contain dicalcium silicate amounting 20-60%. The best way of using such by-products is to utilize them during portland cement gringing, or as secondary fuel, on condition they contain residual kerogen.

Melilit shales have a liquefying capacity when added to raw material cement slimes and can be used, in general, instead of clays.

Shales and solid wastes of their thermal processing may be effectively used in a wide scale as a source of thermal energy and raw materials in the cement industry which is characterized by high heat and mass consumption.

In the Soviet Union promising areas of shale mining, in addition to the Baltic basin, are Carpethians, the Dnieper and Volga regions and the bassin near river Pripyat, there are also considerable deposits in the Komi ASSR.

An advantage of shales in relation to coals is that their kerogen mainly consists of hydrocarbons close in elementary composition to raw oils.

The inorganic mass of shales, the amount of which varies from 40 to 90%, usually includes readily fusible clays or mixtures of carbonates with clays (marls).

The calorific value of most shales varies from 3600 to 10,000 kJ/kg or even higher.

The presence of minerals of laminate structure (montmorillonite, hydromica) with kerogen of the humus type ensures high absorption capacity towards organic ions, from 90-110 mg-eq/100 g of montmorillonite to 25-40 mg-eq/100 g of hydromica [5]. Such shales are characterized by low yield of fuel products when heated to 480-530 °C. Complete removal of kerogen from shales of fraction 2-3 mm is achieved only at 900°C in the presence of oxygen. All other combinations of clayey minerals and carbonates independently of the kerogen release the organic substance at lower energy expenditure and in higher relative yields of fuel products at lower temperatures.

Shales and solid wastes containing organic substance which is difficult to remove are very convenient as a secondary fuel, the oxidation of which begins intensively at temperatures of clay dehydration and is completed in the region of limestone decarbonization.

For combustion in steam generator furnaces of modern power stations shales characterized by calorific value higher than 5800 kJ/kg are used, the mineral mass melt should have viscosity not higher than 200 poise at 1500°C in order to ensure liquid removal of ashes. Fuel shales containing not less than 30% of calcium carbonate and with low or moderate content of alumina display such characteristics.

Solid wastes in the form of slags and ashes are formed when burning such shales in steam generator furnaces. Slags usually contain up to 60% of glass phase and practically do not contain fuel. They are also characterized by enhanced hardness, abrasiveness and high resistance to grinding. Ashes contain up to 2% of residual fuel, are by highly dispersed and do not require additional grinding.

Despite the short period of the combustion process, the high temperature and dispersion of the fuel ensure completion of the clinker formation reaction as a result of which calcium aluminates, ferrites and silicates are formed. Content of the latter mainly in the form of C_2S reaches even 6%. Such slags and ashes may be considered as low-grade cements. At sufficiently high carbonate content in shales, for example more than 60%, such slags mainly contain C_3S and are very close in mineralogical composition to Portland cement clinkers [6]. They may be added to Portland cement during grinding. Due to the high content of clinker minerals a significant amount of these slags may be added during grinding without deterioration of cement quality. Ashes are especially effective as a raw material component during burning of clinker.

A characteristic features of such wastes is high excergy [2] which ensures considerable economy of heat in the production of Portland cement.

Pyrolysis of fuel shales at 480-530°C in most cases does not ensure complete (100%) removal of hydrocarbons. A considerable amount (from 20 up to 50% of initial content) remains in the solid residue, semicoke or ash. Such solid wastes may be effectively used as secondary fuel in clinker burning in units equipped with cyclone heat exchangers.

The raw mix in kilns with cyclone heat exchangers is hested in the first cyclone up to approximately 280°C. When using semicoke or ashes, even in the case of direct contact with oxygen, intensive oxidation of the kerogen does not occur at these temperatures. However since these materials were already subjected to thermal destruction the raw mix as a whole is better prepared. In the second and third cyclones where the temperature is increased to 480 and 650°C, due to direct contact with the oxygen of flue

gases kerogen oxidation is considerably intensified (exothermal effect, Fig.1, curve 2) which facilitates thermal preparation of the material in the kiln.

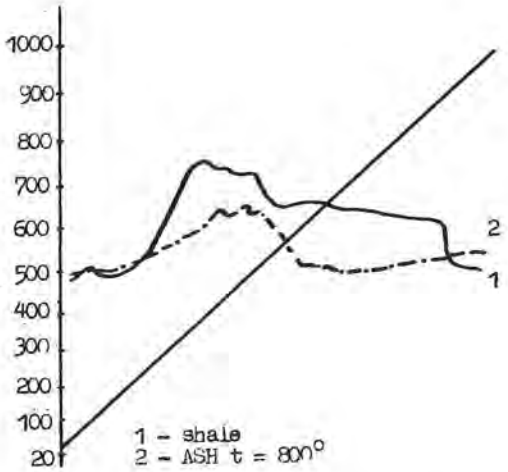

Fig.1. Differential thermal curves

Raw mixes containing natural shales behave slightly differently. The maximum of exothermal effect is shifted towards lower temperatures (Fig.1, curve 1) due to desorption and oxidation at lower temperatures of the light fractions which have higher calorific values. The exothermal effect for most shales begins at 250-300 °C and continues to 700-800 °C and for some shales up to 900 °C (Fig.1, curve 1);

The amounts of shales and their wastes added depends on the chemical and mineralogical composition. Clayey (carbonate free) shales may be added in amounts of only 20-25% (of calcined mass) in the production of common Portland cements. With increase of the amount of carbonates, addition of shales may be increased in proportion to the carbonate fraction.

The use of untreated shales in raw mixes when the cyclone heat exchangers are not used should be restricted on account of possible contamination of the atmosphere with hydrocarbons. The thermal regime may also be considerably distored along the kiln, the redox processes destabilized resulting in changes in mineral composition of the cement clinker.

A distinctive feature of shale pyrolysis in units with solid heating medium is the high degree of extraction of fuel products, up to 85-90% in organic mass.

Such ashes may be used without detrimental effects in existing technologies.

Cement-raw material slags of menilite shales and their semicokes exhibit enhanced fluidity. Ultimate shearing stress of shale slags is 150 mg/cm2 in contrast to 600mg/cm2 of clayey slags at average moisture content of 38-40%.

The technology of cement clinker production with addition of shales does not meet with any difficulties.

Energy consumption from grinding of the raw mix and the effectiveness of the main technological equipment is on the same level as for traditional raw materials.

Correction of the slags does not meet with any difficulties.

There was some apprehension about possible sedimentional stratification of the corrective slags, however addition of a certain amount of clay, and sufficiently fine grinding of the shale provide satisfactory sedimentational stability of the slags.

Calcination of cement clinker in rotary kilns (L=150 m, d=3.0-3.4 m) is more stable for the experimental slag than for a common slag; The clinker formed is characterized by grain sizes less than 10 mm (up to 80%).

Petrographic studies of the clinker showed that synthesis of clinker mineral was completed, free CaO is practically absent. Crystals of clinker minerals have mainly submicroscopic sizes.

A trial cement clinker had the following mineral composition: C_3S - 59.92%, C_2S - 18.30%, C_3A - 6.85%, C_4AF - 14.20% and fully met the requirements for the production of high quality Portland cements.

Physico-mechanical tests of a trial batch of cement clinker and Portland cement established the possibility of stable production of "400" and "500" or even higher grade cements.

Of considerable interest is the scheme of industrial treatment of fuel shales in fluidized state with simultaneous production of cement clinker and generation of steam [5]. Despite relatively low calorific value of the shale used (3832 kJ/kg) the process was very economical.

Some progress has been made in the USSR in the development of the technology of shale combustion with simultaneous production of cement clinker in furnaces of high-power steam generators [6].

Az sufficiently high levels of fuel and carbonate content in the shales a high degree of autothermal combustion may presumably be achieved.

In cement clinker calcination according to existing technologies it is recommended to first extract fuel products, which may be recycled (Scheme, Fig.2), and then subject the shales to pyrolysis. The obtained solid residue (semicoke or ashes) may then be used as a raw mix component.

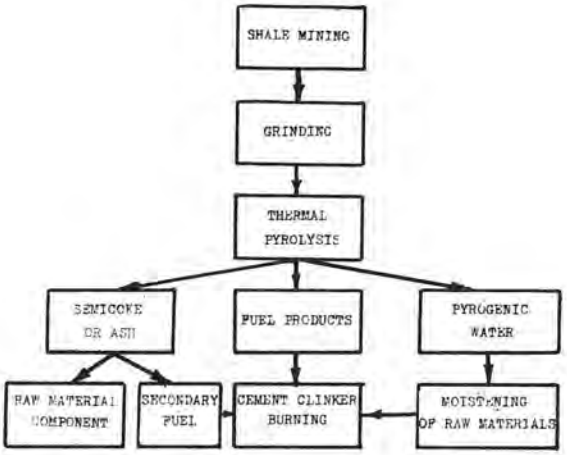

Fig.2. Scheme of complex usage of oil shale

Bearing in mind the increasing cost and decreasing resources of fuel and the abundance of fuel-containing rocks, new plants should be designed for a new type of raw material and fuel basis which will be a guaranteed and stable source of thermal energy and raw materials for many centuries.

REFERENCES

1. Gabinet M.P., Sidorovich Ya.I., Lubentsova V.N., In: Mineralogiya Osadochnykh Porod, Kiev No.4, 1977, pp.101-103.
2. Zhavoronkov N.M.,Boldyrev A.S.,Kogan N.P. Makashev S.D., Mchedlov-Petrosyan O.P., Pashchenko A.A.,Fataliev S.A.,Shchetkina T.Yu., Dokl. Akad.Nauk SSSR, 245 (1979), 666.
3. Ladyzhenskii N.P., Sidorovich Ya;I. et al. Stroitel'nye Materialy i Konstruktsii, 1973, No. 4, 11.
4. Sidorovich Ya.I., Sergatyuk A.F.,Lubentsov V.N., In: Geologiya i Geokhimiya Neftegazonoshykh Provintsii (Geology and Geochemistry of Gas-Beraing Provinces), Naukovo Dumka, Kiev, 1977.
5. Rorbakh R. Proceedings of the First UN Symposium on Development and Use of Fuel Shale Deposits, Tallin 1968, pp.441-446.
6. Tager S.A.,Matin T.I.,Khiga A.A.,et al. Proceedings of the First UN Symposium on Development and Use of Fuel Shale Deposits, Tallin 1968, pp. 447-454.
7. Kikas V.Kh. Proceedings of the First UN Symposium on Development and Use of Fuel Shale Deposits, Tallin 1968, pp.455-461.

THEME II

Hydratation des ciments portland sans constituants secondaires

Hydration of pure Portland Cements

On the process of C_3S hydration in initial period

Etude sur le processus d'hydratation de C_3S à la période initiale

Y.S. MALININE,
V.I. GOUSSEVA,
N.D. KLICHANIS, niitsement, Moscou, URSS.

On a établi la morphologie identique des produits d'hydratation de C_3S et de CaO à la période initiale de l'interaction avec de l'eau. On a également établi que les particles amorphes arrondies, les formations fibreuses et en forme de cigare, les agrégats lamellaires observés dans les microscopes électronique et optique lors de l'hydratation du silicate tricalcique, sont semblables, quant à leurs indices morphologiques, aux produits d'hydratation de CaO pur dans les mêmes délais d'hydratation et représentent les différents stades de cristallisation de $Ca(OH)_2$ et de $CaCO_3$. La formation des hydrosilicates de calcium n'est pas en général une fonction primaire (comme l'affirmaient de nombreux chercheurs) mais une fonction secondaire de la surface de la frange de gel formée autour des grains de départ de C_3S aux points de contact avec $Ca(OH)_2$ dans les délais d'hydratation plus avancés.

The identity of C_3S and CaO hydration products morphology in initial period of interaction with water has been discovered. Spherical amorphous particles, cigar-shaped and fibrous formations, and slaty splices, observable in electron and light microscop during tricalcium silicate hydration have been found to be similar by morphological indications with the products of pure CaO hydration in the same periods of hydration and represent different stages of $Ca(OH)_2$ and $CaSO_3$ crystallization.

In general, calcium hydrosilicate is not the primary, as is clamed by many an invesigators, but a secondary function of gel rim surface around C_3S initial grains in contact points with $Ca(OH)_2$ at later hydration periods.

The mechanisms of hydration and structure formation of the C_3S and CaO hardening grout were studied by the petrographic and selectron microscopy methods.

The hydration mechanism was investigated on slides comprising a fine layer of the cement-water mixture placed between the stage and cover glasses which were bonded to each other with a heated paraffin-rosin mixture.

The suspension water-to-cement ratio was 0.8-10.

All the changes taking part in the hydration processes were observed in the slides which constantly contained water without access of air for a prolonged period of time.

To determine the phase composition of the hydration products, the slides were open and their optical constants were found out by the immersion method.

The replicas of the same slides were investigated on an electron microscope.

The morphology of the hydration products at the grain-to-water contact and in the inter-grain space formed in the course of time was traced which was impossible for a conventional microscope.

The structures of hardened C_3S and CaO samples were studied on transparent polished sections (thinnest slices of hardened samples) by a polarizing microscope and on the replicas of chips of the same samples by the electron microscope.

The contact between the C_3S crystal surface and water was studied on ground slices of the mineral lumps from the moment of establishing said contact and up to 1 day with the use of the optical and electron microscopes.

As a result of the investigations performed, three morphological forms of the C_3S hydration products were detected;

1 - spherical particles;
2 - fibres, cigar- and tree-shaped formations, frequently of the characteristic sheaf-like shape;
3 - large crystals and flaked concretions of CH.

These forms of the hydration products are observed both in the suspensions and in the samples with normal W/C ratios. Such products have been frequently misregarded as calcium hydrosilicates.

However, similar morphologic forms of the hydrate phases were also observed when hydrating pure CaO.

For instance, when C_3S and CaO were hydrated in a suspension, all the above-mentioned forms could be observed on the water surface where first neogenes appeared, obviously owing to surface tension. Initially, there were shapeless isotropic rounded particles, later tight anisotropic spherulites

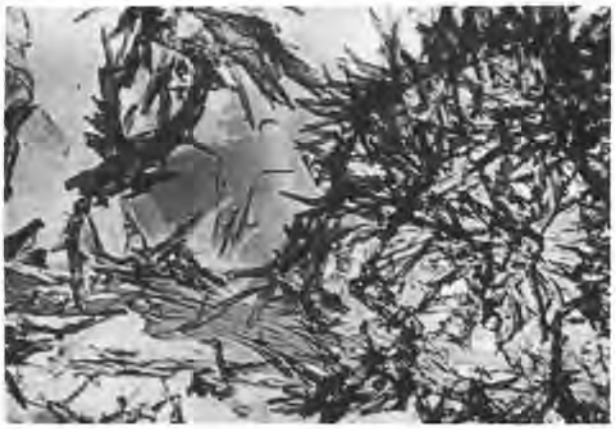

Fig.1. (C_3S). 6h of Hydration. Electron Microscope, X1400

with partial carbonization. While growing, the spherulites disintegrate into separate fibres and "cigars" and get carbonized; Fig.1 (C_3S), Fig.2(CaO) - electron microscopy.

The process of formation of the cigar-shaped particles on the surface of the C_3S grains may be observed by carrying out the gollowing experiment. Pour a freshly crushed C_3S mineral powder onto a water surface, several minutes of hydration in contact with air will result in needle- and cigar-shaped particles on the grain surface, said particles increasing in size and carbonizing with time. These may be observed through an opti-

Fig.2. (CaO). 6h of Hydration. Electron Microscope, X10000

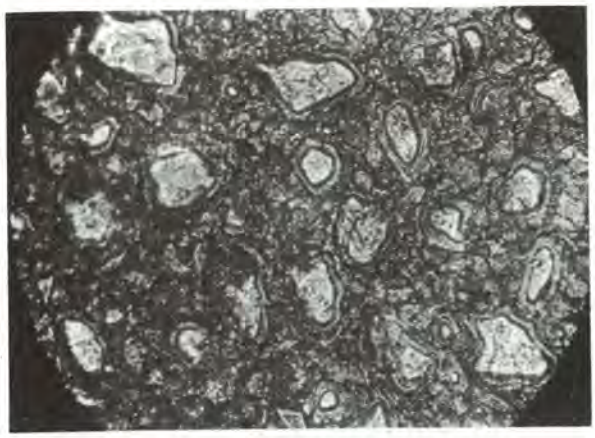

Fig.3. (C_3S). 24h of Hydration. Transmitted Light, without Analyzer, X1200

cal microscope.

The morphological transformations of new formations is also observed in plastic samples with W/C=0.5 on the water surface during water separation.

As regards the internal portions of the samples, the following phenomenon is found there. Water separates ions Ca^{++} from the surface of the C_3S crystals and an isotropic border is formed within the initial grains with time. According to its optical constants the border relates to a silica gel (its N is not below 1.50, whereas the unhydrated core is anisotropic and has refractive indices characteristic of C_3S), Fig.3.

These observations made it possible to suppose that during hydration of C_3S only calcium transfers to the solution, while silica remains in the solid phase in place of the initial grains.

With time (1 day of hydration) cigar- and tree-shaped particles are still found in the inter-grain space, and later large CH crystals.

In case of samples with a low W/C ratio, the proportion of the morphological forms changes. Since the solution is more rapidly saturated with lime, there are few spherical particles in the hardened sample; often fibres and cigar-shaped particles grow directly from the C_3S particle surfaces and large CH concretions are crystallized at oversaturation, Fig.4. The growth of large CH crystals from cigar-shaped and fibrous formations may be also observed at hydration of CaO; This is seen from Fig.5 (the replica of the CaO hardened sample). Hydration of a ground surface of the C_3S lump slice has revealed that immediately on contacting water spherical particles are formed on the surface of the C_3S crystals, said particles

Fig.4. (CaO). 24h of Hydration. Electron Microscope, X14000

converting into polygons rapidly and being essentially portlandite.

Intensive migration of calcium ions from the internal areas of the sample assists in rapid formation of large CH crystals without intermediate forms.

Thus, the spherical, fibrous and cigar-shaped particles observed at the initial period of the C_3S hydration, as well as large crystals and flaked concretions of CH are the products of morphological conversion of CH and $CaCO_3$.

The same regularity was detected at hydration of CaO.

In view of the above, it is possible to

conclude that the primary hydrate phase is CH rather than calcium hydrosilicate which is the secondary function of the silica gel border around the initial C_3S grains at later period of hydration.

Fig.5. (CaO). 24 h of Hydration. Electron Microscope X14000

Influence of organic compounds on the hydration reaction of tricalciumsilicate

Influence de certains composés organiques sur l'hydratation du C_3S.

C. STADELMANN and W. WIEKER, Zentralinstitut für Anorganische Chemie der Akademie der Wissenschaften der DDR - Berlin, R.D.A.

Summary:

The influence of several organic compounds of simple structure on the hydration rate of C_3S was investigated by means of differential calorimetric analysis (DCA).

The results of these measurements in combination with those of further chemical investigations show that hydration rate of C_3S is strongly dependent on the calciumionconcentration in the liquid, water containing, phase.

Lowering the dielectric constant of the water by adding alcohols used in the hydration experiments the reaction rate is always decreased in an amount which corresponds to the dielectric constant in the water-alcohol mixture and the solubility of calciumhydroxide in this medium.

Organic compounds, able to form complexes with calciumions, like organic acids and their sodium salts accellerate the hydration reaction because of the lowered calciumion activity in the liquid phase. At higher concentrations of organic acids or of their sodium salts the hydration rate is decreased as a result of an increase of adsorption of these organic molecules at the grainsurfaces of the C_3S.

The mentioned effect is shown to be dependent on the strength of the complex forming tendency of the added organic compound. To understand fully the influence of organic acids on the C_3S-hydration we must futher assume the formation of a silicagel like cover at the C_3S grains that lower the reaction rate drastically.

RESUME : On a étudié, au moyen de l'analyse calorimétrique différentielle (A.C.D.) l'influence de plusieurs composés organiques sur la vitesse d'hydratation du C_3S. Celle-ci est fortement influencée par la concentration de l'eau en ions calcium.

L'addition d'alcool à l'eau, en abaissant ses constantes dielectriques, diminue cette vitesse d'hydratation, selon la solubilité de la chaux dans cette eau alcoolisée.

Certains composés organiques, susceptibles de former des complexes avec l'ion calcium, peuvent accélérer fortement cette hydratation. Si des gels silicatés se forment autour des grains de C_3S, la vitesse d'hydratation peut être très fortement abaissée.

Introduction

Recent investigations on the mechanism of the hydration of C_3S show that a C-S-H-phase rich in CaO is formed immediately after the beginning of the hydration reaction at the C_3S surface [1,2,3]. By this, its further reaction is prevented so that an induction- or dormant period appears. After the decomposition of this surface C-S-H-cover by a slow release of calcium ions from it into the liquid a very intensive period of hydration takes place, resulting in the formation of C-S-H-phases and $Ca(OH)_2$.
Because the use of admixtures increases in last years very rapidly we tried to investigate the influence of admixtures on the chemical reactions during the first stages of the C_3S-hydration mentioned above.
The investigations were carried out mainly be means of differential calorimetric analysis (DCA). The hydration temperature was 20 °C and the water/C_3S-ratio 0.5. Some alcohols, ketones, several organic acids, the corresponding sodium- and calciumsalts and a cation exchange resin were chosen as admixtures.

Results and Discussion

By adding several aliphatic alcohols to the hydration water (1 mol alcohol/1 hydration water) a retardation of the hydration of C_3S is noted by means of DCA-measurements (fig. 1).

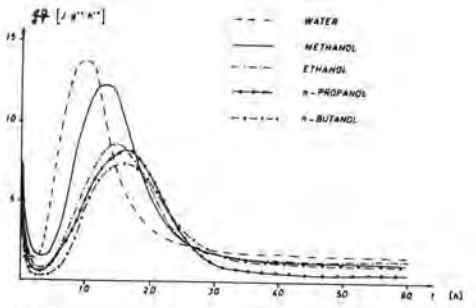

FIG. 1
INFLUENCE OF MONOMER ALIPHATIC ALCOHOLS (1MOL ALCOHOL/L HYDRATION LIQUID) ON HEAT EVOLUTION RATE IN PASTES OF C_3S (LIQUID/C_3S=0.5)

By the determination of the $Ca(OH)_2$-concentrations in the liquid phase during the C_3S-hydration (H_2O/C_3S = 10) it is shown, that supersaturated $Ca(OH)_2$-solutions are produced as well as in experiments with pure water as in those with water-alcohol-mixtures. But the $Ca(OH)_2$-concentrations in the hydration experiments with alcohol-water-mixtures increase much slower and get only smaller values than in the experiments with pure water. These effects are seen in fig. 2 using t- and n-butanol as admixtures.

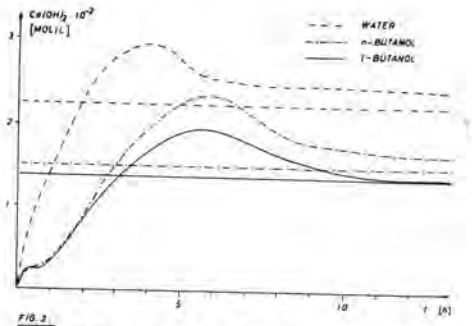

FIG. 2
EFFECT OF THE ADMIXTURE OF n- AND t-BUTANOL TO THE HYDRATION WATER (1MOL ALCOHOL/L HYDRATION LIQUID) ON THE CALCIUM HYDROXIDE CONCENTRATION OF THE LIQUID PHASE IN DEPENDENCE OF THE HYDRATION TIME (LIQUID/C_3S=10) STRAIGHT LINES: $Ca(OH)_2$ - SATURATION LEVELS

From these results we suppose, that the rate of the decomposition of the CaO-rich surface C-S-H-cover is decreased by adding alcohols to the hydration water. That means, that the surface-C-S-H gets stabilized whereby the C_3S-hydration is retarded.
Similar effects are observed by using some other admixtures listed in table 1.

Table 1:
Influence of several alcohols and ketones on the II. DCA-peak during the hydration of C_3S compared with the solubility of calcium hydroxide and the dielectric constants (d.c.) of the water-additive mixtures

additive (all 1mol/l)	II. DCA-peak (h)	$Ca(OH)_2$ (mol/l)	d.c.
water	10.0	$2.21 \cdot 10^{-2}$	80.4
methanol	13.1	2.04 "	78.6
ethanol	14.9	1.70 "	77.4
n-propanol	15.7	1.44 "	76.2
n-butanol	16.0	1.50 "	75.2
i-butanol	15.7	1.37 "	75.8
t-butanol	18.3	1.25 "	74.9
butane-1.3-diol	15.5	1.70 "	77.3
acetone	20.8	1.36 "	77.4
1.4-diazane	19.5	1.43 "	73.4

The results in this table show, that the retarding effect of those alcohols and ketones are evidently attributeable to the decrease of the $Ca(OH)_2$-solubility in the liquid phase caused by the smaller dielectric constants (dc) of the solution phase with respect to pure water.
In contrast to alcohols and ketones, compounds which are able to bind calcium ions, i.e. by complexing reactions, show a complete different influence on the hydration reaction of C_3S.
A very low concentrations shifts of the maximum of the II. DCA-peak to shorter reaction times are observed (acceleration), while at higher concentrations shifts of the maximum of that peak to longer reaction times are found (retardation).
This is shown in Fig. 3 for propionic acid and the corresponding sodium salt as admixtures.

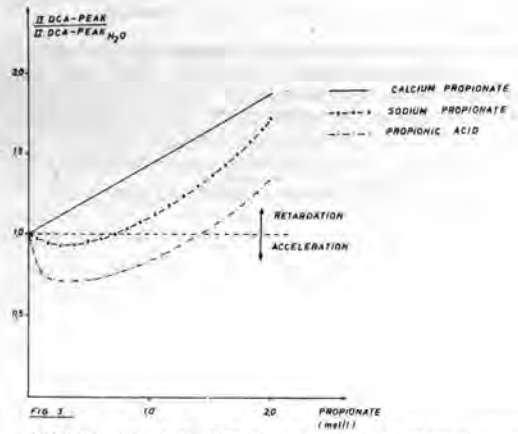

FIG 3

DIFFERENT INFLUENCE OF PROPIONIC ACID, OF CALCIUM AND SODIUM PROPIONATE ON THE II. DCA-PEAK OF THE C_3S HYDRATION IN DEPENDENCE OF THEIR CONCENTRATIONS. IN THE HYDRATION LIQUID (LIQUID / C_3S =0.5) THE DATA ARE RELATED TO THE HYDRATION IN WATER (= 1)

But as can be seen from that figure too, an adding of calcium propionate results at all concentrations only in a retardation of the hydration. The accellerating effect of the acid and the sodium salt we attribute to the formation of complexes with the Ca-ions, resulting in a higher capacity of the aqueous solution for Ca-ions. Therefore the retarding CaO-rich cover at the C_3S grains can't be formed to a great extent or it is decomposed much more faster than in hydration experiments using only pure water. So the acceleration can be explained.

At higher concentrations of propionic acid and sodium propionate at which we found a retardation, we suppose that the organic anions are adsorbed at the grain surfaces. By it a Ca-propionate cover, which hinders the reaction, is formed.
The same effect, we mean, is responsible for the retardation in the hydration experiments with added Ca-propionate. But in that case we have in addition an increased concentration of Ca-ions in the solution, by which the primarily formed CaO-rich C-S-H-phase is stabilized already at low concentrations.
Using α-hydroxyacids (i.e. lactic acid) respectively their salts as admixtures the retarding effect is much stronger. This corresponds to the ability of the lactate-ion to form very stable chelate-complexes with the Ca-ions at the C_3S-surface, resulting in a much more effective blocking of the C_3S-surface.
When adding a cation exchange resin in sodium form to the C_3S hydration experiments there is no possibility that complexforming anions can be adsorbed at the C_3S surface, because they are chemicaly bound to the solid resin. Therefore the admixture of a cation exchange resin should only result in an acceleration as a consequence of the binding of the Ca-ions to the resin and no retarding should occur even at high quantities of the resin added. That this conception fittes in very well is shown in fig. 4.
In contrast to the sodium form of the resin the addition of a protonated resin results in a retardation of the C_3S hydration. We assume, that this effect is the result of an acidifieing of the aqueous solution by the Ca $\rightarrow$ proton exchange processes, which leads to the formation of a silicagel like cover at the C_3S grains. This envelope we mean is capable for the retarding effect, which we also found by adding several acids to the C_3S-hydration.

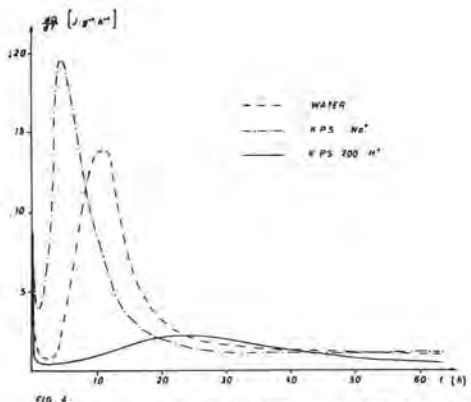

FIG. 4
HEAT EVOLUTION CURVES FOR C_3S PASTES HYDRATED WITH A CATION EXCHANGE RESIN (WOFATIT KPS 200)

Conclusions

These investigations show that the effect of admixtures on the hydration rate of C_3S depends essentially on their influence on the rate of the decomposition of the primarily formed CaO-rich surface C-S-H-cover on the C_3S grains. A stabilization of this C-S-H-phase gives a retardation of the C_3S-hydration, and reverse a fast decomposition of this phase accelerates the hydration.

The following scheme shows several possibilities of the influence of admixtures to the C_3S-hydration. In addition some other effects, which were not discussed in this article in detail are represented at this scheme. A formation of silicate complexes (by adding of pyrocatechol i.e.) or a formation of unsoluble calcium salts (by adding of NaF i.e.) at the C_3S-surface also retards the hydration, while an increase of the crystallization rate of $Ca(OH)_2$ formed during the hydration reaction causes an acceleration of the C_3S-hydration (by adding of $CaCl_2$ or NaCl i.e.).

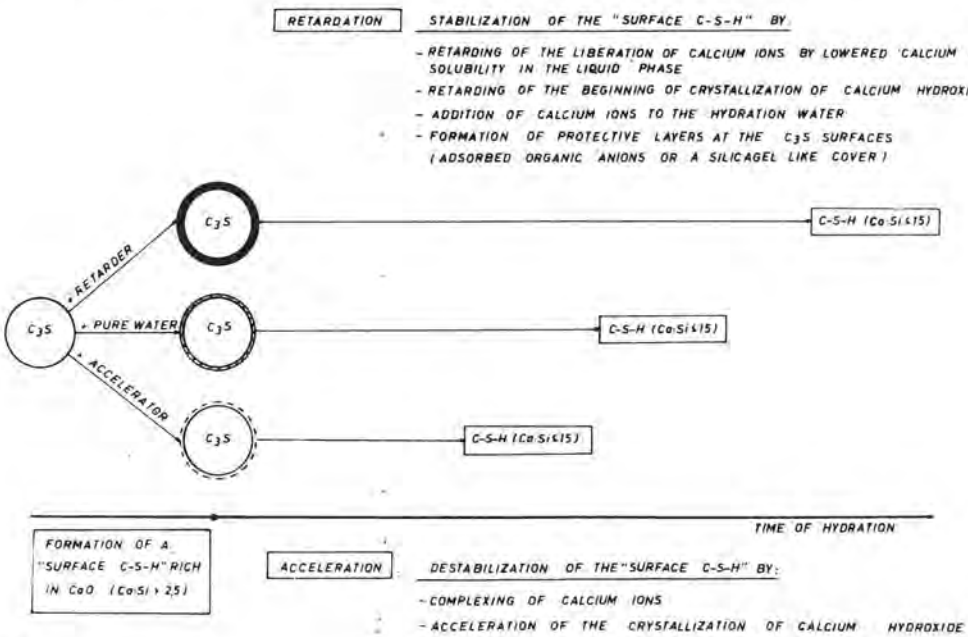

References

/1/ D.MENETRIER, I.JAWED, T.S.SUIV, J.SKALNY Cement and Concrete Research 9 (1979), 473

/2/ J.H.THOMASSIN, M.REGOURD, P.BAILLIF, J.C.TOURAY - C.R.Acad.Sci.Sev.C, 288 (1978), 93

/3/ M.REGOURD, J.H.THOMASSIN, P.BAILLIF, J.C.TOURAY - Cement and Concrete Research 10 (1980), 223

/4/ J.SKALNY, I.JAWED, H.F.W.TAYLOR - World Cement Technology 1978, 183

/5/ M.E.TADROS, J.SKALNY, R.S.KALYONCU J.Amer.Ceram.Soc. 59 (1976), 344

Influence des défauts ponctuels sur l'activité d'hydratation des constituants de clinker

Point defects influence on the hydration activity of clinker minerals

V. V. TIMACHEV,
V.G. AKIMOV, Institut Chimico-Technologique Mendéléev, U.R.S.S.

On a étudié le mécanisme de formation des défauts ponctuels de type p-n dans les solutions solides des silicates de calcium et déterminé leur influence sur l'activité d'hydratation des minéraux. Le type, la concentration et la mobilité des porteurs de charge étaient déterminés d'après la mesure des paramètres de l'effet Hall à la température de 25°C. Les caractéristiques d'hydratation sont déterminées par les méthodes de microcalorimétrie et de résonance magnétique nucléaire (écho de spin).

On a établi expérimentalement que la concentration des porteurs de charge libres atteint 10^{15} à 10^{19} T/m^3, le type de conductibilité par trous dans les minéraux pouvant être changé en conductibilité par électrons par l'introduction dans la composition de la solution solide des ions Fe^{3+}, Co^{2+}, Ni^{2+}. L'augmentation de la concentration des porteurs de charge libres dans les solutions solides du silicate tricalcique de 2,6 x 10^{15} à 3,5 x 10^{18} T/m^3 conduit à l'interaction plus efficace des particules de la phase initiale avec l'eau à la période d'hydratation initiale, ce qui fait que la période d'induction commence 18 minutes plus tôt.

The mecanism of electron-hole point defects developement in calcium silicates solid solutions has been investigated and their influence on the hydrate activity of minerals has been determined. Type, concentration and mobility of charge carriers were determined by taking measurements of Hall effect parameters at 25°C. Hydratation characteristics have been determined by the microcalorimetry method and the nuclear magnetic resonance (spin echo) method.

Experiments ascertained that the concentration of free charge carriers is as great as 10^{15}-10^{19} /m^3, while hole conductivity in minerals can be changed to electron conductivity by incorporation in the solid solution composition of ions Fe^{3+}, Co^{2+}, Ni^{2+}. Increase of free charge carriers concentration intricalcium silicate solid solutions from $2{,}6 \cdot 10^{15}$ to $3{,}5 \cdot 10^{18}$ /m^3 leads to more effective interaction of initial phase particles with water in first hydration period, with the result that induction period sets in 18 minutes earlier.

La défectuosité de la structure cristalline des phases du clinker du ciment portland est un des facteurs déterminant la réactivité du système ciment-eau, les conditions de l'interaction des particules avec l'eau dépendant de la fine structure du constituant pulvérulent (1,2). Les phénomènes qui en résultent se manifestent efficacement sur la surface fortement développée des matières polycristallines et débutent aux centres actifs. L'élucidation des questions liées à une induction artificielle de défauts et au degré de l'influence qu'ils exercent sur l'activité d'hydratation est un problème d'actualité.

Il a été établi (3-8) que dans les solutions solides des phases du ciment il se forme des défauts ponctuels de plusieurs types, dont la concentration est fonction des particularités de la structure du réseau cristallin, du type, de la nature chimique et de la quantité de l'impureté introduite, des conditions de la synthèse, etc. Le présent ouvrage a pour objet la formation des défauts ponctuels à trous électroniques, la détermination de leur influence sur l'activité d'hydratation des minéraux aux premiers stades d'hydratation (ne dépassant pas 180 mn).

Des comprimés d'une charge à composition stoechiométrique ont été cuits sur un support de platine en respectant des conditions de la synthèse identiques pour tous les échantillons. L'identification des solutions solides a été opérée par spectroscopie IR, par analyse thermique différentielle et aux rayons X, par microscopie électronique. Le type, la concentration et la mobilité des porteurs de charge ont été déterminés en mesurant l'effet de Hall à la température de 25 °C. Les études ont été effectuées à une installation pour mesurer la conductibilité électrique, la photoconductibilité et la concentration des porteurs de charge, installation fonctionnant selon le principe de deux champs variables - électrique et magnétique - aux fréquences de 58 et 50 Hz respectivement. Les caractéristiques d'hydratation sont établies par les méthodes de microcalorimétrie et de résonance nucléaire magnétique (écho de spin).

Les recherches effectuées ont confirmé par voie expérimentale l'existence de porteurs de charge libres dans les solutions solides de C_3S, C_2S, C_3A (Tableau 1), le type de conduction étant fonction, comme il a été établi, de plusieurs facteurs. Des particularités de la structure cristalline, des défauts, des écarts à la stoechiométrie font apparaître une conduction par trous (type r) dans les échantillons. L'incorporation d'ions étrangers dans le réseau cristallin lors de la formation des solutions solides, ainsi que le remplacement des radicaux principaux de la structure et des ions Ca^{2+}, Al^{3+}, Si^{4+} modifient considérablement les paramètres du réseau. On constate des changements du caractère ionique ou covalent des liaisons. En outre, la redistribution de la densité électronique des liaisons de valence soit fait augmenter la concentration des porteurs de charges libres de type r, soit conduit au remplacement de ce type de conduction par le type contraire (type p).

L'analyse des résultats obtenus a montré un brusque changement des propriétés des solutions solides lors des conversions d'une variété en une autre (fig.1) et, point le plus important, d'une même variété, ou bien dans le cas d'une redistribution continue de plusieurs phases polymorphes dans les échantillons (fig.2,3).

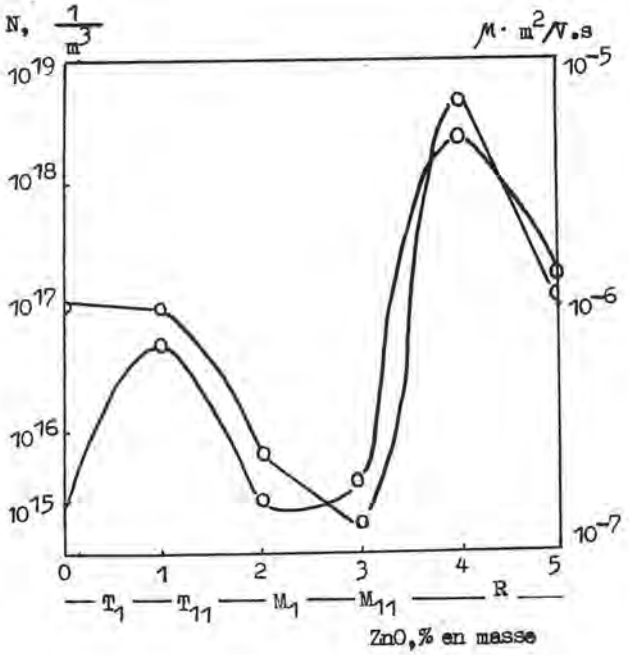

Fig.1. Variation de la concentration des porteurs de charge (N) et de leur mobilité (μ) en fonction de la teneur de C_3S

Ce dernier phénomène se manifeste d'une manière particulièrement prononcé lors de la formation de solutions solides dans lesquelles la concentration de l'impureté varie dans des limites étendues. C'est ainsi que la substitution des ions Mn^{3+} aux ions Ca^{2+} et, dans une faible proportion, aux ions Si^{4+} conduit à la formation de solutions solides de β et α'_L-C_2S occupent les places des cations Ca^{2+} de préférence dans les chaînes du type -Si-O-Ca-Si- , ce qui donne lieu à une variation du paramètre C de la cellule élémentaire, qui passe de 9,19 Å (1% en masse de Mn_2O_3) à 8,98 Å (7% en masse de Mn_2O_3), les valeurs de a (5,50 Å) et de b (6,77 Å) restant invariées pour toutes les solutions solides synthétisées. Les changements concernant les anions sont peu importants. La formation des solutions solides de α'_L-C_2S est due au remplacement des ions calcium

TABLEAU 1

Caractéristiques galvanomagnétiques de certaines solutions solides						
N°s d'ordre	Minéral	Impureté (1% en masse)	Variété	Concentration des porteurs de charge, $1/m^3$	Mobilité des porteurs de charge, m^2/Vs	Type de conduction
1	C_3A	-	cub.	$2,1x10^{18}$	$1,1x10^{-6}$	r
2	C_2S	Mn_2O_3	monocl.	$5,5x10^{17}$	$2,1x10^{-6}$	"
3	C_3S	-	tricl.	$2,6x10^{15}$	$1,2x10^{-6}$	"
4	"	ZnO	"	$6,2x10^{16}$	$1,1x10^{-6}$	"
5	"	Al_2O_3	"	$1,2x10^{17}$	$2,1x10^{-6}$	"
6	"	SO_3	"	$3,3x10^{17}$	$3,9x10^{-6}$	"
7	"	Mn_2O_3	"	$7,9x10^{17}$	$1,2x10^{-6}$	"
8	"	CdO	"	$3,4x10^{18}$	$6,0x10^{-6}$	"
10	"	Fe_2O_3	"	$1,6x10^{17}$	$3,7x10^{-7}$	p
11	"	CoO	"	$5,7x10^{17}$	$3,2x10^{-6}$	"
12	"	NiO	"	$3,5x10^{18}$	$1,3x10^{-5}$	"

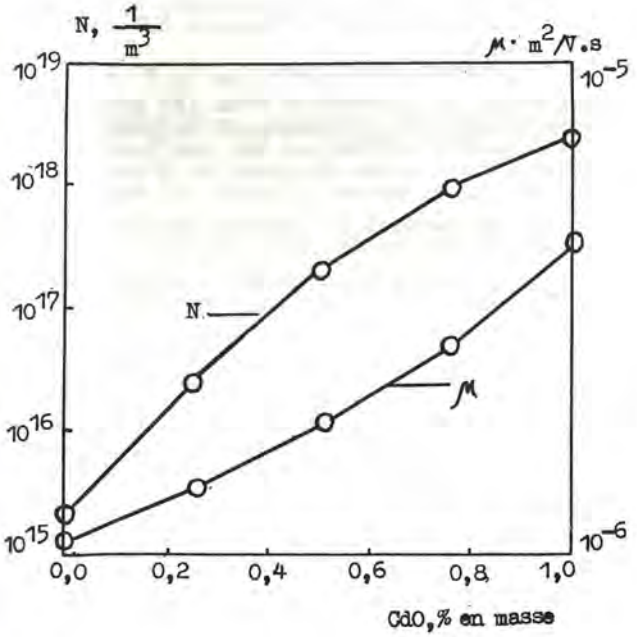

Fig.2. Variation de la concentration des porteurs de charge (N) et de leur mobilite (μ) en fonction de la teneur de C_3S en CdO

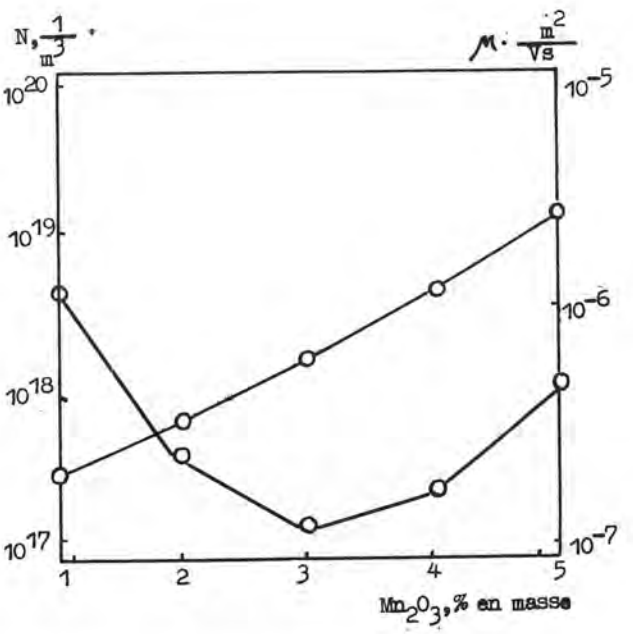

Fig.3. Variation de la concentration des porteurs de charge (N) et de leur mobilite (μ) en fonction de la teneur de C_2S en Mn_2O_3

situés dans les interstices entre les tétraèdres de SiO_4 et des ions silicium dans les tétraèdres eux mêmes. Une telle incorporation de Mn_2O_3 dans la structure de α'_L-C_2S provoque une diminution du paramètre

TABLEAU 2

Caractéristiques des solutions solides de C_2S avec Mn_2O_3

Concentration de Mn_2O_3, % en masse	Proportions des phases dans la composition,		Paramètres élémentaires a	de la cellule, Å		Température de la conversion de la variété β en variété α_L' °C
	β-C_2S	α_L'-C_2S		b	c	
1	100	0	-	-	-	680
3	80	20	10,93	18,22	6,72	690
5	49	51	10,93	16,25	7,00	705
7	40	60	10,93	16,25	7,00	710

b et une augmentation du paramètre C de la cellule élémentaire. La substitution des ions manganèse aux ions calcium par suite de l'incorporation de Mn_2O_3 dans la structure de C_2S fait apparaître la conduction du type r à l'état de valence, qui s'implifie logiquement avec l'augmentation de la concentration de Mn_2O_3. Ce phénomène résulte de la redistribution de la densité électronique des liaisons de valence lors de la substitution de Mn^{3+} à Ca^{2+} dans les chaînes -Ca(Mn)-O-Ca(Mn)- et -Si-O-Ca(Mn)-Si-.

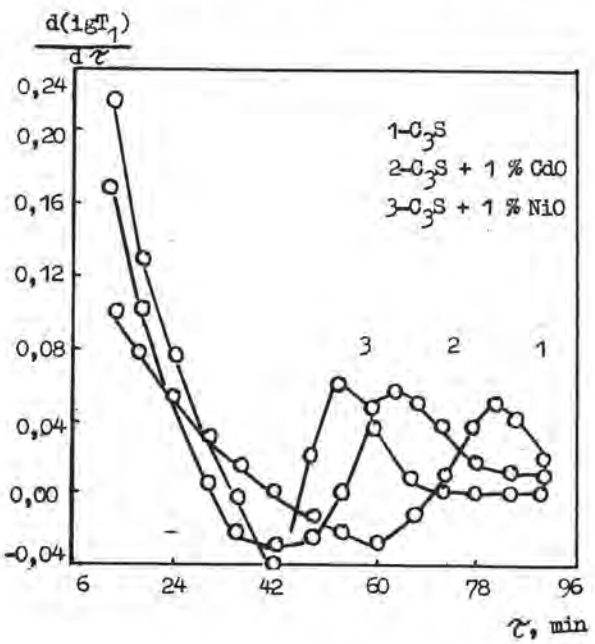

Fig.5. Relation entre la vitesse de la variation du temps de relaxation des protons T_1 (ms) et la durée d'hydratation τ (mn)

L'influence des défauts ponctuels sur la réactivité du liant est particulièrement manifeste lors de l'hydratation des solutions solides de C_3S. L'activité d'hydratation des minéraux a été étudiée par les méthodes de microcalorimétrie et de resonance nucléaire magnétique à impulsions (écho de spin). Cette dernière méthode ne convient pas quand il s'agit d'étudier la mobilité des molécules d'eau au cours de l'hydratation (9,10). On a déterminé les durées de la relaxation longitudinale (T_1) et de la relaxation transversale (T_2) des protons par les méthodes à impulsions (180°-90°) et on a calculé leurs rapports pour de différentes durées d'hydratation. Une poudre aux grains de tailles uniformes (25 à 30 microns) a été gâchée, avant l'expérience, avec de l'eau distillée dont le rapport B/T est égal à 0,5.

Les courbes cinétiques T_1, T_2 et T_1/T_2 sont mises en corrélation avec les courbes représentatives du dégagement de chaleur, l'existence d'inflexions sur ces courbes attestant une nette division de l'hydratation de C_2S en stades (fig.4). Au moment initial de gâchage on observe une brusque diminution des grandeurs T_1 et T_2 des échantillons examinés par rapport à l'eau pure ($T_1 \approx T_2 \approx 3s$); ce qui est dû à un affaiblissement de la mobilité des molécules d'eau par suite de leur adsorption sur les centres actifs de la surface du solide. Etant donné que la grandeur T_1 est fonction de la surface des matières hydratées (11), la décroissement de la durée de relaxation et du rapport T_1/T_2 à la première étape de l'hydratation (jusqu'à 60 mn pour C_2S) est dû à la dissolution de C_3S, au passage, surtout des ions Ca^{2+}, en solution, à leur hydratation et à la formation de l'hydrate $3CaO \cdot SiO_2 \cdot nH_2O$ sur la surface du grain initial. Ensuite, l'hydratation se ralentit brutalement et entre dans une période d'induction, dont le début coïncide avec l'accroissement de T_1 et une inflexion sur la courbe T_2, ce qui peut être dû à la formation d'un hydrate ayant pour formule $1,6CaO \cdot SiO_2 nH_2O$, qui présente un caractère cristallin moins prononcé et une surface unitaire plus développée que l'hydrate $3Ca \cdot SiO_2 nH_2O$. Avec toute nouvelle accélération de l'hydratation, les

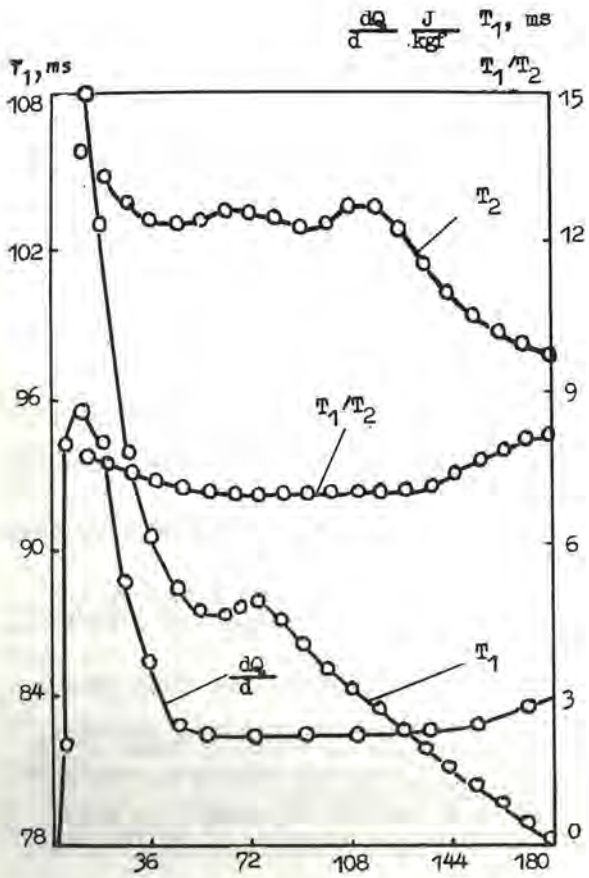

Fig.4.Variations de l'intensité du dégagement de chaleur ($dQ/d\tau$), des durées de relaxation des protons (T_1 et T_2) et de leur rapport lors de l'hydratation de C_3S

durées des relaxations longitudinale et transversale décroissent régulièrement, mais le rapport T_1/T_2 commence à croître par suite de la formation d'une nouvelle couche extérieure de $Ca(OH)_2$ et de cristallohydrates C-S-H dans lesquels les molécules de H_2O ont une faible mobilité.

L'accroissement de la concentration des porteurs de charge libres par incorporation d'ions étrangers à la composition de la solution solide a pour effet une interaction plus efficace des particules de la phase initiale avec l'eau dans la période initiale d'hydratation. Il en résulte que la période d'induction commence plus tot qu'en cas de C_3S pur (fig.5). C'est la conséquence de l'intensification de l'adsorption et de la dissociation des molécules d'eau en ions OH^- et H^+ avec établissement de liaisons entre les ions Ca^{2+} et OH^- et entre O^{2-} et H^+. Il se produit un changement dans la structure électronique des ions en réaction, qui s'accompagne d'un passage d'électrons des ions à charge négative aux ions à charge positive, ce qui entraine un relachement des liaisons dans le réseau cristallin de la phase initiale. L'accroissement de la concentration des porteurs de charges des types r et p contribue au déroulement de ces processus.

Les défauts ponctuels du type à trous influent également sur l'adsorption des molécules d'eau lors de l'hydratation de C_2S, C_3A et de leurs solutions solides, mais la périodicité est la plus manifeste quand on étudie l'hydratation de C_3S par la méthode de résonance nucléaire magnétique.

On constate donc que les défauts ponctuels accentuent les aptitudes réactionnelles des minéraux du clinker au début de l'hydratation et exercent par là une influence sur la mise en forme de la structure de solidification aux étapes ultérieures.

REFERENCES

I. Румянцев П.Ф. Тезисы докладов Всесоюзного Симпозиума по кристаллохимии и фазовым соотношениям в силикатных и окисных системах. Ленинград, 1978, с. 34-35

2. Сычев М.М. Цемент, 1977, № 12, с. 10-12

3. Акимов В.Г., Тимашев В.В., Бойкова А.И. Труды Моск.хим.-технол.ин-та им. Д.И. Менделеева. Силикаты, 1976, вып. 92, с. 112-115

4. Тимашев В.В., Акимов В.Г., Гусейнов М.Б., Якуб Ю.Н. Труды Моск. хим.-технол. ин-та им. Д.И.Менделеева. Силикаты, 1979, вып. 108, с. 122-125

5. Тимашев В.В., Акимов В.Г. Тезисы докладов Всесоюзного Симпозиума по кристаллохимии и фазовым соотношениям в силикатных и окисных системах. Ленинград, 1978, с. 32-33 (en russe).

6. Туркина Л.И., Сычев М.М., Судакас Л.Г. Гидратация и твердение вяжущих. Тезисы докладов и сообщений Всесоюзного совещания, Уфа, 1978, с. 84-85 (en rasse).

7. Maycock J.N., Skalny J., Kalyoncu R. Cem. and Concr. Res., 1974, v.4, p. 835-847.

8. Fierens P., Verhaegen J.P. Cem. and Concr.Res., 1976, v. 6, p. 337-342 (en anglais).

9. Kocuvan I., Uvsic J., Lahajnar G., Blinc R., Silicat ind., 1978, v. 43, p. 223-228.

10. Кудрявцев А.Б., Школьник Я.Ш., Ермаков В.И. Ж.прикл.химии, 1977, т.I, № 5, с. 1024-1027.

11. Blinc R., Burgar M., Lahajnar G., Rozmarin M., Rutar V., Kocuvan I., Ursic L., j. Amer. Cerem. Soc., 1978, v. 61, p. 35-37.

Electron microscope investigation of sulfoaluminate calcium hydration processes at the first stages of solidification

Etude microscopique électronique des processus d'hydratation du sulfoaluminate de calcium dans les premiers délais de durcissement

V.A. DMITRIEVA,
T.V. KOUZNETSOVA, Niitsement, Moscou, U.R.S.S.

On a étudié les produits d'hydratation des particules minces du sulfoaluminate de calcium qui se forment dans les premiers délais du durcissement dans la suspension.

On a relevé plusieurs types morphologiques de formation des phases hydratées dans un seul microvolume, ce qui témoigne de voies différentes de cristallisation:

- les cristaux croissent directement à partir du minéral de départ;
- les nouvelles formations hydratées se trouvent en contact avec la masse amorphe granuleuse secondaire des produits d'hydratation;
- les composés hydratés cristallisés à partir de la solution.

Dans tous les cas on observe des cristaux aciculaires d'ettringite ayant une structure tubulaire. Les données obtenues peuvent être utilisées pour élucider le mécanisme de l'hydratation et de l'expansion des ciments sulfo-alumineux.

Fine sulfoaluminate calcium particles hydration products generating at the first stages of solidification in suspension have been investigated.

Several morphological models of hydration phases in one microvolume have been revealed, what indicates different ways of crystallization: a(crystalls grow up directly from initial mineral; b)hydrate new formations are in contact with secondary granular amorphous substance of hydrate products;c) hydrate combinations, crystallized out of solution.

In all cases needle ettringite crystalls with tubular structure are reported. The data obtained can be used for clearing up the mechanism of hydration and widening of sulfoaluminate cements.

SUMMARY. IN the last few years much interest has been shown in the study of $C_3A_3CS-H_2O$ system owing to the development of special cement production. In spite of the intensive investigation of the calcium sulfoaluminate hydration process its early stage of an interaction with water has not been clearly studied so far.

The present paper investigates the hydration products of the calcium sulfoaluminate fine particles formed in suspension at early ages of hardening.

It has been found that several morphological types of hydrate phases are present in one microvolume :
- crystals grow directly from a starting mineral;
- hydrate new formations are in contact with secondary amorphous grainy mass of hydration products;
-hydrate compounds crystallized out in solution.

Acicular crystalls of ettringite having tubular structure have been observed in all cases. The data obtained can be used for revealing the mechanism of hydration and expansion of sulfoaluminate cements.

INTRODUCTION. Many papers deals with hydration reactions of cement at early stages of hydration. For a long time scientists have considered phase equilibriums in the systems: $CaO-SiO_2-H_2O$ and $CaO-Al_2O_3-H_2O$ and then in more complex systems containing $CaSO_4$, Fe_2O_3 along with CaO, SiO_2 and Al_2O_3. Extensive literature is available on composition of products of a clinker mineral interaction with water (1,2), chemistry of a portland cement hydration process has been studied well (3,4). Scientists are mainly of the same opinion about the composition of hydration products and their studies are reduced to refinement of the ratio Of C/S and C/A, the quantity of crystal water in hydrate compounds.

Up till now there are serious differences in the opinions about the mechanisme of hydration and structure formation (5-8), since a composition of new formations cannot be used as evidence for topochemical and solution mechanisms of a hydration process. At present intensive investigations using different methods are carried out in the area of origin of a hydrate phase and its morphology. Using a mathematical model of a cement stome structure, thermodynamic conceptions of origin of new phase nuclei and data on kinetics of a solution process of a starting phase A.F.Polack (5-5) has shown that cement hydration proceeds through solution of anhydrous compounds and hydrate crystallization mainly on the surface ofa starting grain of cement. L.G.Shpynovy deals with morphology of cement hydration products during long hardening of a cement stone and I.Skalni (10) has recently published the result of investigations of early stages of portland cement hydration with a scanning electrone microscope.

The aim of this work was to investigate morphology of the crystals formed at early stages during an interaction with water of calcium sulfoaluminate of $3CaO \cdot 3Al_2O_3 \cdot CaSO_4$ having great importance in production of rapid-hardening, non-shrink, expansion and tension cements.

MATERIAL OF THE INVESTIGATION. Sulfoaluminate was synthesized from $CaCO_3$, Al_2O_3 and and $CaSO_4 \cdot 2H_2O$, analytical grade, by burning a stoichiometric mixture at 1350°C.The mineral obtained was characterized by the

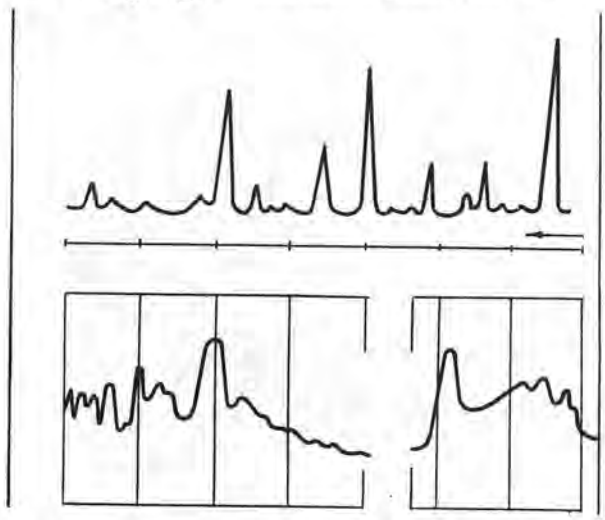

Fig.1. Radiogram (1) and ir-spectrum (2) of calcium sulfoaluminate

refraction index of N=1•571.

The sample radiogram has diffraction lines: cd=3•75; 3.21; 2•89Å; 2•15Å and its IR-spectrum shows absorption bands in the area of 400-500; 1000-1100; 3400-3650 cm^{-1} (Fig.1).

The chemical composition of the sulfoaluminate investigated is represented by (%): CaO=36•7; Al_2O_3 =50•2; SO_3=13•1.

EXPERIMENTAL PROCEDURE. Preparations were made by grinding synthesized calcium sulfoaluminate up to fine particles with thickness of several tens of angstroms (Å). Hydration took place in suspension with the ratio of solid; liquid = 1:50 and in cement paste with w/c ratio equil to its normal density. After a certain time a liquid phase was filtered and the content of CaO, Al_2O_3, SO_3 was determined in it. The filtered solid phase was analized with the X-ray diffraction analysis and differential thermal analysis.

In addition, after a certain time a drop was taken from an upper layer of suspension and placed upon the net strengthened with a carbon film. After drying the preparation was investigated with the UEMB - 100K transmission electron microscope having resolving power of 7 Å at accelerating voltage of electrons of 50 and 75 kW.

RESULTS OF INVESTIGATION. At intervals of 10 min, 30 min, 1 hour, 2 hours, 4 hours and 6 days after preparation of suspension or beginning of sample mixing with water it has been found during investigations of the preparations that several types of crystalhydrates are formed in one microvolume on hydration of C_3A_3CS.

After 10 minutes one can see submicrocrystals oriented in such a way that there are formed a space lattice with closed cells (Fig.2), transparent plates of calcium sulfoaluminate not effected by hydration, fine

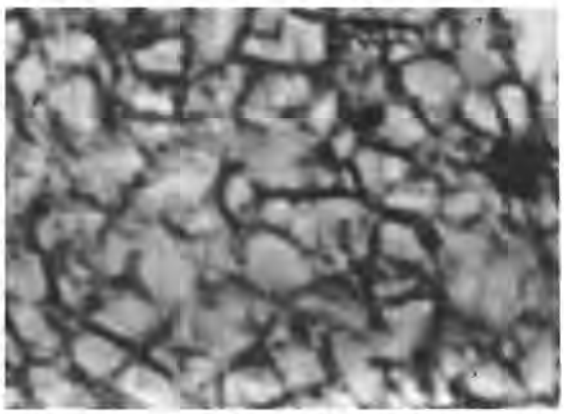

Fig.2. Space lattice from submecrocrystalhydrates (X4000)

whisker crystals and amorphous formations of hydrates.

All four types of hydrate new formations were observed in the subsequent above-mentioned periods.

There, are hawever, some differences residing in the fact that in the course of time the quantity of submicrocrystals forming fine sieve is decreased, as does the quantity of sulfoaluminates particles not effected by hydration while the quantity of gel-like formations and whisker crystals increases.

The later become thicker and while interweaving form a skeleton (Fig;3). Lack of a

Fig.3. Skeleton from interwoven and intergrown pulled crystals of ettringite (X4000)

starting grain in the places of interweaving and intergrowth of submicrocrystals and pulled crystals can demontrate crystal growing of hydration products in solution.

At the same time one can also see intergrowth of pulled crystal-hydrates with calcium sulfoaluminate particles (Fig.4) and gel-like mass of alumina hydroxide (Fig.5). Fig. 3,4 and 5 show a new formation after six days of C_3A_3CS hydration in suspension.

Of interest, to our opinion, is the structure of ettringite crystals in these figures which have a clear tubular structure. In Fig.4 outer diameter of an ettringite crystal tube is about 0.6-0.8 k while wall thickness - 0.01-0.02 k in Fig.5. Ratio of the tube thickness to the outer diameter is $\frac{1}{6} - \frac{1}{4}$ in both examples.

It has been found that tubular crystals sometimes brake down rapidly during preparation drying.

It appears in the fact that pulled crystals become discontinious, like strokes, and defects develop in a matrix.

Table 1 summarizes the results of chemical analysis of a liquid phase on C_3A_3CA hydration.

Table 1

Chemical composition of filtrate

Time of hydration, hours	Content, mg/l		
	Al_2O_3	CaO	SO_3
1	1104	608	432
7	1052	607	175
17	1040	600	137
24	485	308	36

Fig.4. Ettringite crystal intergrown with particle of calcium sulfoaluminate (X75000)

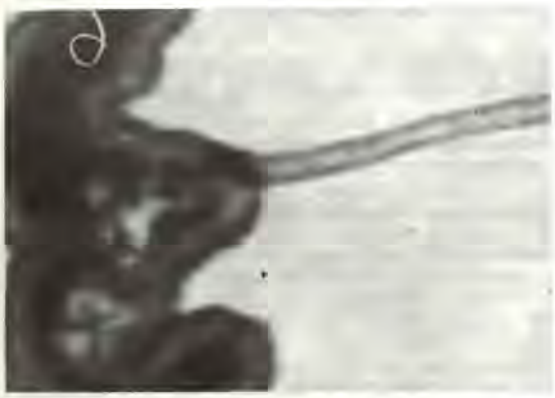

Fig.5. Ettringite crystal intergrown with gel-like mass of alumina hydroxide (X75000)

The results of the liquid phase chemical analysis show that the ratio of C/A in a liquid phase is close to that in starting C_3A_3CS while the sulfate quantity in terms of SO_3 is somewhat lesser than in calcium sulfoaluminate. On further hydration (up to 24 hours) the concentration of CaO, SO_3 and AL_2O_3 decreases sharply. The C/A ratio remains practically unchanged. X-ray diffraction studies have shown that at the first hours calcium hydrosulfoaluminate of trisulfate form is present in a solid residue after siltration of suspension. The quantity of the calcium hydrosulfate grows rapidly with increase in time of hydration. Calcium hydroaluminates have been also found in the composition of hydration products.

Investigations of cement paste have shown that on hardening of calcium sulfoaluminate calcium hexagonal hydroaluminates and ettringite revealed on the radiograms of hydrated samples even after an hour from the moment of preparation of samples are formed. A size of crystals increases by the period of 28 days. To this moment the sample is characterized by a high density. The distinctly formed crystals of new formations are in a close interweaving with each other. The interspaces consisted of the net of acicular crystals are filled with dense mass probably formed from $Al(OH)_3$.

DISCUSSING OF RESULTS

It has been found that regardless of w/c ratio accepted for the investigation of samples hydration products have a similar habit. Morphology of crystals, hydrate compounds typical of an early stage of hydration does not practically change during more prolonged hardening. Increase in the crystal size is only observed. Nature of crystallization of hydration products together with a chemical composition of a liquid phase make possible to say that hydration of C_3A_3CS proceeds through solution of a starting grain and crystal growing of hydrate compounds in solution as well as by water diffusion inside the C_3A_3CS grain and crystallization and growth of tubular ettringite on the surface of an anhydrous starting particle with formation of gel of aluminium hydroxide.

CONCLUSION. On hydration of C_3A_3CS at an early stage two types of hydrate compounds have been discovered: a gel-like phase and tubular crystals which formation was found on the surface of a starting cement particle, on aluminium hydroxide as a substrate and through crystal growing in solution. The data obtained can be used as an explanation of the mechanism of hydration and expansion of cement stone.

REFERENCES

1. Butt Yu.M., Timashev V.V., Portland cement, Moscow, Stroyizdat, 1975 (Russian).
2. Lyudvig U., Investigation on mechanism of hydration of clinker minerals. VI International congress of cement chemistry. Moscow, Stroyizdat, 1976, p.104-119 (Russian).
3. Malinin Yu.S., Lopatnikov L.Ya. Guseva V.I., Klishnis N.D., In book "RILEM", Moscow, Stroyizdat, 1968, p.82-91 (Russian).
4. Taylor H.F.W., Hydrated Calcium Silicates, "Jorn.Chem.Soc.", 1950, p.3682-3690 (English).
5. Polak A.F. Hardening of mineral binders. Moscow, Stroyizdat, 1968 (Russian).
6. Mchedlov-Petrosyan O.P. Chemistry of nonorganic building materials, Moscow, Stroyizdat, 1971 (Russian).
7. Vyrodov I.P. On some basic problems of kinetics of hardening of mineral binders and methods of investigation of products of their hardening. Transactions of Kuban agricultural institute, Krasnodar, 1963 (Russian).
8. Sychev M.M. Conditions of manifestation of binders, Journal of Applied Chemistry, 1971, X IV, 8, p.1740-1745 (Russian).
9. Shpynova L.G., Sinenkaya V.I., Chikh V.I. Electron stereo-microscopy of cement stone of autoclave hardening, Lvov, Publishing House "Vyshcha Shkola", 1978 (Russian).
10. D.Menétrier, L.Jawed, T.S.Sun and J.Skalny. Eska and SEM studies on early hydration.

Utilisation des réactions de formation de l'ettringite pour l'action orientée sur les processus de formation de structure du ciment durci

Use of ettringite formation reaction for directed influence on the structure formation processes of the cement stone

I.V. KRAVTCHENKO, Professeur, Docteur ès Sciences Techniques,
V.L. BERNSTEIN, Collaborateur Scientifique, Candidat ès Sciences Techniques, Niitsement,
Youjguiprotsement, U.R.S.S.

Sur la base des calculs thermodynamiques et des études physico-chimiques complexes on a montré qu'il est possible de commander la réaction de formation de l'ettringite dans le système contenant les aluminates de calcium de diverse basicité - C_3A et CA_2(CA).

On a établi que l'addition contenant les aluminates de calcium faiblement basiques exerce une influence positive sur le processus d'hydratation du ciment, ses indices de résistances et propriétés techniques.

On a déduit les dépendances fonctionnelles des propriétés des ciments vis-à-vis le rapport de C_3A, CA_2 et $CaSO_4 \cdot 2H_2O$ qui participent à la formation de l'ettringite.

Based on thermodynamic calculations and complex physical-chemical investigations, the possibility of ettringite formation reaction in the system containing calcium aluminates of different basicity - C_3A and CA_2(CA) - has been revealed.

Positive influence of the low-basic calcium aluminates containing addition on the cement hydration process, its strength characteristics and construction-technical properties have been find out.

Finctional relationships between cement properties and C_3A, CA_2 and $CaSO_4 \cdot 2H_2O$ ratio in the process of ettringite formation have been deduced.

Le processus de formation de la forme fortement sulfaté du sulfoaluminate hydraté de calcium, l'ettringite, qui a lieu lors de l'interaction du constituant d'aluminate du clinker de ciment portland avec le gypse, exerce une grande influence sur la formation de structure du ciment durci et ses propriétés. Toutefois les possibilités de cette réaction sont loin d'être utilisées complètement, ce qui est lié avant tout à la formation des pellicules de sulfoaluminate hydraté sur la surface des grains d'aluminate tricalcique.

L'objectif visé par nos études est de mettre au point le procédé de commande du processus de formation de l'ettringite par introduction dans la composition du ciment des additions contenant les aluminates. Pour choisir les additions les plus efficaces on a procédé aux calculs thermodynamiques des réactions d'hydratation dans le système aluminates de calcium - gypse - eau -$Ca(OH)_2$. On a établi de cette façon qu'il est ratfonnel d'introduire dans la composition du ciment des additions contenant les aluminates de calcium faiblement basiques - $CaO \cdot 2Al_2O_3$ et $CaO \cdot Al_2O_3$.

Selon les calculs thermodynamiques, dans le système contenant simultanément les aluminates de calcium de diverse basicité: $3CaOAl_2O_3$ et $CaO \cdot 2Al_2O_3$ la formation de l'ettringite aura lieu avant tout grâce à l'interaction du gypse avec C_3A, ce qui est dû à une plus grande valeur absolue de la variation du potentiel isobare-isotherme de cette réaction (-45 kcal/mole). Après que toute la quantité possible de C_3A fut liée, ce qui est limité aux stades d'hydratation précoces par la composition du milieu et les facteurs cinétiques, la fixation du gypse continue grâce à son interaction avec le dialuminate de calcium qui se caractérise par la valeur du potentiel Z égale à -7 kcal/mole. Ceci nous permet de supposer qu'en présence dans le milieu du ciment durcissant des aluminates de basicité différente le processus de fixation du gypse a un caractère continu, ce qui nous permet de commander le processus par variation du rapport des aluminates de calcium et du gypse qui prennent part à la réaction.

Les études physico-chimiques effectuées sur des mélanges différents de matériaux synthétisés avec utilisation de l'analyse aux rayons X, de la spectroscopie infrarouge et de la microscopie électronique ont permis d'établir les faits suivants. Lors de l'interaction du dialuminate de calcium avec le gypse il se forme l'ettringite, produit final de cette réaction, qui reste stable durant un temps prolongé indépendamment du rapport des constituants de départ. Une faible vitesse de cette réaction conditionne la cristallisation de l'ettringite sous forme de gros cristaux de forme prismatique avec un rapport d'axes peu élevé (jusqu'à 3-5). La structure dense du ciment durci est imprégnée du gel $Al_2O_3 \cdot 3H_2O$ qui se dégage lors de la réaction étudiée dont l'équation stoechiométrique peut être représentée sous la forme suivante:

$$CaO \cdot 2Al_2O_3 + CaSO_4 \cdot 2H_2O + \frac{40}{3} H_2O$$

$$\frac{1}{3} 3CaO\ Al_2O_3 \cdot 3CaSO_4 \cdot 31H_2O + \frac{5}{3} Al_2O_3 3H_2O$$

La vitesse de liage du gypse augmente avec l'accroissement du rapport de CA_2 à CSH_2.

Le trait distinctif de ce processus est l'absence de pellicules de sulfoaluminates hydratés sur la surface des grains d'aluminate. La cristallisation de l'ettringite a lieu à travers la solution.

Les méthodes physico-chimiques étaient utilisées pour l'étude de la formation de l'ettringite dans le système où sont présents simultanément deux aluminates de calcium: C_3A et CA_2. Le traitement des données de l'analyse aux rayons X et de la spectroscopie infrarouge, donné sur la figure 1, a permis de confirmer les conclusions des calculs thermodynamiques sur l'ordre d'interaction avec le gypse des aluminates de basicité différente. Le dialuminate de calcium identifié sur les spectrogrammes des rayons infrarouges d'aprés la bande d'absorption de 820 cm^{-1} et sur les radiogrammes d'après les maximums de diffraction avec d=4,44; 2,59 A, entre en réaction avec le gypse après la fixation de la quantité principale (jusqu'à 50-60%) de l'aluminate tricalcique (bande d'absorption de 750 cm^{-1}, d=2,69 A).

L'introduction de $Ca(OH)_2$ ne modifie pas le mécanisme et l'ordre de succession dans lequel les aluminates C_3A et CA_2 entrent en réaction avec le gypse. Cependant,

sa présence dans le milieu du ciment durcissant diminue brusquement le degré de participation de l'aluminate tricalcique à la formation du sulfoaluminate hydraté de calcium aux stades d'hydratation les plus pré-

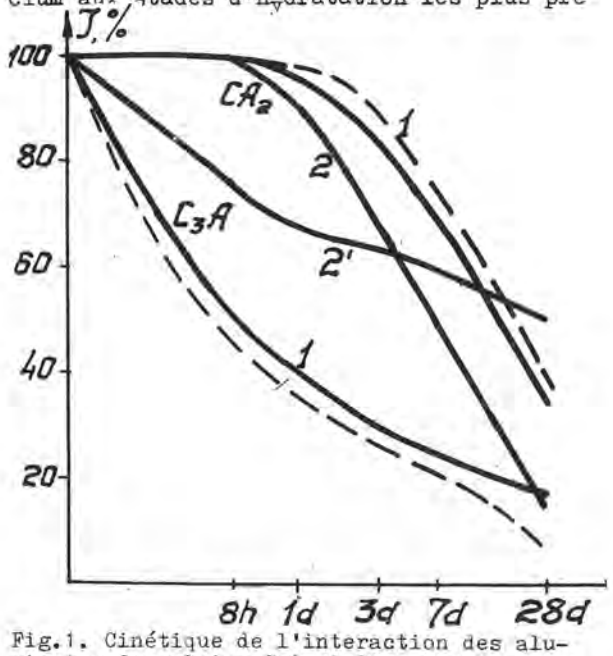

Fig.1. Cinétique de l'interaction des aluminates de calcium C_3A et CA_2 avec le gypse

-------- d'après les données de la spectroscopie infrarouge;

-------- d'après les données de la radiographie;

1- dans le système C_3A-CA_2-$CaSO_4 \cdot 2H_2O$;

2- CA_2 dans le système C_3A-CA_2 - $Ca(OH)_2$-$CaSO_4 \cdot 2H_2O$-H_2O; 2'- C_3A dans le système C_3A-CA_2-$Ca(OH)_2$-$CaSO_4 \cdot CaSO_4 \cdot 2H_2O$-$H_2O$

coces (courbe 2 sur la figure1). L'excès de C_3A aux stades plus tardifs conduit à la décomposition de l'ettringite et à sa transformation en forme de monosulfate (le potentiel Z de cette réaction est égal à -77 kcal/mole). Donc pour augmenter l'efficacité de l'action d'une addition il est rationnel d'introduire dans la composition du ciment une addition minérale active, par exemple le laitier granulé de haut fourneau.

Le caractère continu du processus de formation de l'ettringite à partir des aluminates de basicité différente (C_3A et CA_2) rend possible l'intensification du processus de fixation du gypse aux stades précoces d'hydratation du ciment. Ceci conduit, d'une part, à l'élimination de phénomènesde destruction indésirables accompagnant la cristallisation de l'ettringite aux stades plus tardifs et, d'autre part, la formation d'une quantité supplémentaire de l'ettringite aux stades précoces crée les conditions pour l'expansion du ciment. La formation de l'ettringite à partir de CA_2 sous forme de cristaux de forme prismatique capables de développer des pressions de cristallisation élevées, a permis de prédire que les ciments avec une addition contenant le dialuminate se caractériseront par une valeur d'expan-

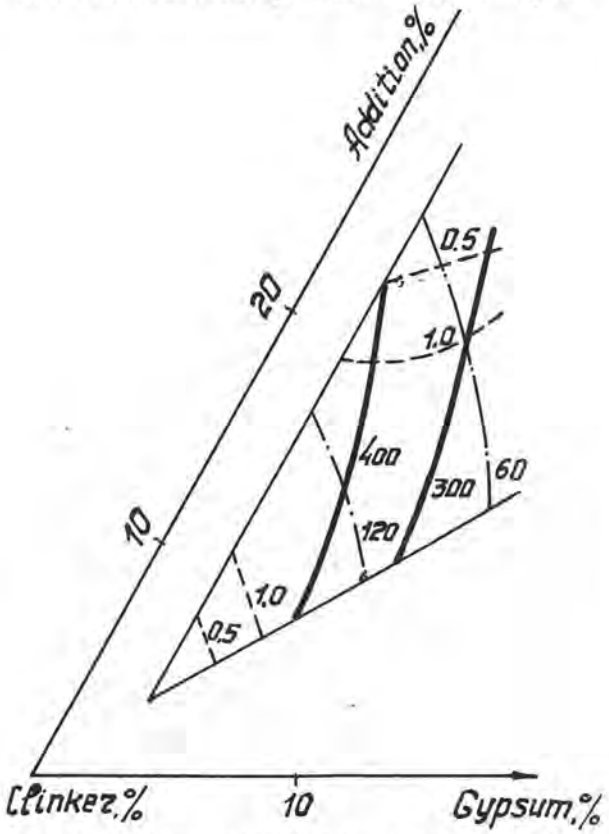

Fig.2. Domaine optimal des compositions des ciments:

------- isolignes de résistance à la compression, kgf/cm2;

------- isolignes de dilatation linéaire,%;

------- isolignes de prise initiale, mn

sion élevée.

Par suite des recherches effectuées on a trouvé des additions efficaces ayant dans sa composition de 60 à 80% du dialuminate calcique.

Vu l'absence de données à priori sur les propriétés des ciment avec addition indiquée, les études des compositions de ciment et la détermination de leur constitution optimale était effectuées avec utilisation de la planification mathématique à deux stades de l'expérience. Sur la figure 2 est représenté le domaine otpimal des compositions des ciments additionnés sur le diagramme "simplex" à 3 constituants "composition (clinker-gypse-addition) - propriété". Les compositions dans le domaine optimal se caractérisent par la résistance à la compression de 30 MPa au minimum, la valeur de la dilatation linéaire de 0,5 à 2,0%, le début de prise pas plus tôt qu'après 1 heure. Le modèle mathématique de la variation de résistance du ciment à l'âge de 28 jours en fon-

ction de la composition minéralogique a la forme suivante:

$$R^{28}_{comp.} = 396,5 - 11,1x_1 + 42,7x_2 + 22,9x_3 + 0,23x_1 \cdot x_2 + 0,078x_1 \cdot x_3 - 2,32x_2x_3 + L,195x_1^2 - 2,58x_2^2 - 2,12x_3^2;$$

où x_1, x_2 et x_3 représentent la quantité du laitier de haut fourneau, du l'addition contenant CA_2 et du gypse (%).

Le traitement des équations de la régression et les études sur les clinkers de composition minéralogique différente ont permis d'établir les rapports optimaux de CA_2/C_3A et de CA_2/SO_3 pour résoudre les problèmes d'accroissement des indices de résistance du ciment (respectivement de 0,8 à 1,5 et de 2 à 4) et pour obtenir une grande expansion au cours du durcissement (0,5 à 1,0 et 0,8 à 1,2).

On a étudié l'influence de l'addition contenant CA_2 sur les processus de formation de structure du ciment durci. L'introduction de l'addition indiquée dans la composition du ciment diminue le temps total de fixation du gypse, cette diminution étant proportionnelle à la quantité de l'addition introduite, ce qui ressort clairement de la figure 3. L'allure de la courbe de fixation de SO_3 varie également: sur la courbe cinétique disparaît la partie horizontale caractérisant la période inductive de fixation du gypse et due à la formation sur la surface des grains d'aluminate tricalcique des pellicules de sulfoaluminate hydraté. Les données de la figure 3 correspondent aux conclusions faites sur la base des calculs thermodynamiques et des études physico-chimiques des monominéraux, sur le caractère continu du processus de fixation du gypse dans le système contenant en meme temps les aluminates de calcium C_3A et CA_2; A l'aide de la microscopie électronique on a démontré l'intensification de la formation de l'ettringite aux stades précoces: pendant la période entre la fin de prise et 1 jour d'hydratation. A notre avis, ceci explique justement la manifestation par les ciments de l'effet d'expansion. La structure du ciment durci se caractérise, lors de l'introduction d'une addition, par une densité élevée. On peut dire que de gros cristaux d'ettringite renforcent la structure dense du ciment en lui conférant une résistance élevée.

L'influence de l'addition contenant CA_2 sur les propriétés techniques des ciments fut étudiée en comparaison du ciment ordinaire. On a établi que le ciment avec addition indiquée se caractérise par l'accroissement accéléré de la résistance tant lors du durcissement normal que lors du traitement à la vapeur humide, et les bétons à base de ce ciment se caractérisent par l'imperméabilité et la résistance au gel élevées. L'étude des déformations du ciment avec addition contenant le dialuminate de calcium a mon montré que dans toute la gamme d'utilisation de l'addition (de 3 à 10%) la stabilisation de l'expansion a lieu durant le premier jour du durcissement. L'effet d'expansion se manifeste lors du durcissement dans l'eau et à l'air.

Le trait distinctif des compositions avec addition contenant le dialuminate est la durée de prise ralentie en comparaison des autres compositions connues des ciments expansifs: prise initiale de 1,5 à 2,0 h, prise finale de 3,0 à 4,0 h.

En meme temps la possibilité d'obtenir des ciments expansifs à prise rapide n'est pas exclue.

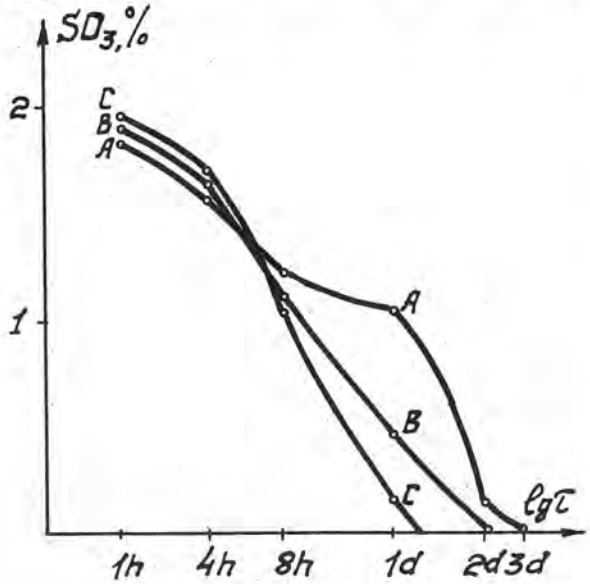

Fig.3. Influence de l'addition contenant CA_2 sur la cinétique de fixation de SO_3: A-ciment sans addition; B-ciment contenant 5% d'addition; C-ciment contenant 10% d'addition.

CONCLUSIONS

L'introduction dans la composition du ciment des additions contenant les aluminates de calcium faiblement basiques modifie le mécanisme de formation de l'ettringite, rend possible la commande du processus de formation de structure du ciment durci dans la direction de la résolution des problèmes visant à accroître les indices de qualité du ciment et à conférer à ce dernier les propriétés spéciales.

Portland cement strength depending on technological factors Micromechanism of destruction

Résistance du ciment portland en fonction des facteurs technologiques et micromécanisme de destruction

B. YOUDOVITCH,
B.D. KLICHANIS, Niitsement, Moscou,
OU. I. PAPIACHVILI, Institut des ingénieurs du Bâtiment par correspondance de l'U.R.S.S., Moscou,
V.G. ABRAMOVA, Institut Polytechnique - Novorossiisk, U.R.S.S.

L'accroissement de la teneur en C_3S et de la dispersion du clinker conduit lors de l'hydratation à la diminution des dimensions moyennes des agrégats cristallins de l'ettringite et de C-S-H(II), des zones de la portlandite et accélère le cheminement des microfissures sous charge. L'amélioration de la morphologie de C_3S ne conduit pas à ces changements, car elle est liée à une moindre tortuosité des frontières entre les blocs de la mosaique-canaux pour la pénétration accélérée de l'eau lors de l'hydratation, ce qui est montré par la méthode de la microscopie électronique à contraste de phase. L'introduction dans le ciment des constituants de cristallisation (crents) simplifie la topographie de la surface de cassure de C-S-H(II), ce qui peut être dû seulement à l'abaissement du niveau des microcontraintes.

During hydration, C_3S content growth and clinker degree of dispersion increase lead to:
a) ettringite and C-S-H(II) crystalline concretions average size decrease;
b) portlandite zones decrease;
c) microcracks development increase under load.

Morphology improvement of C_3S does not lead to such transformations since it is connected with lesser tortuousness of the boundaries between mosaic units (channels for accelerated penetration of water during hydration) - it has been demonstrated by the method of phase-contrast electron microscopy. Incorporation of the crystallizing components (krents) in the cement simplifyes fracture surface C-S-H(II) topography, what can be motivated only by microtension level reduction.

RESUME: The growth of the C_3S content and specific surface of clinker at hydration decreases the average size of the crystalline concretions of ettringite, C-S-H (II), portlandite zones and accelerates formation of microcracks under load. Improvement of the C_3S crystals morphology does not lead to suche changes since it involves more streight boundaries between the mosaic blocks, i.e. channels for accelerated diffusion of water during hydration which is shown by the phase-contrast electron microscopy method. Addition of crystallizing components ("crents") into cement simplifies the topography of the fracture surface of C-S-H (II) that may follow only after the decrease of microstress level.

The present paper deals with the results of the investigations of hardened cement paste submicrostructure (W/C-0.25 and 0.35) of a regular (1) and high-strength (2) portland cements (composition,=C_3S - 61, C_2S -16, C_3A - 6, C_4AF - 15) produced by the Zdolbunovsk plant (see Table 1) performed with the use of the UEMB-100 and 100 K transmission and "Stereoscan-2A" scanning electron microscopes.
Samples for TEM were vacuum dried at 10^{-4} torr during 0.5 h at a temperature of 25°C and aiming self-shaded coal replicas were prepared. A layer of Au was vacuum deposited on the fracture surface before observation of the relief by SEM.

Investigations in the cement pastes of different age show that the submicrostructure is based on a two-component mutually penetrating three-dimensional netting of fibres I (ettringite, AFt;phase) and II (fibrous calcium hydrosilicates), which heals the high-strength cement paste pores after 8-10 h and the pores of a regular cement, after 14-16h; The netting pores starting from the boundaries of the cement initial particles accommodate phase III (portlandite) and phase V (gel-like calcium hydrosilicate zones) which appears 10-12 h later. By the end of the first day phase IV (AFM, in particular C_4AH_{13}) is distributed in the form of loose nodes in the netting cells I+II. By the seventh day phase V fills almost the entire fracture surface of a high-strenght cement paste by the 28th day, of a

Table 1.

Characteristics of Cements

No.	SO_3, %	cm^2/g S	Fraction contents, microns				Compression strength, kgf/cm^2		
			5	5-30	30-60	60	1	3	28
1	2.2	2840	12	44	28	16	112	231	560
2	2.5	4080	23	56	15	6	225	394	673

regular cement paste phase II of the skeleton and phase V are more dispersed in the first case. Domination of angles of 60 (120)-90° in certain knots of netting I+II, pointed out also by D.M.Roy, M.W.Grutzeck and T.Ciach, allows regarding a part of its cells as having a local rhombohedral symmetry. This determines a rhombohedral symmetry of the submicrostructure metric tensor as a whole that includes in the decisive conditions of isotropy of the cement paste nonporous part.

Investigations of the differential porosity by the mercury porometry method indicate reduction of the capillary pores volume (effective radius over 0.5 microns) in a high-strength cement (Fig.1). By the 28 day the latter becomes free from open pores larger than 3-5 microns, as compared with 10 microns at lower specific surface .

Similar investigations were performed to compare hydration structures of cement with different C_3S contents (58 and 65%) and different characteristics of clinker microstructure (average size of alite crystals 20 microns - fine-crystal clinker prepared from a mergel raw mixture, and 50 microns - large-crystal clinker). It was found out that with increase of the alite content the column-shape zones around the cement grains become somewhat thinner, whereas the size and number of portlandite zones increase, the ettringite fibre length shortens and the size of the netting cells of fibres I+II decreases. If alite crystal size is changed, in addition to decrease of the cell I and II size and general acceleration of hydration, the tightness of the hydration submicrostructure increases more intensively. This is seen from changes of the constant of water diffusion rate through the

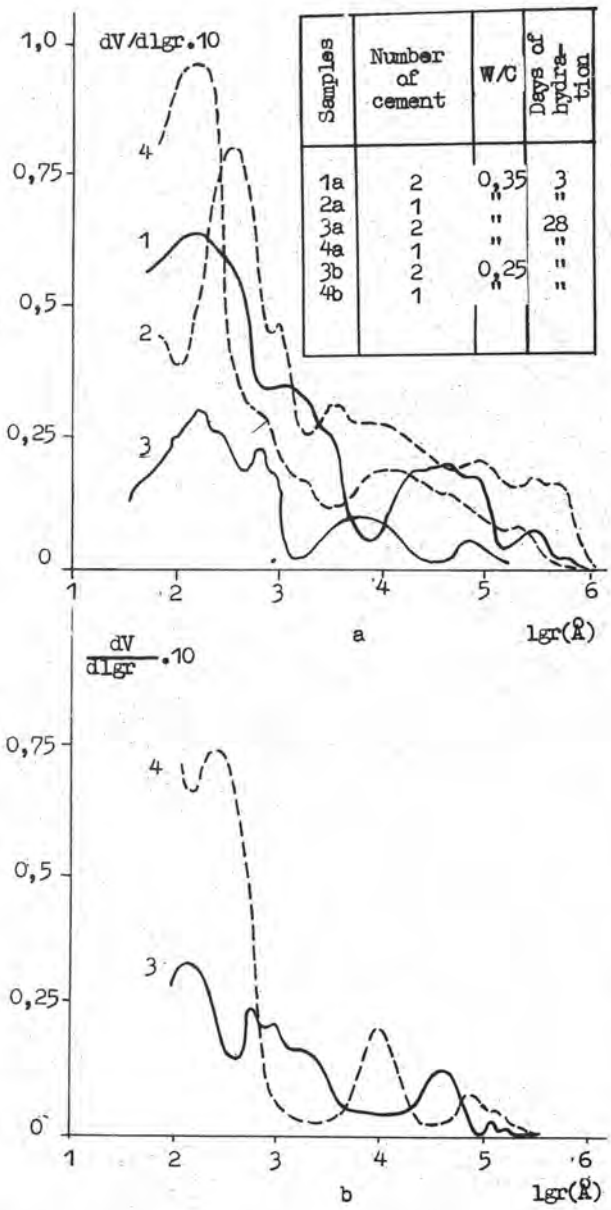

Fig. 1. The differential porosity of hardened cement paste

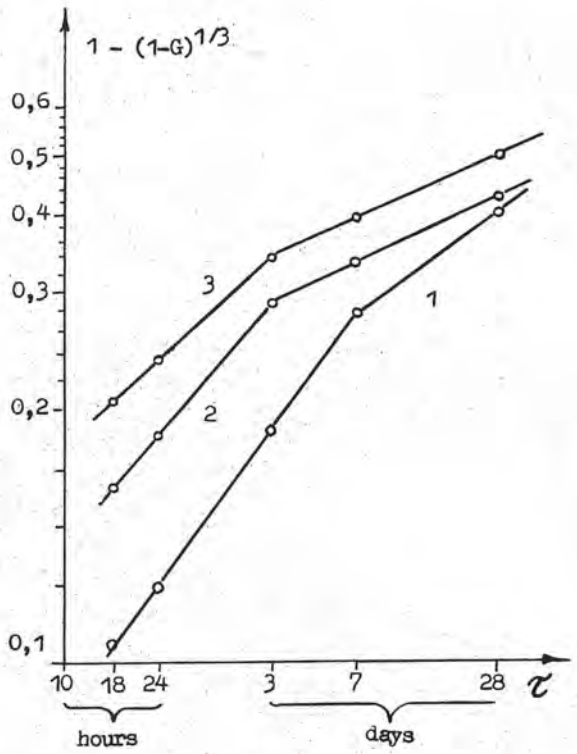

Fig. 2. The kinetics of cements hydration: G - degree of hydration, τ - time, hours and days, 1 - cemevt № 1, 2 - cement № 2, both of clinker with 50 microns alite cristals; 3 - cement from clinker with 20 microns alite crystals, S = 3000 cm^2/g

hydrate membranes (at stage II of the hydration process, Fig.2). A similar phenomenon is observed also when merely increasing the specific surface of cement. Thus, the hydrate membranes of fine-crystal clinkers have higher density, strength and screening ability to water and to obtain the same strenght level the specific surface of cement may be smaller.

N.V.Belov, G.G.Kuznetsova and some authors of this paper had studied the reason of this facts by the method of impregnation of hydrating cement with methylmetacrylate and benzoyl peroxide after vacuum drying and thermal treatment. Black zones is polymethylmetacrylate in places of cement paste pores and channels between the blocks along the external monolayer in the alite crystal. We can conclude that on passing between the blocks, water then separates them from each other and from the remaining part of the crystal which leads to the formation of known globular internal product. Investigations of 20 industrial clinkers have proved that dimensions of alite crystals visible through the optical microscope are directly proportional to the average size of the blocks. The growth of block boundaries density on cement paricle surface leads to said increased tightness of hydrate membranes. This situation changes when introducing crystallizing components; for instance the limit of alite content in clinker (70%) dictated by the increase in the structure portlandite zone dimensions is

Fig. 3. The submicrostructure of metilmetacrylate impregnated cement paste. x 7500: 1 - metilmetacrylate late (parabolic microcrack), 2 - the monolayer of mosaic alite blocks with channels between them

Fig. 4. The microcracks pattern on the betton of capillare pore in phase V.x 2500. The cracks plane is parallel to the traectory of fracture

eliminated. Addition of the crystallizing components, alongside with increasing the amount of ettringite, decreases the number of bends of hydrosilicate flakes on the fracture surface of the C-S-H (II) gel and makes the topography of said fracture more uniform and more similar to the actual gel.

Microcracks under load in hardened cement paste of up to 3 days old concentrate at pores. After 7 days, the interphase cracks around the submicrostructure zones with lower categories of symmetry (parallel concretions III, nodes IV, column shaped zones II) dominate. The parallel crystal bundles near the pores loose stability after shearing and their fracture is indicative of relaxation of stresses owing to instanceous microstrain.

The nature of formation V fracture is very important. We have managed to find out in said formation cylindrical pores with microcracks in the bottoms thereof (Fig.4, 28 days, cement I, SEM). Their location, similar to that occurring in a round plate on a resilient base with peripheral attachment and central loading, shows that phase V is destroyed owing to the lateral rupture in the tensitive zone with the cracks width of 0.1-0.5 microns.

In a number of studies of the concrete fracture mechanism, this phenomenon was attributed to either the influence of the "inter-molecular bonds", which cannot be manifested at such distances, or to plastic "hinges".

The present paper confirms that hardened cement paste and concrete work as a composite material compirsing statistically distributed fibres.

Characteristics of the compositions with low water-demand based on gypsumless portland cement

Propriétés des compositions nécessitant une petite quantité d'eau sur la base du ciment portland sans gypse

S.M. ROYAK,
T.Y. GALPERINA,
Y.N. PERMINOVA,
M.G. DOROGUINA, Vzisi, Sibniiproekttsement, U.R.S.S.

Les compositions nécessitant une petite quantité d'eau furent obtenues sur la base du ciment portland sans gypse, du surfactif (vinasse de sulfite et de levures), du silicate ou du carbonate d'un métal alcalin. La quantité d'eau nécessaire pour ces compositions est de 30 à 40% plus petite que pour le ciment portland ordinaire. Leur résistance est élevée surtout après l'étuvage.

Une petite qualité d'eau exigée par ces compositions est due à la capacité des additions de diminuer la vitesse d'adsorption des surfactifs par les produits d'hydratation C_3A et d'assurer une haute concentration des surfactifs dans la phase liquide de la pâte de ciment. Les produits d'hydratation des compositions ont une dispersité élevée et la composition des phases stable dans le temps, ce qui assure une grande résistance et la durabilité de la pierre de ciment. On a étudié l'influence sur les propriétés des compositions de la minéralogie du clinker, du mode d'introduction des additions et de la composition granulométrique de la poudre de ciment.

Compositions with low water-demand have been got on the base of gypsumless portland cement, surface-active agents (sulfid-yeast malt grains), silicate or carbonate of an alkali metal. They have water-demand 30-40% lower than ordinary portland cement, as well as high strength, especially after steaming.

Low water-demand of the compositions, is caused by the ability of additions to reduce the adsorption rate of SAA by the products of C_3A hydration and to provide high concentration of SAA in liquid phase of cement paste. Products of compositions hydration have high degree of dispersion and phase structure stable in time, what results in cement stone high strength and durability.

The influence of clinker mineralogy, additions introduction method, and cement powder grain formation on the characteristics of the compositions has been studied.

It was established in [1] that addition of lignosulphonate and alkali metal carbonate in optimal amounts to finely ground clinker gives a composite binder of high strength and density and with water consumption by 30-40% less than of usual Portland cement.

We have established that compositions with similar properties may be also obtained on the basis of sulphite-yeast waste (SYW) (a waste of pulp and paper industry) and alkali metal silicate [2]. On addition of up to 1.0-1.5% of SYW and 0.25-1.0% of Na_2SiO_3 to gypsum-free Portland cement with specific surface of about 5000 cm^2/g (according to Tovarov's method) reduces water consumption by 30-40% and gives setting period close to those of compositions with K_2CO_3. The strength of mortar specimens formed according to standard GOST 310.4-76 at W/C = 0.24-0.27 directly after steaming is 60-65 MPa, 28 days ofter steaming 70-80 Mpa. Under normal conditions at early stages (1-3 days) compositions with Na_2SiO_3 harden less intensively than with K_2CO_3, however at the age of 28 days the strength of both reaches 60-70 Mpa.

The positive effect of steaming on properties of compositions with high dosages of SYW is due to low W/O ratio and the nature of the forming pore structure of the cement stone. Study of porosity of mortar specimens by the method of threestep water saturation [3] showed the that porosity of steamed specimens is lower than porosity of normal-hardening speciments. Total porosity and pore volume and the volume of pores capable of being saturated with water at atmospheric pressure is by 1.5-2 times lower than in specimens of usual Portland cement.

The mineralogical composition of the clinkers, the method of introducing the additives and the mix temperature significantly affect the setting periods and strength of gypsum-free Portland cement compositions. Data presented in the Table indicate that in order to obtain compositions with high strength and practicable setting periods it is advisable to use clinker with not less 55% of C_3S, not more than 8% of C_3A and not more than 1.0% of unbounded lime. At high contents of C_3A (9-12%) and of unbound lime in the clinker the setting petiods are sharply reduced.

Acceleration of setting is also caused by increase of the amount of SYW added during grinding of the cement. The best strength and setting values are obtained when the clinker is ground with small additions of SYW (0.1-0.2%) and remaining SYW and K_2CO_3 or Na_2SiO_3 is added with the hydration water

Setting is also accelerated by reduction of the temperature of concrete mixture or mortar from 20-22 °C to 0-5 °C, which is connected with enhanced solubility of $Ca(OH)_2$

The water consumption of gypsum-free Portland cement with additives (SYW + K_2CO_3) or (SYW + Na_2SiO_3) is practically independent of mineralogical composition of the clinker and method of introducing the additives. Of paramount importance is the granular composition of the cement powder. Compositions based on polydispersed cements obtained from open-cycle mills have lower water consumption than compositions based on cements of separator grinding.

In order to elucidate the nature of low water consumption and hydration and hardening features of gypsum-free compositions the processes of SYW adsorption by clinker minerals in the presence of K_2CO_3 and Na_2SiO_3 and products of their hydration with these additives were studied. Investigation showed that of the clinker minerals the determining a effect on the properties of compositions with low water consumption is excerted by C_3A mineral. The dosage of additives and the rates of hydration and hardening of gypsum-free Portland cement depend on its content.

Low water consumption of the compositions is due to the capacity of K_2CO_3 and Na_2SiO_3 to slow down the rate of C_3A hydration and to reduce its adsorption capacity in relation to the plastifying additive. A high concentration of SYW is ensured in the liquid pase of cement paste that facilitates mobility of the paste at low W/C ratios. At high dosages of SYW gypsum becomes ineffective as a decelerator of C_3A hydration and regulator of cement paste setting.

Clinker	Mineralogical composition of clinker, %					Additives. %			W/C paste	Setting time h-min	
	C_3S	C_2S	C_3A	C_4AF	$CaO_{lb.}$	SYW	K_2CO_3	Na_2SiO_3		Beginning	End
I	65	11	5.5	13	0.76	1.0	0.25	-	0.20	0-30	0-40
						1.0	-	0.25	0.20	0-30	0-40
II	57	20	7.5	14	no	1.5	1;0	-	0.22	1-15	1-30
						1.5	-	0.75	0.22	1-00	1-15
III	59	13	7.1	16	0.80	1.5	1.0	-	0.20	0-40	0-50
						1.5	-	0.5	0.20	0-35	0-45
IV	59	16	9.0	16	0.1	1.5	1.0	-	0.20	0-20	0-25
						1.5	-	0.75	0.20	0-20	0-25
V	56	18	11.4	11	0.35	1.5	1.0	-	0.20	0-20	0-30
						1.5	-	0.75	0.20	0-20	0-25

W/C mortar	Spread of mortar, mm	Ultimate strength, Mpa					
		bending			compressive		
		normal hardening, days					
		1	7	28	I	7	28
0.26	118	4.54	-	7.52	19.1	-	56.1
0.26	116	2.0	-	8.03	12.5	-	58.6
0.26	114	6.56	9.08	8.72	38.0	59.0	62.0
0.26	115	1.5	3.12	7.31	10.1	19.5	70.9
0.28	115	6.55	8.03	7.72	30.3	53.6	62;1
0.27	113	2.31	8.58	9.37	11.7	52.7	63.6
0.25	113	3.03	8.46	9.17	17.4	58.0	70.8
0.25	113	1.20	2.44	8.90	12.2	15.5	80.2
0.26	115	6.19	9.95	10.6	45.9	65.1	69.6
0.23	113	5.06	9.51	10.8	32.9	57.1	67.6

Hydration products of Portland cement in the presence of SYW + K_2CO_3 or SYW + Na_2SiO_3 are characterized by very high dispersion. They are represented by X-ray amorphous calcium hydroaluminates C_4AH_{13} and C_2AH_8 and calcium hydrosilicates of the type C_2SH_2. The content of calcium hydroxide in the hydration products is by 1.5-2 times less than in common Portland cement which is connected with the higher basicity of hydrates forming at low W/C ratios.

Recrystallization of hexagonal C_4AH_{13} into cubical C_3AH_6 is not observed during hardening of the compositions. This is in agreement with the accepted notion about the stability of hexagonal calcium hydroaluminates in the presence of SYW [4]. High dispersion and stable phase composition of hydration products allows to obtain cement stone with minimal internal stresses, with high density and strength.

Direct testing of concretes showed that on the basis of compositions with low water consumption easily placable concrete mixtures with very low W/C ratio (0.23-0.27) may be obtained as well as high-strength steamed concretes of grades 700-800 with cement consumption 500-600 kg/m³. Concretes from these compositions display low porosity and high sulphate and frost resistance.

It may be considered that composition with low water consumption containing gypsum-free Portland cement, SYW and alkali metal carbonate or silicate will be effective binders for the production of high-strength steamed concretes with low W/C ratio.

REFERENCES

1. I.Odler, Ya.Skal'ny, S.Brunauer, Properties of the system "Clinker-lignosulphonate-carbonate", 6-th Internation Congress on the Chemistry of Cement, vol.2, part 2, Moscow, 1976 (in Russian).
2. Author's Certificate No.668908, Bulleten Izobretenii, No;23, 1979.
3. G.I.Gorchakov, A.A.Alimov, V.V;Voronin, A;V.Akimov, Dependence of Frost-Resistant Concretes on Structure and Temperature Deformations, Beton i Zhelezobeton, 1972, No.10.
4. O.I.Luk'yanov, Z.A.Abueva, Formation of X-ray Amorphous Phases and Dispersed Structures in Water Suspensions of C_3A, Colloidnyi Zhurnal, 33, 1971.

Ultimate strength, Mpa			
bending		compressive	
steaming, days			
1	28	1	28
6.46	7.49	69.6	73.1
6.80	8.30	68.3	77.3
7.03	8.12	64.0	73.6
6.99	7.72	67.4	72.6
7.10	8.91	65.9	69.9
7.58	7.85	62.8	70,0
7.77	9.03	66.6	80.7
7.09	7.79	74.7	77.0
6.05	7.50	59.7	70.8
6.81	7.90	61.4	75.8

THEME III

Structure des laitiers et hydratation des ciments de laitier

Structure of slags and hydration of slag cements

Laitier phosphorique activé - Matière première pour la production de ciment Portland de laitier

Activated phosphorus slag raw material for slag Portland cement production

A T SOULEIMENOV
T B PARCHIKOVA Institut Chimico Technologique de Kazakhstan, Tchimkent, U.R.S.S.

On a élaboré la technique de transformation complexe du laitier phosphorique par la méthode d'introduction de la poussière secondaire de la cimenterie de Tchimkent lors de la granulation du laitier phosphorique.

On a établi que l'activité hydraulique des laitiers électrothermophosphoriques modifiés augmente lors de l'introduction dans le laitier des oxydes de métaux alcalins.

On a tracé les voies d'utilisation de la poussière capturée en fonction de ses propriétés chimiques et physiques.

Dans les conditions industrielles on a obtenu le liant à base des laitiers phosphoriques activés par la poussière des électrofiltres.

Les laitiers phosphoriques activés de composition proposée se caractérisent par une grande activité hydraulique et peuvent etre utilisés dans l'industrie du ciment en tant qu'addition (jusqu'à 40%) dans la fabrication du ciment portland de laitier.

The technology of phosphorus slag complex workingover with incorporation into it during granulation the secondary dust of Chimkent cement plant has been developed.

The hydraulic activity of modified electrothermophosphorus slags was found to increase with incorporation of alkali metals oxides into the slag.

Means of collected dust using depending on its chemical and physical properties were planned.

Binder based on phosphorus slags activated by the dust from electro-static precipitators was received in industrial conditions.

Activated phosphorus slags of the composition proposed features significant hydraulic activity and can be used in cement industry as an addition up to 40% in the manufacture of slag portland cement.

Much consideration is being given to the use of wastes in the cement production. Of particular interest is the use of electrothermal phosphorus-bearing slags formed in electrothermal production of phophorus.

Phosphite ores are employed as a main raw material in the electrothermal phosporus production. The phosphites (23-25% P_2O_5) with a higher content of impurities compared to that allowed in acid phosphorus production are suitable for electrothermal processing consisting of reduction of phosphate ore into phosphorus in special electric furnaces, burning of phosphorus and hydration of phosphorus anhydride so as to obtain a pure concentrated "thermal" sulphuric acid. Such phosphorus ores usualy comprise a loose sand-claying material with fragments of phosphites. Thus, in addition to a final product electrothermal slag is formed during thermal sublimation of phosphorus.

In the Soviet Union the use of electrothermal slags in the cement production was started on a commercial scale in 1977. In the recent decade the slags have been used as a component of a raw mix at two and as an active mineral additive at nine cement plants. According to the Yuzhgiprotsement developments the cement industry is now producing not only ordinary portland-slag cement with the granulated phosphorus-bearing slags additives but also sulphate-resistance portland-slag cement.

Phosphorus is employed in production of sulphate-resistance portland-slag cement containing 60% of slag due to a specific mineralogical composition (low content of aluminium compounds). The resistance of this cement to an agressive media is higher than that of a standard sulphate-resistant portland cement.

The technology has been developed to produce oil-well cement with the addition of up to 20% of the granulated phosphorus slag.

Among current methods of slag processing the best is granulation having a number of advantages over other methods. It enhances a hydration activity as well as improves labour conditions and reduces operational costs.

The output of the electrothermal slags will be considerably increased owing to the development of phosphorus and mineral fertilizer production in the Central Asiatic Soviet republics and Kazakh SSR of the basis of the local raw material.

In electrothermal production of yellow phosphorus there are produced 10 tons of flame-liquid phosphorus slags per a ton of phosphorus, annual output of the slags being more than 1 million tons at present. In the phosphorus production in electric furnaces using sublimation of the charge consisting of natural phosphites, silica and coke reducer the following reaction takes place:

$$Ca_3(PO_4)_2+SiO_2+5C=3CaSiO_3+2P+5CO$$

The basic components of the slag are calcium oxide and silica which total quantity equils 95%. Electrothermal phosphorus slags differ from blast-furnace slags by a low content of Al_2O_3 (up to 3%) and MgO (3-4%), CaO/Si ratio of 0.8-1.2 as well as by the presence of P_2O_5 (1-3.3%) and F(2-2.4%).The chemical composition of the slags depends on a composition of phosphorus ore and technology of phosphorus production (1,2).

A high stability of the electrothermal slags chemical composition allows their use in cement production. It has been proved by the investigations of Yuzhgiprotsement. The scientists of the institute have carried out statistical processing of the data on the chemical composition of electrothermal slags (1040 samples). In the plant probes taken at an hour interval and in the averaged slag batches shipped to the interprises mean value of P_2O_5 did not exceed 2% and its maximum content in the samples taken at half an hour interval was 2.65%.

Slag hydration is to a grater extent determined by a composition and structure of a glassy phase. Petrographic investigations have shown that a basic phase of electrothermal phosphorus-bearing slags is glass of a wollastonite composition (90-92%). However, the glass of electrothermal phosphorus-bearing slags differs from a pure pseudowollastonite glass by the presence of P_2O_5 and F, Al_2O_3 and MgO which cause structural reconstruction in it.

According to (4), P_2O_5 and F contained in the slags in minor quantities do not have independent phases and enter into the com-

position of pseudowollastonite. These data are proved by the Yuzhgiprotsement investigations (5,6) which using petrographic and X-ray diffraction analysis have revealed the absence of phosphorus-bearing slags in these granulated slags.

Since the glass of a pseudowollastonite composition is a predominent in quantity phase its properties and structure should decisively effect the slag properties. At the same time chemical, petrographic, and X-ray diffraction analysis have shown that slag calcium silicate is basically represented by wollastonite glass of various degree of crystallization. Lower basicity of electrothermal phosphorus-bearing slags results in increase of silicon-oxygen effect, reducing their hydration activity.

However, according to (7), universally adopted conceptions of a glass structure also cover slag glasses. The slag consists of complex anions of $(SiO_4)^{-4}$, $(AlO_4)^{-5}$ and others connected with each other by oxygen bonds into polytetrahedral radicals of a different composition and kind. Cation-modifiers are also connected to these anions according to the scheme -Si -O...Me. During water adsorption by glass an exchange takes place between fairly loosely bound ions-modifiers of alkali and alkali-earth metals from glasses and hydrogen anions of water to water to form on the surface of glass particles films of hydrated silica containing the groups of -SiO,..H. These films hinder a further interaction of slag with water. However, the formation of stable silicates (and aluminates) at the limit concentrations of metal oxide hydrates is accompanied by distruction of the hydrated silica films. As a result, deeper glass sites lie bare and become accessible for water. This in turn is attended by its further hydrolysis and hydration. In these conditions considerable solubility of alumina and calcium aluminates in water favours their dissolution and formation of pores and capillary tubes securing a fruther intensive access for water hydrolyzing glass.

Thus, the introduction of minor quantities of alkali activators creates a specific impact disturbing a thermodynamically unstable balance of slag glass which then during interaction with water spontaneously reorganize itselv to form more stable hydrosilicats, calcium hydroaluminates at the expense of the component of glass itself and these compounds cause setting and hardenning of all the system.

This served as a basis for conducting investigations on enhancing hydration activity of electrothermal phosphorus-bearing slags through a crystallochemical activation method, i.e.the introduction of alkali metal cations into a melt. The dust retained by precipitators of rotary kilns of one of the cement plants containing a considerable quantity of Na and K oxides was used as an ac activator.

The aim of the prelimenary investigations was to obtain clinker with a given mechanical strength. During the investigations there were used Mark 400 clinker (70%) and finely ground electrothermal phosphorus-bearing phosphorus-bearing slag (30%) activated in the laboratory conditions in a melted state with precipitator dust taken from different fields of precipitators. As a result it has been found that activity of experimental portland-slag cement is considerably increased when the slagaactivated with a high alkali content slag is used (Table 1).

The subsequent investigations have revealed that the introduction of dust from the precipitator third field in the quantity of 3% in a greater extent activates thermal phosphorus-bearing slags.

In the course of the further investigations the pilot batch of portland-slag cement has been obtained in commercial conditions. Electrothermal phosphorus-bearing slags were activated by the precipitators dust and, to do this, 5% of the dust from 2 and 3 fields of precipitators were introduced into melted slag before granulation at the temperature of 1450-1600°C. The chemical composition of starting materials (in mass %) is given in Table 2.

The use of activated phosphorus-bearing slag (Table 3) results in increase of portland-slag cement activity especially by 28 days. The activation of the slag by the method described permits the use of 40% of electrothermal phosphorus-bearing activated slags in the portland-slag cement production against 30% used at present.

As it is shown in Table 3 an activated phosphorus-bearing slag is characterized by a considerable hydration activity and can by used in the cement industry instead of shipped blast-furnace slag. It has been found that the slag can be used as an hydraulically active additive during clinker grinding in the quantity of 40%, with possible obtaining of the Mark 500 cement.

Thus, the use of activated phosphorus-bearing slag and dust of the precipitators of the cement plant rotary kilns in the portland-slag cement production will enables one markedly to encrease technical and economical efficiency of production as a whole and utilize the accumulated byproducts and this in turn creates conditions for a complex employment of natural resources and possibility for the development of a low- and waste-free technology.

The use of the activated phosphorus-bearing slags is espected to stimulate not only the expansion of the cement industry raw material base, further economization of production by the change of transported blast-furnace slags for local chemically produced but also improvement of portland-slag cement quality.

The further investigations are directed to optimization of the process of phosphorus-bearing slags activation with alkali-content wastes of the cement production, i.e. dust retained by precipitators on clinker burning in rotary kilns.

References

1.I.A.Kryzhanovskaya, E.E.Kiryaeva,Yu.L. Galchinskaya. Use of electrothermal phosphorus-bearing slags in cement production.

Table 1

Precipitator dust quantity in cement charge,%	Quantity of R_2O, %	Compression strength, megapascals		
		3 days	7 days	28 days
without dust	-	5.4	10.5	28.7
1% of dust from the first field	0.82	7.6	14.0	37
3% of dust from the first field	0.82	12.0	28.8	46
5% of dust from the second field	7.11	11.0	29.2	47
3% of dust from the third field	48.80	14.5	30.4	52

Table 2

Kind of material	Oxides content, %									
	SiO_2	Al_2O_3	F_2O_3	CaO	MgO	SO_3	Na_2O	K_2O	Other	
Phosphorus-bearing slag of Chimkent industrial unification "Phosphorus"	7.73	2.64	2;55	45.20	3.6	10.08	2.6	8.2	17.3	-
	42.46	2.25	0.59	45.10	2.3	0.34	2.28	0.4	-	4.28
Activated slag	41.32	1.97	0.39	45.32	2.17	0.73	2.60	0.79	0.86	6.95

Table 3

Portland-slag cement											
clinker	non-activated slag	non-activated slag	gypsum	Specific surface	Time of setting		Ultimate strength				
					start	end	bending			compression		
							3	7	28	3	7	28
%	%	%	%	cm^2/g	(hours-min)		megapascals					
55	40	-	5	2930	4-05	6-25	3.2	4.15	5.87	19.8	27.8	36.6
55	-	40	5	2930	3-55	6-05	3.4	4.30	6.22	20;2	28.7	77.48

Review information. Moscow, VNIIESM, 1978.

2. A.T.Suleymenov. Environmental protection - improvement of waste-free technology. Review information. Moscow, VNIIESM, 1979.
3. Transactions of NIITsement, Issue 44, New types of special cements and improvement of cement quality. Moscow,1978.
4. L.L.Vladimirova. Slags of phosphorus industry.Chelyabinsk, Uralniistromproekt, 1970.
5. I.A.Kryzhanovskaya, E.E.Kiryaeva,LG.Korotetskaya et el.Transactions of Yuzhgiprotsement, Issue XI,Stroiizdat,1969.
6. I.A.Kryzhanovskaya, E.E.Kiryaeva.Slags of phosphorus industry, Chelyabinsk, Uralniistromproekt,1970.
7. O.A.Edin, P.V.Geld.Physical chemistry of pyrometallurgy processes.Part II, Metallurgy,1966.

Hydratation des ciments portland de laitier à différentes températures

Hydration of blastfurnace cement under different temperatures

S.A. MIRONOV, Prof., Dr. Tech. Sc.,
I.I. KURBATOVA, Cand. Chen. Sc.,
S.A. VYSOTSKY, Cand. Tech. Sc., NIIZhB, Moscow, U.R.S.S.

Par une série des méthodes d'analyse physico-chimique, y compris, l'examen de la composition de la phase liquide et la méthode d'extraction, sont étudiées les caractéristiques de durcissement de hydratation des ciments avec la différente teneur en laitier granulé de haut fourneau (0-80%) dans les conditions normales et sous le traitement thermique à la vapeur.

On a étudié le rapport des facteurs constructifs pendant l'étuvage qui sont conditionnés par l'accélération de la hydratation du liant en comparaison avec le processus de hydratation pendant le durcissement normal, et des facteurs destructifs provoqués par la différence de la dilatation thermique des composants de la pâte ou du béton.

Est éclairci le rôle déterminant de l'activité d'hydratation du liant et de ses composants pour l'obtention des caractéristiques physico-chimiques prescrites des compositions de ciments-laitiers.

Est mentionné une considérable accélération de la dissolution du ciment portland de laitier et une accélération de la vitesse de cristallisation des nouvelles phases sous l'étuvage. Sont étudié les caractéristiques de la composition de phase des produits de la hydratation des ciments avec une différente teneur en laitier et est mis en évidence l'influence de ces caractéristiques sur les propriétés physico-mécaniques des ciments.

Particularities of hydrated hardening of cements with different content of granulated blast furnace slag (from 0 to 80%) during normal condition and steam curing have been studied.by complex methods of physic-chemical analysises including the composition of liquid phase investigation and using the extraction method.

Correlation during steam curing of constructive factors connected with acceleration of cement hydratation in compare with normal hardening and destructive factors stipulated by different thermal expansion of paste or concrete ingredients has been examined.

The main role,of hydrated activity of cement and it components (slag and clinker) in formation of physic-mechanical properties of cement- slag compositions has been discovered.

Significant acceleration of blast furnace cement solution and incresing of cristallization velocity of new phases during steam curing has been noted.

Particularities of phase composition of hydratation products of cement with different content of slag have been examined and their influence on physic-nechanical properties has been shown.

Sont étudiées les particularités de durcissement d'hydratation des ciments avec la différente teneur en laitiers granulés de haut fourneau (0; 20; 40; 60 et 80%) dans les conditions normales et sous le traitement thermique à la vapeur. En réalisant ces essais on a utilisé une série des méthodes (chimique, radiographique, thermodifférentielle, méthode de microscopie électronique, essai dela phase liquide et méthode spéciale d'extraction [1] permettant de déterminer le degré d'hydratation du laitier :

$\varepsilon = (1 - \frac{H_o - n \cdot H_o^k}{H - n \cdot H^k}) 100$ (%), où H et Ho sont les résidus insolubles du ciment non-hydrate et du ciment hydraté additionnés par laitier dans une solution d'extraction, H^k et H_o^k - la même chose pour le ciment de clinker, "n" - la fraction de clinker dans le ciment).

Les études se fondaient sur le fait que le caractère de durcissement des compositions des ciments-laitiers se détermine par l'interaction de deux groupes des facteurs: des facteurs destructifs liés avec la différence de la dilatation thermique des constituants du béton, et des facteurs constructifs conditionnés par accélération d'hydratation du liant en comparaison avec le durcissement normal. Les essais ont montré que la modification des caractéristiques physico-mécaniques du béton en fonction de la teneur en laitier dans le ciment, de son activité, des conditions et du régime de durcissement se détermine, à priori, par l'activité d'hydratation du liant (I).

L'activité d'hydratation du laitier se diffère nettement de celle du clinker. Le degér d'hydratation du laitier, le durcissement étant normal, est extraordinairement médiocre (6 - 8,5% à l'âge de 28 jours) c'est-à-dire ce est 8-9 fois plus petit que celui d'hydratation d'alite. L'analyse des courbes cinétiques de $C_{Ca^{2+}}(\tau)$ et de $C_{R^+}(\tau)$ obtenues pendant l'essai de la phase liquide montre (Fig.1) que les processus de la dissolution du liant de base ainsi que celui de la cristallisation des phases nouvelles et d'hydratation en entier sont considérablement ralentis dans le ciment contenant 80% du laitier. Une haute $C_{Ca^{2+}}$ (60 mg/équiv./l) s'établissant instantanément dans la phase liquide au contact de l'eau de gâchage avec le liant s'abaisse très lentement durant 24 heures et atteint seulement dans 48 heures la valeur égale à 6,3 mg/équiv./l, ordinaire pour les ciments portlands à l'âge de 24 heures (3). Sur la courbe cinétique de $C_{Ca^{2+}}(\tau)$ il n'y a pas de baisse brusque dans la période de 6-8 heures témoignant l'élimination intensive des phases contenant le calcium. La formation d'ettringhite est ralentie. L'allure en pente douce de la courbe $C_{R^+}(\tau)$ confirme la dissolution lente du ciment portland de laitier. Il est nécessaire de mentionner que malgré la basse énergie de liaison des ions des métaux alcalins dans les unités de structure du verre de laitier (par exemple: Na-O-Si -) leur concentration dans la phase liquide caractérise indirectement la participation de tout le laitier dans le processus d'hydratation puisque pendant ce processus ont lieu le rompement d'équilibre dans la structure du verre et l'augmentation de sa capacité réactionnelle. L'enrichissement de la phase liquide par les ions des métaux alcalins pendant 24 heures se passe pratiquement pour le compte de la dissolution de composante de clinker de ciment portland de laitier. Le clinker essayé contient 0,54% de R_2O; les R_2O qui sont facilement dissolubles et qui passent instantanément dans la phase liquide et assurent dans 10 minutes $/C_{R^+}=60,07$ mg/équiv./l font 24% de quantité totale de R_2O. Dans le ciment portland de laitier il y a 0,77% de R_2O y compris 0,66% du laitier, et avec cela il n'y a pratiquement pas d'alcalis facilement dissolubles. La concentration non-élevée /R+/ dans la phase liquide du ciment portland de laitier pendant le processus d'hydratation (9,29 mg/-quiv./l dans 10 min.) presentant environ 0,2 de la concentration /R+/ dans la phase liquide de clinker est conditionnée par le passage dans cette phase seulement des alcalis facilement dissolubles de clinker. Par la suite, les ions des métaux alcalins passent aussi dans la phase liquide venant principalement de clinker et ce n'est que vers 24 heures que l'on peut observer la participation de lai-

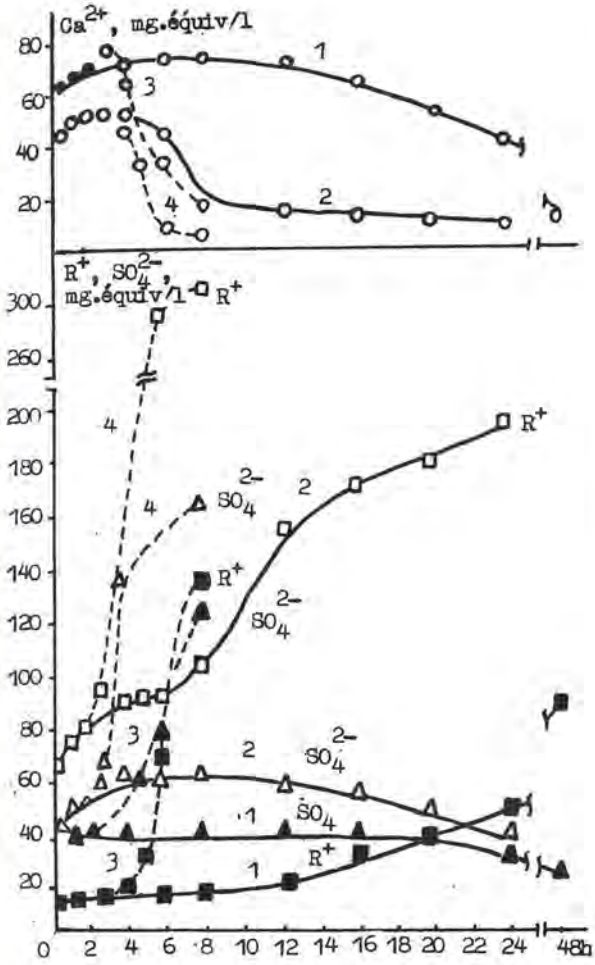

Fig.1. La variation de composition de la phase liquide pendant l'hydratation des ciments dans différentes conditions:
——— durcissement normal;
----- traitement à la vapeur sous 95°C;
1.3-ciment portland de laitier contenant 80% de laitier; 2.4 - ciment de clinker

tier (C_{R^+} dans la phase liquide du ciment portland de laitier dans cette période est plus que 0,2 C_{R^+} clinker).

L'hydratation ralentie des ciments avec la teneur élévée en laitier (40-80%) dans les conditions normales conditionne le formage de la structure poreuse et non-résistante du ciment durci, et explique aussi une effectivité non-importante de leur conservation avant le traitement thermique (2). Dans le ciment durci contenant 80% de laitier à l'âge de 28 jours de durcissement normal prédominent les grains non-hydratés du laitier couverts d'une couche mince des hydrosilicates geleux de calcium avec un espace capillaire rempli par des cristaux d'ettringhite.

Le traitement thermique accélère considérablement l'hydratation et le durcissement des ciments portlands de laitier (2,4). Le degré d'hydratation du laitier sous le traitement à la vapeur pendant 8 heures et sous 80°C augmente jusqu'aux 6-16% en fonction de la basicité, et sous 95°C - jusqu'aux 22% pour des laitiers basiques les plus actifs. Sur la courbe cinétique de $C_{Ca^{2+}}(\tau)$ pour le ciment protland de laitier, le maximum se déplace à gauche et ce fait témoigne l'accroissement de la dissolubilité de la verre de laitier, et une brusque chute postérieure de la courbe témoigne la cristallisation intensive des nouvelles formations. L'hydratation active de laitier sous le traitement thermique est aussi confirmée par le changement de la concentration de $/R^+/$ dans la phase liquide qui non seulement augmente intensivement en fonction de temps mais surpasse dans les périodes du temps correspondants 0,2 de la concentration de ces ions du ciment de clinker.

Les études ont montré que le traitement à la vapeur accélère plus l'hydratation du liant que l'accroissement de son résistance. A mesure d'élévation de la teneur en laitier dans le ciment les déformations de la dilatation du béton (comme la mesure des dérèglements structuraux obtenus au stade d'élévation de la température) s'accroissent; ce fait est lié au ralentissement d'hydratation pendant la période de la conservation préalable et pendant l'élévation de la température, ainsi qu'à la basse résistance de la structure incapable de percevoir sans dérèglements les contraintes qui y surgissent. (Fig.2). En rapport avec ce

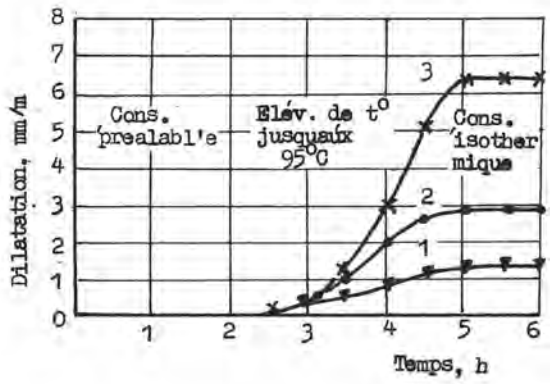

Fig.2. La dilatation thermique du béton avec le E/C = 0,5 sous le traitement à la vapeur: 1 - 0% de laitier; 2 - 40% de laitier; 3 - 80% de laitier

fait, pour les ciments de ce type est efficace le traitement à la vapeur sous recharge et dans le milieu avec la pression excédente.

Il est possible de subdiviser conventionnellement les ciments essayés en 2 groupes: - avec la teneur en laitier modéré (jusqu'aux 40%) qui sont pratiquement équivalents aux ciments portlands dans les conditions du traitement thermique, - et avec la teneur en laitier élevée - plus de 40%. Après le traitement à la vapeur sous 95°C pendant 6-8 heures la quantité de l'eau chimiquement liée et la résistance des ciments du deuxième groupe peuvent dépasser jusqu'aux 20% celles des échantillons à l'âge de 28 jours et durcies dans les conditions normales. Avec cela se forme une structure compacte et homogène des nouvelles formations représentée, essentiellement par les hydrosilicates de calcium de basse basicité apartenant au groupe de CSH (B) et assurant les hautes caractéristiques mécaniques du ciment durci, surtout par rapport à l'action des contraintes de traction, Le traitement à la vapeur des compositions du premier groupe provoque les changements défavorables dans le composé de phase des produits d'hydratation surtout sous 90-95 °C. Dans les conditions données dans ces produits se forme la phase hydro-grénatique avec la teneur en SiO_2 médiocre dont la composition est pareille à celle de C_3AH_6 (d=5,05; 4,38; 3,31; 2,53; 2,26; 2,00 et 1,71 Å) conformément aux données du (5); cette phase range l'agrégat cristallin avec le volume élevé des vides et contribue à l'abaissement de la résistance du ciment durci. La quantité de la phase donnée ainsi que la quantité de $Ca(OH)_2$ divisant les nouvelles formations hydrosiliceuses diminue considérablement dans les compositions contenant plus de 60% de laitier, et dans le ciment durci contenant 80% de laitier elle ne peut pas être captée par la radiographie. Au total les produits d'hydratation des ciments avec la teneur en laitier élevée se caractérisent par un plus grand pouvoir liant confirmé par une grande sorption de vapeur d'eau par le ciment durci calculée par rapport à l'unité de la masse conventionnelle des nouvelles formations.

L'intensification de l'activité des laitiers sous le traitement à la vapeur et les différences mentionnées dans la composition de phase des produits d'hydratation amènent au rapprochement des propriétés mécaniques des compositions avec la teneur en laitier différente; Pourtant, pendant le durcissement postérieur après le traitement thermique l'hydratation des ciments du premier groupe est plus intensive et ceci amène à une "guérissement" partiel des défauts de la structure et à l'obtention d'une résistance plus grande.

Bibliographie

1. S.A.Mironov, S.A.Vyssotsky, I.I.Kourbatova, M.G.Bougrina. "L'influence de l'activité d'hydratation des ciments portlands de laitier sur les propriétés physico-mécaniques des bétons". "Ciment",N 6, 1978.
2. S.A.Mironov, S.A.Vyssotsky, I.V.Bykova. "L'efficacité de traitement thermique des bétons sur les ciments portlands de laitier". "Béton et Béton Armé". N 9, 1976.
3. I.I.Kourbatova. "La chimie d'hydratation du ciment portland"., M.,.Stroyizdat, 1977.
4. S.A.Mironoff. "Die Erhartung des Schlackenportland-Zement-Betons bei verschiedenen Temperaturen". "Zement", N 36, 1936.
5. H.Smolczyk. "Die Hydratationproduckte Huttensandreicher Zement". "Zement - Kalk - Gips", N 5, 1965.

Nouvelles compositions à base de laitiers

New binding compositions based on slags

V.A. BELETSKAJA, Aspirante,
I.G. LOUGININA, Docteur ès Sciences Techniques, Professeur, Belgorod, U.R.S.S.

La diversité des combinaisons alcalines manifestant les propriétés liantes ouvre de grandes perspectives pour la création de nouvelles espèces des composés polyminéraux au spectre étendu d'utilisation.

On a effectué le contrôle expérimental pour établir la présence des propriétés liantes des produits de calcination des compositions existant au système R_2O-RO-R_2O_3, ou R_2O, RO, R_2O_3 - sont les oxydes du 1-e, du 2-e, du 3-e groupe dans le tableau de Mendeléev.

On a obtenu les liantes d'une grande activité.

Le milieu alcalin crée par des oxydes alcalins et les oxydes alcalino-terreux est la condition déterminée pour une synthèse de nouveaux ciments alcalino-métallurgiques mixtes.

On a obtenu les liants alcalino-métallurgiques hydrauliques portant du laitier granulé, métallurgique et électrothermophosphorique.

On a à présent trouvé que les compositions liantes existant au système R_2O-RO-R_2O_3 sont les composants actifs des ciments alcalino-métallurgiques. On a déterminé les proportions optimales, les conditions de la synthèse et les caractéristiques physico-mécaniques des ciments alcalino-métallurgiques.

On a étudié alcalino-métallurgique le composé des produits de l'hydratation du liant.

L'hydratation de nouveaux ciments alcalino-métallurgiques est déterminée par l'alcalinité d'une phase liquide

The variety of alkaline combinations demonstrating binding properties gives great possibilities for the creation of new types of polymineral binding substances having a wide range of application.

An experimental examination of the present binding properties of the products of burning composition existing in the system of R_2O-RO-R_2O_3, where R_2O, RO, R_2O_3 are oxides of the 1-st, 2nd, 3-d groups of Mendeleyev's Periodic System. The binding materials of high activity have been got.

The alkaline medium created by the alkaline and alkaline-earth oxides is a determining condition of the synthesis of new combined slag-alkaline cements. Slag-alkaline hydraulic binding materials based on the granulated metallic and electric thermo-phosphoric slags have been created.

The binding compositions existing in the system of are established to be an active component of the slag-alkaline cements. The optimal correlations of components, the conditions of synthesis and physical-mechanical characteristics of slag-alkaline cements have been determined.

The composition of the products of hydration of slag-alkaline binding materials have been investigated. The hydration of new slag-alkaline cements is determined by the alkaline character of the liquid phase.

Une série de ciments du laitier alcalins à la base des laitiers des compositions différentes est proposée en Union Soviétique. Il est établi que les laitiers basiques aussi bien que les laitiers acides peuvent être utilisés pour leur fabrication à condition que le choix du composant alcalin soit correct (1). L'alcali caustique, les sels non-siliceux de faibles acides, les sels siliceux, les aluminates alcalins sont utilisés le plus souvent pour une fabrication des ciments de laitier alcalins.

Les ciements alcalins et alcalino-terreux, mono- et polyminéraux hydrauliques à la base des compositions des métaux alcalins sont obtenus à l'Institut technologique de Léningrad (2,3). Ces données précédaient une vérification expérimentale de la présence des propriétés visqueuses dans le produit de grillage des compositions existant dans le système R_2O-RO-R_2O_3 ou R_2O, RO, R_2O_3 sont des oxydes du premier, du deuxième et du troisième groupe du système périodique des éléments de Mendéléev.

On avait pour but d'obtenir des ciments de laitier alcalins hydrauliques à la base des compositions des laitiers granulés, métallurgiques, électrothermophosphoriques et visqueux synthétisées au système R_2O-RO-R_2O_3.

Les visqueux sont obtenus au moyen du mouture fine des produits du grillage avant l'agglomération des oxydes indiqués pris en proportions différentes. Les compositions obtenues à la base des composants du potassium sont capables de durcir effectivement dans les conditions aqueuse, aériennes et d'autoclave. Une résistance des visqueux de sodium au durcissement en air atteint 80 MPa. Les visqueux synthétisés ont une grande réfractarité et ne durcissent pas sous l'action de hautes températures.

Pour l'obtention des ciments de laitier alcalins on a utilisé les laitiers des cinq unies dont les compositions chimiques sont citées au tableau 1. Les visqueux synthétisés ont été utilisés en qualité du composant alcalin. Les laitiers était préalablement broyés jusqu'à à la surface spécifique égale à 2900-3100 cm^2/g selon le mesureur de surface -2. Le ciment de laitier alcalin était obtenu sans grillage par le mélange du laitier et du visqueux-excitateur pendant 45-60 min.

Les propriétés physico-chimiques du visqueux était étudiées sur les échantillons (1x1x3 cm) préparés de la pâte au durcissement aqueux et aérien. Un traitement d'autoclave des échantillons (175°C 4 heures) a été fait dans 24 heures après le formage avec le séchage postérieur jusqu'au poids constant à la température 90°C.La durée de la prise des visqueux de laitier alcalins a été déterminée par l'appareil de Vic.

Une microstructure des laitiers a été examinée en lumière passante et polarisée dans les appareils à immersion.
Un analyse radiologique de phase des laitiers et des visqueux de laitier alcalins a été fait à l'aide de la méthode de poudre avec l'enregistrement ionisé des maximums difractionnels à la température ambiante. Les courbes de l'intensité était faites par l'appareil ionisant YPC-50HM à l'utilisation de la radiation cuivrique au filtre de nickel.

Il est établi que la masse importante des laitiers est composée du verre (70-80%). Les indices de son réfraction de lumière sont - de 1.662 à 1,646. Une phase cristallique est présentée par une gélenite et une melelite. Selon les données de l'analyse radiologique de phase, une phase cristallique du laitier N1 est composée d'un -quartz, du ceux N2-N5 est composée de la mélélite surtout.

On peut observer l'influence de la nature des composés des métaux alcalins suivant les propriétés visqueuses du laitier granulé au tableau II, ou il y a des indices de résistance de la pâte de laitier de l'épaisseur normale, contenant des composants alcalins égaux à 3% de R_2O.

En se basant sur les données citées ci-dessus, il convient, que la résistance des visqueux autoclavés dépasse celle des visqueux durcissant pendant les 28 jours dans de l'eau. Une appréciation comparative de la résistance mécanique du pierre de laitier alcalin a permis de tirer une conclusion que l'activité des visqueux de laitier s'accroît dans une série:

ROH RO-R_2O_3 R_2CO_3 R_2O-RO R_2O-RO-R_2O_3

Les durées du durcissement du ciment de laitier alcalin dépendent de la composition d'un composé alcalin : les hydroxydes et les carbonates des métaux alcalins les diminuent, les visqueux synthétisés les augmen-

Tableau 1

Composition chimique des laitiers

Numéro du laitier	Teneur en oxydes %								
	SiO_2	Al_2O_3	Fe_2O_3	CaO	MgO	SO_3	Na_2O	K_2O	P_2O_5
1	41,24	2,90	0,10	46,51	2,15	1,78	-	-	2,58
2	39,60	12,09	0,51	39,53	4,43	1,90	-	-	-
3	37,56	11,02	0,84	46,20	2,24	1,06	-	-	-
4	38,00	8,20	0,20	46,50	4.80	2,20	-	-	-
5	38,30	5,00	0,50	34,20	1,50	0,76	-	-	-

Tableau II

Dependance de l'activité des compositions de laitier de la nature des composés des métaux alcalins

N	Composition de l'additif	Durée du durcissement min		Résistance MPa	
		commencement	fin	après l'évaporisage dans l'autoclave	après le durcissement dans de l'eau pendant les 28 jours
1	NaOH	15	32	20	8
2	KOH	13	25	11	9
3	Na_2CO_3	25	33	49	32
4	K_2CO_3	57	75	35	15
5	Na_2O-RO	142	173	39	33
6	K_2O-RO	42	54	32	34
7	Na_2O-RO-R_2O_3	135	155	45	40
8	K_2O-RO-R_2O_3	35	45	42	34
9	RO-R_2O_3	60	75	24	20
10	RO	58	66	16	28

Tableau III

Activité des visqueux de laitier alcalins

Numéro du laitier	Numéro du visqueux	Résistance après le traitement dans l'autoclave MPa	Résistance après les 6 mois du durcissement dans de l'eau MPa
1	1	48	48
	3	27	37
2	1	63	67
	3	38	43
3	1	40	46
	3	32	41
4	1	37	45
	3	24	27
5	1	51	72
	3	29	77

tent.

Ainsi, les mélanges des visqueux synthétisés dans le système R_2O-RO-R_2O_3 et des laitiers présentent de nouveaux visqueux hydroliques possédant une haute activité.

On essayait d'obtenir un visqueux des laitiers granulés dont la composition chimique est indiquée au tabl.I et du visqueux synthétisé.

Les compositions visqueuses obtenues à cette base (dessin 1) ont une grande durabilité et une résistance à l'eau. Il convient de noter que la substance en état de pierre se formant dans le système durcissant visqueux - laitier conserve sa résistance à l'eau à l'augmentation dans le visqueux de la teneur en R_2O_3 jusqu'au 40 mol % malgré la diminution importante de sa résistance au cas des laitiers basiques aussi bien qu'au cas des ceux alcalins.

Une activité des visqueux de laitier alcalins durcissant dans les autoclaves est citée au tableau III.

Une activité des compositions étudiées augmente en cas du vaporisage dans l'autoclave. Donc dans les conditions naturelles du durcissement une interaction des compositions examinées passe relativement lentement. Ap-

Tableau IV

Dépendance de l'activité du ciment de laitier alcalin de la teneur en visqueux

Numéro du laitier	Quantité du visqueux %	eau/dureté	Résistance au durcissement MPa	
			en air	dans de l'eau
1	5	0,25	6	15
	10	0,25	3	14
	20	0,27	12	26
	30	0,32	22	38
2	5	0,25	7	40
	10	0,25	13	43
	20	0,27	26	56
	30	0,30	51	57

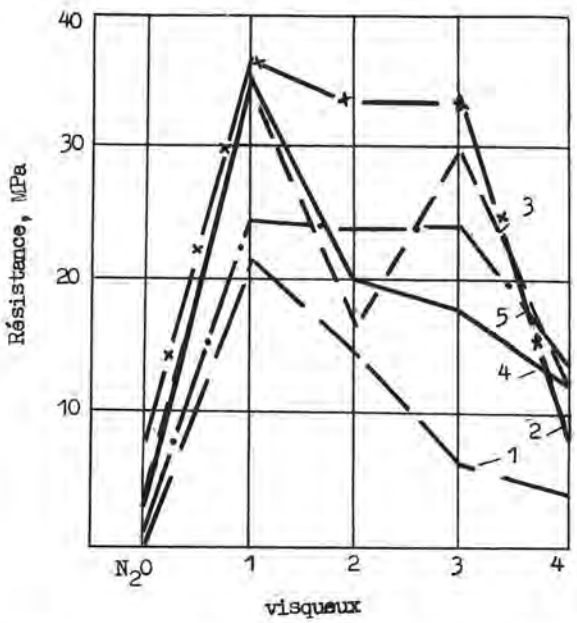

Fig. 1. Dependence de l'activité du ciment de l'espéce de l'exitateur alcalin: 1, 2, 3, 4, 5 - numéro du laitier

ces le durcissement aqueux de longue durée et le vaporisage dans l'autoclave la résistance du pierre à la base du laitier acide avec l'addition du visqueux syntétisé est beaucoup plus grande de celle du pierre de laitier alcalin à la base du laitier basique.

Les indices fixés de la résistance de la pâte de laitier alcalin ne présente qu'une idée générale des possibilités de l'obtention du visqueux à la base des laitiers de différentes usines, car on ne peut pas considérer la proportion choisie parmi les visqueux synthétisé comme optimale.

Une dépendance de l'activité du ciment du débit du composant alcalin a été étudiée pour les compositions "laitier 1,2 - visqueux 1". Les échantillons, préparés dans la pâte durcissaient dans de l'eau et en air pendant les 28 jours, Les résultats sont cités au tableau IV.

Les données du tableau IV montrent que l'activité du ciment s'accroit à l'augmentation du visqueux alcalin débité.

Un analyse différentiel thermique des produits de l'hydratation des visqueux de laitier se fait à l'aide du dérivatographe du système des F.Paulik, I.Paulik,A.Erdei à l'intervale des températures jusqu'à 1000 °C dans un creuset à corindon à l'utilisation du Al_2O_3 comme étalon à la vitesse 20°/min. Selon les données de l'analyse thermographique à l'interaction des visqueux synthétisés et des laitiers se font les mêmes formations nouvelles qui se produisent à l'hydratation du ciment de laitier alcalin synthétisé aupravant (1).

BIBLIOGRAPHIE

1.Gloukovskii V.D.,Pakomov V.A. (1978)."Ciments de laitier alcalins et les bétons", p.184, russ.

2.Fedorov N.F., Volconskii B.V.,Mikailova A.I.,Upolovnikova L.C. (1974), "ciments alcalino-siliceux", r."Ciment",N4,p.8-9; russ.

3.Fedorov N.F. Upolovnikova L.C.,Semeinik N.S. (1977), "Ciments monominéraux siliceux", r."Ciment", N6, p.14-16,russ.

THEME IV

Structure des pouzzolanes et des cendres volantes et hydratation des ciments aux pouzzolanes et aux cendres volantes

Structure of pozzolana and fly-ash and the hydration of pozzolanic and fly-ash cements

---

The use of SiO_2-residues as admixtures for pozzolanic portland cements

Utilisation de résidus siliceux comme pouzzolane des ciments

R. HERR, W. WIEKER and G. PRIEM, Zentralinstitut für Anorganische Chemie der Akademie der Wissenschaften der DDR - Berlin, RDA.

Summary

The residues remaining in a mineral acid extraction process of thermal activated Al-Silicates with layer structure (clay minerals) are rich in SiO_2 and poor in Al_2O_3. These "residues of clay extraction" (RCE) show extraordinary pozzolanic properties. The use of these pozzolanic residues RCE as admixture to portland cement results in a special type of quickly hardening pozzolanic portland cement. In this report the most important chemical and physical properties of the RCE as well as of the pozzolanic portland cements are discussed.

RESUME : Certains procédés d'extraction à chaud de minéraux dans les argiles, au moyen d'acides, laissent des résidus riches en SiO_2 et pauvres en Al_2O_3. Ces résidus ont des propriétés pouzzolaniques extraordinaires. Leur addition à des clinkers Portland permet d'obtenir des ciments pouzzolaniques à forte résistance initiale. On a étudié les propriétés physiques et chimiques les plus importantes de ces résidus, ainsi que la qualité des ciments pouzzolaniques obtenus.

The residues remaining in a mineral acid extraction process of thermal activated Al-silicates with layer structure (clay minerals) are rich in SiO_2 and poor in Al_2O_3 and show pozzolanic activity.
The use of these pozzolanic "residues of clay extraction" (RCE) as admixtures to portland-cement clinker and gypsum results in a special type of quickly hardening pozzolanic portland cement with improved chemical resistence.

Table 1 shows the chemical composition of the investigated RCE.

Table 1: Chemical composition of "residues of clay extraction", resulting from a HCl-extraction process

oxid	concentration (mass-%)
SiO_2	72.....84
Al_2O_3	0,4....15
Fe_2O_3	1 3
CaO + MgO	0,01...0,5
$K_2O + Na_2O$	0,2....1,5
TiO_2	1 3
Cl^-	0,01...0,25
L.O.I.	5 15

According to their chemical composition the RCE are to compare with some types of natural siliceous earthes, for instance diatomite earth /1/, Gliezh-earth /2/ or Sacrofano-earth /3/.

The mineralogical composition of RCE was investigated by the X-ray diffractometric method. In table 2 the qualitative and the quantitative results of the X-ray analysis are placed together.

For the use of the SiO_2-residues as admixtures for pozzolanic portland cements especially the not crystalline, X-ray amorphous parts and the semicrystalline parts of the RCE are of interest. The high chemical activity of RCE in the reaction with $Ca(OH)_2$ can be correllated to these components. The crystalline parts of RCE operate in PC-RCE-pastes as inert microfillers only. Dried RCE contain about 80 to 90 mass-% reactive silicid acid and metakaolinite.

Some physical properties of the RCE are shown in table 3.

The pozzolanic activity of the RCE in the reaction with $Ca(OH)_2$ and portland cement was measured by chemical, physical and mechanical test methods.

Figure 1 shows the results of experiments in which the RCE is treated with $Ca(OH)_2$ in suspensions. The amount of $Ca(OH)_2$ which has reacted with RCE has been estimated by a titrimetric procedure in dependence of the reaction time.

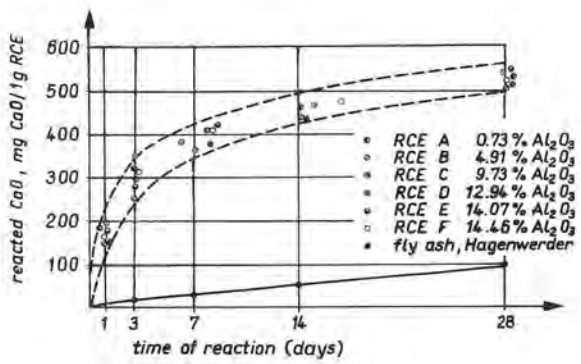

Fig. 1 Time dependence of the reaction of RCE with saturated $Ca(OH)_2$-solution, measured by shaking tests. For comparison the reaction of a lignite fly ash from the power station Hagenwerder (GDR) is also shown.
Test conditions: saturated $Ca(OH)_2$-solution 1,20 g CaO/l; molar ratio $CaO/SiO_2 + Al_2O_3 = 1:1$; temperature 20 °C.

After a reaction time of 1,3 and 28 days the following amounts of $Ca(OH)_2$, calculated in mg of CaO, have reacted with 1 g of RCE.

1	day	140....190 mg CaO/ 1 g RCE
3	days	250....350 mg CaO/ 1 g RCE
28	days	520....560 mg CaO/ 1 g RCE

This shows, that the reactivity of RCE with respect to $Ca(OH)_2$ is much higher than other types of pozzolanas, i.e. ground lignite coal fly ash or pozzolanic tuffs /4/ or trass /5/.

Table 2: Mineralogical composition of RCE remaining in a HCl extraction process

crystallinity	mineral	concentration %
crystalline parts	quartz SiO_2	6 ... 11
	anatase TiO_2	1 ... 3
semicrystalline parts	hydromuskovite metakaolinite	5 ... 30 *
not crystalline parts	$SiO_2 + Al_2O_3 + Fe_2O_3$	
	difference	to 100

*dependend upon the clay extraction conditions

Table 3: Some characteristics of the physical structure of RCE

characteristic	dimension	value
density	$g \cdot cm^{-1}$	2,05....2,34
apparent density of RCE-powder	$g \cdot cm^{-1}$	0.39....0,64
pore size distribution	radius Å	range 20....500
		maximum 1 25
		maximum 2 150
total porosity	%	50....85
specific surface	$m^2 \cdot g^{-1}$	50...250

The pozzolanic portland cements, we have investigated here, were produced by mixing of commercial portland cement (standard type PC 1), milled RCE and small amounts of gypsum to adjust the aluminate-sulfate-ratio of these mixed cements. The pozzolanic portland cements contained up to 30 mass-% RCE.

In figure 2 the results of the compressive strength tests of PC/RCE cement pastes are demonstrated in comparison with the strength development by PC-quartzpowder-pastes.

At constant water-solid-ratios the compressive strength of PC-RCE-pastes increases up to an admixture of about 10 mass-% of RCE to the PC. Above a RCE-content of 10 mass-% the compressive strength decrease slowly, especially in the early stage of hydration. After 28-days-hydration pure PC-pastes and PC-RCE-pastes 75/25 have the same compressive strength. At higher amounts of RCE in the cements the compressive strength decreases rapidly.

In order to get a better insight in the differences of the strength development of RCE and quartzpowder blended portland cements we have analysed the contents of the "free lime" and of acid soluble SiO_2 in the hydrated PC-RCE-pastes.

The free lime content of the samples was determined by the Franke method. The results (Fig. 3) show, that the content of free calciumhydroxide decreases very rapidly with increasing amounts of RCE and the hydration time due to the reaction with the amorphous SiO_2 of the RCE.

This result is underlined by the change in the amount of soluble SiO_2 during the hydration reaction, measured by the Molybdatmethod of Thilo, Wieker and Stade /6/. In table 4 it is shown, that the amount of soluble SiO_2 increases from 16,65 % (resulting from the alite and belite content of the

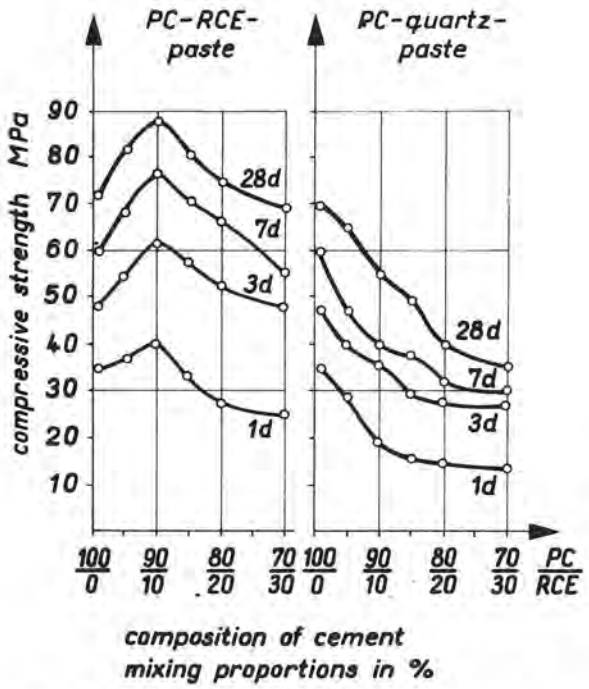

Fig. 2: Compressive strength of PC-RCE-pastes and of PC-quartzpowderpastes after 1, 3, 7 and 28 days

Test conditions: ratio water/PC+RCE = 0,40 = const.; ratio water/PC + quartz = 0,40 = const.; specific surface of the quartzpowder O_s = 8000 cm^2/g (Blaine method); sample storage under water; temperature 20 °C.

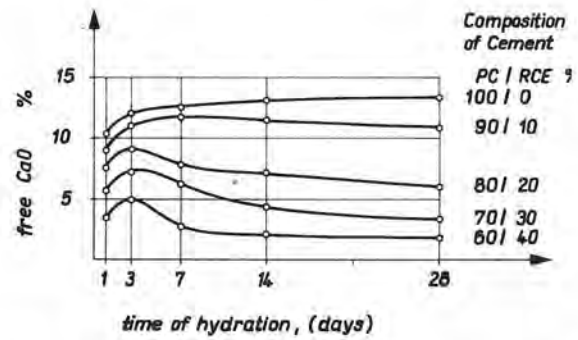

Fig. 3: Lowering of the "free lime content" in hydrated PC/RCE-pastes by increasing amounts of RCE

Test conditions: Alcohol-ether-dried samples, determination of the free CaO by the extraction method of B. Franke

portland cement) up to 30,97 % after 28 days as a result of the conversion of the very high molecular amorphous SiO_2 to low molecular silicate species by the reaction with $Ca(OH)_2$ which is formed by the hydration of the portland cement.

Table 4: Increase of the amount of acid soluble SiO_2 during the hydration reaction of PC/RCE 80/20-pastes (Ratio water/solid 0,50; temperature of storage 20 °C)

time of hydration days	H_2SO_4-soluble SiO_2 %
0	16,65
1	19,22
3	21,16
7	23,41
14	27,05
28	30,97
extrapolation time	33,50

On the basis of these results one must conclude, that during the hydration in the cement pastes additional amounts of CSH-phases and CAH-phases are formed.

The investigation of the PC/RCE-pastes by the Molybdatmethod also shows that the degree of polymerisation of the silicate anions in the CSH-phases increase with increasing amounts of RCE in the cement paste.

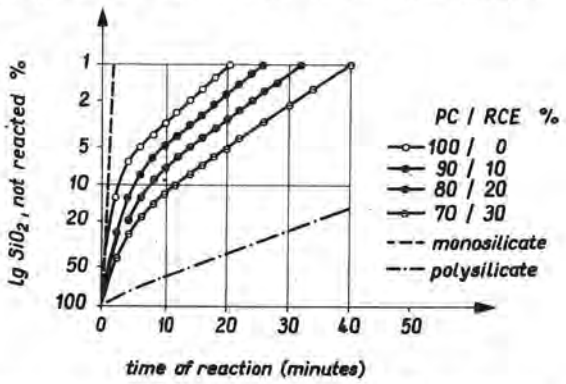

Fig. 4: Effect of RCE-admixture on the degree of polymersation of the silicates in hydrated PC/RCE-pastes, measured by the Molybdatmethod of Thilo, Wieker and Stade.

Storage conditions of the samples: Hydration under water, 28 days, temperature 20 °C.

An important property of the PC/RCE-mix cements is their relativly high resistence against aggressive solutions, i.e. Mg-salt-solutions. The chemical resistence of the mix cements was evaluated by compressive strength tests of the samples (paste cubes 1 x 1 x 1 cm) versus the storage time in the solutions. Some results of the corrosion test show figure 5.

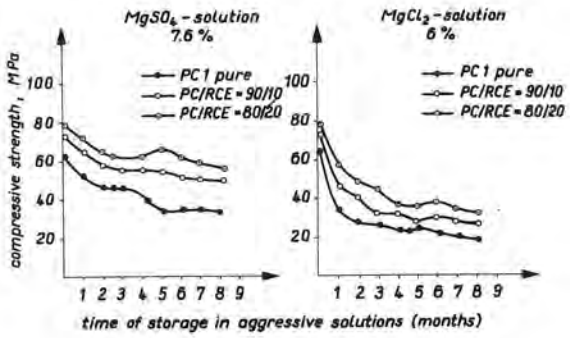

Fig. 5: Compressive strength of 28 days hydrated PC/RCE-pastes in dependence of the time treated by $MgSO_4$- and $MgCl_2$-solutions
Test conditions:
$MgSO_4$-solution 7,6 % = 1,53 % Mg^{2+}
$MgCl_2$-solution 6,0 % = 1,53 % Mg^{2+};
storage temperature 20 °C.

According to our attitude the reasons for the enlarged resistence of PC/RCE-mix cements against chemical attack are due to the deminishing of free lime content, the additional formation of CSH-phases and the increase of the degree of polymerisation of the calciumsilicatehydrates.

References

/1/ Kühl,H. Zement-Chemie, Vol.II,p.51 VEB Verlag Technik Berlin 1961

/2/ Massazza,F. General report III-6, VI. Intern.Symp. on the Chemistry of Cement, Moscow 1974

/3/ Massazza,F. and U. Costa II Cemento (1979) 1, 3-18

/4/ Sersale, R. and co-worker Rend.Soc.Mineral.Ital. 18 (1962) p. 215-218

/5/ Ludwig,U. and Schwiete,H.-E. Zement-Kalk-Gips 16 (1963) 10, p. 421-431

/6/ Thilo,E., Wieker W. and Stade,H. Ztschr. allg. anorg. Chem. 340 (1965) 261-265

Fly ash from Kakanj Power Plant in Cement Production

Production du ciment aux cendres volantes de la centrale thermique de Kakanj

V. KORAC et V. UKRAINCIK, Institut de Génie Civil, Zagreb, YOUGOSLAVIE.

RESUME : Des recherches de laboratoire ont permis de déterminer la composition optimale d'un ciment à faible chaleur d'hydratation, constitué d'un clinker à teneur relativement élevée en C_3A et C_3S, et de cendre volante de la centrale thermique de "Kalkanj".

C'est un ciment unique en Yougoslavie avec l'adjuvant de la cendre volante, qui s'utilise pour bétons hydro-techniques de masse.

Dans la centrale thermique "Kakanj", la poussière de charbon brun est brûlée exceptionnellement à la température d'environ 1600°C, tandis que dans les autres centrales thermiques yougoslaves cette température est d'environ 1000-1100°C.

La cendre volante est composée des constituants principaux suivants : environ 42 % SiO_2, 19 % Al_2O_3, 9 % Fe_2O_3 et 23° CaO. La propriété caractéristique de ce ciment est qu'il diminue le besoin de l'eau et qu'il démontre les propriétés de plastification. Ce qui est particulièrement évident dans le béton frais. Avec un grain de maximum 63 mm du granulat et avec seulement 225 kg ciment/m3 de béton et 108 litres d'eau, on peut produire un béton très ouvrable de la résistance à la compression de 30 N/mm2 après 28 jours.

SUMMARY: On the basis of laboratory research of blended cement having as ingredients portland cement, with relatively high C_3A and C_3S content and fly ash, the optimum composition of low heat cement was chosen. Now, after several industrial trial grindings, fly ash from Kakanj power plant is the only one in Yugoslavia used as addition in production of cement for hydraulic mass concrete.

Extraordinary, in Kakanj power plant, brown coal dust burns at the temperature of about 1600°C, while in the others at 1000-1100°C. Fly ash under consideration containes 42% SiO_2, 19% Al_2O_3, 9% Fe_2O_3 and 23% CaO. The substantial property is that it unusualy decreases the water requirement and its plasticizing effect is expressive. This came strikingly out in fresh concrete mix design. With maximum aggregate grain size 63 mm, with 225 kg/m^3 of blended cement containing 50% fly ash, 108 l of water, well-workable concrete with characteristic 28-days strength of 30 N/mm^2 is obtained.

Several Yugoslav thermo-electric power plants are fired with coal dust obtained from brown coal of more recent geological age.

Because Yugoslav fly ashes have not been adequately and thoroughly studied in terms of their application in the cement industry, practically no use at all has been made of this waste material as an addition to clinker.

However, our systematic studies of a series of cement and concrete batches has shown fly ash obtained from the Kakanj (near Sarajevo) power plant to possess extraordinary good properties as an addition to clinker in cement production in terms of both pozzolanic and physical features. Whereas in other Yugoslav power plants fly ash develops by burning coal dust at the temperature of 1000-1200°C, Kakanj fly ash is produced by burning at 1600-1650°C, which substantially affects its structure and physico-chemical features.

Coal dust is obtained from separated brown coal with a calorific value of about 3200 kcal/kg. Our project entailed the determination - for a new cement plant in the area of the Kakanj power plant - the optimum composition of cement with a low hydration heat for hydraulic engineering applications; accordingly, a series of laboratory cement batches was produced by homogenizing pure Portland cement with 30, 40, 50, 60, 70 and 80 percent of fly ash.

BASIC CHARACTERISTICS OF PRIME MATERIALS

CLINKER

Phase composition

	Bogue	X-ray
C_3S	62.63 %	68.00 %
C_2S	8.54 %	10.00 %
C_3A	11.65 %	6.00 %
C_4AF	12.41 %	11.00 %
Hydraulic modulus:	2.14	
Silicate modulus:	1.75	
Aluminate modulus:	1.71	
Degree of saturation:	99.9	
Free CaO:	1.04 %	
Specific area (Blaine):	3200 cm^2/g	
Density:	3.08 g/cm^3	

FLY ASH

Average Chemical Composition in %

Loss on ignition	1.63
Insoluble	0.30
SiO_2	41.95
Al_2O_3	19.13
Fe_2O_3	0.04
CaO	22.93
MgO	2.02
SO_3	2.01
Na_2O	0.39
K_2O	1.10
free CaO	1.41

The aformentioned chemical composition represents the one-year average of thirty analyses.

The range of standard deviation for the basic components (SiO_2, Al_2O_3, Fe_2O_3 and CaO) was 0.74-1.49, and for the other components 0.09-0.52.

In terms of its chemical composition, according to A.Jarrige (1) this fly ash can be considered atypical because its SiO_2 and Al_2O content brings it close to silicate-aluminum type ashes, while on the other hand it contains much CaO but few sulfates. It is also distinguished by a very low loss on ignition.

X-RAY - DIFFRACTION AND THERMAL ANALYSIS OF FLY ASH

These tests showed fly ash to be of an almost exclusively amorphous glassy structure, without thermal effects, which is indicative of possible pozzolanic properties.

---

(1) A.Jarrige: Les cendres volantes, Editions Eyrolles, 61, Boulevard Saint-Germain, Paris V^C, 1971, p. 63

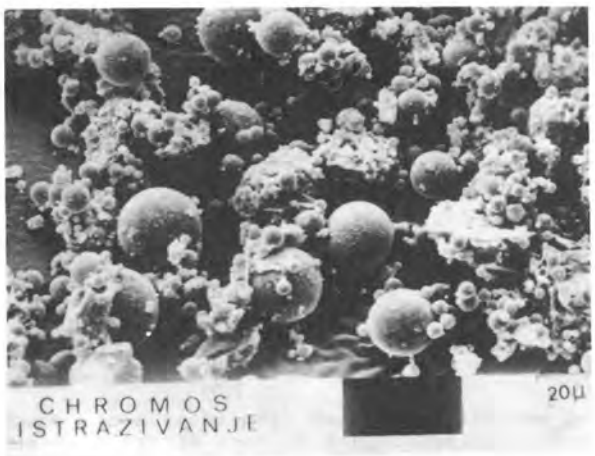

Fig. 1

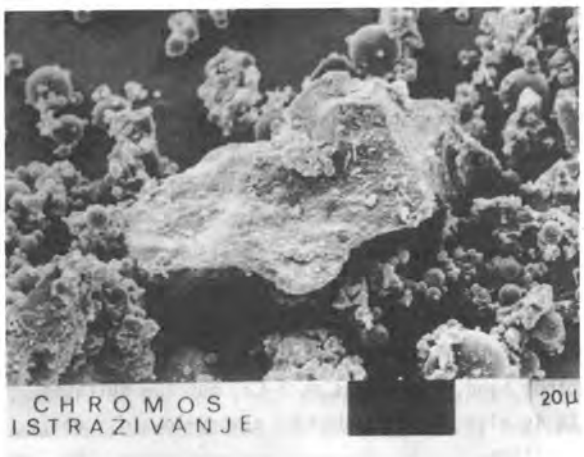

Fig. 2

Fig. 3

Fig. 4

Figures 1 and 2 show the Kakanj power plant fly ash. It consists of very fine glassy, closed, dense and regular spherical particles, with very few unburnt coal particles of an irregular form.

For the sake of comparison we are also enclosing figures 3 and 4, showing fly ash from another Yugoslav power plant, of a very similar chemical composition in terms of the basic component, i.e., SiO_2, Al_2O_3, Fe_2O_3 and CaO content. However, this ash was produced by burning at the temperature of 1000 - 1050°C, and did not melt (apart from the smallest particles) during burning, but was only syntherized. Hence its porous and alveolate structure, resulting in a higher water requirement.

Fly ash sieve analysis

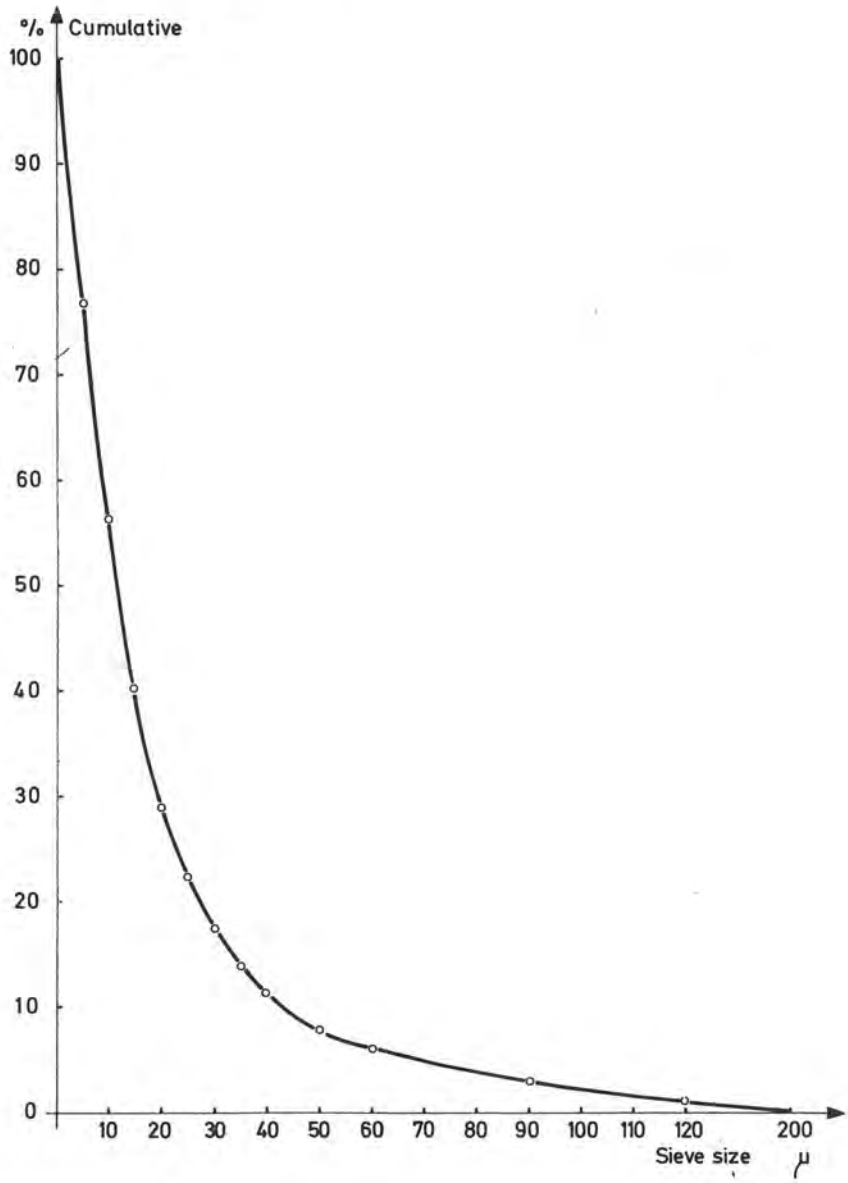

Specific area (Blaine): 4042 cm^2/g
Density: 2.62 g/cm^3

Particles smaller than 40 microns were determined by a Sartorius automatic balance. As shown in the diagram, Kakanj fly ash is distinguished by extremely great particle fineness. Particles larger than 45 microns accounted for only 9,7 %.

Pozzolanic activity according to Fratini (after 8 days)

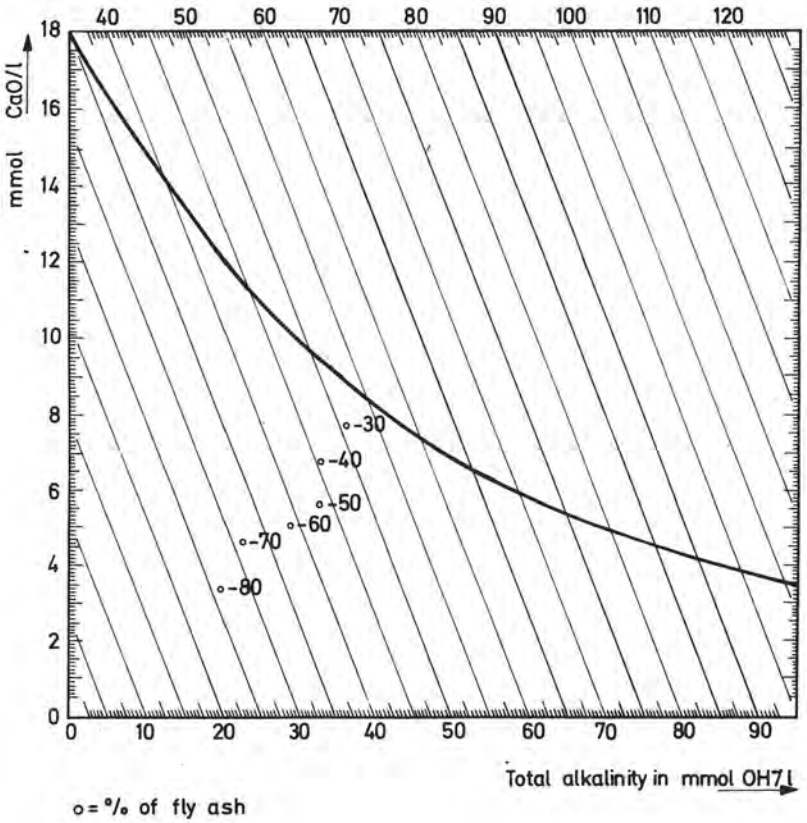

Pozzolanic activity was tested on a variety of cement types containing 30 to 80 % of fly ash.
All the cement types showed a positive pozzolanic activity at the temperature of +40°C as early as after 8 days.

CEMENT TEST RESULTS

TABLE No. 1 Physical Properties of Cements

Sample code		FA-0*	FA-30	FA-40	FA-50	FA-60	FA-70	FA-80
Normal consistency	%	25.0	22.0	21.5	20.7	19.7	19.0	18.5
Setting time:								
Initial	h min	2 50	3 40	4 00	4 30	4 40	5 00	5 50
Final		4 00	5 00	5 30	5 35	5 40	6 30	7 10
Soundness								
Le Chatelier in	mm	1.3	1.8	2.5	7.1	8.5	13.5	30.3
cakes		sound	sound	sound	sound	sound	unsound	unsound
Residue on 90 μ mesh	%	3.6	3.5	3.3	3.1	3.1	2.9	3.1
Blaine	cm^2/g	3200	3663	3675	3744	3894	3943	4070
Density	g/cm^3	3.08	3.02	2.95	2.85	2.83	2.78	2.71
Heat of hydration,	after 7 days	325	284	270	247	230	200	183
Joule/g, after vacuum flask method	after 28 days	357	324	311	288	264	244	225

TABLE No 2 Strength Test Results

Sample Code	Constant w/c ratio=0.5				Constant consistency					
	Compressive strength in N/mm^2 after		Bending strength in N/mm^2 after		Compressive strength in N/mm^2 after			Bending strength in N/mm^2 after		
	7 days	28 days	7 days	28 days	7 days	28 days	90 days	7 days	28 days	90 days
FA - 0*	38.7**	48.5	7.1	8.4	-	-	-	-	-	-
FA - 30	26.0	42.6	5.6	7.7	-	-	-	-	-	-
FA - 40	23.0	36.3	5.3	7.1	24.9	41.5	-	5.5	7.5	-
FA - 50	17.9	30.0	4.3	6.3	20.0	31.3	41.7	4.5	6.2	7.6
FA - 60	13.9	23.9	3.7	5.2	16.7	30.1	41.4	4.0	5.7	7.0
FA - 70	10.7	18.5	3.0	4.2	-	-	-	-	-	-
FA - 80	7.2	13.1	2.1	3.2	8.0	17.8	-	2.1	3.8	-

* The number in sample code indicates the percantage of fly ash in cement.

** The foregoing compressive stregnth testing results are mean values of 6 individual results. The values for bending strength are means for 3 individual results.

COMMENTS

The results of these tests have shown that the addition of 50% od Kakanj fly ash can produce cement having very good characteristics for hydraulic engineering applications:

- standard consistency is low (about 20.7%)
- setting begins after 4 hours
- the cement is sound
- hydration heat values are below the prescribed maximum values for the heat by solution method
- the strength growth rate is very high till 90 days.

CONCRETE APPLICATIONS

Mixed cement with 50% of fly ash has already been used for six months in the production of conrete for the Salakovac dam and Bočac dam hydro-electric power plant. The anticipated advantages of such cement, as determined by laboratory testing, were confirmed again by on-site concrete checks:

- marked plastifying effect
- good workability with only 108 l of water and 225kg of cement per m^3 of concrete, and maximum aggregate size of 63 mm
- maximum temperature within the mass concrete of $49^{o}C$ with initial temperature of fresh concrete $23^{o}C$
- with a w/c ratio of 0.48, concrete compressive strength in N/mm^2 was as follows:

	$\bar{X}$	$\bar{s}$
28 days	44.0	3.5
90 days	52.0	3.5

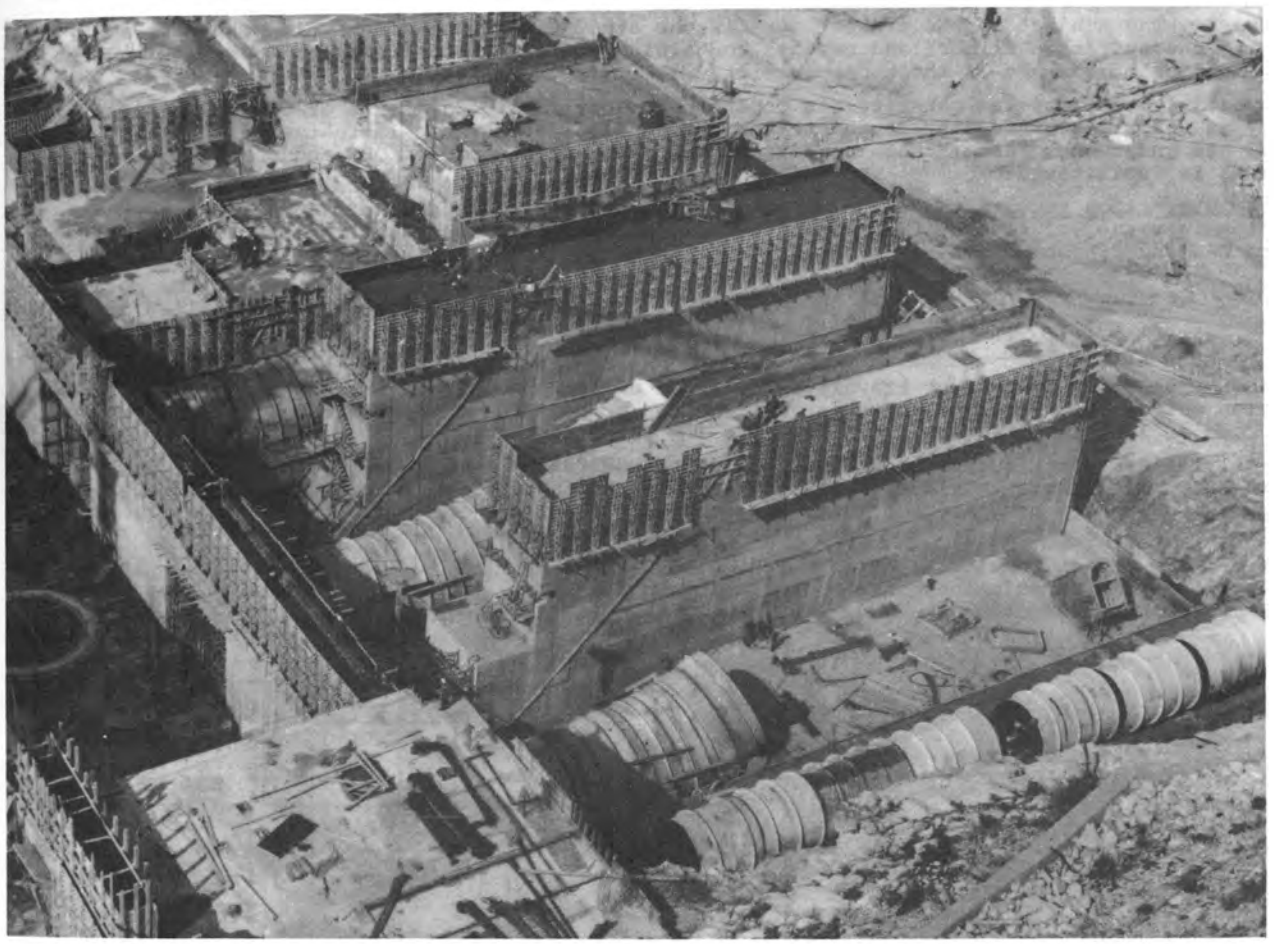

Fig.5 Salakovac hydro-electric power plant

A Study on the mechanism of the reaction of Santorin earth during its hydration with Portland Cements

Etude sur le mécanisme de la réaction de la terre de Santorin pendant son hydratation avec des ciments Portland

Dr. CH. FTIKOS, Dr. G. PARISSAKIS,
HERACLES General Cement Co. - National Technical University of Athens, Lab. of Inorg. and Anal. Chemistry, Greece

SUMMARY : The subject of the present work is the study of the phenomena which take place during the hydration of portland cements containing different proportions of pozzolan and the explanation of the way of their interaction.

The activity of pozzolan constituents depends on their lattice deffects or even on the deficiency in their structure, attributed to various physical or technical treatments that the material has undergone. Under these conditions the interaction between OH^- and pozzolanic constituents is facilitated.

This interaction results the dissolution of Al_2O_3 and SiO_2 in the alkali solution, their transition into the solution by the form of hydroxycomblex ions, and their reaction with Ca^{2+} to form CAH and CSH compounds.

RESUME : Le sujet du présent travail est l'étude des phénomènes qui se passent pendant l'hydratation des ciments Portland contenant différentes proportions de pouzzolane et l'explication du mode de leur inter action.

L'activité des constituants pouzzolaniques dépend des défauts de leur réseau ou même de leur structure déficiente attribuée à divers traitements physiques ou techniques que le matériel a subis. Sous ces conditions l'inter action entre OH^- et les constituants pouzzolaniques est facilitée.

Cette inter action résulte la dissolution de Al_2O_3 et SiO_2 dans la solution alcaline, leur transition dans la solution par la forme d'ions hydroxycomblèxes et leur réaction avec Ca^{2+} pour former des composés de CAH et CSH.

1. Introduction

It is well known (1,2) that the grinding of clinker with Santorin earth or with a pozzolan in general, leads to the production of cements which present some advantages regarding their physical and chemical properties, as compared to those of pure portland cements.

Though the phenomena which take place during the hydration of cement with pozzolan have been studied by many researchers (3,4,5), some of them have not yet been clarified.

The aim of the present work is the study of these phenomena in cements containing different proportions of Santorin earth and the explanation of the way of its interaction.

The hydration phenomena are studied by XRD, EPMA and SEM, as well as by determining the active part of Santorin earth in cement pastes. These pastes have been prepared from two portland cements of different composition in mixtures containing 0,10,20,30 and 40% of Santorin earth respectively, cured in water at $18\pm2^{o}C$ for 7,28,90 and 365 days. Strength development of these blended cements has also been studied.

The results of this study provide useful information about the way in which pozzolans interact during their hydration with portland cement.

2. Experimental

The materials which have been used are two Portland cements (P_1,P_2) of different composition regarding their C_3S,C_2S,CaO_f content and Santorin earth (S.e.) which is a well known natural pozzolan.

Both the chemical and the minerological composition (according to Bogue) of the two Portland cements and the chemical composition of the Santorin earth, as well as their fineness are shown in Table I.

TABLE I: Composition of materials used

	L.O.I.	SiO_2	Al_2O_3	Fe_2O_3	CaO	MgO	Na_2O	K_2O	SO_3
P1	1,60	20,48	5,94	2,82	63,10	3,54	0,85	0,65	2,48
P_2	1,74	21,71	5,44	2,64	60,16	2,20	0,35	0,65	2,42
S.e.	2,40	63,50	15,65	6,10	3,95	1,83	2,87	2,73	Traces

	C_3S	C_2S	C_3A	C_4AF	CaO_f	Sp. surface cm^2/g (Blaine)
P1	50	21	11	9	2	3500
P2	33	38	10	8	1	3500
S.e.	—	—	—	-	-	6000

Specimens have been prepared, according to ISO-RILEM-CEMBUREAU-CEN, by mixing the cements P_1 and P_2 with 0, 10, 20, 30 and 40% of Santorin earth respectively, for the study of strength development. These specimens were cured in water at $18\pm2^{o}C$ for 7, 28, 90 and 365 days.

The results derived from cement mixtures P_1 and P_2, are presented in Fig. 1 and Fig. 2 respectively.

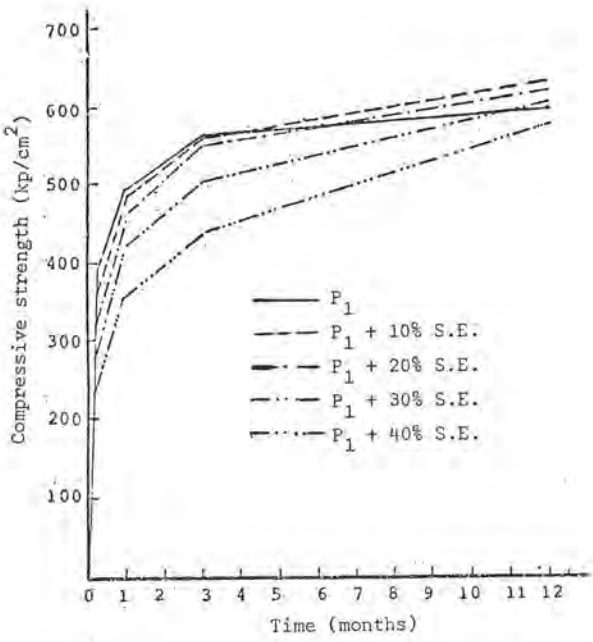

Fig. 1.: Compressive strength development.

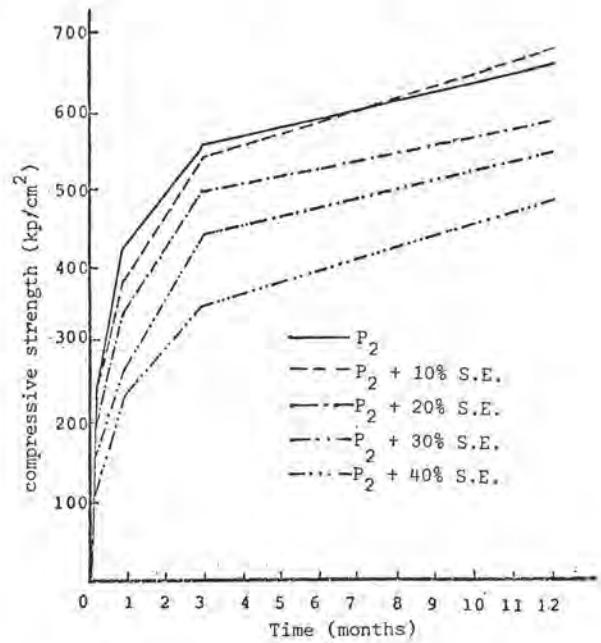

Fig. 2.: Compressive strength development.

Pastes prepared from the above mixtures were also cured under the same conditions. The ratio W/C used for the preparation of the pastes is shown in Table II.

TABLE II: W/C ratio used.

Mixtures	W/C	Mixtures	W/C
P_1	0,27	P_2	0,26
P_1 + 10% S.e.	0,28	P_2 + 10% S.e.	0,27
P_1 + 20% S.e.	0,32	P_2 + 20% S.e.	0,30
P_1 + 30% S.e.	0,34	P_2 + 30% S.e.	0,31
P_1 + 40% S.e.	0,35	P_2 + 40% S.e.	0,32

The hydration phenomena in these pastes have been studied, according to the following methods:

a. Determination of the active part of S.e. by chemical treatment.
b. Study by X-Ray Diffraction (XRD)
c. Study by Electron Probe MicroAnalysis (EPMA)
d. Study by Scaning Electron Microscopy (SEM)

a. Determination of the active part of S.e.

For the determination of the active part of S.e., the cement pastes were ground and treated with hydrochloric acid (HCl) 1:1, at -3°C for 10 min. The residue was treated with hot Na_2CO_3 solution 5% for 5 min. The residue derived after ignition gives the active part of S.e., during its hydration with Portland cement.

It should be mentioned that in anhydrous samples all the contained S.e. appears to be insoluble.

The results after the above mentioned treatment of the mixtures derived from cements P_1 and P_2, appear in Figures 3 and 4 respectively.

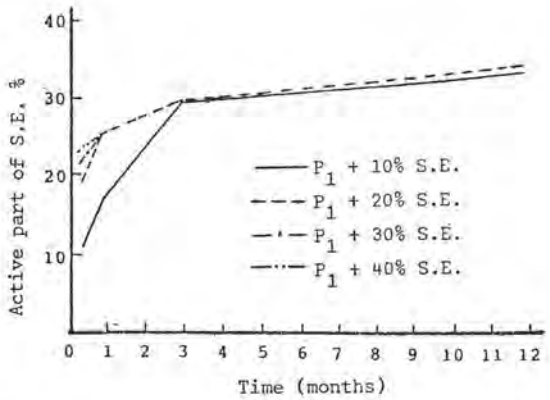

Fig. 3.: Determination of the active part of S.e. % of the added.

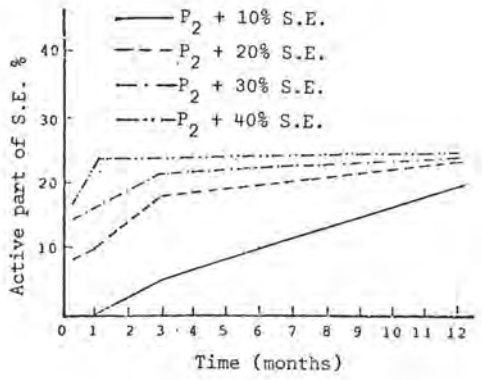

Fig. 4.: Determination of the active part of S.e. % of the added.

b. Study by XRD.

Some of the patterns of the cement pastes examined by XRD are presented in Figures 5 and 6.

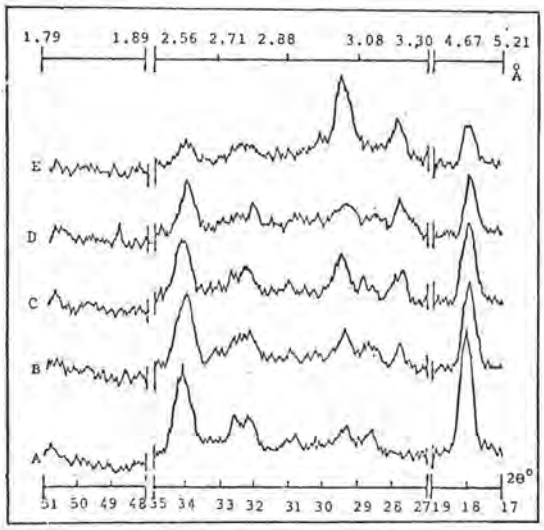

Fig. 5.: XRD patterns of hydrated cement pastes, (A) P_1 (B) P_1+10% S.e. (C) P_1+20% S.e. (D) P_1+30% S.e. (E) P_1+40% S.e. cured in water at 18+2°C for 1 year.

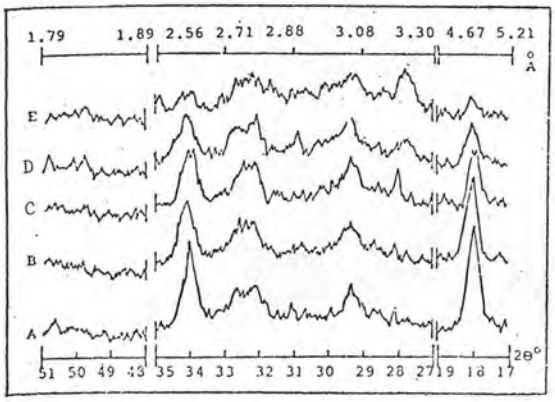

Fig. 6.: XRD Patterns of hydrated cement pastes (A) P_2 (B) P_2+10% S.e. (C) P_2+20%S.e. (D) P_2+30% S.e. (E) P_2+40% S.e. cured in water at 18±2°C for 1 year.

What may be noticed here is the reduced intensity of the peaks of $Ca(OH)_2$ (4.92, 2.63, 1.80 A°), as the S.e. content is increased.

In the patterns of Fig. 5 the increased intensity of the peaks of CSH (3.02, 2.75, 1.83 A°) in the pastes by increased content of S.e. is also noticeable.

c. Study by EPMA

A series of photos are presented in Fig. 7 concerning the examined cement paste prepared from cement P_1, with 40% of S.e. after 1 year time of hydration.

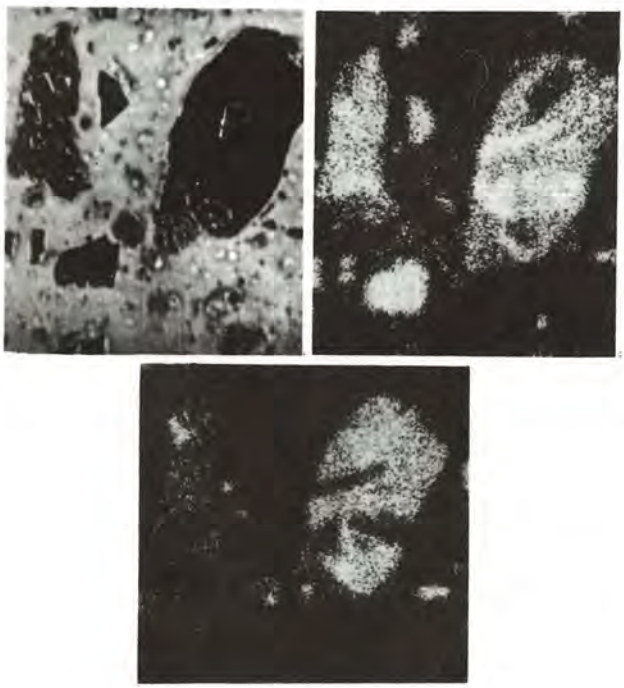

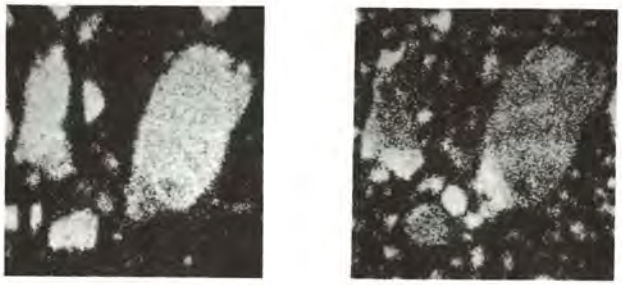

Fig. 7.: Hydrated cement paste (P_1+40% S.e.) cured in water at 18±2°C for 1 year.
Ph_1: Absorbed electrons, 100 μ
Ph_2: Al x-rays Ph_4: Si x-rays
Ph_3: Fe x-rays Ph_5: Ca x-rays

In photo No. 1 a grain of pozzolan (point P) appears reacted with $Ca(OH)_2$. Around this grain the reaction products are observed.

As these photos reveal there is a remarkable heterogeneity even in a small grain of pozzolan. Furthermore, the way of interaction between the pozzolan and $Ca(OH)_2$ may be traced in these pictures,

d. Study by SEM

Two photos are provided concerning the examined cement paste prepared from pure cement P_1 (Fig. 8).

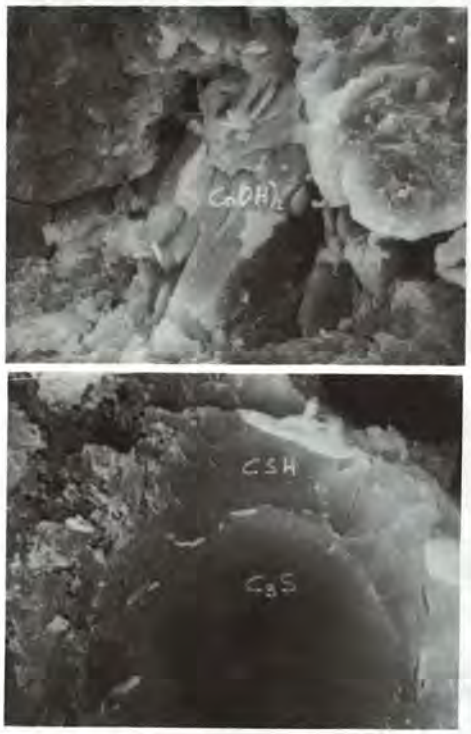

Fig. 8.: Ph_1 M x 2.000 Ph_2 M x 10.000 Hydrated pure portland cement (P_1) paste cured in water at 18±2°C for 1 year.

In photo No. 1 crystals of portlandite grown from CSH. A grain of C_3S with its hydration products may be seen as well. By higher magnification, the same grain of C_3S may be seen in photo No. 2.

A point of special interest in this photo is the zone of reaction around the C_3S grain.

In Fig. 9, the four photos presented concern the examined paste prepared from cement P_1 with 40% S.e. cured for 1 year.

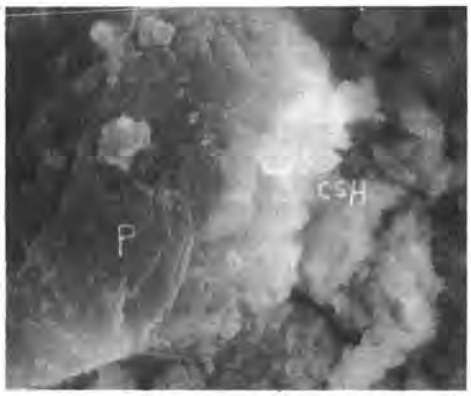

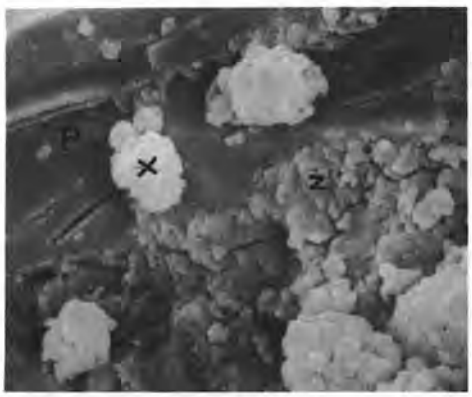

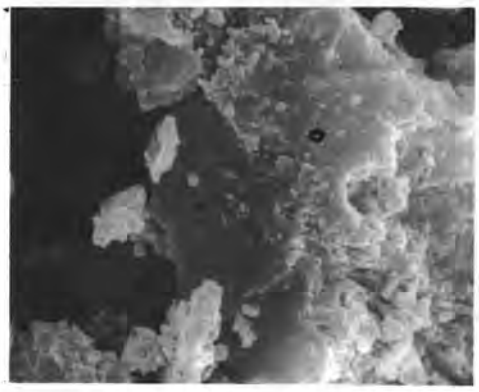

Fig. 9.: Ph_1 M x 10000, Ph_2 M x 10000
Ph_3 M x 10000 Ph_4 M x 10000
Hydrated cement paste (P_1+40% S.e) cured in water at 18+ 2°C for 1 year.

In these photos grains of pozzolan are shown after their interaction with $Ca(OH)_2$. The hydration products appear around these grains.

The remarkable points in these photos are the zone of reaction as well as the cohesion and adhesion of the hydration products.

3. Discussion

The research concerning the mechanism of the action of Santorin earth or of a pozzolan in general, during its hydration with portland cements consists in the study of the behavior of the active constituents of pozzolan in the alkali solution derived during the hydration of clinker constituents.

In the present work the study of the hydration phenomena by the above mentioned methods has been conducted in four periods of time, as follows:

-	1st period	0 - 7	days
-	2nd period	7 - 28	days
-	3rd period	28 - 90	days
-	4th period	90 -365	days

1st period: During this period of hydration they have not yet been observed any remarkable reactions between the constituents of S.e. and Ca $(OH)_2$, which can effect the strength development.
A selective dissolution takes place on the vitreous phase as well as on the low crystallinity constituents of S.E. This selective dissolution is caused by the OH^-, released during the hydration of clinker.

2nd period: The formation of calcium aluminate hydrates (CAH) is now clearly observed, the formation of CSH and the decrease in $Ca(OH)_2$ are begining.

3nd period: The reaction between the Santorin earth active constituents, especially the SiO_2 and $Ca(OH)_2$, are still taking place. Thus, CSH gel and some crystals of tobermorites begin to form.

4th period: The reaction between the Al_2O_3 and SiO_2 of S.e. with $Ca(OH)_2$ is continued to form CSH and CAH compounds at low rate due to the reduced alkalinity because of the binding of $Ca(OH)_2$.
The transformation of the CSH gel in tobermorites of small lattice parameters (d) is remarkable too.
Regarding the pastes prepared from the cement P_2 and S.e, it is concluded that the released amount of $Ca(OH)_2$ is insufficient to react with Santorin earth.

4. Conclusion

The study of the results and remarks provided in the present work, in combination with the mechanism of hydration of portland cement (6,7) gives useful informations of the way of interaction of Santorin earth or of a pozzolan in general, during its hydration with Portland cement.

The activity of the clinker constituents is attributed to the increased ionization of the Ca-O bond with formation of double oxides during clinkerization.

The activity of pozzolanic constituents depends on their lattice deffects or even on the deficiency in treir crystal structure, attributed to various physical or technical treatments that the material has undergone. Under these conditions, the interaction between OH^- and pozzolanic constituents is facilicated.

This interaction results the dissolution of Al_2O_3 and SiO_2 in the alkali solution, their transition into the solution by the form of hydroxycomplex ions, and their reaction with Ca^{2+} to form CAH and CSH compounds.

The most probable form of aluminium transition into the solution is that of $Al(OH)_6^{3-}$. This is concluded from the study of the hydration products and the PH(8,9) values, during hydration.

Taking into consideration the above mentioned alkalinity and the C/S low ratio of the hydration products, it is concluded that the most probable form of silica transition into the solution is that of SiO_2OH^-.

As soon as the concentration of $Al(OH)_6^{3-}$, SiO_2OH^-, Ca^{2+} and $CaOH^+$ in the solution becomes saturated, crystallisation nuclei are created on which the formed hydrated compounds are built. The most probable position of the crystallization nuclei is on the surface of other particles present in the solution.

The above explains the cause of inactivity of some oxides e.g. MgO, which during the hydration of pure Portland cement produce harmful compounds.

BIBLIOGRARHY

1.- NICOLAÏDES, N. (1958) "Technika Chronika" 409-10 327-44.

2.- PARISSAKIS, G., FTIKOS, C. (1975): Proceedings of the 2nd Hellenic Concrete Conference, Thessaloniki, Greece.

3.- TERRIER, P., MOREAU M., (1966) Rev. Mater. Constr. 613, 379-396, 441-451.

4.- DRZAJ, B., HOCEUAR,S. SLOKAN, M., (1978) Cem. Concr. Res. 8, 711-20.

5.- VAN AARDT, J.HP., VISSER J., (1977) Cem. Concr. Res. 7, 39-44.

6.- BERNARD J.P., (1978) Cim. Bet. plant. Chaux, 6, 715, 359-366.

7.- DANILOV V.V., (1974) Proceedings of the 6th International Congress on the Chemistry of cement, Moscow sect. II 1-6, II-1

8.- BABUSKIN V.I., MITVEVEN G.M., MCHEDLOV-PETROSSYAN O.P. (1969) "Thermodynamics of Silicates", Moscow, Stoyivdat p.p. 188, 199, 205.

9.- NARAI-SABO I.(1969) "Inorganic Crystallochemisstry", Budapest, Ac. Sc. Publ.

10.-BECKER H., VON ZANDER H.,(1977) Zem. Kalg Gips, 6, 287-291.

Influence of alkali sulphates on setting and hardening of pozzolanic cements

Influence des sulfates alcalins sur la prise et le durcissement des ciments pouzzolaniques

V. SABATELLI, Assistant Professor and G.L. VALENTI, Assistant Professor
Institute for Applied Chemistry, Faculty Engineering, University of Naples, Italy.

SUMMARY: The hydraulic behaviour of a pozzolanic cement (clinker 58.5%,pozzolana 39.0%, gypsum 2.5%) in presence of accelerators and hardeners, such as lithium, sodium and potassium sulphates has been investigated. The additives were separately added to the mixing water in concentrations ranging from 0.5 to 3.0 weight percent of cement. Reference terms have been the same pozzolanic cement without accelerators and a Portland cement prepared with the same clinker and the same percentage of gypsum, hydrated under the same experimental conditions.

Setting times, water contents for normal consistency, compressive and flexural strengths at 16h, 24h, 3 days, 7 days and 28 days were evaluated.

It has been pointed out that pozzolanic cement in the presence of additives shows considerable increases in mechanical strength, especially at 16 and 24 hours, while the 28 days strengths are practically coincident with those of the same cement without additive. Specimens of Portland cement, containing the same additives, show increases at early ages considerably lower, while at long ages significant reductions in strength often occur. It has been emphasized that alkali sulphates generally accelerate the setting and reduce the water of normal consistency with an effectiveness which depends on the amount of additive and is of the same order for both the cements. Lithium sulphate is generally the most effective additive, while potassium sulphate appears to be the least effective.

The course of hydration process and the characterization of the neo-formed products have been followed by thermal and X-ray diffraction analyses, achieving useful informations on the influence of alkali sulphates on the pozzolanic cement behaviour.

RESUME: On a étudié le comportement hydraulique d'un ciment pouzzolanique (clinker 58.5%, pouzzolane 39.0%, gypse 2.5%) en présence d'accélérateurs tels que sulfates de lithium, sodium et potassium. Les adjuvants ont été dissous séparément dans l'eau de mélange en concentrations comprises entre 0.5 et 3.0 pour-cent du poids de ciment. Deux termes de référence ont été choisis: le même ciment pouzzolanique sans adjuvants et un ciment Portland préparé avec le même clinker et le même pour-cent de gypse, hydraté sous les mêmes conditions expérimentales.

On a évalué le temps de prise, l'eau de consistance normale, la résistance à compression et à flexion après 16 heures, 24 heures, 3 jours, 7 jours et 28 jours.

On a souligné que le ciment pouzzolanique en présence des adjuvants manifeste considérables augmentations de résistance, surtout à 16 et 24 heures, tandis que la résistance à 28 jours coincide pratiquement avec celle-là que le même ciment montre sans adjuvants. Echantillons de ciment Portland qui contiennent les mêmes adjuvants montrent aux échéances brèves augmentations remarquablement inférieures, tandis que à celles-là plus longues il y a beaucoup de réductions significatives de résistance. Les sulfates alcalins en général accélérent la prise et diminuent l'eau de consistance normale avec un'efficacité qui dépend de la quantité d'adjuvant et est du même ordre de grandeur pour les deux ciments. Le sulfate de lithium est en général l'adjuvant le plus efficace, tandis que le sulfate de potassium est le moins efficace.

Le cours du processus d'hydratation et la caractérisation des produits de néo-formation ont été suivis par analyses thermiques et par diffraction aux rayons X, en obtenant informations utiles au sujet de l'influence des sulfates alcalins sur le comportement du ciment pouzzolanique.

1. INTRODUCTION

About 40% of the total cement production in Italy is covered by pozzolanic cements. The interest for these cements derives not only from their high chemical resistance and low heat of hydration which represent useful characteristics in particular applications, but also from the saving of thermal energy involved in their production, due to the substitution of a considerable amount of Portland cement clinker with pozzolana. On the other hand such replacement causes in pozzolanic cements reductions in strength at early ages in comparison with Portland cements. It may be therefore interesting to evaluate the influence of accelerators and hardeners on the hydraulic behaviour of pozzolanic cements.

It is known that alkaline substances present in clinkers or added to cements can considerably influence the hydration process and consequently modify the technical behaviour: significant changes in setting time, shrinkage and expansion under water, as well in mechanical strength are observed.

Literature data on the influence of alkali sulphates on the hardening almost exclusively concern Portland cement and are generally based on the use of a single additive in a single concentration. Alkali sulphates in Portland cement generally cause shortening in setting time, increase in mechanical strength at early ages and decrease at longer ages.

Aim of this work is the evaluation of the hydraulic behaviour of a pozzolanic cement (clinker 58.5%, pozzolana 39%, gypsum 2.5%) in presence of different alkali sulphates, added separately in different concentrations. Two reference terms have been employed: the same pozzolanic cement without additions and a Portland cement prepared with the same clinker and the same percentage of gypsum, hydrated under the same experimental conditions.

2. EXPERIMENTAL

In preparing Portland and pozzolanic cements, an industrial clinker, natural pozzolana and gypsum were employed. Gypsum was added to both the cements in a measure of 2.5% by weight. Fineness of cements was about 4000 cm^2/g (Blaine). The chemical composition of clinker and pozzolana is shown in Tab.I. Clinker/pozzolana ratio in the pozzolanic cement was 1.5.

Sodium, potassium and lithium sulphates were employed as additives. These were dissolved in the mixing water, so as to obtain preselected concentrations in respect to the cement, namely: 0.5%; 1.5%; 3.0%.

The mixing water content required for normal consistency, the initial and final setting times, and the flexural and compressive strengths (at 16 hours, 24 hours, 3 days, 7 days, 28 days of aging) were measured. Tests were performed in accordance with Italian specifications.

TABLE I - Chemical composition of clinker and pozzolana.

%	clinker	pozzolana
SiO_2	22.07	44.47
Al_2O_3	5.87	18.52
Fe_2O_3	3.10	9.99
CaO	66.08	11.96
MgO	1.21	5.49
K_2O	0.98	3.28
Na_2O	0.38	2.02
H_2O^+	-	3.50

Specimens to be submitted to thermal and X-ray analyses were prepared under paste form: water/cement ratio was 0.5. At preselected times of reaction, ranging from 10 minutes to 28 days, the hydration was stopped by aceton and the samples were washed with acetone and dried with diethyl ether. For determining the rate of hydration of the alite fraction X-ray quantitative analysis was employed: the alite peak at 51.8 °2θ CuKα was used.

3. RESULTS AND DISCUSSION

The water content for normal consistency is generally reduced by alkali sulphates for both the cements: the lowest reductions have the same order of magnitude (-9%) but are more frequent in pozzolanic cement.

As regards the setting, potassium sulphate promotes for pozzolanic cement (Fig.1) at the lowest concentration a delay, but at higher concentrations induces an accelerating effect, as the other two sulphates, generally increasing with the amount of additive. In Portland cement (fig.2) no delay occurs and the accelerating effects have the same order of magnitude as in pozzolanic cement; the maximum shortening of setting time is about 75' for pozzolanic cement and 90' for Portland cement. Obviously the shortenings are proportionally more significant for Portland cement whose setting time is lower in comparison with pozzolanic cement.

At all ages, exception made for 28 days, increases in flexural and compressive strengths are found, more considerable at shorter than at longer times. Such increases are growing with the amount of additive: lithium sulphate is generally the most effective additive, while potassium sulphate appears to be the least effective.

At 16 hours (fig.3) lithium and sodium sulphates, for all the employed concentrations, induce mechanical strengths different from zero, generally greater than those shown by the cement without additives after 24 hours of aging. Such circumstance is presented by po-

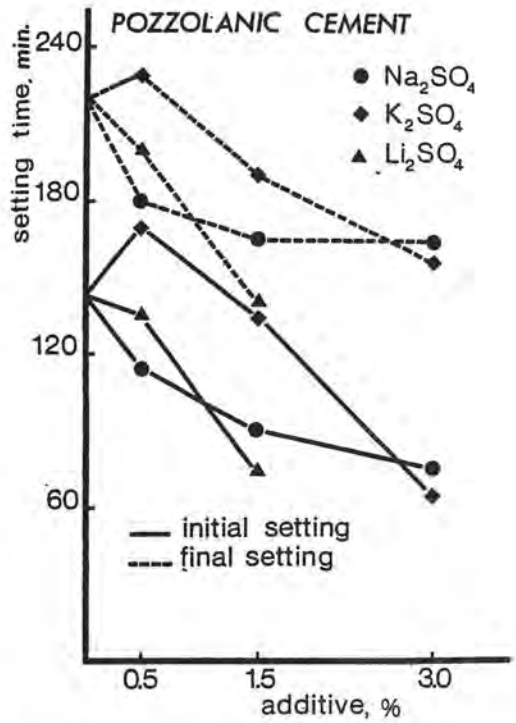

Fig.1 - Setting time of pozzolanic cement.

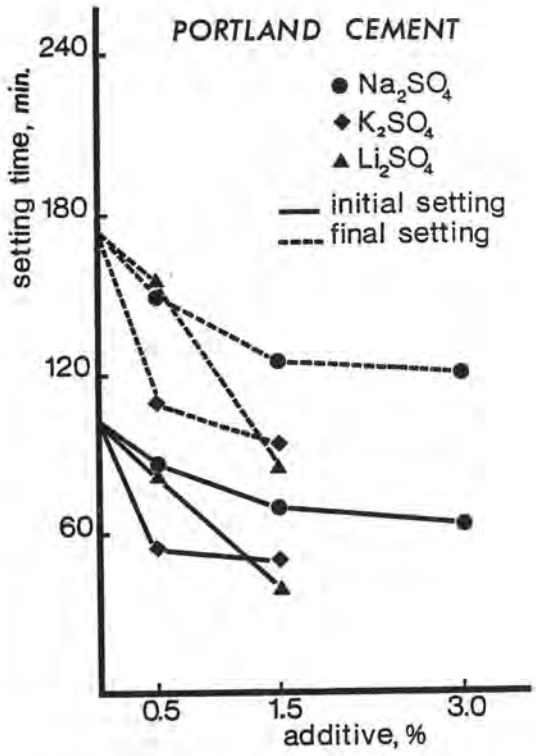

Fig.2 - Setting time of Portland cement.

tassium sulphate only at concentrations larger than 0.5%.

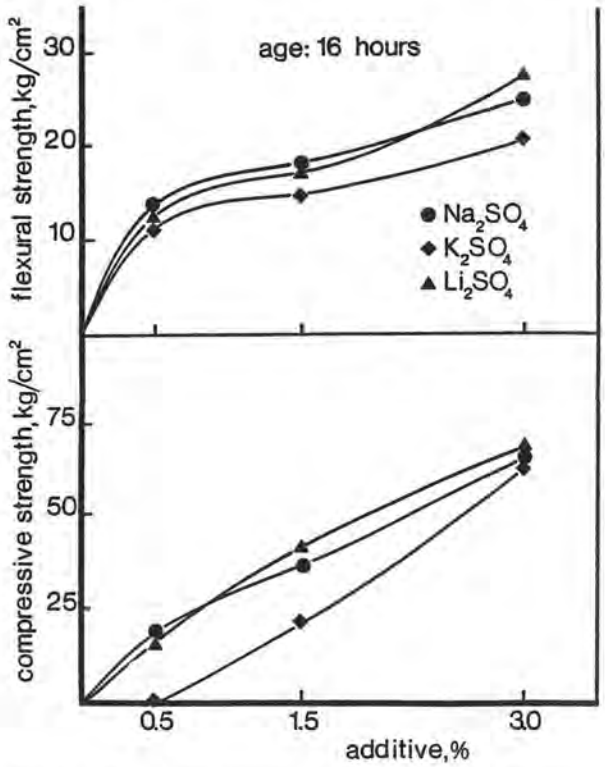

Fig.3 - Pozzolanic cement strength after 16 hours.

At 1 day (fig.4) the greatest increases in strength are ranging, depending on the kind of additive from 100% to 200% for the bending, from 400%to 600% for the compression. The values obtained with lithium sulphate at 3% overcome those shown by the cement without additives after 3 days of aging.

At 3 days (fig.5) the largest increases are 55% for the bending and 85% for the compression; at 7 days (fig.6) are about 30% and 40% respectively.

At 28 days (fig.7) flexural and compressive strengths show different trends: flexural strengths display in every case increases ranging from 5% to about 20%; compressive strengths often show reductions which do not overcome 3% and are increasing with the amount of additive for Na_2SO_4 and K_2SO_4, decreasing for Li_2SO_4. This, on the contrary, at 3% of concentration promotes a rise in strength of 5%.

Like pozzolanic cement, Portland cement shows increases in strength at 16 hours, 1 day, 3 days and reductions in compressive strengths after 28 days of aging (fig.8). Such changes however have for Portland cement a very different order of magnitude: increases in strength up to four time lower and reductions ten times higher may be found. Other important differences conce-

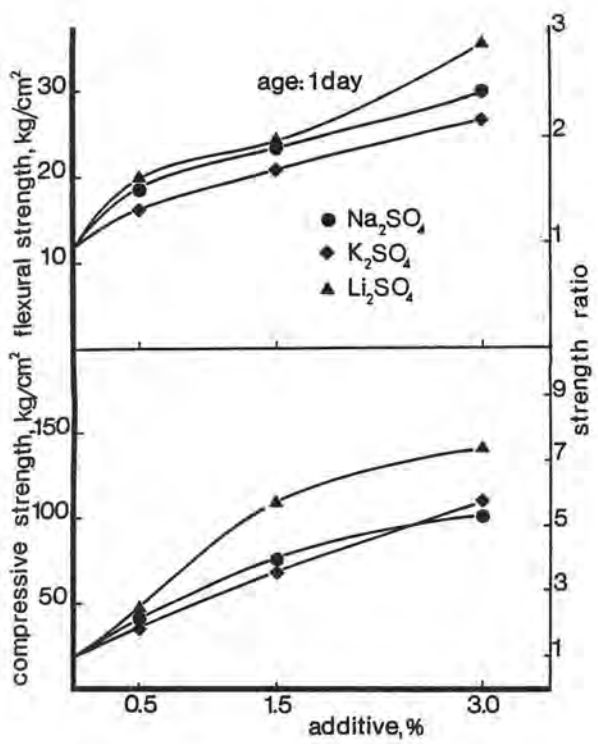

Fig.4 - Pozzolanic cement strength after 1 day.

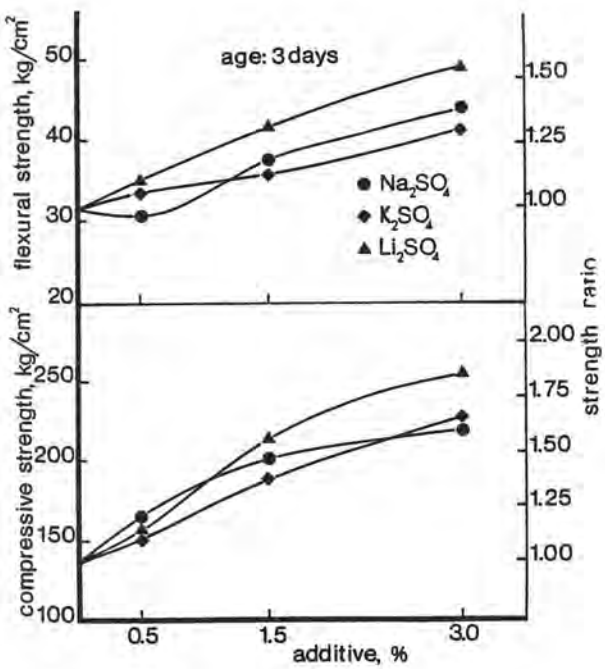

Fig.5 - Pozzolanic cement strength after 3 days.

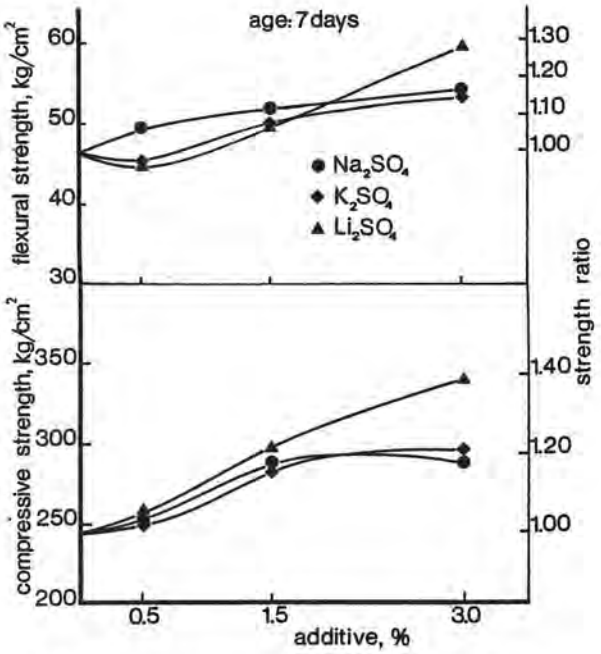

Fig.6 - Pozzolanic cement strength after 7 days.

rn the reduction in strength shown by Portland cement after 7 days and the negative influence of additives on the flexural strengths of Portland cement after 28 days of aging.

During the first 24 hours of reaction the hydration degree of the alite fraction is considerably higher (fig.9) for cement in presence of additive, especially until 11 hours of aging; this effect, common to Portland cement too, is generally more marked in the case of lithium sulphate addition. It is also to be pointed out the positive influence of pozzolana on the hydration rate of the alite fraction present in the cement.

The roentgenografic and thermal analyses, at least in the range of the examined concentrations and preselected times of aging, have not shown significant differences as regards the nature of hydration products, which were basically calcium silicates hydrate, calcium hydroxide and ettringite.

Much more informations are however needed in order to elucidate the relationships between the physical properties already described and the characteristics of the hydration process; further investigations are therefore carrying out.

The writers gratefully thank prof. R. Sersale for his useful discussions and Mr. A. Annetta for his technical assistance.

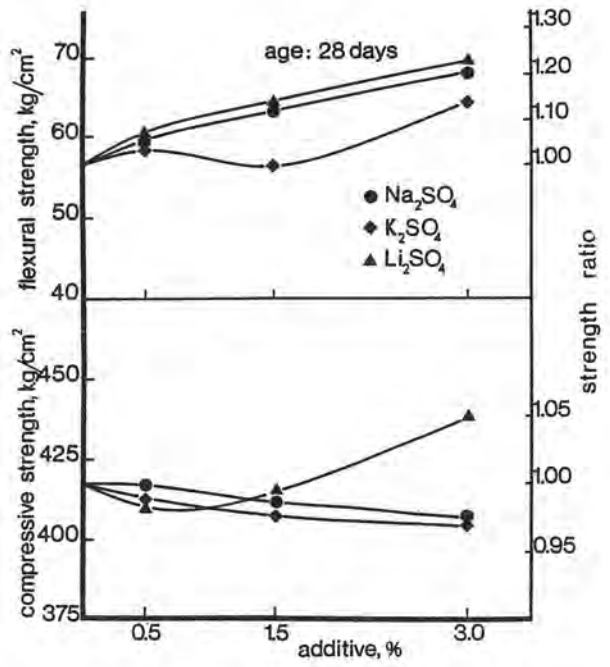

Fig.7 - Pozzolanic cement strength after 28 days.

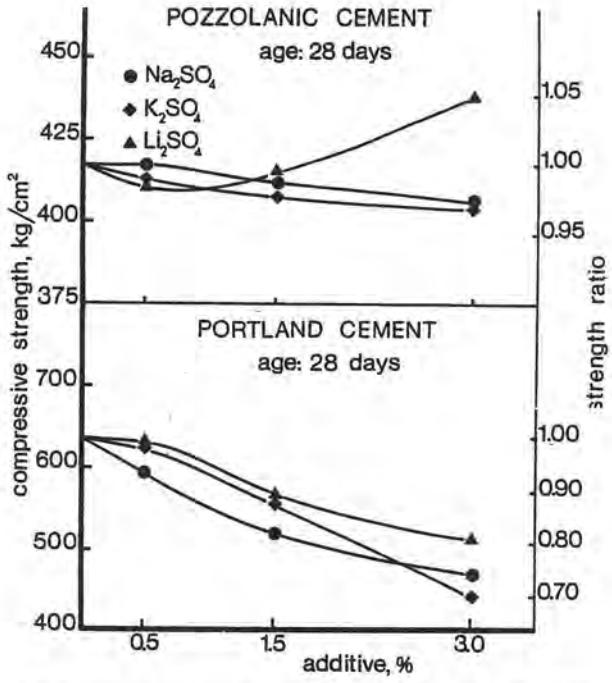

Fig.8 - Compressive strengths of pozzolanic and Portland cements after 28 days.

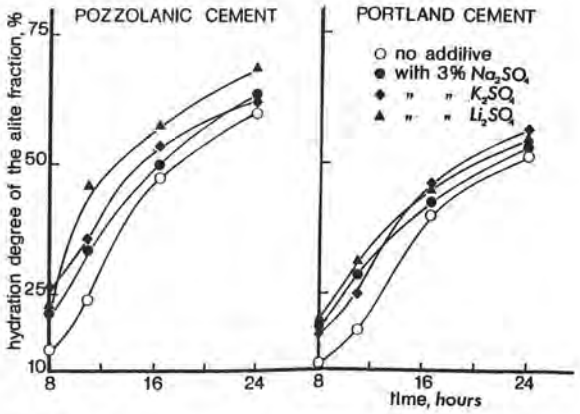

Fig.9 - Hydration degree of the alite fraction in pozzolanic and Portland cements.

REFERENCES

1.- I. JAWED, J. SKALNY (1978), "Alkalies in cement: a review, II. Effects of Alkalies on hydration and performance of Portland cement", Cement and Concrete Research, 8, pp.37-52.

2.- G.L. VALENTI, V. SABATELLI (in press), "The influence of alkali carbonates on the setting and hardening of Portland and pozzolanic cements", Silicates Industriels.

3.- J.M. BUTT, G.S. ROJAK (1956), "On combined accelerators of cement hardening", Zurnal prikladnoj chimii, 1, 7-10.

4.- F. MASSAZZA, U. COSTA (1979), "Aspects of the pozzolanic activity and properties of pozzolanic cements", Il Cemento, 1, 3-18.

5.- A. VAQUIER, A. CARLES-GIBERGUES (1970), "Sur l'importance des sulfates dans le caractère pouzzolanique d'une cendre volante silicoalumineuse de centrale thermique", Revue des Matériaux de Construction, 662, 331-337.

6.- A. CARLES-GIBERGUES, R. STAMBOLIEVA, A. VAQUIER (1973), "Rôle initial des sulfates d'une cendre volante dans son caractère pouzzolanique", Revue des Matériaux de Construction, 31, 29-38.

7.- H.S. SIMONS, J.W. JEFFERY (1960), "An X-ray study of pulverised fuel ash", Journal of Applied Chemistry, 10, 328-336.

8.- H.E. SCHWIETE, P. KASTANJA, U. LUDWIG, P.A. OTTO (1968), "Investigations on the behaviour of Natural and artificial puzzolans", Proc. 5th, International Symposium Cement, Tokyo IV, 135-139.

Aspects chimiques et technologiques de l'utilisation des machefers granulés lors de la fabrication du ciment

Physicochemical and technological aspects of application of furnace granulate slags in cement production

L.Y. GOLDSTEIN, Candidat ès Sciences Techniques, Institut « Guiprotsément », U.R.S.S.

Les travaux entrepris par l'institut "Guiprotsément" au cours d'une série d'années sont liés à l'élaboration des bases physico-chimiques et technologiques de l'utilisation dans la fabrication du ciment des mâchefers granulés obtenus lors de la combustion des différents combustibles solides de l'URSS dans les foyers énergétiques avec évacuation des mâchefers à l'état liquide.

On a étudié l'activité des mâchefers en fonction de leur composition chimique et minéralogique ainsi que des particularités structurales du laitier vitreux. Lors de la combustion de certains charbons bruns, dans les mâchefers obtenus peut se cristalliser, outre C_2S, la phase alitique. On a montré la possibilité de fabriquer le ciment portland et les ciments portlands de mâchefer avec utilisation des mâchefers en tant qu'additions actives. On a révélé certaines propriétés physiques des mâchefers granulés, qui ont une grande importance dans la pratique. On a envisagé également les possibilités d'utiliser les mâchefers en qualité du constituant du mélange cru du ciment.

On a mis au point les schémas types d'utilisation des mâchefers dans la fabrication du ciment.

Over a number of years the Giprocement Institute is engaged in research works aimed on development of physicochemical and technological fundamentals for application in cement production of furnace granulated slags as a product of burning various solid fuels of the USSR in energy furnaces with wet slag disposal.

The subjects studied in the process of the research were activtity and other properties of furnace slags depending on their chemical and mineralogical composition as well as structural peculiarities of slag glass.

Experimental and commercial scale works carried out have proved it practicable to produce portland cement and portland blast-furnace slag cement for various purposes using furnace slags as active additives.

Some physical properties and characteristic features of furnace slags have been revealed which have practical significance as regards technological peculiarities of applying them;

A typical diagram of a plant for taking from the steam electric station and dispatching for consumers of furnace granulated slag of low water content without forced dewatering (drying) has been evolved. Besides typical diagrams have been elaborated for utilizing furnace slags with due account for the ability of these slags to a higher evaporation when stored.

Potentialities of furnace slag application as a component of cement raw mix were also under consideration.

Involving these furnace slags into the rank of the traditional cement materials will contribute to the expansion of the raw material base of the cement industry.

Il est connu (1,2) que les mâchefers granulés sont les produits d'un brusque refroidissement dans l'eau de la partie minérale fondue des combustibles solides, qui se forme lors de la combustion de ces derniers dans les foyers énergétiques avec évacuation des mâchefers à l'état liquide. Une série de centrales thermiques équipées de puissants générateurs de vapeur fonctionnent actuellement en U.R.S.S. avec évacuation des mâchefers à l'état liquide. Les mâchefers à l'état liquide. Les mâchefers se présentent en général sous forme de granules sombres et denses dont les dimensions varient de 0,15 à 15-20 mm; parfois ils ont une forme de plaques et de fils de dimensions de 30 à 35 mm.

La composition chimique de mâchefers granulés est déterminée par les particularités de la composition de la partie minérale des combustibles solides et varie donc (en fonction du type de combustible) dans de très larges limites (1).

Il faut noter que les compositions chimiques des mâchefers se distinguent quelque peu de la composition de la partie minérale des combustibles solides correspondants. Cette distinction s'explique par une certaine redistribution des constituants de la partie minérale du combustible entre le laitier liquide et les cendres volantes. A la différence des cendres volantes, les laitiers ayant les compositions basiques ne contiennent pas de CaO libre et en général n'ont pas de perte de calcination (i.e. ne contiennent pas de particules non brûlées du combustible). La particularité caractéristique de la composition chimique des mâchefers est une teneur élevée (jusqu'à 20 % et meme plus) en oxydes de fer, principalement sous forme bivalente (FeO).

L'absence de conditions de cristallisation équilibrée et un brusque refroidissement des laitiers fondus conduisent à ce que les mâchefers ont en général une structure vitreuse. Dans la phase vitreuse peuvent prédominer les domaines polymérocristallitiques de compositions soit mullitique (teneur en CaO jusqu'à 10%), soit mélilitique ainsi que wollastonitique (teneur en CaO de 10 à 40 %), parfois gehlénitique (teneur en CaO de 40 à 50%). Les phases cristallines peuvent être représentées par la mullite, la gehlénite, la pseudowollastonite, la monticellite ferreuse, le silicate β-dicalcique. La teneur en ce dernier des laitiers schistocendreux peut atteindre 60 à 70 % (fig.1). Lors de la combustion dans les foyers à décrassage en phase liquide de certains charbons dont la partie minérale contient une quantité élevée de CaO, la phase alitique inhabituelle pour les mâchefers peut se cristalliser dans ces derniers (fig.2).

Fig.1. Microstructure des mâchefers granulés schistocendreux (B-bélite, lumière réfléchie, X200)

Compte tenu d'une ressemblance déterminée des caractéristiques chimico-minéralogiques des mâchefers et des laitiers de haut fourneau granulés (en présence de différences tout à fait évidentes avant tout dans la teneur des oxydes de fer) on ne peut pas s'attendre aux différences de principe brusques dans le déroulement des processus de durcissement et les produits basiques d'hydratation des ciments contenant les laitiers de haut fourneau et les mâchefers. Ce point de vue est confirmé par les résultats du travail (3).

Fig.2. Microstructure des mâchefers granulés à alite (A-alite, B-bélite, lumière réfléchie, X200)

Il est naturel que l'activité et d'autres propriétés des machefers soient le mieux caractérisées par leur composition chimico-minéralogique. Toutefois pour plus de commodité on se sert également de caractéristiques modulaires bien connues malgré le caractère conventionnel de ce procédé.

A l'Institut Guiprotsément on a procédé à l'étude de l'activité des mâchefers en fonction de leur composition chimique et minéralogique ainsi que des particularités structurales du verre de laitier.

On a montré en particulier que

1. Avec l'accroissement des valeurs du module de basicité des laitiers (rapport % CaO + % MgO à % SiO_2 + % Al_2O_3) jusqu'à 1,0 pour les valeurs constantes du module d'activité (rapport % Al_2O_3 à % SiO_2) on observe un accroissement de la résistance des ciments à leur base. Un accroissement ultérieur des valeurs du module de basicité s'accompagne d'une certaine diminution de l'activité des laitiers.

2. Avec l'augmentation de la teneur en Al_2O_3 (l'accroissement des valeurs du module d'activité jusqu'à 0,6) l'activité des laitiers augmente. Un accroissement ultérieur des valeurs du module d'activité entraine une diminution de l'activité.

3. Les études physico-chimiques ont montré que la diminution de l'acttivité des machefers vitreux qui se distinguent par la teneur élevée en Al_2O_3 (dans les limites de 21 à 28%) était liée à la modification structurale interne du verre de laitier.

Avec l'augmentation de la teneur en CaO (et respectivement avec la diminution de la teneur en Al_2O_3 et SiO_2) a lieu une modification structurale essentielle des laitiers liée à la dépolymérisation de la carcasse alumo-oxygénée du verre de laitier. On observe en meme temps le passage d'une partie d'ions aluminium de la coordination tétraédrique à la coordination octaédrique avec la diminution de l'énergie de liaison Al-O. Ceci conduit à une diminution de la stabilité chimique et par conséquent à un accroissement de l'activité hydraulique des laitiers (et respectivement des ciments à leur base) (4).

4. L'augmentation de la teneur en fer divalent des laitiers basiques jusqu'à 4% influe peu sur leur activité. Un accroissement ultérieur de la teneur des laitiers en FeO diminue leur activité. A la différence des laitiers basiques une diminution de l'activité des laitiers acides est moins intense (fig.3).

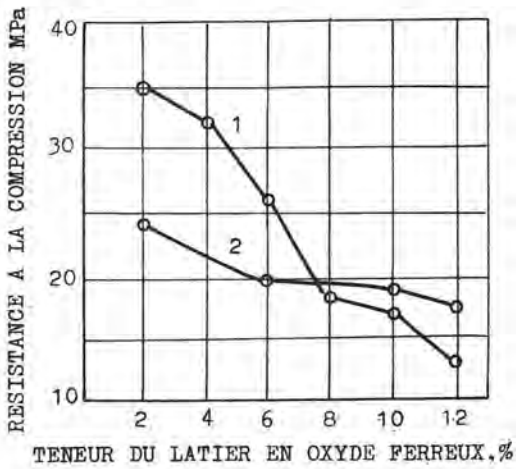

Fig.3. Variation de l'activité des ciments à base des machefers avec l'augmentation de la teneur de ces derniers en oxyde ferreux:
1-Ière série (CaO=48,5 à 48,7%;Ma=0,5);
2-IIième série (CaO=36,3 à 36,5%;Ma=0,5)

En se fondant sur les résultats des travaux expérimentaux et industriels et des travaux d'étude aux cimenteries de Krasnoiarsk et Timluïsk on a démontré qu'il est possible d'utiliser les machefers granulés basiques et acides pour la production tant du ciment portland avec additions minérales activès que du ciment portland de laitier (ordinaires et hydrotechniques, à exothermie abaissée).

Le Tableau 1 donne les caractéristiques comparatives de résistance des ciments portlands de laitier hydrotechniques de la cimenterie de Krasnoïarsk avec addition du machefer (centrale électrique régionale d'Etat Nazarovskaïa) et du laitier de haut fourneau (combinat métallurgique de Magnitogorsk). Les ciments avec addition du machefer ont un dé-

TABLEAU 1

Laitier	Teneur, %			Limite de résistance (MPa) après			
	laitier	SO_3	R_{008}	à la flexion		à la compression	
				7 jours	28 jours	7 jours	28 jours
Mâchefer	35,3	1,24	10,8	4,03	5,32	22,5	39,9
Laitier de haut fourneau	35,8	1,57	10,7	3,97	5,67	23,5	38,1
Mâchefer	37,9	1,75	7,2	3,72	5,18	24,2	40,0
Laitier de haut fourneau	37,8	2,23	11,2	3,56	5,51	18,4	35,2

Nota: La teneur du clinker en C_3S est de 49 à 50%.
La teneur en CaO du mâchefer est de 34,5 à 36,5 % et du laitier de haut fourneau de 40 à 42 %.

gagement de chaleur beaucoup plus petit que celui des ciments au laitier de haut fourneau (3).

Le tableau 2 donne les caractéristiques de résistance du ciment portland de laitier de la cimenterie de Timluïsk avec addition de mâchefers acides de la centrale électrique Goussinooziorskaïa.

Au cours des travaux expérimentaux et industriels on a montré que les mâchefers provenant des crassiers des centrales électriques thermiques et amenés aux cimenteries possédaient une constance tout à fait suffisante de la composition chimique et de phase. On a relevé certaines propriétés physiques spécifiques des mâchefers granulés ayant une grande importance pratique du point de vue des particularités technologiques de leur utilisation. Par exemple, on a montré que les mâchefers absorbent l'eau au moindre degré (par rapport au laitier de haut fourneau) et la cède beaucoup plus facilement non seulement lors du séchage mais au cours du stockage ordinaire (Tableau 3).

La comparaison directe de ces laitiers à l'aide de la méthode de porosimétrie à mercure a montré que la porosité intégrale du mâchefer était beaucoup plus petite que celle du laitier de haut fourneau (fig.4). Il importe de noter que la différence de porosité des laitiers comparés se conserve lors du broyage jusqu'à R_{008}=15%. Le mâchefer peut donc être considéré comme addition pour le ciment, qui exige une petite quantité d'eau.

Sur la base de ces données on a mis au point le schéma type de l'installation pour le prélèvement sur les centrales thermiques et l'expédition aux consommateurs des mâchefers granulés à basse humidité sans leur déshydratation forcée (séchage). On a également élaboré les schémas types de l'utilisation des mâchefers aux cimenteries, qui tiennent compte des particularités physiques indiquées de mâchefers.

Avec le passage à la combustion, pour

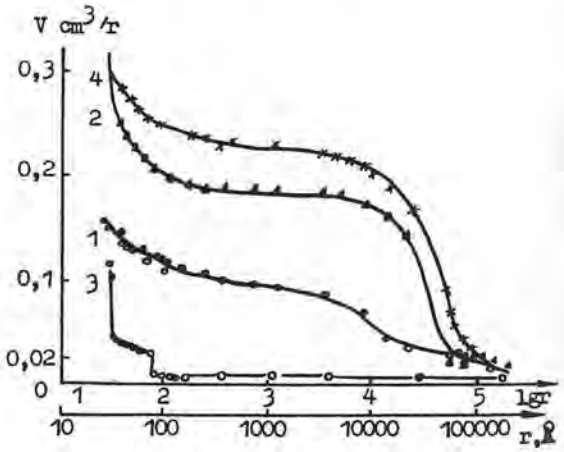

Fig.4.Porosigrammes comparatifs du mâchefer et du laitier de haut fourneau granulés : 1-laitier de haut fourneau; 2-laitier de haut fourneau broyé; 3-mâchefer; 4-mâchefer broyé

l'évacuation des laïtiers à l'état liquide, d'une série de charbons perspectifs de la Sibérie, en particulier des charbons du gisement Bérézovskoïé avec une teneur élevée de la partie minérale en CaO, dans les mâchefers, comme il est indiqué ci-dessus, peut apparaître une nouvelle phase cristalline fortement basique (C_2S) qui assure à ces mâchefers une activité hydraulique élevée (Tableau 4).

En ce qui concerne l'utilisation des mâchefers en tant que constituant du mélange cru, ces problèmes doivent être résolus de

TABLEAU 2

Teneur, %			Résistance (MPa) après			
laitier	SO_3	R_{008}	à la flexion		à la compression	
			7 jours	28 jours	7 jours	28 jours
30,8	2,01	4,08	4,58	6,16	32,4	49,8
30,1	1,76	8,4	4,15	5,56	28,3	42,9
30,1	2,22	12,2	4,14	5,34	25,5	38,2

Nota: La teneur du clinker en C_3S est de 60 à 65%.
La teneur du laitier en CaO est de 4 à 5%.

TABLEAU 3

Temps d'écoulement de l'humidité, heures	0	0,25	0,5	1,0	2,0	4,0	8,0	24,0
Humidité: du machefer (centrale électrique Nazarovskaïa)	18,5	12,0	7,1	6,6	6,4	5,9	5,0	2,5
du laitier de haut fourneau (combinat de Magnitogorsk)	17,3	13,8	10,8	9,9	8,7	7,9	7,6	6,3

TABLEAU 4

Teneur du ciment en laitier,%	S des constituants (machefer: clinker), cm^2/g	Résistance, MPa, %			
		à la flexion		à la compression	
		7 jours	28 jours	7 jours	28 jours
0	3310	4,79/100	5,79/100	23,9/100	33,8/100
60	3320:3310	4,64/97	6,37/110	24,9/104	40,8/120
80	3320:3310	4,84/101	5,04/87	22,8/95	34,0/100
100	3500	3,10/65	5,25/91	13,3/56	25,1/74

Nota: Composition du machefer (%) : SiO_2 - 18,62; Al_2O_3 - 8,46; Fe_2O_3 - 3,96 ; FeO - 2,15; CaO -53,88; alite - 36,0 ; bélite - 31,0.

façon concrète et avant tout du point de vue de l'efficacité technologique et économique de cette utilisation. On doit alors tenir compte du fait que dans une série de cas pour obtenir le clinker de composition de ciment portland normale il faut introduire dans le mélange cru de grandes quantités d'additions de correction. Les études montrent qu'il est plus rationnel d'utiliser à cette fin les machefers à teneur très élevée en CaO ou simultanémenet à teneur élevée en CaO et en Al_2O_3 (1).

L'utilisation des machefers granulés comme matériaux de ciment traditionnels permettra dans certains cas d'obtenir un effet technico-économique important et contribuera à l'élargissement des ressources de matières premières de l'industrie du ciment.

BIBLIOGRAPHIE

1.Goldstein L.Y., Steiert N.P. Utilisation des cendres et des machefers dans la production du ciment. L.,Stroïizdat,1977.

2.Travaux du VI^{ième} Congrès international sur la chimie du ciment, tome III.M., Stroïizdat, 1976. Auteurs: S.D.Okorokov, L.Y.Goldstein, K.V.Gladkikh, K.B.Freïdine.

3. Izvestia des écoles supérieures, série "Construction et architecture", n°6,1971, Auteurs: A.V.Volgenski, B.N.Vinogradov, K.V.Gladkikh, K.B.Freïdine.

4.Okorokov S.D., Goldstein L.Y., Andréev V.V. Travaux de la VIIième Conférence sur le béton et le béton armé en U.R.S.S. L., Stroïizdat, 1972.

5.Travaux de l'Institut Guiprotsément,fasc. 40, L.,Stroïizdat, 1972.Auteurs: L.Y.Goldstein, E.A.Klimova, S.D.Okorokov,A.A.Pariiski.

Alite composition and structure state of ferrum in high-basic furnace slags

Composition de l'alite et état structural du fer dans les machefers à haute basicite

M.B. SVATOVSKAYA,
M.M. SYTCHEV,
L.Y. GOLDSTEIN, Guiprotsement, Itl Lensovet, U.R.S.S.

Lors de la combustion à haute température des charbons du Bassin de Kansk-Atchinsk on obtient des machefers qui se distinguent par l'activité hydraulique élevée. La composition des phases des machefers: alite (jusqu'à 35%) et bélite (jusqu'à 53%). Les études instrumentales montrent que d'après sa caractéristique cristallochimique l'alite se rapporte à la modification hautement symétrique et contient les quantités élevées des ions aluminium et magnésium.

Le rapport stoechiométrique de CdO à SiO_2 dans sa composition était de 3,15 à 3,20. L'état structural du fer bivalent et trivalent dans ces machefers fut étudié sur une série de compositions synthétiques avec le rapport de Fe^{+3} à Fe^{+2} de 1,66 à 0,26. On a étudié les machefers de composition mélilitique: vitreux et cristallins. On a montré que l'amorphisation du système s'accompagne d'une diminution de symétrie de l'entourage local des ions Fe^{+2} et d'une augmentation de symétrie de Fe^{+3}. On a révélé que Fe^{+3} et Fe^{+2} entrent dans la structure de la géhlénite lors de la substitution partielle aux ions Al^{+3} des ions Fe^{+3}. Les résultats obtenus ont permis, dans une certain mesure, d'élucider le mécanisme de la décomposition hydrolytique des machefers lors de leurs interaction avec de l'eau.

When burning at high temperatures coals of certain deposits of the Kansko-Achinsk basin one obtains slags of high hydraulic activity. The phase composition of such slags includes high-basic calcium silicates - alite (up to 35%) and bélite (up to 53%). It has been ascertained through instrument examinations of the alite phase extracted from the furnace slag in a monomineral form by means of a heavy fluid centrifuge process that in its crystallochemical characteristics alite can be ralated to the high-symmetrical modification.

It has been found out as well that furnace slag alite includes a higher amount of aluminum and magnesium ions.

The stoichiometric ratio between CaO and SiO_2 in the furnace slag alite was in the order of 3.15-3.20. The structure state of bivalent and trivalent ferrum in the furnace slags of the Kansko-Achinsk basin was studied on a series of synthetic compositions with a Fe^{+3} to Fe^{+2} ratio varying from 1.66 to 0.26. The investigations were conducted applying NGR spectroscopy. Slags of melilite composition, both glass-like and crystalline, were also under examination. The study showed that the amorphous-prone state of the system is characterized by reduction of the symmetry of the local surrounding of Fe^{+2} ions and by increase of the Fe^{+3} symmetry. It was revealed that Fe^{+3} and Fe^{+2} are a part of the gelenite structure with partial replacement of Al^{+3} ions by Fe^{+3} ions. The results obtained made it possible, to a certain degree, to clear up the mechanism of the hydrolytic decomposition of furnace slags when reacting with water.

High-temperature combustion of coals of the Kansko-Achinskii deposit with removal of liquid slags and subsequent grinding of the silicate melt yields a product which is characterized by the following features:

1. Formation of high-basic calcium silicates, alite and belite.

2. The presence of considerable amounts (3-16%) of ferrous oxide.

The appearance of high-basic calcium silicate (alite) in the composition of a fuel slag, is observed for the first time, and it was interesting to examine the composition and structure of this slag. The alite phase was isolated in mineral form by separation in heavy liquids [1]. For comparison the alite phase was also separated from clinker obtained in the traditional way by sintering and from melted clinker synthesized from calcium carbonate and mineral fraction of Estonian fuel shales. The chemical compositions of the specimens are presented in Table 1.

The composition of alite phase was determined from the difference in content of the main components in fractions enriched with alite and ferrite components.

Separation of the silicate component from the ferrite one was carried out in several stages (extraction in absolute alcohol selective treatment with solvents separation in high-density liquid (ρ=3.32). Due to the specific morphological characteristic of the fuel slag special attention was devoted to selection of solvents. Further enrichment of the phases was carried out by repeated centrifugation of specimens in liquids of various density from ρ=2.49 to ρ=3.32. The degree of enrichment was monitored by microscopic examination. Phases were obtained with the degree of monomineralization in the range of 94-96%.

Chemical compositions of the isolated alite phases are presented in Table 2. The obtained data indicate that the presence of admixture elements in the alites correletes with their presence in the starting material (Table 1).

The content of Mg^{2+} and Al^{+3} in the alite obtained from the fuel slag is higher than in similar phases extracted from the sintered and melted clinkers. The amount of Fe^{+3} cations corresponds to the values determined by instrumental methods [2]. The stoichiometry of the alite phases corresponds to values of 3.04-3.20. Enhanced concentration of Al^{+3} and Mg^{+2} ions in the alite of fuel slag may be connected with high temperature level during combustion of high-calcium coals and also with increase of the degree of inequilibrium of silicate phases due to rapid cooling of the melt.

Crystallochemical study of the fuel slag alite by X-ray diffractometry and optical microscopy in transparent glass cells (Fedorov's table) showed that the phase under study belongs to the highly symmetrical modification [3]. According to several researchers [4] crystallization of alite in the highly symmetrical modification is one of the causes of enhanced hydraulic activity.

Fig.1. Microphotograph of fracture surface of alite-containing fuel slag, electron microscope, carbon replace X10000. The block submicrostructure of alite is distinctly revealed

Estimation of the crystalline microstructure of the fuel slag alite by electron microscopy showed (Fig.1) prevalence of fine and medium-block structure that, as established previously [5], facilitates forma-

Table 2

Chemical Composition of the Alite Phases

Alite isolated from	Oxide content, mass. %								Molar composition
	SiO_2	Al_2O_3	CaO	MgO	Fe_2O_3	TiO_2	Cr_2O_3	MnO	
Fuel slag	23.07	2.99	68.95	2.80	1.23	no	0.12	0.44	$C_{3.2}SiFe_{0.02}Al_{0.09}Mg_{0.02}Mn_{0.02}Cr_{0.002}$
Melted clinker	18.89	2;75	58.84	not determined	1.20	not determined	not determined	not determined	$C_{3.04}SiFe_{0.02}Al_{0.09}$
Sintered clinker	23.82	2.39	70.43	1.40	1.55	0.51	no	no	$C_{3.2}SiFe_{0.02}Al_{0.09}Mg_{0.02}Mn_{0.02}Cr_{0.002}$

Chemical Composition of Specimens Table 1

Material	Oxide content, mass;%											SF
	SiO_2	Al_2O_3	Fe_2O_3	FeO	CaO	MgO	TiO_2	SO_3	S'	MnO	K_2O	Na_2O	
Sintered clinker	22.31	4.42	4.86	-	67.3	0.80	-	0.03	-	-	0.15	0.07	0.93
Melted clinker	21.07	5.55	3.49	1.35	62.65	3.50	0.42	0.22	0,05	-	0.13	0;04	0.89
Fuel slag	18.62	8.46	3.96	2.15	53.88	5.79	0.48	0.90	-	1.19	0.10	0.13	0.74

tion of a more dispersed product during mechanical grinding.

The valent state of iron was studied by nuclear gamma-resonance spectrometry. A series of synthetic slag compositions with calcium oxide content of 38-50% was studied. The Fe^{+3}/Fe^{+2} ratio varied from 1.86 to 0.26. Phase composition changed from glass to crystalline. Measurements were carried out at room temperature in combination with a pulse analyzer AI 40-96. ^{57}Co in palladium was used as a radiation source, activity 10 mC. Variation of Fe^{+3}/Fe^{+2} ratio was accompanied by change of the shape of the Mossbauer spectrum (Fig.2). The Mossbauer spectrum of high-basic fuel slag with Fe^{+3}/Fe^{+2}= =1.86 (Fig.2a) represented by cristalline silicates displayed two quadrupole doublets correspondings to Fe^{+3} in octaand tetrahedral environment. The latter points to inclusion of Fe^{+3} into the aluminoferrite phase with substitution of Al^{+3}, which is in agreement with (6).

δ_1=0.51±0.02 mm/s; Δ_1=1.56±0.03 mm/s[FeO_6];

δ_2=0.33±0.02 mm/S; Δ_2=1.48±0.03 mm/s[FeO_4].

Amorphization of the system is accompanied by change of the shape of Mossbauer spectrum (Fig.2b) and indicates increase of local Fe^{+3} symmetry and lowering of local Fe^{+2} symmetry.

The spectrum of glass-like fuel slag of melilite composition with Fe^{+3}/Fe^{+2}=0.35 is

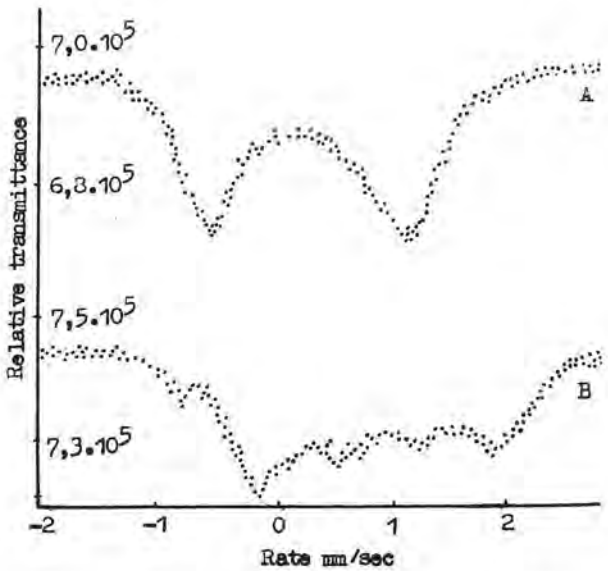

Fig.2. Mossbauer spectra of High-Basic fuel slags: a-crystalline, Fe^{+3}/Fe^{+2}= =1.86; b - glass-like, Fe^{+3}/Fe^{+2}=0.35

represented by supurposition of three quadrupole doublets: two doublets of trivalent iron .

δ_1=0.22±0.02 mm/s; Δ_1=1.53±0.03 mm/s

δ_2=0.52±0.02 mm/s; Δ_2=0.60±0.03 mm/s;

and one doublet of Fe^{+2}

δ=1.15±0.04 mm/s Δ=2.03±0.03 mm/s.

Analysis of this spectrum allows to assume that Fe^{+3} replaces Ca^{+2} in tetrahedral sites of gehlenite glass. Possessing a strong field, it excerts a considerable polarizing effect on the Si-O-Me bond. The latter hinders processes of hydraulic decomposition of high-basic slags containing bivalent iron with water.

CONCLUSIONS

1. The composition, crystal-optical characteristics and microstructure of alite phase isolated from high-basic fuel slag were studied by chemical methods, optical and electron microscopy.
2. NGR spectroscopy was employed to elucidate the structural state of bi and trivalent iron in glass-like and crystalline fuel slags.
3. An explanation of the reduced hydraulic activity of glass-like fuel slags containing iron in +2 oxidation state is given.

REFERENCES

1. Svetovskaya M.B.,Kas'yanova G.N.,Sychev M.M. et al. Separation of mineral phases in heavy liquids. Tsement, 6 (1979).
2. Midgley H.G., Paper at the Fifth Internation Symposium on Chemistry of cement, Tokio, 1968.
3. Svatovskaya M.B., Kas'yanova G.N.,Sychev M.M et al. Clinker and slag alites, Zh. Priklad. Khim.,5 (1977).
4. Ono I., Kavamura Sh.? Sodo I., Fifth International Congress on Chemistry of Cement, Stroiizdat, 1973 (in Russian).
5. Papiashvili U.N., Candidate's Dissertation, Moscow, 1974.
6. Grant R.W. Nuclear Electric Field Gradient at the Iron Sites in $Ca_2Fe_2O_5$ and Ca_2FeAlO_5. J.Chem.Phys., 51,3 (1969),1156.

Influence des matériaux analogues aux pouzzolanes sur la formation de la structure du ciment durci

Influence effects of pozzolana-like materials on structure formation of cement stone

L. KOURASSOVA, Collab. Sc. Super. (NIIZhB, Moscou)
Z. LARIONOVA, Chef de Laboratoire, U.R.S.S.

Les fractions finement dispersées de la plupart des agrégats poreux sont les analogues des pouzzolanes dont les propriétés hydrauliques dépendent du degré de leur dispersité, de leur composition de phase et de leur structure.

Ayant pris comme un échantillon d'exemple le kéramsite dont la composition de phase et la structure sont différentes dans les parties de granule différemment éloignées de son centre, on a étudié l'influence de ses fractions finement dispersées sur la formation de la structure du ciment durci. Est étudié la structure des grains de kéramsite disposés dans des parties différentes de granule. Est mise en évidence la microdureté du ciment durci contenant les particules du kéramsite (ainsi que la microdureté de ces particules, proprement dit) et la phase essentielle de formation de sa structure favorisant l'accroissement de la résistance du ciment durci et son imperméabilité à l'eau.

Est mis à jour le mécanisme de l'interaction des particules du kéramsite finement dispersées avec le ciment durci. Ce mécanisme consiste en formation de la couche de contact du ciment durci, compactée et chimiquement modifiée.

Fine-dispersed fractions of most of porous aggregates are similar to those of pozzolanas the hydraulic properties of which depend on the degree of their dispersity, phase composition and structure. Ceramisite being taken as a specimen of a mineral with, granules noted for their phase composition and structure, the effects of its various fine-dispersed fractions on the structure formation of the cement stone has been studied. The structure of ceramsite poarticles from various parts of its granule.

Microhardness of cement stone with ceramsite particles in it has been revealed, as well as the basic structure forming phase that increases its strength and water impermeabylity.

The mecanisme of physico-chemical interaction between the fine-dispersed ceramsite particles and cement stone has been brought to light.

This mechanism consists in formation of compacted, chemically transformed contact layer of cement stone.

Les fractions finement dispersées de la plupart des agrégats poreux sont les analogues des pouzzolanes dont les propriétés hydrauliques dépendent du degré de leur dispersité, de leur composition de phase et de leur structure. Ayant pris comme un échantillon d'exemple le kéramsite dont la composition de phase et la structure sont différentes dans les parties de granule différemment éloignées de son centre, on a étudié l'influence de ses fractions finement dispersées sur la formation de la structure du ciment durci.

L'étude complexe physico-chimique des composants finement dispersés des zones extérieure et intérieure de granule de kéramsite a été réalisé pour la première fois. Une telle étude différentielle est conditionnée par le fait qu'en fonction de la technologie de la préparation du béton, les uns ou les autres y peuvent prédominer.

Il a été constaté que la composition de phase, la microstructure, la porosité, la masse spécifique et volumique des fractions finement dispersées de zone intérieures et de zone extérieure du kéramsite sont différentes.

La composition de phase de la zone extérieure se diffère principalement de celle de la zone intérieure par la présence de la forme oxyde de fer, ce qui amène à la formation dans cette zone des minéraux de hématite - Fe_2O_3, magnétite - Fe_3O_4.

L'activité hydraulique (déterminée d'après l'absorption de CaO de la solution) des particules de la zone extérieure, d'habitude, est plus grande que celle des particules de la zone extérieure, simultanément leurs masses volumique et spécifique est moins à 4%, S_{sp} étant 3000 cm^2/g, et à 7%, S_{sp} étant = 7000 cm^2/g.

Les particules de la zone extérieure se caractérisent par une surface incohérente et avec une grande quantité des pores 2 mkm. Les particules de la zone intérieure de kéramsite se distinguent par une surface régulière et dans ces particules les pores rares, mais ayant les dimensions plus grandes, égales à 10-12 mkm, prédominent.

La microdureté des cloisons des deux sortes des particules du kéramsite est à peu près égale et est comprise entre 10000 et 14000 MPa en fonction de la composition de phase de la phase de verre du kéramsite. Les valeurs citées correspondent à la microdurecté de minéraux tels, que quartz; ces valeurs sont 2,5 fois plus grandes que les valeurs de microdureté de minéraux de clinker et 10-20 fois plus grandes que la masse hydraté du ciment durci.

Cette différence des particules conditionne la différence de leur action sur le ciment durci, et ce fait, ensuite, amène à une évolution bien différente du processus de la formation de structure.

Par les expériments réalisés spécialement est mis en évidence que la présence des particules finement dispersées du kéramsite (également de la zone extérieure et de la zone intérieure) provoque les changements considérables dans la composition de phase du ciment durci: se forme le hydro-grenat bas-siliceux-$C_3A(F)S\ 0,5^{H}x$, abaissela quantité de $Ca(OH)_2$; avec cela la phase essentielle de hydrates est CSH(I). L'application d'un complexe des méthodes physico-chimiques a permis de mettre en évidence la différence de microstructure du ciment durci additionnée et non du kéramsite. Dans le dernier cas la masse hydratée faiblement cristallisée a une structure incohérente et des fissures de largeur égale à 0,5 mkm. Le ciment durci contenant les particules des zones intérieure et extérieure du kéramsite se distingue par une compacité plus grande, par l'homogénéité de la microstructure il n'y a presque pas de fissures; la quantité des pores est diminuée. Les particules corrodées du kéramsite sont liées avec la phase essentielle des hydrates par des différentes formes cristallines (Fig.1).

Il a été établi que les particules finement dispersées du kéramsite font diminuer la porosité intégrale du ciment durci et autant plus considérablement que leurs dispersité s'accroit; avec cela la quantité des macropores diminue, particulièrement quant aux macropores ayant un rayon R > 5000 A, ce fait doit amener à l'accroissement de l'imperméabilité à l'eau. Dans les compositions contenant les particules avec S_{sp}=2700 cm^2/g (et également sans particules) le maximum est dans les pores ayant un rayon R=100 A et 1250 A. Avec S_{sp}=7000 cm^2/g dans la composition contenant les particules de la zone extérieure R étant, égal à 1250 A le maximum, diminue et la formation d'un nouveau ma-

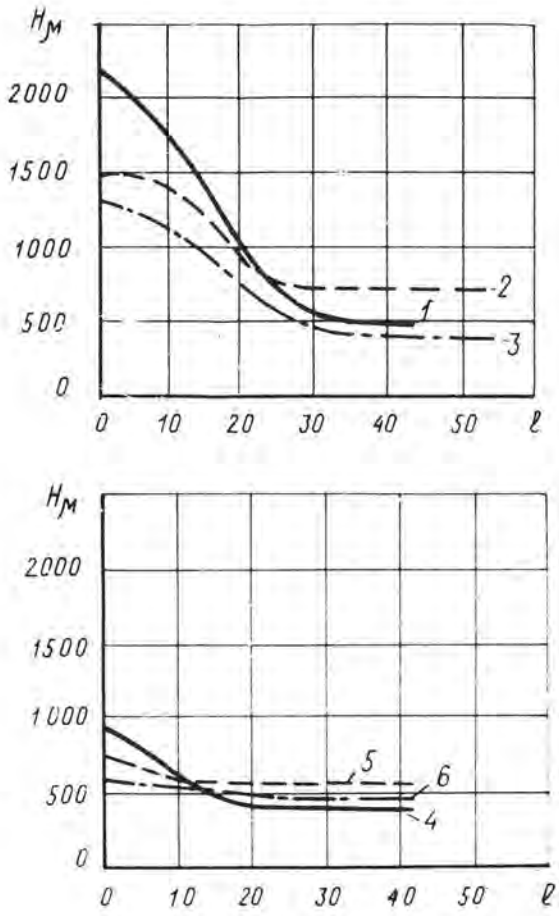

Fig.1. La variation de microdureté $H_м$ (en MПa) lorsque la distance l (en mkm) entre la ligne de contact et les grains ayant les dimensions égales 0,15 mm (1), 0,25 mm, 0,5 mm(3), 1,2 mm(4), 2,5 mm (5), 5 mm (6), s'accroît

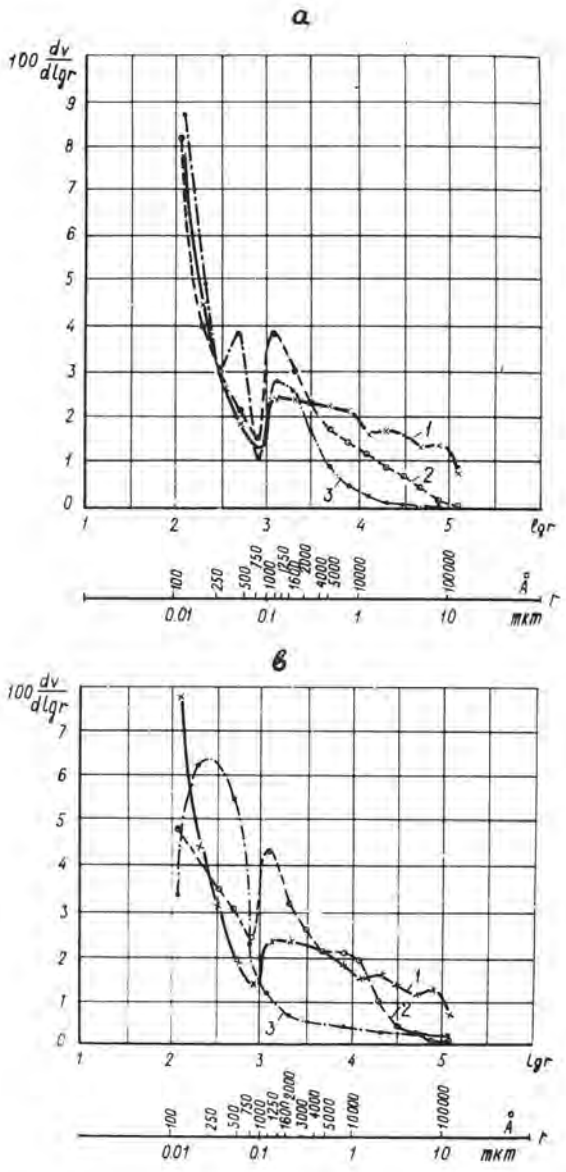

Fig. 2. Programmes des mortiers de cimentables sans particules (1) et avec les particules de la zone exterieure (a) et de la zone intérieure (b) du Keramsite, leure surface spécifique S_{sp} étant égale á 2700 cm^2/g (2) et 7000 cm^2/g (3): v - volume des pores; r - rayon des pores

ximum avec le R=750 A en résulte; dans la composition contenant les particules de la zone intérieure il y a un maximum dans les pores ayant R=200-250 A (Fig.2). Par l'étude donnée a été déterminé le mécanisme de l'interaction physico-chimique des grains hydrauliquement actifs du kéramsite et du ciment durci. Il consiste en formation de la couche de conde contact du ciment durci qui a des modifications chimiques et dont le largeur est égal à 10-30 mkm. Son microdureté autour les particules 10 mkm, qui est 4-7 fois p plus grand que le microdureté de la masse hydratée en volume, est conditionné par la présence de nouvelles formations et des particules plus petites du kéramsite, joints epitaxiquement avec le ciment durci. Le volume des zones consolidées (particulièrement au contact avec les particules de la zone extérieure) est 10-100 fois plus grand que le volume des particules et accroit la résistance du ciment durci. C'est pourquoi l'influence positive des particules de la zone extérieures 10 mkm se manifeste meme si la teneur en ces particules est égale à 1-2% de la masse du ciment. Avec l'augmen-

tation des dimensions des grains la largeur des zones ne change pas, et le volume relatif diminue. Donc, les particules de la zone extérieure du kéramsite avec les dimensions 50 mkm et se caractérisant par leur activité hydraulique et la microstructure spécifique représentent une composante qui est la plus active dans le processus de la formation de structure. Les particules de la zone intérieure du kéramsite sont d'une moindre activité hydraulique; une action positive sont seulement les particules de 10-15 mkm, pratiquement privées de la porosité; ces particules représentent une sorte de centre de la cristallisation des unités des hydrates et sont des éléments consolidants la structure (en remplissant des espaces vides).

Donc, les résultats obtenus ont permis de mettre en évidence le rôle positif des particules finement dispersées du kéramsite dans le processus de la formation de la structure du ciment durci et d'expliquer du point de vue de physique et de chimie l'influence qu'elle exercent sur certaines propriétés techniques du ciment durci, ainsi que sur celles du béton leger.

THEME V

Ciments spéciaux

Special cements

Centres basiques sur la surface des solutions solides du silicate bicalcique

Basic centers on the surface of dicalcium silicate

KAZANSKAIA A.N.,
SYTCHEV M.M., Docteur ès Sciences Techniques, Professeur, SPIROV I.S.. Institut Technologique Lensovet de Leningrad, U.R.S.S.

Par la méthode de l'adsorption du phénol suivie d'une détermination différentielle thermique de la quantité d'une substance chimisorbitisée on a évalué la force et la concentration des centres basiques (propriétés électrono-donatrices) sur la surface du -silicate bicalcique et de ses solutions solides de type β-$C_{2,56}{}^{Sa}{}_{0,047}{}^{Cr}{}_{0,09}$ β-$C_{2,48}{}^{Sa}{}_{0,11}{}^{Cr}{}_{0,09}$.
On a décélé deux types de centres basiques correspondant de toute évidence aux groupes OH^- et O^- sur la surface.
La concentration des centres basiques sur la surface de β-C_2S dépend du traitement préalable de la surface, de la concentration et du type des constituants d'impureté. On peut se représenter que le processus d'hydratation se développe d'après le mécanisme dissociatif généralisé et acido-basique.

Intensity and concentration of basic (electron-donor properties) centers on the surface of -dicalcium silicate and its solid solutions - type β-$C_{2.56}{}^{Sa}{}_{0.047}{}^{Cr}{}_{0.09}$ and β- $C_{2.48}{}^{Sa}{}_{0.11}{}^{Cr}{}_{0.03}$ has been estimated by the method of phenol adsorption with subsequent differential-thermal defenition of the chemisorptioned substance quantity. Two types of basic centers have been discovered, having on the surface, probably, OH^- and O^- groups.
Concentration of the basic centers on the surface β- C_2S depends on previous surface processing, concentration and type of additions. One can imagine, that the hydration process developes according to the generalized dissociation and acid-basic mechanism.

La nature et la concentration des centres actifs apparaissant sur la surface des constituants de clinker au cours de la synthèse à haute température sont dues aux défauts de leur structure cristalline et à la présence de corps étrangers (1), au régime de traitement thermique et au degré de vieillissement de l'échantillon en contact avec les gaz atmosphériques (O_2,H_2O, CO_2) (2 à 4). Pour le silicate tricalcique contenant sous forme d'impureté les ions , on a révélé trois types de défauts ponctuels (5):1) centres électroniques sur les vacances d'oxygène dans les complexes de calcium-oxygène, 2) centres électroniques sur les atomes d'oxygène des tétraèdres en fragments, 3) centres lacunaires sur les atomes d'oxygène en fragments.

Dans le cadre de la théorie (6) l'apparition de centres lacunaires sur la surface des oxydes (en particulier sur le silicagel) en présence de cations étrangers, peut conduire à deux types de structure de ces centres:

1)"en pont" dans le cas des cations de valence minimale (silicagel contenant Al^{3+})

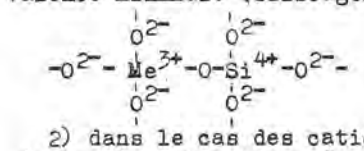

2) dans le cas des cations de valence maximale, les structures des anions-radicaux superficiels finals ayant formellement dans leur sphère de coordination une vacance cationique :

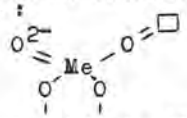

Selon la théorie d'acide base (7, 8) les centres accepteurs d'électrons sont interprétés comme centres acides de Lewis (centres α, OH^- sur la surface des alumosilicates). En présence d'eau ces centres se transforment en centres acides de Bronsted (centres β, OH^- sur la surface) ayant une capacité caractéristique de transfert du proton. Les centres donneurs d'électrons qui transmettent un doublet électronique à l'acide adsorbé (proton) sont définis comme centres basiques. Les atomes d'oxygène chargés négativement, les groupes OH^- peuvent constituer les centres basiques. D'après la fréquence de la vibration principale les groupes hydroxyles acides et basiques se distinguent peu dans les spectres infrarouges. Toutefois, lorsque ce groupe hydroxyle entre en réaction, les différences dans son acidité commencent à se manifester de façon sensible (9).

Selon la théorie des clusters on peut simuler le centre actif avec une force différente de l'acidité de Bronsted en faisant varier dans de larges limites le potentiel d'ionisation des atomes du voisinage immédiat du centre à l'intérieur du cluster (dopage par les cations polyvalents, adsorption des molécules accepteurs et des molécules-donneurs d'électrons, etc.)(10).

La nature du centre actif définit sa réactivité dans les processus d'adsorption, d'hydratation, de polycondensation,etc.Ainsi on observe une corrélation qualitative entre la réactivité des centres lacunaires "en pont" (propriétés d'accepteur d'électrons) et la profondeur à laquelle se trouvent les niveaux accepteurs correspondants dans la zone "interdite" de l'oxyde. Les centres lacunaires finals ont les propriétés du radical libre (6). Pour les groupes OH en pont (groupes OH^- sur la surface des alumosilicates) on peut observer, lors de l'absorption de l'eau, l'adsorption à deux points conduisant à la formation des particules semblables aux ions hydroxonium adsorbés et influant sur la réaction d'échange de protons entre l'adsorbant et l'adsorbat (10):

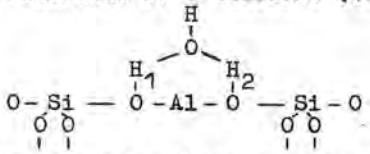

Lors de l'adsorption sur la surface du semi-conducteur (11)le complexe donneur-accepteur formé défaut-molécule adsorbée peut cesser de jouer le rôle du centre de capture de porteurs libres. S'il s'agit de l'adsorption des molécules-donneurs (H_2O)le complexe commence à jouer le rôle du centre de capture des trous. Si le trou est localisé au voisinage de ce complexe d'adsorption la déformation de la molécule d'eau adsorbée devient plus grande. La capture d'un trou aux niveaux donneurs de la molécule d'eau

conduit à la dissociation $H_2O \rightarrow H^+ + OH^-$. Le développement d'un tel processus de dissociations de l'eau aux centres actifs d'un constituant de clinker peut contribuer de façon efficace, selon M.M.Sytchev (12), à la pronotisation des liaisons dans ce constituant.

Par la méthode d'adsorption du phénol (13) suivie de la détermination thermique différentielle de la quantité d'une substance chimisorbée (7) on a évalué la force des centres basiques (propriétés de donneur d'électrons) et on a mesuré leur concentration. Au cours de l'étude de $\beta - C_2S$ (B_2O_3 stab.)les solutions solides de type $\beta - C_{2,56}{}^{SA}O_{0,047}{}^{Cr}O_{0,09}$, $\beta - C_{2,48}{}^{SA}O_{0,11}{}^{Cr}O_{0,03}$ et CaO (étalon de haute basicité) avec les particules de dimension inférieure à 60 μ sous forme de comprimés de poids de 0,5 g étaient traitées dans le vide (dépression de 10^{-4} mm Hg) aux diverses températures (300 et 500 °C) pendant un temps différent (2 à 3 h), ensuite elles étaient refroidies dans le vide jusqu'à 100 °C et soumises à l'adsorption par les vapeurs du phénol (48 h à 50 °C).

La désorption du phénol était réalisée dans les conditions quasi statiques (4 h à 60 °C jusqu'au poids constant de l'échantillon et 5 h à 500 °C) et dans les conditions dynamiques (levé dérivatographique à l'aide du dérivatographe de Paulik et Erday pour la vitesse de chauffage de l'échantillon de 5 degrés/mn jusqu'à 600 °C; la valeur de la charge TG=0,5g et de la sensibilité de l'appareil d'après TG= 20 à 200, d'après ATD = =1/2 à 1/5). L'évacuation d'une plus grande partie du phénol physiquement adsorbé dans les conditions quasi statiques a permis d'augmenter la sensibilité du dérivatographe en TG et de diminuer ainsi l'erreur de mesure de la valeur de la chimisorption.

Les résultats d'étude des propriétés d'adsorption de la surface pour toutes les solutions solides à base de $\beta - C_2S$ et de CaO sont donnés dans le tableau. Il résulte de ce tableau que pour tous les objets étudiés on a décelé la présence de centres basiques (désorption du phénol chimiquement lié dans le domaine de températures de 275 à 550 °C). Dans plusieurs cas (CaO, C_2S (B_2S_3 stab.)et $C_2SAl_nCr_m$ traités à 500 °C dans le vide de 10^{-4} mm Hg pendant 3h) on a révélé deux types de centres basiques (résolution des effets endothermiques sur les courbes ATD).

Les centres basiques faibles correspondant au pic de désorption sur la courbe ATD à plus basse température sont évidemment formés par les groupes OH^- de la surface. Des centres basiques plus forts correspondent à une température plus élevée de l'effet endothermique et il se forme O^- sur la surface. Ainsi pour l'échantillon de $\beta - C_2S$ (B_2O_3 stab.) les centres basiques faibles se caractérisent par la température de désorption du phénol de 275 °C et les centres basiques forts par la température de 425 °C. Les centres les plus forts sont décelés sur la surface de CaO (température du pic de désorption de 550 °C) et pour les solutions solides, sur la surface de $\beta - C_{2,48}{}^{SA}O_{0,11}{}^{Cr}O_{0,03}$ (température du pic de désorption de 470 °C).

La concentration des centres basiques sur la surface du silicate bicalcique β et de ses solutions solides est beaucoup plus petite (0,025 à 0,066 mmol/g) que la concentration des centres basiques sur la surface de CaO (0,55 mmol/g), est en accord avec les donnéees de référence (7, 11),et dépend du traitement préalable de la surface, de la concentration et du type de constituants étrangers. La concentration des centres basiques sur la surface des solutions solides de $C_{2,56}{}^{SA}O_{0,047}{}^{Cr}O_{0,09}$ et de $C_{2,48}{}^{SA}O_{0,11}{}^{Cr}O_{0,03}$ (0,063 et 0,066 mmol/g respectivement) dépasse la même valeur pour $\beta - C_2S$ (B_2O_3 stab.) (0,060 mmol/g).

L'analyse simultanée des courbes ATD et TG du dérivatogramme a permis d'évaluer le rapport quantitatif des centres basiques de force différente d'après la quantité de chaleur nécessaire pour la désorption du phénol (7). Ainsi, la quantité relative des centres basiques les plus forts pour l'échantillon de $\beta - C_2S$ (B_2O_3 stab.;500 °C, 3 h) est de 0,0125 mmol/g pour la concentration totale des centres basiques de 0,060 mmol/g ou 21 % de la quantité totale des centres actifs de type basique.

Ainsi le silicate bicalcique et les solutions solides à base de ce dernier de type $\beta - C_{2,48}{}^{S-A}O_{0,11}{}^{-Cr}O_{0,03}$ et $\beta - C_{2,56}{}^{-S-A}O_{0,047}{}^{Cr}O_{0,09}$ possèdent une basicité sommaire très basse qui est cependant en corrélation avec leur activité dans la réaction d'hydratation (diminution fixée de la concentration et de la force des centres basiques, de l'activité hydraulique et accroissement des temps de prise dans la série) :

$$\beta - C_{2,48}{}^{SA}O_{0,011}{}^{Cr}O_{0,03} > \beta - C_{2,56}{}^{A}O_{0,047}\ {}^{Cr}O_{0,09} > \beta - C_2S\ (B_2O_3\ \text{stab.})$$

Compte tenu des données de Fiereus (2) qui a établi, dans le système silicate de calcium-eau, le fait de participation à la formation des liaisons de chimisorption des électrons dont le donneur est le crops solide, on peut se représenter que le processus d'hydratation se développe selon le mécanisme généralisé dissociatif et acido-basique (11). Dans ce cas les centres actifs (parties de surface autour de l'atome actif) sont responsables de la formation des complexes donneurs-accepteurs défaut-molécule adsorbée d'eau et de la dissociation des molecules adsorbées d'après le schéma $H_2O \rightarrow H^+ + OH^-$. Par la suite le mécanisme de la réaction d'hydratation devient analogue au mécanisme acido-basique avec le transfert d'un doublet électronique au proton sur les centres basiques de la surface (Si-O-Ca-O(H^+)). La protonisation initiale des groupes basiques dif-

TABLEAU

Propriétés basiques de la surface des solutions solides à base de β- C_2S et de CaO

Chiffre de l'objet	Conditions du traitement préalable de la surface			Propriétés basiques de de la surface	
	t, °C	p, mm Hg	τ, h	concentration des centres basiques, mmol/g	force des centres basiques (t° du pic de désorption)
β-$C_{2,56}{}^{SA}{}_{0,047}{}^{Cr}{}_{0,09}$	300	10^{-4}	2	0,025	445
β-$C_{2,56}{}^{SA}{}_{0,047}{}^{Cr}{}_{0,09}$	500	10^{-4}	3	0,063	400; 425
β-$C_{2,48}{}^{SA}{}_{0,11}{}^{Cr}{}_{0,03}$	500	10^{-4}	3	0,066	300; 470
β-C_2S (B_2O_3 stab.)	300	10^{-4}	2	0,026	420
β-C_2S (B_2O_3 stab.)	500	10^{-4}	3	0,060	275; 425
CaO	500	10^{-4}	3	0,55	180; 450; 550

ficilement polarisables - $Si\overset{=}{-}O-$ conduisant à la formation de groupements moins basiques facilite par la suite l'attaque nucléophile du type de substitution (S_{N_1} et S_{N_2}) auprès de l'atome de silicium.

BIBLIOGRAPHIE

1. Тимашев В.В., Акимов В.Г. Определение концентрации точечных дефектов в твердых растворах трехкальциевого силиката.-Тезисы докладов Всесоюзного симпоз.по кристаллохимии и фазовым соотношениям в силикатных и окисных системах. Л., 1978, с.32-33.
2. P.Fiereus, JP. Verhaegen. Propriétés nucléophiles de surfaces de silicate tricalcique. C.C.R., v.6, n°1, 1976, p.103-106.
3. P. Fiereus, J.P. Verhaegen. Induction Period of Hydration of tricalcium silicate. C.C.R., v.6, 1976.
4. P. Fiereus, J.P. Verhaegen.C.C.R., v.8, n°4, 1978, p.397-401.
5. J.Skalny, I.Jawed, H.F.W.Taylor. "Studies on hydration of cement - recent developments". World Cem.Technol., 1978,9,n°6, p.183-195.
6. Казанский В.Б. Кинетика и катализ.1978, № 2, с. 279. - Природа дырочных радиационных дефектов на поверхности окислов и их роль в адсорбции и катализе.
7. Танабе К. Твердые кислоты и основания. "Мир", 1973, с. 9.
8. Сычев М.М. Химия отвердевания и формирования прочностных свойств цементного камня. - Цемент, № 9, 1978, с. 4-6.
9. Казанский В.Б. Физические основы катализа.- Кинетика и катализ, т.XVШ, вып.I, 1977, с. II-I5.
10. Михейкин И.Д. и др. Расчет хемосорбции и элементарных актов каталитических реакций в рамках кластерной модели.-Кинетика и катализ, т.XX, вып. 2, 1979, с. 499-500
11. Киселев А.В. Кинетика и катализ. XIX, вып.6, 1978, с. 1593.
12. Сычев М.М., Сватовская Л.Б. Некоторые аспекты химической активации цементов и бетонов. -Цемент,№4, 1979.
13. Крылов О.В., Фокина Е.А. Об изменении кислотно-основных свойств поверхности. Проблемы кинетики и катализа, АН СССР, 8, 248 (1955).

Mechanical-chemical activation of mixed portland cement with increased content of technogen belite product of alumina industry

Activation mécano-chimique du ciment portland mixte à teneur élevée en produit bélitique technogène de la production de l'alumine

S.D. MAKACHEV,
V.I. AKOUNOV,
T.A. ARBEKOVA,
T.V. KOUZNETSOVA,
B.E. YOUDOVITCH, Niitsement, Moscou, U.R.S.S.

Dans la technologie ordinaire du ciment portland la teneur en produit belitique technogène de la production de l'alumine est limitée à 10-15%.

On a mis au point une nouvelle technologie du broyage et de l'activation mécano-chimique simultanés du ciment portland permettant d'augmenter la teneur en produit bélitique technogène jusqu'à 30%.

Ce ciment a une activité à l'âge de 3 jours: 257 kgf/cm^2 à la compression et 47 kgf/cm^2 à la flexion, à l'âge de 28 jours respectivement 487 kgf/cm^2 et 71 kgf/cm^2, ce qui correspond aux exigences sur le ciment portland à durcissement rapide de marque 500 d'après GOST-10178-76 (URSS).

L'activation du ciment est atteinte grâce à la combinaison optimale de deux mécanismes de broyage: de fragmentation et d'écaillage permettant d'obtenir le système dispersé ayant une composition granulométrique et une morphologie déterminées, réunissant l'état spécifique de la surface avec la destruction suffisante des particules.

It is common in portland cement technology that the content of belite technogen product is limited to 10-15%.

A new technology of combined grinding and mechanical-chemical activation of portland cement has been developed permitting for increase the content of technogen belite product up to 30%.

Such a cement has the 3-day activity: 257 kg/sm^2 compression strength and 47 kg/sm^2 bend strength; and the 28-day activity: 487 kg/sm^2 and 71 kg/sm^2 respectively, meeting the requirements for quick-hardening portland cement (brand 500, according to the USSR GOST-10178-76).

The cement activation is achieved due to optimum combination of two grinding mechanisms: cracking and shelling. This makes it possible to get the dispersed system of a particular granulometric content and morphology, thus combining the specific surface condition and satisfactory particles destruction.

RÉSUMÉ: Decrease of clinker formation and hydration activation energy at jet pulverization considerably increases the degree of utilization of potential physical and chemical energy of such clinker components as technogenic β-C_2S and provides for organizing an economic production of various-activity cement on its basis. The jet pulverization process differs from milling process with free milling bodies by the rate of crack formation in the particles approaching the sonic one and two orders as high and substantially zero mutual abrasion of the particles.

The works by M.Wilson, T.Suzuki (theory) and A;Shand (experiments) show the diagram of increase of winding of the crack path (Fig. 1) when its opening speed approaches the

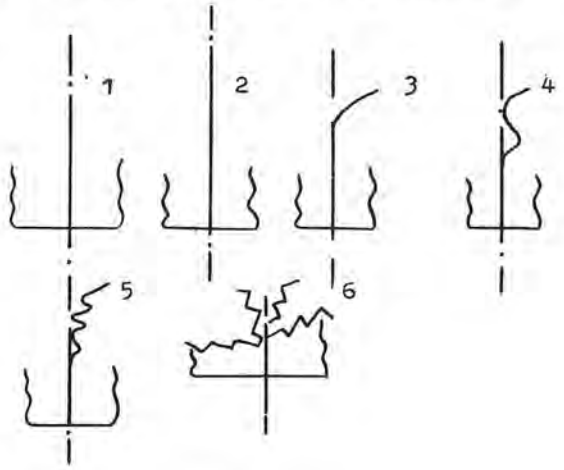

Fig.1. Crack Trajectory in Half-Plane Depending on Opening Rate: 1-0.01s; 2-0.1 s; 3-0.3 s; 4-0.5 s; 5-0.7 s; 6-0.9 s; c-average sound velocity in material

sound velocity in the solid body up to beginning of branching. Therefore, the jet pulverization products should feature a more angular shape of particles and, in particular, particles with inward angles. Investigations of the jet pulverization products with the use of a scanning electron microscope after application of an Au film show (Fig.2) that such inward angles are actually formed on the particles of clinker crushed to a specific surface of 3000 cm^2/g. The microphotos show general view of the particles left on a screen with a me size of 80 microns.

Formation of sharp edges and inward angles increases accessibility of the particle internal regions for chemical reaction, hydration in this case, and determines increased strength of the jet pulverization cements over the ball mill cements, mentioned by some of us in the report at the VIth Congress on Chemistry of Cement in 1974 which discussed production of high-strength and rapid-hardening cements.

The electron microscopy investigations reveal another characteristic feature of the jet pulverization products stemming from high energy stress in the air-pressure mills which is about one order as high (per unit volume) as that of the ball mills. We mean the mechanochemical aggregation of particles (Fig.3) which forms bridges between grains containing mainly intermediate substance in case of clinker. A similar phenomenon is observed in case of jet pulverization of a cement raw mix where the soft carbonate component (chalk) particles are main subject of aggregation.

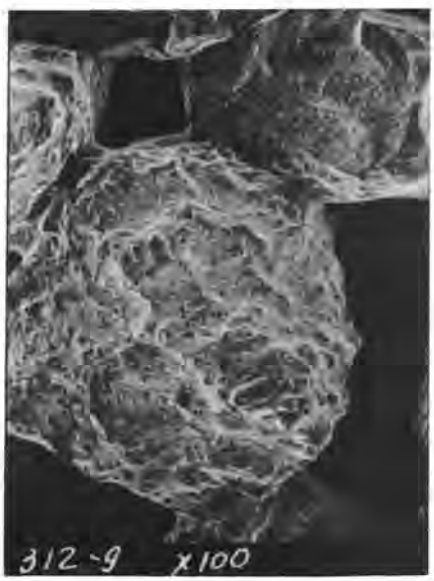

Fig.3. General View of Portland Cement Clinker Jet Pulverization Product Fraction > 80 Microns. Bridges (Jumpers) between Particles are Seen: Scale - 1 micron

The technological importance of this phenomenon as applied to cements resides in the increase of water requirements of the jet pulverization cements. The amount of

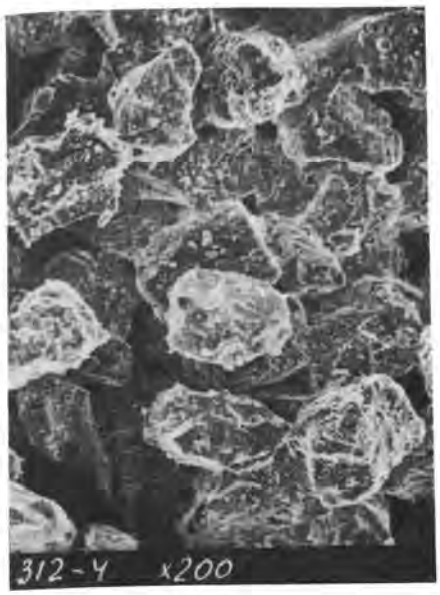

Fig. 2 a

Fig.2. General View of Portland Cement Clinker Jet Pulverization Product Fraction >40 Microns in Scanning Electron Microscope: Scale - 1 micron. Particle with Inward Angle on Top Face is Enlarged

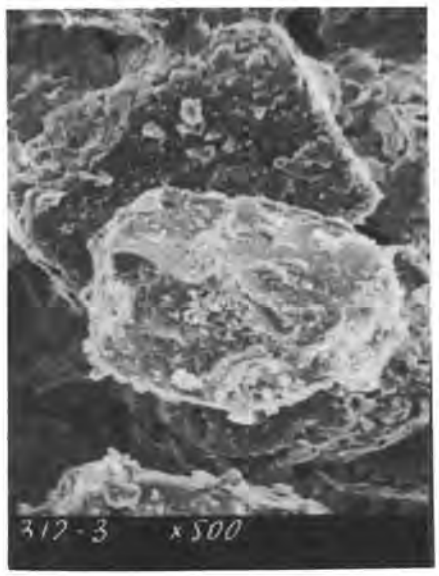

Fig. 2 c

water for the normal thickness grout increases at jet pulverization for 1.5-2 abs. % as compared with the ball mill cements at the same specific surface. As regards the raw materials, aggregation impedes the process of homogenization of the raw mixture

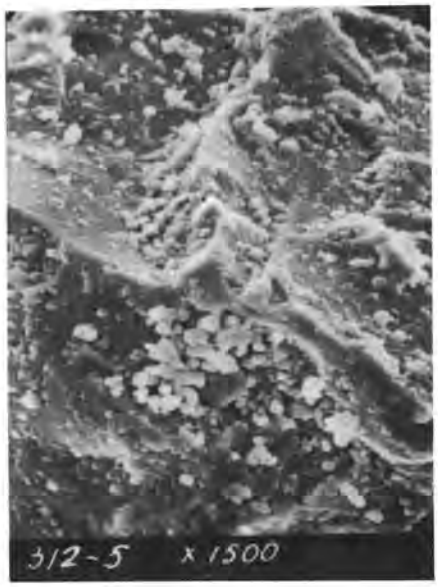

Fig. 2 b

and leads to considerable variations of the mixture dispersion at the mill outlet; therefore the reaction ability of the raw mixture rises at separate jet pulverization of components followed by intermixing or at jet pulverization of one and milling of other components (Table 1).

The theoretical analysis of the stream mill pulverization process the results of which are published in the "Cement" periodical in 1979, Leningrad, reveals that the periodical fluctuations in the dispersion of charges consisting of two components with different crushing ability are more vividly manifested in the stream mills than in the ball ones. Therefore, the stream mills are less suitable for pulverization of multicomponent charges. Further the theory witnesses that owing to only impact crushing and higher level of energy stress the grain composition of the stream mill products should be narrower, whereas the uniformity coefficient in the Rosin-Rammler-Shperling equation for the granulometric composition of said products should approach 1.

These postulates are supported by the experiment (Fig. 4). In view of the conclusion on the correlation between the high strength of cement and the degree of uniformity of its granulometric composition drawn by S.Sprung in his general report at the VIth Congress on Chemistry of Cement, it is clear that a norrower grain composition is one of the factors increasing the strength o of jet pulverization cements. The fact that is somewhat above 1(1.17-1.22 in the data of the experiment, Fig.4) may by explained by multi-phase structure of the material being crushed and stimulated formation of cracks in the inter-phase boundary region. A number of factors mentioned above and decreasing of the jet pulverization products both in the clinker formation and cement hydration pro-

Table 1

Grain Composition and Reaction Ability of Raw Mixtures

Type of milling of three-component raw mixture (chalk+clay+pyrite cinders, KH=0.96; n=2.4; p=1;1)	Screen residue, wt.%			Free lime content after 15-min exposure to 1450°C,%	Alite-formation rate constant, Yander equation	
	No. 008 (80 u)	No. 006 (60 u)	No. 004 (40 u)		abs.	%
Ball 1	3.2	4.0	7.2	5.39	0.0167	100
Ball 2	0.8	1.5	3.5	4.91	0.0176	105
Jet, joint	0.2	0.3	0.8	1.97	0.0276	165
Jet, separate	0.2	0.1	0.1	0.69	0.0373	223
Jet - chalk Ball - clay, cinders	0.3	0.2	1.0	0;79	0.0359	215
Jet - clay Ball - chalk, cinders	0.2	0.8	1.2	1.67	0.0298	178

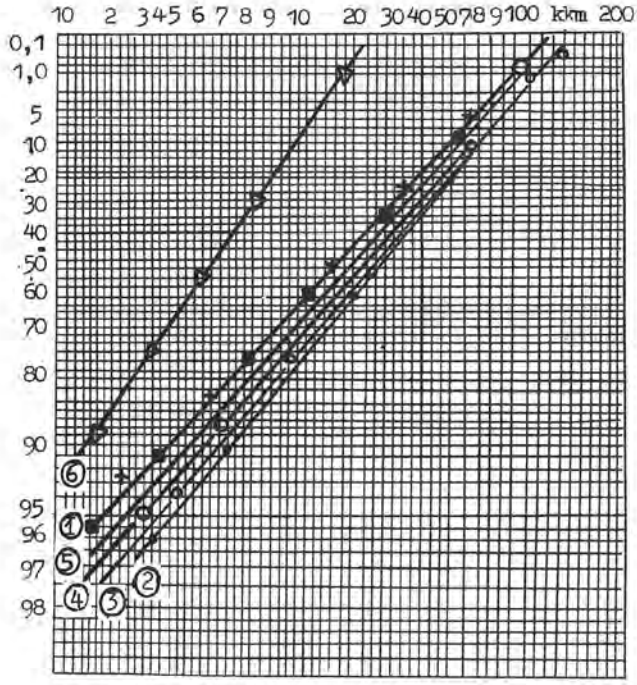

Fig. 4. Granulometric Composition of Stream Mill Pulverization Products in RRSB System: 1 - sand; 2 - cement with 30% slag (1800 cm^2/g; 4 - same, 2120 cm^2/g; 5 - same, 2310 cm^2/g; 6 - separation product, S = 9660 cm^2

cesses may be regarded as providing for the reduction of the activation energy of said p processes and make it possible to believe in activation at jet pulverization of some materials passive as compared with the portland clinker which was pointed out by some of us at this Congress in a written report dealing with technogenic belite products. In addition to the above data it will suffice to report on the test results of the jet pulverization product of the mixture consisting of 70% of the industriel portland cement clinker and 30% of belite slime of the Volkhov combine. The technological advantages of this process reside in that when using overheated steam or hot furnace gases as an energy carrier for the stream mills, there is noneed for pre-drying of the belite slime which is necessary in case of crushing of charge with such a high content of technogenic belite in a ball mill. A 150-kgf/cm^2 higher strength at the age of 28 days - 3 months as compared with a check mix of the ball mill cement proves that the activating effect of the jet pulverization, irrespective of its physical essence of those mentioned above, makes it more technologically preferable for mixed cements than the ball mill method. Thus, in this cas the theoretical limitation linked with fluctuations of the multi-component charge jet pulverization product dispersion is eliminated. The analysis of the composition of separate fractions of the jet pulverization mixed cements reveals that the reason for activation is dictated in this case by the conversion of a more considerable part of the belite material into a fine fraction of the cement than ever registered at ball milling even with preliminary complete drying of the belite products.

A detailed analysis of belite grain resistance to crushing which is being carried out at present provides for drawing a preliminary conclusion that the technogenic belite offers higher resistance to abrasion than clinker minerals but fails to withstand impact loads. Substantial domination of the latter in the jet pulverization process leads to concentration of said material in the fine fractions of the product and its activation in the mixed cements. The corresponding technological process is to be organized at the cement plants of the USSR using or intending to use the technogenic belite products.

Synthèses à basse température de silicates bicalciques actifs

Syntheses at low temperature of active dicalcium silicates

B. MORTUREUX, E. REVERTEGAT, B. THURET, CERILH, Paris, France.

Un intérêt essentiel de la synthèse de C_2S hydrauliquement actif est d'ouvrir une voie de recherche en matière d'économie d'énergie. Plusieurs chercheurs ont obtenu du C_2S actif, même à relativement basse température, comme D.M. ROY qui a mis au point plusieurs techniques de synthèses entre 750°C et 900°C.

ARNOULT et STRUILLOU (1), ont synthétisé un C_2S sulfaté (5% de SO_3) à partir de spongolithe et de nitrate de calcium. Ce C_2S hydrauliquement très actif a des performances voisines de celles d'un CPA. Le nitrate, qui fond vers 680°C permet d'obtenir une réaction rapide et pratiquement totale dès 750°C avec une silice réactive comme la spongolithe.

La méthode nitrate ne constitue pas une voie industrielle en raison de la difficulté de recyclage des vapeurs nitreuses et de la valeur élevée de la chaleur de dissociation du nitrate de calcium qui pèse très lourdement sur le bilan thermique de la synthèse de C_2S. Elle a eu le grand mérite de montrer l'existence d'un C_2S très actif.

L'objet des travaux effectués au C.E.R.I.L.H. était d'examiner si un tel silicate pouvait être obtenu par d'autres moyens, et particulièrement sans faire intervenir le nitrate dont le rôle n'est pas parfaitement élucidé.

On a examiné en premier lieu le domaine de stabilité thermique du produit synthétisé par la méthode nitrate, tout en cherchant à préciser quelques-unes de ses caractéristiques afin de mieux identifier par la suite les solides obtenus par d'autres voies. L'examen par diffraction des rayons X des préparations par voie nitrate, avant et après traitement thermique et trempe a été utilisé à cette intention. Selon la température de traitement on aboutit aux constatations suivantes:

1°) Préparation sans traitement ultérieur (température d'obtention: 750°C).

Les pics de diffraction très larges suggèrent la présence simultanée de α' C_2S et β C_2S mal organisés. La proportion α'/β étant assez variable pour les diverses préparations. On note la présence en faible quantité de quartz et de chaux libre, ainsi que de sulfospurrite 2 C_2S, Ca SO_4 ce dernier caractère n'étant nullement systématique.

2°) Préparation examinée après traitement thermique :

(a) de 800 à 950°C

Les pics correspondant aux phases C_2S, observés dans les préparations initiales, se précisent et se développent, de sorte que les variétés α' et β C_2S deviennent identifiables sans ambiguïté: les formes cristallines de C_2S initialement présentes ont un degré d'organisation croissant avec la température de retraitement. Cette observation est également valable pour la sulfospurrite.

(b) à 1000°C. la phase α' C_2S disparaît.

(c) de 1000 à 1200°C la sulfospurrite se forme dans tous les cas.

(d) après 1250°C la sulfospurrite disparaît et l'anhydrite apparaît comme produit de décomposition.

Ces observations sont en accord avec les travaux de PLIEGO CUERVO et GLASSER (2) sur la stabilité de la sulfospurrite.

Les traitements thermiques altèrent progressivement les propriétés hydrauliques. A 1000°C le phénomène s'accentue, les résistances mécaniques en compression sur pâtes pures étant alors réduites au dixième de leur valeur initiale.

Le domaine de stabilité du produit actif apparaît donc limité aux basses températures. La technique de synthèse a donc été orientée vers la recherche de matières premières très réactives physiquement, en évitant d'introduire des ions étrangers.

La matière crue est obtenue par hydrolyse d'un mélange de silicate d'éthyle et de sulfate diéthyle par une suspension aqueuse de chaux maintenue pendant 16 heures à 90°C. On obtient une sorte de gel de silicate de calcium hydraté. Ce "gel" a été soumis à diverses conditions de cuisson. Un traitement de 24 heures à 750°C conduit à un produit dont les caractéristiques cristallographiques sont identiques à celles du C_2S synthétisé par la méthode nitrate. La teneur en SO_3 du produit ainsi préparé est de 5 %, le rapport C/S étant ajusté à 2.

Une seconde propriété commune aux produits des deux synthèses réside dans la perte de poids caractè-

ristique entre 900° et 1000°C observée en Analyse Thermique Pondérale. Il est intéressant de noter que cette perte ne s'observe pas si le gel cru est directement soumis à l'examen A.T.P. On en conclut que le silicate sulfaté n'a pas le temps de se former dans les conditions de montée en température de l'essai (300°C/H).

Il faut enfin signaler que les produits des synthèses par cuisson du gel donnent des pâtes de résistances très variables suivant les préparations et cette variabilité est vraisemblablement liée à la très grande altérabilité au gaz carbonique du cru; mais les résistances peuvent dans certains cas approcher celles qui sont atteintes par la méthode nitrate spongolithe et sont en tous cas bien supérieures aux résistances de pâtes de β C_2S.

En conclusion, bien que les auteurs de la méthode, nitrate ne mentionnent que la forme β C_2S, il est clair que les points de vue sont convergents pour attribuer en première approche les propriétés hydrauliques observées à une forme de C_2S mal organisée, modifiée par insertion de SO_3 dans le réseau. En ce qui concerne les possibilités de synthèses:

- l'insertion du SO_3 se fait à basse température.

- le silicate sulfaté actif devient instable dès 800°C.

- le nitrate, utile, n'est pas indispensable et ne conditionne pas l'activité du produit formé.

- la phase α' peut jouer un rôle important dans l'insertion et le maintien de SO_3 dans la structure.

Les travaux de REVERTEGAT (3) et REVERTEGAT et CHOISNET (4) donnent un autre exemple de la réactivité d'une phase α'C_2S stabilisée par un ion étranger. En effet, ces auteurs ont pu attribuer à cette phase l'effet bénéfique sur les propriétés mécaniques du clinker de l'introduction de baryum.

C'est pourquoi l'on a tenté d'appliquer les méthodes de préparation décrites précédemment pour synthétiser un éventuel C_2S activé par cet ion. Bien que les travaux ne soient pas suffisamment avancés pour conclure, on peut signaler que l'on a obtenu - par la technique du gel d'hydrolyse du silicate d'éthyle par une solution de chaux + baryte cuit à 800°C - un produit actif à durcissement assez rapide. L'analyse par diffraction des rayons X montre qu'il s'agit d'un mélange de α' C_2S et de β C_2S mal organisés auxquels s'ajoute une phase X: correspondant à un silicate de baryum-calcium $Ba_x\ Ca_y\ SiO_4$ avec x + y = 2.

On obtient par la méthode nitrate un produit de caractéristique cristallographique comparable.

Le traitement thermique ultérieur jusqu'à 900°C provoque une organisation des trois phases. Au-dessus de 900°C on observe une dilatation de la maille de α' C_2S et une diminution de la phase X qui disparaît complètement lorsque la température de retraitement atteint 1300°C.

Références bibliographiques

(1) M. ARNOULT - R. STRUILLOU - J.ROGER - D. BRETON
Rapports de recherches au Ministère de l'Industrie et de la Recherche 1975-1979.

(2) Y.B. PLIEGO-CUERVO et F.P. GLASSER
Cement and Concrete Research - vol 9 pp 51-56
1979

(3) E. REVERTEGAT -
Influence des oxydes MgO, BaO sur la formation et les propriétés des minéraux d'un clinker de ciment Portland.
Thèse 3e cycle Université de Paris-Sud Orsay

(4) E. REVERTEGAT - J. CHOISNET
Influence de l'oxyde de baryum sur les propriétés cristallochimiques et technologiques du clinker de ciment Portland.
à paraître - Annales de Chimie - Science des matériaux.

Processus de formation des minéraux et composition de phase du clinker d'alinite

Mineral formation processes and phase composition of alinite clinker

M. BIKBAOU, Candidat ès sciences techniques, Chef de laboratoire de l'Institut des Recherches scientifiques et des projets des matériaux de construction, Tachkent, U.R.S.S.

RESUME : L'étude de la formation des minéraux du clinker d'alynite obtenu par la cuisson des matières premières en présence de chlorure de calcium a démontré que ces processus sont assez compliqués; nous avons découvert la formation de nouvelles phases minérales : du chlorure de calcium carbonaté, de la spourrite, de l'orthosilicate et de l'aluminoferrite de chlorure de calcium. A l'étape initiale de la cuisson, les phases minérales contiennent une quantité considérable d'atomes de Cl; à l'étape finale, par contre, on n'observe que des minéraux avec un faible Cl (3-4 % de la masse) - l'alite et l'aluminate de chlorure de calcium. Dans ces derniers minéraux, le chlore est solidement lié dans les positions structurales.

A part les minéraux indiqués, le clinker d'alynite contient également de la bélite et du ferrite de calcium, qui peuvent contenir un peu de chlore (1 % de la masse environ) dans leur structure. La contenance quantitative des phases minérales dans le clinker d'alynite varie dans les limites suivantes (% de la masse) :

l'alynite	60 - 80
la bélite	10 - 30
l'aluminate de chlorure de calcium	5 - 10
la ferrite de calcium	2 - 10

Des recherches effectuées ont permis de décrire le caractère de la cristallisation des phases siliciques du clinker, qui ont généralement une structure distincte à grains fins. Nous avons établi que les conditions de la cuisson et de la déchloraison exercent une influence sensible sur le caractère de la cristallisation du clinker d'alynite.

Cette influence s'explique par la genèse des phases intermédiaires de la spourrite, de l'aluminoferrite et de l'orthosilicate de chlorure de calcium.

SUMMARY : The investigation of mineralformation processes of alinite-clinker produced by kilning the raw material together with calcium chloride has shown their considerable complication which leads to the formation of new phases - calcium chloride carbonate, spurrite, orthosilicate and aluminoferrite of calcium chloride.

At the initial stage of kilning new phases with considerable content of the chlorine atoms (about I5% of the mass) -/orthosilicate and aluminoferrite of calcium chloride/-are formed only the minerals containing small quantity of chlorine (3-4% of the mass)-alinite and aluminate of calcium chloride are kept at the final stage. In the above mentioned minerals the chlorine is tightly cohered in structure positions.

Besides the minerals mentioned above, the alinite clinker comprises also belite and calcium ferrite, which could comprise small quantity of chlorine (about I.0% of the mass).

The quantitative content of mineral phases in alinite clinker varies within the following limits (% of the mass):

alinite	60 - 80
belite	I0 - 30
aluminate of calcium chloride	5 - I0
calcium ferrite	2 - I0

The research data have allowed to describe crystallization of silicate phases of the clinker, which are normally characterized by clear but fine-grained structure.

Important dependence of the caracter of cristallization of alinite clinker upon the conditions of kilning and dechlorination has been established.

This dependence is closely connected with the genesis of intermediate phases of the clinker.

La cuisson du clinker de ciment en présence de la fusion des sels de chlorure de calcium provoque des changements radicaux dans la cinétique des processus de la formation du clinker, ainsi que dans sa composition de phase (I). Le présent travail montre les résultats d'une étude sur la suite des processus de la formation du clinker en presence de $CaCl_2$, ainsi que les données sur la composition plus precise des produits intermediaires et finales de la cuisson du clinker d'alynite; ces donnees n'ont pas ete decrites dans les publications speciales.

Des mélanges suivants ont ete prepares:

I. Un mélange des réactifs:

$CaCO_3$	SiO_2	Al_2O_3	Fe_2O_3	MgO	$CaCl_2$
69.2	I6.I	2.5	I.9	I.3	9.0

2. Un mélange de limon de loess, de cendres et des calcaires de l'usine de ciment d'Akhan-garan avec 9% de chlorure de calcium, à raison de CS = 0,92; n = 2,6; p = 3,I+.

Des mélanges ont été preparés sous forme de granules de dimension de 7-8 mm et cuits dans un four électrique de laboratoire. La vitesse de la montée de la température était égale à 5°C ce qui correspond à peu près aux conditions de production industrielle. A partir de 400°C, un échantillon des matériaux a été pris toutes les 50° et refroidi en l'air. A part cela, un essai isothermique aux températures données était employé afin de déterminer la composition de phase des produits de la cuisson.

Le produit cuit a été analysé sur le contenu de l'oxyde de calcium CO_2 libre et du chlore.

La composition de phase des produits de la cuisson a été déterminée par les méthodes quantitative et qualitative de l'analyse optique et celle aux rayons X. La méthode de l'analyse thermique différentielle a aussi été utilisée.

La suite et le contenu des processus de la formation du clinker à basse température se diffère carrément des processus analogiques de cuisson du clinker de ciment portland. La présence de la chlorure de calcium, composante supplémentaire dans le mélange brut servant à produire le clinker à basse température provoque une complication considérable des processus de la formation des minéraux. La présence de la chlorure de calcium abaisse la température du processus final de la cuisson des minéraux de sortie du clinker du ciment d'alynite aussi que tous les processus intermédiaires. Ces processus sont illustrés par les courbes de l'analyse thermique différentielle (courbe ATD) (fig.I). A partir de 500°C, la courbe ATD du mélange brut du ciment change à cause de l'évaporation de l'eau des hydrates.

Nous avons utilisé une méthode d'étude de la composition de phase dans une couche mince qui a permis de découvrir le commencement de l'interaction chimique entre les composantes du mélange brut pour la formation du clinker d'alynite au niveau de 450 - 500°C.

Le processus de la formation des composés complexes commence déjà aux températures de 530 - 600°C grâce à l'interaction de $CaCl_2$ et de $CaCO_3$, le carbonate de la chlorure de calcium ($CaCO_3$ $CaCl_2$).

A 620 - 640°C ce composé se transforme en phase X qui est, peut-être, sa modification de haute température qui existe dans l'intervalle de 630 - 800°C; leurs propriétés chimiques et les paramètres des cellules sont assez proches (voir le tableau).

Dans l'intervalle de 650 - 750°C une décarbonisation plus intense fait apparaître l'oxyde de calcium libre. A ces températures, les composantes acides entrent en action mutuelle ce qui mène à la formation du spurrite dans les produits de la cuisson $2Ca_2SiO_4 \cdot CaCO_3$.

Tableau I

Données de la diffractométrie aux rayons X des phases minérales découvertes dans le système $CaCO_3 - CaCl_2$

$CaCO_3 \cdot CaCl_2$			Phase X		
Cellule cubique à capacité centrée a = 9,720 ± 0,0I5 Å			Cellule cubique à capacité centrée a = 9,965 ± 0,05 Å		
d,Å	hkl	I	d,A	hkl	I
6.88	II0	30	5.00	700	40
3.97	2II	65	3.I8	3I0	50
3.44	220	85	2.675	32I	5
2.8I	222	90	2.485	400	30
2.600	32I	75	2.356	330	I00
2.I74	420	I00	2.II6	332	40
I.984	422	70	I.94I	5I0	40
I.7I6	440	20	I.808	52I	5
			I.654	600	5

+CS - coefficient de saturation, n - module silicique, p - module alumineux

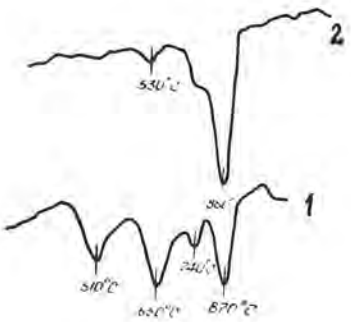

Fig.I. La courbe de la ATD de la formation du clinker d'alynite (I) et du clinker portland (2).

Aux température de 750 - 800°C les produits de la cuisson contiennent, à part le spourrite prédominant, l'alumoferrite et l'aluminate de la chlorure de calcium.

Les diffractogrammes des phases synthétisees intermediaires du clinker sont représentes sur la fig.2.

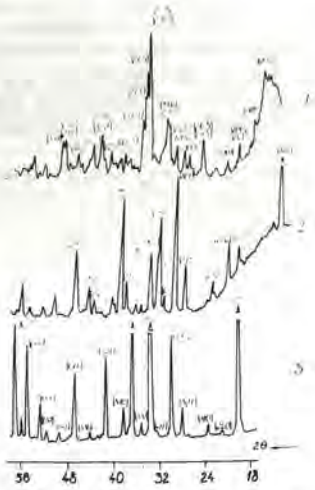

Fig. 2 - Les diffractogrammes des phases intermédiaires du clinker d'alynite:

I - du spourrite;
2 - de l'orthowsilicate de la chlorure de calcium;
3 - de l'aluminate de la chlorure de calcium

C'est dans l'intervalle de 650-850°C que les exoeffets correspondent aux processus exothermiques de la formation de ces minéraux sur la courbe ATD.

Le changement quantitatif de la teneur des phases à chaque étape de la cuisson caractérise le mécanisme de la formation du clinker. Ainsi, la courbe du changement de la teneur d'oxyde de calcium libre dans les produits de la cuisson a deux valeurs extrémales (fig.3). La teneur plus élevée de CaO libre dûe à une température plus haute est en correlation avec la courbe du changement de la teneur de CO_2 - l'oxyde de calcium libre apparaît au cours de la décarbonisation de la calcite.

Pourtant, les températures de 700-750°C provoquent une formation intense du spurrite, dont la quantité atteint le maximum à 800°C (fig. 3).

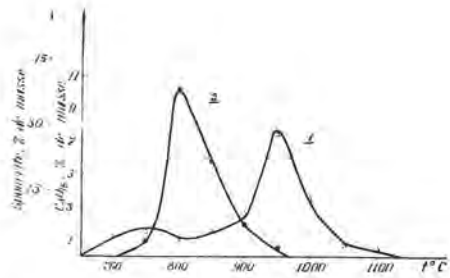

Fig.3. Changement du contenu de CaO libre (I) et du spourrite (2) dans les produits de la cuisson du clinker d'alynite en fonction de la température

La formation du spurrite s'efiectue grâce a la liaison intense entre la silice et l'oxyde se libérant à la decomposition de $CaCO_3$:

$$4\ CaO + 2\ SiO_2 + CaCO_3 \longrightarrow 2\ Ca_2SiO_4 \cdot CaCO_3$$

En même temps une partie de molécules de la calcite participe à la formation du minéral nouveau, spourrite. Il convient de souligner le rôle tres important de $CaCl_2$, agent de dispersion qui intensifie considérablement le processus de la decarbonisation et joue le rôle du milieu catalytique de cristallisation.

Aux températures de 750-800°C, il est intéressant à noter la formation de l'orthosilicate de la chlorure de calcium en présence de la chlorure de calcium. La fig.4 montre les données expérimentales sur le changement de la teneur en orthosilicate de la chlorure de calcium $2\ Ca_2SiO_4 \cdot CaCl_2$ dans le processus de la cuisson.

On peut supposer la possibilité de l'isomorphisme des anions au cours de la formation du spourrite et de l'orthosilicate de la chlorure de calcium quand une partie des d d'atomes de l'oxygene dans la molécule de la calcite du spourrite - $2\ Ca_2SiO_4 \cdot CaCO_3$

est remplacée par les atomes du chlore. Les résultats des experiences sur la séparation du chlore du spourrite synthétique synthétisé en présence de CaCl confirment que le replacement de O par Cl dans le spourrite est possible. Ces expériences ont montré la conservation de 2% de Cl dans le minéral, probablement grâce à l'élevation du Cl dans la structure. Il n'est pas exclu que $2\ Ca_2SiO_4 \cdot CaCO_3$ et $2\ Ca_2SiO_4CaCl_2$ forment des solutions

solides grâce à l'isostructure de ces composés contenant à la base une molécule de Ca_2SiO_4. Ces phases intermédiaires sont stables dans un intervalle déterminé, car à 800-850°C le spourrite commence à se décomposer et aux températures supérieures à 950°C disparaît tout a fait.

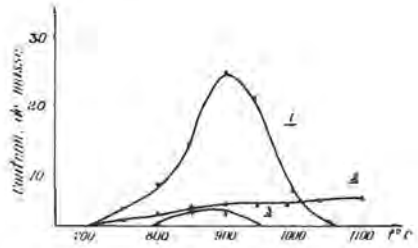

Fig. 4. Changement du contenu de l'orthosilicate de la chlorure de calcium (I), de l'aluminate de la chlorure de calcium (2) et de l'alumoferrite de calcium (3) das les produits de la cuisson du clinker d'alynite en fonction de la température.

Les fig.3-5 montrent des résultats des mesures sur le changement de la teneur quantitatives des phases minérales du clinker d'alynite dans le processus de la cuisson.

Elles sont effectuées à l'aide d'une analyse quantitative aux rayons X. La formation du spourrite et de l'orthosilicate de la chlorure de calcium lie l'oxyde de calcium libre se libérant au cours de la décarbonisation. Sa quantité dans l'intervalle de 700-900°C ne dépasse pas quelques pourcents. Ceci est juste pour la vitesse normale de l'élevation: 5-20% par min. Grâce au nivellement des facteurs cinétiques, le traitement isothermique prolongé aux températures 700-900°C libère tout l'oxyde de calcium du mélange brut, sauf sa quantité liée par le spourrite, l'orthosilicate, l'aluminate et l'alumoferrite de la chlorure de calcium (fig.4); même dans ce cas la quantité de l'oxyde de calcium libre ne dépasse pas IO-I2% ce qui est égal à un cinquieme de sa quantité totale. Ces données sont en accord avec les résultats de la détermination de la teneur en CO_2 des produits de la cuisson. L'aluminate de la chlorure de calcium commence a se former a 700-750°C; il est stable sur toutes les étapes ultérieures de la formation du clinker. Par contre, l'alumoferrite de la chlorure de calcium[+] n'existe que dans un intervalle limité de températures. Il commence à se former à 750-800°C, mais à 950°C il se décompose en ferrite de calcium, un composé stable et en même temps il fournit l'aluminium pour la formation de l'alynite. Il est probable que ce fait explique le commencement de la cristallisation de l'alynite aux températures de l'alumoferrite de la chlorure de calcium, c'est-à-dire à 900-950°C (fig.5).

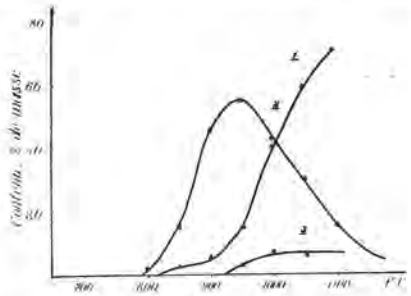

Fig.5. Changement du contenu de l'alynite (I) et du bélite (2) et le ferrit de calcium (3) en fonction de la température.

L'hypothèse citée explique l'effet de forte minéralisation en présence de Fe_2O_3 dans le mélange brut au cours de la cuisson du clinker d'alynite. Grâce a la formation et à la décomposition de l'alumoferrite de la chlorure de calcium, l'aluminium, un des éléments principaux du réseau cristallin de l'alynite, est fourni au moment de la cristallisation de l'alynite. Cela se trouve en accord avec le fait de l'absence de l'alumoferrite de calcium dans le clinker d'alynite.

L'hypothèse proposée explique la nécessite d'une augmentation sensible de la concentration de l'aluminium dans le mélange brut utilisé au cours de la cuisson du clinker d d'alynite blanc. Le bélite se forme à 850-900°C, car la quantité de Cl ne suffit pas à lier toute la substance en orthosilicate de chlore (I5% de chlore dans la structure), aluminate de chlore (4% de chlore dans la structure) et alumoferrite de chlore (I5% de chlore dans la structure).

De cette façon, à 900°C tout le chlore est déjà pratiquement lié en composés, l'alynite se forme à partir de l'orthosilicate de la chlorure grâce a une nouvelle répartition du chlore entre lui et le bélite, pendant que les CaO et Al_2O_3 superflus libérés a la décomposition de l'alumoferrite, sont liés. Ainsi, la cristallisation de l'alynite est suivie du dégagement de HCl grâce a la décomposition thermique de l'alumoferrite et de l'orthosilicate de la chlorure de calcium. Une partie de HCl fournit les particules voisines et participe au processus ulterieur de la formation du minéral en homogéneisant la composition de phase du clinker; une autre partie s'en va avec les gaz grâce à la sublimation. De cette façon, une étude de la suite de la formation du clinker à basses température a demontré une grande importance des phases intermédiaires du clinker dont la formation et la genèse, par notre opinion, exerce une influence décisive

[+]La composition du minéral est, probablement, la suivante: $Ca_4Al_2Fe_2Cl_2O_9$.

sur le caractère de la cristallisation du clinker d'alynite.

Le méchanisme des processus de la formation du clinker à basses températures que nous venons d'examiner nous permets de comprendre les particularités de la composition de phase du clinker d'alynite.

Le clinker d'alynite est représenté par quatre minéraux (% de la masse).

I. L'alynite - $Ca_{II}(Si, Al)_4O_{I8}Cl$ - 60 ÷80

2. Le bélite - β - C_2S - I0 ÷ 30

3. L'aluminate de la chlorure de calcium - Ca_6AlO_7Cl - 5 ÷ I0

4. Le ferrite de calcium-$Ca_2Fe_2O_5$- 2 ÷ I0

La formation du clinker d'alynite s'effectue dans la lutte concurrentielle des atomes et de leurs configurations pour les atomes du chlore qui sont les plus actives aux hautes températures de cristallisation du clinker; ces atomes passent facilement de la phase solide en liquide (fusion), en phase gazeuse et de nouveau solide (chloration).

Cette lutte aboutit à ce que le chlore ne reste que dans l'alynite, ou il est solidement lié dans un motif structural original et entoure étroitement par huit atomes de calcium (2), ainsi que dans l'aluminate de chlorure de calcium, ou il est aussi lié dans les motifs structuraux solides (3).

Le bélite et le ferrite de calcium sont identiques sur tous les indices aux minéraux portlands.

Certaines particularités de la morphologie et de la composition des cristaux sont liées à une faibre solubilité du chlore (I,0-I,5% de la masse) dans le bélite et le ferrite de calcium.

Dans les clinkers obtenues à la base des matières premières aux différentes usines de ciment de l'URSS d'apres la technologie de basse température avec l'utilisation de la fusion catalytique de la chlorure de calcium, l'alynite se cristallise sous forme des plaques hexagonales, des petits prismes allongés dans le même sens et des formations des rayons aiguisés. On peut y observer des grains de forme des rhomboédrique et des tablettes. Les clinkers ont une structure à grains fins irréguliers,la cristallisation de l'alynite est distincte Les dimensions des grains varient de plusieurs mkm à 30-35 mkm. les particules de dimension de I5-20 mkm prédominent.

On y observe des agrégats de l'alynite, quelquefois des macles des grains a l'extinction zonale caractéristique. La birefringence est basse, l'extinction est directe. Les index de refraction varient dans les limites: I.7I0 - I.7I4.

Une autre phase silicique du clinker d'alynite observée dans les materiaux etudies est representée par le bélite (silicate basique bas), qui se diffère de l'alynite par sa forme arrondie, ovale ou celle de lentille; les debris des grains sont le plus souvent incolores, à l'extinction directe.Les index de réfraction sont N = I.724 - I.730. La birefringence et les index de réfraction sont les seuls indices distinctifs des études microscopiques des phases du clinker d'alynite.

Les études minéralogiques des clinkers synthetisés à basse température sont très difficiles à accomplir à cause de la structure microcristallin des phases minérales. Les études au microscope électronique nous ont permis d'étudier le faciès et la morphologie des cristaux dans le clinker.

Le bélite est représente dans le clinker sous forme des grains arrondis et des débris irréguliers; souvent, on l'observe sous forme des incorporations dans les cristaux de l'alynite (fig.6).

Fig. 6. Stéréomicrophotographies+ d'un cristal de l'alynite avec des incorporations du bélite (stéréoskan - 4). Agrandissement - 5000.

Dans le clinker, l'alynite est représenté parles polyèdres bien cristallisés aux facettes distinctes reproduisant de differentes varietestions du faciès tétragono-pyramidal (fig.7).

Une etude des microcristaux de l'alynite dans le clinker par la methode de l'analyse microscopique du spectre aux rayons X a l'aide de l'appareil "Komeka" nous a permis de preciser la composition des ele-

+L'auteur remercie vivement m-me N. Sirotkine d'avoir exécuté une analyse.

a b

Fig. 7. Variétés du faciès des cristaux de l'alynite dans le clinker: a - photos des répliques des clivages des grains de clinker prises au microscope électronique ME - 5, agrandissement de 4000, b - stéréomicrophotographies prises au microscope électronique à balayage, agrandissement de 2800.

ments des cristaux de l'alynite, dont le contenu qualitatif est représenté par Ca, Si, O, Cl, Al, Fe et Mg (fig.8) et le contenu quantitatif par: Ca = 46-47 Si =IO-II Al = I,5-3,0 Mg = I.0-I.5 Fe = I.2-I.3 Cl = 2.5-3.0 O = 35-36.

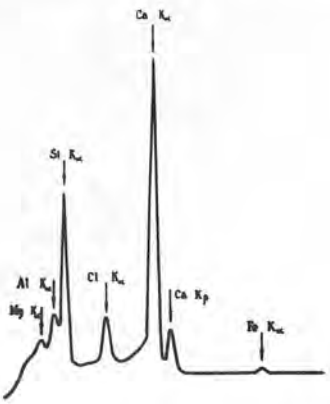

Fig. 8. Spectrogramme d'une grain d'alynite dans le clinker.

CONCLUSIONS:

Le présent travail montre la suite de la formation et des transformations des phases intermédiaires et finales du clinker d'alynite.

A l'étape initiale du processus, les a auteurs ont etabli la formation du carbonate de la chlorure de calcium et de la phase X dont la composition est à peu près la même ils ont déterminé les parametres de leurs cellules élémentaures. Le spourrite,l'alumoferrite et l'orthosilicate de la chlorure de calcium se forment également en tant que les phases intermédiaires du clinker d'alynite.

La contenance quantitative des phases minérales dans le clinker d'alynite varie dans les limites suivantes (% de la masse):

l'alynite	60 - 80
le bélite	IO - 30
l'aluminate de la chlorure de calcium	5 - IO
le ferrite de calcium	2 - IO

Le changement la proportion quantitative des phases minérales intermédiaires et stables dans le processus de la formation du clinker d'alynite est demontré.

Les auteurs donnent la description du caractère de la cristallisation des phases minérales du clinker - alynite; ils soulignent sa dépendanse des conditions de la cuisson des matières premières liée à la genèse des phases intermédiaires du clinker.

BIBLIOGRAPHIE

I. B. NOUDELMAN (I976) VI Congrès international la chimie du ciment "Clinkérisation dans la fusion de sel de la chlorure de calcium", tome I, pp.2I7-22I (russe).

2. V. ILUKHINE,N.NEVSKY, M. BIKBAOU et R. HOWIE (I977). Nature, "Crystal structure of alinite", v.269, n°5627, pp.397-398, english.

3. P. WILLIAMS (I968) V Congrès international sur la chimie du ciment "Crystal structure II • CaO • $7Al_2O_3$ • CaF_2", tome I, pp. I73-I76.

Calculation of strength parameter for hydrated portland cements from hydration heats measured by differential calorimetric analysis (DCA)

Prévision des résistances des ciments portland au moyen de leur chaleur d'hydratation

G. OLIEW, W. WIEKER, Zentralinstitut für anorganische chemie der Akademie der Wissenschaften der DDR, Berlin, R.D.A.

Summary:
Precalculation of compressive strength for hydrated portlandcement is an important question for scientist as well as for practical men.
Setting and hardening of cement is influenced by those factors which also influence the heat liberation, measured by differentialcalorimetric analyses (DCA) too. Small differences in chemical and mineralogical compositions and in burning-and cooling conditions of the clinker lead to different DCA-curves (fig. 1).
Increasing SO_3-content and surface area (BLAINE) determines the position of the 3 rd DCA-Peak (fig. 2). Hydration of PC under steam curring conditions influence considerably DCA-curves (fig. 3).
Hydration heat Q_I (first reaction of cement with water - first DCA-Peak area) and Q_t (t = 24...672 h) clearly depend on surface area and SO_3-content (fig. 4 and 5). Compressive strength depends on surface areas and SO_3-content too (fig. 6).
A set of correlation equations allow to precalculate the strength of hardened cement for 1 up till to 28 days and after hardening under steamcurring conditions already after 1 hour (Q_I) (tab. 1). More reliable results can be calculated from heat developed after reaction times more than 72 hours (Q_t) (tab. 2).
Results of the calculations are to be seen in fig. 7. The factors and constants of these equations must be changed if a cement of another cement is to be investigated.

RESUME : La prévision des résistances des ciments pose un important problème aux chercheurs et aux praticiens. Elle peut se faire grâce à leur courbe d'analyse calorimétrique différentielle. Ces courbes (A.C.D.) sont fortement influencées par la composition minéralogique et le mode de cuisson du clinker, ainsi que par la teneur en SO_3 et la granulométrie du ciment broyé, et même par le procédé de conservation des éprouvettes.

Des formules de corrélation entre les pics et la forme de ces courbes, et la résistance du ciment à 28 jours de conservation normale, ou à 1 heure de conservation dans la vapeur chaude, ont été établies. Elles nécessitent le relevé de ces courbes jusqu'à 72 heures.

Des résultats expérimentaux sont exposés. Les paramètres des formules varient avec les ciments.

The precalculation of strengthparameter for hydrated portlandcements is an important question for scientist as well for practical men. Starting from the fact, that setting and hardening of cement is influenced by those factors which also influence the heat liberation, we tried to precalculate strengthparameter from hydration heats, measured by differentialcalorimetric analysis (DCA).

As it known from literature, small differences in chemical and mineralogical compositions of the clinker lead to different DCA-Curves (fig. 1).

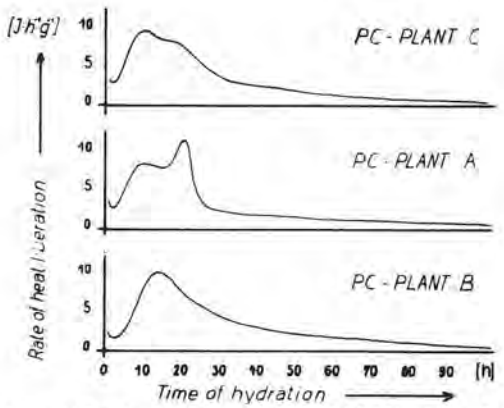

Fig. 1 Heat liberation (DCA)-Curves from PC's of different PC-Plants (W/C = 0,5; temp. = 20 °C)

The differentialcalorimeters which had been used are described in [1,2].

To get correlation functions between the strength developed by portlandcement pastes and the heat of hydration, a set of cements with different SO_3 contents and surface areas are prepared from clinkermaterial of the cement plants A and B. Fig. 2 shows the results of DCA measurements of portland-cement samples with different SO_3-contents and surface areas of the plant B.

From this figure it is to be seen, that with increasing SO_3-content the III. DCA-maximum is shifted to longer reaction times and that with increasing surface of the cement this peak is shifted to shorter hydration times for cements with a constant SO_3 content of 3.8 %.

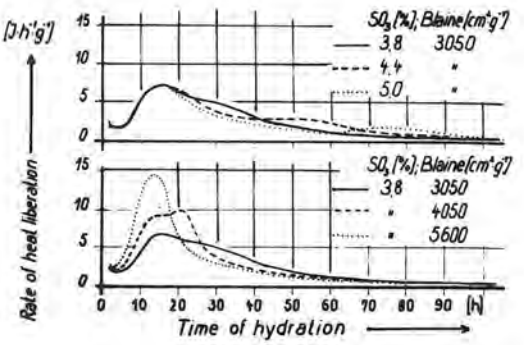

Fig. 2 Hydration of PC-Type B with various contents of SO_3 and various surface area (W/C = 0,5; temp. = 20 °C)

Under commercial aspects there is very often an interest in strength-developement at higher temperatures too. Therefore we have measured the heat liberation of the mentioned cement samples during a programmed temperature treatment with a maximum at 85 °C [2]. The results of these experiments in fig. 3 show, that only at a SO_3-content of 4,4 % there is a shift of the hydration peak to longer hydration times. With increasing surface at a constant SO_3 content of 3,8 % we found at medium surface areas (4050 cm^2/gr) a shift to higher reaction times and at high surface values (5600 cm^2/gr) to shorter reaction times.

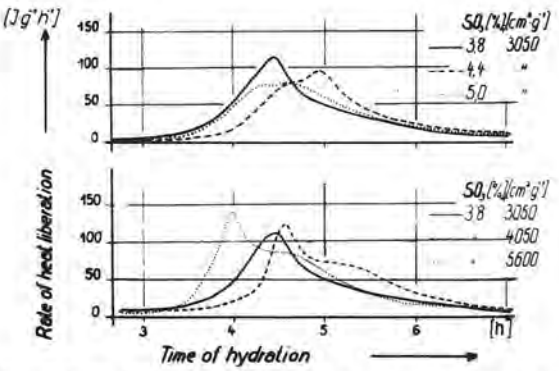

Fig. 3 Hydration of PC-Type B with various contents of SO_3 and various surface area (W/C = 0,5; max. temp. = 85 °C; curing conditions according to TGL 28 103/08).

The reaction heats (Q_t) developed up till 1, 24, 72 hours were calculated from the DCA-curves by direct integration. For the calculation of reaction heats at longer reaction times we used the formula

$$\frac{1}{Q} = \alpha \cdot \frac{1}{t} + b$$

published by SCHWIETE u. ROTH [3].

The results in fig. 4 show, that there is

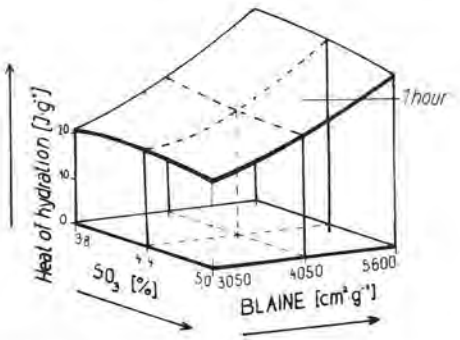

Fig. 4 Dependence of Q_I on SO_3-content and surface area measured by BLAINE method.

already for the heat developed after 1 hour (Q_I = area of the first DCA-peak) a clear dependence from the SO_3-content and the surface area of the tested cement. The same results we got for hydration times up till 28 days (fig. 5).

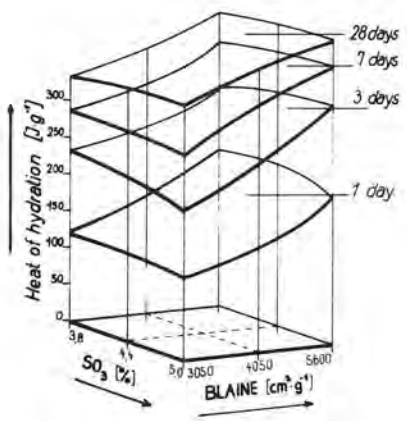

Fig. 5 Heat of hydration Q_t vs SO_3-content and surface area measured by BLAINE method

Beacause there are good correlations between compressive strength measurments and SO_3-content and surface area (fig. 6) too,

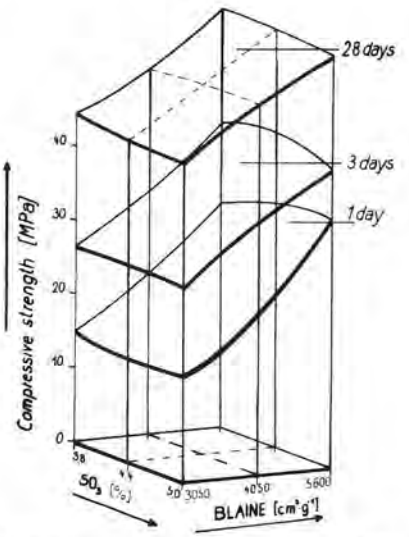

Fig. 6 Compressive strength vs SO_3-content and surface area

it should be possible to get mathematical regression equations between the developed reaction heat (Q) and the compressive strength (D). In table 1 there are given some equations we got for calculation of compressive strength after 24, 72 and 672 hours of hydration at 20 °C using Q_I-values.

Tab. 1 Equations for calculation of compressive strength parameters (D_{24}...D_{672}, D_w, D_{w672}) from hydration heat Q_I (D_t[MPa] ; Q_t[J/g])

Nr.	PC - PLANT A		$\bar{\Delta}D$ [%]	± s
1.	D_{24} = 0,83	Q_I - 2,64	5,5	4,3
2.	D_{72} = 0,67	Q_I + 12,88	3,7	2,3
3.	D_{672} = 0,58	Q_I + 31,61	2,6	4,0
4.	D_w = 0,48	Q_I + 11,45	5,6	2,9
5.	D_{w672} = 0,29	Q_I + 35,06	4,2	3,7
	PC - PLANT B			
6.	D_{24} = 0,72	Q_I + 7,50	7,5	4,4
7.	D_{72} = 0,64	Q_I + 20,00	3,4	2,4
8.	D_{672} = 0,72	Q_I + 28,40	2,5	2,0
9.	D_w = 0,66	Q_I + 15,81	6,7	3,6
10.	D_{w672} = 0,70	Q_I + 26,39	5,7	3,8

Tab. 2 Equations for calculation of compressive strength parameters (D_{24}...D_{672}, D_w, D_{w672} [MPa]) from hydration heat Q_t (t = 1...∞ [J/g])

Nr.	PC - PLANT A		$\bar{\Delta}$ D [%]	± s
1	D_{24}	= 0,08 Q_{24} + 0,1 Q_{72} - 17,49	4,2	4,4
2	D_{24}	= 0,008 BLAINE - 8,91	4,2	4,1
3	D_{72}	= -0,21 Q_{12} + 0,18 Q_{24} + 0,1 Q_{672} - 21	1,3	0,9
4	D_{72}	= 0,07 Q_{168} + 0,004 BLAINE - 4,40	2,0	1,3
5	D_{672}	= 0,03 Q_{168} + 0,004 BLAINE + 20,65	0,8	0,5
6	D_{672}	= 0,38 Q_I + 0,05 Q_{168} + 20,72	1,0	0,8
7	D_w	= 0,10 Q_{24} + 9,77	4,8	3,9
8	D_{w672}	= 0,11 Q_∞ - 3,38	3,0	2,4
9	D_{w672}	= 0,09 Q_{672} + 6,45	3,2	2,9

In addition there are in table 1 two equations to calculate compressive strength of steam curred samples directly after steam-curring (D_w) and 672 hours later (D_{w672}). From the medium error $\bar{\Delta}$ D [%] and standard deviation it is to be seen, that the results are relativly good, for cements of plant A as well as for those from plant B.
More reliable results can be received from calculations in which reaction heats developed after longer reaction times than one hour are used. Some of these equations we got are listed in table 2. The noted values for the medium error and standard deviation shows, that these equations realy give better results than those using Q_I values only.

In fig. 7 measured compressive strength is plotted against the corresponding calculated values. This gives the proof, that there is realy a very good correlation between compressive strength and heat development durnig hydration of a portland cement. Therefore we think that DCA measurments are very convenient for production controll measurments in cement plants and that it will be possible to reduce the extensive number compressive strength measurments in cement plants. But we have to remarc, that the factors and constants given in the equations of table 2 are only valid for cement plant A. If one wants to use these equations on other cement plants one had to estimate these factors and constants by an investigation of a set of cement samples of that special plant.

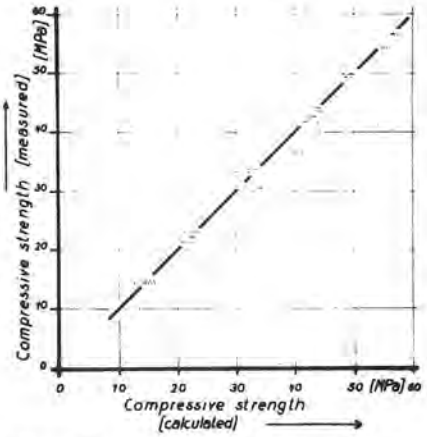

Fig. 7 Measured vs calculated compressive strength of PC-Type B

References:

1 Mtschedlow-Petrossian, O.P.; Sen, A.; Uscherow-Marschak, A.: Zur Untersuchung der Hydratation von Bindemitteln nach den Methoden der Differential-Mikrokalorimetrie. Silikattechnik 20 (1969) H 7, S. 229-232

2 Oliew, G; Schüttauf, St.: Über die Anwendung der Differentialkalorimetrie (DCA) bei der Wärmebehandlung von Portlandzementen. Betontechnik 1 (1980) H.3, S.5-

3 Schwiete, H.E.; Roth, W.: Forschungsberichte des Landes Nordrhein-Westfalen (BRD), Nr. 2269; West.Deutscher Verlag Opladen, 1973, S. 32

THEME VI

Les pâtes de ciment : rhéologie, évolution des propriétés et des structures

Cement pastes : rheology, evolution of the properties and structures

---

The effect of various admixtures on the surface aera and pore structure of Portland cement paste prepared in suspension form

Etude de l'effet de divers mélanges sur la surface spécifique et la structure poreuse de la pâte de ciment Portland préparée en suspension

Professor G.A. GAMLEN, Dr. D. DOLLIMORE, Mr. P.F. RODGERS,
Department of Chemistry and Applied Chemistry, University of Salford, England.

Summary

The effect of the addition of three water soluble polymers. Versicol W13, Dextran and hydroxyethyl cellulose to the mixing water of a bottle hydrated Portland cement was studied. Surface areas obtained from nitrogen adsorption isotherms are presented along with pore size distributions calculated using the method of Dollimore and Heal.

RESUME : On a étudié l'effet de l'addition de trois polymères solubles dans l'eau : le Versicol W 13, le dextrane et la cellulose hydroxyle-éthyliquie, à l'eau de prise du ciment Portland hydraté en flacon. On présente les valeurs des surfaces spécifiques obtenues, en utilisant les isothermes d'adsorption d'azote, aussi bien que les valeurs de la distribution de la structure poreuse calculées à l'aide de la méthode proposée par DOLLIMORE et HEAL.

INTRODUCTION

The surface area of cement pastes obtained from water vapour adsorption are usually larger than those obtained from nitrogen adsorption (1,2). Mikhail et al conclude that either the pores are too small to allow nitrogen in or that 'ink-bottle' pores exist (3,4). Feldman and Sereda believe that the water must, at least in part, be chemically adsorbed, and nitrogen adsorption reflects the true surface (5,6). To remove free water from the hydrate, D-drying is commonly used (7,8) although Lawrence recommends treatment with methanol (9). The adsorption of an organic polymer is thought to occur with the ionic group away from the solid surface (10), but recent work has provided alternative explanations (11).

EXPERIMENTAL

1) Materials

The cement used was ordinary Portland cement (OPC), obtained commercially (phase composition, C_3S, 47.6%; C_2S, 22.55%; C_3A, 11.06%; C_4AF, 7.66%; $C\bar{S}H_4$, 4.65%). The surface area (Blaine) was $3,200 \pm 200$ cm^2 g^{-1}. The polymers investigated were Versicol W13, a nonionic polyacrylamide, (pH 8-9 at 20%). Dextran, a carboxymethyl starch (pH 6.0 at 1%) and hydroxyethyl cellulose (HEC), a nonionic cellulose ether (pH 6.5-8.0 at 1%). The nitrogen used in the adsorption experiment was dry and oxygen free.

2) Preparation of Samples

A sample without the polymers present was first used as a control. In this, 100g of OPC was mixed with one litre of distilled water in a sealed airtight polythene bottle. It was rotated on a ball mill at 87 r.p.m. at 22 ± 2°C for up to 28 days. In experiments involving polymers enough of a 1% solution of each polymer was added to give an initial ratio of 0.08% dry polymer/dry cement. At various times up to 28 days after mixing, about 100 mls of suspension was removed and filtered in a CO_2 free nitrogen atmosphere. After one hour's vacuum pumping the sample was placed in a small polythene bottle and dry excess methanol added. It was further rotated for two weeks, followed by vacuum filtration from the methanol in a nitrogen atmosphere and a 15 minute evaporation of the methanol at 30-35°C. Any calcium hydroxide crystals were removed from the sample by sieving through a BS 200 mesh sieve (75 μm). These crystals were ground in an agate mortar until they also passed through the sieve. They were then remixed thoroughly with the rest of the sample, and it was these samples that were used in the adsorption experiments.

3) Adsorption

Nitrogen adsorption-desorption isotherms (at 77.4 K) were carried out on a volumetric adsorption apparatus (12). The pore size distributions were calculated using the method of Dollimore and Heal (13).

RESULTS AND DISCUSSION

Samples exhibiting definite hysteris loops in the adsorption-desorption isotherms were subjected to the pore size distribution calculation. These were samples beyond seven days hydration. The general observation is that as hydration time increases, then the size of the hysteris loop also increases, along with the volume of nitrogen

adsorbed. The isotherms would be best designated as Type II by the classification of Brunauer et al (14), but the adsorption approaches the value of P/Po = 1 with a large increase in adsorption and a hysteris loop on desorption. The loop closes between P/Po values of 0.3 to 0.5 depending upon the sample. A comparison of the 28 day old samples shows that the effect of the addition of the polymers appears to reduce the volume of nitrogen adsorbed, compared to the control. Surface areas were calculated on the basis of the evacuated weight of the sample taken after the experiment was over. Representative surface areas, total pore volumes and cumulative areas for the control are shown in Table 1. Tables 2, 3 and 4 show surface areas and porosity properties for samples modified with Versicol W13, Dextran and HEC respectively. The results are tabulated as a ratio of the sample result to the corresponding result for the control. In general, it can be seen that the ratio $S_{BET}/S_{BET\ CONTROL}$ is highest for the Dextran modified cement between one day and 14 days hydration. This shows that these samples have the highest surface area of all modified samples. All series show a sharp increase in surface area between ten hours and one day's hydration.

The addition of all polymers reduce the total pore volume compared to the control. This can be seen by the fact that the ratio $V/V_{CONTROL}$ in Tables 2, 3 and 4 are all lower than unity. In the case of samples modified with polymers at ages of 7 and 14 days, the $V/V_{CONTROL}$ ratio increases whilst the $S_{BET}/S_{BET\ CONTROL}$ ratio decreases. It would appear therefore that the addition of water soluble polymers tend to favour the formation of smaller pores that would not ordinarly be present. The model used for the pore size distribution is that of a cylindrical non-intersecting pore. An alternative analysis, based on a slit shaped model will be the subject of a further publication.

References

1. R.Sh. Mikhail and S.A. Abo-el Enein, Cem. Concr. Res., 2 (1972) 401-414
2. J. Skalny and I. Odler, Conf. Silicat. Indus., Proc. 11th, Budapest 1973, 505-519
3. R.Sh. Mikhail, L.E. Copeland and S. Brunauer, Can. J. Chem., 42 (1964) 426-438
4. E.E. Bodor, J. Skalny, S. Brunauer, J. Hagymassy Jr., and M. Yudenfreund, J. Coll. Int. Sci., 34 (1970) 560-570
5. R.F. Feldman, Int. Symp. Chem. Cem., Proc. 5th, Tokyo, 1968, Vol III, 53-66
6. R.F. Feldman and P.J. Sereda, Eng. J. (Montreal), 53 (1970) 53-59
7. L.E. Copeland and J.C. Hayes, ASTM Bull., 194, (1953) 70-74
8. D.L. Kantro and C.H. Weise, J. Am. Ceram. Soc., 62 (1979) 621-626
9. C.D. Lawrence, Cem. Concr. Ass. Tech. Rep. No. 42.520, 1978, pp29
10. F.M. Ernsberger and W.G. France, Ind. Eng. Chem., 37 (1945) 598-600
11. N.B. Milestone, J. Am. Ceram. Soc., 62 (1979) 321-324
12. S.J. Gregg and K.S.W. Sing, Adsorption Surface Area and Porosity, Academic Press, London and New York, 1967, p310-316.
13. D.Dollimore and G.R. Heal, J.App.Chem, 14 (1964) 109-114
14. S. Brunauer, L.S. Deming, W.C. Deming and E. Teller, J. Am. Chem. Soc., 62 (1940) 1723-1732

TABLE 1

Surface Areas and Porosity Properties of Cement Hydrates Control Sample - No Polymer Added

Age of Sample	Surface Area S_{BET} $m^2 g^{-1}$	Total Pore Volume V $ml.kq.N_2 g^{-1}$	Cumulative Surface Area S_{CUM} $m^2 g^{-1}$
1h	6.4		
3h	5.7		
6h	5.8		
10h	5.1		
1d	12.8		
3d	19.0		
7d	29.5	0.622	95.5
14d	28.1	0.3514	86.8
28d	104.5	0.6065	237.1

TABLE 2

Surface Area and Porosity Properties of Hydrates Modifed by the Addition of Versicol W13

Age of Sample	$\frac{S_{BET}}{S_{BET_{CONTROL}}}$	$\frac{V}{V_{CONTROL}}$	$\frac{S_{CUM}}{S_{CUM_{CONTROL}}}$
1h	.3125		
3h	.807		
6h	.9483		
10h	1.51		
1d	1.523		
3d	1.1		
7d	1.529	.34	0.6
14d	1.148	.633	0.914
28d	0.8134	.377	0.519

TABLE 3

Surface Area and Porosity Properties of Hydrates Modified by the Addition of Dextran

Age of Sample	$\frac{S_{BET}}{S_{BET_{CONTROL}}}$	$\frac{V}{V_{CONTROL}}$	$\frac{S_{CUM}}{S_{CUM_{CONTROL}}}$
1h	0.25		
3h	0.228		
6h	0.724		
10h	0.745		
1d	2.023		
3d	1.584		
7d	2.583	0.322	1.084
14d	1.965	0.748	1.529
28d	0.642	0.538	0.48

TABLE 4

Surface Area and Porosity Properties of Hydrates Modified by the Addition of Hydroxyethyl Cellulose

Age of Sample	$\frac{S_{BET}}{S_{BET_{CONTROL}}}$	$\frac{V}{V_{CONTROL}}$	$\frac{S_{CUM}}{S_{CUM_{CONTROL}}}$
1h	0.458		
3h	0.474		
6h	0.948		
10h	0.382		
1d	1.539		
3d	1.905		
7d	1.573	0.303	0.839
14d	0.975	0.553	0.737
28d	0.98	0.62	0.681

Hydration and hardening processes modeling

Simulation des processus d'hydratation et de durcissement des ciments

V.B. TCHERNIAVSKI,
V.Y. DOUBNITSKI, Promstroiniiproekt, Kharkov, U.R.S.S.

On décrit la construction et les résultats de fonctionnement du modèle de la structure du ciment durci et les transformations physico-chimiques qui s'y déroulent par rapport aux stades d'hydratation tardifs. Le principe de construction consiste en ce que les constituants de structure du ciment durci sont groupés en éléments conventionnels réunis compte tenu de l'unité de leur rôle fonctionnel dans le processus de formation des propriétés du ciment durci.

L'objectif visé par le travail est d'optimiser les propriétés de construction du ciment durci en fonction des conditions du milieu ambiant en choisissant les paramètres initiaux de la constitution des compositions ciment-eau. La source d'information principale sur la dynamique réelle du modèle est un ensemble d'études physico-chimiques. Par suite du traitement statistique des données on a effectué l'identification des paramètres des équations du modèle.

Sur la base de la méthode de Monte-Carlo on a étudié le fonctionnement du modèle et résolu une série de problèmes d'optimisation de la structure initiale du ciment durci, permettant de prévoir les propriétés du ciment durci en fonction de la compositon de base et de l'intensité de l'interaction avec le milieu ambiant.

Structure and results of functioning of cement stone texture model and transformations in the late hydration stages of the cement stone has been described. The principle of model structure is that the structural components of cement stone are grouped together in arbitrary units with regard to their functional part in the process of cement stone characteristics formation.

The purpose of the work is to opimize cement stone constructional characteristics depending on the environmental conditions by choosing initial parameters of cement-water compositions.

The main source of information of the model real dynamics is the complex of physical-chemical investigations. The identification of model equations has been developed as a result of data statistical interpretation.

On the base of Monte-Carlo method, functioning of the model has been studied and some problems on the optimization of cement stone initial structure have been solved, and hence there is a possibility of forecasting cement stone charactristics as a function of initial composition and intensity of interaction with environment.

Later stages of cement hydration taking place on the background of intense interaction between cement rock and its environment include complicated processes which are hard to be described analytically. A number of circumstances (multicomponent macro- and microstructure, substantial role of distructive phenomena, deformation and strength characteristics, permeability changing with time) define non-monotonous pattern of change of cement rock properties even though the environment parameters being constant. This makes the change of the material properties fixed at the end phase of early hydration period impossible to be formally extrapolated to later perod.

The development of engineering cybernetics caused a specific method of complex system investigation - simulation[1]. Simulation model is an analog of a complex real phenomenon realized in a computer which permits to discuss consequences of changes in process proceeding conditions and of making decisions concerning the control of properties of the system under study. Such a model is peculiar in the process being described step by step which permits making changes in due time (for control purposes) in the model equations caused by a long-term existence of the real object.

In simulating the process of non-hydrated binder grains hydration in cement rock notions of its structure are used based on grouping multiple structural elements according to their functional properties[2]. Percentage of non-hydrated clinker, slag, pozzolan, ash, etc. grains is designated as V_I, percentage of hydrate, formations as V_2, relative amount of empty "pores" (excluding "gel" pores), capillaries ($r \geq 10^{-7}$cm) as V_3, percentage of corrosion products and other inclusions with sharply reduced strength and deformation characteristics as V_4.

Liquid phase in cement rock represented by chemically fixed, crystallization, adsorption, capillary and gravity forms is taken into account while constructing and evaluating each of the model elements.

The processes taking place at later stages of the cement rock existence in the form of element interaction are summed up in Table I and reflect a creative process (pos. I) and destructive processes (pos.2,3). The latter may be subdivided into those including removal of elementary volumes V_I, V_2, V_4, and those including formation (introduction) of an elementary volume V_4.

Statistical evaluation of quantitive X-ray definitions ascertained that α_{12} is independent upon the kind of clinker mineral (C_3S, C_2S, C_4AF, seldom C A) at later stages (up to 10 years) of cement hydration in water, sulfate-containing solution in water under their continious and batch influence.

Assume all the elements of V_I are uniformly distributed along each coordinate axis, i.e. in each elementary volume all the elements are present in ratio corresponding to the complete volume; connections of any element with other elements are continious and mutually independent. Change of element V_3 is ascribed both to the transformations of V_{3i} and V_{i3} as noted in Table I and to the compensation of volume expansion during transformations of other elements. The intensity of interactions is invariant relative to the coordinates of an elementary unit volume and the macrovolume. The process is viewed upon as determined and monotonous on a segment.

The efficacy of the model proposed has benn verified on real objects (cement rock, concrete). Close connection between change of cement rock strength in time and change of the model components percentage has been established[2]. To evaluate prognostic properties of the model of cement rock as the main component of concrete vectors are formed which include R, V_I, V_3, V_4[3]. The degree of destruction of the material is proposed to be defined as $\widetilde{V}_3 = V_3 + V_4$[4]. It has been shown that at the stage of destruction (irrespective of the type of binder) the vectors $\vec{V}_1 = (V_I, \widetilde{V}_3)$ and $\vec{V}_2 = (R, V_I, \widetilde{V}_3)$ are statistically undiscernable [5].

In practice cement rock in concrete is never isolated from the environment which influence upon the intensity of transformation of cement minerals at later stages of existence of cement rock by accelerating hydrate formation pers ec as well as by partial

Table I

Position	Discription of a process of structural elements interaction	Process formalization, rates of transformations	
		Elementary mutually independent transformations for time Δt	Intensity of transformation $\alpha_{ij}^{xx} = \frac{\Delta V_i}{\Delta t \to 0}$
1	Transformation of V_I into V_2-V_{12}, volume increased	$\Delta V_1 \to K_{12}^{x)} \Delta V_2$	$-\alpha_{12} = \alpha_{21}$
2	Transformation of V_I, V_2, V_4 into V_3-V_{13}, V_{23}, V_{43}	$\Delta V_1 \to \Delta V_3$ $\Delta V_2 \to \Delta V_3$ $\Delta V_4 \to \Delta V_3$	$-\alpha_{13} = \alpha_{31}$ $-\alpha_{23} = \alpha_{32}$ $-\alpha_{43} = \alpha_{34}$
3	Transformation of V_I, V_2, V_3 into V_4-V_{14}, V_{24}, V_{34}, volume preserved and/or increased	$\Delta V_1 \to K_{14} \Delta V_4$ $\Delta V_2 \to K_{24} \Delta V_4$ $\Delta V_3 \to K_{34} \Delta V_4$	$-\alpha_{14} = \alpha_{41}$ $-\alpha_{24} = \alpha_{42}$ $-\alpha_{34} = \alpha_{43}$

x) K_{ij} - factor of volume change during transformation of structural elements ($0 < k < 1$)

xx) positive values of α_{ij} are ascribed to increase of the component designated with the first index

transformation of anhydrous combination into corrosion products. Naturally a period comes when the store of non-hydrated cements becomes insufficient to restore the properties of cement rock. From that time on being in contact with corrosive environment the cement rock begins to destroy irreversibly. To simulate this process differential equations of transformations of V_i into V_j are drawn taking into account α_{ij} - the value proportional to the intensity of the corresponding transformation.

$$V_2^{(m)} - V_2^{(m-1)} = \alpha_{12} V_1^{(m-1)} - \alpha_{23} V_2^{(m-1)}$$

$$\tilde{V}_3^{(m)} \quad \tilde{V}_3^{(m-1)} = \alpha_{13} V_1^{(m-1)} + \alpha_{23} V_2^{(m-1)} \quad (I)$$

Equation (I) is a stepped approximation of a system of equations (I) in [2]. Assume that step of division m corresponds to the time interval between two subsequent measurements made by petrographic method and method of isothermal desorbtion.

Physically the values α_{12}, α_{13}, α_{23}, are not mutually independent because transformations V_i V_j are simultaneous and non-simple. This fact is formally reflected in indeterminate form of thesystem (i) whose solution is a function pf any one of three values α_{ij}. A simultaneous estimation of these values experimentally without additional computing operations is impossible. Therefore, the values of α_{ij} are defined by least square method with a limitation.The value of V_i on each sample was defined experimentally by planimetric method using transparent flat-parallel samples [7]made of cement rock. Mineralogical composition of cement is given in Table 2.

Let

$$\Delta V_2^{(m)} = V_2^{(m)} - V_2^{(m-1)}$$

and

$$\Delta \tilde{V}_3^{(m)} = \tilde{V}_3^{(m)} - \tilde{V}_3^{(m-1)}$$

Then the criterion of least square method for each line of system (I) takes form:

$$U_1 = \sum_{p=1}^{20} (\Delta_{2p}^{(m)} - (\alpha_{12} V_{1p}^{(m-1)} - \alpha_{23}^{(I)}))^2 \to \min, \quad (2)$$

$$U_2 = \sum_{p=1}^{20} (\Delta_{3p}^{(m)} - (\alpha_{13} V_{1p}^{(m-1)} + \alpha_{23}^{(2)} V_{2p}^{(m-1)})) \to \min \quad (3)$$

The solution comes to the problem of definition on a conditional extremum with a limitation represented by equality

$$U_1 + U_2 \to \min \quad (4)$$

at

$$\alpha_{23}^{*(1)} = \alpha_{23}^{*(2)} \quad (5)$$

The symbol (*) designates an estimate of factor α_{23} obtained separately for each equation (2) and (3).

The results of computing the values α_{ij} in fractions of a unit are given in figure 1. It is obvious from this figure that in the course of prolonged contact between cement rock and the active environment three

Table 2

Position	Codes name of cement	Mineralogical composition (weight percent)				
		C_3S	C_2S	C_3A	$C_xA_yF_z$	Gypszm
1	A	51,6	22,7	6,8	10,8	5,0
2	B	58,6	17,9	2,9	15,5	5,0
3	H	54,5	20,2	9,1	11,1	5,0

stages of the process of structural change for the period corresponding to late stage of hydration can be observed.

Stage I: mainly creation when
$\alpha_{12} > \alpha_{13} + \alpha_{23}$

Stage 2 : mainly equilibrium when
$\alpha_{12} \approx \alpha_{13} + \alpha_{23}$

Stage 3: mainly destruction when
$\alpha_{12} < \alpha_{13} + \alpha_{23}$.

The existing methods of experimental definition of the value α_{ij} permit only to obtain a total estimate of V_I transformation into V_2 and V_3. Differentiation between these processes being limited to linear cases became possible to be achieved at only owing to the use of methods of calculation mathematics.

The simulation being performed it has been ascertained that the time of preserving useful properties in cement rock substantially depends upon the values α_{ij}. Under such conditions the structure of the material at each stage is in strict compliance with the relation between elements of the model V_i. In order to define the area of initial structural parameters of cement rock providing the preservation (taking into account the reestablishment caused by the transformation $V_I > V_2$) of its strength properties the problem of optimization of the initial composition of cement rock interacting with the active environment is solved.

Using transformation $V_3 = V_3 + V_4$ present teh system of equations (I) in the form

$$\begin{cases} V_2(t) + \int_0^t (\alpha_{12}(t) - \alpha_{23}(t))dt = V_2(t) & (6.1) \\ \tilde{V}_3(t) + \int_0^t (\alpha_{13}(t) + \alpha_{23}(t))dt = \tilde{V}_3(t) & (6.2) \\ V_1(t) = 1 - (V_2(t) + \tilde{V}_3(t)). & (6.3) \end{cases}$$

Assume that in any given moment the condition of the system is defined by vector $\vec{V}(t) = (V_1(t), V_2(t), V_3(t))$ condition being that

$$V_i(t_o) > 0; \quad i = 1, 2, 3. \qquad (7)$$

The main carrier of the strength properties of cement rock is element V_2. Therefore, it is necessary that by the required moment $t = \tau$ the percentage of element V_2 in the material was maximal. Accordingly, the limitations (.3) and (7) being kept to t_o t in all preceding interval of time.

In this case the purpose function

$$L = V_2(t = \tau) \rightarrow \max. \qquad (8)$$

The conditions (6,3), (7),(8) may be satisfied by the linear programming method.As

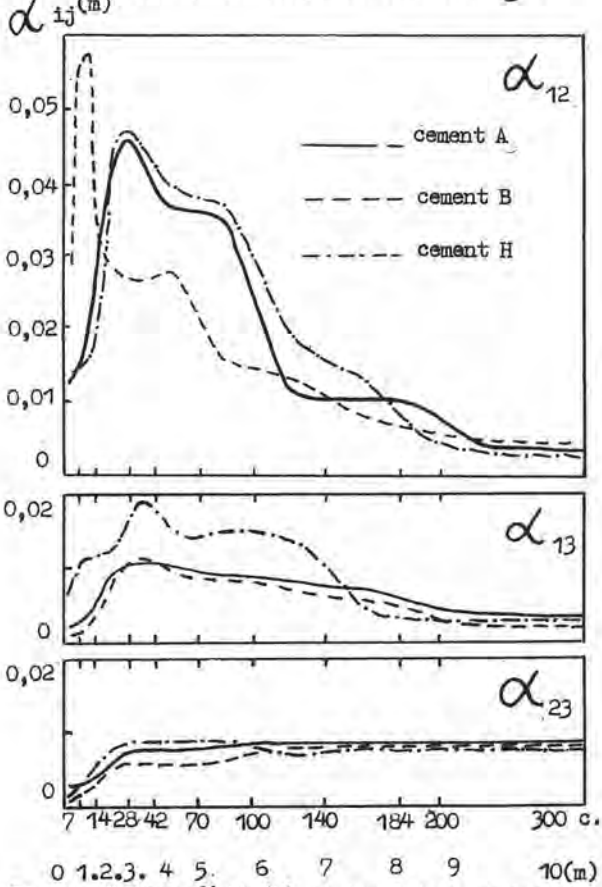

Fig. 1. Values α_{ij} (m) at the latest period of cements hydratation in active medium after n cycles, m steps

a result such values of initial composition $V_i(t_o)$ are abtained which provide the best operating properties by the required moment. Any deviation from the optimum values causes only a decrease in percentage of $V_2(t=\tau)$.

We have optimized the initial correlation between elements of V_i (in fractions of a unit) cement rock in conventional heavy concrete preliminarily hardened under usual conditions of temperature and humidity, made on medium-aluminia alitic cement and placed

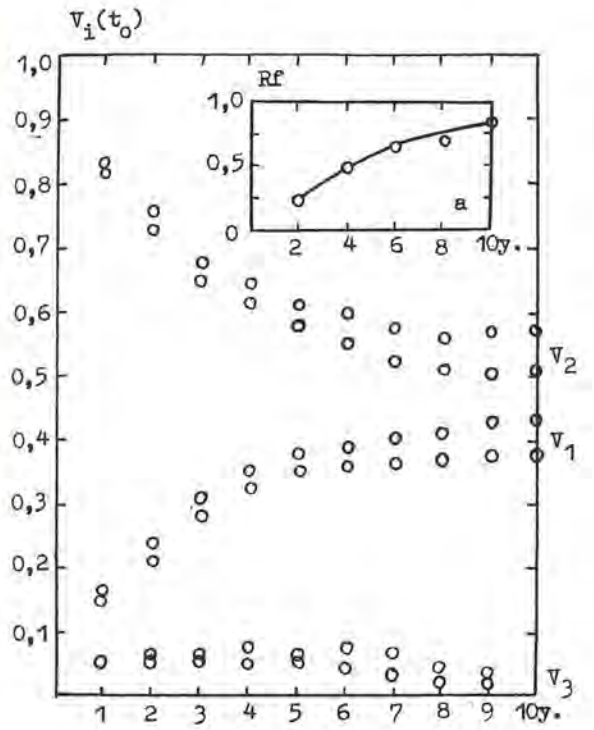

Fig. 2. Values of $V_i(t_o)$ broviding $V_2(t)_{max}$ by the time assumed by optimizing: a) values R_f to the same times

into a sulfate-containing solution. Numerical values of factors dij(t) are chosen on the basis of their identification in system (3) and statistical simulation 6 . The extent of the time interval conforms to condition V_2 max by 1,2...10-th year the step of division being I year. The results of solution are presented as a corridor of permissible values expanding with the course of calculated time (Figure 2).

As we see, the duration of the period of achieving condition V_2 (max) under present conditions is defined by the non-hydrated stors factor $R_f = \frac{V_1}{V_2}$ (Figure 2a). The shorter is the period of achieving V_2 max the lasser is R_f which corresponds to a high degree of hydration. On the contrary, the longer is the planned term of service of the material the larger should be the non-hydrated store and R_f I.

Therefore, the results given permit to assume that the proposed simulation model reflects reliably (in statistical sense) the diversity of creative and destructive processes in cement rock at every stage of its existence these processes being presented in a generalised form. The transformation of any model element V_i into V_j is treated independently of a given mineralogical composition of a property carrier the influence of environment being expressed only in values dij irrespective of the mechanism of process similarly to the estimation of a system phase condition as used in phenomenological thermodynamics.

The authors are grateful to Professor O.P.Mchedlov-Petrosyan for continious attention and support of the work for many years.

REFERENCES

I. Д.Х.Клейнен. Статистические методы в имитационном моделировании. М., "Статистика", I978.
2. О.П.Мчедлов-Петросян, В.Ю.Дубницкий, В.Л.Чернявский, Л.Б.Фридган. О формулировке модели структуры цементного бетона по отношению к старению. Известия ВУЗов, сер. "Строительство и архитектура", № I2, I970.
3. О.П.Мчедлов-Петросян, В.Ю.Дубницкий, В.Л.Чернявский. Использование многомерного статистического анализа для изучения долговечности цементного бетона. Известия ВУЗов, сер. "Строительство и архитектура" № 8, I974.
4. О.П.Мчедлов-Петросян, В.Ю.Дубницкий, В.Л.Чернявский, А.Г.Ольгинский. Статистическое изучение влияния агрессивных грунтовых вод на изменение свойств цементного бетона. Известия ВУЗов, сер. "Строительство и архитектура", № 5, I975.
5. О.П.Мчедлов-Петросян, В.Ю.Дубницкий, В.Л.Чернявский. Применение методов распознавания образцов для выборов режимов ускоренного определения долговечности бетона. Известия ВУЗов, сер. "Строительство и архитектура", № I, I976.
6. О.П.Мчедлов-Петросян, В.Ю.Дубницкий, А.Г.Ольгинский, В.Л.Чернявский. Статистическое моделирование процессов старения в цементном бетоне при его эксплуатации в агрессивной среде. Известия ВУЗов, сер. "Строительство и архитектура", № 9, I975.
7. С.А.Салтыков. Стереометрическая металлография. М., "Металлургия", I970.

Sur la composition des produits d'hydratation des hydroaluminates et les hydrogrenats de calcium et de magnesium

On the quantity of hydroaluminates and hydrogarnets of calcium and magnesium dehydration products

V.I. KORNEEV,
G.N. KASSIANOVA, Institut Technologique Lensovet de Léningrad, U.R.S.S.

Dans le rapport de stand présenté on a exposé les problèmes de déshydratation des hydroaluminates et des hydrogrenats de calcium et de magnésium; Par les méthodes d'analyse physico-chimique on a démontré l'existence en qualité du composé chimique individuel de la phase de l'hydroaluminate de calcium sesquihydraté, on a étudié ses caractéristiques physico-chimiques on a déterminé la composition des phases intermédiaires qui se forment lors de la déshydratation partielle des hydrogrenats de calcium et de magnésium. On a montré dans le travail que la composition des composés de calcium qui se forment dépend de la teneur de l'hydrogrenat en SiO_2 : jusqu'à 0,4 moles de SiO_2 la composition dela phase correspond à la formule $C_3AS_xH_{1,5-2x}$; plus de 0,4 de SiO_2, à $C_3AS_xH_{1,5-x}$. Dans les hydroaluminates et les hydrogrenats de magnésium l'évacuation de l'eau se fait également en deux stades. La composition de l'hydroaluminate de magnésium partiellement déshydraté correspond à la formule $3MgO \cdot Al_2O_3 \cdot 3H_2O$. L'interaction des phases partiellement déshydratées avec de l'eau donne les produits de départ.

Questions of hydroaluminates and hydrogarnets of calcium and magnesium dehydration are reported. With the help of physical-chemical analysis the existence of sesquihydrate calcium hydroaluminate phase as a separate chemical compound has been proved, its physical-chemical characteristics have been studied; composition of intermediate phases producing at partial dehydration of hydrogarnets of calcium and magnesium has been determined. Composition of the resulting calcium compounds depends on the SiO_2 content in hydrogarnet: up to 0,4 mol SiO_2 ⟶ phase composition $C_3AS_xH_{1,5-2x}$, more than 0,4 mol SiO_2 ⟶ phase composition $C_3AS_xH_{1,5-x}$. Dehydration of magnesium hydroaluminates and hydrogarnets has two stages too. Composition of partially dehydrated magnesium hydroaluminate is $3MgO \cdot Al_2O_3 \cdot 3H_2O$. Partially dehydrated phases, on interaction with water, produce initial products.

Les données disponibles sur la composition des produits de dissociation thermique de l'aluminate de calcium hexahydraté (C_3AH_6) sont contradictoires: il existe deux points de vue sur ce processus qui se distinguent par l'évaluation de la possibilité de la formation d'un composé intermédiaire de composition $C_3AH_{1,5}$, l'aluminate de calcium sesquihydraté. Ainsi, d'après les données (1 à 3) ce composé existe, a un indice de réfraction de la lumière de 1,543 et les caractéristiques radiographiques proches de celles pour $C_{12}A_7$; d'après les données (4 à 6) on propose le schéma de déshydratation suivante:

$$7(C_3AH_6) \xrightarrow{330\ ^oC} C_{12}A_7 + 9Ca(OH)_2 + 33H_2O$$

$$Ca(OH)_2 \xrightarrow{500\ ^oC} CaO + H_2O$$

$Ca(OH)_2$ libre étant fixé par les auteurs par la méthode à l'éthyle-glycérine.

Pour élucider un ensemble de problèmes liés à la composition des produits de dissociation thermique des solutions solides dans le système C_3AH_6 - C_3AS_3 on a étudié (12) les grenats de calcium hydratés avec la teneur variable en SiO_2 (0,0 à 1,13 mole). La composition chimique des grenats hydratés est donnée dans le Tableau I.

Les grenats hydratés utilisés dans le travail sont monominéraux à 92-97%. Les phases étrangères sont représentées par les hydrocarboaluminates de calcium de composition $3CaO \cdot Al_2O_3 \cdot CaCO_3 \cdot 11H_2O$, le carbonate de calcium, plus rarement par $Ca(OH)_2$. La caractéristique physico-chimique de C_3AH_6 - γ = = 2,52 g/cm^3, N = 1,600, les maximums de diffraction pour d/n=5,1; 3,34; 2,79; 2,28Å de la bande d'absorption dans le domaine de 540,800 et 3670 cm^{-1} correspondent aux données de référence. Dans les grenats de calcium hydratés l'indice de réfraction de la lumière croît avec la teneur en SiO_2 (7), les maximums de diffraction sur les radiogrammes se déplacent vers les angles 2θ plus grands, les effets endothermiques sur les thermogrammes se déplacent du coté des hautes températures, ce qui témoigne d'une plus grande force de liaison de l'eau dans les grenats hydratés par rapport à $3CaO \cdot Al_2O_3 \cdot 6H_2O$.

L'analyse des produits de déshydratation (8,9) a montré que dans l'intervalle de température de 300 à 450 °C la phase prédominante est représentée par l'aluminate de calcium sesquihydraté. Les preuves de l'individualité du composé obtenu se réduisent au fond à la démonstration de l'absence dans les agglomérés de $Ca(OH)_2$ libre, car la synthèse directe à partir des oxydes d'aluminate de calcium sesquihydraté est pratiquement impossible. La réaction microchimique de Watt, la détermination de $Ca(OH)_2$ libre par les méthodes de Franké et d'immersion n'ont pas relevé de présence de $Ca(OH)_2$; il s'est avéré que le mélange éthyle-glycérine décompose $3CaO \cdot Al_2O_3 \cdot 1,5H_2O$: un des produits de décomposition est représenté par $Ca(OH)_2$ que certains auteurs (5) prenant par erreur pour phase primaire de la dissociation thermique de C_3AH_6. Sur les radiogrammes il n'y a pas de maximums de diffraction caractéristiques de $Ca(OH)_2$. L'hypothèse sur l'identification éventuelle au lieu de $C_3AH_{1,5}$ des solutions solides de $C_{12}A_7$-$Ca(OH)_2$ ou sur la présence dans la composition des phases en cours de formation des microcristaux d'interpénétration de C_3AH_6 de base n'est pas confirmée en partant des valeurs de l'indice de réfraction de la lumière (il doit être de beaucoup supérieur à 1,543) et de la densité de la phase $\gamma C_3AH_{1,5}$ = 2,40 g/cm^3 (ce qui est beaucoup plus petit que pour des mélanges hypothétiques probables). La chaleur de dissolution de la phase obtenue (dans le mélange des acides nitrique et fluorhydrique) est de 548 ± 2 C/g, ce qui est inférieur aux chaleurs de dissolution des mélanges mécaniques $C_{12}A_7$ et CaO (653 ± 15 C/g), $C_{12}A_7$ et $Ca(OH)_2$ (587 ± 12 C/g), ainsi que de $C_{12}A_7$ et de CaO obtenus par cuisson de C_3AH_6 à 700 °C (609 ± 10 C/g). Une preuve supplémentaire de l'individualité de la phase $C_3AH_{1,5}$ est la formation par son hydratation de C_3AH_6 tandis que l'hydratation de $C_{12}A_7$ don-

Composition des composés dans une série					
Chiffre	Teneur en oxydes, %				Formule du minéral, mol
	n.n.n.	CaO	Al_2O_3	SiO_2	
G - 0	29,14	44,5	27,0	-	C_3AH_6
G - 1	26,1	42,4	25,75	3,8	$C_3AS_{0,25}H_{5,5}$
G - 2	21,8	43,07	25,21	8,02	$C_3AS_{0,54}H_{4,9}$
G - 3	21,78	41,86	24,62	8,75	$C_{3,1}AS_{0,61}H_{5,0}$
G - 4	18,34	41,66	24,6	13,49	$C_{3,1}AS_{0,93}H_{4,24}$
G - 5	16,53	38,70	25,16	16,75	$C_{2,8}AS_{1,13}H_{3,7}$

TABLEAU I

ne naissance aux aluminates de calcium hydratés hexagonaux. Tout ce qui vient d'être dit sert d'une preuve assez sûre bien qu'indirecte de l'individualité de la phase d'aluminate de calcium sesquihydraté.

Lors de la déshydratation des grenats de calcium hydratés de composition $C_3AS_xH_{6-2x}$ pour x jusqu'à 1,13 à la température du premier effet endothermique il se forme des phases du type de l'aluminate sesquihydraté qui se distinguent de ce dernier (12) par la composition et le domaine de stabilité thermique. Dans les grenats de calcium hydratés, surtout avec la teneur élevée en SiO_2, une partie de silice se dégage par cuisson sous forme d'une phase autonome dont l'indice de réfraction est de 1,480 à 1,490. La teneur en SiO_2 était déterminée quantitativement par les méthodes d'analyse chimique et pétrographique et prise en considération lors du calcul de la composition des phases. Le schéma de décomposition des grenats de calcium hydratés (exemple) peut être représenté de la façon suivante :

$$3CaO \cdot Al_2O_3 \cdot 0{,}93\ SiO_2 \cdot 4{,}24\ H_2O \xrightarrow{400\ ^\circ C} 3CaO \cdot Al_2O_3 \cdot 0{,}68\ SiO_2 \cdot 0{,}68\ H_2O + 0{,}25\ SiO_2 + 3{,}56\ H_2O$$

Les formules des phases qui se forment après le premier stade de déshydratation sont données dans le Tableau II. On a établi que les grenats de calcium hydratés avec SiO_2 jusqu'à 0,4 mole forment des phases partiellement déshydratées de formule générale $C_3AS_xH_{1,5-2x}$; si la teneur en SiO_2 dépasse 0,5 mole la composition des phases formées correspond à la formule $C_3AS_xH_{1,5-x}$.

Les aluminates et les grenats de calcium partiellement déshydratés sont stables dans l'intervalle de température assez étroit et lors du chauffage au-dessus de 450 °C il se produit la décomposition de l'aluminate hydraté avec la formation de $C_{12}A_7$ et de CaO, qui est fixé par les méthodes chimique et radiographique. Ces phases sont stables dans l'intervalle de 500 à 1000 °C, lorsque la température s'élève (1000 à 1300 °C) il se forme dans les agglomérés C_3A qui devient la phase principale à 1200-1300 °C.

Lors du traitement thermique des grenats de calcium hydratés avec un faible degré de saturation en SiO_2 c'est la phase de composition $C_3AS_xH_{1,5-2x}$ qui est stable dans l'intervalle de 350 à 450 °C et qui se décompose au-dessus de 450 °C avec la formation de CaO et de $C_{12}A_7$. Lors du traitement thermique au-dessus de 1000 °C il y a formation dans les agglomérés de C_3A et de la gehlénité. Dans les grenats de calcium hydratés avec une grande teneur en SiO_2 (>0,5 mole) à 500 °C les phases partiellement déshydratées avec l'indice de réfraction de la lumière de 1,590 à 1,600 se conservent comme phases principales, elles sont également prédominantes à 550-600 °C; la part de $C_{12}A_7$ formé grâce à la décomposition partielle de $C_3AS_xH_{1,5-x}$ ne dépasse pas 10 à 15 %.

Aux températures plus élevées on observe une décomposition sensible des phases intermédiaires, ce processus étant plus intense dans le grenat hydraté avec une teneur élevée en SiO_2 (1,13 mole). Les produits de décomposition des hydrogrenats partiellement déshydratés aux températures élevées (1000 °C) sont la gehlénite, C_3A, CaO, $C_{12}A_7$.

On a procédé à des études analogues avec l'aluminate et le grenat de magnésium hydratés $3MgO \cdot Al_2O_3 \cdot 8H_2O$ et $3MgO \cdot Al_2O_3 \cdot SiO_2(8-2x) \cdot H_2O$ pour x = 0,2 et 0,5. Les composés utilisés sont monominéraux à 85-93 %. Les corps étrangers sont l'hydrocarboaluminate de magnésium, MgO et $Mg(OH)_2$. Sur les radiogrammes les maximums de diffraction les plus prononcés pour d/n = 7,42 à 7,75, 3,76 à 3,81, 2,54 à 2,56, 2,26 à 2,28 Å appartiennent aux aluminates-grenats de magnésium hydratés. L'indice de réfraction des aluminates de magnésium hydratés est de 1,505 à 1,515, pour les grenats hydratés il s'élève jusqu'à 1,525-1,530. En comparaison des aluminates de magnésium hydratés les grenats de magnésium hydratés se caractérisent par le déplacement sur les thermogrammes des effets endothermiques liés à la déshumidification vers les grandes températures et par le déplacement des maximums de diffraction principaux dans le domaine des moindres angles 2θ.

En étudiant les processus de déshydratation de l'aluminate et du grenat de magnésium hydratés on a établi que la déshumidi-

TABLEAU II

Composition des grenats de		Composition des produits de déshydratation calcium hydratés	
Chiffre du grenat hydraté de base	Température du premier effet endothermique sur la courbe ATD	Composition des produits de déshydratation partielle	Indice de réfraction de la lumière
G - 0	360°	$C_3AH_{1,5}$	1,545
G - 1	340°	$C_3AS_{0,07}H_{1,15}$	1,551 à 1,557
G - 2	360°	$C_3AS_{0,37}H_{0,75}$	1,557 à 1,562
G - 3	380°	$C_3AS_{0,44}H_{1,0}$	1,550 à 1,557
G - 4	400°	$C_3AS_{0,68}H_{0,68}$	1,580 à 1,585
G - 5	440°	$C_{2,8}AS_{0,79}H_{0,72}$	1,595 à 1,610

fication avait lieu en deux stades. Notons qu'au premier stade on évacue 5 molécules d'eau et au deuxième les trois molécules restantes, ce qui ne s'accorde pas avec les données disponibles (10, 11) selon lesquelles au premier stade on évacue 7 molécules d'eau et au deuxième, 1 molécule.

D'après nos données, après le premier stade de déshydratation (300 °C) il se forme dans les agglomérés, en tant que phase principale, les aluminates et les grenats de magnésium partiellement déshydratés radioamorphes ayant l'indice de réfraction de la lumière de 1,545 à 1,555. Ces phases sont stables dans l'intervalle de température jusqu'à 450 °C. Aux températures plus élevées (500 à 900 °C) il apparaît dans les produits de traitement thermique, à coté de MgO, la phase intermédiaire radioamorphe dont la composition n'est pas déterminée. L'indice de réfraction de cette phase croît avec l'élévation de la température jusqu'à 900 °C de 1,545 à 1,620 pour l'aluminate de magnésium hydraté et de 1,555 à 1,630 pour le grenat de magnésium hydraté avec 0,5 SiO_2. Dans l'intervalle de température de 900 à 1300 °C les phases principales sont représentées par le périclase et la spinelle.

Lors du gâchage par l'eau des aluminates et des grenats de magnésium partiellement déshydratés il se produit une formation très rapide des aluminates et des grenats hydratés qui ont la meme quantité d'eau chimiquement liée comme ceux de base, dans les grenats de magnésium hydratés l'indice de réfraction étant inférieur à celui de départ, ce qui est lié à la séparation partielle de SiO_2 à partir des grenats de magnésium hydratés par leur traitement thermique.

BIBLIOGRAPHIE

1. Shneider W., Thorvaldson G. "Canadian J.Res", 1941, 123.
2. Majumdar A.I. Roy R. "J.American Ceramic Society", 1956,39,434.
3. Хейкер А.М., Залкинд А.И. Труды ВНИИасбестоцемент, вып. II, 1961.
4. Окороков С.Д., Голынко-Вольфсон С.Л. "Природа эндотермического эффекта, наблюдаемого на термограммах трехкальциевого алюмината при температуре 520-540°С". Труды ЛТИ им.Ленсовета, вып. 56, с.20-25, 1960.
5. Кондрашенков А.А., Жигун И.Г. "Фазовые превращения при нагревании некоторых гидроалюминатов кальция". Сб. трудов УралНИИСтройпроекта, вып.2. Гидратация и твердение цементов. Челябинск, 1974, с. 87-100.
6. Пушнякова В.А., Коцупало Н.П., Бергер А.С. "О термическом разложении гидроалюминатов кальция", ЖПХ, 7, 1975, с.48.
7. Еремин Е.И., Ящунин П.В. и др. "Исследование свойств твердых растворов состава $3CaO.Al_2O_3 \cdot O_2H_2O$", ЖПХ, 6, 1968, с. 1173.
8. Корнеев В.И., Касьянова Г.Н., Кузьмин Б.А. "К вопросу о существовании фазы полутораводного гидроалюмината кальция", Межвузовский сб. научных трудов ЛТИ им. Ленсовета. Химия и технология вяжущих веществ, силикатных и неорганических материалов", Л., 1977.
9. Сизяков В.М., Корнеев В.И., Касьянова Г.Н. и др. "Физико-химические свойства полутораводного гидроалюмината кальция", Труды ВАМИ, 100, Л., 1978.
10. Романов Л.Г., Алькенов П.А., Пономарев В.Д. "Обескремнивание алюминатных растворов с помощью окиси магния", Труды ИМ и ОАН Каз.ССР, т. XXXУП, Алма-Ата, 1970.
11. Волкова Н.С., Аракелян О.И. "Взаимодействие окиси магния с алюминатным раствором", Труды ВАМИ, № 70, Производство глинозема, М., 1970.
12. Корнеев В.И., Сизяков В.М., Касьянова Г.Н. и др. "О составе продуктов термической диссоциации гидроалюминатов и гидрогранатов кальция", "Цветные металлы", № 1, 1980.

Précisions pour la méthode ∝ d'estimation des paramètres de la structure poreuse du ciment durci

Method of the cement stone porous structure parameters estimation ∝ improvements

G.I. GORTCHAKOV,
O.A. MARKOVA,
L.P. ORENTLIKHER,
O.O. PEREBATOVA, Institut des Ingénieurs du Bâtiment Kouibychev de Moscou, U.R.S.S.

Les travaux expérimentaux des dernières années contiennent de nouvelles données obtenues par les mesures directes; Ces données permettent de recalculer les paramètres numériques dans les formules servant au calcul des volumes de pores des différents groupes, utilisés pour l'évaluation de la résistance au gel des produit de ciment. Il s'est avéré possible de préciser également la classification des pores. Il y a une possibilité de calculer séparément les volumes de pores du gel et des intervalles interlaminaires des cristaux de sa phase solide remplis par de l'eau facile à évacuer. Le volume de pores capillaires est calculé comme somme des volumes de l'eau qui n'a pas réagi et du volume libéré par la contraction. Le volume de contraction est considéré en tant que réserve de la résistance au gel; il n'est pas associé comme auparavant à un groupe de pores déterminé mais il est interprété comme déficit de volume de l'eau disposible dans les pores capillaires, de déficit apparaissant par suite de la contraction si l'eau n'arrive pas de l'extérieur.

Les précisions proposées correspondent plus complètement aux concepts actuels de la structure du ciment durci et permettent d'élever la fiabilité du pronostic de la résistance au gel.

Recent works contain new data resulting from direct measurings. These data allow recalculating the numerical parameters in formulae for volume calculation of different groups of pores. The formulae are used for frost-resistance estimation of cement articles. It turned out possible to improve also pore classification. The possibility exists of calculating separately volumes of gel pores and crystalls interlayer gaps of its solid phase, the gaps being filled with readily removable water. The volumeoof capillar pores is the sum of the unreacted water volume and the volume being released during contraction. Contraction volume is considered as a frost-resistance reserve, but is not ascribed, as earlier, to the defenite group of pores, it is looked upon as a volume deficit of water available in capillar pores arising because of contraction in the absence of water coming externally.

The improvements proposed comply in more detail with modern views of cement stone structure, they allow for increasing the frost-resistance forecast reliability.

La technologie d'obtention du ciment durci compact s'appuie sur l'analyse de sa structure poreuse, qui se fonde sur l'utilisation des valeurs expérimentales du degré d'hydratation du ciment α (proposée par G.I.Gortchakov en 1964 [12]). Cette méthode de détermination de la porisité de groupe doit être développée et precisée vu l'accumulation de nouvelles données scientifiques ayant trait aux concepts et aux grandeurs formant la base de la méthode.

Considérons les nouvelles données obtenues par R.F.Feldman et T.K.Powers. En mettant en jeu les méthodes spécialement élaborées dans une expérience montée de façon soigneuse Feldman établit la densité de: a) la phase solide du gel de ciment saturée au maximum en eau interlaminaire, $\rho_{(a)}$ = $2{,}35 \pm 0{,}01$ g/cm^3; b) l'ossature siliceuse de la phase solide du gel qui reste après l'évacuation à partir du gel de l'eau lors du séchange D, $\rho_{(b)} = 2{,}51 \pm 0{,}01$ g/cm^3 [3].

Powers construisit un diagramme très important permettant (voir fig.1) la détermination directe des caractéristiques physico-chimiques nécessaires du gel de ciment. Le point A sur ce diagramme représente la pierre de ciment qui ne se compose que du gel, ce dernier étant caractérisé par la teneur minimale en milieu de dispersion. Le diagramme nous montre qu'au point A correspond E/C = 0,38; W_t=0,45; W_e=0,225. En prenant 1g du ciment + 0,38 g de l'eau on obtient le ciment durci comprenant le gel A (c'est ainsi qu'on notera le gel dans ce qui suit) de masse de 1,45 g. La quantité d'eau supplémentaire (0,07 g) au-dessus de 0,38 g est prise (aspirée) par le gel du milieu ambiant. La teneur totale en eau est W_t=0,45 g.

D'après Powers, le volume de 1,45 g du gel obtenu est égal à:

V_A=0,315 cm^3/g·1 g+0,99 cm^3/g·0,38g=0,691cm^3

(0,315 cm^3/g est le volume spécifique du clinker de ciment: 0,99 cm^3/g le volume spécifique de la solution d'aqueuse saturée de $Ca(OH)_2$).

D'après les données déjà citées de Powers 1g du ciment hydraté fixe W_e=0,225 g de l'eau évaporée si la saturation est totale. Dans le calcul du volume des pores de gel V_3 divisons l'eau W_e en eau interstitielle au

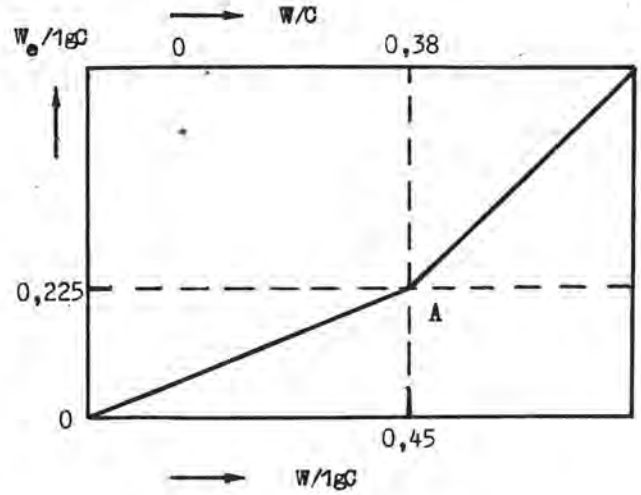

Fig. 1. Diagramme de powers

sens propre de ce mot et en eau interlaminaire. Utilisons à cet effet les données de Feldman et écrivons pour la phase solide du gel:

$2{,}51(1-x) + 1{,}25x = 2{,}35.$

On en tire :

$(1-x)$, la fraction du volume de la phase solide du gel, associée à l'ossature siliceuse, x, la fraction du volume de la meme phase, associée à l'eau interlaminaire

$(1-x) = 0{,}873$ et $x = 0{,}127$.

Trouvons encore le rapport entre l'ossature siliceuse (OS) et l'eau interlaminaire (EI) d'après la masse :

OS:EI=2,51(1-x):1,25x=0,219:0,016,

où 1,25 est la densité de l'eau occupant les interstices entre couches dans les cristaux de la phase solide d'après Feldman [3]. Calculons maintenant la quantité de l'eau interlaminaire liée à l'ossature siliceuse du gel A: $\frac{1{,}225 \cdot 0{,}016}{0{,}219} = 0{,}081$ g;

Ainsi dans le gel

1·1,225+0,081=1,306g - la phase solide à l'état saturé en eau (i.e. avec l'eau inter-

laminaire),
2.0,225-0,081=0,144g - l'eau dans les pores du gel. Le rapport des volumes est alors $\frac{1,306}{2,35\ g/cm^3}$ =0,556 cm^3 - le volume de la phase solide du gel saturée en eau, i.e. comprenant l'eau interlaminaire, et 0,691-0,556=0,135 cm^3 - le vrai volume des pores du gel; désignons-le par $V_{3,vrai}$ à la différence de V_3 comprenant le volume des interstices entre couches de la phase solide. Faisons le bilan. Selon le calcul effectuée, le vrai volume des pores de gel se définit par la formule

$$V_{3,vrai} = 0,135\alpha C\ cm^3 \qquad (1)$$

sans perturbation de cette valeur par l'introduction dans cette dernière du volume des interstices entre couches de la phase solide du gel. En cas de nécessité on peut calculer V_4=0,065αC qui est un volume des interstices entre couches de la phase solide du gel, occupés par l'eau de critallisation interlaminaire si la saturation en eau de cette phase est totale; on peut calculer également V_5=0,556αC qui est un volume de la phase solide saturée en eau du gel.

Passons à la contraction. Le volume de contraction V_2 est déterminée d'après [1,2] à l'aide de la formule

$$V_2=E-(m-1)v_c\alpha C-(E-W_t\alpha C)=(v_c+W_t-mv_c)\alpha C, \quad (2)$$

où m est le coefficient montrant l'accroissement du volume lors de l'hydratation et de la transformation en gel d'un gramme du ciment; v_c-le volume spécifique du ciment. Trouvons d'après les données de Powers

$$m = \frac{0,691\ cm^3}{0,315\ cm^3} = 2,19_3 \approx 2,2.$$

La même valeur était utilisée également dans [1,2] La formule (2) et ses coefficients n'ont pas besoin d'être précisés. On peut seulement simplifier l'expression (2) en substituant les valeurs numériques v_c = =0,315 cm^3/g, W_t=0,45g par 1g du ciment, m=2,20; on a dans ce cas

$$V_2 = 0,07\alpha C.$$

En considérant la valeur V_2 il faut prêter attention sur ce que le gel A aspira du milieu ambiant 0,45-0,38=0,07 g de l'eau grâce à la contraction. Comme on l'a vu, le volume des pores du gel A et $V_{3,vrai}$ = =0,135αC=0,135 cm^3, par conséquent, 0,07g de l'eau aspirée de l'extérieur remplissent une partie de ces pores du gel.

Comme interpréter la grandeur V_2?

La figure 2a montre le système E+C pris pour l'expérience. Les quantités de E et de C sont arbitraires, mais E/C$\leq$0,38. Le moment où par suite de l'hydratation il s'est formé une certaine quantité du gel est représenté sur la figure 2b. Pour plus de commodité on a choisi le moment où il s'est formé 1,45g du gel. Ceci donne la possibilité d'illustrer les schémas de la figure 2 par les données numériques figurant dans le texte. Voyons les changements qui doivent survenir à ce moment dans l'échantillon par rapport à l'état initial représenté sur la figure 2a.

La figure 2c montre la façon dont on divise le volume du gel en volume de sa phase solide et en volume de ses pores. Sur la figure 2d on a dégagé du volume des pores du gel le volume de contraction V_2. Il est montré ici comme une partie du volume des pores du gel. Les figures 2e,f donnent la redistribution des masses d'eau mobiles dans les échantillons de plusieurs années de Powers. Un espace libéré dans le système E+C grace à la contraction fut rempli en fin de compte dans les expériences de Powers par l'eau liquide aspirée dans ce système à partir du milieu ambiant.

Procédons maintenant au calcul du volume des pores capillaires V_1. D'après [1,2] ce volume est calculé à l'aide de la formule

$$V_1 = E - 0,5\alpha C. \qquad (3)$$

Le coefficient 0,5 représente la quantité d'eau W_t se transformant en gel par hydratation d'un gramme du ciment. La figure 2 montre que la formule (3) est à préciser. Comme on le voit sur le dessin,

$$V_1=(E+v_cC)-V_{gel}-v_cC_{reste}=E-(m-1)\alpha v_cC.$$

Substituant m = 2,2 et V_c = 0,315 nous obtenons une formule simple

$$V_1 = E - 0,38\alpha C. \qquad (3')$$

Il est aisé de voir que le volume calculé d'après la formule (3') ne se distingue du volume calculé d'après (3) que par ce que maintenant il comprend, ce qui est de règle d'ailleurs, le volume de contraction.

La figure 3 montre le passage de [1,2] aux grandeurs V_1, V_2, V_3 calculées d'après les formules précisées.

Pour déterminer le volume de contraction, on peut recommander encore, outre la méthode α, la méthode [6], ce qui peut être nécessaire pour des objets dont le volume de contraction ne se détermine pas à l'aide de la formule (2) vu l'utilisation de nouvelles additions, l'accroissement de la température de durcissement de la température de durcissement, etc.

Cette détermination nécessite que l'échantillon soit pris sous forme de gros morceaux, que l'air soit pompé de cet échantillon et que ce dernier soit immergé dans l'eau. Après l'extraction de ces échantillons à partir de l'eau il faut évacuer un excès d'eau restant sur la surface de chaque morceau et peser une charge d'environ 7 à 10 grammes de l'échantillon préparé de la façon décrite. Ensuite il faut déterminer pour cet échantillon les pertes de calcination en les calculant pour 1g du reste calcuné, i.e. pour 1g du ciment de départ. Ces pertes (nnn') représentent les pertes de calcination d'un échantillon saturé en eau et non pas séché comme d'habitude. La valeur de la contraction est obtenue par soustraction des nnn' de l'eau qui était introduite dans la pierre de ciment étudiée au moment de gachage. Tout le calcul du résultat de l'analyse peut etre

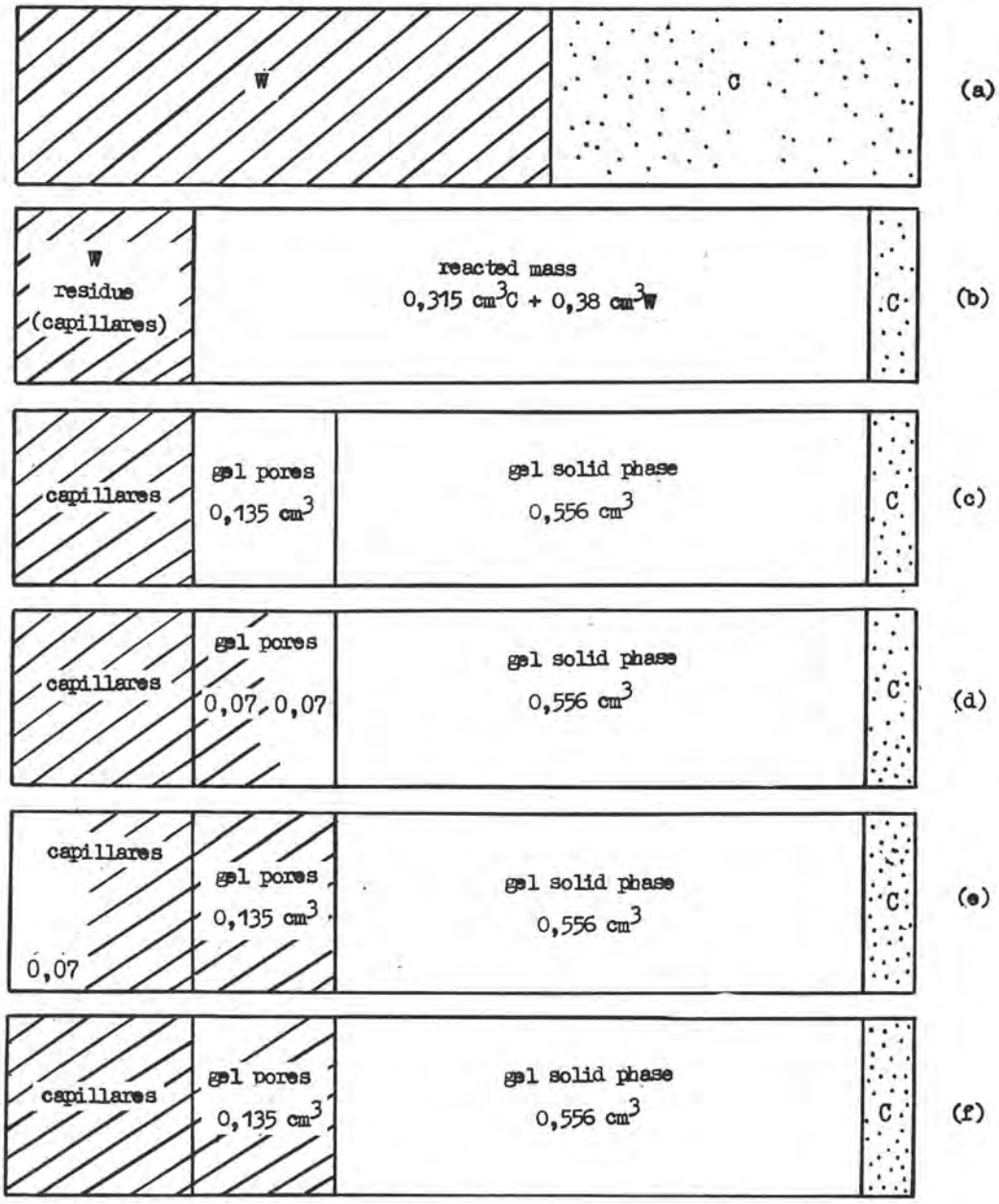

Fig. 2. Contraction et migration de l'eau vers le lieu de la reaction (schema, explications dans le texte)

effectué en pour cent du volume total de
l'échantillon d'après la formule suivante
simple

$V_{contr}=(nnn' - E/C)/(E/C+v_c)$ 100% vol.

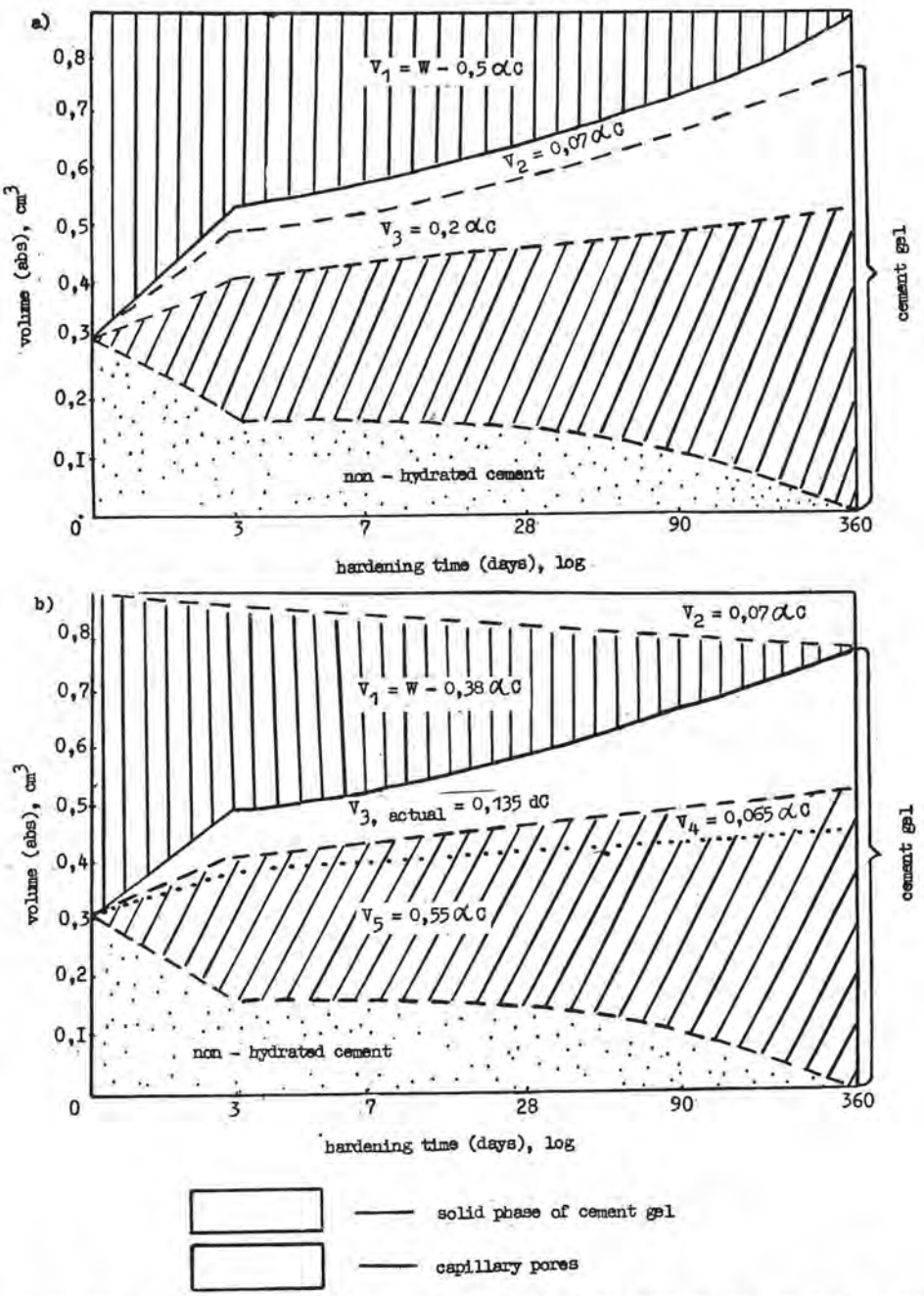

Fig. 3. Volumes des parties constitutives du ciment durci (avec changement au cours du durcissement, E/C = 0,5): a - d'apres 1, 2 et b - selon les precisions effectuees

LITERATURA

I. Горчаков Г.И. Морозостойкость бетона в зависимости от его капиллярной пористости. Бетон и железобетон, I964, № 7.

2. Горчаков Г.И., Кашкин М.М., Скрамтаев Б.Г. Повышение морозостойкости бетона в конструкциях промышленных и гидротехнических сооружений. М., Стройиздат, I965.

3. Feldman R.F. Cement Technology, 3, №1, 1976.

4. Пауэр Т.К. Сб. "Химия цементов" под ред. Тейлора Х.Ф.У. М., Стройиздат, I969.

5. Горчаков Г.И., Маркова О.А., Перебатова О.О. Способ определения концентрации цементной смеси. Заявка № 2724009/33 (022500), М., I979.

Application of physical-chemical and micromechanical formalized models for cement stone pore structure analysis

Application des modèles formalisés physico-chimiques et micromécaniques à l'analyse de la structure poreuse de la pierre de ciment

D.A. UGINCIUS, Vniivodgeo, Kharkov, U.R.S.S.

Le processus de formation et les propriétés mécaniques de la structure poreuse de la pierre de ciment sont envisagés du point de vue des modèles du corps poreux élastique de Mackenzie et du champ réactif d'Onsager. Le processus de consolidation de la structure par diminution de la porosité est décrit par la dépendance exponentielle de Tychkevitch. Les processus de colmatage des pores sont étudiés avec utilisation du modèle microrhéologique de Gutt-Simkhi-Gold et du modèle d'adsorption polymoléculaire BET.

On a montré donc que la relation entre la porosité, les propriétés mécaniques et les propriétés de diffusion du ciment durci peut être estimée non seulement statistiquement mais avec utilisation des modèles formalisés fondamentaux connus physico-chimiques et micromécaniques.

The process of formation and mechanical properties of cement stone pore structure have been considered taking into account Maccensey elastic porous body model and Onzager reactive field model. The process of structure hardening with porosity decrease in is described by Kyshkevich exponent. The processes of pore colmatation have been studied with the use of Gut-Simkhy-Gold microrheological model and BET polymolecular adsorption model.

In this way it is shown that the interconnection of cement stone porosity, mechanical and diffusion properties can be estimated not only statistically, but also with well-known basic physical-chemical and micromechnaical formalized models.

When investigation the structure and properties of hydrated Portland cement having polydispersed sponge porous structure a number of general physico-chemical problems (adsorption, diffusion, abovemolecular formations, structural sensitivity of properties) is inevitably touched upon. It is resonable to consider them using theoretical and semiempirical formalized models describing these phenomena.

Sufficiently strict analytical consideration of porosity influence upon the cement stone stress-strain properties is connected with insuperable difficulties relative to high structural sensitivity of properties of defective bodies [1]. To estimate this influence Mackenzie model [2,3] derived from computations based on Frolich "self-consistency" method [4] has been used. The idea [2] implies that a single isolated pore in the center of a sphere of real material with real shear (G) and bulk (H) moduli is supposed to be surrounded by the spherical "crust of absolutely dense material with hypothetical moduli G_o and H_o.

Consideration of such model deformation under the effect of the homogenious stress has given the following dependence.

$$\frac{G_o - G}{G_o} = \frac{5(3H_o + 4G_o)}{9H_o + 8G_o} + AP^2 \qquad (1)$$

where, A - the factor taking into account mutual influence of structural elements (pores).

Kingery [5] using a number of simplifications on the basis of the dependence (1) obtained the simplified formula which adequately describes the experimental dependences $E/E_o = f(P)$ for a variety of materials with the Poisson's ratio $\mu = 0.5$; for the cement stone the assumption $\mu = 0.3$ is insufficiently correct, since in this case the Poisson's ratio varies over rather wide range [6]. On the basis of generalisation made by Verbeck and Helmuth [7], using data on Yong's modulus, the shear and bulk moduli, as well as Mackenzie dependence (1) the following dependence has been derived:

$$E = E_o(1 - 2.18P + 0.5P^2) \qquad (2)$$

where, E-Yong's modulus of the cement stone;
E_o - Yong's modulus of the cement stone with zero porosity.

The formula (2) is a semiempirical case of the dependence (1) for the idealized cement stone with ovenly distributed spherical equidimensional pores. Likewise the general model (1) the formula (2) is valid when P 0.4, since with greater P values interaction of pores becomes essentual 8 , i.e. the coefficient values at a quadratic term.

The first Lamet's coefficient of porous λ_1 is:

$$\lambda_1 = H - 2/3\,E \quad 0 \qquad (3)$$

This relationship is valid with the lowest value of the coefficient at a quadratic term of 0.5 [9].

Fig.1 gives a comparison between the dependence (2) and Helmuth, Turk [10] with the cement stone of 100% hydration; it is obvious that the structure of the cement stone samples is rather close to the modelled one (2) which takes into account real elastic properties of the mineral phase. Relationship between mechanical strength and porosity of the cement stone is of more complex nature; as Griffith and his followers showed that the size and configuration of pores are of essential significance. Additionally, if to consider the kinetics of crack increase process, Laplace's pressure, the coalencence of pores, on may state that the behavior of porous bodies under stress and porous structure formation are exclusively involved complexes which represents and in some cases competitive elemental processes. Therefore, an interesting work 11 treating intermolecular interaction model on the basis of Lennard-Jones potential 12 as applied to the theory of strength can be considered as a basis for modelong concepts on dispersed structure strength at the molacular level only.

Due to the complexity of the problem strengthening of porous materials under stress or as a result of various technological effects is considered in most general form, for example, on the analogy of some chemical reaction 13 .

Analogous to sintering 9 it is propoused to regard the process of cement materials strengthening as the result of filling its porous spaces with solid phase (hydration hardening, formation new phases when admixtures are added, filling of pores with polymer densifiers etc.) as relaxational process. In this case, using Maxwell equation for

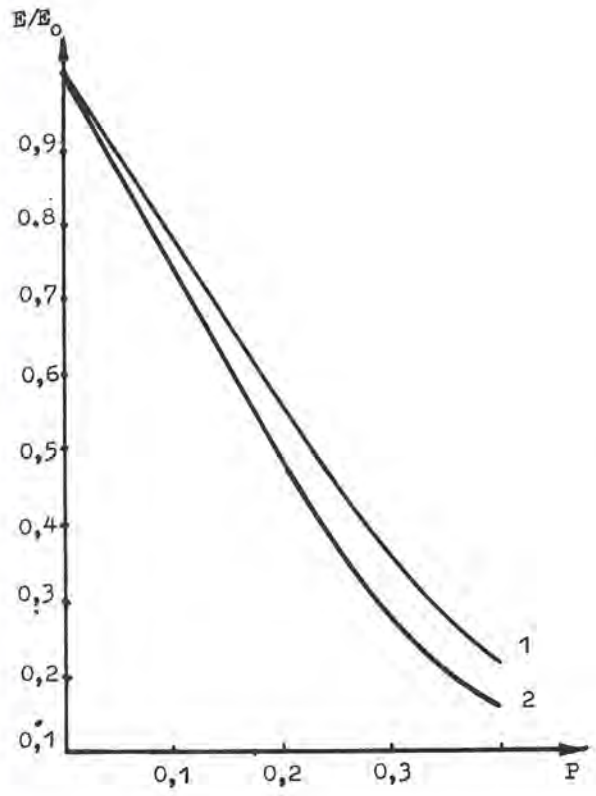

Fig. 1. Dependences $E/E_o = f(P)$ FOR cement stones

viscous-elastic body and assuming P=f(t), deformation as a constant:

$$dR/dP = -nR \qquad (4)$$

and after integration:

$$R = R_o \exp(-n\,P) \qquad (5)$$

Empirically this dependence is derived (for ceramics) by Ryshkewitch [14] and has been well supported with the examination of dependences R=f(P) for ceramics and ceramal.

Modelong concepts on cement stone hardening process on the basis of Ryshkewitch dependence (5) consist in the following:

- P coefficient equivalent to porosity quantitatively reflects the process of cement stone strengthening resulted from filling of pores with solid phase;
- coefficient $n = f(\varphi_1, \varphi_2, \varphi_3, \varphi_4)$ where φ_1 is the function of local densities (pores or ensembles of pores) distribution, φ_2 is the function of pore distribution according to size, φ_3 is the function of pore distribution according to configuration and φ_4 is the function of pore distribution according to orientation to force action;
- R_o - strength of the absolutely dense mineral phase (without pores);

The exponential formula (5) is good for description of the experimental dependences both for ceramics [5,14] and cement stone [15,16] including polymer impregnated cement stone [17] It is necessary to note that dependence (5) can be said adequate porous cement material model only in the case when pores are predominant defects in particular, this dependence is not suitable for properties description of concrete which fails primarily along aggregates or along the contact zone "binder-aggregate". The model postulates the presence of adhesion strength within the contact zone at binder cohesive strength level. Such on assumption might be acceptable only for the cement stone, high-strength fine concrete and polymer impregnated cement materials.

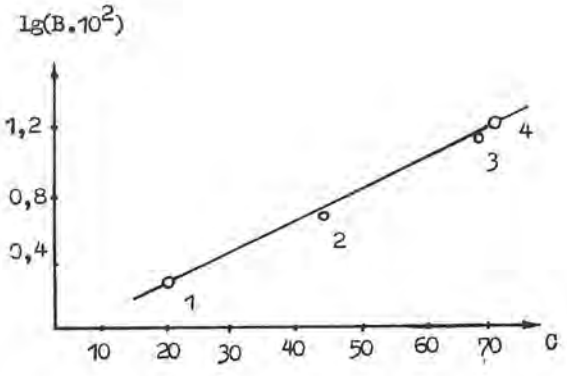

Fig. 2. Generalized dependences $R/R_o = f(P)$

When filling a cement stone porous space with organic polymers hydration products of clinker minerals, posessing high specific surface, actively participate in the structure formation processes of the polymer phase. Morphology above molecular structure reorganization under the influence of the mineral phase has been estimated by means of the Guth-Simha-Gold's microrheological equation 18 , supplemented (Smoluchowski's method 19) by the quadratic term allowing for the interdependence of dispersed particles:

$$E_k/E_n = 1+2.5\varphi + 14,1\varphi^2 \qquad (6)$$

where, E_k - Yong's modulus of composition;
E_n - Yong's modulus of despersion medium (of polymer)
φ - filler volume concentration (of mineral phase).

The equation (6) is invariant to the nature of the filler and matrix surfaces, and therefore it is convenient as a standard for comparison while investigation the polymer

properties in boundary layers. Physico-chemical interaction polymer - mineral backing is expressed in the change of Yong's modulus value calculated according the equation (6), e.i. allowing only for a filling (hydrodynamical) effect. Investigated dependences are approximated by the stright-line equation:

$$Kp = A + B \frac{a}{\varphi_n} \qquad (7)$$

where, a - the adsorption value on a mineral proportional to the specific surface of a mineral phase;

φ_n - polymer concentration in the system.

Value B in the equation (7) is a mesure of the mineral phase physico-chemical activity[20] since it characterizes the rate of polymer reorganization coefficient change K_p;with amineral phase surface unite being introduced.

It is estimated that the activity of interaction between mineral and polymer phases does not depend upon a degree of a specific chemical interaction: portlandite[21] the most active with regard to the donor-acceptor interaction has B value which a very close to the similar characteristics of calcite which does not form complexes with a polymer. On the other hand, the correlation dependency has been established between coefficient B and constant C from the BET equation [22] the constant C is a quantitative measure of the mineral phase adsorption activity (Fig.3). Thus, it can be stated that the polymer structure reorganization in immediate proximity to the cement hydration products surfaces could be accounted for mainly by a physico-chemical interaction (conformal restrictions in adsorption layers), but not by a specific chemical interaction.

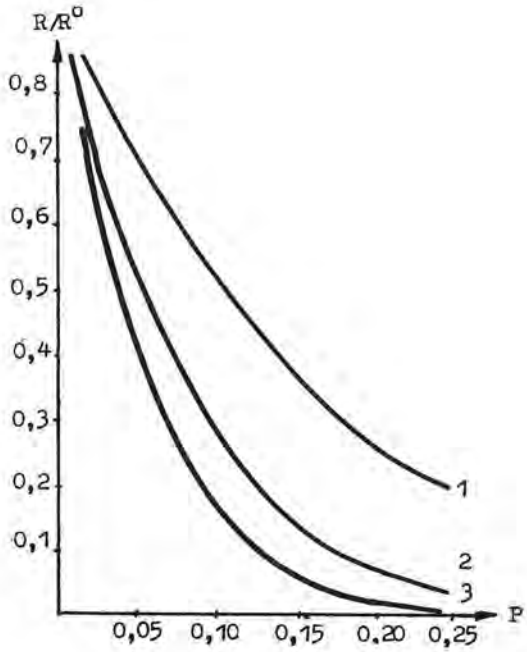

Fig. 3. Dependence between coefficient B from equation (7) and constant C from equation BET

A cement stone being impregnated with various polymer compositions, hydrosilicate gel can display properties of a molecular sieve. This phenomenon has been studies experimentally using a series of organic liquids with an increasing size of molecules (methanol, benzol, butanol, methylmethacrilate, hexane, etc;) Having no data on the radii of this molecules averaged out in all possible conformations, we in the calculations made use of Onsager [23] model of intermolecular interaction. This has made it possible to use simple and suitable for experiment dependences in which molecular sizes are determined by the macroscopic properties of liquids[24] Correlation has been established between the cement stone adsorption volume and Onsager radii of molecules. This correlation quantitatively characterizes the molecular sieve effect which is of great significance from the engineering point view.

Thus, in the investigation of the cement stone structure and properties as a polydispersed porous body, alongside with statistical classical physico-chemical modeling concepts may be successfully made use of.

REFERENCES

1. Geguzin J.E. Macroscopic defects in metals (in Russian) Moscow, Metallurgy Press., 1962.
2. Mackenzie J.K.Proc.Phys.Soc.,1950,B 63, 361,2.
3. Lawrence P.,Majumdar A.J.Nurse R.W.Cem. and Concr.Res.,1971, 1,1,75
4. Frolich H.,Sack R.Proc.Roy;Soc.,1946,A 185, 415.
5. Coble R.L.,Kingery W.D.Journ.Amer.Ceram. Soc.,1956,39,11, 377.
6. Malmeister A.K. Elasticity and non-elasticity of concrete (in Russian).Riga, Latvian Acad.,Sci.Press.,1957.
7. Verbeck G.J.,Helmutch R.A.Chemistry of Cement.Princ.pap.of the V-th Int.Symp., Tokyo,1968,PartIII,Sess.1.
8. Guth E.,Simha R.Kolloid.Z.,1936,74,266.
9. Skorochod V.V.Rheological principles of sintering theory. (in Russian),Kiev, Scientific Thought Press,1972.
10. Helmuth R.A.,Turk I.H.Highway Res.Board, Spec.Rep.,1960,90,135.
11. Yuschenko V.S.,Schukin E.D.(in Russian) Rep.Acad.Sci.USSR, 1978,242,3,653.
12. Lennard-Jones J.E.,Devonshire A.Proc.Roy. Soc.,1937,A 163,53.
13. Pines B.J.Metallophysical essays (in Russiang),Kharkov, Univ. Press;1963.
14. Ryshkewitch E.Journ.Amer.Ceram.Soc.1953, 36,2,65.
15. ROy.D.M.,Gouda G.R. Cem.and Concr.Res., 1973,3;6,807.
16. Kondo R.,Diamond M.(inRussian).Chemistry of Cement.VI Int. Congr.,Moscow,v.II, book 2, 1976,65.

17.Ugincius D.A.(inRussian) Abstr.All-Union Conf. on Polym.Concr.,Tashkent,1978,124.
18.Einstein A.,Ann.der Physik,1911,34,591.
19.Smoluchowski M.Z.physik Chem.1917,92,129.
20.Kerch G.M.,Chirkova E.A.,Irgen L.A. (in Russian) "Thermodinamical and structural properties of polymer boundary layers", Kiev, Scientific Thought Press,1976,73.
21.Spirin Y.A.,Olginski A.G. Mchedlov-Petrosyan O.P., Ugincius D.A. (in Russian) Rep.Acad.Sci.USSR,1978,241,3,654.
22.Brunauer S.,Emmett P.H.,Teller E.Journ. Amer.Chem.Soc.,1938,60,309.
23.Onsager L.J.Amer.Chem.Soc.,1936,58,1486.
24.Bokov O.G. (in Russian) Optics and Spectroscopy, 1973,311,996.

Structures et résistances mécaniques sous des traitements hydrothermiques

Structures and mechanical resistances under hydrothermal treatments

G. TEODORU, ancien rechercheur en chef INCERC Cologne, République Fédérale d'Allemagne.

RESUME : L'étude des bétons ayant subi un traitement hydrothermique fût commencée en 1957 lorsque l'auteur dirigeait le laboratoire d'essais d'une fabrique de précoulage. Des recherches systématiques sur la structure et sur les résistances mécaniques de ces bétons ont été effectuées à partir de 1967.

Les résultats des essais non-destructifs à l'aide des ultrasons (fig. 1 et 2) permettent de conclure que pour les bétons ayant subi un traitement hydrothermique, existent les relations exponentielles V_L-R_c et A-R_c . Les coefficients de corrélation allant de 0,898 à 0,988 sont obtenus.

Les essais laissent entrevoir, d'une manière très évidente surtout dans le cas du traitement à l'autoclave, l'existence des défauts de structure. Les valeurs du module d'élasticité statique des compositions traitées à l'autoclave sont inférieures à celles correspondantes au durcissement normal. Le comportement est sur une grande étendue de la courbe $\varepsilon = f(\sigma)$ élastique (fig. 3) et on a remarqué une réduction importante de l'aire de la courbe de hystéresis pour les cas du traitement à l'autoclave.

Des recherches à l'aide du microscope optique sur des suspensions de ciment, sections minces et sections polies, et d'autre part, à l'aide du microscope électronique sur des "moulages" contrastés avec du platine ont été effectuées.

La compacité cède le rang d'importance à l'obtention des formations nouvelles caractérisant les traitements hydrothermiques sous pression possédant de meilleures qualités liantes. La capacité liante supérieure résulte de l'augmentation des points de contact créés par la dispersion plus élevée des particules quoique la structure ait plus de défauts.

SUMMARY : The study of concretes subjected to a hydrothermal treatment was started in 1957 when the author directed the testing laboratory of a precasting plant. From 1967, systematic researches onto the structure and their mechanical resistances were carried out.

The results of the non-destructive tests with ultrasonic pulse method (fig. 1 and 2) allow to conclude that for concretes having been subjected to a hydrothermal treatment, the relations V_L-R_c and A-R_c are exponential. Correlation coefficients from 0,898 to 0,988 are obtained.

The tests showed very clearly, especially in the case of autoclaving, the existence of structural faults. The values of modulus of elasticity of the autoclaved compositions are inferior to those of cured ones under ordinary conditions. The behaviour of autoclaved mortars had shown the almost linear trend (fig. 3) of the curve $\varepsilon = f(\sigma)$ and an important reduction of the hysteresis area has been noticed for the cases of autoclaving treatment.

With the help of the optical microscope, researches were carried out on cement-water grouts, thin sections and polished sections and, on the other side, with the help of the scanning electron microscope on platinum-contrasted "moulds".

The compacity cedes the rank of importance to the obtaining of new formations characterising the hydrothermal treatments under pressure which have better cementitious qualities. The superior binding capacity results from the increasing of contact points, created by the higher dispersion of the particles although the structure has more faults.

I. INTRODUCTION

La constatation faite lors de quelques expertises de la destruction avec une rapidité surprenante des éléments en béton à agrégats ordinaires traités en autoclave, a déterminé les recherches systématiques poursuivies par l'auteur dans le but de préciser la structure de ces bétons. [1].

II. RECHERCHES EFFECTUEES

A. Essais non-destructifs à l'aide des ultrasons

A partir de 1967, des recherches ont été effectuées dans le but d'étudier l'effet qu'exercent les principaux types de traitement hydrothermique-étuvage (E), traitement en moules chauffants (M) et traitement à l'autoclave (A) - sur les relations de transformation des grandeurs mesurées de manière non-destructive en résistance du béton à la compression à des âges différents [2, 3, 4].

Les recherches ont été exécutées dans une usine de précoulage sur un béton à agrégats de rivière. Les résultats de l'analyse du ciment et les cycles des traitements hydrothermiques se trouvent dans [2].

Les essais non-destructifs par ultrasons ont été effectués avec l'ausculteur SBR2 des Laboratoires Electroacoustiques de Rueil (France), fonctionnant sur le principe de l'émission d'impulsions ultrasoniques à la fréquence de 100 kHz.

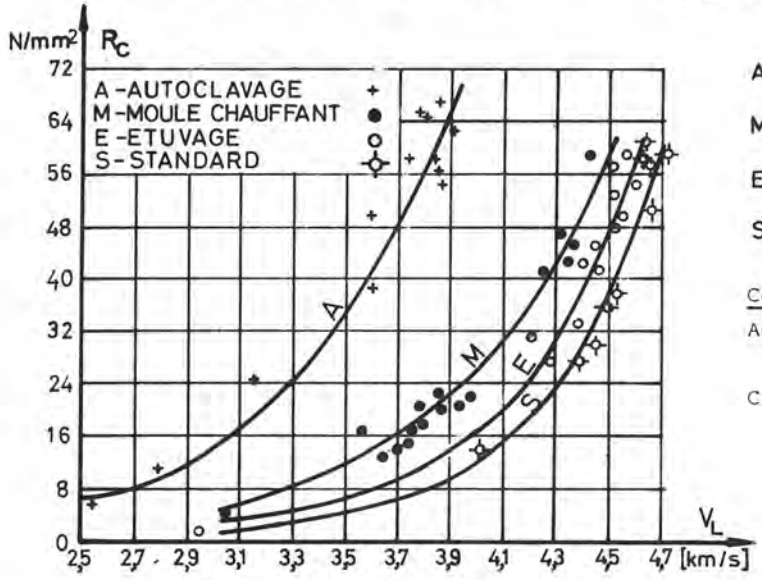

A - $R_c = 0.07765 e^{1.75 V_L}$ r = 0.959

M - $R_c = 0.04014 e^{1.62 V_L}$ r = 0.988

E - $R_c = 0.00483 e^{2.04 V_L}$ r = 0.959

S - $R_c = 0.00121 e^{2.30 V_L}$ r = 0.950

Composition du béton:

Agrégats de rivière	0 - 3 mm	30 %
	3 - 7 mm	20 %
	7 - 15 mm	50 %
Ciment RIM (HRI) 200		350 kg/m³

Fig. 1 Relation V_L-R_c pour le béton à l'âge de 28 jours

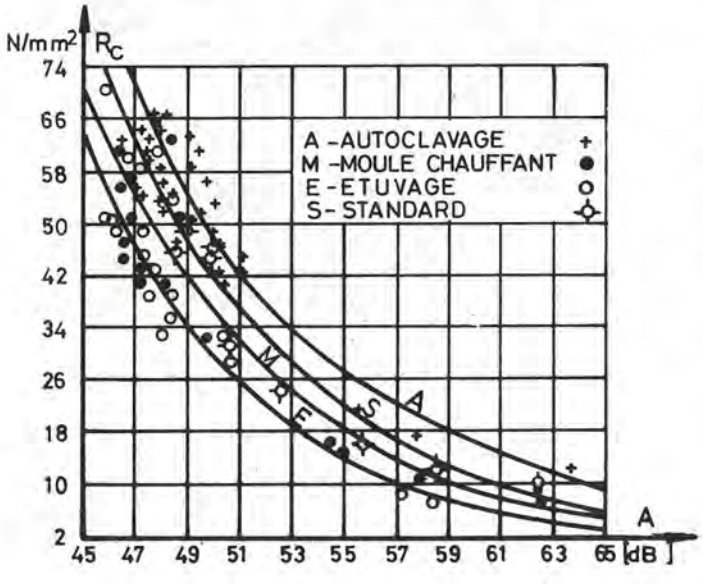

A - $R_c = 11.219\ e^{-0.109A}$ r = 0.924

M - $R_c = 32.181\ e^{-0.136A}$ r = 0.898

E - $R_c = 87.220\ e^{-0.159A}$ r = 0.944

S - $R_c = 27.014\ e^{-0.13A}$ r = 0.970

Composition du béton: voir fig. 1

Fig. 2 Relation A-R_c pour le béton à l'âge de 28 jours

La vitesse de propagation longitudinale et l'atténuation des ultrasons donnent des indications qualitatives et quantitatives sur la structure des bétons traités dans l'autoclave (fig. 1 et 2). L'étalon est constitué par le béton standard (S) ayant durci 7 jours dans l'eau et 21 jours à l'air 20°C et 65% humidité relative. On a démontré que la forme des relations V_L-R_C et A-R_C est exponentielle. Les relations expérimentales établies montrent de très bons coefficients de corrélation r allant de 0,898 à 0,988.

Intéressant à citer sont les résultats des essais à ultrasons sur des pâtes de composents minéralogiques purs traités à l'autoclave. Dans tous les cas, le traitement abaisse la vitesse de propagation sauf pour le C_2S et C_4AF où on note une croissance de la vitesse de propagation (voir tableau I).

TABLEAU I

Comp. miner.	V_L km/s indiv.			Rapp. à C_3S		R_C
	S	Av	Av/S	S	Av	Av/S
C_2S	1,9	2,3	1,18	0,48	0,68	5,00
C_3S	4,0	3,3	0,83	1,00	1,00	0,54
C_3A	2,6	1,8	0,69	0,65	0,55	0
C_4AF	3,6	3,9	1,08	0,90	1,18	2,05

B. Détermination du module d'élasticité de Young

Afin de compléter des indications obtenues par les essais à ultrasons sur la structure formée durant le traitement à l'autoclave, on a déterminé le module d'élasticité statique pour des compositions de mortiers et bétons différant par le rapport E/C et dosage de ciment. Le module d'élasticité a été déterminé sur des prismes 10x10x30 cm. Les déformations ont été enregistrées à l'aide du dispositif Martens et en parallèle à l'aide des tensomètres électrorésistifs. Sur la fig. 3 sont présentés les résultats comparatifs durcissement en autoclave/durcissement dans des conditions normales pour les mortiers ① ② et ③.

On remarque une caractéristique importante pour les structures durcies en autoclave: l'allure très linéaire de la courbe $\varepsilon = f(\sigma)$ sur le domaine presqu'entier avant la rupture. La forme de la courbe montre que la fissuration précédant la rupture se produit, par rapport au béton durci dans des conditions normales, très tard, de façon qu'on peut mieux compter sur un comportement élastique de ce matériel. Cette conclusion est confirmée aussi par la réduction très marquée de l'air de hystéresis suite au traitement à l'autoclave[1]. Les surfaces de rupture des éprouvettes traitées à l'autoclave contiennent un plus grand pourcentage de granulats rompus que les surfaces témoins de béton non autoclavé. Cela indique que les bétons autoclavés, en dehors des résistances supérieures de la pâte de ciment elle-même, possèdent aussi une meilleure adhérence granulat-pâte de ciment.

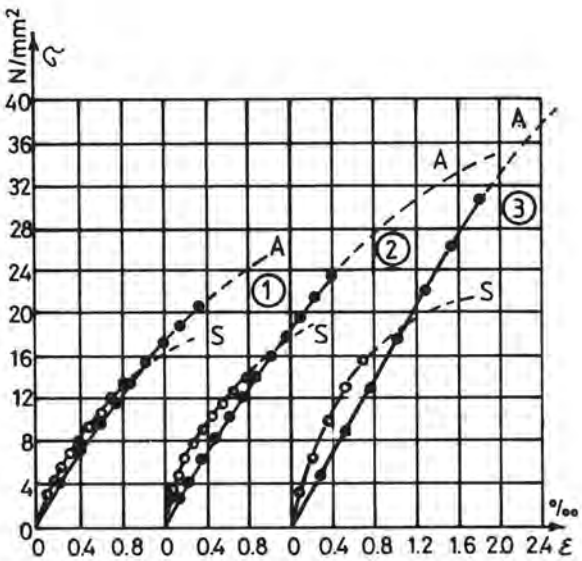

Fig. 3 Courbe $\varepsilon = f(\sigma)$ pour les mortiers ① ② ③

C. Recherches à l'aide de la microscopie optique

Le traitement hydrothermique sans pression a été "simulé" par l'ébullition de la suspension de ciment, parfaitement isolée du milieu extérieur grâce au collage de la lamelle à la lame avec un co-polymère.

Fig. 4 Suspension de ciment RIM (HRI) 200 traitée à 90°C après 72 heures

On observe immédiatement après le traitement des cristaux tabulaires, hexagonaux, sous forme de prismes allongés qui grandissent en permanence (fig. 4). Au moment où ces cristaux atteignent de grandes di-

mensions, on remarque la tendance accentuée de fissuration (fig. 5).

Fig. 5 Suspension de ciment RIM (HRI) 200 traitée à 90°C, après 168 heures

La simulation du traitement à l'autoclave a nécessité des améliorations successives de l'étanchéité des récipients qui, à la fin, ont permis le traitement jusqu'à 220°C.

Les recherches microscopiques - la plupart des résultats se trouve dans [1] - ont démontré (fig. 6) que dans les conditions de traitement à l'autoclave, les formations cristallines possèdent des dimensions beaucoup plus petites que celles obtenues suite aux traitements hydrothermiques sans pression.

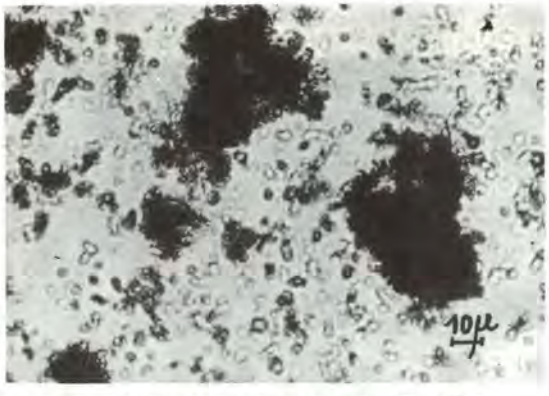

Fig. 6 Suspension de ciment PZ 400 traitée à 12 Atm.

Le développement des cristaux après le traitement est réduit, le processus étant presque terminé à ce moment.

A cause des dimensions très petites, il n'a pas été possible de mettre en évidence - à l'aide de la microscopie optique - l'existence des hydrosilicates de calcium.

Afin de mettre en évidence les réactions de surface entre la pâte de ciment et l'agrégat, on a procédé à l'examination microscopique à la lumière incidente des surfaces polies. Cette méthode est souvent utilisée en pétrographie et métallographie. Les réactions de surface entre la pâte de ciment et l'agrégat sont plus développées dans le cas du traitement hydrothermique (fig. 7 par rapport à fig. 8).

Fig. 7 Interface pâte de ciment/agrégat. Mortier traité hydrothermiquement

Fig. 8 Interface pâte de ciment/agrégat. Mortier (conditions normales)

La liaison entre le SiO_2 du granulat et les phases CH et CSH de la pâte de ciment a, dans le cas du traitement à l'autoclave, un caractère chimique témoigné par le fait que les hautes résistances mécaniques ne varient pas avec l'humidité comme dans le cas des bétons durcis dans des conditions normales.

A l'aide de Phenolphtaleine, on a mis en évidence l'existence de Portlandit autour des agrégats en plus grandes quantités que dans le cas du mortier durci dans des conditions normales. Cette présence est la prémise de la réaction chimique qui peut mener jusqu'aux formations épitaxiques[5].

Des pâtes de ciment durci, ayant E/C = 0,2 ÷0,6 et des mortiers, ayant E/C = 0,45÷0,8, on a extrait des carottes de Ø 50 mm. De ces carottes on a préparé des sections minces (20-25 μm) qui ont servi à effectuer

des mesurages de la surface des pores à l'aide d'un intégrateur microscopique. Les mesurages comparatifs - traitement hydrothermique/durcissement dans des conditions normales - ont démontré que dans le premier cas, les valeurs sont supérieures de 5% à 12%. Il faut quand-même noter que les mesurages du poids volumique n'ont pas mis en évidence des différences sensibles entre les bétons traités à l'autoclave et ceux durcis dans des conditions normales.

Sur la photo 9 on remarque un cas d'"autoguérison", c'est-à-dire le remplissage ultérieur d'un pore avec de nouvelles formations, spécialement de Portlandit dont l'existence a été confirmée par ses caractéristiques optiques.

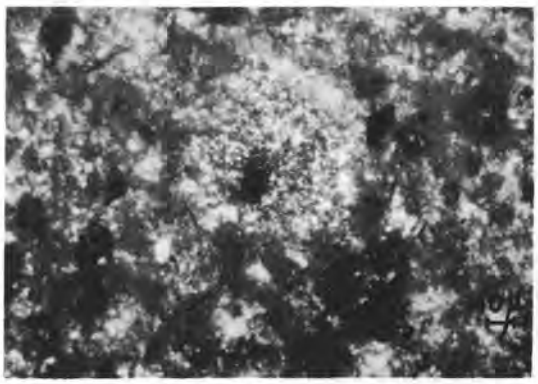

Fig. 9 "Autoguérison"

D. Recherches à l'aide du microscope électronique

On a utilisé la méthode des "moulages" contrastés avec du platine afin de les rendre visibles aux faisceaux d'électrons. Les recherches se sont limitées seulement aux pâtes de ciment et mortiers traités à l'autoclave, ayant comme "témoin" le durcissement dans des conditions normales. Les hydrogrènats, typiques dans le traitement sous pression, peuvent être reconnus sur la photo 1o.

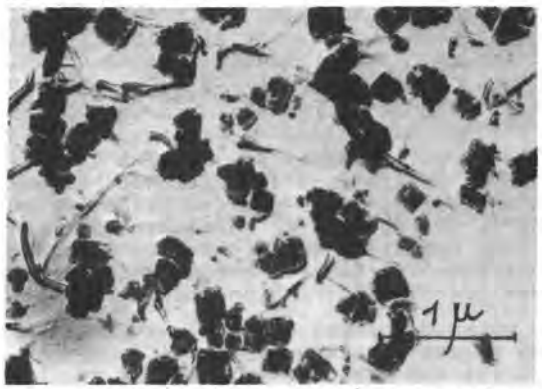

Fig. 10 Hydrogrènats. Mortier traité en autoclave

La photo 11 révèle des caractéristiques trouvées très souvent chez les montiers traités à l'autoclavage.

Il s'agit des surfaces de rupture qu'on peut reconnaître d'après la forme des hydrosilicates de calcium arrachés de la section avec laquelle ils maintiennent encore des "ponts" de liaison. Au vu de ces "ponts", on peut reconnaître la direction de rupture. D'après l'opinion de l'auteur, ces photos témoignent les qualités liantes supérieures des pâtes de ciment durcies à l'autoclave.

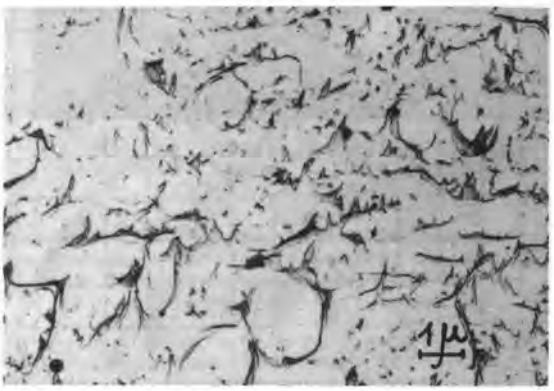

Fig. 11 Surface de rupture avec des phases CSH. Mortier traité en autoclave

Sur la photo 12 on voit des phases CSH avec un rapport C/S = 4/5÷5/6 typique pour la Tobermorite qui caractérisent ces traitements hydrothermiques.

Fig. 12 Tobermorite. Mortier traité en autoclave

III. CONCLUSIONS

Les recherches microscopiques ont mis en évidence le fait que durant les traitements hydrothermiques, se forment des quantités plus grandes de cristaux de $Ca(OH)_2$. Lorsque les cristaux atteignent de grandes dimensions, on remarque la tendance accentuée de fissuration (fig. 5). Les microfissures sont dues aussi bien à la dilatation de l'eau et de l'air durant le processus de chauffage et de refroidissement, qu'à la perte d'eau. La diffusion du Portlandit, favorisée par la haute température, amène une porosité élevée des structures d'hydrosilicates de calcium.

Les recherches faites à l'aide de la microscopie optique et électronique sur des pâtes de ciment et sur des mortiers, traités à l'autoclave, ont mis en évidence que ce traitement donne naissance à de nouvelles formations différentes de celles résultant des autres traitements hydrothermiques et possédant un grand degré de dispersion, ce qui mène à un haut niveau d'énergie potentielle de surface.

En général, on accepte que les résistances finales de la pâte de ciment soient d'autant plus grandes que le contenu en CSH à de longues fibres est plus grand (pour la même compacité de la structure). Cela explique les hautes résistances obtenues par l'hydratation à températures basses, et l'effet favorable des retardeurs de prise. [6]

Dans le cas du traitement à l'autoclave, il paraît que cette hypothèse n'est plus valable.

La grande résistance en compression des bétons traités en autoclave s'explique, d'une part par la quantité plus grande de nouvelles formations qui a son origine dans l'activation du SiO_2 du granulat quartzeux, et spécialement du sable fin et d'autre part, par les meilleures qualités de ces nouvelles formations.

Par ailleurs, cette structure de la pierre de ciment qui se forme d'une manière presque définitive dans un délai de temps extrêmement court, présente plus de défauts, surtout fissures, de manière qu'il paraît être possible qu'en dépit des grandes résistances en compression, l'action des agents physiques la détruise parfois rapidement. Cet aspect est très bien mis en évidence par les essais à ultrasons.

Mais, sans connaître les conditions de durcissement du béton examiné, une interprétation des essais non-destructifs peut mener à de grandes erreurs.

En dehors de la résistance en compression qui est le plus souvent déterminée, la structure et la distribution des pores, les microfissures dans la pierre de ciment et sa capillarité constituent des éléments très importants pour en juger de la compacité, de la résistance aux agents physiques et chimiques extérieurs, en un mot, de sa durabilité.

REMERCIEMENTS

L'auteur désire exprimer ses remerciements aux collègues qui lui ont donné la possibilité d'entreprendre et de poursuivre les recherches microscopiques. En particulier, il est reconnaissant à son ancien professeur, plus tard directeur de sa thèse de doctorat, le feu Professeur Dr. Alex. Steopoe auquel tous ceux qui l'ont connu et qui ont bénéficié de son érudition, lui gardent un souvenir inoubliable.

BIBLIOGRAPHIE

1.- G. TEODORU (1971) "L'essai non-destructif du béton ayant subi un traitement hydrothermique", Thèse de docteur ès Sciences sous la direction du Prof. Dr. A. Steopoe, Bucarest (non publiée) pp. 20-120.

2.- G. TEODORU (1968) "Influence du traitement hydrothermique appliqué au béton sur la relation de transformation de la vitesse de propagation des ultrasons, dans la résistance en compression du béton", RILEM NDT, Varna, pp. 5-21.

3.- G. TEODORU (1971) "Résultats obtenus dans la détermination de la corrélation entre l'atténuation des ultrasons et la résistance en compression du béton ayant subi un traitement hydrothermique", IVème Conférence Internationale de la Préfabrication CNIT (Commission Nationale des Ingénieurs et Techniciens), Bucarest, pp. 273-282.

4.- G. TEODORU (1971) "Utilisation de la méthode de dureté superficielle au contrôle de la qualité du béton ayant subi un traitement hydrothermique, Session scientifique de l'Institut de Constructions, Bucarest, pp. 5-1o.

5.- A. STEOPOE et V. MOLDOVAN (1962) "Sur la qualité de la couche de béton qui protège les armatures", RILEM Durabilité des bétons Colloque international, Prague, pp. 329-331.

6.- W. RICHARTZ (1969) Über die Gefüge und Festigkeitsentwicklung des Zementsteins Beton H5 S. 2o3-2o6 und H6 S. 245-248.

Rheology of setting Portland cement pastes

Rhéologie des pâtes du ciment Portland faisant prise

P.F.G. BANFILL, Department of Building Engineering, University of Liverpool, U.K.

RESUME : Pendant la prise du ciment les phases solides des minéraux hydratés croissent dans le liquide. On peut étudier la prise par les méthodes chimiques, thermiques, électriques ou mécaniques. Nous avons employé un viscosimètre à rotation pour observer les variations des propriétés rhéologiques des pâtes du ciment pendant la prise.

Les pâtes fraîches montrent la destruction par agitation de la structure, mais la pâte cisaillée est un corps de Bingham. A cause des difficultés expérimentales avec les pâtes du ciment dans les cylindres coaxiaux, où une zone immobile peut se produire ou disparaître imprévisiblement, on a employé un nouveau viscosimètre. C'est une pale hélicoïdale qui tourne dans l'axe du cylindre qui contient la pâte.

Les courbes d'écoulement obtenues avec cet appareil indiquent que le seuil de cisaillement décroît au commencement et croît ensuite avec le temps. Si l'on cisaille la pâte continument à vitesse fixe, le couple sur la pale décroît jusqu'à un minimum (T-Tmin), au bout du temps t suivant l'équation :

$$T-Tmin = A\ t^{b}$$

Les accélérateurs et les retardateurs changent la constante A , mais ne changent pas l'exposant b .

Ces résultats indiquent qu'on peut employer cette méthode pour étudier la prise des pâtes du ciment.

SUMMARY : Setting of cement is the growth and interlocking of a solid phase of hydrated minerals within a liquid. It can be studied by chemical, thermal, electrical or mechanical methods. We have used rotational viscometry to observe changes in the rheological properties of cement pastes with time.

Fresh cement pastes shows structural breakdown, but the broken down paste conforms closely to the Bingham model. Because of experimental difficulties with cement pastes in coaxial cylinders, where a stationary plug may form or disintegrate unpredictably a new geometry has been used. This is a helical impeller rotating in the paste contained in a cylinder.

Repeated flow curves using this latter geometry show that yield stress decreases at first and then increases uniformly with time according to a power law. When sheared continuously at constant speed the torque on the impeller decreases to a minimum (Tmin) as the structure breaks down and then increases as the hydration structure builds up. The helical impeller shows slower breakdown than coaxial cylinders due to the complex flow pattern. The increase of torque, (T-Tmin), with time, t, follows a power law relationship of the form:

$$(T-Tmin) = A\ t^{b}$$

The effect of accelerators and retarders is to change the value of A, while b remains constant.

These results show that, with suitable development, the technique can be used to monitor setting of pastes.

INTRODUCTION

Setting is generally agreed to be caused by the interlocking of solid phase hydration products. As these grow through the aqueous phase separating particles the physical manifestation is a change from liquid-like flowing behaviour to solid. This transformation usually coincides with an increase in the rate of hydration. Practically it can be studied by chemical, thermal and electrical methods, or, making use of the change in properties from liquid to solid, a variety of mechanical methods. These latter range from primitive standard penetrometers such as the Vicat needle to the more sophisticated calibrated devices of Bombled (1) and Forrester (2). We have approached the problem using conventional rotational viscometry.

The rheology of cement pastes has been widely studied at early ages. The main techniques used are flow curves, where the speed of rotation increases to a maximum value and then decreases to zero, and continuous shear, where a constant speed of rotation is maintained. In both cases the torque produced by the rotation is measured. Fig.1 shows a typical flow curve. As shear rate increases the shear stress passes through a maximum as the yield value of the structure is overcome, it then declines as the structure breaks down by shearing. The down-curve follows the Bingham relationship (equation 1).

$$\tau = \tau_o + \mu_p \dot{\gamma} \qquad (1)$$

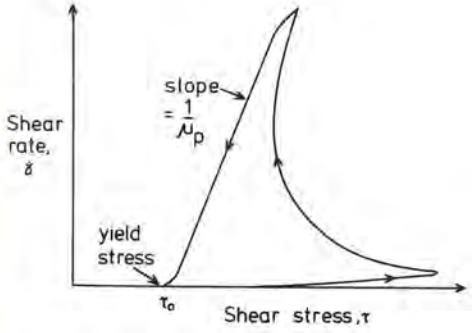

Fig.1 - Cyclic flow curve for cement paste. Arrows indicate shear stress behaviour as shear rate goes up to a maximum and back to zero.

The existence of a hysteresis loop is often taken to mean that the paste is thixotropic. This term means a reversible breakdown of structure, but there is no evidence that the breakdown in cement paste is reversible and subsequent flow curves show stresses below the original at all corresponding shear rates. Accordingly the term thixotropy should not be used. In continuous shear the torque (shear stress) declines as structure breaks down (Fig.2) and Tattersall found that the breakdown followed first order kinetics (3), equation 2:

$$(T - T_e) = (T_o - T_e)e^{-Bt} \qquad (2)$$

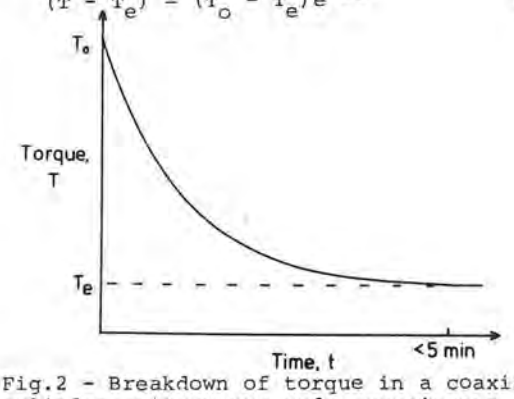

Fig.2 - Breakdown of torque in a coaxial cylinder viscometer under continuous shear.

Very little work has been done at later ages of the paste, though it seems reasonable to expect that paste viscosity will increase again as the hydration structure builds up.

APPARATUS

There are experimental problems with flow of cement pastes in coaxial cylinders (4). A stationary plug of paste forms at the outer cylinder wall with a sheared zone inside. This changes the geometry of the annulus. Additionally the plug may either slide round at some speed below that of the rotating cylinder or disintegrate, in both cases at unpredictable times. To avoid this problem and that of sedimentation during the experiment a helical impeller was designed and constructed (Fig.3.). Direct observation of the flow in this geometry showed that plug flow did not occur, and all stationary zones had been eliminated.

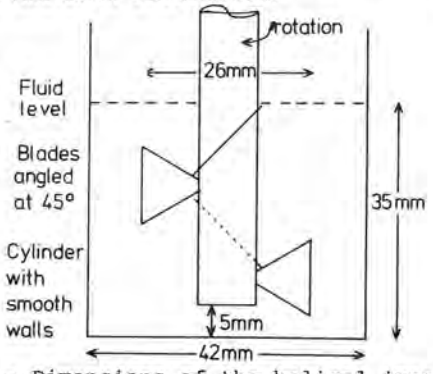

Fig.3 - Dimensions of the helical impeller.

This viscometer geometry was used with a Rotovisco RV2 viscometer with a PG 142 external speed programmer which could produce repeated cycles of shearing. Flow curves, and stress curves in continuous shear were recorded on an X-Y plotter and chart recorder respectively.

EXPERIMENTAL NOTES

All pastes were mixed by hand as follows: 35g of water were added over a period of 1 minute to 100g of ordinary Portland cement (see Appendix) in a crystallising dish. Lumps were broken up and the whole paste stirred with a spatula for 2 minutes before loading into the viscometer. All experiments took place at 20 ± 0.5°C.

RESULTS

Repeated flow curves show that the yield stress and plastic viscosity decrease initially before increasing with time approximately according to a power law relationship. The data shown in Fig.4. were obtained by flow curves repeated every 10 minutes. The maximum speed of rotation was 200 rev/min (equivalent to mean shear rate = 35 sec^{-1}) and the time taken up for an up-and-down cycle was 2 minutes.

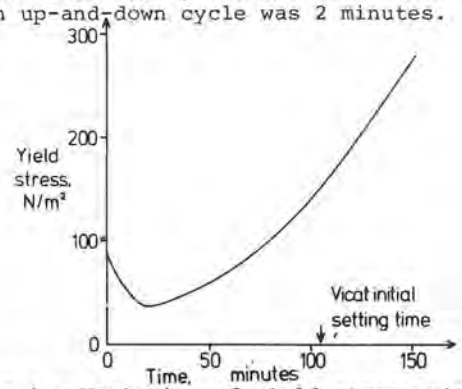

Fig.4 - Variation of yield stress with time, found by repeated flow curves.

In continuous shear the torque on the impeller declines to a minimum value after about 100 minutes when the equilibrium structure has been achieved. Torque then increases as hydration proceeds (Fig.5). The data can be represented by two straight lines on graphs of ln (T-Tmin), the excess torque above the minimum value, and ln t, the time (Fig.6). The hydration section fits an equation:

$$T - T_{min} = At^{b} \qquad (3)$$

Fig.7 shows the effect of admixtures on the build up curves. The slope of the straight lines of ln (T-Tmin) against ln t is unchanged but the whole plot is moved to earlier times by 2% $CaCl_2$ and later times by 0.01 and 0.1% citric acid, i.e. these admixtures change the value of b in equation 3.

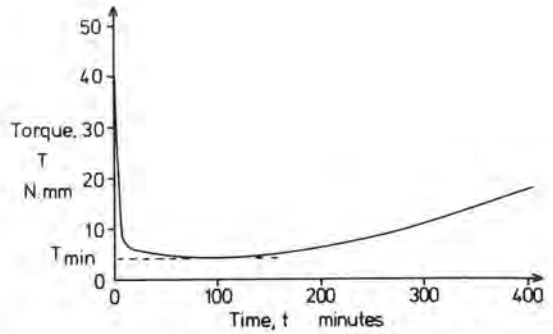

Fig.5 - Breakdown of torque with time in the helical geometry, and subsequent build up as hydration proceeds.

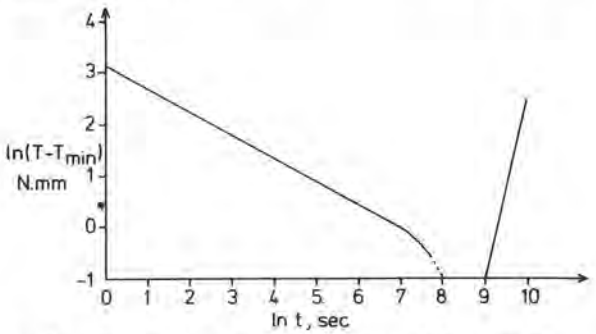

Fig.6 - Logarithmic plot of breakdown and build up in the helical geometry.

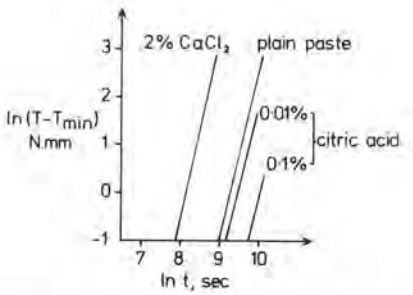

Fig.7. - Effect of admixtures on the logarithmic build up plot.

DISCUSSION

In comparison to the results of other workers using coaxial cylinders (3,4) it takes much longer to breakdown the structure present in the cement paste when mixed. This must be due to the complicated flow pattern in the sample. The range of shear rates in the paste is likely to be wide so that some regions are broken down more rapidly than others. Mixing is also taking place so the torque on the impeller at any time is an 'average' of the torque produced by the different elements of paste. At the same mean shear rate in coaxial cylinders and our helical apparatus the speeds of breakdown differ by about ten times, and since

the speed of breakdown varies with shear rate, we can infer that the breakdown rate and shear rate are related non linearly. In the range of shear rates in the helical apparatus those at the lower end are more important in determining the breakdown rate than those at the top end.

The data of Fig.5 may be interpreted in terms of two superimposed processes, the breakdown of structure at short shearing times due to the destruction of weak bonds between cement particles by shearing, and the building up of structure at longer times by hydration.

During hydration water in the paste reacts chemically to give hydrates and is also immobilised physically by the 'onion-shell' and needle shaped gel products. This process surely starts from the initial contact of cement and water, but in the experiments described here was masked by the breakdown. Subsequently a method of preparing fully broken down pastes was developed. The cement and water were placed in a 250 cm^3 beaker and stirred with a propellor turbine mixer at 2500 rev/min for 7 minutes before loading into the viscometer. Pastes made like this gave no further breakdown in the viscometer and build up of structure by hydration was seen right from the start of the experiment. Fig.8 shows this type of curve obtained at 200 rev/min. The slope is different from Fig.7 which indicates that the kinetics are different. This is under investigation.

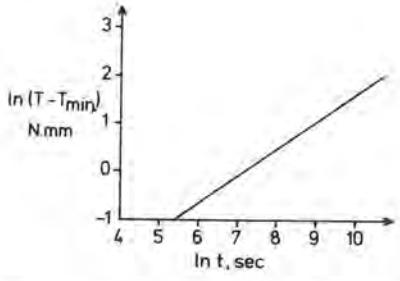

Fig.8 - Build up of torque for a fully broken down cement paste.

The results of Figs. 7 and 8 show that the build up curve may be used as a guide to the hydration behaviour of cement pastes, but in developing the technique we must consider the process of hydration. According to a recently proposed model initial reactions are surface dissolution and formation of a C-S-H gel layer. This retards hydration which can only restart on rupture. The C-S-H gel is selectively impermeable to silicate ion so that osmotic pressure inside the skin builds up until rupture occurs, whereupon the extruded hydrosilicate combines with Ca^{2+} in solution to give secondary C-S-H outgrowths (5). These outgrowths are likely to be damaged by shear-induced collisions with other particles and this might release more hydro-silicate into solution, i.e. the rate of hydration might strongly depend on the rate of shear, and would be higher at higher shear rates.

Comparison of Figs.4 and 6 supports this suggestion. Taking the work done by shearing to be proportional to the product of time and $\dot{\gamma}^2$ the paste of Fig.4 was subjected to about 7% of the shear work of the paste of Fig.6. (0-200 rev/min in 2 minutes repeated every 10 as against 200 rev/min). In these cases the exponents of the power-law relationships between excess yield stress or excess torque and time are 2.3 and 3.5 respectively. Clearly factors affecting the rate of hydration also affect the kinetics of the structural build up curve.

Experiments are currently in progress to find the effect of shear rate on the constants in equation 3, and also to study the effect of the shearing process on the rate of hydration of cement by chemical methods. Preliminary results suggest that the trend is not simple and that there may be an optimum value of shear rate at which the hydration rate is scarcely changed compared to an unsheared paste. If this is confirmed the value of the technique as a monitor of hydration is much enhanced.

Other factors which must be checked are the effects of water/cement ratio, temperature and cement composition. Future work will be to study the effects of admixtures.

CONCLUSIONS

The technique described here permits us to study the hydration of cement pastes through the effect on rheology. The equilibrium apparent viscosity of a fully broken down paste may be reached either by shearing in the viscometer or externally in a high speed mixer. Subsequently the torque on a continuously rotating impeller increases as hydration takes place. The excess torque above the minimum value is a power law function of time and the exponent of the power law is affected by shear rate, while the presence of retarding and accelerating admixtures changes the constant but not the exponent.

APPENDIX

The cement used was of the following composition:

Compound	%
C_3S	65.9
C_2S	7.3
C_3A	7.1
C_4AF	10.1
SO_3	2.3
Na_2O	0.36
K_2O	0.87

REFERENCES

1.- J.P. BOMBLED (1971), "A rheograph for the study of cement setting", Rev. Mat. Constr. No. 673, 256-277.

2.- J.A. FORRESTER and R.W. LAMBE (1980), "Effects of mechanical shear during mixing of cement", 7th International Congress on Chemistry of Cement, Paris, Poster VI-4.

3.- G.H. TATTERSALL (1955), "Rheology of cement pastes", Brit.J.App.Phys., 6, 165-7.

4.- C.R. DIMOND and G.H. TATTERSALL (1976), "Use of the coaxial cylinders viscometer to measure the rheological properties of cement pastes", Hydraulic cement pastes, Conference, University of Sheffield, 118-133.

5.- J.D. BIRCHALL, A.J. HOWARD and D.D.DOUBLE (1980), "Some general considerations of a membrane/osmosis model for Portland cement hydration", Cem.Concr.Res. 10(2), 145-155.

Effects of curing time on the mechanical properties of cement paste

Effets du temps d'étuvage sur les propriétés mécaniques de la pâte de ciment

A. BAJZA, Slovak Technical University, Brastislava, Czechoslovakia.

RESUME: On a étudié les effets du temps d'étuvage et de la température, sous pression de vapeur atmosphérique, sur les propriétes mécaniques de la pâte de ciment. On a suivi en particulier les résistances à la compression, la porosité, et les pourcentages d'eau evaporable.

SUMMARY: The effects of curing time and temperature, under atmospheric steam conditions, on the mechanical properties of cement paste was studied. In particular, compressive strength, porosity and evaporable water contents were monitored.

INTRODUCTION

Increasing energy cost and volume of concrete used in prefabricated structures, as well as the expanded use of accelerated methods of concrete curing, require a more thorough knowledge of the relationship between curing conditions and mechanical properties of elevated temperature-cured concrete. The following work summarizes preliminary data with portland cement pastes; this is to be followed by optimized mortar and concrete studies.

EXPERIMENTAL

A cement of the following composition was used in the study: Portland Cement "400" (Bogue: 64.3% C_3S, 9.5% C_2S, 9% C_3A, 9.1% Fss; 4% $CaSO_4$ added as gypsum; Initial set: 3 hours, final set: 4 hours 10 minutes; Blaine surface area: 3000 cm^2/g). Cement pastes were prepared by mixing cement with water at w/c of 0.3, 0.4 and 0.5 for 3 minutes. Six 2-cm^3 cubes of each mix were molded by vibration for 15 seconds. Samples were subsequently cured at temperatures of 20°, 60°, 70°, 80° and 90°C under atmospheric steam conditions. The control samples (20°C, cured 24 hours in moist room, then in water) were tested after 1, 7 and 28 days. The steam-cured samples were preheated and cured according to the schedule of increasing and isothermal temperatures shown in Fig. 1. The curing temperature was monitored within the cement paste using Cu-constantan thermocouples. The samples were tested at the end of heat treatment, and also after 7 and 28 days of water curing at room temperature. The following properties were measured: density, compressive strength, porosity, and evaporable water at various temperature intervals by simultaneous thermal analysis (DTA/TGA).

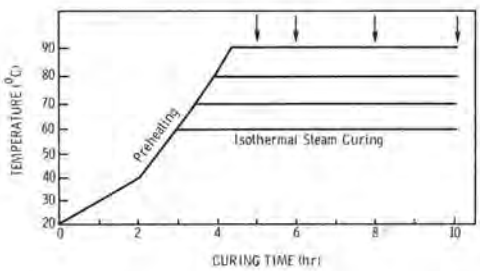

Fig. 1 - Temperature profile of curing

DISCUSSION OF RESULTS

Because of space restrictions, detailed experimental data are not given; they can be found in ref. (1). In brief, the following results were obtained.

Strength at the end of steam curing. For up to 6 hours of heat-treatment, the compressive strengths at the time of demolding increased with increased curing temperature. At longer curing times (e.g., 8 and 10 hours), samples cured at 90°C showed a decrease in strength relative to those cured at 70°C and 80°. An example of this, for pastes made at a w/c of 0.4, is shown in Fig. 2. It has been also noted that the strengths obtained at 60°C, for all curing times, were substantially lower than those for the pastes cured at higher temperatures. As expected, the strengths at demolding were strongly influenced by the w/c used.

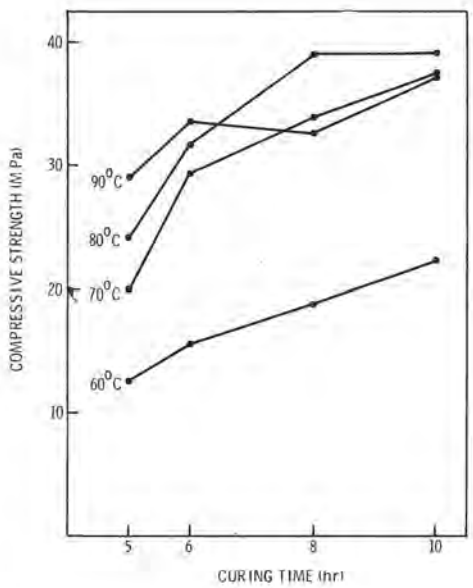

Fig. 2 - Compressive strength development as a function of curing time and temperature; w/c = 0.4

28-day strength. Irrespective of the initial duration of steam curing, the highest 28-day strengths were obtained for specimens cured at 80°C. However, for all of the temperatures studied, the highest 28-day strengths were obtained from those specimens cured for 5 hours.

For specimens cured for longer times the strengths generally decreased (Fig. 3). As was the case with strengths determined at the end of the heat treatment, the 28-day strengths also decreased with increasing w/c.

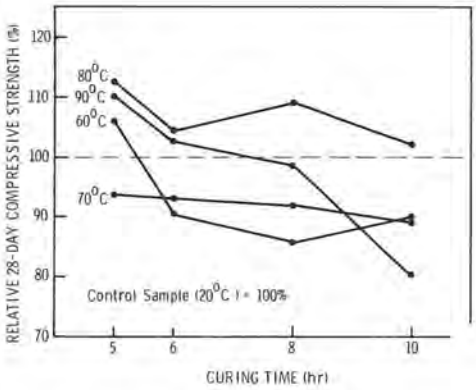

Fig. 3 - Relative 28-day compressive strength as a function of steam curing time and temperature; control sample (20°C) = 100%

Porosity. In agreement with published literature (2,3), a good correlation between the decrease in porosity and increase in compressive strength was found. This was very obvious for the strength-porosity relationship immediately following steam curing and demolding (Fig. 4); the correlation was not as good for samples tested after 28 days of curing because the total porosities, in contrast to strengths, were all very similar. Differences in the distribution of pores may explain the above finding. Understandably, samples prepared at lower w/c had at all times a lower porosity than those prepared at higher water contents. The higher the original w/c, the more rapid is the decrease in porosity.

Evaporable water. The total ignition loss as well as water released in four temperature intervals (20-100°C, 100°-450°C, 450°-600°C, and 600°-1000°C) was measured by simultaneous thermal analysis to give an indication of the relative increase of water content in the main products of hydration. At the end of steam curing and at a given temperature, the amount of water bound in hydrates decomposing below 450°C (e.g., C-S-H, calcium sulfoaluminate hydrates) increased with the temperature of curing. During additional curing in water the amount of bound water

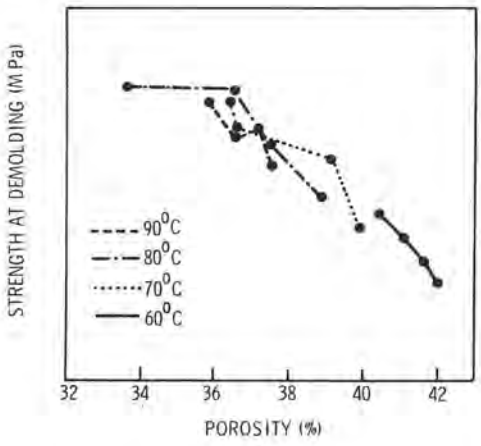

Fig. 4 - Strength at demolding vs. porosity for pastes hydrated at different temperatures

increased. This increase was found to be somewhat higher for samples cured at lower temperatures and for shorter times. It is assumed that evaporable water between 450°-600°C represents water present in the form of calcium hydroxide. The amount of water released in this temperature interval was only slightly affected by the curing temperature, especially at longer hydration times.

From the vast amount of data obtained and briefly summarized above, it became obvious that more emphasis has to be given to better understanding of the porosity versus strength relationship; this is because it is the porosity of the paste that correlates better than any other variable to the strength. Better understanding of the changes in porosity and the distribution of pores with changes in rate and mode of hydration and in the type of hydration products will enable a more technically sound rationale for the design of concrete, via a direct application of generated knowledge to the concept of concrete maturity(4,5).

REFERENCES

1. A. Bajza, Cem. Concr. Res., to be published.

2. P.J. Sereda, R.F. Feldman and V.S. Ramachandran, Principal Report VI-1, Proc. 7th Int. Congr. Chem. Cement, Vol. I, Paris 1980.

3. D.M. Roy and G. Gouda, J. Amer. Ceram. Soc. 56

(1973), 549-550.

4. P. Nerenst, Session C, Proc. RILEM Symposium on Winter Concreting, Copenhagen 1956.

5. G.M. Idorn, General Report VII, Proc. 7th Int. Congr. Chem. Cement, Vol. IV, Paris 1980.

Early Autogeneous Shrinkage of Cement Pastes

Retrait initial des pâtes de ciment

S. ZIEGELDORF, Dr. rer. nat.
H.K. HILSDORF, Professor, Universität Karlsruhe, West Germany

SUMMARY: Results of measurements of early shrinkage of cement paste will be presented. The tests have been conducted in a new dilatometer which has a variety of advantages compared to older systems, the most important being its high accuracy and the possibility to begin recording 8 minutes after mixing.

In the study early shrinkage of cement pastes of different water-cement-ratios with and without admixtures has been studied. During the tests the samples either have been in a sealed condition or open i.e. absorption of additional water was possible during early shrinkage. For open storage the time development of the volume change of cement pastes is independent of the water/cement-ratio when presented as a fraction of the total cement content. Under sealed conditions the volume change as a fraction of cement content is independent of the water/cement-ratio up to the moment at which all the bleeding water has been absorbed by the sample. At this stage some expansion occurs which is followed by further shrinkage however at a slower rate.

It is shown that admixtures as well as the form and dimension of the specimens can have a strong effect on early shrinkage. A hypothesis is presented to explain some of the observed phenomena.

RESUME : Les résultats de mesures du retrait initial de pâtes de ciment sont présentés. Les essais ont été faits avec un nouveau dilatomètre, qui présente de multiples avantages sur les appareils existants; les plus importants sont sa grande précision, et la possibilité de commencer les mesures 8 minutes après le malaxage.

Ont été étudiés les retraits initiaux de pâtes de ciment à diverses teneurs en eau, et contenant divers additifs. Pendant ces essais, les éprouvettes sont placées dans des conditions prédéterminées de relations avec l'extérieur; par exemple, l'absorption d'eau complémentaire est possible. Pour une conservation immergée sans protection, la courbe des variations de volume en fonction du temps est indépendante de la teneur en eau initiale. Pour une conservation sous enrobage hermétique, cette courbe est indépendante de la teneur en eau initiale, jusqu'au moment où toute l'eau de ressuage a été absorbée par l'éprouvette. Ensuite, une certaine expansion se produit, suivie par un nouveau retrait, qui s'effectue à vitesse plus lente.

On a observé que les additifs, ainsi que la forme et les dimensions des éprouvettes, avaient une grande influence sur le retrait initial. Une théorie est proposée pour expliquer ces phénomènes.

1. Introduction

Most authors consider the chance of concrete cracking as a consequence of autogeneous early shrinkage of the cement paste to be almost negligible. More recently, however, some authors postulate such cracking to be of considerable significance (1). Chatterji (2) even proposed that crack formation due to autogeneous early shrinkage may occur in neat hardened cement paste.

One possibility to get a better insight into the mechanisms of crack formation in young concrete is the determination of the shrinkage behavior of the cement paste. However, though the number of publications dealing with this subject is large, there still remain many unsolved questions. Part of these questions are due to the fact that there are different methods to investigate the shrinkage and particularly the early shrinkage of cement paste, each method giving another aspect of the material behavior. The most widely used methods are described in the following, not considering shrinkage due to drying, carbonation or chemical attack.

2. Methods to Determine Shrinkage

Shrinkage experiments on cement paste can be subdivided into two categories: experiments on unsealed specimens, in which case the specimens are able to absorb water or experiments on sealed specimens, in which case the true autogeneous shrinkage is determined.

a) Unsealed Specimens

In the simplest case a certain amount of fresh cement paste is put into a water-filled vessel with a capillary to indicate the volume changes of the paste (3). The shrinkage thus measured is due to the fact that the hydration products have a higher density than the initial products. The shrinkage thus measured is commonly called chemical shrinkage (in french: shrinkage "Le Chatelier").

b) Sealed Specimens

A different approach is possible by using sealed instead of unsealed specimens. Experiments can be done in a volumetric as well as in a unidimensional dilatometer. Recently Detriché and Maso (5) and Buil and Baron (6) performed such measurements on cement pastes and mortar in a unidimensional dilatometer and observed a development of shrinkage as shown in Fig. 1. The development of shrinkage can be subdivided into 3 stages:

I. first shrinkage
II. expansion
III. second shrinkage.

I. The first shrinkage develops before and during setting. Detriché and Maso (5) explain this shrinkage by energetic interactions between the solid, the liquid and the gaseous phases, specially referring to capillary forces, which develop when the surface water has evaporated. Buil and Baron (6) furtheron report that the first shrinkage begins between 2 and 3 hours after mixing. However, it is more probable that the first shrinkage is caused by the hydration reactions occuring during the time until setting. These reactions are for once not influenced by evaporation.

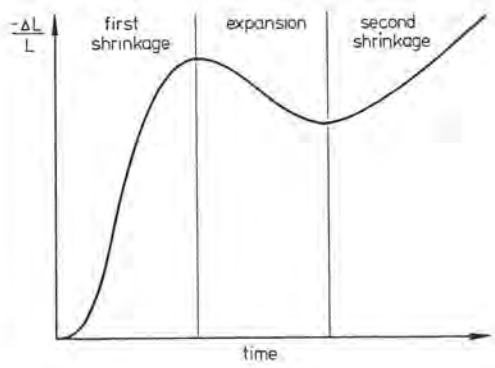

Fig.1: Shrinkage of cement paste in a unidimensional dilatometer

Secondly they begin immediately after mixing, thus causing shrinkage immediately after mixing.

The first shrinkage could be expected to be identical to the so-called plastic shrinkage, i.e. shrinkage before setting. Such plastic shrinkage often had been observed to be the cause for crack formation within the first hours after placing a concrete mix. It must be reminded, however, that plastic shrinkage cracks normally are observed only when the concrete surface is dried by evaporation, thus leading to additional drying shrinkage.

II. The first shrinkage normally is followed by a period of expansion the reasons of which, however, are not yet very clear.

III. The second shrinkage develops in the course of hardening and therefore is often called hardening shrinkage. It may also be referred to as dessiccation shrinkage due to the fact, that this type of shrinkage can be explained by internal dessiccation (1,6). The reasons of this shrinkage predominantly are of physical nature, comparable to the deformations caused by drying shrinkage.

3. Comparison of Methods

Fig. 2 summarizes results from the literature

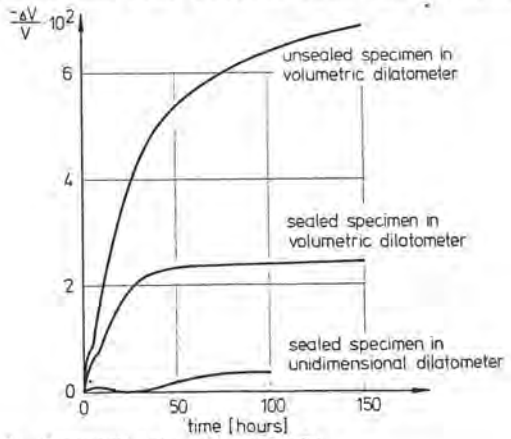

Fig.2: Comparison of methods

on early shrinkage of cement paste for the three experimental methods described above. When comparing these data large differences can be observed. A close analysis, however, shows that the different methods should yield at least partially identical results.

The first point which has to be mentioned in this connection is shrinkage before setting. It should be identical for all three methods introduced here, at least as long as no internal pore formation occurs. Such pore formation is not to be expected in plastic cement paste or concrete, provided that the w/c-ratio is not extremely low.

Another point which has to be analysed more carefully is the role of the bleeding water in the shrinkage experiments. Buil and Baron (6) overcame the problem by using cement pastes with a very low and thus unrealistic w/c-ratio (w/c = 0,27).

Setter and Roy (7) used a different approach: They removed the bleeding water of the sealed specimens 2 hours after mixing. This procedure, too, is problematic since the effective w/c-ratio of the paste is altered, and the removal of all bleeding water is difficult particularly in concretes, where part of the bleeding water is trapped below the aggregates.

When sealed cement paste specimens with bleeding water are examined in a volumetric dilatometer the observed shrinkage should be identical to the chemical shrinkage of unsealed specimens as long as bleeding water does exist. After imbibition of the bleeding water the shrinkage measured thereafter will be a pure bulk shrinkage which thus should be comparable to the bulk shrinkage as measured in the unidimensional dilatometer. Until now, however, experimental evidence does not support this hypothesis.

4. Scope of Investigation

Considering the problems which are unsolved in the area of autogeneous shrinkage of cement paste, mortar and concrete, it was intended to design a dilatometer which should fulfill the following requirements:

- high accuracy, simple and easy to handle;
- volumetric in order to allow comparison of shrinkage of sealed and unsealed specimens;
- permission of the use of specimens with a volume of at least 1000 cm^3, such that the shrinkage of real concrete specimens can be determined;
- permission of the use of variable specimens, in order to make possible the evaluation of the influence of specimen size and specimen form on shrinkage;
- suitable for continuous registration of shrinkage and temperature.

In the following a dilatometer designed according to these requirements is described.

5. Dilatometer

The dilatometer vessels used in this investigation consist of a 3000 cm^3 glass vessel on which a top with openings for a thermometer, for the capillary and for two ventpins is

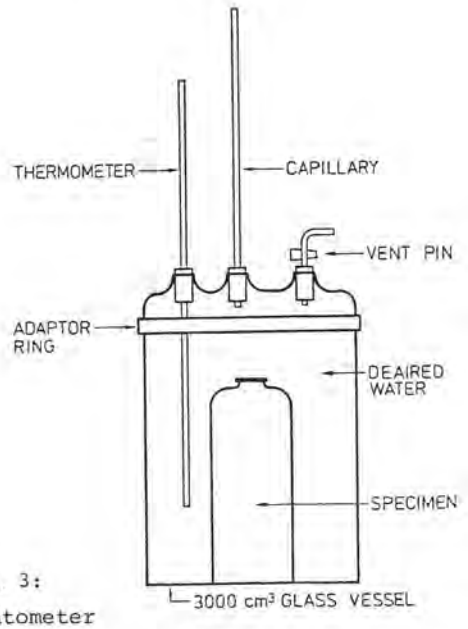

Fig. 3: Dilatometer

fixed by using an adaptor ring (Fig. 3). Six dilatometers are used at a time, such that comparative measurements are easily possible. The dilatometer are filled with deaired water. They operate in a room with a temperature of 21 ± 1°C.

Unsealed as well as sealed specimens have been investigated. The unsealed specimens consist of 3 bowls placed on top of each other in order to obtain a sufficiently large total specimen volume of approx. 600 cm^3 (Fig. 4a). The sealed specimens had various shapes (Fig. 4b). The fresh cement paste is placed in bags made of 0,4 mm-polyethylene sheets which are highly flexible, water-tight and transparent.

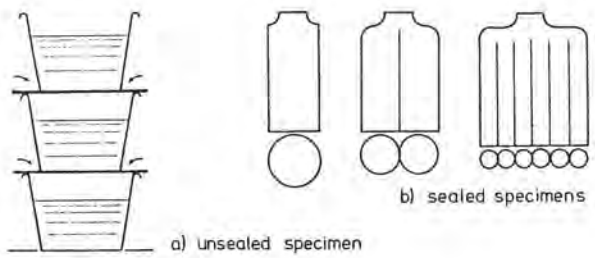

Fig.4: Specimen forms

All materials and apparatus necessary for the experiments are stored in the same constant environment room. Thus the fresh cement paste has the same temperature as the dilatometer water. The latter is mixed with 1 cm^3 of a detergent which reduces the amount of residual air in the dilatometer water. Remaining air is removed completely by shaking the filled dilatometer. All specimens are vibrated before installation into the dilatometer.

Because of the simple construction of the dilatometer the first results can be obtained about 8 minutes after mixing. Another advantage of the set-up is the possibility of continuous temperature registration which renders the dilatometer a type of calorimeter.

6. Accuracy

The temperature registration in the dilatometer is important because small variations of the dilatometer temperature lead to a large amount of ficticious shrinkage. The influence of the variation of the temperature of each dilatometer was taken into account in the calculation of the shrinkage values. Furtheron fluctuations of the room temperature were considered by comparing the temperature of each dilatometer with the temperature of a reference dilatometer without specimen. Thus the temperature variation due to heat development caused by hydration could be distinguished from temperature variations caused by fluctuations of the room temperature.

The first results in our experiments were obtained in the time interval of 8 to 30 minutes after mixing depending on the time necessary for mixing and vibrating. Naturally, the later recording begins after mixing the larger is the portion of first shrinkage which is not recorded. However it had been observed that all shrinkage curves initially show a linear increase with log t with a slope independent of the w/c-ratio, when the shrinkage is related to the cement content of the specimen, i.e. when $\Delta V/100$ g cement is plotted as a function of log t. This relationship was used to correct all shrinkage curves in such a way that shrinkage was considered zero at a time of 10 minutes after mixing. Because of this procedure the scatter of experimental data obtained was small and because of

- identical temperature of all materials and apparatus before mixing;
- no restraint of shrinkage of sealed specimens;
- relatively large specimens;
- no movable parts of the dilatometer.

7. Results and Discussion

7.1 Unsealed Specimens

In Fig. 5 the development of shrinkage and temperature of unsealed portland cement specimens (German specification PZ 35F) with two different w/c-ratios of 0,4 and 0,6 resp. is shown. This result confirms earlier results e.g. from Czermin (3). It is evident that the shrinkage is independent of the w/c-ratio. This, however, holds true only as long as permeability of the hardened paste allows the imbibition of water at a sufficient high rate. In the diagram three regions of the shrinkage-time relationship can be distinguished:

- Stage I, which is characterized by a small rate of shrinkage (dormant period) and by a linear dependence of shrinkage on log t;
- Stage II, which shows a linear increase with log t with a steeper slope;
- Stage III, which is characterized by decreasing rate of shrinkage indicating nearly complete hydration.

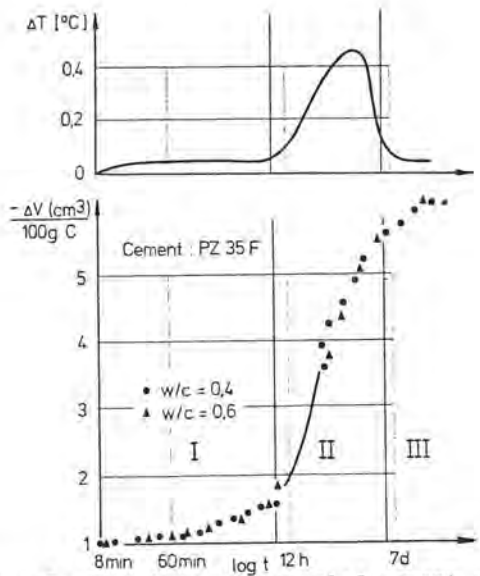

Fig. 5: Shrinkage of unsealed cement paste specimens

The temperature of the dilatometer increases slightly shortly after mixing but remains constant during the dormant period. Following the dormant period the temperature increases rapidly and decreases again after having reached its maximum after about 12 hours.

7.2 Sealed Specimens

In Fig. 6 the shrinkage behavior of sealed specimens is demonstrated. The following characteristics are to be observed:

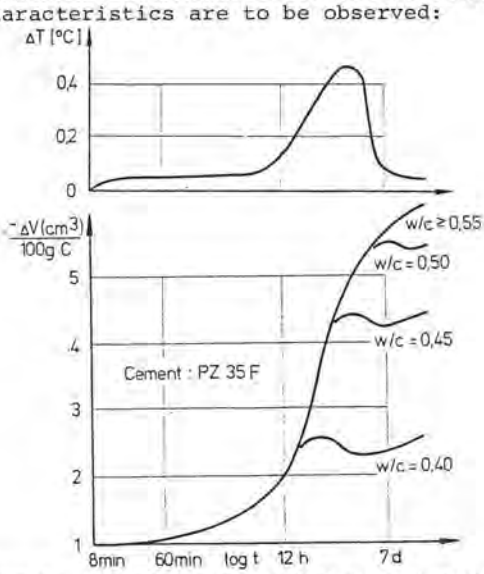

Fig.6: Shrinkage of sealed cement paste specimens

- plastic shrinkage (shrinkage during the dormant period) of sealed specimens is identical to shrinkage of unsealed specimens and independent of the w/c-ratio;
- the shrinkage curve of sealed specimens coincides with the shrinkage curve of unsealed

specimens for a period which is the longer the higher the w/c-ratio. By visual observation of the specimens it was verified that during this period bleeding water could be detected on top of the specimens;
- when the bleeding water was absorbed by the specimens, a period of expansion occurred,which was followed by further shrinkage, however at a slower rate;
- the final value of shrinkage increased with increasing w/c-ratio;
- the temperature curve shows the same characteristics as in the experiments on unsealed specimens (Fig. 5).

Furtheron it is to be noted that the time at which the temperature maximum occurs is independent of the w/c-ratio.

Thus these experiments demonstrate the close correlation between bleeding water and shrinkage of sealed specimens. As specimens with a high water-cement-ratio show strong bleeding their final shrinkage value is high. For w/c-ratios > 0,55 no difference in the shrinkage behavior of sealed and unsealed specimens could be detected within the first 28 days. The results of these experiments do not confirm the statement by Buil and Baron (6) that the expansion period normally is not observed in a volumetric experiment.

Another point can be analysed more clearly on the basis of these results. When performing volumetric shrinkage experiments on sealed cement paste specimens Haas et. al. (8) observed higher shrinkage values (shrinkage given in percent of cement paste volume) for lower w/c-ratios up to about 10 hours. After this time an inverse tendency was observed. Haas et. al. as well as setter and Roy (7) explained this effect by shrinkage caused by ettringite crystals. This explanation seems, however, improbable, as the results of this investigation demonstrate the independence of initial shrinkage on w/c-ratio when shrinkage is related the cement content of the paste. From this result it follows that shrinkage values which are related to the volume of the cement paste must initially be the higher the lower the w/c-ratio.

7.3 Effect of Type of Specimens

In Fig. 7 it is shown that shape and dimensions of the specimens can have a strong influence on the shrinkage of sealed cement paste specimens. In this experiment three different types of specimen made of identical cement pastes have been studied. Type A specimen has a cylindrical form with diameter of 60 mm and a volume of about 600 cm^3. Type B and C specimens only had a volume of 300 cm^3. Both specimens consisted of 8 parallel cylinders (see Fig. 6) each with a diameter of 15 mm. As shown in Fig. 7 the cylinders are in a vertical position for the type B specimen and in a horizontal position for the type C specimen.

Obviously the different specimen forms lead to different shrinkage characteristics of the cement paste. The different behavior can be

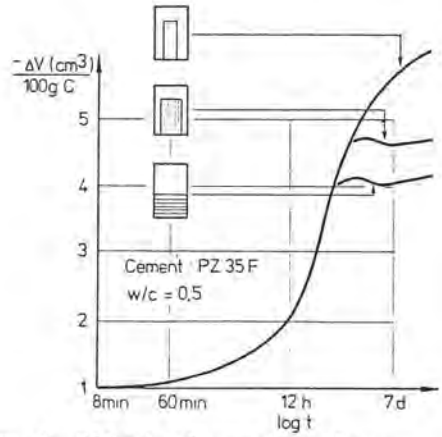

Fig. 7: Effect of specimen form

explained by differences in the amount of bleeding water. It was observed that bleeding was strongest in the type A specimen and weakest in the type C specimen. The high amount of bleeding water in the type A specimen then led to a high final shrinkage value corresponding to the results of Fig. 6, in which the influence of w/c-ratio on shrinkage of sealed specimens had been demonstrated.

7.4 Effect of Admixtures

In a few pilot experiments the effect of admixtures on the shrinkage characteristics of cement paste has been investigated. Three types of admixtures were used:

a) UCR 1/10, a mixture of 10 Vol.-% high polymer resin and 90 Vol.-% ligninsulphonate;
b) UCR 100, the pure high polymer resin, which is used as a plasticiser;
c) polyvinylpropionate.

As shown in Fig. 8 these admixtures had only a slight influence on the shrinkage of the unsealed specimens.

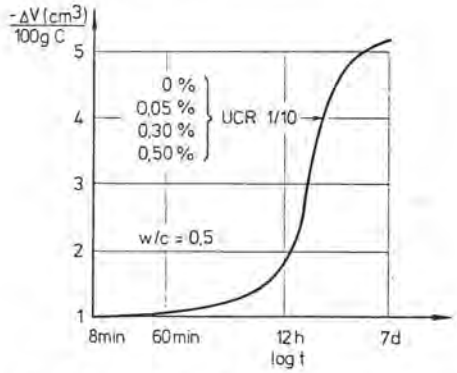

Fig. 8: Effect of admixtures (unsealed sp.)

Fig. 9, on the other hand, shows the result of an experiment on sealed specimens with three different UCR 1/10 concentrations using cement paste with a w/c-ratio of 0,5. In this case, the addition of 0,5% UCR 1/10 slightly

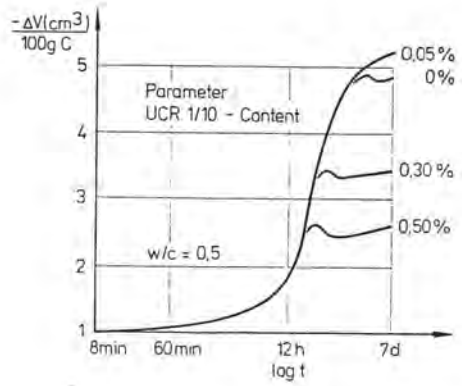

Fig. 9: Effect of admixtures (sealed sp.)

increased the final shrinkage value whereas final shrinkage had been decreased significantly by the addition of larger amounts of admixtures.

The fact that shrinkage of the unsealed specimens with and without admixtures was equal indicates that the admixtures had only a negligible effect (in comparison to the accuracy of the measurement) on the hydration of the different pastes. The shrinkage characteristics of the sealed specimens can be explained - as has been done previously - by different amounts of bleeding water: The addition of 0,5% UCR 1/10 led to a strong reduction of the amount of bleeding water thus decreasing final shrinkage.

8. Outlook

Until now all experiments had been performed by recording each individual data point. Experiments are, however, under way, which will allow continuous reading of shrinkage and temperature. In the final experimental set-up the height of the water in the capillary is recorded by a pressure transducer. Thermocouples determine the temperature in the dilatometer water and in the specimens. The signals of the pressure transducer and thermocouples are processed and recorded by a data recorder. After the experiment the records are connected to a computer which in combination with a plotter will then deliver the final shrinkage plots.

The investigation is being continued. In addition to studies on mechanisms of autogeneous shrinkage and of parameters influencing it, the effect of shrinkage on mechanical properties of concrete is being studied.

References

(1) Baron, J.: Rapp. Rech. Lab. P. et Ch. Nr. 15, 1971.
(2) Chatterji, S.: Cem. Concr. Res. 6 (1976) 145-148.
(3) Czernin, W.: Zement-Kalk-Gips 9(1956), 525-530
(4) Detrichê, C.H.; Maso, J.C.: Mat. et Constr. 12(1979), 185-191.
(5) Buil, M., Baron, J.: 7. Int. Conf. Chem. Cem. 1980, paper VI-37
(6) Buil, M.: Rapp. Rech. Lab. P. et Ch., Nr. 92, 1980.
(7) Setter, N., Roy, D.M.: Cem. Concr. Res. 8 (1978) 623-634.
(8) De Haas, G.D. et al.: Cem. Concr. Res. 5 (1975), 295-320.

THEME VII

Réaction aux interfaces entre ciment et granulat dans les bétons et mortiers

Interface reactions between cement and aggregate in concrete and mortar

---

Etude de l'effet produit sur la déformation des bétons par les alcalis au cours de leur interaction avec la silice dans les agrégats

Investigation of cement alkalis influence on concrete deformations at interaction of the alkalis and silica in aggregates

G. ROYAK, TsNIIS, Moscou, U.R.S.S.

On a étudié l'influence qu'exercent sur la déformation du béton la teneur du ciment en alcalis, la quantité d'opale dans l'agrégat, la taille de ses grains, le facteur eau-ciment et l'activité de l'addition minérale present dans la composition du ciment. On a déterminé les déformations qui se produisent dans le béton en fonction du nombre et du type d'adjuvants minéraux actifs d'origine volcanique et sédimentaire additionnés au ciment.

On a examiné le mécanisme d'interaction entre la phase liquide du ciment et la silice.

On a formulé des propositions concernant la composition minéralogique des ciments et leur teneur en alcalis lors queles agrégats contiennent de la silice active.

Influence on concrete deformations of alkalis quantity in cement, opal in aggregate, size of its grains, W/C factor, activity of mineral addition containing in cement composition has been investigated.

Concrete deformations have been determined as a function of quantity and type of sedimentary and volcanic active mineral additions containing in cement.

The mechanism of interaction of cement liquid phase, with active silica has been considered. Suggestions are made about cement substantial composition and relating to the alkalis contents in the cement with active silica in aggregates.

Dans leur rapport détaillé au 4ième symposium international sur la chimie du ciment qui s'est tenu à Washington en 1960, P.Bredsdorf, G.M. Idorn et coll. (1) ont exposé les différents aspects des réactions chimiques avec les agrégats. Ils ont noté que le type et la structure des minéraux réactifs et le comportement des grains d'agrégats de grande dimension devaient être considérés comme objets d'importance primordiale dans les études de base ultérieures. Il est connu que la réaction avec la silice dans les agrégats commence sur la surface des grains et embrasse les couches plus profondes grâce à la rupture des liaisons Si-O-Si. S.A.Greenberg et D.Sinclair (2) ont abouti à la conclusion que les liaisons siloxane formées par la polymérisation de l'acide monosilicique sont détruites dans l'eau et cette réaction est réversible. Déjà en 1933 B.N.Dolgov (3) a indiqué la possibilité de formation de la liaison siloxane et du polymère à partir de composés organiques oxygénés de silicium avec le dégagement de l'eau :

$$\equiv Si\text{-}O\boxed{H + OH} - Si\equiv \rightarrow \equiv Si\text{-}O\text{-}Si\equiv + H_2O$$

Les échantillons de silice naturelle contenus dans les agrégats surtout sous forme de phases amorphes et microcristallines d'origine sédimentaire possèdent la surface intérieure développée accessible à la pénétration de la phase liquide et à la réalisation rapide des réactions chimiques. La silice formée dans les conditions naturelles sous forme de verre peut aussi contenir des additions d'eau et être caractérisée par la structure défectueuse et l'activité chimique élevée. Des idées analogues peuvent être généralisées aux pouzzolanes utilisées dans la composition des ciments et absorbant activement l'hydroxyde de calcium formé au cours du durcissement. Pour des grains macroscopiques de silice la part d'ions superficiels est trop petite pour que l'hydratation puisse influer sur la composition moyenne d'une particule. La surface des particules colloïdales de silice est tellement grande que l'hydratation est mesurable et on peut parler de la silice hydratée. Le fait connu de diminution de l'expansion si les pouzzolanes entrent dans la composition du ciment, ne trouve pas d'explication assez claire bien qu'on liait la diminution de l'expansion avec la propriété traditionnelle des pouzzolanes d'interagir activement avec l'hydroxyde de calcium (1). I.Powers et N.N.Steinour ont supposé quela réaction des alcalis avec la silice se déroule "sans aucun danger", i.e. ne provoque pas d'expansion, lorsque $Ca(OH)_2$ arrive dans la zone de réaction assez vite pour pouvoir interagir avec la moitié de la quantité de la silice dissoute dans NaOH. Or ceci n'est possible que lorsque la concentration de $Ca(OH)_2$ surla surface extérieure de la couche des produits de la réaction est assez élevée durant tout le temps. On pouvait supposer que le grain isolé de la silice, par exemple de l'opale, ne deviendrait pas plus grand quant à la dimension ou gonflerait de façon limitée lors de l'interaction avec la solution de NaOH et de $Ca(OH)_2$ car les con-

ditions indiquées ci dessus sont observées dans ce cas. La figure 1 montre la variation de la valeur de la solubilité de l'opale dans les solutions de NaOH si ces dernières contiennent un excès de $Ca(OH)_2$. La figure 2 montre l'augmentation de la dimension des

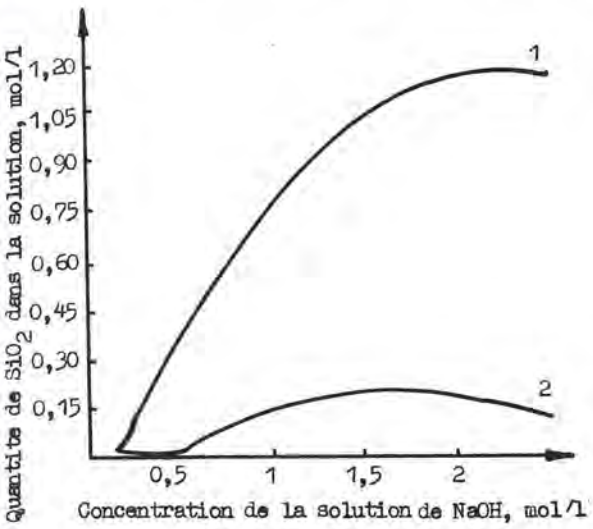

Fig.1. Variation de la concentration de SiO_2 soluble en fonction de la concentration de l'alcali et de la teneur en $Ca(OH)_2$ de la phase solide: 1 - en solution de NaOH; 2 - en solution de NaOH avec $Ca(OH)_2$ solide

grains isolés dans le temps, i.e. leur gonflement, dans différents milieux. Notons le caractère adéquat de l'augmentation de la dimension des grains dans le temps lorsqu'ils se trouvent dans la solution saturée de $Ca(OH)_2$, dans la solution de $NaOH+Ca(OH)_2$ et dans la matrice du ciment durci ou lorsqu'ils se trouvent dans l'eau ou la solution aqueuse de NaOH. Ainsi la diminution de l'expansion lors de l'introduction dans la composition du ciment de la pouzzolane doit évidemment être liée non à la formation du gel "expansif ou non expansif" mais aux conditions telles que l'arrivée des ions Ca^{2+} vers les gros grains soit essentiellement détournée. Dans les gros grains il y a une réserve de la silice réactive pour la réalisation d'une réaction chimique prolongée et du gonflage. On détourne l'arrivée des ions Ca^{2+} vers ces grains par introduction dans la composition du ciment d'une quantité déterminée de la pouzzolane active à grains fins (surface spécifique ~10 000 cm^2/g) dont les particules entreront rapidement en réactions chimiques avec Ca^{2+} et la dépolymérisation

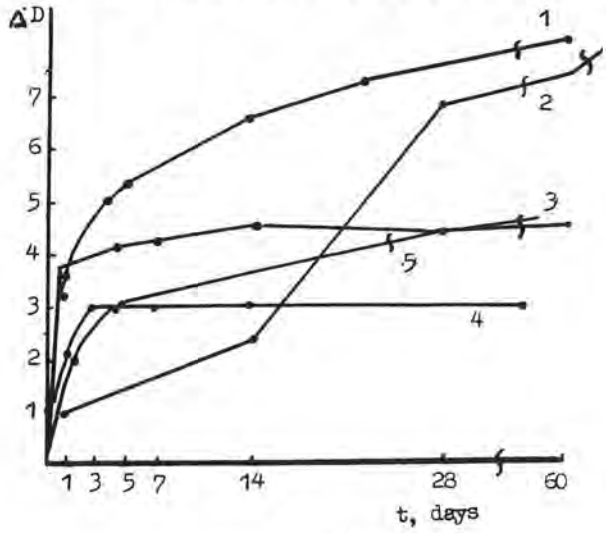

Fig.2. Expansion des grains isolés de l'opale dans les milieux suivants: 1 - solution saturée de $Ca(OH)_2$, avec la teneur de CaO de 1,3 g/l; 2 - matrice du ciment durci; 3 - solution de NaOH, 1 N- 4 - eau; 5 - 1 N solution de NaOH + $Ca(OH)_2$

ultérieure de la silice par les ions OH^-, Na^+ et K^+ conduira à l'expansion initiale limitée des grains suivie d'une dissolution sans aucun indice d'expansion. Dans le Tableau I on trouve les données sur la diminution des déformations d'expansion des ciments avec les pouzzolanes d'origine sédimentaire et volcanique. On voit sur la figure 3 les isolignes des déformations d'expansion pour les pouzzolanes qui se distinguent par le type et la structure de la silice active caractérisés d'après l'absorption de l'hydroxyde de calcium recalculée pour CaO. La figure 3 montre qu'avec l'augmentation de l'activité de la pouzzolane on peut admettre l'accroissement de la teneur des ciments en alcalis sans aucun risque de voir apparaître dans le béton des déformations critiques. Le traitement statistiques des données de l'U.S.A. et de

TABLEAU I

Déformations d'expansion des échantillons contenant les additions pouzzolaniques d'origine sédimentaire et volcanique

nos d'ordre	Addition pouzzolanique	Quantité %	Déformations d'expansion à l'âge de 1 an,%
1	Sans addition	0	0,99
2	Spongolite	17	0,37
		30	0,07
3	Gaize n°1	17	0,62
		30	0,067
4	Gaize n°2	17	0,96
		30	0,09
5	Tuf	17	0,61
		25	0,198
		40	0,110
6	Pierre ponce	17	0,59
		25	0,10
		40	0,09
7	Gliej	17	0,80
		25	0,09
		40	0,06
8	Perlite	17	0,40
		40	0,065
9	Porphyroïde	7	0,54
		40	0,06
10	Laitier	17	0,53
		30	0,10
		60	0,09

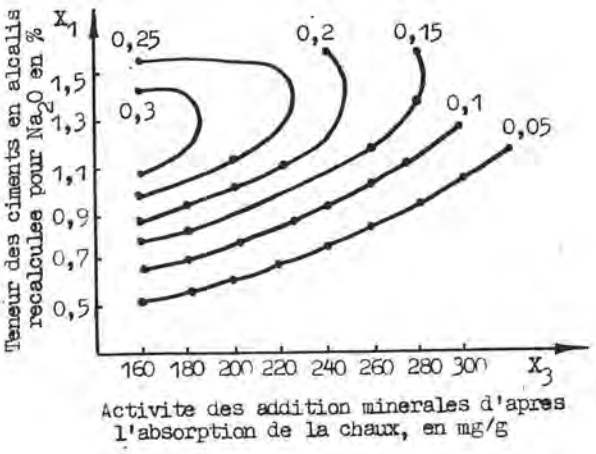

Fig.3. Isolignes des déformations d'expansion. Les chiffres près des courbes représentent les valeurs des déformations en pour cent

l'U.R.S.S. a permis d'obtenir l'équation suivante :

$$y = 32,77 + 0,287\ x - 0,000353\ x^2,$$

où y est la diminution de l'expansion en %, x la diminution de l'alcalinité en mmol/l, permettant, d'après les résultats de détermination de la diminution de l'alcalinité (méthode ATM), de prévoir la diminution de l'expansion lors de l'utilisation dans la composition du ciment des différentes pouzzolanes. Les résultats obtenus permettent d'aboutir à la conclusion suivante : l'approche de la teneur admissible en alcalis du ciment contenant les pouzzolanes doit être mise en dépendance avec l'absorption de la chaux, la quantité de la pouzzolane dans le ciment et sa consommation.

BIBLIOGRAPHIE

1.P.Bredsdorf, G.M.Idorn, Alice Kjaer, Niels Munk Plum and Ervin Panlsen Chemical Reactions involving aggregate ; Proceeding of the Fonrthgh International Simposium of the Chemistry of cement, Washingtоn, 1960.

2. S.A.Greenberg, D.Sinclair, I.Ofphystc Chem. 59, 435 (1955).

3. B.N.Dolgov, Chimie des composés organosiliciés, Goskhimtekhizdat, 1933.

4.Powers T. and Steinour H.H., Proc.Am. Concrete Inst. 51, 497-514 (1955).

La formation de la zone de contact à la limite avec un agrégat poreux

Formation of contact zone on the border with porous aggregate

L. KOURASSOVA, Collab. Sc. Supér., NIIZhB, Moscou
Z. LARIONOVA, chef de Laboratoire. U.R.S.S.

Les facteurs importants exerçant une influence sur la résistance de la zone de contact dans le béton léger sont: l'activité hydraulique de l'agrégat poreux amenant aux formations nouvelles et l'aspiration par cet agrégat de la phase liquide du ciment durci. En fonction de la grandeur des grains del'agrégat poreux ces propriétés se manifestent d'une manière différente. Par un complexe des méthodes physico-chimiques est étudiée la zone de contact avec les grains de kéramsite (du 5 mc à 20 mm)dans les échantillons des mortiers. Est constaté l'accroissement de microdureté du ciment durci sur le contact avec les grains (avec d 2 m.) ce qui s'explique par la formation de la couche consolidée résultant de l'interaction chimique intensive entre les grains de grandeur donnée et les composantes du ciment durci. A mesure que les grains deviennent de plus en plus grands, la microdureté du ciment durci sur le contact decroît, le rôle de l'interaction chimique abaisse et augmente l'influence de l'aspiration qui abaisse la résistance de la structure. Pourtant l'aspiration de la phase liquide est exerce une influence favorable sur la structure de la zone de contact, si elle a lieu avant le début de la vibration du béton frais.

Important factors affecting the strength of the contact zone in lightweight concrete are hydraulic activity of the porous aggregate leading to newformations and extraction by it the liquid phase from the cement stone. Depending on fineness of the porous aggregate particles, these peculiarities reveal themselves in various ways.

Using a several of physico-chemical methods, studies have been made of the contact zone with ceramsite particles (d ranging from 5 mkm to 20 mm) in mortar specimens.

Microhardness of the cement stone contacting with particles (d 1,2mm) increases due to intensive chemical interaction between the particles of this size and the cement stone components.

As the particle size grows, the cement stone microhardness in the contact zone is lessened, the role of the chemical interaction being decreased, while the effect of extraction (that reduces the strength of structure) is stepped up. But extraction of the liquid phase has a favourable effect on the contact zone structure if it takes place before the vibration of the concrete mix.

Les propriétés physico-mécaniques du béton sont considérablement influencées par l'état de la zone de contact, c'est-à-dire par sa structure, sa composition de phase et sa résistance. La zone de contact c'est le microvolume du béton, limité conventionnellement par les deux surfaces qui passent dans le ciment durci et dans le grain d'agrégat à une telle distance de la surface de contact qu'il n'y a pas d'influence des phases contigues.

L'état de la zone de contact dépend de propriétés physico-chimiques d'agrégat ainsi que de processus au contact résultant de l'interaction de l'agrégat avec le ciment durci. Les facteurs importants déterminant la résistance de la zone de contact dans le béton léger sont: l'activité hydraulique de l'agrégat poreux amenant aux formations nouvelles et l'aspiration par cet agrégat de la phase liquide du ciment durci. Nous avons mis en évidence que ces propriétés se manifestent différemment en fonction de grandeur des grains de l'agrégat poreux. Par un complexe des méthodes est étudié la zone de contact avec les grains de l'agrégat poreux - kéramsite (d étant égal à 5 mkm - 20 mm). L'étude des couches de contact du ciment durci à la limite avec les grains du kéramsite non-concassé ayant les dimensions différentes a été réalisée sur les trois séries d'éprouvettes qui se distinguaient par les dimensions des fractions étudiées: 0,15 mm; 0,15-5 mm et 5-20 mm. Pour la détermination de la microrésistance de la zone de contact a été utilisée la méthode des mesures de microrésistance à l'aide d'un microscope dans une lumière réfléchie. Cette méthode est basée sur l'enfoncement statique de la charge dans un volume microscopiquement petit du matériau. La microdureté (H) des couches de contact du ciment durci (diagnostiquées visuellement à l'aide d'un microscope lumineux d'après la peinture de rouille brune) immédiatement à la limite avec les grains de 3-7 mkm était égale à 3000-4700 MPa. A mesure de l'éloignement de la limite la microdureté diminuait et à la distance de 10-20 mkm elle était égale à des valeurs correspondant à H de la masse hydratée du ciment durci en volume (600-700 MPa). Donc, autour les particules dont les dimensions sont égales à 3-7 mkm se forment les microvolumes du ciment durci renforcé; les diamètres de ces volumes sont 7-15 fois plus grands que les dimensions des particules.

L'augmentation de microdureté dans les couches de contact autour les grains de fraction de 0,15-5 mm de sable non-concassé du kéramsite n'était observé qu'à la limite avec les particules de 1,2 mm (Fig.1). A mesure de l'accroissement des dimensions des particules la microdureté diminue à partir de 2200 MPa (pour 0,15 mm) jusqu'aux 900 MPa (pour 1,2 mm), et la largeur de la couche renforcée diminue à partir de 20-25 mkm jusqu'aux 10-15 mkm; c'est-à-dire jusqu'aux 0,01-0,15 du diamétre de la particule. Au contact avec les grains de 2,5-5 mm la microdureté est égal à 650-750 MPa; cette valeur n'excède pratiquement pas de microdureté du ciment durci (400-750 MPa).

Nous considérons que l'aspiration de l'eau du ciment durci par l'agrégat influence favorablement sur la formation de la structure du béton frais seulement jusqu'au moment de son compactage définitif. L'aspiration ultérieure de l'eau porise le mortier et le béton devient d'une résistance moindre. Ce fait a été confirmé par des essais spéciaux, par lesquels on a déterminé l'influence de compactage (vibration) sur la microstructure et la microdureté du ciment durci, contigu à l'agrégat poreux.

Les résultats obtenus correspondent avec nos hypothèses que si la quantité essentielle de l'eau est aspirée par l'agrégat avant le compactage du béton frais (c'est-à-dire la vibration est réalisée 15-20 minutes après la préparation du béton frais) alors l'aspiration de l'eau joue un role positif. Dans ce cas-là la formation du béton frais a lieu justement dans la période où sont déjà terminés l'aspiration de l'eau d'agrégat et l'abaissement de E/C et le compactage du ciment durci liés avec l'aspiration de l'eau. L'aspiration ultérieure de l'eau du ciment durci diminue ou n'existe pas de quoi résulte lefait que la porisation de la couche de contact n'a pas lieu. Dans lesconditions données, les propriétés de microrésistance du ciment durci au contact sont conditionnées, principalement, par la composition et par la microstructure des nouvelles formations. Si le compactage du béton frais est réalisé immédiatement après sa préparation, alors l'aspiration ultérieur de la quantité essentielle de l'eau, qui dure encore 15-25 minute, amène à la porisation de la

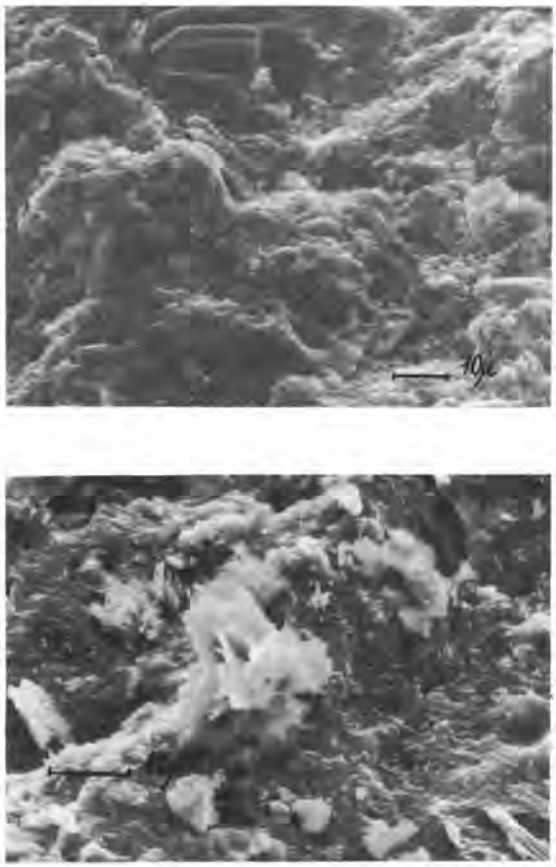

Fig.1. La surface de clivage du ciment durci sans particules (a) et avec les particules de la zone extérieure du kéramsite (b) SEM

couche de contact du ciment durci et à diminution de sa résistance.

Par ces mêmes processus s'explique aussi un tel phénomène que dans les éprouvettes essayés, au contact avec les grains finement disperés du kéramsite dont l'aspiration de l'eau se réalise pratiquement instantanément, est observé le dépassement de microdureté du ciment durci en fois et plus. Avec l'augmentation des dimensions de la fraction du sable quand l'aspiration de l'eau se réalise pendant une période plus longue l'augmentation de microdureté de la couche de contact en comparaison avec le ciment durci en volume ne constitue que 20-25%. Donc, l'augmentation de microrésistance du ciment durci au contact avec un agrégat poreux (particulièrement avec les grains de 1,2 mm) est conditionné par la formation résultant de l'interaction chimique de la zone transitoire renforcée dont la largeur est égale à 10-20 mkm et qui est constituée des nouvelles formations et des particules submicroscopiques d'agrégat, ainsi que de micro-couches ointes d'une résistance élévée qui se forment autour de ces particules. L'abaissement de microdureté, observée au contact, n'est déterminé que par l'accroissement de la porosité du ciment durci qui résulte de l'aspiration de l'eau par l'agrégat continuée après le compactage du béton frais.

En se basant sur les résultats obtenus nous sommes amené à la conclusion suivante: à la limite du ciment durci et du kéramsite ont parallèlement lieu les deux processus qui influencent sur la formation de la zone de contact. Ce sont les processus suivants:

1. L'apparition d'un nombre considérable des phases nouvelles (qui résulte de l'interaction chimique du kéramsite avec le ciment durci) amenant à la formation de la structure cristalline plus compacte et à l'accroissement de microrésistance de la couche de contact.
2. L'augmentation de la porosité du ciment durci résultant de l'aspiration de l'eau par l'agrégat continue après le compactage du béton frais; cette aspiration de l'eau contribue à l'abaissement de microrésistance de la couche de contact.

La résistance finale de la couche de contact est conditionnée par des processus qui ont lieu à cette étape de la formation de la structure du béton léger frais.

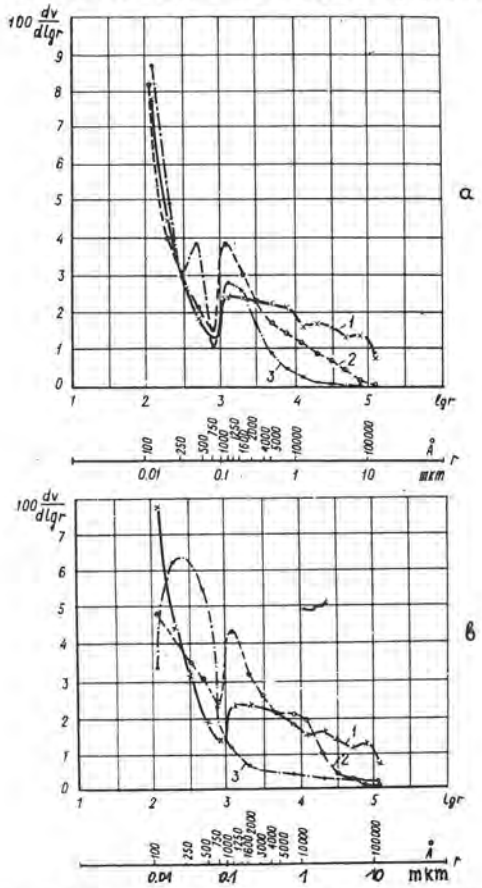

Fig.2. Porogrammes des mortiers de ciment sables sans particules (1) et avec les particules de la zone extérieure (a) et de la zone intérieure (b) du Kéramsite, leur surface spécifique S_{sp} étant égale à 2700 cm^2/g (2) et 7000 cm^2/g (3): V - volume des pores; r - rayon des pores

Investigation of contact zone in cement stone hydrate phases single-crystal concretions and their concretions with aggregates

Etude de la zone de contact dans les agrégats de monocristaux des phases hydratées du ciment durci et dans leurs agrégats avec les matériaux de remplissage

V.V. TIMACHEV,
Y.I. BENSTEIN,
L.V. BALKEVITCH,
N.S. NIKONOVA, MkhTI Mendeleev, Niitsement, U.R.S.S.

On a étudié les agrégats de cristaux des phases hydratées du ciment durci entre eux et les processus de leur cristallisation sur la surface du quartz et de la calcite.

Les agrégats furent étudiés à l'aide de l'analyse structurale aux rayons X d'après la méthode de Laue, de la microscopie optique et électronique.

On a étudié les régularités et déterminé les faces et les angles préférentiels d'agrégation des cristaux de quartz et de calcite. On a découvert l'agrégation épitaxique des cristaux indiqués d'après le schéma de Royé.

On a étudié la zone de contact dans les systèmes réels durcissants où sur la surface des agrégats on a découvert les couches orientées des cristaux de la calcite. On a dégagé trois secteurs principaux de la zone de contact. On a montré que par les méthodes de l'action chimique, mécanique et combinée sur les constituants du mortier composé de ciment et de sable on peut commander les processus de formation de structure des cristaux ayant lieu lors du durcissement des liants.

Concretions of cement stone hydrate phases crystals one with another and process of their crystallization on the surface of quartz and calcit have been investigated. The concretions have been studied through the use of X-ray diffraction analysis by Laue method, and optical and electronic microscopy.

Mechanism of concretion haz been studied and preferred facets and angles of concretion of hydrate phases crystalls one with another and with crystalls of quartz and calcit have been determined. Epitaxic concretion of mentionned crystalls according to Roier have been revealed;

Contact zone in real solidifying systems has been studied. Oriented layers of calcit crystalls have been found on the aggregates surface in the contact zone. Three main regions of contact zone have been distinguished. It was demonstrated that one can control the processes of binder crystallization by the methods of chemical, mechanical and combined influence on the components of cement sand solution.

A comprehensive study of concretion of calcium hydrosilicate and portlandite crystals with each other was carried out together with investigation of CHS crystallization from satured solutions of various stoichiometric composition on quartz and calcite surfaces.

Various methods of crystal growth from aqueous solution and methods of hydrothermal crystallization were used. Concretions of quartz and calcite sith large (1-5 mm) $Ca(OH)_2$ crystals were obtained by the method of diffusion of saturated $CaCl_2$ and KOH solutions in water, placing in the reaction zone plates cut out of quartz and calcite single crystals along different crystallographic directions. Accretion of hydrate phase crystals on substrates was carried out by Belyustin's method. Specific features of concretion and of the contact zone structure were studied by Laue X-ray structure analysis, local X-ray spectral analysis, electron microdiffraction and electron microscopy.

Contact Zone in Concretions of Hydrate Phase Crystals

Crystals of $Ca(OH)_2$ most frequently intergrow along faces of hexagonal and dihexagonal prisms and basis, and twinning planes are faces of ditrigonal scalenohedron and hexagonal dipyramid. Angles between triad axes in concretions change abruptly and are multiple of 15-16°. Most ofthe Laue patterns obtained from the contact zone of concretions show the presence of additional reflections indicating considerable distortion of the crystal lattice and the existence of disoriented microcrystalline blocks in the Contact zone.

Among the synthesized concretions of calcium hydrosilicates (Table 1) ideal laue patterns are observed in concretions of crystals obeying Royer's structure-geometrical principle. Such are practically all cross-shaped concretions (manebach and pericline types) of crystals C_6S_3H, $CaNaHSiO_4$ and of microtwins of calcium chondrodite C_5S_2H. Well-shaped Laue patterns are also displayed by penetration concretions of crystals $Na_2Ca_3Si_2O_{10}$. The strength of contact zone in such concretions is close to the strength of intergrown crystals (Table 2).

The obtained experimental data indicate that a strong crystalline contact in a concretion is formed in the case of apitaxial intergrowth along the general directions of anionic and cationic bonds in accordance with the principle of structure-geometrical conformity of conjugating lattices alongs the planes and directions of most dense packing.

Regular concretions of hydrate new formations in the hardening system are formed not as a result of intergrowth of already formed crystals, but in the process of nucleus formation - growth of nuclea from one point or one face. Strength of the contact zone characterized by microhardness in most cases is higher than the strength of the crystals forming concretions, thus pointing to a high degree of ordering in the contact zone structure (Table 2).

Contact Zone in Crystal Concretions of Hydrate Phases with Quartz and Calcite

Concretions were prepared by keeping quartz and calcite plates in satured solutions of the appropriate phases for 6 months and by the diffusion method.

On all substrates, independent of solution composition, spherical particles and their aggregates are observed (Fig.1).They do not give reflections in electron microdiffraction experiments, that suggests amorphic nature. These particles are the primary form of crystallization of hydrate new formations. Coalescence of particles and thus formation of larger aggregates is observed, indicating weak bonding with the substrate and capacity to migrate along its surface. The particles accumulate on macrodefects of the surface, steps of the cleavage surface, cracks, etc., however frequently their locations are not connected with surface topography. In this case microdefects of crystal-substrate surface play an important role. In addition to these formations crystalline particles of various morphology are observed on substrates.

Superposition of diffraction patterns of crystals comprising the concretion are observed in laue patterns of the concretion zone of portlandite with quartz and calcite. On several patterns of the concretion zone spreading and bifurcation of reflections is observed indicating the presence of stresses

Table 1

Specific Features of Formed Crystalline Concretions of Calcium Silicates and Hydrosilicates

N	Mineral	Single crystal morphology, and concretion		twin type	Orientation of constituent crystals of concretions	Twinning law
1	C_6S_3H $6CaO \cdot 3SiO_2 \cdot H_2O$ $Ca_6 SiO_4 Si_2O_7 (OH)_2$	Elongated prisma, platelets	Cross-tration bined Prisma in polysynthe ning.	shaped pene-twins. Com-aggregates. the case of tic twin-	100_1 $100_2 = 98°$ $(001)_1$ $(001)_2$	Analogue of peri-cline law. Polycry-stalline twinning;
2	C_5S_2H $5CaO \cdot 2SiO_2 \cdot H_2O$ $Ca_5(SiO_4)_2(OH)_2$	Prisms, platelets	-shaped prisms. aggregates. the case twinning.	concretions, Intergrowth Prisms in of micro-	001 1 002 2 70°	Manebache law. Structural micro-twinning.
3	Tricalcium silicate hydrate - TSH	Elongated hexagonal prisms, fibers	Druses, shaped	conical ray-aggregates	Angle at cone apex	Growth druses, felt-like structures
4	$CaNaHSiO_4$	Elongated prisms	Cross-netration Intergrowth	shaped pe-twins. druses.	010 1 010 2 = 122° Twinning along prism faces 110	Aragonite law
5	$Na_2Ca_3Si_3O_{10}$	Planar prisma	Cross-tact twins. aggregates.	shaped con-Star-shaped	010 1 010 2 = 45° 010 1 010 2 010 3 010_4= = 45°	Analogue of aragonite law

Table 2

Microhardness of Contact Zone and of Hydrosilicates		Crystals of Portlandite and Calcium (data of)		
Phase	Microhardness of crystals	Microhardness of contact zone		
		structure	penetration structure	integrowth structure
Portlandite	49.5-258.0	140.0	290.0	84-420
High-basic calcium hydrosilicates	91-801	850.0	460.0	380.0

in the lattices which in its turn points to intergrowth of crystals and not simple mechanical cohesion. Many photographs also show additional reflections which are weaker and randomly distributed, indicating the presence of small disoriented single crystals in the contact zone. This suggests that at the early stages of crystallization variously oriented nuclea are formed, the growth of which is hindered by rapid growth of crystals with more favourable orientations.

Examination of the contact zone of concretions of portlandite with quartz using a scanning electron microscope confirm this suggestion. A smaller crystal grown to the substrate by the hexagonal prism face and scaly formations, possible thin platelets of portlandite grown to the substrate by the basis face, were observed in the contact zone.

Analysis of stereographic projections constructed from laue patterns of portlandite concretions with quartz and calcite showed that intergrowth mainly occurs along faces of hexagonal prisms with angles between triad axes of portlandite and calcite crystals of 21 and 42° (Fig.2) and between triad axes of portlandite and quartz crystals of 0, 38, 48 and 90° (Figs. 2 and 3).

A transition zone between intergrown crystals with smooth variation of Si and Ca concentrations was established by local X-ry spectral analysis in concretions of

Fig. 1. Spherical particles on the surface of aggregates

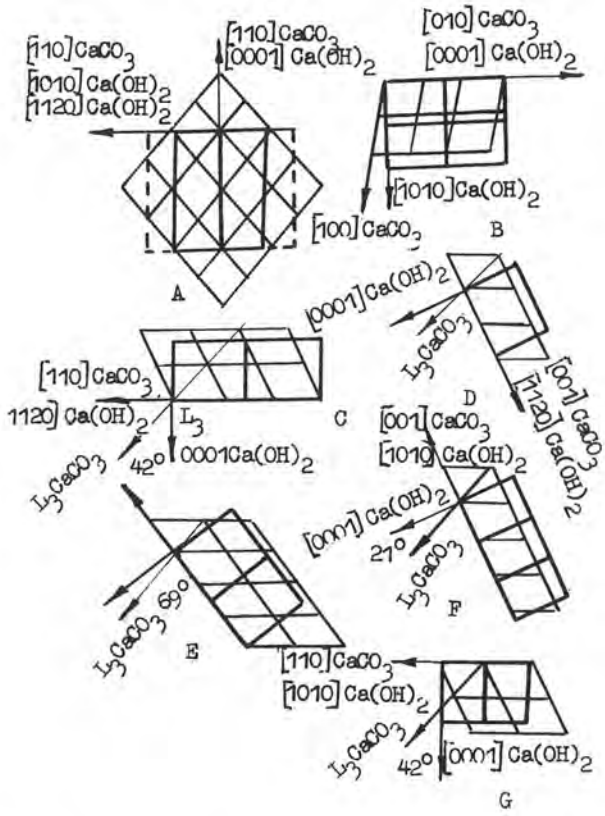

Fig. 2. Schemes of growing together portlandite and calcite. Thick lines - grating of portlandite, thin lines - grating of calcite

quartz with portlandite. The width of this zone is 35-50 μm.

Crystallochemical analysis of quartz, calcite and portlandite structures points to intergrowth according to Royer's scheme along planar grids with equal or multiple parameters.

The conformity of lattice parameters may serve as a criterion of regular intergrowth of quartz with CHS crystals. In calcium hydrosilicates with rhombic or pseudohexagonal cells the parameters "a" and "b" are multiple to parameters "c" and "a" of the quartz cell which determines the possibility of formation of a regular concretion for conjugation of plane (001) of CHS with the hexagonal prism plane of quartz (Fig.4). Coincidence is also observed for conjugation of plane (001) of CHS and quartz basis (001) when the direction of (010) CHS is parallel to direction 1010 quartz. Intergrowth of CHS with the plane of hexagonal prism of quartz is observed more frequently since it possesses a larger reticular plane than the basis plane.

Of interest is crystallization of C_2SH_2 on the calcite surface. New formations decorate slip bands on calcite faces according to a specific regularity (Fig.5). With growth of CHS on calcite conjugation of planes (001) of CHS and (100) of calcite is observed when 100 and [010] of CHS and [110] and [100] of calcite are parallel (Fig.6).

The obtained data allow to suggest the following process of contact zone formation. Nucles of new phase are formed on the substrate in random orientation. In the case of conformity with the structure-geometric principle of Royer and for the appropriate orientation acquired due to migration along the surface, the growing crystals form a concretion with the substrate. Crystals with more favourable orientation for growth (e.g., portlandite crystals with the face of hexagonal prism oriented parallel to the substrate plane) grow more intensively, suppressing growth of nuclea with less favourable orientation. As a result, at the contact of two intergrown crystals a transition zone is formed which includes randomly

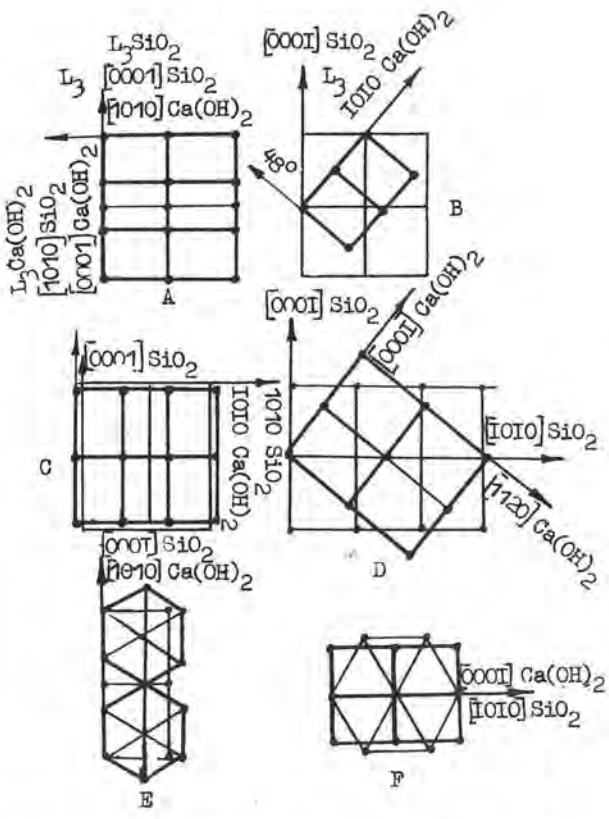

Fig. 3. Schemes of growing together portlandite and quartz. Thick lines - grating of portlandite, thin lines - grating of quartz

oriented small single crystals on which one crystal lattice passes into another in the substitutional form of solid solution with composition continuously varying from one contacting crystal to the other and also sections containing epitaxial inclusions formed as a result of decomposition or formation of solid solutions and isolation of independent phases in epitaxial orientation. The structure and strength of the contact zone depends on the presence of one-dimensional, two-dimensional or three-dimensional similarity of the contacting lattices, the degree of commensurability of parameters, and the possibility of transition from one structure into another during substitutions.

Contact Zone in Real Hardening Systems

Intergrowth contacts were studied on mortar specimens (rods 1x1x3 cm) of composition 1:3, W/C=0.5•C_3S, C_3A and Portland cement were used as binders. Natural single crystals of quartz and calcite ground to 1 mm, in order to exclude the effect of granulometric composition, were used

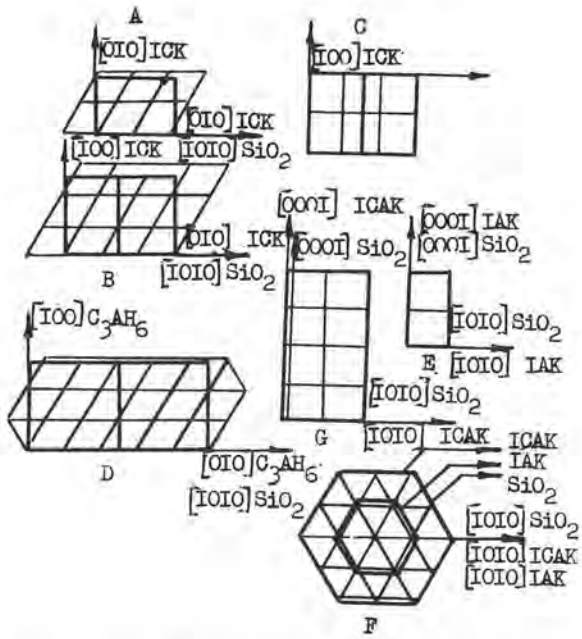

Fig. 4. Schemes of growing together hydrated phases and quartz. Thick lines - grating of gydrated phases, thin lines - grating of quartz.

as aggregate.

The strength of specimens with calcite aggregate was 25-50% higher than for the quartz aggregate. In the case of C_3A and cement this may be explained by formation calcium hydrocarboaluminates in the contact zone, whereas in the case of C_3S increase of strength may be caused only by a larger amount of concretions between hydrate new formations and calcite than in the case of quartz.

Electron microscopic study established on the surface of aggregates in hardening paste of C_3S and Portaldn cement well crystallized rhombohedra of calcite which is the product of carbonization of calcium hydroxide formed during hydrolysis of C_3S (Fig. 7). The ordered arrangement of calcite crystals on surface of aggregates is clearly revealed in the patterns. Calcite rhombohedra grow onto the surface by the face (001), ribs [100] and [010] being parallel. Crystals frequently intergrow along faces (100) and (001) covering large surface areas with a continuous layer. The regular shape of the calcite crystals and their ordered arrangement on the aggregate surface indicate that their crystallization occurs at small supersaturation, presumably at late stages of hardening. Oriented calcite layers on the aggregate surface condense and strengthen the contact layers of the binder, favourably affecting the strength of the

Fig. 5. Decoration pictures on calcite surface

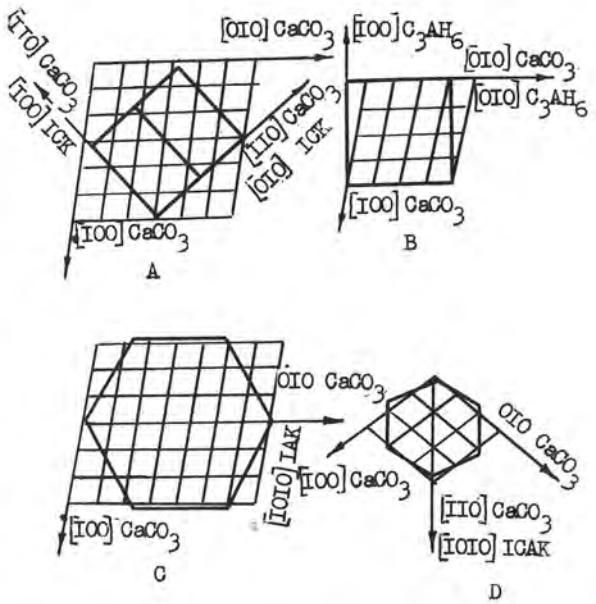

Fig. 6. Schemes of growing together hydrated phases and calcite. Thick lines - grating of hydrated phases, thin lines - grating of calcite

mortar.

Hence, in real hardening systems the contact zone is complex both in phase composition and in structure. Three main sections may be distinguished: a) sections where cohesion of the cement stone with the aggregate is purely mechanical; b) sections where the contact zone is formed by chemical interaction; c) sections where epitaxial intergrowth of crystals of hydrate new formations with crystals of aggregate occurs. All these processes may proceed simultaneously and consecutively. The different strength of cohesion of cement stone with various sections of aggregate surface is thus explained by different mechanisms of contact zone formation.

The strength may be enhanced by creating conditions for active intergrowth of crystal hydrates with each other and with aggregate crystals, i.e. by increasing the number of active centers of crystallization and influencing the surface properties. This may be realized, for example, by chemical action (etching) on the crystal-substrate or by creating fresh cleavage surfaces by mechanical action. Etching removes the surface layer containing impurities which block the active centers on the surface. Moreover, etching of a polycrystalline specimen reveals crystallographic planes of single crystals most p favourable for accretion of crystals of hydrate new formation (e.g., faces of hexagonal prisms of quartz crystals in a polycrystalline sample).

Corrosion des ciments Portland par les gaz contenant du sulfure d'hydrogène

Portland cement hydrosulfide gas corrosion

V.S. DANUCHEVSKI,
A.P. TARNAVSKI, MinKh et GP Goubkine, U.R.S.S.

Dans les différentes constructions les matériaux en ciment portland entrent en contact avec les gaz d'origine naturelle ou tecnogène, qui contiennent l'hydrogène sulfuré en concentrations importantes. Sous hautes pressions du gaz et à la température élevée, ce qu'on observe par exemple dans les sondages à gaz, il se produit une destruction rapide du ciment portland. La corrosion par les gaz contenant le sulfure d'hydrogène a un mécanisme particulier. Lors de la dissolution du sulfrue d'hydrogène dans le liquide interstitiel il se produit sa neutralisation par l'hydroxyde de calcium avec la formation de l'hydrosulfure soluble dans l'eau. Par suite des réactions d'oxydoréduction avec l'oxygéne dissous dans le liquide interstitiel et le composés fortement oxydés du ciment portland (avant tout Fe^{III}), le soufre de sulfure s'oxyde jusqu'au soufre neutre et ensuite jusqu'au soufre de sulfate. La présence de l'ion sulfate diffusé dans la profondeur de la pâte de ciment provoque la formation de l'ettringite, l'expansion et le craquelage de la pierre de ciment. Si l'hydrogène sulfuré continue d'arriver dans le liquide interstitiel, l'ettringite se détruit avec séparation du gypse. La vitesse de la corrosion est déterminée par la pression, la température, la teneur du gaz en sulfure d'hydrogène, le degré de résistance aux sulfates et aux sulfures du ciment donné.

In different building constructions portland cement materials contact with natural and industrial gases containing hydrosulfide of sufficient concentrations. At high temperature and high-pressure gases presence, as in gas-extractive boreholes, quick destruction of portland cement exists. Gas hydrosulfide corrosion has a unique mechanism. Hydrosulfide, on sulution in pore liquid, is neutralized by calcium hydroxid with water-soluble hydrosulfide generation. As a result of reduction;oxidation reactions with oxygen and portland cement high-oxidized compounds (primarily with Fe^{III}) dissolved in pore liquid, sulfid sulfur oxidizes to neutral, and then to sulfate. Diffusing in the depth of cement paste sulfate-ion presence results in ettringite generation, and then expansion and cracking of cement stone. As hydrosulfide subsequently enters the pore liquid, the ettringite becomes destroyed, gypsum being given off. Corrosion rate is determined by pressure, temperature, hydrosulfide content in gas, rate of sulfid - and sulfate - stability of the cement under consideration.

RESUME: Dans les différentes constructions les matériaux en ciment portland entrent en contact avec les gaz d'origine naturelle et technogène, qui contiennent l'hydrogène sulfuré en concentrations importantes. Sous hautes pressions, ce que l'on observe par exemple dans les sondages à gaz, il se produit une destruction rapide du ciment portland. La corrosion par les gaz contenant le sulfure d'hydrogène a un mécanisme particulier. Lors de la dissolution du sulfure d'hydrogène dans le liquide interstitiel il se produit sa neutralisation par l'hydroxyde de calcium avec la formation du sulfure hydraté soluble dans l'eau. Par suite des réactions d'oxydoréduction avec l'oxygène dissous dans le liquide interstitiel et les composés fortement oxydés du ciment portland (avant tout Fe^{III}), le soufre sulfuré s'oxyde jusqu'au soufre neutre et partiellement jusqu'au soufre sulfaté. L'ion sulfate diffuse à l'intérieur du ciment durci où se conserve encore la valeur du pH du liquide interstitiel suffisante pour la formation de l'ettringite, qui s'accompagne d'une destruction de la structure interne du ciment durci, d'une expansion et d'un craquelage.

Si l'hydrogène sulfuré continue d'arriver dans le liquide interstitiel, l'ettringite se détruit avec séparation du gypse. La vitesse de la corrosion est déterminée par la pression, la température, la concentration de l'hydrogène sulfuré dans le gaz, la teneur du ciment en composés susceptibles d'entrer en réactions de réduction et en réactions avec l'ion sulfate.

Comme agent agressif envers le ciment portland l'hydrogène sulfuré est moins étudié que les sulfates, les sels de magnésium ou l'acide carbonique.

Toutefois les derniers temps dans la pratique d'utilisation du ciment portland on rencontre de plus en plus souvent des cas de son contact avec le milieu contenant le sulfure d'hydrogène. Outre les ouvrages de canalisation et d'épuration de différents types, les gaz naturels contenant l'hydrogène sulfuré et exerçant une action sur le ciment portland pour colmatage dans les sondages représentent le cas le plus caractéristique.

Dans les études précédentes (1,2) on a noté que l'hydrogène sulfuré agit sur le ciment portland comme acide faible ou comme source de sulfates secondaires. L'étude le plus détaillée fut entreprise par O.I.Gratcheva et E.O.Barbakadzé (3,4). Ils ont étudié le processus de **corrosion spécifique** de réduction de Fe^{III} **jusqu'à** Fe^{II} détruisant les composés ferrifères de la pâte durcie ainsi que la destruction de l'ettringite sans fer dans le milieu d'hydrogène sulfuré.

En procédant aux expériences où les échantillons de ciments portlands de composition différente ainsi que du liant composé de gypse et de laitier à haute teneur en alumine et du ciment alumineux étaient placés dans le gazoduc de production d'un gaz naturel contenant l'hydrogène sulfuré et ensuite étudiés par les méthodes d'analyse chimique aux rayons X et d'analyse thermique différentielle, nous avons mis en évidence que dans ces conditions de pression partielle élevée de H_2S et en l'absence de l'air a lieu le processus de corrosion intense ayant le mécanisme spécifique. Le gaz naturel contenait en volume 1,5 à 1,6% de H_2S, de 0,5 à 0,6 % de CO_2, 0,4 g/m^3 de H_2O, le reste étant les hydrocarbures. La pression du gaz dans la conduite était de 12 à 14 MPa à la température de 10 à 12 °C. Les échantillons sous forme de cylindres de 18x18 mm étaient disposés dans la zone au voisinage immédiat du gazoduc.

La composition minéralogique des ciments éprouvés est donnée dans le Tableau 1.

Les données sur la variation de la résistance des échantillons à la compression en fonction de la durée de conservation sont représentées sur la figure 1.

La photo de la figure 2 montre le caractère de la destruction des échantillons.

Le Tableau 2 donne les résultats de calcul des changements de composition chimique des échantillons après 3 mois de conservation dans le gaz contenant l'hydrogène sulfuré. Le calcul était effectué sous l'hypothèse que SiO_2 n'entre pas en réaction avec le milieu agressif et reste dans les échantillons en quantité invariable.

La figure 3 représente les diagrammes aux rayons X.

Discussion des résultats. La comparaison des données sur le changement de composition chimique avec les données concernant l'intensité de la diminution de résistance montre que la résistance diminuait plus vite pour le ciment portland n°2 qui se caracté-

TABLEAU 1

n°de la série	Composition minéralogique du clinker, en % pour 100 du ciment						
	C_3S	C_2S	C_3A	C_4AF	CA	CA_2	$CASO_4$
1	60,94	16,20	2,51	18,85	-	-	4
2	55,48	15,65	8,45	17,82	-	-	5
3	58,72	23,29	13,15	1,51	-	-	6
4	-	16,63	-	-	66,0	13,0	18,8
5	-	12,23	-	-	68,82	18,34	-

Nota. 3 - ciment portland blanc, 4 - liant composé de gypse et de laitier à haute teneur en alumine; 5 - ciment alumineux.

TABLEAU 2

n°s des séries	Variation de la teneur, g/100 g							
	SiO_2	Al_2O_3	Fe_2O_3	FeO	CaO	SO_3	S^{2-}	S^0
1	0	-0,86	-2,43	+2,47	-6,25	+6,08	+2,08	+5,73
2	0	-0,95	-4,16	+3,69	-5,50	+8,25	+5,05	+5,70
3	0	-2,54	-0,54	+0,47	-3,75	+3,35	+1,30	+2,85
4	0	+1,0	-0,20	+0,17	-1,20	+1,70	+1,18	+2,00
5	0	+1,5	-0,05	+0,04	-0,80	+0,80	+0,74	+2,53

risait parla somme maximale $C_3A + C_4A$ et la teneur maximale en C_3A malgré une moindre teneur en Fe_2O_3 et en CaO en comparaison du ciment n°1.

Une diminution rapide de la résistance du ciment n°2 s'accompagne d'une accumulation maximale des trois espèces du soufre. L'oxydation du soufre a lieu grâce à la réduction du fer jusqu'à Fe^{II} et à l'interaction avec l'oxygène dissous dans le liquide interstitiel (le contact avec l'oxygène de l'air lors de l'analyse des échantillons n'était pas exclu). Toutefois la comparaison des données sur la quantité du soufre oxydé et du fer réduit montre que dans les conditions données l'oxydant principal est Fe^{III}, car dans les ciments contenant peu de Fe^{III} l'accumulation de S^0 et de SO_3 est beaucoup plus faible. Il était naturel de supposer que l'élimination de Fe^{III} de la composition du ciment augmenterait sa stabilité envers l'hydrogène sulfuré. C'est justement cette supposition qui a servi de base pour l'introduction dans le programme d'essais du ciment portland blanc (n°3). Comme il était prévu, la diminution de sa résistance était d'abord plus lente que pour les ciments portlands n°s 1 et 2 et s'accompagnait d'une accumulation d'une moindre quantité de SO_3. Or, vers 3 mois le degré de sa destruction s'est avéré non inférieur à celui des autres ciments portlands. On peut l'expliquer pas sa sensibilité élevée à l'agression sulfatique à cause d'une teneur très élevée en C_3A liant SO_3 en ettringite.

L'analyse aux rayons X et l'analyse thermique différentielle montrent que dans les ciments portlands soumis à l'action de H_2S on observe une diminution considérable de la teneur en $Ca(OH)_2$, une augmentation de la teneur en ettringite et en $CaSO_4 \cdot 2H_2O$ et l'apparition des sulfates de calcium, d'aluminium et de fer.

A la différence de ce qui était dit, une diminution de la résistance des échantillons de liant composé de gypse et de laitier à haute teneur en alumine s'accompagne d'une décomposition de l'ettringite et d'une augmentation de la teneur en gypse (ou est due à ce fait).

Nous représentons le processus compliqué d'agression gazeuse par l'hydrogène sulfuré du ciment portland de la façon suivante.

L'hydrogène sulfuré contenu dans le gaz se dissout dans le liquide interstitiel du ciment portland solidifié. Si le gaz se trouve sous une grande pression, la quantité de H_2S dissous est assez grande. Il réagit alors avec $Ca(OH)_2$. Dans les conditions indiquées il se forme $Ca(HS)_2$ facilement soluble, la valeur du pH diminue. C'est le premier processus de corrosion. Son action destructive dépend de la teneur du ciment en silicate tricalcique. Les expériences de E.O.Barbakadzé et de O.I.Gratcheva (3) montrent que les échantillons de β-C_2S sont beaucoup plus stables dans le milieu de H_2S que les échantillons de C_3S pur.

Le deuxième processus de corrosion est le passage $F^{III} \rightarrow Fe^{II}$ avec la formation de FeS pratiquement insoluble et colorant les échantillons en noir foncé. Dans ce cas les phases AFm et AFt se détruisent, et la diminution de la résistance résultant de ce processus a lieu d'autant plus vite que la quan-

tité de ces phases dans le ciment durci est plus importante, c'est-à-dire que la somme $C_3A + C_4AF$ est plus grande dans le ciment portland.

En meme temps que la réduction $Fe^{III} \rightarrow Fe^{II}$ a lieu l'oxydation $S^2 \rightarrow S^0 \rightarrow S^{6+}$ avec la formation de SO_4^{2-}. Ceci est dû également à l'action de l'oxygène contenu dans le liquide interstitiel.

L'ion SO_4^{2-} entre en réaction avec Ca^{2+} avec la formation de $CaSO_4 \cdot 2H_2O$, ce qui entraîne encore un type de corrosion. L'accroissement de la teneur des échantillons en ettringite et la stabilité peu élevée du ciment 3 montrent que l'ion diffuse dans la profondeur du ciment durci où l'indice pH est encore insuffisamment élevé pour la formation de l'ettringite.

Ceci provoque la destruction des couches internes, l'apparition de fissures et y ouvre l'accès à l'hydrogène sulfuré. Tous les autres processus corrosifs se trouvent alors accélérés et dans les conditions de la diminution provoquée du pH l'ettringite se décompose. C'est pourquoi le liant composé de gypse et de laitier à haute teneur en alumine stable aux sulfates est instable dans le milieu d'hydrogène sulfuré.

CONCLUSIONS

1. Un ensemble complexe de processus corrosifs dans le milieu gazeux contenant l'hydrogène sulfuré comprend la transformation de $Ca(OH)_2$ en $Ca(HS)_2$ facilement soluble et la diminution du pH, la réduction de Fe^{III} jusqu'à Fe^{II} dans les phases AFt et AFm avec la décomposition de ces phases, la corrosion par sulfoaluminates et gypse due au sulfate secondaire. Le sulfoaluminate hydraté se décompose ensuite par l'hydrogène sulfuré pénétrant.

2. Sur le front de progression de la corrosion le processus primaire est la formation du sulfoaluminate hydraté suivie d'une formation du gypse, d'une décomposition des phases ferrifères, d'une dissolution de $Ca(OH)_2$. La succession temporelle dans une couche fixée est l'inverse de la succession susmentionnée.

3. Le ciment stable à l'hydrogène sulfuré doit être obtenu dans le milieu réducteur, etre stable aux milieux faiblement acides et à la corrosion due aux sulfates.

Fig. 2. Caractere de la destruction des echantillons

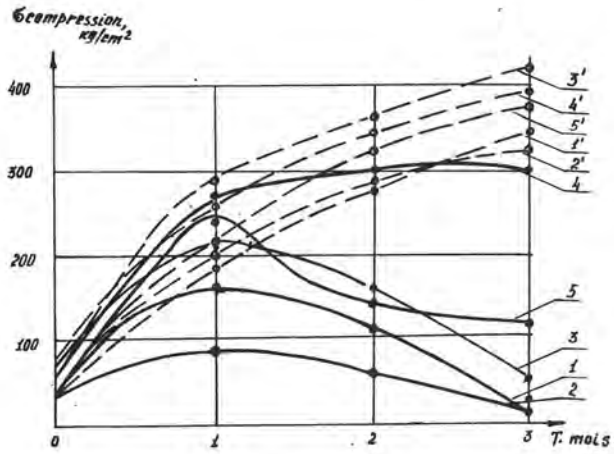

Fig. 1. Diagramme de la resistance des echantillions: 1 - 5 - dans le daz naturelle dans le gaz H_2S; 1 - 5 - dans le gaz inevte

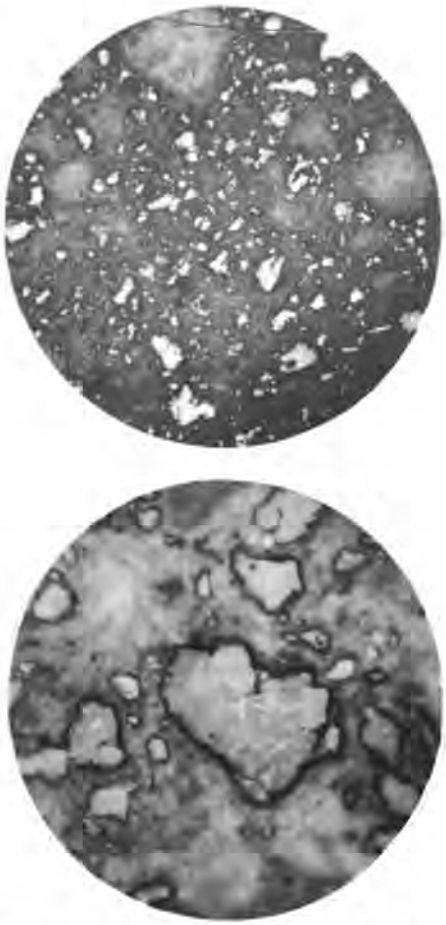

Fig. 3. X-ray - diagramme des echantillons apres 3 mois: 1, 4, 5 - dans le gaz naturel , dans legaz H_2S

A study on the action of sea water on hydrated cement pastes

Etude de l'action de l'eau de mer sur les pâtes de ciments hydratés

Dr. Ch. FTIKOS, Dr. V. KASSELOURIS, Sr. S. TSIMAS, Dr. G. PARISSAKIS,
HERACLES General Cement C° - National Technical University of Athens, Greece,
Lab. of Inorg. and Anal. Chemistry.

RESUME : Dans le présent travail le phénomène de l'action de l'eau de mer sur les pâtes de ciment est étudié.

Les pâtes étudiées furent préparées avec des ciments Portland purs contenant différentes compositions minéralogiques, et avec les mêmes ciments mélangés avec 30 % de terre de Santorin..

L'étude montre que la détérioration des ciments conservés dans l'eau de mer n'est pas seulement due à l'attaque de SO_4^{2-} sur les composés d'aluminate de calcium hydratés, mais à une action combinée des Mg^{2+} et Cl^- contenus dans l'eau de mer sur les composés de CSH.

Les ciments avec de la terre de Santorin (pouzzolane naturelle) sont plus résistants à l'attaque de l'eau de mer.

SUMMARY : In the present work the phenomenon of the action of sea water on the cement pastes is studied.

The studied pastes were prepared from pure Portland Cements with different mineralogical composition as well as from their mixtures with 30% Santorin earth.

The study shows that the deterioration of cements cured in sea water, is not only due to the attack of SO_4^{2-} on the hydrated calcium aluminate compounds but to a combined action of Mg^{2+} and Cl^- contained in sea water on CSH compounds.

Cements with Santorin earth (natural pozzolan) are more resistant to sea water attack.

1. Introduction

Praxis and research have shown that sea water affects on the hydrated cement components.

This phenomenon, which has been stydied by many researchers, (1-5), constists of complicate interactions due to the great number of the hydrated cement components and the ions contained in sea water.

In the present work, which is a part of an extended research program, the action of some ions contained in sea water, on Portland cement of different mineralogical composition as well as on their cogrinded mixtures with Santorin Earth (natural Pozzolan) is studied.

In pastes prepared from these cements, the above mentioned action has been studied by XRD, DTA-TG and SEM. Also, strength development has been measured.

Experimental

The chemical composition of four Portland cements (PCI, PCII, PCIII, PCIV) as well as of Santorin Earth, is shown in table I. The mineralogical composition (according to Bogue) of Portland cements used is shown in table II.

Table I. Chemical composition of materials used.

%	PCI	PCII	PCIII	PCIV	Santorin Earth
L.O.I	0,25	0,20	0,20	1,00	2,50
I.R.	0,25	0,24	-	0,26	-
SiO_2	21,72	23,73	21,55	21,08	61,50
Al_2O_3	4,86	5,27	5,70	4,82	15,80
Fe_2O_3	4,00	3,65	2,70	5,72	5,90
MgO	1,30	2,20	3,95	2,36	1,70
CaO	65,17	63,84	63,55	62,32	3,62
CaO free	3,30	1,56	-	-	-
SO_3	1,42	traces	0,97	1,93	traces
K_2O	traces	traces	traces	0,60	2,72
Na_2O	traces	traces	traces	0,18	3,87

Table II. Mineralogical composition of cements tested (according to Bogue)

Cement type	% C_3S	% C_2S	% C_3A	% C_4AF
PCI	58	19	6	12
PCII	39	39	8	11
PCIII	50	24	10	8
PC IV	47	25	3	17

From the above mentioned cements as well as from their mixtures with 30% Santorin Earth, specimens have been prepared, according to ISO-RILEM CEMBUREAU CEN specifications, for the strength development measurement. These specimens were cured in sea water, at the area of Pagasiticos gulf, for one year.

In table III and figure 1 the results of compressive strength measurement are shown.

Table III. Compressive strengths (Kp/cm^2).

Cement type	Fineness cm^2/g (Blaine)	2 days	7 days	28 days	3 months	6 months	1 year
PCI	2900	186	288	388	397	437	432
PCII	2900	135	266	392	410	463	442
PCIII	2900	245	339	405	397	433	437
PCIV	3000	165	295	409	422	452	423
PCI+30%S.E	3900	135	217	315	386	391	419
PCII+30%S.E	3900	90	199	334	401	422	456
PCIII+30%S.E	3900	162	243	329	388	423	430

From the cements shown in table III pastes have been prepared with a c/w ratio 0,27 and 0,33 for the pure Portland cements and their mixtures with Santorin Earth, respectively.

In these cements, hydration phenomena have been studied by XRD, DTA-TG and SEM.

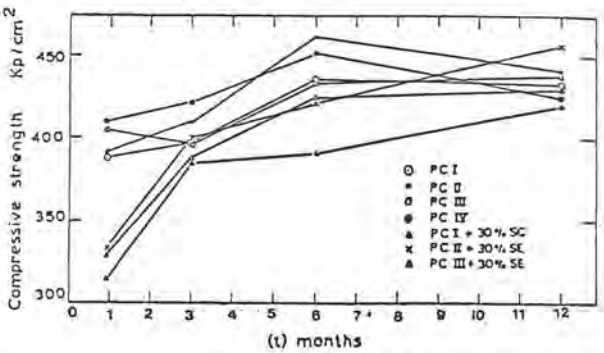

Fig. 1. Compressive strength of pure Portland Cements and their mixtures with 30% S.E.

Study by XRD

In pure Portland cement pastes, the compounds of Ettringite, thaumasite, chloroaluminates, C_4AH_{13}, CAH_{10}, C_3S, CSH and $Ca(OH)_2$ are observed (Fig.2).

The peaks of Ettringite are more intense in the cement paste of PCI, PCII, PCIII than those of PCIV, while the peaks of chloroaluminates are more intense in the cement paste of PCII.

The nonhydrated C_3S content is greater in cement pastes prepared form cements in which it is contained in high percentages.

In blended cement pastes the same compounds are observed. The intensities of the peaks of Ettringite, thaumasite, C_4AH_{13}, CAH_{10} and $Ca(OH)_2$ are lower than those of pure cement pastes while the intensities of the peaks of CSH and chloroaluminates are higher. A part of Ettringite is transformed to monosulfate.

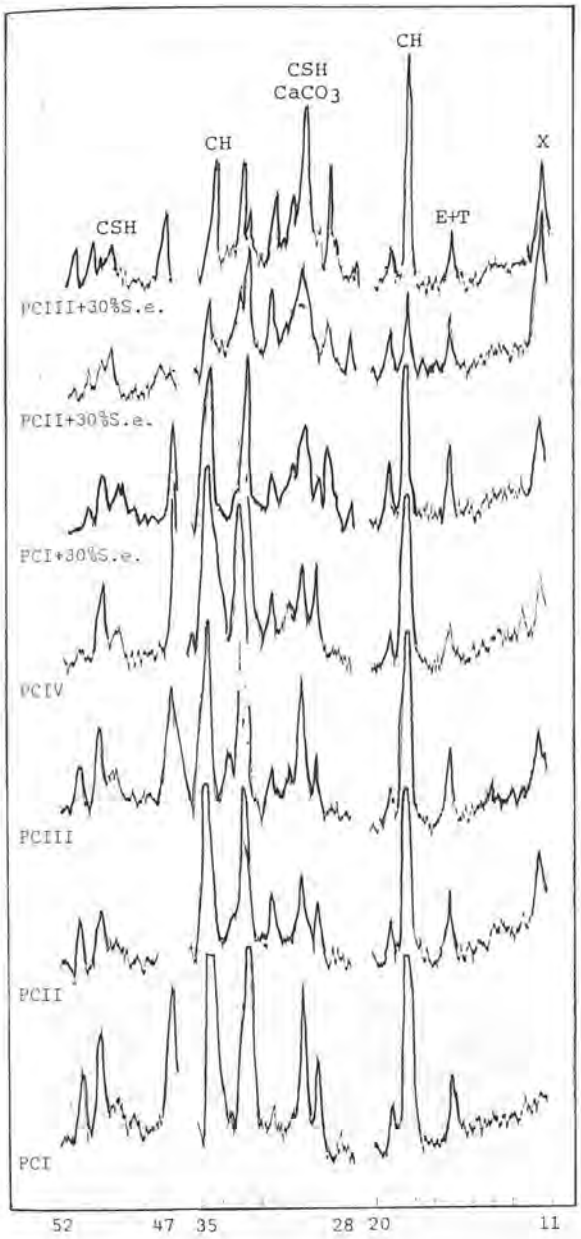

Fig. 2. XRD patterns for cement pastes cured in sea water for one year.
E: Ettringite
T: Thaumasite
X: Chloroaluminates

Study by DTA-TG

In figure 3 thermograms are shown from cement pastes cured for one year. In all pure Portland cement pastes the compounds of Ettringite, chloroaluminates, C_4AH_{13}, $Ca(OH)_2$, CSH(I) and small amounts of $CaCO_3$ are observed.

The exothermic peak at 620° is attributed to thaumasite without any remarkable differentiation in its content.

The pastes of PCII are enriched in chloroaluminates compared to PCI pastes. The highest concentration of $Ca(OH)_2$ is observed in PCI and the lowest in PCII. The presence of Ettringite is less intense in PCIV pastes.

Study by SEM

In figures 4,5,6 and 7 some photos are presented concerning the study by SEM of cement pastes cured for one year. In photo 1 a great number of pores are observed. Crystals of Ettringite are grown in these pores. Photo 2 depicts the reduced amount of Ettringite. The sturcture of CSH is not porous and the Portlandite in the center, is not deteriorated.

In photo 3 a cluster of Ettringite is observed while in photo 4 the great number of chloroaluminatew, the nonporous CSH and the low dispersion of Ettringite and observed. In photo 5 the Ettringite results in the formation of some cracks around it, while in photo 6 the great cohesion in the structure and intence presence of chloroaluminates are observed.

In photo 7 the reticulated CSH and the low dispersion of Ettringite are observed.

Discussion and conclusion

In figure 1 which shows the strength development from 28 days up to one year, it is observed that the affect of sea water on compressive strengths appears after six months with an exception of the mixtures of PCI and PCII containing 30% Santorin Earth.

This phenomenon is more indicative in PCIV despite its low C_3A content. The above mentioned observation leads to the opinion that the sea water attack is not only due to the presence of C_3A, at least in the studied percentage of C_3A.

The study of XRD patterns and the semiquantitative estimation of hydration products by DTA-TG, show that Ettringite and thaumasite are increased in pure Portland cement pastes by increasing of the C_3A content.

Also, the presence of nonhydrated C_3S even after a curing for one year, is observed.

The blended cement pastes contain more chloroaluminats, C_4AH_{13} and CSH and less $Ca(OH)_2$ that the pure Portland cement pastes.

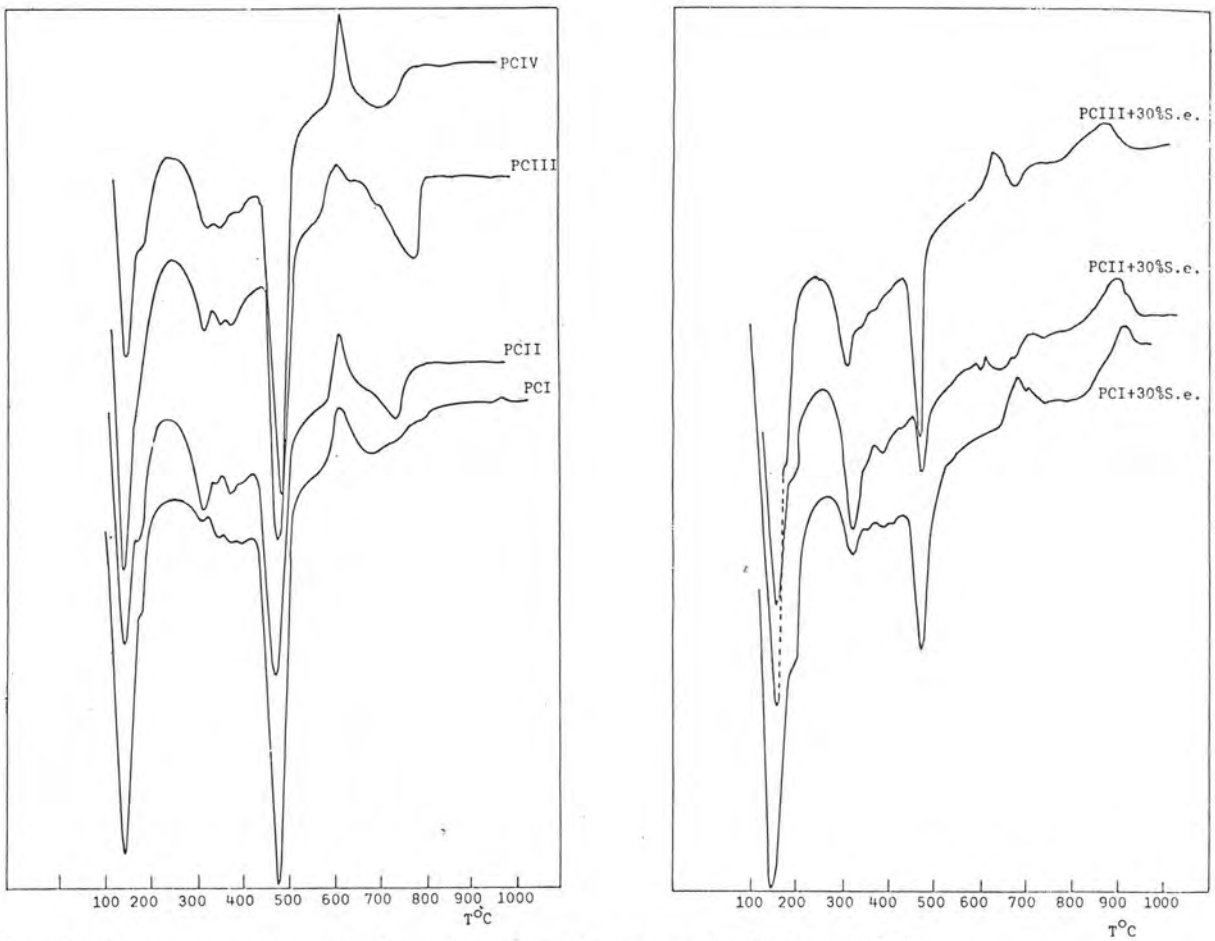

Fig. 3. Thermograms for cement pastes cured in sea water for one year.

Ph. 1. M x 2000

Ph. 2. M x 2000

Fig. 4. PCI and PCI+30% S.E pastes cured in sea water for one year.

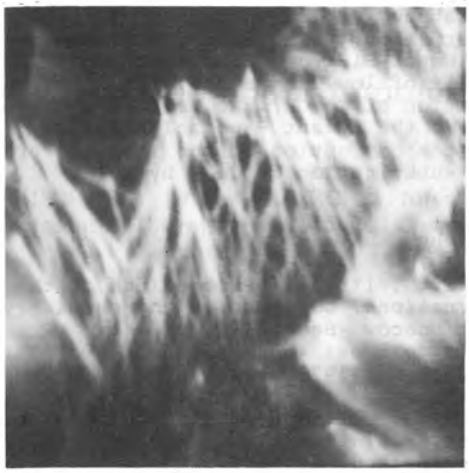

Ph. 3. M x 2000

Ph. 4. M x 2000

Fig. 5. PCII and PCII+30% S.E pastes cured in sea water for one year.

Ph. 5. M x 2000

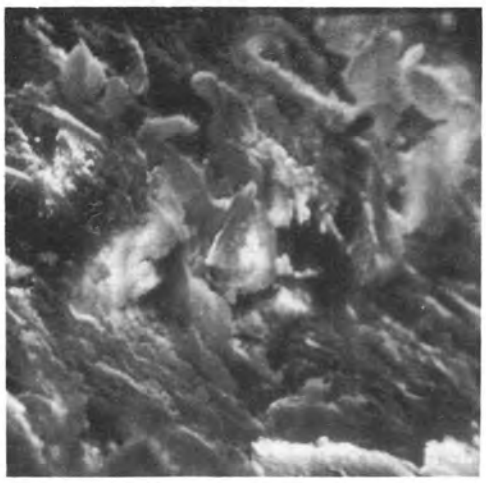

Ph. 6. M x 2000

Fig. 6. PCIII and PCIII+30% S.E pastes cured in sea water for one year.

Ph. 7. M x 2000

Figure 7. PCIV paste cured is sea water for one year.

In addition to the above mentioned observations, the study of the same pastes by SEM, leads to two remarkable conclusions.

a). In pure Portland cements and especially in PCIII, in which C_3A is greater, the cracks are due to the decreased formation of Ettrigite and its structure.

b). The observed structure of CSH is different between the various pure Portland cement pastes as well as between the pure Portland cements and their mixtures with Santorin Earth. Reticulated CSH shows increased possibilities to be formed, in cements with high C_3S content.

The conclusion is that the deterioration of cements cured in sea water, is not only due to the attack of SO_4^{2-} or Cl^- on the calcium aluminate compounds, but to a combined action of the Mg^{2+} and Cl^- contained in sea water on the hydrated calcium silicate compounds.

Cl^- ions accelerate the calcium silicate compounds hydration and lead to the formation of high C/S ratio CSH.

This high C/S ratio and the different K_S between $Ca(OH)_2$ ($Ca(OH)_2 \rightleftharpoons Ca^{2+}+2OH^-$ $K_S=5,5.10^{-6}$, $Mg(OH)_2$ $Mg(OH)_2 \rightleftharpoons Mg^{2+}+2OH^-$ $K_S=1,8.10^{-11}$) facilicate the substitution of Ca^{2+} by the Mg^{2+} in the CSH lattice, resulting in its transformation to the reticulated form and in the formation of nonhydraulic MSH.

Cements with pozzolan are more resistant to sea water attack despite their high content in hydrated calcium aluminate compounds.

This resistancy explained by the different way of CSH formation (6,7). The CSH formed by the interaction of SiO_2 containedin pozzolan and $Ca(OH)_2$, is of low C/S ratio. Thus, the low concentration of $Ca(OH)_2$ as well as the low porosity of the cement - pozzolan pastes, decrease the diffustion of the ions and prevent the substitution of Ca^{2+} by Mg^{2+}.

Bibliography

1.- ISOGAI, S. (1974) : Proceedings of the 6th International congress on the chemistry of cement Moscow Sect. I-6.

2.- REGOURD, M. (1975) : Cilan No 18 4e trimestre.

3.- TAYLOR, M.A, KUWAIRI, A. (1978) : Cem. Concr. Research 8, 491-500.

4.- REGOURD, M., HORNAIN, H., MORTIREUX, B. (1978): Annales de l'Institut Technique du Batiment et des Travaux Publics 358.

5.- GJ ØRV, O.E, VENNESLAND, Ø (1979): Cem. Concr. Research, 9 229-38.

6.- PARISSAKIS, G., FTIKOS, CH (1975): Proceedings of the 2nd Hellenic Concrete Conference. Thessaloniki, Greece.

7.- FTIKOS, CH. (1977) : Study on the pozzolanic action in cement pastes during their hydration process. Diss Thesis Nat. Techn. Univ. of Athens.

The mechanical properties of polymer modified cement paste cured under sea and tapwater

Les propriétés mécaniques de la pâte de ciment modifiée par l'addition de polymères, et conservée dans l'eau de mer ou dans l'eau courante

Dr. D.I. BHATTY, Dr. D. DOLLIMORE, Professor G.A. GAMLEN and M. R.J. MANGABHAI,
Department of Chemistry and Applied Chemistry, University of Salford, Salford - ENGLAND.

RESUME : On a effectué des recherches sur les modifications de la pâte de ciment, dues à l'addition de divers polymeres, tels que le Versicol W13 (polyacrylamide), la cellulose hydroxyle - éthylique (la cellulose - éther) et le dextrane (l'amidon méthylique carboxyle). On a conservé les pâtes du ciment durci sous l'eau de mer ou sous l'eau du robinet pour déterminer leur effet sur les propriétés mécaniques de la pâte, à savoir la résistance à la compression et à la flexion.

On constate que le Versicol W13 augmente la résistance à la compression et à la flexion de la pâte du ciment durci conservée dans l'eau de mer, tandis que la cellulose hydroxyle-éthylique ne montre pas aucun effet important sur ces résistances. Ceci peut être dû à la nature de la cellulose hydroxyle-éthylique et à l'effet des conditions alcalines de la pâte du ciment. Les essais effectués sur la résistance de la pâte démontrent un comportement anormal dans l'eau de mer et dans l'eau du robinet. On a poussé plus loin les recherches pour y inclure l'effet de la durée de la conservation avec divers polymères sur les propriétés mécaniques de la pâte de ciment. On examine ensuite en détail les conséquences de ces études.

Summary

Investigations have been carried out on the modifications of cement paste with various polymeric materials such as Versicol W13 (polyacrylamide), Hydroxyethyl cellulose (cellulose ether) and Dextran (carboxy methyl starch). The hardened cement pastes were cured under sea and tap water to determine their effect on the mechanical properties of the paste related to compressive and flexural strength.

It is shown that Versicol W13 increases the compressive and flexural strength of the hardened cement paste cured under seawater whereas Hydroxyethyl cellulose does not show any significant effect on the strength. This may be due to the nature of the Hydroxyethyl cellulose and the manner in which it is affected by the alkaline condition in the cement paste. The strength tests carried out on paste containing Dextran show anomalous behaviour in the sea and tapwater.

The investigations have been extended to include the ageing affect of the polymers on the mechanical properties of the cement paste and the consequences of these studies are discussed in detail.

INTRODUCTION

The use of water-soluble polymers has not become established in the field of concrete, cement and mortars except in certain restricted cases (1). Polymer additives are known to affect the hydration process and the strength of the hardened paste. The environment is also a factor which affects these two parameters. At present, there are four important types of polymer modifed cement systems: (1) water soluble polymers, (2) fibre-reinforced concretes, (3) polymer impregnated concretes, (4) polymer latex-modified mortars and concretes. The discussion here is confined to type (1), because water soluble polymers are used in this study.

The polymers used can be classified by the function they perform, into two categories, (1) polyorganosiloxanes and (2) polyelectrolytes and their co-polymers, and cellulose and starch ethers. The first group tend to impart imperimeability qualities to the cement, whilst the second give either a plasticizing effect to the flowing cement paste or improve the strength of the hardened paste.

The first category is less important and its uses have been confined to Russia (2), where it is claimed that improvements to strength and water tightness of concretes can be made. In the second category there are two divisions:-

(a) polyelectrolytes and their co-polymers,

(b) cellulose and starch ethers. In this study, polymers from the second category have been used.

The use of cellulose and starch ethers in grouts, mortars and concretes was suggested earlier than the use of polyelectrolytes, but, apart from work done for patent applications, very little has been published about them. Methyl cellulose added to the dry cement composition gives "thin-set, dry-set" mortars. Upon mixing with water there is obtained a high viscosity aqueous phase, which is inhibited (e.g., by ceramic tiles) and substrate at a lower rate than pure water, leaving the water available to the cement for the required hydration reaction (2).

EXPERIMENTAL

1. Materials

The cement used was ordinary Portland cement (OPC) obtained commercially, it had a chemical composition as follows:- C_3S - 47.6%; C_2S - 22.5%; C_3A - 11.06%; C_4AF - 7.66%; $C\bar{S}H_4$ - 4.65%. The polymers investigated were:- a) Versicol W13, a non-ionic polyacrylamide (pH = 8-9 at 20%), b) Dextran, a carboxy-methyl starch (pH = 6.0 at 1%) and c) hydroxyethyl cellulose (HEC), a nonionic cellulose ether (pH = 6.5 - 8.0 at 1%). The seawater used for curing the hardened cement paste was standard seawater (3). The moulds which were used to cast the paste into cubes and beams were made of steel. The dimensions of each cube was 2.54 cm and those of the beams were 15.24 cm x 2.54 cm x 1.27 cm.

2. Experimental Procedure

The w/c ratio was fixed at 0.3 because this gives a good mix which can be handled easily and gives high strength after curing under water compared to higher w/c ratios (4). A standard procedure was used for mixing the cement paste (5).

The cement paste was poured into the moulds and placed on a vibrating table for one minute. The moulds were then placed in a constant temperature room set at $25 \pm 0.5°C$ and 40% rh. The moulds

were covered with a damp hessian cloth and left for 24 hours, after which they were dismantled and the hardened pastes cured under sea water and tap water.

3. Mechanical Testing

3, 9 and 27 days after mixing, five cubes were taken and the compressive strength determined using an AVery-Denison Type T42U compression testing machine at a constant rate of 30 kN min^{-1} until failure occurred. The flexural strength was determined on 3, 9 and 27 day old samples using a 500 lb Howden testing machine operated manually.

RESULTS

The mean of five readings for compressive strength and the mean of three readings for flexural strength were obtained. These results are given in Table 1 a), b) and c) for samples cured under seawater. The results for samples cured under tap water are given in Table 2 a), b) and c) (6).

DISCUSSION

The behaviour of different polymers towards the strength of hardening cement pastes cured under sea and tap water is complex. Versicol W13 shows a general increase in compressive strength of the cubes when its concentration is higher than 0.08% by weight, and the paste is cured under seawater. The strength increases quickly within nine days and then levels off. A polymer concentration of 0.13%, however, shows unusual behaviour and seems to be affecting the compressive strength of the samples in an unexpected manner.

Investigations on the paste modified with W13 and cured under tap water show a parallel behaviour for 0.13% polymer concentration. But the overall effect of polymer addition results in a slight reduction in the compressive strength. In the case of flexural strength of the pastes with W13, an improvement in strength is indicated when the samples are cured under seawater. The tests carried out on similar cement pastes in tap water do not show much improvement in flexural strength. The overall difference in the flexural strength of pastes aged in sea water and tap water is about 60% for pastes containing 0.18% poly.er There is a general trend of increasing strength when the polymer concentration is increased and the curing takes place under sea water.

The effect of HEC on the compressive and flexural strengths of pastes cured under sea and tap water does not show any great difference in strength. (Table 1b and 2b). The neat pastes cured under both sea and tap water have higher strengths than pastes with the addition of HEC. This may be due to the hydrolysis of the HEC by the alkali in the cement paste.

The effect of Dextran on the compressive and flexural strength is anomalous. Thus, when cured under sea water there is a slight decrease in flexural strength, while when cured in tap water there is a slight increase in flexural strength. The compressive strength decreases on samples cured under sea water, but increases on samples cured under tap water. A subsequent publication deals with surface area and adsorption properties.

REFERENCES

1. Concrete Society, Technical Report No. 9, (1975) 13-14.
2. Kudinov, K.A., Khramova, V.I., Ilvin, R.K. and Gorbushina, V.B., Betin i Zhelezobeton No. 3, (1964) 120-122.
3. Handbook of Chemistry and Physics, 59th Edition, 1978-1979, CRC Press.
4. Neville, A.M. Properties of Concretes. Pitman, 1963.
5. ASTM Method C035, ASTM Book Part 13, 1977, p254-256.
6. Rodgers, P.F. The properties of polymer modified cements. 1st year report, University of Salford, 1978.

Table 1 a) Strength of pastes cured under sea water, modified with Verisicol W13.

STRENGTH		CONC. OF POLYMER			
TYPE	DAY	0	0.08%	0.13%	0.18%
FLEX.	3	19.68	18.60	20.19	21.82
	9	19.50	20.90	22.04	23.39
	27	21.65	22.03	23.42	21.82
COMP.	3	72.82	65.72	74.46	76.01
	9	78.49	77.93	77.93	85.02
	27	85.04	87.17	95.33	88.88

Table 1 b) Modified with HEC

STRENGTH		CONC. OF POLYMER			
TYPE	DAY	0	0.08%	0.13%	0.18%
FLEX	3	19.68	17.00	18.68	16.00
	9	19.50	16.21	17.31	18.72
	27	21.65	18.55	18.68	18.28
COMP	3	72.82	66.77	63.40	51.50
	9	78.49	77.16	78.88	60.14
	27	85.04	75.33	81.81	54.84

Table 1 c) Modified with Dextran

STRENGTH		CONC. OF POLYMER			
TYPE	DAY	0	0.08%	0.03%	0.18%
FLEX	3	19.68	17.90	16.97	16.37
	9	19.50	19.92	18.62	20.42
	27	21.65	19.65	18.57	19.04
COMP	3	72.82	60.68	61.61	59.75
	9	78.49	67.92	67.54	57.28
	27	85.04	56.55	54.68	59.18

Table 2 a) Strength of pastes cured under tap water

Modified with Versicol W13

STRENGTH		CONC. OF POLYMER			
TYPE	DAY	0	0.08%	0.13%	0.18%
FLEX	3	12.0	14.8	14.1	13.1
	9	13.7	12.2	13.7	14.8
	27	14.3	14.3	16.0	15.9
COMP	3	58.1	64.7	63.6	56.0
	9	74.7	75.5	65.4	72.7
	27	83.6	82.8	81.7	85.4

Table 2 b) Modified with HEC

STRENGTH		CONC. OF POLYMER			
TYPE	DAY	0	0.08%	0.13%	0.18%
FLEX	3	12.0	12.9	8.7	-
	9	13.7	12.7	11.3	-
	27	14.3	14.5	13.8	-
COMP	3	58.1	57.4	58.4	56.6
	9	74.7	69.4	67.3	67.4
	27	13.6	74.6	78.0	79.4

Table 2 c) Modified with Dextran

STRENGTH		CONC. OF POLYMER			
TYPE	DAY	0	0.08%	0.13%	0.18%
FLEX	3	12.0	13.4	14.8	13.8
	9	13.7	14.6	15.8	14.3
	27	14.3	16.4	15.7	14.0
COMP	3	58.1	65.6	68.3	65.6
	9	74.7	83.8	79.4	83.0
	27	83.6	90.4	93.9	92.9

COMMUNICATIONS *

*** Ces communications, présentées au Congrès, n'ont pu être imprimées dans les volumes II et III pour des raisons de délai.**

Processus de formation des minéraux et composition de phase du clinker d'alinite

Mineral formation processes and phase composition of alinite clinker

M. BIKBAOU, candidat ès sciences techniques, chef de laboratoire de l'Institut des Recherches Scientifiques et des projets de construction, Tachkent, U.R.S.S.

RESUME: L'étude de la formation des minéraux du clinker d'alynite obtenu par la cuisson des matières premières en présence de la chlorure de calcium a démontré que ces processus sont assez compliqués; nous avons découvert la formation des nouvelles phases minérales: du carbonate de la chlorure de calcium, du spourrite, de l'orthosilicate et de l'alumoferrite de la chlorure de calcium. A l'étape initiale de la cuisson les phases minérales contiennent une quantité considérable d'atomes de Cl; à l'étape finale, par contre, on n'observe que les minéraux avec un faible contenu de Cl (3-4% de la masse) - l'alite et l'aluminate de la chlorure de calcium. Dans ces derniers minéraux, le chlore est solidement lié dans les positions structurales.

A part les minéraux indiqués, le clinker d'alynite contient également le bélite et le ferrite de calcium qui peuvent contenir un peu de chlore (1ù de la masse environ) dans leur structure. La contenance quantitative des phases minérales dans le clinker d'alynite varie dans les limites suivantes (% de la masse):

l'alynite	60 - 80
le bélite	10 - 30
l'aluminate de la chlorure de calcium	5 - 10
le ferrite de calcium	2 - 10

Des recherches effectuées ont permis de décrire le caractère de la cristallisation des phases siliciques du clinker qui ont généralement une structure distincte à grains fins. Nous avons établi que les conditions de la cuisson et de la déchloraison exercent une influence sensible sur le caractère de la cristallisation du clinker d'alynite.

Cette influence s'explique par la genèse des phases intermédiaires du spourrite, de l'alumoferrite et de l'orthosilicate de la chlorure de calcium.

SUMMARY: The investigation of mineralformation processes of alinite-clinker produced by kilning the raw material together with calcium chloride has shown their considerable complication which leads to the formation of new phases - calcium chloride carbonate, spurrite, orthosilicate and aluminoferrite of calcium chloride.

At the initial stage of kilning new phases with considerable content of the chlorine atoms (about 15% of the mass) - /orthosilicate and aluminoferrite of calcium chloride/ - are formed only the minerals containing small quantity of chlorine (3-4% of the mass) - alinite and aluminate of calcium chloride are kept at the final stage. In the above mentioned minerals the chlorine is tightly cohered in structure positions.

Besides the minerals mentioned above, the alinite clinker comprises also belite and calcium ferrite, which could comprise small quantity of chlorine (about I.0% of the mass).

The quantitative content of mineral phases in alinite clinker varies within the following limits (% of the mass):

alinite	60 - 80
belite	10 - 30
aluminate of calcium chloride	5 - 10
calcium ferrite	2 - 10

The research data have allowed to describe crystallization of silicate phases of the clinker, which are normally characterized by clear but fine-grained structure.

Important dependence of the caracter of cristallization of alinite clinker upon the conditions of kilning and dechlorination has been established.

This dependence is closely connected with the genesis of intermediate phases of the clinker.

La cuisson du clinker de ciment en présence de la fusion des sels de chlorure de calcium provoque des changements radicaux: dans la cinétique des processus de la formation du clinker, ainsi que dans sa composition de phase (I). Le présent travail montre les résultats d'une étude sur la suite des processus de la formation du clinker en présence de $CaCl_2$, ainsi que les données sur la composition plus précise des produits intermédiaires et finales de la cuisson du clinker d'alynite; ces données n'ont pas été décrites dans les publications spéciales.

Des mélanges suivants ont été préparés:

I. Un mélange des réactifs:

$CaCO_3$	SiO_2	Al_2O_3	Fe_2O_3	MgO	$CaCl_2$
69.2	16.1	2.5	1.9	1.3	9.0

2. Un mélange de limon de loess, de cendres et des calcaires de l'usine de ciment d'Akhan-garan avec 9% de chlorure de calcium, à raison de CS + 0,92; n = 2,6; p = 3,1[+].

Des mélanges ont été préparés sous forme de granules de dimension de 7-8 mm et cuits dans un four électrique de laboratoire. La vitesse de la montée de la température était égale à 5°C ce qui correspond à peu près aux conditions de production industrielle. A partir de 400°C, un échantillon des matériaux a été pris toutes les 50° et refroidi en l'air. A part cela, un essai isothermique aux températures données était employé afin de déterminer la composition de phase des produits de la cuisson.

Le produit cuit a été analysé sur le contenu de l'oxyde de calcium CO_2 libre et du chlore.

La composition de phase des produits de la cuisson a été déterminée par les méthodes quantitative et qualitative de l'analyse optique et celle aux rayons X. La méthode de l'analyse thermique différentielle a aussi été utilisée.

La suite et le contenu des processus de la formation du clinker à basse température se diffère carrément des processus analogiques de cuisson du clinker de ciment portland. La présence de la chlorure de calcium, composante supplémentaire dans le mélange brut servant à produire le clinker à basse température provoque une complication considérable des processus de la formation des minéraux. La présence de la chlorure de calcium abaisse la température du processus final de la cuisson des minéraux de sortie du clinker du ciment d'alynite aussi que tous les processus intermédiaires. Ces processus sont illustrés par les courbes de l'analyse thermique différentielle (courbe ATD) (Fig.1). A partir de 500°C, la courbe ATD du mélange brut du ciment change à cause de l'évaporation de l'eau des hydrates.

Nous avons utilisé une méthode d'étude de la composition de phase dans une couche mince qui a permis de découvrir le commencement de l'interaction chimique entre les composantes du mélange brut pour la formation du clinker d'alynite au niveau de 450-500°C.

Le processus de la formation des composés complexes commence déjà aux températures de 530-600°C grâce à l'interaction de $CaCl_2$ et de $CaCO_3$, la carbonate de la chlorure de calcium ($CaCO_3$ $CaCl_2$).

A 620-640°C ce composé se transforme en phase X qui est, peut-être, sa modification de haute température qui existe dans l'intervalle de 630 - 800°C; leurs propriétés chimiques et les paramètres des cellules sont assez proches (voir le tableau).

Tableau I

Données de la diffractométrie aux rayons X des phases minérales découvertes dans le système $CaCO_3$ - $CaCl_2$

$CaCO_3$ · $CaCl_2$			Phase X		
Cellule cubique à capacité centrée a = 9,720 ± 0,015 Å			Cellule cubique à capacité centrée a = 9,965 ± 0,05 Å		
d, Å	hkl	I	d, Å	hkl	I
6.88	110	30	5.00	700	40
3.97	211	65	3.18	310	50
3.44	220	85	2.675	321	5
2.81	222	90	2.485	400	30
2.600	321	75	2.356	330	100
2.174	420	100	2.116	332	40
1.984	422	70	1.941	510	40
1.716	440	20	1.808	521	5

Dans l'intervalle de 650-750°C une décarbonisation plus intense fait apparaître l'oxyde de calcium libre. A ces températures, les composantes acides entrent en action mutuelle ce qui mène à la formation du spurrite dans les produits de la cuisson

[+]CS - coefficient de saturation, n-mobule silicique, p-module alumineux.

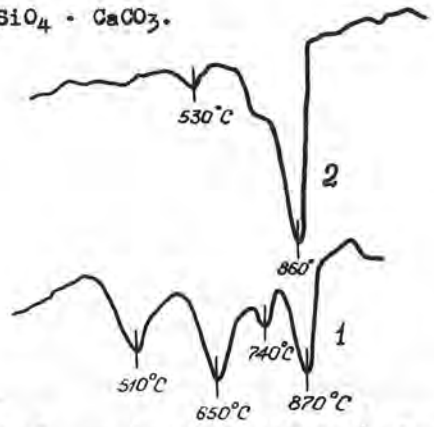

Fig.1. La courbe de la ATD de la formation du clinker d'alynite (I) et du clinker portland (2).

Aux température de 750-800°C les produits de la cuisson contiennent, à part le spourrite prédominant, l'alumoferrite et l'aluminate de la chlorure de calcium.

Les diffractogrammes des phases synthétisées intermédiaires du clinker sont représentés sur la fig.2.

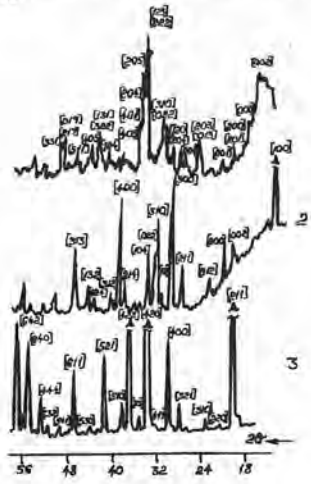

Fig.2 - Les diffractogrammes des phases intermédiaires du clinker d'alynite:

I - du spourrite;
2 - de l'orthowsilicate de la chlorure de calcium;
3 - de l'aluminate de la chlorure de calcium.

C'est dans l'intervalle de 650-850°C que les exoeffets correspondent aux processus exothermiques de la formation de ces minéraux sur la courbe ATD.

Le changement quantitatif de la teneur des phases à chaque étape de la cuisson caractérise le mécanisme de la formation du clinker. Ainsi, la courbe du changement de la teneur d'oxyde de calcium libre dans les produits de la cuisson a deux valeurs extrémales (fig.3). La teneur plus élevée de CaO libre dûe à une température plus haute est en correlation avec la courbe du changement de la teneur de CO_2 - l'oxyde de calcium libre apparaît au cours de la décarbonisation de la calcite.

Pourtant, les températures de 700-750°C provoquent une formation intense du spourrite dont la quantité atteint le maximum a 800°C (fig.3).

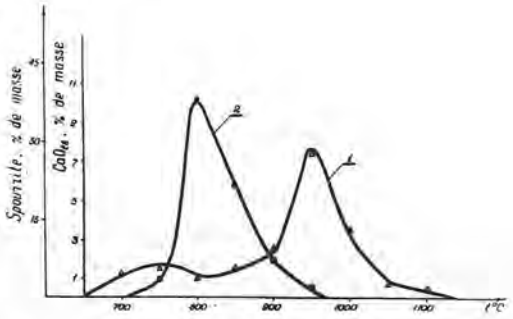

Fig.3 Changement du contenu de CaO libre (I) et du spourrite (2) dans les produits de la cuisson du clinker d'alynite en fonction de la température.

La formation du spourrite s'effectue grâce à la liaison intense entre la silice et l'oxyde se libérant à la décomposition de $CaCO_3$:

$$4\ CaO + 2\ SiO_2 + CaCO_3 \rightarrow 2\ Ca_2SiO_4 \cdot CaCO_3$$

En même temps une partie de molécules de la calcite participe à la formation du minéral nouveau, spourrite. Il convient de souligner le rôle très important de $CaCl_2$, agent de dispersion qui intensifie considérablement le processus de la décarbonisation et joue le rôle du milieu catalytique de cristallisation.

Aux températures de 750-800°C, il est intéressant à noter la formation de l'orthosilicate de la chlorure de calcium en présence de la chlorure de calcium. La fig.4 montre les données expérimentales sur le changement de la teneur en orthosilicate de la chlorure de calcium $2\ Ca_2SiO_4 \cdot CaCl_2$ dans le processus de la cuisson.

On peut supposer la possibilité de l'isomorphisme des anions au cours de la formation du spourrite et de l'orthosilicate de la chlorure de calcium quand une partie d'atomes de l'oxygène dans la molécule de la calcite du spourrite - $2\ Ca_2SiO_4 \cdot CaCO_3$ est remplacée par les atomes du chlore. Les résultats des expériences sur la séparation du chlore du spourrite synthétique synthétisé en présence de CaCl confirment que le replacement de O par Cl dans le spourrite est possible. Ces expériences ont montré la conservation de 2% de Cl dans le minéral, probablement grâce à l'élévation du Cl dans la structure. Il n'est pas exclu que $2\ Ca_2SiO_4 \cdot CaCO_3$ et $2\ Ca_2SiO_4CaCl_2$ forment des solutions solides grâce à l'isostructure de ces composés contenant à la base une molécule de Ca_2SiO_4. Ces phases intermédiaires sont

stables dans un intervalle déterminé, car à 800-850°C le spourrite commence à se décomposer et aux températures supérieures à 950°C disparaît tout à fait.

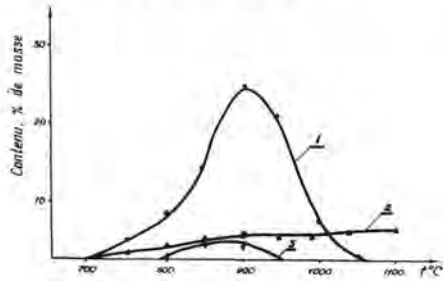

Fig.4 . Changement du contenu de l'orthosilicate de la chlorure de calcium (I), de l'aluminate de la chlorure de calcium (2) et de l'alumoferrite de calcium (3) dans les produits de la cuisson du clinker d'alynite en fonction de la température.

Les fig.3-5 montrent des résultats des mesures sur le changement de la teneur quantitatives des phases minérales du clinker d'alynite dans le processus de la cuisson.

Elles sont effectuées à l'aide d'une analyse quantitative aux rayons X. La formation du spourrite et de l'orthosilicate de la chlorure de calcium lie l'oxyde de calcium libre se libérant au cours de la décarbonisation. Sa quantité dans l'intervalle de 700-900°C ne dépasse pas quelques pourcents. Ceci est juste pour la vitesse normale de l'élévation: 5-20% par min. Grâce au nivellement des facteurs cinétiques, le traitement isothermique prolongé aux températures 700-900°C libère tout l'oxyde de calcium du mélange brut, sauf sa quantité liée par le spourrite, l'orthosilicate, l'aluminate et l'alumoferrite de la chlorure de calcium (fig.4); même dans ce cas la quantité de l'oxyde de calcium libre ne dépasse pas 10-12% ce qui est égal à un cinquième de sa quantité totale. Ces données sont en accord avec les résultats de la détermination de la teneur en CO_2 des produits de la cuisson. L'aluminate de la chlorure de calcium commence à se former à 700-750°C; il est stable sur toutes les étapes ultérieures de la formation du clinker. Par contre, l'alumoferrite de la chlorure de calcium n'existe que dans un intervalle limite de températures. Il commence à se former à 750-800°C, mais à 950°C il se décompose en ferrite de calcium, un composé stable et en même temps il fournit l'aluminium pour la formation de l'alynite. Il est probable que ce fait explique le commencement de la cristallisation de l'alynite aux températures de l'alumoferrite de la chlorure de calcium, c'est-à-dire à 900-950°C (fig.5).

L'hypothèse citée explique l'effet de forte minéralisation en présence de Fe_2O_3 dans le

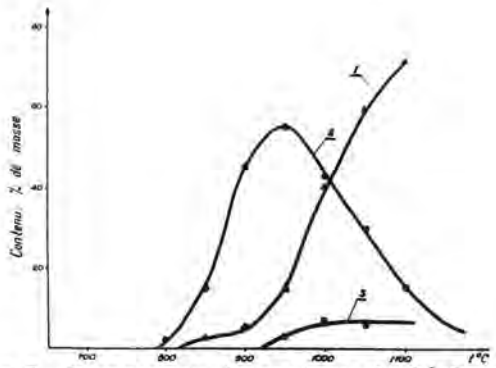

Fig.5. Changement du contenu de l'alynite (1) et du bélite (2) et la ferrite de calcium (3) en fonction de la température.

mélange brut au cours de la cuisson du clinker d'alynite. Grâce à la formation et à la décomposition de l'alumoferrite de la chlorure de calcium, l'aluminium, un des éléments principaux du réseau cristallin de l'alynite, est fourni au moment de la cristallisation de l'alynite. Cela se trouve en accord avec le fait de l'absence de l'alumoferrite de calcium dans le clinker d'alynite.

L'hypothèse proposée explique la nécessité d'une augmentation sensible de la concentration de l'aluminium dans le mélange brut utilisé au cours de la cuisson du clinker d'alynite blanc. Le bélite se forme à 850-900°C, car la quantité de Cl ne suffit pas à lier toute la substance en orthosilicate de chlore (15% de chlore dans la structure), aluminate de chlore (4% de chlore dans la structure) et alumoferrite de chlore (15% de chlore dans la structure).

De cette façon, à 900°C tout le chlore est déjà pratiquement lié en composés, l'alynite se forme à partir de l'orthosilicate de la chlorure grâce à une nouvelle répartition du chlore entre lui et le bélite, pendant que les CaO et Al_2O_3 superflus libérés à lé décomposition de l'alumoferrite, sont liés. Ainsi, la cristallisation de l'alynite est suivie du dégagement de HCl grâce à la décomposition thermique de l'alumoferrite et de l'orthosilicate de la chlorure de calcium. Une partie de HCl fournit les particules voisines et participe au processus ultérieur de la formation du minéral en homogénéisant la composition de phase du clinker; une autre partie s'en va avec les gaz grâce à la sublimation. De cette façon, une étude de la suite de la formation du clinker à basses températures a démontré une grande importance des phases intermédisires du clinker dont la formation et la genèse, par notre opinion, exerce une influence décisive sur le caractère de la cristallisation du clinker d'alynite.

Le mécanisme des processus de la formation du clinker à basses températures que nous venons d'examiner nous permet de comprendre les particularités de la composition de

+La composition du minéral est, probablement, la suivante: $Ca_4Al_2Fe_2Cl_2O_9$.

phase du clinker d'alynite.

Le clinker d'alynite est représenté par quatre minéraux (% de la masse).

1. L'alynite - $Ca_{II}(Si,Al)_4O_{18}Cl$ - 60÷80
2. Le bélite - $\beta - C_2S$ - 10÷30
3. L'aluminate de la chlorure de calcium - $Ca_6Al_7O_{16}Cl$ - 5÷10
4. Le ferrite de calcium - $Ca_2Fe_2O_5$ - 2÷10

La formation du clinker d'alynite s'effectue dans la lutte concurrentielle des atomes et de leurs configurations pour les atomes du chlore qui sont les plus actives aux hautes températures de cristallisation du clinker; ces atomes passent facilement de la phase solide en liquide (fusion), en phase gazeuse et de nouveau solide (chloration).

Cette lutte aboutit à ce que le chlore ne reste que dans l'alynite, où il est solidement lié dans un motif structural original et entoure étroitement par huit atomes de calcium (2), ainsi que dans l'aluminate de chlorure de calcium, où il est aussi lié dans les motifs structuraux solides (3).

Le bélite et le ferrite de calcium sont identiques sur tous les indices aux minéraux portlands.

Certaines particularités de la morphologie et de la composition des cristaux sont liées à une faible solubilité du chlore (I,0-1,5% de la masse) dans le bélite et le ferrite de calcium.

Dans les clinkers obtenues à la base des matières premières aux différentes usines de ciment de l'URSS d'après la technologie de basse température avec l'utilisation de la fusion catalytique de la chlorure de calcium, l'alynite se cristallise sous forme des plaques hexagonales, des petits prismes allongés dans le même sens et des formations des rayons aiguisés. On peut y observer des grains de forme des rhomboedrique et des tablettes. Les clinkers ont une structure à grains fins irréguliers, la cristallisation de l'alynite est distincte. Les dimensions des grains varient de plusieurs mkm à 30-35 mkm. les particules de dimension de 15-20 mkm prédominent.

On y observe des agrégats de l'alynite, quelquefois des macles des grains à l'extinction zonale caractéristique. La birefringence est basse, l'extinction est directe. Les index de refraction varient dans les limites: 1.710 - 1.714.

Une autre phase silicique du clinker d'alynite observée dans les matériaux étudiés est représentée par le bélite (silicate basique bas), qui se diffère de l'alynite par sa forme arrondie, ovale ou celle de lentille; les débris des grains sont le plus souvent incolores, à l'extinction directe. Les index de réfraction sont N = 1.724 - 1.730. La birefringence et les index de réfraction sont les seuls indices distinctifs des études microscopiques des phases du clinker d'alynite.

Les études minéralogiques des clinkers synthétisés à basse température sont très difficiles à accomplir à cause de la structure microcristallin des phases minérales. Les études au microscope électronique nous ont permis d'étudier le faciès et la morphologie des cristaux dans le clinker.

Le bélite est représenté dans le clinker sous forme des grains arrondis et des débris irréguliers; souvent, on l'observe sous forme des incorporations dans les cristaux de l'alynite (fig.6).

Fig.6. Stéréomicrophotographies[+] d'un cristal de l'alynite avec des incorporations du bélite (stéréoskan - 4). Agrandissement - 5 000.

Dans le clinker, l'alynite est représenté par les plyedres bien cristallisés aux facettes distinctes reproduisant de différentes variétés du faciès tétragono-pyramidal (fig.7).

Une étude des microcristaux de l'alynite dans le clinker par la méthode de l'analyse microscopique du spectre aux rayons X à l'aide de l'appareil "Komeka" nous a permis de préciser la composition des éléments des cristaux de l'alynite, dont le contenu qualitatif est représenté par Ca, Si, O, Cl, Al, Fe et Mg (fig.8) et le contenu quantitatif par: Ca = 46-47 Si - 10-11 Al = 1,5-3,0 Mg = 1.0-1.5 Fe = 1.2-1.3 Cl = 2.5-3.0 O = 35-36.

CONCLUSIONS:

Le présent travail montre la suite de la formation et des transformations des phases intermédiaires et finales du clinker d'alynite.

A l'étape initiale du processus, les auteurs ont établi la formation du carbonate de la

[+]L'auteur remercie viement mme N.Sirotkine d'avoir exécuté une analyse.

Fig.7. Variétés du faciès des cristaux de l'alynite dans le clinker: a - photos des répliques des clivages des grains de clinker prises au microscope électronique ME - 5, agrandissement de 4000, b - stéréomicrophotographies prises au microscope électronique à balayage, agrandissement de 2800.

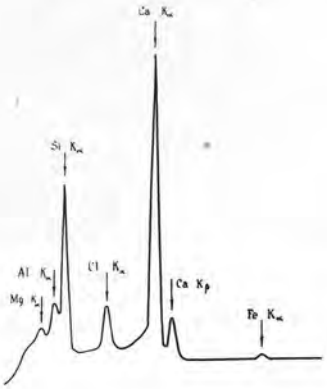

Fig.8. Spectrogramme d'une grain d'alynite dans le clinker.

chlorure de calcium et de la phase X dont la composition est à peu près la même ils ont déterminé les paramètres de leurs cellules élémentaires. Le spourrite, l'alumoferrite et l'orthosilicate de la chlorure de calcium se forment également en tant que des phases intermédiaires du clinker d'alynite.

La contenance quantitative des phases minérales dans le clinker d'alynite varie dans les limites suivantes (% de la masse):

l'alynite	60 - 80
le bélite	10 - 30
l'aluminate de la chlorure de calcium	5 - 10
le ferrite de calcium	2 - 10

Le changement de la proportion quantitative des phases minérales intermédiaires et stables dans le processus de la formation du clinker d'alynite est démontré.

Les auteurs donnent la description du caractère de la cristallisation des phases minérales du clinker - alynite; ils soulignent sa dépendance des conditions de la cuisson des matières premières liée à la genèse des phases intermédiaires du clinker.

BIBLIOGRAPHIE

1. B.NOUDELMAN (1976) VI^{e} Congrès international de la chimie du ciment "Clinkérisation dans la fusion de sel de la chlorure de calcium", tome I, pp.217-221 (russe).

2. V.ILUKHINE, N.NEVSKI, M.BIKBAOU et R.HOWIE (1977). Nature, "Crystal structure of alinite", v.269, N°5627, pp.397-398, english.

3. P.WILLIAMS (1968). V^{e} Congrès international sur la chimie du ciment "Crystal structure II · CaO · 7Al_2O_3 · CaF_2", tome I, pp.173-176.

Quantitative determination of the degree of conversion of high alumina cement

La détermination quantitative du degré de la conversion du ciment alumineux

John BENSTED, Principal Scientist, Head of Materials Section, Blue Circle Industries Ltd. Research Division, ENGLAND.

RESÜME : La détermination quantitative du degré de transformation cristalline du ciment alumineux hydraté a été faite par les différentes techniques de l'analyse thermique. Les imperfections sont discutées avec référence particulière à l'ATD. La valeur de ces mesures est en fait qualitative plutôt que quantitative, mais permet de distinguer les échantillons de ciment alumineux peu, modérément ou fortement transformés.

SUMMARY: Quantitative determination of the degree of conversion of high alumina cement by different thermal analysis techniques is discussed. The shortcomings are discussed with particular reference to DTA. The true value of these tests is shown to be qualitative rather than quantitative in being able to distinguish high alumina cement samples as little, moderately or highly converted.

Thermal analysis methods like DTA, QDTA, DTG, DSC and EGA have been used for quantitative determinations of the degree of conversion of high alumina cement (1-6). Such methods do, however, present a number of shortcomings, which are discussed here specifically for DTA, but they do correspondingly affect the applicability of the other thermal analysis techniques as well when used to obtain percentage conversion factors for high alumina cement samples.

The hydraulic aluminous component is assumed to be CA, which hydrates to CAH_{10}. Formation of C_2AH_8 is assumed to be negligible. In practice, $C_{12}A_7$ is normally present in high alumina cements in amounts ~2-10%. It hydrates to give principally C_2AH_8 together with some alumina gel that crystallises to gibbsite with time. Hydration of CA frequently gives significant C_2AH_8 and also alumina gel which in turn crystallises to gibbsite. Consequently two generations of gibbsite are formed:

(i) as a consequence of C_2AH_8 formation.

(ii) due to conversion.

Hence the height of the AH_3 endothermic peak, which is used as a standard for measuring conversion, is greater than can be explained by conversion alone. This would account for relatively high conversion figures being common for lower age high alumina cement concrete samples.

β-C_2S can be present ~ 2-10% and is said to hydrate to Strätling's compound (C_2ASH_8) in an aluminous medium. Generally < 5% is present in high alumina cements, which also contain some of their silicate in the form of melilite, a solid solution whose end members are gehlenite (C_2AS) and akermanite (C_2MS_2). In practice significant quantities of C-S-H are occasionally present (detectable by infrared spectroscopy) and C-S-H gives an endotherm in a similar position to that of CAH_{10}(7). Hence, when C-S-H is present, the CAH_{10} endothermic peak is exaggerated and this can give rise to a low conversion figure.

Use of the calcium aluminate hydrates CAH_{10}, C_2AH_8 and C_3AH_6 as basic analytical standards for calibration purposes is suspect, because all are highly susceptible to atmospheric carbonation. If prepared pure and used once for this purpose they are probably all right, but if used again there is likely to be significant carbonation due to more contact with air and thus lead to a more uncertain quantity of the respective calcium aluminate hydrate being present in the standard. Only CAH_{10} is normally used as a primary standard. C_3AH_6 is not so used owing to its high susceptibility to carbonation, which is likely to have occurred as well to at least an appreciable extent in many specimens under test. Carbonation converts C_3AH_6 to calcite and alumina gel, which may later crystallise as gibbsite, thereby augmenting further the AH_3 endotherm.

The gibbsite AH_3 peak is one of the basic standards of the techniques, because it is not subject to carbonation during normal atmospheric exposure (8). When conversion first takes place, alumina gel is formed which in turn crystallises to gibbsite. In practice this crystallisation process may take from several months to two years or so, so that if young high alumina cement concrete be examined the AH_3 peak may be depressed because of the occurrence of much alumina gel and in consequence the degree of conversion may be underestimated (9). Other forms of AH_3 such as nordstrandite and/or bayerite may also be present when alkaline hydrolysis has taken place and it is no longer meaningful just to consider the gibbsite peak. Complete resolution of the AH_3 and C_3AH_6 endotherms does not normally take place, so that the precise effect of each one of these upon the other is not known accurately.

Sulphate attack produces ettringite and although in general the peaks due to ettringite and CAH_{10} are clearly resolved enabling a conversion factor to be calculated, this is not always so, and in a few instances the presence of ettringite may produce a peak interfering with that of CAH_{10}. The presence of Portland cement renders the test valueless since there is no means of ascertaining what relative contributions are made to the peak at ~ 100-130°C by CAH_{10} and C-S-H.

Conversion in concrete beams is heterogeneous to a greater or lesser degree and in order to gain some representative insight into the problem, several samples need to be taken from different points in the beam under examination. Conversion at or near the edge of a beam may be greater or less than at the centre, depending upon the particular circumstances of the individual beam. Care should be taken to ensure that suitable samples are taken from the cores of beams for testing. Sampling needs careful drilling or, better, chipping, if the operator be untrained, so that any heat effects, that might themselves give rise to conversion, might be avoided.

The differential thermogram from ambient temperature to 500°C of a partially converted high alumina cement specimen is illustrated in Figure 1. The instrument used was laboratory made (7), with chromel-alumel thermocouples attached to a Kent potentiometric recorder. Dead-burnt alumina was used as the reference standard for heating. The endothermic peaks obtained are characterised in Table 1.

TABLE 1 - Endothermic Peaks for Differential Thermogram in Figure 1

Peak Temperature (°C)	Phase Present
115	CAH_{10}
150	C_2AH_8
230 (shoulder)	C_2ASH_8
285	AH_3
320	C_3AH_6

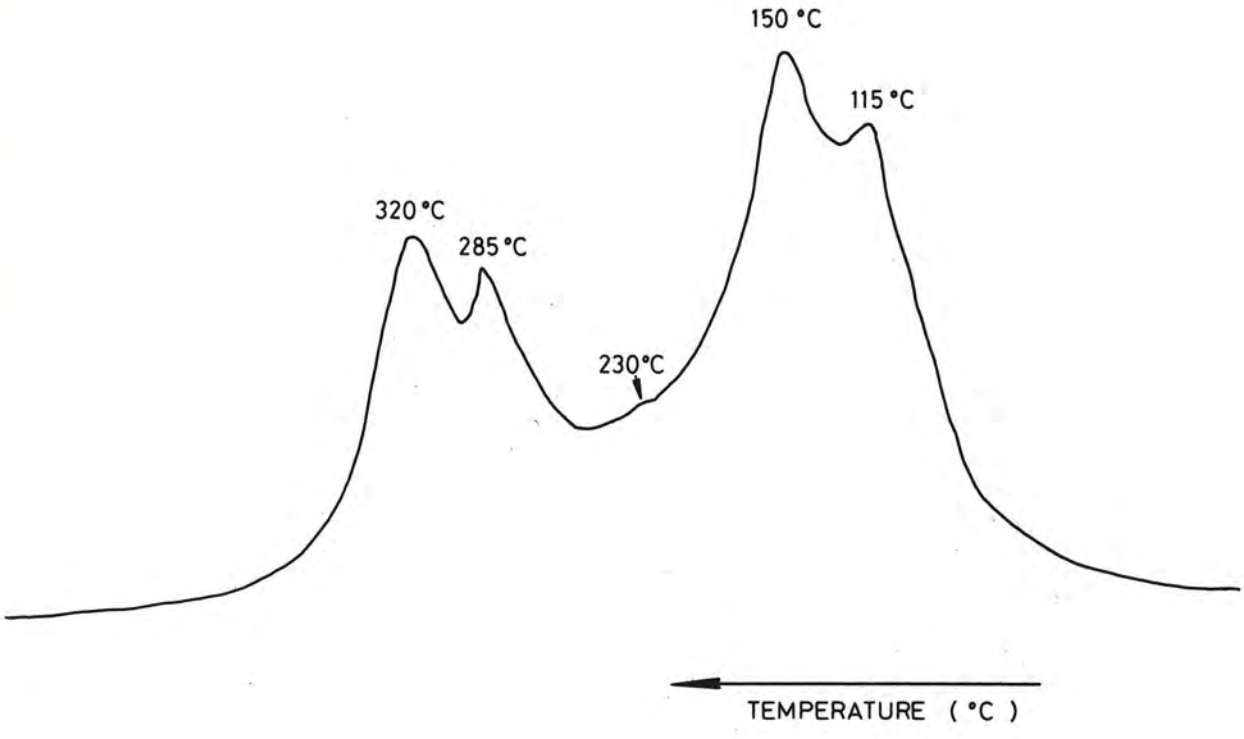

Fig. 1 - Differential thermogram from ambient temperature to 500°C of partially converted high alumina cement specimen.
(Conversion = 40% by the approved DTA method).
HEATING RATE: 20°C PER MINUTE.

The peak height method makes two assumptions (10) that are not valid in all instances:

(i) It is assumed that the peak shapes remain the same for all samples.

(ii) The base line is linear in all cases.

The percentage conversion figure obtained can thus in practice have a much greater uncertainty than ± 5% sometimes claimed. A figure of ± 20% is quite likely in some instances. This percentage conversion figure is not an end in itself, but simply an aid to structural tests. The rate of conversion and not the degree of conversion is what is of prime importance. There is no correlation between degree of conversion and compressive strength. Some beams have failed at low conversions; their weakness was due to the fact that such conversion as had occurred had been rapid; other beams were satisfactory at low conversions. Rate of conversion is a factor which can only be ascertained with time and cannot in consequence always be readily determined. The value of the DTA test is that a high strength highly converted beam is likely to be regarded as safe. It should be remembered that the DTA test is a calibrating and not an absolute method.

The real value of the DTA test is therefore qualitative rather than quantitative, in being able normally to grade high alumina cement samples as little, moderately or highly converted. Similar comments apply to the other thermal analysis techniques such as QDTA, DTG, DSC and EGA.

BIBLIOGRAPHY

1. - H.G. MIDGLEY and A. MIDGLEY (1975) The conversion of high alumina cement. Magazine of Concrete Research 27, 59-77.

2. - H.G. MIDGLEY (1976) "The use of thermal analysis methods in assessing the quality of high alumina cement concrete." Proceedings of the First European Symposium on Thermal Analysis, University of Salford, U.K., 20th-24th Semptember 1976. (Editor D. DOLLIMORE). pp. 378-379. Heyden and Son Ltd., London, New York, Rheine.

3. - B. EL-JAZAIRI (1976) The semi-isothermal thermogravimetry and the determination of the degree of conversion of high alumina cement concrete. Ibid. p. 380-383.

4. - J.P. DIXON (1976) Some applications of the Dupont DSC cell in quantitative analysis. Ibid. p. 390-393.

5. - E.L. CHARSLEY (1976) The application of derivative thermogravimetry to the determination of the degree of conversion of HAC concrete. Paper delivered to the Meeting on the Application of Thermoanalytical Methods to the Testing of High Alumina Cement Concrete, Sheffield, 24th February 1976.

6. - P.A. BARNES (1976) Some studies of HAC using DTG and EGA methods. Paper delivered to the Meeting on the Application of Thermoanalytical Methods to the Testing of High Alumina Cement Concrete, Sheffield, 24th February 1976.

7. - J. BENSTED (1979) Some instrumental investigations of Portland cement hydration. Part II. Differential thermal analysis (DTA). Il Cemento 76 (3), 117-126.

8. - D.C. TEYCHENNÉ (1975) Long-term research into the characteristics of high alumina cement concrete.

Magazine of Concrete Research 27, 78-102.

9. - D. FLETCHER (1976) Differential thermal analysis. Concrete 10 (5), 17.

10. - H.A. DAVIES (1976) Some aspects of the sampling and thermal testing of HAC concretes. Paper delivered to the Meeting on the Application of Thermoanalytical Methods to the Testing of High Alumina Cement Concrete, Sheffield, 24th February, 1976.

Sulfoaluminate cement series

Ciments sulfoalumineux

DENG JUN-AN, GE WEN-MIN, SU MU-ZHEN, LI XIU-YING, Engineers, Cement Research Institute The People's Republic of China.

RESUME : La formation des clinkers des ciments sulfoalumineux cuits à différentes températures, avec différentes valeurs de la saturation en chaux et avec différents rapports alumine/silice et alumine/trioxyde de soufre fut étudiée par rayons X A.T.D., microscope électronique, et analyses chimique et pétrographique. Furent également étudiées les caractéristiques d'hydratation et de durcissement des ciments fabriqués avec ces clinkers. Les résultats montrent que dans le système $CaO-Al_2O_3-SiO_2-SO_3$, la présence de SO_3 inhibant la formation de C_2AS, et à température appropriée de cuisson, 2 $C_2S.CaSO_4$ étant décomposé en C_2S et $CaSO_4$, des clinkers à base de $C_4A_3\bar{S}$ et $\beta-C_2S$ se sont formés. En outre, par addition de différentes quantités de gypse aux clinkers, on peut régler le temps de formation, les quantités d'ettringite et celles des autres phases d'hydratation dans la pâte de ciment, de façon à obtenir toute une série de ciments à propriétés différentes, tels que des ciments à durcissement rapide, à expansion légère, à forte expansion ou à auto-contrainte. Ces ciments qui constituent la série sulfoalumineuse sont maintenant produits sur une échelle industrielle en Chine. Le ciment à auto-contrainte est utilisé pour produire des conduites auto-contraintes, et les ciments à durcissement rapide et à expansion légère sont utilisés essentiellement pour les travaux de réparation urgente, des travaux à exécuter par temps très froid, et pour des ouvrages exigeant une bonne imperméabilité.

Summary: The formation of sulfoaluminate cement clinkers with different lime saturation values, alumina/silica ratios and alumina/sulfur trioxide ratios and burnt under different temperatures was investigated. XRD, DTA, petrographic analysis, EM and chemical analysis were employed in the study. The hydration and hardening characteristics of the cements made from the above clinkers were also studied. Results show firstly, in $CaO-Al_2O_3-SiO_2-SO_3$ system, the presence of SO_3 inhibits the formation of C_2AS and under appropriate burning temperature, $2C_2S\cdot CaSO_4$ is decomposed into C_2S and $CaSO_4$. Hence clinker with $C_4A_3\bar{S}$ and $\beta-C_2S$ as its main constituents are formed; secondly, by adding different amounts of gypsum to the clinker, the time of formation and the amounts of ettringite and other hydrated phases in the cement pastes may be so adjusted that a series of cements of different performance characters i.e., rapid hardening, slightly-expansive, expansive and self-stressing can be obtained. These cements which constitute the sulfoaluminate series are now manufactured on an industrial scale in China. Self-stressing cement is used in making self-stressing pressure pipes while slightly-expansive and rapid hardening cements are used mainly in emergency repair and permeability resisting works and under sub-zero temperatures.

1. Introduction

Calcium sulfoaluminate has been used as an expansive agent in cements by many investigators since the mineral was first proposed by Halstead.[1-5] Some investigators have used sulfoaluminate clinker to make rapid harding cements.[6-8] The studies on the formation of sulfoaluminate cement clinker are mostly concentrated on $CaO-Al_2O_3-SO_3$ system, while less work is done on $CaO-Al_2O_3-SiO_2-SO_3$ system.[9] Recently there have been reports on the formation of $2C_2S \cdot CaSO_4$ in $CaO-SiO_2-SO_3$ system.[10-11]

Much investigations have been made on the hydration of $C_4A_3\bar{S}$, with particular respect to its reaction when it is used as an expansive agent in portland cement. Xue et al[12-13] put forward the view that ettringites may form and even expand under unsaturated $Ca(OH)_2$ solution. The subsequent development of calcium sulfoaluminate cement series in China[14] proves to support this view.

The sulfoaluminate cements as described in this paper used limestone, siliceous bauxite and gypsum as raw materials. Clinker with $C_4A_3\bar{S}$ and $\beta-C_2S$ as its main constituents is formed in the burning. By adding different amounts of gypsum to the clinker in the grinding cements with distinct performance characters, i.e., rapid hardening, slight-expansive, expansive and self-stressing are obtained.

More than one hundred thousand tons of sulfoaluminate cements have been manufactured since 1974. Rapid hardening cement has been used in the manufacture of concrete products (concrete ships, electric poles, railway sleepers, floor slabs, prefabricated beams and pillars and large span trusses), in emergency-repair and permeability resisting work and in frame work joints. Instances of some other applications are joints for prefabricated slabs used in reservoirs and binder for moulding sand. The cement has especial good performance under sub-zero temperatures (-10°C, -25°C, -35°C). Only simple measures are needed to acquire favorable strength gain and to assure no decrease in final strength. In the meantime, more than 2000 kilometers of self-stressing pressure pipes of various diameters have been produced using sulfo-aluminate self-stressing cement.

II. Sulfoaluminate cement clinker

With a view to studying the clinker formation and its mineral composition, 16 raw mixes were prepared having different lime saturation values ($C_m = C/0.7(F+T+\bar{S})+0.55A+1.87S$), alumina/silica ratios ($N=A/S$) and alumina/sulfur trioxide ratios ($p=A/\bar{S}$). Limestone, gypsum and five siliceous bauxites with N=4, 2, 1, 0.2 and one containing 13% Fe_2O_3, were used as raw materials. MgO and graphite powder were mixed into some of the raw mixes to study the influence of MgO and reduced atmosphere on the formation and composition of the clinker. Burning tests were carried out at first in a siliconit tube furnace and later in a small rotary kiln. Surface observation, chemical analysis, XRD and

*Participants of the investigation are: Zheng Wan-lin, Li Pei-quan, Zhang Pei-xin and Li De-dong, Engineers, Cement Research Institute

**The investigation was directed by:
Wu Zhong-wei, chief engineer, Research Institute of Building Materials,
Wang Yan-mou, vice director, Research Institute of Building Materials,
Xue Jun-gan, Vice director, Cement Research Institute.

petrographic analysis were made on clinkers burnt under different temperatures (950,1050, 1250,1300 and 1400°C). Physical properties of some of the cements made from the above clinkers were examined.

Results show that under appropriate conditions clinker with $C_4A_3\overline{S}$ and β-C_2S as its main constituents is obtained. N value does not affect the pattern of formation of clinker minerals but it does affect the relative amount of $C_4A_3\overline{S}$ and β-C_2S. With $C_m=1, p=3.82$, the lime absorption is completed in clinker burnt under 1250°C. By introducing SO_3 into the mixes and under appropriate burning temperature, the formation of C_2AS is inhibited and the decomposition of $2C_2S\cdot CaSO_4$ into C_2S and $CaSO_4$ is promoted. At above 1280°C, $C_4A_3\overline{S}$ and β-C_2S are found to have formed and the intermediate phases C_2AS and $2C_2S\cdot CaSO_4$ disappear. Between 1280-1400°C no appreciable changes in mineral phases have occurred. At above 1400°C, $C_4A_3\overline{S}$ begins to decompose and SO_3 to volatize. For normal raw mixes i.e., $C_m=1, p=3.82$, the clinkering temperature range is fairly wide.

Fig.1 and Fig.2 are plots of clinker

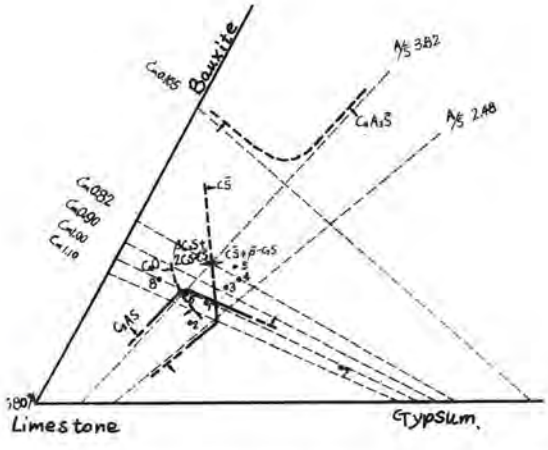

Fig.1 Clinker compositions against constituents of raw mixes at 1250°C.

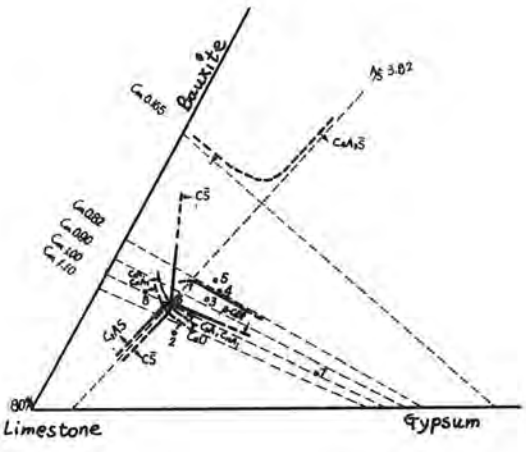

Fig.2 Clinker compositions against constituents of raw mixes at 1300°C.

compositions against the constituents of raw mixes. The latter are prepared from siliceous bauxite, limestone and gypsum. XRD and petrographic analyses have been made on clinkers burnt under 1250 and 1300°C with various C_m and p values. The diagrams are schematic, yet they do illustrate the tendency of the clinker formation and its mineral composition in relation to changes in raw mix constituents.

The addition of as high as 5% MgO, which exists in clinker as extremely small periclase particles, has no distinct influence on the mineral composition of clinker. Reduced atmosphere accelerates the decomposition of $CaSO_4$, give rise to adverse effect on clinker formation and may even decompose $C_4A_3\overline{S}$ already formed.

III. The hydration, hardening and physical properties of sulfoaluminate cements.

Various types of sulfoaluminate cements have been obtained by grinding the above clinker with different amounts of gypsum. While the amount of gypsum needed depends on the content of $C_4A_3\overline{S}$ in the clinker, the mole ratio of $CaSO_4\cdot 2H_2O/C_4A_3\overline{S}$ designated as M

varies from 0.5 to 6,depending on the type of cement to be made. The ratio increases in the order of rapid hardening,slightly-expansive,expansive and self-stressing cement.

In order to study the characteristics of hydration of the different types of sulfo-aluminate cements,various combinations of individual minerals $C_4A_3\bar{S}$,C_2S and $C\bar{S}H_2$ were prepared. Hydration and hardening tests were made both on pastes and suspensions of cements and individual mineral combinations. Table I lists the proportioning and properties of pastes made from the individual mineral combinations. XRD,EM,DTA and chemical analysis were employed in examining specimens of different ages. Results indicate that the hydration of sulfoaluminate cements proceeds

The proportioning and properties of pastes made from individual mineral combinations. Table I

No.	proportioning			W/C	strength N/mm²						
	C_4A_3S	β-C_2S	gypsum		6 hrs	1 day	3 days	7 days	14 days	28 days	2 mons
S_1	100	0	0	.39	15.5	37.0	41.0	31.0	35.0	-	35.0
S_2	73.69	0	23.31	.33	24.0	15.5	d*	-	-	-	-
S_3	45.12	0	54.88	.27	21.5	12.0	d	-	-	-	-
S_4	0	100	0	.36	0	0	0	1.0	1.0	4.0	-
S_5	0	52.31	47.69	.26	0	0	0	0	0	.8	-
S_6	80	20	0	.40	6.0	42.5	46.0	44.0	49.0	-	44.0
S_7	64.35	16.09	19.56	.32	18.0	24.5	30.5	34.5	36.0	-	32.0
S_8	40.55	10.14	49.31	.29	17.0	18.5	25.0	35.5	35.0	-	37.0
S_9	60	40	0	.38	8.5	40.0	34.5	27.5	28.5	29.0	-
S_{10}	50.74	33.83	15.43	.33	22.0	25.0	30.5	29.5	30.5	33.0	-
S_{11}	34.69	23.13	42.18	.29	17.5	22.0	25.5	33.0	35.0	41.0	-
S_{12}	40	60	0	.35	-	27.5	25.0	24.5	17.5	27.0	-
S_{13}	35.66	53.49	10.85	.32	20.0	20.5	22.5	23.0	-	25.0	-
S_{14}	26.91	40.37	32.72	.29	14.0	20.0	30.5	33.5	26.0	37.0	-

* d= disintegrated

as follows:

$$C_4A_3\bar{S} + 2C\bar{S}H_2 + 32H \longrightarrow C_3A\cdot 3(C\bar{S})\cdot H_{32} + 2AH_3$$

$$C_2S + 2H \longrightarrow C\text{-}S\text{-}H\ gel + Ca(OH)_2$$

$$3Ca(OH)_2 + 3C\bar{S}H_2 + AH_3 + 20H \longrightarrow C_3A\cdot 3(C\bar{S})\cdot H_{32}$$

The time of formation,amount and distribution of the resultant phases determine the structure of the cement paste as well as its deformation ability. Hence they influence directly the strength,expansion,self-stressing and compactness of the cement paste. Ettringite behaves differently in different stages of hardening. By adding different amount of gypsum,the time of formation and amount of ettringite may be so regulated that a series of cements with different properties may be obtained. In rapid hardening cement where a small amount of gypsum is added $C_3A\cdot C\bar{S}\cdot H_{12}$ is formed besides $C_3A\cdot 3(C\bar{S})\cdot H_{32}$,$AH_3$ and C-S-H gel.

Ettringite,one of the main hydration products of sulfoaluminate expansive cement and self-stressing cement,is the source of expansion. The p^H value of the liquid phase of the paste as determined is about 10.5. In other words,ettringite here is formed under unsaturated $Ca(OH)_2$ solution. It expands but moderately and together with the cushion effect of AH_3 gel and C-S-H gel,it imparts a

fairly large deformation ability to the cement paste of increasing structural strength. Thereforethe cement has a high self-stress value with good stability.

Fig.3 shows the relationship between the proportions of the three main phases in the cements and the physical properties of the cements. The rapid hardening sulfoaluminate cement has moderate setting time. The

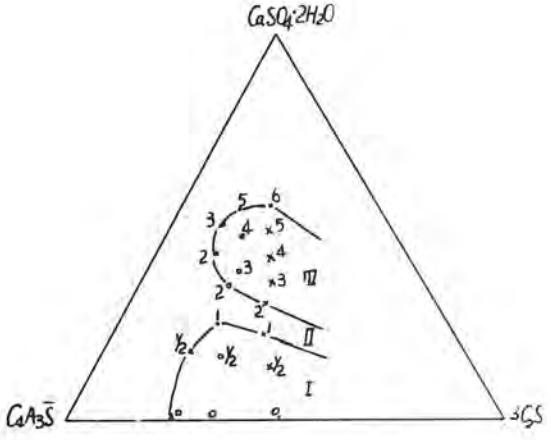

Fig.3 The proportions of the three main phases and the physical properties of the cements.

I. Rapid hardening cement area

II. Slightly-expansive cement area

III. Expansive and self-stressing cement area

interval of initial set and final set is short. The compressive strength of 1:3 earthen dry mortar may attain 30 N/mm^2 in 12 hours and 50 N/mm^2 in three days. Compressive strengths in later ages still increase and high tensile strengths are attained. (Table II). The properties of its concretes are similar to those of mortars. Both are anti-freezing and permeability resistant.

It is worth noting that the rapid hardening sulfoaluminate cement has very good performance under sub-zero temperatures. The strength of a cement frozen in early stage but later cured under normal temperature may approach that of a cement cured under normal temperature from the very beginning. By applying simple heat preservation measures, the strengths of the concrete have developed effectively under -10°C, -25°C and -35°C atmospheric temperatures at winter construction sites in Beijing and Heilungjiang.

For self-stressing sulfoaluminate cement, the self-stressing value may reach 5 N/mm^2 and the strength above 40 N/mm^2 for 1:2 mortars and 1:2 concretes while free expansion is less than 2.5% (Table III). Pressure pipes made from such cement have good performance properties in relation to water imperviousness and air tightness.

The expansion and strength values of the slightly-expansive and expansive sulfoaluminate cements are between those of rapid hardening cement and self-stressing cement. Their expansion may be regulated as required by controlling the amount of gypsum added during finish grinding. These two types of cement are mainly used in permeability resisting works and shrinkage compensating concrete works.

Properties of rapid hardening cement Table II

No.		Strength N/mm^2							
		12 hrs	1 day	3 days	7 days	28 days	3 mons	12 mons	24 mons
3-1	comp	39.5	50.0	58.7	64.7	68.3	76.1	80.3	—
	tens	3.05	3.43	4.03	4.24	4.34	4.34	5.05	5.59
2-1	comp	37.6	50.4	64.0	70.5	79.5	83.6	91.5	94.5
	tens	3.17	3.45	3.70	4.03	4.18	4.86	5.15	5.90

Properties of self-stressing cement — Table III

No.	curing systen	proportioning	free expansion % / self stressing value N/mm²						compressive strength N/mm²						
			1 d	3 d	7 d	14 d	28 d	6 m	*	1 d	3 d	7 d	14 d	28 d	6 m
2-4	40°C x 80'	1:2 concrete	.15 20	.27 38	.67 52	1.04 63	1.23 69	1.29 71	148	282	392	298	463	470	690
B-3.5	40°C x 80'	1:2 mortar	.26 19.9	.91 42.8	1.62 53.5	1.96 59,1	2.02 63.0	- -	139	306	433	444	447	567	-

* immediately after demoulding

References

1. P.E.Halstead,J.Appl.Chem.,1962,Vol.12,413
2. Nobue Fukuda,Proceedings of the Fifth International Symposium on the Chemistry of Cement,Tokyo,1968,Part 4,341
3. P.P.Budnikov,Proceedings of the Fifth International Symposium on the Chemistry of Cement,Tokyo,1968,Part 4,319
4. Report by A.C.I.Committee 223,J.A.C.I., No.8,583,1970
5. P.K.Mehta and M.Polivka,Proceedings of the Sixth International Symposium on the Chemistry of Cement,Moscow,1974,Part 3, 158
6. A.A.Borje,U.S.Pat. 3860433,14 Jan 1975
7. Nobue Fukuda,Jpn.Kokai Tokkyo Koho,76 28116,9 Mar. 1976
8. Yang Jing Cement Factory and Tongji University,Cement,No.5-6,1974
9. Takanori Nakamuka,Giichi Sudoh and Shigeo Akaiwa,Proceedings of the Fifth International Symposium on the Chemistry of Cement,Tokyo,1968,Part 4,351
10. Y.B.Pliego-Cuervo and F.P.Glasser,Cement and Concrete Research,Vol.9,No.1,51,1979
11. Y.B.Pliego-Cuervo and F.P.Glasser,Cement and Concrete Research,Vol.8,No.4,455,1978
12. Xue Jun-gan,Chen Wen-hao and Zhou Shi-fen, Cement and Cement Products,64001 (4) 5-10; 64002 (5) 17-19 (1964)
13. Xue Jun-gan,Chen Wen-hao,Tong Xue-li, Zhao Yu-ping and Xu Ji-zhi,Journal of the Chinese Silicate Society,Vol.7,No.1,58, 1979
14. Cement Research Institute,Research Institute of Building Materials,Journal of Chinese Silicate Society,Vol.6,No.3,123, 1978

The limitation of high pressure mercury porosimetry to the study of hardened cement pastes

Mesures de dimension des pores par pénétration de mercure dans l'étude des pâtes de ciment durci

S. MODRY and J. HEJDUK, Building Research Institute, Praha, Czechoslovakia.

RESUME : La validité des mesures de dimension des pores, par pénétration de mercure, a fait l'objet d'études sur des pâtes durcies. Des essais de pénétration de mercure ont été effectués sur des éprouvettes vierges; puis ils ont été repris, à plus haute pression, sur les mêmes éprouvettes. Il en résulte que les fortes pressions ne provoquent pas de destructions importantes dans ces éprouvettes.

SUMMARY : The validity of results of pore size measurements by mercury intrusion was unvestigated on hardened cement paste. Mercury intrusion measurements were compared for virgin samples and reintruded samples after removal of mercury. Results showed no evidence of sample damage at high pressures.

Since the time the high pressure mercury intrusion porosimeter was introduced by Ritter and Drake /1/, this method has been gaining field first of all due to its undoubt advantages as e.g. relative simplicity and the speed of obtaining of the results The mentioned properties of the method caused its many applications for investigation of pore structure of materials in many scientific and technical areas /2,3,4/. The use of the mercury porosimetry in such a broad scope was also made possible by commercially available equipments produced by several firms in Europe and in the U.S.A. /5/. The application of these instruments /in some of them can pressures reach level as high as 414 MPa/ has raised questions about the effects of high pressures on the pore structure.

This problem have been investigated and discussed by many authors as far back as Drake /1,5/ in 1949 year. From the results obtained by different authors can be concluded that a closer comparison of measured data is unfortunately rarely possible due to the fact that no detail information is available with respect to the mode of preparation etc. In general, however, it is evident that the distortion is dependent on mechanical properties of the solid phase itself, and at the same time on the shape and size of the pores and on the way of their mutual connection.

The question to what extent the pressure damages the sample and alters the pore size distribution is of utmost importance also for hardened cement pastes and concretes.

In the range of pore radii from 10 to 240 μm results measured by mercury porosimetry were compared with those from light microscopy by Chekhovskii and Leirich /6/. Data obtained by these authors shown a reasonable agreement.

The investigation reported here was undertaken to examine the influence of high pressure on pore size distribution of pores with radii under 10 μm in hardened cement paste.

The procedure was to determine the pore size distribution of a hardened cement paste by mercury intrusion and then to distill the mercury out of the sample and remeasure its pore size distribution. Comparison of these distributions will give an indication of any damage to the sample.

EXPERIMENTAL WORK

The sample selected for tests was a hardened cement paste prepared from cement with w/c = 0,45. After 7 days of the water curing specimens were dried to stop the hydratation at the temperature 105 ^{0}C until they reach a constant weight. Dried specimens were crushed and granules of 2 - 3 mm in diameter were used for pore analysis.

Mercury intrusion tests on these specimens were performed with Carlo Erba porosimeter type 65A, capable of reaching pressures of 98,1 MPa.

Prior to intrusion the samples were outgassed at 135 ^{0}C for 7 hours under the vacuum of 0,20 Pa and were cooled to room temperature prior to loading in the porosimeter. The reason for such a temperature treatment was that after an intrusion test on a particular sample the residual mercury was removed under the same temperature and vacuum conditions.

Such a pretreatment seems to be reasonable and makes possible to differentiate changes due to temperature and due to high pressure itself. After an intrusion test a small portion of the mercury could not be removed by described technique. These samples were than retested in the porosimeter in the same manner.

For the conversion of the recorded data to pore size values cylindrical pore model was assumed. Surface tension of the mercury of 480 dyn/cm^{2} and contact angle 140^{0} were assumed for calculation.

RESULTS

Figure 1 shows a set of mercury intrusion pore size distributions for a samples of hardened cement paste.

The curve for the "virgin" specimen /Curve A/ and the one remeasured after removal of the mercury /Curve B/ coincide the entire range of radii. The difference between the curves is comparable of even less than the experimental error.

CONCLUSIONS

The identical course of the integral porosity curves gives the evidence that the pressure up to 98,1 MPa has not caused measurable alteration in the sample.

BIBLIOGRAPHICAL REFERENCES

/1/ Ritter, H.L., Drake, L.C., /1945/, Industrial Engineering Chemistry, Anal. Ed., Vol.17, pp.782-786, English

/2/ Modrý, S., Svatá, M., /1972/, Bibliography on Mercury Porosimetry, House of Technology, Prague, 79 p., English

/3/ Modrý, S., /1975/, Bibliography on Mercury Porosimetry, Supplement I, House of Technology, Prague, 42 p., English

/4/ Modrý, S., /1979/, Bibliography on Mercury Porosimetry, Supplement II, House of Technology, Prague, 43 p., English

/5/ Modrý, S., /1979/, Porosimetry and its Applications, Development and the Present State of Mercury Porosimeter Construction, pp.113-129, Czech.

/6/ Chekhovskii, Yu.V., Leirikh, V.E.,/1964/ Kolloidnyi Zhurnal, Vol.26, pp.518-522, Russ.

.../...

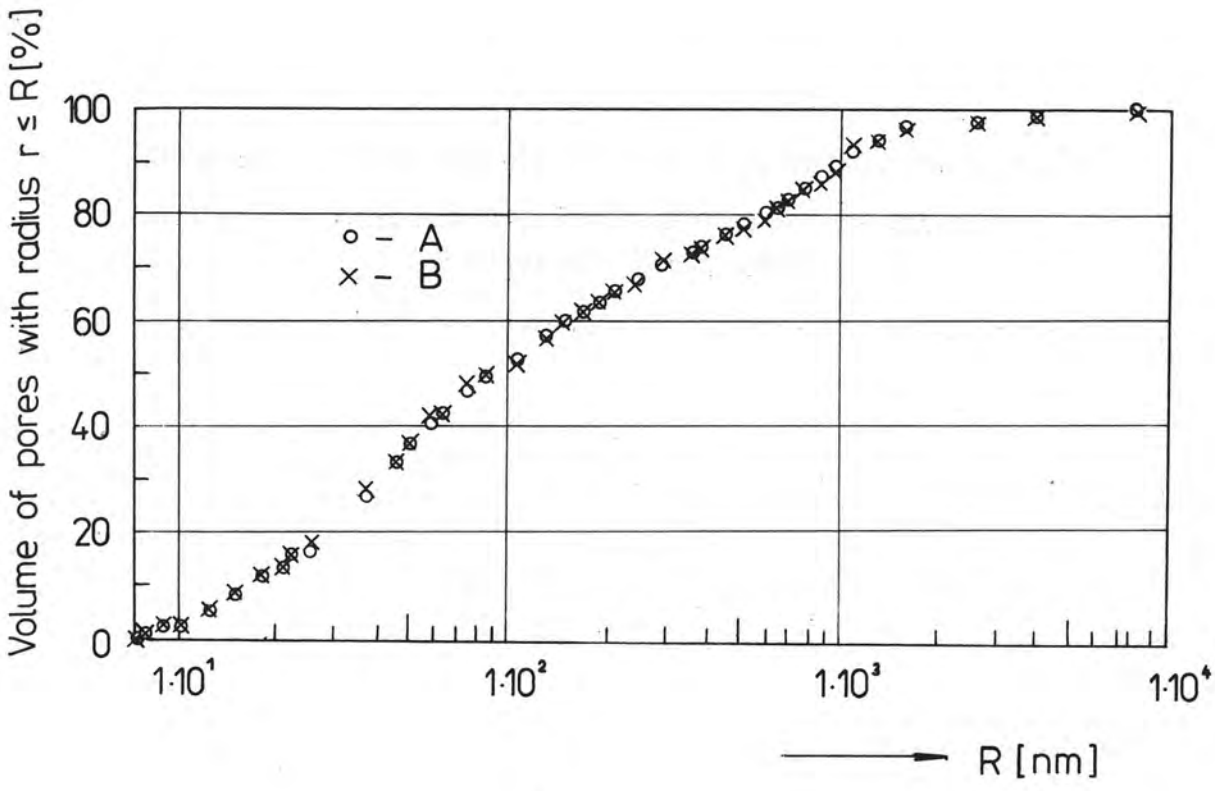
Volume of pores with radius r ≤ R [%]
100
80
60
40
20
0
o – A
× – B
1·10¹
1·10²
1·10³
1·10⁴
R [nm]

FIGURE 1

$Ca(OH)_2$ formation in air voids of cement pastes

La formation des cristaux de $Ca(OH)_2$ dans les vides des pâtes de ciment

O.Z. CEBECI, Assistant Professor, Department of Civil Engineering, King Abdulaziz University, Jeddah, Saudi Arabia.

RESUME : Des recherches ont été faites sur l'influence des ambiances de cure, sur la formation des cristaux de $Ca(OH)_2$ dans les vides interstiels des pâtes de ciment. Les pâtes ont été hydratées, puis conservées, soit sous enveloppe imperméable, soit en atmosphère saturée, soit immergées en eau pure ou en eau saturée en chaux. Quatre morphologies différentes de petits cristaux et de plaquettes de $Ca(OH)_2$ ont été observées au microscope électronique dans les géodes. Ceci indique que la chaux hydratée, libérée par la réaction d'hydratation du ciment, se dégage à l'intérieur des pâtes, sauf pour celles conservées en eau pure, parce qu'une partie de cette chaux migre hors de la pâte durcie.

SUMMARY : Effect of different curing media on the formation of $Ca(OH)_2$ crystals in air-voids of hardened Portland cement pastes was investigated. The pastes were hydrated in impermeable coating, humidity room, clean water and saturated lime solution. Four different morphology of deposits, ranging from small crystals to packing of $Ca(OH)_2$ plates, were observed in air voids by scanning electron microscopy. This indicated that $Ca(OH)_2$ liberated by hydration is accommodated within the pastes cured in impermeable coating, humidity room or saturated lime solution. However, curing of cement pastes in clean water may not faithfully duplicate the curing conditions of concrete in common construction practice, because part of $Ca(OH)_2$ liberated into pore solution is leached out of the hardened paste.

INTRODUCTION

Scientists investigating the structure, properties and behaviour of hardened cement paste, mortar and concrete hydrate their samples in a variety of curing media. Furthermore, standard methods established by various institutions for testing mortar and concrete do not agree in a unique hydration practice. The most common hydration methods may be classified as follows:

1. Placing the fresh paste, with the original mixing water, in a sealed water-impermeable container (1,2).
2. Storing the samples in an environment of high relative humidity (3,4).
3. Keeping the hardened paste immersed in clean water (5,6).
4. Keeping the hardened paste immersed in saturated lime solution (7,8).

The first method is an ideal way of preserving the original water-cement mix for hydration but is not very practical especially for larger mortar and concrete specimens. The second and third methods aim at preventing the evaporation of the original mixing water, or supplying water for hydration, in an enviroment very similar to what common construction practice offers to concrete manufactured in the field. It is usually more convenient to immerse samples in water rather than storing them in moisture cabinets; however, calcium hydroxide liberated by the hydration of cement may be leached away from the hardened paste especially if fresh water has easy access to hydration products (9). A trend developing in recent studies is to hydrate the samples in a saturated lime solution, so that all hydration products are deposited within hardened pastes.

The present study is an attempt to evaluate the effect of different curing media on the formation of calcium hydroxide crystals in the air voids of air-entrained hardened Portland cement pastes. Scanning electron micrographs of the air voids showing various calcium hydroxide deposits are interpreted in order to help the designation of a practical curing method that faithfully represents the curing conditions of concrete in common construction practice.

MATERIALS AND METHODS

Type I Portland cements from two different sources (an American and a Turkish factory) were used in this study. The cements were mixed with distilled water (containing commercial air-entraining agents) in a bench-top mixer at 0.5 and 0.6 water/cement ratios. The fresh pastes (containing about 6 % air by volume) were cast into glass test-tubes (diameter = 1.5 cm, height = 5 cm) and metal cubes (edge = 5 cm). The specimens were kept in a humidity room for 24 hours, then the hardened pastes were demolded. Further hydration took place under various conditions as follows:

1. HR curing in a humidity room at 95 ± 5 % RH and 23 ± 2°C
2. SL curing by coating individual samples with an impermeable layer of epoxy.
3. FW curing in tap water by renewing the water every 2-3 days.
4. SW curing in tap water without changing the water.
5. CH curing in saturated lime solution.

SL, FW, SW and CH curing containers were also kept at 23 ± 2°C in the same room as HR cured samples. After 60 days of hydration (130 days as well in case of CH curing) the hardened pastes were dried at 105 ± 5°C for at least 24 hours and then broken into small pieces for visual and microscopic examination (using JEM-100 B JEOL/Jeolco, and Stereoscan S4-10, Cambridge Scientific Instruments).

RESULTS AND DISCUSSION

Calcium hydroxide deposits observed in the air voids of hardened Portland cement pastes have been classified into four distinct morphologies shown in Figure 1. The differences in the source of cements, water/cement ratio, shape and size of specimens had no effect on the results. The voids containing the deposits (one in every 10-15 void) were randomly distributed through the cross-section of the samples.

Hydration of Portland cements is one of the major areas of great interest to cement chemists. Investigations of hydration mechanisms, hydrate structure and composition have revealed various features of calcium hydroxide crystals formed by the hydration of C_3S and C_2S (10). In general, calcium hydroxide liberated by hydration crystallizes from nuclei formed near or at the surface of cement particles (11) and surrounds air voids and aggregate particles (12,13).

In recent investigations, the interpretation of analytical data on pore solutions expressed from hardened pastes showed that these solutions are saturated with calcium hydroxide up to several months of hydration (11, 15, 16). Marchese observed calcium hydroxide plates in cavities of Portland cement pastes hydrated in tap water (5).

The results of this study implied that the crystals are deposited by capillary pore solutions saturated with calcium hydroxide (14). The solution penetrates air voids if there is a leak in the surrounding calcium hydroxide layer. In order to test this hypothesis some specimens were taken out of curing solutions and broken immediately. Optical examination of the fracture surfaces showed that the voids accommodating the deposits were filled with water whereas other voids contained neither deposits nor liquid.

The effect of curing media on the formation of deposits depends on two factors:

1. The degree of saturation of the pores with solution.
2. The degree of saturation of the pore solutions and curing solution with calcium hydroxide.

In case of SL and HR curing, the pores get unsaturated with solution as hydration continues but the solution is saturated with calcium hydroxide. Hence the result is small crystal deposition in air voids (Fig. 1-a), because the hydration products are accommodated in the vicinity of the reactants (11).

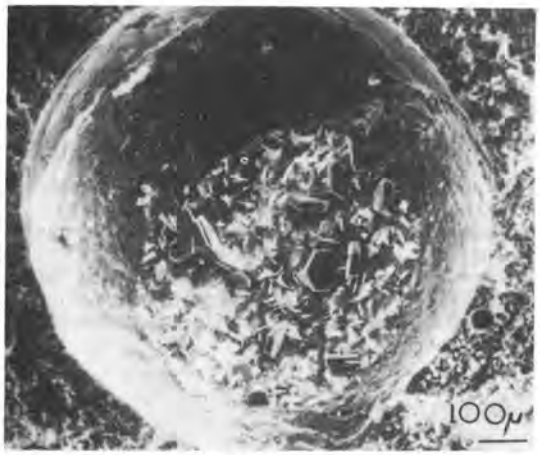

(a) HR and SL curing for 60 days

(b) FW and SW curing for 60 days.

(c) CH curing for 60 days.

(d) CH curing for 130 days.

Figure 1 - Electron micrographs showing calcium hydroxide deposits in air-voids of hardened cement pastes.

The pores are saturated with solution but the saturation of the curing solution with calcium hydroxide is limited in FW and SW curing. This increases the mobility of calcium hydroxide liberated by hydration (10) ; part of which is deposited within the hardened paste and in permeable air voids (Fig. 1-b) ; however part of calcium hydroxide is leached by curing water (9), and hence, further crystal growth in the voids is not possible.

Calcium hydroxide crystals in the air voids of CH cured pastes extended through the entire cross-section of the voids after 60 days of hydration (Fig. 1-c). The voids were packed with calcium hydroxide plates after 130 days of curing in saturated lime solution (Fig. 1-d). The pores of these samples are saturated with solution and the curing solution is saturated with calcium hydroxide. Thus, calcium hydroxide liberated into the pore solution is not leached but deposited within the hardened paste; many plates being easily accommodated in air voids.

Mortar samples were prepared according to the Rilem - Cembureau procedure, and cured in humidity room, water and saturated lime solution for 60 days. The compressive strengths were determined as 29.31 MPa for both FW and SW cured samples and 38.04 MPa for CH cured mortars. HR curing is known to develop less strength than water curing (10). The decrease in the strength of samples cured in water (as compared to the strength of samples cured in saturated lime solution) is regarded as another demonstration of the fact that some calcium hydroxide liberated by hydration is leached away from these samples by the clean curing water.

CONCLUSION

The difference in the morphology of calcium hydroxide crystals deposited in air voids of hardened cement pastes hydrated in different curing media indicated that calcium hydroxide liberated by hydration is accommodated within the pastes cured in humidity room or in saturated lime solution, whereas part of calcium hydroxide is leached by curing water if the pastes are hydrated in clean water. Hence curing of cement pastes in clean water may not faithfully duplicate the curing conditions of concrete in common construction practice.

REFERENCES

1) R.Sh MIKHAIL, L.E. COPELAND, and S. BRUNAUER (1964), "Pore structures and surface areas of hardened Portland cement pastes by nitrogen adsorption" , Canadian Journal of Chemistry, 42, 426.

2) G.G. LITVAN (1976), "Variability of the nitrogen surface area of hydrated cement paste", Cem. Concr. Res. 6, 139.

3) ASTM C-192 : Standard test method for making and curing concrete test specimens in the laboratory.

4) BS 1881 : British standard methods of testing concrete, Part 3: Methods of making and curing test specimens

5) B. MARCHESE (1978), "Microstructure of mature alite phase", J. Am. Ceram. Soc. 61, 349.

6) BS 4550 : British standard methods of testing cement, Part 3: Section 3:4 Strength test.

7) D.N. WINSLOW and S. DIAMOND (1970), "A mercury porosimetry study of the evolution of porosity in Portland cement", J. Mater. 5, 564.

8) ASTM C-109 : Standard test method for compressive strength of hydraulic cement mortars using 2-in or 50-mm cube specimens.

9) W. LERCH and R.H. BOGUE (1927), "Studies on the hydrolysis of compounds which may occur in Portland cement", J. Phys. Chem. 31, 1927.

10) F.M. LEA (1970), "The chemistry of cement and concrete, 3rd. ed.", Edward Arnold Publishers Ltd.

11) R.L.BERGER and J.D. McGREGOR (1973), "Effect of temperature and water-solid ratio on growth of $Ca(OH)_2$ crystals formed during hydration of Ca_3SiO_5", J. Am. Ceram. Soc. 56, 73.

12) B.D. BARNES, S. DIAMOND and W.L. DOLCH (1978), "Contact zone between Portland cement paste and glass aggregate surface", Cem. Concr. Res. 8, 233.

13) B.D. BARNES, S. DIAMOND and W.L. DOLCH (1979), "Micromorphology of the interfacial zone around aggregates in Portland cement mortar", J. Am. Ceram. Soc. 62, 21.

14) S. DIAMOND (1975), "Long-term status of calcium hydroxide saturation of pore solutions in hardened cements", Cem. Concr. Res. 5, 613.

15) P. LONGUET, L. BURGLEN and A. ZELWER (1973), Rev. Mater. Contr. Travaux Publics. Ciments et Betons, 676, 35.

16) K.FUJII and W. KONDO (1979), "Rate and mechanism of hydration of B-dicalcium silicate", J. Am. Ceram. Soc. 62, 161.

Low temperature calorimetry as a pore structure probe

Détermination de la structure des pores, par calorimétrie à basse température

Erik J. SELLEVOLD and Dirch H. BAGER, Building Materials Laboratory, Technical University of Denmark, DK-2800 Lyngby, Denmark.

Summary

Heat flow during cooling and heating of water saturated porous building materials have been measured at temperatures down to -100° C. The relationship between freeze/thaw temperature and pore size is discussed. A number of experimental results, mostly on cement pastes, are given to illustrate the ability of low temperature calorimetry to detect pore structural differences.

RESUME : Des mesures ont été faites jusqu'à des températures inférieures à - 100°C, sur les flux de chaleur, dans les pores saturés d'eau des matériaux de construction, lors de cycles de refroidissement et de réchauffement. Une relation entre la température de gel et la dimension des pores a été établie et discutée. Un grand nombre de résultats expérimentaux, obtenus principalement sur des pâtes de ciment, sont donnés pour illustrer cette aptitude de la calorimétrie à basse température à détecter des différences dans la structure des pores.

Introduction

Since 1976 a large number of calorimetric measurements of ice formation in porous building materials have been carried out at our laboratory. The experimental equipment, procedures, and a number of results have been reported previously (1, 2). In a recent report (3), calorimetric data with implications for frost resistance testing of concrete are discussed.

The present paper presents results on water saturated specimens which illustrate the potential of low temperature calorimetry as a pore structure probe. For cement products we regard this application of calorimetry as important since it may be applied without first drying the test specimen. Other types of experiments have shown that drying of hydrated cement products results in changes in their pore structures, but, as shown in this report, calorimetry provides particularly clear evidence of the character and magnitude of these changes.

Pore Size - Freezing Point of Pore Water

The Kelvin equation relates the meniscus radius of capillary condensed water to the relative vapor pressure it exerts. An analogous equation, given by Defay et al. (4), relates the meniscus radius to the freezing point of the water. Both equations are shown in diagram form in Figure 1. If it is assumed that the contact angle between water condensed in circularly cylindrical pores and the pore wall is zero, both with and without ice in the pore system, then the meniscus radius may be set equal to the pore radius, and Figure 1 may be used to interpret calorimetric ice formation data in terms of pore sizes. For example, assuming that the ice-water interface controls the state of stress in the unfrozen water, then according to Figure 1, the amount of ice formed to -5° C is equal to the volume of pores with radii greater than about 11 nm (110 Å). The geometric assumptions are necessary, but not very realistic. The spreading of the ice front through a pore system with variable cross sections would be controlled by the narrowest parts: the necks. The melting of ice in such a pore system, on the other hand, would be controlled by the size of the pores rather than of the necks. Hence, the hysteresis between cooling and heating curves gives information about the continuity of the pore system.

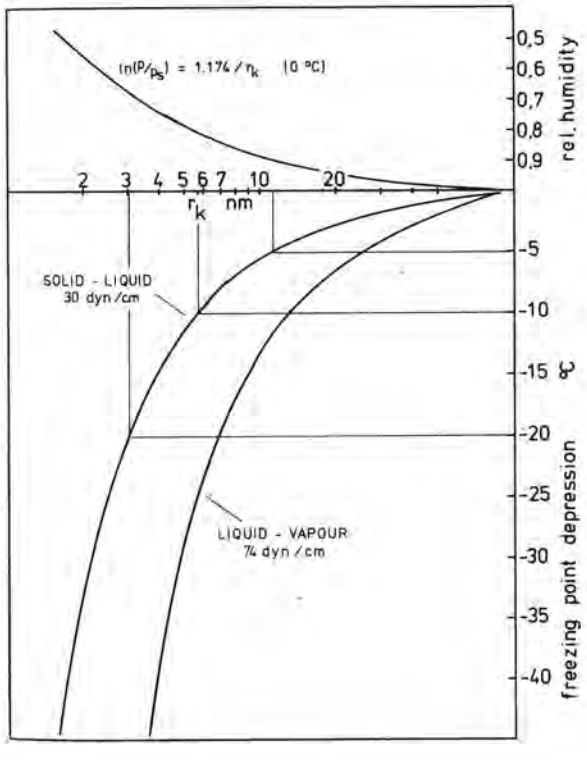

Figure 1. The Kelvin equation (top). The relationship between meniscus radius of capillary condensed water (r_K) and freezing point (bottom) for two interface possibilities.

It should be emphasized that both the calculation of amounts of ice from calorimetric data, and the interpretation of freezing temperatures in terms of pore sizes are based on many assumptions. The results must therefore not be taken too literally. In particular, simple capillary theory is only applicable in pores very large compared to the size of the water molecule. At -10° C (see Fig. 1) the pore diameter is about equal to 40 molecular diameters; possibly not a "very large" number in this connection. Everett (5) suggests that such application of capillary theory is questionable below about 300 molecular diameters. Calculated pore size data are therefore most realistic at large pore sizes (high freezing temperatures). It should also be pointed out that pore size data calculated from sorption isotherms or mercury penetration are subject to many of the same uncertainties mentioned above.

Experimental

Heat flow has been measured using a Low Temperature CALVET Micro-Calorimeter. The measurements are carried out in a scanning mode in the temperature range down to about -55° C. Experiments have shown that practically no freezing takes place below this temperature. In a "normal" experiment heat flow data is collected during both cooling at 3.3° C/hr and heating at 4.1° C/hr.

The test specimens are in the form of circular cylinders with d ≃ 15 mm and l ≃ 70 mm. During an experiment the specimens are enclosed in an air-tight stainless steel specimen cell, slightly larger than the specimens.

During early experiments no freezing took place (even with pure water) at temperatures greater than about -10° C. The amount of super cooling was later reduced substantially by sprinkling a few mg's of AgI powder on the specimens.

The calorimeter block temperature differed of course somewhat from the specimen temperature during a test; separate experiments showed the lag to be 0.4 to 0.8° C in "normal" runs and during periods of small freeze/thaw activity, while the lag could reach several degrees during periods of high activity.

Results and Discussion

Figure 2 shows the cumulative amounts of ice versus temperature for several water saturated materials. The curves are in qualitative agreement with our knowledge of the different pore structures; a) the standard clay brick contains large pores (μm range) and a very small surface area - all the pore water is freezable and freezes right after nucleation; b) the autoclaved, aerated concrete has a very large macroporosity - but also a finely divided C-S-H product with a large surface area to water. This is reflected in the freezing curve, in that there is gradual freezing down to about -50° C and not all the pore water is able to freeze; c) the two mature cement pastes display very gradual freezing and at -55° C only ~15% (w/c = 0.40) and 63% (w/c = 0.70) of the evaporable water is able to freeze.

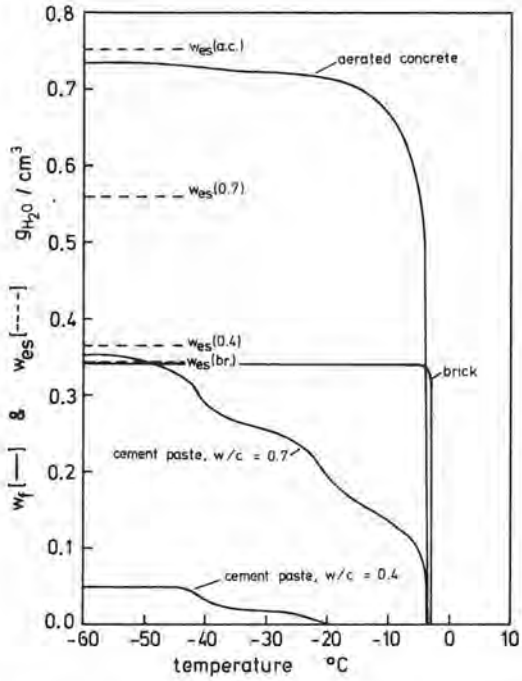

Figure 2. Cumulative ice formation (W_f) curves for water saturated building materials. Dotted lines indicate total evaporable water content (W_{es}) for the materials Cool 3.3° C/hr.

Figure 3 shows cool and heat results for water saturated mature cement pastes. Equivalent results are shown in (1), but no AgI powder was used, which resulted in nucleation temperatures several degrees below the present ones. It is noteworthy that only a few mg's AgI powder sprinkled on the specimen surface is able to trigger ice formation in the whole specimen volume. We therefore believe that freezing takes place by the spreading of an ice front through the pore system from a few nucleation points on the surface.

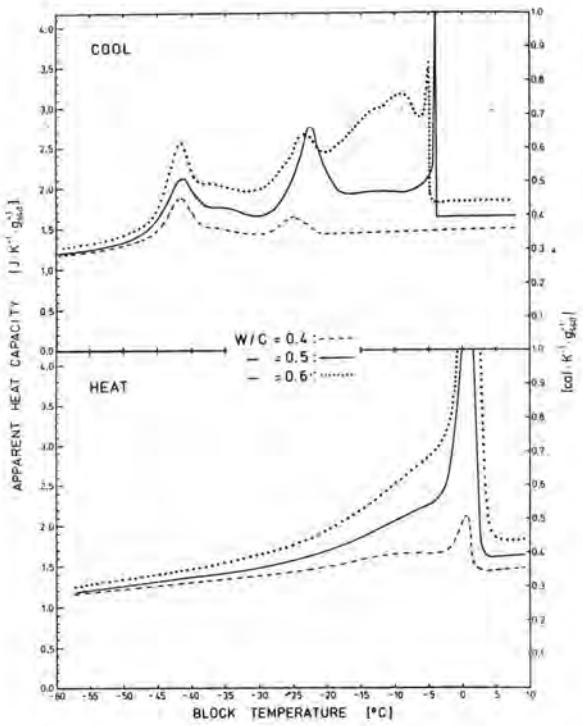

w/c	Age	W_{es}	W_f (-55)	W_{nf} (-55)
.4	486	.213	.030	.183
.5	675	.305	.099	.206
.6	548	.379	.184	.195

Age = days of water curing
W_{es} = evaporable water content at saturation
W_f = frozen water content
W_{nf} = non-frozen water content
All units of g/g_{dry}.

Figure 3. Heat flow during cooling and heating for mature water saturated cement pastes. Cool 3.3° C/hr. Heat 4.1° C/hr.

The main features of the two sets of curves are similar, in spite of the different degrees of supercooling. The large hysteresis between cool and heat, and the "trimodal" nature of the cooling curves indicate the existence of restrictions or necks in the pore system in certain size ranges. The heating curves are more gradual and almost unimodal, indicating a pore size distribution of the same nature. Some details of the curves in Figure 3 differ from the previous results. Based on numerous experiments it is clear that the details of the freezing response of virgin cement pastes are quite sensitive to minor variations in w/c ratio, degree of hydration, and probably other variables. However, the main features, including the amount of "non-frozen" water at -55° C, W_{nf} (-55), change in a very consistent manner with the main structural parameters of cement pastes.

The influence of curing time on pore structure development is shown in Figure 4, (6). After one day of curing almost all the ice forms right after nucleation, indicating few small pores. However, even in this young specimen W_{nf} (-55) is about 30% of the evaporable water. The high values of W_{nf} (-55) for cement pastes (see also Figure 1) are indications of the extreme fineness of the hydration products, whether this water is surface adsorbed, interlayer or gel water. Based on the calorimetric results the evaporable water may be divided into the categories "non-frozen" and "frozen". The cooling and heating curves both give information on the size distribution of the pores containing the latter type of water. These categories of water appear analogous to the traditional "gel" and "capillary" types proposed by Powers. The quantitative relationship between the two descriptions will be given in a future publication.

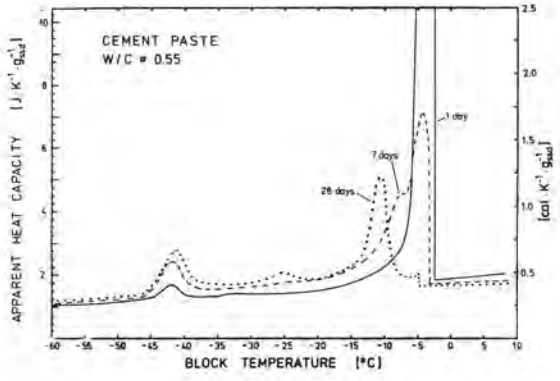

Age	W_n	W_{es}	W_f (-55)	W_{nf} (-55)
1	.09	.434	.311	.123
7	.15	.372	.197	.175
28	.18	.350	.149	.201

W_n = non-evaporable water ($g/g_{ign.}$)
Units g/g_{dry}. Symbols: see Figure 3.

Figure 4. Heat flow during cooling for water saturated cement pastes. 3,3° C/hr.

The curing temperature is known to have a significant influence on the pore structure of cement pastes. That this influence is large is illustrated by the calorimetric data given in Figure 5 for pastes cured at 22° C and 97° C.

The influence of $CaCl_2$ used as an admixture to cement is illustrated in Figure 6. The total frozen and non-frozen water contents are not very different for the two specimens, but the freezing generally takes place at lower temperatures in the specimen mixed with $CaCl_2$. Length change data during cooling for companion specimens are included in Figure 6, to illustrate the qualitative correspondence between calorimetric and dilatometric freezing behavior. Other

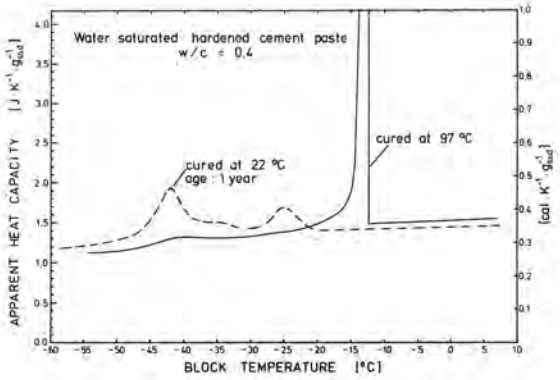

°C	W_n	W_{es}	W_f (-55)	W_{nf} (-55)
22	.18	.235	.157	.078
97	.21	.213	.030	.183

Symbols: see Figures 3 and 4.

Figure 5. Heat flow during cooling for water saturated cement pastes cured at 22° C and 97° C. AgI not used. 3.3° C/hr.

types of experiments have also indicated that cement pastes mixed with $CaCl_2$ obtain finer pore structures (7).

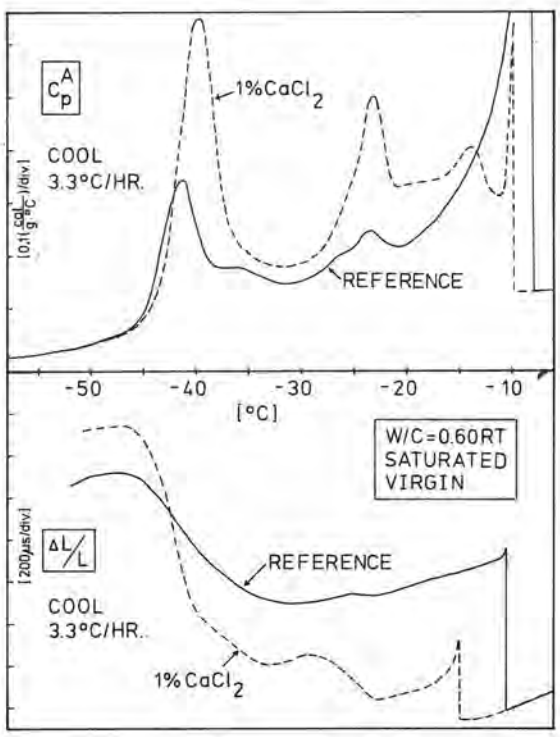

	Age	W_n	W_{es}	W_f (-55)	W_{nf} (-55)
Ref.	488	.21	.391	.190	.201
$CaCl_2$	50	.20	.405	.191	.214

Symbols: see Figures 3 and 4.

Figure 6. Heat flow (top) and length change (bottom) for water saturated cement pastes made with and without $CaCl_2$. No AgI used.

The "instability" of the pore structure in the virgin cement paste is shown in Figure 7. Two heat flow curves are shown in the figure; one for a virgin specimen (the curve is also shown in Figure 1), and one for a companion specimen slowly dried to 58% relative humidity over a period of one year and then resaturated. Two major changes are caused by the drying-resaturation treatment: 1) W_{nf} (-55° C) is decreased, i.e. more water is frozen, and 2) most of the frozen water freezes right after nucleation. The magnitude of these effects depend primarily on the drying time as long as drying takes place below about 60% relative humidity. More results will be published in the near future.

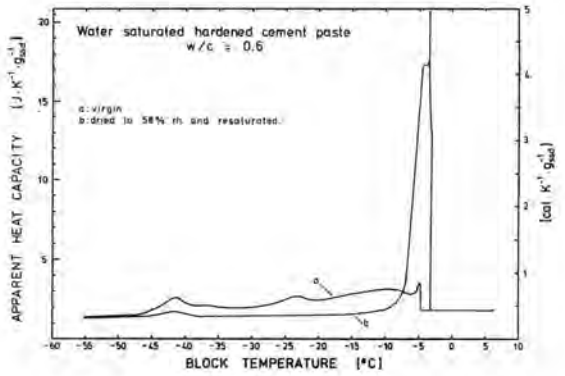

	W_{es}	W_f (-10)	W_f (-55)	W_{nf} (-55)
a	.379	.029	.184	.195
b	.378	.195	.219	.159

Symbols: see Figures 3 and 4.

Figure 7. Heat flow during cooling for a mature virgin and water saturated cement paste (a), and a companion specimen slowly dried to a water content of 0.148 g/g_{dry} at 58% relative humidity before resaturation (b). Cool 3.3° C/hr.

An example of the relationship between cumulative pore size distributions derived from calorimetric (CAL) and mercury penetration (MIP) tests is shown in Figure 8. All tests were made on companion samples of mature cement mortar. The MIP specimens were dried at 92.5° C in the standard manner, as were the resaturated CAL specimen before resaturation. The CAL curves were calculated assuming that the solid-liquid interface controls the freezing-melting process, see Figure 1. The curves are only calculated up to about -5° C. Above this temperature the rate of heat flow is too high during both cool and heat at our standard rates to treat the curves as equilibrium curves. We have not yet carried out calorimetric runs sufficiently slowly to allow calculation of distribution curves above -5° C, but it is quite possible to do so.

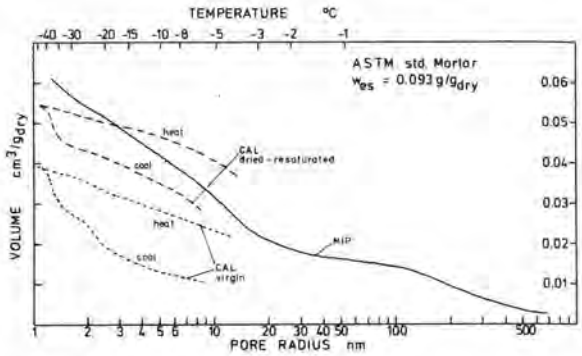

Figure 8. Cumulative pore size distribution curves for cement mortar calculated from mercury intrusion (MIP) and low temperature calorimetry (CAL). The mortar is mature and has a w/c ratio of 0.50. The evaporable water content was the same for all three specimens and equal to 0.093 g/g_{dry}. See text for further details.

Figure 8 shows that there is much better agreement between MIP and CAL curves when the comparison is made for specimens treated the same way; a natural consequence of the drying-resaturation effect.

The cool-heat hysteresis is reduced by the drying-resaturation treatment, but it is still substantial. We have other experimental evidence showing that long-time drying reduces the hysteresis much further, suggesting that the "necks" are eliminated and thereby the continuity in the pore system increased.

References

(1) le Sage de Fontenay, Carl, and Sellevold, E.J., "Ice Formation in Hardened Cement Paste - 1. Mature Water Saturated Pastes". Durability of Building Materials and Components, ASTM STP 691, P.J. Sereda and G.G. Litvan, Eds., 1980. Presented in Ottawa, Canada, Aug. 1978.

(2) Bager, D.H., and Sellevold, E.J., "Ice Formation in Hardened Cement Paste - II. Steam Cured Pastes with Variable Moisture Contents". Durability of Building Materials and Components, ASTM STP 691, P.J. Sereda and G.G. Litvan, Eds., 1980. Presented in Ottawa, Canada, Aug. 1978.

(3) Sellevold, E.J., and Bager, D.H., "Some Implications of Calorimetric Ice Formation Results for Frost Resistance Testing of Cement Products". Technical Report 86/80 - Building Materials Laboratory, Technical University of Denmark, 1980. Presented in Vienna, Austria, June 1980.

(4) Defay, R., Prigogine, I., Bellemans, A., and Everett, D.H., "Surface Tension and Adsorption". Longmans, London, 1966.

(5) Everett, D.H., Complementary information to "Capillary properties of some model pore systems with special reference to frost damage" by Everett, D.H., and Haynes, J.M., RILEM, Bulletin No. 27, June 1965.

(6) le Sage de Fontenay, Carl, Unpublished Results, Building Materials Laboratory, Technical University of Denmark, 1979.

(7) Young, J.F., "Effect of calcium chloride on the capillary porosity distribution in tricalcium silicate pastes". Pore structure and properties of materials, RILEM/IUPAC, Prague, 1974.

Sulphate expansion of cement products made with aggregates containing Ca-rich feldspars

Gonflement sous l'action des sulfates des ciments en contact avec des granulats calcaires riches en feldspath

J.H.P. VAN AARDT and S. VISSER, National Building Research Institute, CSIR, Pretoria, South Africa.

SUMMARY : Work undertaken indicates that at 22°C and 40°C, cement products made with sulphate resisting portland cements and aggregates containing Ca-rich feldspars, show expansion in a 5 per cent sodium sulphate solution. There is more expansion at 40°C than at 22°C. The vulnerability to sulphate attack is probably due to the fact that Ca-rich feldspars in the aggregate and the $Ca(OH)_2$ of the cement react to form C_4A-hydrates which in turn form ettringite in the presence of sulphates.

RESUME : L'étude ci-après montre qu'à 22 et 40° les pâtes de ciment faites avec des ciments résistant aux sulfates, et avec des granulats de calcaire riche en feldspath, gonflent lorsqu'elles sont plongées dans une solution de sulfate de soude à 5 %. Le gonflement est plus fort à 40°C qu'à 22°C. Cette vulnérabilité à l'attaque des sulfates est probablement due au fait que les calcaires riches en feldspath et la chaux hydratée du ciment réagissent pour former des hydrates C_4A, qui, à leur tour, donnent de l'ettringite en présence de sulfates.

INTRODUCTION

It has been indicated (1,2) that feldspars react with calcium hydroxide in the presence of water. At 95°C the reaction products are the silica-containing hydrogarnet, hydrated calcium silicates and alkalies. At 39°C the alkali-feldspars produce tetracalcium aluminate hydrates, alkalies and/or calcium alkali silicate hydrates; the calcium-rich feldspars produce substantially more tetracalcium aluminate hydrates. At 22°C small amounts of the tetracalcium aluminate hydrates were detected at early ages (26 days) and substantial amounts at later ages (760 days). The tetracalcium aluminate hydrates thus formed reacted with $CaSO_4$ to form ettringite (3). Recent experiments with aggregates containing a Ca-rich feldspar seem to substantiate that the use, in the presence of sulphates, of such aggregates in mass concrete which is likely to remain continually damp and which is not likely to become carbonated, in the long term might cause distress.

EXPERIMENTAL

The rock called "norite" used in these experiments is a medium coarse grained gabbro, grey in colour, consisting mainly of labradorite and augite ophitically intergrown. The augite shows twinning in seams. The feldspar shows slight sericitization.

The cements that were used, are an ordinary portland cement (OPC) and various sulphate resisting portland cements (SRPC).

The compound composition of the cements and their chemical analysis as well as the chemical analysis of the crushed norite are given in Table I.

The preparation, storage and examination of mortars made are described by van Aardt (4). Where crushed stone was substituted for natural sand the crushed material was screened and recombined to provide the same grading.

The grading of the crushed stone and of the siliceous sand, the various cements used, the curing conditions and other relevant information are given in Table II.

Since sulphate attack of portland cement concretes and mortars is usually accompanied by an expansion the dimensional change of experimental prisms of mortar and concrete were measured during storage in a sulphate solution. The dimensions of the mortar prisms were 25 x 25 x 281.25 mm and those of the concrete prisms 50 x 50 x 280 mm. The results for the mortar prisms are presented in Figures 1 and 2. Figure 3 shows the expansion observed for concrete prisms stored in a 5 per cent Na_2SO_4 solution at 22°C. The prisms were made with a sulphate resisting portland cement, sand and crushed norite as coarse aggregate in the ratio 1:2.53:3.40.

TABLE I

Chemical analysis and phase composition* of cements and chemical analysis of the norite

	Ordinary Portland Cement (OPC)	Sulphate resisting portland cements (SRPC)			Norite (gabbro)
	A	K	S	G	
SiO_2	23.00	21.6	21.23	19.90	50.88
Al_2O_3	5.76	3.16	2.99	4.26	20.13
Fe_2O_3	2.04	6.24	6.25	6.16	7.66
MgO	1.36	1.1	0.99	0.71	7.15
CaO	63.4	63.8	63.51	63.8	10.42
Na_2O	0.04	0.26	0.19	0.26	2.42
K_2O	0.18	0.49	0.40	0.49	0.28
SO_3	1.65	1.75	1.90	1.86	
MnO	0.07		0.08	0.04	
L.O.I.	1.02	0.9	0.67	0.95	0.38
Total	98.52	99.17	98.21	98.51	99.32
C_3S	36.43	60.38	62.71	65.71	
C_2S	38.09	16.39	13.57	16.39	
C_3A	11.81	-	-	0.89	
C_4AF	6.21	18.99	19.02	18.75	

*Calculated using the Bogue formula

TABLE II

Particulars about mortar specimens

Sieve aperture size (μm)	Percentage, by mass, of material retained on individual sieve			
	Experiment 1		Experiment 2	
	Norite	Sand	Norite	Sand
4750	-	-	-	-
2360	1.4	1.4	1.4	1.4
1180	16.4	16.4	16.4	16.4
600	14.0	14.0	14.0	14.0
300	34.0	34.0	34.0	34.0
150	12.8	12.8	12.8	12.8
75	13.6	13.6	20.6	20.6
45	5.0	5.0	-	-
-45	2.0	2.0	-	-
sand/cement	3:1	3:1	3:1	3:1
water/cement	0.60	0.50	0.50	0.45
Curing	All prisms cured at 95% RH and 22°C for 7 days		All prisms cured at 95% RH and 22°C for 28 days	
Aggressive solution and temperature	All prisms kept at 40°C in 5% Na_2SO_4		A set of prisms each kept at 22°C and 40°C in 5% Na_2SO_4	
Cements	K		A, G and S	

DISCUSSION

After it was established that Ca-rich feldspars react with $Ca(OH)_2$ and $CaSO_4$ to give ettringite, experiments with mortar prisms made with aggregate containing these feldspars, were started. In an attempt to rule out the role of C_3A in the cement, sulphate resisting cements (SRPC) were used. Expansion of specimens at 40°C, led to further experiments with various SRPC and ordinary portland cements (OPC) at 22, 40, 50 and 80°C and in 5 per cent sodium sulphate solutions as well as with saturated sodium sulphate solutions.

At 80°C none of the specimens in a solution of 5 per cent Na_2SO_4 showed expansion. This is thought to be due to the fact that the reaction product at this temperature between Ca-rich feldspar and $Ca(OH)_2$ is the silica-bearing hydrogarnet which shows resistance to sulphate attack (5). The hydrated products of cement are also different from those formed at 22°C. This aspect has been discussed in literature (6). The results obtained were therefore to be expected.

At 40°C the specimens made with norite and SRPC showed a marked expansion. Those made with OPC of course showed more severe expansion than those made with sand and OPC. Specimens made with sand and SRPC showed no expansion, see Figures 1, 2(a) and 2(b).

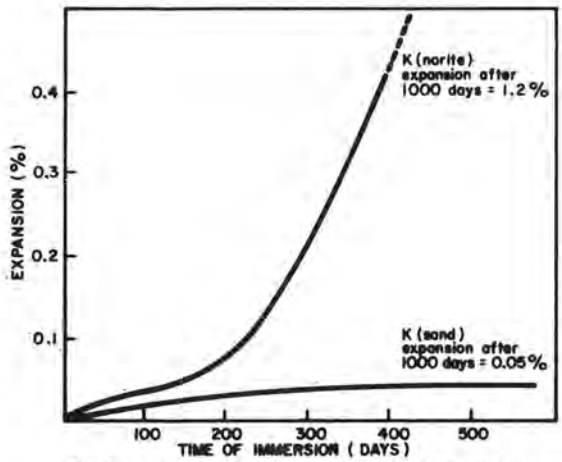

FIG. 1: Expansion at 40 °C in 5 % Na_2SO_4 of prisms made with crushed norite fine aggregate and SRPC : K.

At 22°C the specimens made with norite and SRPC and also those made with sand and SRPC showed little or no expansion after 300 days. However, this exposure time appears to be too short for the prisms made with norite to show expansion because a concrete specimen made with norite (coarse aggregate) and a SRPC showed an expansion of 0.2 per cent after 1000 days at 22°C, see Figure 3.

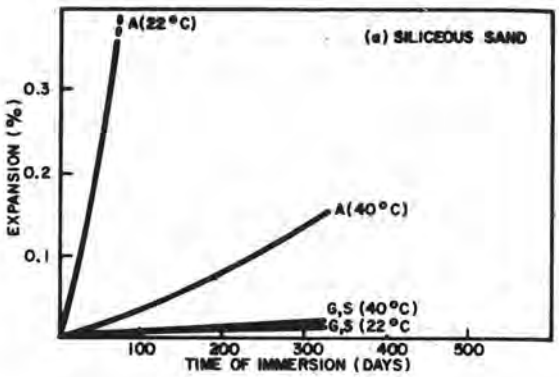

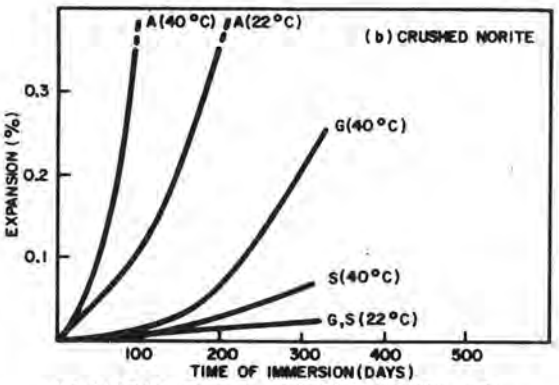

FIG. 2(a)&(b): Expansion at 22°C and 40°C in 5% Na_2SO_4 of prisms made with OPC: A and SRPC: G and S.
(a) Siliceous sand and (b) crushed norite fine aggregate

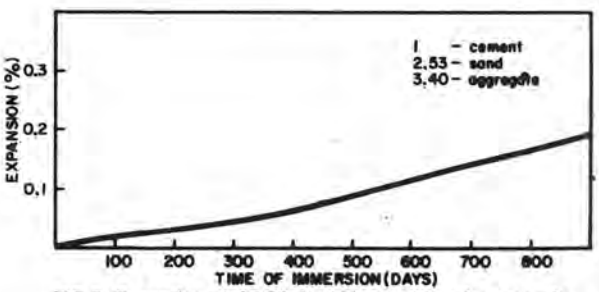

FIG. 3: Expansion at 22 °C in 5 % Na_2SO_4 of a concrete prism made with norite coarse aggregate, sand and a sulphate resisting portland cement.

The specimens made with OPC and sand expanded less at 40°C than at 22°C. This observation has also been discussed in the literature (6). However, specimens made with norite and OPC expanded more at 40°C than at 22°C. It is concluded that a rise in temperature favours the reaction between the Ca-rich feldspar and $Ca(OH)_2$ to produce the C_4A-hydrates in such quantities that with the addition of sulphate, large amounts of ettringite is formed thus causing distress.

Specimens made with norite and OPC which were stored at 50°C in a saturated sodium sulphate solution expanded excessively, and disintegrated completely after 500 days. Large quantities of ettringite were detected. Specimens made with norite and SRPC showed similar expansion curves as were obtained for specimens stored at 40°C in 5 per cent Na_2SO_4. Specimens which were made with sand and either OPC or SRPC showed little expansion in the saturated sodium sulphate solution.

It is interesting to note that the specimens made with norite and SRPC expanded as much as 1.2 per cent in 1000 days without disintegrating although cracks were clearly visible. Normally if mortar specimens made with sand and an OPC with a high C_3A content expand, the expansion is usually accompanied by some localized disruptive cracks while the rest of the specimen still appears to be sound. It appears that in the case of norite mortar the expansion is more general around the grains causing the whole body to expand while in the case of a high C_3A-OPC cement and sand the expansion is more disruptive at localized cracks.

This leads to the thought that exposed surfaces i.e. surface areas play an important role in the reaction between aggregate and the available $Ca(OH)_2$ from the cement and sulphate from an external source. Of course substantial quantities of C_4A-hydrates had been observed after 760 days in slurry mixtures of powdered anorthite and $Ca(OH)_2$ stored at 22°C. See Figure 4.

REFERENCES

1.- J.H.P. VAN AARDT and S. VISSER (1977), "Formation of hydrogarnets : calcium hydroxide attack on clays and feldspars", Cement and Concrete Research, 7, pp.39-44.

2.- J.H.P. VAN AARDT and S. VISSER (1977), "Calcium hydroxide attack on feldspars and clays : possible relevance to cement-aggregate reactions", 7, pp.643-648.

3.- J.H.P. VAN AARDT and S. VISSER (1978), "Reaction of $Ca(OH)_2$ and of $Ca(OH)_2$ + $CaSO_4.2H_2O$ at various temperatures with feldspars in aggregates used for concrete making", 8, pp.677-682.

4.- J.H.P. VAN AARDT (1955), "The resistance of concrete and mortar to chemical attack. Progress report on concrete corrosion studies". Bulletin 13, National Building Research Institute, Pretoria. CSIR 115, pp.44-60.

5.- B. MARCHESE, G. MASCOLO and R. SERSALE (1972), "Relation of composition of hydrogarnet to resistance to sulfate attack", J. Am. Cer. Soc., 55, pp.146-148.

6.- J.D. RICHARDS (1965), "The effect of various sulphate solutions on the strength and other properties of cement mortars at temperatures up to 80°C", Magazine of Concrete Research, 17, pp.69-76.

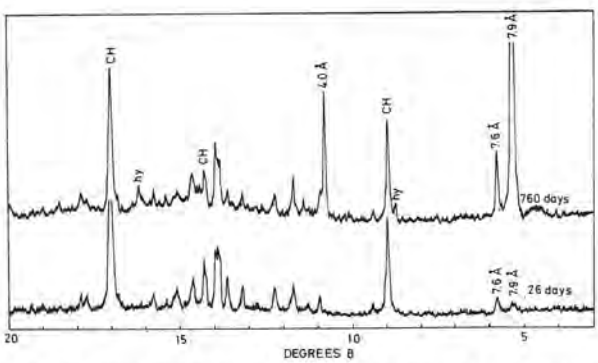

FIG. 4: XRD traces for a mixture of $Ca(OH)_2$ and powdered anorthite stored at 22°C in water.
CH - $Ca(OH)_2$; hy - hydrogarnet
7.9Å and 7.6Å - C_4A - hydrates

THEME VII

Microtexture et résistance mécanique du ciment durci

Microtexture and mechanical resistance of hardened cement

CHTCHOUROV A.F., Docteur ès Sciences Techniques à l'Université de Gorki, U.R.S.S.

RESUME : A l'heure actuelle il n'existe pas de théorie physique de la déformation et de la destruction du ciment durci. L'une des causes principales qui empêche la construction des modèles physiques de la microtexture réside dans le fait que les données expérimentales absolument sûres pour le domaine de 10 à 1000 Å constituant le maillon intermédiaire entre la structure christallochimique et la microstructure font malheuresement défaut. Le domaine des hétérogénéités (particules et pores) des produits hydratés des minéraux de ciment inférieur à 1000Å reste pratiquement inexploré et fait l'objet des discussions. En outre la clarté sur les mécanismes de la destruction et leur relation avec la texture à l'échelle microscopique n'est pas encore faite.

Les techniques physiques d'analyse telles que la diffraction et diffusion centrale des rayons X, la microscopie électronique et la porosimétrie à mercure, des éprouvettes hydratées dans les différentes conditions ont permis d'obtenir les donnés statistiques sur la microtexture et la microporosité de la pâte durci correspondant aux silicates hydratés et à un ciment Portland.

De nombreuses études, par émission acoustique et par fractographie électronique sur la fissuration des éprouvettes de pâte et de beton sous l'action de contraintes mécaniques, ont montré le rôle joué par la microtexture et ont permis de déduire la dépendance entre la résistance mécanique et des caractéristiques statistiques de texture de la pâte hydratée.

SUMMARY : The field of heterogeneties (particles and pores) of the cement minerals hydration products less than 1000 Å is practically not investigated and considered to be the subject of discussion. Besides, the destruction mechanism and its relationship with the texture on the microscopic level are not clear.

Physical analysis methods, such as diffruction and central diffusion of X-rays, electronic microscopy and mercury porosimetry, and also specimen, hydrated under different conditions made it possible to get statistic data about the microtexture and microporosity of hardened paste, that correspond to hydrated silicates and Portland cement.

Numerons investigations, with the help of acoustic emission and electronic fractography, of cracks formation in paste and concrete specimen under the influence of mechanic stresses, showed the role of microtexture and allowed to state the mechanic resistance dependence on statistic structural characteristics of hydrated paste.

Nous proposons dans le présent rapport de présenter les résultats de l'analyse de la microtexture du ciment durci et de montrer l'interdépendance des caractéristiques structurales et de la résistance. Pour l'étude des systèmes monophasés les principaux minéraux de ciment et leurs mélanges avec du sable quartzeux moulu ont été sélectionnés comme matériaux d'origine. La modification du rapport c/s, de même que des conditions du durcissement par autoclave a permis d'obtenir des structures presque monophasées de différente composition.

Pour l'examen de la pierre de ciment Portland nous avons fait appel à des ciments industriels. La modification de la texture a été réalisé dans une large plage des valeurs E/C, par l'emploi des additions chimiques et le changement des conditions de température et d'humidité du durcissement. Nous avons choisi pour notre travail les additions chimiques qui sont bien connues pour leur pouvoir modificateur le plus efficace: AC 1%Na_2SO_4+1%CH_3COONa +0,2%CDB et NNC 1,5%$Ca(NO_3)_2$ + 1,5% $Ca(NaO_2)_2$. L'analyse complexe de la microtexture a englobé les méthodes suivantes: diffractométrie des rayons X (DRX), adsorbtion de l'azote à basse température (BET), porosimétrie à mercure (PM) et microscopie électronique ME La submicrotexture a été explorée par la diffusion centrale des rayons X (DCRX). Afin d'obtenir les caractéristiques statistiques une méthode des cordes a été développé et mis en pratique au moyen d'une calculatrice électronique (1 - 3).

En ce qui concerne le mécanisme de l'hydratation de départ des minéraux de ciment, il avait été exposé dans le travail de l'auteur(4). En vue de présenter de façon précise le modèle de formation du ciment durci nous avons mesuré les dimensions moyennes des cristallistes et des degrès d'hydratation aux étapes diverses du durcissement. La periodicité du mécanisme de l'hydratation, liée à la formation des textures primaires sur la surface des particules, s'est observée par la méthode électrochimique dans des conditions des rapports élevés E/C (jusqu'à 80), le pH de la solution étant en variation (S).

Ces données mettent en évidence que la croissance du cristallite élémentaire se fait directement sur la surface du grain de ciment à partir d'un centre actif; dans beaucoup de cas on peut observer les textures dans lesquelles certains cristaux élémentaires se dirigent radialement vers le centre.

Les données DCRX (tableau I) décelent que les éléments texturaux primaires sont des microcristallites aux dimensions de 20 à 60Å de section et de 100 à 600Å de longueur. Un tel cristallite, croissant depuis le centre actif et ayant atteint une certaine longueur, peut être adsorbé par la surface d'un autre grain ou bien se heurter et se souder avec un autre cristal élémentaire. L'apparition des ces actes engendre la formation par contact entraînant la croissance d'origine du module élastique.

Dès que le paquet de cristallites primaires s'opposera à la naissance des nouvelles mailles de la chaîne, les forces élastiques des chaînes en croissance le chasseront de la surface du grain. Par la suite il peut migrer dans l'espace poreux. Dans l'ensemble ce phénomène apparaît comme la désagrégation de la couche d'origine du silicate - hydraté bas moléculaire (de haute base). Si les cristaux du silicate hydraté se trouvent dans la solution ils se transforment en textures surmoléculaires secondaires. De tels pseudocristallites agrégés sont étalés aux stades avancés de 10^3 à 10^4Å et sont bien vus sur les photos DCRX.

Par suite du durcissement prolongé à haute température des mélanges on voit apparaitre la recristallisation qui fait naître des hydrates dont la microtexture est fonction de la composition, de la température et du temps. Dans le présent travail nous avons exploré les textures surmoléculaires et la

résistance de certains silicates hydratés du calcium et du ciment durci Portland (tableau I).

La diffusion centrale des rayons X est une méthode qui a de bonnes perspectives d'avenir pour l'examen de la texture à fine porosité du gel de ciment et qui permet ensemble avec les méthodes ME et PM d'obtenir l'assortiment le plus complet de caractéristiques structurales statistiques.

les courbes p(l) avec des maximums dans le domaine de 10 à 12 Å et les tailles des cristallites aux environs de 50 à 60 Å correspondent aux silicates hydratés mal cristallisés de type C-S-H dont les diffractogrammes sont démunis de pics sélectifs. En d'autres termes, dès que les couches élémentaires, parallèles à (001) deviennent ordonnées, la part des cordes de longueur de moins de 15 Å diminue fortement dans la

Tableau I

Caractéristiques des textures surmoléculaires

Phases formatrices de texture	Indices intégraux		Texture surmoléculaire primaire		Texture surmoléculaire secondaire		Défauts technologiques
	porosité P, %	surface spécifique S, m^2/g	taille moyenne pores l, m 10^{10}	taille moyenne cristallites t, m 10^{10}	taille moyenne pores l_m, m 10^6	taille moyenne cristallites t_m, m 10^6	d, m 10^6
		1. Silicates hydratés					
C - S - H(P)	37	120	114	138	0,03	3,50	
C - S - H(1)	45	320	47	63	0,02	0,64	
Tobermorite 11A	46	66	150	250	0,05	2,50	depuis
α-hydrate C_2S	45	33	270	430	0,07	5,00	10
silicate hydrate C_3SH_2	42	29	315	530	0,12	5,20	jusqu'à 10^3
Girolite	50	29	382	575	0,08	6,00	
		2. Produits hydratés du ciment Portland					
Gel C - S - H	24	160	55	105	0,04	1,50	
	25	114	74	300	0,07	3,60	depuis
Portlandite	23	280	28	60	0,04	0,70	10
Ettringite	24	119	63	140	0,05	2,1	jusqu'à
	22	480	14	35	0,03	0,5	10^3
	24	70	118	240	0,05	3,2	

L'examen en commun des images de diffraction des rayons X des silicates hydratés de type tobermorite (fig.1b) et des courbes de distribution des cordes p(l) (fig.1c) révèle qu'elles sont étroitement liées ce qui réside dans le fait qu'elles reflètent l'état dispersif du système. Les distributions p(l) avec des maximums dans le domaine des pores de grandes tailles et les gros cristallites (tobermorite 11Å) correspondent aux cristallahydrates parfaits, tandis que

distribution p(l); et vice versa, le maximum est deplacé vers le domaine de 10 à 12 Å lorsque la structure périodique se détériore. De là découle que les cordes, définies par la méthode DCRX, sont des segments de droite, situés entre les faces de vrais cristallites qui sont composés, eux-même, de couches élémentaires parfaitement paquetées. L'évacuation de l'eau de coordination conduit à un réarrangement de la microtexture, à la formation de pores de

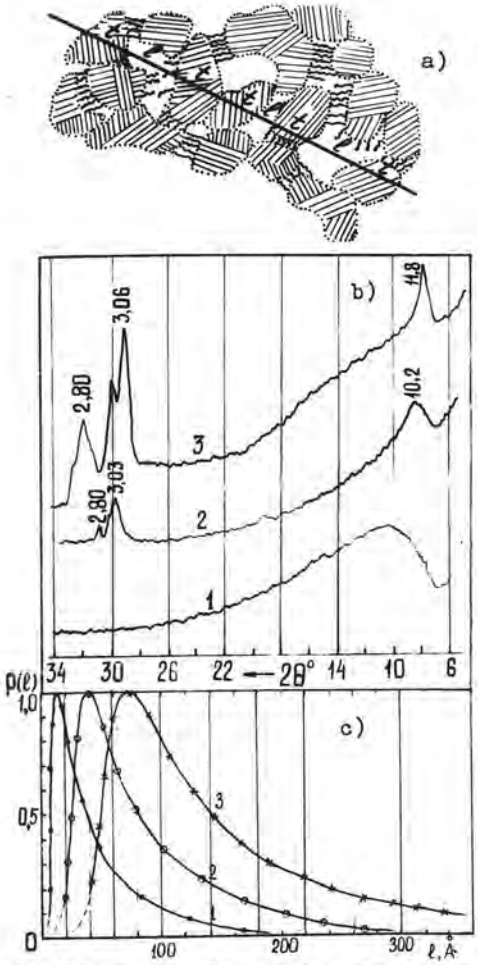

Fig.1.-Alternance des cordes l et t du modèle de la microtexture (a), enregistrement diffractomètrique (b), courbes de distribution des cordes d'après la longueur dans l'espace poreux (c): 1 et 2 - silicates hydratés semi-cristallins C-S-H(II) et C-S-H (I) respectivement; 3 - tobermorite 11 Å.

plus grande taille, de même qu'aux résultats appropriés sur les diagrammes des rayons X à petits angles. Certains éléments structuraux de grande taille, explorés dans les textures C-S-H avec la microscopie électronique, sont généralement des cristaux imparfaits, de faux cristallites, c-à-d des agrégats (paquets, etc) de petits cristallites primaires entre lesquels il y a des espaces intercristallins. De tels pores sont exclusivement décelés par la méthode DCRX. La nature des courbes de distribution des longueurs de cordes dans l'espace poreux du gel de ciment varie de façon notable en fonction des conditions de durcissement et de la présence des additions chimiques. La hausse de la température de durcissement déclenche la croissance des pores de la taille moyenne et des cristallites du gel. L'usage des additions rend impossible la croissance de gros cristallites primaires et favorise la formation d'une texture bien ordonnée lors du traitement de température et d'humidité du ciment durci.

L'analyse des données de distribution des pores et des cristallites d'après leur taille a montré que chaque rang de texture surmoléculaire est doté d'une porosité particulière, c-à-d il a son rang de pores. Les textures du ciment durci, examinées lors du travail, comportent principalement deux rangs de textures surmoléculaires et trois rangs de pores: a) le rang nul de pores (i=0) est limité par la taille des cristallites primaires ($l \leqslant t$); b) le premier rang de pores (i=1) est limité par la taille des textures surmoléculaires primaires et secondaires ($t < l \leqslant t_m$); c) le second rang de pores (i=2) n'est pas directement lié aux textures surmoléculaires et est déterminé par les facteurs technologiques ($l > t_m$).

Les variations des rapports entre les volumes des pores de gel et capillaires, qui s'observent lors du changement des conditions de durcissement, sont dues au réarrangement des textures surmoléculaires. La taille de seuil, observée dans la distribution des pores d'après la taille dans le ciment durci (6), dépend de celle des textures surmoléculaires secondaires.

L'observation du micromécanisme de la destruction, faite à l'aide de la fractographie électronique et de l'émission acoustique, a permis d'établir le rôle que des éléments structuraux jouent dans la désagrégation du ciment durci. La naissance et la croissance des fissures de cisaillement au sein de la texture cristalline constituent le micromécа-

nisme essentiel à l'échelle cristallographique. Le travail, indispensable à la formation du relief de fissure sous forme de degrès et aux déformations plastiques locales apporte la contribution la plus importante à l'énergie efficace des destructions (γ^*) (tableau II). L'influence de la taille des textures secondaires sur la résistance à la compression peut être exprimée par le critère modifié Griffith-Orowan:

$$R_c = K_c t_m^{-1/2}(1 - p)^n,$$

où P - porosité, $K_c = (E\cdot\gamma^*)^{1/2}$ - coefficient d'adhérence, t_m - taille maximale des formations surmoléculaires secondaires, n - a des valeurs de 2,5 à 4,5.

Tableau II

Valeurs des coefficients d'adhérance K_c et de l'énergie efficace de destruction

Ciment durci	E/C	Durcissement normal 28 j.		Vaporisage à 80° C 3-6-10 heures	
		$K_c N/m^{3/2} 10^4$	$\gamma^* J/m^2$	$K_c, N/m^{3/2} 10^4$	$\gamma^*, J/m^2$
sans additions	0,25			45,0	3,05
	0,30	45,5	4,2	40,0	2,90
	0,35	37,6	3,2	30,7	2,10
	0,40	-	-	23,6	1,70
AC	0,30	43,2	3,8	45,3	3,80
	0,35	-	-	37,9	3,20
NNC	0,30	12,7	3,5	48,9	4,35
	0,35	-	-	39,4	3,70

A la différence de la fissure de compression celle de traction, qui apparaît sur le contour d'un gros défaut, se développe de façon instable dans le plan normal à la direction de la force appliquée tout en divisant presque intantanément l'échantillion en fragments. Aussi la résistance à la traction du ciment durci est-elle contrôlée par la taille du défaut le plus dangereux (d) du point de vue de son pouvoir générateur de ruptures et déterminée par la formule:

$$R_p = K_c d^{-1/2}$$

Le modèle mathématique constitue un élément inséparable des essais de matériaux sans lequel il est impossible de planifier l'expérience technologique quelle que soit sa nature. Le rôle de la texture poreuse dans la destruction a été profondément étudié dans le cadre de la mécanique de la destruction fragile, se basant sur le modèle du solide poreux fissuré, proposé par Panassuk V.V. et développé par Goldchtein P.V. et autres. Le modèle tient compte de l'interaction de toutes les fissures considérées qui atteignent le contour des pores voisins. Le modèle généralisé comprend la notion de rangs de pores: le rang nul n'a presque aucune influence sur la résistance; le premier rang est déterioré par suite de la fusion des pores de rang supérieur des champs locaux de surcharge; le second rang conditionne la naissance et la croissance des fissures instables.

La valeur limite de l'effort de compression q est déterminée par la condition où la composante de contraintes σ_y (l'effort de traction sur l'axe aux environs du pore), normale à la surface de fissure, satisfait à l'expression asymtotique:

$$\lim_{a > x \to 0} \sqrt{|x - a|}\,\sigma_y = \frac{K_c}{\sqrt{\pi}}$$

Le critère de la destruction locale pour les fissures de rupture normale $K = K_c$ permet d'établir la dépendance de la charge limite q_c de la longueur de la fissure.

En vue de calculer les charges critiques de compression et celles de traction pour les paramètres différents de texture poreuse nous avons mis au point un algorithme et un programme pour la calculatrice électronique. Les résultats des calculs de la charge limite réduite $q_c\sqrt{\pi}\sqrt{r}/K_c$ en fonction de la longueur réduite de la fissure interne l_1/r sont représentés à la fig. 2a.

Le modèle mathématique de la micromécanique destructive du silicate poreux permet de faire des estimations quantitatives des points paramétriques de la destruction avec l'application des caractéristiques de la microtexture poreuse. En outre, le modèle permet de réveler les régularités importantes du comportement d'un matériau cassant

poreux sous charge en fonction de sa texture réelle.

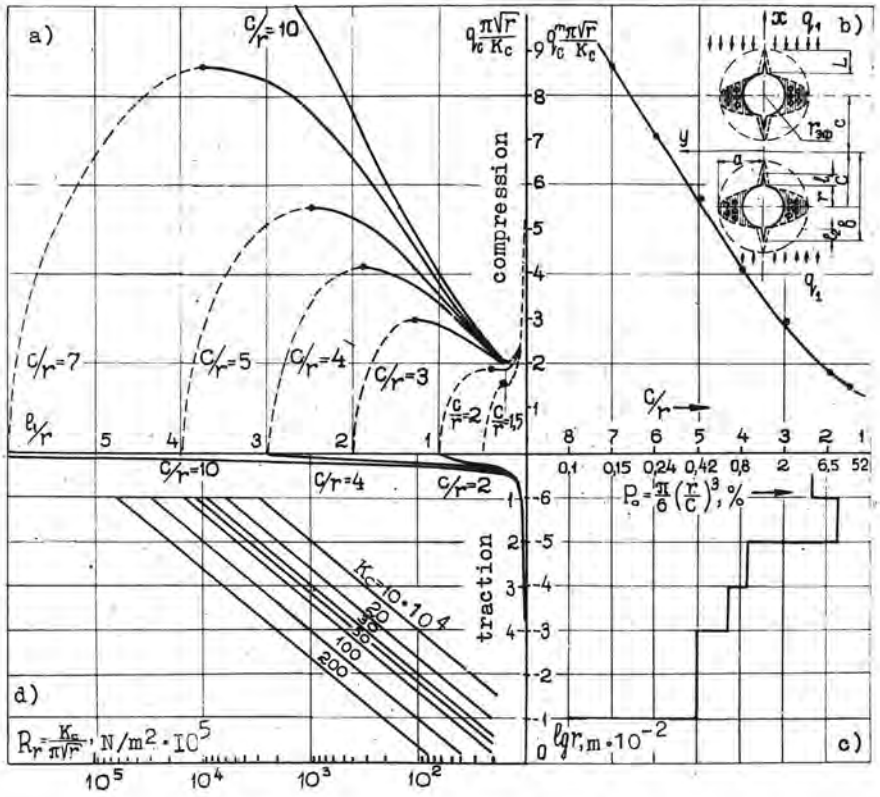

Fig. 2. Graphiques pour le modelage de la destruction du matériau poreux: a - interdépendances de la longueur de la fissure et de la charge; a - modèle du solide poreux et relation des charges maximales aux porosités partielles; c - distribution des porosités partielles suivant les rayons; d - dépendance du paramètre de résistance R_r du rayon des pores et du module d'adhérance.

1. La destruction globale instable du matériau poreux à la compression simple est due à la naissance des fissures magistrales, donnée par la fusion des pores séparés. La contrainte critique, qui assure la fusion des pores, dépend fortement de la porosité (fig.2) ce qui indique d'emblée le sens physique de la relation empirique bien connue "résistance-porosité"(7).

2. La valeur de la contrainte limite de traction est déterminée par la longueur des fissures d'origine paraissant sur le contour des pores, et dépend de la porosité faiblement. Des graphiques fig. 2a, vient que l'augmentation de la porosité fait accroître le rapport R_c/R_p ce qui est prouvé par l'expérience.

Les deux premières conséquences mettent en évidence que les microfissures technologiques de retrait et d'autres réduisent de façon importante la tenue à la traction et sont presque négligeables pour la tenue à la compression.

3. La fusion des pores de rang inférieur des matériaux poreux aux rangs multiples ayant lieu aux endroits de concentration des contraintes (aux environs des pores de rang supérieur) n'entraîne pas de destruction globale, mais diminue la contrainte critique ce qui donne naissance aux fissures magistrales dans les pores de rang supérieur.

Le rôle primordial de la porosité capillaire et du diamètre de seuil dans la résistance du ciment durci, établi expérimentalement dans le travail (8), consiste en ce que les pores capillaires adhèrent, à partir du diamètre de seuil, au système de gros pores bulleux tout en formant avec ceux-ci une texture de destruction autoentretenue à rangs multiples.

4. Les pores et les microfissures qui ne quittent pas les formations surmoléculaires secondaires (pour le ciment durci ce sont les pores de gel ou ceux de rang zéro) ont influence faiblement sur la résistance du ciment durci ce qui est dû au fait que leur croissance est stoppée par la texture cristalline du matériau.

5. Le module d'adhérance est généralement déterminé par les paramètres cristallochimiques et les caractéristiques de la microtexture.

Dans notre travail la vérification expérimentale des régularités principales, resultant du modèle physique de la destruction a été réalisée sur un grand nombre de silicates poreux à nature différente de la liaison chimique.

BIBLIOGRAPHIE

1.- J. Mering, D. Tchoubar (1968) "Interprétation de la diffusion centrale des rayons X par les systèmes poreux", I-J. Appl. Cryst. Vol.1 Part.3, 153-165.

2.- D.R. Lachaud (1973) "Microtexture du ciment durci Données de la diffusion centrale des rayons X de 1 jour à 6 mois d'age", Revue des Matériaux, n°681, 4-10.

3.- A.F.Chtchourov, T.A. Erchova, V.R. Kalinin (1976) - "Calcul par MEC des caractéristiques de texture à base des données de la diffusion centrale des rayons X", Crystallography, Vol.21, n°4, 688-695.

4.-A.F. Chtchourov, M.A. Sorotchkine, T.A. Erchova (1978) "Modèles physiques du durcissement initial des liants", 6-e Congres international de la chimie du ciment, Vol.2, 76-80.

5.- M.A. Sorotchkine, M.B. Linkinde, A.F. Chtchourov (1978)-"Périodicité des mécanismes de l'hydratation du ciment", J.Chim. Vol.51, n°6, 1205-1207.

6.- S. Diamoud (1971) "A critical comparaision of porosimetry and capillary condensation por size distributions of portland ciment paste", Cem. and Corcr. Res., Vol.1, 531-546.

7.- D.M. Roy, G.R. Gouda (1973) "High strength Generation in Cement Pastes", Cem. and Concr. Res. Vol.3, n°6,807-820.

8.- H.G. Smolthik, H. Romberg (1976) - "Discussion" 6-e Congr.Int. de la Chem.des Cim. Vol.2, 343-344.

SEMINAIRES

SEMINAIRE A

Rôle du C_3A sous toutes ses formes dans l'hydratation des ciments et leur attaque par les sulfates

Président : Mme REGOURD (France)

Les 27 communications présentées par 52 auteurs au Séminaire sur l'aluminate tricalcique ont été réparties dans cinq grands thèmes :

Thème 1 : Polymorphisme de C_3A et de ses solutions solides.
Rapporteur Général : Miss A.E. MOORE - Grande-Bretagne.

Thème 2 : Hydratation de C_3A.
Rapporteur Général : Prof. H.N. STEIN - Pays-Bas.

Thème 3 : Hydratation de C_3A dans les ciments.
Rapporteur Général : Prof. U. LUDWIG - République Fédérale d'Allemagne.

Thème 4 : Hydratation de C_3A en présence d'adjuvants.
Rapporteur Général : Dr V.S. RAMACHANDRAN - Canada.

Thème 5 : Rôle de C_3A dans l'attaque des ciments par les sulfates.
Rapporteur Général : Prof. P.K. MEHTA - Etats-Unis d'Amérique.

Le 30 juin 1980, chaque rapporteur général a d'abord exposé les principaux résultats apparus dans les communications. Certains de ces résultats ont suscité de vives discussions.

Parmi les données nouvelles figurent :

1 - L'existence, dans la série des solutions solides $C_3A + Na_2O$, de quatre structures cristallines : deux cubiques C_I et C_{II}, une orthorhombique O et une monoclinique M. La forme de haute température des variétés O et M est orthorhombique. Cette forme, stabilisée à la température ambiante par trempe rapide, n'est que pseudo-tétragonale.

2 - Le rôle de Na_2O, retardateur dans l'hydratation des systèmes $C_3A + H_2O$, accélérateur aux tous premiers instants dans l'hydratation des systèmes $C_3A + H_2O$ + gypse, par passage rapide en solution des ions SO_4^{2-}, Na^+, Al^{3+}.

3 - L'interaction $C_3A - C_3S$ au cours de l'hydratation de mélanges synthétiques et de ciments industriels (formation de silico-aluminates, adsorption d'ions SO_3 sur le C-S-H, développement des résistances mécaniques).

4 - L'interprétation de la fausse prise par une modification de la morphologie des hydrates.

5 - L'action des adjuvants retardateurs sur la cristallisation de l'ettringite et la conversion $C_4AH_{13} \rightarrow C_3AH_6$.

6 - L'apparition à la surface des grains de C_3A, en présence d'adjuvants, de charges électriques qui, répulsives, accroissent la fluidité des pâtes.

7 - L'influence de la concentration d'un adjuvant sur son action accélératrice ou retardatrice de l'hydratation de C_3A dans les mélanges $C_3A + H_2O$, $C_3A + C_3S + H_2O$, ciment + eau.

8 - L'amélioration de la liaison pâte de ciment-granulat calcaire par formation de carboaluminates.

Les points qui n'ont pas été élucidés et qui demandent une étude ultérieure approfondie concernent :

1 - L'existence de la solution solide NC_8A_3 (7,6 % Na_2O).

D'une part NC_8A_3 a été observé en microscopie optique en lumière réfléchie, grâce au maclage de ses grains. D'autre part, NC_8A_3 n'a pu être synthétisé qu'en présence de SiO_2. Dans la série $C_3A - Na_2O$, la limite de solubilité de Na_2O est atteinte à 5,9 % Na_2O quand les sites vacants du réseau cristallin de C_3A sont occupés à 75 % par les atomes de Na.

2 - La congruence de la dissolution de C_3A.

D'après l'analyse de la phase liquide, la composition de l'hydrate couvrant les grains de C_3A dans le système $C_3A + H_2O$ correspond au rapport $C/A = 3$. Ce même rapport est différent de 3 d'après les mesures du potentiel Zêta. Il semble que les concentrations locales au niveau des grains de C_3A soient différentes de celles éloignées des grains anhydres. Ces différences doivent agir que la diffusion des ions en solution, la vitesse d'hydratation de C_3A, la cristallisation des hydrates, l'interaction mutuelle entre les cristaux hydratés dans la forme aqueuse.

3 - La formation de l'ettringite.

L'ettringite est soit amorphe, soit cristallisée. Elle est supposée se former à partir de la solution ou topotactiquement.

4 - L'influence des adjuvants retardateurs sur la cristallisation des hydrates.

Les complexes que forment les adjuvants sont-ils chimisorbés ou formés par l'intermédiaire de la solution puis précipités sur les cristaux de C_3A ?

5 - L'influence de la forme cristalline de C_3A sur la résistance des ciments aux eaux sulfatées.

D'après les études sur des systèmes simplifiés, (mélanges synthétiques et ciments de composition très proche), il peut apparaître que le type de C_3A affecte la vitesse de l'attaque d'un ciment par une solution sulfatée (Na_2SO_4 ou $MgSO_4$) mais aucune conclusion n'a pu être tirée quant à l'influence de la forme cristalline de C_3A sur la résistance à l'action de Na_2SO_4 de 26 ciments portland industriels. L'hypothèse selon laquelle la porosité et la perméabilité des pâtes de ciment contenant C_3A cubique (plus réactif) réduisent l'attaque des sulfates, est à vérifier.

6 - Le mécanisme de l'expansion des pâtes de ciment dans les solutions sulfatées.

L'expansion est attribuée soit à la formation de gypse secondaire par dissolution de $Ca(OH)_2$, soit à la formation d'ettringite colloïdale par absorption d'eau, soit à la formation de monosulfoaluminate par échange d'ions à partir de C_4AH_{13}.

Avant d'encourager vivement toute nouvelle recherche, qu'il me soit permis de remercier ici les rapporteurs généraux, les auteurs de communications et de posters, les participants, les traducteurs, les hôtesses. Chacun d'entre eux a contribué largement au succès de cette journée d'étude sur C_3A, phase mineure qui joue cependant un rôle important dans les propriétés chimiques, physiques et mécaniques du ciment portland.

Dr Micheline REGOURD
Présidente du Séminaire A

Theme 1 - Polymorphism of C_3A and its solid solutions

GENERAL REPORT

By MISS A.E. MOORE, Cement and Concrete Association, Materials Research Department, Slough, U.K.

Polymorphism of C_3A and its Solid solutions:

We have three papers in this section, two on the C_3A - NC_8A_3 series and one on halogen-substituted $C_{12}A_7$ compounds. I will deal with the latter first.

"Non-stoichiometry of solid solutions $C_{11}A_7.CaX_2$, and their properties" by Professor Timachev, Ossokine, Potapova and Nikolski.

Prof. Timachev and his colleagues have prepared $C_{11}A_7.CaX_2$ where X is F, Cl, Br or I, together with non-stoichiometric solid solutions of the fluorine- and Chlorine-containing series.

The structure of a member of the CaF_2 series was determined by Williams (1) and shown to contain a partially occupied site for fluorine, with two adjacent calcium sites also partially occupied, as shown in Fig. 1.

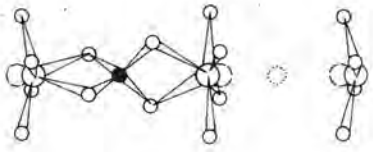

F, Cl, OH or hole
Oxygen
Calcium
Aluminium

Fig. 1. Co-ordination of the calcium atoms in $C_{12}A_7$ type compounds. (Williams)

When the fluorine site is occupied the calcium atoms move towards it, to the positions shown dashed. Williams deduced the composition of his crystal to be $C_{11.56}A_7.0.44\ CaF_2$. It has been assumed that the asymmetric co-ordination of the calcium atoms is responsible for the hydraulic activity of compounds of this type.

Fig.2 shows part of the phase diagram CaO - Al_2O_3 - CaF_2, with $C_{12}A_7$, "$C_{11}A_7$", $C_{11}A_7.CaF_2$ and W the composition deduced by Williams. Compositions synthesised by Timachev et al are marked T; they represent two solid solution series, one with $C_{11}A_7.x\ CaF_2$ and one with $C_xA_7.CaF_2$.

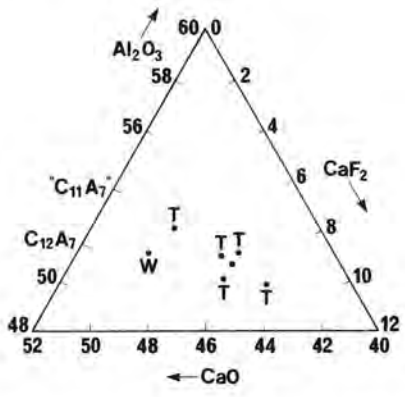

Fig. 2. Part of the system $CaO-Al_2O_3-CaF_2$ (wt%) T = non-stoichiometric solid solutions of $C_{11}A_7.CaF_2$

In both cases, it is the compounds with $C_{11}A_7.0.9\ CaX_2$ that are more reactive than those with either more or less CaX_2.

In Fig. 3(a) some properties of these compositions are shown in a diagram similar to their positions on the phase diagram. In the series with $C_xA_7.CaF_2$ density increases and refractive index decreases as the C:A ratio increases.

Fig. 3(b) shows a comparable diagram of properties for the $C_{11}A_7.CaCl_2$ series of non-stoichiometric compounds showing a smaller range than is possible with CaF_2.

The authors also find that only 0.7 mole of Al can be replaced by Fe in $C_{11}A_7.CaF_2$, giving practically no change in properties.

REFERENCE

1. - P.P. WILLIAMS (1973), "Refinement of the structure of $11CaO.7Al_2O_3.CaF_2$" Acta Cryst. B29, 1550.

(a)

	CaF_2							
	0.5		0.9		1.0		1.3	
$C_{10.8}A_7$					-	1.665		
					2870	-		
$C_{11}A_7$	-	-	-	-	1550	1.600	1550	1.605
	-	34	-	55	2900	50	2950	-
$C_{11.3}A_7$					-	1.595		
					2920	-		

(b)

	$CaCl_2$							
	0.5		0.9		1.0		1.1	
$C_{10.9}A_7$					-	1.634		
					2820	-		
$C_{11}A_7$	-	-	-	-	1520	1.620	1520	1.615
	-	23.5	-	45.6	2850	40.7	2860	-
$C_{11.1}A_7$					-	1.615		
					2850	-		

Key

T_f^o	R.I.	T_f^o = Fusion temperature (°C)
ρ	R_{28}	R.I. = Refractive Index
		ρ = Density Kg/m³
		R_{28} = *Compressive strength at 28 days (MPa)

Fig.3 Properties of some compounds in the systems (a) $CaO-Al_2O_3-CaF_2$ and (b) $CaO-Al_2O_3-CaCl_2$

The C_3A - NC_8A_3 series.

Pure C_3A is cubic (space group Pa 3) with a = 15.262, it has a very strong pseudo-cell at $^a/_4$, because most of the metal atoms lie on this lattice; the aluminium atoms form kinked rings of composition Al_6O_{18} with their axes parallel to the three-fold cell axes and a vacant site at the centres of the rings, which lie at $\frac{1}{8}$, $\frac{3}{8}$, $\frac{5}{8}$, and $\frac{7}{8}$ levels in the cell.

Two non-cubic forms have been shown to occur, orthorhombic and monoclinic. An apparently tetragonal high-temperature form has been shown by Dr Makí (2) to be due to the optic axial angle (2V) becoming zero for a single wavelength of light at a specific temperature and hence the crystal appearing to be uniaxial; at other wavelengths the effect occurs at different temperatures and thus the crystal cannot be uniaxial.

In "Structural aspect of the C_3A-Na_2O solid solution" Professor Takeuchi, Dr Nishi and Dr Maki show that as Na_2O is introduced into the system, a different cubic form, CII, occurs at 2.4% (wt.) Na_2O, when the cell becomes non-centro-symmetric. (space group $P2_13$). The position of the Al_6O_{18} rings is unchanged, but two of the calcium atoms split into groups with different Na/Ca occupancy ratios. These are the two Ca in eightfold (x,x,x) positions, of the same type as the positions of the ring centre vacancies, some of which are now occupied by Na.

The Ca polyhedra that accommodate Na become larger than the corresponding ones in CI (C_3A), and rings that are occupied by Na show a contraction compared with the vacant rings in CI. This produces a decrease in cell volume from CI to CII (See Table 1 in Takeuchi et al).

When the Na_2O content is increased to 3.8% (wt.) a major change in structure, to orthorhombic (Pbca) occurs. The c dimension is retained, but the true cell volume is halved, with $a_o \not\perp b_o$ both approximately $^a c/\sqrt{2}$. The Al_6O_{18} rings now lie with centres at c = 0 and c = $\frac{1}{2}$ only and have their axes all parallel to one pseudo-three-fold axis at c = 0, and another at c = $\frac{1}{2}$. (See Fig.2 in Takeuchi et al.)

The Na atoms lie partly near the centres of these rings and partly replace the calcium atoms that lie in the same planes, c = 0 and $\frac{1}{2}$.

A further minor change in symmetry, to monoclinic ($P2_1/a$) occurs at 5.7% (wt.) Na_2O and again entails splitting of the calcium positions at c = 0 and $\frac{1}{2}$ to give partial occupancies of Na. Within this range of solid solutions, there is no change in the volume of the Al_6O_{18} rings as they become occupied by Na. The calcium polyhedra also remain constant, until they split into two groups at the change to monoclinic, when group A increase and group B decrease in size as they are progressively occupied by Na. This results in a continuous increase in cell volume.

Takeuchi et al find that the monoclinic solid solution range terminates at 5.9 wt % Na_2O, apparently because the limiting occupancy of the ring centres is 75%, and the Ca sites can accept more Na only if some Si is present to replace Al. They examined one crystal with 5.535 Al and 0.475 Si (atom ratios to 18 oxygen) and found that 6.6% Na_2O was accommodated, with higher replacement ratios in the Ca sites. This seems to indicate that the full 7.6% Na_2O replacement for NC_8A_3 would be possible with sufficient silica present. (See their Fig.5)

Another crystal containing both Fe and Si with 3.3 wt % Na_2O was found to be orthorhombic, with less Na in ring sites and more in Ca sites than in the orthorhombic form with 3.8% Na_2O only.

Prof. Tavasci, Prof. Massazza and Dr Costa have explored the stability fields of the anistropic forms of C_3A, using reflected light microscopy on samples quenched from different temperatures.

They found that etching with 2% HNO_3 in alcohol gave a clear distinction between orthorhombic and monoclinic phases, revealing multiple twinning in the monoclinic phase when viewed with sufficiently high magnification.

They found that the composition NC_8A_3, when quenched from 1300°C or 600°C gave all orthorhombic crystals (with no free lime) and when quenched from 500°C gave all monoclinic, but that mixes richer in Na_2O always showed the presence of free-lime and sodium aluminate.

The stability fields for the two forms are shown in Fig.16 of Tavasci et al.

Thus these authors consider that the full replacement of 7.6% Na_2O is possible without the presence of SiO_2. This is a point of disagreement with Takeuchi et al which we should discuss.

REFERENCE

2. - I. MAKI (1976), "Optics and phase relationships of the optically anisotropic C_3A", Cement and Concrete Research, Vol.6, pp 797-802.

Thème 1 - Polymorphisme de C_3A et de ses solutions solides

RAPPORT GENERAL

A.E. MOORE, Cement and Concrete Association, Materials Research Department, Slough, U.K.

Nous avons trois communications dans ce thème, deux sur la série C_3A - NC_8A_3 et une sur les composés $C_{12}A_7$ substitués par les halogènes. Je commencerai par la dernière.

1) Non-stoechiométrie des solutions solides $C_{11}A_7.Ca.X_2$ et leurs propriétés par le Professeur TIMACHEV et OSSOKINE, POTAPOVA et NIKOLSKI

Le **Prof. TIMACHEV** et ses collègues ont préparé les solutions solides $C_{11}A_7.CaX_2$ où X est F, Cl, Br ou I et des solutions solides non-stoechiométriques de la fluorine et de la série contenant du chlore.

La structure d'un membre de la série $C_{11}.A_7CaF_2$ a été déterminée par **WILLIAMS** (1) : elle contient un site partiellement occupé par le fluor avec deux sites calcium adjacents, aussi partiellement occupés, comme le montre la Figure 1. Quand le site fluor est occupé, les atomes de calcium se déplacent vers lui jusqu' aux positions hachurées. **WILLIAMS** en a déduit la composition de son cristal soit $C_{11,56}A_7.0,44\ CaF_2$. La coordination assymétrique des atomes de calcium a été supposée responsable de l'activité hydraulique des composés de ce type.

La Figure 2 montre une partie du diagramme de phase $CaO - Al_2O_3 - CaF_2$ avec $C_{11}A_7$, "$C_{11}A_7$", $C_{11}A_7.CaF_2$ et W la composition déduite par **WILLIAMS**. Les compositions synthétisées par **TIMACHEV** et al sont marquées T. Elles représentent deux séries de solutions solides, l'une avec $C_{11}A_7.xCaF_2$ et l'autre avec $C_xA_7.CaF_2$.

Sur la Figure 3(a), quelques propriétés de ces compositions sont données dans un diagramme correspondant à leurs positions dans le diagramme de phase. Dans la série avec $Ca_xA_7.CaF_2$ la densité croît et l'indice de réfraction décroît quand le rapport $\frac{C}{A}$ croît.

La Figure 3(b) montre un diagramme des propriétés de la série $C_{11}A_7.CaCl_2$ des composés non-stoechiométriques qui présente un domaine plus étroit que celui contenant CaF_2.

Dans les deux cas, ce sont les composés $C_{11}A_7.0,9\ CaX_2$ qui sont plus réactifs que ceux contenant plus ou moins de CaX_2.

2) Polymorphisme de C_3A et de ses solutions solides

La série $C_3A.NC_8A_3$

C_3A pur est cubique (groupe spatial Pa 3), avec a = 15,262 Å. Sa structure présente une forte pseudo-maille de paramètre a/4 parce que la plupart des atomes métalliques s'y trouvent. Les atomes d'aluminium forment des anneaux légèrement gauchis de composition Al_6O_{18} dont les axes sont parallèles aux axes d'ordre 3 de la maille. Un site vacant se trouve aux centres des anneaux dont les positions sont aux niveaux $\frac{1}{8}, \frac{3}{3}, \frac{5}{8}, \frac{7}{8}$ de la maille.

Deux formes non cubiques ont été trouvées, l'une orthorhombique, l'autre monoclinique. Une forme haute température apparemment tétragonale est due, d'après le Dr **MAKI** (2), à la valeur de l'angle 2V des axes optiques égale à zéro, pour une radiation monochromatique de la lumière, à une température spécifique. Pour les autres longueurs d'onde, cet effet se produit à des températures différentes. Le cristal ne peut donc pas être uniaxial.

2.1 Dans "l'aspect structural des solutions solides C_3A-Na_2O", le Professeur **TAKEUCHI**, le Dr **NISHI** et le Dr **MAKI** montrent qu'une seconde forme cubique C_{II} apparaît quand 2,4 % Na_2O (en poids) sont introduits dans le réseau dont la maille devient non centro-symétrique (groupe spatial P 2_13). La position des anneaux Al_6O_{18} est inchangée mais deux des atomes de calcium se divisent en groupe de rapports d'occupation Na/Ca différents. Ce sont les deux calcium dans les positions d'ordre 8 (x,x,x,) du même type que celles des sites vacants au centre des anneaux, certains d'entre eux étant maintenant occupés par Na. Les polyèdres de Ca qui accueillent Na deviennent plus grands que ceux de la structure C_I de C_3A et les anneaux qui sont occupés par Na se contractent par rapport aux anneaux vacants de C_I. Ceci entraîne une décroissance du volume de la maille de C_I à C_{II} (Tableau I).

Quand la teneur en Na_2O atteint 3,8 % (en poids), un changement important se produit dans la structure qui devient orthorhombique (Pbca). La dimension c n'est pas modifiée mais le volume de la vraie maille est divisée par deux avec $a_o \neq b_o$, tous deux approximativement égaux a $c/\sqrt{2}$. Les anneaux Al_6O_{18} se trouvent maintenant dans les positions correspondant à c = 0 et c = $\frac{1}{2}$ seulement et ont, tous, leurs axes parallèles à un pseudo-axe d'ordre 3, l'un à c = 0 l'autre à c = $\frac{1}{2}$ (Fig. 2 dans **TAKEUCHI** et al).

Les atomes de sodium se placent partiellement près des centres de ces anneaux et remplacent partiellement les atomes de calcium qui se trouvent dans les mêmes plans, c = o et c = $\frac{1}{2}$.

Un autre changement de symétrie, mineur, se produit à 5,7 % Na_2O (en poids). La structure devient monoclinique (P $2_1/a$) ce qui entraîne à nouveau un partage des positions de calcium à c = 0 et c = $\frac{1}{2}$ pour une occupation partielle de Na. Dans ce domaine de solutions

solides, il n'y a pas de changement de volume des anneaux Al_6O_{18} quand ils sont occupés par Na. Les polyèdres de calcium restent ainsi constants jusqu'à ce qu'ils se partagent en deux groupes à la transformation orthorhombique → monoclinique. Quand la taille du groupe A croît, celle du groupe B décroît au fur et à mesure de l'occupation par Na. Ceci entraîne un accroissement continu du volume de la maille.

TAKEUCHI et al trouvent que le domaine des solutions solides se termine à 5,9 % Na_2O (en poids) apparemment parce que le taux limite d'occupation des centres d'anneaux suit la règle des 75 % et que les sites Ca ne peuvent accepter plus de Na sauf si Si est présent pour remplacer Al. Ils ont étudié un cristal avec 5,535 Al et 0,475 Si (atomes rapportés à 18 oxygène) et trouvé que 6,6 % Na_2O peuvent être logés avec des rapports de remplacement plus élevés dans les sites Ca. Ceci semble indiquer que la valeur de 7,6 % Na_2O correspondant à NC_8A_3 serait possible en présence d'une quantité suffisante de silice (voir Fig. 5 **TAKEUCHI** et al).

Un autre cristal contenant à la fois Fe et Si avec 3,3 % Na_2O (en poids) a été trouvé orthorhombique avec moins de Na dans les sites des anneaux et plus de Na dans les sites Ca que dans la forme orthorhombique contenant seulement Na (3,8 % Na_2O).

2.2 Le Prof. **TAVASCI**, le Prof. **MASSAZZA** et le Dr **COSTA** ont exploré les domaines de stabilité des formes anisotropiques de C_3A en utilisant la microscopie en lumière réfléchie

Ils ont trouvé que l'attaque avec 2 % HNO_3 dans l'alcool donne une distinction claire entre les phases orthorhombiques et monocliniques, révélant un maclage multiple dans la phase monoclinique pour un grossissement suffisamment élevé.

Ils ont également trouvé que la composition NC_8A_3, trempée à partir de 1300 °C ou de 600 °C donne des cristaux orthorhombiques (sans chaux libre) mais quand elle est trempée à partir de 500 °C, elle donne des cristaux monocliniques. Ceci est un point de discordance entre **TAKEUCHI** et al et **TAVASCI** et al qui devrait être discuté.

Les mélanges plus riches en Na_2O montrent toujours la présence de chaux libre et d'aluminate de sodium.

Les domaines de stabilité pour les deux formes sont donnés dans la Fig. 16 (**TAVASCI** et al).

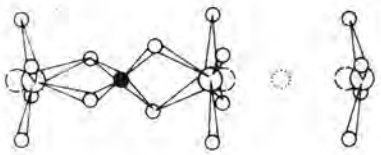

F,Cl,OH, ou site vacant.
Oxygène
Calcium
Aluminium

Fig. 1 : Coordination des atomes de calcium dans les composés du type $C_{12}A_7$ (Williams)

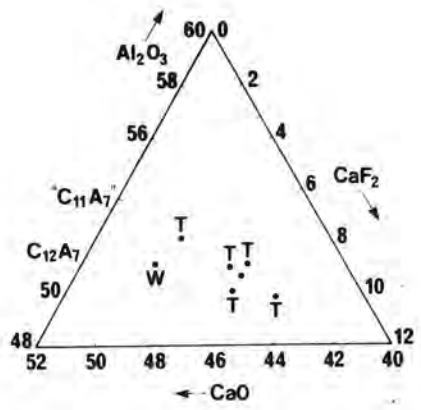

Fig. 2 : Fraction du système CaO - Al_2O_3 - CaF_2 (% en poids). T = solutions solides non stoechiométriques de $C_{11}A_7.CaF_2$.

(a)

	CaF_2					
	0.5		0.9		1.0		1.3	
$C_{10.8}A_7$					- 2870	1.665 -		
$C_{11}A_7$	- -		- -		1550 2900	1.600 50	1550 2950	1.605 -
	-	3/4	-	55				
$C_{11.3}A_7$					- 2920	1.595 -		

(b)

	$CaCl_2$							
	0.5		0.9		1.0		1.1	
$C_{10.9}A_7$					- 2820	1.634 -		
$C_{11}A_7$	- -		- -		1520 2850	1.620 40.7	1520 2860	1.615 -
	-	23.5	-	45.6				
$C_{11.1}A_7$					- 2850	1.615 -		

Code

T_f^o	I.R.
ρ	R_{28}

T_f^o = Température de fusion (°C)
I.R. = Indice de réfraction
ρ = Densité kg/m³
R_{28} = Résistance en compression à 28 jours (MPa).

Fig. 3 : Propriétés de quelques composés dans le système (a) CaO - Al_2O_3 - CaF_2 et (b) CaO - Al_2O_3 - $CaCl_2$.

REFERENCES

1. P.P. **WILLIAMS** (1973), "Refinement of the structure of $11CaO.7Al_2O_3.CaF_2$". Acta Cryt. B29, 1550.
2. I. **MAKI** (1976), "Optical properties of the anniso-tropic C_3A". Cem. Concr. Res. 6 (2), 183-192.

La non-stoechiométrie des solutions solides de $C_{11}A_7CaX_2$ et leurs propriétés

Non-stoichoimetry of solid solutions $C_{11}A_7CaX_2$ and their properties

V.V. TIMACHEV, membre correspondant de l'Académie des sciences de l'U.R.S.S., professeur à l'Institut chimico-technique Mendéléev,
A.P. OSSOKINE, candidat ès sciences techniques,
E.N. POTAPOVA, ingénieur,
E. NIKOLSKI, ingénieur, Moscou, U.R.S.S.

RESUME : La formation des halogéno-aluminates de calcium dans le système $CaO-Al_2O_3-CaX_2$ (où X est F, Cl, Br, I) se produit aux températures comprises entre 900 et 1400 °C et donne lieu à une sublimation intense des halogènes. Les phases bromées et iodées ne se prêtent à la synthèse que dans une ampoule scellée.

La présence, dans la structure des aluminates de calcium, de vides spacieux est à l'origine de la formation de solutions solides à teneur variable en CaO et CaX_2 et conduit au remplacement d'une partie de Al_2O_3 (jusqu'à 0,7 moles) par Fe_2O_3. La sublimation des halogènes lors de la synthèse des minéraux provoque une modification des caractéristiques optiques, de la densité et de l'activité hydraulique de ces derniers. Avec l'accroissement du rayon de l'ion dans la série F - Cl - Br - I, on constate une diminution de la résistance thermique et de la densité des halogéno-aluminates et une baisse de leur température de fusion.

Les minéraux fluorés et chlorés, surtout ceux ayant une composition non stoechiométrique ($0,9CaX_2$), présentent une activité hydraulique augmentée. Les propriétés des solutions solides du type $C_{11}A_{7-x}Fe_xCaX_2$ correspondent à celles du fluoraluminate de calcium.

La régulation des conditions de la préparation des solutions solides de halogéno-aluminates de calcium et des clinkers à leur base permet d'apporter des modifications voulues à leur composition et, en conséquence, aux propriétés des liants obtenus, en modifiant notamment la durée de prise et l'intensité de la genèse de la résistance.

SUMMARY : In the system $CaO-Al_2O_3-CaX_2$ (where X-F, Cl, Br, I) calcium halogen aluminates are formed in the temperature range of 900-1400 °C with intensive volatilization of halogens. Bromine- and iodine-bearing phases are synthesized only in conditions of sealed ampoule.

The presence of large voids in calcium aluminate structure causes the formation of solid solutions with variable content of CaO and CaX_2 as well as part substitution of Al_2O_3 (up to 0.7 moles) for Fe_2O_3. During mineral synthesis the volatilization of halogens brings about changes of optical characteristics density and hydration activity. With increasing of ion radius in the series of F-Cl-Br-I there are reduced thermal stability of halogen aluminats, their melting temperature and density.

Intensified hydraulic activity is the typical of minerals containing fluorine and chlorine and especially of non-stoichoimetry (0.8-0.9 CaX_2) composition. The properties of solid solutions of $C_{11}A_{7-x}Fe_xCaX_2$ type correspond to calcium fluorine aluminate.

The regulation of solid solution synthesis conditions of calcium hylogenaluminates and clinkers on their basis allows to change purposely the composition and hence the properties of cements obtained that is the setting time and intensity of strength growth.

Une condition sine qua non des substitutions hétérovalentes dans le réseau des minéraux du clinker est une compensation des charges qui peut être réalisée par les procédés les plus variés. Pendant la formation de solutions solides et la dissolution d'impuretés dans les minéraux, on observe l'apparition de vacances, la formation d'associations d'atomes et l'insertion d'atomes supplémentaires dans le réseau, ce qui prête à la formation de structures défectueuses.

La présence de vides spacieux dans la structure des aluminates de calcium a pour conséquence une diversité plus grande des schémas de compensation lors des substitutions hétérovalentes, par rapport à l'alite et au bélite. Les substitutions hétérovalentes sont une des causes du dérangement de la stoechiométrie des oxydes contenus dans les minéraux du ciment. On voit ainsi apparaître un moyen de plus de la régulation orientée de la concentration de défauts dans les minéraux du clinker en vue d'augmenter leur activité hydraulique.

Le procédé le plus simple de régulation du degré d'écart à la stoechiométrie dans les halogéno-aluminates de calcium du type $C_{11}A_7CaX_2$ (où X est un halogène) est une sublimation dosée de l'halogène au cours de la synthèse des minéraux conformément aux réactions

$$Al_2O_3 + 3CaF_2 \rightarrow 2AlF_3\uparrow + 3CaO \qquad (1)$$

$$H_2O + CaF_2 \rightarrow 2HF\uparrow + CaO \qquad (2)$$

La formation des halogéno-aluminates de calcium d'une composition $C_{11}A_7CaX_2$ se fait par un mécanisme de substitution de CaX_2 à une molécule de CaO dans la composition du maénite, c'est-à-dire en vertu de la réaction

$$C_{12}A_7 + CaF_2 \rightarrow C_{11}A_7CaF_2 + C \qquad (3)$$

Le réseau des halogéno-aluminates de calcium est caractérisé par une déformation et se distingue quelque peu de la forme cubique du maénite, en provoquant des changements des caractéristiques radiographiques, illustrés pour $C_{11}A_7CaF_2$ par les données du Tableau I. La substitution de deux atomes de fluor à un atome d'oxygène a pour effet un déplacement des atomes de fluor vers la périphérie, ce qui favorise la polarisation de la liaison et l'accroissement de l'activité hydraulique.

La vitesse de dégagement de l'halogène (en calculant en CaX_2), lors de la cuisson des compositions stoechiométriques de $C_{11}A_7CaF_2$ et de $C_{11}A_7CaCl_2$, atteint son maximum ($2{,}5\cdot10^{-2}$ et $4\cdot10^{-2}$ g/mn respectivement) à la température de fusion, alors qu'ensuite, avec l'apparition de la matière fondue, elle décroît et devient constante. Les résultats de l'analyse chimique montrent que la sublimation de l'halogène

TABLEAU I

Caractéristiques radiographiques de $C_{12}A_7$ et de $C_{11}A_7CaF_2$

$C_{12}A_7$		$C_{11}A_7CaF_2$	
d, Å	I/I_0	d, Å	I/I_0
4,895	84	4,862	55
3,791	10	3,783	10
3,201	15	3,190	24
2,994	38	2,982	40
2,675	100	2,661	100
2,560	8	2,550	15
2,442	44	2,440	42
2,183	40	2,178	42
1,945	32	1,940	30
1,660	28	1,655	30
1,600	27	1,594	31

s'effectue non seulement suivant les réactions 1 et 2, mais aussi sous forme de X_2. C'est pourquoi, pour obtenir des phases stoechiométriques, il est nécessaire de cuire les mélanges bruts dans des ampoules scellées ou bien d'introduire dans ces mélanges un excédent de CaX_2 et de Al_2O_3 que l'on dose suivant la durée de maintien isothermique et la température de la cuisson.

Lors de la synthèse de $C_{11}A_7CaF_2$ et de $C_{11}A_7CaCl_2$ selon les régimes représentés par la figure 1, on observait une réalisation à fond des processus de formation des minéraux. Pour les phases bromées et iodées, on n'est pas parvenu à faire passer intégralement à l'état combiné l'oxyde de calcium, de sorte que sa proportion s'élevait à 0,8 à 1,2 %, même dans les conditions d'une ampoule scellée. Et si la réalisation était réalisée à découvert, ces phases ne prenaient pas naissance point du tout, à cause de la faible résistance thermique des sels de calcium correspondants.

La formation des minéraux du groupe de $C_{11}A_7CaX_2$ se fait par l'intermédiaire d'un composé intermédiaire CA.

L'élévation de la température de la synthèse et l'accroissement de la durée de cuisson provoquent un décroissement de la teneur en CA, et on voit apparaître sur les radiogrammes une structure caractéristique des halogéno-aluminates de calcium. Si l'on passe successivement du fluoraluminate à l'iodaluminate de calcium, la densité et la température de fusion (Tableau II) des composés décroissent progressivement, en fonction de l'accroissement du rayon de l'ion à implanter. La résistance thermique varie d'une façon similaire, en décroissant dans la série : $C_{11}A_7CaF_2 \rightarrow C_{11}A_7CaCl_2 \rightarrow C_{11}A_7CaBr_2 \rightarrow C_{11}A_7CaI_2$.

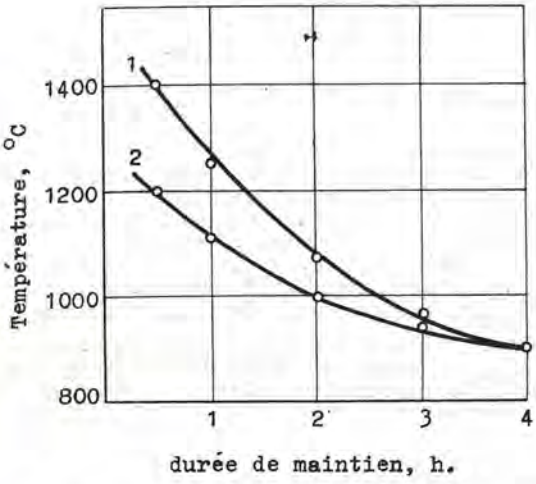

Fig. 1 - Régimes de synthèse de $C_{11}A_7CaX_2$ où X est Cl (1) et F (2)

TABLEAU II

Caractéristiques des halogéno-aluminates de calcium synthétisés

Minéral	Température de fusion, °C	Densité, kg/cm³	Indice de réfraction
$C_{11}A_7CaF_2$	1550	2900	1,600
$C_{11}A_71,3CaF_2$	1550	2950	1,605
$C_{11}A_7CaCl_2$	1520	2850	1,620
$C_{11}A_71,1CaCl_2$	1520	2860	1,615
$C_{11}A_7CaBr_2$	1420	2720	1,681
$C_{11}A_7CaI_2$	1410	2690	1,693
$C_{12}A_7$	1400	2680	1,617

Les minéraux $C_{11}A_7CaBr_2$ et $C_{11}A_7CaI_2$ se décomposent facilement à l'air sous un chauffage relativement faible (200 °C) avec dégagement visible de vapeurs brunes de brome ou d'iode.

La variation de la stoechiométrie d'après l'halogène ne peut se produire que dans un intervalle déterminé, au-delà duquel la structure se décompose avec dégagement de CaF_2, CA et $C_{12}A_7$. La stabilité des solutions solides de $C_{11}A_7 \cdot xCaF_2$ se maintient dans un intervalle $0 \leq x \leq 1,3$. Avec l'augmentation de la teneur en halogène, on voit apparaître sur les radiogrammes des crêtes caractéristiques de CaO. Les radiogrammes de ces solutions solides sont pratiquement identiques et ne diffèrent l'un de l'autre que par l'importance de la crête correspondant à un espacement d'interplan de 4,88 ($C_{11}A_7CaF_2$). Dans le cas des chloraluminates de calcium, la limite supérieure de la teneur en $CaCl_2$ est égale à 1,1. Il s'avère impossible d'évaluer ce chiffre pour $C_{11}A_7CaBr_2$ et $C_{11}A_7CaI_2$, du fait d'une sublimation poussée de l'halogène. L'implantation d'une quantité excédentaire de CaX_2 a pour cause non seulement l'existence de vides spacieux dans le réseau des aluminates mais aussi l'apparition éventuelle, lors de la sublimation de l'halogène, de vacances cationiques (2). La densité des solutions solides dans le domaine des fortes concentrations d'halogène est légèrement plus grande par rapport aux minéraux qui en contiennent une quantité diminuée, ce qui est confirmée par la formation des solutions solides de cette série par le mécanisme de substitution. L'implantation d'une quantité excédentaire de CaX_2, dans les conditions d'une sublimation poussée de l'halogène, conduit à la formation de solutions solides de $C_{11}A_7CaX_2$ avec CaO.

La variation de la stoechiométrie d'après l'oxyde de calcium est limitée, pour le fluoraluminate de calcium, à l'intervalle $C_{10,8}A_7CaF_2$ - $C_{11,3}A_7CaF_2$, au-delà duquel on enregistre l'apparition de CaO libre. Les chloraluminates de calcium sont caractérisés par un intervalle plus étroit : $C_{10,9}A_7CaCl_2$ - $C_{11,1}A_7CaCl_2$. Le décroissement de la teneur du mélange en oxyde de calcium provoque l'apparition des minéraux $C_7A_3CaX_2$ et CA. La preuve de l'existence des solutions solides indiquées est une variation continue des indices de réfraction et de la densité (Tableau III).

TABLEAU III

Caractéristiques des solutions solides du type $C_nA_7CaX_2$ à teneur variée en CaO

Solution solide	Densité, kg/cm³	Indices de réfraction
$C_{10,8}A_7CaF_2$	2870	1,665
$C_{11,3}A_7CaF_2$	2920	1,595
$C_{10,9}A_7CaCl_2$	2820	1,634
$C_{11,1}A_7CaCl_2$	2850	1,615

En essayant de donner une évaluation expérimentale de la possibilité d'obtenir des halogénoferro-aluminates de calcium en vue de pouvoir modifier les propriétés des liants, on a établi que la substitution, dans le réseau du minéral $C_{11}A_7CaF_2$, de l'oxyde ferrique à l'oxyde d'aluminium ne se fait que jusqu'à 0,7 mole. La cuisson des compositions à teneur accrue en oxyde

ferrique (telles $C_{11}A_6FeCaF_2$, $C_{11}A_5Fe_2CaF_2$) conduit à la formation d'un système polyphasé comportant C_4AF, CA et $C_{11}A_7CaF_2$. L'augmentation de la concentration de Fe_2O_3 entraîne un dégagement accru de CA. Si la teneur en oxyde ferrique ne dépasse pas 0,7 mole, une partie des cations fer se répartit dans les interstices des octaèdres de l'aluminium et le remplace en partie dans les polyèdres de coordination. Les solutions solides de la série $C_{11}A_{7-x}Fe_x \cdot CaF_2$ (où $x \leq 0,7$) présentent pratiquement les mêmes propriétés que les halogéno-aluminates.

Les calculs thermodynamiques montrent que le maclage des cristallohydrates peut donner lieu à des germes de croissance, la facilité de la formation desquels est proportionnelle à la densité de défauts. C'est pourquoi le degré d'écart à la stoechiométrie caractérise l'activité hydraulique des minéraux. En l'occurrence, l'écart à la stoechiométrie ne traduit, au fond, autre chose que la facilité de détachement des molécules ou des ions d'avec la surface de la phase solide au cours de l'hydratation (3). L'intensité de l'hydratation est proportionnelle au dégagement de chaleur qui peut servir lui aussi d'indice d'activité hydraulique des minéraux. Les halogéno-aluminates synthétisés se sont montrés beaucoup plus actifs que le maénite (fig. 2).

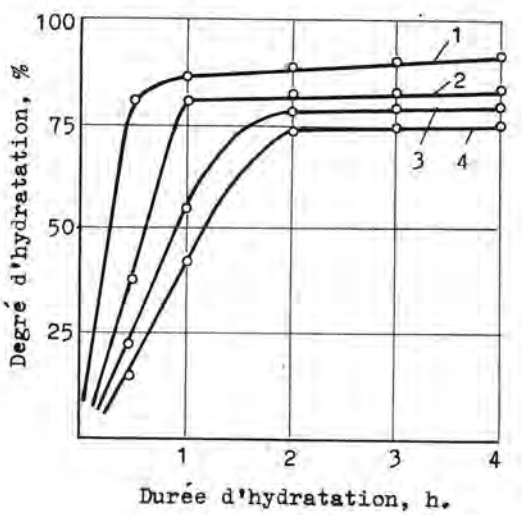

Fig. 2 - Cinétique de la combinaison à l'eau des minéraux hydratables :
1 - $C_{11}A_7CaF_2$; 2 - $C_{11}A_7CaCl_2$;
3 - $C_{11}A_7CaBr_2$; 4 - $C_{11}A_7CaI_2$

Le degré d'hydratation du fluoraluminate de calcium atteint 80 % au bout de 30 à 40 mn après le gâchage, celui du chloraluminate, au bout de 6 à 8 heures.

L'hydratation du fluoraluminate de calcium se déroule schématiquement comme suit :

$$C_{11}A_7CaF_2 + H \rightleftharpoons C_nAH_m + AH_{3-x}F_x$$

avec formation d'hydroaluminates de calcium lamellaires et d'un hydroxyde d'aluminium géliforme à teneur variable en fluor. La phase liquide dégage d'abord des néoformations d'hydroaluminates de calcium : CAH_{10}, C_2AH_8, C_4AH_{13} (fig. 3-a) et un gel d'alumine modifié au fluor $Al(OH)_{3-x}F_x$ (4). Au bout de 6 heures d'hydratation, il y a formation et dégagement de C_4AH_{19} et aussi un début de recristallisation des hydroaluminates de calcium métastables. CAH_{10}, dont l'état cristallin devient plus ordonné, se transforme en C_2AH_8. Ce processus s'achève à la 12-ième heure d'hydratation, ce qui est confirmé par la disparition des réflexions diffractionnelles 7,16 ; 3,56 ; 2,55 Å de CAH_{10}.

Le durcissement du fluoraluminate de calcium en présence de gypse et sans celui-ci se déroule différemment, ce qui retentit sur la cinétique de l'hydratation et de la formation des phases.

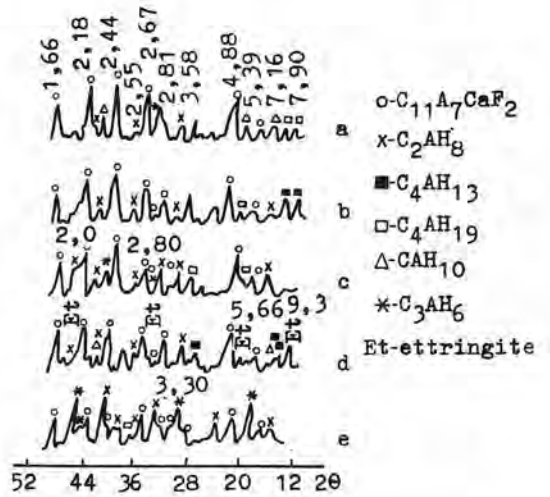

Fig. 3 - Les radiogrammes des produits d'hydratation de $C_{11}A_7CaF_2$ qui a durci :
a - 1 h ; b - 1 h en présence de gypse ;
c - 1 jour ; d - 1 jour en présence de gypse ; e - 7 jours

Lors de l'hydratation de $C_{11}A_7CaF_2$ avec 12 % de gypse à deux molécules d'eau de cristallisation, il se forme au bout d'une heure C_2AH_8, C_4AH_{13}, C_4AH_{19} (fig. 3-b) et un gel

d'alumine $Al(OH)_{3-x}F_x$. En outre, à la différence de l'hydratation de C_3A et de $C_{12}A_7$, il y a formation, en présence de fluor, au lieu d'ettringite, d'une solution solide d'ettringite contenant le fluor.

La formation de la composition en phase s'achève vers la 3-ème journée de durcissement et l'hydratation ultérieure ne fait qu'accumuler dans le système les phases hydratées (C_2AH_8, C_3AH_6, C_4AH_{19}, $AH_{3-x}F_x$) (fig. 3-e).

L'hydratation de $C_{11}A_7CaCl_2$ s'effectue d'une manière analogue.

Les délais de la prise (en minutes) des fluoro et chloraluminates d'une composition $C_{11}A_7O,9CaF_2$ et $C_{11}A_7O,9CaCl_2$ sont de 4/5 et 5/7 (début/fin) contre 4/6 et 6/9 pour les compositions stoechiométriques $C_{11}A_7CaF_2$ et $C_{11}A_7CaCl_2$ respectivement. Les délais de la prise des bromo et iodaluminates de calcium sont proches et se chiffrent par 7/11 et 8/11 respectivement.

Le degré d'écart à la stoechiométrie a une répercussion notable sur la résistance mécanique des minéraux, les délais de la prise et l'activité hydraulique de ceux-ci (Tableau IV).

TABLEAU IV

Résistance des halogéno-aluminates de calcium

	Résistance à la compression, MPa			
	1	3	7	28
$C_{11}A_7CaF_2$	30,4	32,0	39,5	50,1
$C_{11}A_7O,9CaF_2$	32,5	35,0	43,0	55,0
$C_{11}A_7O,5CaF_2$	19,0	25,2	27,1	34,4
$C_{11}A_7CaCl_2$	23,5	27,0	28,4	40,7
$C_{11}A_7O,9CaCl_2$	25,0	30,3	42,1	45,6
$C_{11}A_7O,5CaCl_2$	14,3	18,2	20,7	23,5

Les minéraux caractérisés par une non-stoechiométrie considérable présentent de faibles résistance et activité hydraulique, ce qui a vraisemblablement pour cause une concentration optimale de défauts dans la structure des solutions solides. La pierre de ciment monominérale à base de $C_{11}A_7O,9CaX_2$ avait une résistance maximale, les phases fluorées présentant les meilleures caractéristiques. L'influence de la stoechiométrie sur les propriétés hydrauliques des minéraux s'explique par l'apparition d'une quantité supplémentaire de défauts qui facilitent à l'eau l'accès de la phase à hydrater. En faisant varier la stoechiométrie d'après l'halogène dans certaines limites, on parvient à réguler la résistance, alors que le degré d'écart à la stoechiométrie d'après l'oxyde de calcium donne la possibilité de modifier les délais de la prise du liant monominéral et des ciments à sa base.

CONCLUSIONS

1. Par suite d'une sublimation poussée des hylogènes et en raison de la présence de vides spacieux dans la structure de $C_{12}A_7$, il se forme des solutions solides d'halogéno-aluminate de calcium à teneur variable en CaO, CaX_2 et Fe_2O_3.

2. Dans des conditions industrielles, seules les phases non stoechiométriques prennent naissance, et pour pouvoir synthétiser un liant ayant les propriétés voulues, il faut un dosage précis de la composition du mélange brut, avec prise en considération du régime de synthèse des clinkers qui est responsable du degré de sublimation des halogènes.

3. La préparation des clinkers contenant une phase aluminate d'une composition $C_{11}A_7O,9CaX_2$ permet d'augmenter l'activité hydraulique et la résistance des ciments halogénés.

BIBLIOGRAPHIE

1.- I.A. INLACH (1974), "The influence of heating conditions on the production of fluorine-containing Portland cement clinker", Cement Technology, 5, № 4, 403-406.

2.- М.Т.Власова, Б.Э.Юдович, И.В.Кравченко, В.И.Гусева, Н.В.Иванова (1975) XI Менделеевский съезд по общей и прикладной хим., химия и технология силикатов, I77-I78 (en russe).

3.- Мчедлов-Петросян О.П., Бабушкин В.И. (1969) Термодинамические исследования твердофазных реакций в силикатах (en russe).

4.- Мори С., Утикава Х., Цукияма К., Утида С., (1976) "Гидратация специального сверхбыстротвердеющего цемента при температуре 5°С", Труды УI Международного конгресса по химии цемента, т.3, 34-40 (en russe).

Structural aspect of the C_3A-Na_2O solid solutions

Etude de la structure des solutions solides C_3A-Na_2O

Y. TAKEUCHI, Professor, Mineralogical Institute, Faculty of Science, University of Tokyo,
F. NISHI, Doctor, Mineralogical Institute, Faculty of Science, University of Tokyo, and
I. MAKI, Doctor, Nagoya Institute of Technology, Japan.

SUMMARY : The C_3A-Na_2O solid solution series has been structurally characterized based on four new structures: (i) a = 15.248(2) A , $P2_13$, Z = 8, (ii) a = 10.879(1), b = 10.845(2), c = 15.106(2), Pbca, Z = 4, (iii) a = 10.877(6), b = 10.854(13), c = 15.135(13), γ = 90.1(1)°, $P2_1/a$, Z = 4, and (iv) a = 10.844(2), b = 10.855(2), c = 15.122(4), γ = 90.38(1)°, $P2_1/a$, Z = 4. They respectively contain 2.4, 3.3, 5.7, and 6.6 Na_2O in wt. %. Among these, (ii) contains 0.45 Fe and 0.375 Si, and (iv) contains 0.465 Si per 18 oxygen atoms.

The structure (i) represents the structure type of a hitherto unreported new cubic phase, which is here denoted by CII; the C_3A phase is then denoted by CI. Thus in the C_3A-Na_2O solid solution series, there are four distinct phases, CI, CII, O, and M.

In the CII structure type, Na atoms substitute for Ca at Ca3B and Ca4B which respectively correspond to the Ca(3) and Ca(4) sites in C_3A. Excess Na atoms resulting from the replacement in the Ca/Na ratio of 1/2 go around the centers of the six-membered rings. The substitution gives rise to an expansion of the polyhedra particularly about Ca4B and a contraction of the Al - O bonds.

In the orthorhombic structure type, Na substitutes for Ca only at the Ca5 site. When Si is present in the solid solution, the Na occupancy in the rings is reduced and the solid solution range is extended towards Na-poor range. With increasing Na_2O content, the Ca5 site is differentiated into two non-equivalent sites, Ca5A and Ca5B, which accommodate Na in different amounts , thus generating the monoclinic structure type. When Si is present, Ca5B is fully occupied by Na and the monoclinic solid solution range is extended to more Na-rich region. The monoclinic - orthorhombic transition is caused by an order - disorder process of Ca and Na at the Ca5A and Ca5B sites.

RESUME : La série des solutions solides C_3A-Na_2O a été caractérisée sur la base de quatre nouvelles structures cristallines (i) a = 15,248(2) A, $P2_13$, z = 8, (ii) a = 10,879 (1), b = 10,845 (2), c = 15,106 (2), Pbca, z = 4 , (iii) a = 10,877 (6), b = 10,854 (13), c = 15,135 (13), γ = 90,1 (1)°, $P2_1/a$, z = 4, et (iv) a = 10,844 (2), b = 10,855 (2), c = 15,122 (4), γ = 90,38 (1)°, $P2_1/a$, z = 4. Elles contiennent respectivement 2,4, 3,3, 5,7 et 6,6 % Na_2O (en poids). Parmi elles, (ii) contient 0,45 Fe et 0,375 Si et (iv)contient 0,465 Si pour 18 atomes d'oxygène.

La structure (i) représente le type de structure d'une nouvelle phase cubique qui n'a pas encore été rapportée et qui est notée ici CII ; la phase C_3A est notée CI. Ainsi, dans la série des solutions solides C_3A-Na_2O, il y a quatre phases distinctes CI, CII, O et M.

Dans le type de structure CII, les atomes Na se substituent au Ca dans Ca3B et Ca4B qui correspondent respectivement aux sites Ca(3) et Ca(4) dans C_3A. Les atomes de Na, en excès, résultant du remplacement dans le rapport Ca/Na égal à 1/2, se placent autour des centres des anneaux à six membres. La distribution entraîne une expansion du polyèdre, particulièrement autour de Ca4B, et une contraction des liaisons Al-O.

Dans le type de structure orthorhombique, Na se substitue au Ca seulement dans le site Ca5. Quand Si est présent dans la solution solide, l'occupation de Na dans les anneaux est réduite et le domaine de la solution solide s'étend vers le domaine des faibles valeurs de Na. Quand la teneur de Na_2O croît, le site Ca5 se différencie en deux sites non équivalents, Ca5A et Ca5B qui logent le Na en quantités différentes, engendrant ainsi le type de structure monoclinique. Quand Si est présent, Ca5B est occupé complètement par Na et le domaine de la solution solide monoclinique s'étend vers la région plus riche en Na. La transition monoclinique + orthorhombique est due à un processus ordre-désordre de Ca et de Na, dans les sites Ca5A et Ca5B.

INTRODUCTION

The C_3A-Na_2O solid solution series, $Ca_{9-x/2}Na_x[Al_6O_{18}]$, has been structurally characterized based on four new structures having different Na_2O contents and two reported structures, one is the C_3A structure (Mondal and Jeffery (1)) and the other an orthorhombic structure (x=1.0) (Nishi and Takéuchi (2)). The present paper is to discuss in light of them the structural features of the solid solution series.

CRYSTAL DATA AND NOMENCLATURE

The new structures we determined include: (i) a hitherto unreported cubic structure having, unlike C_3A, a non-centric space group $p2_13$. (ii) an orthorhombic structure containing Si and Fe, and has a composition which falls in the two-phase region between the cubic and orthorhombic solid solutions. (iii) a monoclinic structure with x=1.5, and (iv) a monoclinic structure bearing Si and has an Na_2O content which exceeds over the compositional range for the monoclinic solid solution range. The four specimens are denoted by #1 ~ #4 according to the increasing order of the Na_2O contents. Their chemical compositions and cell dimensions obtained from single-crystal diffractometry are listed in Table I.

We propose to designate the above new cubic phase CII and the C_3A phase CI. In addition to the cubic phases, O (=orthorhombic phase) and M (=monoclinic phase) are known (Regourd et al., (3)). These four phases are the distinct ones in the C_3A-Na_2O series which we have so far recognized. As will be shown later, we have structurally confirmed that the high-temperature form of M is not tetragonal but orthorhombic as pointed out by Maki (4) based on optical studies.

The phases which occur in the compositional range for the orthorhombic metastable extension will be denoted O' in the present paper, and those occurring in the range for the monoclinic extension M'.

The four crystal structures were determined based on diffraction intensity data collected on four-circle single-crystal diffractometer and refined to R=3.7-4.9 %. Note that the structure types of CII and M are ordered derivatives respectively of CI and O. Therefore, in CII, for example, there are two non-equivalent six-membered rings, whereas in C_3A all rings are equivalent. Then we designated atomic sites in these derivatives in the following rule: when a site in a structure is differentiated into two non-equivalent sites in its derivative, the sites are denoted by putting A and B following the site symbol for the fundamental structure; e.g. the Ca(3) site in CI is differentiated into two distinct sites in CII which we denote Ca3A and Ca3B. Full details of the four structures will be reported elsewhere shortly (Takéuchi, Nishi and Maki (5)).

TABLE I

Specimen	m	#1	#2	n	#3	#4
Phase	CI	CII	O'	O	M	M'
Na_2O (wt%)	0	2.4	3.3	3.8	5.7	6.6
x*	0	0.625		1.0	1.5	
Composition**						
M	9Ca	8.688Ca, 0.625Na	8.375Ca, 0.875Na	8.5Ca, 1.0Na	8.25Ca, 1.5Na	7.9CCa, 1.73Na
T	6Al	6Al	T†	6Al	6Al	T▽
Cell dimensions (Å)						
a	15.263(3)	15.248(2)	10.879(1)	10.875(3)	10.877(6)	10.844(2)
b			10.845(2)	10.859(3)	10.854(13)	10.855(2)
c			15.106(2)	15.105(10)	15.135(13)	15.122(4)
γ			-	-	90.1(1)°	90.38(1)°
Pseudocubic subcell						
a	3.816	3.812	3.840	3.842	3.845	3.849
b			3.840	3.842	3.838	3.823
c			3.777	3.776	3.784	3.781
γ			90.2°	90.1°	90.1°	90.4°
Cell volume ($Å^3$)	3555.7	3545.2	$3564.5\times\frac{1}{2}$	$3567.5\times\frac{1}{2}$	$3573.6\times\frac{1}{2}$	$3560.0\times\frac{1}{2}$
Space group	Pa3	$P2_13$	Pbca	Pbca	$P2_1/a$	$P2_1/a$
Z	8	8	4	4	4	4

m: Mondal & Jeffery (1). n: Nishi & Takéuchi (2). *$Ca_{1-x/2}Na_x[Al_6O_{18}]$. **For 18 oxygen atoms.

M = Large cations. T = Tetrahedral cations. T† = 5.175Al, 0.45Fe, 0.375Si. T▽ = 5.535Al, 0.475Si

THE CII STRUCTURE TYPE

In order to elucidate the mode of Na distribution in the cubic phase, an attempt was made of preparing cubic crystals containing maximum possible Na for that solid solution range. Electron microprobe analyses showed the product we obtained contained 2.4 Na_2O in wt. per cent. These are the #1 specimens. Our X-ray study showed that the crystals had the space group, not Pa3, but $P2_13$ and represented a new cubic phase CII.

Of a total of 5 Na in the unit cell of the structure, 2.5 Na are located, substituting for Ca, at the positions corresponding to Ca(3) and Ca(4) sites which occur in the threefold axes in the C_3A structure. The remaining Na atoms go to around the centers of the six-membered rings. The Na atoms in the rings are coordinated by bridge oxygen atoms, giving rise to a contraction of the rings compared to those in C_3A; this situation makes the a periodicity of the CII structure type smaller than that of CI.

As mentioned earlier, the rings are now differentiated into two non-equivalent rings, A and B. The non-centric feature of the structure is well represented by the difference in occupancy of Na in the rings (Table II). In harmony with this, Na atoms in the cation sites mainly substitute for Ca at Ca3B and Ca4B rather than Ca3A and Ca4A. This situation would presumably be the result of attaing local charge balance.

One of marked features of the structure is that the polyhedra that accommodate Na become bigger in size compared to the corresponding ones in C_3A. In particular, the Ca4B site has nine near oxygen atoms at the distances smaller than 3Å and the coordination polyhedra are ninefold, while Ca(4) in the C_3A structure has six Ca-O bonds smaller than 3 Å and three additional bonds longer than 3 Å; the coordination about Ca(4) is essentially sixfold. The mean volume (16.90 $Å^3$) of the octahedra about Ca3A and Ca3B is likewise bigger than the volume (16.58 $Å^3$) of the octahedron about Ca(3) in C_3A. Such a 'swelling effect' of polyhedra that occurs upon replacement of Ca by Na sensibly generates structural distortion and is of basic importance to characterize the structural features of the solid solution series now considered.

It is notable that the mean *Al*-O bond length of the #1 specimen is 1.746(2) Å and smaller than 1.752(2) Å for the C_3A structure. Excepting this case of #1, we find that the mean *Al*-O bond lengths are almost constant throughout the C_3A-Na_2O solid solution series (figure 1).

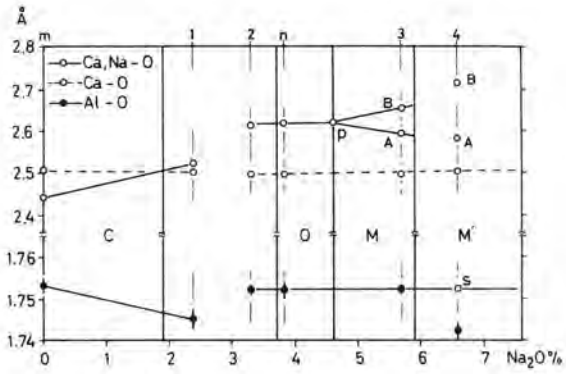

Fig. 1. Variations of mean *Al*-O, Ca-O and Ca(Na)-O bond lengths versus Na_2O content in the solid solution series. The solid solution ranges for C, O and M indicated by heavy vertical lines are those given by Regourd et al. (3); the range of C must be revised so as to indicate those of the two phases, CI and CII. The diagram is based on the data from m (Mondal & Jeffery (1)), n (Nishi & Takéuchi (2)), and #1 - #4 specimens; p is a plot based on calculated Na occupancy (Takéuchi et al. (5)). The open square indicated by S is a plot of mean *Al*-O length corrected for the Si content in #4. The mean value of Ca(3)-O and Ca(4)-O bonds in C_3A was evaluated and plotted separately from that of other Ca-O bonds in the C_3A structure.

TABLE II

Specimen	#1		#2	n	#3		#4	
Ring	A	B			A	B	A	B
Occupancy of Na (%)	26(3)	37(3)	26.7(6)	50(2)	74.6(8)	75.4(8)	52(2)	75(3)
δ*(Å)			0.41(5)	0.30(4)	0.45(2)	0.52(2)	0.41(4)	0.60(4)
Average Na-O distance (Å)	2.86	2.83	2.73	2.68	2.68	2.68	2.70	2.70

n: Nishi & Takéuchi (2). * The separation of a pair of split Na positions.

This situation would probably suggest that the cubic arrangement of the six-membered rings is a stable form basically for C_3A and the effect on the arrangement caused by the replacement of Ca by Na is compensated by reducing the *Al*-O bond lengths. With increasing Na_2O content in the structure, the cubic arrangement of the rings then undergoes a drastic change to yield a new arrangement.

THE MONOCLINIC STRUCTURE TYPE

Geometrically the crystal structure of the monoclinic structure type shares the same feature with that of the orthorhombic structure type (Nishi and Takéuchi (2)); the mode of arrangement of the six-membered rings in M is in principle the same as that of the O phase. So far the type of the arrangement of the six-membered rings is concerned, there are in the C_3A-Na_2O solid solution series only two different types. They are compared in figure 2.

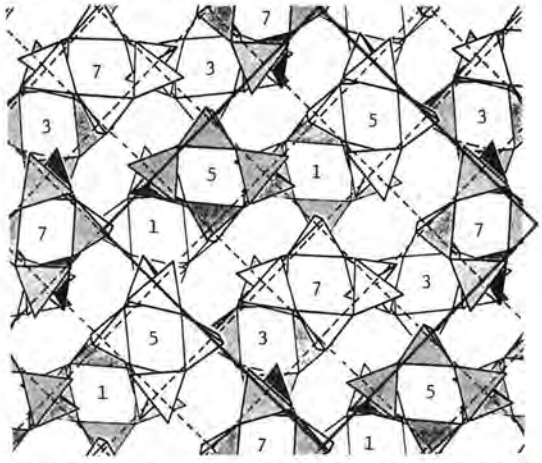

The essential feature that characterizes the monoclinic structure type is in the mode of distribution of Na over the cation positions corresponding to Ca5 in the orthorhombic structure type. The positions are in the monoclinic structure differentiated into two different sets of positions, Ca5A and Ca5B, having different Na occupancies (Table II). Such a cation ordering gives rise to a slight distortion of the orthorhombic cell to yield a monoclinic symmetry. Compared to the Na occupancy at Ca5 (Table III) in the orthorhombic structure, that in the Ca5B in the monoclinic structure of the #3 specimen is increased, while that in the Ca5A is decreased.

TABLE III

#1		#3	
Site	Contents	Site	Contents
Ca3A	0.91(2)Ca 0.09(2)Na	Ca5A	0.803(4)Ca 0.197(4)Na
Ca3B	0.73(2)Ca 0.27(2)Na	Ca5B	0.447(4)Ca 0.553(4)Na
Ca4A	0.97(2)Ca 0.03(2)Na	#4	
Ca4B	0.76(2)Ca 0.24(2)Na	Ca5A	0.902(6)Ca 0.098(6)Na
#2		Ca5B	- 1.000 Na
Ca5	0.696(3)Ca 0.304(3)Na		

In the orthorhombic structure, the Ca5 site has six near oxygen atoms at the distances smaller than 3 Å plus two additional oxygen neighbors at the distances of 3.008 Å and 3.138 Å (Nishi and Takéuchi (2)). In contrast to this, Ca5B has seven near oxygen atoms at the distances smaller than 3 Å and one additional neighbor at a distance of 3.157 Å in the case of the #3 specimen. A calculation excluding the bond lengths longer than 3 Å showed that the mean Ca-O bond lengths for the Ca5B polyhedra are 2.652 Å for the #3 specimen and 2.714 Å for #4; these are considerably bigger than 2.551 Å for the Ca5 polyhedron in the orthorhombic structure. On the other hand, those for the Ca5A polyhedra are 2.521 Å for #3 and 2.622 Å for #4.

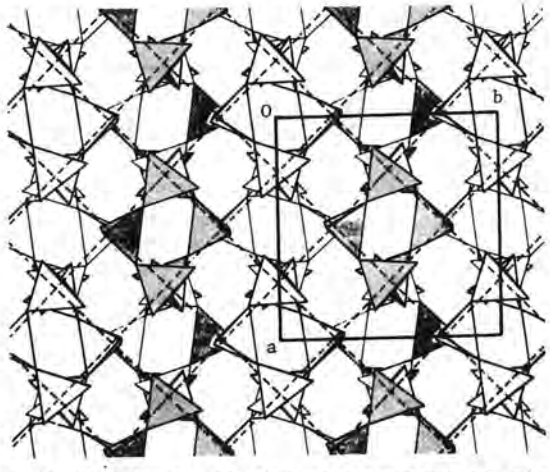

Fig. 2. Two types of the arrangement of six-membered rings. (Left): the arrangement in the cubic structures. Numbers indicate in fractions of eight the height of rings. The rings shown by shaded tetrahedra correspond to B rings in CII, and those shown by open tetrahedra to A (all rings are equivalent in CI). (Right): the arrangement of rings in the non-cubic structures. The rings shown by shaded tetrahedra correspond to B rings in the monoclinic structure type (all rings are equivalent in the orthorhombic structure type). The rings drawn with light lines are at $\underline{z}=0$, and those with heavy lines at $\underline{z}=1/2$. The unit cell is indicated by heavy lines and subcells by broken lines.

The Na atoms in the unit cell other than those in the Ca5A and Ca5B sites are located at around the centers of the six-membered rings. Occupancies of Na at around the centers of A and B rings are nearly the same. These Na atoms are each at a distance of around 3.8 Å from both Ca5A and Ca5B; the Na in the ring will therefore be exchangeable with Na at the cation sites at elevated temperatures.

Each Na atom is not exactly at the center of symmetry on which the ring is located but statistically located at a pair of positioned slightly off the center. The separation, δ, of the pair in each non-cubic structure examined is listed in Table II given previously.

The occurrence of the monoclinic structure type may be rationalized in terms of the mode of Na distribution over the Ca5A and Ca5B sites. As observed in Figure 3, the

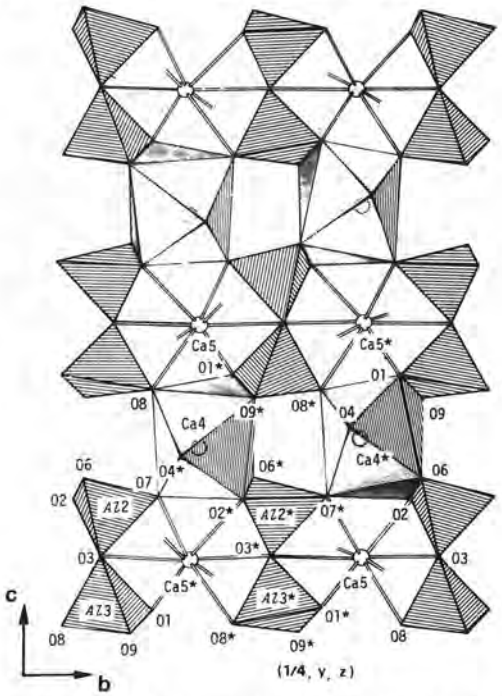

Fig. 3 The structure of the orthorhombic type (the drawing is based on the structure reported by Nishi and Takéuchi (2)), showing the arrangements of polyhedra about cations nearly in the x=1/4 level. The site symbols indicated by stars correspond to B sites in the monoclinic structure type; those not indicated by stars to A sites. Each pair of tetrahedra is portion of a six-membered ring.

Ca5A and Ca5B sites occur in the same z level and the polyhedra about these sites flank on a pair of tetrahedra of each six-membered ring. Note that they occur alternately along the b axis and also along c. If suppose that the Na occupancies at both cation sites were the same and both sets of polyhedra about these sites equally 'expand'. Then the result would bring about strain in the crystal. The mode of Na distribution at the cation sites we found in the monoclinic structure type implies an alternate arrangement of the two kinds of polyhedra about Ca5A and Ca5B, different in size. Such a situation would minimize strain in the crystal.

The monoclinic solid solution range terminates at the Na_2O content of 5.9 wt% (Fletcher et al., (6)). This limitation appears to be explainable structurally. As observed in Table II given previously, the Na-O distances decrease with increasing Na occupancy in the ring. This trend is however only in the range from zero to 50 % Na occupancies in the ring. The distances for the occupancy of 75 % Na are not significantly different from those for 50 % Na. This fact would suggest that the contraction of the six-membered ring brought about by the occupancy of 75 % Na would be the permissible limit for the distortion of the ring. Namely, the occupancy of Na in the ring appears to be limited up to around 75 %. The #3 specimen contains 5.7 % Na_2O which corresponds to the limit of the monoclinic solid solution given by Regourd et al. (3) and the occupancies of Na in the A and B rings are nearly of the same value of 75 % (Table II).

PHASE TRANSITION

Using a crystal piece of the #3 specimen, we recorded with a precession camera the hkO patterns at temperatures from 600°C to 900°C with an interval of 100°C. The result showed that the monoclinic structure was transformed to orthorhombic. Noting that the pair of intensities of $8\bar{1}0$ and 810 reflections are one of the characteristic pairs to distinguish the orthorhombic form from monoclinic, we measured their intensities recorded at 880°C with an automated microdensitometer and compared them in Fig.4 with those at room temperature.

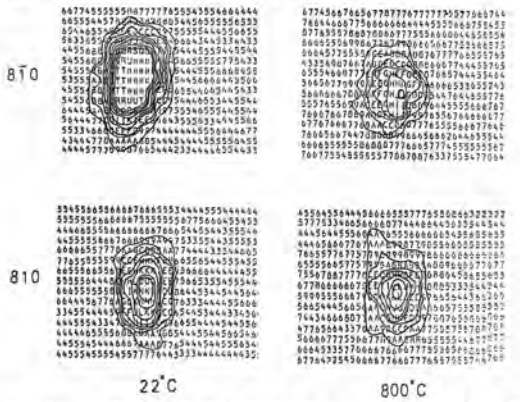

Fig. 4. Portions of computer out put, showing intensities of $8\bar{1}0$ and 810 reflections recorded in film at 22°C and 800°C. Contours are drawn at an arbitraly scale but with equal intervals; those at the central portion of the $8\bar{1}0$ peak at 22°C are omitted. The ratio in observed integrated intensity of this reflection pair was 1.9 at 22°C, and 1.0 at 800°C.

When the crystals were heated above 600°C and quenched to room temperature, they exhibited lamellar twins and gave monoclinic diffraction patterns.

It is highly conceivable that the transition is caused by order-disorder of Na and Ca at the Ca5A and Ca5B sites. If the Na occupancies at these sites in the monoclinic structure type is equalized at elevated temperatures, the structure is simply transformed into orthorhombic; positional adjustment of the six-membered rings required for the transition is almost negligible.

ROLE OF Si IN THE STABILITY OF SOLID SOLUTIONS

A comparison between the structures of the #2 specimens and the reported orthorhombic structure of pure aluminate (Nishi and Takéuchi (2)) shows that the Na occupancy of 30 % at Ca5 in the former is slightly higher than that of the latter (25 %), while the Na occupancy in the rings of the former (Table II) is roughly half of that of the latter (50 %); the excess positive charge introduced by Si in the #2 specimen is mainly compensated by decreasing Na in the rings. It then appears that the Na occupancy in the six-membered rings is related to the stability of the orthorhombic phase. If therefore the orthorhombic structure type permits to contain more Si than that in the #2 specimen, the compositional range would be more widened towards the Na_2O poor region by decreasing Na in the rings. This situation will offer a structural basis for explaining the 'meta-stable' extension of the orthorhombic phase.

Our structural study of the #4 specimen revealed that the presence of Si in the monoclinic solid solution permits the Na occupancy of 100 % at the Ca5B site (Table III) and as the result the occupancies of Na in the rings, which will otherwise increase with increasing Na_2O content (Figure 5), are kept to the values less than around 75 %. As a total effect, the number of Na per cell may exceed over the number permissible for the original monoclinic range and thus the range may be extended to the Na_2O content of 7.59 %.

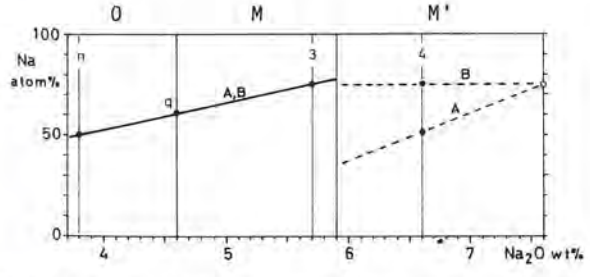

Fig. 5. Variation of the Na occupancy in the rings versus Na_2O content in the non-cubic structures. A and B represent A and B rings; q is a calculated value for the composition having Na_2O of 4.6 %. Broken lines indicate assumed variations in the M' range. Entries are: n=Nishi and Takéuchi (2), 3=#3 specimen, and 4=#4 specimen.

CONCLUSIONS

The conclusions drawn from the present study include:

(i) In the C_3A-Na_2O solid solution series, the existence of four distinct phases, CI (=C_3A), CII, O, and M, has so far been recognized.

(ii) The monoclinic phase is transformed at around 500°C to orthorhombic and the transition is reversible. This transition is of an order-disorder type.

(iii) When a calcium site is replaced by Na, the polyhedron about the site tends to expand. The structural changes from one phase to another with the change in Na_2O contents can be explainable in terms of this effect.

(iv) The occupancy of Na at around the center of a six-membered ring appears to be limited up to around 75 %.

(v) When Si exists in the solid solutions, it plays a role in reducing the Na occupancy at around the centers of the six-membered rings. The extensions of the orthorhombic and monoclinic solid solution ranges can be rationalized based on such a structural characteristics.

BIBLIOGRAPHIE

1. - P. MONDAL and J. W. JEFFERY (1975), "The crystal structure of tricalcium aluminate, $Ca_3Al_2O_6$", Acta cryst. B31, 686-697.

2. - F. NISHI and Y. TAKÉUCHI (1975), "The Al_6O_{18} rings of tetrahedra in the structure of $Ca_{8.5}NaAl_6O_{18}$", Acta Cryst. B31, 1169-1173.

3. - M. RUGOURD, S. CHROMY, L. HJORTH, B. MORTREU and A. GUINIER (1973) "Polymorphisme des solutions solides du sodium dans l'aluminate tricalcique", J. Appl. Cryst. 6, 355-364.

4. - I. MAKI (1976) "Optical properties of the anisotropic C_3A", Cement Concr. Res. 6, 183-192.

5. - Y. TAKÉUCHI, F. NISHI and I. MAKI (1979) "Crystal-chemical characterization of the $3CaO \cdot Al_2O_3$-Na_2O solid solution series". To be published in Zeit. Krist.

6. - K. E. FLETCHER, H. G. MIDGLEY and A. E. MOORE (1965) "Data on the binary system $3CaO \cdot Al_2O_3$-$Na_2O \cdot 8CaO \cdot 3Al_2O_3$ within the system CaO-Al_2O_3-Na_2O" Mag. Concr. Res. 17, 171-176.

Anisotropic forms of C_3A : phase relations

Formes anisotropiques de C_3A : relations de phase

B. TAVASCI, Professor, Politecnico di Milano,
F. MASSAZZA, Professor, Italcementi - Laboratorio Chimico Centrale, Bergamo.
U. COSTA, Doctor of Chemistry, Italcementi, Laboratorio Chimico Centrale, Bergamo.

RESUME: La composition d'équilibre des deux phases anisotropiques de l'aluminate tricalcique contenant du sodium est déterminée en fonction de la température. Ces compositions sont représentées par une couple de courbes qui se joignent en correspondance du composé C_8NA_3, dont on prouve l'existence.

SUMMARY: The equilibrium composition of the two anisotropic phases of tricalcium aluminate containing sodium is determined as a function of temperature. These compositions are represented by a couple of curves joining in the C_8NA_3 compound, whose existence is proved.

1. INTRODUCTION

The origin of this investigation mainly lies in a sentence contained in a paper of two of us (1): "....but none of the researchers who were concerned with this subject found the two anisotropic forms at the same time" (rhombic and monoclinic phases according to Maki (2), or orthorhombic I or tetragonal and orthorhombic II according to Regourd et Al. (3).
It lies also in that, apart from the thermochemical results, not even the mentioned investigation could distinguish the two phases. Consequently one of us proposed to re-examine the problem by using the microscopic observation by reflected light as a research method on samples quenched from different temperatures. Of course the optical properties of the phases are not determined but only their differentiation is sought through the different behaviour towards suitable reagents.
Therefore from now on the phases will be indicated as rhombic and monoclinic, for semplicity's sake, without entering upon their structure.
The starting point is represented by Maki's (2) results which slightly differ from and indeed seem to simplify Regourd, Chromy, Hjorth, Mortureux and Guinier's (3) results. In substance it is question of defining the stability field of the two rhombic and monoclinic phases by determining the couple of curves which represent the composition of the two phases in equilibrium as the temperature changes.
The extension of the rhombic phase towards the cubic one is not of interest here; on the contrary the extension of the two anisotropic phases towards C_8NA_3(•) is considered since, of course, the two curves must join.

2. EXPERIMENTAL

2.1 Preparation of the samples

The solid solutions of sodium oxide in tricalcium aluminate were prepared by homogenizing stoichiometric quantities of r.g. $CaCO_3$, Na_2CO_3 and γ-Al_2O_3 in cyclohexane by an agate jar mill. After evaporation of the liquid, the material was decarbonated for 1 hour at 900°C and afterwards re-homogenized.
Since the sodium volatility is high at the selected firing temperature (1350°C), it was necessary to introduce the material, pressed in small cylinders, into 5 mm diam. sealed platinum tubes.
To prevent the tubes from cracking owing to the thermal expansion of air, they were evacuated by a rotary pump and welded.
To reach the equilibrium with certainty, the fired samples were ground and fired again; after this treatment, their sodium content was determined by atomic absorption spectrometry and optical and X-ray examinations were carried out to ascertain their pureness.
Aliquots of each preparation were closed in platinum tubes and brought to the selected quenching temperature which was maintained for at least 12 hours. After this annealing, the samples were quenched in water. Table I shows the examined compositions expressed by the general formula $C_{3-n}N_nA$ [for C_8NA_3, n is 0.33, exactly 0.3̄].

2.2 Microscopic observations

The microscopic observations were carried out especially on 4 mm diam., 8 mm long cylinders soaked in styrene and afterwards resinified. The cylinders were sectioned and polished along a longitudinal plane.

(•) C = CaO, N = Na_2O, A = Al_2O_3

TAB. I: Examined compositions and quenching temperatures

Composition	calculated Na_2O wt%	found Na_2O wt%	Quenching temperature (°C)							
			25	400	450	475	500	550	600	1350
$C_{2.82}N_{0.18}A$	4.11	4.13	•	•						•
$C_{2.80}N_{0.20}A$	4.57	4.47	•	•						•
$C_{2.79}N_{0.21}A$	4.79	4.77	•							
$C_{2.78}N_{0.22}A$	5.02	5.00	•	•						•
$C_{2.77}N_{0.23}A$	5.25	5.28	•	•						
$C_{2.76}N_{0.24}A$	5.47	5.46	•	•						•
$C_{2.75}N_{0.25}A$	5.70	5.74	•	•						
$C_{2.74}N_{0.26}A$	5.93	5.97	•	•	•	•	•			•
$C_{2.72}N_{0.28}A$	6.38	6.14	•	•			•			•
$C_{2.66}N_{0.33}A$	7.60	7.62	•	•			•	•	•	•
$C_{2.65}N_{0.35}A$	7.97	7.80								•

The pursuit of reagents suitable to distinguish the two phases presented a considerable difficulty, given the very close analogy of the two phases. Several reagents were tried: distilled water, borax at different concentrations, alcoholic solution of H_2SO_4 a.s.o., reagents studied by one of us to investigate the constitution of portland cement (4) or during subsequent research to identify the constituents of celite. The outcome was always negative: the etching was either missing or equal for the two phases. The attention was turned to stronger reagents and, among these, to "nital", an alcoholic solution of HNO_3 (usually at 2%) universally used in the metallography of steels.
The result was quite positive: with an etching of about 30 seconds, one of the phases (the monoclinic) was constantly characterized by very fine stripes of polysynthetic or also multiple twinning. The observation of these stripes requires strong objectives: a numerical aperture below 0.65 is not convenient.
It was noted that also this one is sometimes insufficient.
Stripes, that were visible by a 0.85 aperture objective, became undistinguishable by using a 0.65 aperture. The micrographs reproduced in this paper are all 450X (0.65 N.A. objective).
In the observation and still more in the photography, it was necessary to use all the tricks useful to eliminate blurs, sometimes very frequent, due to internal reflections of the crystals, or more generally, to drawbacks of preparation. To this purpose the photographs were taken by introducing the analyzing nicol and, except for the two last, in oblique illumination.
Coming back to the action of the reagent on the two phases, it is possible to add that the reagent simply defines the single crystals in the rhombic one; single planes of twinning are characterized by a line: no stripes. On the contrary, as regards the monoclinic phase, the reagent evidences also the stripes. However it must be noticed that the eventual lack of stripes does not mean that a given crystal is not monoclinic.
The stripes could be not resolvable by the used objective or the twinning plane could be parallel to the section.

Finally the eventual presence of free lime (or of other constituents), if limited and irregularly distributed (that is lacking in some zones) can be attributed to defects of homogenization; if systematic, it must be considered as a consequence of composition.
Free lime, that the indicated reagent would strongly corrode, can be easily recognized in the simply polished specimen since it appears light against a grey background owing to its higher refractive index.

2.3 Results

It is natural to present them by following the development of this work.
At first the composition was simply changed by passing from n = 0.18 (0.18 N) to n = 0.28 (0.28 N) at an annealing temperature of 400°C. Since the first results of the observations were positive, also the ordinary temperature (slow cooling) and, for some mixes, the annealing temperature of 1350°C were considered.
Subsequently, the composition was maintained constant (0.26 N) and the annealing temperature was changed.
Given the obtained results, this operation was carried out also for n = 0.33 (C_8NA_3).
In the final plot (fig. 16), the different compositions observed under the microscope are represented by rather marked spots.

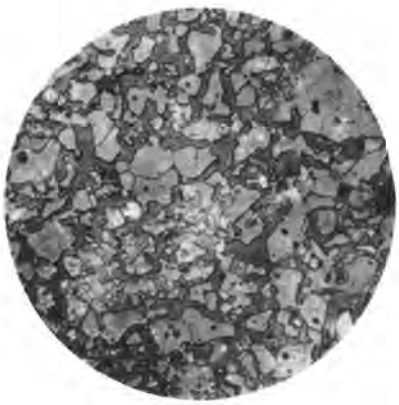

FIG. 1: $C_{2.78}N_{0.22}A$ quenched from 400°C - Nital - 450X

I) Quenching from 400°C. Fig. 1 shows the appearance of the 0.22 N mix, that is n = 0.22. Considering that the dark zone represents the styrene resin, different crystals are noted in the grains, however without stripes: this is obviously the rhombic phase.
Fig. 2 shows the appearance of the 0.26 N mix. Practically all the crystals are striped (monoclinic phase).
Fig. 3 corresponds to the 0.28 N composition and, owing to the similarity of its stripes to those of the previous figure, it evidences that the phase is completely monoclinic already in 0.26 N.
In Fig. 4, corresponding to 0.24 N, some crystals have not stripes and others do, with a certain prevalence of the former: both phases are present. The monoclinic phase begins appearing at about 0.23 N.

II) Slow cooling up to ordinary temperature. The presence of the monoclinic phase begins little below 0.21 N instead of 0.23 N. Fig. 5, corresponding to 0.22 N (cmp. Fig. 1) already shows the evident presence of this phase.

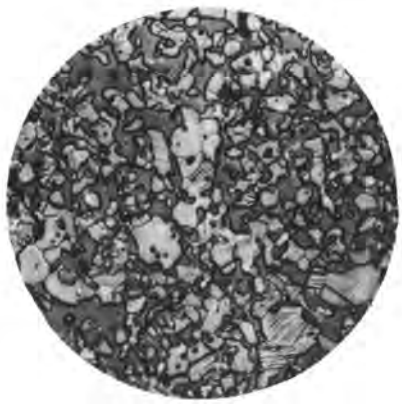

FIG. 2: $C_{2.74}N_{0.26}A$ quenched from 400°C - Nital - 450X

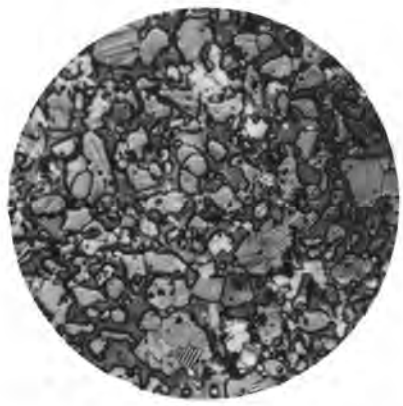

FIG. 3: $C_{2.72}N_{0.28}A$ quenched from 400°C - Nital - 450X

FIG. 4: $C_{2.76}N_{0.24}A$ quenched from 400°C - Nital - 450X

FIG. 5: $C_{2.78}N_{0.22}A$ cooled at room temperature - Nital 450X

FIG. 6: $C_{2.76}N_{0.24}A$ cooled at room temperature - Nital 450X

FIG. 7: $C_{2.75}N_{0.25}A$ cooled at room temperature - Nital 450X

It clearly prevails at 0.24 N (fig. 6). It represents almost the totality at 0.25 N (compare fig. 7 with figures 2 and 3).

III) 0.26 N composition quenched from different temperatures. The rhombic phase is present at the temperature of 450°C (fig. 8). It becomes prevalent at 475°C (fig. 9). It represents the totality at 500°C (fig. 10).
Also a 0.28 N mix was quenched from 500°C. Both phases are present again in it.

IV) 0.33 N composition (C_8NA_3) quenched from different temperatures. The two curves representing the equilibrium composition of the two phases, as defined by the above results, tend to shift rightwards as the temperature increases, nevertheless without joining for Na_2O contents considered up to now.
If the assumption of two individual phases is true, the two curves must necessarily meet in one point, which is already indicated schematically in the paper (1). This point, however, must represent the composition and transformation temperature of an only component.

FIG. 8: $C_{2.74}N_{0.26}A$ quenched from 450°C - Nital - 450X

FIG. 9: $C_{2.74}N_{0.26}A$ quenched from 475°C - Nital - 450X

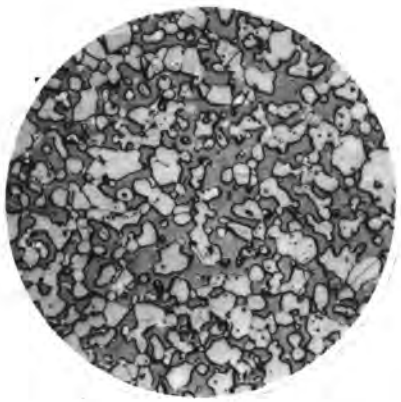

FIG. 10: $C_{2.74}N_{0.26}A$ quenched from 500°C - Nital - 450X

The extrapolation of the two curves led to foresee their joining in the 0.33 N composition and at a temperature ranging between 500° and 600°C. Of course it was necessary to ascertain that the mass of this composition should correspond to a single compound which, at the sought temperature, must appear in two phases simultaneously.
The 0.33 N mix fired and quenched from 1350°C was lacking in free lime or other components: therefore the C_8NA_3 compound exists, notwithstanding the difficulties of its preparation.

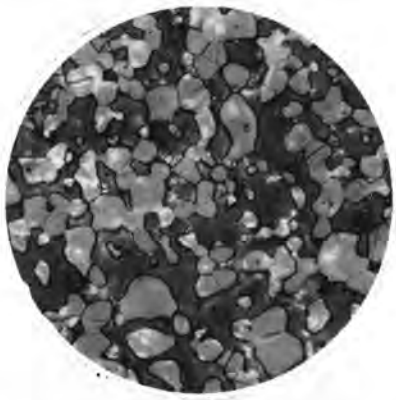

FIG. 11: $C_{2.66}N_{0.33}A$ quenched from 1350°C - Nital - 450X

Fig. 11 represents its micrographic appearance, without stripes. The small light spots inside the crystals are due to internal reflections and not to the presence of free lime that would strongly have been etched.
Fig. 12 shows the same product quenched from 400°C : the stripes are complete.
The quenching from 600°C did not produce stripes, whereas the latter were wholly present for quenching from 500°C.

FIG. 12: $C_{2.66}N_{0.33}A$ quenched from 400°C - Nital - 450X

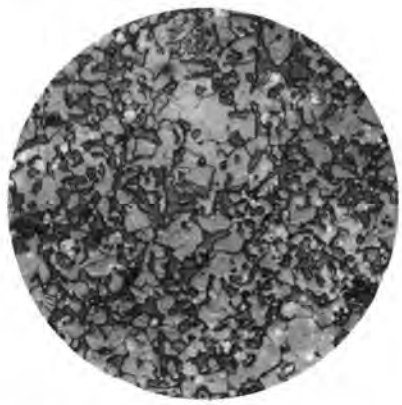

FIG. 13: $C_{2.66}N_{0.33}A$ quenched from 550°C - Nital - 450X

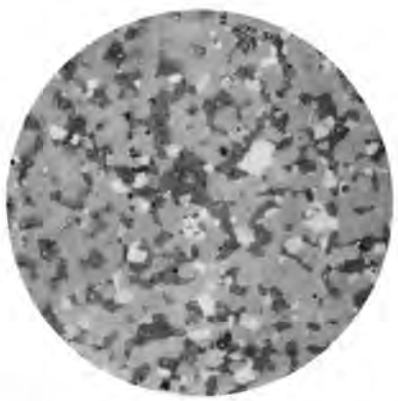

FIG. 14: $C_{2.65}N_{0.35}A$ quenched from 1350°C - Not etched - 450X

The sample quenched from 550°C (fig. 13) appeared to be extremely interesting: both phases are present. Moreover the development of striped roundish crystals of the monoclinic phase was often noticed inside crystals of the rhombic phase. Obviously the temperature of 550°C (apart from experimental errors) corresponds to the temperature of transformation of a phase into the other.

V) 0.35 N composition quenched from 1350°C. One could suppose that the two curves should not join yet at 0.33 N and that, consequently, it should be necessary to examine mixes richer in Na_2O. Instead, there is no need of many quenching tests from different temperatures. The 0.35 N mix, quenched from 1350°C, showed the systematic presence of free lime and, obviously, of sodium aluminate (NA).
Fig. 14 shows that, when the specimen is simply polished, free lime appears (owing to its higher reflectivity than that of aluminate) in clearer (polygonal) grains. The NA compound, having low reflectivity, is almost undistinguishable from the dark resin in the background. Sodium aluminate could be easily evidenced by hydrofluoric acid-based reagents (which do not etch CaO) studied by one of us (4), eventually by restraining their solving action with the addition of alcohol.

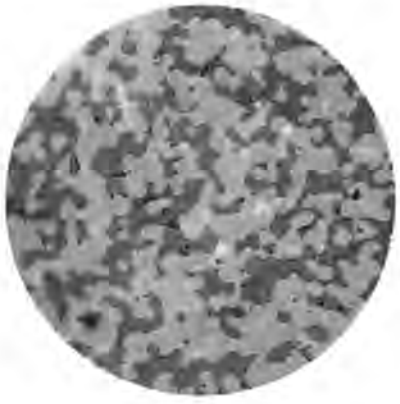

FIG. 15: $C_{2.66}N_{0.33}A$ quenched from 1350°C - not etched 450X

In order to assure that the 0.33 N composition does not contain free lime, the same specimen of fig. 11 is reproduced in fig. 15 which shows its not etched appearance.
The small light spots, having irregular and blurred boundaries, do not represent free lime but internal reflections of the crystals.
Here the mass among the aluminate crystals exclusively consists of resin.
After all, the two equilibrium phases show a varying composition according to two curves joining in C_8NA_3, as indicated in fig. 16.

3. CONCLUSIONS

The compound C_8NA_3 exists. The composition of the two solid anisotropic solutions, that this compound forms as a preponderant part with C_3A, varies according to two co-existence curves.

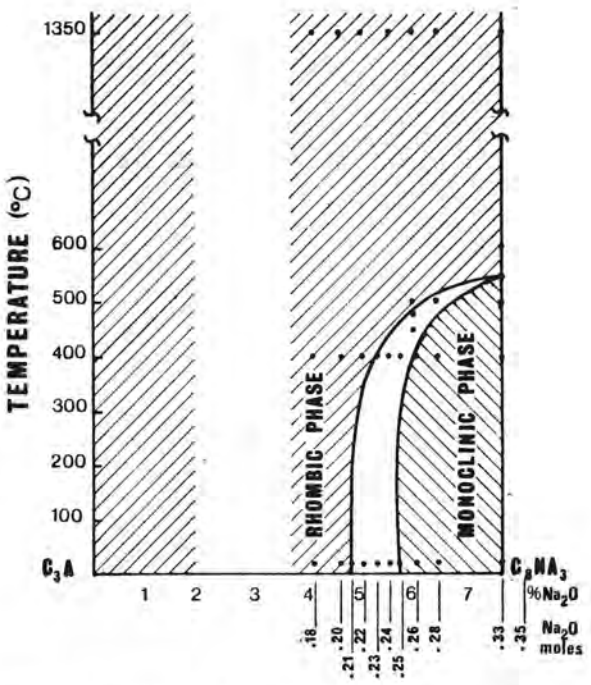

FIG. 16: Phase equilibrium in the part richest in sodium in the system C_3A-C_8NA_3

These have a common point at 550°C corresponding to the pure C_8NA_3 compound; they also present a decreasing trend as the temperature and the sodium content decrease.

REFERENCES

(1) MASSAZZA F., COSTA U. (1978), "Entalpia di formazione delle soluzioni solide 3(CaO, Na_2O)Al_2O_3", Il Cemento, (3), 263-70 (It.)

(2) MAKI I. (1976), "Optics and phase relationships of the optically anisotropic C_3A", Cement and Concrete Research, 6, 797-802 (Eng.)

(3) REGOURD M., CHROMY S., HJORTH L., MORTUREUX B., GUINIER A. (1973), "Polymorphisme des solutions solides du sodium dans l'aluminate tricalcique", J. Appl. Cryst., 6, 355-64 (French)

(4) TAVASCI B. (1934), "Ricerche sulla costituzione del clinker di cementi portland", Giornale di Chimica Industriale ed Applicata, 16, 538-51 (It.)

Theme 2 - The hydration of C_3A

GENERAL REPORT

by H.N. STEIN, Laboratory of Colloid Science, Vakgroep Elecktrochemie, Department of Chemical Engineering, Eindhoven University of Technology, Eindhoven, THE NETHERLANDS.

The papers which have been contributed to the present congress and which are specially related to the hydration of C_3A, concern the following problems:

a. What is happening at the C_3A/water and $C_3A/Ca(OH)_2$ solution interfaces?
b. How is the hydration of C_3A influenced by the presence of Na_2O as solid solution in the C_3A?
c. What is the mechanism of retardation of C_3A hydration in the presence of calcium sulfate?
d. How large is the mutual interaction between calcium aluminate hydrate crystals when present in aqueous solution?

a. Phenomena at the C_3A/water and $C_3A/Ca(OH)_2$ solution interfaces.

Barret and Bertrandie investigated the dissolution of C_3A in water and in $Ca(OH)_2$ solutions by analyzing the liquid after contact with C_3A, for its increase in CaO and Al_2O_3 contents. In a stagnant medium (water or dilute $Ca(OH)_2$ solution), C_2AH_8 is the first solid to precipitate, which leads to a Δ CaO/Al_2O_3 molar ratio > 3 in the liquid phase. This does not, however, signify that the dissolution process itself is incongruent: after very short contact times (effected by passage of liquid through a thin layer of C_3A), the filtrate has a Δ CaO/Al_2O_3 ratio = 3. In more concentrated $Ca(OH)_2$ solutions ($[CaO]>9.10^{-3}$ mol.kg^{-1}), C_4AH_{13} is the first solid to precipitate which leads to Δ CaO/Al_2O_3 molar ratios < 3 in the liquid. The authors describe the dissolution as being determined by the solubility of superficially hydrated C_3A.

Thus, according to Barret and Bertrandie, the first process taking place is the formation of a hydrated layer on the C_3A itself, with Δ CaO/Al_2O_3 molar ratio = 3.

However, it has been found from electrokinetic data reported by the present author, that the calcium aluminate hydrates when formed during C_3A hydration, have a definitely non-stoechiometric surface layer deficient in aluminate ions: the ζ potential of both hexagonal and cubical hydrates is > 0 during C_3A hydration, and the corresponding surface charge increaseswith NaOH concentration, which indicates progressive extraction of aluminate ions from the surfaces of the calcium aluminate hydrates.

There is no real contradiction, however, between the results reported by Barret and Bertrandie, and the ζ potential data, because a surface charge of the required magnitude can easily originate through differences in calcium and aluminate ion dissolution rate which are too small to be detected by analyses of the aqueous solutions.

b. Influence of Na_2O on C_3A hydration

The ζ potential data mentioned have been advanced as a support for an explanation of the influence of Na_2O on the hydration rate of C_3A: extraction of aluminate ions from the hydrated surface layer on C_3A would make its composition approach to that of $Ca(OH)_2$ [1]. This subject has been a rather controversial one. It had been studied previously by Gupta, Chatterji and Jeffery [2], by Regourd and Mortureux [3], by Boikova c.s. [4] [5] and by Butt c.s. [6] [7] with none too consistent results. In reality, two questions are involved here: does Na_2O retard or accelerate the hydration of C_3A; and does Na_2O present as solid solution in the C_3A, act in the same way as an equivalent amount of NaOH added seperately?

Most investigators [1] [2] [3] [4] [5] report a retardation by Na_2O; however, Butt c.s. [6] [7] found an acceleration. This discrepancy is not resolved by the contributions to the present congress: Boikova, Grishchenko and Domansky again report a retardation; Kolbassov, Kozyreva and Dobronravova on the other hand report an acceleration. From the data presented in the communications, no possible reason (e.g. differences in experimental conditions) can be extracted which may be held responsible for the discrepancy. Although part of the results reported by Kolbassov c.s. have been obtained by plastometry, which means that they are influenced not only by the degree of hydration but by the mutual interaction between the calcium aluminate hydrates as well, the authors also find a higher hydration activity of Na_2O containing C_3A by differential thermokinetic curves. Perhaps the difference in results can be explained when details on the experimental procedures employed are exchanged at this congress.

Similarly, the opinions are still divided as to whether Na_2O built into the C_3A structure acts in the same way as an equivalent amount of NaOH added separately. This question is of practical interest, since by a suitable choice of fuel it is possible to either enclose the Na_2O in a Portland cement clinker as solid solution in the C_3A, or to have it present in a separate phase (Na_2SO_4) [7].

Boikova c.s. discern three different stages in the hydration of C_4A; during the first stage, Na_2O built into the C_3A structure retards the hydration strongly because water penetration into C_3A containing Na_2O is hindered by Na^+ ions occupying holes in the C_3A crystal structure. This agrees with Regourd's view [3) 8)], which is, however, not shared by Spierings and the present author [1)]. The latter authors report, in agreement with Gupta c.s. [2) 9)], a strong retardation of C_3A hydration by NaOH added separately. Perhaps the conflicting evidence brought on this point can be conciliated by the statement that in stirred suspensions of large water to solids ratios, the action of NaOH added separately is similar to that exerted by Na_2O built into the C_3A structure, whereas in pastes of low w/s ratio local NaOH concentrations near the hydrating, Na_2O containing, C_3A are much larger than if NaOH is added separately. However, this point clearly needs further elaboration by experiments.

c. Retardation of C_3A hydration in the presence of calciumsulfate

---

Local concentrations deviating from the bulk concentrations also play a dominant role in the discussions of the retardation of C_3A hydration in the presence of $CaSO_4.2H_2O$. To this point, part of the communication of Ghorab, Heinz, Ludwig, Meskendahl and Wolter to the present congress is devoted. The authors confirmed the topo-tactical formation of hedgehog-like ettringite layers on C_3A in pastes $C_3A+CaSO_4+CaO+H_2O$, both with and without the additional presence of $CaCO_3$ or C_3S. Probes cured at rest react (under otherwise identical curing conditions) faster than shaken ones, because in the pastes cured at rest local concentrations lead to conversion of the ettringite layer, e.g. according to:

Ettringite + 2 C_3A + $16H_2O$ → 3 monosulfate

Thus, the ettringite itself is regarded as a retarder.

This is to be contrasted with Chatterji's opinion, that not the ettringite itself, but a hexagonal hydrate layer (C_4AH_{13}) between the C_3A and the ettringite retards the C_3A hydration; according to Chatterji, the role of ettringite is to effect a decreasing sulfate concentration from the bulk solution to the C_3A surface which results in hexagonal hydrate formation adjacent to the C_3A grains. Having reviewed different other mechanisms presented for the retardation of C_3A hydration by $CaSO_4.2H_2O$, Chaterji finishes by stating that "in the ultimate analysis what is considered to be an acceptable explanation depends more on the fashion of the day than anything else".

d. The mutual interaction between calcium aluminate hydrate crystals in aqueous solution.

This subject, a very important one for a material which is used for its mechanical properties, has just been entered upon. By the methods of colloid chemistry (measurement of coagulation rates), a value has been obtained for the so-called Hamaker constant operative between C_3AH_6 crystals (about 0.1×10^{-20} J, rather small in comparison with other substances). More important perhaps is, that in dilute electrolyte solutions the coagulation clearly is not governed by electrostatic repulsion, and that there is, in addition to van der Waals attraction, some other agent effecting a relatively strong attraction between the C_3AH_6 crystals resulting in rapid coagulation. Polyaluminate ions have been held responsible for this effect [10)], but this idea needs further confirmation.

Final Remarks: ideas on future research

The present author does not share Chatterji's pessimism with regard to the possibility of progress in understanding the hydration reactions of C_3A. Although there are still problems to be solved, it is possible to surmount agnosticism. One leading point emerges from the foregoing discussion: the importance of local ionic concentration gradients in the aqueous phase, for determining the reactivity of C_3A. Near the C_3A/water surface, especially in a stagnant aqueous medium, apparently quite different conditions obtain than far away from C_3A grains. Thus, the importance of local concentrations in the formation or conversion of hydrates is stressed by Barret and Bertrandie, by Ghobar c.s., and by Chatterji; and the formation of different hydrates far away from and near the C_3A grains has been demonstrated convincingly by Regourd [8)].

There is a problem here, however. If local concentrations different from those in the bulk solution, are to be maintained, diffusion of ions must be a slow process as compared with other processes occuring. A calculation in this respect [11)] about what porosity (= area available for ion transport per cm^2 C_3A surface) of the hydrate layer should be assumed in order to achieve this situation, leads to 10^{-6} cm^2, a rather low value as remarked by Chatterji. This particular calculation refers to $Ca(OH)_2$ diffusion; however diffusion of other electrolytes concerned is not much slower (a slow diffusion allows the porosity to become proportionally larger ; diffusion coefficients of hydroxides are generally about 1.5 times larger than those of salts with other anions [12)]). Although the remarks made by Chatterji are not convincing (he apparently overlooks the possibilities that the number of C_3A grains decreases during hydration, and that a number of C_3A grains may be shielded from the bulk solution by a common hydrate layer; in addition, his pressure difference, $1.5\ 10^4$ dyne cm^{-2}, amounts to about 0,015 atmosphere which seems quite acceptable), nevertheless a porosity of 10^{-6} is surprisingly low. One of the problems for

future research then appears to be, to obtain a quantitative idea about the effective porosity in hydrate layers formed under different conditions, and consisting of different hydrates.

A second problem, perhaps an even more important one, appears to me a further elaboration of the colloid chemical aspects of hardening cement. Properties such as the rheology of cement pastes and mortars, and creep of systems containing hardening cement, can only be understood if a quantitative idea can be obtained of attraction and repulsion between the hydrate particles.

References

1) G.A.C.M. Spierings and H.N. Stein, Cement and Concrete Research 6, 265-272, 487-496 (1976)
2) P. Gupta, S. Chatterji and J.W. Jeffery, Cement Technology 1, 159-166 (1970)
3) M. Regourd and B. Mortureux, in: Reaction of Aluminate during the Setting of Cements, Summary of Contributions to a Seminar at the University of Technology, Eindhoven, 13-14.4.1977.
4. A.I. Boikova, A.I. Domansky, V.A. Paramonova, G.P. Stavitskaja and V.M. Nikushchenko, Cement and Concrete Research 7, 483 (1977)
5. A.I. Boikova, V.M. Nikushchenko, V.A. Paramonova, A.I. Domansky, N.I.I.Tsement, Trudy Inst., Vypusk 46,p. 3 (1977).
6. J.M. Butt, V.M. Kolbasov, N.A. Kozyreva, Proc.MCTI n.a. D.I. Mendeleev 57, 48-52 (1975).
7. L.A. Dobronravova, J.M. Butt, V.M. Kolbasov, L.L. Astansky, Proc. MCTI n.a. D.I. Mendeleev 57, 44-48 (1975)
8. M. Regourd, Il Cemento 75, 323 (1978)
9. P. Gupta, S. Chatterji and J.W. Jeffery, Cement Technology 4, 146 - 149 (1973)
10. G.A.C.M. Spierings and H.N. Stein, Colloid and Polymer Sci. 257, 171-177 (1979)
11. H.N. Stein, Cement and Concrete Research 4, 1001-1006 (1974)
12. International Critical Tables, vol. 5.

Thème 2 - Hydratation de C_3A

RAPPORT GENERAL

par H.N. STEIN, Laboratory of Colloid Science, Vakgroep Elecktrochemie, Department of Chemical Engineering, Eindhoven University of Technology, Eindhoven, THE NETHERLANDS.

Les communications relatives à l'hydratation de C_3A concernent les problèmes suivants :

a) Que se passe-t-il aux interfaces C_3A/eau et C_3A/ solution de $ca(OH)_2$?

b) Comment l'hydratation de C_3A est-elle influencée par la présence de Na_2O en solution solide dans C_3A ?

c) Quel est le mécanisme du retard de l'hydratation du C_3A en présence de sulfate de calcium ?

d) Quelle est l'importance de l'interaction mutuelle entre les cristaux d'aluminates hydratés dans la solution aqueuse ?

a) Phénomènes aux interfaces C_3A/eau et C_3A/solution de $Ca(OH)_2$

BARRET et **BERTRANDIE** ont étudié la dissolution de C_3A dans l'eau et dans des solutions de $Ca(OH)_2$ en analysant la phase liquide après le contact avec C_3A car sa teneur en CaO et Al_2O_3 croît. Dans un milieu stagnant (eau ou solution de $Ca(OH)_2$ diluée) C_2AH_8 est le premier solide à précipiter ce qui conduit à un rapport molaire CaO/Al_2O_3 supérieur à 3 dans la phase liquide. Cependant ceci ne signifie pas que le processus de dissolution lui-même soit incongruent: après des temps de contact très courts (réalisés par passage du liquide au travers d'une couche mince de C_3A) le filtrat a un rapport $CaO/Al_2O_3 = 3$. Dans des solutions de $Ca(OH)_2$ plus concentrées ($[CaO] > 9.10^{-3}$ $mol.kg^{-1}$), C_4AH_{13} est le premier solide à précipiter ce qui entraîne des rapports molaires inférieurs à 3 dans le liquide. Les auteurs décrivent la dissolution comme étant déterminée par la solubilité du C_3A superficiellement hydraté. Ainsi d'après **BARRET** et **BERTRANDIE**, le premier processus est la formation d'une couche hydratée sur le C_3A lui-même avec un rapport molaire $CaO/Al_2O_3 = 3$.

Cependant, le présent auteur a trouvé à partir des données électrocinétiques que les aluminates de calcium hydratés, qui se forment durant l'hydratation de C_3A, ont d'une manière définie une couche superficielle non-stoechiométrique, appauvrie en ions aluminate : le potentiel Zêta des deux types d'hydrates, hexagonaux et cubiques, est positif au cours de l'hydratation de C_3A et la charge de la surface correspondante croît avec la concentration en NaOH, ce qui indique une extraction progressive d'ions aluminate des surfaces des aluminates de calcium hydratés.

Il n'y a pas toutefois de contradiction réelle entre les résultats rapportés par **BARRET**, **BERTRANDIE** et les données du potentiel Zéta parce que la charge superficielle mesurable peut aisément provenir de différences dans le taux de dissolution des ions calcium et aluminate qui sont trop faibles pour être détectées par les analyses des solutions aqueuses.

b) Influence de Na_2O sur l'hydratation de C_3A

Les données du potentiel Zêta déjà mentionnées ont été utilisées comme support d'une explication de l'influence de Na_2O sur le taux d'hydratation de C_3A : l'extraction des ions aluminate de la couche superficielle hydratée de C_3A rendrait sa composition proche de celle de $Ca(OH)_2$ (1). Ce sujet a été plutôt controversé. Il a été étudié auparavant par **GUPTA, CHATTERJI et JEFFERY** (2), par **REGOURD** et **MORTUREUX** (3), par **BOIKOVA** et al (4, 5) et par **BUTT** et al (6, 7), les résultats ne sont pas concordants.

En réalité, deux questions se posent : Na_2O retarde-t-il ou accélère-t-il l'hydratation de C_3A ? ; Na_2O présent en solution solide dans C_3A agit-il de la même manière qu'une teneur équivalente en NaOH ajoutée séparément ?

La plupart des chercheurs (1, 2, 3, 4 et 5) ont rapporté un retard dû à Na_2O; cependant **BUTT** et al (6,7) trouvent une accélération. Cette contradiction n'est pas résolue par les contributions à ce présent Congrès : **BOIKOVA, GRISHCHENKO** et **DOMANSKY** rapportent à nouveau un retard ; **KOLBASSOV, KOZYREVA** et **DOBRONRAVOVA** rapportent une accélération d'autre part. A partir des données présentées dans les communications, aucune raison possible (par exemple, différences dans les conditions expérimentales) ne peut être extraite qui puisse être responsable de cette contradiction. Bien qu'une partie des résultats donnée par **KOLBASSOV** et al ait été obtenue par plastométrie, ce qui signifie qu'ils sont influencés non seulement par le degré d'hydratation mais aussi bien par l'interaction mutuelle entre les aluminates de calcium hydratés, les auteurs trouvent aussi une activité plus grande dans le C_3A contenant Na_2O, à partir des courbes thermocinétiques différentielles. Peut-être la différence entre les résultats pourra-t-elle être expliquée quand les détails sur les procédés expérimentaux utilisés seront échangés à ce Congrès.

De la même manière, les opinions sont toujours divisées quant à savoir si Na_2O dans la structure de C_3A agit dans le même sens qu'une teneur équivalente de NaOH ajoutée séparément. Cette question est d'un intérêt pratique car par un choix approprié de fuel, il est possible, soit d'inclure le Na_2O dans le clinker de ciment portland en solution solide dans le C_3A, soit de l'avoir présent dans une phase séparée, Na_2SO_4 (7).

BOIKOVA et al discernent trois stades différents dans l'hydratation de C_3A : durant le premier stade, Na_2O dans la structure de C_3A retarde fortement l'hydratation parce que la pénétration de l'eau dans C_3A contenant Na_2O est empêchée par les ions Na^+ occupant les trous de la structure cristalline de C_3A. Ceci est en concordance avec le point de vue de REGOURD, qui n'est cependant pas partagé par SPIERINGS et le présent auteur. Ces derniers auteurs ont rapporté en accord avec GUPTA et al (2, 9) un retard important de l'hydratation de C_3A par NaOH ajouté séparément. Peut-être le conflit évident sur ce point peut-il être concilié par l'opinion que, dans les suspensions agitées à grand rapport eau/solides, l'action de NaOH ajouté séparément est similaire à celle exercée par Na_2O dans la structure de C_3A tandis que dans les pâtes à faible e/s des concentrations locales au niveau du C_3A contenant Na_2O , qui s'hydrate, sont plus élevées que si NaOH est ajouté séparément. Cependant, ce point nécessite clairement une élaboration plus poussée par des expériences.

c) Retard à l'hydratation de C_3A en présence de sulfate de calcium

Les concentrations locales s'écartant des concentrations globales jouent aussi un rôle dominant dans les discussions sur le retard de l'hydratation de C_3A en présence de $CaSO_4.2H_2O$. A ce point est consacrée une partie de la communication à ce Congrès de GHORAB, HEINZ, LUDWIG, MESKENDAHL et WOLTER. Les auteurs confirment la formation topotactique de couches d'ettringite sous forme de hérissons sur C_3A dans des pâtes $C_3A + CaSO_4 + CAO + H_2O$ à la fois avec et sans la présence additionnelle de $CaCO_3$ ou de C_3S. Les échantillons traités au repos (par ailleurs dans des conditions de traitement identiques) réagissent plus vite que les échantillons agités parce que dans les pâtes au repos des concentrations locales entraînent la conversion de la couche d'ettringite suivant la formule :

$$\text{Ettringite} + 2C_3A + 16\ H_2O \rightarrow 3\ \text{monosulfate}$$

Ainsi l'ettringite, elle-même, est un retardateur.

Ceci contraste avec l'opinion de CHATTERJI que ce n'est pas l'ettringite elle-même mais une couche d'hydrate hexagonal (C_4AH_{13}) entre le C_3A et l'ettringite, qui retarde l'hydratation de C_3A. D'après CHATTERJI , le rôle de l'ettringite est d'entraîner une décroissance de la concentration en sulfate de la solution à la surface de C_3A ; il en résulte une formation d'hydrate hexagonal adjacent aux grains de C_3A. Ayant revu d'autres mécanismes différents du retard de l'hydratation par $CaSO_4.2H_2O$, CHATTERJI finit par énoncer "que dans l'analyse ultime, ce qui est considéré comme être une explication acceptable dépend plus du goût du jour que d'autre chose".

d) L'interaction mutuelle entre les cristaux d'aluminate hydratés dans la solution aqueuse

Ce sujet, très important pour un matériau qui est utilisé pour ses propriétés mécaniques, vient juste de débuter. Par les méthodes de la chimie colloïdale (mesure des taux de coagulation), une valeur a été obtenue pour la constante de Hamaker, qui agit entre les cristaux de C_3AH_6 (environ $0{,}1 \times 10^{-20}$ J, valeur plutôt faible en comparaison avec d'autres substances). Plus important, peut-être, dans les solutions d'électrolyte diluées, il est clair que la coagulation n'est pas gouvernée par la répulsion électrostatique et qu'il y a en plus de l'attraction VAN der WAALS, quelque autre agent responsable d'une attraction relativement forte entre les cristaux de C_3AH_6, aboutissant à une coagulation rapide. Des ions polyaluminate ont été rendus responsables de cet effet (10) mais cette idée demande une confirmation ultérieure.

Remarques finales : idées sur des recherches futures

Le présent auteur ne partage pas le pessimisme de CHATTERJI concernant la possibilité de progrès dans la compréhension des réactions d'hydratation de C_3A.

Bien qu'il y ait encore des problèmes à résoudre, il est possible de surmonter l'agnosticisme. Un point principal émerge de la discussion précédente : l'importance des gradients de concentration ionique locale dans la phase aqueuse pour déterminer la réactivité de C_3A. Près de la surface C_3A/eau, spécialement dans un milieu aqueux stagnant, les conditions obtenues sont apparemment différentes de celles éloignées des grains de C_3A. Ainsi l'importance des concentrations locales dans la formation ou la conversion des hydrates est mise en valeur par BARRET, BERTRANDIE , par GHORAB et al et par CHATTERJI. La formation de différents hydrates loin et près des grains de C_3A a été démontrée de façon convaincante par REGOURD (8).

Toutefois, il y a ici un problème. Si les concentrations locales, différentes de celles de la solution sont maintenues, la diffusion des ions doit être un processus lent comparé à celui des autres processus qui ont lieu. A cet égard, un calcul concernant quelle porosité (surface utile pour le transport d'ions par cm^2 du surface de C_3A) de la couche d'hydrate serait affectée dans la réalisation de cette situation, aboutit à 10^{-6} cm^2, une valeur plutôt faible comme l'a remarqué CHATTERJI. Ce calcul particulier se réfère à la diffusion de $Ca(OH)_2$: cependant, la diffusion des autres électrolytes concernés n'est pas beaucoup plus faible [une diffusion faible permet à la porosité de devenir proportionnellement plus grande ; les coefficients de diffusion des hydroxydes sont généralement environ 1,5 fois plus grands que ceux des sels d'autres anions (12)] . Bien que les remarques de CHATTERJI ne soient pas convaincantes (il néglige apparemment les possibilités que le nombre de grains de C_3A décroisse pendant l'hydratation et qu'un nombre de grains de C_3A puisse être protégé de la solution par une couche d'hydrate commune ; de plus, sa différence de pression $1{,}5 \times 10^4$ dyne.cm^{-2} s'élève à environ 0,015 atmosphère ce qui semble tout à fait acceptable), une porosité de 10^{-6} est néanmoins étonnamment basse. Un des sujets de recherche future apparaît être celui d'obtenir une idée quantitative de la porosité effective dans les couches d'hydrates formées dans différentes conditions et composées de différents hydrates.

Un second problème, peut-être même le plus important, m'apparaît être une élaboration ultérieure des aspects de la chimie colloïdale du durcissement du ciment. Des propriétés telles que la rhéologie des pâtes de ciment et des mortiers et le fluage des systèmes contenant le ciment durci peuvent seulement être compris si une idée quantitative peut être obtenue sur l'attraction et la répulsion entre les particules d'hydrates.

REFERENCES

Veuillez vous reporter aux références page 440.

Hydratation de C_3A en présence d'eau de chaux

Hydration of C_3A in lime water

P. BARRET, Professeur à l'Université de Dijon, Directeur du L.A. 23 (Réactivité des Solides),
D. BERTRANDIE, Docteur de l'Université de Dijon, C.N.R.S. (L.A. 23) Dijon, France.

RESUME : La solubilité de C_3A calculée à partir des données thermodynamiques paraît très élevée (9). Mais ce calcul ne tient pas compte du processus d'hydroxylation superficielle par protonation comme celui décrit dans le cas de C_3S et qui est accompagné d'un abaissement notable de l'enthalpie libre, par interaction directe des molécules d'eau avec la surface du solide. Selon certains auteurs, le passage en solution des ions $[Al(OH)_4]^-$ ainsi formés et des ions Ca^{2+} ne serait pas congruent. Si, dans un milieu stagnant, un excès d'ions Ca^{2+} autour des grains peut résulter d'une distribution ionique d'équilibre, en régime dynamique, l'expérience ne conduit pas à un rapport $[C/A]_\ell$ (rapport CaO/Al_2O_3 en phase liquide) croissant au-delà de 3 comme on pourrait s'y attendre si les ions Ca^{2+} passaient sélectivement en solution. Dans l'eau pure ou l'eau de chaux diluée, la précipitation préférentielle de C_2AH_8 en accord avec le diagramme C,A,H , suffirait d'ailleurs à expliquer que $[C/A]_\ell > 3$ même dans l'hypothèse d'une dissolution congruente ; en fait l'analyse X faite sur les échantillons solides après un contact de plusieurs minutes avec le solvant (eau ou eau de chaux) permet de déceler l'hydrate C_3AH_6 avec seulement une faible proportion de monocarboaluminate de calcium. Avec l'eau ou l'eau de chaux diluée ($[CaO] < 9.10^{-3}$ mol.kg^{-1}) comme solvant, on observe $[\Delta C/A]_\ell \geq 3$ mais avec de l'eau de chaux plus concentrée ($[CaO] > 9.10^{-3}$ mol.kg^{-1}) $[\Delta C/A]_\ell \to 2$.

Les essais effectués par flux continu de solvant à travers une couche mince de C_3A sur filtre ont permis également de tracer la partie de la courbe de supersolubilité des hydrates riches en CaO aux grands rapports $[C/A]_\ell$; cette courbe vient compléter la partie que nous avions déterminée, notée (I) dans le domaine des $[C/A]_\ell$ voisins de 1. La similitude avec la courbe (I) que nous avons également construite à partir de C_3S sur le diagramme C,S,H est évidente ce qui établit une analogie fondamentale entre les deux diagrammes, la différence de comportement venant de ce que, dans le cas de C_3A, des hydrates de rapport $[C/A]_S \geq 3$ peuvent précipiter ce qui entraîne $[C/A]_\ell \leq 3$, tandis que, à partir de C_3S, ce sont des C-S-H de rapport $[C/S]_S < 3$ qui précipitent de sorte que $[C/S]_\ell$ ne peut aller qu'en augmentant jusqu'à la précipitation de l'hydroxyde de calcium.

SUMMARY : The C_3A solubility calculated from thermodynamic data seems to be very high (9). But, such a calculation does not take in account superficial hydroxylation process by protonization like that discribed with C_3S and accompanied by a decrease of free enthalpy due to the direct interaction of the solid surface with the water. The dissolution of $[Al(OH)_4]^-$ and Ca^{2+} ions coming from this hydroxylated surface is considered as uncongruent. But, if in a stagnant medium, an excess of Ca^{2+} ions around the grains may result from an equilibrium ionic distribution, in a dynamic state, the experiment did not lead to a $[C/A]_\ell$ (CaO/Al_2O_3 ratio in liquid phase) becoming higher and higher than 3 by a selective transfer of Ca^{2+} ions into solution. In pure water or in diluted lime water, an excess of C_2AH_8 in the precipitate can explain that $[\Delta C/A]_\ell > 3$ according to the C,A,H diagram even if the congruent dissolution is assumed ; in fact by X ray diffraction on solid samples in contact with the solvent (water or lime water) for several minutes, C_3AH_6 cubic hydrate was detected with only a few amount of calcium monocarboaluminate. With water or diluted lime water ($[CaO] < 9.10^{-3}$ mol.kg^{-1}) as solvent $[\Delta C/A]_\ell \geq 3$ was observed but with more concentrated lime water ($[CaO] > 9.10^{-3}$ mol.kg^{-1}) $[\Delta C/A]_\ell \to 2$.

The part of the supersolubility curve of the hydrate rich in lime, corresponding to the high values of $[C/A]_\ell$ ratio, could be plotted from the results obtained by a continuous flow of solvent through a thin layer of C_3A on a filter. The first part of this curve, noted (I) had been previously determined in the range of $[C/A]_\ell$ close to 1. A similar curve was plotted on the C_3S diagram too. This shows a real analogy between the two kinds of diagram, the difference of behaviour being essentially that, with C_3A, hydrates of $[C/A]_S > 3$ ratio may precipitate leading to $[C/A]_\ell \leq 3$, whereas with C_3S, hydrates of $[C/S]_S < 3$ can only precipitate, leading to $[C/S]_\ell > 3$, this ratio increasing by lime accumulation in liquid phase till precipitation of calcium hydroxyde.

INTRODUCTION

Tadros, Jackson et Skalny (1) considèrent la dissolution de C_3A dans l'eau comme non congruente : les ions Ca^{2+} passant préférentiellement en solution. Ils interprètent ainsi leurs résultats expérimentaux obtenus d'une part, par agitation dans l'eau pendant une minute de C_3A dans un rapport solide/liquide (ℓ/s) compris entre 25 et 250, d'autre part, par analyse ESCA et Auger de la surface du solide résiduel. Or, les mesures des concentrations en CaO et Al_2O_3 que nous avons effectuées sur C_3A, tant par agitation dans l'eau pendant la même durée que par flux de solvant (eau et eau de chaux de diverses concentrations) à travers une couche mince de C_3A sur filtre ne sont pas en accord avec ces résultats. C'est pourquoi nous proposons dans ce mémoire de replacer le problème de la dissolution de C_3A et de la précipitation des hydrates dans le cadre du diagramme chaux-alumine-eau (C,A,H) complété par les concepts cinétiques que nous avons développés aussi bien dans le cas de CA que dans celui de C_3S et qui paraissent avoir une portée générale : stade cinétique d'hydroxylation superficielle par interaction directe entre le solide et l'eau, accompagné d'un abaissement de l'enthalpie libre et donc d'une réduction de solubilité ; dissolution congruente en régime établi ; conservation de la congruence pour la dissolution dans l'eau de chaux ; caractère complexe de la réaction globale de formation des hydrates et existence d'un réseau de réactions simultanées ; définition sur les diagrammes d'équilibre de courbes de supersolubilité des phases hydratées délimitant les domaines à nucléation spontanée et les domaines conditionnellement instables et dans ceux-ci, de courbes d'instabilité minimale marquant la transition entre deux hydrates. Il était donc intéressant d'étudier le comportement de C_3A au contact de solutions de plus en plus concentrées en chaux et de chercher à faire apparaître dans les interprétations une unité conceptuelle valable aussi bien pour les systèmes chaux-silice-eau que pour les systèmes chaux-alumine-eau.

ETUDE EXPERIMENTALE

Celle-ci a consisté d'abord à reprendre le même type d'essais que ceux effectués par Tadros, Jackson et Skalny cités ci-dessus (1) et dont les auteurs ne donnent qu'un résultat : $[Ca^{2+}]/[Al^{3+}] = 1,9$ pour $[Ca^{2+}] = 10,5.10^{-3}$ mol.kg^{-1} après 1 min d'agitation dans l'eau, ($25 < \ell/s < 250$). Ceci donne un rapport $[C/A]_\ell = 3,8$ au lieu de la valeur 3 correspondant à la congruence. Nos essais ont été effectués avec $\ell/s = 12,5$, 25, 50, 100 et 250. Ils ont été complétés par des essais de même nature sur un échantillon ayant déjà été agité dans l'eau avec un rapport $\ell/s = 25$ pendant une minute puis lavé à l'acétone et à l'éther et replacé sur un nouveau filtre, ceci afin d'éliminer la chaux non combinée. Le nouvel essai a été effectué également avec $\ell/s = 25$. Puis un ensemble d'essais en système ouvert a été effectué dans le but d'étudier la composition du filtrat prélevé à des instants successifs et celle du filtrat total. Pour cela, a été utilisé un filtre millipore sous pression, d'aire a = 13,85 cm^2. Le flux de solvant était assuré au moyen d'une pompe péristaltique capable d'entretenir une pression hydrostatique de 5 bar . Le flux était réglé à une valeur maximale de : 0,60 ml.s^{-1}.cm^{-2}. Nous avons déjà donné dans d'autres publications, par exemple (2), la définition de ce que nous appelons le temps de contact θ entre chaque tranche de liquide traversant le lit pulvérulent d'épaisseur h et d'aire a avec un débit q supposé constant au cours d'une période Δt. Le temps de contact $\theta = ah/q$ est celui pendant lequel un plan du liquide traverse la couche d'épaisseur h. Le solvant ne se charge pratiquement en ions du solide que pendant ce temps de contact qui peut être réglé très bref en agissant sur le flux q/a et sur l'épaisseur h du solide pour une section a. Le temps de passage τ est le temps total pendant lequel le flux de solvant dure. L'échantillon solide résiduel est susceptible de réagir et de se dissoudre pendant tout ce temps. Si, au cours de la traversée du lit solide, chaque fraction du liquide a le temps d'atteindre une composition telle que la nucléation d'un précipité survienne spontanément, celui-ci reste sur filtre, mais il se peut que la sursaturation du filtrat soit encore suffisante pour que celui-ci soit le siège d'une nouvelle nucléation exigeant une période d'induction plus longue.

Dans chaque prélèvement de filtrat, toute évolution est bloquée en ajoutant une proportion connue d'acide chlorhydrique. Les concentrations en chaux et en alumine sont déterminées par spectrométrie atomique d'absorption de flamme à mieux que 10^{-4} mol.kg^{-1}.

L'intérêt d'une telle méthode vient de ce qu'un état stationnaire ou quasi stationnaire est réalisé, en ce sens que l'attaque du solide est constamment renouvelée au cours du temps par du solvant de même composition.

Une variante de la méthode a été également mise en œuvre en envoyant sur l'échantillon un flux de solvant finement pulvérisé et réglé de telle façon qu'aucune accumulation de gouttelettes ne puisse avoir lieu. Les conditions de faible ℓ/s qui règnent dans une pâte sont ainsi réalisées approximativement.

L'analyse des filtrats est complétée par celle des solides résiduels sur filtre par diffraction X afin de tenter d'identifier les phases hydratées qui sont apparues. En outre des essais d'analyse quantitative de Ca et Al par microsonde à dispersion d'énergie dans le cas où les dépôts d'hydrates sur les grains sont d'épaisseur suffisante pour masquer le substrat sont actuellement en cours. Les aspects caractéristiques des différents hydrates sont également recherchés par microscopie électronique à balayage (SEM).

RESULTATS

C_3A agité 1 min dans l'eau : Les résultats des dosages en CaO et Al_2O_3 sont rassemblés dans le tableau I

TABLEAU I

masse C_3A g	ℓ/s	CaO 10^{-3} mol.kg^{-1}	Al_2O_3 mol.kg^{-1}	$[C/A]_\ell$
1	12,5	9,87	2,32	4,25
"	25	9,57	2,75	3,48
"	50	9,10	3,25	2,80
"	100	6,97	2,57	2,71
"	250	6,40	2,20	2,91
"	25 bis	7,72	2,67	2,89

pour des essais effectués à 20°C sur 1 g de C_3A et à différentes valeurs du rapport pondéral ℓ/s. L'essai sur l'échantillon ayant subi un premier lavage à l'eau à ℓ/s = 25 est noté 25 bis dans la colonne ℓ/s.

Essai d'évolution en système ouvert :

a) Flux de solvant à travers 1,5 g de C_3A sur filtre: L'aire du filtre était a = 13,85 cm^2 et l'épaisseur initiale du lit de poudre h = 0,11 cm. Le flux diminue au cours du temps par suite d'un colmatage progressif du filtre par les produits d'hydratation, ce qui conduit à une augmentation du temps de contact θ du solvant avec le solide. Le volume de filtrat correspondant à chaque prélèvement était de 30 ml dont 2 utilisés pour le dosage de Ca et 25 pour celui de Al. A titre indicatif, avec le débit maximum, $q = 8,31\ ml.s^{-1}$, la durée d'un prélèvement était de 3,6 s.

Deux séries d'essais notés 1 et 2 ont été effectués avec l'eau distillée décarbonatée comme solvant ; leurs résultats sont rassemblés dans le tableau II (essais a). D'autres essais ont été faits en utilisant successivement comme solvant de l'eau de chaux aux concentrations suivantes exprimées en 10^{-3} $mol.kg^{-1}$: 1) 3,10 , 2) 6,06 , 3) 8,31 , 4) 9,37 , 5) 10,87 , 6) 14,00. Les résultats sont consignés dans le tableau III.

TABLEAU II

n° série essais	temps min	J $\frac{ml}{s.cm^2}$	θ s	CaO 10^{-3} mol.kg^{-1}	Al_2O_3 mol.kg^{-1}	$[C/A]_\ell$
essais a (flux de solvant)						
1	1/4	0,58	0,19	8,92	2,97	3,00
2				9,40	3,17	2,97
1	3/4			7,62	2,50	3,05
2				9,15	2,80	3,27
1	2,5	0,48	0,23	3	0,95	3,15
2				6,93	2,25	3,08
1	4,45	0,48	0,23	1,35	0,50	2,70
2		0,24	0,46	4,72	1,51	3,13
1	8	0,36	0,31	0,82	0,36	2,28
2	11	0,10	1,10	2,48	0,82	3,02
1	14	0,29	0,38	0,53	0,25	2,12
2	17	0,07	1,57	1,97	0,66	2,98
1	31	0,18	0,61	0,32	0,15	2,13
2	35	0,04	2,75	1,26	0,46	2,74
1	36			0,32	0,15	2,13
2	45	0,04	2,75	1,03	0,37	2,78
essais b (solvant pulvérisé)						
1		0,020	2,00	5,15	1,68	3,07
2		0,009	4,44	6,35	2,16	2,94

Dans le cas des 2 essais effectués avec l'eau pure, le volume total de filtrat recueilli a été respectivement de 7 ℓ et 5,5 ℓ ; les concentrations en CaO et Al_2O_3 de ces filtrats ont été : essai 1 : $[CaO] = 1,25.10^{-3}\ mol.kg^{-1}$; $[Al_2O_3] = 0,48.10^{-3}\ mol.kg^{-1}$; $[C/A]_\ell = 2,60$. Essai 2 : $[CaO] = 2,72.10^{-3}\ mol.kg^{-1}$; $[Al_2O_3] = 0,94.10^{-3}\ mol.kg^{-1}$; $[C/A]_\ell = 2,89$. Les masses de solide résiduel sur filtre ont été respectivement de 0,6654 g et 0,1164 g et les pourcentages d'eau liée par rapport au produit hydraté : 22,4 et 27,5 %.

TABLEAU III

n° essai	temps min	J	θ s	CaO 10^{-3} mol.kg^{-1}	Al_2O_3 mol.kg^{-1}	ΔC	$[\Delta C/A]_\ell$
1	1/4	0,36	0,31	9,38	2,11	6,28	2,98
2				10,38	1,49	4,32	2,90
3				11,25	1,11	2,94	2,65
4				11,44	0,91	2,07	2,27
5				12,12	0,81	1,25	1,54
6				14,87	0,50	0,87	1,74
1	1			9,31	2,10	6,21	2,96
2				10,44	1,52	4,38	2,88
3				11,50	1,07	3,19	2,98
4				11,50	0,93	2,13	2,29
5				12,30	0,79	1,45	1,84
6				15	0,63	1,0	1,60
1	2			9,06	1,95	5,96	3,06
2				10,56	1,46	4,50	3,08
3				11,43	1,06	2,92	2,75
4				11,44	0,91	2,07	2,27
5				12,12	0,78	1,25	1,60
6				14,62	0,40	0,62	1,55
1	3			8,56	1,82	5,46	3,00
2				10,38	1,44	4,32	3,00
3				11,31	1,05	3,00	2,86
4		0,21	0,52	11,50	0,84	2,13	2,53
5				12,12	0,77	1,25	1,62
6		0,090	1,22	14,81	0,49	0,81	1,65
1	6			7,12	1,37	4,02	2,93
2				10,10	1,20	4,04	3,36
3				11,12	0,93	2,81	3,02
4				11,19	0,75	1,82	2,42
5				12,12	0,74	1,25	1,62
6		0,045	2,40	14,70	0,45	0,70	1,56
1	10			5,81	0,91	2,71	2,98
2				9,22	1,02	3,16	3,09
3				11,0	0,84	2,69	3,20
4		0,10	1,10	10,69	0,60	1,32	2,20
5				12,12	0,65	1,25	1,92
6		0,024	4,58	14,70	0,43	0,70	1,63

b) Solvant pulvérisé : Les essais ont seulement été effectués avec l'eau distillée décarbonatée en utilisant le pulvérisateur de l'appareil de spectrométrie atomique d'absorption de flamme et un diaphragme disposé de telle façon qu'aucune gouttelette ne puisse se déposer sur les parois de l'entonnoir à filtration. L'aspiration de la trompe à eau était mise en route avant le début de la pulvérisation. Les essais ont eu lieu sur des lits de C_3A pulvérulent à raison de 0,5 g uniformément réparti sur l'aire de 12,56 cm^2 du filtre millipore. Les résultats sont donnés dans la partie b du tableau II. Chacun des deux essais a été effectué sur un lit de C_3A frais, avec des temps

de passage τ respectivement de 2 min et 2 min 15 s.

Analyse X du résidu solide sur filtre : L'analyse par diffraction X des résidus solides sur filtre a fait apparaître essentiellement l'hydrate cubique C_3AH_6 accompagné d'un peu de carboaluminate de calcium en raison de la difficulté d'éliminer complètement CO_2. Il est frappant de constater, aussi bien avec l'eau de chaux de diverses concentrations qu'avec l'eau distillée comme solvant que les raies de diffraction de C_2AH_8 et de C_4AH_{13} sont absentes du spectre des échantillons utilisés dans les essais de filtration continue. Les analyses X ont eu lieu seulement à la fin de ces essais qui ont duré respectivement 36 à 65 min avec l'eau comme solvant, mais seulement 10 min avec l'eau de chaux à diverses concentrations. Ce résultat est à rapprocher de celui rappelé par Spierings dans sa thèse (2) d'après Breval (3) et Ciach et Swenson (4). Nous espérons être en mesure de donner oralement des indications complémentaires à partir des études actuellement en cours au moyen de la sonde à dispersion d'énergie.

Courbe de supersolubilité des hydrates : La méthode d'étude par filtration continue permet d'obtenir un filtrat débarrassé des germes dont la nucléation a été pratiquement instantanée. La composition de ce filtrat est donc celle d'une solution sursaturée dans laquelle un faible accroissement des concentrations en chaux et en alumine provoquerait une précipitation immédiate. On peut donc admettre, avec une légère erreur par défaut, que la courbe tracée sur le diagramme C,A,H en joignant les points représentant les concentrations maximales dans de tels filtrats en fonction de la concentration en chaux du solvant est proche de la courbe de supersolubilité des hydrates dans le domaine considéré (Fig. 1). Cette courbe constitue le prolongement de celle que nous avons tracée (2, 6) dans le domaine des concentrations plus faibles en ions calcium et plus élevées en ions aluminates, par adjonction de chaux à des solutions d'aluminate monocalcique.

DISCUSSION

En ce qui concerne les résultats des essais d'agitation de C_3A dans l'eau pendant 1 min, on n'obtient pas, contrairement aux conclusions de Tadros, Jackson et Skalny (1) une valeur de 3,8 pour $[C/A]_\ell$ à toute valeur de ℓ/s comprise entre 25 et 250. A ℓ/s = 50, 100, 250, on peut constater que $[C/A]_\ell \simeq 3$ avec de petites variations de part et d'autre de cette valeur que l'on peut attribuer en partie aux incertitudes expérimentales. C'est seulement pour les valeurs de ℓ/s les plus petites (12,5 , 25) que $[C/A]_\ell$ est nettement supérieur à 3 : respectivement 4,25 et 3,48 à ℓ/s = 12,5 et 25. Mais le fait que $[C/A]_\ell$ apparaisse d'autant plus grand que ℓ/s est plus petit conduit à se demander si de la chaux résiduelle non combinée, lors de la préparation de C_3A, ne pourrait être responsable de cet excédent. C'est pour répondre à cette question qu'un essai complémentaire a été fait en opérant sur un échantillon séché à l'acétone puis à l'éther après un premier contact de 1 min avec l'eau à ℓ/s = 25.

Le résultat est significatif, puisque, dans ces conditions (Tableau II,b), $[C/A]_\ell$ est nettement inférieur à 3. On doit donc craindre que, dans les essais d'agitation dans l'eau pendant un court instant, les résultats ne soient faussés par le passage en solution de chaux non combinée, même si elle se trouve en très faible proportion.

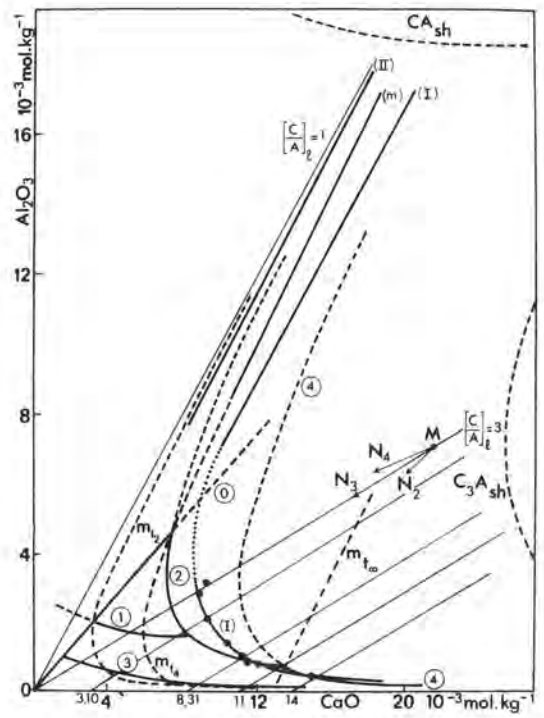

Fig. 1 - Courbes de solubilité : (o) gel d'alumine, (1) CAH_{10}, (2) C_2AH_8, (3) C_3AH_6, (4) C_4AH_{13}. La partie supérieure de la courbe (I) est complétée à l'aide des points expérimentaux obtenus en filtration continue : • . La courbe m_{t_∞} définie par analogie avec m_{t_2}, courbe d'instabilité minimale entre C_2AH_8 et AH_3, apparaît comme une courbe de transition possible entre C_4AH_{13} et C_2AH_8. A droite de cette courbe, C_4AH_{13} n'a pas tendance à se transformer en C_2AH_8. C_3A_{sh} : courbe de solubilité hypothétique.

Les essais en système ouvert par filtration continue ne présentent pas cet inconvénient, car la chaux libre résiduelle est éliminée dans les premières secondes par le flux de solvant.

Les conclusions suivantes se dégagent de ces essais :
1) Les dosages successifs, échelonnés dans le temps, du filtrat qui est passé sur le même échantillon donnent une valeur du rapport $[\Delta C/A]_\ell$ assez constante et reproductible dans le temps bien que les valeurs absolues des concentrations en chaux et en alumine et donc de l'écart ΔC diminuent régulièrement en même temps que le flux, en raison du colmatage occasionné par la formation des hydrates.
2) Le rapport $[\Delta C/A]_\ell$ qui est voisin de 3 avec de petites fluctuations en plus ou en moins dans l'eau pure comme solvant, a tendance à décroître lorsque la concentration en CaO augmente et particulièrement lorsque celle-ci est supérieure à 9.10^{-3} mol.kg^{-1}. Pour une concentration de $10,87.10^{-3}$ mol.kg^{-1} $[\Delta C/A]_\ell \simeq 2$ et ce rapport devient même inférieur à 2 ($\simeq 1,6$) lorsque la concentration en CaO dans le solvant est de l'ordre de 14.10^{-3} mol.kg^{-1}.

Ces résultats montrent clairement, qu'en régime dynamique, une dissolution sélective du calcium de C_3A n'a pas lieu. Les résultats expérimentaux sont au contraire en bon accord avec l'hypothèse d'une disso-

lution congruente de C_3A, non seulement dans l'eau, mais également dans les solutions de chaux.

Cela n'exclut pas que, dans un milieu stagnant un équilibre puisse s'établir entre la phase liquide et la surface hydroxylée de C_3A, de telle sorte qu'un certain écart à la stoechiométrie, par exemple par lacunes d'ions Ca^{2+}, s'instaure dans la couche superficielle ; mais il paraît exclu que cet écart augmente indéfiniment. Du point de vue cinétique, une autorégulation doit s'établir conduisant au transfert interfacial en solution des ions calcium et aluminate dans des proportions quasi stoechiométriques.

Dans nos expériences, le rapport 3 est à peu près conservé tant que la concentration en CaO du solvant est inférieure à 9.10^{-3} mol.kg^{-1}, bien qu'un précipité d'hydrate se forme. Mais comme celui-ci est constitué par C_3AH_6, le rapport $[C/A]_\ell$ après précipitation n'a pas changé. La précipitation d'une petite fraction de monocarboaluminate $3CaO,Al_2O_3,CaCO_3,H_2O$ peut contribuer à faire tendre le rapport $[C/A]_\ell$ vers une valeur inférieure à 3. Si la formation de C_3AH_6 passe par l'intermédiaire de C_2AH_8 et de C_4AH_{13}, il faut supposer que les proportions de ces deux aluminates sont celles de la réaction stoechiométrique :

$$C_2AH_8 + C_4AH_{13} \rightleftarrows 2C_3AH_6 + 12H_2O$$

Il convient également de remarquer, en se rapportant au diagramme C,A,H (Fig. 1) que la courbe (I) se situe en partie dans le domaine sous-saturé par rapport à C_4AH_{13}.

Reprenons la construction graphique que nous avons proposée et utilisée par ailleurs (2, 7), pour représenter sur le diagramme C,A,H les variations de composition de la phase liquide accompagnant les processus de dissolution et précipitation : l'hypothèse de la dissolution congruente de C_3A_{sh} (superficiellement hydroxylé) se traduit, lorsque le solvant est l'eau, par la circulation du point M (Fig. 1) sur la droite $[C/A] = 3$ passant par l'origine. La précipitation d'aluminates hydratés tels que C_2AH_8, C_4AH_{13}, C_3AH_6 entraîne des changements de composition représentés respectivement par des vecteurs tels que MN_2, parallèle à la droite C/A = 2, MN_4, parallèle à la droite C/A = 4, MN_3, colinéaire de la droite C/A = 3. La combinaison de la dissolution congruente de C_3A_{sh} et de la précipitation de l'un ou l'autre de ces hydrates a comme conséquence que le rapport $[C/A]_\ell$ reste égal à 3 si le précipité est formé de C_3AH_6 seul ou d'un mélange équimoléculaire de C_2AH_8 et de C_4AH_{13} qu'il devient > 3 si ce mélange est plus riche en C_2AH_8 qu'en C_4AH_{13} et < 3 dans le cas contraire. Les conclusions restent les mêmes lorsque le solvant est de l'eau de chaux, à condition de remplacer le rapport $[C/A]_\ell$ par le rapport $[\Delta C/A]_\ell$ où ΔC est l'accroissement de concentration en CaO ; le point M circule alors sur une parallèle à la droite $[C/A] = 3$ passant par l'abscisse correspondant à la concentration initiale de l'eau de chaux.

Avec l'eau comme solvant, aux résultats expérimentaux obtenus aussi bien par agitation de C_3A à différentes valeurs de ℓ/s que par filtration continue correspondent des points N situés au voisinage ou au-dessous de la courbe (I) avec des valeurs de $[C/A]_\ell$ très voisines de 3 par excès ou par défaut. Ces valeurs peuvent être justifiées soit par la précipitation directe de C_3AH_6 ce qui est thermodynamiquement possible, soit par celle du mélange quasi équimoléculaire C_2AH_8 et C_4AH_{13}. Cela suppose alors que le point M pénètre largement dans le domaine métastable sursaturé par rapport à C_4AH_{13}, à droite du prolongement en pointillés de la courbe de solubilité (4) de cet hydrate. Mais, dans ce domaine, des considérations expérimentales et théoriques nous ont conduit à prévoir l'existence d'une courbe de transition m_{t_∞} entre C_4AH_{13} solide et C_2AH_8 correspondant à l'équation chimique :

$$C_4AH_{13} \rightleftarrows C_2AH_8 + 2Ca^{2+}_{aq} + 4\ OH^-_{aq} + 2H_2O$$

Sur cette courbe, les valeurs du degré de sursaturation de la solution par rapport à chacun de ces hydrates sont égales et en constituent un minimum commun (8).

Si une telle transition a lieu effectivement, cela signifie que le point M doit aller au-delà de cette courbe pour que se produise la précipitation effective de C_4AH_{13}, ce qui suppose que la solubilité de C_3A_{sh} soit suffisante. (Courbe hypothétique sur le diagramme).

Il existe donc des raisons théoriques pour que C_2AH_8 précipite préférentiellement ce qui permettrait d'expliquer que $[C/A]_\ell > 3$ sans recourir à l'hypothèse d'une dissolution non congruente de C_3A_{sh}.

Avec l'eau de chaux comme solvant, la même situation se présente, mais va en s'atténuant à mesure que la concentration de cette eau de chaux s'approche, par valeurs croissantes de la valeur $[C] = 11.10^{-3}$ mol.kg^{-1}, donnée par l'intersection de l'axe des abscisses avec la parallèle à la droite $[C/A] = 3$ passant par le point d'intersection des courbes d'équilibre de solubilité de C_2AH_8 et C_4AH_{13}. En effet, au-delà de cette valeur, le point M pénètre en premier lieu dans le domaine sursaturé par rapport à C_4AH_{13} avant de traverser le prolongement dans le domaine métastable de la courbe de solubilité de C_2AH_8. En outre, le point M est immédiatement au-delà de la courbe de transition m_{t_∞}, de sorte qu'une précipitation préférentielle de C_4AH_{13} peut être prévue. Mais, naturellement, la solution est également sursaturée par rapport à C_3AH_6 qui peut précipiter. Il est donc logique de s'attendre, en utilisant l'eau de chaux comme solvant, à ce que : $[\Delta C/A]_\ell > 3$ lorsque sa concentration initiale $[C]^o < 11.10^{-3}$ mol.kg^{-1} et à ce que : $[\Delta C/A]_\ell < 3$ lorsque $[C]^o > 11.10^{-3}$ mol.kg^{-1}. C'est bien une telle conclusion qui paraît devoir être dégagée des résultats expérimentaux en filtration continue.

En ce qui concerne la solubilité dans l'eau de C_3A selon l'équation :

$$(1)\ C_3Al_2O_6 + 6H_2O_\ell \rightleftarrows 3Ca^{2+}_{aq} + 2[Al(OH)_4]^-_{aq} + 4\ OH^-_{aq}$$

elle a été exprimée par H.N. Stein (9) à partir de données thermodynamiques permettant de remonter aux valeurs des ΔG^o_{298} de formation des partenaires de cette réaction. Le produit de solubilité est 3.10^8 ou 4.10^{10} suivant la valeur choisie pour $\Delta G^o_{C_3A}$. En prenant la plus petite de ces deux valeurs, on peut se rendre compte de l'ordre de grandeur atteint par $x\gamma^\pm$ où x représente la concentration molaire massique en Ca^{2+}_{aq} et $\gamma^\pm$ le coefficient d'activité ionique moyen. Si l'on appelle y et ψ les concentrations molaires massiques des ions $[Al(OH)_4]^-_{aq}$ et OH^-_{aq}, la relation d'électroneutralité impose :

$\frac{\psi}{2x} + \frac{y}{2x} = 1$ que l'on peut écrire $X + Y = 1$.

La loi d'action de masse s'écrit alors :

$$64(x\gamma^{\pm})^9 x^4 (1 - X)^2 = 4.10^{10}$$

Dans l'hypothèse d'une dissolution congruente :

$[C/A]_{\ell} = 3$, soit $x/y = 1,5$, ou encore :
$1/2(1-X) = 1,5$. On en tire $X = 0,67$, d'où :

$$x\gamma^{\pm} = \left[\frac{2,61.10^8}{64.(0,67)^4.(0,33)^2}\right]^{1/9} = 8,295 \text{ mol.kg}^{-1}$$

Il faudrait $\gamma^{\pm} > 1$, de l'ordre de 2,75 pour obtenir $x = 3$ mol.kg^{-1}, ce qui correspondrait à une solubilité $S_{C_3A} = 1$ mol.kg^{-1}

En fait, le mécanisme d'hydroxylation superficielle que nous avons proposé doit contribuer à réduire notablement cette valeur, mais les données nécessaires pour le calcul font défaut. On peut néanmoins en poser le principe :

L'équation quasi chimique de l'hydroxylation superficielle peut s'écrire en éléments de structure :

$$(2)\ 3\underset{Ca}{Ca} + 2\underset{AlO_3}{AlO_3} + 6H_2O_{\ell} \rightleftarrows 3\underset{Ca}{Ca} + 2\underset{AlO_3}{[Al(OH)_4]^{\cdot\cdot}} + 4(OH_a^-)'$$

et la réaction de transfert interfacial en solution :

$$(3)\ 3\underset{Ca}{Ca} + 2\underset{AlO_3}{[Al(OH)_4]^{\cdot\cdot}} + 4(OH_a^-)' \rightleftarrows 3Ca^{2+}_{aq} + 4\,OH^-_{aq} \ldots$$
$$\ldots + 2[Al(OH)_4]^-_{aq}$$

La somme de ces deux réactions donne évidemment l'équation globale (1). Mais ce qui est en équilibre à la saturation, c'est la réaction (3), d'où $\Delta G_3 = 0$. Comme $\Delta G_1 = \Delta G_2 + \Delta G_3$, il en résulte que $\Delta G_2 = \Delta G_1$.

L'abaissement d'enthalpie libre correspondant à la formation de l'état superficiellement hydroxylé (équation 2) est égal à celui de l'équation globale (1), mais avec une valeur de $x\gamma^{\pm}$ < à la valeur d'équilibre et qui rendrait positive l'affinité chimique de cette réaction.

Rappelons à titre indicatif que dans le cas de CA, les concentrations d'équilibre avec l'état superficiellement hydroxylé sont mesurables en raison de la durée de vie importante de la solution métastable. Un calcul semblable a donné comme valeur de l'abaissement d'enthalpie libre accompagnant la réaction d'hydroxylation superficielle (10) :
$\Delta G' = - 14,71$ KJ.mol^{-1}
et $\Delta G'' = - 12,83$ KJ.mol^{-1} comme valeur de la chute d'enthalpie libre correspondant à la précipitation de CAH_{10} à partir de cette solution.

La valeur de $x\gamma^{\pm}$ calculée pour la solubilité théorique de CA anhydre est 0,078 mol.kg^{-1}. Elle tombe à 0,0113($\gamma^{\pm} = 0,57$) pour celle de CA_{sh}, soit à $x = 0,020$ mol.kg^{-1}.

CONCLUSION :

Les observations et les arguments théoriques ci-dessus développés sont en faveur d'une dissolution congruente, mais de celle de C_3A_{sh} (superficiellement hydroxylé), aussi bien dans l'eau de chaux à diverses concentrations que dans l'eau distillée. En régime dynamique l'accumulation d'ions Ca^{2+} en solution comme cela se produit avec C_3S, semble exclue. Bien au contraire, le rapport $[\Delta C/A]_{\ell}$ voisin de 3 par dissolution de C_3A_{sh} dans l'eau distillée ou l'eau de chaux diluée, tend à diminuer lorsque la concentration de l'eau de chaux utilisée comme solvant augmente. La raison de cette différence de comportement entre C_3A et C_3S doit être recherchée, non dans une dissolution incongruente, mais dans le fait qu'il existe des aluminates hydratés susceptibles de précipiter dans lesquels $[C/A]_S \geq 3$, tandis que cela n'est pas le cas pour les C-S-H dont le rapport $[C/S]_S$ est toujours < 3.

Ce travail a été fait en coopération avec la Société LAFARGE à laquelle nous exprimons nos remerciements.

BIBLIOGRAPHIE

1.- M.E. TADROS, W.Y. JACKSON and J. SKALNY (1976), "Study of the dissolution and Electrokinetic behaviour of C_3A", Col. and Int. Sc., IV, 211.

2.- D. BERTRANDIE (1977), "Contribution à l'étude cinétique de la formation des hydrates dans les solutions aqueuses obtenues à partir du ciment alumineux", Thèse Doctorat d'Université, Dijon, 194.

3.- G. SPIERINGS (1977), "The influence of Na_2O on the formation and colloïd chemical properties of calcium aluminate hydrates", Thèse, Eindhoven.

4.- E. BREVAL (1976), Cem. Concr. Res., 6, 129.

5.- T.D. CIACH and E.G. SWENSON (1971), Cem. Concr. Res., 1, 143.

6.- P. BARRET et D. BERTRANDIE (1979),"Cinétique particulière de précipitation provoquée et spontanée d'une solution métastable de CA", C.R. Acad. Sc. Paris, C, 288, 291.

7.- P. BARRET, D. MENETRIER et D. BERTRANDIE (1977), "Cinétique d'hydratation des aluminates et silicates de calcium", Rev. Int. Htes Temp. et Réfract., 14, 127.

8.- P. BARRET et D. BERTRANDIE (1979), "Courbes d'instabilité minimale d'une solution métastable. Exemples sur le diagramme chaux-alumine-eau", C.R. Acad. Sc. Paris, C, 288, 323.

9.- H.N. STEIN (1972) "Thermodynamic considerations on the hydration mechanisms of Ca_3SiO_5 and $Ca_3Al_2O_6$", Cem. Concr. Res., 2, 167.

10.- P. BARRET et Ph. DUFOUR (1978) "Sur l'existence d'un stade d'hydroxylation superficielle dans le processus de dissolution de CA", C.R. Acad. Sc. Paris, C, 286, 569.

The colloid chemistry of calcium aluminate hydrates

La chimie colloïdale des aluminates de calcium hydrates

H.N. STEIN, Laboratory of Colloid Science, Vakgroep Elektrochemie, Department of Chemical Engineering, Eindhoven University of Technology, Eindhoven, THE NETHERLANDS.

SUMMARY

A review is given on colloid chemical data for calcium aluminate hydrates, both with regard to the state of the surface of the hydrate crystals in aqueous solutions, and with regard to the interaction between hydrate crystals dispersed in aqueous electrolyte solutions. On the basis of these data, some cement chemical problems are discussed.

RESUME

On donne une revue sur les données de chimie colloïdale pour les aluminates de calcium hydratés, tant par rapport à l'état de la surface des cristaux des hydrates dans les solutions aqueuses, que par rapport à l'interaction entre les cristaux des hydrates dispersés dans les solutions aqueuses des électrolytes. En se basant sur ces données, on discute quelques problèmes de la chimie des ciments.

1. INTRODUCTION

Colloid chemistry is a discipline dealing with the properties of systems in which interfaces between phases play an important role. In cement chemistry, the following problems are related to colloid chemistry and can be studied with profit by the experimental methods available in this science:

a. The mechanical and rheological properties of pastes consisting of solid particles embedded in a liquid are influenced by attraction and repulsion between the particles. Colloid chemistry, since the introduction of the well-known Derjaguin-Landau-Verweij-Overbeek theory [1] [2], enables us to determine quantitatieve parameters for these effects.

b. The reactivity of hydrating cement compounds is connected with the physical and chemical character of their surfaces. Colloid chemical data are specifically connected with the situation at the surface, and can thus give evidence about problems such as the retardation of C_3A hydration by hydrate formation, the character of the C_3S surface during the dormant state of C_3S hydration, etc.

In spite of these obvious connections, cement chemists have only occasionally paid attention to colloid chemistry, and colloid chemists have only occasionally paid attention to cement chemistry. The reasons for this latter statement may be understood: the solids encountered in cement chemistry, being isolators, do not allow easy application of some experimental methods employed in colloid science. Thus, AgJ, a solid studied extensively by colloid chemists, is so good a conductor that a AgJ electrode can be made relatively easily; by means of this electrode, changes in overall potential difference over the solid/electrolyte solution interface can be registered. However, with isolating solids such as are encountered in cement chemistry, this is very difficult. Furthermore, the electrolyte concentrations in the aqueous phases present in hydrating cement pastes are rather large as compared with those usually dealt with in colloid chemistry.

Nevertheless, the present author hopes to show that some colloid chemical methods can be used with advantage in cement chemistry.

2. THE NATURE OF THE SURFACE OF CALCIUM ALUMINATE HYDRATES, DISPERSED IN AQUEOUS SOLUTIONS

One colloid chemical parameter, which is readily measured even with isolators as dispersed phases, is the so-called ζ-potential, i.e. the difference in electrical potential between two points in the aqueous phase: one situated in the "bulk" aqueous phase far away from the solid; the other situated at the "slipping plane", the locus where the liquid loses its movability with regard to the solid. The first layer of liquid is attached rigidly to the solid ("no slip" condition, universally accepted in hydrodynamics [3]), and only at the slipping plane the liquid can be moved towards the solid.

The ζ potential can be calculated from elektrokinetic data [4] (from the relative motion of solid and liquid under influence of an electric field as e.g., in electrophoresis, electroosmosis, streaming potential, etc.). From it, the net surface charge behind the slipping plane can be calculated; for a solid suspended in a solution of a symmetrical electrolyte (NaCl, $MgSO_4$, etc.) by the formula [5]:

$$\sigma = \sqrt{2\varepsilon_r \varepsilon_o nkT}\ \left[\exp.\left(\frac{ze\zeta}{2kT}\right) - \exp.\left(-\frac{ze\zeta}{2kT}\right)\right]$$

where

ε_r = the dielectric constant of the liquid phase
ε_o = the permittivity of vacuum (= $8.85 * 10^{-12}$ $C.V^{-1}m^{-1}$),
n = the concentration of the electrolyte (ions per m^3),
k = the Boltzmann constant ($1.38 * 10^{-23}$ $J.K^{-1}$),
T = the absolute temperature,
z = the valency of the ions in the electrolyte solution,
e = the charge of a proton.

It should be realized that the surface charge thus calculated is in general not equal to the surface charge on the solid itself, since ions present in the liquid layer between the phase boundary and the slipping plane will be counted as belonging to the "solid" when the surface charge is calculated from elektrokinetic data.

Thus, if the charge on a solid is negative in say, 0.01 NaOH solution, addition of Ca^{2+} ions will decrease the ζ potential (in absolute sense); the latter may even become positive ("charge reversal"). However, careful planning of experiments is necessary in order to ascertain whether the Ca^{2+} ions are taken up by the solid itself or are only strongly adsorbed ("chemisorbed") on it. It has been reported [6] that C_3A hydrating in excess water has a positive surface charge ($\zeta \approx +34$ mV), which can be

reduced to $\zeta = 0$ but not reversed to a negative surface charge, by adding SO_4^{2-} ions. The finding itself is significant, but it cannot with any claim on certainty be understood in the absence of additional data on the hydrates present on the C_3A surface.

Fig. 1 shows the ζ potential of the hydrates formed during C_3A hydration in NaOH solutions of various concentrations (w/s = 100) [7) 8)]. The data refer to two reaction stages, the first one corresponding to the metastable point of coexistence of $Ca_2Al_2(OH)_{10}.3H_2O$ (=C_2AH_8) and $Ca_2Al(OH)_7.6H_2O$ (= C_4AH_{19}) with solution [9)]. The second stage occurs when the reaction comes finally practically to a standstill [10) 11)].

During stage I, the hexagonal hydrates $Ca_2Al_2(OH)_{10}.3H_2O$ and $Ca_2Al(OH)_7.6H_2O$, and the cubical $Ca_3Al_2(OH)_{12}$ (= C_3AH_6) are present. The ζ potential is positive at all NaOH concentrations investigated. In spite of significant differences between these solids as regards their crystal structure, no difference was noted between them in electrophoresis (the individual particles observed in electrophoresis can be identified by their habitus as being hexagonal or cubical).

During stage II, the cubical hydrate predominates. The ζ potential is still positive, though somewhat less than at stage I. Fig. 2 shows the ζ potential as a function of reaction time, in 0.01 M NaOH solution. The "dip" of the ζ potential after 5 - 10 hours corresponds to conditions shortly after the conversion of the hexagonal hydrates into $Ca_3Al_2(OH)_{12}$. It is found at other NaOH concentrations as well (cf. fig. 1).

Although the ζ potential decreases with increasing NaOH concentration, the net surface charge behind the slipping plane increases (see fig. 3) for both reaction stages.

The large positive ζ potentials and the increasing σ_ζ with increasing NaOH concentration indicate that there exists on the hydrate particles a surface layer, in which the charge of the Ca^{2+} ions is not fully balanced by that of the anions (aluminate and OH^- ions). Such a layer can be envisaged to originate either by withdrawal of aluminate ions from, and only partial replacement of them in the hydrates, by OH^-, or by chemisorption of Ca^{2+} and $Ca(OH)^+$ ions from the solution (chemisorption of Na^+ ions to the extent required is unknown on oxidic surfaces). It is true that the crystal structure of the hexagonal hydrates would give rise to a positive surface charge if layers with overall composition $Ca_2Al(OH)_6^+$ [12)] form the outermost part of the crystal. However, the increasing positive net surface charge with increasing NaOH concentration cannot be explained by this model. Moreover, a net positive surface charge is observed on $Ca_3Al_2(OH)_{12}$ as well, at least in non-equilibrium solutions such as are obtained during C_3A hydration [10) 11)].

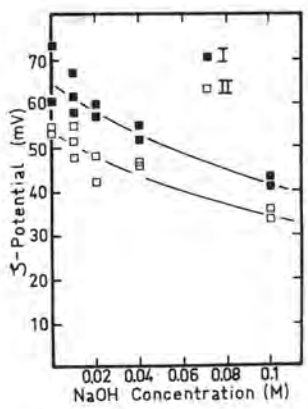

Fig. 1
The ζ potential of calcium aluminate hydrates during the reaction of C_3A with NaOH solutions versus the NaOH concentration [8)].
I : reaction stage I (both hexagonal hydrates and $Ca_3Al_2(OH)_{12}$.
II : reaction stage II ($Ca_3Al_2(OH)_{12}$).

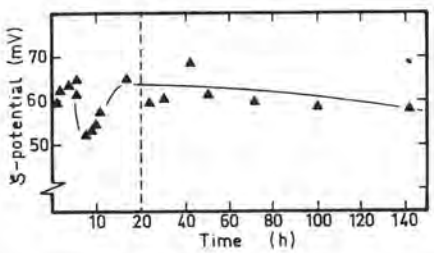

Fig. 2
The ζ potential of the hydrates during the reaction of C_3A with a 0.01 M NaOH solution versus time. [8)]

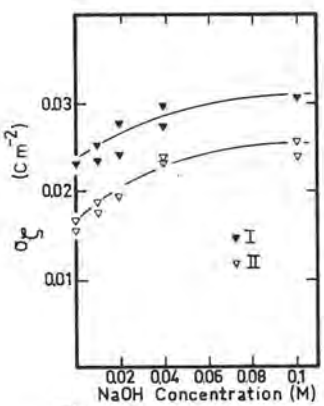

Fig. 3
(for legends of fig. 3 see page 4)

Fig. 3
The net charge behind the slipping plane versus the NaOH concentration for reaction stages I and II (as in fig. 1) [8].

In equilibrium solutions, however, $Ca_3Al_2(OH)_{12}$ has a negative surface charge (fig. 4) which increases in absolute sense (= becomes more negative) with increasing NaOH concentration. The transition of positive into negative surface charge, with gradual establishment of equilibrium, can be followed by registering the ζ potential as a function of time after introduction of $Ca_3Al_2(OH)_{12}$ into a 0.01 M NaOH solution previously saturated towards that compound, (fig. 5). If the $Ca_3Al_2(OH)_{12}$ had been prepared in an autoclave, the transition of the ζ potential into negative values is relatively rapid (curve A). If the $Ca_3Al_2(OH)_{12}$ had been obtained by room temperature hydration of C_3A, the transition is slower (curve B). If $Ca_3Al_2(OH)_{12}$ obtained in an autoclave is placed in a metastable solution obtained during C_3A hydration in 0.01 M NaOH after 6 hours, which is supersaturated towards $Ca_3Al_2(OH)_{12}$ and $\gamma Al(OH)_3$, a very slow transition is found (curve C). The result can be interpreted as indicating that the surface layer becomes disordered similar to that of $Ca_3Al_2(OH)_{12}$ formed during the reaction. The recrystallization is very slow, but at a certain point it is so far advanced that precipitation from the solution can occur; indeed concentration changes have been observed in the solution at that stage.

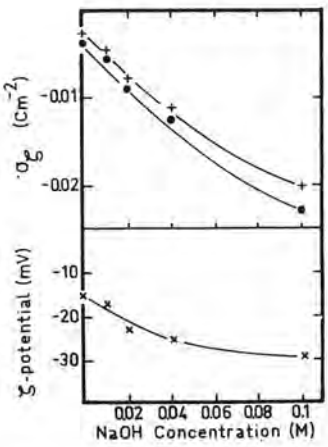

Fig. 4
The ζ potential and charge behind the slipping plane for $Ca_3Al_2(OH)_{12}$ when redispersed in water and NaOH solutions saturated towards it. [8]
- ● charge calculated without taking account of changes in ionic activity coëfficiënts near the solid
- + charge calculated with taking into account these changes.

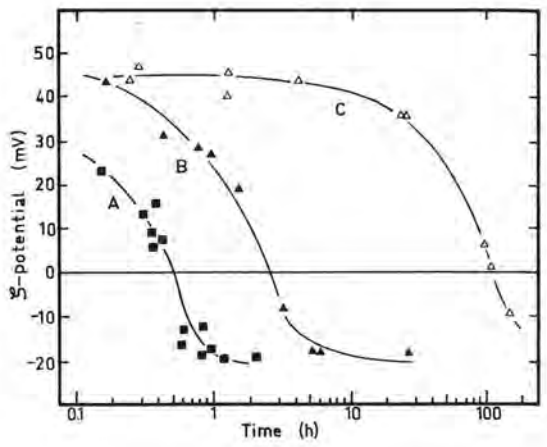

Fig. 5
The ζ potentials versus time [8]
A. $Ca_3Al_2(OH)_{12}$ (autoclave) in a solution of 0.01 NaOH saturated towards $Ca_3Al_2(OH)_{12}$
B. $Ca_3Al_2(OH)_{12}$ (after 140 hr reaction of C_3A + water) in the same solution as A.
C. $Ca_3Al_2(OH)_{12}$ (autoclave) in a solution obtained after 6 hr reaction of C_3A + water.

3. INTERACTION BETWEEN CALCIUM ALUMINATE HYDRATES

Colloid chemistry enables us to draw conclusions on the mutual attraction or repulsion between solid particles embedded in a liquid. The experimental data concerned consist of measurements of the coagulation rate [13) 14)] as a function of electrolyte concentration. A transition is seen between two regimes:

a) "slow coagulation" at low concentration, dependent on the electrostatic repulsion between two solids with surface charge of equal sign, and consequently characterized by a dependency on electrolyte concentration.

b) "fast coagulation" at large electrolyte concentration, where electrostatic repulsion is absent [1) 2)] and where the coagulation rate is independent on the electrolyte content of the solution.

Fig. 6 shows, as an example, some typical data for AgJ in H_2O + ethylene glycol mixtures, with KNO_3 as an electrolyte [16)]. The coagulation is followed by measuring the light extinction (E) as a function of time (t); a large value of dt/dE corresponds to a very slow coagulation rate, hence to a stable dispersion. The transition between "slow" and "fast" coagulation is situated at the critical coagulation concentration, at the intersection between the two straight lines drawn through the experimental data at low and high concentrations, respectively. Thus, for a mixture with x_{EG}, the mole fraction of

ethylene glycol, = .403, the transition is found at log c_{RbNO_3} = 1.85, which means $[RbNO_3]$ = 0.071 M (c_{RbNO_3} is the concentration expressed in m mol.l^{-1}).

For $Ca_3Al_2(OH)_{12}$ in water, different curves are found (fig. 7) [17]. Here, the concentration is expressed by the parameter

$$\kappa = \left(\frac{e^2 \sum N_i z_i^2}{\epsilon_r \epsilon_o kT} \right)$$

well-known from the Debije-Hückel theory of electrolyte solutions. For $NaNO_3$ at relatively large concentrations ($\kappa > 10^9$ m^{-1}, i.e. $[NaNO_3] > 0.1$ M), the expected decrease in dispersion stability with increasing electrolyte concentration is found; transition from "slow" to "fast" coagulation is situated at $\kappa \approx 2 * 10^9$ m^{-1}, from which the constant describing the mutual attraction between $Ca_3Al_2(OH)_{12}$ crystals in water ("the Hamaker constant") can be calculated to be about $0.1 * 10^{-20}$ J.

For NaOH, the stability decrease is shifted towards higher electrolyte concentrations. This is not unexpected because OH^- ions act as "potential determining ions" for oxidic materials [18] so that the surface potential increases in absolute sense (= becomes more negative) with increasing NaOH concentrations. Consistent with this idea are the data on the ζ potentials of $Ca_3Al_2(OH)_{12}$ shown in fig. 5. The increasing potential between $Ca_3Al_2(OH)_{12}$ surface and bulk liquid counteracts coagulation.

The most interesting part of fig. 7, however, is the destabilisation of the $Ca_3Al_2(OH)_{12}$ dispersions with decreasing electrolyte concentration, found at low electrolyte content of the solution. This effect is independent of the type of electrolyte employed being the same for $NaNO_3$, KNO_3, NaOH and $Ca(OH)_2$; it is also independent of the surface potential. It leads to a very low value of dt/dE, i.e. to large coagulation tendency, for $Ca_3Al_2(OH)_{12}$ dispersed in water. Although a definite explanation of this phenomenon cannot at present be given, it has been suggested that it is connected with the formation of polyaluminate ions in the solution of low electrolyte content. The polyions are thought to form bridges between the particles, thus enhancing coagulation. The increasing stability of the dispersion with increasing electrolyte concentration in the concentration range concerned has been ascribed tentatively to the polyions being progressively broken down with increasing κ; the absence of a special role of OH^- ions can be understood if it is assumed that the average charge per Al-ion in a polyion is independent of the degree of polymerization. But at present no independent confirmation of these ideas has been obtained.

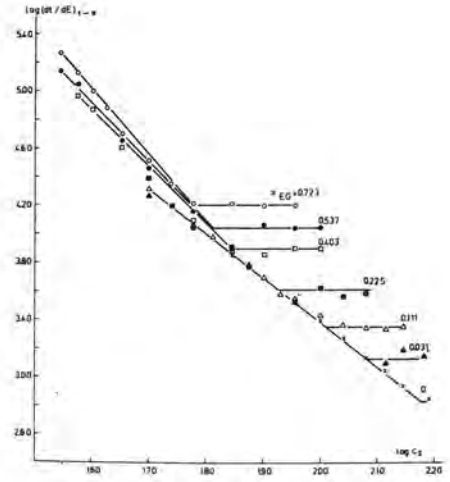

Fig. 6
Rates of coagulation of AgJ sols by KNO_3 in water-ethylene glycol mixtures, [16], pJ = 4.6; x_{EG} = mole fraction of ethylene glycol in in the liquid.

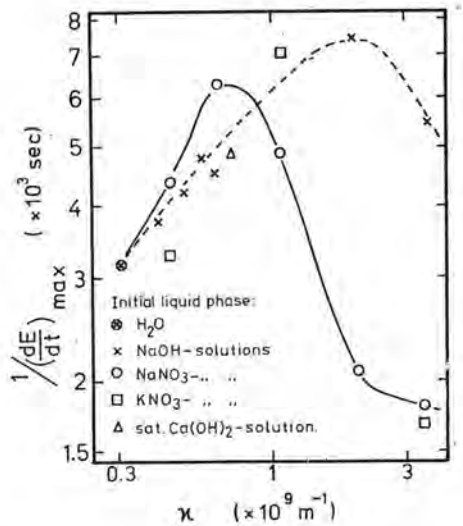

Fig. 7
$1/\left(\frac{dE}{dt}\right)_{max}$ for $Ca_3Al_2(OH)_{12}$ -suspensions in water and NaOH, $NaNO_3$, KNO_3 and saturated $Ca(OH)_2$ solutions, saturated towards $Ca_3Al_2(OH)_{12}$ [17].

4. APPLICATION OF THE DATA TO SOME CEMENT CHEMICAL PROBLEMS

a. The Conversion of C_4AH_{19} and C_2AH_8 into C_3AH_6

$Ca_3Al_2(OH)_{12}$ nuclei accelerate the transition of the hexagonal hydrates into the cubical one [11]. Nevertheless, the aqueous phase which is present when the C_3A hydration comes practically to a standstill, is supersaturated towards the two stable solids: $Ca_3Al_2(OH)_{12}$ and γ-$Al(OH)_3$, in spite of $Ca_3Al_2(OH)_{12}$ crystals being present in abundance [10]. From the results reported in the present paper on the surface of $Ca_3Al_2(OH)_{12}$ crystals it is clear that the latter become inactive as nuclei during the C_3A hydration, because they are covered by a disordered layer.

b. The retardation of C_3A hydration by hydrates

One of the old problems in cement chemistry is: why does $CaSO_4$ retard the hydration of C_3A? Coverage by ettringite crystals [19] [20] and inactivation of the C_3A surface by adsorbed SO_4^{2-} ions [6] are among the theories advanced, the most recent data [21] being in favour of an ettringite coating. However, ettringite layers as formed in hydrating pastes are too incoherent for complete screening of the C_3A [22].

It has been remarked [23] that there is no need to assume such a complete screening. If ettringite is the sole hydrate formed, and counteracts the transport of ions from the bulk solution towards the vicinity of the C_3A sufficiently for a concentration gradient to exist between those regions, there will arise a local SO_4^{2-} shortage near the C_3A. If initially the solution is saturated towards $CaSO_4.2H_2O$, H_2O and $CaSO_4$ reach the C_3A in a weight to weight ratio of 400 : 1; if ettringite precipitates as the sole hydrate, H_2O and $CaSO_4$ are withdrawn from the solution in a weight to weight ratio of 14 : 1. Thus, predominant ettringite formation leads to a local SO_4^{2-} shortage near the C_3A. Nevertheless, the reactivity of C_3A is lower than in SO_4^{2-} free pastes. It has been suggested [23] that amorphous $Al(OH)_3$ is formed because the ettringite crystals tend to grow further when there is no SO_4^{2-} at hand, with $2OH^-$ replacing SO_4^{2-}, causing a locally low pH and Ca^{2+} concentration near the C_3A. Although mixed crystals $Ca_2Al_2(OH)_{12}(SO_4^{2-})_{3-x}(OH^-)_{2x} . 25H_2O$ are not known, the effect sugggested here may be a surface effect rather than a bulk effect.

Earlier [24] it was supposed that the amorphous $Al(OH)_3$ precipitates from the solution. It would be more in line with the colloid chemical data presented in the present paper, to think of a disturbed surface layer on the C_3A similar to the one shown to be present on $Ca_3Al_2(OH)_{12}$. This layer might be formed by preferential extraction of Ca^{2+} from the C_3A and its replacement by H^+. However, it is very difficult to obtain any direct evidence for such a layer, at least in alkaline solution where the C_3A is covered by hydrates. Further research may perhaps bring evidence on this point.

REFERENCES

1) E.J.W. Verweij and J.Th.G. Overbeek, Theory of the stability of lyophobic colloids, Elsevier Publ.Co., New York, etc. 1948.

2) B.V. Derjaguin and L. Landau, Acta Phys. Chim. URSS 14, 633 (1941)

3) H. Lamb, Hydrodynamics, 6th Edition, Cambridge University Press 1932, p. 576.

4) D.J. Shaw, Introduction to Colloid and Surface Science, 2nd Ed., Butterworths & Co(Publ.) Ltd. 1970, p. 156.

5) J.Th.G. Overbeek, in: H.R. Kruyt (ed.), Colloid Science Vol.1 p. 130, Elsevier Publ.Co., Amsterdam etc. 1952.

6) M.E. Tadros, W.Y. Jackson,J. Skalny, in: M. Kerker (ed) Colloid and Interface Science Vol. IV, p. 211 Academic Press Inc. New York, etc. 1976.

7) G.A.C.M. Spierings, Ph.D. Thesis, Eindhoven, 1977.

8) G.A.C.M. Spierings, and H.N. Stein, Colloid & Polymer Sci. 256, 369 (1978)

9) F.E. Jones and M.H. Roberts, Bdg. Res. Curr.Pap. Ser. 1 (1962)

10) J.G.M. de Jong, H.N. Stein and J.M. Stevels, J. Appl. Chem. (London) 19, 25 (1969)

11) H.N. Stein, J.Appl.Chem. (London) 13, 228 (1963)

12) S.J. Ahmed and H.F.W. Taylor, Nature 215, 622 (1962)

13) H. Reerink and J.Th.G.Overbeek, Disc. Faraday Soc. 18, 74 (1954)

14) R.H. Ottewill and J.N. Shaw, Disc.Faraday Soc. 42, 154 (1966)

15) G.R. Wiese and T.W. Healy, J.Coll.Int.Sci. 51, 427 (1975)

16) J. Lyklema and J.N. de Wit, Colloid Polym. Sci. 256, 1110 (1978)

17) G.A.C.M. Spierings and H.N. Stein, Colloid Polym.Sci. 257, 171 (1979).

18) G.A. Parks, Chem.Rev. 65, 177 (1965)

19) H.N. Stein, Rec.Trav.Chim. Pays-Bas, 81, 881 (1962)

20) H.E. Schwiete, U.Ludwig and P. Jäger, Highway Res. Board, Spec.Rep. no. 90, p. 353 (1966)

21) M. Collepardi, G. Baldini, M. Pauri and M. Corradi, Cem. Concr. Res. 8, 571 (1978)

22) P.K. Mehta, Cem.Concr.Res. 6, 169 (1976)

23) C.L.M. Holten and H.N. Stein, Cem. Concr. Res. 7, 291 (1977)

24) H.N. Stein, J. Appl. Chem. (London) 15, 314 (1965).

The peculiarities of initial processes of hydrates forming in C_3A-H_2O systems and the role of its medium in hydrate

Les particularités des processus initiaux de formation des hydrates dans le système C_3A-H_2O et le rôle du milieu dans la formation de la structure des hydrates

V.M. KOLBASOV, Doctor of technology, assistant professor MCTI n.a. D.I. Mendeleev Miusskaja sp. 9, Moscow, U.S.S.R.
N.A. KOZYREVA, Doctor of technology, Head of the Laboratory MCTI n.a. D.I. Mendeleev,
L.A. DOBRONRAVOVA, Engineer, assistant MCTI , n.a. D.I. Mendeleev, U.R.S.S.

RESUME : La présente étude porte sur le rôle du C_3A et du NC_8A_3 (identifié comme une combinaison indépendante) dans les réactions initiales de l'hydratation du ciment et dans les modèles représentant ces réactions.

La formation simultanée de plusieurs phases hydratées, au voisinage et à la surface du C_3A et du NC_8A_3, au tout début de l'hydratation, montre l'interdépendance de ces réactions initiales avec la composition, la symétrie et le degré de saturation de la phase liquide à ce moment, ainsi qu'avec la vitesse de diffusion des ions et les propriétés physiques des minéraux.

La présence de NC_8A_3 dans le clinker est indésirable, car elle peut entraîner une diminution des résistances du ciment hydraté.

SUMMARY: The role of C_3A and NC_8A_3 (identified as an independent compound) is investigated in primary competing reactions of initial process of cement hydration in the systems modelling this process.

Simulteneous formation different hydrate phases near and on the surface of C_3A and NC_8A_3 in first moments of hydration prove the interdependence of primary reactions and composition, symmetry, the degree of oversaturation of primary liquid phase, rate of diffusion of ions and physical properties of minerals.

Presence of NC_8A_3 in Portland cement clinker is undesirable as it may favour the decrease of strength of hardening system "cement-water".

It is known that C_3A and its alkali analogue NC_8A_3 play an important role in initial reactions of cement hydration particularly in the formation of primary structures of hardening in the processes lying in the basis of "false" setting of cement [1].

To detalize the role of C_3A and alkali calcium aluminates in the initial hydration process of cement and to investigate primary competing reactions, the scientists of MCTI named after D.I.Mendeleev carried out some research works of the initial processes of C_3A and NC_8A_3 hydration (by means of a number of physico-chemical methods) in the systems modelling the processes taking place during cement hydration.

Indentification of synthesized minerals was carried by means of chemical, optical, X-ray diffractometry, differential thermal analyses and by means of electronic microscope.

The following facts state that NC_8A_3 is an independent mineral with the ordered arrangement of ions Na in C_3A lattice. The presence of 7% of sodium in the above mentioned mineral, the effect of anysotropy change of refraction index from $N_m = 1.714 \pm 0.03$ to $N_p = 1.700 \pm 0.003$ and $N_g = 1.712 \pm 0.003$; change of frequency and intencity of amplitude in the ranges of 430-540 cm^{-1} and 700-900 cm^{-1}, the appearance of endothermic effect ($t = 1285°C$) and exothermic ($t = 1370°C$) the appearance of unstable regions on the surface of dendrites of NC_8A_3:

New reflections of 4.93; 4.426; 3.432; 3.401; 2.719; 2.625; 2.435; 2.316; 2.050; 1.915; 1.397 Å; instead of completely disappeared reflections of C_3A (4.604, 3.501, 3.332; 3.262, 3.120, 2.993, 2.581, 2.512, 2.138, 2.097; 2.078 Å could be clearly seen on the X-ray diffractograms.

Two reflections of 2.050 and 2.035 appear instead of reflection 2.040 Å. From the remaining group of C_3A reflections the following reflections remain. A group of reflections of C_3A shifs in NC_8A_3 in the following way. for C_3A: 1.405, 1.390, 1.3649, 1.3596, 1.3491, 1.3336, 1.3190; for NC_8A_3: 1.397, 1.348, 1.345, 1.339, 1.337 Å the range of 1.211-1.198 we have poorly formed similar picks 1.1899 and 1.0979 Å of two minerals simultaneously.

The experiments carried out by means of electronic microscope and electron-diffraction microscope aimed at the investigation of initial stages of hydration C_3A and NC_8A_3 beginning with the moment of cement and water interaction (1-5 sec) in rather short intervals of time (1,5,15 and 30 sec; 1,5, 15 and 30 minutes; 1,2,3 and 6 hours) allowed to analyse morphological and phase changes, taking place in the systems, modelling initial processes of hydration [2].

In C_3A-H_2O system calcium hydroaluminates C_4AH_x ($x=19-13$) and $Al(OH)_3$ are formed beginning with the moment of interaction and they dominate up to 2-3 hours with the following forming of C_3AH_6.

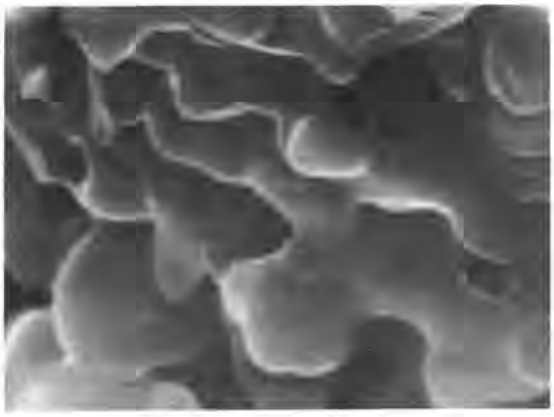

Fig.1. The surface of the mineral C_3A before hydration (x 20 000).

Fig.2. The surface of the mineral NC_8A_3 before hydration (20 000).

Analysing electron-diffraction photographs (period 1 sec - 1 hour of hydration) we can see reflections as diffusion rings 2.88, 2.50, 1.65, 1.60 and 1.24 Å and dot reflexes 1.87, 1.80, 1.60, 1.57, 1.40 Å corresponding in general to C_4AH_{19} and $Al(OH)_3$.

In the system C_3A-$CaSO_4.2H_2O$-H_2O in the moment of mineral and water interaction the formation of prismatic $C_3A.3CaSO_4.31H_2O$ and plate like C_4AH_{13}, $C_3A.CaSO_4.12H_2O$ is typical (Fig.4).

They are characterised by the reflections on the electron-diffraction photographs 3-58-2.95; 3.00-2.87; 2.50-2.45; 2.15-1.80 and 1.71-1.68 Å. They all have the form

of diffusion rings and have the following dot-reflexes 3.23; 3.19; 2.95; 2.86; 1.87; 1.62; 1.59; 1.52 and 1.49 Å.

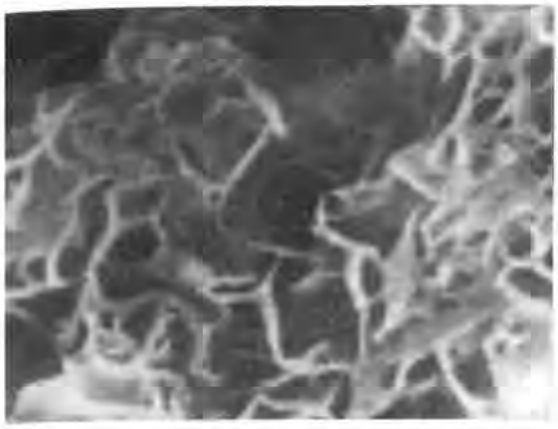

Fig.3. The surface C_3A after 5 seconds of hydration in the system C_3A-H_2O (x 40 000).

Fig.4. The surface of C_3A after 5 seconds of hydration in the system C_3A-$CaSO_4 \cdot 2H_2O$-H_2O (x 20 000).

The presence of ions of Ca^{2+} and SO_4^{2-} in the preliminary liquid leads to simultaneous formation of $C_3A.3CaSO_4.31H_2O$, $C_3A.CaSO_4.12H_2O$; C_4AH_x and $Al(OH)_3$ on the surface of grains of C_3A. This is the evidence of the fact that there are different conditions for crystalformation on the surface of the mineral. The formation of C_4AH_x in the system with two-water gypsum and in the system with the nucleui of C_3A $3CaSO_4 \cdot 31H_2O$ proves that the reaction of C_3A solving with the formation of calcium, hydroaluminates is the very primary stage. Besides it, it reaffirms the idea that $C_3A.3CaSO_4.31H_2O$ is not the only phase that forms on the C_3A grains in the presence of $CaSO_4.2H_2O$ and that this phase exists after all SO_4^{2-} ions have dissappeared from the solution.

In the system with two-water gypsum two main reactions aimed at the formation $C_3A.3CaSO_4.31H_2O$ and C_4AH_x take place and in some local parts of the system if there are no enough SO_4^{2-} ions and in the base of the less oversaturations of the liquid phase. The formation of $C_3A.CaSO_4.12H_2O$ takes place.

Investigations of NC_8A_3 in analogical conditions revealed the difference of the initial process of hydrates formation compared to that of C_3A, i.e. by 5 sec of hydration almost the whole surface of C_3A is covered by hydrates of this or that composition depending on the system. In case of pure NC_8A_3 the hydrates usually have plate-like form and only some parts of the surface are covered by them.

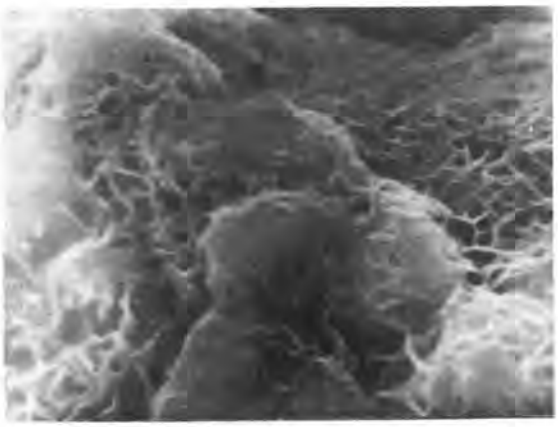

Fig.5. Surface of NC_8A_3 after 5 seconds of hydration in the system NC_8A_3-H_2O (x10000).

In the presence of two-water gypsum the formation of $C_3A.3CaSO_4.31H_2O$ is not noticed, and plate-like phase with the composition C_4AH_x, $C_3A.CaSO_4.12H_2O$ dominates.

The formation of various hydrate phases near and on the surface of the minerals under investigation proves the fact that there is a certain dependence of primary hydration reactions and crystalformation on the composition, symmetry and the degree of oversaturation of the environment, i.e. on the initial liquid phase, rate of diffusion of ions, formed in the process of solving of the basic adhesive mineral and physical properties of the basic mineral.

Fig.6.Surface of NC_8A_3 after 5 seconds of hydration in the system NC_8A_3-$CaSO_4.2H_2O$--H_2O (x 10 000).

The investigation of hydration activity of minerals, kinetics of their solving and heat liberation allowed to find substantial differences in the character of these changes [3] .

Plastometry analyses of monomineral pastes during 10 hours reveal differences in structure formation of hydration products of C_3A and NC_8A_3. The formation of primary structure takes place quicker in the system with the sodium analogue. But after six hours of hydration the increase of plastic strength is more intensive in the system with C_3A.

The curve is devided into two parts, which may be refered to the formation of the primary structure and then to the process of mass crystallization typical for the second period of hydration. Gypsum added to hardening systems (5% of gypsum) influence differently on the structureformation of C_3A and NC_8A_3.Thus resistance to shift deformations in increased by 2 or 3 times in case of C_3A, and in the second case it decreases by 2 times. As the mentioned above investigations by means of electronic microscope show the formation of $C_3A.3CaSO_4.31H_2O$ is not found on the grains of NC_8A_3 and this may lead to a "false" setting.

Differential thermokinetic curves show that in the first 30 minutes the rate of heat liberations of NC_8A_3 is higher. On the curves only one maximum during four hours is fixed. After 1.5 hours the rate of heat liberations decreases 4 times for instance during 4 hours 560.3 kDj/kg and as to C_3A-549.9kDj/kg was liberated; and as to NC_8A_3 hydration occupies only some parts of the surface.

Thus alkali analogue of C_3A in early periods of hydration forms a structure differing from C_3A. Characteristic properties of this structure show that probably there may be formed "false" unstable structures.

Data concerning the change of composition of water medium prove it. When C_3A is hydrated in a suspension with m/s = 10 during 672 hours the concentration of calcium oxide in the solution changes in a "wave-like" way.On the curve we may see 3 maximum points after 2 minutes of mineral and water mixing (067 g/l). After 6 hours - 1.11 g/l and after 168 hours - 1.15 g/l. In case of NC_8A_3 the amount of CaO in the solution is 3-4 times lower and does not change in a "wave-like" manner. It changes with a constant velocity and the concentration of Al_2O_3 is 4-5 times as great as in C_3A system in the first minute of contacting with water. Then for C_3A the amount of Al_2O_3 remains insignificant 0.0%-0.9 mg/l compared to NC_8A_3 where its amount is 50-60 mg/l. After 72 hours of hydration the amount of Na_2O remains constant (6-7 g/l). The excess of Al_2O_3 in the solution prevents hydrolyzation of NC_8A_3 by forming sodium aluminate.

The data given above prove the facts that alkali oxidies take part in sorption and hydrate formation processes in the formation of strong structure during the hydration of the minerals C_3A and NC_8A_3 which takes place at different parameters pH of the liquid medium. In case of NC_8A_3 pH is 12.9 after 1 min of hydration and after 592hours of hydration - 13.4 and as to C_3A hydration these parameters are as follows 11.9 and 12.1.

Various primary conditions of hydration lead to the formation of different primary structures of hardening and influence the kinetics of hydration and this in turn influence the difference in strength parameters.

Thus C_3A mineral by 672 hours of hydration has strength 2.8 MPa (small samples - 1 x 1 x 3 cm), and when folding - 1.1 MPa NC_8A_3 mineral (though its setting is extremely quick) loses its strength as time goes (as if they become liquid) and it leads to the following: in 24 hours it is difficult to take the samples out of the forms and later they do not became strong even in 2 years.

CONCLUSION In C_3A hydration in systems modelling the processes of cement hydration the formation of calcium hydroaluminates proves the fact that the reaction of C_3A solving is a primary one. Besides it proves that in the system various local conditions for hydrate formation in the moment of mixing are created. In the system C_3A-$CaSO_4$.$2H_2O$-H_2O the reactions with the formation of C_4AH_x, $C_3A.3CaSO_4.31H_2O$, $C_3A.CaSO_4.12H_2O$ and $Al(OH)_3$ are primary ones.

NC_8A_3 is an independent mineral. The characteristic features of hydration of this mineral differ greately from those of C_3A.

The presence of NC_8A_3 in Portland cement clinker is obviously undesirable as in the first moments of hardening its presence may give rise to a "false" setting and later it may favour continuous loss of strength of hardening system "cement-water".

REFERENCES

1.G.L.KALOUSEK (1976) "Processes of Hydration at Early Stages of Cement Hardening" Proceeding of the VI-th International Congress on Cement Chemistry, v.5, b.2,65-81 (Russian).

2.J.M.BUTT, V.M.KOLBASOV, N.A.KOZYREVA (1975) "Phase Formation on the Early Stages of Porland Cement Hydration", Proc. of MCTI n.a. D.I.Mendeleev, ed. 57, 48-52 (Russian).

3.L.A.DOBRONRAVOVA, J.M.BUTT, V.M.KOLBASOV, L.L.ASTANSKY (1975) "Alkali Phases of Portland Cement Clinker", Proceeding of MCTI n.a. Mendeleev, ed. 57, 44-48 (Russian).

Hydration of C_3A and solid solutions of various composition

Hydratation de C_3A et des solutions solides de composition variable

A.I. BOIKOVA, Academy of Sciences, Leningrad (U.S.S.R.),
L.V. GRISHCHENKO,
A.I. DOMANSKY.

RESUME :

Des phases aluminates de composition complexe analogues aux phases des clinkers industriels ont été synthétisées et étudiées. Elles représentent des solutions solides multicomposants de C_3A avec Na_2O, K_2O, MgO, Fe_2O_3, SiO_2 et avec de petites quantités de Cr_2O_3, TiO_2, P_2O_5. On a étudié aussi des solutions solides de C_3A avec Na_2O, SiO_2 ; C_3A + K_2O + SiO_2 ; C_3A + Na_2O + K_2O + SiO_2.

On obtient les phases homogènes quand la quantité totale des impuretés n'excède pas 12 à 13 % en poids. Dans les échantillons contenant plus de 5 % en poids de Fe_2O_3, certaines quantités d'aluminoferrites de calcium cristallisent avec les aluminates.

La phase contenant plus de 3 % en poids de Na_2O + K_2O se trouve être orthorhombique. Les aluminates avec une petite quantité d'alcalins sont cubiques. Les paramètres cristallins et les densités des aluminates sont donnés.

On a étudié l'hydratation à court et à long terme. On montre que le processus d'hydratation de C_3A et des solutions solides C_3A + Na_2O peut être considéré comme un modèle par rapport à l'hydratation des solutions solides multicomposants. Les courbes cinétiques d'hydratation permettent de distinguer trois stades du processus. Les particularités d'hydratation à chaque stade sont prédéterminées par un nombre de facteurs corrélés.

L'hydratation des aluminates en présence d'aluminoferrites se poursuit avec moins d'intensité et ne peut être complète même après des temps prolongés.

Dans le cas général, les éléments mineurs en solution solide ainsi que la présence d'autres phases retardent considérablement l'interaction des aluminates avec l'eau. Le degré d'hydratation peut être deux ou trois fois plus faible que dans le C_3A pur.

SUMMARY : Aluminate phases of complicated composition analogous to the phases of commercial clinkers have been synthesized and studied. They represent polycomponent solid solutions of C_3A with Na_2O, K_2O, MgO, Fe_2O_3, SiO_2 and small amounts of Cr_2O_3, TiO_2, P_2O_5. Studies have also been made of the solid solutions of C_3A with Na_2O, SiO_2; C_3A with K_2O, SiO_2; C_3A with Na_2O, K_2O, SiO_2.

The homogeneous phases were obtained when the total amount of impurity oxides did not exceed 12-13 wt %. In samples containing more than 5 wt % Fe_2O_3 some amounts of calcium aluminoferrites crystallized together with the aluminates.

The phase containing more than 3 wt % Na_2O + K_2O appeared to be orthorhombic. Aluminates with a less content of alkalis are cubic. The unit cell parameters and densities of the aluminates are given.

Hydration at early and later ages was studied. It is shown that the hydration process of C_3A and its solid solutions with Na_2O can be regarded as a model with respect to the hydration of polycomponent solid solutions. The hydration kinetic curves permit to distinguish three stages of the process. The peculiarities of hydration at each stage are predetermined by a number of interrelated factors.

Hydration of the aluminates in the presence of aluminoferrites proceeds less intensely and cannot be completed even after long times.

In general case, the impurity components of the solid solution as well as the presence of other phases slow down considerably the interaction of the aluminates with water. The degree of hydration in this case can be twice or thrice as low as in pure C_3A.

ON THE ALUMINATE PHASE IN CEMENT CLINKER

Polycomponent solid solutions of C_3A with Na_2O, K_2O, MgO, Fe_2O_3, SiO_2 are constituents of the aluminate phase of clinker. They can also contain small amounts of other oxides: Cr_2O_3, Mn_2O_3, TiO_2, P_2O_5, SO_3.

Due to the peculiarities of structure, the aluminate phase contains the greatest amount of impurities compared to other cement phases. The presence in the C_3A crystal lattice of a large Ca^{2+} cation and holes exceeding in size any cation provides, on the one hand, the distribution of foreign ions with large radii and, on the other hand, promotes the realization of the different and numerous schemes of heterovalence isomorphic substitutions.

As known, the crystal structure of C_3A is most convenient for Na^+ substituting Ca^{2+}. The compensating additional Na^+ is distributed in the holes. When the aluminate phase is formed in the clinker rich in SiO_2, the balanced substitution $Ca^{2+}Al^{3+} \rightleftharpoons Na^{2+}Si^{4+}$ is possible. That's why the aluminate phases contain considerable amounts of Na_2O and SiO_2; the amount of potassium is smaller, as a rule, compared to sodium.

Fe^{3+} is always present in the aluminate due to the wide-spread substitution $Al^{3+} \rightleftharpoons Fe^{3+}$; Mg^{2+} can also enter the structure as a result of substitutions $Ca^{2+} \rightleftharpoons Mg^{2+}$, $2Al^{3+} \rightleftharpoons Mg^{2+}Si^{4+}$, $3Mg^{2+} \rightleftharpoons 2Al^{3+}$ and occupy positions both of Ca^{2+} and Al^{3+}. Much less are the amounts of Cr^{3+}, Mn^{3+}, Ti^{4+}, P^{5+}, S^{6+}, first of all as they are present in the clinker in small quantities. Besides, Cr, Mn, Ti prefer the crystal lattice of aluminoferrites, and P and S that of belite.

All the foreign ions mentioned were found in the aluminate phase of clinker by means of electron-probe microanalysis. The maximum contents of them depend on the possibilities of the crystal lattice of C_3A and are limited.

However, attention is drawn to the fact that the total amounts of impurity oxides determined by different authors differ considerably and are within the limits of 10-20 wt %. Data obtained by us on the amounts of the main and secondary impuritiy oxides present in the aluminate phases are as follows:

Na_2O	0.3-4.0	TiO_2	0.1-0.4
K_2O	0.3-0.8	P_2O_5	0.04-0.1
MgO	0.8-1.7	SO_3	0.1-0.5
Fe_2O_3	2.9-7.8		
SiO_2	3.5-5.6		

The indicated maximum amount of Fe_2O_3 exceeds, in our opinion, the amount of this oxide that can be distributed in the polycomponent solid solution.

The laboratory syntheses of the aluminate phases of complicated composition analogous to the phases of industrial clinkers showed that homogeneous samples could be obtained when the total amounts of impurity oxides did not exceed 13 wt %. It was observed in this case that if the initial batch contained more than 5 wt % Fe_2O_3, some amount of the aluminoferrite phase always appeared in the synthesis product. Most often the aluminoferrite phase crystallized in the form of thin intergrowths with the aluminate phase.

SYNTHETIC ALUMINATE PHASES OF COMPLICATED COMPOSITION

Table I gives compositions of the aluminate phases synthesized according to the data of chemical analysis. The compositions of samples I, II, VII were chosen using the data of electron-probe microanalysis of the phases of industrial clinkers. The composition of phase VI containing the impurity oxides SiO_2, Fe_2O_3, MgO, Na_2O, K_2O most characteristic of the aluminate was chosen according to /1/. Phases III, IV, V are solid solutions of C_3A with Na_2O, K_2O, SiO_2.

X-ray and microscopic investigations permitted to establish that only the aluminate phase VI containing more than 3 wt % of alkali oxides is orthorhombic, all the others are cubic. According to X-ray analysis, all aluminates resemble each other and are derivatives of pure C_3A (Fig.1). The X-ray diffraction pattern of the orthorhombic aluminate differs from those of C_3A and cubic phases only with splitting of reflections at angles 2θ of 32-34°, 47-49°, 58-60°.

Table II represents unit cell parameters of cubic aluminates and their densities determined by picnometer method.

The unit cell parameters of orthorhombic aluminate VI are : a=10.879(4) Å; b=10.841 (4) Å; c=15.134(5) Å. The density is 3.18 g/cm^3. The greater value of density of the aluminates I, II, VI, VII compared to III, IV, V is due to the presence of iron in their crystal lattice.

Samples I, VI, VII contain small amounts of calcium aluminoferrite which increase with increasing amount of Fe_2O_3 in the initial batch. The greatest amount of aluminoferrite was found in sample VI. According to /1/ the total contents of impurity oxides in this sample should be 19 % with 7.8 % Fe_2O_3 included. However, we failed to obtain the homogeneous aluminate phase of this composition.

In sample VI the compositions of aluminate and aluminoferrite were determined by us using electron microprobe. The data are given in Table III.

The results of the analysis of the aluminate and aluminoferrite formed during the simultaneous crystallization are of interest as evidence of the preferable distribution of the elements in these two phases.

The amount of Fe_2O_3 in the aluminate is about 5 %. This is considerably less compared to clinker aluminates. The same refers to SiO_2.

Of special attention is the behaviour of MgO. In the aluminate crystals analyzed no magnesium was found. In the clinker aluminate phases we also found crystals

TABLE I

Samples / Oxides	Aluminate phases						
	I	II	III	IV	V	VI	VII
CaO	56.68	57.10	59.02	58.62	59.45	52.19	56.88
Al_2O_3	29.31	31.63	36.29	35.73	35.96	26.77	31.86
Na_2O	0.48	0.48	-	0.69	1.67	2.16	1.93
K_2O	0.64	0.69	1.20	0.85	-	1.02	0.41
MgO	0.67	1.11	-	-	-	2.39	0.78
MnO	$\leqslant$ 0.03	-	-	-	-	-	-
Fe_2O_3	5.75	2.90	-	-	-	8.13	4.95
Cr_2O_3	< 0.01	< 0.01	-	-	-	-	< 0.01
SiO_2	5.84	5.40	2.84	3.58	2.07	6.48	3.08
TiO_2	0.12	$\leqslant$ 0.08	-	-	-	-	$\leqslant$ 0.11
P_2O_5	0.08	0.06	-	-	-	-	< 0.001
Loss on ign.	0.35	0.40	0.40	0.29	0.46	0.64	0.24
Σ	99.92	99.77	99.75	99.76	99.61	99.78	100.13
Σ impur.	13.58	10.64	4.04	5.12	3.74	20.18	11.15

TABLE II

Aluminates / Parameters Densities	I	II	III	IV	V	VII
a, Å	15.234(5)*	15.223(5)	15.278(5)	15.283(5)	15.264(5)	15.241(5)
d, g/cm^3	3.14	3.11	3.05	3.05	3.07	3.14

* Standard deviations in unit cell parameters are indicated in brackets.

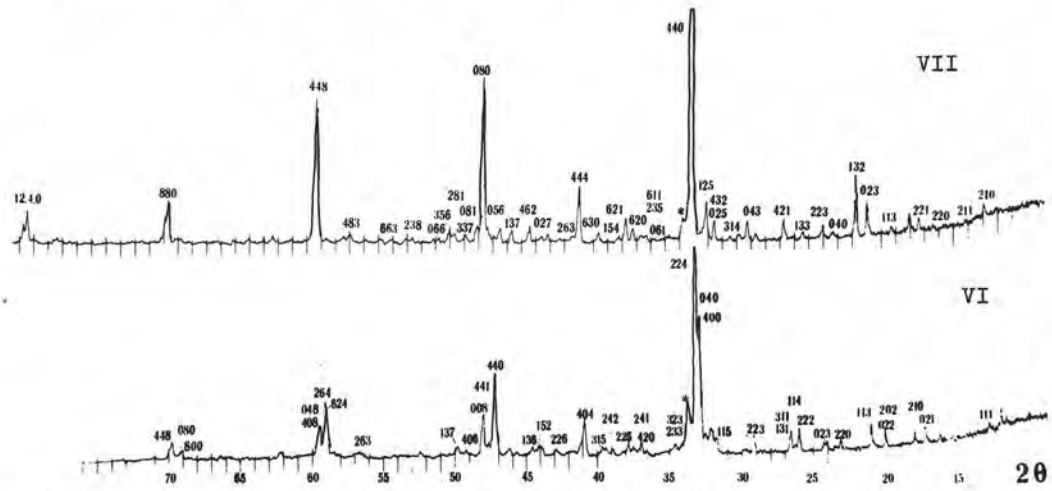

Fig. 1 - X-ray diffraction patterns of the cubic (sample VII) and orthorhombic (sample VI) aluminates. The aluminoferrite reflection is indicated with sign *.

which sometimes contained no magnesium. The fact that among all cement minerals magnesium is distributed first of all in the aluminoferrite is visibly demonstrated by microprobe analysis. As should be expected, sodium is present in a greater amount in the aluminate.

TABLE III

Oxide \ Phase	Aluminate Cryst.1	Aluminate Cryst.2	Aluminoferrite Cryst.1	Aluminoferrite Cryst.2
CaO	56.54	54.99	45.08	44.68
Al_2O_3	33.34	35.59	15.90	15.88
Na_2O	2.00	2.12	0.81	0.48
K_2O	0.34	0.32	0.22	0.12
MgO	0.00	0.00	2.29	3.52
Fe_2O_3	4.70	4.89	23.79	29.51
SiO_2	3.59	3.22	6.16	6.12
Σ	100.51	101.13	94.25	100.31
Σ impur.	10.63	10.55	9.48	10.24

HYDRATION

Hydration kinetic curves for the aluminate phases obtained by means of X-ray diffraction are shown in Fig. 2a. For comparison, the hydration curves for C_3A and crystalline forms of solid solutions of C_3A with Na_2O/2/ are also shown. Analogous results were simultaneously published in /3/.

The hydration process of C_3A and its solid solutions with Na_2O can be regarded as a model which permits the description of the hydration course of any derivative of C_3A.

According to the kinetic curves, three stages of hydration are clearly distinguished at early interaction with water.

The first stage is characterized by an intense reaction course accompanied by a considerable heat liberation and is completed after a short period (to ~ 15 minutes). The intense start of the hydration is due to the peculiarities of the crystal structure of C_3A, first of all to large holes /4/. The decrease of the degree of hydration with increasing amount of sodium in the C_3A crystal lattice and consequently the increase in number of the occupied holes are evidence of the predominant role of the latter at early hydration.

In case of either substitution of Ca^{2+} or Si^{4+} by elements of other valency (what takes place during the formation of the aluminate phase in clinker) the charge balance can be realized not only by Na^+ but also by other ions. This is one of the reasons of a lower value of the degree of hydration of the aluminate phases of complicated composition (Fig. 2a,b), although the Na_2O content in them is less than in the cubic solid solution of C_3A with Na_2O. In other words, together with sodium, other compensating ions can be located in the crystal lattice holes of the aluminate phase.

The second stage of hydration that is completed after ~ 80-100 minutes from the beginning of the process is characterized by a sharp retardation of the reaction and is diffusion-controlled /2,5/. The reason of retardation is a layer of hydration products formed on the surface of hydrated particles. After completion of the period of intense

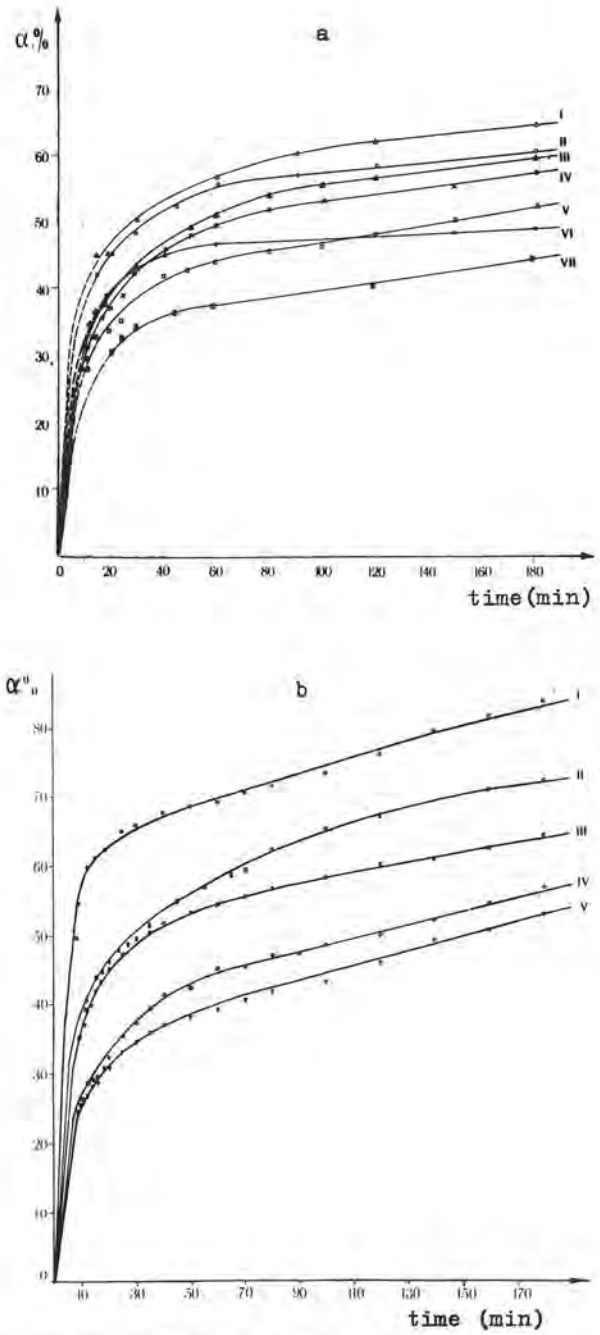

Fig. 2 - Kinetic hydration curves for : (a) aluminate phases of complicated composition (numbers of curves correspond to those of phases in Table I); (b) C_3A(curve I) and solid solutions with Na_2O : curve II - cubic solid solution (2.4 wt % Na_2O) ; III - orthorhombic (3.8 wt % Na_2O); IV - tetragonal (4.8 wt % Na_2O); V - monoclinic (5.7 wt % Na_2O).

reaction the thickest layer of hydrates forms on the surface of C_3A particles. The greater the amount of ions filling the crystal lattice holes of the solid solution, the lower the degree of hydration, the thinner the layer of hydration products that hinders the penetration of the liquid phase into the non-interacted substance.

The third, delayed completing stage is predetermined by the two preceding stages and depends also on the newly formed factors, namely on the kind of reaction products, on the growth of crystallohydrates, their size, orientation, recrystallization etc.

Due to a thinner layer of reaction products on the surface of the solid solution with the maximum filling of the holes, its hydration at the third stage will proceed more intensely compared to any other solid solution. As a result, the curves of degree of hydration can intersect after certain periods of time different for the different samples.

The analysis of the values of degree of hydration shows that after one day hydration the aluminates of the simplest composition containing sodium (samples IV, V) practically hydrated. The degree of hydration for them was ~ 90 %. An analogous sample containing potassium (III) showed a 70 % degree of hydration. The samples of aluminate phase containing Fe_2O_3 (I,II,VI,VII) showed a clear tendency to retardation of the hydration process at the third stage. The aluminate phase with the least amount of Fe_2O_3 (sample II) showed the highest value of degree of hydration after one day hydration and longer to six months (the term to which the observation was made).

The presence of aluminoferrite, although it does not change the general character of hydration, retards much more the hydration at the later stage, as shown by kinetic curves for sample VI. This is probably due to the fact that the layer of a mixture of hydration products of the aluminate and aluminoferrite is more dense compared to the products of hydration of the aluminate alone. As a result, the mineral can remain non-hydrated. Completeness of the reaction in this case depends to a considerable extent on the grain size.

CONCLUSIONS

The clinker aluminate phase is a polycomponent solid solution of C_3A with the oxides of constituent elements of raw materials.

The maximum amount of impurity oxides to be contained in the aluminate phase during the clinker formation does not exceed 12-13 wt% at a Fe_2O_3 content not more than 5 %.

In structural respect, the clinker aluminate phases are derivatives of C_3A and can possess the same crystal forms as solid solutions of C_3A with Na_2O.
The hydration of the aluminate phases proceeds by analogy with C_3A and crystal forms of its solid solutions with Na_2O. However, other components of the solid solution as well as other phases retard considerably the hydration.

The course of hydration at different stages is predetermined by a number of interrelated factors. However, at each stage only some of them play the decisive role.

Thus, in the initial period the hydration activity of the different crystal forms of solid solution depends mainly on the occupancy of lattice holes with foreign ions. The degree of hydration of the solid solution with the highest occupancy of the holes can be twice or thrice as low as in pure C_3A.

At subsequent stages the peculiarities of the interaction process with water depend on the thickness and the nature of the layer of hydration products, on the presence of other phases.

Each of the impurities also plays a definite role. Thus, Fe^{3+} ions, wherever they were (in the lattice of the aluminate solid solution or in the composition of the calcium aluminoferrite), retard the hydration of the aluminate phase. Aluminates of a simple composition containing Na^+ (along with K^+ and Si^{4+}) possess a greater value of the degree of hydration at the third stage compared to all phases investigated.

The choice of a set of impurities in the polycomponent solid solution permits wide variations of the degree of hydration of the aluminate phases of complicated composition.

REFERENCES

1.- G. YAMAGUCHI and SH. TAKAGI (1969), "The analysis of Portland cement clinker", in: Proceedings of the Fifth International Symposium on the Chemistry of Cement, pt.1, v.1, p.181-218.

2.- A. I. BOIKOVA, A. I. DOMANSKY, V. A. PARAMONOVA, G. P. STAVITSKAJA and V. M. NIKUSHCHENKO (1977), "The influence of Na_2O on the structure and properties of $3CaO.Al_2O_3$", Cement and Concr. Res. 7, nº 5, 483-491.

3.- M. REGOURD and B. MORTUREAUX (1977), "Tricalcium aluminate in synthetic solid solutions and in cements". Summaries of contributions to a Seminar at the University of Technology, Eindhoven, the Netherlands, April 13-14, 1977.

4.- P. MONDAL and J. N. JEFFERY (1975), "The crystal structure of tricalcium aluminate $Ca_3Al_2O_6$", Acta Cryst. 31, nº 3, 689-697.

5.- R. KONDO and SH. UEDA (1969), "Kinetics and mechanism of the hydration of cement", in: Proceedings of the Fifth International Symposium on the Chemistry of Cement, pt.2, v.2, 203-248.

Mechanisms of retardation of C_3A : a critical evaluation

Evaluation critique des mécanismes de ralentissement de l'hydratation de C_3A

S. CHATTERJI, M.Sc., D. Phil., Research Scientist, H + H Industri A/S, Lyngby, Denmark.

SUMMARY: The original papers were critically evaluated in order to differentiate between three proposed mechanisms of retardation of C_3A hydration.

(i) Retardation due to "alumina-rich" layer formation:-
From the hydration characteristics of dilute suspensions of C_3A in water and acid, it was concluded that "alumina-rich" layers form on C_3A grains which retard further hydration. Analyses of experimental conditions and results indicate the formation of expected alumina gels. The relevance of these results to pastes of C_3A, particularly in alkaline media, is uncertain especially as, contrary to practice, "$CaCl_2$ was found not to influence the induction (retardation) period".

(ii) Retardation due to alumina gel formation:-
From the hydration characteristics of C_3S+C_3A+gypsum+water pastes, it was concluded that C_3A grains, protected by layers of hydration products which hinder the flow of Ca^{2+} and OH^- but not water, hydrate in a dilute $Ca(OH)_2$ solution forming C_4AH_x and alumina gel and this gel is the actual retarding agent. Subsequently it was calculated that only 3.2×10^2 dyne$\cdot$cm^{-2} pressure differential across the protective layer is sufficient to maintain the required water flow. In the above calculation the number of C_3A grains was underestimated. The insertion of the proper number, without any other change, yields about 1.5×10^4 dyne$\cdot$cm^{-2}. Moreover there was no direct evidence of alumina gel formation.

(iii) Retardation due to water shortage at C_3A surface:-
An electron microscopic study showed that additives, especially $Ca(OH)_2$, reduce the size of hydration products in C_3A pastes. It was postulated that the smaller the hydration products the higher their resistance to water flow and hence smaller volume of water will reach the C_3A grains for further reaction. The presence of C_4AH_{13} instead of C_4AH_{19} in virgin moist pastes substantiates this water shortage. Effects of $CaCl_2$ and organic additives can be easily explained.

RESUME: Les études originales ont fait l'objet d'une évaluation critique afin de différencier les trois mécanismes de ralentissement de l'hydratation du C_3A.

(i) Ralentissement dû à la formation de couches "riches en alumine"
Selon les caractéristiques de l'hydratation des suspension diluées de C_3A dans l'eau et les acides, on a conclu que les couches riches en alumine se forment à partir de granules C_3A, ce qui ralentit toute hydratation ultérieure. L'analyse des conditions expérimentales et des résultats obtenus indique la formation de gels d'alumine. La pertinence de ces résultats en ce qui concerne les pâtes de C_3A, particulièrement en milieu alcalin, peut être mise en doute, surtout après avoir découvert que, contrairement à la pratique, "le $CaCl_2$ n'avait aucune influence sur la période d'induction (ralentissement)".

(ii) Ralentissement dû à la formation de gel d'alumine:-
Selon les caractéristiques de l'hydratation des pâtes C_3S+C_3A+gypse+eau, on a conclu que les granulés C_3A, protégés par les couches de produits de l'hydratation qui empêchent les flux de Ca^{2+} et de OH^- tout en laissant l'eau s'hydratent dans une solution diluée de $Ca(OH)_2$ et forment du C_4AH_x et un gel d'alumine qui est l'agent véritable du ralentissement. En conséquence on a calculé qu'une pression différentielle de 3.2×10^3 dyne$\cdot$cm^{-2} à travers les couches protectrices est suffisante pour maintenir le flux d'eau nécessaire. Dans ce calcul, on a sous-estimé le nombre de granules C_3A. L'introduction du nombre exact, sans faire intervenir d'autres changements, donne une pression de 1.5×10^4 dyne$\cdot$cm^{-2} environ. De plus, il n'y avait pas de preuves directes de formation de gel d'alumine.

(iii) Ralentissement dû au manque d'eau à la surface du C_3A:-
Une étude au microscope électronique a montré que les additifs, notamment le $Ca(OH)_2$, réduisent le volume des produits d'hydratation dans les pâtes C_3A. On a postulé que plus les produits d'hydratation sont faibles, plus leur résistance au flux de l'eau est grande, ce qui entraine une baisse du volume d'eau qui atteindra les granulés de C_3A pour la réaction ultérieure. La présence de C_4AH_{13} au lieu de C_4AH_{19} dans les pâtes humides vierges confirme ce manque d'eau. On peut facilement trouver une explication à l'action du $CaCl_2$ et des additifs organiques.

It is known that finely ground clinker of commercial Portland cement react with water with considerable evolution of heat and the paste is quick setting. In commercial practice the high rate of heat evolution and the quickness of set are controlled by co-grinding clinker and gypsum; although other chemicals can also be used for this purpose. It is generally conceeded that C_3A or related phases are responsible for quick setting. As a result the hydration of C_3A and the effects of different chemicals on its hydration have been studied extensively; and different mechanisms have been proposed to explain the observed effects. The object of this paper is to differentiate among three current mechanisms of retardation of C_3A hydration.

As any reaction mechanism can only be evaluated by comparying its corollaries with observations, so certain aspects of paste hydration of C_3A have been collected below:

(1) C_3A-H_2O system: Hedin was the first to show that about 40% of C_3A hydrates within 3 minutes of water addition but the subsequent hydration rate is much slower (1). Recent quantitative x-ray diffraction (QXRD) results confirmed it (2,3). Fig. 1 is taken from reference 2 and shows this effect clearly. Electron microscopic studies show that well formed hexagonal crystals of C_2AH_8 and C_4AH_x form within 4 minutes of water addition (4,5). With the passage of time, hexagonal crystals grow in size and proportion and C_3AH_6 appears.

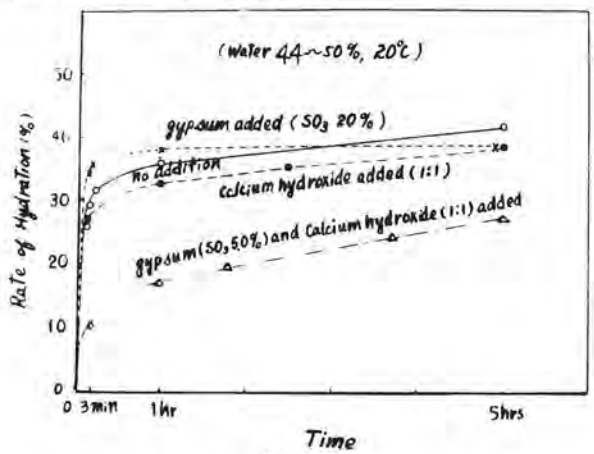

Fig. 1
Rates of C_3A hydration in different media

(2) C_3A-$Ca(OH)_2$-H_2O system: QXRD and other studies showed that the addition of $Ca(OH)_2$ lowers the rate of C_3A hydration (1,2,4,5,6) Plates of hexagonal aluminates, smaller and thinner than in C_3A-H_2O paste, could definitely be identified in a 3 hours sample (4,5); though their formation within 4 minutes could be inferred.

(3) C_3A-$CaSO_4$-H_2O system: QXRD results show that the addition of gypsum does not affect the early rate of C_3A hydration (2). According to Hedin, gypsum is less effective than $Ca(OH)_2$ (1), but according to Collepardi et al gypsum is more effective than $Ca(OH)_2$ (6). Thus the results are not in concordance. Ettringite is the main hydration product in the presence of gypsum although a small amount of hexagonal aluminate could be detected at all times (4,5,6,7). In a 3 hours old sample hexagonal crystals were as thin as in the C_3A-$Ca(OH)_2$-H_2O paste. Monosulfate forms when SO_4 ion concentration in the liquid phase drops below that required by ettringite.

(4) C_3A-$Ca(OH)_2$-$CaSO_4$-H_2O system: It is generally been accepted that lime-gypsum combination is a better retarder than either of the components (1,2,5,6). Ettringite is the main hydration product in the presence of gypsum although hexagonal aluminates can be found at all times. (4,5,6,7). Sizes of the hydration products are very much reduced in this system (5,8).

(5) C_3A-$CaCl_2$-H_2O system: The effect of $CaCl_2$ on C_3A hydration depends on its concentration (1,5). For the same retardation a lower amount of $CaCl_2$ is needed than $Ca(OH)_2$+$CaSO_4 \cdot 2H_2O$ combination; however at a higher concentration $CaCl_2$ is an accelerator (1). Electron microscopic and x-ray diffraction studies show that hexagonal monochloride ($C_3A \cdot CaCl_2 \cdot xH_2O$) forms at low $CaCl_2$ concentration and needle shaped trichloroaluminate ($C_3A \cdot 3CaCl_2 \cdot yH_2O$) forms at high $CaCl_2$ concentration (5).

With the above background information it is now possible to analyse and differentiate between different mechanisms of retardation of C_3A hydration.

(A) Retardation due to "alumina-rich" layer formation:

This mechanism has been proposed by Tadros and Skanly (9,10). The authors concluded that C_3A dissolves incongruently in water or dilute acid solutions forming alumina-rich surfaces on C_3A grains. Calcium ions get adsorbed on this layer forming positively charged particles. "The formation of a structure consisting of an aluminium-rich surface with adsorbed calcium ions, appears to minimize the active dissolution sites and results in reduced rates of dissolution". "In the presence of sulfate ions, adsorption on the positively charged sites further reduces the rate of dissolution. This effect is probably achieved via the blocking effects of sulfate ions on coordination sites which would otherwise be occupied by hydrogen or hydroxyl ions, known to be able to catalyze the dissolution of alumina ..". In order to appreciate their conclusions, it is necessary to analyse their experimental technique and results:

(i) C_3A-water suspensions: In these suspensions water/solid ratios varied between 25 to 250. The liquid phase after one minute of mixing contained 1.05×10^{-2}M Ca

ions and 5.5×10^{-3}M Al ions. As Ca/Al ratio was 1.9 instead of 1.5 of C_3A the authors concluded that C_3A dissolves incongruently. However an examination of $Ca(OH)_2$-$Al(OH)_3$-H_2O phase diagram (11) shows that a liquid phase containing 1.05×10^{-2}M Ca ions in equilibrium can contain only 1.96×10^{-3}M Al ions i.e. the analysed solution was already 2.8 times supersaturated with Al ions. A congruent solution of C_3A, if all Al ions could be kept in solution, would have yielded a Al ion supersaturation of 3.6. It is highly unlikely that such a supersaturation could be achieved in practice. Whether from the above analyses of the liquid phase one can conclude incongruent solubility of C_3A is another matter altogether. In this context it is of interest to note that Hedin who arranged C_3A/water ratio so that both Ca and Al ions could be kept in solution, found Ca/Al ratio of 1.5 over a period of 20 minutes (1).

(ii) C_3A-dilute acid suspensions: Figs. 2 and 3 are taken from reference 9 and show representative results. The time interval between pH 4 and about 11.2 has been termed "induction period". It can be seen that the induction period has been lengthened by SO_4 ions. In some experiments $CaCl_2$ was used instead of $CaSO_4$ and "$CaCl_2$ was found not to influence the induction period". A quantitative analysis of these results will be informative. Consider the case of pure 0.166M HCl first.

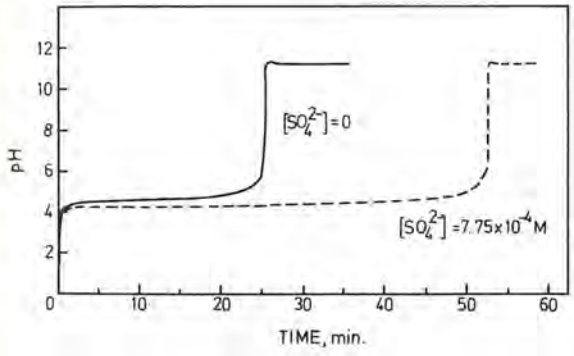

Fig. 2 - Rates of dissolution of 2g C_3A in 75 ml. of 0.166M HCl

(a) From Fig. 3 it can be seen that the initial Ca ion concentration was just below 0.06M and that of Al ion just above 0.02M; for the sake of simplicity assume them to be 0.06 and 0.02 respectively. From Fig. 2, the pH of the solution at that time was 4. If both the metals were in their fully ionized state then Ca ions would have required 0.12M Cl ions and Al ions would have required 0.06M Cl ions i.e. altogether 0.18M Cl ions; whereas the solution contained only 0.166M Cl ions. If the pH of the solution is taken into consideration, a higher Cl ion concentration will be needed to neutralize the positive ions.

It is thus obvious that not all the metals in the solution were in their fully ionized state i.e. at least a part of Al was in a hydrolyzed state

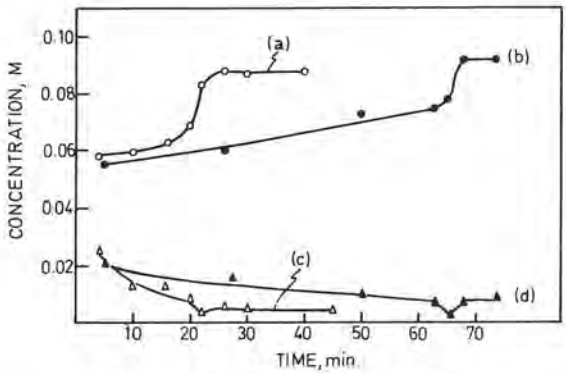

Fig. 3 - Dissolution of 2g C_3A in 75 ml of 0.166M HCl. (a) and (c) for $[Ca^{2+}]$ and [aluminium]; (b) and (d) for $[Ca^{2+}]$ and [aluminium] in the presence of 1.55×10^{-3}M $CaSO_4$ respectively.

(b) Fig. 2 shows that between 2 and 12 minutes the pH of the solution rose slightly above 4. Fig. 3 shows that in the same period Ca ion concentration was effectively constant, however Al ion concentration dropped from 0.02 to 0.01M. A removal of Al ion from the solution should have been accompanied by a change in positive ions i.e. changes in pH and/or Ca ion concentration. In the absence of either, one is forced to think that at least a part of Al was in a finely divided state at the time of the first filtration but had grown subsequently and was removed at the second filtration. This interpretation is consistant with the fact that Al ions start to hydrolyse at pH3 (12,13) and that the solubility of $Al(OH)_3$ at pH4 is $1.\times10^{-4}$ mol/l (14). It is only natural that freshly formed $Al(OH)_3$ will need time to grow sufficiently to be removed by filtration. Incidentally the measured Ca ion concentration of 0.06M is just short of that required to neutralize 0.166M HCl to pH4. It will thus appear that a major part, if not all, of Al released by the action of HCl was hydrolyzed to $Al(OH)_3$ in a very short time. It is expected that adjacent to C_3A grains the pH will be higher than in the bulk liquid phase and a major part of hydrolysis and precipitation of $Al(OH)_3$ will occur there i.e. C_3A grains will be covered by $Al(OH)_3$ layers. The difficulty of material transport through this $Al(OH)_3$ layer will explain the "induction period".

Dissolution of C_3A in HCl in the presence of SO_4 ions could not be analysed in detail, the reason being that Figs. 2 and 3 report results of two different SO_4 concentrations.

However qualitatively the effectiveness of SO_4 ions could be explained on the basis of Schulze-Hardy rule, which states that diavalent SO_4 ions will be very effective in precipitating positively charges $Al(OH)_3$ gel (15). A tightly packed $Al(OH)_3$ gel will hinder the flow of materials through it more than a loosely packed layer.

The authors definitely got $Al(OH)_3$ layers on C_3A grains in their experiments. However their results and hypothesis are at variance with the following characteristics of C_3A paste:

(i) in C_3A pastes hexagonal aluminates or/ and ettringite were found from 30 sec. onwards whereas the authors could not find them,

(ii) the hypothesis suggests that high concentration of $Ca(OH)_2$, in the absence of SO_4 ions, should dissolve aluminous layer thereby increasing C_3A hydration, whereas in practice $Ca(OH)_2$ is a retarder,

(iii) it is difficult to explain the higher efficiency of $Ca(OH)_2+CaSO_4 \cdot 2H_2O$ mixture,

(iv) $CaCl_2$, which the authors found to be ineffective, is in practice a very effective agent.

In view of the above contradictions, the relevance of this experimental set up and the hypothesis to paste hydration of C_3A especially in alkaline medium is very uncertain.

(B) The hypothesis of retardation due to an aluminious hydroxide layer formation:

This hypothesis was proposed by Stein et al (16,17). According to this hypothesis "when C_3A reacts with water, both C_2AH_8 and C_4AH_n are formed" (17). However when C_3A reacts in a solution containing Ca and OH ions the nucleation of C_4AH_x is favoured leading to a local shortage of Ca and OH ions near C_3A grains and formation of $Al(OH)_3$ gel layers on the grains. This gel layer needs a protective layer of C_4AH_x to hinder the flow of Ca and OH ions but not water.

From the measured heat liberation data and the known enthalpy of the following reaction

$$C_3A + Ca^{2+} + 2OH^- + 12H_2O = C_4AH_{13}$$

Stein calculated that for a 0.75g C_3A + 0.25g C_3S paste if C_4AH_x layer had a porosity less than 10^{-6} cm^2/cm^2 of C_3A surface the shortage of Ca and OH ions would be the rate determining factor. Inserting the above porosity and calculated water flow through C_4AH_x layer to maintain the rate of heat liberation in the Hagen-Poiseuille equation Stein calculated that a pressure differential of 3.2×10^3 dynes$\cdot cm^{-2}$ across the C_4AH_x layer would be needed. This low figure indicated the absence of water shortage (17).

In the above calculation Stein used 10^{-6} as the radius of the individual pores. A division of the total pore area by πr^2 gives 3.18×10^8 as the total number of pores in the paste. From the characteristics of their starting materials it can be calculated that 0.75g C_3A contained 1.42×10^9 equal sheres of radius 3.46×10^{-4}cm. Note that the number of spheres is larger than the number of pores. An assumption of size distribution in C_3A should increase the number of particles. From Stein's other data it can be calculated that during the initial stages of hydration the volumes of individual particles were reduced by about 30% i.e. there was no reduction of particle number. The use of this number in the Hagen-Poiseuille equation without any other change gives a pressure differential of 1.5×10^4 dyne$\cdot cm^{-2}$. This is also the pressure on the pore walls tending to disrupt them i.e. C_4AH_x layer. One may wonder if the above assumption of one pore per particle is reasonable especially as Fig. 4 taken from reference 18, shows several pores per 400 μm^2 surface of C_4AH_x layer. The use of pro rata number of pore gives an enormous pressure differential. It is also to be noted that in the case of no water shortage C_4AH_{19} and not C_4AH_{13} should form. The assumptions of the number of pores and the rigidity of C_4AH_x layer depend on ones personal belief. However the followings are independent of personal belief:

(i) there is no independent evidence of $Al(OH)_3$ formation,

(ii) there is independent x-ray evidence of C_4AH_{13} formation in moist paste indicating a water shortage (19),

(iii) as $Al(OH)_3$ is not expected to form in C_3A-water paste (17), this hypothesis can not explain the drop in the rate of C_3A hydration after about 3 minutes,

(iv) it is also difficult to explain the effects of $CaCl_2$ on C_3A hydration.

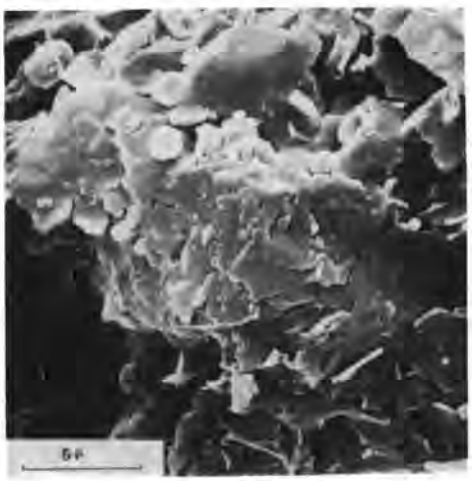

Fig. 4 - C_3A hydrated for 10 minutes in paste (w/s = 1).

(C) The hypothesis of water shortage as the cause of retardation of C_3A hydration:

In this hypothesis (20,21) it has been assumed that (i) the hydration of C_3A depends on the availability of water at the grain surfaces, (ii) water has to flow through hydration products which form round the grains, (iii) the resistance to water flow varies directly with the thickness of the reaction product layer and inversely as the particle size of the product i.e. the flow follows a Kozeny-Carman type equation, (iv) thin plates e.g. C_4AH_x offer higher resistance than needles e.g. ettringite. These authors showed that the addition of $Ca(OH)_2$, gypsum, $Ca(OH)_2+CaSO_4 \cdot 2H_2O$ mixture to C_3A paste causes reduction in the particle size of the reaction products compared to pure C_3A paste. They also showed that at low $CaCl_2$ concentration hexagonal plates of monochloride form and at high $CaCl_2$ concentration needles of trichloride form.

From the above hypothesis it follows that C_3A-water paste will need a thick layer of hydration products before a water shortage will cause a lowering of the hydration rate i.e. the initial hydration rate will be high and once a sufficiently thick layer of hydration products has formed the rate will drop. The retarding and the accelerating effects of $CaCl_2$ at different concentrations can be explained on the basis of the plate and needle shapes of the product, respectively. In the case of C_3A-$Ca(OH)_2$-gypsum paste, the formation and persistance of hexagonal aluminate phases suggests a decreasing gradient of SO_4 ion from the bulk solution to C_3A surface. This gradient results in the formation of the hexagonal phase adjacent to the grains and on top of which a layer of ettringite. Better performance of $Ca(OH)_2$+ gypsum mixture has been attributed to the observed smallness and thinness of the hexagonal crystals.

It should be noted that no other ad-hoc assumption is necessary to explain the actions of lignosulfonate, NaOH etc. (21,22). The direct x-ray evidence of a water shortage at C_3A grain surface has already been referred to (19).

Recently Collepardi et al suggested a modified version of the water shortage hypothesis (6). These authors proposed that the ettringite layer, which forms in the presence of gypsum, has a better retarding effect than a layer of thin and small hexagonal aluminates. Fig. 5, which has been taken from ref. 6, shows that the heat liberation rate of C_3A-gypsum paste has an early peak at about 5 minutes. "After 15 minutes of hydration a peak (in DTG curves) at 120°C assigned to $C_3A \cdot 3\overline{C}S \cdot H_{32}$ is recorded. Traces of calcium aluminate hydrate can be observed". Fig. 5 also shows that the heat liberation rate accelerates again at about 1.5 hours and peaks at about 4.5 hours; the rate has another inflextion at about 6 hours.

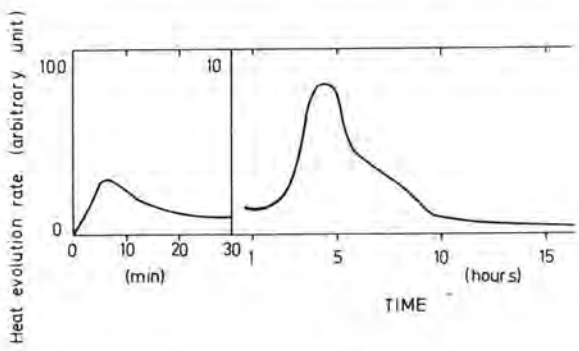

Fig. 5 - Heat evolution in the system $C_3A+Ca(OH)_2+CaSO_4 \cdot 2H_2O+H_2O$.

"At 3-4 hours ettringite is the principal product of hydration while traces of gypsum and hexagonal hydrate can also be observed. At 6-24 hours ettringite tends to decrease and a large peak at 220°C assigned to $C_3A \cdot \overline{C}S \cdot H_{12}$ appears". As ettringite was the principal product upto 3-4 hours, it is obvious that the accelerating rate of heat liberation between 1.5 and 3-4 hours must be due to the accelerating rate of ettringite formation. As ettringite tends to decrease at 6-24 hours monosulfate must also be forming at that time i.e. the inflexion of the heat liberation curve at about 6 hours is due to monosulfate formation. It is rather surprising that a thin layer of ettringite, which according to the authors, could retard C_3A hydration between 0.25 and 1 hour but a thicker ettringite layer could not retard between 1.5 and 3-4 hours. No explanation of this anomaly has been offered.

It is to be noted that the authors have confirmed the formation of hexagonal aluminate hydrate from 15 minutes onwards. The formation of ettringite as the principal product upto 3-4 hours shows that the bulk liquid phase had a high SO_4 ion concentration upto that time. The persistant formation of hexagonal aluminate then means a persistant decreasing gradient of SO_4 ions from the bulk solution to C_3A surface and that the hexagonal aluminates must have formed in between C_3A and ettringite layer. One can of course always claim that an ettringite layer, which can not stop hexagonal aluminate formation, is a more effective retarder than the layer of hexagonal aluminate which forms between the layer of ettringite and C_3A grain. However on the above basis it will be difficult to explain the higher retarding efficiency of hexagonal monochloride over needle shaped trichloride.

The type of analyses carried out in this paper can be further extended and merits or otherwise of different hypothesis can be evaluated. However in the ultimate analysis what is considered to be an acceptable explanation depends more on the fashion of the day, than anything else.

REFERENCES

1. R. HEDIN (1945). "Chemical Processes in the Hardening Portland Cement". Cement and Concrete Research Inst., Stockholm, Sweden.
2. G. YAMAGUCHI et al (1960). "Rate of hydration of cement compounds and Portland cement estimated by x-ray diffraction analysis". Proc. IVth Intern. Symp. Chemistry of Cement, Washington D.C., 495-499.
3. K.E. DAUGHERTY and M.J. KOWALEWSKI (1968). "Effects of organic compounds on the hydration reactions of tricalcium Aluminates". Proc. Vth Intern. Symp. Chemistry of Cement, Tokyo. Part IV, 42-51.
4. S. CHATTERJI and A. GRUDEMO (1961), quoted by A. Grudemo in "The Chemistry of Cements". Ed. H.F.W. Taylor. Academic Press. London. 1964. Vol. 371-389.
5. P. GUPTA et al (1970). "Studies of the effects of various additives on the hydration reaction of tricalcium aluminate: Part I". Cement Technology, 159-166.
6. M. COLLEPARDI et al (1978). "Tricalcium aluminate hydration in the presence of lime, gypsum and sodium sulfate". Cement and Concrete Res. 8, 571-580.
7. H.E. SCHEWIETE et al (1966). "Investigation in the system $3CaO \cdot Al_2O_3 - CaSO_4 - CaO - H_2O$". Highway Research Board. Washington. Special Report No. 90, 353-367.
8. P.K. MEHTA (1973). "Mechanism of expansion associated with ettringite formation". Cement and Concrete Res. 3, 1-6.
9. M.E. TADROS et al (1976). "Study of the dissolution and electrokinetic behaviour of tricalcium aluminate". In Colloid and Interface Science, vol. IV, Ed. Kerker. Academic Press. 211-223.
10. J. SKANLY and M.E. TADROS (1977). "Retardation of tricalcium aluminate hydration by sulfates". J.Amer.Ceram. Soc. 60, 174-175.
11. F.E. JONES and M.H. ROBERTS (1959). "The System $CaO-Al_2O_3-H_2O$ at 25°C". DSIR Building Research Station. Note E 965, HMSO. London.
12. I.M. KOLTHOFF and F.B. SANDELL (1963). "Textbook of quantitative inorganic analysis". Macmillan & Co. Ltd., New York. 318.
13. J.R. PARTINGTON (1961). "General and inorganic chemistry". Macmillan & Co. Ltd., London. 424.
14. R.W. SMITH (1971). "Relations among equilibrium and non-equilibrium aqueous species of aluminium hydroxy complexes" in Nonequilibrium Systems in Natural Water Chemistry. Ed. Hem. Advances in Chemistry Series 106. Am.Chem.Soc.
15. S. GLASSTONE (1966). Textbook of Physical Chemistry. Macmillan & Co. Ltd., London. 1243.
16. W.A. CORSTANJE et al (1973). "Hydration reactions in pastes $C_3S+C_3A+CaSO_4 \cdot 2H_2O$+Water at 25°C". Cement and Concrete Res. 3, 791-806.
17. H.N. STEIN (1974). "A reply to S. Chatterji's discussion on Hydration Reactions in Pastes etc.". Cement and Concrete Res. 4, 1001-1006.
18. G.A.C.M. SPIERINGS and H.N. STEIN (1975). "The influence of Na_2O oxides on the reaction of C_3A with water" in Some Recent Research on Cement Hydration. CEMBUREAU.
19. S. CHATTERJI and J.W. JEFFERY (1964). "Discussion of a paper on "A new hypothesis of sulphate expansion"". Mag. Concrete Research. 16. 239-241.
20. P. GUPTA et al (1973). "Studies of the effects of various additives on the hydration reaction of tricalcium aluminate. Part 5". Cement Tech. 4, 146-149.
21. P. GUPTA (1970). "Studies of the effects of various additives on the hydration reactions of tricalcium aluminate paste". Ph.D. Thesis. London University.
22. S. CHATTERJI (1967). "Electron-optical and x-ray diffraction investigation of the effects of lignosulphonates on the hydration of tricalcium aluminate". Indian Concrete J. 41, 151-160.

Theme 3 - Hydration of C_3A in cements

GENERAL REPORT

by UDO LUDWIG, Institut für Gesteinshüttenkunde, Rwth Aachen, R.F.A.

With the above theme eight papers are submitted for presentation and they deal with

(I) the reactivity of cubic, orthorhombic and monoclinic C_3A (1)

(II) the formation of mono- and trisilico-aluminate hydrates (1, 2)

(III) the hydration of C_3A in pure systems with C_3S, $C\bar{S}$, $C\bar{C}$ and $K\bar{S}$ (1, 3, 4, 5)

(IV) the hydration of C_3A and $C_2(A,F)$ in cements (1, 5, 6, 7, 8)

REGOURD, HORNAIN and MORTUREUX (1) studied the rate of hydration of both cubic and orthorhombic forms of C_3A in the presence of C_3S and gypsum by XRD with a normal paste of 0·35 to 0·5 W/S ratio. They found that in the initial stages of reaction the cubic form was more reactive than that of orthorhombic. The use of NaOH solution instead of distilled water showed no effect on the reactivity of C_3A. From these observations, the authors concluded that the higher density of the orthorhombic form of C_3A is responsible for the lower reactivity. Addition of 3 wt.-% K_2SO_4 to C_3A-C_3S-$C\bar{S}H_2$ paste accelerates the hydration of both the cubic as well as the orthorhombic form of C_3A. - The lower hydration rate of orthorhombic as well as monoclinic C_3A was also observed in pastes hydration of industrial clinker.

J.H.P. VAN AARDT and S. VISSER (2) synthesized a monosilicoaluminate hydrate (10,0 Å) analogous to the calcium monosulphoaluminate hydrate (10·3 Å) by reaction of amorphous silica and lime with a slurry of C_4AH_{19} (10·6 Å) at 5°C. The reaction was followed by XRD.
C_4AH_{19} was prepared from C_3A and $Ca(OH)_2$ at 5°C, which contained a little amount of C_3AH_6 and 8·2 Å hydrate. On the addition of silica or silica with $Ca(OH)_2$, the following reactions took place.

1. silica and $Ca(OH)_2$ formed CSH and
2. silica replaced the OH groups in C_4AH_{19} to form the silicoaluminate hydrate.

On the addition of increasing amounts of silicoaluminate hydrate is formed readily especially when no extra $Ca(OH)_2$ is added. The addition of CSH did not produce the 10 Å hydrate.
At later ages of hydration or by raising the temperature from 5°C to room temperature, 10,0 Å hydrate is converted into C_2ASH_8 (12·6 Å) and CSH.

Under normal conditions, the formation of silicoaluminate hydrate is unlikely in hydrated Portland cement because of the excess $Ca(OH)_2$ present.

On the otherhand with the help of electron microanalysis of the polished sections of the following two hydrated mixtures

76 wt.% C_3S + 19 wt.% C_3A + 5 wt.% gypsum and

80 wt.% C_3S + 20 wt.% C_3A_c.

M. REGOURD, H. HORNAIN and B. MORTUREUX (1) found the following two silicoaluminate hydrates

C_4ASH_{12} and $C_3A{\cdot}3CS{\cdot}H_{31}$.

After seven days of hydration, the formation of poorly crystalline trisilicoaluminate hydrate was observed as pseudomorph of the anhydrous C_3A. The monosilicoaluminate hydrate is formed outside the original C_3A boundary. The C_3A_c reacts faster than C_3A_o.

J. JAMBOR (3) studied the binding properties of C_3A in the presence of $CaCO_3$. The fineness of C_3A and $CaCO_3$ were respectively 2800 and 2480 cm^2/g (Blaine). The experiment was carried out with 2 cm cubes with mixtures of

1. C_3A with graded amounts of $CaCO_3$
2. C_3A with graded amounts of quartz sand and
3. 73 wt.-% C_3A and 27 wt.-% $CaCO_3$ and graded amounts of quartz sand.

After 1 and 28 days curing, bulk density and compressive strengths were determined in wet and dry states (100°C drying). In addition to this the total porosity, average radius of the micropores and ignition loss at 600°C were also determined for dried specimens. The specimens were analysed by XRD, thermal analyses and scanning electron microscopy. The usual hydration products of C_3A form only loose structures with low binding capacity whereas due to additions of $CaCO_3$, the strength is increased 300 times in the wet state. Maximum strength was found to be 29 MPa for a paste with $C_3A/CaCO_3$ ratio of 60/40. XRD and thermal analyses confirmed that the formation of mainly $C_3A{\cdot}CaCO_3{\cdot}H_n$ and the higher rate of hydration of C_3A in the presence of $CaCO_3$ is the cause of increased strength.

I. ODLER (4) studied the interaction between the CSH phase formed in C_3S hydration in the presence of gypsum and the ability of bound gypsum to react

with C_3A. The maximum amount of bound gypsum was found to be 9.8 g/100 g C_3S after 1 day of hydration in a paste with 10 wt.-% calcium sulphate. This ratio of 1 mol SO_3 per 6.1 moles C_3S hydrated corresponds well with the results in literature. Increase in C_3S hydration takes place upto 10 wt.-% of gypsum additions. The bound gypsum can not be detected by DTA and XRD but can easily be quantitatively extracted by lime water or can reactwith C_3A to form ettringite. The bond between calcium sulphate and CSH phase is weak and the author assumes that the calcium sulphate is physically adsorbed at the surface of CSH gel. -

H. Y. GHORAB, D. HEINZ, U. LUDWIG, T. MESKENDAHL and A. WOLTER (5) did new research on the stability of calcium aluminate sulphate hydrates in pure systems and in cements. - Suitable additions of calcium sulphates to cements prevent false setting by formation of an ettringite layer preferably on the surfaces of the C_3A. Investigations in pure systems with C_3A, gypsum or anhydrite and lime with and without additional $CaCO_3$ or C_3S and with industrial plain or blended Portland cements confirm or indicate that ettringite and carboaluminate hydrate are the stable phases at room or lower temperatures. Monosulphate hydrate is the stable phase at elevated temperatures. In consequence an interim formation of instable monosulphate hydrate at normal temperatures or specially at direct, delayed or repeated, wanted or unwanted heat treatment of cement pastes mortars or concretes can cause damage by subsequent ettringite formation accompanied by expansion, cracking and decreased strength. Calcium carbonate additions can increase the damage. Portland cements with limited or without C_3A or Portland cements blended with granulated blast furnace slags or suitable puzzolanas in appropiate amounts reduce or even prevent damage. - But reduction or prevention of damage should not be regarded as the sole task. One should look ahead making use of the knowledge of the reactions of the calcium aluminate hydrates, for instance, for the chemical prestressing of concrete.

B. F. COTTIN (6) studied the kinetics of hydration of the following four different industrial clinkers.

Cement	C_3S	C_2S	C_3A	C_4AF	C_{free}	Alkali-sulphate	$CaSO_4$
A	67	19	8	1	4.4	0.2	0.2
B	59	16	13	7	1.0	1.8	1.5
C	62	19	2	14	1.9	0.7	0.1
D	60	20	7	10	1.1	0.5	0

The clinkers were mixed with 0, 1, 2.5 an 5 wt.-% SO_3 in the forms of gypsum, hemihydrate and burned and natural anhydrite and ground to a fineness of 3000 cm^2/g (Blaine). The W/C ratio during the hydration was kept at 0.5. The kinetics of hydration was followed by an isothermal calorimeter. The calorimetric curves show three exothermic peaks with changing intensity and time of occurence due to

1. early hydration of C_3A (influenced by the presence of C_3S and sulphates)
2. C_3S hydration
3. total sulphate consumption.

The addition of calcium sulphate always lead to a decreased intensity of the first peak except clinker C with hemihydrate. But from the results it seems impossible to have a general correlation between the decrease in heat liberation and the quantity and the nature of the added sulphates. For all clinkers the optimum gypsum content lies between 2.5 to 5 wt.-% of the added SO_3. With the exception of clinker B, sulphate additions resulted in an increased and early heat liberation second peak. This peak which is mainly due to C_3S hydration occurs at early hydration time even in the plain clinker B without any sulphate additions because the clinker itself contains a lot of alkali sulphates. The third peak which is due to total SO_3 consumption was generally very weak and broad. With natural anhydrite this peak was absent.

I. ODLER and R. WONNEMANN (7) studied the effect of different forms of calcium sulphate on the hydration of C_3A present in a laboratory burned clinker. The clinker contained 15 wt.-% C_3A and 5 wt.-% $C_2(A,F)$. The clinker was ground with 3 wt.-% of SO_3 in the form of anhydrite, hemihydrate or gypsum to a fineness of 3000 $\pm$ 100 cm^2/g (Blaine) and hydrated with W/S = 0.5. The ettringite formation was determined up to 30 minutes by DTA. The unreacted fraction of gypsum and hemihydrate was determined by DTA that of anhydrite by QXRD. - The results indicate, that there is no significant influence of the additions and of the form of added sulphate on the hydration kinetics of C_3A. With sulphate addition ettringite is the first hydration product of C_3A to be converted later on to monosulphate hydrate. The ettringite formation is reduced and the conversion to monosulphate hydrate is delayed with anhydrite. - The flash setting of pure clinker (< 1 minute) is not a consequence of rapid C_3A hydration but a consequence of an altered morphology of the hydration products as already suggested by LOCHER, RICHARTZ and SPRUNG. With hemihydrate the measured fast setting is related to the conversion to dihydrate. The higher water requirement with anhydrite is due to the formation of a significant amount of different calcium aluminate hydrates than ettringite.

E. S. JONS and B. OSBAECK (8) investigated the influence of C_3A in cements. They prepared three clinkers each with 60 wt.-% C_3S and 22 wt.-% C_2S. The C_3A and C_4AF contents in each clinker varied respectively from 0 to 16 and 2 to 18 wt.-%. Three cements were made from each clinker by the addition of different amounts of SO_3 in the form of a mixture of equal amounts of gypsum and hemihydrate. Clinkers mixed with sulphates were ground in a ball mill for 15 min. Differences in fineness reflect differences in grindability and remained without consideration. On the other hand corrections were made for strength values arising from the contribution to the measured fineness by the added sulphate. The maximum correction amounts to 6 MPa. Further correction was made for decreased bulk density with increased C_3A content of the clinker. The largest correction attributable to entrained air was 5 MPa. The strength development curves show an optimum amount of both C_3A and added SO_3. There is a positive effect of SO_3 addition on the early hydration of C_3S which corresponds well with the work of other researchers with pure C_3S or alites. The strong retarding effect of excess SO_3 on C_3A hydration is significant. It appears that large amounts of C_3A have a negative effect on C_3S

hydration. By plotting logarithm of compressive strength vs reduced porosity by C_3S hydration, the authors conclude that C_3A gives an independent positive contribution to strength during the entire period of examination. Negative effects are the air entrainment in the mortars and the lower rate of C_3S hydration at more advanced stages of hydration.

Summarizing the submittel papers, the following conclusions can be made:

The orthorhombic and monoclinic C_3A are less reactive as compared to the cubic form. Analogous results are obtained both in pure systems and hydrated cements.

In the presence of water, the reaction between C_4AH_{19} and amorphous silica and as well as between C_3A with C_3S or C_2S showed the formation of

$C_3A \cdot CS \cdot H_{12}$. In the reaction of C_3A with C_3S or C_2S, the formation of $C_3A \cdot 3CS \cdot H_{32}$ was also observed. The formation of silicoaluminate hydrates has also been observed in hydrated Portland cements.

In systems containing sufficient amounts of sulphate ions, the immediate formation of a gel like ettringite layer on the surface of C_3A grains hinders false setting. The monosulphoaluminate hydrate and its solid solutions, formed subsequently, are partly unstable at room or lower temperatures. A renewed ettringite formation, without and - increased - with interim heat treatment, was also observed at later ages. Additional $CaCO_3$ increases this reaction. The renewed ettringite formation was also observed during cement hydration and this can cause damage by expansion, decreased strength and cracking. The Portland cements with limited C_3A or blended cements are less susceptible to this damage.

The sulphate adsorbed on the surface of CSH gel from the reaction of C_3S, $C\bar{S}$ and water can react subsequently with C_3A to form ettringite.

The form and amount of calcium sulphate added to cements will influence the early hydration but it will not change the hydration kinetics significantly.

The hydration products of C_3A will contribute to the strength formation.

REFERENCES

1. - M. REGOURD, H. HORNAIN, B.MORTUREUX, Département Microstructures, C.E.R.I.L.H., Paris, France
"Hydratation de C_3A dans des mélanges synthétiques et dans des ciments portland industriels"

2. - J.H.P. VAN AARDT and S. VISSER, National Building Research Institute, CSIR, Pretoria, South Africa
"Synthesis of a calcium silicoaluminate hydrate at 5°C"

3. - J. JAMBOR, Ing. Dr., Dr., Dr. Sc., Institute of Construction and Architecture, Slovak Academy of Sciences, Bratislava, Tchécoslovaquie
"Influence of $3CaO \cdot Al_2O_3 \cdot CaCO_3 \cdot nH_2O$ on the structure of cement paste"

4. - I. ODLER, Clausthal
Clausthal University, Germany
"Interaction between gypsum and the C-S-H phase formed in C_3S hydration"

5. - H.Y. GHORAB, D. HEINZ, U. LUDWIG, T.MESKENDAHL and A. WOLTER,
Institut für Gesteinshüttenkunde, RWTH Aachen, Germany
"On the stability of calcium aluminate sulphate hydrates in pure systems and in cements"

6. - B.F. COTTIN,
Chef de Service, Laboratoire de Recherche Générale, Lafarge S.A., France
"Cerzaines intéractions entre C_3A et C_3S lors de l'hydratation des ciments portland"

7. - I. ODLER and R. WONNEMANN,
Clausthal University, Germany
"Hydration of C_3A in Portland cement in the presence of different forms of calcium sulfate"

8. - E.S. JONS et B. OSBAECK,
F.L. Smidth & Co. A/S, Vigerslev Alle 77
DK-2500 Valby Copenhagen, Denmark
"The influence of the content and distribution of Al_2O3 on the hydration properties of Portland cement"

Thème 3 - Hydratation de C_3A dans les ciments

RAPPORT GENERAL

par UDO LUDWIG, Institut für Gesteinshüttenkunde, Rwth Aachen, R.F.A.

Dans ce thème, 8 contributions sont présentées et traitent de :

1) la réactivité de C_3A cubique, orthorhombique et monoclinique (1),
2) la formation de mono et trisilicoaluminate hydratés (1, 2),
3) l'hydratation de C_3A dans des systèmes purs avec C_3S, $C\bar{S}$, $C\bar{C}$ et $K\bar{S}$ (1, 3, 4, 5),
4) l'hydratation de C_3A et $C_2(A,F)$ dans les ciments (1, 5, 6, 7, 8).

REGOURD, HORNAIN et MORTUREUX (1) ont étudié le taux d'hydratation des formes à la fois cubique et orthorhombique de C_3A en présence de C_3A et de gypse par DRX dans une pâte normale de rapport eau/ciment égal soit à 0,35 ou à 0,5. Ils ont trouvé que dans les stades initiaux de réaction, la forme cubique est plus réactive que la forme orthorhombique. L'utilisation d'une solution de NaOH à la place d'eau distillée ne montre aucun effet sur la réactivité de C_3A . De ces observations, les auteurs ont conclu que la plus forte densité de la forme orthorhombique de C_3A est responsable de la plus faible réactivité. L'addition de 3% K_2SO_4 à la pâte C_3A-C_3S-$C\bar{S}H_2$ accélère l'hydratation de la forme cubique aussi bien que celle de la forme orthorhombique. Le taux d'hydratation plus faible de la forme orthorhombique et de la forme monoclinique de C_3A a aussi été observé dans l'hydratation de pâtes de clinker industriel.

J.H.P. VAN AARDT et S. VISSER (2) ont synthétisé un monosilicoaluminate hydraté (10,0 Å) analogue au monosulfoaluminate de calcium hydraté (10,3 Å) par réaction d'une silice amorphe et de chaux avec des traces de C_4AH_{19} (10,6 Å) à 5 °C. La réaction a été suivie par DRX. C_4AH_{19} a été préparé à partir de C_3A et $Ca(OH)_2$ à 5 °C, il contenait une faible quantité de C_3AH_6 et un hydrate à 8,2 Å. L'addition de silice ou de silice et de $Ca(OH)_2$ donne les réactions suivantes :

1) la silice et $Ca(OH)_2$ forment C-S-H et
2) la silice remplace les groupes OH dans C_4AH_{19} pour former le silicoaluminate hydraté.

En présence de teneurs croissantes en silice, le silicoaluminate hydraté est formé rapidement, spécialement quand $Ca(OH)_2$ n'est pas ajouté en sus. L'addition de C-S-H ne produit pas l'hydrate à 10 Å.

A plus long terme de l'hydratation ou en élevant la température de 5 °C à la température ambiante, l'hydrate à 10,0 Å est transformé en C_2ASH_8 (12,6 Å) et C-S-H. Dans les conditions normales, la formation d'un silicoaluminate hydraté est peu probable dans le ciment portland hydraté à cause de la présence d'un excès de $Ca(OH)_2$.

D'autre part, à l'aide de la micro-analyse électronique de sections polies des deux mélanges hydratés suivants :

76 % C_3S + 19 % C_3A + 5 % gypse et

80 % C_3S + 20 % C_3A_C (en poids)

M. REGOURD, H. HORNAIN et B. MORTUREUX (1) ont trouvé deux silicoaluminates hydratés :

C_4ASH_{12} et $C_3A.3CS.H_{31}$

Après sept jours d'hydratation, la formation d'un trisilicoaluminate hydraté mal cristallisé a été observéecomme un pseudomorphe du C3A anhydre. Le monosilicoaluminate hydraté est formé à l'extérieur de la bordure du C_3A original. Le C_3A_C réagit plus vite que C_3A_O.

J. JAMBOR (3) a étudié les propriétés liantes de C_3A en présence de $CaCO_3$. Les finesses de C_3A et $CaCO_3$ étaient respectivement de 2800 et 2480 $cm^2.g^{-1}$ (Blaine). L'expérience a été effectuée sur des cubes de 2 cm avec les mélanges de :

1) C3A avec des quantités de $CaCO_3$ calibré,
2) C3A avec des quantités de sable de quartz calibré et
3) 73 % C_3A et 27 % $CaCO_3$ (en poids) et des quantités de sable de quartz calibré.

Après 1 et 28 jours de traitement, la densité volumique et les résistances à la compression ont été déterminées à l'état humide et sec (séchage à 100 °C). En addition à ceci, la porosité totale, le rayon moyen des micropores et la perte au feu à 600 °C ont été aussi déterminés sur les échantillons séchés. Les échantillons ont été analysés par DRX analyses thermiques et microscopie électronique à balayage. Les produits d'hydratation habituels de C3A forment seulement des structures lâches avec une faible aptitude liante tandis que grâce aux additions de $CaCO_3$, la résistance est accrue 300 fois à l'état humide. Le maximum de résistance trouvé a été de 29 MPa pour une pâte avec un rapport $C_3A/CaCO_3$ de 60/40. La DRX et les analyses thermiques confirment que la formation de $C_3A.CaCO_3.H_n$ principalement et le taux d'hydratation plus élevé de C_3A en présence de $CaCO_3$ est la cause de l'accroissement de la résistance.

I. ODLER (4) a étudié l'interaction entre la phase C-S-H formée dans l'hydratation de C_3S en présence du gypse et l'aptitude du gypse lié à réagir avec C3A. La teneur maximale de gypse lié à été trouvée égale à 9,8 g/100 g de C_3A après un jour d'hydratation dans une pâte avec 10 % de sulfate de calcium. Ce rapport de 1 mol SO_3 pour 6,1 moles de C_3S hydraté correspond bien aux résultats déjà publiés.

Le taux d'hydratation de C_3S croît jusqu'à une addition de 10 % de gypse (en poids). Le gypse lié ne peut être détecté ni par ATD ni par DRX mais peut être facilement extrait quantitativement par une eau de chaux, ou peut réagir avec C_3A pour former de l'ettringite. La liaison entre le sulfate de calcium et la phase C-S-H est faible et l'Auteur assume que le sulfate de calcium est adsorbé physiquement à la surface du gel de C-S-H.

M. Y. GHORAB, D. HEINZ, U. LUDWIG, T. MESKENDAHL et A. WOLTER (5) ont fait une nouvelle recherche sur la stabilité des sulfoaluminates hydratés dans des systèmes purs et dans les ciments. Des additions appropriées de sulfates de calcium aux ciments empêchent la fausse prise par formation d'une couche d'ettringite, de préférence sur les surfaces de C_3A. Les études de systèmes purs avec C_3A , gypse ou anhydrite, et chaux, avec ou sans $CaCO_3$ ou C_3S , et avec des ciments portland avec ajouts, confirment ou indiquent que l'ettringite et le carboaluminate hydraté sont les phases stables à la température ambiante. Le monosulfate hydraté est la phase stable aux températures élevées. Par conséquent, une formation provisoire de monosulfate hydraté, instable à la température normale ou spécialement au cours d'un traitement thermique (direct, retardé ou répété, désiré ou indésiré) de pâtes de ciments, mortiers ou bétons, peut entraîner des dommages par formation ultérieure d'ettringite accompagnée d'expansion, de fissuration et de chute de résistance. Des additions de carbonate de calcium peuvent accroître la détérioration. Les ciments portland à teneur limitée en C_3A ou sans C_3A ou les ciments portland au laitier de haut fourneau granulé ou aux pouzzolanes appropriées en quantités convenables, réduisent ou même empêchent la dégradation. Mais la réduction, ou l'empêchement du dommage, ne devrait pas être considéré comme la seule tâche. On devrait aller plus loin en utilisant la connaissance des réactions des aluminates de calcium hydratés, par exemple, pour la précontrainte chimique du béton.

B. COTTIN (6) a étudié la cinétique de l'hydratation des quatre clinkers industriels suivants :

Ciment	C_3S	C_2S	C_3A	C_4AF	C_{libre}	Sulfate alcalin	$CaSO_4$
A	67	19	8	1	4,4	0,2	0,2
B	59	16	13	7	1,0	1,8	1,5
C	62	19	2	14	1,9	0,7	0,1
D	60	20	7	10	1,1	0,5	0

Les clinkers ont été mélangés avec 0,1, 2,5 et 5 % (en poids) de SO_3 sous les formes gypse, hémihydrate, anhydrite naturelle et surcuite, broyées à une finesse de 3000 $cm^2.g^{-1}$ (Blaine). Le rapport e/c a été gardé égal à 0,5 pendant l'hydratation. La cinétique d'hydratation a été suivie par calorimétrie isotherme. Les courbes calorimétriques montrent trois pics exothermiques d'intensité variable et dont le temps d'apparition est dû à

1) l'hydratation initiale de C_3A (influencée par la présence de C_3S et des sulfates),
2) l'hydratation de C_3S,
3) la consommation totale du sulfate.

L'addition du sulfate de calcium entraîne toujours une décroissance de l'intensité du premier pic, excepté dans le clinker C avec l'hémihydrate. Mais à partir des résultats, il semble impossible d'avoir une corrélation générale entre la décroissance de la chaleur dégagée et la quantité et la nature des sulfates ajoutés. Pour tous les clinkers, la quantité optimale de gypse se place entre 2,5 et 5 % en poids de SO_3 ajouté. A l'exception du clinker B, les additions de sulfate entraînent l'accroissement d'intensité et l'apparition plus précoce du second pic de dégagement de chaleur. Ce pic qui est dû principalement à l'hydratation de C_3A se produit plus tôt, même dans le clinker B sans aucune addition de sulfate, parce que le clinker lui-même contient beaucoup de sulfates alcalins. Le troisième pic qui est dû à la consommation totale de SO_3 , est généralement très faible et large. Dans le cas de l'anhydrite naturelle, ce pic est absent.

I. ODLER et R. WONNEMANN (7) ont étudié l'effet de différentes formes de sulfate de calcium sur l'hydratation de C_3A présent dans un clinker préparé en laboratoire. Le clinker contenait 15 % de C_3A et 5 % de $C_2(A,F)$ (en poids). Le clinker a été broyé avec 3 % de SO_3 (en poids) sous la forme d'anhydrite, d'hémihydrate et de gypse à une finesse de 3000 $\pm$ 100 $cm^2.g^{-1}$ (Blaine) et hydraté avec un rapport e/c = 0,5. La formation d'ettringite a été déterminée, par ATD, jusqu'à 30 minutes. La fraction de gypse et d'hémihydrate qui n'a pas réagi a été déterminée par ATD et celle d'anhydrite par diffraction des rayons X. Les résultats indiquent qu'il n'y a pas d'influence significative de l'addition et de la forme du sulfate ajouté sur la cinétique d'hydratation de C_3A . Par addition de sulfate, l'ettringite est le premier produit hydraté de C_3A , qui se convertit plus tard en monosulfate hydraté. La formation d'ettringite est réduite et la conversion en monosulfate hydraté est retardée avec l'anhydrite. La fausse prise du clinker pur (inférieure à 1 minute) n'est pas une conséquence de l'hydratation rapide de C_3A mais une conséquence de l'altération de la morphologie des produits hydratés comme l'ont déjà suggéré **LOCHER, RICHARTZ et SPRUNG.** Avec l'hémihydrate, la prise rapide est reliée à la conversion en dihydrate. La demande en eau plus élevée avec l'anhydrite est due à la formation d'une quantité significative de différents aluminates de calcium hydratés plutôt que d'ettringite.

E.S. JØNS et B. OSBAECK (8) ont étudié l'influence de C_3A dans les ciments. Ils ont préparé trois clinkers l'un avec 60 % C_3S et 22 % C_2S (en poids). Les teneurs en C_3A et C_4AF de chaque clinker variaient respectivement de 0 à 16 et de 2 à 18 % (en poids). Trois ciments ont été préparés à partir de chaque clinker par addition de différentes quantités de SO_3 sous la forme d'un mélange en quantité égale de gypse et d'hémihydrate. Les clinkers mélangés avec les sulfates ont été broyés dans un broyeur à boulets pendant 15 minutes. Les différences de finesse reflètent les différences de broyabilité mais peuvent ne pas être prises en considération. D'autre part, les valeurs de résistance ont été corrigées en tenant compte de la contribution de la finesse mesurée et de l'addition de sulfate. La valeur maximale de la correction était de 6 MPa. Une correction supplémentaire a été faite tenant compte de la décroissance de la densité volumique en fonction de la croissance de la teneur en C_3A du clinker. La correction la plus élevée, attribuée à l'air entraîné, était de 5 MPa. Les courbes de variation de résistance mettent en évidence une teneur optimale de C_3A et de SO_3 ajouté. Il y a un effet positif de l'addition de SO_3 sur l'hydratation initiale de C_3S qui correspond bien aux résultats d'étude d'autres chercheurs sur le C_3S pur et les alites. L'effet retardateur important d'un

excès de SO_3 sur l'hydratation de C_3A est significatif. Il apparaît que des quantités importantes de C_3A ont un effet négatif sur l'hydratation de C_3S. En traçant la courbe du logarithme de la résistance à la compression en fonction de la réduction de la porosité par l'hydratation de C_3S, les Auteurs concluent que C_3A apporte une contribution positive et indépendante, à la résistance, pendant la totalité de la durée de l'étude. Les effets négatifs sont l'entraînement d'air dans les mortiers et le taux plus faible de l'hydratation de C_3S à des stades plus avancés de l'hydratation.

Résumant les contributions ci-dessus, les conclusions suivantes peuvent être tirées :

- Les C_3A orthorhombiques et monocliniques sont moins réactifs comparés à la forme cubique. Des résultats analogues ont été trouvés à la fois dans des systèmes purs et dans des ciments hydratés.

- En présence d'eau, la réaction, entre C_4AH_{19} et la silice amorphe et aussi bien entre C_3A et C_3S ou C_2S, entraîne la formation de $C_3A.CSH_{12}$. Dans la réaction de C_3A avec C_3S ou C_2S, la formation de $C_3A.3CS.H_{32}$ a aussi été observée. La formation des silicoaluminates hydratés a aussi été trouvée dans les ciments portland hydratés.

- Dans les systèmes contenant des teneurs suffisantes en ions sulfate, la formation immédiate à la surface des grains de C_3A d'un gel, tel qu'une couche d'ettringite, empêche la fausse prise. Le monosulfate hydraté et ses solutions solides, formés ensuite, sont partiellement instables à la température ambiante ou aux plus basses températures. Une formation nouvelle d'ettringite sans, et (accrue) avec un traitement thermique transitoire, a aussi été observée à plus long terme. L'addition de $CaCO_3$ favorise cette réaction. La formation nouvelle a aussi été observée au cours de l'hydratation du ciment et elle entraîne des détériorations, par expansion, chute de résistance et fissuration. Les ciments portland à teneur limitée en C_3A ou les ciments avec ajouts sont moins sensibles à cette dégradation.

- Le sulfate adsorbé à la surface du gel de C-S-H au cours de la réaction entre C_3S, $C\bar{S}$ et l'eau peut réagir ansuite avec C_3A pour former l'ettringite.

- La forme et la quantité du sulfate de calcium ajouté au ciment influencent l'hydratation initiale mais ne changent pas la cinétique d'hydratation d'une manière significative.

- Les produits d'hydratation de C_3A contribuent au développement de la résistance.

REFERENCES

1.- **M. REGOURD, H. HORNAIN, B. MORTUREUX**, Département Microstructures C.E.R.I.L.H., Paris (France). "Hydratation de C_3A dans des mélanges synthétiques et dans des ciments portland industriels".

2.- **J.H.P. VAN AARDT and S. VISSER**, National Building Research institute, CSIR, Pretoria, South Africa. "Synthesis of a calcium silicoaluminate hydrate at 5 °C".

3.- **J. JAMBOR**, Ing. Dr., Dr Sc., Institute of Construction and Architecture, Slovak Academy of Sciences, Bratislava, (Tchécoslovaquie). "Influence of $3CaO.Al_2O_3.CaCO_3.nH_2O$ on the structure of cement paste".

4.- **I. ODLER**, Clausthal University (Germany). "Interaction between gypsum and the C-S-H phase formed in C_3S hydration".

5.- **H.Y. GHORAB, D. HEINZ, U. LUDWIG, T. MESKENDAHL and A. WOLTER**, Institut für Gesteinshüttenkunde, RWTH Aachen, (Germany). "On the stability of calcium aluminate sulphate hydrates in pure systems and in cements".

6.- **B.F. COTTIN**, Chef de Service, Laboratoire de Recherche Générale, Lafarge S.A. (France). "Certaines interactions entre C_3A et C_3S lors de l'hydratation des ciments portland".

7.- **I. ODLER and R. WONNEMANN**, Clausthal University (Germany). "Hydration of C_3A in portland cement in the presence of different forms of calcium sulfate".

8.- **E.S. JØNS ET B. OSBAECK**, F.L. Smidth & Co. A/S Vigerslev Alle 77, DK-2500 Valby Copenhagen (Denmark). "The influence of the content and distribution of Al_2O_3 on the hydration properties of portland cement".

Hydratation de C_3A dans des mélanges synthétiques et dans des ciments portland industriels

Hydration of C_3A in synthetic mixtures and in industrial portland cements

M. REGOURD, H. HORNAIN, B. MORTUREUX, Département Microstructures C.E.R.I.L.H. - Paris, France

Résumé

L'hydratation de C_3A et de ses solutions solides avec Na_2O a été suivie par diffraction des rayons X, microscopie électronique à balayage et microsonde électronique. Ces différentes méthodes ont toutes révélé une réactivité décroissante de la forme cubique à la forme monoclinique aux brèves échéances. L'interaction C_3A-C_3S au cours de l'hydratation de mélanges C_3A + C_3S + gypse a été mise en évidence par la formation de silicoaluminates autour des grains de C_3A et par le taux d'hydratation plus élevé de C_3S dans les mélanges C_3S + C_3A cubique. Cette interaction a été retrouvée dans les ciments portlands industriels et le silicoaluminate a été observé également dans des mélanges C_2S + C_3A.

Summary

The hydration of C_3A and its solid solutions with Na_2O has been followed by X-ray diffraction, scanning electron microscopy and electron probe microanalysis. These various methods have all shown a decreasing early reactivity from the cubic form to the monoclinic form. The C_3A-C_3S interaction during hydration of C_3A + C_3S + gypsum mixtures has been put in evidence by the formation of silicoaluminates around the C_3A grains and by the higher degree of hydration in the C_3S + cubic C_3A mixtures. This interaction has been found again in industrial portland cements and the silicoaluminate has also been observed in C_2S + C_3A mixtures.

1. INTRODUCTION

$Ca_3Al_2O_6$, cubique à l'état pur (1), forme des solutions solides notamment avec les alcalins Na et K qui peuvent entraîner des changements de symétrie, cubique → orthorhombique → monoclinique (2, 3). Dans les ciments portlands, C_3A est cubique ou orthorhombique. La forme monoclinique est rarement observée (4).

Les solutions solides synthétiques $C_3A + Na_2O$ ont une réactivité hydraulique inférieure à celle de l'aluminate cubique (5, 6). Il existe, en outre, une interaction C_3A-C_3S : le taux d'hydratation de C_3S dépend de la réactivité de C_3A d'une part, il se forme autour des grains de C_3A des silicoaluminates de calcium d'autre part (7, 8).

Dans cette communication, nous préciserons la réactivité de C_3A en relation avec sa teneur en alcalins. Nous étudierons ensuite la formation de silicoaluminates dans des mélanges $C_3A + C_3S$ et $C_3A + C_2S$.

2. REACTIVITE DE C_3A

Les échantillons étudiés sont des mélanges synthétiques et des ciments portlands. Les produits synthétisés en laboratoire ont une granulométrie comprise soit entre 25 et 40 µm soit entre 40 et 63 µm. Le C_3S est triclinique, le C_3A cubique est pur et le C_3A orthorhombique contient 4,8 % Na_2O. Les poudres sont convenablement homogénéisées et gâchées sous forme de minicylindres de 1 cm de hauteur et 1 cm^2 de section. Différents rapports eau/solide sont utilisés (e/c = 0,35, 0,40 et 0,50). La conservation des éprouvettes a lieu dans l'eau à 20 °C. A chaque échéance choisie, 3 minicylindres sont prélevés et broyés. L'hydratation est arrêtée par lavage à l'acétone-éther et l'eau interstitielle évaporée par cryosublimation. Le taux d'hydratation est mesuré par diffraction des rayons X.

Deux séries de mélanges synthétiques sont étudiées : 80 % C_3S + 20 % C_3A et 76 % C_3S + 19 % C_3A + 5 % gypse. Afin de définir le rôle exact de Na_2O (dans le réseau cristallin ou dans la solution aqueuse) le taux d'hydratation de C_3A a été comparé d'une part dans deux mélanges 76 % C_3S + 19 % C_3A + 5 % gypse contenant l'un C_3A cubique pur, l'autre C_3A orthorhombique, d'autre part dans une pâte du mélange contenant C_3A cubique, gâchée avec une solution de soude contenant l'équivalent des 4,8 % Na_2O de la solution solide orthorhombique, soit 0,55 M NaOH par litre. Les résultats sont groupés dans le Tableau I.

Temps d'hydratation	C_3A_C eau distillée	C_3A_C sol. NaOH	C_3A_O eau distillée
7 jours	0,45	0,47	0,22
14 jours	0,63	n.d.	0,63

Tableau I - Comparaison des taux d'hydratation α de C_3A_C gâché avec une solution de soude (4,8 % eq. Na_2O) et de C_3A_C et C_3A_O gâchés avec de l'eau distillée (mélanges 76 % C_3S + 19 % C_3A + 5 % gypse). e/c = 0,35 ; granulométrie 40-63 µm.

Le tableau I indique qu'à 7 jours, C_3A_C est plus hydraté que C_3A_O. Les taux d'hydratation pratiquement égaux de C_3A_C gâché à l'eau distillée et de C_3A_C gâché avec la solution de soude montrent que les différences de réactivité entre C_3A_C et C_3A sont, à cette échéance, dues à la présence de Na_2O dans un réseau cristallin plus compact que celui de l'aluminate pur. Une deuxième série d'essais effectuée sur des pâtes C_3S + C_3A + gypse, de granulométrie 25-40 µm et gâchée à l'eau distillée confirme la plus grande réactivité de C_3A cubique dès les premières échéances (fig. 1).

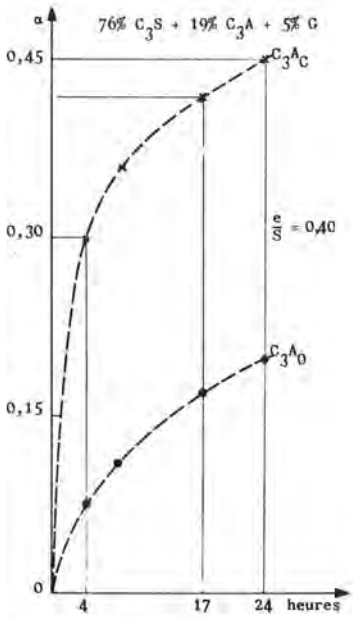

Fig. 1 : Taux d'hydratation de C_3A dans un mélange synthétique $C_3A + C_3S$ + gypse. C_3A cubique s'hydrate plus vite que C_3A_O (4,8 % Na_2O).

Il existe par ailleurs une corrélation très nette entre le taux d'hydratation de C_3A et celui de C_3S : à une hydratation plus rapide de C_3A correspond une réactivité plus grande de C_3S, (Tableau II).

Taux d'hydratation α	$C_3S + C_3A_C + G$	$C_3S + C_3A_O + G$
C_3A	0,63	0,34
C_3S	0,58	0,47

Tableau II - Corrélation entre le taux d'hydratation α de C_3A et celui de C_3S ; 28 jours ; e/c = 0,40.

Afin de nous rapprocher de la composition de ciments portlands dans lesquels le potassium se partage entre C_3A, C_2S et K_2SO_4, nous avons ajouté 3 % de K_2SO_4 aux mélanges $C_3A + C_3S$ + gypse. Dans ce cas, C_3A_O s'hydrate aussi rapidement que C_3A_C dans les pâtes sans K_2SO_4. La différence de réactivité entre C_3A_C et C_3A_O subsiste cependant si les aluminates sont tous deux hydratés en présence de K_2SO_4 (fig. 2). Le Tableau III montre que K_2SO_4 est aussi accélérateur de C_3S.

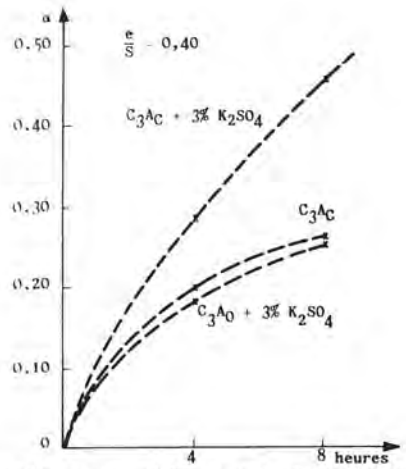

Fig. 2 : Influence de K_2SO_4 sur le taux d'hydratation de C_3A dans un mélange C_3A + C_3S + gypse.

Taux d'hydratation α	C_3A_C	C_3A_C + K_2SO_4	C_3A_O + K_2SO_4
C_3A	0,25	0,46	0,26
C_3S	0,20	0,30	0,30

Tableau III - Taux d'hydratation α de C_3A et C_3S dans les mélanges C_3S + C_3A + gypse (e/c = 0,40) à 8 heures.

Les différences de réactivité des solutions solides de C_3A et l'interaction C_3A-C_3S ont été également observées dans des ciments industriels. Ainsi dans 3 ciments contenant respectivement 7 % de C_3A cubique, 13 % d'un mélange C_3A cubique + orthorhombique, et 16 % de C_3A orthorhombique, les taux de réaction de C_3A, après 7 jours, sont de 0,65 pour C_3A_C , 0,42 pour le mélange C_3A_C + C_3A_O et 0,35 pour C_3A_O.

Des essais ont aussi été effectués sur deux clinkers industriels A et B de compositions voisines (Tableau IV) mais renfermant l'un 12 % de C_3A orthorhombique, l'autre 12 % de C_3A monoclinique. Les taux d'hydratation mesurés par DRX sont rassemblés dans le Tableau V, qui montre que, d'une part C_3A monoclinique s'hydrate plus lentement que C_3A orthorhombique, d'autre part le taux de réaction de C_3S aux courtes échéances est plus élevé dans le cas du ciment A contenant C_3A_O que dans le cas du ciment B contenant C_3A_M.

Clinker	C_3S	C_2S	C_3A	C_4AF	CaO libre
A	61	20 < 15 β / 5 α	12 O	5	1,5
B	60	24 < 15 β / 9 α	12 M	3	0,7

Tableau IV - Composition minéralogique déterminée par DRX des deux clinkers industriels A et B testés.

α	Echéances	A (C_3A_O)	B (C_3A_M)
C_3S	8 heures	0,50	0,42
	24 "	0,64	0,55
	48 "	0,70	0,70
C_3A	7 jours	0,66	0,55

Tableau V - Taux d'hydratation de C_3S et de C_3A dans les deux clinkers industriels A et B ; e/c = 0,50 ; granulométrie 40-63 µm.

3. FORMATION DE SILICOALUMINATES DANS LES MELANGES C_3S-C_3A ET C_2S-C_3A

L'interaction C_3A-C_3S se manifeste également par la formation de silicoaluminates, trisilicoaluminate $C_3A.3CaSiO_3.31H_2O$ ($C_4AS_3H_{31}$) et monosilicoaluminate $C_3A.CaSiO_3.12H_2O$ (C_4ASH_{12}) qui ont été mis en évidence dans des mélanges synthétiques C_3S + C_3A et C_2S + C_3A.

Ces deux hydrates, déjà signalés par FLINT et WELLS (8), peuvent être considérés comme faisant partie de deux séries de composés de formules générales (9) :

$C_3A.3CaX.mH_2O$ ou $C_3A.3CaY_2.mH_2O$ et $C_3A.CaX.nH_2O$ ou $C_3A.CaY_2.nH_2O$

avec X = CO_3, SO_4, S_2O_3 ..., Y = OH, Cl, SiO_3 ... et

m = 30 à 32 , n = 10 à 12.

Avec l'anion SO_4^{2-} on obtient les deux sulfoaluminates bien connus : trisulfoaluminate $C_3A.3CaSO_4.31H_2O$ (ettringite) et monosulfoaluminate $C_3A.CaSO_4.12H_2O$. De même l'aluminate hexagonal C_4AH_{13} peut être assimilé au composé $C_3A.Ca(OH)_2.12H_2O$. FLINT et WELLS ont mis en évidence les deux silicoaluminates dans des solutions où ils ont fait varier le rapport molaire CaO/Al_2O_3 entre 1 et 4. Dans ces solutions se forment d'abord des plaquettes hexagonales correspondant au monosilicoaluminate $C_3A.CaSiO_3.12H_2O$ homologue du monosulfoaluminate $C_3A.CaSO_4 12H_2O$. Le monosilicoaluminate se transforme ensuite lentement en trisilicoaluminate $C_3A.3CaSiO_3.31H_2O$ sous forme de fines aiguilles de structure identique au trisulfoaluminate $C_3A.3CaSO_4.31H_2O$. FLINT et WELLS ont également obtenu le trisilicoaluminate dans des mélanges C_2S_β + C_4AF, C_2S_β + C_3A, C_3S + C_4AF, en suspension dans des solutions saturées de CaO. Ils n'ont pas observé de silicoaluminate dans les suspensions de C_3S + C_3A. Plus récemment, MITUZAS, KAMINSKAS et MITUZAS (10) ont déduit à partir d'analyses chimiques que le composé $C_3A.3CaSiO_3.aq.$ devait exister dans les ciments portlands hydratés. Dans ce sens, nous avons observé les mêmes éprouvettes que celles mentionnées au paragraphe précédent et nous avons étudié également des pâtes C_2S + C_3A traitées dans les mêmes conditions.

3.1 Mélanges 76% C_3S + 19 % C_3A + 5 % gypse

Les examens de sections polies à l'aide de la microsonde de Castaing indiquent que les échantillons évoluent de la façon suivante :
- à deux jours les grains de C_3A sont entourés de cristaux d'ettringite contenant une petite quantité de SiO_2,
- à partir de 7 jours, il se forme par pseudomorphose progressive des grains de C_3A une double couche de silicoaluminates : trisilicoaluminate en contact avec C_3A anhydre, monosilicoaluminate dans la partie externe du grain transformé. A l'extérieur du grain, en

contact avec le silicoaluminate on observe d'abord de l'ettringite qui est remplacée peu à peu par un mélange monosulfoaluminate C_4AH_{13} (fig. 3). Les rapports molaires mesurés à l'aide de la microsonde électronique, à différentes échéances, sont rassemblés dans le Tableau VI

- après 10 mois, seul le monosilicoaluminate est observé. Sa composition semble évoluer ; la concentration en SiO_2 diminue lorsqu'on passe de l'extérieur vers l'intérieur du grain. En outre dès 3 mois, une couronne de monosulfoaluminate est susceptible de se former autour du centre encore anhydre de C_3A par diffusion d'ions SO_4 à travers la couche de silicoaluminate (fig. 4). D'une façon générale on constate que la formation des silicoaluminates est plus rapide avec C_3A cubique que C_3A orthorhombique. A 28 jours, la couche de silicoaluminates est plus importante autour des grains de C_3A_C. A cette échéance les deux silicoaluminates y sont déjà détectés alors que pour C_3A_O, seul le trisilicoaluminate est observé.

En contact avec les grains de C_3S, existe une couche pseudomorphique de silicates de calcium hydratés

Phase	Echéances*	C/S	C/A	S/A	C/(S + A)
Trisilico-aluminate (zone interne)	28 j	2,1	5,6	2,7	1,5
	3 m	1,7	4,4	2,5	1,2
	6 m	2,4	6,2	2,6	1,7
Monosilico-aluminate (zone externe)	28 j	4,0	3,6	0,9	1,9
	3 m	3,7	3,3	0,9	1,7
	6 m	5,2	3,8	0,7	2,2
Monosilico-aluminate centre	10 m	6,3	3,2	0,5	2,1
bord	10 m	4,4	3,3	0,8	1,9

* j : jour ; m : mois.

Tableau VI - Rapports molaires mesurés dans les silicoaluminates des mélanges 76 % C_3S + 19 % C_3A + 5 % gypse ; e/c = 0,35 ; granulométrie 40-63 µm. (résultats à ≈ ± 0,2 près).

Fig. 3 : Section polie d'un mélange C_3A_C + C_3S + gypse. 1 C_3A ; 2 Trisilicoaluminate ; 3 Monosilicoaluminate ; 4 Monosulfoaluminate.

Fig. 4 : Section polie d'un mélange C_3A_O + C_3S = gypse. 1 C_3A ; 2 Monosulfoaluminate ; 3, 4 Silicoaluminate ; 5 Monosulfoaluminate.

C-S-H dont la composition est différente suivant que le grain de C_3S se trouve à proximité ou loin d'un grain de C_3A : près des grains de C_3A les C-S-H sont plus pauvres en SiO_2 et plus riches en chaux ; le rapport molaire CaO/SiO_2 déterminé par microsonde électronique est de 1,4-1,5. Loin de C_3A la teneur en SiO_2 augmente et celle de la chaux diminue ; le rapport molaire est de l'ordre de 0,8 à 1,0. La quantité d'Al_2O_3 dans les C-S-H est d'environ 2 à 3 %.

3.2 Mélange 80 % C_3S + 20 % C_3A cubique

Dans ce mélange la formation des deux silicoaluminates est plus rapide qu'en présence de gypse. A 34 jours la zone de silicoaluminate en contact avec C_3A est très large. A l'extérieur du grain cristallise l'aluminate hexagonal C_4AH_{13}. Par diffraction des rayons X il a été possible de mettre en évidence le monosilicoaluminate qui donne un diagramme identique à celui du monosulfoaluminate (fig. 5). Par contre il n'a pas été observé de pics pouvant être attribués au trisilicoaluminate dont le spectre X serait analogue à celui du trisulfoaluminate. Les examens par microsonde électronique à balayage montrent que, d'une façon générale, les deux silicoaluminates observés dans toutes les pâtes C_3S + C_3A gypsées ou non, ont une apparence amorphe ou faiblement cristallisée. (fig. 6 et fig. 7).

3.3 Mélanges 67 % C_3S + 16,5 % C_3A + 16,5 % gypse.

En présence d'une forte proportion de gypse, les silicoaluminates ne se forment pas. Seuls l'ettringite et C_4AH_{13} sont observés en contact des grains de C_3A.

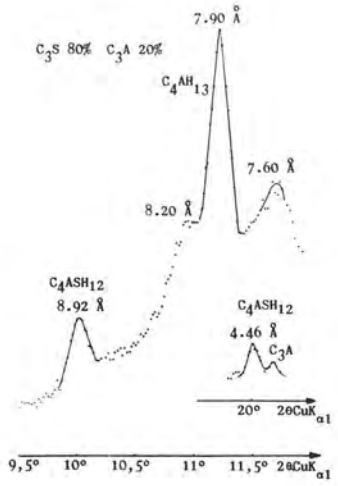

Fig. 5 : Diffractogramme de rayons X pas à pas d'un échantillon contenant C_3ASH_{12}.

Phase	Echéances	C/S	C/A	S/A
Trisilico-aluminate	7 jours	2	5	2,4
Trisilico-aluminate	28 jours	2,1	6,1	3,0

Tableau VII - Rapports molaires mesurés dans les silicoaluminates des mélanges 76 % C_2S + 19 % C_3A + 5 % gypse ; e/c = 0,35 (erreur moyenne absolue ≃ ± 0,2).

Bien que rapide, la formation du silicoaluminate se limite donc au seul trisilicoaluminate (C/S = 2), jusqu'à 28 jours. Elle est peut-être en relation avec la valeur plus faible du rapport C/S du silicate bicalcique comparée à celle du silicate tricalcique qui, à la même échéance, donne déjà du monosilicoaluminate (C/S = 4). Elle implique également une interaction importante entre C_2S et C_3A liée à une diffusion de la silice à travers la solution.

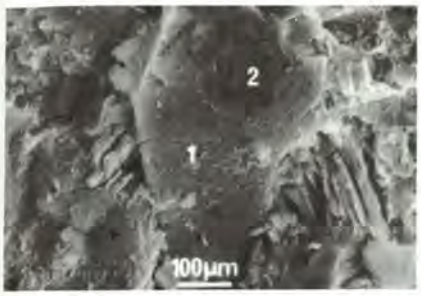

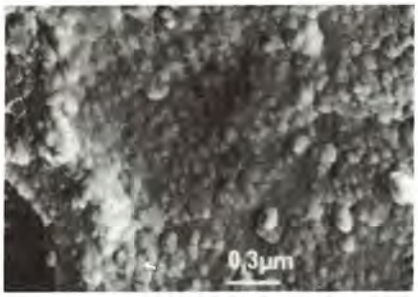

Fig. 6 : a) Trisilicoaluminate (1) au contact de C_3A anhydre (2).
b) Aspect amorphe du trisilicoaluminate.

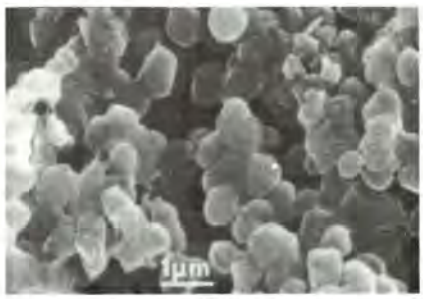

Fig. 7 : Monosilicoaluminate

Par ailleurs les silicoaluminates C_4ASH_{31} et C_4ASH12 ne sont pas stables dans les solutions fortement chargées en sulfates telles que l'eau de mer. Il se forme de l'ettringite.

3.4 Mélanges 76 % C_2S + 19 % C_3A + 5 % gypse

Dans ces mélanges, les silicoaluminates apparaissent plus rapidement. Après 7 jours, il s'est déjà formé une couche relativement épaisse de silicoaluminate de composition proche du trisilicoaluminate, associé à C_4AH_{13} et au monosulfoaluminate. Après 28 jours, contrairement à ce qui avait été observé dans les mélanges avec C_3S, seul le trisilicoaluminate est présent. Le monosilicoaluminate n'est pas observé (fig.8). Les résultats de l'analyse des silicoaluminates obtenue à l'aide de la microsonde de Castaing exprimés en rapport molaires sont groupés dans le Tableau VII.

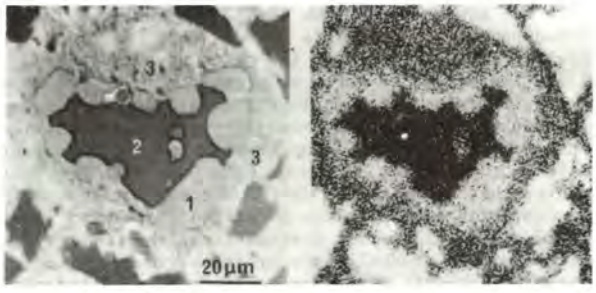

Electrons absorbés

Si

Ca

S

Fig. 8 : Formation de trisilicoaluminate (1) au contact de C_3A (2) dans un mélange de 76 % C_2S + 19 % C_3A + 5 % gypse, hydraté 7 jours. Monosulfoaluminate (3) à l'extérieur du grain.

DISCUSSION

La réactivité de l'aluminate tricalcique dans les mélanges C_3A + C_3S + gypse est en relation avec sa structure cristalline due à la présence d'alcalins en solution solide. Les mêmes résultats ont été obtenus, dès les premières échéances (10 minutes), par BOIKOVA, DOMANSKY, STAVITSKAYA ET NIKUSHCHENKO (6) qui ont étudié quatre solutions solides contenant 2,4, 3,8, 4,8 et 5,7 % Na_2O et dont ils ont comparé la réactivité à celle du C_3A pur. D'après SPIERINGS et STEIN (11), la réactivité de $Na_{2x}.Ca_{3-x}.Al_2O_3$ ne diffère pas d'une manière significative de celle de C_3A pur car un mélange, à part égale, de solutions solides avec x = 0,5 et x = 0,25 donne les mêmes résultats que l'échantillon avec x = 0,15, prouvant ainsi que seule la concentration de NaOH dans la phase liquide est le facteur déterminant du taux d'hydratation de l'aluminate. Dans le même sens, MASSAZZA et COSTA (12) n'ont mis en évidence aucune influence de la forme cristalline sur les enthalpies de formation des solutions solides $3(CaO,Na_2O).Al_2O_3$. Ces résultats, en apparence contradictoires, sur l'influence du sodium dans le réseau cristallin ou dans la phase aqueuse, demandent à être discutés au cours de ce séminaire.

L'interaction C_3A-C_3S est clairement mise en évidence au cours des réactions d'hydratation. Elle est surtout sensible à court terme. Elle se manifeste également par la formation de silicoaluminates. Toutefois la morphologie de ces composés ne correspond pas à celle décrite par FLINT et WELLS (8) : plaquettes hexagonales isomorphes du monosulfoaluminate pour le monosilicoaluminate et cristaux aciculaires isomorphes de l'ettringite pour le trisilicoaluminate. Nos observations au microscope électronique à balayage ont montré que les silicoaluminates apparaissent peu ou pas cristallisés. Seules les analyses par diffraction des rayons X ont indiqué la présence de monosilicoaluminate cristallisé. La formation de ces silicoaluminates est due à une diffusion importante d'ions silicates hydratés à partir des grains de C_3S vers les grains de C_3A. La diffusion inverse des ions aluminates de C_3A vers C_3S est beaucoup plus limitée. Néanmoins, les C-S-H peuvent contenir 2 à 3 % de Al_2O_3. Au stade initial de la réaction, dans les pâtes gypsées, c'est l'ettringite qui se forme en premier mais la présence de silice dans cette ettringite prouve que la diffusion de SiO_2 est déjà amorcée. Cette diffusion devient ensuite prépondérante et on observe le trisilicoaluminate au contact des grains de C_3A. Par suite de l'accroissement de la couche de C-S-H entourant les grains de C_3S et de la diminution du silicate anhydre, la diffusion de la silice est fortement ralentie. Le trisilicoaluminate se transforme progressivement en monosilicoaluminate. La diffusion des ions SO_4^{2-} à travers la couche de silicoaluminate vers le grain anhydre de C_3A redevient prépondérante et il se forme au contact de C_3A une couronne de monosulfoaluminate vraisemblablement aux dépens des sulfoaluminates externes.

Les silicoaluminates sont particulièrement bien mis en évidence dans les mélanges synthétiques C_3S-C_3A ou C_2S-C_3A, de granularité régulière. Ces échantillons constituent un ensemble de microsystèmes (grain de C_3A-grain de C_3S) dans lesquels se produisent des échanges ioniques par l'intermédiaire de la solution : les propriétés électrocinétiques, caractérisées par le potentiel Zéta, attribuent une charge superficielle positive à C_3A (13) et une charge négative à C_3S (14). Nous n'avons pu mettre en évidence aucun des deux silicoaluminates dans les ciments portlands à l'aide de nos techniques physiques d'analyse. En fait, la pâte de ciment est un système beaucoup plus complexe que nos mélanges synthétique C_3A + C_3S. Chaque grain de clinker est polyphasé et la granularité de ses différentes phases est assez étendue. Dans la phase interstitielle, l'aluminate tricalcique est souvent finement cristallisé avec l'aluminoferrite et l'analyse de la zone hydratée autour des grains de C_3A n'est pas aisée. Cependant, d'une part le silicium est détecté dans l'ettringite et l'aluminium dans le C-S-H d'autre part, MITUZAS, KAMINSKAS et MITUZAS (10) ont, à partir des résultats de leur analyse chimique par attaques sélectives, suggéré l'existence du trisilicoaluminate de calcium.

BIBLIOGRAPHIE

1. **P. MONDAL and J.W. JEFFERY** (1975) :"The crystal structure of tricalcium aluminate $Ca_3.Al_2O_6$." Acta Cryst. 31, n° 3, 689-697.
2. **I. MAKI** 51973) :"Nature of the prismatic dark interstitial material in portland cement clinker". J. Cem. and Concr. Res. vol. 3, 295-313.
3. **M. REGOURD and A. GUINIER** (1974) :"The crystal chemistry of the constituents of portland cement clinker". VIth Int. Congress Chem. Cement Moscow. Principal paper I.2.
4. **M. REGOURD** (1978) :"Cristallisation et réactivité de l'aluminate tricalcique dans les ciments portlands". Il Cemento, vol. 75, juil.-août.pp323-336.
5. **M. REGOURD and B. MORTUREUX** (1977) :"Tricalcium aluminate in synthetic solid solutions and in cements". Seminar Cembureau on reaction of aluminates during the setting of cements.
6. **A.I. BOIKOVA, A.I. DOMANSKY, V.A. PARAMONOVA, G.P. STAVITSKAYA and V.M. NIKUSHCHENKO** (1977) :"The influence of Na_2O on the structure and properties of $3Ca.Al_2O_3$". Cement and Concr. Res. 7, n° 5,483-491.
7. **M. REGOURD, H. HORNAIN, B. MORTUREUX** (1976) :"Evidence of calcium silicoaluminates in hydrated mixtures of tricalcium silicate and tricalcium aluminate". Cem. Concr. Res. vol 6,pp. 733-740.
8. **E.P. FLINT, L.S. WELLS** (1944) :"Analogy of hydrated calcium silicoaluminates and hexacalcium aluminate to hydrated calcium sulfoaluminates". J. Res. Nat; Bur. Stand., vol.33, pp. 471-478.
9. **F.M. LEA** (1970) :"The chemistry of cement and concrete".Edward Arnold Ltd 2diteur, 3rd edition, pp. 220-223.
10. **Yu.I. MITUZAS, A.Yu. KAMINSKAS, A.Yu. MITUZAS** (1974) "New data on phase composition of hardening cement stone". The VIth Int. Congress of the chemistry of cement, Moscou, Suppl. paper.
11. **G.A.G.M. SPIERINGS and H.W. STEIN** (1976) :"The influence of Na_2O on the hydration of C_3A". I Paste hydration, Cem. and Concr. res. 6, 265-272.
12. **F. MASSAZZA and U. COSTA** (1978) :"Formation enthalpies of the solid solutions $3(CaO.Na_2O).Al_2O_3$". Il Cemento 3, 263-270.
13. **G.A.C.M. SPIERINGS** (1977) :"The influence of Na_2O on the formation and colloïd chemical properties of calcium aluminate hydrates". Thesis. Eindhoven.
14. **M.E. TADROS, W.Y. JACKSON and J. SKALNY** (1976): "Study of the dissolution and electrokinetic behavior of tricalcium aluminate . Colloïd and Interface science". Ed. M. Kerker, IV, 211.

Synthesis of a calcium silicoaluminate hydrate at 5° C

Synthèse d'un silicoaluminate de calcium hydraté à 5° C

J.H.P. VAN AARDT and S. VISSER, National Building Research Institute, CSIR, Pretoria, South Africa.

SUMMARY : A calcium monosilicoaluminate hydrate analogous to calcium monosulphoaluminate hydrate has been synthesized at 5°C from a mixture of C_3A, calcium hydroxide and amorphous silica. The thin hexagonal plates have a basal d-spacing of 10,0 Å in contrast to the d-spacing of 10,3 Å for the monosulphoaluminate at 5°C. It does not show a clear shift to lower d-spacings like the calcium monosulphoaluminate {10,3 Å (5°C) to 9,6 Å (25°C)} when the temperature is raised from 5°C to 25°C; substances with higher d-spacings, i.e. higher than 10,0 Å, are produced on raising the temperature and in some instances C_2AH_8 (Stratling's compound) and C-S-H hydrates are produced.

RESUME : On a effectué la synthèse d'un monosilicoaluminate de calcium hydraté analogue au monosulfoaluminate de calcium hydraté, à une température de 5°C, à partir d'un mélange de C_3A, d'hydroxyde de calcium et de silice amorphe. La distance-d des plaques minces hexagonales est de 10,0 Å par contraste avec celle du monosulfoaluminate, qui est de 10,3 Å à 5°C. On ne voit pas de déplacement évident aux faibles distances d comme dans le cas du monosulfoaluminate de calcium {de 10,3 Å (5°C) à 9,6 Å (25°C)} quand on éleve la température de 5 à 25°C; on obtient des substances avec des distances-d plus élevées, c'est-à-dire de plus de 10,0 Å, quand on éleve la température, et dans certains cas on obtient C_2ASH_8 (composé de Stratling) et des C-S-H hydratés.

INTRODUCTION

Numerous calcium aluminate complexes of the general formulae $3CaO.Al_2O_3.3CaX.30\text{-}32H_2O$ and $3CaO.Al_2O_3.CaX.8\text{-}12H_2O$ (X represents an acid radical) have been synthesized at ambient temperatures. In 1944 Flint and Wells (1) reported the existence of silico-aluminates. Since then various workers have reported on the presence of these compounds in hydrated mixtures of calcium silicates plus aluminates and in hydrated portland cement (2,3). Van Aardt (4) reported on tetracalcium hydroxyaluminate hydrates and sulphoaluminate hydrates observed at early hydration times of C_3A or C_3AH_6 with $Ca(OH)_2$ and $CaSO_4$ at low temperature (5°C). The sulphoaluminate hydrate (10,3 Å)† was synthesized by adding $CaSO_4$ to C_4AH_{19} (10,6 Å). Subsequently, a silicoaluminate hydrate (10,0 Å) was obtained in a similar manner by adding amorphous silica.

EXPERIMENTAL

C_3A (135 mg) was reacted with $Ca(OH)_2$ (37 mg) in water (100 ml) at 5°C for 19 days. The presence of C_4AH_{19} (10,6 Å) was established by wet X-ray diffraction. To this slurry was then added :-

1. 30 mg SiO_2 + 37 mg $Ca(OH)_2$
2. 60 mg SiO_2 + 74 mg $Ca(OH)_2$
3. 90 mg SiO_2 + 111 mg $Ca(OH)_2$
4. 90 mg SiO_2 + 74 mg $Ca(OH)_2$
5. 30 mg SiO_2 +
6. 60 mg SiO_2 +

The reaction was followed by means of X-ray diffraction. Some solid was filtered off and excess liquid was removed between sheets of filter paper before the still humid solid was scanned. No precaution was taken to keep the temperature at 5°C since no shifting to a lower d-spacing, as with calcium sulphoaluminate hydrate (4,5,6), was observed at ambient temperatures.

RESULTS AND DISCUSSION

Although the reaction between C_3A and $Ca(OH)_2$ at 5°C gave mainly C_4AH_{19} (10,6 Å), a little C_3AH_6 and the 8,2 Å phase were also present.

On adding amorphous SiO_2 or amorphous SiO_2 plus $Ca(OH)_2$ to C_4AH_{19}, see experiments 1 to 6 above, two reactions took place namely $Ca(OH)_2$ and silica reacted to form C-S-H compounds and silica replaced the OH-group in C_4AH_{19} to form a silicoaluminate hydrate phase with a d-spacing of 10,0 Å. Table 1 lists the main compounds detected after 240 days for experiments 1 to 4 and after 120 days for experiments 5 and 6. Figure 1 gives the XRD-traces.

†The d-spacing attributed to the 001 reflection or basal interference of the compound named.

TABLE 1

Oxide ratios of silica and calcium added to one mole of C_4AH_{19} and the compounds detected after 120 and 240 days reaction time at 5°C

Exp. No.	Time (days)	C_4AH_{19}	SiO_2	CaO	Compounds identified by XR-diffraction					
					10,0 Å phase	C_4AH_{19}	C-S-H	8,2 Å phase	C_3AH_6	$Ca(OH)_2$
1	240	1	1	1	-	xxxx*	x	x	x	x
2	240	1	2	2	x	xxx	x	x	x	x
3	240	1	3	3	xxx	x	x	x	x	x
4	240	1	3	2	xxxx	x	x	x	-	-
5	120	1	1	-	xxx	xx	-	x	-	-
6	120	1	2	-	xxxx		-	x	-	-

*Number of x's are in relation to quantity of relevant compound

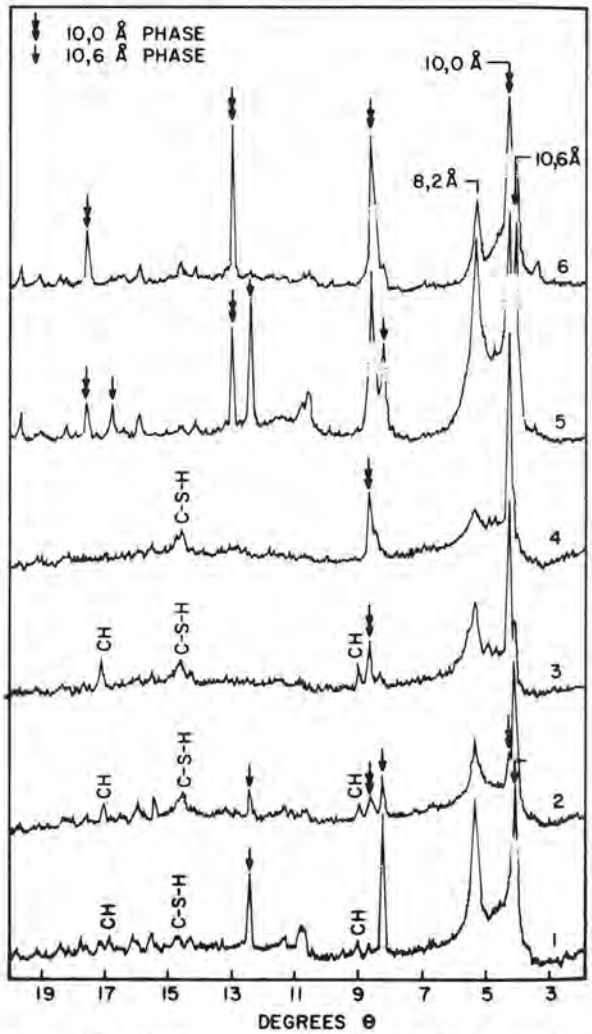

Fig. 1 - XRD-traces for experiments 1 to 4 after 240 days and experiments 5 and 6 after 120 days

The C_4AH_{19} compound persisted where the $Ca(OH)_2$ was in excess, i.e. experiments 1, 2 and 3. With increasing silica additions the 10,0 Å phase seemed to form more readily. In experiments 5 and 6 where no extra $Ca(OH)_2$ was added, the 10,0 Å phase formed much more readily and was detected in large quantities at much earlier times. After 120 days the presence of C_4AH_{19} could hardly be detected especially in experiment 6. At later ages the 10,0 Å phase seemed to decompose and it produced C_2ASH_8 (Stratling's compound) and C-S-H. Figure 2 shows the reaction products for experiment 5 at 240 days; here the breakdown can be detected. The basal reflection of 12,6 Å for Stratling's compound can be seen. Figure 3 gives XRD-traces comparing C_4AH_{19} (10,6 Å), $C_4A\bar{S}H_x$ (10,3 Å) and C_4ASH_x (10,0 Å). The marked difference between the 10,3 Å phase and the 10,0 Å phase becomes pronounced when comparing the higher order of the basal reflections as can be seen from Figure 3.

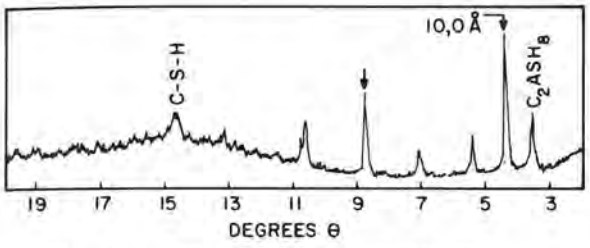

Fig. 2 - XRD-trace for experiment 5 after 240 days showing the presence of C_2ASH_8 and C-S-H

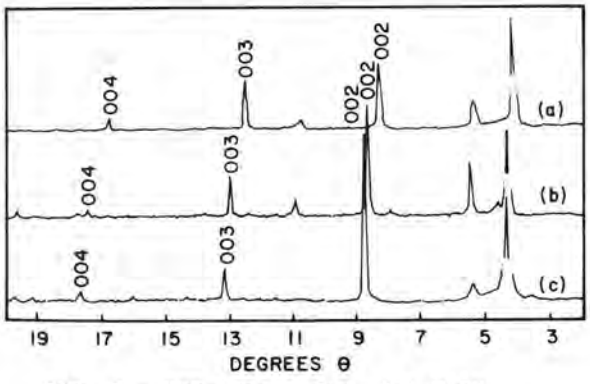

Fig. 3 - XRD-traces for (a) C_4AH_{19}, (b) $C_4A\bar{S}H_x$ and (c) C_4ASH_x

SEM with energy X-ray dispersive analysis shows that the hexagonal crystals obtained in experiment 6 contain silica in their structure. Figure 4 shows the hexagonal morphology of the crystals and Figure 5 shows the energy dispersive analytical results.

Raising the temperature from 5°C to room temperature and higher did not shift the basal reflection of the 10,0 Å phase to lower d-values but a breakdown to C_2ASH_8 and C-S-H was observed.

Fig. 4 - SEM of the 10,0 Å phase showing hexagonal crystals

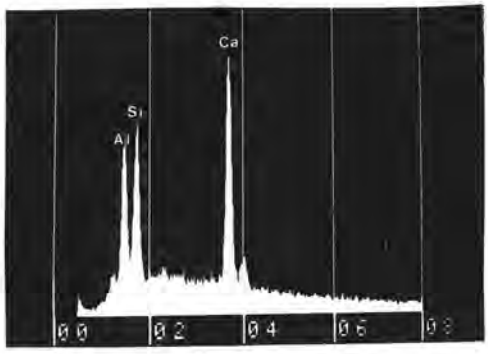

Fig. 5 - Energy-dispersive analysis of the above crystals

In an experiment where $Ca(OH)_2$ and amorphous silica in the ratios of 1 $Ca(OH)_2$ to 1 SiO_2 and 2 $Ca(OH)_2$ to 3 SiO_2 were added together and kept at 5°C, C-S-H compounds were formed and no $Ca(OH)_2$ was observed after 100 days. As can be expected from the previous experiments the addition of the C-S-H compounds to C_4AH_{19} did not produce the 10,0 Å phase. There appears to be a competition between the C_4AH_{19} and the $Ca(OH)_2$ for the silica and the formation of C-S-H compounds is dominant in the system. Also if the ratio of $Ca(OH)_2$ to $A\ell_2O_3$ was high no Stratling's compound, C_2ASH_8, was formed. The delicate balance between reactants to produce the 10,0 Å phase and the meta-stability of its existence is further illustrated by the fact that even when some 10,0 Å phase was present in the initial stages it decomposed at equilibrium i.e. after long periods of storage. These observations could explain why workers in the past had difficulty in preparing the silicon bearing phase. Furthermore, it is unlikely that the phase will exist under normal conditions in hydrated portland cement because of the presence of excess $Ca(OH)_2$.

REFERENCES

1.- E.P. FLINT and L.S. WELLS (1944) "Analogy of hydrated calcium silico-aluminates and hexacalcium aluminate to hydrated calcium sulfoaluminates", J. Research NBS 33, pp. 471-477, R.P. 1623.

2.- M. REGOURD, H. HORNAIN and B. MORTUREUX (1976) "Evidence of calcium silico-aluminates in hydrated mixtures of tricalcium silicate and tricalcium aluminate", Cement and Concrete Research, 6, pp. 733-740.

3.- E.T. CARLSON and H.H. BERMAN (1960) "Some observations on the calcium aluminate carbonate hydrates", J. Research NBS A, Physics and Chemistry, 64A, n° 4, pp. 333-341, July-August 1960.

4.- J.H.P. VAN AARDT (1968) "The influence of temperature on sulphate attack on portland cement mortars", Proceedings, 5th International Symposium on The Chemistry of Cement, Tokyo, Oct. 1968, pp. 249-259.

5.- P. SELIGMAN and N.R. GREENING (1968) "Phase equilibria of cement-water", Proceedings, 5th International Symposium on The Chemistry of Cement, Tokyo, Oct. 1968, pp. 179-200.

6.- W. DOSCH, H. KELLER and H. zur STRASSEN (1968) Written discussion to "Crystal structures and properties of cement hydration products (hydrated calcium aluminates and ferrites)" by H.E. Schwiete and U. Ludwig, Proceedings, 5th International Symposium on The Chemistry of Cement, Tokyo, Oct. 1968, pp. 72-77.

Influence of $3CaO.Al_2O_3.CaCO_3.nH_2O$ on the structure of cement paste

L'influence de $3CaO.Al_2O_3.CaCO_3.nH_2O$ sur la structure de la pâte de ciment

J. JAMBOR, Ing. Dr. Dr. Sc. Institute of Construction and Architecture, Slovak Academy of Sciences, Bratislava, Tchécoslovaquie.

RESUME : Tenant compte des connaissances sur l'influence de $CaCO_3$ sur l'hydratation de l'aluminate tricalcique C_3A, aussi bien que des expériences acquises par la pratique de la technologie du béton, l'auteur a réalisé une recherche dont le but était de vérifier l'influence de la formation de l'aluminate de chaux carbonaté hydraté $C_3A.CaCO_3.H_n$ dans la pâte liante, sur sa structure et sa résistance.

Pour la recherche, on a utilisé des pâtes-liants faites des mélanges de C_3A à teneur variable en $CaCO_3$ broyé et en sable siliceux, qui étaient traitées de la manière habituelle. Après avoir établi les caractéristiques principales des propriétés physico-mécaniques, les pâtes durcies ont été soumises à l'analyse de leur composition de phase et de leur structure poreuse.

Les résultats ont confirmé que, contrairement au sable siliceux, $CaCO_3$ participe activement à l'hydratation de C_3A en causant la formation de $C_3A.CaCO_3.H_n$ comme le produit d'hydratation principal. En comparaison avec des produits habituels d'hydratation de C_3A, c'est à dire C_3AH_6 ou C_4AH_{19} - C_2AH_8, c'est $C_3A.CaCO_3.H_n$ qui présente une capacité liante très élevée. Sa formation dans la pâte liante de C_3A lui donne une structure plus compacte, ayant une valeur jusque 10 fois plus petite du rayon moyen des micropores et une résistance à la compression même jusque 100 fois plus importante.

Ces constatations permettent d'éclaircir les expériences acquises par la technologie du béton, qui indiquent une influence favorable de l'addition de $CaCO_3$, broyé ou de l'emploi des agrégats calcaires sur la résistance du béton. En même temps elles montrent des possibilités nouvelles de l'amélioration de la capacité liante des ciments portland à teneur élevée en C_3A.

SUMMARY : Taking into consideration the experience concerning the influence of $CaCO_3$ on the hydration of tricalcium aluminate - C_3A as well as the experience acquired in the concrete technology, an investigation was carried out, the aim of which was to clarify the influence of the forming of calcium aluminate carbonate hydrate - $C_3A.CaCO_3.H_n$ in the binder paste on its structure and strength.

The hardened binder pastes made of the mixtures of C_3A with a graded amount of ground $CaCO_3$, or quartz sand, cured in usual way, were used for the investigation. After ascertaining the basic physico-mechanical properties the phase composition and the character of pore structure of the tested pastes were investigated.

The achieved results have confirmed, that unlike the quartz sand, the $CaCO_3$ participates in the hydration process of C_3A and causes forming of $C_3A.CaCO_3.H_n$ as a main hydration product. In comparison with the usual hydration products of C_3A - i.e. C_3AH_6 or C_4AH_{19} - C_2AH_8 - the $C_3A.CaCO_3.H_n$ possesses a spectacularly higher binding capacity. The forming of this compound in the hydrating C_3A paste causes a more compact structure - with up to 10-times smaller average micropore radius and up to 100-times higher compressive strength.

These findings permit to explain the experience acquired in practical concrete technology, that indicate a positive effect of ground $CaCO_3$ admixture, or of an use of calcite aggregate on the concrete strengths. At the same time, they provide new possibilities of an improvement of the binding capacity of the portland cements with a higher C_3A content.

INTRODUCTION

Experience shows, that the tricalcium aluminate C_3A and its hydration products of the type C_3AH_6, or C_4AH_{19} - C_2AH_8 contribute only very little to the binding properties of portland cement and in addition to it they affect negatively some other technically important properties of hardened cement paste and concrete /1,2/. For this reason effort is developed to modify the hydration of C_3A in such a way as to obtain hydration products with a much higher binding capacity. This effect comes true partly already by using gypsum as a retarding admixture to the cement. Due to its influence calcium aluminate sulphate hydrates with a higher binding capacity are formed from a part of C_3A present during the hydration process. Taking into consideration the experience acquired in the concrete technology we drew our attention to the investigation of the influence of $CaCO_3$ on the hydration of C_3A and especially of the influence of the developed calcium aluminate carbonate hydrate on the structure and strength of hardened binder pastes.

The effect of various carbonates on the hydration of calcium aluminates and the conditions of forming as well as the relative stability of calcium aluminate carbonate hydrates have been studied by G. Schippa and R. Turriziani /3/, P.P. Budnikow, W.M. Kolbassow and A.S. Pantelejew /4/, K.T. Greene /5/, E.T. Carlson and H.A. Berman /6/, R.F. Feldman, V.S. Ramachandran and P.J. Sereda /7/ and others /8,9/. These authors have proved, that due to the effect of the soluble as well as insoluble carbonates the calcium aluminate monocarbonate hydrate - $C_3A.CaCO_3.H_n$ is formed by the hydration of C_3A and C_4AF at a normal temperature. The amount of bound water in this compound is given mostly by the value of n = 10-12 in dependence on the relative humidity of the medium. Some authors suppose the forming of calcium aluminate tricarbonate hydrate - $C_3A.3CaCO_3.H_{32}$ - under specific condition too, although this assumption was hitherto not confirmed generally.

The influence of the formed $C_3A.CaCO_3.H_n$ on the structure and strength of hardened binder pastes has been investigated relatively little so far. P.P. Budnikow and cowerkers have proved, that the forming of $C_3A.CaCO_3.H_{11}$ causes in C_3A paste a spectacular increase of its strength, whereas in C_4AF paste it does not appear significantly /4/. E. Spohn and W.Lieber have demonstrated a positive influence of the formed $C_3A.CaCO_3.H_{10}$ on the strengths in C_3A pastes as well as in C_4AF pastes. In connection with these findings the mentioned authors have proved the positive influence of the $CaCO_3$ admixture on the strengths of portland cement mortars and concretes, too /9/.

MATERIALS AND METHODS USED

The following materials were used for the tests:

a/ C_3A - prepared by five times repeated burning at 1400°C ± 20°C of pressed mixture of chemically pure $CaCO_3$ and Al_2O_3 in molal proportion 3:1. The C_3A was ground to the maximum grain size of 90 microns.

b/ $CaCO_3$ - prepared by grinding of selected lumps of natural marble to the maximum grain size of 90 microns.

c/ Standard quartz sand for testing of cement corresponding to the specifications of the standard ISO/R 697-1968, or IS 650-1966.

The composition of used materials is given in Table I.

TABLE I

		C_3A	$CaCO_3$
Ignit.loss at 1000°C	%	0.30	43.63
Insoluble residue	%	1.03	0.34
CaO	%	61.42	55.32
Al_2O_3	%	37.24	-
R_2O_3	%	-	0.32
MgO	%	-	0.38
Free CaO	%	0.20	-
Main phase - approx.		98% C_3A	98% $CaCO_3$
Specific density g/cm^3		3.151	2.582
Blaine fineness cm^2/g		2796	2483

For the investigation 2 cm edge test cubes made of thirteen binder pastes were used. Three types of mixtures were used for the preparation of pastes and test specimens: mixtures of C_3A with a graded amount of $CaCO_3$, mixtures of C_3A with a graded amount of quartz sand and mixtures with a graded amount of quartz sand containg the compound of 73% C_3A and 27% $CaCO_3$ as a binder. The pastes and the test specimens were prepared and cured in usual way. After 1 and 28 days of hardening at 20°C twelve specimens of each paste were used for the determination of their bulk density and compressive strength, six of them being tested in their original wet state and six after their drying at 100°C. After the strength tests the crushed specimens were used for the investigation of their phase composition as well as their pore structure.

Compressive strength, bulk density, specific density and total porosity of the test specimens were determined by using usual methods. The phase composition of hardened pastes was investigated by means of X-ray diffraction phase analysis and complex thermal analysis - using a Philips diffractograph with a PW 1050 goniometer and Derivatograph of type OD 102 delivered by MOM Budapest. The pore size distribution was determined by the Guyer - Böhlens method using a Carlo Erba mercury intrusion porosimeter of model 70 H. A stereoscan made by

TABLE II

Paste No.	Composition of dry mixture %	Mixing water %	Curing time in days	In wet state: Bulk density g/cm³	In wet state: Compressive strength MPa	After drying at 100°C: Bulk density g/cm³	After drying at 100°C: Compressive strength MPa	After drying at 100°C: Total porosity %	After drying at 100°C: Average micropores radius nm	Ignition loss at 600°C %
1	C_3A 100	60	1	1.730	0.03	1.240	0.27	53.3	1880	10.9
			28	1.771	0.13	1.276	1.38	51.1	1420	12.0
2	C_3A 85 $CaCO_3$ 15	60	1	1.701	4.26	1.282	13.53	51.5	510	13.2
			28	1.772	7.05	1.367	20.81	47.7	407	14.3
3	C_3A 73 $CaCO_3$ 27	60	1	1.717	11.45	1.332	29.25	45.2	261	16.4
			28	1.797	18.20	1.429	41.60	39.7	204	17.5
4	C_3A 60 $CaCO_3$ 40	60	1	1.709	17.07	1.347	31.36	44.1	250	16.4
			28	1.795	29.12	1.430	56.97	36.2	157	18.3
5	C_3A 50 $CaCO_3$ 50	60	1	1.704	10.64	1.313	24.14	48.0	410	14.7
			28	1.779	21.72	1.405	40.62	41.3	196	16.9
6	C_3A 40 $CaCO_3$ 60	60	1	1.696	6.24	1.276	16.53	49.8	505	12.9
			28	1.762	14.98	1.346	27.13	45.4	288	15.3
7	C_3A 80 sand 20	50	1	1.759	0.06	1.279	0.19	53.7	1750	7.6
			28	1.769	0.14	1.282	0.39	52.2	1590	8.5
8	C_3A 60 sand 40	42	1	1.865	0.10	1.495	0.23	45.1	1620	6.4
			28	1.870	0.19	1.539	0.50	43.7	1490	7.0
9	C_3A 40 sand 60	35	1	2.016	0.07	1.665	0.22	37.4	1650	5.1
			28	2.042	0.20	1.669	0.37	36.9	1510	5.6
10	C_3A 58.4 $CaCO_3$ 21.6 sand 20	50	1	1.766	9.25	1.432	23.02	42.2	320	14.6
			28	1.826	11.76	1.518	40.20	37.5	197	15.7
11	C_3A 43.8 $CaCO_3$ 16.2 sand 40	42	1	1.835	7.22	1.547	20.03	38.0	407	11.5
			28	1.899	9.12	1.614	34.21	33.9	210	13.4
12	C_3A 29.2 $CaCO_3$ 10.8 sand 60	35	1	1.970	6.70	1.750	15.61	32.6	462	8.5
			28	2.028	8.10	1.772	30.49	30.6	236	12.0
13	C_3A 14.6 $CaCO_3$ 5.4 sand 80	25	1	2.116	4.14	1.790	10.51	30.9	525	5.7
			28	2.135	6.79	1.801	14.34	29.3	407	7.6

Cambridge Scientific Instruments Ltd. was used for the scanning electron microscopy.

RESULTS AND THEIR DISCUSSION

The composition of the binder pastes and the ascertained basic properties of test specimens after their 1 and 28 days hardening are given in Table II.

The results of tests prove a decissive influence of the $CaCO_3$ presence in the mixture on the properties of hardened paste. All hardened pastes without $CaCO_3$ and containing only C_3A as a binder - i.e. pastes No. 1,7,8 and 9 have shown in original wet state as well as after drying at 100°C very low compressive strengths only; likewise a very little increase of strength and decrease of total porosity during their 28 days hardening. A relatively coarse-pore structures with an average micropore radius above 1400 nm have been ascertained in these pastes by porosimetric analysis. These results have proved, that C_3A alone and its usual hydration products form only a relatively little compact structure of the paste and possess a very low binding capacity only.

On the other hand all hardened pastes containing $CaCO_3$ in addition to C_3A have shown in wet state as well as after drying up to 100-times higher compressive strengths than compared pastes without $CaCO_3$. The pastes with $CaCO_3$ have also manifested a spectacular increase of compressive strength and bulk density as well as a corresponding decrease of their total porosity during 28 days hardening. In all these pastes a substantially higher content of the water bound in the hydration products has been

ascertained. The porosimetric analyses have proved a more compact fine-pore structure of these pastes - with the values of average micropores radius up to 10-times smaller than those in the pastes without $CaCO_3$. A spectacular difference in the pore structure character of the tested pastes containing $CaCO_3$ and without $CaCO_3$ is shown in Fig.1, in which the integral pore size distribution curves of pastes No. 2,3,4,6 and pastes No. 1,8 after 1 day of their hardening are illustrated.

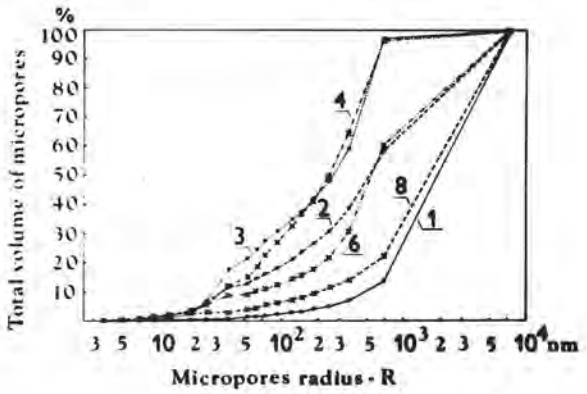

Fig. 1 - Integral pore size distribution curves of pastes No. 1,2,3,4,6 and 8 after 1 day hardening.

The given results already indicate, that in the pastes prepared of the C_3A with $CaCO_3$ mixtures another type of the hydration products is formed, than that formed in the pastes containing only C_3A as a binder. This has been confirmed by the results of XRD - analysis and complex thermal analysis.

In pastes No. 1,7,8 and 9, prepared with C_3A only as a binder, after their 1 and 28 days hardening, the C_3AH_6 as the main hydration product has been identified. Beside that the non-hydrated C_3A, C_4AH_{19} and a small amount of $C_3A.CaCO_3.H_n$ - formed probably due to the effect of air - CO_2 - have been ascertained in these pastes. In the pastes No. 7,8 and 9 /β - quartz have been present.

In pastes No. 2,3,4,5,6,10,11,12 and 13 prepared of the C_3A with $CaCO_3$ mixtures the $C_3A.CaCO_3.H_n$ as the main hydration product has been identified after their 1 and 28 days hardening. The non-hydrated C_3A, C_3AH_6, $CaCO_3$ and /β- quartz /in the pastes No. 10, 11,12,13 only/ in a variable content have been determined in these pastes as the secondary phases. In no paste the presence of $C_3A.3CaCO_3.H_{32}$ has been ascertained. The highest relative amount of the $C_3A.CaCO_3.H_n$ has been found in the pastes No. 3 and 4 prepared of the mixtures, in which the original proportion of C_3A to $CaCO_3$ was closed to that in the compound $C_3A.CaCO_3.H_n$. The characteristic diffractometer traces of the pastes No. 1,3,5,8,11 in their original wet state after 1 day hardening are illustrated in Fig.2.

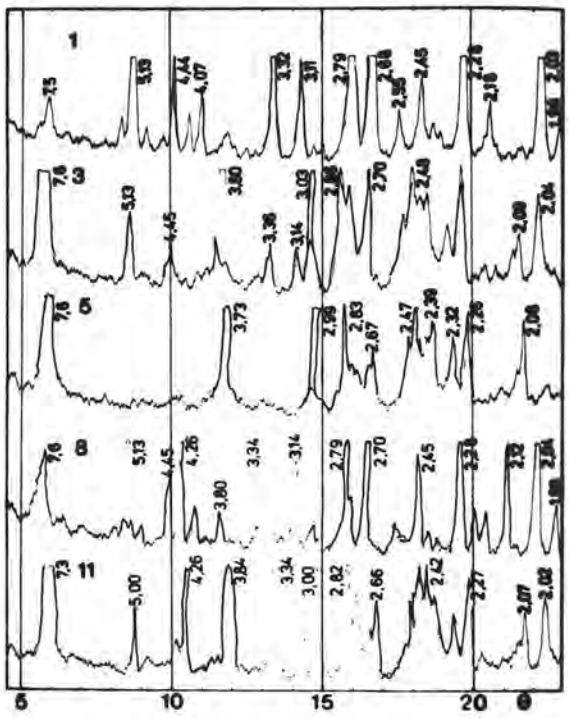

Fig. 2 - Diffractometer traces of pastes No. 1,3,5,8 and 11 after 1 day.

The results of XRD-analyses have been fully confirmed by the results of complex thermal analyses of tested pastes. The characteristic DTA - curves of the pastes No. 1, 2 and 4 after their 1 day hardening are demonstrated in Fig. 3. DTA curve of the paste No. 1 is typical of the C_3AH_6, whereas the DTA curve of the paste No. 4 shows the presence of $C_3A.CaCO_3.H_n$ as the main phase in the paste.

The spectacular differences in the type of hydration products and in the character of the structure of the pastes prepared with or without $CaCO_3$ have been demonstrated by electron scanning microscopy, too. In Fig. 4 a typical structure of paste No. 1 formed mostly of C_3AH_6 and in Fig. 5 a more compact and fine-porous structure of the paste No. 4 formed mostly of $C_3A.CaCO_3.H_n$, is shown.

These results have confirmed, that the forming of $C_3A.CaCO_3.H_n$ is the main cause of the relatively high strengths of the pastes made of C_3A with $CaCO_3$ mixtures. This finding is confirmed indirectly also by the relationship between the compressive strength of the pastes No. 2 to 6 and the relative proportions of C_3A and $CaCO_3$ in the mixtures used for the preparation of these pastes - as illustrated by Fig. 6. This relationship confirms that the highest compressive strengths have been exhibited by

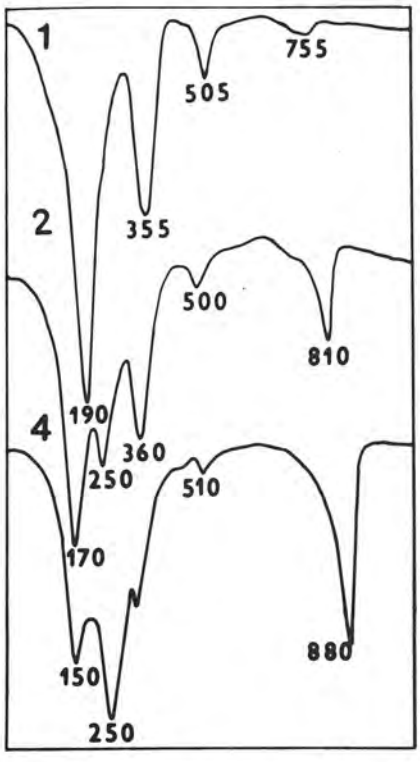

Fig. 3 - DTA curves of pastes No. 1,2 and 4 after 1 day hardening.

Fig. 4 - Fracture surface of hardened paste No. 1.

the pastes made of the mixtures containing 60 to 70% C_3A and 30-40% $CaCO_3$. The fact, that the highest strengths have been obtained in pastes with a moderately higher $CaCO_3$ content than corrosponding to the theoretical composition of $C_3A.CaCO_3.H_n$ may in this case be explained by inperfect reaction of the $CaCO_3$ grains with C_3A.

Fig. 5 - Fracture surface of hardened paste No. 4.

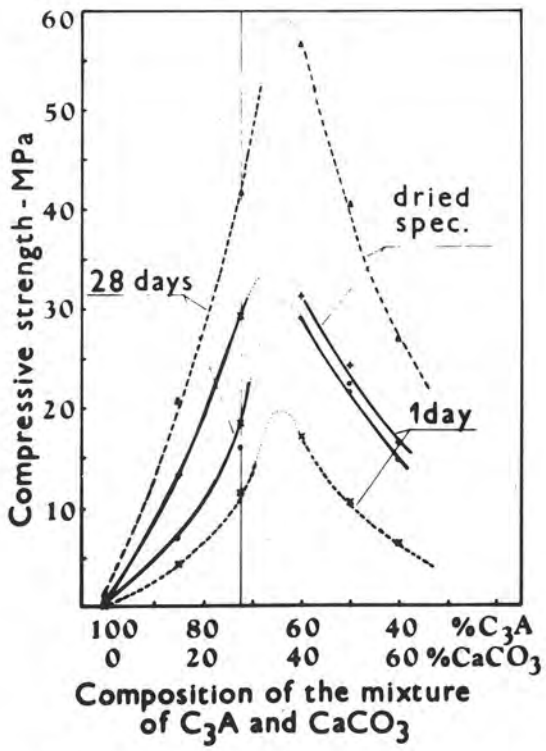

Fig. 6 - Relationship between compressive strength of the paste and composition of used C_3A-$CaCO_3$ mixture.

CONCLUSION

The achieved results have confirmed, that finely ground $CaCO_3$ in hydrating C_3A - pastes participates in the hydration process and causes forming of $C_3A.CaCO_3.H_n$ as a main hydration product. The amount of formed

$C_3A.CaCO_3.H_n$ depends on the proportion of C_3A and $CaCO_3$ in the hydrating mixture and the relatively highest share of this phase has been formed in mixtures containing 60-70% C_3A and 30-40% $CaCO_3$. In comparison to the usual hydration products of C_3A - i.e. C_3AH_6 or C_4AH_{19}-C_2AH_8- the $C_3A.CaCO_3.H_n$ possesses spectacularly higher binding capacity and its forming in the hydrating C_3A paste causes a more compact structure of the paste - with up to 10-times smaller average micropore radius and up to 100-times higher compressive strength. This finding permits to expalin the cause of the usually higher strengths of the concretes made of calcite aggregate and provides new possibilities for improvement of the binding capacity of the portland cements with a higher C_3A content.

REFERENCES

1.- H. KÜHL /1961/ "Cement Chemistry", Vol. III, Berlin 1961, pp. 332-325 /in German/.

2.- J. JAMBOR /1973/ "Influence of Phase Composition of Hardened Binder Pastes on its Pore Structure and Strength", in Pore Structure and Properties of Materials - Proceedings of Int. Symp., Prague 1973, Vol. II, pp. D 75-D 96.

3.- R. TURRIZIANI, G.SCHIPPA /1956/ "Hydrated Calcium Monocarbonate Aluminate", Ricerca Scient., 26, No. 9, pp. 2792-2797 /in Italian/.

4.- P.P. BUDNIKOW, W.M. KOLBASSOW, A.S. PANTELEJEW /1961/ "Reactions of $3CaO.Al_2O_3$ and of $4CaO.Al_2O_3.Fe_2O_3$ with Calcium and Magnesium Carbonates", Silikat Technik, 11, No. 6, pp. 271-272 /in German/.

5.- K.T. GREENE /1960/ "Early Hydration Reactions of Portland Cement", in Chemistry of Cement - Proceedings of Fourth Int. Symp., Washington 1960, Vol. 1, pp. 359-374.

6.- E.T. CARLSON, H.A. BERMAN /1960/ "Some Observations on Calcium Aluminate Carbonate Hydrates", Journ. Res. Nat. Bur. Std., 64A, No. 4, pp. 333-341.

7.- R.F. FELDMAN, V.S. RAMACHANDRAN, P.J. SEREDA /1965/ "Influence of $CaCO_3$ on the Hydration of $3CaO.Al_2O_3$", Journ. Amer. Cer. Soc., Vol. 48, No. 1, pp. 25-30.

8.- H.F.W. TAYLOR /1964/ "The Chemistry of Cements", Vol. 1, London-New York 1964, pp. 273-275.

9.- E. SPOHN, W. LIEBER /1965/ "Reactions between Calcium Carbonate and Portland Cement", Zement-Kalk-Gips, 18, No. 9, pp. 483-485 /in German/.

10.- ISO/R 697-1968 "Method of Testing of Cements Compressive and Fluxural Strength of Plastic Mortar /Rilem-Cemburcan Method/".

Interaction between gypsum and the C-S-H phase formed in C_3S hydration

Interaction entre le plâtre et la phase C-S-H, formée pendant l'hydratation de C_3S

I. ODLER, Institut für Stein und Erden - Clausthal-Zellerfeld, R.F.A.

RESUME :

L'interaction entre le plâtre et la phase C-S-H, qui s'est formée pendant l'hydratation de C_3S, a été étudiée. La quantité de plâtre lié et l'aptitude de ce gypse à réagir avec le C_3A ont été déterminées.

ABSTRACT :

The interaction between the C-S-H-phase formed in C_3S hydration and gypsum was studied. The amount of gypsum bound and the ability of bound gypsum to react with C_3A were determined.

In the study of the kinetics of hydration of a series of portland cements we observed that ettringite was formed even after the total supply of free calcium sulfate in form of gypsum or anhydride, as determined by DTA and/or XRD, was depleted. We tentatively assumed that at this stage calcium sulfate bound to the CSH-phase formed in C_3S hydration can serve as source of SO_4^{2-}-ions needed for ettringite formation. To test this hypothesis the interaction between gypsum and the CSH-phase formed in the hydration of pure tricalcium silicate was studied.

In the first part of our work pastes prepared from pure C_3S and from blends of C_3S and gypsum (w/s = 0,7) were allowed to hydrate in small polyethylene bottles for different periods of time. After stoping the hydration process by D-drying the resultant material was further analysed. The gypsum content as determined by DTA (Mettler 2000 apparatus, 10 mg sample 10 °C/min N_2 atm) and the non reacted C_3S fraction as determined by quantitative XRD on samples preignited to 600 °C are shown in Tab. I. It can be seen that the amount of gypsum detectable by DTA declined with progressing C_3S hydration and dissapeared completely in pastes with long enough hydration time and small enough gypsum additions. Similar results were obtained when gypsum was determined by XRD. Thus it appears that gypsum is bound by the C_3S hydration products in a way that makes it undetectable by the two methods employed. If expressed per unit of C_3S hydrated the amount of "missing" gypsum was not constant. It increased with increasing amount of gypsum added to the original paste and declined with progressing hydration. The maximum amount of bound gypsum i.e. 9,8 g/100 g C_3S found after 1 day of hydration in a paste with 10% calcium sulfate added coorresponds to a molar ratio of 1 mol SO_3 per 6.1 mols C_3S hydrated. This value is in good agreement with those found earlier by Copeland and coworkers (1) on a C_3S paste milled 11 days with 20% gypsum, by Bentur (2) on C_3S pastes hydrated to a degree of hydration of 70% with up to 9% gypsum added, and by Mehta and coworkers (3) on alite cement pastes with 3 an 6% gypsum added.

As to the effect of gypsum on the rate of C_3S hydration it was found that the fraction of C_3S hydrated after any hydration time increased with increasing amount of gypsum added up to 10% $CaSO_4$. These data have to be compared with those of Bentur (2) who also found a positive effect of gypsum on C_3S hydration however only up to about 2-3% gypsum added.

In subsequent work it was tested whether gypsum bound to the CSH-phase and detectable neither by DTA nor XRD can serve as source of SO_4^{2-}-ions for ettringite formation. To do so pastes made from C_3S and gypsum hydrated for various periods of time were ground to a fine powder, blended with C_3A (Mol C_3A : Mol $CaSO_4$ = 1 : 3) and mixed with additional water to obtain thin paste consistency. After different times of further hydration the pastes were dried at 35 °C to constant weight and further investigated by DTA and XRD. As an example, results obtained on a sample of C_3S + 2,5% $CaSO_4$ prehydrated for 28 days and subsequently allowed to react with C_3A for additional 7 days are shown in Fig. 1. It can be seen that within 28 days the endothermic peak belonging to gypsum dissapeared; instead a broad endothermic area belonging to the CSH-phase formed in C_3S hydration became apparent. After adding C_3A and further hydration a new peak belonging to ettringite developed. After additional gypsum addition this compound was again detectable as a separate peak. XRD studies confirmed the formation of ettringite after C_3A addition. Similar results were obtained on all pastes studied. Acomparison of samples that were allowed to react with C_3A for different periods of time revealed that the ettringite peak reached its final intensity within about 3 hours. In samples in which an excess of C_3A was added monosulfate and calcium aluminate hydrate rather than ettringite were detectable.

In the final part of our experimental work the amount of sulfate ions that can be recovered by extraction of the paste with a saturated calcium hydroxide solution was measured. To do so finely ground C_3S pastes containing 2,5 calcium sulfate and hydrated 3, 7 and 28 days were repeatedly extracted for 1 hour with a 100 fold excess of a saturated calcium hydroxide solution. After filtering the concentration of SO_4^{2-} in the liquid phase was determined. About 40 - 60% of SO_4^{2-} present in the paste was recovered in the first extraction; between 3 and 6 additional extractions were needed to recover more than 95% of the total amount of sulfates.

From the data obtained one has to conclude that significant, however not unlimited, amounts of calcium sulfate can be taken up by the hydration products in the hydration of C_3S in presence of gypsum. As a reaction between calcium sulfate and calcium hydroxide, i.e. one of the C_3S hydration products, can be excluded one has to assume that the dissapearing of gypsum from the system is due to a reaction of the latter substance with the second product of C_3S hydration i.e. the CSH-phase. From the observation that the "missing" sulfate can be rather redily recovered by extraction of the paste and can even serve as source of SO_4^{2-} ions for ettringite and monosulfate formation one has to conclude that the bond of calcium sulfate to the CSH-phase is rather weak. It had been suggested by Copeland and coworkers (1) that in the hydration of C_3S in presence of calcium sulfate a CSH-gel is formed in which silicone is partially substituted by the sulphur of sulfate ions. Mehta and coworkers (3) postulated an "absorption" of gypsum by the precipitating calcium silicate hydrates. It seems however unlikely that sulphur atoms bound firmly within the structure of the CSH-phase could enter the liquid phase as quickly and react with tricalcium aluminate as readily as observed in our experiments. Thus we belive that the sulfate ions are just physically adsorbed to the large surface of the CSH-phase and an equilibrium exists between the amount of sulfate ions adsorbed and the calcium sulfate concentration in the liquid phase.

In the light of the results reported the formation of ettringite in portland cement pastes at a time when free calcium sulfate is not detectable anymore becomes understandable. It can be assumed that also here calcium sulfate bound by the CSH-phase can serve as source of SO_4^{2-}-ions for ettringite formation as originally postulated.

Conclusions

1. In the hydration of C_3S in presence of gypsum up to 1/6 mol SO_4^{2-} per 1 mol C_3S hydrated is bound by the hydration products. The bound gypsum can be detected neither by DTA nor by XRD.

2. The gypsum bound by the CSH-phase can by almost quantitatively extracted by water saturated with calcium hydroxide and can react with C_3A to form ettringite.

References

1. L.E. Copeland, E. Bodor, T.N. Chang and C.H. Weise. Reactions of tobermorite gel with aluminates, ferites and sulfates. J. Portland Cem. Ass. Res. Develop. Lab. 9 (1), 61-74 (1967)

2. A. Bentur. The effect of gypsum on the hydration and strength of C_3S pastes. J. Am. Ceram. Soc. 59, 210-213 (1976)

3. P.K. Mehta, D. Pirtz and M. Polivka. Properties of alite cements. Cem. Concr. Res. 9, 439-450 (1979)

Tab. 1

Hydration time (d)	$CaSO_4$ added (as gypsum) (g/100g C_3S)	$CaSO_4$ found (as gypsum) (g/100g C_3S)	$CaSO_4$ missing (g/100g C_3S)	degree of C_3S hydration (%)	$CaSO_4$ missing (g/100g C_3S hydr.)
1	0	-	-	29	
	2,5	0,3	2,2	33	6,7
	5,0	2,4	2,6	34	7,7
	7,5	3,8	3,7	38	9,7
	10,0	6,1	3,9	40	9,8
3	0	-	-	40	-
	2,5	0	2,5	41	6,1
	5	1,5	3,5	46	7,6
	7,5	3,0	4,5	50	9,0
	10,0	5,1	4,9	55	8,9
7	0	-	-	53	
	2,5	0	2,5	60	4,2
	5	1,2	3,8	62	6,1
	7,5	2,9	4,6	68	6,8
	10,0	4,2	5,8	69	8,4
28	0	-	-	79	
	2,5	0	2,5	84	3,0
	5	0,6	4,4	85	5,2
	7,5	2,7	4,8	88	5,5
	10,0	3,8	6,2	90	6,9

Fig. 1: Thermograms of a. C_3S + 2,5% $C\bar{S}H_2$
b. same after 28 d hydration
c. as b. after adding C_3A and further hydration, d. as c. + 1,5% $C\bar{S}H_2$
E = ettringite
G = gypsum CSH = CSH-phase

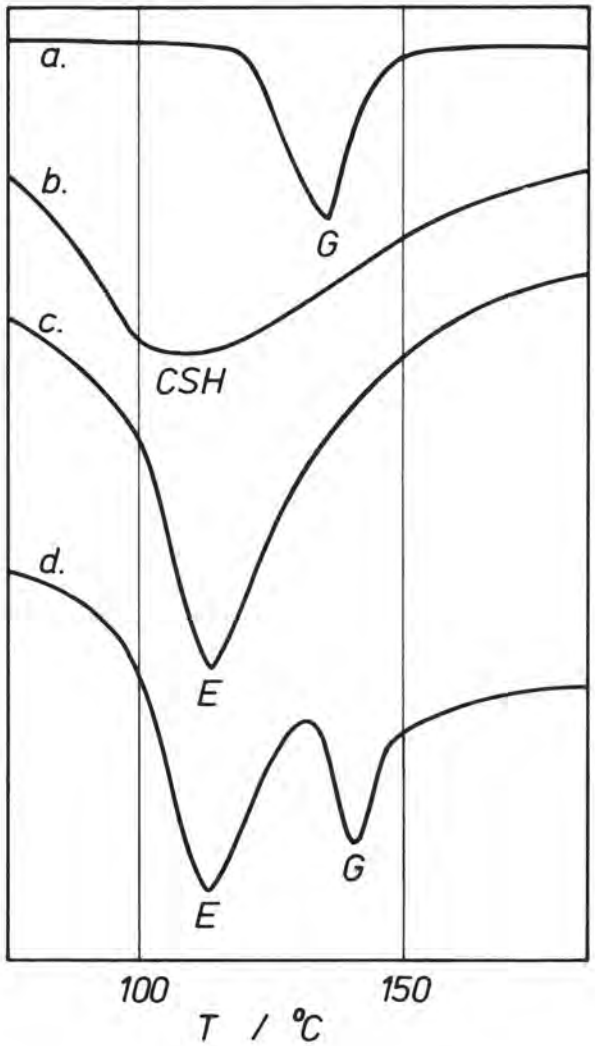

On the stability of calcium aluminate sulphate hydrates in pure systems and in cements

Sur la stabilité des hydrates de calcium-aluminate-sulfate dans des systèmes purs et dans des ciments

H.Y. GHORAB, D. HEINZ, U. LUDWIG, T. MESKENDAHL and A. WOLTER, Institut für Gesteinshüttenkunde, RWTH - Aachen, R.F.A.

RESUME :

Dans des systèmes secs ou humides, l'ettringite se décompose déjà à 18 °C dans le vide de 10^{-6} bar, à 74 °C à l'humidité et sous la pression atmosphérique ordinaire, à 82,5 °C sous le nitrogène humide, mais il résiste au traitement dans l'eau de 100 °C après que l'équilibre ait été obtenu.

Les produits de déshydratation forment des pseudomorphes de l'ettringite avec une porosité ouverte élevée. Sous l'attaque du gaz carbonique, le plâtre, la bayerite et l'aragonite se forment. La porosité ouverte augmente de 46 % en volume par rapport au volume de l'ettringite.

Dans des systèmes humides, des additions convenables de sulfates de calcium aux ciments empêchent la fausse prise par la formation d'une couche d'ettringite sur les surfaces du C_3A. Des recherches récentes sur des systèmes purs avec C_3A, gypse ou anhydrite et chaux et avec ou sans $CaCO_3$ ou C_3S supplémentaire et des recherches sur des ciments industriels confirment ou montrent la formation instantanée de l'ettringite, sa recristallisation postérieure et sa dissolution accompagnée de la formation de monophases avec la réaction du C_3A encore présent et une formation topochimique de l'ettringite renouvelée. Il est montré que dans les systèmes de ciment contenant des sulfates, l'ettringite et le carboaluminate hydraté sont les hydrates plus stables à la température ordinaire et à basse température . Aux températures plus élevées, le monosulfate hydraté devient l'hydrate stable. C'est pourquoi, un traitement thermique direct, retardé ou répété, désiré ou accidentel, des mortiers de ciment ou des bétons peut causer des dégâts sous forme d'expansion, de fissuration et de chute de résistance. Le remplacement total ou partiel du ciment portland ordinaire par du ciment sans C_3A ou par du ciment à faible teneur en C_3A, par des laitiers granulés ou par des pouzzolanes peut réduire ou éviter ces dégâts.

D'autre part, la connaissance de ces corrélations ne devrait pas être utile seulement pour réduire ou éviter des dégâts, mais devrait être utilisée, par exemple, pour la précontrainte du béton.

SUMMARY :

In both dry and moist systems, ettringite already decomposes at 18 °C under vacuum of 10^{-6} bar, at 74 °C under normal humidity and pressure conditions, at 82.5 °C under wet N_2-gas but resists treatment with 100 °C water after equilibrium is reached. The dehydration products form pseudomorphes of ettringite with high open porosity. At CO_2-attack gypsum, bayerite and aragonite are formed. The open porosity increases by 46 vol.-% related to the ettringite volume.

In wet systems suitable additions of calcium sulphate to cements prevent false setting by formation of an ettringite layer preferably on the surfaces of C_3A. New investigations in pure systems with C_3A, gypsum or anhydrite and lime with and without additional $CaCO_3$ or C_3S and with industrial cements confirm or indicate the immediate formation of ettringite, its later recrystallization and dissolution accompanied by formation of monophases with reaction of still present C_3A and a renewed topochemical ettringite-formation. It is confirmed that in sulphate bearing cement systems ettringite and the carboaluminate hydrate are the more stable hydration products at normal and lower temperatures, whereas monosulphatehydrate at elevated temperatures comes to be the more stable hydration product. Therefore, direct, delayed or repeated, wanted ou unwanted heat treatment of cement mortars and concretes can cause damage in the form of expansion, cracking and decreased strengths. Complete or partial replacement of normal portland cement by portland cement without or with limited C_3A content, by granulated blast furnace slags or pozzolanas can reduce or prevent damage.

On the other hand, the knowledge on the given correlations should not only be sufficient to reduce or prevent damage but to make use of it, for instance, for the prestressing of concrete.

INTRODUCTION

The setting retardation of cement pastes is caused by the added calcium sulphates. They form a hedgehog-like layer of ettringite ($C_3A \cdot C\bar{s}_3 \cdot H_{32}$) on the surfaces of the quick reacting clinker component C_3A.[1] This layer scarcely influences the interdependent mobility of the particles and this prevents quick setting (1 - 3). Without addition of calcium sulphates the transformation of C_3A was just as high. The formation of a cards' house-like macro structure, which causes quick stiffening, was observed, however (2).

Hydration in the system $C_3A - C\bar{c} - C - H$ of Portland cements produces, after an initial formation of ettringite, a decomposition of the same and formation of tricalcium aluminate monosulphate hydrate ($C_3AC\bar{s}H_{12}$) or solid solutions with tetracalcium aluminate hydrate (C_4AH_{13}), respectively and hydration of the residual C_3A (4,5). After 60 days' further wet storage at room temperature in some cases a renewed formation of ettringite was observed. The high stability of ettringite at room temperature could be derived from the earlier investigations in the pure system $CaO - Al_2O_3 - CaSO_4 - H_2O$ (6,7) and $CaO - Al_2O_3 - CaSO_4 - CaCO_3 - H_2O$ (8). But no great importance was attached to these observations.

Damage to heat treated concrete products and thick concrete walls of reactors and the observation of interim lower bending strength of mortar bars encouraged further work on the thermal and chemical stability of the calcium aluminate sulphate hydrates and the related compounds.

The experimental work is subdivided into three parts
- thermal dehydration of ettringite,
- chemical stability of calcium aluminate sulphate hydrates in pure systems and
- influence of heat treatment on cement mortars.

THERMAL DEHYDRATION OF ETTRINGITE

Experimental

The ettringite used was prepared by mixing C_3A and gypsum in the stoichiometric ratio and excess water in a vibrating mill. Its chemical composition was $C_{2.8}AC\bar{s}_{2.7}H_{31.4}$. The isothermic dehydration was carried out

- under normal air pressure at temperatures from 50 to 900°C,
- under wet nitrogen gas at temperatures from 46 to 180°C and
- under vacuum at temperatures from 18 to 180°C.

Moreover, the dehydration of ettringite was carried out under normal pressure and humidity conditions dynamically with a heating rate of 5°C/min up to 1000°C and quasi-isothermically (9) up to 900°C by thermoanalytical measurements.

Finally the solubility of ettringite was investigated in the temperature range between 20 and 100°C. More details are given in (10).

[1] The following abbreviations are used:
A - Al_2O_3; F - Fe_2O_3; C - CaO; S - SiO_2;
$C\bar{s}$ - $CaSO_4$; $C\bar{c}$ - $CaCO_3$; H - H_2O

Results

The isothermic dehydration of the ettringite under normal pressure and humidity conditions at temperatures of between 50 and 144°C is shown in Fig. 1.

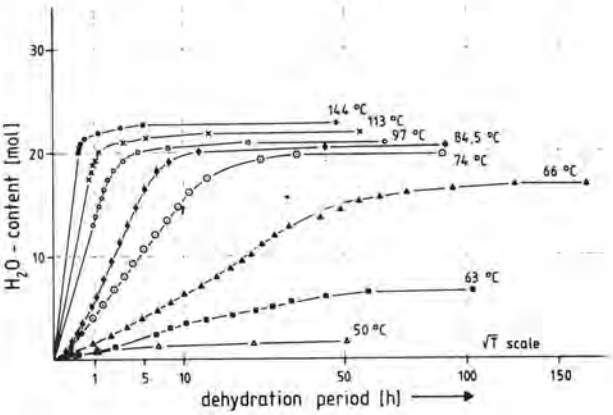

Fig. 1 Isothermic dehydration of ettringite under normal pressure and humidity

To a great extent the curves follow a $\sqrt{t}$ - law. That means the dehydration is diffusion-controlled. This corresponds well with the model of the ettringite structure (11). Increased temperature leads to an increased dehydration velocity.

The dehydration isotherms under normal pressure and humidity, under wet nitrogen and under vacuum are shown in Fig. 2. The enrichment of the rinsing gas with water vapour effects only a small displacement

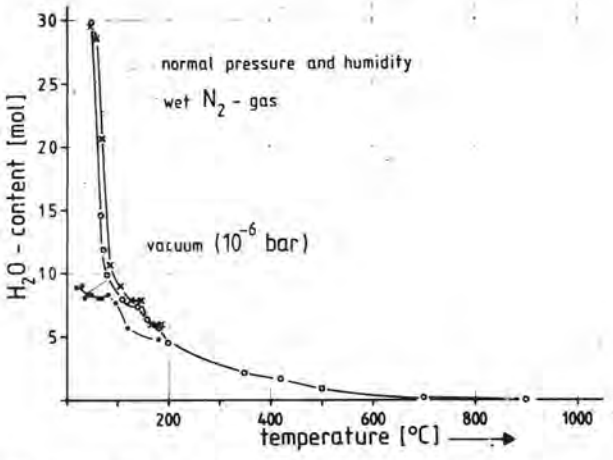

Fig. 2 Isothermic dehydration of ettringite

of the dehydration temperature to higher values. The temperature range from 46 to 50°C effects a loss of 1.4 m H_2O. From 50 to 125°C a further 22 m H_2O are emitted. In the range of 110 to 146°C a hydrate with a residual water content of 8 moles is recognizable.

Between 160 and 180°C a second hydrate stage with 6 m H_2O is observed. At 900°C dehydration is complete. - Lowering of the total pressure to 10^{-6} bar already leads to a water content of only 9 moles at 18°C. In the range of 39 to 85°C the water content amounts to only 8 and up to 120°C to 5.7 moles of water.

The results of the thermo-gravimetric dehydration are shown in Fig. 3. The accurate corresponding of the quasi-isothermic with the dynamic dehydration is evident.

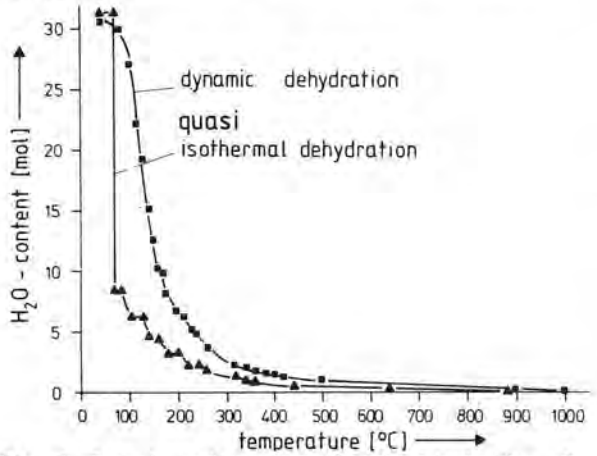

Fig. 3 Dynamic and quasi-isothermic dehydration of ettringite

X-ray diagrams show that the structure of ettringite is already destroyed in a vacuum of 10^{-6} bar at 18°C, at 74°C under normal pressure and at 82.5°C under wetted nitrogen. The restorage to 90 % r.h. leads to the rehydration of ettringite and in the presence of CO_2 from the air to the decomposition products gypsum, bayerit and aragonite. The molecular weight of the decomposition products amounts to only 54 % of that of the ettringite. That means that the carbonization effects a corresponding increase of the open porosity. The decomposition products from dehydration and carbonization products form ettringite-shaped pseudomorphs.

The solubility of ettringite was investigated at 20, 40, 80 and 100°C. It was established that the values of solubility at temperatures ≥ 40°C increase very much with the reaction period and that the equilibrium has not yet been reached after 21 or 49 days stirring. At this time ca. 30 wt.-% of ettringite were solved.

CHEMICAL STABILITY OF CALCIUM ALUMINATE HYDRATES IN PURE SYSTEMS

Experimental

The chemical compositions and the surface areas (BET) of the starting materials are given in Table 1. The investigated systems, the molar ratios of the systems, water/solid-ratios (w/s-ratios), temperatures, reaction periods and curing conditions are given in Table 2. More details are published in (10).

Substance	Chemical components [M.-%]					O_{sp} [m^2/g]	Composition
	CaO	Al_2O_3	SiO_2	CO_2	Ignition loss		
C_3A	58.91	38.56	-	0.34	1.5	0.24	$C_{2.9}S$
C_3S	71.95	-	26.31	0.08	0.3	0.82	$C_{2.9}S$
$CaSO_4 \cdot 2H_2O$	p.a.					0.39	
$CaCO_3$	p.a.					-	
CaO	p.a.					1.30	

Tab. 1 Chemical composition and surface area of the starting materials

System	Sample No.	Molar Ratios					w/s	Hydration		
		C_3A	$C\bar{S} \cdot H_2$	C	$C\bar{C}$	C_3S		Temp. °C	Period	Condition
C_3A - $C\bar{S}$ - C - H	1	1	0.6	1	-	-	2.5	80	1 d	storage
							0.5	20	236 d	"
							1.0	5	4 m	"
	2	1	0.8	1	-	-	1.0	5	4 m	"
	3	1	0.9	1	-	-	5	80	1 d	"
C_3A - $C\bar{C}$ - $C\bar{S}$ - C - H	4	1	1	1	0.5	-	4	20	1 d	shaking
	5	1	1	1	1	-	4	20	95 d	"
							2.5	80	1 d	storage
							5.0	20	3 d	"
C_3A - C_3S - $C\bar{S}$ - C - H	6	1	1	1	-	0.5				
	7	1	1	1	-	1	2.5	80	1 d	"
	8	1	1	1	-	2	0.5	20	236 d	"
	9	1	1	1	-	3				

Tab. 2 Systems, mixtures and curing conditions

Results

The investigations on the stability of the calcium aluminate sulphate hydrates in the three systems

$C_3A - CaSO_4 - CaO - H_2O$
$C_3A - CaSO_4 - CaCO_3 - CaO - H_2O$ and
$C_3A - CaSO_4 - C_3S - CaO - H_2O$

result overall in the ascertainment that ettringite is at room and lower temperature the most stable phase. The topochemical formation of ettringite in lime-saturated solutions is confirmed. Increasing temperatures accelerate the ettringite formation and the recrystallisation of the hedgehog-like layer of very small ettringite particles on the surface of the C_3A grains. At rest cured probes react under otherwise identical curing conditions much faster than shaken ones since the micro heterogeneities in the first case support an earlier formation through solution of monophases under dissolution of the originally topochemically formed ettringite and rapid reaction of the residual C_3A corresponding, for example, to the following mechanisms:

$$C_3AC\bar{S}_3H_{32} + 2C_3A + 16\,H \longrightarrow 3C_3ACsH_{16} \quad \text{or}$$

$$C_3AC\bar{S}_3H_{32} + xC_3A + (x-2)CH + yH \longrightarrow (1+x)C_3A(C\bar{S},CH)H_y$$

The use of equivalent amounts of anhydrite instead of gypsum leads under otherwise identical conditions, because of the slower solution velocity, to a decrease or prevention of the layer formation and thereby to an increase of C_3A - hydration (1,3,13).
The $C_2(A,F)$-components of the clinker react in a similar way but with decreased velocity at decreased alumina content (1,13).

The differentiation of the various monophases in the examined systems was done by drying the samples at equilibrium humidities ranging from 11 to 90 % (Tab.3).

Monophase	Drying [% r.h.]	X-ray d_{0001} [Å]	Thermal analysis
$C_3A \cdot C\bar{S} \cdot aq$	11	8.8	OH at 440°C
$C_3A \cdot (Cs,CH) \cdot aq$ (CO_2 - free)	33 - 90 11	8.8 8.15	OH at 440°C and 470°C
$C_3A \cdot (CH,C\bar{C}) \cdot aq$ (CO_2 - bearing)	11	8.15 - 8.2	OH at 440°C CO_2 at 740°C

Tab. 3 Differentiation of monophases

It is well known that the CO_2-free tetra calcium aluminate hydrate forms solid solutions with monosulphate hydrate. The basic interference of the mixed crystal appears at equilibrium humidities of 11 % at 5.15 Å and at humidities ranging from 33 to 90 % at 8.8 Å. Increased carbonization leads to increased formation of CO_2 containing tetra calcium aluminate hydrate with a basic d-value at 8.1 to 8.2 Å. This interference remains unaffected by humidities between 11 and 90 %. Further carbonization leads to the formation of monocarbo aluminate hydrate. That is at room temperature the most stable monophase. The basal d-value of the monosulphate hydrate at 8.8 Å remains unaffected at 11 % r.h.. Additional differentiation of the monophases are possible by thermoanalytical investigation, mainly by dehydration of portlandite and decarbonization of calcium carbonate. With 0.6 molar $C_3A/C\bar{S}$ ratio the renewed formation of ettringite was established after a curing period of 90 d at a constant 20°C (12).

In the system C_3A - $C\bar{S}$ - C - H the mixtures with 0.6 and 0.8 molar $C_3A/C\bar{S}$-ratio after complete formation of monophases were cured at 5°C. After four month curing a formation of ettringite was established. In the presence of $CaCO_3$ or C_3S the renewed formation of ettringite was found after 1 d curing at 80°C and further wet curing at room temperature.

Fig. 4 shows the renewed formation of ettringite in the system with $CaCO_3$ addition by X-ray diagrams. The starting sample contains ettringite, monocarbo-aluminate hydrate ($C_3AC\bar{C}H_{12}$), portlandite and small amounts of monosulphate hydrate. The one day at 80°C cured sample shows only the interference at 8.8 Å. It remained unaffected at 11 % r.h. and belongs to the monosulphate hydrate. Under these conditions the carboaluminate hydrate and the ettringite are unstable. After only three days curing at room temperature renewed formation of ettringite from monosulphate hydrate is established.

Fig. 5 shows the renewed formation of ettringite in the system with C_3S. After one day's curing at 80°C the X-ray diagram shows the interferences of ettrin-

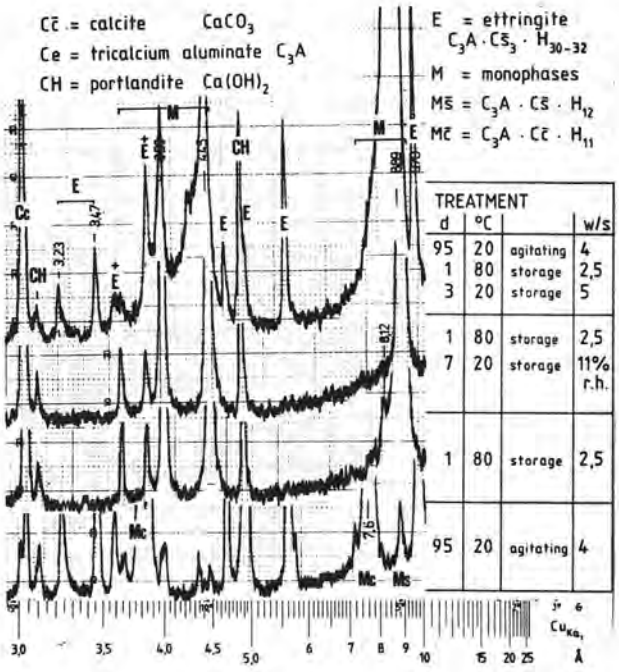

Fig. 4 X-ray diagrams of samples with $CaCO_3$ cured at 80 and 20°C

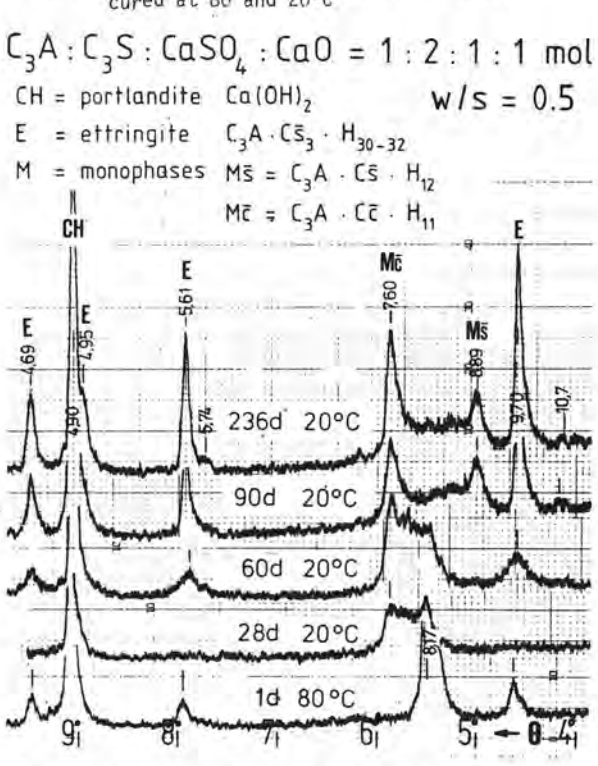

Fig. 5 X-ray diagrams of samples with C_3S cured at 80 and 20°C

gite, monophases and portlandite. After 28 days' storage at 20°C the ettringite was totally converted into monophases. After 60 days' a renewed formation of ettringite was visible. The intensity of the interferences increases up to 90 and 236 days. This behaviour of C_3S-containing mixes was observed for all of the proved mixes with molar C_3S/C_3A-ratios from 0.5 to 3.

INFLUENCE OF HEAT TREATMENTS ON CEMENT MORTARS

Experimental

The investigations on cement mortars were done with two different series of experiments.

The first series was done to prove the influence of the temperature of heat treatment on cement mortars with a high early strength cement type 55. The temperatures used are 60, 70, 80, 90 und 100°C. The hot curing period varied from 12 to 72 h. The weights, lengths and resonance frequencies dependent on the curing period were measured. More details are given in (14).

In the second series special heat treatment was carried out that, with cements that are sensitive to heat treatment, doubtlessly leads to severe expansion and damage to the structure. Fig. 6 shows the treatment used together with an industrial treatment programme. The work was done with the above mentioned

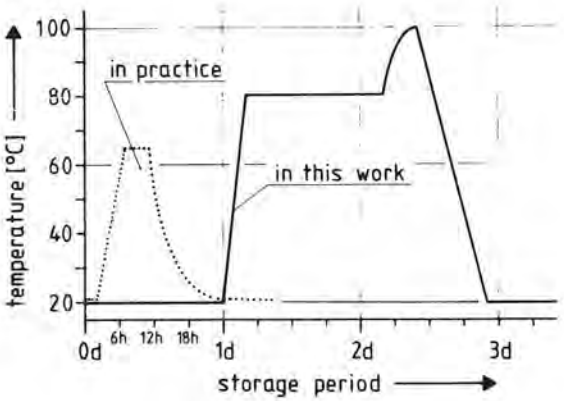

Fig. 6 Heat treatment programmes in practice and in this work

PZ 55. The cement was partly or totally substituted by a Portland cement type 45 HS (high sulphate resistent), by granulated blast furnace slag and by puzzolanas (Bavarian trass and fly ash). The sulphate content of the blended cements was kept at the same value as the type 55 Portland cement. The heat treatment was carried out as shown in Fig. 6 after 1 d, after 1 a or as a renewed treatment on mortars that had already been heat treated. Measurements of weights, lengths, resonance frequencies and strengths were carried out. X-ray diagrams were prepared from enriched cement stone from the mortars.

Results

The results of the investigations on the influence of the period of heat treatment and of the temperature in Fig. 7 show that expansions with the Portland cement type 55 are measured after curing at temperatures

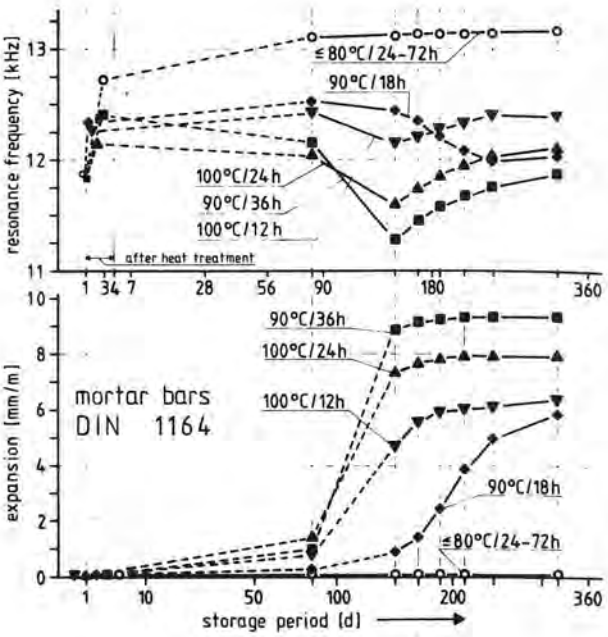

Fig. 7 Influence of heat treatment on cement mortar with type 55 Portland cement

>80°C. The early expansion is increased by increased curing periods and temperatures. After an 11 months' curing period at 20°C the expansions amount to from 6 to 9 mm/m. Analogous to the expansions a lowering of the resonance frequencies was measured. This is a measure for the loss in strength.

The results of the investigations under use of the treatment programme from Fig. 6 are in Fig. 8 to 12.

Fig. 8 shows the behaviour of the PZ 55 at direct, subsequent and renewed heat treatment. First of all it is recognizable that expansions are accompanied by decreased resonance frequencies. A subsequent heat treatment leads to more severe expansions and more reduced resonance frequencies and a repeated heat treatment at later curing stages leads to renewed expansions accompanied by strength's loss and decrease of resonance frequencies. The more severe damaging of the specimens at delayed or repeated heat treatment is caused by the reduced elasticity of the structure at this later stage.

The results of investigations with partial or full exchange of PZ 55 by PZ 45 HS are given in Fig. 9. Expansions and loss in resonance frequencies are even increased by the replacement of 25 and 50 wt.-% of the PZ 55. Only 75 wt.-% replacement gives up to this stage of the investigation (10 months) a sharply reduced reaction. With PZ 45 HS up to now no sign of a reaction is visible. The explanation of the increased reaction, specially with 25 wt.-% replacement of the PZ 55, lies in the compensated sulphate content in the cement. That means that the relative sulphate content related to the C_3A content is higher while the reduced C_3A content is not yet effective.

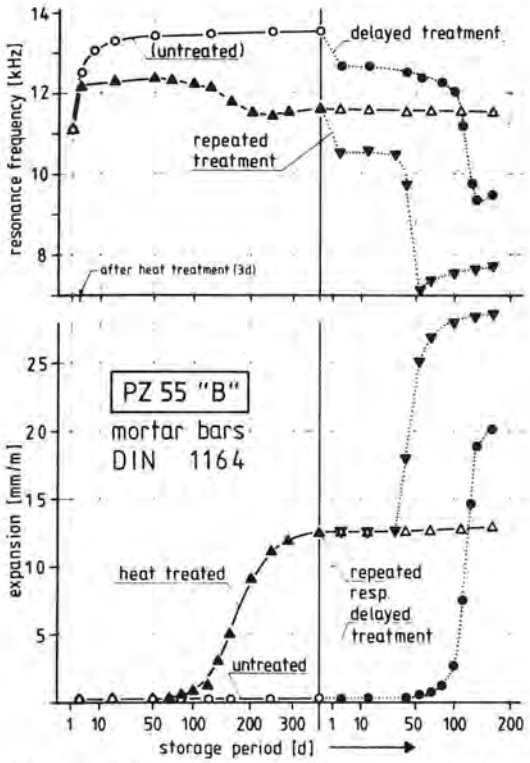

Fig. 8 Expansion and resonance frequency of mortar bars with PZ 55 at direct, delayed and repeated heat treatment

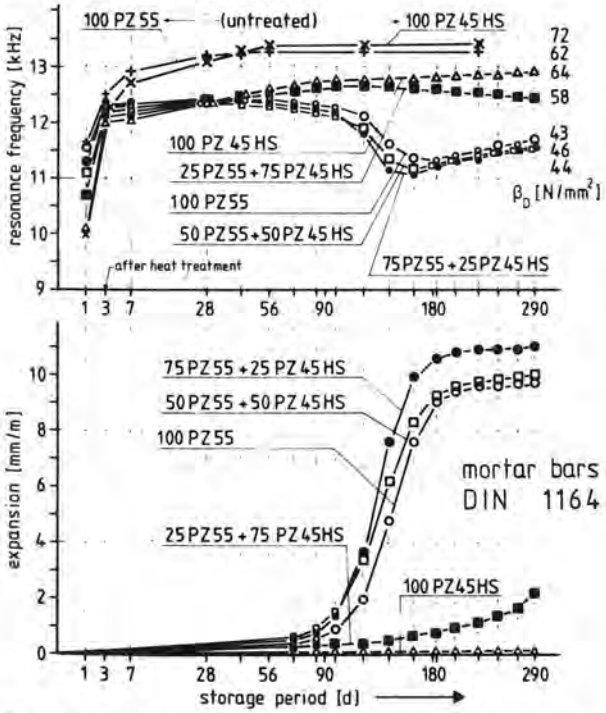

Fig. 9 Expansion, resonance frequency and final compressive strength of mortar bars with partial and full replacement of PZ 55 by PZ 45 HS

A drastically reduced or prevented reaction is achieved by the replacement of the PZ 55 by 25 or 50 wt.-% blast furnace slag (Fig. 10).

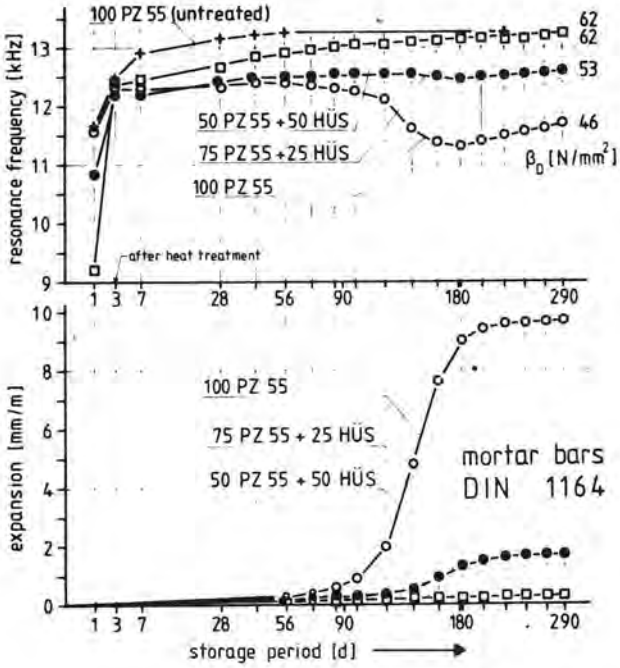

Fig. 10 Expansion, resonance frequency and final compressive strength of mortar bars with partial replacement of PZ 55 by blast furnace slag

The replacement of 15 wt.-% Portland cement by Bavarian trass causes a lowering of the intensity of the reaction accompanied by a shifting of the starting point of the visible reaction to a shorter curing period (Fig. 11). 30 wt.-% exchange of PZ 55 by the trass prevents the reaction totally.

The replacement of PZ 55 by 15 or 30 wt.-% of fly ash is a very effective provision to reduce or prevent sensitiveness against heat treatment (Fig. 12).

The expansions and the loss in strength are caused by the renewed topochemical formation of ettringite from the unstable sulphate-containing monophases. Favoured by a heat treatment, the ettringite formed in the early hydration period becomes unstable and forms monosulphate hydrate and its solid solutions with tetracalcium aluminate hydrate that are themselves unstable at lower temperatures and give rise to the renewed formation of ettringite. Fig. 13 shows in each case on the left (a) the d-values of hydrates formed at a constant curing temperature of 20°C and on the right (b) those of interim heat treated samples. If permanent 20°C curing the basic d-values at 9.7 Å are more or less present at all states of the curing period. This is one of the main interferences of ettringite. - Contrary to this, directly after the heat treatment at a total curing period of three days this interference of the ettringite is not present. With increasing additional curing at 20°C

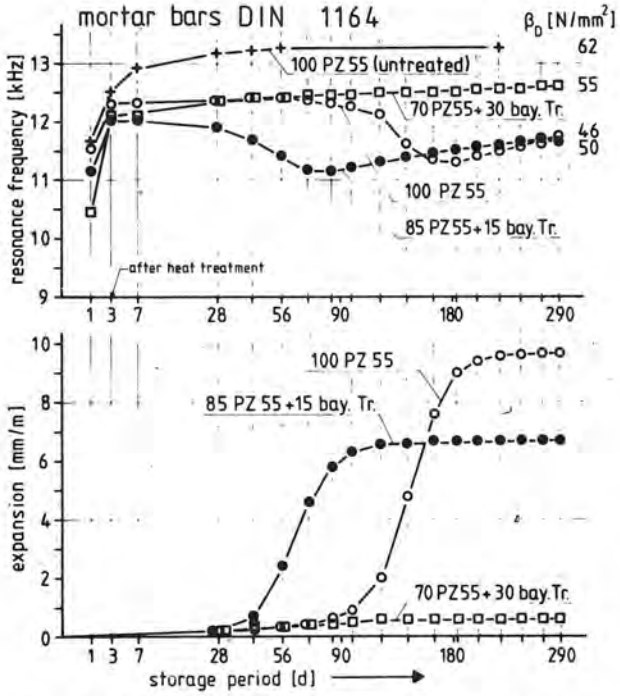

Fig. 11 Expansion, resonance frequency and final compressive strength of mortar bars with partial replacement of PZ 55 by Bavarian trass

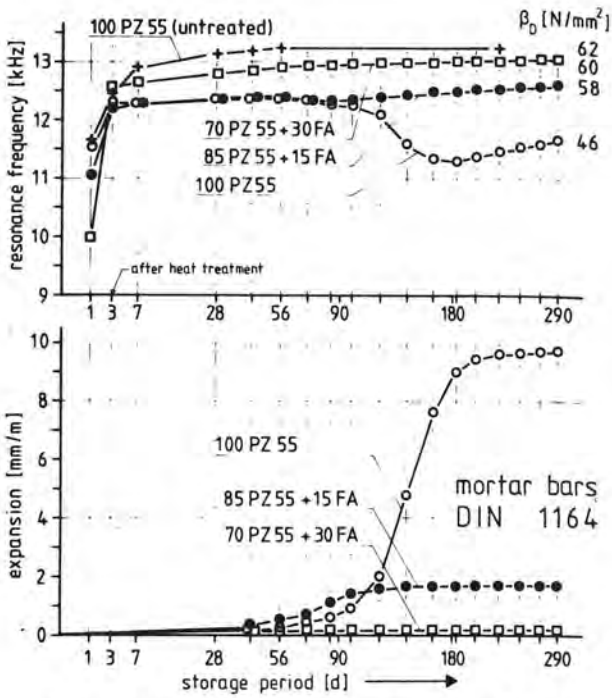

Fig. 12 Expansion, resonance frequency and final compressive strength of mortar bars with partial replacement of PZ 55 by fly ash

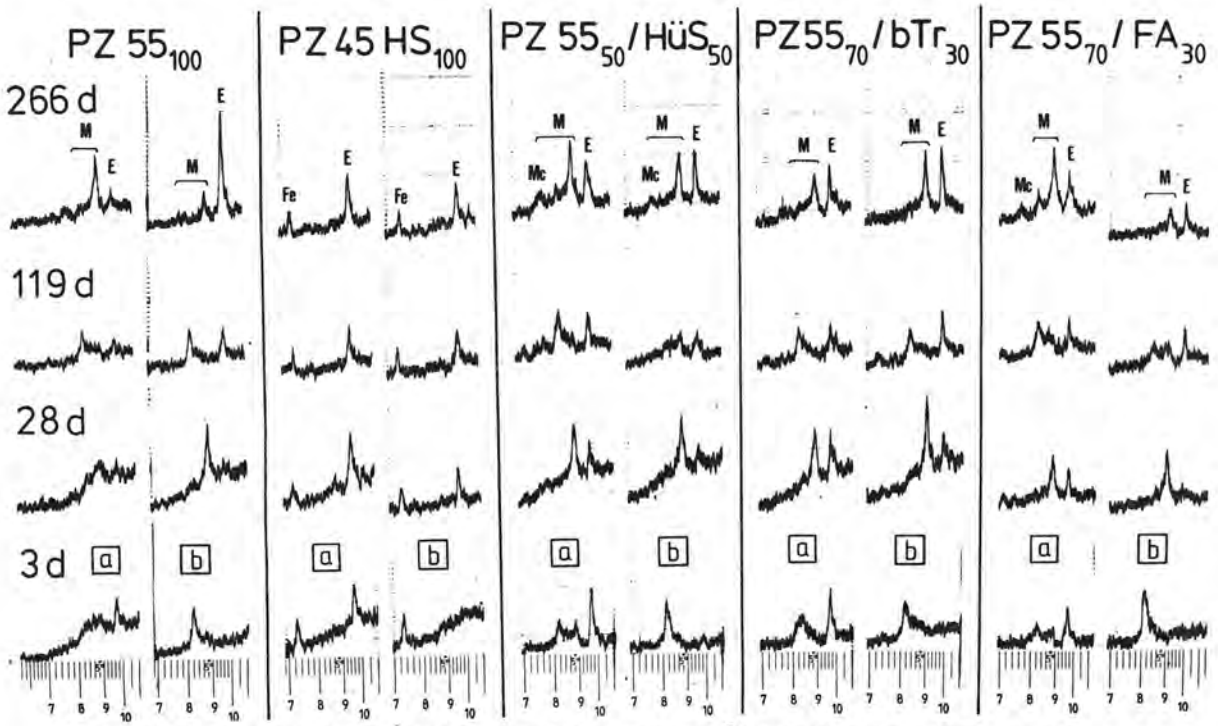

Fig. 13 X-ray diagrams of samples (a) constantly cured at 20°C and (b) interim heat treated. Mortar bars DIN 1164, abbr. accord. to Fig. 4 and 5, Fe = C_2 (A,F)
HüS = granulated blast furnace slag, bTr = Bavarian trass, FA = fly ash

this ettringite interference becomes visible and grows with curing time.

CONCLUSION

The dehydration of ettringite is a diffusion-controlled process which corresponds well with the model of the structure (8). The dehydrated product has the same habitus as the formed ettringite with a very open structure sensitive to carbonization. The volume loss of carbonated ettringite amounts to 46 % and a corresponding decrease of strength.

Ettringite is a very important cement hydration product. It is formed mainly topochemically with the added calcium sulphates and serves the required workability of cement mortars and concretes. This first or early ettringite formation is harmless as long as it is finished in the plastic state of the mortar or concrete. Elongation of ettringite formation period leads to lowering of the early strength accompanied by expansion (12).

The new investigations on pure systems and with plain and blended Portland cement show that ettringite and carboaluminate hydrate are the stable phases at room and lower temperatures and monosulphate hydrate is the stable phase at elevated temperatures. In consequence an interim direct, delayed or repeated, wanted or unwanted heat treatment of cement pastes, mortars or concretes can cause damage by expansion, cracking and decreased strength. Calcium carbonates can increase the damage. Portland cement with limited or without C_3A or Portland cements blended with granulated blast furnace slags or suitable puzzolanas in appropriate amounts reduce or even prevent damage. - On the other hand, reduction or prevention of damage should not be regarded as the sole task. One should look ahead making use of the knowledge of the reactions of the calcium aluminate sulphate hydrates and related compounds.

ACKNOWLEDGEMENT

We are grateful to W. Boenicke and D. Ganser for preparation and measurement on mortar bars and to the Deutsche Akademische Austauschdienst and to the Deutsche Forschungsgemeinschaft in Bonn for the financial support.

REFERENCES

1. - JÄGER, P., LUDWIG, U. and SCHWIETE, H.E. (1964), "Al_2O_3-Untersuchungen im System $3CaO-CaSO_4-CaO-H_2O$", Zement-Kalk-Gips, 17, 229-236.

   - JÄGER, P. (1966), Dissertation, RWTH Aachen.

2. - LOCHER, F.W., RICHARTZ, W. and SPRUNG, S. (1977), "Studies on the behaviour of C_3A in the early stages of cement hydration", Summary of Contributions to a Seminar at the University of Technology, Eindhoven 13.-14. April 1977 Cembureau.

3. - LUDWIG, U. (1968), "Über die Einflußnahme verschiedener Sulfate auf das Erstarren und Erhärten von Zementen, Zement-Kalk-Gips, 21, 81-90, 109-120 u. 175-180, Translation Nr. 143 by Cement and Concrete Ass., 52, 1971, Grosvenor Gardens London SW1.

4. - LUDWIG, U. (1978), "50 Jahre Institut für Gesteinshüttenkunde - 26 Jahre Lehre und Forschung auf dem Gebiet der Bindemittel" Tonind.Ztg., 102, 272-284.

5. - NIEL, E. and SCHWIETE, H.E. (1964), "Untersuchungen über die Reaktionen im System Klinker-Sulfat-Wasser in den ersten Minuten nach der Wasserzugabe, Forschungsbericht des Landes NRW Nr. 1392.

6. - JONES, F.E. (1944), "The quaternary system $CaO-Al_2O_3-CaSO_4-H_2O$ at 25°C", J. phys. Chem., 48, 311-356.

7. - D'ANS, J. EICK, H. (1953), "Das System $CaO-Al_2O_3-CaSO_4-H_2O$ bei 20°C", Zement-Kalk-Gips, 6, 302-311.

8. - PUNZET, M. und LUDWIG, U. (1974), "Über die chemische Stabilität des Ettringit", Tonind.-Ztg., 98, 181-187

   - PUNZET, M. (1973), "Chemische und thermogravimetrische Stabilitätsuntersuchungen an Calciumaluminathydraten", Dissertation, RWTH Aachen.

9. - REYNEN, P., persönliche Mitteilung

10. - GHORAB, H.Y. (1979), "Thermische und chemische Stabilität der Calciumaluminatsulfathydrate" Dissertation, RWTH Aachen.

11. - MOORE, A.E. and TAYLOR H.F.W. (1970), "Crystal structure of ettringite" (1970), Acta Cryst., 26, 386-393.

12. - MESKENDAHL, T. (1979), "Hydratationsverlauf von Tricalciumaluminat in Gegenwart von Calciumsulfat und Kalk bei Raumtemperatur", Diplomarbeit Institut für Gesteinshüttenkunde, RWTH Aachen.

13. - ALBECK, J., LUDWIG, U., SCHWIETE, H.E. (1969), "Bindung von Calciumchlorid und Calciumsulfat bei der Hydratation der aluminatisch-ferritischen Klinkerbestandteile, Zement-Kalk-Gips, 29, 225-234, 4. Ibausil, Weimar, Tagungsbericht Teil 1 (1970), 369-371.

   - ALBECK, J. (1970), Dissertation RWTH Aachen.

14. - HEINZ, D. (1979), "Einfluß der Temperatur bei der Warmbehandlung von Zementpasten auf die Bildung von Calciumaluminathydraten und -sulfathydraten und die Frühfestigkeiten", Studienarbei, Institut für Gesteinshüttenkunde, RWTH Aachen.

Certaines interactions entre C_3A et C_3S lors de l'hydratation des ciments portland

Some interactions between C_3A and C_3S during cement portland hydration

B.F. COTTIN, Chef de Service, Laboratoire de Recherche Générale, Lafarge S.A. France.

RESUME : Quatre clinkers de ciment Portland industriels, de compositions très différentes, ont été broyés à 3000 cm^2/g Blaine et gypsés aux taux de 0 - 1 - 2,5 et 5 % de SO_3 à l'aide de gypse - semi hydrate - surcuit ou anhydrite naturelle. La cinétique d'hydratation des ciments obtenus a été suivie par calorimétrie isotherme.

Les spectres de calorimétrie des ciments Portland révèlent en général trois pics dont l'intensité et l'échéance montrent respectivement l'hydratation d'une partie de C_3A (modifiée par la présence de C_3S et de sulfate de calcium) - l'hydratation de C_3S (influencée par l'hydratation du C_3A : empoisonnement) - la consommation totale des ions SO_4 (dont l'échéance est liée aux deux premières réactions).

Les principales conclusions sont les suivantes :

- Le premier pic (hydratation de C_3A) est toujours diminué par le gypsage. Mais il ne parait pas possible de dégager une loi générale entre cette diminution et la nature et la quantité de sulfate de calcium ajouté.

- Dans tous les cas, le gypsage optimum se situe entre 2,5 et 5 % de SO_3 ajoutés, même avec le clinker le plus riche en C_3A.

- Sauf pour ce dernier clinker, qui est aussi le plus riche en sulfates alcalins, le "désempoisonnement" de C_3S par le gypsage est caractérisé par un pic calorimétrique plus précoce et plus intense. Il est vrai que l'échéance du pic de C_3S du clinker riche en C_3A et sulfates alcalins est inhabituellement précoce.

- Le pic révèlant le moment où la consommation des ions SO_4 est complète n'existe pas lorsque le gypsage est réalisé par addition d'anhydrite naturelle. Dans les autres cas, il est le plus souvent très peu intense et étalé dans le temps.

- L'interaction silicates - aluminates - sulfates de calcium est très complexe. D'autres paramètres interviennent très probablement, comme la teneur et la nature des sels alcalins du clinker, le procédé et l'intensité de la cuisson. C'est la raison pour laquelle les quelques essais réalisés, loin de tout expliquer, soulèvent un lot de nouvelles questions auxquelles seules de nombreuses études pourraient répondre de façon satisfaisante.

SUMMARY : Four industrial Portland cement clinkers were chosen owing to their quite different compositions. They were ground at 3000 cm^2/g Blaine and calcium sulphate added with gypsum - hemi hydrate - anhydrous $CaSO_4$ or native anhydrite at 1 - 2,5 - 5 % SO_3 levels. The kinetics of hydration of these mixes were analysed by isothermal calorimetry.

Generally, the calorimetric curves obtained with Portland cement show three exothermic peaks whose intensity and time of occurence correspond respectively :

- to hydration of a part of the C_3A (modified by the presence of the C_3S and the calcium sulphate)

- to C_3S hydration (possibly "poisoned" by the C_3A)

- to total consumption of SO_4 ions (at a time depending on the two previous reactions).

Our main conclusions are as follows :

- Adding calcium sulphate results always in diminishing the intensity of the first peak (C_3A hydration). But it does not seem possible to define a general law between this decrease in heat liberation and the nature or the quantity of calcium sulphate added.

- In every case, optimum gypsum content takes place between 2,5 and 5 % of added SO_3, even with the C_3A richest clinker.

- Except for this last clinker, which is also the highest in alkaline sulphates, the "dispoisoning" of the C_3S due to calcium sulphate adding results in an earlier and more intense calorimetric peak. It is true that the C_3S peak of the C_3A and alkaline sulphates rich clinker is abnormally early.

- The total consumption SO_4 peak is not present when the added sulphate is native anhydrite. In other cases, this peak is generally very weak and broad.

- The calcium silicates - aluminates - sulphates interaction is very intricate. Probably, other parameters affect the phenomena, as alkaline salts content of the clinker, or the process and intensity of the burning. For this reason, it is not possible to explain everything by our few tests which raise new questions for many future studies to be carried out in this field.

L'influence primordiale de l'aluminate tricalcique sur les propriétés du ciment Portland n'est plus à démontrer. Ce constituant agit en particulier :

a – sur l'aptitude à la mise en place des pâtes, mortiers ou béton, qui peut devenir totalement impossible à cause de l'hydratation très rapide de C_3A. C'est le phénomène de prise rapide ou flash universellement combattu par l'addition de sulfate de calcium.

b – sur leurs cinétiques d'hydratation et de durcissement. En effet, par nature, l'aluminate tricalcique réagit extrêmement rapidement avec l'eau. Ces réactions se déroulent avec un passage plus ou moins important d'alumine en solution, selon la composition globale du ciment. Or, les ions aluminiques en solution ont une forte tendance à retarder l'hydratation des silicates de calcium, par empoisonnement de leur surface.

c – sur leurs propriétés physiques et chimiques. La teneur en C_3A du ciment Portland a des répercussions importantes sur les variations dimensionnelles (retrait hygrométrique ou gonflement sous eau) sur la tenue aux solutions agressives ...

Les essais, dont nous donnons les résultats et qui ne représentent qu'une petite contribution à la connaissance de ces phénomènes, avaient pour but d'étudier les deux premiers points a et b, c'est-à-dire les cinétiques de réaction à courte échéance. En particulier, nous désirions voir comment interviennent sur ces cinétiques les variations de compositions des ciments dues à des provenances différentes de clinkers industriels et à des "sulfatages" différents (taux d'addition de sulfate de calcium et nature de ce sulfate).

PARAMETRES CHOISIS

Nous avons choisi quatre clinkers de compositions aussi différentes que possible :

Clinker A : riche en C_3S et en chaux libre, pauvre en alcalins solubles et en SO_3

Clinker B : à forte teneur en C_3A et sulfates alcalins. Il y a un net excédent de SO_3 par rapport aux alcalins solubles.

Clinker C : sans C_3A et riche en aluminoferrites. Les teneurs en SO_3 et alcalins solubles sont relativement faibles.

Clinker D : d'analyse moyenne. La teneur en SO_3 est insuffisante pour combiner tous les alcalins solubles.

Le tableau n° I donne les analyses chimiques et les compositions potentielles, calculées selon Bogue, de ces clinkers. Les sulfates alcalins ont été calculés d'après les teneurs en alcalins solubles, et le $CaSO_4$ d'après le taux de SO_3 résiduel.

Nous n'avons pas retenu la finesse du clinker comme paramètre, car il est trop évident que la consommation du sulfate de calcium est accélérée par l'augmentation de la surface de réaction. Nous avons adopté la finesse de 3000 Blaine obtenue au broyeur à boulets de laboratoire de capacité 5 kg.

Les taux de SO_3 ajoutés par l'apport de sulfate de calcium ont été de 0 – 1 – 2,5 et 5 % pour chaque clinker. Les quatre sulfates de calcium utilisés furent le gypse pur – le semi hydrate pur – le surcuit pur – une anhydrite naturelle à 96 % de $CaSO_4$.

Les mélanges clinkers – sulfate de calcium ont été très soigneusement réalisés au tamis. Leurs cinétiques d'hydratation ont été suivies en continu jusqu'à 24 heures à l'aide d'un calorimètre isotherme du type CERILH, à la température de 25°C. La quantité d'eau distillée injectée sur le ciment au temps 0 correspondait à un E/C de 0,5.

	Clinker A	Clinker B	Clinker C	Clinker D
SiO_2	24,05	21,05	22,70	22,75
Al_2O_3	2,95	6,25	3,55	4,65
Fe_2O_3	0,25	2,15	4,65	3,25
CaO	71,05	65,15	67,25	67,00
MgO	0,50	2,10	0,65	0,90
SO_3	0,20	1,70	0,35	0,20
K_2O total	0,19	1,00	0,68	0,60
Na_2O total	0,11	0,10	0,05	0,33
CaO libre	4,35	1,00	1,90	1,10
K_2O soluble	0,08	0,89	0,33	0,30
Na_2O soluble	0,02	0,07	0,02	0,07
C_3S	66,8	59,2	61,6	60,2
C_2S	18,5	15,8	18,8	19,7
C_3A	7,5	13,0	1,5	6,9
C_4AF	0,7	6,5	14,2	10,0
Sulfates alcalins	0,20	1,80	0,65	0,45
$CaSO_4$	0,15	1,45	0,10	0

TABLEAU I : Analyse et composition des clinkers

Après les 24 heures d'hydratation, les pâtes hydratées étaient examinées par diffraction X qualitative, et leur eau liée déterminée par perte au feu après lavage acétone-éther.

RESULTATS OBTENUS

Nous ne donnerons que les résultats qui nous paraissent les plus intéressants.

Aspect habituel d'un thermogramme de ciment Portland

Les courbes calorimétriques habituellement obtenues avec les ciments Portland comportent toujours (Graphique 1)

– un premier pic de dégagement de chaleur rapide et limité dans le temps. Son interprétation est complexe car il comprend les chaleurs de mouillage et de dissolution. Mais celles-ci doivent être relativement faibles puisque, pour certains clinkers ou ciments, le premier pic est peu important, alors qu'il n'y a pas de raison que les chaleurs de mouillage et de dissolution soient très différentes d'un échantillon à l'autre. Les variations relatives de ce premier pic sont donc en grande partie dues à une réaction d'hydratation pratiquement instantanée et de courte durée.

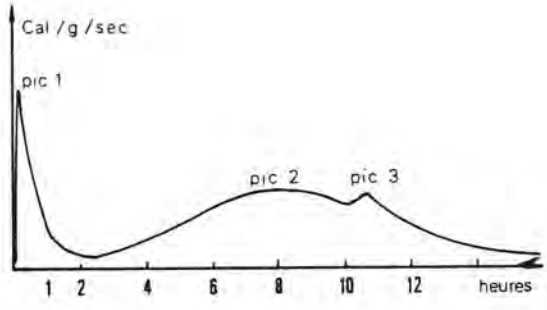

FIG. 1 – Aspect classique d'un thermogramme de ciment Portland

– une période relativement athermique, souvent appelée période dormante.

– un second pic exothermique correspondant à un dégagement de chaleur beaucoup plus important que celui du premier pic, mais très étalé dans le temps. Ce pic est attribué à l'hydra-

tation proprement dite, en particulier des silicates de calcium.

- parfois un troisième pic, toujours peu intense, dont l'échéance est variable, c'est-à-dire que le maximum de ce pic peut se situer avant ou après celui du deuxième pic. Ce pic est attribué aux phénomènes qui se déroulent lorsque le sulfate de calcium a été complètement consommé pour faire l'ettringite. Ces phénomènes sont attribuables, soit à une recristallisation de l'ettringite déjà formée qui ne se trouve plus en équilibre avec la solution appauvrie en SO_4^{--}, soit à la reprise de l'hydratation de C_3A de nouveau disponible par la modification de structure de la couche protectrice d'ettringite, soit à la transformation de l'ettringite en monosulfoaluminate de calcium hydraté.

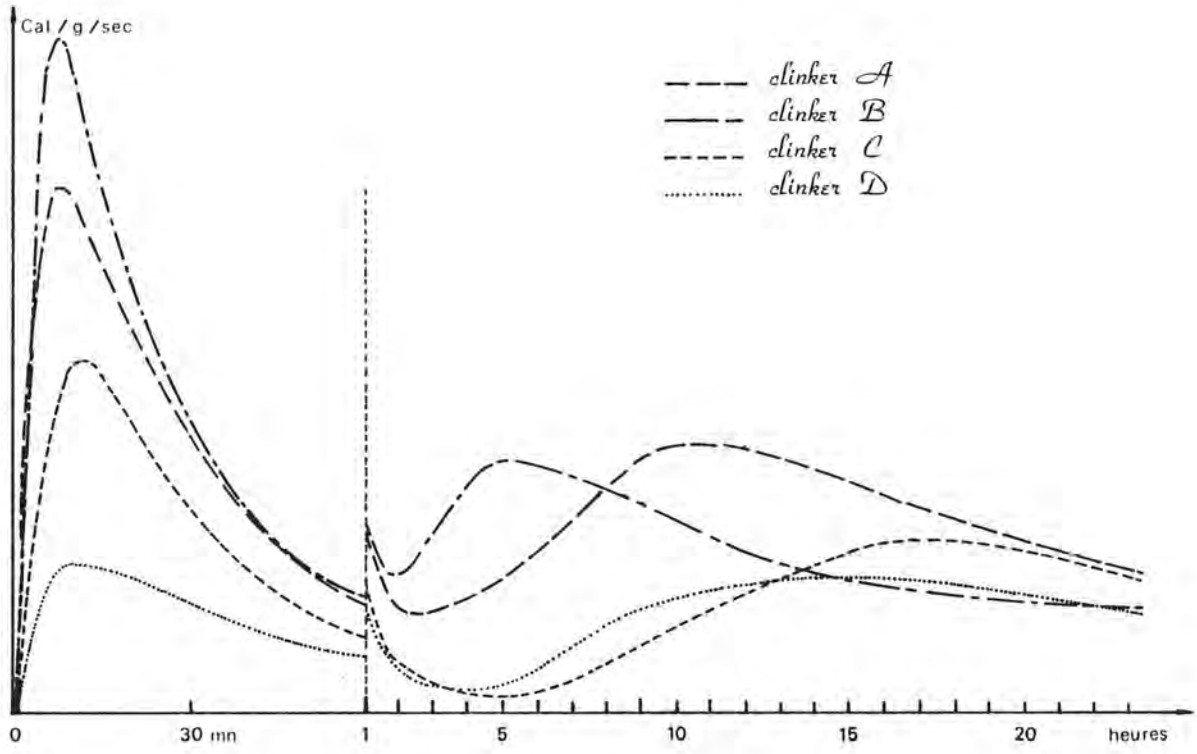

FIG. 2 - Clinkers témoins

Résultats obtenus sur clinkers non sulfatés

Les courbes sont tout à fait conformes au modèle classique. Elles sont reportées sur le graphique 2 (dans lequel les échelles sont modifiées après la première heure : multipliées par 2 pour les dégagements de chaleur, divisées par 10 pour les temps).

L'intensité du premier pic varie beaucoup d'un clinker à l'autre. Ces variations peuvent être attribuées en grande partie à l'hydratation de C_3A, comme le montre le graphique 3 a : hauteur du premier pic en fonction de la teneur en C_3A.

L'intensité et l'échéance du maximum du second pic sont elles aussi très variables. Mais il paraît a priori difficile de définir avec certitude une loi reliant ces valeurs aux divers paramètres chimiques mesurés. Nous avions pu prouver, par des essais antérieurs faisant appel à des techniques tout à fait différentes, que, en absence de sulfate, le C_3A laisse passer en solution suffisamment d'alumine pour empoisonner le C_3S, c'est-à-dire le retarder. Nous avions aussi montré que le sulfate de calcium (ou de potassium) supprime le passage de l'alumine en solution, probablement par formation d'ettringite protectrice autour de C_3A. Si nous appliquons ces théories aux quatre clinkers étudiés ici,

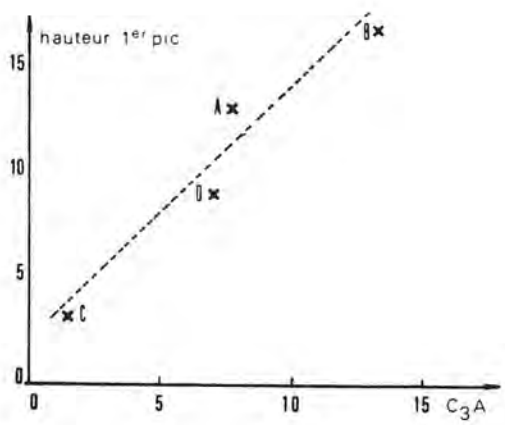

FIG. 3 a - Relation entre la hauteur du 1er pic de calorimétrie et la teneur en C_3A des clinkers non gypsés

nous devrions trouver une relation entre l'échéance du maximum du second pic et la teneur en alumine du clinker corrigée par la teneur en SO_3. Le graphique 3 b montre que cette relation parait convenable pour $A - 3\,SO_3$ (sans que l'on puisse affirmer qu'il y ait une relation entre ce coefficient 3 de SO_3 et le rapport $A/SO_3 = 3$ dans la formule de l'ettringite).

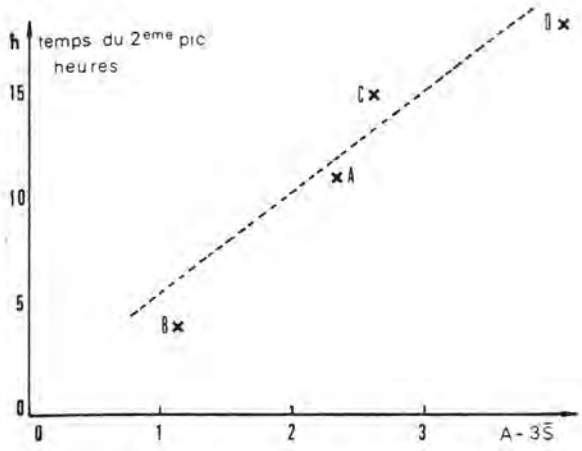

FIG. 3 b - Temps du 2ème pic de calorimétrie en fonction de $C_3A - 3\,SO_3$ des clinkers non gypsés

Les autres constatations que nous avons pu relever sur l'étude de ces clinkers non sulfatés sont les suivantes :

- Les quantités d'eau liée à 24 heures sont aussi très variables d'un clinker à l'autre (20,5 % pour le clinker A - 9,8 % pour le clinker C) et proportionnelles à l'intensité du maximum du second pic de calorimétrie.

- Il est plus difficile de se faire une opinion générale sur l'hydratation des aluminates. Comme il est normal, c'est pour le clinker B que l'on a observé la plus grande quantité d'ettringite après 24 h. d'hydratation. Le clinker A révèle dans les mêmes conditions un très large pic de diffraction X au niveau de C_4AH_n.

Influence du "sulfatage" sur le premier pic de calorimétrie

Le graphique 4 fournit tous les résultats obtenus avec les quatre clinkers et les divers types de "sulfatage".

Le cas du clinker A paraît le plus simple à expliquer : dans tous les cas, la hauteur du premier pic de calorimétrie est diminuée, les extrêmes étant obtenus avec les additions de semi hydrate (le plus soluble et le plus actif) et d'anhydrite naturelle (la moins active car moins rapidement soluble). La proportion d'addition de sulfate ne joue pas significativement. A noter qu'avec les additions de 2,5 et 5 % de semi hydrate, on observe nettement le pic d'hydratation en gypse vers 2 h.

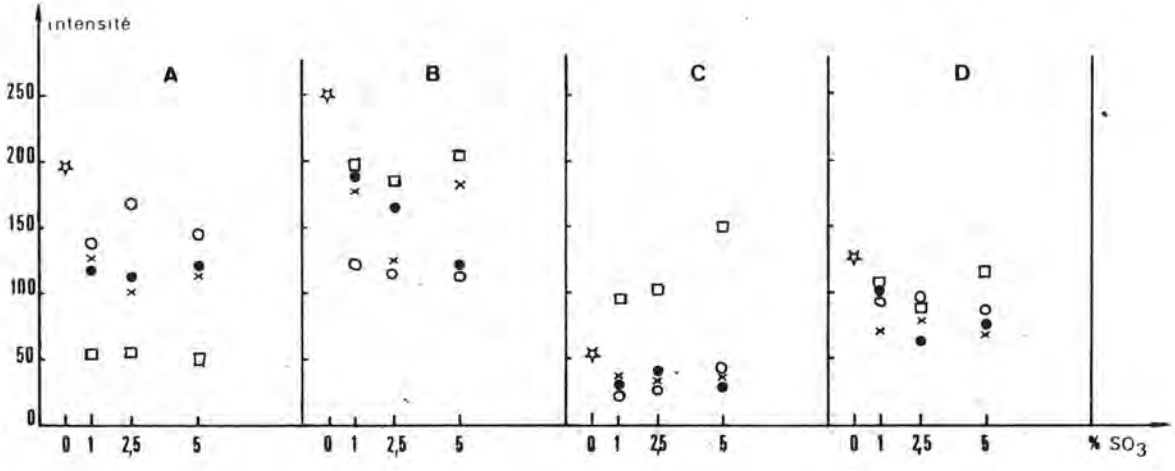

FIG. 4 - Intensité du 1er pic de calorimétrie en fonction du taux de SO_3 ajouté

☆ témoin non sulfaté, ● gypse, □ semi hydrate, × surcuit, ○ anhydrite

Le cas du clinker B est plus complexe à analyser : le gypse diminue la hauteur du premier pic proportionnellement à son addition, les résultats obtenus avec le surcuit sont assez dispersés, par contre c'est l'anhydrite naturelle qui révèle l'action la plus importante, indépendante du pourcentage ajouté. Ce dernier résultat est surprenant compte tenu des caractéristiques de solubilité de ce sulfate de calcium. Les phénomènes sont faussés avec l'addition du semi hydrate dont l'hydratation en gypse est accélérée par la présence du sulfate de potassium dans le clinker : le pic correspondant s'ajoute au premier pic d'hydratation du ciment, et augmente sa hauteur.

Le clinker C non "sulfaté" donne un premier pic de faible intensité. Les additions de sulfate de calcium le laisse à un niveau très bas, sauf lorsqu'il s'agit de semi hydrate à cause de son hydratation rapide en gypse.

Le premier pic du clinker D est relativement peu modifié par toutes les additions de sulfate de calcium réalisées. L'hydratation du semi hydrate est moins accélérée qu'avec les clinkers B et C, de sorte que le pic correspondant n'apparaît que vers 50 minutes, et n'influence pas le premier pic de calorimétrie.

Influence du "sulfatage" sur le second pic de calorimétrie

Le graphique 5 donne l'échéance du maximum du pic dit "des silicates" pour tous les essais réalisés.

Avec le clinker A, ce temps est toujours diminué de 2 à 3 h.,

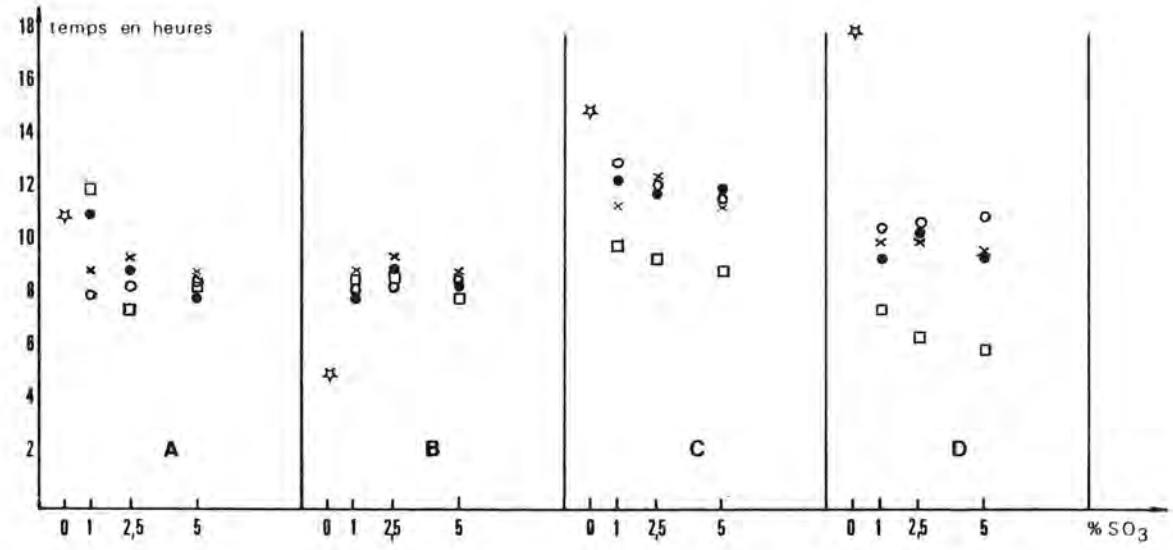

FIG. 5 – Temps du maximum en fonction du taux de SO_3 ajouté

☆ témoin non sulfaté, ● gypse, □ semi hydrate, × surcuit, ○ anhydrite

sauf avec la plus faible addition de gypse et de semi hydrate. On peut noter aussi que par rapport au témoin non sulfaté, la hauteur de ce pic est inchangée avec toutes les additions à 1 % de SO_3, mais augmentée de 40 à 50 % avec les additions à 2,5 et 5 % de SO_3.

Le clinker B se comporte de façon tout à fait différente : alors que le témoin non sulfaté présente un pic d'hydratation des silicates anormalement précoce à 5 heures, tous les essais de "sulfatage" conduisent à rallonger de 3 à 4 heures l'échéance de ce maximum. L'intensité de ce pic reste du même ordre de grandeur.

Les comportements des clinkers C et D sont analogues : le "sulfatage" accélère toujours le pic des silicates, l'action du semi hydrate étant plus importante que celle des autres sulfates de calcium. La hauteur de ce pic est toujours pratiquement doublée par l'addition du sulfate de calcium.

D'une manière générale, on retrouve bien le "désempoisonnement" des silicates lorsque le sulfate de calcium permet de précipiter rapidement l'alumine. Celui-ci se traduit par une accélération du second pic, d'autant plus sensible que le clinker témoin était plus lent, et plus importante avec l'addition de semi hydrate. Une exception cependant à signaler, et qui concerne le clinker B dont le témoin non adjuvanté présente un pic des silicates anormalement rapide, dû peut-être à la grande quantité de sulfates alcalins contenus dans ce produit. L'addition des sulfates de calcium ramène un pic de silicate dont la cinétique est analogue à celles des autres clinkers "sulfatés".

Influence sur le "sulfatage optimum"

La notion de "sulfatage" optimum résulte d'un compromis entre deux phénomènes :

– L'addition de sulfate de calcium permet une hydratation des silicates non entravée par l'alumine en solution, et conduit à la formation d'ettringite très volumineuse, favorable aux résistances. Ces deux actions bénéfiques sont évidemment d'autant plus importantes que le taux d'addition de sulfate est plus grand, jusqu'à une proportion limite à partir de laquelle se produit :

– Un blocage des réactions d'hydratation des aluminates et des sulfates, d'autant plus important que le taux d'addition de sulfate dépasse cette limite. Il reste alors, après le début de durcissement, du sulfate de calcium libre qui finit par s'hydrater en donnant des sulfoaluminates expansifs.

Cette limite, qui correspond aux meilleures résistances initiales et aux variations de dimensions ultérieures minimales des éprouvettes, est appelée "sulfatage optimum". Elle correspond, en première approximation, à un taux d'addition de sulfate de calcium tel que ce sulfate soit complètement consommé en sulfoaluminates de calcium hydratés en moins de 24 heures.

Il paraît logique de penser que le "sulfatage optimum" dépende de la réactivité du sulfate ajouté et de celle du clinker (au moins ses phases alumineuses). Nous n'avons pas la prétention de déterminer le niveau de "sulfatage optimum" à partir de trois essais seulement, mais nous avons été surpris de constater, par diffraction X, que dans tous les cas le "sulfatage optimum" se situe entre 2,5 et 5 % de SO_3 ajouté. En effet, après 24 heures d'hydratation, nous ne trouvons, dans les pâtes hydratées, du sulfate de calcium que pour l'addition correspondant à 5 % de SO_3 : sous forme de gypse avec le gypse et le semi hydrate, sous forme d'anhydrite avec le surcuit et l'anhydrite naturelle.

Par ailleurs, comme nous l'avons expliqué dans la description générale des courbes calorimétriques obtenues sur les ciments, le moment où tout le sulfate de calcium est consommé se traduit parfois par un pic exothermique. Celui-ci n'a évidemment jamais été visible sur nos essais à 5 % de SO_3 ajoutés, puisque le sulfate n'était pas entièrement consommé à 24 heures, fin de nos enregistrements.

Mais dans les autres cas, ils ont été relativement peu souvent mis en évidence, comme le montre le tableau 2 : Ce pic "sulfates" n'a jamais été observé avec l'anhydrite naturelle, ni avec le clinker C. C'est avec le clinker A qu'il a été le plus souvent rencontré. Il paraît difficile de tirer des conclusions ou des tentatives d'explication de ces quelques résultats.

Sulfate ajouté	% SO_3	Clinker A	Clinker B	Clinker C	Clinker D
Gypse	1	très net 3 h	large 10 h	invisible	invisible
	2,5	net 11 h	faible 14 h	invisible	invisible
Semi hydrate	1	très fort 6 h	faible 9 h	invisible	invisible
	2,5	invisible	faible 13 h	invisible	invisible
Surcuit	1	net 7 h	invisible	invisible	net 8 h
	2,5	net 10 h	invisible	invisible	invisible
Anhydrite	1	invisible	invisible	invisible	invisible
	2,5	invisible	invisible	invisible	invisible

TABLEAU 2

CONCLUSIONS

Les comportements des quatre clinkers étudiés vis-à-vis du "sulfatage" sont très différenciés, et le nombre d'essais réalisés est trop restreint pour pouvoir tirer des lois générales sur les interactions entre constitution du clinker - niveau de "sulfatage" - nature du sulfate de calcium. Ceci est d'autant plus vrai que nous ne connaissons pas tous les paramètres susceptibles d'agir.

Les principales conclusions que l'on peut tirer de ces essais sont les suivantes :

- Le premier pic d'hydratation est toujours diminué, mais on ne peut tirer de loi générale reliant cette diminution d'intensité à la nature ni à la quantité de sulfate ajouté.

- Le semi hydrate est très actif pour régulariser la prise du C_3A. Mais son hydratation en gypse peut occasionner des raidissements, ou fausse prise sulfate. Il apparait, d'après nos essais, que si le semi hydrate est pur (exempt de gypse) et si le clinker est pauvre en composés susceptibles d'activer la germination du gypse (sulfate alcalins par exemple), la fausse prise sulfate n'apparaîtra qu'à une échéance où elle ne gênera plus la mise en place.

- Nous confirmons que l'addition de sulfate de calcium empêche bien l'"empoisonnement" des silicates par l'alumine en solution. Cela se traduit par l'obtention d'un deuxième pic de calorimétrie dont l'échéance du maximum est raccourcie et ramenée à peu près au même temps de 8 à 12 heures. Cependant il existe une exception, avec le clinker B riche en sulfates alcalins, pour lequel le maximum du second pic est anormalement précoce, mais ramenée à une valeur habituelle par addition de sulfate de calcium.

- Le troisième pic d'hydratation (pic des sulfates) apparait rarement. Il est plus visible avec le ciment A, le plus pauvre en sultates alcalins. Il n'est jamais mis en évidence lorsque le sulfate ajouté est l'anhydrite naturelle : nous supposons que sa lenteur relative de passage en solution ne doit pas lui permettre de s'épuiser rapidement.

- Nous avons observé par diffraction X un blocage relatif de l'hydratation des aluminates avec les plus fortes additions de sulfate, qui se traduit par une plus grande quantité d'anhydres résiduels après 24 h d'hydratation.

La complexité des phénomènes explique le fait que nous n'ayions trouvé aucune loi valable entre composition de clinker et "sulfatage" d'une part, et cinétique d'hydratation d'autre part.

Nous avons cependant été surpris par le fait que, malgré sa faible réactivité avec l'eau, l'anhydrite naturelle se comporte le plus souvent, vis-à-vis de l'hydratation des aluminates et des silicates, de la même façon que le gypse et le surcuit.

Il reste donc beaucoup à apprendre sur le gypsage du ciment Portland, surtout si l'on songe que la température, l'énergie de malaxage, les adjuvants ou additions doivent jouer un rôle non négligeable sur le déroulement des phénomènes.

Hydration of C_3A in portland cement in the presence of different forms of calcium sulfate

L'hydratation de C_3A de ciment portland en présence de diverses formes du sulfate de calcium

I. ODLER, Institut für Stein und Erden - Clausthal-Zellerfeld, R.F.A.
R. WONNEMAN

RESUME :

L'influence du sulfate de calcium, sous forme d'anhydrite, d'hémihydrate et de gypse sur l'hydratation de C_3A, constituante d'un clinker préparé en laboratoire, a été étudiée. La cinétique d'hydratation et les phases formées ont été déterminées.

ABSTRACT :

The effect of calcium sulfate in the form of anhydride, hemihydrate and gypsum on the hydration of C_3A present in a laboratory made portland clinker was studied. The kinetics of the hydration process and the phases formed were determined.

Within our work the effect of anhydrite $CaSO_4$ ($C\bar{S}$), of calcium sulfate hemihydrate $CaSO_4.1/2H_2O$ ($C\bar{S}H_{0,5}$) and of gypsum $CaSO_4.2H_2O$ ($C\bar{S}H_2$) on the hydration of tricalcium aluminate $3CaO.Al_2O_3$ (C_3A) present in a portland clinker was studied. The aim of the work has been to determine whether the rate of the hydration process and the quality of the hydration products formed is affected by the form of the sulfate employed.

Experimental

The cements studied were prepared from a laboratory burned clinker (1 h at 1350 °C) containing 68,9% CaO, 21,9% SiO_2, 5,9% Al_2O_3 and 3,3% Fe_2O (all other oxides < 0,1%). The clinker contained 15% C_3A and 5% C_2 (AF) as determined by QXRD after concentrating these phases by dissolving the calcium silicates in methanolic maleic acid. The cements tested contained each 3,0% SO_3 in form of anhydrite, hemihydrate and gypsum. For comparison a cement made from pure clinker without calcium sulfate added was studied as well. All cement were ground to a spec. surface area of 3000 ± 100 cm^2/g (Blaine). The cements were allowed to hydrate in paste form (w/s = 0,50) for different periods of time at 20 °C. The hydration process was stopped by grinding the paste with acetone, filtering the resultant suspension and washing the residue with acetone and then with ethyl ether.

The non reacted fraction of C_3A was determined by QXRD after igniting the sample for 1 hour to 600 °C by measuring the intensity of the peak d = 2,70Å. This way the C_3A content of the sample could be determined with an accuracy of about ± 0.5 g/100 g cement.

For quantitative determination of ettringite formed in the hydration of C_3A in the presence of calcium sulfate the DTA method can be employed only in pastes hydrated short time, as in the further course of hydration the endothermic peak belonging to ettringite gets overlapped by an endothermic region having its origin in the decomposition of the CSH-phase formed in the hydration of calcium silicates. Consequently in our experiments ettringite was determined by DTA only up to 30 min of hydration (Mettler 2000 apparatus, sample 10 mg, 10 °C/min, N_2 atm.). For measuring the ettringite content in pastes with longer hydration times the area or the XRD peak d = 9.75Å was determined and the obtained peak area was compared with the area of the 30 min peak for which the corresponding ettringite value has been already known on the basis of DTA determination. The non reacted fraction of calcium sulfate was determined by DTA (gypsum and and hemihydrate) or QXRD (anhidrite).

Results

Fig. 1 shows the amount of C_3A used up in the hydration process as function of hydration time. In the absence of calcium sulfate about 1,5 g C_3A/100 g cement was used up within the first 15 min of hydration; the hydrated amount stayed almost constant up to about 10 hours and started to increase again in the further course of hydration.

The three calcium sulfates affected the rate of C_3A hydration only unsignificantly; here again an initial rapid hydration was followed by a dormant period and a renewed faster hydration after several hours.

Fig. 2: Shows the ettringite content of the pastes as function of hydration time. In all three cements the ettringite content rose up to a maximum and decreased in the further course of hydration. The beginning of the decline of the ettringite content coincided with the appearance of the monosulfate peak at d = 8,92Å in the XRD diffraction pattern of the paste. The rate at which ettringite was formed was not uniform in the three cements It was slowest in the cement containing anhydrite and about equally fast in the two remaining cements. In addition to that the maximum amount of ettringite formed was lower and the beginning of monosulfate formation was delayed in the cement containing calcium sulfate in the anhydrous form. The delayed formation of ettringite and monosulfate in presence of anhydrite as compared to cements containing hemihydrate and gypsum is obvious also from Fig. 3 in which the DTA curves of the cement pastes studied determined after different hydration times are shown.

Fig. 4: Shows the content of nonreacted calcium sulfate as function of hydration time. It appears that the rate at which calcium sulfate was used up was about identical in the case of hemihydrate and gypsum and significantly slower in the case of anhydrite. It may be also noted that, in addition to reacting with C_3A, the hemihydrate was gradually converted to dihydrate; this conversion was completed within about 30 min.

Finally in Tab. I the setting of the cements studied as determined by the Vicat needle penetration test is shown. It appears that both the amount of water needed to obtain normal consistency as well as the beginning and end of setting depended on the form of calcium sulfate present in the system.

Discussion

A comparison of the hydration rates of C_3A in absence and presence of the three calcium sulfates revealed that the rate at which C_3A was used up was non altered significantly by the presence of any of the calcium sulfates in the system. This finding is contrary to the general view (1, 2,, 3, 4, 5, 6) however in line with observations of Locher and coworkers (7) who found equal C_3A hydration rates in absence and presence of gypsum.

Unlike the C_3A hydration rate, the rate of ettringite formation was found to be different in the presence of different calcium sulfate forms, this phase being formed slowliest in the presence of anhydrite and about equally fast in presence of hemihydrate and gypsum. This difference may be due to the slower dissolution rate of the former compound in water. The extended duration of ettringite formation, the slower rate of SO_3 depletion and the delayed beginning of monosulfate formation in the cement containing anhydrite were proably additional consequences of the lower dissolution rate of this calcium sulfate form.

In Fig. 5 the amount of ettringite formed v.s. amount of C_3A used up in the hydration is plotted. The straight line in the figure gives the amount of ettringite formed if the amount of C_3A shown on the abscissa is quantitatively converted to this phase. It can be seen from the figure that in the cements

containing hemihydrate or gypsum a significant fraction of C_3A used up in the hydration process formed ettringite. On the other hand less than one third of C_3A was converted to this phase in the cement containing the same amount of SO_3 in form of anhydrite. It has to be assumed, that in the latter case, most of the C_3A hydrated to calcium aluminate hydrate due to an insufficient dissolution rate of this form of calcium sulfate.

From a comparison of the setting time determination data with the results of quantitative phase determination it appears that the setting time has been not only a function of the amount of C_3A hydrated and that other factors were involved as well. The flash setting of pure clinker was obviously not a consequence of excessive C_3A hydration as about similar amounts of C_3A hydrated in the three cements containing calcium sulfate did not cause setting. The reason for the instant setting of this cement is not obvious; it is conceivable that this phenomenon may be related to an altered crystall morphology of the hydration products formed under these conditions as suggested by (7). In the case of the cement containing hemihydrate one has to assume that its relatively fast setting is related to the conversion of hemihydrate to gypsum rather than to reactions involving C_3A. The shorter setting time and higher water requirements of the cement containing anhydrite as compared to the one with gypsum are probably due to the conversion of a significant part of C_3A to calcium aluminate hydrate rather than to ettringite in the hydration of the former cement.

Conclusions

1. In the hydration of finely ground portland cement clinker in absence of calcium sulfate an intensive hydration of C_3A takes place right after contact with water; the fast initial reaction is succeeded by a dormant period of rather slow hydration and a renewed fast hydration after several hours. An addition of SO_3 in form of anhydrite, hemihydrate or gypsum does not alter the kinetics of C_3A hydration significantly.

2. In the presence of any of the calcium sulfates ettringite is formed as the first product of C_3A hydration to be converted later on to monosulfate. The rate of ettringite formation is significantly reduced and the beginning of the conversion to momosulfate is delayed if anhydrite, rather than hemihydrate or gypsum is employed as SO_3 source.

3. The flash setting of portland cement in absence of calcium sulfate does not appear to be due to excessive C_3A hydration as equal amounts of C_3A hydrated in presence of calcium sulfates do not produce cement setting.

References

1. F.M. Lea: The chemistry of cement and concrete 3rd.ed. Chemical Publishing Co. New York 1971

2. F.W. Locher and W. Richartz: Study of the hydration mechanism of cement (principal paper) VIth.Int.congr. on chemistry of cement. Moscow 1974

3. Reaction of aluminates during the setting of cements (Summaries of contributions to a Seminar at the University of Technology Eindhoven) Cembureau Paris 1977

4. J. Skalny and M. Tadros: Retardation of tricalcium aluminate hydration by sulfates. J.Amer.Ceram.Soc. 60, 174-175 (1977)

5. J. Skalny, I. Jawed and H.F.W. Taylor: Studies on hydration of cement - recent developments. World Cement Technology 9, 181-195 (1978)

6. J.P. Bernard: Hardening of portland cement pastes. Cements Betons Platres Chands 715, 359-366 (1978) (in French)

7. F.W. Locher, W. Richartz and S. Sprung: Setting of cement. Part. I. Reaction and development of structure. Zement - Kalk - Gips 29, 435-442 (1976) (in German)

Tab. 1: Vicat needle penetration test data

Cement	water requirements %	set time (min) beg.	end
no calcium sulfate	-	< 1	-
anhydrite (3% SO_3)	30	115	180
hemihydrate (3% SO_3)	25	15	20
gypsum (3% SO_3)	25	180	220

Captions of the Figures

Fig. 1: Amount of C_3A hydrated as function of hydration time

Fig. 2: Content of ettringite in hydrated cement pastes as function of time

Fig. 3: DTA curves of cement pastes after different hydration times

Fig. 4: Amount of non reacted calcium sulfate (% of SO_3) as function of hydration time

Fig. 5: Amount of ettringite formed v.s. C_3A used up in the hydration process

The figures are on the following page

/...

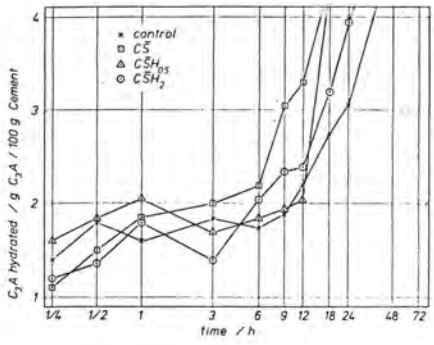

Fig. 1

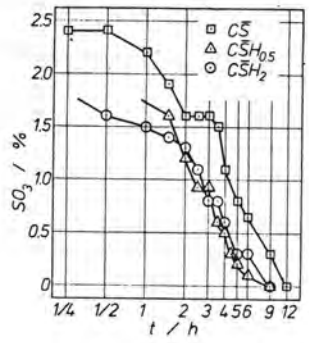

Fig. 4

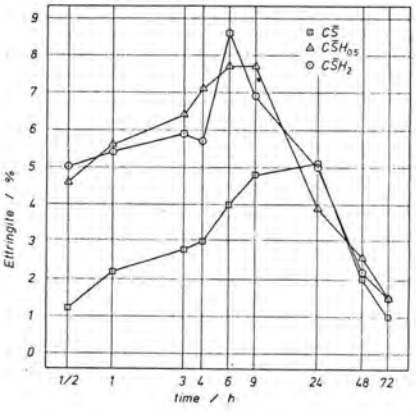

Fig. 2

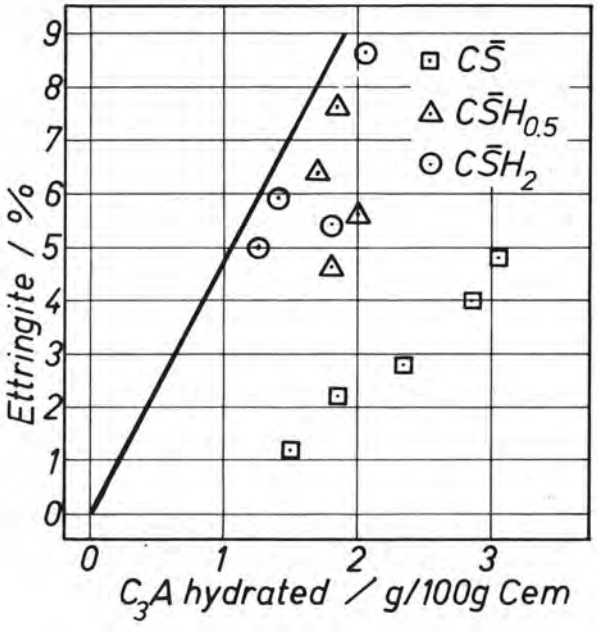

Fig. 5

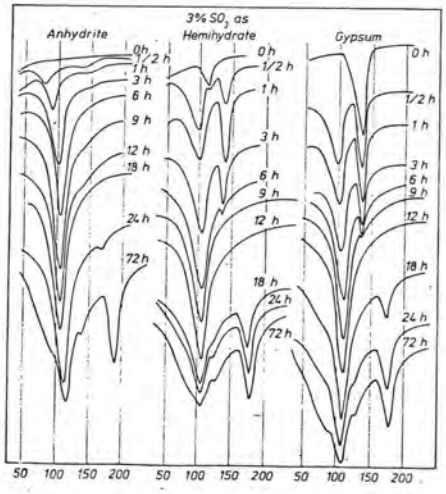

Fig. 3

The influence of the content and distribution of Al_2O_3 on the hydration properties of portland cement

Influence de la teneur et de la répartition de l'Al_2O_3 sur les propriétés d'hydratation du ciment portland

E.S. JONS, F.L. Smidth et C° A/S, Vigerslev Alle 77, et
B. OSBAECK, DK-2500 Valby Copenhagen, Denmark.

RESUME : L'évolution des résistances des ciments Portland est influencée par leur teneur en C_3A. La cause de cette influence n'est cependant pas entièrement établie; elle peut être due à des modifications tant de la composition des hydrates constitués que de leur quantité. La quantité d'hydrates peut être affectée tant par la propre hydratation du C_3A que par les modifications de l'hydratation du C_3S provoquées par le C_3A.

Pour connaître l'importance relative de ces divers effets possibles, plusieurs clinkers cuits en laboratoire ont été examinés. Ces clinkers ont été broyés avec des proportions variables de SO_3. L'évolution des résistances des mortiers et l'allure de l'hydratation des pâtes ont été suivies en recourant à la diffractométrie quantitative par Rayons X.

Il ressort des résultats obtenus que le C_3A de tous les ciments examinés contribue positivement, de lui-même, aux résistances des ciments. En même temps, il semble que le C_3A exerce une influence négative sur le taux d'hydratation du C_3S. Cet effet est dominant pour une forte teneur en C_3A et en fin de prise. Dans cet article sont expliquées les causes possibles des effets ainsi observés.

SUMMARY: The strength development of Portland cements is influenced by their contents of C_3A. The cause of this influence, however, is still controversial and can be due to changes both in the composition, and in the amount, of the hydrates formed. The amount of hydrates can be affected both by the hydration of C_3A itself and by changes in C_3S hydration induced by C_3A.

To elucidate the relative importance of these possible effects, a series of laboratory-burned clinkers have been investigated. From the clinkers, cements with different SO_3-contents have been prepared. The development of strength has been followed in mortars, and the course of hydration in pastes, using quantitative X-ray-diffraction.

From the results obtained it appears that C_3A in all amounts examined gives an independent positive contribution to the strength-producing properties of the cements. Simultaneously, however, C_3A seems to have a negative influence on the rate of C_3S hydration. This effect dominates at high C_3A levels and at late ages. Possible explanations for the observed effects are given.

INTRODUCTION

It is well established that the presence of C_3A* in Portland cement affects its strength producing properties. Qualitatively, C_3A raises the early strength, an effect still observable at 7 and 28 days curing (20°C), but seems to have a negative influence at late ages. The quantitative effect is dependent on which component C_3A is replacing in the cement (1), and also on the amount of SO_3 and alkalies present. A recent review on this topic is given by Schrämli (2).

Many of the explanations given for the effect of C_3A take as a starting point an observed acceleration of C_3S hydration, due to the presence of C_3A. The independent contribution from C_3A to the overall degree of hydration is viewed as unimportant, or even harmful to the strength of the product. (3, 5).

This paper is a further contribution to the understanding of the effect of C_3A, with special reference to the interrelationship between the rates of hydration of C_3A and C_3S in Portland cement.

The following three potential clinker compositions were formulated to permit observations of the hydration-related effects of partial or total replacement of C_4AF by C_3A:

TABLE 1

Planned Clinker Compositions

	BA	B	BF
C_3S	60	60	60
C_2S	22	22	22
C_3A	16	8	0
C_4AF	2	10	18

EXPERIMENTAL

The raw mixtures were formulated from 75% of an industrial material, corrected with 25% analytical grade reagents to the desired compositions. Each mixture was ground to pass a 90 µm sieve.

The heat treatment was carried out in 300 g batches of powdered raw meal in an open platinum crucible. After calcination for 30 min. at 1050°C the crucible was placed in an electric furnace preheated to the desired reaction temperature.

* Throughout the paper the oxide abbreviations C_3S, C_2S, C_3A, and C_4AF are used to designate the solid solutions of the four major clinker minerals.

The bottom of the crucible reached the reaction temperature after about 20 min. Clinker BF and B were kept for 40 min. at 1450°C, while clinker BA required 80 min. at 1500°C to attain a free lime level below 1.5%. The crucible was cooled to 1300°C during 20-25 min. in the furnace; then air-cooled from 1300°C to ambient.

The composition of the clinkers was characterized by the following techniques: Total chemical analysis by X-ray fluorescence, mineralogical composition by X-ray diffraction, chemical composition of the clinker minerals by scanning electron microscopy with EDAX-analyzer, and structure description by optical microscopy.

Three cements were made from each clinker with different levels of SO_3 added as equal amounts of calciumsulphate-dihydrate and calciumsulphate-hemihydrate. The precrushed clinkers (-1 mm) were mixed with the desired amount of SO_3 and ground in a ball mill for 15 min. The differences in fineness thus reflect differences in grindability.

The cements were characterized by determinations of grain size distribution, using Laser granulometry, specific surface according to Blaine, and the total sulphur content.

The strength development of the cements was determined in mortars according to the ISO-RILEM procedure (sand-cement-water, 3 : 1 : 0.5), except that the specimen dimensions were $2 \times 2 \times 5$ cm^3, and the mixing and casting procedures differed slightly. The method used gives results approximately 25% higher than the standard ISO-RILEM procedure. The bulk density of the mortars was measured after 1 day of curing. The compressive strength was determined after 1, 3, 7, 28, and 90 days.

The course of hydration was followed in pastes, using X-ray diffraction. The cements were mixed with 10% analytical grade CaF_2 as internal standard, and cast with a water-cement-ratio of 0.44 in 1 cm^3 cylinders. The paste specimens were cured at 100% relative humidity, which resulted in weak carbonation during hardening.

The residual unhydrated C_3S, C_3A, and C_4AF were determined after 1, 3, and 28 days' during at 20°C. At each fixed time, four cylinders were broken to determine the compressive strength. The results were in agreement with the mortar results, but gave inferior reproducibility.

The crushed specimens were ground with isopropanol and dried at 65°C. (Residual C_3S was determined from the peaks at 30.1°2θ and 51.7°2θ (Cu-K_α-radiation); then the samples were treated with salicylic acid-methanol to remove anhydrous silicates. After a quantitative filtration and drying, C_3A and C_4AF were determined in the residue.

Attempts to develop a sufficiently reproducible procedure for the determination of C_2S consumption were not successful.

RESULTS

The results are shown in figures 1-3 and in tables 2-5. From table 2 it appears that the desired clinker compositions were obtained.

The microanalysis of the clinker minerals in table 3 show that the contents of Al_2O_3 and Fe_2O_3 in the silicate phases depend nearly linearly on the composition of the interstitial phase. The molar sum of Al_2O_3 and Fe_2O_3 (A+F in table 3) seems to be independent of the Al_2O_3/Fe_2O_3-ratio and the fraction of Al_2O_3 (f_A in table 3) is almost the same in the three measured phases.

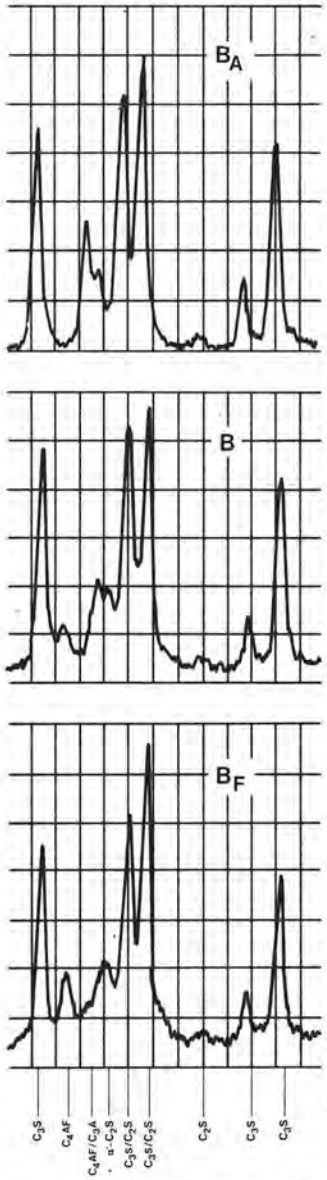

Fig. 1 - XRD-patterns of the clinkers with Cu-K_α-radiation.

The X-ray-diffraction patterns in fig. 1 show that the C_2S is in the ß-modification in the high Al_2O_3 clinker (BA), but is stabilized in a high-temperature modification in the Fe_2O_3-rich clinker (BF). From table 3 it appears that the difference cannot be explained from differences in the K_2O contents.

Fig. 2 shows the micro-structure of the BA and BF clinkers. The C_3S-borders in clinker BA are diffuse, and surrounded by small crystals of C_2S, while the C_3S-borders of the BF clinker appear unaffected. The effect has been described earlier (8) as due to the corrosive behaviour of high Al_2O_3-melts on C_3S during the cooling.

Data obtained from cement testing are shown in table 4. The grain-size distribution are approximated by Rosin-Rammler-distributions, from which the steepness (n) and the calculated

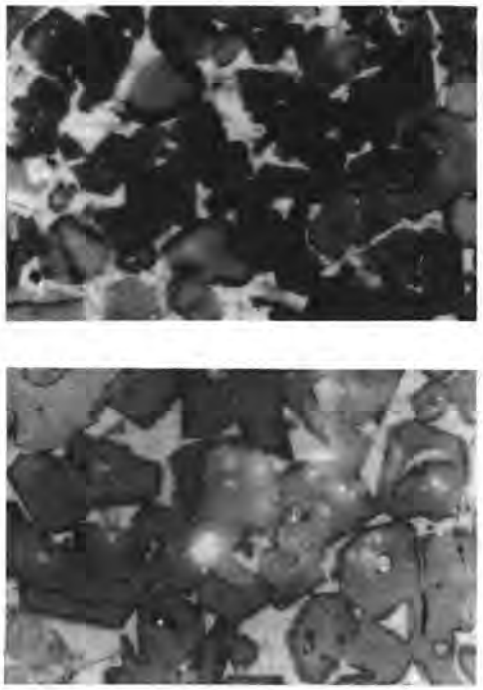

Fig. 2 - HF-etched polished sections of clinker BF and BA. Notable are differences in development of the edges of C_3S crystals (x 500).

residue on 20 µm ($R_{20\mu}$) are given in the table. Also given in the table are the measured specific surface of the cement, bulk density of mortar and the compressive strength.

However, to obtain more comparable strength results, two corrections have been applied, one correcting for differences in fineness, and the other for differences in bulk density. Fig. 3 shows the corrected strength results, together with the measured data. The corrections do not alter the qualitative results, but give the relevant data, which are suitable for direct quantitative comparison.

In order to correct strength values to equal clinker fineness, the contribution to the measured fineness from the added SO_3 is calculated using linear regression. From this a specific surface of each cement is calculated as if it contained 4% added "mixed" gypsum, designated as Blaine, 4% in table 4. These values are used to correct the strength to a 'constant clinker fineness' basis, using empirical constants of 0.045 MPa/m^2/kg at 1 and 90 days and 0.09 MPa/m^2/kg at 3, 7, and 28 days. The largest correction in this set of data is 70 · 0.09 MPa = 6 MPa.

TABLE 2

Chemical Analysis of the Clinkers

Clinker		BA	B	BF
SiO_2,	%	23.14	22.87	23.00
Al_2O_3,	%	6.33	5.02	3.69
Fe_2O_3,	%	0.59	3.15	5.63
CaO,	%	68.05	66.39	65.17
MgO,	%	0.43	0.44	0.45
Loss on ign.	%	0.47	0.54	0.78
Free CaO,	%	0.59	0.59	0.51
K_2O,	%	0.78	0.87	0.87
Na_2O,	%	0.30	0.30	0.29
SO_3,	%	0.17	0.27	0.26
K_2O-sol,	%	0.29	0.33	0.41
Na_2O-sol,	%	0.09	0.06	0.08
M_A		10.7	1.6	0.66
M_S		3.34	2.80	2.47
LSF		93.7	92.2	90.0
C_3S		55.3	55.8	55.5
C_2S		24.9	23.8	24.4
C_3A		15.8	8.0	0.3
C_4AF		1.8	9.6	17.1

TABLE 3

Composition of C_3S, C_2S, and the Interstitial Phase

Clinker		BA	B	BF
C_3S				
CaO,	%	69.7	70.0	69.7
SiO_2,	%	26.3	25.6	26.1
Al_2O_3,	%	1.6	1.2	0.7
Fe_2O_3,	%	0.0	1.0	1.3
K_2O,	%	0.5	0.4	0.4
A + F *		1.6	1.8	1.5
f_A **		1.00	0.65	0.46
C_2S				
CaO,	%	62.2	62.4	62.4
SiO_2,	%	31.9	30.9	30.9
Al_2O_3,	%	2.9	2.0	1.1
Fe_2O_3,	%	0.0	1.6	2.4
K_2O,	%	1.3	1.4	1.4
A + F *		2.9	3.0	2.6
f_a **		1.00	0.66	0.42
Interstitial phase				
CaO,	%	57.8	53.0	48.5
SiO_2	%	7.3	7.2	6.4
Al_2O_3,	%	31.1	22.7	14.8
Fe_2O_3,	%	2.0	15.9	29.2
K_2O,	%	2.2	1.3	1.0
A + F *		32.4	32.8	33.4
f_a **		0.96	0.69	0.44

* (A+F = % Al_2O_3 + 0.64 x % Fe_2O_3)
** (f_A = % Al_2O_3/(A + F)

Corrections for air entrained during mixing and casting are made by adding 5% to the strength value for each 1% air entrained equivalent to a 1% reduction in mortar density. The largest correction attributable to entrained air in the set of data is $5 \cdot (2300-2263)/23 = 8.0\% = 5$ MPa, taking 2300 kg/m^3 as the reference density for all mortars.

Finally, table 5 shows the measured extents of reaction of five selected cements, together with the relevant strenght data, corrected for bulk density but not for fineness deviations. As mentioned earlier, reproducible methods to assess the extent of hydration of C_2S have not been developed. However, for the measurements carried out, there was no measurable reduction in the amount of anhydrous C_2S after 1 og 3 days. The degree of reaction after 28 days averaged 0.25.

DISCUSSION

The replacement of C_4AF by C_3A has simultaneously changed the composition and structure of the silicates. The importance of these changes with respect to cement hydration characteristics cannot be derived from the data given here. However, preliminary results (9) from experiments intended to give such information have not shown measurable effects from changes in C_3S-composition. As regards C_2S the question is open.

TABLE 5

Hydration Data for Selected Cements (using the symbols from table 4

	Degree of reaction of									Bulk density corr.compr. strength		
	C_3S			C_3A			C_4AF			MPa		
	1 d	3 d	28 d	1 d	3 d	28 d	1 d	3 d	28 d	1 d	3 d	28 d
BF 1	0.29	0.50	0.85	-	-	-	0.00	0.05	0.11	9	28	76
BF 4	0.42	0.59	0.81	-	-	-	0.00	0.02	0.06	19	38	78
B 4	0.41	0.66	0.84	0.19	0.46	0.68	0.00	0.09	0.26	22	43	84
BA 6	0.40	0.51	0.62	0.55	0.62	0.78	-	-	-	24	43	66
BA 8	0.36	0.38	0.70	0.07	0.33	0.80	-	-	-	13	21	70

TABLE 4

Cement Testing Data

	Added mixed gypsum %	Total SO_3	Grain size distribution		Specific surface after Blaine m^2/kg	Corrected specific surface Blaine 4% m^2/kg	Bulk density kg/m^3	Compressive strengths in MPa				
			$R_{20\mu}$	n				1 day	3 days	7 days	28 days	90 days
BF 1	1.0	0.68*	31.9	0.94	336	370	2300	9	28	49	76	88
BF 2	2.0	1.24	32.3	0.88	344	368	2310	13	32	53	77	88
BF 4	4.0	2.22*	33.4	0.84	365	361	2309	19	39	62	80	89
B 2	2.0	1.30	36.8	0.84	316	341	2281	12	32	60	84	89
B 4	4.0	2.32*	34.9	0.82	353	352	2281	21	41	66	81	90
B 6	6.0	3.30	34.0	0.83	382	358	2286	24	45	67	80	89
BA 4	4.0	2.24	43.8	0.81	300	300	2263	18	35	43	56	67
BA 6	6.0	3.32*	42.8	0.79	334	305	2266	22	40	48	61	68
BA 8	8.0	4.34*	41.8	0.79	350	311	2279	12	20	45	67	80

(* calculated from clinker-SO_3 and added mixed gypsum)

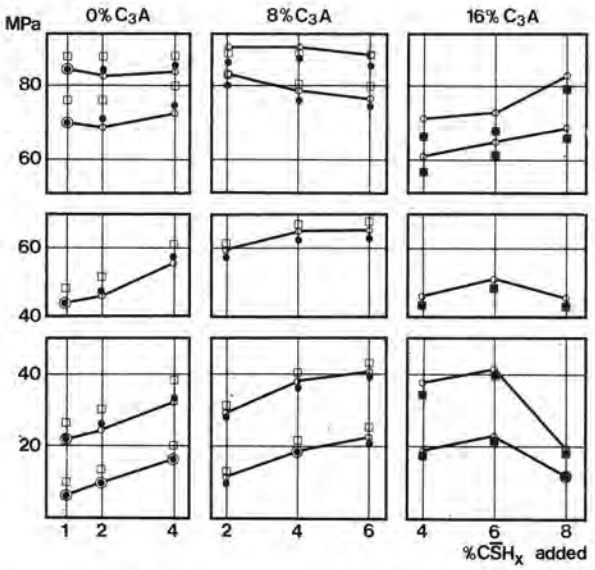

Fig. 3 - Compressive strength results.
Lower square = 1 and 3 days.
Central square = 7 days.
Upper square = 28 and 90 days.
= measured values
= fineness corrected values.
= fineness and bulk density corrected values.

The strength development curves from fig. 3 which are in accordance with the results of Celani and Ish-Shalom (3,10), show a complex pattern with an optimum amount of both C_3A and added SO_3, indicating that several mechanisms act togehter; some of them can be understood by comparing the results of fig. 3 and table 5, as follows:-

The positive effect of SO_3 on the early hydration age (1 and 3 days) of C_3S is seen by comparing early strengths of cement BF 1 with those of BF 4. (7). Also the retarding influence of SO_3 on the early hydration of C_3A is seen by comparing strength results of cement BA 4 with BA 8 (6). The parameter with the greatest influence on the early strength, thus seems to be the content of added SO_3. The effect of C_3A is less clear.

TABLE 6

The Quantitative Effect of Substituting 8% C_3A for 8% C_4AF from 0% to 8% C_3A and from 8% to 16% C_3A.

	From BF to B		From B to BA	
	Bulk density corrected MPa	Only fineness corrected MPa	Bulk density corrected MPa	Only fineness corrected MPa
1 day	2	1.5	0.5	0
3 days	4.5	2	0.5	-0.5
7 days	11	6.5	-15.5	-16
28 days	10.5	5	-15	-17
90 days	7	2	-17.5	-19.5

The quantitative effect of C_3A is seen in table 6. Comparison of the results of BF 2 - BF 4 with B 2 - B 4 shows that B-cements are superior at all ages. However, half of the potential strength gain is lost due to air entrainment. The magnitude of this effect depends on the casting and mixing procedure.

The observed potential strength gains can be explained by the hydration data for BF 4 (0% C_3A) and B 4 (8% C_3A). Since there is no significant difference in degree of reaction of C_3S between the two samples, the strength differences can best be attributed to a larger contribution to the overall degree of hydration from C_3A than from C_4AF.

Further, large substitutions of C_3A for C_4AF give no further strength gains, as seen from a comparison of the strengths of B 4 - B 6 and of BA 4 - BA 6. On the contrary a strength loss is seen at late ages. From the hydration data in table 5 this can be explained as a result of the generally lower degree of reaction of C_3S in BA-cements, which only at early ages can be compensated for by a larger contribution to the overall degree of hydration from C_3A.

It seems, therefore as if C_3A in large amounts has a negative influence on the rate of hydration of C_3S. A possible explanation is that C_3A competes with C_3S for the available water in the mortar. Although C_3A makes up only 16% of the cement, it would require 1/3 of the water in the mortar to be completely converted to monosulphate hydrate, which is the hydrate consuming the least water. This could well lead to local depletion of free water near C_3S surfaces. Consistent with this explanation it is reasonable that the degree of hydration of C_3S at 28 days is larger in BA 8 than in BA 4, since C_3A has been retarded for a longer periode in BA 8. The lack of water thus is felt somewhat later in BA 8.

Summing up we propose the effect of C_3A as being composed of three different partial effects:

The positive effect of C_3A is that it reacts faster than C_4AF, leading to a larger contribution to the overall degree of hydration. This is demonstrated in fig. 4. The initial amount of C_3S (f_{C_3S}) and the degree of reaction af C_3S (α_{C_3S}) are used to calculate the reduction in porosity associated with the consumption of C_3S: (Θ = porosity, $^w/_c$ = 0.5)

$$(1-\Theta)_{C_3S} = \frac{0.25 \cdot f_{C_3S} \cdot \alpha_{C_3S} + 31.75}{31.75 + 50.00}$$

In fig. 4, this parameter, $(1-\Theta)_{C_3S}$, is plotted against the logaritm of the strength results, corrected for bulk density, from table 5. It is seen that the data fall in groups according to the C_3A contents of the cements, demonstrating that C_3A gives an independent positive contribution to strength at all ages.

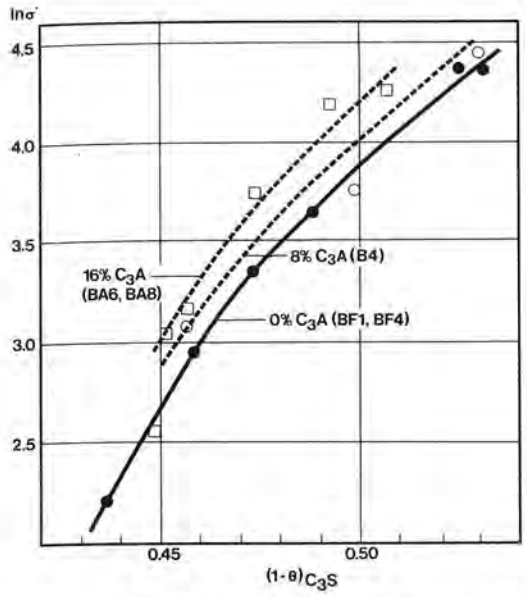

Fig. 4 - Illustration of the independent contribution from C_3A to the mortar strength.

The unfavourable effects of C_3A observed are the entrainment of air in the mortars and the negative influence on C_3S consumption at late ages as seen in the BA-cements.

No unambiguous evidence of a positive influence of C_3A on the early hydration of C_3S was found. It seems as if the major accelerator of the early C_3S-hydration is the cement SO_3.

In this attempt to account for the effect of C_3A on strength primarily in terms of differences in the overall degree of hydration, the authors do not ignore the importance of hydration product quality aspects. These have, however, not been the subject of this investigation.

CONCLUSIONS

When C_3A is substituted for C_4AF in Portland cement it will contribute positively to mortar strength at all ages due to its higher reactivity.

This positive effect is, however, counteracted by two negative effects of increasing the C_3A-content in the cement:

- a tendency of increasing air entrainment, an effect which must be expected to be rather dependent on the testing procedure,

  and

- a negative influence on the degree of hydration of C_3S at late ages, an effect which could be due to the high water needs of C_3A-hydration.

The present investigation does not provide evidence to a positive effect of C_3A on C_3S hydration; however, a positive effect of cement SO_3 is seen.

ACKNOWLEDGEMENTS

The efficient technical assistance of Dorthe Lotz Clasen and Margrethe Møller is gratefully acknowledged. F. MacGregor Miller's critical remarks helped to clarify linguistic and conceptual difficulties.

REFERENCES

1.- C. SCHMITT-HENCO (1973), "Einfluss der Zusammensetzung des Klinkers auf Erstarren und Anfangsfestigkeit von Zement", Zement-Kalk-Gips 26, (2), p.63.

2.- W. SCHRÄMLI (1978), "An Attempt to Assess Beneficial and Detrimental Effects of Performance", World Cement Technology, March, (1978) p. 35.

3.- A. CELANI, P.A. MOGGI, A. RIO (1969), "The Effect of Tricalcium Aluminate on the Hydration of Tricalcium Silicate and Portland Cement", Proceedings of the Fifth International Symposium on the Chemistry of Cement, vol. 2, p. 492.

4.- K.M. ALEXANDER, J.H. TAPLIN, J. WALDLAW (1969), "Correlation of Strength and Hydration with Composition of Portland Cement", ibid, vol. 3, p. 152.

5.- S. POPOVICS (1976), "Phenomenoligical Approach to the Role of C_3A in the Hardening of Portland Cement Pastes", Cement and Concrete Research 6 (3), p. 343.

6.- I. JELENNIĆ, A. PANOVIĆ, R. HALLE, T. GAĆESA (1977) "Effect of Gypsum on the Hydration and Strength Development of Commercial Portland Cements Containing Alkali Sulfates", Cement and Concrete Research, vol. 7, p. 239 - 246.

7.- A. BENTUR (1976), "Effect of Gypsum on the Hydration and Strength of C_3S-Pastes", J. Amer. Ceram. Soc., Vol. 59, No. 5-6, p. 210.

8.- R.H. BOGUE (1955), "The Chemistry of Portland Cement", New York, p. 245.

9.- Unpublished data from F.L. Smidth Laboratories.

10.-M. ISH-SHALOM, A- BENTUR (1972), "Effects of Aluminate and Sulfate Contents on the Hydration and Strength of Portland Cement Pastes and Mortars", Cement and Concrete Research, vol. 2, p. 653-662.

Theme 4 - Hydration of C_3A in the presence of admixtures

GENERAL REPORT

by V.S. RAMACHANDRAN, Division of Building Research, National Research Council of Canada, Ottawa, Ontario, CANADA.

This report summarizes six papers. Although the amount of C_3A present in portland cement is relatively low in comparison with other phases, it exerts a significant influence on the heat development, setting property and early strength development.

COLLEPARDI, CORRADI, BALDINI and **PAURI** investigated two sets admixtures, namely, Na_2CO_3 + Na-lignosulphonate and sulphonated naphthalene formaldehyde on the hydration of C_3A + CH and C_3A + CH + $C\bar{S}H_2$ systems, respectively. At different hydration periods, varying between 5 min and 7 days, the products were examined by DTA, DTG, TG and XRD. Zeta potential measurements were also carried out using a C_3A/solution ratio of 10.

In the C_3A-CH-H_2O system, monitoring of C_3A peak intensity by XRD indicated that the addition of Na_2CO_3 + Na-lignosulphonate retarded the hydration of C_3A. Significant changes in the Zeta potentials were observed in mixtures containing the admixtures. In C_3A-H_2O system, the value was 37.4 mV and by the addition of the admixture combination, it attained a value of -41.5 mV, indicating high dispersion. The change in the Zeta potential was less remarkable when the admixtures were not used in combination. In the C_3A-$C\bar{S}H_2$-H_2O system, the effect of sulphonated naphthalene formaldehyde showed that it neither modifies the rate of formation of ettringite and its subsequent conversion of the low sulphoaluminate, nor the type of hydration products. This admixture changes the Zeta potential from -8.5 to -30.9 mV.

It can be concluded that the flowability in the C_3A-CH-H_2O or C_3A-$C\bar{S}H_2$-CH-H_2O system containing Na_2CO_3 + Na-lignosulphonate or sulphonated naphthalene formaldehyde depends on Zeta potential changes, retardation of the initial stages of reaction and possibly water/solid ratio.

MASSAZZA and **COSTA** have reported the effect of Na-lignosulphonate or alkyl naphthalene sulphonate formaldehyde on the hydration of C_3A + $CaSO_4.2H_2O$ mixtures. The products formed within a few minutes and those up to 3 days were examined by XRD, TG, DSC, thermoluminescence, adsorption and electron microscopic and conduction calorimetric techniques.

Admixtures retarded the hydration reactions. For example, in the absence of admixtures, gypsum is consumed in the reaction in 4 h, in the presence of 1% naphtalene sulphonate formaldehyde gypsum disappears after 7 h and in the presence of 1% Na-lignosulphonate gypsum persists up to 36 h. Adsorption of these admixtures carried out on ettringite and monosulphonate in a non-aqueous medium showed that substantial amounts were adsorbed. An electron microscopic examination revealed that whereas ettringite fibres formed in the absence of the admixtures, smaller size crystals of ettringite, appearing as fine felts, covered the C_3A grains in the presence of the admixtures.

It is concluded that the flowability in the C_3A + $CaSO_4.2H_2O$ + H_2O system is caused by the retardation of ettringite in the presence of admixtures, resulting in a decrease in the water demand. In addition, the admixtures, by decreasing the interlocking of ettringite crystals, enhance the flowability of pastes.

RAMACHANDRAN, in an elucidation of the role of lignosulphonates on the hydration of C_3A, has studied the hydration and adsorption-desorption isotherms of systems containing C_3A, C_3S, C_4AH_{13}-C_2AH_8, C_3AH_6 and C_3S, in the presence of Ca- and Na-lignosulphonates. The products were examined by XRD, DTA and SEM.

In the system C_3A-H_2O-Ca-lignosulphonate, treated with 15, 30, 50, 100 and 200% CLS, a complex gelatinous product is formed containing Al^{3+}. In an aqueous medium both hexagonal and cubic aluminate hydrates adsorb lignosulphonate irreversibly. An evidence for a complex and interlayer adsorption was also obtained in the hexagonal aluminate hydrate. In the non-aqueous medium, only the hexagonal phase irreversibly adsorbs lignosulphonate. Consequently it is suggested that the present tendency of explaining the, retardation action on the basis of adsorption of lignosulphonate on C_3A should be altered to "consumption of lignosulphonate by the hydrating C_3A". The influence of the small amounts of calcium aluminate and its hydrates on the hydration of C_3A in the presence of calcium lignosulphonate can be explained by the relative adsorption effects which are in the order of C_3A > hexagonal phase > cubic phase. As C_3A adsorbs substantial amounts of lignosulphonate it should follow that in commercial lignosulphonates containing sugars, the lignosulphonate should play an important role in retardation effects. Data have been presented to show the sugar-free Na- or Ca-lignosulphonate is as effective as the commercial lignosulphonates in retarding the hydration of C_3A.

It has been concluded that C_3A can interact with lignosulphonate in the presence of water to form a complex compound. Both hexagonal and cubic aluminate hydrates adsorb lignosulphonate irreversibly in an aqueous medium. In a non-aqueous medium, only the hexagonal phase adsorbs lignosulphonate, indicating that for adsorption or interaction of lignosulphonate with C_3A the presence of water is necessary. Sugar-free Ca- or Na-lignosulphonate retards the hydration of C_3A as efficiently as commercial lignosulphonates.

ZIELINSKA and **ZIELINSKI** investigated the effect of $Na_2S_2O_3$ on the hydration of C_3A alone and in portland cement clinker. The mixtures were hydrated to different times between 1 h and 28 days and subjected to exmination by XRD, TG, IR and SEM.

In the hydration of C_3A, $Na_2S_2O_3$ retards the formation of hexagonal phases and their conversion to the cubic phase, changes the morphology of the cubic aluminate hydrate. Complex compounds of the AFm type containing $S_2O_3^{-2}$ group are formed ; the deformed agglomerates of hexagonal phase also result. The polyhydrons of large dimension of C_3AH_6, evident without admixture, are converted to small octahedrons of C_3AH_6 in the presence of $Na_2S_2O_3$. In the clinker, $Na_2S_2O_3$ seems to accelerate the hydration of C_3A. At 8 h in the presence of the admixtures, needles analogous to ettringite are formed, probably a complex compound of the AFt type containing $S_2O_3^{-2}$ groups.

It is concluded that $Na_2S_2O_3$, although a retarder for the hydration of C_3A, acts as an accelerator of C_3A when it is present in the clinker. Certain morphological changes of the hydration products and formation of complex compounds containing $S_2O_3^{-2}$ groups are also indicated.

SERSALE, SABATELLI and **VALENTI** examined the effect of Na-gluconate, copper acetate and aluminum phosphate on the hydration of C_3A up to 48 h, utilizing XRD, DTA, TG and SEM techniques.

All the admixtures retarded the hydration of C_3A, Na-gluconate being the most efficient retarder. At 48 h, the degree of hydration was almost constant in the presence of all admixtures but this value was still lower than that observed for sample hydrated without an admixture. Comparison of the products at 50% hydration showed that in the presence of retarders, hexagonal rather than the cubic phase was present. The micrographs of samples hydrated to the same degree do not show any significant differences.

It is concluded that Na-gluconate, copper acetate and aluminum phosphate retard the hydration of C_3A by stabilization of the hexagonal calcium aluminate hydrate. These admixtures do not alter the morphological features of the products.

REGOURD, MORTUREUX and **HORNAIN** studied the effect of $CaCl_2$ and sucrose on the hydration of C_3A, C_3S, C_3A + C_3S + gypsum and portland cement utilizing XRD and electron microscopic techniques.

Tricalcium aluminate hydrates to hexagonal phase followed by the cubic phase in two days. In the presence of $CaCl_2$, chloroaluminate is formed but the rate of hydration is not affected. Sucrose is a retarder and inhibits the hydration after two days, forming ill-crystallized C_4AH_{13}. A product enveloping the C_3A grains was indicated in the SEM. In the C_3S + C_3A + gypsum system, ettringite forms initially and is converted to monosulphate and finally to a solid solution of monosulphate and C_4AH_{13}. Calcium chloride is an accelerator for C_3S hydration up to seven days. The microstructure of C-S-H is also modified. It is also observed that $CaCl_2$ is a better retarder than gypsum for C_3A hydration. In the presence of $CaCl_2$ hexagonal plates of chloroaluminate are formed. Sucrose retards the hydration of C_3S up to two days and then acts as an accelerator. Sucrose, although a retarder for C_3A hydration, is less effective than $CaCl_2$. In portland cement, $CaCl_2$ acts as an accelerator and sucrose as a retarder between four and sixteen hours. After twenty-four hours, portland cement alone or that with the admixtures shows the same rate of hydration.

It is considered that $CaCl_2$ affects the hydration of cement at the outset by influencing the nucleation of C-S-H and CH. In C_3A-gypsum-$CaCl_2$ system, competition exists between gypsum and $CaCl_2$. Calcium chloride is a better retarder than gypsum up to twenty-eight days. The formation of a coating of chloroaluminate may explain the retardation. Sucrose is a retarder of C_3A hydration and forms ill-crystallized aluminate hydrates.

B. CASU, M. CHIRUZZI, F. TEGIACHI and **G. ZOPETTI** studied the effect of aqueous solutions of some carbohydrates and the corresponding aldonates on the hydrating C_3A. Techniques such as optical rotation, potentiometer, NMR and IRA were used to follow changes occuring from 1 min to 100 min. Within a few minutes after contact of C_3A with reducing glucose and maltose, precipitation occured. Evidence was obtained for the formation of complexes in solution between C_3A and sodium gluconate and this preceded the precipitation on C_3A. The protective layer thus formed retarded the hydration and set.

CONCLUDING REMARKS

Although C_3A content in portland cement is low, it influences significantly many physical, chemical and mechanical properties of the cement such as setting rheology, early strength, sulphate attack, heat effect, carbonation, etc ...Since C_3A seems to adsorb large amounts of different admixtures, it is very essential to study the role of C_3A and C_3A + gypsum + CH systems and their interaction with admixtures. The importance of such studies becomes evident from the number of new admixtures (93, 71, 73 and 88 in 1976, 1977, 1978 and 1979, respectively) that have been developed.

One of the problems encountered in the study of systems containing C_3A is the variation of results reported by different workers. One of the obvious problems is that the hydration is relatively fast. Many factors influence the reaction rate and these include the shape of the bulk sample, size of the material taken for a particular study, pre-exposure conditions, effect of impurities, the difference in the reactivity of samples apparently of same particle size, the W/S ratio, temperature, etc ... This becomes more complex when admixtures and admixture combinations are added to C_3A systems. The influence of the molar concentrations of admixtures in solutions is often neglected and comparisons are generally made on the basis of a particular percentage of admixture with respect to solid C_3A.

It is very important to investigate the influence of admixtures on C_3A and C_3A + gypsum systems but often these results may not be directly applicable to portland cement systems because of the role of other phases and also because C_3A in portland cement contains Na in solid solution.

The limitation of various techniques should also be considered in evaluating results. One of the necessary requirements should be that all published reports should contain the essential information that would characterize the materials and experimental conditions. This may be a starting point for eventual comparison of results obtained in different laboratories and for answer to many questions.

Thème 4 - Hydratation de C_3A en présence d'adjuvants

RAPPORT GENERAL

par V.S. RAMACHANDRAN, Division of Building Research National, Research Council of Canada, Ottawa, Ontario, CANADA.

Ce rapport résume sept contributions. Bien que la teneur en C_3A présent dans le ciment portland soit relativement faible comparée à celle d'autres phases, elle exerce une influence significative sur le dégagement de chaleur, la prise et le développement des premières résistances.

COLLEPARDI, CORRADI, BALDINI et **SAURI** ont étudié deux séries d'adjuvants, à savoir Na_2CO_3 + lignosulfonate de Na et formaldéhyde de naphtalène sulfoné, sur l'hydratation des systèmes C_3A + CH et C_3A + CH + $C\bar{S}H_2$ respectivement. A différentes périodes d'hydratation, variant entre 5 minutes et 7 jours, les produits ont été examinés par ATD, DTG, TG et DRX. Les mesures de potentiel Zêta ont aussi été effectuées en utilisant un rapport C_3A/solution égal à 10.

Dans le système C_3A - CH - H_2O, l'évolution de l'intensité du pic de C_3A par DRX indique que l'addition de Na_2CO_3 + lignosulfonate retarde l'hydratation de C_3A. Des changements significatifs dans les potentiels Zêta ont été observés dans les mélanges contenant les adjuvants. Dans le système C_3A - H_2O, la valeur était de 37,4 mV et par addition de la combinaison d'adjuvants, il atteignait une valeur de -41,5 mV, avec une dispersion élevée. Le changement du potentiel Zêta était moins marqué quand les adjuvants n'étaient pas utilisés en combinaison.

Dans le système C_3A - $C\bar{S}H_2$ - H_2O , l'effet du formaldéhyde de naphtalène sulfoné montre qu'il ne modifie ni le taux de formation de l'ettringite ni sa conversion ultérieure en monosulfoaluminate ni le type des produits d'hydratation. L'adjuvant change le potentiel Zêta de -8,5 à -30,9 mV.

On en conclut que la fluidité des systèmes C_3A - CH - H_2O ou C_3A - $C\bar{S}H_2$ - CH - H_2O contenant Na_2CO_3 + lignosulfonate de Na ou le formaldéhyde sulfoné dépend des changements du potentiel Zêta, du retard des stades initiaux de la réaction et peut-être du rapport eau/solide.

MASSAZZA et **COSTA** ont rapporté l'effet du lignosulfonate de Na et du formaldéhyde d'alkyl naphtalène sulfoné sur l'hydratation de mélanges C_3A + $CaSO_4.2H_2O$. Les produits formés en quelques minutes et ceux formés pendant les trois premiers jours ont été examinés par DRX, TG, DSC, thermoluminescence, microscopie électronique, adsorption isotherme et calorimétrie à conduction. Les adjuvants retardent les réactions d'hydratation. Par exemple, en absence d'adjuvants, le gypse est consommé dans la réaction en 4 heures , en présence de 1 % de formaldéhyde de naphtalène sulfoné, il disparaît après 7 heures et en présence de 1 % de lignosulfonate de Na, il persiste jusqu'à 36 heures. L'adsorption de ces adjuvants effectuée dans un milieu non aqueux montre que des quantités substantielles sont adsorbées, sur l'ettringite ou le monosulfate. Un examen au microscope électronique révèle que, en absence d'adjuvants, l'ettringite cristallise en fibres tandis qu'en présence d'adjuvants, des cristaux de plus petite taille forment un feutrage fin couvrant les grains de C_3A.

On en conclut que la fluidité du système C_3A + $CaSO_4.2H_2O$ est due au retard de la formation d'ettringite en présence d'adjuvants qui entraîne une demande d'eau plus faible. De plus, en réduisant l'enchevêtrement des cristaux d'ettringite, les adjuvants améliorent la rhéologie des pâtes.

RAMACHANDRAN a étudié l'hydratation et les isothermes d'adsorption-désorption des systèmes contenant C_3A, C_3S, C_4AH_{13} - C_2AH_8, C_3AH_6 et C_3S, en présence de lignosulfonates de Ca et de Na afin d'expliquer leur rôle sur l'hydratation de C_3A. Les produits ont été examinés par DRX, ATD et MEB.

Dans le système C_3A - H_2O, traité avec 15, 30, 50, 100 et 200 % de lignosulfonate de Ca, il se forme un complexe gélatineux contenant Al^{3+}. Dans un milieu aqueux, les hydrates d'aluminate à la fois hexagonaux et cubiques adsorbent le lignosulfonate irréversiblement. Un complexe interlamellaire d'adsorption a aussi été mis en évidence dans les aluminates hydratés hexagonaux. Dans un milieu non aqueux, seule la phase hexagonale adsorbe irréversiblement le lignosulfonate. Par conséquent, on peut suggérer que l'action retardatrice fondée sur l'adsorption du lignosulfonate sur C_3A puisse être modifiée en "consommation du lignosulfonate par le C_3A qui s'hydrate". L'influence de petites quantités d'aluminate de calcium et de ses hydrates, sur l'hydratation de C_3S en présence de lignosulfonate de Ca, peut être expliquée par les effets relatifs d'adsorption qui sont dans l'ordre, C_3A > phase hexagonale > phase cubique. Comme C_3A adsorbe des quantités substantielles de lignosulfonates, ceux contenant des sucres, devraient jouer un rôle dans les effets retardateurs. Des résultats publiés montrent que le lignosulfonate de Na ou de Ca, sans sucre, est aussi efficace dans le retard de l'hydratation de C_3A que les lignosulfonates commerciaux.

On en conclut que C_3A peut interagir avec le lignosulfonate en présence d'eau pour former un composé complexe. Les aluminates hydratés à la fois hexagonaux et cubiques adsorbent irréversiblement le lignosulfonate dans un milieu aqueux. Seule la phase hexagonale adsorbe le lignosulfonate indiquant que pour l'adsorption ou l'interaction du lignosulfonate avec C_3A, la présence d'eau est nécessaire. Le lignosulfonate de Ca ou de Na, sans sucre, retarde l'hydratation de C_3A aussi efficacement que les lignosulfonates commerciaux.

ZIELINSKA et **ZIELINSKI** ont étudié l'effet de $Na_2S_2O_3$ sur l'hydratation de C_3A seul et dans le clinker de ciment portland. Les mélanges ont été hydratés à des temps différents entre 1 heure et 28 jours et examinés par DRX, TG, IR et MEB.

Dans l'hydratation de C_3A, $Na_2S_2O_3$ retarde la formation des phases hexagonales et leur conversion

en phase cubique et change la morphologie de l'aluminate hydraté cubique. Il se forme des composés complexes du type AFm contenant le groupe $S_2O_3^{2-}$. Il en résulte des agglomérats de phase hexagonale. Les polyèdres de C_3AH_6, de grandes dimensions, mis en évidence sans adjuvants, sont couverts de petits octaèdres de C_3AH_6 en présence de $Na_2S_2O_3$. Dans le clinker, $Na_2S_2O_3$ semble accélérer l'hydratation de C_3A. A 8 heures, en présence d'adjuvant, des aiguilles analogues à l'ettringite se forment, elles sont probablement un composé complexe du type AFt contenant des groupes $S_2O_3^{2-}$.

On en conclut que $Na_2S_2O_3$ bien que retardateur de l'hydratation de C_3A agit comme un accélérateur de C_3A quand il est présent dans le clinker. Certains changements morphologiques des produits d'hydratation et la formation de composés complexes contenant des groupes $S_2O_3^{2-}$ sont aussi indiqués.

SERSALE, SABATELLI et VALENTI ont étudié l'effet du gluconate de sodium, de l'acétate de cuivre et du phosphate d'aluminium sur l'hydratation de C_3A jusqu'à 48 heures, en utilisant la DRX, l'ATD, la TG et le MEB.

Tous les adjuvants retardent l'hydratation de C_3A, le gluconate de Na étant le retardateur le plus efficace. A 48 heures, le degré d'hydratation est presque constant en présence de tous les adjuvants mais cette valeur est plus faible que celle observée dans l'échantillon sans adjuvant. La comparaison des produits à 50 % d'hydratation montre qu'en présence de retardateurs, la phase hexagonale est présente plutôt que la phase cubique. Les micrographies des échantillons, au même degré d'hydratation, ne montrent pas de différences significatives.

On en conclut que le gluconate de sodium, l'acétate de cuivre et le phosphate d'aluminium retardent l'hydratation de C_3A en stabilisant l'aluminate de calcium hydraté hexagonal. Ces adjuvants n'altèrent que les caractéristiques morphologiques des hydrates.

REGOURD, MORTUREUX et HORNAIN ont étudié l'effet de $CaCl_2$ et du saccharose sur l'hydratation de C_3A, C_3S, $C_3A + C_3S$ + gypse et du ciment portland en utilisant la DRX et le MEB.

L'aluminate tricalcique s'hydrate en phase hexagonale suivie par la phase cubique en deux jours. En présence de $CaCl_2$, le chloroaluminate est formé mais le taux d'hydratation n'est pas affecté. Le sucre est un retardateur et inhibe l'hydratation après deux jours, formant C_4AH_{13} mal cristallisé. Un produit enveloppant les grains de C_3A est observé au MEB. Dans le système $C_3S + C_3A$, $CaCl_2$ agit comme un accélérateur de l'hydratation de C_3A jusqu'à 1 jour. La formation de chloroaluminate semble retarder l'hydratation ultérieure. Le sucre est un retardateur de l'hydratation à la fois de C_3A et de C_3S aux stades initiaux. Dans le système $C_3S + C_3A$ + gypse, l'ettringite se forme initialement puis se convertit en monosulfate et finalement en une solution solide monosulfate - C_4AH_{13}. Le chlorure de calcium est un accélérateur de l'hydratation de C_3S jusqu'à 7 jours. La microstructure de C-S-H est modifiée et il se forme des plaquettes hexagonales de chloroaluminates. On observe aussi que $CaCl_2$ est un meilleur retardateur de l'hydratation de C_3A que le gypse. Le sucre retarde l'hydratation de C_3A jusqu'à 2 jours et ensuite agit comme un accélérateur. Le sucre, bien que retardateur de l'hydratation de C_3A est moins efficace que $CaCl_2$. Dans le ciment portland, $CaCl_2$ agit comme un accélérateur et le sucre comme un retardateur entre 4 et 16 heures. Après 24 heures, le ciment portland seul ou celui avec les adjuvants présente le même taux d'hydratation.

On estime que $CaCl_2$ affecte l'hydratation du ciment au début en influençant la nucléation de C-S-H et de CH. Dans le système C_3A - gypse - $CaCl_2$, une compétition existe entre le gypse et $CaCl_2$. Le chlorure de calcium est un meilleur retardateur que le gypse jusqu'à 28 jours. La formation d'une couche de chloroaluminate peut expliquer le retard. Le sucre est retardateur de C_3S initialement et aussi de C_3A et forme des aluminates hydratés mal cristallisés.

B. CASU, M. CHIRUZZI, F. TEGIACCHI et G. ZOPETTI ont étudié l'effet, sur l'hydratation de C_3A, des solutions aqueuses de quelques carbohydrates et des aldonates correspondants. Les techniques telles que la rotation optique, la potentiométrie, la RMN et l'IR ont été utilisées pour suivre les changements se produisant entre 1 et 100 minutes. Dans les premières minutes après le contact de C_3A avec le glucose et le maltose réducteurs, une précipitation se produit. La formation en solution de complexes entre C_3A et le gluconate de sodium a été mise en évidence et elle précède la précipitation sur C_3A. La couche protectrice ainsi formée retarde l'hydratation et la prise.

CONCLUSIONS ET REMARQUES

Bien que la teneur en C_3A dans les ciments portland soit faible, elle influence, d'une manière significative, les propriétés physiques, chimiques et mécaniques du ciment telles que la prise, la rhéologie, les premières résistances, l'attaque au sulfate, le dégagement de chaleur, la carbonatation, etc... Etant donné que C_3A semble adsorber de grandes quantités d'adjuvants différents, il est essentiel d'étudier le rôle de C_3A et des systèmes C_3A + gypse + CH et leur interaction avec les adjuvants. L'importance de telles études devient évidente en raison du nombre de nouveaux adjuvants qui se sont développés (93, 74, 73 et 88, respectivement en 1976, 1977, 1978 et 1979).

Un des problèmes rencontrés dans l'étude des systèmes contenant C_3A est la variation des résultats rapportés par les différents chercheurs. Un des problèmes évident est celui de la vitesse relativement rapide de l'hydratation. De nombreux facteurs influencent le taux de réaction et ceux-ci incluent la forme de l'échantillon, la taille du matériau pris dans une étude particulière, les conditions de prétraitement, l'effet des impuretés, les différences de réactivité des échantillons apparemment de particules de même taille, de rapport e/c, de température, etc... Ceci devient plus complexe quand les adjuvants ou les combinaisons d'adjuvants sont ajoutés aux systèmes C_3A.

L'influence des concentrations molaires des adjuvants en solution est souvent négligée et les comparaisons sont généralement faites sur la base d'un pourcentage particulier d'adjuvants par rapport au C_3A solide.

Il est très important d'étudier l'influence des adjuvants sur C_3A et sur les systèmes C_3A + gypse mais souvent ces résultats ne peuvent être directement applicables aux systèmes du ciment portland à cause du rôle des autres phases et aussi parce que C_3A dans le ciment contient Na en solution solide.

Les limitations des différentes techniques devraient aussi être considérées dans l'évaluation des résultats. Tous les rapports publiés devraient contenir l'information caractérisant les matériaux et les conditions expérimentales ; c'est une exigence indispensable. Ceci pourrait être le point de départ d'une comparaison éventuelle de résultats obtenus dans différents laboratoires et la réponse à de nombreuses questions.

Hydration of C_3A in the presence of lignosulfonate-carbonate system or sulfonated naphthalene polymer

Hydratation du C_3A en présence de lignosulfonate et de carbonate ou de polymère de naphtalène sulfoné

M. COLLEPARDI*, Professor of Materials Technology and Applied Chemistry, M. CORRADI**, Doctor in Industrial Chemistry, G. BALDINI*, Doctor in Industrial Chemistry and M. PAURI*, Doctor in Industrial Chemistry, Italie.

* Department of Materials Science, University of Ancona.
** Research and Development Laboratory, MAC Mediterranea Additivi Cemento, Treviso.

SUMMARY :

The combined addition of water soluble lignosulfonate and carbonates to Portland clinker without gypsum has been proposed to prepare flowable pastes with low water/cement ratios. On the other hand sulfonated naphthalene polymer (SNP) based admixtures are normally used as superplasticizers to obtain concretes with low w/c ratios.

In the present paper the influence of sodium lignosulfonate (LGS) and carbonate (NC) on the hydration of C_3A with lime and without gypsum was examined. The C_3A hydration rate is retarded by the simultaneous addition of LGS (0.6%) and NC (0.6%), and for some minutes the hydration is completely blocked. It may be speculated that this effect combined with the change in the zeta potential caused by LGS and NC could contribute to the flowability of clinker pastes. By C_3A hydration, hexagonal calcium aluminate hydrates are initially formed and then they are transformed into the cubic hydrate. The same products are obtained in the presence of LGS and NC.

The effect of SNP (0.6%) on the hydration of C_3A with lime and gypsum was also studied. No substantial change in the C_3A hydration rate is observed. The same products (ettringite and then monosulfate) are formed with and without SNP. Changes in zeta potential caused by SNP are recorded. It can be assumed that this is substantially responsible for the increase in flowability of cement pastes.

RESUME :

On a suggéré de préparer des pâtes très fluides avec un faible rapport eau/ciment en additionnant simultanément du lignosulfonate et du carbonate, solubles dans l'eau, au clinker portland sans gypse. Par ailleurs, des adjuvants à base de polymère de naphtalène sulfonée (PNS) sont déjà utilisés pour obtenir des bétons très fluides.

Dans cet article, on a examiné l'influence du lignosulfate de sodium (LGS) et du carbonate de sodium (NC) sur l'hydratation du C_3A avec de la chaux et sans gypse. La vitesse d'hydratation du C3A est ralentie par l'addition simultanée de LGS (0,6%) et de NC (0,6%) et, pour quelques minutes, l'hydratation est complètement bloquée. On pourrait déduire que la combinaison de cet effet avec le changement du potentiel Zêta, causé par le LGS et le NC, pourrait contribuer à rendre fluide les pâtes de clinker. Lors de l'hydratation du C_3A se forment d'abord les aluminates de Ca hydratés hexagonaux qui sont ensuite transformés en hydrate cubique. Les mêmes produits se forment en présence de LGS et de NC.

L'effet du PNS (0,6%) sur l'hydratation du C_3A avec chaux et gypse a également été étudié. On ne note aucune modification significative dans la vitesse d'hydratation du C_3A. Les mêmes produits (ettringite et ensuite monosulfate) se forment avec et sans PNS. On a enregistré des modifications du potentiel Zêta dues au PNS. On peut considérer que ces modifications sont la principale cause de l'accroissement de la fluidité des pâtes de ciment.

INTRODUCTION

The so called superplasticizers are largely used, particularly in Europe and Japan, as additives that permit a concrete to have 20-30% of the mixing water removed without reduction in workability (1) or a strong increase in workability (for instance : from 20 to 220 mm in slump) without significant change in all the properties of the hardened concrete (2). They are substantially based on sulfonated-naphthalene- formaldehyde polymers (SNP) or sulfonated melamine-formaldehyde polymers (3). On the other hand, Brunauer and coworkers (4) studied the combined effect of water soluble lignosulfonates and carbonates on pastes from ground Portland clinker without gypsum. Therefore, superplasticizers based on SNP can be considered as liquefying agents for Portland cement pastes, whereas lignosulfonate-carbonate combinations act as both set regulator and liquefying agent for ground Portland clinker without gypsum. The purpose of the present work was to study the influence of SNP on the C_3A hydration in the presence of lime and gypsum, and the effect of lignosulfonate-carbonate combination on the C_3A hydration in the presence of lime without gypsum. The two systems correspond to the C_3A hydration in Portland cement and Portland clinker respectively.

EXPERIMENTAL

Materials and methods

Tricalcium aluminate (free lime = 0.1% and Blaine fineness of about 3,500 cm^2/g) was prepared according the method described in a previous paper(5). It was blended with reagent grade calcium hydroxide (CH) in order to simulate the aqueous phase present in Portland cement of Portland clinker pastes. The C_3A/CH weight ratio was 5:1 for all the mixes, whereas reagent grade gypsum ($C\bar{S}.H_2$) was present (20% by weight of C_3A) only in mixes C and D as shown in Table I. Reagent grade sodium carbonate (NC), sodium lignosulfonate (LGS), said to be free of sugars or other carbohydrates, and SNP, produced as dry powder by MAC, were dry-mixed with the other ingredients. The percentages of NC, LGS and SNP were 0.6% by weight of C_3A. By taking into account the H_2O/C_3A ratio (0.5) the concentration of the additives in the liquid phase was 12 g/l.

Table I - Composition (in grams) of mixes for paste hydration (H_2O/C_3A = 0.5)

Mix	H_2O	C_3A	CH	$C\bar{S}.H_2$	NC	LGS	SNP
A	5	10	2	-	-	-	-
B	5	10	2	-	0.06	0.06	-
C	5	10	2	2	-	-	-
D	5	10	2	2	-	-	0.06

Hydration at 20°C of these pastes was examined. After a certain time (5 min - 7 days) the hydration was stopped by grinding the pastes with methyl alcohol. The filtered solids were dried at 60°C and analyzed by a Netzsch apparatus in which DTA, DTG and TG curves are obtained simultaneously. Only DTG curves are shown in the present paper. XRD analysis was also carried out by a Philips apparatus and the intensity of the C_3A peak at 1.56 Å was determined.

Zeta potential measurements were performed using a Laser Zee Meter by Pen Kem Inc. which is based on electrophoretic technique (7) and gives the results directly in millivolt. The samples for zeta potential measurements were prepared by mixing for 5 min 100 g of lime saturated water solution with 10 g of C_3A, with or without 2 g of $C\bar{S}.H_2$, 1.2 g of NC, LGS or SNP as shown in Table II. Therefore, the concentration of NC, LGS and SNP in the liquid phase (12 g/l) was the same as used for the paste samples. The liquid phase was separated by vacuum filtration. A small portion of the solid sample was added to the filtered liquid phase and a suspension (10 mg/20 ml) was obtained with the same ionic strength of the original suspension and diluted enough to be observed by the microscope of the Laser Zee Meter.

Table II - Composition (in grams) of mixes for zeta potential measurements

Mix	CH saturated water solution	C_3A	$C\bar{S}.H_2$	NC	LGS	SNP	Zeta potential (mV)
A'	100	10	-	-	-	-	+ 37.4
B'	100	10	-	1.2	1.2	-	- 41.5
C'	100	10	2	-	-	-	- 8.5
D'	100	10	2	-	-	1.2	- 30.9

RESULTS AND DISCUSSION

C_3A - CH system

In Fig. 1 the XRD intensity peak of C_3A as a function of time is shown. When C_3A hydrates in the presence of lime without gypsum the reaction rate is very high. The addition of 0.6 % of LGS and NC to the C_3A-CH system retards the reaction between C_3A and water particularly during the initial period of hydration.

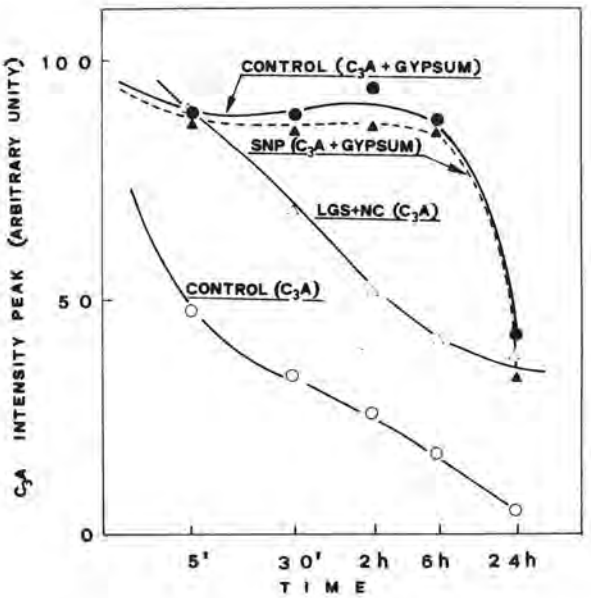

Fig. 1 - XRD intensity peak as a function of hydration time. All the mixes contain CH.

The DTG curves of Fig. 2 confirm this effect and show that the initial hydration of C_3A is substantially blocked by the addition of NC and LGS for 5 min. Similar results are obtained when NC and LGS (0.625%) are added to C_4AF-CH system as the C_4AF hydration is substantially blocked for about 30 min (8). By C_3A hydration (Fig. 2.A) hexagonal calcium aluminate hydrates (C_4AH_x and C_2AH_8) are initially formed with DTG peaks at about 200 and 270°C. The peak at about 100°C, recorded in a previous paper (5), is not observed in the present work as the hydrated samples were dried for a longer time at 60°C before being analysed by DTG. Some cubic hydrate (C_3AH_6) with a DTG peak at about 320°C and a smaller one at about 500°C appears immediately. However, the transformation of the hexagonal calcium aluminate hydrates into the cubic hydrate occurs remarkably after 1 day only. The same products are observed when C_3A hydrates in the presence of NC and LGS (Fig. 2.B) although there is a retardation during the initial period of hydration.

The data reported in Table II show that the zeta potential of C_3A in a lime saturated solution is positive (37.4 mV). This result agrees very well with the data of Tadros et al (9) who found a value of 34 mV for suspensions of 8 g of C_3A in 100 ml water. The high zeta potential would indicate that the C_3A suspension (Mix A' in Table II) is a well dispersed system. The deflocculation of Mix A' was actually confirmed by the difficulty in centrifugal sedimentation and vacuum filtration. On the other hand, the C_3A paste (Mix A in Table I) is a stiff system. It may be speculated that by going from Mix A' to Mix A the ionic strength is changed and the zeta potential decreases towards to zero by favouring thus the flocculation. Alternatively, one could think that Mix A' and Mix A have approximately the same zeta potential, but the clusters formation in

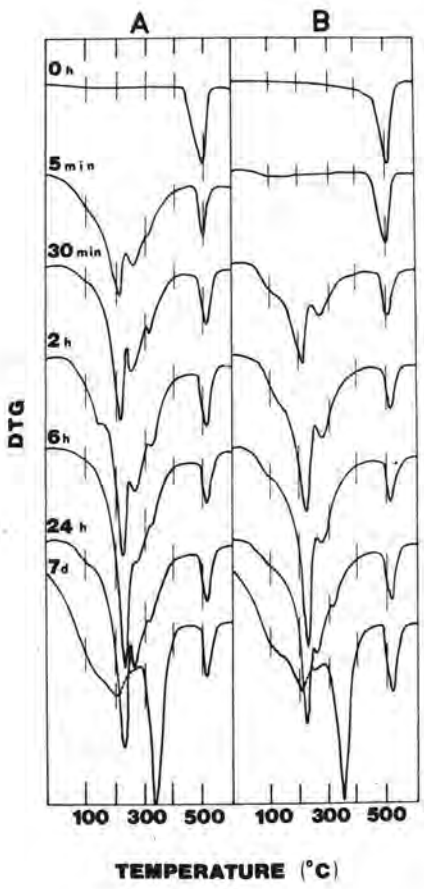

Fig. 2 - DTG curves for C_3A + CH pastes without (A) and with (B) NC and LGS.

the paste - due to hexagonal calcium aluminate hydrates - plays a prominent role in the stiffening of the system. On the other hand, the initial hydration products in Mix A' (Table II) and Mix A (Table I) are different, as the cubic hydrate is mainly formed in the C_3A suspension (Mix A') instead of the hexagonal hydrates in the C_3A paste (Fig. 2.A at 5 min). Traetterberg and Grattan-Bellew (10) and Collepardi et al (11) have found that when, for some reason, the transformation of the hexagonal calcium aluminate hydrates into the cubic phase occurs during the initial period of hydration, the C_3A paste changes from a stiff system to a fluid one. In the present work it seems that a high water/solid ratio, such as that of Mix A', favours the transformation of the hexagonal hydrates into the cubic phase having a high positive zeta potential.

A sharp change of zeta potential to a negative value of -41.5 mV (Mix B' in Table II) is obtained in the presence of NC and LGS (12 g/l). Incidentally, in the presence of LGS (12 g/l) without NC a less remarkable change in zeta potential to about - 20 mV is obtained. On the other hand the change in zeta potential caused by NC addition is still weaker. Similar results were obtained for the C_4AF-CH system (8).

C_3A - CH - $C\bar{S}.H_2$ system

The C_3A hydration is remarkably retarded by the addition of gypsum to the C_3A-CH system particularly during the first 6 hours (Fig. 1). During this period the amount of ettringite (with a DTG peak at about 130°C) increases, whereas the amount of $C\bar{S}.H_2$ (with a DTG peak at about 160°C) proportionally decreases (Fig. 3.C). Then ettringite is transformed into monosulfate (with DTG peaks at about 220 and 270°C) at 6 - 24 hours (Fig. 3.C) and C_3A hydration is remarkably accelerated (Fig. 1). Similar results were obtained by studying the influence of lime and gypsum on the C_3A hydration by an isothermal conduction calorimeter and DTG (5).

The addition of SNP to the C_3A-CH-$C\bar{S}.H_2$ system does not substantially change either the hydration rate (Fig. 1) or the hydration products (Fig. 3.D). Massazza et al (12) found that a SNP based superplasticizing admixture retarded the C_3A hydration. A different composition of the admixture used by Massazza et al could explain the apparent disagreement with the results of the present work.

The zeta potential of the C_3A-CH-$C\bar{S}.H_2$ system (Table II) changes from -8.5 mV to - 30.9 mV by addition of SNP (12 g/l). So, the effect of SNP on the zeta potential of the C_3A-CH-$C\bar{S}.H_2$ system seems to be less remarkable than that of LGS + NC on the zeta potential of the C_3A-CH system. On the other hand, the influence of SNP on the zeta potential seems to be more remarkable in Portland cement paste

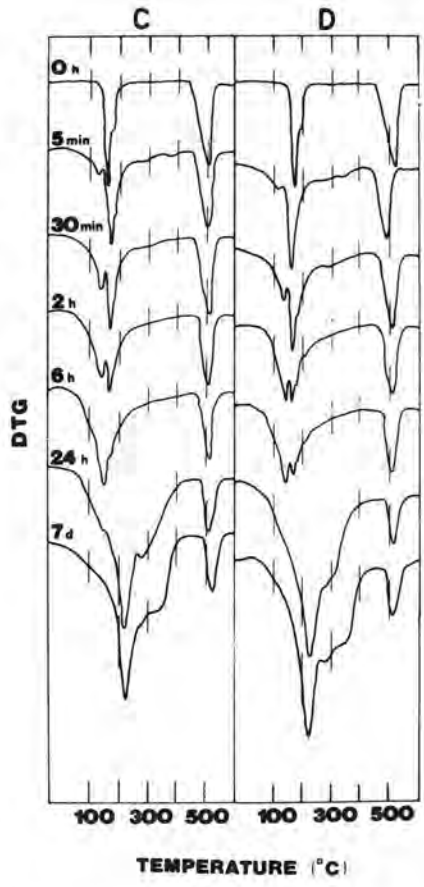

Fig. 3 - DTG curves for C_3A + CH + $CS.H_2$ pastes without (C) and with (D) SNP.

than in the C_3A-CH-$C\bar{S}.H_2$ - H_2O system. When the concentration of SNP in the liquid phase is 7.5 g/l, the zeta potential of Portland cement is about -50 mV (6), so that a still more negative value could be expected with a higher concentration of SNP (12 g/l) as that of the present work.

CONCLUSIONS

By paste hydration of C_3A in the presence of lime, hexagonal calcium aluminate hydrates (C_4AH_x and C_2AH_8) are initially formed and then they are transformed into the cubic hydrate (C_3AH_6) after 1 day. The same products are obtained when LGS and NC (both 0.6% by weight of C_3A) are added to the C_3A-CH system. However, the C_3A hydration is retarded by addition of LGS and NC and in particular the reaction is completely blocked for some minutes. The zeta potential - determined on a C_3A suspension - is remarkably changed from a positive value (37.4 mV) to a negative one (-41.5). Similar effects on the hydration rate and

zeta potential were caused by NC and LGS in the C_4AF-CH system (8). It may be speculated that both the change in zeta potential and the retardation of the initial hydration of C_3A and C_4AF could substantially contribute to the flowability of Portland clinker pastes containing NC and LGS. The high negative value of zeta potential on all the Portland clinker compounds - possibly including C_3S and C_2S - due to the addition of NC and LGS, could cause the mutual repulsion of clinker particles and then their dispersion (13). On the other hand, the formation of large clusters of hexagonal calcium aluminate hydrates sticking together could cause lower workability in a Portland clinker paste without gypsum (14, 15). When this aggregation is prevented, as the C_3A and C_4AF hydrations are completely blocked, more flowable clinker pastes could be obtained. Therefore, the liquefying effect of NC and LGS in Portland clinker pastes without gypsum could be partly ascribed to both the dispersing action caused by a negative zeta potential and the retardation in C_3A and C_4AF hydrations.

In the presence of lime and gypsum ettringite is initially (0-6 hours) formed causing retardation in C_3A hydration (5). When ettringite is transformed into monosulfate (6-24 hours) the C_3A hydration rate is accelerated. No substantial change either in the C_3A hydration rate, type of products or transformations are caused by the addition of SNP (0.6% by weight of C_3A). Therefore, it can be assumed that - as far as the C_3A-CH-$\bar{C}S.H_2$ system is concerned - the increase in flowability of Portland cement pastes, caused by SNP addition, is mainly due to a change in zeta potential resulting in a mutual repulsion of cement particles and then in their dispersion.

ACKNOWLEDGMENTS

The authors are grateful to Miss S. Malgherini for the drawing and to Misses D. Larese for typing the manuscript.

REFERENCES

(1) Proceedings of an International Symposium "Superplasticizers in Concrete" held in Ottawa, Canada, 1978. ACI Publication SP-62, pg. 315.

(2) M. Collepardi, M. Corradi, M. Valente, "Low Slump Loss Superplasticized Concrete", Transportation Research Record, Washington, January, (1979).

(3) Joint Working Party, Cement Admixture Assn & Concr. Assn., Superplasticizers in Concrete, Cem. Concr. Assn., Wexham Springs, UK, 1976.

(4) S. Brunauer et al., Cem. Concr. Res. 2, 313; 2, 331; 2, 463; 2, 577; 2, 731, (1972); 3, 129; 3, 279, (1973).

(5) M. Collepardi, M. Corradi, G. Baldini and M.Pauri, Cem. Concr. Res. 8, 571, (1978).

(6) M. Collepardi, M. Corradi, G. Baldini and M.Pauri, "Influence of Sulfonated Naphthalene on the fluidity of Cement Pastes", VII International Congress on the Chemistry of Cement, Paris, 1980.

(7) T.M. Riddick, Control of Colloid Stability through Zeta Potential, pg. 372, Zeta Meter Inc., New York (1968).

(8) M. Collepardi, M. Corradi, S. Monosi and G. Moriconi "Combined Effect of Lignosulfonate and Carbonate on Pure Portland Compounds Hydration. I. Tetracalcium Aluminoferrite Hydration", pending publication on Cem. Concr. Res.

(9) M.E. Tadros, W.Y. Jackson, J. Skalny, Colloid and Interface Science, 4, 211, (1976).

(10) A. Traetterberg and P.E. Grattan-Bellew, J. Am. Cer. Soc., 58, 221, (1975).

(11) M. Collepardi, M. Corradi, G. Baldini and M.Pauri, Cem. Concr. Res. 8, 741, (1978).

(12) F. Massazza, U. Costa and E. Corbella, "Influence of β-Naphthalene Sulfonate Formaldehyde Condensate Superplasticizing Admixture on C_3A Hydration" Seminar on Reaction of Aluminates during the setting of cements, Eindhoven, The Nederlands, (1977).

(13) M. Daimon and D.M. Roy, Cem. Concr. Res. 8, 753, (1978).

(14) F.W. Locher, W. Richartz and S. Sprung, Zement-Kalk-Gips 29, 435, (1976).

(15) I. Odler, R. Schönfeld, H. Dörr, Cem. Concr. Res. 8, 525, (1978).

Effect of superplasticizers on the C_3A hydration

Effet des superfluidifiants sur l'hydratation du C_3A

F. MASSAZZA, Professor of Applied Chemistry, Italcementi, Laboratorio Chimico Centrale Bergamo, Italy,
U. COSTA, B. Ch. Italcementi, Laboratorio Chimico Centrale, Bergamo, Italy.

RESUME : On a étudié l'hydratation de mélanges de C_3A et de gypse en présence de lignosulfonate de sodium et de condensat de naphtalène sulfoné et de formaldéhyde dans le but d'éclairer les causes de l'action fluidifiante exercée par ces substances sur les pâtes de ciment.
Les adjuvants ralentissent la vitesse de formation de l'ettringite, mais cela ne devrait pas être attribué à leur interaction avec C_3A. En effet l'aluminate non encore hydraté n'adsorbe pas les adjuvants et ne subit même pas de modifications structurales au niveau des centres actifs en thermoluminescence.
Au contraire, les sulfoaluminates hydrates adsorbent des quantités considérables de ces adjuvants et cela cause des modifications morphologiques dans les cristaux d'ettringite. Dans ce cas ils apparaissent, au microscope électronique, sous forme de petites aiguilles et pas comme de gros faisceaux fibreux représentant leur aspect normal en l'absence d'adjuvants.
Ces morphologies différentes peuvent expliquer, au moins partiellement, l'action exercée par ces superfluidifiants sur la rhéologie des pâtes de ciment. Leur présence cause la formation d'un feutre microcristallin sur les grains de C_3A, en empêchant son hydratation. Vice-versa, la morphologie normale, caractérisée par de gros cristaux d'ettringite joignant les différentes particules, justifie la perte rapide de plasticité des pâtes qui s'hydratent en l'absence d'adjuvants. En définitive, l'action des deux fluidifiants sur les ciments peut être attribuée à la réduction initiale de la demande d'eau du ciment et à la plus petite interconnexion entre les particules en cours d'hydratation.

SUMMARY: The hydration of mixes of C_3A and gypsum in the presence of sodium lignosulphonate and naphtalene sulphonate formaldehyde condensate was studied in order to explain the causes of the fluidizing action exerted by these substances on cement pastes.
The admixtures slow down the rate of formation of ettringite but this does not seem to be attributed to their interaction with C_3A. In fact the not yet hydrated aluminate does not adsorb the admixtures and does not even undergo structural changes concerning the active sites in thermoluminescence.
On the contrary sulphoaluminate hydrates adsorb considerable amounts of these additives and this causes evident morphological changes in the ettringite crystals. In this case they appear, under the electron microscope, in the form of small needles and not as large fibrous bundles representing their usual aspect in the absence of admixtures.
These different morphologies can explain, at least partly, the action exerted by these superplasticizers on the rheology of the cement pastes. Their presence causes the formation of a microcrystal felt on the grains of C_3A, hampering its hydration. Viceversa the normal morphology,characterized by large fibrous ettringite crystals connecting the different particles, justifies the rapid loss of plasticity of the pastes hydrating without admixtures. After all the action of the two plasticizers can be attributed to the initial reduction in the water demand of cement and the lower interlock among the hydrating particles.

1. INTRODUCTION

Plasticizers and superplasticizers have usually been employed for some time in the manufacture of concrete but, despite the several studies performed, the mechanism of their action has not yet quite been explained.
Many works reported in the most recent reviews (1) (2)(3) were carried out on the hydration of C_3A since this compound affects to a great extent setting times, water demand, workability and generally rheology of cement pastes.
A more limited number of works was performed on the action of these admixtures on the C_3A hydration in the presence of gypsum.
This work, which is part of a research programme on the mechanism of action of superplasticizers, reports the results obtained in the study of the C_3A hydration in the presence of gypsum, sodium lignosulphonate (L.S.S.) and naphtalene sulphonate formaldehyde condensate (N.S.F.). Lignosulphonate does not appreciably modify the initial rate of reaction of C_3A with gypsum but retards the conversion of ettringite to monosulphate and the formation of aluminate hydrates (4). This retarding action depends on the admixture content (5) and was confirmed by differential thermal analysis (6) and electron microscopic observations (7).
Lignosulphonate does not alter the sequence of the reactions but modifies the morphology of the hexagonal hydrates appearing when gypsum is depleted (8).
Observations by the scanning electron microscope showed that also ettringite undergoes morphological changes (9) like those noticed in the presence of sugar (10).
As for the N.S.F. action, information was not found in the available literature.

2. EXPERIMENTAL

2.1 Materials

Synthetic C_3A, natural $CaSO_4 \cdot 2H_2O$, purified sodium lignosulphonate and commercial alkyl naphtalene sulphonate formaldehyde condensate were used in the present work.
The tests were carried out on mixes consisting of 100 parts of C_3A and 20 parts of $CaSO_4 \cdot 2H_2O$ hydrated with pure water or 1% solutions of the admixtures.

2.2 Course of the hydration reaction

The hydration process was followed by a conduction calorimeter (11) recording the heat evolved by pastes consisting of 1 g mix and 1 ml pure water or containing the admixtures.
The heat evolution curves (figs. 1 and 2) show two peaks: the former, intense but of short duration, is due to the rapid reaction of C_3A with water, the latter, which appears when gypsum is exhausted, indicates the conversion of ettringite to monosulphate (12). Type and dosage of the admixtures affect intensity and position of the latter peak but not those of the former.

2.3 Identification of the phases in the pastes

The identification of the phases present at different stages of reaction was performed by X-ray diffraction, thermogravimetric analysis (TG) and differential scanning calorimetry (DSC).
The hydration was stopped at the established times by dispersing the paste in agate mortar with acetone.
However this treatment caused the removal of some water of crystallisation of ettringite, monosulphate and tetracalcium aluminate hydrate. This fact was pointed out by the change in the intensity and the position of the X-ray diffraction peaks. Ettringite showed extremely weak and broad peaks in some samples.

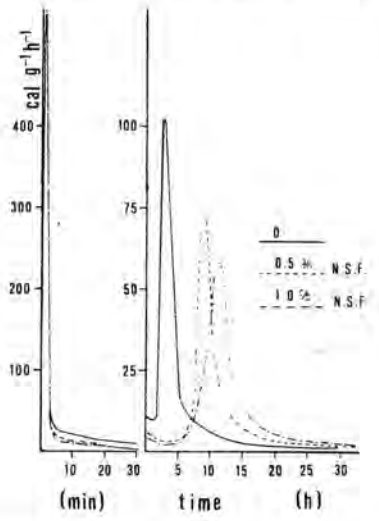

FIG. 1: Heat evolution curves recorded on pastes of C_3A + 20% gypsum containing N.S.F.

To restore the original structure, the samples were stored for some hours at 23°C and 100% R.H. (13).
After this treatment, the samples gave X-ray diffraction patterns corresponding to ettringite $32H_2O$, monosulphate $12H_2O$ and tetracalcium aluminate 19 and $13H_2O$. The last was partially carbonated (14).

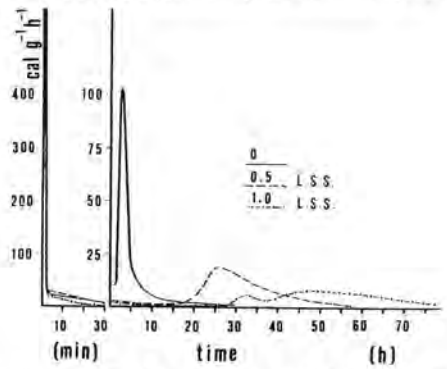

FIG. 2: Heat evolution curves recorded on pastes of C_3A + 20% gypsum containing L.S.S.

The phases identified by X-rays (table I) are in agreement with those detected by DSC (fig. 3).
Ettringite is the first hydration product forming and remains the only one as long as gypsum is present in the paste.
Calcium sulphate disappears in the pastes without admixtures after about 4 hours whereas it should disappear after about 7 hours in the presence of 1% N.S.F., according to the results obtained by conduction calorimetry. On the contrary in the presence of L.S.S., gypsum is found up to 36 hours.
The depletion of calcium sulphate is followed by the appearance of monosulphate forming at the expense of

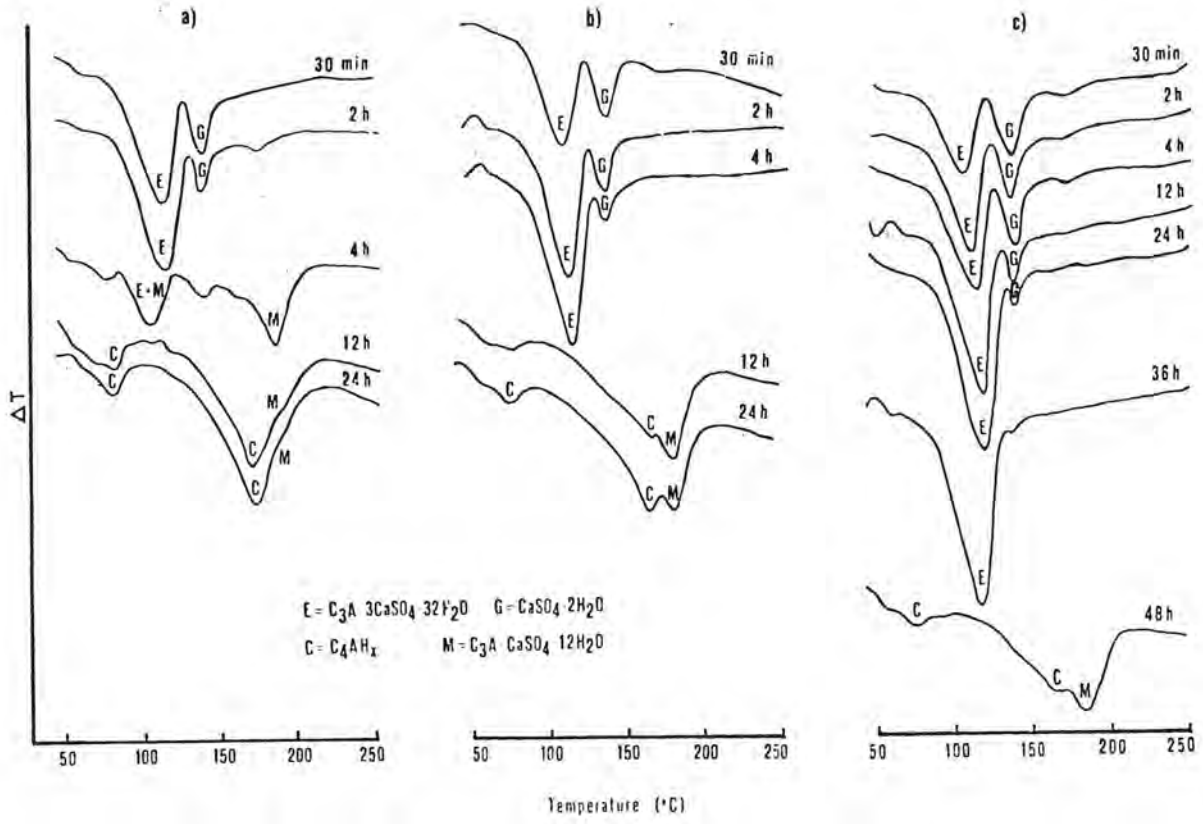

FIG. 3: DSC curves obtained on pastes of C_3A + 20% gypsum: a) without admixture, b) with N.S.F., c) with L.S.S.

ettringite. Then the hydration of the still present C_3A proceeds with the formation of hexagonal hydrates C_4AH_{19} and partially carbonated C_4AH_{13}.
The lattice constants of ettringite do not undergo changes due to the presence of the admixtures, whereas those of monosulphate slightly vary, as it is shown by the line d(0001) passing from 8.84 to 8.93 Å.

2.4 Dosage of ettringite in the pastes

The ettringite content in the hydrating pastes was determined by DSC or TG. The enthalpic effect related to the dehydration peak, that the compound shows at 115°C, was measured by the former method and the corresponding weight loss by the latter. The obtained calorimetric data were converted to concentration on the basis of the known value of the dehydration enthalpy of ettringite (213.9 Kcal/mole (15)).
The ettringite content was calculated from the weight loss measured between 50 and 120°C; at this temperature the compound loses 70% of its water (13). At the selected rate of heating (5°C/min), gypsum slightly affects the exactitude of the ettringite determination since it begings decomposing as from about 120°C.
As table II shows, ettringite is already present in considerable amount after 30 minutes. The content is maximum in the sample without admixtures and minimum in the sample containing L.S.S..

2.5 Interaction among admixtures, C_3A and hydration products

2.5.1 Thermoluminescence (TL) was used to evidence an eventual interaction between admixtures and anhydrous C_3A. In fact the aim was to verify whether

TAB. I: Phase identified by X-rays in the hydrated pastes

		0.5 h	2 h	4 h	12 h	24 h	36 h	48 h
Pastes without admixtures	C_3A	+	+	+	+	+	+	+
	$CaSO_4 \cdot 2H_2O$	+	+	--	--	--	--	--
	$C_3A \cdot 3CaSO_4 \cdot 32H_2O$	+	+	+	--	--	--	--
	$C_3A \cdot CaSO_4 \cdot 12H_2O$	--	--	+	+	+	+	+
	C_4AH_{19}	--	--	--	+	+	+	+
	C_4AH_{13} °)	--	--	--	+	+	+	+
Pastes with 1% N.S.F.	C_3A	+	+	+	+	+	+	+
	$CaSO_4 \cdot 2H_2O$	+	+	+	--	--	--	--
	$C_3A \cdot 3CaSO_4 \cdot 32H_2O$	+	+	+	--	--	--	--
	$C_3A \cdot CaSO_4 \cdot 12H_2O$	--	--	--	+	+	+	+
	C_4AH_{19}	--	--	--	--	+	+	+
	C_4AH_{13} °)	--	--	--	--	+	+	+
Pastes with 1% L.S.S.	C_3A	+	+	+	+	+	+	+
	$CaSO_4 \cdot 2H_2O$	+	+	+	+	+	+	--
	$C_3A \cdot 3CaSO_4 \cdot 32H_2O$	+	+	+	+	+	+	--
	$C_3A \cdot CaSO_4 \cdot 12H_2O$	--	--	--	--	--	--	+
	C_4AH_{19}	--	--	--	--	--	--	--
	C_4AH_{13} °)	--	--	--	--	--	--	+

°) Partially carbonated

the crystal defects always present in this compound (16) could constitute preferential sites for the hydration or adsorption of the admixtures.
To obtain this information, an apparatus with evacuated cell enabling heating rates up to 2°C/s was used. The intensity of the light emission was measured between 20 and 250°C by a single photon counting instrument provided with a photomultiplier sensitive in the 250-680 nm range.

TAB. II: Percentage of ettringite formed in the dried pastes of C_3A + 20% gypsum

Hydrat. time	Pastes without admixtures			Pastes with 1% N.S.F.			Pastes with 1% L.S.S.		
	DSC	TG	% of the theor. amount+)	DSC	TG	% of the theor. amount+)	DSC	TG	% of the theor. amount+)
0.5 h	21	22	61	17	18	49	13	17	43
2 h	23	24	65	22	24	65	18	20	53
3 h	27	31	82						
4 h				30	28	82	20	21	58
12 h							24	27	72
24 h							30	31	86
36 h							35	34	97

+) Complete reaction of gypsum gives a maximum of 35.5% by weight of ettringite

The active centres were excited as far as saturation by the X-rays produced by a tube with chrome anticathod. All the TL curves showed only the two maxima of light emission, belonging to C_3A, which as many electron traps related to crystal defects corresponded to (16).
The characteristics of the traps, namely:
E = depth of the trap (eV)
S = frequency factor (s^{-1})
p = probability of escape of trapped electrons at 25°C (s^{-1})
t = lifetime of trapped electrons (s) = 1/p
were calculated according to Randall and Wilkins' formalism, already successfully applied to the study of the thermoluminescence of the portland cement constituents (17).
Table III shows that the values of the fundamental parameter E, which the others derive from, undergoes random variations attributable to the measurement error. Therefore there are not evident modifications of the active sites of C_3A present in the different samples. The constancy of the characteristics of the traps and the progressive reduction in the intensity of the TL peaks, observed as the C_3A hydration proceeds (18), would lead to exclude that these traps or centres of luminescence play a role in the reactions occurring during the hydration of C_3A with gypsum in the presence or absence of the considered admixtures.

2.5.2 The interaction between admixtures and hydration products of C_3A was studied by determining the adsorption isotherms obtained by dispersing the hydrates in solutions of dimethylsulphoxide (DMSO), already used in similar studies (19).
Ettringite was prepared according to J. D'ANS and H. EICK's (20) method. Monosulphate was obtained by reaction between solutions saturated with calcium hydroxide and calcium sulphate and a solution obtained by shaking CA in water (20)(21). After filtration in atmosphere of inert gas, the precipitates were washed with acetone which was eliminated by vacuum evaporation. The samples were controlled by X-ray diffraction and thermal analysis. One mole of ettringite contained 25÷26 moles of water whereas one of monosulphate did 10 moles.
Anhydrous DMSO is considerable hygroscopic and causes a partial dehydration of sulphoaluminate hydrates.
To eliminate this inconvenience, a small amount of water (8%) was added to the solvent. It proved to be sufficient to stabilize the hydration products without modifying other characteristics.
The adsorption of the admixtures on the hydrates was determined by continuously recording the variations of the electric conductivity of the suspensions.
In fact the electric conductivity of the solutions of the admixtures in DMSO is proportional to their concentration in a rather large range of concentrations (0-10 g/l). All the measurements were performed at 20°C by using a thermostatic conductivity cell connected to a conductimeter working at 400 Hz. They were protracted as far as the attainment of the equilibrium indicated by the stabilization of the electric conductivity.
The equilibrium conductivity was also confirmed in the liquid obtained by filtering the suspensions.
Figures 4 and 5 show that at the equilibrium concentration of 9 g/l, the adsorption values are, for L.S.S., 5.9 wt % of ettringite and 4.3% of monosulphate. For N.S.F. the corresponding values are 4.7% of ettringite and 3.1% of monosulphate.
Monosulphate, differently from ettringite, showed an appreciable increase in its lattice distances after adsorption (18).
The increase in the lattice distances of monosulphate and the invariability in those of ettringite correspond to what occurs for the two compounds when they pass from 10 to 12 and from 10 to 32 water molecules respectively (22)(13).

TAB. III: Characteristics of the electron traps of C_3A

Sample	Hydrat. time	TRAP I				TRAP II			
		E(ev)	$S(s^{-1}) \times 10^{10}$	$p(s^{-1}) \times 10^{-6}$	$t(s) \times 10^{5}$	E(ev)	$S(s^{-1}) \times 10^{10}$	$p(s^{-1}) \times 10^{-9}$	$t(s) \times 10^{7}$
Anydrous C_3A		1.05	91	1.4	7.1	1.15	44	1.4	7.1
Pastes without admixtures	0.5 h	0.90	0.6	5.9	1.7	0.94	0.12	14	0.71
	4 h	0.97	6.2	2.4	4.2	1.29	1200	0.14	71
Pastes with 1% N.S.F.	0.5 h	1.07	135	0.9	11	1.25	447	0.26	38
	15 h	0.88	0.45	5.5	1.8	0.95	0.15	11	0.91
Pastes with 1% L.S.S.	0.5 h	1.19	7300	0.5	20	1.28	1600	0.38	26
	24 h	1.12	650	0.7	14	1.18	86	0.97	10

After all the adsorption data seem to indicate that the admixtures can replace some water in the lattice of sulphoaluminate hydrates.
It was ascertained that anhydrous C_3A shows no adsorption.

2.6 Morphology of the hydration products

The morphology of the hydration products was examined by observing the broken surfaces of the pastes under the scanning electron microscope.
The most interesting results concern the first stag-

es of reaction during which the main hydration pro - duct is ettringite. After 30 minutes its morpholo g y has appeared considerably affected by L.S.S. and N.S. F.

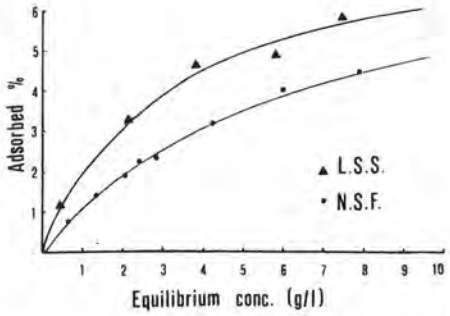

FIG. 4: Adsorption isotherms of N.S.F. and L.S.S.dis solved in DMSO on ettringite

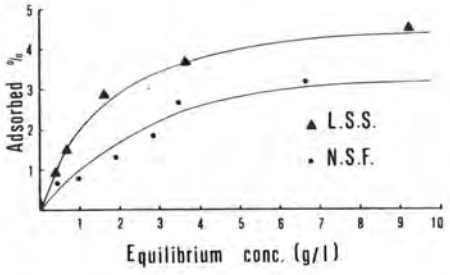

FIG. 5: Adsorption isotherms of N.S.F. and L.S.S. dis solved in DMSO on monosulphate

The micrography of fig. 6, relevant to a mix with pu- re water, shows the presence of large fibrous cry - stals of ettringite forming a sort of tridimensional branching which joins the different grains.
On the contrary the appearance of the pastes m a d e with solutions of the two admixtures is quite diffe- rent: the ettringite crystals have considerably smal ler sizes, they prevailingly appear as a fine felt (figs. 7 and 8) covering the C_3A and gypsum parti - cles but seem unable to form strong and broad inter- locks.
These differences can be considered as the consequen ce of introducing admixture molecules into the lat - tice of ettringite. This explanation is based on t h e results of the adsorption of the admixtures dissolv- ed in dimethylsulphoxide and it is reasonable to ext end it to the aqueous solutions.

3. CONCLUSIONS

The tests carried out showed that sodium lignosulpho nate and naphtalene sulphonate formaldehyde slow down the formation of ettringite. From this standpoint the action of L.S.S. is higher than that of N.S.F..
Whilst C_3A does not adsorb the admixtures dissolved in DMSO, sulphoaluminate hydrates can adsorb appre - ciable amounts. As for monosulphate, the adsorpti o n is accompained by a noticeable variation of the lat- tice distances.
This adsorption is likely to be the cause of the mor

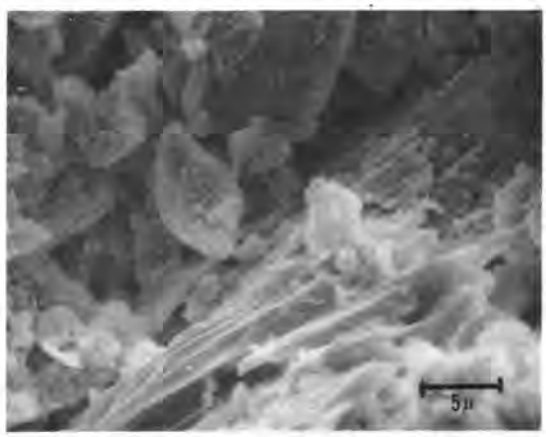

FIG. 6: Large ettringite bundles in pastes of C_3A + + $CaSO_4 \cdot 2H_2O$ hydrated for 30 minutes with pu re water. 3000 X

phological changes noticed in the ettringite c r y - stals.
The fine structure of its crystals observed in t h e pastes containing the admixtures can, in its turn, ju stify the slowing down underwent by the C_3A hydrati - on.

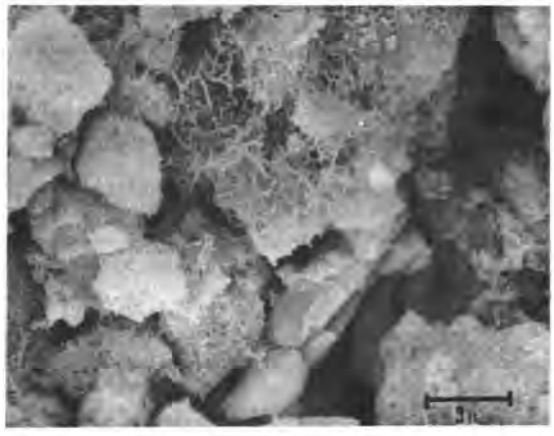

FIG. 7: Ettringite needles in pastes of C_3A + $CaSO_4 \cdot$ $\cdot 2H_2O$ hydrated for 30 minutes with 1% N.S.F. solution. 5000 X

In fact ettringite in the form of small crystals pro tects the C_3A grains from the action of water mo r e than it does when it consists of large fibrous cry - stals.
Viceversa, the large fibrous crystals can exert a mo- re effective mechanical action of interlock amo n g the grains forming the paste.
To conclude, the fluidizing action caused by the two examined products on cement pastes can be attributed, at least partly, to the two following effects:

1. Slowing down of the rate of formation of ettringi

te and therefore reduction in the water demand of cement
2. Decrease in the interlock performed by the ettringite bridges connecting the solid particles and consequent improvement in the rheology of the paste.

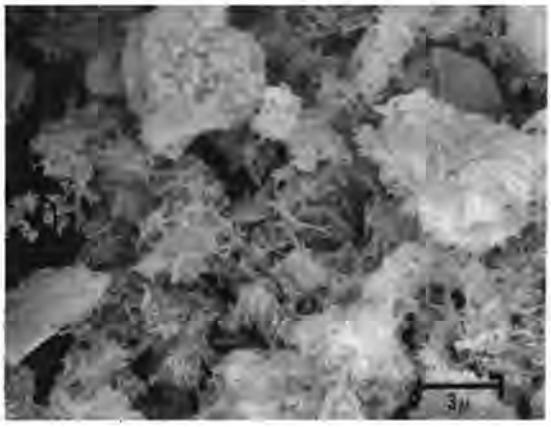

FIG. 8: Ettringite needles in pastes of $C_3A + CaSO_4 \cdot 2H_2O$ hydrated for 30 minutes with 1% L.S.S. solution. 5000 X

REFERENCES

1. - YOUNG J.F. (1972), "A review of the mechanism of set-retardation in portland cement pastes containing organic admixtures", Cement and Concrete Research, 2, 415-433 (Eng.)
2. - YOUNG J.F. (1976), "Reaction mechanisms of organic admixtures with hydrating cement compounds", Transportation Research Record, No.564, 1-9,(Eng.)
3. - RAMACHANDRAN V.S. (1977)(1978), "Chapter 6 - Admixtures", Cements Research Progress 1976, 97; 1977, 119, The American Ceramic Society, Columbus, (Eng.)
4. - SELIGMANN P., GREENING N.R. (1964), "Studies of early hydration reactions of portland cement by X-ray diffraction", High.Res.Record, High.Res.Board, No. 62, 80-105, (Eng.)
5. - GUPTA P., CHATTERJI S., JEFFERY J.W. (1973),"Studies of the effects of various additives on the hydration reaction of tricalcium aluminate: Part 4", Cement Technology, 4, 63-69, (Eng.)
6. - RAMACHANDRAN V.S. (1972), "Elucidation of the role of chemical admixtures in hydrating cements by DTA technique", Thermochimica Acta, 4, 343-366 (Eng.)
7. - CHATTERJI S. (1967), "Electron-optical and X-ray diffraction investigation of the effects of lignosulphonates on the hydration of C_3A", The Indian Concrete Journal, 41, 151-160, (Eng.)
8. - YOUNG J.F. (1962), "Hydration of tricalcium aluminate with lignosulphonate additives", Magazine of Concrete Research, 14, 137-142,(Eng.)
9. - CIACH T.D., SWENSON E.G. (1971), "Morphology and microstructure of hydrating portland cement and its constituents. I - Changes in hydration of tricalcium aluminate alone and in the presence of triethanolamine or calcium lignosulphonate", Cement and Concrete Research, 1, 143-158, (Eng.)
10. - YOUNG J.F. (1969), "Supplementary Paper II-26. The influence of sugars on the hydration of tricalcium aluminate", Proc. of the Fifth Int. Symp. on the Chemistry of Cement (Tokyo 1968), 256-267, (Eng.)
11. - MASSAZZA F., FRANCARDI M.T., COSTA U., (1969) "Quelques méthodes pour le contrôle des phénomènes associés à l'hydratation initiale des ciments", CEMBUREAU - Manifestations Thermiques de l'Hydratation au Cours de la Prise du Ciment - Rapport et Discussion d'un Colloque (Paris),15 pp,(French)
12. - STEIN H.N. (1963), "Some characteristics of the hydration of $3\,CaO.Al_2O_3$ in the presence $CaSO_4 . 2H_2O$", Silicates Industriels, XXVIII, 141-145, (Eng.)
13. - DÄRR G.M., PUNZET M., LUDWIG U. (1977), "On the chemical and thermal stability of ettringite", CEMBUREAU - Reaction of Aluminates During the Setting of Cements, 4 pp., (Eng.)
14. - TAYLOR H.F.W. (1964), "Appendix I - Tabulated crystallographic data", Taylor, The Chemistry of Cements, 2, 347-404, Academic Press - London, (Eng.)
15. - HENNING O., STROBEL U. (1969), "Kalorimetrische Messungen an Kalziumaluminatsulfathydraten mit dem Differential Scanning Calorimeter", Wissenschaftliche Zeitschrift der Hochschule für Architektur und Bauwesen Weimar, 16, 173-176, (Ger.)
16. - FIERENS P., VERHAEGEN A., VERHAEGEN J.P.(1974), "Etude par thermoluminescence de l'hydratation de l'aluminate tricalcique", Cement and Concrete Research, 4, 381-387,(French)
17. - FIERENS P., TIRLOCQ J., VERHAEGEN J.P. (1973), "Luminescence et hydratation du silicate tricalcique", Cement and Concrete Research, 3, 549-560,(French)
18. - Unpublished work
19. - RAMACHANDRAN V.S., FELDMAN R.F. (1971), "Adsorption of calcium lignosulfonate on tricalcium aluminate and its hydrates in a non-aqueous medium", Cement Technology, 2, 121-129, (Eng.)
20. - D'ANS J., EICK H. (1953), "Das System $CaO-Al_2O_3-CaSO_4-H_2O$ bei 20°C", Zement Kalk Gips, 6, 302-311 (Ger.)
21. - TURRIZIANI R., SCHIPPA G. (1954), "Riconoscimento all'ATD ed ai raggi X dei solidi quaternari $CaO-Al_2O_3-CaSO_4-H_2O$", La Ricerca Scientifica, 24, 2356-2363, (Ital.)
22. - TURRIZIANI R. (1964), "The calcium aluminate hydrates and related compounds", Taylor, The Chemistry of Cements, 1, 233-286, Academic Press - London, (Eng.)

Elucidation of the role of calcium lignosulfonate in the hydration of C_3A

Eclaircissement du rôle du lignosulnonate de calcium dans l'hydratation du C_3A

V.S. RAMACHANDRAN, Senior Research Officer of Building Research, National Research Council of Canada, Ottawa, Ontario KIA 0R6 Canada.

RESUME: L'auteur obtient des isothermes d'adsorption et de désorption en exposant de l'aluminate tricalcique (C_3A), de l'aluminate calcique hexagonal (C_4AH_{13}-C_2AH_8) et de l'hydrate d'aluminate cubique (C_3AH_6) à des solutions de lignosulfonate de calcium (CLS) dans de l'eau ou du diméthylsulfoxyde. Dans le milieu non aqueux, le C_3A et le C_3AH_6 absorbent peu ou pas de lignosulfonate; la phase hexagonale adsorbe à peu près 2.2% de CLS. Dans une solution aqueuse contenant une grande quantité de CLS, le C_3A forme un complexe de CLS basique qui est insoluble dans l'eau. Les boucles de balayage dans les isothermes pour le système aluminate hexagonal-CLS-H_2O montrent une complète irréversibilité avec une adsorption de 10% à une concentration d'équilibre de 0.10% de CLS. Une adsorption rapide et irréversible de 2.05% de CLS se produit dans le système C_3AH_6-CLS-H_2O. Les phases C_3A, C_4AH_{13}-C_2AH_8 et C_3AH_6 agissent comme des absorbants pour le CLS dans l'hydratation du C_3S contenant du CLS; l'hydratation du C_3S qui est complètement inhibée en présence de 0.8% de CLS peut être rétablie par l'addition de ces phases d'aluminate. L'efficacité relative avec laquelle l'addition de 5% de ces additifs annule l'influence inhibitrice du CLS est de l'ordre de C_3A>C_4AH_{13}-C_2AH_8>C_3AH_6.

Le Ca et le Na-lignosulfonate ne contenant aucun sucre agissent de façon similaire au lignosulfonate commercial et retardent l'hydratation du C_3A.

SUMMARY: Adsorption-desorption isotherms were obtained by exposing tricalcium aluminate (C_3A), hexagonal calcium aluminate (C_4AH_{13}-C_2AH_8) and cubic aluminate hydrate (C_3AH_6) to calcium lignosulfonate (CLS) solutions in water or dimethyl sulfoxide. In the non-aqueous medium C_3A and C_3AH_6 adsorb little, if any, lignosulfonate; the hexagonal phase adsorbs about 2.2% CLS. In an aqueous medium containing large amounts of CLS, C_3A forms a basic CLS complex that is insoluble in water. Scanning loops in the isotherms for the hexagonal aluminate-CLS-H_2O system show complete irreversibility with an adsorption of 10% at an equilibrium concentration of 0.10% CLS. A rapid irreversible adsorption of 2.05% CLS occurs in the C_3AH_6-CLS-H_2O system. The C_3A, C_4AH_{13}-C_2AH_8 and C_3AH_6 phases act as sinks for CLS in the hydration of C_3S containing CLS; the hydration of C_3S that is completely inhibited in the presence of 0.8% CLS can be restored by the addition of these aluminate phases. The relative effectiveness with which the addition of 5% of these additives counteracts the inhibitive influence of CLS is in the order of C_3A>C_4AH_{13}-C_2AH_8>C_3AH_6.

Both Ca and Na-lignosulfonates containing no sugar behave in a manner similar to the commercial lignosulfonate in retarding the hydration of C_3A.

INTRODUCTION

Lignosulfonic acid and its salts are widely used as water-reducing and retarding admixtures in concrete. They are known to reduce water requirements by about 5 - 10% and setting times by 30 - 60%.

Since only small amounts of lignosulfonate are needed to influence the water-reducing and retarding properties of concrete, it has been concluded that the action of this admixture involves the phenomenon of adsorption. Some attempts have been made to study the adsorption of admixtures on portland cement and the individual cement minerals, viz., C_3S, C_2S, C_3A and C_4AF. Since the C_3A phase plays an important role in the early stages of hydration, considerable work has been directed to a study of the adsorption of lignosulfonate on this phase. In most studies, the amount of the admixture adsorbed by C_3A under so-called equilibrium conditions has been determined by exposure to an aqueous solution. In this method the hydration of C_3A could not have been avoided and, consequently, conclusions drawn from such experiments are questionable.

Another unresolved question concerns the role of lignosulfonate in the retardation of cement hydration. Commercial lignosulfonates invariably contain sugars and it is generally thought that they are, in fact, responsible for the retarding action (1-3). There is strong evidence, however, that lignosulfonate is adsorbed by the hydrating minerals (4-12). This would indicate that the lignosulfonate molecule in a commercial sample should play an important role in the dispersion and retardation of hydration of C_3A.

In view of these questions, it was thought that a more realistic approach to study the adsorption isotherms of lignosulfonates on the aluminate phases should involve measurements under conditions in which the adsorbent does not undergo hydration. This condition could be achieved by using a non-aqueous solvent, viz, dimethyl sulfoxide and adsorbents C_3A, C_4AH_{13}-C_2AH_8 and C_3AH_6 or using aqueous solutions of lignosulfonate with C_4AH_{13}-C_2AH_8 and C_3AH_6. Thus, adsorption-desorption scanning branches emanating at different points on the main adsorption curve would enable a study of the type of surface interaction occurring in the system.

For a further evaluation of the role of lignosulfonate, purified sugar-free lignosulfonate salt of Ca or Na was prepared from the corresponding salts of commercial products and its effect on the relative rates of hydration of C_3A was followed by differential thermal technique.

EXPERIMENTAL

Materials - Tricalcium aluminate was obtained by calcining a mixture of $CaCO_3$ and Al_2O_3; it had a Blaine surface area of 4350 m^2/g. Tricalcium silicate was prepared by calcining a mixture of $CaCO_3$ and SiO_2; it had a Blaine surface area of 3310 m^2/g. The hexagonal calcium aluminates comprising C_4AH_{13} and C_2AH_8 (referred to as the hexagonal phase) were prepared by the hydration of C_3A at 2°C for 5 days. The cubic calcium aluminate hydrate C_3AH_6 (referred to as the cubic phase) was prepared by steam curing C_3A at a pressure of 0.69 MN/m^2 for 24 h. Calcium lignosulfonate sample in the form of powder was supplied by Lignosol Chemical Ltd., Quebec. The sample had 4.5% reducing bodies. Sugar-free Ca or Na lignosulfonates were obtained by fractionation of commercial lignosulfonates by continuous diffusion using a Dowex 50WX2 resin.

Methods - Amounts of lignosulfonate adsorbed by the aluminates were determined by estimation of lignosulfonate, before and after adsorption, by a Perkin Elmer double beam UV spectrophotometer at a wavelength of 275 μm. Details of the method are described in another publication (13).

Differential thermal analysis (DTA) was carried out in N_2 using a Du Pont 900 Thermal Analyser. X-ray diffractograms (XRD) were obtained by a Hilger and Watts unit using CuKα source. Electron microscopic examination was carried out by a Cambridge Stereoscan Mark 2A instrument.

RESULTS AND DISCUSSION

Tricalcium Aluminate-Calcium Lignosulfonate-Water System

Tricalcium aluminate hydrates to the metastable hexagonal hydrate and finally to the cubic form. In the presence of calcium lignosulfonate (CLS) conversion to the hexagonal and cubic hydrate proceeds more slowly, depending on the dosage of CLS (Table I). In portland cement containing 10% C_3A, incorporation of 3% CLS is equivalent to 30% with respect to the C_3A phase and hence it was of interest to study the effect of the addition of 15, 30, 50, 100 and 200% CLS on the hydration of C_3A.

TABLE I - Influence of Calcium Lignosulfonate on the Hydration of C_3A

Lignosulfonate, %	Products Formed			
	1 day	7 days	14 days	28 days
0	cubic	cubic	cubic	cubic
0.5	cubic	cubic	cubic	cubic
1.0	hexagonal	hexagonal + cubic	cubic	cubic
3.0	hexagonal	hexagonal	hexagonal	hexagonal + cubic

A gelatinous mass formed at concentrations equivalent to and greater than 50% CLS. Electron microscopic examination revealed the gel to be a fluffy mass typical of a non-crystalline material, which appeared different from CLS or C_3A (Figs. 1a, b, d) (13). In samples treated with an aqueous solution containing 30% CLS with respect to C_3A, the resultant material exhibited a honeycomb structure (Figure 1c). Using surface area, chemical analysis, DTA and X-ray methods, it was concluded that the gel formed at higher concentrations of CLS was a basic CLS containing some Al^{+++}. Very high adsorption values reported in the C_3A-CLS-H_2O system by Rehbinder and Segalova can be explained by the formation of such a complex (14). In the presence of <30% CLS, a non-crystalline complex results, and this is related to that formed between CLS and the hexagonal phase.

Hexagonal Aluminate Hydrate-Calcium Lignosulfonate-Water System

Adsorption-desorption isotherms of CLS on the hexagonal phase are shown in Figure 2 (15). After a rapid adsorption, the curve tapers off between equilibrium concentrations of 0.05 and 0.15% CLS. The scanning isotherms obtained from various points show complete irreversibility.

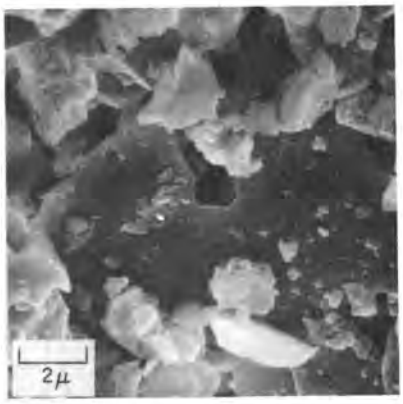

Fig. 1a - Tricalcium aluminate

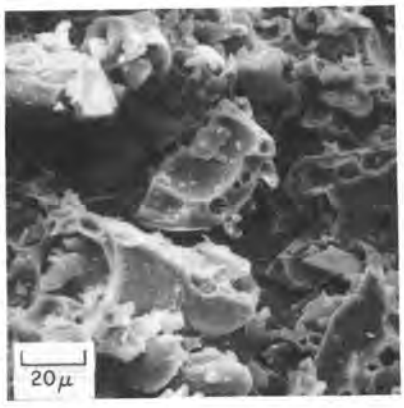

Fig. 1b - Calcium lignosulfonate

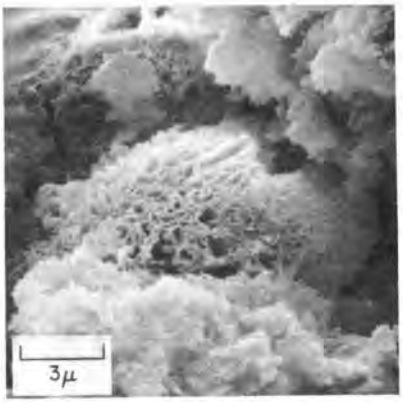

Fig. 1c - C3A treated with 30% calcium lignosulfonate

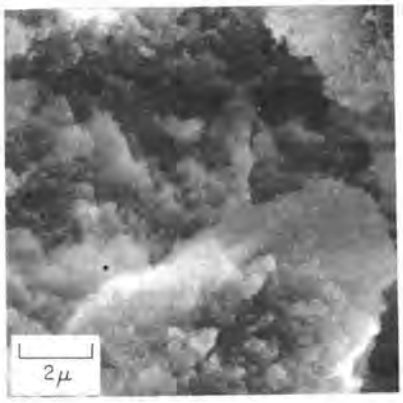

Fig. 1d - Gel-like material from C3A + 100% calcium lignosulfonate

Figure 3 represents X-ray diffractograms of the hexagonal phase and CLS-treated samples on the desorption branch corresponding to a net adsorption value of 10% CLS (13). The hexagonal phase shows a peak at 7.90Å for C_4AH_{13} and two characteristic peaks for C_2AH_8 at 10.5Å and 5.23Å. The sample containing 10% CLS exhibits a sharp peak of larger magnitude at 10.5Å but one of reduced intensity at 7.90Å. The surface area measurements indicated that whereas the hexagonal phase had a value of 11.1 m^2/g, that which had adsorbed 10% CLS had an area of 15.3 m^2/g. The hexagonal phase containing the irreversibly adsorbed CLS was found to be unmistakably different from the normal phase on examination by DTA, thermogravimetric analysis and electron microscopy. These results could be interpreted as follows. A complete irreversibility up to an adsorption value of 10% CLS was due to the formation of a complex between CLS and the hexagonal phase. The increase in the intensity of the 10.5Å peak and a decrease in the intensity of that at 7.9Å in XRD may be due to an increase in the C-axis spacing, as a consequence of CLS entering the interlayer position. Thus, it seems possible that retardation of conversion of the hexagonal to the cubic phase is due to CLS existing as a complex with the hexagonal phase. The interlayer complex may

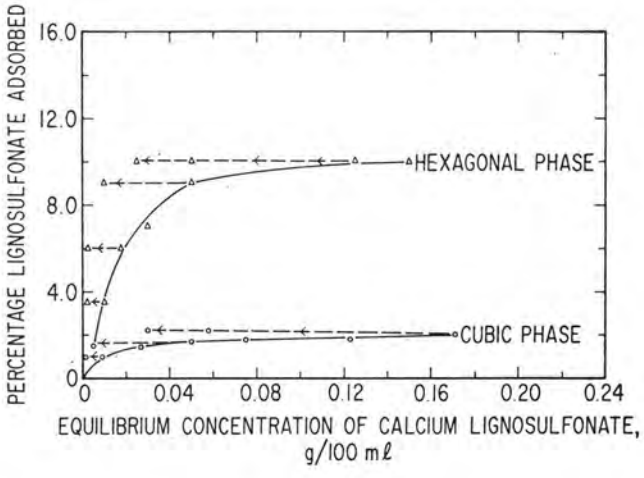

Fig. 2 - Adsorption-desorption isotherms of calcium lignosulfonate on the hexagonal and cubic phases of calcium aluminate hydrates

restrict the free movement of the interlayer ions for conversion to the cubic form.

Tricalcium Aluminate Hexahydrate-Calcium Lignosulfonate-Water System

Adsorption-desorption scanning isotherms of this system are presented in Figure 2. After a rapid, initial adsorption the amount remains almost constant at 2.05%. Scanning isotherms from different points show irreversibility. Surface areas of C_3AH_6 before and after adsorption of CLS were 4.71 and 9.38 m^2/g, respectively. It appears that in the presence of CLS, dispersion of C_3AH_6 and chemi-sorption of CLS are promoted.

Adsorption of Calcium Lignosulfonate on C_3A and its Hydrates in a Non-aqueous Medium

Figure 4 gives the typical adsorption isotherms of CLS (using dimethyl sulfoxide (DMSO) as a non-aqueous solvent) on the hexagonal phase (16). After a rapid adsorption, the value tapers off to a value of 2.2%. The irreversibility, even at low concentrations of CLS, indicates that CLS is strongly complexed with the hexagonal phase. The amount of adsorption of CLS in an aqueous medium is much higher than in DMSO because of the possibility of water with a higher dipole moment entering the interlayer positions and enabling more CLS to enter. In a non-aqueous medium, practically no adsorption of CLS occurs on C_3A or C_3AH_6 phase. The relatively lower surface areas of C_3A and C_3AH_6, the nature of the surfaces and absence of interlayer spaces are probably responsible for the lack of adsorption.

Tricalcium Silicate-Calcium Lignosulfonate-Water System in the Presence of Tricalcium Aluminate and its Hydrates

The adsorption-desorption experiments have shown that the relative amounts of adsorption of CLS in the aluminate phases are in the decreasing order C_3A> C_4AH_{13}-C_2AH_8> C_3AH_6. Ceteris Paribus C_3A hydrates faster than C_3S and, therefore, in cements the hydrating aluminate may act as a sink for CLS. A few experiments were performed to investigate the effect of 5% of these aluminate phases on the hydration of C_3S containing 0.8% CLS. Addition of 0.8% CLS to C_3S completely inhibits its hydration, as evidenced by the absence of $Ca(OH)_2$ formation (Figure 5, A-2) (17). Addition of 5% C_3A is sufficient to promote hydration slowly at first and normally after 3 days because C_3A has the capacity to react with large quantities of CLS (Figure 5, B-2). The hexagonal phase, adsorbing less CLS than the C_3A phase, is relatively less efficient in counteracting the inhibitive action of CLS; the cubic phase is practically ineffective (Figure 5, C-1, C-2, D-1 and D-2). The greater inhibitive action of CLS (on the hydration of C_3S) when added to cements after 5 min of hydration may be explained on the basis of the hydrated products of C_3A consuming less CLS than C_3A itself.

Hydration of Tricalcium Aluminate in the Presence of Sugar-free Calcium and Sodium Lignosulfonates

Figures 6, 7 and 8 compare the thermograms of C_3A hydrated in the presence of 0.1, 0.5, 1.0 or 3%

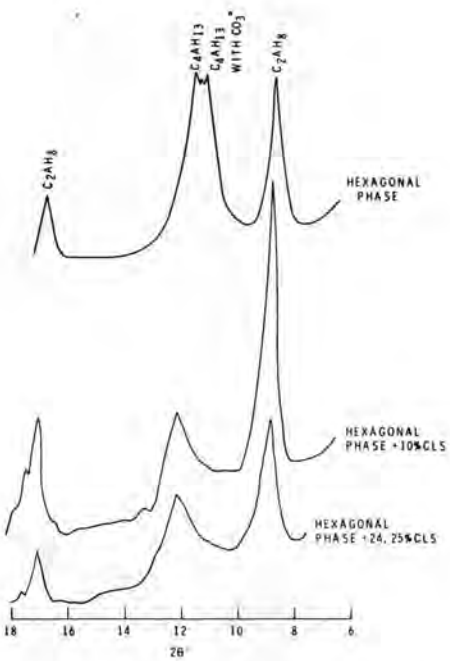

Fig. 3 - X-ray diffractogram of hexagonal phase and that treated with calcium lignosulfonate

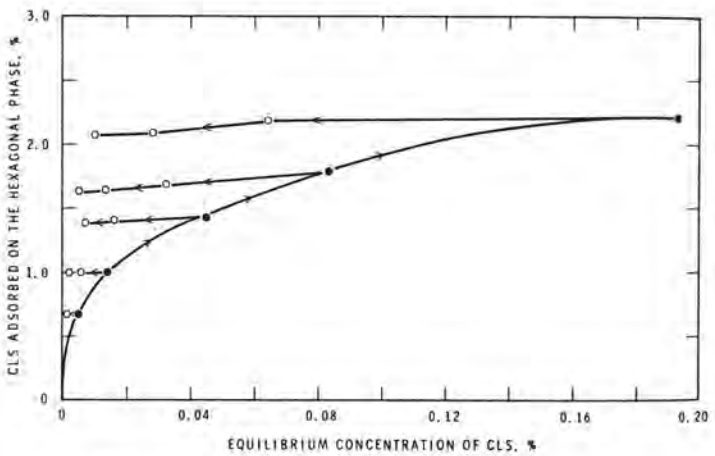

Fig. 4 - Adsorption-desorption isotherms of calcium lignosulfonate on the hexagonal phase

commercial Ca-lignosulfoaluminate (CLS), sugar-free Ca-lignosulfonate (Sf-CLS) and sugar-free Na-lignosulfonate (Sf-NLS), for periods ranging from 1 to 60 days (18). The thermal behaviour of C_3A hydrated in the absence of admixtures (not shown in the figure) indicates, even at 15 min, a large endothermal effect at 300°C denoting the presence of the cubic phase. Slight retardation in the early stages of hydration occurs in the presence of 0.1% admixtures but at 1 day the cubic hydrate is the only dominant phase present. At 0.5% addition, Sf-NLS seems to be the best retarder,

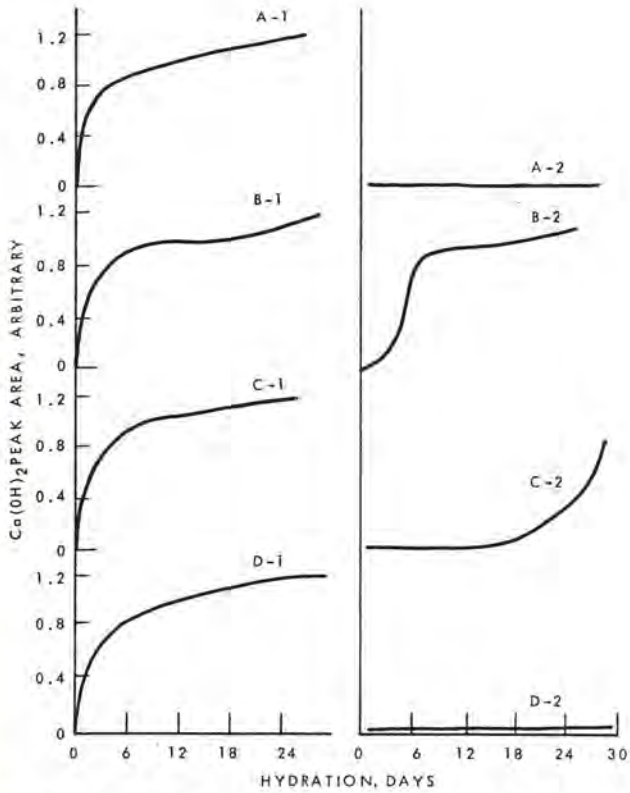

Fig. 5 - Kinetics of the hydration of C_3S in the presence of calcium lignosulfonate, C_3A or its hydrates.
A-1 = C_3S+H; A-2 = C_3S+CLS+H;
B-1 = C_3S+C_3A+H; B-2 = C_3S+C_3A+CLS+H;
C-1 = C_3S+hexagonal phase+H;
C-2 = C_3S+hexagonal phase+CLS+H;
D-1 = C_3S+C_3AH_6+H; D-2 = C_3S+C_3AH_6+CLS+H.

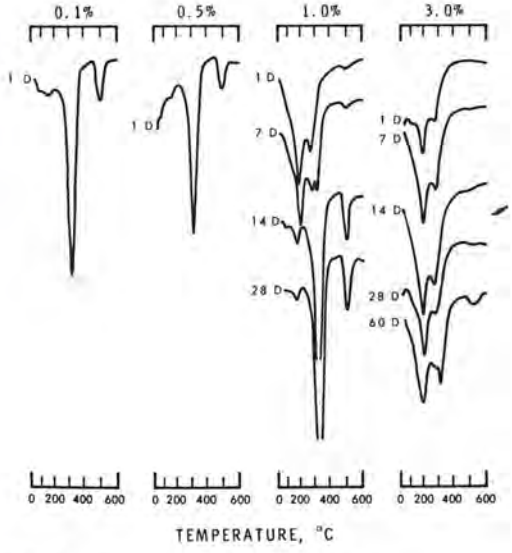

Fig. 6 - DTA of C_3A hydrated in the presence of commercial Ca lignosulfonate.

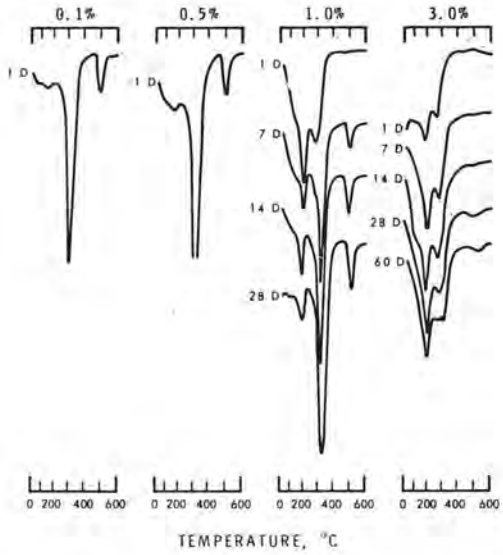

Fig. 7 - DTA of C_3A hydrated in the presence of sugar-free Ca lignosulfonate.

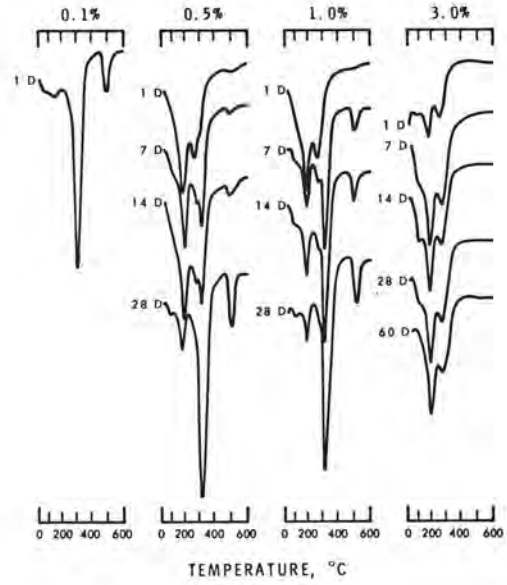

Fig. 8 - DTA of C_3A hydrated in the presence of sugar-free Na lignosulfonate.

as evidenced by the presence of only the hexagonal phase at 1 day (Figure 8). In the presence of 1.0% lignosulfonate, the conversion of the hexagonal to the cubic phase is retarded in all samples. A much more efficient retardation occurs at an addition of 3% admixture. These results demonstrate that sugar-free lignosulfonate, which is presumably adsorbed irreversibly by C_3A and its hydrates, is as efficient as the commercial lignosulfonate in retarding the hydration and interconversions in the C_3A-H_2O system. The XRD and TGA data on these samples were in fair agreement with those obtained by DTA.

CONCLUSIONS

In the C_3A-calcium lignosulfonate (CLS)-H_2O system, at low concentrations of CLS, a surface complex containing C_3A, CLS and H_2O may form, but at higher concentrations of CLS a highly basic CLS compound containing some Al^{3+} results. In the hexagonal aluminate-CLS-H_2O system, scanning loops in the isotherms indicate complete irreversibility due to the formation of an interlayer complex that may be responsible for the retardation of the conversion of the hexagonal to the cubic phase. In the C_3AH_6-CLS-H_2O system, a rapid irreversible adsorption is followed by dispersion.

In the non-aqueous medium, in contrast to the aqueous medium the C_3A does not adsorb CLS. Thus the present tendency of explaining the retarding action on the basis of adsorption of CLS on C_3A should be altered in favour of the concept "the consumption of CLS by the hydrating C_3A."

The inhibitive action of CLS on the hydration of C_3S is modified by incorporation of C_3A, the hexagonal phase or the cubic phase. The phase consuming larger amounts of CLS lowers the inhibitive action of CLS on the hydration of C_3S. Thus, when prehydrated C_3A is added to the C_3S-CLS-H_2O system there is less adsorption of CLS on aluminate phases, and hydration of C_3S is inhibited or retarded more than by the addition of C_3A.

Calcium and sodium lignosulfonates, deplete of sugars, are as effective as the commercial lignosulfonates in retarding the hydration of C_3A, indicating thereby that adsorption of lignosulfonate by the cement compounds is an important mechanism by which hydration is retarded.

ACKNOWLEDGEMENTS

The author thanks G.M. Polomark for the experimental assistance. This paper is a contribution from the Division of Building Research, National Research Council of Canada, and is published with the approval of the Director of the Division.

REFERENCES

1.- S. CHATTERJI (1967), "Electron-optical and X-ray diffraction investigation of the effects of lignosulphonates on the hydration of C_3A", Ind. Concr. J., 41, 151-160.

2.- R.A. KENNERLEY, A.L. WILLIAMS and D.A. ST. JOHN (1960), "Water reducing retarders for concrete", Dominion Laboratory Rept. 2026, Dept. Sci. Ind. Res., Lower Hutt, New Zealand, p. 66.

3.- N.B. MILESTONE (1976), "The effect of lignosulphonate fractions on the hydration of tricalcium aluminate", Cem. Concr. Res., 6, 89-102.

4.- F.M. ERNSBERGER and W.G. FRANCE (1945), "Portland cement dispersion by adsorption of calcium lignosulfonate", Ind. Eng. Chem., 37, 598-600.

5.- J.F. YOUNG (1969), "Influence of tricalcium aluminate on the hydration of calcium silicates", J. Am. Ceram. Soc., 52, 44-46.

6.- B. BLANK, D.R. ROSSINGTON and L.A. WEINLAND (1963), "Adsorption of admixtures on portland cement", J. Am. Ceram. Soc., 46, 395-399.

7.- D.R. ROSSINGTON and E.J. RUNK (1966), "Adsorption of admixtures on portland cement hydration products", J. Am. Ceram. Soc. 51, 46-50.

8. T. MANABE and N. KAWADA (1960), "Actions of calcium lignosulfonate upon portland cement clinker compounds", Rev. 14th Gen. Meeting, Japan Cem. Eng. Assoc., Tokyo, p. 25-26.

9.- N. KAWADA and M. NISHIYAMA (1960), "Actions of calcium lignosulfonate upon portland cement clinker compounds", Rev. 14th Gen. Meeting, Japan Cem. Eng. Assoc., Tokyo, p. 25-26.

10.- W.C. HANSEN (1959), "Action of calcium sulfate and admixtures in portland cement pastes", Symp. Effect of Water-Reducing Admixtures and Set-Retarding Admixtures on Properties of Concrete, ASTM Spec. Tech. Publ. No. 266, p. 3-37.

11.- W.C. HANSEN (1970), "Interaction of organic compounds in portland cement pastes", J. Mater. 5, 842-855.

12.- S. DIAMOND (1971), "Interactions between cement minerals and hydroxycarboxylic acid retarders", J. Am. Ceram. Soc. 54, 273-276.

13.- V.S. RAMACHANDRAN (1972), "Effect of calcium lignosulfonate on tricalcium aluminate and its hydration products", Mater. et Constr., 5, 67-76.

14.- P. REHBINDER and E. SEGALOVA (1957), "Structure formation in the hardening binding materials", Proc. Int. Congr. Surface Activity, London, p. 492-505.

15.- V.S. RAMACHANDRAN (1973), "Differential thermal investigation of the system tricalcium silicate-calcium lignosulfonate-water in the presence of tricalcium aluminate and its hydrates", Proc. III Int. Conf. Thermal Analysis, Davos, Switzerland, Vol. 2, p. 255-267.

16.- V.S. RAMACHANDRAN (1971), "Adsorption of calcium lignosulfonate on tricalcium aluminate and its hydrates in a non-aqueous medium", Cem. Technol., 2, 121-129.

17.- V.S. RAMACHANDRAN (1972), "Elucidation of the role of chemical admixtures in hydrating cements by DTA technique", Thermochemica Acta, 3, 343-366.

18.- V.S. RAMACHANDRAN (1978), "Effect of sugar-free lignosulfonate on cement hydration", Zement Kalk Gips, 31, 206-210.

Influence du thiosulfate de sodium sur l'hydratation du C_3A

Influence of sodium thiosulphate on the hydration of C_3A

E. ZIELINSKA, Professeur-adjoint, Ecole Polytechnique de Varsovie,
B. ZIELINSKI, Docteur ès Sciences Chimiques, Ecole Polytechnique de Varsovie, Pologne.

RESUME: Parmi les constituants du clinker du ciment portland c'est le C_3A qui est le plus actif dans le sens de la vitesse d'hydratation et de la réactivité chimique. Comme son hydratation peut sensiblement être atteinte par la présence d'un autre composé chimique, surtout au début du processus, l'auteur a étudié l'influence exercée sur son cours par le thiosulphate de sodium ($Na_2S_2O_3$), qui d'après ses expériences s'est montré un accélérateur efficace du durcissement des ciments portland.

Les recherches étaient poursuivies sur les pâtes du C_3A pur à l'aide des RX, de la thermogravimétrie, la spectrométrie IR et la microscopie électronique TEM. On a essayé aussi de démontrer l'influence du $Na_2S_2O_3$ sur l'hydratation du C_3A dans le clinker du ciment portland.

On a constaté que le thiosulphate de sodium retarde l'hydratation du C_3A pur durant les premières 24 heures, change la composition de la pâte et modifie la morphologie de l'hydroaluminate de calcium cubique. Les résultats de recherches font suggérer aussi que le C_3A forme en présence du $Na_2S_2O_3$ des sels doubles, avant tout du type AFm, contenant des groupes $S_2O_3^{2-}$.

Dans le cas de l'hydratation du clinker le thiosulphate de sodium n'exerce aucune influence retardatrice envers le C_3A, tout au contraire il semble l'accélérer. La cristallisation accélérée de l'hydroaluminate de calcium cubique est un fait incontestable, ainsi que l'est sa morphologie différente de la morphologie de l'hydroaluminate analogue se formant sous l'action du $Na_2S_2O_3$ dans les pâtes du C_3A pur. La présence du $Na_2S_2O_3$ mène aussi à la cristallisation des formes caractéristiques de morphologie analogue à celle de l'ettringite, et étant d'après toute probabilité un sel double du type AFt, comprenant des groupes $S_2O_3^{2-}$.

SUMMARY: Among the minerals of the clinker of Portland cement, C_3A is the most active in the sense of speed of hydration and of chemical reactivity. Since its hydration may undergo significant changes in the presence of other chemical compounds, particularly in the early stages, the authors examined the possible influence of $Na_2S_2O_3$, which according to her earlier research proved to be an effective activator of hardening of Portland cements.

Research was carried out on pastes of pure C_3A by means of X-ray analysis, thermogravimetry, IR-spectroscopy, and electronic microscopy TEM. An attempt was also made to determine the influence of $Na_2S_2O_3$ on hydration of C_3A in Portland cement clinker.

It was found that $Na_2S_2O_3$ retards the hydration of pure C_3A during the first 24 hrs, changes the phase composition of the paste, an modifies the morphology of the resulting cubic calcium hydroaluminate. The results also indicate that in the presence of $Na_2S_2O_3$, C_3A forms complex compounds, primarily of the AFm type, containing the $S_2O_3^{2-}$ group.

In the case of clinker, $Na_2S_2O_3$ does not retard the hydration of C_3A, and indeed seems to accelerate it. Without doubt the appearance of cubic hydroaluminate is accelerated, and their morphology differs from the morphology of analogous hydroaluminate appearing in pure C_3A pastes under the influence of $Na_2S_2O_3$. In the presence of $Na_2S_2O_3$ characteristic crystalline forms appear, morphologically analogous to ettringite, which are probably complex compounds of the AFt type, containing $S_2O_3^{2-}$ groups.

Le thiosulphate de sodium qui s'est montré un accélérateur efficace du durcissement des ciments portlands (1) exerce une action spécifique sur le processus de leur hydratation, se manifestant avant tout au début de celui-ci et paraissant influencer le plus la phase interstitielle. C'est pourquoi, en vue d'éclaircir plus précisement le mécanisme d'action du $Na_2S_2O_3$ on a poursuivi tout d'abord les recherches concernant l'hydratation du C_3A en présence du $Na_2S_2O_3$, pendant les prémiers 28 jours. Les essais ont été faits pour le C_3A pur ainsi que pour le clinker du ciment portland.

MATERIAUX ET METHODES

Les recherches sur l'hydratation du C_3A ont été effectuées sur les pâtes monominerales, préparées avec 50% d'eau et additionées de $Na_2S_2O_3$ (3% par rapport au C_3A) ainsi que sur les pâtes sans addition, comme temoins. C_3A était synthetisé par traitement thermique a partir des melanges des oxydes. Finesse du C_3A = 2900 cm^2/g. Les observations de l'hydratation du C_3A dans le clinker étaient poursuivies sur des pâtes pareilles, préparées du clinker portland broyé jusqu'à la finesse = 2680 cm^2/g. La composition minéralogique du clinker: 67,4% C_3S, 9,5% C_2S, 10,2% C_3A, 8,5% C_4AF. La concentration du $Na_2S_2O_3$ dans l'eau de gâchage du clinker etait la même que dans le cas des pâtes du C_3A pur.

Les recherches étaient poursuivies a l'aide des RX, de la thermogravimétrie et techniques associées, la spectrometrie IR et la microscopie electronique TEM. L'évolution de la morphologie et microstructure de phases hydratées était étudiée dans le cas du C_3A pur - sur pâtes, et dans le cas du clinker - sur les fractures de grains hydratées dans une solution de $Na_2S_2O_3$ et, parallèlement dans l'eau.

RESULTATS ET DISCUSSION

I. Hydratation du C_3A

Conformément aux résultats obtenus, dans les pâtes temoins - sans addition du $Na_2S_2O_3$ les phases essentielles sont: l'hydroaluminate hexagonal C_2AH_8 et l'hydroaluminate cubique C_3AH_6. En outre on décèle la gibbsite et le carboaluminate de calcium. La teneur des hydroaluminnates appréciée d'après les courbes ATD, DTG et TG varie dans le temps: la quantité de C_2AH_8 diminue de 14% au bout de 24 heures d'hydratation aux valeurs difficiles à déterminer d'après la méthode ci-dessus, tandis que la quantité de C_3AH_6 monte de 47% (au bout de 24 heures) a 51% au bout de 28 jours. Dans les pâtes avec le $Na_2S_2O_3$, se trouvent comme phases essentiels: l'hydroaluminate hexagonal C_4AH_{13} et l'hydroaluminate cubique C_3AH_6 accompagné aussi de gibbsite et de carboaluminate. La teneur en C_3AH_6 varie dans le temps dans un sens inverse par rapport aux échantillons témoins - sa quantité diminue de 34% apres 24 h jusqu'à 21% après 28 jours d'hydratation. La quantité de C_4AH_{13} diminue de 44% après 8 h à 12% après 28 jours. En même temps on observe l'accroissement de la teneur en eau libre de 6% à 14%.

Sur les courbes ATD des pâtes avec $Na_2S_2O_3$ se fait remarquer dès les premiéres heures d'hydratation un pic exothérmique avec un maximum a 460°C d'une intensité croissante dans le temps (figure 1). Aucun changement

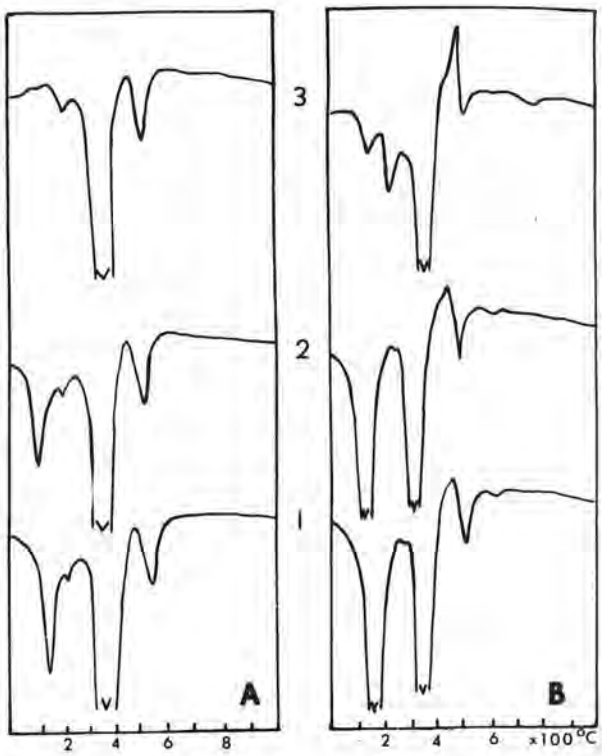

Fig. 1 - Courbes ATD du C_3A hydraté: A - sans $Na_2S_2O_3$, B - avec $Na_2S_2O_3$; 1-8 heures, 2-24 heures, 3-28 jours d'hydratation

de poids ne correspond à cet effet, qui, de plus ne subit nulle modification si les essais sont exécutés dans l'atmosphère d'azote - ce qui fait penser à une cristallisation d'un produit partiellement déhydraté.

Des différence marquantes se font voir aussi entre les spectres IR des pâtes avec et sans $Na_2S_2O_3$ (figure 2). Dans le cas des pâtes additionnées on observe tout d'abord la persistence des bandes du C_3A anhydre, notamment pendant les prémières 24 heures, ce qui prouve un retardement de l'hydratation du C_3A (confirmé d'ailleurs par les RX). Une attention spéciale attire l'apparition sur les courbes du C_3A + $Na_2S_2O_3$ des bandes à 996, 1015, 1130, 1145 cm^{-1} qui, bien que situées dans le domaine des vibration des groupes $S_2O_3^{2-}$ ne peuvent être attribuées au $Na_2S_2O_3$ pur (figure 3). On note aussi l'absence de la bande ν_2 de $S_2O_3^{2-}$ à

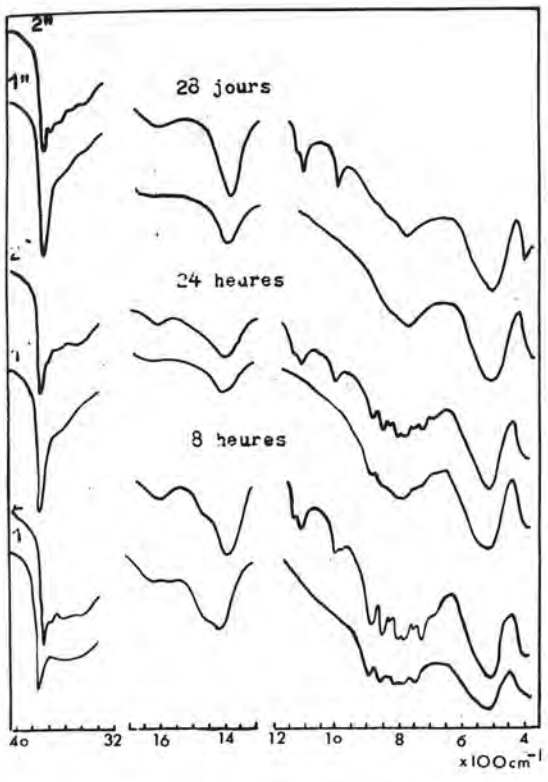

Fig. 2 - Spectres IR du C_3A hydraté sans $Na_2S_2O_3$ (1, 1', 1") et avec $Na_2S_2O_3$ (2,2',2")

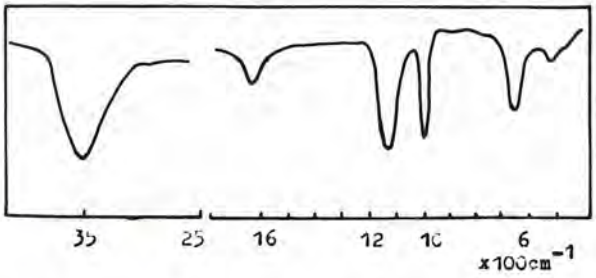

Fig. 3 - Spectre IR du $Na_2S_2O_3 \cdot 5H_2O$

600 cm^{-1} et des changement dans la région de 3400 a 3600 cm^{-1}. Les bandes en question évoluent dans le temps: après 28 jours on n'observe presque plus celle à 996 et à 1149 cm^{-1}, par contre celles à 1015 et à 1130 cm^{-1} paraissent plus intenses et mieux formées. Au plus dans le domaine 3400-3600 cm^{-1}, caracteristique de vibration ν_1 et ν_3 de H_2O ainsi que νOH^- se forment nettement des bandes a 3622, 3550, 3475 et 3400 cm^{-1}.

L'ensemble d'observations des spectres IR fait supposer l'existence evêntuelle d'un composé du type Afm renfermant des groupes $S_2O_3^{2-}$. Les résultats de l'analyse thermique - l'apparition d'un effet exothermique sur les courbes ATD du C_3A + $Na_2S_2O_3$ et, avant tout la diminution de la quantité du C_3A et C_4AH_{13} parallèlement a l'acroissement de l'eau libre dans ces échantillons font envisager aussi une telle possibilité. Le composé en question pourrait se former du C_4AH_{13} (2) a partir d'un mécanisme proposé pour les transformations des aluminates hydratés en présence du gypse, celles-ci menant à la formation du monosulphate de calcium (3,4). La formation d'un sel du type AFm expliquerait aussi le retardement de l'hydratation du C_3A par le thiosulphate de sodium. L'hypotèse prsentée semble être confirmée par les observations microscopiques des produits d'hydratation dans les pâtes du C_3A pur et avec $Na_2S_2O_3$. C'est seulement dans les pâtes additionnées qu'on observe, outre les plaquettes de C_4AH_{13} un nombre important de grandes plaquettes hexagonales fortement déformés, constituant une caracteristique structure stratifiée (figure 4). On remarque aussi que le thiosulphate de sodium modifie la morphologie de l'hydroaluminate cubique. Dans les pâtes du C_3A pur le C_3AH_6 parait sous forme de polyèdres (figure 5) de grande dimension, tandis qu'en présence du $Na_2S_2O_3$ - sous forme d'octaèdres de beaucoup plus petit (figure 6).

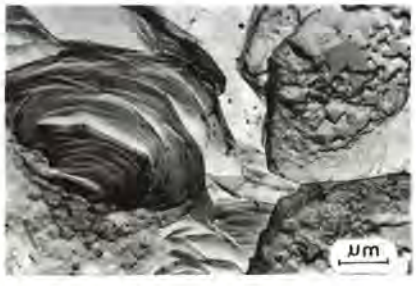

Fig. 4 - Pâte de C_3A + $Na_2S_2O_3$ durcie 24 heures. Agglomerat de plaquettes hexagonales fortement déformés

Fig. 5 - Pâte de C_3A pur durcie 24 heures. Polyèdres de C_3AH_6

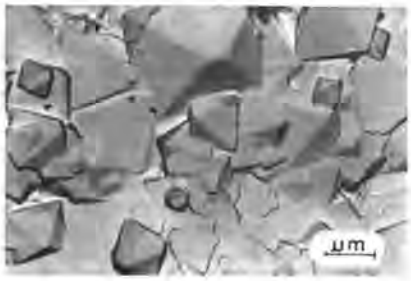

Fig. 6 - Pâte de C_3A + $Na_2S_2O_3$ durcie 24 heures; octaèdres de C_3AH_6

HYDRATATION DU CLINKER

Les observations de l'hydratation du C_3A dans un mélange tel que clinker présente certaine difficulté. Néanmoins les recherches faites ont put démontrer quelques mode d'action du $Na_2S_2O_3$ sur le C_3A.

Tout d'abord aucune action retardatrice du $Na_2S_2O_3$ n'est remarquée. Sur les courbes ATD du clinker hydraté en presence du $Na_2S_2O_3$ (figure 7) on ne voit pas l'effet

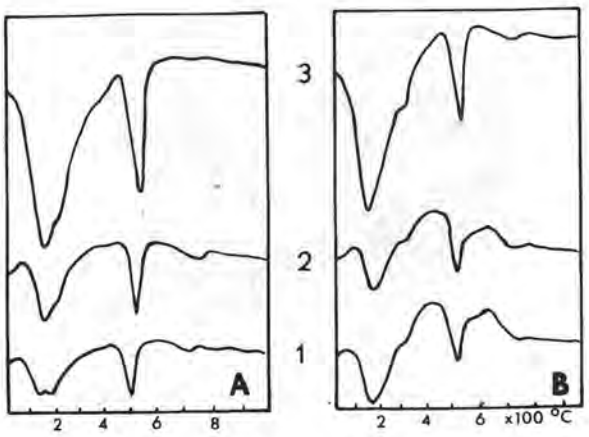

Fig. 7 - Courbes ATD du clinker hydraté: (A) - sans $Na_2S_2O_3$, (B) - avec $Na_2S_2O_3$ 1.-8 heures, 2.-24 heures, 3.-28 jours d'hydratation

exothermique a 460°C présent dans le cas des pâtes du C_3A + $Na_2S_2O_3$; l'effet exothermique avec un maximum à 620°C est lié à l'interaction du $Na_2S_2O_3$ avec les silicates (5). Tout-demême l'apparition d'un pic endothermique avec un maximum à 320°C indique une modification d'hydratation de la phase interstitielle par le $Na_2S_2O_3$.

En comparant les spectres IR du clinker hydraté en présence du $Na_2S_2O_3$ (figure 8) aux spectres du C_3A + $Na_2S_2O_3$ on a attiré une

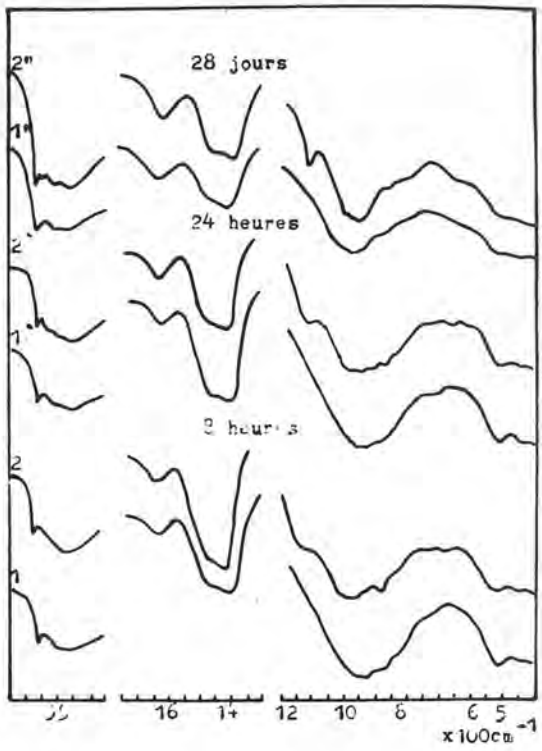

Fig. 8 - Spectres IR du clinker hydraté sans $Na_2S_2O_3$ (1,1',1") et avec $Na_2S_2O_3$ (2,2',2")

attention toute particulière sur le domaine des vibrations du groupe $S_2O_3^{2-}$ et la région 3400-3600 cm^{-1}. On a noté les differences suivantes: Après 8 heures sur les spectres du clinker apparait une bande deformée ("shoulder") à 1100-1300 cm^{-1} et de très faibles bandes à: 1015, 995 et 670 cm^{-1}. Cette dernière n'a pas été aperçue dans le cas des spectres des pâtes du C_3A + $Na_2S_2O_3$ ou par contre apparaisait une bande à 1145 cm^{-1}, absente dans le cas du clinker. Après 28 jours la bande à 670 cm^{-1} a disparu et la bande à 990 cm^{-1} a fortement diminué. Dans la région 1100-1130 cm^{-1} on a pu voir une bande très nette avec un maximum a 1130 cm^{-1}. Dans la région 3400-3600 cm^{-1} la bande apparaisant sur les courbes du C_3A additionné à 3530 cm^{-1} c'est déplacé sur 3540 cm^{-1}, en outre on n'observe pas la bande à 3470 cm^{-1}.

L'ensemble des observations fait supposer, que dans le clinker hydraté avec le $Na_2S_2O_3$ se forme, d'après toute probabilité aussi un sel double contenant des groupes $S_2O_3^{2-}$, mais du type AFt.

Les images des produits d'hydratation obtenus a l'aide du mioroscope electronique TEM confirme cette suggestion. En cas du clinker hydraté dans la solution du $Na_2S_2O_3$

apparaît un grand nombre de cristaux à la morphologie caractéristique, analogue a celle de l'ettringite (figure 9). Les observations microscopiques laissent aussi

Fig. 9 - Fracture de grain de clinker hydratée 8 heures dans une solution de $Na_2S_2O_3$ Aiguilles analogues à l'ettringite

constatter que la crystallisation des hydroaluminates hexagonaux est accélérée en présence du $Na_2S_2O_3$. Après 15 min déja on note la présence de plaquettes hexagonales bien formé, tandis que les produits d'hydratation du clinker hydraté dans l'eau apparaissent dans le même temps uniquement sous forme de gel.

Comme c'etait le cas du C_3A, le $Na_2S_2O_3$ change la morphologie du C_3AH_6, bien-que d'une autre facon.

Dans les produits d'hydratation du clinker le C_3AH_6 se crystallise sous forme de cubes (figure 10), soudés et formant une structure granuleuse.

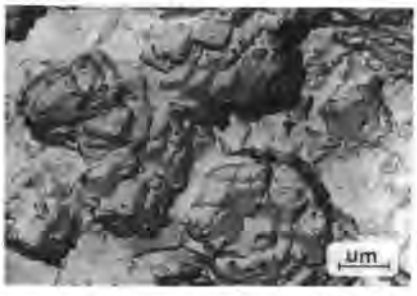

Fig. 10 - Fracture de grain de clinker hydratée 8 heures dans une solution de $Na_2S_2O_3$. Cubes de C_3AH_6

CONCLUSIONS

Les recherches poursuivies ont permis de constater que le thiosulphate de sodium modifie d'une facon marquante l'hydratation du C_3A, dans les pâtes monominerales ainsi que dans le clinker. Cette modification est différente dans les deux cas.

En cas du C_3A en pâte monominerale $Na_2S_2O_3$ retarde son hydratation, change le type de l'hydroaluminate hexagonal ainsi que la morphologie de l'hydrate cubique C_3AH_6. La présence du thiosulphate de sodium mène aussi, d'après toute vraisemblance, à la formation d'un sel double du type AFm contenant des groupes $S_2O_3^{2-}$.

En cas du C_3A dans le clinker on n'observe aucune action retardatrice du $Na_2S_2O_3$. Le thiosulphate de sodium accélère la crystallisation des aluminates hydratés hexagonaux et modifie aussi la morphologie du C_3AH_6. En présence du $Na_2S_2O_3$ semble se former aussi un sel double contenant des groupes $S_2O_3^{2-}$, mais du type AFt.

BIBLIOGRAPHIE

1.- E. ZIELIŃSKA (1973) "L'influence du $Na_2S_2O_3$ sur le durcissement des mortiers de ciments" (en polonais), Prace Instytutu Technol. i Org. Prod. Bud. Politechniki Warszawskiej, n° 5, 217--232.

2.- K. MURAKAMI et H. TANAKA (1968) "Contribution of calcium thiosulphate to the acceleration of the hydration of portland cement and comparison with other soluble inorganic salts", Proc. V Int. Symp. Chem. Cem., Tokio.

3.- N. TENOUTASSE (1970) "Le mécanisme de l'hydratation de C_3A et C_3S en présence du sulfate et du chlorure de calcium", Rev. Mat. Constr. n° 655, 98-102.

4.- T. VASQUEZ MORENO (1976) "Reacciones de hidratacion del cemento portland por espectroscopia infrarroja", La Revista Materiales de Construction, n° 163.

5.- E. ZIELIŃSKA (1979) "L'influence du $Na_2S_2O_3$ sur le processus d'hydratation de l'alite" (en polonais), Cement-Wapno-Gips, n° 10, 314-317.

Influence of some retarders on the hydration, at early ages, of tricalcium aluminate

Influence des retardateurs sur l'hydratation, en tout début, de l'aluminate tricalcique

R. SERSALE, Professor, Institute for Applied Chemistry, Faculty Engineering, University of Naples,
V. SABATELLI, Assistant Professor,
and G.L. VALENTI, Assistant Professor, Italie.

SUMMARY: The Authors give an account of the preliminary results of an experimental research carried out for the purpose of carefully investigating the influence of some set-retarders on the hydration process of tricalcium aluminate pastes.

The evaluation of the hydration degree of the starting product, as well the characterisation of hydration products, has been carried out via X-ray diffraction analysis, while scanning electron microscopy and thermal analysis have been used as complementary techniques.

The effects of the different retarders have been assessed with reference to the same hydration degree of the pastes and some information has been collected on the mechanism involved in the reaction.

RESUME: Les Auteurs rapportent les résultats préliminaires d'une recherche sur l'influence de quelques adjuvants retardateurs de la prise, sur l'hydratation de pâtes d'aluminate tricalcique.

A l'aide de la diffractometrie des rayons X on a évalué le degré d'hydratation des produits de départ, en caractérisant aussi les produits d'hydratation. L'analyse thermique differentielle et la microscopie électronique à balayage ont été utilisées comme techniques de reference.

Les effets des différents retardateurs ont été évalués à égalité de degré d'hydratation, en recueillant des informations sur le mode d'action des retardateurs employés.

1. INTRODUCTION.

The study of the chemistry of the hydration of Portland cement, in the presence of additives, preliminarly requires the careful investigation of the behaviour of the individual phases entering in its composition, even if one must act very cautiously afterwards in extending the results to the more complex system (1).

The purpose of this investigation is therefore to give a contribution to the knowledge on the hydration of tricalcium aluminate in the presence of set retarders, taking into account that this compound, whose content in Italian Portland cements runs upon 7-10%, plays an important role in the whole hydration process and also affects some determinant characteristics of these hydraulic binders.

This investigation attempts therefore to find a correlation between the retardation effect of some chemical products and the nature and morphology of the hydration products of tricalcium aluminate. The selection, restricted at the present to only three retarders, includes: a soluble salt of a complex organic acid: the sodium gluconate; a soluble salt of a simple inorganic acid: the copper acetate; an insoluble salt of a inorganic acid: the aluminium phosphate, which are all indicated in the literature as possible industrial additives (2) and therefore suitable for use in an alkaline environment, such as that characterizing hydraulic binders.

These chemicals have been employed in the form of laboratory reagent grade, in order to prevent the influence of some impurities (3); while two of them are, at least up now, among the additives whose behaviour has been very little investigated.

The study has been carried out on pastes, using the same product with no additives, as reference, with the samples investigated, containing different amounts of additive, hydrated for different time intervals, always within the limits of the early ages, although the comparison of its behaviour concerns a very similar hydration degree. This condition, in our opinion, favours a more homogeneous comparison of the relative results, both in terms of intrinsic characteristics of the pastes (4) and, possibly, in terms of action mechanism.

Recently very interesting investigations have been indeed carried out on the hydration chemistry of the clinker constituent which is more responsible for setting: the C_3A (5), but the most complete works concern the effect of gypsum as set retarder (1) (6) or the effect of sugars and their oxidation products (7). Moreover, the question of the action mechanism is still open, namely, whether the action is to be connected to delay in the nucleation process of the hydration products (8) rather than to the formation of a protective coating (9) which at a definite moment loses its efficiency. Nor is a possible interaction between hydration products and additive to be rejected, resulting in the formation of complexes (10) having a stability which depends on the pH of the environment.

2. EXPERIMENTAL.

2.1. Material

Tricalcium aluminate was prepared by heating a stoichiometric mixture of calcium carbonate and aluminium oxide, both reagent grade, ground previously in an agate ball mill, for four hours at 1375°C. Thereafter the mixture was heated again during twice four hours at 1500°C. Between all firings, the product was ground and the end product was brought to a specific Blaine surface of 3500. The X-ray diffractogram (fig.3) of the product agrees completely with the data mentioned in the literature (11). The percentage of free CaO was less than 1% by weight.

2.2. Pastes preparation.

The pastes were prepared using synthetic tricalcium aluminate as previously reported, with a water/solid ratio of 0.6. When soluble, the additive was added in solution. The relative amounts, referred to the weight of tricalcium aluminate, were: 0.10% for sodium gluconate and 3.0% for copper acetate. The water insoluble aluminium phosphate was instead added as powder, in amount of 5% of the weight of aluminate. The above mentioned amounts were determined by means of experimental tests, in order to keep the values of the hydration degree in a rather restricted band, so as to compare systems having very similar hydration degree.

The pastes containing the retarders, as well those with no additives, were aged for time intervals within 48 hours, in a thermostat at the temperature of 20 ± 1°C, in polythene envelopes, hermetically sealed.

At estabilished times of expiry, the hydration process has been stopped by means of acetone treatment, grinding and successive filtration, followed by washing with ethyl ether. Such treatment furnished the powders that were employed in the different investigations.

X-ray investigation has been carried out by means of a Philips diffractometer, using CuKα radiation, scanning speed 0.5°C 2θ/min., time constant 8 secs. Quantitative evaluation of the percentage of hydrated C_3A were made using the method worked out by Daugherty and Kowalewski (12).

Thermal differential analysis has been made with a Du Pont thermalanalyser, heating rate 10°C/min.

Thermogravimetric analysis has been made by means of a Stanton thermobalance Massflow Mod. MF/H5/20, heating rate 6.6°C/min, using 80 mg of powder.

Scanning electron microscopy analysis has been carried out by means of a Leitz-AMR 1200, using samples previously metallized with carbon and successively with a gold-palladium alloy.

2.3. Results.

The course of the hydration process of the pastes containing the selected additives in the above mentioned percentages, is reported in fig.1. Term of reference is always the paste of tricalcium aluminate with no additive (curve n.4). Besides the retardation effect which is more intense if sodium gluconate is used (curve n.3), one should notice the long induction period in the hydration process, which follows the addition of this retarder, as clearly appears from curve n.3. Fig.1 shows that while the samples prepared using

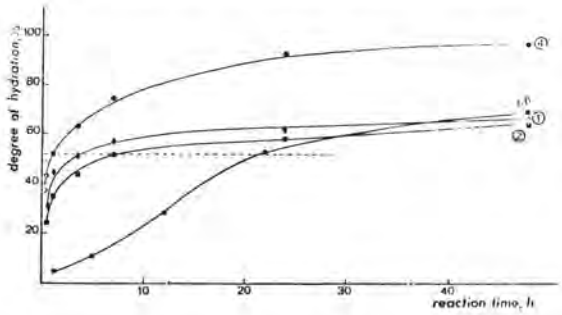

Fig.1 - Hydration degree (%) of C_3A pastes with or without retarders, versus reaction time (hours).

aluminium phosphate (curve n.2) or copper acetate (curve n.1), aged for about five hours, obtain a hydration degree of about 50%, those made with sodium gluconate, tested in the same condition, hardly reach one of 10%.

On the contrary, samples aged 48 hours show that the influence of all the selected additives, in the percentages indicated above, appears to be pretty similar, with a slight inversion for the action of sodium gluconate. The hydration degree of pastes prepared with this retarder surpasses, indeed, even if very little, those of the pastes prepared with the other two additives, respectively.

Fig.2 shows the results of thermal differential analysis, carried out on fraction of pastes prepared with no additives, aged for time intervals within 10 min. and 48 hours. The following five endothermal peaks are to be seen: the first, declining with the increase of the aging and showing considerable amplitude at very early hydration ages, with a maximum between 170 and 180°C, more intense for ages between 30 and 66 min., which can be attributed to dicalcium aluminate hydrated (13); the second, very weak and with a maximum around 250-255°C, this, too, declining with the increase of the aging, which can be attributed to the tetracalcium aluminate hydrated (13); the third, increasing with the aging, with a maximum between 280 and 320°C, which can be attributed to tricalcium aluminate hydrated (13); the fourth, which can be recognized after aging of about seven hours, increasing with the length of aging, with a maximum between 480 and 505°C, which can be attributed to the dehydration of calcium hydroxide, deriving from thermal decomposition of tricalcium aluminate hydrated (13); the fifth, very weak with a

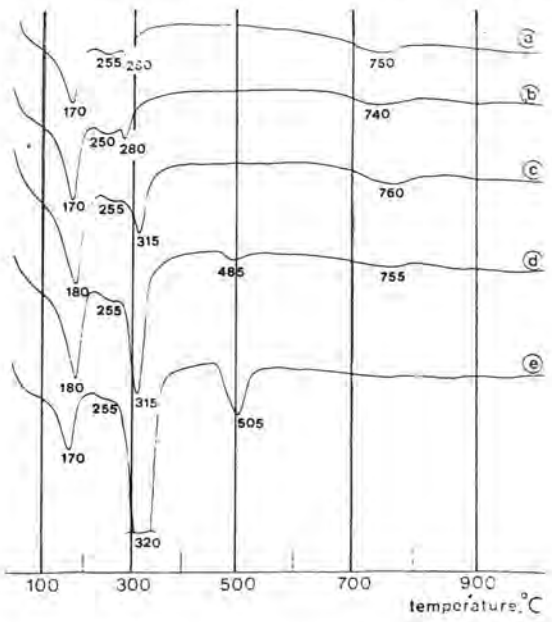

Fig.2 - DTA traces of C_3A pastes with no retarders, aged for: a=10; b=30; c=66 min.; d=7; e=48 hours.

maximum around 760°C, which can be attributed to the presence of slight quantities of calcium carbonate, deriving from thermal decomposition of calcium carboaluminate (14), recognized by X-ray diffraction. The figure, which represents a useful reference for evaluating the behaviour of the starting product in presence of additives, shows that in the experimental conditions that have been selected, the formation of tricalcium aluminate hydrated, together with di-and tetracalcium aluminate hydrated, is to be recognized, just after 10 min of reaction with water. Moreover, after hydration times running about seven hours, the rate at which tricalcium aluminate hydrated is generated, exceeds the rate at which dicalcium aluminate, as well tetracalcium aluminate hydrated, is produced.

Fig.3, 4 and 5 show a selection of the more interesting results of the investigations on pastes prepared with the retarders in the amounts that have been indicated above. Term of reference is always a paste of tricalcium aluminate hydrated with no additive. As has been emphasized above, the comparison is made at a pretty similar hydration degree, in order to restrict the numbers of the factors affecting the behaviour of the system.

Each of the three figures refers chronologically: to a paste containing copper acetate (n.1); aluminium phosphate (n.2); sodium gluconate (n.3), as well to a paste prepared with no additive (n.4). The relative aging are indicated by the points marked in fig.1. In fig.3 the diffractogram of the unhydrated product is

reported in order to make the comparison more easy (n.0).

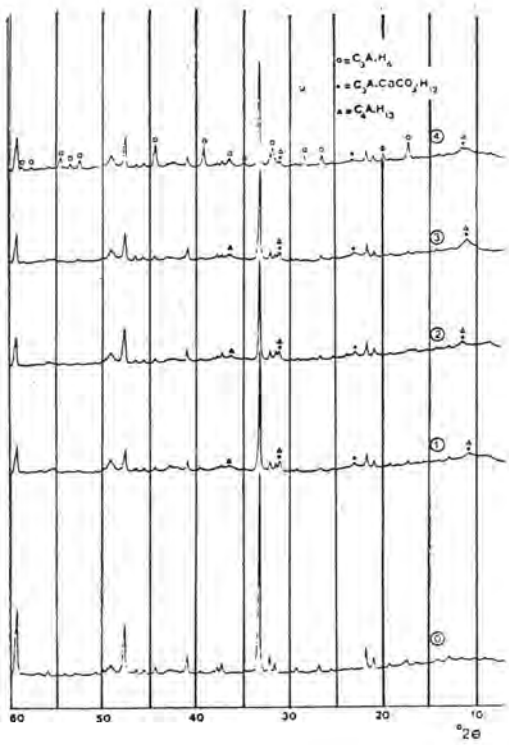

Fig.3 - X-ray patterns of C_3A pastes having similar hydration degree (see fig.1).

The examination of the diffractograms in fig.3 shows that in the presence of additives, the neo-formed phases are characterized by a relative low degree of crystallinity. The only phases that can be recognized are: $C_3A \cdot CaCO_3 \cdot H_{12}$ (lines at 11.63; 23.39; 31.24 °2θ) and C_4AH_{13} (lines at 11.19; 22.49; 31.12 °2θ), excluding the lines that can be attributed to the fraction not yet hydrated and recognizable by a comparison with the diffractogram n.0.

The lines at 17.27; 19.94; 26.50; 28.40; 31.77, etc. 2°θ, in the diffractogram of the paste with no additive (n.4), show the presence of C_3AH_6, together with the phases just indicated.

The diffractograms of the same pastes, aged for times different from those that are mentioned above, show the same lines as these just indicated; the only difference is that C_3AH_6 does not appear when the length of the hydration falls under 66 min.

Fig.4 shows the following endothermic peaks: a peak with maximum at 175-180°C, which can be attributed to the presence of C_2AH_8; a peak, with a maximum between 240-270°C, which can be attributed to the presence of C_4AH_{13}; a peak, with maximum at 320°C, which in the presence of sodium gluconate appears at 280°C, attributable to the presence of C_3AH_6.

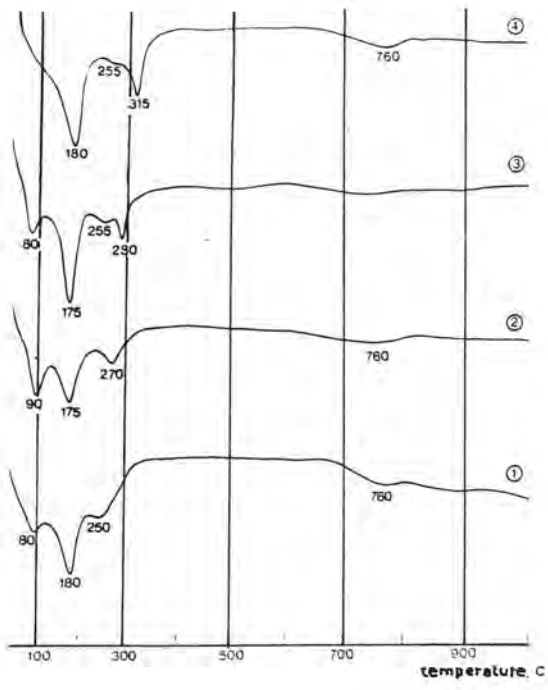

Fig.4 - DTA traces of C_3A pastes having similar hydration degree (see fig.1).

As a significant difference in the presence of additives, there is to be noticed the appearance of peak with maximum around 80°C, which can be attributed to the presence of C_4AH_{19} (7). Its evolution in C_4AH_{13} seems indeed to be inibited, in normal conditions of drying, by the presence of the three retarders selected.

Fig.5 allows one to verify precisely, on the basis of the relative losses of weight, the presence of the phases individuated by X-ray diffraction analysis (fig.4). A lack of the slight loss of weight, before 100°C, in the diagram of the paste with no additive (n.4) is to be seen. This loss can be attributed to the dehydration of C_4AH_{19} and has been observed only in the presence of additives. According to X-ray results, in the temperature interval of 200-300°C (fig.5), there is to be noticed the slight difference in the profile of curves 1 and 2, in comparison to curve 3. Only for this curve may one observe the insertion of a second localized loss at about 280°C, on the continuous loss which begins at about 200°C, according to the two endothermic distinct peaks at about 255 and 280°C in fig.4.

It seems therefore correct to ascribe the anticipation

at 280°C of the dehydration effect of C_3AH_6, which usually can be found at 320°C, to the poor crystallinity of this compound because of the presence of sodium gluconate. Such an interpretation seems to be very

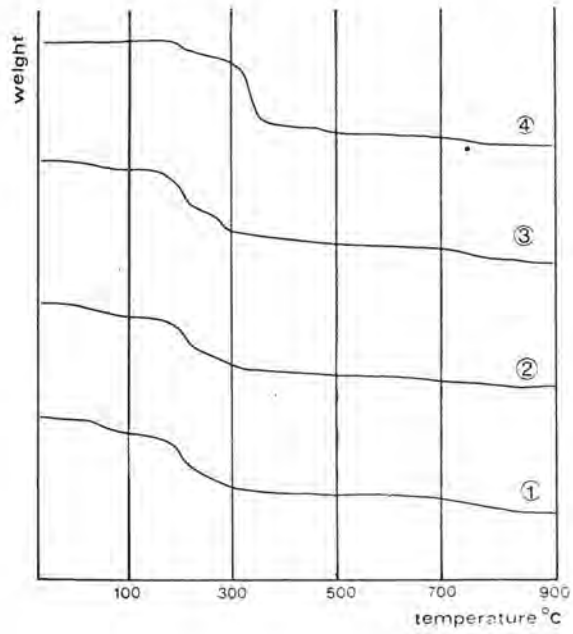

Fig.5 - TGA traces of C_3A pastes having similar hydration degree (see fig.1).

likely, on the basis of the profile of the differential thermal diagrams a and b in fig.2, concerning the dehydration of pastes without retarders, at very early ages, between 10 and 30 min.

Fig.6 shows a selection of the examination of C_3A pastes with or without retarders, by scanning electron microscopy.

Micrographs a and b concern pastes with no additive. Micrograph a shows the presence of irregular lamellar forms and secondarily of forms attributable to a cubic lattice, in a paste aged for about one hour. On the basis of X-ray diffraction analysis and of the complementary techniques, the lamellar forms can be attributed to the calcium aluminates hydrated: C_2AH_8 and C_4AH_{13} (15), the others to tricalcium aluminate hydrated. The last forms become more evident for aging running about 48 hours (micrograph b).

Micrographs c, d and e concern, chronologically, the pastes prepared with sodium gluconate, copper acetate and aluminium phosphate, respectively, in the above mentioned amounts. The comparison of the microstructures is made, as just emphasized, at pretty similar degree of hydration. The microstructures appear to be very similar and the absence of forms attributable to a cubic lattice can be observed. This remark also concerns aging of about 48 hours, as it has been observed, for example, in the micrograph f (paste with aluminium phosphate).

3. DISCUSSION.

Among the three different retarders that have been used in this study, sodium gluconate seems the most active chemical. Its action not only appears to be more effective, but concerns the whole process which in turn seems to be characterized by a long induction period before the chemical decreases its activity. The complex phenomenon seems to involve the nature of the neo-formed phases, too, since if in the presence of all the retarders used we have always observed phases attributable to calcium aluminates hydrated: C_2AH_8 and C_4AH_{13}, only in the presence of sodium gluconate has it been possible to reveal the probable, rapid formation of tricalcium aluminate hydrated, as soon as the induction period stops.

Owing to the mode of formation, this aluminate is characterized by a low crystallinity degree, of the type of phase which it is possible to detect, at very early ages, by hydration of tricalcium aluminate with no retarder.

The selected additives favour the stabilisation of a calcium aluminate hydrated which, according to the temperature of dehydration, could be classified as C_4AH_{19} (7).

The retarders that have been employed do not seem to favour single morphological modifications that are possible to reveal by scanning electron microscopy examination on pastes; so that the microstructure appears to be similar in all the samples prepared with the three different retarders.

In spite of the different chemical nature, the mechanism of the three additives can be brought back to the same pattern and supports the more reliable theory (16) of a stabilisation of hexagonal calcium aluminates hydrated.

The questions concerning the main mechanism responsible for the retardation and the research of the reasons which at a precise moment cancel the stabilising effect, are therefore still open, so investigations in the field must be encouraged.

Acknowledgements. The writers gratefully thank Mr. A. Annetta for his technical assistance. The writers received financial support from the Consiglio Nazionale delle Ricerche, Italia.

REFERENCES.

1.- J. SKALNY, I. JAWED, H.F.W. TAYLOR (1978), "Studies on hydration of cement: recent developments", World Cement Tech., 9, 183-195.

2.- A.J. FRANKLIN (1976), "Cement and mortar additives", Noyes Data Corp., USA, 5-9.

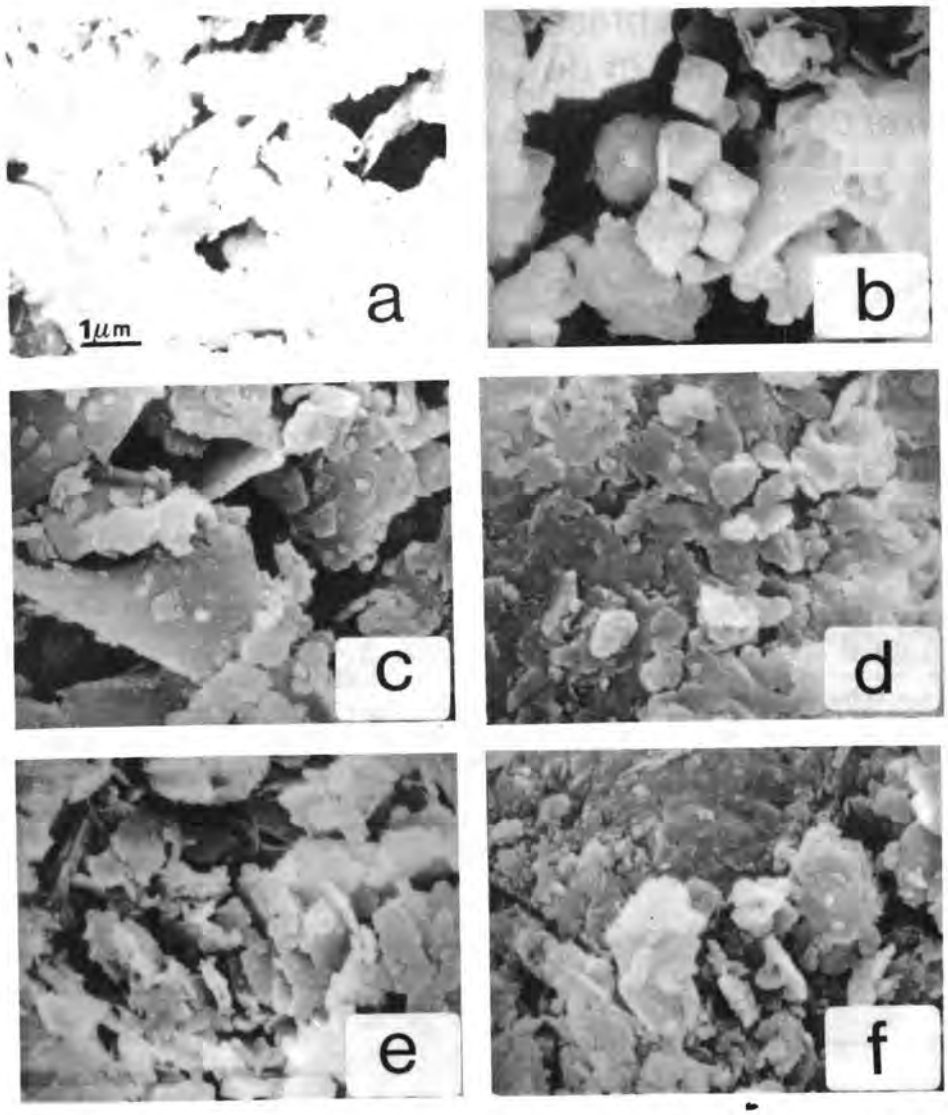

Fig.6 - SEM's micrographs of C_3A pastes with or without retarders.

3.- N.B. MILESTONE (1976), "The effect of lignosulphonate fractions on the hydration of tricalcium aluminate", Cement and Concrete Res., 6, 89-102.

4.- V.S. RAMACHANDRAN, R.F. FELDMAN (1978), "Time-dependent and intrinsic characteristics of Portland cement hydrated in the presence of calcium chloride", Il Cemento, 75, 3, 311-322.

5.- P. GUPTA, S. CHATTERJI, J.W. JEFFERY (1972-73), "Studies of the effect of various additives on the hydration reaction of tricalcium aluminate", Part 2, Cement Technology, 3, 1, 19-25; Part 3, 3, 4, 146-153; Part 4, 4, 2, 63-68.

6.- M. COLLEPARDI, G. BALDINI, M. PAURI (1978), "Tricalcium aluminate hydration in the presence of lime, gypsum or sodium sulphate", Cement and Concrete Res., 8, 571-580.

7.- N.B. MILESTONE (1977), "The effect of glucose and some glucose oxidation products on the hydration of tricalcium aluminate", Cement and Concrete Res., 7, 45-52.
- N.B. SINGH (1976), "Effect of gluconates on the hydration of cement", Cement and Concrete Res., 6, 455-460.

8.- J. SKALNY, M. TADROS (1977), "Retardation of tricalcium aluminate hydration by sulfates", Jour. Amer. Ceram. Soc., 60, 174-175.

9.- H.N. STEIN (1963), "Mechanism of the hydration of $3CaO \cdot Al_2O_3$", J. Appl. Chem., 13, May, 228-232.
- P.GUPTA, S. CHATTERJI, J.W. JEFFERY (1973), "Part 5, A mechanism of retardation of tricalcium aluminate hydration", Cement Technology, 4, 4, 146-149.

10.- J.F. YOUNG (1970),"Effect of organic compounds on the interconversion of calcium aluminate hydrates: hydration of tricalcium aluminate", Jour. Amer. Ceram. Soc., 53, 2, 65-69.

11.- Powder diffraction file (1967), sets 6-10 (revised), 8-5a, pag.281, American Soc. Test. Mat.

12.- K.E. DAUGHERTY, M.I. KOWALEWSKY (1968), "Effect of organic compounds on the hydration reaction of tricalcium aluminate", Proc.5th. Int. Symp. Cement, Tokyo, IV, 42-52.

13.- R.F. FELDMAN, V.S. RAMACHANDRAN (1966), "Character of hydration of $3CaO \cdot Al_2O_3$", Journ. Amer. Ceram. Soc., 49, 5, 268-273.

14.- R. TURRIZIANI, G. SCHIPPA (1956), "Sull'esistenza del monocarboalluminato di calcio idrato", Ric. Sci., 26, 9, 2792-2797.

15.- E. BREVAL (1976), "C_3A hydration", Cement and Concrete Res., 6, 129-138.

16.- V.S. RAMACHANDRAN, R.F. FELDMAN (1972), "Effect of calcium lignosulphonate on tricalcium aluminate and its hydration products", Rev.Mat.Constr., 5, 26, 67-76.

Hydratation de C_3A en présence de saccharose, de gypse et de $CaCl_2$

Hydration of C_3A with saccharose, gypsum and $CaCl_2$

M. REGOURD, B. MORTUREUX, H. HORNAIN, Département Microstructures,
C.E.R.I.L.H., Paris, France.

Résumé

L'étude de l'hydratation de C3A seul et dans les mélanges synthétiques C3A + C3S + gypse a été effectuée en présence d'un accélérateur de C3S, le chlorure de calcium et d'un retardateur de C3A, le saccharose. Le taux d'hydratation a été mesuré par diffraction des rayons X et la morphologie des hydrates observée par microscopie électronique à balayage.

Il existe une compétition gypse-$CaCl_2$ dans l'hydratation de C3A jusqu'à 28 jours (formation de sulfoaluminate et de chloroaluminate). L'interaction C3A-C3S, trouvée dans les conditions normales d'hydratation, est également mise en évidence en présence d'adjuvants accélérateurs et retardateurs.

Summary

Hydration study of C3A and C3A in synthetic mixtures C3A + C3S + gypsum has been done with an accelerator of C3S (calcium chloride) and a retarder of C3A (saccharose). The hydration ratio has been measured by X-ray diffraction and the morphology of the hydrates observed by scanning electron microscopy.

There is a competition between gypsum and $CaCl_2$ during hydration of C3A up to 28 days (formation of sulfoaluminate and chloroaluminate). The C3A-C3S interaction found in normal conditions of hydration, is also shown with admixtures, accelerators and retarders.

1. INTRODUCTION

L'action des adjuvants sur l'hydratation du ciment portland est complexe car elle fait intervenir un grand nombre de paramètres (composition chimique et teneur de l'adjuvant, composition minéralogique et temps d'hydratation du ciment, température) (1).

Afin de décomposer les interactions adjuvant-ciment, des études ont été entreprises sur le rôle des accélérateurs et des retardateurs sur l'hydratation de chacun des constituants du ciment portland (C3S, C2S, C3A, C4AF) puis sur des mélanges C3S + C3A (les deux phases qui s'hydratent en premier) et C3S + C3A + gypse, enfin sur des produits industriels.

Le taux d'hydratation de chaque minéral a été déterminé par diffraction des rayons X (DRX) par la méthode de l'étalon interne. La microstructure des pâtes, au cours de la prise et du durcissement, a été observée par microscopie électronique à balayage (MEB).

L'étude a porté principalement sur le rôle d'un accélérateur, le chlorure de calcium, et d'un retardateur, le saccharose.

2. PREPARATION DES ECHANTILLONS

Afin d'assurer une meilleure répartition de l'adjuvant, celui-ci a toujours été dissous dans l'eau de gâchage. Sa quantité a été mesurée en % pondéral par rapport au poids du ciment (rapport e/c = 0,5).

Les phases pures préparées au laboratoire sont broyées et tamisées de façon à obtenir une granulométrie comprise entre 25 et 40 µm.

Le ciment utilisé provient d'un clinker broyé à la finesse de 3570 $cm^2.g^{-1}$ et additionné de 5 % de gypse.

Les échantillons se présentent sous la forme de micro-éprouvettes cylindriques (phases pures) ou cubiques (ciments). Les éprouvettes sont conservées pendant deux jours dans une atmosphère à 100 % d'humidité relative puis immergées dans l'eau à 20 °C. A l'échéance prédéterminée, elles sont plongées dans l'azote liquide afin d'arrêter les réactions d'hydratation; l'eau est évaporée par cryosublimation. Dans chaque série, les échantillons adjuvantés sont comparés à un échantillon témoin.

Nous retiendrons de l'étude générale des deux adjuvants sur les phases du clinker, l'action du saccharose et du chlorure de calcium sur C3A seul puis sur C3A dans les mélanges C3A + C3S, C3A + C3S + gypse et enfin dans un ciment portland.

3. HYDRATATION DE C3A SEUL

L'aluminate tricalcique réagit très rapidement avec l'eau en donnant les hydrates hexagonaux C2A H8 et C4A H13 qui se transforment en hydrate cubique C3A H6. A deux jours, le témoin est presque entièrement hydraté en gros cristaux (dodécaèdres rhomboïdaux) de C3A H6 (fig. 1).

Fig. 1 : C3A hydraté 2 jours. Dodécaèdres rhomboïdaux de C3AH6 et plaquettes de C4AH13.

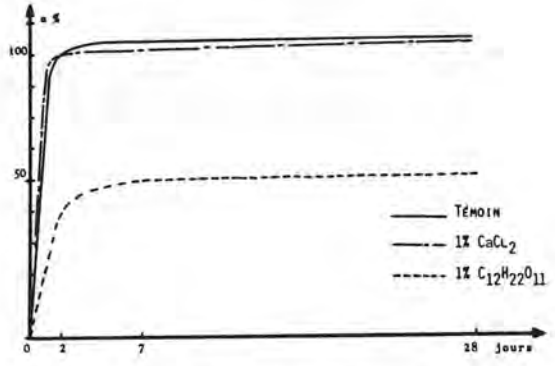

Fig. 2 : Taux d'hydratation α en fonction du temps et de l'adjuvant.

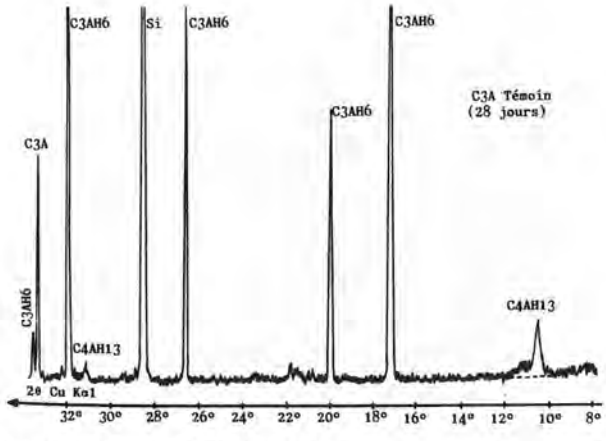

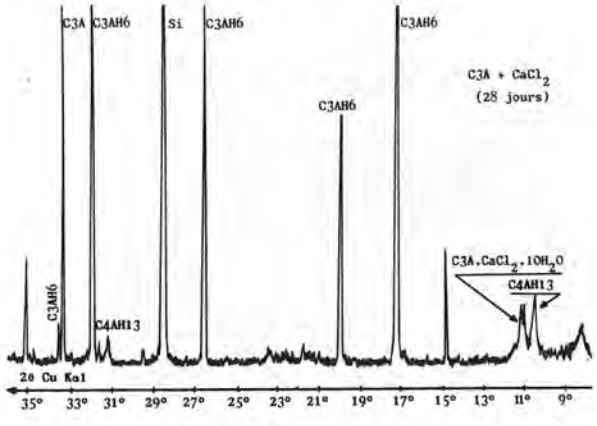

Fig. 3 : Pâte de C3A hydraté 28 jours. Enregistrements diffractométriques X obtenus sur C3A pur et sur C3A + $CaCl_2$.

- (1) **$CaCl_2$ n'a pas d'influence sensible sur le taux d'hydratation de C3A** (fig. 2). Les hydrates formés diffèrent cependant de ceux du témoin : chloroaluminates C3A.$CaCl_2$.12H_2O et C2AH8 identifiés par diffraction des rayons X à 28 jours. Dans le témoin, seuls sont détectés C3AH6 et C4AH13 (en faible teneur) (fig. 3).

- (2) **Le saccharose est retardateur de C3A** (fig. 2). En présence de 1% de saccharose, la prise est instantanée mais l'hydratation est pratiquement bloquée jusqu'à 2 jours. La réaction est ensuite très lente et le taux d'hydratation plafonne à 50% entre 7 et 28 jours. A cette dernière échéance C3AH6 est en très faible proportion d'après la DRX qui, par contre, caractérise l'aluminate C4AH13 par une raie très élargie, preuve d'une moins bonne cristallisation que dans le témoin (fig. 4).

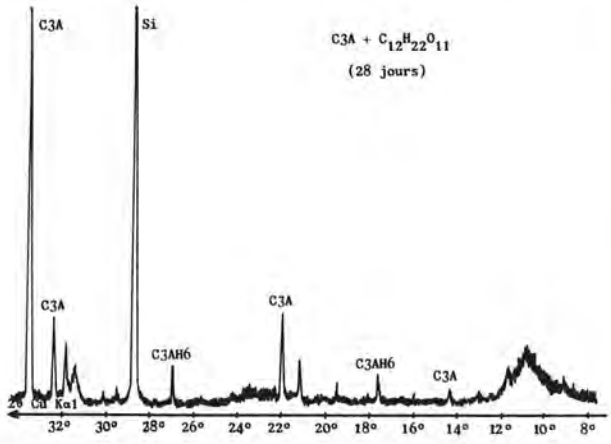

Fig. 4 : DRX - C3A + saccharose hydraté 28 jours.

Le MEB révèle dans les premiers instants la présence d'une membrane qui enrobe tous les grains de C3A (fig. 5), et qui semble être la cause du retard de l'hydratation aux premiers âges. En se fissurant par la suite, elle permet au grain anhydre sous-jacent de s'hydrater mais la réaction reste plus lente que dans le cas du témoin. Les aluminates sont mal cristallisés et la conversion en aluminate cubique est sinon empêchée, du moins considérablement retardée. La formation d'un aluminate hydraté contenant dans son réseau un complexe organique interlamellaire a été suggérée par YOUNG (2), RAMACHANDRAN et FELDMAN (3), MILESTONE (4,5), VAN WALLENDAEL et MAHIEU (6).

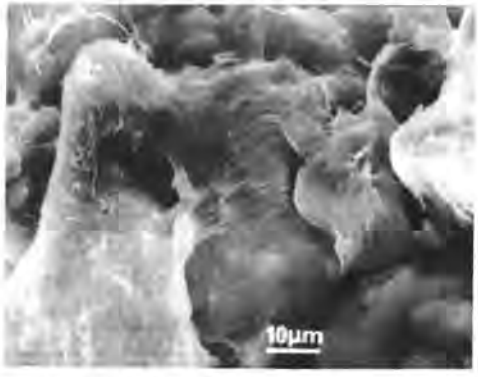

Fig. 5 : Pâte C3A + 1% saccharose.
Membrane recouvrant les grains de C3A.

4. HYDRATATION DU MELANGE C3S (80%) + C3A (20%)

Le C3A du témoin s'hydrate uniquement en cristaux hexagonaux de C4AH13. L'interaction C3A-C3S y est très nette : C3A s'hydrate plus lentement que lorsqu'il est seul (75% du C3A hydraté à 28 jours) ; C3S s'hydrate plus rapidement (45% dès 7 jours contre 30%).

Le taux d'hydratation pondéré du mélange C3S +C3A est donné sur la figure 6. L'action des deux adjuvants appelle les remarques suivantes :

- (1) **$CaCl_2$ est accélérateur de C3A à 1 jour.** Ensuite, les chloroaluminates qui apparaissent en amas autour des grains de C3A retardent son hydratation (fig. 7). Le pourcentage d'anhydre (environ 10%) reste constant entre 2 et 28 jours, l'hydratation est moins avancée que sur le témoin. Les aluminates hydratés se présentent sous forme d'un mélange de chloroaluminates et de C4AH13.

- (2) **Le saccharose maintient un effet retardateur jusqu'à 1 jour pour un pourcentage pondéral de 0,1%** et jusqu'à 4 jours pour 0,2%. Ensuite, il devient nettement accélérateur et le taux d'hydratation dépasse celui des deux autres échantillons (fig. 8 a & b).

L'interaction C3A-C3S est également très nette. L'allure des courbes de variation du taux d'hydratation est la même pour C3S et C3A.

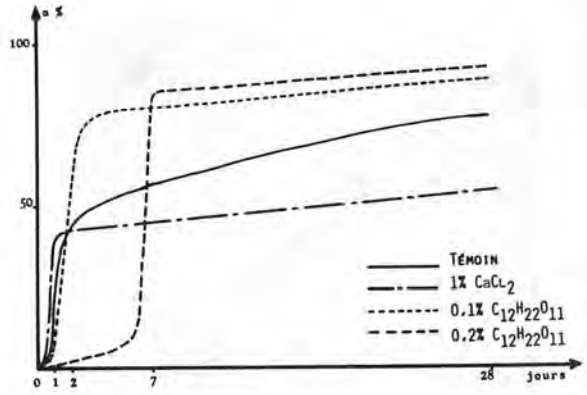

Fig. 6 : Pâtes C3S + C3A - Taux d'hydratation global α en fonction du temps.

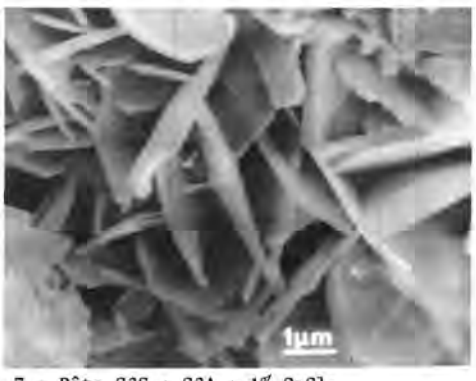

Fig. 7 : Pâte C3S + C3A + 1% $CaCl_2$.
Plaquettes hexagonales de chloroaluminate.

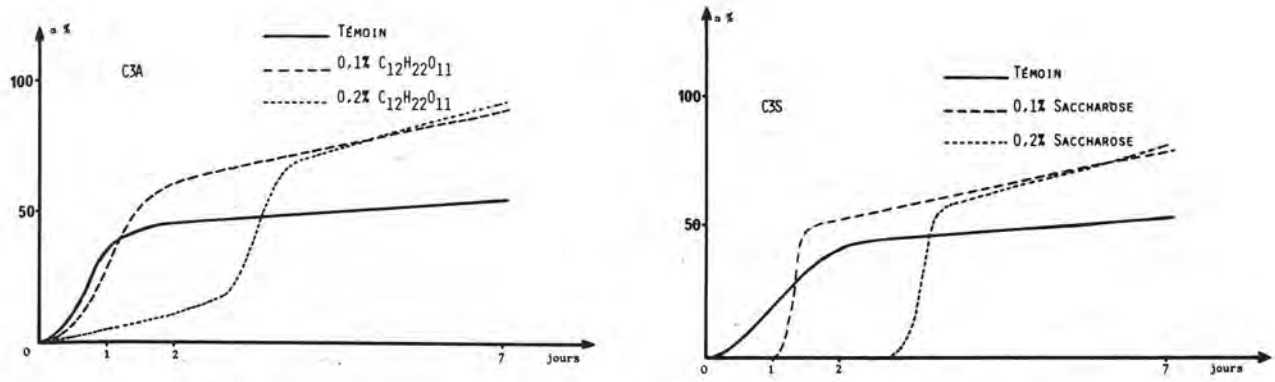

Fig. 8 : Pâtes C3S + C3A - Taux d'hydratation α de C3S et de C3A en fonction du temps.

5. HYDRATATION DU MELANGE C3S (76%) + C3A (19%) + GYPSE (5%)

L'hydratation se rapproche de celle d'un ciment portland. Le gypse est un régulateur de prise. Il retarde la cristallisation des aluminates hydratés hexagonaux par la formation de sulfoaluminates : d'abord, le trisulfoaluminate $C3A.3CaSO_4.32H_2O$, puis le monosulfoaluminate $C3A.CaSO_4.12H_2O$, enfin une solution solide $C3A.CaSO_4.12H_2O$ - C4AH13 (fig. 9).

- (1) **L'action de $CaCl_2$** doit être considérée séparément sur C3S et C3A. $CaCl_2$ a un rôle accélérateur de C3S jusqu'à 7 jours (fig. 10). Cet effet apparaît clairement sur les diagrammes de diffraction des rayons X du mélange avec et sans $CaCl_2$ à l'échéance de 2 jours (fig. 11). Par rapport à la raie de l'étalon interne Si, celles de C3S anhydre sont beaucoup moins intenses en présence de $CaCl_2$. La chaux $Ca(OH)_2$ est caractérisée par les deux raies à 3,11 et 2,63 Å alors qu'elle est à peine détectée sur le témoin. $CaCl_2$ modifie la microstructure du C-S-H qui est réticulé en raison de la présence d'ions Cl^- dans son réseau cristallin. La différence est pratiquement inexistante en ce qui concerne C3A.

Le gypse (témoin) est moins retardateur de l'aluminate tricalcique que $CaCl_2$.

Ces résultats sont illustrés par la figure 12 où sont comparés les taux d'hydratation de C3A dans divers cas : les courbes 1 et 4 montrent l'effet retardateur du gypse ; les courbes 4 et 5 le rôle retardateur de $CaCl_2$ par rapport au gypse.

Dans le témoin les premiers hydrates formés sont de l'ettringite en fines aiguilles disséminées. Dans l'éprouvette contenant $CaCl_2$ on observe des assemblages de plaquettes hexagonales de chloroaluminate $C3A.CaCl_2.12H_2O$.

- (2) **Le saccharose retarde l'hydratation de C3S** jusqu'à 2 jours puis l'accélère, par rapport au témoin, jusqu'à 7 jours. A partir de cette dernière échéance, les deux échantillons (témoin et adjuvanté) ont un taux d'hydratation comparable.

Le C3A est aussi retardé mais moins qu'avec $CaCl_2$. Le taux d'hydratation moindre par rapport au témoin est mis en évidence par la présence d'ettringite à 7 et 28 jours (fig. 13) alors que le témoin contient déjà des monosulfoaluminates (fig. 9).

Fig. 9 : Pâte C3S + C3A + gypse, 7 jours, monosulfoaluminates.

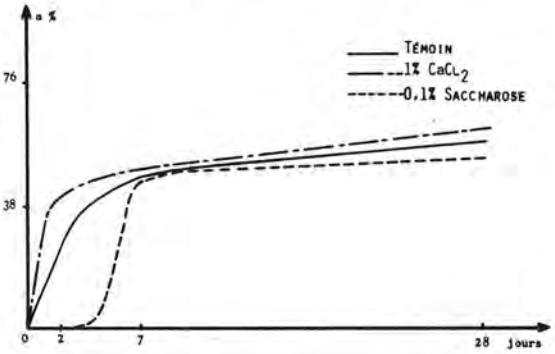

Fig. 10 : Pâte C3S + C3A + gypse - Taux d'hydratation α de C3S en fonction du temps.

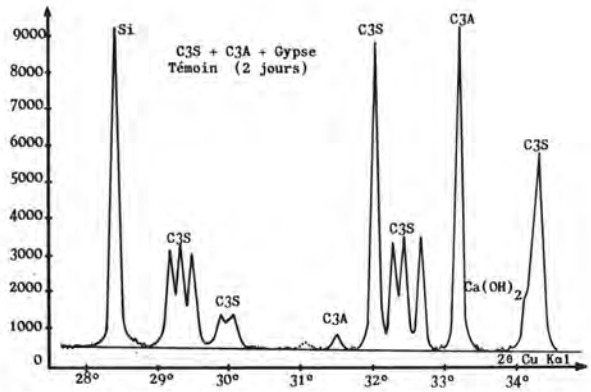

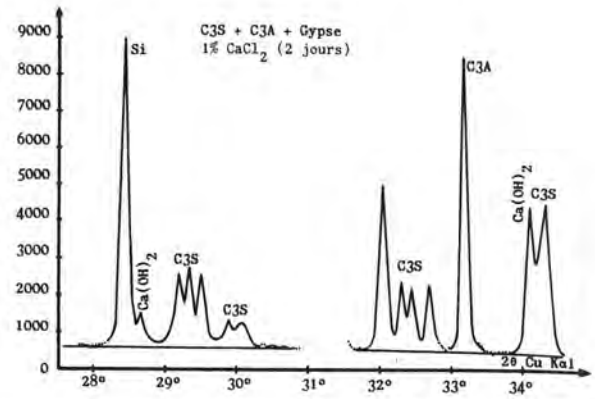

Fig. 11 : Pâte C3S + C3A + gypse. DRX - Enregistrements pas à pas obtenus en présence et en l'absence de $CaCl_2$

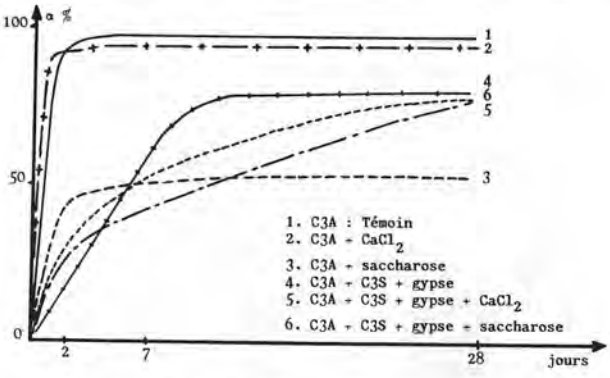

Fig. 12 : Pâte C3A + C3S + gypse. Comparaison des taux d'hydratation α de C3A : C3A seul ou adjuvanté (1,2,3) et mélanges C3A + C3S + gypse avec ou sans adjuvant (4,5,6).

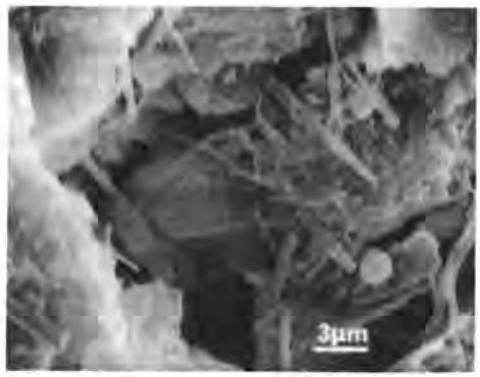

Fig. 13 : C3A + C3S + gypse + 0,1% de saccharose. Ettringite.

6. HYDRATATION DU CIMENT PORTLAND

Le ciment portland étudié contient 62% C3S et 15% C3A. Les résultats des mélanges C3S + C3A + gypse s'appliquent au ciment : $CaCl_2$ est accélérateur, le saccharose est nettement retardateur entre 4 et 16 heures. On note qu'avec $CaCl_2$ la différence affecte surtout C3S comme l'indique le diagramme de diffraction des rayons X à l'échéance de 4 heures (fig. 14) : la raie de C3A a sensiblement la même intensité que dans le témoin. A partir de 24 heures, les trois échantillons, le témoin et les deux adjuvantés (1% $CaCl_2$, 0,1% $C_{12}H_{22}O_{11}$) suivent la même courbe d'hydratation. Cependant, les échantillons contenant le saccharose sont moins compacts que les deux autres, la fracture observée au MEB est plus intergranulaire que transgranulaire.

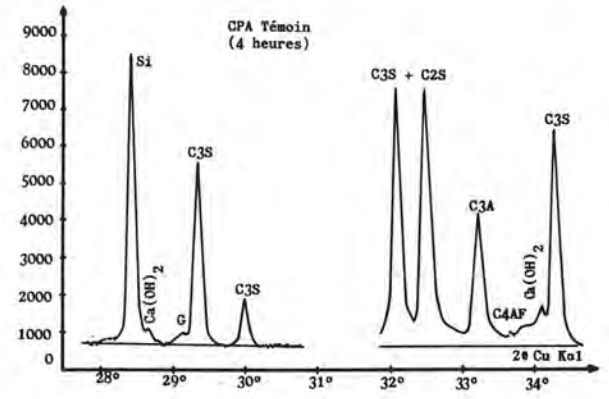

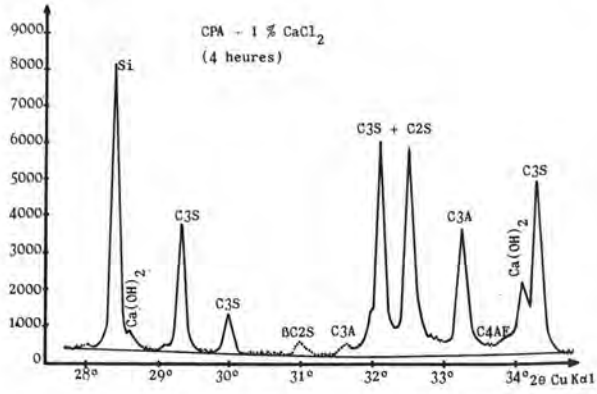

Fig. 14 : CPA. DRX - Enregistrements pas à pas obtenus sur le CPA avec et sans $CaCl_2$. (G = gypse)

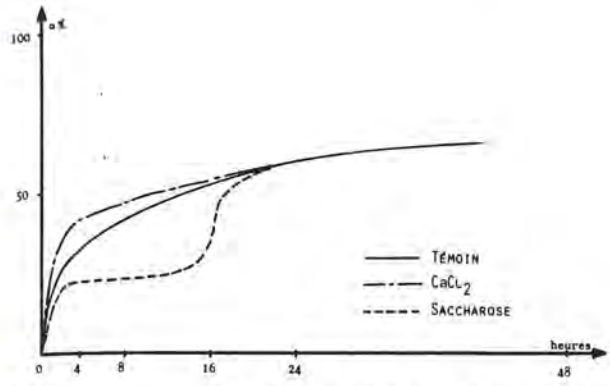

Fig. 15 : CPA. Taux d'hydratation global α en fonction du temps.

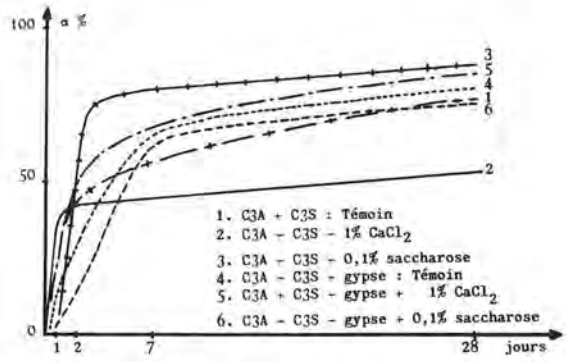

Fig. 16 : C3A + C3S. Influence du gypse sur le taux d'hydratation global pondéré α .

L'hydratation des grains de clinker est plus irrégulière. L'effet retardateur de 0,1% de saccharose sur le C3A dans le ciment portland est détectable par DRX, il est faible jusqu'à 1 jour. Les deux adjuvants considérés ici ont, surtout en présence de gypse, un effet sur C3S (fig. 15).

DISCUSSION

Le chlorure de calcium intervient dans la période précoce de l'hydratation du ciment. Il affecte essentiellement la nucléation des silicates hydratés C-S-H et de la portlandite $Ca(OH)_2$, hydrates du C3S. Au cours de l'hydratation de C3A il existe une compétition gypse-$CaCl_2$. Jusqu'à 28 jours, le sulfate est moins retardateur que le chlorure. Celui-ci forme aux premières échéances un chloroaluminate protecteur dont l'effet retardateur apparaît beaucoup moins en présence de gypse : les courbes de la figure 16 mettent bien en évidence cette influence des deux adjuvants $CaCl_2$ et saccharose en présence et en l'absence de gypse, sur l'hydratation d'un mélange C3S (80%)+ C3A (20%). Les courbes 1, 2, 3 représentent le taux d'hydratation pondéré en l'absence de gypse et les courbes 4, 5, 6 le taux d'hydratation en présence de gypse : l'effet des deux adjuvants est très nettement atténué et $CaCl_2$ agit globalement comme un accélérateur.

Le saccharose est retardateur de C3S aux brèves échéances. Il est également retardateur de C3A par formation d'aluminates mal cristallisés (raie de diffraction des rayons X très élargie à 8,2 Å).

CONCLUSION

La diffraction des rayons X et le microscope électronique à balayage ont permis de suivre l'évolution de la microstructure des produits adjuvantés (phases pures, mélanges synthétiques et ciments industriels). Ces techniques mettent bien en évidence d'une part l'influence des adjuvants accélérateurs et retardateurs sur la cristallisation et la composition des hydrates du ciment, d'autre part l'action différente de ces adjuvants sur un minéral à l'état isolé ou inclus dans un système polyphasé. Dans un ciment, le rôle d'un adjuvant doit tenir compte des interactions C3A-C3S et gypse-adjuvant.

BIBLIOGRAPHIE

(1) **J. SKALNY, J.F. YOUNG** (1980) : "Hydration mechanisms of portland cement". Congrès de Paris 1980. Principal Report.

(2) **J.F. YOUNG** (1968) : "The influence of sugars on the hydration of tricalcium aluminate". Vème Symp. Int. sur la Chimie du Ciment, vol. II, 256-267.

(3) **V.S. RAMACHANDRAN , R.F. FELDMAN** (1972) : "Effect of calcium lignosulfonate on tricalcium aluminate and its hydration products". Matériaux et Constructions, vol. 5, n° 26, 67-76.

(4) **N.B. MILESTONE** (1979) : "Hydration of tricalcium silicate in the presence of lignosulfonates, glucose, and sodium gluconate". J.A.C.S., vol. 62, N° 7-8, 321-324.

(5) **N.B. MILESTONE** (1977) : "The effect of glucose and some glucose oxidation products on the hydration of tricalcium aluminate". Cem. Concr. Res., vol. 7, N° 1, 45-52.

(6) **M. VAN WALLENDAEL, J. MAHIEU** (1973) : "Etude de l'action des "sucres" sur la prise des ciments. Analyse des sucres". RR CRIC 36-f-1973.

Interaction of aluminates with carbohydrates and aldonates

Interaction des aluminates avec les hydrates de carbone et les aldonates

B. CASU*, M. CHIRUZZI**, F. TEGIACCHI** and G. ZOPPETTI*, Research Chemists.

* « G. Ronzoni » Research Institute and **Grace Italiana S.p.A., Milan, Italy.

SUMMARY: The interaction of C_3A (both alone and in cement compositions) with some carbohydrates and the corresponding aldonates, was investigated using optical rotation, potentiometric, NMR and IR methods. Evidence was obtained that stable complexes form first in solution and then precipitate, coating the C_3A granules.
The complexing ability of the carbohydrate was correlated with the flow and resistance properties of cement pastes added of the carbohydrate.

Blocking the anomeric center by formation of a methyl glucoside substantially reduced the complexing ability of the carbohydrate and its water-reducing properties on cement pastes, on the contrary, this ability was substantially enhanced by the corresponding aldonates. The strength of the cement-pastes appear to be affected in a more complex way.

The carboxylate group as well as all the hydroxyl groups of the aldonates, are involved in complexing with C_3A. The availability of suitably oriented hydroxyl groups on contiguous units of disaccharides also appear to favour the formation and stability of the complexes.

RESUME: L'interaction du C_3A (soit lui-même, soit comme composant du ciment) avec quelques hydrates de carbone et les aldonates correspondants fut étudiée en adoptant des métodes de rotation optique, potentiométriques, NMR et IR. Il fut mis en évidence que les complexes stables se forment tout d'abord en solution et ensuite précipitent en revêtant les granules de C_3A.
La capacité complexante des hydrates de carbone a été mise en relation avec les caractéristiques de résistance et d'ouvrabilité des pâtes de ciment contenant des hydrates de carbone.

Au moment où on bloque le centre anomérique, avec la formation d'un méthyl glucoside, on réduit substantiellement la capacité complexante des hydrates de carbone et leurs propriétés de réduction d'eau sur les pâtes du ciment; au contraire, cette capacité était récupérée substantiellement avec les aldonates respectifs. La résistance du ciment semble être influencée d'une façon plus complexe.

Les groupes carboxyliques, d'ailleurs tous les groupes hydrosiliciques des aldonates sont mêlés dans la complexation avec le C_3A.
La disponibilité des groupes oxhydryliques orientés convenablement sur les unités contigues des disaccharides semble favoriser aussi la formation et la stabilité des complexes.

INTRODUCTION

Carbohydrates are well-known set-retarders of cement, and to some extent they also improve the flow properties of cement pastes (1). Although there is a general agreement on the concept that carbohydrates, as well as the corresponding aldonates, act as set-retarders by coating the cement granules thus retarding the hydration of its components, it is still not clear whether the additives are just adsorbed by the granules or precipitate on the granules after complexation with cement components that went into solution. Conflicting conclusions have also been drawn from different types of experiments as regards the role played in the set-retarding process by the "aldehydo" (in fact, hemiacetal) groups of reducing sugars, and of the hydroxyl groups alpha to the carboxylate groups of hydroxyacids (2-7).

To elucidate some of the above aspects, the present work was focused on the interaction of some carbohydrates (and the corresponding aldonates) with cement components in solution, in the presence of an excess of these components in the solid state. Since the effects of additives on the first stages of hydration primarily involve interaction with tricalcium aluminate (C_3A), this component was investigated in more detail. However, experiments were also made with the silicates (C_3S and C_2S) and ferroaluminates (C_4AF).

The investigated carbohydrates were reducing monosaccharides (typically, D-glucose), the di-saccharide maltose (α-D-glucopyranosyl-1,4-D-glucose) and the corresponding aldonates. The non-reducing monosaccharide methyl-α-D-glucoside was used as a model, to investigate the effect of blocking the hemiacetal group. Aldonates other than D-gluconate (D-galactonate and D-mannonate) were also investigated, in order to evaluate the influence of a change in configuration at carbons-4 and -2 relative to D-gluconate.

The influence of the $-CH_2OH$ group at C-6 was indirectly evaluated using an aldonate lacking this group, i.e. D-xylonate.

The structure of D-glucose, maltose and the corresponding aldonates are shown in Figure 1.

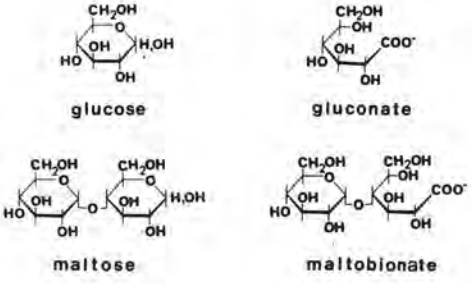

The present approach involved monitoring several physico-chemical parameters of the aqueous phase containing the additive contacted with cement components (especially C_3A), as a function of the time of contact. The main parameter considered was optical rotation. In the absence of complexation with solubilized cement components, the optical rotation values provide a sensitive determination of the optically-active additives that remain in solution at any given time of contact.
In case of an interaction with cement components in solution, these values are also a function of the type and extent of complexing. Together with independent measurements of total (free+complesed) additive in solution, the optical rotation measurements are thus a measure of the extent of involvement of the additive in complexing with solubilized cement components. Total additive was measured by colorimetric and potentiometric methods.

The extent of solubilization of cement components in the presence of the additive was determined by measuring total calcium (by atomic absorption). "Free" calcium was evaluated by potentiometric measurements, using both a calcium-specific electrode and a standard pH electrode. Soluble complexes were also investigated by ^1H-NMR spectroscopy, and solid complexes by IR spectroscopy.

MATERIALS AND METHODS

Monosaccharides, maltose and sodium D-gluconate were chromatographically pure commercial samples (Merck, Darmstadt and C.Erba, Milan). The aldonates of D-galactose, D-mannose, D-xylose and maltose were prepared starting from the corresponding aldoses (8), C_3A, C_3S, C_2S and C_4AF, were prepared by standard procedures.

The optical rotation was measured with a Perkin-Elmer Mod. 141 photoelectric polarimeter, at 436nm. Use of this wavelenght, which doubles the sensitivity as compared with the sodium D-line, was especially required at the lowest concentrations of the aldonates.

The potentiometric experiments were made with a Metrohm pH-meter. The pH was measured with a standard glass electrode, and the Ca^{++} activity with an Orion ion-specific electrode.
The atomic absorption measurements on C_3A-carbohydrate solutions were made on a Perkin-Elmer Mod. 303 spectrophotometer, equipped with a calcium lamp. The IR spectra of solid samples of C_3A + additive (as KBr pellets) were obtained with a Perkin-Elmer Mod. 337 grating spectrophotometer. After contacting with H_2O or carbohydrate (aldonate) solutions, the C_3A granules were air-dried before preparing the pellets. The spectra of the soluble compleses were obtained after evaporating the solvent under vacuum, after filtering the solutions as described for the optical rotation measurements.

The ^{1}H-NMR spectra of sodium gluconate solutions were obtained with a 90 MHz Perkin-Elmer Mod. R-32 spectrometer. A 10% (w/v) solution of gluconate in D_2O (99.7%), alone and saturated with C_3A, was evaporated under vacuum, and the residue redissolved in D_2O. The evaporation-solubilization process was repeated three times, to exchange with deuterium most of active hydrogens of the samples. The spectra of the gluconate+C_3A solutions were obtained within 30' from their preparation, before precipitation of any solid complex.

The physico-chemical parameters of the aqueous systems were measured as follows:
4 g aluminate (or silicate, clinker or cement) were introduced in a 400 ml beaker containing 200 ml H_2O (or the same volume of a solution containing from 0.2 to 10% (w/v) carbohydrate or aldonate). For the optical rotation and atomic absorption measurements, 10 ml aliquots were taken from the solution (vigorously stirred with a magnetic stirrer) at given time intervals, with a syringe equipped with a Millipore 0.45 μ filter.

pH and Ca^{++} activity measurements were made with the electrodes directly immersed in the suspensions. Typical measurements were made after 1', 3', 5', 10', 20', 30', 60', 100' and (occasionally) 1000'.

The total concentration of carbohydrate in solution was determined by the colorimetric anthrone (9) method, on filtered aliquots of the suspensions. Total aldonates in solution were similarly determined by potentiometric titration with 0.1N NaOH, on the eluates from a column of IR-120 (H^+) resin.

The effect of the additives on the flow and strength properties of cement pastes was evaluated on a Portland cement, using standard tests (UNI 7102).

RESULTS

The optical rotation of the reducing carbohydrates suddenly decreased at the very early stages (within a few minutes) of contacting with C_3A. Being paralleled by a concurrent decrease of the carbohydrate concentration (colorimetric analysis), this behaviour clearly reflect precipitation of the carbohydrate. On the contrary, the non-reducing carbohydrate methyl α-D-glucoside did not precipitate (no changes in optical rotation over a period of 100' of contacting with C_3A).

The optical rotation of sodium gluconate solutions is dramatically affected by contacting the solution with solid C_3A. An increase of up to 5 times the original rotation value ($[\alpha]_{436} = +23$) was in fact observed, the actual increase being a function of the time of contact with C_3A. Such a behaviour is illustrated in Figure 2, where the optical rotation changes of solutions of different gluconate content (from 0.2 to 5% w/v) are plotted vs the time of contact with C_3A.

(For the sake of presentation, the curves are "normalized", i.e. the α values are divided by the corresponding concentration of gluconate, and vertically displaced by the same amount relative to each other.)

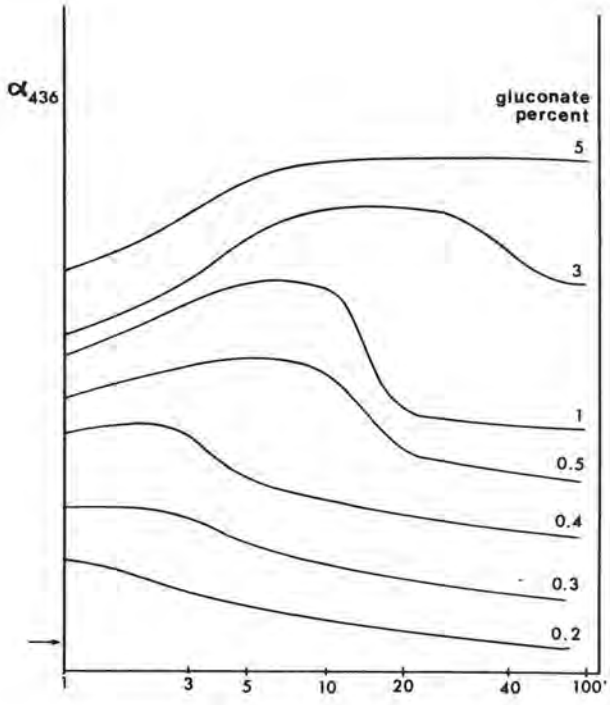

Fig. 2 - Optical rotation (α_{436}) of solutions at different concentrations of sodium gluconate, as a function of the time of contact with C_3A. (The curves are normalized and vertically displaced with respect to each other (see text). The arrow indicates the α value for the 0.2% gluconate solution at time zero).

As shown in the figure, the relative increase in optical rotation at any given time of contact with C_3A is also a function of the gluconate concentration. For 0.2% gluconate solutions, a maximum value of α was already reached after 1 minute contacting with C_3A. The optical rotation then steadily decreased with time, reaching a minimum value after 100'.

As the original gluconate concentration increased from 0.3 to 3%, the maximum α value was displaced toward longer times, followed by a progressively steeper decrease.
Potentiometric analyses indicated that practically all the gluconate present before contacting with C_3A remained in solution up to the time at which a decrea

se of α is observed, and that the drop in α values is clearly associated with disappearance of the gluconate, as it precipitates from the solution. (Such a precipitation was currently observed after a while even from filtered solution, i.e. non longer contacted with C_3A.)
In the presence of C_3A granules, precipitation occurred after 1' for 0.2% gluconate solutions, - 3' for 1% and -25' for 3% solutions. At 5% gluconate, all C_3A used in these experiments (2g) went into solution after -10', originating a clear stable gel.

As shown in Figure 3, also other clinker components produced an increase in optical rotation of gluconate solutions. However, such an increase was observed at times considerably longer than for C_3A. The maximum α values were at - 40' for C_3S, - 1000' for C_4AF and more than 1000' for C_2S. Also, the relative increase of α (as measured on contacting the gluconate solutions with the same amount of each clinker component) was substantially lower than observed for C_3A.

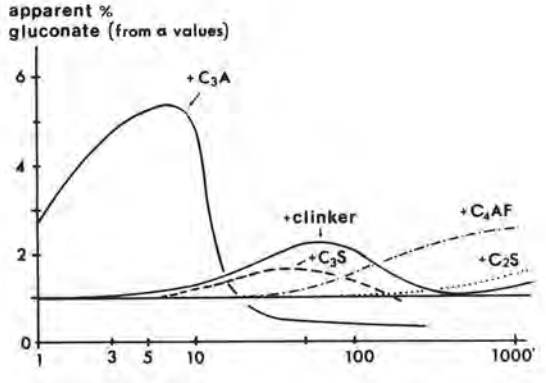

Fig. 3 - Apparent concentration of gluconate as calculated from α_{436} values before contacting with C_3A, as a function of the time of contact with C_3A and other cement components, for a 1% solution of Na gluconate. The curve for a reconstituted clinker (see text) is also shown.

Fig. 3 also illustrates the behaviour of clinker (in fact, a "reconstituted" composition consisting of 4% C_3A, 55% C_3S, 25% C_2S and 16% C_4AF), contacted with 1% gluconate under the same experimental conditions used for the isolated components. It is noteworthy that this experimental α/t curve (with a maximum at - 60') does not correspond to the one calculated by adding up the relative contributions of the individual clinker components.

The calculated curve consists in fact of two curves, with maxima corresponding to the maxima of C_3A (the component that produces the largest increase in α) and of C_3S (the most abundant component in the clinker). As the concentration of gluconate is decreased (to 0.2%) and the C_3A content of the clinker increased (to14%), the separate contributions of C_3A and the other components clearly show up in the experimental curves for reconstituted clinkers.

Addition of gypsum to C_3A shifts the α/t curves toward longer times, without substantially affecting the maximum α values. (For 0.2% gluconate in the presence of 2% solid C_3A + 1% gypsum, the maximum of the curve shifts from - 1' to - 4'.)

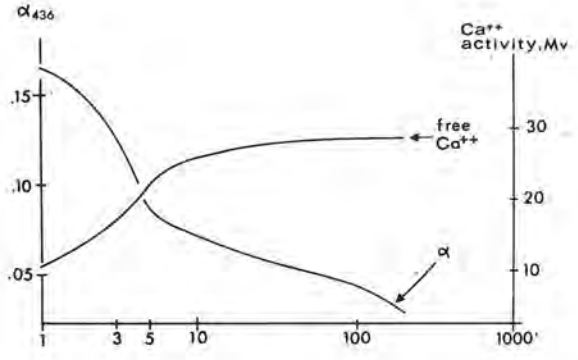

Fig. 4 - Optical rotation (α_{436}) and calcium ion activity for a 0.2% Na gluconate solution, as a function of the time of contact with C_3A.

The curves showing total calcium in the gluconate solutions as a function of the time of contact with the cement components are closely similar to the optical rotation curves.
On the contrary, as shown in Figure 4 for the 0.2% gluconate solution, curves for free calcium are complementary to the optical rotation (and total calcium) curves, i.e. the Ca^{++} activity is minimum for the maximum α value, and levels-off when the α values (and the gluconate concentration) fall below a certain level.
Such a levelling-off of free calcium is quite different from that observed in the absence of additive. In fact, in additive-free systems the Ca^{++} activity is somewhat higher than in the presence of gluconate up to - 10' contacting with C_3A, then sharply

increases with a maximum at ~80'; at 1000', it becomes again close to the values at time zero. The pH of the gluconate solutions contacted with C_3A increase in parallel with the concentration of free calcium. (An increase from 12.5 to ~ 13 was observed for 1-3% gluconate solutions, with a maximum pH value reached after 10'.

As shown in Figure 5 all the ^{1}H-NMR signals of Na gluconate are affected by addition of C_3A. (Assignements (10) refer to hydrogens on carbons at different distances from the carboxylate group.)

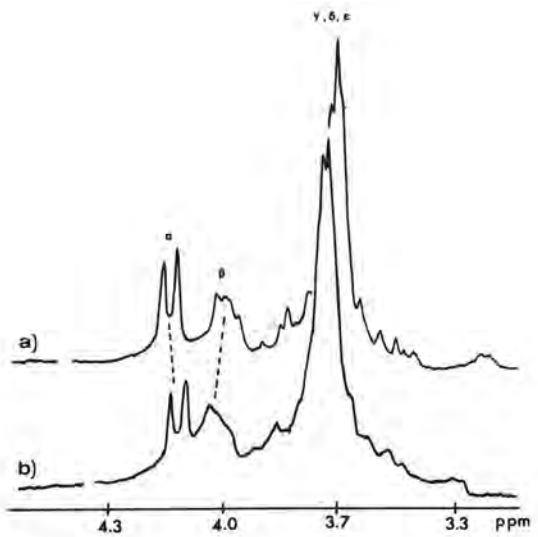

Fig. 5 - ^{1}H-NMR spectra (90 MHz) of a D_2O solution of Na gluconate (a) and Na gluconate added of C_3A (b).

Also aldonates other than D-gluconate interact with C_3A and other cement components. The α/t curve of D-gluconate was quite close to that of D-gluconate. The D-mannonate curve is also to be considered similar to the one of D-gluconate, in spite of its being reseversed in sign, as expected because of the different configuration at C-2. On the contrary, D-xylonate did not show any significant changes of α in the presence of C_3A.
Maltobionate showed a α/t curve similar to the one of D-gluconate, with somewhat bigger $\Delta\alpha$ values at the same molar concentration.

The effect of glucose, maltose and the corresponding aldonates on the flow and strength properties of a Portland cement is illustrated in Table I. Data for methyl α-D-glucoside are also included. While this latter additive did not cause any significant variation in the flow and strength of the cement paste, the other additives substantially increased the flow and retarded the strength development.

Table I - Percent variation of flow and strength of a Portland cement added of 0.1% carbohydrate or aldonate (referred to a blank without additive)

	flow	compressive strength after 1 day
D-glucose	+ 9	- 21
maltose	+ 12	- 38
methyl -D-glucoside	+ 1	- 3
sodium D-gluconate	+ 16	- 43
malto-aldobionate	+ 13	- 54

DISCUSSION

The above results clearly indicate that the reducing carbohydrates glucose and maltose precipitate from their solutions at the very beginning of contacting with C_3A. This behaviour prevented to ascertain whether any complex is formed in solution before the carbohydrate deposits on the C_3A granules. Interaction with C_3A was prevented by blocking the anomeric center by a methyl group, such as in methyl α-D-glucoside.
On the other hand, a clear evidence that complexes in solution are formed was obtained for Na gluconate. The complex with C_3A, which is formed within a few minutes especially for the most dilute gluconate solutions, precipitate on the undissolved granules in a short time after its formation. This time increases with increasing concentration of the gluconate, up to 5% gluconate, which forms a stable gel.

Preliminary IR measurements on the C_3A granules after contacting with aldonate solutions as well as on the aldonate +C_3A recovered from the aqueous phase have confirmed that the gluconate is indeed in a complexed form both in solution and in the solid phase precipitated on the granules.

C_3S, C_2S and C_4AF also form soluble complexes with gluconate. However, these complexes are formed at longer times and are associated to smaller variation ofoptical rotation than with C_3A. Since also sodium aluminate formed a similar complex with C_3A, it is suggested that the complex involves the aluminate part and not the calcium part of this cement component. On the other hand, since the concentration of total calcium in solution parallels the concentration of gluconate (and the optical rotation values), it is inferred that C_3A binds to gluconate as a complexion.

It should be noted that formation of the well -known calcium complex of gluconate brings about a much smaller change in optical rotation than observed for aluminates (i.e., only ~ 17% increase of α as compared with the ~ 500% increase observed in the present experiments with C_3A.)

Aluminates were recently shown to form strong complexes with carbohydrates(11). It is not surprising that aldonates, which retain all the hydroxyl groups of the original carbohydrate except the anomeric one (which is replaced by a good coordinating group such as the carboxylate) can form even stronger complexes. Preliminary experiments with D-glucitol (sorbitol) have shown that this analog of D-gluconate, having a primary hydroxyl group instead of the carboxylate, complexes C_3A less strongly (and affects the flow and resistance of cement substantially less) than gluconate. It is relevant that the ^{1}H-NMR spectral shifts on addition of C_3A indicate that all the hydroxyl groups of gluconate are involved in the complex. (A significant effect of simple Ca^{++} salts was observed only for the α and β hydrogens). It is therefore not surprising that D-xylonate, missing the hydroxyl group at C-6, does not significantly interact with C_3A. On the contrary, an inverted configuration of the hydroxyl group at C-2 (such as in D-mannose) does not prevent the formation of stable complexes.

Maltobionate (consisting of a non-reducing sugar and an aldonate)also forms strong complexes with C_3A, suggesting that the non-reducing, intact glucose ring partecipates is some way in coordination of the complex aluminate ions, possibly involving suitably oriented hydroxyl groups. Also the better complexability observed for the disaccharide maltose as compared to glucose is likely attributable to the above possibility, clearly shown by inspection of molecular models.

Data in Table I show that the additives that complex C_3A improve the flow properties of cement pastes. This complexing ability qualitatively correlates also with the retarding effect on the strength development of the pastes at the early stages.

CONCLUSION

The above findings throw some light on the mechanism of carbohydrate-derived cement additives, the formation of a complex in solution precedes precipitation of the additive on the undissolved granules, and formation of the protective layer that retards hydration (and setting) of cement.

ACKNOWLEDGEMENT. The authors would like to thank Prof. A.Rio of Rome University for the stimulating and helpful discussion.
Thanks are also due to G.Torri and M.Morrone of Ronzoni Institute, and C. Rossetti of Grace Italiana, for their fine work in performing the experiments.

REFERENCES

1) A.Joisel, "Admixtures for cement", 1973.
2) J.H.Taplin, discussion on paper by H.E.Vivian, 4th Int. Symposium on the Chemistry of Cement, Natl. Bur.Standards Monograph . 43 vol.2. 927 (1960)
3) K.E. Daugherty and M.J.Kowalewski, "Effects of organic compounds on the hydration reaction of tricalcium aluminate", 5th Int. Symposium on the Chemistry of Cement Tokio, 42-52 (1968)
4) J.F.Young, "The influence of sugar on the hydration of tricalcium aluminate", 5th Int. Symposium on the Chemistry of Cement, Tokio 256-267 (1968)
5) R.W. Previte, "Some insights on the mechanism of saccharide set retardation of Portland cement", Cement Concr.Res. 1, 301-316 (1971)
6) N.B.Singh, "Effects of gluconates on the hydration of cement", Cement Concr. Res. 6 , 455-460 (1976)
7) N.B.Milestone, "The effect of glucose and some glucose oxidation products on the hydration of tricalcium aluminate", Cem. Concr. Res. 7 , 45-52 (1977)
8) J.W. Green: "The halogen oxidation of simple carbohydrates", Advances Carbohyd. Chem. 3 , 129-184 (1948)
9) J.E.Hodge and B.T. Hofreiter, "Anthrone Colorimetric Method", in L. Whistler and M.L.Wolfrom (Ed. s) "Methods in Carbohydrate Chemistry", Academic Press, New York 1962, 389-390
10) D.T.Sawyer, "Proton magnetic resonance studies of several polyalcohols, hydroxyacids, and derivates of D-gluconic acid" Anal.Chem. 38 , 192-198 (1966)
11) J. A. Rendleman and J.E. Hodge, "Complexes of Carbohydrates with aluminate ion Chromatography of carbohydrates on columns of anion-exchange resin (aluminate form), Carbohyd. Res.44 , 155-167 (1975).

Theme 5 - The role of C_3A in sulfate attack on cements

GENERAL REPORT

by P.K. METHA, University of California, Berkeley, U.S.A

A review of four papers on the role of C_3A in sulfate attack on cements is given in this report. Two papers present new information in the field since the Moscow Congress. The third paper presents test results of sulfate attack on a large number of portland and blended portland cements. The fourth paper contains a literature review on the mechanism of expansion associated with the sulfate attack.

The first paper reviewed here describes an investigation on the significance of the differences in the rates of hydration of various forms of C_3A in regard to attack by magnesium sulfate, which is the principal source of sulfate in seawater. The second paper describes a study in which two hydrated cements were exposed to a sodium sulfate solution, the C_3A in one of the cements being in the cubic form and in the other being predominantly in the orthorhombic form. The third paper describes an investigation on the relative sulfate resistance of 26 different portland cements and several portland pozzolan cements. The last paper presents a critical review of the literature in order to show that it is not the formation of ettringite but monosulfate hydrate which is responsible for expansions associated with sulfate attack on cements.

According to the paper authored by **M. REGOURD, H. HORNAIN and B. MORTUREUX**, 4 different types of C_3A were synthetized for making cements by mixing 50 % alite, 30 % quartz powder, 5 % gypsum and 15% of any one of the four types of C_3A. The following types of C_3A were used : pure C_3A in cubic form, orthorhombic C_3A containing 4,8 % Na_2O, cubic C_3A containing 5 % Fe_2O_3 and orthorhombic C_3A containing 4,8% Na_2O and 5 % Fe_2O_3. Minicylinders (1 cm diameter by 1 cm height) of neat cement paste corresponding to 0.35 water-cement ratio were moist-cured for 3 days and then immersed in a 5 % $MgSO_4$ solution. After 7 days of sulfate immersion all the specimens showed large expansions and were badly cracked. Formation of gypsum, ettringite and brucite in the deteriorated material was confirmed by X-Ray diffraction analysis. It was concluded by the authors that in the presence of quartz, the porosity of the specimens was so high that it was not possible to detect the differences in the sulfate resisting characteristics of the different forms of C_3A. Four new cement compositions were synthesized in which the quartz fraction was replaced with a granulated blastfurnace slag of 3000 cm^2/g Blaine. Also, the authors investigated the effect of two different periods of moist curing, namely 48 hours or 6 hours in fresh water, on the subsequent behavior of cements in sulfate solution. XRD and DTA were used to monitor the rates of hydration of C_3A at various intervals. Evaluation of the degree of sulfate attack was done by visual examination.

For the pastes cured in water for 48 hours, prior to sulfate immersion, it was observed that those made from the cement containing the pure C_3A in cubic form performed better during the sulfate attack. The pastes from the other three cements showed evidence of more sulfate attack. The pastes from the other three cements showed evidence of more sulfate attack which, according to the XRD and DTA data, was due to the transformation of $Ca(OH)_2$ and monosulfate hydrate into gypsum and ettringite, respectively. The authors also found significant differences in the rates of hydration of C_3A present in the 4 cements. For instance, DTA of the pastes hydrated for 3 hours (Fig. 2 of the **REGOURD** et al paper) shows that more ettringite was present in the cement paste containing pure C_3A in cubic form than in the cement paste containing C_3A in the orthorhombic form (4.8 % Na_2O), Similarly, the data from XRD analyses (Fig. 3 of the **REGOURD** et al paper) show that in the pastes cured for 48hours, the degree of hydration of C_3A for the cement containing pure C_3A in cubic form was about 70 % as compared to 55-60 % for the cements containing the other types of C_3A. It was concluded by the authors that the superior performance to sulfate attack of the cement containing pure C_3A in cubic form resulted from the lower porosity of the paste due to the higher rate of hydration of C_3A in the cement.

In the second series of tests in which the pastes were cured in fresh water for 6 hours only prior to the sulfate immersion, it was found that both the cements containing C_3A with 5 % Fe_2O_3 performed better than the cement containing pure C_3A in cubic form or the orthorhombic C_3A containing 4.8 % Na_2O. According to the authors, this was due to the fact that only a small fraction of the C_3A was hydrated in all the cements prior to sulfate immersion. Therefore, the lower reactivity of the anhydrous C_3A containing Fe_2O_3 was favourable for sulfate resistance than the higher reactivity of the others types of C_3A which did not contain Fe_2O_3. The authors concluded that the porosity of a cement paste, as affected by hydration characteristics of the constituents compounds, and history of curing prior to sulfate exposure, are the most important factors in determining its sulfate resistance.

According to the paper authored by **P.K. MEHTA**, two cements containing C_3A in different forms were investigated for relative sulfate resistance. The cements were made from a high-alkali industrial clinker containing 13.6 % potential C_3A. The C_3A in the clinker was predominantly in the orthorhombic form. Cement "A" was made by grinding this clinker with 5 % gypsum to 4000 cm^2/g Blaine. Another clinker having the same potential compound composition, but with C_3A present in the cubic form only, was obtained by heating the industrial clinker at 1350 °C for 30 minutes in a la-

boratory furnace. Cement "B" was made from this heat-treated clinker by grinding it with 5 % gypsum to the same fineness as Cement "A". The sulfate resisting characteristics of the cements were evaluated by an accelerated test procedure according to which neat cement paste cubes and mortar prisms, normally cured for 14 days, were immersed in a 4 % Na_2SO_4 solution. The solution was maintained at a constant pH and sulfate concentration by automatic and continous titration against N/10 H_2SO_4. Changes in compressive strength of the neat cement paste cubes and expansion of the mortar prisms during a 5-week sulfate immersion period were used as criteria for evaluation of the sulfate resistance of the cements. X-Ray diffraction analyses of the neat cement pastes at regular intervals, both before and during the sulfate immersion, were carried out in order to monitor the mineralogical changes.

The compression strength data from the neat cement paste cubes and the expansion data from the mortar prisms (Fig. 2 of the **MEHTA** paper) showed that these were significant differences between the rates of sulfate attack of the two cements. For instance, the sudden increase in the expansion rate of Cement "A" during the third week of sulfate immersion was not observed in Cement "B until the fifth week. From the XRD data of the pastes prior to the sulfate immersion (Fig. 4 of the **MEHTA** paper), it was concluded that the main alumina-containing compounds in the paste of Cement "A" were ettringite and monosulfate hydrate, whereas in Cement "B", besides ettringite, a calcium aluminosilicate was detected. The deteriorated portions of Cement "A" after the 28-day period of sulfate immersion contained more ettringite and less monosulfate hydrate than were present before the sulfate immersion. Also, like **REGOURD** et al, the author found that Cement "B" (the cement containing the cubic C_3A only) hydrated faster, produced most of the potential ettringite within 1 day of normal hydration, and was 15 % stronger in compression than Cement "A" (the cement containing the orthorhombic C_3A).

On the basis of his experimental results, the author concluded that the process of expansion and cracking of high-C_3A portland cement pastes in a sulfate solution can be divided into two stages. In the first stage, called the dormant stage, the chemical reaction between the sulfate solution and unreacted aluminate and aluminate hydrates present in the cement paste is associated with increase in the amount of monosulfate hydrate, and is not accompanied by expansion. This is followed by the second stage during which expansion and cracking occur as a result of conversion of the monosulfate hydrate into ettringite. It was also concluded by the author that high-C_3A portland cements, regardless of the type of C_3A, would eventually show deleterious expansion in sulfate solution, however the rate of sulfate attack was slower in the cement containing cubic C_3A. This was mainly due to the rapid rate of hydration of cubic C_3A which made the cement paste stronger and less permeable, and also led to the formation of aluminosilicate hydrate which was found more resistant to sulfate attack than the monosulfate hydrate.

K. **MATHER** reported the results of an investigation on relative sulfate resistance of 26 industrial portland cements, and several pozzolan cements made from some of the portland cements used in the investigation. Five portland cements contained no potential C_3A content, 6 contained C_3A in orthorhombic and/or tetragonal form, 8 contained C_3A in cubic and orthorhombic or tetragonal form, and 7 had C_3A in cubic form only. Nine of the portland-pozzolan cements contained fly ash from burning of bituminous, sub-bituminous or lignite coals, one contained a calcined natural pozzolan of high silica and glass content, and one consisted of a silica dust which is a byproduct of the ferrosilicon alloy industry. By continuous immersion in 5 % Na_2SO_4 solution, the sulfate resistance was evaluated from changes in length and fundamental transverse frequency of 25.4 mm by 25.4 mm by 285.8 mm prisms made with mortars, containing one part of cement to 2.75 parts graded sand to 0.485 parts of water by weight. The mortar prisms were cured for 24 hours in sealed molds at 35°, then demolded and thereafter cured in saturated lime water at 23 ± 1.7° until the comparison mortar cubes showed 20.7 ± 1.0 MPa compressive strenght. At this time the prisms were immersed in the 5 % Na_2SO_4 solution. Changes in length and fundamental transverse frequency were measured at 7, 14, 21, 28, 56 and 90 days, and thereafter as needed. Each time the prisms were measured for length, the sulfate solution was changed. The criterion for fracture by increase in length was chosen as 0.1 %.

In regard to the portland cements, all the zero-C_3A cements were found sulfate resisting except one which showed 0.085 % expansion in 180 days (and may show more than 0.1 % expansion at one year). The author suspected that the large expansion shown by this cement may be related to hydration of periclase, since the cement contained 4.53 % MgO by chemical analysis. All the 6 cements containing orthorhombic and/or tetragonal C_3A failed except one cement which showed 0.057 % expansion at 180 days of sulfate immersion. Since this cement contained only 2 % MgO, the author seems to suggest that the overall expansion in the test for sulfate attack is influenced by the amount of periclase in cement. At the time of reporting the results, the author found that 7 of the 8 cements containing C_3A in cubic and orthorhombic or tetragonal form had failed by exceeding the 0.1 % expansion limit. Similarly, 5 of the 7 cements containing only cubic C_3A had also failed. From this the author concluded that, contrary to the observations of some earlier investigations, there was no correlation between the type of C_3A present in portland cement and the resistance of the cement to sulfate attack. The author also made interesting observations on the strain capacity (increase in length without fracturing) of various cements. Expansions could not be related directly to the C_3A of the cements because due to rapid strength gain, the cements with higher C_3A content possessed lower strain capacity.

In regard to the effect of the type of pozzolan on the sulfate resistance of portland-pozzolan cements containing from 0.4 to 14.6 % potential C_3A, it was shown (Fig. 1 of the **MATHER** paper) that 30 % cement replacement by volume with either of the 2 reactive pozzolans, namely the calcined volcanic pozzolan and the silica dust from the ferrosilicon industry, made the cements highly resistant to sulfate attack. On the contrary, at this level of cement replacement, none of the 8 sub-bituminous and lignitic fly ashes were able to reduce the expansion in mortar prisms to less than 0.1 % when portland cement of either 13.1 % potential C_3A content (RC 714) or 14.6 % potential C_3A content (RC 756) were used in making the pozzolan cement (Fig. 2 and 3 of the **MATHER** paper). In fact many of the sub-bituminous and lignitic fly ashes increased the sulfate expansion of the central portland cement instead of reducing it. This type of behavior was observed from fly ashes which contained less than 50 % silica, 16 to 26 % Al_2O_3 and 5 to 30 %

CaO. The increase in sulfate expansion of portland-pozzolan cements made with high-C_3A clinkers and fly ashes of high alumina and lime content is attributed to formation of ettringite from the readily available Al_2O_3 and CaO in fly ash.

With portland cement containing 9.4 % potential C_3A, 2 of the 8 fly ashes of the sub-bituminous-lignitic group were able to reduce the sulfate expansion to less than 0.1 % at 365 days (Fig. 4 of the **MATHER** paper). Portland-pozzolan cements made with clinkers containing up to 11 % potential C_3A and about 20 % bituminous fly ash showed substantial improvement in sulfate resistance of mortars as compared to the control portland cements made from the same clinkers. In conclusion, the author has shown that the ability of portland cements and portland-pozzolan cements to resist sulfate attack is affected by the C_3A content of the portland cement and the composition, reactivity, and amount of pozzolan used.

In his paper containing a critical appraisal of the cement literature on mechanism of sulfate expansion, S. **CHATTERJI** presents arguments challenging the widely held belief that the expansion in portland cement pastes on exposure to sulfate solutions is associated with ettringite formation. He also presents arguments in support of **CHATTERJI** and **JEFFERY**'s hypothesis according to which the formation of monosulfate hydrate from C_4AH_{13}, by ion exchange in portland cement pastes exposed to sulfate ions, is responsible for expansion. The literature survey on sulfate generated expansion divided into two categories : free expansion, and restrained expansion. In regard to free expansion, the author cites his own work as well as the work of **SELIGMANN** and **GREENING** on considerable free expansions observed in C_3A-gypsum-lime systems in which monosulfate rather than ettringite was the stable product. Also, from an examination of **MATOUSEK** and **SAUMAN**'s work on expansion of mixtures containing portland cement, metakaoline and gypsum, the author notes that at least 20 % expansion occured after the formation of ettringite had ceased. Citing **MEHTA**'s studies on restrained expansions of Type K, M and S cements, the author points out that the expansions continued even beyond the time when formation of ettringite had ceased and, in fact, ettringite was being transformed into the monosulfate hydrate. In further support of his case for sulfate expansion due to the monosulfate formation, the author notes that there is no expansion in the sulfate resisting portland cement because they do not contain the monosulfate hydrate on hydration. In conclusion, the author says : "It is possible to set down evidence for this or that hypothesis but in the ultimate analysis ones prejudices determine which hypothesis one believes".

Summarizing the main points from the 4 contributions on the role of C_3A in sulfate attack, **REGOURD** et al and **MEHTA** have shown that the rate of sulfate attack in cements can be influenced by the type of C_3A present. Hydrated pastes made from cements containing cubic C_3A were attacked at a slower rate by sulfate solutions than the pastes made from cements containning C_3A in more densely packed structurals. The differences in the rates of sulfate attack were attributed mainly to the more rapid hydration of cubic C_3A which produced stronger and probably less permeable paste prior to the immersion in sulfate solution. **MEHTA** also demonstrated the formation of a calcium aluminosilicate hydrate in the pastes of a portland cement containing cubic C_3A. He suspected that the relatively superior resistance of the calcium aluminosilicate hydrate may be partially responsible for the slower rate of sulfate attack on portland cements containing cubic C_3A. **MATHER** has shown that the high alumina and lime present in lignitic and sub-bituminous fly ashes can increase rather than reduce the sulfate resisting behavior of pozzolan cements made from such fly ashes. **MATHER**'s test results did not confirm the finding of other investigation that the type of C_3A present in a portland cement can influence its resistance to sulfate attack.

In the opinion of this reporter, the contradiction between the findings of **REGOURD** and al, and **MEHTA** on one hand, and **MATHER** on the other, is not real. Whereas **MATHER**'s conclusion was drawn from sulfate immersion up to 365 days, the former investigators made their comments on the basis of 4 to 5 weeks of sulfate immersion. It appears that the type of C_3A affects only the rate of sulfate attack but not the eventual degree of attack. Evidently, more work is needed to confirm the hypothesis that reduced porosity and permeability of the pastes made from cements containing cubic C_3A is responsible for slower rate of sulfate attack on these cements. Also, the need for accelerated and reliable test methods for evaluation of sulfate resistance of cements is self evident. Different curing periods, size of specimens, sulfate solutions, and failure criteria were used in the three investigations reported above, **CHATTERJI**'s contribution makes the point that the question of mechanism of expansion accompanying sulfate attack also deserves more attention in the future. Most of his criticism on the ettringite expansion hypothesis is based on continuing expansion of pastes even after the formation of ettringite has ceased. This argument, instead of being against the ettringite-expansion hypothesis, can be used in support of the hypothesis if the mechanism of expansion is due to swelling of colloidal ettringite by water adsorption. **MEHTA** and **HU** reported that maximum expansions as a result of swelling of ettringite were not observed in their experiment until after about 45 days of exposure of ettringite to water. Clearly, more experimental studies are needed to settle this controversy. **CHATTERJI** is, therefore, correct in stating that ones prejudices often determine which hypothesis one would like to believe. This reporter hopes that before the next Congress the researchers interested in the mechanism of sulfate generated expansion in portland cements pastes, including **CHATTERJI**, would cast aside their personal prejudices and undertake conclusive experimental studies to shed better light on the subject.

Thème 5 - Le rôle de C_3A dans l'attaque des ciments par les sulfates

RAPPORT GENERAL

par P.K. METHA, Université de Californie, Berkeley U.S.A.

Une revue de quatre communications sur le rôle de C_3A dans l'attaque des ciments par les sulfates est donnée dans ce rapport. Deux communications présentent des informations nouvelles dans ce domaine, depuis le Congrès de Moscou. La troisième communication présente les résultats des essais de l'attaque par les sulfates d'un grand nombre de ciments portland et de ciments portland avec ajouts. La quatrième communication contient une revue de la littérature sur le mécanisme de l'expansion associée à l'attaque par les sulfates.

La première communication revue ici décrit une recherche sur la signification des différences dans les taux d'hydratation des formes variées de C_3A à l'égard de l'attaque par le sulfate de magnésium qui est la source principale de sulfate dans l'eau de mer. La seconde communication décrit une étude dans laquelle deux ciments hydratés ont été exposés à une solution de sulfate de sodium, le C_3A dans l'un des ciments étant sous la forme cubique et dans l'autre étant principalement sous la forme orthorhombique. La troisième communication décrit une étude sur la résistance relative aux sulfates de 26 ciments portland différents et de quelques ciments portland aux pouzzolanes. La dernière communication présente une revue critique de la littérature afin de montrer que ce n'est pas la formation de l'ettringite mais celle du monosulfate hydraté qui est responsable des expansions associées à l'attaque des ciments par le sulfate.

D'après la communication de **M. REGOURD, H. HORNAIN** et **B. MORTUREUX**, quatre types différents de C_3A ont été synthétisés pour faire des ciments en mélangeant 50 % C_3S, 30 % de poudre de quartz, 5 % de gypse et 15 % d'un des quatre types de C_3A. Les différents types de C_3A utilisés sont les suivants : C_3A pur cubique, C_3A orthorhombique contenant 4,8 % Na_2O, C_3A cubique contenant 5 % Fe_2O_3 et C_3A orthorhombique contenant 4,8 % et 5 % Fe_2O_3. Des minicylindres (1 cm de diamètre et 1 cm de hauteur) de pâte pure de ciment correspondant à un rapport eau/ciment = 0,35 ont été conservés en atmosphère humide pendant 3 jours et ensuite immergés dans une solution à 5 % $MgSO_4$. Après 7 jours d'immersion dans l'eau sulfatée, tous les échantillons montraient des gonflements importants et étaient très fissurés. La formation de gypse, d'ettringite et de brucite dans le matériau détérioré, était confirmé par l'analyse par diffraction des rayons X. Les Auteurs ont conclu qu'en présence de quartz, la porosité des échantillons était si élevée qu'il n'était pas possible de détecter les différences des caractéristiques de la résistance au sulfate des différentes formes de C_3A. Quatre nouvelles compositions, dans lesquelles la fraction quartz a été remplacée par du laitier de haut fourneau granulé de surface spécifique Blaine égale à 3000 cm^2/g^{-1}, ont été synthétisées. Les Auteurs ont aussi étudié l'effet de deux périodes différentes de traitement en atmosphère humide, à savoir 48 heures et 6 heures dans l'eau, sur le comportement ultérieur des ciments dans la solution de sulfate. La DRX et l'ATD ont été utilisées pour connaître les taux d'hydratation de C_3A à différentes échéances. Le degré de l'attaque par le sulfate était évalué par observation visuelle.

Pour les pâtes conservées dans l'eau pendant 48 heures avant l'immersion dans le sulfate, il a été observé que celles qui contiennent le ciment avec C_3A pur sous la forme cubique résistent mieux à l'attaque du sulfate. Les pâtes des trois autres ciments mettent en évidence une attaque plus forte par le sulfate qui, d'après les données de la DRX et l'ATD, est due à la transformation de $Ca(OH)_2$ et du monosulfate hydraté respectivement en gypse et ettringite. Les Auteurs ont aussi trouvé des différences significatives dans les taux d'hydratation de C_3A présent dans les 4 ciments. Par exemple, le thermogramme des pâtes hydratées pendant 3 heures (Fig. 2, **REGOURD** et al) montre plus d'ettringite dans la pâte de ciment contenant C_3A pur cubique que dans la pâte de ciment contenant C_3A sous la forme orthorhombique (4,8 % Na_2O). D'une manière similaire, les données des analyses DRX (Fig. 3, **REGOURD** et al) montrent que dans les pâtes traitées pendant 48 heures, le degré d'hydratation de C_3A pour le ciment contenant C_3A pur sous la forme cubique était d'environ 70 % comparé à 55-60 % pour les ciments contenant les autres types de C_3A. Les Auteurs en concluent que la performance supérieure à l'attaque par le sulfate du ciment contenant C_3A pur sous forme cubique est le résultat d'une plus faible porosité de la pâte due à un taux plus élevé d'hydratation dans le ciment.

Dans la seconde série d'essais dans laquelle les pâtes ont été traitées dans l'eau potable pendant 6 heures seulement avant leur immersion dans le sulfate, il a été trouvé que les deux ciments contenant C_3A avec 5 % Fe_2O_3 résistent mieux que le ciment contenant C_3A pur sous la forme cubique ou le C_3A orthorhombique contenant 4,8 % Na_2O. D'après les Auteurs, ceci est dû au fait qu'une petite fraction seulement de C_3A s'était hydratée dans tous les ciments avant leur immersion dans le sulfate. Donc, la réactivité plus faible du C_3A anhydre contenant Fe_2O_3 était plus favorable à la résistance au sulfate que la réactivité plus forte des autres types de C_3A qui ne contenaient pas de Fe_2O_3. Les Auteurs concluent que la porosité d'une pâte de ciment affectée par les caractéristiques de l'hydratation de ses constituants et l'histoire du traitement avec l'exposition au sulfate sont les facteurs les plus importants dans la détermination de la résistance au sulfate.

D'après la communication de **P.K. MEHTA**, deux ciments contenant C_3A sous différentes formes ont été étudiés quant à leur résistance au sulfate. Les ciments ont été préparés à partir d'un clinker industriel à haute teneur en alcalins contenant 13,6 % de C_3A potentiel. Le C_3A dans le clinker était d'une manière prépondérante sous la forme orthorhombique. Le ciment "A" a été obtenu en broyant ce clinker avec 5 % de gypse à 4000 $cm^2.g^{-1}$ Blaine. Un autre clinker ayant la même composition potentielle mais avec C_3A présent sous la forme cubique seulement a été obtenu par chauffage du clinker industriel à 1350 °C pendant 30 minutes dans un four de laboratoire. Le ciment "B" a été préparé à partir du clinker traité thermiquement en le broyant avec 5 % de gypse de la même finesse que celle du ciment "A". Les caractéristiques de la résistance au sulfate des ciments ont été évaluées par un test accéléré dans lequel des cubes de pâte pure de ciment et des prismes de mortiers traités normalement pendant 14 jours sont immergés dans une solution à

4 % de Na_2SO_4. La solution est maintenue à une concentration en sulfate et un pH constants par une titration automatique et continuelle à l'aide de H_2SO_4 à N/10. Les changements dans la résistance à la compression des cubes de pâte pure de ciment et l'expansion des prismes de mortier durant une période d'immersion dans le sulfate de 5 semaines ont été utilisés comme critères d'évaluation de la résistance des ciments aux sulfates. Les analyses par diffraction des rayons X des pâtes pures de ciments, à intervalles réguliers, à la fois avant et pendant l'immersion dans le sulfate, ont été effectuées afin de suivre les changements minéralogiques.

Les données de la résistance à la compression des cubes de pâte pure de ciment et les données de l'expansion des prismes de mortier (Fig. 2, **MEHTA**) montrent qu'il y a des différences significatives entre les taux d'attaque au sulfate des 2 ciments. Par exemple, l'accroissement brusque du taux d'expansion du ciment "A" durant la troisième semaine d'immersion dans le sulfate n'est pas observé dans le ciment "B" et ce jusqu'à la cinquième semaine. Des données de la DRX des pâtes avant leur immersion dans le sulfate (Fig. 4, **MEHTA**), il a été conclu que les principaux composés contenant de l'alumine dans la pâte de ciment "A" étaient l'ettringite et le monosulfate hydraté tandis que dans la ciment "B" un aluminosilicate de calcium a été détecté à côté de l'ettringite. Les fragments détériorés du ciment "A", après une période de 28 jours d'immersion dans le sulfate, contenaient plus d'ettringite et moins de monosulfate hydraté qu'avant l'immersion dans le sulfate. Comme **REGOURD** et al, l'Auteur trouve aussi que le ciment "B" (le ciment contenant le C_3A cubique seulement) s'hydrate plus vite et produit plus d'ettringite potentielle pendant un jour d'hydratation normale et que la résistance en compression est 15 % plus forte que celle du ciment "A" (le ciment contenant C_3A orthorhombique).

Sur la base de ses résultats expérimentaux, l'Auteur conclut que le processus d'expansion et de fissuration de pâtes de ciment portland à haute teneur en C_3A dans une solution de sulfate peut être divisé en deux étapes. Dans la première étape, appelée période dormante, la réaction chimique, entre la solution de sulfate et l'aluminate anhydre et les aluminates hydratés présents dans la pâte de ciment, est associée à l'accroissement du taux de monosulfate hydraté et n'est pas accompagnée d'expansion. Ceci est suivi du second stade dans lequel l'expansion et la fissuration apparaissent comme le résultat de la conversion du monosulfate hydraté en ettringite.

L'Auteur conclut aussi que les ciments portland à haute teneur en C_3A, sans tenir compte du type de C_3A montreraient éventuellement une expansion délétère dans la solution sulfatée. Cependant le taux de l'attaque par le sulfate était plus faible dans le ciment contenant du C_3A cubique. Ceci est dû principalement à la vitesse rapide d'hydratation du C_3A cubique qui rend la pâte plus résistante et moins perméable et aussi entraîne la formation d'un aluminosilicate hydraté qui a été trouvé plus résistant à l'attaque par le sulfate que le monosulfate hydraté.

K. MATHER rapporte les résultats d'une recherche sur la résistance relative au sulfate de 26 ciments portland industriels et de quelques ciments pouzzolaniques préparés à partir de quelques uns des ciments portland utilisés dans cette recherche. Cinq ciments portland ne contenaient pas de C_3A potentiel, six contenaient C_3A sous forme orthorhombique ou tétragonale, huit contenaient C_3A sous les formes cubique et orthorhombique ou tétragonale et sept avaient C_3A sous la forme cubique seulement. Neuf des ciments portland pouzzolaniques contenaient des cendres volantes provenant du chauffage de charbons bitumineux, sous-bitumineux ou de lignite, un contenait une pouzzolane naturelle calcinée à haute teneur en verre et en silice et un consistait en une poussière de silice qui est un sous-produit de l'industrie des alliages de ferrosilicium. Par immersion continuelle dans une solution à 5 % Na_2SO_4, la résistance au sulfate a été évaluée à partir des variations de longueur et de la fréquence fondamentale transversale de prismes de 25,4 x 25,4 x 285,8 mm de mortiers contenant une part de ciment pour 2,5 parts de sable calibré et de 0,485 part d'eau, en poids. Les prismes de mortier ont été conservés, à 35°, pendant 24 heures dans des moules scellés, puis démoulés et ensuite traités dans une eau de chaux saturée à 23 ± 1,7° jusqu'à ce que les cubes de mortier de comparaison présentent une résistance à la compression de 20,7 ± 1,0 MPa. A ce moment, les prismes ont été immergés dans la solution à 5 % Na_2SO_4. Les variations de longueur et la fréquence fondamentale transversale ont été mesurées à 7, 14, 21, 28, 56, 90 jours et plus si nécessaire. La solution de sulfate était changée chaque fois que la longueur des prismes était mesurée. Le critère de dégradation par accroissement de longueur a été choisi à 0.1 %.

Dans les ciments portland, tous les ciments à 0 % C_3A ont été trouvés résistants au sulfate excepté un ciment qui a présenté une expansion de 0,085 % à 180 jours (et pouvait montrer plus de 0,1 % d'expansion à un an). L'Auteur soupçonne que le gonflement important de ce ciment pourrait être relié à l'hydratation du périclase puisque le ciment contenait 4,53% MgO d'après l'analyse chimique. Les six ciments contenant C_3A orthorhombique ou tétragonal se sont dégradés, excepté un ciment qui présentait 0,057 % d'expansion après 180 jours d'immersion dans le sulfate. Ce ciment contenant seulement 2 % MgO, l'Auteur semble suggérer que l'expansion totale dans l'essai de l'attaque par le sulfate est influencée par la quantité de périclase dans le ciment. A l'époque de ses derniers résultats, l'Auteur a trouvé que 7 des 8 ciments contenant C_3A sous la forme cubique, orthorhombique ou tétragonale se sont dégradés en dépassant la limite d'expansion de 0,1 %. De la même manière, 5 des 7 ciments, contenant seulement C_3A cubique, se sont également détériorés. De ceci, l'Auteur conclut que, contrairement aux observations précédentes de certains chercheurs, il n'y a pas de corrélation entre le type de C_3A présent dans le ciment portland et la résistance du ciment à l'attaque par le sulfate. L'Auteur a aussi fait des observations intéressantes sur l'aptitude à la déformation (expansion linéaire sans fissuration) de ciments différents. Les expansions ne peuvent pas être reliées directement à la quantité de C_3A dans les ciments en raison de la croissance rapide de la résistance, les ciments plus riches en C_3A possèdent une aptitude à la déformation plus faible.

En ce qui concerne l'effet du type de pouzzolane sur la résistance au sulfate des ciments portland aux pouzzolanes contenant de 9,4 à 14,6 % C_3A potentiel, il a été montré (Fig. 1 **MATHER**) que le remplacement de 30 % de volume de ciment par l'une ou l'autre des 2 pouzzolanes réactives, à savoir la pouzzolane volcanique calcinée et la poussière de silice de l'industrie du ferrosilicium, rend les ciments hautement résistants à l'attaque par le sulfate. Au contraire, à ce taux de remplacement du ciment, aucune des 8 cendres volantes sous-bitumineuses ou de lignite n'est capable de réduire l'expansion dans les prismes de mortier à moins de 0,1 % quand le ciment portland con-

tenant soit 13,1 % de C_3A potentiel (RC 714) ou 14,6 % de C_3A potentiel (RC 756) est utilisé pour fabriquer ces ciments aux pouzzolanes (Fig. 2 et 3, **MATHER**). En fait, beaucoup de cendres volantes sous-bitumineuses ou de lignite accroissent l'expansion au sulfate du ciment portland étalon au lieu de la réduire. Ce type de comportement a été observé à partir de cendres volantes qui contenaient moins de 50 % de SiO_2, 16 à 26 % Al_2O_3 et 5 à 30 % de CaO. L'accroissement de l'expansion au sulfate des ciments portland aux pouzzolanes contenant des clinkers riches en C_3A et des cendres à haute teneur en alumine et en chaux est attribué à la formation d'ettringite à partir de Al_2O_3 et de CaO disponibles dans la cendre volante.

Avec le ciment portland contenant 9,4 % de C_3A potentiel, 2 des 8 cendres volantes du groupe sous-bitumineux et de lignite ont été capables de réduire l'expansion au sulfate à moins de 0,1 % à 365 jours (Fig. 4, **MATHER**). Les ciments portland pouzzolaniques fabriqués avec des clinkers contenant jusqu'à 11 % de C_3A potentiel et environ 20 % de cendres volantes bitumineuses montrent une amélioration substantielle à la résistance des mortiers au sulfate comparée à celle des ciments portland étalons fabriqués avec les mêmes clinkers. En conclusion, l'Auteur a montré que l'aptitude à la résistance au sulfate des ciments portland et des ciments portland aux pouzzolanes est affectée par la teneur en C_3A du ciment portland par la composition, la réactivité et la teneur de la pouzzolane utilisée.

Dans sa communication contenant une évaluation critique de la littérature en cours sur le mécanisme de l'expansion au sulfate, **S. CHATTERJI** présente des arguments contestant la croyance largement reconnue que l'expansion dans les pâtes de ciment portland exposées aux solutions de sulfate est associée à la formation de l'ettringite. Il présente aussi des arguments supportant l'hypothèse de **CHATTERJI** et **JEFFERY** suivant laquelle la formation de monosulfate hydraté à partir de C_4AH_{13}, par échange ionique dans les pâtes de ciment portland exposées aux ions sulfate, est responsable de l'expansion. Une vue d'ensemble de la littérature sur les expansions dues au sulfate révèle une division en deux catégories : expansion libre et expansion restreinte. En ce qui concerne l'expansion libre, l'Auteur cite son propre travail aussi bien que celui de **SELIGMANN** et **GREENING** sur les expansions libres considérables observées dans des systèmes C_3A - gypse - chaux dans lesquels le monosulfate, plutôt que l'ettringite, était le produit stable. A partir également de l'examen du travail de **MATOUSEK** et **SAUMAN**, sur l'expansion de mélanges contenant ciment portland, métakaolinite et gypse, l'auteur note qu'une expansion d'au moins 20 % se produit après que la formation d'ettringite ait cessé. Citant les études de **MEHTA** sur les expansions restreintes des ciments de Type K, M et S, l'Auteur signale que les expansions continuent dans le temps, après que la formation de l'ettringite ait cessé et, en fait, l'ettringite est transformée en monosulfate hydraté. Un support supplémentaire de l'expansion au sulfate due à la formation de monosulfate, noté par l'Auteur, est qu'il n'y a pas d'expansion dans le ciment portland résistant au sulfate parce qu'il ne contient pas de monosulfate hydraté au cours de l'hydratation. En conclusion, l'Auteur dit : "Il est possible de considérer comme évidente telle ou telle hypothèse mais en dernière analyse, l'hypothèse retenue l'est en fonction d'idées préconçues".

Résumant les points principaux des 4 contributions sur le rôle de C_3A dans l'attaque au sulfate, **REGOURD** et al, et **MEHTA** ont montré que la vitesse de l'attaque des ciments par le sulfate peut être influencée par le type du C_3A présent. Des pâtes hydratées de ciments contenant C_3A cubique ont été attaquées à une vitesse plus lente par les solutions de sulfate que les pâtes de ciment contenant C_3A dans des structures plus denses. Les différences dans les taux d'attaque par le sulfate ont été attribuées principalement à l'hydratation plus rapide du C_3A cubique qui produit une pâte plus résistante et probablement moins perméable avant l'immersion dans la solution de sulfate. **MEHTA** a aussi démontré la formation d'un aluminosilicate de calcium hydraté dans les pâtes de ciment portland contenant C_3A cubique. Il soupçonne que la résistance relativement supérieure de l'aluminosilicate hydraté, comparée à celle du monosulfate hydraté, puisse être partiellement responsable du taux plus faible de l'attaque, par le sulfate, des ciments portland contenant C_3A cubique. **MATHER** a montré que les teneurs élevées en alumine et chaux, présentes dans les cendres volantes de lignite et les cendres sous-bitumineuses, peuvent accroître plutôt que réduire le comportement au sulfate des ciments pouzzolaniques fabriqués avec de telles cendres volantes. Les résultats des essais de **MATHER** ne confirment pas les conclusions d'autres chercheurs d'après lesquels le type de C_3A présent dans un ciment portland peut influencer sa résistance à l'attaque par le sulfate.

D'après le rapporteur, la contradiction entre les résultats de **REGOURD** et al et **MEMHTA** d'une part, de **MATHER** d'autre part n'est pas réelle. Tandis que la conclusion de **MATHER** est tirée d'une immersion dans le sulfate jusqu'à 365 jours, les premiers chercheurs commentent sur la base de 4 à 5 semaines. Il apparaît que le type de C_3A affecte seulement la vitesse d'attaque par le sulfate mais pas le degré éventuel de l'attaque. Evidemment, un travail supplémentaire est nécessaire pour confirmer l'hypothèse que la porosité et l'imperméabilité réduites des pâtes de ciment contenant C_3A cubique sont responsables de la vitesse plus faible de l'attaque de ces ciments par le sulfate. La nécessité de tests accélérés et dignes de confiance pour l'évaluation de la résistance des ciments au sulfate est aussi évidente. Différentes périodes de prétraitement, de taille des échantillons, de solutions de sulfate et différents critères de dégradation ont été utilisés dans les trois études rapportées ci-dessus. La contribution de **CHATTERJI** fait ressortir que la question du mécanisme de l'expansion accompagnant l'attaque par le sulfate mérite plus d'attention dans le futur. La plus grande partie de sa critique sur l'hypothèse de l'expansion due à l'ettringite est fondée sur l'expansion continuelle des pâtes, même après que la formation de l'ettringite ait cessé. Cet argument, au lieu d'être contre l'hypothèse de l'expansion due à l'ettringite, peut être utilisé comme support de l'hypothèse si le mécanisme de l'expansion est dû au gonglement d'une ettringite colloïdale par adsorption d'eau. **MEHTA** et **HU** ont rapporté que les expansions maximales résultant du gonflement de l'ettringite n'ont été observées, dans leur expérience, qu'après environ 45 jours d'exposition à l'eau de l'ettringite.

Des nouvelles études expérimentales sont clairement nécessaires pour régler cette controverse. **CHATTERJI** est, néanmoins, correct en déclarant "Les idées préconçues souvent déterminent quelle hypothèse on aimerait retenir". Le présent rapporteur espère qu'avant le prochain Congrès, les chercheurs intéressés par le mécanisme d'expansion au sulfate des pâtes de ciment, **CHATTERJI** compris, se débarasseront de leurs préjugés personnels et entreprendront des études expérimentales concluantes pour éclairer le sujet.

Rôle de C_3A dans l'attaque des ciments par les eaux sulfatées

Role of C_3A in the attack on cements by sulfate solutions

B. MORTUREUX, H. HORNAIN, M. REGOURD, Département Microstructures,
C.E.R.I.L.H. - Paris, France

Résumé

L'évolution de mélanges synthétiques C_3A + C_3S + gypse et de ciments portland à différentes teneurs en C_3A a été suivie par diffraction des rayons X, microscopie électronique à balayage et microsonde électronique. Les facteurs étudiés sont la forme cristalline de C_3A (cubique, orthorhombique), la composition élémentaire des grains de C_3A (teneur en Na_2O, K_2O, Fe_2O_3), l'interaction C_3A - C_3S.

Les résultats montrent que la résistance aux eaux agressives des pâtes de ciment et des mortiers dépend avant tout de leur compacité. A brève échéance, C_3A cubique s'hydrate plus vite que C_3A orthorhombique et donne un matériau moins vulnérable si l'échantillon est immergé dans la solution agressive après un temps d'hydratation suffisamment long. Le rôle bénéfique du fer en solution solide dans C_3A a été confirmé.

Summary

The evolution of synthetic mixtures C_3A + C_3S + gypsum and portland cements with different amounts of C_3A has been followed by X-ray diffraction, Scanning Electron Microscopy and Electron Micro Probe Analysis. The factors which have been studied are the crystalline from of C_3A (cubic, orthorhombic), the elemental composition of C_3A grains (amount of Na_2O, K_2O, Fe_2O_3), the C_3A - C_3S interaction.

The results show that the resistance of cement pastes and mortars to aggressive waters depends before all on their compacity. At short time, cubic C_3A hydrates more rapidly than orthorhombic C_3A and gives a less vulnerable material if the sample is immersed into the aggressive solution after a sufficient time of hydration. The beneficial role iron in solid solution in C_3A has been confirmed.

Les études sur la réactivité de C_3A et de ses solutions solides avec les alcalins ont montré que l'aluminate tricalcique pur cubique s'hydrate plus rapidement que C_3A dopé au sodium sous les formes orthorhombique ou monoclinique (1, 2, 3, 4). Dans les produits industriels, C_3A peut insérer, dans son réseau cristallin, d'autres ions que le sodium : le potassium, le silicium et le fer par exemple.

Le rôle bénéfique du fer dans la résistance des ciments à l'eau de mer ayant été mis en évidence par **FRIGIONE et MARRA** (5), nous avons essayé de comparer le comportement, dans une solution de $MgSO_4$, de mélanges synthétiques C_3S + C_3A + gypse dans lesquels nous avons fait varier la composition de C_3A (C_3A + Na_2O, C_3A + Fe_2O_3, C_3A + Na_2O + Fe_2O_3). La résistance aux eaux sulfatées des ciments et mortiers étant fonction de leur imperméabilité, nous avons aussi comparé l'influence du temps de traitement avant l'immersion dans l'eau agressive. L'évolution des réactions chimiques et de la microstructure du matériau a été suivie par ATD, diffraction des Rayons X et microscopie électronique à balayage.

Préparation des échantillons

Des minicylindres de mélanges synthétiques C_3S + C_3A + gypse ont été préparés avec un rapport eau/solide = 0,35, conservés 24 heures en atmosphère humide puis deux jours dans l'eau potable, enfin immergés dans une solution à 5 % de $MgSO_4$.

Les quatres compositions de C_3A utilisées sont les suivantes :

1. C_3A cubique pur,
2. C_3A orthorhombique avec 4,8 % Na_2O,
3. C_3A cubique avec 5 % Fe_2O_3 (limite de solubilité de Fe_2O_3 dans le réseau cristallin de C_3A),
4. C_3A orthornombique avec 4,8 % Na_2O et 5 % Fe_2O_3.

Une première série d'éprouvettes est constituée de 50 % C_3S + 15 % C_3A + 30 % quartz + 5 % gypse. La granularité de C_3S et de C_3A est comprise entre 20 et 40 µm, celle du gypse inférieure à 40 µm, ceci afin de faciliter les observations microscopiques, le quartz a une surface spécifique de 3000 $cm^2.g^{-1}$.

Dans la seconde série, le quartz a été remplacé par du laitier et deux temps de prétraitement ont été étudiés (2 jours et 6 heures dans l'eau potable).

Etude des mélanges C_3S (50 %) + C_3A (15 %) + quartz (30 %) + gypse (5 %).

Après 7 jours d'immersion dans l'eau sulfatée, tous les échantillons sont en très mauvais état (gonflement et fissuration). La diffraction des Rayons X montre la formation de $Mg(OH)_2$ et de $CaSO_4.2H_2O$ secondaire (Fig. 1). Ces deux nouvelles phases sont dues à la réaction de $MgSO_4$ sur $Ca(OH)_2$ libéré par l'hydratation de C_3S.

Il n'est pas possible de différencier la résistance des différentes formes de C_3A dans ces mélanges dont la porosité devait être trop élevée au moment de leur immersion dans l'eau agressive. Afin de diminuer cette porosité, nous avons remplacé le quartz par du laitier.

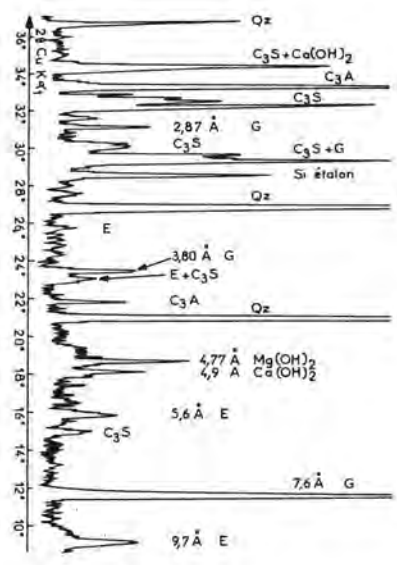

Fig. 1 - Diffraction des Rayons X.
Formation de gypse secondaire et de $Mg(OH)_2$ dans un mélange C_3S (50 %) + C_3A (15 %) + quartz (30 %) + gypse (5 %) après 7 jours d'immersion dans une solution à 5 % $MgSO_4$.
E = ettringite, G = gypse, Qz = quartz.

Etude des mélanges C_3S (50 %) + C_3A (15 %) + laitier (30 %) + gypse (5 %)

Mis à part le laitier qui remplace le quartz, la composition chimique des échantillons reste la même que dans la première série mais deux temps de prétraitement ont été étudiés (2 jours et 6 heures dans l'eau potable après 24 heures en atmosphère humide).

Mélanges C_3S + C_3A + laitier + gypse : 48 heures dans l'eau

La différence de réactivité hydraulique entre les quatre formes de C_3A est montrée dans le thermogramme de la Figure 2 et dans la courbe de la Figure 3 tracée à partir des données de la diffraction des Rayons X. Avant l'immersion dans l'eau sulfatée, C_3A cubique pur est le plus hydraté. Après 26 jours dans $MgSO_4$, C_3A cubique pur est hydraté à 80 % et C_3A + 5 % Fe_2O_3, également cubique, à 64 %.

C_3S est aussi hydraté différemment dans les quatre échantillons. En raison de l'interaction C_3A-C_3S (4, 6), C_3S est hydraté à 60 % dans l'échantillon ① et 50 % dans les échantillons ② et ④ à la fin du prétraitement.

L'échantillon ① est en bon état après 26 jours en eau sulfatée. Les autres échantillons présentent une certaine expansion qui peut être reliée à la dissolution de $Ca(OH)_2$ et à sa transformation en $Mg(OH)_2$ d'une part, à la formation d'ettringite d'autre part. L'ATD (Fig. 4) et la diffraction des Rayons X (Fig. 5) montrent clairement ces transformations.

Il semble donc que dans cette série, l'échantillon ① , plus hydraté que les autres, ait acquis une

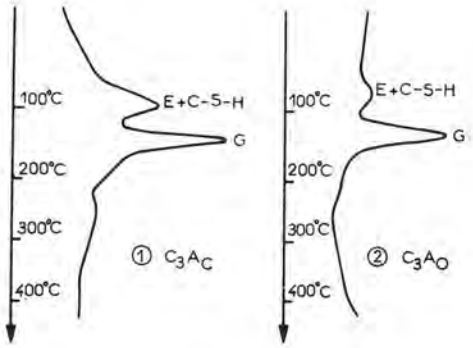

Fig. 2 - Enregistrements ATD des mélanges C_3S + C_3A + laitier + gypse après 3 heures dans l'eau : le mélange ① avec C_3A cubique a donné plus d'ettringite et de C-S-H que le mélange ② avec C_3A orthorhombique.

G = gypse, E = ettringite.

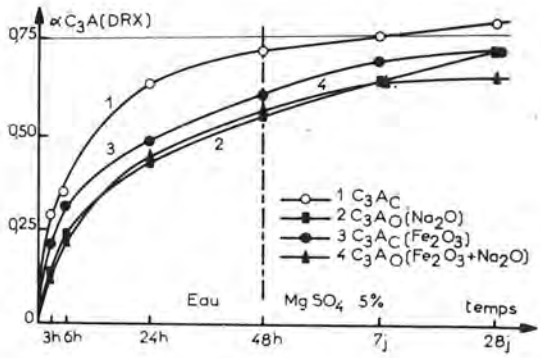

Fig. 3 - Taux d'hydratation α des mélanges C_3S (50 %) + C_3A (15 %) + laitier (30 %) - gypse (5 %), conservés 48 heures dans l'eau puis 26 jours dans la solution à 5 % $MgSO_4$.

Fig. 4 - Enregistrement ATD d'un mélange C_3S + C_3A + laitier - gypse après 2 jours dans l'eau Ⓐ puis 7 jours dans une solution à 5 % $MgSO_4$ Ⓑ .

M = monosulfoaluminate, E = ettringite

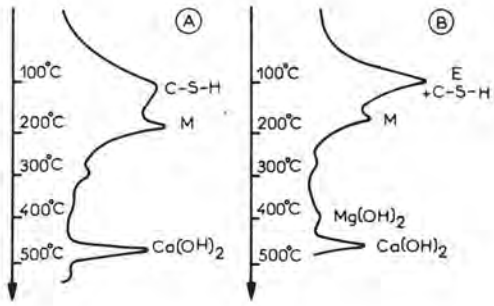

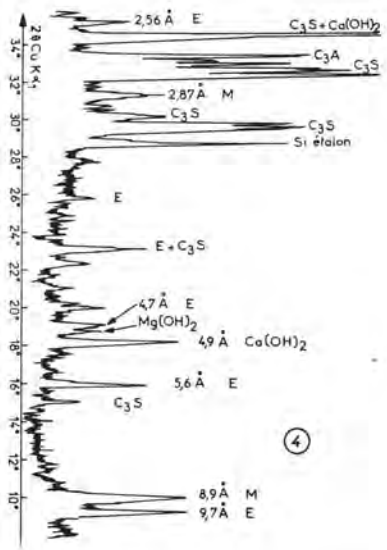

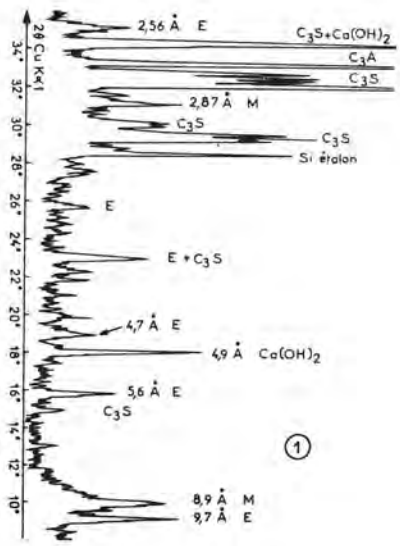

Fig. 5 - Diffraction des Rayons X. Mélanges C_3S + C_3A + laitier + gypse, après 7 jours dans $MgSO_4$. Comparaison entre le mélange ① avec C_3A_C et le mélange ④ avec C_3A_O (Na_2O + Fe_2O_3) : $Ca(OH)_2$ est partiellement transformé en $Mg(OH)_2$ dans l'échantillon ④ seulement.

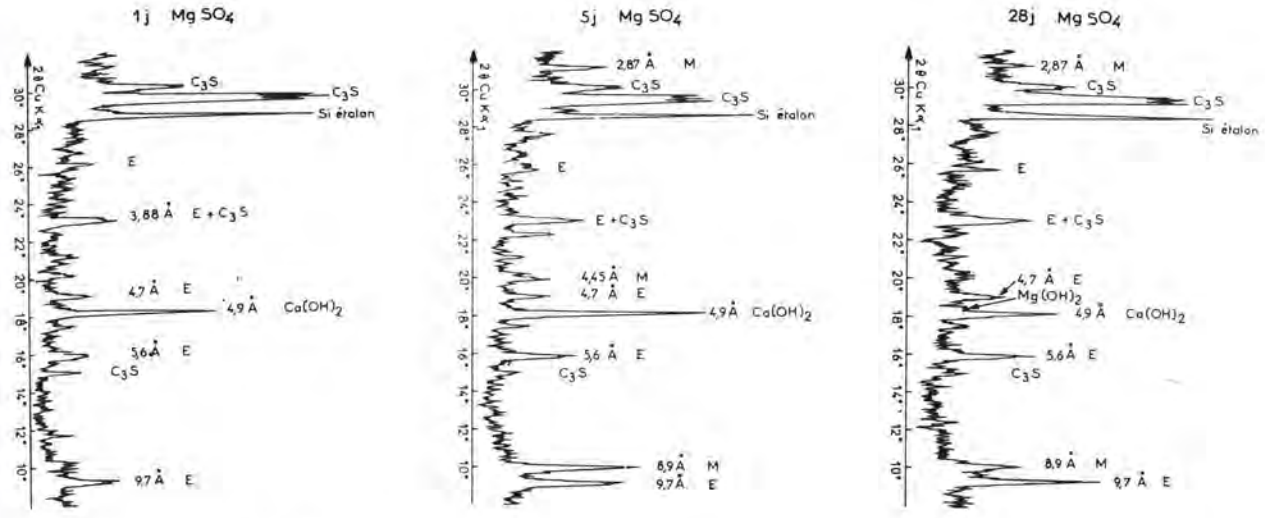

Fig. 6 - Diffraction des Rayons X.
Evolution du mélange ④ C_3S + C_3A (4,8 % Na_2O + 5 % Fe_2O_3) + laitier + gypse dans la solution de $MgSO_4$ après 6 heures dans l'eau potable. La corrosion est visible à 28 jours : décroissance de $Ca(OH)_2$ et apparition de $Mg(OH)_2$, croissance de l'ettringite et décroissance du monosulfoaluminate. Cette corrosion est faible, il reste $Ca(OH)_2$ et le gypse secondaire n'est pas visible.

E = ettringite, M = monosulfoaluminate

imperméabilité suffisante avant l'agression de $MgSO_4$. Contrairement au quartz, le laitier a réagi. Activés par $Ca(OH)_2$, ses grains se sont entourés d'une mince couche de C-S-H favorable à la cohésion.

Mélanges C_3S + C_3A + laitier + gypse : 6 heures dans l'eau

Afin de vérifier l'hypothèse de l'influence de la compacité de l'échantillon (due à un taux d'hydratation élevé de C_3S et C_3A) sur la résistance au sulfate, nous avons immergé une seconde série d'éprouvettes après un temps de traitement plus court, soit 24 heures en atmosphère humide et 6 heures dans l'eau potable.

Avant immersion dans la solution sulfatée, C_3A est hydraté à 30 % dans l'échantillon ① avec C_3A cubique pur et à 20 % dans les échantillons ② et ④ avec C_3A orthorhombique. Après 5 et 28 jours dans la solution sulfatée, les échantillons ③ et ④ sont en meilleur état que les échantillons ① et ② les premiers (③ et ④) ne montrent aucune fissure externe, tandis que les derniers (① et ②) ont partiellement éclaté .

Dans ce cas, il semble que la réactivité de C_3A ait joué un rôle plus important que dans la série précédente. Les mesures par diffraction des Rayons X du taux d'hydratation de C_3A montrent que C_3A + Fe_2O_3 réagit moins vite que C_3A pur entre 1 et 28 jours dans $MgSO_4$:

Echantillon	Après 1 jour dans $MgSO_4$	Après 28 jours dans $MgSO_4$
1. C_3A_c pur	58 %	74 %
2. C_3A_o (4,8 % Na_2O)	53 %	67 %
3. C_3A_c (5 % Fe_2O_3)	65 %	67 %
4. C_3A_o (4,8 % Na_2O - 5 % Fe_2O_3)	53 %	54 %

Après 28 jours dans l'eau sulfatée, on observe une différence importante entre les échantillons ① et l'échantillon ④ . La couche superficielle de l'échantillon ① est composée d'ettringite, de gypse secondaire et de $Mg(OH)_2$; le monosulfoaluminate et la portlandite ont disparu. Au contraire, la couche superficielle de l'échantillon ④ contient encore du monosulfoaluminate et $Ca(OH)_2$ (Fig. 6). Dans ce cas, la réactivité plus faible de C_3A + Fe_2O_3 est plus favorable que celle de C_3A pur qui, peu hydraté avant son immersion dans l'eau sulfatée, a réagi trop rapidement avec $MgSO_4$ et a formé trop d'ettringite expansive.

CONCLUSION

La comparaison entre les différentes séries d'échantillons C_3S + C_3A + gypse + quartz et C_3S + C_3A + gypse + laitier montre clairement que la porosité de l'éprouvette est le facteur le plus important de la résistance du ciment à l'attaque par les sulfates. Une compacité suffisante peut être obtenue à partir d'un C_3A réactif tel que C_3A cubique pur après un temps d'hydratation suffisamment long avant l'immersion dans l'eau agressive. Parce qu'il existe une interaction C_3A - C_3S, C_3S est aussi plus hydraté et

contribue à une réduction de la porosité des échantillons. La dégradation est faible, elle est reliée à la transformation du monosulfoaluminate en ettringite.

Dans le cas d'un temps d'hydratation en eau potable relativement court avant l'immersion dans la solution agressive, la réactivité de C_3A semble être un facteur important. Le C_3A cubique pur s'hydratant plus rapidement que le C_3A orthorhombique contenant du sodium forme, très vite, de l'ettringite qui est expansive.

Bien que de symétrie cubique, C_3A contenant du fer s'hydrate plus lentement que C_3A pur et paraît plus favorable dans le cas d'un prétraitement court.

Ces résultats, obtenus sur des mélanges synthétiques sont très partiels, ils montrent que la composition de C_3A dans les ciments peut jouer un rôle dans la résistance aux sulfates mais d'autres facteurs influençant la perméabilité doivent être étudiés simultanément (temps de prétraitement, granularité, température, ...).

REFERENCES

1. C.A.C.M. SPIERINGS and H.N. STEIN, (1970) "The influence of Na_2O on the hydration of C_3A. I Paste hydration", Cem. and Concr. Res., 6, 265-272.

2. M. REGOURD and B. MORTUREUX (1977) "Tricalcium aluminate in synthetic solid solutions and in cements". Seminar Cembureau on reaction of aluminates during the setting of cements.

3. A.I. BOIKOVA, A.I. DOMANSKY, V.A. PARAMONOVA, G.P. STAVITSKAYA and V.M. NIKUSHCHENKO (1977) "The influence of Na_2O on the structure and properties of $3CaO.Al_2O_3$". Cem. and Concr. res., 6, 733-740.

4. M. REGOURD (1978) "Cristallisation et réactivité de l'aluminate tricalcique dans les ciments portland". Il Cemento, vol. 75, 323-336.

5. G. FRIGIONE and S. MARRA (1975) "Influence of the isomorphous replacement Fe → Al on the technological characteristics of tricalcium aluminate". Il Cemento, 4, 173-180.

Influence of different crystalline forms of C_3A on sulfate resistance of portland cement

Influence des différentes formes cristallines de C_3A sur la résistance aux sulfates du ciment portland

P. K. MEHTA, Professor of Civil Engineering,
University of California, Berkeley, California 94720, USA

SUMMARY: A preliminary investigation was made to determine the effect of different crystalline forms of C_3A present in portland cement on the sulfate resistance of the cement. An industrial portland-cement clinker containing 13 percent potential C_3A, predominantly in the orthorhombic form, was used for this study. In order to redistribute the alkalies and to convert the orthorhombic C_3A into the cubic C_3A, a portion of the clinker was heat treated at 1350°C in a laboratory furnace. The cements made by grinding the two clinkers separately with 5 percent gypsum were evaluated for relative sulfate resistance, using an accelerated test procedure developed at the University of California. According to the test procedure, neat cement paste cubes and small mortar prisms were immersed in 4 percent Na_2SO_4 solution which was held at a constant pH by automatic titration against dilute H_2SO_4. From preliminary results it is seen that the strength loss and expansion due to sulfate attack occurred earlier in the cement containing the orthorhombic C_3A. Higher initial strength of the cement containing the cubic C_3A is considered partially responsible for the lower sulfate resistance shown by this cement.

RÉSUMÉ: Une étude préliminaire a été réalisée afin de déterminer l'effet des différentes formes cristallines de C_3A présentes dans le ciment Portland sur la résistance du ciment aux sulfates. Un clinker de ciment Portland industriel contenant 13 % C_3A, principalement sous la forme orthorhombique, a été utilisé dans cette étude. Afin de redistribuer les alcalins et de convertir le C_3A orthorhombique en C_3A cubique, une partie du clinker a été traitée à 1350°C dans un four de laboratoire. Les ciments préparés par broyage des deux clinkers séparément avec 5 % de gypse ont été évalués en ce qui concerne leur résistance relative aux sulfates à l'aide d'un test accéléré développé à l'Université de Californie. D'après la procédure de ce test, des petits prismes de mortier et des cubes de pâte de ciment sont immergés dans une solution à 4% de Na_2SO_4 qui est tenue à un pH constant par une titration automatique avec H_2SO_4 dilué. A partir des résultats préliminaires, on voit que l'expansion et la chute de résistance due a l'attaque des sulfates se produisent plus tôt dans le ciment contenant C_3A orthorhombique. Une résistance initiale plus élevée du ciment contenant du C_3A cubique est considérée comme partiellement responsable de la résistance aux sulfates plus faible, trouvée dans ce ciment.

INTRODUCTION

It is well known that chemical composition of raw materials and processing conditions influence the crystal structure of the principal compounds of portland cement. It is also known that the differences in hydration characteristics of the various crystalline forms of a cement compound can affect the setting and hardening properties of the cement, and in some instances, its durability in aggressive environments. The results of an experimental investigation on the effect of sulfate attack on two portland cement samples containing different crystalline forms of C_3A is described in this paper.

Several investigators including Moore (1), Maki (2), Regourd and Guinier (3), and Baikova et al (4) have shown that substitution of alkalies in C_3A lattice changes the crystal symmetry. With increasing amount of alkalies, the crystal structure of C_3A changes from cubic → orthorhombic → tetragonal → monoclinic. For instance, Boikova et al (4) reported 2.42, 3.80, 4.83, and 5.70 percent Na_2O in cubic, orthorhombic, tetragonal, and monoclinic C_3A respectively. According to Regourd (5), C_3A is usually cubic or orthorhombic/tetragonal, but rarely monoclinic in industrial clinkers. Splitting of the 440,008, and 844 X-ray diffraction lines of the cubic C_3A can be used for detection and quantitative determination of the various crystalline forms of C_3A present in a cement. Regourd used the splitting of the 440 line for this purpose. According to the author (5), this line splits to a doublet (040, 400) and a single line (224) for the orthorhombic form, and to two lines (040 and 224) for the tetragonal form. The ratio of peak intensities of the 040 and 224 lines is indicative of the amount of orthorhombic or tetragonal C_3A present. This ratio is about 0.5 when no cubic C_3A is present in the cement.

There is some published data on the differences in the hydration behavior of the various crystalline forms of C_3A. Regourd (5) reported that the hydration rates in water are: C_3A cubic > C_3A orthorhombic > C_3A tetragonal. Boikova et al (4) explained that plugging of the structural holes in cubic C_3A by increasing amounts of alkali ions slows down their initial hydration reaction. Both investigators (4,5) found that the differences in hydration rates were confined to early ages, 1 and 3 days, only. After 3 days hydration small differences in the degree of hydration of the four crystalline forms of C_3A were observed. After 28 days there was hardly any difference. Regourd (5) also showed that the presence of alkali sulfates considerably accelerated the hydration of all forms of C_3A.

Regourd (6) reported that the rapid hydration of the cubic C_3A was associated with a corresponding rapid hydration of the C_3S. This probably accounted for the presence of large zones of the trisilicoaluminate hydrate, $C_3A \cdot 3CaSiO_3 \cdot 32\ H_2O$, around the cubic C_3A grains in the 28-day old specimens which were examined by scanning electron microscopy. Much smaller zones of the silicoaluminate hydrate were detected around the tetrogonal C_3A grains in which C_3S hydration was slower. The existence of silicoaluminates of the type, $C_3A \cdot x\ CaSiO_3 \cdot y\ H_2O$ in hydrated cements had been envisaged for a long time, and the silicoaluminate isomorphs of both the monosulfate hydrate and the trisulfate hydrate (ettringite) are suggested in the literature. Except for Regourd's (6) work on the action of sea water on cements, there is little published data regarding the effect of different crystalline forms of C_3A on durability of cement to aggressive environments, such as sulfate attack.

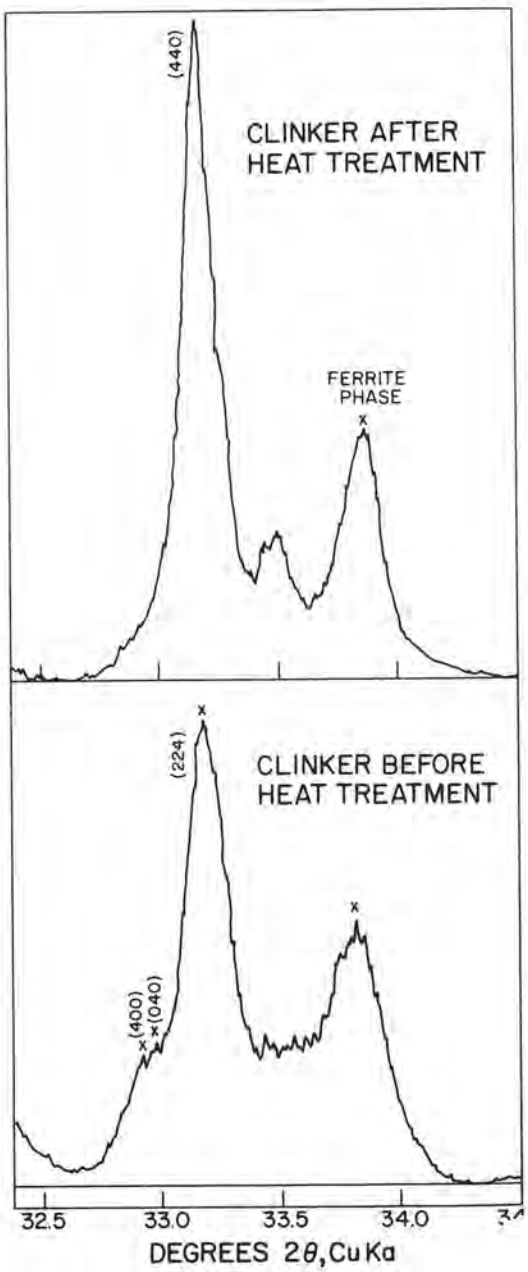

FIG. 1 X-RAY DIFFRACTION ANALYSIS OF MALEIC ACID RESIDUES OF CLINKERS

MATERIALS AND PROCEDURE

An industrial clinker containing 20.9% SiO_2, 6.8% Al_2O_3, 2.6% Fe_2O_3, 63.9% CaO, 2.9% MgO, 1.2% SO_3, 1.1% K_2O, and 0.4% Na_2O was used for making the two cements of this investigation. The potential C_3A in clinker, as determined by the Bogue equation, was 13.6 percent. After dissolving out the silicates by maleic acid, the residue showed that in addition to some cubic C_3A, there was a large quantity of the orthorhombic C_3A present. Another clinker having the same compound composition, but with C_3A present only in the cubic form, was obtained by heating this industrial clinker at 1350°C for 30 minutes in a laboratory furnace. The X-ray diffraction analysis of the maleic acid residue of the heat-treated clinker confirmed that the orthorhombic C_3A had converted to the cubic form. The diffraction patters of the two clinkers are shown in Fig. 1.

From the peak intensity ratio of 040 and 224 lines in Fig. 1, it was determined that the industrial clinker without the additional heat treatment contained about 60% orthorhombic C_3A and 40% cubic C_3A. Also, by chemical analysis of the heat-treated clinker, it was determined that the total alkali content remained unchanged by the heat treatment. Since the apthitalite, NaK_3S_4, peaks became stronger after the heat treatment, probably it was due to the high sulfate content in clinker that the orthorhombic-cubic conversion occurred by redistribution of alkali in the clinker rather than by alkali loss through volatilization. Both the clinkers were ground separately in a laboratory ball mill, with 5 percent added gypsum. The cement containing C_3A predominantly in the orthorhombic form was designated as 'Cement A', and the cement which contained C_3A in the cubic form only was designated as 'Cement B'. Both the cements conformed to about 4,000 cm^2/g Blaine fineness.

The sulfate resistance characteristics of the cements were evaluated by an accelerated test procedure described elsewhere in detail by this author (7,8). According to the procedure, 13 by 13 mm cubes of neat cement paste, and 15 by 15 by 100 mm mortar prisms, both cured for 14 days at room temperature, were immersed in a 4 percent Na_2SO_4 solution which was kept at a constant hydrogen-ion and sulfate concentration by automatic titration against N/10 H_2SO_4. The pH of the immersion solution, which was stirred constantly, was maintained at 7±0·5, and it was replaced by a fresh solution every week. In addition to the small specimen size and the constant sulfate and hydrogen ion concentrations, the acceleration of the sulfate attack was achieved by high permeability of the specimens. For this purpose the neat cement paste cubes were made with 0.5 water-cement ratio, and the mortar prisms were made with 1:1:0·6 proportions by weight of cement, coarse sand (600-850 μm), and water, respectively. Changes in visual appearance and compressive strength of the neat cement paste cubes, and expansion of the mortar prisms were used as criteria for evaluation of sulfate resistance of the cements. X-ray diffraction data was obtained using Cu Ka radiation at 40 kV and 30 mA.

RESULTS AND DISCUSSION

Average values from the compressive strength tests and expansion measurements are plotted in Fig. 2.

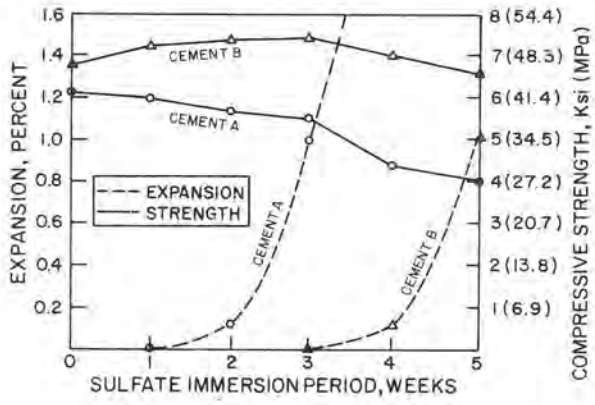

FIG. 2 EFFECT OF SULFATE IMMERSION ON EXPANSION AND STRENGTH

From the mortar expansion data in Fig. 2 it can be seen that Cement A showed only a slight expansion during the first 2 weeks of sulfate immersion; however, during the 3rd week there was a sudden increase in expansion from about 0.1 to 1.0 percent. On the other hand for Cement B, a similar increase in expansion did not occur until the 5th week. Visual appearance and strength changes in neat cement paste cubes also confirmed that the rate of sulfate attack was faster on Cement A than on Cement B. For instance, Cement A showed a gradual loss of compressive strength on the order of about 10 percent during the first 3 weeks of sulfate immersion but, thereafter, during the 3-5 week period lost about 33 percent of the original strength. On the contrary, Cement B showed little strength loss during the first 3 weeks of immersion, thereafter, only 6 percent strength loss was recorded until the end of the test period. Since the strength loss tends to lag behind expansion, further strength loss was expected to occur on prolonging the immersion period. However, it is evident from the test data that Cement A was attacked more readily in the sulfate solution than Cement B.

The first cracks at the corners and edges of the neat Cement A paste specimens appeared at the 18th day of sulfate immersion, which is consistent with the expansion date. Thereafter, the cracks widened rapidly and resulted in surface spalling. The spalled layers of the paste were weak and could easily be broken with fingers. With regard to Cement B, after 4 weeks of sulfate immersion the cement paste cubes were still sound, with sharp edges and corners. A photograph of the typical specimens of Cement A and B on the 28th day of the sulfate immersion is shown in Fig. 3.

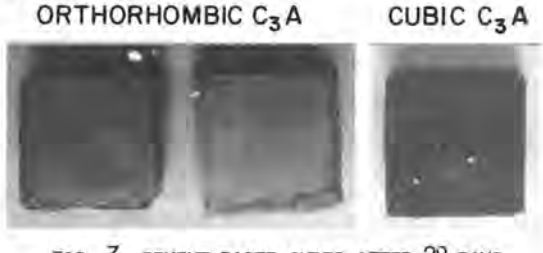

FIG. 3 CEMENT PASTE CUBES AFTER 28 DAYS SULFATE IMMERSION

X-ray diffraction analyses of the neat cement pastes at regular intervals, both before and after the sulfate immersion, were carried out in order to explain the differences between the two cements with regard to their behavior on sulfate attack. On hydration the 1-day old pastes showed ettringite peaks of considerable intensity from Cement B, whereas no such peaks were observed during the same period from hydration of Cement A. This showed that the C_3A in Cement B hydrated faster than the C_3A in Cement A. Also, from examination of peak intensities for alite and $Ca(OH)_2$, Regourd's (6) observation was confirmed that the rate of hydration of alite was closely associated with the C_3A hydration rate, i.e., relatively more alite hydrated in the Cement B paste after 1 day hydration. At 3, 7, and 14 days, some ettringite was detected in the pastes of Cement A, but at no time the peak intensities became as high as they were in the pastes of Cement B. Already at 3 days some low sulfate, $C_3A \cdot C\bar{S}H_{12}$, was detected in Cement A, and much higher peak intensities of this component were found in the 7 and 14-day old samples. On the contrary, the low sulfate peaks were not detected in the 3, 7, and 14-day old pastes of Cement B. Interestingly, instead of low sulfate, another phase corresponding to 8·66Å d-spacing (10.2°2θ, Cu Ka) was observed in the 7 and 14-day hydrated pastes of Cement B. According to the ASTM card file, this peak appears to belong to a calcium aluminosilicate hydrate of the composition, $Ca_6(AlSiO_4)_{12}.30H_2O$. The calcium aluminate hydrates and carboaluminate hydrates do not have peaks in this position, but other calcium aluminosilicate hydrates of the type, C_3A. x $CaSiO_3.yH_2O$, may have main peaks in this region. Regourd (6) reported large zones of $C_3A \cdot 3\ CaSiO_3 \cdot 32H_2O$ around the hydrating cubic C_3A grains, but their identification by X-ray diffraction analysis was difficult. Thus, assuming that the 8.66 A peak is due to a calcium aluminosilicate hydrate, it can be concluded that prior to the sulfate immersion the main alumina - containing compounds in the hydrated paste of Cement B were ettringite and a calcium aluminosilicate hydrate, whereas the corresponded compounds in the hydrated paste of Cement A were ettringite and low sulfate hydrate. This is illustrated in Figs. 4-I and 4-II.

The changes in compound composition as a result of sulfate attack on the hydrated cement pastes were followed by X-ray diffraction analyses of the outer 3 mm thick portions of the specimens. During the first 2 weeks of sulfate immersion, there was no change in the intensity of ettringite peaks in the pastes of both Cements A and B. At the same time there was some increase in low sulfate for Cement B, however, there was a considerable increase in the intensity of low sulfate peaks for Cement A. After two weeks of sulfate immersion, the low sulfate peaks in Cement A started to decrease, with a corresponding increase in the intensity of ettringite peaks. It should be noted that a sudden increase in expansion of the mortar prisms of Cement A was recorded during the same period.

For Cement B, during the first 3 weeks of sulfate immersion there was no change in the intensity of ettringite and the aluminosilicate peaks. However, a gradual increase in the low sulfate peak was observed. After three weeks some decrease in the low sulfate and the aluminosilicate peaks was recorded, with a corresponding increase in ettringite. And this was the same period during which the mortar

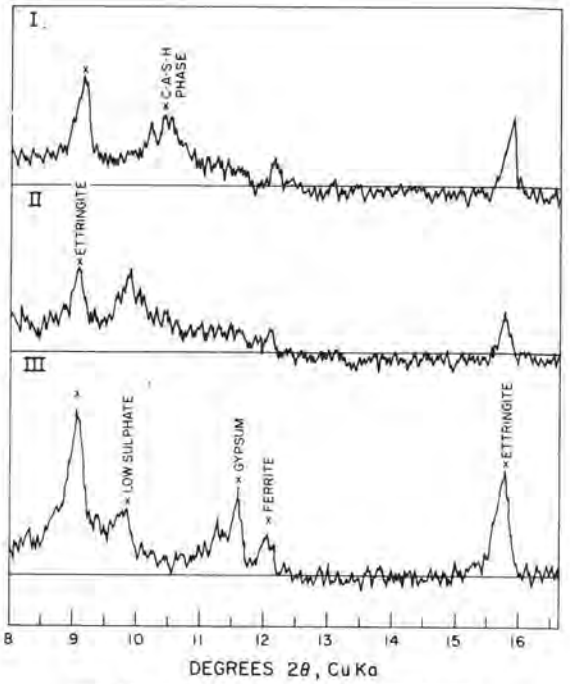

FIG. 4 X-RAY DIFFRACTION PATTERS OF:
I. HYDRATED CEMENT 'B', 14 DAYS
II. HYDRATED CEMENT 'A', 14 DAYS
III. SPALLED LAYER OF CEMENT 'A' AFTER 28 DAYS SULFATE IMMERSION

prisms of Cement B started to show large expansion. It appears from the x-ray diffraction data that, from the standpoint of expansion and cracking of hydrated cements in sulfate solutions, there is an initial dormant period associated with increase in the low sulfate hydrate as a result of chemical reaction between the sulfate and unreacted aluminates or aluminate hydrates present. This dormant period is followed by a period of expansion, cracking and strength loss associated with the conversion of the low sulfate hydrate to ettringite. Also, it appears that transformation of the low sulfate hydrate to ettringite occurred more readily than the similar transformation involving the low aluminosilicate hydrate.

Finally, Fig. 4-III shows X-ray diffraction analysis of a spalled layer of Cement A after four weeks of sulfate immersion. In addition to ettringite and low sulfate, gypsum peaks were detected in the sample. During advanced stage of sulfate attack formation of gypsum, as a result of decomposition of C-S-H and $Ca(OH)_2$, is accompanied by serious weakening of the cementing properties. This is why the spalled material was weak and easily friable. The diffraction pattern from a spalled layer of Cement B exposed to the sulfate solution for 5 weeks also showed peaks due to gypsum and ettringite. Although gypsum peaks were present in the specimen, it was noted that the 8.66Å peak due to the aluminosilicate hydrate was still present. This showed that the compound was more sulfate resistant than the low sulfate hydrate.

On the basis of this work the author believes that at least three factors were involved in the superior sulfate resistance of the cement which contained

C_3A in the cubic form alone, and alkalies present mainly as sulfates. Firstly, the higher reactivity of the cubic C_3A, which was further enhanced by considerable amount of aphthitalite present, was responsible for the formation of most of the potential ettringite during the early hydration period, i.e., within 1 day, when the cement paste was less stiff. Consequently, the tensile stress induced would have been low and the ettringite thus formed contributed to strength, rather than to disruptive expansion. Secondly, since more alite hydrated under these conditions this also contributed to the higher strength of the paste at the time of sulfate immersion (Cement B paste was about 15 percent stronger than Cement A paste). Finally, the hydration characteristics of the cement containing C_3A in the cubic form alone were such that a significant proportion of the aluminate was tied up as aluminosilicate hydrate, rather than the aluminosulfate hydrate or low sulfate ($C_3A \cdot C\bar{S}H_{12}$). The former was found to be more resistant to conversion to ettringite when the hydrated pastes were exposed to the sulfate solution. A combination of the three factors appears to be responsible for the slower rate of sulfate attack on the cement which contained C_3A in the cubic form alone, as compared to the cement containing the orthorhombic C_3A.

CONCLUSIONS

On the basis of a laboratory study on sulfate resistance of two cements having the same compound composition, but with C_3A present either in the cubic form alone or in predominantly orthorhombic form, it is concluded that the rates of expansion, cracking, and strength loss associated with ettringite formation in high-C_3A portland cements can be affected by the crystalline form of C_3A.

Under normal curing conditions it was found that the cement containing the cubic C_3A alone hydrated faster, produced most of the potential ettringite in 1 day, and was 15 percent stronger at the time of immersion in the sulfate solution. Also, the hydration products of this cement, prior to the sulfate immersion, contained a complex calcium aluminosilicate hydrate, which was found to be more resistant to sulfate attack than the low sulfate hydrate present in the hydration products of the cement containing the orthorhombic C_3A. A combination of these factors appears to be responsible for the slower rate of sulfate attack on the cement which contained C_3A in the cubic form alone, as compared to the cement which contained the orthorhombic C_3A.

REFERENCES

1. A. E. Moore, "Tricalcium Aluminate and Related Phases in Portland Cement", Mag. Concrete Res., Vol. 18, No. 55, pp. 58-64, (1966).

2. I. Maki, "Nature of the Prismatic Dark Interstitial Material in Portland Cement Clinker", Cement and Concrete Res., Vol. 3, pp. 295-313, (1973).

3. M. Regourd and A. Guinier, "The Crystal Chemistry of the Compounds of Portland Cement Clinker", Sixth International Congress on the Chemistry of Cement, Moscow, (1974).

4. A. I. Boikova, A. I. Domansky, V. A. Paramonova, G. P. Stavitskaja, and V. M. Nikushchenko, "The Influence of Na_2O on the Structure and Properties of $3CaO.Al_2O_3$", Cement and Concrete Res., Vol 7 pp. 483-492, (1977).

5. M. Regourd, "Crystallization and Reactivity of Tricalcium Aluminate in Portland Cement", Cemento No. 75, pp. 323 - 336, (1978).

6. M. Regourd, "The Action of Sea Water on Cements", Annales de l'Institute Technique du Batiment et des Travaux Publics, No. 329, pp. 86-102, (1975).

7. P. K. Mehta, "Evaluation of Sulfate Resisting Cements by a New Test Method", ACI Journal, Vol. 72, pp. 573-575, (1975).

8. P. K. Mehta, "Performance Tests for Sulfate Resistance and Alkali-Silica Reactivity of Hydraulic Cements", ASTM, STP 691, pp 336-345, (1980).

Factors affecting sulfate resistance of mortars

Facteurs affectant la résistance au sulfate des mortiers

KATHARINE MATHER, Chief, Engineering Sciences Division, Structures Laboratory,
U.S. Army Engineer Waterways Experiment Station, Vicksburg, MS 39180, USA.

SUMMARY : The ability of a mortar made using portland cement, fine aggregate, and water to resist attack by sulfates is affected by the proportions of the mortar (water-cement ratio and cement content), by the maturity, by the amount of tricalcium aluminate in the portland cement, the presence of tricalcium aluminate-sodium oxide solid solutions with different structures and reactivities, and by the composition, reactivity, and amount of pozzolan used together with the portland cement.

Cements investigated included portland cements of Types I, II, III, and V meeting ASTM C 150, blended cements including Type IP's meeting ASTM C 595 that were made from the same clinkers as the Type I's, and Type I's blended with pozzolans including fly ashes produced by burning bituminous, subbituminous, and lignitic coals, calcined natural volcanic glass high in silica, and silica fume. Silica fume forms glassy microspheres that may contain over 90 percent SiO_2; it is a by-product of the production of silicon metal.

Some of the fly ashes produced from subbituminous and lignitic coals replacing 30 percent by volume of cements increased the expansion of mortars containing the blends when stored in sulfate solutions. This behavior reflects SiO_2 below 50 percent, Al_2O_3 16 to 26 percent, and CaO 5 to 30 percent. Other investigations show that Al_2O_3 and CaO in the fly ash glass are readily available to form ettringite. With cement of lower C_3A content some of the subbituminous and lignitic fly ash blends improved the sulfate resistance of mortars, except when SiO_2 in the fly ashes was 38 percent or less.

Type IP blended cements made with portland-cement clinkers containing up to 11 percent calculated C_3A and about 20 percent fly ash show substantial improvement in sulfate resistance of mortars compared with Type I cements made from the same clinkers.

RÉSUMÉ : La résistance au sulfate des mortiers est affectée par le rapport eau/ciment et la teneur en ciment (dont il n'est pas parlé) ainsi que par la quantité d'aluminate tricalcique dans le ciment portland, la présence des solutions solides du sodium dans l'aluminate tricalcique de structures et de réactivités différentes, par la composition, la métastabilité thermique et la quantité de pouzzolane employée pour remplacer une partie du ciment portland dans le but d'augmenter la résistance au sulfate du mortier.

Les ciments hydrauliques étudiés comprenaient les Types I, II, III, et V répondant à la spécification ASTM C 150, les ciments de Type IP répondant à la spécification ASTM C 595 fabriqués à partir des mêmes clinkers que les ciments de Type I, et du Type I comportant de la pouzzolane, y compris les cendres volantes produites par la combustion de charbons bitumineux, subbitumineux et lignitiques, le verre volcanique naturel calciné à haute teneur en silice et les fumées de silice. Les fumées de silice forment des microsphères vitreuses pouvant contenir plus de 90 pour cent de SiO_2; elles sont un sous-produit de la production de métal au silicium.

Les cendres volantes produites par les charbons subbitumineux et lignitiques remplaçant 30 pour cent du volume des ciments à haute teneur en C_3A cubique augmentèrent l'expansion due au sulfate de sodium des mortiers contenant les mélanges. Ce comportement représente SiO_2 au-dessous de 50 pour cent, Al_2O_3 de 16 à 26 pour cent et CaO de 5 à 30 pour cent. D'autres analyses indiquent que Al_2O_3 et CaO présents dans le verre de cendre volante peuvent permettre la formation d'ettringite. Dans le cas des ciments à plus faible teneur en C_3A cubique les mélanges de cendres volantes subbitumineuses et lignitiques améliorent la résistance au sulfate des mortiers, sauf lorsque la proportion de SiO_2 dans les cendres est de 38 pour cent ou moins. Les effets de mélanges de C_3A cubique et orthorhombique I et de C_3A orthorhombiques ou tétragonaux seront également étudiés.

Les ciments mélangés du Type IP produits à partir de clinkers contenant jusqu' à 11 pour cent de C_3A calcu environ 20 pour cent de cendres volantes démontrent une amélioration sensible dans la résistance au sulfat mortiers par rapport aux Types I produits a partir des mêmes clinkers.

INTRODUCTION

The chemical resistance of pastes, mortars, and concretes made using portland cement is affected by the proportions of the mixture (water-cement ratio and cement content), by the presence and amount of various solid solutions of C_3A with different structures and containing Na_2O, K_2O, SiO_2, Fe_2O_3, MgO, etc. If a pozzolan is used together with the portland cement, its composition, reactivity, and proportion in the mixture will affect for good or evil the sulfate resistance of the system.

CEMENTITIOUS MATERIALS

In the work upon which this paper is based, the sulfate resistance of mortars containing portland cements complying with the requirements for Types I, II, III, and V of ASTM C 150-78, Standard Specification for Portland Cement, and also cements complying with the requirements for Types IP and IS of ASTM C 595, Standard Specifications for Blended Hydraulic Cements, were investigated. In most cases we were able to test the Type I and the Type IP and the Type I and Type IS sampled at the same time from the same plant. We also tested four bituminous fly ashes, three subbituminous fly ashes, four lignitic fly ashes, a calcined natural volcanic glass, a glassy silica fume of high silica content that is a waste product in the production of silicon metal, and a sample of Santorin earth. Some of the materials studied are not reported on here.

MORTARS

The mortars were made with one part of cement to 2.75 parts graded standard sand to 0.485 parts of water, by weight. When other materials were used, the water content was changed until the flow of the mortar was equal to that of the mortar containing portland cement alone. Reductions were necessary with some of the portland-pozzolan cements; one pozzolan having very high surface area increased the water-cement ratio by about 3 percent.

TEST SPECIMENS AND INITIAL TESTS

All the specimens cast were 25.4 mm by 25.4 mm by 285.8 mm long with gage studs at both ends. All were cured for 24 hr in sealed molds in water at 35° ± 3°C, then removed from the molds. The initial gage length, 254 ± 2.5 mm, was determined; the fundamental transverse frequency was measured, and the bars were cured in water saturated with CH at a temperature of 23° ± 1.7°C. The same procedure was used for curing cubes of the same mortar which were broken in compression at various ages until the cubes reached the desired strength at which age the mortar bars were to be placed in 0.352 molar Na_2SO_4 solution. Before the bars were placed in sulfate solution, the length and fundamental transverse frequency of each bar was again measured. The strengths at which the bars were placed in sulfate solution were equalized as well as possible so that cements compared in the test for sulfate-resistance would be at the same maturity as measured by compressive strength. The first tests were made with bars having a compressive strength of 27.6 ± 1.4 MPa as measured in equivalent cubes; the next series at 24.1 ± 1.4 MPa; the final choice of strengths was 20.7 ± 1.0 MPa. The decision to lower the strength level was made because many portland, portland-pozzolan, and several portland blast-furnace slag cements survived the test for one year and did not fail by breaking although they expanded well over 1.0 percent of the gage length. There thus seems to be a wide variation in the strain capacity of mortar bars made with different portland, portland-pozzolan, and portland blast-furnace slag cements as well as among those made using blends of different portland cements with 30 or 35 percent replacement of cement by absolute volume of pozzolan.

LATER TESTS

The bars were subsequently measured for length change and tested for fundamental transverse frequency at 7, 14, 21, 28, 56, and 90 days. Thereafter the schedule for measurements was adjusted to the rate at which the expansion was increasing and the relative dynamic modulus of each group of mortar bars was decreasing. Each time the bars were measured, the sulfate solution was changed and since the measurement interval was not constant throughout the test it was not to be expected that a constant amount of sulfate was available to attack the bars during each interval between readings. The volume of sulfate solution to bars was maintained at 3.9 to 1 throughout the test.

FAILURE CRITERIA

The criterion for failure by increase in length was chosen as 0.10 percent; some cements failed by having all of the mortar bars break at expansions which were not determined because the failure occurred between two readings and we only know for example that after an expansion of 0.44 percent at 28 days every bar was broken at 56 days, the time of the next reading. The earliest failures by fracture of any of the bars took place at 28 days. Failures by fracture occurred thereafter at ages up to 180 days, but there was a tendency among the portland cements for failures to occur at relatively low expansions at ages below 90 days or for failures to occur at markedly larger expansions where the bars would already have been judged to have failed simply on the basis of expansion.

TRICALCIUM ALUMINATE DETERMINATIONS

We investigated the form of C_3A or C_3A solid solution with sodium oxide, potassium oxide, magnesium oxide, or silicon dioxide (1) by X-ray diffraction using a diffractometer with nickel-filtered copper radiation; in all cases the portion of the cement examined had been treated with maleic acid in methanol solution stirred for 30 min and then filtered (2).

We have followed the method in Appendix A of Mander et al (2) except that we use as-received cement samples and stir for 30 min in the maleic acid-methanol solution, followed by vacuum filtration over a small piece of nylon stocking under No. 50 Whatman filter paper in a Büchner funnel, three washes with methanol, and evaporation to free-flowing dryness under an infrared lamp. Sulfates are removed by a 10 percent solution of ammonium chloride in water, stirred at laboratory temperature with a magnetic stirrer for 45 min, filtered, and evaporated to free-flowing dryness as are the maleic-acid residues. Mander et al (2) and Regourd, Chromy, et al (4) provide X-ray diffraction spacings for cubic and orthorhombic C_3A and solid solutions of C_3A and sodium oxide. Regourd and Guinier (5) provide more information; we have assumed that Orthorhombique II mentioned

by Regourd et al (4) is equivalent to "Monoclinic" in Regourd and Guinier (5) and Maki (6) except for the necessary differences in indexing. Like Kristmann (7) the diffractometer available to us resolved doublets in the relevant angular ranges of C_3A and solid solutions in C_3A but did not resolve triplets. Therefore, we used in our separations of C_3A the lines in the angular region from 21 to 21.84 degrees two-theta. As a consequence we believe that the separation of cubic C_3A from other C_3A is reliable as is the absence of C_3A from the maleic acid residue. The distinction of the cubic and orthorhombic or tetragonal C_3A from orthorhombic and tetragonal or orthorhombic or tetragonal we suspect may be less reliable.

EFFECTS OF TRICALCIUM ALUMINATE CONTENT

Initially let us consider cements in which no C_3A was detected by X-ray diffraction. Five such portland cements were found. Only one had been tested for one year and it had expanded only to 0.065 percent at that time. The other four cements in which no C_3A was detected have been tested to 180 days at which time one which contains 4.53 percent M by chemical analysis has expanded to 0.085 percent, although it may expand more than 0.10 percent at one year, the influence of the periclase content hydrating to $Mg(OH)_2$ is believed to be the significant feature explaining the expansion of this cement. All of the other three cements contain less possible periclase. Six cements were recognized as containing orthorhombic or tetragonal or orthorhombic and tetragonal C_3A. These include one which in one year reached an expansion of 2.88 percent in mortar bars.

The strain capacity (i.e., the increase in length without fracturing) of this particular cement was the largest shown by any of the portland cements tested. Another cement reached an expansion of 0.861 percent at 146 days but was not measurable at 180 days. Clearly, the strain capacity was substantial but well below that of the cement just discussed. Three other cements reached expansions over 0.10 percent by 180 days. One of those which exceeded 0.10 percent at 180 days contained 4.36 percent M by chemical analysis. The sixth cement which contains slightly over 2 percent M expanded to 0.057 percent at 180 days. The question of the strain capacity of the mortar bars of four of these cements has not yet been answered since all are still under test and none in the four sets has fractured. Cements containing cubic and orthorhombic or tetragonal C_3A or cubic C_3A and one of the other two forms in this group made up eight cements. Seven of those tested have failed by exceeding 0.10 percent expansion and three have failed in fracture, two at quite low expansions, and the others at expansions above 0.58 percent.

Seven portland cements contained only cubic C_3A. One of these reached an expansion of 1.77 percent at 365 days with no mortar bars broken. Another at 90 days had expanded to 0.61 percent with four mortar bars broken. Another has achieved the same expansion at 180 days without any failures by fracture. A fourth expanded to 0.29 percent at 90 days and was unreadable at 146 days. A fifth has expanded beyond 0.20 percent at 180 days without failures in fracture. Two other cements have not failed. One is expected to because although it contains the least cubic C_3A detected it also contains 3.63 percent M by chemical analysis and has expanded to 0.085 percent at 180 days. While we endeavored to find out which substances were present in the 26 portland cements tested, our tests so far suggest, but do not confirm, the opinions of Regourd and Chromy et al (4) that cubic C_3A is more active than the forms with denser packing. Certainly the amount of C_3A in the cement as ranked by X-ray diffraction is not invariably correlated with maximum expansion, usually because the cements with the highest C_3A contents also are cements of quite rapid strength gain and low strain capacity, so that they may fail in 56 to 90 days by exceeding 0.10 percent expansion and by having all of the mortar bars fail in fracture.

BEHAVIOR OF PORTLAND-POZZOLAN CEMENTS

A comparison has been made between C_3A and solid solutions of the several crystal forms ranked by relative amount and the companion IP cements made with the same portland cement clinker and an addition ranging from 15 to possibly 25 percent of fly ash in the cements containing the most cubic C_3A. In the group of portland cements containing the largest amounts of cubic C_3A and their companion IP cements, all of the portland cements failed by expanding from 0.289 percent at 90 days where all fractured, up to as much as 1.77 percent where the bars survived to one year but relative E had fallen to 57 percent. Only one of the three companion IP cements expanded as much as 0.10 percent. One reached one year with an expansion of 0.035; it was the companion of the portland cement that expanded 1.77 percent. The other two cements are still under test with no apparent relation between the expansion of their companion portlands and those of the IP's. In the group of cubic C_3A cements, one portland with a relatively low amount of C_3A has a companion IP. The portland had expanded 0.61 percent at 180 days while the IP expanded 0.06 percent at the same age. In the group containing cubic and either orthorhombic or tetragonal C_3A solid solution or both, two portland cements have in one case two companion IP cements, one made with fly ash and one experimental cement with bottom ash. The other portland cement had a companion portland blast-furnace slag cement. The portland with IP companions is still under test but has substantially exceeded the failure criterion of 0.10 percent expansion. The companion IP still under test at the same age as the portland has expanded 0.08 percent while the experimental cement with bottom ash has already expanded over 0.90 percent at the same age. The portland cement with the companion portland blast-furnace slag cement expanded over 1 percent and failed by cracking and warping at 146 days with a relative E of 49 percent. The portland blast-furnace slag cement reached an expansion of 0.08 percent at 292 days and was terminated. Among cements containing relatively small amounts of cubic and orthorhombic or tetragonal C_3A or solid solutions one Type I cement survived to an age of one year at an expansion of 1.40 percent; the companion cement expanded 0.43 percent at one year. The second portland cement is still under test but has exceeded the failure criterion of 0.10 percent expansion. It had two companion IP cements with different amounts of fly ash in each. One has expanded 0.04 percent and the other 0.05 percent at the same age as the portland; all three are continuing in test. In cements containing orthorhombic or tetragonal solid solutions or both one cement containing an intermediate amount of total C_3A expanded to 2.9 percent at one year with a relative E of 64 percent at that time. Its companion IP expanded 0.11 percent at one year with a relative E of 150 percent. Within the same group of C_3A solid solutions one containing a relatively small amount of total C_3A expanded 0.10 percent at 280 days and is still in test. Its companion which has been in

test for 180 days has expanded 0.05 percent. In the same group of C_3A solid solutions the cement containing the least total aluminate phase has expanded to 0.86 percent at 146 days and was thereafter unreadable. Its companion IP has expanded 0.14 percent and is still under test. Summarizing these results shows that out of a total of 12 portland cements with companion blended cements, almost all blended with fly ash, 11 of the blended cements had expansions substantially reduced from those of the portland cements but in one case the addition of fly ash increased the total expansion but prolonged the life of the blended cement mortar bars from 90 days when all of the portland cement bars had broken to 270 days and the blended cement is still under test. Thus we have a clear case for the utility of Type IP cements.

BEHAVIOR OF BLENDS WITH HIGH-SILICA POZZOLANS

Three cements: RC 756 with 14.6 percent C_3A as calculated from chemical composition, RC 714 with 13.1, and RC 744 with 9.4 were tested alone and with 30 percent replacement by solid volume of each of two high-silica pozzolans. The C_3A in 756 was indicated by X-ray diffraction to be cubic, that in 714 and 744 to be cubic and orthorhombic. The high-silica pozzolans were AD 518, a calcined volcanic glass, and AD 536, a silica fume.

As shown on Fig. 1, the three cements tested alone behaved as follows: RC 714 showed 0.515 percent expansion at 56 days and all the bars disintegrated before the next test age; RC 756 showed 0.868 percent expansion at 90 days and all the bars disintegrated before the next test age; and bars made with RC 744 all survived to 365 days at which time the expansion was 0.808 percent after which the bars began to warp.

With 30 percent silica fume (AD 536) the expansions at 365 days with the three cements were insignificant and insignificantly different: 0.019, 0.016, and 0.018, respectively. With 30 percent calcined volcanic glass the expansions with the three cements remained in the order of expansion of the cements alone but were well below failure at one year being 0.057, 0.041, and 0.034, respectively. It is concluded that either of these two pozzolans at 30 percent replacement can effectively control sulfate expansion using any of these cements in this test; the silica fume is more effective and equally effective with all three cements. The volcanic glass still allows the cements to manifest their inherent differences in sulfate resistance but the expansion is at an innocuous level in all cases.

BEHAVIOR OF CEMENT 714 WITH FLY ASHES

Cement 714, by itself survived to 56 days, had expanded then 0.515 percent, and then disintegrated (Fig. 2). When replaced by 30 percent of each of eight fly ashes the effects varied. With fly ash 509 the specimens only survived 28 days after which they disintegrated, but at 28 days the expansion (0.040 percent) was less than when 511 was used. With fly ashes 506, 510, 511, and 513 the bars survived to 56 days but with widely different expansions at that point (0.427, 0.229, 0.417, and 0.056, respectively) and then disintegrated. With fly ashes 505, 507, and 512 the bars survived to 90 days, again with widely different expansions (1.167, 1.172, and 0.385, respectively). It is concluded that none of the eight fly ashes tested would control sulfate expansion of this cement in this test at 30 percent replacement. It is not positively shown however that any of the eight fly ashes made sulfate resistance significantly worse than it was when the cement was used alone.

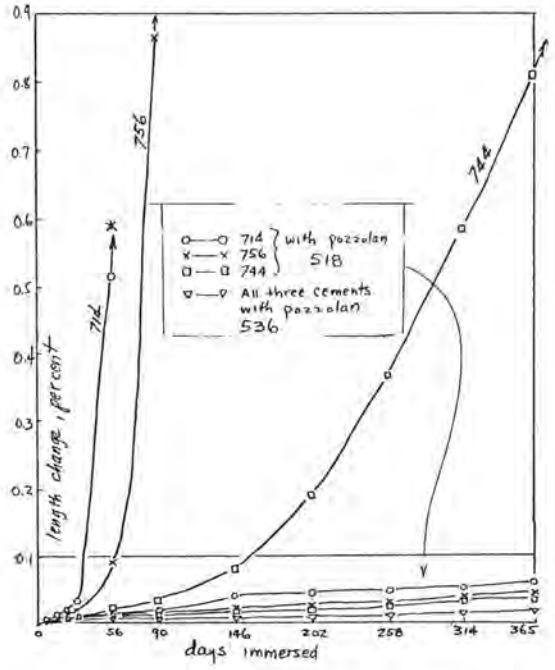

Figure 1

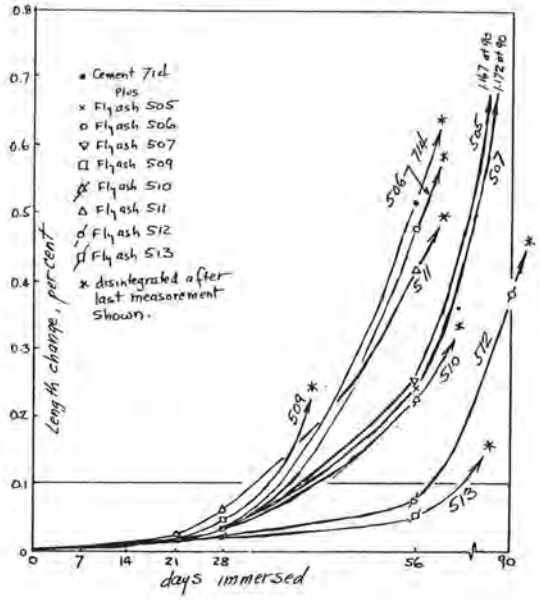

Figure 2

BEHAVIOR OF CEMENT 756 WITH FLY ASHES

Cement 756, by itself survived to 90 days at which time its expansion was 0.867 (Fig. 3). When replaced by 30 percent of each of eight fly ashes, as was to be expected, the effects varied. Five of the fly ashes had an adverse effect on sulfate resistance. In four cases the specimens only survived 56 days at which time their expansions were:

506:	0.634	510:	0.276
509:	0.209	513:	0.031

In the fifth case, with 505, the bars survived to 90 days but with higher expansion (0.939) than the cement by itself. In the other three cases the bars survived as long as the cement by itself, but no longer, and had lesser but still large expansions (0.199, 0.392, and 0.500). It is concluded that none of these fly ashes will control sulfate expansion of this cement in this test at 30 percent replacement; five of the eight actually make the system less sulfate resistant.

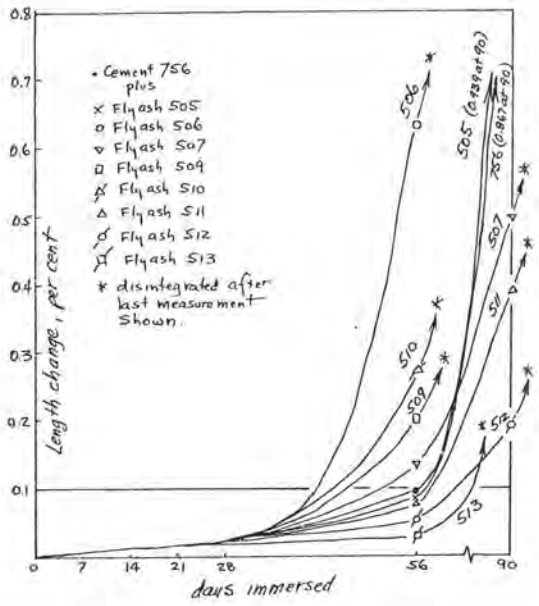

Figure 3

BEHAVIOR OF CEMENT 744 WITH FLY ASHES

Cement 744, by itself survived to 365 days (Fig. 4), at which time its expansion was 0.808 percent. When replaced by 30 percent of each of eight fly ashes the effects varied. In contrast to the behavior of these fly ashes with cement 714, here two of them (510 and 513) did significantly increase the sulfate susceptibility of the system; with both of these fly ashes the specimens only survived to 202 days. With all the other six fly ashes the specimens survived to 365 days and, in all cases, with reduced expansions as compared with cement 744 by itself. However only with 505 and 512 was the expansion at 365 days reduced below 0.10 percent, the failure criterion. It is concluded that of the eight fly ashes, the use of two made the sulfate resistance worse, with two others the sulfate expansion was reduced to a possibly tolerable amount, and with the other four expansion was reduced but by not sufficient to provide protection in the test.

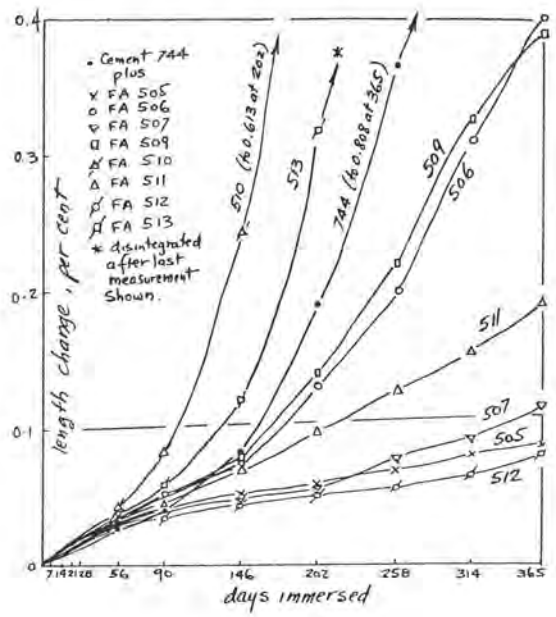

Figure 4

Based on the behavior of these ten pozzolans with the three cements (714, 756, 744), they may be ranked from best to worst with regard to their effects on sulfate resistance as follows:

	With Cement 714	756	744	Weighted Average	
Best	536	536	536	536	(silica fume)
	518	518	518	518	(volcanic glass)
	512	512	512	512	(subbituminous)
	505	511	505	505	(subbituminous)
	507	507	507	507	(subbituminous)
	513	505	511	511	(bituminous)
	510	513	509	513	(lignite)
	511	509	506	509	(lignite)
	506	510	513	510	(lignite)
Worst	509	506	510	506	(lignite)

CONCLUSIONS

1. Although it is possible by the use of an X-ray diffractometer to separate cubic C_3A from solid solutions of C_3A with alkalies and silica when the solid solutions have crystal structures other than cubic, without special provisions to improve resolution of the use of monochromatic radiation, the separation of cubic from not cubic is the most reliable unless a step-scanner

can be used on the diffractometer or a Guinier camera is available.

2. The cubic and orthorhombic I group following the nomenclature of Regourd, Chromy, et al (4) is probably the next most reliable separation as made with a diffractometer, on the basis of the experimentation by Maki (6) that shows that the partial solid solution in cubic C_3A passes with increasing substituents into mixed cubic and orthorhombic solid solutions as the substituents increase to a level of 7 percent Na_2O, modified in commercial portland cements by the SiO_2 content and K_2O content.

3. We had hoped in this work to provide evidence to support or refute the belief of Regourd, Chromy, et al (4) that cubic C_3A should be more reactive than any of the solid solutions with Na_2O which have denser structures. However, our results are not clear regarding this particular question because it developed that bars made using mortars prepared in accordance with ASTM Designation C 109 with constant water-cement ratio and proportions proved to have very different strain capacities, probably as a consequence of the rate of strength gain of the cements even when the C_3A contents were similar. For example, cement 756, containing the most cubic C_3A of any of the cements we tested (14.6 percent C_3A calculated from chemical analysis) in mortar bars exposed in 5 percent Na_2SO_4 solution survived to 90 days and reached an expansion of 0.868 percent; the bars disintegrated before the next reading. When that cement was replaced by 30 percent by volume of each of eight fly ashes, the expansions were reduced in four cases but failure by disintegration of the bars took place earlier than that of the cement; in one case the bars survived as long as the cement by itself but the expansion was greater. In three other cases the bars containing fly ash survived as long as the bars containing the straight portland cement but disintegrated at lower expansions. In this group, only one fly ash increased the strain capacity. Cement 714 contained 13.1 percent C_3A, a smaller amount than in cement 756. In C 109 mortar bars it expanded to 0.515 at 56 days and then disintegrated. As compared with cement 756, it had less strain capacity because the bars disintegrated earlier at a lower expansion. If it were possible to exchange the cubic C_3A of 756 with the lower cubic and orthorhombic C_3A of 714, leaving the rest of each cement as it was, would the greater strain capacity of 756 with the C_3A of 714 lead to a larger expansion of that combination before the bars disintegrated? Would the smaller strain capacity of 714 be further decreased by the larger amount of cubic C_3A from 756? Does strain capacity in sulfate exposure depend on the formation of ettringite and gypsum and the development of tensile strength and creep capacity all pari passu? Does failure by disintegration occur when expansion, strength gain, and creep depart in rate from each other by more than a certain, at present unknown, rate? Cement 744, with 9.4 percent cubic plus orthorhombic C_3A, less than either 756 or 714, survived in bars exposed in sodium sulfate to 365 days when it had expanded to 0.81 percent. Two fly ashes increased the sulfate susceptibility; one caused earlier failure at lower expansion and the other failure at 365 days at lower expansion. Cement 744 is concluded to have the greatest strain capacity of these three cements, but contained less C_3A.

4. Because we did not find cements of equal C_3A content in the cubic, cubic and orthorhombic I, and orthorhombic or tetragonal, or orthorhombic or tetragonal groups, and we did find cements of equal strain capacities in these groups, we can neither confirm nor refute the belief of Regourd, Chromy, et al (4) that cubic C_3A is more reactive than solid solutions of other crystal forms.

BIBLIOGRAPHY

1. A. E. Moore [1966], "Tricalcium Aluminate and Related Phases in Portland Cement," Magazine of Concrete Research, Vol 18, No. 55, pp 59-64, English.

2. J. E. Mander, L. D. Adams, and E. E. Larkin [1974], "A Method for the Determination of Some Minor Compounds in Portland Cement and Clinker by X-Ray Diffraction," Cement and Concrete Research, Vol 4, pp 533-544, English.

3. M. A. Shahat [1952], "The Crystal and Molecular Structure of Maleic Acid," Acta Crystallographica, Vol 5, p 763ff, English.

4. M. Regourd, S. Chromy, L. Hjorth, B. Mortureux, and A. Guinier [1973], "Polymorphisme des Solutions Solides du Sodium dans l'Aluminate Tricalcique," Journal of Applied Crystallography, Vol 6, pp 355-364, French.

5. M. Regourd and A. Guinier [1974], "The Crystal Chemistry of the Constituents of Portland Cement Clinker," preprint of principal paper for the VI International Symposium on the Chemistry of Cement, Moscow, English.

6. I. Maki [1973], "Nature of the Prismatic Dark Interstitial Material in Portland Cement Clinker," Cement and Concrete Research, Vol 3, pp 295-313, English.

7. M. Kristmann [1977], "Portland Cement Clinker: Mineralogical and Chemical Investigations, Part I, Microscopy, X-Ray Fluorescence and X-Ray Diffraction," Cement and Concrete Research, Vol 7, pp 649-658, English.

Mechanism of sulfate expansion : A reappraisal of literature

Mécanisme de l'expansion due au sulfate : une réestimation de la littérature

S. CHATTERJI, M. Sc., D. Phil., Research Scientist. H + H-INDUSTRI A/S, Lyngby, Denmark

SUMMARY: The expansion of Portland cement concrete due to SO_4 ion attack has been attributed either to ettringite formation or formation of monosulfate from pre-existing C_4AH_x. The two mechanisms can be distinguished by noting whether the expansion follows ettringite formation or if it continues even when the proportion of ettringite is decreasing. The relevant literature has been critically surveyed to ascertain the validity of either of the above relationships. In this survey a distinction will be made between free expansion and expansion against a constraint.

The literature on free expansion: Chatterji has noted that in a C_3A-gypsum-$Ca(OH)_2$ paste expansion can occur even when ettringite was disappearing. Analyses of quantitative results of Greening as well as Sauman show that most of the expansion occurs when ettringite is disappearing.

The literature on expansion against a constraint: Mehta has done extensive work on this aspect using all types of expansive cements. Analyses of his papers show that:

(i) M and S type expansive cements develop about half the total expansion at maximum ettringite content; the rest occurs when ettringite is disappearing.
(ii) In K type expansive cement a third of the total expansion occurs by the time free $CaSO_4$ has reacted. During the rest of expansion ettringite and some unstated calcium aluminate hydrate, in the ratio 1:8, form from $C_4A_3\bar{S}$.
(iii) Hydration of $C_4A_3\bar{S}$ in the presence of $Ca(OH)_2$ yields monosulfate and C_4AH_x.
(iv) The expansion continues when either ettringite is decreasing and/or monosulfate is forming.

It is to be noted that ettringite causes no expansion in a sulfate resistant Portland cement.

The role of ettringite in sulfate expansion is uncertain especially as a number of workers, including Mehta, have reported the formation of hexagonal aluminate hydrate even when gypsum is present in the system. In other words, even the early expansion of expansive cements may be due to monosulfate formation. It is to be noted that in a sulfate resistant Portland cement monosulfate does not form.

RESUME: L'expansion du béton de ciment Portland due à l'action des ions SO_4 a été attribuée soit à la formation d'ettringite, soit à la formation de monosulfates à partir de C_4AH_x pré-existant. Que l'expansion suive la formation d'ettringite ou bien qu'elle continue pendant que la proportion d'ettringite diminue, il est impossible de distinguer entre les deux méchanismes. Les ouvrages pertinents sur ce sujet ont été soumis à une lecture critique pour assurer la validité des deux relations décrites plus haut. Dans cette étude nous ferons une distinction entre l'expansion libre et l'expansion soumise à une contrainte.

Les ouvrages sur l'expansion libre: Chatterji a remarqué que dans un C_3A-plâtre-$Ca(OH)_2$ il peut se produire une expansion de la pâte, même pendant la disparition de l'ettringite. Les analyses des résultats quantitatifs obtenus par Greening et Sauman montrent que la plus grande partie de l'expansion se produit quand l'ettringite disparait.

Les ouvrages sur l'expansion soumise à une contrainte: Mehta a fait une étude approfondie sur ce sujet en utilisant différents types de ciments expansifs. Une analyse de son travail montre que:

(i) Les ciments expansifs de type M et S développent la moitié de leur expansion totale quand la teneur en ettringite est maximale. Le reste se produit quand l'ettringite disparaît.
(ii) Les ciments expansifs de type K développent un tiers de leur expansion totale pendant le temps de réaction du $CaSO_4$ libre. Pendant le reste de l'expansion, il se forme de l'ettringite et des hydrates d'aluminate de calcium indéterminés à partir de $C_4A_3\bar{S}$ dans le rapport 1:8.
(iii) L'hydratation du $C_4A_3\bar{S}$ en présence de $Ca(OH)_2$ forme des monosulfates et du C_4AH_x.
(iv) L'expansion continue quand l'ettringite diminue et/ou quand il y a formation de monosulfate.

Il faut remarquer que l'ettringite ne cause pas d'expansion dans les ciments Portland résistants aux sulfates.

Le rôle de l'ettringite dans l'expansion des sulfates est hypothétique, notamment depuis que Mehta et d'autres ont constaté une formation d'aluminates hydratés hexagonaux, même en présence de plâtre dans le système. Autrement dit, l'expansion du début des ciments expansifs peut être due à la formation de monosulfate. On remarquera qu'il ne se forme pas de monosulfate dans les ciments Portland résistants aux sulfates.

It is known that structures containing some types of calcerious cements expand and disintegrate when exposed to sulfate bearing water. For both economic and scientific reasons, the processes leading to the above breakdown, also known as sulfate expansion, have been extensively studied. It is a commonly held belief that the expansion is related to the formation of calcium sulfo-aluminate hydrate. There are two calcium sulfoaluminate hydrates namely monosulfate (low sulfoaluminate) and trisulfate (ettringite); and each of these has been implicated in sulfate expansion. The main object of this paper is to critically evaluate the relevant literature in order to differentiate between the two conflicting hypotheses.

As a preliminary to this evaluation it is in order to recapitulate the salient points of the two opposing hypotheses.

(1) The hypothesis involving monosulfate:

This hypothesis postulates that in a hydrating paste, C_4AH_{13} forms from alumina bearing phases. If exposed to SO_4 ions C_4AH_{13} first changes over to monosulfate by an ion-exchange process. When SO_4 ion concentration increases, monosulfate changes over to ettringite by a "through-solution" process. The conversion of C_4AH_{13} to monosulfate is accompanied by a volume expansion. Depending upon the presence or absence of excess $Ca(OH)_2$, the hardened paste may or may not expand. The formation of ettringite may give rise to second order expansive forces (1).

(2) The hypothesis involving ettringite:

According to this hypothesis the formation of ettringite from alumina bearing phases is responsible for the expansion. The exact mechanism by which ettringite causes the expansion has been variously attributed to (a) a solid state formation of ettringite (2,3), (b) a crystal growth pressure (4), (c) an adsorption of water by colloidal ettringite which forms in the presence of $Ca(OH)_2$ (5). More will be said about each of the above explanations later on. However it is generally been accepted that the presence of free $Ca(OH)_2$ is necessary for expansion (1,2,5).

Since both the hypotheses accept ettringite as the stable calcium sulfoaluminate hydrate in the presence of excess or stoichiometric amounts of sulfate, its presence under these circumstances does not constitute evidence for or against any of these hypotheses. Moreover, as in one of the hypotheses the formation of monosulfate has been given a role analogous to that of free radicals in organic reaction mechanisms, an appropriate experiment has to be performed to reveal its importance. The two hypotheses can be differentiated by

(i) a continued expansion when ettringite formation has stopped especially when it is disappearing or disappeared.

(ii) the absence of expansion in a system containing excess $Ca(OH)_2$ in which ettringite but not monosulfate form.

The relevant literature on sulfate expansion has been critically surveyed keeping the above two criteria in mind. In this evaluation a distinction has been made between free and restrained expansion measurements.

(A) Literature on the free expansion measurements:

It appears that Chatterji was first to report that in C_3A-$Ca(OH)_2$-gypsum-water system, expansion continues even when ettringite is disappearing and monosulfate is forming (1). However a similar inference can be drawn from Meissener's work on sulfate unsoundness of cement (6). Meissener had added upto about 4.9% SO_3 to different types of cements and measured lengths of wet cured mortar prisms made with those cement samples. Unsoundness appeared by about 90 days, long after all gypsum had been consumed.

Matousek and Sauman have reported the expansion characteristics of expanding cements based on Portland cement, metakaolinite and gypsum (7).

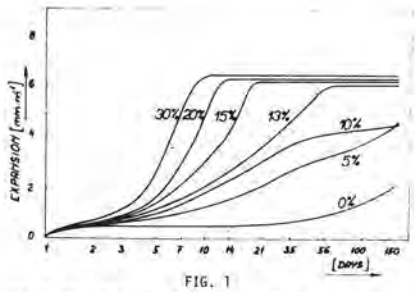

FIG. 1

Influence of the addition of metakaolinite on the volume changes of the cement with a constant gypsum content (10%).

Fig. 1 has been taken from their paper. An analysis of the results (8) indicated that in the mixture containing 20% metakaolinite, complete consumption of gypsum had occurred between 7 and 10 days. From Fig. 1 it can be seen that the expansion continued upto the 14th day i.e. even after ettringite formation had stopped. The last 20% or so expansion occurred against a higher cohesive strength of the cement i.e. the expansive force was stronger than that at the beginning.

However, the most interesting results are those of Seligmann and Greening (9). These authors measured volume changes of wet pastes against a small Hg head in the system C_3A-$Ca(OH)_2$-gypsum having varying SO_3/Al_2O_3 ratios; they also followed their hydration by using an x-ray diffraction technique.

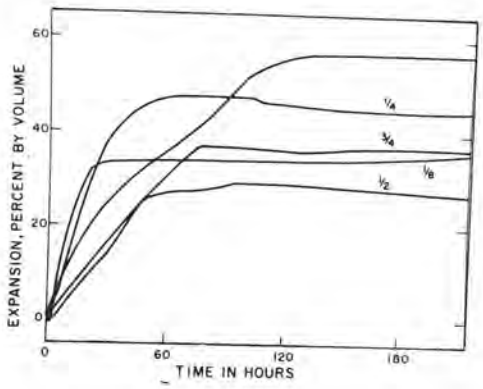

Fig. 2
Expansion characteristics
of C_3A-$CaSO_4$-$Ca(OH)_2$ pastes

Fig. 2 shows their volume expansion results. In the figure 1/2 etc. denote SO_3/Al_2O_3 ratios. In the mixture 1/4 it took about 6 hours for the complete consumption of gypsum and that of ettringite about 9 hours. However from Fig. 2 it can be seen that the expansion continued upto about 40 hours; moreover it also shows that only a minor fraction of the total expansion occured whilst ettringite was forming and most of the expansion occured whilst it was disappearing. This is also true for the mixture marked 3/4. The authors stated "The expansion continued during stages II (consumption of ettringite to form monosulfate) and III (formation of monosulfate-C_4AH_x solid solution) hydration ....."

The results of Seligmann and Greening and Chatterji are of particular interest as the expansion could not be attributed to any other compound and they show that expansion occurs when ettringite is disappearing and monosulfate or its solid solution is forming.

(B) Literature on restrained expansion:

On this aspect Mehta and his co-workers have done extensive work using both pure components and expansive cements of different types.

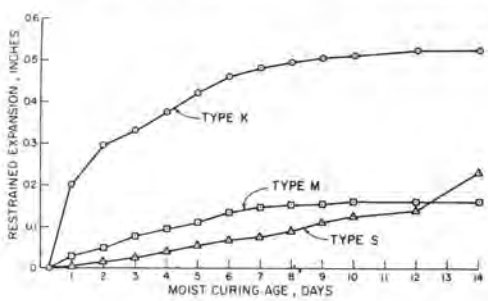

Fig. 3
Expansion characteristics
of expansive cements

Fig. 3 and table 1 have been taken from one of their papers (10). In this paper Mehta and Lesnikoff have studied the expansion characteristics of water cured pastes of K,M and S type expansive cements as well as their hydration reaction by x-ray diffraction technique. The expansive cements were produced by grinding small amounts of expansive agents with Portland cement clinker. Analyses of these results will start with S type cement and end with K type cement.

(i) S type expansive cement: Table 1 shows that ettringite had reached its maximum proportion in between 7 and 10 days. The proportions of ettringite and C_3A decreased between 10 and 14 days. Fig. 3 shows that about half of the total expansion occurred by 10 days and the expansion continued thereafter apparently with acceleration. In other words the later part of the expansion and disappearence of ettringite occurred simultaneously.

(ii) M type expansive cement: In this cement the proportion of ettringite was highest on the 3rd day. Thereafter its proportion decreased as did those of C_3A and CA. Fig. 3 shows that about half of the observed total expansion occurred by the 3rd day and the rest subsequently. Here again the expansion continued whilst ettringite was disappearing.

This cement deserves further attention. In this case, the complete consumption of $CaSO_4$ took about 3 days. In the presence of excess $Ca(OH)_2$, the continued hydration of C_3A and CA must have produced C_4AH_x. Mehta has previously shown that C_4AH_x reacts very fast with ettringite to produce monosulfate (11). For some unknown reasons Mehta and Lesnikoff could not detect the formation of monosulfate or C_4AH_x until about 14 days. Thus half of the total expansion was occurring concurrently with the disappearance of ettringite and formation of C_4AH_x and/or monosulfate.

(iii) K type expansive cement: This is a very interesting case. Table 1 shows that CaO was completely hydrated by 6 hours and in the 24-hour sample no free $CaSO_4$ could be detected. Proportions of $C_4A_3\bar{S}$ and C_3A decreased and that of ettringite increased monotonously with time. This is the only cement sample where the proportion of ettringite increased all the time.

Now SO_4 ions needed for the formation of ettringite after 24 hours must have come from $C_4A_3\bar{S}$. This is somewhat surprising as Mehta and Kline have previously shown that mixtures of $C_4A_3\bar{S}$, CaO and $C\bar{S}$ under similar conditions form monosulfate (mix.nos P and R of ref. 3). However that may be, the stiochiometry of ettringite formation from $C_4A_3\bar{S}$ is informative. As equation 1 shows, each "molecule" of ettringite formation is accompanied by the liberation of 8 "molecule" of $Al_2O_3 \cdot nH_2O$ and 6 of $Ca(OH)_2$

$$3\ C_4A_3\bar{S} + aq = C_3A{\cdot}3CaSO_4{\cdot}32\ H_2O + 8\ Al_2O_3{\cdot}nH_2O + 6\ Ca(OH)_2 \quad \ldots\ldots\ldots 1$$

Table 1

Relative XRD Peak Intensities of Hydrated Cement Pastes

Age of Hydration/ Type of Cement	CaO	$C\bar{S}H_2$	$C\bar{S}H_{1/2}$	$C\bar{S}$	$C_4A_3\bar{S}$	C_3A	CA	Ettringite
Type K:								
0 hr	20	3	9	20	16	19	0	0
6 hrs	–	5	–	7	12	18	–	19
1 d	–	–	–	–	11	16	–	23
3 d	–	–	–	–	10	14	–	27
5 d	–	–	–	–	9	14	–	28
7 d	–	–	–	–	9	14	–	29
10 d	–	–	–	–	6	13	–	30
14 d	–	–	–	–	5	11	–	30
Type M:								
0 hr	0	65	7	0	0	35	18	0
6 hrs	–	16	–	–	–	27	12	10
1 d	–	6	–	–	–	26	10	20
3 d	–	–	–	–	–	25	10	25
5 d	–	–	–	–	–	21	9	23
7 d	–	–	–	–	–	15	7	22
10 d	–	–	–	–	–	17	7	21
14 d	–	–	–	–	–	16	5	18
Type S:								
0 hr	0	3	7	79	0	69	0	0
6 hrs	–	7	–	29	–	60	–	9
1 d	–	–	–	11	–	58	–	18
3 d	–	–	–	11	–	58	–	20
5 d	–	–	–	10	–	47	–	24
7 d	–	–	–	8	–	41	–	25
10 d	–	–	–	–	–	33	–	25
14 d	–	–	–	–	–	32	–	23

As the cement already had enough $Ca(OH)_2$ both from CaO and Portland cement hydration, it is expected that the above "nascent" $Al_2O_3{\cdot}nH_2O$ will form C_4AH_x. Furthermore, the continued hydration of C_3A after 24 hours will add more C_4AH_x to the stock. It is also expected that C_4AH_x will react with ettringite to form monosulfate (11). Thus it is doubly surprising that in this cement the proportion of ettringite went on increasing and no monosulfate or hexagonal calcium aluminate hydrate could be detected until about 14 days.

Fig. 3 shows that about 30% of the total expansion occurred within 24 hours when ettringite may be claimed to be the main sulfoaluminate and the rest, about 70%, occurred when ettringite was forming along with another calcium aluminate hydrate in the ratio 1:8.

Attribution of the continued expansion to ettringite or the other calcium aluminate hydrate depends on ones prejudices. When one notes that the particular K type studied contained CaO as a component, one may wonder if the expansion upto 24 hours logically can be attributed solely to ettringite. It is known that CaO can cause expansion after it has been fully hydrated (12).

It will thus appear that the major part of the restrained expansion of any expansive cement occurs when monosulfate is forming and/or ettringite is disappearing. It is not even certain that the expansion at the initial stages of hydration can be attributed to ettringite. A number of authors including Mehta have reported the formation of monosulfate at the initial stages of hydration even in the presence of excess calcium sulfate (1,3,11,13,14,15). Undetected monosulfate, as it must have happened in the cases of M and K types of expansive cements, might have caused the initial expansions.

(c) Ettringite formation without expansion:

Any theory of sulfate expansion must explain the absence of expansion in the case of sulfate resistant Portland cement. Like ordinary Portland cement, it liberates $Ca(OH)_2$ on hydration and forms ettringite on reacting with sulfate (4,16,17). The particle size of ettringite is similar to those in ordinary Portland cement (18) if not smaller (4). It is difficult to explain why ettringite formation does not cause any expansion in sulfate resistant Portland cement as it does in ordinary Portland cement.

It will be of interest to know if monosulfate forms in sulfate resistant Portland cement. In a cooperative research programme none of the seven participating laboratories could detect it by DTA any time upto 365 days of hydration (19). Kalousek and Benton had previously published similar results (20,21,22). A maximum of two, out of seven cooperative laboratories, could detect trace or possible trace amount of monosulfate at any time upto 365 days by x-ray diffraction technique (23). Noting that the strongest line of monosulfate is at 8.9A and that ettringite has a line of moderate intensity at 8.84A, the detection of trace amounts of monosulfate in the presence of larger amounts of ettringite is somewhat uncertain especially when the intensity of 8.9A line was varying erratically with time. The absence of monosulfate in sulfate resistant Portland cement has been previously noted (16). If this general inability to detect monosulfate in any quantity in sulfate resistant Portland cement is taken at its face value then the absence of expansion in this type of cement is very straightforward - no monosulfate no expansion.

Some comments on the proposed explanations as to how ettringite causes expansion:

Various authors have proposed various explanations as to how the formation of ettringite causes expansion in cements. Some of these will be examined in this section.

(i) Solid state formation of ettringite:

It was proposed that expansion occurs only when ettringite forms through a solid state reaction from alumina-bearing phases in a saturated $Ca(OH)_2$ solution (2). Both transmission and scanning electron microscopic studies showed that ettringite formation is a "through-solution" process irrespective of $Ca(OH)_2$ concentration (5,16, 24). Moreover this does not explain the case of sulfate resistant Portland cement.

(ii) Crystal growth pressure:

It can be shown that a crystal, in contact with its supersaturated solution, will exert a pressure against any constraint provided there is no other crystal in the same system which can grow unhampered. This proviso is difficult to satisfy in any cement paste. Neither can the crystal growth pressure hypothesis explain the observations of Chatterji and those of Seligmann and Greening.

(iii) Expansion due to water adsorption by colloidal ettringite:

This is one of the latest proposals (5,25). According to this proposal ettringite forms in a colloidal state in the presence of $Ca(OH)_2$ and this colloidal ettringite adsorps a large amount of water on its surface causing expansion. However, there seems to be some confusion as regards to the experimental evidence for it. In his 1967 paper questioning the validity of monosulfate hypothesis, Mehta had shown that lime free C_3A-$3C\bar{S}H_2$ paste of water/solid ratio of 0.6 (the theoretical w/s ratio for complete reaction is 0.59) can expand i.e. ettringite which had formed in the absence of $Ca(OH)_2$ and had no access to an external source of water could expand. (11). In his 1973 paper proposing the colloidal ettringite hypothesis, Mehta has shown that "a stoichiometric mixture of $C_4A_3\bar{S}$,$C\bar{S}H_2$, and quicklime ..... with more than enough water to form ettringite" could not expand significantly in the absence of extra water (5). Thus it is difficult to predict for a given case if ettringite will need $Ca(OH)_2$ and/or water to expand or not.

In spite of above confusion, the results of Mehta and Hu (25) deserve closer examination. In this work a stoichiometric mixture of $C_4A_2\bar{S}$, $C\bar{S}$, lime and water, to produce ettringite, was cast in a steel cylinder which was closed at the bottom. After about 1 hour, when the mix had set, a small plastic plate was placed on the top of the mix and a dial gage was brought in contact to measure the subsequent length change continuously.

The mix was allowed to hydrate for 7 days to complete ettringite formation during which time there was a volume decrease. After complete reaction, excess water was added to the top of the paste which then gradually expanded by about 54%. As the paste expanded so much it has to be assumed that most of the ettringite must have formed in the presence of $Ca(OH)_2$, in other words, for most of the time, the reaction condition was similar to mix No. J of ref. 3, which according to Mehta and Kline develop poor bonding property. Furthermore the observed 54% expansion itself is an indication of the poor bonding property of the mix. Present day dial gauges exert a spring load of about 100 g. As in the above experiment this 100 g load was distributed by the plastic plate over the paste surface, it may be inferred that the expansion occurred against a very low pressure. A force which causes an expansion in a low cohesive paste against a low pressure may not be able to expand a high cohesive paste i.e. the experiment has very little relevance to sulfate expansion. Another indication of this irrelevance is that colloidal ettringite can not cause any expansion in sulfate resistant Portland cement.

The irrelevance of the above type of experiments to sulfate expansion is best illustrated by the results of Collepardi et al (15). Using the above experimental technique these authors have shown that a C_3A-gypsum paste can expand even when no $Ca(OH)_2$ is present. Following Mehta and HU these authors have attributed the expansion to water adsorption by ettringite though they could detect hexagonal aluminate in their samples from 15 minutes onwords. If the force monitored by their experiment has any relevance to sulfate expansion then one would expect sulfate expansion in $Ca(OH)_2$ free cement like supersulfated cement, aluminous cement, pozzolana cement etc. Absence of sulfate expansion in any of the above cements illustrates how irrelevant this type of experiment is to sulfate expansion.

A prediction from monosulfate hypothesis:

In a subject as technological as sulfate expansion, a method of decreasing the sulfate expansion of a given ordinary Portland cement will be highly desirable. The monosulfate hypothesis suggests that the addition of finely ground $CaCO_3$ to ordinary Portland cement will decrease its sulfate expansion by decreasing monosulfate formation. This suggestion was found to be valid (26).

In conclusion it can be said that it is possible to set down evidence for this or that hypothesis but in the ultimate analysis ones prejudices determine which hypothesis one believes.

REFERENCES:

1. S. CHATTERJI and J.W. JEFFERY (1963), "A New Hypothesis of Sulfate Expansion" Mag. Concrete Res., 15, 83-86.

2. H. LAFUMA (1929), "Theory of the expansion of cements", Revue Mater. Constr., Trav. Publ., 243, 441.

3. P.K. MEHTA and A. KLEIN (1966), "Investigation on the Hydration Products in the System $4CaO \cdot 3Al_2O_3 \cdot SO_3$-$CaSO_4$-CaO-$H_2O$". Highway Res.Board Special Pub. No. 90, 328-352.

4. G.L. KALOUSEK and E.J. BENTON (1970), "Mechanism of Seawater Attack on Cement Pastes". J. Amer. Concrete Inst. Proc. 67, 187-192.

5. P.K. MEHTA (1973), "Mechanism of Expansion Associated with Ettringite Formation". Cement and Conc. Res. 3, 1-6.

6. H.S. MEISSNER (1950), Amer. Soc. Testing Materials Bull. No. 169, 39.

7. M. MATOUSEK and Z. SAUMAN (1974), "Contribution to the Hydration of Expansive Cement on the Basis of Metakaolinite", Cement and Conc. Res. 4, 113-122.

8. S. CHATTERJI (1974), "A Discussion of Ref. 7", Cement and Conc. Res. 4, 685.

9. P. SELIGMANN and N.R. GREENING (1964), "Studies of Early Hydration Reactions of Portland Cement by X-ray Diffraction", Portland Cement Assoc. Bull. No. 185.

10. P.K. MEHTA and G. LESNIKOFF (1973), "Hydration Characteristics and Properties of Shrinkage-Compensating Cements". Amer. Conc. Inst. Pub. SP-38, 89-105.

11. P.K. MEHTA (1967). "Expansion Characteristics of Calcium Sulfo-aluminate Hydrates", J. Amer. Ceram. Soc., 50, 204-208.

12. V.S. RAMACHANDRAN et al (1964), "Mechanism of hydration of calcium oxide", Nature, 201, 288-289.

13. P. GUPTA, S. CHATTERJI and J.W. JEFFERY (1970), "Studies of the effects of various additives on the hydration reaction of tricalcium aluminate. Part 1". Cement Tech. 1, 59-66.

14. H.E. SCHWIETE, U. LUDWIG and P. JäGER (1966), "Investigation in the System $3CaO \cdot Al_2O_3$-$CaSO_4$-CaO-H_2O". Highway Res. Board Special Pub. No. 90, 353-367.

15. M. COLLEPARDI et al (1978), "Tricalcium Aluminate Hydration in the Presence of Lime, Gypsum or Sodium Sulfate", Cement and Conc. Res. 8, 571.

16 S. CHATTERJI and J.W. JEFFERY (1963), "Studies of Early Stages of Paste Hydration of Different Types of Portland Cements", J. Amer. Ceram. Soc. 46, 268-273.

17. L. HELLER and M. BEN-JAIR (1968), "Effects of Sulfate Solutions on Normal and Sulfate Resisting Portland Cement". J. Appl. Chem. 14, 20-30.

18. S. CHATTERJI and J.W. JEFFERY (1971), "Further studies if the three-dimensional arrangement of hydration products of Portland cements", Indian Conc. J. 45, 167-172.

19. G.L. KALOUSEK and K.T. GREENE (1976), "Differential Thermal Analysis Tests of Hydrated Cements and Individual Hydrates". Transport. Res. Circular No. 176, 30-41.

20. G.L. KALOUSEK et al (1949), "An Investigation of Hydrating Cements and Related Solids by DTA". Proc. Amer. Conc. Inst. 45, 693-712.

21. E.J. BENTON (1959), "Cement-Pozzolan Reaction", Highway Res. Board Bull. 239, 56-65.

22. G.L. KALOUSEK and M. ADAMS (1951), "Hydration Products Formed in Cement Pastes at 25 to 175°C". Proc. Amer. Conc. Inst. 48, 77-90.

23. K. MATHER (1976), "Examination of Cement Pastes, Hydrated Phases and Synthetic Products by X-ray Diffraction". Transport Res. Circular No. 176, 9-30.

24. S. CHATTERJI and J.W. JEFFERY (1966), "Three-dimensional arrangement of hydration products in set cement pastes". Nature 209, 245-247.

25. P.K. MEHTA and F. HU (1978), "Further Evidence for Expansion of Ettringite by Water Adsorption". J. Amer. Ceram. Soc. 61, 179-181.

26. S. CHATTERJI and J.W. JEFFERY (1967), "Further evidence relating to the "New hypothesis of sulfate expansion"". Mag. Conc. Res. 19, 185-189.

RESUMES DE POSTERS

V. BABOUCHKIN, (Kharkov) et A. KOLOMATSKI, Institut Technologique, (Belgorod) - U.R.S.S.

"Thermodynamique de l'hydratation de C_3A et le rôle des hydrates d'aluminium dans les changements de volume de la pierre de ciment pendant le durcissement et la corrosion du sulfate".

Ayant précisé les données thermodynamiques pour les aluminates hydratés C_2AH_8, C_4AH_{13}, C_3AH_6 et pour les sulfo-aluminates hydratés de calcium C_3ACsH_{12}, C_3ACsH_{32}, on a fait des calculs thermodynamiques dans les systèmes C_3A-H_2O et C_3A-Cs-H_2O à la température normale et élevée.

On a établi les domaines de température de la stabilité thermodynamique des sulfoaluminates hydratés de calcium et on a démontré la possibilité de leur transformation réciproque selon les conditions de la réaction.

Dans le système C_3A-Cs-H_2O, on a analysé la préférence des réactions de formation des sulfoaluminates hydratés de calcium en différentes proportions quantitatives des constituants réactifs à l'intervalle des températures 298-398 °K.

On a examiné les conditions de la stabilité de la forme monosulfate du calcium pendant le durcissement et la corrosion du sulfate. On a montré le rôle de l'ettringite dans ce processus, y compris les changements de volume et la destruction.

N. BILANDA *, P. FIERENS *, N. TENOUTASSE ** et J. TIRLOCQ *, * Université de Mons, ** Université libre de Bruxelles - Belgique.

"Hydratation du C_3A dopé au sodium".

Les auteurs ont étudié quatre échantillons de C_3A dopés par différentes quantités de Na_2O. Le dosage a été réalisé en incorporant diverses teneurs de Na_2O aux matières premières avant la synthèse thermique de C_3A.

L'hydratation des échantillons a été suivie par les techniques ci-après : diffraction des R.X., microcalorimétrie isotherme, l'évolution de la concentration des ions de la phase aqueuse et analyse thermogravimétrique.

L'ensemble des résultats permet de constater qu'en absence de gypse, les échantillons dopés sont d'autant moins réactifs que la teneur en Na_2O est plus élevée.

Par contre, la présence de gypse inverse cette séquence.

Notons encore la disparition quasi instantanée du gypse lors de l'hydratation des échantillons dopés.

Ces résultats ont conduit les auteurs à proposer une interprétation originale sur le rôle des ions contrôlant la cinétique de l'hydratation du C_3A en présence de gypse.

M. CONJEAUD, Lafarge, (Trappes) - France.

"Processus d'attaque des ciments portland hydratés par le sulfate de magnésium".

La résistance au sulfate de magnésium de cinq CPA industriels et d'un C_3S synthétique a été testée sur mortier 1/3 à des échéances allant jusqu'à 3 ans. La concentration de la solution agressive est 50 g/l $MgSO_4$, 7 H_2O, soit 1,6 % SO_3 dans la solution, et celle-ci est renouvelée tous les mois. L'analyse des phases formées et de la microstructure a été effectuée par diffraction X et microscopie à balayage. La stabilité des mortiers, comme celle des bétons, dépend de paramètres physiques et chimiques. La compacité et la perméabilité jouent un rôle considérable imbriqué à celui des paramètres chimiques. Le processus d'attaque chimique des mortiers et bétons par $MgSO_4$ passe par la formation bien connue d'ettringite à partir du C_3A résiduel, avec augmentation de volume consécutive. Mais il est mis en évidence que cette ettringite se décompose ensuite rapidement (ce qui s'explique, d'après LEA, par l'instabilité de l'ettringite en présence de $MgSO_4$) en chaux, alumine et gypse avec libération d'eau et création de porosité. D'où une première accélération du processus d'attaque. Puis, on observe la décomposition du C-S-H qui réagit avec la chaux, l'alumine et le gypse, pour former de la "Si-ettringite" gonflante en quantité très importante, et la dégradation du béton devient complète. Dans un tel processus, le C_3A joue un rôle initiateur, d'où son importance.

Mais il faut noter que tous ces résultats ne doivent être extrapolés à d'autres milieux, même contenant $MgSO_4$ comme l'eau de mer, qu'avec beaucoup de précautions, car d'autres phénomènes entrent en jeu ainsi que l'ont montré d'autres études que nous avons faites.

S. DIAMOND, Purdue University, (Lafayette) - U.S.A.

"Hydration reactions of C_3A and anhydrite present within a high-calcium flyash".

A high CaO - content flyash having C_3A, free CaO and $CaSO_4$ as soluble components was found to set hydraulically in pastes consisting only of flyash and water. SEM micrographs displayed show rapid development of ettringite supplemented by calcium monosulfoaluminate bridging between individual flyash spheres to produce a rigid structure. Some C-S-H gel is produced at later ages.

H. HORNAIN, B. MORTUREUX, M. REGOURD, C.E.R.I.L.H., (Paris) - France.

"Formation de silicoaluminates dans des mélanges gypsés C_3A + C_3A et C_2S + C_3A".

La formation de silicoaluminates de calcium dans des mélanges synthétiques gypsés C_3A + C_3S et C_3A + C_2S a été mise en évidence par analyse à la microsonde électronique de Castaing et observation au microscope électronique à balayage. Cette formation est due à une diffusion importante d'ions silicates à partir des grains de C_3S ou C_2S vers les grains de C_3A. Au début de la réaction, la diffusion de la silice se manifeste déjà par la présence de silicium dans la couche d'attringite qui se forme initialement autour des grains de C_3A. Cette diffusion devient ensuite prépondérante et se traduit par la formation d'abord de trisilicoaluminate $C_6AS_3H_{31}$, puis de monosilicoaluminate C_3ASH_{12}, par pseudomorphose des grains de C_3A.

B. MORTUREUX, H. HORNAIN, M. REGOURD, C.E.R.I.L.H., (Paris) - France.

"C_3A dans les clinkers industriels".

L'aluminate tricalcique de 30 ciments portland industriels a été analysé par diffraction des rayons X, microscopie optique et microsonde électronique. Les formes cristallines cubiques et orthorhombiques sont les plus fréquentes, elles coexistent souvent. Une forme monoclinique a été trouvée dans deux cas, elle est riche en alcalins, SiO_2 et Fe_2O_3.

La stabilisation de C_3A_C, C_3A_O ou C_3A_M dépend du taux d'alcalins mais aussi du taux de SO_3 du clinker.

B. MORTUREUX, H. HORNAIN, M. REGOURD, C.E.R.I.L.H., (Paris) - France.

"Comportement de pâtes C_3S + C_3A + gypse et de ciments portland dans les solutions sulfatées".

L'évolution de mélanges synthétiques C_3A + C_3S + gypse et de ciments portland à différentes teneurs en C_3A a été suivie par diffraction des rayons X et microscopie électronique à balayage. Les paramètres étudiés sont la forme cristalline de C_3A (cubique, orthorhombique), la composition élémentaire des grains de C_3A (teneur en Na_2O, K_2O, Fe_2O_3).

Les résultats montrent que la résistance aux eaux agressives des pâtes de ciment et des mortiers dépend avant tout de leur compacité. A brève échéance, C_3A cubique s'hydrate plus vite que C_3A orthorhombique et donne un matériau moins vulnérable si l'échantillon est immergé dans la solution agressive après un temps d'hydratation suffisamment long.

W. RICHARTZ, Forschungsinstitut der Zementindustrie, (Düsseldorf) - Federal Republic of Germany.

"Reactivity of C_3A and setting of cement".

Immediately after mixing the cement with water a reaction starts in which a small amount of the tricalcium aluminate C_3A and the calcium sulfate added as set-controlling agent take part. After approximately 10 to 15 minutes this initial reaction stops to restart again after a "dormant period" of several hours.

On principle, the pattern of this initial reaction is the same with all cements. In the first few minutes there are, however, differences in the amount of C_3A taking part in the reaction. The reason for this is the differing reactivity of the C_3A of the various portland cements. To achieve setting according to the standard, the supply of the sulfate must be adjusted to the reactivity of the C_3A at the start of the hydration. In this case the sole reaction product is ettringite which forms in a thin layer on the surface of the cement grains only. Too low a sulfate supply leads to the formation of monosulfate, too much sulfate to secondary gypsum. In both case the result is early setting, because monosulfate and gypsum crystallize as relatively large plates or laths in the pore space between the cement grains. The adjustment of the sulfate supply to the reactivity of the C_3A may be achieved by the use of a suitably proportioned mix of natural anhydrite $CaSO_4$ and gypsum $CaSO_4.2H_2O$. During the grinding process of the cement the gypsum should be dehydrated completely to hemihydrate $CaSO_4.1/2H_2O$ so that at the start of the hydration there is a suitable mix of anhydrite and hemihydrate.

N. TENOUTASSE, G. WAESSENS, L. VAN HELDEN, Université libre de Bruxelles - Belgique.

"Etude en ATD de l'hydratation de C_3A en présence de gypse".

N. TENOUTASSE, A.M. VOGELS, Université libre de Bruxelles - Belgique.

" Hydratation du mélange C_3S + C_3A en présence de gypse".

N. TENOUTASSE , A.M. VOGELS, Université libre de Bruxelles - Belgique.

"Action des sucres sur l'hydratation des différentes phases du ciment portland. (utilisation de sucres marqués au ^{14}C).

POSTER

A Progress report on analytical electron microscopy studies of the hydration of tricalcium aluminate

Rapport d'avancement sur les études par microscopie électronique analytique de l'hydratation d'aluminate tricalcique

J.E. BAILEY, Professor, Department of Metallurgy and Materials Technology,
University of Surrey - GUILDFORD SURREY,
D. CHESCOE, Great-Britain.

SUMMARY :

Analytical electron microscopy has proved a useful tool in the study of hydrating cement particles. Apart from morphology detail in both TEM and SEM, it is possible with this technique to obtain elemental analysis and diffraction from a single fibre.

In previous work on the hydration of OPC, several different fibre types were observed, of which, the most predominant designated type II, were hollow amorphous calcium aluminate sulphate hydrates.

To obtain a greater understanding of the hydration mechanism, tricalcium aluminate was hydrated with varying quantities of gypsum.

Examination in TEM of hydrated C_3A revealed the expected hexagonal hydrates. As the quantity of gypsum was increased, in addition to the hexagonal calcium aluminate hydrates, fibrous calcium aluminate sulphate hydrates were observed. With low concentration of gypsum, these CASH precipitates were remote from the C_3A particles, but as the concentration increased, so fibres emanating from a C_3A particle surface were observed. It was found, that although the elemental concentration of the remote and surface associated fibres were similar, those emanating from the C_3A were amorphous, this evidence increasing the understanding of the growth mechanism of these fibres.

RESUME :

La microscopie électronique analytique s'est révélée un outil pratique dans l'étude de l'hydratation des particules de ciment. A part le détail morphologique, il est possible d'obtenir avec le M.E.T. (Microscope Electronique à Transmission) et le M.E.B. (Microscopie Electronique à Balayage) l'analyse élémentaire et la diffraction d'une seule fibre.

Dans un travail précédent sur l'hydratation du ciment portland, plusieurs types de fibres ont été observés, le plus fréquent étant le type II, c'est-à-dire des hydrates de sulfo-aluminate de calcium creux et amorphes.

Pour mieux comprendre le mécanisme de l'hydratation, l'aluminate tricalcique a été hydraté avec différentes quantités de gypse.

L'examen au "M.E.T." du C_3A hydraté a révélé les hydrates hexagonaux attendus . Quand la quantité de gypse croît, on constate la présence, non seulement d'hydrates hexagonaux d'aluminate de calcium, mais aussi de sulfo-aluminates de calcium hydratés fibreux. A faible concentration de gypse, ces précipités de CASH se trouvent loin des particules de C_3A , mais à forte concentration des fibres émanant de la surface d'une particule de C_3A ont été observées. Bien que la concentration élémentaire des fibres éloignées et superficielles soit la même, celles émanant du C_3A sont amorphes, cette évidence accroissant la compréhension du mécanisme de croissance de ces fibres.

1. INTRODUCTION

This paper is in the form of a brief report of some recent studies on the nature of the structure of the hydration products obtained from calcium aluminate in the presence of gypsum.

In a recent paper, a technique for examining directly the morphology, crystallinity and chemical composition of hydrated Portland cement was described, see Bailey and Chescoe (1). Three morphologically distinct fibrillar hydration products were observed to form at the surface of Portland cement particles. Perhaps surprisingly, two of these were found to be predominantly calcium aluminate sulphate compositions and were distinctly amorphous and one of these fibres referred to as type II was clearly tubular in form (1).

In this short report, some further observations on the hydration behaviour of calcium aluminate in the presence of gypsum are presented which demonstrate the validity of the technique and demonstrate the ability of the technique to distinguish between amorphous and crystalline products.

2. SPECIMEN PREPARATION AND EXPERIMENTAL TECHNIQUES

For this work tricalcium aluminate (C_3A) was prepared from calcium carbonate and Linde. A alumina and fired to 1400°C for several hours. The Portland cement used was an ordinary Portland cement (OPC), details given below :

	CaO	SiO_2	Al_2O_3	SO_3	Fe_2O_3	MgO	(Na_2O+K_2O)	Free Lime
OPC	63.90	19.70	7.00	3.00	2.10	1.3	0.77	1.3

Calculated (Bogue) percentage compounds:

	C_3S	C_2S	C_3A	C_4AF
OPC	46.5	21.4	15.0	6.4

Specimens for examination in the electron microscope were prepared by coating electron microscope grids with a formvar film. Droplets of the required cement/water mix were pipetted onto these grids which were positioned on a glass microscope slide and then contained by a coverslip after removal of air bubbles. The system was then sealed with a quick-setting epoxy resin. After hydration the seal was broken and the electron microscope grid transferred to a carbon coating vacuum unit and a thin layer of carbon deposited to stabilise the grid for electron microscopy. Specimens of C_3A and C_3A + gypsum were prepared in a similar manner except that for the latter, the materials were ground together before water was added. In all of these experiments the water/cement mix ratio was approximately 0.3.

All specimens were examined in a JEOL 200CX electron microscope. An operating voltage of 100kV was normally used and all specimens were examined in transmission electron microscopy for morphological and electron diffraction studies. In addition to TEM, specimens were always examined in SEM to check the region of interest was on the upper surface of the support film. If the hydration product was on the lower surface, the elemental ratio could be distorted due to absorption of x-rays within the support film. X-ray microanalysis was always performed at low beam current to minimise beam damage to the specimen. It was found, that although the counting statistics were obviously improved at higher beam currents, there was migration of elements along the fibre and the fibre was damaged.

3. RESULTS

A striking example of the fibrillar hydration products observed in Portland cement is shown in Figure 1. The prominent large fibres which have extruded reaction products at their ends are the hollow type II, reported previously (1).

FIGURE 1: OPC Hydrated for 24 Hours

An elemental analysis of the fibres themselves show that they are predominantly calcium aluminate sulphate in composition and the extruded product contains largely calcium, see table 1. Selected area electron diffraction from these areas give only very diffuse rings, indicating an amorphous nature.

In order to investigate further the origin of these tubular growths, a study has been initiated of the hydration of tricalcium aluminate and the effect of gypsum and lime on its hydration behaviour. The hydration products obtained for C_3A are shown in Figure 2. Hexagonal platelets and related structures are observed dispersed randomly and not specifically related to any interface i.e. C_3A surface. Furthermore, the precipitates are crystalline. X-ray microanalysis of these precipitates gives an average Ca/Al ratio of $\sim$ 3 (see table 1).

Table 1

TYPE OF HYDRATE	ELEMENTAL RATIOS $Ca/_{S}$	$Ca/_{Al}$	
$C\bar{A}SH$ in OPC	2.58±0.95	2.59±0.65	
EXTRUSION PRODUCT IN OPC	22.2	24.6	*Typical value
CAH in C_3A		3.19±0.59	
$C\bar{A}SH$ in $C_3A/C\bar{S}$	1.97±0.82	2.84±1.21	

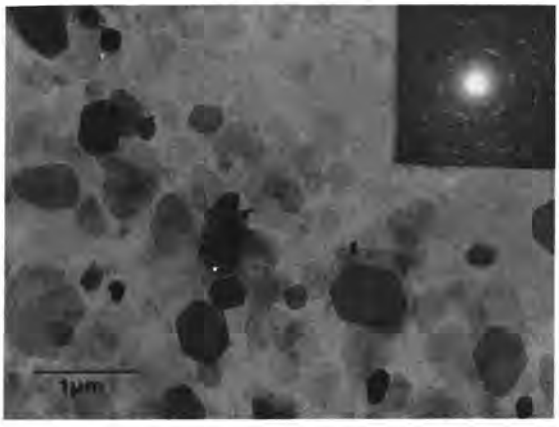

FIGURE 2: C_3A Hydrated for 30 Hours

When C_3A is hydrated in the presence of small amounts of gypsum i.e. a molar ratio of 1.5, two types of precipitate are observed remote from the C_3A interface. The two forms of precipitate can be seen in Figure 3. The precipitates at A crystalline calcium aluminate hydrates as confirmed by elemental analysis (see table 1) and electron diffraction. The precipitates at B were found to be calcium aluminate sulphate and electron diffraction showed them to be crystalline. Figure 4 shows the result of increasing the gypsum content further, the molar ratio being 1. In this case two forms of calcium aluminate sulphate were observed. The interfacial fibrous growths at C were shown to be similar in composition to the type II fibres observed in ordinary Portland cement (OPC). Electron diffraction confirmed that these fibres were amorphous in nature. Once again, the fibres remote from the interface were found to be crystalline and of approximately ettringite composition.

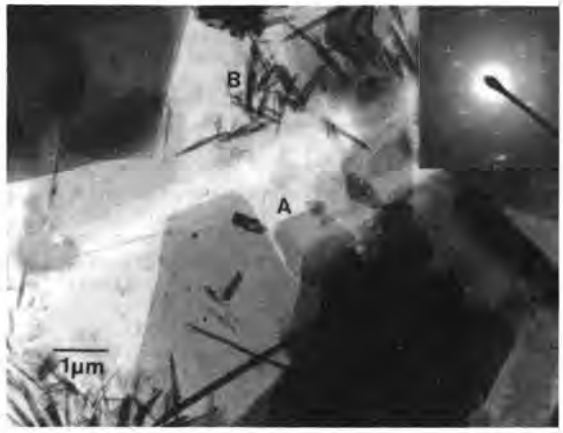

FIGURE 3: $C_3A/C\bar{S}$ = 1.5 Hydrated for 43 Hours

FIGURE 4: $C_3A/C\bar{S}$ = 1 Hydrated for 3¼ Hours

4. DISCUSSION

As reported previously,(1) the observation of amorphous tubular filaments of calcium aluminate sulphate composition in Portland cement leads to the suggestion that amorphous films of $C\bar{A}SH$ form at C_3A surfaces and that these are ruptured by osmotic swelling to produce the tubular filaments. Lea (2), when reviewing explanations of the effects of gypsum on the set of Portland cement suggested such a mechanism by analogy with Power's (3) osmotic pressure model for calcium silicate hydration although in neither case was the formation of tubular filaments proposed. The attractiveness of the membrane precipitation/osmosis model has recently been emphasised by Birchall, Howard and Double (4) and the lack of direct evidence of crystalline ettringite at the C_3A surface does not favour models based on the rupturing of crystalline platelets at that surface and indeed these latter theories do not explain the tubular fibrous growths observed. Skalny and Young (5) in their review of C_3A hydration come to somewhat similar conclusions, commenting that the

evidence indicates that after initial hydrolysis, a CASH gel forms which causes retardation. The osmosis model merely suggests that the gel is ruptured by osmotic pressure to form the observed tubular filaments and possibly other crumpled shapes although direct evidence of the latter have not been observed to date.

In order to study the reactions between C_3A and $\bar{C}S$ we are examining more closely the nature of the precipitated hydration products. As seen in Figure 2, the transmission electron micrographs of hydrated C_3A show an abundance of precipitates remote from C_3A surfaces, favouring a "through solution" precipitation mechanism. There is no evidence in these studies to date of nucleation of aluminate hydrates at a C_3A surface but combined transmission and scanning electron microscopy may provide further information. The elemental analysis was carried out on an area containing a number of individual precipitates and the observed calcium/aluminium ratio of 3 is an average. These precipitates appear hexagonal in nature and the average may result from the presence of the two hexagonal hydrates referred to in the literature, i.e. C_4AH_{13} and C_2AH_8. Further work will be required to determine whether this interpretation is correct or whether in fact conversion to C_3AH_6 has occurred.

At $C_3A/\bar{C}S$ molar ratios of 1.5 which may be comparable to those found in Portland cement, both crystalline calcium aluminate hydrates and crystalline calcium aluminate sulphate hydrates have been observed remote from C_3A surfaces, see Figure 3. It seems reasonable to conclude that in this case also the crystalline calcium aluminate sulphate precipitates have resulted from a "through solution" precipitation mechanism but clearly more detailed work is required.

A small increase in gypsum content, i.e. $C_3A/\bar{C}S = 1$ leads to the observation of two types of calcium aluminate sulphate precipitates suggesting a change in precipitation mechanism and the interesting observation of the simultaneous precipitation of both the amorphous and crystalline CASH compositions, one interfacial and one apparently precipitated from solution, would suggest competing mechanisms.

One important conclusion from these observations is that the analytical electron microscopy technique is able to quite clearly distinguish between amorphous and crystalline forms of these aluminate sulphate hydrates and we have independently demonstrated this by preparing crystalline ettringite by adding calcium sulphate to a solution of sodium aluminate. When examined in the electron microscope this material was crystalline. These observations will be reported elsewhere. It is premature to speculate in detail on the chemical reactions and processes involved until more detailed observations have been made but it would seem from these earlier results that competing mechanisms may be operating in determining the structure and form of the resulting calcium aluminate sulphate hydrates.

5. CONCLUSIONS

It is concluded from these preliminary results that :

(1) The analytical electron microscopy of samples hydrated "in situ" on electron microscope grids is capable of revealing detailed information on the elemental composition, structure and form of the precipitating hydrates in these hydraulic cements.

(2) In Portland cements an amorphous form of calcium aluminate sulphate hydrate precipitates at C_3A surfaces and in part this is tubular in form providing strong support for membrane precipitation/osmosis models of hydration.

(3) The experiments reported on C_3A hydration in the presence of calcium sulphate clearly show that two forms of CASH are observed; one crystalline and one amorphous, which leads to the view that there may be competing mechanisms i.e. membrane precipitation vs "through solution" precipitation, depending upon the chemical and environmental conditions.

(4) The observations on C_3A hydration may explain why both amorphous and crystalline ettringite have been observed in Portland cement.

REFERENCES

1. J.E. Bailey and D. Chescoe (1979) "Microstructure Development during the hydration of Portland cement", Proc. Brit. Ceram. Soc. No. 28, 165-177, Special Edition Conf. Mineralogy of Ceramics, Eds Taylor and Rogers.

2. F.M. Lea (1976) "Chemistry of Cement and Concrete", 3rd Edition p 308.

3. T.C. Powers (1961) "Some physical aspects of the hydration of Portland cement", J. Res. Dev. Labs. Portland Cem. Ass. 3(1), 47.

4. J.D. Birchall, A.J.Howard and D.D. Double (1980) "Some general considerations of a membrane/osmosis model for Portland cement hydration", Cem. Concr. Res., 10, p 145.

5. J. Skalny and J.F. Young (1980) "Mechanism of Portland cement hydration", Int. Cong. on the Chem. of Cem. Vol 1, Principal report II-1.

POSTER

Fibrous growth products in the hydration of portland cement and related systems

Produits de croissance en fibres dans l'hydratation du ciment portland et des systèmes correspondants

A. GHOSE, H.M. JENNINGS, P.L. PRATT and P. BARNES - London, England.

ABSTRACT :

Microscopic observations of hollow fibres in cement hydration lends credence to the idea of osmotic driving forces being responsible for such growths. However, the present results indicate that these fibrous growths are intimately associated with the hydration of the aluminate phases rather than the silicates whose hydration mechanism is different.

RESUME :

Les observations microscopiques de fibres creuses, dans l'hydratation du ciment, confortent l'idée des forces de pression osmotique responsables de telles croissances. Cependant, les résultats présents indiquent que ces croissances en fibres sont intimement associées à l'hydratation des phases aluminates plutôt que des silicates dont le mécanisme d'hydratation est différent.

FIBROUS GROWTH PRODUCTS IN THE HYDRATION OF PORTLAND CEMENT AND RELATED SYSTEMS

A. Ghose, H.M. Jennings and P.L. Pratt,

Department of Metallurgy and Materials Science, Imperial College, London, SW7, England

and

P. Barnes,

Department of Crystallography, Birkbeck College, London, WC1, England.

The observation of hollow tubular growths in cement pastes by Double et al (1) has aroused much interest recently. In their work, hydration was studied "in situ" in a wet cell of a high voltage (1 MeV) microscope using a very high water to cement ratio (about 10:1) though tubular growths have also been observed (2-4) in more realistic cement pastes. A "reverse silica garden" osmotic pump model has been envisaged by Double et al (1) to account for such tubular growths.

The present note reports on the electron-optical investigations of three systems - ordinary Portland cement (O.P.C.), synthetic C_3S and synthetic C_3A in presence of gypsum - undertaken in an effort to pinpointing the origin of hollow cement tubes. The results are summarised below:

1. O.P.C.

Hydration in this system (w/c between 0.5 to 0.7) points to the presence of both hollow and solid fibres (Figures 1-2) after about 4 hours. Many of the hollow fibres exhibited evidence of a past or present internal liquid meniscus (or multiple menisci on occasions - Figure 2) with liquid turbulence being induced inside on concentration of the electron beam. The skeletal morphology of some of the fibres in Figure 1 is a result of beam and vacuum damage in the TEM. Microanalysis of these fibres (both solid and hollow) revealed the presence chiefly of Ca, Al and S in variable proportions with K, Si and Fe being occasionally present (Table 1). These fibres thus appear to be far closer in composition to AFt rather than C-S-H as required by the "reverse silica garden" model. Outgrowths of C-S-H were however observed with a crumpled foil morphology (Figure 3) which in places rolled up to give the appearance of fibrillar growths. The more squat and solid rod-like growths in this micrograph are AFt and they appear like fibre bundles.

2. Synthetic C_3S

Hollow tubular growths have never been seen in this system in our observations. C-S-H fibrillar growths have been observed as with O.P.C. but they do not appear to be hollow (Figure 4). Microanalysis revealed the presence of Ca and Si only in widely varying proportions (Table 1).

Figure 1

Figure 2
TEM micrographs of O.P.C. hydrated for 1 day at w/c 0.6 illustrating both hollow and solid fibrillar AFt growths.

Figure 3. TEM micrograph of O.P.C. hydrated for 5 days at w/c 0.5 illustrating AFt and C-S-H growths.

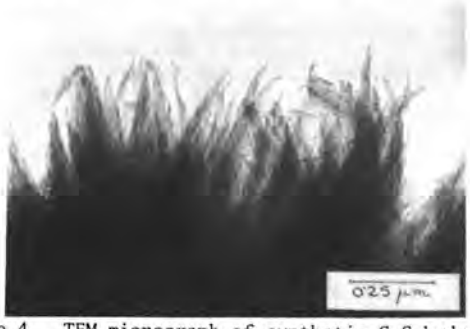

Figure 4. TEM micrograph of synthetic C_3S hydrated for 1 day at w/c 0.6 illustrating the crumpled foil-fibrillar C-S-H morphology.

3. Synthetic C_3A + 20% Gypsum

Hollow and solid fibres (composition close to AFt as revealed by microanalysis - Table 1) were visible in this system after 15 minutes of hydration (Figures 5 and 6). These fibres are morphologically similar to those observed in the hydration of O.P.C.

Our results thus indicate that hollow fibrillar growths is intimately associated with the hydration of the aluminate phase (in conjunction with gypsum) rather than with the silicates as required by the "reverse silica garden" model and that the hydration mechanism of the silicates in fact differs from this. However the concept of osmotic driving forces being responsible for hollow tubular growths appears to account for the presence of hollow AFt fibres. The presence of both hollow and solid AFt fibres is indicative of a combined "through solution" and "topochemical" growth (5), with a topochemically formed layer of ettringite on the aluminate grains possibly acting as the semi-permeable membrane in the osmotic growths.

REFERENCES

1. Double, D.D., Hellawell, A. and Perry, S.J., Proc. Roy. Soc. Lond., A359, 435-451 (1978).
2. Birchall, J.D., Howard, A.J. and Bailey, J.E., Proc. Roy. Soc. Lond., A360, 445-453 (1978).
3. Jennings, H.M. and Pratt, P.L., Proc. Brit. Ceram. Soc., 28, 179-193 (1979)
4. Bailey, J.E. and Chescoe, D., Proc. Brit. Ceram. Soc., 28, 165-177 (1979).
5. Ghose, A., Ph.D. Thesis, University of London, 1980.

Figure 5

Figure 6
TEM micrographs of synthetic C_3A (+20% gypsum) hydrated for 15 minutes at w/c 0.6 showing the presence of both hollow and solid AFt fibres.

Table 1

TEM-Microanalysis results on various hydration products

Specimen	Hydration Conditions (hydration period water:cement ratio)	Growth Product (designated by morphology and composition)	Composition Range					
			Ca	S	Al	Si	K	Fe
OPC	4→24 hrs, w/c 0.5→0.7	C-S-H fibres	6	0→ 0.9	0→ 1.2	0.7→ 5.7	-	-
	4→24 hrs, w/c 0.5→0.7	solid AFt fibres	6	1.0→10.0	1.0→18.4	0→ 7.7	0→4.4	0→0.6
	4→24 hrs, w/c 0.5→0.7	hollow AFt fibres	6	0.9→ 8.3	1.2→21.1	0→ 5.9	0→4.4	0→0.6
C_3S	24 hrs, w/c 0.5→0.7	C-S-H fibres	6	-	-	2.8→48.5	-	-
C_3A + gypsum	1/4 hr, w/c 0.5→0.7	solid AFt fibres	6	3.2→ 5.1	2.5→ 4.0	-	-	-
	1/4→4 hrs, w/c 0.7	hollow AFt fibres	6	1.5→ 7.4	1.1→ 4.3	-	-	-
	4 hrs, w/c 0.7	platey monosulphate	6	0.4→ 2.0	1.9→ 2.7	-	-	-

The ranges of atomic composition quoted are overall ranges for each atomic species and normalised to 6 Ca atoms.
Details concerning specific compositions are given elsewhere (5).

POSTER

Possibility of a catalytic role of C_3A in the hardening of portland cements

Possibilité d'un rôle catalytique de C_3A dans le durcissement des ciments portland

Sandor POPOVICS, Professor, Department of Civil Engineering,
Drexel University, Philadelphia, Pennsylvania 19104 U.S.A.

SUMMARY :

This paper demonstrates that there is an interaction between the calcium silicates and the C_3A in portland cements. It also shows that the effect of C_3A on the strength development of portland cement mortars and concretes can be calculated as if the C_3A acted as catalyst on the calcium silicates. Finally, a quantitative form is proved for the fact widely known in the qualitative form that high C_3A content accelerates the strength development at early ages but hinders it later.

RESUME :

Cet article démontre qu'il y a une interaction entre les silicates de calcium et le C_3A dans les ciments portland. Il montre aussi que l'effet de C_3A sur le développement des résistances des mortiers et bétons peut être calculé comme si C_3A jouait le rôle d'un catalyseur sur les silicates de calcium. Enfin, une forme quantitative est donnée à la forme qualitative bien connue d'après laquelle une haute teneur en C_3A accélère le développement de la résistance aux brèves échéances mais le gêne plus tard.

Is There Interaction Between the Calcium Silicates and C_3A?

When the first attempts were made for the development of a numerical relationship between the strength development of a portland cement and its compound composition (1)-(3), it was a natural assumption that the main constituents contribute their intrinsic strengths without any interaction between each other. This means mathematically that the pertinent formulas are linear creating a linear cement model. It has become obvious later, however, that experimental data do not support adequately either the original linear cement model or its linear modifications, as discussed in details elsewhere in the Proceedings of this Congress. (4) For instance, Figure 1 shows that the effect of the C_3A content on the strength development in a portland cement mortar is much stronger than proportional. Furthermore, Figure 2 demonstrates that the effect of the C_3A content on the ultimate compressive strength, that is, on the strength obtained after very long wet curing, depends also on the C_3S content. This is again a clear indication of an interaction between these two compounds. In addition, an increasing amount of other evidence has been reported that the hydration processes of the calcium silicates are interacted by the C_3A. (9)-(17)

In the light of all this unambiguous evidence, this writer believes that the real question is not any more whether there is interaction between the calcium silicates and aluminate but rather (a) what is the nature of this interaction; and (b) how can one estimate quantitatively the effect of this interaction on the strength development of a portland cement. One would expect that research would answer first the (a) portion of this question and then develop a method for the estimation of its effect; however, it did not happen in this order. While there is no generally accepted view yet concerning the nature of interaction between the calcium silicates and C_3A, the effect of C_3A on the strength development of portland cement, essentially calcium silicates, can be calculated quite well with the exponential cement model.

The Exponential Cement Model

The exponential cement model, probably the first non-linear cement model for the representation of hardening, was introduced in 1967. (5) (6) The mathematical form of this model provides a relationship between the strength developing capability of a portland cement and its simplified compound composition, as follows:

$$f_{rel} = 100\,\frac{1 - pe^{-a_1 t} - (1-p)e^{-a_2 t}}{1 - pe^{-28a_1} - (1-p)e^{-28a_2}} \qquad 1)$$

where

f_{rel} = relative strength of portland cement paste, mortar, or concrete, percent of the 28-day strength,

t = age of the specimen at testing, days,

p = computed C_3S content of the portland cement, percent/100,

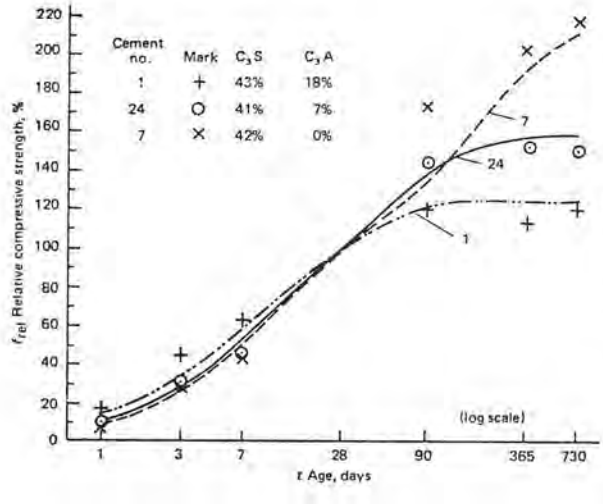

Figure 1 Comparison of experimental and computed values to illustrate the effect of C_3A content on the kinetics of the hardening of portland cement in 1:2.75 mortars. Experimental values are represented by points, and values calculated by Eq. 1) with $a_1 = 0.0067C_3A + 0.10$ and $a_2 = 0.0018C_3A + 0.005$, by lines (5) (6)

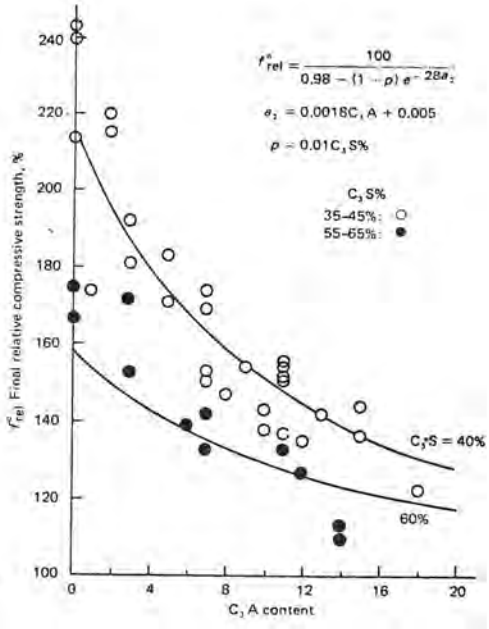

Figure 2 Final relative compressive strength of portland cements in mortars as a function of the compound composition (7) (8)

a_1 and a_2 = rate parameters of the two hardening components which are independent of the strength, age, and C_3S content, but may be a function of the C_3A content, and any other factor that influences the course of hydration (fineness, gypsum content, admixtures, water-cement ratio, temperature, curing and testing methods, etc.), 1/day.

Equation 1) was obtained from the following conditions:

(a) The model consists only of two hardening components; the first component is the C_3S, the second component is a mixture of the other cement ingredients, mainly C_2S.

(b) These two components hydrate simultaneously as first order reactions with differing rates but without any interaction with each other.

(c) The final strength developed by C_3S is the same as the final strength of the second component.

The proportionality factors, which are the $\underline{a}$ parameters in Equation 1), represent the specific rates of hardening, that is, (rate of hardening)/(remaining strength at a given age). The squares of these parameters represent specific decelerations of hardening. The more intensive the early hardening process, the greater is the value of a_1; and the longer and larger is the hardening after 28 days, the smaller becomes the value of a_2 up to a certain limit.

For the sake of simplicity, the model does not take into consideration directly the effect of diffusion on the strength development.

Numerically, the $\underline{a}$ parameters can be obtained by applying a suitable statistical method to pertinent experimental data. For instance, by applying Equation 1) to the previously mentioned test results by Gonnerman (3), the following a_1 and a_2 values were obtained for the compressive strength of 1:2.75 Ottawa sand mortars with wet curing:

$$a_1 = 0.0067C_3A + 0.10 \qquad 2)$$

and

$$a_2 = 0.0018C_3A + 0.005 \qquad 3)$$

where C_3A represents the percent of the potential tricalcium aluminate in the portland cement computed according to the Bogue method.

The application of the presented formulas will be illustrated below.

Example

The compositions of three of Gonnerman's cements are shown in Figure 1. The computed C_3S contents of all three cements are practically the same but the C_3A contents differ.

Illustrate the effect of C_3A content on the relative strength development at various ages by using Eq. 1) along with Eqs. 2) and 3).

The $\underline{a}$ parameters of cement No. 24 are calculated by Equations 2) and 3):

$$a_1 = 0.14 \qquad \text{and} \qquad a_2 = 0.018$$

By substituting these values into Eq. 1) the following is obtained:

$$f_{rel,24} = 100\,\frac{1 - 0.41e^{-0.14t} - 0.59e^{-0.018t}}{1 - 0.41e^{-3.92} - 0.59e^{-0.50}} =$$

$$= 100(1.58 - 0.65e^{-0.14t} - 0.93e^{-0.018t}),$$

Similarly, the equations of the curves for relative compressive strength versus age for the cements Nos. 1 and 7, respectively, are

$$f_{rel,1} = 100\,(1.25 - 0.54e^{-0.22t} - 0.71e^{-0.037t}),$$

and

$$f_{rel,7} = 100\,(2.12 - 0.89e^{-0.10t} - 1.23e^{-0.005t})$$

A group of values calculated by these formulas are presented in Figure 1 by lines along with observed results by points from Gonnerman's experiments.

Note that (a) the a_1 and a_2 values of these three cements are affected strongly by the C_3A content in these formulas; and (b) the fit in Figure 1 between experimental and calculated strengths is good, that is, the exponential model reflects the non-linear effect of C_3A on the strength development quite accurately from the age of one day to two years.

Equation 1) can also be used for the estimation of the ultimate strength, that is, the strength obtained after very long wet curing, expressed as a percentage of the 28-day strength. This equation takes on the following form for great $\underline{t}$ values (7) (18):

$$f^{\circ}_{rel} = \frac{100}{1 - pe^{-28a_1} - (1 - p)e^{-28a_2}} \approx \qquad 4)$$

$$\approx \frac{100}{0.98 - (1 - p)e^{-28a_2}} \qquad 5)$$

where f°_{rel} = relative ultimate strength, percent of the 28-day strength. The other symbols are the same as the symbols of Eq. 1).

As another numerical illustration for the reliability of the exponential model, Figure 2 presents also the calculated relationship between the compound composition of portland cement and the relative ultimate compressive strength. Points represent experimental values reported by Gonnerman (3) for cements of approximately 40 and 60 percent C_3S contents, respectively, with constant (1.8%) SO_3 content, and the same fineness (1440 cm^2/g by air permeability). The lines designate

values that were calculated from Eq. 5) for 40 and 60 percent C_3S contents, respectively, with the a_2 value of Eq. 3). Considering the satisfactory goodness of fit in Figure 2, one may say that Eqs. 1) and 3) not only provide numerically the detrimental effect of the higher C_3A content on the ultimate strength but also show that this effect depends simultaneously on the C_3S content.

Incidentally, a cement model based on the dimensionless relative strength is more suitable for the exploration of the roles of the cement compounds in hardening than one based on actual strength, that is, strength expressed, say, in MPa. This is so because the interfering effects of factors other than the compound composition, such as the conditions of clinkering of the cement, cooling, etc. on the strength development are considerably reduced by the ratio-structure of the model. Note also that f_{rel} is what can be called the "age factor", that is, its product with the actual 28-day strength provides the strength at any t age.

It can be seen from the evidence presented here and elsewhere (5)(6)(19)(20) that the interaction between the calcium silicates and the C_3A is represented quite well numerically by the a factors as exponents in Eq. 1). Even more important, however, is that the formula reveals the nature of this interaction in the cement model, as shown below.

C_3A as Catalyst

As has been shown in Eqs. 2) and 3), the general forms obtained for the two a factors for Eq. 1) were found to be linear

$$a = k + m(C_3A) \qquad 6)$$

where

k and m = parameters which are independent of the strength, C_3S and C_3A contents, and age but may be a function of other factors that influence the strength and hydration,

C_3A = computed tricalcium aluminate content of the portland cement, percent.

In certain cases k or m can be negligibly small; but when m is greater than zero, that is, when the a factor contains the C_3A term, this means according to the theory of first-order reactions that the C_3A acts as a catalyst on the C_3S and/or on the second component of the portland cement model the majority of which is C_2S. In other words, the paste of this cement model hardens as if the C_3A acted on the calcium silicates as a catalyst. (21)

Experimental results discussed above support the applicability of the exponential model within wide limits, which is unlikely to have happened to such extent without a similarity between the hardening process represented by the model and the actual process. Therefore, it may be instructive to summarize what this cement model has to say about the role of C_3A in the hardening process of portland cement.

> The strength of a portland cement paste comes from the hardening of two, more or less, hypothetical components, namely the calculated C_3S, and the rest of the cement which is essentially C_2S.
>
> These two components hydrate simultaneously in the model as first-order reactions, the C_3A acting as catalyst on both components. This means that either the C_3A does act, in reality, as a catalyst on the calcium silicates during hydration, or that the complex role of C_3A, for instance the one advanced by Hansen (9), can be approximated statistically on the basis as if the C_3A acted as such a catalyst.
>
> Each component has a rate of hardening: a_1 for the C_3S and a_2 for the second component. These are predetermined by the C_3A content and fineness of the cement as well as by the composition of the strength specimen, and the curing and testing conditions.
>
> The values of a_1 for different portland cements are about seven to ten times higher than those for a_2 within the usual range of C_3A content.
>
> The squares of the a parameters represent the specific decelerations of hardening of the components, that is, (deceleration of hardening)/(remaining strength development), at a given age. (22) Consequently, the specific rate of hardening is a linear function, and the specific deceleration of hardening is a quadratic function of the C_3A content with a reasonable degree of approximation. In other words, an increase in the C_3A content increases the early strength through an increased specific rate of hardening, but, simultaneously, it increases the deceleration of the hardening quadratically, thus the final strength will be less.

Note that the possibility of fundamental similarities between the hypothetical hardening process of the exponential cement model and the actual hardening process of a portland cement can help cement chemists to aim their research at new, promising goals, such as to establish directly the role of C_3A in the cement hydration and hardening by focusing the investigation to its possible catalytic action.

Conclusion

On the basis of the available experimental evidence it is safe to say that there is interaction between the C_3A and the calcium silicates in a portland cement. The effect of this interaction on the strength development can be estimated by the exponential cement model. Whether the interaction is catalytic as in the model, or some other process the effect of which can be approximated by the assumption of catalytic action is still a question the answer for which is left for future research. In any case, the interaction casts doubts to efforts where experience obtained with the hydration or hardening of pure C_3S or C_2S is attempted to be transferred to portland cement.

References

1. Bates, P. H., and Klein, A. A., "Properties of the Calcium Silicates and Calcium Aluminate Occurring in Normal Portland Cement," Technologic Paper No. 78, National Bureau of Standards, June 9, 1917.

2. Woods, H., Starke, H. R., and Steinour, H. H., "Effect of Cement Composition on Mortar Strength," Engineering News Record, Vol. 109, No. 15, 1932, pp. 435-437.

3. Gonnerman, H. F., "Study of Cement Composition in Relation to Strength, Length Changes, Resistance to Sulfate Waters and to Freezing and Thawing of Mortars and Concrete," Proceedings ASTM, Vol. 34, Part II, 1934, pp. 244-295.

4. Popovics, S., "Calculation of Strength Development from the Compound Composition of Portland Cement," 7th International Congress on the Chemistry of Cement, Vol. III, Editions Septima, Paris, 1980, pp. VI. 47- VI. 51.

5. Popovics, S., "A Model for the Kinetics of the Hardening of Portland Cement," Highway Research Record No. 192, Highway Research Board, Washington, D.C., 1967, pp. 14-35.

6. Popovics, S., "Berechnung der Festigkeitsentwicklung von Morteln und Betonen unter Berucksichtigung der Klinkerphasen des verwendeten Portlandzementes," Referate, (Calculation of the Strength Development of Mortars and Concretes from the Compound Composition of the Portland Cement Used), Betonstein-Zeitung, Vol. 34, No. 11, November, 1968, pp. 587-590.

7. Popovics, S., Effect of Kinetics on the Ultimate Strength of Portland Cement Pastes, (Published in Russian), Beton i Zhelezobeton, Moscow, March, 1972, pp. 23-24.

8. Popovics, S., "Phenomenological Approach to the Role of C_3A in the Hardening of Portland Cement Pastes," Cement and Concrete Research, Vol. 6, No. 3, May, 1976, pp. 343-350.

9. Hansen, W. C., "Interactions of Organic Compounds in Portland Cement Pastes," Journal of Materials, Vol. 5, No. 4, December, 1970, pp. 842-855.

10. Kuhl, H., Zement-Chemie, Band III, Die Erhartung und die Verarbeitung der hydraulischen Bindemittel (Chemistry of Cement, Vol. III, The Hardening and Application of Hydraulic Cements), VEB Verlag Technik, Berlin, 1961.

11. Celani, A., Moggi, P. A., and Rio, A., "The Effect of Tricalcium Aluminate on the Hydration of Tricalcium Silicate and Portland Cement," Proceedings of the Fifth International Symposium on the Chemistry of Cement, Part II, Hydration of Cements, Tokyo, 1968, pp. 492-503.

12. Alexander, K. M., Taplin, J. H., and Wardlaw, J., "Correlation of Strength and Hydration with Composition of Portland Cement," Proceedings of the Fifth International Symposium on the Chemistry of Cement, Part III, Properties of Cement Paste and Concrete, Tokyo, December, 1969, pp. 152-166.

13. Alexander, K. M., "The Relationship Between Strength and the Composition and Fineness of Cement," Cement and Concrete Research, Vol. 2, No. 6, November, 1972, pp. 663-680.

14. Bobrov, B. S., "Mutual Influence of $3CaO-SiO_2$ and $4CaO-Al_2O_3-Fe_2O_3$ in Portland Cement Hydration," Supplementary Paper, II-2, The VI International Congress on the Chemistry of Cement, Moscow, September, 1974.

15. Copeland, L. E., and Kantro, D. L., "Hydration of Portland Cement," Proceedings of the Fifth International Symposium on the Chemistry of Cement, Part II, Hydration of Cements, Tokyo, 1968, pp. 387-421.

16. Verbeck, G., "Cement Hydration Reactions at Early Ages," Journal of the PCA Research and Development Laboratories, Vol. 7, No. 3, September, 1965.

17. Schramli, W., "An Attempt to Assess Beneficial and Detrimental Effects of Aluminate in the Cement on Concrete Performance," Parts 1 and 2, World Cement Technology, Vol. 9, Nos. 3 and 4, March and April, 1978, pp. 35-42 and 75-80.

18. Popovics, S., Concrete Making Materials, McGraw-Hill Book Company, New York, etc.and Hemisphere Publishing Corporation, Washington, etc.,1979.

19. Popovics, S., "Factors Affecting the Relationship Between Strength and Water-Cement Ratio," Materials, Research and Standards, MTRSA, Vol. 7, No. 12, December, 1967, pp. 527-534.

20. Popovics, S., "Comparison of Various Measurements Concerning the Kinetics of Hydration of Portland Cements," Proceedings of the Fifth International Symposium on the Chemistry of Cement, Part III, Properties of Cement Paste and Concrete, Tokyo, December, 1969, pp. 129-137.

21. Popovics, S., "Strength Development of Portland Cement Paste," The VI. International Congress on the Chemistry of Cement, Supplementary Paper, Section II, Moscow, September, 1974.

22. Popovics, S., "Examples for the Application of Mathematics in Concrete Technology," Reports, IV. International Congress on the Application of Mathematics in Engineering, Weimar, DDR. 1967, Vol. I, VEB Verlag fur Bauwesen, Berlin, 1968, pp. 375-382.

POSTER

Hydratation de l'aluminate tricalcique dopé à l'oxyde de sodium

Hydration of tricalcium aluminate doped by sodium oxide

N. BILANDA, P. FIERENS, J. TIRLOCQ, Université de Mons,
et N. TENOUTASSE, Université Libre de Bruxelles, Belgique.

RESUME : Des échantillons d'aluminate tricalcique pur et d'aluminates tricalciques dopés par Na_2O, à des teneurs variables, ont été synthétisés et caractérisés.
L'hydratation de ces échantillons a été suivie par les techniques ci-après : diffraction des RX, microcalorimétrie isotherme, analyse de la phase aqueuse et thermogravimétrie.
En absence de gypse la vitesse d'hydratation est de plus en plus réduite au fur et à mesure que la teneur en Na_2O augmente. Par contre, en présence de gypse une séquence inverse est observée.
Dès que la concentration en ions sodium s'élève dans la phase aqueuse, on assiste à la consommation quasi instantanée du gypse et à la formation simultanée de tous les composés hydratés.
Pour les échantillons fortement dopés, la production d'ettringite est inhibée par la carence en ions calcium.
Ces résultats montrent l'importance de la composition de la phase aqueuse sur la cinétique de l'hydratation de l'aluminate tricalcique dopé au Na_2O.

SUMMARY : Different samples of pure and Na_2O doped tricalcium aluminate have been synthetized and characterized.
Their hydration has been followed by several techniques : XR diffraction, isothermal microcalorimetry, aqueous phase analysis and thermogravimetry.
Hydration rate, without gypsum, decreases when Na_2O concentration increases. On the other hand, in hydration with gypsum, a reverse behaviour is observed.
When Na^+ ions amount increases in the aqueous phase, gypsum vanishes immediately and the different hydrates appear at the same time.
In the highest doped C_3A hydration, ettringite grow is inhibited because of a lack of calcium ions.
Our results show that the aqueous phase composition is an important factor which governs the rate of hydration of C_3A doped by Na_2O.

1. Introduction

Le présent travail a pour but d'examiner systématiquement l'effet du Na_2O sur l'hydratation de l'aluminate tricalcique ; dans le présent article, le sodium se trouve incorporé sous forme de solution solide dans l'aluminate tricalcique.

Des travaux antérieurs effectués par Regourd (1), Butt (2), Spiering (3), Boikova (4), Collepardi (5), et autres ne semblent pas aboutir à des conclusions unanimement acceptées quant à l'effet du sodium sur l'hydratation de l'aluminate tricalcique.

Dans cette étude, nous avons fait appel aux techniques ci-après :

- la Diffraction des RX, la Thermogravimétrie Différentielle (TGD), la Microcalorimétrie et l'analyse de la phase liquide par Absorption atomique et par Néphélométrie.

L'effet du Na_2O sera examiné, lors des hydratations, en eau pure ou après addition de gypse (20 % en poids de C_3A).

2. Résultats expérimentaux

2.1. Synthèse et caractérisation des produits anhydres.

La synthèse de l'aluminate tricalcique pur par la technique classique n'a pas posé de problème (6,7).

Par contre, celle des échantillons dopés à l'oxyde de sodium, sans formation de chaux libre en excès a été peu aisée, d'abord à cause de la volatilité de l'oxyde alcalin observée déjà à 650°C, ensuite à cause de la présence de traces de $C_{12}A_7$ résultant de l'hétérogénéité subséquente du système synthétisé (8).

Trois échantillons d'aluminate tricalcique dopés à l'oxyde de sodium ont été synthétisés à 1350°C avec des teneurs variables en Na_2O :

(I) 1,2 % ; (II) 4,6 % et (III) 5,8 %.

La teneur en sodium, après la synthèse, a été dosée par spectrométrie d'absorption atomique. La chaux libre a été mesurée par la méthode de Franke (9), et la surface spécifique de nos échantillons broyés, déterminée par la méthode de BET (10).

La surface spécifique du gypse, finement broyé, a également été mesurée et vaut 0,7 m^2/g.
La variété allotropique de chaque échantillon de C_3A a été déterminée par diffraction des RX au laboratoire du C.E.R.I.L.H. (M. Regourd).

Les caractéristiques des échantillons sont résumées au tableau suivant :

Tableau I : Caractéristiques des produits anhydres

Produits	%CaO libre	% Na_2O dans le réseau	Surface Spécif. m^2/g.	Variété allotropique
C_3A pur	0,30	0	0,30	Cubique
C_3A dopé I	0,13	1,2	0,24	Cubique
C_3A dopé II	0,15	4,6	0,41	Orthorhomb. I
C_3A dopé III	0,13	5,8	0,48	Orthorhomb.

2.2. Cinétique d'hydratation de C_3A sans gypse

L'effet du sodium sur l'hydratation de C_3A, dans l'eau distillée, a été suivi à 25°C avec un rapport Eau/Solide = 1, par TGD et par DRX. (Diffraction des RX) (6,7).

Dans tous les cas examinés, l'hydrate cubique (C_3AH_6) est présent dès la première minute d'hydratation et son pic de TGD qui apparaît aux environs de 300°C (11) croît en fonction du temps d'hydratation. Les hydrates hexagonaux instables, bien visibles dès le début de l'hydratation, disparaissent progressivement au cours des trois premières heures, dans le cas de l'hydratation du C_3A pur.
Mais, dans celui des échantillons dopés, la présence des hydrates hexagonaux est permanente et simultanée à celle de C_3AH_6 durant les périodes d'hydratation examinées.

De plus, nous avons observé que le spectre DRX du produit hydraté obtenu à partir du C_3A pur ne montre pas la présence de $Ca(OH)_2$, tandis que cet hydroxyde est toujours présent dans les hydrates des échantillons dopés dès les premiers instants d'hydratation.

A partir de la stoechiométrie de formation de C_3AH_6, on peut définir un degré d'avancement α de la réaction et dresser les courbes cinétiques reprises à la figure 1.

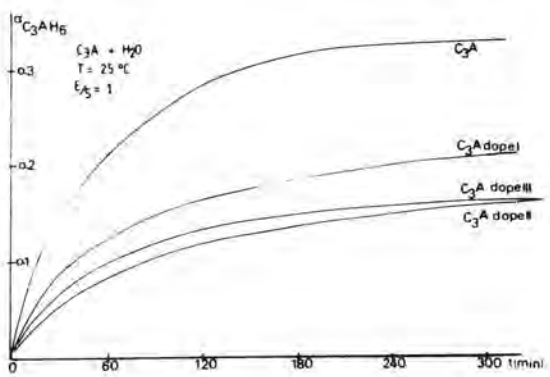

Fig. 1 - Cinétique d'hydratation de C_3A par TGD.

On constate que la cinétique d'hydratation de l'aluminate tricalcique décroît à mesure que la teneur en sodium incorporé dans le réseau augmente ; ce qui conduit à la séquence suivante (3) :

C_3A pur > C_3A dopé I > C_3A dopé II = C_3A dopé III.

Par DRX, nous avons suivi la décroissance de l'intensité de la raie principale à d = 2, 700 Å du C_3A en fonction du temps d'hydratation.

Des courbes cinétiques, représentées à la figure 2 ont été établies, dans chaque cas, grâce à une courbe d'étalonnage construite à partir de mélanges C_3A-C_3AH_6.
Le processus d'hydratation de nos systèmes obéit au modèle de mécanisme réactionnel par diffusion

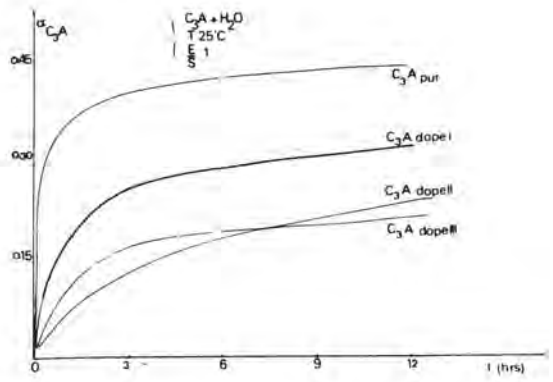

Fig. 2 - Cinétique d'hydratation de C_3A par DRX.

de Jander (12), qui répond à l'équation suivante :

$$D_3(\alpha) = (1 - \sqrt[3]{1-\alpha})^2 = kt$$

α = degré d'avancement de la réaction.
k = constante cinétique de la réaction.
t = temps d'hydratation.

Les graphiques sont illustrés à la figure 3 et les constantes cinétiques au tableau II.

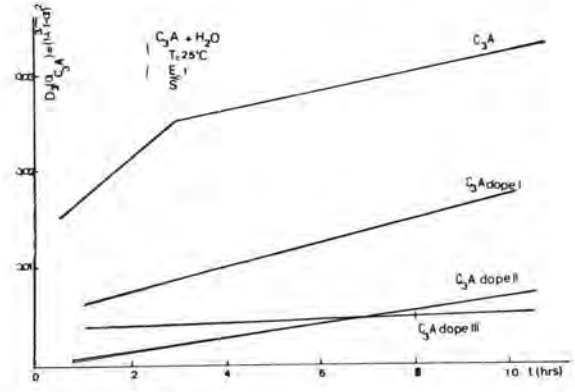

Fig. 3 - Modèle cinétique.

Tableau II : Constantes cinétiques				
Réaction d'hydratation de :	C_3A pur	C_3A dopé I	C_3A dopé II	C_3A dopé III
Constante cinétique (min^{-1})	$6,5.10^{-5}$	$1,8.10^{-5}$	1.10^{-5}	$3,6.10^{-6}$

Au bout de quelques minutes d'hydratation, tous les échantillons obéissent à la loi de diffusion de Jander (12).
De plus, le C_3A pur plus réactif, atteint rapidement un degré d'avancement tel qu'il apparaît une diminution de la constante cinétique ; les échantillons dopés ne présentent pas cette particularité pendant la période d'hydratation étudiée.

D'après Spiering et Breval, la présence de la soude dans le milieu réactionnel favoriserait la formation d'un double hydroxyde alumino-calcique (3) et d'un gel amorphe (13) qui emprisonnerait la solution périphérique dans une enveloppe pseudo-imperméable, dont la consistance croîtrait en fonction de la teneur en soude du milieu.

2.3. Cinétique d'hydratation des C_3A en présence de gypse

L'hydratation de l'aluminate tricalcique pur et dopé, en présence de gypse, a été suivie par microcalorimétrie à conduction, à 25°C, avec un rapport Eau/Solide = 2.

Une étude parallèle de l'hydratation a été réalisée en discontinu, par filtration de la phase liquide après différents temps d'hydratation.

En microcalorimétrie, l'hydratation de C_3A avec 20 % de gypse a donné le résultat classique qui consiste en deux phénomènes exothermiques dont l'un se situe dans les deux premières minutes et l'autre après 30 heures (14,15,16,17).

Par contre, l'hydratation des phases dopées en présence du gypse subit une importante accélération du déroulement des différentes étapes calorimétriques. En effet, l'intervalle de temps entre les émissions exothermiques se réduit très nettement jusqu'à disparaître pour les fortes teneurs en sodium. Les différentes courbes calorimétriques sont représentées à la figure 4.

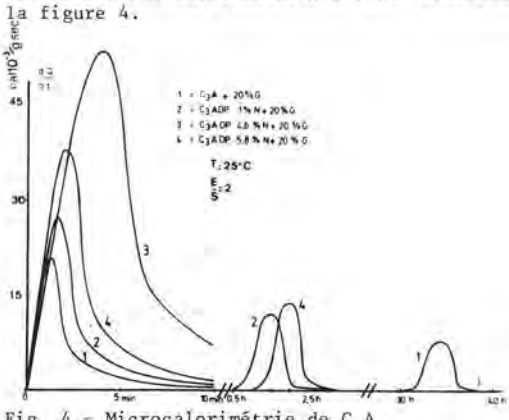

Fig. 4 - Microcalorimétrie de C_3A.

Au tableau III sont consignés les intervalles de temps observés pour chaque hydratation.

Tableau III : Intervalles de temps				
Réactifs	C_3A pur	C_3A dopé I	C_3A dopé II	C_3A dopé III
% Na_2O	0	1,2	4,6	5,8
Intervalle de temps entre les 2 pics calorim.	30 h.	1h30 min	0	2 h.

Lors des analyses de la phase aqueuse, les hydratations ont été arrêtées après différents temps correspondants aux changements d'allure des courbes calorimétriques.

Les éléments Ca, Na, Al de la phase liquide ont été dosés par absorption atomique, les ions sulfates $SO_4^=$ par néphélométrie. Les résultats obtenus sont portés en graphique dans les figures 5, 6, 7 et 8.

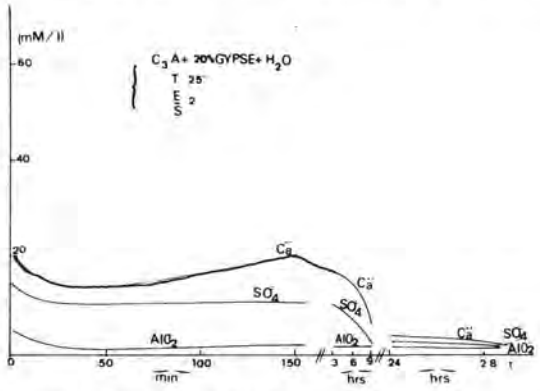

Fig. 5 - Analyse de la phase aqueuse.

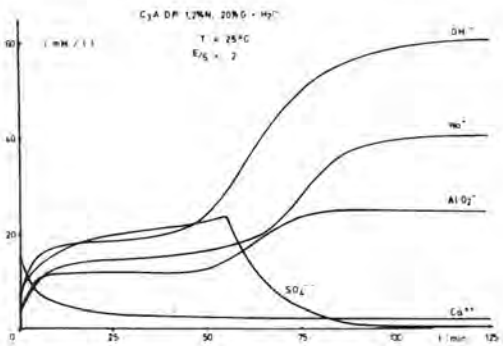

Fig. 6 - Analyse de la phase aqueuse.

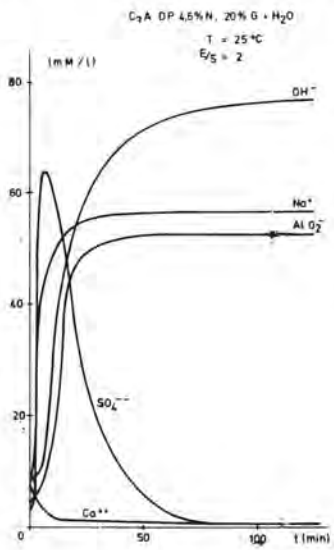

Fig. 7 : Analyse de la phase aqueuse.

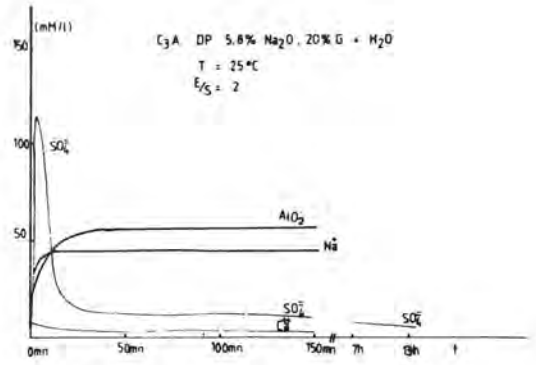

Fig. 8 - Analyse de la phase aqueuse.

Le résidu solide de la filtration, immédiatement lavé à l'acétone et séché, est soumis à l'analyse DRX. Un résultat qualitatif a été obtenu pour l'apparition des hydrates.

Le C_3A qui n'a pas réagi, a été dosé quantitativement.

Un degré d'avancement de la réaction par la consommation de C_3A a été calculé à partir d'une courbe d'étalonnage établie sur base de mélange C_3A-Ettringite (figure 9).

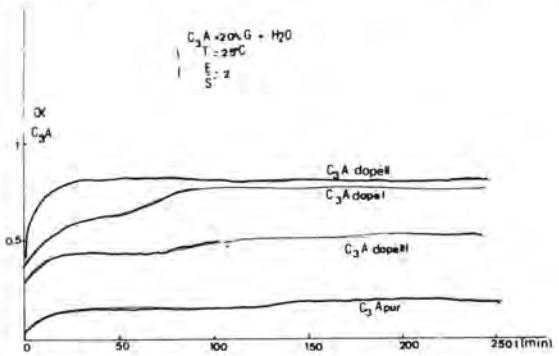

Fig. 9 - Cinétique d'hydratation des C_3A + gypse par DRX.

Discussion des résultats expérimentaux

L'effet du sodium sur l'hydratation de l'aluminate tricalcique en présence de gypse est bien marqué.

L'hydratation est fortement accélérée dès que la teneur en sodium augmente dans la phase aqueuse ; cependant, lorsque la concentration en Na_2O dans l'aluminate tricalcique atteint environ 5 %, on observe une certaine diminution de l'effet du dopant.

Les courbes obtenues par analyse des phases aqueuses ainsi que la cinétique de consommation de l'aluminate tricalcique complètent bien les données microcalorimétriques.

En effet, lors de l'hydratation de l'aluminate tricalcique pur, en présence du gypse, on observe une concentration constante en ions $SO_4^=$ (10 mM/l) pendant la formation de l'ettringite; on remarque

ensuite une diminution rapide de la concentration en ions $SO_4^=$ accompagnée de l'apparition du monosulfoaluminate après 6 heures d'hydratation (Fig.5)

La transformation ettringite-monosulfoaluminate se déroule entre la 6^e et la 24^e heure d'hydratation. Après ce délai on n'observe plus la présence du gypse par D.R.X. Apparaissent alors le C_3AH_6 et les hydrates hexagonaux comme le montrent les spectres RX ainsi que le deuxième pic calorimétrique (Fig. 4).

Dans l'hydratation de l'aluminate tricalcique faiblement dopé (1,2 % Na_2O) la concentration maximale en ions $SO_4^=$ est plus élevée (24,5 mM/l) et atteinte plus rapidement (après 1 heure) que dans l'hydratation de l'aluminate tricalcique pur (3 heures). Cette augmentation accélère la formation de l'ettringite.

Parallèlement, la transformation ettringite-monosulfoaluminate s'opère beaucoup plus tôt (entre la 10^e et la 60^e minute).

Après l'épuisement du sulfate, on décèle par DRX le C_2AH_8.

L'hydratation du C_3A dopé II (4,6 % Na_2O) constitue le cas le plus typique d'accélération de la réactivité des aluminates tricalciques dopés ; on observe en effet la consommation quasi instantanée du gypse et la formation simultanée des différents hydrates : le C_3AH_6, le monosulfoaluminate, l'ettringite et le C_2AH_8.

La concordance entre les résultats de microcalorimétrie, de DRX et de l'analyse des phases liquides est très nette. La chute rapide de la concentration en ions $SO_4^=$ (de 63,5 mM/l à 2 mM/l) indique bien la consommation très rapide du gypse (Fig. 7).

Les deux pics microcalorimétriques se confondent en un seul grand pic exothermique qui apparaît dans les 30 premières minutes.

Les grandes quantités de chaleurs dégagées dans ce processus sont probablement à la base de la formation précoce du C_3AH_6 et du monosulfoaluminate.

Pour l'échantillon fortement dopé (5,8 % Na_2O), on assiste à un changement profond du processus décrit plus haut. Il y a bien une forte concentration en ions $SO_4^=$ dans la phase aqueuse (120 mM/l) ; la teneur en soude et en aluminate est également très élevée, mais nos analyses de la phase aqueuse révèlent une concentration quasi nulle en ions Ca^{++} (due à la présence importante de soude en solution).

Dans ces conditions, on n'observe pas de quantité importante d'ettringite car l'étape limitante devient (exceptionnellement) la concentration en ions Ca^{++}. Celle-ci semble être non seulement un paramètre important pour la formation de l'ettringite, mais elle conditionne également la transformation ettringite-monosulfoaluminate ; l'analyse de la phase aqueuse de l'hydratation des différents aluminates tricalciques révèle en fait que la formation du monosulfoaluminate débute lorsque la concentration en ions Ca^{++} n'est plus que d'environ 2 mM/l.

Conclusions générales

Dans ce travail, nous avons étudié l'hydratation de l'aluminate tricalcique pur et dopé au sodium en présence et en absence de gypse.

Dans le système $C_3A + H_2O$, le Na_2O diminue la vitesse de l'hydratation ; on observe, en outre, une stabilisation des hydrates hexagonaux aux dépens de la formation de l'hydrate cubique.

Dans le système C_3A+Gypse+H_2O, on assiste à un phénomène inverse dû aux modifications profondes de la composition de la phase aqueuse.

En effet, le passage de Na_2O dans l'eau entraîne les modifications ci-après :

(1) Augmentation de la teneur en AlO_2^-.

(2) Augmentation de la teneur en $SO_4^=$.

(3) Diminution de la teneur en Ca^{++}

L'ensemble des résultats montre que pour les échantillons faiblement dopés, la formation de l'ettringite est accélérée, alors que pour l'échantillon fortement dopé, elle est inhibée par manque de Ca^{++}.

Ce travail a permis de montrer le rôle primordial de la composition de la phase aqueuse lors de l'hydratation de l'aluminate tricalcique dopé au sodium.

Nos recherches ultérieures devront montrer si l'hydratation de C_3A pur, en présence de soude, est identique à celle des échantillons dopés contenant Na_2O dans leur réseau.

Remerciements

Nous tenons à exprimer toute notre gratitude à Madame M. Regourd pour la détermination des variétés allotropiques des aluminates tricalciques dopés qu'elle a bien voulu réaliser au laboratoire du CERILH à Paris.

Nous remercions également Madame A.M. Vogel pour sa collaboration scientifique efficace dans l'analyse des phases liquides (Service de Chimie Industrielle - Chimie des Ciments à l'Université Libre de Bruxelles).

Bibliographie

1.- M. REGOURD and B.MORTUREUX,(1977), Tricalcium Aluminate in Synthetic solid solutions and in cements, Seminar at University of Technology, Eindhoven, April 13-14.

2.- L.A. DOBRON, J.M. BUTT, V.M. KOLBASSOV, L.L. ASTANSKY, (1975), Proc. METI n.a. D.I. Mendelew, 57, 44-48.

3.- G.A.C.M. SPIERING and H.N. STEIN, (1975), The influence of Na_2O on the reaction of C_3A with water, Seminar in Koge-Denmark, May 25-26.

4.- A.I. BOIKOVA, A.I. DOMANSKY, V.A. PARAMONOVZ, G.P. STAVITSKAJA and V.M. NIKUSHCHENKO, (1977), Cement and Concrete Research, 7, 485.

5.- M. COLLEPARDI, G. BALDINI and M. PAURI, (1978), Tricalcium Aluminate Hydration in the presence of lime, gypsum or sodium sulfate, Cement and Concrete Research, 8, 571-580.

6.- H.F.W. TAYLOR, (1964), The Chemistry of Cements, I, II, Academic Press, London, New-York.

7.- F.M. LEA, (1970), The Chemistry of Cements and Concrete, Ed. Arnold Publ.

8.- M. REGOURD, S. CHROMY, L. HJORTH, B. MORTUEUX et A. GUINIER, (1973), Polymorphisme des solutions solides du sodium dans l'aluminate tricalcique, J. Appl. Cryst., 6, 356.

9.- EE. PRESSLER, S. BRUNAUER and DL. KANTRO, (1956), Investigation of the Franke Method of determining free calcium hydroxyde, Analytical Chemistry, 20, n° 5, 896-902.

10.- F. CAMBIER, P. FIERENS, G. LAMBIN, (1974), Mesure de surfaces spécifiques par la méthode dynamique améliorée, Silicates Industriels, Vol. 1, 21-26.

11.- V.S. RAMACHANDRAN, (1969), Applications of Differential Thermal Analysis in Cement Chemistry, Chemical Publ. Company, Inc. New-York.

12.- E.A. GIESS, (1963), Equations and Tables for Analysis Solid-State Reaction Kinetics, Journ. of American Ceramic Society, Vol. 8, 374-76, August.

13.- E. BREVAL, (1975), C_3A - Hydration - Experimental Investigations, Cembureau, Seminar in Koge - Denmark, May 25-26.

14.- H.N. STEIN, (1963), Some characteristics of the hydration of $3CaO.Al_2O_3$ in the presence $CaSO_4.2H_2O$, Silicates Industriels, 28, 141-145.

15.- N. TENOUTASSE, (1968), The hydration Mechanism of C_3A and C_3S in the presence of chloride and calcium sulfate, V^e Symp. de la Chimie des Ciments, Tokyo, 6-12 Oct., V.II, Suppl.Pap., 372-378.

16.- U. LUDWIG, (1974), Investigations of the Hydration Mechanism of the clinker Mineral, Intern. Congress on the Chemistry of Cement, Moscow, Sept. 1974, Princip.Pap.

17.- F.W. LOCHER, W. RICHARTZ, S. SPRUNG, (1976), Setting of Cement, Part I : Reaction and Development of structure, Zement - Kalk - Gips, 29, 435.

SHORT COMMUNICATION

« Some considerations on the present state and future trends of knowledge on calcium aluminates, as a possible basis for discussing the future work in this field. »

J. CALLEJA, Instituto Eduardo Torroja (Madrid), Spain.

1. A part of the Principal Paper on **DURABILITY** presented to the Theme VII, and most of the 27 communications presented to the Seminar A of this 7th International Congress on the Chemistry of Cement deal with :

   i) The structure and crystalline forms of aluminates and their solid solutions , mainly of C_3A.
   ii) The hydration of aluminates and their solid solutions, as influenced by different retarders, admixtures and mediums, or by other clinker components , mainly of C_3A, either synthetic or as a component of portland cements.
   iii) The formation, structure, stability and chemical resistance of more or less complex calcium aluminate hydrates , mainly the expansion and sulfate attack of some of them.

2. The principal starting point determining hydration mechanisms of aluminates, and the structure, properties and behaviour of their hydrates is point i).

3. Much research work has been carried out in the last time on anhydrous calcium aluminates and more particularly on C_3A, whihch is the most important aluminous component of ordinary portland cement clinker.

4. A part of this work has been directed to synthetize different crystalline forms of C_3A and to identify them in clinker.
   Another part of the work has been devoted to study the properties and bahaviour of those forms of C_3A, particularly as far as their susceptibility to sulfates is concerned.

5. No doubt that both parts of this work have been attempted and developped mainly as a (scientific) research basic in nature. The interest of it is obvious, as a good mean -and perhaps the better way- to gain and cumulate new solid knowledge on the theme of the chemistry of calcium aluminates.

6. But no doubt as well that the final interest of this necessary and more basic research is to form the support and the starting point for an applied research, more technical in nature, able to give practical results.

7. It is worth while not to forget that for cement makers and cement users calcium aluminates are more interesting as "natural" components of industrial portland cement clinker than considered as isolated "artificial" laboratory synthetic products.

8. In this view, once established -if so- that different forms of C_3A have different nature, properties and behaviour in different technical aspects, two lines of study and action may arise immediately.

9. The one is analytical in nature : to develop reliable, practical easy and rapid methods to detect qualitatively the presence and if possible to determine quantitatively the content of the different forms of C_3A -occasionally of other calcium aluminates- in portland cement clinker.

10. The other line is technical in nature : to develop procedures and techniques to create preferently in industrial portland cement clinker those forms of C_3A -and occasionally of other calcium aluminates- whose behaviour may be better in all or part of the aspects involved in the use and applications of portland cement, i.e., in concrete science and technology.

11. It is thought that so, and only so, the whole chain beginning with the more pure, basic, scientific, fundamental, theoretical or academic research, and finishing with the more applied, technical, practical or industrial research in the field of calcium aluminates may be continuous and complete.

12. This may permit the development and the innovation of the world cement industry. Otherwise the chain is broken and the knowledge gained may be sterile, at least during a long time, for practical pourposes.

13. Probably this second type of research -or this second way to direct the single and unique research for those who prefer to consider it so-, is more difficult than the first type or way to focus and project research in the field of calcium aluminates.

14. But, anyway there is no doubt that it is a tempting challenge for those who like and wish to make progress the cement industry and subsidiarily the concrete technology, i.e., the building and construction industry.

SEMINAIRE B

Insolubilisation à l'aide de liants hydrauliques des ions métalliques contenus dans les boues industrielles

Président : M. MERIC (France)

INTRODUCTION DU PRESIDENT

Chaque année, l'industrie produit de grandes quantités de boues contenant des corps nocifs, essentiellement des ions métalliques. Ces boues proviennent de l'épuration des eaux résiduaires et des effluents gazeux et concentrent un grand nombre d'éléments dangereux pour l'environnement. Parmi ces éléments, les métaux lourds se trouvent être initialement dans la nature sous forme de minerais insolubles. L'homme a extrait ces minerais et a solubilisé les métaux afin de pouvoir les utiliser dans les divers circuits de l'activité humaine. Ces éléments, lorsqu'ils ont rempli leurs fonctions, sont en général recyclés mais ce recyclage s'accompagne toujours de pertes qui se traduisent par des rejets dans le milieu naturel. La présence de ces éléments dans la nature est en général éphémère si l'on se réfère à l'échelle géologique car, tôt ou tard, ils sont fixés à nouveau sous la forme d'un minerai insoluble en rencontrant des sites minéralogiques réactifs. Mais en attendant, ils transitent dans les circuits des eaux de surface et souterraines en concentration parfois importante, ce qui constitue une menace pour la qualité des eaux.

Le rejet de ces éléments en milieu naturel, s'il constitue la seule issue possible, doit donc se faire dans des conditions bien déterminées. Deux solutions peuvent être envisagées. D'abord, le stockage des boues dans des sites réputés étanches à toute infiltration d'eau. Les boues resteront en attente pendant un temps plus ou moins long, mais continueront à présenter un danger potentiel important. L'autre solution est d'accélérer le cycle naturel en mettant les boues en contact avec un minéral réactif afin de les retransformer immédiatement en un minerai insoluble. Le minerai réactif le plus couramment utilisé dans l'industrie et le plus facilement disponible est le ciment ou, plus généralement, les produits appartenant à la famille des liants hydrauliques.

Le ciment permet de reconstituer des pierres dont la durabilité est équivalente et même supérieure à celle des pierres naturelles. Les premiers ciments confectionnés il y a plus de 2000 ans par les romains n'ont rien perdu de leurs qualités avec le temps et ont atteint un équilibre géologique. Lorsque l'on traite des boues industrielles contenant des métaux lourds avec des liants hydrauliques, on vise ce même équilibre géologique pour obtenir une pierre inattaquable et insoluble qui constituera un piège idéal pour les éléments à fixer.

L'action des liants hydrauliques sur les boues est multiple ; elle est d'abord chimique, physique et enfin mécanique, c'est-à-dire qu'il se produit des liaisons au niveau des molécules, que ces molécules s'organisent en réseaux cristallins et que ces réseaux cristallins s'enchevêtrent pour donner des structures résistantes.

L'objectif de ce Séminaire est d'étudier ces liaisons et mécanismes de solidification dans la perspective de prévoir l'évolution à long terme des produits solidifiés. Il est en effet nécessaire de bien comprendre le processus de solidification afin d'évaluer le degré de confiance que l'on peut accorder à ces procédés pour la sauvegarde de notre patrimoine écologique.

Chimie des ciments et traitement des boues minérales

Cement chemistry and mineral sludge processing

P. LONGUET - G. BELLINA, Département « Chimie des Ciments » - C.E.R.I.L.H. - Paris, France.

RESUME

Après avoir situé le sujet vis-à-vis des conséquences écologiques du rejet inconsidéré de déchets minéraux plus ou moins toxiques, on développe les caractéristiques particulières des composés de la chimie du ciment considérés comme réactifs chimiques. Les réactions de neutralisation, de précipitation et de complexation sont particulièrement étudiées soit dans leurs principes, soit sous l'angle de l'application. On précise ensuite les manières d'apprécier l'efficacité d'un traitement principalement vis-à-vis des caractéristiques de l'eau potable.

SUMMARY

After we have set the subject beside ecological consequences of rash rejection of mineral wastes highly poisonous or not, we develop the specific characteristics of cement chemistry compounds regarded as chemical reagents. Neutralization reactions, precipitation and complexation reactions are studied with carefulness and looked at from whether their principles or their applications. Then we clarify the ways to estimate the effectiveness of some processings mainly beside drinkable water charateristics.

I - PRESENTATION

En l'an 2000 la population du globe atteindra six milliards d'êtres humains. L'homme devient donc selon l'expression du professeur Vladimir **VERNADSKY**, spécialiste des sciences de la terre, une puissante force géologique.

Compte tenu de l'intensité des activités humaines actuelles cette force peut provoquer en quelques décades des changements qui auraient demandé des millions d'années pour s'accomplir naturellement.

Indépendamment d'une gestion optimale des ressources terrestres cette rapidité d'évolution pose le problème du traitement des déchets plus ou moins toxiques qui en résultent. Le but de cet exposé est de montrer comment, dans le domaine particulier et limité des boues minérales toxiques, peut intervenir la chimie du ciment pour éviter particulièrement la pollution de l'eau potable et la dispersion des matières premières minérales.

II - LIMITES DE L'EXPOSE ET RAPPEL DE QUELQUES DEFINITIONS

L'exposé concerne essentiellement le traitement des boues compatibles avec les composés de la chimie des ciments c'est-à-dire le plus souvent des déchets d'origine minérale. Il suppose que la nature et la composition de ces déchets s'opposent à leur rejet direct dans le milieu naturel (toxicité certaine) et qu'ils se présentent dans leur état final c'est-à-dire, qu'ils ne peuvent plus pour des raisons techniques, économiques ou toxicologiques subir d'opérations de concentration et que le traitement doit être définitif et durable. Le terme de traitement ultime est souvent utilisé pour définir cette opération.

III - BUTS DU TRAITEMENT

Le traitement cherche d'abord à assurer la solidification du milieu afin de le rendre manipulable et transportable.

Le second point concerne la fixation des substances toxiques présentes afin d'éviter au maximum leur rejet dans le milieu naturel environnant compte tenu des conditions de stockage ou d'utilisation.

Enfin le traitement doit assurer le mieux possible une stabilisation dans le temps, l'idéal étant le retour vers des formes thermodynamiquement stables comparables à des espèces minéralogiques.

L'efficacité du traitement se définit à partir de ces trois paramètres: solidification, fixation, stabilisation.

Il est évident que l'on recherchera une efficacité d'autant plus grande que la toxicité de la boue à traiter sera plus grande. Parallèlement le coût du traitement croît le plus souvent avec l'efficacité.

IV - POSSIBILITES APPORTEES PAR LES COMPOSES DE LA CHIMIE DU CIMENT

Citons d'abord les propriétés classiques bien connues des liants hydrauliques. Gâché en pâte avec l'eau un ciment fait prise et durcit en consommant de l'eau pour former des hydrates de très grande surface spécifique (100 fois environ la surface du solide initial) et générer finalement un solide mécaniquement très résistant et pratiquement inattaquable par les agents naturels habituels. Ces caractéristiques conduisent déjà à proposer les liants hydrauliques pour le traitement des boues minérales aqueuses. Mais l'examen plus approfondi des propriétés des composés de la chimie du ciment met en évidence bien d'autres propriétés intéressantes permettant de réaliser toute une série de réactions bien plus générales que celles rappelées précédemment et qui amènent à considérer le ciment comme un réactif chimique.

- Réactions de neutralisation

Si nous considérons, pour simplifier, que pour notre sujet les deux constituants essentiels du ciment sont le silicate tricalcique (C_3S) et l'aluminate tricalcique (C_3A), nous avons affaire dans les deux cas à des sels d'acides faibles (silice et alumine) et de base forte (chaux). C_3S et C_3A mis en contact avec des acides forts vont se comporter sensiblement comme une base forte en libérant les acides faibles correspondants sous des formes hydroxylées très réactives (cf. exposé de PETIT et ROUXHET). L'effet tampon propre à ce type de neutralisation sera par ailleurs très favorable pour assurer une faible solubilité aux hydroxydes pouvant exister dans la boue à traiter (cf. exposé de BLANCHARD).

Le ciment apparaît donc comme un réactif de choix pour la neutralisation des effluents acides qui représentent d'après les statistiques la plus grande partie des rejets aqueux industriels.

- Réactions de précipitation

Le milieu apporté par le ciment est fortement calcique.Les sels de calcium étant pour la plupart peu ou très peu solubles un grand nombre d'anions susceptibles d'être présents dans la boue à traiter vont précipiter et venir s'insérer dans la texture du ciment hydraté. Citons les fluorures, les zincates, les borates, les arséniates, les phosphates, les plombates, les tungstates, les chromates,...).

Cette possibilité de précipitation de sels de calcium confirme l'intérêt de la neutralisation d'un effluent acide par un ciment à la place de Na_2CO_3 ou NaOH qui augmentent obligatoirement la teneur du milieu neutralisé en sels solubles (bases alcalines).

- Réactions de complexation

Ces réactions sont propres aux phases aluminiques du ciment (C_3A, phases aluminoferritiques). La grande réactivité du C_3A intervient très souvent dans la chimie du ciment (cf. Séminaire A).

Dans le cadre de notre sujet nous nous intéressons aux complexes prenant naissance en milieu fortement alcalin et calcique. Le plus connu est le trisulfoaluminate de calcium hydraté (Al_2O_3 $3CaO,3SO_4Ca$ $31\ H_2O$) que l'on forme volontairement d'une manière tout à fait générale pour régulariser la prise du ciment (gypsage des clinkers). Mais de nombreux anions peuvent aussi former des aluminates de calcium complexes dont les sels de calcium sont peu ou très peu solubles. Citons les ions suivants: sulfate, chromate, séléniate, carbonate, chlorure,bromure, iodure, nitrate, nitrite, permanganate, iodate, formiate, acétate, propionate....(A).

D'autre part les ions aluminium peuvent être partiellement substitués dans ces aluminates complexes par les ions Cr^{3+}, Ti^{4+}, Tl^{2+}.... La phase aluminate, et aussi la phase aluminoferritique qui donne en première approximation des réactions analogues, sont les composés du ciment qui apportent des

possibilités de fixation très diverses pour de nombreux ions toxiques.

Nous n'entrerons pas ici dans les détails des réactions pour lesquels nous renvoyons à la bibliographie commentée de cet exposé. En résumé les composés de la chimie du ciment présents dans les liants hydrauliques sont à considérer comme de véritables réactifs chimiques susceptibles de consommer de l'eau (déshydratation), de neutraliser les milieux acides, de précipiter des sels de calcium, de complexer de nombreux ions toxiques, d'adsorber (adsorption et chimisorption) et de solidifier les suspensions aqueuses minérales (prise et durcissement).

Bien entendu il peut y avoir, et il y a le plus souvent, compétition entre les diverses réactions possibles. Cette compétition soulève, lors du traitement, des problèmes très différents des problèmes classiques de la chimie des ciments et dont l'étude fort intéressante n'a été entreprise que depuis quelques années seulement. Nous avons essayé malgré tout d'indiquer les lignes directrices actuellement suivies pour conduire un traitement.

V - MODALITES D'APPLICATION

- Connaissance du milieu à traiter

Bien qu'essentiel ce point est quelquefois négligé à cause des difficultés analytiques posées par un milieu dont il est souvent très difficile d'établir l'histoire complète (mélange de plusieurs effluents, traitements de produits inconnus, mise en lagune ancienne... et qui dans la plupart des cas présente une hétérogénéité importante). De toute manière il faudra s'efforcer d'obtenir un échantillon aussi représentatif que possible et déterminer sa composition élémentaire complète (anions et cations) et préciser les espèces chimiques présentes: effluents directs plus ou moins acides, effluents déjà traités (décyanuration, réduction de Cr^{6+}, neutralisation avec précipitation d'hydroxydes...). C'est à partir de ces données qu'il convient ensuite de conduire le plus efficacement possible les réactions de base mentionnées. Citons quelques incidences pratiques à considérer:

- Sur les réactions de neutralisation

Une acidité élevée du milieu entraîne une consommation importante de ciment pour sa neutralisation avec la formation éventuelle trop importante d'hydroxydes. (Un ciment portland artificiel précipite environ la moitié de son poids en hydroxydes). Dans ce cas une neutralisation partielle préalable avec du carbonate de calcium ou de la chaux (CaO ou $Ca(OH)_2$) permettra une opération convenable.

- Sur les réactions de précipitation

La difficulté provient ici de la compétition entre les propriétés d'enrobage et de colmatage des sels insolubles de calcium formés qui inhibent plus ou moins totalement la poursuite de l'hydratation du ciment. Il faut alors jouer soit sur des facteurs physiques qui changent les vitesses de réaction (température, dilution...) soit sur des facteurs chimiques (accélérateurs ou retardateurs...) soit sur des facteurs mécaniques (agitation, dispersion ou même traitement en broyeur pour renouveler les surfaces de contact...).

- Sur les réactions de complexation

C'est la teneur en alumine du liant et l'alcalinité du milieu qui interviennent le plus dans ces réactions indépendamment de la formation de composés insolubles traitée au paragraphe précédent. Dans bien des cas le taux de fixation peut être augmenté par addition de laitier granulé de haut fourneau ou quelquefois de cendres volantes de centrale thermique. Il conviendra cependant de bien connaître la teneur du milieu en alcalis libres (NaOH ou KOH) qui peuvent limiter la solubilité de $Ca(OH)_2$ et s'opposer ainsi à la formation des complexes calciques dont le produit de solubilité ne peut ainsi être atteint.

Inversement d'ailleurs la boue à traiter peut avoir une teneur élevée en alumine, il convient alors d'ajouter un anion complexant, sulfate par exemple.

- Sur les réactions de dispersion et d'adsorption

Nous avons déjà signalé l'intérêt du développement important de surface spécifique lié à l'hydratation du ciment. Quelquefois on recherche uniquement l'action dispersante du phénomène c'est ainsi que certaines chaux vives activées seules ou en mélange avec un support minéral, sont utilisées pour disperser des résidus organo-minéraux. Dans ce cas le matériau pulvérulent obtenu doit être compacté et protégé de l'action dissolvante des agents atmosphériques ou réinséré dans une matrice insoluble. Signalons encore l'utilisation des propriétés des échangeurs d'ions (cf. exposés de SUZUKI et Coll. et de FORMANEK).

Ces quelques commentaires sur les modalités de réalisation du traitement des boues montrent la complexité du problème et confirment la nécessité d'une étude préalable avec des essais de vérification pratiquement dans chaque cas (cf. exposés de SUGI et Coll. de RAU et de LEROY).

Sur un autre plan, il est certain que cette nouvelle application des liants hydrauliques aura des conséquences bénéfiques sur notre connaissance de la chimie des ciments.

VI - APPRECIATION DE L'EFFICACITE DU TRAITEMENT REALISE

Lorsque l'étude préalable indique que le traitement est possible il convient de vérifier ses qualités potentielles et d'essayer de prévoir son évolution dans le temps compte tenu du mode de conservation envisagé (fig. B texture d'une boue traitée).

De très nombreux essais ont été décrits. Nous en mentionnerons trois qui correspondent chacun à une préoccupation différente:

- Connaissance de l'état d'équilibre ionique de la solution interne de la boue traitée: on utilise la technique déjà proposée pour le ciment hydraté .

- Connaissance de l'état d'équilibre de la surface externe de la boue traitée avec une eau stagnante: c'est l'adaptation de la méthode préconisée par l'agence nucléaire internationale.

Cet essai correspond à l'effet le plus faible de l'action dissolvante de l'eau.

- Connaissance de l'action d'une eau de ruissellement.

La simulation est obtenue au laboratoire dans un extracteur type Soxhlet perfectionné.

La capsule d'extraction dans laquelle est disposé l'échantillon, conditionné de manière à présenter une surface connue à l'action de l'eau, est maintenue isotherme (C et D).

Cette particularité permet une mesure conductimétrique continue sur la solution d'extraction et permet d'établir un diagramme de solubilité (E).

Cet essai dynamique représente l'action la plus aggressive d'une eau.

L 'analyse élémentaire des solutions extraites permet au moins un classement des traitements réalisés. Les valeurs obtenues ne sont évidemment qu'indicatives et la transposition au cas réel est souvent difficile. En effet la conservation en site naturel fait intervenir un très grand nombre de facteurs tantôt favorables (importance des masses traitées, qui diminue l'effet de surface, action colmatante due à la formation du carbonate de calcium...) tantôt défavorables (acidité des eaux naturelles, mouvements de terrain, alternances climatiques....). Cependant il est toujours intéressant de comparer les valeurs fournies par les essais de laboratoire à celles des tables fixant les limites des teneurs en ions toxiques de l'eau potable.

Ici encore indépendamment des conclusions tirées des essais de laboratoire, ce sera la toxicité initiale de la boue traitée qui pourra orienter les précautions à prendre a priori pour l'utilisation ou le stockage des produits traités. On pourra aller ainsi de l'addition à un béton de préfabrication dans le cas d'une nocivité négligeable jusqu'au stockage sur une aire imperméable permettant le contrôle permanent des eaux de ruissellement ayant été en contact avec la boue traitée (cas des résidus nucléaires par exemple).

CONCLUSION

Suivant la toxicité de l'effluent initial le traitement ultime des boues par les liants hydrauliques apporte, chaque fois qu'il est réalisable, des solutions intéressantes pour la protection de l'environnement:

- Amélioration de la manutention.
- Facilités de mise en décharge.
- Utilisations diverses : charges routières ou autres, béton manufacturé...
- Stockage sans pollution des eaux potables permettant d'éviter la dispersion d'éléments importants dont le retraitement sera possible dans l'avenir....

BIBLIOGRAPHIE succincte

1 - J.P. MERIC - P. LONGUET
Traitement des boues et eaux résiduaires
Aspects économiques et physicochimiques.
Rev. Mat. Const. France - mars-avril 1976 p.79-81

2 - P. LONGUET
La phase liquide du ciment hydraté.

3 - Symposium Sol Déchets - Angers avril 1980
Edité par SEPIC 40 rue du Colisée -
75381 Paris Cedex 08
- Plus de la moitié de ce Symposium est consacrée à la "Mise en décharge des déchets industriels"

4 - J. RODIER
Analyse de l'eau
Dunod Paris 1976.

Table des Figures

A - Complexation
Coprécipitation de sulfo et de chromoaluminates de calcium.

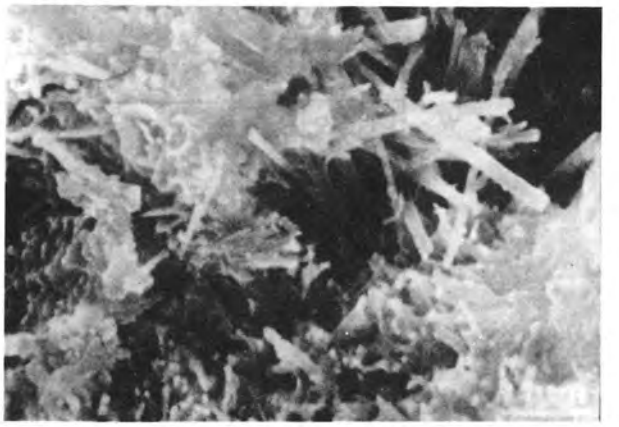

B - Texture d'une boue traitée.

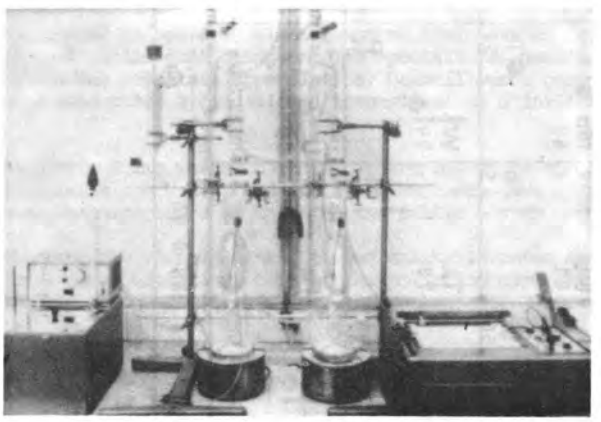

C - Contrôle par extraction continue.

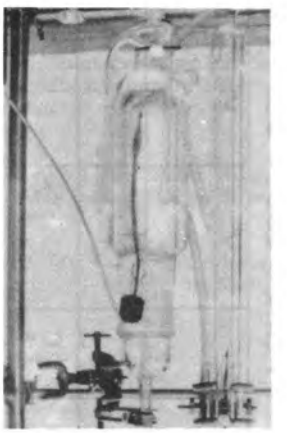

D -Détail de l'extracteur.

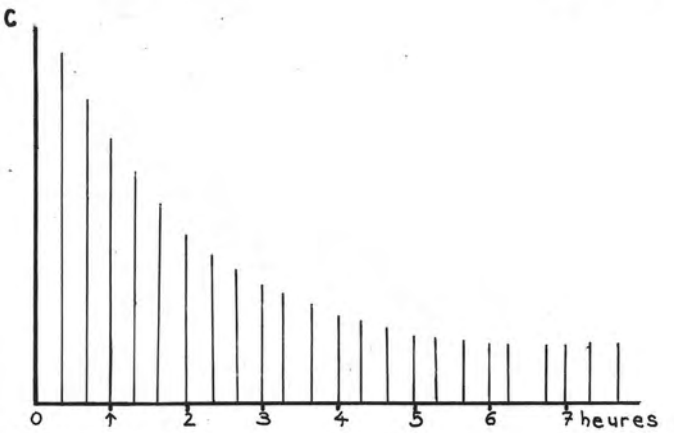

E - Conductogramme d'extraction
Mise en évidence d'une solubilité limite de la boue traitée.

CLASSIFICATION PERIODIQUE DES ELEMENTS

	gr. I	II	III	IV	V	VI	VII	VIII	gr.O	
0									Nn 0	0
1	H 1								He 2	1
2	Li 3	Be 4	B 5	C 6	N 7	O 8	F 9		Ne 10	2
3	Na 11	Mg 12	Al 13	Si 14	P 15	S 16	Cl 17		A 18	3
4	K 19	Ca 20	Sc 21	Ti 22	V 23	Cr 24	Mn 25	Fe 26 Co 27 Ni 28	Kr 36	4
	Cu 29	Zn 30	Ga 31	Ge 32	As 33	Se 34	Br 35			
5	Rb 37	Sr 38	Y 39	Zr 40	Nb 41	Mo 42	Tc 43	Ru 44 Rh 45 Pd 46	Xe 54	5
	Ag 47	Cd 48	In 49	Sn 50	Sb 51	Te 52	I 53			
6	Cs 55	Ba 56	La 57	58 à 71	Hf 72	Ta 73	W 74	Re 75	Os 76 Ir 77 Pt 78	6
	Au 79	Hg 80	Tl 81	Pb 82	Bi 83	Po 84	At 85		Rn 86	
7	Fr 87	Ra 88	Ac 89	Th 90	Pa 91	U 92	93 à 95			7
			97 Cm à 96 103							

Précipitation
Complexation
Adsorption

Lanthanides 58 à 71 — Uranides 93 à 95 — Curides 97 à 103

Figure F

La solidification des déchets : motivations, acquis, perspectives

Solidification techniques, motivations, state of the technology, developments

Philippe J. PICHAT, CdF Chimie-A.P.C., Paris-La Défense, France.

Resumé : Le devenir des déchets toxiques est un sujet qui n'intéresse plus seulement les milieux spécialistes de l'environnement et de la protection des ressources en eau. En effet, plus particulièrement aux Etats Unis, ce sujet, par le biais d'incidents concernant parfois des centaines de personnes, a atteint une dimension nationale, puis a eu une audience internationale. La grande presse a consacré des articles à ce thème techniquement et médicalement délicat en présentant parfois des hypothèses comme des faits.

Cet intérêt des élus, du public est compréhensible, compte tenu de l'importance fondamentale maintes fois soulignée par l'O.M.S. (l'Organisation Mondiale de la Santé) de l'eau pour la santé des humains.

Cet exposé résume les relations entre l'eau et les déchets, une nouvelle filière technologique qui élargit la gamme d'outils dont disposent les spécialistes de l'anti-pollution. La solidification-fixation des déchets a déjà obtenu des résultats appréciables. De meilleures performances à un rapport efficacité-coût intéressant peuvent être escomptées à condition d'intensifier et d'infléchir les premiers efforts.

Summary : Toxic wastes no more concern the alone specialists of pollution control. Problems which took place for example in the U.S.A. and in the Netherlands gave an international size to the topic. The mass media feel concerned. The importance of water to the public health explains these reactions.

This article reminds links between drinkable water and wastes, describes briefly the solidification techniques which are a useful new tool of the pollution control. Results have been obtained. Better performances would be reached along efforts of Research-Development.

1 - L'eau et la protection des ressources en eau

1.1. La biosphère et le cycle de l'eau

La biosphère qui abrite les êtres vivants peut être comparée à une mince enveloppe recouvrant notre globe.

La biomasse (masse totale d'organismes vivants) varie selon les régions de la biosphère dans de fortes proportions (forte dans une prairie normande, faible en haute montagne,...).

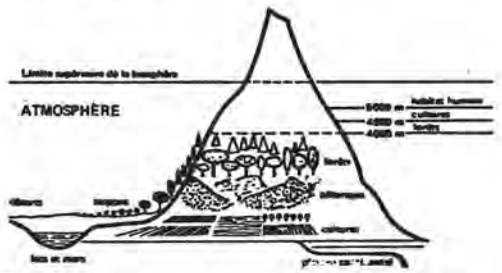

Figure 1

La biosphère n'est pas peuplée de façon désordonnée par les êtres vivants mais par des communautés, associations de microorganismes - végétaux - animaux, installées dans un milieu déterminé et que l'on dénomme "biocoénose". Ce milieu déterminé (un "biotope") de dimensions variables, est caractérisé par des dominantes homogènes (t°, humidité, type de sol...)

On a pu écrire :

Ecosystème = biotope + biocoénose

A la surface des terres émergées, la biomasse est sensiblement proportionnelle au volume des précipitations

Cette eau de pluie, arrivée au sol, peut :

a/ ruisseler jusque dans les océans, en empruntant ruisseaux, rivières, fleuves. Le ruissèlement est important sur les terrains imperméables, par exemple granitiques.

Dans ce cas, l'eau de pluie alimente essentiellement les eaux de surface. Il n'y a pas de ressources en eau souterraine notables(Bretagne, Massif Central). Il en découle que les cours d'eau ont un débit irrégulier, fonction des précipitations.

b/ percoler, s'infiltrer et alimenter les gisements aquifères souterrains.

Il se forme une nappe lorsque l'eau d'infiltration rencontre une assise pratiquement imperméable : argile, roche. Il peut exister dans la même région plusieurs nappes (ou niveaux d'eau) superposées. C'est ainsi que l'on trouve des nappes stampiennes, sauroisiennes, bartonniennes, de la craie sénonienne, de la craie turonnienne, cenovonienne, albienne dans la région parisienne...

c/ s'évaporer, transpirer (ces deux processus sont groupés sous le nom d'évapotranspiration) par l'intermédiaire du système foliaire. Les racines contribuent fortement à ces mouvements ascendants d'eau sol-atmosphère.

On a représenté ci-dessous le schéma simplifié du cycle de l'eau.

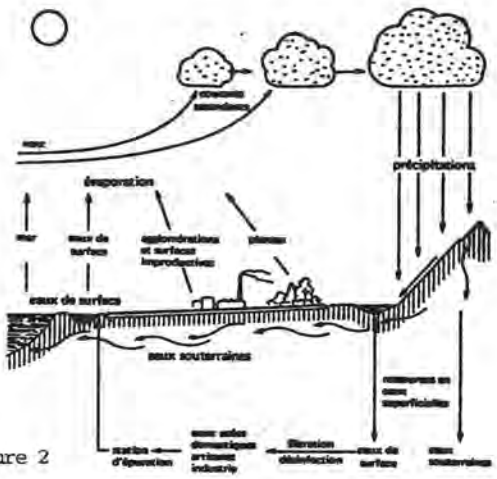

Figure 2

1.2. La vitesse de circulation de l'eau et ses implications

Le processus général de circulation des eaux dans le sol est gravitationnel, freiné par les phénomènes de capillarité. Il se développe des courants analogues à ceux des rivières et des fleuves. Indiquons, pour donner une idée de l'échelle de ces phénomènes, que la vitesse varie entre quelques centaines de mètres et quelques centaines de kilomètres par an.

La circulation diaclosienne donne lieu à de nombreuses variations de vitesse. Par contre, en milieu suffisamment homogène et isotrope, la circulation en milieu poreux peut être représentée par la loi de Darcy : $I = \alpha V$ I étant la perte de charge unitaire et V la vitesse de circulation. Ces vitesses sont en général très faibles, de quelques mètres par an à un mètre par jour, alors que pour un cours d'eau, elles sont de l'ordre du mètre par seconde.

Lorsqu'un déchet liquide (fosse septique, lixiviation de pesticides, agent antigel d'autoroute...) sera déversé au-dessus d'une nappe, la pollution n'apparaîtra que lentement : la contamination peut demander des années, voire des décades à se manifester. Dans le passé, on a supposé que si un site acceptait des sous-produits ou des déchets sans dommage immédiat, on avait réalisé un stockage ultime. Cette façon de voir explique des incidents du genre de LOVE CANAL qui se sont passés aux Etats Unis (1).

Au contraire, dans le cas d'un cours d'eau, la pollution pourra être détectée rapidement au moyen de méthodes physico-chimiques (absorption atomique, chromatographie) ou biologiques (utilisation de poissons sensibles à la pollution, de crustacés du type Daphnies). Les nappes sont alimentées par les eaux de surface. Lorsque ces dernières sont polluées, leur infiltration dans le sol souille les couches aquifères.

1.3. Pollution, "formation" des déchets

La pollution, stricto sensu, est la destruction d'un cycle biologique dans un écosystème, exemple la mort de tonnes de poissons dans la Saône en 1974 par suite des déversements en amont de Lyon.

Chaque utilisateur d'eau, qu'il soit un particulier,

un industriel ou un cultivateur, a tendance à rejeter celle-ci sans trop se soucier des utilisateurs suivants situés en aval, en pensant que la nature s'accommodera de cette eau additionnée de diverses substances.

Les cours d'eau jouent un rôle de convoyeurs de déchets vers la mer. Le résultat est que l'eau est dans certains cas, très polluée.

Cette pollution est soit d'origine :

- organique (égouts urbains, abattoirs, sucreries, laiteries... usines de pâte à papier, hydrocarbures, phénols, détersifs, pesticides...)
- inorganique : métaux lourds, plomb, acides, silico-aluminates provenant de dragages, etc... ;
- bactérienne et virale.

La nature ne peut "assimiler" les déchets qu'en quantité limitée et très variable (selon leurs propriétés physico-chimiques et biologiques) en un point donné. Ce principe essentiel a été trop longtemps oublié alors que l'on assiste à une "concentration" des rejets par suite des phénomènes d'urbanisation et d'industrialisation massifs.

Il y a confusion entre besoins en eau et besoins d'écoulement d'eau. La plus large part du besoin en eau vient de l'habitude d'utiliser l'eau en mouvement comme "vecteur" de transfert de déchets.

Dans ces conditions, il n'y a rien d'étonnant à ce que les déchets contiennent une forte proportion d'eau même dans le cas des boues ou de pseudo-solides pelletables qui peuvent encore atteindre des teneurs de l'ordre de 60 % d'eau libre.

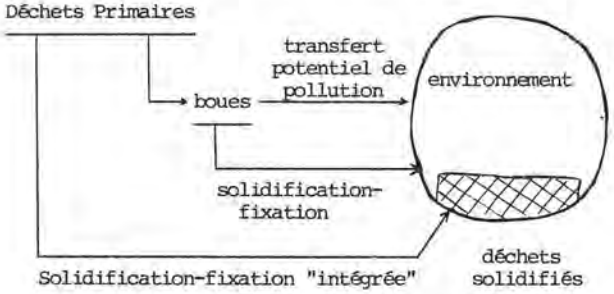

Solidification-fixation "intégrée"

2 - Principe de la solidification des déchets

Lorsque la valorisation, toujours souhaitable, n'est pas possible, il s'agit de transformer un déchet liquide ou une boue en un véritable solide afin de supprimer les dangers (et les coûts d'un point de vue économique) liés au stockage de liquides ou de boues liquides.

D'autre part, le solide ainsi constitué doit relarguer peu d'ions ou de molécules vers le milieu naturel.

Les déchets, par exemple d'un atelier de chromage sont détoxiqués, neutralisés et on obtient une boue "déchets des déchets".

Souvent sous l'action des intempéries, les constituants des boues peuvent être entraînés dans les eaux souterraines ou de surface (Photo P.J. PICHAT)

Les boues si celles-ci ne sont pas judicieusement stockées, sous l'action des intempéries, pourront peu à peu être entrainées dans les eaux de surface ou les eaux souterraines. Une parade est le dépôt des boues dans des sites étanches au point de vue hydrogéologique. (Une conférence patronnée par l'ANRED aura lieu à l'INSA de Lyon (FRANCE) en février 81). Un tel site peut ne pas exister à proximité. Une autre parade qui peut d'ailleurs être complémentaire est de transformer de l'eau libre en eau liée.

L'eau contenue dans le déchet réagira avec le liant hydraulique, mélange constitué principalement de silicates et d'aluminates de calcium anhydres qui vont être transformés en silicates et aluminates de calcium hydratés. (On rappelle, pour mémoire, que d'autres filières technologiques existent : bitumes, thermodurcissables, céramiques, verres).

Ces effets ont lieu soit à l'échelle microscopique, soit à l'échelle macroscopique.

3 - L'acquis, Sommaire de l'état de la technique

Les méthodes de solidification-fixation sont récentes (3, 4). Elles datent d'une dizaine d'années et elles ont été consacrées principalement aux boues de désulfuration des fumées et aux boues toxiques (le cas des déchets radioactifs n'étant pas abordé ici).

En mars 1979, a été organisé par l'A.C.S. (American Chemical Society) et la C.S.J. (Chemical Society of Japan) à Hawaï le premier séminaire consacré exclusivement aux méthodes de solidification-fixation. A peu près simultanément paraissait aux U.S.A. le premier livre consacré à ces techniques (2) qui depuis a été suivi de 2 autres volumes : en quelques années, ces techniques se sont bien développées et un certain nombre d'entreprises, par exemple :

- aux U.S.A. (I.U., DRAVO, CHEMFIX, COTTRELL...)
- en France (SARP Industries, GEREP, PEC-ENGINEERING)

les utilisait

3.1. Phases du traitement

Le tableau ci-dessous rappelle succinctement les phases d'un traitement industriel :

a/ CHOIX D'UNE FORMULATION

Homogénéisation du déchet brut	Echantillonnage (Opération délicate comme le rappellera Monsieur BLANCHARD)	Analyse	Choix d'une formulation

b/ MISE EN OEUVRE

Homogénéisation du déchet brut ⟶ - Dosage de réactifs - Leur addition ⟶ Homogénéisation ⟶ Début des réactions d'hydratation des silicates, aluminates aluminofemités de calcium

qui induisent des réactions de : neutralisation, précipitation, adsorption, complexation, substitution, enrobage.

Mise en place appropriée.

c/ CONTROLE

- Propriétés mécaniques Rp (la résistance à la compression doit être compatible avec le passage d'engins et le stockage sur de fortes épaisseurs sans fluage.
- Propriétés écologiques - essai statique de lixiviation
  - essai dynamique
  - perméabilité

3.2. Principaux paramètres

3.2.1. Influence du traitement primaire - Intégration du traitement ultime dans le processus global de traitement

Les déchets bruts, primaires pour utiliser une autre terminologie sont souvent acides. Ils sont ensuite neutralisés. Le type de neutralisation n'est pas sans répercussion sur la qualité de la solidification ultérieure du déchet. On doit préférer à l'utilisation d'un hydroxyde dont le métal sous forme ionique est très soluble, l'utilisation de l'hydroxyde de calcium. Ce thème sera développé par Monsieur LONGUET.

Il est nécessaire dès le traitement primaire (et à plus forte raison, secondaire) que la production de déchets ait le souci du traitement ultime du déchet, c'est-à-dire du devenir du déchet, ceci dans l'esprit de la loi française des déchets de 1975. On ne peut pas demander au traitement de solidification de "gommer" toutes les erreurs qui ont été faites précédemment.

3.2.2. Type de déchets traités - Flexibilité des procédés - Ambiguité des objectifs

L'incinération des déchets ayant un PEI convenable est pratiquée. Des déchets biodégradables sont traités par les méthodes d'aspersion, d'épandage, voire de landfarming lorsque les caractéristiques du sol et le climat le permettent.

Par contre, les méthodes de solidification semblent particulièrement appropriées avec des produits inorganiques pouvant contenir une certaine proportion de produits organiques, ou biologiques ou organo-métalliques variables selon le procédé et ses conditions d'exploitation.

Il y a probablement un effort à faire dans le sens d'une plus grande adaptation du dosage (avec un procédé donné) au type de déchet considéré (5).

On peut dire qu'il y a eu souvent une tendance à sous-doser en liants hydrauliques pour des raisons économiques bien compréhensibles.

Cette attitude a amené des exploitants à ne pas solidifier des déchets qui, en fait, auraient pu être traités convenablement en abaissant le rapport eau/liant.

Dans ce domaine, il existe d'ailleurs une certaine confusion sur l'objectif à atteindre :

- S'agit-il de solidifier pour stocker à un prix attractif des boues ou des déchets liquides en abaissant par voie de conséquence la lixiviation
- ou s'agit-il de fixer les éléments polluants avec des préoccupations de coût moindres.

Des représentants des pouvoirs publics ont pu peut-être parfois être un peu déçus des performances d'un procédé parce que, pour des raisons commerciales, la première attitude avait dû être adaptée, compte tenu de ce que la détenteur du déchet ne proposait pas un budget suffisant.

3.2.3. Conditions de mise en place et de stockage

Il est important que la mise en place du déchet soit définitive avant sa solidification, c'est-à-dire, en d'autres termes, sans reprise. Une reprise n'est possible, comme en techniques routières, qu'avec un liant à prise lente du genre grave - cendres, et l'expérience montre que dans le domaine de la solidification des déchets, on se trouve en général assez loin de ces conditions.

Les précautions usuelles vis-à-vis du grand froid, du soleil, du vent, lors de coulées de béton sont aussi recommandées lors d'une opération de solidification.

Le résidu doit être placé en couches compactes continues présentant un rapport surface/masse faible de façon à minimiser la lixiviation (du genre tumulus).

3.2.4. Evaluation des résultats

On peut distinguer non sans quelque arbitraire, l'eau stagnante et l'eau de ruissèlement et les essais de lixiviation peuvent être classés dans ces deux catégories.

Souvent ont été utilisés, dans le passé, des tests qui n'ont que des liens trop éloignés avec les réalités industrielles et qui consistaient à faire des essais de solubilité sur des échantillons qui, après avoir été solidifiés étaient broyés ou concassés ou avec des solutions à caractère artificiel au lieu d'eau de pluie. Un béton classique soumis à ce genre de test peut se révéler un matériau toxique !

Le plâtre se révélerait un matériau inutilisable alors que les maisons parisiennes (XVIIè) ont souvent défié les années.

Il existe un besoin de définir avec précision des tests simples (utilisables par les exploitants) qui prennent bien en compte les conditions de stockage du déchet solidifié à l'échelle industrielle.

La Société IU CONVERSION SYSTEMS (Dr RAU) présentera une expérience dans ce domaine (6).

On trouvera ci-dessous à titre d'information les résultats obtenus par un déchet traité par un procédé de solidification "intégrée" ayant les caractéristiques suivantes (en g/l) avec le test statique.

pH	Cu	Fe	Zn	Cr	Cd	Ni	Mn
0	9,4	8,1	7,6	1,6	0,038	0,65	0,65

On obtient une eau de lixiviation ayant les concentrations ci-dessous : (expression en 10^{-3} g/litre)

0,1	0,1	1,2	0,1	0,1	0,1	0,1

L'échantillon avait un an. La durée de contact échantillon - eau a été d'une semaine.

Il y a longtemps que les agronomes utilisent des "lysimètres" pour étudier par exemple l'effet d'un épandage d'engrais, de lisier sur un sol et sa flore.

4 - Evolution des procédés

Un certain nombre de facteurs concourrent à une évolution rapide des procédés : d'une part les nouvelles conditions économiques (augmentation du prix de l'énergie, ralentissement de la croissance), d'autre part la constitution d'une masse critique, d'un capital technologique de Recherche-Développement

De nombreux travaux ont été effectués. On ne compte pas moins de quatre cents publications et brevets. Ces travaux sont récents et restent encore à l'état de Recherche-Développement mais dans les années qui viennent, ils devraient donner naissance à de nouveaux procédés industriels exploités. Rappelons que ce domaine très complexe touche à la physico-chimie de l'eau, des liants hydrauliques, la physico-chimie des surfaces. On peut écrire les schémas suivants :

Eau (pure) + liant hydraulique + agrégat ⟶ mortier

Dans le cas de la solidification des déchets (Eau + Agrégat) est remplacé par une variété considérable d'espèces physico-chimiques. Incidemment pour cette raison on peut escompter des retombées sur la connaissance de l'hydratation des ciments hydrauliques et leur utilisation dans des milieux difficiles (eaux usées, mer...).

Ce domaine intéresse de nombreux scientifiques et techniciens dont les travaux devraient contribuer à l'évolution des techniques.

Les méthodes de solidification/fixation contribuent à protéger l'Environnement (Photo Ph. PICHAT)

CONCLUSIONS

Les techniques de solidification-fixation élargissent la gamme des traitements. Cette filière technologique est d'ailleurs pratiquée depuis des années dans le traitement des déchets dits faiblement radio-actifs.

Seule une élite des entreprises de construction possède les moyens scientifiques et techniques nécessaires pour fabriquer des bétons à hautes performances. Compte tenu de la très grande complexité des méthodes de solidification des déchets, ces techniques ne peuvent actuellement être exploitées avec une fiabilité acceptable que par les quelques entreprises ayant acquis le bagage scientifique et technique indispen-

sable à leur exploitation convenable.

Par ailleurs, la jeunesse de cette technologie fait appel à des efforts importants de Recherche-Développement.

BIBLIOGRAPHIE SUCCINCTE

(1) "The Poisoning of America" TIME, 22/09/1980, p. 34-35

"Groundwater contamination poses growing problems" CHEMICAL and ENGINEERING, 8/09/1980

(2) "Toxic and hazardous wastes disposal" Robert POJAZEK Editor Ann Arbor Publishers USA 1979 I

(3) XIè conférence internationale des Arts Chimiques (Société Chimie Industrielle) 6-9 décembre 1977 PARIS

Conférences de MM J. VERON, J.M. BLANCHARD, A. NAVARRO (INSA LYON)
M. JACHIMIAK (ANRED)
M. B. GONTARD (SARP INDUSTRIE)
Pr FRIPIAT (CNRS ORLEANS)
M. BONNET (BRGM)
Pr DELMON (LOUVAIN Université)
Dr BROMLEY (HARWELL U.K.)
P. LONGUET (CERILH)
P. JARRETT (GREATER LONDON COUNCIL)

Présidences de MM AFFHOLDER (ANRED), Pr CHOVIN

(4) "Traitement ultime des boues" ANDES n°13, Mars 1975 p. 2-12 (Philippe PICHAT)

(5) "Fixation of harmful elements by a high grade special cement " H. UCHIKAWA K TSUKIGAMA Y MINORA Onada Cement TOKYO JAPON Zement Kalb Gips n° 4 1978 195-203

(6) LEACH testing of chemically stabilized waste Steven I Taub Beverly K. ROBERTS 3rd annual conference on treatment and disposal of industrial wastewaters and residus Houston Avril 1978

Incorporation d'ions métalliques dans la silice

Incorporation of metallic ions in silica

L. PETIT et P.G. ROUXHET, Groupe de Physico-Chimie Minérale et de Catalyse, Université Catholique de Louvain, 1, place Croix du Sud 1, B-1348 Louvain-la-Neuve, Belgique (*).

RESUME : L'incorporation d'ions métalliques dans la silice entraîne une perturbation du squelette silicique qui se marque dans le spectre infrarouge (glissement de la bande de vibration de valence SiO vers les faibles fréquences) et dans le diagramme de diffraction des rayons X (étalement vers les valeurs 2θ élevées de la bosse caractéristique de la silice). Ces méthodes permettent d'observer l'incorporation, par coprécipitation avec un sol silicique acide, de l'aluminium à un pH égal ou supérieur à 4 et du calcium à pH égal ou supérieur à 9 en milieu concentré. L'action du calcium sur l'organisation du squelette silicique se manifeste même lorsque l'on procède à une coprécipitation de silice et d'aluminium à pH 9, en partant d'un sol silicique; ceci est confirmé si l'on extrait le calcium et l'aluminium du squelette silicique par carbonatation et titrage acide, respectivement.

Les mêmes méthodes instrumentales confirment l'incorporation de métaux de transition (Fe^{3+}, Ni^{2+}, Cu^{2+}) dans la silice par coprécipitation à pH 7 et 9 avec un sol silicique. Des dosages chimiques montrent que l'incorporation de Cu^{2+} et Ni^{2+} est favorisée par la présence de Al^{3+} et Fe^{3+} et par un passage rapide du pH initial du sol silicique au pH de coprécipitation.

SUMMARY : The incorporation of metallic ions in silica produces a perturbation of the siliceous skeleton, which is revealed by the infrared spectrum (shift towards lower wavenumbers of SiO stretching) and the X-ray diffraction diagram (flattening towards high 2θ values of the hump characteristic of silica). These methods show incorporation of aluminium at pH equal to or higher than 4 and of calcium at pH equal to or higher than 9 in a concentrated medium, by coprecipitation with an acidic silica sol. The influence of calcium on the organization of the siliceous skeleton is even marked when silica and aluminium are coprecipitated at pH 9, starting from a silica sol; this is confirmed if calcium and aluminium are extracted by carbonation and acid titration, respectively.

These instrumental methods confirm incorporation of transition metals (Fe^{3+}; Ni^{2+}, Cu^{2+}) by coprecipitation with silica sol at pH 7-9.Chemical analyses show that incorporation of Cu^{2+} and Ni^{2+} is favored by the presence of Al^{3+} and Fe^{3+} and by a quick rise from the pH of silicic sol to the pH chosen for coprecipitation.

(*) Recherche subventionnée par l'Institut pour la Recherche Scientifique dans l'Industrie et l'Agriculture (I.R.S.I.A.)

INTRODUCTION

Beaucoup de chimistes ne reconnaissent la formation d'un solide comme produit de réaction entre certains réactifs que lorsque la phase formée est cristalline. Il est vrai que la diffraction des rayons X est une méthode particulièrement concluante pour identifier une phase solide et mettre en évidence la formation d'une liaison chimique entre des éléments présents dans celle-ci; cependant c'est également une méthode extrêmement restrictive.

Cette communication vise à illustrer l'incorporation de certains ions (Al, Ca, métaux de transition) dans une matrice silicique et la formation de liaisons entre ces ions et la silice par simple coprécipitation.

La possibilité d'incorporer l'aluminium dans une matrice silicique par coprécipitation ne fait plus de doute. Si le mode d'organisation du solide est mal connu, s'il peut être hétérogène, on admet généralement l'existence d'une phase mixte silice-alumine, qui possède notamment des caractéristiques particulières d'acidité et possède de l'aluminium en substitution du silicium (1-6). Les silicates de calcium anhydres ou hydratés offrent un exemple intéressant d'un autre mode d'association chimique entre un ion et la silice. Si la formation de phases cristallines est possible, les produits de réaction fréquemment obtenus sont mal cristallisés ou amorphes (7,8).

Nous allons montrer comment des méthodes très simples comme la spectroscopie infrarouge et l'observation de la large bande de diffraction des rayons X des produits amorphes silicatés permettent de mettre en évidence l'incorporation d'ions métalliques tels que l'aluminium et le calcium dans un squelette silicique. Nous examinerons ensuite le comportement d'ions de métaux de transition vis-à-vis d'une silice en voie de polymérisation. La formation d'oxydes mixtes silice-oxyde ferrique a été moins étudiée que la formation de silico-alumine; la substitution isomorphique du silicium par le fer, moins favorisée que la substitution du silicium par l'aluminium en raison de la dimension de l'ion ferrique, est suggérée par certains auteurs (9) mais rejetée par d'autres (10,11). L'obtention de silicates basiques contenant du nickel ou du cuivre est délicate et nécessite des températures élevées et des temps de réaction longs (12).

METHODES EXPERIMENTALES

Les produits étudiés ont été préparés par une coprécipitation conduite à un pH donné et à température ambiante, en milieu aqueux fortement agité, d'un sol silicique et de l'ion métallique introduit par un sel soluble ($Al(NO_3)_3$, U.C.B. p.a.; $NiCl_2$, $CuCl_2$, $FeCl_3$, Merck p.a.); ils sont recueillis par filtration sur buchner, sans lavage, et séchés à 120°C.

Le sol silicique est obtenu par passage d'une solution de silicate de sodium (Merck) 1.2 M sur une résine échangeuse d'ions (Amberlite IR-120, BDH) saturée en protons. La base utilisée est un lait de chaux à 10% $Ca(OH)_2$ en poids (Merck p.a.)

Les spectres infrarouge ont été enregistrés à l'aide d'un spectrographe Beckman IR-12; la poudre était dispersée dans une pastille KBr de manière à obtenir une épaisseur effective de l'ordre de 0.4 mg/cm^2. Les diagrammes de diffraction des rayons X ont été obtenus en utilisant un diffractomètre Philips (CuK_α, 34 kV ou CoK_α,28 kV); les réglages de l'appareil sont rigoureusement identiques pour tous les échantillons. Le dosage des ions métalliques a été réalisé par absorption atomique

SYSTEME SILICE-ALUMINIUM-CALCIUM

Les figures 1 et 2 se rapportent à des produits préparés à pH 4 et 9, avec une concentration globale Si + Al = 0.6 M et pour des rapports atomiques Si/Al valant respectivement 100/0, 80/20, 60/40, 40/60.

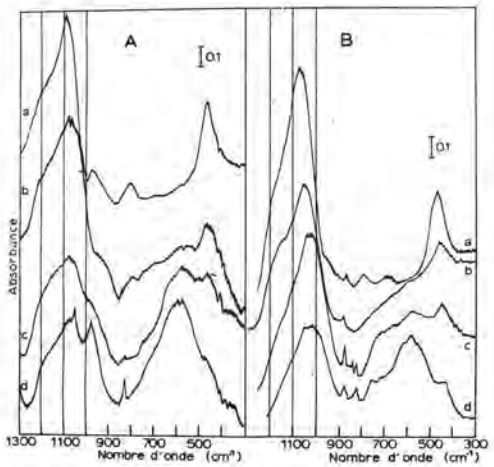

Fig. 1. - Spectres infrarouge de produits obtenus par coprécipitation de silice et d'aluminium à pH 4 (A) et 9 (B); milieu de concentration Si+Al = 0.6 M; rapports Si/Al = (a) 100/0, (b) 80/20, (c) 60/40, (d) 40/60.

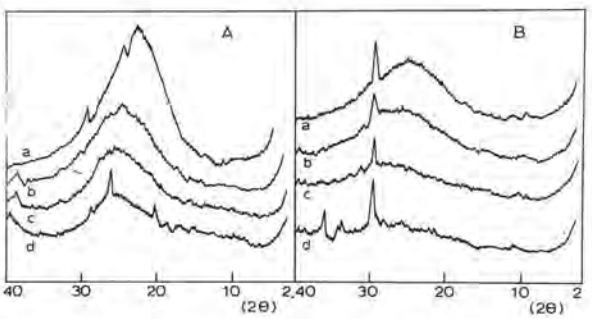

Fig. 2. - Diagrammes de diffraction des rayons X de produits obtenus par coprécipitation de silice et d'aluminium à pH 4 (A) et 9 (B); milieu de concentration Si+Al = 0.6 M; rapports Si/Al = (a) 100/0, (b) 80/20, (c) 60/40, (d) 40/60.

Les spectres infrarouge des produits préparés à pH 4 sont présentés à la figure 1A. La bande donnant deux composantes à 1100 et 1200 cm^{-1} dans la silice pure (spectre a) est due à des vibrations de valence

antisymétriques Si-O-Si; les bandes à 950, 800 et 485 cm^{-1} sont dues respectivement à la vibration de valence Si-O du groupe SiOH, à une vibration de valence symétrique Si-O-Si et à la déformation O-Si-O (13).

Lorsque la précipitation a lieu en présence d'une grande quantité d'aluminium (spectre d) on observe une bande importante à 600 cm^{-1} ainsi qu'une absorption marquée vers 980 cm^{-1}, qui sont probablement dues à une phase libre d'alumine hydratée (13,14). Pour des teneurs intermédiaires en aluminium, on observe un élargissement vers les basses fréquences de la bande à 1100 cm^{-1}. Ce glissement pourrait être dû à une modification des vibrations du squelette silicique (6,13,15) résultant de la substitution de Si par Al; cependant il pourrait également résulter de la présence en quantité croissante d'une phase alumine libre.

Les diagrammes de diffraction des rayons X des mêmes échantillons, présentés à la figure 2A, indiquent un net déplacement vers les valeurs 2θ élevées de la bande de diffusion des rayons X de la silice, qui reflète une perturbation du squelette silicique par l'aluminium et indique donc une incorporation de cet ion. Les fins pics présents sur le diagramme d sont dus au nitrate de calcium.

Le spectre de la silice pure précipitée à pH 9 en présence de calcium (figure 1B, spectre a) présente une bande de valence SiO qui est élargie vers les basses fréquences, en comparaison de la silice précipitée à pH 4. Cet élargissement indique une perturbation du squelette silicique par le calcium; en effet il ne se manifeste pas si le calcium est remplacé par le sodium. La perturbation est confirmée par la comparaison des diagrammes de diffraction de la silice précipitée à pH 4 et 9 (figures 2A et B, diagramme a). Il convient de signaler que cette incorporation de calcium au squelette silicique ne se produit pas si la précipitation à lieu en mettant en oeuvre des réactifs 10 fois plus dilués.

L'évolution de la bande de valence Si-O des produits précipités à pH 9 indique une perturbation très nette du squelette silicique par l'aluminium (figure 1B, spectres b,c,d); cette perturbation est confirmée par l'évolution des diagrammes de diffraction des rayons X (figure 2B). Les pics observés à 2θ = 29.5° à la figure 2B et à 875 cm^{-1} à la figure 1B sont dus à la présence de $CaCO_3$ résultant de l'exposition des échantillons à l'air.

Le traitement d'un coprécipité silice-alumine par HCl donne lieu à une extraction progressive de l'aluminium et à la restauration d'une bande à 1100-1200 cm^{-1} typique de la silice pure. Il est connu que la carbonatation du ciment donne lieu à la production de silice et de carbonate de calcium à partir des silicates de calcium hydratés (16). La figure 3A présente le spectre d'un produit obtenu par précipitation d'un sol silicique à pH 13, de concentration Si=0.4M, avec un rapport molaire CaO/SiO_2 = 3/1; la bande de valence SiO indique que le squelette silicique est nettement plus perturbé que lors de la précipitation à pH 9 (figure 1B, spectre a). Une carbonatation de ce produit a été réalisée en faisant barboter du CO_2 dans la suspension obtenue immédiatement après précipitation, jusqu'à obtention de différentes valeurs du pH. Les spectres infrarouge de ces produits carbonatés (figure 3A) illustrent la restauration d'un squelette silicique non perturbé; le produit obtenu après carbonatation complète donne des bandes de la silice identiques à celles obtenues après attaque acide.

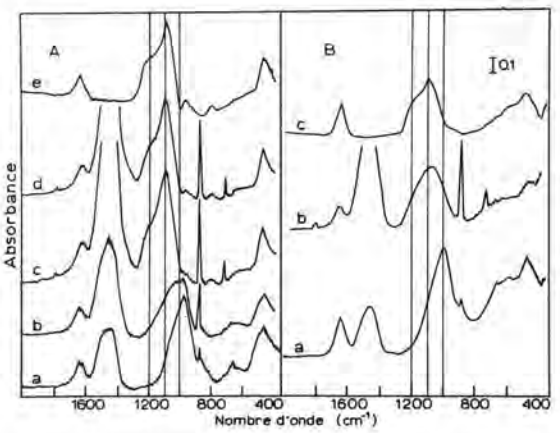

Fig. 3. - Spectres infrarouge :
A - Silice précipitée par la chaux en milieu de concentration Si = 0.4 M et de rapport CaO/SiO_2 = 3 (a); silice précipitée puis soumise à une carbonatation jusqu'à pH 10 (b), 8 (c), 6 (d); silice précipitée, séchée puis traitée par HCl (e).
B - Silico-alumine précipitée à la chaux (Al/Si=0.45, Si+Al=0.5 M, CaO/SiO_2=3) obtenue comme telle (a), soumise à une carbonatation après précipitation (b), traitée à l'acide (c).

La figure 3B permet de bien distinguer la formation de liaisons silice-calcium et silice-aluminium. Le produit de départ a été précipité à pH 13 à partir de réactifs donnant les proportions suivantes Ca/Si = 3, Si/Al=2.2 et une concentration globale Si+Al=0.5 M. Une carbonatation intense de la suspension donne lieu à l'extraction du calcium et à une réorganisation partielle du squelette silicique (spectre b) dont la bande SiO est typique d'une silico-alumine (voir figure 1B, spectres b et c). Une attaque acide complète la réorganisation du squelette silicique (spectre c).

REACTION DE METAUX DE TRANSITION AVEC LA SILICE

Les produits se rapportant aux figures 4 et 5 ont été obtenus à partir d'une concentration Si = 0.07 M dans le milieu réactionnel.

La figure 4A présente les spectres infrarouge de la silice pure, du produit de coprécipitation de la silice avec Fe^{3+} dans un rapport Si/Fe = 3/1 et d'un produit similaire contenant du cuivre et du nickel dans un rapport atomique Si/Ni = Si/Cu = 10/1. La forme de la bande Si-O indique une perturbation du squelette silicique par les métaux de transition, cette perturbation est confirmée par les diagrammes de diffraction des rayons X (figure 5A), qui montrent un étalement marqué de la bande de la silice.

La figure 4B présente les spectres de la silice pure précipitée à pH 9; l'interaction de la silice avec le calcium est très faible en raison de la dilution du milieu. Les autres spectres se rapportent aux produits de coprécipitation correspondant aux rapports atomiques Si/Ni = 10/1, Si/Cu = 10/1 et

Si/(Cu + Ni) = 10/1. Dans tous ces cas on observe un élargissement vers les basses fréquences de la bande SiO, qui reflète une interaction entre la silice et les métaux de transition. Il faut souligner que la perturbation du squelette silicique par Cu et Ni est observée pour un faible rapport ion métallique/Si, de l'ordre de 1/10. Les diagrammes de diffraction des rayons X présentés à la figure 5B montrent que l'incorporation de Ni et Cu est plus marquée à pH 9 qu'à pH 7.

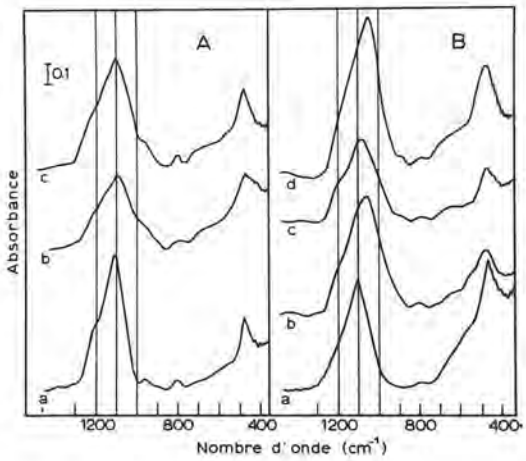

Fig. 4. - Spectres infrarouge de produits précipités en milieu de concentration Si=0.07 M.
A - à pH 7: (a) silice pure; (b) Si/Fe=3/1; (c) Si/(Cu+Ni)=10/1.
B - à pH 9: (a) silice pure; (b) Si/Cu=10/1; (c) Si/Ni=10/1; (d) Si/(Cu+Ni=10/1).

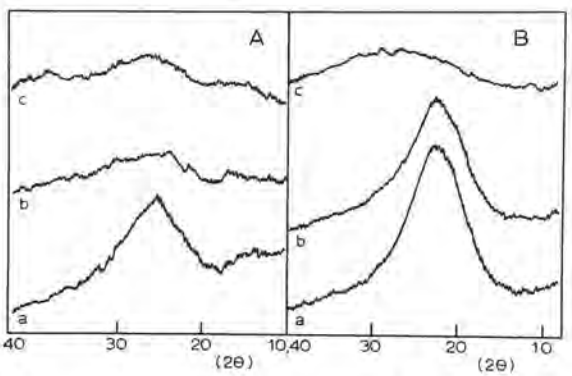

Fig. 5. - Diagrammes de diffraction des rayons X :
A - (CoK_α): (a) silice pure, pH 7; (b) Si/Fe=3/1, pH 7; (c) Si/Fe=3, Si/(Cu+Ni)=10, pH 7.
B - (CuK_α): (a) silice pure pH 7, (b) Si/(Cu+Ni)=10, pH 7; (c) Si/(Cu+Ni)=10, pH 9.

Ces résultats montrent que la rétention de métaux de transition par une silice peut se faire par des liaisons chimiques et n'est pas limitée à une simple adsorption à la surface de particules siliciques (17,18).

Nous avons examiné l'influence du pH de coprécipitation sur le taux de fixation du cuivre et du nickel. A cet effet nous avons mesuré la quantité de ces métaux soustraite à la solution aqueuse lors de la précipitation de silice, de silice en présence d'aluminium avec un rapport Si/Al = 3/1, de silice en présence de fer avec un rapport Si/Fe = 1/1; la concentration initiale du milieu réactionnel était de 10 ppm en Ni et Cu; la quantité de silice mise en oeuvre correspondait à un rapport Si/Ni = Si/Cu = 200.

La figure 6 montre l'évolution du degré d'élimination du nickel et du cuivre en fonction du pH de précipitation. La case A donne, à titre de référence, les résultats attendus sur base d'une simple précipitation des hydroxydes, calculés à partir du produit de solubilité. Ces résultats indiquent que la coprécipitation avec la silice permet l'élimination du nickel et du cuivre à des pH bien inférieurs au pH de précipitation. Il apparaît en outre que la présence d'aluminium ou de fer est favorable à une fixation à plus bas pH.

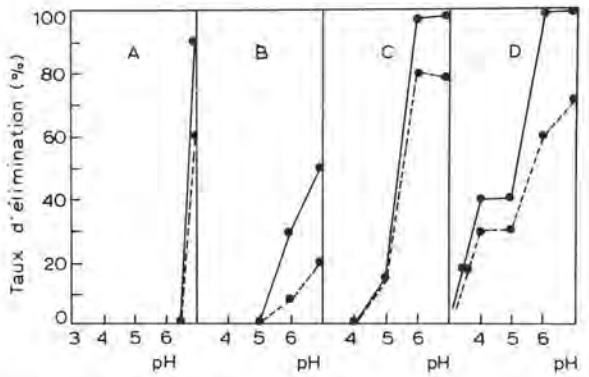

Fig. 6. - Degré d'élimination du nickel et du cuivre à différents pH (10 ppm en Ni et Cu; rapport Ni/Si= Cu/Si = 1/200):
A - résultats attendus sur base d'une simple précipitation;
B - résultats obtenus par précipitation de silice;
C - résultats obtenus par coprécipitation de silice et d'aluminium (Si/Al = 3);
D - résultats obtenus par coprécipitation de silice et de fer (Fe/Si = 1/1).
Traits pleins : Cu, traits discontinus : Ni.

Il ne nous est pas possible de discuter ici les explications de cet effet d'entraînement par l'aluminium et le fer. Il peut être lié aux phénomènes transitoires qui se produisent lorsque le sol silicique est porté au pH imposé pour la coprécipitation; on peut notamment imaginer que, grâce à leur affinité pour la silice à bas pH, ces ions bloquent la polymérisation de la silice et préservent une réactivité qui se manifeste à pH plus élevé.

L'importance de la concurrence entre la polymérisation de la silice et l'incorporation d'autres ions est illustrée par un examen de l'influence des conditions opératoires. Nous avons étudié la précipitation de silice en présence d'aluminium (Si/Al =3/1)

et de nickel et cuivre (Si/Ni = Si/Cu = 20); la concentration du milieu réactionnel en Ni et Cu était de 100 ppm. Outre une coprécipitation à pH 7, nous avons réalisé une neutralisation du sol silicique additionné des métaux par addition d'un lait de chaux à différentes vitesses jusqu'à montée du pH à 7.

Les taux d'élimination du nickel et du cuivre de la solution sont comparés pour différentes conditions opératoires à la figure 7. L'influence sur le cuivre n'est pas marquée en raison de sa faible solubilité à pH 7; par contre il apparaît clairement que l'élimination du nickel est favorisée par une élévation rapide du pH.

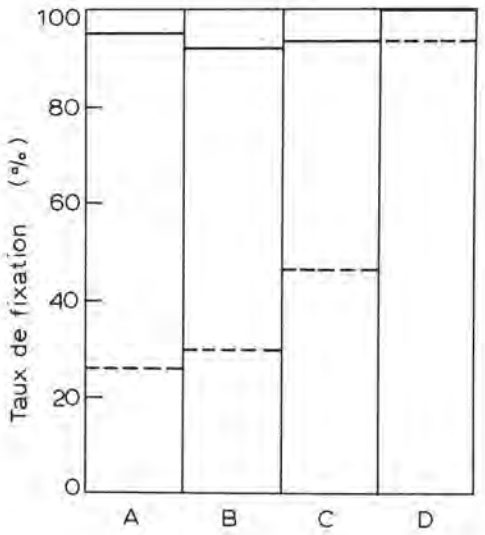

Fig. 7. - Influence du mode de précipitation du système sol silicique-métaux sur le taux de fixation de ces derniers par la silice (Si/Al = 3/1; Si/Ni = Si/Cu = 20): montée jusqu'à pH 7 en 4 jours (A), en 2 jours (B), en 2 minutes (C); coprécipitation à pH 7 (D).
Traits continus : Cu; traits discontinus : Ni.

Nous avons déjà souligné qu'une simple adsorption des métaux lourds sur la surface des particules de gel ne peut rendre compte des caractéristiques structurales des produits obtenus. En raison de ces derniers résultats on ne peut attribuer une part importante de l'élimination des métaux de transition à une induction par la surface silicique de la précipitation des hydroxydes. L'influence du mode opératoire peut s'expliquer par le fait qu'une polymérisation relativement lente, à des pH où les ions Cu^{2+} et Ni^{2+} sont très solubles, produit une silice qui incorpore peu de nickel et de cuivre et est incapable d'en incorporer par la suite. Au contraire une réaction rapide, se produisant d'emblée dans des conditions où les ions Cu^{2+} et Ni^{2+} ne sont pas trop solubles permet à la silice en voie de polymérisation d'incorporer ces derniers.

CONCLUSION

Notre étude montre que la simple précipitation d'une silice en présence d'ions métalliques donne lieu à leur élimination de la solution. Les spectres infrarouge et les diagrammes de "diffraction" des rayons X des solides obtenus montrent qu'il y a une perturbation réelle du squelette silicique par les ions et donc formation de liaisons chimiques entre la silice et les ions; il ne s'agit pas d'une simple adsorption d'ions par la silice ou de l'induction par celle-ci de la formation d'hydroxydes métalliques. Cette incorporation peut se faire à un pH légèrement plus bas que le pH de précipitation des hydroxydes; elle implique que la polymérisation de la silice ne soit pas trop poussée avant que l'on atteigne ce pH.

BIBLIOGRAPHIE

1. - C.L. THOMAS (1949), "Chemistry of cracking catalysts", Ing. Eng. Chem. 41, 2564-2573.
2. - T. MILLIKEN, G.A. MILLS et A.G. OBLAD (1950), "The chemical characteristics and structure of cracking catalysts", Discussions Faraday Soc. 8, 279-290.
3. - J.D. DANFORTH (1960), "Structures and chemical characteristics of cracking catalysts by ion exchange", Actes 2e Congr. Intern. Catalyse, Paris 1, 1271-1286.
4. - A. LEONARD, S. SUZUKI, J.J. FRIPIAT et C. DE KIMPE (1964), "Structure and properties of amorphous silico-aluminas", J.Phys. Chem. 68, 2608-2617.
5. - P. CLOOS, A.J. LEONARD, J.P. MOREAU, A. HERBILLON et J.J. FRIPIAT (1969), "Structural organization in amorphous silico-aluminas", Clays and Clay Minerals 17, 279-287.
6. - P.G. ROUXHET, P.O. SCOKART, P. CANESSON, C. DEFOSSE, L. RODRIQUE, F.D. DECLERCK, A.J. LEONARD, B. DELMON et J.P. DAMON (1976), "The chemistry and surface chemistry of oxides in the silica-alumina range", Colloid and Interface Science, Vol. III (Ed. M. KERKER), Academic Press, New York, 81-94.
7. - H.F.W. TAYLOR (1964), "The calcium silicate hydrates", The Chemistry of Cements, Vol. I, Ch. 5 (Ed. H.F.W. TAYLOR), Academic Press, London,167-227.
8. - P. BARRET, D. MENETRIER et B. COTTIN (1977), "Study of silica-lime solution reactions", Cement Concrete Research 7, 61-68.
9. - D.K. ACQUAYE et J. TRINSLEY (1965),"Soluble silica in soil", Experimental Pedology, (Ed. E.G. HALLSWORTH et D.V. CRAWFORD),Butterworths, London, 126-148.
10. - A.J. HERBILLON et J. TRAN VIN AN (1969), "Heterogeneity in silicon-iron mixed hydroxides", J. of Soil Sci. 20,2, 223-235.
11. - G. PEDRO et A.J. MELFI (1970), "Recherches expérimentales sur le comportement des hydrates ferriques et des constituants silico-ferriques amorphes en milieu lessivé",Pédologie 20,5-33.

12. - R. WEY, B. SIFFERT et A. WOLFF (1968), "Sur la formation de silicates basiques de magnésium, nickel et cuivre. Interprétation des résultats par la théorie des champs des ligands", Bulletin Groupe Français des Argiles, XX, 1, 79-90.

13. - V.C. FARMER (1974), The infrared spectra of minerals, Mineralogical Society, London,pp 539.

14. - C.J. SERNA, J.L. WHITE (1977), "Hydrolysis of aluminium-tri-(sec-butoxide) in ionic and non-ionic media", Clays and Clay Minerals 25, 384-391.

15. - F. HONDA et K. HIROKAWA (1972), "The infrared spectroscopic study of metals intruded into a silica framework", Spectrochimica Acta 28A, 1793-1803.

16. - P.A. SLEGERS et P.G. ROUXHET (1976), "Carbonation of the hydration products of tricalcium silicate", Cement Concrete Research, 6,381-388.

17. - H. BILINSKI, S. KOZAR et M. BRANICA (1976), "Adsorption of heavy metal traces on particulate matter in sea water", Colloid and Interface Science, Vol. III (Ed. M. KERKER), Academic Press, New York, 211-230.

18. - R.K. ILER (1979), The chemistry of silica, John Wiley & Sons, New York, pp. 866.

Caractérisation des boues d'hydroxydes

Characterization of hydroxide sludges

J.M. BLANCHARD, Maître-Assistant, Laboratoire de Chimie Physique Appliquée et d'Environnement, I.N.S.A., 20, avenue Albert-Einstein, 69621 Villeurbanne, France.

RESUME : Préalablement à toute opération de prétraitement visant à solidifier ou à atténuer le potentiel polluant d'un résidu industriel ayant la consistance d'une boue, il est nécessaire de disposer d'une démarche analytique comparative permettant d'apprécier l'impact du déchet initial et du produit résultant du traitement de solidification de ce même déchet.

Cette démarche, que nous avons appliquée aux boues d'hydroxydes, s'inscrit dans une approche scientifique de l'impact de la mise en décharge des résidus industriels.

SUMMARY : Previously to every processing action aimed at solidifying an industrial waste which has a sludge consistence or weakening its polluting potential, it is necessary to have at its disposal a comparative analytical procedure allowing to estimate the impact of the initial waste ant that of the product obtained through the solidifying process of this waste.

This procedure that we applied to hydroxide sludges is inscribed in a scientific approach of the impact of the landfill of industrial wastes.

1.- Aspect théorique - Solubilité des hydroxydes en fonction du pH.

La préparation de surfaces métalliques à base de fer ou d'alliages de métaux de la même famille nécessite souvent une attaque en milieu acide à l'aide de réactifs en solution aqueuse tels que HCl, H_2SO_4, HNO_3 HF, H_3PO_4 pris individuellement ou à l'état de mélange.

Cette attaque des métaux conduit à la formation de sels. Leur dissolution en milieu suffisamment acide donne une solution des ions constitutifs, donc en particulier du cation plus ou moins hydraté.

Si nous ajoutons une solution de base forte, soude, potasse ou comme on le fait souvent dans l'industrie de la chaux, nous allons rendre le milieu progressivement plus basique, et nous constaterons souvent la précipitation d'une espèce nouvelle dont la solubilité est faible, dans les conditions de pH atteintes.

Ce précipité peut ensuite se maintenir ou se dissoudre lorsque nous augmenterons le pH. Il s'agit donc d'un phénomène de solubilité lié au pH qui peut se traduire par les réactions équilibrées suivantes :

$$M^{n+}_{(aq)} + nOH^-_{(aq)} \rightleftharpoons M(OH)_{n(s)} \qquad (1)$$

$$M(OH)_{n(s)} + n'OH^-_{(aq)} \rightleftharpoons M(OH)^{n'-}_{n+n'(aq)} \text{ ou } MO^{\frac{n'-}{n+n''}}_{2} \qquad (2)$$

$(n'' < n')$

Nous avons alors les relations suivantes :

$$K_{S1} = [M^{n+}][OH^-]^n \text{ soit } [M^{n+}] = \frac{K_{S1}}{[OH^-]^n} = K\,[H_3O^+]^n$$

$$\text{avec } K = \frac{K_{S1}}{[OH^-].[H_3O^+]^n} = \frac{K_{S1}}{Ko^n}$$

$$\text{puis } K_{S2} = \frac{\left[MO^{\frac{n'-}{n+n''}}_{2}\right]}{[OH^-]^{n'}} \quad \text{soit :}$$

$$\left[MO^{\frac{n'-}{n+n''}}_{2}\right] = \frac{K'}{[H_3O^+]^{n'}} \quad \text{avec :}$$

$$K' = K_{S2}\,[OH^-]^{n'}[H_3O^+]^{n'} = K_{S2}.Ko^{n'}$$

La solubilité de l'espèce métallique considérée s'écrit :

$$S = [M^{n+}] + \left[MO^{\frac{n'-}{n+n''}}_{2}\right]$$

ce qui permet d'écrire :

$$S = K\,[H_3O^+]^n + \frac{K'}{[H_3O^+]^{n'}}$$

Ce calcul n'est valable bien sûr que lorsque la solution est saturée puisque nous avons établi cette équation à partir des relations données par le produit de solubilité.

S varie en fonction du pH suivant la courbe (1). Les deux branches sont des fonctions exponentielles. La branche de gauche varie surtout comme $K\,[H_3O^+]^n$ ou $K \times 10^{-npH}$, celle de droite comme $K'/[H_3O^+]^{n'}$ ou $K' \times 10^{n'pH}$.

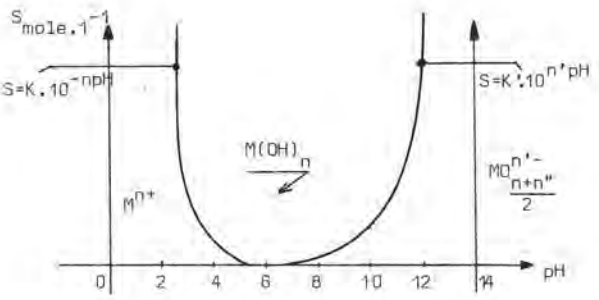

Ainsi, nous avons traité dans son ensemble le problème des hydroxydes amphotères. Les hydroxydes insolubles en milieu plus basique auraient seulement la branche de gauche comme courbe de solubilité.

Enfin, il est intéressant de noter l'effet tampon des hydroxydes ; en considérant la forme de la courbe de solubilité des hydroxydes en fonction du pH, nous voyons que, si nous sommes en présence d'un excès de précipité, le pH de la solution se maintient fixé à une valeur presque constante, tant que l'hydroxyde précipité n'est pas complètement dissous.

Considérons à titre d'exemple 1000 g d'hydroxyde de manganèse $Mn(OH)_2$ qui sont lessivés par 1 l d'eau de pluie renfermant 49 mg d'acide sulfurique par litre (eau de pluie polluée), soit 10^{-3} mole de proton H^+. Que va-t'il se passer ?

Dans l'eau pure on a $[Mn^{++}] = \frac{[OH^-]}{2}$

car on aurait alors $Mn(OH)_2 \rightleftharpoons Mn^{++} + 2OH^-$

$K_S = 4 \times 10^{-14} (\text{mole.l}^{-1})^3$ à 18°C

et donc $\frac{[OH^-]^3}{2} = 4 \times 10^{-14}$ $\qquad [OH^-]^3 = 8 \times 10^{-14}$

$[OH^-] = \sqrt[3]{8 \times 10^{-14}} = 4,31 \times 10^{-5}$

$[H^+] = 2,32 \times 10^{-10}$ $\boxed{pH = 9,63_4}$

Dans l'eau acidulée préalablement $0,5.10^{-3}$ mole de $Mn(OH)_2$ est attaquée selon :

$$Mn(OH)_2 + 2H^+ \longrightarrow Mn^{++} + 2H_2O$$

Donc il reste un excès de $Mn(OH)_2$ et le nouveau pH peut être calculé d'après la réaction de solubilité.

$$4 \times 10^{-14} = [0,5 \times 10^{-3} + \tfrac{x}{2}] [x]^2$$

$\frac{x}{2}$ étant la fraction de $Mn(OH)_2$ provenant de l'équilibre de solubilité. Il vient :

$$x^3 + 1 \times 10^{-3} x^2 - 8.10^{-14} = 0$$

On trouve alors :

$x = 8,9 \times 10^{-6}$ mole.l^{-1} $\boxed{pH = 8,95}$

Il est clair que si le pH a varié de façon relativement importante, cela est dû à la faiblesse des concentrations en Mn^{++} ; mais malgré cela, il va y avoir un apport de 27,5 mg/l de Mn^{++} dans le lessivat.

Ce qui vient d'être dit pour le manganèse est tout aussi valable pour les autres ions métalliques et surtout pour les métaux lourds.

Tout apport d'acide faible ou fort a pour conséquence de libérer des ions métalliques toxiques, même si la quantité libérée est négligeable vis-à-vis de la masse d'hydroxydes. Cette seule considération justifie pleinement la solidification de ces composés dans une matrice minérale présentant des propriétés basiques et difficilement lixiviable dans le milieu naturel.

2.- Aspect pratique. Neutralisation des solutions acides industrielles par la chaux.

a - Cas "idéal"

Il semble a priori relativement simple de neutraliser correctement à la chaux une solution acide contenant seulement plusieurs sels métalliques ; apparemment, il suffirait de maintenir un pH dans la solution tel que la solubilité de tous les différents hydroxydes concernés tende vers une valeur nulle.

En fait le précipité obtenu, une fois décanté et convenablement déshydraté (filtre presse par exemple), s'il est placé tel quel et sans précautions dans le milieu naturel risque sous l'influence des acides humiques, d'acides faibles organiques provenant de fermentation, des eaux de pluies, ou même de réactions d'oxydo-réduction en son sein, de se redissoudre et d'introduire des ions métalliques dans le circuit des eaux naturelles.

L'intérêt d'utilisation de la chaux se trouve à la fois dans son faible coût, mais aussi parce qu'elle permet d'éliminer à l'état de sels de calcium les anions de certains acides (sulfates et fluorures) selon :

$$Ca^{++} + SO_4^{--} \rightleftharpoons Ca\,SO_4$$

$$Ca^{++} + 2F^- \rightleftharpoons Ca\,F_2$$

$$3Ca^{++} + PO_4^{---} \rightleftharpoons Ca_3\,(PO_4)_2$$

Mais à nouveau si le pH redevient acide (pH < 5) la solubilité de ces sels augmente et les ions fluorures sulfates et phosphores repassent en solution, ce qui est extrêmement gênant.

b - La "dure réalité"

En fait, les solutions acides industrielles sont des mélanges extrêmement complexes. Elles renferment généralement :

- des cations métalliques "simples" - Cu^{++}, Ni^{++}, Mn^{++}, Co^{++}, Fe^{++}, Fe^{+++}, Cr^{+++}, qui peuvent déjà poser des problèmes d'oxydo-réduction ;
- des ions minéraux complexes non précipitables à la chaux qu'il faudra préalablement traiter - $Cr_2O_7^{--}$, ($Cr6^+$), NH_4^+, CN^-, ...
- des agents complexants minéraux (NH_4^+ par exemple) ou organiques (pyridine, E.D.T.A. ...) qui entravent la précipitation ;
- des composés organiques plus ou moins toxiques, huiles, hydrocarbures, solvants, des phénols, des détergents.

Il est inutile de préciser que le produit résultant du traitement à la chaux de telles solutions est fort loin des hydroxydes dont nous avons parlé dans le paragraphe 1.

3.- Le problème analytique

La complexité des mélanges obtenus rend illusoire, coûteuse et absurde une analyse physico-chimique complète.

Les seules propriétés intéressant l'élimination d'un tel résidu sont celles qui concernent les interactions de ce dernier et des eaux météorites que l'on peut trouver sur un site de décharge.

Il faut donc disposer d'un test facile à mettre en oeuvre, répétable et peu coûteux pour comparer les potentiels polluants d'un résidu seul et d'un même résidu préalablement solidifié.

C'est en tenant compte de telles constatations que nous avons mis au point une démarche analytique [*] permettant de comparer des échantillons de boues hydroxydes entre eux. Nous avons testé au laboratoire dans le cadre de cette démarche une centaine d'échantillons de boues d'hydroxydes.

---

[*] Contrat I.N.S.A.-M.E.C.V.- Mise au point d'un protocole d'extraction à l'eau des substances solubles ou entraînables contenues dans un déchet solide ou pâteux - Décembre 1979.

Le protocole expérimental que nous avons mis au point consiste à réaliser à l'aide d'une agitation mécanique l'extraction des composés solubles ou entraînables jusqu'à obtention de paramètres physico-chimiques constants (résistivité, pH, mesure d'oxydabilité : C.O.T., D.T.O. ou D.C.O.).

Nous vérifions par une seconde extraction le niveau de solubilité ou d'entraînement des substances extractibles.

L'étude d'un déchet s'effectue alors selon l'organigramme ci-dessous :

1/ IDENTIFICATION préalable { Enquête sur place. Renseignements généraux. Filiation du déchet. Toxiques présumés.

2/ ANALYSES AU LABORATOIRE { Evaluation massique et volumique des phases (eau, boue, huile, émulsion ...). Recherche qualitative des éléments ou combinaisons. EVALUATION DES PARAMETRES CHIMIQUES LIES A LA MISE EN DECHARGE. Test de lixiviation. ANALYSES EAUX USEES.

3/ EXPLOITATION DES RESULTATS { Bilan total des toxiques. Orientation éventuelle des prétraitements. Essais particuliers.

4.- Conclusions pratiques.

Tout d'abord, il faut noter que sous la même appellation plus ou moins précise, se trouve une palette extrêmement étendue de résidus.

Sous l'appellation de boues ferritiques se trouvent toutes sortes de produits de décapage de tôles ou de fûts qui peuvent contenir en plus du fer sous forme $Fe(OH)_3$, des traces de métaux lourds (Pb, Cd, Mo ..), mais aussi parfois jusqu'à 10% d'huile (sur la boue brute), voire même d'autres dérivés organiques (phénols, détergents, agents complexants ...) qui peuvent poser de graves problèmes pour leur mise en décharge.

En plus, si ces boues dites ferriques contiennent des quantités notables de $Fe(OH)_2$ elles s'oxydent à l'air en $Fe(OH)_3$, ce qui a pour conséquence de faire chuter le pH par production de protons et donc de permettre la mise en solution de métaux lourds par exemple.

Enfin, peuvent être considérées en général comme bien traitées, les boues dites de Cr^{3+} qui présentent en général une teneur faible en éléments solubles ou lessivables.

Les problèmes les plus graves sont posés par les boues de centres de détoxication dont la composition varie d'un jour à l'autre et au sein desquelles se trouvent parfois à côté de quantités importantes d'ion ammonium, des complexants organiques (Pyridine, E.D.T.A.) engendrant des fuites chroniques de métaux complexés (Cu, Ni, Cd, ...).

La pollution saline engendrée par les boues hydroxydes est souvent négligeable, sauf accident (cyanures ou Cr^{6+} non éliminés par les traitements préalables à la précipitation des hydroxydes) eu égard à la toxicité potentielle des métaux lourds sous forme ionique.

Ces remarques engendrent deux conclusions précises au niveau des traitements de ces boues :

1/ La nécessité de toujours travailler avec un notable excès de chaux, même si les eaux résultant du traitement ont un pH supérieur à 9 ("fuites" de chaux), car ainsi les boues obtenues ne risquent pas de relarguer rapidement des ions des métaux constituants des hydroxydes.

2/ La solidification d'une boue est une opération difficile car la complexité des mélanges traités conduit à ne considérer que des cas d'espèces.

Importance de l'absorption des ions métalliques sur les surfaces minérales dans le procédé de flottation

Importance of metallic ions absorption on the mineral surfaces in the floating process

V. FORMANEK, Ingénieur E.N.S.C.T., Conseiller Technique de Minemet Recherche (Groupe « IMETAL »), France.

R E S U M E.-

La modulation de la solubilité des ions métalliques est à la base du procédé de valorisation des minerais par flottation.

Les ions métalliques libérés au cours des différentes phases du processus sont neutralisés par l'utilisation de toutes les forces d'origine chimique ou physico-chimique qui se développent à l'interface solide-liquide et par l'addition de réactifs tels que la chaux, les silicates, etc.....

L'importance de l'hydratation et des structures minérales environnantes sur la précipitation des ions métalliques est soulignée.

-:-:-:-

1.- INTRODUCTION.-

L'absorption sélective d'ions minéraux et organiques sur la surface de particules minérales en suspension dans l'eau est à la base du procédé de flottation.

Pour séparer les minéraux de valeur, préalablement libérés de leur gangue par le broyage, l'industrie utilise à grande échelle le procédé de flottation qui fait appel aux différences des propriétés physico-chimiques des surfaces. On utilise des réactifs, qui se fixent spécifiquement sur les minéraux de valeur à récupérer, qui rendent leur surface hydrophobe afin de permettre l'accrochage de bulles d'air.

Ce sont les bulles d'air, finement dispersées dans la pulpe, qui effectuent le tri entre les grains hydrophobes et les grains hydrophiles circulant dans les cuves de traitement.

La plupart des réactifs organiques utilisés pour hydrophobiser la surface forment un composé insoluble avec l'ion du métal à récupérer.

On utilise par exemple des xanthates pour former des composés insolubles avec le plomb, le cuivre, l'argent, etc....., ou encore des acides gras pour former des composés insolubles avec les ions calcium, fer, tungstène etc.... de la surface du minéral.

Ce sont les ions actifs de la surface du minéral qui interviennent directement dans le procédé de flottation.

Mais le minéral de valeur à récupérer par insolubilisation et hydrophobisation de sa surface est environné d'autres minéraux qui libèrent des ions métalliques et non métalliques qui peuvent perturber complètement le procédé de flottation.

La flottation est un système à trois phases : solide - eau - air.

Or, lorsqu'un solide est immergé dans l'eau, il y a intéraction avec les molécules polaires de l'eau et les ions de la surface du solide. Les énergies de liaison hydrogène de l'eau avec les sites non électriquement saturés de la surface du solide conduisent à la formation d'une atmosphère de molécules d'eau dipole fortement orientées ; cette surface est alors hydrophyle.

Plus la surface du solide a une charge électrostatique élevée, plus la surface est hydratée.

La plupart des minéraux immergés dans l'eau possèdent une charge superficielle due :

- soit à des remplacements isomorphiques dans le réseau,

- soit à un déficit ou un excès superficiel d'ions constitutifs du réseau,

- soit à la formation sur la surface d'acides faibles par suite de l'hydratation de groupements superficiels. (Cas des oxydes, des silicates, des carbonates, des phosphates, etc...).

Les solides ont alors un comportement d'échangeurs d'ions. Ainsi dans une eau pure, à la température ambiante, il se dissout :

2,4 mg/litre de sulfate de baryum

14,3 mg/litre de carbonate de calcium

16 mg/litre de fluorure de calcium

Enfin, l'hydratation d'une surface solide peut aboutir à une réaction chimique comme la décomposition de sulfures, formation d'hydroxydes, etc...

Il en résulte qu'un certain nombre d'ions sont mis en solution dans l'eau. Ces ions vont réagir avec les zones des surfaces de minéraux à haut potentiel d'énergie pour tendre vers le point de charge nulle (PCN).

Lorsque la liaison normale est d'origine électrostatique, l'absorption est contrôlée par le pH de la solution.

Selon la nature des charges (électrostatique, chimique ou physique), l'absorption des ions sera réversible ou irréversible.

Les paramètres qui déterminent le degré d'absorption des ions de la pulpe sont principalement la stabilité de la surface (importance et nombre de sites à énergie libre), la surface spécifique, la concentration dans la pulpe de l'absorbant et de l'absorbat, la valeur du pH, les conditions d'agitation.

La quantification des intéractions qui se produisent à l'interface eau-minéral peut être faite par les méthodes électro-cinétiques, par la détermination de la solubilité des composés qui se forment en fonction du pH et de la réaction du réactif collecteur avec le minéral. On utilise de plus en plus les diagrammes de potentiel des systèmes Métal-ion-eau, proposés par Du RIETZ et de POURBAIX, et qui maintenant sont établis sur ordinateur. (1)

D'autres moyens d'investigation électroniques sont en cours de développement pour avoir une meilleure connaissance du mécanisme de l'absorption et du chimisme de l'interface. (2)

(1) M.H. FRONING et E.D. VERINK - "A computer program from calculation of Potential pH Diagrams of metal-ion-water systèms".
Université de Floride - Gainesville (Collège of Engineering) - 1976.

(2) J.L. Cécile et G. BARBERY "Techniques nouvelles de l'étude des interfaces"
Congrès de la Sté de l'Industrie Minérale - Perpignan - 1979.

Il est de première importance dans le procédé de flottation de pouvoir maîtriser à tous les stades du traitement la solubilité des différents ions présents dans l'eau et à l'interface solide-eau.

2.- MODULATION DES IONS METALLIQUES DE LA PULPE AU STADE DU BROYAGE.-

L'importance de la mobilité des ions métalliques apparaît dès la première phase du traitement qu'est le broyage et dont la fonction est de libérer les minéraux de valeur plus ou moins finement imbriqués dans la gangue stérile. En fonction de ses caractéristiques et de son schéma de traitement, le minerai subit un broyage plus ou moins fin, en un ou plusieurs étages.

Le schéma de broyage, les types d'appareils et de corps broyants, les additifs de broyage, auront une influence sur le nombre de sites à énergie libre des particules créées et sur les ions métalliques solubilisés ou précipités.

Le broyeur est un réacteur, où par suite de la formation de surfaces nouvelles, par suite de la transformation de l'énergie en chaleur, par suite des conditions intenses de mélange, par suite de l'aération, se produisent des intéractions importantes à l'interface solide-eau.

Un certain nombre d'ions des substances minérales passent en solution pour être immédiatement plus ou moins réabsorbés sur les surfaces fraiches.

Les sulfures de plomb, de cuivre, de zinc, de fer, sont soumis, sous l'action combinée de l'oxygène et de l'élévation de la température de la pulpe au cours du broyage, à des réactions d'oxydation avec libération d'ions métalliques qui se refixent sur les sites des surfaces à haute énergie libre des surfaces. Ces phénomènes sont accentués lorsque la gangue est basique.

IL en résulte pour le procédé de flottation une diminution importante de la sélectivité et des rendements métalliques.

Les remèdes connus jusqu'à présent consistent à neutraliser in situ les ions métalliques par insolubilisation soit par addition d'un réactif collecteur organique (xanthate, di-thiophosphate), soit par précipitation à la chaux, au carbonate de soude, au silicate de soude, soit par cémentation sur de la poudre de fer métallique ajoutée au broyeur. (*)

(*) M. REY et V. FORMANEK
"Quelques facteurs influançant la sélectivité dans la flottation différentielle des minerais plomb-zinc, particulièrement en présence des minéraux oxydés du plomb".
Congrès de Préparations des Minerais - Londres 1960.

Ces moyens d'insolubilisation des ions métalliques ne sont pas cependant d'une efficacité absolue comme le montrent les essais comparatifs avec des broyages à sec ou en broyeurs autogènes, dans lesquels les ions métalliques ne sont pas autant libérés.

Indépendamment de la modification des niveaux d'énergie, un broyage très poussé, en augmentant considérablement la valeur de la surface spécifique du minéral broyé, peut accroître sa solubilité. Des micro-particules de calcite, d'anglésite, de malachite, etc...., se dissolvent et viennent accroître la quantité de sels solubles qui ont un effet nocif en flottation.

Un autre phénomène prend également plus d'importance dans les broyages fins, c'est le "slime coating". Certaines fines particules se fixent aux particules plus grossières, probablement surtout par des forces d'origine chimique.

La calcite, l'hématite, par exemple, sont fréquemment responsables, par suite du phénomène de slime coating, de mauvais rendements. Nous verrons plus loin que ce "slime coating" peut, par contre, être bénéfique pour le piégeage des ions des métaux lourds dans les boues de décantation, lors des séparations solide-liquide.

Dans certaines conditions de broyage (broyage ultre-fin, broyage dans des systèmes à forte dissipation d'énergie sous forme de chaleur) des surfaces minérales verront leur niveau énergétique homogénéisé vers le niveau le plus bas ; il y aura amorphisation. On aura une insolubilisation des ions métalliques. (*)

L'amorphisation des surfaces n'est pas recherchée ici puisqu'elle détruit les différences de propriétés de surface qui sont précisément utilisées dans les procédés de séparation par flottation.

(*) J.M. CASES, P. DEGOUL, G. GOUJON, JF DELON
"Influence du broyage sur les propriétés superficielles des solides et sur la collection"
Journées d'études de la Section Minéralurgie de la Sté de l'Industrie Minérale - TOULOUSE (octobre 1975).

Discussion de la communication de BRADLY A.H. HURD A., L. LLOYD, P.J.D. et SCHYMURO K.
"Développements in Centrifugal Milling"
European Symposium Particle Technologie - AMSTERDAM 1980.

3.- MODULATION DES IONS METALLIQUES DE LA PULPE AU STADE DE LA FLOTTATION.-

Dans la phase de flottation proprement dite, les minéraux, sous forme d'une suspension aqueuse entre 20 et 50 % de solide, fortement aérée, reçoivent des réactifs modulateurs de l'hydrophilie des différentes espèces de particules : régulateurs de pH, sequestrants ou précipitants des ions métalliques, collecteurs, moussants.

Toutes les surfaces de sulfures métalliques mises en contact avec de l'eau aérée s'oxydent. L'oxydabilité des sulfures métalliques dépend de l'environnement et du type de sulfure ; elle croît dans l'ordre : galène, pyrite, blende, chalcopyrite, pyrrhotine, mispickel.

Dans les pulpes, il y a de nombreux consommateurs d'oxygène : certains sels dissous comme les sels ferreux et cuivreux, le fer d'abrasion des boulets et des revêtements métalliques des appareils, la présence de minéraux fortement oxydables.

Aussi, étant donnée la complexité des phénomènes intervenant simultanément dans la pulpe de la flottation des minerais polymétalliques, la mise au point des conditions opératoires ne peut qu'être facilitée par le suivi du potentiel redox, la teneur en oxygène dissous, et le pH.

Dans toutes ces opérations, il s'agit d'insolubiliser sélectivement les ions des métaux lourds et des alcalino-terreux. On dispose de tout un arsenal de réactifs minéraux et organiques. (Thiosels, acides carboxyliques, alkylsulfates, alkylphosphates, amines, chelatants, cyanure, polyphosphates, silicates, tannins, charbon actif, colloides, etc....).

4.- MODULATION DES IONS METALLIQUES DE LA PULPE AU STADE DE LA SEPARATION SOLIDE-LIQUIDE.-

Dans la phase finale, décantation, séparation solide-liquide, l'insolubilisation des métaux lourds doit être alors non-sélective et aussi totale que possible. En effet, le plus généralement les eaux, après décantation, sont renvoyées par pompage au bassin de stockage des eaux industrielles avant d'être de nouveau recyclées dans l'usine de traitement.

Les réactifs utilisés en cours de traitement sont absorbés tout au long du circuit par le minerai, ou neutralisés.

Des analyses chimiques, biochimiques et toxicologiques montrent qu'on ne les retrouve sous aucune forme dangereuse dans les eaux résiduaires de l'usine.

Les résidus solides sont déversés dans des zones d'épandage spécifiquement aménagées pour éliminer tout risque de pollution mécanique et pour répondre aux normes actuelles relatives à la protection du site et de son environnement.

A titre d'exemple, indiquons que l'usine de Largentière, dans l'Ardèche, avec une production journalière de 2.700 tonnes de minerai brut, sort environ 2.500 tonnes de rejets sous forme de pulpe que l'aire de stockage doit être en mesure d'emmagasiner et de décanter chaque jour ; ceci représente le traitement de près de 200 m^3/heure d'eaux chargées de particules solides très fines. Depuis le démarrage de l'exploitation, plus de 5 millions de tonnes de solides furent ainsi déversés dans la zone d'épandage.

En ce qui concerne la qualité des eaux résiduaires, le tableau ci-dessous, extrait d'une publication récente sur la mine de St SALVY, indique que les teneurs en métaux lourds sont inférieures aux normes actuelles.

Tableau

Qualité des eaux résiduaires de l'usine de traitement de minerais de St SALVY.

Contrôle mensuel des effluents

Août 1978 - Quantités exprimées en mg/l

	Normes SSB	Normes Complément.	Teneurs SSB
pH	5,5 - 8		7,6
MeS	50		4,3
DBO		40	
DCO	100		20
Azote total		12	1,2
H_2S	0,5		0
Cyanures		0,1	< 0,05
Fluorures	15		3,9
Arsenic		1	0,002
Cadmium		3	0,002
Cuivre		2	0
Fer		2	0,1
Plomb		1	0,0004
Zinc		6	0,4
Aluminium		2	0
Cobalt		3	-
Cr total		2,2	0
Etain		2	-
Mercure		0,1	0,0006
Total métaux lourds	15		0,505

Ce tableau est extrait de la "Monographie de la

laverie de Noailhac - SAINT SALVY" (de H. GISTAU et A. MILHAU - publiée dans la revue de l'Industrie Minérale de février 1980).

La faible quantité d'ions métalliques dans les eaux résiduaires des usines de traitement de minerais par le procédé de flottation s'explique, par le contrôle et l'ajustement du pH qui est réalisé de façon à obtenir la précipitation d'ions métalliques sous forme d'hydroxydes; et par l'exploitation des phénomènes d'absorption propres aux fines particules. (slimes).

En effet, l'action du pH seul, par addition de chaux par exemple, n'est pas suffisant car il y a formation de flocs d'hydroxydes volumineux qui sédimentent difficilement.

En présence de slimes minéraux, la situation est fortement modifiée : la précipitation des ions peut être obtenue à un pH beaucoup plus bas et par suite de l'absorption des flocs par le phénomène de "slime coating", ces ions métalliques sont piégés par les substances minérales.

Ce phénomène de "slime coating" varie naturellement en intensité avec le type de minéral utilisé. Les roches de type basique sont préférables aux roches de type acide.

La fluorine, le calcaire, la pyrite (FeS_2), la pyrrhotine (FeS), le feldspath, le quartz, peuvent être, par le phénomène de "slime coating", de remarquables sequestrants des ions métalliques.

Ainsi une tonne de particules, ayant une surface de 20.000 cm^2 par cm^3, séquestrent entre 1 à 2 kg d'ions Mg^{2+}, Cu^{2+}, Pb^{2+}, Zn^{2+}, Cd^{2+}, Fe^{2+}, Fe^{3+}, Cr^{3+}, Mn^{2+}, présents dans les eaux.

Ces propriétés absorbantes des particules minérales, sous forme de slimes, sont précisément utilisées pour purifier des eaux industrielles ou des eaux urbaines. (*).

En SUEDE, l'eau d'un lac au nord-ouest de Stockholm, polluée par des ions mercure provenant d'une usine proche, a été complètement assainie par addition de particules fines de fluorine et de calcaire. Ces substances minérales absorbaient, de façon irréversible, jusqu'à 10 kg de mercure par tonne.

L'absorption du mercure (et de l'arsenic) sur le calcaire ou sur la fluorine est renforcée par la présence de fer, sous forme métal ou sous forme ionique.

Des essais ont montré que la pyrrhotine, à surface spécifique équivalente, pouvait fixer plus de 350 kg de mercure par tonne.

Le mercure est alors bloqué sous forme de sulfures de mercure particulièrement insoluble (produit de solubilité 10^{-53}).

Les slimes de calcite et de fluorine sont également utilisés pour abaisser la concentration des phosphates dans les eaux par formation de phosphate de calcium et de fluorophosphate insolubles.

Pour toutes ces opérations de purification des eaux, il faut utiliser des substances minérales fraichement broyées.

5.- CONCLUSIONS.-

Les minéraux, notamment s'ils sont broyés, présentent, une fois immergés dans l'eau, une surface hétérogène avec des charges superficielles qui ont un rôle déterminant dans les mécanismes de l'absorption sélective des ions métalliques et des tensio-actifs. Ces absorptions sélectives sont à la base de la valorisation des minerais par le procédé de flottation.

C'est par la modulation de la solubilité et de l'absorption des ions métalliques à l'interface minéral-eau qu'il est possible de séparer sélectivement les minéraux de valeur de ceux de la gangue, en jouant sur l'hydrophobie et l'hydrophilie induite par l'addition de réactifs.

Les propriétés absorbantes des surfaces minérales peuvent être considérablement modifiées par le broyage, le temps de séjour dans l'eau, les ions environnants, etc....

Des recherches sont encore nécessaires pour mieux connaître les phénomènes d'hydratation des surfaces et le chimisme de l'interface.

Néanmoins, les intéractions absorbat-absorbant à l'interface eau-substance minérale continuent d'être très largement exploitées à l'échelle industrielle pour la valorisation des minerais et pour la purification des eaux.

-:-:-:-:-

(*) G. BROMAN "Purification of industrial and municipal waste water by means of mineral slime" 11ème International Mineral Processing Congress CAGLIARI - 1975.

Stabilizing industrial sludge for fill applications

Stabilisation des boues industrielles pour comblement d'excavations

J.J. EMERY, Associate Professor, Department of Civil Engineering and Engineering Mechanics, Ms Master University, Hamilton, Ontario, Canada.

RESUME : Un procédé de stabilisation des boues industrielles a été mis au point récemment. La boue obtenue, qui sert à des fins de comblement d'excavations, répond à la fois aux besoins de la protection de l'environnement et à ceux du génie civil. Des mélanges contenant différentes proportions de boues, de cendres volantes, de poussières de fours, et de ciment, sont utilisés dans un procédé combiné "séchage-pouzzolanique-hydraulique", selon le degré de résistance exigé. Des tests de solidification et de solubilité sont décrits ainsi que les détails des essais faits dans des conditions normales et leurs résultats.

SUMMARY: A stabilization process for industrial sludge has been developed that meets both environmental and engineering requirements for use as fill. Various combinations and proportions of sludge with fly ash, waste kiln dusts, and cements are used in a combined drying/pozzolanic/hydraulic process, depending on the desired strength development. Laboratory solidification and solubility testing is described along with details on field trial procedures and results.

INTRODUCTION

Expansion of a steel plant in Hamilton requires both the removal of a large quantity of very soft, high water content, industrial sludge from an old disposal area, and replacement with suitable fill to provide a construction site. Some treatment of the sludge to meet landfill disposal requirements would be required (1), and various stabilization methods have been evaluated in the laboratory and small field trials. It has been found that the sludge can actually be satisfactorily stabilized/solidified to meet both environmental (solubility of toxic constituents) and engineering (bearing capacity) requirements for industrial site fill applications. Thus, the disposal area reclamation process will consist of removing the sludge by stone fill displacement below the water surface and dredging (in progress), stabilization, and then return to the site to act as fill above the water table.

The stabilization process involves a number of possible combinations and proportions of sludge with stabilizing agents - fly ash, waste cement kiln dusts, waste lime kiln dusts, steel slag fines, portland cement, and slag cement - to give various strengths and rates of strength gain for the highly variable sludge. Industrial byproducts have been used where possible, with low level cement additions, to minimize stabilization materials costs. A wide range of these byproducts has also been evaluated to ensure supply continuity. Construction soil stabilization concepts have essentially been adopted involving initial drying by high surface area materials (fly ash, dusts) and then pozzolanic and/or hydraulic reactions as required. For disposal to landfill, just some drying and fairly low strengths (shear strength ≈0.01 to 0.02 N/mm^2, equivalent to soft clay) are desirable, while for fill, initial handling strength and then high strength development (shear strength >0.1N/mm^2, equivalent to very stiff clay) is required.

As the various combinations and proportions of materials used are largely a function of the specific industrial sludge involved, masses of test data will not be given, but rather the methodology, and typical combinations and strengths. For the reader interested in a more complete review of stabilization/solidification technology than can be incorporated here, the volumes edited by Pojasek are excellent (2).

INDUSTRIAL SLUDGE

The industrial sludge involved (approximately 300,000 m^3) had been deposited over a number of years under lake level in an old harbour slip area adjacent to the plant. Geotechnical studies indicate the sludge is fairly consistent in appearance along the slip - very loose, oily, black, organic metallic (mainly iron oxide) waste - but highly variable in moisture content (29 to 75%, weight of water to total weight used throughout), insitu bulk density (1300 to 1650 kg/m^3), and loss on ignition (7 to 31%). While mainly of industrial origin from rolling mills, at early stages the slip received municipal sewage. In summary, a rather unpleasant and variable industrial sludge is involved.

LABORATORY STABILIZATION TRIALS

A simple laboratory procedure for preparing and monitoring stabilized sludge was developed so that a wide range of stabilizing agents and addition rates could be considered to provide information for field trials and costing. This involved mixing the sludge with the selected quantities of stabilizing agents in a small Hobart mixer (or by hand) until consistent, placing this mix in 10 cm diameter by 10 cm high cans, sealing the can with both a twist lid and double plastic bags to maintain moisture conditions, and then taking penetrometer* readings to monitor unconfined compressive strength development with time at 20°C(3). Supplemental tests included pH, moisture content, temperature and bulk density monitoring.

This approach is considered more representative of conditions in a large mass of solidifying sludge than open curing where significant strength development may be due to simple drying, rather than cementitious reactions. Other conditions can be readily simulated in the laboratory such as lowered or elevated temperatures and curing under water.

Some typical laboratory stabilization trials for a 46% moisture content sludge (combinations and proportions by weight, with 1, 7, 14 and 21 day penetrometer strengths in brackets) would include:

80% sludge/15% lime kiln dust (quick)/
5% portland cement
(0.29,0.43, >0.43, >0.43 N/mm^2)
80% sludge/15% lime kiln dust (quick)/
5% slag cement
(0.25, 0.31, 0.41, 0.43 N/mm^2)
80% sludge /15% cement kiln dust (bypass)/
5% portland cement
(0.04, 0.42, 0.43, >0.43 N/mm^2)
80% sludge/15% lime kiln dust/5% portland cement
(0.12, 0.20, 0.22, 0.24 N/mm^2)

*Soiltest Pocket Penetrometer CL-700 which gives a direct measure of unconfined compressive strengths up to 0.43 N/mm^2 (4.5 TSF). For a safety factor of 3, these readings are very close to the safe bearing capacity for a footing at the surface of a cohesive soil. However, care should be taken in extrapolating to the field as correlations have not been checked.

80% sludge/15% fly ash (≈8% carbon)/5% lime kiln dust (quick)
(0.07, 0.12, 0.17, 0.18 N/mm^2)
75% sludge/15% lime kiln dust/10% fly ash (≈8% carbon)
(0.16, 0.27, 0.30, 0.34 N/mm^2)
75% sludge/20% cement kiln dust/5% portland cement
(0.02, 0.20, 0.43, >0.43 N/mm^2)
75% sludge/15% fly ash (≈8% carbon)/5% lime kiln dust/5% portland cement
(0.12, 0.24, 0.43, >0.43 N/mm^2)
75% sludge/15% fly ash (≈8% carbon)/5% lime kiln dust/5% slag cement
(0.04, 0.12, 0.15, 0.31 N/mm^2)

These results for stabilization trials meeting strength requirements for landfill and/or structural fill indicate that the high organic content is not stopping pozzolanic and hydraulic reactions, but probably inhibiting them to some extent. Quick (i.e. unslaked) lime kiln dust is much more efficient than ordinary calcitic or dolomitic lime kiln dust and slag cements require a fair degree of alkaline activators. The additive costs are in the Can.$1.50 to $4.00 range per tonne of final stabilized material. The combinations and proportions for satisfactory stabilization of a wide range of sludge moisture contents have been established.

To check that miniaturization of the laboratory strength gain tests is valid, some large, 90 kg samples were prepared with various stabilizing agents and mixed in an Eirich R-7 mixer using only the drum rotation to simulate a large stabilization plant pugmill. Both sealed curing and curing under a 0.8 m head of water were considered at a 7 to 13°C temperature range to simulate cooler field conditions. Strength development monitored with a penetrometer and probe rod indicated similar results to parallel small samples. These results, particularly for the submerged curing, supported the laboratory test methodology adopted. While bearing capacity is the major geotechnical factor of concern, it is planned to complete laboratory triaxial, consolidation and permeability testing on specimens recovered from the early full-scale stabilization work (4).

SOLUBILITY TESTING

The major environmental concern with any industrial sludge is the potential level of soluble toxic constituents and their significance to the fill design. However, there are a number of solubility testing procedures and acceptable toxic constituent levels to choose from (5-9). The writer has adopted and modified an OECD solubility test procedure (7) as it gives the required solubility rate for each constituent of interest. Selection of the maximum allowable concentrations of toxic constituents is not easy as indicated by the range in Table I for various agencies.

The results for typical solubility tests on the raw and stabilized industrial sludge are given in Table II. Batch kinetics and desorption isotherms indicated a 1 g sludge to 0.05 ℓ distilled water ratio and 24 hour shaking to be appropriate. Unfortunately, the shaking at 3 Hz is rather aggressive, even on stabilized sludge, so there was continuous turbidity in the shaker flasks. After 24 hours, the shaker flask contents were allowed to settle, the supernatant drawn off and filtered, and the filtrate stored in a refrigerator until chemical analysis. This was repeated four more times although only the first, third and fifth shaking results are given in Table II. While not shown here, it is also possible to draw solubility curves from the data for each constituent as cumulative solubility in mg/g against cumulative filtrate in ℓ/g.

The solubility data summarized in Table II indicate that the stabilization has reduced trace element constituent levels in all cases except copper and lead, but these are still well below the maximum allowable (EPA extract or Ontario industrial effluent in Table I for instance). While the alkalinity that results from the stabilization materials is important and very effective in limiting the solubility of many trace metals, this is probably not the case for copper and lead. Since the stabilized sludge was broken up before testing and then continually reduced during shaking (constant rates of solubility indicate this), the solubility test is far too severe to represent field conditions. This is now being checked by using a much gentler shaking action and column tests (6). Cadmium will also be considered in future solubility testing.

Regardless, it is clear that the stabilized sludge is fully acceptable from an environmental viewpoint.

FIELD TRIALS

Field trials to check the possibility of completing the stabilization in-situ (generally under water) without removing the sludge were completed early in the study. This involved the use of a large drag-line to mix waste cement kiln dust into the sludge. Where adequate mixing was achieved there was a noticeable stiffening of the sludge. Unfortunately, this process required too much machine time and there were substantial pockets of unstabilized sludge. It was decided at this stage that the sludge would have to be put through some sort of stabilization plant to produce the desired strength properties, and stabilized material would probably only be used for fill above the water table. A few simple trials using a large grader to mix sludge with waste kiln dusts confirmed that "proper" mixing resulted in the required stabilization. At this stage, the laboratory testing was emphasized to develop a range of suitable combinations and proportions of stabilizing agents.

TABLE I TYPICAL MAXIMUM ALLOWABLE CONCENTRATIONS OF SUBSTANCES IN WATER

Maximum Level in mg/ℓ

Substance[a]	EPA Drinking Water Standards[b]	EPA Extract[c]	Ontario Drinking Water (9)	Ontario Industrial Effluent Discharges (8)
	Interim Primary			
Arsenic	0.05	0.50	0.05	
Barium	1.0	10.0	1.0	
Cadmium	0.01	0.10	0.01	0.001
Chromium (VI)	0.05	0.50	0.05	1.0
Flouride	1.4-2.4		1.2-2.4	
Lead	0.05	0.50	0.05	1.0
Mercury	0.002	0.02	0.002 water quality	0.001
Nitrate (as N)	10			
Selenium	0.01	0.10	0.01	
Silver	0.05	0.50	0.05	
	Secondary			
Chloride	250			
Copper	1			1.0
Iron	0.3			
Manganese	0.05			
Nickel				1.0
Sulphate	250			
Tin				1.0
Zinc	5			
pH	6.5-8.5			5.5-9.5

Notes: a. Only ions and pH listed here. For pesticides, radioactivity, etc., see references cited.
b. EPA interim primary and proposed secondary drinking water standards. For full listing see Reference 5.
c. Extract based on EPA extraction procedure. Levels specified are ten times the EPA national interim primary drinking water standards. For full details and listing see Reference 5.

TABLE II COMPARISON OF SOLUBILITY TEST DATA FOR RAW AND STABILIZED INDUSTRIAL SLUDGE

Sample	Analysis of Filtrate, mg/ℓ											
	Ca	Cu	Fe	Hg	Mn	Mg	Ni	Pb	Zn	Cl^-	$SO_4^=$	pH
R-1	8.3	0.01	0.16	0.00032	0.08	2.5	0.02	<0.01	0.07	5.8	10.9	6.6
R-3	11.1	0.02	0.07	0.00011	0.57	1.5	0.03	<0.01	0.10	0.8	19.6	7.6
R-5	7.2	0.04	0.18	0.00012	0.71	2.2	<0.01	<0.01	0.37	1.3	24.7	7.4
S-1	160	0.04	0.06	0.00008	0.01	0.02	0.02	0.04	<0.01	9.0	2.9	11.9
S-3	81	0.02	0.06	0.00018	<0.01	0.06	<0.01	0.03	<0.01	7.0	1.4	11.5
S-5	111	0.04	0.06	0.00005	<0.01	0.03	<0.01	0.02	<0.01	9.1	3.4	11.7

Notes: a. Using OECD test procedure adopted in Construction Materials Laboratory (7). Solid (70 g) to distilled water (pH 6.4) ratio of 1 g to 0.05 ℓ. Cr <0.01 mg/ℓ in all cases.
b. Raw industrial sludge R. R-1, R-3 and R-5 filtrates from first, third and fifth 24 hour shaking respectively.
c. Stabilized industrial sludge S - 75% wet sludge/15% slag cement/10% lime kiln dust (quick), cured 77 days and crushed. S-1, S-3 and S-5 filtrates from first, third and fifth 24 hour shaking respectively.

Recently, field trials have been completed to prepare for the proposed stabilization process. A rather efficient method has been developed for large field trials that allows a number of batches to be tested each day: a chute has been constructed that allows excavated sludge to be fed into a standard ready-mix truck; then the stabilizing agents are added using a small belt conveyor with the most reactive agent going in last to allow for visual control of initial stiffening; and after mixing, the batch is discharged at a location where strength monitoring can be completed on the stabilized sludge "lump". Samples are also taken for laboratory testing. As the summer weather in Hamilton can be very hot, the stabilized sludge is excavated to below any surface influences before using the penetrometer. In several cases the stiffening has been so rapid that water additions have been necessary to get the stabilized sludge out of the truck. After several days, it is possible to drive vehicles onto the stabilized sludge. This ready-mix truck operation proved so efficient that it has been adopted as an alternative to a large base stabilization plant for the production rates required.

While field evaluations are continuing, some typical results can be given:

72.8% sludge/13.7% fly ash/8.1% lime kiln dust/5.4% portland cement ($0.41\ N/mm^2$ at 6 days)
83.6% sludge/12.9% lime kiln dust/3.5% portland cement ($0.28\ N/mm^2$ at 5 days)
75.7% sludge/11.5% fly ash/9.9% lime kiln dust/2.9% portland cement ($0.22\ N/mm^2$ at 5 days)

Based on these types of field results, final process (large ready-mix truck with central additive storage silos) and stabilization agent selection(s) (i.e. economics and availability, with waste lime kiln dust and slag cement favoured) were completed. It is estimated that the total cost for removal, stabilization and placement as fill is about Can. $5.00 per tonne of stabilized material. This is most favourable compared to sludge disposal and fill material costs.

CONCLUSIONS

It is hoped that at the time of the congress it will be possible to report on the progress of the full-scale field stabilization process and results. The concept of industrial sludge stabilization using industrial byproducts and low cement contents, and construction stabilization technology, appears most attractive. Hopefully other sludge applications will develop.

ACKNOWLEDGEMENT

The assistance of D. Matchett with the experimential work is gratefully acknowledged.

Any opinions expressed in this paper are those of the writer, and not necessarily those of any associated organizations.

REFERENCES

1. MOE (1978), "New reporting system and guidelines for hauled liquid industrial wastes", Ontario Ministry of the Environment, Toronto, December.

2. R.B. POJASEK (1979), Editor, Toxic and hazardous waste disposal, "Volume 1 - Processes for stabilization/solidification", "Volume 2 - Options for stabilization/solidification", (other volumes in press), Ann Arbor Science, Ann Arbor, Michigan.

3. G.A. SNYDER, F.A. ZUHL, and E.F. BRUCH (1977), "Solidification of fine coal refuse", Mining Congress Journal,December, 43-46.

4. ASTM (1978), Recommended practice for use of process waste in structural fill, draft, American Society for Testing and Materials Subcommittee E38.0605, personal communication, June.

5. EPA (1978), "Hazardous waste - proposed guidelines and regulations and proposal on identification and listing", Federal Register, Vol. 43(243), December 18.

6. MOE (1978),"Determination of leaching potential", Ontario Ministry of the Environment, Toronto, July 26.

7. OECD (1977),"Use of waste materials and by-products in road construction", Organization for Economic Cooperation and Development, Paris.

8. MOE (1978),"Objectives for the control of industrial wastes discharges in Ontario", Ontario Ministry of the Environment, Toronto.

9. MOE (1978),"Water Management - Goals, policies, objectives, and implementation procedures of the Ministry of the Environment", Ontario Ministry of the Environment, Toronto, November.

Solidification of sludges with cement-slag-$CaSO_4$

Solidification des boues à l'aide de ciment, de laitier et de gypse

Tomonitsu SUGI, Koji KATAOKA, Shuzo YAMADA, Yutaka ANDO, Japan.

RESUME : Au Japon, il est devenu nécessaire, pour préserver l'environnement et assurer la sécurité des ouvrages à construire sur ces terrains, de traiter les boues qui se sont accumulées sur les bords des lacs et de la mer pendant des années.

Ce rapport a pour but de trouver un matériau de solidification bon marché, apte à traiter les boues en les solidifiant.

24 sortes de ciments ont été utilisées dans ces essais de solidification des boues, en faisant varier les diverses proportions du ciment portland, du laitier et du gypse.
On a observé que les mélanges de ciment et de laitier, dans des proportions allant de 40/60 à 20/80 pour une teneur en $CaSO_4$ de 10 à 20 % avaient la résistance la plus élevée; cette résistance était dix fois plus élevée que celle donnée par le ciment Portland seul. Ces mélanges forment principalement de l'ettringite lors d'hydratation, et on peut penser que celle-ci crée une résistance élevée en se liant efficacement aux hydrates.

Summary: In Japan, it has become necessary to preservation of environment and securing of building lots to deal with the sludge deposited in rivers, lakes and seashores over a long term of years.
In order to find effective and inexpensive solidifying materials for sludge, the authors studied solidifying ability of 24 kinds of mix cements with different mix proportions of portland cement, slag and anhydrite for sludge.
As the result, present cement with mix proportion of cement : slag = 40 : 60 - 20 : 80 and $CaSO_4$ content of 10 - 20% showed high strength the highest of which was 10 times as strong as that of portland cement.
It is known that ettringite, a main product of hydration of the cement, gave the high strength by interlocking effectively with other hydrates.

1. Introduction

Up to now, quicklime (CaO), Slaked lime ($Ca(OH)_2$) and ordinary portland cement have been used for solidifying the sludge deposited in rivers, lakes and seashores. However, the use of quicklime involves problem in conservation of environment as it generates intense heat on hydration. The slaked lime is used in expectation of pozzolanic reaction with clay minerals in the sludge, and in many cases gives no sufficient strength. Solidifying strength of ordinary portland cement extremely decreases with increase of organic components in the sludge.

The authors studied a preliminary experiment mixing several materials with the main object of solving such weak points involved in using conventional sludge solidifying materials as intense heat evolution and insufficient solidification of organic sludge. Out of the materials, it was found that solidifying materials of the ternary system of ordinary portland cement - slag - anhydrite showed very good results.

This report describes the experiments conducted on the basis of the preliminary experiment to find out a optimum composition, which is able to give high strength, safe for use and inexpensive from abovementioned ternary system.

2. Method of experiments

The sludges prepared in the laboratory were following three kinds: Silty sludge which is inactive with cement; clayish sludge that causes pozzolanic reaction with cement; and organic sludge containing humic acid which is harmful to hydration of cement. Beside three kinds of sludges, silty sludge to which 1.0%, 2.0% and 4.0% of acetic acid were added to lower PH was also used in a part of the experiments. The sludges were prepared with Toyoura standard sand pulverized with a test mill, powderly bentonite, humic acid, and prescribed amount of water. Mix proportions and physical properties of each sludge are shown in Table I. Moisture contents were made approximately equal to those of actually existing sludges.

Table I. Mix proportions and physical properties of sludges.

Item	kind	Silty sludge	Clayish sludge	Organic sludge
Mix proportions (%)	sand	100	50	47.5
	bentonite	0	50	47.5
	humic acid	0	0	5
Moisture content (%)		75	300	300
Wet density (kg/m^3)		1,562	1,165	1,165
Grain size distribution (%)	>75 μm	9.9	5.1	4.8
	75 ~ 5 μm	84.3	50.0	47.5
	< 5μm	5.8	44.9	47.7

Solidifying materials of 24 different kinds were prepared by blending ordinary portland cement, granulated glassy blast furnace slag, and anhydrite obtained from the fluoric acid industry. Cement to slag ratios were 100 : 0, 80 : 20, 60 : 40, 40: 60, 20 : 80, 5 : 95 and $CaSO_4$ were 3.4%, 10%, 20%, 30% abovementioned slag - cement mix. Specific gravity, fineness and chemical composition of these materials are given in Table II.

TableII, Chemical composition and physical properties of portland cement, slag and anhydrite.

Item	kind	Portland cement	Blast furnace slag	Anhydrite
Chemical Composition (%)	Ig. loss	0.3	0.3	0.5
	Insol	0.1	0.4	—
	SiO_2	22.0	33.7	—
	Al_2O_3	5.0	15.3	—
	Fe_2O_3	3.2	0.6	—
	CaO	64.3	43.7	40.8
	MgO	1.8	4.0	—
	MnO	—	1.1	—
	SO_3	2.0	1.1	57.4
	Total	98.7	100.2	98.7
Specific surface (cm^2/g)		3,300	4,100	8,430
Residue on 88 μm (%)		1.0	0.5	5.0
Specific gravity		3.15	2.92	2.92

The specimens for solidifying test were prepared by adding 100 kg or 200 kg of solidifying materials to 1 m^3 of sludge, then mixing for 5 minutes with a mixer and molding in ϕ5 x 10 cm mold followed with curing in moisture at 20°C. The unconfined compressive strength of the hardened specimen was determined in conformity to JIS method (JIS A 1216). To identify hydration products, the specimen was crushed, washed with ethanol and dried at 45°C. Identification was made on the sample prepared as above by means of X-ray diffraction, DTA-TGA and SEM. Pore size distribution was also measured on a part of the specimens using a mercury penetrating porosimeter.

3. Results of experiments

Unconfined compressive strength of specimens prepared by adding 200 kg each of 24 kinds of solidifying materials to 1 m^3 of sludge are shown in Fig.1. For silty sludge, solidifying materials proportioned in cement : slag = 20 : 80 and $CaSO_4$ content of 10% and 20% were high in strength, and for clayish sludge, solifying materials proportioned in cement : slag = 40 : 60 and 20 : 80, and $CaSO_4$ content of 10% showed high strength. The results of organic sludge resembled that of clayish sludge.

The strength ratio to portland cement in these optimum compositions was generally 3 - 5 times and in case where 100 kg/m^3 of solidifying material was added to silty sludge, it was 9 - 10 times at age of more than 3 days.

The hydration products were mainly ettringite according to X-ray diffraction, DTA, TGA and SEM, and its quantity increased with increase of $CaSO_4$ content. The relation between the quantity of formation ettringite determined by X-ray diffraction peaks and age is shown in Fig. 2. In the case where $CaSO_4$ content was 10%, the quantity of ettringite was nearly constant from one day on, and when the content was 20% and 30%, the quantity increased with the time elapsed. Monosulphate was

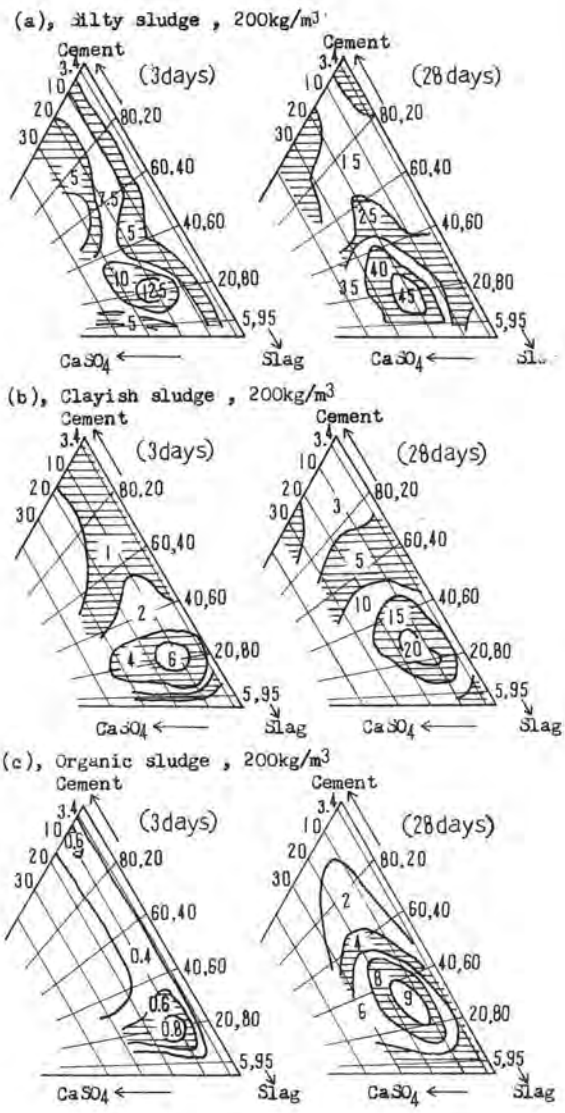

Fig.1. Unconfined compressive strength (kgf/cm^2) of solidified specimens with mix cements blended cement, slag and $CaSO_4$.

formed at $CaSO_4$ content 3.4% and 10%, but it was scarcely recognized in case of organic sludge. $Ca(OH)_2$ was formed at rich amount of cement. $CaSO_4$ remained unreacted at early age in case of 20% and 30% $CaSO_4$ content and disappeared from one week on of age (Fig.2).

Fig.3 shows the pore size distribution of hardened specimens at the age of 13 weeks. No interrelation was recognized between total pore volume and strength. However, it was recognized that the specimens of higher slag content showing higher strength had more pores of small pore radii.

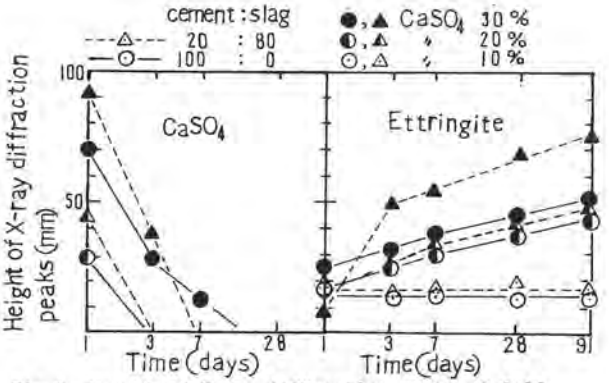

Fig.2, Height of X-ray diffraction peaks of $CaSO_4$ and ettringite, in case of silty sludge and adding 200 kg/m^3 of solidifying materials.

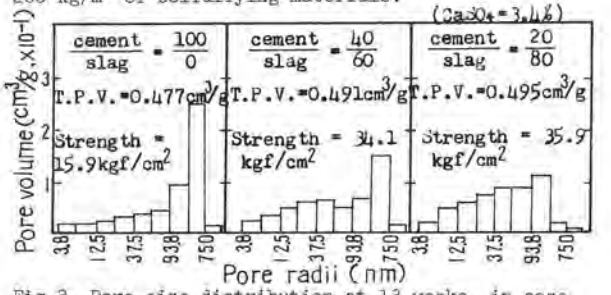

Fig.3, Pore size distribution at 13 weeks, in case of silty sludge and adding 200 kg/m^3 of solidifying materials.

In the case of adding 100 kg/m^3 of solidifying material to the organic sludge, solidification was not effected by the use of solidifying material blended with 3.4% $CaSO_4$ or solidifying material of high slag content. The mix proportion that gave relatively good solidification for the organic sludge was $CaSO_4$ content of 10% or more and rich in cement (cement : slag = 100 : 10 - 60 : 40).

The low PH value, as experienced the organic sludge, was thought to be the main cause of the phenomenon. For the purpose of examining influence of lowering of PH value in these type cement upon strength, solidifications of silty sludge of low PH value were experimented using a solidifying material proportioned in cement : slag = 20 : 80 and $CaSO_4$ content of 10%. The result is shown in Table III. At PH 10, solidification was not effected up to 3 days of age. As seen in Fig. 4, formation of ettringite was not observed at PH 10.

4. Discussion

It was found that in solidifying sludge of high moisture content, solidifying meterials proportioned in cement : slag = 40 : 60 - 20 : 80 and $CaSO_4$ content of 10 - 20% were effective. More ettringite was formed with increasing anhydrite and slag. Behavior of the ettringite is considered to be acting to lower pore water and to increase density of hardened specimens and as a interlocking material in the hardened specimens. These are presumed to be one of principal factors to increase the strength.

When solidifying sludge, formation of

Table III, Unconfined compressive strength of specimens lowered PH value, in case of adding 200kg/m^3 of solidifying material proportioned in cement: slag = 20 : 80 and $CaSO_4$ content of 10%.

Addition of acetic acid	PH after mixing(1hr)	Strength (kgf/cm^2)			
		1 day	3 days	7 days	28 days
1.0 %	11.5	3.1	11.0	11.5	12.9
2.0 %	11.2	2.1	9.9	12.8	16.6
4.0 %	10.2	x	x	7.0	10.0

x------not solidified

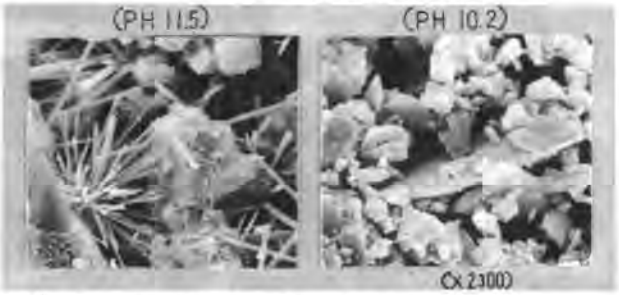

Fig.4, SEM photographes of specimens, at 3 days.

ettringite was greatly influenced by PH of the sludge. In the case where PH after mixing became 10 or thereabout, formation of ettringite was hindered and strength was remarkably lowered. Therefore, when solidifying low PH sludge using these type materials, it is necessary to adjust PH above 11.

A tendency was observed in pore size distribution that the greater the slag content of solidifying materials added to the specimen the greater the number of openings of small pore radii. This can be attributed to the influence of difference in generated hydrates consequent on difference in solidifying material.

As seen in Fig 1 and Fig. 2, interrelation between the strength and the quantity of formation of ettringite cannot be determined distinctly. It is rather considered that in addition to the formation of ettringite, interactions of C-S-H and or C-A-S-H hydrates formed from the slag cement are contributing to the strength.

5. Conclusions

In solidifying sludge of high moisture content with soiidifying materials of portland cement - slag - anhydrite system, high strength was obtained throughout every age by mix proportions of cement : slag = 40 : 60 - 20 : 80, and $CaSO_4$ content of 10 - 20%. The highest strength obtained was 10 times as strong as that using ordinary portland cement.

As stated above, it is possible to solify sludge of high moisture content to give strength several times as strong as that of ordinary portland cement by the use of solidifying materials mixed with a large quantity of blast furnace slag and chemical anhydrite which are supplied in quantities as industrial by-products.

Removal of valuable but toxic ions from waste water by synthetic hydroxyapatites

Utilisation des hydroxyapatites de synthèse pour la récupération d'ions métalliques toxiques

Takashi SUZUKI, Toshiaki HATSUSHIKA and Yasumasa HAYAKAWA,
Department of Applied Chemistry, Yamanaschi University, Takeda-4, Kofu-shi, 400 Japan.

RESUME : La récupération des ions Cd^{++}, Zn^{++} et Ni^{++} dans diverses solutions aqueuses, au moyen d'hydroxyapatites de synthèse, a fait l'objet d'études approfondies, en utilisant plusieurs méthodes d'analyse, telles que : la titrimétrie ATDE, la sélection des ions aux électrodes et la spectroscopie d'absorption atomique. On a montré ainsi que le comportement de ces ions ne consistait pas en un simple effet d'adsorption, mais en un échange d'ions entre les ions à récupérer et les ions Ca^{++} des apatites. L'importance des échanges est plus grande avec les ions Cd^{++} ou Zn^{++} qu'avec les ions Ni^{++}, mais n'est pas complète pour les premiers, même avec une proportion cent fois plus grande d'ions Ca^{++} ; ces ions sont stabilisés sur les apatites.
Ces résultats suggèrent que les apatites ont le pouvoir de sélectionner les cations métalliques ; aussi peuvent-elles être utilisées comme échangeur de cations inorganiques, pour récupérer ou pour fixer les ions de valeur mais toxiques dans les effluents.

SUMMARY : The removal behaviour of Cd^{2+}, Zn^{2+} and Ni^{2+} ions from various aqueous solutions by synthetic hydroxyapatites was probed in detail by using analytical methods such as EDTA titrimetry, ion electrode analysis and atomic absorption spectroscopy. It was elucidated that the behaviour is not a mere adsorption effect but such an "ion-exchange reaction" between the ions (Cd^{2+} etc ...) in the solutions and Ca^{2+} ions on the apatites. The amount of the exchanged Cd^{2+} or Zn^{2+} was larger than that of the Ni^{2+} and the former ions were not eluted with even 100 times Ca^{2+}, i.e., the ions were stabilized on the apatites. These results suggest that the apatites have a selectivity for metallic cations and can be employed as an inorganic cation-exchanger for removing and stabilizing the valuable but toxic ions in waste water.

1. INTRODUCTION

It is well known that hydroxyapatite is not only a main constituent of phosphate rock, but also the major inorganic constituent of bones and teeth. The authors have been investigating surface characteristics[1-5] of various synthetic apatites and have happened to discover a new and important fact that Cd^{2+} ions in the aqueous solution are strongly held on some synthetic hydroxyapatites at room temperature and moreover, the behavior is not a mere adsorption phenomenon but a cation exchange phenomenon between Ca^{2+} ions on the apatites and the Cd^{2+} ions. Starting from the interesting result, the authors intended to examine the feasibility of employing the apatites as inorganic cation exchangers for treatment of waste water containing valuable but hazardous metallic ions.

2. EXPERIMENTALS

Materials.
Various synthetic hydroxyapatites were prepared in the usual way[6,7] by precipitation from hot water and stored in a desiccator over phosphorus pentoxide. All chemicals were analytical grade commercial materials and used without farther purification.

Specific surface area.
The specific surface areas of the apatites were determined by applying BET method to the nitrogen adsorption data obtained at the liquidnitrogen temperature, assuming the cross-sectional area of a nitrogen molecule to be 16.2 $Å^2$.

Crystal structure.
The structural changes of the apatites before and after the uptake phenomena were investigated by X-ray diffraction method.

Procedures.
Each sample (1.0 g) of the hydroxyapatites was mixed and stirred with 400 ml of 100 PPM Cd^{2+}, Zn^{2+} and Ni^{2+} aqueous solutions at various temperatures (20~40°C), and released Ca^{2+} ions in the solutions and adsorbed ions on the apatites were analyzed by measurements with a cadmium ion meter, EDTA titrator and an atomic absorption spectrometer. In addition to the batch operation, column method was also applied to the case of Ni^{2+} and Zn^{2+} solutions.

3. RESULTS AND DISCUSSION

The specific surface areas and Ca/P molar ratios of the apatites are summarized in Table I. From the table, it was found that each of the apatites had relatively large surface area and the molar ratio values close to the ideal value (1.66) calculated from the molecular formula $\{Ca_{10}(PO_4)_6(OH)_2\}$.

Table I. Specific surface areas and Ca/P molar ratios of various synthetic hydroxyapatites.

apatite / measured value	S - 1	S - 2	S - 3
Ca/P molar ratio	1.65	1.63	1.63
surface area (m^2/g)	62.8	60.2	45.3

Table II shows the amounts of uptaken Cd^{2+} on S-1 or S-2 from 400 ml of 100 PPM Cd^{2+} aquous solutions and those of released Ca^{2+} in the solutions at 20°C. Note that the molar ratios (Ca^{2+}/Cd^{2+}) almost equal to an integer 1.0. This means that the Cd^{2+} uptake phenomenon is not a mere adsorption effect but such an ion-exchange reaction between Cd^{2+} in the solution and Ca^{2+} on the apatite as R-Ca system, where R-Ca is a commercial Ca^{2+} form cation exchange resin. The interesting result is very important because the hydroxyapatite has been considered to be an anion exchanger[8] and much attention has not been paid to the divalent cationic characteristics. pH changes of the solutions before and after the addition of the apatites are listed in the table for reference.

Table II. Removal of Cd^{2+} ions by S-1 and S-2.

sample / measured value	S - 1	S - 2	R - Ca
Ca^{2+} mg/400 ml	11.9	9.76	3.82
($\times 10^{-4}$ mol)	(2.96)	(2.43)	(0.95)
Cd^{2+} mg/400 ml	33.2	28.5	11.3
($\times 10^{-4}$ mol)	(2.95)	(2.54)	(1.00)
Ca^{2+} : Cd^{2+} molar ratio	1 : 1	0.96:1	0.95:1
before addition of the apatites pH	5.7	5.7	-
after 30 min. pH	6.0	6.1	
dissolved amount of Ca^{2+} in water (mg/400 ml water)	1.21	1.10	-

Table III contains the amounts of adsorbed Zn^{2+} on the S-1 from 400 ml of 100 or 50 PPM Zn^{2+} aqueous solutions, those of the released Ca^{2+} in the solutions, Ca^{2+}/Zn^{2+} molar ratios and pH changes of the solutions at various temperatures (20~40°C). As indicated in the table, the Ca^{2+}/Zn^{2+} molar ratios are close to an integer 1.0. The result means that the Ca^{2+} ions on the apatites are not peculiarly exchanged with Cd^{2+} ions in the solutions.

Table III. Removal of Zn^{2+} ions by S-1 at various temperatures

system / measured value	Zn^{2+} 100 PPM (400 ml)			Zn^{2+} 50 PPM (400 ml)		
	20°C	30°C	40°C	20°C	30°C	40°C
Ca^{2+} mg/400 ml	14.56	15.68	20.52	7.36	10.24	12.07
Ca^{2+} ($\times 10^{-4}$ mol)	(3.63)	(3.91)	(5.12)	(1.84)	(2.55)	(3.01)
Zn^{2+} mg/400 ml	20.04	25.76	30.08	11.36	15.92	18.57
Zn^{2+} ($\times 10^{-4}$ mol)	(3.52)	(3.94)	(4.60)	(1.74)	(2.43)	(2.84)
Ca^{2+} : Zn^{2+}	1.03 : 1	0.99 : 1	1.11 : 1	1.06 : 1	1.05 : 1	1.06 : 1
pH before addition of the apatite	5.8	5.8	5.9	6.0	6.1	6.0
pH after 30 min.	6.2	6.2	6.3	6.2	6.2	6.2

Concerning Ni^{2+} uptake, it was found in Table IV that the molar ratios of Ca^{2+} and Ni^{2+} are almost close to 1.0 and the difference of exchanged quantities of Ni^{2+} between batch method and column operation was small (S-3 sample was treated by column operation. The flow rate of 100 ml of Ni^{2+} solution with a concentration of 100 PPM is 1 ml/min.).

Table IV. Removal of Ni^{2+} ions by S-1, S-2 and S-3.

apatite / measured value	S - 1	S - 2	S - 3
Ni^{2+} solution	100 PPM 100 ml	100 PPM 100 ml	100 PPM 100 ml
operation	batch	batch	column (1 ml/min.)
Ca^{2+} mg	4.65	4.49	3.87
Ca^{2+} (mol)	(1.16×10^{-4})	(1.12×10^{-4})	(0.97×10^{-4})
Ni^{2+} mg	6.72	6.35	5.80
Ni^{2+} (mol)	(1.14×10^{-4})	(1.08×10^{-4})	(0.99×10^{-4})
Ca^{2+}:Ni^{2+}	1.02 : 1	1.04 : 1	0.98 : 1

Table V contains the quantities of exchanged Ni^{2+} and Zn^{2+} on 1 g of the S-3 from 400 ml of 100 PPM solutions by column method, those of eluted Ni^{2+} and Zn^{2+} from the loaded S-3 with 400 ml of 0.001 N sulfuric acid and so on. From the table, it was found that the amount of the exchanged Zn^{2+} was larger than that of the Ni^{2+}. The result also suggest that the apatite have a selectivity for metallic cations. This consideration is also supported by the difference of the amounts of recovery ratios between Zn^{2+} and Ni^{2+} (cf. Zn^{2+} : 50 %, Ni^{2+} : 65 %). Moreover, the dissolved amounts of P from the S-3 were negligibly small. (cf. Ni^{2+} system ; 0.21 mg, Zn^{2+} system ; 0.22 mg).

Table V. Removal and elution of Ni^{2+} and Zn^{2+} ions by using column method.

system / measured value	S-3 — Ni^{2+}	S-3 — Zn^{2+}
Ca^{2+} mg	5.4	13.4
Ca^{2+} (mol)	(1.34×10^{-4})	(3.3×10^{-4})
Ni^{2+} mg and Zn^{2+} (mol)	7.4 (1.26×10^{-4})	20.8 (3.2×10^{-4})
Ca^{2+} : Ni^{2+} and Ca^{2+} : Zn^{2+}	1.06 : 1	1.03 : 1
P mg	0.21	0.22
P (mol)	(0.068×10^{-4})	(0.071×10^{-4})
eluted amount of Ni^{2+} and Zn^{2+} mg	4.8	10.4
eluted amount of Ni^{2+} and Zn^{2+} (mol)	(0.82×10^{-4})	(1.59×10^{-4})
recovery ratio (%)	65 %	50 %

4. CONCLUSION

In addition to the above results, it was found out that the structural changes of the apatites before and after the uptake phenomena were not detected at least by X-ray diffraction method, the exchanged Cd^{2+} or Zn^{2+} ions on the apatites were not eluted with even 100 times Ca^{2+} ions, i.e., the Cd^{2+} or Zn^{2+} ions were stabilized on the apatites and maximum value of the exchanged Cd^{2+} was 80 mg per 1 g of the S-1. These results suggest that the apatites can be employed as an "inorganic cation-exchanger" for removing and stabilizing the valuable but toxic ions in waste water.

We thank the Ministry of Education of the Japanese Government for financial support

(contract No. 403046) and Mrs. H. Hatsushika for her secretarial help in the preparation of this paper.

REFERENCES

1. T. Suzuki and Y. Hayakawa, Abstracts of Japanese Chemical Society Symposium on Inorganic Chemistry, Sapporo, 28-31, August, 1976, P.3R26.

2. T. Suzuki and Y. Hayakawa, Proceedings of the 1st International Congress on Phosphorus Compounds, IMPHOS Pub. Paris, 1977, P.381.

3. T. Suzuki and Y. Hayakawa, Abstracts of the 40th Annual Meeting of the Chemical Society of Japan, Fukuoka, 18-21, October, 1979, P.3K12.

4. T. Suzuki, N. Ayuzawa and Y. Hayakawa, Abstracts of the 47th Annual Meeting of Electrochemical Society of Japan, Yokohama, 4-5, April, 1980, P.B212.

5. T. Suzuki, T. Hatsushika and Y. Hayakawa, Proceedings of 2nd International Congress on Phosphorus Compounds, IMPHOS Pub. Paris, 1980, in press.

6. Y. Aunimelech, E. C. Moreno and W. E. Brown, J. Res. Nat. Bur. Stand., 1973, 77A, 149.

7. H. Mcdowell, T. M. Gregory and W. E. Brown, J. Res. Nat. Bur. Stand., 1977, 81A, 273.

8. See, for example, I. Zipkin, A. S.Posner and E. D. Eanes, Biochim. Biophys. Acta, 1962, 59, 255 ; G. Montel, G. Bonel, J. C. Trombe, J. C. Heughebaert and C. Rey, Proceedings of 1st International Congress on Phosphorus Compounds, IMPHOS Pub. Paris, 1977, P.321.

The Poz-O-Tec process for fixation of industrial wastes

Le procédé Poz-O-Tec de traitement des cambouis industriels

Dr. Eric RAU, Director of Research and Development, IU Conversion Systems, Inc. Horsham, Pennsylvania, U.S.A.

RESUME : Le procédé Poz-O-Tec permet de traiter complètement les cambouis qui se déposent dans les conduites de gaz désulfurisé. Ces cambouis contiennent du CO_4Ca et du SO_3Ca; mais ils contiennent aussi, d'une façon aléatoire, plusieurs éléments lourds, qui peuvent réagir avec les cendres volantes et la chaux, et produire un matériau à faible perméabilité. Cette réaction peut être utilisée, en la menant convenablement, pour éviter toute contamination des eaux souterraines, à partir des écoulements à la surface des sols. Et même, ces eaux peuvent être réutilisées après traitement.

Ce procédé est utilisé aux U.S.A., où vingt installations, déjà réalisées ou en cours de construction, seront capables de traiter annuellement dix huit millions de tonnes de ces cambouis. La présente communication donne des détails sur le processus chimique et sur l'expérience déjà acquise du procédé.

Ce procédé a aussi été utilisé pour traiter des effluents industriels. Ces derniers ont été classés en effluents traitables ou non traitables par ce procédé, d'après leur réaction avec la pouzzolane. Cette classification est exposée en détail.

SUMMARY: The Poz-O-Tec® process is a complete waste management system for the disposal of flue gas desulfurization sludges. In this system the $CaSO_4/CaSO_3$ sludges, which contain many heavy elements considered hazardous, are reacted with fly ash and lime to produce a material of low permeability. This composition can be landfilled in a manner that assures virtually no contamination of groundwater by leachates nor contamination of surface water by surface runoff. Further, the ground is suitable for re-use after the landfill is closed. The system is in use in the U.S.A., with 20 plants capable of solidifying over eighteen million tons per year of sludge now in operation or under construction. Details on process chemistry and operational experience are presented.

The method had also been adopted to the processing of industrial wastes. These wastes have been classified into materials that affect the pozzolanic reaction which are beneficial, compatible, or incompatible with the systems. Details of the classification are presented.

The Poz-O-Tec® process developed by IU Conversion Systems, Inc. (IUCS), is a system of waste management in which hazardous materials are encapsulated in a pozzolanic matrix formed by the reaction of lime with fly ash. Retention within the matrix may be by chemical as well as physical forces. Chemically bound material is rendered insoluble by the formation of complex calcium silicate alumina compounds. Physically held materials are entrapped in the dense cementitious matrix which is virtually impermeable to water. Thus, the host matrix is able to retain a wide variety of wastes and prevent contact with solvents that might leach the toxics from the matrix.

POZZOLAN CHEMISTRY

By definition, pozzolans are materials which are not cementitious in themselves, but which contain constituents that will combine with lime at ordinary temperatures in the presence of water to form cementitious compounds. Natural pozzolans are usually materials of volcanic origin, but include some diatomaceous earths and, in the broadest sense, soils. Artificial pozzolans are mainly products obtained by heating clay or shale. Today, the primary artificial pozzolan is fly ash, a residue from the combustion of pulverized coal at modern electric power plants.

When lime or lime-based additives are mixed with fly ash in the presence of water, a chemical reaction takes place producing materials whose properties are similar to the reaction products of Portland cement. The major cementitious reaction occurs between silica and lime with some alumina contributions. In addition, sulfur-bearing compounds can react with lime and alumina to form calcium sulfo-aluminohydrates. The chemical equations for these reactions are shown below:

$$SiO_2 + Al_2O_3 + Ca(OH)_2 \longrightarrow xCaO.yAl_2O_3.zSiO_2.wH_2O \quad (1)$$

$$Al_2O_3 + SO_3^- + Ca(OH)_2 \longrightarrow xCaO.yAl_2O_3.zCaO.SO_3.wH_2O \quad (2)$$

The chemical reactions are complex. Initially, the fly ash surface is attached by lime, creating a gel. This gel contains predominantly calcium, aluminum, and silica ions in solution, which combine to form insoluble hydrate complexes. Since the chemical reactions take place on the fly ash surface, the pozzolanic reactivity of the fly ash increases with greater surface area (i.e., smaller particle size).

The pozzolanic reactions described in (2) can be used to chemically fix SO_2 scrubber sludges from electric utilities. These scrubber sludges contain $CaSO_3.\frac{1}{2}H_2O$ and/or $CaSO_4.2H_2O$ depending on scrubber conditions.

Other wastes which may contain hazardous components can be rendered innocuous by this same pozzolanic reaction. The liquid phase of the waste is utilized to form the hydration compounds that are cementitious in nature. The hydration reaction progressively seals off the pore structure in the resultant mass. Permeability is typically reduced to 10^{-6} and 10^{-7} cm/sec. Sulfur compounds may be chemically reacted to form insoluble compounds. Other solid wastes are physically entrapped in the rigid matrix which develops. The basic pH of the pozzolanic reaction renders most heavy metals insoluble. In addition, the hydrating gel provides a large surface area for adsorption and ion exchange processes.

The longevity of these reaction products has been amply demonstrated by structures (such as the Appian Way) built centuries ago during the Roman Empire.

APPLICATION TO FLUE GAS DESULFURIZATION SYSTEMS

With the resurgence of coal as fuel, it has become necessary for utilities to install and operate a growing number of flue gas desulfurization (FGD) systems for SO_2 removal. It is estimated that nearly 60,000 MW of FGD capacity will be installed by 1980.

Among the various FGD scrubber systems available, wet-lime/limestone scrubbing and double alkali (indirect-lime/limestone) scrubbing have gained the widest acceptance. These scrubbing operations produce an enormous volume of low-solids-content sludge, which must be properly treated so that groundwater and surface water are not polluted by unacceptable concentrations of heavy metals and dissolved solids.

A solution to this massive sludge disposal problem is the chemical stabilization of scrubber sludge by the Poz-O-Tec® process to prevent significant environmental damage and minimize land disposal requirements. The Poz-O-Tec® system has received large-scale commercial acceptance on a wide variety of scrubbers. Twenty utilities have contracted to install it.

The Poz-O-Tec® process is a complete waste-management system for coal-fired power plants. It blends fly ash, bottom ash (if desired), scrubber sludge, lime, and other wastes. Concentrated streams from the evaporator and cooling tower sludge can also be incorporated. The stabilized material is a cementitious material, and with proper placement and compaction, exhibits low permeability and superior structural properties.

PROCESS CONSIDERATIONS

The fixation of power plant wastes involves more than just combining the wastes. Each of the waste materials contributes chemically and physically to the process. Variations in those materials must be considered in developing the specific process design.

Fly Ash

Fly ash is utilized in the Poz-O-Tec® process for several reasons. It is a waste material which must be disposed of, and is usually available from the same plant as the sludge waste. It is a fine-particle material and provides the alumina and silica which are necessary for the pozzolanic reactions to bind the sulfur compounds of the sludge.

The quantity of fly ash will also contribute to the final solids content of the product and affect its handling characteristics. Generally, ash-to-sludge ratios of 1:1 or higher will result in an immediately placeable material; those below that ratio will usually require interim stockpile conditioning prior to final placement.

Particle size of the ash also contributes to the process chemistry: the extremely fine particles have more surface area and therefore react faster.

Scrubber Sludge

The chemical composition of a sludge is one of the most important considerations in designing a stabilization system, because it can vary greatly, even

during standard power plant operation. All FGD sludges can be stabilized, but it is important to understand those characteristics of sludge which have the greatest potential effect on stabilization systems.

Sulfite/sulfate proportions primarily affect dewatering. The larger size of the sulfate particles affords easier dewatering. However, given the same ash to sludge ratio, sulfate based sludges require a numerically higher solids content of the final product to be equally handleable than do sulfite based sludges.

The lime or limestone used in scrubbers also has an effect on process design. Poor quality reagent requires greater quantities in the scrubber to achieve the required SO_2 removal, and the high proportion of non-lime materials increases loads on the dewatering equipment. When in the form of grit, it causes extensive wear on piping and process equipment.

Process Additives

Most stabilization processes require that some additive be used to initiate chemical reactions. Although this activator may already be present in some coal, such as lignite, it must be added separately in most cases.

For pozzolanic stabilization, the additive most used is lime, available as pebble lime (which requires crushing), pulverized quicklime, hydrate, or lime slurry. The important considerations for the lime are CaO and MgO content and particle size distribution.

PLANT DESIGN CONSIDERATIONS

Concurrent with the evaluation of process variables to achieve chemical stabilization, the physical processing systems for the plant must also be planned. A stabilization plant is a materials handling system in which liquids, sludges, damp and dry solids are combined into a reactive mass.

Siting

The location of the stabilization facility will depend on land availability, location of the disposal area, and other physical and economic factors. Ideally, the landfill should be located near the power plant to minimize transportation costs for both waste materials and the stabilized product. A 600-800 MW plant producing 1,000,000 tons per year of stabilized material will require about 60 hectares of disposal area 35m high, over a 20-year period.

Dewatering

Dewatering of the sludge is important in dry stabilization systems to produce higher final product solids. Most FGD systems, however, only thicken the sludge to 25-30% solids.

Dewatering in the stabilization facility is usually accomplished by vacuum filtration, although centrifuges have been used in some applications. Scrubber sludge can be vacuum-filtered at rates of 250-500 $kg/m^2/hr.$ depending on the composition of the sludge, the filter medium, and filter aids. Sulfate sludges usually yield higher filtration rates and solids than do sulfites. Conversely, high concentrations of magnesium often result in lower filtration rates and solids. If these conditions are known at the time of design, the filtration equipment and operating parameters can be adjusted to maximize sludge dewatering.

A lime base sludge will usually dewater from 30% solids to 40-60% solids, and limestone-based sludge to 55-60% solids. Oxidized sludges are reported to achieve 80-85% solids, which when mixed with fly ash and additive, would result in a high-solids final product. This product may require water addition to achieve optimum placement density.

Materials Feeding

Feed systems for fly ash and lime involve more than just adding these materials to the sludge. For situations where there is limited ash available, controlled feed is important to conserve ash. This equipment must not only feed accurately but must control flooding.

As lime constitutes a small percentage of a mix on a dry-weight basis and is the activator of the chemical stabilization reactions, accuracy of measurement and uniform dispersion of the lime in the product is absolutely necessary. Dispersion within the mix depends upon accuracy of feed, location of lime feed into the system, particle size, and uniformity of mixing.

Mixing

Mixing is the combining of the waste and additives to permit the fly ash lime to contact all sludge particles so complete chemical action can take place. The mixer must be able to provide the required blending, even though the ratio of wet and dry materials may vary over any given period, and the mixer designed for 200 tons per hour (TPH) may only be operating at 100 TPH due to reduced station load. The specific combination of waste materials to be mixed at a facility must be evaluated for material ratios, solids content, particle size, retention time, type of additive, etc., to ascertain the proper mixing design.

FINAL PRODUCT HANDLING

The achievement of a structurally stable and environmentally compatible landfill requires a detailed materials handling and placing program, landfill preparation, and quality control procedures. In many respects, the disposal and placement procedures are as important to the overall stabilization system as the processing facility itself.

Once the processed sludge leaves the facility, it is usually placed in a surge pile. Normally, a drier final product will require less time in the surge pile prior to handling. For example, final product with solids in the range of 50-58% require initial conditioning of several days before movement. Table I gives a range of final product solids and required conditioning times.

TABLE I: Time required for stockpiling a various processed material solid content.

Solids Range (%)	Stockpile Conditioning (days)
50-58	4+
58-63	3-4
63-70	1-3
70-80	0.1

Temperature can also affect the material cure, handling and placement operations. During winter months, with temperatures below 5°C, the chemical reactions in the material are slowed--as in cement chemistry. As a result, greater curing times may be required for the material in the surge pile before placement in the landfill. Adequate storage capacity in the surge pile area must be included in system design for this requirement.

The processed material is usually moved to its final disposal area by front-end loading directly onto trucks or by direct conveyor to the landfill. In all instances, grading, placing and compacting are required for final placement.

Material is usually placed in 30 to 60 cm lifts. The disposal site should be maintained so that a minimum surface area of fresh material is exposed to the elements. The working face should have a slight grade, so that any rainfall will tend to run off rather than collect in pockets. Should rainwater pockets occur, especially on fresh material, the material stabilization will be adversely affected or stopped completely, creating soft spots in the landfill.

In the landfill, the material can be graded to elevations up to 35m and greater. The landfill is developed in approximately 8m lifts and benched at the outer surface to provide haul roads and prevent erosion. Side slopes can be 2:1 horizontal to vertical, with 15m benches. The finished surfaces should have at least an 0.5m layer of topsoil and be revegetated to retard erosion.

At several of IUCS' installations, long-range plans call for material to be built into small mountains in excess of 35m in height, thus minimizing land area requirements.

The biggest potential environmental impact could be water runoff. For this reason, exposed surface area of freshly placed material should be kept to a minimum. Sedimentation ponds should collect the runoff discharge from the landfill area.

A good landfill operation will use monitoring wells to sample groundwater. These should be installed well in advance of the beginning of operations to obtain background data.

Resource Recovery

Considerable effort has also been expended on finding applications for re-using processed material. It has been used in road base, parking lots, liners, and aggregate for cement blocks. A novel proposed application has been in synthetic reef material for ocean disposal. Opportunity for Poz-O-Tec® utilization depends on the local economics and need for such material.

ENVIRONMENTAL CONSIDERATIONS

The major objective of an FGD waste management program is to protect surface and subsurface water quality and resources. This is achieved by minimizing leachate generation potential, providing adequate runoff control measures and placing the processed material in a structural matrix. To protect surface and subsurface water quality, the landfills are designed to promote rapid surface runoff. The low permeability of the placed material (10^{-6} to 10^{-7}cm/sec) contributes further to promoting runoff. All surface runoff is controlled through swales, paved ditches, piping, and sedimentation basins. Discharges from the sedimentation basins are subject to National Pollution Discharge of Effluents Standard (NPDES) or state discharge criteria for pH, alkalinity, suspended solids, total dissolved solids, sulfates and sulfites. Table II presents the combined results of surface runoff quality monitoring at three disposal sites. IUCS also monitors the eight heavy metals specified in Resource Conservation and Recovery Act (RCRA). The monitoring program results show that no heavy metal contamination is expected from a stabilized FGD sludge surface runoff discharge.[1]

TABLE II (mg/l)

SURFACE RUNOFF QUALITY

	Stabilized FGD Sludge	Discharge Criteria	EPA IPDWS
pH	6.5 - 10	6 - 10	N/A
Alkalinity	7 - 350	0	N/A
Suspended Solids	.01 - 10	30	N/A
TDS	900 - 3400	N/A	N/A
Sulfate	500 - 2200	N/A	N/A
Sulfite	2 - 25	N/A	N/A
Arsenic	.02	—	.05
Barium	.2	—	1.0
Cadmium	.01	—	.01
Chromium	.05	—	.05
Lead	.05	—	.05
Mercury	.001	—	.002
Selenium	.01	—	.01
Silver	.05	—	.05

*EPA Interim Primary Drinking Water Standards, effective October 15, 1979.

The chemical characteristics of a waste material, the method of disposal, and the physical integrity of the in-place waste materials directly influence potential leachate quality. Values were obtained by the proposed American Society for Testing Materials (ASTM) Test Procedure, Leaching Test of Waste Material, Method A, a 48-hour shake test procedure.

TABLE III (mg/l)

	Fly Ash	Sulfate Sludge	Sulfite Sludge	Stabilized FGD Sludge	EPA IPDWS	EPA RSDWS
pH	4-6	6-8.5	10-12.5	9.5-11.5	–	6.5-8.5
TDS	4,000-6,000	16-20,000	16-18,000	700-1,800	–	500
SO_4	800-1,200	7-10,000	7,000-9,000	300-850	–	250
Arsenic	.01-.20	<.02	<.02	.003-.02	.05	–
Barium	<.50	<.5	<.50	< .50	1.0	–
Cadmium	<.01	<.01	.01-.08	.002- <.01	.01	–
Chloride	30-40	–	500-1,000	60-120	–	250
Chromium	<.05	<.05	<.05	< .05	.05	–
Copper	2-6	–	< 1.0	.1-.5	–	1.0
Fluoride	–	–	–	< 1.0	1.4-2.4	–
Iron	80-150	–	<.2	< .20	–	.30
Lead	.2-.5	<.10	<.25	< .05	.05	–
Manganese	–	–	<.10	< .05	–	.05
Mercury	<.002	<.001	<.002	<.001	.002	–
Nitrate	–	–	–	< .50	10.0	–
Selenium	<.06	< .06	< .06	< .01	.01	–
Silver	<.05	< .05	< .05	< .05	.05	–

Table III shows that leachate from an unstabilized fly ash, sulfate sludge, or sulfite sludge disposal site could be expected to exceed the EPA Interim Primary Drinking Water Standards for arsenic, cadmium, lead and selenium, and the recommended secondary standards for pH, total dissolved solids (TDS), sulfates (SO_4), copper, iron and zinc. The values for the same waste materials stabilized show that all of the primary drinking water standards would be met; however, the values for pH, TDS and SO_4 would exceed the recommended secondary standards. Groundwater contamination is not seen as a problem since no leachate or permeate is expected.

The unconfined compressive strength of the stabilized FGD waste materials is a function of the filtercake solids, fly-ash-to-sludge ratio, in-place density, and additive content. For a given plant, the above factors, with the exception of additive content, remain relatively constant on a month-to-month basis. The additive content may vary to compensate for the effect of adverse weather conditions, lowered ambient temperatures, and changes in waste material characteristics and ratios. Figure 1 shows the unconfined compressive strength of laboratory-cured samples versus in-place cured samples with typical fly-ash-to-sludge ratios and additive content.

FIGURE 1

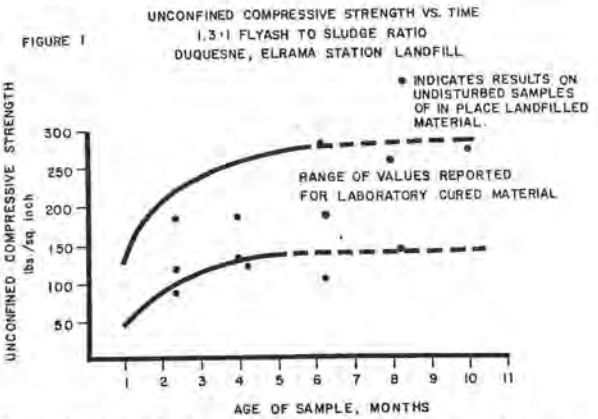

Permeability of the landfilled material was also measured after several periods of time after placement. As shown in Figure 2, the slow pozzolanic reactions are sealing the material with increasing time.

FIGURE 2

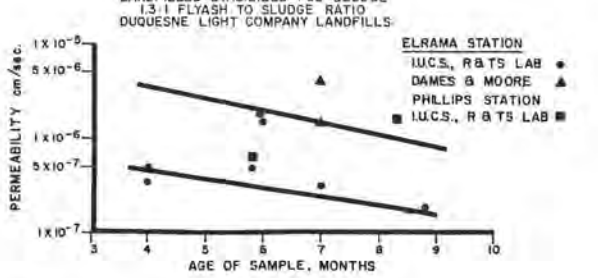

APPLICATION TO INDUSTRIAL WASTES

American industry is estimated to generate 57 million tons of hazardous wastes each year. The promulgation of the Resource Conservation and Recovery Act will have significant impact on the manner in which disposal of this material is carried out. Since disposal of toxics into water is prohibited, wastes will either have to be incinerated or landfilled. Landfilled materials must be buried under safe and secure conditions to assure that no contamination of the environment occurs.

The same fixation technology used for disposal of FGD scrubber sludge can be applied to industrial wastes. Since the type and concentration of hazardous material in these wastes vary widely, IUCS has tested many wastes and classified them into categories so that judgment on treatability could be made. The following kinds of wastes have been examined.

Generic Types of:

Sludges: $CaSO_4/CaSO_3$ sludges result from neutralization of waste battery acid, lagooning of waste gypsum and lime scrubbing of SO_2 gases in industrial or utility operations. Metal hydroxide sludges result from neutralization of acid waters containing heavy metals from steel mill and plating operations.
Dust and Slag: Dust results from the purification of air streams by exhaust devices on the furnaces of ferrous and non-ferrous smelting operations. Cement and lime kiln dusts are also included. Slag is produced in the smelting operations of ferrous and non-ferrous metals industries.
Solid Wastes: This category comprises solid wastes that are not dusts or slags but also cannot be described as sludges. Typical wastes in this category are chrome ore residue, mine tailings, and incinerator ash.
Organic Wastes: Biological sludges result from bacterial treatment used to destroy certain organic compounds. Heavy ends or still bottoms are the viscous, tarry residue from distillation or purification columns. Solvent waste streams are used solvents that have been contaminated by reactants or products from the processes or reactions for which they were the solvents.

These categories account for a majority of industrial waste streams and are useful for classifying industrial waste management options.

Chemical Stabilization of Industrial Waste

It was found convenient to classify the wastes as beneficial, compatible, and excluded, with respect to the stabilization reaction.

Beneficial Wastes

Beneficial wastes are defined as wastes which have a synergistic effect on the lime/fly ash reaction or wastes which can be used as a lime or fly ash substitute.

Several waste products were found to be acceptable fly ash substitutes as received. These include, for example, cement kiln dust, electric furnace dust, spent catalyst, and precipitator fines.

In addition, the following waste materials were acceptable replacements for fly ash when ground to a fine particle size: blast furnace slag, bottom ash, smelter fines, and coal mine tailings.

The blast furnace slag and cement kiln dust cannot technically be called pozzolans because they can react with water alone to produce a cementitious product. In this respect, these waste products are true cement-type compounds.

Considerable work has been performed at the IUCS Research and Technical Services laboratories on the use of cement kiln dust (CKD) and electric furnace dust (EFD) in waste stabilization. These dusts may be used for their lime value.

Compatible Wastes

Compatible wastes are defined as materials which do not contribute significantly to the pozzolanic reaction, do not inhibit or retard the reaction, do not contribute significantly to environmental pollution through leachate or runoff, and can be economically stabilized. The majority of compatible wastes are $CaSO_4/CaSO_3$ sludges and metal hydroxide sludges.

Heavy metal sludges may contain three readily identifiable potential problems. Hexavalent chromium is a soluble anion which is not rendered insoluble by the lime/fly-ash treatment. Reduction of the hexavalent chromium to the trivalent oxidation state is easily accomplished by the addition of ferrous ion in the form of ferrous sulfate. Cyanide may be destroyed by alkaline chlorination or ozone/ultraviolet treatment. Certain metals, chiefly lead and trivalent/arsenic may be solubilized at the high pH values required for the lime/fly ash reaction.

Incompatible Wastes

Incompatible wastes are defined as those materials for which microencapsulation, or microencapsulation alone, is not feasible. Generally, incompatible wastes are soluble salts, organic wastes, biological sludges, low-solids or liquid waste streams, wastes that retard the pozzolanic reaction, or wastes containing hazardous components which are released under high alkalinity.

Organic wastes have not been extensively studied, although several wastes which contain small amounts of organics have been evaluated. Neutral hydrocarbons such as oil, grease, and tars appear to have little effect on the pozzolanic reaction. Up to 8.5% of oil and grease in a lime/fly-ash mix does not decrease the compressive strength, and actually produces slightly greater strength than lime and fly ash alone. Decanter tar from a coke process was stabilized by mixtures of lime or CKD with fly ash or EFD in amounts of up to 20%. Benzene and xylene at 8.5% showed no effect on the pozzolanic reaction, although there is evidence that these organic compounds volatize from the matrix within a few days after compaction. Polar function groups such as the alcohol or carboxylic acid groups inhibit or retard the pozzolanic reaction. Carboxylic acid groups also neutralize the lime and render it useless for the pozzolanic reaction.

Biological sludges deserve separate comment. Biological or activated-sludge treatment utilized microbial enzymes to anaerobically or aerobically decompose organic substances. Some of the end products of this biological degradation are amino acids, organic acids, alcohols, methane, carbon dioxide, water, ammonia, nitrates, hydrogen sulfide, sulfuric acid, and fatty acids. In addition, the sludge may contain organic compounds that are wholly or partially resistant to biological degradation, and the microbial enzymes (dead or alive) themselves. Many of the organic compounds in biological sludges are known to retard cement and pozzolanic reactions. Therefore, attempts at pozzolanic stabilization of bio-sludges have to be approached very carefully with special testing after long-term stability.

CONCLUSIONS

Pozzolanic stabilization is becoming a major process for the disposal of undesirable waste materials. Among the oldest of stone-forming reactions, the known longevity of the reaction products is adequately demonstrated.

The largest-volume application today is the stabilization of SO_2 scrubber sludge and fly ash. Some 18 million tons per year capacity has now been built or contracted with continued growth expected. In this system, sludge, fly ash and lime are combined to form a strong, impermeable landfill material. Since the reaction depends on the chemical and physical properties of the reactants, careful characterization of these is necessary. Plant design must reflect these characteristics, or difficulties in operation will be met. Data obtained from the landfill corroborates design predictions from the laboratory. The results indicate that water discharge criteria for pH, alkalinity, and suspended solids are being met. Monitoring shows no contamination can be expected from the eight heavy metals considered hazardous.

Pozzolanic stabilization has also been applied to industrial wastes. Here it has been found that many wastes containing reactive materials are actually beneficial to the pozzolanic process. Many others are encapsulated by the cementitious material and prevented from leaching by the impermeability of the matrix. Incompatible systems have also been identified.

ACKNOWLEDGEMENTS

I am pleased to acknowledge many contributions from my co-workers at IU Conversion Systems with particular emphasis on those of Dr. A. A. Metry, L. C. Cleveland, L. Ruggiano, E. Poulson, and C. L. Smith.

REFERENCE

1. Geotechnical Evaluation of Stabilized FGD Sludge Disposal by L. M. Ruggiano & E. S. Poulson. Presented at the Second Conference on Air Quality Management in the Electric Power Industry, Austin, Texas, January 1980.

Fixation des boues industrielles avant décharge

Consolidation of industrial sludge before disposal

Jean Bernard LEROY, Ingénieur Principal à la Compagnie Générale des Eaux à Paris, France.

RESUME : Pendant longtemps, la mise en décharge des ordures ménagères puis des déchets de l'industrie a été considérée comme une solution définitive. Certes, on entendait plutôt ce terme dans un sens subjectif considérant qu'il n'y avait plus aucune raison de se soucier des résidus mis à l'écart dès qu'ils ne se manifestaient guère, plutôt que dans un sens objectif, supposant résolue la question de leur évolution ultérieure. Il fallut les récents progrès en matière d'analyse, surtout de celle des eaux profondes, pour que l'on décidât d'examiner de plus près les phénomènes de cheminement des matières nocives dans les décharges. Lors du premier symposium "Sol et Déchets" tenu à Angers en Avril dernier, plusieurs communications ont mis l'accent sur les interactions entre les déchets et le sol, même à travers des couches imperméables à l'eau et entre les déchets eux-mêmes. Des études poussées se poursuivent sur cette importante question. Dès lors qu'un déchet peut rester dangereux même placé en décharge, à des titres et à des degrés d'ailleurs très divers, n'y aurait-il pas une méthode, sinon pour le neutraliser, du moins pour en réduire la nocivité à la limite du mesurable?
La fixation des boues, par gélification au moyen de réactifs où les liants hydrauliques prennent une grande part, méthode que nous pratiquons maintenant depuis plus de cinq ans, semble être une des réponses à ce nouvel aspect de la protection de l'eau et de la nature.
Des essais de lixiviation en laboratoire et en vraie grandeur ont montré l'efficacité de cette méthode commercialisée sous le nom de CHEMFIX. Il existe actuellement une installation fixe à LIMAY, près de MANTES et une autre mobile, prête à intervenir sur n'importe quelle lagune même éloignée.

SUMMARY : The disposal of domestic, and then industrial, waste effluents has, for a long time, been regarded as a definitive solution. With this removal and disposal of wastes has, come a subjective out of sight out of mind way of thinking rather than one based on objective consideration of what happens to these wastes a little further down the road. Recent improved methods in the field of analyses, especially as applied to groundwater, have made possible a much closer examination of movements of toxic substances in waste effluents. At the first symposium on "Soil and Waste Effluents" held last April in Angers, many statements laid stress to interactions between waste effluents and the soil, even across strata that are impermeable to water, and within the effluents themselves. Thorough studies have been made on this important question. Is there note a method, therefore, whereby the various types and concentrations of toxic materials in the waste effluents, from the time of disposal and throughout the period they remain toxic, could be neutralized or at least reduced in toxicity to measurable maximum limits?
Sludge consolidation by gelification with the application of special chemical reactants along with heavy reliance on hydraulic binding agents is a process we have used for the last 5 years and which appears to respond to this new aspect of protecting water resources and the environment in general.
Lixiviation experiments conducted in the laboratory and in the field have demonstrated the efficacy of this method which has been made available commercially under the name of CHEMFIX. There now is a stationary facility at Limay, close to Mantes and another mobile one ready to intervene no matter what sludge lagoon or distance away.

-I-ASPECT THEORIQUE

De nombreuses études ont récemment démontré que l'évolution d'une boue pouvait se poursuivre longtemps après sa mise en décharge. Un des dangers les plus sournois étant la libération de métaux lourds à la suite d'une baisse de pH dûe à une action microbienne. Pour empêcher cela, on peut rassembler les déchets toxiques soigneusement déshydratés dans des fûts qui seront ensuite placés dans des mines désaffectées. On peut aussi opérer une "fixation" dans le but de rendre les boues analogues aux minerais qui ont inclus les éléments les plus toxiques pendant l'étendue des temps géologiques; les plus fréquents de ces minerais étant les silicates à la structure octaédrique particulièrement stable.

-A- Principes du procédé de fixation

La fixation, objet de la présente communication, consiste en un mélange intime des boues à traiter avec un réactif solide constitué essentiellement de ciment auquel est joint un liquide catalyseur à base de silicates. Le procédé est destiné aux boues dont le jus de pressage ne serait pas acceptable pour un rejet dans le milieu extérieur, soit en raison d'une DCO trop forte, soit en raison des métaux lourds qu'il pourrait contenir.

Avant de parler de la mise en œuvre de ce traitement qui relève surtout de la technologie, il a semblé bon de s'étendre sur les caractéristiques du matériau obtenu et sur les résultats d'essais tant en laboratoire que in situ sur des masses plus importantes de boues fixées soumises à des arrivages d'eau parfois acidulée. Ces derniers essais étaient destinés à étudier une évolution possible à long terme, même dans des conditions inhabituelles.

Bien que les réactions qui ont lieu dans le mélange boues-réactifs soient particulièrement complexes, on peut distinguer plusieurs actions simultanées :

- une neutralisation des boues faiblement acides sous l'action du calcaire contenu dans les réactifs solides. Les silicates réagissent dans le milieu basique ainsi formé pour donner des ions de la forme $Si(OH)_6^{=}$ qui se rassemblent sous la forme octaèdrique mentionnée ci-dessus. La silice étant au préalable très divisée, la surface de contact est très grande comme dans le cas de réactifs "activés".
- une précipitation des composés hydratés(hydroxydes), comme toujours en milieu alcalin. Cette précipitation ayant lieu en même temps que la formation des ions d'acides siliciques. Le résultat est la formation de sels complexés et hydratés très insolubles qui incluent les molécules d'eau présentes dans le milieu, la surface de contact est encore accrue au cours de ce processus.
- des réactions d'absorption entre composés ionisés plus ou moins faiblement, les cations étant attirés par les anions du système réticulaire en cours de formation. Cette absorption sera plus importante pour les cations les moins solubles qui sont souvent les plus lourds; c'est un élément favorable. Il est aussi possible qu'il y ait dans la masse en réaction des échanges d'ions :
- la gélification du réseau ainsi constitué se propage de proche en proche, la solidification totale ayant lieu dans un délai de 1 à 3 jours. Les cations métalliques sont enrobés dans des réseaux extrêmement fins et serrés qui donnent une grande stabilité au produit final désigné souvent sous le nom de "pseudo-minéral".

-B- Caractéristiques physiques du matériau obtenu

Les essais et mesures faits sur les eaux de lixiviation seront résumés au chapitre suivant qui traitera de l'efficacité du procédé. Du point de vue purement mécanique, si la boue à la sortie du réacteur a encore un aspect liquide, elle le perd assez rapidement pour prendre l'aspect d'une terre argileuse allant en se durcissant. Des mesures ont donné comme résistance à la compression des valeurs de l'ordre de 2,5 à 3 Bars; un chiffre de 5 Bars a été enregistré aux Etats-Unis. De fait, quelques temps après son épandage, il est possible de marcher sur les boues solidifiées, d'y circuler à bicyclette ou même en voiture. La température a une influence certaine sur le temps de séchage : en été, le temps de prise peut être ramené à quelques heures. En hiver, il est beaucoup plus lent en cas de froid prolongé, même si la réaction n'est jamais complètement arrêtée. La couleur du produit final dépend des constituants des boues à fixer, elle peut varier du jaune au gris-vert, voire au bleu. L'odeur est imperceptible sauf cas tout à fait particuliers. Elle reste d'ailleurs toujours très inférieure à celle de la boue primitive.

Une fois mises en décharge, les boues fixées se comportent comme n'importe quel remblai argileux. Elles ont été souvent recouvertes de terre arable, afin d'être le support d'espaces verts ou de terrains de jeux. La végétation s'y est développée tout à fait normalement ce qui est un excellent indice d'efficacité si l'on se rappelle le caractère toxique de la plupart des ions emprisonnés.

Il faut aussi rappeler le caractère tampon des boues fixées, qui a pour cause la présence de calcaire dans les liants hydrauliques utilisés. Ce caractère tampon est particulièrement précieux dans les décharges où sont reçus conjointement des déchets organiques et des déchets comprenant des ions métalliques plus ou moins nocifs. Un abaissement de pH du sol, qui peut être la simple conséquence d'une activité bactérienne, peut avoir pour résultat le dégagement de mauvaises odeurs (non neutralisation des acides organiques dégagés) et la remise en solution d'ions précipités en milieu basique. Dans de tels sites, l'addition de boues fixées a un double rôle bénéfique : elle constitue une couche parfaitement étanche bloquant ou retardant considérablement l'évolution des déchets entreposés et elle maintient le pH à un niveau suffisamment élevé. Bien qu'évoquée assez rarement, il s'agit

d'une propriété particulièrement intéressante. La rétention de l'eau contenue dans les boues et son bloquage avec les autres constituants montre bien qu'il s'agit d'un procédé "définitif". Cela implique par contre qu'il n'y a aucune réduction de volume; par rapport à la boue primitive, il y a même une augmentation d'environ 20%, tant en raison des réactifs ajoutés qu'au foisonnement du produit final par rapport à certaines boues.

II - EFFICACITE DU PROCEDE - ESSAIS DE LIXIVIATION

De nombreux essais ont été effectués, non seulement en FRANCE mais aussi aux ETATS-UNIS, en ANGLETERRE et au JAPON, pour ne citer que les principaux. Avant d'examiner deux cas particuliers, il est intéressant de tracer les grandes lignes des résultats de laboratoire. Les essais de lixiviation ont été menés par immersion dans des colonnes d'eau.

On a considéré que l'évolution au cours d'une année était obtenue par le passage de 800 cm^3 dans une colone normalisée de manière à ce que le débit corresponde à une année de précipitations en FRANCE (hauteur moyenne de pluie 760m/m). Ces essais ont été menés en faisant descendre le pH de l'eau de lixiviation jusqu'à 3, ce qui est bien rare pour une eau de pluie. La nature de l'acide utilisé à cette fin n'a eu qu'une influence négligeable sur les résultats (on a employé entre autres les acides acétique, hydroxybenzoique, nitrique, chlorhydrique, sulfurique). Pour les métaux suivants : fer, zinc, nickel, plomb et cadium, la teneur de l'eau de lixiviation de boues traitées provenant de l'industrie automobile est restée inférieure à 0,10 g/m^3. Pour le cuivre et le chrome, elle n'a atteint 0,25 que la première "année", dans le cas d'une eau acidifiée à un pH inférieur à 4 au moyen de l'acide chlorydrique. Pour le chrome même à un pH de 1, la teneur en chrome total est restée inférieure à 0,5 g/m^3 après trois ans de "précipitations" simulées comme il a été dit ci-dessus.

En régime de précipitations moyennes, la quantité d'ions métalliques relâchée par mètre carré de terrain revêtu d'une couche moyenne de 60 cm de boues fixées est inférieure à 0,4 g pour le chrome, 0,35 pour le cuivre, 0,05 pour le zinc, elle a été indécelable pour le nickel, ce qui s'explique peut-être par une fixation de cet ion au cours de la percolation. Ce sont des quantités bien inférieures à celles des eaux de ruissellement d'une décharge classique.

Il faut enfin remarquer que les ions métalliques sont eux-mêmes assez dilués dans la boue fixée en place, plus diluées que dans la boue d'origine puisqu'il y a ajoût de réactif.

"Il est évident que ces premières tentatives de contrôle in situ ne sont pas parfaites et demanderaient à être améliorées, mais telles quelles, elles amènent à des conclusions positives. Elles montrent que, si l'insolubilisation totale des éléments toxiques n'est pas possible (ce que tout chimiste aurait pu affirmer à priori avec une certitude parfaite), leur facteur de possibilité de passage en solution est ramené à des valeurs parfaitement compatibles avec la politique actuelle de protection de l'environnement."(M. Longuet-Cérilh).

III - INSTALLATIONS EXISTANTES

-A- Installation fixe

Contrairement aux solutions anglaise et américaine qui ont choisi de placer l'ensemble des appareils nécessaires au traitement dans une seule remorque de grandes dimensions, la SARP-Industries a choisi à LIMAY de construire une installation fixe et cela pour plusieurs raisons. D'abord parce que ce centre produit lui-même des boues en quantités importantes lors de ses opérations de neutralisation et de détoxication. En particulier les effluents de traitement de surface contenant du chrome hexaval ent sont traités par réduction puis précipitation sous forme de chrome trivalent.

Ensuite parce que, la France étant moins étendue mais d'un peuplement plus dense que les Etats-Unis -peut être aussi pour des raisons de tradition industrielle - les lagunes de boues et d'effluents sont rares.

Situé en Région Parisienne, le Centre de LIMAY était destiné à recevoir les effluents de diverses usines, en quantités relativement modestes pour chacune d'elles (une ou deux citernes par mois) mais devant subir un traitement élaboré.

Le Centre de LIMAY possède donc :

a) Une lagune de stockage d'une capacité de 2000 m^3, dans laquelle les boues reconnues aptes à ce type de traitement sont déversées. Elle est étanchéifiée par un revêtement plastique. Les boues entreposées sont homogénéisées par une drague automatique qui retarde en même temps la formation d'une couche de dépôt.

b) Un groupe de pompage qui reprend les boues pour les diriger dans le réacteur.

c) Un ensemble de stockage et d'alimentation du réactif solide pour lequel l'alimentation par fluidisation, trop coûteuse en énergie, a été abandonnée au profit d'une alimentation gravitaire et d'un dosage volumétrique moins précis mais plus fiable que le précédent.

d) Un ensemble de stockage et d'alimentation du réactif liquide pompe doseuse asservie aux pompes d'alimentation.

e) Un réacteur placé sous le silo de réactif solide dans lequel boues et réactifs sont mélangés énergiquement et aspirés par un groupe d'échange.

f) Deux lagunes de solidification de 1000 m^3 chacune dans lesquelles les boues achèvent leur évolution avant d'être reprises par tractochargeur et envoyées en décharge.

g) Un bâtiment de régulation et de contrôle.

Cet ensemble a une capacité nominale de 50 m^3/h soit, pour 2000 heures de travail, une possibilité de 100.000 m^3/an, ce qui permet d'abaisser le prix de revient du traitement dans la mesure où le prix du transport reste acceptable.

-B-Installation mobile

Une installation fixe ne peut toutefois répondre à toutes les demandes, ne serait-ce qu'en raison du prix de transport du déchet. C'est pourquoi un poste de traitement mobile a été mis à l'étude dès que l'installation fixe a pu être mise en marche industriellement.

On a surtout recherché la souplesse, la facilité de mise en place et la fiabilité. Dans cet esprit, les différentes parties du traitement ont été distinguées, leur assemblage n'étant fait qu'au dernier moment.

La plate-forme de traitement a été éclatée en trois parties :

- stockage et alimentation en réactif solide
- stockage et alimentation en réactif liquide
- mélange et contrôle.

Parties auxquelles se joignent naturellement les dispositifs de pompage, de transit et d'évacuation (tuyaux et pompes).

Le réactif solide est introduit par une alimentation gravitaire avec dosage volumétrique. Le réactif liquide est transporté en citerne, le reste de l'installation (mélange, dosage, régulation etc...) tient dans un camion classique. Le train routier se compose donc de trois véhicules dont aucun ne sort du gabarit légal, ce qui est un avantage incontestable.

Pour chaque matériel choisi, une attention particulière a été apportée à sa simplicité et sa solidité. En effet, le matériel mobile peut être amené à travailler dans des conditions difficiles. Tout ce matériel est vendu sur le marché français, ce qui simplifie les problèmes d'entretien.

IV- DOMAINE D'APPLICATION DU PROCEDE

Comme toutes choses en ce bas monde, ce procédé n'est pas universel, environ 10% des échantillons examinés ne sont pas propres à être traités par ce procédé. Il y a des inhibiteurs connus parmi lesquels

- le sucre : qui exclut que l'on traite les boues de vinasse, les mélasses ...
- le chrome hexavalent, les cyanures, l'arsenic, le phénol qui ne sont pas retenus, ce qui implique qu'un traitement préalable puisse être nécessaire pour des boues chromées afin de réduire l'état d'oxydation de ce cation.
- Les sulfures et le mercure sont parfois bien piégés, parfois non, sans qu'il soit toujours possible d'en discerner les causes.
- L'ion ammonium se conduit comme un "poison" de la réaction à partir d'une concentration de 500 g/m^3.

Il est donc indispensable avant de traiter une boue de vérifier son aptitude à la fixation. Cette analyse préliminaire consiste en un essai en laboratoire qui permet en outre de déterminer les taux de réactifs. Après 24h d'attente, on procède à des essais de lixiviation par trois percolations de 800 ml chacune, on a donc les résultats correspondants à trois années de précipitations simulées. L'analyse des métaux est faite par spectrographie. Ces exceptions mises à part, le domaine d'application du procédé est très étendu. On peut citer pêle-mêle : liqueurs de décapage, huiles et goudrons (en solution), boues de neutralisation, boues de collecteurs de poussière, régénération des acides, liqueurs noires, boues de déchromatation, de neutralisation d'acides ou bases forts, toutes boues contenant des métaux lourds, boues de dépigmentation etc...

Sans prétendre à l'universalité, la fixation des boues a donc de grandes possibilités et tient une place importante dans la lutte actuelle pour la sauvegarde de la nature.

V - CONCLUSION

Outre la fixation des boues, le Centre de la SARP-Industries à LIMAY dispose d'installations de neutralisation, de détoxication, de cassage d'émulsions huileuses et de traitement de déchets cuivro-ammoniacaux avec récupération du cuivre. La comparaison des quantités de déchets traités en 1979 est assez instructive (les poids sont exprimés en tonnes) :

Traitement physico-chimique (neutralisation et détoxication)	45.800
Liquides incinérés	17.400
Emulsions huileuses	16.200
Boues fixées	33.150
Déchets de laboratoire et cuivre ammoniacal	850
TOTAL	113.400

Il est symptomatique qu'aucun procédé n'ait de place véritablement prédominante, cela confirme s'il en était besoin le caractère illusoire de la recherche d'une solution "fourre-tout". La fixation des boues est une solution très intéressante parce que "définitive". Elle complète très bien la panoplie actuelle. Mais elle n'a aucune prétention à l'universalité et le meilleur traitement reste celui qui permet de récupérer ce qui peut l'être.

COMPTE RENDU GENERAL DU PRESIDENT J.P. MERIC

Le premier exposé relatif au rôle de la chimie des ciments dans la compréhension et la réalisation du traitement optimum d'une boue donnée a surtout suscité des questions sur le rôle des alcalins sur les réactions de fixation des ions toxiques par le ciment. En fait l'hydroxyde de calcium est une base forte peu soluble dans l'eau (environ 0,025M) dont l'équilibre de solubilité dépend de l'activité des OH^- présents dans la solution:

$$Ca(OH)_2 \rightleftarrows Ca^{2+} + 2OH^-$$

En présence de fortes quantités de bases alcalines (NaOH, KOH) complètement dissociées, la concentration en Ca^{2+} peut s'abaisser au-dessous du produit de solubilité du composé dont on recherche la formation et la précipitation (chloroaluminate de calcium hydraté par exemple, dans ce cas Cl^- reste en solution). On voit combien la connaissance du milieu à traiter est indispensable. Il est possible de regrouper d'une manière très générale les réactions de traitement en fonction des ions à traiter sur un tableau de classification périodique (figure F de l'exposé de P. LONGUET et G. BELLINA)

Ajoutons que certains fabricants ont proposé l'élaboration de liants spéciaux pour le traitement des boues.

L'exposé de Monsieur PICHAT montre les impératifs qui conduisent au traitement, les problèmes économiques posés par l'application des procédés de traitement (centres de traitement ou unités mobiles),les succès et les difficultés de réalisation avec une vue prospective du développement à venir.

L'exposé de Monsieur PETIT soulève des questions sur la nature des liaisons entre les ions fixés et les gels silicique et aluminique présents dans un milieu acide dont on abaisse progressivement le pH. Le manque d'organisation structurale des composés ainsi générés rend délicate la réponse exacte, mais il est bien établi que géologiquement des minerais actuellement parfaitement cristallisés ont eu une génèse identique.

Monsieur BLANCHARD précise que même si la boue toxique se présente sous une forme très peu soluble (hydroxyde), cette forme n'est pas forcément la mieux adaptée au stockage (action des agents atmosphériques acides). Il montre que l'utilisation de la chaux et des liants hydrauliques assurent une bonne stabilisation pratiquement irréversible.

L'intéressant exposé de M. FORMANEK sur l'incidence des solubilités des différents ions à l'interface liquide solide dans la flottation n'a pu être suivi d'une discussion à cause de l'horaire.

Avec l'exposé de Monsieur EMERY on aborde plus directement le domaine des applications. L'auteur relate une étude conduite pour le traitement d'une boue donnée avec des mélanges en quantités variables de poussières de four, de cendres volantes et de ciment. La discussion qui suit cet exposé dégage l'importance des aspects économiques pour ce genre de problème.

Monsieur KATAOKA développe une étude du même genre réalisée dans son cas avec des mélanges de ciment portland, de laitier et d'anhydrite. Ces liants à prise essentiellement ettringite développent des résistances mécaniques fort intéressantes. Malheureusement aucune mesure de lixiviation n'est indiquée dans cet exposé.

L'exposé de Monsieur SUZUKI et collaborateurs n'est pas présenté par les auteurs. Sa lecture publique montre une application originale des hydroxyapatites de synthèse pour la séparation sélective de certains ions métalliques. L'impossibilité d'une discussion est regrettée par les participants.

Monsieur RAU présente le procédé POZ.O.TEC utilisant principalement les cendres volantes et la chaux, procédé qui présente l'avantage d'une longue pratique. La discussion concerne surtout les problèmes de lixiviation des produits traités qui dépend évidemment de la boue initiale et des conditions de stockage. L'auteur signale que sur un remblai recouvert par la suite de végétation aucun rejet dangereux n'a été mis en évidence dans des puits de contrôle disposés autour du terrain traité.

Monsieur LEROY nous fait part de son expérience sur un autre procédé industriel utilisé dans un centre de traitement de déchets en France et qui assure le traitement du tiers environ du tonnage des déchets collectés par ce Centre.

L'examen des divers exposés relatifs à des applications met clairement en évidence la nécessité de pouvoir disposer de méthodes d'essais sur terrain pour apprécier l'efficacité réelle d'un procédé. C'est à partir de tels essais qui restent souvent à établir ou à perfectionner que pourra vraiment se dégager une comparaison objective des nombreux procédés proposés et partant apporter la garantie indispensable au développement du traitement des boues par les liants hydrauliques.

Le Président donne ensuite la parole à Madame ALOISI, Chef de Service au Ministère de l'Environnement et du Cadre de Vie qui nous a fait l'honneur de participer à nos travaux. Madame ALOISI exprime tout l'intérêt porté au problème du traitement des déchets par son Ministère et montre le rôle de l'Administration en France dans la lutte contre les déchets toxiques (incitations légales, aides financières, poursuites judiciaires....).

Le Président dégage ensuite les conclusions essentielles de ce séminaire.

CONCLUSION DU SEMINAIRE PAR LE PRESIDENT

A la lumière des exposés présentés, il apparaît que le traitement des boues industrielles à l'aide de liants hydrauliques permet, au moins en théorie, de fixer définitivement les ions métalliques contenus dans ces boues. De nombreux procédés fondés sur ce principe sont entrés ou sont sur le point d'entrer en application. Ces procédés reposent en général sur des connaissances héritées de la techniques des bétons ou de la chimie classique des silicates. Bien que ces procédés soient dans leur ensemble satisfaisants, des progrès peuvent encore être accomplis par des recherches fondamentales sur les réactions d'hydratation en présence d'une concentration importante de molécules étrangères. Ces réactions conduisent à des produits spécifiques dont la durabilité doit être étudiée. Il s'agit là d'un champ de réflexion très vaste pour les chimistes du ciment, mais il n'est pas nécessaire d'attendre qu'il soit entièrement exploré pour mettre en exploitation les procédés de solidification actuels car, tels qu'ils existent, ils constituent déjà une solution infiniment préférable au rejet pur et simple dans le milieu naturel.

Des débats très animés qui ont eu lieu aujourd'hui à l'occasion de ce Séminaire, on peut tirer un ordre de priorité pour les recherches à entreprendre dans l'avenir :

- D'abord, il faudra définir une procédure de mise en oeuvre de procédés rigoureuse calquée sur celle du béton. En effet, pour garantir la durabilité des ouvrages d'art, on identifie soigneusement les liants utilisés, on analyse l'eau de gâchage, le sable et les granulats afin de déterminer les dosages appropriés. Lorsque l'ouvrage est en cours d'exécution, une surveillance vigilante est exercée. Dans certains cas, des prélèvements conservatoires permettent de retrouver l'origine d'éventuels désordres. Dans le cas de la fixation des boues, cette même procédure pourrait être adoptée pour obtenir une garantie de qualité sur le résultat de l'opération.

- Ensuite, il est nécessaire de définir un test représentatif des phénomènes qui se déroulent sur le site où les produits traités sont entreposés. Ce qui a été proposé jusqu'ici ne constitue qu'un point de départ ; il semble particulièrement utile de tenir compte de l'acidité du milieu naturel. Cette acidité constitue une agression pour le produit solidifié au même titre que pour les bétons courants.

- Finalement, il faut aboutir à une meilleure connaissance des réactions de base qui se déroulent entre les composants de la boue et les phases actives du ciment ; cette connaissance permettra d'établir les limites des procédés et de choisir les réactifs les plus appropriés.

Ce Séminaire, qui a été l'occasion d'une rencontre entre les industriels, les physicochimistes et les représentants de l'Administration, aura donc permis aux différents points de vues de s'exprimer et, je l'espère, de se rejoindre pour un objectif commun qui est la protection de l'environnement.

SEMINAIRE C

Economies d'énergie
Vues prospectives

Président : M. GUY (France)

La chimie solaire à température élevée

High temperature solar chemistry

Geoges URBAIN, Lab. des Ultra-Réfractaires, CNRS, B.P. 5, 66120 Odeillo, France.

Résumé

L'article présente quelques exemples de réactions effectuées avec des réacteurs solaires à temperature élevée en chimie préparative ou énergétique. Ces études sont financées en France par le C.N.R.S.

Abstract

Some examples are given of material research and energetics reactions using high temperature solar reactors. These projects are sponsored by the C.N.R.S. in France.

I. INTRODUCTION.

Les avantages du chauffage au moyen du rayonnement solaire concentré sont les suivants :

- un apport d'énergie sans contamination et en absence de champs magnétiques,
- une densité d'énergie élevée,
- la localisation précise de l'impact énergétique,
- la possibilité d'effectuer ce chauffage en atmosphère oxydante (air)

A ces possibilités intéressantes sont associées des difficultés notables en ce qui concerne :

- la mesure des température des cibles,
- la régulation de l'énergie reçue par la cible,
- le confinement de la cible pour travailler sous vide ou sous atmosphère contrôlée.

Ces difficultés technologiques sont actuellement résolues pour les équipements de laboratoire de quelques kW. Les solutions ainsi utilisées ne sont pas toujours transposables aux installations de plus forte puissance. En particulier les parois transparentes utilisables au laboratoire (Pyrex ou silice transparente) ne seront pas économiquement possibles pour les installations pilotes. Le verre Pyrex supporte un flux de 20 W cm^{-2} et la silice transparente environ 500 W cm^{-2}. A l'occasion de la description de quelques montages précis nous verrons les méthodes utilisées au laboratoire pour résoudre ces difficultés spécifiques.

2. LA CHIMIE SOLAIRE PREPARATIVE.

Les premières années du développement des fours solaires correspondent surtout à des essais destinés à présenter leurs possibilités. Les montages démonstratifs ainsi réalisés exploitent de façon judicieuse les avantages du chauffage solaire par rapport aux techniques classiques d'obtention des températures élevées.

De tels essais ont été effectués de 1958 à 1970 à Montlouis avec un four de 50 kW, depuis ils sont réalisés à Odeillo avec le four de 1 MW et différents montages de 1,5 et 2 kW. Les principaux domaines d'application du chauffage solaire sont :

- les fusions ou préparations de produits réfractaires,
- les traitements de minerais,
- la détermination de grandeurs thermochimiques à température élevée.

Pour les traitements à température élevée citons par exemple:

- des fusions de zircone (T_f = 2710°C) en continu (150 à 250 kg par heure, d'alumine (T_f = 2054°C) à 150 kg par heure et de différents mélanges d'oxydes (zircone et oxydes de terres rares, etc...) qui ont été effectués avec le concentrateur de 1 MW en four tournant (lit brassé). La méthode de fusion en tas avec granulation du produit par soufflage du jet liquide est aussi utilisée. Ces fusions, suivies ou non de granulation, conduisent à un produit fondu ou divisé, particulièrement apte aux opérations de frittage ultérieur. Avec ces techniques ont été traités des bauxites (de 1850 à 1950°C) à 120 kg par heure, des composés alumineux (2000 à 2100°C) à 30 kg par heure et des zircones dopées (20 kg par heure), à l'occasion de contrat avec des groupes industriels intéressés.

Avec les montages de faible puissance (2 kW) mais disposant des mêmes densités d'énergie, des essais de fusion de zone sur nacelle refroidie et de croissance de monocristaux (TiO_2) ont aussi été effectués. Comme exemples de traitement de minerais on peut citer :

- l'élimination du fluor par voie thermique de phosphates apatitiques,
- la décarbonatation de minéraux (phosphates contenant 30 à 40 % de carbonates),
- le grillage de minerais sulfurés (molybdénite),

- la fragmentation par choc thermique (basnaésite).

Les objectifs visés sont alors l'application de techniques solaires (de haute température) pour valoriser des ressources minérales des pays à fort ensoleillement.

Ces techniques sont néanmoins suffisamment simples pour être mises en place sur le site des exploitations minières. Les intérêts économiques de ces pré-traitements sont :

- diminuer les inertes à transporter par élimination des carbonates, etc...
- obtenir un produit de pureté technique (MoO_3 par grillage de la molybdénite),
- économiser une part importante de l'énergie de broyage pour les minerais étonnables thermiquement : basnaésite.

D'autre part les équipements solaires de 2 kW du laboratoire sont utilisés pour des études de thermochimie à température élevée :

- des mesures de pression de vapeur, et de cinétiques d'évaporation de composés réfractaires sous différentes atmosphères sont ainsi réalisées. Les réfractaires (isolants et conducteurs électriques) spéciaux prévus dans les programmes concernant la conversion magnéto-hydro-dynamique (MHD) ont été soumis à des essais de corrosion, d'évaporation, de tenue au choc thermique, sous des atmosphères contrôlées (air, vapeur d'eau, argon + oxygène, etc...).

- l'étude de la dissolution des gaz (oxygène, vapeur d'eau, gaz carbonique) dans des oxydes et des aluminosilicates est aussi menée à bien avec ces fours solaires. La connaissance des équilibres de dissolution (chaleur de dissolution) et des conditions cinétiques du dégazage au cours du refroidissement (influence du chemin de solidification, des solubilités dans les différentes phases et de la viscosité de ces phases) sont très importantes pour les industries utilisatrices de laitiers, scories et réfractaires fondus : métallurgie, sidérurgie, réfractaires électrofondus, etc... Les mécanismes des remontées magmatiques dépendent aussi des variations de solubilité de phases gazeuses (H_2O et CO_2) dans les familles d'aluminosilicates constituant les magmas suivant la pression et la température.

Des montages utilisant un concentrateur parabolique de 2 kW à axe horizontal permettent le tracé de courbes de refroidissement d'oxydes réfractaires. Le montage en autocreuset, en rotation autour de son axe horizontal, permet d'obtenir la mesure des températures d'équilibre solide-liquide avec une bonne reproductibilité.

Ces applications du chauffage par rayonnement (fours à image et fours solaires) utilisent au mieux leurs caractéristiques : rapidité, non contamination, concentration localisée de l'énergie.

On opère souvent de façon dynamique avec des fluctuations notables de la température à la fois dans le temps et l'espace. L'équilibre thermique du matériau irradié est difficile à obtenir. Par contre un état de régime, proche de l'équilibre thermodynamique est obtenu en lit brassé avec le montage en four tournant. Pour des réactions entre phases condensées (solides et liquides) l'expérience vérifie bien, par des mesures de températures de transition par exemple, la réalité d'un régime stationnaire.

3. LA CHIMIE SOLAIRE ENERGETIQUE.

L'objectif est ici de produire un vecteur énergétique à partir du rayonnement solaire. Ce vecteur peut être l'hydrogène, un métal, un oxyde, soit en général le produit d'une réaction réversible. En effet, une condition nécessaire à l'utilisation énergétique du rayonnement solaire est la possibi-

lité de stockage de ce vecteur. L'utilisation différée, grace au stockage, des produits de la réaction se fera avec restitution d'une partie de l'énergie initiale et production de chaleur en un lieu et au moment voulu par le consommateur. Le "génie chimique solaire" comporte les étapes suivantes :

1°) des études thermodynamiques des réactions réversibles possibles. Ce sont des calculs et des modélisations à partir de données expérimentales. Les grandeurs manquantes doivent être estimées ou mesurées. Le résultat est une optimisation des paramètres réactionnels : température, pression et nature de l'atmosphère gazeuse, etc...

2°) l'étape suivante est le choix d'un réacteur adapté au problème posé suivant la nature des phases en présence, de la température et de la pression. Pour un réacteur donné on doit ensuite mesurer ou calculer les transferts thermiques et les bilans de masse. Ce travail suppose connue la cinétique de la réaction choisie. Ce sont des essais à l'échelle du laboratoire, puis l'établissement de modèles qui permettent une transposition à une échelle pilote.
Les trois exemples suivants concernent de tels aspects du génie chimique solaire :

- étude de deux réacteurs (réaction de décarbonatation),
- réaction en phase gazeuse (thermolyse de l'eau),
- réaction entre solide et gaz (grillage).

Etude de deux modèles de réacteurs solaires.

En prenant la réaction bien connue :

$$CO_3Ca \rightleftarrows CaO + CO_2$$

c'est à dire la décomposition du carbonate de calcium, on étudie deux types de réacteurs au foyer des fours solaires de 2 kW à Odeillo :

- un réacteur à lit fluidisé,
- un réacteur tournant à lit brassé.

Le réacteur cylindrique tournant absorbe presque complètement le rayonnement et ses parois sont à température élevée (1500°C). Les gradients thermiques sont élevés (montage en auto-creuset) mais le rendement de la captation de l'énergie rayonnante est bon (40 %). En marche continue, avec une alimentation arrière en produit, avec un temps de passage de 100 secondes, on mesure un taux de décarbonatation de 60 % et un rendement thermochimique global de 15 %.

Le second réacteur testé est un lit fluidisé recevant latéralement le rayonnement au travers d'un tube de silice transparente. La température du lit fluidisé varie entre 800 et 1300°C suivant le coefficient d'absorption du solide divisé. En régime permanent la température en un point du lit fluidisé est bien stable. Une décomposition complète du carbonate est obtenue avec une consommation de l'ordre de 5 kW par kg de carbonate. Le rendement thermochimique est de l'ordre de 20 % en fonctionnement discontinu.

Etude d'une réaction en phase gazeuse à température élevée.

La décomposition thermique de l'eau est obtenue dans une tuyère réfractaire (réfractaire à base de zircone) située au foyer d'un concentrateur solaire à 2200°C. Le choc thermique, puis le refroidissement à la vitesse de 10^6 degré par seconde permet de tremper les constituants de la réaction dont l'hydrogène.

Un semblable traitement (chauffage éclair et trempe brutale) appliqué à du méthane au foyer d'un concentrateur de 1,5 kW (le gaz est porté à environ 1500°C) donne à peu près 10 % d'acétylène.

Etude d'un réacteur solaire pilote pour le grillage de minerais.

Le grillage de minerais sulfurés (molyb-

dénite) en réacteur solaire rotatif à lit brassé devrait permettre :

- d'économiser une fraction importante de la consommation d'énergie pour les broyages,
- d'obtenir directement un oxyde (MoO_3) de pureté technique.

Après l'étude thermodynamique (mesure des enthalpies aux températures élevées) et cinétique de la réaction d'oxydation des produits susceptibles d'être traités en réacteur solaire. Ce travail montre l'intérêt de traiter la molybdénite après un premier enrichissement par flotation (produit à 6 % environ de molybdénite). Le minerai brut à 0,5 % de molybdène entrainerait le chauffage de quantités importantes d'inertes (silice). Le grillage du concentrè à 96 % ne présente aucun intérêt économique. C'est le semi-concentré à 6 % qui présente la granulométrie et la concentration les mieux adaptées au traitement solaire. Les problèmes à résoudre et en cours d'étude sont la réalisation d'un réacteur solaire tournant à lit brassé avec récupération du SO_2 et condensation de l'oxyde de MoO_3 vaporisé. La taille des cristallites de MoO_3 est comprise entre 300 et 500 nm. Cette filtration et cette épuration posent de délicats problèmes technologiques.

Ces trois études sont en cours de développement dans le cadre de contrats passés avec le PIRDES. Elles engagent sis laboratoires et la somme de trois contrats sont le l'ordre de 480 kF pour deux années.

4. CONCLUSION.

Les orientations prises par les laboratoires engagés dans les études de chimie solaire à température élevée sont cohérentes avec les options exprimées par les responsables nationaux (COMES) : études prospectives de faisabilité (niveau laboratoire et pilote de première génération) pour l'horizon 2000, avec des moyens réduits, mais une certaine continuité.

Lectures complémentaires à propos de chimie solaire à température élevée.

1958 - Applications thermiques de l'énergie solaire, Colloque CNRS N°85, Mont-Louis 1958 - Publié en 1961.

1973 - Techniques d'utilisation du rayonnement au foyer des appareils concentrant l'énergie solaire, M.FOEX, Les Hautes Températures, Vol.1, p.245, Masson, Paris, 1973.

1977 - Use of solar energy for direct an two step water decomposition cycles, E.BILGEN et Col., dans Int.J. of Hydrogen Energy, 2, pp.251/257, 1977.

1978 - Décomposition thermique à l'air de la magnétite au foyer d'un four solaire, M.DUCARROIR et Col., Rev.Int. des Hautes Températures et Réfractaires, 15, pp.7/13, 1978.

1979 - Deux articles dans le même numéro de Janv/Fev. de la Revue Entropie :
- *Les réacteurs chimiques solaires, J.VILLERMAUX, pp.25/31.*
- *Energétique chimique et énergie solaire, J.MAHENC, pp.32/42.*

Utilisation d'un sous-produit à très haute teneur en soufre comme combustible dans un four de cimenterie, sans transfert de pollution atmosphérique

Use of a by-product with very high sulphur content as fuel in a cement kiln, without transferring atmospheric pollution

P. ETOC, Ingénieur à la Société des Ciments Français, Professeur à l'Ecole Nle Supérieure Céramique de Sèvres et à l'Ecole de Thermique (I.F.E.), France.

RESUME : En prévision d'avoir à brûler dans l'avenir des fuels extra-lourds à haute teneur en soufre, la Société des Ciments Français a effectué des essais d'utilisation d'un goudron de pétro-léochimie non encore commercialisé comme combustible, sur un four à voie humide de 1 000 t/d de clinker.

Ces essais en vraie grandeur comportaient de gros risques car on ne savait pas si le procédé allait accepter un combustible à teneur en soufre nettement plus élevée que celle du fuel lourd ordinaire, 5 % contre 3,5 %; par ailleurs le goudron est nettement plus visqueux que celui-ci au niveau de la température de pompage et, de plus, fuel lourd et goudron ne sont pas miscibles.

Au moyen d'une tuyère-prototype permettant de brûler simultanément le goudron et un fuel à basse teneur en soufre, il a été possible d'augmenter progressivement la teneur en soufre résultante des combustibles injectés. Finalement, les essais ont montré qu'il était possible de fonctionner à 100 % de goudron sans difficultés d'exploitation et sans modification significative de la qualité du clinker. Depuis Mars 1979, l'utilisation de ce produit est devenue routine d'exploitation.

Le four de cimenterie a confirmé ses propriétés de piège à soufre - on devrait dire de piège à polluants. Rien n'interdit à présent d'envisager de brûler dans un four de cimenterie des combustibles encore plus sulfureux, par exemple des bitumes et, également de détruire de nombreux déchets industriels, sans transfert de pollution, mais avec récupération de la valeur énergétique.

SUMMARY : As it is anticipated that extra heavy fuel oils with a high sulphur content will have to be used in the future, Société des Ciments Français has carried out field trials with steam cracking residue (tar), which is not yet commercialised as fuel, in a 1000 t/d wet process rotary cement kiln.

These full-sized trials involved great risks, as it was not known whether the process would tolerate a fuel with a percentage of sulphur much higher than that of the ordinary heavy fuel, 5% as against 3.5%; also, the viscosity of the tar is notably higher than that of the heavy fuel at pumping temperature and, in addition, heavy fuel and tar do not mix together.

Using a prototype burner which allows the simultaneous firing of tar and low sulphur content fuel oil, it was possible to increase progressively the sulphur percentage of the injected fuels. Finally, the trials showed that it was possible to work with 100% tar without running into operating problems and without significant modification of the clinker quality. Since March 1979 the use of tar has become routine.

It has been proven that the cement kiln has the characteristics of a sulphur trap - or should we say a pollution trap. It now seems perfectly feasible to consider the firing of a cement kiln with fuels of an even higher sulphur content, such as bitumen, and the burning of industrial waste without transferring pollution, whilst recovering its energy value.

I - INTRODUCTION

A partir de 1974, l'alourdissement du fuel-oil lourd ordinaire déjà constaté, la perspective de mise en place dans les raffineries d'unités de conversion avec apparition sur le marché français de combustibles "hors normes", extra lourds, à haute teneur en soufre tels que résidus sous vide, sous-produits de pétroléochimie, l'éventualité d'avoir à brûler divers résidus industriels, nous ont incité à étudier l'utilisation de tels produits comme combustibles dans nos fours. Nous pouvions légitimement penser que cette utilisation ne devait pas conduire à un transfert de pollution, car nous avions déjà à notre disposition les résultats de nos travaux expérimentaux sur les fours des usines de Ranville et de Guerville, montrant que le four de cimenterie se comportait comme un "piège à soufre efficace" (1). Cette étude allait dans le sens de la recherche de la récupération d'énergie et surtout de la substitution de tout combustible au fuel-oil lourd, à laquelle les Cimentiers Français s'étaient engagés en signant le 22.03.76 le premier Contrat Sectoriel d'Economies d'Energie avec le Ministère de l'Industrie.

Aussi, lorsque vers le milieu de 1975, Esso-Chimie a proposé à la Société des Ciments Français des fournitures assez importantes de goudron de pétroléochimie - souvent baptisé "tar" dans les compte-rendus - dont la teneur en soufre pouvait dépasser 5%, il a été décidé de tenter l'expérience.

Les essais ont eu lieu de septembre 1977 à juin 1978 sur le four de 1 000t/d de clinker gris à voie humide à l'usine de Guerville et, en définitive, la fabrication du clinker n'a pas été affectée par l'utilisation du nouveau combustible. Au cours de ces essais, nous avons contrôlé particulièrement les marches à fuel-oil pur, en mixte goudron 60% - fuel-oil 40% et à goudron pur et, de ce fait, nous avons obtenu un grand nombre de résultats nouveaux à verser au dossier du "four de cimenterie piège à soufre"; c'est l'objet du présent mémoire.

Notons que depuis mars 1979, la chauffe au goudron est devenue routine d'exploitation non seulement dans le cas du clinker gris, mais également dans celui du clinker blanc.

II - LE PROBLEME DU GOUDRON A ESSO-CHIMIE

Ce goudron, qui est un sous-produit de la fabrication d'éthylène à l'usine Esso-Chimie de Port-Jérome, est considéré par les Douanes françaises non comme un combustible pétrolier, mais comme analogue à un produit de distillation des goudrons de houille. Il est très aromatique, non miscible aux fuel-oils lourds et sa teneur en soufre est supérieure à celle du fuel-oil lourd n°2.

L'usine de Port-Jérome, dont l'émission totale journalière de soufre est obligatoirement limitée pour raison de lutte contre la pollution atmosphérique, ne pouvait utiliser pour ses besoins propres la totalité du goudron qui pouvait être produit dans des conditions économiques optimales. Plutôt que de ne pas produire le goudron, et par conséquent de limiter ses exportations pourtant assurées d'éthylène, Esso-Chimie a cherché à commercialiser ce combustible "hors normes".

III - LA LEGISLATION FRANCAISE CONCERNANT LA TENEUR EN SOUFRE DES COMBUSTIBLES

La législation française n'interdit pas à proprement parler la vente et l'utilisation d'un combustible non classé administrativement comme un fuel-oil lourd, même si sa teneur en soufre dépasse celle de ce dernier, soit 4 %.

En fait, très vite d'autres contraintes peuvent intervenir :

a) une contrainte technique : l'apparition ou l'augmentation des corrosions à basse température "côté fumées", et l'émission de fumerons acides,

b) deux contraintes administratives :
   - le respect de la "Circulaire ministérielle sur la hauteur des cheminées" du 24.11.70 (J.O. du 13.12.70) : une augmentation du débit d'anhydride sulfureux implique une surélévation de la cheminée,
   - une décision du Comité Interministériel pour l'Aménagement de la Nature et de l'Environnement prise le 27 janvier 1972 de faire mettre en place et d'exploiter un réseau de contrôle du SO_2 par les Etablissements Industriels émettant plus de 0,5 t/h de SO_2 (cette émission est calculée à partir de la consommation annuelle de combustible, de la teneur en soufre de celui-ci et du nombre d'heures d'utilisation).

En fait, ces contraintes ne concernent pas les fours de cimenterie, car sur le plan technique, nous verrons plus loin que le captage des oxydes de soufre par la matière réduit presque totalement les risques de corrosion et sur le plan réglementaire, l'Administration admet que, dans les divers calculs, on utilise les teneur d'oxydes de soufre réellement mesurées.

IV - CHOIX DU SITE DE GUERVILLE

Le four à voie humide de Guerville a été retenu pour les raisons suivantes :

- du fait de sa taille, il peut détruire beaucoup de goudron
- du fait du procédé et de la composition de la matière, il n'est pas exagérément affecté par les anneaux lorsqu'il est chauffé au fuel-oil normal
- il fait partie d'une usine située en bordure de la Seine qui peut être ravitaillée par bateaux de 700 tonnes (capacité retenue dans le cas des livraisons de goudron).

V - CARACTERISTIQUES DES COMBUSTIBLES UTILISES

V-1 Objectif : montée progressive de S %

Pour ne pas avoir à surmonter simultanément, dès le début de l'opération, les problèmes de manipulation d'un combustible inhabituel, très visqueux à

froid, non miscible au fuel-oil lourd et les problèmes dûs au soufre, il a été décidé de brûler en même temps du goudron et du fuel-oil lourd à basse teneur en soufre, de façon à augmenter progressivement la teneur en soufre résultante et de ne pas dépasser la valeur de 4% - teneur limite dans le fuel-oil lourd utilisé jusqu'ici - qu'après avoir maitrisé les problèmes de préparation, de transfert et de combustion du goudron - Ceci a été possible grâce à la mise au point d'une tuyère à circuits séparés.

V-2 Le goudron Esso

Durant les essais, 9 analyses de goudron comprenant les déterminations suivantes : C %, H %, S %, pouvoir calorifique ont été effectuées par des laboratoires extérieurs. Aux résultats rassemblés dans le tableau 1, nous avons ajouté quelques informations complémentaires communiquées par Esso.

Par ailleurs, les mesures de viscosité effectuées par SCF confirment une particularité de la courbe viscosité/température d'un goudron qui avait déjà été mentionnée par Esso. Dans le diagramme log-log habituellement utilisé pour cette représentation graphique, les courbes caractérisant les fuel-oils sont des droites parallèles. Or, la droite relative au goudron a une pente plus élevée et croise celle des fuel-oils. En d'autres termes, le goudron est plus visqueux que les fuel-oils ordinaires au niveau du pompage et du stockage et plus fluide qu'eux au stade de la pulvérisation(figure 1).

V-3 Les fuel-oils lourds

Composition centésimale et pouvoir calorifique des fuel-oils lourds qui ont été utilisés pendant les contrôles sont donnés dans le tableau 1.

Tableau 1 CARACTERISTIQUES DES COMBUSTIBLES UTILISES

		Goudron Esso	Fuel-oil lourd ordinaire	Fuel-oil lourd B.T.S.
Soufre	%	4,6 à 5,2	3,69	1,13
Hydrogène	%	6,5 à 7,1	11	11,79
Carbone	%	84,7 à 89,0	85	86,6
C/H		12,5 à 13,1	7,7	7,35
Pouvoir calor. inférieur	(mth/kg	8 930à 8 960	9 625	9 778
	(kJ/kg	37 380 à 37 500	40285	40925
Asphaltenes	%	env. 20	N.D.	N.D.
Conradson	%	env. 20	N.D.	N.D.

VI - DESCRIPTION DE L'INSTALLATION

VI-1 Ensemble de cuisson

. Four Fives Lille à voie humide à chaines, 1970, 4,80x4,40x150m
Capacité maximale : 1 150 t/d de clinker
Production pendant les essais: 965 à 1 050 t/d
Consommation thermique : 1 270 à 1 370 th/t ck (5320 à 5735 MJ/t ck) à l'époque des essais. Au début de 1980, celle-ci est de 1 200 th/t ck(5025 MJ/t ck)

. Refroidisseur de clinker Fuller, à grille, température d'air secondaire 650°C

. Electrofiltre Elex, émission de poussières : 40 à 50 mg/Nm3.

VI-2 Pâte

Pâte "lourde" dont la teneur en eau est, en 1980, de l'ordre de 30 à 31%, alors qu'elle était de 32 à 33% pendant les essais et de 43% en 1974. Cette réduction, effectuée dans l'optique de la recherche des économies d'énergie, a été obtenue grâce à la mise au point d'un mélange de défloculants et de l'utilisation dans la pâte de cendres de centrale thermique.

VI-3 Préparation du goudron

Pour définir les installations de dépotage, stockage et réchauffage de pulvérisation et la tuyère, nous avons suivi deux recommandations essentielles : ne pas mélanger le goudron et le fuel-oil lourd, même au niveau du pulvérisateur et prévoir un réchauffage à la pulvérisation de 180°C.

L'ensemble d'alimentation comprend trois circuits de combustibles : goudron, fuel-oil lourd B.T.S. et fuel-oil lourd ordinaire, un circuit de rinçage des canalisations de goudron par un solvant spécial et finalement constitue une installation assez complexe.

En définitive, les températures de réchauffage retenues sont les suivantes : . dépotage et stockage 70°C
. pulvérisation 140°C

VI-4 Tuyère

La Société Pillard a spécialement conçu pour cet essai une tuyère à trois injecteurs, aux caractéristiques suivantes :

- Le tube central de Ø 220mm est équipé de trois fourreaux de Ø 70 permettant chacun le passage d'une canne terminée par un injecteur (fig. 2).
- Chaque injecteur est du type MY à deux arrivées de combustible, l'une en rotation, l'autre axiale. En réglant la pression différentielle entre les deux circuits, on peut faire varier l'angle du jet.
- Autour du tube central, un tube concentrique et une rosace permettent de distribuer l'air en rotation. Un dernier tube concentrique, sans rosace, permet d'amener l'air axial. En réglant la pression différentielle entre les deux arrivées d'air, on peut ajuster l'angle de la flamme.
  . débit air primaire 13 000 Nm3/h, soit environ 15% de l'air total de combustion
  . pression air en rotation : 250 mm C.E.
  . pression air axial : 400 mm C.E.
  . pression amont de pulvérisation : goudron et fuel-oil lourd ordinaire 42 bars, fuel-oil lourd B.T.S. 39 bars
  . pression différentielle entre les deux circuits de chaque combustible 1,75 bar(la même pour les trois combustibles).
  . température de pulvérisation 140°C pour le goudron et le fuel-oil ordinaire et 130°C pour le B.T.S.

VII - PROGRAMME EXPERIMENTAL

VII-1 Recherche de la teneur en soufre résultante optimale

Avant les essais, il était acquis que l'ensemble four/matière pouvait "accepter" un fuel-oil dont la teneur en soufre était comprise entre 3,5 et 4%. En utilisant

la tuyère Pillard à deux combustibles, goudron et fuel-oil lourd B.T.S., le pourcentage de goudron utilisé a été progressivement et rapidement augmenté jusqu'à atteindre 60% du débit thermique, ce qui donnait une teneur en soufre résultante voisine de celle du fuel-oil ordinaire. Une longue période de marche dans ces conditions permit de vérifier que le fonctionnement du four était satisfaisant. Enfin, le débit de goudron a été poussé à 100% et il a été vérifié que l'ensemble four/matière "acceptait" le nouveau combustible. A chaque étape de ce programme, plusieurs séries de contrôles portant sur le soufre ont été effectués.

VII-2 Contrôles effectués - Techniques utilisées

VII-21 Généralités

A chacun des trois stades de la montée de la teneur en soufre résultante, il a été effectué un bilan soufre c'est-à-dire un état comptable des entrées et des sorties de soufre :

- entrées : combustible et pâte
- sorties : clinker, poussières captées à l'électrofiltre et fumées.

On considère comme négligeable le soufre contenu dans les poussières s'échappant à la cheminée (rappelons que l'émission est de 50mg/Nm3).

Chaque bilan établi sur une durée de 24 heures comporte donc des mesures de débit et des contrôles sur les matières minérales, les combustibles, les fumées.

/II-22 Mesure sur les matières minérales

En ce qui concerne pâte et clinker, les mesures de débit et les analyses complètes sont des contrôles de routine. On a opéré un prélèvement par poste et analysé le produit aux rayons X. A l'occasion du bilan le même contrôle a porté sur les poussières captées à l'électrofiltre.

VII-23 Contrôle des combustibles

Les débits sont mesurés au moyen de compteurs. Lors de chaque bilan, une analyse a été opérée.

VII-24 Contrôle de routine sur les fumées (sortie four)

Le débit de fumées est calculé à partir de l'analyse et du débit de la pâte, de l'analyse et du débit de combustible, et de l'excès d'air. La connaissance de cette dernière caractéristique implique que l'on mesure la teneur en oxygène des fumées et leur teneur en imbrûlés. Le four est équipé normalement d'un analyseur en continu d'oxygène (basé sur les propriétés paramagnétiques de O_2) et d'oxyde de carbone (absorption de rayonnement infra-rouge).

VII-25 Contrôles relatifs au soufre dans les fumées (après électrofiltre)

Plusieurs déterminations de point de rosée ont été faites au moyen de l'appareil B.C.U.R.A. (2,3). Cet appareil a été conçu pour permettre des mesures de point "acide" dans la zone 120-160°C. En fait, nous avons déjà vérifié (1) sur un four de cimenterie - et nous verrons que cela a été encore confirmé ici - que le point de rosée mesuré est égal au point de rosée "de l'eau" qui, au point de mesure, dépasse rarement 70°C et par suite on peut dire que $SO_3 = 0$ et que le soufre des fumées se trouve sous forme de SO_2 (on sait en effet qu'il suffit de quelques millionièmes de SO_3 pour faire croître considérablement le point de rosée des fumées qui dépasse alors rapidement 120°C(5). A notre avis, l'appareil B.C.U.R.A. est l'appareil le plus sensible pour détecter l'absence de SO_3 dans les fumées. En définitive, cette mesure préalable nous permet de simplifier considérablement l'appareil de mesure d'oxydes de soufre, en supprimant le condenseur à SO_3 en fait à H_2SO_4 (5)(3). Pour chaque analyse, le SO_2 a été capté dans l'eau oxygénée et dosé par acidimétrie. La mesure comprend trois prélèvements au débit de 200 l/h pendant 30mn.

VIII - RESULTATS

VIII-1 Caractéristiques d'exploitation durant les essais

Durant la période considérée octobre 1977 - juin 1978, le four a continué à produire du clinker dans les conditions les plus économiques possibles. De ce fait, certains paramètres ne sont pas restés constants, en particulier la composition de la pâte dont la teneur en eau a été réduite de 36,5% en octobre-novembre, à 32-33% en mai-juin, ce qui a eu pour conséquence de faire passer la consommation thermique moyenne de 1 370 th/t à 1 270 th/t de clinker (5 735 MJ/t à 5 320 MJ/t). L'alourdissement de la pâte semble avoir entrainé un plus grand débit de poussières captées à l'électrofiltre et, par conséquent, apporte un certain changement dans la répartition des sorties de soufre. Nous y reviendrons au paragraphe "discussion".

La combustion du goudron a eu lieu sans imbrûlés et il ne semble pas que l'utilisation du nouveau combustible ait entrainé une augmentation de la consommation thermique. La réduction de consommation évoquée au paragraphe VIII-1 correspond bien à la réduction de la teneur en eau de la pâte. Il n'a pas été constaté de formation d'anneaux et la qualité du clinker n'a pas été affectée de façon significative.

VIII-2 Contrôles relatifs au soufre dans les fumées

Les principaux résultats de mesures de SO_2 et de point de rosée sont résumés dans le tableau 2.

Tableau 2 CONTROLES RELATIFS AU SOUFRE

% goudron	date	Soufre résultant du combustible %	teneur en SO_2 sur fumées sèches 10^{-6} (ppm)	teneur en SO_2 sur fumées humides* 10^{-6} (ppm)	Point de rosée °C	O_2 au point de mesure %
0	31.05.78	3,69	554	384	63	8,4
62,5	5.10.77	3,34	70	50	ND	10,2
58,6	2.11.77	3,20	77	53	60	8,6
100	2.05.78	4,64	354		ND	9,2
100	6.06.78	3,86	361		62	9,5

VIII-21 Le calcul de point de rosée de la vapeur d'eau des fumées donne dans chaque cas des valeurs de l'ordre de 70°C, donc assez proches du point de

rosée mesuré. Comme nous l'avons dit au paragraphe VII-25, $SO_3 = 0$, ce qui explique pourquoi on rencontre fort peu de cas de corrosion à basse température "côté fumées" dans un four de cimenterie.

VIII-22 Il n'apparait pas de relation entre la teneur en soufre résultante du combustible et la teneur en SO_2 des fumées. L'incidence de l'augmentation de cette teneur a peut-être été masquée par l'alourdissement progressif de la pâte; les dernières concentrations dans le temps sont plus élevées.

VIII-23 Les teneurs en SO_2 mesurées sont relativement faibles, 354 ppm le 2.05.78 et 554 ppm le 31.05.78. Le calcul montre que les teneurs théoriques en SO_2, provenant du combustible, dans les mêmes conditions de dilution et sans captage par la matière seraient respectivement de 1 900 et 1 526.

VIII-3 Les bilans-soufre

Six bilans soufre ont été établis sur une durée de 24 heures. Nous présentons dans le tableau 3, les résultats des trois bilans les plus significatifs.

Tableau 3 — BILANS - SOUFRE

Combustible	Fuel-oil lourd ordinaire	{B.T.S. 38,5 goudron 62,5 %	Goudron
date	31.05.78	5.10.77	21.03.78
Soufre résultant %	3,69	3,34	4,78
ENTREES SOUFRE			
Pâte (t/d	1,997	0,963	0,755
Pâte (%	29,7	18,3	10,0
Combustible (t/d	4,723	4,944	6,788
Combustible (%	70,3	83,7	90,0
total entrées (t/d	6,720	5,907	7,543
total entrées (%	100,0	100,0	100,0
SORTIES SOUFRE			
clinker (t/d	1,300	1,426	2,218
clinker (%	19,8	27,6	35,1
poussières (t/d	3,212	3,410	2,443
poussières (%	48,9	65,9	38,6
fumées (t/d	2,051	0,335	1,666
fumées (%	31,3	6,5	26,3
total sorties (t/d	6,563	5,171	6,327
total sorties (%	100,0	100,0	100,0
Indétermination %	- 2,3	- 12,5	- 16,1

On remarque que ces bilans sont déficitaires(moins de sorties que d'entrées de soufre) et que l'indétermination va de 2,3 à 16,1 %. Il est difficile de connaître le ou les postes responsables de l'indétermination quand on connait les difficultés d'analyse ou de pesée. En particulier, les variations de la teneur en soufre de la pâte sont du même ordre que la teneur en soufre elle-même. Il n'en reste pas moins qu'il est évident que la majeure partie du soufre des sorties se trouve dans le clinker et les poussières.

IX - DISCUSSION

IX-1 Remarque générale sur les essais sur four

Nous insistons sur le fait que nous relatons ici des résultats d'essais industriels et non des résultats sur maquette, en laboratoire, Il n'existait pas à Guerville de four à clinker gris disponible, plus petit que le four 7. De ce fait, les essais ont été menés en vraie grandeur sur un four produisant environ 1 000 t/d de clinker et, pendant leur durée, il a fallu continuer à réduire la consommation thermique autant que faire se pouvait par réduction de la teneur en eau de la pâte. Ce manque de rigueur dans le plan de travail a peut-être eu pour conséquence de masquer quelques phénomènes secondaires, mais il a conduit à de substantielles économies.

Notons également que la composition des fumées dans un four n'est pas aussi constante que dans un générateur à fumées séparées du fluide caloporteur par suite des irrégularités de l'écoulement de la matière (formation d'anneaux dans la partie rotative qui se détruisent ensuite, avalanches). Ces retenues de matière font que la composition des fumées ne correspond pas toujours à celle de la matière dans les bilans. Certes, en effectuant un bilan sur une durée de 24 heures, on miniminise ce genre d'erreur, mais on n'est pas sûr de la supprimer.

IX-2 Sur les très faibles émissions d'oxydes de soufre

L'absence de SO_3 dans les fumées ne peut nous surprendre. Il y a en effet 20 ans qu'il a été prouvé expérimentalement que des additifs basiques injectés dans les fumées pouvaient neutraliser le SO_3(6)(4). La matière crue introduite dans le four, constituée principalement de calcaire, joue parfaitement ce rôle. Par ailleurs, du fait des températures rencontrées dans un four de cimenterie, la majeure partie du SO_2 est fixée par les matières calcaires indépendamment de la teneur en alcalins du cru. Cette propriété a été étudiée entre autres par E. VOGEL (7)

IX-3 Comparaison des émissions d'oxydes de soufre par différents générateurs

Dans le tableau 4 ont été rassemblés les résultats obtenus dans la présente étude, ceux enregistrés en 1972 sur le four de Ranville et ceux que l'auteur a obtenus jadis sur des générateurs aussi différents que le sont des chaudières domestiques et industrielles et les fours de briqueterie. L'examen de ce tableau confirme l'intérêt exceptionnel du four de cimenterie pour détruire des produits hautement sulfureux.

Tableau 4 — EMISSIONS D'OXYDE DE SOUFRE PAR DIVERS GENERATEURS

Cas	Soufre du combust. %	Soufre de la matière première %	Point de rosée des fumées °C	Teneur en SO_2 des fumées 10^{-6} (ppm)	Teneur en SO_3 des fumées 10^{-6} (ppm)	Taux de conversion $\frac{SO_3 \times 100}{SO_2 + SO_3}$	N.B. excès d'air au point de mesure (dilution) %
Four de cimenterie voie humide Guerville 965 à 1 000 t/d 1977 - 1978	3,69 à 4,78	0,05 à 0,12	60 à 63	207 à 554	0	0	110 environ
Four de cimenterie voie semi-sèche Ranville 1 200 t/d 1972	3,3	0,17	54	20	0	0	100 environ
Chaudières chauffage domestique 1960	0,5	-	43 à 47	220 à 280	0	0	20 à 50
Chaudières industrielles 1960-1970	3,5	-	130 à 150	1950 à 2100	30 à 60	1,5 à 3	15 à 25
Fours tunnels briqueterie 1966	0,5	0,03 à 0,7	140 à 160	935 à 950	260 à 595	16,1 à 28,6	650 environ

X - CONCLUSIONS

X-1 Les problèmes de dépotage, stockage, transfert et préparation du goudron Esso particulièrement visqueux à froid et non miscible au fuel-oil lourd ont été surmontés.

X-2 La chauffe au goudron à près de 5 % de soufre, seul, après mise au point, a lieu sans difficulté de combustion ou d'exploitation, sans augmentation de consommation thermique, sans modification significative de la qualité du clinker et sans problème de pollution atmosphérique. Elle n'a absolument pas été un obstacle à la poursuite de la recherche de réduction de teneur en eau de la pâte. Depuis un an, la chauffe au goudron Esso est devenue routine d'exploitation dans les fours à clinker gris et à clinker blanc. L'usine de Guerville a brûlé 26 000 tonnes de goudron en 1978 et 48 000 tonnes en 1979.

X-3 La tuyère Pillard à deux arrivées indépendantes de combustible, décrite ici et mise au point spécialement pour ces essais, permet, avec deux produits, l'un hautement sulfureux, l'autre moyennement ou peu sulfureux, de constituer un combustible à teneur résultante en soufre prédéterminée, compatible avec le procédé et le degré de pollution admis. Bien que l'emploi de cette tuyère ne soit pas indispensable pour la marche à 100% goudron, elle garde tout son intérêt pour des applications futures où le procédé serait plus exigeant.

X-4 Le four de cimenterie a confirmé ses propriétés de "piège à soufre" - on peut dire de façon plus générale de "piège à polluants" - Les émissions de SO_2 sont au moins cinq fois plus faibles que ce qu'elles seraient si le goudron brûlait dans un foyer, sans réaction de neutralisation. Rien n'interdit, à présent, de brûler dans un four de cimenterie des combustibles encore plus sulfureux, par exemple du résidu "sous vide" ou des bitumes et de détruire des déchets industriels très gênants, tels que des goudrons sulfuriques, sans transfert de pollution. Cette étude ouvre de larges perspectives sur la récupération de sous-produits ou de déchets industriels ayant une précieuse valeur énergétique.

C'est pour cette raison qu'en novembre 1979, la Société Générale a décerné pour cette étude, à l'équipe de la Société des Ciments Français, constituée de MM. Jean Commène, Claude Mayrargue, Marc Dancoisne et de l'auteur de la présente communication, un de ses prix de l'Energie.

XI - REFERENCES

1 - P. ETOC "Le four de cimenterie, un piège à soufre efficace" - Revue des Matériaux de Construction n° 701, avril 1976

2 - P. F. CORBETT, D. FLINT, R. F. LITTLE JOHN Journal of the Institute of Fuel, nov. 1952

3 - P. ETOC "Techniques modernes d'étude de corrosion" - l'Industrie Céramique, avril 1966

4 - P. ETOC "Cours sur les corrosions à basse température" - Ecole de Thermique (I. F. E.)

5 - H. GØKSOYR et K. ROSS - Journal of the Institute of Fuel, avril 1962

6 - L. K. RENDLE et R. D. WILSDON, Journal of the Institute of Fuel, septembre 1956

7 - E. VOGEL - Silikattechnick, Deutsch, août, octobre, novembre 1958.

Fig. 1 DIAGRAMMES DE VISCOSITE FO n°2 et GOUDRON

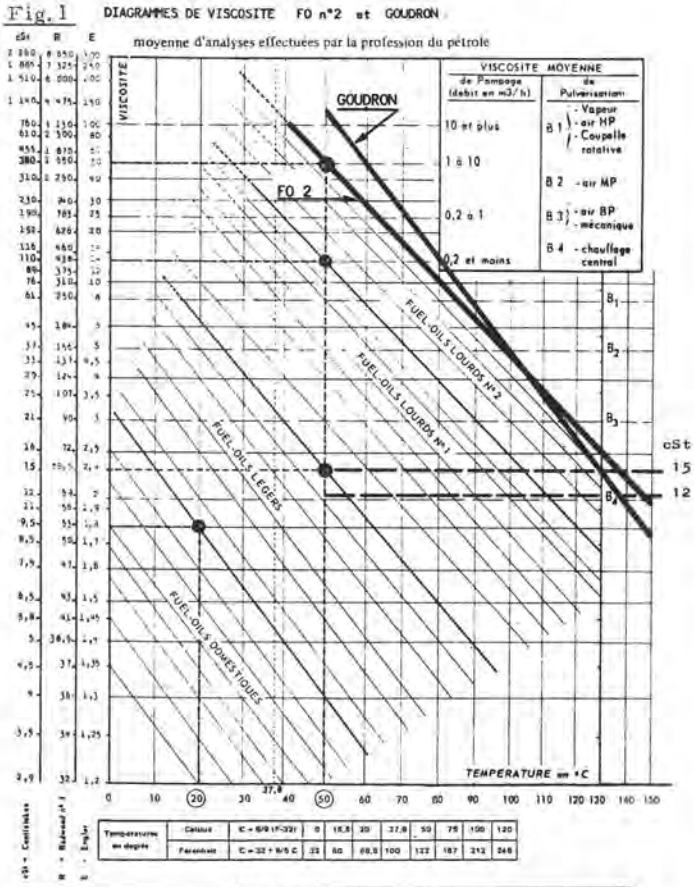

Fig. 2 TETE DE LA TUYERE

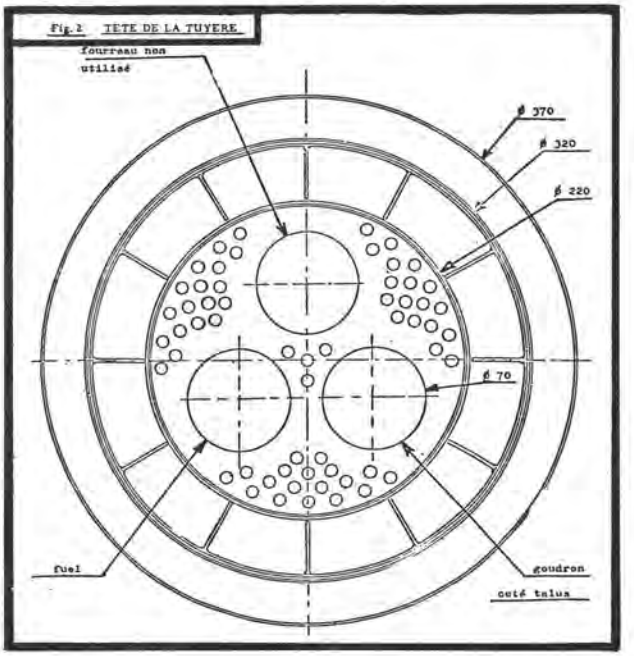

Complex utilization of rotary kiln heat losses

Utilisation complexe des pertes de l'énergie thermique par les fours rotatifs

L. VOROBEICHIKOV, senior scientific worker, candidate of technical sciences,
V. SATARIN, professor, doctor of technical sciences, Yuzhghiprotsement, USSR.

SUMMARY: Rotary kilns operate with low heat efficiency: external losses are 10-25%, with clinker and aspiration air 5-10%, with flue gases 15-20%, etc.
Equipment for complex heat utilization consists of an installation for using the heat of kiln shells and an air-evaporative cooler. These installations have been built and used, with the aim of heat recovery and use for central heating and technological requirements. The service period of lining is increased due to automatic control of coating formation.

RESUME: Le rendement des fours rotatifs est bas:les pertes du groupe de fours dans le milieu ambiant sont de 10 à 25%, avec le clinker et l'air d'aspiration de 5 à 10%, avec les fumées d'échappement de 15-à 20%, etc.
Les installations complexes d'utilisation de la chaleur se composent de: dispositif pour l'utilisation de la chaleur des corps de four, réfrigérant d'évaporation à l'air. On a créé et implanté les installations complexes d'utilisation de la chaleur dans le but d'utilisation et de conservation de l'énergie thermique pour l'alimentation en chaleur et pour les besoins technologiques. Augmentation de la durée de vie du garnissage grâce à la commande automatique de la formation de l'enduit.

Cement industry is a large-scale consumer of thermal energy. Every year more than 100 000 000 tons of conventional fuel is consumed in the whole world.

In cement industry fuel is mainly consumed by clinker burning; it is also consumed by heat supply and some other technological needs which depend on the climatic zone of the country, presence of certain heat consumers, kind of fuel, etc. The heat which is produced in the boiler room is used for the heat supply of the plant, dwelling-houses, production of reinforced concrete and asbestos slate, for mazut heating, for heating greenhouses and for other needs; this heat amounts to 25% of all fuel. In zones with hot climate, heat may be used for mazut heating and for obtaining cold for air conditioning.

Rotary kilns which are the main fuel consumers, have low thermal efficiency. Irretrievable heat losses in rotary kilns are distributed in the following way: environment losses from the kiln body (10-20%); losses in the cooler (5-10%); with waste fumes (15-20%). These heat losses can be successfully used for covering heat needs. Correspondingly, the kiln thermal efficiency increases. The heat surplus, obtained by using secondary power resources, is preserved in the kiln unit.

Complex heat utilization installations, consisting of a cooling device for kiln bodies and means for coating formation, have been theoretically grounded and installed at a number of cement plants in the Soviet Union. These installations have been patented in the USA, Japan, German Federal Republic, France, England, Spain and other countries.

Such installation is mounted on the body in the burning zone and is intended for recovering the lost heat which in the form of hot water with the temperature up to 373 K is used for the needs of heat supply and technological process. The installation has a system of air supercharging which allows to control the coating thickness and almost double the lining operating period. The kiln has movable insulation due to which fuel consumption for clinker burning is reduced

The device for cooling recuperator refrigerators consists of heat exchangers sections and a system of suction of hot air for supplying it to the kiln in hot state which is especially important for mazut burning. The control of the kiln bodies state and of the complex installations work is reliably performed by means of the indications of a recorder which moves along the kiln body and by means of visual inspection. For this purpose there is a special window in the protective housing along the kiln axis.

The devices for clinker burning trap and use the heat of the hot clinker in such a way, that the temperature of the air, supplied for fuel burning, is not reduced. The device for air-evaporative clinker cooling in the grate refrigerator allows to eliminate heat exhaust with suction air and to use the heat of evaporative clinker cooling. In the nearest time scientific work on using the secondary heat of waste fumes will begin.

For the contactless method of heat exchange, which is used in utilization installations, the candidate of technical sciences Vorobeichikov L.T. has elaborated a mathematical model - a system of analytical connections between the parameters of the heat exchanger input and output and the construction parameters. In our case the mathematical model is developed according to the main processes of water heating in heat exchangers of the utilization installation. Here the thermal process for steady-state conditions can be described by the following equation:

$$C \cdot G \frac{dT}{dx} = Q(x) \qquad (1)$$

where C is the heat capacity of the heat exchanger water, J/kg (kcal/kg); G - water mass flow, kg/h; x - coordinate, measured from the tube inlet to the studied section, m; Q(x) - heat flow supplied to the heat carrier per tube length unit of the heat exchanger, J/m h (kcal/m h); T - average water temperature along the tube length, K/°C).

For calculating the value of Q(x), let us examine Fig. 1 where the schematic diagram of the heat exchanger tubes location is given:

S - the distance between the axes of tubes in the bundle, m; D - heat exchanger tube diameter, m; 1 - the external surface of the kiln body, $F_1 \cdot m^2$; 2 - the external surface of the tube, $F_2 \cdot m^2$; 3 - the surface of the inner walls of isolated flaps, $F_3 \cdot m^2$.

For calculating Q we introduce the following assumptions:

1. The average temperature of the heat exchanger tubes surface is assumed to be equal to the average temperature of the heat carrier (heated water).

2. The complex heat exchange between the surfaces 1,2,3 (mainly by radiation and convection) is generalized in the form of heat transfer coefficients ($\alpha_1, \alpha_2, \alpha_3$).

3. The temperature of the rotary kiln body surface is assumed to be independent on the construction and operating conditions of the cooling system (according to measurements data).

Let us introduce the following indices:
$\alpha_{1,2}$ - heat transfer coefficient, J/degree m^2 • h (kcal/m^2 h °C) from the surface with the first index to the surface with the second index. The same indices are used for mutual surfaces of heat exchange.

Now we can write the following equation:

$$Q = \alpha_{1,2} \cdot F_{1,2}(T_1 - T_2) + \alpha_{3,2} \cdot F_{3,2}(T_3 - T_2) \quad (2)$$

It means that the heat flow, which influences the heat exchanger tube, consists of two flows - from the body and from the housing flaps.

For calculating T_3 let us use the following equation:

$$F_{1,3} \cdot \alpha_{1,3}(T_1 - T_3) = \alpha_{3,2} \cdot F_{3,2}(T_3 - T_2) + \alpha_{3,0}(T_3 - T_0) F_{3,0} \quad (3)$$

which represents heat balance of the surface 3, received from the hot body; the heat is consumed by heat transfer to the tube and by losses to the environment.

From eq. (3) we can obtain the value of T_3:

$$T_3 = \frac{\alpha_{3,2} \cdot F_{3,2} \cdot T_2 + \alpha_{1,3} \cdot F_{1,3} \cdot T_1 + \alpha_{3,0} \cdot F_{3,0} \cdot T_0}{\alpha_{3,0} \cdot F_{3,0} + \alpha_{1,3} \cdot F_{1,3} + \alpha_{3,2} \cdot F_{3,2}} \quad (4)$$

When $\alpha \to \infty$, T_3 273 K (0°C), eq. (4) can be freely used in the absence of housing flaps.

Representing eq. (4) and (2), and then the result and eq. (1) we obtain:

$$cG \frac{dT}{dx} = A - BT \quad (5)$$

where $A = \alpha_{1,2} \cdot F_{1,2} \cdot T_1 + \frac{\alpha_{3,2} \cdot F_{3,2}(\alpha_{1,3} \cdot F_{1,3} \cdot T_1 + \alpha_{3,0} \cdot F_{3,0} \cdot T_0)}{\alpha_{1,3} \cdot F_{1,3} + \alpha_{3,2} \cdot F_{3,2} + \alpha_{3,0} \cdot F_{3,0}}$ (6)

$$B = \alpha_{1,2} \cdot F_{1,2} + \frac{\alpha_{3,2} \cdot F_{3,2}(\alpha_{1,3} \cdot F_{1,3} + \alpha_{3,0} \cdot F_{3,0})}{\alpha_{1,3} \cdot F_{1,3} + \alpha_{3,2} \cdot F_{3,2} + \alpha_{3,0} \cdot F_{3,0}} \quad (7)$$

or

$$c \cdot G \frac{dT}{dx} = \alpha_{1,2} F_{1,2} T_1 + \frac{\alpha_{3,2} \cdot F_{3,2}(\alpha_{1,3} \cdot F_{1,3} \cdot T_1 + \alpha_{3,0} \cdot F_{3,0} \cdot T_0)}{\alpha_{1,3} \cdot F_{1,3} + \alpha_{3,2} \cdot F_{3,2} + \alpha_{3,0} \cdot F_{3,0}} - (\alpha_{1,2} \cdot F_{1,2} + \frac{\alpha_{3,2} \cdot F_{3,2}(\alpha_{1,3} \cdot F_{1,3} + \alpha_{3,0} \cdot F_{3,0})}{\alpha_{1,3} \cdot F_{1,3} + \alpha_{3,2} \cdot F_{3,2} + \alpha_{3,0} \cdot F_{3,0}}) \quad (8)$$

For obtaining the output value of T, it is sufficient to solve the eq. (5) - (8) and substitute into the solution, as function "x", the complete length of the tube part.

The calculating formulae will be more convenient, if the temperature reference will be from the conventional zero 273 K, i.e. the temperature in the heat carrier system:

$$T_{x=o} = 0$$

Then eq. (5) will be written as follows:

$$T_{(x)} = \frac{A}{B} \cdot \left[1 - 1_{xp}\left(-\frac{B}{cG} \cdot x\right)\right], \quad (9)$$

and the water temperature at the outlet:

$$T_{(1)} = \frac{A}{B}\left[1 - 1_{xp}\left(-\frac{Bl}{cG}\right)\right] \quad (10)$$

By means of eq. (6, 7, 10) it is possible to calculate the final temperature of the carrier according to the values:

1) kiln body temperature, T_1;
2) ambient temperature, T_0;
3) heat carrier consumption, G.

For this purpose it is necessary to know the heat exchange characteristics α, F and others.

Eq. (10) is one of the possible mathematic models of the analyzed heat exchanger, having six parameters: three of them characterize the dependency of heat exchange on temperature conditions (α), and the other three characterize the system geometry (F). But it is impossible to estimate these values in a pure theoretical way, therefore additional experiments have been performed. In the result of experimental research we have obtained an equation for defining the amount of heat recovered by the utilization installation.

$$Q=10\cdot\varphi D_n\cdot K_{\Delta}Tl-\alpha_{3,0}\cdot F_{3,0}(T_{3,0}-T_{e.a.}) \qquad (11)$$

where 10 is an empirical coefficient; φ-screening degree; D_K - kiln body diameter, m; K - heat transfer coefficient, J/m^2 hK; T - thermal head, K (°C); l - length of sections zone (according to the kiln length), m; $F_{3,0}$ - housing flaps surface, m^2; $T_{3,0}$ - temperature on the housing flap surface, K (°C); $T_{e.a.}$-external air temperature, K (°C).

The obtained main experimental dependences allowed to transform the main equation of the mathematical model (eq. (10)) and to reduce it to a form convenient for engineering calculations.

As the parameters $\alpha_{1,3}$ and $\alpha_{3,2}$, due to the low temperatures of housing flaps, exert small influence on the heat exchange, and because of the difficulties of their exact defining, we substitute them conventionally by $\alpha_{1,2}$ which can be experimentally defined.

Then eq. (10) can be transformed and written in the following form:

$$T_{(1)} = T_{in.}+(T_k-T_{av.v.})\left[1-1_{xp}\cdot\frac{(-\alpha_{1,2}\cdot Q+\alpha_{k\cdot1,2}\cdot Q_k)\varepsilon_k\cdot255\cdot D_n)}{cG\cdot\varphi T}\right] \qquad (12)$$

Substituting in the main equation (12) the value of the criterion dependence $N_u=\varphi(Re)$, we obtain:

$$T_{(1)} = T_{in.}+(T_k - T_{av.v.})\left[1 - - 1_{xp}\left(-\frac{4,8\cdot\lambda\cdot Re\varepsilon_x\cdot2,55\cdot D_n\cdot l_e}{dcG\,\varphi T}\right)\right] \qquad (13)$$

The performed theoretical and experimental research allowed to elaborate the method of thermal estimation, control conditions and thermal schemes of heat utilization.

When the contactless method of rotary kilns heat utilization is used, the heat take-off varies in a limited range. The parameters of the heat, taken from kiln bodies, are in the range 323 - 383 K and are conditioned by the necessary operating schedule of the kiln, at which the necessary coating is formed protecting the lining from quick wear.

Optimum conditions of heat takeoff for summer and winter seasons are finally established during the operating process of utilization installations and depend on the quality of burned raw material, on the kiln diameter, climatic conditions, etc. In the winter heating period the heat carrier parameters and the periods of peak heater boilers joining-up are chosen in dependence of the relation of the quantity of taken-off from the kilns heat Q_n to the estimated - consumed quantity Q_{max}, i.e.

$$\varphi=\frac{Q_n}{Q_{max}},$$

The annual economical effect from using utilization installations differs with kilns dimensions, climatic conditions and heat supply systems. It is achieved due to fuel economy, reducing of capital and operation expenditures and the increase of lining durability. In most cases the expenses are justified in approximately one year. Technical economic indices are shown in Table 1.

Already nowadays there is a practical possibility to economize up to 15% of thermal energy due to the use of the complex method of heat utilization.

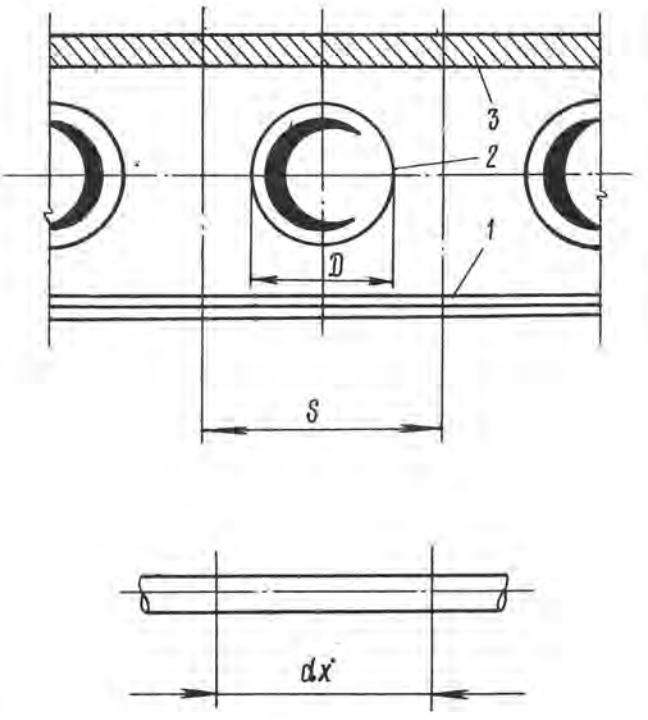

Fig.1

Table 1

Indices	Unit of measurement	Before introducing heat utilization installations	After introducing heat utilization installations
Kiln 3.6x103.9 m			
Annual take-off of secondary heat	thousands Gcal/year	-	11-12
Conservation of heat of the kiln during clinker burning (due to the kiln body insulation)	thousands t/year	-	1.2-1.8
Increase of lining life	days	320	590
Kiln 5x185 m			
Annual take-off of secondary heat	thousands Gcal/year	-	30-35
Conservation of heat in the kiln during clinker burning (due to the kiln body insulation)	thousands t/year	-	5.0
Increase of lining life	days	200	300

Opportunities for energy saving in the cement industry

Les économies d'énergie dans l'industrie cimentière

G.R. GOUDA, Ph. D. manager, Cement Technology, Fuller Company, Bethlehem, Pennsylvania, U.S.A.
G.J. LABELLE, B.S. General manager, Cement Industry Group, Fuller Company, Bethlehem, Pennsylnania, U.S.A.

SUMMARY: Opportunities for energy saving in the cement plants is discussed and the following points are covered:

1. Selection of raw materials
2. Process change to improve efficiency
3. Reduction of heat loss from the kiln system
4. Better sintering process and retention time
5. Waste heat recovery
6. Energy conservation through high efficiency fans
7. Improve combustion, control of temperature, oxygen, and turbulence
8. Kiln insulation
9. Automatic process control
10. Use of alternative fuels and energy supply systems
11. Good maintenance
12. Dust use
13. Clinker quality

In a suspension preheater or a flash calciner system about 340 kcal/kg clinker is wasted. This represents the amount of heat used in excess of the theoretical amount of heat required. A great amount of energy can be saved in the existing plants by (a) controlling: the mix design, (b) improving the sintering process, (c) using high efficiency fans, (d) controlling combustion, (e) using automatic process control, (f) good maintenance and (g) the production of a porous clinker.

RESUME: Cet article s'agit d'une discussion sur la conservation d'énergie dans les fabriques de ciment. Les sujets suivants sont compris:

1. Sélection des matières premières.
2. Changement du procédé pour améliorer l'efficacité
3. Réduction des pertes de chaleur du système du four
4. Un meilleur procédé de clinkérisation et temps de rétention
5. Récupération des chaleurs perdues
6. Conservation d'énergie par des ventilateurs d'haute efficacité
7. Amélioration de combustion, régulation de températures, d'oxygène, et de turbulence.
8. Isolation du four
9. Régulation automatique du procédé
10. Emploi des combustibles et systèmes d'alimentation d'énergie alternatifs
11. Bon entretien
12. Emploi de pousse
13. Qualité de clinker

Environ 340 kcal/kg de clinker est perdu dans un système de préchauffeur à suspension ou de précalcination. Celui-ci représente la quantité de chaleur employée au-dessus de la quantité de chaleur théorique exigée. Une grande quantité d'énergie peut être conservée dans les fabriques existantes (a) en régulant le mélange, (b) en améliorant le procédé de clinkérisation (c) en employant les ventilateurs d'haute efficacité (d) en régulant la combustion (e) en employant la régulation automatique du procédé (f) en éffectuant le bon entretien et (g) en produisant le clinker poreux.

INTRODUCTION

Energy conservation is a vital concern of every industrial company throughout the world because everyone is aware of the energy crisis. The steadily rising dependence on imported oil continues to threaten the economic stability everywhere, due to heavy balance of payment deficits. In the U.S.A., for example, industry shares a large portion of responsibility for energy consumption as it uses nearly 40% of the nation's net energy requirement. Steady improvement in energy efficiency by obtaining maximum energy per Btu, and by establishing long-range energy conservation programs, is mandatory for the improvement of the profitability of industrial operations.

There is no doubt that the success achieved over the last twenty years in cement production, by using the preheater system, is considered a major step in energy conservation, in comparison to the wet process. But, even in the dry process there is still wasted heat; the theoretical amount of heat required to form one kg of clinker is equal to 1040 kcal, while the amount of heat which is recuperated is about 600 kcal/kg clinker. This means that the theoretical heat required to form clinker is about 440 kcal/kg clinker. Practically, it is impossible to reach this fugure, and the average lowest fuel consumption obtainable by an SP (Suspension Preheater) or SF (Suspension Flash Calciner) system is about 780 kcal/kg clinker. About 340 kcal/kg clinker is wasted through heat loss in the kiln and cooler radiations, by heat transmitted by convection, and by the kiln gases and the dust in the gases.

ENERGY CONSERVATION IN THE CEMENT INDUSTRY

The cement industry is in a unique position to play a major role in conserving energy, materials, and the environment. Modernization of existing equipment and conversion of the existing wet process plants to dry process using suspension preheater or suspension flash calciner, can save a substantial amount of energy. Application of mixed cement should be widely used. Additionally, there are various operating techniques which can be modified. These are:

1. Selection of raw materials
2. Process change to improve efficiency
3. Reduction of heat loss from the kiln system
4. Better sintering process and retention time
5. Waste heat recovery
6. Energy conservation through high efficiency fans
7. Improvement of combustion, control of temperature, oxygen, and turbulence
8. Kiln insulation
9. Automatic process control
10. Use of alternative fuels and energy supply systems
11. Good maintenance
12. Dust use
13. Clinker quality

1. SELECTION OF RAW MATERIALS

Selection of the cement raw materials for better clinkerability and quality offer a good opportunity for fuel consumption in the cement industry. Raw mixes with (a) high free silica, (b) low flux content, (c) high moduli (silica modulus and alumina modulus) are sintered at high temperature compared to raw mixes with low free silica, high flux content and low moduli.

Each cement plant should review the mix design, fineness and the additive characteristics in order to achieve optimum energy conservation throughout the entire cement production process, including the cement mills (1 & 2). Better clinker and cement qualities can also be obtained by this energy conservation effort.

Choice of raw materials with low alkali content eliminates the need of an alkali bypass in a clinker producing system. Hence, the fuel wasted by the alkali bypass system is saved.

Raw materials with quartz are harder to crush, grind, and burn than those without a high percentage of quartz (2).

2. PROCESS CHANGE TO IMPROVE EFFICIENCY

Dry process cement manufacturing undoubtedly reduces fuel consumption and provides better utilization of energy, especially when either an SP or SF system is used. But, about 340 kcal/kg clinker is wasted. Now is the time to analyze the cement manufacturing process in order to reduce or eliminate the loss of the 340 kcal/kg clinker. The following are to be considered to minimize wasted heat:

a. Use of a new and efficient process to produce the clinker.
b. Improve the clinker cooler heat recuperation efficiency.
c. Reduce the sintering temperature by using fluxes and/or mineralizers in various ways.
d. Recover the heat loss through the exit gases and the kiln shell radiation.
e. Production of porous clinker, which requires less energy to grind (3).
f. Modify the crushing and the grinding processes, as about 75% of the total power is used for these two processes.
g. Use a five-stage preheater system.

3. REDUCTION OF HEAT LOSS FROM THE KILN SYSTEM

In order to increase the cooler recuperative efficiency, the leaking air should be reduced. It has been found that reducing inleaking or primary air by about 15% of combustion air saves about 25 kcal/kg clinker for a dry SF kiln.

The cooler and the kiln should work with maximum possible efficiency by reducing the inleaking ambient air. This allows a higher volume of hot combustion air to enter the kiln from the cooler and greatly reduces fuel consumption. Priority should be given to reduction of air leaking through the hoods and the combustion chamber and to improvement of the clinker cooler recuperation.

The kiln shell loss, as well as the SP or SF system, greatly influences fuel requirements. Insulation of the kiln, preheater, and cooler reduces, but does not eliminate, the heat loss.

Depending on the capacity of the kiln and the fuel consumption, hood leakage can reach 6% to 15% of the combustion air; this undesirable inleaking air can be reduced by modifying the seal gap and/or hood draft. Density differences of ambient and hot cooler secondary air produces localized pressure differences, which causes a large air exchange. A radiation protection system is required to insure the temperature of the kiln shell remains low despite the high waste gas temperature.

4. BETTER SINTERING PROCESS AND RETENTION TIME

Sintering cement raw materials differ from one plant to another depending on the characteristics of the raw materials. Ideally, each burner should burn the raw materials with the most economic fuel consumption and with the least retention time to obtain a high quality clinker. Overburned clinker is expensive as much fuel is wasted, much energy is required to grind such a clinker, and the cement produced from this clinker is considered poor quality.

Kiln feed should be homogenous and constant. Its chemistry should be adjusted so that it can be burned with a minimum amount of fuel. Evaluation of the clinker microstructure by a scanning electron microscope (4), or by a polarized microscope, is essential to relate raw mix burnability to clinker quality. The most economical burning process can be achieved by continuously examining the clinker microstructure. Thus the optimum in fuel savings, retention time, crystal distribution and size, and cement quality can be determined.

5. WASTE HEAT RECOVERY

The exhaust gases from the kiln and cooler are considered the major components of wasted energy in the cement industry; about 20% of the energy in fuel is wasted in the kiln exhaust gases. The heat from the kiln exhaust gases is recovered, partially or completely in the case of dry grinding raw materials.

Recovery of the kiln and/or cooler exit gases by a heat exchanger serves both as an air pollution function and a method of recovering heat. The heat exchanger helps save capital and conserve fuel. The air-to-air heat exchanger eliminates the need for a baghouse by establishing a closed system of air circulation. Ordinarily, hot dust-laden kiln gases pass through the clinker cooler and a baghouse before being discharged into the atmosphere. In the case of a heat exchanger, the dusty air from the clinker cooler is directed through the heat exchanger and then back to the cooler inlet again without discharge to the atmosphere. The air is cooled in the heat exchanger from 315° to 93° C (600° to 200° F) by atmospheric air flowing over the outside of the tubes carrying the heated air.

A study is required to recover the heat radiated from the kiln shell by a hood system in the form of hot air; this air can be used for space heating in the cement plant or for drying the raw materials.

6. ENERGY CONSERVATION THROUGH HIGH EFFICIENCY FANS

Fans are among industry's largest energy consumers. Evaluation of the compatibility of the fan with its system and analyses of the fan curves should be performed continuously. Any air leakage into (induced draft) and out of (forced draft) the system should be prevented. Every square inch of external ducting must be carefully inspected. Leak air increases the pressure drop and the horsepower which is proportional to the air volume cubed.

Excessive static pressure losses through various components of the air distribution system contributes to needless horsepower consumption. These losses can be caused by pluggage, deterioration of internal components, or absence of turning vanes in critical duct locations.

In the cement plant, the process fans play a very important role as they participate greatly in the chemical and physical modification of the raw material. The fans also have a great influence on the consumption of energy per ton to clinker produced. For example, a kiln with a capacity of 4700 metric ton per day clinker requires a total power of 8810 hp with an overall efficiency of 86% by using a high efficiency fan. In the case of low efficiency fans, 10,400 hp is required, with 73% efficiency. The power saving is 1590 hp. In the U.S.A., the cost of energy is approximately 3.0 cents per kW (0.13 FF). For fans running 7500 hours per year, the savings amounts to $268,000 U.S. (1,163,000 FF).

Besides, the high efficiency fan blades have a higher resistance to stresses and vibrations than the straight radial blades (5).

7. IMPROVE COMBUSTION, CONTROL OF TEMPERATURE, OXYGEN, AND TURBULENCE

Combustion can be improved by using oxygen-enriched air to increase kiln production and to achieve a reduction in fuel consumption. The oxygen-enriched air creates higher flame temperature and reduces the nitrogen concentrations in the combustion products. The flame emissinity is increased and the shell losses per kg of clinker is decreased.

Most efficient combustion is achieved by a short, high energy release flame which generates the maximum flame temperature.

Trimming the fuel/air ratio can produce savings. It is important to have fuel/air ratio controls and burners that can hold operations close to correct fuel/air ratio throughout their entire firing range. Too little air results in unburned gases going up the stack and too much air wastes heat. Optimum fuel combustion depends on the proper fuel and air mixture. Practically 10% excess air would give a flame temperature of about 200 degrees hotter than the 30% excess air, greatly improving heat transfer efficiency (6). Most efficient burning condition is obtained by controlling the fuel/air ratio until the maximum CO_2 is obtained, which are:

in natural gas: 11-12% CO_2
in light oils: 15-15½% CO_2
in heavy oils: 15½-16% CO_2
in case of coal, the CO_2% varies from one coal to another according to the percentage of volatile matter, ash and moisture content.

8. KILN INSULATION

A way to reduce kiln shell losses is by using insulating refractories. In this category it is required to:

a. Improve the kiln installation, by development of new materials to extend the life of the existing lining and/or reducing the heat loss through the kiln shell.

b. Develop new refractories with low thermal conductivity or refractory combinations to lower the overall sensible heat loss from the kiln shell.

This area needs additional research to develop new kinds of bricks which can lower the heat radiated from the kiln.

9. AUTOMATIC PROCESS CONTROL

Undoubtedly, using an automatic process, controlled by a computer, will have a great affect on energy savings and on production of a homogenous clinker (7).

10. USE OF ALTERNATIVE FUELS AND ENERGY SUPPLY SYSTEMS

It has been shown (8) that 15% of pulverized refuse (with a calorific value of approximately 3000 kcal/kg) is used as an alternative fuel. The ash is absorbed into the clinker without any harmful affects. This application should be widely used, and the application of different kinds of energy supplies in various qualities and percentages should be evaluated.

11. GOOD MAINTENANCE

Good maintenance throughout the cement plant will minimize inleaking air and will increase production. This includes the crushing system, raw materials and clinker grinding, and kiln linings, etc. Use of proper grinding balls (size and amount) will reduce the energy consumption for the grinding process. Using classifying liners increases capacity and reduces the required grinding energy kW per ton.

12. DUST USE

The dust in cement plants is a calcined ground raw mix which is too costly to be disregarded. Unless it contains a high percentage of alkalies and chlorides, it should be reused in the process. Research is needed to investigate the feasibility of using the kiln dust, having a high alkali content, in the process once more.

13. CLINKER QUALITY

Clinker produced should be porous, as such clinker is easier to grind and requires less energy. Very dense, hard-burned clinker consumes more energy in comparison to a porous clinker (3). A great amount of energy can be saved by grinding porous clinker rather than non-porous clinker.

CONCLUSIONS

Energy conservation and eliminating energy waste in the cement industry should be considered. Study of the existing technology and development of new processes are recommended in order to produce clinker with the lowest energy consumption. The produced clinker should not be overburned as non-porous clinker consumes more energy in grinding than the porous clinker. An international committee is suggested to coordinate the efforts and the studies required to accomplish energy conservation in the cement industry.

BIBLIOGRAPHY

1.- G.R. GOUDA (1979), "Raw mix: the key for a successful and profitable cement plant operation", World Cement Technology, London England, Vol. 10, Number 9, pp. 337-346.

2.- G.R. GOUDA (1977), "Cement raw materials: their effect on fuel consumption", Rock Products, Vol. 80, No. 10.

3.- G.R. GOUDA (1979), "Effect of clinker composition on grindability", Cement and Concrete Research, Vol. 9, pp. 209-218.

4.- G.R. GOUDA (1979),"Clinker characterization by SEM", Scanning Electron Microscopy, Washington, pp. 387-398.

5.- Personal Communication, Solyvent-Ventec Ltd., Montreal, Quebec, Canada.

6.- R.J. REED (1973), "Development in automatic fuel/air ratio controls for fuel preservation and pollution preventation", Ash Rae Transactions, Part 1, Chicago.

7.- M. ABD-EL-BARY & G.R. GOUDA (1979),"Process control in the cement industry", Annual meeting of the American Ceramic Society, Cincinnati; Cement Division.

8.- P. DAVIS & J.A. STRINGER (1976), "Potential for energy economy in cement operations", The Associated Portland Cement Manufacturers Limited, London, England.

Industrie et électricité dans un proche avenir

Industry and electricity in a near future

BOUCHET Jacques, Contrôleur Général Adjoint à la Direction Générale d'E.D.F., France.

La France n'a pas de pétrole dans son sous-sol ; elle avait un peu de charbon et de gaz naturel, mais leur production est maintenant en décroissance.

Aussi dès 1974, le Gouvernement a-t-il pris des décisions fermes :

- les économies d'énergie devraient être fortement encouragées ;
- il y aurait accroissement du programme de réalisation des centrales nucléaires.

Les premières de ces centrales sont maintenant proches de la mise en service ; aussi la pénétration de l'électricité dans l'industrie doit-elle être activement poussée pour économiser devises et énergie.

Cette pénétration semble dans beaucoup de cas devoir être intimement liée à une forte baisse du rapport : coût moyen de l'électricité sur coût moyen des combustibles fossiles.

Du fait de la mise en service d'un grand nombre de centrales nucléaires au cours de la prochaine décennie, une telle décroissance surviendra très vraisemblablement.

Mais un peu d'électricité sera encore produite dans des centrales à fuel-oil, surtout dans les périodes chargées d'hiver.

De ce fait, l'électricité pourra à ces moments rester à un niveau de prix relativement élevé, contrastant avec des niveaux plus bas les autres saisons.

Ces changements dans les niveaux relatifs de prix pourront entraîner des changements dans la façon d'exploiter les usines ; et la plupart des fois, il y aura au moins deux façons de minimiser les coûts d'exploitation sans compliquer l'optimisation de la qualité des produits. Toutes les deux pourront être des moyens efficaces d'économiser l'énergie.

France has no oil underground;it had some coal and some natural gas, but their production is by now decreasing.

So,as soon as 1974, Government made up its mind :

- energy conservation was to be strongly promoted ;
- there would be an increase in the development of nuclear power plants.

The first of these plants are now close to commissionning ; so electrification of industry must be actively promoted, in order that foreign currencies and energy might be saved.

Such an electrification seems in many cases to be closely related to a strong decrease in the ratio : mean cost of electricity vs mean cost of fossil fuels.

Due to the commissionning of a large amount of nuclear power plants within the next decade, such a decrease is very likely to occur.

But some electricity will yet be produced in oil-fired plants, mainly during winter peak times.

As a result, price of electricity may then remain at a relatively high level in contrast with lower levels during other seasons.

These changes in relative levels of prices may result in changes in how to run a factory ; and most of the times there will be at least two ways to minimize running costs without adding difficulties to how to optimize quality of products. Both may be very efficient ways to conserve energy.

CONTEXTE GENERAL

Depuis quelques années, la France s'est trouvée placée dans un contexte énergétique et dans une situation économique qui imposent des choix -mais aussi offrent des possibilités- qui ont encore peu d'équivalents dans le monde.

Certes, le problème "énergie" n'est pas particulier à la France ; il est mondial et point ne sera besoin de rappeler longuement deux faits majeurs :

. les besoins énergétiques s'accroitront encore fortement, aussi bien du fait de l'accroissement de la population que de celui de l'accroissement de la consommation par habitant, encore à des niveaux très bas dans certains pays ;

. les découvertes d'hydrocarbures ne se font désormais qu'à un rythme inférieur à celui de la consommation ; d'où report obligatoire sur d'autres formes d'énergie, charbon et nucléaire principalement.

La France a été parmi les premières nations à s'industrialiser et l'a fait à partir de ses ressources en charbon et en houille blanche.

Aujourd'hui, ses gisements de charbon économiquement exploitables sont en voie d'extinction et ses sites hydrauliques à peu près tous équipés. Aucun gisement notable d'hydrocarbures -sauf le gaz de Lacq qui arrivera bientôt au terme de son exploitation- n'a été (et ne sera probablement) découvert sur son territoire.

Dans ces conditions, dès le déclenchement en 1973 de la crise pétrolière politico-économique qui nous affectera encore longtemps sans doute, la France s'est trouvée dans l'obligation d'agir vite pour réduire sa dépendance énergétique vis-à-vis de l'étranger. Actuellement, cette dépendance, près de 75 %, porte à la fois sur les hydrocarbures et le charbon -ce dernier étant cependant moins dispendieux en devises.

CHOIX FONDAMENTAUX

Dès 1974, des choix ont été faits, d'égale importance dans leurs effets prévus pour 1985 :

- promouvoir une politique d'économies d'énergie ;
- intensifier le programme de construction de centrales nucléaires.

  Ces centrales, qui nécessitent six à sept ans pour être réalisées, commencent à être mises en service ; désormais, cette formulation des choix doit donc se compléter par :
- reporter les consommations sur l'énergie nucléaire (très peu dispendieuses en devises) aussitôt que le report est techniquement réalisable et économiquement rentable.

Car l'accroissement annuel de production des centrales nucléaires est désormais du même ordre de grandeur que celui des besoins énergétiques globaux, et le restera pendant longtemps. Certains objectent que le recours à l'énergie électrique restera un gaspillage d'énergie et de devises tant que des centrales au fuel-oil resteront en service -et cela du fait du rendement limité de la transformation chaleur-électricité- ; ils en prennent prétexte pour repousser tout usage thermique de l'électricité.

Cela est doublement erroné car :

- au niveau des appareils d'utilisation, les rendements de l'électricité global production-utilisation est, dans la majorité des cas, meilleur que dans les processus à combustibles fossiles ; ceci est dû à la spécificité des formes sous laquelle elle peut être mise en oeuvre (induction, rayonnement, etc.) et à la facilité de contrôle (régulation, automatisation) ;
- la part du fuel dans la production d'électricité va tomber à 10/12 % dès 1985 et 5/7 % vers 1980. La plus grande partie de la production d'électricité va être en France assurée par ce que l'on a coutume d'appeler l'électricité primaire -l'hydraulique et le nucléaire-. Dès 1985, on peut prévoir 20 % d'hydraulique et 50 % de nucléaire ; en 1990, ces chiffres passeront respectivement à 15 % et 70 %.

INTERET POUR LES UTILISATEURS

L'accroissement parallèle des besoins énergétiques et des moyens de production d'électricité nucléaire auront plusieurs conséquences attrayantes pour l'utilisateur de cette forme d'énergie.

La première est une assurance contre les risques de rupture d'approvisionnement de longue durée. Plusieurs raisons contribuent à cette assurance :

- le stockage d'uranium-métal peut aisément (faible prix - faible encombrement) couvrir une ou deux années de besoins ;
- le sous-sol français recèle pas mal de minerai d'uranium (100 000 tonnes à des conditions actuellement compétitives) et ces réserves ne sont, par prudence, que faiblement entamées chaque année grâce à une politique de recours à des importations d'Afrique francophone ;
- la répartition du minerai d'uranium sur le globe est très différente de celle du pétrole et présente a priori moins de risques de non-respect de contrats à longue durée ;
- la mise au point des surrégénérateurs divisera par 50 au moins les besoins en minerai.

La deuxième découle du moindre coût de production du kWh nucléaire -de l'ordre de 13 centimes aux bornes d'une centrale nucléaire fonctionnant en base contre plus de 20 pour une centrale analogue au charbon et près de 24 pour une centrale au fuel-oil (y compris frais de lutte contre la pollution sulfurique). La part du combustible est en gros de 4 centimes pour le nucléaire contre 12 pour le charbon et 16 pour le fuel-oil.

Il y aura donc un intérêt économique évident à faire fonctionner aussi régulièrement que possible les centrales nucléaires et à réserver les centrales thermiques au fuel-oil pour la satisfaction des besoins de pointe. Car la part élevée des amortissements dans la formation du coût du kWh nucléaire rend les centrales thermiques classiques intéressantes pour des utilisations annuelles inférieures à 2 000 heures environ.

Cette évolution des prix de revient et des conditions d'exploitation se répercuteront bien évidemment dans les tarifs. En ce domaine, la politique d'EDF est de refléter d'aussi près que possible dans ses tarifs les variations horaires et saisonnières des coûts de production. Non pas d'ailleurs tellement celles que l'on constate aujourd'hui, mais celles que l'on prévoit à échéance de cinq à dix ans.

Une telle politique, qui tient compte des délais de décision et des durées de vie des installations industrielles, a pour objet d'inciter les industriels à des choix conformes à l'intérêt collectif.

D'où une double tendance :

- globalement une baisse du coût moyen du kWh pour des fournitures types à l'Industrie. Cette baisse était prévue pour s'amorcer franchement vers 1981 après une période de stabilité de 1974 à 1980. En fait, les relèvements de tarifs en francs courants autorisés pendant cette période ont été insuffisants pour respecter la stabilité à francs constants. Cela retardera jusque vers 1985/87 l'époque où l'ensemble des tarifs (certains y sont déjà) reviendra, en francs constants, aux niveaux d'août 1973, avant le début de la crise pétrolière ;
- Plus dans le détail, une forte baisse de l'énergie d'été (heures pleines et heures creuses) et un maintien, voire une légère remontée, du prix de l'énergie d'hiver, surtout pendant les périodes de pointe (4 heures par jour ouvrable pendant trois mois). Il en résultera en heures creuses d'hiver (5 mois par an) une énergie électrique plus chère qu'en heures pleines d'été. Cette tendance s'est déjà concrétisée à l'occasion des deux dernières révisions de tarif.

Est-ce à dire que pour suivre ces principes les structures tarifaires seront à modifier profondément ? Certainement pas. Autant que l'on puisse le prévoir aujourd'hui, le "Tarif Vert" pour les fournitures à l'industrie bénéficiera d'une évolution, mais ne subira pas de bouleversements profonds.

Pour les clients les plus importants, il y aura probablement deux ou trois postes horo-saisonniers de plus, afin de mieux suivre les tendances d'évolution des coûts. Mais pour la très grande majorité des clients industriels, il devrait y avoir simplification, d'autant plus sensible que leur puissance souscrite sera faible, et cela aux niveaux des comptages et facturations aussi bien que du raccordement au réseau.

INDUSTRIE ET ELECTRICITE

Dans ce cadre général, où il y aura assurance d'approvisionnement en une énergie revenue en moyenne à son niveau de prix de 1973 -à francs constants-, quelle pourra être l'attitude des industriels, accoutumés de longue date à recourir surtout à d'autres énergies, qui verront fortement décroître le coût relatif de l'électricité par rapport à celui des combustibles fossiles ?

Il est difficile de préjuger de leur réaction ; elle sera fonction non seulement de la vitesse d'évolution -brutale ou lente- du prix des autres énergies, mais aussi des possibilités techniques et financières de se convertir à des matériels utilisant principalement l'électricité. Ce que l'on peut dire, surtout s'ils sont gros consommateurs d'énergie, c'est qu'ils sont dans l'obligation d'envisager, dès maintenant, dans quelles conditions l'électricité pourrait être utilisée dans leur industrie, que la décision finale soit fonction de facteurs économiques évoluant progressivement ou d'une rupture brutale des possibilités d'approvisionnement.

Plusieurs voies sont d'ailleurs ouvertes dans chaque industrie. En gros surtout lorsque le coût de l'énergie est un poste fondamental des prix de revient, elles peuvent se réduire à deux :

- rechercher des procédés techniquement à l'avant-garde du progrès -très performants et économes en énergie- en profitant des multiples formes sous laquelle l'électricité peut être utilisée (rayonnements, plasma, ...) ;
- se limiter à des techniques simples (par exemple basées sur l'effet Joule), mais bien étudiées en profitant au mieux des avantages tarifaires dont le recours de plus en plus marqué à l'énergie nucléaire permettra de bénéficier à certaines heures et à certaines saisons.

Ces deux voies ne sont nullement exclusives l'une de l'autre, bien au contraire et leur combinaison pourra amener à secouer bien des routines et fera fructifier l'innovation.

Dans la recherche de la solution, il pourra notamment être tenu compte de la saisonnalité de la demande en produits fabriqués, des possibilités physiques -ou financières- de stockage temporaire (parfois sous forme de produits non totalement élaborés encore)- et aussi des facilités d'automatisation d'au moins certaines phases des processus. Il y a là un large champ de possibilités, particulièrement dans les industries du ciment.

Ainsi, l'électricité ajoutera-t-elle à ses attraits de disponibilité, de respect de l'environnement d'amélioration du cadre de travail et, ce qui n'est pas négligeable, de qualité des productions, celui de donner matière à imagination dans la recherche de conditions d'exploitation économiquement optimales. Ce qu'il ne faut pas perdre de vue, ce sont les longs délais nécessaires à un changement profond des techniques, surtout dans les industries lourdes. Aussi les choix d'aujourd'hui doivent-ils prendre en compte les possibilités d'approvisionnement -et les coûts- des énergies à échéance d'une dizaine d'années. Et ne perdant pas de vue cette échéance, nul doute que les industriels ne soient dès aujourd'hui tentés par les possibilités immédiates et les perspectives d'avenir qu'apporte l'électricité.

PENETRATION DE L'ELECTRICITE ET ECONOMIES D'ENERGIE

Dans un séminaire consacré à des vues prospectives sur les Economies d'énergie, on ne peut éviter de souligner l'effet global que pourra avoir une pénétration profonde de l'électricité dans les processus industriels.

Une substitution rationnelle de l'électricité aux combustibles entraîne généralement de sensibles

réductions des consommations d'énergie primaire. Le "handicap" lié au médiocre rendement de la transformation chaleur-énergie mécanique au niveau de la production de l'électricité est plus que compensé par le rendement élevé au niveau des installations de distribution et d'utilisation de l'énergie. Ainsi un kWh peut remplacer un nombre γ de mégajoules supérieur à celui qui aurait été nécessaire pour le produire dans une centrale thermique. Un certain nombre de réalisations et d'études ont confirmé cette affirmation. A titre d'exemple, l'analyse de 38 projets, de puissance unitaire variant de 50 à 7 000 kW, a donné pour γ les valeurs moyennes ci-après :

- Chimie (12 projets de 620 kW en moyenne): 21 MJ
- Agro-alimentaire (12 projets de 380 kW en moyenne) : 26 MJ
- Métallurgie, Mécanique (5 projets de 2 120 kW en moyenne) : 9,5 MJ
- Industries diverses (9 projets de 520 kW en moyenne) : 20 MJ

TOTAL (38 projets de 710 kW en moyenne) γ = 17,5 MJ

En tenant compte que les projets "électriques" sont peut être comparés à des solutions classiques, susceptibles de perfectionnements sur le plan économie d'énergie (gain de 15 % par exemple), le coefficient moyen apparaît de l'ordre de 15 MJ/kWh ; c'est-à-dire en extrapolant, que des besoins actuellement satisfaits par 3,5 Mtep pourraient être satisfaits par 10 TWh, qui ne nécessiteraient pour être produits dans une centrale moderne, brûlant du fuel-oil, que moins de 2,5 Mtep.

La substitution de l'électricité au fuel-oil, surtout dans certaines applications et certains secteurs, peut donc avoir pour premier effet de réduire la demande apparente en énergie primaire exprimée en Mtep.

Point ne sera besoin d'ailleurs de ne recourir qu'à des techniques "de pointe" pour obtenir de tels résultats. La possibilité pour l'électricité d'être utilisée seulement là où il le faut et seulement quand il le faut, l'absence de pertes à la cheminée sur les lieux d'utilisation, permettent dans beaucoup de cas à des procédés basés sur l'emploi judicieux de simples résistances de s'avérer énergétiquement intéressants.

D'autant qu'à l'époque où la substitution pourra être devenue effective de façon appréciable, l'électricité nécessaire ne sera plus, même dans un raisonnement marginaliste, que peu fournie par des centrales au fuel.

Le recours à l'électricité provoquera donc un transfert des consommations primaires vers le charbon, puis de plus en plus, vers le nucléaire.

Ce transfert sera d'autant plus rapide que pour applications visées, les besoins auront de l'importance en heures creuses ou semi-creuses (nuit, week-ends, été, demi-saison).

Et l'automatisation, rendue plus aisée par l'électricité, combinée avec les différenciations des postes horaires tarifaires, aura pour effet de faciliter ces reports en heures "moins chargées", diminuant par là très notablement la charge en devises des consommations énergétiques de l'industrie.

Sauf pénurie brutale en combustibles fossiles, la pénétration de l'électricité semble devoir rencontrer quelques freins à son développement, notamment: difficultés de modifier les habitudes, difficultés de consentir à des renouvellements ou à des transformations de matériel avant leur obsolescence...

On ne peut donc être certain qu'aucun "accident majeur" dans l'approvisionnement en hydrocarbures -liquides ou gazeux- ne pourra survenir avant que la pénétration de l'électricité soit suffisamment profonde pour protéger l'industrie de ses conséquences.

Or, si un tel accident arrivait prématurément, les études et mises au point nécessaires à l'optimisation des processus et des matériels risqueraient de n'avoir pas encore été faites et le matériel adéquat ferait sans doute défaut pour répondre massivement à des besoins immédiats.

Dans ces conditions, des solutions "rustiques" de transfert rapide vers l'électricité ne manqueraient pas de fleurir et il serait hasardeux d'espérer que l'on puisse en espérer des gains en énergie primaire.

Point n'est besoin d'insister sur les répercussions catastrophiques qu'une telle situation entrainerait au niveau de la production industrielle.

Il faut éviter de se trouver dans un tel cas ; et comme on ne peut raisonnablement escompter agir au niveau de "l'accident", il faut pallier ses conséquences par un recours progressif, mais très rapide, à des procédés basés sur un emploi aussi développé que possible de l'électricité : son origine presque exclusivement nucléaire, hydraulique et charbonnière -du moins en France-, sa large disponibilité et son coût modéré seront une bonne protection contre des risques que l'industrie ne peut absolument pas se permettre de courir.

Corrélations entre la proportion de laitier, le type de ciment et les consommations énergétiques dans la fabrication des ciments mixtes

Correlation of slag ratio, cement class and power consumptions in mixed cement production

I. TEOREANU, Professeur, Faculté d'Ingénierie Chimique, Institut Polytechnique de Bucarest,
D. DULAMESCU, Ingénieur, ICPILA, Roumanie.

RESUME : Dans le présent travail, on a examiné l'obtention des ciments mixtes dans le contexte des corrélations qui existent entre la proportion de laitier, les propriétés des ciments et leurs paramètres dispersionnels, en considerant l'influence de ces derniers sur les consommations énergétiques.

On a eu en vue, en même temps, la corrélation du rapport ciment / laitier - paramètres dispersionnels - consommation d'énergie - propriétés des ciments avec la composition minéralogique des clinkers utilisés.

SUMMARY : In the present study were investigated the mixed cement obtained in the context of the correlations of slag ratio, cement properties and their dispersion parameters, taking into account the influence of last mentioned ones upon power consumptions.

It have been taken into consideration, also, the agreement of cement / slag ratio - dispersion parameters - power consumption - cement properties - with mineralogical composition of the used clinkers.

INTRODUCTION

L'industrie de ciment est, actuellement, un grand consommateur d'énergie. Du point de vue statistique, approximativement 20% de la consommation totale d'énergie (75% de la consommation d'énergie électrique) revient à la préparation des matières premières et au broyage du ciment et plus de 75% au procès de calcination-clinkérisation. Dans ce contexte, la fabrication et l'utilisation des ciments aux additifs cimentoids (laitier de haut fourneau) ou hydrauliquement actifs (cendres volante par exemple), dans les conditions d'une plus grande proportion de pareils additifs et sans modification essentielle des propriétés de résistence des ciments durcis, représente, à ce moment, l'une des voies d'intérêt exceptionnel, dans l'ensemble des préoccupations pour la restriction des consommations énergétiques (1-4).

Dans le présent travail, l'obtention de tels ciments a été abordée dans le contexte de la détermination, non seulement des corrélations qui existent entre la proportion de cimentoid et les propriétés du ciment, mais aussi en considérant l'influence des paramètres dispersionnels des ciments sur leurs propriétés physico-mécaniques et sur les consommations énergétiques au broyage. On a considéré, en même temps, la corrélation du rapport ciment/laitier, des paramètres dispersionnels, de la consommations d'énergie et des propriétés des ciments, avec la composition des clinkers.

MATERIAUX UTILISES

Les ciments à laitier ont été préparés à partir des clinkers de fabrique (A et D): un clinker à une plus haute teneur en alite (D) et un autre à une moins haute teneur en alite (A). La composition chimique des clinkers utilisés, ainsi que la composition chimique du laitier de haut fourneau (Z), sont présentés dans le Tableau I.

TABLEAU I

Composition chimique (%)	Clinker		Laitier de haut fourneau
	A	D	
P.F.	0,86	0,72	1,14
SiO_2	21,67	21,37	36,07
Fe_2O_3	4,03	2,36	0,35
Al_2O_3	5,73	5,95	8,27
CaO	62,71	64,53	54,40
MgO	1,30	0,79	5,20
SO_3	1,38	1,83	0,70
TiO_2	0,24	0,19	0,24
Na_2O	0,44	0,58	0,55
K_2O	1,15	1,65	0,55

Dans le Tableau II on présente, pour les clinkers, la composition minéralogique potentielle (calculée d'après Bogue), ainsi que celle réelle (déterminée par diffraction des rayons X).

A partir de ces deux clinkers, on a préparé des ciments unitaires (étalon, sans laitier)

TABLEAU II

Minéraux	Teneur (%) :			
	D'après Bogue		Par diffraction des rayons X	
	A	D	A	D
C_3S	48,6	58,5	40-45	55-60
C_2S	27,5	16,7	30-35	15-20
C_3A	8,4	11,5	12	15
C_4^3AF	12,2	7,0	7-10	5- 7

et mixtes (avec 15%, 30% et 60% laitier); tous les ciments préparés ont été broyés à des surfaces spécifiques Blaine d'approximativement 3000, 4000 et 5000 cm^2/g.

LE COMPORTEMENT AU BROYAGE DES CIMENTS ET DE LEURS COMPOSANTS

Les influences négatives, que, parfois, les additions de laitier peuvent induire dans les valeurs de résistance des ciments mixtes obtenus, pourraient être éliminées ou bien atténuées par un broyage plus avancé.

Le développement plus rapide des résistances mécaniques élevées, en même temp que l'augmentation des surfaces spécifiques des ciments portland, sans ou avec additifs (de laitier ou de puzzolane) est unanimement confirmé; ainsi, on accepte le fait que, dans des mêmes conditions chimico-minéralogiques, la résistance mécanique du ciment portland durci augmente avec la finesse de broyage de celui-ci (dans un spectre granulométrique restreint et uniforme), la limite supérieurs de la surface spécifique étant d'autant plus grande que le ciment est moins actif; dans cette dernière catégorie on inclue aussi les ciments mixtes.

En tenant compte de ce que nous avons montré plus haut, on peut réaliser - pour les ciments à laitier - des surfaces spécifiques qui conduisent à l'obtention des résistances mécaniques comparables à celles du ciment unitaire étalon. Certainement, on doit tenir compte des éventuelles consommations supplémentaires d'énergie au broyage. C'est pourquoi on est necessaire d'examiner les clinkers, le laitier et les ciments à laitier du point de vue de l'aptitude au broyage et de correler les résultats obtenus avec le comportement au durcissement des ciments étalons et mixtes, ayant différentes surfaces spécifiques.

Les informations obtenues concernant la consommation spécifique d'énergie en fonction de la surface spécifique du laitier, des clinkers A et D, ainsi que des ciments mixtes afférents (ciments avec 15%, 30% et, respectivement, 60% laitier) sont présentées dans les figures 1 et 2.

Les données présentées dans les figures 1 et 2 ont été obtenues, en utilisant un broyeur de laboratoire avec les dimensions : Ø 0,5 x 0,5 m, qui fonctionne d'une manière discontinue.

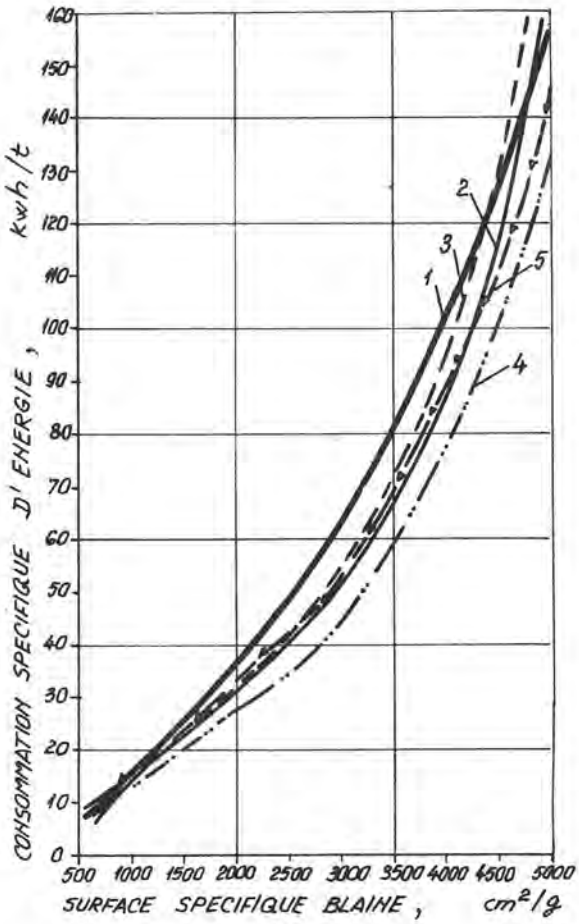

Fig. 1 - Aptitude au broyage
1- laitier ; 2- clinker A ;
3- clinker A + 15% laitier;
4- clinker A + 3o% laitier;
5- clinker A + 6o% laitier;

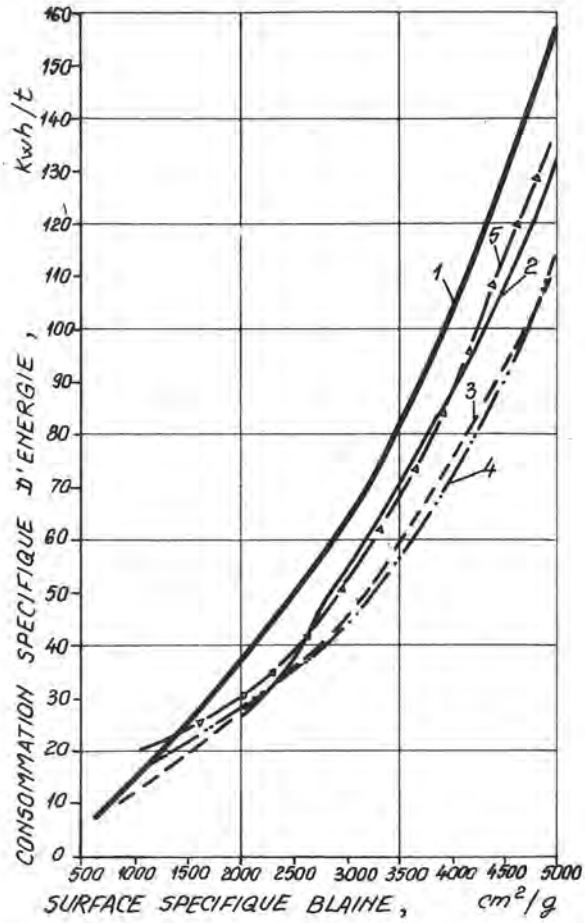

Fig. 2 - Aptitude au broyage
1- laitier ; 2- clinker D ;
3- clinker D + 15% laitier;
4- clinker D + 3o% laitier;
5- clinker D + 6o% laitier;

Pour une surveillance plus facile, les données concernant la corrélation entre la consommation d'énergie électrique et la surface spécifique Blaine des clinkers broyés sont inscrites dans le Tableau III.

TABLEAU III

Surface spécifique Blaine (cm^2/g)	Consommation spécifique d'énergie au broyage (kwh/t) :	
	Clinker A	Clinker D
2ooo	31	27
3ooo	53	53
4ooo	88	87
45oo	117	1o8
46oo	127	115
48oo	148	121

Ces valeurs démontrent que le clinker plus bélitique (A), comme prevu, présente une aptitude au broyage inférieure à celle du clinker plus alitique (D).

Dans le cas du clinker A (à une plus haute teneur en bélite), on constate une importante augmentation de la consommation spécifique d'énergie électrique, correspondante à des surfaces spécifiques, dépassant 4ooo cm^2/g Blaine; en arrivant à plus de 48oo cm^2/g Blaine, pratiquement, la surface spécifique du ciment n'augmente plus, avec la croissance de la consommation d'énergie électrique. Ce comportement est évidemment atténué dans le cas du clinker plus alitique (D). Le comportement différent au broyage des deux clinkers est en concordance avec les résultats de Beke (5), qui a trouvé que, dans le cas des clinkers très bélitiques, le phénomène d'agglomération se manifeste même

à des surfaces spécifiques supérieures à 4400 cm^2/g Blaine, le phénomène d'agglomération, dans le cas de ce clinker étant plus grand que celui du laitier.

Bien que le laitier comme tel montre des aptitudes au broyage, en général, inférieures aux clinkers dont on a préparé les ciments mixtes examinés, elle met pourtant en évidence un effect légèrement additif, d'amélioration de la broyabilité des clinkers avec lesquels on broye en mélange.

On constate aussi, dans le cas des ciments à laitier, un comportement différentié au broyage, en fonction de clinker utilisé (A ou D) dans les ciments. Ainsi, à l'utilisation du clinker A, l'addition de 15% laitier ne détermine pas la réduction de l'intensité du phénomène d'agglomération au broyage (intensité caractéristique au clinker A) et, en totalité, le mélange : clinker-15% laitier se broye plus difficilement que le clinker seul; ce comportement est d'autant plus accentué, que la surface spécifique du ciment est plus grande (fig. 2); par la suite, l'augmentation de la proportion de laitier, détermine des diminuations de la consommation spécifique d'énergie, avec la réalisation d'un minimum de celle-ci. Dans le cas des ciments préparés avec le clinker D, l'effet additif se manifeste même à une addition de 15% laitier.

Pour les ciments à partir des clinkers A et D aussi, la proportion optime de laitier (correspondant à une consommation spécifique minime d'énergie) se déplace vers des valeurs inférieures à l'augmentation de la surface spécifique (fig. 3 et 4).

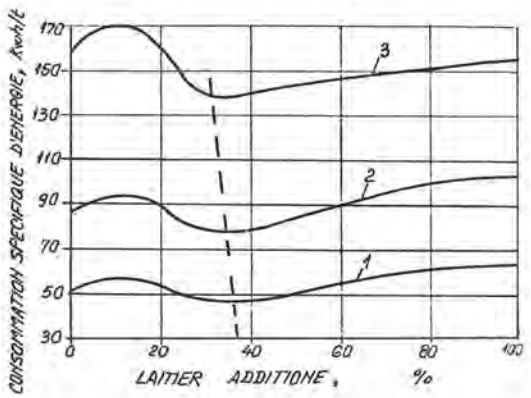

Fig. 3 - L'influence de l'addition de laitier sur la consommation spécifique d'énergie (clinker A)

Surface spécifique Blaine :
1- 3000 cm^2/g;
2- 4000 cm^2/g;
3- 5000 cm^2/g.

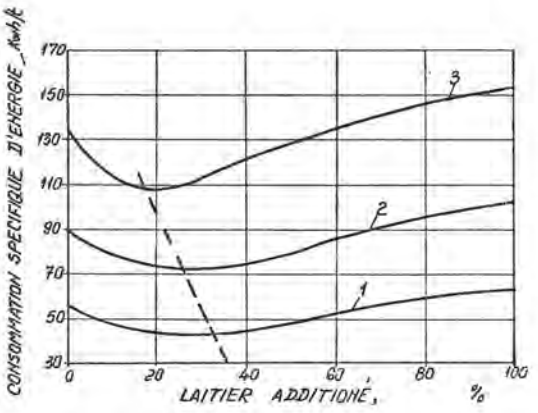

Fig. 4 - L'influence de l'addition de laitier sur la consommation spécifique d'énergie (clinker D)

Surface spécifique Blaine :
1- 3000 cm^2/g;
2- 4000 cm^2/g;
3- 5000 cm^2/g.

LES PROPRIETES DES CIMENTS EN CORRELATION AVEC LEURS CARACTERISTIQUES COMPOSITIONELLES ET DISPERSIONELLES

L'obtention des ciments à laitier ayant des propriétés équivalentes à celles du ciment unitaire étalon, dans les conditions d'une consommation énergétique optimale, suppose la modification simultannée de la proportion du laitier et de la surface spécifique du ciment. En tenant compte de ce qu'on a mentionnée, on a examiné, du point de vue des résistances mécaniques, les ciments mixtes à proportions de laitier et des surfaces spécifiques différentes, préparés de la manière plus haut présentée (voir "Les matériaux utilisés"). Les représentations graphiques des informations obtenues sont données dans les figures 5 et 6. Les courbes des figures 5 et 6 illustrent la correlation simultannée entre les résistances mécaniques, la proportion de laitier et la surface spécifique des ciments; de leur examination il en résulte l'effet négatif de l'addition de laitier sur les résistances mécaniques, dans les conditions de maintien nonmodifié de la surface spécifique du ciment, effet manifesté d'une manière evidente à des périodes courtes de durcissement; pour des termes plus longs de durcissement (28 jours), l'effet mentionné plus haut est atténué, ou bien il cesse même de se manifester dans le cadre de certaines proportions relativement limitées de laitier, ajoutées au broyage des ciments (la proportion limite dépendant de la nature du clinker et de la surface spécifique prise en considération).

Pour éliminer l'effet négatif plus haut mentionné s'impose la modification de la

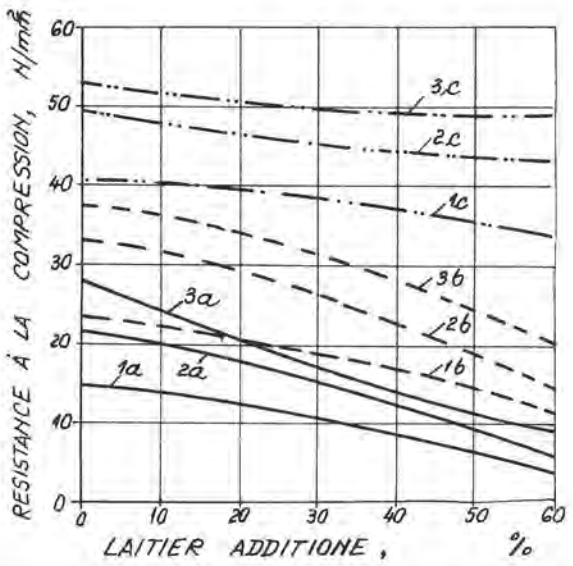

Fig. 5 - L'influence de l'addition de laitier sur la résistance à la compression (clinker A)

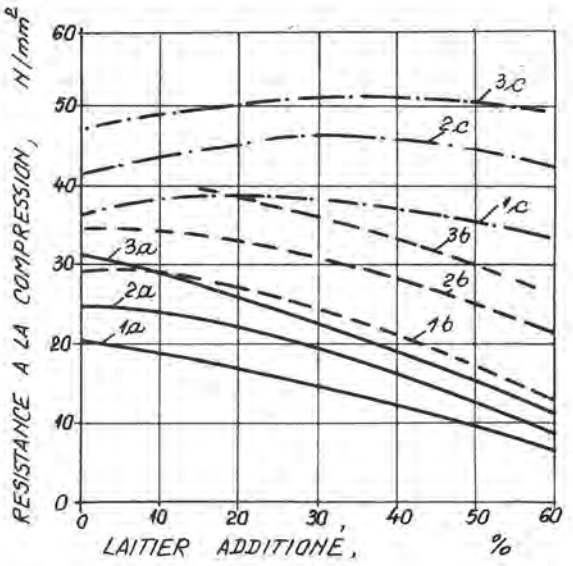

Fig. 6 - L'influence de l'addition de laitier sur la résistance à la compression (clinker D)

1a, 2a, 3a : ciment à surface spécifique de 3ooo, 4ooo et, respectivement, 5ooo cm^2/g à l'âge de 2 jours ;
1b, 2b, 3b : idem à l'âge de 7 jours ;
1c, 2c, 3c : idem à l'âge de 28 jours .

surface spécifique du ciment, en correlation avec la proportion de laitier utilisé et la marque du ciment qui doit être obtenue; ainsi, en vue de l'obtention d'un ciment d'une certaine marque (Pa 35 en conformité avec les standards roumains), il est nécessaire de réaliser - dans les conditions de l'utilisation des clinkers A et D et de laitier Z - les corrélations inscrites dans les Tableaux IV et V (avec les consommations énergétiques correspondantes au broyage). En partant de ces données, on peut établir l'influence globale sur l'énergie consommée à la fabrication des ciments à différente teneur en laitier, sans affecter les propriétés de résistance au durcissement; dans le Tableau VI on présente les résultats obtenus pour les ciments à base de clinker D.

TABLEAU IV

Clinker A			
Addition laitier (%)	Surface spécifique Blaine (cm^2/g)	Consommation spécifique d'énergie électrique (kwh/t)	
		Laboratoire	Industrie
15	31oo	57	42
3o	35oo	61	46
6o	54oo	16o	1o9

TABLEAU V

Clinker D			
Addition laitier (%)	Surface spécifique Blaine (cm^2/g)	Consommation spécifique d'énergie électrique (kwh/t)	
		Laboratoire	Industrie
15	26oo	37	32
3o	3ooo	45	35
6o	5ooo	135	93

TABLEAU VI

Destination de l'énergie	L'unité de mesure	Consommation (économie) d'énergie, correspondant à une tone de ciment à laitier dans le proportion (*) :		
		15%	3o%	6o%
Broyage	kwh	32	35	93
Séchage laitier	kcal	$26,4 \cdot 1o^3$	$52,8 \cdot 1o^3$	$1o5 \cdot 1o^3$
Clinker économisé	kcal	-	$135,8 \cdot 1o^3$	$4o6 \cdot 1o^3$
Economie d'énergie	kcal	-	$1o6,8 \cdot 1o^3$	$274 \cdot 1o^3$

(*) On a considéré comme liant de référence un ciment à 15% laitier, à base de clinker

D. On a gardé la comparabilité, en considérant, pour le laitier, la même humidité et, pour 1 kwh- l'équivalence théorique en kcal.

CONCLUSIONS

Les résultats des recherches, qui ont fait l'objet du présent travail, soulignent d'une manière évidente la possibilité d'obtenir des ciments à laitier, de relativement bonne qualité, dans des conditions de la corrélation optimale de la proportion de laitier, de la finesse de broyage des ciments et de la nature des clinkers et des laitiers utilisés.

La proportion de laitier dans les ciments mixtes, sans affecter les propriétés de résistance de ceux-ci, est limitée autant par l'activité des clinkers et des laitiers utilisés, que par les difficultés technologiques de l'obtention des ciments à grandes surfaces spécifiques. Même dans le conditions du broyage avancé des ciments, en vue de la conservation d'une qualité correspondante de ceux-ci, il en résulte, indubitablement, une économie globale très importante d'énergie pour la fabrication des ciments à laitier.

BIBLIOGRAPHIE

1.- P.K. MEHTA (1978) "Energy, resources and the environment a review of the US cement industry", World Cement Technology, 9, no 5, 144-160.

2.- M.F. PETER, H.F. ERNI et W. SCHRAMLI (1978) "Full production efficiency requires a fresh look at specifications", Rock Products, 81, no 4, 117-122.

3.- (1978) "Contribucion de las industrias de cemento y del hormigon a la conservacion de la energia", Cemento Hormigon, 536, no 8, 818-825.

4.- R.S. LEVMAN (1979) "Puti economii energhii v ţementnoi promîşlennosti", Tementnaia promîşlennosti, no 2, Moscova.

5.- B. BEKE, L. OPOCZKY (1969) "Feinstmahlung von Zementklinker", Zement Kalk Gips, 22, no 12, 541-546.

The latest operation performance of the MFC system

Les résultats récents d'opération du système « MFC »

M. KONDO, Vice President, Mitsubishi Mining and Cement Co., Ltd.
S. FUKUDA, Manager, Research and Development section, Japan.

RESUME : Le système de calcination fluidifiée de Mitsubishi ("Mitsubishi Fluidized Calciner" ou MFC) est un nouvel équipement pour la calcination du ciment au clinker appartenant aux systèmes de NSP sus-mentionnés et est mis en opération depuis 1971 après les développements par Mitsubishi Mining and Cement Co., Ltd. pendant plusieurs ans.

Depuis ce temps 16 équipements chauffés au mazout ont été construits au Japan et aux divers pays, se faisant une excellente réputation pour sa performance. De plus le système a été perfectionné continûment pour répondre aux besoins de l'époque.

Le système de MFC est notamment caractérisé par le fait que la calcination des matières se fait dans une couche fluidifiée montrant une haute efficacité d'échange de chaleur et permettant un long temps de rétention des matières. Par consequent en comparaison du système SP conventionel, celui permet une capacité augmentée de calcination du four, une opération continue et stabilisée du four pendant long temps même avec un combustible solide de combustion lente.

Mitsubishi Mining & Cement Co., Ltd., ayant verifié au moyen des divers essais sur l'équipement industriel que ses opérations peuvent être accomlies d'une manière satisfaisante avec les combustibles solides et que le charbon d'une inférieur qualité de 3,000 - 4,000 kcal peut être seulement utilisé comme le combustible, a établi de fondement de MFC chauffé au charbon. Ici, trois exemples du système MFC sont donnés d'aprés l'opération récente de performance.

Depuis la crise de pétrole dans 1973, dans l'industrie de ciment qui est un consommateur d'une grande quantité d'énergie, le développment d'une technologies d'utiliser une énergie autre que la de pétrole a été un objectif plus important, à cause de la hausse du prix du mazout.

Dans telle situation, nous croyons que l'importance de la technologie de MFC accroîtra de plus en plus.

SUMMARY : Mitsubishi Fluidized Calciner (MFC) system is one of the NSP systems, which has been developed by Mitsubishi Mining & Cement Co., Ltd. (MMCC) after the long efforts and put into practice since 1971.

So far, 16 units of oil/coal fired MFC system have been installed in Japan as well as in foreign countries and have won a reputation for its excellent performance. Furthermore, continuous efforts for the improvement of the MFC system has been done to meet the requirement of the time.

The peculiarity of the MFC system lies in the adoption of fluidized bed which gives high heat exchange efficiency and long retention time of raw meal. Consequently, it makes possible to increase the kiln capacity, to achieve the long stable and continuous kiln operation, and to burn exclusively any kinds of solid fuel having low combustion velocity.

Various kinds of test were performed to apply solid fuel to the MFC system at MMCC's Kurosaki Works. As the results of these test, it has been confirmed that there is no problem for firing in the MFC, even such low grade coals having the calorific value of 3,000 to 4,000 kcal/kg.

In this paper, three examples of the MFC system are described from the latest operation performance.

Since the oil crisis in 1973, the development of energy diversification other than oil has become the most urgent and important subject for cement industries.
At this period, the availability of the MFC technology will be extended further.

INTRODUCTION

Various precalciner systems which have been developed in both Japan and Europe are currently in use. Among them the MFC system is unique because it uses a fluidized bed as the precalciner. So far 16 units of the MFC system have been installed and have won a high reputation for its excellent performance.

Recent steep price rises and unstable supply of oil have forced cement manufacturers to save on energy consumption and to convert from liquid to solid fuel. The MFC system admirably meets both of these requirements.

CHARACTERISTICS OF THE MFC SYSTEM

Fig. 1 shows the general arrangement of the MFC system. Detailed descriptions of the principle, structure and equipment of the MFC system have been given in some papers(1)(2)(3).

The distinct peculiarity of the MFC system lies in the adoption of a fluidized bed which gives high efficiency of heat exchange and combustion.

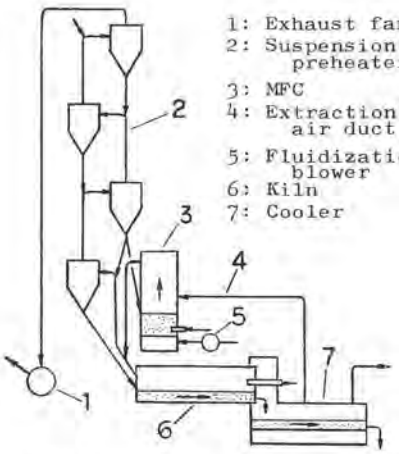

Fig. 1 General arrangement of MFC system

Test operations were carried out to apply solid fuel to the MFC system at Kurosaki Works of MMCC. All of the parameters and criteria necessary for the design of the coal-fired MFC have been obtained through these test operations, and its reliability and stability as a commercial furnace have thereby been comfirmed.

Various grades of coal have been burned in the tests and it has been found that there are no difficulties in using pulverized coal to fire the MFC. Very low grade coal, such as that with a value of 3,000 kcal/kg, can be exclusively used for firing.

Using pulverized coal depends mainly on the high mixing effect and the long retention time of several minutes which can be obtained by forming the fluidized bed.

Though there is a slight difference in the specific gravity between raw meal and pulverized coal, the mixing effect in the fluidized bed is so complete that the behaviour of pulverized coal is almost the same as that of raw meal.

The operating conditions of the MFC and suspension preheater(SP) show no substantial differences, whether oil-fired or coal, if thermally equivalent.

THE LATEST OPERATION RESULTS OF THE MFC SYSTEM

a) Newly installed MFC system with large capacity

Table I shows the newest kiln of MMCC started in Sep. 1979 at Kanda Works. This system belongs to the so-called doubled capacity type.

With a view to the saving of energy and power, some improvements such as the reduction of the air quantity for fluidization, were made in designing this MFC.

The temperature of the SP exhaust gas is 340 °C or so, which is considered to be the same as that of the conventional 4-stage SP kiln.

Table I Specifications and operating condition of Kiln No. 5, Kanda Works, Mitsubishi Mining & Cement, Japan

Kiln size	5.4 mø x 95 mL	
Preheater type	Dopol	
MFC size	5.0 mø x 15 mH	
Fluidization blower	390 m^3/min x 1800 mmAq x 30 °C	
Kiln		
Clinker produced	t-cl/d	6500
Fuel feed	kg-oil/h	10450
Preheater		
Exhaust gas vol.	Nm^3/t-cl	1310
Exhaust gas temp.	°C	340
MFC		
Fuel feed	kg-oil/h	10000
Fluidization air vol.	Nm^3/min	340
Extracted air vol.	Nm^3/min	1640
Fluidized bed temp.	°C	830
Exhaust gas temp.	°C	870
Specific heat consumption	kcal/kg-cl	740

b) Coal-fired MFC system

Table II shows the Samchock Kiln No. 3 of Tong Yang Cement Mfg., Co., Ltd., in Korea, which was constructed in 1967 and modified to the MFC system in 1978.

The conventional SP system had a burning capacity of 1,300-1,350 t/d. The standard capacity according to the design criteria is 1,290 t/d. By replacing the existing suspension preheater with a large preheater and additional installation of the MFC, burning capacity has been increased to an average of 2,200 t/d and a maximum of 2,300 t/d - a 70 % increase over its standard capacity.

Fuel was changed from oil to coal at the end of 1979. To the kiln is fed a small quantity of oil besides the coal, in order to control the burning zone. But, to the MFC is fed only pulverized coal.

The specific heat consumption is 795 kcal/kg-cl in the case of coal firing and 790 kcal/kg-cl in the case of previous oil firing. The raw materials and the chemical composition, and the fineness of the raw meal are kept the same in both cases.

From these operational results, we have estimated that at present there is no difference in the specific heat consumption between both fuels.

Other operating conditions in coal firing showed the same as those in oil firing.

Table II Specifications and operating conditions of Kiln No. 3, Samchock Plant, Tong Yang Cement Mfg., Korea

Kiln size	4.14 mø x 63 mL	
Preheater type	Dopol	
MFC size	4.3 mø x 10.9 mH	
Fluidization blower	310 m^3/min x 1300 mmAq x 20 °C	
Kiln		
Clinker produced	t-cl/d	2210
Fuel feed	kg-coal/h	3230
	kg-oil/h	2240
Preheater		
Exhaust gas vol.	Nm^3/t-cl	1460
Exhaust gas temp.	°C	340
MFC		
Fuel feed	kg-coal/h	4310
Fluidization air vol.	Nm^3/min	159
Extracted air vol.	Nm^3/min	370
Fluidized bed temp.	°C	840
Exhaust gas temp.	°C	860
Coal		
Net calorific value	kcal/kg-coal	6800
Specific heat consumption	kcal/kg-cl	795

Table III shows another example of a coal-fired MFC system which was restarted in Dec. 1979 after the modification. The capacity was increased from 600 t/d to 950 t/d. In this MFC system, low grade coal having the calorific value of 4,000 to 4,500 kcal/kg-coal is the only material used for combustion.

The heat consumption was reduced by almost 100 kcal/kg-cl as compared with the previous SP system.

Table I Specifications and operating conditions of Wadi Kiln No. 1, The Associated Cement Companies, India

Kiln size	3.75 mø x 54 mL	
Preheater type	Dopol	
MFC size	3.2 mø x 11.8 mH	
Fluidization blower	250 m^3/min x 1300 mmAq x 350 °C	
Kiln		
Clinker produced	t-cl/d	960
Fuel feed	kg-coal/h	4590
Preheater		
Exhaust gas vol.	Nm^3/t-cl	1590
Exhaust gas temp.	°C	330
MFC		
Fuel feed	kg-coal/h	3060
Fluidization air vol.	Nm^3/min	74
Extracted air vol.	Nm^3/min	198
Fluidized bed temp.	°C	830
Exhaust gas temp.	°C	860
Coal		
Net calorific value	kcal/kg-coal	4500
Specific heat consumption	kcal/kg-cl	860

CONCLUSION

From the above latest operational results, it can be clearly understood that the MFC system is the most advantageous of all precalciner systems. The especial advantage of this system is that solid fuel, even extremely low calorific fuels that cannot be fired in the kiln, can be burned easily in the MFC and the heat contained in these fuels is used in almost the same way as oil.

Since the oil crisis, diversification in the use of fuels has posed serious problems for the cement industry throughout the world. MFC technology will no doubt be used to help solve them.

REFERENCES

(1) Kondo, M. and Fukuda, S.; Klinkerbrand nach dem MFC-Fliessbett-Verfahren, Zement-Kalk-Gips, 451-456, Nr. 9, 1974

(2) Kondo, M. and Fukuda, S.; Fluidised bed precalciner boosts heat exchange efficiency, Rock Products, 93, May, 1975

(3) Duda, W. H.; Cement Data-book, 350-352, 1975, Bauverlag GmbH

$CaCl_2$ utilization in clinker burning

Utilisation de $CaCl_2$ dans le processus de formation du clinker

W. KURDOWSKI, Professor, Research Centre of the Industry of Binding Materials,
A. GARBACIK, Engineer, Research Centre of the Industry of Binding Materials, Pologne.

SUMMARY : An addition of calcium chloride to the mix of calcium carbonate with silica appears to accelerate considerably the reaction of calcium silicates formation. In this process a series of unstable, intermediate phases are formed.

This effect has been utilized to obtain belite in a rotary kiln. Using an addition of 10% CaCl2, belite was burnt at about 1100°C; the chlorine was found to be practically absent in the product, as it passes to the gaseous phase. In similar conditions also high belite content clinkers were burnt. In the case of raw mixes corresponding with Portland cement clinkers the mineralizing action of calcium chloride occurs as well.

The studies on the burnability of raw mixes with various silica- and iron moduli have indicated, that in the mixes with an addition of 5% $CaCl_2$, burnt at the temperatures as low as 1300° - 1350°C, no free lime is present. In this case the course of the process is more complicated as in the system $CaO-SiO_2-CaCl_2$, since - as is well known - the calcium chloride forms, apart from chlorosilicate phases, also some transient phases with aluminates. All these phases are unstable and at the temperatures of 1000° - 1250°C they decompose, liberating the chlorine to gaseous phase.

Obtained results, as well as the data from literature, indicate the possibility of utilization of $CaCl_2$ to obtain the clinkers of various types at relatively low temperatures. The realization of this conception, however, necessitates resolving the problem of the recovery of chlorine from the gaseous phase. The utilization of the kilns with 100% bypass for this purpose seems to be promising.

RESUME : L'addition de chlorure de calcium à un mélange de carbonate de calcium et de silice accélère sensiblement la réaction de la formation des silicates de calcium à des basses températures. Dans ce processus une série des phases transitoires est formée. Un mélange contenant 10% de chlorure de calcium a été utilisé pour la préparation de la bélite dans un four rotatif à la température de 1000°C environ. Le produit obtenu ne contenait pas de chlore, ce dernier étant échappé avec les fumées. Dans les conditions analogues les clinkers de ciment Portland à haute teneur en bélite ont été cuits également. En cas de mélanges crus correspondant aux clinkers de ciment Portland l'action minéralisatrice du chlorure de calcium se manifeste aussi nettement.

Les investigations de l'aptitude à clinkérisation des mélanges crus à des modules silicique et alumino-ferrique variés ont montré, qu'avec l'addition de 5% de $CaCl_2$ les mélanges cuits à la température allant de 1300° à 1350°C ne contiennent pas de chaux libre. En ce cas le processus est plus complexe que dans le mélange $CaO + SiO_2 + CaCl_2$, le chlorure de calcium formant, comme on le sait, non seulement des phases chlorosilicatées, mais aussi des phases aluminochloriques. Tous ces phases sont métastables et se décomposent à des températures entre 1000° et 1250°C avec l'échappement du chlore.

Les résultats obtenus montrent la possibilité d'utilisation de $CaCl_2$ pour la fabrication des clinkers de différents types, à des températures relativement basses. Cette question nécessite une solution du problème de la récupération du chlore des fumées. Il semble prometteur d'utiliser dans ce but des fours avec un by-pass de 100% des gaz.

1. INTRODUCTION

The energetic crisis, accompagned by a growth of fuel prices, results in a continuous increase of the expenses on energy as well as of their part in whole costs of the cement production. This problem obliges to energy saving, among other by reduction of heat consumption in the burning process. At the present moment, for the burning of Portland cement clinker, short kilns with external heat exchangers, for which the specific heat consumption amounts to 3000-3200 kJ per kg of clinker, are more and more widely used.

The energetic efficiency of these installations is close to the limit obtainable in practice by burning a common clinker /1/. In the kiln systems with precalcining, for example of Polysius-Rohrbach process type /2/, the utilization of poor quality fuels with low heating value gives the prospects for reduction of the costs of fuel consumed in the process of clinker burning /3/. Further savings in fuel consumption are possible for example by making hydraulic binders on the basis of materials substituting for the classical Portland clinker or by the use of mineralizers, markedly intensifying the process of sintering of Portland cement clinker.

One obtains substantial energy savings by the replacement of common Portland cements with the slag- or fly ash addition containing cements. The activation of hydraulic properties of these additions allows to increase their part in the process of hardening of blended cements.

Recently, bigger and bigger interest is gained by the problem of manufacturing the hydraulic binders from unconventional clinkers, viz. high belite clinkers or calcium sulphoaluminate clinkers /4/. The clinkering process of the latter takes place at about 1200°C with energy consumption by 25 per cent lower as the energy necessary for the burning of common Portland cement clinker. Similar meaning has the diminishing of clinkering temperature in the process of Portland cement clinker burning, realized through the employment of mineralizers. It was found, that F^- and Cl^- simple anions reveal a very efficient action, accelerating this process. In this paper the results of investigations of the course of reaction in the mixtures $CaO+SiO_2+CaCl_2$ are discussed and the usefulness of calcium chloride as a mineralizer in Portland cement clinker sintering process is considered.

2. EFFECT OF $CaCl_2$ ON THE COURSE OF REACTION IN $CaO+SiO_2$ MIXTURES AND IN TYPICAL CEMENT RAW MIXES.

The course of reaction in a mixture of $2\text{-}3CaO+SiO_2$ has been found to be substantially accelerated in the presence of $CaCl_2$ /5/. The reaction occurs with a high rate already at the temperature ranging from 500° to 600°C, with formation of a series of unstable, intermediate compounds. In the temperature range given above, well-known, compound chlorosilicate $Ca_3/SiO_4/Cl_2$ is formed /6/, the presence of which in the mixture $CaO+SiO_2+CaCl_2$ was stated already by Le Chatelier /7/. The formation of this compound takes place with participation of a liquid phase, which appears at these temperatures, in $CaO+SiO_2+CaCl_2$ mixture. The reaction advances until the whole quantity of calcium chloride is turned into $Ca_3/SiO_4/Cl_2$. Dicalcium silicate, which starts to be formed at the temperature of about 680°C, coexists with $Ca_3/SiO_4/Cl_2$ up to about 1000°C and above this temperature the decomposition of chlorosilicate takes place into dicalcium silicate and liquid calcium chloride. Heating compounds in atmospheric air leads to a decomposition of the latter with driving off gaseous chlorine.

The decomposition of $Ca_3/SiO_4/Cl_2$ into Ca_2SiO_4 and CaO starts at the temperature 900°C. In the case, the free silica is present in the mix, it reacts in the temperature range of 700° - 800°C with substantial rate with $Ca_3/SiO_4/Cl_2$. The products of this reaction are less basic chlorosilicate phases $Ca_2/SiO_3/Cl_2$ and $Ca_4/Si_2O_7/Cl_2$. The latter compound can be considered to be a chloride analogue of well-known mineral cuspidine $Ca_4/Si_2O_7/F_2$ /8/. These two calcium chlorosilicates are unstable and they decompose with separation of liquid calcium chloride. The decomposition temperature for $Ca_2/SiO_3/Cl_2$ is about 850°C and for $Ca_4/Si_2O_7/Cl_2$ about 995°C.

In carbon dioxide atmosphere in the temperature range of 700° - 850°C besides $Ca_3/SiO_4/Cl_2$ the spurrite $Ca_5/SiO_4/CO_3$ is formed as a succeding, intermediate phase.

Mineralizing effect of $CaCl_2$ on the process of spurrite formation is connected with the formation of liquid phase in the mixture $Ca_3/SiO_4/Cl_2 + CaCO_3$. Spurrite can be formed at the expense of chlorosilicate and is more stable as the latter. In these conditions $Ca_3/SiO_4/Cl_2$ starts to decompose at 910°C and the spurrite at 960°C. Above this temperature Ca_2SiO_4 and CaO remain in the system and the process of chlorine evaporation is completed at about 1200°C.

An excellent mineralizing activity of $CaCl_2$ in the process of dicalcium silicate formation has been confirmed by burning the belite in a laboratory rotary kiln 0,39/0,54x7 m /9/.
The burning was realized at 1000°-1200°C employing 10% addition of $CaCl_2$. Owing to stabilization with small addition of B_2O_3 the phase β-Ca_2SiO_4 was obtained practically without chlorine, which was leaving the rotary kilns with the gases.

Mineralizing action of $CaCl_2$ appeared again by burning the typical Portland cement raw mixes. An addition of 5% $CaCl_2$ accelerates notably the clinkering process /Table I/. The course of reaction in this case is more complex as in the mixture of $CaCO_3+SiO_2+CaCl_2$. $CaCl_2$ apart from chlorosilicate phases forms also intermediate phases with alumina/TableII/

TABLE I

Combination of calcium oxide in the clinkering process of a raw mix with $CaCl_2$ admixture

Mix	$CaCl_2$ content /per cent/	Charakteristics of the clinker			Free CaO content /per cent/ after heating for 20 min at temperature /°C/						
		Kind lime saturation faktor[1/]	silica modulus	iron modulus	1000	1100	1150	1200	1250	1300	1400
1	-	0,88	4,00	1,00	19,7	18,4	17,6	15,7	13,8	13,1	2,3
2	5				10,1	9,7	6,0	2,3	1,5	1,3	0,3
3	-	0,88	4,00	3,00	22,4	21,0	19,2	17,0	15,4	14,5	4,0
4	5				11,9	10,6	8,1	5,3	3,4	2,6	0,3
5	-	0,88	2,50	1,00	18,1	17,6	16,3	14,1	13,4	11,5	0,2
6	5				9,8	9,5	8,0	3,0	2,5	1,6	0,2
7	-	0,88	2,50	3,00	22,4	22,1	20,9	18,2	17,0	14,2	1,8
8	5				12,1	11,8	8,6	5,5	4,8	3,0	0,2

1/ Calculated as $\frac{CaO - /1,65A+0,35F+0,7SO_3/}{2,8SiO_2}$

TABLE II

Composition of the raw mix N° 4 after heating for 20 min at various temperatures

Test	Temperature, °C					
	1000	1100	1150	1250	1300	1400
Phase composition determined by X-ray diffraction 1/	C_2S CaO $Ca_3/SiO_4/Cl_2$ $C_{11}A_7.CaCl_2$ C_4AF	C_2S CaO $C_{11}A_7.CaCl_2$ C_4AF $Ca_3/SiO_4/Cl_2$	C_2S Chl CaO $C_{11}A_7.CaCl_2$ C_4AF	Chl 2/ C_2S $C_{11}A_7.CaCl_2$ C_3S C_4AF CaO	C_3S C_2S $C_{11}A_7.CaCl_2$ Chl C_4AF CaO	C_3S C_2S $C_{11}A_7,CaCl_2$ C_4AF Chl
Chlorine content in the mix after heating %	4,4	3,6	2,6	1,6	0,8	0,6

1/ Phases are enumerated in order of quantity estimated to be present

2/ High-lime calcium chlorosilicate

This compound decomposes at about 1000°C with separation of liquid calcium chloride. The formation - as a result of this process - of salt melt, accelerates rapidly the process of combination of calcium oxide at the temperatures ranging from 1050° to 1250°C. In this reaction an intermediate phase is formed, which constitutes a more basic calcium chlorosilicate /10/.

This phase, as the other chlorosilicates mentioned previously decomposes with evolution of the chlorine, which leaves the kiln with the gases.

In the alite Portland cement clinkers burnt in laboratory rotary kiln with addition of 5% $CaCl_2$ at about 1300°C the chlorine content in the product varied within the limits of 0,2 - 0,5 per cent. In principle,

the chlorine is combined entirely in the $C_{11}A_7.CaCl_2$ phase /11/.

The microscopic view of a clinker burnt with $CaCl_2$ addition shows the phase of alite with irregular habit, with numerous belite inclusions as well as extremely fine-crystalline belite /Fig.1/.

Fig.1 - Reflected light microscopic photograph of normal clinker burnt with $CaCl_2$ admixture, etched with 1-per cent solution of HNO_3 - alcohol. Shows alite crystals and clusters of belite crystals. Enlarged 800 x.

This effect is connected undoubtedly with low clinkering temperature and it can influence the hydraulic activity of the cement. Intensified hydraulic activity of belite is confirmed also by a substantial increase in the strengths between 7-th and 28-th day of hardening of the mortars made with cements high content of this phase /Table III/. A shortcoming of the clinkers burnt with $CaCl_2$ addition is the presence of chlorine, the content of which in the cements destined for reinforced concrete constructions is often limited to 0,1%.

3. PROSPECTS OF TECHNOLOGICAL UTILIZATION OF THE MINERALIZING ACTION OF CALCIUM CHLORIDE

The utilization of $CaCl_2$ addition for clinker burning reduces distinctly the clinkering temperature and intensifies this process. As a result of mineralizing action of $CaCl_2$ it is possible to burn the high belite clinkers at the temperatures ranging from 1100° to 1200° and the normal clinkers at 1250°- 1300°C. In the latter case one acquires a lowering of the clinker burning temperature by 150°- 200°C. It can be assumed, that the clinkering process at so low temperature necessites an energy consumption lower by about 650 - 850 kJ/kg of clinker as the energy necessary for the production of a mineralizer-free Portland cement clinker. Furthermore, because of low clinker burning temperature, the use of realatively poor coal is possible.

The escape of substantial amounts of chlorine into gaseous phase requires however bypassing of 100 per cent of the gases as well as recovering of the chlorine from gaseous phase.

Complete bypassing of the exit gases causes a marked increase in heat consumption in the process of clinker burning. However, the last reports from various manufactures of cement plant equipment, for example from F.L.Smidth Co. /12, 13/, offer the solutions in which complete bypassing of the gases results in heat losses as low as 630 kJ/kg of clinker /Fig. 2/. Such a value of the losses practically cancels the advantages resulting from the reduction of the clinkering temperature.

Acceleration of the clinkering process in presence of the calcium chloride is however so appreciable, that it seems interesting to undertake further works with the aim to verify the possibility of utilization of this mineralizer in unconventional suspension kilns /14/.

TABLE III

Properties of high belite content clinker, burnt with $CaCl_2$ admixture

Clinker				Cement									
Calculated phase composition /percent/				Gypsum addition /per cent/	Specific surface cm^2/g	Paste				Mortar			
						H_2O /per cent/	Soundness Le Chatelier test	Initial set h min	Final set h min	Strength N/mm^2 - compressive, after days			
C_3S	C_2S	$C_{11}A_7.CaCl_2$	C_4AF							1	3	7	28
44	40	7	5	4	3000	26,5	0	1^{40}	2^{10}	8,2	17,3	21,9	36,7
30	50	11	7	4	3000	25,0	0	0^{55}	1^{05}	5,2	9,4	12,7	30,6

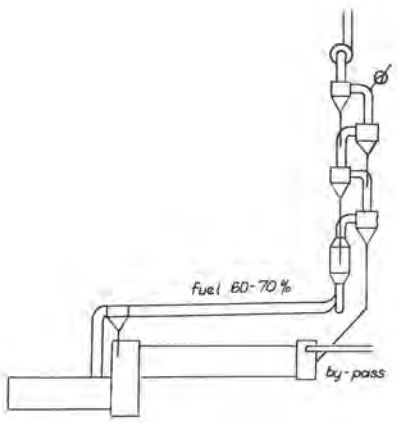

Fig.2 - Kiln system with 100 per cent by-passing of the gases for maximum reduction of alkali content in the clinker

Nevertheless, already for the present $CaCl_2$ can be employed for the production of high belite cements or single belite phase. Such possibilities are the more so interesting, as the soda industry yields substantial amounts of by-products with rather high content of calcium chloride.

BIBLIOGRAPHY

1.- A. FOLLIOT / 1975 /, "L'industrie cimentière et l'énergie", Rev. Mat. Constr. n° 694, 133-135.

2.- H. RITZMANN / 1975 /, "Oil shale fires precalcining preheater", Rock Products, 78, n° 5, 89-130.

3.- E. STEINBIS / 1979 /, "Experience with precalcining with due regard to substitute fuels", Zement - Kalk - Gips, 32, n° 5, 211-222.

4.- P.K. MEHTA / 1978 / "Energy, resources and the envirenment - a review of the US cement industry", World Cement Technology, 9, n° 5, 144-160.

5.- W.KURDOWSKI / 1965 /, "Formation des silicates bi- et tricalciques jusqu'à la température de 1300°", Silicates Industriels, 30, n°9, 500-506.

6.- R.CZAYA / 1970 /, "Darstellung und kristallographische Daten von $Ca_2SiO_4.CaCl_2$" Z. anorg. Chem., 375, n°2, 124-127.

7.- H.LAFUMA / 1952 /, "Expansive cements", Proc. of the Third Int. Symp. on the Chemistry of Cement, Cement and Concrete Association London, p. 583.

8.- C. BRISI / 1957 /, "Role of Cuspidine /$3CaO.2SiO_2.CaF_2$/ in the system $CaO-SiO_2-CaF_2$", J.Am. Ceram. Soc., 40, n° 5, 174-178.

9.- W.KURDOWSKI, A.THIEL, / 1975 /, "Preparation of belite in rotary kiln", Sprawozdania z posiedzeń Komisji Oddziału PAN w Krakowie, PWN, Warszawa-Kraków, t. XVIII/1, pp. 246-248, /in Polish/.

10.- J.S. CZERKINSKIJ / 1979 /, "Properties of clinkers obtained by low-temperature synthesis", Dokł. Akad. Nauk SSSR, 247, 174-178, /in Russian/.

11.- J. JEEVARATNAM, F.P. GLASSER, L.S. Dent GLASSER / 1964 /, "Anion Substitution and Structure of $12CaO.7Al_2O_3$", J. Am. Ceram. Soc., 47, n°2, 105-106.

12.- H. MEEDOM / 1979/, "Precalcining systems in F.L. Smidth kilns", Cement, Wapno, Gips, 32/46/, nr 5, 166-171, /in Polish/.

13.- J. SVENDSEN / 1978 /, "Alkaliarmer Zement aus Hochalkali-Rohstoffen mit energiewirtschaftlich günstiger Verfahrenstechnik", Zement - Kalk - Gips, 31, n°6, 281-284.

14.- W. KURDOWSKI / 1978 /, "The lines of development of cement industry", Cement, Wapno, Gips, 31/45/, nr 12, 335-344 /in Polish/.

Aptitude à la cuisson des crus de cimenterie en fonction de leur finesse de broyage

Burning ability of cement raw materials in relation with grinding fineness

N. MUSIKAS et E. HAAG, Laboratoire Central des Ciments d'Origny,
J.P. HENIN et P. GARDE, Centre de Recherches de Fives-Cail Babcock, France.

RESUME : Dans la première partie de cet article, on fait une étude comparée de différentes méthodes d'estimation de l'aptitude à la cuisson des crus de cimenterie. Il s'est avéré que le plupart de ces méthodes sont trop qualitatives pour permetttre de déboucher sur un critère de prévision du comportement industriel des crus de cimenterie.

Par contre les méthodes adoptées par FCB et par les Ciments d'Origny aboutissent à des résultats directement exploitables, comparables entre eux, et recoupant la réalité industrielle. Dans la deuxième partie, on utilise ces tests de réactivité pour étudier l'influence de la finesse sur la cuisson des crus de cimenterie. Nous avons pu trouver les conditions opératoires permettant d'obtenir des crus de laboratoire de granulométries similaires à celles des crus broyés industriellement et présentant la même aptitude à la cuisson.

A partir de ces travaux, nous sommes à même de définir une finesse optimale de broyage aussi bien pour un projet à partir d'échantillons représentatifs de la carrière que pour affiner les conditions de marche d'une installation existante.

SUMMARY : In the first part of this article, a comparative study is made of the various methods used to evaluate the burning ability of cement raw materials. It has been shown that most of these methods are too qualitative to give a prediction criteria for the industrial behaviour of the raw materials.

On the other hand, the methods adopted by FCB and Ciments d'Origny give results which can be directly employed, they can furthermore be compared between themselves, and they conform to the industrial realities. In the second part of the article, these reactivity tests are used to study the fineness effect on the raw material burning. We could find operative conditions which have given us laboratory raw materials of a grain size identical with that of the ground industrial one and having the same ability to be burned.

As a result of this work, we are able to define a grinding optimal fineness and this for quarry samples as well as for improving the operating conditions of an existing installation.

I INTRODUCTION

I - 1) Paramètres conditionnant l'aptitude à la cuisson.

Pour des crus correspondant à un type de clinker donné, les teneurs en constituants principaux : SiO_2, CaO, Al_2O_3 et Fe_2O_3, ne peuvent varier que dans des limites relativement étroites ; en outre celles des autres constituants de matières premières : MgO, SO_3, alcalins.... sont volontairement maintenues à des pourcentages assez bas en raison des difficultés qu'ils peuvent provoquer en cours de fabrication ou de leur "nocivité" dans le ciment.

Aussi, dans la plupart des cas, les faibles variations de composition chimique entre crus de "même famille" ne suffisent pas à expliquer leur comportement parfois nettement différent en cours de cuisson, ni, a fortiori, à prévoir dans le cas d'une nouvelle installation, l'aptitude à la clinkérisation du cru choisi.

De nombreux paramètres interviennent dans le degré de facilité de cuisson des crus. Parmi ceux-ci, outre la composition chimique du mélange, on peut citer :

- La finesse de broyage,

- l'homogénéité chimique et l'homogénéité minéralogique,

- la nature minéralogique des matières premières et leur degré de cristallinité,

- la proportion et la composition des phases liquides successives auxquelles le cru peut donner naissance au cours de sa cuisson.

La mesure quantitative de l'influence de chacun de ces facteurs est extrêmement difficile et n'a pas été entreprise dans cette étude, sauf en ce qui concerne la finesse de broyage ; par contre on peut chercher à déterminer globalement, à partir d'un test de laboratoire sur un échantillon de cru, l'aptitude à la clinkérisation de ce dernier. Le présent compte rendu résume donc les résultats obtenus sur 14 crus industriels en appliquant diverses méthodes de caractérisation relevées dans la bibliographie, en détaillant plus particulièrement les méthodes utilisées par les Ciments d'Origny d'une part et par FCB d'autre part. On commente également les recommandations pratiques sur la finesse de broyage que l'on peut en tirer.

I - 2) Méthodes d'études

La détermination de l'aptitude à la cuisson des crus peut s'effectuer :

- soit à partir de l'analyse chimique du cru en utilisant des formules empiriques faisant intervenir des grandeurs caractéristiques telles que le module de Kuhl et la teneur en silice libre. (1er groupe de méthodes).

- Soit en pratiquant en laboratoire des cuissons de matières crues suivant un cycle de température déterminé ; le degré de combinaison entre les divers constituants étant estimé par mesure de la teneur en chaux libre du produit calciné (2e groupe de méthodes).

Nous avons plus particulièrement axé notre étude sur ce 2e groupe de méthodes.

II RESULTATS DES ESSAIS EFFECTUES SUR DES CRUS INDUSTRIELS

Tous les résultats obtenus ont été regroupés dans le tableau ci-après :

Crus indust.	Analyses chimiques en %					Modules calculés			Granulométrie Refus en % à			Indice réfractairité à 1450°C		CaO libre à 1450°C	Aptitude à la	CaO libre à 1400°C par FUNDAL			CaO libre clinker
	CaO	SiO_2	Al_2O_3	Fe_2O_3	SO_3	Kuhl	Silic.	A/F	63 µ	90 µ	200µ	BOGUE	GLAUSER	FCB	cuisson ORIGNY	Q	K	X	indust.
1	42,28	14,30	3,67	1,47	0,85	0,92	2,78	2,50	36,6	25,0	6,7	2,28 (3)	2,95 (5)	0,81 (2)	4,44 (2)				
2	43,77	14,30	2,85	2,24	0,25	0,97	2,81	1,27	20	10,0	0,6	2,99 (10)	3,29 (8)	2,18 (8)	2,20 (10)				0,87
3	43,12	13,80	3,26	2,05	0,55	0,975	2,60	1,59	31,6	18,8	4,1	2,75 (6)	3,18 (6)	1,73 (5)	3,26 (3)				
4	42,84	13,80	3,47	1,43	0,12	0,98	2,82	2,43	27,6	17,5	1,6	3,06 (11)	3,81 (11)	1,79 (6)	2,67 (8)				
5	43,68	14,00	3,57	1,20	0,30	0,98	2,93	2,98	27,5	17,5	1,8	3,26 (13)	4,18 (13)	1,79 (6)	2,87 (5)				
6	43,40	14,30	2,86	2,60	0,38	0,955	2,62	1,10	22,5	12,3	0,4	2,65 (5)	2,83 (4)	1,68 (4)	2,73 (7)				0,45
7	44,80	13,80	3,35	3,16	0,20	1,0	2,12	1,06	32,2	20,4	2,2	2,43 (4)	2,59 (3)	2,58 (10)	2,17 (11)				
8	43,68	14,40	3,26	1,69	0,08	0,96	2,91	1,93	20,0	12,1	0,4	2,98 (9)	3,57 (10)	3,58 (12)	2,00 (13)				
9	43,68	14,30	3,26	1,91	0,05	0,965	2,76	1,71	11,5	6,5	1,2	2,75 (6)	3,24 (7)	3,92 (13)	1,89 (14)				1,60
10	44,50	16,40	1,84	0,88	0,10	0,91	6,08	2,08	25,9	16,4	1,5	5,26 (14)	6,26 (14)	2,41 (9)	2,86 (6)				
11	42,28	12,80	3,06	4,34	0,60	0,99	1,73	0,71	25,5	15,6	2,4	1,83 (2)	1,76 (1)	0,56 (1)	6,08 (1)				0,78
Zahana	41,65	14,41	3,34	2,54	0,27	0,90	2,45	1,31	22,0	13,4	0,5	1,77 (1)	2,04 (2)	1,29 (3)	3,14 (4)	1,48	4,69	4,00	0,8 à 1,0
Le Boucau	43,29	14,13	3,32	1,75	0,57	0,96	2,79	1,90	27,6	18,7	3,1	2,80 (8)	3,35 (9)	4,20 (14)	2,05 (12)	2,59	8,52	7,20	0,8 à 1,3
Crugey	41,60	13,90	3,16	1,08	0,88	0,94	3,28	2,93	28,6	17,4	2,0	3,17 (12)	4,04 (12)	2,97 (11)	2,57 (9)	1,02	6,14	4,41	0,5 à 1,0

Les chiffres ( ) donnent le classement par ordre décroissant, relatif à chaque méthode, de l'aptitude à la clinkérisation des crus industriels.

III ANALYSES CHIMIQUES ET GRANULOMETRIQUES DES CRUS INDUSTRIELS EXPERIMENTES

Celles-ci sont données dans le tableau ci-avant. Afin de ne pas surcharger ce compte rendu nous n'avons pas reproduit les analyses complètes.

Ces résultats amènent les observations suivantes :

- Les teneurs en éléments principaux, SiO_2, Al_2O_3, Fe_2O_3, CaO des crus sont comprises dans des fourchettes assez étroites ; on notera toutefois que le cru n° 10, de par la nature minéralogique (calcaire siliceux) de ses matières premières, présente une teneur assez élevée en SiO_2.

- Du point de vue analyse granulométrique on notera la granulométrie grossière trouvée sur le cru n° 1, refus cumulé de 6,7 et 25 % respectivement aux tamis de 200 et 90 μ .

IV APTITUDE A LA CUISSON

IV - 1) 1er groupe de méthodes : méthodes utilisant les résultats des analyses chimiques.

IV - 1 - 1) Méthodes ne faisant pas intervenir la granulométrie (taux de phases liquides et indices de réfractairité).

- Deux modes de détermination ont été utilisés pour calculer le taux de phases liquides à 1450°C, l'un à partir de l'abaque de Terrier, l'autre à partir de la formule : taux de phase liquide = 3A + 2,25F + MgO + alcalins. Les valeurs obtenues n'ont pas été reproduites dans cet article.

- Du point de vue indice de réfractairité, nous avons utilisé la formule :

$$\text{Indice de réfractairité} = \frac{C3S + 0,6C_3A - 0,61C_4AF}{1,12C_3A + 1,45C_4AF}$$

Les indices ainsi obtenus (voir tableau du paragraphe II) diffèrent suivant que l'on utilise les valeurs de composition potentielle trouvées à partir des formules de Bogue ou de Glauser.

- On a constaté qu'il n'y avait pas de corrélation précise entre les valeurs obtenues par ces différentes méthodes et l'aptitude à la cuisson des crus de cimenterie. Ces valeurs peuvent toutefois apporter, dans certains cas particuliers, d'utiles renseignements sur d'autres caractéristiques de la matière à cuire.

IV - 1 - 2) Méthodes faisant intervenir la granulométrie (notamment celle du quartz).

La silice présente dans un cru sous forme de quartz se combine difficilement aux autres constituants et rend le cru d'autant moins réactif que le quartz présent est plus grossier. La granulométrie du quartz peut être estimée par examen minéralogique ou mesurée après attaque sélective. Parmi les méthodes faisant intervenir la granulométrie du quartz, nous retiendrons celle développée par FUNDAL.

Fundal a établi une relation empirique : X = 0,33 LSF + 0,018 MS + 0,56 K + 0,93 Q - 0,349 qui permet de déterminer le taux de chaux libre (X) du cru après 30 minutes de cuisson à 1400°C.

LSF est le standard de Kuhl,
MS est le module silicique
K est le pourcentage de $CaCO_3$ du cru présent dans la fraction granulométrique supérieure à 125 μ .
Q est le pourcentage de quartz du cru présent dans la fraction supérieure à 44 μ .

Cette relation a été appliquée sur les crus de Zahana, du Boucau et de Crugey. Les résultats sont donnés au tableau du paragraphe II.

IV - 1 - 3) Conclusions concernant ce 1e groupe de méthodes

Parmi ces méthodes celle proposée par Fundal nous semble la plus intéressante et elle donne des résultats cohérents avec le 2e groupe de méthode que nous allons étudier dans la suite de ce rapport. Comme elle permet d'analyser l'influence de différents paramètres (en particulier quartz et calcite), elle constitue un complément intéressant aux méthodes du 2e groupe qui fournissent, elles, une mesure directe de la réactivité.

IV - 2) 2e groupe de méthodes : essais de cuisson

Ces méthodes consistent à estimer le degré de combinaison obtenu par cuisson en laboratoire en se basant sur la teneur en chaux libre du produit calciné. Ces essais de laboratoire permettent donc de comparer différents crus quant à leur facilité relative de cuisson. Ils ne permettent toutefois pas de préciser de façon absolue le degré de combinaison des matières dans les clinkers ni la valeur exacte du taux de chaux libre obtenu au four industriel d'une part en raison des conditions différentes de cuisson entre four industriel et four de laboratoire et d'autre part parce que les exploitants règlent la marche de leur four de façon à obtenir un clinker satisfaisant.

IV - 2 - 1) Méthode FCB

Les cuissons ont été réalisées sur 5 g de cru industriel placés dans une nacelle de platine qui est introduite progressivement dans un four porté à la température d'essai ; la nacelle est ensuite maintenue 30 minutes dans la zone de chauffage. Après refroidissement rapide, le produit calciné est ensuite broyé à tout passant à 100μ et traité selon la méthode de dosage à l'éthylène glycol EDTA.

Cette méthode ne tient compte que du taux de chaux libre obtenu après cuisson du cru pendant 30 mn à 1450°C.

Les résultats obtenus sont reproduits au tableau du paragraphe II. Plus la valeur obtenue est faible, plus la cuisson du cru est facile.

IV - 2 - 2) Méthode Origny

On comprime sous 3 T, 2g de cru de façon à réaliser un cylindre d'environ 1 cm^3. Sept de ces cylindres sont disposés dans le four à 700°C et vont subir un cycle de température. A chaque étape, on retire un cylindre et on détermine le taux de chaux libre. L'aptitude à la cuisson est définie comme une fonction inverse de l'intégrale de la courbe CaO libre en fonction de la température (1000,1100, 1200, 1300, 1350, 1400 et 1450°C).

Le tableau du paragraphe II donne les valeurs trouvées par cette méthode pour les différents crus industriels étudiés.

Comme pour la méthode FCB, les valeurs trouvées ne sont que des indices qualitatifs ; plus l'indice est élevé plus la cuisson du cru sera facile.

IV - 2 - 3) Conclusions concernant le 2e groupe de méthodes.

On remarquera que les méthodes FCB et Origny aboutissent à deux classements relatifs des différents crus tout à fait comparables. D'autre part, ces classements correspondent aux estimations des exploitants (on rappelle qu'il n'est pas significatif d'établir une relation directe avec la chaux libre du clinker industriel).

- Pour le test FCB, nous estimons que le cru industriel se "cuira" normalement (température maxi clinker $\simeq$ 1450°C et taux de chaux libre résiduel dans le clinker $\leqslant$1%) si le calciné obtenu en laboratoire (30' à 1450°C) présente un taux de chaux libre résiduel $\leqslant$2,5 %.

- Pour le test Origny, pour un indice voisin de 1,2 à 1,3, le cru est considéré comme très difficile à cuire ; vers 1,7 à 2,0, il est considéré comme normal ; au delà de 2,5 il entre dans la catégorie des crus faciles à cuire. On peut noter que ces limites sont moins contraignantes que celle déterminée par FCB ce qui est normal car le cimentier a toujours la latitude de modifier les conditions de marche de son four pour obtenir un clinker de qualité correct.

V PROBLEMES POSES

Ainsi que nous l'avons vu précédemment, il existe de nombreuses méthodes permettant de caractériser l'aptitude à la cuisson d'un cru industriel, chaque exploitant et chaque engineering constructeur ayant développé la sienne. Nous avons détaillé les méthodes de FCB et des Ciments d'Origny qui donnent des résultats voisins, exploitables industriellement, et qui illustrent deux soucis différents :

- Pour l'exploitant (Ciments d'Origny) il s'agit principalement d'améliorer les qualités des clinkers et les performances des usines existantes utilisant des matières premières données. Les tests de cuisson doivent permettre d'optimiser la composition du cru (ajouts éventuels...) ou la finesse de broyage, et de suivre le comportement de la matière en zone de cuisson par l'observation de la courbe CaO libre en fonction de la température.

- Pour le constructeur responsable des performances d'un four à construire le problème est plus simple (ce qui explique la plus grande simplicité du test FCB), il s'agit, à partir d'échantillons donnés de préconiser une finesse de broyage pour obtenir un clinker de bonne qualité dans des conditions de cuisson normales.

On peut donc dire que dans tous les cas, pour un cru de composition donnée, il s'agit de réduire le broyage au minimum compatible avec une bonne cuisson de façon à diminuer la consommation énergétique de l'usine existante ou projetée. Notons d'autre part qu'un broyage trop poussé d'un cru réactif peut être source d'inconvénients d'exploitation en favorisant les concrétions dans les échangeurs cyclones. Pour bien utiliser le test d'aptitude à la cuisson, il est donc nécessaire de pouvoir broyer au niveau du laboratoire, les mélanges crus à des finesses variables et représentatives de ce que délivrerait un broyeur industriel

Nous présentons donc ci-après, les moyens mis en oeuvre et les résultats obtenus par FCB et les Ciments d'Origny lorsqu'il s'agit d'étudier l'influence de la granulométrie du cru sur sa réactivité.

VI OPTIMISATION DE LA FINESSE DE BROYAGE

VI - 1) Préparation des échantillons.

Des essais ont été effectués sur les matières premières en provenance des Cimenteries de Zahana, du Boucau et de Crugey. Pour chaque cimenterie nous avons reconstitué au laboratoire un mélange, à partir des matières premières préalablement concassées en tout passant à 3,15 mm, ayant une composition chimique

aussi proche que possible de celle du cru industriel.

Les mélanges ainsi préparés ont ensuite été broyés,avec un agent de mouture, au laboratoire : la Société FCB utilise un broyeur Alsing (L = 503 mm, Ø = 720 mm) chargé de 150 kg de boulets de 30 mm ; les Ciments d'Origny utilisent un broyeur Henry (L = 450, Ø = 500) chargé de 160 kg de boulets de 25 mm.

Des échantillons ainsi broyés (sur le broyeur Henry et sur le broyeur Alsing) ont été prélevés au cours du broyage.

VI - 2) Analyses granulométriques (non reproduites dans ce rapport)

Celles-ci ont été effectuées à l'alpine et à l'élutriateur Bahco. On a constaté une bonne concordance entre les échantillons broyés au laboratoire et les échantillons de cru industriel. Des essais préalables ont d'autre part permis de montrer que l'ajout d'un agent de mouture permettait de reproduire plus fidèlement les granulométries industrielles, notamment pour les finesses poussées, en évitant l'agglomération.

VI - 3) Essais de cuisson

Nous avons appliqué sur les échantillons obtenus par broyage en laboratoire, la méthode FCB (cuisson 30 mn à 1450°C) et la méthode Origny (cuisson à plusieurs températures).

Les résultats ont été traduits sous forme de courbes :

- En ordonnées :

pourcentage de chaux libre après cuisson 30 mn à 1450°C (figure 1) ou coefficient d'aptitude à la cuisson déterminé par la méthode Origny (figure 2)

- En abcisse :

pourcentage de refus à 63 μ .

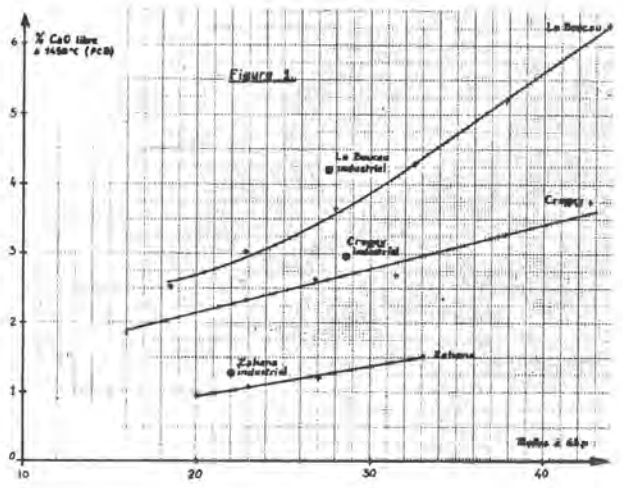

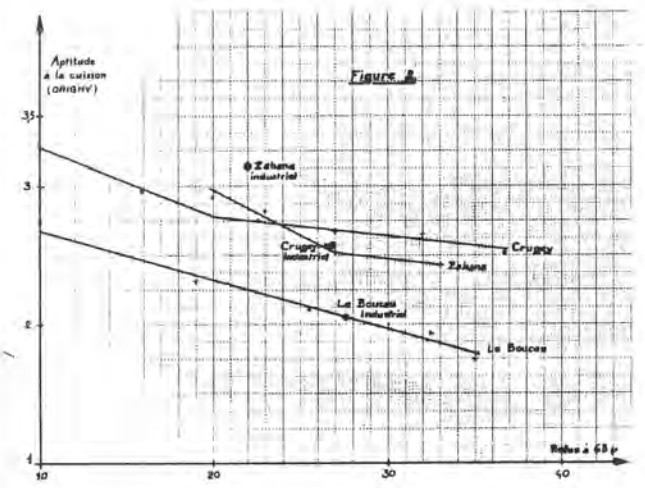

VI - 4) Commentaires sur les essais de broyage.

Ces essais ont montré que l'on pouvait reproduire, sur des broyeurs de laboratoire, un cru ayant une granulométrie et une aptitude à la combinaison tout à fait comparables à celles du cru industriel.

Ces essais ont d'autre part permis de mettre en évidence l'influence de la granulométrie sur l'aptitude à la combinaison d'un cru.

On peut donc à partir d'essais de laboratoire (broyage - essais de cuisson) déterminer la finesse optimum du cru, c'est à dire fixer la finesse de la farine, compatible avec l'obtention d'un clinker de bonne qualité, en évitant le surbroyage.

Les courbes ci-dessus (figures 1 et 2) montrent par exemple que l'on pourrait pour le cru de Zahana se contenter d'un broyage beaucoup plus grossier. Ceci s'est d'ailleurs vérifié lors de la mise en route de cette installation où il a été passé, pendant une période, un cru présentant 20 % de refus à 90 (soit environ 33 % de refus à 63μ) sans que l'on constate d'inconvénients quelconques sur la cuisson et la qualité du clinker obtenu.

VII CONCLUSIONS

De nombreuses méthodes d'estimation de l'aptitude à la combinaison des crus de cimenterie ont été proposées par divers auteurs. Il s'est avéré que la plupart de ces méthodes sont trop qualitatives pour permetttre de déboucher sur un critère de prévision du comportement industriel des crus de cimenterie.

Le choix de la méthode de caractérisation adoptée à FCB s'est porté sur la méthode de cuisson unique à 1450°C. L'adoption de cette méthode se justifie d'une part par la corrélation que l'on a pu faire entre taux de combinaison obtenu en laboratoire et taux de combinaison obtenu industriellement et d'autre part en raison de sa simplicité de mise en oeuvre en laboratoire.

Dans les cas où un cru donné peut être obtenu à partir de différents mélanges de matières premières, la méthode de cuisson unique à 1450°C peut aboutir à des taux de combinaison en laboratoire trop voisins les uns des autres pour justifier le choix de tel ou tel mélange cru. La méthode de cuisson à différentes températures, mise au point par les Ciments d'Origny peut alors permettre de mieux préciser les caractéristiques de chacun des mélanges.

On a d'autre part pu, sur des broyeurs de laboratoire, reconstituer la granulométrie obtenue sur les broyeurs industriels. Ces essais ont ainsi permis de mettre en évidence l'influence de la granulométrie sur l'aptitude à la combinaison d'un cru.

On peut donc à partir d'essais de laboratoire (broyage, essais de cuisson) déterminer la finesse optimum d'un cru, c'est à dire fixer la finesse de la farine compatible avec l'obtention d'un clinker de bonne qualité, en évitant le surbroyage.

Energy savings through better utilization of waste heat

Economie d'énergie par récupération de la chaleur non utilisée

E.M. GARTNER, Senior Research Chemist, Portland Cement Association, Skokie, Illinois, 60077, U.S.A.

RESUME: L'industrie cimentière américaine produit plus de 50% de son ciment par procédé humide. Pour cette raison, ses besoins énergitiques sont élevés comparé à ceux des industries cimentières de l'Europe et du Japon. La conversion des anciens systèmes peu efficaces en systèmes équipés de préchauffeurs et de pré-calcinateurs modernes permettra aux cimenteries américaines de réaliser d'importantes économies d'énergie dans un avenir rapproché. Néanmoins il est déjà possible de réaliser d'importantes économies d'énergie dans les usines actuelles par l'application de methodes améliorées de récupération de chaleur.

Dans le moment, aux Etats-Unis, on a considérablement intensifié la recherche pour produire de l'électricite à partir de la chaleur perdue, à des températures aussi basse que 260°C. Ces systèmes utilisent généralement un fluide organique plutôt que de la vapeur d'eau. De nouvelles idées telle que l'amélioration des méthodes d'emmagasinage de la chaleur sont à l'étude. D'autres idées plus avant-gardistes présentées ici permettront une meilleure récupération de la chaleur des refroidisseurs à clinker et des gaz d'évacuation des fours à procédé humide.

SUMMARY: The U.S. cement industry produces over 50% of its cement by the wet process. For this reason, its specific energy requirements are high compared to the European and Japanese cement industries. Conversion of older, less efficient kiln systems to modern preheater and precalciner kiln systems will probably account for most of the energy savings made by U.S. cement manufacturers in the near future. Nevertheless, there are still opportunities for large energy savings at new and existing plants by means of improved methods of waste heat utilization.

At the present time, a considerable amount of research is being conducted in the U.S.A. in an effort to design high-efficiency electricity generating systems which can use waste heat at temperatures as low as 500°F. These systems generally use organic working fluids instead of steam. Other new ideas include improved methods of heat storage which will permit more efficient use of waste heat. Some more speculative ideas presented here include methods for better recuperation of heat from clinker coolers and also from the exit gases in wet process kilns.

1. Background - The U.S. Cement Industry

As of December 31, 1978, there were 162 cement plants, owned by 49 separate companies, operating in the U.S.A. Of the total of 363 kilns, 206 used the wet process and 157 used the dry process, including 41 kilns with some form of preheater. Of the 73.8 X 10^6 short tons (67 X 10^9 kg) of clinker manufactured in 1978, approximately 55% was produced using the wet process.

In the U.S.A., as elsewhere, the dramatic increases in energy costs over the last six or seven years have led to a decrease in the number of wet plants and an increase in the number of dry plants, especially preheater plants. But we still have a long way to go before all our cement is manufactured by the most energy efficient processes. The North American continent encompasses such a wide range of raw materials and product demand requirements that it is impossible to generalize when considering the design of cement plants for this market. Raw materials with high contents of alkalies, halides, sulfur, and hydrocarbons occur in some areas, and these minor components, combined with frequent specification of low alkali cements, have made U.S. cement manufacturers cautious regarding installation of preheater kilns. The advent of the precalciner kiln, with the capacity for efficient use of high bypass levels, may hasten the conversion to the dry process in the next few decades.

2. Waste Heat Generation in the U.S. Cement Industry

In 1978, 82.9 X 10^6 short tons (7.52 X 10^{10} kg) of finished cement were produced in the U.S., about 94% being made from U.S.-produced clinker. The total fossil fuel use for the U.S. cement industry was 421 X 10^{12} Btu (444 X 10^{15} J), and total electrical power consumption was 11.1 X 10^9 kWh. The fossil fuel requirement for clinker production averaged about 5.70 X 10^6 Btu/short ton (6,630 kJ/kg). The electrical requirement for finished cement production averaged 134 kWh/short ton (0.148 kWh/kg), including grinding of imported clinker. If we assume that the "theoretical" enthalpy requirement for clinker production from typical raw materials averages about 1.5 X 10^6 Btu/short ton (1,740 kJ/kg), this suggests that about 4.2 X 10^6 Btu/short ton (4,880 kJ/kg) of excess heat is lost during clinker manufacture. This amounts to roughly 310 X 10^{12} Btu (330 X 10^{15} J) annually. To some extent, all of this heat may be regarded as "waste" heat. The better use of this heat is the subject of this paper.

3. Current Status of Waste Heat Utilization

The major use of waste heat in U.S. cement plants at present is in raw feed drying. Two minor uses are:

(1) Space heating in buildings, etc.
(2) Electricity generation.

Neither of these two account for a very great percentage of the available waste heat. We estimate that about 4 X 10^8 kWh of electricity are generated annually from waste heat at U.S. cement plants. The average conversion efficiency is not known accurately, but is believed to be about 20%. This implies that about 6.8 X 10^{12} Btu (7.2 X 10^{15} J) of waste heat are used annually in electricity generation. The amount of waste heat used for feed drying is also not known to us. Many U.S. cement plants operate separate fuel-fired dryers instead of using waste heat from the kilns, and the fuel for these dryers is included in the total fuel-use figures for cement production given above. Some cement plants also produce steam or hot water for heating of buildings, etc., but, again, this only accounts for a very small fraction of the available waste heat.

There are two large cement plants in the U.S.A. which currently product significant amounts of electricity from waste heat. There are also one or two small, older plants which have waste heat boilers, but which are near the end of their operational lives. The two large plants both have several dry process kilns, (without preheaters), equipped with steam boilers. Steam from more than one boiler is piped to the turbines for electricity generation. One of the plants has a raw feed, rich in hydrocarbons, which add 0.95 MBtu/short ton (1,105 kJ/kg) to the 4.57 MBtu/short ton (5,314 kJ/kg) of fuel burnt in the kiln. In the past, this was a significant factor in the decision to use waste heat boilers, since this raw feed was unsuitable for use in anything other than a dry-process kiln without preheaters.

One of the major disincentives to the generation of electricity from waste heat in the U.S.A. has been the difficulty in negotiating cogeneration agreements with the local electric power company. Generally, if the cement company sells any power back to the grid, it will only get a small fraction of the price per kWh that it pays when it buys energy. However, this situation is improving slowly, and the Federal government is taking steps to encourage the negotiation of cogeneration agreements which will be fair both to the cogenerator and to the electric company. This is a result of the National Energy Act of 1978.

4. Modern Trends in Electricity Generation from Waste Heat

4.1 Organic Rankine Systems

Currently, there is a resurgence of interest in electricity generation from waste heat. Several North American companies are developing "Organic Rankine Cycle" boilers and generators, which can be used more efficiently than steam-cycle systems, with the low waste heat temperatures typical of the more efficient modern dry-process cement kilns. Most of these units are designed to be "retrofitted" to existing cement plants, without involving drastic changes in the design of the plant. Modern, efficient steam-cycle boiler/generator systems are also being marketed for cement plant installations.

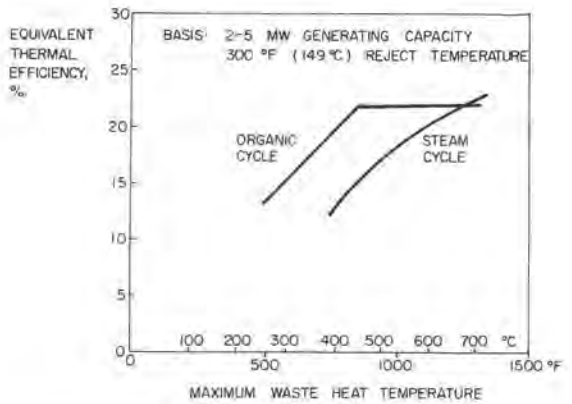

FIGURE 1 - COMPARISION OF ORGANIC AND STEAM SYSTEMS

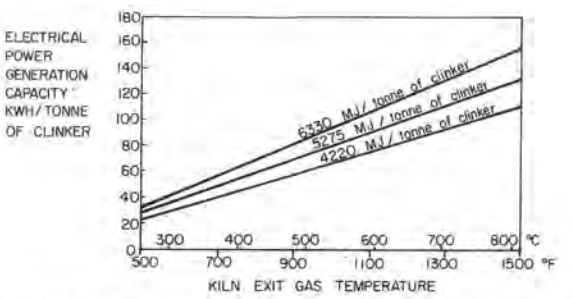

FIGURE 2 - WASTE-HEAT ELECTRICAL POWER GENERATION CAPACITY vs. KILN FUEL REQUIREMENTS
NOTE: CALCULATED FOR DRY PROCESS KILNS, ASSUMING A 20 % CYCLE EFFICIENCY

An idea of the relative efficiencies of organic rankine and steam cycle power generating plants can be obtained from Figure 1. Organic rankine cycles are potentially up to 50% more efficient than steam cycles for waste heat temperatures in the range 500-1000°F, (260-540°C). This is partly because they have the advantage of a less severe "thermodynamic pinch" due to the lower latent heat of vaporization of the organic fluid. Use of some organic fluids also allows the boiler reject heat temperature to be well below 300°F (150°C), which is impractical for most steam cycles.

The fraction of the electrical energy requirement which can be generated within any given cement plant depends mainly on the thermal efficiency of the kiln system. This is shown graphically in Figure 2; the data have been calculated on the basis of a 20% cycle efficiency.(1) The high efficiency of organic rankine cycles at low inlet temperatures means that waste heat boilers can be installed on preheater kilns, where exit-gas temperatures are typically in the range 550-850°F (290-450°C).

4.2 Energy Storage Systems

Together with the use of improved waste heat boilers, there is the possibility of using some form of energy storage to balance power generation against power requirements. This idea has been discussed in a recent report.(2) One of the proposed systems uses "draw salt" (a mixture of sodium and potassium nitrates) as the heat storage medium. The salt mixture melts at 430°F (221°C) and has a high thermal capacity. It can also maintain a high thermal density gradient, which allows both hot and cold salt to be stored in a single tank.

Another possible system is "rockbed" energy storage, basically consisting of a simple bed of gravel through which the hot kiln exit gases can be passed. Air can then be used to reclaim the heat. An economic analysis carried out by Martin Marietta Aerospace(2) concluded that the ability to store up to 24 hours production of waste heat for use in electricity generation would result in an improved economic return as compared to a simple, direct waste heat to electricity conversion system. However, there is some doubt as to the real economic feasibility of these storage systems; it seems probable that they will be sensitive to erosion and corrosion by dust, etc., in the waste gas streams. Moreover, the density of energy storage is too low to allow storage of more than one or two days' waste-heat production. With the current trend towards cogeneration agreements, such system may be unnecessary.

4.3 Use of Waste Air from Clinker Coolers, and Bypass Gases from Preheater Kilns

Most of the recent studies on the use of modern waste heat electricity generating systems on cement plants in the U.S.A. have tended to rule out the use of clinker-cooler waste air as a useful source of heat for electric power generation, since it is generally at a rather low temperature, i.e., 250-450°F (120-230°C). Nevertheless, since most U.S. cement plants are equipped with grate coolers as opposed to planetary coolers, clinker cooler waste air does represent a considerable source of waste heat. It may frequently amount to well over 0.5 MBtu/short ton of clinker (580 kJ/kg) on preheater kilns. This source of heat could be incorporated into some schemes for waste heat electricity generation from kiln exit gases, especially in cases where the kiln exit gases are excessively hot and must be diluted with cold air. This might be the case if bypass gases from a preheater or precalciner kiln were to be used for electricity generation. The presence of low-melting alkali sulfates and chlorides in bypass gases may make it preferable to cool the gases below about 1350°F (730°C) in order that the alkali salts condense to solid particles before reaching the heat exchanger tubes. Use of clinker-cooler waste air for dilution would be especially advantageous if it were at a temperature above the boiler rejection temperature, as it then would contribute some extra heat to the system.

4.4 Corrosion and Erosion of Heat Exchangers

The problem of sulfuric acid attack on boiler pipes is almost negligible in the case of waste heat boilers on cement kilns, because of the alkalinity of the dust and the low SO_3 content of the kiln exit gases. However, the effects of kiln dust are one of the major considerations when designing waste heat boilers suitable for cement plant use. The boilers themselves are bound to act as a trap for dust particles and must be provided with an efficient system for dust removal, including soot blowers, etc. The dust is not generally very corrosive towards steel but it is abrasive. Another problem is the formation of hard build-ups which frequently result from the recarbonation of calcium oxide particles. These particles apparently stick to the boiler pipes in the presence of small amounts of alkali salts. Recarbonation of CaO gives calcite, with a 120% increase in volume. This can give rise to a very hard, dense layer on the tubes, which cannot easily be removed.

5. Future Developments in Waste Heat Utilization

5.1 More Effective Methods of Raw Feed Drying

Although, currently, much research is being directed towards improving efficiency of electricity generation from waste heat, a simpler use of waste heat is in raw feed drying. Of course, many of the newer preheater plants already have systems for using kiln exit gases for feed drying, especially if roller mills are used for raw feed grinding. Hot gases from the kiln (or clinker cooler) pass directly into the roller mill. However, many plants in the U.S. use separate, fuel-fired dryers when they could well be using waste heat from either the kiln or the clinker cooler. There is sufficient suitable waste heat rejected from the clinker coolers at many dry-process plants to remove upto 6% moisture from the raw feed. In theory, it should be possible to make the system serve two purposes simultaneously, by combining the requirements for a clinker cooler dust-collector with that of a raw feed dryer. This would be especially useful for plants which use ball mills to grind the raw feed. A simple outline of such a system is shown in Figure 3.

It is proposed that hot waste air from the clinker cooler be passed directly through the moist, crushed raw feed, supported on a travelling grate. The bed of raw feed acts effectively as a gravel bed filter which is continually being renewed. At the same time, considerable drying of the feed can be achieved.

Moist air from the bed is blown back through the hot zone of the clinker cooler and thus ultimately ends up as secondary combustion air in the cement kiln. The increased moisture content of this air could be advantageous in that it would have a higher heat capacity than ordinary dry air; this may result in an increased rate of clinker cooling. Water vapor may also help heat transfer in the burning zone, due to increased flame emissivity. Both of these secondary effects should help to improve clinker quality. The overall effect of this system would be to use hot waste air as a drying medium and simultaneously to save on the cost of installing and maintaining clinker dust collectors and a waste air stack. The coarse clinker dust could be removed by cyclones for return to the finish mills, and the fine dust would end up as part of the dried kiln feed, and be returned to the kiln. This system would be most useful for fuel efficient plants, and should free more of the hot kiln exit gases, which would otherwise be required for feed drying, for electricity generation if desired.

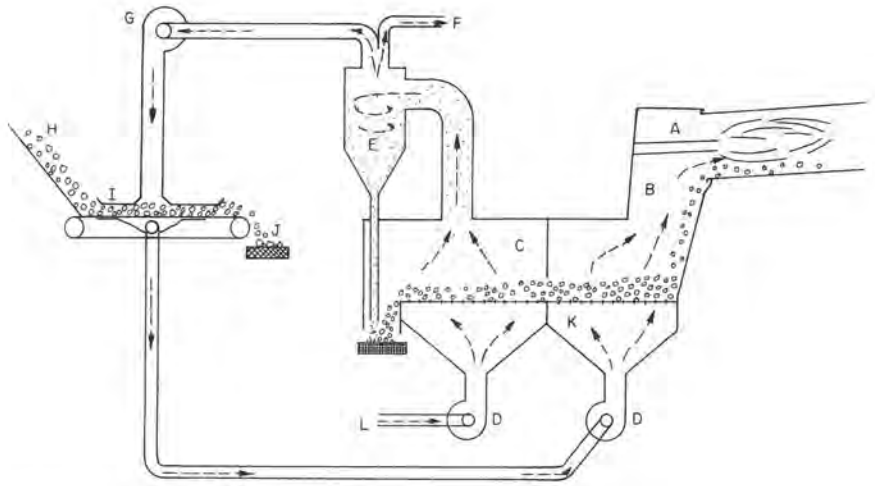

FIGURE 3 – COMBINED CLINKER COOLER DUST COLLECTOR AND RAW FEED DRYER

A – BURNER HOOD; B – SECONDARY AIR TO KILN; C – "WASTE" AIR; D – UNDER GRATE FANS; E – CYCLONE TO REMOVE COARSE DUST (RETURN TO CLINKER BELT); F – HOT AIR TO COAL MILL, IF REQUIRED; G – AUXILIARY FAN, IF REQUIRED; H – CRUSHED FEED; I – FEED DRYER HOOD; J – DRIED FEED TO BALL MILLS; K – DAMP AIR TO CLINKER COOLER; L – FRESH AIR INLET.

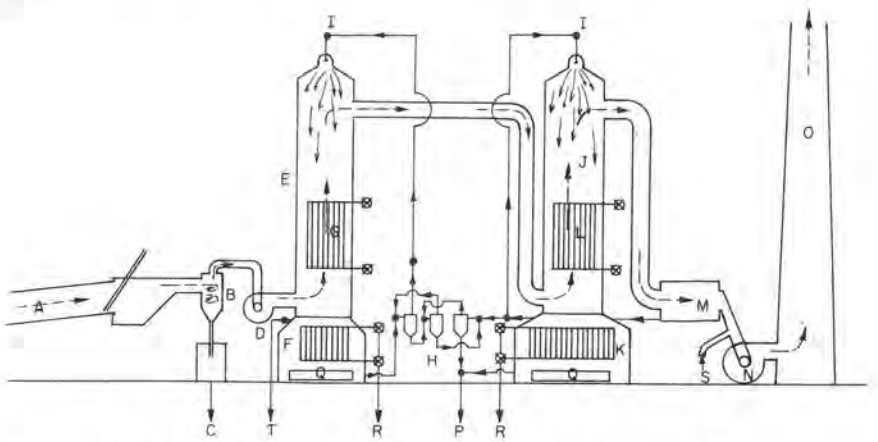

FIGURE 4 – WET SCRUBBER WITH HEAT AND ALKALI RECLAIM

A – ROTARY KILN; B – DRY CYCLONE; C – COARSE DUST FOR INSUFFLATION, IF DESIRED; D – FIRST I.D. FAN; E – FIRST SCRUBBER TOWER (FOR DUST AND ALKALI REMOVAL); F – SLURRY THICKENING TANK; G – AUXILIARY HIGH TEMPERATURE HEAT EXCHANGERS; H – COUNTERCURRENT HYDROCYCLONES FOR SLURRY WASHING TO REMOVE ALKALI SALT SOLUTION; I – SPRAY NOZZLES; J – SECOND SCRUBBER TOWER (FOR LATENT HEAT RECAPTURE); K – HEAT EXCHANGER TANK; L – MAIN HEAT EXCHANGERS; M – DEMISTER; N – SECOND I.D. FAN; O – STACK; P – DILUTE SLURRY RETURN TO RAW FEED MILLS; Q – SLURRY AGITATORS; R – CONNECTIONS TO CLOSED CYCLE HOT WATER SYSTEM FOR SPACE HEATING, ETC.; S – HOT AIR FROM CLINKER COOLER, FOR REHEAT OF CLEAN GASES; T – CONCENTRATED ALKALI SALT SOLUTION BLEED POINT; ⊠ – CONNECTIONS TO HEAT EXCHANGERS; ● – SLURRY PUMPS; ⟶ – LIQUID FLOWS; – – → – GAS FLOWS

5.2 Use of Waste Heat from Wet-Process Plants

One area in which few attempts have been made to fully utilize waste heat is in wet process cement plants, which still produce over 50% of the cement clinker manufactured in the U.S.A. The waste heat, which is mainly in the form of the latent heat of vaporization of water, can be used effectively in low temperature heating, mainly at temperatures below 212°F (100°C). There is a limit to the amount of such heat which is required at any cement plant. However, if the plant were located close to a small community or industrial site which did require such heat for space heating, etc., then it should be possible for the plant to install a complete heat exchanger/condenser system, to extract most of the latent heat from the water vapor in the stack gases. If such a system were to be considered, it clearly should include recycle of the condensed water back into the kiln feed slurry. The hot condensate could be cooled via heat exchange with clean water in a closed loop heat transfer system, the clean water be used to transfer heat to nearby homes, factories, etc. A large reservoir for storage of hot water, or for loss of waste heat by evaporation, may also be helpful to level the heating and cooling load between summer and winter. Such systems may be feasible in certain localities.

Figure 4 is a sketch of a possible system for utilizing waste heat from a wet-process kiln. This system is more complex than a simple condenser. It combines heat recuperation devices with a wet scrubber for kiln dust removal and also a special alkali removal cycle, based on kiln dust leaching theories developed at PCA. The wet, dusty gases pass first through a dry cyclone to remove coarse dust particles, which can be returned to the kiln by insufflation, if desired. The gas is then scrubbed with a concentrated solution of the alkali salts normally found in the dust itself, the solution being generated from the dust initially. Heat exchange at this point is such that the gases are cooled to a temperature slightly above 212°F (100°C), where the concentrated alkali solution is close to equilibrium with the vapor. A large fraction of the kiln dust is removed in this stage of the process; the scrubber is specifically designed for dust removal. The dust slurry is thickened and then washed with water from the second stage scrubber, in countercurrent flow, which decreases the alkali content of the slurry before its return to the raw feed mills. A continuous "bleed off" of the alkali-rich solution enables the alkalies to be removed from the system in a concentrated solution which could be a useful byproduct.

The relatively dust-free gases then pass into the second scrubber, where excess cold water is used to aid condensation of water vapor from the gases, as well as removal of the remaining dust. The main heat exchangers heat the cold return water from the external closed-cycle heat transfer system; the water temperature is then increased further in the first stage scrubber. The condensed water and dust form a dilute slurry which may be combined with the slurry from the first scrubber and returned to the raw feed mills. The pH of the dust slurry is lowered by contact with the CO_2 in the kiln exit gases, which tends to carbonate much of the free lime in the dust and make it more suitable for remixing with the feed slurry. Finally, the cool saturated gases leaving the second scrubber pass through a demister, and can then be reheated, using waste air from the clinker cooler if possible, before leaving the stack.

A rough estimate suggests that a wet-process cement plant of average capacity (100 tons/hour) could provide enough heat to heat 4,000-8,000 typical homes during winter.

6. Conclusions

Some of the systems suggested in this report may seem far-fetched, and indeed it is doubtful if they would be economically justifiable at present. However, with the ever increasing cost of fuel and electricity, complex systems which combine heat recuperation with other useful processes such as dust removal, etc., will become increasingly attractive. It should be remembered that the best use of waste heat and waste materials can generally be made only by combining and optimizing all the possible uses of the various waste streams from the whole manufacturing process. The major problem with such systems is that they are complex both chemically and physically, and it may take time before industry becomes able to sponsor the extra research required to fully develop them.

References

1. Breindel, B., Collamore, F.M. and Goetz, J.L., "Multi-Megawatt Organic Rankine Engine for Power Generation in the Cement Industry," Proceedings of the IEEE Cement Industry Technical Conference, Tampa, Florida, May 1979.

2. Jaeger, F.A., et al, "Application of Thermal Energy Storage in the Cement Industry," U.S. Department of Energy, 1978, Report No. NASA CR-159399.

Bilan énergétique de l'incorporation d'ajouts et des moyens d'activation de ces liants

Thermal evaluation of binder induction and their induction means

J.P. BOMBLED, C.E.R.I.L.H. - Paris, France.

RESUME

L'incorporation de n tonnes de matériaux naturels ou de sous-produits industriels hydrauliques ou pouzzolaniques permet l'économie de n/9 TEP en fabrication.

Outre l'intérêt économique et écologique, l'expérience montre que ces ciments à forte teneur en constituants secondaires ont généralement d'excellentes qualités notamment en ce qui concerne la maniabilité du béton frais et la bonne résistance des bétons durcis en contact avec des milieux agressifs. Néanmoins le principal grief qui leur est reproché est leur moindre vitesse de durcissement pouvant ralentir les cadences de préfabrication ou freiner les chantiers.

L'analyse des séquences de l'hydratation et du durcissement montre que pour les "activer" on peut avoir recours au niveau de la fabrication, au surbroyage ou, au stade de la mise en oeuvre, à des moyens rhéologiques (fluidification et réduction d'eau importante), mécaniques (pressage énergique), thermiques (étuvages ou autoclavages) ou chimiques (adjuvants accélérateurs).

Les essais effectués sur des CPJ 35 ont permis de comparer l'efficacité de ces différents moyens et aussi les effets de leur association deux à deux, ou trois à trois ...

Hormis le cas d'exigences de résistances mécaniques à très brève échéance (quelques heures) le bilan le plus positif joue en faveur du surbroyage et des adjuvants à l'exclusion des moyens thermiques qui peuvent consommer en énergie beaucoup plus que le bénéfice fait lors de la fabrication de ces liants.

L'avenir sera sans doute dans l'étude de nouveaux procédés d'"activation", dans la recherche d'adjuvants plus efficaces et dans la conjugaison des différents moyens d'action.

SUMMARY

Using n tons of hydraulic or pozzolanic natural materials and industrial by-products allows the saving of n/9 fuel oil tons.

In addition to economical and ecological interest, experience shows that cements with high content in secondary components generally have excellent qualities, especially concerning the workability of fresh concrete and the strength of hardenned concrete in contact with agressive environments. A low hardening velocity, which is its main defect, can slow down the rate of precast production or slacken the in situ operations.

Hydration and hardening process analysis shows that they can be accelerated during production : by an overgrinding, or during placing : by rheological means (fluidification and high water reducing), by mechanical means (strong pressure), by thermal means (steam curing or autoclaving) or by chemical means (acceleration admixtures).

Compound Portland Cement (CPJ 35) was used in the experiments permitting the comparison of the efficiency of various means and the effects of their association.

Excluding the requirement of a very early strength (some hours), the most positive evaluation is in behalf of overgrinding and admixture. Exception made for thermal means that can have a higher energy consumption than the profit produced by the fabrication of that kind of binders.

New activation processes will be studied in the future to research more effective admixtures and to the conjugation of various means.

1 INTRODUCTION

Les grandes préoccupations de cette fin de siècle et de millénaire sont essentiellement l'amélioration de la qualité de la vie, la sauvegarde de la nature, la diminution de la peine des hommes et les économies aussi bien de matières premières que d'énergie.

Comme la plupart des industries, la cimenterie a été confrontée à toutes ces exigences, qu'il est parfois difficile de concilier.

Le problème prioritaire est sans aucun doute le souci d'économiser les thermies et les kWh nécessaires à la fabrication du ciment et beaucoup d'efforts ont déjà été fournis dans ce sens.

Un des moyens pour économiser le combustible de cuisson du clinker est évidemment de remplacer celui-ci dans toute la mesure du possible par des matériaux naturels ou des sous-produits industriels hydrauliques ou pouzzolaniques. Or il se trouve que la politique de l'ajout de ces constituants secondaires peut aussi être favorable pour certains des autres objectifs qualitatifs cités ci-dessus.

Néanmoins il est indispensable que la qualité de ces ciments composés (CPJ des nouvelles normes, CPM, CHF ...) soit suffisante pour satisfaire aux exigences des cadences des chantiers ou des usines de préfabrication faute de quoi le recours à des procédés thermiques d'accélération du durcissement par exemple, risquerait de compromettre le bénéfice énergétique escompté; c'est par conséquent ce bilan que nous allons essayer d'examiner.

2 INTERET DE L'INCORPORATION DES SOUS-PRODUITS

La politique de fabrication des liants contenant des sous-produits industriels a démarré il y a déjà très longtemps en France, avec le développement des ciments de laitier et des ciments à la pouzzolane naturelle (gaize par exemple) ou artificielle (cendres volantes), ceci non seulement pour des raisons économiques lors de périodes difficiles mais aussi souvent à cause des qualités particulières de ces liants.

Si l'on définit les taux d'ajout par :

$$\tau = \frac{\text{tonnage de liant produit}}{\text{tonnage de clinker consommé}} = \frac{L}{K} = 1 + \frac{A}{K} \qquad (1)$$

A = tonnage d'ajout incorporé

$$\text{et} \quad \alpha = \frac{A}{L} = 1 - \frac{1}{\tau} \qquad (2)$$

pour fixer les idées, le taux α a oscillé ces dernières années entre 0,20 et 0,25 et τ a été très voisin (tous liants réunis) de 1,3.

L'incorporation de sous-produits et de déchets industriels présente des avantages économiques, écologiques et techniques.

2.1 Economie d'énergie

La substitution du clinker qu'il n'aura pas été nécessaire de cuire par des matériaux disponibles, procure une économie directe de combustible à laquelle il faut ajouter l'économie de kWh (donc d'équivalent pétrole) faite sur la préparation du cru et en particulier sur le broyage des matières premières qui auraient été nécessaires pour la fabrication du clinker économisé :

$$E = \alpha\left[\overbrace{C_1}^{\text{cuisson}} + \overbrace{\underbrace{K a C_2}_{\text{cru}} - \underbrace{K C_3 \frac{\Delta S}{1000}}_{\text{surbroyage du ciment}}}^{\text{broyage}} + \overbrace{\alpha C_4 d}^{\text{transport de l'ajout}}\right] \qquad (3)$$

Avec :

- E = économie d'équivalent fuel par tonne de ciment.
- α = teneur en ajout.
- C_1 = kg de fuel pour la cuisson d'une tonne de clinker ($\simeq 105$).
- C_2 = kWh par tonne pour le broyage du cru.
- a = quantité de cru par tonne de clinker ($a \simeq 1,6$).
- C_3 = consommation spécifique (kWh/t) pour le surbroyage éventuel du clinker.
- ΔS = surbroyage nécessaire.
- C_4 = consommation de fuel par tonne-km pour le transport des ajouts.
- d = distance de transport.
- K = consommation moyenne de fuel par kWh à la centrale électrique ($\simeq 0,25$ kg/kWh)

En négligeant la dépense de transport, très variable suivant les conditions, on peut écrire :

$$E = \alpha\left[105 + 0,25\ (1,6 \times 20)\right] - 0,25 \times 11 \times \frac{\Delta S}{1000}$$

$$= 113\,\alpha - \frac{\Delta S}{364} \qquad (4)$$

Pour une teneur moyenne α de 23 % et en remarquant que la part du surbroyage reste généralement faible, on aboutit en moyenne à un gain de 26 kg de fuel par tonne de ciment c'est-à-dire qu'une tonne d'ajout fait gagner plus de 110 kg de fuel et l'emploi en cimenterie de n tonnes de sous-produits fait économiser environ n/9 tonnes de fuel.

L'incorporation annuelle de sept millions de tonnes de constituants secondaires correspond donc à une économie générale en fabrication, de l'ordre de 750 000 tonnes de fuel soit pratiquement le double de celle estimée lors de l'instauration de l'heure d'été.

2.2 Valorisation des déchets et protection de l'environnement

La valorisation de ces sous-produits se situe non seulement dans la lutte contre le gaspillage de matières premières mais représente pour les industries d'amont une économie certaine puisque la commercialisation des déchets évite des dépenses non négligeables pour l'évacuation, l'entassement et la surveillance des décharges et crassiers (outre la difficulté de plus en plus grande de trouver des terrains appropriés).

Par ailleurs au niveau de la cimenterie la substitution du clinker dans les liants fabriqués en France par près de 7 millions de tonnes d'ajouts par an évite d'extraire de l'ordre de 10 millions de tonnes de matières premières annuellement c'est-à-dire, permet de laisser en place chaque année environ 5 millions de m^3 ce qui, outre l'économie d'extraction, n'est pas négligeable pour la sauvegarde de la nature, la conservation des sites et la protection de l'environnement.

Ajoutons que sur le plan purement économique, en dehors des économies déjà indiquées, l'incidence sur les coûts de fabrication de l'emploi des déchets qui n'exige qu'un volume d'investissement de l'ordre de 1/5 de celui qu'il faudrait pour fabriquer le même tonnage de clinker.

2.3 Qualités des ciments à constituants secondaires

Ajouté aux considérations ci-dessus et contrairement à l'idée parfois répandue, il convient de souligner sur le plan technique que les liants contenant des constituants secondaires sont d'excellents ciments présentant des propriétés et des qualités spécifiques.

Maintes fois démontrées et bien qu'il sortirait du cadre de ce travail de les développer en détail, nous les résumons rapidement :

- qualités du béton frais : dans la plupart des cas la présence de constituants secondaires améliore la maniabilité et la plasticité des bétons frais, toutes choses égales par ailleurs; cela peut se concrétiser par une amélioration de la mise en oeuvre et du serrage ou par une diminution de l'exigence en eau à maniabilité égale. Tout cela peut conduire à des gains de compacité, d'étanchéité et de résistance sur le matériau durci.
- béton durci : on sait que le point faible des hydrates du ciment portland est la portlandite ; or la teneur en chaux plus faible des ciments à constituants secondaires et la possibilité de son insolubilisation dans les réactions pouzzolaniques rendent les mortiers et les bétons durcis moins sensibles aux actions dissolvantes des eaux pures ou aux attaques des eaux agressives ou chargées.

Par ailleurs un certain nombre d'ajouts à caractère pouzzolanique qui ne sont pas saturés peuvent fixer et insolubiliser une part des alcalins avec les conséquences que cela entraîne : atténuation du retrait hygrométrique à long terme, suppression du risque de réaction alcali-granulats, limitation de la carbonatation.

Outre la bonne maniabilité, facteur de serrage, la masse volumique plus faible de ces ciments conduit, à dosage pondéral égal, à des volumes plus grands de pâte liante ce qui milite en faveur d'une bonne étanchéité donc contribue à la résistance aux attaques, au gel, à la corrosion, bref est favorable à la durabilité.

- autres qualités : leur faible chaleur d'hydratation doit diminuer les contractions thermiques ; la plus grande déformabilité de la pâte interstitielle doit atténuer les contraintes dues aux retraits gênés ; certains ajouts peuvent jouer le rôle de stabilisateur dimensionnel à l'égard des éléments expansifs éventuels du clinker utilisé : tout cela conduit à un moindre risque de fissuration dans certains emplois. Ajoutons aussi une bonne aptitude de ces ciments à la plupart des traitements thermiques et généralement une bonne tenue au feu.

En revanche les inconvénients et points faibles habituellement reprochés à ce type de liant, surtout ceux à forte teneur en ajout, sont les vitesses de prise et de durcissement plus faibles que celles de nombreux portland purs. Cette lenteur qui peut freiner la cadence des chantiers ou des usines de préfabrication est nuisible pour les bétonnages à basse température, en hiver, ou dans les pays de climat rigoureux.

Il peut résulter de cette sujétion, non seulement un "surprix" (évalué entre 2 et 8 %) pour le coût du béton mais aussi la possibilité d'une consommation supplémentaire d'énergie, si l'on a recours à des traitements thermiques par exemple, qui risquent d'annuler une partie du bénéfice réalisé en fabrication. D'où la nécessité d'étudier les moyens d'"activer" ces liants.

3 RECENSEMENT ET EVALUATION DES MOYENS D'"ACTIVATION" DES CIMENTS A FORTE TENEUR EN AJOUTS

3.1 Généralités

La séquence des phénomènes qui constituent l'hydratation et la prise d'un liant hydraulique est rappelée dans le TABLEAU I avec les moyens théoriques d'action à chaque niveau : mouillage, floculation, pénétration ou non, hydrolyse, dissolution, solvatation, diffusion des ions hydratés, sursaturation et précipitation.

On peut noter dans le tableau la fréquence d'apparition de la température, de la surface du contact solide-liquide et d'adjuvants potentiels.

Tableau I

Phase de l'hydratation	Phénomènes physico-chimiques	Action physique ou chimique efficace	Intervention possible en fabrication	Intervention possible à l'utilisation
Mouillage	Tension superficielle de l'eau	Inutile (les ciments sont hydrophiles)	-	-
Floculation (ou défloculation)	Potentiel électrocinétique de l'interphase	Adjuvants ioniques	-	Défloculants ou fluidifiants pour réduire les espaces intergranulaires
Pénétration	Viscosité de l'eau	Température	-	Chauffage
	Surface d'action	Accroissement de la surface ext. Défauts et failles int. des grains.	Broyage Trempe	-
Hydrolyse	Surface d'action	idem	Broyage ou trempe	-
	Affinités chimiques	ions convenables "catalyseurs"	Teneur en C_3A	Adjuvants
Dissolution	Forces de séparation des ions Agitation thermique Surface d'action "Solvants"	Constante diélectrique Température Défaut de cristaux ions convenables	- - Broyage, trempe -	- Chauffage - Adjuvants
Diffusion	Agitation thermique Dimensions des ions Gradient de concentration	Température Concentration, dosages.	- -	Chauffage E/C et serrage
Précipitation et Cristallisation	Sursaturation Germination Morphologie des cristaux	Ions convenables, température Architecture réticulé (accueil de cristallisation) Concentrations	- Fillers -	Adjuvants chaulfage Germes fillers E/C et serrage

Si par ailleurs on essaie de démonter les rouages de l'hydratation et du développement des résistances, on aboutit à une relation schématique telle que celle de la formule (5) qui même si elle n'est pas rigoureuse permet une représentation simple des phénomènes et surtout de mettre en relief les différents facteurs qui peuvent influer et donc où il faudra agir pour accélérer le processus :

$$R = KS\,(\theta+a)^n\, b\,(1+\psi)\,\frac{C}{E+\varepsilon}\,f_{(t)} \qquad (5)$$

R = résistance en cisaillement ou en traction
avec : b et ψ : teneur en C_3S et C_3A
S : aire volumique du ciment
θ : température du liquide interstitiel
C, E et ε : volumes relatifs du ciment, de l'eau et des vides.

Cette relation qui a en définitive la forme de la formule de Feret dont elle explicite le coefficient K_t montre non seulement l'importance de S et θ mais aussi le problème "spatial" représenté par le volume des hydrates (et leur résistance propre évidemment) en rapport avec les espaces à remplir, auparavant occupés par l'eau de gâchage et qu'auront à franchir les liaisons, c'est-à-dire en définitive les problèmes rhéologiques de plasticité, d'exigence en eau et du serrage.

3.2 Moyens d'actions pratiques

Il ressort de la relation (5) que l'on devrait pouvoir agir :

- en fabrication : en jouant sur S (surbroyage) et sur b et Ψ (et le gypsage) dans une certaine mesure.
- lors de la mise en oeuvre : en jouant sur C, E et ε c'est-à-dire les dosages et la rhéologie et sur θ.

En pratique on pourra envisager différents moyens:

3.21 Moyens mécaniques

Il s'agit essentiellement du surbroyage et dans des cas très particuliers de broyage sélectif (broyeur à jet) ou de broyage humide d'un coulis de ciment envoyé directement à la Centrale du béton; comme le broyage des CPJ consomme entre 30 et 40 kWh/t, un surbroyage de 1 000 cm^2/g Blaine pourra coûter un supplément de 50 % soit entre 4 et 5 kg de fuel (à la Centrale électrique).

Le broyage séparé des constituants et leur homogénéisation ultérieure est parfois un moyen efficace pour accroître la réactivité de l'une des phases seulement alors qu'en broyage simultané on broie inégalement en fonction des broyabilités des composants et l'on n'est par conséquent pas maître du résultat.

Les agents de mouture peuvent aussi apporter un gain énergétique d'autant plus marqué que l'on vise des finesses plus élevées et que l'on a des matériaux très "agglomérants".

3.22 Moyens d'actions rhéologiques

Il s'agit de réduire les distances intergranulaires et les vides interstitiels :

- en diminuant la quantité d'eau de gâchage (fluidifiant réducteur d'eau)
- en diminuant la quantité d'air soit en améliorant la maniabilité (plastifiants) soit en augmentant l'énergie de serrage (pressage par exemple).
- éventuellement en augmentant l'énergie de malaxage de la phase eau-ciment (malaxage à haute turbulence) qui désagglomère et "décape" les grains par attrition et augmente la surface réactive.

3.23 Moyens thermiques

La chaleur intervient sur la viscosité de l'eau et sur la diffusion des ions pour accélérer la dissolution et partant l'hydratation et le durcissement. On peut avoir recours à différentes techniques :

- préchauffage du béton lequel peut consommer de 5 à 10 kg de fuel/m^3 pour atteindre 60 °C par exemple
- auto-étuvage par la chaleur d'hydratation ce qui est intéressant mais nécessite des moules parfaitement calorifugés et des ciments à forte chaleur d'hydratation ce qui n'est généralement pas le cas des ciments à forte teneur en ajout.
- étuvage par de nombreux moyens (effet joule, fluides caloporteurs, vapeur perdue, micro-ondes etc) le TABLEAU II montre l'intérêt énergétique évident du chauffage électrique lequel sera encore plus intéressant au niveau national lorsqu'une grande part des kWh seront d'origine non pétrolière.
- autoclavage lui-même gourmand en énergie et coûteux en investissements.

L'avantage incontestable des traitements thermiques est qu'ils peuvent fournir des résistances suffisantes à très brève échéance, 5 ou 6 heures par exemple, ce que ne peuvent pas donner la plupart des autres moyens.

En revanche ils peuvent engloutir les économies de fuel faites en fabrication (cf4) et conduisent toujours à un déficit de résistance à longue échéance et parfois à des gonflements ou à des produits plus poreux.

3.24 Moyens chimiques ou physico-chimiques

- adjuvants accélérateurs de durcissement : l'intérêt des adjuvants est de ne pas exiger d'installations et d'investissements coûteux et dans la plupart des cas (mais encore faut-il le vérifier en étudiant les produits de base et leurs procédés de fabrication) ils sont plus économiques que les moyens précédents sur le plan énergétique.
- moyens divers (pour mémoire) : germes, eau magnétisée ..., ont été maintes fois proposés mais n'ont jusqu'à présent pu faire les preuves de leur efficacité.

Tableau II

Mode de chauffage		Quantité d'énergie	Coût de l'énergie **	Investissement
Electricité		60 KWh *	0,15 F x 60 = 9 F	base de 1
Vapeur perdue	Fuel domestique	45 litres	0,75 F x 45 = 33,75 F	environ 1
	Fuel lourd	45 litres	0,40 F x 45 = 18 F	environ 1
Fluides caloporteurs	Fuel domestique	25 litres	0,75 F x 25 = 18,75 F	2 à 4
	Fuel lourd	25 litres	0,40 F x 25 = 10 F	2 à 4

* Soit 15 litres de fuel lourd à la centrale (Doc EDF)
** Prix mars 1978

4 COMPARAISON ET ASSOCIATION DES DIFFERENTS MOYENS POUR ACCROITRE LES RESISTANCES INITIALES

4.1 Comparaison de quelques procédés

Les figures 1, 2, 3 et 4 montrent l'action de quelques-uns des moyens indiqués sur les résistances en compression d'un CPJ 35 en pâte pure et la figure 5 permet de les comparer.

Même si ces résultats donnent une idée sur l'action comparée de ces différents modes d'accélération sur un même ciment il faut bien se garder d'extrapoler à tous les ciments, ceux-ci pouvant réagir différemment selon la composition de leur clinker et la nature des ajouts.

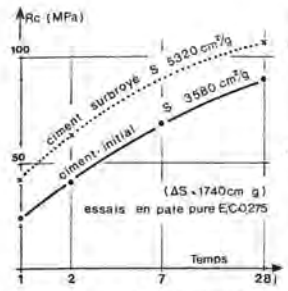

Fig 1 . Influence du surbroyage .

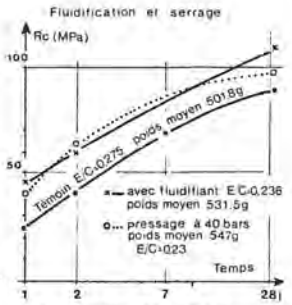

Fig 2 . Action rhéologique .

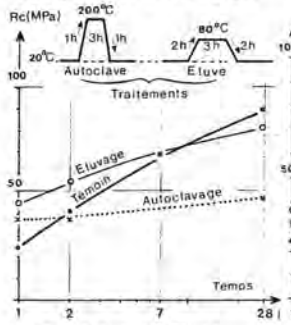

Fig 3 . Action thermique

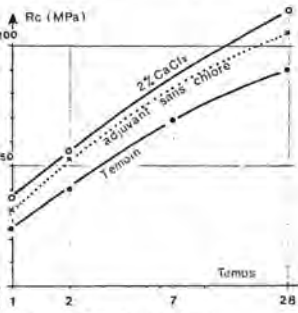

Fig 4 . Action chimique

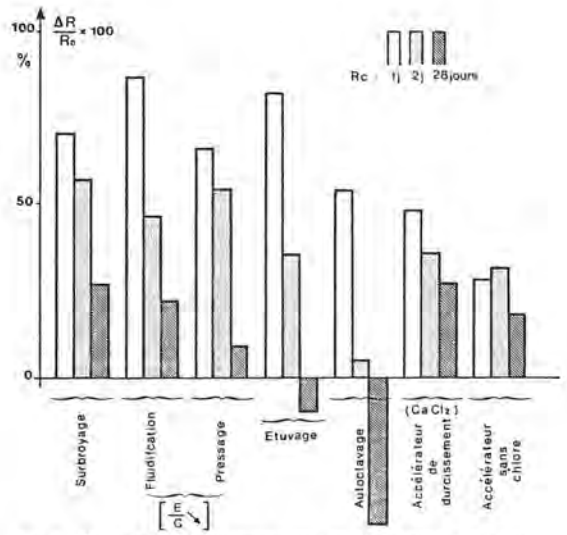

Fig 5 . Comparaison de différents moyens d'accélération sur un CPJ 35 (ciment aux cendres)

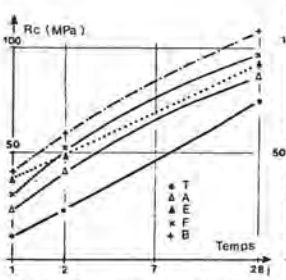

Fig 6 . Traitements simples .

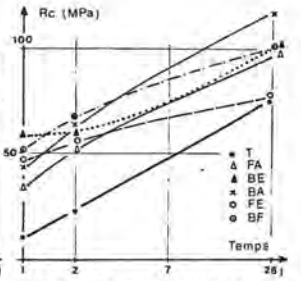

Fig 7 . Traitements doubles

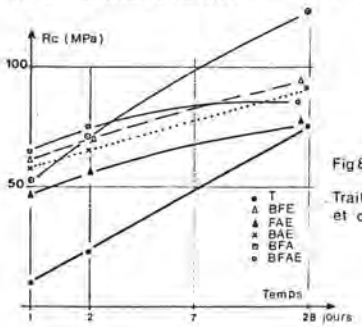

Fig 8 . Traitements triples et quadruple .

Pour simplifier on a sélectionné seulement les quatre modes d'action suivants :

A : adjuvant accélérateur sans chlorure
B : surbroyage
E : traitement thermique par étuvage (même cycle que figure 3)
F : abaissement de la teneur en eau par un fluidifiant efficace
T : témoin sans traitement.

La figure 9 permet la comparaison des résultats obtenus.

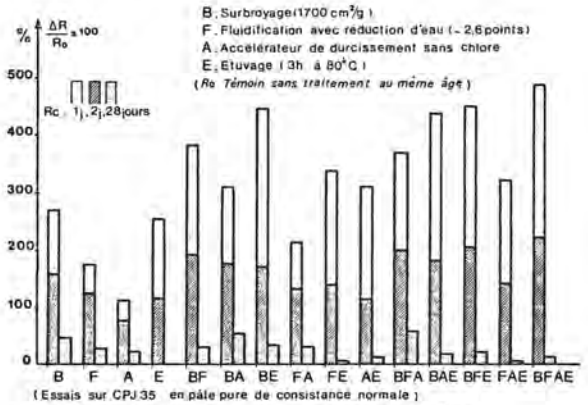

Fig 9 . Association de quelques moyens d'activation .

4.2 Association de plusieurs moyens

Ces essais ont été effectués sur un autre CPJ 35 ; les résultats sont groupés sur les figures 6, 7 et 8.

4.3 Récapitulation et bilan sommaire

Le TABLEAU III résume les consommations énergétiques correspondant aux quatre modes d'activation

choisis précédemment.

Tableau III

		Consommation énergétique			
		B Surbroyage	F Fluidification	E Etuvage	A Accélérateur ($CaCl_2$)
Coût spécifique en énergie		20 KWh par tonne pour $\Delta S = 1000 cm^2/g$ (au voisinage de $4000 cm^2/g$)	33 Kg de fuel et 50 KWh par tonne d'adjuvant naphtalénique **	60 KWh électrique ou 25 à 45 litres de fuel pour chauffage par chaudière pour 1 m^3 de béton	1,36 Kg de fuel et 40 KWh par tonne de $CaCl_2$ **
Kg de fuel (0,25 kg/kWh)	par tonne de ciment	5 Kg	1,1 Kg	37,5 Kg ou 62,5 à 112 Kg	2,9 Kg
	par m^3 de béton *	2 Kg	0,5 Kg	15 Kg ou 25 à 45 Kg	1,2 Kg

* dosé à 400 Kg de ciment m^3 — ** 2 % d'adjuvant en poids de ciment

On peut noter l'intérêt évident des adjuvants avec toutefois la réserve faite en 3.23 dans le cas d'exigences à très brève échéance (6 à 8 heures par exemple).

La relation (3) du paragraphe 2.1 peut en définitive s'écrire :

Fabrication du ciment — Utilisation

$$E = \alpha\left[C_1 + (K.a.C_2)\right] - \left[KC_1\frac{\Delta S}{1000} + (aC_4d) + \frac{K}{\gamma}(C_5 + C_6) + \Sigma\,\beta_i.C_i\right] \qquad (6)$$

Cuisson — Broyage du cru — Surbroyage du ciment — Transport des ajouts — Traitements thermiques du béton — Adjuvants

Economies — Dépenses supplémentaires

Outre la signification des symboles déjà donnée en 2.1 on a :

γ : dosage en ciment (tonne/m^3 de béton),
β : dosage en adjuvant "i".
C_i : consommation d'énergie pour élaborer l'adjuvant "i".
C_5 : consommation en kWh/m^3 * pour chauffer le béton frais.
C_6 : consommation d'énergie pour étuver le béton.

(* ou en kg de fuel, il faut alors supprimer k)

Un calcul simple montre que l'économie faite par l'incorporation de 25 % de sous-produits est voisine de 24 kg de fuel par tonne de ciment mais le terme négatif pourra atteindre 40 kg de fuel en cas d'étuvage électrique d'un béton dosé à 400 kg/m^3. Le bilan est donc fortement négatif dans ce cas (le surbroyage ne comptant que pour 2 kg).

5 CONCLUSION

Il semble résulter que l'"activation" des liants à ajouts qui économisant l'énergie en fabrication passe par le surbroyage (éventuellement séparé) et par la recherche d'adjuvants de durcissement et de fluidifiants ainsi que par l'association de ces différents moyens entre eux, les procédés thermiques devant être réservés aux cas (à limiter dans la mesure du possible à des besoins très particuliers) où des résistances élevées sont indispensables après quelques heures.

L'avenir sera sans doute dans l'étude de nouveaux procédés d'activation, dans la recherche d'adjuvants plus efficaces et dans la conjugaison des différents moyens d'action.

Fuel oil saving by IHI-SF precalciner-kiln process

Economies de combustible pétrolier au moyen du procédé IHI-SF au four de précalcination

N. NAKAMURA, Manager, Cement Plant Engineering Department, Ishikawamima-Harima Heavy Industries Co, Ltd, Japan.

SUMMARY : The application of NSP kilns has seen rapid increase in recent years. Pioneer manufacturer of NSP kilns, IHI has already delivered 50 units of its SF system kilns in eight years since 1971, when the IHI-SF precalciner kiln process was developed by IHI.

Ever since the first installation of a commercial SF plant, IHI has spent much effort in further reducing fuel consumption through a number of improvements brought to the process and component equipment. To meet the needs raised by the spiralling rise in oil prices and the accompanying instability of supply sources, IHI has developed new combustion techniques associated with the SF process, to open the way to the utilization of substitute materials such as spoil from coal mines and oil shale, as well as coal to replace part or all of the petroleum fuel hitherto used as heat source.

The heat required to produce 1 kg of cement clinker is about 800 kcal. This specific heat consumption, hitherto depending almost entirely on petroleum fuel, can be reduced with application of the IHI-SF kilns adapted to burn substitute combustible matter, as evidenced by the following successful examples:

1) Use of spoil from coal mines to replace part of the clay, with savings in oil up to 50 kcal/kg clinker.
2) The realization of a 3 000 t/d IHI-SF kiln designed to burn 100% coal, which is providing completely stable operation.
3) Development of a kiln to utilize oil shale as clay substitute, which promises oil savings amounting to 400 kcal/kg-clinker. An industrial installation incorporating the results of this development, of a capacity of 4 000 t/d, is expected to be completed in October 1980.

RESUME : L'application des fours NSP (nouveau système de préchauffage à particules en suspension) a vu une augmentation rapide au cours de ces dernières années. Première à se lancer dans la fabrication des fours NSP, la société IHI a déjà fourni 50 exemplaires de son système SF dans les huit ans depuis 1971, l'année dans laquelle le procédé IHI-SF de four à précalcination a été mis au point.

Depuis la réalisation de la première installation commerciale d'un four SF, la société IHI s'est évertuée à réduire davantage la consommation de combustible, au moyen de maintes améliorations apportées au procédé et à ses éléments constitutifs. Afin de prévenir les besoins suscités par la montée en flèche des prix de pétrole, et l'instabilité concomitante de la disponibilité de cette source d'énergie, l'IHI mit au point de nouvelles techniques alliées au procédé SF, qui ouvrirent la voie à l'utilisation des succédanés tels que déblais de houille, schiste bitumineux, aussi bien que la houille, pour remplacer tout ou partie du pétrole utilisé auparavant en tant que combustible.

La chaleur requise pour produire 1 kg de clinker s'élève à 800 kcal. Cette consommation spécifique, qui dépendait auparavant presqu'entièrement du pétrole, peut être réduit en appliquant le procédé IHI-SF adapté à brûler ces succédanés, témoin les exemples réussis de:-

1) L'utilisation du déblais de mine de houille, pour remplacer une partie de l'argile en tant que matière première, ce qui a réalisé des économies s'élevant jusqu'à 50 kcal par kg de clinker produit.
2) La réalisation d'un four de 3 000 t/j conçu pour brûler la houille à 100%, et qui fonctionne avec une stabilité complète.
3) Mise au point d'un four utilisant le schiste bitumineux en tant que succédané d'argile, qui promet une économie de pétrole s'élevant à 400 kcal/kg de clinker. Une installation industrielle comportant les résultats de ces études, d'une capacité de 4 000 t/j doit être achevée en octobre 1980.

1. INTRODUCTION

Since the commissioning in 1971 of a 2000 t/d SF kiln plant by Ishikawajima-Harima Heavy Industries Co., Ltd. (IHI), the advantages of the SF Process have come to be highly appreciated by the cement industry, and fifty IHI-SF kilns have already been installed within a period of 8 years.

The experience gained with numerous SF kiln plants has served as basis for IHI to develop a new SF Process (NSF), of which the first unit successfully entered service in 1979. The aim held in view in developing the NSF was to further reduce its fuel consumption, and the development has been accompanied by many new features incorporated in the cyclones, clinker coolers and other equipment to become an outstanding energy-saving process.

The present paper covers an outline of the SF and NSF Processes, followed by descriptions of examples in which these Processes have been applied to firing spoil, coal, oil shale and other fuel to substitute heavy oil.

2. DESCRIPTION OF PROCESS

2.1. Original SF Process

The equipment of the original IHI-SF Process comprises: Suspension preheater such as in the conventional preheater processes, calcining furnace called "Flash Furnace", rotary kiln and clinker cooler (Fig. 1). The raw meal fed to the uppermost (first) stage is gradually heated up to 750°C as it passes through the three preheater stages; the preheated raw meal is then fed into the Flash Furnace -- the main feature of the SF Process.

The Flash Furnace is constituted mainly of a reaction chamber (upper part) and a vortex chamber (lower part). The raw meal inlet is located on the ceiling of the reaction chamber, and multiple burners are arranged horizontally round its lower part. Combustion air for the Flash Furnace is provided by air heated to about 750°C in the clinker cooler. The heated air is introduced into the reaction chamber of the Flash Furnace through the vortex chamber below, where it mixes with the kiln gas.

About 60% of the overall fuel consumption of the clinker burning process is utilized in the Flash Furnace, and the raw meal is calcined to 85 - 90% before proceeding toward the kiln. After leaving the Flash Furnace, the calcined meal passes into the rotary kiln through the last-stage cyclone, where it is separated from the gas.

The remaining 40% of the fuel is fired in the front end of the kiln, where it is mixed with combustion air heated to about 1 050°C in the hot end of the clinker cooler.

The clinker cooler is so arranged to supply the hottest air to the rotary kiln, where the highest temperature is required for the sintering, and to send the next hottest to the Flash Furnace through the air duct.

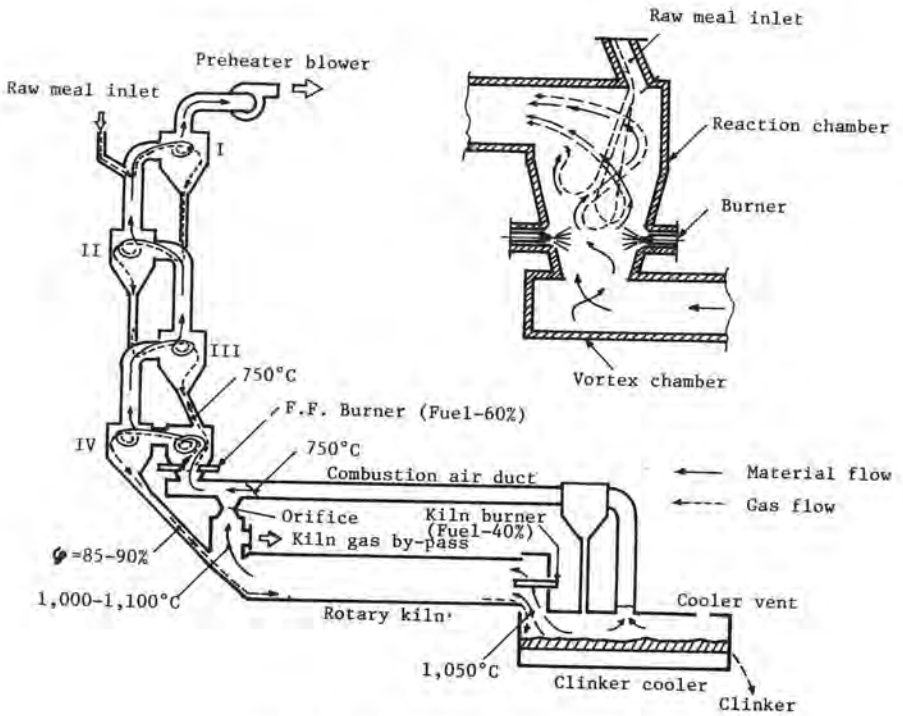

Fig. 1 Flow sheet of SF Process

2.2. Energy Saving Provided by the NSF

2.2.1. The new Flash Furnace

The aim held in view in developing the NSF Process was to answer the current needs of energy conservation and conversion from heavy oil to coal and other substitute fuels.

The difference between the original and new Flash Furnaces are as follows (see Fig. 2):

(1) The hot air from the cooler is introduced through the vortex chamber separately from the kiln gas; the kiln gas joins the hot air, rising vertically upward from the riser duct.

(2) A large part of the raw meal is fed into the flue gas in the riser duct.

(3) The fuel is injected into the vortex chamber by burners arranged to ensure ignition of the fuel by the swirling hot air.

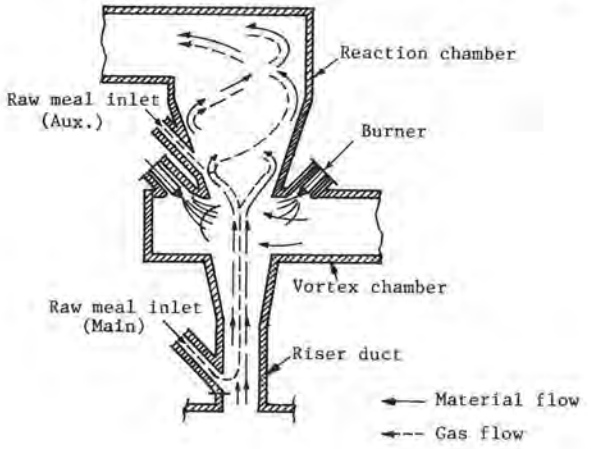

Fig. 2

This new arrangement of the Flash Furnace ensures more stable combustion of the fuel, and the enhanced thermal efficiency of the new Flash Furnace provides for reduced fuel consumption; it also opens up possibilities for the firing of coal and other substitute fuels more difficult to burn, without requiring to increase furnace size.

The first industrial NSF unit was installed at the Ibuki Works of the Osaka Cement Company, and entered service in February 1979, since when this 3 000 t/d plant is operating to the owner's full satisfaction.

Figure 3 outlines the NSF production line of this Works. The temperatures indicated in this diagram for the outlets of the four cyclones represent a lowering of 20 - 30°C compared with the corresponding temperatures of the original SF, and the heat consumption has registered a rate as low as 740 - 750 kcal/kg-clinker.

Another notable feature of this plant is -- as shown in Fig. 3 -- the provision of a gas circulating grate cooler, combined with a waste-heat boiler, to ensure energy economy of the Works as a whole.

The grate cooler, of horizontal three-stage type, is equipped with a breaker between its second and third stages. The heated air issuing at about 260°C

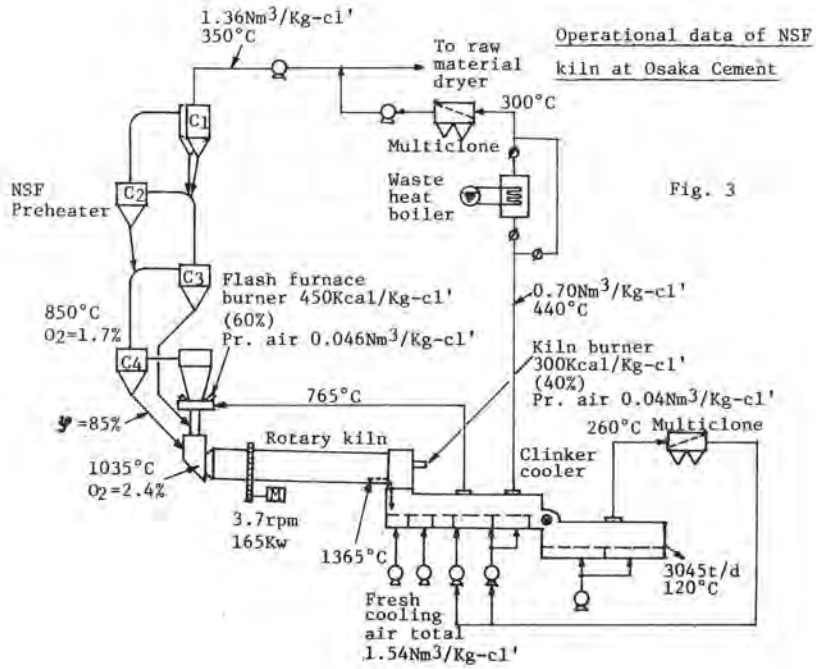

Operational data of NSF kiln at Osaka Cement

Fig. 3

from the third stage of this cooler is cycled back into the second grate, to be further heated to about 440°C. The heat acquired by this air is recovered, first in a waste heat boiler, where it cools to about 300°C. The air then joins the exhaust gas from the preheater and is used in the raw meal dryer for secondary heat recovery.

In the present instance, the waste heat boiler serves to supply utility steam, but if the boiler were used for generating power, its capacity should suffice to furnish all the electric power consumed by the cooler and ancillary equipment.

2.2.2. Low pressure loss cyclone

To improve preheater performance, the most straightforward means is to increase the number of cyclones. This however would increase the loss of pressure in the precalcining stages, resulting in increased power consumed by the induced-draught fan. With an orthodox cyclone design, four stages is usually the limit for optimum overall economy.

To increase the number of stages while maintaining overall energy economy, IHI developed the extra low pressure loss cyclones shown in Fig. 4.

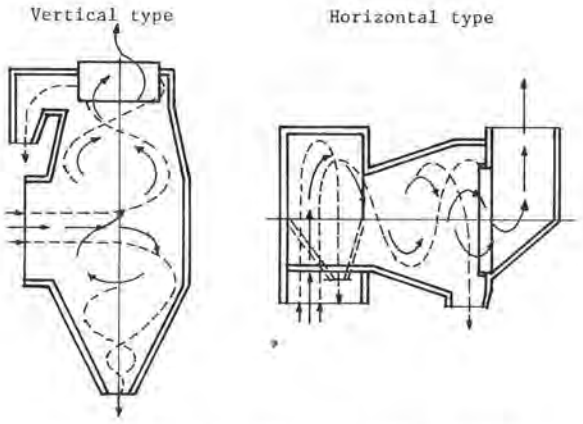

Fig. 4 Figure of low pressure loss cyclone

The performance of these cyclones is presented in Fig. 5. The plots reveal that, as compared with conventional cyclones, the new types provide significantly lower values of pressure loss, at a small sacrifice of cyclone efficiency.

In the NSF system, these new low pressure loss cyclones are planned to be adopted for the intermediate stages, while the conventional models will be retained for the top and lowest stages, where the cyclone efficiency is of consequence.

Two actual plants have been trially equipped with the new cyclones in the second stage of a five-stage preheater system. Both plants are operating satisfactorily, and are providing the expected performance, as evidenced by a fuel consumption of 720 kcal/kg-clinker for a throughput of 2 400 t/d.

3. FIRING WITH SUBSTITUTE FUELS

3.1. Spoil

Spoil, accompanying mined coal, has a chemical composition that parallels clay, and also contains some coal. It has a heating value of around 1 000 kcal/kg, which could be effectively utilized to economize fuel consumption, if spoil were used to replace part of the clay as raw material.

The spoil is ground together with the other raw materials and charged into the first stage of the preheater. The amount of spoil charged would depend on the composition of the spoil; it is usually limited to about 100 kg/t-clinker, beyond which it is liable to raise the impurity contents in raw meal to the extent of causing clogging trouble in the cyclones and to increase the exhaust gas temperature, with concomitant loss of heat.

The spoil passing through the preheater hardly burns in this stage, on account of the low content of available oxygen, while it burns completely upon entering the Flash Furnace. Some amount of volatile combustible matter contained in the spoil will inevitably be lost from the preheater, but despite this loss, the savings in fuel oil obtained with the use of spoil can amount to 30 - 50 kcal/kg-Cl.

3.2. Coal

In cooperation with the Mitsui Mining Company, IHI has been performing tests on pulverized coal combustion in the Flash Furnace, using the pilot plant in the IHI Research Institute.

These tests proved that with the old type Flash Furnace, coal could not provide combustion performance equal to that of heavy oil, but excellent results were obtained on coal with the NSF Furnace. These results have induced Mitsui Mining to reconstruct their 5.0m dia. x 75m long Repol Kiln of

Fig. 5

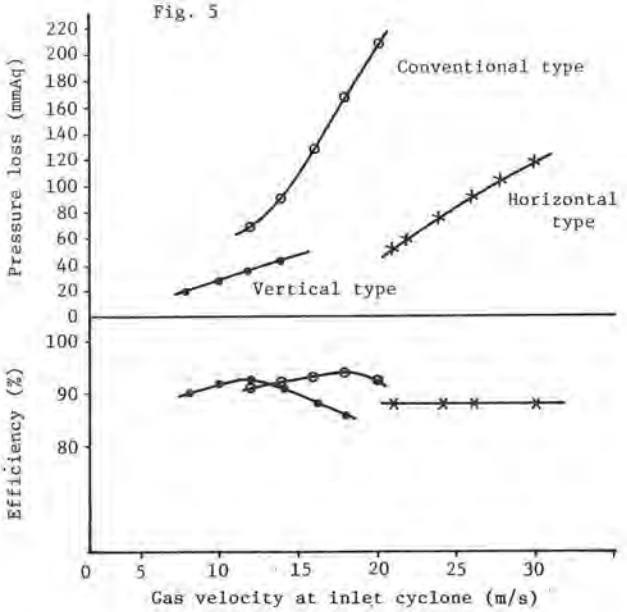

Fig. 6

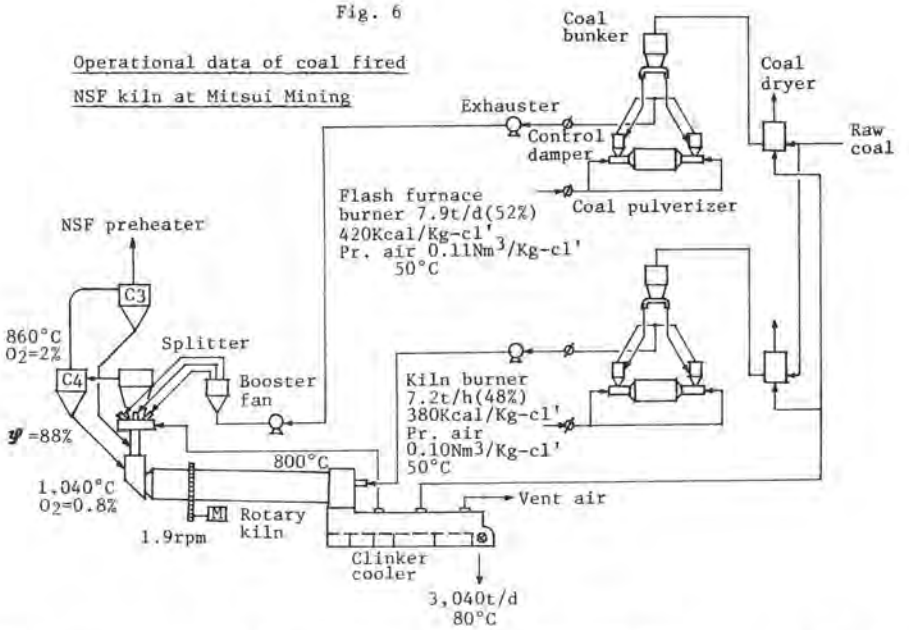

2 000 t/d capacity to incorporate the NSF Process arranged for coal firing, and have its capacity increased to 2 700 t/d.

A throughput of 5 000 t/d would have been possible with this size of kiln by incorporating the NSF Process, but the capacity was limited to the above figure, with the view of utilizing the already existing coal grinding mill and other ancillary facilities. The plant entered operation in April 1979, and has since been satisfying all expectations, with a sustained throughput exceeding of 3 000 t/d, representing the maximum design capacity.

The operating characteristics of the coal-fired installation are as indicated in Fig. 6.

3.3. Oil shale

Oil shale is produced in South-East Asia, Latin America, Canada and other countries. Its composition is almost identical with the clay used in cement manufacture, added to which it contains a considerable amount of petroleum, so that it is very aptly suited for use as substitute for clay with the aim of economizing fuel oil.

Following basic experiments conducted on oil shale, IHI proceeded with tests on oil-shale-fired cement manufacture with use made of the Research Institute pilot plant, to develop a process that has been incorporated in a 4 000 t/d plant now under construction.

Figure 7 represents the schematic flow sheet of this plant. It is seen that before being charged into the preheater, limestone and oil shale are processed separately. We will here limit our description to the treatment of oil shale.

The wide fluctuations in quality -- a general property of oil shale -- requires it to be blended in a mixing bed, to stabilize its quality. The moisture content also calls for drying before charging into grinding mill.

In the grinding mill, the oil shale is mixed with iron, sand and other additives, whose amounts are

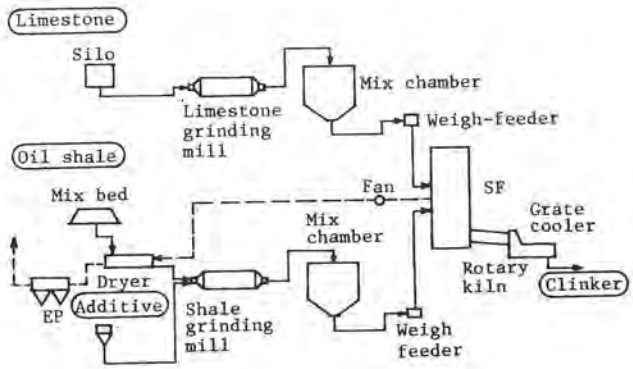

Fig. 7

determined according to the quantities and composition of the limestone being treated separately, in order to place within a given range the values of H.M., S.M., I.M. and L.S.D. to produce cement clinker of the required quality.

The previously ground and blended oil shale is further mixed and stored in the mix chamber, before being fed into the preheater via a weigh feeder of high accuracy. The final proportion between limestone and oil shale to be fed into the SF is determined by the chemical composition of the mixture issuing from the mixing chamber. This regulation is automatically ensured by a feed-back circuit incorporating an automatic sampling device and continuous X-ray analyzer connected to a computer.

The foregoing regulation of the feed rate of oil shale would naturally affect the amount of heat generated by this oil shale, but fluctuations in the heat generation in SF are offset by automatic control of the oil burners in the Flash Furnace.

The amounts of oil saving foreseen with the use of oil shale in the plant are as follows:-

- Calorific value of oil shale: 600 - 1 000 kcal/kg-shale
- Total raw meal feed required: 1.6 kg-raw meal/kg-clinker
- Mixing ratio of shale: 25%.

Hence, the calorific value of oil shale burned to obtain 1 kg of clinker is:

(600 - 1 000)x1.6x0.25 = 240 - 400 kcal/kg-clinker.

Repeated tests with the oil shale in an experimental installation have proved that, with a modified IHI-SF Process, the heat carried by oil shale, as represented by the calorific values cited above, can be utilized to 100%.

The total heat required to produce 1 kg of clinker is about 800 kcal, meaning that economies in fuel oil up to 30 - 50% can be expected with the adoption of the IHI-SF Process arranged for utilizing oil shale.

This 4 000 t/d industrial unit under construction is expected to enter service in October 1980. Its performance, expected to fully meet the design values, will be reported on a future occasion.

3.4. Other substitute fuels

Apart from the various fuels described above, various other substitutes are being actually utilized in SF kilns. Examples include used tyres, waste powdered coke, sludge, bark. Used tyres, in particular, are being utilized by many cement manufacturers in Japan. The oil savings obtained are reported to be 20 - 30 kcal/kg-clinker.

The procedure for feeding kilns with used tyres is to manually feed the material through a gate provided on the kiln inlet chamber between kiln and preheater. From this gate the tyres pass into the kiln. The tyres are raised to the chamber floor by means of a lift available for persons and cargo. The supply of used tyres is ensured by a car scrapping company which offers to deliver the tyres free of charge, as a means of disposal of what to them is unwanted waste.

The current oil situation points toward increasing prices of petroleum combined with continuing instability of supply, so that the range and quantities of petroleum substitutes for fuelling cement kilns would be expected to increase with the years to come. To meet this situation, IHI is continuing its efforts to improve the NSF Process with the view of further enhancing the versatility of this Process.

L'utilisation des additifs aux différents stades du processus peut apporter une économie importante d'énergie lors de la fabrication du ciment

The use of additives at different stages of the process can bring in an important economy of energy at the time of cement manufacturing

F. FIALA, Directeur des Etudes, Travaux et Recherches - S.A. Ciments d'Obourg,
A. RIVAL, Ingénieur Développement, Belgique.

Les additifs peuvent intervenir à deux stades différents de la fabrication du ciment :

1. Lors de la préparation du cru en voie humide, il est possible de diminuer la teneur en eau de la pâte en moyenne de 25 % en valeur relative, tout en maintenant ses caractéristiques rhéologiques . Cette réduction d'eau s'obtient par addition de produits chimiques à la pâte dans des proportions variant de 0,01 à 0,06 % . L'efficacité du carbonate de soude est connue depuis longtemps, mais, actuellement, on utilise aussi des lignosulfites, des polyphosphates ou d'autres composés mais toujours associés au carbonate de soude . Pour chaque cru, il faut déterminer qualitativement et quantitativement les additifs qui, économiquement, donneront le meilleur résultat . Vu que la composition chimique et minéralogique des matières premières varient dans le temps en fonction de l'avancement de leur extraction, la consigne relative aux additifs devra être revue soit en fonction d'une étude préalable du gisement, soit lorsque des variations significatives de la teneur en eau de la pâte auront été mise en évidence . Il semble que l'action des additifs ait lieu au niveau des micelles et soit liée à la nature minéralogique de la fraction argileuse du constituant principal du cru, la craie ou le calcaire . Une variation des forces électrostatiques au voisinage des particules en suspension déterminerait le mode d'action de ces additifs en réduisant l'épaisseur moyenne du film d'eau entre ces particules .

Pour un four donné, la diminution de la teneur en eau de la pâte dans les proportions ci-dessus modifie le comportement rhéologique de la matière en voie de déshydratation, l'allule de cette dernière et le dégagement de poussières . La conception des échangeurs de chaleur de ce four devra être modifiée en fonction du pourcentage d'eau qui aura été atteint .

L'économie d'énergie réalisée dépendant de plusieurs facteurs, comme de la teneur en eau avant et après l'emploi d'additifs, la température des fumées à la sortie du four, la quantité de poussières dégagées, l'aptitude à la cuisson de la matière crue, il n'est pas possible de la chiffrer d'une manière générale . On peut néanmoins l'estimer, suivant les cas, entre 10 et 15 % de la consommation énergétique totale nécessaire pour la cuisson en voie humide . L'économie ainsi réalisée pourrait varier entre 540 et 800 kJ par kg de clinker .

2. Lors de la mouture du ciment, l'emploi d'adjuvants, adaptés à la nature chimique et minéralogique du clinker, conduit à une diminution de la consommation spécifique d'énergie pouvant aller de 10 à 15 %, ce qui représente, pour un ciment ordinaire, 11 à 16 kJ/kg Ces adjuvants, qui agissent à des dosages sur clinker compris entre 0,01 et 0,1 %, peuvent être des amines ou des sels d'amine, des polyols, des lignosulfites ou des acides organiques faibles . Ils ne sont pas décomposés à la température de broyage et n'ont pas d'action importante sur les résistances des mortiers et bétons . La quantité d'adjuvant nécessaire semble augmenter avec la finesse du ciment .

Leur mode d'action serait le suivant :

Ils évitent le colmatage des boulets et des plaques de blindage . Ils empêchent la formation d'agglomérats contenant à la fois des particules fines et des particules grossières . Il en résulte une augmentation de l'efficacité des séparateurs à air .

Lors de leur emploi, il y aurait réduction des forces électrostatiques sur le blindage, les boulets et les particules de matière broyée .

Les adjuvants améliorent également les propriétés d'écoulement des ciments, ce qui entraîne une diminution de la consommation d'énergie lors de leur soutirage et de leur manutention .

Il faut remarquer que l'air humide est un adjuvant : il facilite l'évacuation des fines particules, diminue le temps de séjour de la matière dans le broyeur et concourt au refroidissement de celle-ci . La vitesse de l'air dans le broyeur ne peut dépasser 1,8 m/sec. Le solde de chaleur sera évacué par l'évaporation de l'eau injectée dans le broyeur .

La solution idéale consiste à combiner, dans un circuit de mouture, l'emploi d'un adjuvant avec une augmentation du débit de ventilation ; l'adjuvant empêche l'agglomération des fines particules et l'air de ventilation les entraîne hors du circuit de broyage .

Une connaissance plus approfondie de leur mécanisme d'action devrait aboutir à une diminution plus importante de la consommation spécifique des installations de mouture .

Pour conclure, on peut dire que les économies d'énergie les plus importantes s'obtiendront, pour la fabrication du ciment en voie humide, par la réduction de la teneur en eau du cru, et, pour la fabrication en voie sèche, par la diminution de la consommation spécifique d'énergie lors de la mouture .

Intensification of the burning process by using components with high exergy in the raw mix

Augmentation du processus de cuisson par utilisation des composés à haute énergie dans les matières premières

N.P. KOGAN, Candidate of Technical Science,
O.P. MCHEDLOV-PETROSYAN, Doctor of Technical Science, Yuzhgiprotsement, USSR.

SUMMARY: The method of exergic analysis is used for technical evaluation of oxides and compounds which are contained in cement raw mix components. This method enables the determination of maximum work of the substance in the process, the final state of which is determined by conditions of thermodynamic equilibrium with the surrounding medium. The normal chemical exergy has been calculated from the phase composition. Increasing of Al_2O_3- and C_2S-content in slags causes substantial increase of slag exergy. Iron in the form of FeO possesses much greater exergy than in that of Fe_2O_3. Materials with greater exergy, able to melt at lower temperatures and to form silicate melts with low viscosity, can be used in raw mixes as coarse-grained components thus forming an independent physico-chemical system. Slag enthalpy determined by M.A. Pavlov's formula includes heat consumption for heating them to the melting temperature. Calculations have shown that slag admixture to the cement raw mix increases heat capacity and enthalpy of the liquid phase.

Classical method of thermal balances is known to be based on the first thermodynamic law - the law of energy conservation and transformation. According to the second thermodynamic law, the state of chaos and entropy of a closed system, containing a great quantity of individual particles with irregular movement, can be increased or remain unchanged. In such a system there can proceed spontaneously only processes which approach it to the equilibrium state. The exergic method of making out the process balance takes into consideration the second thermodynamic law. While being the measure of potential resources exergy defines the maximum technical ability of the substance to fulfil the work in the process, the final state of which is in thermodynamic equilibrium with the surrounding medium. In the given technological process the normal chemical exergy of compounds (reaction products) is that they must be taken out of the process, as it happens e.g. with blastfurnace slag during cast iron production. However in another process the exergy of such compounds can be still utilized with great technical-and-economical efficiency.

The paper /1/ doesn't give the value of the normal chemical exergy of raw mix components and doesn't take into account devaluation compounds and reactions.

For technical evaluation of oxides and compounds of cement raw mix components we have used the method of normal chemical exergy calculation developed by Ya. Shargut /2/. Devaluation reactions of compounds of reference have been made out on data /2/ for gaseous and solid compounds that may be components and reaction products of clinkering.

While making out devaluation reactions of individual components or clinkering process as a whole it is necessary to take into consideration the phase composition. Carbonate rocks are supposed to contain SiO_2 admixture represented by quartz, MgO represented by carbonate $MgCO_3$. In clayish compounds SiO_2 is combined into aluminosilicates and can partially be in the form of quartz.

The phase composition of metallurgical slags was defined on the basis of X-ray and petrographic determinations.

For calculation of normal chemical enthalpy of devaluation reaction there has been made out the normalized reaction in which compounds appear at $T_n = 298.15$ K and $P_n = 0.101$ N/mm^2.

The following formula was used for calculation of enthalpy of chemical compound devaluation

$$d_n = i_n + \sum_j I_{nj} - \sum_k I_{nk} \qquad /1/$$

where:

d_n = devaluation enthalpy in kJ/kmol;

i_n = normal specific (i.e. absolute) enthalpy of the considered compound in kJ/kmol;

I_n = normal enthalpy of the compound of reference (per unit of the considered compound quantity);

j,k = indexes of additional and resulting compounds of reference.

Values of standards enthalpy of compound formation from elements H_{298} are taken from the monograph /3/.

The entropy of devaluation reaction was determined according to the formula:

$$\sigma_n = s_n + \sum_j s_{nj} - \sum_k s_{nk}, \qquad /2/$$

where:

σ_n = normal devaluation entropy of compound considered in kJ/kmol·K;

$\sum_j s_{nj}$, $\sum_k s_{nk}$ = the sum of normal chemical entropies of initial and final compounds in kJ/kmol·K.

When table values of normal entropies of solid compounds are absent S°_{298} is determined according to the formula /4/:

$$S^\circ_{298} = A \lg M + B, \text{ kJ/kmol·K} \qquad /3/$$

where M is molecular weight; A and B are constants characteristic for each kind of compounds.

Free devaluation entropy is determined as difference between the devaluation entropy and the product of (298.15 x σ_n).

The normal chemical exergy of chemical compounds of initial and final products of clinkering process is determined according to table data /2/. In case of absence of proper data this exergy is determined according to the formula:

$$l_n = d_n - T_n\sigma_n - R_u T_n\left(\sum_j n_j \ln k_j - \sum_k n_k \ln k_k\right) \qquad /4/$$

The latter member in this equation denotes residual chemical exergy.

Table 1 shows calculation results of normal chemical exergy of materials for cement production according to literature data /2/ and to our own calculations.

On the basis of data indicated it is possible to make out the normalized clinkering reaction in which components content in mols is used as initial compounds; clinker minerals, CO_2, and H_2O content in mols is used as final products. On the basis of this equation it is easy to determine the theoretical heat consumption and the normal chemical exergy. The most devaluated initial compounds obviously give the maximum theoretical heat consumption.

The exergy of compounds forming slags composition is greater than that of raw mix natural components. Calcium silicates, calcium aluminosilicates, and magnesium silicates contain the main quantity of slags

exergy. The exergy increases with CaO content. The exergy of FeO is much greater than that of Fe_2O_3.

Materials with greater exergy, able to melt at lower temperatures and to form silicate melts with low viscosity, can be used in raw mixes as coarse-grained (unground) components thus forming an independent physico-chemical system /5/. This is accompanied by liquid phase changes in quality and quantity and substantial acceleration of heat-and-mass transfer.

The greater quantity of the liquid phase with increased heat capacity and enthalpy under clinkering conditions in a rotary kiln allows substantial decrease of energy consumption during clinker production. Adding unground slags with great exergy into raw mix results in theoretical heat consumption of less than 880 kJ/kg of clinker.

CONCLUSION

Technical evaluation of cement raw materials and of burning process products is made on the basis of exergic analysis. Natural components exergy is shown to be substantially less than that of waste products of pyrometallurgical industry.

Theoretical heat consumption for clinkering mixes containing compounds with increased exergy is sustantially lower than that for clinkering mixes composed of natural materials.

Materials with increased exergy can be used in raw mix in unground form permitting the decrease of not only specific heat consumption for clinker burning but also energy consumption for raw mix preparing.

BIBLIOGRAPHY

1. - FRANKENBERGER (1967). "Die exergtische Beurteilung des Zementbrennens", Zement-Kalk-Gips, N1, S. 24-30, Deutsch.
2. - Ya. SHARGUT, R. PETELA (1968). Exergy, Russian.
3. - V.I. BABUSHKIN, G.M. MATVEYEV, O.P. MCHEDLOV-PETROSYAN (1962).
4. - Chemist's reference book (1963), v. I, Russian.
5. - N.P. KOGAN, O.P. MCHEDLOV-PETROSYAN, A.I. ZDOROV, N.F. DREPIN (1978). "Intensification of cement clinker production process due to the burning of raw mix consisting of independent initial physico-chemical systems", DAN, v. 238, No. 2, p. 408-410, Russian.

.../...

Table 1

Free Devaluation Enthalpy and Normal Chemical Exergy of Cement Materials and Burning Products

Compound	Free devaluation enthalpy, kJ/kmol	Normal chemical exergy, kJ/kmol
Carbonate components		
$CaCO_3$ - calcite	0	12430
$CaCO_3$ - aragonite	+1080	13470
$MgCO_3$	0	14160
$CaCO_3 \cdot MgCO_3$ - dolomite	-12664	13904
$CaSO_4 \cdot 2H_2O$ - gypsum	0	25820
$CaSO_4$ - anhydrite	+18280	20570
$CaCl_2$	+90000	98700
Clayish components		
$Al_2O_3 \cdot 2SiO_2 \cdot 2H_2O$ - kaolinite	120695	139824
$Al_2O_3 \cdot 2SiO_2 \cdot 4H_2O$ - halloysite	130427	171224
$Al_2O_3 \cdot 4SiO_2 \cdot 2H_2O$ - montmorillonite	63042	107563
$Al_2O_3 \cdot 2SiO_2 \cdot 2H_2O$ - dickite	115972	156770
$KAl_3Si_{10}(OH)_2$ - muscovite	43740	89977
Slags and ferriferous additives		
$3Al_2O_3 \cdot 2SiO_2$ - mullite	+294561.97	338914
$CaO \cdot SiO_2$ - wollastonite	+40710	34810
$2CaO \cdot 2SiO_2 \cdot MgO$ - akermanite	+133632.75	115818
$2CaO \cdot Al_2O_3 \cdot SiO_2$	+249215.78	2499090
$CaO \cdot MgO \cdot SiO_2$	+75361.38	63449
$MgO \cdot Al_2O_3$ - spinel	+152021.86	159555
$2MgO \cdot SiO_2$ - forsterite	+151590	141430
$MnO \cdot SiO_2$	+85810	106800
Fe_3O_4 - magnetite	+97400	126960
Fe_2O_3 - hematite	0	20370
$FeCO_3$ - siderite	+91040	120410
Burning process products		
$3CaO \cdot SiO_2$	+273420	251990
$2CaO \cdot SiO_2$	+137570	123900
$3CaO \cdot Al_2O_3$	+591240	581490

.../...

Table 1 (continued)

Compound	Free devaluation enthalpy, kJ/kmol	Normal chemical exergy, kJ/kmol
$4CaO \cdot Al_2O_3 \cdot Fe_2O_3$	+794469	797320
$12CaO \cdot 7Al_2O_3$	+2733003	2734624
$CaO \cdot Al_2O_3$	+339820	334050
$CaO \cdot Fe_2O_3$	+52130	64730
$2CaO \cdot Fe_2O_3$	+223220	228070
SiO_2 - crystobalite	+1420	3280
CaO	+129960	122170
MgO	+6553	59610
MnO_2	0	21110
CO_2	0	20170
H_2O	-8620	3150

On reduction of fuel consumption during burning of cement clinker

Sur la réduction de consommation de combustible pendant la cuisson du clinker de ciment

O.I. AVRAMENKO, Candidate of Technical Science,
A.I. ZDOROV, Candidate of Technical Science,
V.M. KOPELIOVICH, Candidate of Technical Science, Yuzhgiprotsement, USSR.

SUMMARY: Results of investigations ensuring fuel consumption decrease for cement clinker production through slurry moisture decrease, intensification of slurry drying and dehydration by means of heat-exchanging units, kiln rotation speed increase, proper fuel combustion, and utilization of kiln secondary heat are given.

Kiln rotation speed increase is found to favour heat exchange particularly in processes with great endothermal effect and to increase total heat transferred to the material by 10% on average.

Proper fuel combustion is achieved by gas burners with diffusion flame position and length control what affects clinker size distribution.

Process regularities found are given.

Various methods of fuel saving for clinker burning in rotary kilns have received wide use in the cement industry of the U.S.S.R.

One percent decrease of slurry moisture content (W_{sl}) decreases fuel consumption for burning by 28 - 35 kcal per kg of clinker or by 1.7 - 2 % /I/, since in a W_{sl} range of 36-48 % the heat consumption for water evaporation varies from 550 to 900 kcal/kg.

The decreasing of moisture content is most advantageous at $W_{sl} > 40$ %, since a relative quantity of evaporating water at this value is higher.

When mechanical methods of dewatering are used, so called partial dewatering seems rational. Average moisture content of thus treated raw mix fed into the kiln is 30-35 %. In this case, a required filtration area substantially decreases and the process gets simplified.

The use of thinning agents is the cheapest way of decreasing W_{sl}. Depending on raw materials kind, on account of thinning agents based on human acids, W_{sl} can decrease by 3-7 %, which saves 6-10 % fuel. Addition of sulcor, oxidated lignine, sodium metasilicate and others can decrease slurry moisture content by 4-9.5 % /2/.

As for intensification of slurry drying and dehydration by installation of rational heat-exchanging units in rotary kilns, our investigations have shown that it is most effective when a system of built-in heat-exchanging units is used. The system includes a drum-type slurry filter-heater, a chain curtain with a developed surface of heat exchange and a metal cellular heat-exchanger installed in succession. The system worked out ensures stable operation of 4.5 x 170 m and 5 x 185 m kilns with an exit gases temperature of 160-180 °C and 210-230 °C, respectively. That saves 2-2.5 % fuel. In addition, the filter-heater decreases total dust losses from the kiln by 10-15 %.

There are used garland chain systems, curtain systems, in which only one end of the individual length is fastened to the shell, and mixed-type chain systems at the cement plants of the U.S.S.R. Though, compared with the curtain systems, the garland chain systems have higher coefficient of heat emission from a unit of chain surface to material (α_F), the possibility of chain surface (F_{ch}) increase is limited by construction factors (maximum admissible superficial coefficient of suspension density K_F is 3.8 m^2/m^2). As a result, high values of F_{ch}, of volume coefficient of suspension density K_V and of steam removal ρ_B can not be achieved. These three parameters are very important for intensification of kiln operation, especially when W_{sl} is high (more than 42 %). As for the free-ended chain systems, the possibility of K_F and K_V increase is little limited by construction factors. As a result, it is possible to create a large chain surface in kilns, to obtain high values of α_V (the volume coefficient of heat transfer in the chain zone) and ρ_B, to lower easily the exit gases temperature to 160-200 °C (depending on type-and-size of a kiln), to decrease the specific consumption of fuel for burning.

The free-ended chain systems are considerably simpler in operation, erection and repair.

In our opinion, the optimum operation conditions of slurry drying in the chain zone are those, under which material leaves the zone with 2-5 % moisture content and a temperature of not higher than 120-130°C /I/. A material moisture content after the chains of 8 %, and according to the offer of some researchers that of 15-20 %, is not desirable, as already at the material moisture content of 8 % the relative quantity of water not evaporated from the slurry will be 13 % and at that of 15-20 % it will be 27-38 %, respectively. Under such operation conditions the degree of material preparation is artificially limited, the evaporating capacity of the chain curtain is not fully used, while the process of material drying in the hollow kiln is 3-5 times less intensive.

The metal cellular heat-exchanger with reliability protects the discharge part of the chain curtain from burning out and prolongs its service life and at the same time successfully ensures fuller utilization of the kiln inner volume. As the investigations have shown, in the 4.5 x 170 m kilns with a heat-exchanger length of 11.5 m the passing along material heats by 350-400°C; whereas in the hollow kiln the temperature increases only by 70-100°C.

Increase of the kiln rotation speed influences both geometry of the material layer and the very process of thermal treatment. As a result of theoretic analysis the heat rate of the material layer in the kiln has been determined:

$$m = 3a \left(\frac{4\mu_{1,1}^2}{B_1 - C_1 n} + \frac{4\mu_{1,2}^2}{B_2 - C_2 n} + \frac{4\mu_{1,3}^2}{L^2} \right) \qquad (I)$$

where: B_1, B_2, C_1, C_2 = coefficients,

n = rotation speed, s^{-1},

a = coefficient of temperature conductivity, m^2/s,

L = material layer length, m

μ = radicals of the following characteristic equation:

$$\operatorname{ctg}\mu = \frac{L}{B_i} \cdot \mu$$

B_i = Bio criterion.

The equation shows that the heat rate of a body increases with n.

The heat-engineering calculations of n influence on heat transfer and the material

layer thickness in 2.4 to 5 m dia. kilns over the material temperatures range of 115-1300°C have shown that the charge ratio (φ) decreases and the heat quantity transferred to the material (g_M) increases with increase of n. In this case, the minimum increase of g_M is 8-10 % when n increases by 1.5-2 times.

At present, increase of n of various type-and-size kilns with a length from 100 to 185 m is widely spread in the U.S.S.R. That ensures 1-3.5 tph output increase and simultaneous decrease of specific fuel consumption by 2-5 kg per 1 t of clinker.

Improvement of fuel combustion conditions is a practicable way of fuel saving and improvement of kiln operation conditions.

During last 10-15 years in the fuel balance of the U.S.S.R. cement industry the use of fuel oil increased. In this connection, a set of measures has been developed which allows considerable increase of efficiency of fuel preparation and fuel combustion in furnaces:

- development and commissioning of efficient burner units - two-channel fuel-oil burners - in various type-and-size kilns; these burners ensure fine dispersion of fuel oil and its combustion with small α= 1.05-1.1 without chemical underburning. They have a wide control range of flame length and volume;
- rise of temperature of fuel oil heating before combustion to 120-140°C and use of the system for control and stabilization of fuel oil viscosity at a set level (2-3° relative viscosity);
- development of a method for combustion of water-containing fuel oil by making fine-dispersed water-fuel-oil emulsions; the use of these emulsions in rotary kilns gives not only a uniform water distribution in fuel oil, but also almost instantaneous evaporation of dispersed water drops ("microbursts") which considerably intensifies fuel oil dispersion;
- supply of hot aspiring air from coolers into burners as primary air;
- installation of continuously operating fuel oil flow-meters and erection of special stands for their calibration.

Execution of above-mentioned measures will allow saving of 4-5 kg of fuel oil per a ton of clinker.

The "YGC" type gas burner /3/ developed by the Institute "Yuzhgiprotsement" ensures efficient combustion of gaseous fuel. This burner forms the minimum flame divergence angle due to absence of gas flow swirless and due to the new curvilinear shape of the nozzle and the core. The carried out investigations of flame length influence on clinker burning with a constant consumption of natural gas in various type-and-size kilns confirm the possibility of localization of material inadequate preparation by changing the length and position of the diffusion flame and production zones in the rotary kiln without output decrease and fuel consumption increase.

Flame length control with a minimum divergence angle does not cause coating deterioration what promotes lining service life increase and heat losses decrease from the kiln shell into surroundings. Double air passage and increased bed thickness of clinker in the grate cooler ensure heat losses decrease during clinker cooling.

Experimental investigations of clinker cooling in a bed resulted in the equation of heat exchange intensity which is characterized by heat transfer coefficient value (α_F) dependent on cooling air velocity (w), its temperature (T), and equivalent diameter of clinker particles (d):

$$\alpha_F = 4210 \frac{w^{1.29}}{d^{1.59} \cdot T^{0.94}} \cdot \frac{\lambda \cdot \nu^{0.59}}{c^{0.54}} \qquad (2)$$

where:

λ = heat conduction,
ν = kinematic viscosity,
c = heat capacity of air.

Rational cooling of clinker in a bed of 0.5-0.6 m thickness in "Volga-CA" type grate coolers is found to reduce heat losses by 20-30 kcal/kg of clinker.

Complex utilization of kilns secondary heat lost by the kiln shell (10-25 % of total heat consumption), in waste gases (20-25%), in aspiring air from coolers and in clinker (5-10%) can result in substantial decrease of total heat consumption for clinker burning. Installations for recovery of heat radiated from rotary kilns shells operate in the U.S.S.R. providing for annual 15 000-20 000 Gcal heat removal by each installation depending on kiln type-and-size. The characteristic feature of such installations is the possibility for coating formation control and thus for increase of lining durability and of calendar time of kiln operation as a whole.

Above-mentioned methods of fuel saving are recommended for wide use in the future.

BIBLIOGRAPHY

1. - G.S. VAL'BERG, I.K. GRINER, V. Ya. MEFODOVSKII. (1971), "Intensification of cement production", Russian.
2. - V.V. TIMASHEV, L.M. SULIMENKO. (1978), "Fluidization of cement raw slurries", Russian.
3. - I.G. MOS'PAN, B.M. MEL'NIK. (1976), "Rational application of controlled gas burner", Russian.

Economie d'énergie lors de la cuisson du ciment par utilisation intégrale de déchets et de combustibles de moindre qualité

Helmuth RECHMEIER, Diplom-Chemiker,
Portlandzementwerk Dotternhausen, Rudolf Rohrbach KG, RFA.

Resume:
Les procédés modernes de cuisson du ciment permettent d'atteindre des rendements thermiques de l'ordre de 50 %.
Des rendements thermiques plus élevés nécessitent une amélioration considérable du rendement du radiateur. De telles améliorations ne sont pas projetées à l'heure actuelle.

Trois alternatives s'offrent pour une production plus économique du ciment, particulièrement au niveau de ce facteur de coûts qu'est le combustible:

1. L'utilisation de combustibles pauvres permettant un déroulement très rapide de la combustion dans la mesure où l'on respecte les particularités touchant au mélange du combustible avec les gaz d'échappement du four rotatif, à l'échauffement du combustible et au processus de combustion un peu modifié. Ici, l'impulsion de la farine chargée (farine brute, comme combustible) joue un rôle particulier.

2. L'utilisation de combustibles plus riches, tels que les pneus de véhicules, les déchets plastiques, les solvants, etc.. Afin de pouvoir les utiliser et les exploiter de façon optimale, ces combustibles doivent être amenés à une forme aptes à la combustion, ce qui peut avoir lieu par traitement dans la couche fluidisée. L'utilisation de telles matières permet de lier dans le clinker des substances nocives qui, autrement, sont difficiles à éliminer.

3. La production d'additifs hydrauliques au ciment par réaction à l'état solide en dessous de la température de frittage et sans grande consommation de chaleur. Les procédés ayant recours à des matières comportant déjà leur combustible, comme c'est le cas du schiste bitumineux, du calcaire bitumineux ou des schistes de lavage, sont particulièrement avantageux ici.

   Les conditions définies de température et de temps de séjour nécessaires à la production de telles matières peuvent être établies de façon optimale dans une couche fluidisée, laquelle permet également l'utilisation de combustibles à très faible capacité calorique.

   Dans ce procédé, la chaleur excédentaire provenant du lit fluidisé peut servir à la production d'énergie électrique, ce qui favorise l'économie, selon le prix de l'électricité devant être achetée et le pouvoir calorifique des combustibles à utiliser.

Ces trois alternatives sont actuellement utilisees à l'échelle industrielle, ou du moins partiellement, dans les usines de ciment portland, Rudolf Rohrbach KG de Dotternhausen.

La fabrication du clinker est un processus nécessitant beaucoup d'énergie. Les procédés les plus économiques requièrent des quantités de chaleur allant de 3140 à 3350 J par kg de clinker, ce qui correspond approximativement à 75 ou 80 kg de fuel-oil par tonne de clinker.

Le rendement thermique des fours à dispositif de préchauffage par mise en suspension dans les gaz se situe aux environs de 50 %. La chaleur de recuperation est le rayonnement des différentes parties du four, la chaleur perdue du clinker et le gaz perdu à température relativement faible (350 à 360°C) provenant de l'air d'échappement du radiateur et du four.
Le rendement calorifique pourrait être amélioré par un système de radiateur exploitant mieux la chaleur dégagée par le clinker puisque les gas d'échappement du four sont déjà utilisés en grande partie pour le séchage du matériau brut.

Jusqu'à présent, tous les efforts entrepris pour améliorer le rendement des systèmes de radiateur sont restés vains. Il est vraisemblable qu'aucune amélioration sensible ne puisse être actuellement apportée au rendement thermique du système de cuisson du clinker.

Une meilleure rentabilité du procédé de cuisson peut être obtenue par utilisation de combustibles bon marché, tels que les combustibles naturels comme le schiste bitumineux, le calcaire bitumineux et autres ainsi que de combustibles de récupération de haute qualité.
Cependant, le pouvoir calorifique d'un combustible n'est pas le seul facteur déterminant pour le processus, encore faut-il que ce combustible permette d'atteindre la température de flammes nécessaire.

Afin de réduire suffisamment le temps de formation du clinker lors de sa cuisson, il fut que la température de flamme calculée des brûleurs doit dépasser 2000°C.

Une température inférieure à cette valeur peut entraîner des coefficients de transmission thermique si faibles qu'il devienne impossible de cuire du clinker dans le four considéré.

Pour cette raison, les combustibles à très faible pouvoir calorifique ne peuvent donc pas être utilisés dans la zone de frittage car leur faible valeur calorifique ne permettrait pas d'obtenir la température de flamme indispensable.

Afin de tirer malgré tout parti de ces combustibles, ils doivent être utilisés là où une forte énergie thermique est certes exigée mais où la température de flamme requise n'est pas très élevée. Dans la cuisson du clinker, il s'agit ici de la zone de désacidification.
La température nécessaire ici est relativement faible, à savoir de l'ordre de 900° C au maximum.

Il est donc judicieux d'introduire les combustibles de moindre qualité dans l'échangeur de chaleur et de les y brûler. La zone la plus appropriée ici est celle avec la température la plus élevée, à savoir celle qui va de l'admission du four tubulaire rotatif au premier cyclone d'échangeur de chaleur.
Dans cette zone, le combustible doit être échauffé, mélangé à l'oxygène contenu dans le gaz résiduel du four tubulaire rotatif (env. 10 %/vol.) et brûlé.

Les combustibles médiocres ne peuvent brûler dans la zone de réaction pendant leur temps de séjour relativement court (env. 2 s) et libérer leur énergie que s'ils sont intensément mélangés aux gaz, chauffés suffisamment vite et s'ils peuvent entrer rapidement en réaction avec l'oxygène disponible.

Au cas où l'une de ces conditions ne serait pas remplie, l'énergie potentielle serait dilapidée dans l'échangeur de chaleur, ce qui conduirait en fin de compte à une consommation de chaleur exagérée.

Afin d'obtenir un mélange homogène du combustible d'alimentation avec les gaz chauds et visqueux, impulsion nécessaire au mélange doit être procurée au combustible lors de son chargement.

L'impulsion nécessaire ne pouvant pas être transmise au combustible comme dans une flamme au moyen du gaz porteur, il doit être enfourné à une vitesse aussi grande que possible générée par une hauteur de chute importante avant son arrivée dans la zone de combustion et par concentration en un seul chargement.

L'impulsion contenue dans la farine brute de l'étage cyclone suivant à l'entrée dans le réacteur peut être exploitée pour le mélange par une disposition adéquate des deux zones d'admission. La combustion du combustible pauvre ne doit avoir lieu que là où l'énergie calorifique peut être absorbée par désacidification de $CaCO_3$.

Abstraction faite des processus de combustion, la vitesse d'échauffement est étroitement liée au transfert de chaleur entre la gaz et les particules. La plus grande partie du transfert de chaleur consistant, pour les températures en question, en une chaleur rayonnante, la vitesse d'échauffement dépend de la différence de température existant entre le gaz et les corps solides s'élevant environ à $(T)^4$ et peut être calculée selon la formule suivante:

$$Q = C \cdot F \cdot \left[\left(\frac{T1}{100}\right)^4 - \left(\frac{T2}{100}\right)^4\right] J/h$$

L'échauffement des particules est donc extrêmement rapide (une fraction de seconde).

La quantité de chaleur nécessaire à l'échauffement est tout d'abord prélevée sur la capacité calorique des gaz d'échappement du four.

Si l'on admet que les gaz d'échappement quittent le four à une température de 1100° C, leur capacité calorique est donc de 335 J/Nm^3 environ entre 1100 et 960° C, ce qui équivaut à environ 307 J par kg de clinker. La proportion de poussières contenue dans les gaz d'échappement du four n'est pas prise en considération dans ce calcul. Environ 200 J sont nécessaires à l'échauffement de 200 g de combustible pauvre de 0 à 900°. La capacité calorique des gaz d'échappement du four suffit donc amplement pour amener le combustible à la température de désacidification sans que cela nécessite une combustion.

Dans les zones de réaction, les processus de combustion tels qu'ils ont lieu entre le four tubulaire rotatif et le premier cyclone sont vraisemblablement quelque peu différents et un peu plus compliqués que ceux normalement observés dans les fours tubulaires rotatifs.
En général, la combustion du carbone se déroule de la facon suivante:

une couche mince appelée couche limite hydrodynamique est toujours en repos à la surface du grain du combustible, même lorsque le grain est soumis à des turbulences dans de l'air.

La vitesse de diffusion des gaz participant à la combustion détermine la vitesse de combustion. Ici, la réaction primaire à la surface du grain est la réaction du CO_2 avec du carbone par rapport à CO, alors que la combustion proprement dite, à savoir la réaction de CO avec O_2 a lieu dans la couche limite hydrodynamique.

Sans s'étendre sur les vitesses des différentes réaction, il est possible d'admettre que la vitesse de combustion se déroule, à température constante de la surface du grain, de façon proportionnelle à la concentration de CO_2 à la surface du grain. A son tour, cette concentration est proportionnelle à la vitesse de diffusion de l'oxygène, ce qui fait que la vitesse diminue donc en fonction de la diminution de la concentration d'oxygène.

Partant de ces considérations, la combustion d'un combustible pauvre dans le réchauffeur devrait ralentir dès que la teneur en oxygène diminue.

Pourtant, comme nous l'avons vu, la vitesse de combustion est parallèle à la pression partielle du CO_2 à la surface du combustible.
Il existe donc un autre processus pouvant devenir primordial pour la vitesse de combustion, à savoir la pression partielle du CO_2 dans le grain désacidifié, lequel est en même temps support de combustible. A 900° C environ, cette pression partielle est de l'ordre de 760 mm Hg. Pour comparaison: lors de la combustion du carbone, la pression partielle du CO_2 régnant dans le compartiment des gaz en présence d'air comme gaz combustible est de l'ordre de 160 mm Hg, ce qui équivaut à 21 % seulement de la pression ci-dessus.

Ceci signifie que, lorsque la température de désacidification est atteinte et maintenue, la réaction primaire doit se dérouler à une vitesse 5 fois plus grande que lors d'une combustion normale sans CO_2.

La pression partielle du CO_2 sur le grain étant fonction de la température du grain, le temps d'échauffement est, en fin de compte, décisif pour la vitesse de combustion. La pression partielle intégrale du CO_2 est pratiquement disponible dans le compartiement à gaz immédiatement après le chargement des composants et la conversion avec le carbone peut avoir lieu à une vitesse très élevée.

Les considérations ci-dessus sont valables pour un combustible pauvre dont les cendres comportent du $CaCO_3$ en proportion importante.
Si cela n'est pas le cas, la combustion ne sera, certes, pas aussi rapide qu'en présence d'une grande proportion de $CaCO_3$; pourtant, la proportion de CO_2 contenue dans les gaz d'echappement du four et provenant de la désacidification de la farine brute est si élevée qu'une pression de diffusion considérable est générée à la surface du grain, ce qui fait que la conversion se déroule plus vite que ne le permettrait la basse pression d'oxygène partielle.

La seconde alternative s'offrant pour économiser une énergie chère et précieuse réside dans l'exploitation d'une énergie de haute qualité tirée de déchets tels que: huile usée, pneus de véhicules, déchets de papier, bois et plastiques, vernis, peintures, solvants, restes de cuir, écorces d'arbres éventuellement, bagasse résultant du traitement de la canne à sucre.
Alors que les déchets liquides, pour autant qu'ils puissent être amenés à une forme atomisable, comme l'huile lourde, peuvent être diffusés et brûlés avec elle, les déchets pâteux et solides doivent être amenés à une forme combustible. Certains matériaux comme les pneus se désagrègent très vite sous l'effet de la chaleur. Ils peuvent alors être ensuite grossièrement broyés et brûlés dans le réchauffeur; les armatures en acier des pneus peuvent être également brûlées dans le four tubulaire rotatif et se retrouvent ensuite dans le clinker sous forme de Fe_2O_3.
Sinon, elles doivent être thermiquement décomposées dans des installations à couche fluidisée puis enfournées.

Une telle installation à couche fluidisée permet une conversion rapide de la plupart des déchets combustibles en des combustibles aptes à la combustion. Il est important de noter ici que, suite aux températures de combustion élevées régnant dans le four tubulaire rotatif, l'environnement n'est pas soumis à des nuisances olfactives. La gazéification se déroule selon la réaction de Boudouard ou encore du gaz à l'eau. Par fonctionnement en dessous du point de Curie du fer, des particules de fer peuvent être magnétiquement retirées de la couche.

Les composants anorganiques, principalement le ZnO et le soufre, sont entièrement liés au clinker. Le soufre sous forme d'alcali ou de sulfate alcalino-terreux et le ZnO sous une forme n'influençant pas négativement la résistance du ciment.

Dans l'échangeur de chaleur, seule la moitié environ du combustible nécessaire peut, au maximum, être utilisée.

La troisième possibilité d'économiser de l'énergie consiste dans le production d'adjuvants hydrauliques au ciment par traitement thermique de marnes ou d'argiles dans la couche fluidisée selon la température et le temps de séjour. En présence de composants marneux, des aluminates et des silicates calcaires à activité très élevée peuvent être obtenus ici à l'état solide.
Certaines argiles peuvent également être activées par de tels procédés. De tels procédés sont surtout intéressant à partir du moment ou le combustible nécessité est déjà contenu dans les composants comme le schiste bitumineux par exemple. La chaleur perdue résultant de tels procédés peut alors être utilisée pour la production de courant électrique. Il est pratiquement possible de prétendre que les coûts d'investissements nécessaires à la fabrication d'une tonne d'additifs hydrauliques activés, production de courant y comprise, ne sont pas plus élevés que pour la production d'une tonne de clinker.

Nota - L'unité utilisée ici est le J .
L'unité habituelle est le KJ .

Saving energy during cement burning by complete utilization of waste material and low-grade fuels

Helmuth RECHMEIR, Diplom-Chemiker,
Portlandzementwerk Dotternhausen, Rudolf Rohrbach KG, RFA.

Summary:
Today, with a modern process of cement burning, it is possible to reach a thermal efficiency of about 50 %.
Higher thermal efficiencies require essential improvements of the cooler efficiency. Such improvements are not yet available.

For more economical production of cement there are three possiblities, concerning the costs of combustibles:

1. The use of poor graded combustibles is possible, if the special conditions concerning the mixing with kiln exhaust gases, the heating of the combustibles and the different conditions of combustion are taken into consideration. The combustion takes place in a short time. It is important to pay attention to the impulse of the feeded meal.

2. Relatively high graded waste combustibles, tires, plastics, liquid solvents can be used. They must be converted into a suitable state for combustion. This is made by upgrading in a fluidized bed. During combustion of such materials there may arise air polluting problems which are difficult to overcome. In cement production, many air polluting substances can be combined to the cement clinker in a harmless way.

3. The production of artificial pozzolanes, by reaction in solid state, below the sinterring temperature with a low heat requirement. Especial advantage is gained with processes where substances are used, containing fuel, like oil shale, bituminous limestone or washery slates.

The conditions which are needed for the production of such substances, referring to temperature and treating time can be favorably maintained in a fluidized bed system. The use of very low grade fuels is possible.

In this process it is possible to use the surplus heat for production of electric energy. According to the price of the electric energy, which is to buy, and the calorific value of the used combustibles it is possible to cut down expenses.

At the Portlandzementwerk Dotternhausen, Rudolf Rohrbach KG, these possibilities are technically used in full scale or will be also used in full scale in the near future.

Manufacturing cement clinker is a process that entails a great deal of energy. In the case of those processes which are the most economical with respect to energy consumption, amounts of heat energy of between 3,140 and 3,350 J/kg of clinker are necessary. This corresponds to approximately 75 - 80 kg of heavy fuel oil per ton of clinker.

The thermal efficiency of furnaces incorporating suspensiontype heat exchangers is approximately 50 %. The heat loss consists of radiation from the various furnace sections, heat loss through the clinker and exhaust gas at a relatively low temperature (350° to 360° C) from the cooler - and furnace exhaust.

Improving the thermal efficiency could be achieved by using a cooling system making better use of the waste heat from the clinker as the furnace exhaust gases are, for the most part, already used for drying the raw materials.

Up until the present, all attempts to develop a cooler system operating at an improved level of thermal efficiency, have failed. Proceeding from this, we may assume that no essential improvements leading to increased thermal efficiency of the system when burning cement clinker can be expected at the present time.

An improvement in the burning process efficiency may be achieved by using more priceworthy fuels. Fuels in this class include low-grade natural fuels such as oil shales, bituminous limestone, and the like, as well as high-grade waste fuels.

However, it is not only the calorific value of the fuel but also the flame temperature achievable when using the fuel which is the crucial factor in the process.

In the case of cement clinker burning especially, a computed flame temperature of over 2,000° C in the burner flame must be achieved in order to be able to carry out the process of clinker formation in a sufficiently short time.

If the temperature is lower than this, the heat transfer coefficients may be so small that it is impossible to burn clinker in the furnace in question. For this reason, fuels with a very low calorific value cannot be used in the sintering zone. This is because an insufficiently high flame temperature is reached owing to the low calorific value.

In order to be able to use such fuels despite this fact, they must be used where there is, admittedly, a high thermal requirement but, however, where there is no need for a high flame temperature. In the case of clinker burning, this is the decarbonating zone.

In this zone a relatively low temperature is required, i.e. a maximum of 900° C.

This therefore provides an opportunity to supply the heat exchanger with low-grade fuels and, thereby, combust them. For this purpose, the highest temperature zone, i.e. the section extending between the inlet to the rotary kiln and the first heat exchanger cyclone is the most suitable section.

It is in this section that the fuel supplied has to be heated and both mixed and combusted with the oxygen present in the residual gas from the rotary kiln (approximately 10 % of the volume).

Low-grade fuels are only able to burn and make available their energy during the relatively short dwell period in the reaction zone (approximately 2 sec), if they are intensively mixed with the gases and heated sufficiently rapidly and also only if they are able to react rapidly with the available oxygen.

If any one of these conditions is not satisfied, the available energy is dragged through the heat exchanger, thereby leading to increased heat consumption in the long run.

To bring about thorough mixing of the fuel to be supplied and of the hot viscous gases, the energy required for mixing must be supplied to the fuel in the form of an impulse during charging.

In order to do this, the fuel must be supplied from as high a vertical position as possible before entering the combustion section and must be supplied at as high a speed as possible by concentrating the fuel in <u>one</u> charge since the fuel, unlike a flame, is unable to receive momentum by means of the carrier gas.

The impulse possessed by the raw meal from the next higher cyclone stage when entering the heat exchanger can be made available for the mixing process if a correct arragnement of both input locations is provided. The low-grade fuels must not be combusted until the heat energy can be absorbed by the decarbonating process of $CaCO_3$.

If we temporarily disregard the processes of combustion, the rate of heating is a matter of heat transfer between gas and particles. Since radiant heat constitutes the major proportion of heat transfer in the case of the temperatures in question, using the formula:

$$Q = C \cdot F \cdot \left[\left(\frac{T1}{100}\right)^4 - \left(\frac{T2}{100}\right)^4\right] J/h$$

the rate of heating is dependent upon the temperature difference between gas and solids at approximately $(\Delta T)^4$.

For this reason, the particles are heated extremely rapidly (within a fraction of a second).

The quantity of heat required for heating is, firstly, absorbed from the heat content of the kiln exhaust gases.

Assuming that the kiln exhaust gases leave the kiln at a temperature of 1.100° C, their heat content between 1.100° C and 960° C will be approximately 335 J/Nm^3, i.e. approximately 307 J/kg of clinker. This does not take into account the dust content of the kiln exhaust gases.

In order to heat up 200 g of low-grade fuel from 0° to 900°, approximately 200 J are required. The heat content of the kiln exhaust gases is, therefore, more than sufficient to heat the fuel to decarbonating temperature without combustion being required.

The combustion processes in reaction sections such as those between the rotary kiln and the first cyclone are probably somewhat different and somewhat more complicated than can normally be observed in rotary kilns. Carbon combustion normally proceeds in the following manner:

Even if the particles are in turbulent motion in the air, there will be a thin quiescent layer on the surface of the fuel particles, the socalled hydrodynamic interface. The diffusion rate of the gases involved in combustion determines the rate of combustion.

In this process, the primary reaction on the surface of the particles is the reaction of CO_2 with carbon to form CO, whilst "actual" combustion, i.e. the reaction of CO with O_2 takes place in the hydrodynamic interface.

Without examining the rates at which the individual reactions take place, we may assume that at constant temperature of the surface of the particles, the combustion rate will proceed proportionally to the concentration of CO_2 on the particle surface, which in turn, will be proportional to the oxygen diffusion rate. This therefore means that with a decrease in oxygen concentration, the rate of combustion will also decrease.

Using this approach, the combustion rate of low-grade fuels in the pre-heater would have to decrease with decreasing oxygen content.

However, as we have seen, the combustion rate runs parallel to the CO_2 partial pressure at the fuel surface.

So there is another process which is decisive, and indeed crucial, to the rate of combustion, i.e. the CO_2 partial pressure of the decarbonating particles, which are, at the same time, the fuel carrier. At a temperature of approximately 900° C, this partial pressure is approximately 760 mm Hg. By way of comparison: during carbon combustion, the CO_2 partial pressure in the gas chamber using air as the fuel gas is approximately 160 mm Hg, i.e. only approximately 21 % of the above pressure.

This means that, if the decarbonating is reached and maintained, the primary reaction must proceed at five times the rate for normal combustion without carbonate CO_2.

As the CO_2 partial pressure in the particles is a function of the particle temperature, in the final analysis, the heating rate will be the decisive factor determining the combustion rate. The complete CO_2 partial pressure is available practically straight away after the components have been supplied to the gas chamber and reaction with the carbon may, for this reason, proceed at a very high rate.

The above considerations apply to low-grade fuels whose ashes contain considerable proportions of $CaCO_3$.

In other cases, combustion will, admittedly, not proceed at quite as rapid a rate as in the case of a high $CaCO_3$ content, but, however, the CO_2 content of the kiln exhaust gases is so high, owing to the decarbonization of raw meal that a considerable diffusion pressure occurs at the particle surface. This therefore means that the reaction proceeds more rapidly than would be expected in view of the low oxygen partial pressure.

The second possible method of saving expensive, high-grade energy is by using high-grade waste energy. The relevant energy sources in question for this purpose include:

Oil recovered from waste oils and fats, car tires, plastic-, wood- and paper waste, lacquers and varnishes, solvents, waste leather and even, possibly, tree bark and residue bagasse from sugar cane processing.

Whilst the liquid waste products, providing they are able to be converted into a form useable in an atomizer, like fuel oil, are able to be atomized together with the fuel oil and combusted, the pasty and solid waste must be converted to a combustible form.

Amongst them are materials, such as tires, which very rapidly disintegrate under the influence of heat. They may accordingly either be combusted in coarsely comminuted form in the preheater, whereby the steel linings of the tires are combusted along with the rest of the tire in the rotary kiln, appearing again as Fe_2O_3 in the clinker or, they must be thermally decomposed e.g. using fluidized bed systems and then fed to the kiln.

In fluidized bed plants, the majority of combustible waste materials are able to be converted in rapidly combustible fuels. One important point to bear in mind, is that owing to the high combustion temperatures in rotary kilns no odorous substances can reach the atmosphere.

Gasification proceeds following the Boudouard or watergas reaction process. By allowing the iron to drop to its Curie point, iron sections may be removed magnetically from the charge.

The inorganic constituents, chiefly ZnO and sulphur, are completely bonded into the clinker. Sulphur as alkaline or alkaline earth sulphates and ZnO in a form which is not detrimental to the development of cement strength.

No more than approximately half of the necessary fuel is able to be used in the heat exchanger.

The third way of saving energy is by producing hydraulic material to be admixed to the cement by heat treatment of marls or clays in the fluidized bed, the heat treatment process being matched to the temperature and dwell. Using this process, calcium aluminates and calcium silicates of very high activity are achieved in the presence of marly constituents by reaction in a solid state.

Certain clays may also be activated using this process. Such processes are Particularly attractive if the required fuel is already contained in the components, such as, e.g. oil shales amongst others. This means that the heat given off by such processes may be used to produce electrical power.

We may start from the fact that the investment costs for the manufacture of one ton of hydraulically activated aggregates including power generation are no higher than the costs of producing one ton of cement clinker.

NB. The dimensions of energy requirements are given in J. Correctly dimension must be in KJ .

Utilization of combustible wastes in cement manufacture

Utilisation des déchets combustibles dans la fabrication du ciment

T.M. LOWES, B.Sc., PhD, Deputy Manager, Engineering R and D, B.C.I.,
B. TETTMAR, B.Sc., PhD, Manager, Engineering R and D, B.C.I., Grande-Bretagne.

RESUME : Des grandes quantités de déchets combustibles tels que des ordures municipales se trouvent fréquemment disponibles tout près des cimenteries. L'utilisation de ces déchets dans la fabrication de ciment permet d'économiser des combustibles primaires aussi bien que fournir une méthode peu couteuse d'élimination qui n'augmente pas la pollution atmosphérique. Les experiences de B.C.I. de l'utilisation directe de déchets combustibles sont examinées et on fait allusion particulière aux ordures combustibles municipales et aux effets de déchets matériau sur l'ensemble des opérations d'une usine. On recommande des limites d'utilisation pratiques en ce qui concerne las substitution de déchets combustibles qu combustible primaire et on propose un schème pour la production totale de ciment de l'énvgie des déchets combustibles.

SUMMARY : Large quantities of combustible waste materials such as domestic refuse are frequently available near a cement works. The utilisation of these wastes in cement manufacture can save prime fuel as well as providing a relatively cheap method of disposal, which does not increase the pollutant emission. B.C.I.'s experience in the direct use of waste fuels, is reviewed with special reference to municipal refuse and the effect of a waste fuel on overall works operation. Practical limitations to the prime fuel replacement by the direct use of waste fuels are recommended. A scheme to produce cement totally from the energy from waste fuels is suggested.

1.0 INTRODUCTION

In recent years the rising costs and decreasing resources of prime fossil fuels, have caused National Government and Private Industry to re-examine their energy usage and look for alternative sources of energy. Governments have had to become involved with long term strategic planning of energy usage, in order to develop energy policies which would take account of the finite reserves of the various prime fuels. Meanwhile, industry is directing its efforts to a shorter time scale; to reduce energy consumption so that production costs can be reduced or maintained at a reasonable level when other costs are rising.

Cement manufacture is an energy intensive process; the cost of energy is the largest single item in running a cement works. In 1978 the fuel and electrical costs associated with the production of OPC by Blue Circle Cement (BCC), was almost half the production costs. While many industries are now looking actively at the reduction of their energy consumption, the fact that it represents such a high proportion of the costs of cement production, has encouraged cement manufacturers to pursue actively this area long before the energy crisis of the mid-70's. Figure 1 shows the reduction in fuel consumption in BCC since 1965. This reduction has generally been achieved via good housekeeping (e.g. low back-end oxygen, reduction of inleaking air) and the application of improved technology (e.g. reduction of slurry moisture and kiln chain design). The above principles have generally been applied fully to BCC and therefore with the exception of the conversion of wet to semi-wet or dry process, the only significant changes in energy consumption in the manufacture of OPC that are left to BCC are generally associated with the implementation of innovative research.

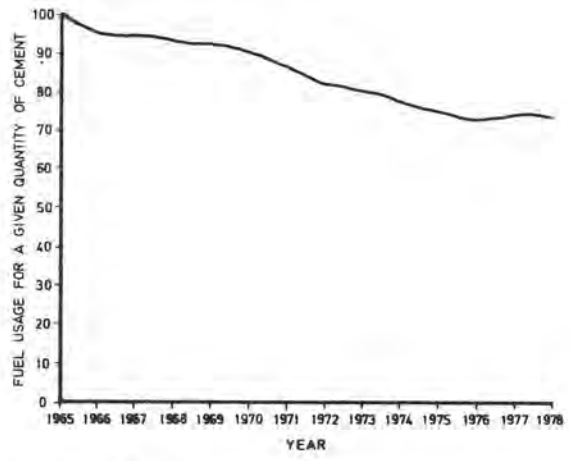

Figure 1 - Reduction in fuel usage by B.C.C. in the making of OPC.

Unfortunately, the cost of replacing a wet process with a semi-wet or dry process is high. An even higher rate of increase in relative energy costs than has occurred in recent years is required to make it a reasonable commercial investment. Therefore, the cost effective reduction of energy consumption via innovative research is required. Current research work is aimed at reducing fuel consumption by up to approximately 75 kcals/kg via an optimum firing system design for low primary air opeation, and the electrical consumption by up to 30 kWh/ton via flame and mill optimisation and external electricity generation from waste heat. These reductions are representative of most of the feasible improvements in energy consumption for the dry process. This statement also applies to the wet process once the slurry moisture has been reduced to its lowest practical value. However, even with reductions in energy consumption via innovative research, associated investment costs must be considered as the work progresses, as these often make the energy saving uneconomic from a commercial viewpoint.

An alternative method of reducing the energy costs associated with cement manufacture is to use a less expensive fuel. BCC already produce all of their OPC using a medium ash pulverised coal as a fuel, therefore, savings arising from the cost of the fuel can only come from the use of higher ash coals or low grade fuels. Techniques are being developed for firing higher ash coals (e.g. 35-45% ash) while maintaining product quality. These techniques are also being extended to low grade fuels, into which category can be included a large number of combustible wastes. This paper is based on BCI's experience and indicates how waste fuels could be used currently and in the future, to reduce energy costs in cement manufacture. Specific reference is made to Blue Circle Industries (BCI) use of municipal refuse as an auxillary fuel.

2.0 WASTE MATERIALS AS ENERGY SOURCES

As a general rule the use of waste as a fuel cannot compete commercially with dumping. However, as the availability of viable dumping areas decreases and alternative methods of disposal are considered, the use of waste as a fuel becomes a possibility. Generally, there is between 5 and 8% (1) of a Nation's annual energy consumption available in the form of combustible waste. As this amount of energy is significant in terms of the cement industry, and the process of cement manufacture is one of the few industrial processes that could utilise the energy in combustible wastes in its different forms, consideration of this area of energy cost reduction can be fruitful to the cement manufacturer.

The energy in wastes can, in theory, be utilised in a process in 4 ways, i.e.:-

a) Directly, via pretreatment and injecting in a similar manner to a prime fuel.
b) Semi-directly, via a gasification/pyrolysis and then using as a prime fuel.

c) Semi-indirectly, combusting externally in a fluid bed or combustor and using as hot combustion products or preheated air.
d) Indirectly, via electricity generation from a combustor.

The decision as to which route is most suitable depends on process constraints and the properties of the waste material itself. Each mode of energy utilisation can be employed in principle in cement manufacture. Figure 2 shows how they could be used to produce cement entirely from the energy in the waste material.

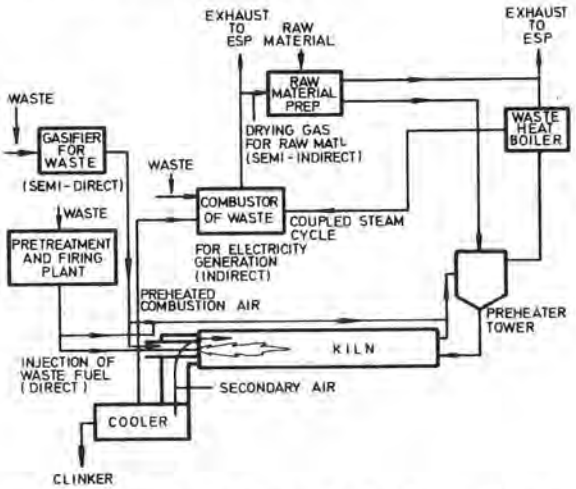

Figure 2 - Schematic diagram for the potential use of the modes of energy generation from wastes in cement manufacture.

Unfortunately, development work is still required on gasifiers and combustors, before a free choice can be made of energy type. Therefore, the current commercial viability of many potential applications can be somewhat low due to uncertainties of "success" and the cost of the required development to the cement manufacturer. However, development work outside the cement industry on fluidised beds e.g.(2) and cyclone combustors e.g.(3), could make the semi-direct and semi-indirect modes of energy generation attractive to the cement manufacturer in a few years. Currently, BCI are employing the direct method to reduce energy costs on some of their Works, by the introduction of pretreated waste into their burning zone via appropriate firing systems. Consideration is also being given to the economics and the required research and development associated with the semi-direct method.

3.0 DIRECT USE OF WASTE AS A FUEL IN A CEMENT KILN

The cement kiln has several inbuilt advantages for the direct use of waste as an auxiliary fuel, i.e.
- the flame temperature is in excess of 2000°C, which can stand some reduction via the introduction of waste as an auxiliary fuel without any major detrimental effect on the process.
- the large and high temperature combustion chamber is capable of completely destroying odoriferous and toxic organic compounds.
- the raw materials act as a natural calcium carbonate scrubbing system to remove acid gases.
- the kiln is already fitted with an efficient waste gas de-dusting device.

Despite all these advantages it is not possible to supply shovel in waste and forget about it. The waste must be subjected to similar types of storage, blending, comminution, feeding and firing operations as a prime fuel. It is important that the pretreatment plant supplies the firing plant with an "adequately" prepared waste fuel, which is then supplied to the kiln at a "uniform" calorific value and chemical composition, where it has no "significant" detrimental effect on production or product quality. The exact definitions of and difficulties in achieving "adequately", "uniform" and "significant" depend on the fuel and the cement making process. It is important that product quality and production capacity is maintained, dangers must be avoided, costs and general inconveniences assessed to make sure that they do not outweigh the benefits derived from payments for taking the waste and from prime fuel saving. Generally, a waste without substantial beneficiation has insufficent combustion and heat transfer intensity, to be able to supply the energy requirements of a process via its direct use. Therefore, as these beneficiation processes are not yet viable commercially, wastes are normally used as auxiliary fuels.

3.1 THERMODYNAMIC RELATIONSHIPS

Two of the most important aspects of kiln operation are the fuel consumption and clinker output. The use of a waste as an auxiliary fuel can adversely affect both these parameters. The fuel consumption can be increased when using waste as an auxiliary fuel due to; the conveying air used for transporting the waste, increased exhaust losses due to lower heat transfer in the burning zone, higher exhaust mass flows and moisture associated with the waste. In considering the financial benefits associated with the prime fuel saving when using a waste as an auxiliary fuel, it is necessary to consider these above affects, in terms of an "effective" calorific value of the waste fuel. The output of cement kilns can be adversely affected by decreased heat transfer rates in the burning zone and increased exhaust gas volume.

Simulation programmes have been developed, based on plant trials, which predict changes in output and the fuel consumption together with "effective" calorific value, when wastes are used as auxiliary fuels in wet, dry and semi-dry processes.

3.2 PRODUCT QUALITY

While the waste material must be adequately prepared to give a similar combustion pattern to the prime fuel being used and then injected into

the cement kiln with a constant thermal input in order to maximise its thermal value; further constraints are introduced by the requirement to maintain product quality. It is important that a constant thermal input and combustion stoichiometry are maintained to ensure that the cement clinker is burnt at a consistent temperature to a specific free lime. Additionally, both chemical and thermal reducing conditions have to be avoided in order to minimise the effect of the waste fuel on strength/growth characteristics, grindability and workability of the cement. Special care has to be taken to avoid reducing conditions in the burning zone when the clinker has a high C_3A. The constant thermal input and combustion stoichiometry is maintained via the appropriate design of the pretreatment plant and feeding part of the firing plant. The combustion intensity can be achieved via adequate material preparation and injecting the waste via a specially designed burner system, which has the momentum flux that is calculated to produce the gas recirculation ratio, which is required to minimise the chemical reducing conditions in the burning zone. Additionally, the combustion intensity of the waste material should be maximised via its injection along the axis of the kiln through the centre of the flame formed from the prime fuel, preferably through a swirl induced reverse flow zone. The burner configuration and the gas recirculation pattern is shown in figure 3.

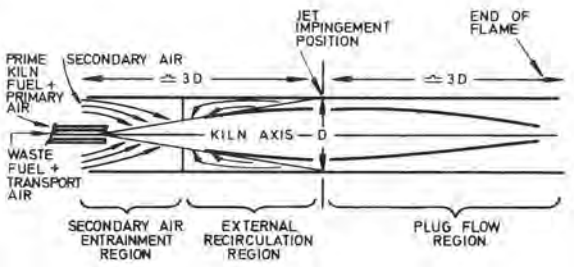

Figure 3 - Gas flow pattern in the burning zone of a cement kiln.

Waste materials which have significant ash contents must be prepared so that the incombustible material is reduced to an appropriately small particle size after it has passed through the flame region, and the injection system designed so that the ash is homogeneously incorporated into the kiln feed. A burner system which maximises the combustion intensity of the waste, by injecting it along the axis is usually optimum for incorporating the ash homogeneously into the kiln feed, as it eliminates interaction with the externally recirculating gases. Failure to produce an adequately small particle size of the ash or to homogeneously incorporate it into the kiln feed, gives rise to the necessity to burn the clinker at a higher temperature in order to achieve combination, which can result in thermally reduced and over burnt clinker. In addition to being homogeneously incorporated into the feed, the ash must be of relatively constant chemical analysis, in order that the cement raw material mix may be adjusted to maintain clinker quality. Fortunately, the chemical analyses of the ash from most wastes do not vary significantly in the short term. A variation in terms of percentage ash is more usual. Such a variation can be allowed for via the design of an adequate blending system.

In addition to product quality problems due to: combustion intensity, variable thermal input, ash variability and heterogeneity, significant product quality problems can occur due to relatively minor constituents. The inputs of volatile compounds such as alkalis, chlorides and sulphates have to be assessed in the light of similar inputs from the normal kiln fuel and raw materials to anticipate their possible effects on kiln operation and product quality. The level of volatile compounds which can be tolerated is known technology and depends on the type of cement making process used. Other minor, but potentially harmful constituents have to be considered. Special laboratory work has to be undertaken and related to full scale trials, to anticipate their behaviour and eventual destination when introduced into the kiln system, in order to determine possible effects on production quality and kiln operation. With minor constituents, common problems are that their range of variation in waste materials are not known. Furthermore, it is not easy to get representative samples of the waste.

3.3 ATMOSPHERIC POLLUTION

The raw material calcium carbonate scrubbing system associated with each Works usually means that there will be little problem with exhaust emissions when waste is successfully used as a fuel. However, each waste needs to be considered carefully.

3.4 WORKS' OPERATION

The pretreatment and firing plant must be suitably designed to prevent inconvenience to Works' personnel, to meet statutory requirements and to a maintain acceptable working conditions. At the same time these plants must be capable of providing the kiln with uniform quality of waste fuel at a cost effective rate. In commercial considerations the real effect on Works' operation of running the waste fuel plant has to be carefully identified.

4.0 PRACTICAL APPLICATION OF DIRECT FIRING OF WASTE

While it is possible to completely replace a prime fuel with a waste in firing a cement kiln, this

can only be achieved for a good quality OPC at a reasonable fuel consumption and output if the waste is in fact a high grade fuel (e.g. refinery tail gas) or it has been highly beneficiated. Generally, however, there is either insufficient supply of the waste to supply completely the fuel requirements of the kiln or the beneficiation process is not commercially attractive. Many combustible wastes which are available in sufficient quantities have a significant ash content, e.g. colliery minestone, municipal refuse. The ash content is usually the limiting factor in their replacement of the prime fuel, once adequate pretreatment has taken place and an appropriate firing plant is available. In order to maintain an acceptable clinker quality the maximum ash on clinker that could normally be considered for introduction via the flame is approximately 10%, providing the ash's particle size distribution after combustion is similar to that which occurs with pulverised coal. Depending on the waste and cement making process used, prime fuel replacements of 10-25% can be achieved.

BCI has evaluated, carried out trials, and in some cases brought into operational fruition, the use of wastes as an auxiliary fuel in a cement kiln. Typical examples are: charcoal fines, power station grit, rice husks, colliery minestone, wood-waste, coconut shells, Fullers Earth, battery cases, rubber tyres/chars, municipal refuse, waste oils, acid tar and solvent recovery residues. The scope of the paper does not allow detailed description of each evaluation. Generally, however, if they are not currently being successfully applied, the overall "cost" of using the waste is too high compared to the prime fuel saving. This can be due to many reasons; however, the investment and operating costs of the pretreatment plant required to maintain cement quality and output, combined with the potential disposal fee often predominate. More details of the evaluation procedure, which is based on R & D analysis that should be applied to assessing the commercial viability of a waste as an auxiliary fuel is given in reference (4).

A typical successful example of the use of a waste as an auxiliary fuel in BCI, is that of municipal refuse. Initial trials were carried out in 1971(5) on a 4.5 t.p.h. experimental cement kiln and involved repulverising refuse from a nearby municipal pulveriser plant and mixing with the normal coal before firing into the kiln. The trial showed that the method of disposal was practical but that the method of addition was difficult to control. Trials were carried out to develop adequate pretreatment and firing plants on 20 and 40 t.p.h. wet process kilns. The process developed is currently in commercial operation at a minimum of 60,000 t.p.a. of refuse on a coal fired wet process Works. Figure 4 shows a schematic diagram of the installation which passes the refuse on an as-received basis through a two stage milling process.
The primary stage reduces the refuse to 80%< 50mms and the second stage to essentially all minus 50mms. It is particularly important that few "streamers" and little ferrous metal penetrates

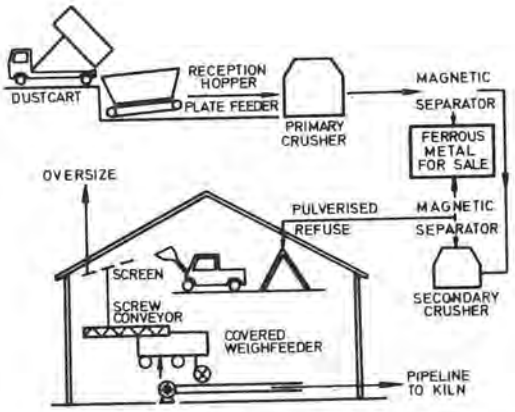

Figure 4 - Typical flow sheet for a pretreatment and firing plant for municipal refuse.

into the firing plant. The pulverisers and process line were chosen accordingly. The streamers are avoided by using a Hazemag Universa 16/20 as a primary pulveriser and a Hazemag EM 1000/1500 or a Gondard "Civic" as secondary pulverisers. Over-band magnets after each pulverisation remove approximately 90% of the ferrous metal. The pretreated refuse is then fed to the firing plant, where it is injected into the kiln via a screw feeder, weight belt, rotary valve and burner. Provisions exist to increase the refuse input providing the cement quality can be maintained. It should, however, be noted that the maximum coal ash that one would normally consider incorporating into the raw material via the flame is 10% of the clinker output. At 60,000 t.p.a. refuse, it's ash plus the ash in the coal gives an ash on clinker level is approximately 6%.

There is an increasing preponderance throughout the world of dry process kilns, including many firing with fuel oil. Therefore, the most recent commercial trials have been carried out in such a kiln in the UK. A mobile pretreatment plant was used to supply nominally 100%< 50mm refuse to a firing plant which comprised of an elevator, screen, weigher, screw, rotary valve and a double concentric, swirling oil/refuse burner. Appropriate adjustments were made to the cement chemistry to accommodate the ash from the refuse. The trials showed that:-

- the use of refuse as an auxiliary fuel in the dry process can be compatible with the manufacture of good quality cement.
- the amount of refuse which may be insufflated depends on its chloride content.
- the amount of refuse which can be used as an auxiliary fuel when not restricted by chlorine level, is largely dictated by its fineness.

- with the appropriate chloride levels and fineness significant replacements (6) of fuel oil can be achieved.

Unfortunately the major drawback in the use of refuse as an auxiliary fuel is the capital and operating costs of the pretreatment plant. The fuel equivalent of the refuse on its own is not an attractive investment, therefore it is important that a realistic price be paid by the local Waste Disposal Authority (W.D.A.) for its disposal. This process is less costly to the W.D.A. than incineration and makes maximum use of its fuel value without any significant increase pollutant emission (6).

The major limitations governing the increased use of refuse as an auxiliary kiln fuel, are associated with its combustion intensity, ash and chloride levels. Future work will concentrate initially on increasing the combustion intensity and decreasing the ash on clinker level, via a simple beneficiation process which takes out the heavier fraction. For the longer term, process developments which would facilitate the use of refuse for cement manufacture (or indeed any other waste) in other than the direct form of energy will be followed, with specific attention being given to the semi-direct method. This latter development could give rise to cement kilns being fired entirely by a waste fuel. As there is usually sufficient municipal refuse in a country to supply all the necessary energy for cement making, the fact that its disposal via cement making competes favourably with incineration and has reduced overall pollutant emission, could make the disposal method part of a countries strategic plan to reduce their consumption of prime fuel at the same time as reducing their overall pollutant emission.

5.0 CONCLUSIONS

1) Wastes having a significant calorific value can be used as an auxiliary fuel to provide energy directly to the cement making process, provided they are subjected to the appropriate pretreatment and introduced into the process via a suitably designed firing plant.

2) Even with an appropriate pretreatment and firing plant, the direct firing of waste is normally limited to an auxiliary fuel rôle due to product quality and process operation considerations.

3) The fuel savings arising from using solid waste as a fuel does not normally made the investment/development costs of the pretreatment plant commercially viable. A disposal charge for the waste has normally to be made.

4) The limitations imposed by the use of waste as a direct source of energy, may be overcome by the development of suitable gasifiers or combustors. However, development and operating costs could be a problem.

REFERENCES

1. - T.M. LOWES and A.D. LORIMER (1979). "Waste as a Fuel". International Energy Managers Conference, N.E.C. Birmingham.

2. - N. HODGKINSON (1979) "Burning of waste in fluidised beds". Energy for Waste Burning Symposium, Portsmouth.

3. - N. SYRED (1979) "Burning of low calorific value gases in flames". Energy from Waste Burning Symposium, Portsmouth.

4. - G.G.S. DAVIES (1974) "The R.P.D. system for Project Planning under Uncertainty". International Conference on Project Management in the Seventies. Paris.

5. - British patent No.1405294.

6. - C.A.C. HALEY "Use of Domestic Refuse as a Fuel in Cement Manufacture". International Recycling Congress, Berlin.

SEMINAIRE D

Influence des caractéristiques du ciment sur les propriétés du béton

Président : M. MCHEDLOV PETROSSYAN, URSS
Correspondant français : M. BARON

INTRODUCTION AU SEMINAIRE D

Le ciment, en réagissant avec l'eau, forme la colle du béton. On doit donc s'attendre à ce qu'il y ait une relation entre les propriétés du béton et les caractéristiques du ciment. Les communications qui suivent montrent que cette relation est souvent loin d'être claire ; parfois, elle semble ne pas exister ; parfois encore, d'un auteur à l'autre, elle est contradictoire.

Exemple 1

Pour un béton riche en ciment, le dosage en eau nécessaire pour obtenir une consistance donnée, peut être décomposé en deux parties, l'une attribuable au ciment, l'autre au granulat inerte :

$$e = Ac + Dg$$

A et D caractérisent le ciment et le granulat inerte ; c et g sont les volumes de ciment et de granulat dans le mélange.

Toutes choses égales par ailleurs (c, D et g), il existe alors une relation entre e et A, donc entre une propriété du béton et une caractéristique du ciment. En particulier si le ciment est plus fin, A est plus grand et le dosage en eau du béton, nécessaire pour avoir une consistance donnée, est plus grand.

Pour les dosages en ciment usuels, la relation ci-dessus n'est plus valable ; le dosage en eau dépend toujours de la finesse du ciment mais il dépend aussi de la porosité du granulat inerte, c'est-à-dire de la répartition granulométrique de l'ensemble des grains. Augmenter la finesse du ciment peut alors, suivant le cas, augmenter ou diminuer, ou encore ne pas changer le dosage en eau nécessaire pour avoir un béton de consistance donnée.

Exemple 2

Influence du moment de mise en place sur la résistance à 28 j. Le moment optimal de mise en place dépend du ciment et de la température interne. Le choix d'un moment arbitraire peut fausser la comparaison entre les ciments adjuvantés ou non.

Exemple 3

Il n'existe pas un rapport fixe entre le retrait au jeune âge du béton et celui de sa pâte (le granulat étant toujours le même par ailleurs). Suivant les ciments, ce rapport varie entre 0,1 et 0,25. Cela est probablement dû, en partie, aux microfissures qui se forment dans le béton au jeune âge entre la pâte et les granulats. Quoi qu'il en soit, la valeur de ce rapport dépend de la cinétique de durcissement de la pâte de ciment, de la répartition granulométrique des grains du granulat et du ciment, des caractéristiques élastiques du granulat ainsi que des conditions mécaniques imposées aux limites de l'éprouvette. Compte tenu de tout cela, une pâte de ciment au retrait supérieur peut donner un béton au retrait plus faible.

On pourrait multiplier ainsi les exemples. Mais cela n'est pas nécessaire pour être convaincu que la relation entre les propriétés des bétons et les caractéristiques des ciments ne peut être étudiée qu'au travers de modèles physiques schématisant le fonctionnement global.

En Union Soviétique, on a vu ces dernières années le développement de modèles semi-empiriques, prenant en compte l'influence de très nombreux paramètres (caractéristiques du ciment, des granulats, des proportions du mélange, des conditions de mise en oeuvre, des conditions atmosphériques). Le développement de ces modèles est possible grâce aux progrès des moyens de calcul.

D'un point de vue pratique, ces modèles permettent une optimisation globale du béton qui peut être une source de progrès et d'économies importantes.

Le Séminaire a été organisé selon 5 thèmes, organisé chacun par un rapporteur :

1 - Influence de la composition chimico-minéralogique et de la finesse du ciment - M. J.P. BOMBLED

2 - Influence des constituants secondaires (cendres volantes, laitiers, pouzzolanes, etc ...) - M. LUDWIG

3 - Influence des traitements thermiques - M. L.J. PARROT

4 - Influence des adjuvants - M. O. HENNING

5 - Influence des effets extérieurs et de leur association - M. O.P. MCHEDLOV PETROSSYAN

Thème 1 - Influence de la composition minéralogique et de la finesse du ciment sur les propriétés du béton

par J.P. BOMBLED, C.E.R.I.H.L, Paris, France.

I Introduction

Dans un béton hydraulique le ciment représente pratiquement la fraction la plus fine donc, par unité de volume, de béton l'élément solide présentant le plus grand nombre de points de contact et la plus grande surface d'échange avec ce qui l'entoure c'est-à-dire au début, l'eau de gâchage ; par ailleurs, le ciment forme avec cette eau l'élément actif de cet ensemble et aussi, à l'état frais, l'élément déformable.

Il est par conséquent assez logique de penser que les caractéristiques du ciment influenceront en grande partie les propriétés du béton frais ou durci.

Toutefois il ne faut pas aller trop loin dans ce raisonnement et attribuer au ciment toutes les qualités et pourquoi pas aussi tous les défauts d'un béton : ne perdons pas de vue qu'une réalisation en béton et sa bonne tenue c'est aussi le résultat :
- du soin dans la conception de l'ouvrage,
- du choix d'une composition du béton,
- de la présence d'autres composants y compris des adjuvants,
- de la qualité de la mise en oeuvre,
- du déroulement des traitements éventuels,
- des conditions de travail ou d'environnement immédiates ou ultérieures.

Certains de ces points font d'ailleurs l'objet d'autres thèmes de ce séminaire.

Le thème I concerne "L'influence de la composition minéralogique du clinker et de la finesse du ciment sur les propriétés du béton".

Auparavant pour essayer d'avoir une vue globale de l'etat de nos connaissances il est bon de se reporter au Tableau I formant une matrice dont les colonnes correspondent aux propriétés du béton que j'ai divisées en cinq groupes :

"Caractéristiques" du ciment	"Propriétés" du Béton				
	Etat frais : maniabilité	Evolution : prise et raidissements	Performances mécaniques	Variations dimensionnelles fissuration	Durabilité
Constitution minéralogique et chimique du clinker (y compris éléments mineurs)	??	≈	≈	??	???
Composition du ciment (en tenant compte des divers composants laitier, pouz. zolane)	?	~	~	?	???
Finesse de mouture.	B	B	B	B	≈
Dosage en ciment dans le béton.	B	~	B	B	B

? domaine où il reste des questions plus ou moins nombreuses à resoudre.
~ domaine où il existe un acquit important mais encore des zones d'ombre à éclaircir.
B domaine où on peut admettre avoir une bonne connaissance de l'essentiel pour comprendre et agir pratiquement.

- les propriétés à l'état frais,
- l'évolution depuis l'état initial pendant les premières heures de la vie du matériau (prise, raidissements...),
- les performances mécaniques à plus longue échéance,
- les variations dimensionnelles et les risques de fissuration qui leur sont souvent associés,
- la durabilité.

Les lignes correspondent à des caractéristiques ou des facteurs liés au ciment :
- La composition minéralogique du clinker [et chimique en ce qui concerne des éléments dits "mineurs"] .
- La composition du ciment en tenant compte des constituants en dehors du clinker : laitier, pouzzolanes naturelles ou artificielles ... et le gypse.
- La finesse de mouture soit par son aspect synthétique de l'aire massique soit par son aspect analytique de la granulométrie.
- Et, bien que ce ne soit pas une propriété intrinsèque du liant, son dosage dans le béton.

Dans ce tableau j'ai essayé de faire le point de nos connaissances en les estimant en trois niveaux :

1 Celui que j'ai symbolisé par un ou plusieurs points d'interrogation pour signifier qu'il reste encore dans ce domaine beaucoup de questions à élucider par les chercheurs.

2 Dans quelques cas le symbole ondulé veut dire que nous disposons déjà d'un certain acquit mais qu'il reste des zones d'ombre à éclaircir et sans doute des synthèses à effectuer.

3 Enfin dans le troisième niveau indiqué par la lettre B ce sont les domaines où j'ai estimé notre connaissance satisfaisante.

Les appréciations portées dans ce tableau sont évidemment très subjectives et peuvent donner lieu à des discussions, on peut ne pas être d'accord et je laisse à chacun le soin de les modifier à son gré.

Néanmoins on peut penser que cette forme de présentation a le mérite de nous mettre sous les yeux un panorama de nos connaissances et de nos lacunes. Evidemment chaque colonne et chaque ligne peuvent elles-mêmes se subdiviser en plusieurs facteurs ou éléments.

Les différentes colonnes du tableau formeront les têtes de chapitre, de cette courte présentation du Thème I. Mais pour ce thème I qui est mon sujet, il faut faire abstraction des lignes 2 et 4 qui ressortissent des autres sujets qui seront abordés par les autres rapporteurs.

II Caractéristiques du ciment et propriétés du béton frais

Les recherches sur le comportement rhéologique du béton frais et les composants de l'ouvrabilité (cohésion, viscosité, frottement interne) ainsi que sur les facteurs qui les influencent, commencent à nous permettre d'entrevoir les mécanismes.

On connait en particulier assez bien l'influence soit sur la cohésion, soit sur l'effet lubrifiant de la pâte interstitielle, soit sur la lutte contre les risques de ségrégation etc, l'influence de la proportion d'éléments fins et, par conséquent, de la finesse de mouture du ciment d'une part et du dosage de celui-ci dans le béton d'autre part.

Dans ce domaine de la finesse on s'est aperçu par ailleurs que le mode de broyage n'était pas sans répercussions rhéologiques et c'est un problème à l'étude actuellement.

En ce qui concerne l'influence de la composition du clinker, on est beaucoup moins fort mais des études sont en cours sur la floculation, sur la thixotropie, sur le potentiel zeta en relation avec la constitution du clinker et les ions présents dans la phase aqueuse.

On sait néanmoins que la teneur en C_3A dont la vitesse de dissolution est grande, doit jouer un rôle prédominant puisque si son hydratation rapide et les liaisons précoces qui peuvent en résulter ne sont pas correctement ralenties, on risque de voir augmenter rapidement la résistance au cisaillement du béton frais et de voir ainsi la prise empiéter sur la période de mise en oeuvre.

On a commencé aussi à mieux comprendre le rôle des sulfates de calcium et du gypse en particulier, floculants, réducteurs de solubilité des aluminates, comme sulfo-aluminate, colmateurs de certaines plages des grains, accélérateurs des silicates ; selon la teneur en C_3A du clinker l'incorporation du gypse pourra soit produire un effet pseudo-fluidifiant soit au contraire pour une teneur en C_3A faible, conduire à une diminution de maniabilité ou à une exigence en eau plus grande à caractéristique rhéologique égale.

L'action des alcalins dépend non seulement du cation mais aussi de l'anion toutefois ils présentent généralement deux effets contradictoires l'un fluidifiant l'autre accélérateur de prise, et dans ce cas peuvent contribuer à diminuer rapidement l'ouvrabilité ; si les alcalins sont en trop grande proportion c'est ce dernier effet qui risque de prédominer.

Tout ceci commence à être mieux connu et il faut remercier Monsieur GEBAUER de son étude très intéressante et très instructive fondée sur une grande quantité d'observations et un grand nombre de ciments.

Cette communication propose une relation qui permet de calculer l'exigence en eau à consistance normale, en fonction de trois facteurs qui sont parmi ceux que nous venons de mentionner.

Nous l'avons vérifiée avec quelques ciments et elle nous a donné de bons résultats. Toutefois on peut s'étonner de deux choses : l'absence du terme sulfate et le fait que la finesse est caractérisée par la fraction 10/30 µm. Remarquons que pour le sulfate, comme la teneur optimale en gypse est fonction de la teneur en C_3A, en alcalin et de la finesse, on conçoit que l'influence du gypse soit difficile à dissocier des autres facteurs pour les ciments commerciaux.

Un autre enseignement du travail de Monsieur GEBAUER est de montrer combien les variations rhéologiques liées au facteur ciment sont assez faiblement répercutées et fort atténuées sur la maniabilité du béton ; c'est un avantage mais aussi un inconvénient. :

- Ceci devrait d'abord nous conduire à une certaine modestie et décourager ceux qui proposent de mesurer une maniabilité intrinsèque du ciment alors que c'est toujours de maniabilité du béton qu'il s'agit.
- En revanche ceci nous interdit de transposer sans précaution les résultats des essais rhéologiques obtenus sur pâte ou sur mortier à des bétons, et pour les laboratoires c'est toujours une charge très lourde et une difficulté que d'effectuer toutes ces mesures sur béton d'autant plus qu'il n'existe pas de béton normalisé.

III Evolution initiales et caractéristiques du ciment

Il s'agit de la deuxième colonne du tableau ; cette évolution peut se manifester de trois manières :

- par une prise habituelle après une période dormante ou d'induction plus ou moins longue
- par une perte d'ouvrabilité progressive mais quelquefois assez rapide (et qui peut être parfois fort gênante).
- par des raidissements prématurés qui sont rédhibitoires pour une bonne mise en oeuvre.

Il va de soi que ce sont les éléments rapidement solubles qui interviennent à ce stade ; on sait bien aussi comment la finesse de mouture influe sur la vitesse de prise.

En ce qui concerne la composition du clinker ce sont essentiellement C_3A et les éléments alcalins qui agissent soit comme, constituants à prise rapide soit pour les alcalins généralement comme accélérateurs, la conjonction des deux pouvant évidemment entraîner des temps de prise très courts ou des raidissements prématurés.

L'action modératrice des sulfates de calcium (gypse, anhydrite, semi-hydrate) dépend de la vitesse de dissolution de ceux-ci et de celle des différents éléments en présence, laquelle conditionne cette compétition qui régit la cinétique d'hydratation dans les premiers instants laquelle sera influencée :

- par la concentration des éléments en présence,
- par la nature et la mobilité des ions qui apparaissent,
- par l'état d'hydratation et de solvatation des éléments dissous,
- par la température qui agira entre autres sur la diffusion etc.

Nous commencons à comprendre certains de ces mécanismes ce qui ne veut pas dire qu'il ne reste pas encore des points à préciser ; il reste en particulier à mieux élucider l'influence d'un certain nombre d'éléments dits "mineurs" dont la cinétique de dissolution et dont les effets que j'appellerai faute de mieux "catalytiques" peuvent déplacer notablement les équilibres ioniques qui régissent tous ces systèmes.

Un point important sur lequel nous sommes beaucoup moins forts et qui pourtant nous pose des problèmes fréquemment, est celui des raidissements prématurés ; on a pu leur trouver un certain nombre de causes mais il reste beaucoup à faire pour démonter tous les mécanismes : il est d'ailleurs surprenant qu'aucune communication ne se soit intérressée cette question ; peut être a-t-on quelque pudeur à reconnaître notre ignorance.

Dans le domaine de la prise nous trouvons la très intéressante étude de Monsieur le Professeur TAM de Thaïlande qui étudie en particulier l'influence des éléments alcalins notamment dans le cas où l'on incorpore des adjuvants dont le but est justement de modifier la vitesse de prise.

On peut toutefois s'interroger sur la validité de conclusions tirées de l'addition d'hydroxyde de sodium aux alcalins déjà présents dans le clinker, dont le passage en solution est sans doute plus lent (l'ordre d'incorporation des additions peut d'ailleurs généralement intervenir) mais aussi parce que l'anion as sans doute aussi son mot à dire et joue un rôle non négligeable dans les états d'équilibre dont j'ai parlé

Néanmoins la recherche de l'influence des éléments alcalins sur la solubilité et sur la cinétique de dissolution des autres constituants, est très intéressante et peut aider à comprendre les répercussions éventuelles dans le cas d'incorporation de certains adjuvants.

IV Caractéristiques du ciment et résistances

Je serai relativement bref sur ce point pourtant important car beaucoup est déjà connu et a été fait.

La relation entre la finesse de mouture et en particulier la granularité et la cinétique de durcissement a fait l'objet de fort nombreux travaux. On sait que la résistance entre 0 et 24 h est directement proportionnelle à la surface spécifique, on sait aussi quelles sont les tranches granulaires qui donnent les premières résistances et l'intérêt d'un spectre granulométrique resserré.

Mais la corrélation entre finesse et résistance n'est pas sans dépendre elle aussi de la composition car la constitution des différentes fractions granulaires est liée à la broyabilité de chaque minéral : par exemple plus un clinker est dur à broyer, plus les fines seront riches en C_3S.

Pour ce qui est de l'influence de la composition minéralogique ,le C_3S est l'élément essentiel des résistances finales. Par ailleurs n'oublions pas les possibilités d'intéraction, des effets de synergie, entre différents constituants, C_3A et C_3S par exemple, et il ne faut pas se borner à additionner les propriétés séparées de chacun.

Mais dans ce domaine la composition n'est pas tout et on commence à entrevoir que la morphologie des cristaux peut influer notablement ; ainsi on a pu entendre dire çà et là que des alites en cristaux hexagonaux ou prismatiques, des bélites en cristaux arrondis donneraient les meilleurs résultats.

En outre la dimension des cristaux a aussi son importance : des petits cristaux de quelques dizaines de microns, peu différents de la grosseur des grains qui résultent du broyage, donnent généralement de très bons résultats du fait qu'à ces dimensions le broyage entraînerait des contraintes plutôt génératrices de défauts et de failles ce qui est favorable à l'hydratation en augmentant la vitesse de pénétration de l'eau. Notons ici que les conditions de refroidissement et de trempe du clinker ne sont pas non plus sans importance.

Pour les éléments mineurs, en schématisant, un ciment riche en alcalins donnera des résistances initiales plutôt plus élevées (effet accélérateur de durcissement) ce qui ne sera plus le cas des résistances finales ; par ailleurs l'insertion et l'inclusion de certains éléments mineurs peuvent être bénéfiques.

N'oublions pas que la résistance mécanique d'un béton outre la résistance propre de la pâte interstitielle de ciment hydraté fait intervenir l'adhérence de celle-ci aux granulats et cette adhérence mécanique par les multiples queues d'arondes qui réalisent une infinité d'ancrages est liée d'une part à des problèmes rhéologiques, la pénétration dans ces anfractuosités, et d'autre part à l'état de surface des grains : la communication de Monsieur AYAPOV nous montre des tentatives de traitement de granulats notamment des laitiers par des actions chimiques.

Par ailleurs il faut dire que la plupart des propriétés des pâtes de ciment durcies sont en relation avec leur porosité et plusieurs communications (qui ne relèvent pas essentiellement du Thème I d'ailleurs) sont consacrées à ce point.

Enfin, bien que cette communication relève de bétons spéciaux (refractaires) il faut citer l'interressant travail de Monsieur TOREANU et collaborateurs qui trouve quelques liens avec ce que nous avons dit plus haut.

V Propriétés du ciment et variations dimensionnelles

Je serai très bref, ici aussi, car il n'y a pas eu de communication traitant de ce sujet, ce qui pourrait laisser penser que tout est connu alors que beaucoup de recherches s'effectuent encore dans ce domaine et celui de la fissuration.

On a trop souvent tendance à relier retrait entravé du ciment et fissuration du béton alors que l'on sait très bien que les causes de fissuration des ouvrages sont multiples et que la plupart du temps le retrait hygrométrique à long terme du ciment, celui que l'on mesure habituellement, n'y a qu'une très faible part. Si le retrait hydraulique d'une pâte de ciment est une grandeur facilement mesurable, en revanche, la fissurabilité qui dépend de très nombreux facteurs intrinsèques ou extrinsèques au béton n'a qu'un caractère aléatoire et ne peut être en aucune manière une caractéristique propre des ciments.

Pour les facteurs qui interviennent sur le retrait d'une pâte de ciment on connait bien l'influence de la finesse de mouture mais moins bien celle de la composition du clinker : il est certain que les alcalins solubles sont connus comme facteurs de retrait, il semble que l'influence de la teneur en C_3A, négligeable jusqu'à 7 ou 8 %, joue au-delà dans le sens d'un accroissement de retrait hydraulique.

Quant aux causes d'expansion elles ont donné lieu à de nombreux travaux et, outre les facteurs extérieurs font intervenir les constituants du ciment tels que chaux ou magnésie libre (périclase), excès de sulfate, réaction avec les granulats; mais on aborde ici les problèmes de la 5ème colonne du Tableau I c'est-à-dire ceux de la durabilité.

VI Composition du ciment et durabilité du béton

Pour ce qui concerne la composition du clinker de base du ciment, il existe une littérature abondante qui confirme que les bétons sont d'autant plus vulnérables à la plupart des milieux agressifs, que la teneur en C_3A du ciment augmente.

On admet souvent qu'au dessous de 7 à 8 % de C_3A il y a fort peu à craindre et en revanche beaucoup au dessus de 10 %, la zone frontière pouvant donner lieu à des discussions.

N'oublions pas toutefois trois remarques qui peuvent être fort importantes :

- Qu'il peut exister des différences relativement notables selon les moyens de chiffrer ou de doser les constituants minéralogiques du clinker et donc le C_3A.
- Qu'ici aussi la forme cristallographique des minéraux peut intervenir au moins autant que leur teneur.
- Qu'enfin ce n'est pas le C_3A anhydre qui est attaqué mais les hydrates parfois fort complexes où l'insertion d'éléments "mineurs" n'est pas sans jouer un rôle.

On peut ajouter deux choses importantes sur lesquelles tout le monde est d'accord :

- Une bonne résistance à la carbonatation et une bonne protection des armatures exigent une forte teneur en chaux et pour les aciers un enrobage suffisant d'un matériau imperméable.
- Deuxièmement l'unanimité est faite sur l'importance de la perméabilité dans les problèmes de durabilité des bétons : il faut donc avant tout réaliser des pièces en bétons compacts et étanches donc des bétons maniables, non ségrégeables, richement dosés en ciment et bien serrés, si cela est réalisé le plus important est fait le reste apparait secondaire.

L'importance de ces divers points de la perméabilité est bien rappelée par la communication de Monsieur MATOUSCHEK.

VII Conclusions

Les résumés que nous avons reçus des travaux de Monsieur SZEKELY de Hongrie et de Monsieur SHESTOPYROV et collaborateurs confirment combien on cherche actuellement

- D'une part à bien mettre en relief le rôle du ciment dans le béton,
- D'autre part combien on souhaite et on recherche des moyens et des critères de prévision des qualités du béton,
- Enfin de la nécessité de connaître parfaitement les relations entre les nombreux facteurs en jeu.

Nous avons vu que si l'on connait généralement assez bien l'influence de la finesse de mouture il reste beaucoup à faire pour bien connaître d'une façon certaine l'influence de la composition : sur le Tableau II j'ai essayé de regrouper ce que l'on croit savoir aujourd'hui : ici aussi ce sont surtout des tendances et vous êtes libres de ne pas être d'accord avec ce qui est indiqué.

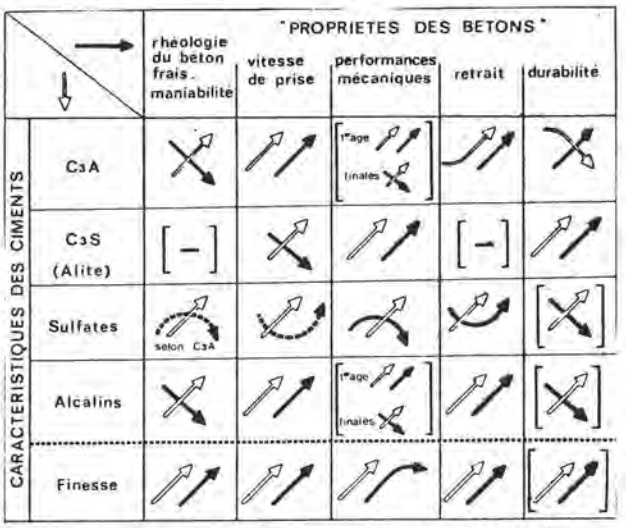

Nota: il s'agit surtout de tendances car il ne faut pas oublier l'interdépendance de nombreux facteurs.

On a beaucoup parlé des alcalins, des sulfates et surtout de C_3A mais on est maintenant sûr que ce n'est pas seulement la teneur de ce composant qui joue mais bien d'autres choses dont les polymorphismes les inclusions, le mode de formation etc ...

En réalité les variables liées à la composition du clinker ne sont pas indépendantes et il y a une telle interdépendance qui commence déjà à partir de la clinkérisation et va bien entendu jusqu'à l'hydratation qu'il est pratiquement impossible de ne faire varier qu'un seul facteur à la fois et surtout on risque d'observer des corrélations qui n'en sont pas ou qui sont hasardeuses sur le plan des mécanismes physico-chimiques.

Néanmoins même s'il reste encore beaucoup de points à éclaircir et de synthèses à effectuer, je pense que l'on peut être optimiste devant le développement de nos connaissance dans ce domaine ces dernières années.

Influence of cement on the properties of fresh concrete

Influence du ciment sur les propriétés du béton frais

Dr. J. GEBAUER, Chimiste, Chef du Groupe « Application du Ciment » du Département Matériaux de la « Holderbank » Gestion et Conseils S.A., 5113 Holderbank, Suisse.

RESUME : L'effet de la composition et de la finesse du ciment sur la consistance, la perte de consistance et le raidissement du béton est discuté à partir d'une investigation compréhensive effectuée sur un grand nombre de ciments industriels et différentes proportions de mélanges de béton.

Au cours de l'investigation, on a utilisé des méthodes d'essai standardisées telles que : besoin en eau pour pâte normale, temps de prise selon Vicat et en plus la résistance à la pénétration à l'aide du pénétromètre Francardi. Les mesures de consistance effectuées sur béton sont : affaissement, degré de compactibilité DIN, étalement DIN, ainsi que la perte de consistance à différents intervalles dès le malaxage et mesure continue de la vitesse de la propagation de l'ultrason durant les premières 24 heures.

Les caractéristiques du ciment influencent significativement les propriétés des pâtes fraiches de ciment. Les facteurs principaux d'influence sont : les teneurs en aluminate, en alcalis et en sulfate du clinker, l'ajout de sulfate de calcium et la granularité du ciment. Les effets du ciment, qui sont facilement mesurables sur pâte, sont fortement affaiblis dans le béton. Par conséquent, on a trouvé, en général, une relation faible entre les propriétés de la pâte et du béton. Certaines relations ont été observées entre l'évolution de la résistance de la pâte à la pénétration, mesurée par pénétromètre, et le raidissement du béton.

SUMMARY : The effect of cement composition and fineness on the consistency, loss of consequency and stiffening of concrete is discussed on the grounds of a comprehensive investigation carried out on a large number of industrial cements and various mix proportions of concrete.

In the investigation standardized test methods on paste were used : water requirement of the standard consistency, Vicat setting time and penetration with the Francardi penetrometer. The tests performed on concrete were: consistency, namely Slump, compacting factor DIN, flow test DIN, as well as loss on consistency at various time intervals after mixing and continuous measurement of ultrasonic pulse velocity during the first 24 hours.

The cement characteristics significantly influence the properties of fresh cement paste. The main influencing factors are : the aluminate - alkali - und sulfate-content of clinker, the calcium sulfate admixture and the particle size distribution of cement. The effects of cement, which can easily be measured on paste, are greatly diminished in concrete. Consequently, the relation between the properties of paste and concrete was generally found to be poor. Some relations were observed between the penetration of paste, as measured by means of the penetrometer, and the stiffening of concrete.

1. INTRODUCTION

The influence of cement upon the properties of fresh concrete is frequently examined on cement paste by means of standard methods on the assumption that there is a close relationship between the properties of cement paste and those of fresh concrete: the water requirement of cement paste is related to the water requirement or workability of concrete, the stiffening rate of cement paste to the loss of workability and stiffening rate of concrete.

The testing methods using cement paste offer the advantage of allowing a better differentiation and thus better comparison between the different cement qualities. A disadvantage consists in the fact that the relationships between the properties of cement paste and those of fresh concrete are sometimes doubtful.

Our investigation was concerned with the influence of the cement upon the properties of both cement paste and fresh concrete. It is based on the comprehensive testing of 48 ordinary portland cement samples from 48 different cement plants. Each cement sample complied with the requirements of the ASTM and DIN standards for type I and type Z 35 F, respectively.

2. INFLUENCE OF CEMENT UPON THE PROPERTIES OF CEMENT PASTE

The water requirement of cement paste of normal consistency depends mainly upon the aluminate and alkali content of clinker and upon the fineness of cement. The following relation was derived from a multiple regression analysis carried out on the 48 portland cements:

$$\text{Water requirement } (\%) = 17.4 + 0.15\,A + 0.26\,B + 0.52\,C$$

A = particle size fraction 10 - 30 µm in weight percent

B = C_3A-content in weight percent

C = total alkali content in weight percent

The correlation coefficient was 0.829.

The stiffening rate of cement paste is influenced by both the composition and fineness of cement; the sulphates and phosphates of clinker generally retard while the aluminate of clinker and the increased fineness of cement accelerate it. The gypsum, if dehydrated during grinding or storage of cement, may cause false set. A calcium sulphate deficiency leads to fast stiffening of the paste which is called flash set.

The stiffening of the cement paste was measured by means of the Francardi penetrometer. The penetrometer continuously measures the stiffening rate of the cement paste, starting immediately after mixing. The false set, as well as other unfavourable types of setting, can easily be recognized by the penetration measurement (see Fig. 1).

The regression analysis of the 48 cement samples did not reveal a satisfactory correlation between the composition of cement and the stiffening rate of cement paste, thus making a reliable prediction of the stiffening rate of paste based on the composition of cement impossible.

3. INFLUENCE OF CEMENT UPON THE PROPERTIES OF FRESH CONCRETE

The correlation between the properties of cement paste and those of concrete was found to be rather poor. Let me illustrate this by a few results of our investigation.

Figure 2 shows the correlation between the water requirement of cement paste and that of concrete, expressed as W/C ratio of concrete of specified consistency. For this testing 13 cements with distinct composition, each being representative for a specific group of cements, were selected from the 48 cements under investigation. A standardized concrete of plastic consistency (slump 7.5) containing 300 kg of cement per m^3 and natural aggregate graded according to Fuller was used for all the concrete tests. The different cement qualities, with a water requirement of the cement paste varying between 24.5 and 28.5%, showed a deviation of the water/cement ratio of concrete of only 0.03.

A comparison between the influence of cement and that of other factors on the water requirement or workability of concrete shows that the impact of cement is rather insignificant. The results of another comparative study on the quality of ready mixed concrete indicated that a substantially greater influence upon the water requirement of concrete is exerted by the aggregate in particular by the sand. In many ready mix plants variations in the water/cement ratio being due to variable batching accuracy have an influence which may not be neglected.

In Figure 3 the possible influences of cement, aggregate, admixture and batching on the water/cement ratio of concrete with specified consistency are compared.

Figure 4 shows the relation between the stiffening rate of cement paste and the loss of workability of concrete. The loss of workability was measured by means of the slump loss after 45 minutes. Again we failed to find a significant correlation between the stiffening rate of paste and the slump loss of concrete. Although it seems obvious that cement with a fast stiffening rate would also have a faster slump loss, the contrary may be true: a cement with false set properties on cement paste showed the lowest slump loss in concrete under our particular testing conditions, i.e. vigorous mixing of concrete in a laboratory pan mixer during three minutes.

As suspected, the attempt to find a correlation between the composition and the properties of fresh concrete - in particular workability and loss of workability - was unsuccessful.

The only distinct correlation between cement paste and fresh concrete was observed between the stiffening rate of paste and that of concrete after placing, measured by means of ultrasonic pulse velocity. The measurement of the ultrasonic pulse velocity in fresh concrete showed a sharp rise in the sound velocity between 2 and 5 hours after mixing (see Fig. 5). The time of this sudden increase in the sound velocity in concrete closely corresponds to the setting time of cement paste

CONCLUSION

The composition and fineness of cement, provided that it complies with the specifications for portland cement, exert only a limited influence upon the properties of fresh concrete, particularly upon the workability and loss of workability.

The pure cement paste reflects the effect of the influence of the cement quality to a much greater degree than concrete. The influence of cement upon the properties of fresh concrete is weakened by "other" factors and by the interaction of these factors. These "other" factors include fine and coarse aggregates, chemical admixtures, fine fillers or active additives, proportioning of concrete, particularly the W/C ratio, temperature of concrete, mixing, transport and placing.

The introduction of special testing methods on cement paste in order to achieve a more differentiated classification of the cement quality with respect to the properties of fresh concrete is hardly advantageous and should be discouraged.

Fig.1

MEASUREMENT OF PENETRATION

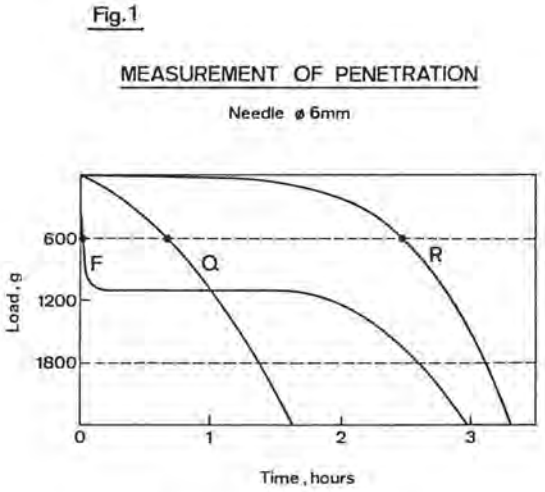

R = REGULAR SET
F = FALSE SET
Q = QUICK (FLASH) SET

Fig.2 RELATION BETWEEN WATER REQUIREMENT OF CEMENT PASTE AND CONCRETE

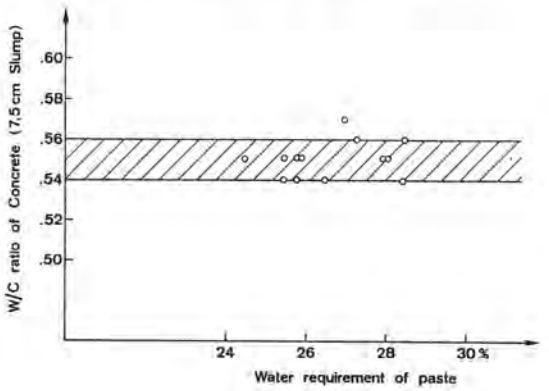

Fig.3 EFFECT OF COMPONENTS OF CONCRETE, PROCESS AND TEMPERATURE ON WATER REQUIREMENT OF CONCRETE

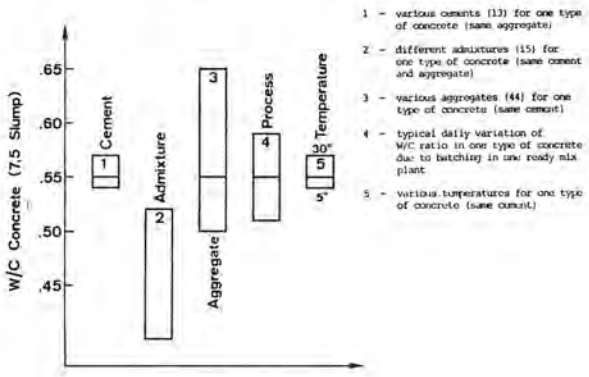

Fig.4

RELATION BETWEEN PENETRATION OF CEMENT PASTE AND SLUMP LOSS OF CONCRETE

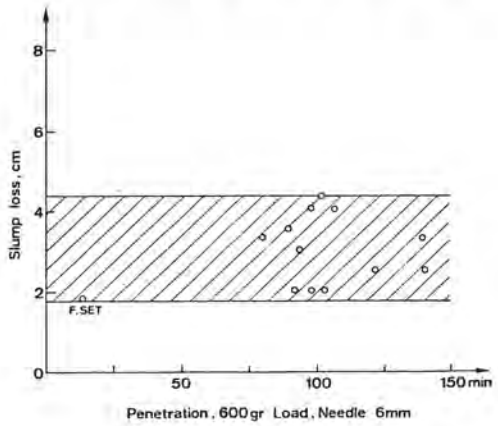

Fig.5

ULTRASONIC PULSE VELOCITY IN CONCRETE

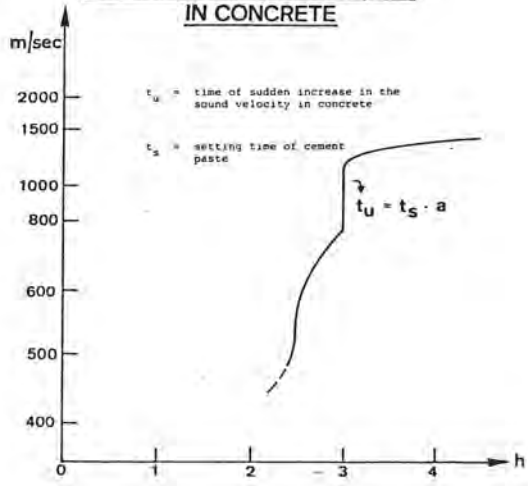

Influence des caractéristiques du ciment sur les propriétés du béton et de sa résistance à la corrosion atmosphérique

The influence of cement properties on the concrete behaviour and its resistance to the atmospheric corrosion

M. MATOUSEK, Chargé de cours, Docteur ès Sciences Techniques, Institut de Technologie des matériaux, Université Technique de Brno, Tchécoslovaquie.

RESUME : La corrosion du béton parsuite des gaz nocifs présents dans l'atmosphère est réglée par les lois de perméabilité. La résistance du béton à la corrosion peut être jugée le mieux d'après son coefficient de résistance à la perméabilité.

La profondeur de la corrosion du béton après un certain temps dans des conditions égales en reste dépend indirectement même de la teneur en CaO réactif dans le béton.

Selon cette réalité il faut donc faire le choix du ciment pour les constructions qui, plus que les autres, sont soumises à la corrosion atmosphérique.

SUMMARY : The concrete corrosion through deterious gases from the atmosphere is governed by the laws of permeation. The concrete resistance to the corrosion can be appreciated the best by the coefficient of permeation resistance.

The depth of concrete corrosion after certain period of time under the same conditions depends also indirectly on the contents of reactionable CaO in the concrete.

Therfore it is necessary to chose the cement for building structures, which are particularly loaded by the atmospheric corrosion.

Les influences atmosphériques agissant sur les matériaux de construction, surtout les bétons, sont assez différents. Il y prédomine cependant l'influence de l'humidité de l'air ainsi que celle de gaz carbonique et de l'anhydride sulphureux. La résistance du béton à ces deux derniers est réglée par d'autres lois qu'il n'en est au cas de la corrosion du béton parsuite des solutions aqueuses, et dans un milieu liquide en général. Les travaux exécutés à l'Institut de technologie de la fabrication des matériaux de bâtiment à l'Université Technique de Brno ont prouvé que la corrosion du béton produite par les gaz nocifs à réaction acide dans les conditions réelles des constructions des bâtiments est réglée surtout par l'état de la structure poreuse capillaire du béton.

Au cas de la corrosion du béton produite par les influences atmosphériques, les gaz se propagent en forme de perméabilité. Pour ce phénomène on peut alors appliquer avec une grande précision la loi de Fourier et la première loi de Fiçk. En examinant plus exactement ces lois d'une façon semblable à celle qui est usuelle dans la technique termique on peut constater que la pénétration des gaz nocifs dans le béton dépend indirectement de la valeur du coefficient de résistance à la perméabilité du béton, évent. du mortier.

Le coefficient de résistance à la perméabilité nous indique combien de fois la résistance à la perméabilité du béton est supérieure à la résistance à la perméabilité de l'air à la même épaisseur et la même température. Au laboratoire on peut le mesurer assez facilement, p.ex. à l'aide des soi-disant méthodes de coupe. De nos expériences il résulte que l'appréciation de la résistance du béton à la corrosion d'après son coefficient de résistance à la perméabilité est tant de fois plus sensible et sûre qu'il n'en était jusqu'à présent d'après sa densité, son poids volumétrique etc.

D'après ce qu'on vient de dire, les lois de la perméabilité sont les meilleures à caractériser la résistance du béton à différent gaz atmosphériques. Ce sont donc des lois physiques. On peut cependant démontrer qu'en même temps on peut y découvrir même des caractéristiques chimiques du ciment employé et de la composition du béton frais, surtout la teneur en anhydride de calcium réactif du ciment. A savoir que si l'on exprime la soi-disant profondeur de carbonatation du béton d'après la loi de Fick comme

$$d = K.\sqrt{\tau} \quad [\,m\,],$$

le coefficient K accompagnant la racine carrée du temps τ [s] sera égal à :

$$K = \sqrt{\frac{2 \cdot D \cdot p}{b \cdot \mu \cdot R \cdot T}} \quad [\,m \cdot s^{-\frac{1}{2}}\,],$$

où D = coefficient de la diffusion du gaz nocif dans l'air [$m^2.s^{-1}$],
p = pression du gaz nocif dans l'atmosphère [Pa],
b = quantité du gaz pouvant se lier dans 1 m^3 de béton [$kg.m^{-3}$],
μ = coefficient de la résistance à la perméabilité du béton [-],
R = constante de gaz de la vapeur d'eau par rapport à 1 kg de vapeur [$J \cdot kg^{-1} \cdot K^{-1}$],
T = température absolue [^oK].

Le coefficient K sera donc inversement proportionnel non seulement à la racine carrée du coefficient de la résistance à la perméabilité du béton, mais encore à la racine carrée de la quantité du gaz nocif donné, p.ex. du gaz carbonique nécessaire pour la carbonatation d'un mètre cube de béton. Cette quantité peut être déterminée, par la méthode stéchiométrique, de la concentration de l'anhydride de calcium qui est contenu dans le béton et qui provient du ciment employé.

Le résultat principal de l'analyse effectuée consiste dans le fait, que le ciment Portland à la teneur supérieure en CaO, fournira avec le même dosage et le même serrage des bétons plus résistants à l'influence des anhydrides carbonique et sulphureux, et d'autres gaz nocifs faisant partie de l'air que les bétons fabriqués avec des ciments à une moindre teneur en CaO, p.ex. avec des ciments contenant du laitier de haut fourneau, de la cendre volante etc.

Un mesurage de longue durée des vieilles constructions en béton réalisé à notre Université Technique a pleinement attesté cette dépendance, c'est à dire que la résistance du béton à la corrosion atmosphérique dépend de la composition du ciment usé. L'expérience a plutôt démontré quen ce cas là, dans les conditions réelles des constructions des bâtiments, l'influence de la teneur en CaO dans le ciment et, parsuite de cela, même l'influence du choix de la sorte de ciment est plus considérable, parce que l'anhydride de calcium se formant grâce à l'hydratation du ciment et présent dans la solution entrecellulaire dans les pores capilaires du béton en plus grande profondeur sous sa surface passe peu à peu vers la surface du béton carbonatant ce qui est dû à la chute de concentration. C'est ici qu'il se lie avec le CO_2 en diffusion tout en formant des cristaux de CO_3Ca appartiennent surtout en modification de calcite. Les néoplasmes cristalliques réduisent le diamètre des capillaires ce qui produit une ultérieure retardation, évent. même l'arrêt d'une ultérieure influence nocive des gaz sur le béton.

Ce fait atteste donc, lui aussi, que les ciments qui, grâce à leur composition ou à la présence des ingrédients, ne font pas de solutions intercellulaires dans les pores du mortier en ciment présentant une assez grande et durable concentration de hydroxyde de calcium pourront servir à préparer seulement des bétons lesquels, dans des conditions en reste égales, auront toujours une moindre résistance à la corrosion produite par les gaz contenus dans l'atmosphère.

Influence of chemical interaction of cement and aggregates on the properties of concrete

Influence de l'interaction chimique et des agrégats sur les propriétés du béton

U. AYAPOV, U.R.S.S.

Positive effect of accelerated chemical interaction of aggregates made from blast-furnace and phosphoric slag with cement on concrete properties was shown. This interaction was accelerated by preactivation of grains surface of aggregates with water solutions of H_2SO_4.

Quantity of the studies on surface grain activization of aggregates and fine-grained additives to concrete and mortars is not so large though the actuality of this problem is not disputed.

It is shown in the study of Yurkul/I/ that during treatment of aggregates by polyhydrociloxane emulsion ГКЖ-94 /GKZh-94/ new growth in the contact zone of aggregates with cement paste in the form of polyorganocalciumsiloxane appears which expands adhesion.

Ljubimova/2/ has suggested to treat the sand from quartzite by 10 % HCI and distillated water and following activation of it by the saturated solution of calcium oxide. Such treatment in the author's opinion makes far better crystallization of calcium hydrosilicates on the more large particles of quartz sand which increases the strength of mortars.

It was shown in /3/ that surface treatment of large aggregates with phthalic acid was enlarging the adhesion strength of mortars to 20–40 %.

According to USA Patent No. 395222/4/ the treatment of fly ash by water solutions of inorganic acids for example by 10% HCI concrete strength in the age of 72 hours has been increased almost 2 times. But it is necessary to point out that ash after acid treatment was not washed with water. Therefore the increase of the concrete strength in the earlier dates of hardening is possible to relate with acceleration of concrete hydratation and hardening.

The treatment of aggregates from blast-furnace slags with HCI solution du-

ring 24–48 hours before the concrete preparation has also increased the bending strength of concrete to 15 %/5/.

The effect of increasing of adhesion strength of mortars with the surface of lining ceramic tiles was also found during theatment of surface of these tiles with the 5 % solution of HCI.

According to /7/ freashly crushed materials are having increased adhesion strength with mortar which is explained by increased chemical activity of their surface

Application of clinker from Portland cement as aggregates is increasing concrete strength to one order because of appearing of chemical bonding between aggregates and cement paste/8/.

Taking into consideration that GKZh-94 and phthalic acid are expensive and scarse materials we have studied the influence of aggregates activization with water solutions of HCI which was comparatively cheap and not scarse product. Aggregates were prepared by the crushing of crystallized phosphoric and blast-furnace slags.

Blast-furnace slags consisted as a rule from melilite and gehlenite and phosphoric slags - from pseudo-wallastonite. P_2O_5 content in it was ~ 2 % and F-content ~ 2,5 %.

In order to obtain optimal parametres of slag activization the kinetics of their destruction by water solutions of HCI was studied and phase composition of new growths was defined. In all cases the quantity of HCI solution was taken equal to Zh / T= 0,5 by volume.

For the preparation of concrete samples Portland cement -400 and sand from slag and natural sand with standardized grain composition were used.

Standard methods of preparation, hardening and testing of concrete samples were used.

Slag destruction rate was measured by the temporal pH values of water solution of H_2SO_4 in comparison with the results of SO_4^{2-}-ions content determination in solution by chemical analysis.

Adhesion strength of grains of slag aggregates with cement paste was determined by testing of samples made in the form of number 8 in the middle of which prisms from aggregates with the dimensions corresponding to minimal cross-section of number 8 were placed.

Reaction kinetics between slags and water solutions of H_2SO_4 is satisfactorily discribed by the first order equation:

$$k = \frac{1}{\tau} \ln \frac{c}{c_o}$$

where c_o = initial concentration of H_2SO_4

c = concentration at the moment τ

Limiting stage of the reaction possibly is H_2SO_4 diffusion through the layer of hard-dissoluble new growth /gips and silica-gel/ formed on the grains surface.

Dependance of reaction rate constant from temperature in the Figure I shows that at the temperature 20-80°C this factor has insignificant meaning. Con-

sequently process of aggregates activization is possible to carry at usual temperatures without special lowering of its intensity.

It was found out by X-ray, petrographic and thermographic analyses that products of slag destruction by H_2SO_4 are basically silica gel and gips which preferably are precipitated on the surface of grain aggregates.

Values of adhesion strength of activated aggregates from phosphoric and blast-furnace slags are given on the Figures 2 and 3. It is seen from them that there are optimal concentrations and period of preparation of aggregates. For example, for the aggregates from slags the best adhesion strength with cement paste is seen for the water solution of H_2SO_4 with concentration 0,I M and with the maintaining of aggregates in this solution during I2-48 hours.

During these periods of time difference between adhesion strength of aggregates with cement is not significant.

Adhesion strength of activated aggregates with cement is increasing more than 2 times after 7 days of concrete hardening and to 85 % after 28 days in comparison with the values for the non-activated aggregates. The effect of adhesion strength increase with cement for aggregates made from blast-furnace slags was on the average I0 % lower than for the aggregates from phosphoric slags.

When the concentration of H_2SO_4 /0,5--I,0 M/ solution increases adhesion strength of aggregates with cement paste lowers and the thickness of contacting layer increases. Thickness of zone in contact equal to 60-200 μm corresponds to maximum positive effect. At the bigger concentrations of reagent stratification within contacting zone is taken place/Figure 4/. It is possible that at the bigger thicknesses of contacting zone its adhesion is determined exclusively by cohesion of new growths in solid state appearing during treatment of aggregates by the reagent. At optimal thicknesses of contacting zone its strength is conditioned by adhesion of low-based hydrosilicates with aggregates; these hydrosilicates are appearing as a result of interaction of hydrolyzed calcium oxide of cement with silica gel which is near the grains' surface of preactivated aggregates; therefore they in its turn are having more strong ion bond with original matter of aggregates.

It is necessary to consider paper of reference /9/ where it is shown that strength of adhesion coupling between aggregates and cement paste lowers as thickness of contacting layer increases.

Study of phase composition of new growths in contact zone of preactivated aggregates with cement paste has shown that they were as a rule gypsum, silica gel and gel-like calcium hydrosilicate C-S-H. Portlandite and calcium hydrosul-

foaluminate are also present. Contents of gypsum, silica gel, and C-S-H increases with the increase of H_2SO_4 solution concentration and treatment time and contents of portlandite lower what is seen from from thermographical and radiographical data/Figures 5 and 6/. Analogous data were received during study of contacting zone between preactivated aggregates from blast-furnace slags and cement paste.

Data concerning water demands of concrete mixtures on the basis of activated phosphoric-slag aggregates are given in Table I.

It is possible to conclude from the data in Table I that aggregates activation considerably lowers water-demand of concrete mixtures. Concrete mixtures with concentration 0,I-0,5 M have the lowest water demand during seasoning equal to I-3 hours.

Further increase of solution concentration and elongation of treatment lowers positive effect.

Data concerning stability of concrete made with activated aggregares from phosphoric slags are given on Figure 7.

It follows from these data that concretes with activates aggregates have strength which is I,4-I,6 times/ by I00-200 kg/cm^2 / more than concretes made with non-activated aggregates.

For the preparation of steamed concretes positive effect of aggregates activization is higher when cement expenditures are higher. Optimal parametres of activation process of slag aggregates are: H_2SO_4 solution concentration- 0,I-0,5 M; period of seasoning of aggregates- I-3 hours. Solution quantity is 0,5 ton/m^3.

Positive effect of slag aggregates activization may be used both for the obtaining of high-strength concretes of grades 5oo-6oo using common cement of grade 4oo by widely used technology of vibroformation and for the lowering of cement expenditures for concretes to 20-30 %.

Determination of strength and deformation properties of concretes with activated aggregates has shown that they at equal indications of strength are the same that the properties of concretes with usual aggregates. Special interes has various increase of adhesion strength of concretes on activated aggregates with steel framework/Table 2/, which allows to use activated aggregates for the preparation of pre-stressed concretes and constructions with steel framework.

Concrete mixture on the basis of activated phosphoric slag aggregates is recognized as the invention/I0/.

Conclusions

It is shown that activation of surface grains of aggregates from blast-

furnace and phosphoric slags by maintaining them in weak water solutions of H_2SO_4 considerably increases adhesion strength of them with cement paste, lowers water-demand of concrete mixtures or increases packability and causes increase of adhesion strength of concretes I,4–I,6 times or allows to lower cement expenditures to 20–30 %.

Optimal parametres of activation of slag aggregates were elaborated. It was shown that new growth in the form of silica gel on grain surface of activated aggregates quickly reacted with hydrolysed calcium oxide of cement forming C-S-H- gel. Silica gel layer of 200. μm on the surface of aggregates grains was causing increased adhesion strength of it with cement paste and with original aggregates grains providing ion bond in contact zone.

It is possible to make chemical activation of concrete aggregates and solutions of every chemico- mineralogical composition using special methods and reagents which makes this branch rich in perspectives.

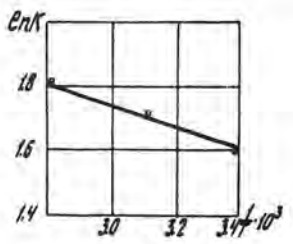

Fig. 1

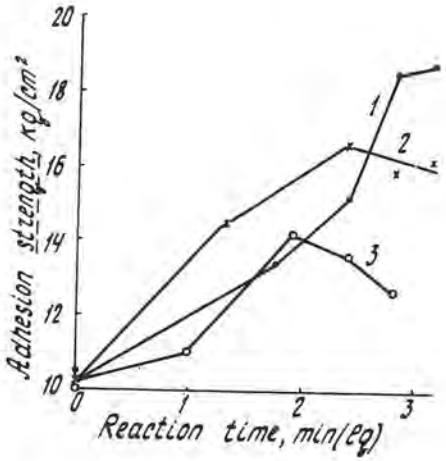

Fig. 2

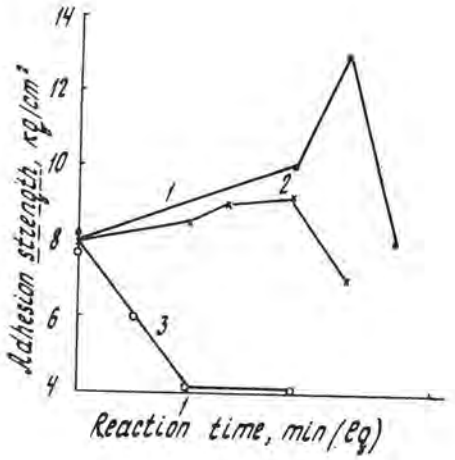

Fig. 3

REFERENCES

I. Yurkul M.A. Vliyanie obrabotki zapolnitelya rastvorami PAV na svoystva betonnoi smesi i betona. Avtoreferat dissertatsii na soiskanie uchenoi stepeni kandidata tehnicheskih nauk. Odessa, I976.

2. Lyubimova I.Yu. Vliyanie sostoyaniya poverhnosti kvartsevogo zapolnitel'a na kristallizatsionnoe tverdenie tsementa i svoistva tsementnogo kamnya v zone kontakta. "Kolloidnyi zhurnal", v. 29, No. 4, I964, p.546.

3. Shteiert N.P. Izuchenie stsepleniya tsementnogo testa s zapolnitelem. Avtoreferat dissertatsii na soiskanie uchenoi stepeni kandidata tehnicheskih nauk. L., I950.

4. USA Patent C1 I06-97 (C04B, 7/02) No. 395222, filed I0.04. I974 (Ser.No. 459587), patented 27.04.I976. Bainton John W. Addition of acidulated pozzolan to concrete and concrete products.

5. Leshchinskij M.Yu. O soprotivlenii k izgibu betonov na zapolnitel'ah iz domennyh shlakov. Kiev, Stroiizdat, I958.

6. Belyaeva G.M. Issledovanie stroitel'nyh rastvorov dlya oblitsovochnyh plit. Avtoreferat dissertatsii na soiskanie uchenoi stepeni kandidata tehnicheskih nauk. Kiev, I958.

7. Adamchik K.A. Materialy nauchno-koordinatsionnogo soveshchaniya po avtomatizatsii i usovershenstvovaniyu protsessov prigotovleniya i uplotneniya betonnyh smesei. M., NShZhB, I962.

8. Kuntsevich O.V., Makarevich O.E. "Sbornik trudov Leningradskogo Instituta inzhenerov zheleznodorozhnogo transporta", I976, Vyp 398, str. II4-I2I.

9. Matveenko A.D., Leshchinskij M.Yu., Chernyshev Yu.M. "Izvestiya vysshih uchebnyh zavedenij", Seriya "Stroitel'stvo i arhitektura", I960, No.4, Moskva.

I0. Ayapov U.A., Timashev V.V., Rodionova A.A., Yankovskaya G.N. Betonnaya smes'. Avtorskoye svidetel'stvo SSSR, No. 662521, Ofitsial'nyi byulleten', No.I8, I979.

Figures

Fig.I. Dependance of rate constant of slag destruction by H_2SO_4 from temperature.

Fig.2. Adhesion strenfth of activated phosphoric slag aggregates with cement paste after hardening during 28 days in usual conditions. I. Solution concentration/C/ = 0,I M; 2. C=0,5 M; 3. C=I,0 M.

Fig. 3. Adhesion strength of activated blast-furnace slag aggregates with cement paste after hardening during 28 days in usual conditions. Symbols are the same as in the Fig. 2.

Fig.3. Micrographs of contact zone between aggregates activated during 24 hours and cement paste. a) aggregates from non-activated phosphoric slag; b) with concentration/C/ of H_2SO_4 = 0,I M; c) C=0,5 M; d) C= I,0 M.

Fig.5. Thermograms of new growths in contact zone between activated phosphoric slag aggregates and cement paste. a) non-activated aggregates; b) aggregates activated with H_2SO_4 solution concentration/C/ = 0,I M; c) C=0,5 M; d) C=I,0 M.

Fig.6. X-ray diagrams of new growths in contact zone. Symbols as in Fig. 5.

Fig. 7. Compression strength of concrete made with activated aggregates. a) samples in 24 hours after steaming; b) samples in 28 days after steaming; c) samples in 28 days after nardening at usual conditions; I. activation period of aggregates /τ/ I hour; 2. τ = 3 hours; 3. τ = 24 hours;

—— projected grade of concrete /M/ 500;

- - - M= 300

-.-.-. M= 200

Table I

Water-demand of concrete mixtures on the basis of preactivated aggregates at settling of Abrams cone of 2-4 cm.

planned concrete grade	w/c for concretes made from non-activated aggregates	solution concentration M	w/c for concretes made from activated aggregates		
			activatai on period /hours/		
			I	3	24
500	0,32	0,I	0,26	0,26	0,28
400	0,40		0,32	0,32	0,33
300	0,5I		0,40	0,40	0,42
200	0,67		0,5I	0,5I	0,53
500	0,32	0,5	0,26	0,26	0,28
400	0,40		0,32	0,32	0, 4
300	0,5I		0,40	0,40	0,44
200	0,67		0,5I	0,5I	0,56
500	0,32	0,I	0,28	0,29	0,32
400	0,40		0,36	0,38	0,44
300	0,5I		0,43	0,44	0,48
200	0,67		0,56	0,57	0,62

Table 2

Adhesion strehgth of concretes on activated aggregates with steel framework

Solution concentration M	exposition period hours	w/c of concretes	adhesion strength, kg/cm^2	
			at the age of 28 days after steam treatment	after normal hardening during 28 days
0	0	0,40	45	48
		0,67	26	29
0,I	I	0,34	84	86
		0,54	55	57
	3	0,34	92	II0
		0,54	63	70
0,5	I	0,34	93	I02
		0,54	62	65
	3	0,34	I03	I20
		0,54	67	78

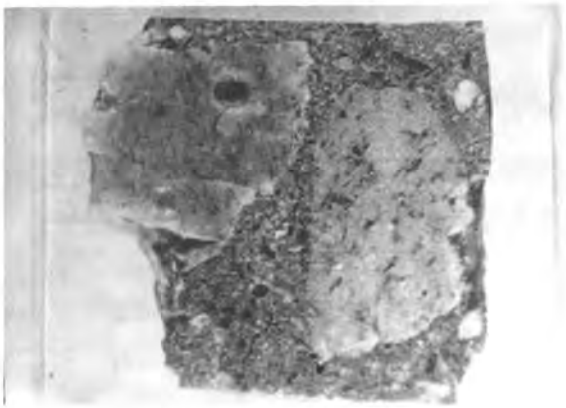

Fig. 4a

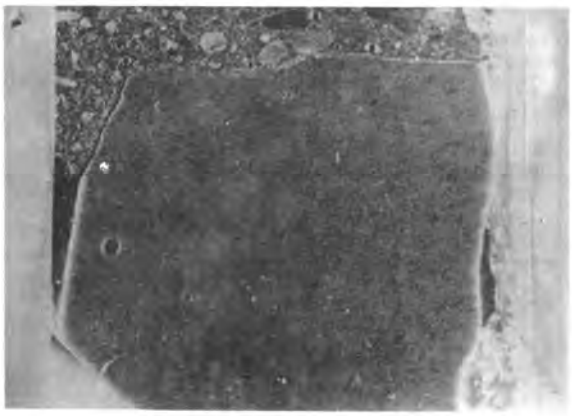

Fig. 4b

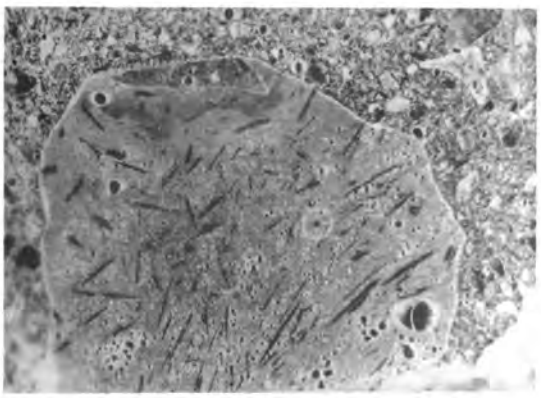

Fig. 4c

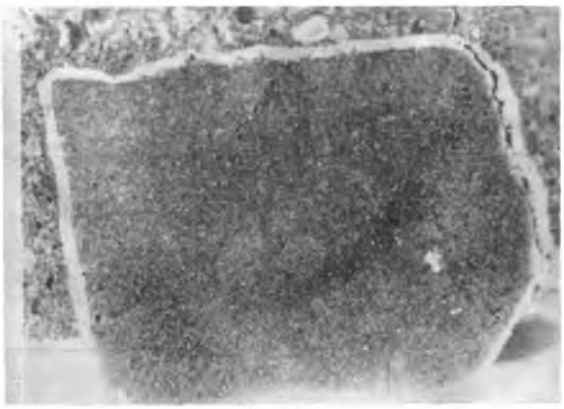

Fig. 4d

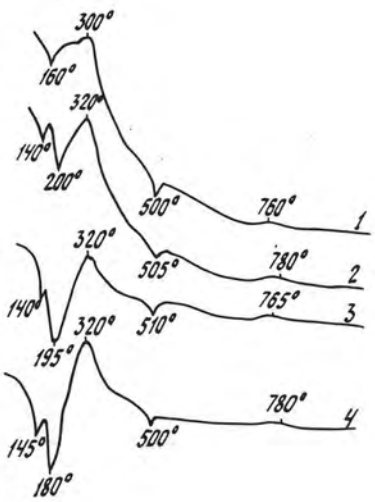

Fig. 6

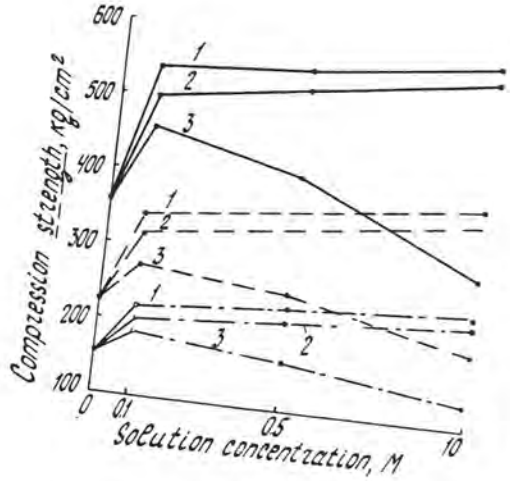

Fig. 7a

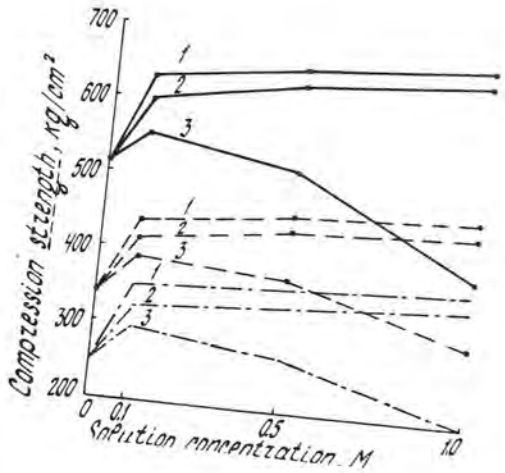

Fig. 7b

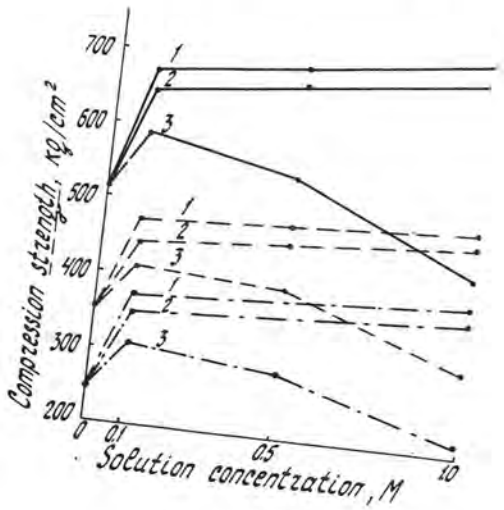

Fig. 7c

The development of porosity in hydrated pastes and water-cement ratio

Evolution de la porosité dans les pâtes hydratées et rapport eau-ciment

V. LACH, Professor Department of Building Material Technology, Technical University, Brno
M. ROSOVA, Assistant Department of Building Material Technology, Technical University Brno, Tchécoslovaquie.

SUMMARY : The development of porosity was studied on the pastes prepared from various cement samples and from cement clinker. The variables were: the water-cement ratio w (0.30, 0.35, 0.40 and 0.50) and the time of curing (7, 14, 28 and 56 days).

The microstructure of hardened pastes was determined by means of mercury porosimetry, X-rays diffractometry, thermography and observed by scanning electron microscope as well.

The various water-cement ratio w were manifested as follows:
- the porosity increases with water-cement ratio and decreases with the time of curing. The correlation could be expressed mathematically;
- the chemical and mineralogical composition and the fineness of cement influences the initial porosity more then the time of curing;
- with high water-cement ratio the hydrated components form coarser crystals as the product of "outer" hydration and
- the contact between the hydration products are not so frequent;this was found out by the scanning electron microscope.

RESUME : L'évolution de la porosité a été étudiée sur les pâtes préparées de ciments differents et de pure clinker de ciment. Les variables ont été: le rapport eau - ciment (0.30, 0.35, 0.40 et 0.50) et la periode retenue (7, 14, 28 et 56 jours).

La microstructure des pâtes durcies ont été determinées par la porosimetrie de mercure, diffraction X, l'analyse thérmique et aussi observées dans le microscope électronique à balayage.

Les rapport differents eau-ciment ont manifestés comme suivit:
- la porosité s'agrandit avec le rapport eau-ciment et diminuit pendant le temps de la consérvation. La correlation peut être exprimée mathématique;
- la composition chimique et minéralogique et la granulometrie influencent la porosité plus que le temps de la consérvation;
- avec grand rapport eau-ciment les composents hydratés forment les grands crystals comme les produits de la hydratation "extérière" et
- les contacts entre les produits de la hydratation ne sont pas si fréquents, ce qui était trouvés par le microscope à balayage.

INTRODUCTION

The properties of hardened Portland cement pastes depend not only on the amount and character of the solid phase, but also on the volume, diameter and shape of the pores (1). During the hydration and formation of the cement stone, a part of the water is more or less firmly bound into the solid phase and a part remains in the capillaries of the hardening paste. This water exerts a decisive influence onto the changes of the porous system in the microstructure of the cement paste during the hardening and influences the ratio between the solid and "zero" phase which together with the diameter and the shape of the pores determine eg. the strength characteristics of the cement stone, as has been shown by numerous authors, eg. Powers (2), Grudemo (3), Kondo and Daimon (4), etc.

The kinetics of pore system formation in the cement stone, dependent on its hardening time and conditions, on the mineralogical composition and the fineness of the cement, was studied eg. by Diamond (5), Chekhovsky and Berlin (6), etc. So far, however, it has not been sufficiently clarified.

The volume and the pore size distribution in hardened pastes can be determined by two methods: a) by calculation from either adsorption or desorption isotherms, or b) by calculation from the relationship between the pressure and volume of mercury intruded into the hardened paste. The results of these two methods deffer and are limited by the diameter of the determinable pores, i.e. below 300 Å in the first case and in the range of 0.0075 to 7.5 /um in the mercury method. It is assumed that the total pore volume as measured by mercury intrusion is more nearly equal to the volume of evaporable water in saturated pastes (1).

In the cement stone microstructure can be found pores of various sizes. They are named in different ways according to their location and sizes. So far no unified classification has been worked out, so that the marking and division of pores differ from author to author (4).

On the basis of the previous as well as our own findings we divided the pores in a simplified manner according to their location in the microstructure into a) internal pores which appear in the gel and in the crystallites of the hydration products, and be external pores formed between the gel and crystallite grains. With the division is also connected the diameter of the pores and the method of its determination (7).

Internal pores are determined by adsorption methods (small d < 12 Å, large d > 12 Å), external pores by mercury porosimetry (small d < 0.2 /um, medium d = 0.2 - 1.0 /um, large d = 1.0 - 15 /um). With regard to the fact that in this way can be determined pores up to a size of d = 75 Å, it is possible to classify according to the method employed the pores in the above manner.

In this study we are not dealing with internal pores that represent only a part of the total pore volume and are limited to the formed C-S-H phases, but with external pores. These pores are in the course of the cement stone formation subjected to considerable changes that are connected with the hydration of clinker minerals and their volume is also influenced by the employed water-cement ratio.

It follows from the above that with the aid of mercury porosimetry we are determining the volume and distributoin of external pores, limited up to a diameter of d = 15 /um, and we thus obtain knowledge about the formation and strengthening of the microstructure in the course of the hardening of the cement paste on the basis of changes of the pore system, in this case also with special reference to the effect of the water-cement ratio (w).

EXPERIMENTAL

The samples chosen for the present studies were various Portland cements, slag-Portland cements and cement clinker. The properties of the samples are given in Table 1.

Pastes of a water-cement ratios w = 0.30, 0,35, 0.40, and 0.50 were prepared in the form od prismatic rods with the dimensions 10 x 10 x 30 mm. After 24 hours the prismatic rods were removed from the mould and conditioned under water. At the time of testing (7, 14, 28 and 56 days), the samples were dried for a period of 24 hours at 105 °C and analyzed.

The development of pores in the microstructure of the hardened pastes was determined by mercury porosimetry. Apart from that, the samples were studied by means of thermal analysis, X-ray diffractometry and observed in the scanning electron microscope.

Mercury porosimetry

The total pore volume TPV and the individual pore distribution IPD were determined in all samples. The minimum TPV were always obtained for a water-cement ratios of w = 0.5 after 56 days of conditioning, the maximum TPV with ratios of w = 0.5 after 7 days of conditioning. The clincer sample exhibited in both cases the smallest TPV, the slag-portland cement samples M and H SPC 250 the highest TPV values.

Analysing the results it follows that the greatest influence onto the external pore volume is exerted by the water-cement ratio, as can be seen from a comparison of TPV values at w = 0.30 and w = 0.50 for a conditioning period of 7 and 56 days, respectively (Table 2).

The microstructure of the samples with w = 0.30 exhibited roughly half the TPV value than for w = 0.50. It should be noted that the M PC 400 sample appeared as anomalous and approached the behaviour of slag-portlabd cement.

If we compare the investigated renge of the water-cement ratio w = 0.30 and 0.50, we find that already a small change in w causes

Table 1. Chemical and mineralogical composition of samples								
Sample	M PC 475	M PC 400	H PC 400	B PC 400	M JPC 450	M SPC 250	H SPC 250	M clincer
Ign.loss	1.86	3.93	1.46	2.15	1.54	3.95	7.09	1.27
SiO_2+in.r.	21.87	21.86	22.27	21.04	22.04	28.00	23.91	21.09
Al_2O_3	5.36	5.09	5.78	5.75	5.35	5.94	5.96	5.48
Fe_2O_3	2.86	2.59	2.60	3.05	2.92	1.90	2.06	3.29
TiO_2	0.21	0.21	0.23	0.23	0.19	0.23	0.19	0.22
CaO	61.91	60.57	63.54	62.36	62.94	50.55	53.65	65.28
MgO	1.44	1.12	1.30	1.75	0.97	4.46	2.48	1.07
K_2O	0.98	0.86	0.78	0.85	0.91	0.78	0.87	0.95
Na_2O	0.29	0.30	0.14	0.12	0.35	0.40	0.21	0.29
SO_3	2.80	3.08	1.51	2.28	2.43	2.86	3.05	0.71
	99.58	99.61	99.61	99.58	99.64	99.07	99.47	99.65
Insol.res.	1.99	1.97	1.14	1.52	1.04	2.88	4.05	0.24
Bogue C_3S	45.67	42.49	46.82	50.93	48.56			63.90
C_2S	28.26	30.63	28.54	21.91	26.57			12.27
C_3A	9.37	9.11	10.92	10.08	9.24			8.95
C_4AF	8.71	7.88	7.91	9.28	8.89			10.01
Blaine cm^2/g	3350	3220	2790	3650	3690	3170	4490	3230

Table 2. TPV in mm^3/g after 7 days			
	w = 0.50	w = 0.30	%
M PC 475	286	123	43
M PC 400	346	176	51
H PC 400	293	111	38
B PC 400	253	111	44
M JPC 450	286	119	41
M SPC 250	329	156	47
H SPC 250	356	188	45
M clincer	225	102	45
TPV in mm^3/g after 56 days			
M PC 475	186	98	52
M PC 400	237	117	49
H PC 400	155	82	52
B PC 400	186	83	44
M JPC 450	18o	87	48
M SPC 250	215	137	63
H SPC 250	257	115	44
M clincer	134	61	45

Table 3 Pore volume of d<0.20/um-7 days				
	w 0.3	% of TPV	w 0.5	% of TPV
M PC 475	11.3	9	132.9	46
M PC 400	85.3	48	248.1	72
H PC 400	16.9	15	143.5	49
B PC 400	7.7	7	110.9	44
M JPC 450	11.2	9	131.4	46
M SPC 250	83.6	54	251.6	76
H SPC 250	29.9	16	197.2	55
M clincer	20.4	30	97.0	43
Pore volume of d< 0,20/um -56 days				
M PC 475	10.5	11	34.0	18
M PC 400	14.1	12	127.3	54
H PC 400	12.0	15	19.0	12
B PC 400	4.9	6	26.0	14
M JPC 450	9.9	11	20.4	11
M SPC 250	16.2	12	101.0	47
H SPC 250	11.3	10	53.0	21
M clincer	6.3	10	32.2	24

a large change of TPV. When the water-cement ratio is reduced e.g. by 0.01, TPV drops by 2.5 to 2.75%, i.e. absolutely 6 - 9 mm^3/g after 7 days and 3 - 6 mm^3/g after 56 days of conditioning. This fact confirms a considerable sensitivity of the water-cement system onto the amount of added water and the favourable effect of additives that reduce this water amount.

Not only the total pore volume TPV, but also the individual pore distribution exhibits for various water-cement ratios w considera-

ble differences. The greatest changes occur for pores with a diameter of d = 0.20 /um through 15 /um, as can readily be seen from Table 3.

The pores with the size d = 0.2 /um represent for w = 0.50 after 7 days conditioning practically half of all the measured pores (43 to 55 %). This proportion of pores drops for w = 0.30 to 7 - 15 % for Portland cements, with the exception of the anomalies observed in M PC 400. For slag-Portland cements it is different (54 and 16 %).

The proportion of pores d = 0.20 /um can decreased markedly for w = 0.50 after 56 days (11 to 21 %) and approached the values for w = 0.30.

The reduction of the total pore volume TPV is caused by the filling of the pores with hydration products and partly also by the overall shrinkage of the hardened paste. The hydration products are readily formed in the region of water filled pores, so that the large pores are reduced and the small ones even filled up. Since for w = 0.50 has occurred in contrast with w = 0.30 a considerable decrease of the d > 0.20 /um pore volume, it can be assumed that the hydration products are crystalically better developed due to the influence of the present liquid phase. In other words, in this case prevails the "outer" hydration over the "inner" hydration which leads rather to gel and imperfectly developed products (8).

As is generally known, a reduction of the water-cement ratio w leads to the growths of strengths. With regard to the previous findings, this is caused on one hand by a smaller total pore volume TPV and thus by a denser microstructure, on the other hand also by a greater tendency for the formation of gel and imperfectly developed hydration products. Cohesion and adhesion are caused by surface forces, especially by the influence of the huge surface of the C-S-H gel, whose proportion in the microstructure also increases the strengths of the hardened paste. The crystalline products exhibit on the other hand a smaller specific surface and thus also a smaller number of contacts, so that the mechanical properties show a decrease.

The total pore volume TPV was influenced also by the type of cement. The group of Portland cements forms microstructures which have smaller TPVs than slag-Portland cements. As long as differences exist among Portland cements, this can be attributed to the influence of the fineness of grinding. An exception is represented by the Portland cement M PC 400.

Both slag-Portland cements have TPVs in comparison with Portland cements larger by 21 and 45 % (w = 0.50) and by 58 and 32 % (w = 0.30), respectively, after 56 days of conditioning. The filling of pores with hydration products occurs more slowly also for w=0.50. That means that slag-Portland cements do not exhibit such a tendency for the formation of hydration products that grow into the pores, and that hydration takes place more slowly even for a higher w. The larger porosity of the microstructure of slag-Portland cements is caused by the presence of slag and its slow hydration. This is the reason why the formed gel and sparsely crystalline hydration products, despite their favourable binding properties, are not able to compensate the low compactness of the microstructure of the hardened paste. This explains the worse mechanical properties of the slag-Portland cements and also the phenomenon that only after a very long period of conditioning they approach with their porosity the Portland cements. The differences in the volume and distribution of pores between the two slag-Portland cements are caused by a different "activity" of the slag and their fineness of the cement.

The total pore volume TPV for the M clinker attained the smallest values. The microstructure of the hardened paste was in all cases the most compact.

The influence of the conditioning period was the same in all the samples. The total pore volume TPV gradually dropped, until it reached the smallest values after 56 days. The water-cement ratio exhibited no substantial influence onto the course of TPV reduction, as can readily be seen from Table 4.

Table 4 Total pore volume TPV for w = 0.50

	7 days	56 days	%
M PC 475	286	186	65
M PC 400	346	237	68
H PC 400	293	155	53
B PC 400	255	186	73
M JPC 450	286	181	63
M SPC 250	329	215	65
H SPC 250	356	257	72
M clinker	225	134	60
Total pore volume TPV for w = 0,30			
M PC 475	123	98	80
M PC 400	176	117	66
H PC 400	111	82	74
B PC 400	111	83	75
M JPC 450	119	87	73
M SPC 250	156	137	88
H SPC 250	188	115	61
M clinker	102	61	60

From this follows the important conclusion that TPV depends even after a long conditioning period on the starting TPV, and that the porosity dependent properties of the hardened paste can by conditioning be improved only to a certain extent, as the pores are gradually depleted.

We have tried to express the development of

pore matematically. By plotting TPV against time, the curves of an exponential character were obtained (Fig. 1), for which holds true

$$TPV = a \cdot e^{-\alpha \tau} + b \qquad (1)$$

where TPV is the total pore volume, τ the conditioning period and α, a, b are constants.

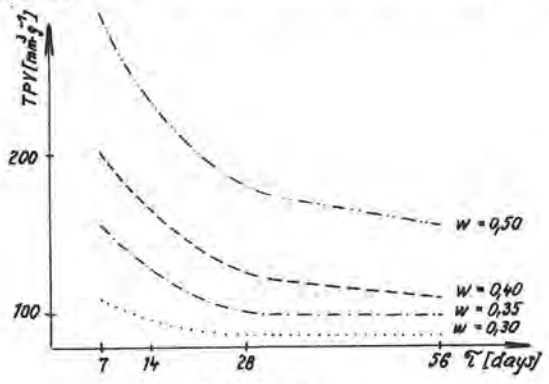

Figure 1

It can be assumed that the total pore volume TPV will not practically change any more with time after 56 days and it can therefore be used as the orientational value b. By introducing the water-cement ratio into the calculation and from the known values of TPV, τ and the orientational value b were determined the values a, b and α for each water-cement ratio and shown graphically (Fig. 2).

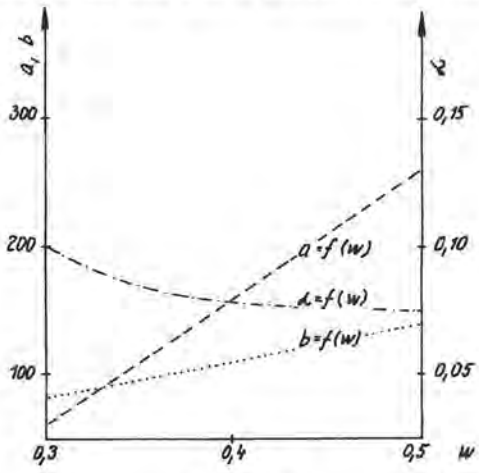

Figure 2

The plots a = f(w) and b = f(w) can be taken as straight lines and expressed by the relationships

$$a = (Aw + B) \qquad (2)$$

$$b = (Cw + D) \qquad (3)$$

The relationship $\alpha = f(w)$ was expressed by a parabola according to the relationship

$$\alpha = (p_2 w^2 + p_1 w + p_o) \qquad (4)$$

This dependence can also be expressed exponentially by the relationship

$$\alpha = (p + q^{-rw}) \qquad (5)$$

By substituting the constants a, b and α into equation (1) are obtained the following TPV depletion equations against time τ and the water-cement ratio w:

$$TPV = (Aw+B).e^{-(p_2 w^2 + p_1 w + p_o).\tau} + (Cw+D) \qquad (6)$$

$$TPV = (Aw+B).e^{-(p+q^{-rw}).\tau} + (Cw+D) \qquad (7)$$

The above equations were verified on the actual case of the H PC 400 sample and the following parameters were calculated:

$$a = -219.46 + 945.75\ w \qquad (2')$$

$$b = -26.73 + 350.35\ w \qquad (3')$$

$$\alpha = -0.3364 + 1.1506 - 1.2743\ w^2 \qquad (4')$$

By substituting into equation (6), we obtained for this sample the equation

$$TPV = (945.75w-219.46).e^{-(0.3364-1.1506w+1.273w^2).\tau} + (350.35w - 26.73) \qquad (6')$$

The calculated and determined TPV values shown in Table 5 indicate a good agreement of the two values and confirm the significance of the water-cement ratio w and the starting pore volume TPV.

Table 5 The calculated and measured values of total pore volume (TPV_c and TPV_m)

w		TPV_c	TPV_m	Δ TPV	%
0.30	7	109.5	111	-1.5	1.35
0.30	14	93.1	98	-4.9	5.09
0.30	28	81.8	84	-2.2	2.57
0.30	56	78.7	82	-3.3	4.02
0.35	7	155.6	158	-2.4	1,52
0.35	14	127.8	90	+37.8	mist.
0.35	28	105.1	102	+3.1	3.04
0.35	56	96.8	101	-4.2	4.15
0.40	7	204.3	202	+2.3	1.14
0.40	14	165.4	167	-1.6	0.96
0.40	28	130.5	123	+7.5	6.09
0.40	56	115.0	109	+6.0	5.50
0.50	7	293.0	293	0	0.00
0.50	14	231.8	234	-2.2	0.95
0.50	28	176.0	181	-5.0	2.75
0.50	56	151.0	155	-4.0	2.58

Thermal analysis

The thermal analysis was suitable for the determination of $Ca(OH)_2$ and $CaCO_3$. The amount of $Ca(OH)_2$ increased with the water-cement ratio and with the conditioning period τ up to 28 days. After that they do not change any more. With slag-portland cement the amount of $Ca(OH)_2$ did not change

practically after 14 days and grew slightly with a larger water-cement ratio w. It was possible to ascertain that the quantity of bound water has grown with the conditioning period τ and the water-cement ratios w in all the samples on the average by 30 to 45%.

X-ray diffractometry

By X-ray diffractometry the presence of C-S-H phases, portlandite and calcite, apart from non-hydrated clinker minerals, especially β-C_2S, was identified. Also weak lines belonging to ettringite and C_4AH_{13} were found. In certain Portland cement samples were also determined weak lines d_{hkl} = 11 Å.

Scanning electron microscopy

The examination of fracture surfaces on selected samples showed that differences exist in the morphology of the microstucture, in the arrangement and appearance of the hydration products. These differences were caused mainly by the type of cement and the water cement ratio w. Samples with w = 0,50 contained a larger quantity of crystalline phases that formad a maize of rods and similar aggregations as a result of the "outer" hydration. The contacts between these hydrations products were not as frequent as in the "inner" hydration products. Great differences in the microstructure were found between Portland and slag-portland cement. In all the samples could be seen a heterogenity of the microstucture and changes in the micro-ragions given by the mineralogical composition of the cement and the presence of the water in the above region.

CONCLUSIONS

The studies of external pores in the hardened cement pastes have shown that their volume and distribution depend on
- water-cement ratio w
- curing time τ
- type and fineness of cement

The water-cement ratio w influences the total starting external pore volume TPV which is reduced exponentially with the conditioning period τ, as has been shown mathematically. Hardened pastes with a higher water-cement ratio w have after the same time τ higher TPV's than pastes with a smaller water-cement ratio. The above holds true for w = 0.30 to 0.50.

The total pore volume TPV depends also on the mineralogical composition and the fineness of the cement. With the same w, various types of cement have a different initial total pore volume TPV which though uniformly reduced with the conditioning period τ, still leads again to differences in the final TPV values. Greater differences were found between Portland cement on one hand and slag-portland cement on the other hand. With a high water cement ratio (w = 0.50) the better cristalized hydration products in the form of rods and similar aggregates were formed in the microstructure of hardened cement pastes. The portlandite crystals were in the larger form. But the contacts among these products were not as frequent as in the "inner" hydration products.

Because the mechanical properties of hardened pastes depend to a considerable extent on the porosity, the results about the development of pores during hardening very important. In this case have been investigated only external pores in the range of d=0.015 to 15 µm by means of mercury porosimetry. The results have confirmed that in this range a sugnificant proportion of pores lies in the hardened paste so that trough them can be characterized the development of porosity. The knowledge about microstructure with respect to the total volume, diameter, shape and orientation of the pores contributes to the understanding of the behaviour and properties of the hardened cement during the hydration and represents a valuable contribution to the application of the cement in the practice.

REFERENCES

1.- L. E. COPELAND and C. J. VERBECK (1974), "Structure and properties of hardened cement pastes", Principal Paper, 6th Int. Congress on the Chem. of Cement, Moscow.

2.- T. C. POWERS (1958), "Structure and physical properties of hardened portland cement paste", J. Amer. Ceram. Soc. 41,1, 1-6.

3.- A. GRUDEMO (1974), "Strength vs. structure in cement pastes", Supplementary Paper Section II 6th Int. Congress on the Chem. of Cement, Moscow.

4.- R. KONDO and M. DAIMON (1974), "Phase composition of hardened cement", Principal Paper, 6th Int. Congress on the Chem. of cement, Moscow.

5.- S. DIAMOND (1971), "A critical comparison of mercury porosimetry and capillary condensation pore size distribution of Portland cement pastes", Cement and Concrete Res.,1, 531 - 546.

6.- Yu. V. CHEKHOVSKY and L. E. BERLIN (1974) "On kinetics of pore structure formation in cement stone", Supplementer Paper Section II 6th Int. Congress on the Chem. of Cement, Moscow.

7.- V. LACH (1977), "Correlations between the microstructure of hardened cement pastes and their properties", Res. Report, Technical University, Brno.

8.- V. LACH (1976), "Die Mikrostruktur - das Kernproblem der Silikate", Tonind. Ztg., 100, 7 - 13.

9.- R. B. WILLIAMSON (1970), "Solidification of Portland cement", Report UC-SESM 70-23, University of California, Berkeley.

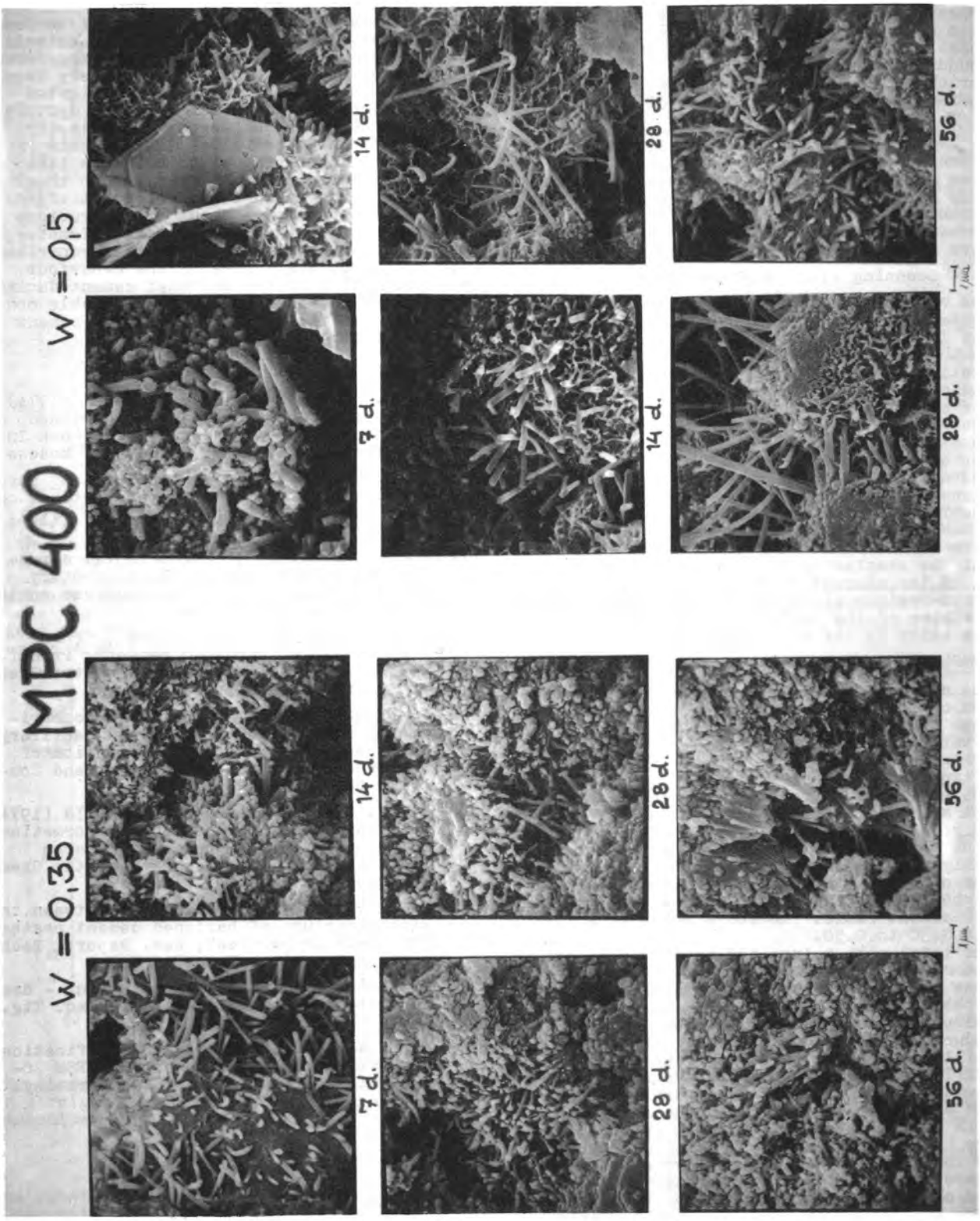

Figure 3
SEM-micrograph of hydrated cement pastes (w=0,35 and 0,5b) after 7, 14, 28 and 56 days of curing.

Pore structure of cement stone and its influence on the mechanical properties of concrete

Structure poreuse du ciment durci et son influence sur les propriétés mécaniques du béton

G. BOZHINOV, Senior Res. Associate, M. Sc., C.E.,
N. BAROVSKY, Junior Res. Associate, C.E., Bulgarie.

RESUME : En vue de programmer des expériences et d'élaborer un modèle mathématique, on a cherché à déterminer l'influence de facteurs technologiques généraux sur la porosité du ciment durci. On a aussi recherché la relation entre la résistance à la compression du béton et le volume total de ses pores.

Les facteurs technologiques pris en compte sont : le rapport E/C - la teneur en gypse ajouté - la finesse de mouture du ciment - et la durée de l'hydratation à la vapeur. La porosité est représentée par le volume total des pores et par les volumes des pores dont les rayons sont inférieurs à cent et à mille Å. Ces volumes sont rapportés aux facteurs ci-dessus. On a cherché à déterminer l'influence de chacun de ces facteurs, pris isolément, ou considérés ensemble, sur ces volumes de pores.

On a constaté l'influence dominante du rapport E/C sur la porosité du ciment durci. L'augmentation de la finesse de mouture du ciment diminue le volume total des pores, et surtout diminue fortement les deux autres volumes partiels. L'influence combinée du rapport E/C et de la finesse de mouture est beaucoup plus compliquée et varie avec le temps.

La relation entre la résistance à la compression et la porosité du béton a été représentée graphiquement. Elle a été examinée, en tenant compte du mode de formation des pores, de la composition du béton et des caractéristiques superficielles du granulat.

SUMMARY : On the basis of the method of experimental design and mathematical modelling an attempt is made to evaluate the influence of the main technological factors on the porosity of cement stone. The relation between total pore volume and compressive strength of concrete is established as well.

The factors involved are: water/cement ratio, gypsum additive, dispersity of cement and duration of steam curing. The porosity of cement stone is presented by the total pore volume and partial pore volumes of pores with radii up to 10^2 Å and 10^3 Å respectivelly. This pore volumes are considered as functions of observable responses being affected by the factors mentioned above. Their individual and joint effects on the pore structure of cement stone are evaluated.

It is shown that the W/C ratio plays a dominant role in the process of pore structure formation. Dispersity of cement causes some reduction of the porous space. Its effect is strong exceptionally on the partial pore volumes. The joint effect of W/C ratio and fineness of cement is more completely and should be regarded in time.

The strength/porosity relation of concrete is discussed in terms of the pore structure formation, composition of concrete and features of contact zone.

INTRODUCTION

The mechanical properties of cement stone and concrete are strongly dependent on the structure of their porous space (1,2,3). It is also shown, that the mechanical behaviour of cement stone is influenced both by the total pore volume and pore size distribution (4). The latter is defined by means of the volumes of pores with radii up to 10^2 Å (V_p^x) and 10^3 Å (V_p^{xx}).

In this paper some results are presented and discussed to estimate the complex influence of the main technological factors on the pore structure formation of cement stone. For that purpose the method of experimental design and mathematical modelling is used (5,6). The relation between total pore volume and compressive strength of concrete is given as well.

EXPERIMENTAL PROCEDURE

A pure clinker cement (ZP - 78) is used with following mineral composition (%) : C_3S = 60,24; C_2S = 18,30; C_3A = 6,63 and C_4AF = 8,78. The factors involved in experiments are as follows: water/cement ratio (W/C); gypsum additive (SO_3); Blaine fineness (S_B) and duration of steam curing at $358 \pm 5^\circ$ K (τ). Their levels are presented in Table 1.

TABLE 1

X_i	Factors and dimenssions	Levels		
		$X_{i,min}$	$X_{i,o}$	$X_{i,max}$
X_1	W/C ratio	0,30	0,40	0,50
X_2	SO_3 (%)	2,50	3,00	3,50
X_3	S_B (m^2/g)	0,22	0,36	0,50
X_4	τ (hours)	6	8	10

A parallel experimental block of specimens including the factors X_1, X_2 and X_3 is cured under water ($T = 293 \pm 2^\circ$ K). These specimens are tested at 1,3 and 28 days.

The factors X_i mentioned above are coded into nondimentional co-ordinates x_i by the formula:

$$x_i = \frac{X_i - X_{i,o}}{\Delta X_i} \qquad (1)$$

where:

$$\Delta X_i = 0{,}5(X_{i,max} - X_{i,min}). \qquad (2)$$

The function of observable responses Y_p is searched as polynomial of second order in the form:

$$Y_p = b_o + \sum_{i=1}^{n} b_i x_i + \sum_{i=1}^{n} b_{ii} x_i^2 + \sum_{i<j} b_{ij} x_i x_j \qquad (3)$$

where: Y_p is characteristic of the porosity ($\ln V_p$ and $\ln V_p^{xx}$ - for water cured specimens; $\ln V_p$ and $\ln V_p^x$ for steam cured specimens);

n = 3 for water curing;

n = 4 for steam curing.

The total pore volume (V_p) of cement stone is determined by using both the mercury pressure porosimetry and a physico-chemical method according to the relation:

$$V_p = \left[1 - \frac{C_o(1 + n_t)}{\rho_{c,s}} \right] .100 \quad (\%) \qquad (4)$$

where: C_o is quantity of the cement in $1cm^3$ cement paste (g/cm^3);

n_t - chemical bound water (g/g);

$\rho_{c,s}$ - specific gravity of cement stone (g/cm^3).

The partial pore volumes (V_p^x and V_p^{xx}) are calculated from the integral curves of porosity obtained by means of the mercury porosimeter "CARLO ERBA",mod.1540.

The concrete specimens (cubes sized 10x 10x10 cm) are prepared using the same cement with S_B = 0,5 m^2/g and SO_3 = 3,5 %, and with different water/cement ratios 0,45 - 0,65, sand/cement ratios by weight K = 1 - 3 and gravel/cement ratios L = 3 - 4. Pure quartz sand with fineness modulus 2,86 and river gravel with D_{max} = 20 mm are used

The total volume of pores in concrete V_p^c is calculated from the following relation:

$$(5) \qquad V_p^c = \frac{V_p(1-V_a)}{1 + \frac{C_o K}{\varrho_s} + \frac{C_o L}{\varrho_g}} + V_a \quad (\%)$$

where: V_a is air content (%);
ϱ_s and ϱ_g are specific gravity of the sand and gravel respectively.

The evaluation for the individual and joint influences of the factors investigated on the total and partial pore volumes of cement stone is made on the basis of the values and signs of coefficients of re - gression equations.

The relation between the total pore volume and compressive strength of concrete is presented grafically. The curves are drown on the basis of the Chebishev's polynomial of second order.

RESULTS AND DISCUSSION

The chage of the coefficients of regression equations during the time for water cured specimens is shown in Fig. 1.

It can be seen that the total porosity of cement stone decreases during the time, while the partial pore volume V_p^{xx} increases. In the centre of experimental block (W/C = 0,40; SO_3 = 3,0 %; S_B = 0,36 m^2/g) their values are very close ($b_o \approx b_o^{xx}$).

The total porosity increases with increasing of W/C ratio and the influence of this factor is intensified during the time. This is likely due to the larger free space in which new hydrate products arise. The effect of the same factor is demonstrated more clearly on the partial pore volume (see curve b_1^{xx}).

The smaller the W/C ratio in the earlier stage of hardening the bigger is the partial pore volume. This effect is also intensified during the time, remaining smaller than it is on the total porosity.

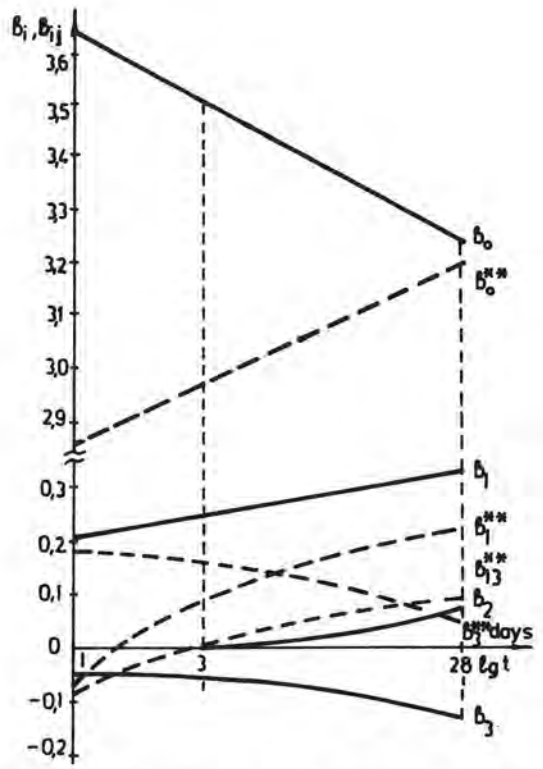

Fig. 1 - Coefficients of regression equations vrs. the time. Compact curves - V_p, dotted curves - V_p^{xx}.

In general the influence of water/cement ratio on the pore structure formation is dominant.

The increase of dispersity of cement causes some reduction of the porous space, which is due to the larger reactve surface of cement grains. The effect of this factor at earlier ages is exceptionally strong on the partial pore volume V_p^{xx}. It remains as a dominant factor up to 5 - 6 days (cross - point of lines b_3 and b_3^{xx}).

The joint influence of W/C ratio and fineness of cement on the partial pore volume is illustrated by the coefficient b_{13}^{xx}. It can be seen that this effect changes its direction during the time. It means that the positive joint effect of these two factors on V_p^{xx} could be obtained either by combination of lower W/C and higher dispersity of cement at 1 day, or higher values

of W/C ratio and Blaine fineness of cement at 28 days.

During the first 3 days of hardening gypsum additive does not effect observably the porosity of cement stone. The higher values of this factor lead to some increasing of total porosity at 28 days, which is probably due to the ettringite destruction under conditions considered.

The regression equations for the steam cured specimens are as follows:

$$(6)\quad \ln V_p = 3{,}429 + 0{,}251\, x_1 - 0{,}030\, x_3 - 0{,}038\, x_4 ;$$

$$(7)\quad \ln V_p^x = 1{,}881 + 0{,}286\, x_3 + 0{,}290\, x_4 + 0{,}112\, x_3^2 - 0{,}191\, x_4^2 + 0{,}104\, x_2 x_3 .$$

The total pore volume V_p is dependent mainly on the W/C ratio, while the influence of dispersity and duration of steam curing is quite feeble (eq.6).

More complicated is the influence of the factors considered on the partial volume of pores with radii up to 10^2 Å (V_p^x)(eq.7). Positive individual effects on V_p^x are demonstrated by the dispersity (x_3) and du - ration of steam curing (x_4). The presence of quadratic effects, however, deform essentially the influence of these factors: in the first case (x_3) the effect is reinforced, while in the second case (x_4) the effect is strongly redused. The prolonged steam curing leads to some decrease of dispersity of hydration products, which reflects into decreasing of partial volume V_p^x.

The effect of gypsum additive is only manifested jointly with the dispersity of cement. It is shown that the simultaneous increase of the factors causes increasing of V_p^x.

The relation between the total porosity and compressive strength of concrete is presented in Fig.2 and Fig.3.

The experimental points relate to concretes with different compositions (varied ratios: W/C; K and L) and corresponding pore volumes after formula (5). In general the results presented confirm the well-known character of strength/porosity relation.

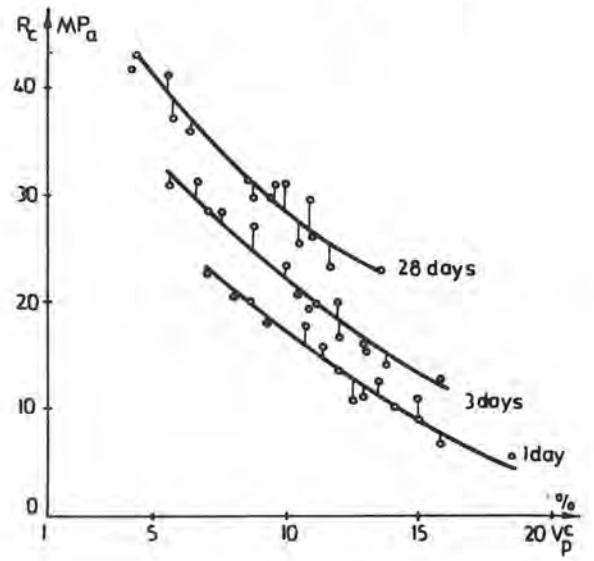

Fig.2 - Strength/porosity relation for concrete cured under water

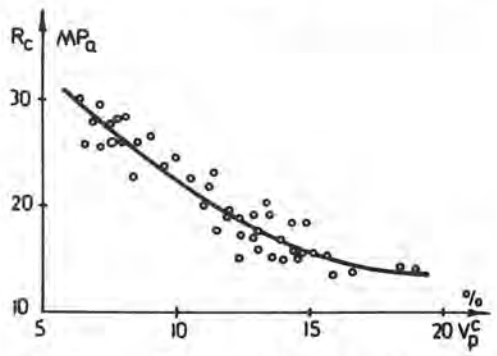

Fig.3 - Strength/porosity relation for concrete at steam curing

It should be pointed out that such a relation is not only determined by the total porosity, but is also necessary to take into account the pore size distribution and the thickness and properties of contact zone. It means that the relation between strength and total porosity is also affected by the quantity and surface of the aggregates, adsorbed water, etc. The total pore volume decreases with increasing the ratios K and L, and the contact surfaces increase too. Both they stimulate the increa-

sing of the strength of concrete. During the time total porosity of cement matrix decreases, a redistribution of pore size takes place and this also leads to the increasing of compressive strength (Fig.2). In addition the contact zone in the steam cured specimens is weaken to a greater extend and this affects adversely the strength of concrete (Fig.3). A comparison of the results presented in Fig.2 and Fig.3 shows that the relation "strength/porosity" for steam cured specimens is very close to the same relation for water cured specimens at 3 days.

CONCLUSION

The individual and joint effects of the main technological factors on the total and partial pore volumes of cement stone are evaluated. It is shown that the W/C ratio plays a dominant role in the process of formation of pore structure of cement stone. Dispersity of cement causes some reduction of the porous space. Its effect is strong exceptionally on the partial pore volume V_p^{xx}.

The joint effect of W/C ratio and fineness of cement is more completely and should be regarded in time.

Gypsum additive demonstrates its effect at the later ages of hardening (28 days).

The influence of the factors considered on the total porosity of steam cured cement stone is analogous to that conserning the water cured specimens. In this case, however the effect of dispersity is quite feeble.

The partial pore volume here is presented by the volume of pores with radii up to 10^2 Å (V_p^x). It is shown, that the presence of quadratic effects deform essentially the effect of dispersity of cement and duration of steam curing.

The effect of gypsum additive is only manifested jointly with the fineness of cement.

The relation between the compressive strength of concrete and its porosity is presented grafically and discussed in terms of the pore structure formation, composition of concrete and features of contact zone.

REFERENCES

1.- C.D.LOWRENCE (1973), "Porosity/strength relationship for portland cement pastes", Proc. of the Int. Symp. Pore structure and properties of materials, Vol. V, Prague, pp. 167-176.

2.- V.RATINOV, T.ROSENBERG, T.KOZIENKO, G. KUCHERJAEVA, V.TOKAR (1973), "Structure of the concrete pore space with CNN and CNNC admixtures", Proc. of the Int. Symp. Pore structure and properties of materials, Vol.III, pp. 205-215.

3.- S.POPOVICS (1969), "Effect of porosity on the strength of concrete", Journal of Materials, IMLSA, Vol.4, No.2.

4.- N.BAROVSKY, G.BOZHINOV (1979), "Influence of the pore size distribution on the mechanical properties of cement stone", Proc. of II National Conference on Mechanics and Technology of Composite Materials,Publ. House of Bulg. Acad. of Sciences, Sofia, pp. 538-541.

5.- V.A.VOSNESENSKII (1974), "Statistical methods for experimental design in technical and economical investigations (in russian), Statistica, Moskow, pp. 62-106.

6.- N.BAROVSKY, G.BOZHINOV, Zh. ENCHEVA, (1979), "Experimental design for investigation of pore structure of cement stone", Proc. of II National Conference on Mechanics and Technology of Composite Materials, Publ. House of Bulg. Acad. of Sciences, Sofia, pp. 534-537.

Behaviour of reinforced concrete under the action of flue gases as a function of the cement composition

Comportement du béton armé sous l'action des gaz de fumée en fonction de la composition du ciment

W. TISCHER, Dr. rer. nat., University-Lecturer, Technische Hochschule Leipzig, DDR.

SUMMARY : Chemical changes by the action of flue gas on reinforced concrete take place first of all by the reactivity of the sulphur oxides with the components of the hydrated cement. Their damaging influence consists first of all in the formation of crystalline phases in the structure of the hydrated cement caused by the sulphite and sulphate formation, above all of the calcium. Analogous to the term of the carbonatisation the change of the cement concrete caused by the action of gaseous sulphur oxides is designated with sulphatisation. Contrary to the carbonisation it is no process happening naturally at the concrete because the sulphur oxides do not belong to the normal components of the air, but come in the flue gas only by combustion processes of sulphureous compounds of the fuels or arise by chemical conversions in other large-scale processes, so that the air in industrial areas contains, in general, increasingly sulphur oxides. In an accummulated form these sulphur oxides are contained as components of the flue gases of lignite furnaces which are particularly discussed in this paper.

1. Sulphatisation

As to the course of the sulphatisation there is an extreme parallelism with the carbonisation. In the same way as in the carbonisation it happens a neutralisation of the basic environment and thus a reduction of the pH value in the hydrated cement up to in ranges, in which a natural protection of the reinforcing steel does not exist. But owing to the stronger acid properties of the sulphur oxides as compared with the carbon dioxide some deviating modes of behaviour must be observed.

The oxides of the sulphur and their acids do not only convert with the strongly basic calcium hydroxide, but also with the less basically reacting salts of the hydrated cement subjected to the hydrolysis as well as with the product of the carbonisation, the calcium carbonate. The oxides of the sulphur with an acid reaction disturb the hydrolysis equilibria of the hydrated cement and owing to the low solubilities of the hydrolysis products a slow structural change takes place:
e.g.

$$CaO \cdot SiO_2 \cdot (H_2O)_x + 2\ H_2O \longrightarrow Ca(OH)_2 + H_2SiO_3 \cdot (H_2O)_x$$

$$Ca(OH)_2 + SO_2 \longrightarrow CaSO_3 + H_2O$$

$$H_2SiO_3 \cdot (H_2O)_x \longrightarrow SiO_2 + n \cdot H_2O$$

As a result of the water being available only to a limited extent and the temperatures exceeding 50 °C there is a fundamental difference between the action of sulphur oxides and the concrete corrosion caused by sulphate ions in aqueous solution and arising because the formation of ettringite. The observation that at the penetration of the concrete with moisture a carbonatisation is excluded seems not to hold in the same strict measure with regard to the sulphatisation as the oxides of the sulphur possess a very good solubility in the water and the acids arising react already in the dilute state with the basic substances. That became obvious from the material change of concrete cubes hung in the chimney mouth and frequently penetrated with moisture, at which an outer layer of some millimetres of thickness with a high content of calcium was arisen. The sulphatisation is always the change of the hydrated cement structure occuring after the carbonatisation and then passing together with it. As to the sulphation velocity there are analogous considerations as with the carbonatisation. The concrete possesses by the arising calcium sulphate a greater diffusion resistance to penetrating gases than in the carbonatisation because the final product of the conversion possesses a volume being enlarged by 124 % as compared with the solid starting material and thereby may lead to the bursting corrosion.

For the reactivity of the gas with the solid matter the presence or the absence of water is decisive. If no water is present, also not in the gaseous phase, no chemical conversion, e.g. between $CaCO_3$ and SO_2, is virtually detected in the temperature range up to 150 °C / 1 / . The sulphur dioxide is only physically adsorbed on the solid matter surface. In the presence of water and sulphur dioxides it happens a mixed adsorption on the solid matter surface. In this case the sulphur dioxide reacts with calcium sulphide or calcium hydrogen sulphide and an oxidation to the sulphate may secondarily happen. Ettringite which arises in the presence of sulphateous solutions in the concrete was not detected after flue gas action at temperatures up to 200 °C. From this behaviour it is derived that the corrosion of the cement concrete in the flue gas cannot be equated with the process in solutions containing sulphate ions. That has consequences as to the cement selection with regard to the C_3A content at such aggressive stresses. Indeed, the sulphur trioxide is contained in the flue gas in a considerably smaller concentration than the sulphur dioxide, yet in particular because of the strong and stable sulphuric acid arising from it as well as of the raise of the acid dew point resulting from the presence of the sulphur trioxide it is a highly important component to the concrete corrosion in the flue gas atmosphere.

2. Action of Sulphur Oxides on Pure, Hydratised Cement Clinker Minerals

Owing to the very versatile composition of the cements and the hydrated cement resulting from them it is very difficult to determine on which its chemical resistance is dependent. In order to detect more exactly with which components the sulphur oxides do mainly react, their reactivity to the pure, hydrated main clinker materials is investigated / 2 / . In laboratory tests hydrated C_3S, C_2S, C_3A and C_4AF were exposed in the presence of water at a temperature from 125 to 130 °C in closed glass flasks to the action of gaseous sulphur dioxide and after a longer period their sulphate content determined.

Table 1: Change of the concrete properties by sulphatisation

Concrete Properties	Influence by Sulphatisation
Corrosion protection of the reinforcement	Decomposition of the passive layer on the steel owing to the reduction of the pH value and action of sulphate ions
Compressive strength	Increase of strength in the initial stage by incorporated $CaSO_4$, bursting corrosion is possible in the later stage, above all at subsequent moisture action, formation of cracks
Permeability	In the initial stage reduction by incorporation of calcium sulphate, in the later stage increase by developing micro-flaws
pH value	Decrease by conversion of the basic components of the concrete with sulphur oxides with acid reaction
Efflorescences	Reduction, easily soluble, surface-near calcium hydroxide is converted into sulphite or sulphate being more hardly soluble
Bond of protective layers	Improvement of the bond with alkali-sensitive protective layers such as polyester or polyurethanes by neutralisation

Table 2: Sulphate content in hydrated cement clinker minerals (approximate values)

Cement Clinker Mineral	Sulphate Content in Weight Percentage	
	after 12 months of period of action	after 36 months of period of action
C_3SH_x	29	57
C_2SH_x	15	59
C_3AH_x	9	46
C_4AFH_x	14	50

During the twelve months of period of action of the sulphur dioxide a reaction takes preferably place with the hydrated cement clinker minerals which split off the strongly basic calcium hydroxide. The hydrated C_3A reacts at the temperatures up to 130 °C first only on a small scale with the sulphur oxides. If the period of action goes on, indeed, the sulphur absorption increases considerably, but in the final result C_3AH_x contains after 36 months of period of action of the sulphur oxides the smallest part of combined sulphur of the four main clinker minerals.

3. Conclusions from the Investigations

From the results of investigation it can be concluded that the action of gaseous sulphur oxides on cement concrete cannot be equated with the action of solutions containing sulphate ions. That is due to their reaction in the presence of only a small quantity of water and the temperatures as high as about 200 °C. Under these conditions the hydrous calcium sulphate aluminate hydrate (ettringite) being instable at temperatures above 50 °C cannot arise and is instable. If concrete is used under these conditions, the C_3A content may have the values of a normal portland cement and a C_3A-poor cement must not be used.

References:

/ 1 / Sprung, S.:
The behaviour of the sulphur during the firing of cement clinkers.
Schriftenreihe der Zementindustrie, no. 31 (1964)

/ 2 / Polak, A.F.; Jakovlev, W.W.:
Corrosion of the concrete and reinforced concrete in an aggressive environment. Papers on the VI Conference on the Protection of the Building against Corrosion, Bratislava 1978.

Influence du dosage et de la nature du liant sur les propriétés de certains bétons réfractaires

Influence of dosage and binder type on the properties of some refractory concretes

I. TEOREANU, Professor, Faculty of Chemical Technology, Bucharest Polytechnical Institute,
N. CIOCEA, Scientific researcher, Bucharest Polytechnical Institute, Roumanie.

RESUME: On présente les propriétés de certains bétons réfractaires, à teneur élevée en Al_2O_3, lorsque la proportion de liant hydraulique varie entre 15 et 25 %. On met en évidence surtout, le role de la finesse de broyage et de la composition chimico-minéralogique du ciment sur les propriétés des bétons.

Les propriétés de ces bétons ont été déterminées par les échantillons gardés à l'air, ainsi qu'après leur cuisson à de divers températures.

SUMMARY: The properties of some refractory concretes of high alumina content, if the hydraulic binder ratio there is in the range 15 - 25 % are shown . The effect of grinding fineness and cement chemical - mineralogical composition upon concrete properties is presented.

The properties of these concretes were determined both on unfired samples kept in air and on samples fired at different temperatures.

Dans de diverses applications industrielles, on sollicite des bétons réfractaires à résistance satisfaisante à l'attaque chimique ou bien à l'errosion de certaines poudres, dans des conditions des températures elevées ou intermédiaires (1-5). Conformèment à de pareilles exigences on peut utiliser des bétons réfractaires à base de ciment alumineux, avec des agrégats, dont la granulation maxime est de moins de 3 mm (2, 6) . En vue de la réalisation de pareils bétons, dans le travail ci-présent, on a examiné l'influence, sur leurs caractéristiques, de la composition chimico-minéralogiques, de la finesse de broyage et du dosage du ciment employé.

La caractérisation des ciments utilisés. Pour la préparation des bétons qui ont constitué l'objet des investigations de ce travail, on a utilisé 5 types de ciments alumineux, dont les compositions minéralogiques, ainsi que les caracteristiques initielles de dispersion, l'eau de consistance normale et le temps de prise sont présentés dans le Tableau I

avec les calculs des compositions minéralogiques (dont les résultats sont inscrits dans le Tableau I).

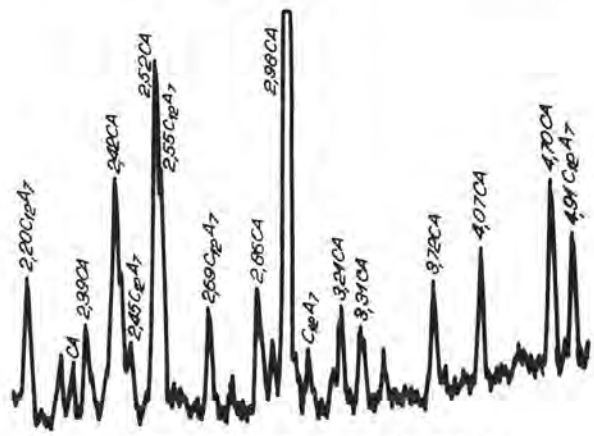

Fig. 2- Roentgénogramme du Ciment 2

TABLEAU I

Symbole du ciment	Al_2O_3 %	Composition minéralogique (déterminée par calcul)x)	Finesse de broyage, refus sur le tamis de 0,06 mm %	L'eau de consistance normale, %	Le temps de prise, heures-minutes	
					Commencement	Fin
1	60,0	35 % $C_{12}A_7$ + 65 % CA	16,3	33,0	15 min	30 min
2	62,0	20 % $C_{12}A_7$ + 80 % CA	5,7	33,5	23 min	50 min
3	64,5	100 % CA	0,0	32,2	1 h 40 min	3 h
4	67,0	80 % CA + 20 % CA_2	0,0	30,0	1 h 50 min	3 h 15 min
P	70,0	60 % CA + 40 % CA_2	27,6	29,5	2 h	3 h 40 min

L'analyse roentgenographique des ciments pris en considération (les figures 1-5) est en bonne concordance

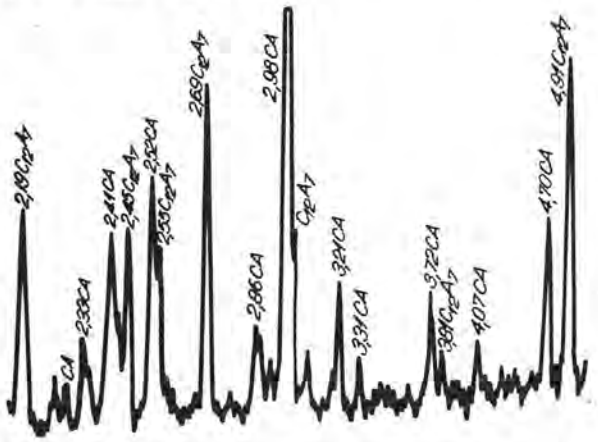

Fig. 1.- Roentgénogramme du Ciment 1.

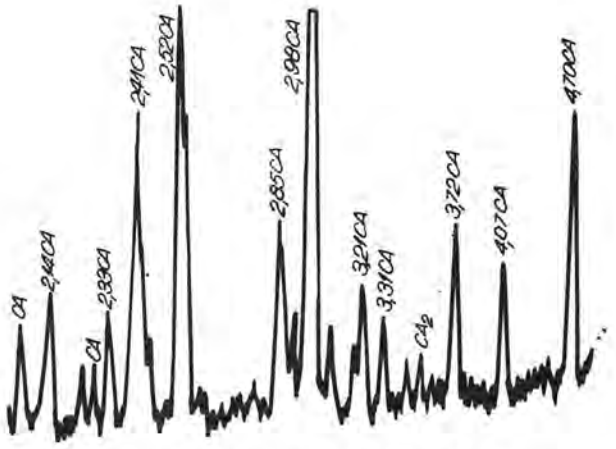

Fig. 3- Roentgénogramme du Ciment 3

On mentionne que, pour l'obtention des caractéristiques initielles de dispersion,

x) On a utilisé les notations .C= CaO; A= Al_2O_3

les ciments 1-4 ont été broyés dans les mêmes conditions (en utilisant les mêmes corps de broyage, le mêmes rapport boulets/liant et le même temps de broyage), pendant que le

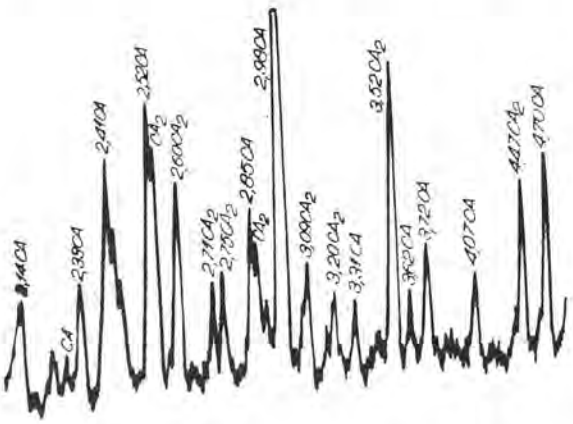

Fig. 4. - Roentgénogramme du Ciment 4

ciment P a été broyé dans de differentes conditions.
Pour suivre l'influence de la finesse de broyage des ciments de composition chimico-minéralogique differente sur les propriétés des bétons, certains ciments ont été broyés supplémentairement, en obtenant les caractéristiques présentée dans le Tableau II.

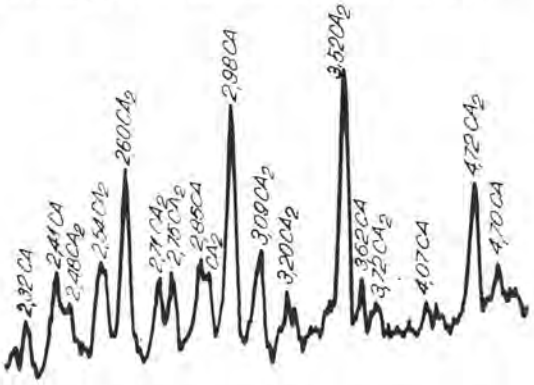

Fig. 5 - Roentgénogramme du Ciment P

L'aptitude au broyage des clinkers, appréciée par les résidus sur les tamis et les surfaces spécifiques correspondantes (Blaine) est défavorisée au fur et à mesure qu'on passe vers des clinkers moins alumineux. Le plus facilement on broye les clinkers alumineux du type CA + CA_2. Dans le même contexte, on remarque la plasticité extrêmement

TABLEAU II

Symbole du ciment	Les principales composants minéralogiques	Le temps supplementaire de broyage, minutes	La finesse de broyage			
			Refus sur le tamis de o,o6 mm, %	Refus sur le tamis de o,o56 mm, %	Sous o,o56 mm %	La surface spécifique correspondante, cm^2/g
1	35 % $C_{12}A_7$	-	16,3o	29,6o	7o,4o	238o
S_1	+	3o,o	5,35	26,8o	73,2o	252o
S_2	65 % CA	6o,o	o,38	11,28	88,72	31oo
S_3		9o,o	o,oo	o,25	99,75	377o
2	2o % $C_{12}A_7$	-	5,7o	27,oo	73,oo	245o
A_1	+	1o,o	3,67	26,67	73,33	258o
A_2	8o % CA	3o,o	1,85	11,68	88,32	3oo o
A_3		6o,o	o,oo	1,33	98,67	326o
3	1oo % CA	-	o,oo	o,6o	99,4o	334o
4	8o % CA + 2o % CA_2	-	o,oo	o,oo	1oo,oo	47oo
P	6o % CA	-	27,6o	48,oo	52,oo	198o
P_1	+	3o,oo	2,5o	8,25	91,75	31oo
P_2	4o % CA_2	6o,o	o,oo	o,oo	1oo,oo	422o

élevée, qui a été observée, dans le cas de l'utilisation des mélanges de bétons réalisée avec le ciment 4, dont la surface spécifique est d'approximativement 4700 cm^2/g

Bétons réfractaires à haute teneur en Al_2O_3.
Dans les bétons réfractaires, formés à la base des types de ciments plus haut mentionnés, ont été utilisés des agrégats d'alumine tabulaire avec les granulations suivantes : 8-14 mesh, 28-48 mesh, - 100 mesh et - 325 mesh.
Pour suivre l'influence du dosage de ciment sur les propriétés des bétons, on a utilisé 3 variantes de recettes, qui sont présentées dans le Tableau III.

TABLEAU III

La dénomination des composants solides des bétons	Dosage, %		
	Variante		
	I	II	III
L'alumine tabulaire	75	80	85
Ciment alumineux	25	20	15

Avec les ciments obtenus après le premier broyage, ayant les granulations présentées dans le Tableau II (et notées symboliquement : 1, 2, 3, 4 et P) , on a realisé les 3 variantes de recettes . Leurs caractéristiques sont présentées dans le Tableau IV

plus grand de ciment en béton, la quantité d'eau est plus grande elle-aussi, tandis que le rapport eau/ciment est plus petit.
La masse volumique des échantillons noncuits augmente, généralement, en rapport avec le baissement de la proportion de ciment (l'augmentation de la proportion de Al_2O_3 du béton) et de l'eau de mise en oeuvre.
La résistance mécanique des bétons (appréciée par la résistance à la traction et à la compression) après un jour et trois jours de conservation dans une atmosphère humide varie en rapport avec la proportion de ciment.
Les plus grandes variations sont enregistrées, surtout, dans le cas des ciments faiblement broyés .
De même,les bétons exécutés avec des ciments faiblement broyés ont aussi des résistances mécaniques plus baisses. Pour cela, pour suivre l'influence de la finesse de broyage du ciment sur la résistance mécanique des bétons durcis, après la conservation à l'air et après le séchage et leur cuisson, on a préparé aussi des bétons avec les types de ciment broyés à une plus grande finesse .
Dans le Tableau V on peut observer l'influence simultanée de la nature du ciment, de sa finesse et son dosage sur les résistances à la compression des bétons obtenus des ciments 1-4 et P (on garde les mêmes dosages de ciments que plus haut : I-25 % ; II - 20 % et III -15 %, mais on utilise tous les ciments, broyés à de divers finesses, qui sont données dans le Tableau II:

TABLEAU IV

Symbole du bétom	La proportion de ciment, %	L'eau de mise en oeuvre, %	Le rapport eau/ciment	La masse volumique du béton durci, kg/dm^3	La resistance à la traction, daN/cm^2		La resistance à la compression, daN/cm^2	
					1 jour	3 jours	1 jour	3 jours
I - 1	25	9,6	0,39	2,92	93,5	101,0	180	400
II- 1	20	8,3	0,41	2,94	88,0	98,0	160	320
III-1	15	7,1	0,47	2,94	75,0	96,0	100	200
I - 2	25	9,6	0,39	2,90	98,5	106,0	230	440
II- 2	20	8,7	0,43	2,96	90,0	101,2	180	350
III-2	15	8,0	0,53	2,98	80,0	98,0	170	220
I - 3	25	10,0	0,40	2,93	101,0	110,0	390	600
II- 3	20	8,5	0,42	2,98	98,3	100,0	380	550
III-3	15	7,5	0,50	2,98	96,0	98,5	300	500
I- 4	25	10,0	0,40	3,00	105,0	110,0	410	650
II- 4	20	8,7	0,43	3,04	100,0	102,5	400	520
III-4	15	7,8	0,52	3,02	100,0	106,0	380	500
I - P	25	10,0	0,40	2,96	65,5	96,0	170	400
II- P	20	8,3	0,41	2,97	61,0	75,0	130	300
III-P	15	7,5	0,50	2,97	57,0	63,5	100	150

Comme on peut constater de ce tableau l'eau de mise en oeuvre, déterminée par la methode "ball in hand" a varié,généralement, avec la proportion de ciment. Au contenu

1, S_1-S_3, 2, A_1-A_3, 3, 4, et P-P_2.

Dans tous les cas, les echantillons soumis

TABLEAU V

L'échantillon de béton	La résistance à la compression, daN/cm^2							
	Avant la cuisson		Après le séchage et la cuisson à la température					
	1 jour	3 jours	200°C	600°C	800°C	950°C	1100°C	1400°C
I - 1	180	400	400	320	250	180	240	500
II- 1	160	320	300	250	170	150	200	520
III-1	100	200	200	150	130	100	160	470
I - S1	230	460	-	400	350	200	250	-
II- S1	180	350	-	350	300	180	200	-
III-S1	150	240	-	240	210	130	175	-
I - S2	280	515	-	450	400	240	280	-
II- S2	260	400	-	400	350	200	240	-
III-S2	250	300	-	300	280	150	200	-
I - S3	350	500	520	450	420	270	320	550
II- S3	350	460	480	460	350	250	280	510
III-S3	310	400	400	400	340	240	270	180
I - 2	230	440	450	380	350	250	280	-
II- 2	180	350	320	300	300	200	250	-
III-2	170	220	230	175	200	130	190	-
I - A1	270	500	-	400	370	250	290	-
II- A1	210	450	-	370	350	240	250	-
III-A1	200	380	-	340	260	200	215	-
I - A2	370	590	-	500	400	270	300	-
II- A2	350	500	-	410	350	240	300	-
III-A2	300	420	-	400	275	200	250	-
I - A3	380	580	600	480	410	300	300	525
II- A3	360	520	540	440	380	275	310	500
III-A3	340	480	480	410	300	250	240	500
I - 3	390	600	600	500	400	270	300	-
II- 3	380	550	500	400	380	250	270	-
III-3	360	500	480	400	250	250	250	-
I - 4	410	650	620	530	390	290	310	-
II- 4	400	520	530	430	320	260	265	-
III-4	380	500	500	400	280	230	250	-
I - P	170	400	450	300	200	150	180	350
II- P	130	300	370	210	160	100	130	300
III-P	100	150	200	100	50	50	70	230
I - P1	210	425	-	340	300	240	240	400
II- P1	200	360	-	300	250	220	230	400
III-P1	180	330	-	210	150	110	170	375
I - P2	400	650	650	520	400	280	300	500
II- P2	400	500	550	410	340	250	260	450
III-P2	380	500	510	400	300	270	230	400

à un traitement de chauffage (avec une conservation à la température respective de séchage et de chauffage de 5 heures) ont eu une période de 3 jours de conservation dans l'atmosphère humide, avant d'être introduits au chauffage.

De l'analyse du Tableau V, il en résulte que les résistances mécaniques à la compression sont fortement influencées par la finesse de broyage du ciment.

L'influence de la surface spécifique est corrélée avec la composition minéralogique et le dosage de ciment, elle étant plus accentuée dans le cas des ciments plus alumineux (à une teneur plus élevée en CA_2, dont la vitesse d'interraction avec l'eau est plus petite que celle des aluminates de calcium plus basiques) et des dosages plus petits de ciment. Comme suite, l'influence positive de l'augmentation du dosage de ciment, dans les limites examinées devient elle-aussi plus importante dans le cas de l'utilisation de certains ciments à surfaces spécifiques élevées. De même, les ciments plus alumineux (à teneur en CA_2)(7) développent des résistances mécaniques plus élevées que les ciments plus basiques, dans des conditions équivalentes de surface spécifique mais à des valeurs plus élevées de celle-ci.

Les résistances mécaniques de tous les bétons cuits atteignent un minimum dans le domaine de température 950-1100°C, après quoi elle connaissent une nouvelle augmentation, comme suite du commencement de la syntérisation et de la réalisation de la liaison céramique. Des déterminations présentées dans le Tableau V, il parait que les plus grands baissements de résistance, qui sont enregistrés à 950°C, sont possédés, dans la majorité des cas, par les bétons à une teneur plus élevée en ciment (si on compare la résistance à la compression, déterminée sur des échantillons conservés trois jours, dans l'atmosphère humide, avec celle déterminée sur des échantillons cuits à 950°C).

Les additifs de syntérisation (frittage), en correlation avec la nature, la finesse et le dosage du ciment, peuvent améliorer le

comportement à des températures intermédiaires des bétons réfractaires à la base de ciment alumineux.
Les éclats de verre finement broyés sont souvent utilisés. Dans ce présent travail, l'influence des additifs de syntérisation, on a suivi sur les recettes avec 25 % et, respectivement 15 % ciment S_2 . Dans le Tableau VI, on a inscrit les résistances mécaniques des échantillons des béton à additif de verre finement broyé.

TABLEAU VI

Symbole d'échantillon	Proportion de ciment %	Proportion de verre %	Résistance à la compression (daN/cm²), après la conservation				
			1 jour	3 jours	cuisson à: °C 800	950	1100
I- N1	25	1,0	200	230	250	160	240
I- N2	25	3,0	220	350	274	200	300
I- N3	25	5,0	200	200	250	180	250
III-N1	15	1,0	350	400	300	200	280
III-N2	15	3,0	300	350	300	235	380
III-N3	15	5,0	300	320	290	260	430

Des données présentées, il en résulte que l'addition de verre finement broyé n'exercite pas une influence favorable sur les résistances des bétons à 25 % ciment; en échange introduit dans les bétons à dosage plus faible de ciment (15 %), elle détermine une amélioration des valeurs des résistances .

CONCLUSIONS

L'analyse de l'influence du dosage et du type de liant sur les propriétés de certains bétons réfractaires à haute teneur en Al_2O_3 a démontré que l'amélioration des résistances mécaniques de ceux-là peut être réalisée par de diverses voies.
Dans ce sens on doit prendre en considération, premièrement, la composition chimico-minéralogique du ciment utilisé; les plus grandes résistances sont obtenues ainsi dans le cas des ciments contenant CA et CA_2.

On peut obtenir l'augmentation des résistances mécaniques aussi par l'augmentation de la finesse de broyage des ciments. Cette augmentation de la finesse de broyage est plus importante, surtout, dans le cas des bétons à la base des ciments plus alumineux et préparés avec un dosage plus réduit de ciment.
L'influence des additifs de syntérisation se trouve dans une évidente correlation avec la nature, la finesse ou le dosage du ciment.

BIBLIOGRAPHIE

1.- J.T. SHAPLAND (1964) "Study of abrasion resistant steelplmt castables", Blast Furnace and Steel Plant, n° 2, 154-162.

2.- M.S. CROWLEY (1969) "Influence of particle size on erosion resistance of refractory concretes", Amer. Ceram. Soc. Bull., n° 7, 707 - 710 .

3.- L. PROST (1973) "Les réfractaires moulables", L'Industrie Céramique, n° 4, Vol. 661, 279 - 286.

4.- R. P. HEILICH, G. MACZURA, F.J. ROHR (1971) "Precision cast 92 -97 % alumina ceramics bonded with calcium aluminate cement", Amer. Ceram. Soc. Bull. Vol. 50, n° 6, 548 - 554 .

5.- I. TEOREANU, N. CIOCEA (1977) "Lianți, mase și betoane refractare" Editura Tehnică, 191 - 206.

6.- R. W. GRIMSHAW, (1968) "Castables and mouldables ", Klei Keram, 18 (11), 298 - 306.

7.- M. JUNG (1973) "Propriétés hydrauliques des ciments à haute teneur en alumine" Bull. de la Soc. Franç. de Céramique , n° 98, ian - mart., 11 - 20 .-

Catalogue des ciments

On cements catalogue

S.V. CHESTOPIOROV, A.N. IZMAILOV, L.A. FEDNER, V.S. CHESTOPIOROV, U.R.S.S.

RESUME :

L'assortiment des ciments portland est trés varié. L'ingénieur-bétonier ne peut pas s'y orienter facilement. Les paramètres de départ de ciments, très importants pour le longévité, la résistance au froid, etc, sont souvent cachés derriére les difficutés liées à leur àpolyminéralité, polydispersité et polyagrégation, àla composition minéralogique agissante lors du durcissement des minéraux. Les ciments de diverses usines bien que pareils par leur minéralogie, sont au fond sensiblement différente. Et vice versa. Il convient de chercher des procédés faciles à l'aide desquels on peut pronostiquer, en fonction des propriétés des ciments, la qualité durable des batiments. Les conditions de la formation des structures de la pierre de ciment doivent se combiner manière organique avec les possibilités potentielles du ciment. Le cataloguement doit se baser sur les propiétés du ciment à durcir au maximum lors de la technologie chimique progressive pour l'obtention du béton.

Le cataloguement de tous les ciments fabriqués dans le pays non d'après leurs propriétés isolées dans le béton mais d'après un groupe de propriétés, i.e. d'après le type complexe, est un problème important d'actualité.

Pour réaliser les travaux de bétonnage dans diverses conditions d'utilisation des constructions il ne suffit pas de prendre en considération seulement la résistance standard du ciment, car ceci conduit à son utilisation irrationnelle, ne révèle pas de liaisons du type de ciment avec toutes les complexités des processus de formation de structure dans le ciment durci qui doit être stable à l'action des conditions extérieures spécifiques dans chaque cas concret.

Pour résoudre le problème de cataloguement des ciments, exigeant beaucoup de temps et de travail, sur la base de l'étude de leurs propriétés techniques on ne peut pas se limiter au problème de détermination des propriétés isolées des ciments fabriqués par n'importe quelle cimenterie. Le problème principal est l'étude des causes déterminant ces propriétés, la recherche des lois régissant la liaison de ces propriétés avec la qualité des matières premières et la technologie de la production, ce qui rend possible le changement essentiel de tout le complexe de propriétés.

L'analyse de nombreux résultats des expériences conduit à la conclusion principale que sur la base des divers procédés courants d'évaluations standards de la résistance et d'autres indices on ne peut pas obtenir une information complexe si nécessaire pour la construction.

En procédant à de nombreuses expériences on a établi que les ciments de différentes cimenteries fabriqués à partir de matières premières différentes et d'après la technologie différente avec la composition minéralogique à peu près identique déterminée par les méthodes conventionnelles existantes, confèrent aux bétons une combinaison essentiellement différente de propriétés techniques. Il est difficile de choisir des exemples où les différents ciments de même composition donneraient les bétons analogues d'après toutes les propriétés. Les différences commencent à se manifester dès le stade de préparation du pâté de béton, lorsqu'on observe les désaccords de la plasticité et de la séparation de l'eau. À mesure que les processus de durcissement deviennent plus profonds les particularités d'abord peu sensibles deviennent de plus en plus profondes. Ceci entraîne une perte de possibilités du contrôle le plus complet de la qualité du produit fini (le béton), de la prévision de son comportement lors de son utilisation dans les différentes conditions variables du milieu ambiant.

Il est également connu que certains ciments portlands livrés par des cimenteries différentes, qui se distinguent par la minéralogie et la dispersité, montrent, lors des essais dans les bétons, des résultats assez proches en ce qui concerne certaines propriétés mécaniques. Il est évident que l'étude de ce problème sur les causes de la simulitude des propriétés de ciments à première vue différents est liée aux particularités individuelles du déroulement des processus d'hydrolyse et d'hydratation suivis d'une formation de structure dans la pierre de ciment, ce qui est lié également à la composition minéralogique agissante du ciment. C'est justement dans cette direction de l'étude de structures fines qu'il faut chercher des bases physico-chimiques profondes pour résoudre le problème de cataloguement des ciments.

Pour cinq ciments étudiés proches d'après l'activité, la composition chimico-minéralogique, la consistance normale et certaines autres caractéristiques standards, on a obtenu une série d'indices nettement différents de propriétés importantes du béton. Ceci témoigne que les données initiales utilisées ne traduisent pas complètement les propriétés essentielles des ciments déterminant la qualité du béton. Ainsi, en particulier, l'étude de la résistance du béton durcissant dans des conditions différentes a montré que la différence de manque de résistance des bétons préparés avec des ciments différents lors du durcissement à l'air sec en comparaison du durcissement à l'air humide (conditions normales) peut varier dans de larges limites (de 20 à 50 %).

Dans quelques cas, à une étape déterminée les différentes parties constitutives de la structure dans les échantillons à base de ciments différents peuvent être formées identiquement et également ; c'est justement ce fait qui déterminera certaines propriétés du béton. Dans ce cas la cinétique tant des processus physico-chimiques que des processus mécaniques peut varier fortement pour des ciments différents, autrement dit, les propriétés techniques de ces bétons ne peuvent pas au fond être identiques.

Le problème d'économie du ciment et de diminution du contenu des matériaux dans le béton et le béton armé dans la construction est directement lié à l'utilisation de l'activité du ciment dans des délais différents de son durcissement. C'est pourquoi il est nécessaire de savoir évaluer la résistance d'après la courbe de son accroissement et non seulement d'après un seul indice de résistance standard.

Evidemment on peut être certain que dans la formation de la résistance mécanique et d'autres propriétés du ciment c'est la structure silicique qui joue le rôle décisif. Toutefois la présence dans le ciment des phases de substance intermédiaire corrige la formation des structures à partir de minéraux siliciques. En envisageant le rôle de C_3A il faut noter que jusqu'à présent l'on ne prête pas assez d'attention à l'étude du rôle de la substance intermédiaire, ce qui concerne en

premier lieu le verre faisant partie de la composition de la substance intermédiaire et ayant une capacité de rétention d'eau élevée.

En fonction du rapport entre le minéral C_3A et l'addition de gypse dihydraté il se forme dans la pierre de ciment de l'ettringite ainsi que, grâce à ce processus, il y a formation de la structure de coagulation en C_3A hydraté, qui diffère par ses propriétés et qui se forme en plus grandes ou plus petites quantités à un rythme accéléré ou ralenti.

Il faut également tenir compte de l'action sur la vitesse de formation de l'ettringite de la morphologie du clinker, de la répartition près de la surface des particules du ciment des substances minérales mères séparées et de leur cristallochimie.

Les facteurs succinctement énumérés déterminent tant la quantité de l'ettringite formée que ses particularités dans la structure du ciment durci. Il est évident que l'ettringite formée de façons si différentes différera par ses propriétés fonctionnelles et influera sur les propriétés du ciment durci de manière tout à fait différente. Notons que ce n'est pas l'ettringite, constituant instable et peu résistant du ciment durci, qui importe mais le fait de destruction des structures de coagulation fixé par la formation de l'ettringite.

Les aluminates de calcium hydratés qui existent sous forme de structures de coagulation et qui se forment principalement vu le manque du gypse dihydraté respectivement pour la teneur élevée du ciment en aluminates et les finesses de broyage correspondantes du clinker, empirent notablement les propriétés techniques du béton. Notons que ce résultat identique peut être obtenu par suite de causes premières tout à fait différentes.

L'étude de la composition du ciment durci aux différentes étapes de son hydratation à l'aide de la dérivatographie montre que sur les courbes DTG on peut déceler la présence d'effets des aluminates de calcium hydratés C_4AH_{13} dans les intervalles de température de 155 à 185 °C et au-dessus. Dans d'autres intervalles de température on enregistre la fixation du gypse et l'augmentation simultanée de la quantité d'ettringite. L'apparition dans le ciment durci des hydrates est décelée également d'après un autre indice. Simultanément avec l'hydratation de C_3A on voit apparaître de la chaux hydrolytiquement détachée qui sature la solution et augmente le pH du milieu. Mais $Ca(OH)_2$ change également la basicité des aluminates de calcium hydratés qui se forment en apportant des changements dans les structures de coagulation, ce qui se répercute inévitablement sur les propriétés du béton à partir du moment de gâchage et de formation du mélange, bien que le cas où les ciments contiennent la même quantité de minéral C_3A et le gypse dihydraté est introduit en proportion nécessaire, soit également possible.

D'autres particularités, par exemple l'éventement du ciment conduisant à la corrosion de la surface de ses particules, en particulier du constituant alitique, diminue le pH du milieu et la possibilité de la formation de l'aluminate tétracalcique hydraté, ce qui entraîne des écarts correspondants dans les structures de coagulation et les propriétés du béton.

L'introduction d'additions hydrauliques actives exerce une influence sur la composition de la phase liquide au cours de l'hydratation du ciment. Dans ce cas la chaux hydrolytiquement détachée est activement absorbée, la séparation de l'eau du mélange est réglée. Par suite les structures de coagulation instables subissent des changements morphologiques, ce qui se répercute directement sur les propriétés du béton des ciments initialement similaires.

L'élaboration du problème des liaisons des propriétés du béton pour la comparaison de ciments différents tant d'après les indices techniques que d'après les caractéristiques des structures fines et des particularités des compositions du ciment durci, est possible dans la direction indiquée ou dans d'autres directions. Les comparaisons données sont possibles à condition que les mélanges choisis soient tels qu'une grande distinction dans la répartition de l'eau, sa coupure, la sédimentation du ciment d'après la grosseur des grains, n'aura pas lieu, car ceci influe considérablement sur la formation de la structure des pores (y compris les pores de contraction remplis d'air ou les pores inondés par l'eau) et finalement, sur toute une série de propriétés techniques.

En développant ce qui était dit plus haut sur les structures en phases de la substance intermédiaire il faut établir d'une manière certaine les types des structures qui se forment en leur présence et les hydrates qui améliorent certaines propriétés des bétons. Des essais mécaniques standards habituels ne permettent pas d'obtenir une telle information nécessaire. Il importe de savoir en quelle relation se trouvent entre elles certaines propriétés du béton et comment les particularités spécifiques de la structure des constituants de clinker modifient le déroulement des processus de durcissement. Notons que sous forme existante le ciment portland n'est pas un liant universel. On peut le voir en particulier en comparant les résistances des échantillons durcissant dans les conditions normales et à l'air sec.

La mise en évidence des mécanismes des relations indiquées au niveau des structures d'hydrates ouvrent de bases scientifiques profondes pour le catalogument des ciments.

Pendant de nombreuses années de travail on n'a pas trouvé de procédés sûrs d'évaluation d'une série de propriétés impor-

tantes du ciment. L'analyse du phénomène de contraction et de son liaison avec une série de propriétés importantes du béton est insuffisante. Quant aux problèmes de formation des structures du ciment durci en pâte de ciment (suspension concentrée) on leur accorde injustement peu temps. Cependant l'étude des processus d'hydrolyse et d'hydratation à toutes les étapes de la formation de structure doit être précédée par l'étude de la propriété du ciment de séparer une quantité d'eau différente dans les compositions du béton variées. Une étude plus détaillée montre que la propriété du ciment de séparer l'eau est liée à la présence de surfactifs (SDB), les processus de séparation de l'eau étant influencés par les additions minérales contenues, le dosage du gypse et sa relation avec la quantité de C_3A, la granulométrie du ciment, son "éventement" (pertes de calcination) et par un nombre d'autres facteurs. Généralement on ne prend pas en considération l'évaluation des particularités de l'"agglutination" de ciments différents et des causes de la différence d'hydratation des ciments lors de l'introduction dans le paté de béton d'électrolytes différents, accélérateurs du durcissement. Les causes d'une plastification différente des ciments séparés par les modifications de surfactifs, des particularités de leur action sur les propriétés des ciments, de l'autoplastification de la pâte de ciment, de l'entraînement de l'air sont peu étudiées. Il convient d'élargir les renseignements disponibles sur le fluage, le retrait et la résistance au gel des bétons. On n'utilise pas les possibilités de la vibration réitérative multiple du paté de béton ainsi que son maintien jusqu'au début du compactage et le rôle de ces procédés dans les processus de durcissement des bétons. Un large développement de la production du béton armé préfabriqué inscrit à l'ordre du jour le problème d'étude des causes de la différence de résistance, de déformabilité et de résistance au gel des bétons après leur traitement à la vapeur humide.

Pour résoudre ces problèmes et bien d'autres on doit mettre en jeu tant les méthodes actuelles de l'analyse physico-chimique que les procédés simples de l'analyse rapide, faciles à réaliser dans les conditions de laboratoire et argumentés du point de vue scientifique et méthodique, dont l'utilisation complexe assurerait l'obtention de l'information nécessaire, ce qui est très important pour la prise en compte approfondie des propriétés des bétons lors du catalogument des ciments (voir le schéma du catalogue des ciments).

La pratique de plusieurs années montre que l'utilisation correctement élaborée du ciment d'après le type complexe du béton détermine la longévité des constructions et l'utilisation rationnelle du ciment. Dans ce cas il est possible d'obtenir une diminution de contenu des matériaux dans les structures en béton d'après la masse du ciment jusqu'à 10 %.

L'argumentation scientifique et technique du catalogument des ciments se fait sur la base de la vérification des résultats obtenus, des recommandations de différents chantiers et usines de structures en béton armé et de la révision des normes.

SCHEMA DU CATALOGUE DES CIMENTS
(Variante possible)

n°s	Propriétés du ciment déterminant le type complexe du béton	Directions de l'utilisation d'après leurs changements possibles
1	Cinétique du durcissement	D'après le type de la dépendance analytique R = f(t)
2	Attitude envers le durcissement pour différentes humidités de l'air	Différences de cinétique du durcissement à l'air humide et à l'air sec
3	Efficacité du durcissement en cas du traitement à la chaleur humide	D'après les écarts dans la cinétique du durcissement après le traitement à la chaleur humide en régimes différents
4	Efficacité de l'utilisation de différentes additions (surfactifs, électrolytes, etc.)	Détermination du groupe de plastification du ciment et du domaine d'application, choix des additions nécessaires et de la technologie de leur introduction
5	Déformabilité (retrait, module d'élasticité, fluage) et résistance au gel	Prévision des valeurs attendues d'après la composition minéralogique agissante du ciment et les processus initiaux de formation de la structure
6	Correspondance du ciment à la technologie de la préparation du paté de béton et à l'équipement utilisé, aux procédés et actions	Etablissement du domaine d'application optimal, variation des paramètres technologiques ou particularités lors de la réalisation des travaux

Dependence of high-strength and rapid-hardening cements optimum granulometry from W/C and hardening conditions

Rapport entre le E/C et les conditions de durcissement et granulométrie optimale de ciments à haute résistance et de nouveaux ciments à prise rapide

I. KRAVCHENKO, prof., doc. of tech. sciences,
M. VLASOVA, cand. of tech. sciences,
B. YUDOVICH, cand. of tech. sciences, NIITsiment - Moscow, U.S.S.R.

SUMMARY: On the basis of precondition of strength reduction as a result of local disturbances of hydration products medium density analitical dependencies according to an optimal strength criterion of "x" small and medium fraction of cement (less than 5 and 5-30 μk) have been plotted against a starting w/c ratio and hydration degree of these fractions considering their composition and quantity of larger fraction. There also shown that "x" should be increased with gain in w/c ration and strengthening requirements to cement early strength values. With w/c = 0.4 and medium fraction hydration degree of 0.9 (28 days) the experimental values of x = 0.195 - 0.21 are close to the calculated of 0.208 - 0.218. Analitical calculation of rational granulometry is thus possible according to the data on a starting w/c ratio and its hydration degree by a given age of hardening.

RESUME: Partant des conditions de la chute de résistance due aux perturbations locaux de la densité moyenne des produits d'hydratation, on a établi des dépendances analitiques de la proportion "x",optimale quant au critère de résistance,entre les fractions fine et moyenne dans le ciment (moins de 5 et 5-30 μk) par rapport au E/C initial et au dégré d'hydratation de ces fractions compte tenue de leur composition et de le quantité de fraction plus grosse. On a montré qu'un accroissement du E/C et/ou celui de la résistance précoce du ciment doivent être suivis d'une augmentation de "x".Avec un "E/C"=0,4 et un degré d'hydratation de la fraction moyenne 0,9(28 jours),les données expérimentales "x"=0,195-0,21 sont proches des calculs theoriques 0,208-0,218.
On en conclut sur le possibilité du calcul analytique d'une granulométrie rationnelle pour le ciment portland à partir des donnés sur le E/C initial et le degré de son hydratation à un delai de durcissement voulu.

The attempts have been repeatedly made to calculate an optimal granulometric composition of portland cement on the basis of hydration rate of its individual fractions. It has been thus found that cement fraction dispersed by the air with moisture content of more than 40% and with cement specific consumption of more than 0.3 m^3/kg considerably changes its hydration activity.

In addition, an optimal granulometric composition of cement must depend on concrete density first of all and on a starting w/c ratio. The report presents a method of calculation of cement granulometric composition with the given amendments; the task does not coincide with the seminar theme but is also urgent.

Starting items. Strength of cement (concrete) reaches a maximum on filling of capillary pores by hydration products. 2. As this takes place, suitable average density also reaches a maximum. 3. Local disturbances of average density will develop if absolute volume of hydration products considering contraction exceeds capillary pore volume. 4. Cement is considered as a composition of three fractions: small - not less than 5 μk, average fraction - 5-30 μk and large - more than 30 μk. 5. In the case of random placing ofcement particles in a process of forming and compaction of cement paste (concrete) the small fraction fills voids in placing of average fraction and the large is speckled in the placing of the others. It has been experimentally proved on the basis of the fact that an efficient diameter of two modes of capillary pore volume size distribution in early age (up to one day) cement stone (about 1 and 8 μk) is less than weighted mean diameters of particles of the small and average fractions of cement (about 1.2-1.8 μk and 11-13 μk, correspondingly).

Legent. Let Θ and V be density and volume of particle layer, γ and v - density and specific volume of particles itselfes, m - fraction content in cement in parts per unit, G - hydration degree, indices "sm., av., l., lr, mf, c" relate to small, average and large fractions, layer, fraction mixture and cement, correspondingly, x - ration of small and average fraction in weight, ε - porosity in parts per unit, W_n - weight content of water bound on hydration of cement, $W_{n,\,max}$ - the same on G = 1, W_t - the same by a given moment of hydration t.

Calculation of x without hydration. Let us consider a mixture of the small and average fractions. Then, following T. Powers and starting density analysis from the compositions of its placing which are rich with average fraction we have:

$$\Theta_c = \Theta_{av} + \Delta\Theta,$$

where $\Delta\Theta$ - density increment as a result of the small particles disposition among the average, according to equation $\Delta\Theta = m_{sm}/(\gamma_{sm} \cdot V_{sm})$. If all the voids of the average fraction placing are filled with the small then according to: $V_{sm} = m_{av}/(\gamma_{av} \cdot V_{av})$ and substituting (1) this in (1) we shall obtain:

$$\Theta_c = \Theta_{av} + \frac{m_{sm} \cdot \gamma_{av} \cdot \Theta_{av}}{m_{av} \cdot \gamma_{sm}} \qquad (2)$$

Starting analysis from the compositions riched with the small fraction we shall similarly obtain for layer volume:

$$V_c = \frac{m_{sm}}{\gamma_{sm} \cdot \Theta_{sm}} + m_{av}/\gamma_{av},$$

and particle volume in a layer: $V_p = m_{sm}/\gamma_{sm} + m_{av}/\gamma_{av}$, where from, by definition,

$$\Theta_c = V_p/V_c = \frac{m_{sm}/\gamma_{sm} + m_{av}/\gamma_{av}}{m_{sm}/\gamma_{sm}\Theta_{sm} + m_{av}/\gamma_{av}} \qquad (3)$$

when $\gamma_{sm} = \gamma_{av}$ and $x = m_{sm}/m_{av}$ the equations (2) and (3) are transformed into:

$$\Theta_c = \Theta_{av}(1 + x), \qquad (4)$$

$$\Theta_c = \frac{x + 1}{x + \Theta_{sm}}\,\Theta_{sm}. \qquad (5)$$

The equations (4,5) characterize increase in density of placing of the average fraction - on filling voids by the small fraction and of the small fraction - in changing conglomerate of its particles spaces between them by the particles of average fraction. It is evident that the equations (4, 5) are hyperbolas (Fig. 1), correspondingly, refering to the arguments m_{sm} and m_{av} considering that Θ_{sm} and Θ_{av} - constant.

Ratio of $x_{optimal}$ for maximum density of the mixture of the small and average fractions will be the following, determining an intersection point of hyperbolas in Fig. 1, i.e. equating (4) to (5):

$$x_{optimal} = \Theta_{sm}/\Theta_{av} - \Theta_{sm}. \qquad (6)$$

In ideal case of spherical particles Θ_{sm} equals to Θ_{av}, then

$$x_{optimal} = 1 - \Theta_{sm} = \varepsilon,$$

i.e. an optimal ratio of the small and average fractions numerically equils to placing porosity. With the increase of the later due, for example, to the growth of w/c ratio, the optimal content of the small fraction in

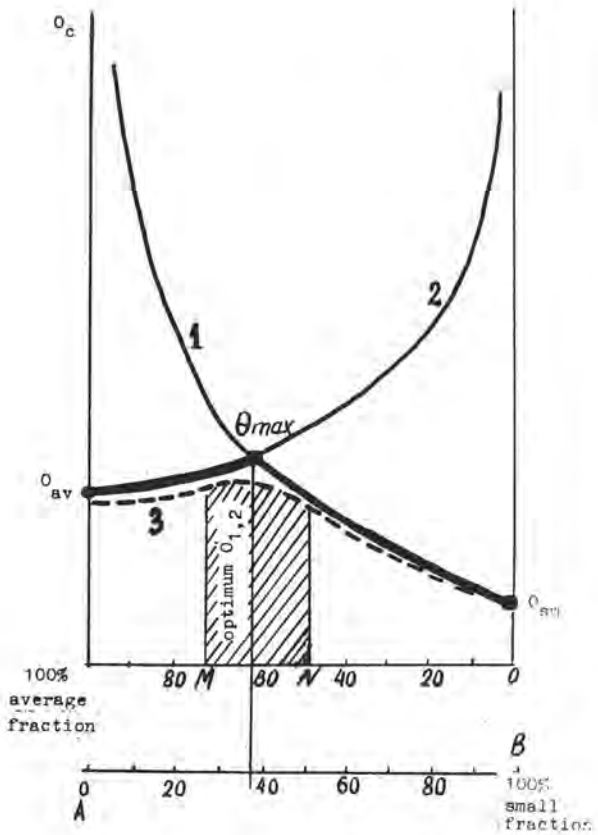

Fig. 1. Placing density of mixtures of cement small and average fractions.

1 - curve according to equations (3,5);
2 - curve according to equations (2,4);
bold curve - calculated placing density;
3 - experimental placing density;
MN - area of optimum (shaded);
B - calculated optimum.

cement should increase and it ash been experimentally proved. In particular, in the USSR when passing from the cement tests in rigid consistancy samples to the tests in plastic consistancy samples and changing w/c ration of the standard mortars from 0.25-0.28 to 0.4, correspondingly, the average data on cement strength growth with increase in specific surface area from 3000 to 4000 cm^2/g constitute about 110 kgF/cm^2 with w/c ratio = 0.4 against 70 kgF/cm^2 with w/c ratio = 0.28, correspondingly, i.e. "contribution" of cement dispersity into its strength is increasing with the growth of w/c ratio. For the case of $\gamma_{sm} = \gamma_{av}$ we can obtain:

$$x_{optimal} = (\theta_{sm}/\theta_{av} - \theta_{sm})\,\gamma_{sm}/\gamma_{av}. \quad (7)$$

Large fraction effect. Volume of layer of mixture of all fractions equals:

$$V_{mf} = \frac{m_{sm} + m_{av}}{\gamma_{sm}\,\theta_{mf}} + m_l/\gamma_l,$$

while in the particle volume:
$V_p = m_{sm}/\gamma_{sm} + m_{av}/\gamma_{av} + m_l/\gamma_l$, then

$$\theta_c = \theta_{mf}/\left[1 - m_l(1 - \theta_{mf})\right]. \quad (8)$$

This suggests that in placing of the large particles with the method - "particle after particle", as in mosaic where space is available for every large particle the close x to $x_{optimal}$ and the lower ξ, the less its positive effect on layer density. Really, there are no voids corresponding to the large particles and when placed on random they have to move apart available voids; A. Weymouth was the first to establish this fact. The moving apart process can be estimated with the Gerts equation for middistance between particles in random placing:

$$D = 0.55\, n^{-1/3},$$

where n - coordination number $\approx \gamma_l/\gamma d^3$, d - particle diameter. Having introduced the coefficients $B = k_1 d_1^{-1.5}$ and $A = k_2 d_{mf}^{-1.5}$ we shall obtain after conversion:

$$\theta_{mf} = B\left[(0.2+0.8\, m_1^{1.5}) \cdot (1 + A\, m_1^{-0.5} - m_1)^{-1}\right].$$

The equation proves the fact that density decreases in random placing of the average and small fractions when the large fraction is introduced into it, the larger size of its particles and lesser total porosity the greater decrease in density. It should be noted that a positive effect of the large fractions on cement technical properties found in a number of the previous experiments, such as the experiments of H. Kühl, Ch. Bruer or G. Burrows, was likely conditioned by the far from optimal ratio of the small and average fraction (lack of the average fraction) used in cements and high values of w/c ratio.

Calculation of placing density considering hydration. By definition, $\theta = 1 - \xi$, therefore available calculation methods for estimating content of different group pores in cement stone are suitable for calculation of θ and, thus, - for granulometry of cement.

If on the basis of the experiments we assume $W_{n,max} = 0.5$, $v = 0.32$, gel pore volume in cm^3/g of cement $q = 0.2$ and volume of contraction $j = 0.09$ cm^3/g then a summary of the calculated equations given in the Table will be obtained.

In the Table the values of W_n, $W_{n,max}$, q and j are selected according to the experimental data; a is a correction for deviation

of a coordinating number in a layer from a mean value. According to the experiment $a_{sm} = 1.2$.

Projecting of cement granulometric composition. On the basis of the equation (7) and considering the aforesaid the following system of the three equations is sufficient to projecting of cement granulometry:

$$m_{sm}/m_{av} = (\theta_{sm}/\theta_{av} - \theta_{sm})\gamma_{sm}/\gamma_{av},$$
$$m_{sm}/m_{1} = (\theta_{sm}/\theta_{1} - \theta_{sm})\gamma_{sm}/\gamma_{1};$$
$$m_{sm} + m_{av} + m_{1} = 1.$$

Solutions to this system with the following symbols:

$$E = \theta_{sm}\gamma_{sm}(1-\theta_{av})(1-\theta_{1}) + \theta_{av}\gamma_{av}(1-\theta_{1}) + \theta_{1}\gamma_{1}(1-\theta_{av}) \text{ are:}$$

$$\left.\begin{aligned} m_{sm} &= \theta_{sm}(1-\theta_{av})(1-\theta_{1})\gamma_{sm} \cdot E^{-1}; \\ m_{av} &= \theta_{av}(1-\theta_{1})\gamma_{av} \cdot E^{-1}; \\ m_{1} &= \theta_{1}(1-\theta_{av})\gamma_{1} \cdot E^{-1}; \end{aligned}\right\} \quad (10)$$

m_1 considering the above estimation from (9).

Here specific mass of fractions and density of placing should be calculated considering values of hydration degree of individual fractions which can be calculated according to the data on values of hydration degree of a combination of not less than 3 cements having known but different grain composition at various ages of hardening and using a diffusion equation and an additivity law assuming $G = 1$ and $t \geq 1$ day.

The values of $G_{sm} < 1$ when $t > 1$ day commonly met in calculations testify the reality of non-evaporated water extract from hydration products of the small fraction for hydration of the average and large fractions of cement.

Table 5

Equations for calculation of cement stone placing density

Porosity	Small fraction	Average and large fraction
Capillary	$D_{I\,sm} = \dfrac{a_{sm}(w/c) - W_{t,sm} \cdot G_{sm}}{a_{sm}(w/c) + V_{sm}}$; $D_{I\,sm} = \dfrac{1.2(w/c) - 0.65G_{sm}}{1.2(w/c) + 0.34}$;	$D_{I\,av,1} = \dfrac{a_{av,1}(w/c) - w_{t.av,1} \cdot G_{sm,1}}{a_{av,1}(w/c) + V_{av,1}}$ $D_{I\,av,1} = \dfrac{0.97(w/c) - 0.5G_{av.,1}}{0.97(w/c) + 0.32}$
Contraction	$D_{2\,sm} = \dfrac{q_{sm} \cdot G_{sm}}{a_{sm}(w/C) + V_{sm}}$; $D_{2\,sm} = \dfrac{0.08\ G_{sm}}{1.2(w/c) + 0.34}$;	$D_{2\,av,1} = \dfrac{q_{av,1} \cdot G_{av,1}}{a_{av,1} \cdot (w/c) + Y_{av,1}}$ $D_{2\,av,1} = \dfrac{0.09\ G_{av,1}}{0.97(w/c) + 0.32}$
Gel	$D_{3\,sm} = \dfrac{j_{sm} \cdot G_{sm}}{a_{sm}(w/c) + V_{sm}}$; $D_{3\,sm} = \dfrac{0.19\ G_{sm}}{1.2(w/c) + 0.34}$;	$D_{3\,av,1} = \dfrac{j_{av,1} \cdot G_{av,1}}{a_{av,1}(W/C) + Y_{av,1}}$ $D_{3\,av,1} = \dfrac{0.2\ G_{av,1}}{0.97/w/c) + 0.32}$

Table 5 (continued)

Porosity	Small fraction	Average and large fraction
Common	$D_{common,sm,1} = \frac{a_{sm,av,1}(w/c) - (W_{t\ sm,av,1} - q_{sm,av,1} - j_{sm,av,1} \cdot G_{sm,av,1})}{a_{sm,av,1}(w/c) + V_{sm,av,1}}$	
	$D_{common,sm} = \frac{1.2(w/c) \cdot 0.38\ G_{sm}}{1.2\ (w/c) + 0.34}$;	$D_{common,av,1} = \frac{0.97(w/c) - 0.21\ G_{av,1}}{0.97\ (w/c) + 0.32}$
Placing density	$\Theta_{sm} = 1 - D_{common} = \frac{V_{sm} + (W_{t.sm} - q_{sm} - j_{sm})G_{sm}}{a_{sm}(w/c) + V_{sm}}$; $\Theta_{sm} = \frac{0.34 + 0.38\ G_{sm}}{1.2(w/c) + 0.34} = \frac{1.1\ G_{sm} + 1}{3.5\ (w/c) + 1}$	$\Theta_{av,1} = 1 - D_{common,av,1} = \frac{V_{av,1} + (W_{t.av,1} - q_{av,1} - j_{av,1})G_{av,1}}{a_{av,1}(w/c) + V_{av,1}}$; $\Theta_{av,1} = \frac{0.32 + 0.21\ G_{av,1}}{0.97(w/c) + 0.32} = \frac{0.65\ G_{av,1} + 1}{3(w/c) + 1}$.

The possibility of the extract has been firstly postulated by H. Kühl but it turned out that opposite to his opinion expressed in the papers of 1928-32 the greater efficiency of this extract, the slower growth of cement strength. This enables the destruction role to be ascribed to the extract process and many investigators believed this starting from T. Powers (1949).

The equations (10) show that small fraction content must be higher with the decrease of placing density of the rest fractions whether it is conditioned by short ages of hardening required for concrete to reach necessary strength (this suggests high dispersity of the new particularly rapid-hardening cements), increased value of w/c ration, or delayed clinker hydration due to its undesired composition and structure.

Example. When w/c ratio = 0.4 and $G_{av} = 0.9$ (28 days) the experimental values of $x_{optimal} = 0.195-0.21$ for clinker characterized in the stand report of B. Yudovich et al., are close to the calculated values of 0.208-0.218.

Theme 2 - Influence of secondary components

by M. CORRADI, Mac Mediterranea, Treviso, Italy.

INTRODUCTION

The interest in fly ashes, pozzolanas and slags has greatly increased in the last few years because of the potential economical and energetic saving they allow.

The shortage of oil has not emphasized only the problem of energy saving, but also urged many countries to a diversification of energy sources. So many thermoelectric power plants are being changed to the use of coal instead of oil. The production of hundreds of tons of fly-ashes all over the world has induced researchers to deepen the study of the possible used of this combustion residual product. The use of fly ashes together with cement in the concrete production is a good combination which, besides solving the problems of waste disposal, enables a substantial energy saving per cubic metre of concrete produced.

POZZOLANAS AND POZZOLANIC CEMENT

Composite binders containing Portland cement and natural or artificial pozzolana are widely manufactured in many countries and are mostly standardized as Portland pozzolanic cements.

Fly ash is an artificial pozzolana, the combustion process residue of power plants using coal.

While the quality of pozzolana is generally constant, at least for the one coming from the same source, fly ash quality differs according to quality, fineness, method of burning pulverized coal, collecting facilities etc.

The standardization of fly ash characteristics and the development of the technique of its addition to concrete on one hand and the standardization of pozzolanic cement characteristics on the other, give a good guarantee of constant quality of composite binder.

The Influence of Fly Ashes on Concrete Properties

It is well-known that fly ashes and pozzolana influence among the other properties of concrete the following :

- Workability, which is generally improved when a good quality fly-ash is used, while is generally reduced with the use of most of natural pozzolana. On the other hand natural pozzolanas will reduce bleeding rate.
- Strength, which generally lowers at early ages and improves at longer ages, the effect being related to the percentage of cement replaced by pozzolana or fly ashes.
- Heat of hydration, which lowers when a portion of cement is replaced by fly ashes or pozzolana.
- Durability against sulphates, which increases when part of the cement is replaced by fly ashes or pozzolana.

POZZOLANIC REACTION

Pozzolanic activity is the ability to react with calcium hydroxide in presence of water and to form hydrated products with binding properties. In the case of addition of pozzolana or fly ashes to Portland cement, the hydroxide necessary for the pozzolanic reaction comes from the hydration of cement and/or free lime.

The reaction products of the lime/pozzolana/water combination are substantially analogous to the hydration products of Portland cement. But some free lime consuming during the pozzolanic reaction, the final product contains a lower amount of $Ca(OH)_2$ and a higher amount of hydrated silicates.

This partly explains the lower strength of pozzolanic cement at early ages compared to Portland cement, and its higher strengths at longer ages. In fact, at early ages at ambient temperature the contribution of the pozzolanic reaction is practically nil; therefore strengths are affected by the lower quantity of the silicates C_3S and C_2S present because of the substitution of pozzolana in place of clinker. At longer ages the hydrated silicates from the pozzolanic reaction add to the silicates of the clinker reaction, strengths being then equal to those of pure Portland cement.

Paper received

The paper presented by P.L. Owens and F.G. Buttler, called "The Reaction of Fly-ash and Portland Cement with Relation to the Strength of Concrete as a Function of Time and Temperature", investigates the influence of concrete temperature rise, due to cement hydration, on strength. Owens points out the difference in strengths between a concrete poured into small standard specimens, cured at 20°C in laboratory, and large volume pours of the same concrete where temperatures higher than 60°C are reached because of the heat of hydration.

Mortar specimens, based on a 1:3 cement/sand ratio, with sufficient water to attain an ASTM flow consistency of 100-110 % were prepared by replacing the cement content by fly-ashes up to 75 %. The proportion of mix water required was then reduced from 0.495 to 0.39. The specimens have been cured at different curing cycles, ranging between 20 and 80°C, thus simulating typical temperature/time profiles of mass concrete pours.

The author notices that at 20°C the early strength of mortars, cured for 11 days, is reduced by increasing the amount of fly ashes. The calcium hydroxide, produced by calcium silicates hydration, is reduced too by increasing the amount of fly ashes. The reduction in both strength and calcium hydroxide is proportional to the reduction of cement thus indicating there is a little pozzolanic reaction between $Ca(OH)_2$ and fly ashes. However, at 28 days the reduction in strength is lower than one could expect from those reductions in cement. This agrees with a pozzolanic reaction of $Ca(OH)_2$ and fly ashes found at 28 days.

Some specimens have been early cured at high temperature and then normally cured at 20°C. For mortars which do not contain fly ashes the 28-day strength after the early curing at 80°C is 32 % lower than the strength of the same mortar constantly cured at 20°C. It is well-known that this reduction is mainly due to the heat developed by cement hydration. Because of the different thermal expansion of air, water, cement paste and aggregates in the mix, cracks occur in mortar or concrete. When the cement is replaced by fly ashes the pozzolanic reaction speed at high temperatures is higher than at ambient temperature. The 28-day strength after an early curing at high temperatures is greater than the corresponding strength at 20°C. In particular, with 75 % of fly ashes the 28-day strength after an early curing at 80°C is more than doubled compared to the 28-day strength at 20°C. The pozzolanic reaction together with the water/cement + fly ash ratio reduction, which occurs when fly ash is used, are responsible for the strength improvement found by the authors.

In mortar tests (cement/sand 1:3) the water/cement plus fly ashes ratio varies from a maximum of 0.495, when pure cement is used, to a minimum of 0.390 when 75 % of the cement is substituted by fly ashes. But calculating the water/cement ratio it follows that it is 0.495 when pure cement is used, up to 1.56 when 75 % of the cement is substituted by fly ashes. This means that till the reaction of fly ashes with lime does not start, the substitution of cement with fly ashes causes a remarkable increase of the water/binder ratio because fly ashes behave as an inhert. This furtherly explains the low strengths at early ages when cement is substituted by fly ash.

At longer ages when the reaction between fly ashes and lime starts both hydration products and a reduction of the water/binder ratio make strengths increase.

The more the fly ashes will react with lime the higher the reduction of the water/binder ratio will be The water/binder ratio, then, is a variable ratio whose influence is the more beneficial, the quicker and the more fly ashes react with lime.

Nevertheless, notwithstanding the evident pozzolanic reaction, the residual amount of lime in the cement paste is sufficient to maintain a pH high enough to prevent corrosion to embedded reinforcement. Some problems could rise if carbonation occurs.

The authors' results indicate, in conclusion, that by adding fly-ash to the mortar subjected to curing temperatures, similar to those that can occur in practice in mass concretes, the adverse effect of high curing temperatures on the strength of Portland cement mortars is counteracted by a pozzolanic reaction acceleration. The optimum strength improvement is to replace 35 % of cement with fly ashes.

Mr. M. Matousek's paper entitled "The Influence of Cement Properties on Concrete Behaviour and its Resistance to the Atmospheric Corrosion" investigates the corrosive effect of atmospheric acid gases on concrete. The corrosive action of these gases is generally ruled by the concrete capillary pore structure. Therefore Fourier's Law and Fick's first law can be used for the diffusion of gases in the concrete. According to these laws, the penetration of aggressive gases into the concrete is inversely proportional to the coefficient of concrete permeability resistance. The author defines this coefficient as the permeability resistance of aggressive gases compared to the permeability resistance of the air diffusing through the same thickness of concrete and at the same temperature.

If aggressive gases react with the basic component of the concrete (lime), as carbon dioxide does, the thickness of carbonated concrete, according to Fick's law, is expressed by :

$$D = K \sqrt{t}$$

where D is the thickness of carbonated concrete (meter), t is the time (seconds), and K is inversely proportional not only to the square root of permeability resistance coefficient of concrete but also to the square

root of the quantity of aggressive gas fixed by the unit volume of concrete. For example the quantity of CO_2 required for the carbonation of one cubic meter of concrete.

The author's conclusion is that Portland cement concretes with high content of $Ca(OH)_2$ provide a better resistance to aggressive CO_2 attack.

In this respect composite cements, containing fly-ash or pozzolana which through a pozzolanic reaction reduce the content of $Ca(OH)_2$ cause a lower resistance of the concrete to acid gas corrosion.

SLAGS AND SLAG CEMENTS

Granulated blast furnace slags are mainly composed of glassy materials with a composition which varies according to the parameters of the production process. Unlike pozzolana they possess latent hydraulic properties which are promoted by alkaline activators. Combining the slag with Portland cement, the calcium hydroxide, produced by silicate hydration, activates the reaction of slag with water.

The alkaline activators are thought to increase the permeability of silica and alumina gels, formed as initial products by the reaction of slag with water, allowing the reaction to proceed furtherly.

All slag-Portland cements can be grouped into two classes. The cements of the first group contain slags in the proportion of 20 to 40 % and are usually used alternatively to Portland cement. The cements of the second group contain higher amounts (up to 80 %) of slag. These cements are generally used for hydrothermal curing, works in hot climates or where good sulphate resistance properties are required. Slag cement hydration heat, in fact, is lower than Portland cement's, the reduction depending on the relative proportion of cement and slag. The durability of a concrete, prepared with slag cement, to aggressive sulphate is also improved especially if cements containing high quantities of C_3A are used. On the other hand, if the slag, which generally contains CaO, SiO_2, Al_2O_3 and MgO as main components, has a very high content of alumina, the sulphate resistance generally lowers. The sulphate resistance of slag cement pastes is thought to be mainly related to the lower $Ca(OH)_2$ content, and to the lower content of C_3A available to react with $CaSO_4$ and to form solfoaluminate.

PAPER RECEIVED

Mr. U. Ayapov's paper, entitled "Influence of Chemical Interaction of Cement and Aggregate on the Properties of Concrete" investigates the properties of concretes when slag is used as aggregate instead of binder with hydraulic properties.

The slag aggregates are pretreated before being used in concrete in order to improve the properties of concrete. Previous studies on aggregate surface treatment reported that concrete strength is improved when normal aggregates are treated. For example, with polyhydrosiloxane, diluted hydrocloric acid or phthalic acid. This improvement is generally explained by the increase in the aggregate/cement paste surface of contact or by a better crystallization of calcium hydrosilicates of the cement paste on the aggregate surface.

Crystallized phosphoric slags or blast furnace slags have been crushed and then activated by an acid treatment. The author investigates the optimum parameters of slag activation through the kinetic of dissolution of the slag aggregate in an acid solution. Using diluted H_2SO_4 as slag aggregate activator, the author shows that the rate of dissolution is very slightly dependent on temperature, in the range of 20-80°C, while it is influenced by the time of treatment and by the acid concentration. Measures of adhesion strength between slag aggregates and cement paste are determined after treatments at different activation conditions.

An optimum adhesion strength was found in the slag-aggregate treatment with 0.1 M sulphuric acid for periods of over 12 hours. After seven days of curing the adhesive strength of activated aggregate with cement paste was doubled and slightly less than doubled after 28 days of curing, compared with non-activated aggregates. Activated blast furnace aggregates showed 10 % lower adhesive strength than phosphoric slag aggregates. By increasing the sulphuric acid concentration over 0,5 - 1 M the adhesive strength of aggregates with cement paste decreases. This is probably related to an excessive thickness of the treated aggregate layer. The optimum thickness of the treated aggregate layer has been found in the range of 60 - 200 μm. By an X-ray petrografic and thermal analysis the author found that the treated aggregate layers are mainly constituted of silica gel and gypsum precipitated on aggregate surface. The products formed on the treated layer in contact with the cement paste are mainly composed of gypsum, silica gel and calcium hydrosilicate gel.

Concrete mixes, whose composition is not given, prepared with Portland cement PZ 400, slag sand and natural sand also showed an approximately 26 % lower water demand, when slag aggregates were activated for 1 - 3 hours with 0.1 - 0.5 M sulphuric acid solution.

The same concrete also showed a much higher strength (1,4 ÷ 1.6 times) than concretes prepared with non-activated aggregates. Beneficial effect of activated aggregates was found by the author also in the adhesion of concrete to steel.

In conclusion, by activating slag aggregates at the optimum conditions of 0.1 - 0.5 M sulphuric acid water solution, for 1 - 3 hours, it is possible to improve considerably concrete mechanical properties or, at constant performances, to obtain a cement saving.

CONCLUSIONS

The chemistry of cement secondary components and the interactions they have with cement hydration products have been long studied in the last decade. Many aspects of the development of the binding function of these secondary components have been clarified even if one of the main problems is still the slower development of strengths at early ages when the cement is partially substituted by pozzolana, fly ash or slag. A deep investigation on thermic parameters - both endogenous and exogenous - as reported by Owens and Butler's paper, could optimize the use of composite binders.

One of the problems that faces us on this subject is the possibility of effectively reducing the water/binder ratio so that at early ages - when the secondary component has not yet started reacting - an effective reduction in the water/cement ratio could be obtained. Another aspect of the problem which should be investigated is the study of the possibility of accelerating - catalytically or thermically - the pozzolanic reaction or slag hydration, so that secondary components can develop their binding action since very early ages.

The economical and energy saving needs will certainly stimulate some research on this subject in the next years.

The reactions of fly ash and portland cement with relation to the strength of concrete as a function of time and temperature

Les réactions de la cendre volante et du ciment portland en rapport avec la solidité du béton en fonction du temps et de la température

P.L. OWENS, Technical Manager, Pozzolanic Limited, Chester,
F.G. BUTTLER, Chemistry Department, Teeside Polytechnic, Middlesbrough, UK.

RESUME : Quand le béton de portland subit des élévations de température occasionées par la chaleur de l'hydration du ciment, la solidité et la durabilité prolongées sont ordinairement mal affectées. En outre quand le béton de portland subit les grandes élévations de température, i.e. plus que 60°C, aux phases premières, le produit est un béton d'une solidité restrainte qui est formé avant biens des jours, par contraste avec le produit qu'on attend si le béton est submergé dans l'eau à 20°C pendant longtemps.

Par la simulation d'un nombre de traitements vieillissants typiques des traitements que le béton peut subir, on peut rapporter la solidité de l'hydrates des divers âges et des portions différentes du portland et de la cendre volante de qualité réglée a la quantité de la chaux, presente comme $Ca(OH)_2$, qui est trouvée dans la structure de l'hydrate. On trouve aussi que tant que la portion de la cendre volânte grandit, il y a non seulement un perfectionnement de la solidité qui s'agrandit avec la température du vieillissement, mais aussi une réduction de la quantité de la chaux.

De l'examen des systèmes où 0% à 75% du ciment est remplacé par la cendre volante, on trouve la solidite la plus grande après un vieillissement de 28 jours à une température de 80°C quand presque 30% du ciment est remplacé. Cela coincide avec une réduction de presque 50% de la chaux dans l'hydrate. Cette quantité de la chaux est, pourtant, plus qu'il n'en faut pour donner la protection suffisante aux renforcements enfouis d'acier.

SUMMARY : Where Portland cement concrete is subjected to rises in temperature , due to the effect of the heat of hydration of the cement, the long term strength and durability of that concrete is usually adversely affected. Further when Portland cement concrete is subjected at early ages, to excessively large temperature rises i.e. exceeding 60°C, the result is a concrete of restricted and limited strength reached within days, in contrast to that which is expected from the long term storage of concrete in water at 20°C.

By simulating different typical curing regimes to which concrete can be subjected the strength of the hydrate at different ages, with various combinations of Portland cement and controlled quality fly ash, can be related to the quantity of lime, as $Ca(OH)_2$, found in the structure of the hydrate. It was also found that as the proportion of fly ash increased not only was there an improvement in strength, which increased with temperature of curing, but that in the hydrate there was an incidental reduction in the quantity of lime.

Within the range from nil to 75% fly ash as a proportion of the cement content, at about 30% fly ash, a maximum strength was attained at 28 days from curing at 80°C, this coincided with a reduction of about 50% in lime content of the hydrate. However, this amount of lime is more than sufficient to provide adequate protection to embedded steel reinforcement.

1.0 INTRODUCTION

1.1 When concrete made with Portland cement undergoes an early age temperature rise, such as that caused by the heat of hydration of the cement, the strength at 28 days is reduced in proportion to the size of the temperature change (1).

1.2 This reduction of strength can be partly explained by the combination of the impaired bond at the interface of paste and aggregate, known as micro-cracking (2) and by the macro-fracture of the gel structure by the expansion of air and water (3). However, if these phenomenon normally occur in concrete, how can the significant increase of strength be explained that occurs to concrete by the use of a composite cement, such as made of Portland cement and fly ash.

1.3 Research has shown that under comparable high temperature curing conditions, the 28 day strength of Portland cement concrete can be 60% or less of that made with a composite cement (4). This indicates, that whilst concretes made with different types of cement can undergo similar orders of temperature change, during hydration, there could be a significant difference in the chemical structure of the hardened paste.

2.0 EXPERIMENTAL

2.1 For this research to have practical application the test specimens required conditions of curing typical of that known to occur in concrete at early ages (5). The profiles of temperature and time known to be caused as a result of cement hydration are mainly dependant on the quality of cement and the dimensions of the element. Thus both the greater the cement content and/or size of the element, the greater will be the profile of temperature with time.

2.2 Figure 1 illustrates four profiles of temperature and time that are typical for a range of different conditions. Profile A represents for instance the standard curing of test specimens at 20°C, and profile D which could be typical of that within an element that has dimensions exceeding 2.5m x 2.5m x 2.5m, cast with concrete made with 450 kg/m^3 Portland cement.

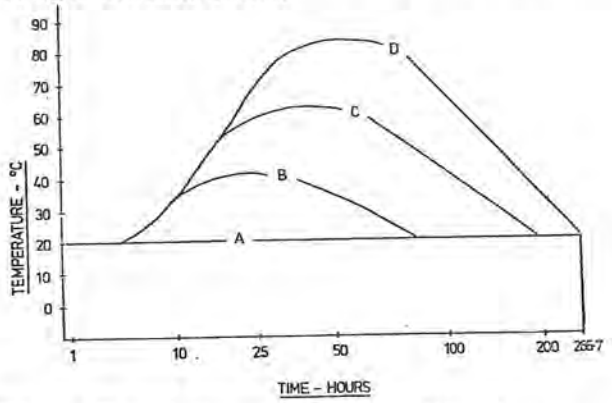

Fig. 1 - Typical temperature/time profiles for concrete.

2.3 The technique for inducing the temperature rise in the test specimens, similar to that of the profiles in Figure 1 was to match by similation the different curing regimes. This was done by having a series of 7 water baths each held at a constant temperature of 20, 30, 40, 50, 60, 70 & 80°C. Then by the transfer of sealed test specimens at various predetermined times the heating and cooling cycles of each profile of temperature could be similated to those shown in Figure 2.

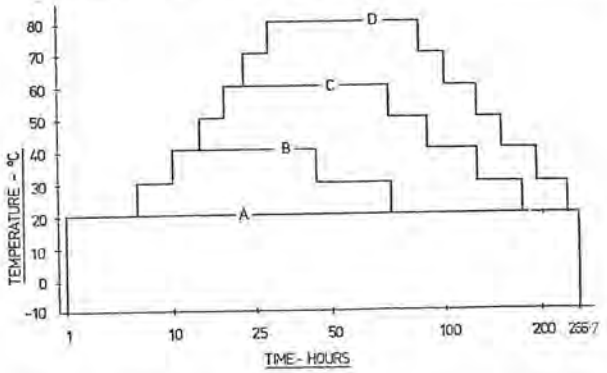

Fig. 2 - Curing cycles simulated to typical temperature/time profiles.

2.4 The authors have also observed from other research

i) Other than under adiabatic conditions the peak temperature experienced in most concrete elements usually occurs within 50 hours after casting.

ii) At 20°C the pozzolanic reaction between Portland cement and fly ash commences usually at about 11 days.

2.5 The means of correlating the effects of the different temperature profiles with both the maturity and the test results of the specimens, was to assume the equivalent period at 20°C was to the base temperature of -10°C (6). Thus the relative maturity of specimens cured by different regimes of temperature could be assessed to approximately 11 days or 8000°C hours (266.67 hours at 20°C.) Then by making the curing regimes conform with convenient factors of maturity i.e. 1.0, 1.125, 1.5 & 2.0, the test results could be correlated to 8000°C.

2.6 In conjunction with the primary test age at 11 days, the test times at 50 hours and 28 days were included so that crushing strength, the more conventional method of assessment, could be related to the different levels of maturity.

3.0 DETAILS of materials, mixes and tests

3.1 The criteria for the Portland cement selected was that it should be from a source with characteristics as close to the mean of that for all UK produced Ordinary Portland cements. Details of the cement used together with the mean and range of variability of 25 UK sources (excluding N. Ireland) are shown in Table 1.

See Table 1 at the end of the communication.

3.2 The fly ash conformed with UK Agrement Board Certificate ABC 75/283 (7). The results are compared in Table 1 with

i) the typical chemical composition of UK fly ash, calculated to 3.0% loss on ignition, after (8) and

ii) the mean quality of fly ash to ABC 75/283 produced during the period July, 1978 to June, 1979.

3.3 The mix was mortar, based on 1:3; cement:sand, to BS 4550 Part 6 quality. The mortar was machine mixed by a standard procedure, with sufficient water to attain a measured ASTM flow consistency of 100 - 110%. In each mix the fly ash substituted a proportion of the Portland cement in increments from nil to 15, 30, 45, 60 & 75%. In consequence the proportion of gauging water required was reduced relative to the amount of fly ash used from 0.495 for the control mix with no fly ash to 0.465, 0.445, 0.415, 0.40 & 0.39 respectively

3.4 From each mix 18 No. 50 mm cube specimens were made, compacted by vibration in 2 layers, then sealed and stored immediately, still in the mould, in water at 20°C. All specimens were removed from the moulds at 22 hours, sealed in polythene air evacuated envelopes and returned to the respective curing regime. At the appropriate time 3 specimens from each mix were tested for the determination of crushing strength and $Ca(OH)_2$ content.

3.5 The technique used for the determination of $Ca(OH)_2$ content was by the carbonation method of thermal analysis (9). This was effected by drilling to the centre of each of 3 cubes and immediately testing each of the drillings.

4.0 TEST results

4.1 The results of the crushing tests at 50 hours, 11 days and 28 days are shown diagramatically in Figures 3, 4, & 5.

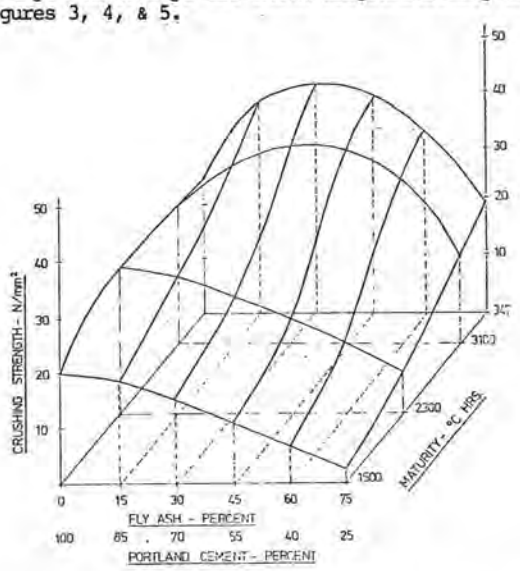

Fig. 3 - Effect of fly ash on the 50 hour strength as affected by maturity.

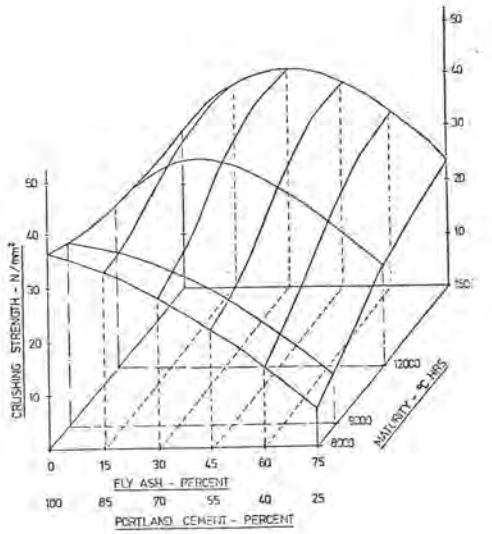

Fig. 4 - Effect of fly ash on the 11 day strength as affected by maturity.

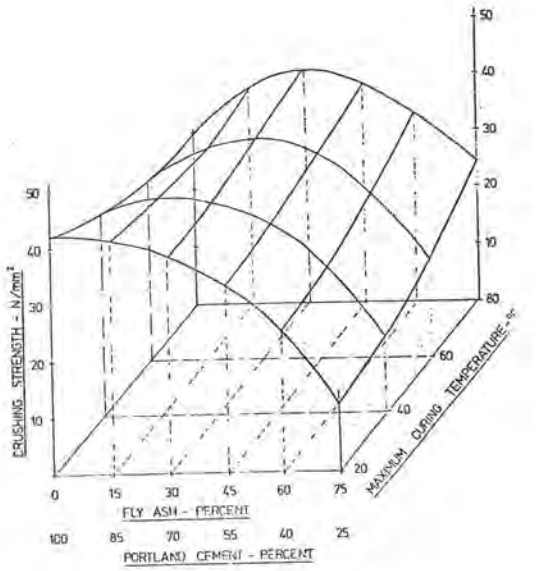

Fig. 5 - Effect of fly ash on the 28 day strength as affected by maximum curing temperature

4.2 The results for the amount of $Ca(OH)_2$ present at 11 days are shown diagramatically in Figures 6, 7, & 8.

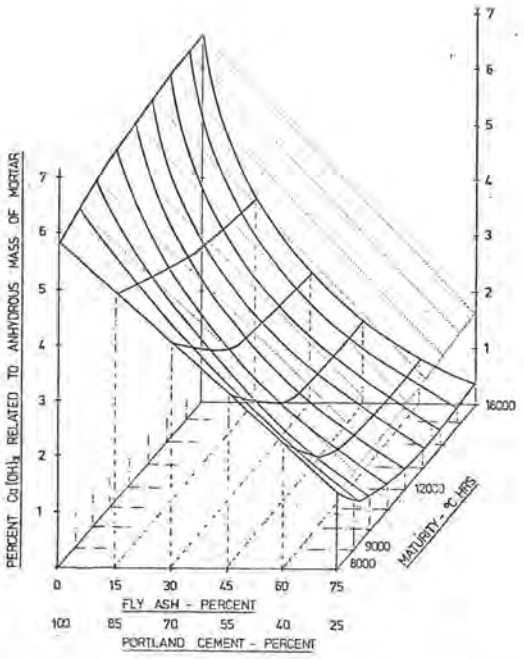

Fig. 6 - Calcium Hydroxide in mortar at 11 days

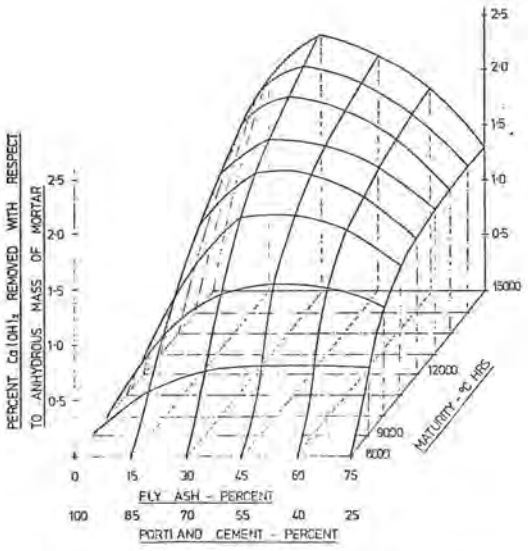

Fig. 7 - Percent Calcium Hydroxide removed in mortar at 11 days.

5.0 DISCUSSION of the results

5.1 The crushing strength of the mortar with no fly ash cured at 20°C at 50 hours, 11 and 28 days was 19.1, 36.3 & 41.8 N/mm^2 respectively. Although the mortar was different in every respect i.e. mix proportions, size of aggregate and water/cement ratio, very close agreement was obtained to the respective concrete crushing strength shown in Table 1.

5.2 The reduction of 32 percent in 28 day crushing strength of the mortar, with no fly ash, cured at more than 60°C is similar in magnitude to that found by other research (1).

5.3 For comparable curing conditions, at and exceeding 60°C, the 28 day crushing strength of the mortar with no fly ash was less than 70% of that made with 30% fly ash, this follows the effects found in (4).

5.4 Figure 3 shows that

i) The strength at 20°C decreases proportionally with the percentage fly ash.

ii) The increase in strength with maturity of the mortar with no fly ash is not maintained above 2750°C hours, where increased maturity reduces the strength.

iii) Corresponding with increases in both fly ash content and maturity, the strength of the mortar increases. The optimum strength occurs with about 35% fly ash at a maturity of 3470°C hours. This approximates with a 2.64 factorial increase in strength for 2.33 factorial increase in maturity.

5.5 As Figure 4 shows at 11 days the trend is similar to that at 50 hours, in that:

i) The crushing strength at 20°C proportionally decreases with the amount of fly ash, indicating little or no pozzolanic reaction.

ii) The reduction in strength with increasing maturity for the mortar containing no fly ash is in agreement with other research (1).

iii) By doubling the maturity and increasing the fly ash to 50%, twice the strength is obtained. However, the maximum strength obtained corresponds with about 30% fly ash.

5.6 Figure 5 shows the effect of fly ash on the 28 day crushing strength as affected by the early curing regimes and that:

i) The crushing strength at 20°C is no longer proportional to the increase in fly ash, and there is indications of a strong pozzolanic reaction at all percentages of fly ash.

ii) The strength, as affected by the early age curing regime of mortar without fly ash, is decreased, but increased at all percentages of fly ash, particularly at 75% where the 20°C strength is doubled by curing at 80°C.

5.7 Figure 6 shows the percentage Ca(OH)$_2$ plotted with respect to both the percentage fly ash and the maturity in °C hours. The Ca(OH)$_2$ is expressed as a percentage of the anhydrous weight of the sample, as the total loss on ignition of each sample was known from the thermogravimetric analysis.

The surface denoted by the solid lines in Figure 6 shows the amount of Ca(OH)$_2$ found to be present, and the surface denoted by the dashed lines the amount of Ca(OH)$_2$ that would have been present, from the cement, if there had been no reaction with the fly ash.

With each of the curing regimes the amount of $Ca(OH)_2$ present, is proportional to the amount of Portland cement used and, therefore the amount of $Ca(OH)_2$ formed for each concentration of Portland cement was calculated from the results obtained with no fly ash.

5.8 It is apparent from Figure 6 that:

i) For samples cured at 20°C for 11 days there is a straight line relationship between the percent $Ca(OH)_2$ and the percentage fly ash, indicating no pozzolanic reaction, which confirms the strength observations in 5.5.i.

ii) For all other samples, in which both the maximum temperature attained and the period the samples experienced temperatures in excess of 20°C, the linear relationship ceases to exist between the percent $Ca(OH)_2$ and the percentage of fly ash. In every case the fly ash reduced the amount of $Ca(OH)_2$ present when compared with similar samples cured at 20°C.

iii) Where no fly ash was used there was an increase in the percentage of $Ca(OH)_2$ when the curing temperature exceeded 20°C.

5.9 The difference between the two surfaces illustrated in Figure 6, corresponds with the amount of $Ca(OH)_2$ which has been removed by reaction with the amount of fly ash present. This difference is shown in Figure 7 where the percentage $Ca(OH)_2$ removed is plotted with respect to both the amount of fly ash and the maturity at 11 days. Figure 7 also shows that the greatest amount of $Ca(OH)_2$ was removed from specimens containing about 30% fly ash. Since the amount of $Ca(OH)_2$ removed must have reacted with the fly ash, and if it is assumed that such a reaction increases the strength of the mortar, then this result implies that the greatest increase in strength with the curing regimes used, should occur with this amount of fly ash. This conclusion is seen from Figure 4 to be in very good agreement with the strength of the mortars at 11 days.

5.10 Figure 8 shows the amount of $Ca(OH)_2$ that has been removed expressed as a percentage of that available from the cement. It is evident that the quantity removed increases with the percentage of fly ash. With the greatest percentage of fly ash very little free $Ca(OH)_2$ remained in the hydrate. Such evidence is important when considering the necessity of having sufficient $Ca(OH)_2$ present from the cement for good corrosion protection to the steel reinforcement of structural concrete. However, it should be noted that although some 50% percent of the available $Ca(OH)_2$ has been removed when using about 35% fly ash, the amount of $Ca(OH)_2$ remaining is more than sufficient to maintain a pH of about 12.5 with good corrosion protection.

6.0 CONCLUSIONS

6.1 By subjecting mortars to curing temperatures similar to those that can occur in practice the effects on concrete strength can be simulated.

6.2 The adverse effects of high curing temperatures on the strength of Portland cement mortars can be related to the amount of lime in the hydrate.

6.3 If high temperatures are likely to be experienced in practice, gains in strength are likely to occur with cements composed of Portland cement and fly ash.

6.4 The amount of residual lime in the hydrate, even when 75% fly ash was used, is sufficient to afford inhibition of corrosion to embedded steel reinforcement.

REFERENCES

1. - VERBECK, G.J. & HELMUTH, R.H. Structures and physical properties of cement paste. From the proceedings of the 5th International Symposium on the chemistry of cement, Tokyo, 1968, Part 3, Properties of cement paste and concrete.

2. - FORRESTER, J.A., Discussion, Propagation of cracks and their detection under short and long-term loading. The structure of concrete and its behaviour under load, Proceedings of an International Conference, London September, 1965 pp 157 to 160, Cement & Concrete Association, 1968.

3. - ALEXANDERSON, J. Strength losses in heat cured concrete. Swedish Cement and Concrete Research Institute, Stockholm, 1972 pp 135. Handlingar Nr 43.

4. - BAMFORTH, P.B., In-situ measurement of the effect of partial Portland cement replacement using either fly ash or ground granulated blast furnace slag on the early age behaviour of mass concrete. Taylor Woodrow Research Report No. 014J/77/1939, October, 1977(Project on behalf of Building Research Establishment).

5. - HARRISON, T.A., Early-age temperature rises in concrete sections with reference to BS 5337 : 1976. Cement and Concrete Association ITN5, November, 1978.

6. - MALHOTRA, V.M., Maturity concept and the estimation of concrete strength - a review. Department of Energy, mines and Resources (Ottawa, Canada, November, 1971, Catalogue No.M38-3/277.

7. -THE AGRÉMENT BOARD CERTIFICATE No 75/283 "Pozzolan - a selected fly ash for use in concrete".

8. - SMITH, M.A. & HALLIWELL, F., The application of the BS 4550 test for pozzolanic cements to cements containing pulverized-fuel ashes. Department of the Environment, Building Research Establishment. Magazine of Concrete Research, Volume 32, Number 108. September, 1979. Cement and Concrete Association.

9. - BUTTLER, F.G. & MORGAN, S.R., A thermoanalytical method for the determination of the amount of Calcium hydroxide formed by hydration of Portland cement. Contribution to this Congress.

TABLE 1

Details of the chemical and physical properties of the Portland cement and fly ash used compared with the UK typical characteristics for those materials

Property Description	PORTLAND CEMENT			FLY ASH		
	Sample	Typical 1978 UK Ordinary Portland cement to BS 12.		Sample	Typical UK fly ash calculated to 3.0% Loss on ignition	
		mean	Std. Deviation		mean	Std. Deviation
Lime Saturation Factor	0.94	0.96	0.03	-	-	-
Bogue Compound Composition % C_3S	56.4	54.0	5.25			
(assuming nil free lime) C_2S	15.2	18.0	5.56			
C_3A	10.5	9.5	1.92			
C_4AF	7.8	7.7	1.61			
Chemical Composition % Silica as SiO_2	20.13	20.48	0.87	52.5	50.00	2.54
Insoluble residue	0.40	0.44	0.26	-	-	-
Alumina as Al_2O_3	5.60	5.29	0.59	27.5	27.23	2.91
Iron as FeO	-	-	-	-	2.40	0.67
Fe_2O_3	2.56	2.53	0.52	9.50	6.75	2.32
Lime as CaO	63.10	64.26	0.71	1.8	2.52	1.08
Magnesia as MgO	2.25	1.39	0.48	1.9	1.76	0.31
Alkalis as Na_2O	0.18	0.21	0.08	0.9	1.04	0.57
as K_2O	0.78	0.70	0.24	3.8	2.96	1.00
Sulphate as SO_3	2.92	2.57	0.23	0.7	0.84	0.37
				Fly ash to ABC 75/283 (1978 / 79)		
Colour Index	3	3.04	0.73	4.0	3.2	1.50
Loss on Ignition %	1.18	1.52	0.41	3.0	2.7	1.33
45 µm sieve residue %	12.0	12.9	4.0	5.8	6.5	1.97
Specific Surface Area m^2/kg	345	345	31	405	385	97
Density kg/m^3	3225	3180	47	2325	2320	80
Concrete Strength N/mm^2 50 hours	20.1	-	-			
0.60 w/c ratio, 20mm Aggregate 3 days	23.0	23.0	2.60			
310 kg/m^3 Portland cement 11 days	34.7	-	-			
28 days	41.3	43.9	2.46			

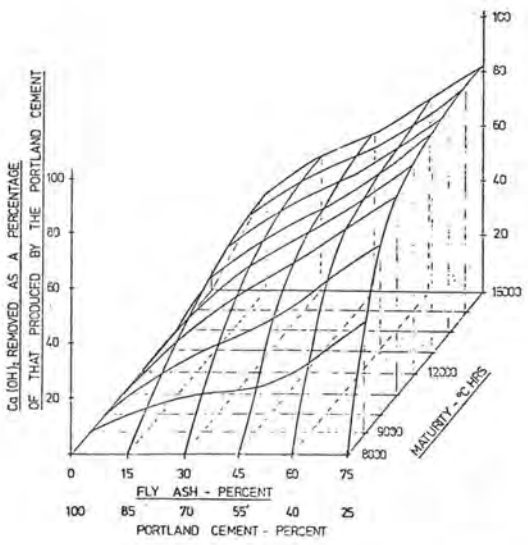

Fig. 8 - Percent Calcium Hydroxide remaining at 91 days.

Theme 3 - The influence of thermal treatment upon the creep of cement systems

by Leslie J. PARROTT, Cement and Concrete Association, England.

INTRODUCTION

The use of concrete in building components and in-situ structures that are subjected to elevated temperatures has increased in recent years. Thermal stresses can arise if potential thermal movements are restrained and such stresses are of concern in nuclear pressure vessels, crude oil storage vessels and bridges subjected to solar radiation. Calculation of stresses requires a general model for the deformation of concrete. Since no reliable model is available concrete properties are normally obtained by experiments in which the concrete mix and the test environment simulate the expected conditions as closely as possible. The results of direct simulation tests are of limited use in developing a general model of thermal creep so basic studies were initiated recently which had the short-term objectives of improving the prediction of thermal creep and assisting the planning of simulation tests. A longer-term aim is to improve general models of creep in concrete. The following sections of this paper indicate recent progress towards these objectives.

IRRECOVERABLE THERMAL CREEP

In many applications concrete is subjected to rises and falls of temperature and the reversibility of deformation under these conditions is an important factor in controlling long-term stresses. In an elastic material the time-dependence of thermal stresses are controlled by the rate of temperature equilibration and removal of a temperature profile returns the material to its original stress. A viscoelastic material would develop stresses at a rate dependent upon the rate of temperature equilibration and the rate of creep but removal of a temperature profile would again return the material to its original stress. However, in a material that develops irrecoverable creep, stresses develop at rates dependent upon the rates of temperature equilibration and creep but removal of the temperature profile would induce a residual stress. This effect of irrecoverable creep can be a serious problem with cyclic temperature changes and can lead to stresses that are opposite in sign to those calculated from an elastic analysis.

LITERATURE ON THERMAL CREEP COMPONENTS

Recent work by Illston and Sanders (1,2) showed that thermal creep was a function of the time between the start of heating and the start of stressing. An increase in the period of preheating reduced the thermal creep that was subsequently measured. Unfortunately this fact had not been appreciated in many studies of thermal creep and in consequence the results are of limited use. Illston and Sanders conducted their creep tests on cement mortar loaded in torsion. This approach simplified a number of testing problems but it was not clear if the results obtained would prove valid in the more practical case of concrete loaded in compression. The torsion results were analyzed, as illustrated in Figure 1, by dividing the load-induced strains into the following components:

a) Elastic Strain. This was proportional to stress and increased with temperature. A secondary effect of elevated temperature was that it increased cement hydration.

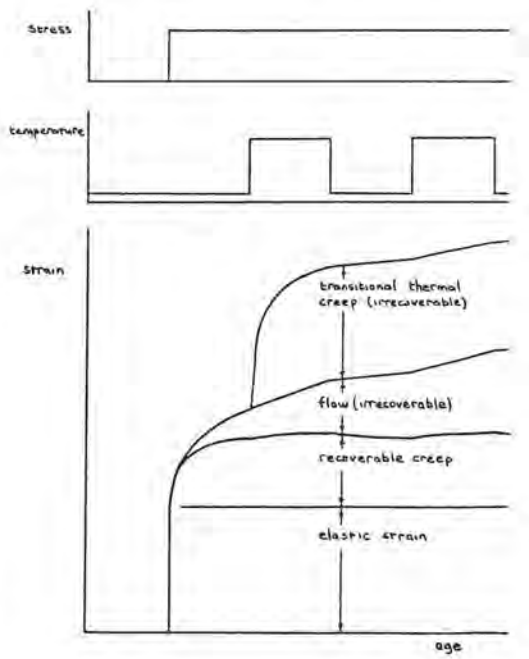

Figure 1. Components of load-induced strain.

This caused some moderation of the increase in elastic strain with increasing temperature. The overall effect of temperature in the range 20 to 80°C upon elasticity was not large.

b) Recoverable Creep. This was similar in many ways to elastic strain but it took a few weeks for its development to stabilize.

c) Flow (Irrecoverable). Flow developed over a prolonged period and was proportional to stress. Its rate of development was dependent upon the current temperature and did not depend upon temperature history apart from a small indirect effect upon the development of the cement paste microstructure.

d) Transitional Thermal Creep (Irrecoverable) This component dominated creep if the mortar had not been heated previously. It developed fairly rapidly after heating (i.e., within one month) and there were no subsequent increases in creep with a reduction in temperature or a second increase.

Deformation results from concrete loaded in compression under various temperature regimes could also be divided into the four components given above (3). The components of compressive creep were incorporated into the analysis of a flexurally-restrained concrete wall that was periodically subjected to a temperature gradient. The analysis successfully predicted experimental results from a full scale wall element and this suggested that a better understanding of the components of thermal creep would be of practical benefit. For example if the effects of mix proportions, aggregate type, cement type or age of heating upon thermal creep were known to be significant some control would be possible. As a preliminary step towards understanding the components of thermal creep we will now consider the effects of elevated temperature upon the microstructure of concrete and its cement paste phase.

POSSIBLE EFFECTS OF HEATING UPON MICROSTRUCTURE

It is appropriate for many practical applications to consider moist concrete subjected to temperatures up to 80°C but even with these limitations a number of microstructural changes are possible. Although most aggregates are not altered by heating some thermal stress and cracking could develop at the aggregate/cement paste interface as a result of thermal expansion coefficient differences. Furthermore the cement paste matrix can be modified chemically and physically. The main chemical effects are an acceleration of cement hydration and an increase in the level of silicate polymerization within the cement hydrates. There is also a possibility that some cement hydrates may dehydrate at elevated temperature. Physical changes can arise from what may be regarded as coagulation of hydrate particles. This would cause a change in the pore size distribution. The porosity would diminish if any additional cement hydration occurred.

CAUSES OF IRRECOVERABLE THERMAL CREEP

A preliminary stage in understanding thermal creep is to clarify the role of aggregate/cement paste thermal incompatibility. The simplest approach was to compare the thermal creep of cement paste and concrete or mortar. The results of such a comparison (4) suggested that the thermal creep of concrete was dominated by the response of the cement paste matrix. Each of the strain components mentioned earlier in Section 3 were present in the cement paste results. Measurements of physical and chemical structure indicated that the irrecoverable thermal creep correlated with an increase in polysilicate formation in the cement hydrates (5,6). Some experimental results are illustrated in Figure 2a and they suggest that acceleration of the molecular rearrangement that is associated with silicate polymerization greatly enhances creep. The similarity between the results for 20 and 60°C in Figure 2a suggests that there is no difference in mechanism between "flow" and "transitional thermal creep." Increases in creep can be found in other materials if they undergo a phase change whilst loaded.

Although the results in Figure 2a were encouraging it was possible that some unmeasured change in the complex microstructure of the cement paste was responsible for the increase in creep. The effect of silicate structure upon creep was therefore studied using a very simple cement; hydrated

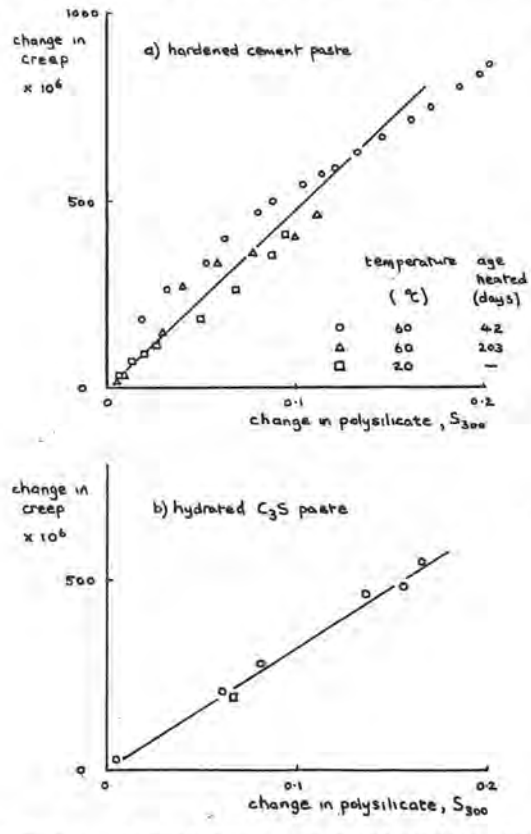

Figure 2. Thermal creep versus polysilicate formation as indicated by S_{300} (7)

calcium silicate. The primary components in this system are calcium silicate hydrates and calcium hydroxide. The results obtained so far (Figure 2b) again show that thermal creep development is associated with changes in polysilicate formation. Indeed if allowance is made for the slight difference in stress level used in the cement and tricalcium silicate tests the slopes of the lines in Figures 2a and 2b are virtually the same. This similarity indicates that thermal creep in cement paste (and in structural concrete) is caused by the response of the calcium silicate hydrates.

It should be emphasized that heating concrete, hardened cement paste or hydrated calcium silicate before stressing will reduce thermal creep because the potential for microstructural changes in a subsequent thermal creep test will thereby be reduced (1,2,3,4,6). The reduction in thermal creep will depend upon the duration of preheating since the changes in microstructure take a few weeks to develop. Published results for cement paste (4) and current results for hydrated calcium silicate show that prolonged rest periods at 20°C can cause some regeneration of thermal creep potential.

RESPONSE OF HYDRATED TRICALCIUM SILICATE TO HEATING

In addition to the gross changes in polysilicate formation indicated by S_{300} (7) a more detailed analysis of silicate structure was undertaken together with studies of nitrogen adsorption, x-ray diffraction, thermogravimetric analysis and water sorption. The detailed silicate structure analysis (7) demonstrated that the proportion of polysilicate and its degree of condensation increased with the duration of heating as shown in Figure 3. The increase in polysilicate content was accompanied by reductions in the amounts of monomeric and dimeric silica. The reaction curves in Figure 3b were computed by subtracting the monosilicate and disilicate contributions from the total silica complexed and normalizing the residual polysilicate contribution to unity (7). The decrease in slope of the reaction curves in Figure 3b is indicative of an increasing degree of condensation with duration of heating.

Nitrogen adsorption measurements showed that heating caused minor surface area changes that did not correlate with the thermal creep results. The x-ray diffraction results indicated that heating at 60°C at an age of 42 days accelerated hydration but the changes were small during the period that the main part of thermal creep developed. Furthermore first heating at an age of 175 days caused substantial thermal creep but had no significant effect upon hydration. Calculated values of lime/silica ratio in the calcium silicate hydrates were in the normal range of 1.6 to 1.9 for heated and non-heated samples. Thermogravimetric analysis indicated that there were no major changes in the shape of the weight loss/temperature curves with heating at 60°C. This implies that there were no major changes in the products of hydration. However a slight increase of weight loss was noted in the thermogravimetric temperature range 200 to 440°C for samples treated at 60°C. A similar increase was noted in previous work with hardened cement paste (8).

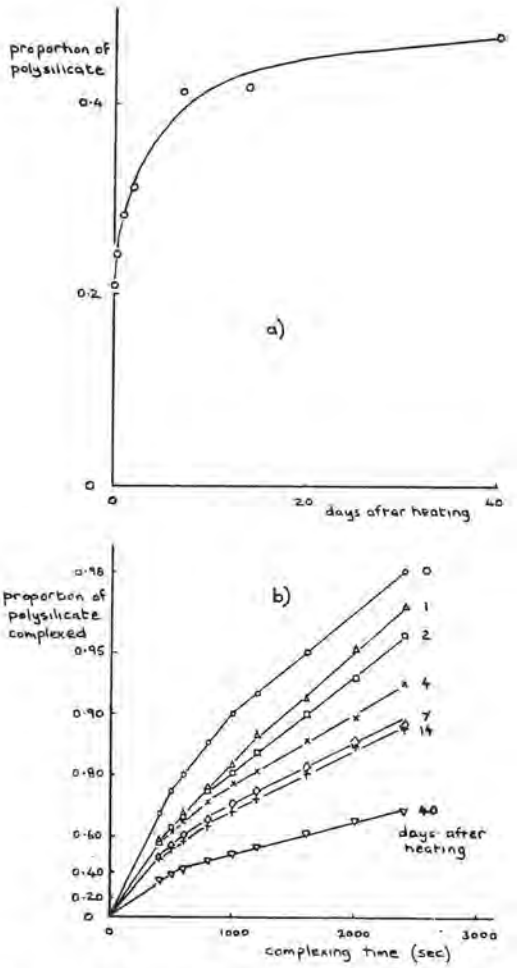

Figure 3. Polysilicate development in hydrated tricalcium silicate paste heated to 60°C at an age of 42 days a) proportion of polysilicate and b) molybdate complexing curves.

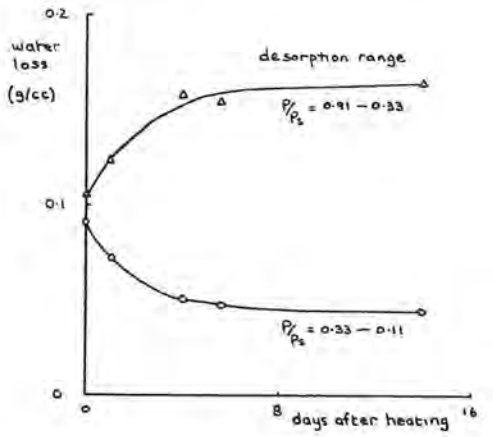

Figure 4. Effect of heating hydrated calcium silicate paste to 60°C at an age of 42 days upon subsequent desorption behavior.

Water sorption studies included first desorption and first adsorption measurements of the type obtained earlier for cement paste (8). The first desorption results for hydrated calcium silicate (Figure 4) suggested, like those for hardened cement paste, that the volume of larger pores increased and the volume of smaller pores decreased with an increase in the duration of heating. The kinetics of these changes in water desorption characteristics were similar to those for thermal creep and silicate polymerization. The first adsorption results suggested, like those for hardened cement paste, that there was no major effect of heating. This difference in sensitivity to heating between first desorption and first adsorption characteristics presumably arose because heating and drying had similar effects upon pore structure.

CONCLUSIONS

Some conclusions from the data presented in this report are listed below:

i. Irrecoverable thermal creep in concrete is a consequence of the basic constituent of the cement binder - the calcium silicate hydrate. Thus thermal creep is not likely to be greatly altered by normal variations of aggregate type, cement type or mix proportions.

ii. One obvious way of controlling thermal creep is to heat prior to stressing, although this may be of limited use because of the possible regeneration of some thermal creep potential with prolonged rest periods at 20°C.

iii. Modelling of thermal creep is likely to be more successful if it reflects the observed changes in microstructure.

iv. Thermal creep is associated with changes in silicate polymerization and pore structure.

ACKNOWLEDGEMENTS

The author gratefully acknowledges the discussions and substantial experimental assistance provided by colleagues at the Cement and Concrete Association.

REFERENCES

1. Illston, J. M. and Sanders, P. D., "The effect of temperature change upon the creep of mortar under torsional loading." Magazine of Concrete Research, 25, 84, 136-144 (1973).

2. Illston, J. M. and Sanders, P. D., "Characteristics and prediction of creep of a saturated mortar under variable temperature." Magazine of Concrete Research, 26, 88, 169-179 (1974).

3. Parrott, L. J. and Symmons, R. M., "Deformation properties of an oil storage vessel concrete subjected to fluctuating stresses and temperatures," Concrete in the Oceans, CIRIA Report P3/I4 (1978).

4. Parrott, L. J., "A Study of transitional thermal creep in hardened cement paste," Magazine of Concrete Research, 31, 107, 99-103 (1979).

5. Parrott, L. J., "Influence of temperature history upon the structure and creep of hardened cement paste," Theme VI, 7th International Congress on Chemistry of Cement, Paris (1980).

6. Parrott, L. J., "Basic creep, drying creep and shrinkage of a mature cement paste after a heat cycle," Cement and Concrete Research, 7, 597-604 (1977).

7. Parrott, L. J. and Taylor, M. G., "A development of the molybdate complexing method for the analysis of silicate mixtures," Cement and Concrete Research, 9, 483-488 (1979).

8. Parrott, L. J., "Changes in saturated cement paste due to heating," Cement and Concrete Association Technical Report 528, August 1979.

Theme 4 - Influence of admixtures

by O. HENNING - HAB - Weimar, DDR,
V.B. RATINOV - MAI - Moscow, USSR.

I Introduction

Starting-point of development and application of chemicals for the use in the production of concrete is the fact that the improvement of cements is limited not only by raw materials but also by technology of cement production.

Moreover there is an actual demand to economize energy, which can be accomplished either by reducing specific cement contents of concrete, i.e. to produce more concrete by using the same quantity of energy intensive cement, or by omitting heat treatment of concrete.

After it was empirically established that many natural and synthetic compounds affect the setting process, at present the mechanism of the processes are being investigated in order to systematically develop more effective admixtures.

In recent years many investigations have been performed in several countries in the field of concrete admixtures. The aim of these investigations was to improve some properties of concrete, to reduce costs of production of concrete, and to avoid secondary effects which impair concrete.

Because during hydration concrete is a continually changing system of many compounds the results of all efforts have been small so far. Nevertheless some exact relationships and regularities have been found.

II Classification of admixtures

It has to be considered that each admixture has several effects but only one effect is most distinctive. For instance, the accelerator calcium chloride also acts as an antifreezing admixture for winter concreting. The plasticizer lignosulfonate also acts as a retarder.

Admixtures for concrete can be classified into two main groups:

- admixtures affecting hydration behaviour
- admixtures affecting flowability behaviour

Beside the two main groups there is a third group of admixtures with special effects. To this group belong antifreezing agents, corrosion inhibitors for reinforcing steel etc.

To the group of admixtures affecting hydration behaviour belong accelerators and retarders. Accelerators shall either shorten the time until setting starts to a few minutes (e.g. sodium fluoride, iron(III) chloride, sodium aluminate / potassium carbonate / sodium sulfate) or increase the initial development of strength or make the heat treatment of concrete more effective resp., by reducing the starting period, lowering the maximum temperature, and reducing stopping time (e.g. calcium chloride, calcium nitrate / calcium nitrite).

Retarders were used in order to extend the setting time or to reduce the hydration, resp. Compounds such as sodium phosphates and borates result in the possibility of washing out the concrete at the surface of concrete elements, which leads to good surface effects of exposed concrete.

To the group of admixtures affecting flowability behaviour of fresh concrete belong plasticizers and superplasticizers. These additives are mainly used to improve the following concrete properties:

- improved workability without increasing water content (dispersing effect)
- decreased water content at the same workability (increased strengths)
- improved penetration and pumpability
- reduced unit costs of concrete

It has been shown that both short-chain and long-chain surfactants can be used as cement dispersing agents. They can be made synthetically or be obtained from natural products. It seems to be essential that not the length of chains but the presence of hydrophylic and hydrophobic groups in definite distribution is most important. These compounds are adsorbed at the cement surface and cause a reduction of the attractive forces between cement particles. The maximum effect is obtained with monomolecular covering. Higher concentrations lead to a considerable retardation of hydration rate causing an obstruction of the water diffusion to the cement surface.

III Papers received

In the following it will be given a short survey of the presented papers which belong to the sub-theme 'Influence of admixtures'. These papers are:

- The combining of sodium chloride and calcium chloride by hardened portland cement compounds C_3S, C_2S, C_3A and C_4AF, by E.M. THEISSING, T. MÖBIUS-VAN DE LAAR and C. DE WIND
- Influence of sulfonated naphtalene on the fluidity of cement pastes, by M. COLLEPARDI, M. CORRADI, G. BALDINI and M. PAURI
- Influence of cement composition on setting time of concrete containing a set-retarding admixture, by C.T. TAM
- Effect of surfactants on the hydration properties of cements, by O. HENNING and L. GORETZKI

The contribution by THEISSING et al. informs about an interesting non-destructive method which allows the experimental measurement of the amount of chloride ions dissolved in the pore solution of hardened cement compounds setting in the presence of sodium chloride and calcium chloride. The equilibrium between the pore solution and the equilibrating solution is considered to be a liquid/liquid equilibrium. That means that the equilibrium concentrations in the equilibrating solution and the pore solution are equal. That it is possible to calculate the dependence of the amount of chloride combined by the compound on the total amount added to the compound. Knowledge of the amount of free chloride in the pore water is necessary to predict corrosion of steel reinforcement.

The paper presented by COLLEPARDI et al. concerning the effect of sulfonated naphtalene in monomeric and polymeric form on cement pastes confirms the theory suggested above. It has been shown that with a dry polymeric addition of 0,25 - 0,50 % by weight of cement the dispersing effect is good enough without any significant retarding effect in the hydration rate. With higher quantities of 1,0 - 1,5 % the retarding effect is significantly increased whereas the flowability ist not substantially improved.

The paper by TAM deals with the effect of a retarder of unknown composition depending on the alkali content of cements. The results indicate that tricalcium aluminate and alkali content influence both the absolute setting time and the delay in setting. A change in equivalent alkali content in excess of 0,25 % alters the delay in setting significantly.

The paper of HENNING et al. gives a summarizing survey of cement dispersing agents and shows the development of an effective plasticizer on the basis of succinic acid. The plasticizers used were synthetized from anhydride of maleic acid, sodium hydrogensulfite, aliphatic alcohols (C_{16} - C_{18}), and ethylene oxide (5 - 40 mole). Using the WASHBURN equation for the flow of liquid through a capillary it was possible to calculate from the rate of penetration the magnitude of the advancing contact angle (fig. 1) and the energy of adhesion between the liquid and the cement powder (fig. 2). With increasing concentration of optimum plasticizer the contact angle decreases and within a definite range of concentration it becomes zero. At higher concentration the angle rises again. The calculated energy of adhesion is at its maximum using a medium concentration.

Finally it should be added that a comprehensive paper concerning the present theories of the mechanism of cement hydration and its interaction by admictures is presented by SKALNY and YOUNG as report to the sub-theme II-1 of this congress.

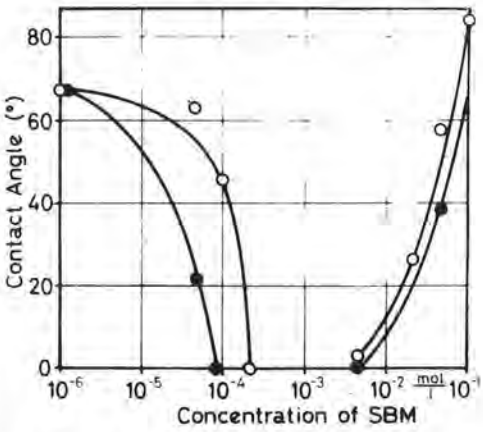

Fig. 1 - Contact angle of solutions of admixtures on cement powder as a function of concentration

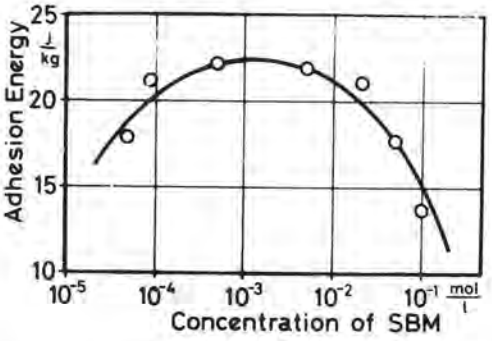

Fig. 2 - Adhesion energy of solutions of admixtures as a function of concentration

The combining of sodium chloride and calcium chloride by the hardened portland cement compounds C_3S, C_2S, C_3A and C_4AF

Les propriétés combinatoires des constituants du ciment portland par rapport à NaCl et $CaCl_2$

E.M. THEISSING, T. MEBIUS-VAN DE LAAR, G. DE WIND,
DELFT University of Technology, Dept. of Civil Engineering, Materials Science Group, Stevin Lab.,
Delft, The Netherlands.

SUMMARY : A non-destructive method is presented to study the combining properties of hardened C_3S, C_2S, C_3A and C_4AF for NaCl and $CaCl_2$. The compounds hardened with solutions of NaCl and of $CaCl_2$ are equilibrated in solutions of these electrolytes in a special way. To interpret the results the equilibrium between the pore solution and the hardened compound is taken as a general solid/solution equilibrium. The equilibrium between the pore solution and the equilibrating solution is considered to be a liquid/liquid equilibrium. That means that the equilibrium concentrations in the equilibrating solution and the pore solution are equal. Thus it is possible to calculate the dependence of the amount of chloride combined by the compound on the total amount added to the compound.

RESUME : On décrit une méthode non-destructive pour déterminer les propriétés combinatoires par rapport à NaCl et $CaCl_2$ des constituants durcis du ciment portland C_3S, C_2S, C_3A et C_4AF. Les constituants durcis avec des additions de NaCl et $CaCl_2$ sont équilibrés dans des solutions de ces sels d'une manière spéciale. Dans le but d'interpréter les résultats expérimentaux on considère l'équilibre entre le constituant durci et le liquide interstitiel comme un équilibre général entre une matière solide et une solution. L'équilibre entre la solution interstitielle et la solution equilibrante est considéré comme un équilibre liquide/liquide. Cela signifie que les concentrations des électrolytes dans ces solutions sont les mêmes en l'état d'équilibre. Cela rend possible de calculer la relation entre la quantité de chloride, combinée par le constituant et la quantité totale de chloride dans le constituant.

INTRODUCTION

The behaviour of chlorides in concrete has aroused much interest throughout the years especially because of their special properties as to the hardening acceleration of cement and the corrosion of steel reinforcement. It is therefore that one is interested in the amount of free chloride in the pore water and in the amount of chloride combined by the cement when chlorides have been added to the mixing water.

It has been known for many years that both NaCl and $CaCl_2$ can be combined by cements. A number of authors investigated the combining properties of hardened cement (mostly portland cement). They determined the amount of combined chloride by extraction of free chloride in the pore water of the hardened cement by means of water or an organic liquid. For a review of the literature we refer to Theissing, van Hest-Wardenier and de Wind (1).

All these extraction methods are in fact destructive methods with all their drawbacks as disturbance of sorption and chemical equilibria between the pore water solution and the pore surfaces in the hardened cement. We consider these methods to be unsuitable for the said purpose. Moreover, the solubilities of some compounds present in the pore water are only slightly soluble in organic liquids. They may precipitate, thus disturbing the precipitation.

Theissing, van Hest-Wardenier and de Wind (1) reported on a non-destructive method to determine the combining properties of hardened cement paste. That method does not have the drawbacks of the extraction methods.

We applied this non-destructive method to the main portland cement compounds C_3S, C_2S, C_3A and C_4AF aiming at determining the relative contribution of these compounds to the overall combining properties of portland cement.

In the following sections we will describe the method used and report on the results.

METHOD

When hardened cement compound has been equilibrated with a chloride solution, there are two overall-equilibria in the case. First, there is the equilibrium between the free chloride in the pore water and the solids in the cement and second, that between the chloride in the pore water and in the equilibrium solution.

This can schematically be depicted as:

$$\text{hardened compound} \overset{Cl^-}{\underset{I}{\rightleftharpoons}} \text{pore water} \overset{Cl^-}{\underset{II}{\rightleftharpoons}} \text{solution}$$

In this equation no other ions are being taken into account.

The first equilibrium (I) consists of a chemical, a sorption, a solid solution/liquid equilibrium or a combination of these three. The overall-equilibrium is generally represented by a curved equilibrium isotherm.

The second equilibrium (II) we consider to be a water/water partition equilibrium. That means that the equilibrium concentrations in the pore water and in the chloride solution are equal, assuming that pore water generally spoken has bulk water properties. Thus its equilibrium isotherm is a straight line bisecting the right angle between the axes.

To be able to calculate the amount of chloride, combined by the compound hydrates, one has to measure three quantities. These are the total chloride content of the compound Cl_t, the amount of its pore water w_p, and the concentration of the equilibrium solution Cl_e. The quantity of combined chloride Cl_c can then be calculated by subtracting $w_p Cl_e$ from Cl_t i.e. $Cl_c = Cl_t - w_p Cl_e$.

The described method may produce somewhat uncertain results in the lower concentration range, whenever the cement is prone to react as an ion exchanging material i.e. when ion exchanging groups are fixed on the pore walls. This phenemenon generally is of influence, as far as the concentration in the equilibrium solution is comparable to the concentration of these groups, calculated on the quantity of pore water. In that case a Donnan equilibrium is established. For details on this phenomenon we refer to textbooks on physical chemistry, as for instance Moelwyn-Hughes's treatise (2).

EXPERIMENTAL METHODS AND RESULTS

MATERIALS

Analytical grades of NaCl, $CaCl_2$ and $Ca(OH)_2$ have been used throughout the investigations. All cement compounds have been supplied by the Portland Cement Ass., Skokie, Ill., (USA).

The analyses as far as available are presented in Table I.

METHODS and results

The cement compounds are thoroughly mixed with salt solutions of known concentrations. The water/compound ratios (w.c.r.) are 0.35 for C_3S and C_2S, 0.5 for C_4AF and 0.7 for C_3A.

The following hydration is carried out in test tubes, tightly closed with rubber stoppers. After a period of 28 days the hardened paste is broken into small lumps. A few of these lumps are weighed and then placed in solutions of either NaCl or $CaCl_2$ of known concentrations. In order to prevent extraction of $Ca(OH)_2$ from the cement during equilibration the salt solutions have been saturated with this compound. The solution/compound ratio is 5. After an equilibration time of 10-14 days, the supernatant solution is titrated for chloride. The system has not been thermostatted. The ambient temperature is 21 ± 2°C.

TABLE I

	CaO	SiO_2	Free CaO	Al_2O_3	Fe_2O_3
C_3S	72.60	26.06	0.57		
C_2S					
C_3A	61.48	0.83		37.07	
C_4AF	45.82			20.43	32.65

Analysis of the portland cement compounds (wt.%)

Whenever the solution concentration after that time interval is equal to be initial concentration, it is considered to be the equilibrium concentration. New lumps are placed in solutions of higher or lower concentrations, whenever the concentration of the supernatant solution, determined after the specified time interval, has decreased or increased resp. This procedure is repeated, until the concentration of the equilibrating solution has not changed after 10-14 days of contact with the compound.

Pore water content is determined on seperate samples after the 28 days hardening period, by heating them in a stove at 105°C to constant weight. The whole of the compound is considered to be in equilibrium with the pore solution, including the surfaces of its cracks and pores containing air. This means that, when solution of equilibrium concentration penetrates these voids, chloride is neither taken up nor liberated by the cement. The accuracy of the results is estimated to be ca. 5%.

The results for the compounds are recorded in Tables II-V.

TABLE II

Cl_t a		Cl_e a		Cl_c a	
C_3S	C_2S	C_3S	C_2S	C_3S	C_2S
1.04		0.50	0.38	0.97	0.96
2.08		2.00	1.08	1.81	1.85
3.16		4.90	3.96	2.51	2.32
4.25		7.00	5.68	3.32	3.02
5.37		10.05	8.53	4.03	3.48
6.51		15.10	12.40	4.40	3.79

Cl_t b		Cl_e b		Cl_c b	
C_3S	C_2S	C_3S	C_2S	C_3S	C_2S
1.04		0.50	0.38	0.97	0.96
2.08		2.00	1.08	1.81	1.85
3.16		4.90	3.96	2.51	2.32
4.25		7.00	5.68	3.32	3.02
5.37		10.05	8.53	4.03	3.48
6.51		15.10	12.40	4.40	3.79

Total content of $CaCl_2$, Cl_t (in % by wt. of compound), equilibrium solution concentration, Cl_e (in % by volume of solution) and calculated combined $CaCl_2$, Cl_c (in % by wt. of compound) for a hardened C_3S and b hardened C_2S.

TABLE III

Cl_t a		Cl_e a		Cl_c a	
C_3A	C_4AF	C_3A	C_4AF	C_3A	C_4AF
1.30	1.52	0.01	0.01	1.30	1.52
2.62	3.06	0.02	0.01	2.62	3.06
3.98	4.64	0.02	0.02	3.98	4.64
5.35	6.25	0.02	0.03	5.35	6.25
6.76	7.90	0.02	0.04	6.75	7.90
8.19	9.57	0.03	0.04	8.18	9.56

Cl_t b		Cl_e b		Cl_c b	
C_3A	C_4AF	C_3A	C_4AF	C_3A	C_4AF
1.30	1.52	0.01	0.01	1.30	1.52
2.62	3.06	0.02	0.01	2.62	3.06
3.98	4.64	0.02	0.02	3.98	4.64
5.35	6.25	0.02	0.03	5.35	6.25
6.76	7.90	0.02	0.04	6.75	7.90
8.19	9.57	0.03	0.04	8.18	9.56

Total content of $CaCl_2$, Cl_t (in % by wt. of compound), equilibrium solution concentration, Cl_e (in % by volume of solution) and calculated combined $CaCl_2$, Cl_c (in % by wt. of compound) for a hardened C_3A^c and b hardened C_4AF.

TABLE IV

Cl_t a		Cl_e a		Cl_c a	
C_3S	C_2S	C_3S	C_2S	C_3S	C_2S
1.36		2.98	2.96	0.95	0.81
2.76		5.20	5.37	2.05	1.74
4.18		10.34	10.28	2.69	2.20
5.62		12.36	12.47	3.90	3.03
7.10		17.94	18.51	5.18	3.23
8.62		20.50	21.01	6.93	4.24

Cl_t b		Cl_e b		Cl_c b	
C_3S	C_2S	C_3S	C_2S	C_3S	C_2S
1.36		2.98	2.96	0.95	0.81
2.76		5.20	5.37	2.05	1.74
4.18		10.34	10.28	2.69	2.20
5.62		12.36	12.47	3.90	3.03
7.10		17.94	18.51	5.18	3.23
8.62		20.50	21.01	6.93	4.24

Total content of NaCl, Cl_t (in % by wt. of compound), equilibrium solution concentration, Cl_e (in % by volume of solution) and combined NaCl (in % by wt. of compound) for a hardened C_3S and b hardened C_2S.

TABLE V

Cl_t a		Cl_e a		Cl_c a	
C_3A	C_4AF	C_3A	C_4AF	C_3A	C_4AF
1.72	1.52	0.008	0.02	1.72	1.52
3.47	3.06	0.09	0.05	3.44	3.05
5.26	4.64	0.24	0.10	5.19	4.63
7.08	6.25	0.40	0.18	6.96	6.22
8.95	7.90	0.65	0.42	8.77	7.83
10.85	9.57	0.99	0.65	10.56	9.45

Cl_t b		Cl_e b		Cl_c b	
C_3A	C_4AF	C_3A	C_4AF	C_3A	C_4AF
1.72	1.52	0.008	0.02	1.72	1.52
3.47	3.06	0.09	0.05	3.44	3.05
5.26	4.64	0.24	0.10	5.19	4.63
7.08	6.25	0.40	0.18	6.96	6.22
8.95	7.90	0.65	0.42	8.77	7.83
10.85	9.57	0.99	0.65	10.56	9.45

Total content of NaCl, Cl_t (in % by wt. of compound), equilibrium solution concentration, Cl_e (in % by volume of solution) and combined NaCl (in % by wt. of compound) for a hardened C_3A and b hardened C_4AF.

In figs. 1 and 2 total $CaCl_2$ and NaCl contents of the compounds C_3S, C_2S, C_3A and C_4AF are plotted against solution equilibrium concentrations of these salts. It has to be noted that the solution equilibrium concentration of the salt is considered to be equal to the equilibrium salt concentration in the pore water.

In figs. 3 and 4 combined amounts of $CaCl_2$ and NaCl are plotted against equilibrium solution concentrations.

DISCUSSION

As to the question whether by our method equilibrium is attained, we refer to ref. 1. We reported there that the differences between Cl_e values after one year and short term equilibrations (as applied in our experiments) for a number of cement samples were all smaller than 0.5%, calculated on the short term values. We therefore assume that in our cement compound experiments equilibrium has been attained.

We will discuss the results for a C_3S and C_2S b C_3A and c C_4AF separately.

a C_3S and C_2S.

The mechanisms by which the electrolytes can be combined are chemical reactions, solid solution formation

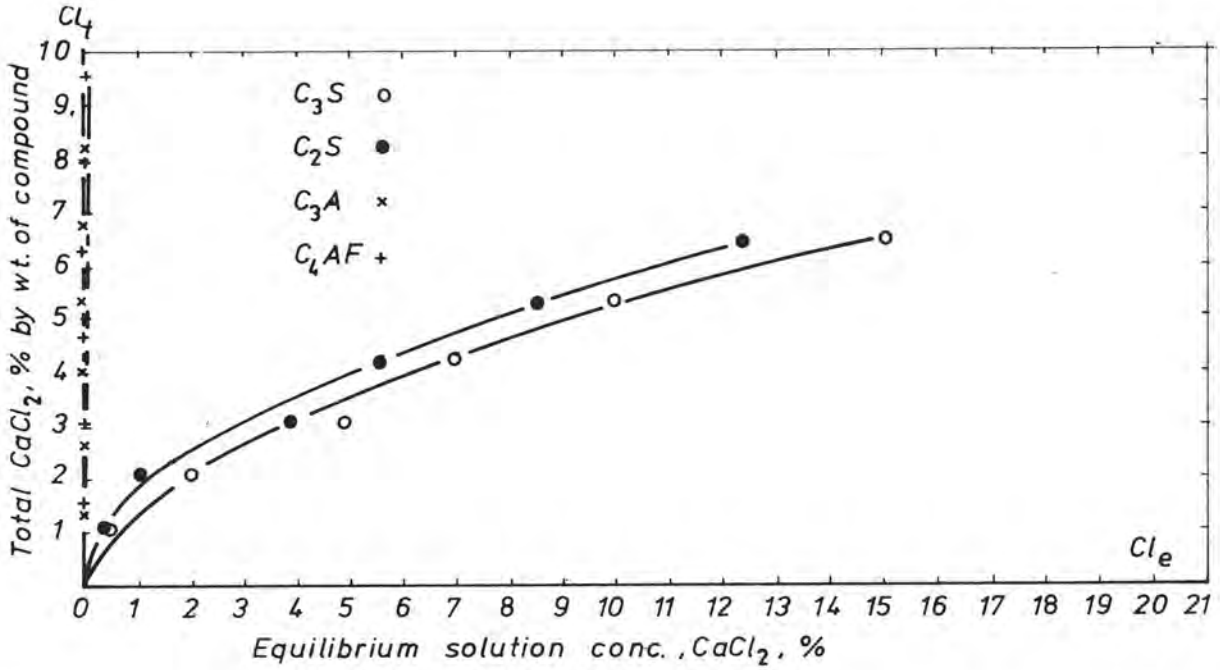

Fig. 1 - Dependence of total $CaCl_2$ content of hardened C_3S, C_2S, C_3A and C_4AF on equilibrium concentration of $CaCl_2$.

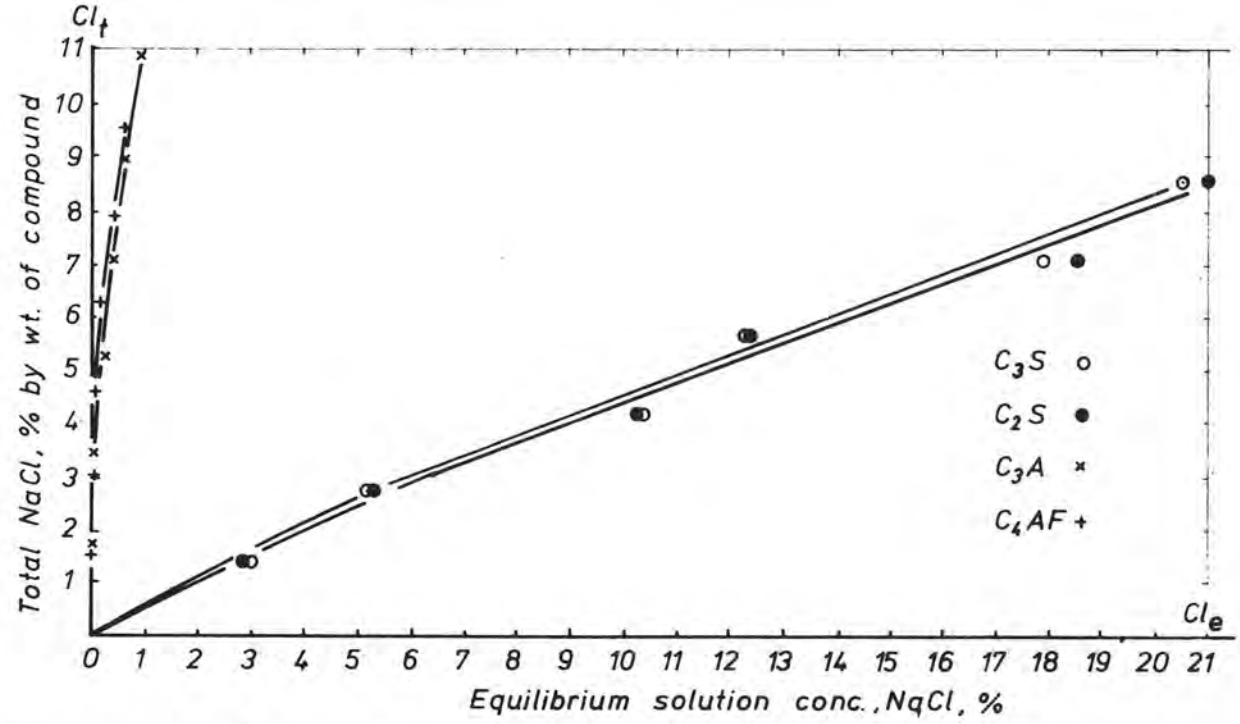

Fig. 2 - Dependence of total NaCl content of hardened C_3S, C_2S, C_3A and C_4AF on equilibrium concentration of NaCl.

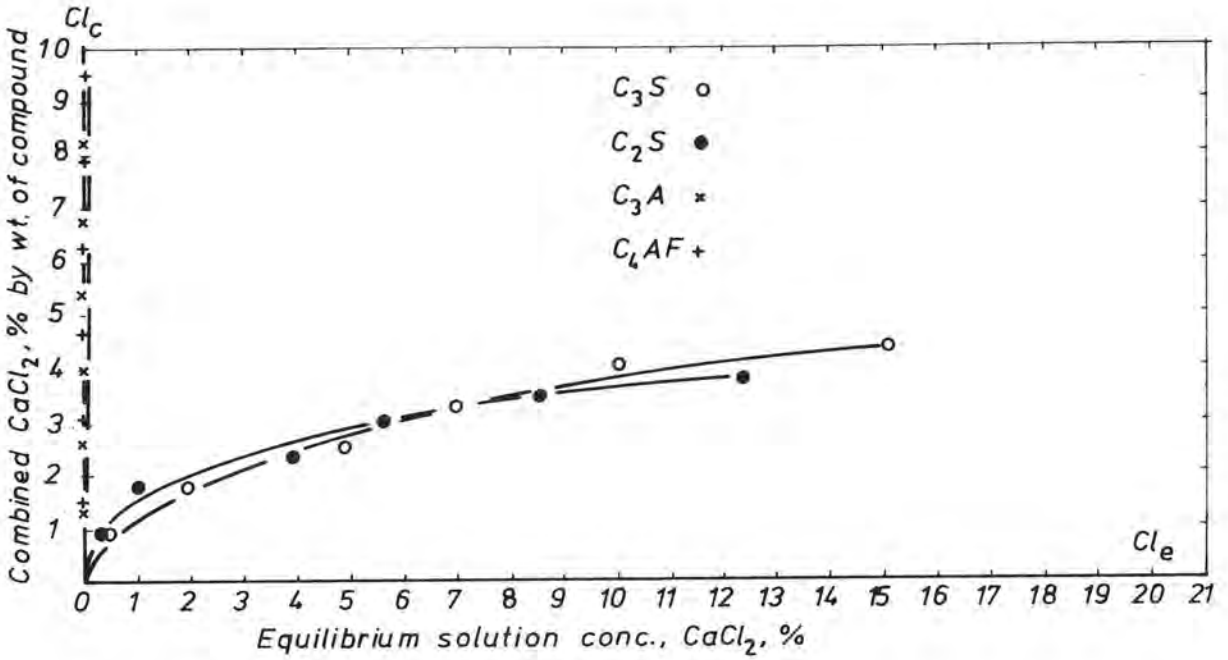

Fig. 3 - Dependence of calculated combined $CaCl_2$ by hardened C_3S, C_2S, C_3A and C_4AF on equilibrium concentration of $CaCl_2$.

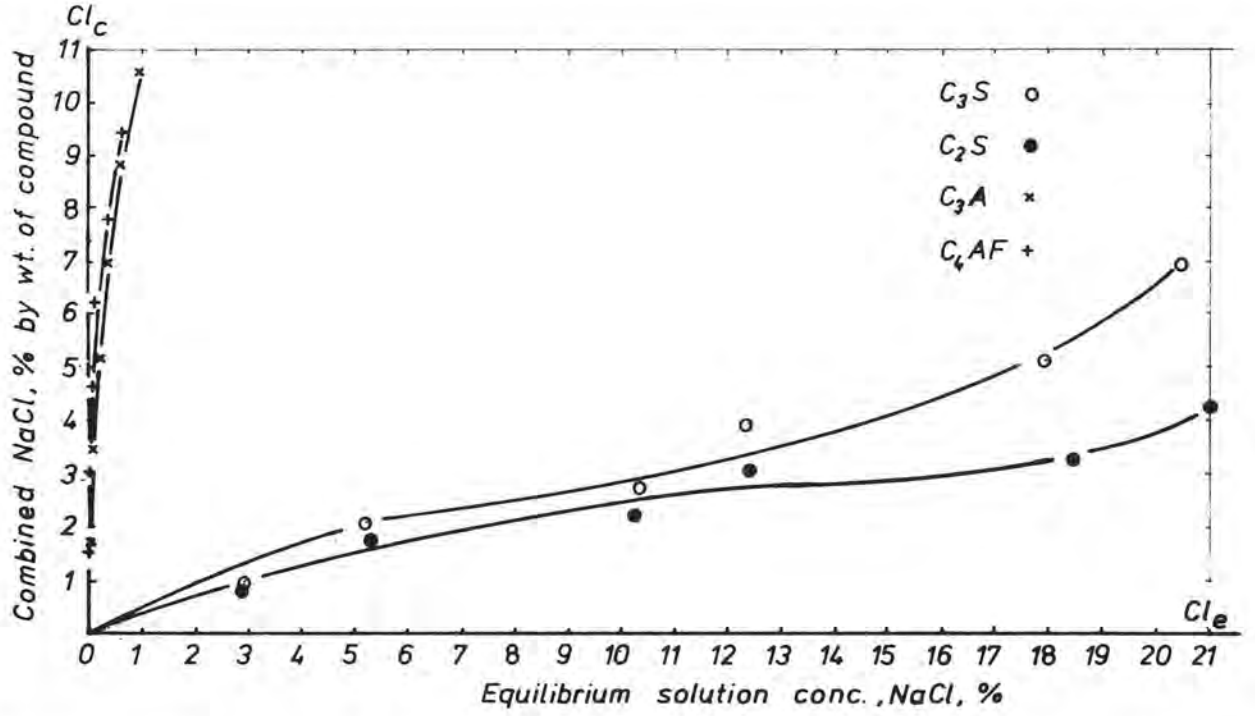

Fig. 4 - Dependence of calculated combined NaCl by hardened C_3S, C_2S, C_3A and C_4AF on equilibrium concentration of NaCl.

and sorption on the pore walls. The method reported here does not enable us to differentiate between these mechanisms.

The electrolyte concentrations in our experiments are too low to allow forming complex compounds of $Ca(OH)_2$ and $CaCl_2$. Compare also the literature review in ref. 1. Using Richartz's results (3), however, it is possible to roughly calculate the amount of $CaCl_2$ sorbed on the pore walls of hardened C_3S. This investigator completely hardened C_3S in solutions of $CaCl_2$ (w.c.r. 5). To determine the amount taken up into the hydrate lattice, the samples were next thoroughly extracted with water. At a concentration level of the mixing water of 1.33% $CaCl_2$ the $CaCl_2$ content of the hardened C_3S sample turned out to be 0.47% (by wt. of C_3S). Considering the final solutions of Richartz's hydration experiments to be equivalent to our equilibrium solutions one can calculate the equilibrium concentration in Richartz's final hydration solution. It is 1.34% $CaCl_2$ (by wt. of vol.). Interpolation in Table II leads to a total amount of $CaCl_2$ i.e. electrolyte taken up into the hydrate lattice and electrolyte sorbed on the hydrate surface, Cl_c, of 1.45% (by wt. of compound). That means that about 1% $CaCl_2$ is sorbed on the hydrate surface. It has to be noted, however, that Richartz's samples had been completely hydrated. The extent of hydration of our samples was not determined.

Comparing C_3S to C_2S we found the equilibrium concentrations i.e. the pore water concentrations, to be higher for C_3S than for C_2S. The pore water contents of the C_3S samples are lower than those of the C_2S samples. We assume that that means that the extent of hydration of the latter samples is lower. Hydration water figures are not available, however.

We compared the C_3S and C_2S results to the results for portland cement (PC) (ref. 1) for the lower range of $CaCl_2$ additions. We suppose the PC to consist of 60% C_3S, 15% C_2S, 10% C_3A and 10% C_4AF ("synthetic PC"). Moreover, we suppose that the silicates react independently of the other compounds in the cement. In Table VI the figures are recorded for C_3S and C_2S. For the "synthetic PC" they were obtained by interpolation in Table III in ref. 1.

The figures in Table VI show that more $CaCl_2$ is combined by PC than is calculated for a "synthetic PC". We suppose that the rest is combined by C_3A and C_4AF (compare b and c).

As to the difference between NaCl and $CaCl_2$, $CaCl_2$ is generally somewhat stronger combined then NaCl on a weight basis.

TABLE VI

PC			"PC synthetic"		
Cl_t	Cl_e	Cl_c	Cl_t	Cl_e	Cl_c
1.30	0.22	1.23			
i 2.08	0.56	1.95	2.08	1.36	1.13
2.59	0.78	2.42			
5.33	4.22	4.42			
i 5.37	4.23	4.44	5.37	7.33	2.94
6.74	7.82	5.06			

Total $CaCl_2$ content, Cl_t (in % by wt. of cement), equilibrium concentration Cl_e (in % by volume of solution) and combined $CaCl_2$, Cl_c (in % by wt. of cement) for portland cement and "synthetic portland cement" (i = interpolated for PC).

b C_3A.

The experiments show that chlorides very strongly combine with hydrated C_3A, $CaCl_2$ even more strongly than NaCl. We therefore assume that in any case part of the discrepancy between PC and "synthetic PC" is caused by free C_3A and C_4AF hydrates. The chlorides are only combined by the cement when all the sulphate has been combined by the the hydrates of C_3A and C_4AF as investigations by e.g. Schwiete, Ludwig and Albeck (4) showed when cement is hardened with solutions of $CaCl_2$.

A w.c.r. of 0.70 has been taken for the hydration of C_3A. Mixtures with lower w.c.r. could not be handled because of their very high rate of hardening.

$CaCl_2$ is more strongly combined than NaCl, especially at the higher concentration levels. The combining capacity of C_3A hydrate for both $CaCl_2$ and NaCl is much higher than that of C_3S and C_2S.

c C_4AF.

The combining properties of the hydrate of this compound are equal to those of C_3A to within the accuracy of the measurements. The w.c.r. has been taken as 0.5. A value of 0.70 would have been preferable. Mixtures of that composition were to wet to handle, however.

CONCLUSIONS

NaCl and $CaCl_2$ are combined by both hardened C_3S and C_2S. The greater part of the combined amount of electrolyte is very probably bound by sorption on the pore walls in the hardened compound.

The calculated amount of $CaCl_2$ combined by a mixture consisting of quantities of C_3S and C_2S as present in an average portland cement is smaller than the measured amount of $CaCl_2$ combined with a portland cement. That is probably caused by those parts of the hydrated C_3A and C_4AF not having reacted with the sulphate present in the cement.

Hydrated C_3A and C_4AF combine much more strongly with both NaCl and $CaCl_2$ than do hydrated C_3S and C_2S.

$CaCl_2$ is somewhat more strongly combined than NaCl by both hydrated C_3A and C_4AF.

REFERENCES

1.- E.M. THEISSING, P. VAN HEST-WARDENIER, G. DE WIND (1978), "The combining of sodium chloride and calcium chloride by a number of different hardened cement pastes", Cem. Concr. Res. 8, 683-692.

2.- E.A. MOELWYN-HUGHES (1961), Physical chemistry, 2nd. Rev. Ed., p. 1106, Pergamon Press, Oxford, U.K.

3.- W. RICHARTZ (1969), "Die Bindung von Chlorid bei der Zementerhartung", Zem.-Kalk-Gips 22, 447-456.

4.- H.E. SCHWIETE, U. LUDWIG, J. ALBECK (1969), "Bindung von Calciumchlorid und Calciumsulfat bei der Hydratation der aluminatisch-ferritischen Klinkerbestandteile", Zem.-Kalk-Gips 22, 225-234.

Influence of cement composition on setting time of concrete containing a set-retarding admixture

L'influence de la composition du ciment sur la durée d'affermissement d'un béton qui renferme un mélange retardant la prise

C.T. TAM, Singapour.

RESUME : Le temps de prise d'un béton, défini par l'essai de pénétration sur le mortier obtenu par tamisage de ce béton, est l'un des critères de choix des additifs chimiques. La durée absolue du temps de prise et le retard provoqué par l'additif retardateur ont été tous deux étudiés en utilisant une méthode modifiée, dans laquelle le mortier est malaxé séparément. Quatre sortes de ciments, contenant des proportions fixes d'additifs, ont été étudiés dans la série A.
Dans la série B, l'effet d'une augmentation de l'alcalinité par addition d'hydrate de soude pur a été étudié. Dans ces deux séries, on a comparé les résultats des essais avec et sans additif. Les résultats montrent que les teneurs en aluminate tricalcique et en alcali influencent le temps de prise et le retard de prise. Une variation de la teneur en alcalis de 0,25 % modifie beaucoup le temps de prise.

SUMMARY : Setting time of concrete as determined from penetration resistance of mortar wet-sieved from a concrete mix is one of the acceptance criteria for chemical admixtures. Both the absolute setting time and the delay in setting due to the addition of a set-retarding admixture were investigated using a modified approach in which the mortar was directly mixed. Four different brands of cement at constant mix proportions were studied in Series A.

In Series B, the effect of increasing alkali content of a cement was observed by adding sodium hydroxide of reagent grade. For each series, plain and admixture treated mixes were compared. The results indicate that tricalcium aluminate and alkali content influence both the absolute setting time and the delay in setting. A change in equivalent alkali content in excess of 0.25 percent alters significantly the delay in setting.

INTRODUCTION

The setting of Portland cement is a complex process. In practice, the setting time is defined as the time taken for a cement paste of standard consistency to reach an arbitrary degree of stiffness, for example by the Vicat apparatus. Similarly, the setting time of concrete is defined as the time from the completion of mixing for the wet-sieved mortar from the concrete mix to reach a chosen penetration resistance. The main purpose of the test is for measuring the change in setting time due to the presence of a chemical admixture. The effect of cement composition on the ability of a retarder to delay setting is the main theme of this paper.

SETTING TIME TEST

The development of the setting time test for concrete was based on the work by TUTHILL and CORDON (1) using the Proctor Penetrometer. This has been incorporated in ASTM C 403, (2) Test for Time of Setting of Concrete Mixtures by Penetration Resistance. The penetration resistance is not measured directly on the concrete mix but on the mortar fraction wet-sieved from the mix. Two setting times are defined. The initial set is taken to be at a penetration resistance of 3.5 N/mm^2 (500 p.s.i.) which according to TUTHILL and CORDON (1) corresponds to the vibration limit of concrete, i.e. the mix cannot be made plastic by revibration. The final set is at the penetration resistance of 27.6 N/mm^2 (4,000 p.s.i.). At this stage the concrete starts to harden, having a compressive strength of about 0.7 N/mm^2 (100 p.s.i.).

The test method prescribed in BS 5075: 1974 (3) is basically similar to that of ASTM C 403 (2). It specifies two stages of the setting process, one at 3.5 N/mm^2 which corresponds to the initial set in ASTM C 403 (2), and the other at a much lower penetration resistance value of 0.5 N/mm^2 (73 p.s.i.). According to FLETCHER and ROBERTS (4), this earlier stage corresponds to the extreme limit of workability for placing and compacting the concrete. There are other differences in the details of conducting the setting time test between the methods of ASTM C 403 (2) and BS 5075: 1974 (3). A comparison of these two methods of testing and comments on their relative merits are in the course of preparation (5).

EXPERIMENTAL PROGRAMME

The programme of study was divided into two series of mixes to investigate the different parameters as follows:-

Series A - four different brands of ordinary Portland cement at constant mix proportions (sand-cement ratio = 2.0 and water-cement ratio = 0.40).

Series B - increase in alkali content by the addition of reagent grade sodium hydroxide at 0.25, 0.50 and 0.75 percent by weight of cement with constant mix proportions as those in Series A.

For each series plain mixes and corresponding mixes with the addition of a water-reducing set-retarding admixture at the recommended dosage were investigated.

Materials

The materials for the two series were not always identical. However, within each series all materials were kept constant except for Series A where the cement brand forms the variable parameter. The sands used were always in the oven dry condition. One brand of water-reducing set-retarding admixture was used in Series A and a different brand of admixture, but of the same class, was employed for Series B. In all cases the admixture was added at the recommended dosage. Details of the various cements, sands and admixture for the programme are listed in Appendix A. The combinations of materials used are indicated in the respective table of results.

Testing method

For the setting time test, both ASTM C 403 (2) and BS 5075: 1974 (3) call for the mortar sample to be wet-sieved from the concrete mix. However, in this programme all mortar mixes were batched directly in their chosen proportions. OKABE, NAKAJIMA and YOSHIHARA (6) have found that similar results may be produced for either method of obtaining the mortar sample by suitable adjustment to the method of mixing the mortar directly. This was not attempted in the present study. However, for a particular case where data for both methods of preparation are available, it is observed that although the absolute values of setting time are different, the resultant delay in setting is similar. Appendix B shows a summary of the data for this case.

The method employed in mixing the mortar directly was standardised as follows:

(a) 90 percent of the total mixing water was thoroughly mixed with the sand in a mechanical mixer of the epicyclic type.
(b) the balance of the water, with the admixture thoroughly mixed into it if used, was then added while the mixer was still running.
(c) cement was added within the next minute while the mixer was kept running for 2½ minutes at low speed.
(d) the mixer was stopped and materials on the side of the bowl was scrapped down.
(e) the mixer was then restarted at medium speed and allowed to run for ½ minute to complete the mixing.

In order to compromise between different detailed requirements of ASTM C 403 (2) and BS 5075 (3) the conduct of the penetration resistance test was in accordance with BS 5075 (3) up to a penetration resistance just beyond 3.5 N/mm^2 (500 p.s.i.), and after this, in accordance with ASTM C 403 (2). For Series A only single runs were conducted. For Series B two duplicate batches were tested. The average of the two runs is reported in the results. This is in agreement with BS 5075 (3) but ASTM C 403 (2) calls for the average of three duplicates. Since by mixing the mortar directly the degree of control is much better than by wet-sieving, this is considered satisfactory. CHEW and CHOOI (7) reported achieving a standard deviation of 15 minutes for plain mixes and 20 minutes for mixes containing a water-reducing set-retarding admixture. The range for four duplicate batches was within 45 minutes in both cases. These compare favourably against the corresponding values of 25 minutes and 84 minutes respectively as permitted

by ASTM C 403 (2) for three duplicates.

Full details on the conduct of the penetration resistance test are described in both standards and will not be repeated here. The apparatus used in the later part of this study differs from those described in the standards only in the load indicating device. A sensitive proving ring mounted on a drill press records accurately the applied force to improve the precision of the results.

RESULTS AND DISCUSSIONS

In reporting the setting time both ASTM C 403 (2) and BS 5075 (3) specified a common penetration resistance of 3.5 N/mm^2 (500 p.s.i.). However, the time to reach this value has to be estimated from readings taken below and above this exact value. The two standards employ slightly different technique to arrive at this time. In general, the difference has been found to be negligible as discussed in Reference (5). Hence only one value is reported for the time to reach this penetration resistance, and referred to as initial set as in ASTM C 403 (2). Similarly the time to reach 27.6 N/mm^2 (4,000 p.s.i.) is referred to as final set as in ASTM C 403 (2). The time to reach the much lower penetration resistance of 0.5 N/mm^2 (73 p.s.i.) specified in BS 5075 (3) is tentatively called the "workability limit" in view of the statement by FLETCHER and ROBERTS (4) regarding the behaviour of the concrete corresponding to this stage of stiffness. Besides the absolute setting times, the delay time, i.e. the increase in setting time due to set-retarders is reported for checking against compliance with specification, e.g. BS 5075 (3) and ASTM C 494 (8).

Series A - cement composition

In this series of experiment four brands of ordinary Portland cements of varying composition were used with the same admixture. The mix proportions were kept constant at water-cement ratio of 0.40 and sand-cement ratio of 2.0.

Table I shows the results for this series together with the tricalcium aluminate and equivalent sodium hydroxide contents of each cement. These two components have been reported by POLIVKA and KLEIN (9), NEWLON (10) and TAM (11) as the major components in cement which affect the effectiveness of a water-reducing and set-retarding admixture. It can be seen that the results in Table I reflect the importance of these parameters similar to that reported in the references quoted above. An increase in either or both components will reduce the effectiveness of the admixture to delay set. However, it is difficult to correlate these parameters with the setting times quantitatively because of several factors. Firstly, the calculated tricalcium aluminate content by Bogue's method does not allow for the effect of the actual cooling rate of the clinker, nor the formation of solid solutions and the influence of minor compounds. The total alkali content as obtained from chemical analysis does not indicate the soluble alkali content. It is this portion that is effective in influencing the behaviour of the fresh cement paste. The lack of correlation between soluble and total alkali contents has been studied by McCOY and ESHENOUR (12).

In spite of the above, the results in Table I follow the trend dictated by the tricalcium and alkali contents. However, it should be noted that although all four brands of cement meet the requirement of BS 5075 (3) with respect to setting time, all except Cement C, show excessive delay time. ASTM C 494 (8) limits this to less than 3½ hours. This situation poses a rather interesting question in acceptance testing as discussed in Reference (5).

TABLE I

EFFECT OF CEMENT COMPOSITION ON SETTING TIMES

Cement	A	B	C	D
C_3A content - %	11.5	10.9	12.3	9.8
Equivalent Na_2O - %	0.20	1.04	0.68	0.39
Workability limit-hr				
Plain	2.9	2.1	1.7	1.7
With admixture	7.8	6.1	4.1	6.3
Initial set-hr				
Plain	4.3	2.9	2.4	2.7
With admixture	9.3	7.1	5.3	8.7
Final set-hr				
Plain	6.5	4.3	3.6	4.0
With admixture	11.2	8.7	6.5	10.4
Delay time-hr				
Workability limit	4.9	4.0	2.4	5.6
Initial set	5.0	4.2	2.9	6.0
Final set	4.7	4.4	2.9	6.4

Mining sand used in all mixes with water-cement ratio of 0.40 and sand-cement ratio of 2.0 and admixture Y added when used.

Series B - alkali content

In order to study the effect of alkali content alone, reagent grade sodium hydroxide was introduced to increase the alkali content of Cement E. Only fractional percentages were added thus there is little change in the relative percentage of the rest of the oxide composition of the cement. Since the original equivalent sodium hydroxide content of the cement is 0.53 percent, a maximum of 0.75 percent was added to keep the total alkali content below 1.30 percent, the upper end of the normal range in Portland cements. The results of this series are presented in Table II. The increase in alkali content has very little effect on the setting times for the plain mixes, showing but a slight reduction in the final set. However, its effect on mixes treated with the admixture is severe. Hence there is similarly a serious reduction in the delay time. Fig. 1 shows a plot of the delay time for various percentages of added alkali content. It can be seen that an increase in excess of 0.25 percent leads to a significant reduction in delay time.

The influence of alkali content on the concentration of the various ions in the liquid phase of cement paste was studied by FORSEN (13). A high alkali content in cement tends to increase the solubility of the aluminates thus promoting faster rate of reaction. LERCH (14) attributes this to the neutralizing action of the alkali on gypsum thereby reducing its retarding influence on the aluminates. LEA (15) suggests that a certain minimum concentrations of lime and calcium sulphate in solution are necessary for the proper retardation of the alumi-

nates. The presence of the chemical retarder reduces the rate of hydration of the silicates. This slows down the release of calcium hydroxide into solution thereby allowing the direct hydration of the aluminates and resulting in abnormally quick setting.

TABLE II

EFFECT OF ALKALI CONTENT ON SETTING TIMES

Added alkali content - %	0.0	0.25	0.50	0.75
Workability limit-hr				
Plain	0.9	1.0	0.9	0.7
With admixture	1.7	2.0	1.3	0.3
Initial set-hr				
Plain	2.0	2.0	1.9	1.6
With admixture	3.6	3.3	2.7	1.1
Final set-hr				
Plain	3.2	3.0	2.8	2.4
With admixture	4.7	4.4	3.8	2.4
Delay time-hr				
Workability limit	0.8	1.0	0.4	-0.4
Initial set	1.6	1.3	0.8	-0.5
Final set	1.5	1.4	1.0	0.0

Cement E and mining sand used in all mixes with water-cement ratio of 0.40 and sand-cement ratio of 2.0 and admixture X added when used. Equivalent Na_2O content of Cement E is 0.53 percent.

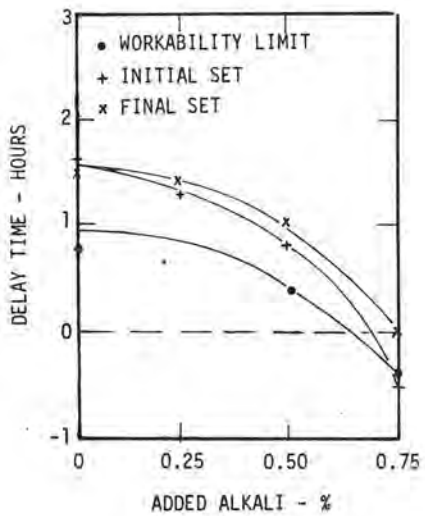

(Original equivalent sodium hydroxide content is 0.53%)

FIG. 1 EFFECT OF ALKALI CONTENT ON DELAY IN SETTING

Cements from different sources and even between batches from the same manufacturer may possess variations in alkali content equal to those investigated in this study. Table III summarises the computed potential compounds and equivalent alkali content of four brands of cement, some with several batches, supplied to the Department of Civil Engineering University of Malaya over a period of five years. It can be observed that cement from different works may have a difference in alkali content of nearly 1.0 percent. Even cement from the same manufacturer may have a variation up to 0.5 percent. In practice, suitable dosage of admixture is obtained from past performance or trial mixes. Subsequent changes in alkali content in the cement delivery may cause erratic setting behaviour in admixture treated mixes. Quality control at cement works involves only the behaviour of plain mixes. Thus the variation in alkali content does not manifest its effect in routine quality control at cement works but only affect the concrete producer employing a set-retarder, e.g. the ready-mixed concrete industry.

TABLE III

COMPOUND COMPOSITION OF CEMENTS

Cement brand	Sample number	Computed potential compounds				Equivalent Na_2O
		C_3S	C_2S	C_3A	C_4AF	
P	1	53.0	14.9	10.9	9.7	1.04
Q	1	69.2	2.0	12.3	10.8	0.68
Q	2	56.6	12.2	9.4	12.3	0.36
Q	3	67.4	4.9	10.0	10.7	0.72
R	1	42.8	31.4	11.5	8.3	0.20
R	2	65.0	8.4	8.1	9.7	0.52
R	3	63.0	9.9	9.8	9.5	0.58
R	4	58.5	14.0	11.3	9.3	0.58
S	1	40.5	29.3	9.8	9.9	0.39
S	2	48.9	18.2	11.5	10.4	0.97
S	3	55.4	17.7	9.6	10.2	0.39
S	4	61.4	9.7	12.2	10.9	1.00
S	5	60.2	10.0	12.5	10.9	0.70

C_3S = Tricalcium silicate

C_2S = Dicalcium silicate

C_3A = Tricalcium aluminate

C_4AF = Tetracalcium aluminoferrite

Equivalent Na_2O content = $\%Na_2O + 0.658 \times \%K_2O$

SUMMARY AND CONCLUSIONS

The effect of cement composition on setting times and their influence on the effectiveness of a water-reducing set-retarding admixture are discussed. This is by no means the only factor influencing setting times. Other significant parameters include different types of cement, fineness of cement, gypsum content, temperature of the mix, ambient environment, different types of chemical admixtures as well as dosages for a given admixture. Many of these have been investigated and documented in publications such as ASTM STP 266, Symposium on Effect of Water-reducing Admixtures and Set-retarding Admixtures on Properties of Concrete,

1959 and RILEM International Symposium on Admixtures for Mortar and Concrete, 1967. The present study draws attention to factors not previously reported. Cement composition is subject to variations even under good practice of quality control in cement and concrete production. An understanding of the factors influencing the absolute setting times and the delay time is important to ensure suitable quality of the mix exists during the process of transporting, placing, compacting and finishing of the concrete.

In conclusion, this study has indicated that:-

1. An increase in alkali content of cement reduces to a small extent only the absolute setting times of plain mixes.

2. The corresponding increase in alkali content of cement may produce a much more severe reduction in absolute setting times of admixture treated mixes, thereby shortening seriously the delay time. For the cement studied, an increase in excess of 0.25 percent changes significantly the delay in setting.

ACKNOWLEDGEMENTS

The author wishes to acknowledge the contribution by Mr. Chew, T.P., Mr. Chooi, H.L., Mr. Chew, S.Y., Mr. Yip, C.Y., Mr. Ng, B.C. and Miss Yap, A.C. from whose project reports the bulk of the data for this paper has been extracted. The permission of the University of Malaya, at which the author formerly worked, to publish this paper is also gratefully acknowledged.

REFERENCES

1. TUTHILL, L.H. and CORDON, W.A., "Properties and Uses of Initially Retarded Concrete", ACI Journal, Proceedings Vol. 52, No. 3, November 1955, pp. 273-283.

2. ASTM C 403-70: Test for Time of Setting of Concrete Mixtures by Penetration Resistance, Books of Standards, American Society of Testing and Materials, 1970.

3. BS 5075: Part 1: 1974: Concrete Admixtures, British Standard Institution, London, 1974.

4. FLETCHER, K.E. and ROBERTS, M.H., "Test Methods to Assess the Performance of Admixtures in Concrete", Concrete, Vol. 5, No. 5, May 1971, pp. 142-148.

5. "Comparison and Comments on Setting Time Test of Concrete" (in preparation).

6. OKABE, J., NAKAJIMA, K. and YOSHIHARA, T., "Investigations on the Methods of Test for Setting Time of Concrete Especially for Concrete Containing Water-reducing Admixture, "Fifth International Symposium on Chemistry of Cement, Tokyo, Vol. IV, 1968, pp. 58-64.

7. CHEW, T.P. and CHOOI, H.L., "Effect of a Retarder on the Setting Time of Mortar", Graduation Thesis, Bachelor of Engineering, University of Malaya, 1975.

8. ASTM C 494-71: Specification for Chemical Admixtures for Concrete, Books of Standards, American Society for Testing and Materials, 1971.

9. POLIVKA, M. and KLEIN, A., "Effect of Water-reducing Admixtures and Set-retarding Admixtures as Influenced by Portland Cement Composition", ASTM STP 266, 1959, pp. 124-139.

10. NEWLON, H.H., "Water-reducing Admixtures as Influenced by Cement Composition", 19th Annual Convention of ASSHO, Biloxi, Mississippi, November 1960.

11. TAM, C.T., "The Effect of a Lignin-based Admixture on Properties of Concrete", Ph.D. Thesis, University of Calgary, Canada, 1972.

12. McCOY, W.J. and ESHENOUR, O.L., "Significance of Total and Water Soluble alkali Contents of Cement", Fifth International Symposium on Chemistry of Cement, Tokyo, Vol. II, 1968, pp. 437-442.

13. FORSEN, L., "The Chemistry of Retarders and Accelerators", Second International Symposium on the Chemistry of Cements, Stockholm, 1938, pp. 298-363.

14. LERCH, W., "The Influence of Gypsum on the Hydration and Properties of Portland Cement Pastes", Bulletin 12, Research and Development Laboratories of Portland Cement Association, Skokie, Illinois, 1946.

15. LEA, F.M., "The Chemistry of Cement and Concrete", 3rd Ed., Edward Arnold, 1970.

.../...

APPENDIX A

PROPERTIES OF MATERIALS

1. Cement

Cement	A	B	C	D	E
CaO	64.14	61.93	66.19	63.55	64.43
SiO_2	22.18	19.10	18.87	20.98	20.02
Al_2O_3	2.73	3.19	3.56	3.25	5.08
Fe_2O_3	6.08	6.16	6.92	5.79	3.18
MgO	1.56	N.A.	N.A.	1.04	2.00
SO_3	1.72	2.79	2.03	2.36	2.23
K_2O	0.15	1.04	0.20	0.55	0.18
Na_2O	0.10	0.35	0.55	0.03	0.41
C_3S	42.8	53.0	69.2	40.5	65.0
C_2S	31.4	14.9	2.0	29.3	8.4
C_3A	11.5	10.9	12.3	9.8	8.1
C_4AF	8.3	9.7	10.8	9.9	9.7

2. Sands

   a. River sand : Zone 2 to BS 882, 1201: 1954
      Fineness modulus 3.06

   b. Mining sand : Zone 2 to BS 882, 1201: 1954
      Fineness modulus 2.59

3. Admixture

   a. For Series B, admixture X is lignosulphonate based and conforms to ASTM C 494 Type D. The recommended dosage of 1/135 by weight of cement was used.

   b. For Series A, admixture Y is of the same type and material but of a different brand. It was used at the recommended dosage of 1/120 percent by weight of cement.

APPENDIX B

SETTING TIMES FOR WET-SIEVED AND DIRECTLY MIXED MORTAR

Mortar	Wet-sieved*	Directly mixed
Water-cement ratio		
Plain	0.55	0.55
With admixture	0.47	0.47
Sand-cement ratio		
Plain	2.0	2.0
With admixture	2.0	2.0
Workability limit-hr		
Plain	-	4.0
With admixture	-	4.9
Initial set-hr		
Plain	3.8	5.3
With admixture	4.6	6.6
Final set-hr		
Plain	5.2	6.8
With admixture	6.5	8.0
Delay time-hr		
Workability limit	-	0.9
Initial set	0.8	1.3
Final set	1.3	1.2

Cement A and river sand used in all mixes with admixture X added when used.

* From concrete mix of 1:2:4 by weight, 20 mm crushed granite coarse aggregate.

Effect of surfactants on the hydration behaviour of cement pastes

Effet des substances qui sont actives sur la surface à la réaction d'hydratation des pâtes de ciment

O. HENNING, Prof. Dr. rer. nat. habil. et L. GORETZKI, Dipl.-Chem.,
Hochschule für Architektur und Bauwesen Weimar, DDR.

SUMMARY

Surfactants, which are used as water reducing agents or cement dispersing agents, influence also the hydration mechanism of cements. A systematic review about the known cement dispersing surfactants is given. Particularly the chemical structure, the molecular size, and the origin of surfactants were taken into consideration.

One group of short-chain surfactants investigated by us are composed of sulphonated dicarboxylic acids esterified by several aliphatic alcohols. In addition the chain length of ester groups was systematically increased by ethoxylation.

The results show dependences of the effect of agents on the hydration and the structure of agents. Rheological properties such as workability and apparent viscosity show the effect of plastification of cement pastes depending on the degree of ethoxylation and the chain length of alcohols. The wettability of cement powder, depending on the contact angles determined by capillary tests, is largest on medium ethoxylation degrees. Strengths after 1 day and 28 days are highest if 5 to 10 molecules of ethylene oxide were incorporated into the alcohol rest of the ester group.

RESUME

Combinaisons, qui sont actives sur la surface, qui sont utilisées en qualité des agents pour réduire l'eau ou agents qui dispersent le ciment, influence sur le mechanisme d'hydratation des ciments. Une discussion systematique sur les combinaisons qui sont actives sur la surface, qui nous connaissons, est donée. Spécialement la structure chemique, la grosseur des molécules et l'origine des agents qui sont actives sur la surface, on prit en considération.

Un groupe des agents qui sont actives sur la surface, que nous avons exploré, est composé des acides sulfamides dicarboxyliques qui sont esterfié par divers alcools aliphatiques. La longeur de chaîne des groupes des esters etait augmenté systematique par l'éthoxylation.

Les resultats montrent les dépendances de l'effet des agents sur la hydratation et la structure des agents. Les propriétés rhéologiques comme la maniabilité et la viscosité apparente montrent l'effet de la liquifaction des pâtes du ciment qui dependent du degré d'éthoxylation et de la longeur de chaîne des alcools. La mouillabilité de la poudre du ciment, qui est determiné fermée en dependance de l'angle de contact par des expériences capillaires, est le plus large médium en degrés d'éthoxylation. La résistance après 1 jour et après 28 jours est la plus haute si 5 molécules de l'oxyde d'éthylene ont éte absorbé dans le reste d'alcool du groupe d'ester. Plus ou moins de 5 - 10 molécules mènent à une resistance diminuée.

INTRODUCTION

In recent years many investigations have been performed in several countries in the field of concrete admixtures. The aim of these investigations was to improve some properties of concrete and to reduce the costs of production of concrete (1 - 8).

Concrete additives are mainly used to improve the following properties:

1. Improved workability without increasing water content (dispersing effect)
2. Decreased water content at the same workability (increased strength)
3. Improved penetration and pumpability
4. Reduced unit cost of concrete (9)

CEMENT DISPERSING AGENTS

It has been shown that both short-chain and long-chain surfactants can be used as cement dispersing agents. They can be made synthetically or obtained from natural products. A general review including an indication on the most important groups is shown in fig. 1.

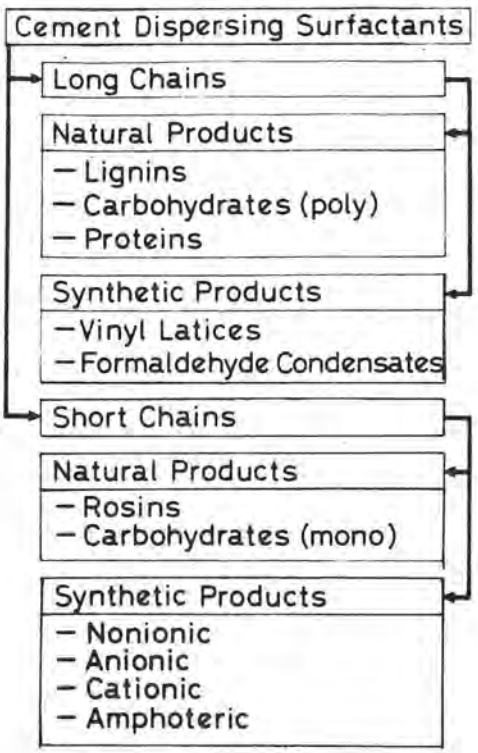

Fig. 1 - Cement dispersing surfactants

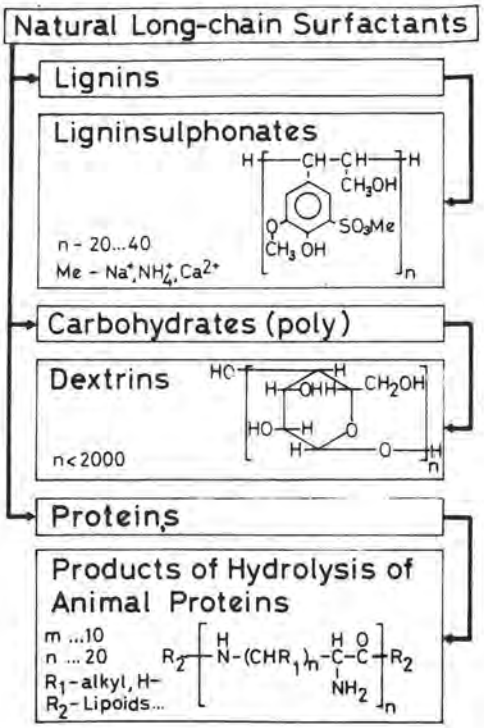

Fig. 2 - Natural long-chain surfactants with cement dispersing properties

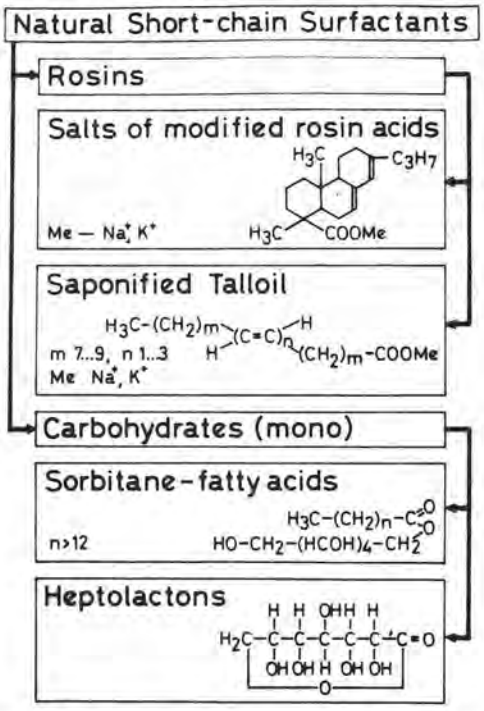

Fig. 3 - Natural short-chain surfactants with cement dispersing properties

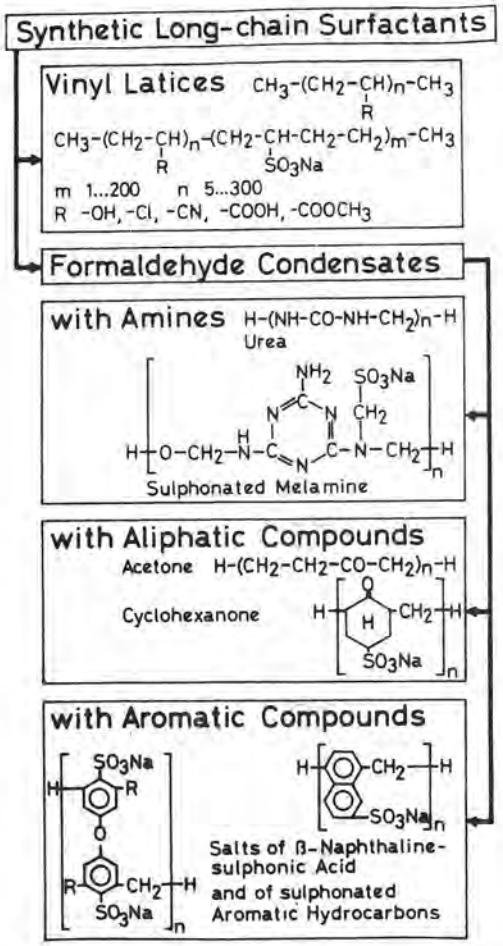

Fig. 4 - Synthetic long-chain surfactants with cement dispersing properties

A closer investigation into individual examples of long-chain and short-chain surfactants (figs. 2 - 5) indicates that a specific molecular structure is required for a dispersing action on water/cement systems.

It seems to be essential that not the length of chains but the presence of hydrophylic and hydrophobic groups in definite distribution is most important.

For the characterization of the dispersing action the degree of plastification α_v was used which is defined as

$$\alpha_v = \frac{AM_w - AM_o}{AM_w}$$

AM_o slump without admixture

AM_w slump with admixture using the same mortar

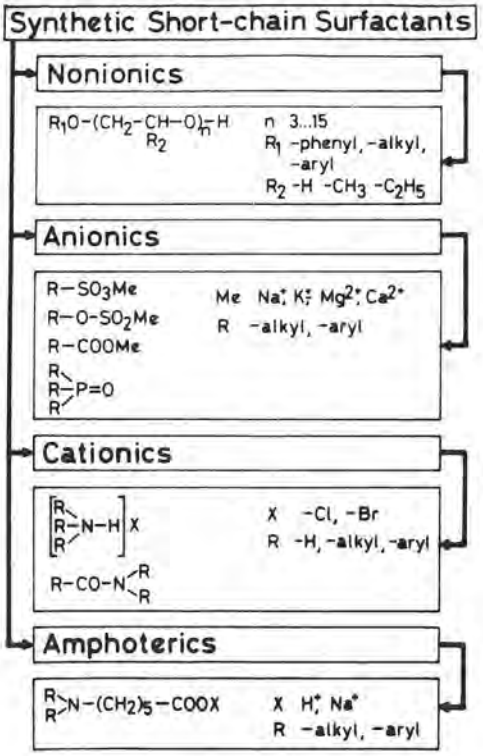

Fig. 5 - Synthetic short-chain surfactants with cement dispersing properties

TABLE I

Surfactant	α_v	Author
Ligninsulphonate	0,33	LEWANDOWSKI
Dextrin	0,40	OHSMANN
Proteins	0,50	BONIN
Melamine-Formaldehyde Condensates	0,33	HATTORI
ß-Naphthaline-Formaldehyde Condensates	0,58	HATTORI
Propylene/Ethylene Adducts	0,41	DEBUS
SBM-10	0,42	this paper

Table I shows optimum degrees of plastification of some surfactants. A vigorous plastificating action is effected by long-chain organic molecules of large molecular weight having a high portion of hydrophilic groups distributed over the whole molecule.

At decreasing molecular weight, decreasing degree of cross-linking, and only a few hydrophilic groups placed at the ends of molecule, the action of plastification of long-chain molecules decreases.

Moreover the formation of pores had to be considered when surfactants are used. Resulting micropores have an unfavorable effect on the strength of concrete. Stable micropores have a plastifying effect (ball bearing model). Surfactants having such an effect are mainly short-chained substances.

The effect of long-chain surfactants can only depend on another mechanism because in this case a good plastification occurs when only a few pores are present. As an explanation a different model has to be taken using the adsorption behavior.

There are some surfactants which are based on both kinds of mechanism (dispersing and air-entraining agents).

EXPERIMENTAL

The aim of our investigation was to find and prepare cement dispersing surfactants which are expected to must have a particularly good effect. Compounds of the following structure were prepared:

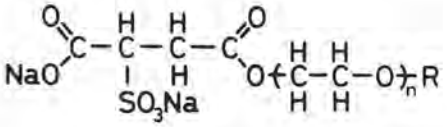

These compounds were synthetized from the anhydride of maleic acid, sodium hydrogensulfite, aliphatic alcohols and ethylene oxide. Twelve different compounds were prepared (Table II).

TABLE II

Name	R	n
SBM-1	$-C_{12}H_{25}\cdots-C_{14}H_{29}$	0
SBM-2	"	3
SBM-3	"	5
SBM-4	"	10
SBM-5	"	20
SBM-6	"	40
SBM-7	$-C_{16}H_{33}\cdots-C_{18}H_{37}$	0
SBM-8	"	3
SBM-9	"	5
SBM-10	"	10
SBM-11	"	20
SBM-12	"	40

For testing the efficiency, the wetting behavior, the rheological properties, and the behavior of strength were examined.

The wetting behavior was determined by means of a method based on the unopposed penetration of the liquid into a plug of cement powder in a glass tube. Using the WASHBURN equation for the flow of liquid through a capillary (10) it was possible to calculate from the rate of penetration the magnitude of the advancing contact angle and the energy of adhesion between the liquid and the cement powder (fig. 6).

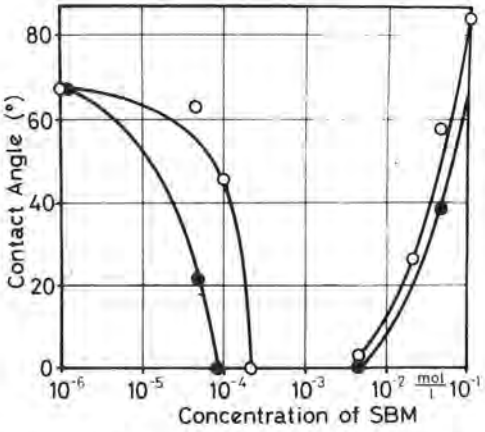

Fig. 6 - Contact angle of SBM solutions on cement powder as a function of concentration

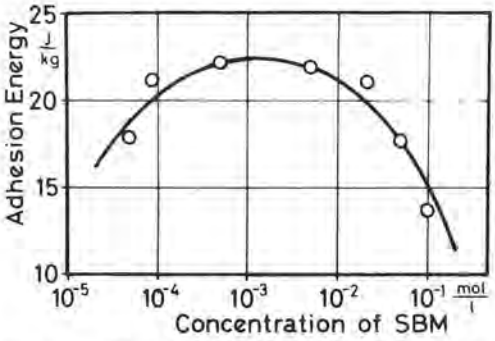

Fig. 7 - Adhesion energy of SBM-3 solutions as a function of concentration

With increasing concentration of SBM the contact angle decreases and within a definite range of concentration it becomes zero. At higher concentration the angle rises again. This behavior is typical of all SBM admixtures. The calculated energy of adhesion is at its maximum using medium concentration (fig. 7).

The influence of admixtures on the flow behavior can be measured by suitable rheological methods (11). In this paper

the slump was used to obtain the degree of plastification. The slump increases at constant water/cement ratio as it occurs with all plasticizers. Reducing the water/cement ratio at constant concentration of the admixture the slump decreases and at a definite w/c ratio the same slump is reached as with a system without admixture at a w/c ratio of 0,5 (fig. 8).

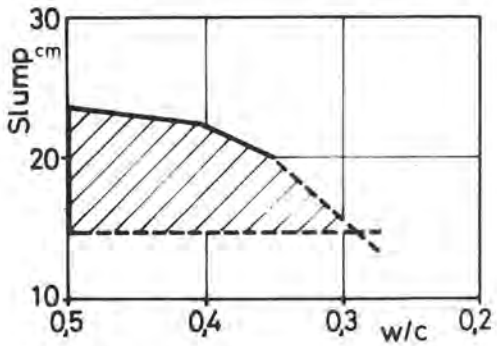

Fig. 8 - Principal connection between w/c ratio and slump on the addition of plasticizers

There is a non-linear function between the slump and the concentration (fig. 9) within a range of concentrations at which the slump changes only slightly.

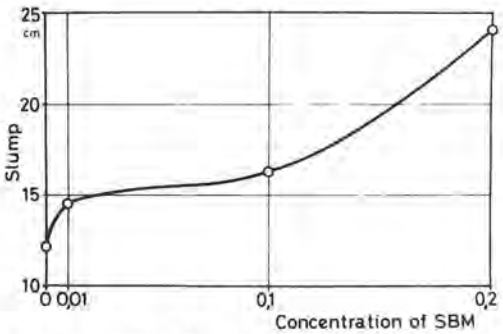

Fig. 9 - Slump of mortars as a function of the concentration of SBM additives

At an increasing degree of ethoxylation the effect of plastification becomes more effective as shown in fig. 10. The shearing stress was determined by means of a special shearing device. An optimum effect of plastification occurs at the inserting of 5 - 10 molecules of C_2H_4O (Table III).

The slump at w/c ratios smaller than 0,5 (to 0,3) is still greater than without admixtures (see fig. 8). But compressive strengths show the expected increase at reduced water/cement ratios as is shown in fig. 11.

In addition an increase of the initial strength at constant w/c ratios caused by the action of the admixtures was found to occur.

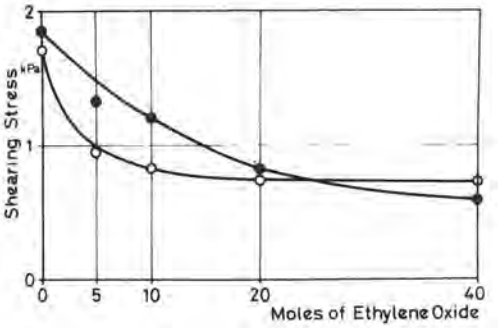

Fig. 10 - Shearing stress of cement pastes as a function of the content of ethylene oxide
o SBM-1...SBM-6 • SBM-7...SBM-12

TABLE III	
Admixture	α_v
SBM-1	0,11
SBM-3	0,38
SBM-6	0,36
SBM-7	0,25
SBM-10	0,42
SBM-12	0,38

Degree of plastification of SBM admixtures

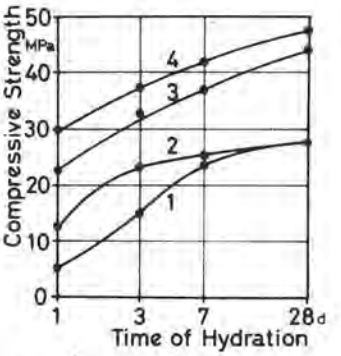

Fig. 11 - Compressive strengths of cement pastes as a function of water/cement ratio
1 without addition, w/c = 0,50
2 0,01 mol/l SBM-3, w/c = 0,50
3 " w/c = 0,40
4 " w/c = 0,35

CONCLUSIONS

Based on a summerizing survey of the cement dispersing agents used, some general aspects of the structure of cement dispersing substances were deduced. Starting from this, corresponding compounds were synthetically prepared, which are expected to have a good efficiency.

Starting point was a basic molecule containing carboxylic and sulphonic groups, which was systematically modified. By means of rheological and strength investigations the expected efficiency was confirmed. Moreover a relationship between the plastifying effect and the wetting behavior of the cement was found.

This paper deals with problems which are part of the research programme at the VEB Fettchemie Karl-Marx-Stadt DDR.

REFERENCES

1.- V. MOLDOVAN (1978), "Concrete Additives", Ed. Technico, Bukarest

2.- M. RIXOM (1978), "Chemical Admixtures for Concrete", Ed. Spon., London

3.- V.B. RATINOW et T.J. ROZENBERG (1973), "Dobavki v beton", Stroijzdat, Moskva

4.- O. HENNING et L. GORETZKI (1975), "Über die Anwendung von Zusatzmitteln im Bauwesen. II. Spezielle Probleme der Anwendung von Mörtel- und Betonzusatzmitteln", Wiss. Zeitschr. HAB Weimar 22, 301

5.- N.S. RAMACHANDRAN (1979), "Admixtures - Cements Research Progress", Nat. Res. Council of Canada

6.- R. LEWANDOWSKI et P. PETERFY (1974), "Superverflüssiger und Fließbetonherstellung", Bauwirtschaft 29/34

7.- G. BABATCHEV (1976), "Komplexe chemische Zusätze zur Beschleunigung der Dampfhärtung von Beton", Baustoffind. 19 B, 20-22

8.- J. KAZIMIR (1979), "Zvysenie pevnosti agloporitoveho betonu plastifikatormi", Spravodaj VUIS No. 8-10

9.- B. MATHER (1971), "Gide for Use of Admixtures in Concrete" ACI-Journ. 68/56, 646-676

10.- J.T. DAVIES et E.K. RIDEAL (1963), "Interfacial Phenomena", Academic Press, New York, p. 423

11.- O. HENNING et L. GORETZKI (1979), "On the Rheological Behavior of Cement Paste", Proc. II. Conf. Mechanics and Technology of Composite Materials, Varna

Air entrained pores in concrete

Air occlus dans le béton

Dr. Hans MARTIN, 4400 Steyr, Autriche.

RESUME

C'est un fait bien connu que la résistance au gel et au sel antigel du béton peut être atteint seulemnt par l'introduction artificielle d'air sous forme de bulles fines. La quantité d'air entraînée sous forme de bulles fines est déterminée aujourd'hui par des procédés macroscopiques assez bien perfectionnés, en général par 200 essais de gels et de dégels successifs dans une machine frigorifique. Quant aux petits chantiers, pour lesquels telle dépense serait trop élevée, il y a assez de règles pour une détermination empirique.

L'Autriche est située dans la zone limite variable entre le climat atlantique et le climat continental et c'est la raison pour laquelle il faut tenir compte d'une sollicitation alternée gel-dégel très fréquente pour les ouvrages. Durant des mois le point de congélation est dépassé environ deux fois par jour. Pour les barrages dans la haute-montagne les fluctuations de température quotidiennes peuvent atteindre 60°C/140°F. C'est là surtout que la question de l'air entraînée est brûlante. L'influence du gel permanent sur le béton est moins iportante.

La formation de bulles d'air peut avoir lieu seulement dans la portion du ciment. En Autriche on utilise pour la plupart du ciment Portland seulement, avec des additifs à savoir laitier, cendres volantes et trass. Il est à présumer que le procédé de la prise est un fait bien connu. Il a lieu d'après les lois de la physique des corps solides. Les travaux y rélatifs ont été recherchés par un microscope électronique à transmission et publiés il y a bien longtemps.

Quant à l'introduction d'air dans le ciment durci, on n'en sait rien. Pour cette raison le ministère de la construction d'Autriche a passé commande pour une recherche scientifique au "Zentrum für Elektronenmikroskopie" Graz. Cet institut est engagé d'une part à l'université et d'autre part à l'industrie. Chef de l'institut est le professeur Grasenick. Les recherches ont pour but la détermination de la forme des bulles d'air, leur comportement par rapport à leur milieu - le béton de ciment - ensuite les modes d'introduction possibles à savoir les types aptes à former des bulles d'air. En outre, le comportement de l'air occlus sous l'influence du dégel et de gel sera à l'étude. Ces recherches ne sont pas encore terminées etant donné qu'il s'agit de problèmes techniques et et expérimentaux très difficiles. De plus, il aura lieu de déterminer l'aspect des bulles d'air au bout de plusieurs années et de constater si elles se ferment ou si elles restent préservées. On a fait des essais dans le microscope électronique à balayage sur des éprouvettes de béton agées de plus de 20 ans et prélevées à des centrales d'énergie et des autoroutes. Les problèmes seront commentés en s'appuyant sur les essais effectués et on présentera des photos y relatives du microscope électronique à balayage sur l'affiche.

SUMMARY

It is well known that resistance against freezing and against thawing salts in concrete can only be obtained by means of introducing air pores. The amount of air pores to be entrained is today already determined with well-defined methods, in general by 200 freezing - thawing cycles in a freezing machine. For smaller building sites for which this method would be uneconomical there exist sufficient empirical rules for determining the required amount.

Austria is situated at the flowing boundary of atlantic (oceanic) and continental climate, thus a very frequent change between freezing and thawing has to be taken into account. For months the freezing point is crossed at least twice daily. At dams across valleys in the high mountains (Alps) daily temeratur fluctuations may amount to 60 centigrade (140°F). There the problem of air pores is especially important. Long-lasting frost, however, is of less influence upon concrete.

Air pores can only be formed in the cement portion of the concrete. In Austria nearly exclusively Portland cement mostly with addition of slags, flue dust, and optionally trass is used. The setting process of concrete is well known. It runs off according to the laws of solid-body physics. Papers on this item habe been worked out in the TEM and habe been published some time ago.

There is practically nothing known, however, about the incorporation of air pores into hardened cement. Therefore, the Research Centre for Electron Microscopy in Graz, Austria, obtained a research order by the Austrian Ministery for Structures (Buildings). That Institute is shared in equal parts by the University and by the industry, respectively. Head of the Institute is Prof.Grasenick. According to the Research Order the shape of the air pores, their behaviour with respect to their environment i.e. the cement stone, and also the possible ways to introduce them (possibilities of forming air pores) should be determined and studied, respectively. In addition, the behaviour of the air pores under the influence of thawing salts and at the ice formation is studied. The last-named studies are not yet terminated because of the difficult technical-preparative problems involved. Also, it should be determined how the air pores look like after periods of years, whether they grow together or remain unaltered. Over 20 year old concrete samples form high-way-roads and power stations have already been examined in the scanning electron microscope. The problems mentioned shall be discussed by aid of the conducted experiments and relating scanning-electron-microscopic pictures will be shown in posters.

In principle, the conglomerate concrete is a ternary compound. Due to external conditions, air may be added, however, as a fourth component to the components PC, aggregate and water. This does not mean air being present in the mixture because of insufficient compaction or an excess of water in the mixture, but air that is introduced artificially over various media. These air bubbles always have an approximately spherical form.

The enthalpy of formation is high, due to the high temperatures used in the burning of PC, and correspondingly also the inner potential plateau in PC is high. The generally known basic components C_3S etc. are unstable compounds.

Water is a very mobile combination, perhaps the most mobil at all. The transitions from molecule to ion are achieved in periods from 10^{-11} to 10^{-13} seconds. This also explains the high ability for solution with many substances. Now, if water is mixed with PC, the marginal layers of the cement grain are released from the bond as ion or molecule. Tests with isotopes of Ca, Si and Fe have shown that these particles are able to overcome large distances in short periods of time. It should be mentioned, however, that during the tests 2 cm had been considered as a very large distance, while under practical conditions the distance will be only about 100 to 1000 nm.

The solution is first saturated, then oversaturated and by recrystallisation now formations of growing up crystals are produced. Since the matrix is cognate, on the etched surfaces of the cement grains most of the new crystals will be of epitaxial kind, the rest topotaxial. In accordance with the laws of solid-state physics, the new formations should have a geometrical system of growing up crystals, but here they cannot have this kind of growth since the space is restricted. Therefore, they must grow statistically and this is also confirmed by pictures of the electron microscope.

Previously formation of gel in the marginal zone of the cement grain had been assumed as a working hypothesis. This certainly originates from the evaluation of the light-optical microscope which, however, by no means is in a position to supply the magnifications required to clarify the marginal conditions of the cement grain. The formation of gel is impossible at the transition from the cement grain to cement stone, for this would be in contradiction to the laws of solid-state physics. In order to obtain a maximum energy gain the elementary crystal must form itself in accordance with certain rules. Any further monocrystals are added in such a way that more and more energy is won. This is also the reason for the high strenght values of new formations.

Cement is burned from products which due to their geological compositions contain à large number of different minerals. This causes dislocations in new formations which, as a consequence, lead to a differing formation of the crystallization forms. An exact mineralogical definition is possible in a few cases only.

Crystallization leads to an interlocking of the cement grains and after a short time the crystal system shows higher strenghts than the cement grain itself. In the case of a break, the cement grain and not the crystal system will be torn apart.

There are no capillaries in the cement grain; this is clearly proved by great magnifications. The linkage is exclusively achieved by new formations. Le Chatelier's assumption has proved to be absolutely correct.

According to pictures made in the TEM the distance between the cement grains is approximately 100 nm after hardening. However, the release of marginal particles of the cement grain in water continues, the crystal system solidifies and this explains the increasing strenght caused by aging. Interlacement in the cement stone is so dense that the latter may be considered as watertight. On the other hand, the system is permeable formed by the constant transformation of water. They may pass and thus settle on all parts of the cement stone. Movement is then provided by temperature differences on the outside layers.

The bonding of cement stone to the aggregate is likewise achieved by recrystallization. Since, conditioned by the aggregate, the matrix differs greatly, the growth may be of epitaxial nature, but in most cases it will be topotaxial. In both cases the grown up product must have a statistical structure, since there is not enough space for geometrical systems. The cement-water solution in many respects is the outstanding bonding agent. It can form itself to a solid body, it can bind to aggregate, it penetrates through the oxide layers of steel and builds up a rigid connection on the metalically bound iron. Inspite of its high strenght it has a weakness: it can resist to crystallization pressures in its interior only to a limited extent. In many regions this is of no significance, for instance when there is no frost or when there is only permanent frost. However, if concrete is exposed to many changes of frost to thawing weather and vice-versa efforts must be made to protect him.

Somewhere about the year 1938 it had been found in the USA that, when using certain types of cement in road construction, freeze-proof concrete could be produced, with others not.

During that time we had lost contact with international science and thus we learned about works of this type only about 1950.

Austria is a country which is subject to a large number of changes in the zero-centigrade border due to the transition from the atlantic to the continental climate and the Alpine meteorogical devide.

Every power station, every bridge, every patch of motorway concrete has to be adapted to winter conditions. Moreover, Austria is a transit country, therefore motorway cincrete has to be treated, in addition, with thawing salt in order to keep the roads open for traffic.

Both freezing water and thawing salt produce high crystallization pressures in the interior of cement stone. As already mentioned above, the crystal systeme which generally provides the connections in the cement stone and in concrete, is permeable for water ionic form. Then it can-and it does in fact again change to the molecular conditions also. In every case it may freeze. Only ice I is involved, either as ich I_c or I_h. Ice I_c may be considered as metastable. For economic reasons, almost exclusively NaCl is used as

thawing salt, only at very low temperatures $CaCl_2$. Ionically dissolved both compounds penetrate into concrete up to a certain depth, then they recrystallize. As chemical compounds, they are without influence on concrete, but the crystallization pressure is to mention.

Crystallization pressure above ice formation and recrystallization of thawing salts are very high, they may be absorbed by concrete (most prominent component: cement stone) only to a limited extent.

By artifically introduced air bubbles it is possible to absorb these crystallization pressures. As a matter of fact, it was by mere chance that they discovered in the USA that by using Vinsol, concrete for road construction can be made freeze-proof.

Somewhere about the year 1950, they started also in Austria to introduce air bubbles into concrete which is endangered by frost. Initially tensides such as for instance spent sulfite liquor or Vinsol had been used. Over the long run spent sulfite liquor did not perform very well since its quality is too production-dependent. Depending on the type of wood used and the type of processing, mixtures of hexoses and pentoses will result which may have a detrimental effect since sometimes sugar has a good, in most cases, however, an unfavourable effect on concrete. It is difficult to control it anyway. Although as a natural product subjected to certain fluctuations, Vinsol is the most customary tenside and also the most used one. A prerequisite is that it must be basified: it should have a p_H value of more than 10.

Many tensides are obtained in the chemical industry as by-products which could gain importance, but among thousands of possibilities marginal conditions are given.

A tenside that should be introduced as an air-bubble-carrying material into concrete must ensure a certain bubble diameter, the bubbles must not be destroyed during the transport from teh mixer to the site, and they also have to resist to compaction. In such a case also the price is of significance, for in an order of many millions of cubic metres of concrete the use of air-bubble entraining agents is also an element which has to be taken into account also from a financial point of view.

The economic researches and the use and the required amount of additives will be determined macroscopically in the Test Institute or by the sitelab.. However, the combined effect of air bubbles and cement stone cannot be solved in such a way, for high magnifications are necessary in such a case. Here it is of importance to recognize the interrelationships in order to classify the various possibilities for the entraining of air bubbles.

These considerations prompted the Federal Ministry of Works in Austria to give to the Centre for Electron Microscopy in Graz a research assignment for exploring the behaviour of air bubbles in concrete. The director of that institute is F. Grasenick, the preparation, the direction of picture-shooting and the supervision of the microscopes used was in the hands of Mrs. J. Blaha.

From approximately 2000 pictures made of cement, aggregate, steel, and air bubbles it resulted that for pictures on which cement should be perceived a magnification below the 20,000-fold does not supply any definite information, but only - at most - a general idea. Useful are magnifications between the 60,000- and the 100,000-fold. Such pictures can be taken in the TEM only, preparation requires special experience.

This is different when taking pictures of artificially introduced air bubbles. In order to perceive the bubble at all, you must operate within a range of 1,000- to 7,000-fold magnification. For this pupose the REM is most suitable. It works very fast, an instantaneous shot may be made, and, moreover, a microanalysis which may be evaluted immediately. After having obtained a general idea, it is useful to make a picture of the inerior zones of the air bubbles with the maximum magnification to be achieved with the REM. However, an identification of the marginal zones of the air bubble requires much higher magnifications which can only be obtained in the TEM. For their evaluation great practical knowledge is needed.

Perfect investigations on cement stone can be made on fractured surfaces only. Cuts and subsequent grinding destroy the marginal zones, leave a heap of rubble on the bottom of the air bubble, the field of observation will be soiled to such an extent that neither pictures taken with the REM or the TEM nor a microanalysis will supply any conclusive evidence.

The preparation of fractured surfaces for TEM and TEM is difficult and requires great care. For the REM, gold-sputtering was chosen for the samples to be tested. Difficulties arise from the height and depht differences caused by the fracture.

In the TEM these differences of height and depht become still more apparent. By the fracture the air bubble suffers a sharp break, for its irradiation a Carbon-layer has to be applied which in many cases is torn off at the edge of the air bubble, even if gold-reinforced.
But this is of no importance if only the marginal zone remains undamaged. Thus, pictures could be taken which with a 600,000-fold magnification supplied information about the state of this marginal zone.

There are many possibilities to introduce artificial air bubbles into concrete. In general, this is achieved by means of tensides corresponding to the previously mentioned conditions. However, it is also possible to use prefabricated hollow bodies with a shell consisting of thermoplast or polyurethans.

In the subject tests the behaviour of air bubbles introduced via Vinsol, then via a tenside produced by Hüls-Marl, a thermoplast hollow body from AKZO and a PU hollow body from Bayer have been investigated. Although all of these products show different structures it was a great suprise that under load they all behave in the same manner.
In tensides the molecules turn with their hydrophilous part towards the outside, the hydrophobe part keeps away water so that a waterfree space is created which indicates the air bubble. Yet this molecularly formed "hedgehog" could not endure permanently, it needs support. As usual, cement stones is formed on the outside according to its

crystalline structure and keeps at first its shape. Simultaneously on the inside of the air bubbele margin a tiny, but very dense support structure is formed which fixes the air bubble. There is no doubt that the tenside layer allows ions to pass, and the same is surely true also for the support structure. Whether or not these two layers allow also molecules to pass cannot be said as yet, however, this problem is of minor imoortance because almost all components of cement, thawing salt and, of course, also water may be figuring ionically. Likewise it cannot be clarified as yet whether or not tensides are persisting after their use, here magnifications of at least 1 nm will be required. The microscopes certainly can do the job, but the problem of preparation is still unsolved. But this is not an important question, what matters is only that the air bubble fulfils its function.
The permeability of the tenside layer and of the support structure means that ionically solved water and thawing salt may penetrate into the air bubble.

Crystallization pressures are very high, but the enlargement of volume caused by them is relatively insignificant. Only little hollow space is required to allow well prepared cement stone to absorb the rest of the crystallization pressure.
This task is performed by the artificially introduced air bubble.

This is proved by pictures taken from samples of more than 20 years old concrete. Water may penetrate into the air bubbles and freeeze without doing damage to cement-stone, just like thawing salt simmers down in the pore. The process must be reversible for it is repeated often.

After thawing water is withdrawn from the air bubble to such an extent that only the rest (corresponding to the steam pressure) is left. As shown by pictures, thawing salt forms topotaxies on the inside of the air bubbel which, however, remain within certain limits.

To investigate old air entrained concrete, samples had been drilled out of the concrete used in the power station of Ybbs an der Donau (200 MW, 1250 GWh) built from 1954 to 1957, and from two patches on the motor highway A 1 where the concrete had been laid during the same period. In order to avoid any damaging, the samples had been removed by diamond bits. It was intended to find out whether or not the air bubbles are still efficient after such a long time.

Every river is moving finest particles in its boulder drifts. The Danube - within the Upper Austrain territory might be classified as a torrent - produces a lot of small material due to turbulences. Concrete samples had been drawn from the sluice wall, the pier wall and a weir pillar.
The pictures taken in the REM have shown for the sluice wall that the air bubbles are provided with a thick interior lining of fine mud up to a depht of approxinately 2 cm. This proves that the air bubble - at least after some time - is also permeable for material beyond the molecule range. Perhaps in this case also the outside stress is decisive, the strain by the numerous lock lifts is high. In a depht of more than 3 cm the air bubbles were free of any fine particles, the natural interior grown up crystals were clearly.discernible, the reduction of the volume of the air bubble is affected only very little.

The examined weir pillar is subject to different outside effects. By the continuous flow of water around the pillar there is no fine mud, the air bubbles are free from it.
Also here, within the area of rapid fluctuations of the water level, only the usual subsequent crystals will be found in the interior of the pore, they affect the volume of the air bubble only slightly.

On the above mentioned places of the motor hinghway A 1 - they are located within the section Enns-Linz-Sattledt, in a zone which is heavily affected by a change of frost and thawing - it was intended to determine the long-term stresses of ice pressure and simultaneously the effects of thawing salt. The combination of crystallization pressures from ice and thawing salt causes a lot of changes of the interior pressure so that surprises had to be expected. Then it was surprising that in spite of ice, recrystallization of thawing salt and the usual calcium oxide hydrates the volume of the air bubbles was reduced only up to a maximum of 30 %.

Due to the high processing speed of the concreting machine units, the air bubbles are smashed in the uppermost concrete layer and the laitance is drawn upwards. This uppermost layer is then also the weakest part of the roadway-platform concrete which, however, is quickly removed by the braking and acceleration manoeuvres of heavy motor vehicles. This unfortunately results in track grooves. After the removal of this thin upper layer a perfect, freeze-resistant and thawing-salt-proof road top layer will be left.

We are able to prove these facts clearly in the REM an the TEM.

Essai d'action d'addition polyfonctionnelle sur les bétons

Study of action of multi-purpose admixture upon concretes

BAGENOV Y., professeur, docteur d'état, chef de chaire,
RATINOV B., professeur, docteur d'état,
ROSENBERG T., docteur d'état,
TCHUMAKOV V., docteur d'état, directeur de l'Institut du béton armé, URSS.

Résumé

Les additions complexes qui se composent de deux et plus matières organiques et minérales permettent renforcer entrainement de l'air, augmenter la plasticité de bétons frais, la compacité et la résistance au gel des bétons. Combinaison de deux additions hydrophobes (abietat de sodium et brai de goudron de bois saponifiable) renforce entrainement de l'air. La valeur d'entrainement de l'air est additif.

Les additions complexes se composent de matières homonènes augmentant la plasticité de bétons frais conformément á principe d'additivité.

L'effet de renforcement réciproque existe en cas d'utilisation d'additions de composants dont le mécanisme de plastification est différent.

Les additions complexes qui se composent de matières organiques ralentissent la prise du béton.

L'utilisation d'additions qui se compose de matière organique et électrolyte permet de diriger le prix du béton en utilisant le propriété d'électolyte d'accélérer la prise du béton.

Les additions qui se composent d'électrolytes et d'adjuvants entraineurs d'air augmentent la compacité du béton. Les additions qui se composent d'électrolytes, nitrites - nitrates - chlorures de calcium (NNHK) abietat de sodium (SNB) augmentent la résistance au gel du béton.

En examinant l'action d'additions sur les liants minéraux on considère le schéma cristallin pour le durcissement de celles-si. Selon ce schéma les phases métastables se dissoudrent avec formation de solutions sursaturées par rapport de composées hydratées qui cristallisent sous les phases finales et intermédiaires.

Par conséquent les processus d'hydratation de liants minéraux on peut considérer comme un ensemble de processus dont la vitesse est limitée par solubilisation des phases initiales.

La résistance de pierre de ciment de la dispercité est faciée de produits d'hydratation et aussi de liaisons entre eux.

L'espèce de contacts essentiels est coagulant jusqu'à la formation de structure capillaire et poreuse. Par la suite sur le fond se forment les contacts cristallins "atomiques" et contacts cristallins "de phase", qui assure la formation au début la carcasse cristalline et par la suite sa consolidation. Les contacts d'assemblage direct prédominent dans les liants monominéraux.

La structure de liants polyminéraux se forme en résultat d'engrenage et d'enchevêtrement des cristaux.

L'espèce poreux se forme en même temps que la phase solide. Celui-ci et les forces d'adhésion entre la pierre de ciment et de granulats ont une grande influence sur la propriété des bétons.

Essai d'action d'additions différents sur les processus de dursissement de liants minéraux permet choisir la composition d'additions multicomposants. Ci-dessous on fait l'analyse de l'influence d'additions multicomposants sur l'entrainement de l'air, la plasticité, la durée de prise et la structure de pierre de ciment ce que détermine la résistance à la compression et la résistance au gel des bétons.

1. L'entrainement de l'air

Les additions qui s'adsorbent sur les liants et ensuite sur les cristaux de nouvelles phases possèdent la propriété d'entrainement de l'air. Ce phénomène dépend de tension superficielle à la frontière liquide - air - σ_{12}.

Moins grande est la valeur de tension superficielle plus grand est la valeur d'entrainement de l'air.

La plus grande valeur d'entrainement de l'air donne l'addition hydrophobe qui participe dans les réactions chimiques avec les produits d'hydratation de liants minéraux.

L'introduction des deux additions hydrophobes comme par exemple abietat de sodium et brai de goudron de bois saponifiable peut provoquer l'entrainement de l'air dont la valeur est additive en présence de petite quantité d'additions ou moins d'après le principe d'additivité en présence de grand quantité d'additions. Cet effet s'explique par présence dans le deuxième cas de "concurrence" entre les additions. (tabl.1).

Ceci s'explique de ce que dans le dernier cas l'addition dont les propriétés tensio-actifs sont plus grands détermine la valeur d'entrainement de l'air.

L'addition hydrophile donne le même résultat.

L'utilisation de mélange d'additions, celle hydrophile (SDB) et hydrophobe dont la valeur est additive provoque l'entrainement de l'air.

La combinaison d'additions hydrophiles et hydrophobes nous permet obtenir l'entrainement de l'air stable dont la valeur et dimensions de bulles d'air ne dépendent de consommation du ciment.

Les additions-"superplastifiants" (des produits de condensation acide naphtalène - sulfonique ou acide mélamine - sulfonique avec formaldéhyde) ne changent pas la valeur de σ_{12}.

Ils n'ont pas d'influence sur la valeur d'entrainement de l'air ou bien le diminuent dans le cas d'utilisation acide sulfonique mélamine - formaldehyde.

L'utilisation des "superplastifiants" avec d'adjuvants entraineurs d'air nous permet conserver des propriétés de chaque composant.

2. L'effet plastifiant d'addition complexe

Les additions plastifiants, ce sont en général les matières organiques qui absorbent sur la frontière des phases et qui diminuent la valeur σ_{12} ou l'énergie sur la frontière solide-liquide σ_{32}.

Les additions "superplastifiants" possèdent des propriétés analogues. Ils provoquent l'effet de désagrégation des particules de ciment et de graissage hydrodynamique.

Mais aussi il y a des additions (poudre d'aluminium) qui provoquent l'effet de plastification en résultat de formation des bulles d'air qui jouent un rôle de graissage. Il existe aussi l'effet de plastification d'électrolytes, par exemple chlorures de calcium etc.

En étudiant l'effet de plastification d'addition complexe on a établi des régularités suivantes.

a) Si les additions complexes se composent de même classe elles provoquent l'effet de plastification additive ou en tout cas plus grand que ceci de chaque composant (tabl.2).

Premièrement, par conséquant, l'utilisation en qualité d'addition des fractions de produits chimiques dont les capacités de plastification sont considérables peut augmenter leur activité spécifique, mais elle a une limite d'après ce signe et ne peut pas donner augmentation importante de plasticité de béton frais.

Deuxièmement, le mélange de plusieurs additions plastifiants de même type ne donne pas la possibilité d'obtenir un addition "superplastifiant" par l'effet de renforcement d'action de chaque composant d'addition complexe.

L'utilisation de cet espèce de mélange est raisonnable au cas que soit la possibilité de diminuer le prix.

b) On peut renforcer l'effet de plastification au cas que l'addition complexe se compose de constituants dont les mécanismes de plastification sont différents, par exemple électrolyte et plastifiant naphtalène formaldehyde (NF) (tabl.3).

On a utilisé dans cette recherche comme additions électrolytes chlorures de calcium et nitrites - nitrates de calcium en rapport de 1:1, nitrites - nitrates - chlorures de calcium en rapport de 1:1:2, acétate et sulfates socium en rapport de 1:1.

3. La durée de prise de béton avec les additions complexes

Les agents tensio-actifs augmentent la durée de prise de ciment en ralentissant la solution /1/.

Le facteur compensateur est désagrégation des particules du ciment /5/ ce qui a une grande valeur avec utilisation de "superplastifiants" mélamine - naphtalène - formaldéhyde.

La désagrégation augmente la surface de réaction ciment - eau et la vitesse de solution des particules du ciment.

Le facteur compensateur est aussi la formation de particules dispersionneles avec la dimension critique d'après l'équation Kelvine

$$r_{cr} = \frac{2Vc}{RT \ln \frac{C}{C_\infty}} \sigma_{32} \quad (1)$$

V_c - volume moléculaire

R - constante des gaz

T - température absolue

$\frac{C}{C_\infty}$ - sursaturation

L'action positive sur la cinétique d'hydratation peut avoir augmentation de vitesse de cristallisation dont la possibilité montre l'équation Gibbs - Folmar

$$\alpha = A \cdot \exp^{-\frac{\Delta Z \max}{RT}} \quad /2/$$

α - valeur proportionnelle de vitesse de formation de germe cristallin

A - multiplicateur préexpotentiel

$\Delta Z = \frac{4}{3} \pi \frac{r^2_{kp}}{RT}$ - énergie libre

R, T et Z_{kp} - les mêmes que dans l'équation /1/

Les certaines additions organiques peuvent augmenter la vitesse d'hydratation en résultat de réaction d'échange des ions ou coordination (acides carboniques, certaines amines etc.).

L'effet de frénage de processus d'hydratation qui augmentent avec la concentration d'addition prédomine pour la plupart d'additions organiques á l'exeption d'additions "superplastifiants".

Cela permet augmenter la dose de celles-ci sans appréhension de ralentir la durée de prise de béton.

Deux additions organiques ou plus ralentissent la durée de prise du béton plus qu' une addition. Mais l'effet de synergie est absent dans ce cas. Si la consentration d'une des additions (p.ex.addition hydrophobe) est moins que de l'autre (p.ex. addition hydrophile) cette dernière addition détermine la durée de prise.

La combinaison d'additions organiques et d'électolyte nous permet de changer considérablement la durée de prise de béton (Fig.1).

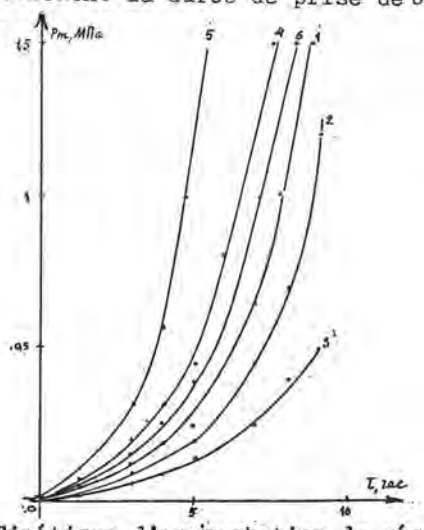

Fig.1. Cinétique d'augmentation de résistance plastique de mortier en présence d'additions.
1. Echantillons sans additions
2. 0,15 SDB : 3-0,7% NF
3. 0,7% NF + 2% NNHK
4. 2% NNHK, 5.0,15%SDB+0,7NF+2%NNHK

Cela nous donne la possibilité de diriger la cinétique d'hydratation.

4. La formation de structure de pierre de ciment avec l'introduction d'additions complexes

Les additions-électrolytes augmentent la compacité de pierre de ciment en grandissant la quantité de micropores et de pores de gel dans le volume de pores de pierre de ciment (tabl.4, fig.2).

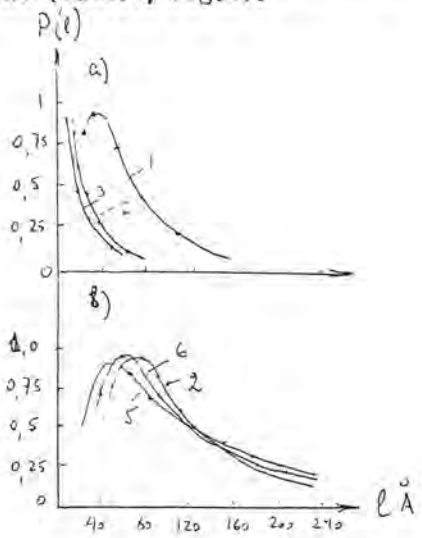

Fig.2. Résistance au gel de béton étuvé en dépendant de continue volumique de gel.
1. Béton sans additions
2. 2%ННХК+0,15% SDB; 2%ННХК+0,02%CHB.

Les additions qui composent sulfates, chlorures ou nitrates - ions (p.ex. nitrite - nitrate - chlorure de calcium) renforcement par des cristaux de sels de hydrates (hydrosulfo, hydrochlorures et hydroaluminates de calcium). Ces cristaux forment la structure primaire de pierre de ciment avec son renforcement par hydrocilicates et hydroaluminates de calcium. Tout cela agrandit la compacité et l'imperméabilité à l'eau de pierre de ciment. L'amélioration de la structure de pierre de ciment par la compacité avec l'introduction d'additions plastifiants et d'électolytes ainsi que l'abaissement de la température de congélation de glaces en présence de ces additions augmente la résistance au gel du béton.

L'action d'adjuvants entraineurs d'air ou d'additions génératrices de gaz se distingue de l'action d'électrolytes et additions plastifiants. La combinaison d'adjuvants entraineurs d'air et d'électrolytes permet utiliser l'avantage de celles-ci et des autres et obtenir les parois de pores plus denses et résistants avec la conservation de caractère de leur distribution par rayons et dimensions moyennes obtenues á l'aide d'adjuvants entraineurs d'air.

Les recherches ont montré que l'utilisation d'additions complexes d'électrolyte et de matières tensio-actives (p.ex. abietat de natrium CHB, lignosulfonat de calcium CDB) augmentent considérablement résistance au gel du béton que l'introduction d'une addition ou l'utilisation des bétons sans additions.(Fig.3)

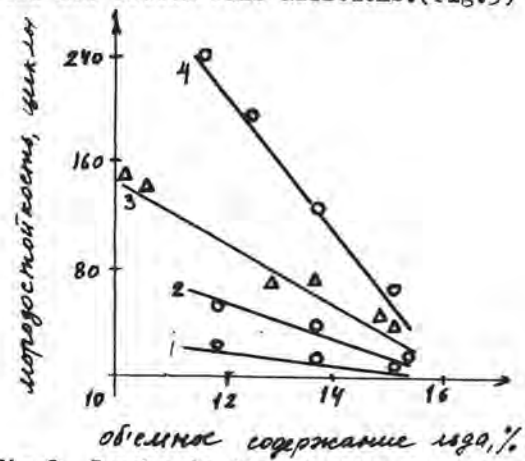

Fig.3. Courbe de distribution de dimensions de pores dans la pierre de ciment.
a) durcissement normal;b)étuvé de 80°C
1 et 2 - sans additions
3 et 4 - 1%CH_3COONa+1%Na_2O_4+0,2%SDB
5 et 6 - 3% НХК

BIBLIOGRAPHIE

1. - RATINOV V.,ROSENBERG T."Additions pour les bétons", Stroiizdat, 1973
2. - NOVGORODSKY W., RATINOV V., STANTSEL I. "Formation de structure des liants minéraux en présence d'additions complexes", TSNIIselstroi, № 19, 1977.
3. - RATINOV V. et autres. "Additions complexes pour les bétons". Bulletin de recherches № 38.
4. - TAOUBE P., TCHUMAKOV Y., RATINOV V. "Variation de dispersité de ciment hydraté en présence d'additions"., "Ciment" № 2, 1980
5. - BAGENOV Y., MAMAIEVSKY V. et autres. "Béton á haute résistance avec additions complexes".

Tableau 1

Augmentation de porosité du mortier avec additions organiques

Addition	Consentration d'addition, %% de masse de ciment						
	0,05	0,1	0,15	0,2	0,3	0,4	0,5
SDB	0,8	1	1	1,2	2	3,5	4
SNB	3,8	4,8	5,8	6,5	7	7,7	8
Brai de goudron de bois savonné	0,2	1	1,6	3	5	6	6,5
SDB + SNB 1:1	4,2	5,5	7	7,8	10,5	12,8	14,8
Brai de goudron de bois savonné + SNB 1:1	3,8	5	5,8	6,5	9,4	11	12
Brai de goudron de bois savonné + SDB 1:1	1,4	3	5	6,5	8,2	9,2	10,2

Tableau 2

Plasticité du mortier (ciment:sable 1:4 E/C = 0,65) en présence d'additions hydrophiles

Ciment	Addition %% envers la masse de ciment		Plasticité, mm
	NF	SDB	
M - 400	abs.	abs.	106
	0,7	abs.	145
	-	0,15	126
	0,7	0,15	162
M - 400	abs.	abs.	114
	1	-	143
	-	0,15	124
	1	0,15	149
	-	0,3	139
	1	0,3	170

Tableau 3

Plasticité de mortier de ciment de composition 1:4 (ciment - sable) E/C = 0,65 avec additions complexes

Addition %% de masse de ciment				Plasticité en mm	
NF	NNF	$CaCl_2$	MNXK	fact.	Attandu ayant en vue additivité d'action d'addition
-	-	-	-	114	-
1	-	-	-	145	-
-	-	1	-	123	-
-	-	2	-	125	-
-	-	7	-	120	-
1	-	1	-	159	154
1	-	2	-	165	156
1	-	7	-	184	151
-	7	-	-	121	-
-	10	-	-	115	-
1	7	-	-	177	152
1	10	-	-	200	146
-	-	-	1	120	-
-	-	-	2	123	-
-	-	-	3	121	-
-	-	-	7	121	-
1	-	-	1	150	151
1	-	-	2	168	154
1	-	-	3	180	152
1	-	-	7	195	152

Tableau 4

Indices de structure du béton á l'age de 28 jours selon le genre d'additions x)

Addition	Porosité ouverte intégrale	Volume de l'air entrainée xx)	Dimension moyen de pores	Rayon moyen des pores
Abs.	14	1,1	1,7	520
3%NNHK	13,6	0,4	1,6	370
3%NNHK + 0,15 SDB	12,8	2,6	1,3	420
0,15% SDB . +0,03%SNB	12,7	8,8	1,1	3700
3%NNHK + 0,03% SNB	13,4	6,6	0,8	1200

x) Consommation de ciment - 440 kgs/m^3, E/C = 0,5

xx) On détermine le rayon moyen des pores en utilisant la mesure des pores á mercure. Le rayon á la dimension jusqu'á 10^5 A^0.

Propriétés du béton et activation chimique du durcissement

Concrete properties and chemical activation of solidification

L.B. SVATOVSKAIA, M.M. SYTCHEV, V.Y. ANDRIEVSKAIA, P.G. KOMOKHOV,
M.S. BARVINOK, Leningrad, U.R.S.S.

RESUME: Dans la communication on a envisagé l'enfluence des activateurs-plastificateurs inorganiques sur le durcissement des mélanges de béton. On a montré que l'introduction des chromates et des thiosulfates et de leur mélanges conduit à l'accroissement de la résistance précoce et standard du ciment durci, à la diminution du rapport E/C, à l'augmentation de l'imperméabilité à l'eau, à la diminution des déformations de retrait, à l'accroissement de la résistance à la corrosion des béton.
L'action des compositions combinées élève les propriétés techniques râce à la formation du soufre à l'état amorphe, trés fin.

SUMMARY: The effect of inorganic activator-plastifiers on hardening of concrete mixtures is studied. It is shown that introduction of chromates and thiosulphates and of their mixtures results in increase of early and grade strength of concrete stone and of water impermeability and corrosion resistance of concretes and in decrease of W/C ratio and shrinkage strains.
Combined compositions also increase technical properties due to formation of sulphur in amophous highly dispersed state.

Pour augmenter la résistance lors de l'étuvage et dans les conditions de durcissement normal, abaisser le rapport e/c et améliorer d'autres propriétés techniques des bétons on peut utiliser les activateurs inorganiques d'action polyfonctionnelle qu'on choisit en partant des faits suivants. Pour l'intensification du durcissement l'oxydation des composés introduits en tant qu'activateurs est indésirable (1 à 3). Au contraire, l'introduction dans le système durcissant de corps simples et composés contenant des éléments à hauts degrés d'oxydation (permanganates, chromates, bichromates) conduit à la plastification du mélange de béton et à l'accroissement de la résistance précoce (à l'âge de 1 ou 2 jours) et standard.

Les données du Tableau I montrent que le chromate de potassium et le thiosulfate de sodium servent d'activateurs du durcissement ; notons que, la plasticité du mélange de béton restant la même, on peut observer la diminution du rapport eau/ciment, ce qui conduit à un plus fort accroissement de la résistance.

Le Tableau II pour les bétons et les Tableaux III et IV pour les mortiers montrent que l'introduction du chromate de potassium peut éliminer l'étuvage du béton en abaissant la perméabilité à l'eau et les déformations par retrait. Ainsi le béton sans addition se caractérise par la perméabilité à l'eau de 2 atm (B = 2). Le béton avec addition de l'activateur de durcissement en quantité de 2 % de la masse du ciment a supporté la pression de 10 atm (B = 10).

Les déformations par retrait des bétons étaient déterminées sur trois échantillons-jumeaux de dimension de 10x10x30 cm. La base de mesure du retrait était de 300 mm. Les essais étaient effectués dans une chambre spéciale (avec le régime de réglage automatique) à la température de 30 °C ± 2 °C et à l'humidité de 55 % ± 3 %. Les déformations par retrait étaient mesurées par l'indicateur à cadran dont la valeur de la division était de 0,01 mm. Parallèlement à la mesure des déformations on a contrôlé la perte en poids des échantillons de béton. Les résultats concernant la cinétique de variation des déformations par retrait et de la perte en poids du béton ont montré que l'introduction de K_2CrO_4 (2 % de la masse du ciment) diminuait sensiblement la valeur des déformations par retrait. Ainsi le béton sans addition à l'âge de 60 jours avait le retrait de $80 \cdot 10^{-5}$ et le béton avec addition, de $45 \cdot 10^{-5}$, i.e. pour le béton avec addition le retrait diminue presque de 2 fois. L'addition dans le béton stabilise le développement du retrait vers 28 jours de durcissement. Pour le béton sans addition la stabilisation du retrait s'observe vers 50 jours. Les données concernant la perte en poids des échantillons de béton sont en bon accord avec le développement des déformations par retrait.

Les données relatives à la résistance au gel des échantillons (Tableau V) témoignent qu'avec l'introduction du chromate la résistance au gel ne s'empire pas et pour certains ciments elle augmente sensiblement. L'efficacité de l'utilisation des additions contenant le chrome peut être augmentée en partant de l'idée de la réalisation du processus d'oxydo-réduction dans le système avec l'introduction simultanée de composés contenant le chrome et de thiocomposés (4). Dans ce cas, à côté d'une diminution encore plus importante du rapport eau/ciment on peut assister à la séparation du soufre à l'état amorphe très fin :

$$3Na_2S_2O_3 + 2K_2CrO_4 + 5H_2O =$$
$$= 4KOH + 2Cr(OH)_3 + 3Na_2SO_4 + 3S$$

$$3Na_2S + 2K_2CrO_4 + 8H_2O =$$
$$= 4KOH + 2Cr(OH)_3 + 3S + 6NaOH$$

Les données du Tableau VI montrent que cette voie assure un grand effet plastifiant, l'accroissement de la résistance et l'amélioration d'autres propriétés techniques liées à l'augmentation de la densité du béton grâce au colmatage des pores par le soufre et à la diminution du rapport eau/ciment. Les compositions des bétons avec addition de sulfures n° 8, Tableau VI, montrent une prise rapide, ce qui rend possible leur utilisation en tant que compositions Torkret de résistance élevée.

Les études physico-chimiques ont montré que l'accroissement de la résistance s'accompagnait d'une augmentation de l'eau chimiquement liée et des changements dans la composition des phases des échantillons.

TABLEAU I

n°s d'ordre	Activateur	% du poids du ciment	Consommation du matériau par 1 m³ du béton, kg				E/C	Résistance à la compression, MPa, à l'âge, jours			
			ciment*	sable	gravillon	eau		1	2	7	28
1	-	-	300	990	1041	170	0,6	3,6	7,5	11,0	18,0
2	K_2CrO_4	1	300	990	1041	170	0,6	8,0	14,0	20,0	24,0
3	K_2CrO_4	1,5	300	990	1041	170	0,6	9,2	15,0	21,5	24,5
4	-	-	292	893	1007	166	0,57	-	8,0	11,0	20,0
5	K_2CrO_4	1	292	893	1007	166	0,57	-	18,5	25,0	26,0
6	-	-	250	772	1152	170	0,68	2,5	12,5	13,6	18,2
7	$Na_2S_2O_3$	1,5	250	772	1152	170	0,68	5,0	12,7	15,0	26,5

* Ciment de type "400", durcissement normal.

TABLEAU II

n°s d'ordre	Types de ciment	Type et quantité de l'activateur, % de la masse du ciment	Consommation du matériau par 1 m³ du béton, kg			Eau-ciment	L	Résistance à la compression, MPa				
								Durée de stockage, jours				
			C	MSG	G			1	2	3	7	28
1	Ciment M-500	Témoin, sans addition	292	893	1007	0,57	19	4,0	10,5	13,5	18,0	28,9
2	"	0,8 % K_2CrO_4	"	"	"	0,57	14	9,7	18,0	21,5	27,4	25,6
3	"	1 % K_2CrO_4	"	"	"	0,54	14	11,5	18,5	24,0	27,0	28,5
4	"	2 % K_2CrO_4	"	"	"	0,54	12	9,6	18,0	24,2	26,3	28,0
5	"	3 % K_2CrO_4	"	"	"	0,54	19	7,5	18,0	21,0	36,0	28,5
1	Ciment M-500	Témoin, sans addition	380	735	1103	0,48	11	7,5	12,0	16,2	25,2	27,0
2	"	0,5 % K_2CrO_4	"	"	"	0,46	11	17,5	26,2	-	37,0	42,3
3	"	1 % K_2CrO_4	"	"	"	0,44	11	19,2	27,3		39,1	45,5
4	"	2 % K_2CrO_4	"	"	"	0,43	11	19,6	30,3		40,3	43,2
5	"	3 % K_2CrO_4	"	"	"	0,42	11	19,1	30,9		39,1	40,4

TABLEAU III

E/C	Plasticité (affaissement du cône), mm	Quantité de $Na_2S_2O_3$, %	Résistance à la compression et à la flexion, MPa, après			
			1 jour	3 jours	7 jours	28 jours
0,43	125	sans addition	10,9 / 2,8	26,9 / 4,7	33,1 / 6,0	45,2 / 6,2
0,40	"	1,0	13,6 / 3,4	27,6 / 6,0	38,5 / 6,8	48,0 / 7,9
0,39	"	2,0	17,7 / 4,0	31,5 / 6,6	39,4 / 6,6	50,6 / 8,3

Suite du Tableau III

E/C	Plasticité (affaissement du cône), mm	Quantité de $Na_2S_2O_3$, %	Résistance à la compression et à la flexion, MPa, après			
			1 jour	3 jours	7 jours	28 jours
0,39	"	3,0	18,2 / 4,2	37,1 / 6,9	43,0 / 6,9	55,0 / 8,7
0,375	"	4,0	17,7 / 4,5	40,1 / 6,8	44,7 / 7,7	54,5 / 8,5

TABLEAU IV

E/C	Plasticité (affaissement du cône), mm	Quantité de K_2CrO_4, %	Résistance à la compression (numérateur) et à la flexion (dénominateur) MPa, à l'âge de			
			1 jour	3 jours	7 jours	28 jours
0,45	125	sans addition	12,3 / 3,05	25,0 / 4,9	28,6 / 5,7	51,2 / 7,0
0,42	"	0,5	15,3 / 4,0	35,0 / 6,1	35,4 / 6,8	51,3 / 7,1
0,42	"	1,0	16,2 / 4,0	30,5 / 6,3	35,4 / 7,0	51,8 / 7,6
0,41	"	1,5	20,5 / 4,6	36,0 / 6,9	40,3 / 8,2	52,0 / 8,7
0,40	"	2,0	23,1 / 4,3	35,2 / 7,2	40,3 / 8,3	50,7 / 8,5
0,41	"	3,0	19,5 / 4,5	30,9 / 7,1	36,9 / 8,1	51,0 / 8,9
0,42	"	4,0	18,5 / 4,2	28,6 / 6,8	34,0 / 7,3	46,7 / 7,5

TABLEAU V

Caractéristique du béton	Consommation du du ciment, kg/m³	E/C	Résistance à la compression, MPa, après			Résistance à la compression, MPa, après			Résistance à la compression, MPa, après		
			10 RG	contr.	coeff. RG	20 RG	contr.	coeff. RG	30 RG	contr.	coeff. RG
Sans addition, ciment Volkhovski	380	0,48	29,9	31,7	0,94	28,4	33,3	0,85	24,2	37,8	0,64
Avec addition de K_2CrO_4, 2% de la masse du ciment	380	0,43	34,4	37,5	0,92	35,4	40,5	0,86	27,6	42,2	0,65

TABLEAU VI

n^os d'ordre	Type de l'activateur-plastificateur	Quantité de l'addition, % de la masse du ciment	Consommation des matériaux par 1 m³ du béton, kg			Eau, l	E/C	L, s	Résistance à la compression, kg/cm², après			
			ciment	sable	gravillon				1 jour	2 jours	7 jours	28 jours
1	-	-	400	760	1090	164	0,42	25	75	215	325	395
2	K_2CrO_4	3	400	760	1090	0,38	0,38	25	155	384	440	440
3	K_2CrO_4+$Na_2S_2O_3$	2 + 3	400	760	1090	136	0,34	25	165	330	400	400
4	$Na_2S_2O_3$	2	400	760	1090	120	0,36	25	120	265	313	380
5	-	-	250	772	1158	170	0,68	20	25	125	140	200
6	K_2CrO_4+$Na_2S_2O_3$	2 + 3	250	772	1158	125	0,5	20	110	256	390	400
7	-	-	250	772	1158	137,5	0,55	20	63	185	225	370
8	K_2CrO_4+Na_2S	3 + 1	250	772	1158	137,5	0,55	20	123	200	240	350

CONCLUSIONS

Afin de diminuer le rapport eau/ciment, d'augmenter la résistance précoce et standard du béton dans les conditions de stockage normales, de diminuer les déformations par retrait et d'accroître l'imperméabilité à l'eau il est recommandé d'utiliser les activateurs-plastificateurs inorganiques : chromates, thiosulfates et leurs mélanges. Les compositions à base des chromates sont en même temps des inhibiteurs de corrosion de l'armature en acier.

INDEX DES AUTEURS

AUTHORS INDEX